

Q
1
S3
V. 83
1980

Sai

PAMPHLET BOX

Physics Abstracts

Science Abstracts Series A
July-December 1980

Subject Index (A - L)

U.I.C.C.
MAR 8 1981
LIBRARY

inspec
The Institution of Electrical Engineers

CONTENTS

Title page	i	Subject index	S1809
Abbreviations and acronyms	iii		

SIX-MONTHLY INDEXES TO SCIENCE ABSTRACTS

Cumulative indexes to Science Abstracts are published twice a year covering the period January-June and July-December. They comprise author and subject indexes and some specialised or 'small' indexes. For Physics Abstracts and Electrical & Electronics Abstracts the Author Index and Subject Index are published as separate volumes. In this case the Small Indexes are included in the Author Index volume.

Cumulative author and subject indexes for preceding years are also available. For details please see inside back cover.

Subject Index

The Subject index provides an alphabetical subject key to the articles included in the abstracts journal. Some general guidance on its use is given below:

1. Look in the index for the name of the specific subject in which you are interested. In most cases this name will be a heading in the index and you will find relevant articles listed under it. The majority of the subject headings fall into the following categories: property, phenomena, substance or named objects, instrument, device, theory, method, process, application, event.
2. Occasionally you will be directed from the subject heading chosen to a different heading under which the relevant or additional articles are listed.
3. If you do not find the subject heading you first chose, try a more general heading.
4. Each entry under the heading relates to an article appearing in the abstracts journal and gives the serial number of that article in the journal preceded by the last digit of the current year, e.g. 0-12345; i.e. Abstract number 12345 in the abstracts journal for 1980.

The language of the article, if it is not in English, is also indicated. e.g. digital frequency meter jamming, distribution function determ. (Russian) 0-41575.

Each entry starts with a Keyword or Keyphrase considered to be most relevant to the heading. On sorting these Keywords, the qualifying prefixes are usually ignored. (e.g. α -brass, 5-sulphosalicylic, 31 Cygni, n-Ge are sorted under brass, sulphosalicylic, Cygni, Ge respectively).

There are three main Keyword lists; alphabetical A-Z, elementary particles, and chemical symbols (organic substances are written and not given as chemical formula). More than one Keyword list may be present under each subject heading.

For document on, say, 'photoemission of germanium' at least two access points 'photoemission' and 'Germanium' are provided. Under the heading 'photoemission' the Keyword will be 'Ge' and under 'germanium' the Keyword will be 'photoemission'.

In a case like this, it is advisable and quicker to use the heading 'photoemission' and go straight to the chemical symbol list for 'Ge'.

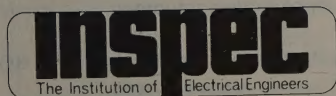
Intermetallic compounds are indexed under the appropriate alloy headings. The chemical formula is used as Keyword. However, it is important to realise in searching the chemical symbol list that, at present, alloys and intermetallic compounds are sorted separately. For example FeCo is sorted at the end of the Fe- list e.g. Fe-Al, ... Fe-Co, ... Fe-Si, ... Fe-Si-B, ... FeCo, ... FeSi and so on in this order.

Physics Abstracts

Science Abstracts Series A

July-December 1980

Subject Index (A - L)



Physics Abstracts is published twice monthly by the Institution of Electrical Engineers. Twice-yearly subject and author indexes covering the period January-June and July-December are included in the subscription. Printed by Unwin Brothers Ltd., Old Woking, Surrey, England. Second class postage paid at Piscataway, NJ 08854 USA. POSTMASTER: Send address changes to INSPEC/IEEE SERVICE CENTER, 445 Hoes Lane, Piscataway, NJ 08854

© 1981: THE INSTITUTION OF ELECTRICAL ENGINEERS

Abbreviations and Acronyms

Abbreviations and acronyms are used in the modifiers in all INSPEC Cumulative Subject Indexes. Individual terms should be readily understood in the context of the subject headings. **Inorganic substances** are usually given by their chemical formulae. Iron and aluminium garnets appear in the formulae lists as MIG and MAG (where M is metal element, e.g. YIG and YAG); (Pb,La)(Zr,Ti)O₃ and Ce₂Mg₃(NO₃)₁₂ appear as PLZT and CMN respectively. **Organic substances** including **liquid crystals** are not given as formulae but common abbreviations are used.

ABS resin	acrylonitrile-butadiene-styrene	CRO	cathode ray oscilloscope
AC	alternating current	CRT	cathode ray tube
ACV	air cushion vehicle	CS	coupled states
A/D	analogue-to-digital	CSM	continuous slowing down models
ADP	administrative data processing	CTR	controlled thermonuclear reactor
AES	Auger electron spectra(ology)	CVD	chemical vapour deposition
AF	audio frequency	CW	continuous wave
AFC	automatic frequency control		
AFL	abstract family of languages	D/A	digital-to-analogue
AGC	automatic gain control	DBR	distributed Bragg reflector
AGR	advanced gas-cooled reactor	DC	direct current
AM	amplitude modulation	DDC	direct digital control
ANS	Astronomical Netherlands Satellite	DDL	diode-diode logic
APACHE	accelerator for physics and chemistry of heavy elements	DECENT	distribution of exact classical energy transfer
APR	acoustic paramagnetic resonance	DESY	Deutsches Electron Synchrotron
APS	appearance potential spectra(ology)	DF	Dirac-Fock
APW	augmented plane wave	DFB	distributed feedback
ATR	attenuated total reflection	DH	double heterostructure
ATS	applications technology satellite	DIL	dual-in-line
ATWS	anticipated transients without scram	DITE	divertor in torus experiment
AVC	automatic volume control	DLTS	deep level transient spectra(ology)
		DM	delta modulation
BARITT	barrier injection transit time	DMSO	dimethylsulphoxide
BBEA	4-butoxybenzal-4'-ethylaniline	DMSS	Defence Meteorological Satellite System
BCC	body centred cubic	DOBAMBC	p-decyloxybenzylidene p'-amino 2-methyl butyl cinnamate
BCD	binary-code decimal		
BFO	beat-frequency oscillator	DODS	different orbitals for different spins
BWO	backward wave oscillator	DORIS	Dopple-ring-Speicher
BWR	boiling water reactor	DOVETT	double velocity transit time
BWT	backward wave tube	DP	data processing
		DPCM	differential pulse code modulation
CAD	computer aided design	DPPH	diphenylpicrylhydrazyl
CAI	computer assisted instruction	DPSK	differential phase shift keying
CARS	coherent antiStokes Raman scattering (spectra)	DSC	differential scanning calorimetry
CATV	community antenna TV	DTA	differential thermal analysis
CB	citizen band	DV-X α	discrete variational X α method
CBOOA	cyanobenzylidene octyloxyaniline	E1,E2	electric dipole, quadrupole
C-CD	charge-coupled device	EAS	extensive air shower
CDI	collector diffusion isolation	EB	exponential Born
CDM	code division multiplexing	EBBA	4-ethoxybenzylidene-4'-n-butylaniline
CDW	charge-density wave	EBR	experimental breeder reactor
CEM	channel electron multiplier	EBT	Elmo Bumpy Torus
CEPA	coupled electron pair approximation	ECC	emergency core cooling
CERN	Conseil Européen pour la Recherche Nucléaire	ECELR	epithermal critical experiment laboratory reactor
CESR	conduction electron spin resonance	ECG	electrocardiography (-gram)
CGTO	contracted Gaussian-type orbital	EDA	ethylene diamine
CHF	coupled Hartree-Fock	EDP	electronic data processing
CI	configuration interaction	EDTA	ethylene diamine tetra-acetic acid
CIEH	charge iterated extended Huckel	EEBAC	ehtyl-4-(4'-ethoxy-benzylidene-amino) cinnamate
CIHY	configuration interaction Hylleras		
CNDO	complete neglect of differential overlap	EEG	electroencephalography (-gram)
COC	cholesteryl oleyl carbonate	EELS	electron energy loss spectra
COM	computer output to microform (fiche or film)	EFM	extended Flygare method
COOB	4,4'-cyano-octyloxy-biphenyl	EHD	electrohydrodynamics
CP	charge, parity	EHF	extremely high frequency
CPA	coherent potential approximation	EHP	electron-hole potential method
CPSK	coherent phase shift keying	EHT	extended Huckel theory
CPT	charge, parity, time	EHV	extra high voltage
		ELDOR	electron electron double resonance

ELF	extremely low frequency	HOMO	highest occupied molecular orbitals
EM	electromagnetic	HORM	hybrid orbital rehybridisation method
EMC	electromagnetic compatibility	HTGR	high temperature gas-cooled reactor
EMF	electromotive force	HV	high voltage
EMG	electromyography(-gram)	HVEM	high voltage electron microscopy
ENDOR	electron nuclear double resonance	HWR	heavy water reactor
EOS	earth observatory satellite		
EPEN	empirical potential energy function based on interactions of electrons and nuclei	IAEA	International Atomic Energy Authority Agency
EPMA	electron probe microanalysis	IBPBAC	isobutyl 4-(4'-phenylbenzylideneamino) cinnamate
EPR	electron paramagnetic resonance		
ERG	electroretinography(-gram)	IC	integrated circuit
ERPS	extramolecular relaxation polarisation shift	ICDF	intermediate coupling Dirac-Fock
ERTS	earth resources technology satellite	IDT	interdigital transducer
ESCA	electron spectroscopy for chemical analysis	IEPA	independent electron pair approximation
ESCAR	experimental superconducting accelerating ring	IF	intermediate frequency
ESFI	epitaxial silicon film on insulator	IGFET	insulated gate field effect transistor
ESS	electronic switching system	IKO	Institute v. Kernph Ouder Amsterdam
EUV	extreme ultraviolet	I ² L	integrated injection logic
EXAFS	extended X-ray absorption fine structure	I ³ L	isoplanar I ² L
		ILS	instrument landing system
		IMPATT	impact avalanche transit time
FBR	fast breeder reactor	INDO	intermediate neglect of differential overlap
FCC	face centred cubic	INDOR	internuclear double resonance
FDM	frequency division multiplex(ing)	ING	intense neutron generator
FDNC	frequency dependent negative conductance	INO	iterative natural orbital
FDNR	frequency dependent negative resistance	INTELSAT	international telecommunications satellite consortium
FEM	field emission microscopy		
FET	field effect transistor	I/O	input/output
FFHR	fusion-fission hybrid reactor	IOC- ω	inclusion of the overlap charges in the omega
FFT	fast Fourier transform		
FFTF	fast flux test facilities	IR	infrared
FIM	field ion microscopy	IRDO	intermediate retention of differential overlap
FM	frequency modulation		
FPT	finite perturbation theory	ISABELLE	intersecting storage and acceleration
FSK	frequency-shift keying	ISR	intersecting storage ring
FSGO	floating spherical Gaussian orbitals	ISX	impurity study experiment
FTR	fast test reactor	ITEP	Institute of Theoretical and Experimental Physics
		IU	Indiana University
		IVO	improved virtual orbitals
GAMBIT	gate modulated bipolar transistor		
GANIL	grand accélérateur national a ions Lourds	JET	Joint European torus
GARP	global atmospheric research programme	JAERI	Japan Atomic Energy Research Institute
GATE	GARP Atlantic tropical experiment	JINR	Joint Institute for Nuclear Research
GCFR	gas-cooled fast breeder reactor		
GCM	generator coordinate method	KEK	Japan National Laboratory for High Energy Physics
GHF-NO-CI	generalised Hartree-Fock/natural orbital/configuration interactions	KKR	Korringa-Kohn-Rostoker
GIAO	gauge-invariant atomic orbitals	LAMPF	Los Alamos meson physics facility
GO	Gaussian orbitals	LC	inductance-capacitance
GOO	generalised Overhauser orbitals	LCAO	linear combination of atomic orbitals
GPM	ground potential model	LCBO	linear combinations of (semi-localised) band orbitals
GSO	general spin orbitals		
GTO	Gaussian-type orbitals	LCGO	linear combination of Gaussian orbitals
GVB	generalised valence bond	LCP	large coil program
		LCRO	linear combination of Rydberg orbitals
HAM	hydrogenic atoms in molecules	LEC	liquid encapsulated Czochralski
HBAB	hexyloxybenzylidene-p' aminobenzonitrile	LED	light emitting diode
HBT	N-(p-hexyloxybenzylidene)-p-toluidene	LEED	low energy electron diffraction
HCDA	hypothetical core disruptive accident	LEP	large electron positron
HCP	hexagonal close packed	LET	linear energy transfer
HEED	high energy electron diffraction	LF	low frequency
HF	high frequency or Hartree-Fock	LMC	Large Magellanic Cloud
HFB	Hartree-Fock-Bogoliubov	LMFBR	liquid metal fast breeder reactor
HFER	hot fuel examination facility	LMTO	linear combination of muffin tin orbitals
HFIR	high flux isotope reactor	LOCA	loss of coolant accident
HFO	Hartree-Fock-Overhauser	LOCE	loss of coolant experiment
HFS	hyperfine structure	LOFT	loss of flow test facility
HLW	high level waste (radioactive)	LPE	liquid phase epitaxy
HMO	Huckel molecular orbitals	LSA	limited space charge accumulation
HOAB	heptyloxyazoxybenzene		
HOBHA	p-n-heptyloxy-benzylidene-p-n heptylaniline		

LSD	local spin density	ODMR	optical detection of magnetic resonance
LSI	large-scale integration	OER	oxygen enhancement ratio
LTE	local thermodynamic equilibrium	OGO	orbiting geophysical observatory
LUMO	lowest unoccupied molecular orbitals	OPHF	orbital polarised Hartree-Fock
LV	low voltage	OPW	orthogonal plane wave
LWR	light water reactor	OR	operations research
MADO	Mulliken approximation for differential overlap	ORELA	Oak Ridge electron linear accelerator
M1,M2	magnetic dipole, quadrupole	ORNL	Oak Ridge National Laboratory
MBBA	4-methoxybenzylidene-4'-n-butyl-aniline	OSO	orbiting solar observatory
MBE	molecular beam epitaxy	OTF	optical transfer function
MBPT	many body perturbation theory	PAA	paraazoxyanisole
MCD	magnetic circular dichroism	PABX	private automatic branch exchange
MCPESCF	multiconfiguration paired excitation SCF	PAC	perturbed angular correlation
MCZDO	multi-centre zero differential overlap	PAHR	post accident heat removal
MEDO	multipole expansion of diatomic overlap	PAM	pulse amplitude modulation
MESFET	metal-semiconductor field effect transistor	PAMPUS	photons for atomic and molecular processes and universal studies
MF	medium frequency	PAP	paraazoxyphenetole
MFP	mean free path	PBF	power bursts facility
MHD	magnetohydrodynamics	PBR	pebble bed reactor
MIC	microwave integrated circuit	PBX	private branch exchange
MIEHM	modified iterative extended Huckel method	PC	printed circuit
MIM	metal-insulator-metal	PCAC	partially conserved axial currents
MIS	metal-insulator-semiconductor or management information system	PCB	printed circuit board
MIT	Massachusetts Institute of Technology	PCGVB	pairwise correlated generalised valence bond
MMF	magnetomotive force	PCILOCC	perturbative configuration interaction using localised orbitals for crystal calculation
MNOS	metal-nitride-oxide-semiconductor	PCM	pulse code modulation
MO	molecular orbitals	PCX	plasma confinement experiment
MOCIC	molecular orbital constraint of interaction coordinates	PDX	poloidal divertor experiment
MODPOT	model potential	PEP	positron electron proton
MOS	metal-oxide-semiconductor	PETRA	positron electron tandem ringbeschleuniger anlage
MOSFET	metal-oxide-semiconductor field effect transistor	PF	power factor
MOST	metal-oxide-semiconductor transistor	PFM	pulse frequency modulation
MRD	multi-reference double excitation	PHWR	pressurised heavy water reactor
MRINDO	modified Rydberg INDO	PID(P,I,PD)	proportional+integral+differential (derivative)
MSI	medium scale integration	PLA	phase locked arrays
MSR	molten salt reactor	PLC	programmable logic control
MSU	Michigan State University	PLL	phase locked loops
MTBF	mean-time between failures	PLT	Princeton Large Torus
MTF	modulation transfer function	PM	pulse modulation
MTX α	muffin-tin X α	PMMA	polymethylmethacrylate
MUF	maximum usable frequency	PMDR	phosphorescence microwave double resonance
MWH	Mulliken-Wolfsberg-Helmholz-semi-empirical method	PND0	partial neglect of differential overlap
NAL	National Accelerator Laboratory	PNO-CI	pair natural orbital configuration interaction
NAND	not-and(logic)	POL	pair orthogonalised Lowdin
NC	numerical control	POPAE	protons on protons and electrons
NCMET	non-closed shell many electron theory	POPOP	phenyl-oxazoly-phenyl-oxazoly-phenyl
NDDO	neglect of diatomic differential overlap	POS	point of sale
NDT	nondestructive testing	PPDP/S	Pariser-Parr-Del Bene-Pople/Segal calculations
NEMO	non-empirical molecular orbitals	PPI	plan position indicator
NEVE	non-empirical valence-electron	PPM	pulse position modulation or parts per million
NIC	negative impedance convertor	PPP	Pariser-Parr-Pople
NMR	nuclear magnetic resonance	PRDDO	partial retention of diatomic differential overlap
NNNDO	neglect of non-neighbour differential overlap	PRF	pulse recurrence (repetition) frequency
NOR	not-or(logic)	PROM	programmable read-only-memory or Pockels readout optical modulator
NPOST	non-perturbative open-shell theory	PS	proton synchrotron (CERN)
NPSO	non-paired spatial orbitals	PSK	phase shift keying
NQR	nuclear quadrupole resonance	PTFE	polytetrafluoroethylene
NRC	nuclear regulatory committee	PTM	pulse time modulation
NRM	natural remanent magnetisation	PVC	polyvinyl chloride
NTO	natural transition orbitals	PWM	pulse width modulation
OAO	orbiting astronomical observatory	PWR	pressurised water reactor
OCR	optical character recognition		

QCD	quantum chromodynamics	TCR	temperature coefficient of resistance
QDMBPT	quasi-degenerate many-body perturbation theory	TDHF	time dependent Hartree-Fock
QED	quantum electrodynamics	TDM	time division multiplex(ing)
QPSK	quaternary phase shift keying	TDMA	time division multiple access
RAM	random access memory	TDPAC	time differential perturbed angular correlation
RBE	relative biological effectiveness	TE	transverse electric
RC	resistance-capacitance	TEA	transversely excited atmospheric
RCNDO	Rydberg CNDO	TEM	transverse electromagnetic or transmission electron microscopy
R & D	research and development	TEXT	Texas Experimental Tokamak
RF	radio frequency	TFTR	Tokamak fusion test reactor
RFI	radio frequency interference	TGFB	triglycine fluoroberyllate
RHEED	reflection high energy electron diffraction	TGS	triglycine sulphate
RINDO	Rydberg INDO	TGSe	triglycine selenate
RKKY	Rudermann-Kittel Kasuya-Yosida	TJS	transverse junction stripe
RLC	resistance-inductance-capacitance	TLD	thermoluminescent dosimeter(-ry)
RMS	root-mean-square	TM	transverse magnetic
ROM	read-only memory	TMMC	tetramethylammonium manganese chloride
RPA	random phase approximation	TOP	transient overpower accident
RPM	relaxation potential model	TNS	The next step
SAMO	simulated ab initio molecular orbitals	TRAPATT	trapped plasma avalanche triggered transit
SAS	small astronomy satellite	TREAT	transient reactor test facility
SAW	surface acoustic waves	TRM	thermoremanent magnetisation
SCF	self consistent field	TSC	thermally stimulated currents
SCL	space charge limited	TSEE	thermally stimulated exo-electron emission
SCPT	self consistent perturbation theory	TTF	tetrathiofulvalinium
SCR	silicon controlled rectifier	TTL	transistor transistor logic
SDM	space division multiplexing	TTT	tetrathiotetracene
SDO	shielded diatomic orbitals	TUCA	transient undercooling accident
SEHF	spin extended Hartree-Fock	TV	television
SEM	scanning electron microscope	TW	travelling wave
SFE	solar-flare effect	TWT	travelling wave tube
SGHWR	steam generating heavy water reactor		
SHF	superhigh frequency	UCHF	uncoupled Hartree-Fock
SHG	second harmonic generation	UHF	ultra high frequency unrestricted Hartree-Fock
SIMS	secondary ion mass spectrometer		
SIN	Swiss Institute of Nuclear Research	UHV	ultra high voltage
SINDO	scaled INDO	UKAEA	United Kingdom Atomic Energy Authority
SISAM	spectrometer with interference selective amplitude modulation	ULF	ultra low frequency
		UMD	unitised microwave devices
SMC	Small Magellanic Cloud	UPS	ultraviolet photoelectron spectra
SMS	synchronous meteorological satellite	US	ultrasonic
S/N	signal-to-noise	UV	ultraviolet
SOG	strongly orthogonal geminal		
SOS	silicon on sapphire	VB	valence bond
SPA	separated pair approximation	VCR	video cassette recorder
SPC	stored program control	VDM	vector dominance model
SPEAR	Stanford positron electron asymmetric ring	VDU	visual display unit
		VHF	very high frequency
SPHF	spin polarised Hartree-Fock	VLBI	very long base line interferometry
SPIN-CIPSI	spin symmetry adapted generalisation of CIPSI	VLF	very low frequency
SPS	super proton synchrotron (CERN)	VLSI	very large scale integration
SQUID	superconducting quantum interference device	VOR	VHF omnidirectional range
SRMCASE	symmetry-restricted-multiconfiguration annihilation of single excitations	VPE	vapour phase epitaxy
		VRC	visual record computer
SSB	single sideband	VRDDO	variable retention of diatomic differential
SSC	sudden storm commencement	VSF	vestigial sideband
SSI	supersonic transport	VSEPR	valence shell electron pair repulsion
STD	salinity-temperature-depth or subscriber trunk dialling	VSFR	voltage standing wave ratio
		VTOL	vertical take-off and landing
STEM	scanning transmission electron microscopy	VTR	voltage transformation ratio or video tape recorder
STO	Slater-type orbitals		
STOL	short take-off and landing	VUV	vacuum ultraviolet
STP	Slater-transfer Preuss	VVER	water moderated water cooled reactors
SUHFC	spin unrestricted Hartree-Fock with local approximation for correlations		
		WVER	water moderated water cooled reactors
SW	short wave		
SWR	standing wave ratio	XPS	X-ray photoelectron spectra
SXAPS	soft X-ray appearance potential spectrum		
		ZEBRA	zero energy breeder reactor assembly
TBBA	terephthal-butylaniline	ZGS	zero gradient synchrotron
TCNE	tetracyanoethylene	ZPPR	zero power plutonium reactor
TCNQ	tetracyanoquinodimethane		

Subject Index

1/f noise see random noise

A-centres

- alkali halides, F-centres, ESR in different states of relaxed configuration 0-108067
- Ag halides, fundamental absorption, nature and function of A-centres determ. the extra band at the long wave edge (*Russian*) 0-76060
- CsBr:Cu⁺, excitation and absorpt. spectra 0-108255
- KCl, additively coloured photochromic crystals, spectral sensitivity (*Russian*) 0-91871
- KCl:Cu⁺ excitation and absorpt. spectra 0-108255
- KCl:Li, X-irrad., F_A centres, thermolum. studies 0-80878
- KCl:Li (F₂⁺)_A centres, tunable CW laser action 0-87399
- KCl:Li F_A(II) centre laser, pumped by flashlamp-pumped dye laser 0-102737
- KCl:Sr, positron annihilation and trapping in A-centres 0-84802
- NaCl:Sr, positron annihilation and trapping in A-centres 0-84802
- RbCl:Li F_A(II) centre laser, pumped by flashlamp-pumped dye laser 0-102737
- Rbl, luminesc. spectra induced by pulsed Ne⁺ and electron beams and X-rays 0-80851
- n-Si, defect charge states, complex form., gamma-ray effects 0-96564
- Si:O, A centre, theoretical study 0-75521
- Si:Se, impurity states, A- and B-centres, electron, hole thermionic emission rates 0-96813
- n-SiC, thermal defects, ESR study 0-88876
- ZnS:Pb, blue luminesc., photoexcited EPR spectrum 0-108070

A/D conversion see analogue-digital conversion

ab initio calculations

- acetaldehyde, dichroic effects, computational expts. 0-83424
- adenine, tautomeric forms protonation, ab initio HF Roothaan SCF calcs. 0-78534
- alkynyl cations, struct., charge distrib., ab initio population anal. calcs. 0-58407
- 1H-alloxazine, and derivatives electronic struct., photoelectron spectrosc. and ab initio study 0-106261
- aminoborylpolyynes, intermolecular interaction through triple bonds, internal rot. 0-106370
- aminopolyynes, intermolecular interaction through triple bonds, internal rot. 0-106370
- atom, one-centre integrals of exact effective valence shell Hamiltonian 0-74128
- atomic and molecular processes, developments in ab initio methods 0-63550
- benzaldehyde, and isomeric phthalaldehydes, dipole moments meas., config., ab initio MO calc. 0-58410
- benzene, dipole polarisability, finite-field SCF MO calcs. 0-83255
- benzenes, substituted, electronic struct., ab initio calcs., photoelectron spectra 0-58314
- binary complexes, small H-bonded mols. electronic structs., ab initio calcs. 0-74108
- carbenes, heterosubstituted, singlet-triplet splitting depend. on heteroatom electronegativity and conform. 0-63553
- 2-chloroethyl radical, struct., ab initio calcs. 0-83252
- chloromethyl formate, conformation potential energy surfaces, ab initio calcs. 0-69065
- crystal Hartree-Fock theory, ab initio effective potentials 0-103290
- cyclic 3- and 4-membered ring cpds., saturated, ab initio struct. anal. 0-58192
- cyclopentanone, n- π^* transition, vibr. band intensities 0-74116
- diatomic isovalent systems, pot. curves, ab initio MRD-CI method 0-83293
- diatomic molecules, hydrides, oxides and BeF, spin orbit coupling const., ab initio calcs. 0-63537
- dicyanoketene, and isomeric forms, heat of form., ab initio STO-3G calcs. 0-58190
- dimethylamine-HCl systems, H-bonded complexes studied by ab initio MO method, dipole moments determ. 0-83253
- dodecahexenes, sudden polarisation effect, ab initio and CI calcs. 0-58160
- ethane cation, relative stability of ²A₁, ²E_g states 0-58140
- ethene, dipole polarisability, finite-field SCF MO calcs. 0-83255
- ethylene, pot. energy and dipole moment surfaces, polarisation effect, ab initio CI calcs. 0-106272
- ethylene ozonide, ab initio gradient and MC SCF calc., conformational anal. 0-83290
- ethylidene, rearrangement to ethylene, barriers, ab initio MO calcs. 0-104424
- floating orbital geometry optimisation with floating outer-shell basis functions 0-95517
- fluoroformaldehyde, pot. energy surface characts., substitution effect 0-89505
- fluoromethyl formate, conformation potential energy surfaces, ab initio calcs. 0-69065
- formaldehyde, ³A" state, zero-field splitting param., ab initio CI calcs. 0-99454
- formaldehyde, electronic struct., dipole moments, mol. polarisability, force fields, ab initio calcs. 0-78531
- formaldehyde anion radical, hyperfine coupling consts., vibr. depend., ab initio calcs. 0-87150
- formamide, force consts. and dipole moment derivatives, ab initio MO calcs. 0-95521
- formamide-glyoxal, charge transfer theory, Mulliken population, ab initio calc., multiconfiguration scheme 0-106392
- trans-formic acid geometry, force fields and fundamental vibr. freq., ab initio study 0-87040
- graphite, electronic struct. exact exchange HF calcs. 0-65438
- guanine, tautomeric forms protonation, ab initio HF Roothaan SCF calcs. 0-78534
- 2-haloethanols, torsional interaction, IR spectra, ab initio calcs., 2-dimens. model 0-74160
- hydrocarbons, average elec. polarisabilities and mag. susceptibilities, ab initio valence electron calcs. 0-87033
- β -hydroxy acrolein, lower excited states, electronic struct. and H-bonding, ab initio SCF and CI calcs., photochemical mechanism 0-83278
- imidazole, quadrupole coupling consts. interpretation, ab initio field gradient calcs. 0-58282
- inert gas, atomic photoionisation, Dirac-Fock calcs., branching ratios and angular distrib. in p shells 0-63601
- 10H-isalloxazine, and derivatives electronic struct., photoelectron spectrosc. and ab initio study 0-106261
- isoelectronic sequence, X-ray spectra 0-87071
- isopropyl radical, pot. energy surfaces, ab initio UHF calcs. 0-106258
- β -lactam antibiotics, ab initio SCF-MO-LCAO calcs., amidic bond breaking, methoxy substitution effect 0-78533
- large molecules, mol. fragment basis, generalisation, for ab initio calcs. 0-91438
- linear mols., π orbital electron energy contrib. to reaction heat 0-76539
- metalloenzymes, model for biological active sites, ab initio calcs. 0-104551
- methane, coord. bond calcs. 0-58129
- methane, orbital relax. energy for single and double ions. from valence shells 0-106253
- methane cation, photodissoc., ab initio RHF and MRD CI calcs. 0-95695
- methanol, coord. bond calcs. 0-58129
- methyl fluoride, coord. bond calcs. 0-58129
- methyl fluoroformate, isomer conformation, CNDO and ab initio STO calcs. 0-58151
- methyl halides, mol. force field at SCF ab initio levels, quantum-mechanical calc., LCAO-MO method 0-106319
- N-methyl m-fluoroaniline, conformational anal., microwave spectra obs. 0-58247
- s-methyl nitrite, methyl group rot. barriers in cis and trans forms, ab initio calcs. 0-74111
- methyl radical, hyperfine coupling consts., vibr. depend., ab initio calcs. 0-87150
- methylamine, affinities for H⁺(Li⁺)(K⁺)(CH₃⁺), ab initio SCF calculations 0-102443
- methylamine, coord. bond calcs. 0-58129
- methylamine-HCl systems, H-bonded complexes studied by ab initio MO method, dipole moments determ. 0-83253
- methylene, B₁-A₁ separation, ab initio 0-106251
- methylene, singlet-triplet excitation energy, relativistic correction 0-69059
- methylene peroxide, struct., energy levels, ab initio UHF and MRUHF NO CI calcs. 0-83287
- molecular electron scattering, theory and calc. techniques 0-63841
- molecular static polarisability, ab initio SCF wave functions 0-74106
- multi-config. SCF super-CI calc., density matrix formulation 0-78547
- naphthalene, dipole polarisability, finite-field SCF MO calcs. 0-83255
- oxirane cation, struct. rearrangement following vertical ionisation, ab initio CI calc. 0-58191
- oxoniomethylene cation, rearrangement to hydroxymethyl cation, barriers, ab initio MO calcs. 0-104424
- papain models, active site α -helix and ion pair stability 0-74265
- periodic systems electronic struct., LCAO SCF ab initio HF calcs. method 0-65419
- phenol-phenyl complex, electrostatic mol. pot. contour maps, MODPOT and VRDDO calcs. 0-102463
- polyenes, photoisomerisation, triplet pot. energy surfaces and normal mode anal. 0-108700
- polyynes, intermolecular interaction through triple bonds, internal rot. 0-106370
- protein, structure and bonding, quantum theory, ab initio calcs. 0-61509
- pyridines, monosubst., H₂O complexes, n- π^* transitions, H bonding, MO theory 0-95550
- pyrrole-acetonitrile, H-bonded complex, ab initio MO calcs. 0-102440
- second-row hydrides, nucl. spin-spin coupling consts., ab initio calcs. 0-95647
- 1,3-sigmatropic rearrangements, ab initio calcs., basis set and electron correl. effects 0-104428
- solid electrolyte, mobility paths for ML₄⁻³ clusters, ab initio electronic struct. calcs. 0-70458
- spirohydrocarbons, strained, bond angles, interatomic distances, semiempirical and ab initio calcs. 0-95533
- TCNE-benzene, charge transfer theory, Mulliken population, ab initio calc., multiconfiguration scheme 0-106392
- thioformaldehyde, electronic struct., dipole moments, mol. polarisability, force fields, ab initio calcs. 0-78531
- thiourea, struct., hydration, ab initio SCF calcs. 0-58142
- three-electron bonds, strengths, ab initio LCAO MO CI calcs. 0-87046
- toluene, mol. struct., ab initio calcs. 0-106262
- transition metal atoms, neutral and ion val. states, electron correlation, ab initio effective val. Hamiltonian calc. 0-99449
- triatomic dihydride molecules, Walsh's rules and small bond angle states 0-106255
- unsaturated hydrocarbons, dipole polarisabilities, STO-4G calcs. 0-83255
- water-imidazole, H bond interrupted chain, cooperative effects, STO-3G ab initio calcs. 0-63535
- Ag, electronic and mag. structure calcs. of mag. impurities 0-80213
- Al₂(Al₂⁺)(Al₂⁺) configurations, ab initio study, LCAO, STO, MO-SCF and CI calcs., binding energy (*French*) 0-91447
- Al₁Mg_{1-c} liquid alloys, vols. and entropies of mixing, calc. 0-75363

ab initio calculations continued

- Ar+HHe⁺, ab initio pot. energy data, SCF-LCAO calcs. 0-63530
 Ar₂ van der Waals dimer, intermol. pot., SCF CI ab initio calcs. 0-106274
 Au⁺, ab initio SCF calcs. using relativistic effective core pot. 0-95524
 BH₃, Walsh's rules and small bond angle states 0-106255
 BN, electronic struct., exact exchange HF calcs. 0-65438
 B₂O₃, bipyramidal struct., stability, ab initio SCF-MO calcs. 0-99446
 Ba II, 5p excitation, relativistic anal., multiconfig. Dirac-Fock calcs. 0-69240
 Ba, quantum defect param., ab initio calcs. 0-78525
 Be complexes, binding and orbital energies, biological systems ab initio calc. 0-102442
 BeF, A² state config., ab initio MO calcs. 0-95532
 BeF, spin orbit coupling const., ab initio calcs. 0-63537
 (Be(OH)(NH₃)₂)⁺ model for biological active sites, ab initio calcs., comparison with Zn complex 0-104551
 Be₂(Σ_g⁺), binding energy, ab initio pot. curves, interacting correlated fragments method 0-63557
 C, one-centre integrals of semiempirical theories of valence, ab initio calcs. 0-102441
 C₃, ground state pot. surfaces, analytical functions 0-83304
 CH, one-centre integrals of semiempirical theories of valence, ab initio calcs. 0-102441
 CH⁺, a¹II-b²Σ⁺ transition moment, ab initio calcs. 0-87047
 CH⁺, excited states, pot. curves and transition moments determ. by ab initio CI methods 0-106286
 CH₂⁺, Walsh's rules and small bond angle states 0-106255
 C₂H₂+HF, interaction, struct. and stability, ab initio calcs. 0-58347
 CN⁺, spectrosc. consts. for ground and excited states, ab initio, CI calcs. 0-78551
 CO, polarisability derivatives, bond length depend., SCF and CI calcs. 0-58162
 CO₂, collision-induced Raman spectrum, theoretical studies 0-63646
 CO₂, stretch-stretch interaction force const., electron correlation influence, ab initio CI study 0-58161
 CO₂+H₂, rot. transfer, ab initio intermol. pot. energy surface 0-58354
 CO₂+He, rot. inelastic collision, ab initio SCF, electron gas and pot. energy surfaces 0-83468
 CO₂+Ne, intermol. pot. in repulsive short-range region, ab initio 0-69204
 Ca, quantum defect param., ab initio calcs. 0-78525
 Cl₂, inner shell excited states, X-ray absorpt. spectra, HF calcs. 0-78536
 ClNSO, ground state geometry, ab initio calcs. 0-106259
 ClO₂⁺, ClO₂⁻ and ClO₂⁻ (n=1 to 3), ab initio calcs., localised MO and nature of Cl-O bond 0-69070
 Co, Auger spectrum, ab initio MO LCAO SCF CI calc. many electron contrbs. 0-87169
 CrOCl₃, electronic structure and valence ionisation energies, obs. by ab initio and SW-Xα methods 0-69073
 Cu, electronic and mag. structure calcs. of mag. impurities 0-80213
 Cu/Ni coherent modulated structures, electronic struct. and magnetism 0-103620
 CuCl, electronic struct. by LCAO and LMTO methods, direct gap semiconductor 0-59868
 CuCl₂, ESCA satellite intensity, ab initio SCF calcs. 0-74103
 CuCl₂(Cl₂²⁻)(Cl₄²⁻), electronic struct. studies by SCF, MSXα and INDO method 0-74119
 CuF₂(F₄⁴⁻), electronic struct. studies by SCF, MSXα and INDO methods 0-74119
 CuSO₄·5H₂O, EXAFS, rel. between Debye-Waller factor and thermal parameters meas. by neutron diff. 0-84803
 D+H₂ reaction, transition state theory calculations, kinetic isotope effect explanation 0-66784
 D₃, Rydberg states, spectroscopic B₀ consts. 0-74109
 D₃⁺, rot.-vibr. spectrum, ab initio calcs. 0-95595
 DOD, vibr. intensities, ab initio and empirical calcs. 0-78592
 DOD, vibr. intensities, ab initio and empirical calcs., band strengths 0-78593
 F, ab initio effective valence shell Hamiltonian for neutral and ionic valence states 0-74117
 F, isoelectronic sequence, X-ray spectra 0-87071
 F₂, electron impact excitation, dissociation of lowest electronic state 0-63839
 FNNF, mol. struct., cis effect 0-91434
 F₂O, geometry, electron spectrum, vert. ionis. pot. ab initio calc. 0-58187
 Fe₂⁺ and Fe₂⁺ hydrate clusters, aq. electron exchange reaction, ab initio RHF MO calc. of inner shell reorganisations, vibr. freq. 0-102564
 GaAs (110), chemisorption of O and Al, ab initio theory 0-75612
 GeH₂, struct. determ., restricted HF calcs. 0-87030
 GeH₃⁺, electronic struct., electron affinity, inversion barrier, ab initio SCF Gaussian basis calc. 0-63552
 H atom finite chains, HF solns. stability and symmetry breaking, independent particle model calcs. 0-87035
 H, electron scattering, optical pot. methods 0-102569
 H+D₂ reaction, transition state theory calculations, kinetic isotope effect explanation 0-66784
 H⁺+CO (Σ), ground state pot. energy surface, ab initio SCF calc., protonated equilib. geometry 0-83301
 H⁺+H₂, rot. and vibr. excitation, energy loss obs. 0-63773
 H⁺+H₂, vibr. excitation, ab initio CI pot. energy surface calcs. 0-74228
 H⁺+H₂, vibr.-rot. excitation, ab initio CI pot. energy surface calcs. 0-74229
 H₂, electron repulsion matrix elements, asymptotic form, adiabatic representation 0-87038
 H₂ molecule dimer, ab initio SCF intermolecular interaction energy calcs. 0-78537
 H₂, triplet state, molecular polarisability calcs. 0-63860
 H₂-H₂, intermol. pair pot., ab initio SCF-CI surface 0-91457
 H₃, Rydberg states, spectroscopic B₀ consts. 0-74109
 H₃⁺, rot.-vibr. spectrum, ab initio calcs. 0-95595
 H₄, pot. energy surfaces, valence bond calcs. 0-74129
 (H-He)⁺, ab initio calcs. 0-63799
 HCN, ground state pot. surfaces, analytical functions 0-83304
 HCN-CO complex, charge transfer theory, Mulliken population, ab initio calc., multiconfiguration scheme 0-106392
 HF, orbital relax. energy for single and double ionis. from valence shells 0-106253
 H₂F₂ and H₂F₃ clusters, molecular structures, ab initio calcs. 0-83532
 HNF₂ and DNF₂, photoelectron spectra, vibr. struct. obs., ionisation pot. determ., ab initio calcs. of ionic geometry 0-83418

ab initio calculations continued

- HNO, isomerism, low lying electronic states, ab initio MRD-CI calcs. 0-83291
 H₂O affinity for Li⁺(Na⁺)(K⁺), ab initio SCF calcs. 0-58125
 H₂O, core 1s and 1b, photoelectron bands, vibr. excitations, ab initio calcs. 0-63543
 H₂O, orbital relax. energy for single and double ionis. from valence shells 0-106253
 HOD, vibr. intensities, ab initio and empirical calcs. 0-78592
 HOD, vibr. intensities, ab initio and empirical calcs., band strengths 0-78593
 HOT, vibr. intensities, ab initio and empirical calcs. 0-78592
 HOT, vibr. intensities, ab initio and empirical calcs., band strengths 0-78593
 HPN-HNP, isomerisation energies, ab initio MRD-CI calcs. 0-106271
 HS_n⁺, n=1-4, electronic struct., ab initio Hartree-Fock-Slater calcs. 0-74107
 HS_n²⁺, n=1-4, electronic struct., ab initio Hartree-Fock-Slater calcs. 0-74107
 H₂S_n⁺, n=1-4, electronic struct., ab initio Hartree-Fock-Slater calcs. 0-74107
 HSO-HOS, isomerisation energies, ab initio MRD-CI calcs. 0-106271
 HSiC-HCSi, isomerisation energies, ab initio MRD-CI calcs. 0-106271
 H₂SiO, electronic struct., dipole moments, mol. polarisability, force fields, ab initio calcs. 0-78531
 He, electron scattering, optical pot. methods 0-102569
 He-LiH, rot. inelastic collisions, ab initio pot. energy surface calcs. 0-87208
 He+ArH⁺, ab initio pot. energy data, SCF-LCAO calcs. 0-63530
 He+H₂, pot. energy surface, ab initio calcs., van der Waals const. determ. 0-106372
 He+H⁺, differential scatt., 1-12 eV, high resolution beam meas. 0-58348
 He+LiH, rot. inelastic collisions, dynamics 0-87209
 He+LiH, rot. inelastic collisions, state-to-state cross sections determ. 0-87210
 Li complexes ((C₂H₂X₂)₂Li)⁺ where X=S, O, binding and orbital energies, biological systems ab initio calc. 0-102442
 Li⁺-H₂O complex, charge transfer theory, Mulliken population, ab initio calc., multiconfiguration scheme 0-106392
 Li⁺-ligand complexes, NMR appl. ⁷Li chemical shifts, expt. and ab initio studies 0-63670
 Li⁺+ether(thioether)(amide), pair pots., ab initio LCAO SCF MO calcs. 0-58184
 Li₂⁺, Σ_g⁺, Σ_u⁺ excimer emission, ab initio calcs. 0-91608
 LiBF₄, nonrigid mol. struct. and stability, ab initio calcs. 0-83259
 LiBeF₃, pot. energy surface, struct., stability and internuclear distances, ab initio calc. 0-58147
 LiCa, laser chemiluminesc. 0-93759
 Li₂Cl₂²⁺, energy cluster expansion convergence 0-91715
 Li₂F₂, struct., force fields and normal mode freqs., ab initio calcs. 0-83260
 LiH-NH₃(ethylene)(acetylene), struct. and props., SCF ab initio calcs. 0-106250
 LiH+He, rot. inelastic collisions, rigid shell models 0-99545
 (LiH)₃ complex, SCF interaction energy nonadditivity 0-91437
 N, ab initio effective valence shell Hamiltonian for neutral and ionic valence states 0-74117
 N₂, ab initio MO-LCAO-SCF and Gordon-Kim intermolecular pot. for seven different orientations 0-95522
 (N₂)₂, Van der Waals molecule, struct. and internal rot. barriers determ., interaction pot. from ab initio calcs. 0-91626
 NH₃, pot. energy curves of X²B₁, A²A₁, ²B₂ valence-shell and π_u²3s-type Rydberg states calc. by CI 0-74138
 NH₃, affinities for H⁺(Li⁺)(K⁺)(CH₃⁺), ab initio SCF calculations 0-102443
 NH₃, affinity for Li⁺(Na⁺)(K⁺), ab initio SCF calcs. 0-58125
 NH₃, lone pair contributions to the IR intensities 0-63630
 NH₃, orbital relax. energy for single and double ionis. from valence shells 0-106253
 NH₃, vibr. excitation in soft X-ray emission and core ESCA spectra 0-69163
 NH₃⁺, two-mode Jahn-Teller effect calcs. 0-83297
 NO₂, ground state pot. surface, ab initio LCAO MO SCF calcs. 0-102461
 NO₂⁺, gas phase equilib. geometry, force consts., vibr. freq., dipole moment function MCSCF/CI calcs. 0-78520
 NOH isomerism, low lying electronic states, ab initio MRD-CI calcs. 0-83291
¹⁴N quadrupole coupling consts., ab initio calcs. 0-58283
 Na I, isoelectronic sequence, X-ray spectra 0-87071
 Na+Xe+hν, collisions in presence of nonresonant lasers 0-99567
 Na₂⁺, Σ_g⁺, Σ_u⁺ excimer emission, ab initio calcs. 0-91608
 Ne+H⁺(D⁺), electron detachment, dynamical phenomenon 0-106305
 Ni, ferromagnetic, electronic struct. and hyperfine field of nonmag. impurities, calc. 0-70658
 Ni, M₁₁₁₁ spectrum, ab initio calculation 0-83276
 Ni surface, (001), H₂ dissociative adsorption, calc. 0-101036
 NiCu molecule, electronic states determ. by ab initio HF and CI methods 0-69087
 Ni(001) surface states, surface magnetisation, electron spin polarisation 0-88612
 O, ab initio effective valence shell Hamiltonian for neutral and ionic valence states 0-74117
 O I, isoelectronic sequence, X-ray spectra 0-87071
 O+H₂, classical trajectory calcs., ab initio surface, singlet state, rate consts. 0-66786
 O+H₂, pot. energy surfaces and reaction rates, ab initio calcs. 0-63531
 O₂, ¹Δ_g diabatic Rydberg states, ab initio CI calcs. 0-95554
 O₂, Rydberg states, Σ_g⁺, Σ_u⁺, Π_g⁺, Π_u⁺, Σ_g⁺ symm., ab initio CI study 0-99460
 O₃, ab initio UHF and UHF-natural orbital CI studies 0-102452
 O₃, line and band strengths in IR spectra, variational calcs. 0-87112
 O₂ molecule, SCF-CI calcs. 0-78517
 OH+H₂-H₂O+H, reaction product vibr. distrib., quasiclassical trajectory, calcs. 0-85162
 O₃H⁺, isomeric structs. ab initio MO calcs. 0-83270
 ONCl, vibr. freq., anharmonic ab initio/empirical pot. energy functions 0-99457
 O⁺(S)+N₂(X¹Σ⁺)-NO⁺(X¹Σ⁺)+N(S), MCSCF potential energy surface for collinear ²Σ pathway 0-63540

ab initio calculations continued

- P, ab initio effective valence shell Hamiltonian for neutral and ionic valence states 0-74117
 Pb, ab initio band struct. calcs. 0-75502
 PbS(PbSe), ab initio SCF calcs. using relativistic effective core pot. 0-95524
 S, ab initio effective valence shell Hamiltonian for neutral and ionic valence states 0-74117
 S²⁺ and S²⁻, structure investigation by ab initio calcs. 0-69066
 Si, ab initio effective valence shell Hamiltonian for neutral and ionic valence states 0-74117
 SiH₃ radical, hyperfine coupling consts., vibr. depend., ab initio calcs. 0-87150
 SiH₃X (X=H, F, NH₂, OH), coord. bond calcs. 0-58129
 SnH₂, struct. determ., restricted HFM, calcs. 0-87030
 Sr, quantum defect param., ab initio calcs. 0-78525
 TCNQ, ab initio SCF LCAO band struct. calc. 0-70608
 TOT, vibr. intensities, ab initio and empirical calcs. 0-78592
 TOT, vibr. intensities, ab initio and empirical calcs., band strengths 0-78593
 TTF, ab initio SCF LCAO band struct. calc. 0-70608
 Ti, neutral and ion val. states, electron correlation, ab initio effective val. Hamiltonian calc. 0-99449
 TiCl, ground-state props., Wannier functions, and electronic struct., ab initio self-consistent calc. 0-80178
 TiH, ab initio SCF calcs. using relativistic effective core pot. 0-95524
 Xe subshell photoionisation, multichannel k-matrix calc., spin orbit interactions 0-63600
 Xe₂, dispersion damping functions and interaction energy calcs. 0-78673
 XeF₃⁺, pseudopot. SCF MO studies, steric aspects of struct. and force fields, Jahn-Teller effect 0-99444
 XeF₆, pseudopot. SCF MO studies, steric aspects of struct. and force fields, Jahn-Teller effect 0-99444
 (Zn(OH)(NH₃)₂)⁺, model for biological active sites, ab initio calcs., comparison with Be complex 0-104551

abacs see nomograms**aberrations**

- aberrations in optics and particle optics only*
see also lenses; optical instrument testing; particle optics
 annular aperture, light distrib. from diffr., aberration correction using mirror lenses (*German*) 0-69325
 aplanatic waxicon insensitive to tilt errors, for high power laser beam transport 0-74460
 apodising filters, numerical exam., second moment of the point spread function 0-106611
 catadioptric objective, development (*German*) 0-102796
 cathode lens having a quasispherical field 0-95782
 caustic point displacement due to generalised bending, third-order approx. 0-83656
 chromatic aberrations of real rays, role of each lens in optical system 0-102655
 chromatic-aberration-free microscope optics 0-86395
 coherent fast IR wavefront aberration sensor interference problems 0-74499
 coherent information processing by a pair of lenses in spherical wave illumination 0-95816
 colour image evaluation from tristimulus values transfer functions measurements 0-87333
 coma corrector for parabolic reflector telescope off-axis guiding 0-82196
 computation accuracy of aberrational diffr. images 0-87328
 condenser objective, single field, advantages and limitation for min.-exposure 0-87292
 confocal scanning microscope, image form. 0-68249
 crossed lenses, electron optical charact., trajectory anal., aberrations from axial pot. profile 0-63909
 crossed lenses, theoretical and expt. study of electron-optical lenses 0-95780
 deflection effect of light reflected from moving mirror in ether theory 0-91749
 diffraction and aberration effects, wave optical calc. 0-83549
 diffraction pattern obs. with computer-generated holograms 0-102681
 diffraction patterns for optical systems with pupils of non-uniform transmittance 0-87470
 diffuser, weak, speckle pattern, spherical aberration effect 0-87476
 discharges, selfluminous, schlieren system for time and space resolved photography 0-87471
 electron beam deflection error assessment, expt. technique 0-78757
 electron beam scanning systems, aberration elimination 0-78756
 electron lens, magnetic, min. spherical aberration 0-87287
 electron lenses between TEM specimen and an electron spectrometer for energy-loss spectral resolution optimisation 0-101886
 electron microscope, chromatic aberration effects on lattice images of defects 0-107210
 electron microscope spiral distortion correction double-lens system 0-68327
 electron microscopy, aberration correction 0-86531
 electron microscopy, field emission transmission, sub-angstrom resolution 0-82851
 electron optical systems, reduction by optimisation techniques 0-87290
 electron probe, compensation, dynamical focusing with stigmator 0-87291
 electron probe forming systems, optimisation with respect to aberrations and vertical beam landing 0-68291
 electrostatic energy filter, telescopic, with cylindrical mirror analysers 0-87296
 eye, chromoretinoscopy and its instrumentation 0-94201
 field emission gun SEM column electron-optical performance obs. and model 0-68328
 flat-field spectrograph design, holographic grating appl. 0-68264
 Foucault, phase edge and wire optical test 0-96046
 four-element lens systems of Cooke-triplet family design considerations 0-57404
 generalised ray tracing, caustic surfaces, bending and merit function for optical design 0-102612
 Hadamard spectrometer, curved slits used to increase throughput 0-95149
 higher order chromatic aberrations, pupil coordinates (*Chinese*) 0-69335
 hologram lens, axial, on spherical substrate with remote pupil, aberrations 0-95849
 holograms, Fresnel copies, aberration props. 0-99676
- aberrations continued**
 holographic diffraction grating on toroidal substrate, astigmatism 0-58482
 holographic elements, axisymmetrical, third order aberrations 0-69341
 holographic image deformation, optical modification at reconstruction 0-83567
 holographic image magnification, new methodology 0-95851
 holographic optical elements, third-order aberration theory and generalised aplanatic condition 0-74314
 holographic optical elements for incoherent polychromatic imaging 0-69349
 holography, aberration coefficient estimation 0-63949
 holography advantages for physical structure meas. and recording 0-95843
 hyperchromatic lens, expressions for first order chromatic aberrations 0-91879
 illumination, relative, easy calc. 0-63920
 image contrast loss in presence of chromatic magnification difference, numerical estimate 0-95823
 image reconstruction, computerized, fragment size choice 0-78785
 ion optical props., aberration, crossed toroidal elec., mag. fields as mass spectrometer (*Chinese*) 0-82843
 IR coating nonuniformity effect on precision optical systems, compensation by auxiliary laser 0-78926
 large-aperture interferometer with low-resolution holographic corrector plate 0-74315
 laser, double-current-confinement channelled-substrate struct., near-field and beam-waist position 0-106553
 laser beam expander design corrected for Petzval curvature 0-74461
 laser beam printer scanning system with f- θ lens 0-78942
 lens, double Gaussian objective, design (*German*) 0-64134
 lens, gradient-index rod, aberrations in multimode optical fibre devices 0-69487
 lens, gradient-index rod, appl. in optical fibre communication systems 0-69488
 lens, gradient-index rod, evaluation by imaging 0-69485
 lens, gradient-index spherical, design for optical pickup systems 0-69483
 lens, photographic gradient singlet, design techniques based on total aberrations 0-69479
 lens, radial gradient-index, with zero Petzval aberration, third-order aberrations 0-69484
 lens design, least squares fitting of Zernike's polynomials to wave aberration function 0-83660
 lens design with simultaneous image spot, optical path difference, diffraction MTF and Seidel aberration minimisation 0-74459
 lens system, distortion by means of numerical transformation (*German*) 0-64132
 lens wavefront aberration, interferometric examination techniques 0-69498
 longitudinal, calc. by stereo-self-collimation method (*Russian*) 0-91878
 Luneberg apodization problem 0-87302
 magnetic einzel lens, satisfying anastigmatic and achromatic conditions 0-87288
 magnetic energy filter, without second-order aberrations 0-86524
 magnetic imaging filter, electron optical experiments 0-87295
 magnetic lens, by foil lens, appl. to STEM 0-87294
 magnetic lens aberration formulae 0-95781
 magnetic prism, design, for TEM energy filter 0-86523
 magnetic spectrometer, corrected second-order aberrations 0-87013
 mechanically ruled and holographic concave diffr. grating parameter relationships 0-87543
 metallic thin film apodising and attenuating filters, phase shifts and aberrations 0-87552
 monochromator, telescopic, in CTEM, with cylindrical mirror analysers 0-87296
 monochromator mounting with ruled diffr. grating at 45° off-plane 0-87479
 monochromator using concave holographic grating and plane mirror, imaging props. 0-99856
 objective lens, with compensated axial chromatic aberration, for electron microscope 0-87293
 ophthalmic lenses, longit. spherical aberration and its effect on visual acuity 0-99816
 optical storage focus error detection, skew beam and Foucault knife-edge techniques 0-102649
 optical system, automatic correction routine 0-58464
 optical system planning and design (*Italian*) 0-69490
 optical system tolerancing, encircled energy performance prediction 0-78935
 optical systems, entropy and neguentropy (*French*) 0-102608
 pancratic objectives, aberration stabilisation during focusing 0-102799
 precision optical element testing by phase meas. interferometry 0-74520
 projection system, wavelength and coherence effects 0-64136
 quadratic structure functions describing random tilted phase fields 0-95799
 round lens aberration correction 0-78758
 scalar diffraction theory, exact solns. 0-78778
 Selfoc lens, aberration improvement by glass composition and ion exchange process parameter choice 0-69486
 Selfoc lens as imaging system, chromatic aberration 0-69480
 sextupole corrector limitations 0-102604
 single-polepiece magnetic lens axial field distrib. 0-69317
 single-polepiece objective and projector lenses for electron microscope 0-68326
 Space Telescope pointing control fine guidance subsystem design 0-82201
 speckle interference fringes, lens aberration effects 0-105700
 spectacle lenses, astigmatic, technological construction (*Russian*) 0-99817
 spectacle lenses, hard resin, comparative study of bitoric effect 0-91877
 spectrograph, with transparent holographic grating 0-57395
 spectrophotometer, UV-visible, high throughput, optical and optomechanical design 0-95155
 STEM, defocus and astigmatism, automatic correction method 0-68298
 superachromatic triplets, design method 0-64133
 telescope-spectrometer combination, optical props. 0-87455
 three-lens cemented component calcs., reduced secondary spectrum 0-102800
 triple monochromator a spectrometer in Raman scatt. (*French*) 0-96007
 UV holographic microinterferometer and probe beam design for plasma probing 0-59270
 wavefront aberration polynomial, calc. 0-102614
 wavefront interpretation with Zernike polynomials 0-78776

aberrations continued

Zernike polynomial generalisation, optimum balanced wavefront aberrations for annular apertures 0-95805
 CO₂ laser Antares fusion system optical diffraction computation 0-74424
 Ge, polycrystalline thermal-imaging lens, optical requirements 0-69495
 SF₆, multiwavelength phase conjugation using multiline CO₂ TEA laser 0-91847

abrasion

see also hardness; wear

active abrasive conc. determ. by static method based on etch figure stars count 0-74544
 composite materials, water lubrication, wear studies 0-60984
 cutting tools, diffusive wear, mag. field effect 0-60985
 glass, surface damage by abrasive contact, effect on strength 0-85066
 granular materials, abrasive, failure and strength characts. in US field, test unit 0-85112
 graphite, sliding against C, dusting wear regime 0-97595
 grinding resist. materials, review 0-108586
 Hayes alloy no.716, Fe-Cr-Ni-Co-W-Mo-Si-C-B (26, 22, 12, 3.5, 3, 1.2, 1.1, 0.4 wt.%), hardfacing alloy 0-100802
 high speed rubbing, thermomechanical interactions 0-83769
 high-speed friction, intensity calc. 0-103416
 instrumentation engineering, laser beam appls. in drilling, welding, cutting, definite abrasion and surface treatment (*German*) 0-108608
 metal surfaces, abrasive wear theory based on shear effects 0-89363
 metal-insulator pairs, sliding behaviour 0-66671
 monocrystal surface layer damage depend. on abrasive working parameters (*Russian*) 0-76368
 non-magnetic material wear in presence of magnetic field 0-60982
 optical surface shaping, contact problems 0-74540
 PMMA, quartz- and glass-particle reinforced, abrasive wear 0-97594
 PTFE, wear, sliding speed, contact press. and rubbing surface temp. 0-76372
 quartz dental composites, acrylic acid grafted on particles by gamma-radiation 0-66840
 slab, surface displacements for high speed rubs 0-83767
 sliding contact, friction, wear, temp. anal. 0-93659
 steel, inclusion chemistry control for machinability enhancement 0-85067
 steel, type Kh12M, rel. between structural inhomogeneity and wear resist. (*Russian*) 0-66672
 steel, wear resistance of low temp. nitriding treatment 0-89357
 topography of abraded surfaces rel. to contact area and abrasion mechanism 0-58986
 white cast Fe, abrasive wear 0-108587
 Al-steel mixture, wear resistant, produced by compaction by discrete shock waves 0-84882
 Al₂O₃ rod, damaged, mech. strength, surface defects effect, appl. as insulators (*German*) 0-76330
 Fe, cast, surface temperature effect on dry sliding wear 0-60983
 Fe-C alloys abrasion resist. materials, review 0-108586
 Fe-Cr-Mo, white cast, optimising fracture toughness and abrasion resist. 0-85042
 Fe-Cr-Mo alloy castings, thick-section, factors affecting 0-108374
 Fe-TiC pseudofused composite magnetoabrasive powders, props. 0-100926
 GaAs-(GaP) single cryst., defect distrib. near abraded surface 0-92533
 GaP single cryst., defect distrib. near abraded surface 0-92533
 MgO single cryst., impact wear characts. 0-76374
 Mo alloy sphere, three-body abrasive wear with small size diamond abrasives 0-76373
 Na₂O-B₂O₃-SiO₂ glass fibre, plastic coating influence on strength 0-58697
 Na₂O-CaO glass, abrasion-resistant, high strength 0-76369
 Si, near (111), fracture by painted indenter, SEM study 0-71734
 Ti-Al-Cr-Mo, type VTZ-1, machinability, using different abrasive materials (*Russian*) 0-97593
 Ti-Al-Mo, type VT14, machinability, using different abrasive materials (*Russian*) 0-97593
 WC-Co hard alloys, hot-pressed, wear resist. under abrasive friction, heat treatment effect 0-66555

abrasive wear *see abrasion***absolute gravity** *see gravity***absolute pressure measurement** *see pressure measurement***absolute temperature** *see temperature***absorbers (surge)** *see surge protection***absorption**

for absorption of substances see sorption

see also acoustic wave absorption; electromagnetic wave absorption
 gas flow, recirculating, in packed columns, mass transfer and mixing, cell model 0-69913
 LiBr absorption, solar air conditioning system, low and high temp. cycles 0-81425

absorption spectra *see spectra***abundance ratio** *see element relative abundance; isotope relative abundance***acceleration**

see also acceleration measurement; accelerometers
 auroral electrons acceleration mechanisms 0-77210
 crystal resonators with increased immunity to acceleration fields in any shock/vibration environment 0-91953
 rigid body rotation in 3D space from body fixed linear acceleration meas. 0-68040

acceleration measurement

electrocapillary acceleration meters, electrolyte composition selection 0-73331
 electrocapillary acceleration meters with electrolyte in gel form 0-73330
 falling objects accel. due to gravity, Doppler effect, student microwave expt. 0-105472
 gravitational, appl. of desk calculator 0-73336
 gravity, inertial navigation, covariance analysis of periodic traversing 0-95087
 low-reactive meas. of motion, transducer effects on body under investigation (*German*) 0-105621
 piezoelectric acceleration sensors, lower limiting frequency and indication threshold (*German*) 0-95093
 piezoelectric accelerometers, effect of strain sensitivity on accel. meas. of flexural vibrations 0-58991
 sensor device for recording vibrations of tall structures 0-95084

accelerators (particle) *see particle accelerators***accelerometers**

see also acceleration measurement

Cactus accelerometer on Castor satellite, flight results synthesis for accels. below 10⁻⁹g 0-77251
 chronobiological movement transducer (*Spanish*) 0-89902
 electrocapillary acceleration meters, electrolyte composition selection 0-73331
 electrocapillary acceleration meters with electrolyte in gel form 0-73330
 EM accelerometer with adjustable rigidity and damping, static/dynamic accel. detect. (*German*) 0-105625
 piezoelectric, effect of strain sensitivity on accel. meas. of flexural vibrations 0-58991
 signature verification, data recovery 0-101791
 Si accelerometer, batch fabricated 0-73328

accidents

see also electric shocks; explosions; safety

accidents during work, mapping of reasons using error beams by function sensed computations of admission probabilities (*German*) 0-68027
 car accidents, correl. of field injuries and GM Hybrid III dummy responses 0-108939
 criticality accidents, dosimetry using activations of blood and hair 0-89857
 FBR notional accidental releases, effect of duration on consequences 0-94296
 Harrisburg reactor accident in 1979, lessons to be learned (*German*) 0-91233
 LMFBR, inherent safety features 0-106145
 nuclear, emergency planning and preparedness 0-57887
 nuclear accident dosimetry, blood-Na meas. 0-57979
 nuclear accident dosimetry system, Czechoslovakia 0-57978
 nuclear power plant safety, West German policy (*German*) 0-57865
 nuclear power plants risks assessment, German Risk Study (*German*) 0-57866
 nuclear power station, Three Mile Island, accident, malfunction development, prevention (*Hungarian*) 0-68846
 nuclear power station leak, ¹³³Xe from Three Mile Island 0-89696
 nuclear power stations, HTGR risk assessment, operator actions, event and fault tree anal. 0-63330
 nuclear power stations (*Portuguese*) 0-68844
 nuclear reactors, LOFT, contribution to safety 0-106139
 nuclear reactors, radioiodine air sampling system, separation into gaseous and particulate fractions 0-57962
 nuclear reactors, radiological emergency monitoring and instrumentation, Federal guidance 0-57961
 plutonium, biologically important physicochemical props. and methods of human contamination (*French*) 0-98004
 PWR accident prevention, extra instrumentation for Ringhals 2 station, Sweden 0-63369
 radioactive materials, IAEA transport information collection system, influence on improved safety measures 0-63413
 radioactivity incidents, national arrangements, review 0-102355
 Three Mile Island, lessons learned in maintenance and reliability 0-57929
 Three Mile Island incident, Atmospheric Release Advisory Capability, response and support 0-57889
 Three Mile Island incident, operator/instrumentation interactions 0-57890
 Three Mile Island incident, Pennsylvania's emergency preparedness and response 0-57888
 Three Mile Island malfunction, monitoring, radiation exposure 0-57960
 Three Mile Island nuclear power station, viewpoint of member of Commission of Enquiry 0-83190

accommodation coefficient *see sorption***accumulation layers**

p-n heterojunctions, forward-biased, charge accumulation 0-107902
 semiconductor surface space charge layers, subband struct., perturbation theory 0-84497
 p-CdTe-Langmuir film interface, prep., characters. and MIS struct. 0-92998
 GaSb, localised carrier interaction with LO phonons, Raman interference lineshapes 0-93338
 InAs, two dimensional accumulation layer, Anderson localisation 0-107871
 InSb (110), cleaved, gap states, field effect meas. 0-84501
 InSb, localised carrier interaction with LO phonons, Raman interference lineshapes 0-93338
 p-InSb MIS struct., field effect studies 0-80386
 Pb_{1-x}Sn_xTe epitaxial films, adsorption-induced accumulation layer form. on surface 0-60117
 Si, thermally oxidised surfaces, electron mobility in inversion and accumulation layers, MOS devices 0-103753

accumulators *see secondary cells***acidity** *see pH***acids, organic** *see organic compounds***acoustic analysis**

auditory analysis of sound, review 0-104593
 automatic speaker verification by cepstral analysis 0-91998
 random response of identical, one-dimensional coupled subsystems 0-102915
 signal rate of change distribution, gramophone player 0-79083
 synthesis of sound by continuous spectral transformation (*French*) 0-79100
 time selector for acoustic spectrosc. 0-87660
 time-delay spectrometry, practical appl. in field 0-79082
 US tone-burst spectroscopy, influence of phase cancellation and pulse shape artifacts 0-81276

acoustic applications

see also ultrasonic applications

atmosphere acoustic and radio acoustic exploration, effects of sound non-linear absorpt. (*Russian*) 0-94567
 atmosphere sounding, appl. to boundary layer obs. from top of steep mountain 0-98409
 beacon guidance system for walking blind aid 0-81676
 fracture toughness testing using acoustic emission monitoring 0-100918
 granular media, density measurement, plane strain conditions, acoustic method (*Polish*) 0-62635
 imaging, visualization and characterization, conf., Houston, TX, USA (Dec. 1979) 0-106672

acoustic applications continued

- imaging aid for the blind 0-104810
- levitation system, parametric study 0-74692
- plasma coatings, elastic properties, acoustic meas. (*Russian*) 0-97519
- reactor fuel pin rupture detection system, using meas. of time differential of acoustic emissions 0-102282
- research over past 50 years, review 0-96151
- rock structure analysis method (*Russian*) 0-85760
- submarine sediments, automatic recognition by sonoprobe survey, acoustic reflection pattern model (*Japanese*) 0-85776
- thermosonimetric investigation, of crystn. in metallic glasses 0-75180

acoustic arrays

- adaptive beam forming processor formulation 0-91967
- adaptive beamforming algorithm for resolving directions of sources in correlated field incident on array 0-64297
- broadband parametric array with Gaussian primary directivity patterns 0-96066
- clustered sensor array, turbulent boundary layer induced noise suppression 0-96121
- crossarray beamforming with a parametric receiving array and a line array 0-79078
- CW coherence meas. at low freq. for long underwater paths 0-106654
- eigenvector decomposition of correlation matrices 0-96118
- element failure and random errors effect on sidelobe level for linear array 0-106670
- environmental influences on acoustic array design and performance in shallow water 0-83721
- gain limitations of passive vertical line array in shallow water 0-96117
- Gaussian acoustic signal detection using array processors, performance eval. 0-83696
- high-efficiency narrowband transducers and arrays, development 0-58880
- high-gain, nonstationary and nonuniform oceanic background 0-64263
- holographic piezoelectric integrated array, system anal. 0-79067
- IC transducer array using electronically-addressed bulk acoustic wave Fourier transform device 0-74637
- in-line reflective array compressor 0-74626
- linear, waveguide attenuator using Helmholtz resonators, design calc. for zeroth normal mode 0-87602
- linear scanning with zone plate comparison with cylindrical focalisation 0-79091
- maximum entropy spectral estimation of frequency and arrival angle 0-96129
- multielement, characterisation by acousto-optic diffraction 0-99911
- noise correlation functions for arbitrary receiver orientation and steering direction in vertically anisotropic, azimuthally isotropic noise fields 0-58864
- noisy acoustic signal sources, optimal meas. of coords. by group of acoustic arrays 0-87659
- optimum range and bearing estimation with randomly perturbed arrays 0-96119
- parametric, beam pattern and propag. curve for air (*Japanese*) 0-83693
- parametric, characterisation of materials at oblique angles 0-96164
- parametric, effect of finite aperture 0-106648
- parametric, suppression of finite-amplitude primary wave attenuation, use of bubbles 0-74563
- parametric arrays with intermediate directivity in water, expt. study 0-74569
- parametric receiving array response to transducer vibration 0-74570
- partitioned signal detection by discrete cross-spectrum analysis 0-91966
- passive tracking acoustic array evaluation, nonlinear filtering lower bound algorithms 0-96088
- periodic dot arrays, selective reflection of SAW 0-74624
- phase arrays, multi-mode operation using noise signals 0-96157
- phase-shift beamformer, narrowband, suitable for IC implementation 0-58865
- phased, infinite periodic, investigation of acoustic field 0-58836
- radiation patterns of acoustical arrays with quantized time delays 0-74566
- random and partially random, statistical props. of beampatterns 0-64301
- reflective dot array for high-performance signal processing, development 0-74623
- robust sequential detection of weak signals in undefined noise 0-58861
- sonar systems, digital beam forming 0-91950
- sound source reconstructions using a microphone array, holographic technique 0-96132
- statistical array-synthesis problem, general soln. 0-87646
- thickness-extensional trapped energy mode transducer array, increased bandwidths and mode shapes 0-74633
- underwater acoustic source location and motion estimation, joint reduction of bias and variance 0-96087
- US receiving array having power response 0-74653
- US transducer, broadband directional reception 0-96126
- wideband Fresnel focusing array response, echography appls. 0-74640

acoustic delay lines

- see also ultrasonic delay lines*
- quartz, doubly-rotated-cut, SAW and SBAW 0-74584
- SAW, towards an ideal photon correlator 0-68252
- LiNbO₃-gap coupled Schottky diode memory correlator, grating coupled optical imaging 0-64143

acoustic detectors *see acoustic transducers***acoustic devices**

- see also acoustic delay lines; acoustic generators; acoustic microscopes; acoustic microwave devices; acoustic parametric devices; acoustic radiators; acoustic receivers; acoustic resonators; acoustic transducers; bells; surface acoustic wave devices; ultrasonic devices*
- elliptic lenses, history 0-96158
- filtering schemes for signals propagating through random multipath medium 0-58862
- Lamb wave focusing device 0-79093
- levitation devices for processing materials, limitations 0-74694
- photographic flash unit triggered by acoustic shock wave, cct. details 0-101862
- research over past 50 years, review 0-96151

acoustic dispersion

- see also ultrasonic dispersion*
- gyrotropic tensor, in crysts., activity rel. to cryst. class 0-107378
- metals, sound absorption and dispersion temp. depend. associated with Fermi surface plateaus (*Russian*) 0-65166
- Al, nonlinear sound wave interactions, sound attenuation in weak superconducting state (*Russian*) 0-75310

acoustic dispersion continued

- Ga, nonlinear sound wave interactions, sound attenuation in weak superconducting state (*Russian*) 0-75310
- Si guided-wave acousto-optical devices 0-102864

acoustic echoes *see echo***acoustic emission**

- see also ultrasonic materials testing*
- acoustic emission, amplitude distrib. anal. 0-66713
- Admiralty Metal, transgranular stress corrosion crack propag. 0-89402
- amplitude distrib., information content 0-108666
- applications (*Japanese*) 0-93726
- automatic digital equipment for recording acoustic emission signals 0-102948
- bone mammalian, testing 0-76783
- composite materials, crack growth, conc. criterion 0-65146
- data acquisition system for processing and recording of signals, on-line 0-57266
- defect development, temporal and spatial variation of elastic constant 0-85127
- defect dimension determination by acoustic emission 0-104381
- earthquake precursory acoustic emission, sound source direction formula (*Chinese*) 0-89961
- failure prediction on basis of acoustic emission 0-104382
- fatigue damage monitoring of 0-97673
- fatigue detection and rating by acoustic emission, review 0-104380
- glass, acoustic emission obs. during heating through glass temp. 0-84253
- glass fibre reinforced plastic, acoustic emission 0-104294
- granite microfracture, source process rel. to earthquake prediction 0-104919
- locator, receiving channels, selection of number 0-108676
- materials testing appl., plastic strain and growing cracks identification 0-81252
- nuclear reactor components, NDT using acoustic emission (*Spanish*) 0-57871
- piezoelectric receivers, amplitude-freq. response determ. for acoustic emission 0-87699
- piezoelectric transducers, single acoustic signal distortion 0-87637
- polymeric liquid, viscoelastic, gas bubble pulsations and assoc. dissipation effects 0-59079
- pressure vessels, AE during fatigue crack expansion 0-108675
- pulse shape, relaxation and acceleration pulses 0-64250
- SEM, combined deformation/heating stage, acoustic emission role meas. 0-101892
- signals, unit for recording and reproduction 0-79039
- solids, acoustic wave emission, absorpt. and propag. in THz range 0-65164
- sonic pulses generated during boiling of underheated liquid, time and spectral characteristics 0-107373
- spectra, laboratory comparisons 0-108658
- spherical void expansion into isotropic elastic medium 0-102914
- statistical investigation of acoustic-emission pulse distrib. 0-87638
- steel, acoustic emission sources and dislocation patterns 0-61040
- steel, ferritic, magnetomechanical acoustic emission for residual stress NDT 0-71149
- steel, high-strength castings, AE study of intercrystalline crack form. 0-104403
- steel, low alloy, isothermal tempering effect on acoustic emission during ductile fracture 0-85047
- steel, mild, 1019 AISI, acoustic emission generated during deform. 0-60921
- steel, stainless, austenitic type 304, martensite transform, acoustic emission identification, opt. microscopy obs. 0-81062
- steel, stainless type SUS 304, diffusion welded joints, sound emission during tensile testing (*German*) 0-61062
- steel, structural, elastic limit determ. by acoustic emission 0-66716
- steel laminate, acoustic emission rel. to fracture at 77K (*Russian*) 0-93633
- test apparatus 0-61041
- timber drying process 0-102940
- transducer calibration (*Czech*) 0-106697
- transient recorders for acoustic emission studies 0-83717
- US materials testing, beam shaping effects and optimisation (*German*) 0-85122
- vibrating body acoustic field calc. via Schenck numerical method (*French*) 0-69589
- welded structure reliability estimation, appls. 0-93702
- welding, crack formation monitoring equipment and acoustic emission method 0-89451
- Al alloy 7039, AE spectra, laboratory comparisons 0-108658
- Al alloy electrode, corroding, acoustic emission 0-60997
- Al anodic films, acoustic and electron-emission during deform. 0-80143
- Cu-NbTi, composite conductor, acoustic emission 0-97032
- β -CuZn, acoustic emission rel. to stress induced martensitic transformation 0-81061
- Fe, magnetomechanical acoustic emission for residual stress NDT 0-71149
- LaNi₅Fe, H₂ absorpt. cracking, acoustic emission characts. (*Japanese*) 0-66631
- NbTi-Cu, composite superconductor, acoustic emission 0-84546
- steel, C, magnetomechanical acoustic emission for residual stress NDT 0-71149
- Ta, acoustic emission induced by hydride formation 0-76257

acoustic equipment

- see also acoustic arrays; acoustic wave interferometers; ultrasonic equipment*
- active sound-suppression system, single-mode waveguide, bandwidth meas. 0-87605
- digital audio systems, future prospects (*Japanese*) 0-83725
- Fresnel zone and diffraction fields anal. near bore sight of acoustic radar antennas 0-64318
- GenRad 2512 portable digital spectrum analyser, simplicity of operation due to interactive display, technical specifications 0-64326
- level meas. in nuclear waste liquor tanks using acoustic pulse-reflection meter 0-86265
- levitation and manipulation method for controlling liquid samples in microgravity expts. 0-74666
- measuring instrum. over past years, review 0-96152
- microscope, acoustic zone plate variable-illuminating-angle system 0-106684

acoustic equipment continued

- radar systems, appl. of microcomputers 0-106685
- sound analyser, undergraduate lab. expts. 0-82600

acoustic field

- 3-D objects, calc. by integral eqn. methods 0-74558
- acoustic diffuser characteristics for amateur user, concert hall appl. (*Italian*) 0-91961
- arbitrarily electroded piezoelec. plate acoustic spatial response determ. 0-99910
- axisymmetric transducers, with various boundary conditions, single integral computer method for Green's function 0-87591
- baffled piston transducer, analytical model for nearfield 0-96168
- coherent optics methods appl. to acoustic field investigations 0-106691
- concert hall design, lateral and ensemble reflection requirements 0-91964
- diffuse vibration field propag. in structs. with periodic inhomogeneities 0-86093
- edgetone sound, prediction of amplitude 0-74568
- factorization by means of 2 concentric spherical sensing surfaces 0-64247
- Fredholm integral equation, 1st kind for acoustic diffraction calc. (*Russian*) 0-58834
- geological materials, acoustic fluidisation prod. by strong transient wave field, theory and appls. 0-85653
- horn loudspeaker, anal. of acoustic radiation by finite element method 0-96171
- intersection of pipe with plenum, acoustic inertial end correction 0-64246
- Lamb wave optical detect. in fused SiO₂ 0-106690
- microsphere probe for pressure field meas. up to 10 MHz 0-96159
- multielement acoustic array characterisation by acousto-optic diffraction 0-99911
- narrow-strip transducer, radiation pattern theory 0-96165
- noise correlation functions for arbitrary receiver orientation and steering direction in vertically anisotropic, azimuthally isotropic noise fields 0-58864
- phased arrays, infinite periodic 0-58836
- piezoelectric transducers, single acoustic signal distortion 0-87637
- point source in rectangular space bounded by thin elastic walls, acoustic field 0-96050
- Raman Nath parameter calc. for entire field of baffled planar transducer 0-74689
- reflectivity field reconstruction from line integrals over circular paths 0-58863
- rigid sphere vibrating parallel to plane wall, near field 0-102910
- spherical, acoustic radiation pressure on rigid sphere 0-64251
- spherical and ellipsoidal Huygens surfaces, discrete approx. for suppression of sound fields 0-87594
- three dimensional objects, stable soln. for integral eqn. formulation 0-106647
- transient, microphone method for energy meas. 0-102942
- US fields, Gaussian-Laguerre description for circular piston 0-64239
- US pressure and interference fields (*German*) 0-89436
- vibrating rigid body, calc. via Schenck numerical method (*French*) 0-69589
- wedge with curved faces, field near edge 0-87592
- LiI₂ single crystal, surface acoustic wave parameter meas., coherent optics method 0-106691

acoustic generators

- see also earphones; loudspeakers; photoacoustic effect*
- biomedical noise generator for masking click stimuli 0-108980
- Doppler thermooptical source of US waves 0-58852
- Helmholtz resonator as high-power deep-submergence LF source 0-74576
- horn excited by Hartmann-Sprenger tube, aeroacoustical phenomena 0-91948
- infrasound and pressure waveform generator, compact, for small cavity appls., animal research 0-104830
- laser thermooptical sound source in liquid, anal. of wave zone 0-87631
- motor car horn diaphragms, free vibr. anal. 0-74687
- moving point sources, intensity of acoustic fields (*German*) 0-102879
- optoacoustic sound focusing device using YAG laser 0-87692
- piezoceramic transducers for generation of acoustic pulses having prescribed shape 0-87691
- piezoelectric ceramic buzzers for high sound levels 0-92005
- PMOS programmable sound generator, microprocessor-compatible, electronic music appls. (*German*) 0-79092
- SAW generation using CW laser, NDT appl. 0-87683
- sphere impacting on thin square plate, acoustic generation mechanism 0-74591
- transducer-receiver configuration, flexible, activated by laser 0-83724
- vortex, separation of acoustic energy and spent-air jets 0-102953

acoustic holography

- biomedical applications, state of art and future 0-67175
- imaging technique without wavelength resolution limit 0-99898
- long-wave imaging with super-resolution by wavelength diversity 0-102675
- near-surface defects, US detection and analysis (*German*) 0-93728
- phase samples, improved image quality (*French*) 0-79088
- piezoelectric integrated acoustic array, system anal. 0-79067
- sound source reconstructions using a microphone array 0-96132
- two-dimensional target imaging using multifreq. hologram matrix, 1 MHz ultrasound expts. 0-64305
- US hologram numerical reconstruction in NDT (*German*) 0-97667

acoustic imaging

- see also acoustic holography*
- 2-D acoustic Fourier transform of optical images 0-74308
- aid for the blind 0-104810
- B-scan imaging with automated water-delay system 0-98041
- biomedical US B-scanning, computer simulation 0-81675
- cellular mechanical and chemical analysis, recommendations of workshop on future of biomedical instrum. 0-81776
- coherent optics methods appl. to acoustic field investigations 0-106691
- cylindrical transducer scatter scanner for medical ultrasonographic imaging 0-96154
- data collection aperture, based on long-wavelength imaging system 0-99905
- diagnostic US, prospects and limitations 0-98040
- diffraction tomography, experimental results 0-76818
- dynamically focused electronic sector scanner based on CCDs 0-98042
- echo-tomographic imaging with SAW processing, ultrafast 0-74639
- echographic phased array for medical diagnostics, dynamically focused insonification 0-89813
- electronic ccts., book 0-99899

acoustic imaging continued

- electronically-addressed bulk acoustic wave Fourier transform device 0-74637
- foetal growth estimation from US image meas. 0-101239
- gallstones, acoustic shadow formation 0-98047
- generalized image synthesis from projections 0-67579
- grating acoustic scanner characteristics measured by an optical probe 0-74662
- Lamb wave optical detect. in fused SiO₂ 0-106690
- linear scanning with zone plate comparison with cylindrical focalisation 0-79091
- mammographic US image correlation with histopathologic sections 0-101240
- medical, shadowing due to calculi and gas collections, differentiation 0-98048
- medical, transmission media for ultrasonography 0-98050
- medical B-scan US, technical factors influencing the imaging of small anechoic cysts 0-98049
- medical US, spread energy method, use of time gain control 0-108988
- medical US imaging, improvement of sensitivity or reduction of dose 0-74641
- medical US imaging light intensity perception charact., stochastic noise influence 0-98053
- medical US phantoms, water-based gels 0-81671
- multiplicative and additive processing comparison 0-64303
- narrow-strip transducer, radiation pattern theory 0-96165
- nematic liquid crystal retinas for direct 2D acoustic images (*French*) 0-69617
- objects buried in seafloor sediment using focused US transducer 0-79036
- optically-controlled acoustic transducers, piezoelect. and electrostrictive 0-74638
- opto-acoustic transducers, improved equivalent cct. 0-74658
- phantom for imaging biological fluids by US and computerised tomography scanning 0-104692
- phase samples, improved image quality (*French*) 0-79088
- piezoelectric elements of array, tall, narrow, vibration mode 0-74690
- SAW transducer array for surface defect imaging in metals 0-74660
- scanning electron microscopy, US imaging technique 0-95192
- scanning of optical images using acoustoelectric memory correlator struct. 0-74632
- seismic imaging of faults in multi-moded coal seams 0-85778
- super-resolution passive imaging system using algebraic reconstruction 0-79081
- thermographic-photographic technique for US intensity pattern characterisation 0-106689
- tissue quantitative characterisation by US, review 0-81670
- US, backscatter enhancement from collagen microspheres, dog liver, erythrocyte suspension 0-94281
- US, intraoesophageal, heart dynamics 0-94303
- US, single-channel reduced-bandwidth SAW-based processor 0-74636
- US B-mode images of human tissue, real-time speckle reduction 0-74634
- US B-scan, pancreas scans of cystic fibrosis sufferers, amplitude anal. 0-94302
- US B-scan, theory of image formation, technique for restoration 0-94300
- US biomedical micro-array technology for improved image quality (*German*) 0-98052
- US imaging modalities for medical appls. 0-81669
- US imaging system, digitally controlled, electronically scanned and focused 0-74659
- US tissue characterization in vivo, broadband integrated backscatter 0-74635
- US transmission tomography 0-94301
- US visualization and characterization, conf., vol.8, Key Biscayne, FL, USA (May-June 1978) 0-83720
- visualization and characterization, conf., Houston, TX, USA (Dec. 1979) 0-106672
- wavefront reconstruction acoustic imaging using two dimensional arrays 0-74661
- wideband Fresnel focusing array response, echography appls. 0-74640
- LiI₂ single crystal, surface acoustic wave parameter meas., coherent optics method 0-106691

acoustic impedance

- see also acoustic wave velocity*
- absorbers, dimensioning of facings for acoustically effective structural elements (*German*) 0-74600
- filled polymer materials, simple approx. method, US velocity meas. 0-64314
- hearing, impedance and tone screening of schoolchildren 0-108985
- horns, quasi-standing waves 0-79071
- influence of grazing flow, cylindrical wall cavity 0-69784
- Kundt's tube, determination of wall impedance by means of FM transmitter signal (*German*) 0-102878
- line transfer and line drive admittance approx., free wavenumbers, fluid-loaded panels 0-64432
- measurement, pulse-tube and direct point meas. methods 0-96164
- measurement using const. vol. vel. sources 0-74651
- neonatal acoustic reflex, static and dynamic impedance obs. 0-104597
- nondestructive eval. using unipolar transducers 0-76471
- pulse echo waveform rel. to acoustic characteristics of continuous medium 0-67145
- radiation impedance of pistons operating in homogeneous layer 0-87596
- rigid sphere vibrating parallel to plane wall 0-102910
- tissue structures characterisation, method of obtaining an impedance profile 0-67171
- tube, meas. combustion process admittances 0-64320
- W-PVC composites, fabrication rel. to performance 0-76218

acoustic insulating materials *see noise abatement***acoustic intensity**

- see also acoustic noise; loudness*
- moving point sources, intensity of acoustic fields (*German*) 0-102879
- moving source in semi-space with stratified medium 0-87617
- resolution and relation to loudness matching 0-108908

acoustic intensity measurement

- air-handling ducts and plants, direct sound intensity measurement method (*German*) 0-102944
- ear protectors, use of sound levels for assessing adequacy 0-104771
- multielement acoustic array characterisation by acousto-optic diffraction 0-99911
- nondirectional sound sources in layer of fresh-water reservoir 0-58845
- room acoustics correction, using Shure analyser (*German*) 0-58873

acoustic intensity measurement continued

- schlieren optical filtering for light diffracted from US beam 0-87672
- structure-borne sound, procedure for meas. sensitivity of building structures to stationary excitation (*German*) 0-64287
- transient sound fields, microphone method for energy meas. 0-102942

acoustic magnetic resonance

- see also *acoustic nuclear magnetic resonance; acoustic paramagnetic resonance*
- No entries

acoustic measurements see *acoustic variables measurement***acoustic microscopes**

- acoustical imaging, US visualization and characterization, conf., vol. 8, Key Biscayne, FL, USA (May-June 1978) 0-83720
- ceramic components nondestructive testing, comparison with SEM and optical microscopy results 0-58875
- dark field acoustic microscopy 0-96149
- imaging, visualization and characterization, conf., Houston, TX, USA (Dec. 1979) 0-106672
- LSI surface analytical techniques applied to electronic components [Si LSI chip inspection] 0-81392
- photoacoustic, thermal wave microscopy, physical processes 0-74652
- photoacoustic thermal-wave microscopy, high resolution studies 0-74647
- planar acoustic microscope lens using Rayleigh to compressional conversion 0-87668
- scanning, acoustic contrast of structs. buried inside object 0-74664
- scanning, with ZnO film concave transducers 0-74663
- scanning acoustic microscopy for study of interfaces in solid-state devices 0-99907
- transmission, phase measurement using AM carrier 0-74665
- transmission scanning, single lens 0-87669
- zone plate variable-illumination-angle system 0-106684
- SiO₂ sputtered film performance as acoustic antireflection coating at sapphire-H₂O interface 0-106686

acoustic microwave devices

- see also *acoustic transducers; surface acoustic wave devices*
- 2.148 GHz SAW oscillator 0-74680
- photoacoustic detection system for investigation of ferromag. resonance in films 0-80613
- SiC delay line at 9.43 GHz, acoustic props. study 0-65169

acoustic mode of crystals see *lattice dynamics***acoustic noise**

- absorption, panel system design 0-87649
- acoustically excited jet, discrete noise spectrum, vortex pairing 0-74847
- aeroacoustics of advanced turbopropellers, noise prediction 0-69598
- aerodynamic sound generation by unsteady subsonic flows around rigid bodies 0-69798
- air bubbles, production, pulsation and damping, in dil. polymer solns. 0-69879
- air traffic, general control measures, case study of Torrance Municipal Airport (California) 0-83702
- aircraft, noise, basic aeroacoustic research, industrial appl. 0-69596
- aircraft, Siemens airport noise monitoring systems 0-99895
- aircraft, the Netherlands, legal and economic factors 0-72112
- aircraft noise propag., review 0-64258
- airfoil trailing edge noise, near-wake struct. and unsteady pressures at trailing edge 0-69794
- airfoil trailing edge noise, pressure field at trailing edge: effect on radiated noise 0-69795
- analysis, Cranfield Institute of Technology, SPAG minicomputer system 0-96162
- annoyance, performance, and mental health related to noise 0-96104
- auditory perception nonlinear model with autocorrel. feedback 0-81615
- auditory system, pitch of amplitude-modulated low-pass noise and predictions by temporal and spectral theories 0-67095
- auditory threshold assessment in extended HF range, with impedance measurements 0-61592
- biological effects, autonomic system activities 0-83700
- biological effects, autonomic system activity and performance on a psychomotor task in noise 0-89790
- biomedical noise generator for masking click stimuli 0-108980
- built-up urban environments, propag. of sound generated by point source 0-58841
- clustered sensor array, turbulent boundary layer induced noise suppression 0-96121
- compressible axisymmetric jet sound radiation by instability waves 0-69792
- core noise and jet noise separation, mean square pressures 0-69779
- diesel electric locomotives, SD40-2 noise under various operating conditions 0-102924
- diesel engine noise generation, diagnosis and control 0-58857
- diesel engine powered installations, noise reduction programme 0-96106
- diesel engines, piston slap, assessment of contribution to overall noise and vibration 0-79055
- discrete frequency sound generation by fluid flows 0-69812
- duct, supersonic flow downstream oscillations from abrupt cross section increase, nozzles 0-74976
- ear protectors, relation of attenuation to noise spectra 0-96100
- effect on performance of a psychomotor task, sorting during 90 dB(A) of pink noise 0-64283
- electrical equipment, noise generation mechanisms and characs., selecting quiet equipment and correcting noisy devices 0-64286
- engine intake noise, high freq., ray-theory approach 0-69595
- environmental, relationship to air pollution levels 0-69594
- environmental, tendencies in subjective assessment 0-72111
- environmental noise system, statistical anal. of mutual relation between two-component noises 0-102917
- excess noise from supersonic underexpanded jets in flight 0-69815
- factor of safety, calc. method and appl. to air and noise pollution 0-94140
- fanjet engines, discrete freq. noise reduction modelling 0-106652
- flight effect of Michalke and Michel vis-a-vis Lighthill's model 0-59018
- flow acoustic interaction near a plane heat conducting compliant boundary 0-69809
- gas turbine combustors, noise source mechanisms, expt. determ. 0-69597
- Gaussian intensive noise spectrum evolution, plane wave in lossless fluids 0-69581
- generation by steady airflow down corrugated duct 0-106660
- ground-borne, building vibration control, use of natural rubber mounts 0-87643
- hearing reflex threshold for noise stimuli 0-108916

acoustic noise continued

- hearing threshold levels of N.Carolina industrial employees, race and sex variations 0-97939
- helicopter rotors, sound radiation props. for free field and near absorptive plane surface 0-102885
- higher order mode effects in circular ducts and expansion chambers 0-96058
- hydroacoustics, role of surface shear stress fluctuations 0-69808
- impulse and impact, review of current knowledge 0-79056
- impulsive noise reduction on gramophone records 0-87689
- induced vibration, fatigue cracks in aircraft skin panels, prediction of edge crack growth 0-69737
- induced vibration in buildings, propag. model 0-74602
- industrial, monitoring workers' hearing 0-81621
- industrial noise onset effects on physiological and psychological functions 0-91959
- industrial process burners, suppression methods 0-74597
- insulation, domestic roofing, expt. facilities of meas. laboratory, test details 0-79058
- insulation, multiple layer walls, prediction of output probability distribution of noise level 0-69593
- insulation, window-glasses, most effective window configurations 0-87655
- jet aeroplane noise, effects on facial expression, EEG and manual responses, human subjects 0-98006
- jet flow turbulence generated, edge dissipation 0-103020
- jet mixing noise generation, eval. of Lighthill analogy using LV turbulence, source location and spectral noise data 0-69803
- jet noise, cross-spectral densities, extension of Ribner's theory 0-69804
- jet noise and large scale instability waves, effect of upstream tones 0-69790
- jet noise in flight, prediction, importance of jet temp. 0-69814
- jet noise in flight prediction from static tests 0-61490
- jet noise prediction, nonlinear Lilley equation 0-69805
- linear predictive coded speech digitisers, background noise spectral subtraction 0-96140
- loudness discomfort level and acoustic reflex threshold for speech stimuli 0-76762
- loudness discomfort level and acoustic reflex threshold for normal and sensorineural hearing-impaired subjects 0-76763
- low frequency noise breakout from air conditioning ducts, abatement 0-74594
- low frequency sound radiation due to the interaction of unsteady flows with a jet pipe 0-69787
- low Mach number aerodynamic noise theory 0-69796
- low Mach number duct flows, combustion noise generation by chemical inhomogeneities 0-92237
- maximum likelihood detection and estimation for harmonic sets 0-96116
- minimum acoustical requirements for school buildings 0-79059
- multiple input/scalar output problem, source identification 0-96105
- multivariate joint probability expression of general random processes, finite expansion terms 0-69592
- noise, aerodynamically generated, fluid flow eqns. (*French*) 0-74848
- noise generation by transonic open rotors 0-69599
- open-plan offices, role of acoustic screening 0-87650
- opencast coalmining, principal noise sources 0-81505
- physiological acoustics and health 0-96103
- power press, relationship between force waveform and sound radiation 0-74596
- pulsation noise damping from small air bubbles in water 0-64253
- radiated noise level calc. of mechanical impact using tapping machine (*French*) 0-87639
- radiation properties of a turbulent jet excited by a sinusoidal acoustic disturbance 0-69789
- railway passenger coaches, structure-borne noise suppression (*German*) 0-91957
- relationship between sound power level and sound pressure level, laboratory and domestic environments, use of noise data 0-74599
- road traffic, a socioeconomic approach to subjective responses 0-67022
- road traffic, close proximity vehicle noise survey method 0-102926
- road traffic, close to light motor vehicles 0-83701
- road traffic, control of noise level of moving vehicles 0-99894
- road traffic, correct building placement, noise emitted by single source in open space 0-87647
- road traffic, highway noise barrier perceived benefit 0-102920
- road traffic, highway noise barriers, optimum weight with respect to effectiveness and cost 0-67021
- road traffic, kerbside study of vehicles 0-79050
- road traffic, meas. accuracy using digital instrums. 0-79075
- road traffic, meas. radiating height of cars and lorries, effectiveness of sound barriers 0-64325
- road traffic, relationships between multidimens. correlation props. of intensity and higher order information, Stratonovich's stochastic theory for random points system 0-87645
- road traffic, subjective annoyance, lab. expt. on students 0-102921
- road traffic, traffic passing through road intersections controlled by roundabouts, model 0-64280
- road traffic, traffic-induced building vibration 0-96098
- road traffic, use of sloped barriers for noise abatement 0-102925
- road traffic Monte Carlo simulation methods, effect of vehicle spacing on results 0-72110
- round free jet, aerodynamic noise, propagation of wavelike disturbances 0-69806
- shear layer instability noise produced by various jet nozzle configurations 0-69791
- signal detection and localization, Fourier series method appl. to signal in noise background, comments 0-106671
- site selected variables effect on human responses to traffic noise 0-61491
- site selected variables effect on human responses to traffic noise 0-61492
- sonic boom of supersonic transport aircraft, effects on ecological environment 0-106661
- sonic booms, pressures inside room with open window 0-69602
- sonic pulses generated during boiling of underheated liquid, time and spectral characteristics 0-107373
- sound generation and propagation in flows, inhomogeneous convected wave equation 0-69813
- sound generation and simulated emission by vortex flows 0-69797
- sound generation by flow-acoustic coupling 0-69793
- sound generation by head-on collision of two vortex rings 0-69801
- sound generation in flows, conf. Göttingen, Germany (Aug. 1979) 0-69797
- sound insulation, domestic roofing systems 0-96109

acoustic noise continued

- sound isolation tests of residential buildings, correlation with subjective privacy opinions, standard sound source requirements 0-64323
- sound levels, use for assessing adequacy of hearing protectors 0-104771
- sound radiation from a simulated jet flow, calc. of vortex configuration and sound field 0-69786
- sound sinks in flows, low freq. sound absorpt. of jets 0-69788
- sound source location techniques 0-69802
- sound spectra radiated by gas jets, influence of closely located solid surfaces 0-69800
- speaker verification algorithm for noisy utterances 0-91992
- speech adaptive noise cancellation by short-time Fourier transform 0-91976
- speech intelligibility, noise effects in cases of presbycusis 0-96139
- speech noise suppression filter for narrowband vocoder 0-91977
- speech wideband noise reduction by spectral weighting 0-96146
- steam turbines, 200 MW, with accessories, noise reduction research and development 0-91958
- STOL aircraft engine-wing system jet flap impact noise meas. 0-96101
- Strouhal number influence on flight effects on jet noise radiated from convecting quadrupoles 0-69781
- subsonic jet in simulated motion, sound radiation 0-74846
- supersonic air flow through high press. gas valves into atm., noise and flow pattern obs. 0-59067
- surface effect vehicles, design problems 0-74598
- surface generated noise in stratified ocean, spatial correlation 0-87620
- surface noise from turbulent hot jet, temperature effects 0-69782
- transmission lines, high-voltage, coronal discharge noise depend. on instantaneous rainfall rate 0-98471
- turbojet, internal 0-87644
- turbulence generated, acoustic radiation from bodies in unsteady flows 0-69799
- turbulence generated sound, mean flow calcs. of large eddy struct. and flow-acoustic interaction 0-69785
- turbulence-generated, air flow in pipes with various fittings 0-74849
- turbulent flow noise generation, role of tornado-like vortices 0-69811
- turbulent jet flow, aeroacoustic interaction, review 0-87765
- underwater noise spectra produced by fishing boats affecting albacore catch, comment 0-58844
- underwater sound, theoretical model of ambient noise in low-loss, shallow water channel 0-64265
- US transmission line of probe for hot metal inspection, spurious signals 0-66754
- vortex pairing in jet noise generation 0-69807
- wall jet flow, compliant walls, influences of flow convection and refraction on sound radiation 0-74595
- wall-pressure spectrum in turbulent boundary layer, rel. to noise generation by boundary layer-surface interactions 0-69810
- waveguide with monopole radiators and dipole receivers, active noise suppression 0-102928
- wing in forward motion, trailing edge acoustic source radiation 0-69780

acoustic noise measurement

- air-handling ducts and plants, direct sound intensity measurement method (*German*) 0-102944
- artificial head system, transmission errors causes and improvements (*German*) 0-106700
- atmospheric probing, appls. of external noise spectrum model 0-58858
- bat detection instruments 0-69609
- buses, noise levels in New York City and Albany metropolitan areas 0-76684
- cavitation tunnel hydroacoustic transfer function, meas. and anal. (*Croatian*) 0-92002
- correlation measurement method for rotating sources of noise 0-64279
- electric machines, meas. errors (*Hungarian*) 0-96102
- environmental random noise distrib., prediction using generalized time-discrete Fokker-Planck eqn. 0-102918
- fluctuating noise, meas. and anal. system (*French*) 0-64316
- fluid power equipment, noise analysis and control, PDP 11/40 minicomputer dynamic analysis system, graphical presentation of results 0-64327
- helicopter noise rating, development of proposed impulse correction 0-96107
- high speed unequally spaced fan rotor, method 0-96163
- impulsive and continuous noise, combined dose meas. 0-102929
- induction motors, 3-phase, laminated cores, sound level theory, meas., and results (*Polish*) 0-92004
- noise and number index, definitions of parameters 0-61489
- noise level meas. using optical fibre interometric hydrophone 0-87673
- ocean, spatial, noise spectrum meas. in ocean for small observation baseline 0-102902
- optical fibre interometric hydrophone appl. 0-87673
- outdoor noise of coal-fired power plants 0-76683
- quarrying, use of electronic transient recorders for meas. explosion noise and vibration 0-67023
- railways, meas. on noise protection screens (*German*) 0-102916
- regulations and methods for noise measurement (*German*) 0-69610
- Rome road traffic noise, 24-hour obs. and statistical analysis (*Italian*) 0-87651
- sound level meter display attachment, small no. of samples metering 0-79076
- sound level meter output measurement, use of digital voltmeter 0-79077
- Space Shuttle, prediction of acoustic environment in payload bay 0-102919
- underwater sound, measurement of acoustic noise effects on behaviour of marine organisms 0-106657
- unsteady noise from letter-handling machines, automatic classification of noise levels 0-79085

acoustic nuclear magnetic resonance

- liquids, spin lattice relaxation, sound coherence 0-97128
- multiple-scan direct and lock-in detection schemes, metal single cryst. appls. 0-66050
- Sn, white, nuclear acoustic reson., Knight shift 0-71204

acoustic paramagnetic resonance

- cubic crystals, pseudo-tetragonal APR spectra 0-88861
- degenerate semiconductor, conduction electron acoustic spin resonance, oscillations of absorbed power 0-108075
- dielectric crystal, Jahn-Teller effect, study of paramagnetic ions 0-84634
- liquids, spin lattice relaxation, sound coherence 0-97128
- semimetal, degenerate, conduction electron acoustic spin resonance, oscillations of absorbed power 0-108075

acoustic paramagnetic resonance continued

- KMgF₂:Fe²⁺, anomalous acoustic relax. absorpt. and APR 0-88864
- MgO:Cr²⁺, APR under applied stress 0-88865

acoustic parametric amplifiers

No entries

acoustic parametric devices

- see also *acoustic parametric amplifiers; acoustic parametric oscillators*
- arrays, beam pattern and propag. curve for air (*Japanese*) 0-83693
- arrays with intermediate directivity in water, expt. study 0-74569
- radiating parametric antennas, review 0-102898
- receiving array response to transducer vibration 0-74570

acoustic parametric oscillators

No entries

acoustic radiators

- see also *acoustic generators; Doppler effect*
- arbitrary shape, directivity pattern calc., near-field press. meas. on surface of finite circular cylinder 0-87677
- circular duct with hyperbolic horn, sound radiation modes 0-96096
- cylindrical steel shells in water, thick-walled (*German*) 0-102899
- elastic shell, appl. FEM to coupled structural-acoustic radiation system 0-83691
- estimation of source motion from time delay and time compression measurements 0-58860
- gas-jet generators, design characts. 0-87695
- horn and silencer design, FEM anal. of acoustic transmission/radiation systems 0-87589
- ill-posed diffraction problem and quasiresolution 0-87593
- moving sources, radiation props. in free field and near absorptive plane surface, helicopter blade noise 0-102885
- parametric, liquid containing gas bubbles 0-87615
- parametric antennas, review 0-102898
- piezoelectric radiator of longitudinal acoustic waves with an inhomogeneous elec. field 0-87693
- piston, operating in homogeneous layer, radiation impedance 0-87596
- plane waveguide with one perforated wall, calc. of radiation characts. 0-102886
- point source between thin elastic plates, fluid immersed, roots of dispersion relations 0-87601
- power output, calc. by integrating energy flux over distant control surface 0-87587
- radiation impedance of infinite-elliptical cylinder in system of like radiators 0-102911
- spherical and ellipsoidal Huygens surfaces, discrete approx. for suppression of sound fields 0-87594
- strip radiator, power output considerations 0-69577
- AI plate excited by free turbulent jet, generation of vibrs. and atmospheric sound (*German*) 0-102908

acoustic reactance see *acoustic impedance***acoustic receivers**

see also *microphone*

- medical ultrasonics, piezoelectric materials study 0-76819
- transducer-receiver configuration, flexible, activated by laser 0-83724

acoustic resistance see *acoustic impedance***acoustic resonators**

- combustion driven oscillators, plane wave theory anal. 0-102951
- cylindrical piezoelec. transducer, influence on spectrum of natural freqs. 0-87694
- definition of quality factor, errors in Q from width of an input impedance peak 0-69572
- distributed, model for a two dimens. resonator 0-64275
- flow-tone effects, forced oscillations of separated shear layer 0-64256
- influence of depth on acoustical props. 0-58838
- non-rectangular reverberation chambers, resonance freq. and eigenfunctions, calculation by finite element analysis 0-64324
- SAW, radiation losses formed by interdigital type reflectors 0-69603
- second-harmonic generation in resonator of multilayered interference filter type 0-58840
- side-branch pipe resonators, flow-induced tones 0-64243
- tetrahedral, exact soln. of natural mode problems 0-64248

acoustic streaming

- intravascular thrombus induction in vivo using localised hydrodynamic shear stresses 0-97997
- MBBA nematic liquid crystals excited by 20 MHz US surface waves 0-76003
- nematic liquid cryst., acousto-optic effect, acoustic streaming 0-88964
- nematic liquid cryst., response to acoustic field, streaming component and instability 0-80747
- nonsteady quasi-one-dimensional acoustic streaming in unbounded volumes with hydrodynamic nonlinearity 0-87611

acoustic superradiance

No entries

acoustic surface wave devices see *surface acoustic wave devices***acoustic surface waves** see *surface acoustic waves***acoustic transducers**

- see also *acoustoelectric transducers; ultrasonic transducers*
- acoustical imaging, US visualization and characterization, conf., vol. 8, Key Biscayne, FL, USA (May-June 1978) 0-83720
- backscattering formula 0-96064
- baffled piston transducer, analytical model for nearfield 0-96168
- calibration (*Czech*) 0-106697
- combustion driven oscillators, plane wave theory anal. 0-102951
- efficiency measurement using self-reciprocity techniques 0-58881
- fibre optic acoustical detector probe 0-91916
- imaging, visualization and characterization, conf., Houston, TX, USA (Dec. 1979) 0-106672
- intermetallic compound, TbFe₂ elastic modulus magnetic field dependence 0-87698
- laser-activated transducer-receiver, flexible configuration 0-83724
- level transducers resistor type, coupled with AC supply amplifier systems, theoretical and experimental behaviour (*Italian*) 0-79051
- narrow-strip transducer, radiation pattern theory 0-96165
- piezoelectric transducer, composite, of low freq. acoustic flaw detector, natural freq. calc. 0-89450
- Cu-NbTi, composite conductor, acoustic emission 0-97032
- R-Fe octagonal transducer 0-74684
- Si-Zn integrated acoustic transducer arrays 0-74683

acoustic variables measurement

- see also *acoustic intensity measurement; acoustic noise measurement; acoustic wave velocity measurement; Q-factor measurement; ultrasonic measurement*
- acoustic coupling between rooms, meas. system using decrease in sound level method (French) 0-69611
- acoustic emission rate, combined deformation/heating stage, for SEM 0-101892
- architectural acoustics measurements by impulsive excitation (Japanese) 0-64292
- auditory system, pitch of amplitude-modulated low-pass noise and predictions by temporal and spectral theories 0-67095
- broadcasting studio, 'Deutsche Welle' building construction and meas. (German) 0-106668
- combustion process admittance measurement, acoustic impedance tube technique 0-64320
- cultural centre reconstruction, acoustic tasks and measurements (Hungarian) 0-106666
- direction location of infrasound waves, meas. on jet planes (German) 0-92000
- directivity pattern, near-field press. meas. on surface of finite circular cylinder, arbitrarily-shaped acoustic radiators 0-87677
- ear static acoustic-impedance measurements 0-76758
- electret condenser microphones, design for meas. purposes 0-79086
- impulse response meas. of acoustic transmission system, digital computer processing (German) 0-91999
- manual and Bekesy thresholds, noise-exposed subjects, test-retest reliability 0-81622
- optical determ. of low US powers of circular piston transducers 0-64319
- pitch, poststimulatory pitch shifts for pure tones 0-97934
- pitch extraction method based on peak detection and AMDF (Korean) 0-102935
- power, use of semiconductor strain gauges, US medical probes 0-87679
- power of plane sound waves, method and apparatus (Polish) 0-79087
- power response of loudspeakers using monitor 0-87674
- radiation fields, complex values of pressures on two concentric spheres 0-96161
- signal rate of change distribution, gramophone player 0-79083
- solutions in alcohols, ultrasonic vel. and density meas. used to calc. compressibility, intermol. free length and salvation no. 0-96150
- stereophony, artificial head, tone meas. (German) 0-106702
- time-delay spectrometry, practical appl. in field 0-79082
- transfer characteristics, acoustic systems with long reverberation, narrow-band digital signal processing (Japanese) 0-64304
- transient recorders for acoustic emission studies 0-83717

acoustic velocity see *acoustic wave velocity***acoustic wave absorption**

- see also *noise abatement; ultrasonic absorption*
- active, broad-band, duct carrying uniformly flowing fluid 0-74556
- airborne sound, damping by laminated building components (German) 0-102877
- architectural acoustics 0-64288
- atmosphere, nonlinear absorpt. of sound in problems of acoustic and radio acoustic exploration (Russian) 0-94567
- atmospheric absorpt. of wave train producing freq. shift 0-64255
- backscattering, cross section for an absorbent sphere 0-64236
- baffles in closed spaces, dependence of effectiveness on nature of closed space, economic and annoyance factors 0-67019
- ceramics containing volatiles, mechanisms for attenuation 0-74560
- coefficient, locally reacting patch of arbitrary shape 0-79049
- combustion duct, attenuation by fuel droplets and soot particles 0-74549
- compressional wave attenuation in deep ocean sediments 0-79033
- conductors, quantum acoustic bleaching, acoustic zones 0-70324
- constrained viscoelastic damping composites, FEM analysis 0-83743
- critical binary mixtures, sound propag., mode coupling theory, validity breakdown 0-65159
- dilute magnetic alloys, electron sound absorpt., disordered mag. impurities, spin glasses (Russian) 0-80503
- dimensioning of facings for acoustically effective structural elements (German) 0-74600
- domestic roofing sound insulation, expt. facilities of meas. laboratory, test details 0-79058
- ear protection systems, attenuation produced at each normal freq., Noise Reduction Rating calc. (Spanish) 0-109041
- elastic floor coverings, effect of thickness and hardness on impact sound insulation props. (Japanese) 0-79053
- equivalent absorpt. area of room in steady-state condition and reverberation (German) 0-102931
- floor sound insulation, analysis using L_C and L_A (Japanese) 0-79054
- fluids, one and two dimensional, hydrodynamics, viscosity, heat conductivity, kinetics (Russian) 0-79972
- gas-bearing sediments, eqns. based on model of resonating gas bubbles 0-87630
- gas-bearing sediments, eqns. based on model of resonating gas bubbles 0-87670
- gases, liquids and solids, relationship with props., research during past 50 years, review 0-96089
- in-duct acoustic props. meas., transfer function method, expt. 0-106688
- in-duct acoustic props. meas., transfer function method, theory 0-106644
- metal, Pippard sound-attenuation oscillating angular depend. (Russian) 0-103613
- metals, HF sound propagation, nonlinear effects, review 0-88279
- metals, sound absorption and dispersion temp. depend. associated with Fermi surface plateaus (Russian) 0-65166
- multitone decay variance in reverberation room 0-87653
- noise control panels, system design 0-87649
- open-cell polyurethane foam, induced mass of an equilateral triangular cylinder moving in an incompressible irrotational fluid 0-64237
- perforated facings on porous backings, calculation of specific normal impedance 0-64281
- personal computer program for air absorpt. 0-96065
- porous materials vibrations, radiations anal. 0-87640
- porous plates in fluids, sound absorpt. props. near rigid walls 0-87730
- rectangular rooms, reverberation time dependence on wall diffusion and room shape (German) 0-102932
- road traffic noise, highway noise barriers, optimum weight with respect to effectiveness and cost 0-67021
- sand, water-saturated, broadband meas. of acoustic attenuation 0-83719
- SAW and anomalous sound absorpt. for fluid-fluid interface 0-74562

acoustic wave absorption continued

- schoolroom acoustic insulation check allowing for boundary absorption (Hungarian) 0-106664
- screens, role in open-plan offices 0-87650
- seawater, chemical relaxation studies using resonator method 0-96073
- semiconductors, HF sound propagation, nonlinear effects, review 0-88279
- single monopole noise source in air duct, very low freq. noise abatement, diesel engine exhaust 0-64282
- sound attenuation in magnetic field at the $2/\lambda$ -order phase transition (Russian) 0-100487
- sound panels, estimation of transmission loss by statistical energy analysis 0-64278
- sound sinks in flows, low freq. sound absorpt. of jets 0-69788
- sound-absorbing wedge, reflection characts., glass wool props. (Japanese) 0-64322
- structure borne sound in ducts by impedances attached to side (German) 0-102876
- tangential momentum accommodation coeff. meas. by acoustic vel. and absorpt. obs. for He, He on W 0-66867
- viscous attenuation in suspensions and high-porosity marine sediments 0-74577
- waterfilled US testing tanks, appl. of filled rubber material system to echo absorpt. 0-96059
- window-glasses, most effective window configurations 0-87655
- CdS, acoustic wave attenuation, phonon viscosity and dislocation drag 0-70319
- CdS(Se), piezoelec. semicond., sound absorption 0-60051
- GaSB, acoustic wave attenuation, phonon viscosity and dislocation drag 0-70319
- H₂O, acoustic relaxation in critical region (Russian) 0-92609
- LiNbO₃-CdSe layer structure, SAW absorpt., elec. field effects 0-65355
- O₂-CO₂ mixture, temp. difference of molecular vibr. relaxation freq. from 300 to 675K 0-74238
- O₂-H₂ mixture, temp. dependence of molecular vibr. relaxation freq. from 300 to 675K 0-74238
- O₂-He mixture, temp. dependence of molecular vibr. relaxation freq. from 300 to 675K 0-74238

acoustic wave amplification

- see also *acoustoelectric effects*
- size-quantised films under ESR conditions 0-70322
- TGS, ferroelec. single crystal, low freq. nonlinear effects 0-84490
- Al, nonlinear sound wave interactions, sound attenuation in weak superconducting state (Russian) 0-75310
- Ga, nonlinear sound wave interactions, sound attenuation in weak superconducting state (Russian) 0-75310

acoustic wave attenuation see *acoustic dispersion; acoustic wave absorption; acoustic wave scattering; acoustic wave transmission; ultrasonic absorption***acoustic wave diffraction**

- see also *ultrasonic diffraction*
- absorbant wall panels, modal analysis (French) 0-79060
- acousto-optic modulator efficiency optimisation, sound diffraction profile model and expt. 0-106615
- axisymmetric transducers, with various boundary conditions, single integral computer method for Green's function 0-87591
- circular cylinders encased in partial annular layers 0-58837
- cylindrical pulse diffr. by metallic half plane, boundary value problem, direct transform technique 0-69573
- diaphragm in circular waveguide, scattering matrices 0-87598
- Fredholm integral equation, 1st kind for acoustic diffraction calc. (Russian) 0-58834
- HF, non-linear effects in tubes 0-87614
- ill-posed diffraction problem and quasissolution 0-87593
- impedance cylinders of large wave dimensions 0-64249
- Lamb waves by finite crack in elastic layer 0-64244
- optical theorem, plate-fluid system 0-87595
- parabolic reflector 0-58835
- perforated screen, sound diffraction, vortex shedding influence 0-69849
- plane, grating of acoustically compliant circular cylinders partially coated with perfectly compliant material 0-87604
- plane pulse diffraction by thin arbitrarily shaped obstacles 0-96053
- rectangular aperture in soft plane screen 0-96055
- SAW filter design with diffraction compensation 0-74672
- seismic signal processing using inverse diffraction technique 0-74608
- simultaneous Wiener Hopf eqns., Fredholm integral type soln. wave diffraction appl. 0-57100
- spherical, ground models 0-74555
- wedge with curved faces 0-87592
- KH₂PO₄ electro-optic modulator crystals, piezoelec. induced acoustic transients 0-70316

acoustic wave diffusion see *acoustic wave scattering***acoustic wave effects**

- see also *acoustic magnetic resonance; acousto-optical effects; acoustoelectric effects; biological effects of acoustic radiation; sonoluminescence; ultrasonic effects*
- aerosol particles, ellipsoidal, relative velocity in acoustic field 0-58854
- aerosol systems, acoustic field effects 0-89529
- cavitation, fluid-solid boundary, US cleaning and cavitation erosion 0-65158
- displacement of infinite elastic plate submerged in ideal liquid, examination of displacement field 0-74557
- geological materials failure, role of acoustic fluidisation 0-85653
- induced vibration, fatigue cracks in aircraft skin panels, prediction of edge crack growth 0-69737
- influence of grazing flow on the acoustic impedance of a cylindrical wall cavity 0-69784
- interaction of induced sound with flow past a square leading edged plate in a duct 0-69783
- levitation of liquid drops, calc. of nonspherical distortion 0-74693
- linear acoustic loading in straight pipes 0-96060
- liquid dispersion, suspended impurities effects on wave excitation in sound field 0-81372
- ⁴He solid-liquid interface mobility under 1 MHz sound wave (French) 0-100373

acoustic wave interference

- see also *acoustic wave interferometers; acoustic wave interferometry*
- birdsong, consequences of interference patterns 0-102881
- correlation of the phase and amplitude fluctuations between direct and ground-reflected sound 0-96067

- acoustic wave interference** continued
underwater sound in shallow sea, influence of bottom on interference struct. of acoustic field 0-102900
US pressure and interference fields (German) 0-89436
- acoustic wave interferometers**
see also acoustic wave interferometry
No entries
- acoustic wave interferometry**
see also acoustic wave interferometers
US attenuation or velocity meas. 0-58874
- acoustic wave propagation**
see also acoustic dispersion; atmospheric acoustics; Doppler effect; liquid helium sound propagation; seismic waves; shock waves; surface acoustic waves; ultrasonic propagation; underwater sound
aircraft noise propag., review 0-64258
architectural acoustics, field and model expts. on solid-borne sound (Japanese) 0-64290
asymptotic solution for sound propag. above impedance boundary 0-87582
beam displacement, cycle distances, and attenuations for rays and normal modes 0-74580
bent thin-walled waveguides, attenuation and pre-bend build-up 0-69576
caustics and spreading of adjacent acoustic rays 0-64241
CDW, quasi two dimens., phason and sound wave coupling 0-92839
circular pipes, mode-selective energy transfer to pipe wall vibration 0-87586
closed tube, nonlinear resonant acoustic oscillators, finite rate theory 0-92171
compressible inviscid linearly-sheared parallel flow, characterisation of acoustic disturbances 0-69848
conical, excitation of an elastic half-space by a buried line source 0-64245
correlation of the phase and amplitude fluctuations between direct and ground-reflected sound 0-96067
critical binary mixtures, sound propag., mode coupling theory, validity breakdown 0-65159
diffuse vibration field propag. in structs. with periodic inhomogeneities 0-86093
discontinuous or layer media, unidimensional propag. of transient signals 0-87265
duct with varying cross section and viscous mean flow, acoustic wave propag. 0-96267
ducts, acoustic characts. of bends 0-74554
ducts, sound propagation in parallel sheared flows, mode estimation 0-79026
elastic bars, phase boundary propagation, dynamic elastic bar theory, sound wave interactions 0-69706
ferromagnet magnetisation, influence of high intensity longitudinal sound waves 0-103875
ferromagnetic conductor, cylindrical, acoustic wave propag., EM field behaviour 0-88857
field suppression beyond narrow slit in rigid baffle, long wave approx. 0-102890
finite-length fluid cylinder, surface wave interpretation of eigenfrequencies 0-58831
frequency shift of wave train due to atmospheric absorpt. 0-64255
Galaxy, hot interstellar matter effect of sound wave propagation in hot gas 0-109511
gas, dissociating, sonic wave propagation, formation of shock waves 0-64672
gas filled tubes, thermoviscous regions for principle and higher modes 0-96057
gas with porous medium obstacle, scalar Helmholtz eqn. 0-74552
Gaussian beams, nonlinear propag. 0-87609
ground, spherical wave diffraction model 0-74555
guided, rigorous asymptotic theory of evanescent waves 0-64238
hard sphere system, surface tension, compressibility, bulk modulus press. coeffs. and Rao's acoustical parameter 0-80027
HF, non-linear effects in tubes 0-87614
higher order mode effects in circular ducts and expansion chambers 0-96058
horn loudspeaker, anal. of acoustic radiation by finite element method 0-96171
in-duct acoustic props. meas., transfer function method, expt. 0-106688
in-duct acoustic props. meas., transfer function method, theory 0-106644
layered systems, direction control 0-103557
Mandel'shtam and sound propagation in microscopically inhomogeneous media 0-101704
metals, HF sound propagation, nonlinear effects, review 0-88279
metals, sound pulse spike like transport near acoustic cyclotron resonance (Russian) 0-100617
modal theory, broad-band active sound absorption in a duct carrying uniformly flowing fluid 0-74556
moving thermal source, acoustic perturbations in medium 0-87597
multipath channels, comments on coherence estimates 0-58832
nonlinear propag. of sound beams with uniform amplitude distrib. 0-102896
nonlocal diffusion theory of wave propagation in highly viscous liquids 0-102897
ocean, internal waves, acoustic refractive index modulation, parabolic moment eqns. 0-83698
ocean, two-point coherence function models with inhomogeneous background and anisotropy 0-81922
ocean ducts, range dependent, acoustic flux formulae 0-96075
oceanic guided waves, acoustic flux methods 0-96077
outdoor sound, ground and building scattered sound fields, black body radiation analogue 0-69579
parabolic waveguide, statistical theory of propag. 0-102887
parallel jets exhausting from ducts 0-64257
piecewise uniform ducts, momentum and energy theorems 0-74550
piezoelectric crystals, acoustic waves, group vel. characts. 0-92613
plane harmonic waves, infinite isotropic medium having embedded doubly periodic array of cylindrical fibres 0-87607
point source in certain built-up urban environments 0-58841
point source in one-dimensional, randomly inhomogeneous medium, with specularly reflecting walls 0-105514
quartz, acoustoelectric methods 0-84359
radiation by plane structures with diffuse flexural-wave field 0-102912
rectangular ducts with sinusoidal undulations 0-74551
- acoustic wave propagation** continued
ribbed cylindrical shell immersed in liquid, dispersion curves and coeffs. of distribution function 0-87736
rigid 3-dimens. waveguides, anal. of propag. using eigenfunction expansion of Helmholtz eqn. 0-83690
rigid planar sharp bends and bifurcation ducts 0-87585
sand, water-saturated, broadband meas. 0-83719
sediment shear wave effects on ocean bottom refl. loss, ray path anal. 0-96084
semiconductors, HF sound propagation, nonlinear effects, review 0-88279
solar atmosphere, acoustic waves interaction with mag. flux tubes 0-85911
solids, how the structure of a medium is seen by an acoustic wave 0-65163
sound propagation along an impedance surface, numerical calcs. 0-87590
space-time structure of acoustical field anal. by means of optical Fourier transform (French) 0-87583
spark-gap, electrodes, acoustic phenomena in erosion 0-64796
structure-borne sound, procedure for meas. sensitivity of building structures to stationary excitation (German) 0-64287
thermoacoustic waves in cylindrical porous tube, Rijke tube limit (French) 0-74553
thermooptically excited acoustic pulses propag. 0-102891
turbulent jets using organ pipe flue 0-91946
two-dimensional solids and hexatic liq. crystals., nonlinear hydrodynamic props., theory 0-100169
underground gas-filled pipes, accompanying surface displacements 0-83692
underwater, intensity fluctuations spectrum in internal wave freq. range 0-64268
underwater, temp. variation of acoustical props. of laboratory sediments 0-96069
vapour-liquid mixture, propagation of acoustic disturbances, model 0-103058
wall jet flow, compliant walls, influences of flow convection and refraction on sound radiation 0-74595
wave-theory peaks in range-averaged channels of uniform sound velocity 0-96076
CdS, electro-acoustically active, AC impedance meas. 0-103726
³He-He II dilute solution, fourth sound velocity 0-70498
⁴He superfluid films, geometry induced third sound splitting 0-96712
InSb, magnetoacoustic wave excitation by acoustic wave propagation 0-88597
KH₂PO₄ electro-optic modulator crystals., piezoelec. induced acoustic transients 0-70316
- acoustic wave reflection**
see also echo; reverberation; ultrasonic reflection
2-dimensional reflecting medium over circular domain, exact soln. of reconstruction 0-64299
architectural acoustics 0-64288
boundary between piezoelec. ceramic and water 0-87588
cochlea, one-dimensional model illustrating resonance 0-61581
concert hall design, lateral and ensemble reflection requirements 0-91964
concert hall design for orchestral balance in seats behind stage 0-91963
concert hall problem, coherence length and diffuse reflection formulation 0-91962
corrugated surface, Rayleigh and Waterman theories 0-96063
ducts, acoustic characts. of bends 0-74554
fluid-solid boundary, cavitation effects, bubble collapse, US cleaning and cavitation erosion 0-65158
gas-bearing sediments 0-87630
in-duct acoustic props. meas., transfer function method, expt. 0-106688
in-duct acoustic props. meas., transfer function method, theory 0-106644
N-wave reflection at open end of circular pipe, nonlinear reflection meas. 0-79027
narrow beam sound waves, rigid cylindrical tube 0-69578
obstacle in one-dimens. medium with random inhomogeneities 0-58839
obstacle in waveguide, acoustic wave transmission and reflection 0-102893
ocean bottom, technique for meas. plane-wave refl. coeff. 0-96081
ocean bottom and surface, correlation measurement of reflection coeff. 0-58848
ocean bottom-reflected pseudonoise signals, correlation with transmitted signal 0-58846
outdoor sound, ground and building scattered sound fields, black body radiation analogue 0-69579
pseudo-steady single-Mach reflection, reconsideration of shock polar soln. 0-99893
Rayleigh waves from periodic corrugations of surface in oblique incidence 0-58850
raypath reflection model for layered media with source and receiver in different layers 0-83704
reciprocity principle in duct acoustics 0-74545
reconstruction of reflectivity field from line integrals over circular paths 0-58863
rolled sheet, artificial surface cracks, reflection of normal shear waves 0-89448
spark-gap, electrodes, acoustic phenomena in erosion 0-64796
spherical waves, reflection from locally reacting plane surface, numerical calcs. 0-87590
torsional waves in semi-infinite cylindrical rod connected to elastic half space 0-96095
underwater detonation wave, reflection from water surface 0-87628
underwater pulse reflected from water surface, spectrum 0-87627
underwater sound, scattering by sea surface 0-106656
underwater sound refl. from bottom with sound vel. and density gradients 0-102901
waveguide reflectors, effectiveness study 0-87599
KH₂PO₄ electro-optic modulator crystals., piezoelec. induced acoustic transients 0-70316
SiO₂ sputtered film performance as acoustic antireflection coating at sapphire-H₂O interface 0-106686
- acoustic wave refraction**
see also acoustic dispersion; ultrasonic refraction
No entries
- acoustic wave scattering**
see also ultrasonic scattering
backscattering, cross section for an absorbent sphere 0-64236
backscattering from a plate with a thickness discontinuity 0-96056
combustion duct, dispersion by fuel droplets and soot particles 0-74549

acoustic wave scattering continued

- convex shell, sound wave scatt. pattern, high freq. asymptotics 0-96051
- cylinder, direct and inverse scatt. problems, Dirichlet boundary conditions 0-95774
- cylinder, inverse scattering problem, determ. of shape from far field data 0-83543
- echosonde signals, excess attenuation 0-83694
- Eckart's formulation, surface correlation effect on average scattered pressure 0-96070
- elastic and viscoelastic obstacles immersed in fluid, acoustic wave scatt. 0-69583
- finite elastic cylinder in water 0-96062
- fish backscattering cross section, swimbladder effect in gadoid and macerel 0-89787
- impedance cylinders of large wave dimensions 0-64249
- impulse response meas. in sound scattering from sphere in air (*French*) 0-87581
- inhomogeneity of medium, determination by means of sound signals 0-87610
- layered elastic and viscoelastic obstacles in water 0-96061
- matrix method of optimal truncation, scalar wave illustration 0-62479
- multilayered elastic body embedded in infinite material, acoustic wave scatt. theory 0-69584
- ocean, two-point coherence function models with inhomogeneous background and anisotropy 0-81922
- ocean bottom-reflected pseudonoise signals, correlation with transmitted signal 0-58846
- ocean surface probing for measurement of directional-frequency spectrum 0-79032
- ocean-surface directional-frequency spectra, inverse scattering problem 0-79031
- one-dimensional vel. inversion, numerical results 0-64240
- optical theorem for scatt. of strain waves by inhomogeneities of plane boundary of solid 0-102888
- physical optics farfield inverse scatt., mathematical inversion technique for nondestructive eval. 0-69580
- piecewise uniform ducts, momentum and energy theorems 0-74550
- Rayleigh surface waves, propag. along corrugated solid boundary 0-87600
- Rayleigh waves from periodic corrugations of surface in oblique incidence 0-58850
- resonant scattering of elastic waves from spherical solid inclusions 0-74547
- resonating fields inside elastic scattering objects 0-106645
- room-acoustic directional diffusivity model (*Hungarian*) 0-106665
- rough interface between two fluids, coherent acoustic scatter 0-96074
- sea surface inhomogeneities, sound scatt. phase function shape in shadowing conditions (*Russian*) 0-94530
- smooth elastic obstacle, adaptation of transition matrix method 0-87584
- sound field calculation, three dimens. objects, integral equation methods 0-74558
- source above rough absorbent plant 0-64289
- statistically rough surface, wave scatt., book 0-73116
- submerged plate with finite number of reinforcing ribs 0-74586
- submerged plate with one reinforcing rib 0-74585
- transducer, backscattering formula 0-96064
- underwater scattering by marine organisms, review 0-64269
- underwater sound, scattering by sea surface 0-106656
- wide-band plane wave scattering and transmission by fluid loaded plates 0-106646
- KH₂PO₄ electro-optic modulator crystals, piezoelec. induced acoustic transients 0-70316

acoustic wave transmission

- see also *ultrasonic transmission*
- airborne sound coupling into earth, freq. dependence 0-74567
- architectural acoustics 0-64288
- boundary between piezoelec. ceramic and water 0-87588
- building elements, use of thin plates for improving transmission loss 0-102930
- concrete plate junctions 0-87652
- deep ocean, anal. of acoustical effects of receiver-source motion at intermediate ranges 0-96082
- diffracted and penetrating, acoustic pathways through barriers 0-102880
- displacement of infinite elastic plate submerged in ideal liquid, examination of displacement field 0-74557
- ducts, circular, with compressible mean flows 0-74900
- gas with porous medium obstacle, scalar Helmholtz eqn. 0-74552
- gas-bearing sediments 0-87630
- horn and silencer design, FEM anal. of acoustic transmission/radiation systems 0-87589
- impulse response meas. of acoustic transmission system, digital computer processing (*German*) 0-91999
- inhomogeneity of medium, determination by means of sound signals 0-87610
- LF sound pressure at various Reynolds numbers 0-87613
- noise transmission through stiffened panels 0-102922
- obstacle in waveguide, acoustic wave transmission and reflection 0-102893
- oceanic, calc. of strength and diffraction parameters 0-74572
- pipe walls, presence of flow, use of reverberation chambers 0-102883
- reciprocity principle in duct acoustics 0-74545
- reverberant sound, transmission through orthotropic viscoelastic multilayered plates 0-102884
- structure-borne power flow, beams and pipes, cross spectral density methods 0-106742
- wide-band plane wave scattering and transmission by fluid loaded plates 0-106646
- CO₂ pulsed laser system, acoustic suppression 0-74378

acoustic wave velocity

- see also *acoustic dispersion; liquid helium sound propagation; shock waves; ultrasonic velocity*
- beamforming when the sound velocity is not precisely known 0-96123
- e-chlorophenol-acetone (ethyl methyl ketone), thermodynamic and transport props. 0-92686
- clathrate hydrates, longitudinal acoustic vel. 0-88275
- compressible classical Heisenberg chain, phonon dynamics and sound velocity 0-96604
- computer model for generating World ocean sound velocity profile 0-87624

acoustic wave velocity continued

- cylindrical steel shells in water, thick-walled, distrib. of normal surface vel. (*German*) 0-102899
 - filled polymers, dynamic shear modulus and acoustic velocity, filler content depend. 0-60900
 - gas-bearing sediments, eqns. based on model of resonating gas bubbles 0-87630
 - gases, liquids and solids, relationship with props., research during past 50 years, review 0-96089
 - liquid, Gruneisen parameter rel. to Rao's acoustical parameter 0-92581
 - metals, sound pulse spike like transport near acoustic cyclotron resonance (*Russian*) 0-100617
 - one-dimensional vel. inversion, numerical results 0-64240
 - polydimethylsiloxanes, rubbery and liq., hypersonic sound vel., Brillouin spectra meas. 0-75308
 - polydisperse, vapour-liquid mixtures, acoustic velocity, damping decrement 0-66881
 - polymers, aliphatic and aromatic, mean mol. orientation factors, from IR spectra and acoustic method 0-70142
 - porous solid, generalised α - α model, eqn. of state, sound vel. 0-65154
 - solids, evaluation of finite strain eqns. of state using lattice models 0-96620
 - tangential momentum accommodation coeff. meas. by acoustic vel. and absorpt. obs. for He, He on W 0-66867
 - underwater velocity inversion in a stratified medium with separated source and receiver 0-96071
 - CeSn₃, mode softening and elastic const., acoustic vel. meas. 0-88242
 - ⁴He, gas, second virial coeff., acoustic determ., 1.28-2.13K 0-69965
 - K₂ReCl₆, elastic constants, softening of acoustic modes, obs. by Brillouin scattering 0-71440
 - K₂SnCl₆, elastic constants, softening of acoustic modes, obs. by Brillouin scattering 0-71440
 - Li₂O₂SiO₂, ceramic, prep. of oriented microstructure by unidirectional solidification of melts 0-71614
 - NH₄H₂PO₄, Z-cut, SAW props. 0-84358
 - (NH₄)₂SiF₆, elastic constants, softening of acoustic modes, obs. by Brillouin scattering 0-71440
 - (NH₄)₂SnCl₆, elastic constants, softening of acoustic modes, obs. by Brillouin scattering 0-71440
 - Pb, thermodynamic characterisation at high temp. 0-103494
 - PbO-containing binary systems, acoustooptic props. from comp. and density 0-76000
 - Se, trigonal, normal mode calcs. 0-84259
 - Si amorphous film, acoustic study using Rayleigh waves 0-75312
 - SiO₂, amorphous films, acoustic study using Rayleigh waves 0-75312
 - SiO₂, thin film on YZ-LiNbO₃, SAW props. 0-84356
 - Te-Se liquid mixtures, sound vel. meas., adiabatic compressibility determ. 0-65161
 - TmSe, first obs. of negative elastic const. 0-103409
 - YIG, sound vel., temp. depend., phonon scatt. processes 0-96598
- acoustic wave velocity measurement**
- see also *ultrasonic velocity measurement*
 - clapping method 0-82620
 - Fresnel zone and diffraction fields anal. near boresight of acoustic radar antennas 0-64318
 - gas-bearing sediments 0-87670
 - sand, water-saturated, broadband meas. 0-83719
 - seawater, microprocessor-based instrument 0-67440
- acoustic waveguides**
- active noise suppression in waveguide with monopole radiators and dipole receivers 0-102928
 - bent thin-walled, acoustic wave propag., attenuation and pre-bend build-up 0-69576
 - circular, acoustic diffraction by diaphragm, scattering matrices 0-87598
 - evanescent waves for guided propag., rigorous asymptotic theory 0-64238
 - finite-length fluid cylinder, surface wave interpretation of eigenfrequencies 0-58831
 - linear array of Helmholtz resonators, design calc. for zeroth normal mode 0-87602
 - obstacle in waveguide, acoustic wave transmission and reflection 0-102893
 - parabolic, statistical theory of propag. 0-102887
 - plane waveguide with one perforated wall, calc. of radiation characts. 0-102886
 - point acoustic source between thin elastic plates, fluid immersed, roots of dispersion relations 0-87601
 - reflectors, effectiveness study 0-87599
 - rigid 3-dimens. waveguides, anal. of propag. using eigenfunction expansion of Helmholtz eqn. 0-83690
 - side-branch pipe resonators, flow-induced tones 0-64243
 - single-mode, bandwidth of active sound suppression system 0-87605
 - single-mode transmission and backscatter measurements in laboratory waveguide 0-64259
 - space-time structure of acoustical field anal. by means of optical Fourier transform (*French*) 0-87583
 - straight pipes, linear acoustic loading 0-96060
 - US transmission line of probe for hot metal inspection, spurious signals 0-66754
- acoustic waves**
- see also *acoustic emission; magnetoacoustic effects; shock waves; surface acoustic waves; ultrasonic waves*
 - CW far-infrared laser scattering from a laboratory plasma ion acoustic wave 0-106974
 - direction location of infrasonic waves, meas. on jet planes (*German*) 0-92000
 - Doppler research in the nineteenth century 0-86070
 - EPR spin system saturation characts., acoustic wave excitation (*Russian*) 0-66013
 - generation by strip propellers, non-uniform liq. stream 0-96094
 - inhomogeneous, visual characts., optical holographic interferometry 0-102943
 - material properties associated with dynamic deformation of matter, acoustics and the props. of materials 0-64234
 - negative-energy waves, investigation of normal modes 0-102889
 - nonlinear sonic wave, excitation by quasi-monochromatic Alfvén pumping 0-106649
 - open pipe exits, flow during acoustic resonance, vortices and boundary layers 0-92224
 - production in polar medium, by radiation, possible detection method appl. 0-63493

acoustic waves continued

- radiated, vibrating strip, power output considerations 0-69577
- solar atmosphere, penetrative instabilities theory in presence of thermal dissipation 0-109406
- sphere impacting on thin square plate, acoustic generation mechanism 0-74591
- stellar atmospheres, short period acoustic wave mechanism for chromospheric heating (*German*) 0-109421
- transonic gas flow, optical excitation of intense acoustic waves 0-74564
- turbulent shear layer, instability waves, radiation of sound 0-79341

acoustical laboratories

- see also *anechoic chambers; reverberation chambers*
- No entries

acoustics

- see also *acoustic applications; acoustic devices; acoustic equipment; acoustic noise; anechoic chambers; architectural acoustics; atmospheric acoustics; audio acoustics; hearing; musical acoustics; photoacoustic effect; sound reproduction; ultrasonics; underwater sound; vibrations*
- Acoustical Soc. America, plenary sessions celebrating 50th anniversary, Cambridge, MA, USA (Jun. 1979) 0-94914
- Acoustical Soc. of America in historical perspective 0-96047
- conference on acoustics, speech and signal processing, Denver, CO, USA (Apr. 1980) 0-83689
- contemporary papers references, 1980 0-96049
- future accomplishments, summary of conjectures based on plenary sessions of ASA 50th anniversary 0-96048
- numerical evaluation of singular integrals in interface separation, new quadrature formulae 0-74559
- quantum, liquids, spin lattice relaxation, sound coherence 0-97128
- stability of difference schemes for multidimensional equations of acoustics 0-105512

acousto-optical devices

- see also *acousto-optical effects*
- active optical devices, seminar, San Diego, CA, USA (August 1979) 0-101664
- Bragg deflector, wideband guided-wave, using tilted-finger chirp transducer 0-74510
- broadband chirp transducers for integrated optics spectrum analyzers 0-74514
- broadband matching of piezo-transducers for acousto-optical devices (*Russian*) 0-64329
- correlator with two-dimensional reference transparency, testing 0-106485
- deflector, bandwidth increase method 0-99861
- fibre loss, dispersion and polarisation meas. by acousto-optical tunable filter 0-102855
- fibre optic acoustic sensor, modulation processes 0-58771
- fibre optic acoustic sensor, single coiled monomode fibre 0-102826
- fibre optic interferometric sensor for acoustic detect., thermally induced optical phase effects 0-74479
- frequency shifter for CO₂ laser velocimeter 0-100042
- gap-coupled Schottky diode array/LiNbO₃ imager for scanning of optical images 0-74632
- gas analyser with acoustooptic detector and semiconducting generator based on Gunn diode (*Russian*) 0-101141
- guided-wave, with appls. to wideband communications and signal processing, progress review 0-58801
- hydrophone, fibre-optic, description and advantages 0-58770
- image and hologram convertor based on acousto-optical effect in liquid crystals. 0-76002
- image processing using space-to-temporal freq. conversion 0-87340
- integrated optic spectrum analyser, design of Bragg cell 0-74515
- integrated optics A/D convertor based on bulk acousto-optic interaction 0-69552
- laser spectrometer, high resolution, appl. to H₂O vapour spectrum 0-86450
- memory correlator based on photoinduced surface storage of SAW patterns in LiNbO₃ 0-74309
- modulator efficiency optimisation, sound diffraction profile model and expt. 0-106615
- modulator for CO₂ laser rangefinder using heterodyne detect. 0-102825
- modulator for mode-locked CW Nd:YAG laser 0-87419
- modulator using coupled plane waveguides 0-69527
- monochromatic light source with electronically variable wavelength 0-102791
- movie camera, laser based, operation and applications 0-57405
- multimode fibre coupler-type acoustic sensor, optical intensity modulation 0-102945
- nematic liquid cryst., isotropic phase, pulse acoustic-optic modulator 0-95993
- noncollinear UV acousto-optical tunable filter 0-102832
- opto-acoustic transducer struct., recent investigations 0-74688
- particle motion detection in transparent liquids, Fourier transform acoustooptical system performance 0-87680
- programmable acousto-optic tunable filter 0-74511
- Q-switch, ultrasonic, for Nd:glass laser 0-64034
- Raman-Nath standing-wave mode-locking switch, modulation index 0-78980
- RF target simulator 0-102843
- SAW Broadband modified chirp transducers for integrated optics spectrum analyser 0-58802
- SAW integrated optics spectrum analyser, development progress 0-58803
- SAW time integrating correlator 0-64295
- signal processing, time-integrating, acousto-optic 0-102641
- signal processing system architectures and applications 0-102652
- signal processors based on light polarization discrimination techniques 0-74310
- signal processors using multichannel SAW correlation and convolution 0-74611
- surface-wave acousto-optic signal processors 0-102640
- time-integrating acousto-optical correlator design and performance 0-106618
- tunable filter, guided-wave, using collinear TE-TM mode conversion 0-102852
- tunable filter based on collinear acousto-optic interaction in ZnO thin film opt. waveguides 0-74509
- tunable filter spectrometer development 0-101848
- US-optical correlator for spatial freq. meas. 0-95995
- wideband programmable filter 0-102842
- Ge acousto-optical deflector performance at 10.6 μ m 0-102835

acousto-optical devices continued

- LiNbO₃-gap coupled Schottky diode memory correlator, grating coupled optical imaging 0-64143
- LiNbO₃-Ge acousto-optic modulator for 10.6 μ m CO₂ laser 0-99776
- LiNbO₃-Ge acoustooptic modulator (*Japanese*) 0-69542
- LiNbO₃-pn-diode airgap convolver struct. optical scanner using single SAW pulse 0-64144
- Si guided-wave acousto-optical devices 0-102864
- TeO₂ acousto-optic laser beam deflector using shear wave propag. slightly off (110) crystal axis (*Japanese*) 0-102818
- TeO₂ acousto-optical tunable filter with microcomputer control 0-102833
- TeO₂ shear wave acousto-optical device with polarisation filtering 0-106619
- TeO₂ time-integrating acousto-optical correlator for chirp spectrum analyses 0-106474

acousto-optical effects

- see also *acousto-optical devices*
- 2-D acoustic Fourier transform of optical images 0-74308
- anthracene, mol. crystal, meas. of US attenuation coeff. by optoacoustical methods (*French*) 0-70317
- apatite type crystals, acousto-optical props. 0-100644
- bonded interface defect testing by differential interferometric Stoneley wave meas. 0-76444
- Brillouin scattering by Stoneley waves, elasto-optic and surface ripple mechanisms 0-71435
- coherent optics methods appl. to acoustic field investigations 0-106691
- cyclobutane, absorpt. of pulsed IR radiation and decomp., joulemeter and opto-acoustic obs. 0-58328
- diffraction of laser light, nonlinear liquids, ultrasound propagation 0-64270
- diffraction of light on ultrasound, phase geometry variation analysis 0-106441
- diffused waveguide, generalised parameters describing acoustooptic interaction 0-91924
- ferroelectric bodies, deformable, coupled acousto-optic modes 0-96093
- Gaussian light beam, diffr. by plane acoustic waves at oblique incidence 0-69326
- impurity relaxation in nonresonance field, phonon amplification (*Russian*) 0-100310
- integrated, numerical procedure 0-91944
- interaction efficiency calc. 0-103940
- Lamb wave optical detect. in fused SiO₂ 0-106690
- laser beam spatial coherence control by progressive US wave 0-78885
- laser radiation intensity distrib. meas. using Bragg diffraction of light 0-64092
- laser speckle reduction in image plane by US modulation of spatial coherence 0-106459
- light diffraction, adjacent US beams 0-87629
- light wave diffr. by complex spectral composition US 0-95939
- liquid crystals., effect due to anisotropic attenuation, new developments and appls. 0-76002
- MBBA nematic liquid crystals excited by 20 MHz US surface waves, acousto-hydrodynamic effects 0-76003
- multielement acoustic array characterisation by acousto-optic diffraction 0-99911
- multifrequency acousto-optic diffraction in optically birefringent media 0-74300
- multiple plane-wave scatt., explicit formalism 0-99621
- naphthalene, mol. crystal, meas. of US attenuation coeff. by optoacoustical methods (*French*) 0-70317
- nematic liquid cryst., acousto-optic effect, acoustic streaming 0-88964
- nematic liquid cryst., response to acoustic field, streaming component and instability 0-80747
- nematic liquid crystals, homeotropically oriented, spectral studies of acoustooptical interaction 0-88965
- nonreciprocal effect, during light passage through US beam 0-106443
- optical coherence modulation by US waves, partial coherence depend. on US parameters 0-58453
- parametric effects anal., in optics 0-102619
- photoelasticity, nonlinear, in impure crystals, theory 0-108179
- Raman-Nath parameter for entire sound field, calc. for baffled planar transducer 0-74689
- solids, high speed anal. of light spectrum (*French*) 0-95156
- stimulated acoustooptical effects due to nonlinear photoelasticity 0-103941
- strong field interaction, Gaussian beams 0-95790
- temporal modulation of light beam, diffraction by real stationary US field in liquid 0-83551
- triphenylphosphite, acoustically induced birefringence 0-93274
- Al, Brillouin spectra, light scatt. cross section for surface ripples 0-71434
- Al₂O₃ s, acoustically induced birefringence 0-93274
- GaAs, Brillouin spectra, light scatt. cross section for surface ripples 0-71434
- Gal, Brillouin spectra, light scatt. cross section for surface ripples 0-71434
- LiI₂ and quartz, piezoelectric transducers, acoustic field distrib., Bragg diffr. method, quartz crystals 0-97231
- LiIO₃ single crystal, surface acoustic wave parameter meas., coherent optics method 0-106691
- LiNbO₃ light induced ultrasonic wave velocity change, refractive index 0-97236
- LiNbO₃ optical waveguide surface, acoustooptical interaction for TE modes, metallisation effect 0-69541
- LiNbO₃, photoinduced surface storage of SAW patterns 0-74309
- LiNbO₃ pure and Fe doped, IR induced acousto-photorefractive memory effect 0-80746
- LiNbO₃, SAW, suppression of harmonic generation, light diffr. determ. 0-84355
- Ni, Brillouin spectra, light scatt. cross section for surface ripples 0-71434
- Pb₂(GeO₄)(PO₄)₂, crystals, acousto-optical props. 0-100644
- Pb₂(GeO₄)(VO₄)₂, crystals, acousto-optical props. 0-100644
- PbO-containing binary systems, acoustooptic props. from comp. and density 0-76000
- Pb₂(SiO₄)(VO₄)₂, crystals, acousto-optical props. 0-100644
- Te, acousto-optical props. at wavelength of 10.6 μ m 0-76001
- ZnO thin film opt. waveguide, collinear acousto-optic interaction and appl. to tunable opt. filter 0-74509

acoustoelasticity *see elasticity*

acoustoelectric devices

see also acoustoelectric transducers

- driven equilibrium Fourier transform sensor operating at 100 MHz 0-74612
- transmission scanning acoustic microscope, single lens 0-87669
- LiNbO₃ acoustoelectric memory correlator struct. for scanning of optical images 0-74632
- LiNbO₃-gap coupled Schottky diode memory correlator, grating coupled optical imaging 0-64143
- LiNbO₃-pn-diode airgap convolver struct. optical scanner using single SAW pulse 0-64144
- ZnO/Si SAW devices 0-80332

acoustoelectric effects

- backward waves and acoustic scanning, nonlinear interaction of vol. and surface waves 0-79040
- charged-particle stream, wave interaction, nonlinear effect 0-80310
- domain injection, semiconductors (*Japanese*) 0-91945
- electron drag by coherent Lamb phonons in quantising magnetic field 0-80330
- ferroelectric bodies, deformable, coupled electroacoustic eqns. 0-96092
- laminar piezodielectric-dimensionally quantised semiconductor film struct., acoustoelectric effects 0-75607
- α -LiIO₃ powders, temp. depend. of electro-acoustic echo 0-66115
- metals, EM generation of ultrasound, theory 0-103727
- parametric excitation of acoustic waves in presence of electron currents (*Russian*) 0-80328
- piezo-semiconductor plates, effect of diffusion of charge carriers (*Russian*) 0-65633
- piezoelectric-semiconductor struct., nonlinear acoustoelectric effects for large amplitude SAW 0-92942
- piezosemiconductors, second harmonics of acoustoelectric current 0-80329
- powders, phonon electroacoustic echoes, storage mechanisms 0-75606
- quartz, SAW propagation, acoustoelectric methods 0-84359
- semiconductor, n-type, lightly doped, hopping acoustoconductivity mechanism 0-65635
- semiconductor, planar acoustomagnetoec. effect, theory 0-60052
- semiconductor film, US propagation in quantised elec. field (*Russian*) 0-60050
- semiconductors, degenerate, acoustodielectric effect, permittivity modulation by acoustic wave in resonance conditions 0-92944
- semiconductors, nonlinear electroacoustic echo 0-92943
- shear SAW in high permittivity three-layer system (*Russian*) 0-80048
- solids, transverse SAW in microwave field 0-92945
- TGS, ferroelec. single crystal, low freq. nonlinear effects 0-84490
- ultrasonic pulsed measuring instrum., signal shape anal. 0-87678
- Ag₃SbS₃(AsS₃), electroacoustic echo, ultrasonic wave attenuation (*Russian*) 0-88280
- n-AlSb, acoustoelectric effect due to piezoelectrically active wave 0-80331
- Au film, ultrathin evaporated, acoustoelectric meas. of electron mobility and diffusion 0-65707
- CdS, acousto-voltaic effect, asymmetric electron ejection from trap levels (*Russian*) 0-65634
- CdS, electro-acoustically active, AC impedance meas. 0-103726
- CdS, single crystals, rel. to US luminesc. 0-76092
- CdS(Se), piezoelec. semicond., sound absorption 0-60051
- n-GaP, acoustoelectric effect due to piezoelectrically active wave 0-80331
- LiIO₃, transverse gap elastic waves, expt. 0-59576
- LiNbO₃, piezoelec., SAW interaction with secondary electrons 0-80708
- LiNbO₃-Si, acoustoelectric memory, effect of band-bending 0-70771
- Se, trigonal, acoustoelectric current saturation 0-60053
- Se₂Te_{1-x}, acoustoelectric current saturation 0-60053
- SiO₂-GaAs, vacuum evaporated system, acoustoelec. signal, interface props. 0-75646
- ZnS, prebreakdown electrolum., domain form. and negative resist. effects 0-84788

acoustoelectric transducers

see also earphones; headphones; hydrophones; loudspeakers; microphones

- ferrofluids, appl. as acoustic transducer material 0-58877
- grating-array acoustic-surface-wave transducers and reflectors 0-58884
- US tone-burst spectroscopy, influence of phase cancellation and pulse shape artifacts 0-81276

acoustooptics *see acousto-optical effects*

actinide alloys

see also actinide compounds; plutonium alloys; uranium alloys

- silicides, atomic volume deviations and supercond. T_c 0-75203
- Bi-Th system, heats of form. 0-89517
- Ni-Th (1 at.%), surface comp., temp. and O₂ exposure effects, AES study 0-80914
- NpCo₂Si₂, mag. struct., neutron diff. determ. 0-93084
- NpCu₂Si₂, mag. struct., neutron diff. determ. 0-93084
- Th-Cr, supercond., press. meas. to 20 kbar 0-88667
- Th-Cu, amorphous, thermal stability, crystn., DSC and elec. resist. study 0-107060
- Th-Dy, dil., type I superconductor, paramag. Dy moment relax., Mossbauer spectra study 0-65755
- Th-Gd(Tb)(Dy)(Ho)(Er)(Tm)(Lu) (1 at.%), Heisenberg exchange, residual resist. meas. 0-75558
- Th-Pu (20 wt.%) metal fuels, compatibility with cladding alloys for FBR appls. 0-102242
- Th-Pu-U-Zr (20, 4, 8 wt.%) metal fuels, compatibility with cladding alloys for FBR appls. 0-102242
- Th-U (20 wt.%) metal fuels, compatibility with cladding alloys for FBR appls. 0-102242
- ThBe₃, lattice spacings and susceptibilities 0-65778
- Th₂Co₃, effect of absorbed H₂ on mag. behaviour 0-60184
- Th₂Ni₃, effect of absorbed H₂ on mag. behaviour 0-60184

actinide compounds

see also compounds of individual actinides, e.g. uranium compounds

see also actinide alloys

- ferromagnetic properties, book contrib. 0-75727
- monopnictides, anomalous mag. props., planar coupling theory 0-60245
- neutron scatt. studies 0-75716
- silicides, atomic volume deviations and supercond. T_c 0-75203
- thermal reactor fuel cycles, actinide wastes toxicity limitations (*German*) 0-99220

actinide metal compounds *see actinide compounds*

actinide metals *see actinides*

actinides

see also individual actinides, e.g. uranium

- ferromagnetic properties, book contrib. 0-75727
- health effects of man-made actinides rel. to natural radionuclides 0-61647
- radioactive waste, biological hazards, consequences for LMFBR fuel recycling 0-86960
- radioactive waste, decay heat estimation, summation calcs. and Standard eqns. 0-63317
- solutions, differential alpha radiography using solid state track detectors 0-71932
- transmutation of by-product actinides to reduce high-level radwaste storage times 0-95384

actinium

see also nuclei with

No entries

actinium compounds

- dihydrides, structs. and stabilities 0-107146

actinometers *see radiometers*

actinometry *see radiometry*

activation analysis *see chemical analysis by nuclear reactions and scattering*

active filters

- spectroscopy, noise reduction by low pass filter for DC signal, appl. chlorophyll-a fluoresc. 0-87249

active nitrogen *see nitrogen*

active oxygen *see oxygen*

actuators

see also electric actuators

- helenoid actuators applied to deformable mirrors 0-74454

adaptive control

see also adaptive optics; adaptive systems

- biological control mechanisms for complex motor systems 0-81573
- image bandwidth compression, scene analysis algorithms and rule-based controller 0-95819
- polymers, molecular weight distribution 0-58434
- prosthesis control system, complete hand/arm 0-109059
- spacecraft, nonstationary, coordinate-parametric control via multi-dimensional asymptotically stable adaptive systems 0-101522

adaptive optics

see also optical phase conjugation

- circular membrane reflector made by surface bending due to electrostatic tension 0-91876
- deformable mirror design for wavefront correction in CO₂ laser fusion system 0-74427
- deformable mirror for wavefront error correction in Gemini CO₂ laser fusion system 0-74426
- deformable mirror system using polyvinylidene fluoride piezoelec. film 0-74455
- deformable mirrors for wavefront error correction, piezoelectric material requirements 0-78928
- focusing of light in inhomogeneous nonlinear medium, interf. criteria 0-99633
- helenoid actuators applied to deformable mirrors 0-74454
- heterodyne receivers for atmospheric optical communications 0-58663
- interferometer, radial grating lateral shear heterodyne, for real-time wavefront meas. 0-78743
- laser and electro-optical systems, conf., San Diego, CA, USA (Feb. 1980) 0-62392
- multidither hillclimbing adaptive optical system, secondary intensity maxima correction 0-106593
- pattern recognition, hybrid parallel optical and serial digital processing systems 0-99657
- reading machine, multifont adaptable automatic, for blind people 0-104814
- real-time optical processing using the liquid crystal light valve 0-63936
- resonator, annular, adaptive mirror effects on performance 0-58596
- single mode fibre polarisation stabilisation 0-58724
- systems analysis using two-dimensional FFT algorithm 0-78986
- thermal blooming cell design for use in evaluating adaptive optics 0-102780
- thermal defocusing of light beams, phase conjugation compensation method 0-64123
- thermal self-action problems and their compensation 0-106579
- wavefront sensing by phase retrieval 0-106478
- Pb(Zn,Ti)O₃ piezoelectric electrically deformable diffraction grating 0-78963

adaptive systems

see also adaptive control; adaptive optics; cognitive systems; learning

systems; pattern recognition; self-adjusting systems

- beam forming processor formulation 0-91967
- multi-dimensional asymptotically stable adaptive systems, appl. to nonstationary spacecraft coordinate-parametric control 0-101522
- natural terrain scenes, segmentation-based boundary-modelling processor 0-99661
- nonstatistical parameter estimation adaptive algorithms 0-91995
- seismic signals deconvolution, adaptive filter structs. 0-98451
- speaker verification algorithm for noisy utterances 0-91992
- speech adaptive noise cancellation by short-time Fourier transform 0-91976
- time-varying images, object displacement estimation adaptive algorithm 0-99668
- voice amplification, adaptive method for feedback suppression (*German*) 0-106676

adding machines *see calculating apparatus*

adherence *see adhesion*

adhesion

- Araldite, high vacuum sealant at liq. N₂ temp. 0-57319
- bond strength, and stressed state during breaking (*Russian*) 0-76478
- bonded interface defect testing by differential interferometric Stonely wave meas. 0-76444
- cemented carbides, physical and chem. nature 0-76265
- ceramic/metal layer adhesion mechanism for metallization of electronic ceramics, elec. props. (*German*) 0-76381
- composites, adhesion between two crystals, theory 0-104417
- concrete, strength, shrinkage strain and deterioration down to -160°C (*Japanese*) 0-100886

adhesion continued

- α -cyanoacrylate adhesive in first monolayer on bulk Al surface, IR spectra, H-bond form., stretching vibr. 0-87119
 E-glass textile filaments, wetting chars. 0-80030
 elastic sphere, deformation and sticking to a rigid plane, mol. force effect 0-106720
 elastomers, surface roughness, friction and adhesion 0-66674
 epoxy resin adhesives, capillary flow and bond strength 0-71883
 epoxy resin bond layer, prep. methods, ultimate thickness 0-71884
 ethylene-methyl acrylate, random copolymer, review 0-108330
 galvanic coatings, adhesion after strain hardening, test device 0-71837
 glass fibres-resin interface studies 0-93531
 ion plating, evaporation sources, gaseous media, and transport modes 0-80984
 laser CVD, film physical props. and applications 0-93493
 metal cutting, direct SEM obs. of adhesion and frictional sliding 0-104412
 metal-polymer, ply-separation resist. polymer polarity effect (*Russian*) 0-61064
 Mylar film/adhesive/Al foil laminate, mech. interactions 0-81112
 polymer adhesion ability enhancement by block copolymer incorporation (*Russian*) 0-61065
 polymer systems for adhesive applications, radiation curing, lap shear strength props. 0-66842
 polymer-metal adhesive bonds, shear resist., polymer crystn. effect 0-89462
 polystyrene-polyethylene block copolymer, deformation ratios, Poisson ratio and adhesion, dilatometric obs. 0-60937
 polyurethane cement, viscosity and shear strength, components influence (*German*) 0-93729
 rubber-metal interface, adhesion mechanism, XPS study 0-65382
 solar cells design, with improved glass, adhesives and heat dissipation 0-76636
 solid-fluid interface, wetting and adhesion, thermodynamic aspects 0-89525
 solids, stickiness 0-88438
 sputtered refractory carbides, adhesion to metal substrates, improved 0-76481
 steels, stainless, surface characterisation rel. to adhesive bonding chem. etching, SEM, AES, XPS and electron probe microanal. 0-88416
 surface anal. techniques appl. 0-65381
 surface and interfacial aspects, review 0-108690
 surface chemistry studies, anal. appls. 0-88440
 thin films, adhesion determination, electron and laser beam appls. 0-71833
 thin films, meas. device 0-66720
 transducer bonding material investigations, US delay lines (*Japanese*) 0-79097
 urea-formaldehyde resin/wood materials, book 0-73114
 US bond evaluation, anal. of problem 0-71847
 vesicles, large, anal. of adhesion to surfaces, expt. procedure 0-109063
 wet particulate systems, pendular band strength between unequal-sized spherical particles 0-104418
 Ag, film, chem. deposited, agglomeration, SEM and TEM obs. 0-59828
 Ag film, on amorphous C and Si substrates, dispersion force contrib. to adhesion (*French*) 0-59842
 Al and Al alloy anodised oxide films, for adhesive bonding appls., AES and SEM study 0-66689
 Al film, on amorphous C and Si substrates, dispersion force contrib. to adhesion (*French*) 0-59842
 Al-steel mixture, wear resistant, produced by compaction by discrete shock waves 0-84882
 Au film, on amorphous C and Si substrates, dispersion force contrib. to adhesion (*French*) 0-59842
 B(C) fibre reinforced matrix, matrix-fibre interaction depend. on metallic dopants (*Russian*) 0-76479
 Co, particle formation by evap., electron microscopy obs. of interaction processes 0-104053
 Cr film, trivalent, cathodic deposition, as bonding interface between Cu and polyethylene 0-76201
 Cu film, on amorphous C and Si substrates, dispersion force contrib. to adhesion (*French*) 0-59842
 Fe, particle formation by evap., electron microscopy obs. of interaction processes 0-104053
 Fe-Ni-Cr-Al-Y, oxidation mechanism, Y addition effect on kinetics and oxide adherence 0-76223
 Ni films, adhesion on graphite 0-80141
 Ni, particle formation by evap., electron microscopy obs. of interaction processes 0-104053
 Ni-SiC coating adhesion to Al alloy, metal interdiffusion (*Russian*) 0-66697
 PLZT/TFPD thermal/flash protective lens assembly, polarised delamination investigation 0-78929
 Pd membrane, sorption of H_2 , adhesion and penetration probabilities, extreme values 0-101040
 Ti metal-metal interface, adhesion energy, surface treatment and ion implantation effects 0-107660

adiabatic compression, plasma see *plasma heating*

adiabatic demagnetisation see *magnetic cooling*

adion see *adsorption*

admittance, electric see *electric admittance*

admittance, electric, measurement see *electric admittance measurement*

ADP (ammonium dihydrogen phosphate) see *ammonium compounds*

adsorbed layers

see also *monolayers*

- acetic acid, on Cu (100), interaction with formic acid, EELS study 0-76120
 acetonitrile, on MgO, IR and TPD study 0-70528
 acetylene adsorbed on Fe containing segregated C, hydrogenation, C-1s XPS spectra obs. 0-84366
 acoustic phonons, obs. method using Brillouin scatt. in adsorbed monolayers 0-59804
 adatom valence-level position variation on metal surface 0-88611
 adatom-surface interaction potential, vibr. spectrum 0-103581
 adsorbed film monolayer melting, dual symm. systems, periodic struct. (*Russian*) 0-107405
 adsorbed monolayer parameter determ. by full current spectroscopy method (*Russian*) 0-70539
 Ag, on AgCl cryst., luminesc. fatigue 0-66281
 alumin, on polystyrene, contact angle meas. 0-61508

adsorbed layers continued

- atoms, surface band splitting, theory, with appl. to He/graphite 0-60058
 autoionisation bands due to one-centre resonances in adsorbed layers, theory 0-59790
 benzene, deuterated and chemisorbed on glass, vibr. bands, Raman scatt. study 0-84737
 benzene, on Al_2O_3 , Raman spectroscopy study 0-65358
 benzene adsorbed on graphite, melting and orientation, NMR study 0-100403
 benzene adsorbent mesopores, capillary evaporation and struct. 0-107614
 1-butene, on δ - Al_2O_3 , isomerisation, IR study 0-76554
 1-butene adsorption on delta alumina, microgravimetric-IR study 0-75432
 capillary condensation theory, adsorbates liq. or gaseous props. 0-80028
 chemisorbed phases, phase transitions 0-107656
 commensurate-incommensurate transition and domain walls 0-107654
 commensurate-incommensurate transitions, substrate defects effect 0-75437
 condensed adsorption layers, effect on electrode reaction rates 0-93769
 correlation effects, s-d hybridization in substrate 0-107886
 density of states, impurity atom effects 0-92958
 dye molecules adsorbed on Ag, Au and Cu films, absorpt. and luminesc. study 0-103981
 elastic interaction between adatoms near distortive phase transition 0-80080
 electrode, anisotropy of optical props. 0-60534
 electron-impact vibr. excitation, specular selection rule 0-80051
 electron-stimulated desorption ion imaging of adsorbate distrib. 0-103572
 electronic transforms, near boundary separating mag. and nonmag. states 0-92961
 enhanced Raman scattering by adsorbates on metals, including nonlocal metal response, nonradiative modes excitation 0-88994
 fibrinogen, on polystyrene, contact angle meas. 0-61508
 formic acid, on Cu (100) interaction with acetic acid, EELS study 0-76120
 formic acid, on Ni surface, decomp., dipole interactions effects 0-61143
 gases on solid surfaces, mobile and localized adsorption, theory 0-65379
 interface total reflection and surface wave obs. 0-108292
 IR photoacoustic spectroscopy of solids and surface species 0-90909
 IR spectroscopy, reflection-absorption, of adsorbed layer systems, review, book contrib. 0-84747
 isoquinoline, adsorbed on Ag, surface enhanced Raman spectrum 0-100400
 LEP, electron positron storage ring, vac. chamber, glow discharge surface cleaning 0-58010
 medical polymers, chem. problems, conf., Prague, Czechoslovakia (Aug. 1977) 0-56996
 metal, modification of surfaces, effect on electrocatalysis, review 0-61110
 methane adsorbed submonolayer on graphite, structural transitions between epitaxially ordered phases 0-96740
 methane-d₄ monolayer films on graphite, neutron diff. studies of phases 0-96739
 methylpyridine adsorbed on Ag, surface enhanced Raman spectra 0-83376
 mobility of adatom on metal surface, density functional approximation calc. 0-103577
 molecular clusters adsorbed on conductor surfaces (*Russian*) 0-80078
 molecule, angle-resolved and variable impact energy electron vibr. excitation spectroscopy 0-76119
 molecule, in electrochem. systems, Raman scattering 0-60563
 molecules, Raman and fluoresc. enhancement by surface roughness 0-102511
 monolayer on graphite, neutron scatt. studies 0-107655
 monolayers, Lennard-Jones system, melting in external field 0-65362
 monolayer adsorbed films, mol. theory 0-80058
 Ni, adsorption residual C removal by electron beam irradiation and heat treatment (*Chinese*) 0-88421
 one-dimensional incommensurate structures at finite temperatures 0-103567
 one-dimensional model crystals, surface density of states, rel. to adsorbed molecule 0-107889
 order-disorder transition, effect on work function 0-59791
 order-disorder transition, Ising model, LEED superlattice beam intensity distrib. 0-65371
 photoelectron diff. aximuthal patterns, struct. sensitivity 0-107644
 polymer chains, surface restricted self avoiding walks span, mol. weight depend. 0-65360
 protein adsorbed layers on field-emitter tips, removal by UV radiation 0-104836
 pseudopotential of adparticle on substrate near second-order phase transition 0-80065
 pyridine, adsorbed on Ag, 210-243 cm^{-1} mode in surface enhanced Raman scatt. 0-89003
 pyridine, on Ag electrode with graphitic C overlayer, Raman spectra obs. 0-103954
 pyridine, on Ag surface, enhanced Raman scatt., ultrahigh vac. study 0-88993
 pyridine, on Ag surface, Raman active librational modes 0-65359
 pyridine, on Au substrate with Ag monolayer, giant Raman effect 0-63637
 pyridine adsorbed on Cu (110) surface, photoemission selection rules 0-100751
 Raman scattering from molecules adsorbed on metal surfaces 0-65374
 rare gas adsorbates on simple metals, optical excitation, configurational switching, charge transfer 0-107643
 rhodamine 6Zh, on stilbene mol. cryst., role of excitonic and radiative mechs. of energy transport 0-108276
 rhodamine B, on Ag electrode, anisotropy of optical props. 0-60534
 semiconductor/adsorbate system, local density of states calcs. (*German*) 0-60062
 solid surface, mol. dynamic processes interaction with laser radiation 0-71943
 surface atomic and electronic struct. studied with synchrotron radiation 0-80945
 surface defects and thermodynamics of chemisorbed layers 0-80068
 surface diffusion calcs. 0-107633
 surface diffusion of adsorbed species 0-80070
 surface enhanced Raman scatt. on rough metal surfaces 0-93307
 surface enhanced Raman scattering surface plasmon model 0-108211
 surface enhanced Raman spectra, image dipole description, critical review 0-87125

adsorbed layers continued

- surface film phase transitions, conf., Erice, Sicily, Italy (Jun. 1979) 0-105429
 surface reactions, dipole interactions effects 0-61143
 tetramethyltin, on graphite, nature of 2 D diffusion 0-84372
 tribenzylmethylammonium sulphate, condensed adsorbed layer, effect on electrode reaction rate 0-93769
 trimethyl tin chloride adsorbed on grafoil, Mossbauer study 0-80643
 triphenyl tin chloride adsorbed on grafoil, Mossbauer study 0-80643
 Van der Waals film adsorbed on graphite, two-dimensional phase transitions 0-107653
 vibrations, large-angle inelastic electron scatt., theory 0-75427
 water, chemisorbed on Pt (111), EELS spectra, vibr. freqs. 0-80920
 water, on Al_2O_3 , Raman spectroscopy study 0-65358
 XPS, core ionisation, negative shake-up energy 0-100749
 Ag, on AgCl cryst., luminesc. fatigue 0-66281
 AgBr emulsion grains, adsorbed dyes, light-induced ESR spectra 0-88862
 Ar, on Al, differential refl. spectroscopy, local field effect 0-80811
 Ar, on graphite, multilayer adsorbed films, mol. theory 0-80058
 Ar-N₂ liquid soln., selective adsorption on graphite, struct. study, mol. dynamics calc. 0-59806
 Au, on AgBr dispersion in gelatin, transient absorpt. spectra, latent image form. and decay 0-66837
 Br, on Si single cryst., X-ray standing waves obs. at cryst. surface 0-96417
 Br₂, chemisorbed on zeolites, Raman spectra 0-93301
 Br₂, chemisorption on V, layer struct., Na adsorption effects 0-101039
 Br₂, on Au electrode, anisotropy of optical props. 0-60534
 C, on Fe(100), adsorbate coverage determ. by LEED, AES and XPS 0-103566
 C, on Ni surface, location of adsorbed atoms, surface channelling meas. 0-84373
 CN⁻, on Ag surface, Raman active librational modes 0-65359
 CO, adsorbed c(2×2) layer on Ni, Cu(001), struct. 0-88428
 CO, adsorbed layer, electron impact, electron impulsive ionisation spectroscopy obs. 0-60720
 CO adsorbed on Ag, Au films, enhanced Raman scatt. mechanism in ultrahigh vacuum 0-107645
 CO adsorbed on graphite, fluid-registered solid transition 0-59796
 CO, adsorbed on jellium, surface plasmon relax. energies 0-70537
 CO adsorbed on Ni, valence band photoemission, SCF MO CNDO calc. 0-100754
 CO adsorbed on Pd surface, Penning ionisation by metastable He beam, theory 0-60735
 CO adsorbed on W, electron-stimulated ion desorption 0-59797
 CO adsorbed on W, electron-stimulated desorption, photoemission, relax. energy 0-100401
 CO, c(2×2) on Ni(001), struct. by LEED, self-consistent scatt. pot. 0-70536
 CO, catalytic oxidation on ferrites, IR spectrosc. investig. 0-89524
 CO, chemisorbed on Al_2O_3 -supported Rh-Cu catalysts, IR spectra (French) 0-60559
 CO chemisorbed on Fe, low energy vibr. modes studied by tunnelling spectroscopy 0-78590
 CO, chemisorbed on Ni (111), bond energies 0-100398
 CO chemisorbed on Pt, IR refl.-absorpt. spectra, adsorbate island struct. 0-84385
 CO chemisorption on Pd, Ag, PdAg, SIMS, XPS study 0-84382
 CO molecular adsorbed on Mo (110) surface, electronic states, photoemission spectra 0-65363
 CO, on Cu (100), vibr. excitation cross-sections 0-75441
 CO, on Mo (100), surface kinetics, photoemission study method 0-80941
 CO on Pd (111) surface, metastable He impact, electron emission, energy and ang. distrib. 0-60744
 CO, on Pd/ Al_2O_3 , IR study 0-108193
 CO, on Si (111), ion scatt. obs. 0-59810
 CO, oriented molecule, photoelectron ang. distrib., energy depend. 0-76152
 CO, oxidation on Ir films, IR absorpt. spectroscopy 0-71398
 CO, reaction with H₂ on Ni(001), extended muffin-tin orbital theory 0-76557
 CO₂, on Al_2O_3 , Raman spectroscopy study 0-65358
 Cl overlayer on Cu (100), adatom bonding effects, photoemission study 0-104044
 Cs on graphite, dissolution, lamellar cpd. form. (French) 0-100399
 D, on graphite (0001), vibr. spectrum, at. beam scatt. obs. 0-92779
 Fe₂O₃ amorphous layer on graphite, Mossbauer spectra, superparamag. props. 0-60474
 Ga on W and Mo (001), struct., FIM obs. 0-103576
 GaP:Cs-O simultaneous adsorption, oxidation interface chemical struct. 0-103584
 H adsorbed on Nb, distrib., electron-stimulated desorption ion imaging 0-103572
 H atoms, chemisorbed on cluster, indirect interactions, Grimley-Pisani model and tight-binding calc. 0-65370
 H, chemisorbed atom, surface charge fluctuations effect on spectral density 0-65368
 H, chemisorbed on transition metals, effect of surface spin fluctuations 0-75613
 H, in contact with He surface, Bose condensation, adsorption isotherms and stability 0-107638
 H, on graphite (0001), vibr. spectrum, at. beam scatt. obs. 0-92779
 H on Ni (110), adatom configuration, He diff. study 0-103569
 H on Pt (111) surface, backscattering, channelling spectra, H adsorption, surface relaxation 0-71552
 H, on W (100) and Ni (111), angle-resolved and variable impact energy electron vibr. excitation spectroscopy 0-76119
 H₂ adsorption on Rh-TiO₂ catalyst, surface states, NMR spectrosc. investig. 0-103891
 H₂, chemisorbed on W, vibr. spectra charact., adsorption sites 0-70535
 H₂, ortho-para conversion, magneto-catalytic reaction, quantum formulation 0-108750
 H(1×1), on W (100), H ν , vibrational mode, IR study 0-60582
 He film, adsorbed, NMR measurements 0-107605
 He, on graphite, band struct. effects in heat capacity 0-59788
 He on graphite, band struct. and thermodynamic props. 0-80349
 He, on graphite surface, anisotropic He-C pair interaction 0-96738
 He on W surface, accommodation coeffs. calcs. 0-66866
³He, adsorbed monolayers, nuclear magnetic relaxation for two dimensional systems 0-103534
³He-⁴He mixture, adsorbed film, systematic exptl. study 0-107603

adsorbed layers continued

- ⁴He film growth on graphite, MgO, and Mylar substrates, vap. press. meas. 0-70499
 Hg adsorbed on W, thermal desorption kinetics, theory 0-59792
 I adsorbed on Ag(111), photoelectron diff. aximuthal patterns, struct. sensitivity 0-107644
 I chemisorbed on Au, AES and LEED study 0-100405
 I₂, chemisorbed on zeolites, Raman spectra 0-93301
 In, chemisorption of O₂, XPS and static SIM spectral study 0-80055
 K adsorbed on W, field emission flicker noise power 0-59795
 K, on Fe(100), adsorbate coverage determ. by LEED, AES and XPS 0-103566
 Kr adsorbed on graphite, commensurate-incommensurate transitions, low temp. theory 0-103582
 Kr, on graphite, commensurate to incommensurate transition 0-80079
 N₂ adsorbed on W(100), vibr. spectra, bonding struct., LEED study 0-84387
 N₂, adsorbed mesopores, capillary evaporation and struct. 0-107614
 N₂, on Ni, valence band photoemission, SCF MO CNDO calc. 0-100754
 NH₃, on Ir (111), mol. adsorbate structs. from angular-resolved photoemission 0-76141
 NO, adsorbed layer, electron impact, electron impulsive ionisation spectroscopy obs. 0-60720
 NO, on Cu, ultrahigh vacuum ESR studies 0-97729
 Na adsorbed on Ni, photoemission, directional memory effects 0-100753
 Na adsorbed on Ni(100), photoelectron diff. aximuthal patterns, struct. sensitivity 0-107644
 Na adsorption on V, effect on Br₂ chemisorption 0-101039
 Na, on Al, adatom valence-level position variation 0-88611
 Na, on Cu (111), UPS study of surface electronic struct. 0-80350
 Na, on Ni(001), photoelectron diff. effects in core-level photoemission 0-76144
 Ni, electrocrystallisation, reaction mechanism, appl. of impedance meas. (French) 0-103597
 Ni(001) surface N adsorption due to ion beam irradi., surface struct. LEED study (Chinese) 0-84364
 O adsorbed on Al (111) surface, surface struct., LEED and SEXAFS data 0-92782
 O adsorbed on CdS, EPR of O radicals, temp. depend. 0-80612
 O adsorption on Cu (001) surface, effect on surface barrier, LEED study 0-84378
 O chemisorption on Cu(100) surface, angle-resolved UPS study 0-84384
 O on Cu vicinal surfaces, LEED study 0-103575
 O, on Fe(100), adsorbate coverage determ. by LEED, AES and XPS 0-103566
 O, on Ni (111), adlayer phases and binding sites 0-80069
 O on Ni {100}, crystallographic effects in low energy ion scatt., local ion-atom neutralisation 0-84377
 O, on Ni surface, location of adsorbed atoms, surface channelling meas. 0-84373
 O, on Pt (111), chemisorbed and oxide states, low energy ion scatt. obs. 0-65372
 O, on Si (111), ion scatt. obs. 0-59810
 O₂ adsorption on Ni(110) surface, LEED and ion scatt. study 0-84386
 O₂ adsorption on Pt (111) surface, UPS, EELS and thermal desorption study 0-100409
 O₂ layer on W, Ar⁺(Ar^{+m})(Ar²⁺) impact, electron emission obs. 0-60740
 O₂ on Cu (100) surface, LEED study 0-100408
 O₂, two-dimensional, on graphite, props. calc. 0-103568
 Pb monolayer, double layer with Sn, growth on Al (111), struct. 0-70567
 Pb, monomolecular film on Ag electrode, anisotropy of optical props. 0-60534
 Pb on Cu vicinal surfaces, LEED study 0-103575
 Pb, underpotential adsorption, cathodic deposition, on Ag(111) and (100) (German) 0-108363
 Pd on W (110), long range interatomic interactions with coadsorbed Re, W 0-59789
 Pd on W (110) surface, growth, struct., stability, desorption 0-59794
 Re on W (110), long range interatomic interactions with coadsorbed Pd 0-59789
 S, on AgBr dispersion in gelatin, transient absorpt. spectra, latent image form. and decay 0-66837
 S on Cu vicinal surfaces, LEED study 0-103575
 S, on Fe(100), adsorbate coverage determ. by LEED, AES and XPS 0-103566
 SiO₂ on BeO, effect on TSEE 0-76159
 Sn, monolayer, double layer with Pb on Al (111), layer growth, struct. 0-70567
 Sn on W and Mo (001), struct., FIM obs. 0-103576
 Te, on Ni(001), photoelectron diff. effects in core-level photoemission 0-76144
 Tl, underpotential adsorption, cathodic deposition, on Ag(111) and (100) (German) 0-108363
 W, diatomic cluster migration on W {100} plane, elementary displacement steps 0-88436
 W on W (110), long range interatomic interactions with coadsorbed Pd 0-59789
 W on W(001), struct., FIM obs. 0-103576
 Xe adsorbed on Cu, NaCl, stepped and disordered surfaces, two-dimens. phase transformations 0-103580
 Xe adsorbed on graphite (0001) surface, monolayer liquid and solid struct. 0-65400
 Xe adsorbed on Pd (110), anomalous 5p photoemission, electron binding energies 0-100750
 Zn, electrocrystallisation, reaction mechanism, appl. of impedance meas. (French) 0-103597

adsorption

see also heat of adsorption

- acetate ions adsorbed on Ag particles in aqueous soln. Raman spectra 0-69148
 adsorbed layers, general principles of construction of structural models 0-84351
 aerosols, atmospheric, gaseous nitrates adsorption by particles in urban and rural area 0-94123
 aerosols, flowing, attachment of ²²⁰Rn decay products using aerosol centrifuge 0-61167
 n-alkanes, adsorption into bimolecular lipid layers 0-88435
 atomic interaction dipoles, perturbation theory 0-78680

adsorption continued

- binary mixtures flowing through activated C, adsorpt. interference 0-107635
 black foam films stability, review 0-104463
 charcoal filters, NDT of residual adsorption capacity 0-89523
 charged system, two-dimens. comparison with neutral particle adsorption 0-80077
 colloids, rel. to thermodynamic stabilisation 0-81369
 copper phthalocyanine film, electron acceptor surface states due to O₂ adsorption 0-88586
 diffusion-controlled reactions on a two-dimensional lattice 0-71940
 N,N-dimethyl aniline, adsorpt. on Ag colloids, surface enhanced Raman spectra obs. 0-97251
 dynamical and geometrical effects on the physisorption of atoms 0-70531
 electrical double layer, ion adsorpt. and discrete charge effects, self-consistent calcs. 0-76516
 electrocatalysis, surfaces modified by metal adatoms, review 0-61110
 electron microscope contamination by surface diffusion of adsorbed hydrocarbon mols., theory 0-99013
 factor VIII, native and modified, surface adsorption and mol. interactions, ellipsometric obs. 0-104555
 fibrinogen, native and modified, surface adsorption and mol. interactions, ellipsometric obs. 0-104555
 film boiling, effect of adsorption characts. on minimum temp. 0-79114
 FIM, gas supply function, expt. determ. from adsorption rate 0-100402
 finite harmonic oscillator chain with surface impurity, dynamics 0-59776
 fly ash particles, water accretion, refract. index and accreted layer thickness 0-58462
 formate ions adsorbed on Ag particles in aqueous soln. Raman spectra 0-69148
 gas, installation for studying static characts. of porous and nonporous materials 0-81361
 gas atmosphere quantitative analysis adsorption chamber 0-85234
 glass, adsorption of Au, AES study, electron bombardment effects 0-65380
 grain boundaries decohesion energy, solute adsorption influence 0-65009
 grain boundary cohesion, resulting from solute segregation, pair bonding theory 0-88166
 graphite, adsorption of CO, fluid-registered solid transition 0-59796
 graphite, of He, surface band splitting, theory 0-60058
 graphite, of inert gas microcluster, temp. depend., mol. dynamics study 0-80056
 graphite, of neopentane, quasi two-dimens. fluid, NMR 0-102525
 graphite, of O₂, partially localised, partially mobile monolayer films, adsorption isotherms 0-107646
 graphite, sliding against C, dusting wear regime 0-97595
 graphite (0001), ⁴He selective adsorption, level crossings 0-71556
 graphite (0001), inelasticity in He scatt. 0-76127
 graphite (0001), scattering and selective adsorption of H₂ (D₂) 0-71553
 graphite selective adsorption from Ar-N₂ liquid soln., mol. dynamics calc. 0-59806
 graphite surface, adsorbed Cs, dissolution, lamellar cpd. form. (French) 0-100399
 hydrogen embrittlement, adsorpt. model. and equilibrium crack growth meas. 0-108574
 hydrocarbons, on activated C, rel. between adsorption and polarizabilities 0-76558
 III-V semiconductor-oxide interface states, photoemission obs. of energy levels induced by adsorpt. 0-93000
 immiscible incompressible fluids, interfacial convective instability, diffusional exchanges, adsorption-desorption processes 0-70504
 inert gas ion milling processes, etch-rate ratio of oxides to nonoxides, increase using halocarbon gases 0-93663
 interface atomic structure, interface roughness, calc. (Russian) 0-103587
 interfacial cohesion, adsorption-induced losses 0-65010
 interfacial tension var. with supersaturation, one-layer adsorpt. model 0-103563
 intermolecular surface forces in plane densely packed hexagonal model 0-59785
 island film growth, cluster size distrib. 0-107665
 isotherm equation based on vacancy solution theory 0-65356
 lipid bilayer membranes, spectrophotometric and elec. corrs. of cyanine-dye adsorpt. 0-85358
 liquid film, falling, O₂ adsorpt. with zero order react. in entrance region 0-64652
 mean sojourn time of molecules on surfaces, meas. in practical vacuum system (Japanese) 0-57315
 metal oxide, of molecules, UPS studies, review 0-84374
 metal surface region, electrostatic energy and screened charge interaction for different Fermi surface shape 0-70631
 metal surfaces, radioactive contamination 0-68771
 metal-electrolyte interfaces, optical reflectance spectra, interpretation 0-93263
 metal-H system, hydride formation in high press. range 0-65235
 metallic membrane interface, mass transfer 0-81366
 metallic substrate, metal atom adsorption, enthalpy calc. 0-100406
 metals, adsorption potential in hydrodynamical model 0-100396
 metals, of atoms, Green's function formalism for studying electronic struct., local density of states calc. 0-107884
 mixed gas adsorption, homogeneous solid surface, adsorbate-adsorbate assoc. model 0-96742
 molecular adsorption, effective reson. Raman spectra 0-97730
 molecular sieves, adsorpt. of atmospheric gases, comparison of 13X and 4A at low temp., press. (German) 0-88423
 molecules adsorbed on rough surfaces, Rayleigh, Mie and Raman scatt. 0-83378
 monolayer films, partially localised, partially mobile, adsorption isotherms, temp. depend., theory 0-107646
 monolayer-covered surface, surfactant adsorpt., Gibbs eqn. calcs. 0-59781
 multicomponent surface phase, comp. determ. from gas adsorption data 0-88417
 N₂O refrigerator, thermodynamics and thermoelectric condenser design 0-108809
 neutron scattering from adsorbed mols., surfaces and intercalates, review, book contrib. 0-84394
 nickel phthalocyanine film, electron acceptor surface states due to O₂ adsorption 0-88586
 nonisothermal one-component sorption in adsorbent particle, interparticle heat transfer 0-70523
 nonpolar molecules, adsorption into lipid bilayer membranes 0-61517
 partial localisation model (French) 0-70526

adsorption continued

- particle absorption rates at high cell concs., Monte Carlo simulation 0-94141
 physical adsorption, vacuum microbalance studies 0-76551
 polymer charcoal, adsorpt. isotherms of organic vapours 0-96731
 polymeric molecules adsorption, statistical mechanics appln. 0-84365
 polymers, of molecules, Green matrix local impurity SCF calcs. 0-92778
 polymers in mixed solvents, preferential adsorpt. coeff. rel. to mol. dimens. 0-103237
 polystyrene, γ -Fe₂O₃ powder filled, mag. films, packing and particle orientation (Japanese) 0-104115
 polystyrene, of albumin and fibrinogen, contact angle meas. 0-61508
 polyvinyl acetate, γ -Fe₂O₃ powder filled, mag. films, packing and particle orientation (Japanese) 0-104115
 polyvinyl butyral, γ -Fe₂O₃ powder filled, mag. films, packing and particle orientation (Japanese) 0-104115
 pore size measurement, comparison of methods 0-62622
 precursor intermediates in adsorption, desorption and reaction 0-108731
 proteins, on polymer surfaces, structural changes 0-89712
 Pyrex glass capillary tubes, effect of adsorbed water vapour on liq. water flow 0-92759
 pyridine, adsorpt. on Pt/Al₂O₃, electron accepting sites 0-71947
 radioactive waste, geologic storage, effect of adsorption of Tc and I radioisotopes by minerals 0-83203
 radioactive waste, sorption of actinides in igneous rocks 0-95367
 radiotracer method investig. appls. 0-70525
 silicate glass, hydration in steam atmosphere 0-85211
 solid electrolyte-metal interface adsorption layer capacitance calc. (Russian) 0-59697
 solid surfaces, surface processes, and solid/gas interactions 0-73125
 solid/liquid adsorption equilb., kinetic studies using isotopic mol. exchange method 0-88427
 solutes in aqueous fissures in porous rocks, effects of adsorption on transport 0-94553
 spherical particles adsorption, statistical mechanics appln. 0-84365
 steel, segregation and adsorption of S, influence on carburisation and nitrogeneration 0-66701
 surface, adsorbed atoms thermal desorption, one dimens. microscopic model, weak binding case 0-96729
 surface adsorbed molecules, internal optic modes, mol. dipole model 0-100395
 surface dipole layers, forces between plates 0-70793
 symmetrical adsorption thermodynamics, case of noninert adsorbent 0-80059
 thermodynamic theory 0-93794
 thioindigo, adsorbed on Al₂O₃, photoisomerisation 0-89503
 vacancy solution theory of adsorption from gas mixtures 0-65357
 γ -Al₂O₃, physisorption and reaction of Mo(CO)₆, IR spectra obs. 0-80064
 Ag (110) surface, adsorption of mol. O₂ species 0-103578
 Ag (111), adsorption of acetic and propanoic acids, LEED obs. 0-80073
 Ag (111) surface, ethylene adsorption, XPS and UPS investigation 0-103573
 Ag, adsorpt. of acetonitrile, surface enhanced Raman spectra obs. 0-97251
 Ag, adsorpt. of benzene (deuterobenzene), surface enhanced Raman spectra obs. 0-97251
 Ag, adsorpt. of pyridine, surface enhanced Raman spectra obs. 0-97251
 Ag coating on refractory metals, energy struct. determ. at two monolayer thickness 0-100392
 Ag electrode, enhanced inelastic light scatt. caused by adatoms 0-89013
 Ag film, ellipsometric response to CO adsorption 0-103571
 Ag, of ethylene and propylene, enhanced Raman spectra obs. 0-95607
 Ag, of monomolecular films of Pb, anisotropy of optical props. 0-60534
 Ag, of pyridine, on (110) surface, UPS, AES and flash desorption meas. 0-92776
 Ag, of rhodamine B, anisotropy of optical props. 0-60534
 AgI aerosol, ice forming activity, UV irradi. effect 0-71950
 AgI surface, of water, effective pair pot. model 0-100394
 Al (111), angle-resolved UPS obs. of 2-dimens. band structs. of S, Se and Te 0-60059
 Al surface, hydrazine and NH₃ adsorption and decomp., XPS obs. 0-92783
 Al-Al₂O₃-Au device, adsorption of Cl₂, effect on current-voltage characts., press. depend. 0-65704
 Al₂O₃, inelastic electron tunnelling spectroscopy of adsorbates, MgO comparison 0-88686
 γ -Al₂O₃ interface with electrolyte solns, adsorption of ions, surface conductance, ion mobility and surface pot. 0-75622
 Al₂O₃, of Cs, Sr, Eu, Co, and Cd 0-99240
 Al₂O₃, Raman spectroscopy study of adsorbed molecules 0-65358
 β -Al₂O₃-Na₂O, of Na, surface electronic struct. calcs. 0-75431
 Au film, adatom surface diffusion at low temps., elec. resist. study (French) 0-65376
 Au film, evap., temp. change and gas adsorpt. effect on opt. consts., ellipsometric obs. (German) 0-89081
 Au of Br₂, anisotropy of optical props. 0-60534
 Ba monoatomic film on W (110), characteristic electron energy loss 0-100720
 BaTiO₃ polymorph, hexagonal, low temp. and surface CO₂ adsorption and desorption 0-80713
 Bi film, adatom surface diffusion at low temps., elec. resist. study (French) 0-65376
 C, activated, adsorption in countercurrent flow 0-70524
 C polymeric chains, reduced from poly(tetrafluoroethylene), N adsorption 0-89488
 CO₂, adsorption and capillary condensation on clays rel. to Mars volatile storage and atmospheric history 0-72833
 CaHPO₄, powder and granules with starch mucilage binder, compressed, low temp. N adsorption obs. of surface area 0-80998
 CaO, of O₂, O₂⁻ ion form. 0-61155
 CeNi₂Al, mag. susceptibility, H adsorption-desorption cycle effects 0-107990
 Co, adsorption-desorption kinetics of CO, surface carbide form. effects 0-103574
 Cr, photon emission due to Ar⁺ ion bombard., adsorbed and recoil-implanted O effect 0-80872
 Cs ion source, SF₆ adsorpt., thermionic emission 0-71557
 Cu adsorption of O₂, N₂O on (100) surface, reaction with CO 0-103583
 Cu, electrolytic coating, brightness and adsorption of surface-active additives 0-100963

adsorption continued

- Cu, of H₂O and Br₂, on (100) face, Helmholtz layer model system 0-92777
 Cu polycrystals, oxidation, secondary ion energy spectra 0-71788
 Cu surface, (001), O₂ adsorption effect on surface barrier, LEED study 0-84378
 Cu surface, (110), methanol adsorption, XPS, UPS and thermal desorpt. study 0-84388
 Cu surface (100), adsorption of O₂, LEED study 0-100408
 Cu vicinal surfaces, LEED study, S, O and Pb adsorption effects 0-103575
 Cu-Ni, of H₂+CO, interaction in (110) single cryst. surface, TDS and UPS obs. 0-80052
 Cu-Ni (110), of CO and H₂, UPS, thermal desorption, AES, and LEED study 0-80087
 CuO powder, surface area determ. by adsorpt. of stearic acid and pyridine 0-107636
 Fe (110), coadsorption of K and O₂, XPS, UPS, AES, and LEED study 0-80084
 Fe, evaporated, adsorbed acetylacetone, XPS study 0-76133
 Fe, H₂ embrittlement and H₂ adsorption 0-89401
 Fe, of acetic acid and ethylenediamine, XPS study 0-76132
 Fe, of O₂, oxidation 0-108730
 Fe, polycrystalline, H₂ adsorpt. and embrittlement, work function changes 0-96741
 Fe, segregation and adsorption of S, influence on carburisation and nitrogenation 0-66701
 Fe surfaces, adsorption, segregation and reactions of non-metal atoms, LEED and AES obs. 0-59783
 Fe-As melts, surface tension, density, adsorption (*Russian*) 0-92757
 Fe(100), of CO and H₂, C, O, S and K adlayer effects 0-71573
 Fe(110), of K, UPS and XPS meas. 0-95675
 GaAs, of O₂, influence of cleavage defects on interaction 0-66684
 GaP, adsorption and desorption of Cs, LEED, AES, and photoemission meas. 0-70532
 GaSb, adsorption and desorption of Cs, LEED, AES, and photoemission meas. 0-70532
 Ge (111) clean surface, of O₂, and electron work function 0-59779
 Ge heteroepitaxial film, ethanol pulsed adsorption effect on elec. cond. 0-93014
 H₂ embrittlement adsorption or decohesion, mechanism 0-97643
 HF adsorption, by smelter-grade aluminas, during Al smelting 0-80075
 Ir, adsorbed gases, field desorption from field ion tips 0-59793
 LiF (001), multiple Debye-Waller effects at selective adsorption in atom-surface scattering 0-76126
 MgCr₂O₄-TiO₂, porous ceramics, humidity-sensitive electrical conduction 0-107782
 MgO, inelastic electron tunnelling spectroscopy of adsorbates, Al₂O₃ comparison 0-88686
 MgO, of acetonitrile, IR and TPD study 0-70528
 MgO powder, surface area determ. by adsorpt. of stearic acid and pyridine 0-107636
 MgO:Mo, of propylene, oxidation reactions, surface structs., IR absorpt. spectra obs. 0-66868
 MnO₂ coated Al₂O₃ and SiO₂ supports, N adsorption obs. of dispersion modes 0-81363
 MnO₂ porous powders, Al₂O₃ and SiO₂ coated, changes in surface free energy for N adsorption 0-84363
 MnO₂:Li(Mo)(V), of Zn²⁺ ions, kinetics, ⁶⁵Zn γ -ray scintillation investig. 0-70529
 Mo (100), condensation of Cu and Ag, early stage comparison with W(100) 0-80072
 Mo (111) planes, of NH₃, preferential nitriding, FEM study 0-66877
 Mo, ion bombard., ion and photon yields, CO adsorption effect 0-89098
 Mo, of O₂ and C₂, simultaneous adsorption struct., emission props., thermal stability 0-66878
 Mo surface, clean and gas covered, He⁺ impact, deexcitation, pot. energy transfer mechanism 0-60743
 NaCl₄ on Pt and Ir surfaces, adsorption kinetics 0-84393
 Nb, adsorbed O₂, effect on polarised Balmer radiation from scatt. H²⁺ 0-99569
 Nb, of H, sticking coeff. calc. 0-59803
 Ni (001), of N₂, c(2 \times 2) struct. form 0-80083
 Ni (001) surface, electronic struct. of ordered S overlayers 0-84835
 Ni (100), dissociative chemisorption and mol. adsorption of NO 0-65373
 Ni (100), of O₂, and reduction of surface oxide by H₂ 0-108741
 Ni (100) surface, coadsorption of Sn on Pb, P or O contaminated surface, AES study 0-88437
 Ni (111) and (110), laser-induced charge transfer to adsorbed CO, photoemission expts. 0-59798
 Ni, atmospheric corrosion, moisture adsorption and indoor corrosion rates 0-71799
 Ni, evaporated, adsorbed acetylacetone, XPS study 0-76133
 Ni film, interaction with O₂, AES, EELS, work function, and gravimetric meas. 0-75433
 Ni films, of ethylene, adsorpt. and decomposition, coverage depend. meas. 0-96743
 Ni, ion bombard., ion and photon yields, CO adsorption effect 0-89098
 Ni, of acetic acid and ethylenediamine, XPS study 0-76132
 Ni, of N₂, photoemission and electronic struct., cluster calcs. 0-97403
 Ni, of O₂, oxidation 0-108730
 Ni, photon emission due to Ar⁺ ion bombard., adsorbed and recoil-implanted O effect 0-80872
 Ni small clusters, of Na, local densities of states 0-88466
 Ni surface, (110), O₂ adsorption, LEED and ion scatt. study 0-84386
 Ni, surface, single-atom self-diffusion FIM study, hydrogen adsorption effects 0-103548
 Ni-Fe, of O₂, oxidation 0-108730
 NiO, (100) surface interaction with SO₂, electron diff. and Auger spectrosc. obs. (*French*) 0-97728
 NiO, prepared by thermal decomp. of Ni(OH)₂, microporosity and irreversible water vapour adsorption 0-80060
 Pb_{1-x}Sn_xTe epitaxial films, adsorption-induced accumulation layer form. on surface 0-60117
 Pd (110) surface, adsorption of S, characterised by LEED (*French*) 0-88422
 Pd cluster, adsorption/desorption of CO, AES and thermal desorption meas. 0-75436
 Pd film, work function changes due to adsorbed H₂, surface and interface dipoles 0-96972
 Pd ribbon, of H₂, thermal desorption and work function meas. 0-70538

adsorption continued

- Pd/Al₂O₃, of CO, IR study 0-108193
 Pt (100) (5 \times 20) and (1 \times 1) surfaces, stability and reactivity, adsorption of H 0-75434
 Pt (111), adsorption of acetic and propanoic acids, LEED obs. 0-80073
 Pt (111), interaction with water, thermal desorption, UPS, and XPS study 0-80088
 Pt (111), of NO, EELS, thermal desorption, LEED, and AES study 0-80086
 Pt (111) and Pt(S)-12(111) \times (111) surfaces, of O, thermal desorption, AES, XPS, and LEED study 0-70534
 Pt, adsorption and catalytic reactions of H₂, CO, and O₂ 0-81362
 Pt, of CO, mol. internal optic modes, mol. dipole moment 0-100395
 Pt, of CO(NO), on SiO₂-supported surface, IR spectrosc. obs. 0-92780
 Pt, of O₂, on (110) surface, Ar⁺ bombardment effects on reactivity 0-89099
 Pt, oxide layers on electrode surface anisotropy of optical props. 0-60534
 Pt, surface, (111), O₂ interactions, UPS, EELS and thermal desorption study 0-100409
 Pt surface, CO oscillatory oxidation, theory 0-85215
 Pt surface, CO oscillatory oxidation, theory 0-85216
 Pt-Pd, of CO(NO), on SiO₂-supported surface, IR spectrosc. obs. 0-92780
 Pt(111), of K, UPS and XPS meas. 0-95675
 Re, adsorption, oxidation, and hydrogenation of CO, XPS, UPS, and thermal desorption study 0-71571
 Re(0001), of O₂, CO, NO, and H₂O, XPS, UPS and temp. programmed desorption 0-71574
 Rh (111), co-adsorption of H₂ and CO segregation of co-adsorbed species 0-65361
 Rh dispersed on Al₂O₃, of CO, ¹³C NMR obs. of adsorbed states 0-96733
 Rh, of CO and H₂, on (111) surface, 2-dimens. phase separation 0-107634
 Ru (0001), of CO, IR spectra, LEED, and thermal desorption meas. 0-70533
 Ru (001), of CO, temp. depend. ordering processes 0-80773
 Ru (1120), of O₂, H₂, and CO, ellipsometry-LEED study 0-103570
 Sc (0001), H adsorption, geometric vs. electronic factor in surface electronic structure 0-70788
 Si (100), H adsorption, MeV ion scatt. study 0-80071
 Si (111), O and CO sorption, ion scatt. obs. 0-59810
 Si (111) surfaces, cleaved, electronic structure following Al adsorption 0-75610
 Si, CVD from SiH₄-HCl-H₂ system, rate-determining reactions and surface species 0-84405
 Si, photon emission due to Ar⁺ ion bombard., adsorbed and recoil-implanted O effect 0-80872
 SiO₂, P-doped amorphous, porous and hydrophilic, water adsorpt. and IR spectra obs. 0-80061
 Si(111), ion-bombard., O₂ adsorption, SIMS study 0-70522
 SrTiO₃, of O₂, electron energy-loss spectra obs. 0-89521
 Ta, simultaneous interactions with Cl₂ and O₂ under low press. and high temp. 0-71938
 Te_{50-x}Se_{50-x}Sn_x, thin films, elec. cond. and thermoelectric power meas. (*French*) 0-80335
 Ti (0001), H adsorption, geometric vs. electronic factor in surface electronic structure 0-70788
 Ti, photon emission due to Ar⁺ ion bombard., adsorbed and recoil-implanted O effect 0-80872
 TiO₂, rutile, pure and SiO₂-coated, adsorption of N₂ and Ar, 77.4K, microcalorimetry obs. 0-80062
 TiO₂ suspension, adsorption-desorption of IO₃⁻ 0-93804
 TlTe, melt, elec. cond., surface tension, microhardness, influence of impurities 0-88551
 W (001), of N₂, effect on LEED electron spin polarisation and intensity profiles 0-65377
 W (100), condensation of Cu and Ag, early stage comparison with Mo(100) 0-80072
 W (100), H adsorbate low energy electron vibrational excitation 0-84375
 W (100), total hemispherical emissivity meas., sensitivity to O₂ adsorption 0-79964
 W (110), of Be, film growth and struct. 0-75477
 W (110) and (111) surfaces, KCl adsorption-desorption behaviour 0-75442
 W (110) mobility and two-dimens. compressibility of adsorbed Xe, field emission current fluctuation method 0-80089
 W (110) stepped surface, of O, electron stimulated desorption, atomic steps and defects influence 0-80091
 W (111), field adsorption of He, array model 0-59800
 W, adsorbed gases, field desorption from field ion tips 0-59793
 W, coadsorption of La and B, field emission and field ion microscopy 0-104049
 W faces, of Ba and Cu atoms, work function changes during simultaneous adsorption 0-65378
 W, of Ba and Ti, work function meas. 0-100411
 W, of Dy, Ho, Er, field emission electron study 0-100393
 W, of NO and NO₂, FEM obs. 0-84390
 W, powder, gas adsorption and desorption (*Russian*) 0-75429
 W surface, (100) adsorbed N₂, vibr. spectra, bonding struct., LEED study 0-84387
 W surface, polycryst., N₂ adsorption states 0-100404
 W, surface adsorption processes following electron excitation, cathodoluminescence studies 0-100390
 W, surface diffusion of adsorbed O, secondary electron emission study 0-76117
 W(100), I adsorption at room temp., LEED and AES study 0-84389
 W(110), substrate strain induced interaction of adatoms 0-96744
 ZnO, adsorbing p- and n-type dyes, surfaces pot., UV light illum. effect 0-75624
 ZnO, of isopropyl alcohol, (acetone), decomp., IR and kinetic obs. 0-59780
 ZnO polar surfaces, H and O₂ exposed, ion irradi., and heat treated, cond., EELS study 0-71525
 ZnTe clean and adsorbed O₂ (110) surfaces, UV photoemission spectra (*Japanese*) 0-93456
 Zr, adsorption and absorpt. of CO, NO, N₂, O₂, and D₂, dissoc. and diffusion 0-80085

adsorption continued

- Zr, photon emission due to Ar^+ ion bombard., adsorbed and recoil-implanted O effect 0-80872
 Zr(BH_4)₂ catalytic reactions on Al_2O_3 , inelastic electron tunnelling spectra 0-75425

aerials *see* **antennas****aerodromes** *see* **airports****aerodynamics**

- see also* hypersonic flow; jets; shock waves; supersonic flow; transonic flow; turbulence; wind tunnels
 aerofoil, incompressible potential flow, second order approx. theory 0-69860
 aggregates, solid, aerosols, dynamic shape factors meas. appls. 0-61165
 air pollution, contaminant movement, Galerkin finite element method 0-74902
 airfoil flow, unseparated, potential distrib. and circulation, non-mapped complex variable method 0-83811
 atmosphere, dissipative effects, convective instability (French) 0-77058
 atomisation units for powder metallurgy, gasdynamic and acoustic props. 0-66451
 axial turbine blades, spatial streamline flow calcs. using pot. flux of incompressible liq. 0-59000
 bird flight, wake behind finch 0-81629
 blades, three-dimens. annular array, aerodynamic forces with nonsteady flow 0-99991
 blades, vibr. due to rotating stall, aerodynamic force meas. 0-92172
 boundary layer, laminar, subsonic, strong slot injection, triple deck theory 0-74831
 compressed gas, nonsteady transonic flow, modified Khokhlov method study 0-79347
 Darrieus rotor, aerodynamic analyses comparison 0-61264
 dissociating gas, relativistic flows, growth and decay of weak waves, shock wave formation 0-69949
 Drive and Ascent Satellite, aerodynamic characts. rel. to lower ionosphere research programme 0-77252
 flight effect of Michalke and Michel vis-a-vis Lighthill's model 0-59018
 gas dynamics eqn. boundary conditions in Chapman-Enskog Boltzmann eqn. soln. 0-96284
 H-shaped section cylinder in laminar and turbulent flows, aerodynamic charact. 0-106813
 hypersonic source flow field, aerodynamical anal. of body in hypersonic source flow field (Chinese) 0-59066
 hypersonic three-dimensional shapes, optimal surfaces and total drag coeffs. 0-59068
 incompressible flows, 2-D, potential flow past aerodynamic body, sub-surface panel method 0-74901
 inviscid gas, expansion into near vacuum, contact front-primary shock regime, particle path formulation 0-59070
 isothermal gas, straight compression wave due to pressure pulse driven flat piston 0-69873
 mass transfer and mixing in packed columns, recirculating gas fraction, cell model 0-69913
 noise, aerodynamically generated, fluid flow eqns. (French) 0-74848
 nonuniform parallel stream, slender wing theory, flow and lift 0-74830
 nuclear power plants, aerodynamic and thermodynamic effects on environment (German) 0-61469
 operating theatre, air flow patterns 0-94439
 operating theatre, air flow patterns 0-94440
 oscillating airfoils with controls in ventilated wind tunnels, aerodynamic interference, subsonic flow 0-74905
 parallel circular cylinders, finite height 0-103013
 perfect gas, vortex sheet, separation from smooth body at large Reynolds number (French) 0-74908
 piston, magnetic field effect, self-similar magnetogasdynamic problem with radiative heat transfer 0-64578
 pollutant transport eqn., 3-D, numerical algorithm 0-106811
 Savonius rotor, aerodynamic performance testing in wind tunnel 0-61266
 shock wave localisation, by shock-capturing results of computation of gas dynamics problems 0-83815
 shocks, magneto-radiative, axisymmetric, equatorial propagation 0-79349
 short-fetch wind waves, aerodynamic lift and drag from Lagrangian wind and current vectors 0-72553
 simple bodies in two-phase flow, aerodynamic drag 0-96294
 slots, circumferential gas streams in running channels (Russian) 0-74980
 sound wave transmission through nonuniform circular ducts 0-74900
 spacecraft, optimal aerodynamic attitude control 0-77250
 stable flow past a wing, appl. of method of discrete vortices 0-74889
 subsonic flow, diverging, stability aspects, time-dependent method 0-74906
 subsonic flow past an oscillating cascade with finite mean flow deflection 0-74907
 subsonic rotational and transonic mixed flows, numerical simulation using fast super-dashpot time-dependent technique 0-83813
 supersonic air flow through high press. gas valves into atm., noise and flow pattern obs. 0-59067
 supersonic gas stream, stationary, conical flow about plane wedge and circular cone 0-74912
 Timoshenko bar, aerodynamic stability, time- and space-harmonic balance (German) 0-83812
 transonic flow, unsteady, turbulence modelling, compression waves developing into shock wave 0-74909
 tube, cylindrical, sudden expansion, turbulent flow meas. by laser Doppler velocimeter 0-75003
 turbulent flow of incompressible liquid in planar channel, axial curvature effects 0-87762
 unsteady airfoil, Kutta condition (Japanese) 0-92155
 unsteady laminar separation and stall from aerodynamic surfaces 0-59090
 wind turbines, machine performance and rotor aerodynamics 0-74904
 wing in forward motion, trailing edge acoustic source radiation 0-69780
 wings near ground, nonlinear unsteady one dimensional theory 0-79344

aeronomy *see* **meteorology; terrestrial atmosphere; upper atmosphere****aerosols**

- see also* foams
 acid sulphate in atmosphere aerosol, detection from S/N ratio 0-61494
 acoustic field effects 0-89529
 aerosols of marine air, submicron size distrib. and CCN supersaturation 0-77041
 aggregates, solid, aerosols, dynamic shape factors meas. appls. 0-61165
 air particulate element conc. over USA 0-76679

aerosols continued

- airborne particulates sources, identification and relative importance estimation 0-72105
 Aitken range size distrib. meas. in N.Atlantic 0-98404
 Antarctic, particle anal., comp. 0-77091
 aqueous aerosol cloud containing medium, light beam propag., thermal self-interaction 0-91750
 atmosphere, above Black Sea, spectral transmission and sky brightness (Russian) 0-94603
 atmosphere, aerosol particles induced error in satellite retrieved temp. profiles 0-98449
 atmosphere, aerosol scattering indicatrices under clear sky conditions in 0.55 to 2.4 μ spectral region (Russian) 0-94600
 atmosphere, Al particles from space rocket launching 0-81503
 atmosphere, Antarctic aerosol origins and props. 0-90197
 atmosphere, charge of aluminosilicate pollutant particles, depend. on thermal history 0-97840
 atmosphere, composition meas. for Florida by time series anal. 0-89688
 atmosphere, condensation nuclei and weather on Mount Kenya 0-82012
 atmosphere, dust grains mean radius rel. to transparency meas. on Maidanak mountain (Russian) 0-72627
 atmosphere, effect on contrast reduction in remote sensing of Earth surface 0-101431
 atmosphere, gas-particle conversion meas. for coal fired power station plumes 0-81502
 atmosphere, gaseous nitrates adsorption by particles in urban and rural area 0-94123
 atmosphere, H_2SO_4 constituent reaction with O_3 , N_2O 0-90168
 atmosphere, H_2SO_4 particulate form. in coastal area 0-90113
 atmosphere, hexagonal ice crystals as cause of 46° halo and its arcs 0-82065
 atmosphere, IR transparency window, 10-13 μm , H_2O and aerosol effects in winter and summer (Russian) 0-105048
 atmosphere, large particle scatt. coeffs. approximation for total O_3 determ. 0-82091
 atmosphere, light scatt. coeff. of marine boundary layer 0-82052
 atmosphere, low-level aerosols as cause of anomalous gray shades in DMSP visible imagery 0-77111
 atmosphere, maritime aerosol near Europe, albedo and 632.8 nm absorpt. 0-90136
 atmosphere, mol. and aerosol scatt. rel. to effects of diffuse radiation on O_3 photodissoc. 0-109210
 atmosphere, near IR absorpt. due to soot particles (Russian) 0-82055
 atmosphere, new particle formation in presence of existing aerosol 0-81962
 atmosphere, obs. at Barrow, Alaska, effect of wind direction 0-85704
 atmosphere, obs. of Denver Brown Cloud 0-81961
 atmosphere, particulate nitrate and HNO_3 in air of equatorial Pacific 0-85702
 atmosphere, S level meas. using continuous flame photometric detect. system 0-81508
 atmosphere, Saharan dust affecting radiative transfer rates, model 0-90149
 atmosphere, scavenging of aerosol particles by cloud drops and small rain drops, elec. field effect 0-82001
 atmosphere, size-fractionated aerosol comp. in Charleston, W.Virginia 0-89687
 atmosphere, sky brightness fluctuations in daytime (French) 0-81959
 atmosphere, steel mill plume, ice nuclei and aerosol obs. 0-89693
 atmosphere, thunderstorm ice nucleation study, Colorado, USA 0-90135
 atmosphere, trace element concs. over Lake Michigan 0-81968
 atmosphere, urban, aerosols distrib. rel. to mixing depths numerical simulation 0-105024
 atmosphere, urban, radiative effects of elevated aerosol pollutant layers on temp. struct. in urban atmosphere, radiative effects of elevated pollutant layers 0-97841
 atmosphere, urban, soot determ., by optical absorption technique 0-108824
 atmosphere, visibility, turbidity and light scatt. obs. 0-105047
 atmosphere aerosol, mass concentration from Lidar-solar radiometer expt. 0-90171
 atmosphere aerosol, study of chemical components in Kashmir region 0-94594
 atmosphere boundary layer, fog and haze, visibility and particle size distrib. 0-109195
 atmosphere composition, Nigeria during dry dusty season 0-81960
 atmosphere H_2SO_4 , extinction, absorpt., backscattering and mass content relations 0-101403
 atmosphere ice platelets, IR radiation attenuation 0-66141
 atmosphere obs. revealing volcanic activity of Mauna Loa, Hawaii 0-76950
 atmosphere off W.African coast, Na, Cl and Br composition 0-77053
 atmosphere particulate matter, role in anthracene photooxidation 0-61487
 atmosphere salinity used to determine ocean salinity flux 0-104986
 atmosphere soil-derived dust, Christiansen effect in IR spectra, Rayleigh limit 0-105046
 atmosphere sulphate aerosol, meso-scale transport obs. in rural East Midlands, England 0-94124
 atmospheric, microscopic samples molecular analysis, using Raman microprobe 0-57391
 atmospheric, simultaneous Al, Si determ. by neutron activation anal. 0-72116
 atmospheric, solar radiation absorpt., visual photometric meas. technique 0-85750
 atmospheric aerosol extinction measurements, multiple scatt. corrections 0-98445
 atmospheric aerosol size distribution determ., optical attenuation meas. (Chinese) 0-72570
 Atmospheric Cloud Physics Laboratory simulation, vorticity transport eqn. solns. 0-94690
 atmospheric environmental research, appl. of lasers (German) 0-97849
 atmospheric nonspherical aerosol particle characterisation with electrooptical nephelometry 0-77106
 binary gas mixture, drop thermophoresis 0-93806
 biomedical influence, conf., Dusseldorf, Germany (Oct. 1979) 0-94915
 bleached zone, probe radiation propag., intensity and phase fluctuations 0-67411
 chemical composition measurement, use of laser induced mass spectrosc. instrument 0-97848
 climate model, zonally averaged, aerosols affecting temperature 0-77102

aerosols continued

- cloud condensation nuclei, meas. using horizontal thermal gradient spectrometer 0-77158
 cloud condensation nuclei in urban environment, effects on cloud microphysical model 0-82004
 clouds, ice nucleation by aerosol particles 0-61864
 coagulation, initial size distrib. effect 0-104469
 coagulation rate measurement, of high Knudsen number aerosol 0-71954
 coastal meas. by 1.06 µm Mie lidar scatt. 0-98403
 condensation nuclei counters at South Pole, calibration 0-98470
 correl. with N.Hemisphere average temps. during Little Ice Age 0-82050
 counter, photoelectric, calibration by sedimentation method 0-99031
 cylindrical surface, aerosol particle capture, thermophoresis forces 0-103060
 deposition in entrance of parallel-plate channel, gravity effect 0-83834
 deposition of particles in model airways 0-72192
 differential scatt. coeff. to mass conc. ratio, spectrophelometer, cascade impactor obs. 0-72628
 dispersity analysis, automatic photoelec. analyser for size range 0.3-40 µm 0-57251
 dust storm in Israel, dust property obs. 0-90162
 dye solution aerosols as laser active media 0-95887
 electro-aerosols, precipitation in the airways, effect of electrostatic scatter 0-108929
 ellipsoidal aerosol particles in binar binary gas mixture, diffusophoresis under hydrodynamic conditions 0-66888
 ellipsoidal particles in acoustic field, relative velocity 0-58854
 fibrous media, dendritic deposition of aerosol particles, inertial impaction and interception 0-74945
 flowing, attachment of ²²⁰Rn decay products using aerosol centrifuge 0-61167
 fog, thermal emissivity 0-95795
 global surface irradiance, effect of aerosol props. and surface reflectivity 0-76611
 hygroscopic particle humidification process, electrooptic scatt. meas. 0-77107
 IR radiation scattering, atmos. heating and cooling rates 0-72630
 IR spectrometry, theory and appl. to spectroscopic effects of atmospheric constituents 0-101428
 laminar tube flow, gravitational deposition of growing aerosol particles 0-59099
 liquid particles, aerosol and hydrosol, separation by size in thermal fields 0-101044
 lung, deposition of inhaled particles, airway generations of normal subjects 0-67125
 mammalian lung airways, aerosol deposition in anatomical models, theoretical evaluation 0-81627
 mass extinction coefficients estimated for nonabsorbing spherical aerosol particles in the geometric scattering regime 0-87310
 middle atmosphere aerosol, remote sensing techniques 0-109269
 midlake region, aerosol mass conc. and scattering coeff. 0-61839
 monodisperse, mass concentration, laser monitoring 0-98878
 multiple light scattering, theory for dispersive media with spherical particles (*Russian*) 0-94599
 Neptune atmosphere, aerosol particles rel. to UV albedo 0-82295
 optical coherence, atm. effects 0-82064
 optical component protection in dusty environments, electrostatic techniques 0-58657
 optical device for examination of mixed phase aerosols 0-86404
 particle optical constants and disperse aerosol comp., phase scattering function (*Russian*) 0-61898
 particle size classifier with parallel plate electrostatic device 0-95070
 particle size distribution meas. using electronic cascade impaction 0-72652
 particle size measurement, optical particle counter calibration by Doppler shift spectrometry 0-68173
 particle size measuring device, using spectral transparency and small angle scatt. methods 0-95069
 particles in flow type chamber, coagulation, deposition 0-69908
 pipe, turbulent aerosol flows at high wall temps., heat transfer 0-74862
 planetary atmospheres, aerosol effect on radiative transfer 0-109383
 pollution in Beijing, China, effect of weather conditions (*Chinese*) 0-108825
 polydisperse aerosol number and mass conc. meas. by elect. aerosol anal. 0-108753
 radioactive aerosol surveillance system evaluation 0-57984
 scattering function determ. with telephotometer 0-105055
 sea salt aerosol, atmospheric temp. sensors contamination 0-82095
 single droplet, size and mass meas. using electrodynamic balance 0-89535
 size distribution by inverting spectral turbidity data 0-95796
 smoke aerosols, optical absorption to extinction ratio, photoacoustic determ. 0-58459
 smoke/dust cloud temporal analysis algorithm 0-98484
 soil-derived atmospheric dusts, particle absorption contributions to mass extinction coefficients 0-61896
 soot conglomerate destruction dynamics in pulsed laser radiation field 0-58617
 spark discharge generator for laser Doppler measurements in turbulent flames 0-59139
 spectrometer using two-pulse Fraunhofer holography, fibrous particle motion anal. 0-58476
 Stokes drag forces for small particles, kinetic corrections to aerosol gravitational collisional efficiency 0-95386
 stratosphere, multi-ion complexes, implications for aerosols and trace gases 0-61872
 stratosphere, satellite monitoring systems, SAM II and SAGE 0-82082
 stratosphere aerosol, modification by supersonic transport and space shuttle operations, climatic implications 0-98408
 stratosphere aerosol content var., rel. to atm. transparency and direct solar radiation 0-82035
 stratosphere sulphate aerosol, kinetics of growth by condensation in homogeneous medium (*Russian*) 0-94566
 stratosphere sulphate aerosol layer, processes, models, obs. and simulations 0-109212
 sulphate and nitrate mixing ratios obs. near tropopause 0-61835
 suspensions of charged particles, laminar tube flow, entrance deposition 0-59100
 thin flat, EM wave scatt. and absorpt. 0-91723
 trace constituents in Indian west coast SW monsoon aerosols 0-81967

aerosols continued

- tropical N.Atlantic Ocean, aerosols water-soluble K, Ca and Mg contents 0-72598
 troposphere, trace gases in summer, background levels in Greenland 0-72609
 troposphere light scattering, particle shape influence 0-90220
 Uranus atmosphere, aerosol particles rel. to UV albedo 0-82295
 urban aerosols at St. Louis, pollutant source strength-rainfall relationships investigation 0-77059
 Venus, cloud microstructure, optical props., H₂SO₄ atmosphere-aerosol study 0-72808
 Venus atmosphere, aerosol model 0-101545
 Venus atmosphere, B-layer and C-layer aerosols rel. to UV cloud model, polarimetric evidence 0-82250
 volcanic dust veils causing Earth surface temp. drops 0-85726
 volcanic Fuego eruption, aerosol density, temp. and particle content determ. 0-90050
 X-ray absorption spectra for chem. characterisation of atmospheric aerosols 0-61501
 X-ray absorption spectra for chem. characterisation of atmospheric aerosols 0-72121
 AgI aerosol, studies of ice-forming activity, verification of theory 0-101406
 AgI aerosol particle size, struct. rel. to ice forming activity 0-61164
 AgI, ice forming activity, UV irr. effect 0-71950
 AgI surface, adsorption of water, effective pair pot. model 0-100394
¹⁴⁴CeO₂, effects of repeated inhalation exposure, mouse obs. 0-104676
¹⁴⁴CeO₂, inhalation exposed mice, toxicity, dosimetry and ¹⁴⁴Ce retention 0-89874
 H₂O-H₂SO₄-ion aerosol particles, ultrafine, stratospheric form., ion-induced nucleation 0-72608
 H₂SO₄ aerosol, filter sampling of air, possible artifacts 0-82079
 H₂SO₄ in atmosphere, heterogeneous reactions and role as tropospheric sinks 0-72612
 H₂SO₄-H₂O aerosols nucleation rate in presence of ionisation source 0-104464
 Na-fire aerosol filtration in nuclear reactors 0-68853
 NaCl monodisperse aerosols, appl. in cloud droplet nucleation expts. 0-82003
 NaCl-gas reactions, atmospheric, in situ TEM studies 0-104544
 P, red, atmospheric aerosol, absorption to extinction coeff. ratio meas. 0-90217
²³⁹PuO₂ inhaled by rhesus monkeys, cytogenetic and other biological effects 0-108968
 Rn daughters in atmospheric air, efficiency of HV-70 filters for sampling 0-108827
 S aerosol, of S. American troposphere 0-67401
 SO₂ and sulphates, residence times under non-steady-state conditions 0-77092
 SnO₂ aerosols, Lamb-Mossbauer factor (*French*) 0-81375
- aerospace**
 see also aerospace computing; aerospace control; aerospace instrumentation; aerospace propulsion; aerospace simulation; aerospace test facilities; aircraft; ground support systems; space research; space vehicles; terrestrial atmosphere
 No entries
- aerospace applications of computing** see aerospace computing
- aerospace computer control**
 see also aerospace computing
 unmanned (or manned) vehicles, automatic rendezvous with space station 0-77249
- aerospace computing**
 see also aerospace computer control
 Salyut-6 spacelab, data acquisition and logging system incl. speech 0-61979
 satellite navigation, Chebyshev approximations for compression of Ephemerides 0-61993
 shells of revolution under axisymmetric and asymmetric loadings, linear elastic dynamic analysis program using finite element analysis (*Japanese*) 0-106719
- aerospace control**
 see also attitude control
 astrodynamics conf. (Provincetown, MA, USA, June 1979) 0-82583
 coordinate-parametric control of nonstationary spacecraft, multi-dimensional asymptotically stable adaptive systems appl. 0-101522
 Drive and Ascent Satellite, orbit control for lower ionosphere research 0-77252
 optimisation algorithm for spacecraft flight trajectory between Earth and Moon 0-72754
 spacecraft charging, neutralisation via electron emitter (*Japanese*) 0-94673
- aerospace engines**
 noise reduction modelling, discrete freq. noise 0-106652
 turbo-jets, fan noise reduction by single- and double-wall barriers 0-87648
 turbojet, internal noise generation 0-87644
 Ni alloy protection against hydrogen embrittlement, by Cu electroplating 0-76416
- aerospace ground equipment** see ground support equipment
- aerospace instrumentation**
 see also aircraft instrumentation; Langmuir probes
 airborne system, for vertical air vel. meas. 0-77159
 cryogenic systems for spacecraft 0-86319
 electron emitter, appl. to spacecraft charge neutralisation (*Japanese*) 0-94673
 Hadamard transform X-ray telescope, characts. (*Japanese*) 0-94714
 Lyman α camera, for high resolution solar Lyman α filtergrams 0-82323
 magnetometer, ring-core type, for space vehicles, geomag. fluctuations high-sensitivity obs. (*Japanese*) 0-94671
 satellite-gyrostat reorientation, optimal attitude control 0-61980
 scatterometer for investigating underlying surfaces, optimization of characts. 0-67436
 solar instruments for Solar Maximum Year review 0-90404
 space optics, conference Huntsville, Alabama (1979 May 22 to 24) 0-62385
 space optics, imaging X-ray optics workshop, Huntsville, Alabama (1979 May 22 to 24) 0-62384

- aerospace instrumentation continued**
space suit cooling, automatic control of human thermal comfort 0-109046
Space Telescope pointing control fine guidance subsystem design 0-82201
- aerospace propulsion**
see also aerospace engines
Drive and Ascent Satellite, on-board propulsion subsystem rel. to lower ionosphere research programme 0-77252
ion beam injection into magnetosphere, from solar power satellite engine 0-82149
- aerospace simulation**
see also aerospace test facilities
flight simulator viewing lens, triplet design 0-74457
large-aperture holographic visual simulator 0-102679
long arc simulated lightning attachment testing using 150 kW Tesla coil 0-70074
moving atmosphere simulation by rotating phase plate 0-79021
RF target simulator using acousto-optical device 0-102843
step-state spaceborne optical system image motion compensation 0-90322
step-state spaceborne optical system smear compensation by focal plane manipulation 0-82172
- aerospace test facilities**
see also wind tunnels
airframe material defectometry, quantitative test specifications (German) 0-89427
solid propellant stress transducer evaluation 0-81245
- a.f. amplifiers** *see audio-frequency amplifiers*
- AFC** *see automatic frequency control*
- afterglows**
decaying plasma, nonequilib. props. during afterglow modulation by acoustic waves 0-103144
diagnostics, instantaneous triple-probe method for direct display of plasma parameters in low density continuum plasma 0-84000
flowing afterglow plasma ion source, appls. 0-87955
lower hybrid waves, propag. in toroidal plasma 0-83927
marine green alga, *Ulva fenestrata*, afterglow in the ms and ds intervals of attenuation 0-104636
molecular photodissociation, recomb. afterglow, quenching var., activator penetration to region inaccessible to quencher 0-64813
nonisothermal plasma electron ensemble, nonstationary behaviour, kinetic description 0-59171
radiation escape kinetics, radiation captured by plane optically thick layer 0-95593
Ar decaying pulsed discharge plasma, acoustic waves density modulation 0-103143
Cu/CuCl double pulse laser, dissoci. pulse, afterglow, and laser pulse model 0-91775
 $H_2O^+(D_2O^+)$ plasma, dissociative ion electron recombination, rate coeffs. 0-63747
He+CS₂, metastable atoms, energy transfer processes 0-83466
He+OCS, emission spectra in He afterglow 0-87139
He, high press. afterglows, reviews 0-64823
Hg(6³P₀)+Hg(6³P₂), line excitation and population decay in afterglow 0-74242
KCl:Eu²⁺ crystals, photostimulated afterglow investigation at room temp. 0-108259
N₂+Ar(Xe), A¹S_u⁺ state energy pooling in flowing afterglow, Herman IR system 0-83503
N₂⁺(B²S_u⁺), N₂(C²Π_u) and N₂(C²Π_g) molecules, emissions obs. in yellow N₂ afterglow 0-63649
Ne+CS₂, metastable atoms, energy transfer processes 0-83466
α-SiC, afterglow stimulated by IR radiation (Russian) 0-89066
Sn hollow cathode laser, emission obs. from Sn II, I transitions 0-106509
- AGC** *see automatic gain control*
- age (Earth)** *see geochronology*
- age determination, radioactive** *see radioactive dating*
- age hardening** *see precipitation hardening*
- ageing**
see also precipitation hardening; strain ageing
Al-Zn-Mg (5.1 wt.%), decomp. process, TEM study 0-71660
alloys, disordered, residual resistivity due to clustering, ageing effects 0-65521
β-brass, spinodally decomposed, morphology and characts. 0-60863
cellulose fibre, gamma-irrad., and storage effects on props. (Russian) 0-61121
ceramic/metal layer adhesion mechanism for metallization of electronic ceramics, elec. props. (German) 0-76381
composite insulating materials, fatigue behaviour, influence of superposition of elec., mech. and environmental stresses 0-97590
creep modelling incorporating initial strain and ageing 0-58939
creep theory problems for ageing bodies with growing slits and cavities 0-69678
CW stripe lasers, thermal-impedance ageing characteristics 0-64018
electrochemically formed layers, kinetic and structural consequences 0-61109
epoxy resin insulation, adapted models selection problems for electric ageing (German) 0-89365
Geiger counter, self-quenching, anode surface changes with ageing 0-58025
glass fibre reinforced plastic greenhouse sheets, ageing behaviour, natural and artificial weathering (German) 0-81226
glass fibre reinforced plastic laminates, strength and deformability, artificial ageing effect 0-60893
glass fibre reinforced plastics, ageing by boiling in water, effect on physico-mech. props. 0-60892
glass reinforced polyamide 6, fatigue strength after heat treatment, ageing and coating of Al-containing lacquer (Polish) 0-89347
graphite fibre filled polyimide composite prepreg laminates, room-temp. ageing effect 0-81093
Hastelloy, C-276, H transport rel. to ageing treatment 0-75384
Hastelloy, H₂, embrittlement in H₂S environments, impurity segregation effects 0-71724
high molecular weight polyethylene for HV cables, characterisation using size exclusion chromatography 0-66897
island films, coalescence kinetics, ageing rate, Kahlweit approx. (Russian) 0-59838
metal strips, welded, aged, reduction of deformations (Russian) 0-97508
metals, quenched, vacancy cluster form. process 0-92706
Metglas 2826 ribbon, voids formation during crystallisation 0-108428
- ageing continued**
Nimonic 80A, order hardening, comparison between revised theory and expt. 0-93565
optical fibre, UV cured epoxy acrylate coated, zero stress ageing effect on strength 0-58753
optical fibre splice, using arc fusion method, protection and reliability 0-69565
optical fibres, GeO₂-B₂O₃-SiO₂, ageing effects of moisture on fatigue and tensile strength 0-66539
polydimethyl siloxane-b-styrene-b-dimethyl siloxane block copolymer, morphology, mech. props. 0-64930
polymer glasses, enthalpy relax., scanning calorimetry technique 0-90851
polymers, atmospheric resistance, distrib. function determ. and anal. (German) 0-81225
polyvinylidene fluoride film, biaxially oriented, charact. for transducer appl. 0-88931
PVC surfaces, natural and stabilised, composition, ageing, oxidation and weathering, ESCA obs. (French) 0-61139
secondary cells with C-air electrodes in alkaline electrolytes, ageing mechanism study 0-101087
spark switches, high repetition rate, with Al and brass electrodes, surface ageing 0-106997
steel, alloy, hardened, electrochem. characts. and stress corrosion cracking, ageing and cold treatment effects 0-108639
steel, austenite, carbide strain hardened, strength and plasticity, effect of Mn content (Russian) 0-97500
steel, austenitic, ageing and plastic deform. effect on struct. and mech. props. of N15Kh5G3T3 (Russian) 0-71691
steel, austenitic Fe-Mn-V-C, ageing characts., discontinuous precip. nature 0-84940
steel, austenitic stainless, creep props., effect of high temp. ageing, SEM 0-97516
steel, austenitic stainless, MC precipitate comp., APFIM study 0-104161
steel, Co-Cr-Mo type HY-180M, mech. props. and SCC, overageing effect 0-108634
steel, Cr-Mn(Ni), Mn and Ni additions, effect on corrosion resistance and hardness 0-104342
steel, Cr-Mo (2.25, 1.0 wt.%), temper embrittlement, effect of P, Sn, comp. and carbide precip. 0-85036
steel, Cr-Mo (2.25, 1.0 wt.%), temper embrittlement, effect of Mn, Si, comp. and carbide precip. 0-85037
steel, ferritic stainless, embrittlement 0-85041
steel, high-strength low alloy, Nb(CN) precipitation and coarsening during hot compression 0-97514
steel, maraging, ageing kinetics and struct. of N12K7M5TYu, effect of high temp. deform. of austenite (Russian) 0-84960
steel, maraging, intermetallic phases precip. study by electron microscopy (Polish) 0-89217
steel, maraging 18%Ni, calorimetric anal. of ageing (Japanese) 0-89264
steel, martensitic, ageing, effect of H₂ on stresses in process of γ-α transformation (Russian) 0-76252
steel, martensitic-ageing, etching technique, for revealing struct. inhomogeneities 0-61035
steel, Mo, energy structure X-ray anal. using TEM 0-84036
steel, Ni-Cr, temper embrittlement, intermediate tempering treatments 0-60944
steel, stainless, sensitization, C content and ferrite morphology effect 0-89400
steel, stainless, stress relieved, microstruct. transformations resulting from ageing 0-71644
steel, stainless 304 sol. of annealed and thermally-aged, high-cycle fatigue behaviour 0-100923
steel, steam pipes, 12Cr1MoV, selection of allowable stresses based on minimum possible strength data 0-104237
steel, type IN-787, for use in Arctic, low temp. effects on mech. props. 0-76310
steel, type Kh13N9D2MT martensitic aged, struct. and mech. props. (Russian) 0-93600
steel turbine casings, residual life determ. 0-93585
steels, low-C, aged after quenching, rel. between micro-cracks and coxing effect (Japanese) 0-81159
steels, nitrided age-hardened, for blanking punches, chipping resist. props. (Japanese) 0-89340
viscoelastic contact, ageing 0-64486
Zircaloy-2, yield pts. obtained by ageing at two stresses 0-81091
Ag film, Ge coated, electrical resistance and ageing (Russian) 0-103759
AgI hydrosols, kinetics and mechanics of colloid systems formation 0-101045
(Al,Ga)As double-heterostructure lasers degraded, deep-level changes during accelerated ageing at high temps. 0-74356
Al-Ag, type-II superconductor, torque oscillations in mag. field (Russian) 0-103800
Al-Cu (3 wt.%), stress aged, GP zone struct. by X-ray diffuse scatt. meas. (Japanese) 0-71653
Al-Cu (3 wt.%) single cryst., stress aging, oriented precipitation (Japanese) 0-71652
Al-Cu (4 wt.%), supersaturated and aged conditions, high strain deform. 0-60907
Al-Cu (4 wt.%) alloy, reversion process of Guinier-Preston zones, ⁶³Cu NMR obs. 0-60871
Al-Cu (4.6 wt.%), cold work and ageing influence on ductility and fracture behaviour (Japanese) 0-89295
Al-Cu-Mg type 2036, thermomech. treatment, flow stress anal., effect in mech. props. 0-93584
Al-Cu(Mg), low freq. internal friction during plastic deform. (Chinese) 0-103420
Al-Li-Mn (2.8, 0.3 wt.%), recrystallised sheet, fracture behaviour, SEM and TEM study 0-97566
Al-Mg, Si alloy, void form. under different precip. conditions, after Al ion irradi. 0-59529
Al-Mg-Si, ageing sequence study by electron microdiff. 0-81068
Al-Mg-Li alloy, metastable S'-phase, struct. (Russian) 0-103291
Al-Mg-Si, type 6010, microstruct. characts. influence on formability, heat treatment 0-81090
Al-Si-Cu-Zr, ageing kinetics (Russian) 0-76274
Al-Zn (10 wt.%), ageing at low temp., effects of fluctuation of solute conc. 0-76287
Al-Zn (10 wt.%), ageing at low temp., effects of fluctuation of solute conc. 0-76288
Al-Zn (38 at.%), TEM study of precipitation processes or different microstructures during ageing 0-93561

ageing continued

- Al-Zn (8-25 wt.%), solid solns., residual resist. during clustering 0-97483
 Al-Zn-Mg, TEM and calorimetric study 0-76290
 Al-Zn-Mg (3.6, 1.95 wt.%), ageing and plastic deform., effect on structure, electron microsc. and X-ray diff. study (*Russian*) 0-81108
 Al-Zn-Mg alloy, Ag addition and pre-precipitation treatment, influence on GP zone growth 0-71658
 Al-Zn-Mg granules and bands rolled from them, heat treatment 0-100862
 AlGaAs DH laser, self-pulsations due to proton bombarded region self-annealing during ageing 0-99728
 Al₂O₃ humidity sensor, ageing improvement (*Japanese*) 0-100863
 AlZn, disordered, residual resistivity due to clustering, ageing effects 0-65521
 Au-Fe ion implanted alloy, Mossbauer conversion electron scatt. 0-88898
 Be, fracture and strength properties, dynamic ageing effects 0-81202
 Co-Ni-Cr-Mo (35, 20, 10 wt.%), MP35N, TEM study of phase transformations 0-81054
 Co-Ni-Cr-Nb (40, 18, 1.8 wt.%), precipitation behaviour of NbC, effect of ageing temp. on morphology 0-89227
 Co-Ti-Fe (3, 1 to 2 wt.%), spinodal decomposition 0-100839
 Cu-Al-Ni Marmen alloys, rapid solidification and ageing 0-76245
 Cu-Be, SCC in NH₃ 0-104326
 Cu-Be (2 at.%), plastic deform. and dislocation substruct. 0-76307
 Cu-Fe system, ageing and reversion phenomena study 0-89274
 Cu-Ni-Sn (15, 8 wt.%), prior deform. effect on spinodal age hardening 0-108465
 Cu-Ni-Zn-Mn fine grained precipitation-hardenable alloy, high strength and ductility 0-100805
 α -Fe, nitrated, aging at room temp. 0-71679
 Fe-Al(Ti), O containing, mag. aftereffect and disaccommodation meas., time depend., activation energy, and ageing props. 0-88836
 Fe-Al(24.3 at.%) C-alloy, magnetic permeability disaccommodation, 260-400K 0-93144
 Fe-Co-Si(B), amorphous ferromagnet, mag. after effect on soft mag. props. 0-84626
 Fe-Cr-Co, ductile magnet alloys, mech. props. 0-85001
 Fe-Cr-Co, magnetic domain walls, Lorentz microscopy 0-103854
 Fe-Cr-Co (28, 10.5 wt.%) ductile magnet alloy, humidity-induced H₂ embrittlement 0-89406
 Fe-Cr-Co alloys, (5-9 wt.% Co), obtained by slow cooling under mag. field, permanent magnet props. 0-75797
 Fe-Mo (13-20 at.%) binary alloys, spinodal decomp. on ageing, TEM and X-ray diff. study 0-97503
 α -Fe-N, supersaturated solid solns., N atom precip. kinetics, resist. meas. 0-60864
 Fe-Ni-Al-(Cu) (12, 0.5, 0.5 to 3 wt.%), Cu addition strengthening at 77K, mech. props. 0-60875
 Fe-Ni-Co-W(Mo) (18.65, 8.99, 4.87 wt.%), ageing characts., 380-530°C 0-60876
 Fe-Ni-(Cu) (12, 0.5 to 3 wt.%), Cu addition strengthening at 77K, mech. props. 0-60875
 Fe-Ti-C, rapidly quenched by splat-cooling 0-84923
 Fe₂Ni₃Cr₁₄P₂B₆ metallic glass, effect of pre-ageing on glass transition temp. 0-100326
 GaAlAs/GaAs kink-free narrow-stripe proton-isolated injection DH lasers 0-85534
 Ga_{1-x}Al_xAs DH laser diode, long-lived, high-power, facet coated 0-85564
 InGaAsP/InP injection lasers for long wavelength (1.1 to 1.6 μ m) optical communication 0-58582
 InGaAsP-InP buried heterostructure lasers emitting at 1.3 μ m, accelerated ageing characts. 0-95898
 InGaAsP-InP DH LED, high temp. aged, dark-spot defects, TEM obs. 0-66300
 KCl:Pb, impurity distrib., light scatt. and microhardness study, heat treatment 0-96562
 LiF, refractive index, effect of ageing, wavelength range 460-1000 nm 0-84707
 LiF:Co, flow stress changes during precipitation 0-92594
 LiF:OH, neutron irradi., interstitial H-centres, ESR obs. 0-93175
 LiNbO₃:Fe spatial holograms, use of thermal fixing (*Russian*) 0-74311
 Mg-Zn alloy, aged, one dimensional transition phase β_2' , crystallographic obs. (*Chinese*) 0-60865
 MgCd wire, elongation during disorder-order transform. (*Russian*) 0-104148
 MgF₂-Na₂AlF₆ thin film deposits, quenched ageing by chopping 0-97364
 Na₂O-SiO₂:Au + CeO₂, Au particle nucleation 0-81066
 Nb-W-Mo-Zr (5, 2.1, 0.92 wt.%), creep resist., high temp. ageing in vacuum 0-71716
 Nb-Zr-C welding solid solutions, ageing kinetics, influence of inclusion elements (*Russian*) 0-100853
 Ni-Al, order hardening, comparison between revised theory and expt. 0-93565
 Ni-Al-Mo (12.7, 21.6 wt.%), directionally solidified eutectic composite, precipitation 0-108454
 Ni-Co-Al alloys, continuous precip., SEM, TEM, X-ray diff. study 0-89220
 Ni-Cr-Mo-W-Al-Ti, heat-resist., phase comp. 0-76250
 Ni-Fe-Cr superalloy 718, heat treatment effect on room temp. and elevated temp. fracture toughness response 0-100922
 Ni-Fe-Nb-Al (11.2, 8.09, 79.66 wt.%), modulated struct. growth process rel. to ageing (*Chinese*) 0-66541
 Ni-Zn, physical-chemical metallurgy (*German*) 0-108390
 PLZT ceramic, ageing, dielec. props. 0-88940
 Pb-Ag (0.068 wt.%), Ag precipitation kinetics and activation energy 0-66517
 Pb-As (~0.01 wt.%), enhanced precip. phenomena, invest. of mechanism by elec. resist. meas. 0-104162
 Pb-Sb-As (1.1-1.8, ~0.01 wt.%), enhanced precip. phenomena, invest. of mechanism by elec. resist. meas. 0-104162
 Pb(Zr,Ti)O₂ ceramic, surface barrier electroreflectance, hysteresis, ageing 0-80752
 Pb(Zr,Ti)O₃ ceramics, DC field sintering preparation, piezoelectric props., ageing behaviour 0-81211
 Pb(Zr,Ti)O₃:Fe(Nb) ceramic, elec. and electromechanical props., depend. on dopants 0-81212
 Pd-Ni-Si amorphous alloys, crystn. process during isothermal ageing 0-89275
 Se, amorphous films, evaporated, ageing and crystn., DTA 0-65413

ageing continued

- Si ion-controlled diodes, acid-base exposure effects, Si-SiO₂ interface state density 0-96984
 Si-SiO₂ interface, thermally grown, surface pot. inhomogeneities after stress ageing 0-92993
 Si₃N₄ thin film, reactively sputtered, struct. and elec. props. 0-88656
 Sn-Pb surfaces ageing, detrimental effect in PC fabrication 0-108625
 Sr_{0.75}Ba_{0.25}Nb₂O₆, ceramic ageing dielec. props. 0-88940
 Ta-Al-N thin film resistors with improved elec. props. 0-100544
 Te₆₀Ge₁Pb₃, DSC sensitivity to controlled ageing in glass transition region 0-71673
 Ti, yield pts. obtained by ageing at two stresses 0-81091
 Ti/Cu/(Au) thin films thermocompression bonds degradation by thermal ageing 0-66546
 Ti-Al-Mo-Cr alloy weldment containing orthorhombic martensite, auto-tempering behaviour and alpha precip. strengthening 0-84976
 β -Ti-Mo, thermal instability, hardness and tensile deform. (*Japanese*) 0-71703
 Ti-Mo-Zr-Sn (11.5, 6, 4.5 wt.%), β III, mech. props. rel. to heat treatment 0-84961
 Ti-Mo-Zr-Sn (11.5, 6.0, 4.5 wt.%) alloy, struct. as affected by processing history 0-84972
 β -Ti-Mo-Zr-Sn (11.5, 6, 4.5 wt.%), metastable phase III, microstruct. and age hardening response 0-84945
 Ti-Mo-Zr-(Al) (15, 5 (3) wt.%), quenched and aged metastable β -phase, crystallography, morphology and decomposition 0-76262
 U-Nb (14 at.%), martensitic and polymorphic transformations 0-60861
 V₃Ga, supercond. A15 phase, prep. by controlled precip. 0-81000
 Y, polycrystn., plastic deform. at different deform. speeds, dislocation glide (*Russian*) 0-93598
 Zn-Al(22 wt.%), alloy sheet, superplastic, cold-rolling effects on mech. props. and microstructure (*Japanese*) 0-71671
 Zr, yield pts. obtained by ageing at two stresses 0-81091
 ZrO₂, partially stabilised ceramics, strengthening, post-sintering heat treatment 0-97518

ageing characteristics see ageing

agriculture

see also farming

- air pollution by N₂O from fertiliser, causing atmos. warming 0-94579
 animal wastes, pollutant transport in runoff water, review 0-97831
 crop and soil bidirectional reflectance factor calibration, remote sensing field research 0-86382
 field burning practice, downwind particulate pollution 0-97836
 flood inundation of agricultural land, LANDSAT digital image anal. 0-61913
 geothermal hot water for controlled horticulture 0-108783
 growing season length as climatic indicator, fluctuations 0-61887
 growing season variations in China in historical past, from written records (*Chinese*) 0-109246
 horizontal-axis wind-turbine system for pumping duties in Third World agriculture, design 0-61259
 irrigation in Karnataka State, in India, wind power and potential appls. 0-108782
 land-use mapping, evaluation of LANDSAT image data 0-101443
 New Zealand, temp. record, historical data and agricultural implications of climatic var. 0-61886
 photosynthesis bioenergetics 0-61521
 power station waste heat utilisation for fish farming and agriculture (*German*) 0-101080
 prairie region of Canada, hailstorm damage problem 0-109204
 remote sensing, agricultural cover types separability in spectral channels and wavelength regions 0-98468
 soil moisture IR thermography remote sensing through agricultural crop 0-109147
 solar technology and methods for appl. of solar energy to European agriculture 0-76616
 space-borne remote sensing (*Italian*) 0-109333
 NH₃, in troposphere, effect of nitrate fertilisers 0-85701

air

see also terrestrial atmosphere

- acetylene-air flame, Li(Na)(K)(Mg)(Ca) damping consts., Lorentz collisions, mag. field effect 0-66805
 adsorption of atmospheric gases on mol. sieves 13X and 4A at low press. and temps. (*German*) 0-88423
 aerosol composition, Nigeria during dry dusty season 0-81960
 air-acetylene flame, multichannel apparatus detect. limits using atomic absorpt. spectra 0-76586
 air-dielectric interface, EM wave reflection and transmission in terms of polarisation, education 0-105458
 air-H₂O, two phase upflow across horizontal tube bundles, void fraction and flow pattern 0-92201
 arc, wall-stabilised, step and sinusoidal current change response 0-103209
 arc temp. meas. by N₂⁺ integrated emission coeffs. 0-59314
 atmospheric, pure rot. CARS obs. 0-99511
 blast waves, cylindrically converging, in normal atm. conditions 0-92180
 blunt flat plates, air flow, 2-D, thermal boundary layer characteristics, nose shape effects 0-92121
 buoyancy demonstration 0-67988
 coal fired power station affecting downwind air quality, Montana, USA 0-108821
 diffusion rate in Au thin layers 0-100359
 dissociation by field-accelerated electrons, macroscopic props., rel. to pure O₂ 0-61118
 electrons, field-accelerated, in dry air and pure O₂, macroscopic props. comparison (*French*) 0-59161
 enthalpy meas. by LiCl humidity sensors 0-90858
 formaldehyde, in marine air and rainwater, wet season obs. 0-85703
 gas, heated, elec. breakdown parameters 0-103202
 heated, optical breakdown, mol. ion reactions influence 0-96341
 multichannel spark form. 0-87976
 optical breakdown, interferometric investigation 0-100064
 particulate element conc. over USA 0-76679
 particulate nitrate in marine air of equatorial Pacific 0-85702
 particulates in Montana air, element composition, background study 0-77034
 plasma, optical absorpt. coeff. at 1000 atm, 13000K, N₂⁻ photodissoc. 0-64691
 plasma, optical emission, localised oscill. mode obs. 0-83903
 plasma, radiowave interaction, electron velocity, collision cross-section depend. 0-103155

air continued

- plasma, slow burning gasdynamics, due to Nd laser beam (*Russian*) 0-108715
 plasma, TEA CO₂ laser-produced, using solid targets, induced shock waves 0-64729
 positive column of high-voltage diffuse discharge, nonstationary processes 0-64802
 sound generator, vortex, separation of acoustic energy and spent-air jets 0-102953
 space charges in rod-to-plane gap, impulse voltage meas. (*Japanese*) 0-87970
 turbulent flow in heated channel, effect of gravitational field 0-64533
 volcanic contamination indicating volcanic activity of Mauna Loa, Hawaii 0-76950
 water-air plug-train system, press. wave propag. characts. 0-59058
 Yaounde, Cameroon, particulates in urban and rural air (*French*) 0-61478
 Ar-air, transformer plasmatron, LF discharge, electrical and energy props. 0-103200
 HNO₃ in marine air of equatorial Pacific 0-85702
 NH₃ content Southern Ocean air 0-61871
 O₃ conc. affected by hydrocarbon emission from car factory 0-76674
 O₃ conc. at ground-level, Oslo, Norway, summer 1977 obs. 0-81965

air bases *see* **airports****air bubbles** *see* **bubbles****air compressors** *see* **compressors****air conditioning***see also* **ventilation**

- air assisted thermolec. air conditioner humidifier (SATEACH) 0-108802
 astronomical observations, building design effect on photographic zenith tube obs. 0-85856
 broadcasting station, 'Deutsche Welle' building construction and meas. (*German*) 0-106668
 BWR, heating, ventilation and air conditioning systems (*Japanese*) 0-91212
 energy saving control system, using heat storage tank (*Japanese*) 0-72087
 laboratory temperature control, modified window air conditioner 0-68192
 low frequency noise breakout from air conditioning ducts, abatement 0-74594
 noise abatement for induction motors in air/air heat-exchangers for ventilation (*Hungarian*) 0-102923
 PWR nuclear power station, heating, ventilating and air conditioning systems (*Japanese*) 0-91213
 solar, heating and air conditioning 0-61290
 solar absorption refrigeration 0-76651
 solar air conditioning, LiBr absorption 0-81425
 solar air conditioning with solid absorbents, earth and underground water cooling 0-72018
 solar evaporation and refrigeration units, assurance of specified energy parameter values, statistical analysis 0-93848
 solar heat pump plant for space heating in winter, air conditioning in summer 0-76615
 solar heating and cooling system for domestic use (*Japanese*) 0-108787
 solar Rankine cycle air conditioner (*Japanese*) 0-72076

air permeability *see* **permeability****air pollution***see also* **air pollution detection and control**; **smoke**

- aerosols, trace element conc. over Lake Michigan 0-81968
 NW.Africa, snowfield acidity (1977-79) 0-98370
 aluminosilicate particles, charge state depend. on thermal history 0-97840
 atmosphere, Al particles from space rocket launching 0-81503
 Beijing, China, weather conditions effect on pollution (*Chinese*) 0-108825
 biomass burning, C flux between biosphere and atmos. 0-97838
 Bombay heavy metal particulates due to road traffic 0-97837
 buildings, indoor airborne radioactivity calcs. 0-63305
 buoyant plume in stably stratified boundary layer, max. ground conc. 0-72573
 carbon tetrafluoride, atmospheric content, sources and residence time 0-61879
 Charleston, W. Virginia, size-fractionated aerosol composition 0-89687
 chemistry of polluted air reactions at 55°N 0-98382
 chlorofluorocarbons in stratosphere, O₃ layer depletion calc. using two-dimensional model 0-109221
 chlorofluoromethane, computer based policy analysis to reduce human health impacts 0-89698
 chlorofluoromethane induced IR cooling, effect on general circulation model 0-90122
 chlorofluoromethane photolysis in stratosphere, effect on O₃ conc. 0-109197
 climate, human influence, conference, Manlo Park, California (1979 February 21 to 22) 0-62381
 coal conversion technologies, health and environmental effects 0-81493
 coal fired power station affecting downwind air quality, Montana, USA 0-108821
 coal fired power station plumes, gas-particle conversion meas. 0-81502
 coal-fired power station, heavy metal fallout to nearby pond 0-76667
 coal-fired power station, particulate nitrates in plume 0-81498
 combustion engine exhaust pollution in Netherlands (*Dutch*) 0-101138
 conference, proceedings of 14th international colloquium, Paris (May 1980) 0-98760
 conference, Rochester, NY, USA (May 1979), polluted rain 0-82585
 cooling tower plumes, interaction with atm., numerical model simulation (*French*) 0-94126
 cooling tower plumes simulation, model calibration at Meppen power station (*German*) 0-94130
 cooling towers affecting rainfall, statistical study 0-109202
 damage to material objects, economic evaluation 0-76692
 data uncertainty rel. to environmental decisions 0-104535
 Denver Brown Cloud, obs. of C particles in aerosol 0-81961
 dichlorofluoromethane pollution, conc. obs. in background troposphere air 0-97843
 dispersal from point source into boundary layer, Ekman-type model 0-105039
 dispersal in tropical region, use of stability and freq. wind roses 0-97846
 dispersal of pollutants over complex terrain, steam plant in Tennessee valley 0-97833
 dispersing plume, crosswind geometry, second-order reaction 0-61480
 dispersion from elevated source in convective boundary layer 0-85312

air pollution continued

- dispersion from ground-level source, appl. of mixed-layer similarity scaling 0-105021
 dispersion from tall stack, into shore line environment 0-97832
 dispersion model (gaussian), incorporating temporal vertical stability variations 0-104526
 dispersion of pollutants, Gaussian moment-conservation diffusion model 0-85317
 dispersion parameters, tracer expts. and theory 0-76680
 Drax coal fired power station, CEC remote sensing campaign results 0-76681
 N.W. England, coastal site, ambient air quality determ. 0-89690
 NW.England, pollution at rural site, transport of tropospheric photochemical ozone 0-61481
 factor of safety, calc. method and appl. to air and noise pollution 0-94140
 field burning practice in farming, downwind particle obs. 0-97836
 fission products and ²²²Rn in N.Atlantic air 0-77074
 Florida, aerosol composition meas. by time series anal. 0-89688
 fly ash particles, water accretion, refract. index and accreted layer thickness 0-58462
 formaldehyde+Br, reactions, rate consts. by EPR 0-93736
 formaldehyde+F reactions, rate consts. by EPR 0-93736
 gas phase chemical reactions in atmosphere, evaluated kinetic and photochemical data 0-101671
 Gaussian plume model, parameters for ground-level and elevated sources from diffusion eqn. 0-82010
 halocarbon depletion of O₃ layer, climate effects 0-98436
 hydrocarbon emission from car factory affecting O₂ level, Wisconsin, USA 0-76674
 industrial area pollution, occurrence affected by wind direction 0-89691
 Lake Michigan, sulphate deposition in stable atmos. conditions 0-81494
 lead alkyls concentration obs. 0-85313
 long range pollutant transport, Lagrange model 0-61851
 long-range transport modeling review 0-108823
 Los Angeles, particulate sulphate and air quality, annual data multivariate analysis 0-61483
 Los Angeles Reactive Pollutant Program (LARPP), anal. of processes affecting oxidant and precursors 0-61479
 material damage functions 0-76693
 Merseyside, England, assessment difficulties for area values and trends 0-104538
 mesoscale dispersion expts., trajectory-diffusion modelling 0-61837
 metals, airborne, in industrial districts, conc. rels., dust anal. 0-72107
 metals, Pb, Cd, Cu, Zn, Ag, in deposited snow, atmospheric pollution, effect of human activity compared to volcanoes (*French*) 0-67018
 meteorology of air pollution conf., New Orleans, USA (March 1980) 0-90603
 methane, troposphere vertical profile, eastern USA in winter 0-77035
 Netherlands, SO₂ conc., source areas, dispersion model 0-61482
 New York, particulate sulphate and air quality, annual data multivariate analysis 0-61483
 New York State, possible anthropogenic causes of local climate trends in four cities 0-105044
 nitrate in suspended particulates, rel. to weather, S.Ontario, Canada 0-76678
 nitrates, gaseous, concentrations, investigations in urban and rural area 0-94123
 nuclear industry, radiation doses, health risks from various power sources 0-57899
 nuclear reactors, Three Mile Island malfunction, monitoring, radiation exposure 0-57960
 oil refinery plume chemical composition, obs. in Los Angeles, USA 0-104524
 organic compounds photooxidation, rates, reactivity and mechanism for reaction with OH radicals 0-72104
 particulate element conc. over USA 0-76679
 Pb concentration variation at two stations in Perth, 1974-76 period 0-94127
 pesticides and heavy metals in Bavarian snow 0-61488
 photochemical air pollution formation simulation 0-81504
 photochemical air pollution potential form. in United Kingdom, numerical estimation method. form. in United Kingdom 0-76682
 plume dispersion model (gaussian), compared to obs. of NO_x from HNO₃ works 0-104525
 plume from steel mill, ice nuclei and aerosol obs. 0-89693
 point source pollution dispersion, meas. and modelling of conc. 0-81973
 pollutant gas analysis, linear regression math. model defining conc. relationships 0-61486
 pollutants long distant transport, analytical diffusion model 0-94125
 polynuclear aromatic hydrocarbons and particulate conc. in urban air 0-76675
 radiation exposure due to exhaust air of nuclear fuel reprocessing plant (*German*) 0-57940
 radiative transfer in polluted atmosphere, conference, San Diego, California (1979 August 29 to 30) 0-62376
 radioactive ¹³³Xe in plume from Three Mile Island nucl. reactor 0-89696
 radioisotopes, resuspended, possible importance of short-term exposure 0-85501
 radionuclides from nuclear facilities, diffusion calcs. (*German*) 0-61484
 radionuclides in N.European air due to Chinese nucl. explosions 0-108826
 Rijnmond, Netherlands, SO₂ concs., comparison with Gaussian plume model obs. 0-85314
 road traffic, relationship to noise pollution levels 0-69594
 Rome, obs. of urban heat island during summer season 0-85717
 smoke plumes in surface layer, cross section diffusion (*Russian*) 0-104532
 soot in urban atm., determ. by optical absorption technique 0-108824
 St. Louis, Missouri, pollutant source strength-rainfall relationships investigation 0-77059
 St. Louis, Missouri, USA, incident solar radiation, urban-neural differences 0-109247
 stratosphere, effects of pollution on sulphate aerosol layer on global climate 0-109212
 stratosphere, trace gas concs. during 1976 in N.Hemisphere 0-67016
 stratosphere aerosol, modification by supersonic transport and space shuttle operations, climatic implications 0-98408
 stratosphere chlorofluorocarbons, possible O₃ depletions and Earth surface UV radiation changes 0-94577

air pollution continued

- sulphate conc. in N.W. United States, 'STATE' program of the EPA 0-76673
 transport, air quality models development for limited wind fetch 0-104533
 transport, contaminant movement, Galerkin finite element method 0-74902
 transport and structure in laser troposphere 0-85319
 transport between troposphere and stratosphere 0-105034
 transport eqn., 3-D, numerical algorithm 0-106811
 transport in atmospheric turbulent boundary layer, finite-element numerical modelling 0-77061
 tropopause, sulphate and nitrate mixing ratios obs. 0-61835
 troposphere aerosol, trace gases in summer, background levels in Greenland 0-72609
 turbulent diffusion model, K-theory 0-89697
 turbulent mass transfer in boundary layer, plume dispersion (French) 0-81850
 W. United States, acidic precipitation, pH value obs. 0-89695
 urban aerosol, effects on cloud microphysical model 0-82004
 urban atmosphere, radiative effects of elevated pollutant layers on temp. struct. and pollutant dispersion 0-97841
 vehicle emission rate depend. on road speed, mass balance techniques 0-97839
 Venetian region, air pollution episodes real-time forecasting, advection-diffusion model 0-77096
 Venetian region, real-time forecasting of air pollution episodes via Kalman predictor 0-82046
 Venice region, real-time forecast, advection-diffusion model 0-72102
 Venice region, real-time forecast, Kalman predictor 0-72103
 Yaounde, Cameroon, particulates in urban and rural air (French) 0-61478
 Br compounds in stratosphere, O₃ depletion due to chem. reactions 0-98391
 CO from vehicle emission in urban area cold engine startups 0-104527
 CO generated from road traffic, rel. to traffic parameters 0-81500
 CO, troposphere vertical profile, eastern USA in winter 0-77035
 CO₂ and climate, model of geographically nonuniform effects 0-90143
 CO₂ and global warming, effect on regional climate 0-77099
 CO₂, climatological significance of doubling of atmospheric conc. 0-101426
 CO₂ from fossil fuel burning and global C budget 0-77080
 CO₂ in atmosphere, ¹³C/¹²C vars. in last 22 yrs. 0-104530
 CO₂ in atmosphere, climate-C budget model 0-98381
¹⁴C released to atmosphere, dynamic model for estimating radiation dose to world population 0-89852
 HNO₃, obs. of lower atmos. pollution in W.Europe 0-72106
 HONO (nitrous acid), obs. in urban atmosphere by differential optical absorpt. 0-76677
 H₂S in troposphere, photochem. production reactions 0-90112
¹³⁷I concentrations in air, milk and antelope thyroids in southeastern Idaho 0-89871
⁸⁵Kr conc. 0-93756
 NH₃ fluxes into free atmosphere over W.Germany evaluation 0-94132
 NH₃, in troposphere, effect of nitrate fertilisers 0-85701
 NO₂, emission inventory for Canada 0-97835
 NO₃, detect. in polluted troposphere by differential optical absorpt. 0-77036
 NO₃ in troposphere, obs. of content in mountain air 0-72582
 N₂O from fertiliser, causing atmos. warming 0-94579
 O₃ in troposphere, evidence for significant in situ photochemical source 0-72619
 O₃ in urban air at night, Jerusalem and Tel-Aviv 0-89689
 O₃ layer depletion 0-104534
 Pb, atmospheric long range transport to Denmark 0-94131
 Pb in subalpine pond sediments, anthropogenic source var. 0-85315
²²²Ra short lived daughter disequilibrium in a mixed maritime and continental atmosphere 0-108822
 Rn, atmospheric, accumulation in calcite caves 0-104531
 Rn daughter concentrations in different atmospheres 0-85316
²²⁰Rn decay products attachment to flowing aerosols using centrifuge 0-61167
²²²Rn, conc. in free air (Hungarian) 0-94128
²²²Rn concentration in tunnel air, atmospheric press. and precipitation effects (Japanese) 0-78445
 S and N, acid precipitation in the Pittsburgh, Pennsylvania area 0-94129
 S budget of eastern N.America, anthropogenic and natural contribs. 0-97834
 S compounds, meso-scale transport obs. in rural East Midlands, England 0-94124
 S, in deposited snow, effect of human activity compared to volcanoes (French) 0-67018
 S oxide pollutants, SURE/MAP3S obs. comparison with regional model predictions 0-81501
 S pollutant removal from atmosphere by rain, modeling method 0-85318
 SO₂ at ground level, air pollutant dispersal, Forth Valley, Scotland 0-81497
 SO₂, emission inventory for Canada 0-97835
 SO₂, movement in atmosphere (Dutch) 0-97844
 SO₂ oxidation to SO₄ in urban atmosphere 0-81964
 SO₂ oxidation to sulphate in troposphere, model predictions 0-81963
 SO₂ pollutant dosages in urban areas 0-81499
 SO₂ pollution in Montreal, Canada, anal. of meteorol. and source factors 0-104537
¹³⁶Xe, A=133,135, interference with low-energy meas. systems 0-89872

air pollution detection and control

- ²²²Rn flux through multilayered covers cover U mill tailings 0-95487
 absorption spectrum Fourier transform for air pollutant meas. 0-81514
 acid sulphate in atmosphere aerosol, detection from S/N ratio 0-61494
 aerosol S content, continuous flame photometric detection system 0-81508
 aerosols, Aitken range size distrib. meas. in N.Atlantic 0-98404
 aerosols, meas. by horizontal thermal gradient cloud condensation nucleus spectrometer 0-77158
 airborne mineralogical dusts, metallic elements determ. by energy dispersive X-ray fluorescence anal. 0-76569
 ambient air analysis, area survey and sampling mobile laboratory 0-104528
 automated environmental monitoring system for pollution studies 0-81513

air pollution detection and control continued

- automatic analysis of pollution, spectroscopic methods (Spanish) 0-81516
 biological surveillance of pollutants using plants 0-76689
 chimney stack sampling, traverse point location for HP calculator program 0-94139
 chlorinated hydrocarbon, dry aerial deposition rate, meas. techniques 0-81506
 cigarette smoke, diode laser meas. of methane, ethane and H₂O vapour concs. 0-97847
 coal, combustion, radiological aspects 0-61485
 condensation nuclei counters at South Pole, calibration 0-98470
 differential absorption lidars, reference range 0-89700
 diffusion battery, screen type, theory 0-95208
 electret fibre appl., non-woven, high efficiency 0-76691
 electron capture detectors operating in tandem, theory 0-61493
 emission measurement design with respect to urban sanitation (German) 0-104536
 environmental chemistry, anal. techniques, conf., Barcelona, Spain, (Nov. 1978) 0-88038
 ethylene, air pollution monitoring, computer controlled CO₂ laser absorpt. system 0-89699
 factor of safety, calc. method and appl. to air and noise pollution 0-94140
 filter media suitable for air pollutant analysis (HNO₃, nitrates and acidity) 0-104541
 gas analyser with acoustooptic detector and semiconducting generator based on Gunn diode (Russian) 0-101141
 gas trace monitor, control of toxic gases 0-61499
 gaseous criteria pollutant methodology and standards for USA Clean Air Act 0-94133
 gaseous pollutants, analytical control, review 0-101140
 halogen air pollution gauge, apparatus based on secondary emission of Pt 0-85320
 high-volume preparation of air to standard quality for zeroing analyzers 0-90829
 HV-70 filters, efficiency for sampling short-lived Rn daughters 0-108827
 industrial atmospheres, pollutant analysis, pollution prevention (French) 0-89692
 interferential detector of atmospheric pollutants 0-108830
 laser application to atmospheric environmental research (German) 0-97849
 laser gas analysers, freq. modulation appls. 0-85246
 laser-Raman microprobe anal. of suspended particulates 0-76687
 lichen indicator appl. in PIXE and NRA environmental studies 0-61744
 measuring apparatus and systems, problems connected with development (Rumanian) 0-72117
 Merseyside, England, assessment difficulties for area values and trends 0-104538
 metals determ. in air particulates, graphite furnace atomic absorption spectrometry app. 0-94134
 methanol trace detection using phase fluctuation optical heterodyne spectroscopy 0-68266
 monitoring, instrumentation and methods 0-72118
 monitoring systems for radioiodine and inert gases, evaluation 0-95480
 multiple gaseous air pollutants, point monitoring method by tunable laser (Japanese) 0-81515
 nitrate determ. using HNO₃ collection on NaCl impregnated filters 0-81509
 nitrosamine, air sampling sorbents testing 0-77026
 noise considerations in millimeter-wave spectrometers, air pollution detection appl. 0-57367
 nuclear reactors, radioiodine air sampling system, separation into gaseous and particulate fractions 0-57962
 particulate chem. composition, use of laser induced mass spectrosc. instrument 0-97848
 particulate size distrib. and refr. index, new lidar-radiometer method 0-77153
 particulates sources, identification and relative importance estimation 0-72105
 personal sampling devices for atmospheric contamination monitoring (French) 0-57986
 plume transport and diffusion studies using fluoresce. lidar 0-101139
 point source pollution dispersion, meas. and modelling of conc. 0-81973
 pollutant gases, monitoring from space using passive microwave techniques 0-76690
 pollutant ground-level concentration, field meas. of benefits of increased stack height 0-76676
 precipitation acidity measurement, error anal. applied to indirect methods 0-72108
 radioactive aerosol surveillance system evaluation 0-57984
 radioactive gaseous effluents, release trends from US PWR reactors 1977 0-95481
 Raman microprobe appl., microscopic samples molecular analysis, particle characts. determ. 0-57391
 relative Raman scatt. cross-sections of pollutant gases and vapours 0-100061
 rocket fuels, CO₂ laser absorption spectra and photoacoustic detection 0-104540
 RWE environment protection organisation outline and functions (German) 0-101552
 sodar acoustic echo sounder for use in air pollution meteorology, low level stability and wind velocity monitors 0-108828
 soot particle conc. meas. by near IR extinction coeff. (Russian) 0-82055
 spectral image analysis device, Chromotron 0-83683
 tacks shade sampling to measure airborne radioactivity (Hungarian) 0-94136
 trace-gas remote analysis, optoacoustic radiometry limitations 0-108759
 transuranic elements in air at nuclear reprocessing plant, monitoring system 0-63409
 USSR environmental pollution obs. and monitoring system 0-85322
 variable selectivity photoionisation analyser, hydrocarbon vapour detection 0-81511
 Venetian region, industrial emissions real-time control using Kalman predictor 0-82046
 vinyl chloride, air pollution monitoring, computer controlled CO₂ laser absorpt. system 0-89699
 visibility at ground level, two meas. methods 0-82078
 X-ray absorption spectra for chem. characterisation of atmospheric aerosols 0-61501
 X-ray absorption spectra for chem. characterisation of atmospheric aerosols 0-72121

air pollution detection and control continued

- Zephyr radar system for meteorological measurements 0-90228
 Al, simultaneous determ. with Si in atmospheric aerosols by neutron activation anal. 0-72116
 C in suspended particulates, meas. technique 0-76686
 CO, determ. by portable IR tester 0-89569
 CO, remote sensing using freq. doubled CO₂ laser radiation 0-67025
 CO₂, atmospheric environmental control technology 0-104529
 CO₂, IR laser velocimetry, processing techniques and applications 0-87831
 HNO₂, obs. by UV differential optical absorpt. 0-72106
 HNO₃, particulate nitrate and acidity measurement in ambient air filter media 0-104541
 H₂SO₄ aerosol, filter sampling of air, possible artifacts 0-82079
 H₂SO₄ and particulate strong acidity measurement techniques, evaluation 0-104542
 H₂SO₄ mist monitor, semicontinuous 0-61495
 H contamination monitoring using centralized control (*French*) 0-63407
 NH₃, gas conc. meas. using ring oven technique 0-81507
 NH₃ monitoring using Stark microwave cavity resonator 0-61500
 NO measurements in CH₄-O₂-N₂ flame by laser fluorescence 0-61178
 NO photometric process analyser using resonance absorption method 0-57360
 NO_x emissions from coal-fired MHD power plants, simplified correlations for prediction 0-97842
 NO_x removal by absorption reaction, using MARTZCLEAN reagents based on NaClO₂ and K₂CO₃ (*Japanese*) 0-61147
 O₃, total content meas. using Dobson spectrophotometer 0-72643
 Pb salts, inorganic 0-77081
 Pu fallout detection using fission tracks prod. with neutron irradiation spectra 0-95479
 Ra, annual rate of release to atmosphere as result of coal combustion in UK 0-93787
²²⁰Rn daughters, 2-count filter method for meas. in air 0-63480
²²²Rn concentration meas. by plastic detectors to determ. environmental α -emitters from natural sources 0-91292
²²²Rn daughter prods. meas. using diffusion sampler 0-81510
 SF₆, trace detection using phase fluctuation optical heterodyne spectroscopy 0-68266
 SO₂, absorption spectrum, meas. using frequency doubled pulsed dye laser 0-87144
 SO₂, absorption spectrum, meas. using frequency doubled CW dye laser 0-87145
 SO_x removal by absorption reaction, using MARTZCLEAN reagents based on NaClO₂ and K₂CO₃ (*Japanese*) 0-61147
 Si, simultaneous determ. with Al in atmospheric aerosols by neutron activation anal. 0-72116
 SnO₂ gas sensor, fast-detecting, prep. 0-61497

air pumps *see compressors***air terminals** *see airports***air traffic**

- noise, general control measures, case study of Torrance Municipal Airport (California) 0-83702
 solar power station hazards, photometric photography of dazzling heliostat mirrors (*French*) 0-61295

aircraft

- see also aerospace control; aerospace instrumentation; helicopters*
 aeroacoustics of advanced turbopropellers, noise prediction 0-69598
 airframe material defectometry, quantitative test specifications (*German*) 0-89427
 ambient and cabin air O₂ conc. simultaneous determ. 0-90198
 fibre reinforced composite aircraft materials, design allowables 0-81204
 flight effect of Michalke and Michel vis-a-vis Lighthill's model 0-59018
 graphite fibre filled phthalocyanine composites, cure cycle investigation 0-81030
 IR segmented composite window design 0-106621
 jet noise in flight prediction from static tests 0-61490
 metal fatigue crack detection using nondestructive evaluation (NDE) methods 0-71826
 noise, basic aeroacoustic research, industrial appl. 0-69596
 noise, Siemens airport noise monitoring systems 0-99895
 noise, UK noise and number index, definitions of parameters 0-61489
 noise generation by transonic open rotors 0-69599
 noise in flight, prediction, importance of jet temp. 0-69814
 noise propag., review 0-64258
 STOL aircraft engine-wing system jet flap impact noise meas. 0-96101
 supersonic, sonic booms, pressure inside rooms and effect on plaster/wood walls 0-69602
 supersonic transports operations, stratospheric aerosol modification and climate implications 0-98408
 US inspection system for composites 0-81274
 Al aircraft alloy, fatigue resistance improvement by laser shock 0-93654

aircraft instrumentation

- aviation, meteorology, forecasting systems, TECAM '79 conf. 0-94569
 scanner, multispectral, optical system design 0-74458

airfields *see airports***airglow**

- see also atmospheric spectra; aurora; nightglow; sky brightness; twilight*
 electron precipitation causing 630 nm emission enhancement, high-altitude auroral zone 0-85803
 F-region airglow, anal. of consistency of ground-based obs. with 0-98496
 Fabry-Perot spectrometer for airglow studies, with large aperture and high resolution 0-67424
 ionosphere, equatorial, airglow data rel. to irregularity patch form., motion and decay 0-67456
 spectrometer, Fabry-Perot instrument for daytime use 0-77156
 temperature measured by obs. of emission lines, using new interferometer aperture 0-82075
 twilight spectrum, new diffuse emission bands obs. 0-72662
 UV dayglow, mesosphere and thermosphere H distrib. from Lyman α and β obs. 0-109290
 VUV global observations made by satellite, 110-290 nm region 0-90272
 N, far UV dayglow emissions 0-90271
 N₂, far UV dayglow emissions 0-90271
 NO₂ density profile from airglow obs., 72-120 km altitude 0-105094
 O, 557.7 nm spectral emission mechanism at 100 km altitude 0-61933
 O atom corona, of fast atoms during solar max., airglow obs. 0-101469
 O emission rel. to shortwave radio absorpt. in winter 0-77184
 O, green line intensity rel. to O atom density (*Chinese*) 0-90269

airglow continued

- O, spectral line shape in upper atm. following dissociative excitation 0-105097
 O₂, 1.27 μ m airglow, middle latit. meas. rel. to mesospheric O₃ concs. 0-72606
 O₂, (0-1) spectral emission band in upper atmos. 0-61933
 O(¹D) formed by N(²D)+O₂ reaction in thermosphere, 6300 Å dayglow implications 0-90270
 O⁺(²P) airglow, meas. rel. to ionisation freq. vars. during solar cycle 21 0-77195

airports

- 25 kW Fresnel lens/photovoltaic concentrator application experiment at Dallas-Fort Worth Airport 0-89647
 aircraft noise, the Netherlands, legal and economic factors 0-72112
 control tower cab, optical design 0-58661
 helicopter environmental noise impact obs. and evaluation 0-104539

alarm systems

- industrial IR detector markets and device limitations 0-86432
 IR forest fire alarm system 0-86429
 motion picture rerecording, warning system devices and electronic digital counter utilisation (*Russian*) 0-95177
 technology, IR applications 0-86431

albedo

- NW.America albedo increase following Pleistocene explosive eruptions, climatic effects 0-61789
 Callisto, IR emission spectra 0-82264
 Deimos, normal albedo and photometric function from Viking orbiter images 0-72838
 Earth, albedo rel. to effects of diffuse radiation on atmospheric O₃ photodissoc. 0-109210
 Earth, global albedo, contrib. from troposphere nonspherical aerosol 0-90220
 Earth albedo, anthropogenic changes and effects on climate 0-81893
 Earth climate affected by land surface albedo changes 0-98434
 Earth surface, albedo rel. to aerosol scatt. indicatrices determ. in 0.55 to 2.4 μ m region (*Russian*) 0-94600
 Earth surface, remote sensing, contrast reduction due to haze 0-101431
 Earth surface UV reflectance, meas. from airborne platform 0-98453
 ice age beginning, instantaneous glacierisation, albedo rate change and feedback effects 0-105006
 ice caps, albedo feedback effects on global climate, 2-D energy balance model 0-67407
 Jupiter, Lyman α albedo, Copernicus UV obs. 0-94747
 Jupiter, Lyman alpha albedo calo. from hydrocarbon and H I photochemistry 0-105194
 Lyman α albedo of Jupiter rel. to solar activity 0-98601
 Mars, longit. var. of radiometric albedo, thermal inertia and 2.8 cm brightness temp. 0-105191
 Mars, soil density map rel. to surface albedo, topography and geology 0-109388
 Moon, effect of transient lunar events, possible mechanisms 0-82238
 Moon, true normal albedo, photometric function and three-dimensional scatt. indicatrix 0-101538
 Neptune, UV albedo meas. 0-82295
 neutron, level meas. method 0-106097
 Phobos, normal albedo and photometric function from Viking orbiter images 0-72838
 planetary atmosphere, single-scatt. albedo determ. for Rayleigh-scatt. atmosphere with true absorpt. 0-94704
 radiative transfer, inverse soln. by F_N and Monte Carlo methods 0-109352
 random media, active remote sensing, depolarisation effects 0-82090
 Sahel region, Africa, surface albedo vars. investigation during recent drought (1967 to 1974) 0-76981
 Saturn, limb darkening and brightness temp., 1.30 cm interferometry obs. 0-82279
 Saturn rings, model constraints from radar obs. of polarisation and albedo 0-82277
 spheroidal particles, randomly oriented, light scatt. 0-58461
 Uranus, albedo and spectral features from IR obs. 0-82299
 Uranus, UV albedo meas. 0-82295

alclad *see aluminium alloys***Alfven waves** *see magnetohydrodynamic waves; solid-state plasma***algebra**

- see also Boolean algebra; linear algebra; matrix algebra*
 connected partially ordered set of events in time measurement 0-77640
 education, exterior algebra and exterior differential forms for electromagnetic problems 0-57037
 free scalar charge field, local nets of algebra of observables 0-99039
 Galileian formulation of spin, explicit realisations 0-62505
 generalized Grassmann algebras with applications to Fermi systems 0-57174
 normal varieties of algebras, Ω -algebras (*Russian*) 0-68019
 para-Grassmann algebras with applications to para-Fermi systems 0-57175

algorithm theory

- see also computational complexity*
 Kalamboukis tests of Davidson algorithm, comments, nuclear structure 0-86822

algorithms (computer listings) *see subroutines***aliphatic compounds** *see organic compounds***alkali metal alloys**

- see also caesium alloys; lithium alloys; potassium alloys; rubidium alloys; sodium alloys*
 dilute binary alloys, equilib. at. vol. and compressibility 0-70295

alkali metal compounds

- see also alkali metal alloys; alkali metal halides; caesium compounds; francium compounds; lithium compounds; potassium compounds; rubidium compounds; sodium compounds*
 borate glasses, Raman study at high temps. 0-93306
 borate glasses, single and mixed, viscosities 0-92701
 borosilicate glasses, phase separation obs. using SEM-EDX technique 0-76224
 carbonates, fused, electrochemical oxidation of H₂ and CO, fuel cell anode appl. 0-72040
 chalcogenides, electronic polarizabilities and ion sizes 0-59432
 cyanides, mol. excitons, X-ray excited emission spectra obs. 0-66287
 dihydroferrates (III), electronic struct. and hyperfine interactions, X α calcs. 0-100448

alkali metal compounds continued

- fluoroaluminates, dissoc. enthalpies, mass spectrometric determ., heat of form. 0-97720
 germanate crystals and glasses, struct. and stability, IR spectra meas. 0-64911
 glass, rapidly quenched, alkali ion cond. 0-107559
 hydride molecules, pot. energy function, rot. const., vibr. const., and binding energy 0-99532
 hydrides, lattice props. from interaction pot. energy function 0-100199
 hydroxides, clusters in gas phase, high press. mass spectrometry, atmospheric implications 0-58436
 hyperoxides, ionic π -electron systems, magnetogyration 0-93155
 intercalated graphite, C XXV Auger lineshape anal. 0-104019
 intercalation and substitution-intercalation cpds. in dichalcogenide hosts, factors affecting ion mobility 0-59707
 ionic conductors with sheet structures, ion mobility and influences 0-107522
 metaborates, vapour over heated solid, XPS, obs. 0-87171
 metaphosphate glass phosphors, $M_2O \cdot R_2O_3 \cdot P_2O_5$ ($R=Y$ or rare earth), fluoresc. props., activator conc. effect 0-89058
 metaphosphate glasses, $M_2O \cdot R_2O_3 \cdot P_2O_5$ ($R=Y$ or rare earth), glass transition temps. and coeffs. of linear thermal expansion 0-88343
 nitrates, molten, Rb^+ and Cs^+ ion tracer diffusion coeffs. meas. 0-70437
 polyether-alkali metal salt adducts, cond. investigation rel. to use as solid electrolytes 0-59708
 rare earth double orthophosphates with alkali metals, conc. depend. of luminesc. props. 0-100673
 rare earth double orthophosphates with alkali metals, spectroscopic obs., struct. and chem. nature 0-100674
 silicate glass, isothermal mech. loss spectrum, appl. of Rheovibron 0-88260
 silicate glasses, high temp. relax. mechanisms 0-70134
 silicate glasses, secondary relax. transitions 0-88261
 silicate glasses, struct. and thermal props. 0-84075
 tetrachloroaluminates, vapor characterisation by photoelectron spectrosc. 0-81388
 tetrafluoroaluminates, vapor characterisation by photoelectron spectrosc. 0-81388
 $CsMHoF_6$, ($M=Na, K, Rb$), mag. behaviour (*German*) 0-65774
 Eu double metaphosphates with alkali metals or H, luminesc. props. 0-100675

alkali metal halides

- see also compounds of individual alkali metals, e.g. sodium compounds*
 activated, physical phenomena and optical data processing appl. (*Russian*) 0-80819
 aggregation process of divalent metal impurities, order of reaction, fractional time conc. depend. 0-107308
 air enthalpy meas. by LiCl humidity sensors 0-90858
 alkali halide:alkaline-earth cations, defect structs. examined by methods based on Mott-Littleton techniques 0-59487
 alkali halide: Cr^{3+} , Szegedi charge and correl. with hyperfine coupling const. 0-96831
 alkali halide: $H^-(D^-)$, local modes and colour centre absorpt. bands, analogy 0-60632
 alkali halides: cation with s^2 ground-state configuration, absorption bands assignment 0-97310
 aqueous solutions, IR absorpt. ν_1 (CN) band parameter temp., conc. study (*Russian*) 0-80801
 bulk modulus, temp. variation 0-92588
 chloride: Mn^{2+} , spin Hamiltonian parameters, binding energies for cation vacancy complexes 0-96461
 chloride crystal, F centre energy level shift and splitting in O^- field 0-70640
 chloride-MgCl₂ system, solid and molten states, struct. props., Raman spectra 0-76011
 chlorides, molten, Ag^+ impurity diffusion 0-59685
 chlorides, photofragment spectra, bond energies and excited state symmetries 0-87190
 crystal binding energy, long and short range forces 0-75200
 damage by UV laser radiation 0-76110
 defect production in cation sublattice, mechanisms 0-96510
 dipole pseudo-spin glasses, collective excitations 0-59617
 dislocation dynamics studied by nucl. spin relax. meas. 0-108091
 doped, thermal expansion at low temps., rel. to glasses 0-96672
 dynamics of nonrelaxed and self-trapped holes (*Russian*) 0-80607
 elastic constants, temp. depend., pseudopot. calc. 0-65120
 elastic const., anomalous temp. depend., phonon-lattice interaction 0-107354
 elastic dielectrics, Gruneisen parameter, effective ionic charge volume derivative 0-84273
 electron emission, photo- and thermostimulated, ultrahigh vacuum conditions (*Russian*) 0-66383
 emission band of F-centre 0-76071
 F-centre accumulation, radiation induced, temp. depend. 0-59460
 F-centres, ESR in different states of relaxed configuration 0-108067
 F-centres, saddle-point configuration, molecular model parameter 0-107234
 F-colouring, role of impurities 0-64995
 g-tensor analysis of S^- and Se^- centres, ESR 0-84650
 heteronuclear XY^- defects, spin Hamiltonian parameters anal. 0-88509
 hole self-localization and capture, temp. depend. 0-92526
 hologram, high-efficiency recording by selective colloidal centre destruction 0-63955
 interionic repulsive short-range interaction pot., lattice energy calc. 0-96466
 ionic crystals, impulse compression temps. 0-100307
 irradiated, first-stage F-centre prod. 0-107231
 irradiated, formation of Z centre 0-103326
 irradiated at room temperature, stored energy 0-79839
 irradiation stability obs. using X-ray emission meas. (*Russian*) 0-66326
 irradiation-induced defects 0-107316
 island metal films, effect of ionisation of condensing flux and transverse electric field on nucleation 0-107675
 lattice dynamics, long wavelength optical mode freq. and Anderson-Gruneisen parameter 0-65182
 lattice dynamics using breathing shell model 0-88285
 luminescence mechanism, gamma and additively coloured crystals, dissolving in pure water 0-100693
 matter transport rel. to point defect parameters 0-107488
 melting and boiling points vs. Coulomb pot., parabolic behaviour 0-70375

alkali metal halides continued

- microhardness and atomic vibr. freq. relation 0-75297
 mixed, impurity centre local vibrs., comp. depend. of spectral parameters 0-79898
 mixed, U-centre localised modes 0-100319
 mixed crystals, volume thermal coeff. of expansion, calc. 0-96671
 molecular centre symm. groups, roto-vibronic spectra (*Russian*) 0-88283
 molecular ion cluster emission in SIMS, parity rule appls. (*French*) 0-63882
 molecule, electronic polarisability, ionic radii and repulsive pot. parameters, mol. const. 0-87242
 molecule, zero point Compton profile anisotropies and bond polarities, correl. 0-78659
 molecules, force const. and vibr. amplitudes calc. using electron gas model 0-87245
 molten, mode coupling theory of charge fluctuation spectrum 0-92451
 photoelastic const., short range polarisability effect 0-80748
 photoemission, energies and lineshapes 0-89119
 Poisson ratio and Gruneisen parameter, vol. depend. anal. 0-96614
 polarization, photoinduced, rel. to exchange between vacancy and impurity 0-59914
 polycrystalline, use as IR optical waveguide fibres 0-58750
 radiation damage, mechanisms, review 0-107315
 refractive index calculation 0-88949
 repulsive hardness parameters, crystal-independent 0-64947
 repulsive softness parameter anal. 0-107102
 solid solns., lattice parameter and heat of form. 0-79739
 solubility press. coeffs. and solvent isotope effect 0-96649
 surface, Au clusters, size depend. of valence bands, XPS study 0-65647
 thermally stimulated depolarisation of NCO^- centres 0-80678
 thin films, high-field electron injection, ionic cond., photocond. 0-75665
 triboluminescence spectra 0-66312
 U-centre electronic struct., cluster-Bethe-lattice calc. 0-107737
 UV high-power laser material, refractive props. and optical constants 0-106555
 UV photodissoc., metal-atom resonance-line lasers 0-58529
 V_K -centres, vibr. modes, calc. 0-84269
 X-ray induced colour centre and halogen aggregate form. 0-96565
 Z^- -centres, peculiarities of thermolum. 0-103999
 Eu^{2+} cation vacancy complexes, binding energies 0-96513
 Eu^{2+} -doped, spin-Hamiltonian parameters, superposition model calcs. 0-96830
 NaCl-type crystals, ionic polarisabilities, pseudopot. calc. 0-88913

alkali metals

- see also caesium; francium; lithium; potassium; rubidium; sodium*
 atom, near-resonant two-photon ionis., non-Coulomb phase shifts of photoelectron partial waves 0-106302
 atom, radioisotopes, hyperfine spectroscopy, nucl. props. 0-57677
 atom, Stark and photoabsorption spectrum, density of oscillator strengths, atom c.f. semiconductor spectra 0-83318
 atom+H, interaction potentials 0-63736
 atom (ion)+inert gas, collision studies of quasi-one-electron systems 0-63750
 atoms, charge exchange, exciplex or excimer form. in plasma 0-75026
 atoms, excited state, laser photoionisation theory, hyperfine coupling effect 0-102493
 atoms, highly excited Rydberg states, fine struct. 0-58402
 atoms, outer p shells multiplet and satellite struct., photoelectron spectra 0-87039
 atoms, spin-polarised, near-reson. two-photon ionis., light polarisation effects 0-106308
 atoms, vapour states, laser spectroscopy and applic., review 0-68260
 atoms+ H^+ , charge exchange, eikonal approx. calcs. 0-78703
 atoms+molecules reactions, electronically excited atoms and alkali metal atoms analogy 0-76490
 bulk modulus and eqns. of state under press. 0-88293
 cation pairs, luminesc. with dichromate anion 0-83409
 clusters in gas phase, high press. mass spectrometry, atmospheric implications 0-58436
 cohesive energy, teaching 0-90630
 compressibility, contrib. of John Bardeen 0-57057
 condensed phase, free energy, Debye-Huckel theory calcs. 0-79958
 contact term, use of local spin density functional method 0-58158
 crystalline and alkaline, eqns. of state, zero compression isotherms (*Russian*) 0-103446
 dense plasma ionisation and cohesion, critical density and press., approx. formulas 0-59253
 effective ion-ion potential, compressibility and force const. 0-70158
 elastic moduli, chem. trends, pseudopot. method 0-107355
 electrical and thermal cond. in weak mag. fields 0-65535
 equation of state, partial press. contrib. 0-107401
 Fermi surface topological changes due to uniaxial stresses 0-92810
 ground state alkali molecules, mag. shielding and spin-rot. interaction 0-87186
 Gruneisen parameter, temp. variation 0-107396
 Gruneisen parameters, influence of press. on lattice anharmonicity and temp. depend. 0-79905
 heat of desorption from refractory material surfaces 0-75430
 homologous ions series, Stark broadening trends 0-105157
 internal energy, heat of mixing, entropy, dielectric function 0-88340
 lattice dynamics, dispersion curves using second-order perturbation theory 0-79893
 lattice excitation dispersion relations 0-100314
 liquid, Fermi energy, density of states, electronic props., exchange and correl. effects 0-96774
 liquid, O_2 pot. and O_2 distrib. coeffs. between alkali and struct. metals 0-65231
 liquid, reactions with refractory metals and oxides, relevance to reactor technology 0-85173
 magnetic property volume depend., Knight shifts, electron spin response 0-88729
 migration and accumulation in Si-SiO₂, interface struct. 0-107574
 phonon dispersion, binding energy, compressibility, elastic const., electron screening and Ashcroft pot. calcs. 0-65174
 thermopower and elec. cond., relationship at low temps. (*Russian*) 0-92882
 vapour, IR image upconversion using two-photon resonant optical four-wave mixing 0-58632
 vapour arc discharge, source for pumping YAG:Nd³⁺ laser 0-78924
 vapour discharge, low-press., energy balance eqns. 0-87969

alkali metals continued

- CaF₂:alkali metal cation, thermal depolarisation study 0-108147
 CaF₂:Li(Na)(K)(Rb), dielec. relax., activation energy, rel. to vacancy pair reorientation 0-88917
 H-alkali metal vapour plasma, charge exchange role in optical props. 0-59284

alkaline earth alloys

- see also barium alloys; beryllium alloys; calcium alloys; magnesium alloys; strontium alloys
 No entries

alkaline earth compounds

- see also barium compounds; beryllium compounds; calcium compounds; magnesium compounds; radium compounds; strontium compounds
 chalcides with NaCl-type structure, third-order elastic consts. 0-70292
 chalcogenides, electronic polarisabilities and ionic radii of metal and chalcogenide ions in cryst. state 0-100198
 chalcogenides, interionic repulsive short-range interaction pot., lattice energy calc. 0-96466
 diatomic alkaline earth halides, multiplet splitting, extended Huckel approach 0-74127
 fluoride, doped with trivalent rare earths, migration entropy for bound fluorine motion 0-71303
 fluoride based solid solns., ion transport 0-107545
 fluorides, cryst. growth in reactive atmosphere 0-80962
 fluorides, orbital binding energy and ionicity relations, XPS meas. 0-97399
 halides, electronic polarizabilities and ion sizes 0-59432
 halides, refractive index, wavelength and temp. derivatives 0-88948
 metaphosphate glass phosphors, MO-R₂O₃-P₂O₅ (R=Y or rare earth), fluoresc. props., activator conc. effect 0-89058
 metaphosphate glasses, MO-R₂O₃-P₂O₅ (R=Y or rare earth), glass transition temps. and coeffs. of linear thermal expansion 0-88343
 mixed fluoride crystals, nucl. radiation effects 0-80831
 molybdates, U activated, scheelite struct. luminesc. props. vibr. modes and quenching temp. 0-60651
 oxide, irradi. stability obs. using X-ray emission meas. (Russian) 0-66326
 oxide based phosphors, photon multiplication and secondary electron-hole pairs generation (Russian) 0-66262
 oxides, emission props. in CO₂ stream 0-100742
 oxides, surface emission active centres 0-100741
 perovskite oxides, point defects, elec. cond., and electron energy spectra 0-70706
 tungstates, U-doped, perovskite struct., luminesc. quenching, QMSCC calcs. 0-71470
 Al₂O₃-SiO₂-MO-Fe₂O₃ glass, M=Ca, Mg, Ba, Sr, UV and EPR absorpt. spectra 0-89018
 BaB₂O₇-RF₂, R=Mg, Ca, Sr, Ba, glass form., struct. and props. 0-84077
 PbO-MoO₃-MO and PbO-WO₃-MO systems, M=Ca, Ba, Mg, Sr, perovskite type cpds. detection 0-108404
 ZnB₂O₇-RF₂, R=Mg, Ca, Sr, Ba, glass form., struct. and props. 0-84077

alkaline earth metals

- see also barium; beryllium; calcium; magnesium; radium; strontium
 alkali halide:alkaline-earth cations, defect structs. examined by methods based on Mott-Littleton techniques 0-59487
 homologous ions series, Stark broadening trends 0-105157

alkalinity see pH**allotropism** see polymorphism**alloy steel**

- A533B1, neutron irradi., flow growth characts. by acoustic monitoring 0-100918
 A533B, fatigue crack growth of irradiated pressure vessel steels in simulated, reactor-grade water environment 0-97582
 acoustic emission, amplitude distrib. anal. 0-66713
 austenitic, ageing and plastic deform. effect on struct. and mech. props. of N15Kh5G3T3 (Russian) 0-71691
 austenitic, heavily doped, linear expansion meas. 0-103501
 bainitic transformation, suppression in steels (Russian) 0-76247
 ball bearing, fatigue damage, influence of dispersed phases in martensitic matrix 0-108549
 bearing, induction hardened, rolling contact strength (Japanese) 0-93568
 bearing type En 31, surface-ground, residual stress and fatigue property comparison 0-60975
 bimetal with austenitic stainless steel, H permeability 0-107572
 boride coatings, spectroscopic thickness determ. 0-85099
 brittleness, elastic props., abrasive wear stability of type Kh12M steel (Russian) 0-66672
 C-Cr (1.0, 1.5 wt.%), 52100 bearing steel, control of surface residual stress by heat treatment 0-97501
 cast, heat-resist., subcrit. crack growth 0-97581
 cementite phase dispersion change during tempering (Russian) 0-93577
 chemicothermal treatment, diffusional basis 0-104343
 cold worked, original struct. effect on softening during heating 0-60882
 composite with 30% TiC, sintered, wear resist. 0-100815
 concentration of B, solubility depend. on introduction of rare earth metals (Russian) 0-65226
 Cr-Mo:P (2.25, 1 wt.%), stress relief cracking, effect of P segregation 0-89324
 Cr-Mo(V), microstruct. effect on high-temp. props. (Czech) 0-89300
 Cr-Ni-(Mo), cast, intercritical heat treatment (Czech) 0-89268
 Cr-Ni-Mo, resist. to corrosion and corrosion-fatigue in seawater 0-104346
 creep limit and long-term strength, parametric eval. method, for X8CrNiNb1613 0-100996
 Croloy steel for LMFBR steam generator, meas. of T permeation 0-68775
 deformation, rapid dynamic, at -196°C 0-104220
 deformation broaching, of type 38KhMYuA and 38KhNMYuA bushings 0-108473
 density and thermal expansion in liq. and solid states 0-96668
 determination of minor impurities and alloying constituents, appl. of inductively coupled plasma spectrometry 0-90903
 dislocation structure changes, susceptibility to damage in type 12Kh1MF steel after thermomechanical working (Russian) 0-66545
 electrical, mag. hysteresis representation in numerical modelling of mag. fields 0-88813
 emissivity, integrated normal with low heat conductivity coeffs. of type Kh23Ni18 0-103504

alloy steel continued

- fatigue crack growth, in presence of welding residual stresses (Russian) 0-71739
 ferrite, transform. kinetics, grain size, alloying element effect, carbide precip. 0-93560
 ferrite/martensite dual phase, compositional anal., TEM 0-85253
 ferritic, Cr-Mo, corrosion behaviour in reducing environment of coal fired MHD generator 0-104322
 ferritic, Cr-Mo (2.25, 1 wt.%), C and Nb influence on structural transformations (French) 0-84925
 ferritic, surface hardening by gas nitriding, process improvements 0-97499
 ferritic Cr-Mo type, microanalysis of precipitates using TEM 0-108688
 fracture mechanics parameters, influence of specimen thickness on tests Rst 37-2, st52-3, StE70 and 30CrNiMo8 (German) 0-66614
 fracture of 10G2S1, subjected to low-temp. fatigue 0-89350
 fracture toughness, single specimen determ. for J_{1c} 0-100989
 hardenability, role of B and P segregation 0-97486
 hardened, electrochem. characts. and stress corrosion cracking, ageing and cold treatment effects 0-108639
 heat treatment, mag. quality control method of 30KhN2MFA and 40Kh 0-108662
 heat-treated, crack resist. in seawater 0-104347
 high speed, fixed time integration-emission spectral anal. and employment of high freq. induction melting-centrifugal casting samples (Japanese) 0-89567
 high speed steel powder, S and O reduction in a H₂ gas stream 0-61015
 high strength, produced by extrusion of Ni-coated steel powder, enhanced fracture resist. 0-81169
 high strength, treatment effect on ductility and strength 0-60880
 high-alloy, creep, expt. investigation above 900 degrees C 0-81134
 high-C, amorphous, mech. props. and thermal stability 0-76361
 high-speed, low-temp. mag. cycling effect on ferromag. struct. 0-100928
 high-speed, struct. changes investigation by hot hardness and quench dilatometry (French) 0-76249
 high-speed tool, properties, powder metallurgy prep. method (Czech) 0-60800
 high-strength, fatigue, interaction effects between trace impurities and environment 0-66651
 high-strength low alloy, H₂ attack, 350-510°C 0-97636
 Hugoniot parameters to 320 GPa, dynamic yield strengths and phase transition press. 0-75331
 low alloy, creep damage and the remaining life concept 0-59574
 low alloy, ferritic-pearlitic, carbonitride hardening 0-104174
 low alloy, high strength, hot compression dynamic precip. and coarsening of Nb(CN) 0-97514
 low alloy, isothermal tempering effect on acoustic emission during ductile fracture 0-85047
 low alloy, Mn-P, temper brittleness, rare earth mischmetal effect (Chinese) 0-104249
 low alloy, particle coarsening reactions, effect of cold deform. 0-71664
 low alloy, S and Mn influence on high temp. strength and ductility after solidification from melt (German) 0-81106
 low alloy, strength, Cr and N effects 0-104277
 low alloy, temper embrittlement and ternary equil. segregation 0-60958
 low alloy, type A553B, fracture toughness meas. using elect. potential method (Japanese) 0-93722
 low C, 15Kh2MFA and 15Kh2NMFA, neutron irradi. embrittlement, effect of P, Sb and Sn impurities 0-85055
 low C, low alloy, ferritic-pearlitic, high temp. mech. treatment, cooling effect 0-104193
 low-alloy, 35KhN2VL, cold resistance determination, quick method 0-100997
 low-alloy, bearing, mech. props., carbide behaviour effect (Korean) 0-93615
 low-alloy, creep, expt. investigation above 900 degrees C 0-81134
 low-alloy, etchant for revealing austenite grain boundaries 0-85098
 low-alloy, fracture toughness characts., loading rate effect 0-100897
 low-alloy, hardened deoxidised, delayed failure, influence of internal adsorpt. of impurities 0-60974
 low-alloy, high strength, deforms. during cold crack developments in welded joints 0-81142
 low-alloy, plastic deform. mechanisms under dynamic loading 0-100883
 low-alloy, residual elements, effect on props. 0-66643
 low-alloy structural 16G2 and 16GFR, struct. and props. after quenching and tempering 0-76280
 low-alloyed, C-content influence on high temp. strength and ductility after solidification from melt (German) 0-81105
 low-Mn low-C, susceptibility to brittle fracture 0-76340
 machining, 12L14, effect of Pb and Te on hot-shortness mechanism 0-104190
 maraging, Fe-Cr-Co-Mo, phase transforms. during high temp. austenitisation and solid soln. decomp. (Russian) 0-66524
 maraging, intermetallic phases precip. study by electron microscopy (Polish) 0-89217
 maraging 18%Ni, calorimetric anal. of ageing (Japanese) 0-89264
 martensitic, alloying element effect on coarsening behaviour of cementite particles in ferrite 0-66518
 martensitic, heavily doped, linear expansion meas. 0-103501
 mechanical props. meas. by acoustic methods, chem. composition influence 0-104384
 microalloyed, types V1599, V1600, V1286, NbCN precipitation in undeformed austenite 0-89230
 Ni-Cr-Mo, electroslag refined, fracture toughness and fatigue behaviour 0-81171
 nitrided age-hardened, for blanking punches, chipping resist. props. (Japanese) 0-89340
 nondestructive mag. quality control method in heat treatment of 30KhN2MFA and 40Kh 0-108662
 nuclear reactor pressure vessel steels, optimum chem. comp. rel. to props. 0-93517
 oxidation of Cr-Mn alloy, sub-cinder layer role as protective coating (Russian) 0-93686
 oxidation resistance, N effect 0-66706
 pearlitic, creep-induced micropore healing kinetics of 12MKh and 15Kh1M1F, TEM obs. (Russian) 0-71690
 peritectic transformations, influence on initial struct., solidification, grain boundaries (Russian) 0-66621
 plastic deformation depend. on grain size in type 08KP low C steel (Russian) 0-66580

alloy steel continued

- plastic deformation of 15KhM1 and 20KhM1 with thermal cycling 0-89310
- powder forged, fatigue, surface treatment effect 0-85048
- precipitation behaviour under high temp. conditions, photoemission electron microscope obs. 0-108456
- pressure vessel, irradiated type A533B-1, reference fracture toughness curves 0-100921
- quenched carbonitrided, multicycle fatigue failure 0-104283
- rolling wear study of misaligned cylindrical contacts 0-108590
- secondary recrystallisation props. of multilayered types St2kp and 10Kh18N10T steel (*Russian*) 0-66533
- segregation embrittlement 0-60958
- sheet, crack-propag. resist. in heat-affected zone in presence of H, rolling direction and preliminary plastic tensile strain effects 0-60971
- spring alloys, microplastic deform. and endurance limit 0-81197
- steel, 35NiCr18, bainite transformation, study with aid of hot stage microscope 0-76253
- steel, ferritic and austenitic, microstruct. study by means of replicas taken from components at 100°C 0-81256
- steel, HSLA, V and N effect on recovery and recrystn. during and after hot working 0-84973
- steel, medium C, Mn, type 42Mn2 cylinders, flake immunisation by hot working (*Chinese*) 0-66540
- structural, macroscopic and microscopic features of fracture 0-81179
- structural, wide plate tensile testing eval. (*German*) 0-100969
- structural steel, type St3S, hardness, random functions 0-76329
- structure steels 4Kh4VMFSSh and 45Kh3V3MFSSh, grain size, hot deform. and austenitising effects 0-76286
- surface quality improvement, thermomech. treatment 0-61020
- temper embrittlement, comp. influence 0-66658
- tensile test, regulated, strength and deform. characteristic values, consistency (*German*) 0-93712
- testing cracked specimens for impact bending, expt. planning method appl. 0-71831
- tool, high speed, wear, effect of magnetisation on tool life 0-89361
- tool, type Kh12M structural inhomogeneity rel. to wear resist. (*Russian*) 0-66672
- TRIP steels, fatigue strength 0-108552
- AI killed, density changes, void growth in biaxial stress fields, plastic deformation 0-71692
- AI semikilled, (Fe,Mn_{1-x})O.Al₂O₃ inclusions, deoxidation, thermodynamic conditions 0-60830
- AI-Cr, FeO.(Al,Cr_{1-x})₂O₃ inclusions, thermodynamics 0-60831
- AI-killed, fatigue life for program loading of multiple repeated two step stresses (*Japanese*) 0-66632
- AI-steel, cementite isolation, Mossbauer anal. 0-93225
- AI-Ti-Nb-(Mo), low-alloy, toughness improvement through Ti additions 0-66525
- AI-Ti-V-(Mo), low-alloy, toughness improvement through Ti additions 0-66525
- AI-Ti-(Mo), low-alloy, toughness improvement through Ti additions 0-66525
- AI-V-(Mo), low-alloy, toughness improvement through Ti additions 0-66525
- B, depth distrib. meas. using time of flight method and ¹¹B(p,n)¹¹C reaction 0-71986
- B-Si, Cu addition effect on mag. props. 0-89366
- BN extraction, and identification, IR anal. 0-85254
- C-Mn-V-Cb-N, high strength low alloy, controlled-rolled 0-100803
- Co-Cr-Mo, type HY 180, correl. between advanced NDT evaluation methods and fracture mech. parameters 0-97675
- Co-Cr-Mo HY 180M, SCC in NaCl, temp. effect 0-108633
- Co-Cr-Mo type HY-180M, mech. props. and SCC, overageing effect 0-108634
- Co-W-Mo-Cr-V, high-speed tool, splat quenching, props. and struct. 0-76294
- Cr (0.5 wt.%), austenite-pearlite transformation 0-97480
- Cr (10 wt.%), precip. free ferrite form., STEM 0-84941
- Cr (2%), austenite decomp., phase diagrams and struct. form. kinetics 0-76223
- Cr, carburising kinetics, in endothermal atm. 0-76410
- Cr, carburising with high-activity carburiser 0-76412
- Cr, coated with TiC, prep. and props. 0-76414
- Cr, cold roll, frictional heating surface damage 0-76289
- Cr, lower bainite transform., significance of carbide precip. 0-97476
- Cr turbine casings, residual life determ. 0-93585
- Cr with metastable austenite, wear resist., temp. effect 0-76370
- Cr-C (1, 1 wt.%), hot ductility and S segregation 0-66594
- Cr-Cr-Mn (Ni), struct. prop. rel., design of struct. steels for high strength and toughness 0-97491
- Cr-Cu-Mo, ductile fracture, microvoid effects (*Japanese*) 0-108542
- Cr-Mi-Mn type 4340, hydrogen bearing environment effect on K_{Iscc} 0-104325
- Cr-Mn, low-cycle fatigue at 20 and -196°C 0-81196
- Cr-Mn, strain hardening, 4.2 to 293K 0-81076
- Cr-Mn type, martensite struct. after quenching and HTMT, X-ray diff. obs. 0-84975
- Cr-Mn(Ni), Mn and Ni additions, effect on corrosion resistance and hardness 0-104342
- Cr-Mo, effect of Mo on high-temp. props. 0-85005
- Cr-Mo, ferritic, grain boundary segregation, X-ray microanal. by STEM 0-66740
- Cr-Mo, H embrittlement in H₂S environment, Mo effect 0-76415
- Cr-Mo, impact fatigue crack growth at low temps. (*Japanese*) 0-104266
- Cr-Mo, notched specimens, fatigue strength distrib. (*Japanese*) 0-66633
- Cr-Mo, oxidised, mechanism of crack decoration of oxides by electrodeposition 0-97560
- Cr-Mo, quenched, carbide reactions during tempering 0-89229
- Cr-Mo (2.25, 1 wt.%), creep and high temp. low-cycle fatigue tests 0-85061
- Cr-Mo (2.25, 1 wt.%) pipe, high temp. fatigue and creep strength 0-85060
- Cr-Mo (2.25, 1.0 wt.%), fracture-mechanisms, tensile specimens 0-85039
- Cr-Mo (2.25, 1.0 wt.%), Mn and Si effect on temper embrittlement, comp. and carbide precip. effects 0-85037
- Cr-Mo (2.25, 1.0 wt.%), P and Sn effect on temper embrittlement, comp. and carbide precip. effects 0-85036
- Cr-Mo (2.25, 1.0 wt.%), time of flight atom probe, quantitative microanal. metallurgical appl. 0-86498

alloy steel continued

- Cr-Mo (2.8, 1.6 wt.%), atom probe anal. of bainitic phase boundaries 0-71990
- Cr-Mo low-alloy, additive remedy for temper brittleness 0-66659
- Cr-Mo steel types JIS SCMV 2, SCMV 3 and SCMV 4, high-temp. high-cycle fatigue props., press. vessel appls. (*Japanese*) 0-93650
- Cr-Mo weld metal, reheat cracking, residual elements and microstruct. influence 0-66553
- Cr-Mo weld metal, trace element embrittlement suppression by creep strength effects 0-66656
- Cr-Mo-Mn-Si-W (3, 1.95, 1.55, 1.45, 0.95 wt.%), struct. and props. 0-104175
- Cr-Mo-Ni-V, dynamic stress intensity factor meas., possibilities and limits (*German*) 0-93719
- Cr-Mo-Ni-WV (6, 4, 3, 2 wt.%), tempering and secondary hardening, TEM obs. (*Chinese*) 0-104245
- Cr-Mo-V, strength and ductility in creep, purity influence 0-66598
- Cr-Mo-V, stress rupture, notch influence, temp. depend. (*German*) 0-60945
- Cr-Mo-V (1, 0.5, 0.25 wt.%), stress relax. data anal. using total strain-time parametric method (*Japanese*) 0-104198
- Cr-Mo-V low-alloy, high-temp. ductility and crack growth, impurities effect 0-66652
- Cr-Mo-V low-alloy, mech. props. and stress relief cracking, effects of impurities and deoxidation practice 0-66599
- Cr-Mo-V low-alloy, prior austenite grain boundary embrittlement by B 0-66657
- Cr-Mo-V low-alloy, stress relief cracking, impurity and alloy content effects 0-66654
- Cr-Mo-V low-alloy with high residual element content, cavitation control 0-66663
- Cr-Mo-V pressure vessel, microstruct. parameters and yielding rel. to plastic deform. 0-89318
- Cr-Mo-V-Nb, supercooled austenite isothermal decomp., struct., strength and fracture characts. 0-60966
- Cr-Mo-W, splat quenched, formation of metastable austenite 0-84974
- Cr-Mo-W-V-Ti-B, transformation mechanism and fine structure of (M-A) phase, TEM study (*Chinese*) 0-66500
- Cr-Mo-(V) austenitic, creep resist., high-temp. props. residuals effect 0-66600
- Cr-Mu-W, carbide form., W effect 0-76259
- Cr-Ni, pendant drop melt extracted, struct. and props. 0-76242
- Cr-Ni, strain hardening, 4.2 to 293K 0-81076
- Cr-Ni, type 4340, high-strength, new inhibitors for crack arrestment in corrosion fatigue 0-100941
- Cr-Ni-C (3, 1, 0.6 wt.%), grain boundary sulphide precip. and hot ductility (*Japanese*) 0-71654
- Cr-Ni-Mn, type 4340, H₂ embrittlement, stress state, thickness and delayed failure in bending 0-71746
- Cr-Ni-Mn, type AISI 4340, correl. between advanced NDT evaluation methods and fracture mech. parameters 0-97675
- Cr-Ni-Mo, 'spots' (*Chinese*) 0-104248
- Cr-Ni-Mo 40KhN2MA, magnetostriction used in inspection after heat treatment 0-108673
- Cr-Ni-Mo-Mn, wetting of TiC, expt. planning investigation 0-60822
- Cr-Ni-Mo-V, austenite form. during heating, influence of recrystn. during tempering (*Russian*) 0-104188
- Cr-Ni-Si (18.15, 17.64, 2.4 wt.%), rare-earth additions effect on impact fracture (*Chinese*) 0-66617
- Cr-Si, oxidation resist. in high pressure CO₂, Si effect 0-66704
- Cr-Si-Mn-Ni-Mo-C, resist. to deform. and fracture, C effect 0-71757
- Cr-W, quenched, carbide reactions during tempering 0-89229
- Cr-W-Mo-Co, high-speed, from atomised powders, mech. and cutting props. 0-66556
- CrMoV, creep resistant, quantitative struct. parameter use in props. prediction (*Czech*) 0-108481
- CrMoV, low alloy, coarsening rate and activation energy of M₄C₃ and M₇C₃ carbides (*Czech*) 0-108480
- Cu-Ni-Mo (2, 2, 0.25 wt.%), sintering, kinetic characts. 0-60805
- Fe-Mn-V-C austenitic, ageing characts., discontinuous precip. nature 0-84940
- Fe-Si (3 wt.%), Bauschinger effect, computerised evaluation method 0-93625
- Fe-Si (3 wt.%) high-permeability grain-oriented steel, quenching effect on primary recrystn. texture development 0-84956
- Fe-V-C (1, 0.2 wt.%), austenite formation 0-84927
- Mn (high), austenitic, creep rupture, p addition and two-step soln. heat treatment effects (*Korean*) 0-93646
- Mn, sintered, production, effect of initial Fe powder struct. on mech. props. 0-104095
- Mn-B-V, low alloy, transform. singularities (*Russian*) 0-104116
- Mn-Mo, castings, mech. props., Cu and Sn trace elements effect 0-66596
- Mn-Mo-Ni, embrittling effects of residual elements 0-66655
- Mn-Mo-Ni (A533 B), ductile-brittle transition, material fracture temp. depend., Gauss distrib. function 0-97574
- Mn-Nb-Al-C, crack prop. and hot ductility during straightening concast strand 0-66646
- Mn-Si, fatigue, level of prior cyclic stresses effect 0-89348
- Mn-Si, thin sheet impact strength study (*Czech*) 0-59571
- Mn-Si-Cr-Mo, dual phase, as-rolled, continuous cooling transformation diagram to optimize composition 0-100829
- Mn-Sn-(Nb), extra low C, shear transformation struct. (*German*) 0-60873
- Mn-V, nitrated age-hardened, for blanking punches, chipping resist. props. (*Japanese*) 0-89340
- Mn-V (0.04 to 0.06 wt.%), strain ageing characts. rel. to mech. props. 0-84969
- Mo, energy selective X-ray anal. using TEM 0-84036
- Mo-Cr-Ni-Mn alloy with TiC, optimum comp. and manufacture conditions, Mn effect 0-84896
- Nb,(V), (Al), hot rolling, laboratory simulation, recrystn. of austenite 0-97512
- Nb, deform., recrystn. and precip. interaction 0-97515
- Nb, microalloyed, hot rolled, Nb(CN) precip. and austenite recrystn. 0-97513
- Nb microalloyed dual phase, etching technique 0-71809
- Nb-Mn, Molytor 53, Bauschinger effect, computerised evaluation method 0-93625
- Ni, 11.6%, quenched cylinder residual stresses, boring/turning and X-ray diff. obs. (*German*) 0-93586

alloy steel continued

- Ni, 9 wt.%, welded joints on LNG carriers mech. props. and fracture toughness 0-85017
 Ni (17 wt.%), martensitic deform. temp., cryst. struct. effect (*Russian*) 0-66576
 Ni, high-strength, impact fatigue strength, heat treatment conditions effect 0-76285
 Ni-Co-Cr, high-strength medium C, Cr effect on props. 0-76339
 Ni-Co-Mo, dynamic stress intensity factor meas., possibilities and limits (*German*) 0-93719
 Ni-Cr, anodic dissoln. in NaCl solns. at high current densities (*Russian*) 0-76396
 Ni-Cr, Sb doped, solute segregation and brittle fracture 0-85033
 Ni-Cr, solute segregation and intergranular brittle fracture 0-108568
 Ni-Cr, temper embrittlement, intermediate tempering treatments 0-60944
 Ni-Cr, type AC/HT-2, grain diameters, US attenuation 0-89429
 Ni-Cr-Fe base, radiation enhanced precip. and dissolution of precipitates, point defect kinetics and dislocation obs. 0-108467
 Ni-Cr-Mo, cyclic creep under increasing stress condition, constitutive eqn. 0-93593
 Ni-Cr-Mo, ductile fracture, microvoid effects (*Japanese*) 0-108542
 Ni-Cr-Mo SNCM8, delayed fracture, specimen thickness and threshold stress intensity effect (*Japanese*) 0-104268
 Ni-Cr-Mo-V, corrosion fatigue crack growth in NaOH soln., cathodic pot. effect 0-89403
 Ni-Cr-Mo-V, hydrogen bearing environment effect on K_{Isc} 0-104325
 Ni-Cr-Mo-V low-alloy, additive remedy for temper brittleness 0-66659
 Ni-Cr-Mo-V turbine disc steel in NaOH soln., corrosion fatigue crack growth rate, applied pot. effect 0-60998
 Ni-Cr-S-P-Mn-Si, residual stress meas. by X-ray diffr. 0-71688
 Ni-Mo-C (2.0, 0.2, 0.4 wt.%) sintered, struct. transforms. and mech. props. after quenching 0-66557
 Ni-Mo-C (5, 0.5, 0.5 wt.%), sintered effects of powder and sintering variables on props. 0-104093
 Ni-Mo-Cr, embrittling effects of residual elements 0-66655
 Ni-Mo-V, fatigue crack growth, H_2 gas environment effect (*Japanese*) 0-104340
 NiCrMo, medium, C, overheated, fractographic study (*Chinese*) 0-66616
 Si (3 wt.%), corrugated texture perfection, mag. anal. 0-88745
 Si (3 wt.%), struct. and preferred orientation, annealing parameters influence (*Czech*) 0-89248
 Si (3 wt.%), textured, secondary recrystn., precip. annealing effect (*Japanese*) 0-71662
 Si (low), martensite struct. and mech. props. (*Korean*) 0-93614
 Si, grain-oriented, high permeability, dissoln. and precip. of AlN and MnS 0-89223
 Si, permeability change due to stress variation after demagnetization in Rayleigh region 0-88854
 V, precip. and transform. kinetics, effect of N 0-97485
 V-Nb, supercooled austenite isothermal decomp., struct., strength and fracture characts. 0-60966
 W (12%), eutectic carbides struct. and comp. during heating 0-76283
 W, microstruct. and hardness, splat quenching effect 0-76293
 W-Co-Mo-Cr-V-C (8.5, 8.1, 4.5, 3.5, 2.2, 1.02 wt.%), phase composition, struct. and props. 0-104163
 W-Cr-V, high-speed tool, splat quenching, props. and struct. 0-76294
 W-Mo-Co, high-speed tool, struct. and props., cooling rate effect at primary crystn. temp. 0-76241
 W-Mo-Cr-V tool steel, laser surface melted, struct., heat treatment effect 0-76424

alloying additions

- alloys, temper embrittlement, impurities and alloying elements role, review 0-66649
 Alnico 5 alloy, S and Ti additions effect rel. to non-metallic inclusions, coercive force and grindability 0-89375
 ferrite, transform. kinetics, grain size, alloying element effect, carbide precip. 0-93560
 Inconel, type 600, Li corrosion inhibitions by Al additions 0-108646
 metals and alloys, trace element detection by atom probe microanalysis 0-66910
 oxidation resistance, high-temp., improvement by alloying additions 0-66702
 restoration carbonisation in one and two phase states (*Russian*) 0-65225
 steel, Al-Ti-(Mo), Al-Ti-V-(Mo), Al-Ti-Nb-(Mo) and Al-V-(Mo) low-alloy, toughness improvement through Ti additions 0-66525
 steel, alloy, temper embrittlement, comp. influence 0-66658
 steel, aluminiuming, thermodynamic anal. of phase transforms. 0-76413
 steel, austenitic stainless, in boiling MgCl₂ solns., alloying elements effect on stress corrosion cracking and K_{Isc} (*Japanese*) 0-93692
 steel, austenitic stainless, N-alloyed 0-108490
 steel, austenitic stainless, stacking fault energy, effect of N 0-107279
 steel, austenitic stainless Ni-Cr, heat resist. and comp. of non-metallic inclusions, effect of La, Nd, Pr and Ce 0-76315
 steel, austenitic type EL-69, carbide transformations on precipitation of C from austenite (*Russian*) 0-97487
 steel, B-Si, grain-oriented, high induction, Cu impurity effects 0-89366
 steel, Cr-Mn(Ni), Mn and Ni additions, effect on corrosion resistance and hardness 0-104342
 steel, Cr-Mo, effect of Mo on high-temp. props. 0-85005
 steel, Cr-Mo, H embrittlement in H₂S environment, Mo effect 0-76415
 steel, Cr-Mo, Mn and Si effect on temper embrittlement, comp. and carbide precip. effects 0-85037
 steel, Cr-Mo (2.25, 1.0 wt.%), temper embrittlement, effect of P, Sn, comp. and carbide precip. 0-85036
 steel, Cr-Mo and Ni-Cr-Mo-V low-alloy, additive remedy for temper brittleness 0-66659
 steel, Cr-Mo-(V) austenitic, creep resist., high-temp. props. residuals effect 0-66600
 steel, Cr-Mu-W, carbide form., W effect 0-76259
 steel, Cr-Ni-Sr (18.15, 17.64, 2.4 wt.%), rare-earth additions effect on impact fracture (*Chinese*) 0-66617
 steel, Cr-Si, oxidation resist. in high pressure CO₂, Si effect 0-66704
 steel, ferritic, Cr-Mo (2.25, 1 wt.%), C and Nb influence on structural transformations (*French*) 0-84925
 steel, ferritic, creep resist., high-temp. props. residuals effect 0-66600
 steel, high Mn austenitic, creep rupture, p addition and two-step soln. heat treatment effects (*Korean*) 0-93646
 steel, high-speed tool, VC additions, properties, powder metallurgy prep. method (*Czech*) 0-60800

alloying additions continued

- steel, HSLA, V and N effect on recovery and recrystn. during and after hot working 0-84973
 steel, low alloy, 15Kh2MFA and 15Kh2NMFA, neutron irradiation embrittlement, effect of P, Sb and Sn impurities 0-85055
 steel, low alloy, S and Mn influence on high temp. strength and ductility after solidification from melt (*German*) 0-81106
 steel, low alloy, strength, Cr and N effects 0-104277
 steel, low-alloyed, C-content influence on high temp. strength and ductility after solidification from melt (*German*) 0-81105
 steel, low-C containing Ti, sheets, recrystn. texture effects on plastic strain ratio and deep-drawing (*Chinese*) 0-66527
 steel, machining, 12L14, effect of Pb and Te on hot-shortness mechanism 0-104190
 steel, martensitic, alloying element effect on coarsening behaviour of cementite particles in ferrite 0-66518
 steel, mild, cold rolled, texture and plastic anisotropy rel. to alloying and precipitation (*French*) 0-108475
 steel, Nb(V), (Al), hot rolling, laboratory simulatory recrystn. of austenite 0-97512
 steel, Ni-Co-Cr, high-strength medium C, Cr effect on props. 0-76339
 steel, rail, toughness, effect of Sn, SEM exam. 0-97569
 steel, stainless type 316 0-108646
 steel (*French*) 0-66670
 steels, nuclear reactor pressure vessel steels, optimum chem. comp. rel. to props. 0-93517
 Zircaloy-4, elastic props., O additions effect 0-66565
 Ag-Zn, internally oxidized, elec. contact characts., alloying additions effect (*Japanese*) 0-88619
 AgZn, $\beta \rightarrow \gamma$ transformation, effect of additional elements 0-66507
 Al alloys, columnar struct. of alloys solidified in flowing melt in centrifugal casting 0-71640
 Al-(Mn), effects of Mn on electrode or free corrosion potentials 0-100942
 Al-Cu-Mn (1.5-2, 0-0.6 wt.%), N alloying and comp. effect on mech. props. (*Bulgarian*) 0-71719
 Al-Zn-Mg alloy, Ag addition and pre-precipitation treatment, influence on GP zone growth 0-71658
 Al-Zn-Ti(Mn), mech. props., Ti or Mn addition effect (*Korean*) 0-93613
 CC Fe-Ni-Cr (35, 15 wt.%): Nb(Ti)/Mo, corrosion in HTGR He environment 0-61021
 Co vacuum condensates, Cr alloying addition effect on texture characts. (*Russian*) 0-108471
 (Co₉₃Fe_{0.77})₇₅₋₂Cr₁₅B₁₀ amorphous alloy, thermal stability, Cr conc. effects, DTA expts. 0-59395
 Cr₃C₂ fibre reinforced Ni-based composite, oxidation and creep, Y additions effect 0-66685
 Cu, microalloyed with B, elec. cond. and strength props. (*Polish*) 0-89285
 Cu-Ni, cast, strength and hot ductility, alloying and residual elements effect 0-66595
 Cu-Ni-Al, cast, strength and hot ductility, Al effect 0-66595
 Cu-Ni-Fe, cast, strength and hot ductility, Fe effect 0-66595
 Cu-Ni-Mn, cast, strength and hot ductility, Mn, effect 0-66595
 Cu-Ni-Si, cast, strength and hot ductility, Si effect 0-66595
 Cu-Sn alloy system, long period superlattice obs. and impurity effects 0-103297
 Fe, cast, grey, fracture surface after dynamic fracture, Mg conc. effect 0-100909
 Fe, cast, tensile strength, Al addition effects (*Korean*) 0-71736
 Fe, cast, white, high Cr, phase composition, B effect 0-104172
 Fe, liquid, N solubility depend. on added elements, mechanism (*Russian*) 0-65223
 Fe, segregation of impurities, physico-chemical aspects (*Czech*) 0-60866
 Fe-Cr-Ni (12, 15 wt.%) austenitic alloy, Ni⁶⁺ irradiated, void swelling and phase stability, Si and Ti effects 0-65055
 Fe-Cr-Si, oxidation resist. in high pressure CO₂, Si effect 0-66704
 Fe-Cr(W)-M, (M=Si, Mo, Ni, Mn, P, Cr), cellular growth of S-pearlite formed by carburisation 0-108486
 Fe-Mn-B, B effect on intergranular embrittlement 0-108555
 Fe-Ni-Al-(Cu) (12, 0.5, 0.5 to 3 wt.%), Cu addition strengthening at 77K, mech. props. 0-60875
 Fe-Ni-B-Mo, crystn. temp. and elec. cond. correl., Mo effect 0-75179
 Fe-Ni-C martensite morphology, butterfly-lenticular transition temp., Cr addition effect (*Japanese*) 0-81053
 Fe-Ni-Cr (35, 15 wt.%) superalloy, stress rupture and tensile props., C and B additions effect (*Chinese*) 0-104244
 Fe-Ni-Cr-Al-Y, oxidation mechanism, Y addition effect on kinetics and oxide adherence 0-97623
 Fe-Ni-Cr-Y, Y addition effect on selective oxidation/diffusion phenomena relationship (*French*) 0-108623
 Fe-Ni-Mo(Si), austenite, annealing effect on atom redistrib., Mossbauer anal. (*Russian*) 0-66529
 Fe-Ni-Ti-(Cu) (12, 0.25, 2 wt.%), Cu addition strengthening at 77K, mech. props. 0-60875
 Fe-Ni-V-(Cu) (12, 2, 2 wt.%), Cu addition strengthening at 77K, mech. props. 0-60875
 Fe-Ni-(Cu) (12, 0.5 to 3 wt.%), Cu addition strengthening at 77K, mech. props. 0-60875
 Fe-Si (3 to 5 wt.%) sinters, mag. props., Si and Fe-Si additions effect 0-71104
 Fe-Ti, Ti as H trap for embrittlement control 0-66662
 Fe₂B₃Si₄, chill block melt-spinning process, geometry depend. 0-97448
 (Fe₉₀Ni₁₀)₃₃B₁₃, amorphous, crystn. 0-75176
 Ir-W (0.3%), grain boundary comp., trace element additions effect 0-66661
 LaNi₄Al, solubility and sorption props. of H₂, effect of Al 0-103482
 Mo alloys, dil. additions, HVEM bombarded, neutron damage simulation, defect cluster and dislocation obs. 0-107330
 Mo-Nb-C, mech. props., effect of alloying and Mo cryst. orientation (*Russian*) 0-71706
 Ni, alloying, influence on recrystn. and grain growth (*Russian*) 0-81071
 Ni alloys, aluminiuming, thermodynamic anal. of phase transforms. 0-76413
 Ni-Al-Cr₂, eutectic alloy, directionally solidified, oxidation resistance, influence of Y 0-89409
 Ni-Al-(Si), diffusion, lattice parameter, microhardness, and constitution, effect of Si additions (*Russian*) 0-84316
 Ni-based superalloys, hot workability, effect of S, Ca, Mg, Y and Zr minor elements 0-66552
 Ni-Cr-Co-Al-W-Mo-Ti-Ta, heat resist. and struct., Ta effect 0-76312

alloying additions continued

- Ni-TaC, eutectic alloys, chem. incompatibility of ceramic nitrides for directionally solidifying 0-81046
 Pb(Ag) alloys, effect of Ag content on yield strength 0-76322
 Pt alloys, influence of Rh, Au, Mo, W, Zr, Hf alloying elements on creep activation energy at high temp. (*Chinese*) 0-66573
 Pt-Au, dil., recovery spectrum after thermal neutron irradi., Au effect and defect conc. depend. 0-65057
 Ta(C,N)-Ni-VC, sintering behaviour, VC effect 0-93520
 Ti-Al, elec. spark Al doping of VT-18, surface struct. and props. (*Russian*) 0-76398
 Ti-Er(Y), effects of Er and Y additives on deformation behaviour 0-81121
 Ti-Fe-Al(Mn), homogeneity and lattice parameters, Mn and Al effect on hydriding compd. FeTi 0-108400
 Ti-Nb alloys, Ta and Zr additions effect on supercond. props. 0-93059
 Ti-Nb-Zr-Fe, supercond. and paramag. props., effect of Fe additions (*Russian*) 0-65730
 TiC-(Mo-Cr-Ni-Mn) steel alloy, optimum comp. and manufacture conditions, Mn effect 0-84896
 α -Zr-Sn(Mo), creep characts., influence of Sn and Mo (*Czech*) 0-81119

alloys

- alloys such as Au-Cu, Au-Cu-Zn are indexed under components of the named elements i.e. gold alloys; copper alloys; zinc alloys in these examples
 see also actinide alloys; alkali metal alloys; alkaline earth alloys; alloying additions; aluminium alloys; antimony alloys; arsenic alloys; bismuth alloys; boron alloys; cadmium alloys; dilute alloys; eutectic alloys; gallium alloys; germanium alloys; indium alloys; lead alloys; liquid alloys; mercury alloys; rare earth alloys; selenium alloys; silicon alloys; solid solutions; superalloys; tellurium alloys; thallium alloys; tin alloys; transition metal alloys; zinc alloys
 amorphous, exhibiting Mossbauer spectra, elec. props. (*French*) 0-80244
 amorphous, Mossbauer spectrometry (*French*) 0-80660
 amorphous, struct. determ. by energy dispersive X-ray diffraction 0-84063
 amorphous alloys, density of states of n-components 0-80153
 axial shadow pattern, width and shape, thermal and static displacements effect (*Russian*) 0-107024
 BCC lattice, crit. embrittlement temp., struct. parameters effect (*Russian*) 0-66618
 binary, 50-50, singularities at metal-insulator transition, CPA calc. 0-84428
 binary, constitution diagrams, computer calc. (*Russian*) 0-84909
 binary, elec. resist. near crit. point 0-96847
 binary, magnetic, interface struct., Monte Carlo simulation 0-60317
 binary, marker displacements as result of diffusion 0-92724
 binary, nonstoichiometric, mean field theory, improved approx. 0-79910
 binary, order-disorder transition kinetics, computer simulation 0-92643
 binary, supercond. transition temp. lowering by nonmagnetic impurities 0-100546
 binary, surface segregation kinetics 0-80044
 binary, with arbitrary mole fraction, order disorder transition in case of FCC lattice 0-88295
 binary alloy, solidification chemical inhomogeneity (*Russian*) 0-75335
 binary alloys, acoustic modes in random and correlated alloys, order-disorder transform. 0-65189
 binary alloys, directional solidification, theory of dendritic growth 0-70145
 binary alloys, ferromagnetism and spatial long-range order 0-60159
 binary alloys, initial transient segregation during unidirectional solidification in a furnace with thermal damping 0-70146
 binary alloys, quenched, vacancy concs. 0-107212
 binary alloys, surface conc. profile and surface energy 0-84350
 binary alloys, two phase region calcs. in solidifying melt (*Russian*) 0-65195
 binary linear chain, electronic props., short-range order effects 0-96769
 binary thermodynamic data 0-104121
 chemicothermal treatment, mathematical modelling 0-100955
 cohesive energy, semiempirical model, heat of form. expressions 0-70160
 colour and colour stability as alloy design criteria 0-101005
 Cowley short-range order parameters, distance dependence restrictions 0-103294
 creep cavitation control, intergranular precipitates role 0-66664
 creep failure criteria for high temperature alloys 0-65150
 criteria of chemical inhomogeneity 0-59670
 critical shear stress, for alloys with ordered domains and disordered regions (*Russian*) 0-107237
 critical temperatures determination, elec. resist. method, IMASH-SS-69 installation 0-71827
 cryogenic, creep, review 0-104222
 dislocation climb, in modulated structs. under irradiation conditions 0-70195
 dislocation stress-velocity depend. 0-96537
 disordered, electron localisation, temp. depend. 0-80219
 disordered, interatomic distances, coord. numbers, and mean relative displacements, EXAFS anal. 0-89087
 disordered alloy, residual resistivity due to clustering, ageing effects 0-65521
 disordered alloys, electronic density of states in muffin tin model 0-88467
 disordered binary alloys of ferromag. crystals, mag. dipole fields at interstitial sites 0-97176
 disordered metal ribbon production by ultrarapid quenching 0-71612
 dispersion hardened, work hardening due to Orowan loops, temp. depend. (*Japanese*) 0-66534
 dispersion hardened alloys, strengthening theories 0-97498
 electron diffraction and imaging, at high resoln., characterisation of alloys and ceramics 0-104050
 electron irradiation in HVEM, solute redistrib. calcs. 0-107324
 embrittling residuals categorisation by Auger electron spectroscopy 0-66739
 emissivity determination, using low-inertia opt. dilatometry 0-59684
 engineering, intergranular fragility index 0-66637
 fatigue life distrib. theoretical obs. near fatigue limit 0-59569
 fatigue limit, static and cyclic loading 0-71755
 FCC, hardening by spinodal modulated structure 0-60874
 FCC, interstitial diffusion, theory (*Russian*) 0-65296
 FCC, stacking faults, long-range oscillatory interactions and stability 0-65012

alloys continued

- FCC base hard materials, low temp. toughness (*Japanese*) 0-100916
 ferromagnetic, disordered cryst. and amorphous, mag. dipolar field distrib., computer simulation 0-65790
 ferromagnetic alloys, surface spin waves, cluster Bethe lattice approach 0-70983
 ferromagnetic disordered alloys, spin wave and ferromag. reson. linewidth 0-66045
 film, rate controlled deposition using electron impact emission spectroscopy based instrument (*German*) 0-89152
 force-and-mass disordered alloys, vibr., average local-information transfer approx. 0-88290
 gas turbine engine, substitution of ceramics for high temp. alloys 0-97678
 hard alloy insert jig brushes, wear resist. (*Russian*) 0-60977
 HCP, stacking faults, long-range oscillatory interactions and stability 0-65012
 high-concentration alloy analysis by optical emission spectrometers 0-104477
 HTR material, oxidation and carburization in He 0-108645
 intermetallic phases, B2 struct., substitutional and triple defects, enthalpies of formation 0-96520
 intermetallic phases, struct. description (*German*) 0-88090
 interstitial alloys, interstitial atomic arrangement and mobility at high degrees of interstice filling (*Russian*) 0-107223
 ion-implanted, integral Gaussian profile determ. method 0-107313
 ion-implanted alloys, surface props. effects and appls. 0-79824
 liquidus and solidus temperatures, determ. by γ -ray method 0-65193
 machining damage, depth of surface layers determ. 0-85094
 magnetic, binary, spinodal decomp., computer simulation study of interface behaviour 0-84913
 magnetic alloys, conc., density of states, Kondo effect, theory 0-65780
 magnetic anisotropy, influence of local symmetry (*Russian*) 0-93109
 magnetic localisation and charge oscillations, spin glasses 0-75781
 martensitic phase transition in β -phase alloys 0-108444
 mechanical properties, electric current effect, test device for 4.2-300K 0-66719
 memory alloy engine, efficiency 0-71648
 metal metal system, glass formation 0-64921
 ordered, spinodal decomposition, theoretical basis 0-60862
 ordered, superlattice fringe images, computer simulation 0-103296
 ordering, nonlinear critical relaxation of the Ginzburg Landau field coupled to a conserved density 0-90803
 oxidation behaviour in the environment, appl. to GCFR fuel claddings 0-104350
 oxidation resistance, high-temp., improvement by alloying additions 0-66702
 phase transition premonitory phenomena, exam. by electron diffr. and microscopy (*French*) 0-59651
 random, equilib. and transport props., single-site approxs. 0-92801
 random binary alloys, quantum percolation 0-80156
 rapid hardening from liquid state, apparatus 0-76275
 rapidly quenched crystalline, struct., and heat treatment effects 0-76292
 rapidly quenched metals, conf., Brighton, England (July 1978) 0-67934
 resistivity evolution during decomposition, theory (*French*) 0-75546
 segregating phases identification, single crystals., radiographs computer calc. 0-84934
 segregation, non-equilib., review 0-66516
 segregation studies by imaging atom probe microscopy 0-66911
 selection for cryogenic resistors with low temp. coeff. 0-98922
 shape memory alloy, martensite boundaries, lattice imaging study 0-107359
 shape memory effect, device for testing in bending 0-66723
 shock wave effect on martensitic transform. (*Russian*) 0-96595
 solid-liquid metallic binary alloy, interfacial tension, chem. adsorption and temp. depend. 0-59777
 solidification, multidimensional three-phase free boundary problems 0-75340
 solidification, planar interface stability (*Czech*) 0-89212
 spinodal decomposition, review 0-96657
 spring alloys, microplastic deform. and endurance limit 0-81197
 strain rate history, endochronic theory of viscoplasticity 0-65122
 stress ageing embrittlement, under short term thermally stressed cycle (*Russian*) 0-60885
 substitutional, electrical resist., long and short range orders effect 0-107761
 substitutional, self consistent cluster theory for off diagonal disordered systems 0-84272
 substitutional alloys of intermediate valence systems, static mag. susceptibility con. and temp. depend. 0-84586
 substitutionally disordered, optical cond., intraband transitions 0-103933
 surface composition after fabrication by SIMS 0-65351
 surface composition modification by high-power CW lasers 0-93699
 temper embrittlement, impurities and alloying elements role, review 0-66649
 tenacity parameters 0-60973
 ternary BCC alloys, ordering process, effect of short-range order (*Russian*) 0-84908
 thin film, thickness depend. of CPA electronic densities of states 0-65644
 thin film alloys, surface magnetism props., Curie temp., Ising model 0-108039
 trace element detection by atom probe microanalysis 0-66910
 twinning, HCP struct., relative orientation of cryst. lattices 0-84181
 undersaturated, irradiated, solute segregation kinetics, via drift and defect-solute complexes 0-60872
 unidirectional memory effect (*French*) 0-66606
 work hardening phenomena and screw dislocation dipole clusters 0-100845
 X-ray analysis, energy selective, TEM appls. 0-84036
 X-ray fluorescence correction in thin foil analysis 0-85256
 X-ray microanalysis, thin foils, data correction for absorpt. effects 0-85255

alnico alloys see iron alloysAl₂O₃ see aluminaAl₂O₃- α see corundum α -Al₂O₃ see corundum**alpha-decay**

see also alpha-decay theory; alpha-particle spectra

²⁹⁴110, naturally occurring superheavy element search, alpha emission half-life 0-63139

alpha-decay continued

- ²³⁸114, high spin pot. energy surfaces, fission barrier, α -, γ -decay half lives, yrast spectrum 0-73764
coherent rotational states, alpha decay, α -emission probability 0-102155
giant halo radioactive inclusions in minerals 0-94524
monazite, α -spectra evidence for natural activity at 6.52 to 9.07 MeV 0-67363
rare earth nuclei, high spin isomer α -decay search 0-102158
(^d,^eLi), A=144-238, alpha-cluster transfer from alpha-decaying nuclei 0-91166
²⁴³Am half life and α -activity 0-102159
^AAt, A=198m,198g,199, alpha branching ratios 0-99154
¹⁸⁸Bi alpha decay half lives 0-57749
²⁴⁵Cm decay, ²⁴¹Pu level structure and γ -transitions 0-105980
^AFr, A=201-203, alpha decay, branching ratios, mass excess and half life 0-99154
¹⁴⁶Gd region, proton subshell effects from α -decay and spectroscopy, self-consistent study 0-57748
^AHg, A=182-184, alpha decay branching ratio 0-57749
⁷Li- α virtual decay vertex constant from (d,t), (p, α) 0-78231
^ALu, A=158, 159, alpha decay and gamma transitions 0-73827
^APb, A=183,184, alpha decay half lives 0-57749
²⁰⁸Pb(^eLi,d), 90 MeV, alpha-cluster transfer from alpha-decaying nuclei 0-91166
^APt, A=178,179, alpha decay branching ratio 0-57749
²⁴¹Pu half life from α -spectrometry and ²⁴¹Am ingrowth 0-68609
¹⁹⁹Rn and ¹⁹⁹Rn^m alpha decay signatures from ¹⁶⁵Tm(³⁵Cl,5n) 0-68610
²³⁰Th alpha-decay half life from specific activity method 0-102157
²³⁸U, radioactive series decay, computer simulation 0-102160
²³⁸U, radioactive series decay, computer simulation 0-102160
^AYb, A=158, 159, alpha decay and gamma transitions 0-73827

alpha-decay theory

- see also *alpha decay*
conference on nuclear physics, Mikolajki, Poland (2-14 Sept. 1979) 0-101662
deformed and superdeformed nuclei from heavy ion reactions, α -decay amplification 0-102156
heavy nuclei, alpha cluster formation at and outside nuclear surface 0-63138
⁵⁶Ni from HI reactions, superdeformed nucleus decay, α -decay amplification 0-68608
²¹⁰Po, nucl. alpha decay, electron inner shell vacancy creation, semi quantal approach 0-68607
¹⁴⁹Tb from HI reactions, superdeformed nucleus decay, α -decay amplification 0-68608

alpha-particle absorption

- stopping power of liquids for alpha particles, meas. apparatus 0-88224

alpha-particle angular distribution

- see also *alpha-particle spectra*
¹⁸O(γ , σ_0), 19-32 MeV, E1 and E2 cross section, E1-E2 phase difference 0-63172
¹⁵⁹Tb(¹⁴N,X), 95 MeV, fast α -particle ang. distrib. 0-63207

alpha-particle attenuation see *alpha-particle absorption***alpha-particle detection and measurement**

- see also *alpha-particle spectrometers; radioactivity measurement*
air ionisation probe for α , β , γ hand and shoe monitor 0-58084
air monitoring system for α -activity and nuclide specific noble gas meas. 0-63408
cellulose acetate solid state track detectors, catalytic oxidation sensitization (Chinese) 0-102399
cellulose acetate solid state track detectors, swelling sensitisation (Chinese) 0-99422
cellulose nitrate, energy loss critical rate 0-74082
cellulose nitrate nuclear track detectors, energy resolution enhancement for alpha particle detection 0-91392
cellulose nitrate thin foil manufacture for α particle track detector (Spanish) 0-74091
energy loss measurements for slow particles, 0.01 to 1.0 MeV, multiple scatt. corrections 0-95511
imaging alpha detector, radioactive contamination monitoring appl. 0-102384
microprocessor controlled long lived alpha emitter monitor 0-58069
multielement α -spectrometry for individuals and environment monitoring 0-58024
on-line radiation monitoring at a nuclear fuel reprocessing plant 0-95469
parallel plate avalanche counters for registration of light charged particles 0-91369
personal dosimetry instrument for airborne radon daughter meas. (French) 0-57989
phosphate fertilizer, specific activity of U and Th rel. to particle size 0-106244
position-sensitive detectors, use of the SnO₂-Si heterotransition 0-91375
self-scanning photodiode array for fast ion detection 0-87018
smear samples, simple and rapid meas. of α -rays using air luminesc. 0-106243
solid state nuclear track detectors, alpha sensitive plastic films for Rn gas conc. meas. 0-94618
solid state track detector for differential alpha radiography of actinide solutions 0-71932
solid state track detectors in solutions of actinides, α track registration 0-63486
SSNTD, alpha sensitive plastic detectors for Rn gas conc. meas. 0-94617
surface-barrier Au(Si) detectors, protective glass walls 0-91374
transuranic aerosol measurement system and its field results 0-58068
 α -emitting effluents from nuclear processing plant, detection and meas. 0-95468
Pb poisoning in human teeth, determ. using alpha-sensitive plastic track detector 0-94433
²²³Rn concentration meas. by plastic detectors to determ. environmental α -emitters from natural sources 0-91292
²²²Rn gas detection using Track Etch system for U exploration 0-98488
Si diffused junction detector for alpha air monitoring instrumentation 0-58083
Si heavy ion surface barrier detector, plasma delay times, electron back-scattered from fission fragment or alpha particle 0-58095

alpha-particle effects

- bacterial cells, heavy ion irradi., long range effects, comparison with γ -irrad 0-101236
benzene, soln., fluoresc., quenching in pulsed proton and alpha particle irradi., radiation quality effects 0-66259

alpha-particle effects continued

- breeding performance of female mice, comparative effects of ⁶⁰Co γ -rays and ²³⁹Pu α -particles 0-72231
Chinese hamster cells, enhanced killing by ²³⁸Pu α -particles in the presence of cordycepin 0-72233
chromosome aberrations, dose-effect relationship, population exposed to increased natural radioactivity 0-72254
creep, irradi. induced, 60 MeV alpha particles 0-92597
diamond, light ion damage, channelling investigation 0-65068
E. coli, value of photoreactive component after exposure to ionising radiation 0-72224
lung, carcinogenic effect of localised fission fragment irradi., rat expts. 0-81656
lung parenchyma irradiated by inhaled ²³⁸PuO₂ particles, collagen localisation, Syrian hamsters 0-72252
mammalian cells, lethally damaged, proliferation obs. after irradi. by various particles 0-108971
plagioclases, volcanic, α -particle dose evaluation rel. to thermoluminescence dating 0-98475
soft errors and oxide damage induced in LSI/VLSI cells, geometric anal. 0-59528
VMOS dynamic memory, 65536-bit, investigation of alpha-particle induced soft errors 0-88223
Al foil, irradi. under fusion reactor conditions, He bubble alignment during deform. 0-107345
Al, foil, secondary electron emission due to α -particle irradi. (Russian) 0-66344
Nb, swelling correlation with local gas concentration following He irradi. 0-70271
Ni-Cr-Fe alloys, radiation enhanced precip. and dissolution of precipitates, point defect kinetics and dislocation obs. 0-108467
²³⁸Pu 4.4 MeV α -particles, mutagenicity and cytotoxicity rel. to X-rays 0-72265
Si, energy loss and multiple scattering of non-channelled α -particles (German) 0-59544
Sn, supercond. tunnel junction, quasiparticle excitation by α -particles 0-103791
- alpha-particle interactions** see *alpha particle-nucleus reactions*
- alpha-particle model** see *nuclear cluster model*
- alpha-particle-nucleus reactions**
for inelastic alpha particle-nucleus scattering, see '*alpha particle-nucleus scattering*'
¹⁰⁷Pd(α ,2n γ), 20-27.5 MeV, ¹⁰⁴Cd quasirot. ground state band and γ -transition 0-105955
fissionability, target mass depend. for π , γ , α , p, cascade-evaporation and liquid drop calcs. (Russian) 0-106089
light relativistic ion-target interactions, particle emission 0-102193
nucleus-nucleus total cross section energy depend. 0-106071
relativistic nuclear collisions, p, d, and t inclusive energy spectra 0-63199
(α ,2 α), A=9, 12, 16, 20, 22 0-68629
(α , α X), inelastic interaction cascade model for Z=3-13, 29-82 0-106064
(α ,¹²C), 90.3 MeV, multi- α -cluster transfer and direct pickup cross sections 0-57760
(α ,d), double stripping core independ. 2-nucleon transfer, Tang-Herndon effective interactions 0-73836
(α ,³HeX), 1 GeV/N, momentum distrib. after high energy fragmentation, spectator peak 0-99164
(α ,³He), composite particle scatt. breakup mechanism 0-83105
(α ,N), microscopic finite-range anal. 0-63181
(α ,n), on B, C, N, Mg, Al, P, activation anal. appl. 0-61206
(α ,p), on B, C, N, Mg, Al, P, activation anal. appl. 0-61206
(α ,X), complete fusion barrier and evaporation from ¹⁹⁴Hg 0-68715
(α ,X), relativistic collisions, slow and fast fragment correlations, multiplicity association 0-86886
(α ,xn), 640, 710 MeV, n ang. and energy distrib., intranuclear cascade model 0-83109
¹⁰⁷AgZZ 0-95329
¹⁰⁷Ag(α ,2n γ), ¹¹¹In 21/2⁺ isomeric state g-factor and relaxation time 0-73794
²⁷Al(α ,d), 27.2 MeV, ²⁹Si levels and ang. distrib., DWBA anal. 0-78157
³⁸Ar(α ,n γ), ⁴¹Ca, spin and parity from angular distrib. and linear polarisation of γ 0-63079
¹⁹⁷AuZZ 0-95329
²⁰⁷AuZZ 0-95329
¹¹B(α ,p)¹⁴C, subsurface production of ¹⁴C, groundwater dating 0-85690
⁹Be(α ,³He), 65 MeV, ¹⁰Be levels and differential cross sections, DWBA and coupled channel anal. 0-102121
⁹Be(α ,n)¹²C, ¹²C gamma line Doppler broadening at 4438 keV 0-91147
⁹Be(α ,t), 65 MeV, ¹⁰B levels and differential cross sections, PWBA and coupled channel anal. 0-102121
²⁰¹Bi(α ,f), 23-140 MeV, τ_{crit} from fragment ang. distrib. anal. 0-106087
²⁰⁹BiZZ 0-95329
²⁰⁹Bi(α ,n), excitation functions and isomer ratios of ²¹²At 0-83039
²⁰⁹Bi(α ,np), excitation functions and isomer ratios of ²¹¹Po 0-83039
²⁰⁹Bi(α ,p), excitation functions and isomer ratios of ²¹²Po 0-83039
²⁰⁹Bi(α ,t), 40 MeV, effective residual interaction matrix elements, spectroscopic factors, cross sections 0-99134
⁸¹Br(α ,2n), 19-25 MeV, ⁸³Rb band struct., spin assignments and transitions 0-73774
⁸¹Br(α ,2n), 19-25 MeV, ⁸³Rb high spin states, J π and transitions 0-105949
¹²C(α ,X), 4.2 GeV/c, multitudes of secondary negative particles, momentum distrib. ratios (Russian) 0-63178
⁴²Ca(α ,n)⁴²Ti, reaction rates in stars 0-82183
¹⁰⁸Cd(α ,2np), 44 MeV, ¹⁰⁹In high spin states, γ -transitions, ang. distrib. 0-73783
¹¹⁰Cd(α ,2n γ), ¹¹²Sn 6⁺ isomeric state, g-factor and relaxation time 0-73794
¹⁴⁰Ce(α , xn), 85 MeV, ^{138,139}Nd high spin states, J π , γ -cascades and shape transition 0-102090
¹⁴⁰Ce(α , xn), 86 MeV, ^ANd, A=138,139, high spin states, isomers and γ -cascade 0-78120
⁵⁹Co(α ,xnyp), 20-172.5 MeV, cross sections excitation functions, hybrid model, pre-equilib. effects 0-57784
¹⁶⁴Dy(α ,4n γ), 51 MeV, ¹⁶⁴Er high spin props. in multiple band crossing region 0-83023
¹⁷⁰Er(α ,2n) 27 MeV, ¹⁷²Yb levels, bands, J π and T_{1/2} 0-91127
¹⁹F(α ,n), 5.4 MeV, ²²Na 0⁺ level mean life, isovector mag. dipole transition 0-68595

alpha particle-nucleus reactions continued

- ⁵⁴Fe(α , γ), 18-27 MeV, ⁵⁷Ni high spin yrast cascade, decay modes J assignment 0-68514
⁵⁶Fe(α , γ), ⁵⁹Co level energies, branching ratios lifetimes and spins 0-63093
 Ga(α ,p), 25 MeV, ^{72,74}Ge O₂⁺ levels, struct. transition between N=40 and 42 0-73800
 Gd(α , xn) Dy, K-shell ionisation cross-sections meas. 0-78687
¹⁵²Gd(α ,4n), 60 MeV, ¹⁵²Dy 60 ns isomer deexcitation E2 x- (or Δ) transition, half life, γ -coincidence 0-86859
 Gd(α ,xn), 47-130 MeV, Dy K-shell internal conversion yields, gamma transition multiplicities 0-78215
 Gd(α , xn) Dy, K-shell ionisation cross-sections meas. 0-78687
⁷⁶Ge(α ,p), 26 MeV, ⁷⁹As levels, J⁺ and ang. distrib. 0-78161
¹H(α , α X), 1.74, 2.57 GeV, low mass π N enhancement, cross section t-depend. 0-63193
²H(α ,ap), 9.22-11.3 MeV, ⁶Li excited states, final state interactions, three-body force effects 0-57692
 Hd(α ,t), ¹Pm, A=143-153, odd-A, spectroscopic factors, shell model anal. 0-78137
⁴He(α , α X), 4.5 GeV/c, Thomas Reiche Kuhn sum rule appl., mean energy losses 0-91192
⁴He(α ,ad), 119 MeV, excited states, J⁺ and γ -ang. correlations 0-86809
¹⁶³Ho(α ,2n) ¹⁶²Tm, levels and transitions 0-73766
¹⁶³Ho(α ,2n γ), 21-27 MeV, ¹⁶²Tm rotational bands, J⁺, γ -transitions and branching ratios 0-86781
¹⁶³Ho(α ,2n γ), ¹⁶²Tm, energy level scheme (*German*) 0-68576
¹²⁷I(α ,4n), ¹²⁷Cs collective quadrupole dynamics, band struct., transitions, collective model anal. 0-78112
 Kr(α ,xn), ^{81,83}Sr yrast and high spin states of neutron deficient isotopes 0-73776
¹³⁹La(α ,4n), ¹³⁹Pr medium spin states, J⁺, transitions and shape 0-86779
²⁶Mg(α ,⁶He), ²⁶Mg ground and γ -bands, direct and multistep processes 0-102094
¹⁴⁶Nd(α ,xn), A=144,146, 20 to 43 MeV, ^{146,147}Sm excited states, energy levels, spin, parity, shell and cluster-vibration models 0-57683
¹⁴²Nd(α ,4n), 60 MeV, ¹⁴²Sm isomers, lifetimes and transitions 0-78122
⁶⁰Ni(α , γ), 10 MeV, ⁶³Cu low excitation states, level struct. and lifetimes 0-86813
⁶¹Ni(α ,X), 35.5 MeV, ⁶⁶Zn* composite particle emission, ang.-distrib., exciton-coalescence model 0-78265
⁶¹Ni(α ,n γ), 8.6, 9.35 MeV, ⁶⁴Zn high spin states, J⁺, T_{1/2}, γ -decays 0-73767
¹⁶O(α , γ), CC ²⁰Ne 8⁺ level radiative width, resonance strength 0-83065
¹⁶O(α , γ), uncorrelated target, optical pot. unitary content, DWIA and Glauber theory 0-105947
²⁰⁸Pb(α ,n), exam. of neutron yield 0-86912
²⁰⁸Pb(α ,n), excitation functions and isomer ratios of ²¹¹Po 0-83039
²⁰⁸Pb(α ,t), 40 MeV, effective residual interaction matrix elements, spectroscopic factors, cross sections 0-99134
 Pb(α ,X), 3.6 GeV/N, secondary particle ang. and vel. distrib., π ,p,d,t prod. (*Russian*) 0-63194
¹⁰⁴Pd(α ,p γ), ¹⁰⁶Ag low-lying excited states 0-57693
¹⁴¹Pr(α ,4n), ¹⁴¹Pm medium spin states, J⁺, transitions and shape 0-86779
⁸³Rb(α ,2n γ), 24-36 MeV, ⁸⁷Y level struct., γ -spectroscopy and J⁺ 0-83040
⁸⁷Rb(α ,3n), 40.1 MeV, ⁸⁸Y 14 ms 8⁺ isomeric state, g-factor 0-63080
¹⁰³Rh(α ,3n γ), 33-55 MeV, ¹⁰⁴Ag levels, J⁺, T_{1/2}, bands and transitions 0-102093
¹⁰³Rh(α ,4n γ), 35-52 MeV, ¹⁰³Ag high spin states, bands transitions, intermediate deformation Coriolis coupling 0-105944
¹⁰³Rh(α ,n γ), ¹⁰⁶Ag low-lying excited states 0-57693
²⁸Si(α ,⁶He), ²⁴Si, Q value and mass excess 0-86795
²⁸Si(α ,n) ³¹S, cross sections and thermonuclear reaction rates 0-73852
¹⁴⁴Sm(α ,2np), 50 MeV, ¹⁴⁵Eu high spin levels, isomers and in-beam γ -spectroscopy 0-78124
¹⁴⁴Sm(α ,3n), 50 MeV, ¹⁴⁵Gd levels, J⁺ and transitions, neutron hole coupling to ¹⁴⁶Gd core 0-78164
¹⁵⁰Sm(α , 2n), 19, 27 MeV, ¹⁵²Gd β - and octupole bands, downbending moments of inertia 0-91131
¹⁵⁴Sm(α ,⁶He), ¹⁵²Sm ground and γ -bands, direct and multistep processes 0-102094
 Sm(α ,n γ), 28.50 MeV, ¹⁵²Gd N=88 nuclei quasirot. bands and J⁺ 0-83025
¹¹⁸Sn(α ,2n γ), ¹²⁰Te quasi-rot. band based on proton 4p-2h state, level scheme, transitions 0-78119
 Sr(α ,xn), ⁸³Zr yrast and high spin states of neutron deficient isotopes 0-73776
¹⁸¹Ta(α ,X), 4.2 GeV/c, multitudes of secondary negative particles, momentum distrib. ratios (*Russian*) 0-63178
²³²ThZZ 0-95329
²³⁸UZZ 0-95329
⁷⁰Zn(α ,p), 26 MeV, ⁷³Ga levels, J⁺ and ang. distrib. 0-78161
⁹¹Zr(α ,t), 35.4 MeV, ⁹²Nb low lying multiplets, DWBA anal. for spectroscopic factors 0-57685

alpha particle-nucleus scattering

- internal S-matrix dynamics and internal deflection function 0-78307
 N=85 isotones, bands and transitions from α and H¹ excitation, in-beam study 0-78123
 (α), folding potentials, Woods-Saxon and squared Woods-Saxon parameterisations 0-102195
 NN interaction, local density dependence, double-folding calcs. 0-83114
²Ba(α , α') A=135,137, 9.7-12.2 MeV, Coulomb excitation, transition probabilities, γ -rays and level collectivity 0-78201
⁹Be(α , α'), 65 MeV, levels and differential cross sections, optical anal. 0-102121
¹²C(α , α'), generator coordinate multichannel calc., levels and resonances 0-78149
¹²C(α , α'), 1.37 GeV, S-matrix expansion from Glauber multiple scatt. theory 0-91191
¹³C(α , α'), 22, 36 MeV, resonant state line shapes 0-91148
⁴Ca(α , α'), 24,29 MeV, A=40,42,44,48 backward ang. distrib. anomaly, coupled and channel anal. 0-86911
⁴Ca(α , α'), A=40, 42, 44, 48, 104 MeV, cross sections and optical pots., nuclear size 0-68524
⁴Ca(α , α'), A=40, 42, 44, 48, 104 MeV nuclear size and density distrib. from folding model anal. 0-68525
⁴Ca(α , α'), A=40, 48, nuclear matter density distrib., saturation effect, optical potential 0-63115

alpha particle-nucleus scattering continued

- ⁴⁰Ca(α , α'), 1.37 GeV, S-matrix expansion from Glauber multiple scatt. theory 0-91191
⁴Gd(α , α'), 30 MeV, A=144,146,147,148, high spin isomer g-factors yrast traps 0-78146
⁴He(α , α'), 4.32, 5.07 GeV/c, Glauber multiple scatt. theory comparisons 0-63192
⁴He(α , α'), large amplitude collective motion, adiabatic TDHF calcs. 0-86786
⁴He(α , α'), nuclear separable plus Coulomb interaction 0-83106
⁴He(α , α'), s-wave, Coulomb amplitudes from generator coordinate theory 0-83107
⁴He(α , α'), size change of α effect on phase shift, generator coordinate and variational methods (*Chinese*) 0-68683
¹⁴N(α , α'), 1.5, 1.6 MeV, ¹⁸F resonances, α -widths, isospin and parity mixing, R-matrix anal. 0-91162
⁵⁸Ni(α , α'), radial sensitivity of optical pot. 0-86869
⁵⁸Ni(α , α'), 50.2 MeV, composite particle optical pot. discrete ambiguities, partly Pauli-forbidden states 0-86870
¹⁶O(α , α'), hyperfine dynamic mag. field effects 0-68689
¹⁶O(α , α'), uncorrelated target, optical pot. unitary content, DWIA and Glauber theory 0-105947
²⁰⁸Pb(α , α'), 172 MeV giant monopole and quadrupole resonances, multipole excitations 0-106031
²⁰⁸Pb(α , α'), levels, B(E3), transition density and nuclear pot., folding model anal. 0-86812
²⁰⁸Pb(α , α'), 172 MeV, giant resonance structures 0-91163
¹⁰²Ru(α , α'), 8.5, 9.0 MeV, Coulomb excitation, 2⁺ state electric quadrupole moment 0-73793
⁴Sc(α , α'), levels, J⁺, transitions and lifetimes 0-63091
 Si, energy loss and multiple scattering of non-channelled α -particles (*German*) 0-59544
¹¹⁶Sn(α , α'), 96, 129 MeV, giant resonance excitation, isoscalar breathing mode state, nuclear incompressibility 0-68620
⁵⁰Ti(α , α'), 140 MeV, model independent description limits from local optical pots. 0-102196
⁴Zn(α , α'), A=64, 66, 129 MeV, isoscalar giant monopole resonances, nuclear incompressibility 0-83083
⁹⁰Zr(α , α'), 96, 129 MeV, giant resonance excitation, isoscalar breathing mode state, nuclear incompressibility 0-68620
⁹⁰Zr(α , α'), form factor, coupling between real and imaginary optical potential 0-68680
- alpha-particle scattering** *see alpha particle-nucleus scattering*
alpha-particle spectra
see also alpha-particle angular distribution
 LWR spent fuel, alpha spectrometric meas. for SNM verification 0-78424
 monazite, α -spectra evidence for natural activity at 6.52 to 9.07 MeV 0-67363
¹⁹⁷Au(²²Ne, α X), 178 MeV, max. α -particle energy at forward angles 0-68698
²³³U(ρ ,f), alpha-particle angular and energy spectra, cross-section anisotropy 0-57809
- alpha-particle spectrometers**
see also alpha-particle spectra
 magnetic analysis of charged particles, α -, β - and mass spectrometers (*Russian*) 0-87011
- alpha-particles**
see also cosmic ray alpha-particles and helium nuclei
 Tokamak reactors, role of α -particles review 0-86971
⁵⁸Ni(⁴⁰Ar,X), 280 MeV, deep inelastic, light fragments, thermal equilib., ang. momentum transfer 0-63203
¹⁶O(^{12,13}C, α X), 140 MeV, fast α prod. and molecular resonance search 0-106066
- alpha-radiation** *see alpha-particles*
alpha-rays *see alpha-particles*
alpha-rhythm *see bioelectric potentials*
alpha-rhythm measurement *see electroencephalography*
alternators
 fusion reactor, TEXT, motor-generator power supply system 0-99292
altitude measurement *see height measurement*
alumina
see also corundum
 α -phase, growth and microstruct. on Ni-Al alloys 0-108626
 additive for Pb(Zn_{1/3}Nb_{2/3})O₃-PbTiO₃-PbZrO₃ ceramics, HF filters appl. (*Japanese*) 0-60507
 adsorbed 1-butene isomerisation, IR study 0-76554
 adsorbed molecules, Raman spectroscopy study 0-65358
 adsorption of 1-butene, microgravimetric-IR study 0-75432
 adsorption of Cs, Sr, Eu, Co, and Cd 0-99240
 adsorption of ethylene glycol, inelastic electron tunnelling spectroscopic study rel. to lubrication 0-70302
 adsorption of thioindigo, photoisomerisation 0-89503
 β -Al₂O₃-Cu₂O, phys. and chem. props., use in determ. of thermodynamics of Cu-Sn alloys 0-107502
 angular particle impact erosion of reaction-bonded SiC 0-89362
 anodic, passified, inhibition of reaction with water 0-89390
 anodic film, behaviour of emulsion particles during electrodeposition 0-104357
 anodic film, trapped O₂ and effect on dielec. stability 0-100634
 anodic films, trapping levels study using TSC 0-103768
 anodisation for surface passivation of GaAs and InP, MIS characts. 0-93004
 atomically sharp cracks, TEM study 0-71729
 cement grog bodies, high Al₂O₃ content, creep characts. obs. 0-66578
 ceramics, high rate reactive ion etching 0-85070
 ceramics, sintering mechanism and kinetics, glass-forming additives effect 0-89187
 clay, Al₂O₃ and SiC recovery by C reduction 0-108704
 conduction and dielec. loss mechanisms, paired interstitiality model 0-107468
 confined arc, ablation-induced effects 0-70073
 deformed by prismatic slip, HV TEM obs. of dislocations 0-108517
 dispersion in polycryst. NaCl, diffusive creep 0-97531
 elastic moduli measurement, US method for up to 2000K (*French*) 0-104373
 electro-erosional prep. (*Russian*) 0-81297
 electron tunnelling spectroscopy, inelastic, of adsorbates, MgO comparison 0-88686

alumina continued

- fast ion transport and electrochem. storage in beta aluminas 0-61324
film, anodic, H conc. profiles meas. 0-75261
film, anodic, trapping of ^3He and ^4He ions at room temp. 0-84221
film, etching in carbon tetrachloride plasmas 0-76407
film, switching times and arc cathode emitting site lifetimes 0-59332
fracture toughness determ. using four-point-bend specimens 0-108536
gel particles, ultrafine, form. from $\text{NH}_3\text{-AlCl}_3$ soln. 0-93807
glass- Al_2O_3 seals, diffusion of Al, electron microprobe study 0-107577
grain boundary thickness obs. using electron diff. techniques 0-79811
high-frequency phonon lifetimes 0-70338
hot isostatic press. 0-108377
hot pressed, fracture stress-reflecting spot relations 0-71731
hot-pressed, transparent and translucent polycrystals 0-60533
integrally coloured oxide films on Al, optical properties 0-93420
interface of γ -phase with electrolyte solns., adsorption of ions, surface conductance, ion mobility and surface pot. 0-75622
irradiation stability obs. using X-ray emission meas. (Russian) 0-66326
layer on stainless steel in water, leaky wave generation 0-75419
Madelung pot. determ. by Ewald method 0-92475
MIS Schottky structures, photovoltaic response 0-101115
 β - $\text{Na}_2\text{O-Al}_2\text{O}_3$ low temp. ultrasonic vel. meas., temp. depend. 0-79885
phase transformations and microstruct., in boehmite derived transition Al_2O_3 0-60857
phosphors, photon multiplication and secondary electron-hole pairs generation (Russian) 0-66262
polarised luminescence in neutron- and proton-irradiated single crystals of α -phase 0-66271
polycrystalline, effects of space charge, grain-boundary segregation and mobility differences on conductivity 0-79979
polycrystalline, stress-strain data up to 1.25 GPa 0-100899
porcelain, crack propag. data applicability to failure prediction 0-81154
porous transparent films as antiref. coatings for glass surfaces, low refr. index 0-74448
powder support for MnO_2 catalyst, N adsorption obs. of dispersion modes 0-81363
recombination luminescence mechanism 0-71477
refractories, fracture, J-integral meas. 0-108537
rod, damaged, mech. strength, surface defects effect, appl. as insulators (German) 0-76330
semisintered, shear strength at high press. 0-76308
shrink-free high Al_2O_3 compounds, prod. method using slips made from clay, orthophosphoric acid 0-66460
simultaneous reduction with Nb_2O_5 by CaH_2 , Nb_2Al prep. 0-100809
single cryst., self-diffusion of O, isotope exchange investig. 0-100348
sintering, effect of SrO , MgO and Y_2O_3 additives on α - Al_2O_3 mineralisation 0-89186
sintering, role of MgO 0-81010
sintering as function of phase comp. 0-66464
sintering temperature effect of titanate additions 0-60808
solid electrolyte, beta phase, optimisation of fabrication process, for Na/S load levelling batteries 0-72035
solid electrolyte β - and β' -phases, defect struct. obs. by high resolution TEM, battery ageing relevance 0-107501
solid electrolyte based Na/S traction batteries, development progress and problems, review 0-61326
solid electrolyte for Na/S battery, GEC development program 0-61327
solid electrolytes, β - and β' -type, resist. obs. 200-1000°C 0-107500
solid electrolytes, elec. cond. and activation energy (Chinese) 0-79987
STEM, Pt on Γ - Al_2O_3 , atomic number contrast, supported catalyst particles 0-79651
substrate, tape-casted, fracture strength analysis 0-60948
substrates for Ni-Cr/Au films, interdiffusion processes and oxidation phenomena 0-59735
superionic conductor, Haven ratio, temp. depend., correl. effects role 0-107504
supermicrogrid preparation and props. for use as support film in high resolution electron microscopy 0-99010
supported Rh-Cu catalyst, chemisorbed CO, IR spectra (French) 0-60559
surface, of γ - Al_2O_3 , physisorption and reaction of $\text{Mo}(\text{CO})_6$, IR spectra obs. 0-80064
surface of γ - Al_2O_3 , OH layer, IR spectra, outgassing temp. effects 0-66175
surface $\text{Zr}(\text{BH}_4)_4$ catalytic reactions, inelastic electron tunnelling spectra 0-75425
suspended particles, behaviour on solidification of Al-Cu (33%) under reduced gravity (German) 0-60853
thin film used in inelastic electron tunnelling spectroscopy, X-ray photoelectron spectrum 0-108319
vacuum condensate, struct. and mech. props., second phase effect (Russian) 0-71705
wetting by Cu-Ti ternary alloys 0-76171
3 Al_2O_3 - GeO_2 - SiO_2 , reduction by C, mixed diffusional-kinetic regime (Russian) 0-66771
Ag- β - Al_2O_3 , test for solid electrolyte by EMF meas on Ag/Au couples (German) 0-104307
Ag $_2$ O-Al $_2$ O $_3$ -MgO-Na $_2$ O, β'' -alumina, structure, X-ray determ. 0-107148
Ag $_2$ O-MgO-Al $_2$ O $_3$, ionic cond. 0-107480
Al/Al $_2$ O $_3$ /Al, dielec. props. 0-80404
Al/Al $_2$ O $_3$ /Al structures with organic monomolecular layer, cond. at high elec. fields 0-80402
Al-Al $_2$ O $_3$, dispersion hardened, creep (Czech) 0-108463
Al-Al $_2$ O $_3$ -Au device in Cl_2 atmosphere, current-voltage characts., press. depend. 0-65704
Al-Al $_2$ O $_3$ -Dy thin junctions, Poole-Frenkel effect obs. and cause 0-80398
Al-Al $_2$ O $_3$ -GaAs backwall MIS Schottky barrier solar cell, anal. model 0-85289
Al-Al $_2$ O $_3$ -Pb contacts, tunnelling spectroscopy, band struct. of Pb 0-80169
Al-Al $_2$ O $_3$ -Si structure, study of charge trapping 0-60097
Al-Al $_2$ O $_3$ -SiO $_2$ -Si capacitors, physical and elec. props. of RF plasma grown Al_2O_3 0-100530
Al-Al $_2$ O $_3$ -p-GaAs MOS diode, capacitance-voltage characts. 0-107914
 β -Al $_2$ O $_3$ -MgO $_6$, X-ray diffuse scatt. obs. of struct. 0-107186
 β -Al $_2$ O $_3$ -(Na,Li) $_2$ O, NMR, Raman and IR spectra, and X-ray diff., heat treatment induced changes 0-107508
Al $_2$ O $_3$ (96 wt.%), fractographic criteria for subcritical crack growth boundaries 0-81155
Al $_2$ O $_3$, anodic, passified, inhibition of reaction with water 0-89390
Al $_2$ O $_3$ bioceramic synthesis, for orthopedic purposes, props. (Polish) 0-66465

alumina continued

- β -Al $_2$ O $_3$, defect props. and ionic transport 0-107486
Al $_2$ O $_3$, fine grained, basal slip and nonaccommodated grain boundary sliding 0-60916
Al $_2$ O $_3$, fine grained, interface-controlled diffusional creep 0-60915
 α -Al $_2$ O $_3$, grain boundary segregation, electron microscopy 0-103361
Al $_2$ O $_3$ humidity sensor, ageing improvement (Japanese) 0-100863
 β -Al $_2$ O $_3$, internal friction and Na transport 0-59578
 β -Al $_2$ O $_3$, long-period strucls., electron microscope obs. 0-92501
 β'' -Al $_2$ O $_3$, Mg- and Li-stabilised, high-resol. electron microscopy images 0-107277
 η -Al $_2$ O $_3$ outgassed at 400, 650°C, heat of adsorpt. of pyridines from soln., surface acidity 0-61154
Al $_2$ O $_3$, polycrystn., high-temp. fatigue and strength 0-60954
 β -Al $_2$ O $_3$, polycrystn., with preferably orientated grains, prep. (Japanese) 0-81012
 α -Al $_2$ O $_3$ scales, early stages of development on Fe-Cr-Al and Fe-Cr-Al-Y alloys at high temp. 0-89413
Al $_2$ O $_3$, single cryst., O self diffusion, ion-probe meas. 0-59701
 β -Al $_2$ O $_3$ structures, superionic props., IR spectra 0-107483
Al $_2$ O $_3$ -Cr, pure and doped, electron irradi. induced cond., TSC and EPR study 0-80277
Al $_2$ O $_3$ -Cr photoexcited crystals, cooperative thermoluminescence quenching (Russian) 0-80881
Al $_2$ O $_3$ -Cr $^{2+}$, HF phonon spectroscopy using supercond. tunnel junctions 0-65178
Al $_2$ O $_3$ -Cr $^{3+}$, Jahn-Teller system, zero-phonon line broadening due to non-radiative transitions 0-108258
Al $_2$ O $_3$ -Fe, pore form. during oxidative annealing, grain growth slowing 0-100856
Al $_2$ O $_3$ -Li, TSEE, Li doping effects 0-80953
Al $_2$ O $_3$ -MgO, grain boundary segregation of Ca and Mg X-ray spectrosc. and STEM study 0-107269
Al $_2$ O $_3$ -Mn $^{2+}$, Jahn-Teller Mn $^{3+}$ ions, phonon spectroscopy and thermal cond. meas. 0-88282
Al $_2$ O $_3$ -Mn $^{2+}$ under uniaxial stress, Jahn-Teller model 0-88521
 β -Al $_2$ O $_3$ -NH $_4^+$ (Nd $_4^+$), polarised Raman scatt. 0-103947
Al $_2$ O $_3$ -Si(Ti), sensitised TLD phosphor, photon energy dependence 0-78498
Al $_2$ O $_3$ -V $^{3+}$, Jahn-Teller effects, ground state 0-75528
Al $_2$ O $_3$ -V $^{3+}$, spin-phonon coupling, rot. mode role 0-70329
Al $_2$ O $_3$ -V $^{3+}$ (Fe $^{2+}$), hyperfine splitting and magnetoelastic const., freq. crossing spectroscopy 0-107392
 α -Al $_2$ O $_3$ -V $^{3+}$ (V $^{4+}$)(Co $^{3+}$)(Co $^{2+}$), optically and thermally stimulated reactions, absorpt. spectra 0-80825
Al $_2$ O $_3$ -Zr ceramic, elec. props., additives effect, and interaction with steel melt 0-104305
 β -Al $_2$ O $_3$ -(K,Li) $_2$ O, ionic cond. and Raman spectra 0-107509
 β -Al $_2$ O $_3$ -(K,Sr) $_2$ O, ionic cond. and Raman spectra 0-107509
 β -Al $_2$ O $_3$ -(Na,K) $_2$ O, equil. distrib. of ionic species 0-107511
 β -Al $_2$ O $_3$ -(Na,K) $_2$ O, model calcs. of cond. anomalies, pot. energies of cation arrangements 0-107510
 β -Al $_2$ O $_3$ -(Na,Li) $_2$ O, first-order quadrupole NMR obs. of cation distrib. and ion motion 0-108113
 β -Al $_2$ O $_3$ -(Na,Li) $_2$ O, ionic cond. and Raman spectra 0-107509
 β -Al $_2$ O $_3$ -(Na,Li) $_2$ O, ionic motion obs. using NMR and internal friction 0-108099
 β -Al $_2$ O $_3$ -(Na,Li) $_2$ O solid electrolyte, Li motion and activation obs. using ^7Li NMR 0-108100
 β -Al $_2$ O $_3$ -Ag $_2$ O, Haven ratio, temp. depend., Ag diffusivity and ionic cond. 0-107503
 β -Al $_2$ O $_3$ -Ag $_2$ O, stoichiometric and nonstoichiometric, structure comparison, phase transitions in stoichiometric compound (French) 0-60856
 β -Al $_2$ O $_3$ -Ag $_2$ O, stoichiometric A phase, X-ray diffuse scatt. obs., subattice phase transition 0-64944
 β -Al $_2$ O $_3$ -Ag $_2$ O(D $_2$ O)(NH $_4^+$) 0-107512
 β' -Al $_2$ O $_3$ -Ag $_2$ O(H $_2$ O)(K $_2$ O)(Li $_2$ O)(NH $_4^+$)(Na $_2$ O), ionic cond. at room temp. 0-107513
 β -Al $_2$ O $_3$ -Ag $_2$ O(K $_2$ O)(Li $_2$ O)(Na $_2$ O), low-energy excitation spectra, localised modes 0-59606
 β'' -Al $_2$ O $_3$ -Ag $_2$ O(K $_2$ O)(Li $_2$ O)(Na $_2$ O)(Rb $_2$ O), single cryst. Raman scatt., cond. mechanism and cryst. struct. 0-66209
Al $_2$ O $_3$ -Al, sintered, plastic props. (Russian) 0-58923
 β -Al $_2$ O $_3$ -D $_2$ O, anhydrous, prep. and struct. of DAl_2O_3 0-107187
Al $_2$ O $_3$ -H $_2$ O $^{+}$, β and β'' phases, protonic, conductance and spectroscopy 0-70450
 β'' -Al $_2$ O $_3$ -H $_2$ O $^{+}$ (Na $_2$ O), struct. basis for superionic cond. 0-107498
 β -Al $_2$ O $_3$ -K $_2$ O-MgO, cryst. struct., nonstoichiometry, ion-ion correlations 0-88129
 β -Al $_2$ O $_3$ -Li $_2$ O-Na $_2$ O, spin-lattice relaxation and Li motion 0-70451
Al $_2$ O $_3$ -Mo cermet, ZrO $_2$ and mullite whisker reinforced, strength var. with temp. 0-104232
 β -Al $_2$ O $_3$ -NH $_4^+$, PMR relax. time obs. of ionic motion 0-71213
 β -Al $_2$ O $_3$ -NH $_4^+$, single cryst. characts. and AC cond. obs. 0-107514
 β -Al $_2$ O $_3$ -NH $_4^+$, single cryst. PMR and proton motion 0-108101
 β -Al $_2$ O $_3$ -NH $_4^+$, proton dynamics neutron scatt. study 0-59408
 β'' -Al $_2$ O $_3$ -NH $_4^+$ -H $_2$ O $^{+}$, single cryst. PMR and proton motion 0-108101
 β' -Al $_2$ O $_3$ -Na $_2$ O, ^{23}Na NMR obs. of ionic diffusion, 180 to 800K, attempt freq. 0-108097
 β -Al $_2$ O $_3$ -Na $_2$ O, ^{23}Na NQR and two-dimens. diffusion, model analysis 0-108111
 β -Al $_2$ O $_3$ -Na $_2$ O, ^{27}Al NMR obs., Na motion and cond. characts. 0-108096
 β -Al $_2$ O $_3$ -Na $_2$ O, AC impedance, microstruct. and strength 0-100349
 β -Al $_2$ O $_3$ -Na $_2$ O, AC ionic cond., dielec. and NMR relax. 0-59713
 β' -Al $_2$ O $_3$ -Na $_2$ O, absorbed water effect on NMR lineshape and spin-lattice relax. time 0-108098
 β -Al $_2$ O $_3$ -Na $_2$ O, adsorbed of Na, surface electronic struct. calcs. 0-75431
 β -Al $_2$ O $_3$ -Na $_2$ O, anomalous Na behaviour obs. using pulsed and CW NMR 0-108095
 β -Al $_2$ O $_3$ -Na $_2$ O, colour centre ESR by localised tunnelling states 0-108073
 β -Al $_2$ O $_3$ -Na $_2$ O, cond. plane struct. and energetics 0-92715
 β -Al $_2$ O $_3$ -Na $_2$ O, development for Na/S battery 0-71615
 β -Al $_2$ O $_3$ -Na $_2$ O, ENDOR meas. of defects 0-66074
 β -Al $_2$ O $_3$ -Na $_2$ O, ionic cond. temp. depend., comparison with NASICON 0-107520
 β -Al $_2$ O $_3$ -Na $_2$ O, low-temp. ^{23}Na satellite spectra, Na ion motion 0-108112
 β -Al $_2$ O $_3$ -Na $_2$ O, motion of charge carrying ions, mol. dynamics simulation 0-107506

alumina continued

- β^* - Al_2O_3 - Na_2O , NMR of ^{23}Na , elec. quad. interaction, 185 to 419K, ion motion obs. 0-108110
- β^* - Al_2O_3 - Na_2O , nonstoichiometric, correl. effects in diffusion, Haven ratio, point defect interactions 0-107505
- β - Al_2O_3 - Na_2O , potential energy distrib. and ionic motion 0-70455
- β - Al_2O_3 - Na_2O , protonic, conductance and spectroscopy 0-70450
- β - Al_2O_3 - Na_2O , single cryst., non-Debye capacitance 0-107497
- β^* - Al_2O_3 - Na_2O , solid electrolyte, behaviour at high current density, sodium heat engine mode 0-61330
- β - Al_2O_3 - Na_2O , X-ray induced defects, EPR and ENDOR study 0-60456
- β - Al_2O_3 - Na_2O doped with transition metal ions, complex plane anal. of impedance and admittance 0-70452
- β^* - Al_2O_3 - Na_2O solid electrolyte, tube fabrication from cast ceramic tape 0-60819
- β^* - Al_2O_3 - Na_2O solid electrolyte, processing and phys. props. 0-60820
- β^* - Al_2O_3 - Na_2O solid electrolyte, strength degradation under electrolytic conditions 0-61329
- β^* - Al_2O_3 - Na_2O solid electrolyte, heat treatment effects on ionic cond. and microstruct. 0-65293
- Al_2O_3 -NiCr composite, plasma sputtering of electroheating coatings, elec. props. (Russian) 0-108350
- Al_2O_3 -NiO reaction at substrate-film interface, Rutherford backscatt. obs. 0-59733
- β - Al_2O_3 - OH_2^+ proton dynamics neutron scatt. study 0-59408
- Al_2O_3 - P_2O_5 - Cr^{3+} glass, absorpt. spectra, Fano antireson. and vibronic Lamb shift 0-71458
- Al_2O_3 -Pt metal-ceramic reaction, micro/macro obs. 0-66467
- Al_2O_3 - SiO_2 (3 wt.%), J-integral meas. at high temps. (German) 0-93624
- Al_2O_3 - SiO_2 refractory, creep, viscosity, resist. to inelastic deform. 0-89309
- Al_2O_3 - SiO_2 refractory concrete, elastic props. 0-89280
- Al_2O_3 - SiO_2 system, evidence for metastable miscibility gap 0-71632
- Al_2O_3 - SiO_2 - ZrO_2 refractories, corrosion behaviour in glassmelting furnaces (Polish) 0-71783
- Al_2O_3 -TiC, composite, fracture behaviour in three-point bending 0-60951
- Al_2O_3 -TiO₂ powder, plasma-prepared, morphology and phase constitution 0-100833
- Al_2O_3 - Y_2O_3 , melting behaviour and metastability determ. by optical DTA 0-92648
- Al_2O_3 - Y_2O_3 , sintering kinetics, influence of minor additions of Y_2O_3 0-84868
- Al_2O_3 (H_2O)_n, uniform colloidal dispersion, prep. by chem. reactions in aerosols 0-97735
- 3.5 Al_2O_3 -2 SiO_2 , mullite, decomposition by SiO_2 volatilisation 0-61082
- 3 Al_2O_3 -2 SiO_2 - ZrO_2 composites, sintered, in situ-reacted, fracture props. 0-81158
- BaO - TiO_2 - Al_2O_3 system, subsolidus equilibria, X-ray powder diffr. 0-108413
- CaF_2 - AlF_3 - Na_3AlF_6 -(Al_2O_3), phase equilibria, X-ray diffr. and DTA meas. 0-108409
- CaF_2 - CaO - Al_2O_3 , phase diagram contribution (German) 0-100830
- CaO - Al_2O_3 - SiO_2 0-89187
- CaO - MgO - Cr_2O_3 - Al_2O_3 - ZrO_2 - SiO_2 system, subsolidus region characts. 0-97466
- CaO - Al_2O_3 , thermodynamic stability, reaction with Ti, Cr and Zr oxides 0-92687
- CoO - Al_2O_3 - P_2O_5 glass, γ -irrad., EPR study 0-84639
- CoO - Al_2O_3 , isoelectric point meas. 0-88609
- CoO - Al_2O_3 , prep. from film forming soln. 0-60811
- Cr - Al_2O_3 powder targets for plasma-ion spray deposition of resistance films 0-84897
- Cr_2O_3 - Al_2O_3 solid soln., Vickers micro-hardness 0-66629
- Cs-SiO_2 - Al_2O_3 system interactions, getter development for radiocaesium 0-83208
- $\text{Cu-Al}_2\text{O}_3$ alloy, internally oxidised, plastically deformed, influence of particle form on primary loop nature (French) 0-103344
- $\text{Fe-Al}_2\text{O}_3$ granular films, superparamagnetism and relax. effects 0-71118
- Fe_2O_3 - Al_2O_3 mixed oxide, X-ray diffr. and elec. cond. 0-79954
- films, DC reactively sputtered, struct. 0-96764
- $\text{HA}(\text{Al})_{0.7}$, H β -alumina, IR absorpt. study 0-100655
- HF adsorption, by smelter-grade aluminas, during Al smelting 0-80075
- K- β - Al_2O_3 , far IR absorpt., Bevers-Ross sites, interstitials 0-66240
- K₂O-MgO-Al₂O₃, ionic cond. 0-107480
- Li_2O - Al_2O_3 - Cr_2O_3 system, subsolidus equilibria 0-60843
- Li_2O -MgO-Al₂O₃ system, subsolidus phase equilibria 0-81036
- MgO-Al₂O₃ spinel, plastic deformation at T<1000°C, slip systems 0-108505
- MgO-Al₂O₃-P₂O₅ system glass, heat treatment of aluminium metaphosphate influence on thermolum. 0-108285
- MgO.1.1 Al_2O_3 spinel, high temp. deform., cryst. orientation effect 0-107263
- MnO₂ porous powders, Al_2O_3 and SiO_2 coated, changes in surface free energy for N adsorption 0-84363
- MnO-Al₂O₃-SiO₂ spin glass materials, mag. field dependence of susceptibility peak 0-103840
- Na_2 - β - Al_2O_3 , far IR absorpt., Bevers-Ross sites, interstitials 0-66241
- Na_2O -Li₂O-Al₂O₃, local electrode current density and flow decoration 0-100935
- Na_2O -Li₂O- β - Al_2O_3 -H₂O, water mol. vibr., IR and Raman spectra 0-89006
- Na_2O -MgO-Al₂O₃, β^* -alumina, high-resolution electron microscopy 0-75208
- Na_2O -MgO-Al₂O₃, ionic cond. 0-107480
- Na_2O .11 Al_2O_3 , Cr, impurity ion struct., ESR study 0-80605
- Ni/Al₂O₃ catalysts, coprecipitated methanation type, metal-support interaction, XPS obs. 0-80936
- Ni-Co-Cr/Al₂O₃ catalyst, IR spectra of adsorption and interaction with pyridine 0-71946
- Ni-Cr-Al₂O₃ powder targets for plasma-ion spray deposition of resistance films 0-84897
- β -NiAl, oxidation, α - Al_2O_3 growth and microstruct. 0-108627
- Pd/Al₂O₃, adsorption of CO, IR study 0-108193
- Pt/Al₂O₃, electron accepting sites by pyridine absorpt. 0-71947
- Si_3N_4 - Y_2O_3 - Al_2O_3 (4-17, 4 wt.%), sintering 0-81009
- SiO_2 -Al₂O₃ porous catalysts, EPMA quantitative anal., new correction calc. method, modified ZAF method (Japanese) 0-93822
- SiO_2 -Al₂O₃-CaO-MgO-B₂O₃, E-glass, acid resist. studies 0-60991
- SnO_2 -Cu₂-ZnS-Mn₂Cu-Al₂O₃-Al₂O₃ light-emitting struct., cond. and electrolum., heat treatment 0-97345
- (Zn_{0.2}Co_{0.8}(Ni_{0.8}))O-Al₂O₃, ZnO evaporation in vac. 0-59640

alumina continued

- ZnO-Al₂O₃, isoelectric point meas. 0-88609
- ZrN-Al₂O₃ composites, strength rel. to solid-, liquid-phase sintering 0-100823
- ZrSiO₄-Al₂O₃ suspensions for slip casting, prep. and props. 0-104103

aluminium

- see also nuclei with
- (100), oxidised surface structure anal., extended appearance potential fine struct. study. 0-75411
- (111) surface, Pb, Sn monolayer, double layer growth, struct. 0-70567
- abundance in cool halo stars implications for galaxy abundance 0-105232
- adhesive bonds with polymers, shear resist., polymer crystn. effect 0-89462
- adsorbed Ar, differential refl. spectroscopy, local field effect 0-80811
- adsorbed Na, adatom valence-level position variation 0-88611
- adsorption and decomp. NH₃ and hydrazine XPS obs. 0-92783
- adsorption on cleaved Si (111) surfaces, effect on electronic structure 0-75610
- anode spot of vacuum arc 0-107006
- anodic films, acoustic and electron-emission during deform. 0-80143
- anodic films, flaw obs. 0-93696
- anodic oxidation, in H₂SO₄, pH-values effect (German) 0-76419
- anodisation, high voltage barrier, Cl⁻ ion effects 0-104327
- anodised oxide films, for adhesive bonding appls., AES and SEM study 0-66689
- anodising, behaviour of emulsion particles during electrodeposition 0-104357
- anodising, porous films formed in chromic acid 0-100966
- anomalous intensity ratios in H like L_α doublet in optically thick laser prod. plasmas 0-103186
- atmosphere, Al particles from space rocket launching 0-81503
- atom, autoionisation reson. determ. from photoelectron polarisation meas. 0-58221
- atom, incoherent scatt. factors calc. by direct integration over impulse approx. Compton profiles 0-102475
- atom, K-shell ionisation by ultrarelativistic electrons, density effect 0-99576
- Auger, RHEED and TEM combined obs., specimen transfer device 0-70093
- Auger spectra, KLL and KLV, screening effects and plasmon gains 0-80913
- Auger spectra induced by 100 keV Ar⁺ impact 0-84820
- bicrystal, high resolution electron microscopy obs. of dislocations 0-103347
- bicrystal, plastically deformed, slip heterogeneities 0-79858
- bicrystals, isoxial, fatigue crack initiation in grain boundary affected regions (Japanese) 0-89338
- Bordoni relaxation, microdeform. 0-104204
- boundary lubrication, inelastic electron tunnelling spectroscopic study 0-70302
- Brillouin spectra, light scatt. cross section for surface ripples 0-71434
- charge-exchange effects in energy-loss straggling for low mass particles, A<16 0-65104
- chemisorption on GaAs (110), ab initio theory 0-75612
- classical plasma frequency in long-wavelength limit, quantum correction 0-107728
- coated Ni-Cr-(Co) alloys, microstruct. and chem. 0-76189
- coating prod. by thermal decomp. of Al alkyls 0-104076
- coating reflectivity in vacuum UV, heating effect 0-95981
- coatings on polyethylene terephthalate, thickness determ. using photometry 0-62626
- cold rolling, inhomogeneous texture 0-89251
- cold rolling of 1100 plates, substruct. development 0-108476
- cold worked, internal friction peaks 0-97520
- commercial purity, density changes, void growth in biaxial stress fields, plastic deformation 0-71692
- composite, SiC fibre reinforced, plasma-formed semifinished products, props. 0-84890
- constitutive equation for porous materials with strength, press. effects 0-79875
- corrosion, general and pitting, Mo and Ar ion implantation effects 0-71794
- corrosion by carbon tetrachloride, IETS obs. 0-81230
- corrosion inhibition of liq. Li cooling system of fusion reactor by Al addition 0-108646
- creep, stationary, in HVEM, cell struct. evolution 0-104242
- creep, threshold stress importance in anal. of data 0-64389
- creep behaviour, at high temp., influence of oxidation 0-97538
- creep under step stress changes, viscous viscoelastic model for type 2618 0-81138
- crystal potential, low-order Fourier coeff., modified thickness fringe method 0-75130
- cyclic loading, change in mech. props. rel. to heat treatment 0-104282
- Debye temp., X-ray diffr. determ., anharmonic parameters of pot. function 0-100320
- deformation parameters, ultrasonically induced resonance, new technique 0-97676
- deformation temperature effect, on stage IV deform. in (100) single crystals. (Japanese) 0-66587
- deformed in uniaxial and equibiaxial tension, dislocation arrangements 0-108516
- determination by activation anal. (α ,n), (α ,p) reacts. investig. 0-61206
- determination with Si in atmospheric aerosols by neutron activation anal. 0-72116
- diffraction grating, concave, Al-coated, polarisation anomalies 0-69519
- diffusion thermopower, inelastic electron-phonon interaction 0-96851
- dislocation loops, interstitial, size distrib. for metal irradiated in high voltage electron microscope (Russian) 0-103335
- dispersed in epoxy resin RDGE MPDA hardened, holographic correlometer study 0-74321
- electroplastic stress curve propag. (Czech) 0-108507
- electrochemical nucleation and growth, of Cu, TEM 0-104451
- electrode, electrical breakdown of water in μ s region 0-103917
- electrode, in high repetition rate spark switches, surface ageing 0-106997
- electrodes, charge effects on insulating films obs., PET and SiO₂ 0-75625
- electromagnetic wave propagation, demonstration 0-73149
- electron backscattering by bulk target, theoretical model (French) 0-60722

aluminium continued

- electron irradiated, selfinterstitial atomic defect interaction radii, recovery expts. and error sources 0-65049
electron microprobe local anal. of light elements, ultrasoft X-ray spectroscopy 0-99027
electroslag welding, using plate electrodes for Al busbar component parts welding 0-81083
energy and elastic constants 0-59435
energy losses and straggling for H^+ and He^+ beams (*Russian*) 0-84226
erosion by solid particle impingement at normal incidence, SEM obs. 0-104304
etching wastes, appl. to corundum ceramics prod. 0-108376
ethylene- O_2 - N_2 -Al particle mixture, two-phase detonation and combustion (*French*) 0-61097
fatigue, high temp., cyclic grain boundary migration phenomena 0-85053
fatigue crack initiation, pre-existing subgrain effect 0-97565
fatigue crack propagation, quantifying the parameters 0-100891
fatigue life, influence of cyclic loading conditions 0-76350
FCC crystals, compressively activated slip, theoretical latent hardening 0-65128
film, deform. under He ion bombardment 0-65073
film, dislocation observation by electron microscope using convergent beam (*French*) 0-96532
film, electron transmission, calc. 0-60724
film, energy losses of electrons, microcalorimetric meas. 0-59543
film, etching in carbon tetrachloride plasmas 0-76407
film, granular, transition to localisation, elec. resist. 0-70877
film, intrinsic stress meas. 0-71696
film, lattice and bulk heat capacity meas. for normal and supercond. states 0-92684
film, on amorphous C and Si substrates, dispersion force contrib. to adhesion (*French*) 0-59842
film, on CdS, bonding and interdiffusion, XPS obs. 0-80000
film, polycrystalline, trapping of 3He and 4He ions at room temp. 0-84221
film, superconducting transition temp. and lattice dynamics 0-93028
film, wave front reversal, holography applications (*Russian*) 0-58483
film and polished bulk specimens, initial stages of oxidation obs. using SIMS 0-81239
film in microwave radiation field, resistive state transition (*Russian*) 0-93038
film on Si(111) substrate, struct., props. depend. on vapour flow, ionisation (*Russian*) 0-75453
film on Si substrate, eutectic point displacement on annealing (*Russian*) 0-100850
films, resistance changes due to bombardment by N, C, or Ar ions 0-103670
foil, α -particle irradiation under fusion reactor conditions, He bubble alignment during deform. 0-107345
foil, deformation, laser optical scanning obs. 0-100995
foil, electrical conduction, electron mean free path, surface scatt. 0-88535
foil, influence of O_2 -pressure on oxidation rate, TEM study 0-104355
foil, internal friction changes during low temp. plastic deform. (*Russian*) 0-100304
foil, laser irradiation, fracture props. (*Russian*) 0-108523
foil, secondary electron emission due to α -particle irradiation. (*Russian*) 0-66344
foil, solar wind ion bombardment, lunar surface modification 0-109325
foil electrolytic perforation, surface film phase composition obs. (*Russian*) 0-61004
foil fuse, electrically exploded, surrounding medium effect 0-103207
foil-excited ion, X-ray spectra and satellite classification 0-95567
foils, high strength, vapour deposited on curved surfaces, quantitative characterisation 0-80144
fracture mechanism 0-100903
fracture speed during phase explosion due to electron beam irradiation. (*Russian*) 0-76336
grain boundaries movement, 3-fold nodes, in high temp. creep. 0-89317
grain boundary internal friction after recrystn. annealing (*Russian*) 0-66561
grain boundary migration, TEM obs. on mechanism 0-79812
granular bridges, with different thicknesses and widths, crit. current, temp. depend. 0-88688
granular films, inhomogeneous supercond. transitions, microwave meas. 0-103789
granular films, self-ion implantation supercond. transition temp. enhancement 0-103774
granular films, vortex noise at supercond. transition 0-84530
granular supercond., normal state cond. 0-88529
granular superconducting bolometer as mol. beam detector 0-73524
heat of soln. of H, spherical model 0-96656
hot extrusion, nonsteady state temp. distrib., numerical method 0-60886
implantation into Cu for corrosion protection 0-71789
implantation on Cr-Ni Nb stabilized austenitic stainless steel surface, effect on oxidation behaviour 0-71791
implanted Xe behaviour during anodic oxidation 0-71800
implementation of Fe-Cr-Al FeCrAlloy stainless steel surface, effect on oxidation behaviour 0-71790
inhomogeneous granular, superconductivity 0-103795
initial interaction of O with single cryst. faces, LEED, AES and work function study 0-84392
interstitial loop form., effects of repeated electron irradiation. 0-75220
ion beam milling, amorphous sputter yield behaviour 0-108624
ion implanted, electron beam annealing, ion backscatt. and TEM meas. 0-59500
ion irradiated with Al ions, void swelling and annealing of voids, electron microscopy study 0-88216
ion-induced electron emission, ion charge depend. 0-108315
K X-ray absorption, K-emission spectrum, band struct. using APW method 0-97380
Kovar-silicon oxynitride-aluminium cathode, local electron emission and electroluminesc. patterns obs. 0-108327
L-shell ionisation by 80 keV electrons, transmission electron energy loss spectrometry 0-60721
laser fusion target simulation, press. ionisation 0-63374
laser plasma, high-Z, temp. meas. from bremsstrahlung emission 0-87914
laser pulse irradiation of Al targets, absorpt. studies 0-79455
laser radiation absorption in craters on metal targets 0-97386
laser strengthening, struct., hardness and dislocation density (*Russian*) 0-76399

aluminium continued

- laser target, multiple-pulse thermal coupling at 3.8 μm wavelength 0-96371
Lifshitz constant for calc. of van der Waals force between two solids (*French*) 0-107658
liquid, dynamical struct. factor calc. 0-64880
liquid, spreading behaviour on Fe-Si 0-84345
liquid, structural details, molecular dynamics calcs. (*Russian*) 0-64879
liquid, thermoelectric power, pseudopotential calc. 0-59959
liquid and polycryst., density fluctuations, neutron scatt. anal. 0-70349
liquid impact erosion and cavitation erosion comparison 0-104302
magnetic susceptibility, model pot. theory 0-75710
magnetoresistance, longitudinal, meas. on single crystals 0-75550
magnetoresistance, path integral method calc. 0-65537
magnetoresistance, temp. depend., impurity effects 0-70682
magnetoresistance and Matthiessen's rule departure, temp. depend., linear lattice defects role (*Russian*) 0-84456
magnetron sputtering in Ar and Ar/ O_2 mixtures, discharge characts. 0-89145
melt-NaF filter material interaction mechanism (*Russian*) 0-108743
melting curve and Gruneisen coeff. at high press. 0-65200
melting theory for small particles, Helmholtz free energy 0-59629
membrane, lifetime prediction and design 0-71752
metallic, phonon freq., binding energy, compressibility, elastic const. and energy band gap calcs., linear pot. 0-88284
metalised amorphous GeSe junctions, electrical contact effects on properties (*German*) 0-93010
metalised coating on polyethylene terephthalate film, fracture under laser irradiation. (*Russian*) 0-76333
MHD laminar flow, longitudinal dynamic effects determination for Al (*Rumanian*) 0-64792
microcrack propagation and plastic strain 0-81187
molten, dissoln. kinetics and diffusion coeffs. of Fe, Co and Ni 0-59666
molten, showering cryst. form. in mould cooled from top (*Japanese*) 0-66498
molten, thermal expansion meas. to 1300K 0-65254
muon diffusion, LAMPF results 0-71285
narrow superconducting bridges, microwave radiation stimulated T_c enhancement 0-84537
neutron damage, positron annihilation 0-65056
nonlinear conductivity of thin films in mixed state (*Russian*) 0-80464
nonlinear sound wave interactions, sound attenuation in weak superconducting state (*Russian*) 0-75310
notched bars, deform. behaviour and strength having biaxial state of stress at notch root (*Japanese*) 0-81116
nuclear spin lattice relaxation measurements in small superconducting particles. 0-88681
nucleosynthesis, isotopic yields from C and Ne zones in explosion of massive star 0-90406
overlay film on quartz for SAW device temp. compensation 0-79043
overlayers on GaAs (110), interfacial electron states, UPS and LEED obs. 0-80377
oxidation of (111) surface, initial stages, LEED anal. 0-80082
oxidised surface, light emission from sputtered O atoms or ions 0-58199
pack aluminisation of Ni based Rene 80 superalloy 0-76188
photoacoustic effect from thermally thin solid 0-75304
photoemission cross-sections for 2s and 2p levels 0-93453
photon penetration, photon backscatt. incidence angle depend. 0-104008
pipe diffusion along segment of faulted dislocation loops during annealing 0-107256
plane coalescence, at grain boundaries 0-70221
plasma, hot, dense, line emission obs. 0-79456
plasma, laser produced, reflectance meas. 0-79568
plasma, laser-produced, high-Z, X-ray diagnostics 0-75074
plasma, photon reabsorption attenuated radiation emission 0-64776
plasma, transfer eqn. soln. using freq. and angle averaged photon escape probabilities 0-64688
plasma etching, undercutting phenomena 0-97635
plasma formation, CO_2 laser pulse interaction with Al target in air 0-96374
plastic deformation, initial stages (*Japanese*) 0-93618
plastic deformation thermal activation parameters from creep kinetics and stress relaxation 0-71717
polycrystalline, implanted with Cu(Pb), doping profile after laser pulse irradiation 0-88194
positron annihilation and vacancy formation, Doppler broadening study 0-60708
positron penetration depth and energy loss 0-92578
powders, electric-pressure sintering onto cylindrical parts in fluidised bed 0-100960
pressure shear impact in transverse displacement interferometer, plastic flow in 6061-T6 Al 0-81137
projected range distrib. of 5-25 keV $^4He^+$ 0-65094
proton irradiation, Al atomic displacement position study 0-103401
reaction kinetics of liquid with B_2C 0-84344
reaction with H_2 , influence of surface reactions on rate (*Russian*) 0-66683
recycling, effect on comp. 0-66455
resistivity and thermoelec. ratio, electron-electron scatt. contrib. 0-70670
review (*Spanish*) 0-84544
rhodamine 6G laser radiation interaction with Al 0-97387
seawater Al content controlled by inorganic processes 0-61815
self-consistent spin density functional calcs. for 3d impurities 0-70635
SEM exam., ultra-high vacuum secondary electron emission dependence on electron beam density dose, surface interactions from AES and ELS 0-61209
shell, explosive expansion, rupture behaviour 0-85063
shield, thick-walled, conducting, for biomag. expts. 0-104845
shielded room for biomag. meas. 0-104846
shock compression at high press., neutron irradiation. (*Russian*) 0-88264
shock compression at high press. (*Russian*) 0-92608
shock wave data, 'solid Hugoniot' rel. to 'fluid Hugoniot' 0-65155
short range order amongst cond. electrons 0-107040
 n^+ -Si-Al ohmic contacts, metallisation structs. for very shallow n^+ /p junctions 0-60084
single cryst., latent hardening in tension 0-60878
single crystals, relation between axial orientation rotating and deform. banding 0-104206
sliding behaviour, against polymers laminates and coated surfaces at cryogenic temps. 0-66671
slip, work of C. Crussard 0-62443

aluminium continued

- small spheres, bulk plasmons damping 0-75561
 soft X-ray emission edge, temp. depend. 0-89090
 solid electrolytic capacitors, pit etching method for improving freq. and temp. characts. 0-100944
 solidification, high press. effects 0-66499
 spark gaps with Al parallel plane electrodes, erosion characts. 0-70076
 specular reflectance standards for visible and infrared region using thin Al film vacuum deposited on optical flats (*Japanese*) 0-102789
 spraying Si semiconductor plates, for control of quality of surface treatment 0-60989
 sputter deposit PIXE expt. 0-61196
 sputtering, planar magnetron, H_2 effect on Ar discharge 0-80970
 sputtering, under D^+ and He^+ bombardment, microstruct. effects study 0-84821
 stability and strength of FCC metal using Morse pot. 0-59430
 steel fibre reinforced Al, thermophys. props. 0-59745
 strain rate sensitivity and ductility, trace element conc. effect 0-66597
 stress-strain curves, cyclic loading initial stage, commercial purity (*Japanese*) 0-93617
 stress/strain constitutive equation, constitutive eqn. covering wide range of strain rates (*Japanese*) 0-79862
 substrate for Zn film deposition, TEM and electron diffr. obs. 0-75460
 subsurface flaw detection by photoacoustic microscopy 0-66725
 superconducting cylinder, order parameter enhancement by microwave irradi. 0-70896
 superconducting film, order-parameter variation meas. 0-103797
 superconducting film, transition to zero vorticity, long-range topological order 0-93039
 superconducting granular films as weak link in Josephson devices 0-88685
 superconducting thin film, crit. temp. enhancement (*Russian*) 0-93021
 superpure, creep, rate-controlling processes 0-85009
 surface, 4He backscatt., Rutherford scatt. cross section correction test 0-66369
 surface, α -cyanoacrylate in first monolayer, IR spectra, H-bond form., stretching vibr. 0-87119
 surface, (001), enhanced photoexcitation 0-80937
 surface, (111), adsorbed O, surface struct., LEED and SEXAFS data 0-92782
 surface, He atom scattering pot., surface electron density depend. 0-104027
 surface, luminesc. accompanied by ion implantation 0-60683
 surface, multiply charged ion interactions, laser plasma 0-70007
 surface, negative affinity, narrow beam emission of slow positrons 0-89091
 surface, obs. of positron Bragg refl. 0-103221
 surface, plasma cleaning and etching, removal of C 0-97645
 surface, positronium emission 0-80897
 surface, rough, reflection loss for s and p polarised waves near surface plasmon freq. (*French*) 0-97225
 surface, thermal desorption of oxide film, influence of grain boundaries and recrystn. 0-61023
 surface (111), angle-resolved UPS obs. of 2-dimens. band structs. of S, Se and Te 0-60059
 surface (111), bonding of O, electronic struct. calcs., rel. to UPS data 0-59801
 surface (111), oxide layer amorphous to cryst. surface transition, slow positron obs. 0-75417
 surface bombardment by fast H^+ 0-66376
 surface chemical characterisation, by SIMS glow discharge spectrometry and other techniques 0-66907
 surface damage, meas. and detect. after static contact loading 0-64495
 surface deformation and wear track obs. using analytical electron microscope 0-108687
 surface films, Cr^{6+}/Cr^{3+} colloidal SiO_2 , TEM/XPS studies 0-85090
 target interaction with pulsed CO_2 laser beam, pulse shape importance 0-108307
 thermal strain meas. in Al plate, one-beam laser speckle interferometry method 0-103005
 thick probes, subthermal neutron transmission curves for grain size and texture eval. (*German*) 0-71667
 thin conducting film, electromigration under superimposed DC and noise powers 0-107879
 thin film, elec. resist., effect of annealing In electrodes 0-80416
 thin film, micrometeoroid penetration expts. performed in laboratory 0-77292
 thin film, thermal cond. meas., size effect 0-65715
 thin film deposited on Si, work function (*French*) 0-80353
 thin film deposition using solar furnace 0-89148
 thin film stripes, electromigration lifetimes width depend. 0-92799
 thin films, H incorporation effects on stress and electromigration 0-80139
 thin films evaporated on rough quartz substrates, surface irregularities, light scattering measurements (*Polish*) 0-88450
 tilt boundary, $\Sigma=5$, struct. and atomic vibr., computer simulation 0-70223
 tubes, type HT30, crushed between rigid plates, large deformation compression 0-66579
 tunnel junctions, superconductivity enhancement by microwaves 0-107956
 ultimate tensile strength for brief impact 0-70309
 ultrafine particles, optical props., 0.3-2.5 μm 0-76020
 US torsional vibrations in metals, measurement of absorpt. 0-58856
 US velocity, meas. method for isotropic nondispersive solids 0-69616
 US velocity, temp. depend., stress effects 0-75307
 vacuum arc, excited state density from line intensities 0-96404
 vacuum arc, excited state density theory 0-100107
 valence band Auger spectra, surface effect 0-80915
 VLSI metallisation, Al and Al alloy metallisation sputter deposition 0-66429
 wear under reversed friction, temp. effect 0-108588
 wire drawing plastic deform. in Al and dil. alloys 0-108508
 wire fibre reinforced Al, stress-deformed state, elastic, strength props. (*Russian*) 0-76303
 workhardened thin specimens, fracture, anisotropy coeff. role (*French*) 0-104276
 X-ray Huang diffuse scatt. from dislocation loops on {111} planes 0-79797
 Z dependence of thick target β -ray backscattering 0-76118
 Ag:Al $_2$ O $_3$:Al tunnel-junction struct., surface polariton mean free path, roughness 0-93008

aluminium continued

- Al I, laser stimulation optimisation for intracavity spectroscopy 0-77881
 Al II near IR laser transitions, large diameter hollow cathode Ne-Al discharge 0-102715
 Al, molten, impurity diffusion of fourth period solutes and homovalent solutes (*Japanese*) 0-70436
 Al, oxide films, metal and O $_2$ transport, AES and inert marker, techniques 0-97641
 Al, polycrystn., HVEM in-situ investigation of creep mechanism 0-104214
 Al XIII, $1s2p^3P_2$ and $1s2p^3P_0$ levels, radiative lifetimes and hyperfine induced decay 0-74149
 Al $^{3+}$, static dipole quadrupole polarisabilities and shielding factors calc. using HF scheme 0-99450
 Al:Ca (Ga), ion implantation, defect structures obs. 0-59494
 Al:Ga, pulsed electron-beam annealing, lattice site location improvement 0-107303
 Al:O, $^{18}O^+$ ion implantation in channelling directions, expt. conditions and range profile obs. 0-65022
 Al:O single crystal, $^{18}O^+$ ions implantation in channelling directions, stopping power meas. from max. range 0-65078
 Al:O supercond. film, RF complex impedance meas., dynamic pinning 0-84573
 Al/Al $_2$ O $_3$ /Al, dielec. props. 0-80404
 Al/Al $_2$ O $_3$ /Al structures with organic monomolecular layer, cond. at high elec. fields 0-80402
 Al/AlCl $_3$ -NaCl/FeS $_2$ secondary cell, preliminary study 0-108793
 Al/AlO $_x$ /La-rare earth metal tunnel junctions, cond. meas., cryst. field effects 0-88694
 Al/As $_2$ Se $_3$ /Sb structures, rectifying effects 0-75654
 Al/Cu thin film couples, TEM study of intermetallic nucleation at interface 0-65305
 Al/GaAs contacts, metallization of surfaces covered with adsorbed S (*French*) 0-107909
 Al/Pd thin film couples, thermal reactions 0-59830
 Al/SiO $_2$ /pSi MIS solar cells, stability 0-85287
 Al-Al $_2$ O $_3$, dispersion hardened, creep (*Czech*) 0-108463
 Al-Al $_2$ O $_3$, sintered, plastic props. (*Russian*) 0-58923
 Al-Al $_2$ O $_3$ -Au device in Cl $_2$ atmosphere, current-voltage characts., press. depend. 0-65704
 Al-Al $_2$ O $_3$ -Dy thin junctions, Poole-Frenkel effect obs. and cause 0-80398
 Al-Al $_2$ O $_3$ -GaAs backwall MIS Schottky barrier solar cell, anal. model 0-85289
 Al-Al $_2$ O $_3$ -Pb contacts, tunnelling spectroscopy, band struct. of Pb 0-80169
 Al-Al $_2$ O $_3$ -SiO $_2$ -Si capacitors, physical and elec. props. of RF plasma grown Al $_2$ O $_3$ 0-100530
 Al-Al $_2$ O $_3$ -p-GaAs MOS diode, capacitance-voltage characts. 0-107914
 Al-AlF $_3$ -Al thin film structures, dielec. and elec. props. (*Slovak*) 0-100536
 Al-AlN-SiO $_2$ -Si capacitors, physical and elec. props. of RF plasma grown AlN 0-100530
 Al-amorphous Ge-n-Si, photoelectric props. 0-70822
 Al-anodised Ta $_2$ O $_3$ /native oxide-n-GaAs MOS structure evaluation 0-84514
 Al-Au couple, electroformed, nonohmic characts. and electron emission 0-60066
 Al-B fibre-D16 alloy welded composites, structure, strength and fracture props. (*Russian*) 0-108524
 Al-brass tubes, passivation treatment for atmospheric corrosion protection during storage and transport 0-85079
 Al-Cr, thin film metal contact, sheet resistance changes 0-80356
 Al-Formvar-Sn coupled films, Ginzburg's excitonic supercond. model 0-97039
 Al-Ge(001) interface, struct., total-reflected X-ray diffr. 0-88441
 Al-In multicomponent binding layers, acoustic light modulator 0-87546
 Al-In $_2$ S $_3$ -Si layered struct., Hall effect, I-V characts., surface states (*Russian*) 0-97001
 Al-insulator-In $_x$ Mg $_x$ film tunnel junction, resistance zero-bias anomalies 0-107925
 Al-Mg (4 wt.%), struct. and strengthening in hot working 0-84968
 Al-Nb, tunnelling expts. on normal metal backed by Al 0-65751
 Al-Nb superimposed metallic layers, ionic movements during anodization, Rutherford backscatt. and nuclear microanal. 0-71913
 Al-PbBi superconducting tunnel junctions, optically illuminated, quasiparticle energy distribution 0-75688
 Al-Permalloy two-layer films, mag. anisotropy, grain boundary diffusion (*Russian*) 0-71122
 Al-poly-Si Schottky-barrier solar cells, grain boundary effects on electrical behaviour 0-85279
 Al-Si MIS solar cells, depth conc. profiles, elec. and optical props. of Al films 0-94076
 Al-Si system, Si regrowth minimisation through overlying Al or Al alloy film 0-70569
 Al-Si $_3$ N $_4$ -Ge, thermally stimulated depolarisation current meas. 0-88643
 Al-Si $_3$ N $_4$ -SiO $_2$ -Si, MNOS structures degradation under UV irradiation effect 0-107923
 Al-Si $_3$ N $_4$ -Al thin film cathode, physical model from expt. study 0-100535
 Al-SiC cermet elasticity, porosity meas. by US means 0-81101
 Al-SiO $_2$ interface in MOS capacitors, conductivity effects of oxidation temperatures 0-100518
 Al-SiO $_2$ -Si, pyroelectricity 0-100524
 Al-SiO $_2$ -Si MOS structures, charge motion, TSC meas. 0-100534
 Al-SiO $_2$ -p-Si solar cells, comparison of majority- and minority-carrier silicon MIS solar cells 0-85280
 Al-SiO $_2$ -Si MOS solar cells, open-cct. voltage var. with oxide layer thickness 0-81434
 Al-SiO $_2$ -(p-Si) barrier structs., minority carrier injection ratio meas., MIS solar cell model 0-93007
 Al-silicon oxynitride-Al cathode, LF noise sources and reduction 0-108328
 Al-stearic acid-Al, low-loss thin film capacitor 0-71317
 Al-steel mixture, wear resistant, produced by compaction by discrete shock waves 0-84882
 Al-Ta $_2$ O $_5$ -Al, healing of defects in dielec. film by anodisation 0-65406
 Al+H $^{+}$, K-shell ionisation 0.5 to 40 MeV, meas. and PWBA-BEA calcs. 0-78699
 Al+He(C)(N)(O), inner-shell multiple ionisation systematics, X-ray obs. 0-63790

aluminium continued

- Al₂⁺(Al₂)⁺ configurations, ab initio study, LCAO, STO, MO-SCF and CI calcs., binding energy (*French*) 0-91447
 AlIX-XII, plasma, X-ray line radiation, radiation transport eqns., calc. method 0-64777
 Al, MoS₂, Chevrel phase, synthesis, stability and characts. 0-71608
 α-Al₂O₃ fibre FP reinforced Al and Mg composites, fabrication and props. 0-81004
²⁶Al from red giant stars 0-67712
²⁶Al nucleosynthesis in novae and supernovae outbursts 0-62143
²⁶Al, synthesis in explosive H burning 0-85929
²⁷Al, in minerals, use as probe nucleus in NQR techniques appl. to geo-sciences 0-67426
 Au/Al thin film, Al diffusion studied by attenuated total reflection method 0-92722
 Au-Al thermocompressional contacts, diffusional zones, phase growth during annealing (*Russian*) 0-75389
 Au-Al/GaAs interfaces, atomic interdiffusion, soft XPS studies 0-65302
 B fibre reinforced Al, impact damage tolerance and reliability 0-81177
 B fibre reinforced Al, thermophys. props. 0-59745
 B fibre reinforced matrix, matrix-fibre interaction depend. on metallic dopants (*Russian*) 0-76479
 C fibre reinforced Al, matrix-fibre interaction depend. on metallic dopants (*Russian*) 0-76479
 CdSb:Al, p-n junction formation by laser emission, photoelectric effects (*Russian*) 0-70815
 CdSb:Al, p-n junction formation by laser radiation 0-96983
 CdSnAs₂-Al, surface barrier junction, elec. props., temp. depend. 0-65686
 Co implantation, replacement collision probability at 4.2K 0-70237
 Cu-Al thin film multistructure, Xe⁺ ion beam cratering 0-66708
 EuIG:Al, mag. anisotropy, magnetisation meas. 0-60240
 Ge:Al, shallow acceptor spectral line intensities 0-88517
 HF adsorption, by smelter-grade aluminas, during Al smelting 0-80075
 Hg_{1-x}Cd_xTe:Al, ion implanted, damage and lattice location study 0-103381
 InP-Al interface struct., low temp. interaction, AES study 0-107661
 MgO:Al, and nominally pure single crystal, thermally stimulated luminesc. rel. to temp., and EPR (*Russian*) 0-84789
 Nb-Al-Ge-Cu, rapidly quenched, comp. and phase equil. 0-76235
 NiO:Al, Ni self-diffusion, vacancy-impurity complex effects 0-107493
 Si:Al, CC Si:Al(Ga), O₂ diffusion, conc. profile meas. 0-79990
 Si:Al, compensated substrates for solar cells, effects of Fe and Al 0-94009
 Si:Al, electron irradi. induced defects, transient capacitance study 0-59516
 Si:Al, localised exciton bound to isoelectronic trap 0-66283
 Si:Al, polycryst. film, grain boundary diffusion, Auger sputter profiling 0-75388
 Si:Al, spreading resist. calibration using Si:B 0-103690
 Si:Al epitaxial layers, nuclear microanalysis of Al impurities ²⁷Al(d,α)²³Mg 0-61193
 p-Si:Al, ohmic contacts, Si dissoln. and recrystn. effects, computer calc. 0-103749
 Si-Al-Al₂O₃ system, solid phase Si regrowth on sapphire 0-100413
 Si-Cr₂O₃-Al, current-voltage characts., oxide film effects 0-70841
 Si-SiO₂-Al, interface barrier energies for tunnel oxides, internal photoemission meas. 0-84512
 Si-SiO₂-Al, internal photoemission, pot. barrier height determ. 0-65699
 Si-SiO₂-Al MOS surface channel influence on channel-to-contact diode charact. 0-92994
 Si-SiO₂-Al with thick dielec. layer, photoelec. props. 0-92979
 Si-TiO₂-Al, current-voltage characts., oxide film effects 0-70841
 Si-V₂O₅-Al, current-voltage characts., oxide film effects 0-70841
 SiC fibre reinforced Al, thermophys. props. 0-59745
 SiC fibre reinforced Al, synthesis by liquid pressing method 0-100816
 SiC:Al,N (6H), ODMR for effective-mass-like acceptor 0-93213
 SiC-coated C fibre, compatibility with Al (*Japanese*) 0-71700
 Si_{1-x}H_x:Al, amorphous, co-sputtered Al modification, electronic and optical props. 0-100461
 SnO₂-Cu₂S-ZnS:Mn,Cu-Al₂O₃-Al, light-emitting struct., cond. and electrom., heat treatment 0-97345
 VO₂:Al, photoacoustic effect study of phase transitions 0-69615
 Zn:Al, ion implantation, temp. and time depend. 0-65013
 Zr/Al, getter for TFTR Flexibility Modification, in-torus surface pumping 0-95451

aluminium alloys

see also *aluminium compounds*

- adhesion with Ni-SiC coating, metal interdiffusion (*Russian*) 0-66697
 AE spectra, laboratory comparisons 0-108658
 Al-Zn-Mg (5.1 wt.%), decomp. process, TEM study 0-71660
 Alnico 5 alloy, S and Ti additions effect rel. to non-metallic inclusions, coercive force and grindability 0-89375
 Alnico 8, permanent magnetic alloy, topography of precipitate phase (*Chinese*) 0-66512
 Alnico type YUNDK25DA alloy permanent magnets, thermal mag. hysteresis 0-75818
 anodised oxide films, for adhesive bonding appls., AES and SEM study 0-66689
 binary, rapid quenching, struct. and decomp. 0-76244
 cavitation-erosion by hydraulic liquids, assessment using ultrasonic disintegrator 0-71832
 corrosion behaviour evaluation, for heat exchanger appls. 0-85092
 crack growth rate prediction under creep conditions 0-85107
 crack initiation at high strain rates, uniaxial and biaxial tests 0-85141
 crack tip opening under cyclic loading, effect of environment and R ratio (*French*) 0-65145
 creep behaviour prediction, physically consistent method for type 2618-T61 0-66610
 creep crack growth 0-60976
 creep of materials with different properties in tension and compression 0-81129
 creep-rupture tests over long-times 0-76434
 cyclic and monotonic crack propag. in high toughness type 7010-T7651 0-108528
 dilute, cold worked, internal friction peaks 0-97520
 dilute, diffusion thermopower, inelastic electron-phonon interaction 0-96851
 dilute, elec. transport and deviations from Matthiessen's rule 0-65524
 dilute alloys, elec. resist., impurity and temp. depend. 0-65526

aluminium alloys continued

- ductile fracture, microvoid effects in type 2024-T4 (*Japanese*) 0-108542
 Duralumin rod, dynamic bending and residual deformation (*Russian*) 0-75293
 electrode, corroding, acoustic emission 0-60997
 failure kinetics, method for investigating under long-term static loading in corrosive medium 0-85110
 fatigue, low cycle, prior treatment effect on type RR58 at 423K 0-104254
 fatigue crack initiation, computer simulation 0-100893
 fatigue crack propagation, stress ratio effect in types L73 and L88 0-71733
 fatigue crack propagation, under variable stresses (*Japanese*) 0-86028
 fatigue resistance improvement by laser shock 0-93654
 fatigue test method, accelerated 0-100981
 FIM and microanalysis, developments 0-100155
 fracture relief formed in fatigue crack growth, rel. to failure mechanism 0-76347
 fracture toughness, split Hopkinson pressure bar application 0-85140
 fusion welding of Al alloys, weld susceptibility to hot cracking 0-81143
 granules, lubricants for rolling 0-60980
 HYCOSOL chemical heat pump, low grade heat enhancement using LaNi_{5-x}Al_x 0-61467
 Indal 3S, corrosion behaviour evaluation, for heat exchanger appls. 0-85092
 membrane, lifetime prediction and design 0-71752
 microcrystalline, rapidly quenched particulates, appl. 0-84887
 noncontinuum crack tip deform. of surface cracks 0-104273
 notched, cyclic stress/strain behaviour, random fatigue life (*German*) 0-100907
 precipitate free zones, X-ray microanal. 0-108768
 rare earth intermetallics, AlAl₃, orbital and spin polarisations of cond. electrons 0-65791
 rare earth-transition metal alloys, RM_{4+x}Al_{8-x}, magnetism and hyperfine interactions, magnetisation and Mossbauer effect studies 0-75892
 rare earth-transition metal-aluminium intermetallics, RT₆Al₆, T=Cr, Mn, Fe, Cu, cryst. struct. 0-107110
 seals with phosphate glass, elec. and mech. props., glass transition 0-81018
 SEM characterization of surfaces anodized in phosphoric acid 0-81241
 steel, Al-Ti-(Mo), Al-Ti-V-(Mo), Al-Ti-Nb-(Mo) and Al-V-(Mo) low-alloy, toughness improvement through Ti additions 0-66525
 steel, aluminium, thermodynamic anal. of phase transforms. 0-76413
 steel, cementite isolation, Mossbauer anal. 0-93225
 steel, Mn-Nb-Al-C, crack prop. and hot ductility during straightening concast strand 0-66646
 steel, Nb₂(V), (Al), hot-rolling, laboratory simulation, recrystn. of austenite 0-97512
 steel, stainless, Fecralloy, creep-rupture props., 650-800°C 0-97535
 stress corrosion cracking, active phase formation 0-85077
 stress corrosion cracking, role of H₂, state of art review 0-61017
 structural alloys for superconducting magnets in fusion energy systems, props. at 4K 0-86976
 Temp-1 system for the ultrasonic inspection of bulky aluminium alloy plates 0-66755
 thermomechanical treatments, effects on microstruct. 0-100858
 US flaw detection of ingots, struct. effect 0-66722
 wire drawing plastic deform. in Al and dil. alloys 0-108508
 Ag-Al (26 at.%), massive transform, β-ζ, crystallography and morphology 0-97475
 Al alloy sheets, type 7075-T6 used in aircraft, early detection of fatigue cracks 0-66730
 Al alloy-mica particle composite, cast prep. and mech. props., bearing appl. 0-71613
 Al alloys, columnar struct. of alloys solidified in flowing melt in centrifugal casting 0-71640
 Al-(Mn), effects of Mn on electrode or free corrosion potentials 0-100942
 Al-Ag, force-and-mass disordered alloys, vibrs., average local-information transfer approx. 0-88290
 Al-Ag, type-II superconductor, torque oscillations in mag. field (*Russian*) 0-103800
 Al-Ag (7.27 wt.%), peculiarities exhibited during fatigue loading (*Chinese*) 0-71723
 Al-Al₂Pt₃ eutectic alloys, unidirectionally solidified, struct. study 0-108394
 Al-Al₃Ni eutectic, temp. gradients, microstructural changes 0-84971
 Al-Al₃Ni eutectic alloy, electrolytic prep. of Al₃Ni fibres, SEM and anodic polarisation studies 0-100817
 Al-Al₃Ti, directionally solidified, thermal stability during annealing, 435-660°C 0-108393
 Al-Bi(Cd)(Pb)-Ti, containing low-melting pt. inclusions, mech. props. 0-93632
 Al-C interstitial solid solns., atomic static displacements and deform. interaction (*Russian*) 0-64953
 Al-Ca-Zn (5.5 wt.%) superplastic sheet alloy, mechanical properties, superplastic forming behaviour 0-60920
 Al-Cr, dil., supercond., nucl. spin relax. and quasiparticle excitations 0-88680
 Al-Cu, dil., core and valence band spectra, XPS study 0-84837
 Al-Cu, high strength, type 2024-T3, crack growth, fatigue induced surface deform., holographic detect. 0-85120
 Al-Cu, liq. alloys, with zero superheat, fluidity 0-70289
 Al-Cu, molten, showering cryst. form. in mould cooled from top (*Japanese*) 0-66498
 Al-Cu, solidification, solid-liq. interface, solute conc. effects 0-59632
 Al-Cu, superconducting amorphous films of high stability 0-70889
 Al-Cu, type 1100, synchrotron radiation microradiography 0-85121
 Al-Cu, type 2036-T4, plane-strain work hardening, meas. and anal. 0-81073
 Al-Cu, type 2219-T851, fracture mechanics and surface chemistry of fatigue crack growth 0-81168
 Al-Cu (0.5 wt.%), evaporated layers, electromigration, linewidth depend. 0-65277
 Al-Cu (1 wt.%), electron irradiated, dislocation damage, HVEM study 0-103389
 Al-Cu (1.9 at.%), solute fluctuations, EXAFS study 0-79949
 Al-Cu (2-5 wt.%), precipitation total surface influence on resistivity (*French*) 0-71650
 Al-Cu (3 wt.%), stress aged, GP zone struct. by X-ray diffuse scatt. meas. (*Japanese*) 0-71653

aluminium alloys continued

- Al-Cu (3 wt.%) single cryst., stress aging, oriented precipitation (*Japanese*) 0-71652
- Al-Cu (33 wt.%) eutectic, solidification under reduced gravity, behaviour of suspended Al_2O_3 particles (*German*) 0-60853
- Al-Cu (3.97 wt.%), containing Guinier-Preston zones, high resolution lattice images 0-107114
- Al-Cu (4 wt.%), high temp. cyclic deform., θ' particle dissolution obs. 0-108515
- Al-Cu (4 wt.%), neutron irradi., weak-beam dark-field obs. of dislocations near θ' precipitates 0-107333
- Al-Cu (4 wt.%), reversion process of Guinier-Preston zones, ^{63}Cu NMR obs. 0-60871
- Al-Cu (4 wt.%), supersaturated and aged conditions, high strain deform. 0-60907
- Al-Cu (4.3 wt.%), containing Guinier-Preston zones, high resolution lattice images 0-107115
- Al-Cu (4.6 wt.%), cold work and ageing influence on ductility and fracture behaviour (*Japanese*) 0-89295
- Al-Cu alloy dendritic solidification kinetics 0-81041
- Al-Cu alloy metallisation sputter deposition for VLSI 0-66429
- Al-Cu alloys, coarsening mechanisms of secondary dendrite arm, and organic analogue 0-81049
- Al-Cu dilute alloys, vein closing mechanism in fluidity tests 0-84924
- Al-Cu films, DC sputtered, Cu distrib. 0-80113
- Al-Cu type 2024 alloy, erosion in cavitating venturi 0-108602
- Al-Cu-Mg, type RR55, high strength, creep behaviour, effect rel. to anodic coatings, SEM study 0-97542
- Al-Cu-Mg, type D16T, thin-wall cylinder cold rolling method 0-66535
- Al-Cu-Mg (4, 1.5 wt.%), mica dispersed, wear characts., and bearing performance 0-108591
- Al-Cu-Mg type 2036, thermomech. treatment, flow stress anal., effect in mech. props. 0-93584
- Al-Cu-Mg/mica particulate composite mech. props. 0-100919
- Al-Cu-Mg-Li alloy extrusions, microstruct., embrittlement and fracture props. 0-60965
- Al-Cu-Mg-Mn-Si-Fe, torsional vibrations decrement, deformed vol. effect 0-76326
- Al-Cu-Mn, long term strength and creep 0-60925
- Al-Cu-Mn, type 2219, synchrotron radiation microradiography 0-85121
- Al-Cu-Mn alloys, effect of comp. and N alloying on mech. props. (*Bulgarian*) 0-71719
- Al-Cu-Si-Mg, deform. simulation using torsional test, elastoplastic constitutive eqn. 0-93594
- Al-Cu-Si-Mn, type 2017S-T4, crack initiation at root of circumferential notch of round bar specimens (*Japanese*) 0-60947
- Al-CuAl, eutectics, microstruct. after solidification, heat pipe influence 0-76243
- Al-Cu(Mg), comparison of liquid impact erosion and cavitation erosion 0-104302
- Al-Cu(Mg), dil. binary alloy, planar interface stability during solidification (*Slovak*) 0-108424
- Al-Cu(Mg), liquid impact erosion 0-108598
- Al-Cu(Mg), low freq. internal friction during plastic deform. (*Chinese*) 0-103420
- Al-Cu(Si)(Mg) binary and ternary alloys, dimensional changes in heat treatment. 0-89271
- Al-Cu(0-10 wt.%) sintered alloys using composite powder 0-76210
- Al-Cv (0.3 wt.%), moving solid-liq. interface, diffusion in liq. 0-107456
- Al-Fe, dil. solid soln., vacancy-trapped Mossbauer impurity Debye Waller factor 0-60468
- Al-Fe (49 at.%) quenched alloy, neutron diffuse scatt., diffuse ω phase obs. 0-84141
- Al-Fe-X-Si (X=transition metal), struct. and comp. by electron microscopy 0-88093
- Al-Ge, dil., magnetoresist., temp. depend. 0-70682
- Al-Ge (0.1 wt.%), channelling meas. of Al interstitial atom trapping by Ge atoms 0-59537
- Al-Li-Mg-Be alloys, phase composition of surface films, oxidation protection mechanism (*Russian*) 0-65417
- Al-Li-Mn (2.8, 0.3 wt.%), recrystallised sheet, fracture behaviour, SEM and TEM study 0-97566
- Al-Mg, alloy A5083-O, fatigue crack prop. and crack closure behaviour under plain strain conditions (*Japanese*) 0-81160
- Al-Mg, dil., ang. correlation of annihilation radiation from impurity trapped positrons 0-104010
- Al-Mg, dilute, dislocation loops, interstitial, size distrib. for metal irradiated in high voltage electron microscope (*Russian*) 0-103335
- Al-Mg, dynamic uniaxial tension and compression curves 0-100884
- Al-Mg, foil, oxidation in O_2 atm., TEM study 0-104356
- Al-Mg, fracture resistance at low temps. 0-104284
- Al-Mg, oxidation control study, electron opt. techniques eval. 0-85089
- Al-Mg, Si alloy, void form. under different precip. conditions, after Al ion irradi. 0-59529
- Al-Mg, solidification, solid-liq. interface, solute conc. effects 0-59632
- Al-Mg, type AMg6, pool metal solidification kinetics in welding with electromag. stirring 0-71636
- Al-Mg, type A5083P-O effects of anisotropy in cutting mechanism (*Japanese*) 0-89232
- Al-Mg (0.1 at.%), neutron damage, positron annihilation 0-65056
- Al-Mg (0.3 wt.%) single cryst., dislocations obs. by high voltage electron microsc. 0-79796
- Al-Mg (2 wt.%), hardening and fracture characts., β -phase dissolution role 0-81178
- Al-Mg (2.5wt.%) sheet, surface oxide state and weldability 0-59769
- Al-Mg (4 wt.%), struct. and strengthening in hot working 0-84968
- Al-Mg (7 wt.%), bare surface reaction rates in aq. solns. 0-101022
- Al-Mg alloy, nitridation process study 0-61013
- Al-Mg sheet, artificial stress raiser effect on strength and local plasticity of weld joint 0-81130
- Al-Mg-Si, ageing sequence study by electron microdiff. 0-81068
- Al-Mg-Si, STEM microdiff. obs. of precip. struct. 0-104167
- Al-Mg-Li alloy, metastable S'-phase, struct. (*Russian*) 0-103291
- Al-Mg-Si, cast, precip.-rich zones on grain boundaries, soln. heat treatment conditions effect on mech. props. 0-104176
- Al-Mg-Si, type 6010, microstruct. characts. influence on formability, heat treatment 0-81090
- Al-Mg-Si, type 6061-T6, 6063-T6, effective stress range factor in fatigue 0-100924
- Al-Mg-Si alloy, dispersion hardened, concentrators, US waveguides appl. (*Polish*) 0-89237

aluminium alloys continued

- Al-Mg-Zn alloys, Al-rich, weld metal comp. effect on microsegregation and eutectic phase segregation (*German*) 0-108455
- Al-Mg-Zn alloys, evaporation effect of alloying elements Mg and Zn in in-situ EM studies 0-103388
- Al-Mg-Zn-Cu, type 7050, calorimetric study of fatigue induced microstructural changes 0-85034
- Al-Mg(Cu)(Si), (5.0(4.5)(11.8) wt.%), ingots, vibr. effect during solidification on porosity formation 0-108426
- Al-Mg(Zn-Mg), long term strength and creep 0-60925
- Al-Mn, dil., core and valence band spectra, XPS study 0-84837
- Al-Mn, dil., supercond., nucl. spin relax. and quasiparticle excitations 0-88680
- Al-Mn (1 wt.%), single crystals, rolled to (123)[412], recrystn. textures 0-104183
- Al-Mn sheet, artificial stress raiser effect on strength and local plasticity of weld joint 0-81130
- r-Al-Mn-C, permanent magnetism and microstruct. 0-75811
- Al-Ni, dil., core and valence band spectra, XPS study 0-84837
- Al-Ni (3-18wt.%), gun-quenched from melt, struct. 0-76225
- Al-Ni (6 wt.%), fine-grained, deform. in tension and torsion 0-85008
- Al-Ni (6 wt.%) misorientation between subgrains, second-phase particles role, STEM microdiff. obs. 0-104415
- Al-Ni multiphase system, simultaneous diffusion in cylindrical symm. (*Russian*) 0-100357
- Al-Ni solid, liquid mixture, diffusion processes (*Russian*) 0-107563
- Al-Ni(Cd)(Fe)(Si), cold worked, struct. and props. 0-71666
- Al-Ni(Pt)(Zn), rapidly solidified, twinned dendrites 0-70572
- Al-Sc, elec. resist. determ. 0-92876
- Al-Si, DC magnetron-sputtered, residual gas influence on props. 0-80968
- Al-Si, eutectic, quasiisotropic, rheological deformation theory 0-79165
- Al-Si, graphite dispersed, wear characts. (*Korean*) 0-93658
- Al-Si (0.57 at.%), Si precipitate dissolution kinetics 0-84935
- Al-Si (1.2 wt.%), dispersion hardened, work hardening due to Orowan loops, temp. depend. (*Japanese*) 0-66534
- Al-Si (25.4 wt.%), solidification, high press. effects 0-66499
- Al-Si (2.4 wt.%), liq. fluidity in solid-liq. zone 0-108429
- Al-Si alloy metallisation sputter deposition for VLSI 0-66429
- Al-Si eutectic, irregular, branching limited growth 0-81042
- Al-Si eutectic alloy, banded struct., SEM and optical microscopy 0-104144
- Al-Si melt, microheterogeneity (*Russian*) 0-103238
- Al-Si melts, spreading behaviour on Fe 0-84345
- Al-Si-Cu, fracture resistance at low temps. 0-104284
- Al-Si-Cu alloy metallisation sputter deposition for VLSI 0-66429
- Al-Si-Cu-Zr, ageing kinetics (*Russian*) 0-76274
- Al-Si-Mg alloy metallisation sputter deposition for VLSI 0-66429
- Al-Si-Y alloy, phase equilibria in Al rich region (*Russian*) 0-93537
- Al-Si(Ge) eutectic alloys in screened ohmic contacts for solar cells 0-94090
- Al-Si(9.3, 12) with graphite particles seizure resistance study using Hohman wear tests 0-89360
- Al-Ti, mechanical props. improvement, by work hardening (*French*) 0-97502
- Al-Ti, molten, showering cryst. form. in mould cooled from top (*Japanese*) 0-66498
- Al-Ti alloy spark alloying, cathode weight change and hardened layer obs. (*Russian*) 0-61005
- Al-Ti system, interdiffusion coeffs. determ. 0-70477
- Al-V, dil., supercond., nucl. spin relax. and quasiparticle excitations 0-88680
- Al-Y, specific elec. resist., variation with Y conc. 0-84455
- Al-Zn, dil., magnetoresist., temp. depend. 0-70682
- Al-Zn, grain boundary reaction sites, determ. of struct. aspects, by electron microscopy 0-103359
- Al-Zn, spinodally decomposing, main wavelength of conc. fluctuations calc. 0-97459
- Al-Zn, type 7075-T6, coldworked hole specimens, residual stresses, fracture mech. anal. 0-97587
- Al-Zn, X-ray diff. after omnidirectional compression (*Russian*) 0-88262
- Al-Zn (10 wt.%), ageing at low temp., effects of fluctuation of solute conc. 0-76287
- Al-Zn (10 wt.%), ageing at low temp., effects of fluctuation of solute conc. 0-76288
- Al-Zn (38 at.%), alloy, TEM study of precipitation processes or different microstructures during ageing 0-93561
- Al-Zn (6.8 wt.%), Guinier Preston zones internal struct., study by X-ray diffraction, α_2 phase comparison (*French*) 0-66472
- Al-Zn (70, 30 wt.%), decomp. study, 25-160°C (*Czech*) 0-89225
- Al-Zn (8-25 wt.%), solid solns., residual resist. during clustering 0-97483
- Al-Zn alloys, interfacial stability of planar solid-liq. interface during solidification 0-104145
- Al-Zn alloys, interfacial holes distrib. at beginning of interfacial instability in solidification 0-104146
- Al-Zn thin film, prep. using Sn-Zn evaporant source 0-100789
- Al-Zn-Mg, age-hardenable, precipitation and dissolution processes, positron annihilation and X-ray small-angle scattering comparison 0-89238
- Al-Zn-Mg, atmosphere effect on fatigue crack prop. (*Japanese*) 0-81161
- Al-Zn-Mg, crack-arrest markings on intergranular stress corrosion fracture surfaces 0-89405
- Al-Zn-Mg, oriented growth of precipitates on dislocations, model 0-108448
- Al-Zn-Mg, TEM and calorimetric study 0-76290
- Al-Zn-Mg, TEM characteris. of precipitates 0-104166
- Al-Zn-Mg, type 7075-T651 plate, thickness direction inhomogeneity of mech. props. and fracture toughness 0-100892
- Al-Zn-Mg, type V-95, ultimate tensile strength for brief impact 0-70309
- Al-Zn-Mg (3.6, 1.95 wt.%), ageing and plastic deform., effect on structure, electron microsc. and X-ray diff. study (*Russian*) 0-81108
- Al-Zn-Mg (3.87, 1.79 wt.%), oriented growth of precipitates on dislocations, TEM obs. 0-108447
- Al-Zn-Mg (91, 6, 3, wt.%), H embrittlement and trapping, HVEM obs. 0-76364
- Al-Zn-Mg alloy, Ag addition and pre-precipitation treatment, influence on GP zone growth 0-71658
- Al-Zn-Mg alloy AA-7039, stress corrosion cracking, SEM obs. 0-104323
- Al-Zn-Mg alloys, grain boundary segregation, implications to stress corrosion cracking 0-84936
- Al-Zn-Mg granules and bands rolled from them, heat treatment 0-100862

aluminium alloys continued

- Al-Zn-Mg superplastic alloy, cavity growth under creep conditions 0-60940
- Al-Zn-Mg type 7N01-T4, weld, SCC in NaCl-H₂O₂ soln. (*Japanese*) 0-108631
- Al-Zn-Mg-Cu (6, 2.5, 1.5 wt.%), deform. simulation using torsional test, elastoplastic constitutive eqn. 0-93594
- Al-Zn-Mg-Cu (6.2, xwt.%) type alloy, fatigue crack propag., Cu content and recryst. effect 0-60960
- Al-Zn-Mg-Cu type 7075, heat treatment optimisation 0-60888
- Al-Zn-Ti(Mn), mech. props., Ti or Mn addition effect (*Korean*) 0-93613
- Al-Zr (1-13 wt.%), rapidly quenched, extended solid solubility, grain refinement and age-hardening 0-76266
- (Al-Cu)/Si system, Si regrowth minimisation through overlying Al or Al alloy film 0-70569
- (Al-Si)/Si system, Si regrowth minimisation through overlying Al or Al alloy film 0-70569
- AlAg, Auger spectra, 4d bandwidth effect 0-89093
- AlB₂, thermochemistry and stability 0-97723
- Al₁₁Be_{0.6}B₂₂, metal distrib., X-ray diff. study 0-75204
- Al₂₀NiCo (5 at.%), θ' hardened, creep mechanism 0-85013
- Al₃(Cu)₂Zr₃₅, metallic glass, inelastic deform., free energy spectra 0-71699
- AlH₃, electronic struct. and electron-phonon interaction, hydrogenation effect, rel. to supercond. 0-107694
- Al₃Mg₂, diffusionless phase transformation 0-104150
- Al₃Mg₁₋₂, liquid alloys, vols. and entropies of mixing, calc. 0-75363
- Al₃(Ni, Co)₃ ternary phase in Al-Ni-Co system, cryst. struct., vacancy controlled phase (*Chinese*) 0-70164
- Al₃Ni, cryst., theoretical morphology and comparison with observed habits (*French*) 0-79732
- AlZn, disordered, residual resistivity due to clustering, ageing effects 0-65521
- Be-Al, plastic deform., flow stresses, fracture (*Russian*) 0-108496
- (Ce,La)Al₃, collective phenomena 0-65933
- (Ce,Y)Al₃, collective phenomena 0-65933
- CeAl₃, antiferromag. ordering and Kondo behaviour, ²⁷Al NQR study 0-71231
- CeAl₃, collective phenomena 0-65933
- CeAl₃, magnetic ordering, 24 component Ginzburg-Landau model 0-97095
- CeAl₃, multiple- q structure or coexistence of different mag. phases, neutron diff. study 0-107985
- CeAl₃, resistivity and volumetric meas., phase diagrams, comparison with CeS 0-107789
- CeAl₃, sp. ht., Kondo effect and ferromag. order coexistence 0-65927
- Ce₂Al₁₁, competition between ferro- and antiferromag. interactions 0-60258
- Ce₂Al₁₁, sp. ht., Kondo effect and ferromag. order coexistence 0-65927
- CeNi₄Al, mag. susceptibility, H adsorption-desorption cycle effects 0-107990
- Co-Al, dendritic segregation 0-76260
- Co-Al, multilayer martensite phases, illustration of polytype structures 0-84932
- Co-Al, X-ray K-absorption spectrum 0-97378
- Co-CoAl, two phase, interaction between deform., fracture initiation and propag. 0-85006
- Co_{1-x}Al_x, ordered β -phase, enthalpy of formation are defect struct. descript. 0-89519
- Co,HfAl, hyperfine fields of Fe impurities, Mossbauer spectra 0-71255
- CoTi₂-Al, mag. and electronic props., ferromag. and paramag. state 0-65814
- Co₂TiAl, hyperfine fields of Fe impurities, Mossbauer spectra 0-71255
- Co₂VAl, hyperfine fields of Fe impurities, Mossbauer spectra 0-71255
- Cr-Al-C, ternary system, phase relationships 0-76230
- Cu-Al, dislocation core cut-off parameter, estimation from stacking fault nodes 0-103370
- Cu-Al, dislocations, dissociated, climb mechanism, nucleated loops, Burgers vectors 0-65002
- Cu-Al, disordered alloys, interatomic distances, coord. numbers, and mean relative displacements, EXAFS anal. 0-89087
- Cu-Al, HV electron microscopy, crit. voltages depend. on comp., temp. and short-range order 0-100146
- Cu-Al, irradi. in HVEM, climb of dissociated dislocations and point defect absorpt. 0-107257
- Cu-Al, linear dislocation multipoles, weak-beam TEM 0-75233
- Cu-Al, liq., elec. cond., temp. and conc. depend., model interpret. and alloy struct. (*Russian*) 0-88528
- Cu-Al, ordered, superlattice fringe images, computer simulation 0-103296
- Cu-Al, planar faults, faint electron microscopic image contrast obs. 0-107283
- Cu-Al, short range order and static distortion contribution to residual elec. resistivity (*Russian*) 0-70672
- Cu-Al (10, 16 at.%), dislocation interactions, influence of jogs on extension of dislocation nodes 0-84176
- Cu-Al (11 at.%) single cryst., dislocation reactions during deform. twinning 0-79795
- Cu-Al (14.3 wt.%), ¹¹⁰Ag diffusion in β/γ_2 interphase boundary 0-79989
- Cu-Al (4 at.%), anneal hardening mechanism 0-60879
- Cu-Al (5 wt.%), subjected to tension-compression fatigue, deform. and fracture strength (*Japanese*) 0-93644
- α -Cu-Al (6 to 17 at.%), short-range order investigated by diffuse X-ray scatt. (*Russian*) 0-104187
- α -Cu-Al (9.13, 13.56, 14.76, wt.%) short-range ordered, characterisation of locally ordered regions 0-79747
- Cu-Al bulk and thin-film forms, reflecting surface absorpt. coeffs. at 10.6 μ m 0-95984
- Cu-Al films, elec. cond. of vacuum condensates depend. on composition, annealing (*Russian*) 0-65709
- Cu-Al-Co liquid alloys, constant Co-content of 5 wt.%, mag. props. (*German*) 0-88720
- Cu-Al-Mn liq. alloys, susceptibility behaviour 0-93077
- β -Cu-Al-Ni (14, 3 wt.%), single crystal, thermal effect due to stress induced martensite formation 0-81059
- Cu-Al-Ni (14.1, 3 wt.%), autooscillations and nonlinear anelasticity 0-70307
- Cu-Al-Ni Marmen alloys, rapid solidification and ageing 0-76245
- Cu-Al-Sn system, coexistence of different and brass like phases 0-89206
- Cu-Mn-Al, Heusler alloys, ferromag. inclusions, mag. props. and struct. study (*Russian*) 0-80570

aluminium alloys continued

- Cu-Mn-Al alloys, displaced hysteresis loop and microstructure obs. 0-84613
- Cu-Ni-Al, cast, strength and hot ductility, Al effect 0-66595
- Cu-Ni-Al (5, 2.5 at.%), precip. hardening (*Japanese*) 0-71663
- Cu-Sn-Al, deform at high temps. (*Polish*) 0-89284
- Cu-Ti-Al, wetting of Al₂O₃, alloying effects 0-107617
- Cu-Zn-Al, β_1' martensite crystal crossing rel. to reversible shape memory effect (*Japanese*) 0-108499
- Cu-Zn-Al, reversible shape memory effect (*Japanese*) 0-108500
- Cu-Zn-Al martensite, lattice dynamics, neutron scatt. meas. 0-88286
- CuMnAl₃, hysteresis, spin orbit scattering effect on anisotropy in spin glass state, rel. to Al impurity conc. 0-71095
- Cu₂MnAl-Pd₂ MnAl mixed Heusler alloys, mag. props. 0-60269
- Cu_{3-x}Mn_xAl, and Cu₂Mn_{2-x}Al_x, Heusler alloys, order-disorder transitions 0-59619
- Cu₃MnAl_{3-x}Sn_x, Mossbauer effect study 0-60473
- DyCo₂-DyAl₃ system, mag. and structural studies 0-108006
- Dy_{1-x}Gd_xAl₃, ordered alloys, hyperfine field, anomalous con. depend. NMR 0-75868
- Er_{1-x}Gd_xAl₃, effective mol. field at ¹⁶⁷Er, NMR meas. 0-71197
- Eu₂La_{1-x}Al₃, cryst. fields and exchange parameters, ESR meas. 0-71175
- Eu₂La_{1-x}Al₃, dil. EPR, cryst. fields and effective exchange interaction 0-66029
- Fe, cast, tensile strength, Al addition effects (*Korean*) 0-71736
- Fe-Al, domain struct. and magnetostriction, heat treatment effect 0-60398
- Fe-Al, mag. aftereffect meas., phenomenological description 0-88835
- Fe-Al, O containing, mag. aftereffect and disaccommodation meas., time depend., activation energy, and ageing props. 0-88836
- Fe-Al, ordered, superlattice fringe images, computer simulation 0-103296
- Fe-Al, planar faults, faint electron microscopic image contrast obs. 0-107283
- Fe-Al, single crystals, deform. at high temps. 0-81125
- Fe-Al (4 wt.%), mag. anisotropy induced by cold rolling (*Russian*) 0-84595
- Fe-Al (40 at.%) and Fe-Al (50.5 at.%) ordered alloys, 20K neutron irradi. effects, stoichiometry depend., resist. obs. (*French*) 0-84215
- Fe-Al-Si (6.22, 9.63 wt.%), bending test under high press., high temp. 0-85057
- Fe-Al (24.3 at.%) C alloy, magnetic permeability disaccommodation, 260-400K 0-93144
- Fe-Co-Al-Cu-Ti (40, 14, 7.5, 4.5 wt.%), metastable equilibrium, high coercive state (*Russian*) 0-66476
- Fe-Co-Ti-Al alloy type γ -FeNDK magnets, metallographic method of distinguishing cracks 0-85096
- Fe-Cr-Al, HOS 875, oxidation, cyclic, role of thermal shock 0-97640
- Fe-Cr-Al, Kanthal films, vac. deposited, evaporation characts., comp., struct. and elec. props. 0-88646
- Fe-Cr-Al, scales, α -Al₂O₃, early stages development at high temp. 0-89413
- Fe-Cr-Al (12, 3 wt.%), internal friction and rigidity modulus, strain amplitude depend. (*Japanese*) 0-92606
- Fe-Cr-Al (7, 5 wt.%), expt. stainless alloys, phys. and mech. props. 0-97637
- Fe-Cr-Al liquid alloy, thermodynamical anal. of O₂ solubility (*Russian*) 0-92676
- Fe-Cr-Al-Y, oxidation resistance, heat treatment and Al⁺ ion implantation 0-71785
- Fe-Cr-Al-Y, scales, α -Al₂O₃, early stages development at high temp. 0-89413
- Fe-Ni-Al-Co-Cu-Ti YuNDK type, S effect on mech. props. 0-60927
- Fe-Ni-Al (Cu) (12, 0.5, 0.5 to 3 wt.%), Cu addition strengthening at 77K, mech. props. 0-60875
- Fe-Ni-Cr-Al-Ti-W-Mo (35, 15, 2.4, 2.3, 2.2 wt.%) wrought superalloy, freckles (*Chinese*) 0-104137
- Fe-Ni-Cr-Al-Y, oxidation mechanism, Y addition effect on kinetics and oxide adherence 0-97623
- Fe-Ni-Cr-Ti-Al, with thermoelastic control coeff., comp. and heat treatment influence on props. (*French*) 0-81074
- Fe-Si-Al, Sendust, ribbon-form, prep. by rapid quenching, mech. and mag. props. 0-71611
- Fe-Si-Al, surface oxide layer struct., AES study 0-89396
- Fe-Si-Al (2.8-3.4, 0-0.86 wt.%) oxidation, annealing 0-89395
- Fe-Si-Al (9.6, 5.4 wt.%), ribbon-form Sendust alloy, mag. props., annealing effects 0-88800
- Fe-Si-Al ribbon-form Sendust alloy made by rapid roll quenching, mag. props., recording head appls. 0-81001
- Fe₃-Al, solid soln., rheological study of crystallographic order on creep (*French*) 0-97548
- Fe₃Al, alloys, superlattice-fringe imaging theory, images formed from two beams 0-79649
- Fe₃Al, electrical resistivity and LRO, energy gap formation in Fermi surface 0-88533
- Fe₃Al, electronic structure, X-ray spectra comparison with band struct. calcs. 0-97383
- Fe₃Al, electronic structure, magnetic moments 0-107695
- Fe_{3-x}Co_xAl, site preference and local environment effects, Mossbauer and NMR meas. 0-71264
- Fe₃Co₂B₂₀Si₁₀Al₃, stress-induced variation in magnetisation and dynamic magnetostrictive charact. 0-88855
- Fe_{3-x}Mn_xAl, ordering of Fe atoms, X-ray diff. meas. and mid gamma reson. anal. (*Russian*) 0-96469
- (FeNi)₈₀Bi_{17.5}Al₂Si_{0.5}, stress-induced variation in magnetisation and dynamic magnetostrictive charact. 0-88855
- (Fe₂Ni₃)₇₅P₁₅B₂Al₃, amorphous, crystn. temp., press. and heating rate depend. 0-70132
- Ga-Al, amorphous, mag. and elec. props. 0-80499
- Gd(Al,Fe)_{1-x}, intermetallic compounds, pseudobinary, Mossbauer studies 0-75887
- Gd_{1-x}Ca_xAl₃, mag. props. and phase relations 0-107991
- Gd(Fe,Al)_{1-x}, mag. behavior 0-108079
- Gd,La_{1-x}Al₃, cryst. fields and exchange parameters, ESR meas. 0-71175
- GdMn₂-GdAl₃ system, mag. and structural studies 0-108006
- Gd₂Ni_{17-x}Al₃, EPR of Gd³⁺ ions 0-97139
- (Gd_{1-x}Al_x)Al₃, ferromag. and spin glass like behaviour, magnetisation meas. 0-75734
- Hf-Al-C, phase diagram and lattice constants, X-ray diff. method 0-89207
- (La,Gd)Al₃, spin glass materials, mag. field dependence of susceptibility peak 0-103840

aluminium alloys continued

- (La,Gd)Al₃ spin glasses, time depend. mag. props. 0-65909
 La-Al amorphous alloys, internal friction, relaxation process 0-92607
 LaAl₃, calc. of energy band-structure and Fermi surface by APW method 0-70590
 LaAl₃, doped with Tb, Nd, or Pr, crystal field effects, tunnelling within mK range 0-70907
 LaAl₃, electronic struct., APW method and local-spin-density approx. 0-65434
 LaAl₃, supercond. and normal states, anomalous US attenuation and velocity change 0-80446
 LaNi₄Al, solubility and sorption props. of H₂, effect of Al 0-103482
 LaNi₅-Al, use in hydride conversion and storage system chemical heat pump 0-72077
 La_{1-x}Tb_xAl₃, competing paramag. anisotropy from cryst. field and indirect quadrupolar coupling 0-60180
 Li-Al system, Li solubility and chem. diffusion in Al, electrochem. study 0-107432
 LiAl, anomalous elec. resistivity near critical composition 0-103673
 7LiAl, cryst. growth, Stockbarger method, struct. and homogeneity 0-89137
 β -LiAl, optical dispersion, room temp. reflectance spectra 0-66195
 LiAl single crystals, growth by Tamman technique 0-66422
 LiAl, transport props., rel. to semimetallic band struct. 0-88581
 LiAl/FeS, battery system research developments at ANL 0-61323
 LiAl/FeS experimental cells with molten salt electrolyte, self-discharge behaviour 0-104501
 LiAl/Fe(S₂) battery developments for electric vehicle propulsion and load levelling appls. 0-61325
 Mg-Al-Zn (94.3, 3.9, 1.8 wt.%), precip. on dislocations, weak-beam TEM 0-76264
 Mg-Al-Zn-Mn (8, 0.5, 0.3 wt.%) casting alloy, penetration resistance 0-100901
 Mn-Al-C, ferromag. alloy, transform. kinetics 0-76229
 Mn-Al-C, fine-grained cast struct., remanence and coercive force 0-60365
 Mn-Al-C, metallic magnets investigations, present state (Polish) 0-107987
 Mn-Al-C (70, 29.5 wt.%) alloy magnet, Almax, anisotropic, mag. props. (Japanese) 0-60371
 τ -MnAl, estimated theoretical limit of mag. moment 0-97072
 MnAlGe film, mag. domains and amorphous to cryst. phase transition, electron microscopy obs. 0-71129
 Mo-Al-Ge, phase equilibria, X-ray and microstructural anal. 0-93536
 Nb-Al, diffuse electron scatt. (Russian) 0-103438
 Nb-Al-C, phase diagram and lattice constants, X-ray diffr. method 0-89207
 Nb₃(Al,Ge) and Nb₃(Al,Si), liq. quenched, supercond. props. 0-84580
 Nb₃Al, A-15 struct., converted from cold worked BCC struct., crit. currents 0-75697
 Nb₃Al, A15 cpd., normal state, low temp. resist. 0-107762
 Nb₃Al, complex refractive index meas. 0-93264
 Nb₃Al film, electron-beam coevaporated, prep. and characts. 0-76187
 Nb₃Al, NQR freq. temp. depend., supercond. transition temp. 0-93207
 Nb₃Al, prep. by reduction of Nb₂O₅ and Al₂O₃ by CaH₂, thermodynamic calc. 0-100809
 Nb₃Al, supercond. props. and lattice parameter, comp. and neutron irradiation effects 0-70880
 Nb₃Al, temp-depend. of elec. resist. 0-103675
 Nb₃Ge, Al_{1-x}, ternary supercond. alloys, comp. variations 0-97022
 Ni alloys, aluminising, thermodynamic anal. of phase transforms. 0-76413
 Ni-Al (2 and 6 wt.%), oxidation, α -Al₂O₃ growth, microstruct., precip. 0-108626
 Ni-Al, itinerant electron ferromagnet, magnetovolume effects 0-60397
 Ni-Al, order hardening, comparison between revised theory and expt. 0-93565
 Ni-Al, solid soln., rheological study of crystallographic order on creep (French) 0-97548
 Ni-Al (12.8 at.%) foil, ion irradiation, surface effects on precip. morphology 0-104168
 ζ -Ni-Al system, solid soln., interdiffusion (Japanese) 0-70476
 Ni-Al-Cr₂Cr₃, eutectic alloy, directionally solidified, oxidation resistance, influence of Y 0-89409
 Ni-Al-Mo (12.7, 21.6 wt.%), directionally solidified eutectic composite, precipitation 0-108454
 Ni-Al-Nb ternary system, electron microprobe analysis of nickel-rich region at 1473K 0-71631
 Ni-Al-Ta dendritic monocrystals, directionally solidified, coarsening kinetics 0-108425
 Ni-Al-(Si), diffusion, lattice parameter, microhardness, and constitution, effect of Si additions (Russian) 0-84316
 Ni-Co-Al alloys, continuous precip., SEM, TEM, X-ray diffr. study 0-89220
 Ni-Co-Cr-Mo-Al-Ti (17.5, 15.1, 4.9, 4.15, 3.25 wt.%), creep and stress rupture behaviour in air and vacuum 0-60918
 Ni-Cr-Al (20, 4 wt.%), tensile stress effect on high temp. oxidation (Japanese) 0-89393
 Ni-Cr-Al sintered alloy, hot vac. pressure, fracture and mech. characts. 0-66667
 Ni-Cr-Al-TaC, eutectic composite, microstructure, fatigue props. 0-85038
 Ni-Cr-Al-Ti, stress corrosion cracking, factors influencing susceptibility 0-97617
 Ni-Cr-Co-Al-W-Mo-Ti-Ta, heat resist. and struct., Ta effect 0-76312
 Ni-Cr-Co-Ti-Mo-W-Al (14, 9.8, 5, 4, 3.9, 3 wt.%), low cycle fatigue, prior heat treatment effect 0-60962
 Ni-Cr-Mo-W-Al-Ti, heat-resist., phase comp. 0-76250
 Ni-Cr-W-Co-Al, high-temp. sulphide corrosion 0-76408
 Ni-Cr-W-Mo-Ti-Al, heat-resist., recovery and recrystn. 0-76268
 Ni-Fe-Cr-Mo-Ti-Al, PE 16, thermally activated domain wall motion 0-88777
 Ni-Fe-Nb-Al (11.2, 8.09, 79.66 wt.%), modulated struct. growth process rel. to ageing (Chinese) 0-66541
 Ni-Fe-Nb-Mo-Al, head material for mag. recording, DC and AC mag. props. 0-88812
 Ni-Ti-Al superalloy, pendant drop melt extracted, struct. and props. 0-76242
 Ni₃(Al, Nb) single crystal, yield stress, orientation and temp. depend. 0-108511

aluminium alloys continued

- γ -Ni₃(Al,Ti), single crystal, dislocation movement, HVEM obs. (Japanese) 0-108503
 β -NiAl, electronic struct. and optical props. 0-97228
 NiAl, nonstoichiometric, interstitial defect cluster obs. 0-107226
 β -NiAl, ordered, hardness after-effect studied by anelastic relaxation 0-66570
 β -NiAl, oxidation, α -Al₂O₃ growth and microstruct. 0-108627
 β -NiAl, oxide films, metal and O₂ transport, AES and inert marker, techniques 0-97641
 Ni₃Al, off-stoichiometric alloy, inverse mag. susceptibility rel. to defect conc. 0-60216
 Pr_{1-x}Ca_xAl₃, mag. props. and phase relations 0-107991
 Pt₃Al, Li₂ ordered alloy, positive temp. depend. on strength, phase destabilization 0-81203
 ScAl₃-Eu, intermediate valence on Eu ions, Mossbauer isomer shift 0-84587
 Si-Al C fibre composite technological coatings, liquid phase method preparation (Russian) 0-108375
 Ta-Al-C, phase diagram and lattice constants, X-ray diffr. method 0-89207
 Ta-Cr-Si-Al, heat resistive films prepared by sputtering, lifetime meas. 0-80132
 Tb_{1-x}Gd_xAl₃, effective mol. field at ¹⁵⁹Tb, NMR meas. 0-71197
 Ti-Al, elec. spark Al doping of VT-18, surface struct. and props. (Russian) 0-76398
 Ti-Al-C, ternary system, phase relationships 0-76230
 Ti-Al-Cr-Mo-V, VT22 alloy, metastable β -phase decay under continuous heating, plastic strain effect (Russian) 0-71656
 Ti-Al-Kh18 steel, O₂ solubility thermodynamical anal. (Russian) 0-92676
 Ti-Al-Mo, type BT22, phase transformations under step-by-step heat treatment (Russian) 0-108436
 Ti-Al-Mo-Cr, weldment containing orthorhombic martensite, auto-tempering behaviour and alpha precip. strengthening 0-84976
 Ti-Al-Mo-Cr (4.5, 5, 1.5 wt.%), weld metal, α/β interphase sliding 0-108512
 Ti-Al-Mo-V (8, 1, 1 wt.%), Widmanstätten colonies, fracture toughness 0-85031
 Ti-Al-Mo-Zr, compressor disk, surface plastic deform., optimal method 0-60924
 Ti-Al-Mo-Zr, type VT-9, creep eqns. rel. to extension and compression props. 0-100875
 Ti-Al-Sn, alloy 6242, dynamic effects of flow and fracture during isothermal forging 0-76343
 α -Ti-Al-Sn, alloy Ti-679, electron diffr. anal. of Ti₃Si phase (Chinese) 0-64845
 Ti-Al-Sn-Zr, Ti-680, O contamination under high temp. (Chinese) 0-66688
 Ti-Al-Sn-Zr-Mo (6.2,4,6 wt.%) fusion weldment, substruct. characts. 0-84183
 Ti-Al-V, friction coeff. reduction on injection with TiC particles 0-85086
 Ti-Al-V, fusion reactor blanket structures, radiation resistance 0-63379
 Ti-Al-V (6, 4 wt.%), fretting corrosion of orthopaedic implant materials by bone cement 0-104813
 Ti-Al-V (6, 4 wt.%), texture depend. stress corrosion cracking 0-104334
 Ti-Al-V (6.4 wt.%), cyclic temp. creep, transition effect 0-97539
 Ti-Al-V (6.4 wt.%), β -annealed, subsurface fatigue crack initiation 0-108553
 Ti-Al-V (6.4 wt.%), effect of air exposure on fracture characts. 0-100890
 Ti-Al-V (6.4 wt.%), H related fatigue fracture 0-76344
 Ti-Al-V (6.4 wt.%), ion irradiated, microstruct. study using TEM 0-96572
 Ti-Al-V (6.4 wt.%), microstruct. effect of base metals on diffusion welding (Japanese) 0-82926
 Ti-Al-V (6.4 wt.%), porous compacts, determ. of effective stress in hot pressing 0-100807
 Ti-Al-V (6.4 wt.%) superplastic alloy, maximum attainable ductility 0-60919
 Ti-Al-V (6.4 wt.%) cast alloy, with improved microstruct., mech. props. (Japanese) 0-71701
 Ti-Al-V-Be-B, melt-extracted polycryst., mech. props. 0-76360
 Ti-Al-V-Fe-Cu, melt-extracted polycryst., mech. props. 0-76360
 Ti-Al-V-Sn (5.5, 5.5, 2 wt.%), crack growth, slow, H-induced 0-104272
 Ti-Al-V-Sn (6.6, 2 wt.%) fusion weldment, substruct. characts. 0-84183
 Ti-Al-Zr-Mo-Si (6, 5, 0.5, 0.25 wt.%), β -processed, fatigue props., hold time effect 0-60961
 Ti-Al-(Mo), phase relations 0-108398
 Ti-Fe-Al, homogeneity and lattice parameters, Al effect on hydriding compd. FeTi 0-108400
 Ti-Mo-V-Al-Cr-Fe (4.8, 4.7, 5.2, 1.1, 1.0 wt.%), structural changes during heating up to 1000°C, DTA study (Russian) 0-93552
 Ti-Mo-Zr-Al (15, 5, 3 wt.%), quenched and aged metastable β -phase, crystallography, morphology and decomposition 0-76262
 Ti-V-Fe-Al (10, 2, 3 wt.%), fracture toughness and stress corrosion resistance 0-100994
 TiN coated, tribological anal. 0-108600
 UAl₃, spin fluctuations, mag. field effect, electronic sp. ht. and elec. resist. 0-108026
 UAl₃, surface comp. and electronic struct., photoemission study 0-66382
 UAl₃, dispersion nuclear fuels, development and irradiation performance 0-78368
 V-Al-C, ternary system, phase relationships 0-76230
 V(Nb)-Al-Cu, rapidly quenched, comp. and phase equilib. 0-76235
 Yb-Al mixed valent film form., XPS study 0-80943
 YbCuAl, mixed valence cpd., dynamic susceptibility, neutron inelastic scatt. 0-65807
 YbCuAl, mixed-valent cpd., thermal expansion and magneto-volume effects 0-66005
 Yb_{1-x}Y_xCuAl, disordered extended Anderson model, CPA-alloy analogue treatment 0-65506
 Zn-Al, electroless plating of Ni, baths and activating solns. (Japanese) 0-71604
 Zn-Al (0.4 wt.%), intergranular slip during in situ superplastic deform. 0-96538
 Zn-Al (1.1 wt.%) superplastic alloy, grain size determ. (Czech) 0-81118
 Zn-Al (22 wt.%), eutectoid, low stress and superplastic creep behaviour 0-81120
 Zn-Al (22 wt.%) superplastic alloy, grain growth texture 0-81075
 Zn-Al-Cu casting alloys, mech. props. and dendritic morphology, Al content effect (Korean) 0-93612
 Zn-Al(Cu), mech. and technological props. (Polish) 0-89286

aluminium alloys continued

- Zn-Al (22 wt.%), alloy sheet, superplastic, cold-rolling effects on mech. props. and microstructure (*Japanese*) 0-71671
 Zr-Al (8.6 wt.%), dimensional stability struct. and mech. props, effects of neutron irradiation 0-92563
 Zr-Al (8.6 wt.%), fast neutron irradiated, tensile props. and fracture toughness 0-84994
 Zr-Al getter modules, transient getter scheme for Tokamak fusion test reactor 0-79584
 Zr-Al-C, phase diagram and lattice constants, X-ray diffraction method 0-89207
 ZrAl₃, X-ray energy spectrum of valence electrons (*Russian*) 0-108304
 Zr₂Al₃, X-ray energy spectrum of valence electrons (*Russian*) 0-108304
 Zr₃Al, deformed and irradiated, lattice defects obs., superlattice dislocations and defect clusters 0-107261
 Zr₃Al, ordered, oxidation, weight gain and metallography 0-89398
 Zr₃Al ordered alloy, ion bombardment damage, TEM 0-100287
 Zr₄Al₃, X-ray energy spectrum of valence electrons (*Russian*) 0-108304
 Zr(Fe_{1-x}Al_x)₂, Curie temp., magnetisation, and crystal struct., conc. depend. 0-75730

aluminium compounds

- see also alumina; aluminium alloys
 Al_{0.5}Ga_{1-x}As/Al_{0.5}Ga_{1-y}As heterostructure lasers, prep. characts., and CW reliability 0-58586
 AlGaAs laser array with Si detector array for stabilization 0-58817
 bauxites, analysis, comparison of atomic absorption, X-ray fluorescence, and other classical methods 0-89551
 chalcogenate and chalcogenite double salts, form. laws and acid-base props. 0-101070
 Ga_{0.1}Al_{0.9}As, optically oriented electron, nuclei spin instability (*Russian*) 0-70660
 Ga_{0.1}Al_{0.9}As-GaAs DH laser material crystal cathodoluminescence, SEM analysis 0-97349
 guanidine aluminium sulphate, lattice charge contribution to coordination polyhedron crystal potential 0-103651
 guanidine aluminium sulphate hexahydrate:Cr³⁺, ESR spectra fine struct. 0-93169
 guanidinium aluminium sulphate hexahydrate, surface obs., SEM and AES expts. 0-71362
 kaolinite:Cr, high temp. reduction reactions, thermodynamic anal. 0-104426
 kaolinite rare-earth complexes, relax., molar free energy of activation for dipole relax. 0-88919
 laterites, Venezuelan, analysis, comparison of atomic absorption, X-ray fluorescence, and other classical methods 0-89551
 oxides and hydroxides, electro-erosion prep. (*Russian*) 0-81297
 (Al, Ga)As DH lasers, water role in gradual degradation 0-74379
 (Al, Ga)As DH lasers, superlinear emission characts., negative resist. obs. 0-95895
 (Al, Ga)As double heterostructure laser, comparison of deep and shallow proton bombardment fabricated devices 0-99724
 (Al, Ga)As double-heterostructure lasers degraded, deep-level changes during accelerated ageing at high temps. 0-74356
 (Al, Ga)As:Zn planar stripe lasers with deep Zn diffusion, guiding mechanisms controlled by impurity concs. 0-78853
 Al/AlCl₃-NaCl/FeS₂ secondary cell, preliminary study 0-108793
 Al₂O₃/La-rare earth metal tunnel junctions, cond. meas., crystal field effects 0-88694
 Al-Al-SiO₂-Si capacitors, physical and elec. props. of RF plasma grown AlN 0-100530
 Al-Ge-SiO₂ solar selective absorber surfaces, optical behaviour at high temp. 0-101130
 Al-Si-N-O system, comps. corresponding to β'-sialon phase reaction hot-pressing 0-84891
 p-AlAs, saturation characts. over CO₂ laser spectrum 0-83646
 AlAs(Sb), fine structure of lowest exciton state (*Russian*) 0-96801
 AlB₁₂, abrasive, effect on machinability of Ti alloys (*Russian*) 0-97593
 AlB₁₂, α- and β-forms, elec. props. at high temps. and in strong elec. fields, thermistor appls. 0-92903
 AlC, precipitates in Ni-base superalloy, STEM microanal. 0-81067
 AlC₃, vaporisation, thermodynamics, 1321-1607K 0-66859
 AlC₃-Be-C-SiC system, phase analysis and TEM struct. obs. 0-108420
 AlCl₃, pseudopot. calcs. 0-91446
 AlCl₃, aq. soln., HCl additive effects on ²⁷Al spin-lattice relax. 0-66058
 AlCl₃-NaCl melt, n-TiO₂ electrode, electrochem. and photoelec. props. 0-81328
 Al₂Cl₆, matrix isolated, vibr. spectra, isotopic fine struct. and valence force field calcs. 0-58258
 Al₂Cl₆ molten, nuclear mag. relax., mol. rot. 0-71209
 AlF₃, pseudopot. calcs. 0-91446
 AlF₃, ⁴He⁺ ion scatt. spectrometry below 5 keV 0-108313
 AlF₃ based glasses, chem., thermal and optical props. (*French*) 0-70139
 AlF₃ in Al-AlF₃-Al MIM thin film structures, dielec. and elec. props. (*Slovak*) 0-100536
 AlF₃-M₂F glasses, M=alkaline earth, density-of-states and structural forms, Raman spectra study 0-97255
 AlF₃-MF (M=Li, Na, K, Rb or Cs), ion-molecule equilibria studied by mass spectrometric method, heats of dissociation and form. calc. 0-104479
 AlGaAs buried heterostructure lasers, gain and absorption spectra meas. 0-91792
 AlGaAs DH injection phase-locked laser, coherence 0-102726
 AlGaAs DH laser, self-pulsations due to proton bombarded region self-annealing during ageing 0-99728
 AlGaAs DH laser epilayer struct. optimization for integrated optical circuits 0-99879
 (Al, Ga)As DH lasers, catastrophic optical damage generation mechanism, TEM obs. of dark line defects 0-100239
 (Al, Ga)As DH lasers, comparison of 'normal' lasers and lasers exhibiting light jumps 0-106519
 AlGaAs heterojunction diode as light source for fibre optical communication 0-58653
 AlGaAs heterojunction laser, lightwave sources and detectors 0-64068
 AlGaAs heterojunctions, nonradiative recomb. vel. estimate from edge luminescence, props. 0-65668
 AlGaAs heterojunction photocell with luminescence wavelength converter 0-108800
 AlGaAs injection laser, large optical cavity, with multiple active regions 0-106538
 AlGaAs laser array on Si heat sink, optical power detection 0-74383

aluminium compounds continued

- (Al, Ga)As laser system, VPE growth and degradation mechanisms 0-99748
 AlGaAs lasers, CW high-power single-mode constricted DH lasers with large optical cavity 0-64076
 AlGaAs mode-locked diode laser, optical pulse generation 0-95907
 AlGaAs p-n diodes, I-V characts., tunnelling 0-100510
 AlGaAs semiconductor lasers, single-mode stabilisation by traps 0-95893
 (Al, Ga)As strip buried heterostructure lasers, mode locking using external cavity 0-91791
 (Al, Ga)As stripe geometry, proton-bombardment delineated DH laser, lifetime 0-106520
 AlGaAs stripe-geometry DH laser, filament displacement and refr. losses 0-58536
 AlGaAs transverse junction stripe laser with distributed Bragg reflector 0-106535
 AlGaAs/GaAs monolithic series-connected solar cell arrays 0-97794
 AlGaAs-GaAs proton irradiated solar cells, deep level defects and recombination parameters 0-94032
 Al_{0.35}Ga_{0.65}As-GaAs cascade solar cell structures, spectral response and junction characts. 0-93926
 Al_{0.35}Ga_{0.65}As-GaAs N-p heterojunction diodes, current suppression by cond. band discontinuity 0-80362
 Al_{0.42}Ga_{0.58}As-GaAs-Al_{0.42}Ga_{0.58}As, etalon, optical bistability and modulation 0-58628
 Al_{0.5}Ga_{0.5}As CW heterolaser, 10000 hr. lifetime tests, degradation of mirror surfaces 0-106542
 Al_{0.5}Ga_{0.5}As CW multiwavelength TJS laser, MBE, single-longitudinal modes 0-64049
 Al_{0.5}Ga_{0.5}As, compensated, electron mobility temp. depend. 0-96868
 Al_{0.5}Ga_{0.5}As, electron mobility illumination, compensation, space charge regions, carrier scatt. 0-70691
 Al_{0.5}Ga_{0.5}As epitaxial film, microstruct., effect on elect. characts. of Schottky diode (*Russian*) 0-107671
 Al_{0.5}Ga_{0.5}As epitaxial layers on GaAs, struct. study by scanning Auger electron microscopy 0-80110
 p-Al_{0.5}Ga_{0.5}As film, variable-gap photo-EMF 0-65626
 n-Al_{0.5}Ga_{0.5}As, ion implanted films, optical and luminescence, props. 0-60699
 Al_{0.5}Ga_{0.5}As, modified-strip buried-heterostructure lasers, CW electro-optical properties 0-74359
 Al_{0.5}Ga_{0.5}As, p-n junction solar cells, effect of interface recombination on photoluminescence and current 0-93893
 Al_{0.5}Ga_{0.5}As, pure and Ge doped, shallow acceptor photoluminescence 0-76064
 Al_{0.5}Ga_{0.5}As semitransparent photocathode, LPE, quantum efficiency spectrum 0-76153
 Al_{0.5}Ga_{0.5}As triggerable semiconductor lasers made by deep proton bombardment 0-69408
 Al_{0.5}Ga_{0.5}As:Cu, variable-gap semicond., impurity props., carrier recomb. 0-96907
 p-Al_{0.5}Ga_{0.5}As:Ge-p-GaAs:Ge-n-GaAs:Sn heterostructure solar cells, LPE growth techniques 0-66977
 Al_{0.5}Ga_{0.5}As-Al_{0.5}Ga_{0.5}As DH IR-visible (0.89-0.72 μm) MBE grown lasers 0-64058
 Al_{0.5}Ga_{0.5}As-GaAs, quantum-well heterostructure laser diode, temp. depend. of threshold current 0-87395
 Al_{0.5}Ga_{0.5}As-GaAs DH injection laser, active region internal parameters determined, composite resonator use 0-106548
 Al_{0.5}Ga_{0.5}As-GaAs DH laser diode, I-V characts., variation of ideality factor 0-64027
 Al_{0.5}Ga_{0.5}As-GaAs DH laser operation, phonon contrib. 0-102724
 n-Al_{0.5}Ga_{0.5}As-GaAs heterojunctions, selectively doped, FET 0-80364
 Al_{0.5}Ga_{0.5}As-GaAs heterostructure, quantum-well, hot electrons and phonons 0-84505
 Al_{0.5}Ga_{0.5}As-GaAs heterostruct., varizional, parameter determined by photoluminescence method (*Russian*) 0-108291
 Al_{0.5}Ga_{0.5}As-GaAs large-quantum-well heterostructures, induced phonon-sideband laser operation 0-95888
 Al_{0.5}Ga_{0.5}As-GaAs quantum-well heterostructures, phonon-assisted recombination and stimulated emission 0-74358
 Al_{0.5}Ga_{0.5}As-GaAs quantum-well heterostruct., exciton in recombination 0-103990
 p-Al_{0.5}Ga_{0.5}As-p-GaAs-n-GaAs heterophotocells, optimal parameters for high solar-excitation level 0-93872
 AlGaAsSb LPE growth, lattice-matched to GaSb, characterisation 0-60794
 AlGaAsSb-GaSb heterojunction injection laser, radiative props. 1.4 to 1.8 μm range 0-91798
 Al_{0.5}Ga_{0.5}AsZn-GaAs solar cells by LPE, open circuit voltage, fill factor 0-101108
 Al_{0.5}Ga_{0.5}P, LPE, crystallographic obs. and electrochem. 0-88445
 Al_{0.5}Ga_{0.5}P, proportional ingredient content determined by X-ray fluorescence 0-97747
 Al_{0.5}Ga_{0.5}Sb solid soln., electrochem. deposition of Ni and Pd 0-93505
 Al_{0.5}Ga_{0.5}Sb, soln.-grown, photolum. 0-71476
 Al_{0.5}Ga_{0.5}Sb-Pd contacts, struct., preparation elec. props. 0-65684
 Al_{0.5}Ga_{0.5}Sb-Pd contacts, band gap depend. of barrier height 0-65685
 AlH₃, pseudopot. calcs. 0-91446
 AlH₃⁺, spectrum at 3632 Å, rot. anal. 0-78632
 AlH₃, nucl. spin-spin coupling constants, ab initio calcs. 0-95647
 AlH₃, synchronous photochem. processes in lattice 0-101029
 Al³⁺(H₂O)_n (n=1,2,4,6), FSGO-pair-pot. calcs. (*German*) 0-74278
 Al(IO₃)₃.8H₂O, crystal structure, thermal vibr. parameters, X-ray study 0-64979
 Al₂Mn₂Si₂O₁₂, amorphous insulating spin glass, susceptibility and magnetisation meas. 0-88765
 AlN, absorption edge shape interpretation, Wannier excitons absorption in charge impurity elec. field 0-66233
 AlN filamentary crystal reinforced mullite-corundum ceramics, filaments strength, eval. 0-104230
 AlN film, oriented c-axis, low temp. deposition by reactive magnetron sputtering 0-76180
 AlN film, thermodynamics and kinetics of CVD 0-108354
 AlN films, RF glow discharge deposited, current-voltage characts. 0-84515
 AlN films, RF reactive ion-plating, struct. and morphology 0-104074
 AlN films on glass substrate, prep. by reactive DC magnetron sputtering technique, c-axis orientation 0-89146
 AlN, luminescence excitation spectrum and band struct. 0-84783
 AlN, piezoelectric film, low temp. growth by RF reactive planar magnetron sputtering method 0-76175

aluminium compounds continued

- AlN, polycrystalline, stress-strain data up to 1.25 GPa 0-100899
 AlN thread-like crystals reinforced mullite-corundum ceramics, props. 0-108525
 AlN-Mo cermets, ZrO_2 and mullite whisker reinforced, strength var. with temp. 0-104232
 AlN-Si₃N₄-Be₃N₂ system, phase equilibria 0-60844
 Al₂O₃ molecule, mass spectrometric study 0-89563
 Al(OH)₃, from Al etching wastes, firing to prod. corundum ceramics 0-108376
 Al(OH)₃, precip. from solns. containing Li ions, X-ray diffr. patterns and comp. determ. 0-76502
 γ -AlOOH and γ -AlOOD, IR and Raman spectra obs., struct. and D_{2h}¹⁷ space group anal. 0-89000
 γ -AlOOH, boehmite, proton pair obs. from NMR absorpt. spectra 0-75866
 AlOOH, diaspor, cryst. struct. refinement and electron density distrib. 0-79758
 AlP(As)(Sb), surface (110), energy distrib. of dangling-orbital surface states 0-80347
 Al(PO₃)₃-BaF₂-Al₂O₃ glasses, opt. props., group I-III fluorides effect 0-66143
 α -AlPO₄ as SAW substrate material, piezoelec. props. 0-80710
 α -AlPO₄, berlinite, H₂O conc. determ. by Raman scatt. 0-76572
 α -AlPO₄ crystal, totally symm. high-freq. fund. vibrs., identification refinement 0-100656
 AlPO₄, synthetic berlinite, electron irradi. effects, ESR, ENDOR, optical spectral study 0-80608
 AlS, B^{II}-X^{II} transition, assignment of UV bands, vibr. and rot. anal. 0-58278
 Al₂(SO₄)₃·(NH₄)₂SO₄·24H₂O, crystn. kinetics in an MSMRP crystalliser 0-100185
 n-AlSb, acoustoelectric effect due to piezoelectrically active wave 0-80331
 AlSb, laser pulse annealing, induced nucleation, crystal growth 0-84966
 p-AlSb, saturation characts. over CO₂ laser spectrum 0-83646
 AlSb Schottky barrier solar cells, characteristics and efficiency of Czochralski-grown crystals 0-61366
 AlSb solar cell material, epitaxy, ionicity and bond struct. 0-61367
 AlSb, thin film growth on insulating substrates, by metal organics CVD 0-60786
 θ -Al_{0.35}V₂O₅, NMR of ⁵¹V 0-71232
 (Al_{1-x}V_x)₂O₅, impurity doping effects, elec. props. obs. 0-75609
 Al₂(WO₄)₃:Cr(Eu), and undoped crystals, luminesc. obs. 0-89047
 Au-Al_{0.5}Ga_{0.5}As -GaAs heterojunction Schottky-barrier solar cells, barrier height enhancement 0-85284
 Au-Ga_{1-x}Al_xSb Schottky barriers, barrier height 0-96986
 Au-n-AlGaAs-n-GaAs Schottky-barrier solar cells, band readjustment effect 0-81458
 Au-n-Ga_{1-x}Al_xAs-n-GaP narrow-band variable-gap surface-barrier photodetector 0-96944
 Ba(PO₃)₂-AlF₃-CaF₂ glass, elec. cond. and IR spectra 0-89005
 Ba(PO₃)₂-AlF₃-MgF₂ glass, elec. cond. and IR spectra 0-89005
 Be₃Al₂[Si₂O₁₈]:Cr³⁺, artificial emerald, distrib. of Cr³⁺ impurity 0-95905
 BeF₂-KF-CaF₂-AlF₃-EuF₃ fluoroberyllate glass, Eu³⁺ fluoresc. linewidth 0-66285
 CaF₂-AlF₃-Na₃AlF₆(-Al₂O₃), phase equilibria, X-ray diffr. and DTA meas. 0-108409
 12CaO.7Al₂O₃, composition of gases released on heating, crystallisation (Russian) 0-93820
 CsLi_{0.5}(Al,Fe)_{1.5}F₆ pyrochlore, Mossbauer contrib. to exam. of cationic order (French) 0-93224
 Cs₂SO₄·Al₂(SO₄)₃·24H₂O, ⁵³Cr³⁺ ENDOR Lines, RF ENDOR power and modulation freq. effects 0-75884
 Cu-Al ferrite films, LPE growth 0-96752
 Er₂Al_{5-x}Ga_xO₁₂, LPE, spectroscopic props. 0-93419
 (Fe_{6-x}Al_x)O₉, IR spectra, lacunar γ -phase to corundum α -phase transform. 0-108199
 (Fe₂Cr_{4-x}Al_x)O₉, IR spectra, lacunar γ -phase to corundum α -phase transform. 0-108199
 (Ga, Al, As) heterostructures and compounds, electronic props., empirical pseudopot. calc. 0-80366
 (Ga, Al)As laser diode, operation and gain meas., importance of gap shrinkage effects 0-66257
 (Ga,Al)As narrow double-current-confinement channelled-substrate planar laser fabrication, double etching technique 0-74371
 (Ga,Al)As:Si, Ge, epitaxial layers, radiative recomb., compensation, cathodolum. study 0-66307
 GaAlAs actively mode-locked laser, bandwidth limited picosecond pulses 0-95905
 GaAlAs DH injection laser, half-ring, room temp. operation 0-58558
 GaAlAs DH laser, narrow stripe geometry, spontaneous carrier lifetime 0-87392
 (GaAl)As DH laser, threshold current density, growth terraces effect 0-99723
 GaAlAs DH laser diodes, small signal modulation, junction capacitance effect 0-83625
 GaAlAs DH laser diode, edge coupling to planar LiNbO₃:Ti waveguide 0-87559
 (GaAl)As DH laser wafer, photoluminesc. improvement with buffer layer 0-64014
 GaAlAs DH lasers, SiO₂ insulated, characts. and near field 0-64019
 GaAlAs DH lasers, self-sustained pulsation suppression, effect of SiO₂ facet coating films 0-95894
 (GaAl)As injection laser operating in external cavity, intensity self-pulsations 0-64013
 (GaAl)As injection lasers operating with optical fibre resonators 0-91812
 (GaAl)As, LPE, GaAs dissolution kinetic in undersaturated isothermal solns. in Ga-Al-As system 0-80106
 GaAlAs laser nonlinearities, harmonic distortion 0-74357
 GaAlAs light intensity modulators using p-n junctions 0-99871
 (GaAl)As low-beam-divergence CW DH laser, grown by low press. metal-organic CVD 0-74376
 GaAlAs, luminescence circular polarisation, electron optical orientation resonant variation (Russian) 0-84782
 GaAlAs mode stabilised separated multilayer stripe geometry DH laser, optical waveguide 0-64051
 GaAlAs on GaAs thin film stacked multiple-bandgap solar cell struct., prep. using CVD techniques 0-94083
 GaAlAs, surface vacancies, bound state energy levels calc. 0-80340

aluminium compounds continued

- GaAlAs terraced substrate laser, visible-light-emitting, characts. 0-106523
 (GaAl)As:Be implanted DH stripe geometry laser 0-64044
 GaAlAs/GaAs solar cells, efficiency optimisation at high and low current levels (French) 0-61348
 GaAlAs/GaAs solar cells, Be and Zn behaviour 0-101111
 GaAlAs-GaAs DH injection laser, external cavity operated angled-stripe geometry, CW operation 0-64078
 GaAlAs-GaAs heteroface solar cells, high open-cct. voltage, full-factor and efficiency 0-94081
 GaAlAs-GaAs heterojunction solar cells, high temp. props. 25 to 300°C 0-94035
 GaAlAs-GaAs lasers, channelled substrate, prepared by combination of organometallic pyrolysis and LPE 0-99745
 (GaAl)As-GaAs narrow stripe laser, improved optical communication system performance 0-102733
 Ga_{0.1}Al_{0.9}As LPE layers containing low-cond. regions, charging effects in SIMS anal. 0-66348
 Ga_{1-x}Al_xAs, LPE layers, electron mobility, scatt. processes 0-84519
 Ga_{1-x}Al_xAs:Zn, acceptor energy level and elec. props. 0-65482
 Ga_{1-x}Al_xAs, appl. of theory of electroepitaxy of multicomponent systems 0-65396
 Ga_{1-x}Al_xAs, band struct. from I-V, C-V meas. on Schottky diodes 0-96989
 Ga_{1-x}Al_xAs based layer structures, optimum growth conditions, comp. and struct. perfection 0-104069
 Ga_{1-x}Al_xAs DH injection laser, FM at microwave freq. rates 0-58610
 Ga_{1-x}Al_xAs DH laser diode, long-lived, high-power, facet coated 0-58564
 Ga_{1-x}Al_xAs, epitaxial, radiative deep states 0-76061
 Ga_{1-x}Al_xAs heterostructure, LPE prep., growth and dissolution kinetics, thermodynamic and kinetic models 0-75456
 Ga_{1-x}Al_xAs, intervalley energy gaps, temp. junction, exptl. determ. 0-80179
 Ga_{1-x}Al_xAs laser, SHG with KNbO₃ 0-74431
 Ga_{1-x}Al_xAs low threshold stripe geometry DH laser, Be implanted, on semi-insulating substrate 0-69409
 Ga_{1-x}Al_xAs, semiconductor defects, spectroscopic study of electronic props. 0-84446
 Ga_{1-x}Al_xAs structures, STEM and scanning deep level transient spectroscopy in defect centre anal. cathodoluminesc. techniques 0-103642
 Ga_{1-x}Al_xAs, varizone layer photoelectron yield depth estimation 0-100745
 Ga_{1-x}Al_xAs visible diode lasers, degradation mechanisms 0-64026
 Ga_{1-x}Al_xAs visible diode lasers, degradation due to macroscopic defects (<730 nm) and facet oxidation (>740 nm), life tests 0-99729
 n-Ga_{1-x}Al_xAs:Si, room-temp. cond. and band struct. 0-96869
 Ga_{1-x}Al_xAs-GaAs DH injection lasers grown by metalorganic CVD, props. 0-99751
 Ga_{1-x}Al_xAs-GaAs p-n and p-p-n heterojunction solar cells, high efficiency, prep., eval. and characts. (Japanese) 0-61342
 Ga,Al_{1-x}As-GaAs heteroepitaxial layer distortion characterisation by X-ray multiple diffr. 0-96754
 Ga,Al_{1-x}As, photodetector diode on GaAs substrate dark currents, tunnelling, energy gaps, effective masses 0-70805
 Ga_{1-x}Al_xAs_{1-x}P_x, epitaxial layer heterojunction, nonradiative recombination at misfit dislocations 0-96901
 GaAlAsSb-GaSb low bandgap solar subcell for high efficiency multiband-gap converters, LPE growth 0-93927
 Ga_{1-x}Al_xN heteroepitaxial films, photoluminesc., cathodoluminesc. 0-66292
 Ga_{1-x}Al_xP varigap struct., crystallation 0-80993
 Ga_{1-x}Al_xP:N epitaxial films, ion implanted, cathodoluminescence study 0-60684
 Ga_{1-x}Al_xSb, surface oxidation, Raman spectra, residual Sb layers 0-71419
 GaAs-(GaAl)As injection lasers with circular resonator 0-74377
 GaAs-Al_{0.3}Ga_{0.7}As n-n heterojunction, LPE grown, cond. band discontinuity, C-V profiling meas. 0-70801
 GaAs-Al_{0.1}Ga_{0.9}As, current transverse junction lasers, low threshold, MBE prep. 0-83614
 GaAs-Al_{0.1}Ga_{0.9}As buried-heterostructure lasers, current injection confinement, MBE/LPE hybrid technique 0-74374
 GaAs-Al_{0.1}Ga_{0.9}As DH laser, MBE grown, CW electro-optical props. 0-102725
 GaAs-Al_{0.1}Ga_{0.9}As electro-optic frequency- and polarisation-modulated injection laser 0-91810
 GaAs-Al_{0.1}Ga_{0.9}As heterojunction interface, two-dimensional hole gas obs., Shubnikov-de Haas meas. 0-80357
 GaAs-Al_{0.1}Ga_{0.9}As heterostructures, real-space electron transfer by thermionic emission, analytical model 0-100512
 GaAs-Al_{0.1}Ga_{0.9}As MOS rib waveguide polarizers 0-64207
 GaAs-Al_{0.1}Ga_{0.9}As MOS rib waveguide polariser, modulator and isolator 0-64217
 GaAs-Al_{0.1}Ga_{0.9}As multilayers, two-dimens. transport at high mag. fields 0-65724
 GaAs-Al_{0.1}Ga_{0.9}As-GaP photocathodes, minority carrier diffusion length determ. by photoluminesc. 0-103992
 GaAs-AlAs mixed crystals, valence charge distrib. and elec. field gradients 0-80239
 GaAs-AlAs superlattice, folded acoustic phonons obs., Raman scatt. 0-88996
 GaAs-AlGaAs DH injection laser with stripe contacts, radiation pulse stepped shape 0-91799
 GaAs-AlGaAs DH laser structure, defect assessment by differentiated cathodolum. topography 0-59819
 GaAs-AlGaAs heterojunction superlattices, inelastic light scatt. by two-dimens. electron gas 0-93360
 GaAs-AlGaAs solar cells (Rumanian) 0-93877
 n-GaAs-Ga_{1-x}Al_xAs, heavily doped superlattice, electronic props., perpendicular low temp. mobility 0-65660
 GaAs-Ga_{2-x}Al_xAs:Be, LPE, diffusion of Be into GaAs substrate 0-103517
 GaAs-GaAlAs bipolar transistor and heterostruct. laser, monolithic integration 0-102858
 GaAs-GaAlAs DH lasers, strain-enhanced luminesc. degradation, photoluminesc. obs. 0-69392
 GaAs-GaAlAs DH laser, O⁺ isolation compared with SiO₂ isolation 0-74382

aluminium compounds continued

- GaAs-GaAlAs injection lasers, narrow-stripe proton-implanted, high bit-rate modulation 0-91824
 GaAs-GaAlAs multilayer struct., Hall mobility enhancement 0-100511
 GaAs-GaAlAs superlattices, metalorganic VPE growth, in sites ellipsometry monitoring 0-70547
 GaAs-GaAlAs wafers, defects and degradation, transmission cathodolum. evaluation 0-65395
 GaAs-GaAlAs-GaAs rectifying semicond. struct., prep. by MBE and characts. 0-65657
 n-GaAs-n-Al_xGa_{1-x}As rectifying heterojunction, cond. props. study 0-88626
 (GaAs)_n(AlAs)_m multilayers, MBE, interdiffusion, X-ray diffr. study 0-70474
 GaAsSb/GaAlAsSb DH lasers, growth and props. 0-69412
 HgCr₂-Al₂Se₃, temp. depend. of ESR linewidth, 105-300K 0-71161
 In_{1-x}Al_xAs, band gap, IR absorpt. spectra meas. 0-66205
 In_{0.5}Al_{0.5}P, proportional ingredient content determ. by X-ray fluorescence 0-97747
 KCrAl_{1-x}(SO₄)₂·12H₂O, EPR of single crystals, zero-field splitting of Cr³⁺ 0-66015
 K₂O-Al₂O₃-P₂O₅-TiO₂, structural role of Ti, kinetic study of chem. destruction 0-88055
 Li-Al-Cl system, thermodynamic props., phase equil. 0-89211
 LiAlSiO₄, β-eucryptite one-dimens. fast ion cond., temp. depend. of cryst. struct. 0-107191
 LiAlSiO₄-Cu, β-eucryptite solid electrolyte, Cu²⁺ EPR obs. of ion exchange props. 0-108056
 LiF-AlF₃, mixture at 1293K, thermodynamic function 0-104134
 Li₂O-Al₂O₃-GeO₂, glass, interdiffusion coeffs. of Li and Na 0-88369
 MgO-CaO-FeO-Fe₂O₃-SiO₂-Cr₂O₃-Al₂O₃ spinel refractories, physicochem. prod. conditions 0-89185
 NH₃-AlCl₃ solution, Al₂O₃ ultrafine gel particle form. 0-93807
 Na₂Al₂Si₂O₇(NaX)_{2n}, X=Cl, Br or I, sodalites, thermal destruction of colour centres (*Russian*) 0-84169
 Na₂Al₂Si₂O₇(NaX)₂₋₃, (X=Cl, Br, I), X-ray irradi., thermal-erase cathodochromism and dihalide mol. centres (*Russian*) 0-66236
 RbAl(SO₄)₂·12H₂O, spin-Hamiltonian with trigonal S³I terms for describing ⁵⁷Fe ENDOR spectra 0-75885
 SbCl₃/AlCl₃ molten mixtures, Raman spectra 0-93305
 Si-Al-Be-C-N system, phase equilibria 0-60839
 Si-Al-O-N ceramic, grain boundary desegregation and intergranular cohesion 0-100872
 Si-Al-O-N system, phase analysis and TEM struct. obs. 0-108420
 Si-Al-O-N system, stable phase cryst. struct. and microstruct. obs. using TEM 0-108421
 SiAlON, prepared from siliceous sand and Al powder, hot pressing, steatite contamination effects (*Japanese*) 0-93528
 Ta-Al-N thin film resistors with improved elec. props. 0-100544
 Ti₂O₃-Al₂TiO₃, solid solubility, X-ray phase and optical microscopic exam. 0-59657
 V₂O₅-AlNBO₄ system, interfacial reactions, efficient boundary conditions and solid state reactivity 0-76542
 Y₂O₃-AlN-SiO₂ oxynitride glasses, elec. props. 0-80267

aluminosilicate glasses

- alkali borosaluminosilicate system, self-focusing fibres with aperture of 0.18 0-87548
 aluminosilicate glass:Co (14.3 wt.%), AC susceptibility meas. 0-88771
 ceramic surface streaks and blisters, UV fluoresc. study 0-84347
 polishing, surface characts. using X-ray reflection grazing (*French*) 0-65533
 sittal cylindrical shell reinforced with internal stiffening ribs, stress-strain state under external press. 0-71684
 vibrational spectra and glass structure 0-84732
 Ag halide photochromic glasses, optical properties, effect of Cu ions 0-93364
 Al₂O₃-B₂O₃-SiO₂ sheet glass, solar energy appl., optical and mech. props. 0-87447
 Al₂O₃-CaO-SiO₂-(B₂O₃)-(Na₂O) composite glasses, high strength, prod. by overlayering 0-89193
 Al₂O₃-SiO₂-MO-Fe₂O₃ glass, M=Ca, Mg, Ba, Sr, UV and EPR absorpt. spectra 0-89018
 CaO-Al₂O₃-B₂O₃-SiO₂-FeO, glass, IR spectra at room and melt temp. 0-88986
 CaO-Al₂O₃-SiO₂ additive to zircon ceramic, sintering and mech. props. 0-60814
 CaO-Al₂O₃-SiO₂ glasses, density-of-states and structural forms, Raman spectra study 0-97255
 CoO-Al₂O₃-SiO₂, amorphous, remanent magnetisation short time depend. 0-65919
 K₂O-Al₂O₃-2SiO₂-BaO plasma emitter 0-96368
 Li, containing Cu and halogen impurities, ESR spectra 0-66027
 LiO₂-Al₂O₃-SiO₂, containing ZrO₂, cryst. process 0-103253
 Li₂O-Al₂O₃-SiO₂, phase separation of initial stages of sitalisation 0-88053
 Li₂O-Al₂O₃-SiO₂, study of elastic props. 0-104205
 Li₂O-Al₂O₃-SiO₂ C_∞:C Cd⁺, γ-irrad., EPR study 0-84639
 Li₂O-Al₂O₃-SiO₂ glass-ceramic, near-zero thermal-expansion heat treatment effect in fracture behaviour 0-66537
 Li₂O-Al₂O₃-SiO₂ glass, crystallised, grain size and internal strain 0-103259
 Li₂O-Al₂O₃-SiO₂:Cd²⁺, ESR study 0-103879
 Li₂O-Al₂O₃-SiO₂-TiO₂ system glasses, Raman spectra obs. of glass-ceramics form. 0-60825
 Li₂O-MgO-Al₂O₃-SiO₂ glass scintillator for pulsed neutron detection 0-87019
 Li₂O-Na₂O-B₂O₃-Al₂O₃-SiO₂ glass, Young's modulus and density, ion exchange effects 0-84982
 Li₂O-TiO₂-Al₂O₃-SiO₂ glass, γ-irrad., struct. position of Ti, EPR study 0-84644
 MgO-Al₂O₃-SiO₂, sintered, cordierite, mineralogy and props. 0-60827
 MgO-TiO₂-Al₂O₃-SiO₂, γ-irrad., struct. position of Ti, EPR study 0-84644
 Mn₂Al₂Si₂O₁₂, amorphous, spin-glass, insulating, Mn²⁺ mag. reson. 0-65918
 MnO-Al₂O₃-SiO₂, amorphous, remanent magnetisation short time depend. 0-65919
 MnO-Al₂O₃-SiO₂, amorphous spin glass, AC susceptibility 0-80520
 Na₂O-Al₂O₃-B₂O₃-SiO₂-AgCl(Br), photochromic glass, kinetics of thermal decolorisation 0-103931

aluminosilicate glasses continued

- Na₂O-Al₂O₃-SiO₂, glass, nucleation, crystn., ceramic form. 0-84082
 Na₂O-Al₂O₃-SiO₂-(K₂) glasses, ion exchange kinetics and interdiffusion mechanisms 0-80003
 Na₂O-BaO-Al₂O₃-SiO₂, glass, nucleation, crystn., ceramic form. 0-84082
 Na₂O-CaO-Al₂O₃-SiO₂ glass, crystn. for the purpose of obtaining vitroceramics (*French*) 0-75163
 Na₂O-K₂O-Al₂O₃-SiO₂, structure of modified surface layer, internal friction method 0-103258
 Na₂O-TiO₂-Al₂O₃-SiO₂, γ-irrad., struct. position of Ti, EPR study 0-84644
 Si₃N₄-Al₂O₃-SiO₂ systems, glass forming regions 0-84070
 SiO₂ fabric, prep. from E-glass, structural stability rel. to brittleness, X-ray diffr. and IR spectrosc. studies 0-96634
 SiO₂-Al₂O₃, vitreous US vel. and absorption 0-107380
 SiO₂-Al₂O₃ (8 mol.%) glass, heat treated, devitrified phases 0-66469
 SiO₂-Al₂O₃-B₂O₃ glass mech. strength increased by etching 0-97609
 SiO₂-Al₂O₃-CaO-B₂O₃-SrO-ZnO-Na₂O-K₂O-B₂O₃, glaze effect of P₂O₅ additions 0-60824
 SiO₂-Al₂O₃-CaO-MgO-B₂O₃, E-glass, acid resist. studies 0-60991
 SiO₂-Al₂O₃-CaO-Na₂O-Fe³⁺, optical absorpt. due to Fe³⁺ ligand field and charge transfer 0-89020
 SiO₂-Al₂O₃-Cu₂O glass alkaline durability, corrosion rate, heat capacity and elastic moduli 0-93673
 SiO₂-Al₂O₃-K₂O glass ceramic interaction with Pb borosilicate glaze 0-84398
 SiO₂-Al₂O₃-MgO-TiO₂ devitrificates, microstruct. and props. (*Polish*) 0-70141
 SiO₂-Al₂O₃-Na₂O-BaO-TiO₂, glass ceramic interaction with Pb borosilicate glaze 0-84398
 SiO₂-Al₂O₃-Y₂O₃-La₂O₃-TiO₂ glasses with high elastic moduli, alkaline durability 0-85071
 SiO₂-B₂O₃-Li₂O-Al₂O₃ (28, 2, 1 wt.%) glass, dielec. const. at 3 GHz 0-93233
 SiO₂-Li₂O-Al₂O₃ glass, luminesc., polarisation degree distrib. 0-108257
 SiO₂-MgO-CaO-Al₂O₃-Ce, Fe, redox equil., expt. 0-85171
 SiO₂-NaAlSi₃O₈ glasses and devitrificates, prep. and vibr. spectroscopy study (*Polish*) 0-93530
 SiO₂-PbO-B₂O₃-Al₂O₃-CaO-Na₂O-K₂O glaze, interaction with aluminosilicate glass-ceramics 0-84398
 TiO₂-Al₂O₃-SiO₂ system, ternary glass-forming region and phys. props. 0-84919

a.m. (modulation) see amplitude modulation

ambient temperature see temperature

americium

see also nuclei with

- 5f-electron delocalisation 0-70595
 oxalate precipitation for separation of Am, Cm, and trivalent lanthanides 0-83202
 phase transformation at high press., X-ray diffr. obs. 0-107422
 radioactive effluent, Pu and Am inventory of ecosystem near a nuclear facility 0-97820
²⁴¹Am, concs. in sediments from coastal basins off California and Mexico 0-98303
²⁴¹Am, gamma-ray meas. of Pu and Am in molten salt residues for nuclear materials safeguards 0-83165
²⁴¹Am, radioactive waste, sorption in igneous rocks 0-95367

americium compounds

No entries

ammeters

pick-up for titrimetric chem. analyser (*Russian*) 0-71984

ammonia

- abundance on Jupiter and Saturn from visible obs. 0-82269
 adsorption of NH₃ and ND₃ on CaCl₂ and CaBr₂, complex formation, IR and far IR spectra obs. 0-80063
 adsorption on Al surface, NH₃ decomp., XPS obs. 0-92783
 adsorption on Mo (111) planes, preferential nitriding, FEM study 0-66877
 affinities for H⁺(Li⁺)(K⁺)(CH₃⁺), ab initio SCF calculations 0-102443
 affinity for Li⁺(Na⁺)(K⁺), ab initio SCF calcs. 0-58125
 in atmosphere, NH₃ and particulate NH₄⁺ fluxes evaluation over W.Germany 0-94132
 atmosphere composition, Southern Ocean air 0-61871
 atmosphere concentration measurement, ring oven technique 0-81507
 atmospheres of Uranus and Neptune, estimation of ammonia and water vapour contents 0-90366
 chemisorbed on Ir (111), mol. adsorbate structs. from angular-resolved photoemission 0-76141
 chemisorption on Ni (111) and reaction, LEED, desorption and photoemission expts. 0-59799
 Earth's early atmosphere, NH₃ photochemically produced in small quantities 0-109208
 effect on low-cycle fatigue of bronze 0-104348
 electron Coulomb profile beyond impulse approx. 0-87083
 far IR emissions by IR pumping using N₂O laser 0-74345
 fuel cell, high temperature solid electrolyte, overpot. and product selectivity characts. 0-104504
 gas, phase conjugation via degenerate four-wave mixing 0-106566
 gas, weak IR absorpt. meas. using double-beam Fourier spectrometer 0-105725
 gaseous ammonia in Saturn troposphere 0-94748
 impurity in H₂-air-H₂PO₄ fuel cells, effect on performance 0-108795
 inversion lines from nonmetastable rotational levels, SHF obs. of Kleinmann-Low nebula 0-73016
 on Jupiter, longitudinal variability in atm. visible spectra 0-82270
 laser, CW far IR emissions, CO₂ laser pumping and Stark tuning 0-106508
 laser, for 16 μm range, review (*Rumanian*) 0-87408
 laser, high-power efficient optically pumped, tunable over 770 to 890 cm⁻¹ range 0-91780
 laser, subMM 81.5 μm, freq. meas. by CO₂ laser difference freq. comparison 0-74415
 laser, synchronous pumping, ultrashort pulse generation at 151 μm 0-102705
 laser 12.8 μm source, 60% efficient SHG in Te cryst. 0-83640
 laser action 11-13 μm, optical pumping by continuously tunable CO₂ laser 0-83596
 laser lines, CW far IR, CO₂ laser pumping and Stark tuning 0-69382
 laser transitions, CW, two-photon pumped 0-99702

ammonia continued

- molecular cloud in NGC 2264, NH₃ line emission mapping, SHF and UHF 0-94847
- molecular energy quantities from localised charge densities, dependence on geometry and basis set 0-63525
- molecular groups in solids, stochastic jumps, group theoretical method 0-79714
- molecule, ¹⁴N quadrupole coupling consts., ab initio calcs. 0-58283
- molecule, absorpt. coeffs. meas. in Nd laser emission band 0-78620
- molecule, absorpt. cross sections at CO₂ laser wavelengths, temp. and press. depend. 0-78613
- molecule, bond bending, bond orbitals rel. to nucl. motion 0-95513
- molecule, core 1s shakeup study, XPS and Alpha calcs. 0-69064
- molecule, correl. energy, fourth order diagrammatic, many body Rayleigh Schrödinger perturbation theory 0-63556
- molecule, electron impact, 35 keV, Bethe surface and Compton profile 0-87235
- molecule, electron impact ionisation, total and partial cross sections meas. 0-95729
- molecule, expansion cooled, mol. photoionisation, rot. struct., rot. predis. soc. of excited states 0-91611
- molecule, ground state, microwave inversion lines 0-87098
- molecule, high-resolution absorpt. spectra obs. using pressure-tuned diode laser 0-82835
- molecule, intermolecular interaction energies calcs. using minimal basis sets 0-78681
- molecule, inversion spectrum collisional line broadening, general theory 0-87184
- molecule, inversion spectrum press. broadening by He and Ar, linewidths calc. 0-95599
- molecule, IR spectra, fine struct. of rot.-vibr. bands 0-102504
- molecule, lone pair contributions to infrared intensities, ab initio calculations 0-63630
- molecule, mapping in L 183 (L 134 N) dust cloud high density core, SHF obs. 0-105307
- molecule, mol. Rydberg S—S and S—T transitions, semi-empirical SCF MO calc. 0-91453
- molecule, nucl. elec. shielding tensor calcs. 0-83296
- molecule, orbital relax. energy for single and double ionis. from valence shells 0-106253
- molecule, transverse relax. time, T₂, of inversion doublets from free induction decay 0-58281
- molecule, vibr. excitation in soft X-ray emission and core ESCA spectra 0-69163
- molecule+Rydberg atom, reaction channels, expt. vs. theory 0-63755
- monitor using Stark microwave cavity resonator 0-61500
- phase conjugation in an inhomogeneously broadened medium 0-83642
- production by ocean thermal energy conversion 0-66988
- pure gas, enthalpy, Carlson-Thodos van der Waals eqn. calcs. 0-83878
- Raman lasing, far IR CW 0-83595
- solar energy storage system, ammoniated salt heat pump using MgCl₂, CaCl₂, NH₄Cl 0-81484
- solar thermochemical cavity absorber based on NH₃ dissociation, design and cost anal. 0-81489
- solid, melting curves, Lennard-Jones Devonshire theory 0-65201
- solid film, absorpt. coeffs. determ. 50 to 7000 cm⁻¹ 0-97356
- spectrophotometer, IR, effective spectral slit width determ. using NH₃ absorpt. line 0-95167
- stimulated hyper-Raman scattering in a molecular gas via a three-photon process to obtain IR and far IR radiation 0-58633
- surface water continuous analysis by NH₄⁺-sensitive plastic membrane electrode 0-89701
- synthesis, industrial, using N₂ reducing solar cells 0-89632
- troposphere, vertical distrib. by photochem. model 0-85701
- troposphere vertical profile, daily and seasonal variation 0-85700
- vapour, supercrit. and subcrit., 0-59162
- vertical density profiles in Jupiter and Saturn atm. from emissivity data 0-82267
- CO-H₂O-NH₃-methanol, solid mixture vibr. modes, IR spectra 0-90504
- CaCl₂-NH₃ dry absorption for solar refrigeration 0-61310
- Li-NH₃ concentrated solution, NMR relaxation of ⁷Li 0-108084
- NH₃⁺, two-mode Jahn-Teller effect calcs. 0-83297
- ¹⁵NH₃ far IR laser emission at 153, 375 μm, optically pumped by ¹³C¹⁶O₂ laser 0-58507
- NH₃-AlCl₃ solution, Al₂O₃ ultrafine gel particle form. 0-93807
- NH₃-Ar mixture, thermal cond., viscosity, Senftleben-Beenakker effect 0-100054
- NH₃-CaCl₂, isothermal dissociation and regeneration, appl. to solar refrigeration (French) 0-61300
- NH₃-He mixture, viscosity, Senftleben-Beenakker effect 0-100054
- NH₃-LiH, struct. and props., SCF ab initio calcs. 0-106250
- NH₃+CO₂(N₂), collisional broadening of NH₃ inversion spectrum lines 0-69521
- NH₃+Cl⁺, reactions at room temp. 0-93749
- NH₃+D₂O⁺(D₂O)_n, binary reactions, rate coeffs. and product ion distributions determ. 0-81305
- NH₃+H₂, NH₃ inversion transition, linewidths and T₁/T₂ ratio 0-99499
- NH₃+H₂O⁺(H₂O)_n, binary reactions, rate coeffs. and product ion distributions determ. 0-81305
- NH₃+He(Ne)(Ar)(Kr), pure rot. line, press. broadening calcs. 0-78656
- NH₃+Hg(P₁), quenching rate constants determ. with nanosecond light pulser with Hg vapour 0-100111
- NH₃+methyl cation, reaction kinetics, 0.04-1 eV (French) 0-66768
- NH₃+NH₃(He)(Ar)(N₂)(O₂), vibr. energy transfer temp. depend. 0-63763
- NH₃(ND₃) in solid Ar, UV absorption spectra, temp. depend. of matrix spectra 0-63652
- ¹⁵N labelled NH₃ production for medical appl. 0-72327
- ¹⁵NH₃ intravenous injection, absorbed radiation dose calcs. 0-94375
- ¹⁵NH₃, Doppler-free optical double reson. spectroscopy using single-freq. laser and modulation sidebands 0-68274
- ¹⁵NH₃ far IR CW laser, optically pumped with ¹³C¹⁶O₂ laser 0-78866
- O(D₂)+NH₃→OH(v,N)+NH₂, bimodal OH rot. distrib. obs. and energy disposal 0-76501
- Xe(nf Rydberg state)+NH₃, n- and l-changing and ionising collisions 0-58360

ammonia clocks see atomic clocks**ammonium compounds**

- ammonia Rochelle salt, temp. depend. of optical axis angle, phase transitions (Russian) 0-97216

ammonium compounds continued

- ammonium Rochelle salt, thermodynamics of ferroelec. transition 0-84702
- ammonium alginate, aq. solns., laminar flow heat transfer in helical coils 0-59030
- halides, phase transitions by Monte Carlo method using cubic Ising model 0-70408
- halides, phonon dispersion, cohesive and dielec. props. in three body force shell model 0-79892
- lithium ammonium tartrate dihydrate, ferroelectric-elastic phase transition, theoretical model and expt. (Russian) 0-75961
- methylammonium bromide, solid, phase transitions, PMR, DTA study 0-107421
- (Rochelle salt)_{1-x}(ammonium Rochelle salt)_x, phase transitions, hydrostatic press. effects 0-93246
- steel, mild, cyclic strain enhanced dissolution in NH₄NO₃, corrosion fatigue props. 0-85083
- tetrachloroaluminate, vapor characterisation by photoelectron spectrosc. 0-81388
- thermal decomposition, appl. to solar storage 0-76656
- [(NH₄)₂H(SO₄)₂]_{1-x}(ND₄)₂D(SO₄)_x system, ferroelectric transitions 0-108160
- β-Al₂O₃-NH₄⁺, neutron diffr. obs. of struct. 0-107512
- β-Al₂O₃-NH₄⁺, PMR relax. time obs. of ionic motion 0-71213
- β-Al₂O₃-NH₄⁺, single cryst. characs. and AC cond. obs. 0-107514
- β-Al₂O₃-NH₄⁺ and β"-Al₂O₃-NH₄⁺-H₂O, single cryst. PMR and proton motion 0-108101
- β-Al₂O₃-NH₄⁺, proton dynamics neutron scatt. study 0-59408
- β"-Al₂O₃-NH₄⁺-H₂O, ionic cond. at room temp. 0-107513
- Al₂(SO₄)₃ (NH₄)₂SO₄·24H₂O, crystn. kinetics in a MSMPR crystalliser 0-100185
- CH₃NH₂·Ga(SeO₄)₂·12H₂O, dielec. relax. near transition temp. 0-60493
- CeNH₄P₂O₇ and Ce(NH₄)₂(PO₃)₅, synthesis by solid-phase reaction, characs. 0-60778
- Fe(NH₄)₂(SO₄)₂·4H₂O, rehydration kinetics, Mossbauer effect study 0-61081
- LiNH₄SO₄, DC elec. cond. 0-88603
- Mg(NH₄)₂(SO₄)₆·H₂O·VO(H₂O)₂²⁺, proton ENDOR meas. used to determine hyperfine coupling tensors 0-66075
- Mg(NH₄)₂(SeO₄)₂·6H₂O·Mn²⁺, EPR spectra 0-100608
- (ND₄)₂BeF₄, incommensurate phase, ⁹Be NMR study 0-75973
- ND₄Br·Cu²⁺, pseudo-Jahn-Teller effect manifestation in ESR spectrum 0-71168
- ND₄D₂AsO₄, protonic cond. near antiferroelec. Neel temp. 0-59703
- (ND₄)₂D₃IO₆, neutron diffr. study 0-88098
- ND₄D₂PO₄, cryst., transverse and longit. elec. susceptibilities, modified Ising model calcs. 0-97203
- ND₄DSeO₄, crystals, struct., IR spectra, dielec. props. 0-75919
- ND₄I, Raman spectrum, press. effects 0-97261
- ND₄IO₄, Raman spectra, libration lattice modes 0-60575
- NH₄AlF₆, single cryst., prep. and struct. (French) 0-79762
- NH₄⁺, mol. consts. and mean vibr. amplitudes calcs. 0-106318
- NH₄⁺, particulate, fluxes into free atmosphere over W.Germany evaluation 0-94132
- NH₄⁺ ion rotation, quantum effect on spin-lattice relax. time 0-75875
- (NH₄)₂SO₄, ferroelectricity, triple 60 Hz D-E hysteresis loops 0-71364
- NH₄Ag₂I₅, superionic cond., pressure effect on phase transitions 0-70405
- NH₄Ag₂I₅, superionic solid film, surface diffusion coeff. 0-92709
- NH₄Al₂I₅, superionic phase transition, dynamical and crit. pt. props. 0-107535
- NH₄BF₄, ionic radii and chem. shifts, correl. with electronegativity 0-66054
- (NH₄)₂BeF₄, elastic props., US damping 0-84229
- (NH₄)₂BeF₄, far-infrared and submillimetre dielectric response 0-80782
- (NH₄)₂BeF₄, ferroelectricity, triple 60 Hz D-E hysteresis loops 0-71364
- (NH₄)₂BeF₄, incommensurate phase, ⁹Be NMR study 0-75973
- (NH₄)₂BeF₄, linear and nonlinear optical props. in incommensurate phase 0-69452
- (NH₄)₂BeF₄, order-disorder phase transitions with many-minimum potential, thermodynamic props. 0-96623
- (NH₄)₂BeF₄, paraelec. phase, X-ray and neutron diffr. cryst. struct. anal. 0-84159
- NH₄Br, heat capacity meas. near order-disorder transition 0-88332
- NH₄Br, NH₄⁺ rot. motion, quasielastic neutron scatt. obs. 0-96492
- NH₄Br, supercooled, polymorphic transform., struct. correspondences and mechanisms 0-107097
- NH₄Br·Cu²⁺, luminesc., orientation phase transition 0-100687
- NH₄Br·TiI₃ and pure crystals, luminesc., VUV irradiated at 80K (Russian) 0-84763
- NH₄Br·Cl₂, heat capacity meas. near order-disorder transition 0-88332
- (NH₄)₂Cd₂(SO₄)₃, dielec. and spontaneous polarisation, -195 to -180°C, particle size depend. 0-97200
- NH₄Cl, ¹⁵N zero point vibr. energy from nuclear photon scattering 0-59593
- NH₄Cl, acoustic absorption by soft modes of defects 0-59584
- NH₄Cl, activation coefficients and solvation numbers in mixed methanol solvents 0-81334
- NH₄Cl, coexistence states during first order transition, optical obs. 0-75350
- NH₄Cl, crit. behaviour near tricritical point, phenomenological interpretation 0-70389
- NH₄Cl, dendrite development and growth in very small crystals, Monte Carlo study 0-107683
- NH₄Cl, piezoelec. effect near nonferroelastic phase transition 0-66116
- NH₄Cl Raman spectra, pressure effects 0-97268
- NH₄Cl, submicron particles, density, morphology 0-61166
- NH₄Cl·Ni²⁺, EPR spectrum, spin Hamiltonian, zero-field splitting effects 0-97135
- NH₄Cl·H₂O, solidification microstructs., effect of reduced gravity 0-96632
- NH₄Cl·H₂O solidification model for showering cryst. form. in molten metal cooling (Japanese) 0-66498
- NH₄Cl(Br), effect of NH₄⁺ internal motion on elec. and optical props. 0-100454
- NH₄ClO₄, AC elec. cond. temp. and freq. depend., obs. and unified defect struct. model 0-88554
- NH₄ClO₄, polymorphism phase transition mechanism 0-79737
- NH₄Cl·3NH₃·NH₄Cl, solar energy storage system heating and cooling 0-81484
- (NH₄)₂Cr₂O₇, crystal hypomorphism and hypermorphism 0-59427
- (NH₄)₂CuBr₄·2H₂O, hyperfine and super-exchange interactions 0-103654

ammonium compounds continued

- $\text{NH}_4\text{Cu}_2\text{Cl}_2(\text{I}_2-\text{Cl}_2)$, highly conducting solid electrolyte 0-65280
 $(\text{NH}_4)_2\text{CuCl}_4 \cdot 2\text{H}_2\text{O}$, hyperfine and super-exchange interactions 0-103654
 $(\text{NH}_4)_2\text{FeF}_6$, one-dimensional antiferromag. systems, Mossbauer studies 0-71266
 $(\text{NH}_4)_2\text{GeF}_6$, cryst., highly bent H bonds, IR spectrosc. investig. 0-93292
 $\text{NH}_4\text{H}_2\text{PO}_4$, blue tunable picosecond pulse generation by synchronous mixing of Nd:glass laser with sideband radiation 0-87431
 $\text{NH}_4\text{H}_2\text{PO}_4$, cryst., transverse and longit. elec. susceptibilities, modified Ising model calcs. 0-97203
 $\text{NH}_4\text{H}_2\text{PO}_4$, cryst. growth in presence of Mn ions 0-93468
 $\text{NH}_4\text{H}_2\text{PO}_4$, crystal growth kinetics, in situ X-ray topography study 0-76167
 $\text{NH}_4\text{H}_2\text{PO}_4$, filiform crystals at low temp., tensile strength determ. 0-100877
 $\text{NH}_4\text{H}_2\text{PO}_4$, SHG method pulse width meas. of Nd:YAG laser (*Chinese*) 0-87432
 $\text{NH}_4\text{H}_2\text{PO}_4$ single crystal evidence for spiral growth on pyramidal faces 0-84120
 $\text{NH}_4\text{H}_2\text{PO}_4$ thin crystal, intracavity SHG of synchronously mode-locked CW dye laser 0-95945
 $\text{NH}_4\text{H}_2\text{PO}_4$, Z-cut, SAW props. 0-84358
 $\text{NH}_4\text{H}_2\text{PO}_4$, ^{57}Fe , Mossbauer study, Fe^{3+} effect in habit 0-100627
 $(\text{NH}_4)_2\text{H}(\text{SO}_4)_2$, phase transitions, dielec. study at low temps. 0-88902
 NH_4HSeO_4 , cryst. struct., dielec. and ferroelec. props. 0-60528
 NH_4HSeO_4 , ferroelec. phase transition, pyroelec. props. 0-60513
 NH_4HSeO_4 , ferroelec. props. rel. to struct. 0-71345
 NH_4HSeO_4 , ferroelec., phase transitions, permittivity and pyroelectricity meas. 0-71350
 $\text{NH}_4\text{H}(\text{SeO}_3)_2$, single crystal, ^{77}Se magnetic shielding, chemical shift tensors 0-71207
 NH_4I , Raman spectrum, press. effects 0-97261
 NH_4IO_4 , Raman spectra, libration lattice modes 0-60575
 NH_4LiSO_4 , point group symm. at high press. phase 0-70150
 $(\text{NH}_4)_2\text{M}(\text{SO}_4)_2 \cdot 6\text{H}_2\text{O}$, $\text{M} = \text{Ni}, \text{Co}, \text{Mg}$, IR spectra 0-97280
 NH_4NO_3 crystals, NH_4^+ ion symmetry in phases II-V, Raman spectra obs. 0-66200
 NH_4NO_3 , IR spectra and vibr. bands 0-69144
 NH_4NO_3 , phase III, cryst. struct., neutron powder diffractometer study 0-107134
 NH_4NO_3 , shock-induced intramol. bond breaking, XPS and EPR study 0-76512
 $(\text{NH}_4)_2\text{Ni}(\text{BeF}_4)_2 \cdot 6\text{H}_2\text{O}$, X-ray cryst. struct. determ. 0-107137
 $(\text{NH}_4)_2\text{PcR}_2\text{O}_{16}$, cryst. struct., $(\text{PcR}_2\text{O}_{16})^{3-}$ anion geometry 0-107157
 $\text{NH}_4\text{PbI}_2 \cdot 2\text{H}_2\text{O}$, X-ray cryst. struct. determ. 0-64958
 $(\text{NH}_4)_2\text{PtF}_6$, X-ray cryst. struct. determ. 0-107125
 $(\text{NH}_4)_2\text{Rb}_2\text{SO}_4$, isomorphic impurity effect on dielec. and nonlinear optical props. 0-88911
 $(\text{NH}_4)_2\text{ReCl}_4(\text{IrCl}_6)$, proton relaxation near antiferromagnetic phase transitions 0-80640
 NH_4ReO_4 (ND_4ReO_4), nuclear electric hexadecapole interactions 0-65513
 NH_4ReO_4 , heat capacity and thermodynamic props., 8 to 304K 0-100335
 $(\text{NH}_4)_2\text{SO}_4$, order-disorder phase transitions with many-minimum potential, thermodynamic props. 0-96623
 $(\text{NH}_4)_2\text{SO}_4$, paraelectric, N-quadrupole coupling meas. by proton-N double resonance 0-60459
 $(\text{NH}_4)_2\text{SO}_4$ polydisperse aerosol number and mass conc. meas. by elect. aerosol anal. 0-108753
 $(\text{NH}_4)_2\text{SO}_4$, static and dynamic dielec. behaviour 0-71337
 $(\text{NH}_4)_2\text{SO}_4 \cdot \text{MnO}_4$, X-ray irradi. damage, optical absorpt. spectra study 0-66246
 $(\text{NH}_4)_2\text{S}_2\text{O}_7$ etchant, for NbC, TaC and HfC 0-85097
 $(\text{NH}_4)_2\text{S}_2\text{O}_8 \cdot \text{HCl} \cdot \text{H}_2\text{O}$ dislocation etchant for β -brass crystals 0-65004
 $(\text{NH}_4)_2\text{SiF}_6$, cryst., highly bent H bonds, IR spectrosc. investig. 0-93292
 $(\text{NH}_4)_2\text{SiF}_6$, elastic constants, softening of acoustic modes, obs. by Brillouin scattering 0-71440
 $(\text{NH}_4)_2\text{SnBr}_6$, structural phase transitions study by Raman scatt. 0-93318
 $(\text{NH}_4)_2\text{SnCl}_6$, elastic constants, softening of acoustic modes, obs. by Brillouin scattering 0-71440
 $(\text{NH}_4)_2\text{SnF}_6$, cryst., highly bent H bonds, IR spectrosc. investig. 0-93292
 $(\text{NH}_4)_2\text{TiF}_6$, cryst., highly bent H bonds, IR spectrosc. investig. 0-93292
 $\text{NH}_4\text{Ti}(\text{SeO}_4)_2$, $(\text{NH}_4)_3\text{Ti}(\text{SeO}_4)_3$, and $(\text{NH}_4)_4\text{Ti}(\text{SeO}_4)_4$, cryst. struct. (*French*) 0-84148
 $(\text{NH}_4)_2\text{ZnCl}_6$, commensurate-incommensurate phase transition, ^{35}Cl NQR study 0-75966
 $(\text{NH}_4)_2\text{ZnCl}_6$, ferroelectricity and incommensurate-commensurate phase transitions 0-60523
 $(\text{NH}_4)_2[\text{VF}_6\text{O}]$, X-ray cryst. struct. determ. 0-107128
 $(\text{NH}_4)_2[\text{ZnCl}_4]$, X-ray cryst. struct. determ. 0-107138
 $\text{NiCl}_2 \cdot 6\text{NH}_3$, low temp. sp. ht. and mag. ordering 0-75784
 $\text{Tb}(\text{NO}_3)_3 \cdot \text{Fe}(\text{NO}_3)_3 \cdot (\text{NH}_4)_2\text{CO}_3 \cdot \text{H}_2\text{O}$ system, cpd. form., comp. and props. 0-100832
 $\text{Zn}(\text{NH}_4)_2(\text{SeO}_4)_2 \cdot 6\text{H}_2\text{O} \cdot \text{Mn}^{2+}$, EPR spectra 0-100608

amorphisation

- amorphisation due to ion bombardment, SRO struct. 0-79844
 α -quartz, electron irradi., defect struct. and radiolysis 0-107321
 D_2O with soluted NaOD, collective excitations in liquid and amorphous state, 77 to 300K 0-92636
Ge, ion bombardment-induced photon emission as function of target temp. 0-100698
Ge surface, (111), ion-bombarded and annealed, spectroscopic ellipsometry study 0-103543
Si, amorphous, substrate orientation effect on regrowth by laser pulses, channeling, backscatter 0-84409
Si film, ion bombarded, crystalline-to-amorphous transition, defect-rich film prep. 0-65071
Si layers amorphized by molecular ions, laser annealing 0-103379
Si:N(P), ion implanted, IR transmission and rel. spectra study 0-108244
 SnO_2 :P, CVD films, elec. props., cryst. to amorphous transition effects 0-107933
 SnO_2 :P, CVD growth and etching characts., doping effects 0-107667
ZnS ion beam etching, topographic changes, amorphisation, luminescence study 0-76078
 Zr_3Al ordered alloy, ion bombardment damage, TEM 0-100287

amorphous magnetic materials *see magnetic properties of amorphous substances*

amorphous semiconductors

- see also chalcogenide glasses; electrical conductivity of amorphous semiconductors and insulators; insulators*
amorphous, high field transport, impact ionisation, carrier mobility 0-80286
amorphous, photogeneration, thermalisation model calcs., band gap (*French*) 0-75595
amorphous film, glow discharge deposited, for low cost solar cells 0-61355
applications in electrophotography, thin film electronics and solar cells 0-107693
conference, Masnuy-St-Jean, Mons, Belgium, Oct. 1979 0-82570
copper phthalocyanine-iodine, amorphous cpd. prep. by I_2 diffusion in polycryst., triplet EPR signals obs. (*Russian*) 0-66016
defects, band gap states 0-80215
density of states determ. from field effect data 0-107688
diamagnetic, photostructural changes, mechanism 0-92557
disordered system in mag. field, frequency dependence of conductivity tensor, theoretical investigation 0-70725
doped, electronic props. 0-80283
electronic phenomena, book 0-77551
electronic states, theoretical methods 0-80167
field effect and capacitance-voltage meas. anal., localised density of states 0-103686
film, laser induced nucleation, long wavelength instability 0-84126
II-VI amorphous semiconductors, electronic states, sublattice one-band Hamiltonian transform. 0-59861
III-V amorphous semiconductors, electronic states, sublattice one-band Hamiltonian transform. 0-59861
ill-condensed matter, summer school, Les Houches, France (July-Aug. 1978) 0-82561
ionised centre diffusion accel. by electrostatic fields 0-70473
laser crystallisation, for production of large grained sheets for solar cells 0-93570
localised states and cond. mechanism (*Japanese*) 0-84467
luminescence 0-80862
modulated photocurrent, analysed for trap-limited case (*Japanese*) 0-60030
Mossbauer effect, props. and investigation methods (*French*) 0-80652
optical absorption, theory 0-80818
oxide semiconducting glasses, electronic cond. mechanism 0-65562
polycarbonate: tri-p-tolylamine, chemical control of conductivity 0-59984
review of structural and electronic props. 0-64901
short-range order, theory and probes 0-79698
Al-amorphous Ge-nSi, photoelectric props. 0-70822
As, amorphous, absence of photodarkening 0-103970
As, amorphous, short-range order, theory and probes 0-79698
As, defects, band gap states 0-80215
As₂Ge amorphous film, far IR absorpt. spectra, refractive index 0-80785
As₂S₃ film, evaporated, switching effects 0-96952
BaO-V₂O₅-CuO semiconducting glasses, impurity effects, elec. resist. and EPR study 0-103692
C-H films, amorphous, elec. props., chem. modifications 0-84523
Cd₃As₂ film on NaCl substrate, vacuum deposition, growth morphology, microstructure 0-75479
CdS(Se)(Te), determ. of wurtzite, zincblende and rocksalt phases 0-100219
CdSe-Sb₂Se₃ heterojunction, photoelec. props. 0-70816
CuInSe₂ amorphous thin film, flash evaporation, struct., stoichiometry 0-89150
EuS, on W, memory effect in field emission 0-89126
Fe₈₀P₁₅C₇, amorphous and crystalline, electrochemical and semicond. behaviour (*Russian*) 0-101021
GaAs, amorphous layers, ion-implanted, low-temp. epitaxial regrowth 0-92790
Ge amorphous film, bright-field hollow cone images 0-75136
Ge amorphous film, crystn. front velocity during scanned laser crystn. 0-107662
Ge, amorphous film, DC sputter deposited, effect of trapped Ar on minimum temp. for impulse stimulated explosive crystallisation 0-100422
Ge amorphous film, disorder induced phonon absorpt. meas. using double beam Fourier spectrometer 0-105725
Ge, amorphous film, persistent photoconductivity, dangling bonds 0-84487
Ge amorphous films, structural relaxation and crystallisation 0-100170
Ge black, selective absorber characterisation 0-80112
Ge, defects, band gap states 0-80215
Ge, ideal surface, definition and characts. 0-107623
Ge:O, Cu, amorphous thin film, impurity effects on struct. 0-107054
Ge-Ga amorphous alloy, co-evaporated elec. and optical props. 0-70860
GeSe₂ amorphous film, laser induced oscillatory phenomena 0-84711
In₂Se₃-SnO₂ amorphous film-SnO₂ system, photovoltaic spectra, annealing effect (*Japanese*) 0-92926
Na₂O-B₂O₃-SiO₂-As₂O₃(As₂O₅) glasses, DC and AC resist., bipolaronic hopping cond. 0-88558
S-based amorphous semicond. film, prep. by plasma decomp. of H₂S-N₂-NH₃, and characterisation 0-80422
SbSBr glass, IR reflectivity spectra 0-71403
Se, amorphous, bulk, Raman scatt. near T_g 0-60596
Se, amorphous, bulk, reson. Raman scatt. 0-60597
Se, amorphous, electronic struct. and optical props., pseudopot. calc. 0-65428
Se, amorphous, US attenuation at low temp., internal friction peak 0-65152
Se, amorphous film, dielec. activity obs. near glass transition temp. 0-75933
Se, amorphous film, highly disordered, UPS study 0-76148
Se, amorphous films, evaporated, ageing and crystn., DTA 0-65413
Se, appl. to xerography 0-57415
Se film, amorphous, empirical formula for temp. depend. of dielec. loss peaks 0-97197
Se, film, influence of wavelength on optical quenching of photoconductivity 0-60046
Se, layer, localised states in band gap 0-59928
Se, localised electronic states, photoluminesc. and ESR studies 0-65501
Se, luminescence 0-80862
Se, modulated photocurrent, analysed for trap-limited case (*Japanese*) 0-60030

amorphous semiconductors continued

- Se, mol. structure, local atomic arrangement at intrinsic bonding defects 0-59374
 Se, Raman spectra, crystn. processes 0-60608
 Se, trigonal and amorphous, electronic struct. and nonempirical calc. of struct. props. 0-59866
 Se, trigonal and amorphous, positron lifetimes, positronium form. 0-60711
 Se, US relaxation and retardation of deform. near T_g point 0-84256
 Se, vac. deposited on polymeric substrates, with dynamic coating device 0-100792
 Se:As, amorphous film, dielec. activity obs. near glass transition temp. 0-75933
 Se:As X-ray plates, electronic transport (*German*) 0-80290
 Se:I, vitreous, crystn. kinetics determ. (*German*) 0-79936
 Se:As alloys, appl. to xerography 0-57415
 Si, amorphous, doped, electronic props. 0-80283
 Si, amorphous, glow discharge produced, defect creation, high optical excitation 0-97327
 Si, amorphous, hydrogenated, electron drift mobility meas. 0-75565
 Si, amorphous, hydrogenated film, electroreflectance study 0-88967
 Si, amorphous, hydrogenated and deuterated, struct. 0-103245
 Si, amorphous, hydrogenation using DC and HF plasma treatment 0-59497
 Si, amorphous, implanted, recrystn. induced by scanning CW laser, reaction rates, analytical model 0-66334
 Si, amorphous, ion implantation method, B and P ions 0-100274
 Si, amorphous, opaque, surface phonon attenuation, Brillouin scatt. 0-80808
 Si, amorphous, prep. by reactive RF sputtering in Ar-silane mixtures, undoped, n-type and p-type targets 0-76182
 Si, amorphous, pure and H doped, picosecond relax. of optically induced absorption 0-97302
 Si, amorphous, pure and hydrogenated, far IR absorption coeff. meas. 0-108213
 Si, amorphous, scanning TEM studies of cryst. inclusions 0-79699
 Si, amorphous, substrate orientation effect on regrowth by laser pulses, channeling, backscatter 0-84409
 Si, amorphous, UHV evaporated, annealing behaviour of spin density 0-93163
 Si, amorphous, undoped, photocond., continuous illum. effect 0-84486
 Si, amorphous and crystalline, heating by Q-switched laser radiation 0-84963
 Si, amorphous and crystalline, ion implanted, UPS meas. 0-97411
 Si, amorphous evaporated, picosecond optoelectronic detect., sampling and correlation meas. 0-100478
 Si amorphous film, anisotropic etching phenomenon, appl. as solar selective absorber surfaces 0-72054
 Si, amorphous film, glow discharge deposition, rate enhancement by mag. field 0-65412
 Si, amorphous film, RF plasma deposition from $\text{SiCl}_4\text{-H}_2$, characterisation 0-66435
 Si, amorphous film, selective laser recrystn. over heavily doped lines 0-84947
 Si, amorphous films, RF sputtering prep. at high Ar press., props. obs. 0-80418
 Si amorphous films, switching, electrothermal model 0-80407
 Si, amorphous hydrogenated solar cells, field depend. quantum efficiency, electron-hole recombination 0-66971
 Si amorphous layer recrystallisation by laser beam 0-93566
 Si amorphous layers, glow-discharge, laser-annealed, elec. props. 0-75661
 Si, amorphous layers, RF-sputtered on sapphire, crystallisation by CW ion laser annealing 0-80109
 Si amorphous p-n junctions, high current, characts. 0-70807
 Si based alloys, amorphous, photovoltaic behaviour, solar cell appl. 0-94051
 Si, co-sputtered doped, photovoltaic material appl. 0-93488
 Si, defects, band gap states 0-80215
 Si, EPR and spin-dependent effects 0-80592
 Si, effect of disorder on H content 0-75258
 Si, epitaxial regrowth, structure and impurities effect 0-84401
 Si film, acoustic study using Rayleigh waves 0-75312
 Si film, analytical techniques, review 0-80120
 Si, film, EELS microanalysis 0-100722
 Si film, hydrogenated, preparation by SiH_4 decomposition 0-80956
 Si film, ion bombarded, crystalline-to-amorphous transition, defect-rich film prep. 0-65071
 Si film, low press. CVD prep., struct., elec. and optical props. 0-70548
 Si, glow discharge deposited, mobility edge calc. 0-80220
 Si, hydrogenated amorphous, laser annealing 0-100713
 Si, hydrogenated amorphous, gap states, comparison of photoemission and photocond. results 0-103724
 Si, ideal surface, definition and characts. 0-107623
 Si, ion implantation, negative magnetoresist., localised mag. states 0-70731
 Si ion implanted, amorphous to crystalline transition due to laser irradi. 0-103451
 Si, ion penetration, computer program 0-88185
 Si, ion-implanted, laser epitaxial recrystallisation threshold energy 0-70571
 a-Si, laser induced crystallisation mechanism, epitaxial regrowth 0-84962
 Si, Lifshitz constant for calc. of van der Waals force between two solids (*French*) 0-107658
 Si, luminescence 0-80862
 Si noncrystalline film, struct., interatomic distances, SRO 0-107053
 a-Si p-i-n and c-Si p-n junction solar cells, design concept differences 0-94031
 Si, random-network model, charge-density variation 0-80165
 Si solar cells, barrier props. determ. by differential I-V characts. meas. 0-94053
 Si solar cells, current collection and electrical shorting problems 0-93969
 Si solar cells, design considerations 0-85277
 Si solar cells, perform. parameters of amorphous and polycryst. thin film cells 0-93882
 Si, sputtered, resist. control by ion implantation 0-100262
 Si, structural and electronic props., review 0-64901
 Si, transient electrical transport, general and unified treatment 0-59977
 Si wafer, thin surface layers, amorphous to cryst. transform., obs. technique 0-107288
 Si:Ar, ion-implanted, epitaxial regrowth by laser annealing, microstruct. 0-84404

amorphous semiconductors continued

- Si:As (P^+) ion implanted, laser annealed, correlation of struct. and elec. props 0-70855
 Si:Au, O(H), film, amorphous, elec. cond. meas. 0-80423
 Si:B(P), ion implanted crystalline and amorphous laser annealing 0-97509
 Si:F, amorphous, heat resistant, prep., elec. cond., IR absorpt., annealing 0-65719
 Si:F,H, amorphous, elec. and optical props. 0-60031
 Si:F,H, amorphous efficient carrier generation for solar photovoltaic energy conversion 0-92906
 Si:H, amorphous, 2p level shift, XPS obs. 0-97401
 Si:H, amorphous, Auger electron spectrosc. obs. 0-76112
 Si:H, amorphous, band tail absorpt., photocurrent meas. for Schottky barrier solar cell 0-60032
 Si:H, amorphous, defect photoluminesc. meas. 0-97334
 Si:H, amorphous, geminate recombination model for photoluminescence decay 0-71481
 Si:H, amorphous, HV photovoltaic cells, design parameters 0-101105
 Si:H, amorphous, horizontal cascade type integrated photovoltaic cell module 0-94091
 Si:H, amorphous, image pickup devices 0-100481
 Si:H, amorphous, optical studies of excess carrier recomb., evidence for dispersive diffusion 0-76059
 n-Si:H, amorphous, photoelectromagnetic effect 0-107845
 Si:H, amorphous, Pt film growth, AES and LEED study 0-88447
 Si:H, amorphous, Schottky diodes, elec. props., light-induced effects 0-103741
 Si:H, amorphous, short-range order, theory and probes 0-79698
 Si:H, amorphous, solar cells using ultrathin active layer to increase conversion efficiency 0-94030
 Si:H, amorphous, solar cells, trap spectroscopy using transient current techniques 0-104508
 Si:H, amorphous, solar-cells, charge collection and spectral response 0-85275
 Si:H, amorphous, sputtered on $\text{Gd}_2(\text{MoO}_4)_3$, ferroelec. domain wall motion, image scanning 0-83663
 Si:H, amorphous, sputtered Schottky barrier solar cells, conduction mechanism 0-104506
 Si:H, amorphous, stacked solar cells, development 0-94050
 Si:H, amorphous, surface states distribution using MOS tunnel junctions 0-103735
 Si:H, amorphous, temp. depend. of photolum. 0-89063
 Si:H, amorphous Schottky solar cells, prep. and characts. of diode RF reactive cathodic sputtered films (*French*) 0-61347
 Si:H, amorphous thin film, ion plating, IR absorpt. meas. 0-84857
 Si:H, amorphous thin film solar cells 0-81478
 n-Si:H, bulk density of deep states, DLTS meas. 0-88518
 Si:H, defect states, luminesc. and ESR obs. 0-76075
 Si:H, depletion width determ. by analytical model 0-100445
 a-Si:H, influence of H on optical props., H conc. and H bonds 0-76098
 Si:H, photoelectrochem. behaviour 0-81480
 Si:H, Li, amorphous, photoluminescence obs. 0-66280
 Si:H, amorphous, solar cell structure, optical absorption by gap states 0-94052
 Si:H amorphous films, IR spectrum and struct. 0-97277
 Si:H amorphous MIS solar cell, loss mechanisms and photovoltaic parameters, overview 0-93923
 Si:H film, amorphous, plasma-deposited, small angle X-ray and neutron scatt. studies 0-59826
 a-Si:H film, glow discharge deposited, H profiles, doping level 0-84202
 Si:H film, H-associated disorder modes, PMR spin-lattice relax. time meas. 0-93202
 Si:H films, reactively sputtered, prep. and characterisation 0-100785
 a-Si:H highly homogeneous, for low-cost solar cell fabrication 0-72053
 Si:H:F, depletion width determ. by analytical model 0-100445
 Si:O,H amorphous, time resolved luminesc. 0-66288
 Si:P, ion implanted, regrowth of damage structs. by laser annealing 0-107289
 Si/ $\text{In}_2\text{O}_3\text{-SnO}_2$ thin film junctions, polarity dependent memory switching effects 0-70814
 Si/Pd system, solid phase epitaxial growth control by C ion implantation 0-75466
 Si:F,H amorphous solar cells, DC glow discharge fabrication 0-72041
 Si-Ge solar cells, tandem multiple gap 0-94029
 Si-H, amorphous, sputtered, photolum. obs. 0-80856
 Si-H, structural and electronic props., review 0-64901
 Si-H:P amorphous film, dark cond., struct., Raman scatt. 0-88588
 Si:C,H amorphous reactively sputtered film, H content effect on film props. 0-75459
 $\text{Si}_{1-x}\text{C}_x\text{-H}$ glow discharge films, local atomic struct., XPS and AES study 0-93448
 SiC_{1-x} , luminescence 0-80862
 SiH_x , amorphous, solar cells, short circuit-currents and collection efficiencies 0-94028
 $\text{Si}_{1-x}\text{H}_x\text{-Al}$, amorphous, co-sputtered Al modification, electronic and optical props. 0-100461
 Si(111):Pb ion implanted amorphous layers, recrystallisation, impurity out-diffusion model (*Chinese*) 0-88363
 $\text{SnO}_2\text{-Sb}$ film, electrotransport phenomena obs., under DC electric field 0-59840
 Te, amorphous, electronic struct. and optical props., pseudopot. calc. 0-65428
 Te, Raman spectra, crystn. processes 0-60608
 Te, trigonal and amorphous, electronic struct. and nonempirical calc. of struct. props. 0-59866
 V_2O_5 amorphous film, photochromism and thermochromism 0-93254
 V_2O_5 , amorphous semicond., solubility and fibrous texture 0-75162
 $\text{V}_2\text{O}_5\text{-P}_2\text{O}_5\text{-Cs}_2\text{O(Na}_2\text{O)}$ glasses, enhanced secondary electron emission yield 0-93441
 $\text{V}_2\text{O}_5\text{-P}_2\text{O}_5\text{-Nb}_2\text{O}_5$ glasses, switching 0-88604
 $\text{WO}_3\text{-B}_2\text{O}_3\text{-ZnO}$ glasses, DC cond. and optical absorpt. 0-107783

amorphous state

- see also electrical conductivity of amorphous metals and alloys; electrical conductivity of amorphous semiconductors and insulators; electron energy states of amorphous solids; magnetic properties of amorphous substances; vitreous state
 alkyl halide, amorphous, depolarisation thermocurrents and dielectric relaxation time distrib. (*French*) 0-60490
 alloys, struct. determ. by energy dispersive X-ray diffraction 0-84063

amorphous state continued

- alloys, struct. end plastic flow, review 0-84090
 bisphenol A-phthalic anhydride epoxy resin, diglycidyl ether, Rayleigh scatt., Brillouin and IR spectra 0-66211
 trans-1,4-chlorobromocyclohexane, liquid, crystalline and amorphous state, conformation and vibr. spectra, IR obs. 0-60568
 trans-1,4-chloriodocyclohexane, liquid, crystalline and amorphous state, conformation and vibr. spectra, IR obs. 0-60568
 EXAFS, determ. of struct. of disordered regions (*French*) 0-80905
 ion-implanted alloys, surface props. effects and appls. 0-79824
 irradiation induced crystalline to amorphous transition, Gibbs energy 0-70371
 metallic glasses, production and properties, technological appl. 0-71105
 metals, geometric struct. models and diffraction exam. techniques 0-79700
 metals, superconducting properties rel. to ordering 0-65735
 Metglas 2826 ribbon, voids formation during crystallisation 0-108428
 Mossbauer effect, props. and investigation methods (*French*) 0-80652
 pentacene, disordered solid layer, absorpt. spectra 0-93417
 polycarbonate, amorphous, yield behaviour in oriented and unoriented condition, effect of temp. 0-97537
 Raman intensities, connection with EXAFS Debye-Waller factors in amorphous solids 0-108214
 rapid quenching, techniques for determ. very short room temp. lifetimes of amorphism 0-84981
 steel, alloy high-C, amorphous, mech. props. and thermal stability 0-76361
 stochastic geometry, review, book contrib. 0-73269
 structured defects, computer simulation study 0-88040
 summer school on ill-condensed matter, Les Houches, France (July-Aug. 1978) 0-82561
 surface, energy profile and binding energy, computer simulation 0-100381
 TEM, filtered electron image contrast for elastic scatt., calc. 0-107026
 TEM, tilting and defocus effects in high resolution dark field images 0-79652
 tetracene, disordered solid layer, absorpt. spectra 0-93417
 vapour quenching techniques, high-rate, use in amorphous phase prep. 0-80977
 X-ray K-absorption edge chemical shifts 0-80904
 a-As, second and third order elastic const., ultrasonic velocity meas. 0-103408
 Au₃₅Ni₆₅, vapour quenched amorphous alloy, atomic arrangements 0-100173
 Au₃₅Si_{1-x} amorphous alloy, crystallisation, elec. cond. study 0-103246
 BaFe₂O₄ amorphous film, prep. by RF sputtering, crystallisation 0-76183
 BaTiO₃ ceramics, PTC-type, grain boundary study using TEM 0-107267
 Bi, amorphous metal films, crystallisation with and without mag. field 0-70570
 C, amorphous film, spin resonance, IR spectra, microhardness 0-71157
 C, Lifshitz constant for calc. of van der Waals force between two solids (*French*) 0-107658
 Co-Fe-B, amorphous, crystn. and thermal stability 0-107057
 Co-Ni-Mo-C, amorphous alloys, med. props. and thermal stability (*Japanese*) 0-85049
 Co₇₀Fe₃₀Si₁₀B₁₀, amorphous, crystn. and thermal stability 0-107057
 Co₇₀Si₃₀B₁₀, amorphous, crystn. and thermal stability 0-107057
 Cu₅₇Zr₄₃, amorphous alloy, computer simulation of atomic structure 0-70125
 α-Fe, vibrational states, phonon dispersion, phonon softening 0-88289
 Fe-Ti, C induced amorphous surface layers 0-107287
 Fe-B, amorphous, crystn., metal or metalloid exchange influence 0-75172
 Fe-B amorphous ribbons formation, high-speed photography investigation 0-76216
 Fe-Co-Mo-C, amorphous alloys, med. props. and thermal stability (*Japanese*) 0-85049
 Fe-Ni-Mo-C, amorphous alloys, med. props. and thermal stability (*Japanese*) 0-85049
 Fe-Ni-P-B amorphous ribbons, form. by melt spin technique 0-76215
 Fe₈₀B₂₀ amorphous ribbon, initial susceptibility time lag 0-100579
 (Fe_{0.95}Co_{0.05})₇₅Si₈B₁₄ amorphous ribbon, anomalous mag. aftereffect 0-100602
 FeNi amorphous films, fast phase transition investigation by TEM method 0-107029
 Fe₈₀Ni₁₀C₁₀P₁₀, amorphous film, dislocation and mag. struct., neutron diff. study 0-70956
 (FeNi)PB amorphous wires, surface oxidation and annealing influence on induced anisotropy 0-100957
 FePC molten and amorphous alloys, struct. factors 0-79674
 Ga, amorphous metal films, crystallisation with and without mag. field 0-70570
 Gd-Co amorphous films, mag. struct., mag. bubbles, electron diff. study (*Chinese*) 0-71126
 (Gd_{1-x}Co_x)_{1-x}Ar, amorphous mag. film, elec. and mag. prop. depend. on Ar 0-80410
 La-Al amorphous alloys, internal friction, relaxation process 0-92607
 La-B, amorphous, B-rich, low freq. modes, Raman scatt. obs. 0-108202
 La-Sm-Au, amorphous, surface effects on Sm valence, XPS and X-ray absorption meas. 0-108325
 La₇₆Au₂₄, disordered ribbons, production of quenched samples using arc furnace 0-71612
 La₇₀Cu₃₀, disordered ribbons, quenched samples production using arc furnace 0-71612
 Na-A zeolite, struct. obs. by high-resolution electron microscopy 0-84175
 Nb-Ge, amorphous supercond. alloy, resistivity, transition temp. 0-60126
 Nb₂Ge, supercond. film, amorphous content, X-ray diff. study, rel. to transition temp. 0-75668
 Nb₂Ge(Si), RF sputtered films, amorphous atomic scale struct. 0-84064
 Nb₂Si Al₅ phase from amorphous Nb-Si alloys, high-press. synthesis 0-93516
 Ni-Cr-P, amorphous, corrosion behaviour, immersion tests and electrochem. meas. (*Japanese*) 0-85085
 Ni-P, amorphous, low P, struct. study using high-angle X-ray diff. 0-107055
 Ni-P, amorphous, prod. by ion implantation 0-75257
 Ni-Ti-P, amorphous, corrosion behaviour, immersion tests and electrochem. meas. (*Japanese*) 0-85085
 P, amorphous, struct. by electron microscopy 0-84065
 P, prepared by chem. transport in low-press. H₂ plasma, radial distrib. function 0-64899

amorphous state continued

- PbTiO₃, amorphous, crystallisation process, DTA and Raman spectroscopy meas. 0-75161
 Pd-Ni-Si amorphous alloys, crystn. process during isothermal ageing 0-89275
 Pd-Si, amorphous thin films, laser irradi., metastable phases 0-96622
 Pd₈₀Si₂₀, vapour quenched amorphous alloy, atomic arrangements 0-100173
 Pr₂La_{80-x}Au₂₀, amorphous, low temp. excitations, specific heat 0-100337
 Pt-Si, amorphous thin films, laser irradi., metastable phases 0-96622
 R_{1-x}Co_x, rare earth amorphous alloys, thermal stability, elec. cond. enthalpy 0-100172
 Se, liquid and amorphous, struct. modelling using Monte Carlo method 0-59391
 Si, CVD amorphous films, effect of surface characts. on visible and UV optical props. 0-60698
 SiH₄, amorphous films, internal photoemission, metal contacts 0-96964
 Si₃N₄, Si(LVV) Auger spectra, ion bombardment, electron energy loss spectra 0-80911
 SiO₂, amorphous, ³⁰Si diffusion (*French*) 0-59696
 SiO₂, amorphous film, Si(LVV) Auger spectra, ion bombardment, electron energy loss spectra 0-80911
 SiO₂, amorphous layer in multilayer target for channelled ion stopping power meas. 0-63431
 SiO₂, CVD layer, high current injection from Si rich SiO₂ film 0-80430
 SiO₂, cryst. and amorphous, laser-induced breakdown, electron avalanche damage mechanism 0-100711
 SiO₂, diffusion of ³⁰Si, SIMS (*French*) 0-107482
 SiO₂, fibres, LF optical phonons, Raman spectra 0-80789
 SiO₂, P-doped amorphous, porous and hydrophilic, water adsorpt. and IR spectra obs. 0-80061
 SiO₂, sp. ht., time-dependent, 0.1 to 1K 0-100338
 SiO₂-water system, inorg. polymer struct. form., globular crystn. 0-101042
 SiO₂, amorphous films, acoustic study using Rayleigh waves 0-75312
 Sm-Au, amorphous, surface effects on Sm valence, XPS and X-ray absorption meas. 0-108325
 Ti-Nb-Si, amorphous alloy, supercond. props. and crystn. behaviour, TEM and DTA study (*Japanese*) 0-84536
 V-S₂, amorphous, electrochemistry in Li cells 0-76626
 WO₃, amorphous anodic film growth on W in acidic soln. 0-81232
 WO₃, film, struct. and crystn., TEM obs. 0-103606
 Y-B, amorphous, B-rich, low freq. modes, Raman scatt. obs. 0-108202
 Y₂GdIG film, amorphous, mag. bubbles obs. and structural transformation 0-75824
 Yb, amorphous metal films, crystallisation with and without mag. field 0-70570
 Zr-Co, amorphous and crystalline, d-band struct., alloying effects 0-59862
 Zr-Ni, amorphous and crystalline, d-band struct., alloying effects 0-59862
- amorphous state structure** *see noncrystalline state structure*
- amplification**
see also acoustic wave amplification; amplifiers
 thin-film multimode waveguides, higher order mode amplification 0-96012
- amplification measurement** *see gain measurement*
- amplifiers**
see also amplification; audio-frequency amplifiers; d.c. amplifiers; intermediate-frequency amplifiers; operational amplifiers; parametric amplifiers; power amplifiers; preamplifiers; pulse amplifiers; ring lasers; wideband amplifiers
 back diode amplifier, use at low temp. 0-57324
 dynamic load line construction amplifiers, tutorial 0-67963
 electronics for the physicist with applications, book 0-62403
 logarithmic amplifier, schematic diagram 0-57047
 MOSFET amplifier, fabrication on Si wafer, integrated acoustic transducer arrays 0-74683
 noise figure, measurement by connecting source resistance between input and output (*French*) 0-68214
 normalising, modulation spectroscopy and other meas. appl. 0-73470
 spike train special purpose amplifier, insect taste cells 0-72394
- amplifying** *see amplification*
- amplitude modulation**
see also pulse amplitude modulation
 auditory system, pitch of amplitude-modulated low-pass noise and predictions by temporal and spectral theories 0-67095
 carrier for phase measurement in transmission acoustic microscopy 0-74665
 electrooptic radiation modulators utilizing semiconductor ridged waveguides 0-91925
 ferromagnet light modulation by microwave using magnetodynamic resonance 0-71393
 laser interferometers, AM and FM operation and applications (*German*) 0-86389
 magnetised semiconductor plasma, EM wave amplitude modulation and demodulation 0-84482
 optical second harmonics 0-78908
 ruby laser, ultrashort pulse generation by internal phase and amplitude modulation 0-106551
- analogue computer applications** *see analogue simulation*
- analogue computer circuits**
see also function generators; operational amplifiers
 vented box loudspeaker analogue model using operational amplifiers 0-92015
- analogue computer methods** *see analogue simulation*
- analogue-digital conversion**
see also digital-analogue conversion
 A/D converter with special appl. to medium precision Pt resist. thermometry 0-86297
 analog signal processing, book 0-86047
 astronomical images, interactive program for digital display (*Italian*) 0-98559
 astronomical instrumentation, X-ray XUV telescope/white light coronagraph expt., quadratic A/D converter 0-62024
 contracted orbital formulation of many-body perturbation theory 0-87026
 digitisers of time and pulse height, monolithic flash A/D convertor 0-63475
 digitizer and image analyzer, microcomputer-controlled 0-86270

analogue-digital conversion continued

- gas chromatography mass spectrometry appls. of wide dynamic range system 0-62788
 high rate liquid Ar calorimeter electronic systems, design and operating experience 0-58087
 Hough-Powell digitizer for processing film from bubble chamber Mirabelle in K⁺p expt. at 32 GeV/c 0-69040
 integrated optics A/D convertor based on bulk acousto-optic interaction 0-69552
 klirr-factor unit dimension meas., errors evaluation 0-98873
 multichannel digitizer for routine monitoring of ion emission from laser-driven implosions 0-57268
 optical fibre laser plate for digital image processing, all-optical parallel logic operation 0-106463
 proportional step size tracking A/D convertor 0-57269
 stereo image digitiser for automatic feature extraction 0-106614
 temperature measurement, using A/D convertors TL505/507 and TMS 1000 microprocessor (French) 0-57290

analogue memories *see analogue storage***analogue simulation**

- acoustic defectoscopes, low freq., elec. simulation of compound piezoelec. transducers 0-102956
 laser beam heat flux and power profiling, using swept null point calorimetry 0-69439
 nuclear fuel production, continuous gas flow control simulation (German) 0-78416
 vented box loudspeaker analogue model using operational amplifiers 0-92015

analogue storage

- ferroelectric memory, matrix-addressed analogue, on Gd₂(MoO₄)₃ cryst. 0-103926
 photoferroelectric image storage in antiferroelectric-phase PLZT ceramics 0-71353

analytical chemistry *see chemical analysis***anaphoresis** *see electrophoresis***Anderson model**

- asymmetric Anderson Hamiltonian, ground state 0-65503
 asymmetric Anderson model, ground state, perturbation approach 0-65504
 dilute alloy, perturbation expansion for the asymmetric Anderson Hamiltonian 0-80202
 disordered alloy, electron localisation, temp. depend. 0-80219
 disordered electronic systems, low-dimensionality, Anderson localisation, resist. 0-84491
 disordered extended Anderson model, CPA-alloy analogue treatment 0-65506
 disordered systems, Anderson localisation, appl. of recursion method 0-107744
 electron gas, screening of proton, Anderson model calc. 0-59895
 electron-electron interaction effects on Anderson transition 0-65453
 ground state, var. trial function approach 0-59913
 impurity pair interactions, local moment form., var. method 0-92854
 inflowing structure, Anderson localisation, elec. cond. temp. depend. (Russian) 0-103639
 intermediate valence compounds, dynamic susceptibilities 0-70653
 localisation, mean field theory and ϵ -expansion 0-80203
 metal inhomogeneous granular, superconductivity 0-103795
 metal-semiconductor disordered interface, supercond. transition temp. enhancement by bipolaron interface centres 0-84528
 metals, Kondo effect, Anderson hamiltonian 0-60187
 mixed valence compounds, dynamic susceptibility, RPA study of Anderson lattice 0-97075
 mixed valence cpds., elec. cond., periodic Anderson model, memory function approach 0-84458
 naphthalene, in naphthalene-d₈, Anderson-Mott transition model for excitation transport 0-96812
 naphthalene, in naphthalene-d₈, energy trapping from localised states 0-100440
 non-orthogonal elec. resist. 0-59947
 one dimensional disordered system, cond. and electron localisation 0-103658
 orbitally degenerate, exchange coupling in atomic limit 0-108000
 periodic Anderson Hamiltonian, alloy analogy treatment for mixed valence states 0-75527
 random systems, localisation 0-80218
 rare earth alloys and cpds., intermediate valence, models for anomalous systems 0-96827
 rare earth metal impurity in metallic host, exchange interaction, electrical resistivity 0-84453
 rare earth systems, Kondo singularity, Anderson-Smith model 0-80479
 real-space renormalisation group theory, decimation method 0-88461
 scaling theory based on renormalisation group ideas 0-70646
 self-consistent diagrammatic theory 0-107746
 semiconductor, doped, metal-insulator transition, anal. 0-88478
 semiconductor with transition metal impurity states, EPR linewidth calc. 0-80599
 semiconductors, amorphous, electronic states, theoretical methods 0-80167
 semiconductors, doped, shallow impurity states, Hubbard bands and donor excitonic states, HF calc. 0-100443
 spatially disordered systems, Anderson localisation and metal-insulator transition 0-59926
 substitutional alloys of intermediate valence systems, static mag. susceptibility con. and temp. depend. 0-84586
 superconducting proximity effect sandwiches, appl. of Anderson theorem to elastic scatt. 0-84568
 thin wires, explt. study of Anderson localisation 0-96849
 Cu-Al-Co liquid alloys, constant Co-content of 5 wt.%, mag. props. (German) 0-88720
 H₂WO₃ bronzes, Anderson transition, XPS 0-107705
 InAs, two dimensional accumulation layer, Anderson localisation 0-107871
 NiFe₂O₄, electronic phase transition 0-65640
 Si vacancy, electron states, Anderson negative-U system 0-96820
 Ta_{1-x}Ti_xS₂ (1T), magnetoresistance in the Anderson localized states near the metal-nonmetal transition 0-88479
 Ta_{1-x}Ti_xS₂ (1T), magnetoresist. near metal-nonmetal transition at ultra low temps. 0-88600
 TmSe, Anderson lattice resist. for antiferromag. ordering 0-65556

Anderson model continued

- WV₂O₆, magnetic susceptibility, behaviour in terms of quasi-isolated binuclear units 0-97073
 Yb_{1-x}Y_xCuAl, disordered extended Anderson model, CPA-alloy analogue treatment 0-65506
- anechoic chambers**
 3 GHz surface and lateral EM wave meas. 0-103742
 waterfilled US testing tanks, appl. of filled rubber material system to echo absorpt. 0-96059
- anelastic relaxation**
see also Bordoni effect; creep; elastic aftereffect; internal friction; Snoek effect; stress relaxation; Zener relaxation
 alkali silicate glass, isothermal mech. loss spectrum, appl. of Rheovibron 0-88260
 alkali silicate glasses, secondary relax. transitions 0-88261
 butadiene styrene elastomers, cross-linked, mech. relax. behaviour (German) 0-84986
 elastic amorphous medium, relax. by defect diffusion 0-58925
 elastomers, soot filled, mech. relax. behaviour (German) 0-84985
 internal stress measurement, in creep, anelasticity influence 0-70306
 LF fluctuation, dissipation and relaxation properties, universality 0-84687
 long-range diffusion, review 0-60904
 polycrystalline materials, effect of grain boundary sliding on anelasticity 0-96592
 stress relaxation theory, for plastic deform. (Hungarian) 0-97661
 Nb, solute trapping of H, symmetry of O-H pair 0-108488
 Nb₃Ta₂, elastic const. charge caused by H addition, hydrostatic press. effect 0-75287
 Ni, hardness after-effect studied by anelastic relaxation 0-66570
 β -NiAl, ordered, hardness after-effect studied by anelastic relaxation 0-66570
 Pd-H system, α and $\alpha+\beta$ phases, annealed and deformed, anelastic effects 0-66567
 Ta-H(D), anelasticity due to long-range diffusion 0-60904
 V, elastic const. charge caused by H addition, hydrostatic press. effect 0-75287
 V-H(D), anelasticity due to long-range diffusion 0-60904

anelasticity

- see also anelastic relaxation*
 damaged body, unknown boundary value problem explicit solution (French) 0-79166
 internal stress, stochastic model for dip test in steady-state creep 0-58915
 internal stress measurement, in creep, anelasticity influence 0-70306
 nonlinear anelasticity, and autooscillations 0-70307
 Cu-Al-Ni (14.1, 3 wt.%), autooscillations and nonlinear anelasticity 0-70307

anemometers*see also laser velocimeters*

- bivane anemometer, Reynolds stress defl. and elevation angle sensing 0-109265
 boundary layer meas. system for wind and temp. obs. (German) 0-94616
 cups, propellers and lasers for wind speed and direction meas. 0-90264
 digital anemograph, for wind direction and average speed meas. (Czech) 0-77174
 hot wire, single rotating slanting, meas. of Reynolds stress tensor in curved duct expt. 0-75006
 hot wire, supersonic rarefied gas flow vel. meas. 0-100040
 hot-film probe velocity measurements in liquid metal MHD duct flow experiments 0-75009
 hot-wire, const. temp., comments on determination and optimization of freq. response in supersonic flows 0-87832
 hot-wire, constant-temp., effect of varying resistance ratio on behaviour 0-59141
 hot-wire, freq. response of constant temp. anemometers in supersonic flow 0-59149
 hot-wire, influence of humidity changes 0-75007
 hot-wire, use of triple-sensor probes for turbulent flow-field investigations 0-100043
 hot-wire, very low velocity calibration 0-75008
 hot-wire, wall proximity meas. corrections 0-74841
 laser, for periodic fluid flow measurement, periodic sampling 0-64657
 laser anemometry, fundamental limitation and accuracy 0-87829
 laser Doppler anemometer, directionally sensitive two-component 0-75004
 laser Doppler anemometer, meas. of turbulent vortex flow 0-79412
 laser transit anemometer signals, semiclassical processing 0-59145
 laser-Doppler anemometry and photon correlation for turbulence length scales 0-87828
 liquid flow rates through pipes, applicability of experimental meas. methods 0-100044
 reflected-beam laser anemometry using photon correlator 0-106861
 spectral analysis of signals from a laser Doppler anemometer operating in the burst mode 0-100041
 thermistors, thermally compensated, math. models (French) 0-90227
 thermosiphon solar water heaters, transient flow meas. using laser doppler anemometer 0-61413
 upper atmosphere wind, meas. with airglow Fabry-Perot spectrometer 0-77156

angle measurement *see angular measurement***angular correlation techniques**

- molecular biophysics, conformational changes and mol. dynamics in bovine serum albumin 0-81538

angular measurement*see also angular velocity measurement*

- butterfly-valve inductive orientation detector 0-68193
 capacitive position indicators (German) 0-57256
 circular scale calibration by reflection grating polygon (German) 0-86250
 cutoff angle of piezoelec. quartz wafers using X-ray comparator 0-105755
 diffraction grating used for angle measurement between edges of distant objects 0-86259
 in-plane motion measurements with Fourier lensless holography 0-77746
 instrument for checking autocollimators 0-77832
 laser interferometric auto-correcting system of high precision thread grinder 0-90830
 light beam deflection angle determ. from holographic shear interference patterns 0-95848
 machine tool industry, angle measurement, automatic testing of precision dividing heads (German) 0-82740
 microcomputer based laser interferometer for instrument graduation (Polish) 0-90816

angular measurement continued

- non-contacting transducer, IR source and fibre optic probe 0-86257
- optical instrument, target position meas., statistical model 0-101778
- optoelectronic meas. devices, error anal. method (*Russian*) 0-95066
- orientation angle calc. using image matrix transformation (*Russian*) 0-73314
- pendulums, random interactions, error anal. (*Russian*) 0-73313
- repeater gyrocompass, digitiser construction principle (*Russian*) 0-73311
- stepping motor for timber volumetric meter (*Russian*) 0-57253
- tilt of diffusely reflecting surfaces, real-time measurement by electronic speckle correlation 0-57252

angular momentum

- binary system, close, with mass and ang. momentum loss, period changes 0-72998
- cylindrical gas system, rotating and self gravitating, thermodynamic instability 0-82191
- Earth atmosphere, angular momentum fluctuations and day length changes 0-85715
- galaxies, ang. momenta rel. to form. by gravit. instability 0-98722
- mass relationship for cosmic objects, Ambartsumian's proto-matter hadronic nature determ. 0-77528
- multiply charged ions, $2p_{1/2}3p_{3/2}$ config., level widths, relativistic calc., S-matrix method 0-63546
- particles, angular momentum in centre-of-mass frame, teaching 0-90631
- star cluster, spherically symmetric, total ang. momentum rel. to struct. and dynamics 0-62215
- star formation protostellar cloud ang. momentum problem, mag. breaking 0-82342
- stars, pre main sequence, effect of ang. momentum on evolution in gravit. contraction phase 0-62133
- static EM angular momentum, in vacuo obs. 0-73631
- stellar orbits in Galaxy, ang. momenta rel. to applicability of approximate third integral of motion 0-67798
- ^3He , superfluid A-phase, mass current, intrinsic orbital angular momentum 0-84338

angular momentum theory

- see also *quantum theory; Regge poles and trajectories*
- 3j and 6j coefficients, symmetries 0-62506
- Abraham-Minkowski controversy, EM momentum in static fields, teaching 0-101678
- angle-angular momentum variables in quantum mechanics, commutation relations 0-86112
- atom, transition metal Racah parameters, atomic screening parameter Slater and Clementi-Raimondi values 0-69071
- atoms, P-state collisions, quantum mechanical treatment, angular momentum coupling 0-99541
- body-fixed frames and angular momentum projection operators 0-86122
- equivalent electrons, J allowed values in jj coupling, teaching 0-90624
- geometry of the quantization of angular momenta (l,s,j) in fields of central symmetry 0-105330
- isotropic harmonic oscillator in ang. momentum basis, algebraic formulation 0-94983
- operator product of traces, derivation from operator identities 0-73202
- operator props. through three-dimens. rot., teaching 0-105469
- orbital angular momentum and parity 0-77564
- recurrence relations for angular momentum traces 0-98816
- spins, arbitrary no., quantum mech. vector addition 0-57134
- trace problem, use of ang. momentum operators between ladder and rot. operators 0-62533
- Wigner-Eckart theorem for an arbitrary group of Lie algebra 0-86124
- HBr, photoelectron angular distrib. 0-58318
- HI, photoelectron angular distrib. 0-58318

angular velocity measurement

- DC motor, contactless method (*Russian*) 0-73329
- fibre optic rotation sensor with low drift 0-69530
- nonuniformity, magnetic resonance appl. (*Russian*) 0-62637
- strobe light with variable pulse length over 22-360 Hz frequency range 0-58716
- viscosity meas. using Couette-type viscometer, capacitor assembly for meas. small rotational vels. 0-100046

animal communication see *biocommunications***anisotropy, magnetic** see *magnetic anisotropy***anisotropy, magnetocrystalline** see *magnetic anisotropy***annealing**

- see also *graphitising; magnetic annealing; recrystallisation annealing; solution annealing; stress relaxation*
- A15 compounds, disordered, reordering kinetics 0-96678
- alkali halides, divalent metal impurities, aggregation process, order of reaction, fractional time conc. depend. 0-107308
- alloys, supplementary annealing during rapid hardening from liquid state, apparatus 0-76275
- amorphous semiconductor film, laser induced nucleation, long wavelength instability 0-84126
- anthracene, ultrathin films on fused quartz and sapphire 0-59812
- α -brass, polycryst., deformed in tension or rolling, anneal hardening (*Japanese*) 0-93564
- abras, single cryst., yielding behaviour rel. to low temp. annealing treatment (*Japanese*) 0-93582
- [CC] Ag-(100)InP, metal-semicond. cathode contact, metallurgical, physical, chemical processes 0-107911
- chalcogenide glasses, O-free, cooling rate influence on optical consts. 0-88952
- conference, Masnuy-St-Jean, Mons, Belgium, Oct. 1979 0-82570
- contact film absorption on plastic deform. of contacting bodies (*Russian*) 0-93596
- crystalline samples, temp. control system design (*Spanish*) 0-73362
- diamond:Sb, implanted, radiation damage and annealing study 0-100263
- diamond, thermal conductivity, high temp., electron irradi. effects 0-65318
- diffusion-controlled defect annealing, theory 0-92520
- ductile fracture, strain hardening and damage relationship 0-108564
- ethylene-vinyl alcohol copolymer, drawn samples, annealing effect around T_g temps. on shrinkage and mol. orientation 0-79712
- faulted dislocation loops induced by elastic interaction, climbing motion 0-75227
- ferrite, 350 NNI, for use in superhigh vacuum systems 0-108478
- ferroelectrics, domain structure as vacuum state for poling procedure 0-80728
- film on Si substrate, eutectic point displacement on annealing (*Russian*) 0-100850

annealing continued

- fluorophosphate optical glass development 0-106588
- fusion reactor, first wall, life extension by periodic annealing 0-102344
- glass, annealed and tempered, impact damage, strength 0-85025
- Incoloy 800, steam oxidised, oxide coating anal. 0-89399
- Inconel, caustic stress corrosion cracking resistance, processing variables effect 0-71796
- Inconel 600, thermal treatment, grain boundary microstruct. and SCC resistance 0-71675
- iron phthalocyanine, annealed, elec. cond., daylight exposure and thickness effect (*French*) 0-84484
- laser, Au diffusion barrier formation, at metal-semiconductor on metal-metal interface 0-80373
- laser annealing for improved stacked-struct. oxide quality 0-65386
- laser annealing mechanisms, continuous and pulsed laser impact, melting 0-84964
- laser annealing parameters, in thermal working (*Russian*) 0-100848
- laser applications in materials processing, seminar, San Diego, CA, USA (Aug. 79) 0-90609
- metal colloid, irradiation-induced defects in alkali halide crystals 0-107316
- metal-tunnel oxide-Si junctions, processing condition depend. 0-80380
- metallic glass, current exptl. data on struct., review 0-88058
- metallic glasses, annealing behaviour, thermal stability and crystn. 0-75167
- metals, radiation defect treatment at annealing stages V and VI (*Russian*) 0-71676
- mica, natural, high γ - and electron-irrad. doses effect on annealing behaviour, thermal decomp. resist. 0-60897
- MNOS p-channel transistor, memory characts., H_2 anneal effects 0-80388
- MNOS structures, electron-beam-irrad., interface defects, high temp. H_2 anneal 0-96745
- MOS structures, radiation-induced positive charge, thermal annealing 0-75648
- n $^+$ -p-p $^+$ bifacial back surface field solar cells, optimisation of p $^+$ doping level by ion implantation 0-97784
- Nafion, densities and expansion coeffs. as function of various parameters 0-79711
- Nylon 6 gut yarn, fine struct. change in twisting, annealing and untwisting, microbeam X-ray obs. 0-81026
- Nylon 6 gut yarn, fine struct. change in twisting, annealing and untwisting, X-ray and electron microscopy obs. 0-84904
- Permalloy, 50NP, and 79NM, magnetic properties and structure, environment effect during annealing 0-60366
- pigeonite, annealing expts. rel. to antiphase domains exptl. coarsening 0-81886
- PMMA, optical damage threshold, alteration methods 0-99814
- polycarbonate, glassy state, enthalpy relax., thermal density fluctuations 0-59678
- polyethylene, dielectric props., investigation for morphology changes created by mechanical drawing and annealing 0-84697
- polyethylene oxide, nascent and annealed, X-ray study of crystal structure 0-64922
- polyethylene terephthalate, oriented, amorphous, stress-induced crystn., shrinkage meas. 0-92466
- polyolefine, liq., memory effect 0-103268
- polypropylene, isotactic, low temp. annealing, differential scanning calorimetry obs. 0-60895
- polystyrene, atactic, indentation recovery 0-84988
- polystyrene, shear bands, morphology and annealing behaviour 0-100873
- porphyrin films, methine bridge substituted, surface photovolt. depend. on fabrication method 0-60119
- PVC, oriented mouldings, struct. order 0-60896
- quartz, electron irradiation effects on optical, dielec., elastic props. 0-59521
- radiation enhanced, dose rate dependent effects of total ionising dose irradiation 0-70249
- sapphire, neutron bombard., F-centre fluorescence, photoluminescence 0-100676
- semiconductor, ion implanted, pulsed laser and electron beam annealing comparison 0-92547
- semiconductor, kinetics of defect cluster annealing 0-84209
- semiconductors, ion implanted, laser annealing 0-65023
- solar cells, ion implantation and annealing technology 0-93996
- sparks, fission track annealing, fission track age-temp. relationship 0-98316
- spin glasses, annealing and mag. remanence 0-60308
- stainless steel, machine faceted, low-energy ion erosion studies 0-80923
- steel, austenitic, Cr-Mn-N, plastic deformation influence on internal friction, relaxation processes (*Russian*) 0-100870
- steel, austenitic stainless, supercond. magnets, mech. and phys. props. at 4K 0-86976
- steel, austenitic stainless types 304 and 316, environment effect on crack growth, under creep and fatigue conditions 0-85035
- steel, cold strained, defects interaction with carbide strengthening phases, carbide decomp. degree (*Russian*) 0-84955
- steel, cold worked, original struct. effect on softening during heating 0-60882
- steel, CrMoV, low alloy, coarsening rate and activation energy of M_2C_3 and M_2C , carbides (*Czech*) 0-108480
- steel, eutectoid, mech. behaviour, thermomech. treatment effects 0-84970
- steel, ferritic stainless, embrittlement 0-85041
- steel, high strength, failure stress, structural relationships 0-81190
- steel, high-speed, low temp. mag. cycling effects on ferromag. struct. 0-100928
- steel, low C, cold rolled, graphite precip. and S segregation, AES investigation (*Japanese*) 0-89222
- steel, low C, cyclic loading, change in mech. props. rel. to heat treatment 0-104282
- steel, low C, high cycle fatigue, crack initiation model (*Japanese*) 0-104258
- steel, martensitic-aged, plastic deformation influence in type N17K12M5T steel on mech. props. (*Russian*) 0-76305
- steel, mild, solderability, annealing effect (*Japanese*) 0-89244
- steel, P, deep-drawing, spatial orientation distrib. of crystallites in cold-rolled and in annealed sheets 0-81079
- steel, plastic loosening and deform. defect healing during recovery annealing of 12Kh18N10T (*Russian*) 0-66530
- steel, Si, nonoriented sheet prod. with texture of {100} (owv) 0-89246

annealing continued

- steel, Si (3 wt.%), struct. and preferred orientation, annealing parameters influence (*Czech*) 0-89248
- steel, stainless, austenitic, deform. substruct. and annealing, stacking fault tetrahedra form 0-107282
- steel, stainless, Cr-Ni-Mo, phase anal. of carbide phases after isothermal annealing (*Czech*) 0-89224
- steel, stainless, highly protective film development by surface treatment 0-66699
- steel, stainless, O₂ desorpt. during laser irradi., etching, AES study 0-66338
- steel, stainless, sensitization, C content and ferrite morphology effect 0-89400
- steel, stainless, surface chem. rel. to metallurgical props., SIMS, XPS and AES (*French*) 0-80045
- steel, stainless, type 304, viscoplastic behaviour, strain rate sensitivity, creep, relaxation, tensile tests 0-66727
- steel, stainless, type EP838 ion irradiated, surface structure changes during post-irradiation heating (*Russian*) 0-75272
- steel, steam pipes, 12Cr1MoV, selection of allowable stresses based on minimum possible strength data 0-104237
- steel, type AISI 316, thermal passivation in controlled vacuum 0-76276
- steel, types 60G, ShKh15, structural changes near holes and inclusions due to pulsed currents (*Russian*) 0-108459
- steel bearing rings, optimisation of thermomechanical working parameters (*Russian*) 0-93579
- steel sheets, surface composition, degreasing and batch annealing effects 0-66700
- steels, tempered with different Ni contents, scaling behaviour obs. 0-71817
- substitutional solid solutions, new phase nucleation mechanism 0-61135
- surfaces, laser-annealed, characterisation by ellipsometry 0-103544
- TGS, autostabilised state, elec. second harmonic generation 0-103921
- TGS, internal bias field, hysteresis loops (*Chinese*) 0-84705
- TGSSE, autostabilised state, elec. second harmonic generation 0-103921
- titanomagnetites, temp. depend. cation distrib., mag. prop. obs. 0-85647
- vermiculite, fission track annealing and dating 0-81885
- web dendrites, dislocations, stacking faults, X-ray topographic study (*Chinese*) 0-88148
- Zircaloy, unirrad., stress corrosion cracking, I₂-induced, effect of test temp., alloy comp. and heat treatment 0-97632
- Ag film, void growth, TEM obs. 0-59833
- Ag-Cu metastable solid soln., form. by ion-beam mixing 0-75244
- Al, Al ion irradiated, void swelling and annealing of voids, electron microscopy study 0-88216
- Al alloys, (5083, 6061, 2219), supercond. magnets, mech. and phys. props. at 4K 0-86976
- Al, cyclic loading, change in mech. props. rel. to heat treatment 0-104282
- Al, neutron damage, positron annihilation 0-65056
- Al, pipe diffusion along segment of faulted dislocation loops during annealing 0-107256
- Al/Ga, pulsed electron-beam annealing, lattice site location improvement 0-107303
- Al/Sb(Zn), ion implanted electron beam annealing, ion backscatt. and TEM meas. 0-59500
- Al/Pd thin film couples, thermal reactions 0-59830
- Al-Al₃Ti, directionally solidified, thermal stability during annealing, 435-660°C 0-108393
- Al-Cr, thin film metal contact, sheet resistance changes 0-80356
- Al-Cu films, DC sputtered, Cu distrib. 0-80113
- Al-Ge (0.1 wt.%), channelling meas. of Al interstitial atom trapping by Ge atoms 0-59537
- Al-Mg (0.1 at.%), neutron damage, positron annihilation 0-65056
- Al-Mn (1 wt.%), single crystals, rolled to {123}[412], recrystn. textures 0-104183
- Al-Ni multiphase system, simultaneous diffusion in cylindrical symm. (*Russian*) 0-100357
- Al-Si eutectic alloy, banded struct., SEM and optical microscopy 0-104144
- Al-Si₃N₄-SiO₂-Si, MNOS structures degradation under UV irradiation effect 0-107923
- Al-Zn (70, 30 wt.%), decomp. study, 25-160°C (*Czech*) 0-89225
- AlGaAs DH laser, self-pulsations due to proton bombarded region self-annealing during ageing 0-99728
- β -AlO₂(NaLi)₂O, NMR, Raman and IR spectra, and X-ray diff., heat treatment induced changes 0-107508
- Al₂O₃/Fe, pore form. during oxidative annealing, grain growth slowing 0-100856
- AlSb, laser pulse annealing, induced nucleation, crystal growth 0-84966
- As₂S₃ and As₂S₄ vapour-deposited films, valence states, thermal and photo-induced changes UPS study 0-93459
- Au, deformed, annealing kinetics of vacancies (*Japanese*) 0-88139
- Au film, adatom surface diffusion at low temps., elec. resist. study (*French*) 0-65376
- Au-Al thermocompressional contacts, diffusional zones, phase growth during annealing (*Russian*) 0-75389
- Au-Co, electron scatt., spin-orbit effects 0-65533
- Au-Pd (150 wt.%), quenched, vacancy annihilation and short-range order formation, elec. resist. 0-108487
- Au-Ti_{0.3}W_{0.7}, thermal annealing study of metallisation on Si 0-80134
- Au-W-GaAs Schottky barrier, elec. and chem. props., AES 0-96973
- Au-Cu-Al thin film bilayer system, phase formation, backscattering spectra 0-96728
- Au₁₁Mn₄ ordered phase formation, electron diff. and microscopy study 0-107418
- BC, sintered, struct. and props. 0-104181
- BP:Zn(Se)(Cd), epitaxial layers, ion implantation, defects and lattice locations, channelling obs. 0-88179
- BaFe₂O₉, powder, milled and annealed, phase composition, lattice conts. and crystallite size 0-71677
- Ba₂RF₇, (R=Dy, Ho, Er, Tm, Yb, Lu, Y), superstructure phases, prep., thermal characterisation and X-ray powder diff. 0-96494
- BaTiO₃ film, dielectric props. depend. on sinusoidal elec. field 0-71318
- Bi film, adatom surface diffusion at low temps., elec. resist. study (*French*) 0-65376
- Bi-Te thin thermoelectric films prep. by solid state reaction method 0-108361
- Bi-S₂-Bi₂Se₃ and Bi₂Te₃-Bi₂Se₃ systems, thermal cond. change during phase transitions 0-100368

annealing continued

- CaF₂/Er, defect structure, quenching effect, dielec. relax. and optical absorption 0-65031
- CaF₂/Eu, CaF₂/Eu,Mn(Gd), single crystal predisintegration phenomena, SEM cathodolum. obs. 0-59502
- CaF₂/Mn, CaF₂/Eu,Mn, single crystal predisintegration phenomena, SEM cathodolum. obs. 0-59502
- CaSO₄/Dy, TLD-900, thermolum. stability at low radiation doses 0-101272
- CaSO₄/Dy, thermoluminescent glow peaks, post γ -irrad. annealing study 0-89077
- Cd-Sn alloy, superconductivity and microstructure 0-107949
- CdCr₂Se₄/Ag, magneto-optical effects in impurity spectral region 0-97313
- CdS, surface energy struct. changes during ion cleaning and thermal annealing 0-92962
- CdS:Na, Hagemark theory, green edge emission line intensity 0-75517
- CdSe film polycryst., thermal diffusion of Cr, 240-400°C 0-80001
- CdSe thin film transistor on Cr substrate, cryst. struct., substrate defect effects 0-70563
- p-CdSiAs₂, electron irradi. elec. props. annealing, lattice defects 0-100465
- p-CdTe, nonpolar, heat treatment in vacuum, dissociation obs. effects on struct. and props. (*Japanese*) 0-60662
- CdTe:As(P), ion implanted, elec. props. 0-65021
- CdTe:In precipitation and out-diffusion of solute during cooling 0-100840
- CdTi₂Se₄/Au, solubility meas. by microhardness method 0-96650
- (Co,Fe)₈₀B₂₀ glass, induced anisotropy and time changes of permeability 0-75815
- Co-B-Si amorphous alloy, liq. quenched, elec. resist. and cyclic deform. 0-59949
- Co-Fe-V-Ni, mag. and mech. props., heat treatment and stress effects 0-60363
- Co-Gd-Mo amorphous films, resist. and extraordinary Hall effect, thermal annealing effect 0-70852
- Co-Gd-Mo films, sputtered, O effects on mag. props. during annealing 0-89374
- Co-Nb-C, obtained by liq. quenching, superconductivity 0-75699
- Co₇₀Fe₄₀Si₁₀B₁₀, amorphous, mag. aftereffect spectra and annealing props. 0-88831
- Co₂(Ni_{0.5}Cu_{0.5})_{1-x}Fe₂O₄ ferrite, relation between elec. cond. and mag. anisotropy 0-75548
- CoP amorphous alloy, heat treatments influence on opt. props., struct. and DC resist. obs. 0-80892
- Cr black solar selective absorbers, thermal degradation 0-61417
- Cr film, obtained by thermo ionic precipitation, phase composition, lattice parameters (*Russian*) 0-96756
- Cr-Fe-Ni, γ -solid soln., thermodynamic activity determ. at 1500K 0-108397
- Cr-Si interfaces, metallurgical and electrical props. 0-60081
- Cu, annealed, plastic strain during non-proportional loading 0-89291
- Cu, cyclic loading, change in mech. props. rel. to heat treatment 0-104282
- Cu, electron irradi., migration and thermal conversion of defects, 100 to 330K 0-59519
- Cu, electron-irradiated, monovacancy migration during stage III annealing, NQR study 0-107576
- Cu film, diffuse optical scattering from variable roughness surfaces 0-100704
- Cu foils, electron-irradiated, point defect agglomerates, HVEM invest. during in-situ annealing 0-84213
- Cu, irradiation with O₂ ions, defect production and annealing 0-88214
- Cu, near Σ 9 grain boundary properties, boundary dissociation 0-100251
- Cu, oxidation kinetics, influence of intermediate annealing treatment 0-89412
- Cu single crystals Au ion implanted, pulsed electron beam irradi. 0-65019
- Cu single crystals, deformed, HVEM study of recrystn. texture 0-104179
- Cu, solderability, annealing effect (*Japanese*) 0-89244
- Cu:Co precipitates, mag. anisotropy, precipitate shape, coercive force 0-80500
- Cu:In, He, lattice defect struct., PAC meas. 0-70190
- Cu-Al, short range order and static distortion contribution to residual elec. resistivity (*Russian*) 0-70672
- α -Cu-Al (9.13, 13.56, 14.76, wt.%) short-range ordered, characterisation of locally ordered regions 0-79747
- Cu-Al films, elec. cond. of vacuum condensates depend. on composition, annealing (*Russian*) 0-65709
- Cu-Al(Au)(Ga)(Ni)(Pd)(Rh)(Zn) (4 at.%), anneal hardening mechanism 0-60879
- Cu-Au alloys, vacancy and divacancy migration activation energies, elec. cond. meas. 0-88140
- Cu-Cr (0.75 wt.%), deformation characts., fully reversed cyclic strain with fatigue cracks and dislocation struct. 0-81148
- Cu-Fe system, ageing and reversion phenomena study 0-89274
- Cu-Ga (17 wt.%), elec. resist. and TEM studies 0-108604
- Cu-Nb multifilamentary composite, dislocation resistivity 0-70671
- CuInS₂ films, RF sputtered, growth and props. 0-80124
- CuInTe₂ single crystals, directional freezing growth and doping, resist. changes on annealing 0-60768
- r-CuMn, annealing ordered phase study by neutron diff. 0-89265
- Cu₂MnIn_{1-x}Sn_x alloy, compositional SRO, hyperfine interactions 0-71065
- Cu₄₀Nb₃₀X₃₀ (X=Ti, Zr, Hf), superconductors with metastable ordered structs. 0-108484
- Cu₂O, Cu inclusions and annealing, optical and IR absorpt. obs. 0-60630
- Cu₂O:Mn, photomemory mobility components, charged centre conc. 0-103725
- Cu₆₀Zr₄₀, amorphous, ductility and stress relief, low-temp. annealing effects 0-76296
- Fe, cast, austenitic grain size determ. 0-81255
- Fe, cast, graphite content determ. by X-ray diff. method 0-100977
- Fe, cast, grey, fracture surface after dynamic fracture, Mg conc. effect 0-100909
- Fe, creep at 77, 295K, formation of five struct. 0-60926
- Fe dilute alloys, irradiation softening, isochronal annealing of yield stresses 0-76319
- Fe, grain growth, normal and abnormal, statistical distrib. of linear grain sizes 0-93581
- Fe, high purity, boriding with cryst. B powder 0-84951
- Fe, internal friction in plastic deformation process (*Chinese*) 0-88259

annealing continued

- Fe, irradiated with electrons then annealed, magnetoresistance at 20K (French) 0-103677
- α -Fe, neutron irradiated, mobile C atom trapping, anelastic and magnetic relaxations 0-100306
- Fe polycrystals, grain misalignment, electron microscope determ. (Russian) 0-103358
- Fe powder, final reduction annealing in vibrating bed 0-84883
- Fe powder, reduction annealing, comminution of sintered cakes 0-66456
- Fe-B, amorphous alloy, mag. props. 0-84618
- Fe-B amorphous alloy, annealed, microstruct. and mag. domain changes 0-75790
- Fe-B metallic ribbons, correl. between quenching temp. and mech. and mag. props. 0-89373
- Fe-B ribbon, microhardness, and static coercive force, melt overheating effect 0-84978
- Fe-B-C, amorphous, effects of replacement of B by C on mag. props. 0-84621
- Fe-B-Si amorphous alloy, liq. quenched, elec. resist. and cyclic deform. 0-59949
- Fe-C-Si, cast, graphite nodularization during annealing, Mg and S effects (Japanese) 0-81087
- Fe-Co-V(Ni), annealing effect on microstruct. rel. to mag. and mech. props. 0-89267
- Fe-Cr, influence of annealing on hyperfine interaction parameters, Mossbauer effect 0-71263
- Fe-Cr-Co (28, 10.5 wt.%) ductile magnet alloy, humidity-induced H₂ embrittlement 0-89406
- Fe-Mn cast alloys, homogenisation annealing and chemical diffusion (Czech) 0-66551
- Fe-Ni, Invar, Curie point, annealing effects and time depend. 0-80508
- Fe-Ni alloys, enthalpy change between α' - γ and α - γ transformations 0-93550
- Fe-Ni alloys, heat treatment variations effect on surface conditions and on Hg wetted switch behaviour 0-66547
- Fe-Ni Invar alloys, sput. quenched, mag. props. 0-75799
- Fe-Ni-C, quenched martensite, annealing during cathodic hydrogenation, 200°C (French) 0-93573
- Fe-Ni-Cr (30.6, 21.3 wt.%), Alloy 800, high temp. oxidation at low O₂ press., SEM, AES and electron probe microanal. study 0-93688
- Fe-Ni-Cr-Ti-Al, with thermoelastic control coeff., comp. and heat treatment influence on props. (French) 0-81074
- Fe-Ni-Mo, martensitic transformation, annealing, influence on struct. of austenite (Russian) 0-81057
- Fe-Ni-Mo(Si), austenite, annealing effect on atom redistrib., Mossbauer anal. (Russian) 0-66529
- Fe-Ni-P-B, metallic glasses, struct. relax., annealing effects on mag. props. 0-89261
- Fe-Si, mag. props., stress and reannealing effects 0-88844
- Fe-Si cast alloy with spherical graphite, transform. investigation during tempering (Russian) 0-97479
- Fe-Si-Al, Sendust, ribbon-form, prep. by rapid quenching, mech. and mag. props. 0-71611
- Fe-Si-Al, surface oxide layer struct., AES study 0-89396
- Fe-Si-Al (2.8-3.4, 0-0.86 wt.%) oxidation, annealing 0-89395
- Fe-Si-Al (9.6, 5.4 wt.%) ribbon-form Sendust alloy, mag. props., annealing effects 0-88800
- α -Fe-Ti, ion implanted, microstruct., ion beam anal. and TEM study 0-107294
- α -Fe-Ti, ion implanted, with C impurity, microstruct. of TiC precip. 0-66513
- Fe₈₀B₂₀, amorphous, crystn. 0-75187
- Fe₈₀B₂₀, amorphous, mag. permeability aftereffect during annealing 0-88834
- Fe₈₀B₂₀ amorphous ribbon, initial susceptibility time lag 0-100579
- Fe₈₀B₂₀ amorphous wire, crystn. by annealing at 780°C 0-100177
- Fe₈₀B₂₀ metallic glass, crystn. and struct. relax., Mossbauer effect study 0-75182
- Fe₈₀P₁₀B₁₀ and Fe₈₀B₂₀, Metglas 2826 and 2605, amorphous ribbon, power loss variation with freq. and applied stress 0-88849
- (Fe_{1-x}Co_x)₇₈Si₁₈B₄, amorphous, roll mag. anisotropy 0-75757
- (Fe_{100-x}Ni_x)₈₃B₁₇, amorphous, crystn. 0-75176
- Fe₄₀Ni₄₀B₂₀, amorphous, phase transforms., resistometric anal. 0-75538
- Fe₄₀Ni₄₀B₂₀, amorphous ribbon, power loss variation with freq. and applied stress 0-88849
- Fe₄₀Ni₄₀B₂₀ and Fe₄₀Ni₄₀P₁₀B₁₀, amorphous, mag. aftereffect spectra and annealing props. 0-88831
- (FeNi)PB amorphous wires, surface oxidation and annealing influence on induced anisotropy 0-100957
- Fe₄₀Ni₄₀P₁₀B₁₀, amorphous, resistometric study of short-range ordering rel. to heat treatment 0-70140
- Fe₄₀Ni₄₀P₁₀B₁₀ amorphous alloy, temper embrittlement 0-76295
- Fe₄₀Ni₄₀P₁₀B₁₀, amorphous, mag. polarisation in approach to ferromag. saturation 0-80560
- Fe₄₀Ni₄₀P₁₀B₁₀, amorphous, steady-state creep rate, cryst. effect 0-81102
- Fe₄₀Ni₄₀P₁₀B₁₀, amorphous, mag. permeability aftereffect during annealing 0-88834
- Fe₄₀Ni₄₀P₁₀B₁₀, metallic glass, bending tests, evidence of ideal elastic-plastic deform. 0-97543
- Fe₂O₃ films, DC reactively sputtered, for selectively semitransparent photomasks, deposition conditions and optical props. 0-60782
- Fe₂Pt austenites, ordering kinetics 0-104155
- Fe₂Pt-Sn Invar alloy, Mossbauer shift temp. depend. 0-100626
- Fe(Sb_{1-x}Te_x)₃ system cpds., prep., cryst. struct., elec. and mag. charac. 0-108349
- Ga-As-O, equilib. phase diagram, GaAs oxidation 0-104130
- GaAs, defect cluster annealing, pot. barrier height determ. 0-84209
- GaAs, electroluminescent study of irradi. induced struct. damage, athermal annealing 0-102820
- n-GaAs, electron irradi. defects, carrier removal rate, annealing effects 0-75269
- GaAs, electron irradi. induced defect levels, hydrostatic press. effect 0-92858
- GaAs epitaxial layers, surface impurity gradients, Schottky barrier capacitance meas. 0-70782
- GaAs, epitaxial layers, electron irradi. deep level trap energy depend. 0-80205
- GaAs, ion beam induced annealing effects 0-59530
- GaAs, ion damage, TEM study of laser annealing 0-88215
- GaAs, ion implanted, capless annealed and dielectrically annealed, comparison of doping profiles 0-100278

annealing continued

- GaAs, ion implanted, laser annealing 0-107296
- GaAs, ion-implanted layers, close contact capless annealing, elec. props. 0-84192
- GaAs, point defects, laser annealing 0-107224
- GaAs solar cells, electron and proton radiation damage 0-94034
- GaAs solar cells, simultaneous radiation damage and annealing 0-94033
- GaAs, surface cryst. regularity by X-ray photoelectron diff. 0-89112
- GaAs thin film polycrystalline solar cells, props. and prep. 0-81437
- GaAs, undoped epitaxial layer growth from nonstoichiometric solns., O₂ contamination sources 0-108362
- GaAs:Cr, Cr²⁺ and Cr³⁺ centres, thermal treatment effects, EPR 0-65492
- GaAs:Cr, ion implanted, implantation damage profiles, laser annealing, ellipsometry study 0-79819
- GaAs:Cr, low temp. gettering 0-96549
- GaAs:Cr, redistrib. of Cr during laser annealing 0-88192
- GaAs:Cr, semi-insulating, Cr redistrib. during thermal annealing as function of encapsulant and implant fluence 0-84199
- GaAs:Cr, semi-insulating, damage gettering of Cr during annealing of Cr and S implants 0-107304
- GaAs:Cr,Se, ion-implanted, semi-insulating effects of Cr redistrib. on elec. charac. 0-59982
- GaAs:Cr capless annealed, under As press., Cr redistrib., SIMS obs. 0-59503
- GaAs:Se, Ga, dual species ion implantation, elec. charac. 0-103377
- GaAs:Se, low dose Se²⁺ ions implanted, DLTS study of laser annealing 0-80204
- GaAs:Se ion implanted samples, Q-switched ruby laser annealing, improvement in elec. props. 0-100460
- GaAs:Se ohmic contacts, pulsed electron beam annealing donor density, mobility 0-65678
- GaAs:Se(Si), ion-implanted, capless annealing by melt-controlled ambient technique 0-75251
- GaAs:Si, activation by multiply scanned electron beams 0-75246
- GaAs:Si, ion implantation, thermal annealing, Hall meas., SIMS atomic profile meas. 0-75243
- GaAs:Si(Sn), ion implanted, laser annealed, high doping levels 0-88181
- GaAs:Sn thermal diffusion from spin-on SnO₂/SiO₂ source 0-96691
- GaAs:Zn, implanted, furnace annealed, electrical, Rutherford backscattering and TEM meas. 0-100272
- GaAs:Zn, implanted, laser annealing, elect., Rutherford backscattering and SEM meas. 0-100273
- GaAs:Zn, ion implanted, TEM study after laser and furnace annealing 0-70234
- GaAs-Si ion implanted, impurity profiles elec. props. 0-96550
- GaAs-(GaP) single cryst., defect distrib. near abraded surface 0-92533
- GaP, complex ¹¹⁹Sn impurity-defect, Mossbauer study 0-75898
- GaP crystals, radiation defects, TSC obs. 0-65588
- GaP single cryst., defect distrib. near abraded surface 0-92533
- (GaSb)_{1-x}(Ge)_x films, single-cryst. metastable semicond., growth and phase stability 0-80115
- (Gd_{1-x}Co_x)_{1-y}Ar, amorphous mag. film, elec. and mag. prop. depend. on Ar 0-80410
- (Gd_{1-x}Co_x)_{1-y}Ar, amorphous films, effective anisotropy field, ferromag. reson. obs. 0-71123
- Ge, acceptor complex spectra, tunnelling H systems 0-89036
- Ge amorphous films, structural relaxation and crystallisation 0-100170
- Ge crystals, electron beam induced changes of real struct., HVEM 0-103390
- Ge epitaxial film, ion implantation and electron beam anneal effects on carrier conc. 0-75255
- Ge epitaxial film, vac. deposited on GaAs, doping effect of annealed GaAs surface 0-65718
- Ge, laser pulse annealing, induced nucleation, crystal growth 0-84966
- Ge, neutron irradi., absorpt. edge 0-93320
- Ge, neutron-irradiated, positron lifetime 0-97374
- Ge surface, (111), ion-bombarded and annealed, spectroscopic ellipsometry study 0-103543
- Ge thin films on glass substrates, annealing by Ar ion bombardment 0-80136
- Ge-Bi-Te system, thermal cond. change during phase transitions 0-100368
- Ge-S glass, melt-quenched photoinduced ESR, annealing behaviour and glass comp. depend. 0-71156
- Ge-Si alloys, n-type, phosphorus doped, precipitation effects due to heat treatment 0-107833
- GeSe, amorphous, film, thermally induced effects, UPS study 0-104042
- GeSe₂, amorphous, film, thermally induced effects, UPS study 0-104042
- Hg electric field gradients at different Be lattice sites, gamma-spectral study 0-80224
- Hg_{1-x}Cd_xTe, epitaxial layers, elec. properties in the range 4.2 to 300K (French) 0-65721
- Hg_{1-x}Cd_xTe, grown from melt, Kirkendall and Frenkel effects 0-100365
- Hg_{1-x}Cd_xTe, implanted with Hg, Al, damage and lattice location study 0-103381
- Hg_{1-x}Cd_xTe, segregation, compositional characterisation 0-107434
- HgCr₂Se₄, electronic props. rel. to departure from stoichiometry 0-100472
- In electrode, annealing, effect on elec. resist. of metallic thin film 0-80416
- In_{0.3}Ga_{0.7}P, N free and implanted, photoluminescence study 0-97322
- In_{0.3}Sn_{0.7}O₂ thin film, Hall mobility, temp. depend., grain boundary effects 0-75658
- InP (110) surfaces, cleaved and polished-sputtered-annealed, LEED and AES study 0-103550
- InP film, electron-beam annealed, surface conduction 0-84500
- n-InP, γ -ray and electron irradi., annealing of radiation point defects, elec. cond. and Hall coeff. meas. 0-65051
- n-InP, heat treatment in controlled P vapour 0-88137
- InP, ion-implanted layers, close contact capless annealing, elec. props. 0-84192
- InSb, absorpt. edge, exciton struct. 0-93321
- InSb, galvanomagnetic props. of annealed single crystals 0-96909
- InSb, Raman scattering study of unoxidised Sb in anodic oxide films 0-88985
- InSb_{1-x}Bi_x films, single-cryst. metastable semicond., growth and phase stability 0-80115
- In₂Se₃-SnO₂ amorphous film-SnO₂ system, photovoltaic spectra, annealing effect (Japanese) 0-92926

annealing continued

- In_2SnO_3 film, effect of ambient atmosphere during annealing, elec. props. 0-97510
 InTe thin films, flash evaporation, electrical props. 0-65722
 $\text{KBr}(\text{Cl})\cdot\text{OH}^-$, cc U_2 to H_2O^- defects conversion after UV photodecomp. 0-107230
 $\text{KCl}:\text{Ba}^{2+}$, localised stress relaxation in excess vacancy system, prismatic loops (*Russian*) 0-88160
 $\text{KCl}:\text{Ba}^{2+}$, solid solution periodic precipitation in inhomogeneous conc. field 0-103485
 $\text{KCl}:\text{Ca}^{2+}$, Z₂-centre thermolum. 0-80879
 $\text{KCl}:\text{Li}$, X-irrad., F₂ centres, thermolum. studies 0-80878
 $(\text{La}_2\text{O}_3)_{1-x}(\text{CeO}_2)_x$, Mn, valence state of Mn, effect of annealing in H₂ atm., ESR obs. (*French*) 0-71164
 Li_2AlO_4 , Li_2FeO_4 and Li_2GaO_4 , additives and moisture effect on ionic cond. 0-107523
 LiF, γ -irrad. induced defects, positron capture and annealing obs. 0-60707
 LiF TLD phosphor, γ -irrad. induced sensitisation, UV effects 0-108286
 LiF TLD phosphor, residual thermoluminescence effect on sensitisation 0-108287
 Li_2GeO_4 - Zn_2GeO_4 , solid electrolyte system, phase diagram 0-66489
 LiInS_2 , blue-band emission 0-76062
 $\text{Li}_2\text{O}-\text{Al}_2\text{O}_3-\text{SiO}_2$ glass-ceramic, near-zero thermal-expansion heat treatment effect in fracture behaviour 0-66537
 $\text{Li}_{1+x}\text{Ti}_{2-x}\text{O}_4$, high temp. spinel-Ramsdellite transform. 0-70407
 Mg-Ag, ion implanted, recovery stage characterisation by electron irrad. 0-107295
 MgAl_2O_4 , radiation damage, optical absorpt., F-centres 0-64994
 MgF_2 obs. of radiation induced point defects, cross-relaxation processes, polarised β -active nuclei 0-60431
 Mn thin film, DC resist., activation energy, thickness depend. 0-84518
 Mn-Al-C, ferromag. alloy, transform. kinetics 0-76229
 Mn-Ni, thermal expansion, mag. susceptibility, lattice consts. 0-100341
 Mn-SiO₂, annealed cermet films, elec. resist., composition depend. 0-97007
 Mn-SiO₂ cermet thin film, DC resist., activation energy, thickness depend. 0-84518
 MnBi film, electrical props., in situ annealing effect 0-65708
 MnBi films, prep. by ionised-cluster beam deposition technique, magneto-optical props. 0-100790
 $\text{Mn}_{1-x}\text{Zn}_x\text{Fe}_2\text{O}_4$, prepared by wet method, neutron diffr. and high field Mossbauer expts. 0-75719
 Mo film, evaporated, annealing behaviour, SEM obs. 0-65397
 Mo film, sputtered, elec. resist., annealing and struct. effects 0-60109
 Mo, gamma irradiated defects, interaction with positrons (*Russian*) 0-93732
 Mo, neutron irrad., radiation anneal hardening mechanism 0-71678
 Mo, plastically deformed single cryst., mag. susceptibility (*Russian*) 0-93074
 Mo polycrystals, grain misalignment, electron microscope determ. (*Russian*) 0-103358
 Mo powder, influence of powder reduction processes on props. 0-89175
 Mo-Re(Os)(Ru), recovery after deform. and annealing, destrengthening mechanism (*Russian*) 0-97546
 Mo-Si sputtered contacts, contact resistance 0-92970
 Mo-W-N system, nitrided annealed samples, W replacement of Mo 0-76227
 MoS_2 , homogeneity size estimation, stacking fault conc. effect 0-96661
 MoSi_2 , refractory formation by As^+ ion beam bombardment 0-107286
 $\text{Na}_6\text{Al}_2(\text{Si}_2\text{O}_6\text{GeO}_6)_2\text{O}_{24}\cdot 2\text{NaBr}$, Ge-doped sodalite powders, UV absorpt. band 0-71452
 $\text{NaCl}:\text{Eu}$, secondary Eu phase dissolution, EPR and optical absorpt. study 0-96655
 $\text{NaCl}:\text{Mn}^{++}$, Mg^{++} , doubly doped, ionic thermocurrent study of linear dimer 0-79977
 $\text{Na}_2\text{O}-\text{SiO}_2$ glass, microcracking about NiS inclusions, fracture mech. description 0-89333
 Nb films, ion beam sputtered, supercond., laser annealing effects 0-97024
 Nb, neutron irradiated, radiation anneal hardening (*Japanese*) 0-89243
 Nb single crystals, for tunnel meas., annealing in ultra high vac. device (*German*) 0-89169
 Nb, US attenuation, hysteresis near and below H_{c1} , annealing effects 0-75676
 Nb-Si(-V)(Zr)(Mo)(Ta)(W)(C)(B)(Ge), ductile amorphous, superconductivity 0-60131
 Nb_2Al , complex refractive index meas. 0-93264
 Nb_2Al , supercond. props. and lattice parameter, comp. and neutron irrad. effects 0-70880
 $4\text{NbO}_{0.76}$ thin film, FCC cell struct. investigation 0-92796
 Nb_3Si A15 phase from amorphous Nb-Si alloys, high-press. synthesis 0-93516
 Ni, creep at 77, 295K, formation of five struct. 0-60926
 Ni ferrite, quenched, Neel temp. and initial-susceptibility 0-75762
 Ni films, adhesion on graphite 0-80141
 Ni, oxidation kinetics, influence of intermediate annealing treatment 0-89412
 Ni precipitates, isothermal annealing influence on structural state, X-ray diffr. anal. (*Russian*) 0-100849
 Ni, push-pull fatigued polycrystals, point defects, elec. excess resist. meas. 0-100910
 Ni-In, He, lattice defect struct., PAC meas. 0-70190
 $\text{Ni}-\text{Al}$ system, solid soln., interdiffusion (*Japanese*) 0-70476
 Ni-Cr, (30 wt.%), collective dislocation movements, in situ study 0-100243
 Ni-Cr-Fe alloys, radiation enhanced precip. and dissolution of precipitates, point defect kinetics and dislocation obs. 0-108467
 Ni-Cu, electron-irrad., neutron-scatt. studies 0-75268
 Ni-Nb-C, obtained by liq. quenching, superconductivity 0-75699
 Ni-Ti/Cu composite, plastic deform. influence on internal friction (*Russian*) 0-100871
 NiClO_4 , neutron activated, radiation annealing 0-93569
 Ni_2Fe , change of H₂ diffusivity with order-disorder transformation 0-59729
 Ni_2Fe , compression induced magnetic anisotropy, annealing effect 0-93112
 Ni_2Fe , magnetocryst. anisotropy, annealing temp. depend. 0-103828
 $\text{Ni}_{36}\text{Fe}_{23}\text{Cr}_{14}\text{P}_{12}\text{B}_6$ metallic glass, mech. props. and thermal stability 0-76362
 NiFe_2O_4 ferrite, mag. props., neutron irrad. 0-103858

annealing continued

- Ni_{98}M_2 , M=impurity metal, formation of MH(D)-complexes 0-65236
 Ni_3Mn , change of H₂ diffusivity with order-disorder transformation 0-59729
 NiP amorphous alloy, heat treatments influence on opt. props., struct. and DC resist. obs. 0-80892
 Ni_2Pt , change of H₂ diffusivity with order-disorder transformation 0-59729
 $\text{Ni}_{100}\text{Sb}_{0.04}$, surface segregation, XPS and AES obs. 0-76135
 Pb_{12} , first-order 2H-4H polytype transition, exciton spectroscopic study 0-59647
 $\text{Pb}_{0.95}\text{Sn}_{0.05}(\text{Zr}_{1-x}\text{Ti}_x)\text{O}_3-\text{Nb}_2\text{O}_5$, phase coexistence range, lattice consts. 0-92680
 n-PbTe, low temperature electrical transport, Hall effect 0-84478
 PbTe-Ga₂Te₃, phase interaction, DTA, XPA and microstructural anal. 0-96625
 PbTiO_3 , amorphous, crystallisation process, DTA and Raman spectroscopy meas. 0-75161
 Pd, H phase hardened, recrystallisation study 0-60883
 Pd, silicide formation due to laser and electron beam annealing 0-84849
 Pd-Si structure, epitaxial silicide growth, LEED and AES study 0-103590
 $(\text{Pd}_{80}\text{Au}-\text{Si}_{15})/\text{Fe}_{30}$, compositionally modulated amorphous film, diffusion, struct. relax. 0-103518
 β -PdDx ($x=0.710, 0.742, 0.754, 0.780$), structural changes in temp. region of 50K anomaly 0-100131
 $(\text{Pd}_{85}\text{Si}_{15})_{61}/(\text{Fe}_{85}\text{B}_{15})_{39}$, compositionally modulated amorphous film, diffusion, struct. relax. 0-103518
 $\text{Pd}_{1-x}\text{W}_x$, calc. of short-range order parameters from X-ray scatt. data (*Russian*) 0-75367
 Pt (997) surface, partial faceting, He beam scatt. and LEED study 0-103547
 Pt, neutron damage, positron annihilation 0-65056
 Pt, silicide formation due to laser and electron beam annealing 0-84849
 Pt-Si Schottky barriers on Si, laser formation and characts. 0-60079
 PtSi film formation by ion sputtering and annealing, form. and exam. problems 0-100782
 Pu, oxidation, binding energies, Auger and X-ray photoelectron spectra study 0-76550
 Sb_2Te_3 - Bi_2Te_3 and Sb_2Te_3 - Sb_2Se_3 systems, thermal cond. change during phase transitions 0-100368
 Se powder compacts, sintered, electrical cond. 0-70693
 Si (001) wafer, pyramidal hillocks, TEM obs. during chemical etching 0-70508
 Si, ambient effect of O precipitation, self interstitial mechanisms, IR spectra, TEM study 0-66510
 Si, amorphous, sputtered, resist. control by ion implantation 0-100262
 Si, amorphous, substrate orientation effect on regrowth by laser pulses, channeling, backscatter 0-84409
 Si, amorphous, UHV evaporated, annealing behaviour of spin density 0-93163
 Si, amorphous films, hopping conduction, dangling bond generation by high temp. annealing 0-60115
 Si amorphous layers, glow-discharge, laser-annealed, elec. props. 0-75661
 Si, amorphous layers, RF-sputtered on sapphire, crystallisation by CW ion laser annealing 0-80109
 Si, annealed, neutron-irradiated, EPR centre ($S=1$), characts. 0-71177
 Si, annealed, photoluminesc. anal. of defects 0-80836
 Si, annealing, using laser pulses, impurity incorporation at melt-cryst. interface 0-59504
 Si, annealing during Czochralski growth, influence on defect density 0-60769
 Si, cast polycryst., laser annealed for solar cells 0-93918
 Si, crystal defects and impurities interaction obs. by electron microscopic methods 0-65003
 Si, Czochralski grown, oxide precip. homogeneous nucleation 0-65221
 Si, Czochralski grown, oxide precipitates, diffusion-limited growth 0-97484
 Si, Czochralski grown crystal, O precip., nucleation behaviour and dislocation loop form. (*Japanese*) 0-59664
 Si, dense plasma dynamics during pulsed laser annealing, carrier density, recombination 0-84479
 Si, electron beam annealing, beam voltage effect modeling 0-75275
 Si, electron beam scan annealed, deep levels 0-65481
 Si epitaxial layer regrowth due to laser annealing mechanism, liquid and solid phase regimes 0-100712
 Si, epitaxial wafer, saucer pit microdefects reduction by intrinsic gettering 0-75450
 Si, graphoeptitaxy on fused SiO_2 using surface micropatterns and laser crystn. 0-70554
 Si, high dislocation density crystals, photoelectret state investigation 0-97191
 Si, high dose self-irrad., spatial correl. between primary and secondary defect profiles 0-59536
 Si, hydrogenated amorphous, laser annealing 0-100713
 Si, implanted crystal, laser induced annealing and diffusion behaviour 0-88202
 Si, implanted semiconductors, laser annealing, review 0-107301
 Si, ion damage TEM study of laser annealing 0-88215
 Si ion implanted, amorphous to crystalline transition due to laser irrad. 0-103451
 Si, ion implanted, annealing of heavy ion cascade damage, channelling meas. 0-89255
 Si, ion implanted, annealing by ion beam heating 0-103382
 Si, ion implanted, damage struct. obs. using TEM and cross section specimens 0-107298
 Si, ion implanted, interstitial generation and loop form. during annealing in oxidising medium 0-107225
 Si, ion implanted, scanning CW and pulsed laser annealing 0-92549
 Si, ion implanted, self implanted, self annealing using high ion current density treatment 0-89254
 n-Si, ion-implanted, elec. characts. after laser annealing 0-88562
 Si, ion-implanted, impurity activation monitoring by SAW techniques 0-65020
 Si ion-implanted dopant redistribution under laser annealing 0-70242
 Si ion-implanted laser-annealed solar cells 0-93881
 Si ion-implanted solar cells, factors controlling efficiency 0-81451
 Si, laser annealing, nonlinear dynamic transport processes 0-93437
 Si, laser annealing mechanisms, disordered overlayers, crystalln. 0-84967
 Si laser annealing of SiO_2 layers 0-97505
 a-Si, laser induced crystallisation mechanism, epitaxial regrowth 0-84962

annealing continued

- Si layer, on buried SiO₂ layer formed by high-dose, O ion implantation, TEM, AES, and XPS obs. 0-88172
- Si layers amorphized by molecular ions, laser annealing 0-103379
- Si materials, advanced, preliminary evaluation for space solar cells 0-94006
- Si, n⁺-p diode, γ -radiation defects, annealing and recomb. props. 0-65045
- Si n⁺p solar cells, effect of elec. bus during 1 MeV electron irradi. and isochronal annealing, elec. characts. and deep level pop. 0-94086
- Si, non thermal laser induced ordering, plasma life time, phonon interactions 0-84481
- Si on sapphire film, laser annealing non-thermal theory expt. test 0-89273
- Si, oxidation stacking faults, shrinkage and growth, bulk O₂ effects 0-96546
- Si, P implanted low pressure CVD polycryst. films, elect. characts. 0-60114
- Si, plasma effects during pulsed laser annealing 0-84480
- Si, point defects, laser annealing 0-107224
- Si, polycrystalline, As segregation at grain boundaries, elec. props. meas. 0-75259
- Si polycrystalline film resistivity reduction by Nd:YAG laser annealing 0-100539
- Si, polycrystalline solar cells, fabricated from metallurgical grade Si 0-81441
- Si polycrystalline solar cells fabricated from refined metallurgical-grade Si, impurity gettering 0-94011
- Si processing technology, appls. of scanning CW lasers and electron beams 0-100932
- n-Si, quenched, fast electron irradiated, annealing of defects 0-89259
- Si, reflectivity time dependence during pulsed laser annealing 0-66214
- Si, screw dislocation networks, TEM study 0-70204
- Si, single crystal solar cell manufacturing process, laser annealing of implanted area, energy saving 0-97791
- Si, slip dislocation nucleation during laser annealing 0-84179
- Si solar cell processing, pulsed laser techniques for annealing ion-implantation damage 0-81453
- Si solar cells, high open circuit voltage, P implantation 0-89642
- Si solar cells, ion implanted grating type 0-101102
- Si solar cells, ion-implanted, furnace annealing 0-81452
- Si solar cells, ion-implanted, expt. study of efficiency controlling factor 0-93997
- Si solar cells, laser annealing, conversion efficiency improvement (*French*) 0-66976
- Si solar cells, n⁺-p, Li-counterdoped, radiation damage 0-94000
- Si solar cells, radiation damaged, origin of reverse annealing 0-76630
- Si solar cells, radiation damage annealing mechanisms and low temp. annealing 0-94003
- Si, surface, pulsed electron beam processing, doping, annealing 0-75254
- Si, surface topography changes due to pulsed laser annealing 0-84348
- Si, TEM and EELS identification of oxide precipitates 0-100723
- Si, temperature during CW laser heating, Raman scatt. meas. 0-76109
- Si, V-grooves formed by etching, phosphosilicate glass bridge struct. 0-104312
- Si wafer, ion implanted, electron beam annealing, computer simulation 0-96569
- Si: As(Pb), high-dose ion implanted and annealed, implant redistribution 0-107309
- Si:Ar, As, ion implanted, laser annealing, doping profiles, channelling 0-97506
- Si:Ar(Ne)(O)(N), ion-implanted, defect reverse annealing, 550-650°C 0-88875
- Si:As, CW CO₂-laser annealing, comparison with thermal annealing 0-84193
- Si:As, diffused, laser irradi., stability study 0-65547
- Si:As, ion implanted, laser annealed, lattice defects, epitaxial regrowth 0-103334
- Si:As, ion implanted, low temp. thermal annealing 0-96552
- Si:As, ion implanted, pulsed ion beam annealing 0-103395
- Si:As, scanning electron beam annealing, spreading resistance, junction depth 0-75267
- Si:As, shallow junctions by high-dose implants 0-96694
- Si:As, solid solubility and thermal behaviour of metastable 0-75359
- Si:As high-dose implanted single crystals., pulsed electron-beam annealing 0-103373
- Si:As ion implanted layers, annealing by CO₂ laser, doping profile shift 0-84965
- Si:As⁺, implanted, CW laser annealing, electron-beam induced current 0-100709
- Si:As⁺(P⁺) ion implanted, laser annealed, correlation of struct. and elec. props. 0-70855
- Si:As(P), ion implanted, TEM study after laser and furnace annealing 0-70234
- Si:As(Sb), ion implanted, lattice location of impurities after pulsed laser annealing 0-88196
- Si:B, high conc. effects in ion implantation 0-75245
- Si:B, implanted laser annealed, lattice strain, X-ray study 0-96554
- Si:B, ion implanted, structure defects formation and behaviour under annealing in various ambients 0-65033
- Si:B, layer resist. depend. on implanting and annealing conditions (*German*) 0-96551
- Si:B (0.2 wt.%) ion implanted, B atom displacement due to low temp. irradi. 0-88234
- Si:B radiation damage and minority carrier lifetime, SEM-EBIC obs. 0-96573
- Si:BF₃⁺, ion implantation appl. in semicond. device production 0-103383
- p-Si:B(Al), radiation defect form. and annealing study using Hall effect, cond. and carrier diffusion length 0-84214
- Si:B(P), ion implanted crystalline and amorphous laser annealing 0-97509
- Si:B(P)(As)(Sb)(Cu)(Fe), ion implanted, doping profile, pulsed laser annealing effects 0-88197
- Si:Be, ion implanted, correl. of atomic distrib. and implantation induced damage profiler 0-88199
- Si:Bi, ion implanted, channelling obs. of pulsed Q-switched ruby laser annealing 0-59542
- Si:F, amorphous, heat resistant, prep., elec. cond., IR absorpt., annealing 0-65719
- Si:Fe, ion implanted, laser annealing studies using Mossbauer spectroscopy 0-79827

annealing continued

- Si:H, amorphous, discharge prod., optically induced cond. changes 0-96937
- Si:H amorphous films, IR spectrum and struct. 0-97277
- p-Si:In, ion implanted, doping profiles from capacitance-voltage characts. 0-88203
- Si:N, laser-annealed, Jahn-Teller distorted donor, EPR meas. 0-84642
- Si:N wafers, Si₃N₄ layer growth by high dose implantation and annealing, elec. props. 0-70227
- Si:N(P), ion implanted, IR transmission and rel. spectra study 0-108244
- Si:O(C), implant redistribution, annealing effects, SIMS meas. 0-96561
- Si:P, implanted low temp. annealed, elec. activation, damage depend. 0-88182
- Si:P, incoherent light flash annealing, elec. props., backscattering spectra 0-97504
- Si:P, ion implanted, regrowth of damage structs. by laser annealing 0-107289
- Si:P, ion implanted with small doses, defect annealing by nanosecond laser pulses 0-107297
- Si:P implanted, multiscanning electron beam annealing 0-75242
- Si:P(As)(B), nonequilibrium solid solutions obtained by heavy ion implantation and laser annealing 0-92544
- Si:Sb, high dose Sb ion implantation, buried layer appls. 0-88186
- Si:Sb, ion implanted and annealed, influence of implantation temp. on dislocation generation 0-88158
- Si:Sb,P, double implants, residual defect reduction after damage anneal 0-88170
- Si:Sb vacuum deposited coating, p-n junction, pulsed electron beam annealing doping, diffusion 0-75480
- Si:Sb(Ga)(Bi)(In), dopant solubility limit, laser irradi. effects 0-84295
- Si/Pd system, solid phase epitaxial growth control by C ion implantation 0-75466
- Si-Au system, ion implanted induced giant gettering, annealing effects 0-88221
- Si-Pd₈₀Si₂₀, amorphous, Pd₂Si layer form., shallow contact 0-103586
- Si-SiO₂, ion implantation through SiO₂ film, recoil implantation of O, EPR study 0-88180
- Si-SiO₂, two layer system, P⁺-ion penetration tails, expt. and computer anal. 0-75249
- Si-SiO₂, interface in MOS solar cells, operational characts. and struct. 0-93901
- Si-SiO₂, interface states, deposition of H containing layers and annealing 0-92991
- Si-SiO₂, MOS capacitors, relationship between trapped holes and interface states 0-70830
- Si-SiO₂, structures, B ions implanted, energy spectra of shallow traps at various implantation energies 0-80392
- SiC ion implanted, laser induced ordering and defects 0-84754
- SiC, radiation defect annealing, recovery of LEED maxima 0-65075
- SiC:H amorphous reactively sputtered film, H content effect on film props. 0-75459
- Si₃N₄, dielectric films made by NH₃-silane reaction, TEM study 0-84413
- SiO₂, As-implanted, electron trapping and detrapping characts. 0-65692
- SiO₂ film, attenuated total reflectance study, impurity spectra 0-97311
- SiO₂ films, Si-rich, amorphous Si region obs. 0-84400
- SiO₂, fused, surface crystn. by Li⁺ ion implantation and annealing 0-89383
- SiO₂, ion implanted, radiation defects and optical props. 0-107293
- SiO₂, layer used for MOSFETs, electron trapping behaviour 0-92981
- SiO₂:As⁺ implanted layers in MOS struct., electron trapping and detrapping characts. 0-92982
- Sm, electron radiation damage, elec. resistivity change rates 0-59954
- Sm₂Co₁₇, coercive force depend. on annealing temp. 0-65964
- Sm₂Co₁₇, sintered magnets, coercive force and constitution, annealing temp. depend. (*Russian*) 0-88786
- Sn, film, superconducting fluctuations, transition temp. (*Russian*) 0-65740
- Sn_{1-x}Pb_xSe(Te) films, oxidation rel. to annealing temp. and time, Mossbauer spectra, X-ray and microstruct. obs. 0-104311
- SnTe, annealed, iodide method of prep., props. meas. 0-71591
- SnO:Co, noncentral and interstitial ion complexes, ESR obs. 0-71169
- Ta₂N₅ and TaN_x films, thermal oxidation and resist. 0-60125
- 2Ta₂O₃ thin film, FCC cell struct. investigation 0-92796
- TaSi₂ refractory formation by As⁺ ion beam bombardment 0-107286
- Ti, commercial, texture depend. stress corrosion cracking 0-104334
- α -Ti sheet, texture dependent stress corrosion cracking in Br₂-methanol soln. 0-71803
- Ti-Al-Mo, type BT22, phase transformations under step-by-step heat treatment (*Russian*) 0-108436
- Ti-Al-V (6, 4 wt.%), texture depend. stress corrosion cracking 0-104334
- Ti-Al-V (6.4 wt.%), microstruct. effect of base metals on diffusion welding (*Japanese*) 0-89296
- Ti-Ni, multiplicity of structural transitions, phase diagrams, elec. cond. meas. 0-71649
- Ti-Ni (48 to 53 at.%), heat treatment and deviation from stoichiometry 0-104192
- Ti-Ni-Fe, multiplicity of structural transitions, phase diagrams, elec. cond. meas. 0-71649
- TiO₂-Ni (100) interface, electronic props., struct., comp., chemical bonding 0-84499
- TiO_{2-x} reduced, crystallographic shear planes, dislocation struct. 0-107175
- Ti₂Te₃-Ti₃SnTe₃-Ti₄PbTe₃, phase equilib., DTA, SPA and microhardness meas. 0-96628
- Tm₂O₃ film, between Al electrodes, prep. and elec. props. 0-60103
- α -U, strain rate effect on tensile flow and fracture 0-84992
- UAl₃(Co₂), surface comp. and electronic struct., photoemission study 0-66382
- V, dehydrogenation by annealing with Zr foils, internal friction meas. 0-96736
- V, electron-irradiated, positron annihilation study 0-70259
- V film, vac. evaporated, elec. props. 0-80414
- W (100), clustering of Kr, He desorption spectrometry 0-77908
- W, plastically deformed single cryst., mag. susceptibility (*Russian*) 0-93074
- W wire, AKS-doped, second phase particle obs. by TEM, SEM and atom probe microanalysis 0-108457
- W-Zr field emitter, time-of-flight atom-probe study 0-80949
- WC-Co hard alloys, hot-pressed, wear resist. under abrasive friction, heat treatment effect 0-66555

annealing continued

- WSi₂ refractory formation by As⁺ ion beam bombardment 0-107286
 WSi₂, sputtered, props. for MOS IC appl. 0-70831
 (Y,Sm,Ca)₂(Fe,Ge)₂O₁₂ epitaxial films, mag. props., growth condition effects 0-97124
 Y, electron radiation damage, elec. resistivity change rates 0-59954
 YAG laser trimmer for wafer level products 0-87428
 YCo₃ amorphous films, ⁵⁹Co spin echo study 0-80636
 YFe_{2-x}Al₂O₁₂, impurity redistrib. kinetics, temp. depend., vacancy effects 0-75263
 YFe_{2-x}Ga₂O₁₂, impurity redistrib. kinetics, temp. depend., vacancy effects 0-75263
 YIG, electron and γ -irrad., photomagnetic effect 0-103877
 YIG:Ca, oxidising effects of high temp. annealing in reducing atmosphere 0-66696
 (YSmLuCa)₂(FeGe)₂O₁₂, epitaxial films, LPE grown, annealing effects on mag. anisotropy 0-66548
 Yb, electron radiation damage, elec. resistivity change rates 0-59954
 Zn-Al (1.1 wt.%) superplastic alloy, grain size determ. (Czech) 0-81118
 Zn-As system, homogeneity range of ZnAs₂ and electrophys. props. 0-60833
 ZnO RF sputtered films, post deposition annealing behaviour 0-100416
 Zn₃P₂, elec. cond., Hall effect, P interstitial effects 0-84465
 ZnS, ion implantation effects on luminesc., thermo-EMF 0-88178
 ZnSe cryst., IR absorpt., annealing effect 0-80774
 ZnSe, in liq. Pb, photoluminescence 0-60661
 p-ZnSiAs₂, electron irrad. elec. props. annealing, lattice defects 0-100465
 ZnTe, ion implantation defect introduction, cathodolum. studies 0-75250
 ZnTe, irradiation induced radiative centers obs. 0-66290
 ZnTe:Bi, laser annealing, channelling, reflectivity spectra 0-66215
 ZnTe:P(As), ion implanted, cathodoluminescence emission spectrum 0-108281
 Zr alloys, irradiation growth, influence of microstructure and test conditions 0-92561
 Zr, H(D) implanted, superconductivity enhancement obs. 0-70884
 Zr, irradiation growth, influence of microstructure and test conditions 0-92561
 Zr-Nb (2.5 wt.%) pipe, fracture resistance, hydrogenation effect 0-104279
 ZrCu, constitutional and struct. studies, by mag. susceptibility, metallography and X-ray diff. 0-70166

annealing, magnetic see *magnetic annealing***anodes**

- contraction region modeling in high intensity arcs 0-103210
 Geiger counter, self-quenching, anode surface changes with ageing 0-58025
 graphite arc, in Ar flow, meas. of anode voltage drop 0-84022
 ion beam extraction, computer simulation, finite element method 0-96387
 plasma electron emitter with constricted arc discharge, characts., anode spots effects 0-70040
 X-ray tube, high continuous power, with Rh-W disc bonded to graphite (German) 0-105760
 X-ray tube rotary anode, by transition metal carbides (German) 0-105759
 Al anode spot of vacuum arc 0-107006
 Cd₂GeO₄ anode for H₂O photoelectrolysis 0-108716
 CdIn₂O₄ anode for H₂O photoelectrolysis 0-108716
 CdSe photoanodes, S substitution during operation and mech. of surface protection 0-107906
 Cd₂SnO₄ anode for H₂O photoelectrolysis 0-108716
 Kr water-cooled arc lamp, anode, temp. distrib. along length, anode geometry effects 0-106994
 Pt, oxide film growth in H₂SO₄ solns., temp. study 0-71802
 S-tolerant components development for molten carbonate cell 0-89611
 W monocrystals in alkaline electrolyte, surface orientation, effect on anode current (Russian) 0-75360

anodes, electrochemical see *electrochemical electrodes***anodic machining** see *electrolytic machining***anodisation**

- steel, mild, anodic polarisation behaviour in hot alkaline sulphide solns. 0-100949
 Al anodic oxidation fabrication of Al/Al₂O₃/p-GaAs MOS diodes 0-107914
 Al, anodisation, high voltage barrier, Cl⁻ ion effects 0-104327
 Al, behaviour of emulsion particles during electrodeposition 0-104357
 Al, implanted Xe behaviour during anodic oxidation 0-71800
 Al-Mg (7 wt.%), bare surface reaction rates in aq. solns. 0-101022
 Al-Nb superimposed metallic layers, ionic movements during anodization, Rutherford backscatt. and nuclear microanal. 0-71913
 Al-Ta₂O₅-Al, healing of defects in dielec. film by anodisation 0-65406
 Al₂O₃, anodic, passified, inhibition of reaction with water 0-89390
 Bi, anodic oxide film capacity in various soln. 0-104320
 Bi₂Te₃, anodic film form., in situ ellipsometric study 0-104318
 Cu anode, passivating behaviour and illum. effects in alkaline soln. 0-104449
 Fe, anodic behaviour in 1M H₂SO₄, influence of straining 0-97612
 GaAs anodisation, ellipsometric study (Japanese) 0-97610
 GaAs, anodisation at low substrate temp. by low pressure O₂ plasma 0-104314
 GaAs, anodisation in HF O₂ plasma, oxide film form. mechanism and kinetics (Japanese) 0-93667
 GaAs MOS solar cells by anodisation in active region 0-101107
 GaAs MOS structures, native oxide growth by wet anodisation 0-70832
 GaAs surface, low temp. thermal nitridation 0-97607
 GaAs/anodic oxide interface, characterisation of proposed model 0-103754
 GaSe, anodic film form., in situ ellipsometric study 0-104318
 InGaAsP, anodic oxidation, refractive indices 0-97601
 InSb MIS diode, anodised, C-V characts., effect of high elec. field pulse 0-60092
 Nb, mono- and polycrystn., crystallographic orientation, etching technique determ. 0-71814
 Nb-Al superimposed metallic layers, ionic movements during anodization, Rutherford backscatt. and nuclear microanal. 0-71913
 Nb-Ta superimposed metallic layers, ionic movements during anodization, Rutherford backscatt. and nuclear microanal. 0-71913
 Ni, role of oxide defects in anodic oxidation 0-76403
 Pb electrode, in situ surface phase study by laser Raman spectroscopy 0-103542
 Si, anodic oxidation in RF induced O plasma 0-100931

anodisation continued

- Si, anodisation at low substrate temp. by low pressure O₂ plasma 0-104314
 Si, high electronic current density in anodic oxidation 0-89386
 Si, p-n junction, electrolytic anodic oxidation method of decoration 0-60069
 SiO₂ films, DC plasma Si anodisation, dielectric const., O₂ pressure influence 0-70564
 Ta-Nb superimposed metallic layers, ionic movements during anodization, Rutherford backscatt. and nuclear microanal. 0-71913
 WO₃ amorphous anodic film growth on W in acidic soln. 0-81232
- anodised coatings** see *anodised layers*
- anodised layers**
 ellipsometer obs. interpretation using film form. models 0-101828
 Hastelloy B-2, corroded surface, electron bombardment effect during Auger electron anal. 0-61014
 Al alloy surfaces anodized in phosphoric acid, SEM characterization 0-81241
 Al and Al alloy anodised oxide films, for adhesive bonding appls., AES and SEM study 0-66689
 Al anodic films, acoustic and electron-emission during deform. 0-80143
 Al anodic films, flaw obs. 0-93696
 Al anodising, porous films formed in chromic acid 0-100966
 Al-Cu-Mg, type RR55, high strength, creep behaviour, effect rel. to anodic coatings, SEM study 0-97542
 Al₂O₃, anodic film, trapped O₂ and effect on dielec. stability 0-100634
 Al₂O₃ anodic films, H conc. profiles meas. 0-75261
 Al₂O₃ anodic films, trapping levels study using TSC 0-103768
 Al₂O₃, integrally coloured oxide films on Al, optical properties 0-93420
 Al₂O₃ supermicrogrid preparation and props. for use as support film in high resolution electron microscopy 0-99010
 FeS amorphous films, on mild steel during anodic polarisation in alkaline sulphide solns. 0-100949
 GaAs anodic films, XPS study 0-71562
 GaAs anodic oxide, states, electrochemical meas. 0-80176
 GaAs anodisation, ellipsometric study (Japanese) 0-97610
 GaAs oxide, prep. by low pressure O₂ plasma, refractive index and elec. props. 0-104314
 GaAs, surface passivation using composite Al₂O₃ and native oxide, MIS characts. 0-93004
 H₂WO₃, formation on Na₂WO₃ surface 0-71767
 InP, surface passivation using composite Al₂O₃ and native oxide, MIS characts. 0-93004
 IrO₂ anodic film electrochromic cell, fabrication and display device use 0-61320
 IrO₂ anodic films, electrochromism and ionic cond., model 0-59706
 IrO₂ anodic films, electrochromic props. and device uses 0-61319
 IrO₂ anodically grown film as electrochromic material 0-71377
 IrO₂, electrochromic, oxidation state changes and struct. 0-100950
 Ni, anodic passive film form. in NaOH soln., refl. and ellipsometric study 0-104447
 NiO film, formed by Ni galvanic oxidation in borate buffer soln., struct. 0-100948
 Rh oxide film, anodic, two-colour electrochromic system 0-66150
 Si, anodic oxidation in RF induced O plasma 0-100931
 Si oxide film, prep. by low pressure O₂ plasma, refractive index and elec. props. 0-104314
 Si, porous layer form. mechanism by anodisation in HF soln. 0-71769
 Ta₂O₅ anodic films, elec. cond. mechanism, admittance meas. 0-70705
 Ti-Mo alloy, thin anodic oxide, AES depth profile 0-71801
 WO₃ electrodes, electrochromic processes, digital simulation model 0-76518
 WO₃, anodic oxide films, quadratic electro-optic and electrostrictive effects, ellipsometry 0-108184
- anodised thin films** see *anodised layers*
- anolytes** see *electrolytes*
- anomalous skin effect**
 metal, cyclotron reson. on open electron orbits (Russian) 0-88878
 metal, surface impedance near anomalous skin-effect limit, electron-electron N processes 0-100497
 metal film, Umklapp processes of charge carriers and anomalous transmittance in RF range (Russian) 0-70851
 metals, cyclotron resonance depend. on surface, anomalous skin effect (Russian) 0-75860
 RF anomalous penetration in collisionless plasma 0-64730
 superconductors, type I, surface impedance, anomalous skin effect, surface supercond. regime (Russian) 0-80459
- antenna arrays**
 see also *antenna phased arrays; directional couplers; microwave antenna arrays*
 large-aperture radio system for meteor studies 0-85870
 microwave arrays for localised tumour heating 0-94308
 passive, tracking continuous-wave transmitting projectiles 0-94955
 radio antenna arrays, incoherent optical 1-bit cross-correlators, radioastron. appls. 0-98555
 resonant antenna system, anomalous radiation and electrodynamic characts. 0-69302
 ULF wave generation by peninsular loop currents 0-90247
- antenna lobe patterns** see *antenna radiation patterns*
- antenna patterns** see *antenna radiation patterns*
- antenna phased arrays**
 acoustic, multi-mode operation using noise signals 0-96157
- antenna radiation patterns**
 dipole antenna in magnetoactive plasma EM field distrib. 0-100079
 meteor recording freq., influence of form and orientation of antenna directivity diagram (Russian) 0-67665
 resonant antenna system, anomalous radiation and electrodynamic characts. 0-69302
 Seasat scanning multichannel microwave radiometer, antenna pattern corrections error analysis algorithm 0-94683
 wave radiation by oscillating electric dipole in moving warm plasma 0-87868
- antenna theory**
 dipole antenna in magnetoactive plasma EM field distrib. 0-100079
 EM wave diffraction problem solution using antenna potential method (Russian) 0-63899
 finite elements in electrical and magnetic field problems, book 0-62399
 hemispherical monopole surrounded by plasma layer, Tonks-Dattner reson. and input admittance 0-87887

antenna theory continued

- horizontal antennas above infinite plane Earth, input impedance and current distrib. 0-90259
- moving collisional plasma and moving plasma with intrinsic spatial dispersion, emission of longit. waves 0-87848
- optical analogue processing system, antenna systems design appl. (*Spanish*) 0-95822
- radiocommunication, propag. problems connected with special source structs. 0-87272
- transponder dipole antennas in and near three-layered body 0-98181
- ULF wave generation by peninsular loop currents 0-90247

antennas

- see also antenna radiation patterns; dipole antennas; directive antennas; microwave antennas; radar antennas; reflector antennas
- ELF, ferrite rod, for Magion satellite for 0.1 to 16 kHz freq. range (*Czech*) 0-85775
- oceanography buoy transmitting antennas, selection criteria (*Russian*) 0-109253
- passive antenna system for atmosphere elec. cond. meas., comparative study 0-85762
- quasi-static potential oscillations of thin conductor, instability 0-87900
- Sun, gravitational lens for interstellar radiocommunication 0-62040
- VLF wave measurement at ground station, antenna pickup for vertical elec. field 0-105063

antibaryons see baryons**anticorrosion coatings** see corrosion protective coatings**antiferromagnetism**

No entries

antiferroelectric materials

- see also antiferroelectricity; ferroelectric materials
- photoferroelectric image storage in antiferroelectric-phase PLZT ceramics 0-71353
- squaric acid, antiferroelec., struct. phase transition mechanism 0-75969
- squaric acid, layered, phase transition mechanism 0-97210
- squaric acid, two dimensional antiferroelec., Brillouin scatt. at structural phase transition 0-71430
- squaric acid, two-dimens. phase transition, Raman scatt. study 0-71401
- BiFeO₃-LaFeO₃, solid solns., antiferroelec.-antiferromag., magnetoelectric effect at antiferroelec. transition 0-100637
- Cs₂PO₄, pseudo-one-dimensional ferroelec. and antiferroelec. transitions, phase diagram obs., soft modes 0-93245
- HUO₂AsO₄·4H₂O and HUO₂PO₄·4H₂O layered cpds., struct. investigs. below antiferroelec. transition temps., H bond ordered structs. 0-107416
- HUO₂AsO₄·4H₂O and HUO₂PO₄·4H₂O layered cpds., single and polycryst., proton cond. behaviour w.r.t. antiferroelec. transition temps. 0-107481
- KCN, dynamics of CN⁻ ions near phase transitions at 83K 0-80717
- ND₂D₂AsO₄, protonic cond. near antiferroelec. Neel temp. 0-59703
- ND₂D₂PO₄, cryst., transverse and longit. elec. susceptibilities, modified Ising model calcs. 0-97203
- NH₄H₂PO₄, cryst., transverse and longit. elec. susceptibilities, modified Ising model calcs. 0-97203
- NaNO₂, incommensurate antiferroelec. phase, Brillouin scatt. freq. shift 0-93349
- PbCo_{1/2}Ti_{1/2}O₃, antiferroelec., high-frequency permittivity, temp. depend. 0-71325
- Sr_x(Na_{0.5}Bi_{0.5})_{1-x} solid solutions, piezoelec. and ferroelec. props. (*French*) 0-108158
- Tb(MoO₄)₃ cryst. struct. in ferroelec., ferroelastic, antiferroelec. and paraelastic phases 0-75205
- TiD₂PO₄, antiferroelectricity, permittivity, electric field double hysteresis loops 0-60512

antiferroelectricity

- see also antiferroelectric materials
- ferrites, coupled magnetoelec. oscills. and high freq. susceptibility tensor (*Russian*) 0-93152
- paraelectric-ferroelectric-antiferroelectric phase transitions, electrostrictive effects 0-97209

antiferromagnetic Curie temperature see Curie temperature**antiferromagnetic-ferromagnetic transitions** see ferromagnetic-antiferromagnetic transitions**antiferromagnetic-paramagnetic transitions** see paramagnetic-antiferromagnetic transitions**antiferromagnetic properties of substances**

- see also antiferromagnetism; magnetic semiconductors
- actinide elements and compounds, mag. props., book contrib. 0-75727
- alkali hyperoxides, ionic π -electron systems, magnetogyraton 0-93155
- α -bis (N-methylsilylaldiminato) copper II, one-dimens. spin-1/2 Heisenberg antiferromag., high-field spin dynamics 0-71224
- Brillouin-Mandelstam scattering from thermal and excited magnons 0-70980
- copper, benzoate, one-dimens. antiferromag., heat capacity, field-induced crossover of spin-dimensionality 0-97099
- copper acetate, deuterated, dimeric, single crystals., inelastic neutron scatt. 0-92867
- copper benzoate, low-dimensional Heisenberg antiferromag., high field magnetisation 0-80558
- copper formate tetrahydrate, antiferromag. phase, neutron diffr. study 0-93085
- copper tetraamine sulphate, two-dimensional Heisenberg antiferromag., high field magnetisation 0-80558
- dialkylammonium iron tetrachloride, antiferromag., mag. susceptibility meas. 0-60220
- diethylammonium manganese chloride, Heisenberg magnet, spin diffusion, EPR study 0-66019
- diisopropylammonium copper chloride, mag. interactions, susceptibility, 2-230K 0-60237
- dimethyl ammonium manganese chloride, quasi one-dimensional mag. systems, impurity effects 0-71015
- dimethylamine iron tetrachloride, antiferromag., mag. susceptibility meas. 0-60220
- dimethylammonium copper manganese chloride, two-dimens. mixed magnet, EPR 0-66030
- dimethylammonium copper tetrabromide, quasi two-dimensional antiferromag., mag. behaviour 0-97098
- dimethylammonium copper tetrachloride-tetrabromide mixed cryst., mag. transition 0-65874
- dimethylammonium manganese tetrachloride, antiferromag. and spin-flop resonance obs., 70 to 100 GHz 0-71190

antiferromagnetic properties of substances continued

- dimethylammonium manganese trichloride: Cd(Cu), impurities in quasi-one-dimens. Heisenberg systems, anisotropy effect 0-80502
- dipropylammonium manganese tetrachloride, two-dimens. weak ferromagnet, AC susceptibility 0-65823
- manganese formate dihydrate, Zn- and Mg-substituted, anomalous crit. phenomena 0-60316
- NiWO₄, antiferromag., low symmetry exhibited during spin-flop phase transition 0-60263
- polyvinyl alcohol film containing Cu²⁺ complexes, photoconductivity 0-107849
- quinolinium (TCNQ)₂, random exchange Neisenberg antiferromag. chain, intermediate field magnetisation meas. 0-103857
- rare earth amorphous alloys, random anisotropy magnetism 0-65853
- rare earth-transition metal alloys, amorphous, ferrimag., spin arrangements in large fields 0-75718
- semiconductors, magnetic, spin wave electron amplification theory 0-97083
- TCNQ complexes, disordered, thermodynamics of random exchange models 0-103826
- TCNQ salt, dibenzo-TTF-TCNQCl₂, one-dimens. mag. semicond., mag. and elec. props. 0-88601
- TMMC, antiferromag., nuclear spin-lattice relax. by solitons 0-97159
- TMMC, crossover transition, effects on susceptibility and EPR shift 0-71047
- TMMC, Cu-substituted, spin dynamics, neutron scatt. cross section 0-60312
- TMMC, linear antiferromag., mag. phase diagram, expt. and theoretical study 0-10308
- TMMC, low-symmetry spin distrib. effect on EPR line 0-66018
- TMMC, one-dimens. antiferromag., nonlinear dynamics 0-80521
- TMMC, one-dimens. magnet, local magnon modes 0-65829
- transition metal 3d monoxides, specific vol. and mag. moment calcs. 0-65822
- transition metals and alloys, superconductivity, relevance of mag. interactions 0-100545
- trimethylammonium cobalt trichloride, metamagnet, AC susceptibility and exchange consts. 0-70961
- trimethylammonium manganese trichloride, Heisenberg antiferromag. chain, specific heat and EPR 0-65931
- TTF-CuBDT, inter- and intra-chain exchange couplings, proton spin-lattice relax. time meas. 0-71220
- weak ferromagnet, domain wall dynamics, nonlinear waves, mag. solitons (*Russian*) 0-75793
- AuMn, mag. struct., phase transition, and magnon spectrum, random anisotropy effects 0-88722
- B₂O₃-Fe₂O₃-nMO, (n=2 or 4, M=Mg, Co, Ni, Cu), mag. props., transitions 0-75763
- Ba₂CoS₃, linear chain antiferromag., mag. susceptibility meas. and Mossbauer spectra 0-107992
- Ba₂FeS₃, linear chain antiferromag., mag. susceptibility meas. and Mossbauer spectra 0-107992
- BaLaMRuO₆, (M=Mg, Fe, Co, Ni, Zn), cubic ordered perovskites, Mossbauer and mag. susceptibility meas. 0-75889
- BaMnF₄, pure and Co doped, ferroelec. antiferromag., dielec. anomalies 0-71288
- BaMnF₄, spectroscopy near ferroelec. transition, dielec. anomalies near mag. ordering temp. 0-75965
- Ba₂MnS₃, linear chain antiferromag., mag. susceptibility meas. and Mossbauer spectra 0-107992
- Ba₂Ni₂F₁₀, cryst. struct. and antiferromag. props. 0-107153
- BaNi₂(PO₄)₂ and BaNi₂(AsO₄)₂, mag. props., neutron diffr. and sp. ht. meas. 0-70948
- BaSrCa_{1-x}Fe₂O₆, substituted hexagonal ferrites, mag. split Mossbauer spectra obs. and X-ray struct. data 0-71250
- BaTiO₃-BiFeO₃ solid solns., ferroelec.-antiferromag., magnetoelectric effect at ferroelec. transition 0-100637
- BiFeO₃, ferroelec., antiferromag., cryst. and mag. struct., neutron diffr. study 0-65786
- BiFeO₃-LaFeO₃, solid solns., antiferroelec.-antiferromag., magnetoelectric effect at antiferroelec. transition 0-100637
- CaLaFeO₄, two-dimens. mag. ordered, structural and mag. props. (*French*) 0-70173
- CaLaFeO₄, two-dimens. mag. props. rel. to cryst. struct. 0-75776
- Ca₃Mn₂Ge₂O₁₂ garnet, metamagnetic transition, high anisotropy peculiarities (*Russian*) 0-60274
- Cd_{1-x}Mn_xTe, semimagnetic, exchange interactions between localised and delocalised electrons 0-97245
- CEAl₂, antiferromag. ordering and Kondo behaviour, ²⁷Al NQR study 0-71231
- CEAl₂, magnetic ordering, 24 component Ginzburg-Landau model 0-97095
- CEAl₂, multiple-q structure or coexistence of different mag. phases, neutron diffr. study 0-107985
- Ce₂Al₁₁, competition between ferro- and antiferromag. interactions 0-60258
- Ce₈₀Au₂₀, metallic glass, mag. ordering and cryst. field effects, speromagnetism 0-80531
- Ce₂, mag. props. 0-108008
- Ce₂Dy_{1-x}C₂, mag. props. 0-108008
- CeIn₃, mag. struct., neutron diffr. study 0-80481
- CeSb, antiferromag., first-order transitions, mag. phase diagram 0-60252
- CEtI₃, mag. susceptibility, magnetisation, neutron diffr., elec. resist., and sp. ht. meas. 0-75733
- Co complex, Co(II)(1,2,4-triazole)₂(NCS)₂ quasi two-dimens. canted S=1/2 antiferromag. 0-70976
- Co-CoO films, evaporated, exchange anisotropy 0-88841
- Co₂(AsO₄)Cl, temp. depend. of mag. susceptibility 0-70962
- CoBr₂·6(0.48D₂O, 0.52H₂O) spin-flop system, intermediate phase existence, sublattice magnetisation reorientation 0-80510
- CoBr₂·6[(1-x)H₂O·xD₂O], mag. intermediate phase, magnetisation and neutron scatt. meas. 0-60195
- Co(C₂H₃NO)₂(ClO₄)₂ [(BF₄)₂], X-Y antiferromagnet, Neel temp., spin correlation functions 0-60345
- CoCo₃, Brillouin-Mandelstam light scatt. obs. of spin wave spectra 0-93358
- CoCo₃, LF exciton and Raman spectra, one-magnon and two-magnon scatt. 0-93333
- CoCo₃, light scatt. from magnons and phonons excited by microwave pumping 0-66213
- CoCo₃, linear magneto-optical effect, birefr. 0-66155

antiferromagnetic properties of substances continued

- CoCO₃, mag. props., microscopic level calcs. (*Russian*) 0-97078
 CoCO₃, spin excitation energies, quantum theory (*Russian*) 0-88735
 CoCO₃, two-sublattice noncollinear antiferromag., exciton-magnon light absorpt. mechanisms (*Russian*) 0-89017
 CoCO₃, weakly ferromag., light absorpt. dichroism and mag. config. 0-66223
 CoCl₂, antiferromag., phase diagram, heat capacity meas. 0-93126
 CoCl₂·2H₂O, Ising antiferromag., high field transverse magnetisation meas. 0-93143
 CoF₂, antiferromag. crit. props., neutron scatt. obs. 0-88749
 CoF₂, linear magneto-optical effect, birefr. 0-66155
 Co_{1-x}Te, fluctuating localised mag. moments, d band motion, Mossbauer study 0-65768
 CoTiO₃, antiferromag., mag. anisotropy, magnetisation meas. 0-65856
 Co_{1-x}Zn_xF₂, antiferromag. crit. props., neutron scatt. obs. 0-88749
 Co₂Zn_{1-x}Rh_xO₄, mag. props., EPR spectra, antiferromag. order 0-75736
 Co(urea)₂Cl₂·2H₂O, two-dimens. mag. props., cryst. struct., specific heat 0-75777
 Cr alloyed with d-transition elements, magnetic transformations, triple point (*Russian*) 0-88747
 Cr, antiferromagnetic, muon diffusion, spin relax. and coherent motion 0-71281
 Cr, antiferromagnetic, US attenuation and phase diagram 0-103831
 Cr, antiferromagnetic structure, mag. field effect, spin density wave model (*Russian*) 0-70953
 Cr, Fermi surface under press., de Haas-van Alphen effect meas. 0-75499
 Cr, hyperfine interactions on ¹¹¹Cd-probe nuclei, TDPAC meas. 0-75904
 Cr, mag. phase diagram, near, spin-flip temp., US attenuation 0-60267
 Cr, mag. struct., phase transition, and magnon spectrum, random anisotropy effects 0-88722
 Cr, Neel temperature and Fermi energy, nonmag. impurity effects 0-65888
 Cr, Q-vector locking, press. induced hardening 0-103870
 Cr, spin density wave, Nambu-Eliashberg eqns. for k-state electron-hole pairing 0-97050
 Cr, spin density wave phases, domains 0-103871
 Cr, spin density wave state, phenomenological free energy density description 0-75720
 Cr, spin-flip transition temperature, press. depend. from elastic const. meas. 0-65944
 Cr, transverse magnetoresist., electron interference oscills. 0-65534
 Cr-Co, dil., antiferromag., elec. resist. min., press. and impurity effects 0-59970
 Cr-Co, phase transformations and magnetostriction (*Russian*) 0-103869
 Cr-Fe, dil., antiferromag., elec. resist. min., press. and impurity effects 0-59970
 Cr-Fe, dil., magnetisation, Fe local moments 0-60215
 Cr-Fe (6.5 wt.%), atomic clustering and mag. defects, mag. moments 0-60246
 Cr-Re, phase transformations and magnetostriction (*Russian*) 0-103869
 Cr-Re (0.18 wt.%), mag. excitations in longitudinal and transverse SDW phases 0-70946
 Cr-Si, dilute alloy, mag. susceptibility and Neel temp. meas. 0-71017
 Cr-Si-V, (2, 0.1 at.%), paramag. to commensurate spin density wave transition 0-65875
 Cr-V, itinerant electron antiferromag., spin fluctuations, low temp. specific heat 0-107439
 CrAs, high press. paramag. antiferromag. transitions, elec. props., band model development (*Russian*) 0-60277
 CrB₂, itinerant antiferromag., spin fluctuations, NMR study 0-108119
 CrCo, dil., low temp. specific heat meas., 1.5 to 4K 0-60328
 Cr_{1-x}Fe_xOOH, 0 ≤ x ≤ 10, prep., Mossbauer effect, Neel temp. 0-108134
 Cr,Mn_{1-x}As, mag. susceptibility anomaly at displacive phase transition 0-93091
 CrN, antiferromagnetic EPR spectra, binding energy, isotropic exchange and ordering (*German*) 0-80604
 Cr₂O₃, dielec. const. in mag. field, nonlinear magnetoelec. effect in Neel pt. region 0-66006
 Cr₂O₃, muon spin rotation expts. 0-71282
 Cr₂O₃, muon states, local mag. fields 0-75911
 Cr_{0.995}Pt_{0.005} alloy, mag. struct., neutron diff. study 0-60198
 CrSb_{1-x}As_x, press. effect on Neel point 0-71147
 Cr_{3-x}Se₄, struct., elec. and mag. props. 0-107160
 CsCoBr₃, 1D Ising antiferromagnet, spin dependent Raman scattering from phonons and electronic excitations 0-103948
 CsCoBr₃, quasi 1D Ising antiferromag., polarised Raman scatt. from mag. excitations 0-66182
 CsCoCl₃, spin dynamics, neutron scatt. study 0-80493
 Cs₂FeF₇, mag. struct. and one-dimens. antiferromagnetism 0-60209
 CsLi_{0.5}(Al_{1-x}Fe_x)_{0.5}F₆ pyrochlore, Mossbauer contrib. to exam. of cationic order (*French*) 0-93224
 CsLi_{0.5}Fe_{1-x}F₆ pyrochlore, Mossbauer contrib. to exam. of cationic order (*French*) 0-93224
 CsMnCl₃, antiferromagnetic resonance, parametric spin wave excitation (*Russian*) 0-93183
 CsMnCl₃·2H₂O, antiferromag. insulator, self-trapping of excitons 0-70619
 CsMnCl₃·2H₂O, mag. phase diagram near bicritical point 0-71021
 CsMnCl₃·2H₂O, quasi one-dimensional mag. systems, impurity effects 0-71015
 CsMnCl₃·2H₂O, subthreshold two-magnon absorpt., depend. on freq., temp. and mag. field, exchange coupling const. (*Russian*) 0-71184
 CsMnCl₃·2H₂O, thermal cond. in mag. field 0-70481
 CsMn_{1-x}Co_xCl₂·2H₂O, random mag. mixture, oblique-antiferromag. phase obs. 0-93142
 CsMn_{1-x}Co_xCl₂·2H₂O, random mag. mixture, mag. torque and sp. ht. expts. 0-60323
 CsMn_{1-x}Cu_xCl₂·2H₂O, impurities in quasi-one-dimens. Heisenberg systems, anisotropy effect 0-80502
 CsMnF₃, antiferromag., variation of spin wave spectrum in interaction between magnons 0-65841
 CsMnF₃, exciton migration, excitation and luminesc. study (*Russian*) 0-66264
 CsMnF₃, exciton-magnon interactions in optical transition, absorpt. and emission spectra meas. 0-70981
 CsMnF₃, mag. struct., phase transition, and magnon spectrum, random anisotropy effects 0-88722
 CsMnF₃, parametric excitation of magnons, effect of RF modulation of mag. field 0-65842

antiferromagnetic properties of substances continued

- CsMnF₃, parametric nuclear magnon excitation, mag. field modulation (*Russian*) 0-107999
 CsNiF₃, quasielastic neutron scatt. around Neel-point 0-75768
 CsNiFe₂ pyrochlore, Mossbauer contrib. to exam. of cationic order (*French*) 0-93224
 Cu complex, Cu₂Cl₂(H₂O)₂·2 tetramethylsulphone, mag. interactions, susceptibility, 2-230K 0-60237
 Cu, nuclear antiferromagnetism, low temp. NMR study 0-66049
 Cu-Mn (8 to 75 at.%), spin correl., neutron polarisation anal. study 0-65905
 Cu₂(AsO₄)Cl, temp. depend. of mag. susceptibility 0-70962
 CuCl₂, anhydrous, mag. phase transition 0-80506
 CuCl₂·2D₂O, cryst. struct., mag. and reson. props. 0-60424
 CuCrSe₂, influence of excess Cu on physical props. 0-103836
 Cu_{1-x}Cr_xSe₄, influence of excess Cu on physical props. 0-103836
 CuFeS₂, antiferromag., NQR local mag. field effects 0-71234
 Cu₂NiSi₂S₇, X-ray cryst. struct. determ., mag. props. 0-107172
 CuSO₄·5H₂O, low freq. spin dynamics, proton relax. study 0-71218
 CuSeO₅, strongly antiferromag. coupled Cu linear chain, orbital props. 0-100580
 CuWO₄, elec. cond., thermoelectric power and dielectric constant temp. depend. 0-96886
 Dy, magnetic domain structure, hysteresis, thermal modulation study 0-71082
 Dy, magnetocaloric effect and mag. phase transitions, 80 to 300K 0-60279
 DyAG, antiferromag., induced staggered mag. fields 0-65810
 DyAG, antiferromag., induced staggered magnetic fields, microscopic mech. 0-80527
 DyAsO₄, phase transitions obs. 0-70412
 DyCo₂Si₂, mag. props. 0-107988
 DyFeO₃, field induced spin reorientation, Mossbauer spectroscopy 0-65878
 DyFeO₃, spin reorientation transitions induced by magnetic fields, Mossbauer study 0-71246
 DyFeO₃, weak ferromagnet, μ SR study 0-93226
 DyNi₂Si₂, mag. props., 4.2-200K 0-84602
 Dy₂O₃SO₄, mag. ordering, magnetisation, AC susceptibility and Zeeman effect meas. 0-60205
 DyPO₄, mag. transitions under hydrostatic press., neutron diff. study 0-71030
 Dy_{1-x}Sm_x, magnetoresist. of polycryst. specimens in fields up to 44 kOe (*Russian*) 0-92880
 DyVO₄, phase transitions obs. 0-70412
 ErCo₂Si₂, mag. props. 0-107988
 ErFeO₃, field induced spin reorientation, Mossbauer spectroscopy 0-65878
 ErFeO₃, weak ferromagnet, μ SR study 0-93226
 EuB₆, ferromag. and antiferromag. sp. ht. meas., 1.8-77K 0-65948
 EuSe(Te), magnetic phase transitions, thermal modulation spectroscopy study (*French*) 0-97301
 EuSe_{1-x}Te_x, transferred hyperfine fields at Eu nuclei, NMR meas. 0-71195
 Eu₂Sn₂Si₂, mag. and thermodynamic props., metamagnetism 0-60273
 EuTe, antiferromag. semicond., Raman scatt., spin-phonon interactions 0-66185
 EuTe, mag. 'Bragg' scatt. obs. through Raman scatt. 0-66179
 EuTe, spin order and fluctuations, Raman scatt. study 0-97273
 Eu_{1-x}Yb_xTe, (0 < x < 1), mag. semicond., elec., mag. and optical props. 0-97070
 Fe complex, Fe(1,2,4-triazole)₂(NCS)₂, quasi-2-dimens. S=1/2 antiferromag., mag. props., hidden canting 0-107986
 Fe complex (2, 9-dimethylphenanthroline) sulphate, mag. props., Mossbauer spectra 0-66081
 Fe-Ni-Cr, mag. props. in weak mag. fields (*Russian*) 0-75771
 Fe, As, mag. props., Mossbauer study 0-88897
 FeBO₃, mag. linear dichroism and absorpt. spectra, exciton-magnon absorpt. mechanism 0-66160
 FeBO₃, spin-reorientation phase transition (*Russian*) 0-93122
 FeCl₂, antiferromag., magnon-phonon interactions in thermal cond. 0-65315
 FeCl₂, collinear metmag., mag. phase diagram 0-71035
 FeCl₂, magnetic transition and sublattice mag. moment rotation nonequivalence (*Russian*) 0-100586
 FeCl₂, reorientation of mag. moments under mech. stresses at 0K 0-93153
 FeCo_{1-x}Cl₂, metmaget, mag. phase diagram by mag. induced light scatt. 0-65883
 Fe_{1-x}Co_xCl₂·2H₂O, random mixture with competing spin anisotropies, tetracrit. behaviour 0-60324
 (Fe,Cr_{1-x})₂O₃, corundum-type solid solution single crystal growth, chem. vapour transport 0-93465
 FeF₂ antiferromag., anomalous anti-Stokes/Stokes Raman scatt. intensity ratio 0-66177
 FeF₂, interacting phonon-magnon states, theory of Raman scattering and IR obs. 0-71426
 FeF₂, mag. sp. ht. near Neel temp. mag. susceptibility meas. 0-60341
 FeF₂:Mn, antiferromag., NMR relax., impurity bonding 0-66061
 FeF₂:Mn, antiferromag. reson. and local magnon mode, FIR laser study 0-66042
 FeF₂:Mn, Heisenberg antiferromag., impurity banding and mag. reson., theory 0-93181
 FeF₂:Mn, Heisenberg model, impurity band resonance at 0K, theory 0-66041
 FeF₃, amorphous, struct. and mag. props., computer model 0-96446
 FeGe₂, antiferromag., Fermi surface, stress effects, oscillatory magnetotri- and torque meas. 0-103616
 FeI₂, spin waves and two magnon bound states, mag. field IR absorption meas. 0-65840
 (Fe_{1-x}M_x)₂O₃, yH₂O, M=Cr,Cu,Ni, crystal growth, characterisation by Mossbauer spectroscopy, mag. meas. and electron microscopy (*French*) 0-80655
 FeMO₄S₄, Mossbauer investigation, Neel point, superparamag. effects 0-97170
 Fe₂Mg_{1-x}Cl₂, metmaget, mag. phase diagram by mag. induced light scatt. 0-65883
 Fe_{1-x}Mn_xCl₂, disordered, Raman scatt. from Fe²⁺ and Neel temp. 0-60579
 Fe_{1-x}Mn_xCl₂, low-lying electronic excitations in antiferromag. and paramag. phases Raman scatt. study 0-71414

antiferromagnetic properties of substances continued

- $\text{Fe}_{1-x}\text{Mn}_x\text{Sn}$, spin reorientation, Mossbauer study, 77 to 400K 0-97172
 FeNbSe_2 , transport props. and mag. ordering 0-65527
 $\alpha\text{-Fe}_2\text{O}_3$, Mossbauer spectra near Neel temp., critical indices, magnetisation (Russian) 0-66094
 $\alpha\text{-Fe}_2\text{O}_3$, muon spin rotation expts. 0-71282
 $\alpha\text{-Fe}_2\text{O}_3$, muon states, local mag. fields 0-75911
 $\text{Fe}_2\text{O}_3\text{-BaO-B}_2\text{O}_3$, magnetic props. of Fe-rich amorphous oxide (French) 0-80511
 Fe_2O_4 , muon states, local mag. fields 0-75911
 $\text{Fe}_2(\text{PO}_4)\text{Cl}$, temp. depend. of mag. susceptibility 0-70962
 FePt_3 , metamagnetic transitions in external fields 0-60272
 FeSO_4 , α - and β -forms, magnetic interactions, neutron inelastic scatt. study 0-107980
 $\text{Fe}_{1-x}\text{Sb}_x$, nonstoichiometry influence on mag. props. (Russian) 0-65813
 $\text{Fe}_{1-x}\text{Te}_x$, fluctuating localised mag. moments, d band motion, Mossbauer study 0-65768
 $\text{Fe}_{2-x}\text{Ti}_x\text{O}_4$, $0.5 \leq x \leq 1$, mag. props. of antiferromag. phase 0-70960
 $\text{Fe}_{1-x}\text{Zn}_x\text{F}_2$, dil. antiferromag., electronic and mag. props., Raman scatt. and optical absorpt. study 0-108207
 $\text{Fe}_{1-x}\text{Zn}_x\text{F}_2$, electronic Raman scatt., mag. anisotropy 0-66184
 $\text{Fe}_2\text{Zn}_{1-x}\text{F}_2$, Neel point and short range order, dilution effects, mag. birefr. obs. 0-71019
 $\text{Gd Ni}_2\text{Si}_2$, mag. props., 4.2-200K 0-84602
 Gd-Y alloys, mag. crit. temp. gap 0-60260
 GdAlO_3 , canted antiferromagnetic, Mossbauer meas. 0-97171
 $\text{GdAlO}_3\text{:La}$, antiferromag., random-field crit. and multicritical behaviour 0-65939
 $\text{GdAlO}_3\text{:La}$, random antiferromagnets, crit. and multicritical props. 0-60332
 GdB_2 , single crystals, mag. behaviour and structure change at low temp. 0-71018
 GdCo_2Si_3 , mag. props. 0-107988
 $\text{Gd}_2\text{Ga}_2\text{O}_7$, mag. phase diagram, AC susceptibility meas. 0-60265
 $\text{Gd}_2\text{Mo}_2\text{Se}_8$, coexistence of supercond. and long range antiferromag. order 0-84534
 GdN , and $\text{GdN}_{1-x}\text{O}_x$, mag. interactions 0-60218
 $\text{GdN}_{1-x}\text{O}_x$, magnetic interaction and carrier conc. 0-71005
 ^3He , BCC solid, nucl. mag. order and paramag. susceptibility 0-59757
 ^3He , FCC, vacancy induced spin polarons 0-59756
 ^3He , liq., exchange model 0-88387
 ^3He liquid, exchange model, antiferromagnetic exchange field, susceptibility-specific heat ratio (French) 0-80019
 $\text{Hg}_{1-x}\text{Mn}_x\text{Te}$, non-parabolic zero-gap semiconductor, indirect exchange interaction 0-80498
 $\text{Hg}_{1-x}\text{Mn}_x\text{Te}$, semimagnetic, exchange interactions between localised and delocalised electrons 0-97245
 HoAlO_3 , electronic and nucl. mag. ordering, mol. field approx. 0-60157
 HoAu_3 , mag. phase diagram 0-75761
 HoCo_2Ge_2 , crystal and magnetic structure obs. 0-64976
 HoCu , resist. and magnetoresist., mag. ordering obs. 0-70677
 HoCu_2 , mag. struct. and elec. resist., neutron diff. obs. 0-60206
 HoCu_2 , resist. and magnetoresist., mag. ordering obs. 0-70677
 HoFeO_3 , field induced spin reorientation, Mossbauer spectroscopy 0-65878
 $\text{Ho}(\text{IrRh}_{1-x}\text{Co}_x)_4\text{B}_4$ pseudoternary system, supercond. and mag. ordering 0-70876
 $\text{Ho}_2\text{O}_3\text{SO}_4$, mag. ordering, magnetisation, AC susceptibility and Zeeman effect meas. 0-60205
 HoSb , mag. phase diagram, quadrupolar interactions 0-65820
 HoTiO_3 , magnetic structure determination, neutron scatt. study 0-65809
 $\text{Ho}_2\text{Y}_{1-x}\text{Sb}_x$ system, magnetisation, elec. resist., and sp. ht. meas. 0-60213
 KCoF_3 , antiferromag. domain wall motion under external stress 0-80583
 KCoF_3 , with residual orbital moment, nucl. mag. relax. 0-71215
 K_2CoF_4 , 2-dimens. Ising antiferromag., mag. excitons, Raman scatt. obs. 0-66181
 K_2CoF_4 , two-dimens. Ising antiferromag., nearest neighbour correl. function, birefr. expts. 0-71386
 KCuF_2 , linear chain Heisenberg antiferromag., nearest neighbour correl. function, birefr. expts. 0-71386
 KCuF_2 , one-dimens. antiferromag., spin waves, neutron scatt. study 0-65848
 $\text{K}_2\text{FeCl}_4(\text{H}_2\text{O})$, antiferromag., press. depend. on spin-flop transition 0-80505
 K_2FeF_4 , antiferromagnet, two-dimensional, mag. excitations 0-80492
 K_2FeF_4 , two dimensional easy plane antiferromag., neutron scatt. expts. 0-65838
 K_2FeF_4 , two-dimensional antiferromag., with easy-plane anisotropy, mag. excitations and two-magnon Raman scatt. 0-65839
 K_2FeF_4 , two-dimensional antiferromag., cryst. field effects, Mossbauer spectroscopy 0-71254
 K_2FeF_4 , mag. struct. and one-dimens. antiferromagnetism 0-60209
 K_2FeF_4 , one-dimensional antiferromag. systems, Mossbauer studies 0-71266
 $\text{K}_3\text{Fe}_2\text{F}_7$, two-dimensional antiferromag., cryst. field effects, Mossbauer spectroscopy 0-71254
 K_2FeO_4 , crit. slowing down of spin fluctuations, Mossbauer spectra and relax. theory 0-65882
 KMnF_3 , specific heat near Neel temp. (Russian) 0-100340
 K_2MnF_4 , ordered quadratic-layer Heisenberg antiferromag., nucl. spin-magnon relax. 0-71217
 $\text{K}_2\text{MnF}_4\text{:Zn(Mg)(Ni)}$, mag. effects of impurities 0-65869
 $\text{K}_2\text{MnF}_4\text{:Zn(Mg)(Ni)}$, local magnetisation, NMR and Green's function study 0-65870
 $\text{K}_3\text{Mn}_2\text{F}_7$, crit. EPR line broadening near Neel temp. 0-71165
 $\text{K}_3\text{Mn}_2\text{F}_7$, quadratic double layer antiferromag., two-magnon Raman scatt. 0-66183
 $\text{KMn}_{1-x}\text{Ni}_x\text{F}_3$, antiferromag. crit. props., neutron scatt. obs. 0-88749
 KNiF_2 , ^{19}F spin-lattice relaxation 0-93211
 KNiF_2 , magnetostriction, X-ray diffractometry and strain gauge meas. 0-65997
 K_2NiF_4 , ordered quadratic-layer Heisenberg antiferromag., nucl. spin-magnon relax. 0-71217
 $\text{K}_3\text{Ni}_2\text{F}_7$, quadratic double layer antiferromag., two-magnon Raman scatt. 0-66183
 La_2CoO_4 , mag. behaviour obs. 0-70971
 $\text{La}_2\text{MnFeS}_3$, antiferromag., mag. props. and mag. struct., neutron diff. and magnetisation meas. 0-65801
 La_2NiO_4 , La_2CuO_4 , magnetic properties obs. 0-70937
 $\text{La}_{2-x}\text{Sr}_x\text{CoO}_4$, mag. behaviour obs. 0-70971

antiferromagnetic properties of substances continued

- La_2FeSi_6 , antiferromag., neutron diff. study 0-70954
 $\text{LuCrO}_3\text{:Er}^{3+}$, doping effect on ^{51}Cr NMR in domain walls 0-71219
 $\gamma\text{-Mn}$, antiferromagnetic, self-consistent bandstructure calcs. 0-88475
 $\gamma\text{-Mn}$, collinear spin structure stability 0-107984
 $\delta\text{-Mn}$, paramag., antiferromag. and ferromag., magnetic moment calcs. 0-60223
 $\gamma\text{-Mn-Cu}$ (10 at.%), spin wave studies using neutron diffraction 0-70991
 Mn-Ni , thermal expansion, mag. susceptibility, lattice consts. 0-100341
 $\text{MnAs}_{1-x}\text{P}_x$, mag. susceptibility anomaly at displacive phase transition 0-93091
 $\text{MnAs}_{1-x}\text{P}_x$ mixed crystals, metallic magnetically ordered, Hall effect 0-65536
 $\gamma\text{-MnAu}$, phase diagram, X-ray diff. and Young's modulus meas. 0-71024
 MnAu_2 , helical antiferromag., optical absorpt., density of states 0-66224
 MnB_2 , polycryst., magnetoresist. and mag. props. (Russian) 0-92907
 $\text{Mn}(\text{Br}_{1-x}\text{Cl}_x)_2\cdot 4\text{H}_2\text{O}$, antiferromagnetism, controllable anisotropy 0-93116
 $\text{Mn}(\text{CN})_3(\text{H}_2\text{O})_{0.57}$, mag. interactions, theory 0-97085
 MnCO_3 , parametric excitation of magnons, effect of RF modulation of mag. field 0-65842
 $\text{MnCl}_2\cdot 4\text{H}_2\text{O}$, antiferromag., low temp. thermal cond. 0-65320
 MnCO_3 , parametric nuclear magnon excitation, mag. field modulation (Russian) 0-107999
 $\text{Mn}_{1.88}\text{Co}_{0.12}\text{Sb}$, antiferromag.-ferrimag. transition, neutron crit. scatt. and crossover effect 0-71023
 $\gamma\text{-MnCu}$ crystals, antiferromag. Zochralski growth 0-97420
 MnF_2 , antiferromag., mag. space groups, Clebsch-Gordan coeff. calcs. 0-79731
 MnF_2 , antiferromag. and piezomag. domain struct., neutron topography study 0-71088
 MnF_2 , parallel pumping studies of magnon damping 0-70990
 MnF_2 spin wave lifetime, theory compared with expt. 0-60228
 $\text{Mn}_{2-x}\text{Fe}_x\text{Si}_3$, elec. resist. and mag. susceptibility, ferromag. to antiferromag. transition 0-80504
 Mn_2GaN , sp. ht., 6 to 350K, mag. and crystallographic phase transitions 0-71060
 $\text{Mn}_{1-x}\text{Mg}_x\text{Se}$, mag. and struct. phase transitions, mag. susceptibility and X-ray diff. study 0-71022
 MnO , antiferromag., temp. depend. of elastic consts., US study 0-79854
 MnO , magnon-sideband lineshape, exciton-phonon interaction effects 0-65846
 MnS , thermal cond., temp. depend., paramag.-antiferromag. transition effects 0-65321
 MnSO_4 , mag. struct. and phase transitions, neutron diff. study 0-60208
 $\alpha\text{-MnSe}$, mag. and struct. phase transitions, mag. susceptibility and X-ray diff. study 0-71022
 $\alpha\text{-MnSeO}_4$, magnetic interactions, neutron inelastic scatt. study 0-107980
 $\text{Mn}_2\text{Zn}_{1-x}\text{F}_2$, Neel point and short range order, dilution effects, mag. birefr. obs. 0-71019
 Mn_2ZnN , sp. ht., 6 to 350K, mag. and crystallographic phase transitions 0-71060
 $(\text{NH}_4)_2\text{FeF}_6$, one-dimensional antiferromag. systems, Mossbauer studies 0-71266
 $\text{N}_2\text{H}_4\text{FeF}_6$, one-dimensional antiferromagnetism, Mossbauer study 0-65872
 $(\text{NH}_4)_2\text{ReCl}_6(\text{IrCl}_6)$, proton relaxation near antiferromagnetic phase transitions 0-80640
 $\text{Na}_2(\text{Fe,Mg})_2\text{Si}_2\text{O}_7(\text{OH})_2$, riebeckite, low temp. Mossbauer obs. of oriented single cryst. behaviour and mag. props. 0-84674
 NaFeF_2 , Mossbauer and low-temp. dilatometry study (French) 0-80662
 $\alpha\text{-Na}_2\text{Fe}_2(\text{PO}_4)_3$ orthophosphate, cryst. and vitreous, Mossbauer spectroscopy and mag. susceptibility (French) 0-80657
 NaMnCl_3 , antiferromag. insulator, self-trapping of excitons 0-70619
 NaMnCl_3 , mag. struct. and spin-flip transition, powder neutron diff. exam. 0-60210
 Nb_2Ge film, superconductivity, relevance of mag. interactions, EPR study 0-100545
 Nd , magnetic-structure, neutron and X-ray diff. study 0-60197
 NdAg , low temp. mag. meas. 0-107989
 Nd_2NiO_4 , Nd_2CuO_4 , magnetic properties obs. 0-70937
 Ni ferrite, quenched, Neel temp. and initial susceptibility 0-75762
 Ni , stress induced cross-over effect near Curie point (German) 0-103873
 Ni , stress induced crossover effect near Curie point (German) 0-103874
 Ni-I single crystals, mag. and dielectric props. 0-93095
 NiBr_2 , commensurate and incommensurate mag. struct., neutron diff. study 0-97067
 NiBr_2 , low-temperature magnetic phase, incommensurate spin structure 0-93082
 $\text{NiCl}_2\cdot 6\text{NH}_3$, low temp. sp. ht. and mag. ordering 0-75784
 $\text{Ni}_3\text{Co}_{1-x}\text{Cl}_{2-x}\text{H}_2\text{O}$, mixed uniaxial planar antiferromag., magnetisation process 0-88788
 $\text{Ni}_3\text{Co}_{1-x}\text{O}$, composition depend antiferromagnetic-ferrimagnetic ordering, mag. susceptibility meas. 0-70973
 NiF_2 , thermal expansion and magnetostriction, 55K to room temp. 0-80586
 NiO , antiferromag. ordering, mag. transition-state approach 0-80507
 NiO , linear birefringence in S-domains near antiferromag. phase transition 0-60261
 NiO , mag. struct., neutron Laue diff. method 0-70951
 $\text{Ni}(\text{PiCl}_6)\cdot 6\text{H}_2\text{O}$, singlet-ground-state magnets, ESR at low temps. 0-97132
 NiS_2 , weak ferro- and antiferromag., magnetisation and neutron diff. meas. 0-65794
 $\text{NiSnCl}_6\cdot 6\text{H}_2\text{O}$, singlet-ground-state magnets, ESR at low temps. 0-97132
 $\text{Ni}_{1-x}\text{Te}_x$, fluctuating localised mag. moments, d band motion, Mossbauer study 0-65768
 NiTiO_3 , antiferromag., mag. anisotropy, magnetisation meas. 0-65856
 NiWO_4 , AC elec. conductivity, thermoelec. power and dielec. const. 0-70736
 $\text{Ni}_{1-x}\text{Zn}_x\text{Fe}_2\text{O}_4$, polycryst., domain wall energy rel. to anisotropy 0-71090
 NpCo_2Si_2 , mag. struct., neutron diff. determ. 0-93084
 $\alpha\text{-O}_2$, antiferromagnetic polycrystal, splitting of exciton absorpt. lines in mag. field (Russian) 0-103943
 $\alpha\text{-O}_2$, 'cryst.', exciton, exciton-magnon, and biexciton absorpt. at 1.5K 0-84750
 $\alpha\text{-O}_2$ crystals, spin ordering effect on light absorpt. (Russian) 0-89029
 O_2 monolayers, on graphite, mag. α -phase and α - β -phase transition 0-70530

antiferromagnetic properties of substances continued

- (Pd_{0.9965}Fe_{0.0035})_{1-x}Mn_x, mag. behaviour at Fe sites, Mossbauer effect meas. 0-66085
 Pd₂MnIn_{1-x}Sn_x and Pd₂MnIn_{1-y}Sb_y, Heusler alloys, mag. order, disorder effects 0-88723
 PrCo₂Ge₂, crystal and magnetic structure obs. 0-64976
 Pr₂NiO₄, Pr₂CuO₄, magnetic properties obs. 0-70937
 Pt-Fe alloy, ordered, T-c phase diagram, antiferro- and ferromagnetism (Russian) 0-65871
 Pt-Fe ordered alloy, multiply mag. phase transitions 0-60264
 RbCoF₄, 2-dimens. Ising antiferromag., mag. excitons, Raman scatt. obs. 0-66181
 Rb₂Co₂Mg_{1-x}F₄ mag.-nonmag. two-dimens. antiferromag. Ising system, spin fluctuations 0-80545
 Rb₂Co₂Mn_{0.5}F₄, two dimens. random antiferromag., excitations 0-107997
 RbFeCl₃·2H₂O, pseudo-one-dimensional canted Ising antiferromag., spin-cluster excitations 0-70989
 RbFeCl₃·2H₂O, spin cluster excitation expts. 0-66039
 Rb₂FeF₄, antiferromagnet, two-dimensional, mag. excitations 0-80492
 Rb₂FeF₄, two-dimensional antiferromag., with easy plane anisotropy, mag. excitations and two-magnon Raman scatt. 0-65839
 Rb₂FeF₄, mag. struct. and one-dimens. antiferromagnetism 0-60209
 Rb₂FeF₄, one-dimensional antiferromag. systems, Mossbauer studies 0-71266
 RbMnCl₃, specific heat near Neel temp. (Russian) 0-100340
 RbMnCl₃, twinning struct., cryst. domains, orientation mag. transition (Russian) 0-107275
 Rb₂MnCl₄, quasi-2D-antiferromag., linear birefr. and optical absorpt. spectra 0-71385
 RbMnF₃, spin wave lifetime, theory compared with expt. 0-60228
 RbMnF₃, spin wave widths 0-97081
 RbNiF₃, spin lattice, susceptibility, Heisenberg model (Russian) 0-65893
 Sm₂CuO₄, magnetic properties obs. 0-70937
 SrLaFeO₄, two-dimens. mag. props. rel. to cryst. struct. 0-75776
 Sr_{0.5}La_{1.5}Li_{0.5}Fe_{0.5}O₄, high spin configuration stabilisation for Fe⁴⁺ (French) 0-88519
 TMMC, 3-D ordering temp. controlled by solitons and defects, mag. field depend. 0-60275
 Tb, magnetisation intensity in antiferromag. state and mag. field induced phase transforms. (Russian) 0-65811
 TbAu₃, mag. phase diagram 0-75761
 TbH_{2-x}TbD_{2-x}, mag. susceptibility conc. depend. 0-70968
 TbNi₂Si₂, mag. props., 4.2-200K 0-84602
 TBP (As)(Sb)(Bi), mag. transitions, quadrupolar interaction effects 0-80512
 TeCr₂O₆, exchange interactions within binuclear entity (Cr₂O₁₀)¹⁴⁻ 0-60236
 (Ti_{1-x}V_x)₂O₃, metallic antiferromag. struct., neutron studies 0-65797
 TlMnCl₃, specific heat near Neel temp. (Russian) 0-100340
 TmFeO₃, acoustic vel. and attenuation shifts at spin reorientation phase transition 0-65986
 TmSe, Anderson lattice resist. for antiferromag. ordering 0-65556
 TmSe, elec. resist. under press. at very low temp. 0-96878
 TmSe, intermediate valence cpd., susceptibility, single-jon approach 0-70935
 TmSe, mag. ordering under press., neutron diff. obs. 0-70947
 TmSe, magnetoresist. and Hall effect, stoichiometry effects 0-65597
 TmZn₂, Mossbauer effect meas. in antiferromag. and paramag. states 0-71265
 UAs, search for lattice distortions at low temps. 0-79759
 UBr₃, cryst. field levels, neutron scatt. determ. 0-65509
 UN, search for lattice distortions at low temps. 0-79759
 UN-ZrN, Young's modulus antiferromagnetic anomaly 0-92583
 UO₂, electronic transitions, crystal field effects and phonons, phase transition 0-97303
 USB, search for lattice distortions at low temps. 0-79759
 U₂Th_{1-x}As_x, mag. phase diagram, magnetisation meas. 0-60271
 V₁, MCD spectra, interpretation rel. to mag. struct. 0-66222
 V₁, mag. 'Bragg' scatt. obs. through Raman scatt. 0-66179
 V₁, spin-dependent Raman scatt. from phonons 0-97274
 V₂O₅, metal-insulator transition, external mag. field effects 0-92819
 V₂S₄ and V₂S₈, itinerant antiferromag. spin fluctuations, NMR studies 0-93198
 V₂Se₄, itinerant antiferromag., spin fluctuations, NMR study 0-75874
 V₂Se₈, itinerant antiferromag., spin fluctuations, NMR study 0-75874
 VTe, mag. and elec. transport props. 0-92897
 WCr₂O₆, exchange interactions within binuclear entity (Cr₂O₁₀)¹⁴⁻ 0-60236
 WV₂O₆, exchange interactions within binuclear entity (V₂O₁₀)¹⁴⁻ 0-60236
 WV₂O₆, magnetic susceptibility, behaviour in terms of quasi-isolated binuclear units 0-97073
 ZnCr₂Se₄, screw spin structure, method of controlling the sense, polarised neutron diff. study 0-70944
 ZnCr₂Se₄, screw spin structure, magnetoelectric effect 0-75827
 ZnCr₂Se₄In, magnetoresist. and elec. resist. above and below Neel temp. (Russian) 0-88576
 ZnGa₂O₄Cr³⁺, weak exchange interaction determ., ESR study 0-93107
 (Zr_{1-x}Nb_x)Fe₂, antiferromag. spin struct., Mossbauer effect study 0-66086

antiferromagnetic resonance

- Brillouin-Mandelstam scattering from thermal and excited magnons 0-70980
 dimethylammonium manganese tetrachloride, antiferromag. and spin-flop resonance obs., 70 to 100 GHz 0-71190
 easy-plane antiferromagnet, coupled spin wave branches (Russian) 0-93096
 easy-plane magnet, antiferromag. reson. linewidth and relax., theory 0-71189
 Heisenberg impure antiferromagnetic, impurity banding and mag. reson., theory 0-93181
 Heisenberg magnet, impurity band resonance at 0K, theory 0-66041
 random antiferromagnets, theory of mag. excitations, antiferromag. reson. 0-97146
 weak ferromagnet, collective excitations in transverse mag. field, AFMR spectrum 0-93100
 CoCO₃, light scatt. from magnons and phonons excited by microwave pumping 0-66213

antiferromagnetic resonance continued

- CsMnCl₃, antiferromagnetic resonance, parametric spin wave excitation (Russian) 0-93183
 CsMnCl₃·2H₂O, subthreshold two-magnon absorpt., depend. on freq., temp. and mag. field, exchange coupling const. (Russian) 0-71184
 CsNiF₃, subthreshold parallel pumping of magnons and antiferromag. reson. 0-71185
 CuCl₂·2D₂O, cryst. struct., mag. and reson. props. 0-60424
 FeF₂·Mn, antiferromag. reson. and local magnon mode, FIR laser study 0-66042
 FeF₂·Mn, Heisenberg model, impurity band resonance at 0K, theory 0-66041
 RbFeCl₃·2H₂O, spin cluster excitation expts. 0-66039
- antiferromagnetism**
 see also *antiferromagnetic properties of substances; exchange interactions (electron); metamagnetism*
 amorphous, spin waves, exchange fluctuations, calc. 0-65847
 amorphous Heisenberg and Ising chains, thermodynamics 0-108022
 amorphous Heisenberg magnet, antiferromag. coupling, ground state and frustration, theory 0-65766
 amorphous Ising antiferromagnetic model, frustration effects 0-103838
 Berezinski transition, effective temp. (Russian) 0-65889
 bond-diluted antiferromagnetic triangular cactus tree, ordered phase 0-71037
 classical mag. moment system, antiferromag. phase transition, secular dipole interactions 0-80551
 de Haas-van Alphen effect, field depend. spin-splitting zero 0-84450
 disordered metamagnets, random field effects 0-60318
 disordered spin flop, bicritical behaviour, critical experiments 0-65899
 easy-plane, coupled spin wave branches (Russian) 0-93096
 exciton motion in antiferromagnets, magnon approx. 0-70617
 Fermi liquid, critical phenomena, neutron scatt., Neel point (Russian) 0-71077
 ferroelectric antiferromagnets, phase transformations (Russian) 0-93114
 ferromagnets and spin glasses, supercond. and mag. order 0-93029
 ground state energy for linear antiferromagnetic Heisenberg chain, neighbour interactions 0-84606
 Heisenberg antiferromagnet, Green function theory 0-107975
 Heisenberg antiferromagnet, one-dimens., autocorrelation function, low freq., temp. and field depend. 0-65929
 Heisenberg antiferromagnet, one-dimens., impure, mag. susceptibility 0-60168
 Heisenberg antiferromagnet, s=1/2 linear, zero-temp. dynamics in mag. field 0-65764
 Heisenberg bicritical points in antiferromagnets, universality tests 0-84604
 Heisenberg chain, alternating, appl. of zero temp. quantum renormalisation group 0-80526
 Heisenberg chain, classical, nearest-neighbour, low temp. dynamics 0-80524
 Heisenberg impure antiferromagnetic, impurity banding and mag. reson., theory 0-93181
 Heisenberg model, anisotropic, finite cell calcs. 0-60164
 Heisenberg one-dimensional magnet, classical, nonlinear dynamics 0-71056
 induced staggered magnetic fields in antiferromagnets, microscopic mech. 0-80527
 insulators, lattice thermal cond. 0-65319
 interphase boundary dynamics, domain wall motion and scatt. (Russian) 0-108032
 intrinsic semiconductors, indirect exchange interaction, finite temp., valence bands and energy gaps effect 0-59943
 IR absorption on impurity excitations near upper edge of spin-wave band of antiferromagnet 0-80829
 Ising antiferromag. phase boundaries, hard-core lattice gas calcs. 0-80542
 Ising antiferromagnet, crit. props., calc. 0-65946
 Ising antiferromagnet, FCC, nearest neighbour interactions, Monte Carlo method 0-80544
 Ising antiferromagnet, nonlinear response to high freq. mag. field, quantum theory (Russian) 0-93066
 Ising antiferromagnet, two-dimens., mag. susceptibility calc. 0-60225
 Ising FCC antiferromagnet, mag. phase diagram, ordering, Monte Carlo calc. 0-103833
 Ising ferromagnet and antiferromagnet, two-dimens. square, ground state, apparent 3-spin interactions 0-88709
 Ising model, antiferromag. case, modified Kadanoff variational renormalisation method 0-88710
 Ising model, bond random, ferromagnetic-antiferromag. mixture, triangular cactus tree, statistical theory 0-75702
 Ising model, with transverse field, ferromagnetic and antiferromagnetic susceptibilities 0-60160
 Ising model with competing interactions, critical properties and exact results 0-93129
 Ising spin glass, d-dimensional, frustration effect 0-108019
 itinerant antiferromagnet, paramag. impurity effects on Neel temp., calc. 0-60257
 itinerant electron model, susceptibility, local exchange approx. calc. 0-60169
 lattice systems with short-range and Coulomb interactions 0-82715
 linear-chain antiferromagnet, sine-Gordon solitons 0-80543
 magnetic phases, spin configurations in external field 0-70955
 magnetoacoustic resonance of domain boundaries (Russian) 0-65636
 magnetoelastic soliton propag. 0-66003
 magnon damping in zero external mag. fields, magnon-magnon interactions 0-70988
 metal, antiferromag., thermoelec. power in mag. field 0-70686
 metal, magnetoelastic coupling effect on magnetoelc. reson. 0-75837
 nonlinear waves in antiferromagnets, domain boundary description 0-84612
 nuclear spin oscillations, interaction with lattice vibrs. 0-70996
 nuclear spin wave relax. 0-65850
 one dimensional anisotropic Heisenberg model, spin 1/2, Ising like antiferromag., dynamic correlation function 0-75704
 one-dimensional antiferromagnet, nonlinear dynamics 0-80521
 one-dimensional antiferromagnet, renormalisation group nearest neighbour interactions 0-60357
 pair interaction and arbitrary fields, correlation inequalities, Ginibre-Percus double variables method 0-68147
 pseudo-one-dimensional antiferromagnets, thermodynamic variables 0-65935

antiferromagnetism continued

- quantum critical dynamics with mode coupling 0-108024
 quantum spin systems, ground state energies, renormalisation techniques
 appls. 0-93132
 random antiferromagnets, crit. and multicritical props. 0-60332
 rhombohedral antiferromagnet, spin-reorientation phase transition (*Russian*) 0-93122
 spin density wave antiferromagnet, neutron scatt. by magnons, modulated
 spin amplitudes 0-75722
 spin glasses, dilute ferromagnets, ferromagnetic modes 0-93133
 spin-1/2 cubic lattice, with anisotropic exchange, configs. 0-65926
 staggered magnetisation in antiferromagnets, crit. fluctuations, AC suscep-
 tibility meas. 0-60219
 superconductor, antiferromag., isolated vortex line 0-70912
 surface spin-waves, long-wavelength 0-88737
 susceptibilities of $S=1/2$ XY model on the square lattice at $T=0$
 0-88732
 two-dimensional antiferromagnet, with easy-plane anisotropy, mag. excita-
 tions and two-magnon Raman scatt. 0-65839
 two-dimensional antiferromagnets, expansion for susceptibilities 0-70963
 two-sublattice Neel-type, stable spin configurations, external mag. field
 and single-ion orthorhombic anisotropy effects 0-60249
 uniaxial antiferromagnet, nonuniform spin configurations 0-97109
 uniaxial antiferromagnetic, phase diagram, spin flop transition (*Russian*)
 0-100587
 vacancy distribution along mag. sublattices in β -brass type ferro and
 antiferromagnetic alloys (*Russian*) 0-79783

antihyperons see hyperons**antimony**

see also nuclei with

- cleavage faces, evaporation pattern determ. by decoration method in elec-
 tron microscopy (*German*) 0-107626
 clusters, 2 to 500 atoms, nucleation, mass spectra 0-102596
 core level binding energies 0-71564
 desorption properties on GaAs (100), AES obs. 0-80074
 diamond:Sb, implanted, radiation damage and annealing study 0-100263
 discontinuous thin films, cluster shape models 0-100419
 electron microscope irradiation effects, agglomeration of point defects, dis-
 location climb and loops (*French*) 0-59518
 electronic struct., depend. on hydrostatic pressure 0-80158
 impurities in low alloy steels, effect on neutron irradi. embrittlement
 0-85055
 impurity in Cr-Mo-V low-alloy steel, effect on high-temp. ductility and
 crack growth 0-66652
 impurity migration from doped Si sources in epitaxial layers (*Russian*)
 0-107570
 liquid, diffusion of O_2 , activity coeff. 0-65267
 optical phonon anharmonicity and melting, light scatt. study 0-60621
 phase transformation due to high press. and shear stress 0-75357
 thin film, elec. cond., grain boundary scatt. effects 0-103766
 thin films, vacuum deposited on Si, solar cells prep. by laser induced
 diffusion 0-93998
 Al:Sb, ion implanted, electron beam annealing 0-59500
 Cu-Sb thin film couples, room temperature interactions 0-96699
 GaAs:Sb, resonance levels of isoelectronic impurities 0-107740
 Ge:Au, Sb, Hall mobility, temp. dependence 0-96919
 p-Ge:Au,Sb,Hg(Zn), radiation-defect form., Au influence 0-92911
 Ge:Mn, Sb, recombination waves, convective instability development
 0-70721
 Ge:Sb, electron-hole drop lifetime, quenching temp. influence 0-59889
 Ge:Sb, excited donor states, double optical transitions, reson. absorpt.
 meas. 0-93371
 Ge:Sb, γ -irrad., carrier trapping and recomb. at point radiation defects
 0-107810
 Ge:Sb, heavily doped, mass anisotropy, and multiple scattering effects
 0-107802
 Ge:Sb, heavily doped semicond., scatt. mechanism, resist, and Hall coeff.
 maxima 0-75586
 n-Ge:Sb, high-field Hall effect spectroscopy 0-65600
 Ge:Sb, kinetics of strain-confined large electron-hole drop and its clinging
 exciton system 0-75508
 Ge:Sb, Ni(Mn), recombination wave spectrum, two-level traps 0-96906
 Ge:Sb, thermal phonon scatt., piezo-thermal cond. 0-70482
 Ge:Sb, Zn(Hg), photoelec. props., 70 to 300K 0-65621
 Ge:Sb,Cu, high resist. compensated, impurity of photocond., pulsed uni-
 polar injection carriers 0-92935
 Ge:Sb,Cu, photoelec. props., fast electron irradi. effects 0-60036
 Ge-Sb, far IR emission stimulation by impact ionisation 0-66301
 Pb,Sb, $_{1-x}O_x$:Sb films, DC sputtered, elec. props. 0-80426
 Sb VII, spectrum obs. 600 to 2100 Å, analysis of $4d^8s-4d^85p$, $4d^9-4p^34d^{10}$
 transitions 0-102471
 Sb/As $_2$ SeTe $_2$ /Al structures, rectifying effects 0-75654
 ^{124}Sb , diffusion in Cu 0-65301
 Si epitaxial layers, grown in vac. at low temps. P and Sb doping 0-88189
 Si n/n^+ epitaxial layers, anomalies of Sb distrib. 0-65035
 Si:Sb, donor-polarizability enhancement as the insulator-metal transition is
 approached from the insulating side 0-80184
 Si:Sb, dopant solubility limit, laser irradi. effects 0-84295
 Si:Sb, high dose Sb ion implantation, buried layer appls. 0-88186
 Si:Sb, ion implanted, annealing of heavy ion cascade damage, channelling
 meas. 0-89255
 Si:Sb, ion implanted, doping profile, pulsed laser annealing effects
 0-88197
 Si:Sb, ion implanted, lattice location of impurities after pulsed laser
 annealing 0-88196
 Si:Sb, ion implanted, Sb diffusion during oxidation, snow-plough effect
 0-88366
 Si:Sb, ion implanted and annealed, influence of implantation temp. on
 dislocation generation 0-88158
 Si:Sb, laser doping, evaporation loss and diffusion of Sb, under pulsed
 laser irradi. 0-59508
 Si:Sb, low energy ion implantation, profile determ. 0-88176
 Si:Sb, low energy ion implantation Schottky barrier diodes and resistors
 0-88177
 Si:Sb, MBE film, doping technique 0-79821
 Si:Sb, Mossbauer spectra of ^{119}Sn defect struct. 0-97174
 Si:Sb, produced by ion implantation and laser annealing, Sb behaviour
 above solid solubility 0-88200
 Si:Sb,P, double implants, residual defect reduction after damage anneal
 0-88170

antimony continued

- Si:Sb vacuum deposited coating, p-n junction, pulsed electron beam
 annealing doping, diffusion 0-75480
 SnO $_2$:Sb film, amorphous, electrotransport phenomena obs., under DC
 electric field 0-59840
 SnO $_2$:Sb film on glass substrates, elec. props. 0-88652
 SnO $_2$:Sb sprayed film, growth mechanism and cryst. struct. 0-89143
 Te:Sb, impurity spectroscopy 0-65499
 Te:Sb, photoconductivity in strong mag. fields, doping effects, impurity
 levels 0-75602
- antimony alloys**
 see also antimony compounds
 steel, martensitic, alloying element effect on coarsening behaviour of
 cementite particles in ferrite 0-66518
 Ag-Sb alloy coating, electrolytes for deposition (*Bulgarian*) 0-93763
 As $_2$ Sb $_{1-x}$, semimetal, thermopower, thermomagnetic power, 4.5 to 77K
 0-107825
 Au-An-Sb, and Au-Ge-Ni-Sb low resist. ohmic contacts to GaP 0-70825
 Bi-Sb, crystallisation temp., overcooling temp. (*Russian*) 0-97472
 Bi-Sb, thermal EMF giant quantum oscils. (*Russian*) 0-59960
 Bi-Sb (1 at.%) alloy single cryst. growth solid-liq. interface study
 0-107073
 Bi-Sb (12 at.%), cryst. growth from melt, impurity distrib. control by
 electrotransfer method (*Russian*) 0-66418
 Bi-Sb (6 at.%) whiskers, persistent metallic behaviour, elec. resist. meas.
 0-75544
 Bi-Sb alloys, metal-semimetal point contacts, volt-ampere characteristics
 (*Russian*) 0-65683
 Bi-Sb-Te melt, Sb and Te distribution coeffs. during crystallisation (*Rus-
 sian*) 0-93472
 Bi-Sb-(As), band struct., effects of Sb and As, mag. susceptibility meas.
 (*Russian*) 0-65775
 BiSb (>20 wt.%), electronic band struct. 0-107698
 BiSb, alloys, semimetallic, camera, dispersion relations 0-59854
 Bi $_{1-x}$ Sb $_x$, deformation calculations, band struct. variation, electron phase
 transitions due to deform. (*Russian*) 0-65137
 Bi $_{1-x}$ Sb $_x$, semiconducting alloy, band struct. study, Shubnikov-de Haas
 effect (*Russian*) 0-80181
 Cu $_{1-x}$ Pd $_x$ MnSb, mag. phase transition 0-60268
 Fe-Sb, dil., short range order, NMR study 0-71237
 Fe-Sb amorphous films, Mossbauer effect study 0-75896
 Fe-Sb-Ni(Cr), dil., short range order, NMR study 0-71237
 Fe-Sb-Ti(V)(Cr)(Mn)(Co)(Ni), interactions and segregations, Mossbauer
 and X-ray diffr. study 0-70415
 HoSb, mag. phase diagram, quadrupolar interactions 0-65820
 Ho $_2$ Y $_3$ -Sb system, magnetisation, elec. resist., and sp. ht. meas.
 0-60213
 In-Sb, cryst. struct. after appl. of high press., supercond. transition temp.
 0-70169
 In-Sb liquid alloy, mixing enthalpy, temp. depend. (*German*) 0-84298
 Mn $_{1.88}Cr_{0.12}Sb$, antiferromag.-ferrimag. transition, neutron crit. scatt. and
 crossover effect 0-71023
 MnSb, magnetic losses, ferromagnetic resonance and antiresonance
 0-100618
 Mn $_2$ Sb, spin-wave dispersion relations, exchange interactions, neutron in-
 elastic scatt. 0-65832
 MnSb $_{1-x}$ Sn $_x$ films, Faraday rotation, optical absorpt. coeffs. 0-97242
 Ni $_{0.96}Sb_{0.04}$, surface segregation, XPS and AES obs. 0-76135
 Pb-Sb, thermal analysis in non-faceted/faceted eutectic systems 0-71637
 Pb-Sb-As (1.1-1.8, ~0.01 wt.%), enhanced precip. phenomena, invest. of
 mechanism by elec. resist. meas. 0-104162
 Pb $_{1-x}$ Sb $_x$, liquid alloys, local fluctuations and quadrupolar relaxation
 0-66060
 Pd $_2$ MnIn $_{1-x}$ Sb, Heusler alloy, mag. order, disorder effects 0-88723
 Pd $_{1-x}$ MnSb Heusler alloys, magnetic hyperfine fields on ^{111}Cd , TDPAC
 and magnetisation meas. 0-93219
 Pd $_{2-x}$ MnSb, struct., appl. as improved neutron polariser 0-60199
 Pt $_2$ Sb, L $_1$ ordered alloy, positive temp. depend. on strength, phase destab-
 ilization 0-81203
 Rh $_2$ MnSb, hyperfine fields, ferromag., NMR and Mossbauer effect studies
 0-71259
 Sb-Ce system, heats of form. 0-89517
 Sn-Sb, small κ supercond., phase transitions higher than second order
 0-88668
- antimony compounds**
 see also antimony alloys
 polyacetylene:SbF $_6$, elec. cond. meas. 0-60055
 polyparaphenylene:SbF $_6$, metallic, absence of Pauli paramagnetism, mag.
 susceptibility meas. and ESR obs. 0-97060
 β -Sb $_2$ O $_3$, Raman spectra, vibr. anal. 0-93312
 Ag $_{19}Sb_{11}Te_{22}$, single-phase, thermoelectric efficiency 0-107826
 As-Se-Sb, crystallised glasses, struct. from Mossbauer spectra 0-64917
 As $_2$ Sb $_{1-x}$ SI mixed crystals, phonon coupling, ferroelectric phase transition,
 Raman study 0-108165
 As $_2$ Sb $_2$ Se $_3$ glassy semiconductors, electronic props. 0-103712
 (Ba,Sb $_{1-x}$)TiO $_3$ 0-60514
 (Bi,Sb) $_2$ (Te,Se) $_3$, thermoelectric alloys, phase diagrams, and imperfection
 chemistry 0-108422
 Bi $_{1-x}$ Sb $_x$, EM wave prop. for rot. of mag. field from Faraday to Voigt
 config. 0-84419
 Bi $_{1-x}$ Sb $_x$, solid soln., temp. depend. of weak-field galvanomag. coeffs.
 (*Russian*) 0-70724
 Bi $_{18}Sb_{12}$ Te, single crystal, dispersion of magnetoplasma waves (*Russian*)
 0-70739
 Bi $_{1-x}$ Sb $_x$ Te $_{2-x}$ Se $_x$, elec. cond. and thermoelec. props., neutral defects
 influence 0-60017
 Bi $_2$ Te $_3$ -Bi $_2$ Se $_3$ -Sb $_2$ Te $_3$, solid solution, single crystal, elec. cond., thermoelec-
 tric props. 0-88550
 (Bi $_2$ Te $_3$) $_0$ (Sb $_2$ Te $_3$) $_0.5$ (Sb $_2$ Se $_3$) $_{0.05}$ n-type alloy for thermogenerators,
 thermo-EMF, elec. cond. and thermoelec. efficiency factor, 300-600K
 0-70735
 (Cu,Ag) $_2$ Se/(Bi, Sb) $_2$ Te $_3$, P type selenide segmented element fabrication,
 thermoelectric props. 0-107835
 (GaSb) $_{1-x}$ Ge $_x$ films, single-cryst. metastable semicond., growth and phase
 stability 0-80115
 Ge-Sb-Se glass, elec. props. comp. depend. 0-70697
 GeSe $_2$ -As $_2$ Se $_3$ -Sb $_2$ Se $_3$, elec. cond. over wide range of temp. 0-88564
 GeTe-Sb $_2$ Te $_3$, solid solutions, cond., density of states 0-88472
 PbS-Sb $_2$ Se $_3$, semicond., optical and photoelec. behaviour 0-96938
 Sb-O-Cl(Br)(I), glass-forming regions 0-88057

antimony compounds continued

- Sb-S glasses, activation energy of crystn. 0-64920
 SbCl₃, bond polarisability and force constants 0-69260
 SbCl₃, nuclear electric hexadecapole interactions 0-65513
 SbCl₃/AlCl₃ molten mixtures, Raman spectra 0-93305
 SbF₆-graphite intercalation cpl., synthesis and elec. props. 0-70781
 SbF₆-benzyl chloride, chemi-ionis. reaction, temp. depend., flow tube investig. 0-108701
 SbF₆⁻, produced from fast Cs+(SbF₆)_n collisions, ionisation cross section energy depend. 0-81300
 Sbl, decay branching ratios meas., transition probabilities derivation 0-95642
 Sb_{0.20(4)}MoO_{3.1}, synthesis, struct. and oxidation state (*French*) 0-64971
 Sb₂O₃, standard free energy of formation, by EMF method with solid oxide electrolyte at low temps. (*Japanese*) 0-88338
 Sb₂O₃ thin film overlay, glass lightguide boundary refraction expts. 0-106639
 Sb₂O₃·H₂O, crystalline, ¹H NMR study of proton transport 0-60446
 Sb₂O₃I₂, Raman spectra, vibr. anal. 0-93312
 Sb₂O₃·nH₂O acid membranes, synthesis and characterisation 0-81027
 Sb₂S₃, defect drift in elec. fields and bistable switching 0-92947
 Sb₂S₃ film, coevaporated, elec. cond. meas. 0-65726
 Sb₂S₃, glassy, photoconductivity dependences applied elec. field 0-107857
 Sb₂S₃ spherulite crysts., direct lattice resolution obs. of defect struct. 0-107255
 SbSBr glass, IR reflectivity spectra 0-71403
 SbSBr, single crystals, birefringence meas., ferroelec. transition obs. 0-88933
 SbSl, absorption edge, elec. field effect rel. to ferroelec. props. 0-97240
 SbSl, anomalous photovoltaic effect 0-70749
 SbSl, ferroelec. phase transition and nonlinear props. 0-75988
 SbSl, ferroelectric, dark current and spontaneous polarisation, ferro-paraelectric transitions obs. 0-60521
 SbSl, photoelectric states in real time spatial light modulators, photorefractive effect 0-80676
 SbSl, photolum. spectra in ferroelec. phase, 600-800 nm., 14-100K 0-71468
 SbSl, struct. comparison with Co₂Si, Co₂P, and PbCl₂ (*French*) 0-84155
 SbSl-SbSBr system, ferroelec., anharmonic effects in far IR reflectivity spectra 0-76014
 SbSl_{0.7}Br_{0.3}, anomalous photovoltaic effect 0-70749
 SbS₂, amorphous thin film high field charge transport and quasi-Fermi level location 0-70863
 Sb₂Se₃ crystals, mag. and elec. props. 0-96873
 Sb₂Se₃, glassy, photoconductivity dependences applied elec. field 0-107857
 Sb₂Se₃-CdSe heterojunction, photoelec. props. 0-70816
 (Sb₂Se₃)_{0.7}(Bi₂Se₃)_{0.3}, solid soln., prep. and elec. properties of layered crystals 0-70762
 Sb₂Te₃, cleavage faces, evaporation pattern determ. by decoration method in electron microscopy (*German*) 0-107626
 Sb₂Te₃, stoichiometric, Hall effect and thermoelec. power studies 0-100470
 Sb₂Te₃, thermoelectric properties and phase transition, under hydrostatic pressure up to 9 GPa 0-65609
 Sb₂Te₃-Bi₂Te₃ and Sb₂Te₃-Sb₂Se₃ systems, thermal cond. change during phase transitions 0-100368
 Sb₂Te₃-Bi₂Te₃ solid solns., single cryst. growth and thermocouple construct. 0-104056
 Se-Te-Sb glasses, electronic transport 0-88579
 SeCl₂-SbCl₅ systems, Raman spectra (*German*) 0-93324
 Te-(Bi_{0.1}Sb_{0.9})₂Te₃ system eutectics, crystn. rate effect on electrophys. props, mutual solubility effect 0-60774
 Te-(Bi_{0.1}Sb_{0.9})₂Te₃ eutectic, electrophys. props., directed crystn. conditions influence and comp. depend. 0-107827
 Te_{0.6}Ge_{2.4}-Sb_{0.4}, DSC studies of struct. phase transformation 0-66505
 Ti-Bi-Sb-Te system, peritectic reactions in TiBiTe₂-TiSbTe₂ cross section, crystn. character 0-108406

antineutrinos see neutrinos**antineutrons see neutrons****antinucleons see nucleons****antiphase boundaries**

- electron wave function in vicinity of planar defect 'on edge' 0-88002
 α -In₂Te₃, I phase, order-disorder transform. for DO₂₂ struct., thermodynamic study 0-70155
 ordered alloys with periodic struct., decomp. invest. (*Russian*) 0-93558
 pyroxenes, contrasting props. and behaviour 0-79813
 Ag₃Mg, periodic antiphase boundaries, electron microscopy study (*French*) 0-59481
 Au₁₁Mn₄ ordered phase formation, electron diffr. and microscopy study 0-107418
 Au₃Mn thin films, electron diffr. study 0-92793
 CsCl-type lattice, (111) superlattice screw dislocation motion, computer simulation 0-79793
 Cu-Sn alloy system, long period superlattice obs. and impurity effects 0-103297
 Cu₃Au thin films, fine-grained and disordered, low temp. ordering 0-97433
 Cu₃Au-Ni, antiphase domains morphology 0-108460
 Cu₃Pd, periodic antiphase boundaries, electron microscopy study (*French*) 0-59481
 Cu₃Pt, antiphase domains morphology 0-108460
 CuZn, planar faults, faint electron microscopic image contrast obs. 0-107283
 Fe-Al alloy, planar faults, faint electron microscopic image contrast obs. 0-107283
 FeCo, planar faults, faint electron microscopic image contrast obs. 0-107283
 Pb₂(VO₄)₂, ferroelastic, phase transitions, boundary walls 0-107419

antiphase domains

- see also antiphase boundaries
 γ -brass type alloys, superstructures and defect obs. 0-107284
 ferroelectric substances, electron microscopy investigations, review (*Japanese*) 0-71366
 pyroxenes, contrasting props. and behaviour 0-79813
 Fe-Co-V-(Ni), annealing effect on microstruct. rel. to mag. and mech. props. 0-89267
 Gd₂(MoO₄)₃, electron microscopy investigs. of ferroelec. substances, review (*Japanese*) 0-71366

antiprotons see protons**antireflection coatings**

- ablative optical recording, computer modelling 0-91752
 alkali-borosilicate glasses, antireflection film production by heat and chem. treatment 0-66677
 evaporator, tubular-type radiation-heated, ZnS film deposition 0-76191
 fusion reactor, neutral beam injecto cryogenic pumping panel chevron baffles, black coating materials, selection 0-95456
 graded-index antireflection coatings, high laser damage threshold 0-83628
 IR thin film plasma deposition processes 0-87466
 layer thickness calcs., thin-layer achromatic coatings 0-87468
 multilayer achromatic, extended region of low reflection coeff. values 0-95982
 multilayer coatings, high-refl. or antirefl., vol., interface absorpt. and scatt. losses 0-63915
 oxide, porous transparent films as antirefl. coatings for glass surfaces, low refr. index 0-74448
 quartz high-transmittance antirefl. film, vacuum-etched 0-74449
 reflection coefficient partial derivatives, matrix calc. (*French*) 0-89080
 removal by Al₂O₃ powder and NH₄HF₂ soln. 0-74521
 resistive wall coating's parameter determ. in short pulse accelerators 0-63418
 solar cell coating, high-efficiency InP homojunction cell 0-104505
 solar cell fabrication, photovoltaic process based on thick film technique 0-94016
 solar cells, inversion layer, surface passivation 0-101098
 thin film technology, appls. in energy, optics, and electronics, review 0-78932
 two-layer, error considerations in design 0-74477
 wideband optical disc data recorder systems 0-102751
 Al₂O₃ porous transparent films as antirefl. coatings for glass surfaces, low refr. index 0-74448
 GaAs homojunction solar cells, large-grained, passivation method to improve open-circuit voltage 0-94070
 GaAs laser diode, spontaneous emission reduction 0-95904
 GaAs/(GaAl)As channelled substrate narrow stripe lasers, with quarter-wavelength facet coatings 0-99746
 Ge-As-Se IR transmitting glass composition, prep. and props. 0-69474
 Ge₃₀As₁₇Te₃₀Se₂₃-As₂S₃, two-layer, error considerations in design 0-74477
 In₂O₃ films, electron beam evaporation, elec. and optical props. (*Japanese*) 0-60784
 p-Si, heavily doped contact layers on IR detectors, IR transmissivity 0-108190
 Si solar cells, proton irradiated, processing influence on elec. performance 0-94001
 Si solar cells with fire through contacts printed on anti-reflection coating 0-93993
 Si₃N₄ antireflection coating for solar cells, reactive plasma process for forming metal grid patterns 0-93990
 SiO₂ sputtered film performance as acoustic antireflection coating at sapphire-H₂O interface 0-106686
 SnO₂/n⁺-pSi heterojunction solar cells, fabrication by paint-on-diffusant method 0-94048
 TiO₂, for Si solar cells by spray deposition, review 0-104511
 TiO₂, spray-on antireflection coatings for Si solar cells 0-80963
 TlI laser window films, stoichiometry, Rutherford backscatt. study 0-59831
 ZnSe laser windows, AR coated, photoacoustic chopping freq. studies using CO₂ laser 0-83629
 ZnSe laser windows, photoacoustic signal var. with chopping freq. 0-75309
- API gravity see density**
apodisation see acoustic imaging; optical images
apparatus see instrumentation; instruments
apparent porosity see porosity
appearance potential see ionisation potential
appearance potential spectra
 rare-earth metals, SXAPS with sealed-off analyser tube 0-80908
 Al(100) oxidised surface structure anal., extended appearance potential fine struct. study. 0-75411
 Ni(100) oxidised surface structure anal., extended appearance potential fine struct. study. 0-75411
 V, extended fine struct. above APS thresholds, effect of central atom. pot. 0-66329
- appearance potential spectroscopy**
 AES, apparatus 0-101888
 extended fine struct. above APS thresholds, effect of central atom. pot. 0-66329
 teaching laboratory and lecture demonstrations 0-105477
 V₂O₅, electron beam induced decomposition, appearance pot. spectroscopy 0-85203
- Appleton layer see ionosphere**
appliances, domestic see domestic appliances
applied mechanics see mechanics
approximation theory
 see also function approximation; interpolation; least squares approximations
 EM wave scattering using successive approximation method for scattering from round dielectric cylinder (*Russian*) 0-63889
 four term WKBJ approx., appl. to Varshni V and Lennard-Jones pot. 0-58113
 generalised Pade approximation, explicit solns. 0-73623
 gravity field analysis, approximation of Stokes and Vening-Meinesz eqns. allowing for initial data errors 0-101459
 light scattering from macromolecular soln. in alternating elec. field, low angle approx. 0-84721
 mathematical physics students teaching 0-105474
 multiple approximations, Hilbert-Pade method, appl. to Gaussian function 0-82707
 near resonant oscillating systems, integration in slow-fluctuation approx. 0-62483
 planets rectangular coordinates, approximation via Chebyshev polynomials (*Russian*) 0-62033
 quasistatic approximation for atmospheric dynamics, characterisation (*German*) 0-98383
 relaxation distribution function, approx. methods and num. inversion of Laplace transform. 0-84720

approximation theory continued

- scattering, approximate coupled equation method 0-73215
- superfluous, meas. elimination, precision evaluation 0-90805

apr see *acoustic paramagnetic resonance***APW calculations**

- disordered system electron energy system, calc. methods 0-75485
- linearised relativistic APW method, using approx. pure spin basis functions 0-70581
- Al, K X-ray absorption, K-emission spectrum, band struct. using APW method 0-97380
- AlH₃, electronic struct. and electron-phonon interaction, hydrogenation effect, rel. to supercond. 0-107694
- Au, energy band structure, X-ray N-emission spectra, relativistic APW calcs. 0-70596
- Au, energy band structure, X-ray emission spectra, APW calc. 0-92811
- Be, eqn. of state, solid-state models, comparison 0-75332
- CdCr₂Se₄, energy band struct. calc. by augmented plane wave method 0-103621
- Cu, single particle lifetime 0-103612
- EuB₆, ferromag., spin-polarised energy band struct., APW calc. 0-96779
- Fe₂Si(Al), electronic structure, X-ray spectra comparison with band struct. calcs. 0-97383
- inert gases, solid, Compton profiles, APW-X α calc. 0-80894
- Ir, energy band structure, X-ray emission spectra, APW calc. 0-92811
- LaAl₃, calc. of energy band-structure and Fermi surface by APW method 0-70590
- LaAl₃, electronic struct., APW method and local-spin-density approx. 0-65434
- LaB₆, electronic struct., APW method and local-spin-density approx. 0-65434
- MnP, spin polarised energy band struct., electronic specific heat, APW calcs. 0-65431
- MnSi, electronic energy band struct., self-consistent APW calc. 0-65433
- Mn₂Si, electronic structure, X-ray spectra comparison with band struct. calcs. 0-97383
- Nb, electron-phonon interaction, relativistic, APW calc. 0-92837
- NbC, band struct. and X-ray emission spectra, APW and X α calc. 0-70605
- Ni (100) films, spin density by self-consistent linear APW method 0-65710
- NiSb, bandstructure and density of states calc. 0-70580
- Os, electronic energy band struct. 0-107697
- Pb, ab initio band struct. calcs. 0-75502
- Pt, energy band structure, X-ray emission spectra, APW calc. 0-92811
- SMS, band struct. and semicond. metal phase transition 0-80180
- Si, semi-empirical APW calc. of band structure 0-84424
- Sr, monochalcogenides, electronic energy band struct., APW calcs. 0-65439
- Ta, electron-phonon interaction, relativistic, APW calc. 0-92837
- TaN, energy band struct. calc., symmetrised APW method 0-96784
- V, electron-phonon coupling constant calc. (Russian) 0-70624
- W(001), surface states and surface resonances, self-consistent electronic struct. 0-96960
- Xe, condensed at high press., electron-band theory and fluid theory calcs. 0-59875
- YS, band struct. and X-ray emission spectra, APW and X α calc. 0-70605

arc discharges see *arcs (electric)***arc furnaces**

- disordered metal ribbon production by ultrarapid quenching 0-71612
- floating-zone melting with viscous torque control 0-89140
- Xe arc lamp imaging furnace for Y₂O₃(:Nd) floating zone growth 0-60777

arc heaters see *arc furnaces***arc lamps**

- alkali metal vapour, source for pumping YAG:Nd³⁺ laser 0-78924
- capillary-arc light source employing mixture of deuterium with neon 0-95971
- Kr water-cooled arc lamp, anode, temp. distrib. along length, anode geometry effects 0-106994
- Li heat-pipe arc lamp as spectroscopic source 0-102787
- Na, light-induced ignition method 0-77599
- Xe, air-water cooling system, DKsSh-1000 high pressure lamp (USSR) 0-74452
- Xe short-arc lamp, current modulated, arc forms and instability 0-96399

arc welding

- acoustic emission method and development of equipment for monitoring crack formation during welding 0-89451
- electric discharge low pressure plasma arc, energy parameters experimental study 0-75117
- EM forces effect on plasma flows, calc. 0-83912
- molten pool solidification and bead formation 0-75341
- pool metal solidification kinetics in welding with electromag. stirring 0-71636
- steel, austenitic stainless, weld, ferritic-austenitic solidification mode 0-89214
- three-phase high performance, power source external volt-ampere characts. determ. using graphical analysis method 0-79594
- VT6 Ti alloy, diffusion welding with constrained deformation 0-81104
- welding arcs, gas velocity fields modelling 0-75039
- Ti-Al-Mo-Cr alloy weldment containing orthorhombic martensite, auto-tempering behaviour and alpha precip. strengthening 0-84976

archaeology

- archaeoastronomy, New Mexico site marking solstices and equinoxes 0-72794
- artefacts, chemical analysis techniques 0-89575
- artefacts, obs. using automated PIXE-PIGME anal. system 0-61199
- bone dating by ESR technique 0-95209
- ceramic materials, thermoluminesc. dating, comparison of results 0-84791
- dating, appl. of luminesc. of calcite under N₂ laser excitation 0-60685
- dating method with digital ESR 0-86542
- flint implements, provenance determ. possible appl. of SIMS 0-61197
- geomagnetic field record in Egyptian adobe bricks (3000-0BC) 0-104862
- geomagnetism study of ceramics from Peru 0-94455
- Indian ceramics, Hueco and Guadalupe Mountain, delayed neutron activation analysis of U content 0-85230
- Java, tektite-like material in remains 0-101365
- megalithic lunar site a Callanish, Lewis 0-77300

archaeology continued

- Mercury silver statuette from Bonn 1896, particle induced X-ray emission analysis 0-85228
- Namoratunga II site in NW Kenya, astronomical dating 0-72793
- pottery, B and Li distrib. in glaze, appl. of (n,p) and (n, α) reactions 0-61200
- Rhodes, discovery of Santorini (Thera) tephra from 1450 BC eruption 0-109129
- Sarawak gold artifacts, X-ray fluorescence and at. absorpt. analysis 0-85229
- sword, 2500-yr-old, obs. using PIXE with external beam 0-61198
- thermoluminescence and age determination (German) 0-105076
- Au in thin Ag objects, quantitative analysis by γ -ray differential absorpt. 0-85227

architectural acoustics

- see also *anechoic chambers; echo; noise abatement; reverberation*
- absorbers, dimensioning of facings for acoustically effective structural elements (German) 0-74600
- acoustic coupling between rooms, meas. system using decrease in sound level method (French) 0-69611
- acoustic diffuser characteristics for amateur users concert hall appl. (Italian) 0-91961
- acoustic wave diffraction at edges of absorbent wall panels, modal analysis (French) 0-79060
- AF vibration, transmission by building columns 0-74602
- ambiophony, practical aspects and appl. in Capitol Theatre, Washington 0-96113
- auditoria and studios, meas. reverberation time, digital instrum. (Japanese) 0-64321
- automated computer optimisation design for concert halls, quantitative criteria 0-87654
- baffles in closed spaces, dependence of effectiveness on nature of closed space, economic and annoyance factors 0-67019
- band-limited power flow into enclosures 0-58859
- broadcasting studio, 'Deutsche Welle' building construction and meas. (German) 0-106668
- built-up urban environments, propag. of sound generated by point source 0-58841
- concert hall design, lateral and ensemble reflection requirements 0-91964
- concert hall design for orchestral balance in seats behind stage 0-91963
- concert hall problem, coherence length and diffuse reflection formulation 0-91962
- concert halls, connection between subjective judgements and criteria of room acoustics (German) 0-102933
- concert halls, factors necessary for warm string tone 0-74603
- concert halls, sound reinforcement system, Nippon Budokan Hall (Japanese) 0-64291
- converted-church theatre rebuilding and acoustic treatment (Hungarian) 0-106667
- cultural centre reconstruction, acoustic tasks and measurements (Hungarian) 0-106666
- Demey metro station, noise level increase due to echoes from passing vehicles (French) 0-69600
- design of music practice rooms, user requirements 0-74606
- domestic roofing sound insulation, expt. facilities of meas. laboratory, test details 0-79058
- eigenmode analysis of the interference patterns in reverberant sound fields 0-96112
- equivalent absorpt. area of room in steady-state condition and reverberation (German) 0-102931
- floors, elastic coverings, effect of thickness and hardness on impact sound insulation props. (Japanese) 0-79053
- impulse responses in concert halls, new method using deconvolution 0-96111
- loudspeaker design for domestic appls. (Italian) 0-91960
- measurements by impulsive excitation (Japanese) 0-64292
- music stage design 0-74605
- noise insulation by multiple layer walls, prediction of output probability distribution of noise level, road traffic noise 0-69593
- noise transmission through stiffened panels 0-102922
- open-plan offices, role of acoustic screening 0-87650
- railway passenger coaches, structure-borne noise suppression (German) 0-91957
- recording studios, shortcomings of apparently improved acoustic designs 0-69601
- reduction of road traffic noise, correct building placement, noise emitted by single source in open space 0-87647
- reverberation time dependence on wall diffusion and room shape (German) 0-102932
- reverberation time for two-dimens. enclosures, iterative calc. 0-102934
- reverberation time measurement using Fourier transforms 0-74601
- review of international standards (Japanese) 0-64294
- road traffic-induced building vibration, Greater London area 0-96098
- room acoustics and human communications 0-96110
- room acoustics correction, using Shure analyser (German) 0-58873
- room having effect on plaster/wood walls open window, pressure due to sonic booms 0-69602
- room-acoustic directional diffusivity model (Hungarian) 0-106665
- school buildings, min. acoustical requirements 0-79059
- schoolroom acoustic insulation check allowing for boundary absorption (Hungarian) 0-106664
- singer and auditorium interactions 0-74604
- solid-borne sound, propagation characts., field and model expts. (Japanese) 0-64290
- sound absorption, perforated facings on porous backings, calculation of specific normal impedance 0-64281
- sound effects transmission, uniplanar and biplanar eidophony (German) 0-106699
- sound fields and acoustic design in rooms, review of subjective effects (Japanese) 0-64293
- sound insulation, domestic roofing systems 0-96109
- sound insulation between buildings, meas. standards 0-96108
- sound isolation tests of residential buildings, correlation with subjective privacy opinions, standard sound source requirements 0-64323
- sound reduction by barriers in rooms 0-79057
- sound transmission, absorption and reflection 0-64288
- sound transmission at the corner of concrete plates 0-87652
- source above rough absorbent plane, analysis of scattering 0-64289
- structure-borne sound, procedure for meas. sensitivity of building structures to stationary excitation (German) 0-64287

architectural acoustics continued

thin infinite panel, sound insulation dependence on effective loss coeff. 0-87737
transmission loss improvement by thin plates in certain distance of building elements 0-102930
window sound insulation, glasses, most effective window configurations 0-87655

arcing see arcs (electric)

arcing, switches see circuit-breaking arcs

arcs (electric)

see also arc furnaces; arc lamps; arc welding; circuit-breaking arcs
ablation stabilised arc theory 0-70072
air, wall-stabilised arc, step and sinusoidal current change response 0-103209
air arc temp. meas. by N_2^+ integrated emission coeffs. 0-59314
alumina confined arc, ablation-induced effects 0-70073
anode-vapour vacuum arc with permanent hollow cathode 0-79616
cap-and pin-type insulators, resistance to high current arcing for 110 and 400 kV power transmission lines (Polish) 0-70049
constant-current vacuum, ignition by plasma steam cathode spot excitation 0-75111
cylindrical, radiant energy transfer, temp. profiles with boundary reflection corrections 0-79600
cylindrical arc column, channel model 0-106995
DC arc plasma, alterations in spectral line intensities due to external mag. fields 0-79621
DC C-arc for excitation temp. meas. of self-absorpt.-free FeI spectral lines 0-87965
dense plasma, radiative thermal cond. and elec. cond. coeffs. determ. in arc discharge 0-75033
dielectric materials spacecraft, surface discharge arc propag. and damage 0-71314
discharge low pressure plasma arc, energy parameters experimental study 0-75117
electric machines, volts-per-bar and flashover, causal mechanisms and preventive measures 0-92408
electron density meas. by far IR laser beam deflection 0-59296
free burning arc characteristic formulae 0-70068
fusion reactor, TFTR, neutral beam source, arc current modulator design 0-102379
graphite, in Ar flow, meas. of anode voltage drop 0-84022
helical form model 0-103199
high speed ground transportation vehicles gas-flow-controlled arcs for power collection 0-70054
high-current arc electrode vapour influence and estimation 0-70070
high-current free burning arcs, approximate model 0-70069
high-intensity, anode boundary layer, one-dimens. anal. 0-96401
horizontal, in graphite tube, in inhomogeneous mag. field, mass spectrometric anal. 0-79620
impulse spark study using two-wavelength interferometry 0-86391
insulators, HV for transmission lines, power arcs occurring in networks and laboratories, comparisons 0-87983
ion source for fusion reactor, 1000-kVa arc power supply 0-99396
joule heating in emitting sites on various nonrefractory arc cathodes 0-100106
long arc simulated lightning attachment testing using 150 kW Tesla coil 0-70074
luminous colour control methods in pulsed arc discharges in Ne-Hg lamps (Japanese) 0-103214
metal cathodes, oxidised and clean, basic erosion processes 0-103211
microarcing studies in low temp. RF-plasma 0-96407
moving arc-air interface, double vortex flow, optical anal. 0-100108
moving arc-air interface, leading edge thermal wave description 0-100109
origin of arcing in a Tokamak 0-92414
partial thermodynamic equilibrium, plasma state 0-79608
perplex confined arc, ablation-induced effects 0-70073
plasma electron emitter with constricted arc discharge, characts., anode spots effects 0-70040
plasma parameters of unipolar arc and spectral lines intensity dependence on Li additive 0-73478
plasma transport functions by precision arc expts., H Balmer spectrum 0-103187
plasma-electrode contact processes, microplasma diagnostics 0-59325
plasmatron, discharge stabilised, by gas blown through porous wall 0-75105
selfluminous, schlieren system for time and space resolved photography 0-87471
snubber using transformer core, theory 0-59315
stabilised, elec. field intensity meas., plate probe meas. 0-75095
steady state, energy eqn. soln., boundary value problem 0-79601
switchgear, SF₆-insulated metal-clad, arcing, decomposition products and pressure rise 0-100101
switchgear, SF₆-insulated substations, insulation design and co-ordination 0-100102
synthetic resins, arc resistance tests in various gas insulators (Japanese) 0-81250
temperature estimation from self-reversed spectral lines 0-75110
thin arc, stability boundary theory 0-59324
three-phase high performance, power source external volt-ampere characts. determ. using graphical analysis method 0-79594
Tokamak, electrically isolated target, formation of arcing, role of runaway electrons 0-64764
Tokamak, T-10, arc tracks, wall erosion by unipolar arcs 0-64811
vacuum arc plasma flow in plasma-optical system (Russian) 0-106992
wall-stabilised, free recovery with imposed laminar and turbulent flows 0-59321
welding arcs, gas velocity fields modelling 0-75039
wire-plane electrodes, breakdown voltage, effect of vacuum conditions 0-64798
xenon filled DC arcs, with and without focal spot, electric behaviour (German) 0-64800
Al anode spot of vacuum arc 0-107006
Al, vacuum arc, excited state density from line intensities 0-96404
Al, vacuum arc, excited state density theory 0-100107
Al₂O₃, film, switching times and arc cathode emitting site lifetimes 0-59332
Ar arc heating, high-pressure complex heat exchange expt. (Russian) 0-75112
Ar arc plasma, partial LTE for lower excited levels of ArI 0-79565
Ar arc plasmas, steady-state and decaying, mol. gas impurities 0-103177

arcs (electric) continued

Ar, high current, interferometric and spectroscopic study 0-59275
Ar II arcs, transition probabilities, statistical inference 0-106357
Ar, wall-confined, nonequilibrium effects 0-70058
Cs, Knudsen arc, electron beam heating and ionisation 0-75114
Cu cathode vacuum arc, cathode spot and cell areas, meas. 0-96405
H spark gap arc discharges, laser-triggered, electron density meas. 0-64822
He continuum radiation, 109 to 540 nm, meas. in arc plasma (German) 0-106932
Kr arc discharge, radiative characts. computational model requirements 0-64812
Kr, plasma, high-press. arc discharge, elec. cond. 0-59181
Mo-Cu cathode, spot motion and nature in UHV 0-79597
N, high intensity arcs, anode contraction region modeling 0-103210
N₂-Cu arc plasma, transport coeffs. 0-96344
N₂-H₂ arc, bent and rot., flow mechanism 0-70047
SF₆ temp. determ. accounting for demixing 0-70057
U₁₀ arc emission discharges, compared to UI plasma emission coeff. 0-64693
W electrodes, C segregation and arc damage 0-64795
Xe arc discharge, radiative characts. computational model requirements 0-64812
Xe, plasma, high-press. arc discharge, elec. cond. 0-59181
Xe short-arc lamp, current modulated, arc forms and instability 0-96399

area measurement

spot size estimate in diff. pattern of scattered field 0-95789
tibia, human, simplified method of radiographic anal. of its cross-section, anthropometric correls. 0-89827
CuO powder, surface area determ. by adsorpt. of stearic acid and pyridine 0-107636
MgO powder, surface area determ. by adsorpt. of stearic acid and pyridine 0-107636

argons

see also nuclei with
adsorbed on Al, differential refl. spectroscopy, local field effect 0-80811
adsorbed on graphite, multilayer adsorbed films, mol. theory 0-80058
adsorbed on graphite, overlayer-substrate spacing, LEED determ. 0-103579
adsorption on pure and SiO₂-coated TiO₂, 77.4K, microcalorimetry obs. 0-80062
arc, graphite, in Ar flow, meas. of anode voltage drop 0-84022
arc, high current, interferometric and spectroscopic study 0-59275
arc heating, high-pressure complex heat exchange expt. (Russian) 0-75112
arc plasma, partial LTE for lower excited levels of ArI 0-79565
arc plasmas, steady-state and decaying, mol. gas impurities 0-103177
arcs, transition probabilities, statistical inference 0-106357
atmosphere isotopic composition in pre-Cambrian, degassing from shungite 0-85749
atom, 2p⁶ shell, oscillator strength, photoionisation cross sections, electron shell alterations determ. (Russian) 0-58144
atom, approximate relativistic Hartree-Fock eqns., soln. using Slater-type functions 0-58168
atom, CI calcs. using modified virtual orbitals 0-58163
atom, closed shell, Jastrow wave functions, var. calcs. 0-83249
atom, electron energy loss spectra 0-62740
atom, electron impact, L X-ray spectrum, radiative Auger transitions 0-58227
atom, first excited config., intermediate coupling coeff. 0-83450
atom, incoherent scatt. factors calc. by direct integration over impulse approx. Compton profiles 0-102475
atom, inner shell alignment following electron impact ionisation, distorted wave approx. calcs. 0-91682
atom, L-shell internal excitation accompanying L-capture 0-95726
atom, metastable, excitation of N₂(C²II_g), symmetry, propensity rules and alternation intensity, rot. spectrum 0-87135
atom, outer p_{1/2} subshell photoionisation, polarised electrons, relativistic RPA calcs. 0-83331
atom, photoelectron asymmetry parameters 0-95684
atom, photoionisation, absolute cross-sections, exptl. meas. techniques 0-63598
atom, spin-polarised photoelectrons by circularly polarised synchrotron radiation 0-91516
atom+H(D), ion pair formation, curve crossing model 0-87216
atom+multicharged ion collisions, one electron capture from inner shells 0-58376
atom beam W surface direct inelastic scatt., vel. distrib. meas. 0-66351
atoms, absorpt. spectra, field induced autoionisation near ionisation threshold 0-106301
atoms, classical many-body collision model incorporating Heisenberg and Pauli principles 0-63511
atoms, Compton profiles, Xalpha wavefunctions 0-106265
atoms, electron energy loss spectra, Compton defect characterised by shift and asymmetry parameters 0-95723
atoms, electron scatt. and ejection, electron energy loss spectra 0-58394
atoms, inner-shell level energies, absorpt. spectroscopy with synchrotron radiation 0-99583
atoms in Ne matrix, radiative and nonradiative lifetimes in excited states 0-69106
beam source, high-flux 0-58416
binary collision-induced light scatt., rot. Raman scatt. 0-78660
binary collisions induced light scatt. 0-83428
broad beam ion source used for sputtering and etching 0-69002
Clausius-Mossotti second virial coefficient 0-79426
cluster containing tetracene molecules, excited state intramol. dynamics, laser-induced fluoresc. spectra obs. 0-78674
cluster formation and homogeneous nucleation, comparison of expt. and theory 0-79925
compressed gas, PVT meas. at high press. 0-98927
condensed, electron drift, Davydov electron energy distribution function, diffusion (Russian) 0-80339
CW optical discharge in laser plasmatron mode 0-75078
desorption, on Pt (111), gas surface interactions, 3-D generalised Langevin model appl. 0-107637
diffusion rate in Au thin layers 0-100359
dilute gas, transport props., simple pair pot. model 0-87835
discharge, high-freq., excited atoms concentration determ., using spectral method (German) 0-70053
discharge, ion density profile, reson. laser light meas. 0-92401

argon continued

- discharge, two-temperature, transport eqns., transient phenomena 0-96402
- electron avalanche development, exact Boltzmann eqn. anal. 0-59318
- electron energy deposition in Ar, Monte Carlo calcs. 0-69242
- energetic electron degradation spectra and initial yields 0-95724
- entropy change on melting of simple substances, thermal expansion, configurational entropy 0-59630
- equation of state, hard core fluid with two-Yukawa tail 0-59618
- excitation by pulsed electric discharge, luminescence obs., time resolved spectra meas. 0-102482
- excited atom+molecules reactions, electronically excited atoms and alkali metal atoms analogy 0-76490
- filament lamps, Kr-Ag-N gas mixture, thermal conduction coefficient calculational methods (*Russian*) 0-96335
- flowing Ar spark gaps, electric breakdown study, improved method 0-64821
- fusion reactor first wall protection, response to spherical blast waves 0-91245
- gas, compressed, Rayleigh-Brillouin spectrum, hydrodynamic region 0-100063
- gas, compressed, Rayleigh-Buillouin spectrum, scaling 0-100062
- gas, heated, elec. breakdown parameters 0-103202
- gas, liquid, solid, refractive index, density and dielectric const. 0-66138
- gas, positron annihilation decay rates, high temp. behaviour 0-58389
- gas, viscosity meas. at very high press. 0-59155
- gas atoms, electron thermalization time and position distribution meas. 0-93771
- glow discharge, cathode dark space ionisation avalanche with cold cathode (*Russian*) 0-84013
- hollow cathode, glow discharge, current balance and secondary electron emission 0-75108
- implantation in Fe, effect on corrosion by H₂SO₄ soln. 0-71793
- ion, energy and ang. distrib. in passing through C, Cu, Ag films 0-100292
- ion laser, ¹²⁷I₂ stabilised, beat freq. intercomparisons at 514.5 nm 0-74338
- ion laser, appls. in research, industry and medicine (*French*) 0-83590
- ion mobilities in He gas at 82K 0-75023
- ion source, HF, proton yield increase, influence of various admixtures to H₂ obs. 0-57422
- K648, halo planetary nebula, low Ar abundance meas. 0-82443
- laser, new IR laser transitions, 3.725 to 17.233 μ m, 5.804 μ m laser line identification 0-83734
- laser with passively locked modes, excitation of dye laser for picosecond pulse generation 0-95930
- liquid, binary non-additive particle interaction, self diffusion and at. motion, mol. dynamics method 0-59372
- liquid, comparison on interaction induced light scatt. and IR absorption 0-60561
- liquid, compressed, excess electron mobility theory 0-80338
- liquid, compressional viscosity and vibrational relaxation 0-70311
- liquid, critical exponent, η , X-ray scatt. 0-92660
- liquid, depolarized Rayleigh scatt. at triple point, mol. dynamics simulation 0-60617
- liquid, diffusion coefficient for model potentials through mean square displacement 0-70098
- liquid, equation of state studied using statistical theory results 0-84276
- liquid, modified droplet model, mean droplet interaction below T_c 0-70363
- liquid, quasi-crystalline structure, role of vacancies in dynamics 0-92438
- liquid, relative motions in molecular dynamics investigation 0-92439
- liquid, surface study, ellipticity coeff., ellipsometric method 0-84343
- liquid, surface tension and width, density functional theory 0-103537
- liquid-vapour interface, surface of tension near triple point, theory 0-100375
- low-press. glow discharge, elec. characts. of positive column 0-100112
- mass spectroscopic chemical anal. using quadrupole mass spectrometer for fissile material accounting 0-63300
- matrix for O₃+Zn(Cd) matrix reactions, IR, Raman and visible spectra 0-87110
- melting transitions, thermodynamic props., positional disordering energies 0-96452
- methanol+Ar, methoxy radical prod., UV emission spectra 0-91572
- methyl cyanide-Ar mixture, thermal cond. in mag. field 0-100058
- molecule, Hulburt-Hirschfelder pot. function 0-63612
- momentum eigenfunctions in complex momentum plane, Hartree Fock functions 0-63517
- neutral system, complete saturation phase excited state population density 0-106284
- nonequilibrium condensation and surface tension in supersonic jet flow (*Russian*) 0-65210
- optical gas breakdown, reduced threshold in two-freq. field 0-64819
- physisorbed monolayer on graphite, neutron scatt. studies 0-107655
- PK 108-76°1, 49+88°1, halo planetary nebulae, low Ar abundances meas. 0-82443
- plasma, decaying pulsed discharge, acoustic wave density modulation 0-103143
- plasma, dense, shock-heating, calc. of equilibrium props. (*Japanese*) 0-79513
- plasma, low density, shock-heated, effective collision freq. calcs., electron temp. meas. 0-75025
- plasma, photon reabsorption attenuated radiation emission 0-64776
- plasma arc, wall-confined, nonequilibrium effects 0-70058
- plasma jet, optical studies using Schlieren and shadow methods 0-59279
- plasma parameters, microwave scanning technique 0-64773
- relativistic ion beam laser, continuously IR to X-ray tunable, in negative temp. state (*Chinese*) 0-87373
- saturated solutions, NO₂ effect on spectral distribution and intensity of sonoluminescence 0-76091
- secondary scintillation under mag. fields, effect in gas proportional counters 0-58055
- shock heated, absorpt. line broadening of Ca and Ba (*Japanese*) 0-83464
- shock-tube end-wall boundary layer 0-79348
- solid, diffusion processes in plastic deform. (*Russian*) 0-92591
- solid, energy bands, depend. on choice of exchange-correlation pot. 0-70607
- solid, equil. props., uncorrel. pairs approx. 0-84303
- solid, high-temp. thermal expansion characts. 0-59680
- solid, many-body contributions to OK binding energy 0-84135
- solid, vacancy conc., X-ray study at const. vol. 0-64991

argon continued

- solid, X-ray induced point defects 0-59514
- starting gas, Hg discharge, high pressure, NaI and TlI additives, line broadening and radiative transport 0-74199
- supersonic pulsed flow from conical nozzle 0-103056
- thermal conductivity, at high press. 0-103099
- total scattering cross sections for low-energy electrons 0-58417
- triple point sealed cells using stainless steel envelope 0-95099
- Venus atmosphere, O₂, Ar, CO abundances, error of Pioneer Venus chromatography obs. 0-105189
- Ar, bath gas, Br₂, long-lived A³Π(1_u) state, quantum-resolved dynamics of excited states 0-69178
- Ar plasma formation in crossed electric and magnetic fields, optical spectra 0-79452
- Ar⁺ and Ar⁺-Kr⁺ ion lasers, I₂ stabilized, beat frequency 0-95916
- Ar⁺ bombardment of Pt(110), O₂ adsorption, effect on reactivity 0-89099
- Ar⁺, conversion to mol. ions, three body association coeffs. determ. using drift-tube mass spectrometer 0-108699
- Ar⁺ ion laser, active mode locking study 0-91827
- Ar⁺ laser 582 THz stabilisation by I₂ cell, improvements 0-102741
- Ar^{16,17+} filled glass shell, symmetric laser compression 0-64759
- Ar⁶⁺, static dipole quadrupole polarisabilities and shielding factors calc. using HF scheme 0-99450
- Ar⁸⁺, second order correl. energy, Z depend. of irreducible-pair energies 0-91417
- Ar¹⁺, (i=1, 2, 3, 4, 5), absolute electron impact ionisation cross section 0-83496
- Ar-N₂O, O(¹S) photodissociative prod., photoluminesc. excitation spectra, excitation energy transfer 0-89508
- Ar-O₂ (6%) cryst., vibr. Raman spectra 0-60558
- Ar-OCS, liq. dissoc. studies 0-78716
- Ar-OCS, O(¹S) and S(¹S) photodissociative prod., photoluminesc. excitation spectra, excitation energy transfer 0-89508
- Ar-acetylene van der Waals molecule, radiofreq. spectroscopy and Stark effect meas., equil. struct. and props. 0-91543
- Ar-air, transformer plasmatron, LF discharge, electrical and energy props. 0-103200
- Ar-CH₄ proportional counter, light emission obs. 0-78488
- Ar-CO glow discharges, positive ion spectra, ion clusters obs. 0-64807
- Ar-CO₂ mixture, Ar* prod. by electron excitation, transfer reaction kinetic study 0-63824
- Ar-Cs plasmas, electron momentum transfer cross section, cyclotron reson., temp., cond., and v_l meas. 0-106930
- Ar-H₂O vapour mixture, H₂O droplets nucleation rate const. 0-61131
- Ar-HBr, intermol. pot. energy surfaces calcs. 0-91625
- Ar-Hg-Cl₂, elec. discharge, electron inelastic collision props. 0-79617
- Ar-Kr-F₂ discharge, inelastic electron collisions, energy distrib. and rate consts. 0-87980
- Ar-Kr-F₂ mixture, nucl. induced excimer fluoresc. for I laser excitation 0-78846
- Ar-Kr-F₂ nuclear pumped laser, high energy beam deposition 0-63999
- Ar-Kr(Xe)(N₂), electron beam ions., low temp. plasma prod. 0-87908
- Ar-like atoms, gradient expansion of atomic kinetic energy functional 0-95530
- Ar-N₂ liquid soln., selective adsorption by plane homogenous surface and C atoms, mol. dynamics calc. 0-59806
- Ar-N₂ mixture, electron beam pumped, lasing obs. at 337, 358, 380 and 406 nm 0-102700
- Ar-N₂ mixture, lasing at four lines 0-99713
- Ar-Ne(H₂), liquid solution, dielectric props., intermolecular interactions (*Russian*) 0-88904
- Ar-O₂ mixtures, positronium form. and quenching, orthopositronium quenching cross section determ. 0-74261
- Ar-Xe high press. transverse discharge laser using Xe IR transitions 0-63978
- Ar-Xe IR laser pumped by electron beam stabilised discharge, lasing parameters 0-102698
- Ar+acetylene, vibr. relax. study using laser-induced fluoresc. 0-74219
- Ar+Ar partially stripped ion, stopping power 0-91651
- Ar+Ar⁺, charge exchange, Σ oscill. and spin change 0-74247
- Ar+Ar⁺(Ar⁺)(Ar⁺), electron stripping cross-sections meas. 0-83477
- 2Ar+Ar⁺(Kr⁺), three body reaction, rate coeffs., temp. depend., 100 to 300K 0-108703
- Ar+Ar²⁺(Ne²⁺), single electron capture excitation, photon emission, VUV spectroscopy 0-58379
- Ar+BaO, in Ar flame, rot. and translational relax. by sub-Doppler optical double reson. 0-95583
- Ar+Be⁺, Be II 2²P excitation, alignment and orientation 0-91647
- Ar+Br₂ dissociation reaction, trajectory study by ensemble method 0-66765
- Ar+D₂, state-resolved $\Delta j=2$ rot. transitions 0-63772
- Ar+F⁺, inner-shell ionisation, X-ray cross sections 0-58369
- Ar+Fe, Fe I reson. line, collisional broadening at high temp. (*German*) 0-106298
- Ar+formaldehyde, mol. isolated Voigt line, off-peak spectral absorpt. coeff. 0-106355
- Ar+H, collisional coherent excitation, meas. of Lyman α -photons 0-99552
- Ar+H, electron energy loss 0-87217
- Ar+H, H α and H β emission cross sections 0-63782
- Ar+H⁺, endothermic charge transfer reaction, low energy crossed beam study 0-95720
- Ar+H⁺, low energy proton transfer reactions, crossed beam studies 0-108697
- Ar+H⁺, H α and H β emission cross section 0-63783
- Ar+H⁺ charge exchange excitation, alignment tensor components, coincidence method 0-63795
- Ar+HCl, differential cross section, quasiclassical close coupling approx. 0-63743
- Ar+HCl, inelastic scatt. exponential perturbation theories 0-74217
- Ar+HF, state-to-state cross sections for rot. to translational energy transfer determ. 0-91644
- Ar+HHe⁺, ab initio pot. energy data, SCF-LCAO calcs. 0-63530
- Ar+H(2S), excitation and ionisation contributions to sum-rule Born cross sections 0-99551
- Ar+Kr, (4p⁵5p) and (4p⁵5p²) states, radiative lifetimes and two-body collisional deactivation rate consts. 0-95572
- Ar+Kr⁺+F⁺, three body ion-ion recombination probability, Monte Carlo simulation 0-85160
- Ar+Kr(Xe), collision induced microwave absorpt. spectra 0-74216

argon continued

- Ar+LiF, polarisation cross section, close-coupling calcs. 0-69214
 Ar+Li*(2P_{1/2}), collision induced fine struct. transition 0-74220
 Ar+methane-d₄, vibr.-translational relax. 0-99537
 Ar+N₂, inelastic scatt. exponential perturbation theories 0-74217
 Ar+N₂(O₂, CO), molecular fluid mixtures, equilibrium props. 0-64867
 Ar+N₂(TiF), sudden approx. of Cross, computational tests, cross section factorisation, scatt. phenomena 0-58352
 Ar+NH₃, pure rot. line, press. broadening calcs. 0-78656
 Ar+NO, NO γ(0,0) band, oscillator strength and line broadening 0-106356
 Ar+Na, 3³P-3²D line broadening obs. 0-78684
 Ar+Na, non-Lorentzian spectral line shape 0-106297
 Ar+Na₂, differential cross sections meas. for rot. energy transfer process, obs. of halos 0-91643
 Ar+O, magnetically selected O(3P) state scatt. 0-99543
 Ar+proton, charge transfer, target K-shell electron capture, impact parameter depend. 0-102552
 Ar+S¹⁸⁺, (q=6-16), K X-ray prod., charge-state depend. 0-106391
 Ar+SO₂, dissoci. rate meas. behind shock wave, laser Schlieren method 0-81296
 Ar+UF₆, UF₆⁻ internal excitation 0-106386
 Ar+UO²⁺(UO₂⁺), collision-induced dissoci. cross section and threshold 0-95706
 Ar+Xe⁺, XeAr⁺ form., dissoci. energy, reaction equilib. and rate consts. 0-61071
 Ar⁺+Ar, charge transfer, fine-structure transitions 0-63808
 Ar⁺+He, integral elastic scatt., repulsive potentials derivation 0-63744
 Ar¹²⁺+Ne, highly charged very slow Ne recoil ions, K X-ray transition 0-91649
 Ar²⁺+Ar(Kr)(Xe), single electron capture excitation, photon emission, VUV spectroscopy 0-58379
 Ar²⁺+inert gas, low energy reactions, SIFT and drift tube obs. 0-97705
 Ar⁶⁺+H₂, collisions, ionisation and excitation resulting from electron capture 0-78683
 Ar¹⁷⁺+He, electron capture into different excited states in plasma 0-64679
 Ar¹⁴⁺+H₂(H₂), electron capture by heavy multicharged ions at low velocities total cross sections meas. 0-99548
 Ar₂, van der Waals dimer, intermol. pot., SCF CI ab initio calcs. 0-106274
 Ar(I), 3p²4p config., level lifetimes meas. 0-102490
 Ar²⁺Li, electron capture excitation, VUV spectroscopy 0-63810
 Ar(P₀)₂+H⁺(C⁺S), energy transfer collisions, Lyman-α emission profile obs., in microwave discharge and reaction cell 0-58359
 Ar⁺(C₂P₂)+H₂(D₂), Ar⁺ two spin orbit state, reaction cross section, direct determ. 0-93748
³⁸Ar, low abundant, isotope shift meas., time averaging using dye laser spectrometer 0-101850
⁴⁰Ar, excess, in Alpine biotites, evolution from ⁴⁰Ar-³⁹Ar anal. 0-94521
 Ar/³⁸Ar/³⁶Ar in Type I diamond from Arkansas 0-94493
⁴⁰Ar/³⁹Ar age and irradiation history of Luna 24 basalts 0-82245
⁴⁰Ar/³⁹Ar age and thermal history of Kirin H5 chondrite meteorite 0-101567
 Ar*+Fe(CO)₅, chemiionisation and chemiluminescence reactions, Penning ionisation and fluorescence obs. 0-97689
 Ar*+H, assoc. ionis., rovibronic struct. in electron energy spectrum 0-106380
 Ar*+H, collisional quenching rates 0-95548
 Ar*+Ne*, associative ionisation studied by merging-beams technique 0-91646
 Ar*+Ne*, Penning ionisation studied by merging-beams technique 0-91646
 Ar*+O₂, ion pair form. explained by charge transfer model 0-99546
 Cs-Sr(He) mixtures, photocond. at atm. press. 0-87844
 D₂ lamps, influence of Ne and Ar on spectral parameters 0-86460
 H+O₂+Ar, HO₂ free radical prod., rate const. calc. 0-101026
 H₂-Ar, states velocity auto-correl. function, relax time, neutron scatt. obs. 0-58401
 H₂-Ar, vibr. energy relax. 0-106384
 He-Ar, Ar I TEA lasers, energy characteristics 0-63977
 He-Ar ion lasers, hollow cathode, CW operation and excitation mechanism 0-69363
 He-Ar mixture, RF discharge, mass spectroscopy, floating double probe meas. 0-84016
³He-Ar, nucl. lasing, population inversion mechanism 0-63980
³He-Ar plasma, electron temp. and density, estimation method 0-64785
³He-Ar volume pumped nuclear laser survey of lasing 0-63979
³He-Ar volumetric nucl. pumped laser, dominating processes and reaction physics 0-63981
 Kr-Ar, phase matched, generation of Lyman-α radiation 0-91845
 N₂-Ar, liquid, high resolution CW CARS spectra 0-63635
 NH₃-Ar mixture, thermal cond., viscosity, Senftleben-Beenakker effect 0-100054
 O₂-seeded Ar plasma supersonic free jet expansion flow, population density measurements (Japanese) 0-96351
 SF₆-R-He(Ar) ternary mixtures, formation of inert gas fluorides in AC discharge 0-64817
 SeO₂+Ar, radiative lifetime and quenching rates 0-95685
 Si, high-dose Ar implantation, X-ray topographic obs. of strains and damage 0-59496
 Si:Ar, As, ion implanted, laser annealing, doping profiles, channelling 0-97506
 Si:Ar, ion implanted, nature of defect reverse annealing 0-88875
 Si:Ar, ion-implanted, epitaxial regrowth by laser annealing, microstruct. 0-84404

argon compounds

- ArF, discharge pumped multiwavelength lasers (Chinese) 0-102703
 ArF excimer laser, electron-beam pumped, efficiency and gain 0-78844
 ArF excimer laser multiphoton ionisation mass spectra 0-81381
 ArF, inert gas halide lasers, 60-ns electron beam excitation 0-74340
 ArH, excited states, theoretical pot. curves 0-95548
 ArH⁺, transition moments, perturbation calcs. 0-102542
 ArH⁺+He, ab initio pot. energy data, SCF-LCAO calcs. 0-63530
 ArH₂, van der Waals mols., rot. predissoc. 0-63721
 ArHBr, ArHCl, and isotopic forms, rot. spectra, mol. struct., mol. consts. 0-58246
 ArN₂, van der Waals mols., rot. predissoc. 0-63721
 ArSO₃, weakly bound complex, struct., MBER obs. 0-95701

argon compounds continued

- Ar.HCl, Van der Waals mols., SCF energies and dispersion forces 0-74279
 Ar.HF, Van der Waals mols., SCF energies and dispersion forces 0-74279
 Ar.H₂O, Van der Waals mols., SCF energies and dispersion forces 0-74279
armouring (cables) *see cable sheathing*
aromatic compounds *see organic compounds*
arrays (antenna) *see antenna arrays*
arsenic
see also nuclei with
 amorphous, absence of photodarkening 0-103970
 amorphous, defects, band gap states 0-80215
 amorphous, short-range order, theory and probes 0-79698
 diffusion in solids, double, gettering of impurities 0-75383
 electric field gradient, temp. and press. variation 0-93205
 impurity in Cr-Mo-V low-alloy steel, effect on high-temp. ductility and crack growth 0-66652
 ion implantation in laminar Si-SiO₂ systems struct. change investig. by MSSl (Russian) 0-107918
 loss peaks elimination using Ga in metal-GaAs contacts 0-80370
 water pollution, arsenic in freshwater fish traced to fly ash leachate using neutron activation analysis 0-97827
 As I, level identification and Zeeman effect obs. 0-95571
 a-As, second and third order elastic consts., ultrasonic velocity meas. 0-103408
 As VI, VII, spectra 100 to 300 and 500 to 1200 Å ranges 0-83307
 As(III) and As(V), redox stability in aq. soln. 0-61068
 As(III)+Br₂ reaction, flow coulometry, with ring-disk electrode 0-71966
 CdTe:As, ion implanted, elec. props. 0-65021
 Ge:As thermal phonon scatt., piezo-thermal cond. 0-70482
 Pt-Si:As, silicide form. during laser irradi., p-n junctions and ohmic contacts 0-84397
 Se:As, amorphous film, dielec. activity obs. near glass transition temp. 0-75933
 Se:As X-ray plates, electronic transport (German) 0-80290
 Si:Ar, As, ion implanted, laser annealing, doping profiles, channelling. 0-97506
 Si:As, CVD, doping using SiH₄-H₂-AsH₃ system 0-79823
 Si:As, CW CO₂-laser annealing, comparison with thermal annealing 0-84193
 Si:As, diffused, laser irradi., stability study 0-65547
 Si:As, diffusion model, degeneracy and partial ionisation effects 0-96693
 Si:As, donor-polarizability enhancement as the insulator-metal transition is approached from the insulating side 0-80184
 Si:As, heavily As-diffused, Hall mobility and resist. rel. to carrier conc. 0-107815
 Si:As, heavy-doping effects and impurity segregation during high-press. oxidation 0-65014
 Si:As, high-dose ion implanted and annealed, implant redistribution 0-107309
 Si:As, ion implanted, annealing of heavy ion cascade damage, channelling meas. 0-89255
 Si:As, ion implanted, doping profile, pulsed laser annealing effects 0-88197
 Si:As, ion implanted, formation of As complexes 0-59511
 Si:As, ion implanted, laser annealed, lattice defects, epitaxial regrowth 0-103334
 Si:As, ion implanted, lattice location of impurities after pulsed laser annealing 0-88196
 Si:As, ion implanted, low temp. thermal annealing 0-96552
 Si:As, ion implanted, pulsed ion beam annealing 0-103395
 Si:As, ion implanted, pulsed laser annealing, partial solid-state regrowth 0-103591
 Si:As, ion implanted, TEM study after laser and furnace annealing 0-70234
 Si:As, ion-implanted, impurity redistrib. during laser irradi. 0-100280
 Si:As, laser-doped, impurity distrib., Rutherford backscatt. and channelling anal. 0-59507
 Si:As, MBE with simultaneous ion implant doping 0-66432
 Si:As, nonequilibrium solid solutions obtained by heavy ion implantation and laser annealing 0-92544
 Si:As, polycrystalline, As segregation at grain boundaries, elec. props. meas. 0-75259
 Si:As, scanning electron beam annealing, spreading resistance, junction depth 0-75267
 Si:As, shallow junctions by high-dose implants 0-96694
 Si:As, solid solubility and thermal behaviour of metastable 0-75359
 Si:As high-dose implanted single crystals, pulsed electron-beam annealing 0-103373
 Si:As ion implanted layers, annealing by CO₂ laser, doping profile shift 0-84965
 Si:As ion implanted shallow junction 0-70228
 Si:As laser annealing, heat and mass transport model 0-92546
 Si:As⁺, implanted, CW laser annealing, electron-beam induced current 0-100709
 SiO₂, As-implanted, electron trapping and detrapping characts. 0-65692
 SiO₂:As⁺ implanted layers in MOS struct., electron trapping and detrapping characts. 0-92982
 Te:As, impurity spectroscopy 0-65499
 Te:As, photoconductivity in strong mag. fields, doping effects, impurity levels 0-75602
 ZnTe:As, ion implanted, cathodoluminescence emission spectrum 0-108281
 ZnTe:As, shallow-acceptor, donor, free-exciton, and bound-exciton states 0-60667

arsenic alloys

- see also arsenic compounds*
 As,Sb_{1-x}, semimetal, thermopower, thermomagnetic power, 4.5 to 77K 0-107825
 Bi-Sb-As, band struct., effects of Sb and As, mag. susceptibility meas. (Russian) 0-65775
 Fe-As, dil., short range order, NMR study 0-71237
 Fe-As melts, surface tension, density, adsorption (Russian) 0-92757
 Fe-As system, mag. props., Mossbauer study 0-88897
 Ni-As, dil., ferromagnetic, hyperfine field and relax. time obs. of impurity heavy nuclei 0-75533

arsenic alloys continued

- Pb_{1-x}As_x, liquid alloys, local fluctuations and quadrupolar relaxation 0-66060
 Zn-As system, homogeneity range of ZnAs₂ and electrophys. props. 0-60833

arsenic compounds*see also arsenic alloys*

- chalcogenides, deep levels, photoluminesc. and photocond. 0-70641
 graphite-AsF₅ intercalated species, fractional ionisation and identification 0-97397
 polyacetylene:AsF₅, AES, XPS, UPS, and X-ray induced 0-66400
 cis-polyacetylene:AsF₅, conductivity meas., non-Ohmic effects 0-96891
 polyacetylene:AsF₅, electronic excitations, momentum depend., EELS study 0-76121
 polyacetylene:AsF₅, soliton doping mechanism, mag. susceptibility meas. 0-107979
 polyacetylene:AsF₅, synthesis, elec. cond., thermoelec. power 0-60016
 polyacetylene:AsF₅, thermopower and transport props. 0-65611
 As-Ge-Te, chalcogenide glass, elec. cond. and dielec. const. 0-75567
 As-S, melt struct., orientation birefr., viscosity, refr. index, and density 0-84713
 As-S amorphous chalcogenide thin film, transient photoinduced phenomena 0-80884
 As-S-Tl, glass, viscosity and elastic props. 0-100180
 As-Se amorphous system, photocond. props. 0-88587
 As-Se amorphous system, Raman scatt. 0-88984
 As-Se glasses, elec. transport studies 0-103695
 As-Se-Ge(-S), photostructural change in Urbach tail 0-76021
 As-Se-S-Ge chalcogenide amorphous film, computer-generated holograms using electron beam irradiation 0-95846
 As-Se-Sb, crystallised glasses, struct. from Mossbauer spectra 0-64917
 As-Te-Ge/n-Si, film on cryst., heterojunction, elec. and photovolt. props. 0-100514
 As-Te-In, glass-forming, density and microhardness 0-103257
 As-Te-Si-Ge amorphous chalcogenide semiconductor, thin film interface, elec. charact. (Korean) 0-97014
 AsCl₃, bond polarisability and force constants 0-69260
 AsF₃, inversion barrier, STO SCF calc. 0-63567
 AsF₃ doped poly(p-phenylene), highly cond. charge transfer complexes, elec. and optical props. 0-70778
 AsF₃ doped polyacetylene films, photocond. and junction props. 0-70770
 AsF₃ doped polyacetylene, X-ray absorpt. meas., 5K to room temp. 0-71516
 AsF₃ intercalated with graphite, quantum oscillatory phenomena 0-107823
 AsF₃-graphite intercalation cpd., synthesis and elec. props. 0-70781
 AsF₃-graphite intercalation compound nature 0-103308
 AsGe amorphous film, far IR absorpt. spectra, refractive index 0-80785
 As₁₀Ge₁Te₇₅Ag_x glass, elec. and dielec. props., Ag additions effect 0-65558
 AsI₃, X-ray cryst. struct. refinement 0-64961
 As₂I₄, ¹²⁷I, ⁷⁵As NQR freqs. meas. 0-58285
 As₂O₃ in (K₂O)_x(SiO₂)_{1-x} glass, Raman study of As 0-84733
 As₂O₃, vitreous, X-ray diff. study of struct. 0-92464
 As₂S₃ barrier layer for As₂Se₃-Ag photosensitive semiconductor-metal systems (Russian) 0-62777
 As₂S₃, amorphous, luminescence 0-80862
 As₂S₃, amorphous, time resolved luminesc. 0-66288
 As₂S₃ chalcogenide glass films, photographic Ag photodoping to produce negative relief image 0-59490
 a-As₂S₃, energy gap meas., by Faraday rotation 0-66161
 As₂S₃ film, amorphous, photo-induced dynamical changes 0-66142
 As₂S₃ film, evaporated, switching effects 0-96952
 As₂S₃ film, hologram recording using total-internal-refl., polarisation depend. 0-106491
 As₂S₃ film, optical recording, light scatt. enhancement due to coherence 0-97362
 As₂S₃ film waveguide, microgratings for guided-beam deflection, electron-beam direct-writing fabrication 0-102856
 As₂S₃ glasses, DC elec. cond. and thermo-elec. power 0-96865
 As₂S₃ glassy, photoconductivity dependences applied elec. field 0-107857
 As₂S₃ glassy, photoinduced defects, EPR and absorpt. spectra 0-59398
 As₂S₃ glassy, photosensitive etching in nonoxidising etchants 0-78813
 a-As₂S₃, time-resolved photoluminescence study 0-89057
 As₂S₃, two photon light absorpt. dispersion, induced linear light absorpt. (Russian) 0-66231
 As₂S₃ vapour-deposited films, valence states, thermal and photo-induced changes UPS study 0-93459
 As₂S₃, vitreous, thermal capacity, 300 to 600K 0-103492
 As₂S₃-Ag glassy films, optical transmission spectra, photodoping effect 0-66317
 As₂S₃-Ge₃₀As₁₇Te₃₀S₂₃, two-layer antirefl. coating, error considerations in design 0-74477
 As₂S₄, amorphous, struct., vibr. and electronic spectra 0-64908
 As₂S₄ vapour-deposited films, valence states, thermal and photo-induced changes UPS study 0-93459
 As₂S_{100-x} amorphous films, optical props. and photoinduced changes 0-60700
 As₂S_{100-x} glasses, Raman spectrum and structure 0-60593
 As₂S_{100-x} localised states density near valence band edge (Russian) 0-103638
 (As_{0.4}S_{0.6})_{100-x}Cu_x, glassy, struct. and elec. cond. study 0-59399
 As₂S₃-Se_x, amorphous, picosecond relax. of optically induced absorption 0-97302
 AsSbO₄, X-ray cryst. struct. determ. 0-107127
 As_{0.5}Sb_{0.5}Si cryst., ferroelec., soft mode Raman and IR spectroscopy 0-76016
 As₂Sb_{1-x}SI mixed crystals, phonon coupling, ferroelectric phase transition, Raman study 0-108165
 As₂Sb₂Se₆ glassy semiconductors, electronic props. 0-103712
 As₂Se₃, amorphous, ionicity dependence of defect reactions and negative-U states in glasses 0-88511
 As₂Se₃, amorphous, luminescence 0-80862
 As₂Se₃, amorphous, transient electrical transport, general and unified treatment 0-59977
 As₂Se₃, amorphous radiative interband recombination 0-66286
 As₂Se₃, cryst., electroabsorption on indirect gap 0-80812
 As₂Se₃ glass, mol. struct. model 0-100179
 As₂Se₃ glassy, photoconductivity dependences applied elec. field 0-107857

arsenic compounds continued

- As₂Se₃, glassy defect electron states, tight binding calc. 0-96818
 As₂Se₃ glassy films, current-voltage characts., temp. depend., SCL current 0-92902
 As₂Se₃, modulated photocurrent, analysed for trap-limited case (Japanese) 0-60030
 As₂Se₃, monoclinic, chem. bonds rel. to electronic and vibr. states 0-64951
 As₂Se₃, single crystals, fine struct. of direct gap from electrorefl. spectra 0-93280
 As₂Se₃, thermally reversible photodarkening effects obs. 0-103970
 As₂Se₃, vitreous, thermal capacity, 300 to 600K 0-103492
 As₂Se₃-Ag amorphous, freq. depend. cond. 0-88565
 As₂Se₃-Pt, vitreous, effect of impurities on elec. props. 0-103699
 As₂Se₃-Ag photosensitive semiconductor-metal systems, effect of As₂S₃ barrier layer (Russian) 0-62777
 As₂Se₃-Ge glassy thin films, flash photoresponse 0-107863
 As₂Se₃-GeSe₂ glass, bulk and impurity IR absorpt. 0-71455
 As₂₀Se₈₀ and As₂₀Se₈₀ semicond. glasses, densified, photoluminesc., inelastic deform. effect 0-66293
 As₂Se_{100-3x} localised states density near valence band edge (Russian) 0-103638
 As₂Se₃-Ag, glassy semicond. film, prep. by photodiffusion of Ag, negative photocond. 0-92934
 As₂SeTe₂, between Al and Sb electrodes, rectifying effects 0-75654
 As₂Se_{1.5}Te_{0.5}, thermally reversible photodarkening effects obs. 0-103970
 As₂Te₃ and As₂Te₂Ge, amorphous, AC cond. at low temps. 0-80269
 As₂Te₃, vitreous, thermal capacity, 300 to 600K 0-103492
 Ge₃As₂S₁₅Te₂₅, chalcogenide thin films, coupled carrier theory test, high field conditions 0-100466
 Ge₃₀As₇Te₃₀Se₃₅As₂S₃, two-layer antirefl. coating, error considerations in design 0-74477
 GeSe₂-As₂Se₃-Sb₂Se₃, elec. cond. over wide range of temp. 0-88564
 Ge₂Si₆As₂Te₃Ga₁₀, chalcogenide thin films, coupled carrier theory test, high field conditions 0-100466
 Na₂O-B₂O₃-SiO₂-As₂O₃(As₂O₃) glasses, DC and AC resist., bipolaronic hopping cond. 0-88558
 Se-As, photoelectric behaviour, in glass transition region 0-60045
 Se₁Te₄₃As₂₉Ge₁₀ semiconductor amorphous films, field effect, trapping 0-84472
 Ti₃AsSe₃, refractive index, thermal expansion temp. depend. 0-97223
 V₂O₅-As₂O₃-RO, R=Ba, Ca, Pb, semicond. glass, electronic props. 0-88557

art

- cinematography film production, use of different computer techniques 0-77887

articulation (speech) *see speech***artificial hearts *see artificial organs*****artificial intelligence**

- see also adaptive systems; biocybernetics; brain models; heuristic programming; learning systems; neural nets; self-adjusting systems*
 heat transfer, problem solver, system design outline 0-99916
 microscopes, recent and near-future advances 0-98166
 NMR spectra, computer-aided interpretation using artificial intelligence system 0-62701

artificial kidneys *see artificial organs***artificial limbs**

- adaptive control system for a complete hand/arm prosthesis 0-109059
 connector, flexible, reduced skin stresses achievement 0-76863
 control signals and transducers for the control of upper extremities in plegic patients, computer controlled experiment (Slovak) 0-109061
 knee-ankle mechanism, polycentric, for above-knee prostheses 0-94413
 phantom hand sensations elicited by afferent nerve stimulation, discrimination in below-elbow amputees 0-97892

artificial organs*see also prosthetics*

- blood cell-vessel wall interaction, fluid dynamic aspects 0-97998
 electronic eye for blind people, implementation through the optical nerve (Croatian) 0-109060
 extracorporeal oxygenation, blood trauma, conf., Stolberg, Germany (Nov. 1978) 0-94922
 heart, microcomputer based automatic controls 0-67289
 heart, transfer function governing ventricular ejection in assisted circulation 0-104817
 heart blood heat exchangers with radioisotopic power supplies 0-85532
 hollow fibre dialyser, mass transfer 0-66873
 implantable middle ear, development prospects (Japanese) 0-81775
 kidney, automatic extrasomatic dialysis system 0-98177
 membranes, DECHEMA symposium, Tutzing, Germany, (Mar. 1978) 0-62373
 platelet stimulation under influence of high shear stresses in tube flow 0-97996
 red blood cell mechanical disruption 0-98001

artificial satellites

- analytical satellite theory in extended phase space 0-67524
 anomalous period, solar radiation press. effects 0-77255
 astronomical observatory, Ariel 5 X-ray astronomy, Cos-B γ -ray astronomy satellites 0-90317
 Atmosphere Explorer B, remote sensing of middle atmospheric aerosol 0-109269
 Atmosphere Explorer C, simultaneous obs. of field-aligned currents and plasma drift vels. 0-72681
 atmosphere temperature sounding data, impact on weather forecasts 0-77028
 ATS-6, ionospheric scintillations assoc. with features of equatorial ionosphere 0-77191
 attitude control, inertially fixed pitch stabilisation by solar radiation press. 0-101523
 Bhaskara, flux-gate magnetometer flight performance 0-72746
 Castor satellite, Cactus accelerometer flight results synthesis for accels. below 10⁻³g 0-77251
 charge neutralisation, electron emitter neutralisation (Japanese) 0-94673
 clock synchronization using Symphonie satellite 0-68184
 conference on satellite Doppler tracking and geodetic appl., London, England (Oct. 1978) 0-77264
 COS-B, instrument description (Danish) 0-82544
 Cosmic Background Explorer, instrumentation 0-61988
 critical inclination problem with small eccentricity 0-67525

artificial satellites continued

- despinning with continuous axial thrust, Geos-1 dynamic experiment 0-61982
- Dive and Ascent Satellite, programme for lower ionosphere research 0-77252
- DMSP visible imagery, causes of anomalous grey shades 0-77111
- Doppler tracking and polar motion determ., MEDOC 0-101445
- Earth Radiation Budget Satellite, climate appls. 0-109283
- Earth scene dynamics, satellite-borne mosaic sensor performance 0-90321 at Earth-Moon libration points, search for natural or artificial objects 0-98647
- Earth-resources satellite using optical preprocessor 0-67430
- electric charge build up in sunlight, model of photosheath 0-90316
- electrostatic charge buildup on ATS 6 and 1976-059A 0-72744
- ELF antenna, ferrite rod, for Magion satellite for 0.1 to 16 kHz freq. range (Czech) 0-85775
- energy storage, Ni-H₂ battery appl. 0-81430
- ephemerides representations, Chebyshev approximation, satellite navigation 0-61993
- European Space Agency programmes, developmental or operational status 0-72742
- EXOS-A, fifth scientific satellite 'KYOKKO' (Japanese) 0-101525
- EXOS-B, sixth scientific satellite JIKIKEN (Japanese) 0-101526
- EXOS-B (JIKIKEN), obs. and comparative study of VLF emissions and high energy electron flux (Japanese) 0-94652
- French satellites, research applications (French) 0-82170
- future applications, reliability and cost considerations (Italian) 0-109334
- geodetic networks connection problems, stiffening problem, error anal. 0-81799
- geodetic satellites, basic mechanical principles of gravimeters and gravity gradiometers (German) 0-101461
- geodetic satellites, longitude-averaged meridional profile of Earth pear-shaped section 0-94450
- geodynamic research techniques using satellites 0-109282
- Geos 3, altimeter data on coincident orbits rel. to ocean transients 0-72535
- GEOS-3 proposed mission to far geomagnetic tail 0-82163
- geostationary, use in determ. of geocentre position var. 0-82083
- geostationary meteorological, role played in Global Weather Expt. 0-77256
- geostationary satellite, orbit determ. by single ground station tracking 0-109329
- geostationary satellite investigation of gravitational Doppler effect 0-109351
- geostationary satellites, appl. to incident solar radiation of Earth surface estimation 0-82006
- geostationary satellites, severe scintillation of VHF and GHz waves during mag. storm 0-109302
- gyrostatic satellite in Kepler orbit, rot. motions 0-86080
- HEAO-B, high-energy astrophysical satellite lab., X-ray observ. facilities (Dutch) 0-61986
- HIPPARCOS, astronomic obs. from space (Polish) 0-67519
- HIPPARCOS, global astrometry by space techniques 0-109369
- Hipparcos, meas. of stellar distances (French) 0-94688
- Hipparcos satellite, proposed space-astrometry mission 0-82164
- Infrared Astronomical Satellite, features and performance 0-61989
- Interkosmos program and Magion satellite project 0-98535
- International Sun-Earth Explorer (ISEE) mission, review 0-90320
- International Ultraviolet Explorer (IUE) second European conference (Tubingen, Germany, 1980 March 26 to 28) 0-82584
- ion beam injection into magnetosphere, from solar power satellite engine 0-82149
- ionosphere satellite wake, assessment ion current distrib. 0-101527
- ionosphere-satellite interaction, ion density in wake of O⁺ plasma 0-82136
- IR detector cooling by multimission solid cryogen cooler 0-86423
- IUE preliminary results, workshop, Udine, Italy (1978 October 12) (Italian) 0-86033
- Jikiken, obs. of mini-substorm and long-period Pi 2 event, (1978 December 11) (Japanese) 0-94653
- JIKIKEN (EXOS-B), plasmopause and propag. waves meas. using stimulated plasma wave results (Japanese) 0-94650
- JIKIKEN (EXOS-B), stimulated plasma wave expts. in magnetosphere (Japanese) 0-94649
- JIKIKEN (EXOS-B), terrestrial and planetary radio and plasma waves obs. (Japanese) 0-94675
- JIKIKEN (EXOS-B), terrestrial kilometric radiation obs. (Japanese) 0-94648
- JIKIKEN (EXOS-B), VLF Doppler shift meas. (Japanese) 0-94651
- JIKIKEN (EXOS-B) scientific satellite, magnetosphere obs. (Japanese) 0-94674
- JIKIKEN satellite, electron beam emission for magnetosphere beam-plasma interaction expt. (Japanese) 0-94655
- JIKIKEN scientific satellite, magnetosphere charged particle fluxes (Japanese) 0-94654
- non-Keplerian orbit, Keplerian representation 0-90324
- Lageos, semimajor axis secular decrease, atmospheric drag 0-94628
- LAGEOS orbit, long-term evolution 0-94676
- Landsat D wideband communications system 0-101529
- LANDSAT data anal. for geological structure research (Italian) 0-109281
- LANDSAT geoexploration, digital mosaicking and lineament enhancement (Japanese) 0-82169
- LANDSAT images, processing method for geological faults and other linear features detect. 0-77177
- Landsat-D systems, design and implementation progress 0-77259
- large structures, construction in space 0-98533
- laser ranging system, Space Borne Event Timer, meas. of Earth movement along San Andreas fault 0-61984
- LASSO experiment on Spiro-2 spacecraft laser synchronisation from stationary orbit 0-82211
- Magion, design and construction 0-98536
- Magion satellite, ELF ferrite rod antenna for 0.1 to 16 kHz freq. range (Czech) 0-85775
- magnetosphere contamination at geosynchronous orbit 0-72701
- magnetosphere research, Ariel 3, 4, Geos, ISEE satellites 0-90317
- material charging in space environment 0-109327
- Meteosat, ocean surface temperature measurements, derivation from Meteosat image data 0-76985
- METEOSAT 1 weather satellite pictures, amateur facsimile reception (German) 0-81982

artificial satellites continued

- METEOSAT project, interactive image system 0-109330
 - METEOSAT project overview (Italian) 0-109331
 - Meteosat remote sensing equipment for atm. general circulation obs. 0-94595
 - Meteosat-1, research uses of early data, review 0-77257
 - Meteosat, wind deviation from cloud motion 0-109244
 - Miranda (X4) satellite, Earth radiance obs., IR expt. design and performance 0-72745
 - MS-T3, TANSEI-3 test satellite (Japanese) 0-101524
 - multispectral scanner, high resolution, for Earth obs., optical design 0-82174
 - Nimbus 6, SCAMS liq. water data over NE.Pacific Ocean, rel. to United States west coast rainfall 0-82005
 - NIMBUS-6, microwave remote sensing over W.Australia 0-98485
 - oceanography remote satellite, USA proposal for 1986 launch 0-105088
 - Ogo 4, VLF signals reception, numerical study using waveguide concepts 0-90282
 - orbit determination, Green's functions appl. 0-61992
 - orbits, short periodic drag perturbations 0-67522
 - orbits, third and fourth-order perturbations rel. to flattening of planet 0-67529
 - orbits with resonance lunisolar perturbations, dependent on inclination 0-90326
 - OTS payload performance, in-orbit RF meas. 0-82167
 - P78-1 satellite, high resolution γ -ray spect. 0-58019
 - Phase 3A satellite, Ariane three-stage launcher, AMSAT Oscar 9 designation following ejection 0-98534
 - photographic tracking, astronomical method (Chinese) 0-77254
 - polar satellite motion and short-wavelength gravity vars. 0-98216
 - remote sensing and ranging systems from space, conf., Rome, Italy (March 1980) 0-105432
 - remote sensing satellites, error in atmospheric temp. profiles due to aerosol particles effects 0-98449
 - reorientation of satellite-gyrostat, optimal attitude control 0-61980
 - satellite solar cell power plant, operating experience 0-94055
 - Seasat, altimeter sensor file algorithms 0-94680
 - Seasat, Gulf of Alaska expt., comparison data set winds 0-94570
 - Seasat, microwave instrum., history 0-94678
 - Seasat, performance evaluation 0-94677
 - Seasat, radar altimeter, initial performance assessment 0-94679
 - SEASAT, radar altimeter resolution capability estimates 0-72645
 - Seasat, scanning multichannel microwave radiometer, antenna pattern corrections 0-94683
 - Seasat, scanning multichannel microwave radiometer, calibration algorithm development 0-94682
 - Seasat, scanning multichannel microwave radiometer, description and performance 0-94681
 - Seasat, scatterometer evaluation 0-94684
 - Seasat, scatterometer scattering coeff. algorithm 0-94685
 - Seasat, synthetic aperture radar system 0-94686
 - Seasat, visible and IR radiometer 0-94687
 - second order perturbation soln. (Chinese) 0-77270
 - Shuttle Orbiter re-entry, remote IR imagery and tracking 0-82171
 - sky survey project EXUV 10-1000 Å waveband, proposed mission 0-82165
 - Skylab 1 rocket, 1973-27B, orbit determ. and anal., geopotential resonance 0-67515
 - Skylab conical multispectral scanner IR data statistics 0-90223
 - SMS, geostationary satellite, soil thermal inertia and humidity cartography over Africa 0-76980
 - Solar Maximum Mission Satellite, for Solar Maximum Year project 0-90404
 - Solar Mesosphere Explorer mission description (1981-2), O₃ and related chemistry 0-105096
 - solar occultation sounding of middle atm. 0-105079
 - solar power satellite, theoretical anal. of nonlinear interaction between strong microwaves and ionosphere (Japanese) 0-94634
 - solar power satellites, effect of transmissions on radio-astronomical research 0-61291
 - solar power satellites microwave power transmission system rectennas, Yagi-Uda receiving elements design, characteristics and economics 0-66938
 - solar power satellites technical considerations 0-72014
 - solar power station, multi-gigawatt, in space, progress review in field since 1979 (German) 0-81424
 - space station, scheme for automatic rendezvous with unmanned (or manned vehicle) 0-77249
 - Space Telescope, scientific instruments 0-61987
 - space-manufactured satellite power systems, costs anal. using lunar materials 0-97767
 - spacecraft heat rejection improvements using thermoelectric devices 0-108810
 - spin-stabilised spacecraft, optimal aerodynamic attitude control 0-77250
 - step-stare spaceborne optical system smear compensation by focal plane manipulation 0-82172
 - Thematic Mapper of Landsat-D, optical component design 0-77260
 - TIROS satellite program of meteorological research 0-109328
 - TIROS-N, meteorological satellite, early operational temp. soundings evaluation 0-77133
 - TIROS-N, polar-orbiting meteorological satellite, operational vertical sounder 0-77132
 - TIROS-N microwave sounder unit for global temp. distribution meas. 0-90265
 - weather forecasting systems, local short-period forecasts 0-94558
- asbestos**
- aerosol spectrometer using two-pulse Fraunhofer holography, fibrous particle motion anal. 0-58476
 - fibre counting by automatic image analysis 0-73538
 - fibre reinforced cement, strength and fracture props. 0-108533
 - fibres concentration meas., in air and liquid, analytical methods review 0-72120
 - insulation, evaluation by polarised light microscopy 0-95134
- asdic** see sonar
- aspherical lenses**
- see also aberrations
 - cylindrical lens surface generation, grinding and polishing machinery design 0-79023
 - cylindrical mirror and lens optical figure characterisation with conventional interferometer 0-78944

aspherical lenses continued

- EKTRAMAX camera lens design and performance 0-77894
 Fresnel lens optical design and utilisation, advantages and limitations 0-78936
 hyperboloid lens manufacturing technique 0-96039
 multiplexer/demultiplexer, low-loss, using interf. filters and rod lenses 0-58728
 night vision goggles, military low-cost, design and development 0-78990
 plastic lenses, aspherical-surface, for large screen TV, optical design and evaluation 0-78937
 polishing technique with equal polishing rate distrib. 0-58818
 refracting objectives for 8 to 13 μm 0-86421
 rod lens analysis and application to optical fibre communications 0-87549
 testing, in-line and carrier freq. holograms, comparison 0-87349
 testing in reflected light using blazed synthetic holograms 0-91881
 LiNbO_3 , diamond-turned aspheric geodesic waveguide lenses 0-58804

assembling

- fusion reactor, ASDEX, assembly and commissioning, review 0-102334
 fusion reactor, PDX, assembly, description 0-99308
 fusion reactor, TFTR, assembly 0-102335
 fusion reactor, TFTR, gas injection assembly 0-99342
 IR scanning system modular design, assembly and alignment 0-78989

assembly lines *see assembling***assembly methods** *see assembling***association**

see also association of liquids; associative ionisation

- acetaldehyde, carbonyl addition, model transition states, vibr. anal. 0-71898
 anthracene, ultrathin films on fused quartz and sapphire 0-59812
 bis(9-anthryloxy)polyoxaalkanes, intramolecular excimer form. and photodimerisation, kinetic anal., rate constants determ. 0-66800
 atomic radiative binding in slow collisions into molecules in a laser field (*Russian*) 0-93753
 2-benzyl-5-benzylidenecyclopentanone, and substituted form, topochem. single-cryst.-to-single-cryst. photodimerisation 0-66819
 biopolymers, electro-optical changes, chem. and rotational contribs. 0-85352
 bisphenol A-phthalic anhydride epoxy resin, diglycidyl ether, Rayleigh scatt., Brillouin and IR spectra 0-66211
 t-butyl alcohol, mixtures, assoc., thermodynamic study using 2-constant model 0-66789
 carboxylic acid systems, H(D) complexes and dimers, ν_{CO} IR band intensities 0-63715
 cartilage proteoglycan, association with hyaluronic acid, elec. birefringence obs. 0-85332
 chloroform-d, intermol. assoc. with solvent molcs., Raman spectra 0-63636
 cluster ions, formation and reactions, SIFT study, review 0-58435
 clusters, small, formation, struct. and props. 0-58437
 collagen, polarisation, contribution of permanent and induced dipole moments, elec. birefringence 0-85351
 colloidal photochromic dyes, quasi-crystals produced in applied electric field 0-85225
 decanoic acid, associated vapours, homogeneous nucleation 0-96638
 dense interstellar clouds, radiative association reactions 0-82441
 diffusion controlled reaction, passage time approach 0-71903
 ferrofluids, agglomeration, review 0-61162
 fluorescein dye, halogen substituted, in dimethyl sulphoxide, spectral evidence for anion-counterion association 0-71909
 fluoroanthene in micelles soln., fluoresc., halide ion induced quenching and enhancement 0-95672
 gas mixture, self sustained volume photoionisation discharge existence conditions 0-79610
 graphitised viscose fibre, fluorination, change in struct. 0-88039
 heptanoic acid, associated vapours, homogeneous nucleation 0-96638
 II-VI semiconductors, thin epitaxial layer, direct synthesis (*German*) 0-104070
 inert gas Van der Waals dimers, electron impact ionis. 0-58400
 ion + molecule association density of quantum states and temp. depend. of rate coeff. 0-101015
 ion-molecule association rate calc. 0-81282
 lithium oligopentadienyl and complexes, IR spectra (*Russian*) 0-71424
 membrane surfaces, antibody association kinetics with spin-label haptens 0-66787
 methyl-(d_3) ions, association reactions, isotopic exchanges, SIFT study, review 0-58435
 methyl ion + H_2O (He) ternary association reaction in energy range 0.04-0.1 eV 0-71896
 myoglobins, Fe-, Co-substituted, O_2 binding, comparisons, thermodynamic investig. 0-67030
 myristic acid, associated vapours, homogeneous nucleation 0-96638
 nitrosofluorene-lipid adducts, mutagenicity, ESR spectra investig. 0-91583
 poly- γ -benzyl-L-glutamate, synthetic polypeptide, nonlinear dielectric effect in nonpolar medium 0-84682
 rhodamine 6G, molecules in solution, photoluminescence study, fluorescence decay time 0-80832
 tetraphenylsilane, crystn. from chem. transport reaction 0-104439
 vinylidene + H_2 , addition reaction, MINDO/3 study 0-108705
 zero range Fermi method, appl. to assoc. detachment processes 0-63798
 $\text{Ag}_3\text{S} + \text{Ln}_2\text{S}_3$, powdered mixtures, reaction rate, production of ionic semiconductors 0-93741
 Al oxides and hydroxides, electro-erosional prep. (*Russian*) 0-81297
 Ar^+ , conversion to mol. ions, three body association coeffs. determ. using drift-tube mass spectrometer 0-108699
 $2\text{Ar} + \text{Ar}^+(\text{Kr}^+)$, three body reaction, rate coeffs., temp. depend., 100 to 300K 0-108703
 $\text{Ar} + \text{Xe}^+$, XeAr^+ form., dissoc. energy, reaction equilib. and rate consts. 0-61071
 C^+ , association reactions, isotopic exchange, SIFT study, review 0-58435
 $\text{CaCeAl}_3\text{O}_7$, mellitic struct., prep. and props. 0-93524
 Cs-H₂ vapour, resonant character of laser induced formation of particles 0-89481
 $\text{Cu}_2\text{S} + \text{Ln}_2\text{S}_3$, powdered mixtures, reaction rate, production of ionic semiconductors 0-93741
 $\text{H} + \text{Cl}^- \rightarrow \text{HCl} + \text{e}$, associative reaction, product vibr. state distrib. 0-66794
 $\text{H} + \text{OH} \rightarrow \text{H}_2 + \text{hv}$, radiative association reaction for mol. synthesis in interstellar clouds 0-90509

association continued

- $\text{HO}_2 + \text{HO}_2$, gas phase reaction mechanism, FT IR spectrosc. obs. 0-85163
 He^+ , conversion to mol. ions, three body association coeffs. determ. using drift-tube mass spectrometer 0-108699
 He^+ , electron scatt., reson. state assoc., incomplete spectrum of Hamiltonian matrix 0-99568
 $2\text{He} + \text{He}^+(\text{Ne}^+)$, three body reaction, rate coeffs., temp. depend., 100 to 300K 0-108703
 ^4He , threshold condition for forming atomic trimer 0-63741
 LaB_6 -Cu, form. by wetting of LaB_6 with Cu 0-100813
 LaN_3 , form. conditions 0-101019
 Ne^+ , conversion to mol. ions, three body association coeffs. determ. using drift-tube mass spectrometer 0-108699
 SmN , form. conditions 0-101019
 Sr_2 dimer, photoassoc., photoluminesc., collisional dissoc. 0-58303
 TaC and Ta₂C, self-propag. high-temp. synthesis 0-60815
 SnSb, orientated crystn. conditions during reaction diffusion (*Russian*) 0-70558
 ZrB₂-Nb, reactions between components 0-100812
association factor (liquids) *see association of liquids*
association of gases *see association*
association of liquids
see also colloids
 acetone-toluene-tetrachloromethane, mol. interaction and thermodynamic props. 0-71935
 acetonitrile-toluene-benzene, mol. interaction and thermodynamic props. 0-71935
 alcohols in organic solvents, H₂O absorption 0-66788
 t-butyl alcohol, self-assoc., linear and nonlinear dielec. effects obs. 0-60484
 3-butyne-1-ol, vibr. spectra, assignments, rot. isomerism 0-58257
 cholinesterase-acetylcholine soln., anion-cation site interactions, solvent effects on aggregate stability 0-61070
 glycerol, highly viscous state, static and dynamic Kerr effect obs. 0-60545
 2(4)-monooxypyrimidines, gaseous, matrix, soln., tautomeric equilib., IR and UV absorpt. spectra 0-58256
 PMMA, syndiotactic, solns. in toluene, NMR obs. of struct. and dynamics of associates 0-75867
 pyridine N-oxide, in benzene, dipolar assoc. investig. 0-107035
 toluene, in benzene soln., mol. motion, correl. functions 0-96431
 vinyl polymers, precip. from solns., temp. determ. (*German*) 0-85208
 In-As, melt, mutual diffusion of components 0-88345
associative ionisation
 associative ionisation, merging beams experiment 0-63789
 collisional ionisation, Penning and associative ionisation produced by laser field 0-63802
 electronic and at. collisions, conference, Kyoto, Japan (Aug.-Sept. 1979) 0-62394
 excited atoms, merging-beams experiments 0-63789
 Ar^+ , conversion to mol. ions, three body association coeffs. determ. using drift-tube mass spectrometer 0-108699
 $\text{Ar}^* + \text{H}$, assoc. ionis., rovibronic struct. in electron energy spectrum 0-106380
 He^+ , conversion to mol. ions, three body association coeffs. determ. using drift-tube mass spectrometer 0-108699
 He , high press. afterglows, reviews 0-64823
 Na + Na, crossed-beam collision, laser-induced Penning and assoc. ionisation, struct. obs. 0-83476
 Ne^+ , conversion to mol. ions, three body association coeffs. determ. using drift-tube mass spectrometer 0-108699
 $\text{Ne}^* + \text{Ar}$, associative ionisation studied by merging-beams technique 0-91646
 $\text{Ne}^* + \text{H}$, assoc. ionis., rovibronic struct. in electron energy spectrum 0-106380
astatine
see also nuclei with
 No entries
astatine compounds
 No entries
asteroids
 1932 HA (Apollo), ephemerides for 1930, 1941, 1964 and (1966) 0-105193
 1936 CA (Adonis), ephemerides for 1943 and (1984) 0-105193
 1979 YA, nonexistence and cancellation of designation 0-77320
 1980 LB, improved orbital elements rel to 2:1 Jupiter libration hypothesis 0-94744
 1980 LB, precise posns., orbital elements and ephemeris (1980 June-July) 0-82259
 1980 PA, fast-moving asteroidal object, discovery and semi-accurate positions (1980 August 6 to 7) 0-94745
 1980 PA, positions, improved orbital elements and ephemeris 0-98597
 1980 PA, posns., elements and ephemeris (1980 August) 0-94746
 1980 PA, precise posns., improved elements and ephemeris (1980 Sept.-Oct.) 0-101548
 1980 QA, fast-moving asteroidal object in Capricornus, discovery and positions (1980 August 16 to 18) 0-98598
 2101 Adonis, orbital problem soln. 0-72842
 1943 Anteros, spacecraft rendezvous potential target, request for photometry and spectrophotometry 0-90356
 1862 Apollo, close approach and ephemeris (1980 Nov.-Dec.) 0-109389
 astrometric 1978 positions from ESO GPO obs. 0-72841
 astrometry (1975-1978), Uppsala southern station obs. 0-85883
 astrometry for 74 objects in 1977, Swedish obs. 0-62065
 astrometry in 1978 April, ESO obs. 0-85882
 belt existence beyond Neptune, cosmogony (*Russian*) 0-82237
 binary systems, detect. and form., occultation and light curve anal. 0-77322
 Ceres, diameter, interferometric meas. (*Russian*) 0-67634
 close encounters with Jupiter, mass distrib. throughout Solar System implications 0-77329
 commensurabilities in solar system 0-109418
 conference on celestial mechanics and positional astronomy, Washington, DC, USA (Nov.-Dec. 1978) 0-90605
 corrections to FK4 zero points from minor planet obs. (*Russian*) 0-82228
 65 Cybele, occultation of AGK + 19°0599, 1979 October 18, obs. using photoelectric photometer (*Chinese*) 0-105172
 349 Dembowska, IR spectral obs., candidate for meteorite parent bodies 0-98595

asteroids continued

- development from comets, Monte Carlo orbit evolution simulations 0-82261
- 78 Diana, occultation of SAO 75392, 1980 September 4, predicted central path revision 0-101547
- differentiation, petrography and chemistry of igneous lithic clasts from mesosiderites and howardites 0-72890
- dynamics and evolution, review 0-82260
- ephemerides, orbits computation using Chebyshev polynomials (*French*) 0-61997
- 45 Eugenia, rot. period and photoelec. light curve determ. 0-72846
- family detection by new criterion, orbital data 0-82256
- 624 Hektor, light curve indicating elongated shape 0-98600
- 532 Herculina, satellite detect from occultation obs. 0-67629
- hyper-periods and Kirkwood Gaps 0-105153
- hypothetical observations giving equinox and equator determ. 0-94742
- impacts at high velocities, catastrophic destruction mechanism 0-82257
- IR reflectance spectra, obs. rel. to search for water of hydration 0-77318
- 216 Kleopatra, photometry rel. to comp., diameter, elongated shape and possible stellar occultations 0-94743
- 68 Leto, rot. period and photoelec. lightcurves determ. 0-98594
- 18 Melpomene, rot. period from photoelec. obs. 0-82258
- meteorite parent body, impact melting rel. to origin of Fe meteorites of groups IAB and IIICD 0-109404
- Minor Planet Center, history and future 0-94712
- Minor Planet Circular 5333-5390, precise posns., elements, ephemerides, new nos. and names 0-77325
- Minor Planet Circulars 5189-5248, precise posns., elements, ephemerides, new nos. and names 0-67631
- Minor Planet Circulars 5249-5286, precise posns., elements, ephemerides, new nos. and names 0-67632
- Minor Planet Circulars 5287-5332 precise posns; elements, ephemerides, new nos. and names 0-67633
- Minor Planet Circulars 5391-5422, precise posns., elements, ephemerides, new nos. and names 0-85884
- Minor Planet Circulars 5423-5454, precise posns., elements, ephemerides, new nos. and names 0-98599
- minor planets, 1978, April, astrometric positions determ., ESO GPO obs. 0-77319
- 51 Nemausa, astrometric posns. for coord. system error reduction 0-72849
- opposition effect, similarity among asteroids 0-62064
- orbit determ. for some unnumbered Purple Mountain Observatory minor planets 0-72848
- orbit determination using Chebyshev's approx. (*French*) 0-94720
- orbital elements from Munich meridian obs. (1941-61) (*German*) 0-77306
- orbital perturbations, regular proximities concept and approximate perturbation methods 0-72843
- origin, initial rotation periods and relative formation times (*Chinese*) 0-105182
- peculiar direct motions, loops made by objects in strange orbits 0-109346
- photographic photometry during 1977 and 1978, light curves and rot. periods 0-72844
- position determination in April 1979, data reduction (*French*) 0-72845
- positions in 1978, visible obs. 0-67630
- positions in August 1977 from Observatorio Nacional, Rio de Janeiro (*French*) 0-94740
- positions of minor planets from Torino Observatory (1977-1979) 0-94739
- 16 Psyche, opposition effect and surface structure (*Russian*) 0-67635
- radii, absolute mags., and discovery distribts. 0-109390
- relative observations, use in accuracy improvement of fundamental system of star position and motion 0-94692
- satellite detect. from occultation obs. 0-67629
- satellites, occulting of stars 0-94741
- shape after collisions with meteoroids, theoretical anal. 0-77321
- solar wind sputtering rate 0-85835
- 563 Suleika, rot. period and photoelec. lightcurves determ. 0-98594
- surface studies from Earthbound obs., technique 0-77324
- 115 Thyra, astrometry and orbit improvement (*German*) 0-85881
- Trojan group, discovery of new members, orbital elements and ephemerides 0-72847
- Trojans with large orbital inclination, dynamics 0-77323
- truncation of asteroid belt, theory of tidal torques on infrequently colliding particle discs in binary systems 0-98596
- Vesta, diameter, interferometric meas. (*Russian*) 0-67634
- Vesta, IR spectral obs., candidate for meteorite parent bodies 0-98595

astigmatism see aberrations

astrobiology see extraterrestrial life

astrometry

- 1309-216, probable BL Lacertae object with absorpt. red shift 1.49, precise position 0-67856
- 1978 P 1, speckle obs. rel. to orbital radius and system mass and density 0-109394
- 1980 LB, precise posns., orbital elements and ephemeris (1980 June-July) 0-82259
- 1980 PA, positions, 1980 August 8 to 17, improved orbital elements and ephemeris 0-98597
- 1980 PA, precise posns., improved elements and ephemeris (1980 Sept.-Oct.) 0-101548
- 1980 S 10, precise positions, 1980 March 15 to 16, and relation to Dione 0-85893
- 1980 S 1, 3, 6, 25, new Saturnian satellites, positional obs., (1980 March 9 to 14) 0-94749
- asteroid position determination in April 1979, data reduction (*French*) 0-72845
- asteroid positions in 1978, visible obs. 0-67630
- asteroids, from ESO GPO obs. 0-72841
- asteroids, Munich meridian obs. (1941-61), orbital elements determ. (*German*) 0-77306
- asteroids, orbit determ. for some unnumbered Purple Mountain Observatory objects 0-72848
- asteroids, precise posns. for 74 objects in 1977, Swedish obs. 0-62065
- asteroids, Trojan group, discovery of new members, orbital elements and ephemerides 0-72847
- asteroids (1975-1978), Uppsala southern station obs. 0-85883
- asteroids in 1978 April, ESO obs. 0-85882
- binary stars, obs. by speckle interferometry 0-90477
- binary systems, speckle interferometric obs. with Haute-Provence 1.93 m telescope 0-90475

astrometry continued

- bright nearby stars, astrometric anal. from Sproul 61 cm refractor plates 0-61991
- Brorfelde transit circle, diameter corrections 0-105164
- CC 1299 (BD+27°4120), unresolved astrometric binary, orbital anal., mass and parallax 0-109464
- Cepheids, ultrashort period, classification from photometric and astrometric data 0-62135
- charge injection device as stellar tracking sensor 0-85861
- Charon (1978 P 1), posns. in 1980 April rel. to probable occultation 0-67651
- Charon (1978 P 1), satellite of Pluto, positions and dynamical parameters 0-62069
- Comet Bowell (1980b), precise positions, elements and ephemeris (1980 March-July) 0-62075
- Comet Cernis-Petruska (1980k), antitail, precise posns., parabolic elements and ephemeris 0-105206
- Comet Cernis-Petruska (1980k), positions, 1980 August 2 to 16, orbital elements and ephemeris 0-98614
- Comet Cernis-Petruska (1980k), precise position, (1980 August 17) 0-101556
- Comet Kohler (1977m), precise positions, (1977 October 5 to 19) 0-105203
- Comet Meier (1978 XXI), position from 1979 April 21 to 30, meas. and reduction (*French*) 0-72884
- Comet Meier (1978f), precise positions meas. at ESO, La Silla, in (April 1979) 0-105204
- Comet Russell (1980l), precise positions, 1980 September 6 to 8, and ephemeris 0-101559
- Comet Torres (1980e), precise posns., elements and ephemeris (1980 June-July) 0-85900
- conference on celestial mechanics and positional astronomy, Washington, DC, USA (Nov.-Dec. 1978) 0-90605
- 78 Diana, astrometric obs. rel. to central path of occultation of SAO 75392, (1980 September 4) 0-101547
- double stars, position angles and separation, Venezuelan obs. (*French*) 0-77450
- double stars, separation and position angle obs. 0-98691
- extra-solar planetary systems, detection by Space Telescope 0-109356
- extrasolar planetary systems, dynamical instability and detection 0-82429
- fitting procedures for stellar positions on Schmidt photographs 0-72783
- FK4, corrections to zero points from minor planet obs. (*Russian*) 0-82228
- FK5, equinox and equator of new fundamental reference coord. system 0-109341
- fundamental system of star position and motion, accuracy improvement using asteroid obs. 0-94692
- Greenwich Obs. Time and Latitude Service, Time Report (January to March 1979) 0-72749
- Greenwich Obs. Time and Latitude Service Time Report (April-June 1979) 0-72750
- HIPPARCOS, global astrometry by space techniques 0-109369
- Hipparcos, meas. of stellar distances (*French*) 0-94688
- Hipparcos satellite, proposed space-astrometry mission 0-82164
- Jupiter and Galilean satellites, astrometric position determ. 0-77327
- Jupiter and Galilean satellites, image photometric anal. technique (*French*) 0-85880
- Jupiter and Galilean satellites, position determ. (1977) (*French*) 0-77326
- KUV09313+4052, variable UV excess object, discovery, position and photometry 0-62159
- Mars, positions, with Danjon astrolabe at San Fernando Observatory (Jan. to Feb. 1978) (*French*) 0-94736
- Mars, rot. period determ. from transits of albedo stations across central meridian (1659 to 1971) 0-98588
- meridian instrument pivot irregularities meas. method 0-94718
- Minor Planet Circular 5333-5390, precise posns. for asteroids and eight comets 0-77325
- Minor Planet Circulars 5189-5248, precise posns. for asteroids and 13 comets 0-67631
- Minor Planet Circulars 5249-5286, precise posns. for asteroids and six comets 0-67632
- Minor Planet Circulars 5287-5332, precise posns. for asteroids and eight comets 0-67633
- Minor Planet Circulars 5391-5422, precise posns. for asteroids and eight comets 0-85884
- Minor Planet Circulars 5423-5454, precise posns. for asteroids and seven comets 0-98599
- minor planets, 1978, April, astrometric positions determ., ESO GPO obs. 0-77319
- minor planets, hypothetical observations giving equinox and equator determ. 0-94742
- minor planets, positions from Torino Observatory (1977-1979) 0-94739
- minor planets, positions in August 1977 from Observatorio Nacional, Rio de Janeiro (*French*) 0-94740
- narrow field optical astrometry, atmospheric turbulence limitations 0-109340
- nearby stars, space astrometry 0-67518
- 51 Nemausa, astrometric posns. for coord. system error reduction 0-72849
- NGC 6494 (M23), open star cluster, membership from astrometry with PDS microdensitometer 0-98697
- observations from space-borne platform (*Polish*) 0-67519
- parallax and proper motion meas. for seven stars 0-62109
- Period Comet Brooks 2 (1980f), recovery, positions and perihelion passage correction 0-85899
- Periodic Comet Chernykh (1977l), precise positions and definitive orbit at first apparition (1977 to 1978) 0-62079
- Periodic Comet Encke, precise posn. for 1980 Oct. 8 and perihelion passage correction 0-109398
- Periodic Comet Harrington (1980m), recovery and precise positions (1980 September 4 to 9) 0-101558
- Periodic Comet Reinmuth 2 (1980n), recovery posns. and appearance (1980 Sept.) 0-101560
- Periodic Comet Tuttle (1980h), recovery and precise position (1980 July 14) 0-85901
- Periodic Comet Wild 3 (1980d), discovery posns., orbital elements and ephemeris (1980 April-June) 0-67657
- Periodic Comet Wild 3 (1980d), precise positions, (1980 May 9 to 17) 0-72885
- photographic star positions obtained with wide-angle astrographs, astrometric influences on precision (*Russian*) 0-72748

astrometry continued

- Photographic Zenith Tube at Tokyo Astron. Observatory, observational errors anal. 0-98547
 photographic zenith tube obs., building design effect 0-85856
 planetary position determ., Mars, Jupiter, Saturn, Jovian satellites (*French*) 0-72809
 planets, Danjon obs. (*French*) 0-94715
 planets, Munich meridian obs. (1941-61), orbital elements determ. (*German*) 0-77306
 Pluto (1973 to 1979) 0-85894
 PSR 1913+16, optical candidate, astrometry and high-speed photometry 0-101609
 pulsars, periods, positions and proper motion determ. from pulse arrival times, UHF, obs. 0-77431
 PZT stars, mean posns. and proper motions for 304 stars, obs. at Ondrejov 0-82175
 radio interferometric differential meas. of coordinates, influence of troposphere 0-67581
 radio source positions, astrometric catalogues 0-105180
 radio sources, galaxies and quasars, optical counterparts, astrometry 0-90551
 radio sources, positions, reference catalogue 0-105176
 reduction of 19th century obs. of Uranus and Neptune positions, method comparison 0-94691
 Saturn, satellites, astrometric obs. from McCormick Observatory (1977) 0-105200
 saturn, satellites 1966 S 2 and 1980 S 15-18, separations 0-67645
 Saturn, satellites I to IX from McDonald Observatory (1975-1976) 0-105199
 Saturn satellites, 1966 December and 1980 March positions for five objects 0-94750
 VY Sculptoris, novaklike variable, precise position 0-101597
 selenodetic reference network construction, choice of coordinate system (*Russian*) 0-72797
 sky photography programme with wide-angle astrographs, for stellar positions and proper motions (*Russian*) 0-72747
 SN 1572 (Tycho's supernova), small dia. radio source discovery and precise position 0-98680
 SN 1979C in M100 (NGC 4321), precise position 0-85962
 SN 1979c in NGC 4321 (M100), radio position 0-82402
 Space Telescope appls. 0-105175
 Space Telescope astrometry from CCD images 0-109370
 space-borne interferometers, astrometry and planetary detection 0-109357
 star positions, comprehensive general catalogue construction 0-105178
 stars, absolute declinations system construction for entire sky using high-latit. obs. 0-67520
 stars of southern sky, reference photographic catalogue introduction (*Russian*) 0-72789
 stellar position determ. on Schmidt plate, standard coord. and Stevenson's method 0-82176
 stellar trigonometric parallaxes, freq. distrib. and systematic effects 0-94785
 115 Thyræ, orbit improvement (*German*) 0-85881
 Tokyo Astronomical Obs., Time and Latitude Bulletins (April/June 1979) 0-72752
 Tokyo Astronomical Obs., Time and Latitude Bulletins (Jul-Sep 1979) 0-82177
 Tokyo Astronomical Observatory Time and Latitude Service, Bulletin (January to March 1979) 0-72751
 Uranus satellites, astrometric obs. 0-67654
 vidicon appl. to low intensities meas., with Si-intensified target (*German*) 0-98545
 visual binaries, orbital elements and masses for 18 pairs 0-62180
 visual binaries with variable components, orbital elements, visible obs. (*Russian*) 0-77455
 W3(OH), interstellar OH maser components absolute positions from VLBI synthesis obs. 0-105368
 zenith telescope, use as astrolabe for time and latitude meas. 0-98550

astronautics see space research**astronomical catalogues**

see also astrometry

- Abell galaxy clusters catalogue, cluster props. distortion by inclusion of spurious clusters 0-101643
 B-type stars, catalogue of photometric data rel. to surface mag. fields 0-85873
 4C radio sources between declinations 20° and 40°, samples 0-73057
 clusters of galaxies, catalogue inhomogeneity, cluster props. distortion, statistical anal. method 0-67888
 comets, ancient and naked-eye objects (2314 BC-AD 1970) 0-105181
 conference on star catalogues, Washington, DC, USA (Nov.-Dec. 1978) 0-90605
 dark nebulae in M31, catalogue 0-72787
 Equatorial Infrared Catalogue No.2 astronomical source distrib. 0-90346
 extragalactic objects, statistical anal. 0-94875
 faint star clusters in LMC, survey, visible obs. 0-73011
 FK4, corrections to zero points from minor planet obs. (*Russian*) 0-82228
 FK5, equinox and equator of new fundamental reference coord. system 0-109341
 galaxies, compact and bright-nucleus, in S.hemisphere, spectroscopic survey 0-94725
 galaxies with UV continuum, twelfth list 0-67585
 galaxies with UV excess, second list 0-67584
 galaxy morphological types in rich clusters 0-85872
 Hauck-Mermilliod catalogue of early type star four colour data, astrophysical parameter determ. 0-72951
 IR bright stars in region of galactic centre, catalogue and photometry 0-77299
 IR sources in Cygnus X region 0-82538
 Jupiter, disturbances and dislocations (1857-1975) 0-72867
 late-type stars, revised MK spectral types for G, K, and M stars 0-82226
 Luyten proper motion catalogues, nearby star suspects selection using Luyten's magnitude estimates 0-82353
 Moon transient phenomena observations, fourth list (1821 to 1978) 0-62038
 OTL radio sources, position and struct. determ. from 327 MHz lunar occultation obs. 0-73061
 OTL radio sources, position and struct. determ. from 327 MHz obs. 0-73060

astronomical catalogues continued

- OTL radio sources, position and struct. determ. from 327 MHz lunar occultation obs. 0-73062
 periodic comets, major semi-axis less than 30 AU 0-72791
 planetary nebulae, catalogue of new and misclassified objects 0-109378
 Ptolemy's star catalogue in Syntaxis, position meas. method 0-67586
 QSOs and BL Lacertae objects, revised optical catalogue 0-105177
 radio continuum sources near galaxies, catalogue and obs. at 11 cm 0-94872
 radio sources, extragalactic, confusion-limited survey at 4.755 GHz, source list and areal distrib. 0-98577
 radio sources observed during continuum interferometric obs. of interstellar dark clouds, catalogue 0-98699
 radio source positions, reference catalogue derivation 0-105176
 radio sources, astrometric catalogues 0-105180
 RC1 galaxies, nuclei, lenses, rings diameters for 532 galaxies 0-90525
 RSO 1 catalogue cross correl. with IRC, AFGL and EIC catalogues 0-77511
 SNR candidates in nearby galaxies 0-62037
 southern sky, reference photographic catalogue introduction (*Russian*) 0-72789
 spectroscopic binaries, seventh catalogue, statistical analysis 0-82422
 star positions, comprehensive general catalogue construction 0-105178
 star positions, general catalogue compilation, material evaluation 0-109375
 stars, general magnitude eqn. between FK4 and southern catalogues 0-67705
 stars with Ca II H and K emission lines (*Polish*) 0-82227
 stellar photometric catalogues: present and future 0-105179
 stellar relative radial vels. for 500 stars near southern open clusters (*German*) 0-94724
 stellar spectrophotometric data, energy distrib. in Hayes-Latham calibration 0-72790
 US Naval Observatory data associated with stellar parallax determ. 0-72788
 uvby β photoelectric photometric catalogue 0-62036
 Vinius photometric catalogue of stars on mag. tape, description 0-98578
 18W catalogue of radio sources in Abell 2197 and 2199, Westerbork survey at 610 MHz 0-67883
 29, 30 and 31W catalogues, Virgo cluster galaxies 0-98721
 28 W sources and catalogue in NGC 7000 IC 5070 H II region complex 0-105308
 Fe/H abundance in 628 stars 0-98579
 He rich stars, intermediate and extreme, spectral atlas in 3700 to 4600 Å range 0-94806
- astronomical ephemerides**
- 1932 HA (Apollo), ephemerides for 1930, 1941, 1964 and (1966) 0-105193
 1936 CA (Adonis), ephemerides for 1943 and (1984) 0-105193
 1980, general ephemerides for Belgium (*French*) 0-72767
 1980 LB, precise posns., orbital elements and ephemeris (1980 June-July) 0-82259
 1980 PA, positions, improved orbital elements and ephemeris, (1980 August 25 to September 30) 0-98597
 1980 PA, posns., elements and ephemeris (1980 August) 0-94746
 1980 PA, precise posns., improved elements and ephemeris (1980 Sept.-Oct.) 0-101548
 1862 Apollo, close approach and ephemeris (1980 Nov.-Dec.) 0-109389
 V342 Aquilæ, eclipsing binary, orbital period changes and eclipses ephemeris 0-67791
 asteroids, Trojan group, discovery of new members, orbital elements and ephemerides 0-72847
 I Carinae, Cepheid variable, Fourier anal. of light var. and ephemeris 0-90442
 Chebyshev approximations, satellite navigation 0-61993
 Comet Bowell (1980b), precise positions, elements and ephemeris (1980 March-July) 0-62075
 Comet Cernis-Petruska (1980k), antitail, precise posns., parabolic elements and ephemeris 0-105206
 Comet Cernis-Petruska (1980k), orbital elements and ephemeris (1980 August 4 to September 28) 0-98614
 Comet Russell (1980l), discovery posns. and ephemeris (1980 September) 0-101557
 Comet Russell (1980l), ephemeris (1980 Sept.-Dec.) 0-105207
 Comet Russell (1980l), parabolic orbital elements and ephemeris, (1980 September 12 to October 2) 0-101559
 Comet Torres (1980e), precise posns., elements and ephemeris (1980 June-July) 0-85900
 Galilean satellites, improved ephemerides for Voyager mission 0-62066
 Jupiter, triple shadow phenomena caused by Galilean satellites (AD 1900-2100) ephemerides 0-67641
 SW Lacertae, W Ursae Majoris star, photoelectric obs. and updated ephemeris 0-62196
 β Lyrae, orbital period variability and ephemeris (1971 to 1990) 0-72997
 Mars, rot. period determ. and albedo markings longits. in N.A.3 ephemeris system 0-98588
 Minor Planet Circular 5333-5390, ephemerides for 92 asteroids 0-77325
 Minor Planet Circulars 5189-5248, ephemerides for 60 asteroids and six comets 0-67631
 Minor Planet Circulars 5249-5286, ephemerides for four asteroids 0-67632
 Minor Planet Circulars 5287-5332, ephemerides for 11 asteroids and ten comets 0-67633
 Minor Planet Circulars 5391-5422, ephemerides for nine asteroids and three comets 0-85884
 Minor Planet Circulars 5423-5454, ephemerides for seven asteroids 0-98599
 minor planets ephemerides, orbits computation using Chebyshev polynomials (*French*) 0-61997
 AU Monocerotis, eclipsing binary, ephemerides for overlapping photometric phenomena 0-77448
 Neptune, ephemeris, 1612 December 28 to 1613 January 30 rel. to obs. by Galileo 0-105485
 Periodic Comet Encke, ephemeris (1980 Oct.-Dec.) 0-105209
 Periodic Comet Halley, orbit parameters and ephemeris, 1759-2024 period 0-62076
 Periodic Comet Olbers, orbit parameters and ephemeris, 1759-2024 period 0-62076
 Periodic Comet Stephan-Oterma (1980g), recovery positions, elements and ephemeris 0-82307

astronomical ephemerides continued

- Periodic Comet Tuttle (1980h), ephemeris (1980 Oct.-1981 Feb.) 0-105208
 Periodic Comet Wild 3 (1980d), discovery posns., orbital elements and ephemeris (1980 April-June) 0-67657
 Periodic Comet Wild 3 (1980d), improved orbital elements and ephemeris (1980 May 31 to August 9) 0-72885
 planetary ephemerides construction, rectangular coordinates approximation by Chebyshev polynomials (*Russian*) 0-62033
 Pluto, no occultation of star on 1980 April, 6 ephemeris 0-62070
 Saturn ring disappearances (1600 to 2100) 0-72876
 RY Scuti, eclipsing binary, ephemeris and UVB obs. 0-94832
 solar position, formulae (*German*) 0-77367
 X-ray sources occultations by Moon, first and last dates (1980 to 1985) 0-77513

astronomical instruments

- see also astronomical observations; astronomical techniques; astronomical telescopes; radiotelescopes*
 active coded aperture for direction meas. of high energy γ -rays 0-62022
 Advanced X-ray Astrophysics Facility, results obtained 0-109366
 airborne far IR Fabry-Perot astronomical spectrometer 0-109371
 airborne far IR Fabry-Perot spectrometer for astronomical fine structure lines 0-62026
 astrophotographs, wide angle, sky photography programme (*Russian*) 0-72747
 astrophotographs, wide-angle, astrolimatic influences on precision of photographic star positions (*Russian*) 0-72748
 automatic CCD measuring machine for star images (*Japanese*) 0-82212
 bandpass interference filters for 1-3 mm window 0-109368
 Berkeley stellar spectrometer and EUV Explorer, Wolter-Schwarzschild optics 0-82197
 Brorfelde transit circle, diameter corrections 0-105164
 C-CD camera, appl. to Einstein X-ray Observatory fields RI photometry 0-62315
 C-CD camera, description performance and calibration 0-73499
 C-CD camera on Galileo Jupiter Orbiter Mission 0-85859
 Cassegrain scanning system for IR images 0-82204
 CCD spectrometer for 500 to 900 nm range 0-82207
 charge injection device as stellar tracking sensor 0-85861
 chopping photometer to eliminate auroral sky background 0-72776
 cold camera, description 0-72779
 compact solar camera, student project 0-67975
 CORAVEL, Cassegrain spectrophotometer for stellar radial vel. determ. 0-82210
 correlator back-end for Culgoora radioheliograph, advantages and disadvantages 0-85865
 Cosmic Background Explorer, satellite instrumentation 0-61988
 Danjon astrolabe, planetary obs. (*French*) 0-94715
 digital system for image processing (*Italian*) 0-98558
 double astrophotometric system, investigation of colour eqns. (*Russian*) 0-72771
 electronic detectors to enhance optical information from telescopes, image intensifiers and CCDs (*French*) 0-67569
 electronic metronome for astrophotography 0-67572
 EUV spectrometer, reliability anal. technique appl. 0-85864
 Fabry-Perot etalon, optically contacted, stability to cosmic radiation 0-98544
 Fabry-Perot imaging device TAURUS for radial velocity field maps 0-82205
 Fabry-Perot spectrometer for solar vel. field meas. 0-90333
 far IR calibration source for balloon-borne telescopes 0-62027
 fluxgate magnetometer on Pioneer Venus Orbiter, design and operation 0-67496
 focal coronagraph detection of new Saturn ring (*French*) 0-72772
 focal grating photometer for magnitude difference determ. of double stars 0-67567
 focal plane IR detector arrays for planetary missions 0-85862
 focal reducer using Fresnel lens, appl. to stellar photometry 0-67568
 FOCAS, faint object classification and analysis system, galaxy counts 0-105350
 Gamma Ray Observatory instrums. and operations 0-109365
 gamma-ray spectrometers with cooled Ge sensors on P78-1 satellite 0-58019
 gradiometer systems for lunar gravity meas. 0-94730
 graphic processor for pseudo-colour images representation (*Italian*) 0-98562
 grating spectrometers and spectrographs, design method 0-62742
 high pressure gas scintillation spectrometers for X-ray astronomy 0-105166
 highly polarised objects detection device (*Japanese*) 0-82209
 imaging gas scintillation counter for X-ray astronomy 0-98551
 imaging photon detectors 0-86405
 IMPATT source, frequency-stabilised, 115 GHz 0-67573
 Infrared Astronomical Satellite, features and performance 0-61989
 integrating wide-field IR photometer for globular clusters study 0-62029
 IR and submillimetre astronomy, book (*Russian*) 0-72773
 IR detectors, trends in low-temp. thermal and photon detectors (*Russian*) 0-72778
 IR Michelson interferometer on Voyager 0-77290
 Joyce-Loeb microdensitometer, computer control for objective-prism spectra meas. 0-105173
 low-background astronomical integrated IR detector array development 0-85860
 Lyman α camera, for high resolution solar Lyman α filtergrams 0-82323
 magnetometer, ring core, for mag. meas. in interplanetary space during Halley-Venus mission (*Japanese*) 0-94672
 meridian instrument pivot irregularities meas. method 0-94718
 Michelson Fourier transform stellar spectrometer 0-98552
 micrometeoroid detector film, penetration expts. 0-77292
 optical instrumentation, advances and appl. to planetary nebulae studies 0-109522
 optical surface shaping process automation 0-105169
 pattern recognition in digitalised images (*Italian*) 0-98554
 PDS microdensitometer, astrometric meas. technique and appl. to membership of cluster (NGC 6494) 0-98697
 phase-tracking stellar interferometer, first fringe meas. 0-82215
 photodiode detectors, thermal background subtraction 0-90342
 photoelectric photometer, appl. to occultations obs. (*Chinese*) 0-105172
 photographic plate scanner, description 0-72780
 Photographic Zenith Tube at Tokyo Astron. Observatory, observational errors anal. 0-98547

astronomical instruments continued

- photometer, with repetitive filter cycle and sky background compensation 0-62025
 photometer for rapid stellar light variation, microprocessor controlled (*Spanish*) 0-82222
 Pioneer Venus, Orbiter and Multiprobe spacecraft instrumentation 0-67491
 Pioneer Venus Bus and Orbiter, Bennett ion mass spectrometers 0-67499
 Pioneer Venus Bus neutral gas mass spectrometer 0-67513
 Pioneer Venus entry probes, atmosphere structure instruments 0-67562
 Pioneer Venus Orbiter, electron temp. probe 0-67500
 Pioneer Venus Orbiter, radar mapper design and operation 0-67495
 Pioneer Venus Orbiter Gamma Burst Detector 0-67505
 Pioneer Venus Orbiter radiometer (VORTEX) 0-67504
 Pioneer Venus Orbiter UV spectrometer, design and operation 0-67503
 Pioneer Venus small probes net flux radiometer experiment 0-67512
 Pioneer Venus Solar Flux Radiometer 0-82198
 Pioneer Venus Sounder and small probes nephelometer instrument 0-67511
 Pioneer Venus Sounder Probe gas chromatograph 0-67507
 Pioneer Venus Sounder Probe IR radiometer 0-67509
 Pioneer Venus Sounder Probe neutral gas mass spectrometer 0-67506
 Pioneer Venus Sounder Probe Particle Size Spectrometer 0-67510
 Pioneer Venus Sounder Probe Solar Flux Radiometer 0-67508
 plasma analyser experiment on Pioneer Venus Orbiter 0-67498
 plasma wave instrument on Pioneer Venus Orbiter, design and performance 0-67497
 pulse counting photometer modified for occultation obs. 0-72921
 radio spectrograph, appl. to interplanetary scintillation spectra obs. 0-72741
 resonance absorption spectrometer for monitoring profile of solar He I 58.4 nm line 0-62019
 Reticon spectrophotometer at Asiago Observatory, data anal. procedure (*Italian*) 0-98565
 rocket borne imaging detector and grating spectrograph far UV spectrophotometry 0-62014
 scanning Fabry-Perot interferometer, for high-resolution meas. of solar spectral lines 0-77298
 SEC Vidicon photometer, appl. to photometry of ω Centauri main sequence 0-90491
 solar double-pass monochromator, with digital device for obs. and spectrum processing automation (*Russian*) 0-72777
 solar interference spectrograph 0-109362
 Solar Thermal Test Facility, description appl. to stellar astronomy 0-77301
 solar visual and photographic survey instrument (*Chinese*) 0-77291
 solid state detector for spectra obs. of binary stars 0-109469
 space experiments for Solar Maximum Year, review 0-90404
 space optics, conference Huntsville, Alabama (1979 May 22 to 24) 0-62385
 space optics, imaging X-ray optics workshop, Huntsville, Alabama (1979 May 22 to 24) 0-62384
 Space shuttle, X-ray astronomical instrums. and expts. 0-109363
 Space Telescope, scientific instruments 0-61987
 spectral image analysis device, Chromotron 0-83683
 spectropolarimetry with an intensifier-dissector-scanner 0-109367
 UVB photometer, double head, for simultaneous fast photometry 0-72775
 vacuum-cold camera, appl. to astronomical near IR photography 0-90341
 X-ray camera, wide field for astronomy, design, sensitivity and performance 0-85863
 X-ray spectrometer-telescope system for solar corona studies 0-105168
 X-ray transmission gratings for 7-304 Å operation, efficiency and resolution 0-82195
 Zeeman analyzer system on McDonald 2.7 m telescope's coude spectrograph 0-62021
 InSb IR detectors, integrating preamplifier 0-90337

astronomical observations

- see also gamma-ray astronomical observations; infrared astronomical observations; radioastronomical observations; ultraviolet astronomical observations; visible astronomical observations; X-ray astronomical observations*
 1610-771, radio QSO with steep optical spectrum, obs. 0-94887
 R Aquarii, UV, visible and 85 GHz continuum obs. 0-85946
 η Aquilae, Cepheid variable, absolute energy distrib. in radiation spectrum (*Russian*) 0-72974
 e Aurigae, photometry during 1955-57 eclipse rel. to wavelength-depend. fluctuations 0-62190
 KR Aurigae, X-ray source nearby, X-ray, IR and visible obs. 0-67742
 Be-stars, IUE obs. 0-82838
 XX Camelopardalis, R Coronae Borealis star, photometry in optical and IR ranges 0-101601
 γ Cassiopeiae, Be star, rapid linear polarisation variability (*Russian*) 0-77417
 UV Cassiopeiae, R Coronae Borealis star, photometry in optical and IR ranges 0-101601
 U Cephei, excess light obs. rel. to accretion discs 0-82412
 Circinus X-1, changes in optical, IR and radio emission 0-67910
 cosmic rays, short-term fluctuations obs. 0-67483
 cosmic rays, studies using gas Cherenkov counter with ionisation spectrometer 0-94662
 V645 Cygni (AFGL 2789), spectroscopic and photometric obs. 0-73066
 HR Delphini (Nova 1967), simultaneous X-ray, UV and optical obs. 0-109440
 galactic cosmic ray intensity out to 18 AU, Pioneer 10 and 11 obs. 0-90297
 galactic cosmic rays, Fe nuclei isotopic comp. 0-72729
 HD 10783, Ap star, spectrophotometric obs. 0-98663
 HD 219150, F0 V star with remarkable UV excess, optical and UV photometry and spectrum 0-90429
 HD 45677, peculiar Be-star, 0.12-12.6 μ m obs. 0-72957
 interplanetary shock wave, He⁺ obs. in driver gas 0-72735
 Jupiter, ion fluxes out to 1200 R_J, Voyager 1 and 2 obs. 0-94667
 Jupiter, magnetosphere, tailward directed ion beam, Voyager-2 obs. 0-72854
 Jupiter, magnetosphere low energy plasma, Voyager obs. 0-72855
 Jupiter, phase effect for disc features brightness coeff. 0-98602
 Jupiter as source of electrons observed at Earth orbit 0-90357
 Jupiter magnetosphere, electrostatic waves obs. 0-72865

astronomical observations continued

- Jupiter magnetosphere, kilometric radiation spatial and temporal studies 0-77328
 Jupiter magnetosphere disturbed by Ganymede, Voyager-2 obs. 0-72856
 M32, absolute spectrophotometry rel. to galaxy spectral synthesis and age 0-67842
 Markarian 3, 231, Seyfert galaxies, optical polarisation obs. 0-90533
 Mars, magnetic minerals, obs. by Viking extended mission 0-72830
 micrometeoroids of inner solar system, Helios 1 obs. 0-77355
 minor planets, hypothetical observations giving equinox and equator determ. 0-94742
 NGC 3227, 3516, Seyfert galaxies, optical polarisation obs. 0-90533
 NGC 3293, open cluster, UBVRI photometry and relation to OB complex in Carina 0-90490
 X Persei (4U 0352+30), Be star, photoelectric photometry rel. to 6-year periodicity 0-109446
 Pic du Midi Observatory, history 0-72770
 QSOs from Molonglo Deep Survey, optical spectra 0-94884
 quasars, faint red 3C QSO candidates spectrophotometry and red shifts 0-67897
 reduction of 19th century obs. of Uranus and Neptune positions, method comparison 0-94691
 Roberts 22, bipolar nebula with OH emission, visual, radio and IR obs. 0-94859
 Saturn, phase effect for disc centre brightness coeff. 0-98602
 V818 Scorpii (Scorpius X-1), UV, visible, IR and X-ray obs. 0-82541
 Seyfert galaxies, photometry and thermal emission vars. 0-67865
 SN 1979c in M100, coordinated obs. (1979 April-June) 0-101604
 solar cosmic rays, obs. of events with high relative ³He abundances during 1976 November to December 0-61972
 solar heavy-ion-rich particle events, ³He/⁴He ratios energy depend. and temporal evolution, ³He/⁴He in heavy-ion-rich solar energetic particle events, energy depend. and temporal evolution 0-90299
 solar wind, upstream particle events close to bow shock and 200 R_E upstream 0-77247
 solar wind electrons epithelial dumbbell distrib. Prognoz 7 obs. following shock wave 0-109321
 solar wind flow observed by satellites, 0.6 to 1.6 AU 0-90303
 stellar photometry, secondary standards spectrophotometric obs. rel. to Ap stars HD 10783 and CU Virginis 0-98663
 stellar spectrophotometry, Moscow and Alma-Ata data comparison with multicolour photometric systems 0-101590
 Sun, luminosity variation (solar const.), direct obs. from rockets 0-90386
 symbiotic star candidates in LMC, optical spectroscopy and IR photometry 0-62139
 ζ Tauri, Be star, rapid linear polarisation variability (*Russian*) 0-77417
 SU Tauri, R Coronae Borealis star, photometry in optical and IR ranges 0-101601
 Vela star cloud, large scale photometric survey 0-90482
 Venus ionosphere composition, meas. by ion mass spectrometers on Pioneer Venus Bus and Orbiter 0-67499
 Venus magnetic tail field structure, role of unipolar induction effects 0-62060
 Venus plasma environment, study via plasma analyser expt. on Pioneer Venus Orbiter 0-67498
 Venus upper atmosphere, N detect. 0-77310
 CU Virginis (HD 124224), Ap star, spectrophotometric obs. 0-98663

astronomical observatories

- building design effect on photographic zenith tube obs. 0-85856
 Cloudcroft Observatory 0-77289
 Kanzelhöhe solar observatory, sunspot obs. (*German*) 0-98631
 Kitt Peak National Observatory telescopes, cost effectiveness in terms of publications and citations 0-90334
 Kitt Peak Observatory, seeing meas. 0-61899
 Louisbourg Observatory and the Marquis de Charbert (1724-1805) 0-68010
 Meudon solar tower, coelostat pointing method 0-90338
 Minor Planet Center, history and future 0-94712
 Mt. Hopkins Observatory, Multiple Mirror Telescope and ground-based astronomy, conference, Arizona (1979 May 9) 0-62386
 Ondrejov Observatory, Czechoslovakia (*Norwegian*) 0-82193
 Paris Observatory, history 0-77288
 satellites Ariel 5, Cos-B, X-ray and γ -ray astronomy respectively 0-90317
 Tokyo Astronomical Observatory, Photographic Zenith Tube observations errors anal. 0-98547

astronomical spectra

- see also atmospheric spectra; stellar spectra*
 49+88.1°, halo planetary nebula, photoionisation models for line emission spectrum rel. to chemical abundances 0-109507
 108-76.1°, halo planetary nebula, photoionisation models for line emission spectrum rel. to chemical abundances 0-109507
 0957+561A, B, double quasar, unusual IR spectral energy distrib. 0-73065
 1309-216, probable BL Lacertae object with absorpt. red shift 1.49, optical spectrum 0-67856
 1610-771, radio QSO with steep optical spectrum, obs. 0-94887
 Abell 1060 galaxy cluster, X-ray spectrum obs. by (HEAO A-2) 0-82518
 Abell 399/Abell 401, X-ray binary galaxy cluster, radial vels. and mass 0-90546
 Abell cluster radio sources, spectra and optical identification, SHF obs. 0-98729
 asteroids, IR reflectance spectra obs. and search for water of hydration 0-77318
 automated reduction by microcomputer based system 0-77296
 B 35, bright rimmed molecular cloud, CH obs. 0-62238
 background radiation spectrum meas. in near-mm region 0-62327
 black hole, massive, radiation spectrum of gas debris from tidally disrupted star 0-90467
 bright galaxy nuclei, optical and radio survey, sample selection and obs. 0-73039
 broad line regions, luminosity and radio emission in active nuclei and quasars 0-105340
 5C1 radiosources, optical identification by photographic photometry and spectra 0-77503
 3C 111, radio galaxy, 1.38 cm obs. and instantaneous radio spectrum of nuclear source (*Russian*) 0-109558
 3C 120, radio galaxy, vars. in optical spectrum (*Russian*) 0-90540

astronomical spectra continued

- 3C 120, Seyfert galaxy, spectrophotometric obs. of assoc. nebulosity 0-67890
 3C 147, 3C 286, quasars, spectral indices from VLBI obs. at 329 MHz 0-67898
 3C 273, quasar, detailed UV obs. with IUE 0-94886
 3C 405 (Cygnus A), 1.38 cm obs. and instantaneous radio spectrum of nuclear source (*Russian*) 0-109558
 Callisto, IR emission spectra 0-82264
 Cassiopeia A, supernova remnant, explanation of secular flattening of radio spectrum 0-101637
 Centaurus A (NGC 5128), 1.38 cm obs. and instantaneous radio spectrum of nuclear source (*Russian*) 0-109558
 Centaurus galaxy cluster, X-ray spectrum obs. by (HEAO A-2) 0-82518
 β Cephei stars, line profile variables, Si III 456.7 nm line modelling 0-85951
 Cepheus IV star formation region, continuum and recomb. lines, SHF obs. 0-90501
 CG 135+1, gamma ray source, spectrum obs. 20 keV-25 MeV 0-105398
 Cloud 2, mol. cloud, detect. of HC₃N (cyanodiacetylene) and HC₅N (cyanohexatriyne), SHF obs. 0-101627
 clusters galaxies, redshift determ. using Image Dissector Scanner, visible spectra 0-90544
 GQ Comae Berenices, QSO or N galaxy, spectrophotometry obs. 0-77488
 Comet Bennett (1970 II), CN (0-0) band brightness profile obs. rel. to CN prod. 0-82303
 Comet Bradfield (1979I), spectroscopic and photographic obs. in near IR 0-105205
 Comet Bradfield (1979I), UV spectrum, UE obs. 0-90371
 Comet Kohoutek (1973 XII), CN violet (0,0) spectra 0-82308
 comet tail spectrum, ¹³C¹⁸O⁺ (2,0) band rot. anal. 0-74157
 Comet West (1976 VI), CN (0-0) band brightness profile obs. rel. to CN prod. 0-82303
 Comet West (1976 VI) ionosphere CO⁺ brightness profile 0-85896
 comets, neutral species brightness profiles, average random walk model for mol. photodissociation 0-77351
 compact thermal sources, linear polarisation spectrum appl. to mag. fields determ. (*Russian*) 0-90344
 cosmic background radiation spectrum, early energy release distortion in Rayleigh-Jeans region 0-73077
 cosmic microwave background spectrum, distortion by pregalactic dust 0-67916
 cosmological microwave black body radiation spectrum, implications for Population III stars 0-67915
 Crab Nebula, spectral index at decametre wavelengths from lunar occultation obs. 0-62248
 Cygnus Loop, fast shock wave detection, optical spectra 0-82467
 Cygnus Loop, SNR, abundances and filament shock vel., UV obs. 0-94848
 Cygnus Loop, SNR, soft X-ray spectra emission line features obs. 0-94849
 Cygnus Loop, supernova remnant, X-ray spectra var. with position 0-82472
 Cygnus X-1, accretion disk round black hole, temp. var., X-ray obs. 0-109561
 dark clouds, formaldehyde obs., 5 GHz survey 0-73028
 30 Doradus nebula, emission line spectrum rel. to chemical comp. and density struct. 0-62226
 ELSPEC/2, interactive procedure for spectrogram processing (*Italian*) 0-98566
 emission line galaxies, spatial distrib. rel. to clusters, visible spectra obs. 0-73046
 emission line spectra, automatic reduction 0-77294
 ESO 012-G21, type I Seyfert galaxy, Ariel V X-ray spectra 0-90539
 ESO 263-PN 02, spectroscopic obs. of southern planetary nebula 0-101626
 extended emission line source radial vel. maps, TAURUS imaging device 0-82205
 extragalactic H II regions, spectra anal. and models 0-73024
 extragalactic sources with strong mm components, simultaneous radio obs. 0-73055
 G333.6-0.2, Ne II 12.81 μ m forbidden line obs. at high resolution 0-85983
 galactic centre, Prognoz-6 obs. of X-ray fluxes and energy spectra (*Russian*) 0-109562
 galactic nonthermal radio spectrum, rel. to cosmic ray electrons spectrum and gamma-rays prod. 0-62257
 galactic nuclei, bright line emission, contrib. of H II regions and shock waves 0-109552
 galactic radio spectrum, influence of primordial black holes 0-62179
 galaxies, bright nuclei activity, emission line sources and radio sources 0-98709
 galaxies, compact and bright-nucleus, in S. hemisphere, spectroscopic survey 0-94725
 galaxies, distance scale from IR magnitude/H I vel.-width relation 0-82480
 galaxies, elliptical, vel. dispersions rel. to mass to light ratios 0-98707
 galaxies, IR magnitude/H I vel. width relation rel. to distance scale and Universe expansion rate outside Local Supercluster 0-105325
 galaxies, large, H I mapping survey and line profiles 0-94870
 galaxies, nearby, interstellar CO survey 0-62276
 galaxies, spectral inversion technique for stellar population synthesis 0-90339
 galaxies, spectroscopy and photometry rel. to evolution of faint objects 0-105353
 galaxies active nuclei, extreme nonthermal radiation physics rel. to spectral parameters 0-90531
 galaxies assoc. with QSOs, spectroscopic search 0-105355
 galaxies in rich clusters, redshifts 0-85872
 galaxies with UV continuum, spectra 0-67585
 galaxies with UV excess, morphological descriptions and spectra 0-67584
 galaxies with UV excess and double and multiple nuclei, spectral study 0-67848
 Galaxy gamma-ray emission, fluxes determ. from cosmic ray electron spectrum 0-62257
 galaxy nuclei, stellar populations and H II regions, spectral anal. 0-98708
 Galilean satellites, water ice existence, IR spectral reflectance obs. 0-82263
 gamma ray spectroscopy 0-67582

astronomical spectra continued

- gamma rays from galactic disc, obs. between $-45^\circ < l < 45^\circ$ in 80 keV to 8 MeV energy range 0-82540
 gamma-ray burst, distance and spectrum of 1972 April 27 event 0-67903
 GL 2636, star form. region in Cygnus-X, IR obs. 0-105302
 IC 342, Scd galaxy, H I radial vel. field and large-scale struct. 0-67857
 IC 418, planetary nebula, UV spectra and C abundance 0-67832
 instantaneous spectra determ. by inversion technique 0-82218
 interplanetary H I, La emission profiles reanal. rel. to local interstellar gas temp. and vel. 0-105141
 interstellar C in mol. clouds, 492 GHz line detection 0-90508
 interstellar C IV and Si IV column densities 0-73018
 interstellar cloud towards gamma Arae, model from stellar spectra anal. 0-105312
 interstellar clouds, H_2 and C I absorpt. rel. to UV radiation field (*Russian*) 0-73026
 interstellar extinction, 2200 Å extinction hump prod. by porous graphite grains 0-62228
 interstellar extinction curve, comparison with visible and UV extinction of silicate, C and SiC smokes 0-82180
 interstellar extinction feature at 220 nm and diffuse 443 nm band, ANS obs. 0-62244
 interstellar grain composition constraints from 10 μm data 0-82471
 interstellar H_2O maser emission, new sources detect. 0-62298
 interstellar H_2O masers in NGC 6334, positions and spectra rel. to star form. 0-73025
 interstellar HCN, absorpt. lines obs. towards Cassiopeia A 0-101624
 interstellar HCO^+ , shock enhancement of abundance in supernova remnant (IC 443) 0-82464
 interstellar lines towards 15(=S) Monocerotis, UV obs. 0-90494
 interstellar matter, hot component information from np^+ ions 0-83305
 interstellar medium, far IR fine structure line obs. 0-62253
 interstellar molecular transitions, rest freqs. 0-62218
 interstellar molecules in grain mantles, IR absorpt. line interpretation 0-90504
 interstellar OH main line maser pumping mechanism 0-67824
 interstellar Se II in ζ Ophiuchi spectrum, abundance upper limit 0-82445
 interstellar thioformaldehyde (H_2CS), 3 GHz absorpt. transition obs. 0-67837
 Io, UV spectrum rel. to global SO_2 abundance upper limit 0-77332
 Io plasma torus, radiative cooling and spectra 0-72850
 Io plasma torus props. from Voyager EUV data 0-82262
 IR sources, galactic, 3 μ spectral feature identification 0-62227
 IR sources, unidentified emission features, possible mechanism 0-82452
 Jupiter, atmosphere constituents, comparison with Saturn, visible spectra obs. (*French*) 0-101550
 Jupiter, C/H and D/H ratios from 8-9 μm IR spectrum 0-67638
 Jupiter, Lyman α albedo, Copernicus UV obs. 0-94747
 Jupiter, methane and NH_3 bands, longitudinal variability, visible obs. 0-82270
 Jupiter, methane line profiles near 1.1 μ as probe of cloud struct. and C/H ratio 0-62067
 Jupiter, NH_3 abundance from visible obs. 0-82269
 Jupiter, NH_3 vertical density profiles from IR and radioelectric emissivity data 0-82267
 Jupiter, S II forbidden line emission nebula studies 0-67636
 Jupiter, S II forbidden line emission round planet, distrib. and intensity 0-85885
 Jupiter, S II torus, longitudinal asymmetry visible spectra 0-82271
 Jupiter decametre radio emission, dynamic spectrum modulation lines origin 0-67643
 Jupiter disc features spectral reflectivity, phase effect 0-98602
 K 648, halo planetary nebula, Ar III line obs. and low Ar abundance meas. 0-82443
 K 648, halo planetary nebula, photoionisation models for line emission spectrum rel. to chemical abundances 0-109507
 Kepler's SN 1604 remnant, spectrum 0-85982
 Kepler's supernova remnant, X-ray obs. from Einstein Observatory 0-82465
 Kerr black hole, low freq. EM and gravit. radiation spectra from infalling particle 0-62176
 BL Lacertae objects, absence of redshifted C IV absorpt. lines rel. to distances 0-62267
 line formation, asymptotics of partial redistrib. in non-LTE radiative transfer 0-62008
 Lupus Loop, X-ray spatial extent and spectrum of SNR 0-82457
 inner M101 galaxy group, H I spectra rel. to galaxies total masses 0-67885
 M31, line intensity distrib., contour maps, vel. profiles, 21 cm HI line survey 0-73038
 M31 and M81 nuclei, UV continua, spectrophotometry obs. from ANS satellite 0-77478
 M32, absolute spectrophotometry rel. to galaxy spectral synthesis and age 0-67842
 M4-18, spectroscopic obs. of compact planetary nebula 0-67829
 M82, H125 α recomb. line, SHF obs. 0-82486
 M82, nuclear source nature from IR obs. 0-82485
 M87, interstellar gas vel. dispersion rel. to presence of large central mass 0-94873
 M87, UV spectrum, IUE obs. 0-82502
 M87 (NGC 4486), vel. dispersion from a population model 0-77490
 M87 halo, Compton-scattered X-ray spectrum calc. from radio emission Faraday rot. 0-67844
 Magellanic Clouds, UV brightness maps and UV spectra 0-85994
 Markarian 231, Seyfert galaxy, substructure with UV excess, UV and visible obs. 0-82512
 Markarian 325, irregular galaxy, emission clumps observational props. 0-67869
 Markarian 3, 231, Seyfert galaxies, optical emission lines polarisation 0-90533
 Markarian 3, class 2 Seyfert galaxy, visible spectra obs. 0-85999
 Markarian 464, type I Seyfert galaxy, Ariel V X-ray spectra 0-90539
 Markarian 59, supergiant H II region in SBm galaxy NGC 4861 spectrum and struct. 0-98705
 Markarian 668 (=OQ 208), Seyfert, H83 α and H99 α radio recomb. lines detect. 0-94864
 Mars, reflectance spectroscopy rel. to surface comp. 0-72834
 MCS 1307+121, BL Lacertae object, radio spectrum shape, VHF and SHF obs. 0-67866
 MCG-6-30-15, type I Seyfert galaxy, X-ray and optical obs. 0-82479
 MCS 141, 232, 275, quasars, spectra interpretation, visible obs. 0-90562

astronomical spectra continued

- methane, liquid, laboratory optical absorpt. spectra rel. to detectability on outer planets 0-93278
 microwave background, spectrum distortions 0-62334
 microwave background longward of 3 mm, spectral distortions 0-62326
 microwave background spectrum 0-105406
 MSH 11-54 (H1122-59), supernova remnant, X-ray spectrum 0-82463
 N132 D, SNR in LMC, rapidly moving material, visible and UV solns. 0-82449
 N51D, giant filamentary shell in LMC, nature and dynamics 0-105343
 N70, giant filamentary shell in LMC, line profiles rel. to dynamics 0-90511
 near IR mapping spectrometer design and testing for Galileo Jupiter Orbiter 0-90336
 nebulae, emission-line spectrum from a slab of hydrogen at moderate to high densities 0-72759
 Neptune, UV albedo wavelength var. 0-82295
 Neptune rotation period, correction, photometric and spectroscopic results comparison 0-82301
 NGC 1023 galaxy group, H I obs. and possible intergalactic H I cloud discovery 0-67886
 NGC 1055, 681, 4594, galaxies, optical spectra rel. to rot. curves and mass distrib. (*Russian*) 0-90541
 NGC 1068, type 2 Seyfert, recombination spectrum and reddening 0-90519
 NGC 1851, 6624, globular cluster, abundance gradients spectroscopic investigation 0-82437
 NGC 2366 H II region visible and radio obs. 0-77475
 NGC 2536, spiral galaxy, radial vars. of emission line ratios 0-82497
 NGC 253, nuclear source nature from IR obs. 0-82485
 NGC 2903, spiral galaxy, nucleus identification and visual energy distrib. 0-62273
 NGC 3115, S0 galaxy, rotation and mass of inner 5 kiloparsecs 0-105326
 NGC 3227, 3516, Seyfert galaxies, optical emission lines polarisation 0-90533
 NGC 3227, Seyfert galaxy, photoelectric and spectroscopic study and comparison with galaxy chain (VV 150) 0-98724
 NGC 3242, 7009, 6210, high excitation planetary nebulae, high dispersion EUV obs. 0-77466
 NGC 3516, SBO type Seyfert galaxy, extended nebulosity, UV and visible obs. 0-82487
 NGC 3686 galaxy quartet, spectra and rot. curves rel. to mass distrib. and group stability 0-62297
 NGC 4151, Seyfert galaxy, gamma-ray emission, Compton scatt. model 0-98711
 NGC 4485/90 interacting galaxies, radio continuum and H I obs. 0-62274
 NGC 488, Sb galaxy, rotation curve from emission line spectra 0-62266
 NGC 4945, late-type spiral galaxy, spectrum rel. to excited gas kinematics 0-109547
 NGC 5236, spiral galaxy peculiar nucleus continuum and reddening 0-73031
 NGC 5728, barred spiral, vels. and mass distrib., visible spectra obs. 0-94863
 NGC 604, 5471, giant extragalactic H II regions, IUE UV spectra 0-77467
 NGC 604, H II region in M 33, H α line profile width rel. to core-halo struct. 0-85984
 NGC 6302, emission nebula, forbidden Ne V 3426 Å wings rel. to energetic stellar wind 0-67835
 NGC 6888, filamentary nebula, optical spectra calc. 0-105304
 NGC 6888, ring nebulae around Wolf-Rayet star HD 192163, spectra of filaments and smooth gas (*Russian*) 0-90515
 NGC 7000 (North America Nebula), rocket UV imagery 0-82440
 NGC 7027, planetary nebula, 3.3 microns unidentified feature, high resolution spectra 0-82466
 NGC 7027, planetary nebula, H γ emission spatial distrib. obs. 0-98698
 NGC 7027, planetary nebula, He I 2.0 μm line strength rel. to He I 584 Å transfer problem 0-67550
 NGC 7027, planetary nebula, UV spectrum rel. to physical conditions and CNO elements abundances 0-82459
 NGC 741, 1316, 7626, radio galaxies, optical spectra and dynamics 0-94871
 NGC 7538 and Shermless 159, H II region/mol. cloud complex, H I aperture synthesis obs. 0-90510
 NGC 7541, rotation curve and mass distrib. in spiral galaxy (*Russian*) 0-94874
 NGC 7582, narrow emission line X-ray emitting nucleus, UV spectra 0-101640
 NGC 7662, planetary nebula, photoionisation model with charge transfer reactions rel. to emission-line spectrum 0-62233
 NGC 7822, NGC 281, bright rimmed mol. clouds, CH obs. 0-62238
 NGC 925, barred spiral galaxy, high-resolution H I spectra and vels. 0-105329
 North Polar Spur, SNR, soft X-ray spectra emission line features obs. 0-94849
 objective-prism spectra meas., computer control of Joyce-Loebl microdensitometer 0-105173
 OH 205.1-14.1, unusual OH maser, left circularly polarised 1667 MHz line obs. during flare 0-98734
 OH 471, OX 057, quasars, millimetre wave spectra and variability (*Russian*) 0-90559
 Omega Nebula (M17, W38, NGC 6618), S III, O III, N III, IR obs. 0-90495
 Ooty occultation extragalactic sources radio spectrum obs. in SHF 0-105371
 ρ Ophiuchi dark cloud, ^{13}CO self absorpt., EHF obs. 0-90500
 Orion A, methanol 84.5 GHz and 96.7 GHz lines obs. 0-62245
 Orion methanol masers, interferometric and multitranstional study 0-67891
 Orion Nebula, forbidden Cl II and forbidden Fe II near IR high resolution mapping 0-62217
 Orion Nebula, IUE obs. of UV continuous spectrum 0-90499
 Orion Nebula, macroscopic motions from atomic line vels. 0-62243
 Orion Nebula (NGC 1976), long-slit spectroscopy in rocket UV 0-105297
 Periodic comet Schwassmann-Wachmann 1 (1974 II), outburst and CO^+ detect. spectrophotometric obs. 0-72881
 PG 1115+08, triple QSO, spectroscopic obs. and gravit. lens model 0-86012

astronomical spectra continued

- PHL 1092, narrow line quasar, discovery of extreme Fe II emission 0-77508
 Pioneer 10 and .11 radio signals, spectral broadening by ionospheres of Jupiter and Saturn 0-109391
 PK 108-76°1, 49+88°1, halo planetary nebulae, Ar III line obs. and low Ar abundances meas. 0-82443
 PKS 0735+178, flat radio spectrum, 0.3-90 GHz obs. of BL Lacertae object 0-94880
 PKS 2155-304, BL Lacertae object, spectral slope from far UV obs. 0-82509
 PKS 2155-304, BL Lacertae object, no evidence for redshifted forbidden O III emission 0-73035
 planetary nebulae, abundances from weak diagnostic spectral lines 0-109531
 planetary nebulae, emission-line fluxes rel. to O/H ratios and Galaxy O enrichment 0-105328
 planetary nebulae, H β fluxes rel. to distances determined from ionised mass/radius relation 0-101625
 planetary nebulae, H and He II spectra rel. to central stars temps. and evolution 0-67724
 planetary nebulae, He II Ly α photons absorpt. rel. to forbidden lines intensities 0-67833
 planetary nebulae, interpretation of UV spectra 0-109524
 planetary nebulae, ionisation models rel. to spectra 0-109529
 planetary nebulae, IR line and continuum spectra 0-109525
 planetary nebulae, radio recomb. lines and mol. emission lines obs. 0-109526
 planetary nebulae, S abundance from IR and visible line meas. 0-82444
 planetary nebulae, theoretical models, low to medium excitation objects 0-67817
 planetary nebulae, theory of physical processes rel. to spectra 0-109527
 planetary nebulae, UV continuum and line spectrum obs. and theory 0-109523
 planetary nebulae central stars, interpretation of UV continuum radiation 0-109524
 planetary nebulae in Magellanic Clouds, spectra rel. to excitation classes and comps. 0-109519
 planetary nebulae optical spectra, effects of inhomogeneous struct. 0-109522
 planetary nebulae spectra, effects of He shell flashes in nuclei 0-73021
 plasma, high temp., thermal bremsstrahlung radiation and spectral emission rate 0-94697
 plasma clouds, comptonisation of X-rays, radiation spectra 0-85850
 PN 173+3.1, planetary nebula near galactic anticentre, coords., radial vel. and orbit 0-105309
 primaeval radiation, polarisation and spectrum in anisotropic universes 0-82552
 Puppis A supernova remnant, X-ray spectra var. with position 0-82472
 Q0353-383, QSO absorption anomalies, UV and visible spectral obs. 0-82532
 QSO 0957+561, double quasar, visible spectrophotometry, gravitational lens interpretation 0-82533
 QSO 0957+561 AB, double quasar, IR spectrum confirms gravitational lens 0-77510
 QSO absorption lines and intergalactic clouds 0-62311
 QSO absorption spectra origin 0-105387
 QSO resonance lines as luminosity calibrators 0-105388
 QSOs, absorpt. from clouds in emission-line regions 0-62308
 QSOs, absorpt. line redshift distrib. 0-90563
 QSOs, redshifted clouds, 21 cm line studies 0-105389
 QSOs from Molonglo Deep Survey, optical spectra 0-94884
 quasars, Cherenkov line radiation, QSO emission-like spectra (*Chinese*) 0-105378
 quasars, Comptonised spectrum, Monte Carlo simulation 0-90566
 quasars, CTIO Curtis Schmidt survey -40° zone, discoveries and spectrophotometry 0-73064
 quasars, faint red 3C QSO candidates spectrophotometry and red shifts 0-67897
 quasars, IR spectra, H I line ratios 0-105391
 quasars, large red shift, spectra, implications of neutrino rest mass for H I obs. problem (*Russian*) 0-105414
 quasars, low redshift X-ray selected, visible spectra and UDVR photometry 0-105397
 quasars, Lyman α absorpt. line distrib., intergalactic origin 0-67899
 quasars, Mg II and Fe II lines excitation 0-67896
 quasars, narrow line absorpt. systems, form. model 0-82535
 quasars, permitted Fe II lines form. and low excitation region parameters 0-62278
 quasars, systematic surveys with slitless spectrum technique 0-105384
 quasars, X-ray spectral indices rel. to contrib. to X-ray background 0-82551
 quasars absorption redshifts, evidence for large-scale uniformity of physical laws 0-73079
 quasars in CTIO 4 m survey, visible and UV spectrophotometry 0-86009
 quasars spectra, absorpt. effects due to intergalactic pyrolytic graphite whiskers 0-94866
 radio galaxies components, radio continuum spectra rel. to fly away velocities (*Russian*) 0-62306
 radio recombination lines, high-n, Zeeman splitting 0-58210
 radio sources, compact, extragalactic, interpretation of spectra 0-62299
 radio sources, form. of universal and diffusion regions of relativistic electrons non-linear spectra 0-109555
 radio spectroscopy (*Japanese*) 0-62031
 radiogalaxies from B2 Catalogue, optical identification, radio positions and redshifts 0-86005
 resonance line scattering in absorbing medium, scaling laws 0-98538
 Roberts 22, bipolar nebula with OH emission, visual, radio and IR obs. 0-94859
 Sa type spiral galaxies, redshifted 21 cm line profiles, radio obs. 0-73041
 HM Sagittae, near-IR spectrographic obs. of young planetary nebulae 0-94810
 Sagittarius B2, He recombination line obs. interpretation 0-62300
 Sagittarius B2, methanol 84.5 GHz and 96.7 GHz lines obs. 0-62245
 Sagittarius B2, mol. cloud, detect. of HC₃N (cyanodiacetylene) and HC₃N (cyanohexatriene), SHF obs. 0-101627
 Saturn, atmosphere constituents, comparison with Jupiter, visible spectra obs. (*French*) 0-101550
 Saturn, NH₃ abundance from visible obs. 0-82269
 Saturn, PH₃ abundance, IR obs. 0-82278
 Saturn disc centre spectral reflectivity, phase effect 0-98602

astronomical spectra continued

- Sc galaxies, rot. props. from major axis visible spectra obs. 0-90517
 SchuWe-3, spectroscopic obs. of southern planetary nebula 0-101626
 Seyfert 1 galaxies, H I Balmer lines correl. with disk struct. 0-82503
 Seyfert 1 galaxies, O I 8446 Å emission excitation mechanism, visible and IR obs. 0-85991
 Seyfert 1 galaxy 1224+04, discovery from spectrophotometry obs. 0-77488
 Seyfert 2 X-ray galaxies, nucleus spectra and photometry obs. 0-98712
 Seyfert galaxies, Mg II and Fe II lines excitation 0-67896
 Seyfert galaxies, nearby, H β line width correl. with morphology 0-82478
 Seyfert galaxies, type 1, permitted Fe II lines form. and low excitation region parameters 0-62278
 Shababian 1 group of galaxies, spectroscopic obs. rel. to dynamics 0-67878
 Sharpless 106 IR sources, 8-13 micron spectrophotometry 0-105305
 Sharpless 159 and NGC 7538, H II region/mol. cloud complex, H I aperture synthesis obs. 0-90510
 SN 1006 remnant, X-ray spectrum 0-82457
 SNR radio shells, spectral index distrib. 0-77462
 SNR X-ray spectra, two component appearance 0-82475
 solar wind, low freq. continuum from ISEE 3, thermal electrostatic noise, LF obs. 0-101519
 stellar atmospheres, spherical transonic flow, reson. line radiative transfer 0-94698
 supernova remnant optical emission spectra, effect of shock wave intermediate zone radiative cooling 0-109517
 supernova remnants, far UV spectrophotometry and astrophysical interpretation 0-90498
 synchrotron radiation, radio and electron components, effect of interstellar mag. field inhomogeneities 0-85849
 T Tauri nebula, ionisation and emission line spectrum calc. 0-67820
 Tololo emission line galaxies, size, morphology and spectroscopy, visible obs. 0-73044
 Uranus, albedo and spectral features from IR obs. 0-82299
 Uranus, UV albedo wavelength var. 0-82295
 Uranus visible and near IR spectrum, appl. of methane band-model parameters 0-98609
 UV galaxies, double nuclei, visible spectra obs. (*Russian*) 0-77495
 Vela SNR, IUE UV spectrum 0-101635
 Venus, O₂, $\Delta g \rightarrow \Sigma g$ band, prod. mechanisms 0-82251
 Venus dayglow spectrum, 1250 to 1430 Å, Pioneer Venus obs. 0-77311
 Virgo cluster spiral galaxies, H I deficiency from 21 cm obs. 0-62277
 VV 126, multicomponent interacting galaxies, visible spectroscopy obs. (*Russian*) 0-77494
 VV 150, galaxy chain, photoelectric and spectroscopic study 0-98724
 VV 493 (UGC 07910), unusual extragalactic object, morphology and spectrum rel. to probable nature 0-98718
 VV 794 H II regions, photographic and spectral obs. (*Russian*) 0-77493
 W3 H II region, CO, CS and HCN obs. LF obs. 0-82446
 W49A, W51A, compact H II regions, H109 α recomb. line, aperture synthesis obs. 0-10534
 W50, supernova remnant, optical spectrum 0-90557
 W51-IRS 2 and W49 NW, compact H II regions, IR spectra obs. 0-90497
 X-ray heated medium phase transfer, optical spectral line emission bursts (*Russian*) 0-77286
 X-ray pulsars, cyclotron line formation in accretion column 0-67901
 X-ray sources, time-dependent Comptonisation and X-ray reverberations rel. to fluctuations spectral evolution 0-86013
 X-ray spectra, direct deconvolution method 0-85867
 C abundance in Orion Nebula and IC 418 from visible and UEI obs. 0-82451
 CO J=1-0 and 2-1 obs. of Lynds 1551 dark interstellar cloud 0-105318
 CO⁺ in Periodic Comet Schwassmann-Wachmann 1 near minimum brightness 0-82305
 Fe II UV lines in QSOs, spectrophotometry obs. 0-73063
 H I absorption in galactic centre direction 0-77465
 H I in field of elliptical galaxy NGC 1052, 21 cm emission mapping and line profiles 0-98719
 H I near Orion Nebula, obs. of absorpt. line vels. and 21 cm emission distrib. 0-105322
 H I regions, high latit., search for OH 18 cm absorpt. line spectra 0-67841
 H I regions towards extragalactic radio sources, 21 cm emission, and absorpt. obs. 0-94854
 H I survey, contour maps, 21 cm obs. 0-85986
 H II regions, ¹²C¹⁸O and ¹³C¹⁸O J=2-1 transitions obs. 0-73022
 H II regions, H166a recomb. line obs. at 1425 MHz 0-90512
 H II regions in barred spiral galaxies NGC 1313, 5236 and 7552 visible obs. 0-82510
 H II regions near nucleus of spiral galaxy NGC 3310, absolute and relative line intensities 0-62235
 HCl in diffuse interstellar clouds, abundance and chem. models 0-91570
 H₂O maser source in Orion A, radio flux density and line width during outburst (*Russian*) 0-105320
 H₂O maser sources near Herbig-Haro objects 7-11, 22 GHz obs. 0-73019
 He I 584 Å in quasars and gaseous nebulae, line transfer problem and line strength 0-67550
 N V, hot interstellar gas diagnostic, IUE obs. 0-101634
 O II, relative intensities and lifetimes in nebulae, conventional radiation theory 0-109513
 OH astronomical maser sources OH 231.8+4.2, CY Canis Majoris, M1-92, UHF obs. 0-90550
 OH radio emission sources, type IIc, in W33, obs. (*Russian*) 0-62247
 SiH⁺, oscillator strengths and dissoc. energy determ. from time resolved precision spectroscopy 0-58272

astronomical spectroscopy see astronomical spectra; spectroscopy

astronomical techniques

- see also astrometry; radioastronomical techniques
 active aperture imaging for direction meas. of high energy γ -rays 0-62022
 AKAIHOSHI flexible real time software system for radio astronomy obs. 0-82214
 amplification of optical stellar images by atm. turbulence 0-72782
 asteroid family detection by new criterion, orbital data 0-82256
 asteroid surface studies from Earthbound obs., technique 0-77324
 asteroids orbital perturbations, analytical integration using regular proximities concept 0-72843

astronomical techniques continued

- astrometry, astroclimatic influences on precision of photographic star positions obtained with wide-angle astrophotographs (*Russian*) 0-72748
- astrometry, PDS microdensitometer meas. appl. to NGC 6494 (M23) cluster membership determ. 0-98697
- astrometry, reference photographic catalogue of southern sky (*Russian*) 0-72789
- astrometry, sky photography programme with wide-angle astrophotographs (*Russian*) 0-72747
- astrometry, stellar absolute declinations system construction for entire sky using high-latitude obs. 0-67520
- astrometry and planetary detection using space-borne interferometers 0-109357
- atmosphere surface layer optical inhomogeneities, investigation via acoustic method 0-67434
- automated faint galaxy counts and galactic evolution 0-105350
- automatic reduction of low dispersion objective prism stellar spectra (*Italian*) 0-98567
- automatic reduction of nebular emission line spectra 0-77294
- autoregressive technique, appl. to astronomy and geodynamics (*Chinese*) 0-85869
- B-type stars detect. in interstellar clouds, use of interstellar molecules distrib. (*Russian*) 0-105321
- background subtraction problem in panoramic photometry (*Italian*) 0-98570
- binary stars, stellar wind and gas streams obs. using multichannel spectropolarimetry 0-109471
- close binary systems, radial vel. curves anal. 0-94829
- Bragg mode analyser potassium acid phthalate, Bragg refl. coeff. obs. 0-95204
- celestial mechanics, 2101 Adonis problem soln. by recurrent power series integration 0-72842
- Cepheid binary detection from U-V curve obs. 0-98667
- Cepheid variables, phase shift technique for determining incidence of duplicity 0-90453
- classification criteria for stars and star clusters, statistics from co-occurrence matrix (*Italian*) 0-98574
- close binary stars, obs. by H I α and β line photometry 0-109470
- close binary systems, radial vel. curves anal. 0-90470
- coelostat pointing method 0-90338
- cometary equations of motion, recurrent power series integration 0-72882
- computer aided calibration technique for EUV instruments 0-85839
- CORAVEL, Cassegrain spectrophotometer for stellar radial vel. determ. 0-82210
- cosmic ray detection methods for energies $>10^{10}$ eV 0-82157
- COSMOS machine for automatic photographic plate image meas. 0-77293
- deconvolution by maximum entropy, appl. to M87 jet optical photograph 0-62032
- deconvolution method and appl. to lunar occultations 0-105174
- design method for field corrector for parabolic reflector, design method (*Chinese*) 0-85857
- distance determ., Baade's method for pulsating stars 0-73082
- dust complexes in spiral galaxies, optical anal. method, visible obs. 0-101638
- eclipsing binaries light curve analysis, new techniques and appl. to V444 Cygni 0-82417
- eclipsing binaries photometric peculiarities anal., appl. to AU Monocerotis 0-77448
- eclipsing binary stars, light curve analysis by Fourier techniques 0-72993
- eclipsing binary stars, light curve analysis by Fourier techniques 0-72994
- eclipsing variables, light curves linear analysis, fractional light loss anal. 0-82416
- electron-positron pair track analysis in multilayer gamma-ray telescope 0-63469
- ELSPEC/2, interactive procedure for spectrogram processing (*Italian*) 0-98566
- exospheres of Moon and Mercury, Monte Carlo simulation methods 0-67588
- exospheres of Moon and Mercury, Monte Carlo simulation methods 0-67589
- extragalactic distance scale calibration, appl. to distance of giant spiral galaxy (M 101) 0-67852
- extraterrestrial civilisations signals search, simulation approach 0-62039
- fitting procedures for stellar positions on Schmidt photographs 0-72783
- fine grating photometer obs. of southern visual star magnitude differences 0-67785
- galaxies distance scale, determ. from IR magnitude/H I vel. width rel. to expansion rate outside Local Supercluster 0-105325
- galaxies stellar population synthesis, spectral inversion technique 0-90339
- galaxy covariance function shape determ. at small scales 0-82506
- galaxy mass determination from binary galaxies, anal. of Turner's (1976) sample 0-67849
- galaxy surface photometry, numerical mapping by interactive procedure (*Italian*) 0-98572
- global astrometry by space techniques, HIPPARCOS 0-109369
- globular star cluster age and distance determ. method 0-82435
- gravitational radiation, seismometer detection possibility 0-86196
- grid photography, appl. to NGC 4565 halo photometry 0-62261
- ground-based astronomy, future, conference, Arizona (1979 May 9) 0-62386
- hierarchical clustering techniques, appl. to NGC 1023 galaxy group membership 0-82521
- high-resolution astronomical imaging, results 0-82225
- holography, twin-image, chromatic lens system, astron. appls. 0-87346
- image photometric analysis for astrometry, appl. to Jupiter and Galilean satellites (*French*) 0-85880
- image processing, digital system (*Italian*) 0-98558
- image processing by digital filtering (*Italian*) 0-98573
- image reconstruction, iterative computer method 0-102634
- imagery multiple analysis at JPL's Image Processing Laboratory 0-82219
- images digital display, interactive program (*Italian*) 0-98559
- imaging of extrasolar planetary systems 0-82426
- information processing methodologies, conference, Trieste, Italy (1979 February 23 to 24) (*Italian*) 0-94917
- integrated IR photometry and wide field techniques for globular clusters 0-67574
- interplanetary dust, density and phase function determ. 0-109324
- interstellar reddening law and dust content determ. in nearby extragalactic systems, new method (*German*) 0-67850

astronomical techniques continued

- interstellar scintillation method for quasar and galaxy superfine radiostructure (*Russian*) 0-77297
- inversion technique for determ. of instantaneous spectra 0-82218
- IR flux method for stellar temps. and diameter determ. 0-62030
- IR image production, high resolution, use of totally computer controlled telescope 0-72785
- near IR photography, with vacuum-cold camera 0-90341
- iterative nonlinear pulsation theory, extension to double mode case for Cepheids 0-82369
- Jovian centre location in Voyager image transformation 0-101534
- Jurkevich period search method, appl. to southern δ Scuti stars AI, WZ and XX Sculptoris 0-90452
- laser range-differencing, Earth pole posn. and rotation determ. 0-101312
- least squares method, generalisation 0-62028
- light curve analysis for eclipsing binary stars appl. to V444 Cygni 0-109374
- line profile computation methods for stellar envelopes 0-85868
- local non-polar terms determ. by Okuda's method, discussion (*Chinese*) 0-85842
- luminosity function determination method from preselected random samples, appl. to quasars 0-94719
- lunar core samples, technique for thermal cond. meas. 0-72781
- lunar crater image edge determ. 0-98581
- lunar features, absolute heights from photographs, computer processing technique (*Russian*) 0-109380
- lunar occultations scans, object shape retrieval from new algorithm 0-105149
- lunar surface rock comp. remote sensing, regolithic radioactivity in Mare Crisium 0-62045
- magnetic fields detection in late-type dwarf stars, line profiles Fourier deconvolution method 0-72949
- magnetic fields of compact thermal sources, determ. via linear polarisation spectrum (*Russian*) 0-90344
- magnetic measurement in interplanetary space during Halley-Venus mission, Planet-A project (*Japanese*) 0-94672
- mean latitude non-polar var., techniques anal. (*Chinese*) 0-85841
- meridian instrument pivot irregularities meas. method 0-94718
- metal abundance determ. using CORAVEL radial vel. scanner for dwarf stars 0-94791
- meteors, simultaneous visible and radar obs. technique 0-77354
- methane, liquid, detectability on outer planets, laboratory optical absorpt. spectra 0-93278
- minor planet orbit determ. using Chebyshev's approx. (*French*) 0-94720
- MK spectral classification from uvby β photometry, general case 0-82216
- Monte Carlo model, N-body, for galaxy correl. functions evolution 0-62292
- nearby star suspects selection from Luyten proper motion catalogues, use of Luyten's magnitude estimates 0-82353
- occultations photometry, photoelectric photometer appl. (*Chinese*) 0-105172
- opacity sampling technique for early B-star LTE model atm. 0-90414
- optical data processing methods for solar granulation spectral analysis 0-101570
- optical testing of Schmidt camera aspheric corrector, simple null test 0-91940
- orbit determination for cosmic object, Green's functions appl. 0-61992
- photodiode detectors, thermal background subtraction 0-90342
- photoelectric photometry, UVB obs. method and reduction 0-72784
- photographic plate background fitting, interactive procedure (*Italian*) 0-98571
- photometry, appl. of single repetitive filter cycle photometer with sky background compensation 0-62025
- photometry, data collection with aid of microcomputer (*Czech*) 0-67570
- photometry, investigation of double astrophotograph system (*Russian*) 0-72771
- photometry of compact galaxies near M3 and M92 with two telescopes, selection and statistics 0-77485
- picture processing, appl. to Venus cloud layer struct. determ. from Venera 9 televised pictures 0-67604
- planet thermal radiation intensity field modelling; principles 0-62056
- planetary atmosphere single-scatt. albedo determ., theory for Rayleigh-scatt. atmosphere with true absorpt. 0-94704
- planetary nebulae, distances determ. through nebular ionised mass/nebula radius relation 0-101625
- planetary nebulae central star, far UV flux determ. from nebula ionisation state 0-72945
- planetary nebulae distance scale, meas. techniques 0-109521
- planetary orbits computation using Chebyshev polynomials, appl. to minor planets (*French*) 0-61997
- planets rectangular coordinates, approximation via Chebyshev polynomials (*Russian*) 0-62033
- plasma X-ray diagnostics 0-59282
- polarimetric method for nature of cataclysmic binary stars (CBS), critique and appl. to (Cygnus X-1) 0-109486
- polarimetry with Norikura Observatory coronagraph (*Japanese*) 0-82223
- proton flux from solar flares, determ. from ^3He in lunar rocks 0-98576
- pseudo-colour images representation, graphic processor appl. (*Italian*) 0-98562
- radial vel. determ., survey of different methods 0-73006
- radiometry in quasi-isotropic atmosphere 0-90345
- radioresources, method for distance determ. 0-109559
- reduction of 19th century obs. of Uranus and Neptune positions, method comparison 0-94691
- relativistic electron spectra, inference from meas. of inverse Compton radiation 0-90339
- reliability analysis appl. to EUV spectrometer 0-85864
- RI photometry with CCD camera, appl. to Einstein X-ray Observatory fields 0-62315
- satellite photographic tracking, astronomical method (*Chinese*) 0-77254
- second order perturbation theory for inner planets (*French*) 0-72801
- selenodetic reference network construction, choice of coordinate system (*Russian*) 0-72797
- self consistent FORTRAN subroutines for Earth motion determ. 0-85845
- sky background estimation on starfield plate 0-67577
- slitless spectroscopy for quasars 0-86009
- slitless spectrum technique for quasar systematic surveys 0-105384
- solar chromosphere active regions, bidimensional spectroscopy obs. with birefringent filter (*Italian*) 0-98568
- solar chromosphere flares, initial phase parameters determ. method 0-62104

astronomical techniques continued

- solar constant determ. methods 0-77376
- solar coronal plasma density, determ. from reson. lines fine struct. components 0-101581
- solar flares, radio brightness distrib. processing in one-dimensional synthesis (Italian) 0-98628
- solar granulation mean vertical vel. determ., spectrograms correction function 0-62094
- solar magnetic field above flocculus, determ. from radio obs. 0-98635
- solar photosphere, vel. gradients retrieval from line asymmetries, linearised approach 0-62093
- solar photosphere microturbulent vels. and damping const. determ., errors (Russian) 0-72899
- solar spectra, line profiles, rough reconstruction from series of narrow-band filtergrams (Italian) 0-98564
- solar spectral lines, high-resolution meas. using scanning Fabry-Perot interferometer 0-77298
- solar wind MHD discontinuities, identification method 0-109322
- solar wind parameter measurement using charged-particle spectrometer, instability of analyzing voltages 0-67565
- Space Telescope pointing control fine guidance subsystem design 0-82201
- speckle interferogram masking, holography and phase flipping 0-109373
- speckle interferometry, appl. to binary stars obs. 0-90477
- speckle interferometry, obs. of binary stars with Huat-Provence 1.93 m telescope 0-90475
- speckle interferometry image processing technique requiring no reference point 0-98556
- spectra reduction by microcomputer based system 0-77296
- spectral anal. analytical method for solar flare impulsive hard X-ray burst (Chinese) 0-85919
- spectral line polarisation meas. in solar VUV spectra, technique and data reduction 0-67691
- spectrophotometric data processing by large scale interactive one dimens. array processing system 0-82220
- standard candle location, giant elliptical galaxy selection 0-105353
- star counts, indicator of galaxy struct. and quasar evolution 0-82507
- stars space densities derivation, new method 0-85932
- statistical methods for star field and config. anal. 0-82224
- stellar $\Delta\alpha$ -photometry, appl. to meas. of 5200 Å feature in Ap stars 0-67734
- stellar absolute luminosity calibration using binary stars, relevance and consistency 0-62111
- stellar absolute magnitudes determination, comparison between Geneva photometric boxes and MK spectral types 0-77385
- stellar gravity and effective temp. determ. by automatic procedure 0-98557
- stellar interferometry, first fringe meas. 0-82215
- stellar magnetic fields measurement techniques 0-82213
- stellar MK spectral classification from photometric obs., appl. to uvby δ photometry with assumed luminosity class 0-67700
- stellar motion and vel. from previous surveys 0-82395
- stellar open clusters, age determ. methods (Italian) 0-90489
- stellar photoelectric photometry, efficiency as function of image quality 0-62034
- stellar photometry, absolute calibration of spectral energy distrib. of 16 stars in 3500 to 7500 Å region 0-67710
- stellar photometry, appl. of focal reducer using Fresnel lens 0-67568
- stellar photometry, photographic, digitalised image processing, reduction procedures (Italian) 0-98569
- stellar simultaneous UVB photometry, by fast double head photometer 0-72775
- stellar spatial distrib. in globular star clusters, recovery method (Russian) 0-94722
- stellar speckle interferometer data for astronomical object reconstruction, iterative method 0-106475
- stellar spectral synthesis, appl. to broad flux depressions of Ap stars and comparison with spectrophotometry 0-67735
- stellar spectrophotometry, Moscow and Alma-Ata data comparison with multicolour photometric systems 0-101590
- stellar spectroscopy, appl. of linear filtering theory to line profiles (Italian) 0-90340
- stellar structure theory, appl. of Clairaut coordinates to vibr. stability of distorted stars 0-90408
- Sun, use of MHD pulses as diagnostic technique 0-109405
- sunspot mag. flux tubes, method for magnetostatic equil. solns. 0-98637
- SURF storage ring calibrations for NASA stratosphere and climate programs 0-94721
- synthetic spectra calc. method for hot stars with circumstellar clouds 0-77382
- synthetic-aperture radar on satellites, digital processing techniques 0-61914
- telescope optics testing by Hartmann method, estimation of reliability of results 0-67564
- television-electronics study of faint astronomical objects, review 0-82208
- timing method for astrophotography 0-67572
- unstable systems, absolute and convective instabilities discrimination method 0-98539
- wave tilt sounding of multilayered structures on planetary surfaces 0-61926
- white dwarfs magnetic fields measurement, anal. of atomic spectra in intense mag. fields 0-105160
- X-ray astronomy, point source imaging via automodulation collimator telescope (Russian) 0-62018
- X-ray detection of cosmological objects 0-62323
- X-ray spectra deconvolution 0-85867
- Zeeman line profile, mag. field determ. by radiative transfer method 0-82221
- H II regions density fluctuations, statistical approach 0-77468
- H II regions' exciting stars mean temp. determ. method 0-73024

astronomical telescopes

- see also radiotelescopes
- 25 m equivalent aperture, optical and IR, design concepts 0-82203
- 80 cm X-ray telescope, facilities and observational possibilities (German) 0-109358
- altazimuth mounted, primary mirror deflection and stress anal. 0-58659
- autoguiders and acquisition systems for optical telescopes 0-82206
- Cassegrain telescope design and tolerancing optimisation 0-82199
- catoptric Schmidt telescope correcting mirrors, aspherication by elastic relax. (French) 0-98515

astronomical telescopes continued

- coelostat, star pointing, Meudon solar tower 0-90338
- cosmic ray telescope, solid state, detection system for heavy ions, element and isotope separation 0-67563
- double astrophot photometric system, investigation of colour eqns. (Russian) 0-72771
- far IR telescopes, balloon-borne, calibration source 0-62027
- field corrector for parabolic reflector, design method (Chinese) 0-85857
- gamma-ray telescope, large sensitivity, energy and angular resolution 0-62016
- gamma-ray telescope, spark chamber, scintillation counter time-of-flight system 0-62017
- gamma-ray telescope spark chamber, e^+e^- track analysis 0-63469
- gearless telescopic drive, transference from elec. motor to polar axis 0-67571
- giant mirrors, telescope design for 1990s, conf. report and review 0-105170
- Hadamard transform X-ray telescope, characts. (Japanese) 0-94714
- HIPPARCOS, global astrometry by space techniques 0-109369
- image contrast of diffraction-limited telescopes for circular incoherent sources of uniform radiance 0-82194
- IR sky survey telescope, wide field photography 0-105167
- Kitt Peak National Observatory telescopes, cost effectiveness in terms of publications and citations 0-90334
- KSC 60 cm reflector, data recording system (Japanese) 0-94717
- Lixiseq, X-ray and gamma-ray telescope system 0-62020
- meridian instrument pivot irregularities meas. method 0-94718
- mirror testing using autocollimation method with multiple pendulum mirrors 0-102792
- Multiple Mirror Telescope and ground-based astronomy, conference, Arizona (1979 May 9) 0-62386
- multiple-mirror telescope systems, astronomical appls. 0-94713
- Nanjing lightweight 4 m telescope design and construction 0-105162
- optical table 10 m telescope 0-105163
- optics testing by Hartmann method, estimation of reliability of results 0-67564
- Palomar Hale telescope, first 30 years 0-72774
- parabolic reflector, coma corrector for off-axis guiding 0-82196
- Salyut 6 submm. telescope with InSb receiver 0-67566
- Schmidt camera, simple null test for aspheric corrector plate 0-91940
- secondary mirror centering of Tingo telescope 0-105133
- Space Telescope, adaptation to Space Shuttle capabilities 0-109364
- Space Telescope, design and projected performance 0-105165
- Space Telescope, scientific instruments 0-61987
- Space Telescope astrometry from CCD images 0-109370
- Space Telescope astrometry project 0-105175
- Space Telescope detection of extra-solar planetary systems 0-109356
- Space Telescope pointing control fine guidance subsystem design 0-82201
- Space Telescope spectrograph Digicons 0-85858
- UV high-resolution optical telescope design 0-90335
- vidicon appl. to low intensities meas., with Si-intensified target (German) 0-98545
- Wolter-Schwarzschild optics for Berkeley stellar spectrometer and EUV Explorer 0-82197
- X-ray spectrometer-telescope system for solar corona studies 0-105168
- X-ray telescope, HEAO-2 Observatory, protective design considerations, system reliability 0-61983
- X-ray telescope, new design using automodulation collimator (Russian) 0-62018
- X-ray XUV telescope/white light coronagraph expt., quadratic A/D converter 0-62024
- XUV solar telescope and white light coronagraph, CCD camera systems and support electronics 0-62023
- zenith telescope, use as astrolabe for time and latitude meas. 0-98550

astronomy see astronomy and astrophysics**astronomy and astrophysics**

- see also astronomical catalogues; astronomical instruments; astronomical observations; astronomical observatories; astronomical spectra; clusters of galaxies; cosmology; extraterrestrial life; galaxies; gamma-ray astronomy; infrared astronomy; intergalactic matter; interplanetary matter; interstellar magnetic fields; occultations; radioastronomy; solar system; stars; ultraviolet astronomy; X-ray astronomy
- Ambartsumian's proto-matter hadronic nature from ang. momentum-mass relation 0-77528
- Ann Arbor school of astronomers, foundation, 1852-63 0-86062
- anti-matter, possible role in high energy astrophysics 0-94705
- archaeoastronomy, Namoratunga II site in NW.Kenya, astronomical dating 0-72793
- archaeoastronomy, New Mexico site marking solstices and equinoxes 0-72794
- Asian-South Pacific regional meeting in astronomy, Wellington, New Zealand (1978 December 5 to 8) 0-77538
- Astronomical Society of India, fifth meeting, Nainital, India (1979 November 6 to 9) 0-101658
- atom motion in very strong mag. fields, mass anisotropy effect (Russian) 0-67557
- atomic collision, coherence and correlation, book 0-90615
- axions, very low mass, astrophysical bounds and stellar-energy loss 0-109353
- balloon and rocket programs, conf. Bournemouth, England (1980, Aug.) 0-105433
- beta strength function, half life and delays, nuclear- and astro-physics consequences 0-102149
- beta strength function structures, nuclear- and astro-physics consequences 0-99152
- charge transfer reactions, appl. to photoionisation model of planetary nebula (NGC 7662) 0-62233
- Compton scattering by unmagetised electrons in ambient mag. field, vacuum polarisation effects 0-86631
- condensed matter in huge magnetic fields, astrophysical problems 0-82187
- conference, general congress, Societe Francaise de Physique, Toulouse, France (June 1979) 0-77536
- conference, New Delhi, India (Jan. 1979) 0-94912
- conference of American Astronomical Society, proceedings of 155th meeting, San Francisco (Jan. 1980) 0-73091
- constellation concept and projective classical group 0-62869
- convection, turbulent, in Boussinesq fluids, viscosity, conductivity and power spectra 0-98543

astronomy and astrophysics continued

- cosmology, sources luminosity evolution from scale parameter for Friedmann models 0-77527
dense matter in laser driven fusion, laboratory expts. 0-75077
dense matter physics, conference, Paris, France (1979 September 17 to 21) 0-73094
dense plasmas and nuclear reactions, astrophysical appls. 0-77281
dense plasmas transport coefficients, kinetic theory 0-77280
Einstein's contribution to cosmology 0-77530
extrasolar planetary systems, direct imaging 0-82426
FK5, equinox and equator of new fundamental reference coord. system 0-109341
fluid theory, universality in short range struct. in simple classical fluids 0-75141
fundamental system of star position and motion, accuracy improvement using asteroid obs. 0-94692
gravitational radiation, collapsed objects and exact solns., Einstein Centenary Summer School, Perth, Australia, 1979 January 0-105434
Gray, Stephen (1666-1736) 0-77601
ground-based astronomy, future, conference, Arizona (1979 May 9) 0-62386
heavy Majorana particles, cosmological and astrophysical implications 0-90331
high energy astrophysics, handbook 0-73113
historical astronomy, Latin terminology relating to aurorae, comets, meteors and novae 0-62437
hydrodynamics, absolute and convective instabilities distinction and appl. to interstellar medium 0-98539
hydromagnetic free convection flow in Stokes problem, for porous vertical limiting surface with const. suction 0-90328
Indian epicyclic astronomy, history and chronology of treatises 0-62448
interstellar radiolink, using Sun as gravitational lens antenna 0-62040
inverse Compton radiation sources, inference of relativistic electron spectra 0-90339
ionic mixtures, phase separation 0-77279
Israel Physical Society 1980 annual meeting, Rehovot, Israel (April 1980) 0-94909
Kukarkin, Boris Vasil'yevich (1909-77), Russian astronomer (*Russian*) 0-101701
Langmuir waves, turbulent bremsstrahlung process 0-62009
line sources, elec. and mag., interaction with moving magnetoplasma slab, EM radiation 0-67537
magnetic oblique rotator, EM field prod., exact vacuum soln. 0-58442
Marquis de Charbert (1724-1805), biography and link with Louisbourg Observatory 0-68010
megahertz lunar site a Callanish, Lewis 0-77300
methanol-d₁, (CH₂DOH), microwave torsional-rot. spectrum, rel. to interstellar search 0-99498
methanol-d₁, laboratory freqs. of J=2-1, a-type transitions 0-63624
Minor Planet Center, history and future 0-94712
multicharged ion thermal charge exchange reaction, rel. to astrophysics 0-63815
neutrino and photon emission from blackbody, thermodynamic laws 0-105451
neutrino astrophysics, review, book contrib. 0-72769
nuclear astrophysics, introduction to form. and evolution of matter in Universe, book 0-105447
observational astronomy, contrib. of Tobias Mayer 0-62438
optical spectral line emission bursts in X-ray heated medium (*Russian*) 0-77286
particle acceleration near singular line of mag. field, energy spectrum (*Russian*) 0-90332
planetary nebulae, advances in theory of physical processes 0-109527
planetary nebulae, atomic and molecular data for heavy particle processes 0-109528
planetary nebulae, observations and theory, IAU Symposium 76, Ithaca, New York, USA (1977 June 6 to 10) 0-105435
plasma, interaction of knowledge from magnetospheric, astrophysical and lab. plasmas 0-59166
plasma, relativistic modes of tearing instability in background plasma 0-62012
plasma, rotating, effect of suspended particles on gravit. instability 0-109347
plasma, self-gravitating, isotropic pressure, gravit. instability 0-72763
plasma astrophysics, nonthermal processes in diffuse magnetised plasmas, wave physics, book 0-105446
plasmas, di-electronic recombination (*French*) 0-82188
radiative transfer, comoving-frame transfer eqn. soln. in spherically symmetric relativistic flows 0-82181
seeing, meas. at Kitt Peak 0-61899
SETI at 18 cm, high sensitivity search 0-82229
shock waves, plane, relativistic, propag. in slowly moving medium 0-62005
Smyth, Charles Piazza (1819-1909) at Cape of Good Hope 0-68011
space optics, conference Huntsville, Alabama (1979 May 22 to 24) 0-62385
spectral line formation depth in mag. field, theory (*Chinese*) 0-105159
star fields and configurations, anal. by statistical methods 0-82224
Stark broadening, trends in homologous ions series 0-105157
stochastic phenomena 0-105161
Stokes problem, effects of free convection on oscillatory flow past infinite porous vertical limiting surface 0-109348
Stokes problem, for infinite vertical plate with const. heat flux 0-79108
superdense celestial bodies, theory 0-67773
thermal-convective instability of partially ionized plasma, radiative transfer, medium porosity and collisional effects 0-67538
thermonuclear reaction rates, thick target meas. 0-73108
Thomson scattering in strong mag. field, vacuum polarisation effects 0-86632
Weinberg-Salam model and extensions, ν EM form factors and mag. moments, neutral currents, astrophysics appls. (*German*) 0-62904
Zeeman splitting of high-n recomb. lines, theory 0-58210
H, longit. excited states in intense mag. fields, rel. to pulsars 0-91469
Mg XI resonance lines, dielectronic satellite lines atomic parameters calcs. 0-78567
Mn abundance meas. by sun model 0-91501
Ni IX to Ni XII, wavelengths of transitions between lower configurations 0-99474
ZrO, singlet-triplet separation meas. 0-78623

astronomy computing

- see also computerised instrumentation*
AKAIHOSHI flexible real time software system for radio astronomy obs. 0-82214
automatic reduction of low dispersion objective prism stellar spectra (*Italian*) 0-98567
CDCA-Nice software package, implementation in Italian institutes implementation in Italian institutes (*Italian*) 0-98561
data analysis, procedure for Asiago Reticon spectrophotometer (*Italian*) 0-98565
digitised images, anal. via interactive data processing system (CIPS) (*Italian*) 0-98560
digitized images, structural pattern recognition (*Italian*) 0-98554
Easter date determ. for any year, program for HP 29C 0-77268
eclipsing binaries light curve analysis, new techniques and appl. to V444 Cygni 0-82417
eclipsing binary light curves soln. using LIGHT computer program 0-77454
eclipsing variables, light curves linear analysis, fractional light loss anal. 0-82416
ELSPEC/2, interactive procedure for spectrogram processing (*Italian*) 0-98566
EUV instruments, computer aided calibration technique 0-85839
galaxy surface photometry, numerical mapping by interactive procedure (*Italian*) 0-98572
image processing, digital system (*Italian*) 0-98558
images digital display, interactive program (*Italian*) 0-98559
information processing methodologies, conference, Trieste, Italy (1979 February 23 to 24) (*Italian*) 0-94917
Jovian centre location in Voyager image transformation 0-101534
large scale interactive one dimens. array processing system, spectrophotometric appl. 0-82220
lunar crater image edge determ. 0-98581
lunar features, absolute heights from photographs, computer processing technique (*Russian*) 0-109380
minor planets ephemerides, orbits computation using Chebyshev polynomials (*French*) 0-61997
MK spectral classification from uvby β photometry, general case 0-82216
orbit computation in galaxy models, algorithms 0-67797
orbital motion on an interactive-graphics terminal, teaching appl. 0-73152
photographic plate digitalised image, object detect. using FINDER program (*Italian*) 0-98575
photometry, data collection with aid of microcomputer (*Czech*) 0-67570
planetary, solar and lunar positions, low-precision formulae 0-61990
planetary and satellite systems evolution 0-77308
planetary system evolution, simulations 0-94733
planets rectangular coordinates, approximation via Chebyshev polynomials (*Russian*) 0-62033
pseudo-colour images representation, graphic processor appl. (*Italian*) 0-98562
radiotelescope antenna array performance, simulation of super-synthesis telescope 0-98548
self consistent FORTRAN subroutines for Earth motion determ. 0-85845
spectra automated reduction by microcomputer based system 0-77296
teaching aids in schools 0-73126
- astrophysics computing**
see also computerised instrumentation
spectroscopic data, real-time acquisition and preprocessing via RETIC interactive package (*Italian*) 0-98553
- asynchronous electric machines** *see asynchronous machines*
- asynchronous generators**
60 m diameter wind turbine generator, appl. 0-61262
variable speed wind power generator, control strategy for 3-phase output (*French*) 0-76591
windpower development programme in Sweden, appl. 0-61237
- asynchronous machines**
see also asynchronous generators; induction motors
precision measuring table with hollow rotor asynchronous motor, digital control system 0-105607
- asynchronous motors** *see induction motors*
- atmosphere, solar** *see solar atmosphere*
- atmosphere, terrestrial** *see terrestrial atmosphere*
- atmosphere, upper** *see upper atmosphere*
- atmospheric acoustics**
aerosol systems in acoustic field, exptl. study 0-89529
aircraft noise propag., review 0-64258
backscatter in GATE, effect of wind shear and moisture fluctuations 0-85709
boundary layer, simultaneous horizontal and vertical sounding obs. 0-61846
boundary layer gravity waves, acoustic sounding obs. 0-61847
correlation of the phase and amplitude fluctuations between direct and ground-reflected sound 0-96067
echosonde signals, excess attenuation 0-83694
frequency shift of wave train due to absorb. 0-64255
nonlinear absorption of sound, rel. to atmosphere acoustic and radio acoustic exploration (*Russian*) 0-94567
radioacoustical sounding, expression for scatt. signal freq. spectra (*Russian*) 0-94612
sounding, appl. to boundary layer obs. from top of steep mountain 0-98409
surface layer, acoustic method for optical inhomogeneities fluctuations 0-67434
thunder propag., status of current research 0-87618
tornado over Delhi, of 1978 March 17, sodar obs. 0-109188
- atmospheric boundary layer**
Aberdeenshire, mesoclimate of Upper Don Basin 0-61889
acoustic sounder observations, from top of steep mountain 0-98409
acoustic sounding obs., simultaneously in horizontal and vertical directions 0-61846
air-sea interface, heat transfer coeffs. meas. 200 km from land 0-72552
airflow transformation over nonuniformly heated underlying surface 0-82031
Birmingham, England, heat island synoptic climatology (1965-74) 0-85740
bulk model, for wind and pot. temp. 0-77030

atmospheric boundary layer continued

- buoyant plume in stably stratified boundary layer, max. ground conc. 0-72573
- convective boundary layer, boundary layer, appl. of mixed-layer similarity scaling to observed dispersion from ground-level source 0-105021
- convective disturbance thermodynamic struct. 0-81978
- cumulus capped planetary boundary layer, numerical model (*French*) 0-94574
- diabatic heating profile, rel. to preferred mode of Ekman conditional instability of second kind (CISK) 0-72617
- diurnal var. of R_n and mixing height for USA Gulf Coast 0-101404
- eddy flux measurement of various quantities corrected for density fluctuations 0-72576
- fog and haze microphysics, visual range obs., and particle size distrib. 0-109195
- formaldehyde, in marine air and rainwater, wet season obs. 0-85703
- GATE aircraft measurements, their value 0-82071
- geostrophic flow over shallow topography 0-90120
- gravity waves observed by acoustic sounding 0-61847
- ground surface temperature prediction, force-restore method investigation 0-98469
- heat fluxes, latent and sensible, from lakes, prediction from surface water temps. 0-72562
- hill affecting airflow, overspeed effect 0-72577
- hill crest, obs. of wind speed, shear and turbulence 0-85722
- horizontal roll vortices, two dims. numerical obs. 0-101409
- Indian Ocean, surface temp. rel. to Indian summer monsoon intensity 0-90121
- interaction of boundary layer with free atmos. (*Russian*) 0-77037
- jetlike wind at 100-600 m altitude over open coast, mesoscale nocturnal phenomena 0-81971
- Lake Michigan, cold water modifying boundary layer struct. 0-72571
- light scattering variability over N. Atlantic rel. to humidity and aerosol 0-82052
- marine atmosphere, surface layer stability rel. to oceanic whitecaps and sea state 0-72554
- marine boundary layer along California coast, instability rel. to marine fog and fog-stratus systems 0-77060
- marine layer, shipboard use of low-level atmospheric thermograph in fog and stratus investigation 0-105073
- marine layer at San Diego, California, depth and moisture content rel. to cool season precip. forecasts in Arizona 0-101395
- marine surface layer, air-sea exchange of heat and water, model 0-61809
- Mohliner Feld (east of Basle), topoclimate investigations (*German*) 0-61890
- Monin-Obukhov similarity functions, from closure model 0-81972
- monsoon airstream at 12 metres height, temp. fluctuations 0-61845
- mountain barrier baroclinity effect on wind direction, Alaskan arctic coast 0-90118
- mountain in airflow, 2-D numerical simulation (*Russian*) 0-81986
- mountainous terrain, atmosphere turbulent kinetic energy budgets 0-105022
- nighttime boundary layer, vertical struct. obs. 0-61848
- nighttime turbulence, wind and temp. obs. compared with model calcs. 0-85707
- ocean, Lagrangian wind and current vectors very close to short-fetch wind-swept sea surface 0-72553
- ocean atmosphere interaction, mean wind speeds and turbulence at coastal site and offshore location 0-98406
- optical inhomogeneities, investigation via acoustic method 0-67434
- orography, influence on atmospheric movement with Coriolis force included (*Russian*) 0-94565
- parameterisation of convective and nonconvective planetary boundary layers, for use in numerical models 0-82009
- parameters of boundary layer determined solely from vel. profile 0-81970
- particle cloud, dispersion in boundary layer, theory 0-61842
- planetary boundary layer, above ocean, stratification parameter 0-82037
- planetary boundary layer similarity profile by turbulence closure model 0-72574
- planetary waves, feedback with stochastically driven ice sheet, model 0-77025
- pollutant dispersal from point source, Ekman-type model 0-105039
- pollutant dispersion from elevated source 0-85312
- pollution dispersion from point source 0-81973
- pollution dispersion from tall stack, into shore line environment 0-97832
- psychrometry, appl. of portable differential system 0-105072
- radiative cooling rate and flux, theory 0-85711
- rapid morning boundary-layer transition, case study from Haswell, Colorado, expt. 0-81996
- refractive index in atmospheric boundary layer, structural charact. vertical profiles (*Russian*) 0-94597
- shear flow instability, Kelvin-Helmholtz and reson. overreflection modes, vortex pairing interactions 0-90129
- shoreline escarpment affecting boundary layer turbulence, wind profile etc. 0-109243
- smoke plumes in surface layer, cross section diffusion (*Russian*) 0-104532
- soil-atmosphere boundary, heat and moisture transport 0-77023
- sounding system for meas. of wind speed and direction, and temp. (*German*) 0-94616
- stationary mesoscale fields, method of calc. from remotely sensed data 0-85734
- steam fog in Fenlands, obs. after heavy rain, (1979 May 1) 0-98431
- sunrise effect on elec. pot. near ground, origin in upper atmos. 0-61866
- surface and soil temperature anals. in humid tropics, case study from Sierra Leone 0-109242
- surface fluxes, scheme for computation from mean flow obs. 0-77031
- surface layer, organised motion features 0-72602
- surface temperature, determ. of diurnal var. in mountainous terrain 0-82011
- temperature fluctuations, heat flux and struct. functions meas. with acoustic Doppler sodar 0-105023
- temperature forecasting for nighttime, short-range model 0-109200
- temperature profile determ., ground-based microwave radiometry (*German*) 0-82097
- temperature structure coeff. detect. by acoustic radar 0-98386
- tropical cyclone, model of ocean-atmos. boundary layer interaction 0-109231
- turbulence and waves in planetary boundary layer, Doppler radar obs. 0-90184
- turbulence coeff. vertical profile 0-85733

atmospheric boundary layer continued

- turbulent boundary layer, finite-element numerical modelling 0-77061
 - turbulent mass transfer, plume dispersion (*French*) 0-61850
 - turbulent mixing, rel. to use of passive antenna system as cond. meas. device 0-85762
 - urban atmosphere, numerical simulation of mixing depths 0-105024
 - urban atmosphere, radiative effects of elevated pollutant layers on temp. struct. and pollutant dispersion 0-97841
 - urban environment, cold air drainage effects on temp. fields, case study of topographical influence on climate 0-94555
 - urban heat island, Rome, obs. during summer season 0-85717
 - urban microclimate of Alma-Ata, significant factors 0-101418
 - urban valley micrometeorology of N. Saskatchewan river valley 0-61843
 - urban-scale wind fields, three-dimensional, construction, objective anal. technique 0-101407
 - vertical eddy flux representation for weather forecast model 0-61844
 - vertical frictional motions on varying scales (*Russian*) 0-105027
 - weather forecasting numerical model, parameterisation of boundary layer 0-72572
 - wind and isotropic turbulence lateral coherence 0-72575
 - wind and temp. profile prediction model, for diabatic layer 0-77032
 - wind flow over water, determ. from phase speeds of upwind and downwind travelling short gravity waves 0-98332
 - wind in planetary boundary layer, 3-D field obs. width radar 0-90183
 - wind in rough time terrain, derivation of mass-consistent flow field from wind obs. 0-105013
 - wind interaction with dry snow and bare ice surface 0-109181
 - wind profile curvature of surface layer, rel. to Richardson number 0-81974
 - wind shear hazard in boundary layer, radar detection feasibility 0-90256
 - wind shear measurement, using pulsed Doppler laser 0-67415
 - wind surface stress estimation, mathematics of vel. scaling parameter 0-61849
 - H_2 composition of marine air of N. Atlantic 0-77057
 - SO_2 at ground level, air pollutant dispersal, Forth Valley, Scotland 0-81497
- atmospheric chemistry**
see also atmospheric composition
- acid precipitation in W. United States, pH value obs. 0-89695
 - acidity of NW. Africa snowfields, 1977-79 obs. 0-98370
 - aerosol off W. African coast, Na, Cl and Br composition evolution 0-77053
 - aerosol particle formation in presence of existing aerosol 0-81962
 - ancient atmosphere, fate of OH and O_3 , origin 0-77116
 - anthracene, photooxidation on atmospheric particulate matter 0-61487
 - aurora, N(D) emission and ion chemistry, satellite obs. 0-72673
 - chlorofluoromethane photolysis in stratosphere, effect on O_3 conc. 0-109197
 - clean air chemistry at 55°N, compared with polluted air reactions 0-98382
 - D-region, NO^+ cluster ion formation, temp. control 0-61931
 - D-region ion chemistry during intense radiowave heating 0-61952
 - data uncertainty rel. to environmental decisions 0-104535
 - dimethyl sulphide + $O(^3P)$, fast flow reson. fluoresc. obs. of absolute rate const. 0-61077
 - earthquake lights, proposed for study by chemiluminesc. NO air pollution apparatus 0-61906
 - F-region, Atmosphere Explorer photochemistry rel. to airglow obs. 0-98496
 - F-region, winter anomaly causes 0-85793
 - formaldehyde, chem. of stratosphere, UV absorpt. spectra implications 0-109209
 - formaldehyde + Br $_2$ reactions, rate const. by EPR 0-93736
 - formaldehyde + ClO radical, expt. showing no reactivity, stratospheric implications 0-90119
 - formaldehyde + F reactions, rate const. by EPR 0-93736
 - heterogeneous reactions, role of H_2SO_4 aerosols as tropospheric sinks 0-72612
 - ion composition and ionisation rates 0-61885
 - ionosphere, lower, photodetachment as source of reflecting layer below classical D-region 0-98508
 - methylhydroperoxide, UV absorpt. spectra of vap. 0-69159
 - middle atmosphere, effects of energetic particle precip. on O_3 catalytic removal 0-109213
 - negative ion photodissoc. and photodetachment 0-69199
 - oxidant and precursors, anal. in Los Angeles Reactive Pollutant Program (LARPP) (operation 33) 0-61479
 - ozoneosphere, photochemical-dynamical model rel. to maintenance of zonal mean O_3 distrib. in N. Hemisphere 0-109220
 - peroxynitrates, UV absorpt., spectra, photodissoc. lifetime meas. 0-83386
 - photochemical air pollution, initiation by HONO (nitrous acid) in urban air 0-76677
 - photochemical air pollution potential form. in United Kingdom, numerical estimation method. form. in United Kingdom 0-76682
 - photochemical data and kinetics of gas phase chemical reaction in atmosphere 0-101671
 - photochemical tropospheric O_3 transport, effect on pollution at rural site 0-61481
 - photochemistry, stratosphere and mesosphere O_2 and O_3 photodissoc. through solar UV radiation absorpt. 0-109248
 - photodissociation rate affected by Rayleigh scatt. 0-61921
 - photooxidation reactions, rates, reactivity and mechanism for organic compounds reaction with OH radicals 0-72104
 - reactive N in unpolluted troposphere, stratospheric source 0-94561
 - stratosphere, chem. of meteor trail metal ions 0-72580
 - stratosphere, CO_2 - O_3 coupling in Cl free atm., photochemical-radiative column model 0-85723
 - stratosphere, NO and ClO at twilight rel. to interpretation of conc. meas. via solar occultation 0-85756
 - stratosphere aerosol, modification by supersonic transport and space shuttle operations, climatic implications 0-98408
 - stratosphere O_3 - CO_2 coupling, photochemical radiative column model with Cl chemistry 0-85724
 - stratosphere sulphate aerosol layer, physical and chemical processes models and simulation 0-109212
 - trace gas transport and photochemistry rel. to greenhouse effect (*Russian*) 0-81989
 - troposphere, evidence for significant in situ photochemical O_3 source 0-72619

atmospheric chemistry continued

- lower troposphere modelling, chemical kinetic data needs, conference, Reston, Virginia (1978 May 15 to 17) 0-62383
 upper atmosphere at nighttime, 400-450 km altitude, anal. of Ogo 6 data 0-90267
 Van der Waals molecules comp. of lower atmos. 0-85699
 Br chemistry of stratosphere, and O₃ depletion 0-98391
 ClO₂ in stratosphere, possible existence and chemistry 0-77066
 HNO₃, air pollution obs. in W.Europe 0-72106
 HO₂+ClO, reaction product distrib. 0-72586
 H₂S in troposphere, photochem. production reactions 0-90112
 H₂SO₄ vapour pressure rel. to gas-particle conversion 0-94560
 H₂SO₄+O₂(N₂O₄), collisional reaction probabilities 0-90168
 Li⁺ diffusion and ion-neutral interactions, laser sounding obs. (*French*) 0-82115
 N fixation by lightning 0-90147
 N fixation in lightning channels, theory 0-90148
 N production in upper atmos., model of far UV dayglow 0-90271
 N⁺+H₂, electron capture and ion-loss cross-section, 2.4-24.3 keV 0-58373
 N⁺+O₂, electron capture and ion-loss cross-section, 2.4-24.3 keV 0-58373
 N₂⁺ upper atmos. photochem. rel. to solar cycle phase 0-85783
 N₂+O₂, electron capture and ion loss cross-section, 2.4-24.3 keV 0-58373
 NH₃+O₃, reaction rate const., rel. to atmospheric processes 0-85155
 NH₃ in troposphere, vertical distrib. by photochem. model 0-85701
 NH₃→NH₄⁺ conversion, in atmosphere, pseudo first-order reaction rate const. 0-94132
 NO, production by lightning, shock and channel heating methods 0-72581
 NO₃ in polluted troposphere, spectroscopic detect. and possible sinks 0-77036
 NO₃ in troposphere, obs. of content in mountain air 0-72582
 N(³P) in auroral arc, excitation and collisional deactivation processes 0-72658
 Na excitation and abundance in nightglow 0-98497
 O⁺ to NO⁺ conversion in dayside auroral oval, rel. to rocket-borne VLF and ELF waves meas. 0-98504
 O⁺+N₂, charge exchange collision, rate coeff. and ionosphere implications 0-87224
 O⁺+N₂(O₂), excited ion reactions, charge transfer coeffs. at thermal energy 0-95721
 O⁺+O₃, charge exchange collision, rate coeff. and ionosphere implications 0-87224
 O₃ and related chemistry in mesosphere, Solar Mesosphere Explorer mission description (1981-2) 0-105096
 O₃ content evolution, one-dimensional coupled chemistry-flow model 0-98400
 O₃ in lower atmosphere, transport processes 0-109196
 O₃ in stratosphere, seasonal composition variation at high-latitude 0-77051
 O₃, instantaneous global balance including observed NO₂ 0-109211
 O₃ layer, depletion and chemistry 0-104534
 O₃ layer, photochemistry rel. to possible O₃ reductions and Earth surface UV radiation 0-94577
 O₃ layer depletion by chlorofluorocarbons, calc. using two-dimensional model 0-109221
 O₃ photodissoc., annual var. of effects of diffuse solar radiation 0-109210
 O₃ photodissoc., O(¹S) yield at 1700-2000 Å 0-97714
 O₃ photolysis by sunlight, rate constants at ground level 0-61836
 O₃(¹D) in thermosphere, quenching by electrons 0-94630
 O(¹D) formed by N(⁴D)+O₂ reaction in thermosphere, 6300 Å dayglow implications 0-90270
 O⁺(²D)+N₂, thermal rate coeff., products and branching ratios 0-82117
 O⁺(²D)+N₂, charge exchange, rate coeff. temp. depend. 0-77179
 OH+gaseous S compounds, lower atmos. chem. 0-61870
 OH+RH→H₂O+R, radical substitution reaction 0-81321
¹⁸O¹⁶O, photodissociation as source of atmospheric O₃ 0-94559
 O⁺+N₂(O₂), metastable ion reactions, rate consts. and ion mobility at 300K 0-95722
 S budget of eastern N.America, anthropogenic and natural contris. 0-97834
 S chemistry of lower atmosphere, reactions with OH 0-61870
 SO₂ oxidation to SO₃ in urban atmosphere 0-81964
 SO₂ oxidation to sulphate in troposphere, model predictions 0-81963

atmospheric composition

- see also atmospheric chemistry: atmospheric structure*
 acid sulphate in aerosol, detection from S/N ratio 0-61494
 aerosol, Nigeria during dry dust season 0-81960
 aerosol, size fractionated, comp. in Charleston, W.Virginia 0-89687
 aerosol above Black Sea, spectral transmission and sky brightness obs. (*Russian*) 0-94603
 aerosol air composition at Barrow, Alaska, wind direction depend. 0-85704
 aerosol Al composition after rocket launch 0-81503
 aerosol in Florida, time series anal. 0-89688
 aerosol off W.African coast, Na, Cl and Br composition evolution 0-77053
 aerosol samples, trace substance concs. rel. to sources identification and relative importance estimation 0-72105
 aerosols, IR spectrometry theory and appl. to spectroscopic effects of atmospheric constituents 0-101428
 aerosols, trace element conc. over Lake Michigan 0-81968
 aerosols in Kashmir region, study of chemical components 0-94594
 aerosols in marine air near Europe, 632 nm light absorpt. obs. 0-90136
 aerosols in urban atmosphere, distrib. rel. to mixing depths numerical simulation 0-105024
 aerosols of Antarctica, origins and props. 0-90197
 aerosols over tropical N.Atlantic Ocean, water-soluble K, Ca and Mg contents 0-72598
 aircraft ambient and cabin air O₃ conc. simultaneous determ. 0-90198
 ancient atmosphere, fate of OH and O₃ origin 0-77116
 Antarctic aerosols particle anal., comp. 0-77091
 anthracene, photooxidation on atmospheric particulate matter 0-61487
 aurora modelling, time-depend. study 0-72672
 Brazil, precipitable water, distrib. maps 0-77075
 carbon tetrafluoride, atmospheric content, sources and residence time 0-61879
 cloud condensation nuclei, obs. over N.Atlantic 0-77074

atmospheric composition continued

- cloud condensation nuclei in urban environment, comp. effects on cloud microphysical model 0-82004
 coastal atmosphere, H₂SO₄ aerosol, form. of particulates 0-90113
 D-region, ion composition at midlatitude in quiet conditions, model 0-109307
 D-region, NO density enhancement on winter anomalous day at S. Uist 0-82130
 dichlorofluoromethane pollution, conc. obs. in background troposphere air 0-97843
 differential absorption lidar, complementarity of UV and IR systems for atmospheric species meas. 0-72634
 dust deposition in N.Nigeria, Harmattan dust (1978-79) 0-94578
 dust fallout in Kuwait, summer 1978 obs. 0-81966
 dust in stratosphere, of interplanetary origin, optical absorpt. spectra 0-101554
 N.W. England, coastal site, ambient air quality determ. 0-89690
 F₁-layer, ion comp. and temp. profiles from incoherent scatter radar studies 0-72654
 F₁-layer at nighttime, ion composition near mag. equator 0-72683
 F-region, bottomside, mol. ion densities rel. to airglow anal. 0-98496
 F-region, N atoms and O ions in dynamic model 0-72693
 filter media suitable for air pollutant analysis (HNO₃, nitrates and acidity) 0-104541
 formaldehyde, in marine air and rainwater, wet season obs. 0-85703
 gas phase inorganic ion clusters 0-77068
 Greenland, summer aerosols and trace gases 0-72609
 inert gas composition, Earth's origin from solar nebula 0-61785
 inorganic clusters, gas phase 0-58436
 ionosphere, metallic ions of meteor origin effect in VHF forward scattering, contribution to sporadic-E formation 0-67461
 ionosphere, O⁺/(NO⁺+O₂⁺) ratio in dayside auroral oval rel. to rocket-borne VLF and ELF waves meas. 0-98504
 ionosphere and plasmasphere at midlatitude, computer model 0-105120
 lower thermosphere, compositional modelling taking account of airglow tidal variation 0-109288
 magnetosphere, contamination by spacecraft at geosynchronous orbit 0-72701
 magnetosphere ion composition during mag. storm, high-altitude region 0-82144
 mesosphere, O₃ concs. meas. from 1.27 μm O₂ airglow at middle latit. 0-72606
 mesosphere at Thumba from in situ UV absorpt. photometry obs. 0-105051
 methane, stratosphere content at mid-latitude, simultaneous N and S hemisphere obs. 0-77052
 methane, troposphere vertical profile, eastern USA in winter 0-77035
 middle atmosphere chemical comp., importance of energetic particle precip. 0-109213
 minor constituents transport between troposphere and stratosphere 0-105034
 nitrate determ. using HNO₃ collection on NaCl impregnated filters 0-81509
 nitrates, gaseous, concentrations, investigations in urban and rural area 0-94123
 organic compounds photooxidation, rates, reactivity and mechanism for reaction with OH radicals 0-72104
 oxidant and precursors, anal. in Los Angeles Reactive Pollutant Program (LARPP) (operation 33) 0-61479
 particulate element conc. over USA 0-76679
 particulate nitrate, pollution of S.Ontario, Canada, rel. to weather 0-76678
 particulate nitrate in marine air of equatorial Pacific 0-85702
 particulate size distrib. and refr. index, new lidar-radiometer method 0-77153
 particulates in Cameroon air, Yaounde, urban and rural (*French*) 0-61478
 particulates in Montana air, element composition, background study 0-77034
 peroxy nitrates, UV absorpt., spectra, photodissoc. lifetime meas. 0-83386
 pollutant concentrations in urban atmosphere, radiation effects of elevated pollutant layers 0-97841
 pollutant ground-level concentration, field meas. of benefits of increased stack height 0-76676
 pollutants, concentrations from analytical diffusion model for long distance transport 0-94125
 pollutant, Gaussian plume model parameters for ground-level and elevated sources 0-82010
 rainfall in Trinidad conc. determ. 0-82045
 ring current ion composition at L>4, Prognostic-7 obs. 0-98517
 snow in Kashmir region, study of chemical components 0-94594
 stratosphere, CO₂-O₃ coupling in Cl free atm., photochemical-radiative column model 0-85723
 stratosphere, gas concentrations from limb sounding radiometry, inversion algorithm 0-82000
 stratosphere, halocarbons and N₂O height profile meas. at several latits. 0-72601
 stratosphere, HCl and HF volume mixing ratios simultaneous meas. 0-72587
 stratosphere, multi-ion complexes, implications for aerosols and trace gases 0-61872
 stratosphere, temp. and O₃ vars. (1958 to 1977) 0-109222
 stratosphere, trace constituents, laser heterodyne spectroscopy 0-109257
 stratosphere, trace gas concs. during 1976 in N.Hemisphere 0-67016
 stratosphere aerosol content var., rel. to atm. transparency and direct solar radiation 0-82035
 stratosphere NO₂ and O₃ variations during solar eclipse 0-105017
 stratosphere NO and ClO meas. via solar occultation, influence of concs. vars. at twilight 0-85756
 stratosphere sulphate aerosol, kinetics of growth by condensation in homogeneous medium (*Russian*) 0-94566
 stratosphere sulphate aerosol layer, processes, models, obs. and simulations 0-109212
 thermosphere, empirical model of temp. and composition 0-77183
 thermosphere, middle, ion comp. and temp. profiles from incoherent scatter radar studies 0-72654
 thermosphere, N and NO conc. depend. on solar activity 0-77178
 thermosphere, tidal dynamics model with O-N₂ diffusion effects 0-101465
 thermosphere O(¹D) content, role of N(²D)+O₂ reaction 0-90270

atmospheric composition continued

- trace constituents in Indian west coast SW monsoon aerosols and rain 0-81967
 trace elements in UK, 1978 survey 0-90208
 trace gas transport and photochemistry rel. to greenhouse effect (*Russian*) 0-81989
 tropopause, sulphate and nitrate mixing ratios obs. 0-61835
 troposphere, O_3 mixing ratio meas. rel. to stratospheric-tropospheric exchange at polar latitudes in summer 0-72599
 lower troposphere modelling, chemical kinetic data needs, conference, Reston, Virginia (1978 May 15 to 17) 0-62383
 Van der Waals molecules comp. of lower atmos. 0-85699
 water vapour, Raman lidar meas., daytime atmosphere 0-85718
 water vapour vertical profile in stratosphere (*French*) 0-77033
 Ar isotopes in ancient atmos., shungite Ar degassing 0-85749
 ^{10}Be as a tracer for helio-geophysical phenomena 0-98525
 C in suspended particulates, meas. technique 0-76686
 C particles in aerosol, obs. of Denver Brown Cloud 0-81961
 CO, pollution from road traffic, street level conc. 0-81500
 CO, stratosphere content at mid-latitude, simultaneous N and S hemisphere obs. 0-77052
 CO, troposphere vertical profile, eastern USA in winter 0-77035
 CO, affected by biomass burning 0-97838
 CO, air composition at Barrow, Alaska, wind direction depend. 0-85704
 CO₂, atmospheric content, climatological consequences (*Dutch*) 0-98411
 CO₂ concentration doubling, climatological significance 0-101426
 CO₂ concentrations, meas. via solar occultation sounding using narrow-band radiometers 0-98452
 CO₂ content of polar ice, 20000 yr BP 0-61891
 CO₂ from fossil fuel burning and global C budget 0-77080
 CO₂ induced atmospheric temp. rise, Arctic sea ice decay 0-61802
 CO₂, stratosphere content at mid-latitude, simultaneous N and S hemisphere obs. 0-77052
 $^{13}C/^{12}C$ in atmosphere CO₂, vars. in last 22 yrs. 0-104530
 ^{14}C , cosmogenic, diffusion distrib. in dynamic reservoir 0-101510
 ^{14}C variability due to variable Sun 0-85730
 ClO composition of stratosphere, balloon borne in situ reson. fluoresc. obs. 0-90167
 H in mesosphere and thermosphere, UV dayglow Lyman α and β obs. 0-109290
 H₂, composition of marine air and surface water in N. Atlantic 0-77057
 HCl, atmospheric measurements using ground based IR spectroscopy (*French*) 0-81975
 HCl, stratosphere content at mid-latitude, simultaneous N and S hemisphere obs. 0-77052
 HF, atmospheric measurements using ground based IR spectroscopy (*French*) 0-81975
 HF, stratosphere content at mid-latitude, simultaneous N and S hemisphere obs. 0-77052
 HNO₂, obs. of lower atmos. pollution in W. Europe 0-72106
 HNO₃ in marine air of equatorial Pacific 0-85702
 HNO₃, stratospheric composition, in situ obs. 0-105077
 H₂O dimer, conc. in H₂O vapour of different temps. and vapour press. (*Chinese*) 0-109237
 H₂O in stratosphere, maintenance of extreme aridity 0-105028
 H₂O in stratosphere, mixing ratio profiles from IR solar spectra obs. 0-105015
 H₂O isotopic sampling apparatus for troposphere (*French*) 0-94614
 H₂O mixing ratio, in-situ obs. using NOAA UV fluoresc. instrument 0-90137
 H₂O, stratosphere content at mid-latitude, simultaneous N and S hemisphere obs. 0-77052
 H₂O, stratospheric composition, in situ obs. 0-105077
 HONO (nitrous acid), obs. in urban atmosphere by differential optical absorpt. 0-76677
 H₂S in troposphere, photochem. production reactions 0-90112
 H₂SO₄ aerosol, filter sampling of air, possible artifacts 0-82079
 H₂SO₄, aerosols heterogeneous reactions and role as tropospheric sinks 0-72612
 ^{85}Kr conc. 0-93756
 N, in equatorial thermosphere, seasonal and diurnal variation 0-85782
 N production in upper atmos., model of far UV dayglow 0-90271
 N₂ in thermosphere, seasonal-latitudinal tidal struct. and mass density 0-101467
 NH₃ content of Southern Ocean air 0-61871
 NH₃ fluxes into free atmosphere over W. Germany evaluation 0-94132
 NH₃ in troposphere, vertical distrib. by photochem. model 0-85701
 NH₃, troposphere vertical profile, daily and seasonal variation 0-85700
 NO and NO₂ mixing ratio profiles of stratosphere from IR sunset spectra 0-94563
 NO densities in upper atmosphere, rel. to global ionospheric absorpt. meas. on board ships 0-98500
 NO, density profile from airglow obs., 72-120 km altitude 0-105094
 NO in middle atmosphere, role of eddy diffusion in mesosphere and lower thermosphere 0-109198
 NO, production by lightning, shock and channel heating methods 0-72581
 NO, thermosphere UV spectral absorpt. and density profile 0-85781
 NO⁺ cluster ion formation in D-region, temp. control by ion obs. 0-61931
 NO₂, atmospheric abundance meas. using solar absorpt. method (*Japanese*) 0-94556
 NO₂ in stratosphere mixing ratio profiles from IR solar spectra obs. 0-105015
 NO₂, stratospheric, ground based obs. 0-85697
 NO₃, detect. in polluted troposphere by differential optical absorpt. 0-77036
 NO₃ in troposphere, obs. of content in mountain air 0-72582
 N₂O, atmos. warming due to N₂O release from fertiliser 0-94579
 N₂O, meas. in marine air over tropical E. Pacific Ocean 0-94542
 N₂O, stratosphere content at mid-latitude, simultaneous N and S hemisphere obs. 0-77052
 N(²P), auroral arc conc. and altitude distrib. 0-72658
 Na abundance from nightglow obs. of Na I D doublet 0-98497
 Na enhancement and nightglow, space lidar obs. 0-101466
 NaCl-gas reactions, atmospheric, in situ TEM studies 0-104544
 O atoms in exposure, polar corona atom distrib. 0-82120
 O I(²P) in lower thermosphere, nighttime conc. obs., using new rocket borne instrument 0-105066
 O in thermosphere, seasonal-latitudinal tidal struct. and mass density 0-101467

atmospheric composition continued

- O in upper atmos., atom density rel. to airglow green line (*Chinese*) 0-90269
 O, O_2 abundances, effects of nearby supernova 0-94584
 O profile of mesosphere and lower thermosphere 0-72660
 O₂ density in thermosphere, solar flux var. 0-72659
 O₂ density profile in upper atmosphere rel. to O_3 atmospheric and OH Meinel bands in nightglow (*Japanese*) 0-94631
 O₃, air composition at Barrow, Alaska, wind direction depend. 0-85704
 O₃ and related chemistry in mesosphere, Solar Mesosphere Explorer mission description (1981-2) 0-105096
 O₃ conc. affected by hydrocarbon emission from car factory 0-76674
 O₃, conc. at ground-level, Oslo, Norway, summer 1977 obs. 0-81965
 O₃ conc. in troposphere rel. to general weather situation 0-101397
 O₃ concs. over Australia, review 0-109223
 O₃ content, evolution 0-98400
 O₃ depletion in stratosphere, space-time distrib. and UV radiation changes at Earth surface 0-94577
 O₃, determ. by Chappuis-band absorpt. 0-77063
 O₃ enhancement by jet stream (*Russian*) 0-94568
 O₃, in lower atmos., Uccle, Belgium, April-June 1979 obs. (*French, Flemish*) 0-98385
 O₃, in lower atmos., Jan.-March 1979, obs. over Uccle, Belgium (*French, Flemish*) 0-94571
 O₃ in lower stratosphere, Nimbus 4 remote sensing method 0-77154
 O₃ in mesosphere and stratosphere, obs. by satellite IR limb scanning method 0-105086
 O₃ in stratosphere, depleted by chem. reactions involving bromine 0-98391
 O₃ in stratosphere, seasonal composition variation at high-latitude 0-77051
 O₃ in stratosphere and troposphere, vertical distrib. during polar front passage 0-94582
 O₃ in troposphere, evidence for significant in situ photochemical source 0-72619
 O₃ in troposphere, implications of stratosphere vertical flux 0-101402
 O₃ in urban air at night, Jerusalem and Tel-Aviv 0-89689
 O₃, instantaneous global balance including observed NO₂ 0-109211
 O₃ layer, depletion and chemistry 0-104534
 O₃ layer depletion by chlorofluorocarbons, calc. using two-dimensional model 0-109221
 O₃ line parameter data, 10 μm and 4.8 μm regions 0-61895
 O₃, maintenance of zonal mean distrib. in N. Hemisphere 0-109220
 O₃, nighttime concentration (15-68 km), Nimbus 6 obs. comparison with OAQ-3 obs. 0-105016
 O₃, obs. of meridional flux by transient eddies in 0 to 30 km height range 0-109224
 O₃ overabundances over Pacific Ocean during Gametag, August 1977, stratospheric source 0-72600
 O₃, stratosphere content at mid-latitude, simultaneous N and S hemisphere obs. 0-77052
 O₃ total content, determ. using satellite meas. 0-77027
 O₃ total content, Dobson spectrophotometer meas. errors 0-72644
 O₃ total content determination, large particle light scatt. coeffs. approximation 0-82091
 O₃, total content meas. using Dobson spectrophotometer 0-72643
 O₃ transport mechanisms, general circulation model 0-109196
 O(²D) in thermosphere, quenching by electrons 0-94630
 O(²D) in thermosphere, role of N(²D)+O₂ reaction 0-90270
¹⁸O concentration in Amazon Basin water, evidence for recycling 0-81955
¹⁸O/¹⁶O ratio in precipitation, correl. with temp. and altitude 0-77067
¹⁸O/¹⁶O, photodissociation as source of atmospheric O₃ 0-94559
 Pb concs. in bulk precipitation in Denmark rel. to atmospheric long range transport 0-94131
 Rn, diurnal var. in boundary layer, for USA Gulf Coast 0-101404
 S aerosol, of S. American troposphere 0-67401
 S budget of eastern N. America, anthropogenic and natural contribs. 0-97534
 S compounds, meso-scale transport obs. in rural East Midlands, England 0-94124
 S oxide pollutants, SURE, MAP3S obs. comparison with regional model predictions 0-81501
 SO₂ and sulphates, residence times under non-steady-state conditions 0-77092
 SO₂ at ground level, air pollutant dispersal, Forth Valley, Scotland 0-81497
 SO₂ conc. downwind of coal fired power station, Montana, USA 0-108821
 SO₂ concentration for Rijnmond, Netherlands, comparison with Gaussian plume model obs. 0-85314
 SO₂, movement in atmosphere (*Dutch*) 0-97844
 atmospheric density see atmospheric pressure and density
 atmospheric disturbances see atmospheric movements; thunderstorms
 atmospheric duct see atmospheric electromagnetic wave propagation
 atmospheric dynamics see atmospheric movements
 atmospheric electricity
 see also atmospheric electromagnetic wave propagation; atmospheric ionisation; atmospheric; aurora; electrojets; ionosphere; lightning; thunderstorms
 aerosol, scavenging of particles by cloud drops and small rain drops, elec. field effect 0-82001
 aurora irregularities, overnight north-south movements obs. at 42 MHz 0-67449
 auroral arc during quiet conditions, electrostatic model 0-72669
 auroral arc electric fields, radar obs. 0-72692
 auroral arcs, Birkeland currents and polar cap elec. fields rel. to arcs global form. 0-67446
 auroral Birkeland current, determ. from plasma line meas. at Chatanika 0-98507
 auroral currents and potentials, generation by magnetosphere correction elec. field divergence 0-67453
 auroral elec. field, non-neutral field-aligned current sheet, theory 0-77196
 auroral electric field obs., comparative rocket obs. 0-85789
 auroral electric fields, implications of extreme thinness of pulsating auroral structures 0-72667
 auroral oval, daytime, elec. fields meas. 0-98501
 auroral oval, daytime, elec. fields rel. to neutral wind profiles between 115 and 175 km altitude 0-98494

atmospheric electricity continued

- auroral oval, dayside, evidence for parallel elec. field particle accel. 0-98503
 auroral oval, dayside, ULF elec. field fluctuations obs. 0-98505
 auroral radio backscatter at 42 MHz, amplitude rel. to Doppler shift 0-91955
 auroral zone, electrodynamic struct. of evening sector 0-72691
 auroral zone currents, obs. in morning sector pass 0-98510
 auroral zone electric currents, ground-based obs. using two-dimensional magnetometer array 0-90245
 Birkeland currents and auroral structure 0-77209
 charge separation, rel. to secondary ice crystal prod. 0-81998
 charge separation laboratory meas., associated with secondary ice crystal production, thunderstorm electrification exam. 0-72623
 daily mag. variations meas. in Alaska, atmos. current system 0-85590
 droplet collision efficiency enhanced by elec. field 0-61863
 E_z-layer ionisation at high latitude, quiet and disturbed conditions 0-61941
 E-region luni-solar currents, electron density distortion meas. using group and phase height meas. 0-109299
 Earth's negative charge, supply mechanism 0-61758
 earthquake lights, proposed for study by chemiluminesc. NO air pollution apparatus 0-61906
 F-region, current convective instability, rel. to localised nighttime auroral zone scintillation enhancements 0-98506
 F-region, horizontal elec. fields rel. to equatorial spread-F seasonal and solar cycle vars. in American zone 0-109298
 F-region auroral elec. fields and convection obs. over $60^\circ \leq \Lambda \leq 75^\circ$, Millstone Hill results 0-67454
 field aligned current above auroral arc, e⁻ and H⁺ precipitation obs. 0-77215
 field aligned current distribution, from S_p⁰ obs. in Alaska 0-85813
 field-aligned current closure and Joule heating near Harang discontinuity 0-72682
 global diurnal variations over continents 0-82039
 ionosphere, auroral electron flux obs. 0-67466
 ionosphere, cond. and electron density of reflecting layer below classical D-region 0-98508
 ionosphere, eastward elec. field rel. to equatorial anomaly form in E Asia and India 0-109301
 ionosphere, elec. field configuration rel. to Ps 6 mag. disturbances seasonal and diurnal var. 0-67477
 ionosphere, elec. fields induced by ion drag and substorms 0-77199
 ionosphere, electron concentration profile, vert. struct. 0-61936
 ionosphere, global distrib. of elec. fields and currents produced by magnetosphere field-aligned currents 0-109303
 ionosphere, global scale electrodynamic coupling of high-latit. and low-latit. regions 0-77194
 ionosphere, high-altitude auroral zone, electron temp. enhanced by electron current 0-85803
 ionosphere, high-latit., field-aligned current sources 0-72674
 ionosphere, midlatitude obs. of ALADDIN rocket 0-101488
 ionosphere, polarisation electric field vert. distrib. in topside 0-61935
 ionosphere, reversal of horiz. elec. field assoc. with VHF scintillation 0-101489
 ionosphere, simultaneous obs. of field-aligned currents and plasma drift vels. by Atmosphere Explorer C 0-72681
 ionosphere currents, obs. by S-310-S rocket (*Japanese*) 0-94635
 ionosphere disturbance dynamo, caused by thermospheric wind 0-82134
 ionosphere during auroral substorm expansion, riometer absorpt. of spikes obs. 0-85799
 ionosphere field-aligned currents at subauroral latitude, assoc. with convection elec. fields 0-90278
 ionosphere fine structure at low latitude from impedance obs. at 406 kHz 0-67468
 ionosphere inhomogeneity formation, influence of elec. field temporal variation 0-105105
 ionosphere polar cap, elec. fields rel. to slant-E condition and plasma flow entry region position 0-67472
 ionosphere waveguide, effect of weak disturbance of permittivity on ray trajectories 0-61966
 ionosphere-magnetosphere, high-latit., average parallel elec. field from perpendicular elec. field vars. below 8000 km 0-72706
 ionosphere-magnetosphere system, induced elec. fields, review 0-94647
 lightning, elec. field changes rel. to optical radiation obs. from above and below clouds 0-85698
 lightning, generation of strong RF radiation, elec. field pulse obs. 0-98401
 magnetic storm main phase ring current, origin by inward displacement of preexisting particles 0-72708
 magnetosphere, Birkeland current sheets in dayside polar region 0-90289
 magnetosphere, Birkeland currents at high-latitude, suprathermal electron contrib. 0-90290
 magnetosphere, elec. field on disturbed days, at mid-latitude 0-77230
 magnetosphere, elec. fields parallel to mag. lines, studied by electron injection expts. 0-72702
 magnetosphere, equatorial elec. field during storm, obs. of whistlers 0-85817
 magnetosphere, fluctuating elec. fields rel. to counterstreaming electron beams over auroral zone 0-67474
 magnetosphere, 'kilometric radiation' elec. fields meas. by JIKIKEN (EXOS-B) satellite (*Japanese*) 0-94648
 magnetosphere, magnetic-field-aligned elec. fields generation mechanisms 0-77233
 magnetosphere boundary layer, field-aligned currents theory 0-67473
 magnetosphere boundary layer, model involving interaction with ionosphere 0-85808
 magnetosphere convection electric field, divergence rel. to auroral currents and elec. pots. and precip. generation 0-67453
 magnetosphere electric field, influence on thermosphere N.Polar Cap winds 0-67445
 magnetosphere equatorial electric field at L=2.3, power density 0-82146
 magnetosphere field-aligned electric currents, global distrib. of induced ionospheric fields and currents 0-109303
 magnetosphere longitudinal currents, dynamic processes in turbulence development 0-67469
 magnetosphere open model, current sheets rel. to plasma populations 0-90295
 magnetosphere polar cap, elec. field and convection after interplanetary mag. field becomes northward 0-94658

atmospheric electricity continued

- magnetosphere substorm and simultaneous thunderstorm, elec. fields, electron precip. and VLF radiation 0-67392
 magnetosphere-ionosphere current system, generating Pi ULF waves 0-85819
 magnetosphere-ionosphere electrical coupling, two-dimens. model 0-61938
 magnetotelluric apparent resistivity, effect of localised source 0-72429
 magnetotelluric methods, use of geomag. depth sounding below surface magnetometer array 0-98486
 micropulsations near plasmapause, elec. field obs. 0-85814
 particles of aluminosilicate, charge state depend. on thermal history 0-97840
 passive antenna system, comparative study for use as elec. cond. meas. device 0-85762
 Pc5 pulsation theory, consequences of ionosphere Hall current 0-105129
 Pc5 pulsation theory, consequences of N. and S. hemispheres ionosphere electricity 0-109316
 Pc5 pulsations, model of magnetosphere and ionosphere elec. and mag. fields 0-77234
 plasma sheet, magnetised plasma slow convection rel. to mag. field aligned currents 0-109312
 plasmasphere, large scale elec. fields and currents, related geomag. vars., review 0-105121
 point discharge from ground surface objects, annual charge change per km² 0-77077
 radio aurora (diffuse), rel. to field-aligned currents and particle precipitation 0-105119
 ring current behaviour during mag. storm 0-82144
 ring current during quiet field variability, mid-latitude 0-72714
 ring current dynamics, role of proton-cyclotron instabilities in non-uniform loss-cone plasma 0-90286
 S_z variation, magnetosphere or ionosphere dynamo? 0-109090
 Sq currents of N. and S. hemispheres affecting equator mag. variations 0-76904
 static electrification, by electrolytic process 0-72624
 storm clouds, observed by elec. field sensor (*French*) 0-85712
 stratosphere, ion mobility and conductivity, comparison balloon and rocket obs. 0-72605
 substorm variation field modeling, current system anal. 0-105130
 sunrise effect on elec. pot. near ground, origin in upper atmos. 0-61866
 thermosphere, lower, electric current and atmospheric motion, symposium, Seattle, Washington, 1977 August to September 0-62371
 thundercloud, positive streamer velocities meas., in quasi-uniform electric fields 0-72625
 thunderstorm, charge generation and time-depend. elec. field 0-72595
 thunderstorm electric charge separation, model 0-77076
 thunderstorm electrification, field expt. 0-72622
 thunderstorms near Langmuir Laboratory, airborne and ground based studies 0-85725
 transmission lines, high voltage, depend. of coronal discharge power loss on instantaneous rainfall rate 0-98471
 upper atmosphere electrical coupling to lower atmos., quasi-static model 0-61865
 warm cloud electricity, shallow axisymmetric cloud model 0-81999

atmospheric electromagnetic wave propagation

- see also *atmospheric light propagation*; *ionospheric electromagnetic wave propagation*; *magnetospheric electromagnetic wave propagation*; *tropospheric electromagnetic wave propagation*
 backscattered pulse shape, small-angle multiple scatt. in random media 0-77079
 classical radiowave propagation criteria, attenuation 0-67390
 clear air radar echo mechanisms 0-90181
 cloud liquid H₂O obs. from 28 GHz satellite signal absorpt. 0-94623
 conference, IR and MM waves and appls., Miami Beach, USA (Dec. 1979) 0-57009
 Earth-ionosphere waveguide, program to compute EM fields in irreg. spheroidal model 0-94638
 ELF sferics in polar region during solar proton event, June 1968 Antarctic obs. 0-90291
 ELF waves in Earth-ionosphere cavity, field eqn. for inhomogeneous ionosphere 0-61950
 ground wave propagation of Loran-C signal, theoretical review 0-94580
 hydromagnetic wave rotation between magnetosphere and ground 0-61969
 LF radio navigation signal affected by variable meteor ionis. 0-82309
 long-delay echoes, 28 MHz amateur band obs. 0-90277
 mesosphere VHF radar signal scattering, tropical latitude 0-90193
 microwave Earth-space link rain cell attenuation 0-94586
 microwave propagation, rel. to pollutant gases monitoring from space using passive sensing techniques 0-76690
 microwave refr. and absorpt. coeffs., optimal orthogonal expansion props. 0-98414
 middle atmosphere, 50 MHz radiowave depolarisation on backscattering 0-85729
 middle atmosphere, radar obs. at UHF and VHF, review of obs. 0-90180
 Mie scattering improved algorithms 0-78771
 millimetric and submillimetric atmospheric scintillation theory 0-61884
 MM wave radiometry conducted at Appleton Laboratory 0-67442
 MM wave systems, atmospheric attenuation factors 0-67405
 problems connected with special source structures, review 0-87272
 propagation problems connected with infinitesimal point source, review 0-90194
 radar scatter from waves of short-period, 13-25 km altitude 0-90192
 radar signal scatt. from turbulent air, VHF and UHF 0-85728
 radiative transfer, fixed cloud-top temp. and fixed cloud-top altitude approximations for temp. profile 0-72616
 radio emission of the atmosphere in the 5-13 cm⁻¹ band 0-61878
 radio noise statistical models for reception in VLF band 0-72611
 radioacoustical sounding, expression for scatt. signal freq. spectra (*Russian*) 0-94612
 radiowave, ground wave attenuation function for a spherical Earth with arbitrary surface impedance 0-94585
 radiowave propag., rel. to mass distrib. by latitude 0-90115
 radiowave propagation studied by FM-CW radar 0-90186
 radiowave refraction corrections for exponential atmosphere, real-time computational method 0-98432
 radiowave scattered by 1-D power law phase screen 0-77220
 scattering in presence of background slab, algorithm for profile reconstruction 0-94644
 Schumann resonances in Earth-ionosphere cavity, book 0-86050

atmospheric electromagnetic wave propagation continued

- stratosphere, radar signal refl. and scatt. from refr. index structs. 0-90182
 stratosphere turbulence near tropopause, review of radar obs. 0-90179
 thunderstorm location by single station techniques, improved method, radiowave propag. effects 0-67438
 turbulence, Doppler radar clean-air echo, intensity 0-90190
 VLF signals, numerical study of satellite reception using waveguide concepts 0-90282
 X-band, dielectric constant of dust, effect of moisture content 0-72578
 ν sea, cosmological, EM wave propagation, torsionic background 0-77283

atmospheric electron precipitation

- see also aurora; radiation belts*
 artificial aurora, conjugate to a Hawaiian launched electron accelerator 0-82124
 aurora in F-region, assoc. with magnetospheric cusp 0-90273
 auroral elec. field, non-neutral field-aligned current sheet, theory 0-77196
 auroral electron flux, rel. to field aligned elec. pot. difference 0-72684
 auroral electron modulation at 2.2 Hz, geomagnetic equatorial origin 0-94632
 auroral electron precipitation regions, generation by magnetosphere convection elec. field divergence 0-67453
 auroral electron transport and energy degradation 0-77219
 auroral electrons, implications of extreme thinness of pulsating auroral structs. 0-72667
 auroral electrons acceleration mechanisms 0-77210
 auroral forms relationship with high latit. particle precip. 0-77189
 auroral hiss, nearly reson. whistler amplified Cherenkov radiation, limitations 0-101482
 auroral luminosity rel. to geomag. field changes 0-77187
 auroral oval, dayside, electron precip. rel. to rocket-borne VLF and ELF waves meas. 0-98504
 auroral particle dumping into ionosphere and magnetotail structure 0-109313
 auroral particle precipitation, rel. to turbulence at 500 mb level 0-77218
 auroral zone microburst precipitation phenomena 0-77208
 auroral zone precipitation and convection reversal, satellite obs. 0-101479
 cusp region of magnetosphere, rel. to interplanetary mag. field 0-90288
 cusp region on dayside, field line topography, precipitation implications 0-85822
 diffuse aurora equatorward boundary, electron precipitation interpretation 0-72668
 dynamics and auroral morphology, photometric data interpretation 0-82141
 field aligned current above auroral arc, e^- and H^+ precipitation obs. 0-77215
 inner magnetosphere penetrated by energetic particles during storms 0-72716
 inner radiation belt electron precipitation, meas. 0-67452
 inverse loss cone electrons, temp. anisotropy quasi-linear relaxation due to interaction with electrostatic waves (*Russian*) 0-109314
 ionosphere, auroral electron flux obs. 0-67466
 ionosphere, electron precip. rel. to radio waves winter absorpt. anomaly at middle latits. 0-67459
 ionosphere, high-altitude auroral zone, electron temp. enhanced by electron current 0-85803
 magnetosphere electron precipitation, obs. during simultaneous substorm and thunderstorm 0-67392
 nighttime global zones of energetic particle precipitation 0-61947
 Pc 4-5, obs. showing ULF mag. fields affect precipitation 0-82147
 pulsating aurora, obs. of precipitating electrons 0-85794
 pulsating aurora electrons, evidence for limiting flux 0-72666
 radio aurora (diffuse), rel. to field-aligned currents and particle precipitation 0-105119
 rapid auroral fluctuations, obs., classification 0-77186
 SAR arc event, soft electron flux as excitation source 0-77217
 sporadic events in local dusk sector of auroral zone, X-emission obs. 0-101480
 substorm associated precipitation, hydromagnetic wave modulated 0-105113
 widespread electron precipitation morphology, from X-ray bremsstrahlung obs. 0-77205
 N_2 gas, electron energy degradation, Monte Carlo study 0-69969

atmospheric energetics *see atmospheric movements***atmospheric humidity**

- see also hygrometers*
 boundary layer, eddy flux meas. corrected for density fluctuations 0-72576
 Brazil, precipitable water, distrib. maps 0-77075
 cloud temperature and humidity changes and overcloud inversion 0-77083
 enthalpy meas. by LiCl humidity sensors 0-90858
 evapotranspiration of continents real land surface, Penman concept calcs. (*German*) 0-98368
 Fenlands, temp. and humidity meas. rel. to steam fog form. criterion 0-98431
 fluctuations, as cause of errors in sea salt contaminated temp. sensors 0-82095
 free atmosphere, temp. and humidity effects on theoretical and exptl. long-wave IR radiation fluxes (*Russian*) 0-94598
 hygroscopic particle humidification process, electrooptic scatt. meas. 0-77107
 ice platelets, IR radiation attenuation 0-66141
 lidar scattering and relative humidity 0-77113
 marine boundary layer, humidity fluctuations affecting light scatt. 0-82052
 marine layer at San Diego, California, depth and moisture content rel. to cool season precip. forecasts in Arizona 0-101395
 moisture content determ. of cloudless atmosphere, microwave radiation meas. 0-94624
 moisture fluctuations, effect on acoustic backscatter in GATE 0-85709
 Orange Lake, Florida, humidity fluctuations rel. to lake latent and sensible heat fluxes prediction 0-72562
 NE-Pacific Ocean, clouds liq. water data rel. to United States west coast rainfall 0-82005
 psychrometry, appl. of portable differential system 0-105072
 remote sensing, water vapour content retrieval from scanning multichannel microwave radiometer obs. 0-90261
 remote sensing by satellite, thermal radiation obs. 0-85660

atmospheric humidity continued

- Rome, effect of urban heat island on humidity during summer season 0-85717
 Southern Hemisphere, moisture conditions and precipitation efficiency 0-98424
 stratosphere, H_2O mixing ratio determ. using NOAA UV fluoresc. instrument 0-90137
 stratosphere, water transport rel. to sulphate aerosol growth by condensation (*Russian*) 0-94566
 stratospheric composition, in situ obs. of H_2O 0-105077
 stratospheric H_2O , maintenance of extreme aridity, review 0-105028
 thermocouple psychrometry, effect of and correction for different wet and dry bulb response 0-98472
 troposphere, total column moisture content meas. by TIROS-N operational vertical sounder 0-77132
 water heat transport, rel. to ocean temperature-salinity curve 0-72534
 water vapour, influence on atmospheric scintillation at millimetre and sub-millimetre wavebands 0-61884
 water vapour content, rel. to diurnal var. of underwater irradiances on horizontal surfaces 0-72549
 water vapour IR continuum absorpt., appl. of aerosol IR spectrometry theory 0-101428
 AgI surface, adsorption of water, effective pair pot. model 0-100394
 NaCl-gas reactions, atmospheric, in situ TEM studies 0-104544

atmospheric ionisation

- see also atmospheric radioactivity; ionosphere*
 aurora, $Ni^{2+}D$ emission and ion chemistry, satellite obs. 0-72673
 aurora, pulsations of electron and ion intensity 0-61934
 aurora modelling, time-depend. study 0-72672
 D-region, electron detachment and loss coeff. at S. Uist 0-82130
 D-region, enhanced electron conc. at mid-latitude, positive-ion model 0-105115
 D-region, ion composition at midlatitude in quiet conditions, model 0-109307
 D-region, ionisation enhancements rel. to radio waves winter absorpt. anomaly at middle latits. 0-67459
 D-region, solar X-ray control of ionisation 0-77198
 E₁-layer, creation, effect of variable meteor particle sizes 0-105108
 E₁-layer ionisation at high latitude, quiet and disturbed conditions 0-61941
 E-region, blanketing layer type ionisation irregularities, growth and decay 0-101477
 equatorial anomaly, counter electrojet assoc. changes, upward drifts reversal 0-109292
 F₁-layer at nighttime, ion composition near mag. equator 0-72683
 F₂-layer, parameters at high latitude during quiet conditions 0-105106
 F₂-layer, seasonal difference in ionisation and height due to neutrals 0-61951
 F-region, interhemispheric ion transport induced by neutral zonal winds 0-98509
 F-region, ionisation enhancements rel. to localised nighttime auroral zone scintillation enhancements 0-98506
 F-region, N atoms and O ions in dynamic model 0-72693
 F-region, winter anomaly causes 0-85793
 F-region peak electron density, diurnal and solar cycle variation 0-61949
 gas phase inorganic ion clusters 0-77068
 ion+ molecule reactions, atmospheric ion chemistry 0-61885
 ionosphere, bubbles in equatorial spread F, nonlinear evolution 0-85801
 ionosphere, calc. technique for ground and satellite obs. 0-90275
 ionosphere, electron gas effective energy reception per created ion electron pair 0-67463
 ionosphere, ionisation irregularity drift motion from spaced fading and scintillation obs. 0-82133
 ionosphere, lower, ionisation model for reflecting layer below classical D-region 0-98508
 ionosphere, O^+ and H^+ equal ionisation level, during max. of solar activity 0-90280
 ionosphere, plasma cloud striations, study of outer scale size 0-90279
 ionosphere, primary ion-electron prod. rates change with solar EUV flux 0-72675
 ionosphere, total electron content fluctuations rel. to scintillation of VHF and GHz waves 0-109302
 ionosphere, winter, thermal electrons energy distrib. obs. by S-310-5 rocket (*Japanese*) 0-94636
 ionosphere D and F-regions, effect of geomag. storms 0-101474
 ionosphere equatorial anomaly, dissimilar forms in E.Asia and India 0-109301
 ionosphere plasma line enhanced by HF radiowave heating 0-82140
 ionosphere-state interaction, ion density in wake of O^+ plasma 0-82136
 ionospheric records over Shanghai, March 1953 to June 1955, effective coefficient of recombination (*Chinese*) 0-77192
 IR brightness obs. 0-94629
 magnetosphere, ionisation ducts of detect. via JIKIKEN (EXOS-B) satellite VLF Doppler shift meas. (*Japanese*) 0-94651
 measurement by automated environmental monitoring system 0-81513
 meteor rate seasonal var., atmos. ionisation effect on LF radio navigational signals 0-82309
 meteors ionisation columns, initial radii meas. 0-94762
 negative ion photodissoc. and photodetachment 0-69199
 plasma bubbles in nighttime equator region, field-aligned characts. 0-109308
 plasmasphere, mid-latitude, nighttime electron content, geophysical disturbance effects, 1974 August to November 0-94642
 plasmasphere total electron content, ATS-6 radio beacon obs. over Europe and USA 0-77201
 radio aurora (diffuse), rel. to field-aligned currents and particle precipitation 0-105119
 SITEC disturbances (1966-1977), rel. to solar flare occurrence 0-90276
 sporadic meteors, ionisation height meas., VHF obs. 0-82312
 stratosphere, ion conc., comparison of rocket and balloon results 0-72605
 stratosphere, multi-ion complexes, implications for aerosols and trace gases 0-61872
 virtual height-freq. curves, nocturnal, reduction method using ionisation models (*Chinese*) 0-105099
 $H^+(H_2O)_n$ ion-induced water clusters, mass spectra, IR continuum absorpt. 0-87257
 Li^+ diffusion and ion-neutral interactions, laser sounding obs. (*French*) 0-82115

atmospheric ionisation continued

- $O^+(D)$ in thermosphere, quenching by electrons 0-94630
- $O^+(P)$, ionisation freq. vars. during solar cycle 21 from airglow meas. 0-77195

atmospheric light propagation

- aerosol layer at 3 km causing sky brightness fluctuations in daytime (French) 0-81959
- aerosol light scattering turbidity and visibility obs. 0-105047
- aerosol mass from Lidar concentration-solar radiometer expt. 0-90171
- aerosol medium bleached zone, probe radiation propag., intensity and phase fluctuations 0-67411
- aerosol particle characterisation with electrooptical nephelometry 0-77106
- aerosol scattering indicatrices under clear sky conditions in 0.55 to 2.4 μ spectral region, determ. (Russian) 0-94600
- aerosols, differential scatt. coeff. to mass conc. ratio, spectronephelometer, cascade impactor obs. 0-72628
- aerosols, in situ meas. of absorpt. coeff./extinction coeff. ratio 0-90217
- aqueous aerosol cloud containing medium, light beam propag., thermal self-interaction 0-91750
- astrometry, astrolimatic influences on precision of photographic star positions obtained with wide-angle astrographs (Russian) 0-72748
- astronomical seeing, influence of spatial resolution on Ca⁺ K-line width and shift in solar prominence 0-77364
- attenuation of HF/CO₂ laser beam by water vapour 0-61905
- band radiation pyrometry for error reduction in transmission coeff. calc. of IR radiation energy depend. on atmospheric props. (German) 0-105649
- clouds, light pulse reflection, height meas. (Russian) 0-82056
- clouds, mathematical model of radiative transfer 0-90215
- clouds, thick, light pulse propag., pulse width expression for scatt. slab 0-82059
- diffuse solar radiation below overcast sky, ang. distrib. 0-85719
- diffusion equation derived from space-time transport equation 0-78772
- dust, soil derived atmospheric, IR spectra, Christiansen effect, Rayleigh limit 0-105046
- extinction of sunlight in mountainous regions 0-90202
- fog, spectral transmission data, IR propag. and performance modelling 0-90218
- haze, radiative transfer model rel. to anomalous gray shades in DMSP visible imagery 0-77111
- heterodyne optical radar S/N ratio in atmospheric turbulence 0-106558
- hydroscopic particle humidification process, electrooptic scatt. meas. 0-77107
- ice clouds, visible and LR optical props. from lidar and radiometer meas. 0-82060
- ice crystals, light scatt. expts. (Russian) 0-94601
- intensity fluctuations and fourth-order coherence function in random media 0-78774
- IR broadband transmission rel. to meteorological events 0-85744
- IR long-wave (8 to 13 μ) radiation in free atmosphere, comparison of theoretical and experiment fluxes (Russian) 0-94598
- IR radiation, attenuation by ice platelets 0-66141
- IR radiation propag. aerosol. effects rel. to error in satellite retrieved temp. profiles 0-98449
- IR transmission at Mauna Kea, determ. from obs. of H Paschen α in P Cygni and other OB-type stars 0-62156
- IR transparency window, 10-13 μ , H₂O and aerosol effects in winter and summer (Russian) 0-105048
- large particles scattering coefficients, approximation for total O₃ determ. 0-82091
- laser application to atmospheric environmental research (German) 0-97849
- laser beam, intensity fluctuations in snowfall (Russian) 0-94602
- laser beam amplitude fluctuation statistics in turbulent atmosphere 0-106458
- laser beam arrival angle fluctuations meas. apparatus using telescope 0-109258
- laser beam off-axis propag. in low visibility weather conditions, non-small-angle scatt. 0-102621
- laser beams, coaxial beams technique for increasing range of visibility of laser beacons in fog 0-101434
- laser-radiation-intensity fluctuations in rainfall, statistical characts. 0-101433
- lidar equation for inhomogeneous atmos. (Russian) 0-82054
- lidar scattering and relative humidity 0-77113
- marine boundary layer, humidity fluctuations affecting light scatt. 0-82052
- maritime aerosol near Europe, albedo and 632.8 nm absorpt. 0-90136
- measurement using CO₂ laser radar 0-90225
- middle atmosphere, solar occultation expt. rel. to aerosol remote sensing 0-109269
- middle atmosphere, solar UV radiation absorpt. rel. to numerical model of zonal mean circulation 0-109218
- monochromatic atmospheric transmission determination, laser heterodyne spectrometry 0-72653
- mountain and desert atmospheric MTF comparison 0-82063
- multiple scattering, Hovenier's exit function eqn., numerical props. 0-62054
- multiple scattering, theory for dispersive media with spherical particles (Russian) 0-94599
- narrow field optical astrometry, atmospheric turbulence limitations 0-109340
- optical parameters determ. by aerial photography at sunset 0-90219
- partially coherent beam intensity fluctuation calc. in turbulent atmosphere 0-78775
- phase correlation scale effects rel. to atmospheric imaging characts., theory 0-94604
- photodissociation fluxes, tropospheric and stratospheric, Mie scatt. contrib. improved model 0-77103
- polarised light transfer problem in presence of absorpt., soln. 0-67561
- radiative transfer, atmospheric effects on remote sensing and laser propag., conference, San Diego, California (1979 August 29 to 30) 0-62376
- radiative transfer eqn., appl. to satellite remote sensing of phytoplankton 0-77105
- Rayleigh scattering, optical thickness values 0-90216
- refraction determination by automatic obs. of meteorological elements (Japanese) 0-82110
- refractive index in atmospheric boundary layer, structural charact. vertical profiles (Russian) 0-94597

atmospheric light propagation continued

- remote imaging of Earth surface with nonuniform albedo, contrast reduction due to haze 0-101431
- satellite solar occultation sounding of the middle atmosphere 0-105079
- scattering corrections for atm. aerosol extinction measurements 0-98445
- scattered light intensity and polarisation degree in model atm., mol. anisotropy effect 0-77104
- scattering, by optically thin spherically symmetric atmosphere rel. to brightness at zenith near terminator 0-109382
- scattering medium, stratified, narrow beam propagation theory 0-106455
- scintillation of astronomical bodies, determ. of stratosphere density inhomogeneity struct., Salyut obs. (Russian) 0-109186
- semi-empirical theory 0-90220
- solar radiation, propag. rel. to direct beam solar irradiance and illuminance 0-90174
- solar radiation atmospheric attenuation, effect of O₃ and H₂O vapour content and atmos. turbidity 0-93855
- solar UV radiation, absorpt. in mesosphere and stratosphere 0-109248
- soot particle absorpt. of near IR (Russian) 0-82055
- speckle propagation statistics through turbulent atm., log-amplitude covariance function effect 0-82058
- spherical wave propagation, effect of turbulence 0-82066
- stratosphere, simulated radiances for ClO and NO concs. determ. via solar occultation meas. 0-85756
- stratosphere aerosol, radiation transport model rel. to climatic effects of aerosol layer modification 0-98408
- surface layer optical inhomogeneities, investigation via acoustic method 0-67434
- thermal blooming, continuum-lens model 0-78918
- thermal defocusing of light beams, phase conjugation compensation method 0-64123
- transmittance, algorithm accuracies 0-101429
- transmittance functions generated by numerical methods, trace gas appls. 0-98455
- transparency, meas. on Maidanak mountain during autumn and winter (1977 to 1978) (Russian) 0-72627
- turbulence and aerosol effects on optical coherence 0-82064
- turbulence effects on IR and near-millimetric-wave propagation 0-61902
- turbulent atmosphere, beam props. of partially coherent curved beam waves 0-95798
- visibility at ground level, two meas. methods 0-82078
- H₂SO₄ aerosol, extinction, absorpt., backscattering and mass content relations 0-101403
- He-Ne laser transmitter/receiver to measure optical parameters of turbulent atmosphere 0-98450

atmospheric measuring apparatus

- see also air pollution detection and control; ionospheric measuring apparatus; meteorological instruments
- acoustic Doppler sodar, appl. to atmospheric temp. fluctuations heat flux and struct. functions meas. 0-105023
- acoustic instrument, for atmosphere surface layer optical inhomogeneities investigation 0-67434
- aerosol S content, continuous flame photometric detection system 0-81508
- air pollution automatic analysis, spectrosc. methods (Spanish) 0-81516
- airborne lidar system for geophysical and atmospheric expts. (Italian) 0-109277
- altazimuth sky scanner optical system, polarization characts. 0-77123
- Atmospheric Cloud Physics Laboratory simulation, vorticity transport eqn. solns. 0-94690
- automated environmental monitoring system for pollution studies 0-81513
- boundary layer meas. system for wind and temp. obs. (German) 0-94616
- chlorinated hydrocarbon, dry aerial deposition rate, meas. techniques 0-81506
- cloud condensation nucleus spectrometer, new design 0-85765
- cloud condensation nucleus spectrometer, with horizontal thermal gradient 0-77158
- COCHISE, cryogenic apparatus for IR excitation studies 0-95166
- differential absorption lidar, complementarity of UV and IR systems for atmospheric species meas. 0-72634
- diffraction and stray fields measurement, angular and amplitude characteristics (Russian) 0-67433
- Dobson instrument, optical stop and focusing faults 0-101454
- Dobson spectrophotometer, for total O₃ content 0-72643
- Dobson spectrophotometer meas. errors in O₃ total content determ. 0-72644
- dual-Doppler radar, coverage area as function of meas. accuracy and spatial resolution 0-82093
- echosonde, excess attenuation of signals 0-83694
- electrical aerosol analyzer for number and mass conc. meas. 0-108753
- electron analysers on ATS 6 and 1976-059A satellites, charge buildup study 0-72744
- Fabry-Perot interferometer, multiple-zone aperture design for airglow temp. 0-82075
- Fabry-Perot spectrometer for airglow studies, with large aperture and high resolution 0-67424
- Fabry-Perot-interferometer imaging system for thermospheric temp. and wind meas. 0-101441
- field meas. Fourier transform spectrometer 0-86470
- Fourier transform spectrometer for atmospheric trace molecules spectroscopy, optical design 0-82099
- Illinois climate centre, review 0-77118
- interference spectrometer, selective modulation, far IR, design and appl. to atmospheric absorpt. meas. 0-57397
- International Sun-Earth Explorer (ISEE) mission, payload instruments 0-90320
- laser application to atmospheric environmental research (German) 0-97849
- laser beam arrival angle fluctuations meas. apparatus using telescope 0-109258
- low-level atmospheric thermograph, shipboard use in fog and stratus investigations 0-105073
- magnetometer, ring-core type, for space vehicles, geomag. fluctuations high-sensitivity obs. (Japanese) 0-94671
- magnetosphere proportional counter, with thin mica windows, for low-energy particles 0-109260
- MATEC (matched tandem etalon camera), appl. to auroral obs. 0-101442

atmospheric measuring apparatus continued

- Michelson interferometer, cryogenic, rocket-borne, for EXCEDE II expt. 0-95133
 MM wave radar system for remotely sensing atmospheric pressure from satellite 0-67443
 OPEN program for investigation of origins of plasma in Earth's neighborhood 0-109318
 operational vertical sounder, on TIROS-N polar-orbiting meteorological satellite 0-77132
 particulate chem. composition, use of laser induced mass spectrosc. instrument 0-97848
 passive antenna system, comparative study for use as elec. cond. meas. device 0-85762
 pyrliometers of the UK Meteorological Office, and radiation reference scales 0-109206
 radiometers for rain attenuation measurements at X, K bands communication appl. 0-68254
 rocket-borne cryogenically cooled field-widened interferometer for the 2 to 8 μ m spectral region 0-95163
 Salyut 6 submm. telescope with InSb receiver 0-67566
 snowfall by dual-gauge and Wyoming shield systems 0-61928
 spectrometer, laser heterodyne four-channel, monochromatic atm. transmission determ. 0-72653
 surface pressure measured using microwave signals transmitted from orbiting satellite 0-94581
 telephotometer for aerosol scattering function determ. 0-105055
 temperature sensors, humidity effects and sea salt contamination 0-82095
 thermocouple psychrometers, effect of and correction for different wet and dry bulb response 0-98472
 TIROS-N microwave sounder unit for global temp. distribution meas. 0-90265
 two-scatter-plate low-speckle-noise integrator for atmospheric laser beam transmission meas. 0-90252
 UV fluorescence water vapour instrum. for stratospheric aircraft 0-82100
 vertical air velocity, airborne meas. system 0-77159
 VLF wave measurement at ground station, antenna pickup for vertical elec. field 0-105063
 CO₂ laser radar used to measure average atmospheric temp. 0-90225
 H₂O isotopic sampling apparatus for troposphere (French) 0-94614
 H₂SO₄ aerosol, filter sampling of air, possible artifacts 0-82079
 InGaAsP LED sources, for near-IR absorpt. meas. 0-77135
 NH₃, gas conc. meas. using ring oven technique 0-81507
 NaCl aerosol generators, for cloud droplets nucleation expts. 0-82003
 Nd:YAG laser as source for airborne lidar system for atmospheric expts. (Italian) 0-109278
 O I(P) in lower thermosphere, nighttime conc. obs., using new rocket borne instrument 0-105066
²²²Rn daughter prods. meas. using diffusion sampler 0-81510

atmospheric measuring instruments *see atmospheric measuring apparatus***atmospheric motion** *see atmospheric movements***atmospheric movements**

- see also atmospheric turbulence; wind*
 accelerating flow horizontal divergence, turning vorticity eqn. anal. 0-77013
 adaptation processes in rot. atmospheric motion (Chinese) 0-67387
 advection-diffusion model, for real-time forecasting of air pollution episodes in Venetian region 0-77096
 E.African jet, dynamics, July mean conditions simulation 0-77045
 E.African jet dynamics, transients 0-77046
 African wave disturbances, convection role, linear primitive eqn. model 0-77043
 air pollutants long distant transport, analytical diffusion model 0-94125
 airflow transformation over nonuniformly heated underlying surface 0-82031
 angular momentum fluctuations and day length changes 0-85715
 Arabian Sea, atm. circulation feedback with sea cooling 0-104979
 aurora irregularities, overnight north-south movements obs. at 42 MHz 0-67449
 auroral convection over 60° \leq Δ \leq 75°: Millstone Hill incoherent scatter obs. 0-67454
 auroral electrojets, movements during high-latit. substorms 0-109315
 baroclinic atmosphere, two dimensional, dynamics (Russian) 0-94564
 baroclinic instability of short-wavelength two-layer Eady model 0-72593
 baroclinic waves, influence of static stability and wind shear time changes 0-109226
 baroclinic waves (unstable), finite-amplitude dynamics 0-72592
 baroclinic waves of finite amplitude, four-layer models 0-98387
 barotropic systems, low order, with forcing and dissipation, steady states and stability props. 0-72614
 boundary layer gravity waves, acoustic sounding obs. 0-61847
 boundary layers, convective and nonconvective, parameterisation for use in numerical models 0-82009
 bubbles seen in topside soundings of spread F, characts. 0-85800
 Cape Verde Islands, hurricane form., general circulation from Meteosat 0-105042
 NE.China, persistently low summer temp., causative circulation pattern (Chinese) 0-109235
 circulation, nonlinear axially symm., in nearly inviscid atm. 0-109190
 circulation driven by diurnal heating in Po Valley 0-85716
 circulation index rel. to solar activity 0-104853
 cloud updraughts, microphysical model sensitivity to urban environment 0-82004
 cold front, obs. of 3-D circulation, precipitation and wave motions 0-90142
 cold front of midlatitude cyclone, air flow assoc. with mesoscale rain bands 0-109192
 contaminant movement, Galerkin finite element method 0-74902
 convection assoc. with pyroclimulus cloud over North Canterbury, New Zealand, anal. 0-109240
 convection, fixed cloud-top temp. and fixed cloud-top altitude approximations for temp. profile 0-72616
 convection and mesoscale motions during Phase III of GATE 0-90153
 convection currents in axisymmetric cyclone 0-77084
 convection dynamics equations, non-Archimedean approach 0-77048
 convection meas. of heat flux and struct. functions of temp. fluctuations with acoustic Doppler sodar 0-105023
 convection with cloud formation and development, numerical model (Russian) 0-81987
 convective instability, Brunt-Vaissala frequency (French) 0-77058
 atmospheric movements continued
 convective mesoscale wave disturbance during GATE investigated by spectral methods 0-101398
 convective motion perturbed stochastically, model 0-92146
 cumulus scale motion assumptions, effect on cloud mass and heat flux 0-90155
 cusp region of magnetosphere, ion convection rel. to interplanetary mag. field 0-90288
 diffusion coefficients and criterion determ. (German) 0-94576
 dispersion expts. in Sydney region using SF₆ as tracer 0-67389
 dispersion from ground-level source, appl. of mixed-layer similarity scaling 0-105021
 dynamic model of low atmos., low-order spectral difference type 0-98415
 dynamics in quasistatic approximation, characterisation of approximation (German) 0-98383
 E-region gravity waves, obs. of Es 0-72657
 E-region plasma waves, radiofreq. cosmic noise absorpt. 0-82139
 Earth's negative charge, supply mechanism 0-61758
 eddy diffusion, models for mesosphere and lower thermosphere 0-109198
 eddy fluxes of conserved quantities by small-amplitude waves 0-61858
 Ekman conditional instability of second kind (CISK), preferred mode 0-72617
 electrojet induced press. and vel. fluctuations 0-82118
 electrojet influenced by lunar tide, semimonthly variation 0-61937
 electrojet strength, rel. to ionospheric drift variability above Tiruchirappalli 0-82129
 equatorial anomaly, counter electrojet assoc. changes, upward drift reversal obs. 0-109297
 equatorial F-region, drift measurement of Ba cloud, spaced receiver technique 0-72678
 equatorial stationary zonal circulation, numerical calcs. 0-85732
 equatorial waves in cloud vel. field over Pacific 0-67395
 NW Europe, polar air outbreak, subsynoptic disturbance case study 0-101408
 F-layer, ion convection at high-latitude, nighttime 0-85797
 F-region, interhemispheric ion transport induced by neutral zonal winds 0-98509
 F-region, neutral zonal winds rel. to interhemispheric ion transport 0-98509
 F-region, post sunset rise rel. to equatorial spread-F seasonal and solar cycle vars. in American zone 0-109298
 F-region, upward drifts reversal, evidence from equatorial anomaly counter-electrojet assoc. changes 0-109292
 F-region gravity wave effects, obs. of TID at nighttime 0-77206
 F-region plasma cloud, intermediate wavelength E \times B gradient drift instability 0-105114
 flow, kinetic energy three power law kinematic props. 0-77087
 forced Rossby waves on a zonal shear flow, model 0-77072
 forward air flow effect on evolution of convection 0-90116
 front formation over central Europe, internal processes 0-81979
 front position, precise determination from temp. and press. field data 0-98426
 frontogenesis, Hoskins-Bretherton model and surface frontal zone anal. 0-94572
 general circulation, eqns. of kinetic and available pot. energy evolution in wave-number freq. space 0-109227
 general circulation, hemispheric model 0-81976
 general circulation, many-year fluctuation rel. to Earth annual polar motion many-year var. (Chinese) 0-104848
 general circulation, polar motion excitation function power spectral anal. (Chinese) 0-104849
 general circulation, prediction rel. to long-range weather forecasting 0-109184
 general circulation at mid-latitude, fluctuations seen in rawinsonde data 0-81980
 general circulation by GLAS model, cumulus friction and Jan. Hadly circulation 0-72588
 general circulation from Meteosat obs. 0-94595
 general circulation in N.hemisphere, features assoc. with poor summers in British Isles 0-109241
 general circulation model, involving estimation of nonlinear energy transfer spectra 0-98389
 general circulation model, response time rel. to ocean surface temp. change 0-98422
 general circulation model, sensitivity to chlorofluoromethane induced IR cooling 0-90122
 general circulation model (NCAR), response to sea surface temp. change 0-98390
 general circulation of midlatitude troposphere, NCAR and GFDL models 0-61856
 general circulation of N.hemisphere in winter, horiz. transport by transient eddies 0-72589
 general circulation response to addition of waste heat 0-89694
 geopotential height fluctuations, geographic variation of vertical struct. 0-90132
 geostrophic adjustment theory, large-scale motion of atmosphere, adaptation, turning and equilibration 0-67404
 SW.Germany, Mediterranean warm air advection rel. to heavy rainfall (1978 May 22 to 24) (German) 0-61869
 global seasonal circulation, evidence for seesaw behaviour rel. to quasi-cycles in meteorology 0-109239
 gravity wave propagation, 'potential' well treatment 0-67396
 gravity waves, effect on ionosphere causing VLF anomalies 0-82127
 gravity waves, interpretation for Mitra drift near travelling ionospheric disturbances 0-82128
 gravity waves in ionosphere, radar obs. of electron density 0-77182
 gravity waves in upper atmosphere, possible effect on Loran-C 100 kHz signals 0-109304
 heat heat transport, rel. to ocean temperature-salinity curve 0-72534
 Hebei Plain, summer drought and flood rel. to atm. circulation seasonal var. 0-90203
 N.Hemisphere transient motions, RMS 1000 and 500 mb geopotential height 0-90163
 N. hemisphere winter circulation, general circulation model, comparison with obs. 0-109189
 India, westerly upper air troughs rel. to western disturbances development 0-90173
 initial vorticity field in short-range numerical weather forecasting, effect of subjective enhancement 0-82008
 intense tropical convective system, mesoscale motion contrib. to convective fluxes 0-90156

atmospheric movements continued

- internal gravity waves and upper atmosphere emissions 0-105093
 internal waves, hydrodynamic instability (*Russian*) 0-61852
 inviscid flow on sphere, statistical mech. 0-90152
 ionisation irregularity drift motion from spaced fading and scintillation obs. 0-82133
 ionosphere, bubbles in equatorial spread F, nonlinear evolution 0-85801
 ionosphere, elec. fields and plasma convection in dayside auroral oval 0-98501
 ionosphere, global scale electrodynamic coupling of high-latit. and low-latit. regions 0-77194
 ionosphere, gradient drift instability, Ba cloud release study 0-85802
 ionosphere, low latitude, total electron content nighttime enhancements motion 0-72677
 ionosphere, plasma convection at high latitudes, model rel. to incoherent scatter obs. 0-72687
 ionosphere, prompt striation of Ba cloud due to plasma instability 0-72685
 ionosphere, simultaneous obs. of field-aligned currents and plasma drift vels. by Atmosphere Explorer C 0-72681
 ionosphere, sporadic-E and F₂ layers, disturbances, electron density fluctuation origin 0-101475
 ionosphere, wave meas. via satellite-borne cross-power spectrum analysers 0-94621
 ionosphere and plasmasphere at midlatitude, computer model 0-105120
 ionosphere auroral zone precipitation and convection reversal, satellite obs. 0-101479
 ionosphere plasma, lower hybrid drift instabilities, electron collisional effects 0-101484
 ionosphere plasma instability, driven by auroral electron distrib. secondary peak 0-82135
 jet flow baroclinic instability in frontogenesis 0-61855
 jet streams, rel. to satellite-derived radiance gradient 0-98447
 K-stability index, rel. to thunderstorms and severe local storms automated 12 to 36 hour probability forecasts 0-77062
 Kelvin-Helmholtz instability, jet stream generated, radar obs. and model 0-90165
 Kelvin-Helmholtz wave, large amplitude, struct. determ. from altocumulus billows 0-72621
 large-scale travelling Rossby waves 0-94588
 lee wave clouds, S.W. airflow over Bank's Peninsula, New Zealand 0-85739
 linear and jet profiles of lower atmos., baroclinic instability 0-90126
 long period oscillations, homogeneous vertical struct. problem soln. 0-90125
 long range pollutant transport, Lagrange model 0-61851
 long waves in polar-plane approx. to Earth's spherical geometry 0-105019
 lower atmosphere instability in different seasons, correl. with solar corpuscular activity 0-61881
 lower thermosphere, compositional modelling taking account of airglow tidal variation 0-109288
 lower thermosphere gravity wave obs., 5-90 minute period 0-61930
 lunar tide, solar modulation anal. 0-94593
 magnetosphere, convection intensification, effect on mid-latitude ionosphere 0-105122
 magnetosphere, plasma flow and populations in simple open model 0-90295
 magnetosphere, plasma mantle flow rel. to plasma sheet thinning during substorms 0-72705
 magnetosphere, plasma stability during storm conditions 0-82150
 magnetosphere, polar cap convection after interplanetary mag. field becomes northward 0-94658
 magnetosphere, polar cap plasma flow entry region longit. position 0-67472
 magnetosphere, variability of plasma sheet dynamics assoc. with substorms 0-98518
 magnetosphere boundary layer, plasma flow rel. to field-aligned currents 0-67473
 magnetosphere boundary layer at low-latitude, fluid mech. model 0-85808
 magnetosphere convection causing auroral latitude, assoc. with convection elec. ionosphere field-aligned currents 0-90278
 magnetosphere convection electric field, divergence rel. to auroral currents and elec. pots. and precip. generation 0-67453
 magnetosphere hydromagnetic wave rotation between magnetosphere and ground 0-61969
 magnetosphere plasma convection, assoc. with type Pi pulsations at high latitude 0-77226
 magnetosphere plasma sheet, plasma flows rel. to discrete auroras occurrence and lifetimes 0-67447
 magnetospheric boundary layer, hydromagnetic waves driven by vel. shear 0-105133
 marine atmosphere, surface layer stability rel. to oceanic whitecaps and sea state 0-72554
 marine boundary layer along California coast, instability rel. to marine fog and fog-stratus systems 0-77060
 marine layer at San Diego, California, vertical motion field rel. to cool season precip. forecasts in Arizona 0-101395
 mass distrib. by latitude, seasonal changes 0-90115
 mean meridional circulations of stratosphere and mesosphere, monthly mean planetary wave fluxes 0-109219
 mean zonal flows accel. by planetary waves 0-105033
 mesoscale convective systems, inertial instability 0-90131
 mesoscale dispersion expts., trajectory-diffusion modelling 0-61837
 mesosphere, gravity waves component in partial refl. drift obs. 0-81993
 mesosphere, long-period waves at 60 to 90 km altitude 0-77056
 mesosphere, Southern hemisphere, wind speed quasi 2-day wave obs. 0-109207
 mesosphere dynamics, obs. by incoherent radar scatt. 0-90117
 meteor region, winter motions meas. in S. hemisphere 0-109287
 middle atmosphere, interaction between radiatively damped planetary wave and zonally averaged circulation 0-109217
 minor atmosphere constituents transport between troposphere and stratosphere implications for pollutant transport 0-105034
 moist convection, six-component spectral model 0-61859
 monsoon, model of large scale seasonal struct. 0-98393
 monsoon circulation over Bay of Bengal, 1976, winter to spring 0-82038
 monsoon disturbances over India, quasi-geostrophic model 0-98394
 monsoon driving mechanisms, model of seasonal struct. 0-98392
 mountain waves, effect of non-uniform shear 0-90127

atmospheric movements continued

- normal mode linear initialisation on sphere 0-77042
 numerical dynamic model atmosphere on a spherical Earth, used in forecasting 0-101416
 ocean tide caused by meteorological conditions, energy transfer calc. (*Russian*) 0-76988
 optical properties of moving atmosphere, simulation by rotating phase plate 0-79021
 orography, influence on atmospheric movement with Coriolis force included (*Russian*) 0-94565
 ozonosphere, photochemical-dynamical model rel. to maintenance of zonal mean O₃ distrib. in N.Hemisphere 0-109220
 Pacific and E.Asia, average vertical circulation in winter 0-90199
 NW.Pacific Ocean, low-freq. propagating disturbances rel. to press. and sea level vars. 0-101415
 W.Pacific subtropical high, summer, form. and struct. simulation (*Chinese*) 0-109233
 palaeo-atmosphere, coupled chemistry-flow model for O₃ content evolution 0-98400
 planetary boundary layer, waves obs. by radar in clear air conditions 0-90184
 planetary wave causing sudden stratospheric warming, model 0-90150
 planetary wave secondary circulation, vertical air exchange implication 0-72584
 planetary waves, effect on eddy momentum and heat fluxes 0-85720
 planetary waves, feedback with stochastically driven ice sheet, model 0-77025
 planetary waves, upward propag. rel. to ionospheric equatorial anomaly in E.Asia and India 0-109301
 planetary waves, zonal mean states baroclinic instability 0-90124
 planetary waves blocking mid latitude westerly winds 0-105036
 planetary waves in stratosphere global propag. in spherical atmos. 0-90139
 plasma convection in polar regions, model calcs. 0-82151
 plasma drift in radial direction at nighttime, and coupling to ionosphere 0-77239
 plasma sheet, magnetised plasma slow convection theory 0-109312
 plasmasphere, geophysical disturbances effect on ionisation downward flow and nighttime electron content 0-94642
 pollutant dispersal from point source into boundary layer, Ekman-type model 0-105039
 pollutant dispersion in urban atmosphere, radiative effects of elevated pollutant layers 0-97841
 pollutant transport and struct., in lower troposphere 0-85319
 pollutants diffusion, field meas. of benefits of increased stack height 0-76676
 pollutants transport, objective anal. technique for three-dimensional urban-scale wind fields construction 0-101407
 pollutant, Gaussian plume model parameters for ground-level and elevated sources 0-82010
 pollution dispersal, Gaussian moment-conservation diffusion model 0-85317
 pollution dispersion from elevated source in convective boundary layer 0-85312
 pollution long-range transport modeling review 0-108823
 pollution transport, air quality models development for limited wind fetch 0-104533
 protons of inner radiation belt, radial diffusion rel. to energy and pitch angle distrib. 0-67471
 quasi-geostrophic flow over anisotropic mountain 0-61860
 quasi-geostrophic flow over mountains 0-90128
 quasi-stationary wave maintenance mechanism in quasi-geostrophic model 0-90140
 realistic models, computation of waves, instabilities and eddy transport 0-90164
 Rossby neutral mode, secular stability 0-81983
 rotating fluids, Rossby and Kelvin waves, open boundary conditions 0-61810
 rotating stratified fluid, parallel shear flow, baroclinic and barotropic instability 0-98328
 semiannual oscillation in tropical middle atmosphere, review of observational evidence 0-109216
 solar semidiurnal tide influenced by zonal wind, theory 0-61853
 solar semidiurnal tide influenced by zonal wind, theory 0-61854
 squall line at midlatitude, thermodynamic and kinematic struct. obs. 0-109191
 stratosphere, circulation in circumpolar vortex, model 0-77082
 stratosphere, interaction of O₃ with circulation over Australia, review 0-109223
 stratosphere, Lagrangian motion of air parcels 0-109215
 stratosphere, southern hemisphere, spring transformation from cyclonic to anticyclonic circulation 0-98420
 stratosphere, sudden warming forced by mountain 0-72583
 stratosphere, travelling planetary waves 0-105030
 stratosphere and troposphere waves of short-period, radar obs. 0-90192
 stratosphere circulation, meas. via solar occultation sounding using narrowband radiometers 0-98452
 stratosphere O₃ net vertical flux, implication for troposphere O₃ budget 0-101402
 stratosphere temperature wave propagation, polar region in winter 0-72597
 stratosphere warmings, thermal and kinetic interactions with troposphere 0-105031
 stratosphere-troposphere exchange at polar latits. in summer, from O₃ concs. meas. 0-72599
 stratospheric H₂O, maintenance of extreme aridity 0-105028
 surface layer, organised motion features 0-72602
 surface pressure waves, 10 to 20-day westward propag. mode rel. to breaks in monsoons 0-94592
 symmetric instability of stratified geostrophic flow 0-98425
 thermals models, scales of motion rel. to self-similarity soln. 0-109228
 thermosphere, lower, electric current and atmospheric motion, symposium, Seattle, Washington, 1977 August to September 0-62371
 thermosphere, middle, incoherent scatter radar studies rel. to energy and mass transport 0-72654
 thermosphere, seasonal-latitude longitudinal tidal struct. 0-101467
 thermosphere, tidal dynamics model with O-N₂ diffusion effects 0-101465
 thermosphere tides, semidiurnal and terdiurnal 0-82119
 TID phenomena in F-region, influences of thermosphere winds 0-109305
 tide, solar semidiurnal, obs. of surface press. oscill. 0-77054

atmospheric movements continued

- tide (solar semi-diurnal), zonal motion and meridional temp. gradient effects 0-98399
 tides, theoretical work since 1970, review 0-94589
 tides at meteor altitudes, CTOP radar obs. 0-77181
 topographic wave clouds in central and northern Urals, characts. 0-101413
 topside ionosphere, H^+ and O^+ ion transport obs. 0-61940
 topside ionosphere, polar wind in mag. quiet conditions 0-72713
 trace gas transport and photochemistry rel. to greenhouse effect (*Russian*) 0-81989
 trajectories, discrete model concepts appl. 0-85706
 transient inertio-gravity waves, induced mean motion 0-105029
 tropical transient planetary waves in general circulation model, seasonal var. 0-90151
 troposphere, radar obs. of vel. and irregularities, spaced antenna VHF method 0-90185
 troposphere, stratospheric air intrusion rel. to 7Be var. 0-98525
 troposphere circulation patterns, affected by stratosphere wind spring reversal date 0-82021
 troposphere circulation patterns, influenced by stratosphere winter strength 0-82021
 troposphere gravity waves, effect on condensation initiation and growth 0-90159
 tropospheric circulation in N.Pacific rel. to sea surface temp. anomaly gradient 0-85674
 ultralong waves forced on cyclone scale, numerical expt. 0-61857
 upper atmosphere, coupled time-dependent diffusion eqns., numerical method using self-diffusion coeff. 0-109285
 upper atmosphere, ion drag effects on winds in N.Polar Cap thermosphere 0-67445
 upper atmosphere, rot. rate and density, obs. of satellite orbit 0-85785
 upper atmosphere perturbations due to mountain ridge air flow (*Russian*) 0-105018
 upper westerly waves, interaction with intertropical convergence zone rel. to Zambian weather during rainy season 0-90175
 upward sensible heat flux by synoptic-scale transients, observational study 0-94591
 urban atmosphere, numerical simulation of mixing depths 0-105024
 urban environment, cold air drainage effects on temp. fields, case study of topographical influence on climate 0-94555
 urban heat island convergence in calm periods, St. Louis USA 0-90169
 vertical air velocity, airborne meas. system 0-77159
 vertical diffusion from meteorological tower meas. 0-61838
 vorticity area index at 500 mb, geomagnetic disturbance effects 0-61873
 vorticity response to IMF sector boundary crossing, at 500 mb level 0-109199
 warm frontal clouds in midlatitude cyclones, air motion and precipitation 0-109193
 water heat transport, rel. to ocean temperature-salinity curve 0-72534
 wave overreflection and baroclinic instability 0-90141
 wave/mean flow interaction, introduction to generalised Lagrangian-mean distribution 0-109214
 waves in upper troposphere (tropical), dynamical anal. 0-98388
 westerly jetstream, effects on summer weather and climate 0-72620
 western boundary currents and detached shear layers in rot. liq. 0-81984
 winds in meteor region, periodic fluctuations of recurrent nature 0-90266
 zonal climate models, inclusion of meridional motion and large eddies 0-90138
 zonal flows and planetary waves in multi-level models on sphere, baroclinic instability 0-90123
 zonal mean circulation of middle atmosphere, numerical model 0-109218
 ^{13}C , cosmogenic, diffusion distrib. in dynamic reservoir 0-101510
 F_2 -layer, plasma ambipolar diffusion and vertical drift at low latitude 0-101472
 Li^+ diffusion and ion-neutral interactions, laser sounding of upper atmosphere (*French*) 0-82115
 NH_3 fluxes into free atmosphere over W.Germany evaluation 0-94132
 O_3 layer, role of dynamic and radiative processes in O_3 depletion by chlorofluorocarbons 0-109221
 O_3 layer, transport rel. to chemistry and depletion 0-104534
 O_3 , obs. of meridional flux by transient eddies in 0 to 30 km height range 0-109224
 O_3 , of stratospheric origin, measured over Pacific Ocean, source and large-scale wave transport 0-72600
 O_3 transport mechanisms, general circulation model 0-109196
 Pb , atmospheric long range transport to Denmark 0-94131
 S compounds, meso-scale transport obs. in rural East Midlands, England 0-94124
 SO_2 , movement in atmosphere (*Dutch*) 0-97844

atmospheric noise *see* **atmospherics****atmospheric optics**

- see also* **airglow**; **atmospheric light propagation**; **sky brightness**; **sunlight**; **twilight**
 46° halo and its arcs, prod. by hexagonal ice crystals 0-82065
 absorption, far IR, appl. of selective modulation interference spectrometer 0-57397
 aerosol, solar radiation absorpt., visual photometric meas. technique 0-85750
 aerosol above Black Sea, spectral transmission and sky brightness obs. (*Russian*) 0-94603
 aerosol light scattering turbidity and visibility obs. 0-105047
 aerosol scattering of IR radiation, atmos. heating and cooling rates 0-72630
 aerosols, coastal meas. by 1.06 μm Mie lidar scatt. 0-98403
 anethic arcs, comments on appearance 0-105050
 astronomical seeing, meas. at Kitt Peak 0-61899
 backscattered pulse shape, small-angle multiple scatt. in random media 0-77079
 cloud, solar radiation absorpt., vertical and horiz. distrib. 0-72596
 cloud extinction coefficient, estimation from multiwavelength lidar backscatter meas. 0-98446
 cloud layer IR radiative transfer 0-72629
 clouds, optical props., similarity criteria (*Russian*) 0-85745
 Denver Brown Cloud, obs. of C particles in aerosol 0-81961
 diffraction image intensity in turbulent atm., Huygens-Kirchhoff principle calcs. 0-63926
 DMSP visible imagery, causes of anomalous grey shades 0-77111
 dust haze of African Harmattan wind, 1962-1973 visibility obs. 0-61900
 extinction, no effects on 160-min. solar oscillation obs. 0-105216

atmospheric optics continued

- extinction variations for UVB photometry, transformations 0-67408
 fog and haze, visibility range obs. 0-109195
 glory, diffr. model 0-82053
 halo phenomena, deviation produced by anisotropic prisms 0-63916
 Harmattan dust rel. to visibility 0-94578
 heterodyne receivers for atmospheric optical communications 0-58663
 ice crystals, light scatt. expts. (*Russian*) 0-94601
 imaging of Earth surface, haze and nonuniform albedo affecting image contrast 0-101431
 IR radiative cooling rate due to H_2O vapour bands, calc. 0-90161
 IR transmittance spectrum, 2.8 to 14 μm 0-85743
 IR transparency window, 10-13 μm , H_2O and aerosol effects in winter and summer (*Russian*) 0-105048
 level surveying, atoms. refr. correction (*Russian*) 0-77127
 lidar equation for inhomogeneous atmos. (*Russian*) 0-82054
 light scattering, by optically thin spherically symmetric atmosphere rel. to brightness at zenith near terminator 0-109382
 mesosphere, light scatt. coeff. correl. to atmos. stratification (*Russian*) 0-105049
 Monte Carlo methods, book 0-77115
 moving atmosphere simulation by rotating phase plate 0-79021
 outgoing IR radiation, in CO_2 absorpt. bands (*Russian*) 0-77109
 particle optical constants and disperse aerosol comp., phase scattering function (*Russian*) 0-61898
 particulate size distrib. and refr. index, new lidar-radiometer method 0-77153
 phase correlation scale effects rel. to atmospheric imaging characts., theory 0-94604
 pollution affecting solar radiation incident on St. Louis, USA 0-109247
 radiative transfer eqn., soln. using Elsasser scheme 0-77112
 radiometric imaging from space, atmosphere effects problems 0-98323
 rainbow, anomalous arc due to refl. image of Sun from water surface 0-77114
 Rayleigh scattering in lower atmos. affecting photodissoc. rates 0-61921
 scintillation intensity in turbulent boundary layer, influence of refr. index structural charact. (*Russian*) 0-94597
 scintillation of astronomical bodies, determ. of stratosphere density inhomogeneity struct., Salyut obs. (*Russian*) 0-109186
 semi-empirical theory 0-90220
 soil-derived atmospheric dusts, particle absorption contributions to mass extinction coefficients 0-61896
 soot particle absorpt. of near IR (*Russian*) 0-82055
 stellar images, amplification by turbulent atm. 0-72782
 stratosphere aerosol content, preliminary results of SAGE and SAM II satellite monitoring 0-82082
 sunpillar formation, theory of light scatt. off cloud ice crystals 0-85747
 turbulence effect on sunspot fine struct. image form. 0-77108
 turbulent atmosphere, light propag. rel. to use of multiple-mirror telescope systems in astronomy 0-94713
 UFO sightings explained by refr. of light, Novaya Zemlya effect 0-77110
 visibility at ground level, two meas. methods 0-82078
 visibility trends, appl. of ridit anal. 0-82051
 VUV solar scatt. radiance, aurora and nightglow, satellite obs. 0-90272
 water vapour, Raman lidar meas., daytime atmosphere 0-85718
 H_2O , weak spectral absorpt. of vap., visible and near IR 0-82062

atmospheric pollution *see* **air pollution****atmospheric precipitation**

- see also* **atmospheric electron precipitation**; **atmospheric proton precipitation**; **ice**; **rain**; **snow**
 acid precipitation in W. United States, pH value obs. 0-89695
 acid rain, Pittsburgh (Pennsylvania) area 0-94129
 acidity measurement, error anal. applied to indirect methods 0-72108
 N.America, Quaternary temps. and precip. for NW. coast region 0-98438
 angular scattering of water drops and ice particles [electromagnetic interference], electromagnetic interference at freq. above 10 GHz appl. 0-109183
 annual precipitation series, stochastic anal. rel. to effects of urbanisation 0-98407
 auroral oval, dayside, evidence for parallel elec. field particle accel. 0-98503
 auroral particles, source regions rel. to dayside auroral morphology at 6300 Å, 5577 Å and 3914 Å 0-85786
 Brazil, precipitable water, distrib. maps 0-77075
 Britain, water balance, 50000 yr BP to present day 0-72566
 cloud seeding, studies of AgI ice-forming activity, verification of theory 0-101406
 Colorado Rockies, affects of Climax and Wolf Creek Pass cloud seeding expts. 0-82094
 correlation with annual streamflow record 0-81950
 daily precip. amounts, modelling with Markov-I chain 0-101401
 dust deposition in N.Nigeria, Harmattan dust (1978-79) 0-94578
 Earth's negative charge, supply mechanism 0-61758
 energetic particle precip., contrib. to middle atmosphere chemical comp. 0-109213
 forecasting in Arizona, rel. to marine layer depth and moisture content at San Diego, California 0-101395
 hail cell detection, for cloud seeding criteria, radar method 0-90170
 hail growth in supercell cloud, theory 0-98419
 hailstone formation within cloud, microphys. recycling 0-90146
 hailstone growth studies, wind tunnel expts. and thin sectioning 0-90160
 hailstorm, finger radar echoes, form. mechanism (*Chinese*) 0-109234
 Hebei Plain, summer drought and flood rel. to atm. circulation seasonal var. 0-90203
 Indian region, rain and snow correl. with tree growth rel. to tree-ring anal. appl. in palaeoclimatology 0-90212
 ion precipitation events in morning auroral oval, evidence for solar wind ion injections 0-98502
 Jerusalem, seasonal precip. temporal fluctuations 0-72618
 magnetosphere ions at high-altitude, particle origin during mag. storm 0-82144
 microwave signal attenuation by rain cell, Earth-satellite link 0-94586
 particle precipitation, energetic, nighttime global zones 0-61947
 radar polarisation techniques for precip. props. determ. 0-61925
 rain and drizzle, scavenging effect on cloud condensation nuclei, meas. by horizontal thermal gradient spectrometer 0-77158
 rime deposits as indicators of wind direction 0-98428
 riming process, laboratory expts. 0-105037

atmospheric precipitation continued

Southern Hemisphere, moisture conditions and precipitation efficiency 0-98424
tornado activity rel. to precipitation, assessment 0-61882
Ukraine, statistics of spatial distrib. of precip. on Experimental meteorological test range 0-101414
warm frontal region, wind and precipitation struct., Doppler radar study 0-81995
Agl surface, adsorption of water, effective pair pot. model 0-100394
¹⁸O/¹⁶O ratio, correl. with temp. and altitude 0-77067
Pb in rain water and dustfall, meas. in Denmark rel. to atmospheric long range transport 0-94131
²²²Rn concentration in tunnel air, atmospheric press. and precipitation effects (*Japanese*) 0-97845

atmospheric pressure see atmospheric pressure and density

atmospheric pressure and density

500 mb height, anal. error development, (1946 to 1969) 0-72615
N.Atlantic weather forecasting, multiday, for press. field 0-98417
auroral oval, dayside, press. gradient rel. to neutral wind profiles between 115 and 175 km altitude 0-98494
available potential energy in atm. in press coords. (*Russian*) 0-109187
Beaufort Sea, mesoscale press. distrib. 0-101366
Brussels-Uccle region, press. records 1833 to 1952 period (*French*) 0-82028
charged particle drag on Lageos, semimajor axis secular decrease 0-94628
convection dynamics equations, non-Archimedean approach 0-77048
forecasting of sea-level press. with allowance for surface press. tendency 0-85738
geopotential along 50°N on 500 mb level 0-101399
NE. Gulf of Alaska, development of synoptic climatology 0-98405
N.hemisphere, press. distrib. assoc. with poor summers in British Isles 0-109241
Hurricane Gladys (1975), subcloud layer energy transformations 0-77089
India, westerly upper air troughs rel. to western disturbances development 0-90173
ionosphere, plasma bubbles spatial relationship with 1 m equatorial spread-F irregularities 0-67457
ionosphere total electron content, nighttime enhancements at low latits. 0-72677
lunar tide, solar modulation anal. 0-94593
mass distrib. by latitude, anal. 0-90115
mesosphere and lower thermosphere, profiles based on obs. of Lyman- α extinction 0-77180
meteorological conditions by radiothermal sounding at 5 mm (*Russian*) 0-77038
NW.Pacific Ocean, relation between atmospheric press. and sea level 0-101415
W.Pacific subtropical high, summer, form. and struct. simulation (*Chinese*) 0-109233
pressure effects of water level in wells tapping deep unconfined aquifers 0-81953
remotely sensed pressure, satellite-borne MM wave radar system 0-67443
stratosphere, southern hemisphere, temp. and press. field spring transformation anal. 0-98420
stratosphere, temp. and press. profiles meas. via solar occultation sounding using narrowband radiometers 0-98452
stratosphere density inhomogeneity struct. determ. from Salyut obs. of astronomical scintillation (*Russian*) 0-109186
stratosphere density oscills. rel. to gamma-ray quasi-periodic intensity variations (*Russian*) 0-90177
surface pressure field, lower atmosphere instability correl. with solar corpuscular activity 0-61881
surface pressure measured using microwave signals transmitted from orbiting satellite 0-94581
surface pressure waves, 10 to 20-day westward propag. mode rel. to breaks in monsoons 0-94592
surface wind of Arizona cool season, correl. to press. gradients 0-98379
thermosphere, mass density, O and N₂ composition, seasonal-latitudinal tidal struct. 0-101467
tide, solar semidiurnal, obs. of surface press. oscill. 0-77054
tropical E.Atlantic, press. and wind fields from TROPEX data 0-82040
upper atmosphere, density depend. of bright meteors ionisation columns initial radii 0-94762
upper atmosphere, density distrib. from Cactus accelerometer flight result on Castor satellite 0-77251
upper atmosphere, rot. rate and density, obs. of satellite orbit 0-85785
weather forecasting for central Asia, for short-term press. field 0-98416
O, upper atmos. atom density, rel. to airglow intensity (*Chinese*) 0-90269
O₂ density in thermosphere, solar flux var. 0-72659
²²²Rn concentration in tunnel air, atmospheric press. and precipitation effects (*Japanese*) 0-97845

atmospheric propagation see atmospheric electromagnetic wave propagation

atmospheric proton precipitation

see also aurora; radiation belts
aurora in F-region, assoc. with magnetospheric cusp 0-90273
auroral particle precipitation, rel. to turbulence at 500 mb level 0-77218
auroral protons, energy rel. to N₂⁺ 1 NG emissions anomalous vibr. distrib. 0-67448
auroral zone precipitation and convection reversal, satellite obs. 0-101479
cusp region of magnetosphere, rel. to interplanetary mag. field 0-90288
cusp region on dayside, field line topography, precipitation implications 0-85822
dynamics and auroral morphology, photometric data interpretation 0-82141
field aligned current above auroral arc, e⁻ and H⁺ precipitation obs. 0-77215
inner magnetosphere penetrated by energetic particles during storms 0-72716
IPDP field fluctuations and proton precipitation, simultaneous obs. 0-77238
magnetosphere, precip. due to proton-cyclotron instabilities in non-uniform loss-cone plasma 0-90286
nighttime global zones of energetic particle precipitation 0-61947
radio aurora (diffuse), rel. to field-aligned currents and particle precipitation 0-105119

atmospheric radiation

see also aurora
Aberdeenshire, mesoclimate of Upper Don Basin 0-61889

atmospheric radiation continued

auroral hiss, nearly reson. whistler amplified Cherenkov radiation, limitations 0-101482
auroral location, visual and radio emission 0-82122
auroral O I 6300 Å emission production efficiency by energetic electrons 0-72671
cirrostratus clouds, IR emissivity meas. by remote sounding 0-82061
cirrus, radiative transfer model for IR region 0-98397
cirrus cloud, IR reflectance of cloud base 0-98397
cirrus clouds, IR emissivity calc. from lidar and radiometer meas. 0-82060
clear atmosphere, radiative transport and thermal turbulence (*French*) 0-82018
clear sky conditions, solar radiation and illumination simultaneous meas. 0-81985
climate, energy balance models, global and one dimens., stability comparison 0-94596
climatology of global solar radiation in California and an interpolation technique based on orthogonal functions 0-67402
cloud, solar radiation absorpt., vertical and horiz. distrib. 0-72596
cloud cover influence on atmos. top radiation budget 0-98398
clouds, radiation rel. to diurnal var. of underwater irradiances on horizontal surfaces 0-72549
clouds, stratiform, modelling and effect on radiation balance (*French*) 0-82017
cyclotron soliton theory of Earth's kilometric radiation 0-94657
daily solar total irradi. fluctuations, temporal statistical anal. (*French*) 0-61292
damping of temp. waves in finite non-grey atmosphere (*Russian*) 0-81990
diffuse solar radiation below overcast sky, ang. distrib. 0-85719
diffuse solar radiation effects on O₃ photodissoc., annual var. 0-109210
direct solar energy, Markov chain simulation with one minute binning (*French*) 0-61293
Earth Radiation Budget Satellite, climate appls. 0-109283
Earth surface thermal radiation effects of doubling of atmospheric CO₂ conc. and climatological significance 0-101426
earthquake lights, proposed for study by chemiluminesc. NO air pollution apparatus 0-61906
global solar radiation est. and prediction by stepwise multiple regression anal. for Greece (1961 to 1975) 0-61880
global spectral distrib. determ. using rapid spectral radiometer for solar cell appls. 0-61369
global surface irradiance, effect of aerosol props. and surface reflectivity 0-76611
greenhouse effect, component contrib. 0-101544
hiss associated with active auroral arcs, sounding rocket obs. 0-98512
ionosphere, auroral, ELF radio signals generation by LF and MF transmissions nonlinear demodulation 0-94639
ionosphere, rocket-borne VLF and ELF waves meas. in dayside auroral oval 0-98504
IR and microwave radiances meas. from TIROS-N processing for temp. sounding 0-77133
IR brightness obs. 0-94629
IR emission, effects on IR propagation and system performance modelling in fog 0-90218
IR long-wave (8 to 13 μ m) radiation in free atmosphere, comparison of theoretical and experiment fluxes (*Russian*) 0-94598
IR properties relevant to building envelope heat losses 0-58895
IR radiance (15 μ m), aerosol particle effects rel. to error in satellite retrieved temp. profiles 0-98449
IR radiation flux in upper atmosphere, meas. in 4 to 6 μ m spectral range 0-61929
IR radiation intensity, satellite meas. appl. to atmosphere total O₃ content determ. 0-77027
IR radiative energy exchange in troposphere from six-layer general circulation model 0-101432
IR radiative transfer in cloud layer 0-72629
Israel, estimation of solar radiation and ambient temps. 0-76607
kilometric radiation from auroral zone, coherent nonlinear theory 0-101495
kilometric radiation from auroral zone, propagation direction 0-101497
kilometric radiation generation, inner magnetosphere auroral zone 0-105128
Lake Victoria, incident global solar radiation, 1970-1974 obs. 0-81940
lightning, RF radiation generation, elec. field var. obs. 0-98401
lightning, simultaneous obs. of optical radiations from above and below clouds 0-85698
luminous efficacy of daylight at Tokyo (*Japanese*) 0-72631
magnetic noise of low-freq., generated on auroral field lines 0-101494
magnetosphere, elec. field in VLF to HF range, EXOS-B obs. 0-67478
magnetosphere, quasi-periodic ELF-VLF emissions assoc. with Pc 3-4 mag. pulsations, geomag. conjugacy 0-67475
magnetosphere, wave emissions prod. by JIKIKEN electron beam-plasma interaction expt. (*Japanese*) 0-94655
mesosphere at Thumba from in situ UV absorpt. photometry obs. 0-105051
meteorite fireball, deduction of props. from behav. in atoms 0-82311
methane and N₂O greenhouse effects, climate model 0-90211
middle atmosphere, IR cooling rel. to numerical model of zonal mean circulation 0-109218
MM wave radiometry conducted at Appleton Laboratory 0-67442
moisture content determ. of cloudless atmosphere, microwave radiation meas. 0-94624
outgoing IR radiation, in CO₂ absorpt. bands (*Russian*) 0-77109
plane parallel atmospheres, radiative transfer eqn. soln. 0-67409
planetary wave in middle atmosphere, radiative damping rel. to interaction with zonally averaged circulation 0-109217
plasmasphere, wave-particle interactions, ELF-HF obs. from EXOS-B 0-67467
pollutant layers, elevated, radiative effects on urban atmosphere temp. struct. and pollutant dispersion 0-97841
radiation intercepted by a tilted surface, estimation of daily, clear sky, spatial distrib. 0-81423
radiative processes and thermal structure 0-82016
radiative transfer eqn., soln. using Elsasser scheme 0-77112
radio emission of cloudy atmosphere, expt. characts. of fluctuation 0-67399
radio emission of the atmosphere in the 5-13 cm⁻¹ band 0-61878
rainfall measurement, combined usage of radar and radiometry techniques (*Chinese*) 0-109272
Saharan dust affecting radiative transfer rates, model 0-90149

atmospheric radiation continued

- satellite-derived radiance gradient, rel. to upper tropospheric/lower stratospheric winds 0-98447
 sky brightness at zenith near terminator, light scatt. theory for optically thin atmosphere 0-109382
 solar, atmospheric attenuation, effect of O₃ and H₂O vapour content and atmos. turbidity 0-93855
 solar, mesoscale mapping of available solar energy at the Earth's surface by use of satellites 0-72613
 solar and terrestrial radiation dependent on the amount and type of cloud 0-67403
 solar anisotropic diffuse insolation, calc. of instantaneous flux on tilted surfaces 0-101412
 solar diffuse irradiance measurement using shadowband, corrections 0-101410
 solar direct irradiance at the ground, parametric modelling 0-101411
 solar energy utilisation, global and sky radiation estimates for Austria 0-93861
 solar energy utilisation, prediction of hourly diffuse solar radiation from measured hourly global radiation on a horizontal surface 0-93864
 solar irradiance, model for determining the spectral quality of daylight on a horizontal surface at any geographical location 0-93856
 solar irradiance on horizontal surface, estimation of totals from UK average meteorological data 0-81422
 solar radiation incident on St. Louis, Missouri, USA, urban-neural differences 0-109247
 solar radiation measurement, reference scales 0-109206
 solar radiation statistics, linear spatial interpolation 0-93859
 solar UV radiation, absorpt. in mesosphere and stratosphere 0-109248
 soot particle absorpt. of near IR (*Russian*) 0-82055
 stratosphere, gamma-ray quasi-periodic intensity variations (*Russian*) 0-90177
 stratosphere, radiometric obs. using superpress. balloon 0-85763
 stratosphere, simulated radiances for ClO and NO concs. determ. via solar occultation meas. 0-85756
 surface and atmospheric radiation balance from satellite data 0-101396
 terrestrial solar spectral irradiance distrib. variations, sensitivity of solar transmittance, reflectance and absorbance 0-82739
 thermal radiation, ground based obs. of temp. distrib. (*Chinese*) 0-82041
 thermal radiation observations from satellites, moisture content characts. 0-85660
 thermosphere, NO radiative cooling 0-72656
 tropical region, heat budget estimate of ocean and atmosphere 0-104968
 troposphere, radiative cooling rate and flux, theory 0-85711
 United States, solar climates 0-76612
 upper atmosphere, IR emission at high latitudes from Meteor satellite, radiometer obs. 0-72655
 vacuum UV background, meas. 0-90221
 Van der Waals mols. in lower atmos., IR emission and absorpt. 0-85699
 VLF emission modulation freq. shift relative to geomagnetic pulsation freq. 0-77229
 VLF radiation during simultaneous magnetospheric substorm and thunderstorm, rel. to elec. fields and electron precip. 0-67392
 VLF wave events at L=4 correl. to optical emission 0-101468
 VLF wave measurement at ground station, antenna pickup for vertical elec. field 0-105063
 VLF waves, magnetospheric, obs. and comparison with high energy electron flux by EXOS-B satellite (*Japanese*) 0-94652
 VLF waves triggered by natural whistlers 0-98521
 VUV solar scatt. radiance, aurora and nightglow, satellite obs. 0-90272
 whistler precursor emissions and whistlers, ducted propagation 0-85809
 X-ray bremsstrahlung from widespread electron precipitation 0-77205
 X-rays from electron precipitation events in local dusk sector 0-101480
 H₂O vapour band, IR radiative cooling rate, calc. 0-90161
 H₂O, weak spectral absorpt. of vap., visible and near IR 0-82062
 O₃ layer, role of dynamic and radiative processes in O₃ depletion by chlorofluorocarbons 0-109221

atmospheric radioactivity

see also fallout

- radionuclides in N.European air due to Chinese nucl. explosions 0-108826
 fission products, ²²²Rn and cloud nuclei particles in N.Atlantic air 0-77074
⁸⁵Kr conc. 0-93756
²²²Rn daughter prods. meas. using diffusion sampler 0-81510
²²²Rn, props. and behaviour of short lived daughter nuclides in the atmos. (*Japanese*) 0-72339
¹³⁵Xe, plume from Three Mile Island nucl. reactor 0-89696

atmospheric spectra

see also atmospheric optics

- absorption continuum in the near IR near 1 μ m 0-61894
 aerosol above Black Sea, spectral transmission and sky brightness obs. (*Russian*) 0-94603
 aerosol IR spectrometry, theory and appl. to spectroscopic effect of atmospheric constituents 0-101428
 aerosol scattering indicatives under clear sky conditions in 0.55 to 2.4 μ m spectral region, determ. (*Russian*) 0-94600
 airglow, F-region, anal. of consistency of ground-based obs. with satellite results 0-98496
 airglow spectrometer, Fabry-Perot instrument for daytime use 0-77156
 airglow studies using large-aperture, high-resolution Fabry-Perot spectrometer 0-67424
 atmosphere, spectral transmissivity, rel. to direct beam solar irradiance and illuminance 0-90174
 auroral spectrum observations, appl. of matched tandem etalon camera (MATEC) 0-101442
 daylight, model for determining spectral quality on horizontal surface at any location 0-93856
 dust, soil derived atmospheric, IR spectra, Christiansen effect, Rayleigh limit 0-105046
 fog, spectral transmission data, IR propag. and performance modelling 0-90218
 formaldehyde, mol., UV absorpt. cross-section, and stratosphere chem. 0-109209
 Fourier transform spectroscopy from South Pole 0-98448
 hydrazine, rocket fuel in ambient air, CO₂ laser absorption spectra and photoacoustic detection 0-104540
 interplanetary dust in stratosphere, visible absorpt. spectra 0-101554
 ionosphere, UV fluoresc. at 391.4 nm excited by electron beam 0-77214

atmospheric spectra continued

- ionosphere plasma line, meas. at Chatanika with high-speed correlator and filter bank 0-98507
 IR mosaic background obs. from balloon altitude expt. 0-90222
 IR radiative energy exchange through strong lines wings 0-101432
 magnetopause, energetic electron spectrum meas. from Prognoz 3 0-72697
 magnetosphere kilometric radiation, emission spectrum fine struct. from JIKIKEN (EXOS-B) satellite obs. (*Japanese*) 0-94648
 mesosphere at Thumba from in situ UV absorpt. photometry obs. 0-105051
 meteor train, long-lived, IR brightness obs. 0-94629
 methylhydroperoxide, UV absorpt. spectra of vap. 0-69159
 nightglow, rocket meas. of O₂ atmospheric system and OH Meinel bands (*Japanese*) 0-94631
 peroxy nitrates, UV absorpt., spectra, photodissoc. lifetime meas. 0-83386
 photon, spectra of gamma rays backscattered by infinite air (skyshine) 0-101436
 plasmasphere, wave-particle interactions, ELF-HF obs. from EXOS-B 0-67467
 pollutant gases microwave spectra, monitoring from space using passive sensing techniques 0-76690
 pressure-scanning millimetric-wave dispersion spectrometer expt. 0-61904
 radar echoes, type 1, from equatorial electrojet, with double-peaked Doppler spectra 0-67458
 silver clouds, visible spectroscopic investig. from Salyut-4 orbit 0-82014
 Skylab conical multispectral scanner IR data statistics 0-90223
 stratosphere, HCl and HF near IR absorpt. spectra and volume mixing ratios meas. 0-72587
 stratosphere, trace constituents, laser heterodyne spectroscopy 0-109257
 stratosphere NO₂ and H₂O, mixing ratio profiles from IR solar spectra obs. 0-105015
 stratosphere trace molecule Fourier transform spectrometer optical design 0-82099
 transparency spectrum, meas. on Maidanak mountain during autumn and winter (1977 to 1978) (*Russian*) 0-72627
 troposphere, IR transmittance in region of NH₃ 927 cm⁻¹ absorpt. 0-85700
 twilight spectrum, new diffuse emission bands obs. 0-72662
 UV dayglow, mesosphere and thermosphere H distrib. from Lyman α and β obs. 0-109290
 vacuum UV background, meas. 0-90221
 Van der Waals mols. in lower atmos., IR emission and absorpt. 0-85699
 water vapour, Raman lidar meas., daytime atmosphere 0-85718
 water vapour continuum absorption (3.5 to 4 μ m) temp. dependence obs. 0-61903
 water vapour submillimetric-wave absorption obs. with photoacoustic cell 0-61901
 CO₂, 4.3 μ m band absorption, solar occultation sounding for temp. and press. profiles meas. 0-98452
 HCl, atmospheric measurements using ground based IR spectroscopy (*French*) 0-81975
 HF, atmospheric measurements using ground based IR spectroscopy (*French*) 0-81975
 H⁺(H₂O)_n ion-induced water clusters, mass spectra, IR continuum absorpt. 0-82757
 HNO₃, IR spectra, 865.5-871.0 and 884.5-887.0 cm⁻¹ regions, equiv. width meas., atm. spectrum appl. (*French*) 0-87114
 H₂O dimer, continuum absorpt. spectra in 8-13 μ m range (*Chinese*) 0-109237
 H₂O vapour band, IR radiative cooling rate, calc. 0-90161
 H₂O, weak spectral absorpt. of vap., visible and near IR 0-82062
 HONO (nitrous acid), obs. in urban atmosphere by differential optical absorpt. 0-76677
 N₂⁺ 1 NG emissions from proton aurora, anomalous vibr. distrib. 0-67448
 N₂⁺, auroral Meinel band excitation rel. to pulsating structs. extreme thinness 0-72667
 NH, IR emission studied using Fourier spectroscopy 0-95628
 NO and NO₂ mixing ratio profiles of stratosphere from IR sunset spectra 0-94563
 NO, thermosphere UV spectral absorpt. and density profile 0-85781
 NO₂, atmospheric abundance meas. using solar absorpt. method (*Japanese*) 0-94556
 NO₂, detect. in polluted troposphere by differential optical absorpt. 0-77036
 N₂O, gaseous, integrated band intensity data, stratospheric detection implications 0-58250
 N(²P) in aurora, UV spectra of metastable atom 0-77185
 N(²P) in auroral arc, excitation and collisional deactivation processes 0-72658
 Na I D doublet in nightglow, Na excitation and abundance 0-98497
 NaD, nightglow spectral intensity changes, correl. with O₂ spectra 0-61932
 O 2.53 μ m line, Zeeman splitting rel. to geomagnetic field vars. 0-77124
 O, 557.7 μ m spectral emission mechanism at 100 km altitude 0-61933
 O, airglow intensity of green line rel. to atom density (*Chinese*) 0-90269
 O I 7774 Å multiplet obs. of nightglow over Arcicibo during magnetic storm 0-72663
 O, spectral line shape in upper atm. following dissociative excitation 0-105097
 O₂, 1.27 μ m airglow, middle latit. meas. rel. to mesospheric O₃ concs. 0-72606
 O₂, 60 GHz absorpt. spectra for lower atmos. temp. 0-77172
 O₂ (¹ Δ_g) auroral emission, vibr. excitation process 0-82125
 O₂ (0-1) spectral emission band in upper atmos. 0-61933
 O₂ absorption of solar Lyman- α in mesosphere and lower thermosphere 0-77180
 O₂, electric quadrupole transitions detection in A band 0-85746
 O₂, mag. dipole transitions, line positions and strengths from stratospheric emission spectra 0-78604
 O₂, nightglow spectral intensity changes correl. with NaD spectra 0-61932
 O₂, UV bands rel. to solar UV radiation absorpt. in stratosphere and mesosphere 0-109248
 O₃, Chappuis-band absorpt. rel. to conc. determ. 0-77063
 O₃, IR absorption rel. to atmosphere total O₃ content determ. using satellite meas. 0-77027
 O₃ line parameter data, 10 μ m and 4.8 μ m regions 0-61895
 O₃ spectrum for atmosphere total O₃ determ., large particle scatt. coeffs. approximation 0-82091

atmospheric spectra continued

- O₃, UV bands rel. to solar UV radiation absorpt. in stratosphere and mesosphere 0-109248
 OH nightglow, photometric obs. to find mesosphere neutral temp. 0-82121
 O⁺(²P) airglow, meas. rel. to ionisation freq. vars. during solar cycle 21 0-77195
¹⁸O¹⁶O, Schumann-Runge bands transmission rel. to photodissoc. and O₃ prod. 0-94559
 SO₂, absorption spectrum, meas. using frequency doubled pulsed dye laser 0-87144
 SO₂, absorption spectrum, meas. using frequency doubled CW dye laser 0-87145

atmospheric structure

- see also *atmospheric composition*
 500 mb height, anal. error development, (1946 to 1969) 0-72615
 altocumulus billows, example of large amplitude Kelvin-Helmholtz wave 0-72621
 aurora, dayside morphology from large scale obs. at 6300 Å, 5577 Å and 3914 Å 0-85786
 aurora pulsating structures, implications of extreme vertical thinness 0-72667
 auroral oval, obs. of high-latit. mag. substorms 0-109315
 auroral zone, nighttime scintillation localised enhancements struct. 0-98506
 barotropic systems, low order, with forcing and dissipation, steady states and stability props. 0-72614
 boundary layer, acoustic sounder obs. from top of steep mountain 0-98409
 boundary layer turbulence, boundary layer, appl. of mixed-layer similarity scaling to observed dispersion from ground-level source 0-105021
 dynamic tropopause, isentropic anal. rel. to polar stratosphere-troposphere exchange in summer 0-72599
 inclinations of atmospheric layers, determ. from sounding data (*Russian*) 0-72569
 intertropical convergence zone, interaction with upper westerly waves rel. to Zambian weather during rainy season 0-90175
 inversion height in urban atmosphere, determ. from numerical simulation of mixing depths 0-105024
 ionosphere, auroral zone, irregularities, simultaneous rocket probe, scintillation and incoherent scatter radar obs. 0-94640
 ionosphere, bottomsides, mid-latitude trough discovery 0-109300
 ionosphere, dynamics of equatorial irregularity patch form., motion and decay 0-67456
 ionosphere, equatorial, features assoc. with radio scintillations 0-77191
 ionosphere, evidence for reflecting layer below classical D-region 0-98508
 ionosphere, irregularities at mag. equator rel. to long-term 1.5 GHz amplitude scintillation meas. 0-85792
 ionosphere, plasma bubbles spatial relationship with 1 m equatorial spread-F irregularities 0-67457
 ionosphere currents, obs. by S-310-5 rocket (*Japanese*) 0-94635
 ionosphere electron density equatorial anomaly, dissimilar forms in E.Asia and India 0-109301
 ionosphere equatorial bubbles, model computations of assoc. radio wave scintillation 0-94641
 ionosphere fine structure at low latitude from impedance obs. at 406 kHz 0-67468
 magnetosphere, high-latit., plasmapause and polar cap boundary and parallel elec. field below 8000 km 0-72706
 magnetosphere, open model plasma populations 0-90295
 magnetosphere, whistler duct struct. and formation 0-94659
 Manabe-Wetherald radiative convective model, fixed cloud-top temp. and fixed cloud-top altitude approximations 0-72616
 marine layer at San Diego, California, depth and moisture content rel. to cool season precip. forecasts in Arizona 0-101395
 mass distrib. by latitude, anal. 0-90115
 mesosphere, Southern Hemisphere, quasi 2-day wave vertical and horizontal struct. 0-109207
 mesosphere at Thumba from in situ UV absorpt. photometry obs. 0-105051
 middle atmosphere (mesosphere) 0-98412
 plasma sheet, cause of thinning during magnetospheric substorms 0-72705
 inner radiation belt trapping zone boundary, electron flux boundaries displacement during substorms 0-67470
 refractive index in atmospheric boundary layer, structural charact. vertical profiles (*Russian*) 0-94597
 stratosphere, quasi-biennial oscills. in temp. and O₃ conc. (1958 to 1977) 0-109222
 stratosphere, zonal mean winds vars. rel. to planetary wave props. and links with troposphere 0-109225
 stratosphere density inhomogeneity struct. determ. from Salyut obs. of astronomical scintillation (*Russian*) 0-109186
 subsynoptic scale vorticity perturbations, influence on short-range numerical weather forecast 0-82008
 surface layer, organised temp. struct. as signature of organised motion 0-72602
 temperature fluctuations, heat flux and struct. functions meas. with acoustic Doppler sodar 0-105023
 thermal structure, effects of nearby supernova 0-94584
 tropical middle atmosphere, observational evidence of semiannual oscillation 0-109216
 tropopause height rel. to sunspot activity 0-77090
 urban atmosphere, radiative effects of elevated pollutant layers on temp. struct. and pollutant dispersion 0-97841

atmospheric techniques

- see also *air pollution detection and control; geophysical equipment; ionospheric measuring apparatus; ionospheric techniques; meteorological instruments*
 500 mb height measurement, anal. error development, (1946 to 1969) 0-72615
 acoustic and radio acoustic exploration, effects of sound nonlinear absorpt. (*Russian*) 0-94567
 acoustic probing, appls. of external noise spectrum model 0-58858
 acoustic sounding, appl. to boundary layer obs. from top of steep mountain 0-98409
 adaptive optics, real-time atm. compensation, using lateral shear heterodyne interferometer 0-77843
 aerological sounding, appl. to atmospheric layers inclinations determ. (*Russian*) 0-72569

atmospheric techniques continued

- aerosol, middle atmospheric, remote sensing techniques 0-109269
 aerosol containing acid sulphate, detection using S/N ratio 0-61494
 aerosol IR spectrometry, theory and appl. to spectroscopic effect of atmospheric constituents 0-101428
 aerosol mass conc., meas. by lidar-solar radiometry expt. 0-90171
 aerosol number and mass conc. meas. 0-108753
 aerosol scattering function determ. with telephotometer 0-105055
 aerosol size distribution determ., optical attenuation meas. (*Chinese*) 0-72570
 air pollution automatic analysis, spectrosc. methods (*Spanish*) 0-81516
 air pollution episodes in Venetian region, real-time forecasting via advection-diffusion model 0-77096
 air pollution episodes in Venetian region, real-time forecasting via Kalman predictor 0-82046
 air quality models development for limited wind fetch, method 0-104533
 airborne particulates sources identification and relative importance estimation, regression model 0-72105
 aircraft ambient and cabin air O₃ conc. simultaneous determ. 0-90198
 airglow spectrometer, Fabry-Perot instrument for daytime use 0-77156
 atmosphere temperature profile, IR remote sounding, error anal. and data acquisition (*Chinese*) 0-109273
 auroral spectrum observations, appl. of matched tandem etalon camera (MATEC) 0-101442
 automatic observation of meteorological elements for atm. refr. determ. (*Japanese*) 0-82110
 available potential energy in press. coords. (*Russian*) 0-109187
 balloon altitude mosaic measurements programme, IR mosaic background meas. 0-90222
 balloon and rocket programs, conf. Bournemouth, England (1980, Aug.) 0-105433
 boundary layer, eddy flux meas. corrected for density fluctuations 0-72576
 boundary layer meas. system for wind and temp. obs. (*German*) 0-94616
 boundary layer temp. profile determ. from ground-based 60 GHz radiometry (*German*) 0-82097
 boundary layers, convective and nonconvective, parameterisation for use in numerical models 0-82009
 buoy for data acquisition, using Meteostat data transmission (*German*) 0-90224
 climate data archiving and quality control by computer 0-61907
 climate from tree ring width interpretation, South Africa Widdringtonia cedarbergensis anal. 0-98439
 climatology, hydrology, atmospheric research and meteorology from space, conference, Ajaccio, Corsica (1979 November 12 to 16) 0-62397
 cloud condensation nucleus spectrometer, new design 0-85765
 cloud extinction coefficient, estimation from multiwavelength lidar backscatter meas. 0-98446
 cloud height meas. using light pulse reflection (*Russian*) 0-82056
 cloud liquid content measurement, ground based microwave instrument 0-94623
 cloud seeding, anal. of Florida Area Cumulus Expt. (FACE) rainfall results, natural variability effects 0-82002
 cloud seeding, Climax and Wolf Creek Pass expts. 0-82094
 cloud seeding, studies of AgI ice-forming activity, verification of theory 0-101406
 cloud seeding studies application of lidar remote sensing 0-109203
 cloud study chamber, study of ice nucleation by aerosol particles 0-61864
 cloud winds over oceans, satellite technique verified by aircraft obs. 0-85764
 cloudy atmospheric parameter determination using microwave radiometric method 0-67435
 double theodolite measurements, control of inherent uncertainties 0-77160
 dynamics and auroral morphology, photometric data interpretation 0-82141
 Earth surface temperature in mountainous terrain, diurnal var. prediction and errors 0-82011
 earthquake lights, proposed for study by chemiluminesc. NO air pollution apparatus 0-61906
 electrical conductivity measurement by passive antenna system, comparative study 0-85762
 electrostatic charges meas. and localisation, neutralised during lightning flashes 0-77097
 filter media suitable for air pollutant analysis (HNO₃, nitrates and acidity) 0-104541
 forecasting nocturnal temperature, short-range model 0-109200
 forecasting of thunderstorms and severe local storms, automated 12 to 36 hour probability forecasts 0-77062
 GATE aircraft measurements, their value 0-82071
 GATE ship surface meas. systems, anal. or drift 0-82070
 geomagnetic field variations, remote sensing at mesospheric heights 0-77124
 ground surface temperature prediction, force-restore method investigation 0-98469
 ground wave attenuation function, computation methods 0-94585
 hail cell detection, for cloud seeding criteria, radar method 0-90170
 hailstone thin sectioning technique, for growth study 0-90160
 humidity 0-85660
 hurricane detection by Doppler radar for coast of U.S.A. 0-67414
 incoherent scatter radar sounding, appl. to daytime middle thermosphere 0-72654
 laser heterodyne spectroscopy for stratospheric trace constituents meas. 0-109257
 lidar equation for inhomogeneous atmos. (*Russian*) 0-82054
 lightning, direction finding at close range, VHF method 0-98481
 lightning direction finding, by mag. method 0-77078
 long-range weather forecasting, appls. of quasi-cycles in meteorology 0-109239
 long-range weather forecasting, art and science 0-109184
 magnetosphere, elec. fields parallel to mag. lines, studied by electron injection expts. 0-72702
 magnetosphere, local electron density and mag. field meas. via JIKIKEN (EXOS-B) satellite stimulated plasma wave expts. (*Japanese*) 0-94649
 magnetosphere sounding, beam-plasma interaction expt. by JIKIKEN satellite (*Japanese*) 0-94655
 magnetotelluric methods, methods to study crust cond. beneath magnetometer array, review 0-98486
 marine wind velocity, remote sensing using oceanic whitecaps 0-72554

atmospheric techniques continued

- meteorological conditions, press. and geopot. by 5 mm radiothermal sound-
ing (*Russian*) 0-77038
meteorological data analysis, interpretation of asynchronous data
0-109271
meteorological data sets, form. from first GARP Global Experiment
(FGGE) obs. 0-101437
meteorological field analysis and forecasting pattern-recognition theory
methods appl. 0-98421
meteorological radar equipment signals processing, interpretation device
(*Russian*) 0-67432
meteorology radar, airborne pulse Doppler method 0-85757
METEOSAT project overview (*Italian*) 0-109331
microwave sensing from satellites, appl. to meteorological meas. over
W.Australia 0-98485
moisture content determ. of cloudless atmosphere, microwave radiation
meas. 0-94624
moving atmosphere, optical simulation by rotating phase plate 0-79021
nephelometry, electrophotical, characterisation of nonspherical atm. aerosol
particles 0-77106
normal mode linear initialisation method 0-77042
optical properties of turbulent atmosphere, determ. via He-Ne laser trans-
mitter/receiver 0-98450
paleoclimatology, Quaternary temps. and precipitation determ. from pol-
len factors 0-98438
paleoclimatology, role of tree-ring anal. in Indian region from prelimi-
nary survey 0-90212
particle size distribution meas. using electronic cascade impaction
0-72652
particulate size distrib. and refr. index, new lidar-radiometer method
0-77153
Pc 1, short-term prediction of pulsation occurrences 0-109317
photochemical air pollution potential form. in United Kingdom, numerical
estimation method. form. in United Kingdom 0-76682
photometric technique for aerosol absorption meas. 0-85750
pollutant gases, monitoring from space using passive microwave techniques
0-76690
pollutant measurement techniques, for H_2SO_4 and particulate strong acid-
ity 0-104542
pollution, factor of safety calc. method 0-94140
precip. time struct., daily precip. amounts modelling with Markov-I chain
0-101401
precipitation acidity measurement, error anal. applied to indirect methods
0-72108
precipitation forecasting in Arizona, rel. to marine layer depth and mois-
ture content at San Diego, California 0-101395
precipitation properties using radar polarisation techniques 0-61925
psychrometry, appl. of portable differential system 0-105072
quasistatic approximation for atmospheric dynamics, characterisation (*Ger-
man*) 0-98383
radar echoes from distributed targets, averaging of time, angle and range
0-109264
radar for observing middle and upper atmosphere, Yaggi antenna array
design 0-90255
radar meas. of upper atmosphere 0-72661
radar observation of lower atmos., MST radar at Poker Flat, Alaska
0-90254
radar signal processing, for SOUSY-VHF-radar, using preprocessor
0-85774
radar studies of strato- and mesospheres, review 0-90180
radar techniques for middle atmos. dynamic struct. 0-105078
radio propag. methods, quasi-single freq. Doppler-Faraday technique
0-77128
radioacoustical sounding, expression for scatt. signal freq. spectra (*Rus-
sian*) 0-94612
radiometry of stratosphere, use of superpress. balloon 0-85763
rain attenuation, radiometric determ. at millimetre wavelengths, multi-
ple-scatt. effects metric determ. at millimetre wavelengths, multiple-
scatt. effect 0-90260
rain estimation, using geostationary satellite data from extratropical region
0-90244
rain measurement and forecasting in UK using radar as part of integrated
system, progress and plans 0-98490
rain measurement by dual-polarisation radar, drop size and fall rate
0-72650
rainfall, convective, meas. over small areas using high-density raingauges
and radar 0-77157
rainfall estimation by satellite borne microwave radiometry 0-105085
rainfall instantaneous rate, meas. technique and influence on high-voltage
transmission lines 0-98471
rainfall measurement, combined usage of radar and radiometry techniques
(*Chinese*) 0-109272
rainfall measurement by radar, methods and interpretation of data
0-81969
rainfall on convective days, analysed with respect to radar obs. atmos.
parameters 0-109205
rainfall prediction over United States west coast, appl. of Nimbus 6 liq.
water data over NE.Pacific Ocean 0-82005
Rayleigh scattering effect determ. method 0-61921
remote sensing, by TIROS-N operational vertical sounder 0-77132
remote sensing, parameters retrieval from scanning multichannel micro-
wave radiometer obs. 0-90261
remote sounding of high clouds, visible and LR optical props. from lidar
and radiometer meas. 0-82060
satellite image gridding, line scan method 0-61915
satellite remote sensing, temp. profiles error due to aerosol particles effects
0-98449
satellite solar occultation sounding of the middle atmosphere 0-105079
short-range numerical weather forecasting, effect of subjectively enhancing
initial vorticity field 0-82008
smoke/dust cloud temporal analysis algorithm 0-98484
solar absorption spectrum method, appl. to atmospheric NO_2 abundance
meas. (*Japanese*) 0-94556
solar irradiance outside atmosphere, Bouguer method for ozonometer
determ. (*Russian*) 0-61918
solar occultation sounding, appl. to press. and temp. profiles meas.
0-98452
solar radiation measurement, reference scales 0-109206
soot particle conc. meas. by near IR extinction coeff. (*Russian*) 0-82055
sounding techniques in IR and microwave regions, recent progress
0-82096

atmospheric techniques continued

- spectral multiplication, props. as viewed in physical space, meteorological
appls. 0-94607
stochastic analysis, appl. to annual rainfall data affected by urbanisation
0-98407
stratosphere, H_2O mixing ratio determ. using NOAA UV fluoresc. instru-
ment 0-90137
stratosphere aerosol, satellite monitoring systems, SAM II and SAGE
0-82082
stratosphere and mesosphere temp. and O_3 , satellite IR limb scanning
method 0-105086
stratosphere NO and ClO meas. via solar occultation, influence of concs.
vars. at twilight 0-85756
stratosphere turbulence struct., using 430 MHz Arecibo radar 0-90258
SURF storage ring calibrations for NASA stratosphere and climate pro-
grams 0-94721
surface layer optical inhomogeneities, investigation via acoustic method
0-67434
synoptic climatology development for NE.Gulf of Alaska, automated
correl. technique appl. 0-98405
TEM, in situ meas. of aerosol-gas interaction 0-104544
temperature fluctuations, heat flux and struct. functions meas. with acous-
tic Doppler sodar 0-105023
temperature measurement in fog and stratus, shipboard use of low-level
atmospheric thermograph 0-105073
temperature sounding from TIROS-N, early operational soundings evalua-
tion 0-77133
thermocouple psychrometry, effect of and correction for different wet and
dry bulb response 0-98472
thermosphere temperature and wind measurement Fabry-Perot-
interferometer imaging system appl. 0-101441
thunderstorm location by single station techniques, improved method,
radiowave propag. effects 0-67438
tornadoic storm research, implications for dual-Doppler radar spacing of
effective coverage area anal. 0-82093
trace gas analysis of stratosphere, based on in situ ion composition obs.
0-105077
transmittance functions, generation by numerical methods 0-98455
triggering lightning by pulsed laser 0-72626
tropical cyclone intensity measurement from tropospheric aircraft
0-67416
troposphere, radar obs. during clear air conditions, review 0-90178
troposphere, radar obs. of vel. and irregularities, spaced antenna VHF
method 0-90185
turbulence parameters from Doppler radar clear-air echo intensity
0-90190
turbulent boundary layer, finite-element numerical modelling 0-77061
ULF wave generation by peninsular loop currents 0-90247
upper atmos., 391.4 nm light excited by electron beam from sounding
rocket 0-77214
upper atmos. temp. and wind, meas. with Fabry-Perot airglow spec-
trometer 0-77156
visibility at ground level, two meas. methods 0-82078
weather charts transmission by facsimile for military appls. 0-90206
weather forecasting, conditional probabilities prediction method (*Chinese*)
0-109238
weather forecasting games at American Universities, survey 0-98770
weather forecasting processing of radar and satellite imagery data
0-109252
weather forecasts, impact of satellite temp. sounding data 0-77028
weather maps, structural description of contour maps 0-101419
wind direction meas. by vane, graphic recording and averaging 0-82098
wind fields, mesoscale, satellite-derived, covariance anal. 0-82013
wind fields, urban-scale, three-dimensional, construction 0-101407
wind in lower atmos., clear air Doppler radar methods, vertical component
0-72642
wind in rough time terrain, derivation of mass-consistent flow field from
wind obs. 0-105013
wind local climate, determ. using trees as indicators 0-82007
wind measurement (absynoptic scale) using dual Doppler radar and vel.
azimuth display 0-109263
wind measurement by radar, technique for strato- and troposphere
0-90257
wind pattern determ. from rime deposits 0-98428
wind profile radar obs., tropo-stratosphere, Poker Flat MST radar
0-72579
wind shear hazard in boundary layer, radar detection feasibility 0-90256
wind shear measurement, using pulsed Doppler laser 0-67415
winds in upper troposphere/lower stratosphere, determ. from satellite-
derived radiance gradient 0-98447
Zephyr radar system for meteorological measurements 0-90228
C in suspended particulates, meas. technique 0-76686
 CO_2 record in polar ice, CO_2 extraction method 0-61891
 ClO composition of stratosphere, balloon borne reson. fluoresc. method
0-90167
HCl, atmospheric measurements using ground based IR spectroscopy
(*French*) 0-81975
HF, atmospheric measurements using ground based IR spectroscopy
(*French*) 0-81975
 H_2SO_4 aerosol, filter sampling of air, possible artifacts 0-82079
 NH_3 , gas conc. meas. using ring oven technique 0-81507
 O_3 , determ. by Chappuis-band absorpt. 0-77063
 O_3 in lower stratosphere, Nimbus 4 remote sensing method 0-77154
 O_3 total content, determ. using satellite meas. 0-77027
 O_3 total content, Dobson spectrophotometer meas. errors 0-72644
 O_3 total content determination, large particle light scatt. coeffs. approx-
imation 0-82091
 O_3 , total content meas. using Dobson spectrophotometer 0-72643

atmospheric temperature

- see also *atmospheric thermodynamics*
500 mb temperatures, rel. to cloud top temps. and Climax and Wolf
Creek Pass cloud seeding expts. 0-82094
Aberdeenshire, mesoclimate of Upper Don Basin 0-61889
aerosol IR radiation scattering, calc. of heating and cooling rates
0-72630
airglow temp. measurement, with new interferometer aperture design.
0-82075
Alaska, climate reconstruction from modern climate-tree ring relations
0-101425

atmospheric temperature continued

- N.America, Quaternary temps. and precip. for NW. coast region 0-98438
 Beaufort Sea, winds and surface temps. rel. to August ice cover vars. 0-101366
 Birmingham, England, heat island synoptic climatology (1965-74) 0-85740
 boundary layer, temp. dimensionless structural charact. rel. to refr. index profiles (*Russian*) 0-94597
 boundary layer, temperature structure coeff. detect. by acoustic radar 0-98386
 boundary layer measurement system, for wind and temp. struct. (*German*) 0-94616
 boundary layer temp. fluctuations of cloud-laden airstream 0-61845
 boundary layer temp. profile determ. from ground-based 60 GHz radiometry (*German*) 0-82097
 boundary layers, convective and nonconvective, parameterisation for use in numerical models 0-82009
 British spring weather, survey (1950 to 1979) 0-98427
 British winters (1659 to 1979), study of temp. correl. with precipitation 0-98444
 California coast, marine fog and fog-stratus systems rel. to marine boundary layer inversion development 0-77060
 China, agricultural growing season vars. in historical time (*Chinese*) 0-109246
 NE.China, persistently low summer temp., causative circulation pattern (*Chinese*) 0-109235
 climate model including aerosol effects 0-77102
 climate of central England, 1660-1977, air temp. variability 0-98437
 cloud temperature and humidity changes and overcloud inversion 0-77083
 Coningsby, Lincolnshire, temp. rise assoc. with snow rollers form. (1979 January 2) 0-72568
 D-region, temp. control of NO⁺ cluster ion formation 0-61931
 distribution from ground based obs. of thermal radiation (*Chinese*) 0-82041
 E-region, electron temp. compared to neutral temp., 100-120 km altitude 0-77211
 E-region, temps. and collision freq. in polar regions, incoherent scatter meas. 0-72688
 Earth surface temperature, climatological significance of doubling of atmospheric CO₂ conc. 0-101426
 Earth surface temperatures, implications of stratospheric aerosol modification by supersonic transports and space shuttle 0-98408
 exosphere temperatures at high latits., geomag. activity effects 0-109286
 F₁-layer, ion comp. and temp. profiles from incoherent scatter radar studies 0-72654
 F-region, electron density and ion temp. profiles rel. to airglow ground-based obs. anal. 0-98496
 F-region, electron temp. model, Aeros-A data compared to radar obs. 0-67465
 F-region, energetic electrons spectra meas. by Hadamard energy spectrometer (*Japanese*) 0-94637
 F-region, global electron temp. distrib. model, 300-700 km altitude 0-67464
 F-region, winter anomaly causes 0-85793
 Fenlands, temp. and humidity meas. rel. to steam fog form. criterion 0-98431
 fluctuations, heat flux and struct. functions meas. with acoustic Doppler sodar 0-105023
 flux used to determine oceanic temp. flux 0-104986
 forecasting max. and min. temp., use of probabilities 0-82020
 forecasting nocturnal temperature, short-range model 0-109200
 free atmosphere, temp. and humidity effects on theoretical and exptl. long-wave IR radiation fluxes (*Russian*) 0-94598
 Fresnel zone and diffraction fields anal. near boresight of acoustic radar antennas 0-64318
 global temp. distrib. from TIROS-N microwave sounder unit meas. 0-90265
 Greenland Sea area, climatic normals 0-77100
 ground surface temperature prediction, force-restore method investigation 0-98469
 halocarbon depletion of O₃ layer, climate effects 0-98436
 N.hemisphere, sea surface temps. assoc. with poor summers in British Isles 0-109241
 ice albedo feedback with temp., one dimens. radiative convective climate model 0-109245
 Indian region, temp. correl. with tree growth rel. to tree-ring anal. appl. in palaeoclimatology 0-90212
 ion temp., International Reference Ionosphere 1978 rel. to Vertical-6 rocket meas. 0-90285
 ion temp., Vertical-6 rocket flight results 0-90268
 ionosphere, effect of recomb. processes and plasma nonisothermability on thermal parametric instability 0-61967
 ionosphere, electron density and temp. rel. to primary ion-electron prod. rates changes 0-72675
 ionosphere, high-altitude auroral zone, electron temp. enhanced by electron current 0-85803
 ionosphere, topside, electron temp. models for low and medium solar activity conditions 0-67460
 ionosphere, winter, thermal electrons energy distrib. obs. by S-310-5 rocket (*Japanese*) 0-94636
 ionosphere and plasmasphere at midlatitude, computer model 0-105120
 ionosphere electron temp., calc. technique for ground and satellite obs. 0-90275
 IR remote sounding, error anal. and data acquisition (*Chinese*) 0-109273
 lapse rate, control of inherent uncertainties in double theodolite meas. 0-77160
 Little Ice Age, N.Hemisphere average temp. obs. rel. to model calcs. 0-82050
 Manabe-Wetherald radiative convective model, fixed cloud-top temp. and fixed cloud-top altitude approximations 0-72616
 marine layer, temp. profiles meas. in fog and stratus using low-level atmospheric thermograph 0-105073
 mean temperature of thickness layers along 50°N 0-101399
 measurement by automated environmental monitoring system 0-81513
 mesosphere, OH nightglow emission obs. 0-82121
 mesosphere, pot. temp. field rel. to eddy diffusion models 0-109198
 mesosphere and lower thermosphere, profiles based on obs. of Lyman- α extinction 0-77180

atmospheric temperature continued

- mesosphere and stratosphere, obs. by satellite IR limb scanning method 0-105086
 middle atmosphere, temps. calc. from numerical model of zonal mean circulation 0-109218
 middle atmosphere (mesosphere) 0-98412
 Mohliner Feld (east of Basle), cold air distrib. rel. to topoclimate (*German*) 0-61890
 Mount Kenya, vertical temp. struct. rel. to condensation nuclei concs. 0-82012
 New York State, ambient temp. decrease rel. to local snowfall trends in four cities 0-105044
 New Zealand, temp. record, historical data and agricultural implications of climatic var. 0-61886
 Orange Lake, Florida, temp. fluctuations rel. to lake latent and sensible heat fluxes prediction 0-72562
 palaeotemperature, O isotopes of mid-Wisconsin limestone cave deposits 0-82069
 precipitation, ¹⁸O/¹⁶O ratio correl. with temp. and altitude 0-77067
 psychrometry, appl. of portable differential system 0-105072
 pyrocumulus cloud over North Canterbury, New Zealand, air temp. due to heating by surface fires 0-109240
 radiational damping of temp. waves in finite non-grey atmosphere (*Russian*) 0-81990
 rapid morning boundary-layer transition, case study from Haswell, Colorado, expt. 0-81996
 remote sensing, by TIROS-N operational vertical sounder 0-77132
 Rome, effect of urban heat island on air temp. during summer season 0-85717
 satellite temperature sounding data, impact on weather forecasts 0-77028
 satellite-retrieved temperature profiles, error due to aerosol particles effects 0-98449
 sounding from TIROS-N, early operational soundings evaluation 0-77133
 stratosphere, diurnal variation of wind and temp. in equatorial region 0-82022
 stratosphere, O₃ behaviour and thermal structure during S. Hemisphere spring 0-105014
 stratosphere, southern hemisphere, temp. and press. field spring transformation anal. 0-98420
 stratosphere, sudden warming forced by mountain 0-72583
 stratosphere, temp. and O₃ vars. (1958 to 1977) 0-109222
 stratosphere, temp. and press. profiles meas. via solar occultation sounding using narrowband radiometers 0-98452
 stratosphere, vars. during total solar eclipse 0-105017
 stratosphere sudden warming, caused by planetary wave secondary circulation 0-72584
 stratosphere temperature wave propagation, polar region in winter 0-72597
 surface and soil temperature anys. in humid tropics, case study from Sierra Leone 0-109242
 surface layer, temp. traces and features of organised motion 0-72602
 surface layer temperature, fluctuations investigation via acoustic method 0-67434
 surface temperature, determ. of diurnal var. in mountainous terrain 0-82011
 thermal structure, effects of nearby supernova 0-94584
 thermosphere, empirical model of temp. and composition 0-77183
 thermosphere, lower, pot. temp. field rel. to eddy diffusion models 0-109198
 thermosphere, middle, ion comp. and temp. profiles from incoherent scatter radar studies 0-72654
 thermosphere, NO radiative cooling 0-72656
 thermosphere temperature and wind measurement Fabry-Perot-interferometer imaging system appl. 0-101441
 tide in temperature of stratosphere due to Moon, NIMBUS 5 obs. 0-101405
 tropical cyclone, intensity inferred from troposphere temp. 0-67416
 tropical middle atmosphere, observational evidence of semiannual oscillation 0-109216
 troposphere temperatures and winds, evidence for solar cycle signal 0-72604
 troposphere/stratosphere, temp. rel. to radiance gradient and jet streams 0-98447
 United States, 1896-1975 interannual temp. variability 0-61888
 upper atmos. temp. meas. with Fabry-Perot airglow spectrometer 0-77156
 upper atmosphere at nighttime, 400-450 km altitude, anal. of Ogo 6 data 0-90267
 urban atmosphere, numerical simulation of mixing depths 0-105024
 urban atmosphere, radiative effects of elevated pollutant layers on temp. struct. and pollutant dispersion 0-97841
 urban environment, cold air drainage effects on temp. fields, case study of topographical influence on climate 0-94555
 volcanic eruption, dust causing temp. drop at Earth surface 0-85726
 wave-wave interactions in vel. and temp. fields, kinetic and available pot. energy evolution 0-109227
 CO₂ laser radar used to measure average atmospheric temp. 0-90225
 CO₂ model run in tandem with climate model, 1800-2100 AD 0-98381
 CO₂-induced atmospheric temp. rise, Arctic sea ice decay 0-61802
 N₂O pollution causing atmos. warming, interaction with O₃ 0-94579
 O₂ microwave absorpt. at 60 GHz 0-77172

atmospheric thermodynamics

see also atmospheric temperature

- aerosol scattering of IR radiation, atmos. heating and cooling rates 0-72630
 air-sea sensible and latent heat transfer coeffs., meas. 200 km from land 0-72552
 airflow turbulent kinetic energy, budgets in mountainous terrain 0-105022
 available potential energy in atm. in press coords. (*Russian*) 0-109187
 baroclinic atmosphere, two dimensional, zonal flows convective instability (*Russian*) 0-94564
 boundary layer, bulk model for wind and pot. temp. 0-77030
 boundary layer, lakes latent and sensible heat fluxes prediction from surface water temps. 0-72562
 boundary layer during convective disturbance, thermodynamics 0-81978
 boundary layers, convective and nonconvective, parameterisation for use in numerical models 0-82009
 cirrus, radiative transfer model for IR region 0-98397

atmospheric thermodynamics continued

- cloud layer cooling by IR radiative transfer 0-72629
- cyclone at temperature latitude, water vap. and energy budget 0-85731
- diabatic heating profile, rel. to preferred mode of Ekman conditional instability of second kind (CISK) 0-72617
- diurnal heating in Po Valley, dynamic circulation 0-85716
- eddy fluxes of conserved quantities by small-amplitude waves 0-61858
- energy balance climate models tests 0-77098
- energy budget of equatorial atmosphere, meridional heat transfer (*Russian*) 0-81988
- equatorial mesosphere and stratosphere, vertical vel. determ. from Diurnal Experiment 0-77047
- equatorial trough zone, heat balance 0-81977
- evapotranspiration of continents real land surface, Penman concept calcs. (*German*) 0-98368
- general circulation, eqns. of kinetic and available pot. energy evolution in wave-number freq. space 0-109227
- greenhouse effect, component contrib. 0-101544
- greenhouse effects of methane and N₂O, climate model 0-90211
- heat exchange between atmosphere and land surface, force-restore method for ground surface temp. prediction 0-98469
- heat fluxes, zonal and meridional var. long planetary wave induced 0-85720
- heat transport, rel. to ocean temperature-salinity curve 0-72534
- heat release, effect on atm. general circulation and climate 0-89694
- heat transfer causing density effects in CO₂ or water flux, corrections 0-85721
- Hurricane Gladys (1975), subcloud layer energy transformations 0-77089
- ionosphere, topside, protonospheric heat flux rel. to electron temp. models 0-67460
- ionosphere auroral zone, ion heating by electrostatic ion cyclotron waves 0-72686
- IR cooling, chlorofluoromethane induced, effect on general circulation model 0-90122
- IR radiative cooling rate due to H₂O vapour bands, calc. 0-90161
- magnetosphere open model, current sheets rel. to plasma populations 0-90295
- Manabe-Wetherald radiative convective model, fixed cloud-top temp. and fixed cloud-top altitude approximations 0-72616
- mean meridional circulations of stratosphere and mesosphere, monthly mean planetary wave fluxes 0-109219
- middle atmosphere (mesosphere) 0-98412
- monsoon in winter over warm ocean current, heat and moisture budgets 0-72590
- monsoon over Indian region, energy anal. by baroclinic model 0-77073
- W.Pacific subtropical high, summer, form. and struct. simulation (*Chinese*) 0-109233
- planetary wave in middle atmosphere, radiative damping rel. to interaction with zonally averaged circulation 0-109217
- radiation problems, thermal struct. 0-82016
- radiative transfer eqn., soln. using Elsasser scheme 0-77112
- Saharan dust affecting radiative transfer rates, model 0-90149
- sea-air heat exchange, rel. to poleward heat flux by ocean gyre 0-85668
- squall line at midlatitude, thermodynamic and kinematic struct. obs. 0-109191
- steam fog in Fenlands, temp. and humidity meas. rel. to fog form. criterion 0-98431
- stratosphere, sudden warming forced by mountain 0-72583
- stratosphere, zonal mean winds vars. rel. to planetary wave props. and links with troposphere 0-109225
- stratosphere warmings, thermal and kinetic interactions with troposphere 0-105031
- sudden stratospheric warming initiated by planetary wave, model 0-90150
- temperature fluctuations, heat flux and struct. functions meas. with acoustic Doppler sodar 0-105023
- thermals models, scales of motion rel. to self-similarity soln. 0-109228
- thermosphere, heating by solar UV, efficiency at mid-latitude 0-85780
- thermosphere, NO radiative cooling 0-72656
- tide (solar semidiurnal), zonal motion and meridional temp. gradient effects 0-98399
- tropical depression, synoptic scale kinetic energy source, cumulus cloud convection 0-77088
- tropical region, heat budget estimate of ocean and atmosphere 0-104968
- troposphere, radiative cooling rate and flux, theory 0-85711
- troposphere jet stream-frontal system, pot. vorticity, role of turbulence 0-77044
- upward sensible heat flux by synoptic-scale transients, observational study 0-94591
- urban heat island, Rome, obs. during summer season 0-85717
- urban heat island convergence in calm periods, St. Louis USA 0-90169
- weather forecasting, atmospheric prediction models, computing and numerical methods 0-77095
- zonal mean circulation of middle atmosphere, numerical model 0-109218

atmospheric turbulence

- aircraft generated turbulence obs. by FM-CW radar 0-90186
- amplification of optical stellar images 0-72782
- auroral oval, dayside, low-amplitude turbulence rel. to ULF elec. field fluctuations obs. 0-98505
- auroral particle precipitation, rel. to turbulence at 500 mb level 0-77218
- baroclinic instability, wave overreflection mechanism 0-90141
- baroclinic instability of short-wavelength two-layer Eady model 0-72593
- boundary layer, horizontal roll vortices, two dims. numerical obs. 0-101409
- boundary layer, lateral coherence of isotropic turbulence and wind 0-72575
- boundary layer, turbulence coeff. vertical profile 0-85733
- boundary layer, turbulence rel. to refr. index structural charact. (*Russian*) 0-94597
- boundary layer, vertical eddy flux representation 0-61844
- boundary layer, vertical frictional motions on varying scales (*Russian*) 0-105027
- boundary layer at nighttime, case study comparison with model calcs. 0-85707
- boundary layer at nighttime, vertical struct. obs. 0-61848
- boundary layer during convective disturbance, thermodynamics 0-81978
- boundary layer turbulence, boundary layer, appl. of mixed-layer similarity scaling to observed dispersion from ground-level source 0-105021
- boundary layer turbulence, finite-element numerical modelling 0-77061

atmospheric turbulence continued

- buoyant plume in stably stratified boundary layer, max. ground conc. 0-72573
- clear atmosphere, radiative transport and thermal turbulence (*French*) 0-82018
- cloud, eddy viscosity parameterisation in two-dims. model 0-85708
- cooling tower plumes, interaction with atm., numerical model simulation (*French*) 0-94126
- correlation of the phase and amplitude fluctuations between direct and ground-reflected sound 0-96067
- cumulus convection, vorticity horizontal transport parameterisation 0-90158
- current convective instability in auroral F-region 0-72680
- diffraction image intensity in turbulent atm., Huygens-Kirchhoff principle calcs. 0-63926
- eddies, transient, in 0 to 30 km height range, O₃ flux obs. 0-109224
- eddy diffusion, models for mesosphere and lower thermosphere 0-109198
- eddy fluxes, zonal and meridional var., long planetary wave induced 0-85720
- eddy fluxes of conserved quantities by small-amplitude waves 0-61858
- effects on IR and near-millimetric-wave propagation 0-61902
- electrojet, equatorial, type II irregularities, nonlinear theory 0-61958
- electrojet induced press. and vel. fluctuations 0-82118
- F-region, collisional Rayleigh-Taylor instability in equatorial spread F 0-82138
- flux of CO₂ or water, correction for density effects 0-85721
- GATE sub-cloud layer, eddy fluxes and spectra 0-105035
- general circulation of N.hemisphere in winter, horiz. transport by transient eddies 0-72589
- heat turbulence effect on sunspot fine struct. image form. 0-77108
- heterodyne optical radar S/NP ratio in atmospheric turbulence 0-106558
- heterodyne receivers for atmospheric optical communications 0-58663
- hill affecting airflow, in boundary layer, overspeed effect 0-72577
- hill crest, obs. of wind speed, shear and turbulence 0-85722
- Hurricane Gladys (1975), subcloud layer energy transformations 0-77089
- IMF sector boundary crossing affecting 500 mb level atmos. of southern hemisphere 0-109199
- ionosphere, auroral, turbulence rel. to irregularities obs. via rocket probe, scintillation and incoherent scatter radar 0-94640
- ionosphere, auroral inhomogeneities revealed by VLF propag. 0-105107
- ionosphere, bubbles in equatorial spread F, nonlinear evolution 0-85801
- ionosphere, partially ionised plasma, strong turbulence 0-79499
- ionosphere auroral zone, ion heating by electrostatic ion cyclotron waves 0-72686
- ionosphere inhomogeneity formation, influence of elec. field temporal variation 0-105105
- Kelvin-Helmholtz instability, jet stream generated, radar obs. and model 0-90165
- laser beam amplitude fluctuation statistics in turbulent atmosphere 0-106458
- laser beam arrival angle fluctuations meas. apparatus using telescope 0-109258
- light spherical wave propagation, effect of turbulence 0-82066
- longitudinal turbulence and mean wind speed, comparison at coastal site and offshore location 0-98406
- lower thermosphere, compositional modelling taking account of airflow tidal variation 0-109288
- magnetosheath, turbulence rel. to solar wind ion injections in morning auroral oval 0-98502
- magnetosphere, turbulence generation by proton-cyclotron instabilities in non-uniform loss-cone plasma 0-90286
- magnetosphere longitudinal currents, dynamic processes in turbulence development 0-67469
- magnetosphere plasma sheet, variability of turbulent dynamics 0-98518
- mass transfer in boundary layer, plume dispersion (*French*) 0-61850
- mesoscale, $k^{-5/3}$ law inertial range to two-dims. turbulence 0-72594
- mesosphere turbulent structure, spectral range (*Chinese*) 0-105092
- middle atmosphere, VHF radar obs. 0-105032
- middle atmosphere (mesosphere), eddy energy dissipation rel. to energetics and thermal struct. 0-98412
- mixing, rel. to use of passive antenna system as cond. meas. device 0-85762
- mountain and desert atmospheric MTF comparison 0-82063
- mountainous terrain, atmosphere turbulent kinetic energy budgets 0-105022
- narrow field optical astrometry, atmospheric turbulence limitations 0-109340
- optical coherence, atm. effects 0-82064
- optical effects, rel. to use of multiple-mirror telescope systems in astronomy 0-94713
- optical propag. through turbulent atmosphere, He-Ne laser transmitter/receiver 0-98450
- ozonosphere, eddy transport rel. to maintenance of zonal mean O₃ distrib. in N.Hemisphere 0-109220
- partially coherent beam intensity fluctuation calc. 0-78775
- partially coherent curved beam waves in turbulent atm., beam props. 0-95798
- particle cloud, dispersion in boundary layer, theory 0-61842
- planetary boundary layer, Doppler radar obs. in clear air conditions 0-90184
- planetary boundary layer, tapped with cumulus, numerical model (*French*) 0-94574
- planetary boundary layer similarity profile by turbulence closure model 0-72574
- pollutant turbulent diffusion model, K-theory 0-89697
- radar detection of turbulence parameters, from clear-air echo intensity 0-90190
- radar signal scatt. from turbulent air, VHF and UHF 0-85728
- rapid morning boundary-layer transition, case study from Haswell, Colorado, expt. 0-81996
- shear flow instability, Kelvin-Helmholtz and reson. overreflection modes, vortex pairing interactions 0-90129
- shoreline escarpment affecting boundary layer turbulence, wind profile etc. 0-109243
- smoke plumes in surface layer, cross section diffusion (*Russian*) 0-104532
- snowfall, turbulence rel. to laser beam intensity fluctuations (*Russian*) 0-94602
- solar mag. sector rel. to tornadoes and similar phenomena, 1955-77 period 0-77094
- Somali jet, planetary boundary layer model 0-72591

atmospheric turbulence continued

speckle propagation statistics through turbulent atm., log-amplitude covariance function effect 0-82058
spectral theory of stratified turbulent shear flow, interactions between motion fields 0-90114
spread-F plasma bubbles in equatorial topside region 0-72694
stratified turbid medium, small-angle approx. soln. of radiative transfer eqn. (*Russian*) 0-82057
stratosphere, turbulent layer struct., 2380 MHz radar obs. 0-90191
stratosphere turbulence near tropopause, review of radar obs. 0-90179
stratosphere turbulence struct., using 430 MHz Arecibo radar 0-90258
structural characts., meas. using spatially limited laser beam 0-98413
symmetric instability of stratified geostrophic flow 0-98425
temperature field structure, new formula (*Chinese*) 0-109236
thermal defocusing of light beams, phase conjugation compensation method 0-64123
thermosphere turbulent structure, spectral range (*Chinese*) 0-105092
troposphere turbulence, influence on radio-interferometric differential meas. of astronomical coordinates 0-67581
troposphere turbulence effect on pot. vorticity in jet stream-frontal systems 0-77044
troposphere winds, radar obs. made at Kwajalein Atoll, equatorial Pacific 0-90188
tropospheric long-distance propag., multiple scatt. effect 0-109229
wave induced eddy transport, computation in realistic atm. model 0-90164
wavelike eddies in zonal flows with shear props., cyclone model perturbation anal. 0-81994
wind generator design, atmospheric turbulence structural influences 0-61247
wind simulation, wind tunnel expts., turbulent boundary layers on rough surfaces, simple roughness elements 0-69774
CO₂ IR laser velocimetry, processing techniques and applications 0-87831

atmospheric wind see wind

atmospherics

see also atmospheric electromagnetic wave propagation; whistlers
auroral oval, dayside, rocket-borne VLF and ELF waves meas. 0-98504
cyclotron soliton theory of Earth's kilometric radiation 0-94657
diffraction and stray fields measurement, angular and amplitude characteristics (*Russian*) 0-67433
ELF radio signals is auroral ionosphere, generation by LF and MF transmissions nonlinear demodulation 0-94639
ELF sferics in polar region during solar proton event, June 1968 Antarctic obs. 0-90291
equatorial hiss in topside ionosphere, obs. 0-61939
ground wave atmospherics generated by lightning return strokes, initial peaks, model 0-61876
kilometric radiation characts., initial results from JIKIKEN (EXOS-B) satellite obs. (*Japanese*) 0-94648
lightning, 2200 MHz atmospherics, rel. to optical radiation obs. from above and below clouds 0-85698
magnetosphere, determ. of mode of propag. electrostatic and radio waves using stimulated plasma wave results (*Japanese*) 0-94650
magnetosphere, elec. field in VLF to HF range, EXOS-B obs. 0-67478
magnetosphere, quasi-periodic ELF-VLF emissions assoc. with Pc 3-4 mag. pulsations, geomag. conjugacy 0-67475
magnetosphere, radio and plasma waves obs. during JIKIKEN (EXOS-B) satellite initial phase (*Japanese*) 0-94675
magnetosphere, VLF plasma waves obs. and comparison with high energy electron flux by EXOS-B satellite (*Japanese*) 0-94652
magnetosphere, wave emissions prod. by JIKIKEN electron beam-plasma interaction expt. (*Japanese*) 0-94655
plasma sphere, wave-particle interactions, ELF-HF obs. from EXOS-B 0-7467
radio noise statistical models for reception in VLF band 0-72611
Schumann resonances in Earth-ionosphere cavity, book 0-86050
simultaneous obs. made in Japan and Thailand propag. study 0-98520
thunderstorms in Asia, anal. of errors of location 0-101421
tropical regions, atm. noise data 0-61875
VLF anomalies, rel. to rainy days over Calcutta 0-82127
VLF chorus, cause of apparent longit. variation, OGo 3 obs. 0-72720
VLF hiss from auroral zone, direction find method and obs. 0-85777
VLF radiation during simultaneous magnetospheric substorm and thunderstorm, rel. to elec. fields and electron precip. 0-67392

atom-atom collisions

includes reactive collisions
2p π orbital transitions Auger study (*Russian*) 0-91639
atomic radiative binding in slow collisions into molecules in a laser field (*Russian*) 0-93753
charge exchange, quantum mechanical and impact parameter capture amplitude 0-87226
collision systems $\alpha(Z_1+Z_2)\geq 1$, quasimolecular 1 s σ orbital, excitation and spectroscopy 0-87199
collisional intense-field fluoresc., Zeeman degeneracy effects 0-99477
collisional ionisation, Penning and associative ionisation produced by laser field 0-63802
energy transfer, reaction dynamics and collisional ionisation, review 0-63801
excited atom ionisation due to collisions in their own gas (*Russian*) 0-91654
gas laser, output power profile collision induced asymmetry, simplified model 0-87366
inert gas+alkali metal, collision studies of quasi-one-electron systems 0-63750
inert gas collisional perturbation of 6³D₁, 6¹D₂ Hg levels 0-74223
inert gas mixture, collision induced microwave absorpt. spectra 0-74216
interacting atoms, retarded energy shift and pair polarisability, field theoretical perturbation theory 0-102560
laser excitation mechanisms for atomic and ionic lasers, book contrib. 0-106512
laser induced Penning ionisation two step optical collisional perturbation sequence 0-63778
laser-induced collisional energy transfer, level crossing expansion 0-83461
mol. target internal motion 0-78697
neutral+high Rydberg atom, thermal collisions, review 0-63756
neutral atom collisions, hyperfine component broadening and shift of spectral lines 0-74136
P-S state atomic collisions, quantum mechanical treatment, decoupling approx. 0-99542

atom-atom collisions continued

P-state collisions, quantum mechanical treatment, angular momentum coupling 0-99541
recombination reactions, energy transfer mechanisms studied using trajectory calcs. and Monte Carlo method 0-66785
resonant impurity gas, translational nonequilibrium in resonance optical field (*Russian*) 0-106865
resonant ionisation spectroscopy, chem.-physics appls. 0-68259
Rydberg atom+atom (photon), separation of Rydberg electron and ion core 0-63754
superheavy and intermediate atomic collision systems, UNILAC expts. 0-63751
two photon ionisation, radiative collision effect 0-106388
Z₁+Z₂>120, 1s σ excitation probability, scaling law, expt. confirmation 0-58365
Ar+Ar, stopping power 0-91651
Ar+Kr, (4p²5p) and (4p³5p) states, radiative lifetimes and two-body collisional deactivation rate consts. 0-95572
Ar+H, assoc. ionis., rovibronic struct. in electron energy spectrum 0-106380
Ar+H, collisional quenching rates 0-95548
Ba in shock heated Ar, absorpt. line broadening obs. (*Japanese*) 0-83464
Ba+Ti, dipole-quadrupole radiative collisional fluoresc. 0-83315
Ba+Ti, radiative collisional fluoresc. obs. from thermally excited atoms 0-102480
Ca in shock heated Ar, absorpt. line broadening obs. (*Japanese*) 0-83464
Ca+Ca(Mg)(inert gas), metastable ³P-state, quenching reactions, fluoresc. meas. 0-102477
Ca+inert gas, ¹P₁-³P₁ excitation transfer 0-102559
Ca+Xe, collision-induced dipole transition due to long range interaction, absorpt. obs. 0-63779
Cd, broadening of 5¹P₁ level 0-83479
Cd+He, Penning ionisation cross section of target atom, for He(2³S₁) 0-63777
Cl atoms, photorecombination, rate constants determ., identification of spectral distribution of recombinative emission intensity 0-85195
Cs+Cs, spin destruction, obs. 0-63781
Cs+He, interaction pot. and oscill. strength 0-91645
Cs+inert gas, three body interaction, fluoresc. spectra principal series lines and secondary satellites 0-83313
Cu+Cu collisions, K α X-ray energy shifts, target thickness depend. 0-83311
D+Ar(Kr)(Xe), ion pair formation, curve crossing model 0-87216
Eu+Sr, absorptive collisional energy transfer, laser induced excitation spectra 0-63584
Eu+Sr, laser induced collisional energy transfer profile, high resolution study 0-83471
Fe+Ar, Fe I reson. line, collisional broadening at high temp. (*German*) 0-106298
Fe+H in type I Seyfert galaxies and quasars, collisional ionisation rel. to permitted Fe II lines 0-62278
H, gaseous, high-resolution mag. reson. study, 1 to 1.3K 0-95560
H+alkali metal atom, interaction potentials 0-63736
H+Ar, H α and H β emission cross sections 0-63782
H+Ar(Kr)(Xe), ion pair formation, curve crossing model 0-87216
H+Cs(Rb)(K)(Na), single-electron capture total cross sections 0-91656
H+D, close coupling calc., resonant spin-flip process, Ramsauer-Townsend effects 0-99547
H+H, electron loss cross section, four-body trajectory calcs. 0-99566
H+H, spin-exchange and freq. shift cross sections at low temps. 0-83452
H+H interaction, second order dispersion energy, Borel integral investigation 0-74218
H+H*, electron loss cross section, four-body trajectory calcs. 0-99566
H+He(Ar), collisional coherent excitation, meas. of Lyman α -photons 0-99552
H+Ne(Ar), electron energy loss 0-87217
H⁰+Cs collisions, H⁻ production cross sections 0-78698
H⁺+Ar, charge exchange excitation, alignment tensor components, coincidence method 0-63795
H(S)+Ar(³P_{0,2}), energy transfer collisions, Lyman- α emission profile obs., in microwave discharge and reaction cell 0-58359
H⁺+H(Li), resonant ionisation, cross section and ionisation probability 0-63785
He, depolarising collision cross sections, quantum beat obs. 0-87203
He+2I \rightarrow I₂+He, energy transfer mechanisms studied using trajectory calcs. and Monte Carlo method 0-66785
He+Ne, 2¹S₀-level excitation, rate const., temp. depend. 0-87218
He*+He, excitation exchange and collisional relax. 0-69226
He(2¹S, 2³S)+Ne(e⁻), transition probs., pots. 0-58371
Hg(6³P₀)+Hg(6³P₂), line excitation and population decay in afterglow 0-74242
K+He, 4²P state j₁m₁-j₂m₂ Zeeman transition, total cross section energy depend. 0-83475
⁸⁶Kr, discharge, metastability-exchange cross section 0-99464
⁸⁶Kr-⁷⁸Kr, discharge, metastability-exchange cross section 0-99464
Li+Li*(H*), resonant ionisation, cross section and ionisation probability 0-63785
Li*(2²P₁)+He(He)(Ar)(Kr)(Xe), collision induced fine struct. transition rate coefficients determ. 0-74220
Na+H(He)(Kr) vel.-changing collisions, effect on 2 photon and stepwise absorpt. line shape 0-87221
Na+inert gas, non-Lorentzian spectral line shape 0-106297
Na+inert gas, Rydberg states transitions, broadening cross-sections meas. 0-69110
Na+Na, crossed-beam collision, laser-induced Penning and assoc. ionisation, struct. obs. 0-83476
Na+Na, electronic-field pot. curves determ. for large interatomic distances, excitation cross sections calc. 0-95704
Na+Ne(Ar)(Xe), 3³P-3³D line broadening obs. 0-78684
Na+Xe+fw, collisions in presence of nonresonant lasers 0-99567
Ne+He⁺, He(3¹P) level excitation, total emission cross section, fast oscills. obs. 0-58362
Ne+Ne, (He) low pressure broadening and shift of Ne line, Lennard-Jones pot. 0-102554
Ne₂, collision induced Raman spectra and diatom polarisability 0-63647
Ne(²P_{1/2})+Ne, differential cross sections 0-58370
Ne* 5882 Å line, Doppler free spectra, press. broadening and shifts, saturation spectroscopy 0-78565
Ne*+H, assoc. ionis., rovibronic struct. in electron energy spectrum 0-106380

atom-atom collisions continued

- Ne($2p^3$) states, radiative lifetimes, collisional deactivation rate consts. 0-69107
 O+Ar(Kr)(Xe), magnetically selected O(3P) state scatt. 0-99543
 $^{17}O+^{16}O$, fractionation by chemical equil. 0-89513
 $^{18}O+^{16}O$, fractionation by chemical equil. 0-89513
 O^2+ inert gas, electron transfer meas., 60-200 keV 0-83480
 Pb+Cu, $1s\sigma$ excitation probability, scaling law, breakdown at very small internuclear distances 0-58365
 Rb in Xe, collision-induced dipole transitions, absorpt. meas. 0-95718
 Rb+He, single-electron capture total cross sections 0-91656
 Rb+H₂, quasielastic and inelastic collisions in S and D Rydberg states 0-83462
 Rb+Rb, radiatively excited states, chemi-ionisation, ionisation rate consts. determ. 0-58363
 Rb+Rb*, freq. shift, line broadening, phase interference effects, Doppler free two photon spectra 0-58200
 Sr+inert gas, $^1P_1-^3P_1$ excitation transfer 0-102559
 Tl+Ba, radiative collisional fluoresc. obs. from thermally excited atoms 0-102480
 Tl+Cs, Tl $6^2P_{3/2}$ -state relax., NMR obs. 0-95653
 Xe+Ne, quenching of excited Xe*(2P_2 , 3P_1 , 1P_1) states 0-63578
 XeF₂(C) state lifetime, quenching rate consts., photolysis in inert gas atmospheres 0-66816

atom-ion collisions

- includes reactive collisions*
see also charge exchange
 collision system, pot. curves at low collision energies, beam studies 0-61088
 drift tube technique in ion-neutral collisions, cross sections determ. 0-63748
 electronic and at. collisions, conf., Kyoto, Japan (Aug.-Sept. 1979) 0-57011
 electronic and at. collisions, conference, Kyoto, Japan (Aug.-Sept. 1979) 0-62394
 emission electron angular and energy distribution 0-87222
 heavy ion+atom collisions, small impact parameters, K-vacancy prod., molecular theory 0-69229
 heavy-ion collisions, charge transfer, target K-shell electron capture, impact parameter depend. 0-102552
 highly excited states, decay spectra 0-63780
 impact ionisation, inner shell alignment calcs. 0-83473
 inert gas atom+alkali ion, collision studies of quasi-one-electron systems 0-63750
 inert gas atom+Ne $^{2+}$ (Ar $^{2+}$)(Kr $^{2+}$)(Xe $^{2+}$), low energy reactions, SIFT and drift tube obs. 0-97705
 inner shell excitation 0-63749
 interstellar molecules synthesis, laboratory studies of ion-atom reactions 0-67812
 ion kinetics in high-pressure laser plasmas 0-64002
 laser excitation mechanisms for atomic and ionic lasers, book contrib. 0-106512
 light ion+heavy atom, inner-shell ionisation, adiabatic effects 0-99561
 multielectron collisions, charge transfer at intermediate energy, atomic model 0-91652
 multielectron target+multiply charged ion, electron capture, review 0-63812
 multiply charged ion+atom, autoionisation, electron and photon emission 0-63813
 multiply charged ion+one-electron target, electron capture, review 0-63811
 negative ion+atom, electron detachment, zero range Fermi approach 0-63798
 negative ions, at. and mol. collisions electron detachment for energies near threshold 0-63797
 superheavy ion-atom collisions, quasiats., K-vacancy form., positron emission 0-63753
 third-row elements, at. K-shell X-ray prod. by $^{14}N^+$ bombardment 0-91482
 wake-bound electron contrib. to convoy electron vel. distrib., effect of ionic field 0-60729
 Ag+H $^+$, excited X-ray polarisation, Born approx. calcs. (Russian) 0-78566
 Al+H $^+$, K-shell ionisation 0.5 to 40 MeV, meas. and PWBA-BEA calcs. 0-78699
 Ar+Ar partially stripped ion, stopping power 0-91651
 Ar+Ar $^+$, charge exchange, Σ oscil. and spin change 0-74247
 Ar+Ar $^+$ (Ar $^{2+}$)(Ar $^{3+}$), electron stripping cross-sections meas. 0-83477
 2Ar+Ar $^+$ (Kr $^{+}$), three body reaction, rate coeffs., temp. depend., 100 to 300K 0-108703
 Ar+F $^+$, inner-shell ionisation, X-ray cross sections 0-58369
 Ar+H $_2^+$, endothermic charge transfer reaction, low energy crossed beam study 0-95720
 Ar+HHe $^+$, ab initio pot. energy data, SCF-LCAO calcs. 0-63530
 Ar+multicharged ion collisions, one electron capture from inner shells 0-58376
 Ar+proton, charge transfer, target K-shell electron capture, impact parameter depend. 0-102552
 Ar+Xe $^+$, XeAr $^+$ form., dissoci. energy, reaction equil. and rate consts. 0-61071
 Ar $^+$ +Ar, charge transfer, fine-structure transitions 0-63808
 Ar $^+$ +He, integral elastic scatt., repulsive potentials derivation 0-63744
 Ar $^{2+}$ +Ar (Kr)(Xe), single electron capture excitation, photon emission, VUV spectroscopy 0-58379
 Au, X-ray production cross sections for protons, fluoresc. obs. 0-102476
 Au+light and heavy ions, L-shell X-ray production and subshell ionisation cross sections meas. 0-91637
 Be $^+$ +He(Ne), ns-np excitation, alignment and orientation, impact, parameter theory 0-91648
 Be $^+$ +He(Ne)(Ar), Be II 2^2P excitation, alignment and orientation 0-91647
 Be $^+$ +Ne, 180 degree phase jumps for Be $^+$ (2s-2p) excitation amplitudes, coherence obs. 0-63793
 C+H $^+$ collision, electron capture cross section 0-63804
 C+proton, charge transfer, target K-shell electron capture, impact parameter depend. 0-102552
 $^{106}Cd+H^+$, simultaneous nucl. and K-shell excitation, ^{107}In lifetime meas. 0-63130
 Cl $^{19}+$ +Cu, K X-ray production and radiative electron capture, fluoresc. yield determ. 0-99553

atom-ion collisions continued

- Cu+H $^+$, K-shell ionisation 0.5 to 40 MeV, meas. and PWBA-BEA calcs. 0-78699
 D $^+$ +atoms (Z=27 to 34), K shell ionisation, nuclear Coulomb effect 0-91650
 Fe group elements, singly ionised, charge transfer, rel. to laser action 0-74246
 Fe II+H in type I Seyfert galaxies and quasars, collisional excitation rel. to permitted Fe II lines 0-62278
 H+Cl $^-$ →HCl+e, associative reaction, product vibr. state distrib. 0-66794
 H+H $^+$, H excitation, angular differential cross sections 0-63784
 H+He $^{2+}$, electron transfer, plane-wave factor, mol. state treatment 0-63807
 H+O n^+ (N n^+)(Cn $^+$)(B n^+), charge transfer cross sections, oscillatory behaviour in low-energy collisions 0-63806
 H+Xe n^+ (Ar n^+)(Fe n^+), electron capture by heavy multicharged ions at low velocities total cross sections meas. 0-99548
 H $^-$ +H(He), electron detachment in adiabatic regime, mechanisms 0-63800
 H $^-$ +He, electron detachment, theoretical obs. 0-63799
 H $^-$ +inert gas, negative ion detachment cross section determ. 0-63796
 H 0 +N $^{2+}$, electron loss cross section 0-63805
 H $^+$ +Ag(Zr)(Fe)(Cu)(Ti), K-shell ionisation cross-section, 85 to 790 keV 0-106390
 H $^+$ +alkali metal, charge exchange, eikonal approx. calcs. 0-78703
 H $^+$ +Ar, H α and H δ emission cross section 0-63783
 H $^+$ +atoms (Z=27 to 34), K shell ionisation, nuclear Coulomb effect 0-91650
 H $^+$ +Cs(Rb)(K)(Na), single-electron capture total cross sections 0-91656
 H $^+$ +H, ionisation and electron capture to continuum 0-58366
 H $^+$ +H high energy collision, excitation multipole moments, classical trajectory approx. 0-106389
 H $^+$ +Li, charge exchange, eikonal approx. calcs. 0-78703
 H $^+$ +Li $^+$, charge transfer and ionisation, total cross sections for production of Li $^{2+}$ determ. 0-91657
 H $^+$ +Ar, low energy proton transfer reactions, crossed beam studies 0-108697
 $^A H$, A=1,2,3, \bar{p} radiative atomic recombination, antiprotonic atoms 0-83527
 H(2S)+He(N)(Ar), excitation and ionisation contributions to sum-rule Born cross sections 0-99551
 He ions +Ti(Fe)(Cu), K-shell ionisation cross-section, 85 to 790 keV 0-106390
 He-like target+fast projectile, electron capture cross-sections 0-69231
 He+ArH $^+$, ab initio pot. energy data, SCF-LCAO calcs. 0-63530
 He+H $^+$, differential scatt., 1-12 eV, high resolution beam meas. 0-58348
 He+He $^+$, 0.7-2 MeV, charge-changing collisions, electron capture 0-58372
 He+He $^+$, double collision spectroscopy 0-58378
 He+He $^+$, low energy collisions, excitation of 2 1S , 2 1P and 3 1P , 3 3P levels 0-58342
 2He+He $^+$ (Ne $^+$), three body reaction, rate coeffs., temp. depend., 100 to 300K 0-108703
 He+He $^+$ (Ne), tensor polarisabilities of 1s and 1D level, fluoresc. depolarisation obs. 0-69099
 He+Li $^+$ autoionisation, electron spectra 0-91653
 He $^+$ +He, autoionisation electrons and scatt. ions, ang. correl. determ. 0-63792
 He $^+$ +inert gas, collisional quenching cross sections, two-state theory calcs. 0-69217
 He $^+$ +Xe, internal energy distrib. at 100 eV 0-99564
 He $^{2+}$ +Li collisions, soft X-ray emission obs. 0-83591
 K+K $^+$ collisions, charge exchange cross section 0-58374
 Kr+F $^+$, inner-shell ionisation, X-ray cross sections 0-58369
 Kr+Kr $^+$, quasimolecular Kr $_2^+$, Auger transitions obs. by electron-scattered-ion coincidence method 0-74243
 Li+doubly charged ions, electron capture excitation, theoretical predictions in fusion plasma 0-63810
 Li+H $^+$, Li core excitation cross section, correlation and reorganisation effect 0-87215
 Li $^+$ +Ne collisions, vel. dependence of Ne 2s and 2p, vacancy production, electron spectroscopy 0-58344
 Mg+H $^+$ $2p_{3/2}$ vacancy alignment electron capture role 0-83465
 Mg $^{2+}$ +He(Ne), ns-np excitation, alignment and orientation, impact, parameter theory 0-91648
 Na+H $^+$, $2p^3s^2p_{3/2}$ state alignment, collisionally induced, impact parameter calc. 0-83474
 Na+He $^+$, crossed beams, l-changing collisions, n-depend. 0-58345
 Ne+He $^{2+}$, optical transition excitation function and cross sections 0-63877
 Ne+C N^+ (N n^+)(O n^+), charge exchange contribution to K-vacancy production 0-102553
 Ne+H $^+$ (D $^+$), electron detachment, dynamical phenomenon 0-106305
 Ne+heavy ion, highly charged very slow Ne recoil ions, K X-ray transition 0-91649
 Ne+proton, charge transfer, target K-shell electron capture, impact parameter depend. 0-102552
 Ne $^+$ +Ar integral elastic scatt., repulsive potentials derivation 0-63744
 Ne $^{2+}$ +Ar (Kr)(Xe), single electron capture excitation, photon emission, VUV spectroscopy 0-58379
 Ne $^{2+}$ +Xe, electron capture collisions, 15 to 50 keV, excitation 0-102566
 Ne $_2$ +atom (molecule), bimolecular and termolecular reaction rate coeffs. 0-81308
 O n^+ +He, charge exchange measurements using double-tandem accelerator-decelerator source of low-energy highly-stripped O ions 0-81317
 Pb, X-ray production cross sections for protons, fluoresc. obs. 0-102476
 Rb+H $^+$, single-electron capture total cross sections 0-91656
 S+F $^+$, inner-shell ionisation, X-ray cross sections 0-58369
 S $^{18}+$ +O $_2$ (Ar)(He), (q=8-19), K X-ray prod., charge-state depend. 0-106391
 Si+F $^+$, inner-shell ionisation, X-ray cross sections 0-58369
 Ti $^{19}+$ +O $_2$ (Ar)(He), (q=8-19), K X-ray prod., charge-state depend. 0-106391
 UO $^{2+}$ +Ar, collision-induced dissoci. cross section and threshold 0-95706
 UO $^{2+}$ +Ar, collision-induced dissoci. cross section and threshold 0-95706
 Xe $^+$ +He $^{2+}$, optical transition excitation function and cross sections 0-63877
 Xe $^+$ +Xe, XeI reson. line excitation 0-87220

atom-molecule collisions

- see also *atom-molecule reactions*; *molecular rotational-vibrational energy transfer*
- acetylene+inert gas, vibr. relax. study using laser-induced fluoresc. 0-74219
- atom+diatom, energy correction of infinite order sudden approx., improved phase shift approach 0-95710
- atom+diatom, energy transfer, reaction dynamics, review 0-63801
- atom+diatom collisions, vibr. to electronic energy transfer, semiclassical decoupling scheme 0-95714
- atom+diatomic molecule, restricted 2-D Morse oscillator model, semiclassical calcs. for mol. dissociation 0-74222
- atom+diatom kinetic cross section, ES, CS and IOS approx. with translational-internal coupling, viscomag. effect 0-63764
- collisional relax. of highly excited states, laser-induced fluoresc. obs. 0-58205
- intermolecular potential, rot. energy transfer, sensitivity anal. 0-63762
- Morse oscillator collisional collision, inelastic vibr. energy transfer, mol. continuum influence 0-106383
- Penning ionisation processes investig. by electron spectroscopy 0-58364
- rotational rainbow maxima: a time dependent study 0-58353
- Rydberg atom+molecule, reaction channels, expt. vs. theory 0-63755
- tetrafluoromethane+He gas mixture, collision induced for IR translational spectra 0-83353
- toluene+OH(D), vibrational and rotational energy effect 0-76497
- 1,3,5-trimethylbenzene+OH(D), rotational and vibrational energy effect 0-76497
- Ar+BaO, in Ar flame, rot. and translational relax. by sub-Doppler optical-optical double reson. 0-95583
- Ar+Br₂ collisions, dissociation reaction, trajectory study by ensemble method 0-66765
- Ar+HCl, differential cross section, quasiclassical close coupling approx. 0-63743
- Ar+HCl, inelastic scatt. exponential perturbation theories 0-74217
- Ar+HF, state-to-state cross sections for rot. to translational energy transfer determ. 0-91644
- Ar+methane-d₄, vibr.-translational relax. 0-99537
- Ar+N₂, excitation of N₂(C²Π_g), symmetry, propensity rules and alternation intensity, rot. spectrum 0-87135
- Ar+N₂, inelastic scatt. exponential perturbation theories 0-74217
- Ar+Na₂, differential cross sections meas. for rot. energy transfer process, obs. of halos 0-91643
- Ar+Fe(CO)₅, chemionisation and chemiluminescence reactions, Penning ionisation and fluoresc. obs. 0-97689
- Ar*+O₂, ion pair form. explained by charge transfer model 0-99546
- Ba+HBr, laser induced fluoresc. study at different collision energies 0-91632
- Ba+HCl, laser induced fluoresc. study at different collision energies 0-91632
- Ba+HF, product rot. and vibr. distributions and reaction cross sections depend. on reagent translational energy 0-93745
- Br+H₂, proximity induced electric dipole moment effect in laser field 0-83456
- CO₂+He, rot. inelastic collision, ab initio SCF, electron gas and pot. energy surfaces 0-83468
- CO₂+Ne, intermol. pot. in repulsive short-range region, ab initio 0-69204
- C(2¹S₀)+H₂(O₂)(ethylene) 0-74241
- Cd+molecule collisions efficient cross-sections determ. 0-58338
- Cd+N₂, vap., creation of inverse population of atomic Cd 6²S and 5³P₂ levels 0-58219
- CS+methyl cyanide, collisional ionisation obs. 0-95716
- CS+O₂, collisional ionisation, energy spectra of forward and backward directed positive and negative ions 0-87200
- CS+O₂, mol. target internal motion 0-78697
- CS+UF₆, ionisation reactions, absolute cross sections 0-99565
- D*+N₂, fast collisions, impulse approx. 0-106281
- ¹⁸F+hexafluoropropylene nonequilibrium effects in moderated nuclear recoil experiments 0-89509
- ¹⁸F+methane, nonequilibrium effects in moderated nuclear recoil experiments 0-89509
- F*+H₂, quenching of excited state, semiclassical studies, comparison between reactive and nonreactive processes 0-106375
- H+Cl₂, stochastic-collision complex model theory 0-108696
- H+D₂, collisional motion, energy transfer and dissociation, collision dynamics 0-99563
- H+H₂, reactions and collisions in IR laser field, collision-induced absorpt. spectra 0-76499
- H+H₂(ν₁=1), exchange reaction, integral and differential cross sections determ. 0-85153
- H+HF, low barrier quantum model, vibr. deactivation 0-69216
- H+methane, abstraction and exchange reaction, barrier height calc. using POL-Cl wave functions 0-81304
- H+O₂(N₂), collisional coherent excitation, meas. of Lyman α-photons 0-99552
- H+O₂, reaction mechanism studied using photoionisation mass spectrometer, form. of O₂(a¹Δ_g) 0-85168
- H₂+H, exponential gap relation, rot. inelasticity 0-78693
- H₂+He, exponential gap relation, rot. inelasticity 0-78693
- H₂+He, vibr. relax. cross section 0-99494
- H₂+Li, exponential gap relation, rot. inelasticity 0-78693
- HCl+Cl(Br)(H), vibr. relaxation and reaction rates determ. 0-108698
- HCl+inert gas, weak collisions, HCl spectral line broadening of IR spectra 0-74161
- H₂O+He, collisional excitation of interstellar molecules, rate consts. 0-67816
- He-LiH, rot. inelastic collisions, ab initio pot. energy surface calcs. 0-87208
- He+CO₂, collisional atom-triatom transition probabilities for anharmonic triatom pots., quantum mech. calcs. 0-83455
- He+CO₂, translational-vibrational energy transfer, quantum dynamical study 0-63746
- He+CS₂, metastable atoms, energy transfer processes 0-83466
- He+H₂, adiabatic distorted-wave infinite order sudden approx. 0-99558
- He+H₂, inelastic scatt., vibr. adiabatic basis functions calcs. 0-102551
- He+H₂, inelastic scatt. exponential perturbation theories 0-74217
- He+H₂, mol. energy transfer by quasiclassical trajectory methods, vibr. relax. and dissociation, rot. effect 0-99557
- He+H₂, vibr. inelastic integral cross-sections, transitions to ν=2 level 0-99539
- He+HCN, HCN excited vibr. state, T₂ meas. 0-102498

atom-molecule collisions continued

- He+HCN, translational-vibrational energy transfer, quantum dynamical study 0-63746
- He+I*, low energy collisions, energy redistrib. 0-63765
- He+LiH, rot. inelastic collisions, dynamics 0-87209
- He+LiH, rot. inelastic collisions, state-to-state cross sections determ. 0-87210
- He+N₂, rot. inelastic scatt., appl. of sudden approx. 0-95705
- He+NO, multiphoton ionisation spectra in supersonic expansion, laser entrained collisional effects 0-83459
- He+Na₂, rotational inelastic scatt., uniform semiclassical sudden approx. 0-99544
- He+NaK collisions studied using circularly polarised laser fluorescence, molecular reorientation obs. 0-69215
- He+OCS, emission spectra in He afterglow 0-87139
- He+OCS, translational-vibrational energy transfer, quantum dynamical study 0-63746
- He+CS₂, dissociation, charge-transfer, CS⁺(B²Σ⁺-A²Π_g) emission prod., Morse pot. Franck-Condon factors calc., vibr. anal. 0-99539
- He+OCS, dissociation, charge-transfer, CS⁺(B²Σ⁺-A²Π_g) emission prod., Morse pot. Franck-Condon factors calc., vibr. anal. 0-99539
- ⁴He+H₂, inelastic collision, R-matrix study 0-87204
- Hg+Cl, +hν→HgCl*+Cl, laser-induced harpooning reactions 0-83458
- HgBr+O₂(N₂)(H₂)(He)(Ne)(Ar)(Kr)(Xe), vibr. relax., rate coeffs., fluoresc. obs. 0-63697
- I₂+He(Ne), energy depend. of collision induced intramolecular energy transfer 0-83470
- K+alkyl halide potentially reactive collisions, electronic excitation 0-74239
- K+CO, rotational inelastic scatt., uniform semiclassical sudden approx. 0-99544
- K+H₂S(DS), collisional ionisation, positive and negative ion energy spectra obs. 0-63775
- K+methyl cyanide, collisional ionisation obs. 0-95716
- K+NaK reactive collisions studied using circularly polarised laser fluorescence 0-69215
- K+O₂, collisional ionisation, energy spectra of forward and backward directed positive and negative ions 0-87200
- K+O₂, mol. target internal motion 0-78697
- K+UF₆, ionisation reactions, absolute cross sections 0-99565
- Kr+CO₂ 0-83455
- LiF+Ar, polarisation cross section, close-coupling calcs. 0-69214
- LiH+He, rot. inelastic collisions, rigid shell models 0-99545
- Li*(²P₁)+H₂(D₂), collision induced quenching and fine struct. transition rate coefficients meas. 0-74221
- Li(2p)+H₂(N₂), Li(2p) excitation, alignment and orientation obs. 0-63794
- N₂+Ar(Xe), Λ³Σ_g⁺ state energy pooling in flowing afterglow, Herman IR system 0-83503
- N₂⁺+He, N₂⁺ selectively excited, collisional deactivation 0-83338
- NH₃+He(Ar), inversion spectrum press. broadening, linewidths calcs. 0-95599
- NH₃+He(Ne)(Ar)(Kr), pure rot. line, press. broadening calcs. 0-78656
- Na+methyl iodide, anisotropic interactions from double rainbow struct., interaction pot. meas. 0-99540
- Na+t-butyl bromide, anisotropic interactions from double rainbow struct., interaction pot. meas. 0-99540
- Na+t-butyl chloride, anisotropic interactions from double rainbow struct., interaction pot. meas. 0-99540
- Na+t-butyl iodide, anisotropic interactions from double rainbow struct., interaction pot. meas. 0-99540
- Na₂+He, rotationally inelastic scatt., state-to-state differential cross sections 0-74234
- Na₂+Xe rate const., energy corrected scaling laws 0-69225
- Ne+CO₂, energy transfer rate consts., semiclassical method 0-91640
- Ne+CS₂, metastable atoms, energy transfer processes 0-83466
- Ne+D₂, anisotropic inversion pot., rot. inelastic cross sections 0-78696
- Ne+D₂, anisotropic potentials, direct inversion methods calcs. 0-69090
- Ne+D₂, energy-loss scaling in 0.5-3.5 keV 0-63768
- Ne*+Fe(CO)₅, chemionisation and chemiluminescence reactions, Penning ionisation and fluoresc. obs. 0-97689
- Ne*+H₂O, pot. energy surfaces, MO and CI calcs., Penning ionisation electron spectra 0-106376
- O(³P)+dimethyl disulphide, absolute reaction rate const. determ. 0-89472
- Rb+methane (and deuterates), 5²P_{1/2}→5²P_{3/2} excitation transfer, isotope effects, temp. depend. 0-91630
- SeO₂+Ar, radiative lifetime and quenching rates 0-95685
- Sr+HF, endothermic reaction, comparison of effectiveness of vibr. and translational excitation 0-93746
- U+molecule, collisional relax. of highly excited states, laser-induced fluoresc. obs. 0-58205
- Xe+Cl₂, classical trajectory calcs., energy threshold for collision induced dissociation, determ. 0-95709
- Xe+Na₂*, rot. energy transfer, vel. depend. 0-95715
- XeCl+inert gas atom, ground state destruction, quenching rate consts. 0-63758
- XeF₂(C) state lifetime, quenching rate consts., photolysis in inert gas atmospheres 0-66816
- XeF*+F₂+Xe, temp. dependent quenching rate constants 0-63701
- Xe(nf)+SF₆, l-changing collisions obs. 0-91633
- Xe(nf Rydberg state)+NH₃, n- and l-changing and ionising collisions 0-58360

atom-molecule reactions

see also *atom-molecule collisions*

- AB+M→A+B+M, nonequilibrium gas at low press., dissociative instability, role of vibr. energy 0-74227
- alkali metal atoms+molecules reaction, electronically excited atoms and alkali metal atoms analogy 0-76490
- atom+diatom, collisional quantum mech. reactive scatt., hyperspherical coords. 0-108694
- atom+diatom reactions, semiclassical tunnelling probabilities, trajectory calc. 0-71886
- atom+diatom reactive scatt., DWBA transition amplitude kernel 0-81310
- atom+polyatom systems, rotation-vibration, symmetry correlation 0-61074
- benzene+O(³P), phenol radical prod., crossed mol. beam investig. 0-71902

atom-molecule reactions continued

- benzene-d+O(³P), phenol radical prod., crossed mol. beam investig. 0-71902
 dynamics, translational energy effects, reviews 0-76489
 excited atoms+ molecules reactions, electronically excited atoms and alkali metal atoms analogy 0-76490
 F+dichloromethane, reaction products, modulated mol. beam mass spectrosc. obs. 0-97742
 formaldehyde+Br reactions, rate consts. by EPR 0-93736
 formaldehyde+F reactions, rate consts. by EPR 0-93736
 hot atom+mol. reaction, steady state vel. distrib., Boltzmann eqn. with BGK elastic collision model 0-66856
 inert gas atom+halogen mol., halide form., relax. and quenching 0-81314
 inert gas metastable atom+HgBr₂, dissociation excitation 0-63774
 methanol+Ar(Kr) methoxy radical prod., UV emission spectra 0-91572
 perhalo-compounds, labelled, high yields from ¹⁸F and ³⁶Cl reactions with CCl₄, F₂, and C₂F₆ 0-109025
 toluene+OH(D), vibrational and rotational energy effect 0-76497
 1,3,5-trimethylbenzene+OH(D), rotational and vibrational energy effect 0-76497
 Ar+SO₂, dissociation, rate meas. behind shock wave, laser Schlieren method 0-81296
 Ar*(³P₁)+H₂(D₂), Ar⁺ two spin orbit state, reaction cross section, direct determ. 0-93748
 Ar*+CO₂, CO* prod., use in laser systems 0-63824
 Ar*+Fe(CO)₅, chemiionisation and chemiluminescence reactions, Penning ionisation and fluoresc. obs. 0-97689
 Ba+CO₂(O₂), crossed beam kinetics, BaO recoil velocity spectra 0-76500
 Ba+Cl₂→BaCl⁺+Cl⁻, chemi-ionis. reaction, mol. beam obs. 0-104434
 Ba+HBr, laser induced fluoresc. study at different collision energies 0-91632
 Ba+HCl, laser induced fluoresc. study at different collision energies 0-91632
 Ba+HF, product rot. and vibr. distributions and reaction cross sections depend. on reagent translational energy 0-93745
 Ba+HF→BaF+H, dual mol. beam excitation difference spectroscopy, state-to-state vibr. resolved dynamics 0-89474
 Br₂+H reaction Br prod., matrix isolated ESR 0-106336
 CH+O reaction, absolute rate const. 0-97690
 Ca+O₂ reaction, chemiluminesc. absolute cross sections, photon yields and CaO dissociation energy 0-97697
 Ca*+HCl, reaction performed under high resolution, luminescence obs. 0-95662
 Cd+H₂→CdH+H, product initial rot. state distrib., pump and probe laser obs. 0-85158
 Cd+O₃, matrix reactions, IR, Raman and visible spectra in Ar and N₂ matrices 0-87110
 Cl+fluoromethane, photochlorination electron and oscill. energy 0-81320
 Cl+formaldehyde, photolysis, Fourier transform IR studies, metastable species detection 0-81293
 Cl+vinyl bromide-d₃ reaction, IR chemiluminesc. 0-102506
 Cl₂+muonium (H)(D), pot. energy surfaces, inversion calcs. 0-93734
 Cs+(AuF₃)_n, prod. of AuF₃⁺, ionisation cross section energy depend. 0-81300
 Cs+(SbF₅)_n→Cs⁺+SbF₆⁻+SbF₄+ (SbF₃)_{n-2}, ionisation cross section energy depend. 0-81300
 Cs⁺+benzyl chloride, beam reactions for 5.8 eV collision energy, mechanism 0-66777
 Cu+Cl₂(Br₂)(I₂), beam-gas chemiluminesc. reactions 0-85151
 Cu+F₂, chemiluminesc. reactions, mol. beam study 0-97702
 D+FD(H), low barrier quantum model, vibr. deactivation 0-69216
 D+H₂ reaction, transition state theory calculations, kinetic isotope effect explanation 0-66784
 D+H₂ rearrangement collision, vibr. excitation effects 0-71910
 D+HX(H=Cl,I), HX dissociative ionisation, H⁺ signal origin, mol. beam obs. 0-66778
 D+PTFE, DF* prod., Fourier transform IR spectroscopy 0-87105
 D+T₂, H-exchange studied by crossed molecular beam experiments 0-93747
 D₂+Y, high temp. equilib. meas. 0-66780
 F+CO in Ar matrix, vibr. and electronic spectra, valence force potential determ., mol. photodissoc. obs. 0-85170
 F+ethylene (benzene) derivatives, deuterated, IR chemiluminesc. 0-102506
 F+H₂, reactivity-selectivity, bounds derivation 0-66763
 F+H₂(D₂), rate consts., temp. depend. 0-81302
 F+H₂(D₂)ZZ 0-81303
 F+H₂→HF+H, DWBA transition amplitude kernel 0-81310
 F+HCl(HBr)(DBr)(HI), H abstraction reactions, temp. depend., laser photolysis IR fluoresc. obs. 0-93744
 F+HCl→HF+Cl, time resolved vibr. chemiluminesc. and rate consts. 0-61069
 F+O₂ reaction, FO(X²Π) radical VUV photoelectron spectra 0-104455
 Ge+N₂O, chemiluminesc. reaction, HTFFR kinetics study 0-76496
 H+CH₃, IR matrix isolation spectra 0-97706
 H+CN(NC)(NSi), bimolecular exchange reactions, dynamical-statistical method calcs. 0-104435
 H+Cl₂, stochastic-collision complex model theory 0-108696
 H+D₂ reaction, transition state theory calculations, kinetic isotope effect explanation 0-66784
 H+FH(FD), low barrier quantum model, vibr. deactivation 0-69216
 H+H₂, collinear quantum mech. reactive scatt., hyperspherical coords. 0-108694
 H+H₂, collinear reaction, Delves radial coord. S-matrix propag. calcs. 0-108695
 H+H₂, reaction probability, max. entropy derivation, statistical theories 0-66781
 H+H₂, reactions and collisions in IR laser field, collision-induced absorpt. spectra 0-76499
 H+H₂, scatt. wave function modal struct. and global behaviour 0-81307
 H+H₂, sudden rot. reactive scatt., 3-dimens., approx. quantum mech. calcs. 0-76498
 H+H₂(Cl₂), reactivity-selectivity, bounds derivation 0-66763
 H+H₂(D₂)(T₂) reactions, accurate pot. energy surface, isotope effects, quasiclassical trajectory study 0-97698
 H+H₂(v_r=1), exchange reaction, integral and differential cross sections determ. 0-85153
 H+H₂→H₂+H three dimens. chem. reaction, distorted-wave calcs. 0-81294

atom-molecule reactions continued

- H+HCO→H₂+CO, classical trajectory study 0-93750
 H+HCl, semi-empirical pot. energy surfaces calc. by diatomics-in-molecules method 0-95556
 H+LiF, laser-induced nonadiabatic collision process, classical model 0-97701
 H+methane, abstraction and exchange reaction, barrier height calc. using POL-Cl wave functions 0-81304
 H+O₂+Ar, H₂ free radical prod., rate const. calc. 0-101026
 H+O₃, reaction mechanism studied using photoionisation mass spectrometer, form. of O₂(a¹Δg) 0-85168
 H+O₃→HO₂+O(³P), yields 0-71900
 H+T₂, H-exchange studied by crossed molecular beam experiments 0-93747
 H₂+Cl(Br)(I)(F), gas phase H-atom transfer reactions, struct.-reactivity correl., pot. energy surfaces 0-104433
 H₂+D(O)(Cl)(Br), relax. and chem. reaction, time resolved IR fluoresc. and mass spectrometry obs. 0-69177
 H₂+H(D)(T) reactions, accurate pot. energy surface, isotope effects, quasiclassical trajectory study 0-97698
 H₂+Y, high temp. equilib. meas. 0-66780
 HCl+Cl(Br)(H), vibr. relaxation and reaction rates determ. 0-108698
 HCl+D(O)(Cl)(Br), relax. and chem. reaction, time resolved IR fluoresc. and mass spectrometry obs. 0-69177
 He+OCS, emission spectra in He afterglow 0-87139
 He⁺+SO₂, dissociation charge transfer reaction, SO⁺ (A²Π-X²Π_g) emission 0-95659
 He*, inert gas, optical absorpt. spectra and kinetic behaviour 0-95635
 Hg+Cl₂+hν→HgCl*+Cl, laser-induced harpooning reactions 0-83458
 K+NaK reactive collisions studied using circularly polarised laser fluorescence 0-69215
 Kr+F₂, KrF form., relax. and quenching 0-81314
 Li+HF→LiF+H, pot. energy surface, SCF and CI calcs. 0-71904
 N+H₂SO₄, atmosphere chemistry, collisional reaction probabilities 0-90168
 Ne*+Fe(CO)₅, chemiionisation and chemiluminescence reactions, Penning ionisation and fluoresc. obs. 0-97689
 O+CS₂→CS+SO, vibrational distribution of CS, laser-induced fluorescence meas. 0-71895
 O+H₂, classical trajectory calcs., ab initio surface, singlet state, rate consts. 0-66786
 O+H₂, pot. energy surfaces and reaction rates, ab initio calcs. 0-63531
 O+H₂O→OH+OH, energy partitioning 0-101009
 O+H₂SO₄, atmosphere chemistry, collisional reaction probabilities 0-90168
 O+NaO, nightglow, excitation and abundance of Na 0-98497
 O+saturated hydrocarbon, chem. reaction dynamics. OH prod. investig. 0-101016
 O+saturated hydrocarbon, reaction dynamics, model pot. surfaces, quasiclassical trajectory calcs. 0-97696
 O+saturated hydrocarbon→OH+alkyl radical, reaction dynamics, mol. beam-laser induced fluoresc. obs. 0-97695
 O(D₂)+NH₃→OH(v,N)+NH₂, bimodal OH rot. distrib. obs. and energy disposal 0-76501
 O(P)+dimethyl disulphide, absolute reaction rate const. determ. 0-89472
 O(P)+dimethyl sulphide, fast flow reson. fluoresc. obs. of absolute rate consts. 0-61077
 O(P)+methane, barrier height and transition state geometry, POL-Cl calc., H abstraction reaction 0-66782
 S+CS₂(OCS)(CH₄), electronically excited atom, reson. fluoresc. 0-99476
 SF₆+Rydberg atom, reaction channels, expt. vs. theory 0-63755
 Sc+NO₂, chemiluminesc., nonequilibrium product distrib. 0-101014
 Sr+HF, endothermic reaction, comparison of effectiveness of vibr. and translational excitation 0-93746
 Sr+HCl, reaction performed under high resolution, luminescence obs. 0-95662
 T+HD, variational transition field theory and unified statistical model 0-97700
 T₂+Y, high temp. equilib. meas. 0-66780
 UF₆, laser chemistry 0-69198
 UO⁺+Ar, collision-induced dissociation cross section and threshold 0-95706
 UO⁺+Ar, collision-induced dissociation cross section and threshold 0-95706
 Xe+Br(CCl₄), excitation functions and rotational polarisation, chemiluminesc., crossed beam study 0-76491
 Xe+Cl₂(F₂), XeCl(X²Π) form., relax. and quenching 0-81314
 Zn+O₃, matrix reactions, IR, Raman and visible spectra in Ar and N₂ matrices 0-87110

atom probe field ion microscopy

- metallic film characterisation technique, APFIM, time-of-flight spectroscopy 0-75138
 metallurgical applications (Dutch) 0-96425
 metals, individual atomic events on surfaces, quantitative examination 0-75409
 metals and alloys, segregation studies by imaging atom probe microscopy 0-66911
 metals and alloys, trace element detection by atom probe microanalysis 0-66910
 pulsed laser atom-probe FIM, development and appls. 0-66402
 solid-solid interface chemistry, characterisation, theory 0-75448
 specimen field corrosion caused by polymer gaskets 0-57425
 steel, austenitic stainless, MC precipitate comp., APFIM study 0-104161
 steel, Cr-Mo (2.8, 1.6 wt.%), atom probe anal. of bainitic phase boundaries 0-71990
 time of flight atom probe, quantitative microanal., metallurgical appl. 0-86498
 Al alloy, FIM and microanalysis, developments 0-100155
 Fe-Ti (0.15 wt.%), Ti distrib., investigation, FIM anal. 0-84200
 Ga ion source, high intensity, emission characs. 0-80950
 Ni-Cr-Co superalloy, combined TEM, FIM, atom probe microanalysis of precipitates and carbide phase comp. 0-100844
 Ni-Cu, surface segregation, computerised atom-probe FIM study 0-75412
 Pt-Au, surface segregation, comp. depth profiles meas. using atom-probe field ion microscope 0-100380
 W wire, AKS-doped, second phase particle obs. by TEM, SEM and atom probe microanalysis 0-108457
 W-Zr field emitter, time-of-flight atom-probe study 0-80949

atom-surface impact

- see also **sputtering**
 anthracene surface, Ar impact, Penning ionisation electron spectra and photoelectron spectra 0-66352
 atomic beam diffraction from solid surfaces, struct. studies 0-65349
 capture of gas atoms on solid surface, non-one-dimens. interaction effects 0-60726
 conference, atomic collisions in solids, Hamilton, Canada (Aug. 1979) 0-62375
 diffractive scatt., specular intensity near bound-state reson. 0-80928
 elastic collision with crystal, shell effects 0-89106
 exospheres of Moon and Mercury, Monte Carlo simulation of regolith interaction 0-67588
 gas-metal interactions, scatt. dynamics 0-92787
 graphite, ⁴He interaction and scatt. 0-60732
 graphite (0001), ⁴He selective adsorption, level crossings 0-71556
 graphite (0001), inelasticity in He scatt. 0-76127
 graphite surface, ⁴He low-energy scatt., inelastic effects 0-100738
 monatomic solids, redefined scatt. cross sections 0-70274
 neutral atom scattering, long range, from solid cylinders, quantum theory 0-71549
 neutrals, keV, energy determ. method 0-89100
 one-electron resonant processes in presence of surface sub-monolayer 0-93445
 physisorption of atoms, dynamical and geometrical effects 0-70531
 rainbow effects and energy exchange, calc. 0-84825
 solid surface, mol. dynamic processes interaction with laser radiation 0-71943
 sputtered atoms, energy distribution, ion mass and target temp. effects 0-66361
 Ag (111) surface phonon dispersion, He atom scatt. meas. 0-75426
 Ag surface, Ne scatt., rainbow effects and energy exchange, calc. 0-84825
 Ag surface, scatt. of He, Debye-Waller factors, expt. 0-60736
 CO adsorbed on Pd surface, Penning ionisation by metastable He beam, theory 0-60735
 Cu surface, (100) coherent elastic scatt. of He, Ne, thermal attenuation 0-89105
 D, adsorbed on graphite (0001), vibr. spectrum, at. beam scatt. obs. 0-92779
 H, adsorbed on graphite (0001), vibr. spectrum, at. beam scatt. obs. 0-92779
 He atom-surface scattering pot., surface electron density depend. 0-104027
 LiF (001), multiple Debye-Waller effects at selective adsorption in atom-surface scattering 0-76126
 LiF (001), surface phonon obs. in He atom inelastic scatt. 0-80927
 LiF, (001) surface, diffractive scatt. of H atoms, 78K 0-76124
 LiF surface, He atom inelastic scatt., phonon coupling 0-71554
 Mo surface, clean and gas covered, He* impact, deexcitation, pot. energy transfer mechanism 0-60743
 Ni (110), adsorbed H, adatom configuration, He diffr. study 0-103569
 Pd (111) surface, clean and CO covered, metastable He impact, electron emission, energy and ang. distrib. 0-60744
 Pt, of Ar, gas surface interactions, 3-D generalised Langevin model appl. 0-107637
 Pt, of Xe, gas surface interactions, 3-D generalised Langevin model appl. 0-107637
 Pt(111) plane and stepped surfaces, H₂ interaction, bond breaking activity, model pot. 0-108744
 Re surface, long range and temp.-depend. interaction with alkali metal atom, theory 0-59802
 Si (100) reconstructed surface struct. study using thermal energy He diffr. 0-60731
 W, Ar beam direct inelastic scatt., vel. distrib. meas. 0-66351
 W, sorption of Ne and He, tangential momentum accommodation coeff. meas. by acoustic vel. and absorpt. obs. 0-66867

atomic absorption spectroscopy

- air-acetylene flame, multichannel apparatus detect. limits using atomic absorpt. spectra 0-76586
 bauxites, analysis, comparison of atomic absorpt., X-ray fluoresc. and other classical methods 0-89551
 brine sulphate anal. by atomic absorpt. 0-89556
 burner system for atomic absorpt. spectrophotometers 0-73468
 cathode lamps for atomic absorpt. spectrometry, method of modifying used lamps 0-90898
 droplets produced by pneumatic nebulisers, size meas. method 0-71992
 flame spectrometry interfs., elimination and control, theoretical anal. 0-81395
 flame spectroscopy, droplet size distrib., impact beads, mixer paddle and oxidant effects 0-93810
 graphite furnace atomic absorpt. spectrometry heated by capacitive discharge, determ. of elements 0-66892
 inductively coupled plasma and atomic absorption spectroscopy combined 0-104478
 laterites, Venezuelan, analysis, comparison of atomic absorpt., X-ray fluoresc. and other classical methods 0-89551
 metals determ. in air particulates, graphite furnace method appl. 0-94134
 multichannel apparatus for material analysis using atomic spectra 0-76586
 noise meas. in atomic absorpt. flame spectrometry, single and double beam instrum. comparison 0-76584
 pulsed Nd laser, use in atomic absorpt. spectroscopy for direct anal. of metallic and nonmetallic solids 0-76582
 radio-frequency excited pulsed hollow-cathode lamp, absorpt. and emission characteristics 0-89550
 selectivity evaluation 0-89561
 steel sheet, surface anal. by ion etching and atomic absorpt. spectroscopy (German) 0-81377
 tubes design with hollow cathode, for Mo, Fe, and Si analysis (Bulgarian) 0-85232
 UV and visible spectra of solids using integrating sphere 0-61188
 X-ray fluorescence and at. absorpt. analysis 0-85229
 Zeeman, appls. 0-76567
 Zeeman effect appls. 0-85245
 Zeeman effect appls. to atomic absorpt. spectrophotometer, development of spectral-line sources 0-76583
 Cr in urine, determ. by electrothermal atomic absorpt. spectrophotometry 0-61175

atomic absorption spectroscopy continued

- Cu determination in serum/tissue specimens using flameless atomic absorption spectroscopy, effects of sample prep. and matrix 0-98200
 CuInS₂ films, RF sputtered, growth and props. 0-80124
 ErD₂ thin film, degradation during film processing, investigation 0-101047
 Fe, purification, recrystn. temp. and elec. resistivity (Japanese) 0-100780
 H, Rydberg consts., saturated absorpt., spectroscopy meas. 0-105604
 Hg resonance line, 253.7 nm for atomic absorpt. meas. 0-78556
 OCSe, quantum yields for Se, ¹S₀, ¹D₂, and ³P_{0,1,2} atoms determ. in photolysis, lifetime and quenching rate meas. 0-97741
 Pb traces in human blood plasma, atomic absorpt. anal., nonspecific absorpt. correction using Zeeman effect 0-76881
 SeH₂, atomisation in cool H₂-O₂ flame burning in quartz tube atomiser 0-76581
- atomic beam electric resonance**
 H⁻ resonances in electric field 0-63607
- atomic beam magnetic resonance**
 laser-RF double reson. spectroscopy of nucl. quadrupole moments, ⁵⁵Mn and ⁵⁰V appls. 0-57682
 Ba, atomic beam and resonance spectroscopy 0-58180
⁴³Ca, atomic beam and resonance spectroscopy 0-58180
 He fine structure interval ²P_{1/2}-²P_{3/2}, optical microwave atomic beam mag. resonance meas. 0-102585
- atomic beams**
 see also **atom-molecule reactions**; **atom-surface impact**; **atomic beam electric resonance**; **atomic beam magnetic resonance**; **particle velocity analysis**; **plasma-beam interactions**
 coaxial electron and atomic beams sequential multiple scatterings, random walk approach 0-99574
 deceleration and monochromatisation laser radiation press. 0-102491
 excited atoms, merging-beams experiments 0-63789
 fast atomic beam, optical reson. detect. by at. fluoresc. 0-102479
 focusing by reson. radiation press., quantum fluctuations influence 0-58217
 high-flux beam source for He, Ne and Ar metastable atoms 0-58416
 maser with beam of inflying atoms, spectral line broadening mechanism 0-106503
 neutral beam armour for Doublet III vacuum vessel 0-95462
 neutral beam injecto cryogenic pumping panel chevron baffles, black coating materials, selection 0-95456
 neutral beam injector for Doublet III, material vacuum props. 0-95457
 neutral beam injector vacuum system transient simulation anal. 0-95453
 Princeton Cyclotron data acquisition system 0-102415
 quantum state selected atomic and molecular beams production, developments in techniques 0-63871
 Ba (5d6p)³D₃ state, lifetime meas. by dye laser spectrosc. 0-78577
 BaI resonance transitions, hyperfine struct. and isotope shifts, atomic beam laser spectroscopy 0-102141
 Cs atomic clock using laser optical pumping of Cs beam 0-101785
 H₂ and H₃ spectral profiles from neutral beams and plasmas in high mag. fields 0-83999
 N, associative ionisation, merging beams experiment 0-63789
 Na atoms cooling by resonant laser radiation (Russian) 0-74155
 O₂ supersonic nozzle beam source development 0-58016
 Sml, laser atomic beam spectroscopy, isotope shifts, hyperfine struct., transitions 0-102468
 Tm I, hyperfine struct., high resolution spectrosc. meas. 0-87238
- atomic clocks**
 see also **frequency measurement**; **time measurement**
 1 metre primary Cs clocks, design and performance 0-98894
 Cs primary clock stand CS1, uncertainty eval. 0-98895
 GDR atomic time scale 0-98892
 Majorana effect on atomic frequency standards 0-98897
 maser oscillator, thermal noise effect meas. on amplitude of oscillation 0-98898
 noise in standard frequency sources 0-98899
 quantum clocks, time meas., teaching 0-90632
 Rydberg atom microwave and far IR spectroscopy 0-63564
 standards development at Shanghai Observatory, China 0-105617
 time measurement, errors, accuracy of watches and clocks, time standard 0-90821
 time scale instability, contrib. of computation algorithm 0-98890
 unbiased clock variance calc. in uncalibrated atomic scale algorithms 0-105620
 CS beam freq. standard, new dipole beam optic 0-98896
 Cs atomic clock using laser optical pumping of Cs beam 0-101785
 Cs, experiments to reduce cavity phase shift errors in the Cs beam tube 0-98893
¹³³Cs, freq. standard, optimum conditions for population inversion for 0-0 transition 0-78824
 H, collision-dependent frequency shift 0-98871
 H maser, frequency changes due to nonuniform magnetic field 0-99687
 H masers, with automatically tuned resonators 0-95859
 H₂ maser freq. standard using dual modulation 0-98900
 H₂ maser wall shift and unperturbed hyperfine freq. of ground state of H₂ atom 0-98901
 Rb⁸⁷ frequency standard 0-98902
- atomic clusters**
 Ag clusters, latent image particles, electronic effects 0-82840
 cluster superlattices in Na-type X zeolite matrix, N and S type volt-ampere characs. (Russian) 0-70665
 metal atom cluster compounds, bonding calc. using d-orbital overlap model, SCF-Xa-SW calc. 0-102595
 metal surface chemisorption theory, electron localisation, surface interactions 0-84376
 metallic, 2 to 500 atoms, nucleation, mass spectra 0-102596
 metals, individual atomic events on surfaces, quantitative examination 0-75409
 rare gas, small clusters, structure thermodynamic properties 0-88341
 unified theory of atoms and atomic aggregates, self consistent theory 0-102418
 Ag-Au clusters, latent image particles, electronic effects 0-82840
 Ag-S clusters, latent image particles, electronic effects 0-82840
 Ar, cluster formation and homogeneous nucleation, comparison of expt. and theory 0-79925
 Au, on W support film, computer simulation of phase contrast 0-100150
 Au-Fe alloys, magnetism and atomic clustering 0-103810
 Be₄ (Be₄⁺), atomic clusters, electronic struct., LCAO-MO-SCF and HF calcs. 0-63880

atomic clusters continued

- C, film, image contrast rel. to inelastic scattering 0-100154
 C⁺, association reactions, isotopic exchange, SIFT study, review 0-58435
 Cr-Fe (6.5 wt.%), atomic clustering and mag. defects, mag. moments 0-60246
 H atoms, chemisorbed on cluster, indirect interactions, Grimley-Pisani model and tight-binding calc. 0-65370
 He(He) clusters, metastable electronic states, electron impact excitation, time of flight spectra 0-106411
 He ground state binding energy, near threshold behaviour in 2 and 3 dims. 0-91716
 He₄, tetramer bound state binding energy, pot. model 0-63883
 Mg₄(Mg₄), atomic clusters, electronic struct., LCAO-MO-SCF and HF calcs. 0-63880
 Mo-Be solid solutions, superconducting transition, temp. changing peculiarity due to press. (*Russian*) 0-70878
 NaA neolyte, Hg cluster transition to paramagnetic state due to mag. field (*Russian*) 0-60183
 Ne, metastable electronic states, electron impact excitation, time of flight spectra 0-106411
 Ni (001) surface, electronic struct. of ordered S overlayers 0-84835
 Re, Br₉, electronic struct. and photoelectron spectra 0-69287
 ReCl₉, electronic struct. and photoelectron spectra 0-69287
 (Re₂Cl₁₂)³⁻, electronic struct. and photoelectron spectra 0-69287

atomic collision processes *see atomic inelastic collisions; elastic scattering of atoms and molecules***atomic electric moment**

- dynamic multipole polarisability 0-74252
 identical atoms, dispersion intermolecular pot. anomaly prod. by intense radiation field 0-58336
 inert gas mixture, collision induced microwave absorpt. spectra 0-74216
 neutral atom collisions, hyperfine component broadening and shift of spectral lines 0-74136
 Ar, K inner-shell level energies, absorpt. spectroscopy with synchrotron radiation 0-99583
 Bi, Faraday effect and magnetic circular dichroism 0-83399
⁴³Ca, atomic beam and resonance spectroscopy 0-58180
 Cs⁺ dipole and quadrupole polarisability fine struct. intervals and g-factor interval 0-91477
 Eu+Sr, laser induced collisional energy transfer profile, high resolution study 0-83471
 H atoms, energy levels and bound-bound transitions in strong mag. field 0-58134
 H⁺+H high energy collision, excitation multipole moments, classical trajectory approx. 0-106389
 He, isoelectronic sequence, E1 and E2 oscillator strengths, MCHF calcs. 0-106292
 Kr, K inner-shell level energies, absorpt. spectroscopy with synchrotron radiation 0-99583
 Li⁺, core-excited bound states 0-91468
 Na vapour, superradiance, quantum beat spectra 0-106311
 Ne, electron impact K-shell excitation, EELS 0-106396
 Xe, L₁, L₂, L₃ inner-shell level energies, absorpt. spectroscopy with synchrotron radiation 0-99583

atomic electron configuration interactions *see atomic electron correlations***atomic electron correlations**

- absorption bands, vibronic intensification obs., floating-orbital method 0-63619
 acetone, absorption bands, vibronic intensification obs., floating-orbital method 0-63619
 atomic collision, coherence and correlation, book 0-90615
 atoms on semi-infinite linear chain, chemisorption theory and superoperator formalism 0-93800
 Brillouin theorem, proof 0-91415
 coherence and correlation in atomic collisions, book 0-90615
 correlation coefficient and electron correlation 0-78552
 coupled HF-perturbation theory of atomic and mol. props., correl. corrections 0-106269
 electron impact excited line radiation, polarisation, long-range electron corrs. effects 0-91683
 excitation energies calc., using renormalised Green's function method (*Japanese*) 0-83295
 light atoms (up to Ni), contact term, use of local spin density functional method 0-58158
 many-body perturbation theory with radially restricted basis functions 0-78526
 modified virtual orbitals, for config. interaction calc. 0-58163
 Politzer-Parr partitioning, electron correl., isoelectronic, isonuclear, spin and excitation aspects 0-78522
 rare earth metal ions, 3d and 4f energy level parametrisation, Slater parameters and correl. corrections 0-87041
 spin-coupled particle-hole excitation, general matrix element formulas 0-69086
 ten-electron systems, correl. energy, fourth order diagrammatic, many body Rayleigh Schrodinger perturbation theory 0-63556
 transition metal atoms, neutral and ion val. states, electron correlation, ab initio effective val. Hamiltonian calc. 0-99449
 transition metal ions, 3d and 4f energy level parametrisation, Slater parameters and correl. corrections 0-87041
 two electron atoms, three-body problem 0-83286
 two-body corrs., variational approach 0-91455
 valence correlation energies, contributions of triply- and quadruply excited states determ. using perturbation theory 0-78545
 Ar, CI calcs. using modified virtual orbitals 0-58163
 Ba II, 5p excitation, relativistic anal., multiconfig. Dirac-Fock calcs. 0-69240
 Be, correl. contribs. to dipole polarisability, coupled HF-perturbation theory 0-106269
 Ca, forbidden transitions, radiative lifetimes, MCSCF and CI calcs., time of flight spectra for metastable state 0-91498
 Ca I excitation series, potential barrier effects, single configuration HFC 0-78558
 Cl, photoionisation cross section and reson. theory, many body perturbation theory, 3p and 3s subshells 0-69114
 Fe, fine struct. levels fitting, config. interaction effect, spin-orbit and electrostatic interaction parameters 0-69248
 He, correl. contribs. to dipole polarisability, coupled HF-perturbation theory 0-106269
 He-like target+fast projectile, electron capture cross-sections 0-69231

atomic electron correlations continued

- Hg, 5d level open shell interactions, 304 Å photoelectron spectrum 0-87087
 In, VUV photoelectron spectra, pseudo-atomic beam technique 0-58225
 Li isoelectronic sequence of three electron atoms, pair correlation study 0-74096
 Li⁺, core excited bound states in beam foil expts., CI calcs. 0-78559
 Lw, ground state config., relativistic prediction, multiconfig. Dirac-Fock calcs. 0-106277
 Mn, fine struct. levels fitting, config. interaction effect, spin-orbit and electrostatic interaction parameters 0-69248
 Ne, correl. contribs. to dipole polarisability, coupled HF-perturbation theory 0-106269
 Ne, even-parity levels, double excited energy levels, frozen-core superposition, config. calcs. 0-106273
 O II, relative intensities and lifetimes in nebulae, conventional radiation theory 0-109513
 O V, E1 transition probabilities, lifetimes, CI calc. 0-83321
 Pb, 5d level open shell interactions, 304 Å photoelectron spectrum 0-87087
 Pb, photoelectron spectra, electron correlations and spin-orbit interaction influence 0-102495
 Pr³⁺, elec. multipole polarisabilities, discrete basis set calcs. 0-91456
 Si (III), excitation thresholds and oscillator strength calc. using CI wavefunctions 0-91496
 Sn II, cool plasma, isolated lines, Stark broadening, semi-empirical impact approx. calcs. 0-59186
 Sr I excitation series, potential barrier effects, single configuration HFC 0-78558
 Ti, fine struct. levels fitting, config. interaction effect, spin-orbit and electrostatic interaction parameters 0-69248
 Ti, neutral and ion val. states, electron correlation, ab initio effective val. Hamiltonian calc. 0-99449
 Ti, 5d level open shell interactions, 304 Å photoelectron spectrum 0-87087
 Ti, VUV photoelectron spectra, pseudo-atomic beam technique 0-58225
 V, fine struct. levels fitting, config. interaction effect, spin-orbit and electrostatic interaction parameters 0-69248
- atomic electron impact excitation**
see also electron spectra
 ab initio methods for atomic and molecular processes 0-63550
 collisional cross-sections determ. for low and intermediate energy processes 0-99579
 distorted wave calcs. for Io plasma torus 0-82262
 electron plasma relax. characts., 3-30 eV 0-79612
 electron scattering, free free processes 0-63834
 electron-collision cross-section data for atom or molecule, rel. to radiation physics 0-63829
 electron-photon coincidence expts., interpretation 0-83489
 electronic and at. collisions, conf., Kyoto, Japan (Aug.-Sept. 1979) 0-57011
 electronic and at. collisions, conference, Kyoto, Japan (Aug.-Sept. 1979) 0-62394
 gas mixture, self sustained volume photoionisation discharge existence conditions 0-79610
 inert gas nuclear pumped lasers, electron impact cross section meas. 0-63985
 ion+electron collision, resonant electron bremsstrahlung (*Russian*) 0-102580
 ion electron impact detachment, ionisation, excitation, dissociation and recombination 0-63832
 laser excitation mechanisms for atomic and ionic lasers, book contrib. 0-106512
 laser field, photon correl. effects 0-83481
 line radiation, polarisation, long-range electron corrs. effects 0-91683
 neutral atoms, bremsstrahlung of low-energy electrons, polarisation effects 0-102577
 nl-(n+1)l' collisional transitions, inelastic form factors and Born cross sections 0-58390
 resonant phenomena, complex stabilisation method 0-78515
 Rydberg atom, electron collisions 0-63833
 Rydberg states, Schwinger's variational principle 0-78713
 Rydberg states, transitions following electron impact excitation (*French*) 0-78711
 spin dependent phenomena in electron-atom collisions 0-63830
 target atom decay, scatt. projectile and photon coincident detect coherence effects 0-63791
 wave packets, radial, appl. to target distortion 0-87234
 Ag electron excited L_α emission spectra 0-102481
 Ar, electron impact, L X-ray spectrum, radiative Auger transitions 0-58227
 Ar, electron scatt. and ejection, electron energy loss spectra 0-58394
 Ar, excitation by pulsed electric discharge, luminescence obs., time resolved spectra meas. 0-102482
 Ar, positron annihilation decay rates, high temp. behaviour 0-58389
³⁷Ar, L-shell internal excitation accompanying L-capture 0-95726
 Ba, electron impact step-wise excitation (*Russian*) 0-83497
 Be isoelectronic sequence, electron impact excitation of reson. transitions 0-63825
 Be⁺, absolute cross sections and polarisation of electron-impact excitation of resonance multiplet 0-99577
 C, electron excitation cross section calc., Born approx. with Slater wave functions 0-69243
 C V, electron impact collision rates, reinterpretation of solar emission line ratios 0-98624
 Cd, ⁵³Pi, autoionising state, 150 eV electron impact excitation, (e, 2e) ang. distrib. study 0-83495
 Cs²⁺, electron impact excitation studies by intersecting beam method 0-69239
 Cs(Ar-Cs) plasmas, electron momentum transfer cross section, cyclotron reson., temp., cond., and vel. meas. 0-106930
¹³¹Cs, L-shell internal excitation accompanying L-capture 0-95726
¹⁶⁵Er, L-shell internal excitation accompanying L-capture 0-95726
 Eu, electron impact excitation cross section, Born and Ochkur approx. 0-87230
 Fe, K_α satellite lines following electron bombardment 0-69097
 Fe¹⁹⁺, electron collision strengths calcs. 0-67545
⁵⁷Fe, L-shell internal excitation accompanying L-capture 0-95726
⁷⁷Ge, L-shell internal excitation accompanying L-capture 0-95726

atomic electron impact excitation continued

- H, $1s \rightarrow 2s$ transition, electron impact excitation, exact second Born amplitude 0-102572
H, electron elastic scatt. at low intermediate energies 0-106393
H, electron impact, $1s \rightarrow 2s$ and $1s \rightarrow 2p$ excitation, electron-photon coincidence meas. 0-87233
H, electron impact excitation, cross-sections, multipole moments, quasiclassical calcs. 0-63828
H, electron impact excitation, electron-photon coincidence, large angle expt. 0-83500
H, electron impact excitation of $n=2$ to $n=3$ transition, algebraic variational method close coupling calcs. 0-91678
H, electron scatt. information obtained using symmetrically coupled partial differential eqn. 0-102574
H, matrix elements by Faddeev approach 0-78714
H-like ions, $n=2 \rightarrow 1$ transitions, collision strength Z-dependence 0-91675
H(1s) electron scattering, variable-charge Coulomb-projected Born approximation 0-58392
He, 2^1P -state electron impact excitation, 40 to 500 eV, alignment and orientation 0-83499
He, 2^3S -state, electron impact excitation, reson. form. mechanism 0-99463
He, 3^3P level, excitation and decay study up to high press. pumped by intense relativistic electron beam 0-74250
He, $(2p^2)^3P$ state, electron impact excitation, parity unfavoured transition 0-91680
He, electron impact, $1^1S \rightarrow 2^1S$ and $1^1S \rightarrow 2^3P$ excitation 0-91679
He, electron impact excitation, electron-photon angular correlation meas. 0-63826
He electron impact threshold excitation of $n=2$ state 0-83490
He, electron scatt., inelastic Feshbach resons., quasi projection operator calc. 0-58395
He, electron-photon ang. meas. for 2^1P state 0-102575
He II excited states in optically thin plasmas, role of direct ionisation-excitation 0-102579
He⁺, electron impact excitation cross-sections, reson. parameters calcs. 0-91686
He⁺, electron scatt., reson. state assoc., incomplete spectrum of Hamiltonian matrix 0-99568
He⁺, $n=2$, 3 , electron impact excitation, Coulomb-Glauber-Ochkur approx. appl. 0-69238
He-like ions, electron impact excitations 0-78712
He-like ions, $n=2 \rightarrow 1$ transitions, collision strength Z-dependence 0-91675
He-like ions, triplet-state, electron impact excitation cross sections obtained by Coulomb Ochkur Rudge approx. 0-102576
³He(He) clusters, metastable electronic states, electron impact excitation, time of flight spectra 0-106411
Li, electron excitation cross section calc., Born approx. with Slater wave functions 0-69243
Li electronic impact excitation, energy level calcs. (Chinese) 0-83488
Li II, electron impact excitation, distorted wave approx. 0-91689
Li⁺, electron scatt., inelastic Feshbach resons., quasi projection operator calc. 0-58395
Mg, $4sn$ autoionising states ejected electron spectra, low energy impact two electron excitation 0-83494
Mg isoelectronic sequence, electron impact excitation of reson. transitions 0-63825
N, electron impact excitation, near threshold, cross-sections for $(2s^2 2p^3 3s)^4P$ and $(2s^2 2p^3)^3P$ states 0-91684
N II, electron impact excitation cross sections, rel. to solar corona abundance 0-58391
Na, electron impact, crossed beam study 0-91672
Na, overlapping autoionisation lines, interference effects 0-91677
Ne, electron impact excitation of $2s^2 p^3 3s$ and $2s^2 p^3 3p$ configs., energy loss obs. 0-91685
Ne, electron impact K-shell excitation, EELS 0-106396
Ne, metastable electronic states, electron impact excitation, time of flight spectra 0-106411
O III, electron impact excitation cross sections, independent particle model calcs. 0-63823
O VII, electron impact collision rates, reinterpretation of solar emission line ratios 0-98624
O⁺(²D) in thermosphere, quenching by electrons 0-94630
¹⁹³Pt, L-shell internal excitation accompanying L-capture 0-95726
SI III, electron impact excitation of $3s^2 1S$ - $3s3p^3P$ transition 0-102578
¹⁷⁹Ta, L-shell internal excitation accompanying L-capture 0-95726
¹⁵⁷Tb, L-shell internal excitation accompanying L-capture 0-95726
Yb, electron impact excitation cross section, Born and Ochkur approx. 0-87230
Zn isoelectronic sequence, electron impact excitation of reson. transitions 0-63825

atomic electron impact ionisation

- see also electron spectra
autoionising states, electron impact ionisation obs., distortion effects calcs. 0-83491
coherence and correlation in atomic collisions, book 0-90615
collisional cross-sections determ. for low and intermediate energy processes 0-99579
electron coincidence spectroscopy, binding energy charge density meas. 0-63817
electron impact detachment, ionisation, excitation, dissociation and recombination 0-63832
electron plasma relax. characts., 3-30 eV 0-79612
electronic and at. collisions, conf., Kyoto, Japan (Aug.-Sept. 1979) 0-57011
fifth-row elements, L₁ electron ionisation cross section, relativistic plane wave Born approx. 0-87229
high-Z atoms ($Z=48-104$), electron impact, K-shell ionisation cross sections calcs. 0-63827
hydrogenic ions, break-up processes, eikonal approach 0-91676
hydrogenic ions, highly charged, electron ionisation of $4s$, $4p$, $4d$ and $4f$ sublevels 0-91681
interstellar medium, local, electron impact rel. to ionisation state 0-90502
Io atmosphere, electron impact ionisation rate rel. to interaction with plasma torus 0-98604
isoelectronic sequence, electron impact ionisation cross section 0-91688
polarization phenomena in electronic and atomic collisions, review 0-83501
positive ions, electron impact ionisation, Coulomb-Born approx. 0-74249

atomic electron impact ionisation continued

- Rydberg atom, electron collisions 0-63833
wave packets, radial, appl. to target distortion 0-87234
Ag, electron (positron), impact, K- and L-shell ionisation, K α and L X-rays meas. 0-99575
Ag, photoionisation cross sections, electron-impact inverse mean free paths, and stopping powers for each subshell 0-69113
Al, K-shell ionisation by ultrarelativistic electrons, density effect 0-99576
Ar, electron scatt. and ejection, electron energy loss spectra 0-58394
Ar, energetic electron degradation spectra and initial yields 0-95724
Ar, energy deposition, Monte Carlo calcs. 0-69242
Ar, inner shell alignment following electron impact ionisation, distorted wave approx. calcs. 0-91682
Ar neutral system, complete saturation phase excited state population density 0-106284
Ar⁺, ($i=1, 2, 3, 4, 5$), absolute electron impact ionisation cross section 0-83496
³⁷Ar, L-shell internal excitation accompanying L-capture 0-95726
Au, electron impact M-shell ionisation, 60-600 keV, absolute cross sections meas. 0-83493
Ba II, $5p$ excitation, relativistic anal., multiconfig. Dirac-Fock calcs. 0-69240
Bi, electron impact M-shell ionisation, 60-600 keV, absolute cross sections meas. 0-83493
Cd, $4d^1 5p^1 P$ autoionising state, electron impact ionisation obs., distortion effects calcs. 0-83491
Cl, K-shell ionisation by ultrarelativistic electrons, density effect 0-99576
¹³¹Cs, L-shell internal excitation accompanying L-capture 0-95726
Cu, K-shell ionisation cross sections, slow electron impact 0-83498
¹⁶⁵Er, L-shell internal excitation accompanying L-capture 0-95726
Fe, inner-shell vacancies, cascade decay, multiple ionisation and X-ray emission calcs. 0-87072
Fe ions, Li-like Auger contris. to electron impact ionisation 0-87231
⁵²Fe, L-shell internal excitation accompanying L-capture 0-95726
⁷⁷Fe, L-shell internal excitation accompanying L-capture 0-95726
H, eikonal exchange amplitude in Coulomb break-up processes 0-87232
H, electron impact ionisation, polarised Coulomb-projected Born approx. 0-106395
H, electron scatt., atomic optical potential model 0-99578
He, electron scatt. at intermediate energy, quantum mechanical treatment 0-91687
He, metastable states, electron and proton impact ionisation, autoionisation 0-102573
Hg electron resonant elastic and inelastic scatt. (Russian) 0-78710
Li isoelectronic sequence, electron impact ionisation cross section 0-91688
Li⁺ positron, positronium formation in highly excited states, first Born approx. 0-58420
Mg, K-shell ionisation by ultrarelativistic electrons, density effect 0-99576
Mn, K-shell ionisation cross sections, slow electron impact 0-83498
Na, K-shell ionisation by ultrarelativistic electrons, density effect 0-99576
Ne plasma, electron collision ionisation, electron kinetic behaviour during elec. field perturbation (German) 0-64676
Ne⁺, absolute electron impact ionisation cross section 0-83496
O ions, Li-like Auger contris. to electron impact 0-87231
O⁺, absolute electron impact ionisation cross section 0-83496
O⁴⁺, electron impact ionisation, close coupling calcs. 0-106293
Pb, electron impact M-shell ionisation, 60-600 keV, absolute cross sections meas. 0-83493
¹⁹³Pt, L-shell internal excitation accompanying L-capture 0-95726
¹⁷⁹Ta, L-shell internal excitation accompanying L-capture 0-95726
¹⁵⁷Tb, L-shell internal excitation accompanying L-capture 0-95726
Xe, valence orbital, electron impact ionisation, absolute cross-section 0-69241
Xe⁺, absolute electron impact ionisation cross section 0-83496
- atomic electron scattering** see atomic electron impact excitation; atomic electron impact ionisation; elastic scattering of electrons by atoms and molecules
- atomic emission spectroscopy**
DC arc plasma, alterations in spectral line intensities due to external mag. fields 0-79621
DC plasma atomic emission spectrometry system, characterisation of interference enhancement effect 0-89549
DC plasma excitation source, interference effects 0-86434
droplets produced by pneumatic nebulisers, size meas. method 0-71992
inductively coupled plasma and atomic absorption spectroscopy combined 0-104478
inductively coupled plasma and DC atomic emission spectrometry, tabulation of spectral interferences 0-71991
laser emission spectroscopy, quantitative microanalysis of reactor graphites 0-81384
laser excited atomic fluoresc. spectrosc., appl. to determ. of Ni and Sn 0-93811
radio-frequency excited pulsed hollow-cathode lamp, absorpt. and emission characteristics 0-89550
selectivity evaluation 0-89561
steel, stainless, oxidised, sputtering yield meas. by atomic fluoresc. spectroscopy 0-80922
trifluoromethane plasma etching of SiO₂, optical spectroscopy appl. 0-87940
Ag, Auger spectra, $4d$ bandwidth effect 0-89093
AlAg, Auger spectra, $4d$ bandwidth effect 0-89093
MgAg, Auger spectra, $4d$ bandwidth effect 0-89093
Na in air-acetylene flame, harmonic saturated spectroscopy for at. fluoresc. detect. 0-104472
Ni, determ. using laser excited atomic fluoresc. spectrosc. 0-93811
SiO₂-GeO₂-B₂O₃-P₂O₅, optical waveguide glass, comp. determ., plasma emission spectra 0-87446
Sn, determ. using laser excited atomic fluoresc. spectrosc. 0-93811
TiO₂, sputtering defects, associated surface electron states, UPS, XPS and AES obs. 0-60755

atomic energy see nuclear power**atomic excited states**

- see also atomic metastable states; atomic resonant states
alkali atoms, excited state, laser photoionisation theory, hyperfine coupling effect 0-102493
alkali atoms, highly excited Rydberg states, fine struct. 0-58402
bound and free, inner charge defect method calcs. 0-78511

atomic excited states continued

- Cd+molecules collisions 0-58338
education, Na Rydberg states, anomalous fine struct., perturbation model 0-57035
effective excitation cross-sections for atoms in meteors 0-101565
electron+ion scattering, Schwinger's variational principle, Rydberg states 0-78713
electronic and at. collisions, conference, Kyoto, Japan (Aug.-Sept. 1979) 0-62394
excitation energies calc., using renormalised Green's function method (*Japanese*) 0-83295
excited atom ionisation due to collisions in their own gas (*Russian*) 0-91654
fast projectile electron loss forward peak oscill. struct. as autoionisation 0-69227
force on atom in electrostatic field, Feynman-Hellmann theorem and oscillator strengths 0-65275
heavy ion+atom collisions, small impact parameters, K-vacancy prod., molecular theory 0-69229
highly excited atoms, blackbody radiation effects 0-58176
highly excited atoms, review 0-58174
inert gas atom, first excited config., intermediate coupling coeff. 0-83450
inert gas atom+halogen mol., halide form., relax. and quenching 0-81314
inert gas collisional perturbation of 6^3D_1 , 6^3D_2 Hg levels 0-74223
inert gases, atomic alignment in positive column (*Russian*) 0-87981
ion+atom collision produced highly excited states, decay spectra 0-63780
ion collisions, electron capture, atomic excited state polarisation, optical detection 0-58377
Landau condensation in atomic physics 0-74098
laser excited, reactive collisions 0-66793
multichannel threshold structures in scattering theory 0-58334
multiply charged ion, electron capture into different excited states in plasma 0-64679
muonium hyperfine structure of ground state, magnetic moments, muonium-antimuonium conversion, excited states 0-69273
N-electron system, Schrodinger eqn. soln. using antisymmetrisation 0-106246
neutral+high Rydberg atom, thermal collisions, review 0-63756
neutral particles, electrostatic trapping 0-102485
oscillator strengths calcs., influence of wave function determ. method 0-99478
perturbation and SCF calcs. 0-102455
positronium formation in highly excited states, first Born approx. 0-58420
rare earth elements, atomic partition functions, Chebyshev approximations 0-67544
Rydberg atom, electron collisions 0-63833
Rydberg atom+atom (photon), separation of Rydberg electron and ion core 0-63754
Rydberg atom+molecule, reaction channels, expt. vs. theory 0-63755
Rydberg atom microwave and far IR spectroscopy 0-63564
Rydberg atoms, teaching approach 0-77570
Rydberg states, autoionisation with large orbital angular momentum 0-87052
Rydberg states, Coulomb and Yukawa pot., wave functions and quantum defects, Schwinger's var. principle 0-63549
Rydberg states, transitions following electron impact excitation (*French*) 0-87811
sputtered atoms in excited states, vel. meas. 0-63561
superfluorescence initiation, master equation study, microscopic description 0-63577
superradiant, excitation by pulse of quantum field 0-87359
transition metal atoms, neutral and ion val. states, electron correlation, ab initio effective val. Hamiltonian calc. 0-99449
transitions, excitation by monochromatic laser radiation, Doppler-broadened transitions 0-78582
two electron atom, energy levels, classical first order perturbation theory 0-58118
two photon excitation, time depend. emitted light spectra, perturbation theory 0-63605
two-electron atoms, doubly excited resonances assoc. with $N=4$ hydrogenic threshold 0-106283
two-level atom, interaction with radiation, photon number time evolution 0-58216
valence correlation energies, contributions of triply- and quadruply excited states determ. using perturbation theory 0-78545
vapours, three-level system, collisional effects in saturation spectroscopy, appl. to Na 0-78579
Al, plasma, transfer eqn. soln. using freq. and angle averaged photon escape probabilities 0-64688
Al, vacuum arc, excited state density from line intensities 0-96404
Al, vacuum arc, excited state density theory 0-100107
Ar neutral system, complete saturation phase excited state population density 0-106284
Ar, optical gas breakdown, reduced threshold in two-freq. field 0-64819
Ar, outer $p_{1/2}$ subshell photoionisation, polarised electrons, relativistic RPA calcs. 0-83331
Ar+Kr, $(4p^55p)$ and $(4p^55p')$ states, radiative lifetimes and two-body collisional deactivation rate consts. 0-95572
Ar $^{2+}$ +Ar (Kr)(Xe), single electron capture excitation, photon emission, VUV spectroscopy 0-58379
Ar*, electron excited in Ar-CO $_2$ mixture, transfer reaction kinetic study 0-63824
Ba, hyperfine splitting and isotope shift of high lying levels, Doppler-free 2-photon laser spectroscopy 0-58215
Ba II, 5p excitation, relativistic anal., multiconfig. Dirac-Fock calcs. 0-69240
Ba, quantum defect param., ab initio calcs. 0-78525
Ba+Ti, dipole-quadrupole radiative collisional fluoresc. 0-83315
Ba+Ti, radiative collisional fluoresc. obs. from thermally excited atoms 0-102480
Be III, doubly excited states, triplet spectra 0-87069
Be isoelectronic series, excited states, oscill. strengths calcs., influence of wave function determ. method 0-99478
Bi Rydberg series from Bi $_2$ three photon excitation 0-106280
C II line excitation by C I photoionisation 0-58223
C IV (CV), UV line identifications and lifetime meas. 0-106288
Ca, 4s4p 1P_1 level Hanle effect density depend., lifetime 0-91494

atomic excited states continued

- Ca I excitation series, potential barrier effects, single configuration HFC 0-78558
Ca, quantum defect param., ab initio calcs. 0-78525
Cd, 1S , 3P , 1P states, dipole polarisabilities from compact variational trial functions 0-63568
Cd, n^1S_0 and n^1D_2 levels lifetimes, time-resolved spectrosc. obs. (*French*) 0-102456
Cd+N $_2$, vap., creation of inverse population of atomic Cd 6^3S and 5^3P_2 levels 0-58219
Cs, excited state, laser photoionisation theory, hyperfine coupling effect 0-102493
Cs, Rydberg states, diamag. and collisional perturbations 0-58181
Cs $^+$ excited levels, hyperfine struct. and lifetimes 0-63590
 ^{133}Cs , first excited D-level, hyperfine struct. meas. by cascade, fluoresc. spectrosc. 0-69101
D ** +N $_2$ fast collisions, impulse approx. 0-106281
F ** +H $_2$, quenching of excited state, semiclassical studies, comparison between reactive and nonreactive processes 0-106375
H, 2p state production by H $_2$ photolysis in Ne matrix 0-93372
H, longit. excited states in intense mag. fields, rel. to pulsars 0-91469
H Rydberg level selective excitation by three-photon absorption 0-58640
H, Stark effect, high orders of perturbation theory for excited states 0-87079
H $^-$, double excited states below $N=3$ threshold, arrangement of resonances in series converging exponentially 0-99462
H+Ar, H α and H β emission cross sections 0-63782
H+H $^+$, H excitation, angular differential cross sections 0-63784
H 0 +N $^{3+}$, electron loss cross section 0-63805
H $^+$ +Ar, H α and H β emission cross section 0-63783
H $^+$ +H(Li), resonant ionisation, cross section and ionisation probability 0-63785
H(2S)+He(N)(Ar), excitation and ionisation contributions to sum-rule Born cross sections 0-99551
He, 2^1S -state, electron impact excitation, reson. form. mechanism 0-99463
He, $(2p^2)^1P$ state, electron impact excitation, parity unfavoured transition 0-91680
He, electron impact excitation, electron-photon angular correlation meas. 0-63826
He energy levels, classical first order perturbation theory 0-58118
He, hollow-cathode type discharge, spectroscopic obs., laser light source appl. 0-95335
He, laser spectroscopy in intense magnetic fields 0-62738
He, polarised light emission after HeH $^+$ impact on C foil 0-58361
He-Cd vapour excitation in hollow cathode discharge 0-64815
He+He $^+$, low energy collisions, excitation of 2^1S , 2^1P and 3^1P , 3^3P levels 0-58342
He+He $^+$ (Ne), tensor polarisabilities of $1snd$ 1D level, fluoresc. depolarisation obs. 0-69099
 ^3He , hyperfine-induced singlet-triplet mixing obs. 0-106399
 $^3\text{He-Xe}$ nuclear pumped laser, small signal gain coeff. and power output, theory comparison with expt. 0-63983
He $^+$ +He, excitation exchange and collisional relax. 0-69226
He(2s-3p transitions), beam foil spectra, emitted light polarisation, depend. on foil tilt angle 0-63786
Hg, 1S , 3P , 1P states, dipole polarisabilities from compact variational trial functions 0-63568
Hg electron resonant elastic and inelastic scatt. (*Russian*) 0-78710
Hg, two photon excitation, time resolved spectroscopy 0-87075
Ho I, Ho II, excited level lifetimes and oscillator strengths, visible spectra 0-63573
K, isotope shifts of individual nS and nD levels 0-102489
K+He, 4^4P state $j_1m_1 \rightarrow j_2m_2$, Zeeman transition, total cross section energy depend. 0-83475
 ^{39}K , first excited D-level, hyperfine struct. meas. by cascade, fluoresc. spectrosc. 0-69101
Kr, 6p levels, two-photon excitation, time resolved fluoresc., quenching, lifetimes and photoionisation cross section 0-78587
Kr, outer $p_{1/2}$ subshell photoionisation, polarised electrons, relativistic RPA calcs. 0-83331
Kr VII, beam-foil excitation, 4s4p $^1P_1^0$ level decay simulation 0-78578
Kr VIII, excited state energies and lifetimes, beam foil spectra 0-63591
Kr+F $_2$, KrF form., relax. and quenching 0-81314
Li core excited even parity 2P states, fluoresc. 0-69100
Li $^+$, core excited bound states in beam foil expts., CI calcs. 0-78559
Li $^+$, optical transition between bound states, beam-foil spectrosc. obs. 0-91476
Li $^+$, 3P and 3S states, fine (hyperfine) struct., dye laser saturation spectroscopy, beam expt. 0-58169
Li+Li $^+$ (H $^+$), resonant ionisation, cross section and ionisation probability 0-63785
Li($2^1P_{1/2,3/2}$), laser induced flame chemistry, saturated mode fluoresc. meas. 0-89491
Li(2p)+H $_2$ (N $_2$), Li(2p) excitation, alignment and orientation obs. 0-63794
Mn I, collisional and radiative excited, lifetime meas. 0-91501
N, electron impact excitation, near threshold, cross-sections for $(2s^22p^33s)^4P$ and $(2s2p^4)^4P$ states 0-91684
 ^{16}N II, 2p3p 1P_1 , hyperfine struct. after ion beam surface impact at grazing incidence 0-58403
Na, $3^2S_{1/2}$ - $3^2P_{1/2}$, spectral distrib. and collisional depolarisation of laser light, D $_2$ -fluorescence 0-58209
Na, excited, electron scatt. at low energy, total cross section 0-63821
Na, excited 4D and 5S state, absolute photoionisation cross-section 0-99488
Na, high Rydberg states, quenching in strong 1.06 μm laser field 0-95559
Na, photofragment of NaBr, non-Gaussian line shape, level shifting and velocity inversion 0-58182
Na, Rydberg states, millimetre spectrosc. 0-99469
Na+H $^+$, $2p^33s^2P_{3/2}$ state alignment, collisionally induced, impact parameter calc. 0-83474
Na+H(Ne)(Kr) vel.-changing collisions, effect on 2 photon and stepwise absorpt. line shape 0-87221
Na+He $^+$, crossed beams, l-changing collisions, n-depend. 0-58345
Na+inert gas, Rydberg states transitions, broadening cross-sections meas. 0-69110
Na+Na, electronic-field pot. curves determ. for large interatomic distances, excitation cross sections calc. 0-95704

atomic excited states continued

- Na($3^2P_{1/2,3/2}$), laser induced flame chemistry, saturated mode fluoresc. meas. 0-89491
 Ne, even-parity levels, double excited energy levels, frozen-core superposition, config. calcs. 0-106273
 Ne+He⁺, He(3^1P) level excitation, total emission cross section, fast oscils. obs. 0-58362
 Ne²⁺+Ar (Kr)(Xe), single electron capture excitation, photon emission, VUV spectroscopy 0-58379
 Ne²⁺+Xe, electron capture collisions, 15 to 50 keV, excitation 0-102566
 O III, electron impact excitation cross sections, independent particle model calcs. 0-63823
 O V, E1 transition probabilities, lifetimes, CI calc. 0-83321
¹⁶O ions, mag. hyperfine interactions, PAC meas. 0-95734
 Pb, L-shell photoelectric photon absorpt. cross section, energy depend. 0-106279
 Pb Rydberg series from Pb₂ three photon excitation 0-106280
²¹⁰Po, nucl. alpha decay, electron inner shell vacancy creation, semi quantal approach 0-68607
 Rb in Xe, collision-induced dipole transitions, absorpt. meas. 0-95718
 Rb, radiative lifetimes up to n=12 excited states, pulsed dye laser and superradiance excitation 0-83322
 Rb+He, quasielastic and inelastic collisions in S and D Rydberg states 0-83462
 Rb+Rb, radiatively excited states, chemi-ionisation, ionisation rate consts. determ. 0-58363
 Rb+Rb⁺, freq. shift, line broadening, phase interference effects, Doppler free two photon spectra 0-58200
^{85,87}Rb, first excited D-level, hyperfine struct. meas. by cascade, fluoresc. spectrosc. 0-69101
 S+CS₂(OCS)(CH₄), electronically excited atom, reson. fluoresc. 0-99476
 Sc I to Sc XXI, energy level tables derived from atomic spectra anal. 0-101672
 Si (III), excitation thresholds and oscillator strength calc. using CI wavefunctions 0-91496
 Si, excited states lifetimes, fluoresc. decay curves 0-58175
 Si(Si⁺)(Si²⁺)(Si³⁺), excited levels, radiative lifetimes, beam foil spectra 0-58368
 Sr I excitation series, potential barrier effects, single configuration HFC 0-78558
 Sr, quantum defect param., ab initio calcs. 0-78525
 Sr, 4s3d³ and 3d⁴ states, HF descriptions, alternative orbital config. 0-63534
 Ti atoms sputtered from Ti, Ti oxides, photon emission, nonradiative transition effects 0-58208
 Ti, neutral and ion val. states, electron correlation, ab initio effective val. Hamiltonian calc. 0-99449
 Ti, Tokamak plasma, atomic struct., highly ionized states 0-75086
 TiXIV(TiXV)(TiXVII), Tokamak discharge, ground state, mag. dipole transitions, UV spectra obs. 0-63575
 Ti+Ba, radiative collisional fluoresc. obs. from thermally excited atoms 0-102480
 Tm I, hyperfine struct., high resolution spectrosc. meas. 0-87238
 U+⁴He(⁴He)(Ne), collisional relax. of highly excited states, laser-induced fluoresc. obs. 0-58205
 U+molecule, collisional relax. of highly excited states, laser-induced fluoresc. obs. 0-58205
²³⁵U, ground and 1st excited states, hfs, laser fluoresc. and laser-RF double reson. spectroscopy 0-58170
 Xe, outer p_{1/2} subshell photoionisation, polarised electrons, relativistic RPA calcs. 0-83331
 Xe+Cl₂(F₂), XeCl(XeF) form., relax. and quenching 0-81314
 Xe(nf Rydberg state)+NH₃, n- and l-changing and ionising collisions 0-58360
 Yb, highly excited levels, odd and even parity spectra, multichannel quantum defect anal. 0-58133
 Yb highly excited levels, reson., visible two photon absorpt. spectra obs. 0-58228
 Yb I, high Rydberg levels of 4f¹⁴ 6snd configs., very high resolution obs. 0-106300
 Zn, ¹S, ³P, ¹P states, dipole polarisabilities from compact variational trial functions 0-63568

atomic explosions see nuclear explosions**atomic fine structure**

- alkali atoms, highly excited Rydberg states, fine struct. 0-58402
 autoionising states, electron angular distribution, fine and hyperfine struct. 0-58222
 education, Na Rydberg states, anomalous fine struct., perturbation model 0-57035
 k ordering of atomic and ionic energy levels 0-74095
 metastable autoionising states, ang. distrib. of electrons which decay via fine and hyperfine struct. interactions 0-102492
 multiple anticrossings in atomic spectrosc. 0-87091
 P-S state atomic collisions, quantum mechanical treatment, decoupling approx. 0-99542
 P-state collisions, quantum mechanical treatment, angular momentum coupling 0-99541
 two-level system, spontaneous emission in bichromatic reson. field 0-69093
 Al₂Cl₆, matrix isolated, vibr. spectra, isotopic fine struct. and valence force field calcs. 0-58258
 Ar, absorpt. spectra, field induced autoionisation near ionisation threshold 0-106301
 Ar+Ar⁺, charge exchange, Σ oscil. and spin change 0-74247
 Ar⁺+Ar, charge transfer, fine-structure transitions 0-63808
 Ba I, quasi-Landau spectrum, semiclassical strong field mixing models 0-63847
 Ba, X-ray spectra, high energy L γ satellites 0-102474
 C, ground state fine struct., laser mag. reson. obs. 0-87062
 Cs, Rydberg states, diamag. and collisional perturbations 0-58181
 Cs⁺ dipole and quadrupole polarisability fine struct. intervals and g-factor interval 0-91477
 F, spin-orbit splitting and ²P_{1/2} radiative lifetime, absorpt. spectrosc. meas. 0-87063
 Fe, fine struct. levels fitting, config. interaction effect, spin-orbit and electrostatic interaction parameters 0-69248
 H, Rydberg consts., saturated absorpt., spectroscopy meas. 0-105604
 H fine structure ³S_{1/2}-³D_{5/2} interval, separated oscillatory field meas. 0-99482

atomic fine structure continued

- H⁺, gyromag. ratio and fine struct. meas. by meas. distance between wires, using laser interferometer 0-74253
 He, ³D level, fine struct. changing collisions in glow discharge 0-58346
 He fine structure interval ²P₀-²P₂, optical microwave atomic beam mag. resonance meas. 0-102585
 He plasma, satellites of He 492.2 nm line, fine struct. interpretation 0-59235
 Kr, absorpt. spectra, field induced autoionisation near ionisation threshold 0-106301
 Kr VIII, excited state energies and lifetimes, beam foil spectra 0-63591
 Li⁺, ³P and ³S states, fine (hyperfine) struct., dye laser saturation spectroscopy, beam expt. 0-58169
 Li*(²P_{1/2})+H₂(D₂), collision induced quenching and fine struct. transition rate coefficients meas. 0-74221
 Li*(²P_{1/2})+He(Ne)(Ar)(Kr)(Xe), collision induced fine struct. transition rate coefficients determ. 0-74220
 Mn, fine struct. levels fitting, config. interaction effect, spin-orbit and electrostatic interaction parameters 0-69248
 Mn I, collisional and radiative excited, lifetime meas. 0-91501
 Na, ²P photodissoc. product, fine struct. anal. 0-78665
 Rb, ²P photodissoc. product, fine struct. anal. 0-78665
 Sr I, quasi-Landau spectrum, semiclassical strong field mixing models 0-63847
 Ti, fine struct. levels fitting, config. interaction effect, spin-orbit and electrostatic interaction parameters 0-69248
 V, fine struct. levels fitting, config. interaction effect, spin-orbit and electrostatic interaction parameters 0-69248
 Xe subshell photoionisation, multichannel k-matrix calc., spin orbit interactions 0-63600
 Zr IV, energy levels, spectrum obs. 440 to 2670 Å 0-99470
- atomic fluorescence**
 antibunching phenomena on single-scatterer fluorescence in weak-field limit 0-63580
 atom+atom collisional intense-field fluoresc., Zeeman degeneracy effects 0-99477
 collisional relax. of highly excited states, laser-induced fluoresc. obs. 0-58205
 cooperative resonance fluorescence and atomic interactions 0-91486
 delayed quantum beat subnatural linewidth spectroscopy 0-77879
 dressed atom system, energy levels and reson. phenomena, universal algorithm 0-69111
 dressed atom system, phase represent. applic. to reson. fluoresc., universal algorithm 0-69112
 electron impact excited line radiation, polarisation, long-range electron corrs. effects 0-91683
 fast atomic beam, optical reson. detect. by at. fluoresc. 0-102479
 flame temperature meas., 5 laser-excited fluoresc. methods, theoretical basis 0-101793
 K-emission photons, calc. of number generated by monoenergetic electrons and β -particles 0-63581
 n-photon resonance phenomena, finite laser bandwidth effect 0-58230
 Na, fluoresc. study, reson. radiation illum. 0-83314
 near resonant scatt. and collision induced (Chinese) 0-63582
 nonlinear optical phenomena in system of colliding atoms, atomic fluoresc. 0-99788
 photoionisation, fluoresc. radiation polarisation 0-87076
 photon antibunching in resonance fluorescence in the presence of atomic number fluctuations 0-91764
 polarisation of atomic fluorescence produced by laser-induced dissociation of Na₂ 0-78569
 quantum beats in two-photon resonance fluorescence 0-91488
 quantum interference method of distinguishing 0 and 2 π rotations 0-91485
 Raman scattered light, Hanle effect influence 0-83323
 resonance fluorescence, collective effects (Russian) 0-91490
 resonance fluorescence, photon correlation laser linewidth effects 0-83316
 resonance fluorescence and Rayleigh scattering at high intensities, effect of collisions 0-102478
 resonance fluorescence of two-state atom, collisional broadening 0-91484
 resonance fluorescence of two-state atoms irradiated by monochromatic light, collisional broadening 0-91483
 resonance light scattering, spectral props. and photon corrs. 0-91510
 resonance Raman lineshapes and fluorescence in strong radiation fields 0-87074
 sputtered excited states, secondary photon emission, role of transition probability 0-102483
 superfluorescence, delay-time statistics and inhomogeneous line broadening 0-99684
 superfluorescence beats, theory incl. quantum fluctuations and finite sample size 0-102686
 superfluorescence initiation, master equation study, microscopic description 0-63577
 three level atom at high photon densities, reson. fluoresc. interference effects 0-87073
 three-level system, 2-photon reson. fluoresc. 0-87077
 two level atom system, coherently driven, cooperative fluoresc. 0-87357
 two photon excitation, time depend. emitted light spectra, perturbation theory 0-63605
 two-atom resonance fluoresc. spectrum, cooperative effects 0-78570
 two-level atom, driven by reson. multimode laser, light scatt., statistical props. 0-91489
 two-level atom, radiation by intense laser beam, resonance fluorescence, photon antibunching, Doppler shift 0-74146
 two-level atom, reson. fluoresc., atomic operators 0-63579
 two-level atom, reson. fluoresc. spectrum of intense amplitude modulated laser light 0-91487
 two-level atoms, inhomogeneously broadened, superfluoresc. and amplified spontaneous emission 0-106499
 Ag electron excited L α emission spectra 0-102481
 Ag, K-fluorescence yield determ. from K-Auger electron emission rates 0-95569
 Ar+Kr, (4p⁵5p) and (4p⁵5p') states, radiative lifetimes and two-body collisional deactivation rate consts. 0-95572
 Ar*, electron excited in Ar-CO₂ mixture, transfer reaction kinetic study 0-63824
 Au, X-ray production cross sections for protons, fluoresc. obs. 0-102476
 Ba⁺ ions confined in cylindrical RF trap, lifetime meas., laser probing 0-95573
 Ba+Ti, dipole-quadrupole radiative collisional fluoresc. 0-83315

atomic fluorescence continued

- Ba+Ti, radiative collisional fluoresc. obs. from thermally excited atoms 0-102480
- BaI resonance transitions, hyperfine struct. and isotope shifts, atomic beam laser spectroscopy 0-102141
- Ca, laser saturation broadening in flames, fluoresc. excitation profile obs. 0-95568
- Ca, stable and radioisotopes, hfs, isotope shifts, dye laser saturation spectroscopy, beam expt. 0-58169
- Ca+Ca(Mg)(inert gas), metastable 3P -state, quenching reactions, fluoresc. meas. 0-102477
- Cd(3P_1) radiation imprisonment lifetime, inert gas effect, phase-shift method 0-58213
- Cs cell, laser beam excitation, multipass, optical pumping and weak neutral current parity violation 0-58207
- Cs+inert gas, three body interaction, fluoresc. spectra principal series lines and secondary satellites 0-83313
- ^{133}Cs , first excited D-level, hyperfine struct. meas. by cascade, fluoresc. spectroscopy 0-69101
- Cu vapour pulsed laser, spectral comp. of superradiance, stimulated and spontaneous radiation 0-102713
- Eu+Sr, absorptive collisional energy transfer, laser induced excitation spectra 0-63584
- ^{57}Fe metastable states, hyperfine struct. meas. by laser RF double-resonance 0-58404
- ^{152}Gd $L_{2,3}$ subshell X-ray fluorescence and Coster-Kronig yields from ^{152}Eu decay 0-69102
- H detection by reson. fluoresc., coherent tunable VUV generation near Ly- β transition 0-99798
- H, diffusion coeff., in H_2 , luminesc. intensity meas. 0-103098
- H+He(Ar), collisional coherent excitation, meas. of Lyman α -photons 0-99552
- H+O(N_2), collisional coherent excitation, meas. of Lyman α -photons 0-99552
- H_2 +D(O)(Cl)(Br), relax. and chem. reaction, time resolved IR fluoresc. and mass spectrometry obs. 0-69177
- HCl+D(O)(Cl)(Br), relax. and chem. reaction, time resolved IR fluoresc. and mass spectrometry obs. 0-69177
- He, collisional excitation transfer for 3P and D states 0-106387
- He+He $^+$ (Ne), tensor polarisabilities of $1snd$ 1D level, fluoresc. depolarisation obs. 0-69099
- He $^+$ +N $_2$, collisional excitation processes, visible emission, cross-sections 0-99571
- He $^+$ +Xe, internal energy distrib. at 100 eV 0-99564
- ^3He , hyperfine-induced singlet-triplet mixing obs. 0-106399
- Hg ions, relaxation two constants meas. of optically pumped stored Hg ions 0-106287
- Hg, two photon excitation, time resolved spectroscopy 0-87075
- ^{155}Er $L_{2,3}$ subshell X-ray fluorescence and Coster-Kronig yields from ^{163}Er decay 0-69102
- In, K-fluorescence yield determ. from K-Auger electron emission rates 0-95569
- In, laser saturation broadening in flames, fluoresc. excitation profile obs. 0-95568
- ^{39}K , first excited D-level, hyperfine struct. meas. by cascade, fluoresc. spectroscopy 0-69101
- Kr, 6p levels, two-photon excitation, time resolved fluoresc., quenching, lifetimes and photoionisation cross section 0-78587
- Li core excited even parity 2P states, fluoresc. 0-69100
- Li, sputtered from Li and LiF, kinetic energies 0-66373
- Li($2^1P_{1/2,3/2}$), laser induced flame chemistry, saturated mode fluoresc. meas. 0-89491
- Mn I, collisional and radiative excited, lifetime meas. 0-91501
- N, ($2^3S_{3/2}$), kinetic study by time resolved atomic resonance fluorescence 0-95557
- Na, $^3S_{1/2}$ - $^3P_{3/2}$, spectral distrib. and collisional depolarisation of laser light, D $_2$ -fluorescence 0-58209
- Na beam, laser beam irradi., reson. fluoresc. intensity, Bloch model calcs. 0-58206
- Na, laser saturation broadening in flames, fluoresc. excitation profile obs. 0-95568
- Na, muonic, $2s^{1/2}$ level decay channel concurrence, neutral current effects observation (Russian) 0-83526
- Na, single atoms, fluoresc. selective detect. by laser radiation 0-83312
- Na, sputtered from NaCl, kinetic energies 0-66373
- Na($3^1P_{1/2,3/2}$), laser induced flame chemistry, saturated mode fluoresc. meas. 0-89491
- Ne $^{2+}$ +Xe, electron capture collisions, 15 to 50 keV, excitation 0-102566
- O(3P) prod. by O $_3$ photolysis, quantum yield determ. 0-78568
- O(3P)+dimethyl sulphide, fast flow reson. fluoresc. obs. of absolute rate consts. 0-61077
- Pb, L-shell photoelectric photon absorpt. cross section, energy depend. 0-106279
- Pb, X-ray production cross sections for protons, fluoresc. obs. 0-102476
- Rb+methane (and deuterates), $5^2P_{1/2}$ - $5^2P_{3/2}$ excitation transfer, isotope effects, temp. depend. 0-91630
- ^{85}Rb , first excited D-level, hyperfine struct. meas. by cascade, fluoresc. spectroscopy 0-69101
- S+CS $_2$ (OCS)(CH $_4$), electronically excited atom, reson. fluoresc. 0-99476
- Se trace amount determ. by hydride generation-nondispersive flame at. fluoresc. spectroscopy 0-89553
- Si, excited states lifetimes, fluoresc. decay curves 0-58175
- Sr atomic beam, time correlations between two sidebands of reson. fluoresc. triplet, multiphoton processes 0-95570
- Sr, laser saturation broadening in flames, fluoresc. excitation profile obs. 0-95568
- Sr-Cs mixture, laser induced collisional two-photon ionisation, fluoresc. monitoring 0-91515
- Ti atoms sputtered from Ti, Ti oxides, photon emission, nonradiative transition effects 0-58208
- Tl+Ba, radiative collisional fluoresc. obs. from thermally excited atoms 0-102480
- TlI, atomic fluorescence, D $_2$ pressure effect on width and shift 0-99475
- U+molecule, collisional relax. of highly excited states, laser-induced fluoresc. obs. 0-58205
- ^{235}U , ground and $1st$ excited states, hfs, laser fluoresc. and laser-RF double reson. spectroscopy 0-58170

atomic fluorescence spectroscopy see atomic emission spectroscopy

atomic forces

- anharmonically coupled oscillators, semiclassical calcs. of eigenvalues 0-95514
- diatomic mols., electronegativity, bond charge and chemical pot. approach 0-91703
- electrostatic pot.-electronic density relationships 0-69206
- hydrogenic ion lines, red shift in plasma 0-103128
- interaction dipoles, perturbation theory 0-78680
- microcosm and macrocosm, discrete modelling 0-82643
- neutral atoms, stimulated Coulomb interaction in external resonance field 0-83449
- polyatomic mols. in liqs., vibr. energy relax. 0-63611
- Schwinger and Kohn variational phase shift calculations, comparison 0-78672
- screened Coulomb pots., perturbation theory approach 0-63524
- surface, adsorbed atoms thermal desorption, one dimens. microscopic model, weak binding case 0-96729
- surface processes, interatomic forces, theories 0-107632
- Ca+Xe, collision-induced dipole transition due to long range interaction, absorpt. obs. 0-63779
- H, low density atomic gas props., dil. hard sphere Bose gas model calc. 0-87194
- He-He, Born Oppenheimer pot. using Hylleraas-type electronic wave functions 0-91442
- He $_2$, ground state, interaction energy, many-body perturbation theory calcs. 0-69210
- ^4He , threshold condition for forming atomic trimer 0-63741
- NaKr, red wing radiation and pot. 0-87180
- ^{87}Rb + ^{129}Xe , spin-exchange cross-section meas. 0-78686

atomic hyperfine structure

- see also Lamb shift
- alkali atoms, excited state, laser photoionisation theory, hyperfine coupling effect 0-102493
- alkali metal radioisotopes, hyperfine spectroscopy, nucl. props. 0-57677
- autoionising states, electron angular distribution, fine and hyperfine struct. 0-58222
- excited nuclear levels, polarisation induced by at. orientation 0-91144
- first row atoms and ions, LSD approx., density functional calcs. 0-78720
- kaonic atoms, quadrupole hyperfine structure 0-78726
- metastable autoionising states, ang. distrib. of electrons which decay via fine and hyperfine struct. interactions 0-102492
- multiple anticrossings in atomic spectroscopy 0-87091
- muonium hyperfine structure of ground state, magnetic moments, muonium-antimuonium conversion, excited states 0-69273
- neutral atom collisions, hyperfine component broadening and shift of spectral lines 0-74136
- ponic atoms, quadrupole hyperfine structure 0-78726
- RF superradiance optical pulse generated under photon-echo conditions 0-95588
- spin exchange collisions, Pauli principle effects 0-99535
- two step reson. photoionisation, multimode and level degeneracy effects 0-78583
- two-level system, hyperfine struct. transitions, weak interaction meas. (Russian) 0-58196
- Ag electron excited $L\alpha$ emission spectra 0-102481
- Al XIII, $1s2p^2P_2$ and $1s2p^2P_0$ levels, radiative lifetimes and hyperfine induced decay 0-74149
- Ba, atomic beam and resonance spectroscopy 0-58180
- Ba, hyperfine splitting and isotope shift of high lying levels, Doppler-free 2-photon laser spectroscopy 0-58215
- Ba II, $5d^2D_{3/2,5/2}$ isotope shifts, hyperfine struct., collinear fast beam laser spectroscopy 0-83310
- Ba, radioisotopes, at. beam laser spectroscopy, hyperfine struct., nucl. moments and radii 0-57678
- BaI resonance transitions, hyperfine struct. and isotope shifts, atomic beam laser spectroscopy 0-102141
- Bi, Faraday effect and magnetic circular dichroism 0-83399
- C, $^5S_{3/2}$ and $^3S_{3/2}$ transitions, ^{13}C isotope shift 0-58201
- Ca, stable and radioisotopes, hfs, isotope shifts, dye laser saturation spectroscopy, beam expt. 0-58169
- ^{43}Ca , atomic beam and resonance spectroscopy 0-58180
- Cd, $5s5^3P_1$ - $5s^2$ 1S_0 intercombination line, press. broadening and shift 0-95564
- Cs, excited state, laser photoionisation theory, hyperfine coupling effect 0-102493
- Cs $^+$ HFS pressure effect determ. from absorption coeff. profiles 0-106299
- Cs $^+$ excited levels, hyperfine struct. and lifetimes 0-63590
- ^{133}Cs , first excited D-level, hyperfine struct. meas. by cascade, fluoresc. spectroscopy 0-69101
- Dy, visible spectra obs., hyperfine struct., mag. dipole and electric quadrupole interaction const. anal. 0-91698
- Fe series atoms and ions, LSD approx., density functional calcs. 0-78720
- ^{57}Fe metastable states, hyperfine struct. meas. by laser RF double-resonance 0-58404
- H, double-quantum saturation spectroscopy, laser and RF 0-77880
- H hyperfine splitting inside paraboloidal surfaces 0-99445
- H+D, close coupling calc., resonant spin-flip process, Ramsauer-Townsend effects 0-99547
- He, Doppler-free two-photon high resolution spectroscopy 0-58197
- He, muonic, formation and hyperfine struct. 0-91707
- ^3He atom forbidden singlet-triplet anticrossings, D levels 0-99491
- ^3He , hyperfine-induced singlet-triplet mixing obs. 0-106399
- I atomic vapour, self-induced transparency and reson. self focusing 0-64114
- ^{129}I , hyperfine struct. and isotope shift of 1.3 μm transition 0-102486
- ^{39}K , first excited D-level, hyperfine struct. meas. by cascade, fluoresc. spectroscopy 0-69101
- ^{83}Kr , weak hyperfine component detect., time averaging using dye laser spectrometer 0-101850
- ^{139}La II $5d^2$ 4F_4 - $5d4f$ $^3F_4^0$, hyperfine structure, $\Delta F=\pm 2$ transitions, three-quantum process 0-63848
- Li ground state, HFS 0-91699
- Li $^+$, 3P and 3S states, fine (hyperfine) struct., dye laser saturation spectroscopy, beam expt. 0-58169
- ^ALu , $A=175,176$, $5d6s^2D_{3/2}$ - $5d6s6p^4F_{3/2}$ transition; isotope shift and hyperfine struct. 0-83309
- Mg $^+$ laser cooled ions bound in Penning trap, high-resolution optical spectra 0-102487

atomic hyperfine structure continued

- Mn, $3d^4 4s^1 D_{1/2-9/2}$ hfs from laser-RF double reson. spectroscopy 0-57682
 ^{14}N II, $2p^3 P_1$, hyperfine struct. after ion beam surface impact at grazing incidence 0-58403
 Na vapour, superradiance, quantum beat spectra 0-106311
 ^{16}O ions, mag. hyperfine interactions, PAC meas. 0-95734
 P I, IR spectra and HFS 0-91478
 Pr, metastable, $F=7-6$ Hfs, laser-RF double reson. spectroscopy 0-58170
 $^{85,87}\text{Rb}$, first excited D-level, hyperfine struct. meas. by cascade, fluoresc. spectrosc. 0-69101
 Sm, and isotopes, hfs, laser-RF double reson. spectroscopy 0-58170
 SmI, laser atomic beam spectroscopy, isotope shifts, hyperfine struct., transitions 0-102468
 Tm I, hyperfine struct., high resolution spectrosc. meas. 0-87238
 ^{235}U , ground and 1st excited states, hfs, laser fluoresc. and laser-RF double reson. spectroscopy 0-58170
 Yb I, high Rydberg levels of $4f^{14} 6s$ nd configs., very high resolution obs. 0-106300

atomic inelastic collisions

- see also atom-atom collisions; atom-ion collisions; atom-molecule collisions; atom-molecule reactions; beam-foil spectra; ionisation of atoms*
 analysis using charact. noise of strong EM wave 0-99492
 angular correlations, summary of review papers 0-63577
 atoms, general adiabatic-diabatic transformation matrix, electronic non-adiabatic transitions 0-93751
 atoms in solids, focusing and defocusing collisions model 0-82618
 chemical ionisation, classical description, complex interaction pot., exponential representation 0-99570
 classical many-body collision model incorporating Heisenberg and Pauli principles 0-63511
 coherence and correlation in atomic collisions, book 0-90615
 collisional and radiative damping effects in Rayleigh and reson. fluorescence scatt. at high intensities 0-102478
 diatomic transition operators, L^2 basis expansions 0-63519
 electron scattering, free free processes 0-83834
 excitation, target atom decay, scatt. projectile and photon coincident detect., coherence effects 0-63791
 lasers, atomic and molecular, appl. to collision physics 0-63596
 muonic D+Y, muon transfer mechanism from free muonic deuterium 0-69218
 muonic H+Y, muon transfer mechanism from free muonic hydrogen 0-69218
 nonlinear optical phenomena in system of colliding atoms, atomic fluoresc. 0-99788
 one-electron atom, rearrangement collisions in laser radiation field 0-74225
 optical collisions, solvable model 0-91638
 polarisation in atomic and nuclear physics 0-63162
 potentials, anisotropic, from rotationally inelastic and elastic cross sections, direct inversion method 0-69090
 radiative collisions, solvable model 0-91638
 reduced phase space approach calcs. 0-83438
 three-state atom, saturated two-photon absorpt. in perturber gas 0-106310
 two-state atom, resonance fluoresc. spectra, collisional broadening 0-91484
 two-state atoms irradiated by monochromatic light, reson. fluoresc. spectra, collisional broadening 0-91483
 two-state collision problems, distorted-wave formula for transition probabilities 0-69212
 vapours, three-level system, collisional effects in saturation spectroscopy, appl. to Na 0-78579
 X-ray and UV lasers appls. 0-64787
 Ar, gas, electron thermalization time and position distribution meas. 0-93771
 Cd, $5s5p^3 P_1-5s^2 \text{ } ^1S_0$ intercombination line, press. broadening and shift 0-95564
 (D,T), reaction rate parameter, temp. dependence, fusion process in Maxwellian DT plasma 0-59254
 ^{151}Eu (^{153}Eu) excitation transfer, effect on selective photoionisation 0-99538
 H, electron-photon angular correlation meas. for excitation of 2P state 0-91636
 H like atom alignment due to electron capture in particle-atom collisions (Russian) 0-106379
 H, Stark effect, scatt. theory methods obs. 0-63586
 He, 3^3D level, fine struct. changing collisions in glow discharge 0-58346
 He, collisional excitation transfer for 3^1P and D states 0-106387
 He I 2^3P-3^1D intercombination line, collision-induced, obs. by laser absorpt. spectroscopy 0-58194
 He- ^3He mixture, relax. of 2^3S_1 metastable atoms 0-102469
 K Rydberg states, optical excitation, collision ionisation processes 0-102561
 Kr, gas, electron thermalization time and position distribution meas. 0-93771
 Na, D-lines, inert gas broadening, photon echo meas. 0-91475
 Na+Ne, potential curves from a model potential (French) 0-78685
 Ne, $1s_2$ metastable, velocity-changing collisions, study by time resolved saturated absorption 0-82832
 Ne, gas, electron thermalization time and position distribution meas. 0-93771
 $^{87}\text{Rb}+^{129}\text{Xe}$, spin-exchange cross-section meas. 0-78686
 Sr-Cs mixture, laser induced collisional two-photon ionisation, fluoresc. monitoring 0-91515
 Ti, 535.0 nm line shift by H_2 perturber 0-91506
 Xe, gas, electron thermalization time and position distribution meas. 0-93771

atomic magnetic moment

- see also gyromagnetic ratio*
 muonium hyperfine structure of ground state, magnetic moments, muonium-antimuonium conversion, excited states 0-69273
 Bi, Faraday effect and magnetic circular dichroism 0-83399
 H atom, form factor for arbitrary states, dipole moment component matrix element calcs. (Russian) 0-58143
 ^4He , muonic, formation and hyperfine struct. 0-91707
 I atomic vapour, self-induced transparency and reson. self focusing 0-64114

atomic magnetic moment continued

- O II, relative intensities and lifetimes in nebulae, conventional radiation theory 0-109513
 TiXIV(TiXV)(TiXVII), Tokamak discharge, ground state, mag. dipole transitions, UV spectra obs. 0-63575
- atomic mass**
see also isotopes; mass spectra; nuclear mass
 reaction with time and expansion of Universe 0-90588
- atomic metastable states**
 metastability exchange collisions, Pauli principle effects 0-99536
 metastable autoionising states, ang. distrib. of electrons which decay via fine and hyperfine struct. interactions 0-102492
 multiphoton transition detection 0-58231
 Penning ionisation processes investig. by electron spectroscopy 0-58364
 Ar plasma, radial distrib. of excited atoms prod. by surface wave (French) 0-96349
 Ar($^3P_{0,2}$), excitation of $\text{N}_2(\text{C}^3\Pi_u)$, symmetry, propensity rules and alternation intensity, rot. spectrum 0-87135
 Ar($^3P_{0,2}$)+H(2S), energy transfer collisions, Lyman- α emission profile obs., in microwave discharge and reaction cell 0-58359
 Ar*+Fe(CO) $_5$, chemiionisation and chemiluminescence reactions, Penning ionisation and fluoresc. obs. 0-97689
 Ar*+H, assoc. ionis., rovibronic struct. in electron energy spectrum 0-106380
 Ar*+H, collisional quenching rates 0-95548
 Ar*+O $_2$, ion pair form. explained by charge transfer model 0-99546
 Ba ($5d6p^3$) D_3 state, lifetime meas. by dye laser spectrosc. 0-78577
 Ba, atomic beam and resonance spectroscopy 0-58180
 C(2^1S_0)+H $_2$ (O $_2$)(ethylene), collisional behaviour, kinetic study 0-74241
 Ca, forbidden transitions, radiative lifetimes, MCSF and CI calcs., time of flight spectra for metastable state 0-91498
 Ca+Ca(Mg)(inert gas), metastable 3P -state, quenching reactions, fluoresc. meas. 0-102477
 ^{43}Ca , atomic beam and resonance spectroscopy 0-58180
 Ca*+HCl, reaction performed under high resolution, luminescence obs. 0-95662
 Cd(3P_0)+CO(CO $_2$)(NO), absolute quenching cross section, phase-shift method 0-58340
 Dy, isotope shift meas. using laser atomic beam technique specific mass shift determ. 0-91497
 ^{57}Fe metastable states, hyperfine struct. meas. by laser RF double-resonance 0-58404
 H($2s$), optical model approach to elastic scattering of electrons, polarisation effects 0-58382
 He, $2S$ metastable states, singlet and triplet; two and three photon ionisation cross section, absolute determ. 0-83329
 He, Doppler-free two-photon high resolution spectroscopy 0-58197
 He, metastable, multiphoton transition detection, n^3S-n^3D splitting meas. 0-58231
 He metastable state, two- and three-photon ionisation 0-91518
 He, metastable states, electron and proton impact ionisation, autoionisation 0-102573
 He, positive column plasmas, metastable atom density meas. by improved self absorpt. method 0-87968
 He- ^3He mixture, relax. of 2^3S_1 metastable atoms 0-102469
 He+CS $_2$, metastable atoms, energy transfer processes 0-83466
 $^3\text{He}(^4\text{He})$ clusters, metastable electronic states, electron impact excitation, time of flight spectra 0-106411
 He*, impact on Mo surface, clean and gas covered, deexcitation, pot. energy transfer mechanism 0-60743
 He* impact on Pd (111) surface, clean and CO covered, electron emission, energy and ang. distrib. 0-60744
 He*-Ne*, Penning ionisation of metastable He* 0-83472
 Hg(6^3P_1)+Hg(6^3P_2), line excitation and population decay in afterglow 0-74242
 ^{86}Kr , discharge, metastability-exchange cross section 0-99464
 ^{86}Kr - ^{78}Kr , discharge, metastability-exchange cross section 0-99464
 Li $^-$, core-excited bound states 0-91468
 N(2D), 2P metastable production by electron collisions in DC glow discharge 0-59274
 Ne, $1s_2$ metastable, velocity-changing collisions, study by time resolved saturated absorption 0-82832
 Ne ($2p^3 3p$) states, radiative lifetimes, collisional deactivation rate consts. 0-69107
 Ne, metastable electronic states, electron impact excitation, time of flight spectra 0-106411
 Ne positive column plasmas, metastable atom density meas. by improved self absorpt. method 0-87968
 Ne-N $_2$, AC discharge, pulse to continuous mode transition, Ne metastable effects (German) 0-84011
 Ne+CS $_2$, metastable atoms, energy transfer processes 0-83466
 Ne($^3P_{0,2}$)+Ne, differential cross sections 0-58370
 Ne(3P_2) elastically scattered, metastable, ang. distrib., conventional rel. to Doppler shift methods 0-58418
 Ne* 5882 Å line, Doppler free spectra, press. broadening and shifts, saturation spectroscopy 0-78565
 Ne*+Ar, associative ionisation studied by merging-beams technique 0-91646
 Ne*+Ar*, Penning ionisation studied by merging-beams technique 0-91646
 Ne*+Fe(CO) $_5$, chemiionisation and chemiluminescence reactions, Penning ionisation and fluoresc. obs. 0-97689
 Ne*+H, assoc. ionis., rovibronic struct. in electron energy spectrum 0-106380
 Ne*+H $_2$ O, pot. energy surfaces, MO and CI calcs., Penning ionisation electron spectra 0-106376
 O $^+$ +N $_2$ (O $_2$), excited ion reactions, charge transfer coeffs. at thermal energy 0-95721
 O $^+$ (4D) in thermosphere, quenching by electrons 0-94630
 O $^+$ (4D) metastable state, temp. depend. of rate coeff. for charge exchange with N $_2$ 0-77179
 O $^{++}$ +N $_2$ (O $_2$), metastable ion reactions, rate consts. and ion mobility at 300K 0-95722
 Pr, metastable, $F=7-6$ Hfs, laser-RF double reson. spectroscopy 0-58170
 Sr*+HCl, reaction performed under high resolution, luminescence obs. 0-95662
 Tm I, hyperfine struct., high resolution spectrosc. meas. 0-87238
 Xe+Br(CCl $_4$), excitation functions and rotational polarisation, chemiluminesc., crossed beam study 0-76491

atomic metastable states continued

Xe+Ne, quenching of excited Xe^{*}(³P₂, ³P₁, ¹P₁) states 0-63578
Xe(nf)+SF₆, l-changing collisions obs. 0-91633

atomic orbitals *see atomic structure***atomic orbitals calculations**

see also GO calculations; GTO calculations; STO calculations
correlated wave functions anal. gradients from two particle density matrix and unitary group 0-78548
correlation coefficient and electron correlation 0-78552
dynamic multiple polarisability, dispersion forces and oscillator strengths, Coulomb approx. 0-63520
education, Na Rydberg states, anomalous fine struct., perturbation model 0-57035
electron+ion scattering, Schwinger's variational principle, Rydberg states 0-78713
ethane, CH bond orbitals, internal rot. barriers, antisymmetrization effects 0-63529
excited atomic states, bound and free, inner charge defect method calcs. 0-78511
extended Numerov method for the numerical solution of the Hartree-Fock equations 0-83245
heavy ion+atom collisions, small impact parameters, K-vacancy prod., molecular theory 0-69229
HF model, nucl. charge rel. to orbital contribution to values $\langle r_{12}^{-n} \rangle^{1/n}$ 0-58115
hydrogenic functions, Gaussian expansions involving few variational parameters 0-91420
hydrogenic Gaussian lobe functions 0-74102
many-body perturbation theory with radially restricted basis functions 0-78526
modified virtual orbitals, for config. interaction calc. 0-58163
momentum eigenfunctions in complex momentum plane, Hartree Fock functions 0-63517
Mossbauer atoms, electron densities at nuclear centre and surface, calcs. using Dirac-Fock eqn. 0-74100
perturbation var. calc. with contact interaction, effect of approx. zero order wavefunctions 0-58107
quadrupole shielding factors calc. using elec. field variant orbitals 0-106276
second row atoms, contracted Gaussian basis sets for mol. calcs. 0-83264
singlet-triplet energy difference and singlet generalised oscillator strength, Lassetre-Dillon relation 0-63508
Slater's calculations, improved screening-loss parameter calc. 0-83271
spherical harmonics problems, identities 0-63515
total electronic energy, atoms and mols., SCF binding energy, Z⁻¹ perturbation theory 0-83268
transition metal atoms, neutral and ion val. states, electron correlation, ab initio effective val. Hamiltonian calc. 0-99449
two electron atom, energy levels, classical first order perturbation theory 0-58118
two-electron wave functions with monopole interaction, asymptotic forms 0-78528
X α method with pseudopotentials 0-83282
Ar, momentum eigenfunctions in complex momentum plane, Hartree Fock functions 0-63517
C, one-centre integrals of semiempirical theories of valence, ab initio calcs. 0-102441
Cl, photoionisation cross section and reson. theory, many body perturbation theory, 3p and 3s subshells 0-69114
Cl⁻, contracted Gaussian basis sets for mol. calcs. 0-83264
Eu, electron impact excitation cross section, Born and Ochurk approx. 0-87230
F, ab initio effective valence shell Hamiltonian for neutral and ionic valence states 0-74117
H, electron elastic scatt., exchange perturbation theory 0-78709
H, Stark and photoabsorption spectrum, density of oscillator strengths, atom c.f. semiconductor spectra 0-83318
H, Stark spectrum and field ionisation, density of continuum states, normalised wavefunctions 0-83317
H⁻, many-body perturbation theory with radially restricted basis functions 0-78526
HD, perturbation var. calc. with contact interaction, effect of approx. zero order wavefunctions 0-58107
He energy levels, classical first order perturbation theory 0-58118
He-He, Born Oppenheimer pot. using Hylleraas-type electronic wave functions 0-91442
Li electronic impact excitation, energy level calcs. (*Chinese*) 0-83488
Li isoelectronic sequence, self-consistent relativistic density-functional theory 0-91441
Li⁻, core excited bound states in beam foil expts., CI calcs. 0-78559
N, ab initio effective valence shell Hamiltonian for neutral and ionic valence states 0-74117
Na+H⁺, 2p³3s²2p_{1/2} state alignment, collisionally induced, impact parameter calc. 0-83474
Ne, momentum eigenfunctions in complex momentum plane, Hartree Fock functions 0-63517
O, ab initio effective valence shell Hamiltonian for neutral and ionic valence states 0-74117
O V, E1 transition probabilities, lifetimes, CI calc. 0-83321
P, ab initio effective valence shell Hamiltonian for neutral and ionic valence states 0-74117
P⁻, contracted Gaussian basis sets for mol. calcs. 0-83264
S, ab initio effective valence shell Hamiltonian for neutral and ionic valence states 0-74117
S⁻, contracted Gaussian basis sets for mol. calcs. 0-83264
Si, ab initio effective valence shell Hamiltonian for neutral and ionic valence states 0-74117
Ti, 4d^{3d} and 3d⁴ states, HF descriptions, alternative orbital config. 0-63534
Ti, neutral and ion val. states, electron correlation, ab initio effective val. Hamiltonian calc. 0-99449
⁹²U, self-consistent relativistic density-functional theory 0-91441
Yb, electron impact excitation cross section, Born and Ochurk approx. 0-87230

atomic polarisability

atom+atom collisional intense-field fluoresc., Zeeman degeneracy effects 0-99477
atoms, polarisation of electrons and nuclei in resonant multiphoton ionisation 0-99486

atomic polarisability continued

contact term, link with polarisability, use of local spin density functional method 0-58158
dipole polarisability 0-58148
dynamic multiple polarisability, dispersion forces and oscillator strengths, Coulomb approx. 0-63520
first-row atoms, SCF calcs. using cusped-Gaussian basis sets, polarisation effects 0-74118
interacting atoms, retarded energy shift and pair polarisability, field theoretical perturbation theory 0-102560
ion collisions, electron capture, atomic excited state polarisation, optical detection 0-58377
Kirkwood-Pople-Schofield method, appls. to polarisabilities calcs. 0-83272
photoionisation, fluoresc. radiation polarisation 0-87076
quantum systems, at. or spin two level, reson. EM wave excitation, free induction decay oscils. 0-63562
quinazolines, enzyme inhibitory, structure-activity quantitative study 0-78540
ring laser, collision model, averaged, in active medium polarizability theory 0-95924
surface-atom polarisability derivation from field-ion energy deficits 0-76155
Be, correl. contribs. to dipole polarisability, coupled HF-perturbation theory 0-106269
Cd, ¹S, ³P, ¹P states, dipole polarisabilities from compact variational trial functions 0-63568
Cs⁺ dipole and quadrupole polarisability fine struct. intervals and g-factor interval 0-91477
H interacting with EM vacuum fluctuations, ground state energy in multiply connected universes 0-87050
H-like atoms, dipole polarisability of arbitrary hybrid bound states 0-87237
H(2s), optical model approach to elastic scattering of electrons, polarisation effects 0-58382
He, correl. contribs. to dipole polarisability, coupled HF-perturbation theory 0-106269
He, electron scatt. at intermediate energy, quantum mechanical treatment 0-91687
He, static multiple polarisabilities, integral equation approach to scaled 1/Z expansion 0-63846
He triplet states, doubly excited, spectrum and polarisation 0-99472
He+He⁺(Ne), tensor polarisabilities of l_{nsd} ¹D level, fluoresc. depolarisation obs. 0-69099
Hf IV, 6s ²S_{1/2}-6p ²P_{1/2,3/2} transition, relativistic oscillator strengths, influence of core polarisation 0-58132
Hg, ¹S, ³P, ¹P states, dipole polarisabilities from compact variational trial functions 0-63568
K⁻, photodetachment and at. polarisability 0-91522
Li(2p)+H₂(N₂), Li(2p) excitation, alignment and orientation obs. 0-63794
Lu III, 6s ²S_{1/2}-6p ²P_{1/2,3/2} transition, relativistic oscillator strengths, influence of core polarisation 0-58132
Mg isoelectronic sequence, static dipole quadrupole polarisabilities and shielding factors calc. using HF scheme 0-99450
Na, saturation spectra, crossover signals, effect of atomic alignment, optical pumping 0-58202
Ne, correl. contribs. to dipole polarisability, coupled HF-perturbation theory 0-106269
Ne, dipole dynamic polarisabilities and two-photon photoionisation cross section calc., R-matrix approach 0-102444
Pr³⁺, elec. multiple polarisabilities, discrete basis set calcs. 0-91456
Yb, 4f¹⁴6s6p ³P₁ and ³P₁ levels, Stark effect, tensor polarisabilities 0-87080
Yb II, 6s ²S_{1/2}-6p ²P_{1/2,3/2} transition, relativistic oscillator strengths, influence of core polarisation 0-58132
Zn, ¹S, ³P, ¹P states, dipole polarisabilities from compact variational trial functions 0-63568

atomic positron scattering *see atomic electron impact excitation; atomic electron impact ionisation; elastic scattering of electrons by atoms and molecules*

atomic power *see nuclear power*

atomic reactors *see fission reactors*

atomic resonant states
atom resonant scattering by light, quantum struct. (*Russian*) 0-78580
dressed atom system, energy levels and reson. phenomena, universal algorithm 0-69111
dressed atom system, phase represent. applic. to reson. fluoresc., universal algorithm 0-69112
hole-burning in at. vel. distrib. by EM radiation 0-64674
ionisation spectroscopy, reson. chem.-physics appls. 0-68259
multichannel threshold structures in scattering theory 0-58334
multicharged ion thermal charge exchange reaction, rel. to astrophysics 0-63815
n-photon resonance phenomena, finite laser bandwidth effect 0-58230
quantum systems, at. or spin two level, reson. EM wave excitation, free induction decay oscils. 0-63562
resonance eigenvalues, accuracy criteria 0-91423
resonance partial widths and partial photodetachment rate using the rotated-coordinate method 0-91428
rotated-coordinate method, rel. to stabilisation method 0-74097
Rydberg spectra, Landau standing wave form. 0-102466
semiclassical two electron atom, appl. of semiclassical equivalent of Hylleraas var. method 0-58111
Stark resonances, stabilisation method calcs., convergence 0-91492
two level atom in low freq. EM field, quasienergetic states (*Russian*) 0-91471
two-level atom, radiation by intense laser beam, resonance fluorescence, photon antibunching, Doppler shift 0-74146
two-level atom, reson. fluoresc., atomic operators 0-63579
two-level system, hyperfine struct. transitions, weak interaction meas. (*Russian*) 0-58196
two-level system, optimal control of resonance radiation processes 0-106498
wavefunctions of complex coord. method 0-106282
Al, autoionisation reson. determ. from photoelectron polarisation meas. 0-58221
Ba I, quasi-Landau spectrum, semiclassical strong field mixing models 0-63847
Be⁻, ²P shape resonances, shift potential calcs. 0-69089

atomic resonant states continued

- C, ground state fine struct., laser mag. reson. obs. 0-87062
 Ca II H-K solar lines, non-mag. polarisation 0-63569
 Cl, photoionisation cross section and reson. theory, many body perturbation theory, 3p and 3s subshells 0-69114
 Cs-H₂ vapour, resonant character of laser induced formation of particles 0-89481
 Cu vapour laser, energy conversion efficiency, reson. levels excitation 0-99715
⁵⁷Fe metastable states, hyperfine struct. meas. by laser RF double-resonance 0-58404
 H I s reson., stabilisation method calcs., convergence 0-91492
 H detection by reson. fluoresc., coherent tunable VUV generation near Ly-β transition 0-99798
 H₂, double-quantum saturation spectroscopy, laser and RF 0-77880
 H⁺, ^p(1) and ^p(1) resonances associated with n=3 hydrogenic threshold 0-78557
 H⁺ resonances in electric field 0-63607
 He, 2^S-state, electron impact excitation, reson. form. mechanism 0-99463
 He, appl. of semiclassical equivalent of Hylleraas var. method appls. 0-58111
 He, spectral lines, singlet, self-broadening, resonant interaction 0-63574
 He⁻, inelastic Feshbach resons., quasi projection operator calc. 0-58395
 He⁺, electron scatt., reson. state assoc., incomplete spectrum of Hamiltonian matrix 0-99568
 Hg resonance line, 253.7 nm for atomic absorpt. meas. 0-78556
 I II, reson. lines, oscill. strengths determ. by absorption method 0-58214
 Li, inelastic Feshbach resons., quasi projection operator calc. 0-58395
 Mg⁺, shape resonances, shift potential calcs. 0-69089
 Mg⁺ laser cooled ions bound in Penning trap, high-resolution optical spectra 0-102487
 Na, four- and six-photon resonance spectra (Russian) 0-91527
 Na I solar D-lines, non-mag. polarisation 0-63569
 Ne⁺ scatt. electron spectra, distinction from neutral autoionising states 0-83482
 O VI, 2s²-2p² reson. lines, wavelength determ. 0-102470
 Rb, situated in external elec. field, near zero energy reson. anal. 0-63563
 Sr I, quasi-Landau spectrum, semiclassical strong field mixing models 0-63847
 Th, reson. localised 5,f continuum state, giant reson. 0-91467
 Tl, autoionisation reson. determ. from photoelectron polarisation meas. 0-58221
 U atomic beam, two laser irradi., two photon reson. effects., visible spectra 0-63604
 Xe, autoionising reson., Stark effect 0-58198
 Xe, resonantly enhanced multiphoton ionis., photoelectron energy anal. 0-63597
 Xe⁺+Xe, Xe I reson. line excitation 0-87220
 Yb highly excited levels, reson., visible two photon absorpt. spectra obs. 0-58228
 Zr VIII, reson. transitions in UV 0-91479

atomic scattering factors see *crystal atomic structure; crystallography; lattice dynamics*

atomic spectra

- see also *atomic fluorescence; atomic hyperfine structure; atomic spectral line breadth; atomic structure; beam-fol spectra; conversion electron spectra; radiative corrections; Russell-Saunders coupling; Stark effect; Zeeman effect*
 A=1-257, nuclear excitation by atomic electron transitions, nuclear levels 0-78191
 air, plasma, optical absorpt. coeff. at 1000 atm, 13000K, N₂⁻ photodissoc. 0-64691
 alkali metals, Stark and photoabsorption spectrum, density of oscillator strengths, atom c.f. semiconductor spectra 0-83318
 atomic scatt. factors and momentum densities, asymptotic form 0-74105
 atoms, 70≤Z≤82, Kα X-ray linewidths and relative intensities, energy dispersive meas. 0-99483
 atoms, reson. radiation force, quantum mech. fluctuations, influence on at. motion 0-58233
 collision systems α(Z₁+Z₂)≥1, quasimolecular 1 sσ orbital, excitation and spectroscopy 0-87199
 double radiooptical resonance, signal propag. and shape 0-87360
 free atoms, diagram Auger electron spectra 0-78585
 gaseous molecules, persistence of p, d, f and g orbitals, ang. functions, Schrodinger's eqn. and cardinal number anal. 0-102426
 high resolution two-photon FM laser spectroscopy of gas atoms, free of Doppler broadening 0-95748
 highly excited atoms, review 0-58174
 homologous ions series, Stark broadening trends 0-105157
 hook spectra, evaluation limitations 0-90905
 inert gas mixture, collision induced microwave absorpt. spectra 0-74216
 ion+atom collision produced highly excited states, decay spectra 0-63780
 k ordering of atomic and ionic energy levels 0-74095
 laser interaction, high intensity, Faisal's theory refinement (Chinese) 0-58195
 line wings, polarized radiative transfer, excited state interference 0-105158
 strong magnetic field effects, theory rel. to spectra of dense stars 0-105160
 Moseley's expts.: Kα line freqs., rel. to at. number, reinterpretation 0-82616
 multiple anticrossings in atomic spectrosc. 0-87091
 muonic atoms, X-ray emission polarisation (German) 0-69268
 muonic X-rays, circular polarisation (German) 0-69266
 near threshold struct. in K-shell spectra, photoionisation or fast charged particle ionisation 0-87064
 np³ ions, forbidden lines, balance and line intensity ratios 0-83305
 oriented atoms, electronic Raman reson. scatt., statistical theory 0-102467
 photoionisation, selective, use in laser isotope separation and spectrosc., review 0-83332
 pionic atoms, electron screening and inner shell refilling, X-ray 0-78729
 planetary nebulae, theory of physical processes rel. to emission line spectra 0-109527
 protonium, atomic X-ray yields 1s and 2p level shifts and widths, cascades, calc. 0-78730
 radiation lifetime laws in spectral series of atoms and ions 0-74150

atomic spectra continued

- radiation trapping, analysis using charact. noise of strong EM wave 0-99492
 rare gas adsorbates on simple metals, optical excitation, configurational switching, charge transfer 0-107643
 Rydberg spectra, Landau standing wave form. 0-102466
 spontaneous radiation, near field calcs. 0-99493
 three-state atom, saturated two-photon absorpt. in perturber gas 0-106310
 two level atom, coherent and Raman scatt. spectra, secondary emissions 0-69449
 two level atoms, absorption spectra of optical bistability with dispersion 0-102757
 two-level atom, interaction with radiation, photon number time evolution 0-58216
 two-level system, hyperfine struct. transitions, weak interaction meas. (Russian) 0-58196
 Ag, polarised photoelectron yields in VUV region 0-106307
 Ag+H⁺, excited X-ray polarisation, Born approx. calcs. (Russian) 0-78566
 Al spectral line, hollow cathode discharge, pulse feeding 0-64797
 Al, vacuum arc, excited state density from line intensities 0-96404
 Al³⁺ foil-excited ion, X-ray spectra and satellite classification 0-95567
 Ar, K inner-shell level energies, absorpt. spectroscopy with synchrotron radiation 0-99583
 Ar, absorpt. spectra, field induced autoionisation near ionisation threshold 0-106301
 Ar, electron impact, L X-ray spectrum, radiative Auger transitions 0-58227
 Ar II arcs, transition probabilities, statistical inference 0-106357
 As I, level identification and Zeeman effect obs. 0-95571
 As VI, VII, spectra 100 to 300 and 500 to 1200 Å ranges 0-83307
 Ba (5d6p)³D₃ state, lifetime meas. by dye laser spectrosc. 0-78577
 Ba II, 5d²D_{3/2,5/2}, isotope shifts, hyperfine struct., collinear fast beam laser spectroscopy 0-83310
 Ba, saturation spectroscopy with laser optical pumping 0-83324
 Be III, doubly excited states, triplet spectra 0-87069
 C, ³S₃P₂ and ³S₃P₁ transitions, ¹³C isotope shift 0-58201
 C, ground state fine struct., laser mag. reson. obs. 0-87062
 C I 1101 Å absorpt. edge in A-type stars, effect of C+H⁺→C⁺+H charge transfer 0-90423
 C II, Zeeman splitting of high-n recomb. lines 0-58210
 C II line excitation by C I photoionisation 0-58223
 C IV (CV), UV line identifications and lifetime meas. 0-106288
 C plasma, spectral and absorpt. coeffs. 0-69985
 C V, electron impact collision rates, reinterpretation of solar emission line ratios 0-98624
 Ca, 4p² ¹S₀-4s4p ¹P₁-4s² ¹S₀ cascade rate, two photon coincidence meas. technique 0-95576
 Ca II H-K solar lines, non-mag. polarisation 0-63569
 Ca+Xe, collision-induced dipole transition due to long range interaction, absorpt. obs. 0-63779
 Cd, 5s5p²P₁-5s² ¹S₀ intercombination line, press. broadening and shift 0-95564
 Cd IV, UV spectral analysis 0-83306
 Co, n=2-2 transitions in XUV spectra, anal. 0-102472
 Co, X-ray transitions in laser produced plasma 0-100093
 Co XI-XVII laser 3s²3p³-3s3p⁴ transition arrays, UV spectra classification 0-63570
 Cr, multiphoton ionisation and absorpt. 0-95575
 Cr, n=2-2 transitions in XUV spectra, anal. 0-102472
 Cr, X-ray transitions in laser produced plasma 0-100093
 Cr(II) lines, oscill. strengths in 2413-2718 Å wavelength range 0-106294
 Cs atomic clock using laser optical pumping of Cs beam 0-101785
 Cs, hook spectra, evaluation limitations 0-90905
 Cs, two photon ionisation, destructive interference effect 0-74153
 Cs⁺ excited levels, hyperfine struct. and lifetimes 0-63590
 Cs²⁺, electron impact excitation studies by intersecting beam method 0-69239
 Cs+He, interaction pot. and oscill. strength 0-91645
 Cu I, high-dispersion absorpt. spectrum obs. 1570 to 2500 Å 0-78564
 Cu IV, wavelength region 700-1200 Å, extended analysis 0-99473
 Cu-like ions, 4s-4p reson. lines and transitions obs. by means of laser prod. plasma, appl. to Tokamaks 0-99468
 Cu+Cu collisions, Kα X-ray energy shifts, target thickness depend. 0-83311
 D, adsorbed on graphite (0001), vibr. spectrum, at. beam scatt. obs. 0-92779
 Dy, isotope shift meas. using laser atomic beam technique specific mass shift determ. 0-91497
 Dy, visible spectra obs., hyperfine struct., mag. dipole and electric quadrupole interaction const. anal. 0-91698
 F, spin-orbit splitting and ²P_{1/2} radiative lifetime, absorpt. spectrosc. meas. 0-87063
 Fe, fine struct. levels fitting, config. interaction effect, spin-orbit and electrostatic interaction parameters 0-69248
 Fe I, a³F₂ levels, relative oscillator strengths 0-63572
 Fe, Kα satellite lines following electron bombardment 0-69097
 Fe, n=2-2 transitions in XUV spectra, anal. 0-102472
 Fe XV, line intensity and linewidths at high electron density, generalised population ratio 0-99481
 Fe XV, transition probabilities and collision strengths 0-78562
 Fe XX, in solar flares and tokamak plasmas, new atomic data 0-67545
 Fe⁺, Fe²⁺, synthetic spectra rel. to radioactive excitation source model for late time spectra for Type I supernovae 0-105264
 Fe²⁵⁺ line emission in Hercules X-1 (HZ Herculis), theory of emission during X-ray source low state 0-105393
 FeVIII-XXVI energy level tables and Grotian diagrams 0-74142
 H, Rydberg consts., saturated absorpt., spectroscopy meas. 0-105604
 H, adsorbed on graphite (0001), vibr. spectrum, at. beam scatt. obs. 0-92779
 H fine structure 3²S_{1/2}-3²D_{5/2} interval, separated oscillatory field meas. 0-99482
 H, gaseous, high-resolution mag. reson. study, 1 to 1.3K 0-95560
 H I Balmer lines, formation in bright prominences spectra (Russian) 0-77377
 H II, Zeeman splitting of high-n recomb. lines 0-58210
 H, infinitely magnetised, spectrum rel. to props. of pulsar crust 0-77282
 H L_α line breadth, Cherenkov line radiation, QSO emission-like spectra (Chinese) 0-105378

atomic spectra continued

- H, mesic, atomic X-ray yields 1s and 2p level shifts and widths, cascades, calc. 0-78730
 H, Stark and photoabsorption spectrum, density of oscillator strengths, atom c.f. semiconductor spectra 0-83318
 H-like ions in solar corona, reson. lines fine struct. components intensity ratios 0-101581
 H⁺, polarised Balmer radiation due to scatt. from Nb surface, adsorbed O₂ effects 0-99569
¹H, pionic, pion mass high accuracy meas. from transitions 0-106406
 He, ³P level, excitation and decay study up to high press. pumped by intense relativistic electron beam 0-74250
 He I 2³P-3¹D intercombination line, collision-induced, obs. by laser absorpt. spectroscopy 0-58194
 He II, Zeeman splitting of high-n recomb. lines 0-58210
 He, muonic, 3p-3d transitions calcs., energy splittings 0-87253
 He parity-violating elec. dipole transitions 0-69094
 He plasma, satellites of He 492.2 nm line, fine struct. interpretation 0-59235
 He positive column discharge, IR optogalvanic spectrosc. using F-centre laser 0-78563
 He triplet states, doubly excited, spectrum and polarisation 0-99472
 He, Voigt profile, absorpt. line calcs. for the 396.5, 361.4, 318.7, 492.2, 587.6 and 447.1 nm lines 0-99471
 He⁺ + Xe, internal energy distrib. at 100 eV 0-99564
 HeI 2s-2p transition at He⁺ and HeH⁺ impact on C foil 0-58343
 Hf IV, 6s ²S_{1/2}-6p ²P_{1/2,3/2} transition, relativistic oscillator strengths, influence of core polarisation 0-58132
¹⁹⁹Hg, 6¹S₀-6³P₀ forbidden transition absorpt. at 265.6 nm, A coeff. and self-press. broadening determ. 0-95562
 Ho I, Ho II, excited level lifetimes and oscillator strengths, visible spectra 0-63573
 I II, reson. lines, oscill. strengths determ. by absorption method 0-58214
 I(P_{1/2,3/2}), from ICN A-state photolysis, branching ratio wavelength depend. 0-81335
¹²⁹I, hyperfine struct. and isotope shift of 1.3 μm transition 0-102486
 In, s²p-sp²(P)np transitions, absorpt. spectra in 100-150 nm region 0-87067
 In, sputtering in Ar-N₂ discharge, mechanism, optical spectra study 0-89107
 In sputtering in N₂-O₂ discharge, mechanism, optical spectra study 0-89108
 Kr, absorpt. spectra, field induced autoionisation near ionisation threshold 0-106301
 Kr IV emission spectral lines, classification 0-95563
 Kr, K inner-shell level energies, absorpt. spectroscopy with synchrotron radiation 0-99583
 Kr V, emission spectral lines, classification 0-95563
 Kr VIII, excited state energies and lifetimes, beam foil spectra 0-63591
 Kr XI-XIV, X-ray and UV spectra, 30-300 Å range 0-95566
¹³⁹La II 5d² ³F₄-5d4f ³F₆ hyperfine structure, ΔF=±2 transitions, three-quantum process 0-63848
 Li⁺, optical transition between bound states, beam-foil spectrosc. obs. 0-91476
 Lu I, 5d6s6p-config., laser spectrosc. investig. 0-69096
 Lu III, 6s ²S_{1/2}-6p ²P_{1/2,3/2} transition, relativistic oscillator strengths, influence of core polarisation 0-58132
¹⁴⁰Lu, A=175.176, 5d6s²D_{3/2}-5d6s6p³F_{3/2} transition, isotope shift and hyperfine struct. 0-83309
 Mg, I-XII, energy levels and optical spectra 0-87065
 Mg III-V, beam-foil spectra, 100-450 Å 0-83308
 Mg XI resonance lines, dielectronic satellite lines atomic parameters calcs. 0-78567
 Mg⁺ laser cooled ions bound in Penning trap, high-resolution optical spectra 0-102487
 Mg²⁺, foil-excited ion, X-ray spectra and satellite classification 0-95567
 Mn, fine struct. levels fitting, config. interaction effect, spin-orbit and electrostatic interaction parameters 0-69248
 Mn, n=2-2 transitions in XUV spectra, anal. 0-102472
 Mo XIII-XVIII, spectrum 20 to 90 Å from laser-prod. plasma and low-inductance vac. spark 0-102473
 Mo XIV to Mo XXIX, extreme UV spectra 0-87068
 Mo (2²S_{1/2}), kinetic study by time resolved atomic resonance fluorescence 0-95557
 N, far vac. UV spectra, oscillator strengths for 3s, 4s, 5s, 3d and 4d ⁴P₁-2p³ ⁴S_{3/2} 0-74178
 N I, spectra in Ar inductively coupled plasma 0-91474
 N IX to Ni XII, wavelengths of transitions between lower configurations 0-99474
¹⁴N II, 2p3p ¹P₁, hyperfine struct. after ion beam surface impact at grazing incidence 0-58403
 Na, D-lines, inert gas broadening, photon echo meas. 0-91475
 Na, four- and six-photon resonance spectra (Russian) 0-91527
 Na, high Rydberg states, quenching in strong 1.06 μm laser field 0-95559
 Na I, atomic spectrum, series formulas 0-99466
 Na I solar D-lines, non-mag. polarisation 0-63569
 Na II, spectrum, config. superposition and transition probabilities calcs. 0-87082
 Na, matrix isolated in Ne, absorpt. and emission spectra 0-99465
 Na, Rydberg states, millimetre spectrosc. 0-99469
 Na, saturation spectra, crossover signals, effect of atomic alignment, optical pumping 0-58202
 Na+H(Ne)(Kr) vel.-changing collisions, effect on 2 photon and stepwise absorpt. line shape 0-87221
 Nb XIII, energy levels, spectrum obs. 0-63571
 Nd I, isotope shifts in energy levels of neutral Nd atom 0-69095
 Ne+⁴He²⁺, optical transition excitation function and cross sections 0-63787
 Ne²⁺+Xe, electron capture collisions, 15 to 50 keV, excitation 0-102566
 Ne* 5882 Å line, Doppler free spectra, press. broadening and shifts, saturation spectroscopy 0-78565
 Ni I, UV lines, oscillator strengths from hook method and absorpt. meas. in furnace 0-83319
 Ni I isotope shift for stable isotopes, nuclear charge radii 0-99484
 Ni, n=2-2 transitions in XUV spectra, anal. 0-102472
 Ni, X-ray transitions in laser produced plasma 0-100093
 Ni XII, XIII, XIV, XV, 3s-3p and 3p-3d transitions, oscillator strength and energy levels calcs. 0-83251
 Ni XII-XVIII solar 3s²3pⁿ-3s3pⁿ⁺¹ transition arrays, UV spectra classification 0-63570

atomic spectra continued

- Ni XVII transition probabilities and collision strengths 0-78562
 NiVI, sixth spectrum analysis 220-335 and 890-1325 Å regions 0-95565
 O, atom or ion sputtered from SiO₂ and oxidised Al surfaces, light emission 0-58199
 O I 7774 Å multiplet obs. of nightglow over Arecibo during magnetic storm 0-72663
 O V, 2s²2s²2p³P₁° intercombination line wavelength determ. 0-102470
 O VI, 2s²2s²2p³P₁° reson. lines, wavelength determ. 0-102470
 O VII, electron impact collision rates, reinterpretation of solar emission line ratios 0-98624
 OI, spectra in Ar inductively coupled plasma 0-91473
 O(³P₁) state, direct obs. from O₃ photolysis at 248 nm 0-101028
 O(³S) yield from O₃ photodissoc. at 1700-2000 Å 0-97714
 P I, IR spectra and HFS 0-91478
 P I, spectra and term anal. 0-91481
 Pb stable isotopes, 2-photon spectroscopy, isotope shift of 6-²³P₀-7p³P₀ transition 0-87070
 Rb II, lifetimes in 4p⁵5p config., precision meas. and calc. 0-102488
 Rb in Xe, collision-induced dipole transitions, absorpt. meas. 0-95718
 S IV, 3s²3p³P-3s3p² ⁴P multiplet, energy levels and transitions, appl. to solar atm. 0-87028
 S⁹⁺+O₂(Ar)(He), (q=8-19), K X-ray prod., charge-state depend. 0-106391
 Sb VII, spectrum obs. 600 to 2100 Å, analysis of 4d⁸5s-4d⁸5p, 4d³4p⁵4d¹⁰ transitions 0-102471
 Sc I to Sc XXI, energy level tables derived from atomic spectra anal. 0-101672
 Sc II, visible spectra and ionisation limit 0-74143
 Sml, laser atomic beam spectroscopy, isotope shifts, hyperfine struct., transitions 0-102468
 Te VII, 4d⁶6s configuration spectrum obs., line identifications 0-106289
 Te VIII, 4d⁶5s, 4d⁸5p and 4d⁴4d¹⁰ config. spectrum obs., line identifications 0-106289
 Ti, fine struct. levels fitting, config. interaction effect, spin-orbit and electrostatic interaction parameters 0-69248
 Ti III, IV, V, radiative lifetime meas. using beam-foil technique, 700 to 1900 Å 0-78574
 Ti, pionic, pion mass high accuracy meas. from transitions 0-106406
 Ti⁹⁺+O₂(Ar)(He), (q=8-19), K X-ray prod., charge-state depend. 0-106391
 TiXIV(TiXV)(TiXVII), Tokamak discharge, ground state, mag. dipole transitions, UV spectra obs. 0-63575
 TI, ionisation limit and oscil. strength in VUV absorpt. spectra 0-74152
 Tm I, hyperfine struct., high resolution spectrosc. meas. 0-87238
 U atomic beam, two laser irradi., two photon reson. effects., visible spectra 0-63604
 U III, IV, line identification on relative intensity basis 0-95561
 UI, precision isotope shifts meas. in visible, near IR 0-63587
 UV, energy levels and UV spectral anal. 0-106290
 V, fine struct. levels fitting, config. interaction effect, spin-orbit and electrostatic interaction parameters 0-69248
 V VII, VIII, IX, X, 3s-3p and 3p-3d transitions, oscillator strength and energy levels calcs. 0-83251
 W, multiphoton ionisation and absorpt. 0-95575
 Xe, autoionising reson., Stark effect 0-58198
 Xe, L₁, L₂, L₃ inner-shell level energies, absorpt. spectroscopy with synchrotron radiation 0-99583
 Xe, photoabsorption, local field effects 0-74151
 Xe VI, emission spectral lines, classification 0-95563
 Xe+⁴He²⁺, optical transition excitation function and cross section 0-63787
 Xel, visible lines, absolute transition probabilities 0-69108
 Yb, 4f¹⁴6s6p ³P₁ and ¹P₁ levels, Stark effect, tensor polarisabilities 0-87080
 Yb, highly excited levels, odd and even parity spectra, multichannel quantum defect anal. 0-58133
 Yb highly excited levels, reson., visible two photon absorpt. spectra obs. 0-58228
 Yb I, high Rydberg levels of 4f¹⁴ 6snd configs., very high resolution obs. 0-106300
 Yb I isotope shift studies in 3900 to 6500 Å region 0-74144
 Yb II, 6s ²S_{1/2}-6p ²P_{1/2,3/2} transition, relativistic oscillator strengths, influence of core polarisation 0-58132
 Zn-like ions, 4s-4p reson. lines and transitions obs. by means of laser prod. plasma, appl. to Tokamaks 0-99468
⁶⁶Zn, 2s-2p muonic X-ray transition obs. 0-74264
⁶⁶Zn muonic atom, dynamical E0 excitation, E0 resonances, muonic X-rays 0-95749
 Zr IV, energy levels, spectrum obs. 440 to 2670 Å 0-99470
 Zr IX, 4s²4p⁵-4s4p⁴ transitions, in VUV 0-91480
 Zr VIII, reson. transitions in UV 0-91479

atomic spectral line breadth

- atomic systems, coherent transients theorem 0-99808
 atoms, 70≤Z≤82, K_α X-ray linewidths and relative intensities, energy dispersive meas. 0-99483
 delayed quantum beat subnatural linewidth spectroscopy 0-77879
 discharge, high-freq., excited atoms concentration determ., Ne or Ar, using spectral method (German) 0-70053
 double radiooptical resonance, signal propag. and shape 0-87360
 foreign gas induced line shifts, thermodynamics 0-106295
 Lorentzian Raman lines, eqn. for correcting finite slit width effect 0-63593
 multimode radiation, many-photon atomic excitation 0-74154
 multiply charged ions, 2p_{1/2}3p_{3/2} config., level widths, relativistic calc., S-matrix method 0-63546
 n-photon resonance phenomena, finite laser bandwidth effect 0-58230
 Na, fluoresc. study, reson. radiation illum. 0-83314
 neutral+high Rydberg atom, thermal collisions, review 0-63756
 neutral atom collisions, hyperfine component broadening and shift of spectral lines 0-74136
 optical Autler-Townes effect, time depend., finite bandwidth laser appl. theory 0-91499
 plasma, nonequilibrium, kinetic theory of spectral line broadening 0-59187
 power broadened two-photon ionisation, reson. lineshape and photoelectron spectra 0-58229
 profiles in Orion Nebula, intensity and vel. calibrations 0-62243
 proutium, atomic X-ray yields 1s and 2p level shifts and widths, cascades, calc. 0-78730

atomic spectral line breadth continued

quantum systems, at. or spin two level, reson. EM wave excitation, free induction decay oscills. 0-63562
rare gas adsorbates on simple metals, optical excitation, configurational switching, charge transfer 0-107643
solar chromosphere line profiles from OSO-8 satellite 0-67690
subnatural linewidth spectra by optical double reson. with two-photon pumping 0-74200
superfluorescence, delay-time statistics and inhomogeneous line broadening 0-99684
three-level spectra, lineshapes in intense laser field, theory 0-69109
three-state atom, saturated two-photon absorpt. in perturber gas 0-106130
transient line narrowing, laser spectroscopic technique yielding resolution beyond natural linewidth 0-82834
two-atom resonance fluoresc. spectrum, cooperative effects 0-78570
two-level atoms, dynamics and spontaneous radiation in bichromatic EM field 0-91502
two-level atoms, inhomogeneously broadened, superfluoresc. and amplified spontaneous emission 0-106499
two-level Doppler-broadened medium in Fabry-Perot, optical bistability 0-102759
van der Waals interaction, spectral line broadening, growth curves 0-102548
vapours, three-level system, collisional effects in saturation spectroscopy, appl. to Na 0-78579
X-ray line shape broadening anal., least squares method 0-63588
Zeeman line profile, mag. field determ., appl. of radiative transfer problem soln. 0-82221
Al, plasma, transfer eqn. soln. using freq. and angle averaged photon escape probabilities 0-64688
Ar, electron scatt. and ejection, electron energy loss spectra 0-58394
Ba, atomic beam and resonance spectroscopy 0-58180
Ba II lines in solar spectra, non-mag. polarisation, centre-to-limb var. 0-67678
Ba in shock heated Ar, absorpt. line broadening obs. (*Japanese*) 0-83464
C IV 1548 Å line profiles of impulsive EUV bursts, OSO-8 obs. 0-90401
C IV (C V), UV line identifications and lifetime meas. 0-106288
C plasma, spectral and absorpt. coeffs. 0-69985
Ca 657.3 nm line saturated absorption spectroscopy, photon-recoil component resolution 0-86457
Ca I, Ca II lines in solar spectra, non-mag. polarisation, centre-to-limb var. 0-67678
Ca II K-line, formation of optically thick solar, profile 0-94767
Ca II K-line in quiescent solar prominence, influence of spatial resolution on line width and shift 0-77364
Ca in shock heated Ar, absorpt. line broadening obs. (*Japanese*) 0-83464
Cd, $5s5p^3P_1-5s^2\ ^1S_0$ intercombination line, press. broadening and shift 0-95564
Cd, broadening of 5^1P_1 level 0-83479
Cs atom, oscillator strength meas. by tunable laser interferometry 0-105697
Cs HFS pressure effect determ. from absorption coeff. profiles 0-106299
Cs+inert gas, three body interaction, fluoresc. spectra principal series lines and secondary satellites 0-83313
Cu vapour pulsed laser, spectral comp. of superradiance, stimulated and spontaneous radiation 0-102713
Eu+Sr, absorptive collisional energy transfer, laser induced excitation spectra 0-63584
Fe I lines in solar spectrum, damping const. determ. preliminary results (*Russian*) 0-72900
Fe II lines, permitted, in type I Seyfert galaxies and quasars, form. and relative intensities 0-62278
Fe II lines in quasars and Seyfert galaxies, excitation and line strength 0-67896
Fe XV, line intensity and linewidths at high electron density, generalised population ratio 0-99481
Fe+Ar, Fe I reson. line, collisional broadening at high temp. (*German*) 0-106298
H fine structure $3^3S_{1/2}-3^3D_{3/2}$ interval, separated oscillatory field meas. 0-99482
H I and He I lines in ν Eridani, δ Cephei type star, visible obs. 0-67739
H I Balmer α emission line core formation in chromosphere of T Tauri-type variables 0-94792
H I Balmer γ line profiles and masses of DA white dwarf stars 0-77399
H I Balmer lines, formation in bright prominences spectra (*Russian*) 0-77377
H I line profiles in RY Persei spectra, visible obs. 0-67795
H L_{α} line breadth, Cherenkov line radiation, QSO emission-like spectra (*Chinese*) 0-105378
H line broadening and shift due to plasma ions (*Russian*) 0-96350
H, mesic, atomic X-ray yields 1s and 2p level shifts and widths, cascades, calc. 0-78730
H⁺, DC Stark broadening of $^1P^o$ shape reson. 0-63585
H+Ar, H α and H β emission cross sections 0-63782
H⁺+Ar, H α and H β emission cross section 0-63783
H α and H β spectral profiles from neutral beams and plasmas in high mag. fields 0-83999
H(S)+Ar($^3P_{0,2}$), energy transfer collisions, Lyman- α emission profile obs., in microwave discharge and reaction cell 0-58359
H α and H β , Stark profiles, ion-motion effect 0-63592
H α emission line in active binary star II Pegasi (HD 224085), equivalent width vars. and profile 0-90480
He I 584 Å in quasars, line strength prediction 0-67550
He I 584 nm line profile, monitoring using resonance absorption spectrometer 0-62019
He I line profiles in RY Persei spectra visible obs. 0-67795
He II, 4686 Å line, Stark broadening, meas. and calcs. 0-91504
He, spectral lines, singlet, self-broadening, resonant interaction 0-63574
He, Voigt profile, absorpt. line calcs. for the 396.5, 361.4, 318.7, 492.2, 587.6 and 447.1 nm lines 0-99471
He-Ar, Ar I TEA lasers, energy characteristics 0-63977
He-Kr, Kr I TEA lasers, energy characteristics 0-63977
He-Xe, Xe I TEA lasers, energy characteristics 0-63977
Hg vapour, resonance line shape in presence of Hg(6^1P_1)-Hg(6^1S_0) interactions 0-78572
 ^{199}Hg , $6^1S_0-6^1P_1$ forbidden transition absorpt. at 265.6 nm, A coeff. and self-press. broadening determ. 0-95562
Kr⁺ mode-locked ion laser, pulse width and linewidth meas. 0-102696
Mg I and II in Sun, line profiles comparison with theoretical spectra, visible obs. 0-82320

atomic spectral line breadth continued

Mg II 280 nm line in Persei, profile, calcs. and UV obs. 0-82421
Mg II k-line formation of optically thick solar chromospheric line, profile 0-94767
Mg II lines in quasars and Seyfert galaxies, excitation and line strength 0-67896
Mo, $\text{N}_2\text{N}_3\text{N}_4$, super Coster Kronig processes 0-106303
Mo, X-ray spectra, K α hypersatellites 0-63576
Na, D-lines, inert gas broadening, photon echo meas. 0-91475
Na I lines in solar spectra, non-mag. polarisation, centre-to-limb var. 0-67678
Na, photofragment of NaBr, non-Gaussian line shape, level shifting and velocity inversion 0-58182
Na+H(Ne)(Kr) vel.-changing collisions, effect on 2 photon and stepwise absorpt. line shape 0-87221
Na+inert gas, non-Lorentzian spectral line shape 0-106297
Na+inert gas, Rydberg states transitions, broadening cross-sections meas. 0-69110
Na+Ne(Ar)(Xe), 3^3P-3^3D line broadening obs. 0-78684
Nb, $\text{N}_2\text{N}_3\text{N}_4$, super Coster Kronig processes 0-106303
Ne V, forbidden 3426 Å emission in nebula NGC 6302, broad wings obs. rel. to energetic stellar wind 0-67835
Ne+Ne, (He) low pressure broadening and shift of Ne line, Lennard-Jones pot. 0-102554
Ne* 5882 Å line, Doppler free spectra, press. broadening and shifts, saturation spectroscopy 0-78565
Ni, $M_{\text{II,III}}$ spectrum, ab initio calculation 0-83276
O, line shape following dissociative excitation of O $_2$, CO $_2$, CO and NO 0-105097
Rb+Rb⁺, freq. shift, line broadening, phase interference effects, Doppler free two photon spectra 0-58200
Rh, $\text{N}_2\text{N}_3\text{N}_4$, super Coster Kronig processes 0-106303
Ru, $\text{N}_2\text{N}_3\text{N}_4$, super Coster Kronig processes 0-106303
Sn II, cool plasma, isolated lines, Stark broadening, semi-empirical impact approx. calcs. 0-59186
Te VII, $4d^6s$ configuration spectrum obs., line identifications 0-106289
Te VIII, $4d^8s$, $4d^8p$ and $4d^8d^{10}$ config. spectrum obs., line identifications 0-106289
TiI, atomic fluorescence, D $_2$ pressure effect on width and shift 0-99475
Xe 3.51 μm laser amplifiers, spectral narrowing and saturation induced rebroadening optical heterodyne obs. 0-63976
Xe I three-level system, level splitting within natural width, saturation spectrum 0-106291
XeI, visible lines, absolute transition probabilities 0-69108

atomic structure
see also atomic electron correlations; atomic excited states; atomic fine structure; atomic orbitals calculations; atomic polarisability; atomic spectra; nuclear screening; Russell-Saunders coupling; triplet state
l-matrix energy functionals, extension to all ensemble representable l-matrices 0-99442
adsorption of atoms on metals, Green's function formalism for studying electronic struct., local density of states calc. 0-107884
atomic scatt. factors and momentum densities, asymptotic form 0-74105
atoms, 5^1P^o and 5^1D^o config., parametric study 0-91444
average electron density, isoelectronic changes, rel. to X-ray scatt. intensity 0-91424
binding energies, determ. from fund. theorems involving electron density, $\langle r^{-1} \rangle$ and Z^{-1} perturbation expansion 0-63521
binding energy and rest mass of constituents, total symmetry effects (*French*) 0-63068
bound-state properties calcs., theoretical error estimates 0-102425
classical many-body collision model incorporating Heisenberg and Pauli principles 0-63511
closed-shell atoms, Jastrow wave functions, var. calcs. 0-83249
dressed atom system, energy levels and reson. phenomena, universal algorithm 0-69111
electronic degrees of freedom, classical models 0-63507
electronic densities, analytic expressions 0-99437
electronic energies, homogeneity prop. 0-63539
electronic structure calcs., self-consistent, accelerating convergence of iterative process 0-87037
electrostatic pot.-electronic density relationships 0-69206
exchange energy as function of electron density 0-91426
exchange energy density functional, gradient expansion, rel. to at. energy functional 0-99441
expectation values, rigorous and approx. relations 0-74099
in external AC and DC fields, complex dressed states determ. 0-63585
fractional parentage coefficient identities, atomic, molecular spectroscopy applications 0-69050
gaseous molecules, persistence of p, d, f and g orbitals, ang. functions, Schrodinger's eqn. and cardinal number anal. 0-102426
high-Z atoms ($Z=48-104$), electron impact, K-shell ionisation cross sections calcs. 0-63827
homologous ions series, struct.-related trends in line strengths and Stark widths 0-105157
hydrogenic and atomic observables, time resolved spectra; time reversal symm. 0-91418
hydrogenlike atoms, spin-orbit terms derivation 0-73148
isoelectronic series, Politzer's energy rel. determ. using HF data 0-91425
Kirkwood-Pople-Schofield method, appls. to polarisabilities calcs. 0-83272
Landau condensation in atomic physics 0-74098
many-electron atoms, foundations of relativistic theory, Hamiltonian H_+ and h_+ and related relativistic HF eqn. derivation 0-99458
many-electron atoms in mag. fields, total energy and atom spin calcs., spin rearrangement 0-83267
many-fermion systems, partial level density for widely varying values of the range of interaction 0-58120
Moseley's expts.: K α line freqs., rel. to at. number, reinterpretation 0-82616
multicharged ions, transitions between energy levels in strong external field, relativistic calcs. (*Russian*) 0-63547
multiply charged ions, $2p_{1/2}3p_{3/2}$ config., level widths, relativistic calc., S-matrix method 0-63546
near threshold struct. in K-shell spectra, photoionisation or fast charged particle ionisation 0-87064
neutral atoms in plasma background, strong EM radiation effects 0-103157
one-electron atom in curved space-time 0-78509
phase integral approximations, advantages over JWKB approx. 0-87027

atomic structure continued

- Politzer-Parr partitioning, electron correl., isoelectronic, isonuclear, spin and excitation aspects 0-78522
 quantum chemistry, conf., Kyoto, Japan, 29 Oct.-3 Nov. 1979 0-101659
 quantum mechanical perturbation problems, resolution using integral eqn. 0-58112
 quasiparticle formalism, atomic shell operators, Lie algebra 0-91414
 rare earth chlorides, glass transition temp. meas., inner-sphere coordination number change effect on soln. props. 0-83239
 rare earth elements, atomic partition functions, Chebyshev approximations 0-67544
 rare earth perchlorates, glass transition temp. meas., inner-sphere coordination number change effect on soln. props. 0-83239
 relativistic theory of P violation in many-electron atoms 0-91042
 rotated-coordinate method, rel. to stabilisation method 0-74097
 scaling and Pade approximants, perturbation theory 0-91429
 spin-density functional formalism, correl. energies calcs., appls. and corrections 0-91433
 spin-dependent correlated atomic pseudopotentials 0-107686
 superheavy and intermediate atomic collision systems, UNILAC expts. 0-63751
 swift ions, electron state energy shift in passing through solids 0-65107
 three-electron dynamics, hyperspherical coord. anal. 0-83241
 3d-transition metal ions, s-doublet struct., appl. of exchange correlation mass operator approx. 0-106266
 transverse electron-electron interaction calc. 0-91430
 two-body correls., variational approach 0-91455
 two-electron atom, lower band to ground state decay 0-78508
 two-electron atom, trial wave function for ground state 0-78510
 unified theory of atoms and atomic aggregates, self consistent theory 0-102418
 universal variational functionals of electron densities, first-order density matrices, and natural spin-orbitals and solution of the ν -representability problem 0-95516
 AIS, $B^1\Pi-X^2\Sigma^+$ transition, assignment of UV bands, vibr. and rot. anal. 0-58278
 Ar,K inner-shell level energies, absorpt. spectroscopy with synchrotron radiation 0-99583
 Ar, $2p^6$ shell, oscillator strength, photoionisation cross sections, electron shell alterations determ. (*Russian*) 0-58144
 Ar, inner shell alignment following electron impact ionisation, distorted wave approx. calcs. 0-91682
 Ar(I), $3p^4$ config., level lifetimes meas. 0-102490
 Ba, $4d^{10}$ shell, photoionisation cross sections, electron shell alterations determ. (*Russian*) 0-58144
 Be₄ (Be₄⁻), atomic clusters, electronic struct., LCAO-MO-SCF and HF calcs. 0-63880
 Ca, $4p^2\ ^1S_0-4s4p\ ^1P_1-4s^2\ ^1S_0$ cascade rate, two photon coincidence meas. technique 0-95576
 Cd, 1S , 3P , 1P states, dipole polarisabilities from compact variational trial functions 0-63568
 Cl⁻, atomic core states, antishielding effects calcs. 0-83299
 Cs, $4d^{10}$ shell, photoionisation cross sections, electron shell alterations determ. (*Russian*) 0-58144
 Cs I, $n^2S_{1/2}$ and $n^2D_{3/2,5/2}$ states, energies 0-87066
 D₃ Rydberg states, spectroscopic B₀ consts. 0-74109
 Fe XXII, coupling energy levels, oscillator strengths, electron collision energies 0-69068
 Fe¹⁹⁺, new atomic data rel. to solar phase spectra 0-67545
 H atom, Dirac and Klein-Gordon relativistic eqns., energy level splitting 0-77938
 H atom, form factor for arbitrary states, dipole moment component matrix element calcs. (*Russian*) 0-58143
 H atoms, energy levels and bound-bound transitions in strong mag. field 0-58134
 H bound states in strong mag. field 0-99438
 H, degenerate 3s-3d levels, in mag. field, eigenvalues, Bender-Wu formulas 0-83275
 H, electron-photon angular correlation meas. for excitation of 2P state 0-91636
 H, in static multipole field, logarithmic perturbation expansion 0-91431
 H, infinitely magnetised, energy levels rel. to props. of pulsar crust 0-77282
 H, n-dimensional atom, Kepler problem, dynamical symmetries 0-58121
 H, photon emission, Bohr theory covariant eqns., teaching 0-105482
 H, quasi-stationary states in field of strong monochromatic wave, perturbation theory calcs. (*Russian*) 0-58145
 H, relativistic energy levels in strong mag. fields 0-102454
 H₂+ e^+ (N⁺)(O⁺), reactant ion electronic states, effect on charge transfer cross sections 0-63809
 H₃, Rydberg states, spectroscopic B₀ consts. 0-74109
^AH, A=1,2,3, muonic atoms, ground state energy levels from quasipot. eqn. 0-87251
 Hg, 1S , 3P , 1P states, dipole polarisabilities from compact variational trial functions 0-63568
 Kr, K inner-shell level energies, absorpt. spectroscopy with synchrotron radiation 0-99583
 Li atom, effective potentials, energy levels 0-106263
 Li, optical oscil. strengths calcs. 0-91495
 Li+H⁺, Li core excitation cross section, correlation and reorganisation effect 0-87215
 Lu I, 5d6s6p-config., laser spectrosc. investig. 0-69096
 Mg (Mg⁺), lifetime meas., beam foil spectra, comparison with numerical coulomb approx. calc. 0-58367
 Mg, I-XII, energy levels and optical spectra 0-87065
 Mg XI resonance lines, dielectric satellite lines atomic parameters calcs. 0-78567
 Mg²⁺ atomic core states, antishielding effects calcs. 0-83299
 Mg₄(Mg₄⁻), atomic clusters, electronic struct., LCAO-MO-SCF and HF calcs. 0-63880
 Na atom, effective potentials, energy levels 0-106263
 Na I, atomic spectrum, series formulas 0-99466
 Na⁺, atomic core states, antishielding effects calcs. 0-83299
 Ne, electron impact excitation of 2s2p³s and 2s2p⁶3p configs., energy loss obs. 0-91685
 Ne⁻ scatt. electron spectra, distinction from neutral autoionising states 0-83482
 Ni films, electronic struct. calc., effects of chemisorption; contact pot. and surface magnetisation 0-103734
 Ni I isotope shift for stable isotopes, nuclear charge radii 0-99484

atomic structure continued

- Ni XII, XIII, XIV, XV, 3s-3p and 3p-3d transitions, oscillator strength and energy levels calcs. 0-83251
 Ni-Fe, electronic struct. calc., effects of chemisorption; contact pot. and surface magnetisation 0-103734
 O ions, non-equilibrium charge state distrib. charge exchange cross-sections in solid targets 0-65109
 Re₃Br₉, atomic clusters, electronic struct. and photoelectron spectra 0-69287
 (Re₃Cl₉)³⁻, atomic clusters, electronic struct. and photoelectron spectra 0-69287
 Re₃Cl₉, atomic cluster, electronic struct. and photoelectron spectra 0-69287
 reactant ion electronic states, effect on charge transfer cross sections 0-63809
 S IV, 3s²3p²P-3s3p² ⁴P multiplet, energy levels and transitions, appl. to solar atm. 0-87028
 Sb VII, spectrum obs. 600 to 2100 Å, analysis of 4d⁹5s-4d⁹5p, 4d⁹-4p²4d¹⁰ transitions 0-102471
 Sc II, visible spectra and ionisation limit 0-74143
 U⁴⁺ electron configuration from nuclear information 0-58146
 UV, energy levels and UV spectral anal. 0-106290
 V VII, VIII, IX, X, 3s-3p and 3p-3d transitions, oscillator strength and energy levels calcs. 0-83251
 Xe, 4d¹⁰ and 3d¹⁰ shell, photoionisation cross sections, electron shell alterations determ. (*Russian*) 0-58144
 Xe, 5s² shell, oscillator strength determ. (*Russian*) 0-58144
 Xe, L₁,L₂,L₃ inner-shell level energies, absorpt. spectroscopy with synchrotron radiation 0-99583
 Xe like ions (I, Cs⁺, Ba²⁺, La³⁺) 3d⁹4f config., collapse of 4f electron, X-ray spectral obs. (*Russian*) 0-58204
 Zn, 1S , 3P , 1P states, dipole polarisabilities from compact variational trial functions 0-63568
 Zn XX, energy levels and one electron transitions, relativistic calculations 0-87051

atomic structure, crystals see *crystal atomic structure*

atomic weight see *atomic mass*

atoms

see also *exotic atoms; helium atoms; hydrogen neutral atoms; positronium*
 No entries

attaching see *joining processes*

attenuation see *absorption; dispersion (wave); scattering; transmission*

attenuation measurement

- compressional wave attenuation in deep ocean sediments 0-79033
 microwave propagation at 10, 11 GHz, radiometric measurement of rain attenuation 0-67397
 optical attenuator metrological certification methods 0-91941
 optical fibre attenuation, bandwidth, and refractive index meas. methods compared 0-64190
 optical fibre attenuation measurement comparison among USA manufacturers 0-58747
 optical fibre characterisation techniques compared 0-64202
 optical fibre total loss spectra, precise meas., automatic meas. system 0-64169
 optical fibres, backscatter meas. theory (*German*) 0-91921
 optical fibres, backscattering method for attenuation and connection insertion loss meas. anal. 0-58675
 optical fibres, fault location and backscattering meas. 0-64183
 optical fibres using bench equipment 0-58695
 optical waveguides, power decay evaluation using backscatter technique 0-106599
 radiowave propagation at X, K bands, microwave radiometers for rain attenuation measurement 0-68254
 radiowave propagation attenuation due to water vapour, microwave radiometer study at 22.235 GHz 0-72610
 LiNbO₃, aluminum-coated YZ, measurements of SAW attenuation 0-74619

attenuators

see also *waveguide attenuators*

optical attenuator metrological certification methods 0-91941

attitude control

- magnetic sensor in Bhaskara satellite 0-72746
 satellite-gyrostat reorientation, optimal attitude control 0-61980
 satellites attitude control, inertially fixed pitch stabilisation by solar radiation press. 0-101523
 Space Telescope pointing control fine guidance subsystem design 0-82201
 spacecraft, optimal aerodynamic attitude control 0-77250

audio acoustics

- see also *audio recording; audio systems; hearing; speech*
 acoustical communication theory, computation of modulation and carrier functions of an arbitrary audio signal 0-79064
 application of communication theory to acoustics, separation of sound carrier and modulating signal 0-79063

audio amplifiers see *audio-frequency amplifiers*

audio equipment

- see also *audio-frequency amplifiers; gramophones; loudspeakers; microphones; pick-ups*
 electronic 0-106682
 four-channel percussion synthesiser using 5700 type modules, construction details 0-106681
 production association Ecran, 25 years of achievement in cinematographic, TV industry (*Russian*) 0-62770

audio-frequency amplifiers

- medium-scale live concert sound reinforcement system requirements 0-92012
 outdoor classical music sound reinforcement systems compared 0-92011
audio recording
 cinematography, magnetic sound records release print KMP-23 (*Russian*) 0-90918
 cinematography, post-synchronization recording equipment KZM-24 (*Russian*) 0-86482
 holographic disc with high data transfer rate, audio response memory appl. 0-58477
 impulsive noise reduction on gramophone records 0-87689
 motion picture sound track, freq. distortion and two dimens. sound record scatt. (*Russian*) 0-95175
 motion picture sound track films, appl. of computer program simulation of recording and reproducing system 0-62767

audio recording continued

- photographic sound negative film, Eastman sound recording II film, 5373/7373 0-62768
- physics homework solutions, recording methods 0-77573
- read head for magnetic tape recorders using magneto-resistance principle 0-87688
- stereophony, artificial head, tone meas. (*German*) 0-106702
- studios, shortcomings of apparently improved acoustic designs 0-69601
- symphonic music, practical and aesthetic microphone techniques, comments 0-79073

audio systems

- see also *acoustic devices; acoustic equipment*
- concert hall sound system for touring quartet 0-92013
- digital, future prospects (*Japanese*) 0-83725
- loudspeaker system amplitude and phase response rel. to driver alignment on baffle 0-92010
- medium-scale live concert sound reinforcement system requirements 0-92012
- outdoor classical music sound reinforcement systems compared 0-92011

auditory activity see *hearing***auditory perception** see *hearing***Auger effect**

- adhesion, surface anal. techniques appl. 0-65381
- AES, ionisation enhanced diffusion effect obs. 0-71497
- alkali intercalated graphite, C XVV Auger lineshape anal. 0-104019
- alloys, embrittling residuals categorisation by Auger electron spectroscopy 0-66739
- appearance pot. spectrometer design, demonstrations 0-105477
- appearance potential spectroscopy, apparatus 0-101888
- atomic collision, coherence and correlation, book 0-90615
- brass, nondestructive determ. of in-depth profile 0-93836
- α -brass, stress corrosion fracture surface anal. by AES 0-104321
- carriers bound to centres involving phonons, Auger recomb. 0-107805
- composition depth profiling sputtering times, conc. gradient effect (*French*) 0-76116
- crystalline solids, electronic industry, chem. anal. instrumental methods progress 0-66903
- electron-hole droplet phonon wind 0-107707
- electronic and at. collisions, conf., Kyoto, Japan (Aug.-Sept. 1979) 0-57011
- electronic material and device characterisation using surface-sensitive analytical techniques 0-65341
- extra-atomic relax. energies, rel. to Auger parameters 0-87090
- field emission micro SEM, for UHV surface anal. 0-86519
- free atoms, diagram Auger electron spectra 0-78585
- glass, adsorption of Au, AES study, electron bombardment effects 0-65380
- glass-metal seals, Auger spectroscopy study of interface 0-76587
- glasses, high vol. low cost, as solar reflectors, compositions and weathering effects 0-106589
- grain boundary segregation, critical assessment 0-75362
- graphite monolayer on Ni (110) surface, oxidation mechanism 0-101037
- graphite surface, adsorbed Cs, dissolution, lamellar cpd. form. (*French*) 0-100399
- guanidinium aluminium sulphate hexahydrate, surface obs., SEM and AES expts. 0-71362
- Hastelloy, H₂ embrittlement in H₂S environment impurity segregation effects, AES study 0-71724
- Hastelloy B-2, corroded surface, electron bombardment effect during Auger electron anal. 0-61014
- inner-shell vacancy creation, ionised fragments probability distrib. 0-83274
- ion bombardment induced, main features 0-100730
- ion impact induced in metals 0-71545
- ions emerging from C foils, mean-charge, inner-shell vacancy effects 0-87219
- LEED/Auger spectroscopy system, retractable rear viewing system 0-57434
- light atom collisions, 2p π orbital transitions Auger study (*Russian*) 0-91639
- lineshape anal. of molecules and solids 0-76113
- LSI surface analytical techniques applied to electronic components [Si LSI chip inspection] 0-81392
- metal silicides, fabrication technique and characterisation (*Japanese*) 0-60779
- metal-semiconductor interfacial reaction, AES study (*Japanese*) 0-96701
- metallurgical applications of XPS, AES, and SIMS (*French*) 0-81253
- metals, narrow-band, Auger line shape 0-60719
- micro Auger analysis, using field emission source 0-104020
- microanalysis, in SEM 0-101058
- microcomputer controlled Auger microprobe 0-81414
- MIS solar cells, interface problems, AES, SIMS and XPS study 0-89627
- narrow gap semiconductors, recombination mechanisms, review 0-96905
- Ni-Co, H₂ embrittlement, heat treatment and impurities effect, Auger anal. 0-76331
- oxidation induced by ion or electron bombardment, AES-SIMS study 0-108606
- p⁺-n -n⁺ pulsed diodes, forward pulsed case, voltage transient response 0-60071
- p 0-80072
- PDX vacuum vessel, glow discharge conditioning 0-79607
- photoelectron spectra, Auger electron spectra of atomic Fano resonances 0-93454
- photovoltaics and absorber/reflectors, diffusion, chemical reactions, contamination, AES and SIMS 0-72066
- pionic atoms, Auger electron emission from C, N, O, Ag, Br (*Russian*) 0-69271
- pionic atoms, electron screening and inner shell refilling, X-ray 0-78729
- polyacetylene:AsF₆, AES, XPS, UPS, and X-ray induced 0-66400
- quantitative AES, backscattering effects, review 0-81398
- quantitative AES, Monte Carlo calc. 0-84813
- radioisotope Auger electrons, use in low energy electron range meas. 0-70257
- rare earth hydrides, form. by rare earth reaction with H₂O vapour 0-76504
- scanning Auger electron microscope, calc. of effects of backscattered electrons on spatial resolution 0-81412
- scanning Auger microscopy, developments 0-101909
- scanning Auger microscopy, effects of backscattering on resolution 0-104021

Auger effect continued

- scanning Auger microscopy, resolution, quantification and sensitivity 0-81411
- scanning Auger microscopy for analysis of biological material 0-73535
- scanning Auger microscopy of Pd on UHV-cleaved mica substrate 0-80149
- scanning microprobe, approach to damage-free anal. 0-89581
- scanning microprobe, backscattered electron images, tailored modulation techniques appl. 0-68305
- scanning microprobe, with computerised image processing 0-68304
- scanning microscope using microprobe with thermal field emission source 0-68297
- scanning microscopy, S/N aspects 0-71993
- SEM microanalysis techniques, review 0-71995
- semiconductor, Auger recombination rate, nonequilib. carrier distrib. 0-65578
- semiconductors, cryst. growth and defects, appl. of analytical techniques for observation 0-73546
- semiconductors, impact ionisation, Auger recombination involving traps 0-80912
- semiconductors, intervalley electron-electron scattering effect on optical transitions 0-108267
- single crystals with lowered work function, secondary and Auger electron emission anisotropy 0-100716
- solar cell, Auger recombination limit on efficiency at high level of illumination 0-108797
- solid laser dynamics, Auger recombination effects 0-69398
- solid-solid interface chemistry, characterisation, theory 0-75448
- specimen charging control for SIMS and AES of insulators 0-101875
- spectrometry, electron gun beam current control for improved stability 0-84814
- spectroscopy, Au-refractory film interdiffusion obs., in combination with other scattering techniques 0-65308
- sputter, depth profile improvement using two ion guns 0-71964
- stainless steel, austenitic, surface, interaction with O₂, AES and work function obs. 0-65364
- steel, austenitic, Cr-Ni, ion-implanted N, chem. state study by AES and XPS 0-79825
- steel, cold-rolled sheet, surface chemistry 0-61146
- steel, continuously cast, segregation at halfway cracks 0-60869
- steel, Cr-Mo:P (2.25, 1 wt.%), stress relief cracking, effect of P segregation 0-89324
- steel, Cr-Ni-Mo, 'spots' (*Chinese*) 0-104248
- steel, industrial, surface chem. characterisation by SIMS, glow discharge spectrometry and other techniques 0-66907
- steel, low C, cold rolled, graphite precip. and S segregation, AES investigation (*Japanese*) 0-89222
- steel, Ni-Cr, temper embrittlement, intermediate tempering treatments 0-60944
- steel, stainless, corrosion and grain boundary penetration on exposure to coal gasification environment 0-61003
- steel, stainless, heat treated, oxide comp. and corrosion susceptibility of grades 410 and 430, AES study 0-66692
- steel, stainless, O₂ desorpt. during laser irradi., etching, AES study 0-66338
- steel, stainless, type 316, surface comp. rel. to crevice corrosion initiation 0-93680
- steel, stainless casts, creep ductility, Auger spectroscopy study 0-60917
- steels, stainless, surface characterisation rel. to adhesive bonding chem. etching, SEM, AES, XPS and electron probe microanal. 0-88416
- surface analysis techniques and appls., symposium, Dayton, USA (Jun. 1979) 0-62363
- surface analytical techniques, quantification, review 0-65342
- surface layers, photon induced ion desorption, surface atom core ionisation, Auger decay 0-59809
- surface microstructure determ. and microanalysis by ultrahigh vacuum field emission gun SEM 0-96423
- surface segregation, effect on metallurgical props, SIMS, XPS and AES (*French*) 0-80045
- surfaces and interfaces, analysis by combined Auger, X-ray and SEM studies 0-81413
- surfaces and thin film studies by combined system of SIMS, AES and XPS 0-86536
- synchrotron radiation techniques for studying atomic physics 0-63583
- synchrotron sources for low energy AES 0-77913
- tensile fracture device for Auger electron spectroscopy 0-73530
- thin film, sputter profiling, combined Auger-X-ray anal. 0-66909
- thin films, surface anal., survey of ESCA, AES, SIMS, and ISS (*Hungarian*) 0-70544
- tinplate surfaces, Auger depth profiling and anal. 0-59768
- Tokamak gettering, Ti thin films, H absorption and desorption, Auger electron spectrosc. 0-75092
- ultra-high vacuum SEM technique exam., secondary electron emission dependence on electron beam density dose 0-61209
- XPS Auger lines, generation by bremsstrahlung 0-87174
- zinc phthalocyanine, resonant two hole bound state at 3p core threshold 0-60750
- Ag (110), ethylene-O₂ interaction, LEED and AES obs. 0-89520
- Ag, adsorption of pyridine, UPS, AES and flash desorption meas. 0-92776
- Ag film, epitaxial growth on Pd, AES and LEED obs. of growth modes and substrate influences (*French*) 0-84408
- Ag film, vacuum deposition on Pb (111), substrate diffusion effects, RHEED, LEED, AES 0-65410
- Ag film growth on Pd substrate, interface cpd. form., AES study (*French*) 0-80131
- Ag, K-fluorescence yield determ. from K-Auger electron emission rates 0-95569
- Ag-Pd alloys, inert gas ion bombardment, dynamic surface composition changes, AES obs. 0-60745
- Ag₂S-K₂SO₄ mixtures, surface comp., AES and XPS obs. 0-81386
- Al and Al alloy anodised oxide films, for adhesive bonding appls., AES and SEM study 0-66689
- Al, annealed and powder sintered (SAP 895), sputtering under D⁺ and ⁴He⁺ bombardment, microstruct. effects study 0-84821
- Al, Auger spectra, KLL and KLV, screening effects and plasmon gains 0-80913
- Al, Auger spectra induced by 100 keV Ar⁺ impact 0-84820
- Al, initial interaction of O with single cryst. faces, LEED, AES and work function study 0-84392

Auger effect continued

- Al, oxide films, metal and O₂ transport, AES and inert marker, techniques 0-97641
 Al sheet surfaces, chem. characterisation by SIMS, glow discharge spectrometry and other techniques 0-66907
 Al, specimen transfer device for combined AES/RHEED and TEM obs. 0-70093
 Al, valence band Auger spectra, surface effect 0-80915
 Al/Pd thin film couples, thermal reactions 0-59830
 Al-Cu films, DC sputtered, Cu distrib. 0-80113
 Al,Ga_{1-x}As epitaxial layers on GaAs, struct. study by scanning Auger electron microscopy 0-80110
 Ar, electron impact, L X-ray spectrum, radiative Auger transitions 0-58227
 Au, Auger spectra, N_{4s}N_{6,7}N_{6,7} and N_{4s}N_{6,7}O_{4s} 0-89094
 Au coins, surface anal. by X-ray fluoresc., SEM and scanning Auger spectroscopy 0-89552
 Au film growth on Mo (110) surface, AES, LEED, thermal desorption study 0-80130
 Au surface, chemisorption of I, AES and LEED study 0-100405
 Au-Si interface, critical Au-film thickness obs. for room temp. interfacial reaction 0-75390
 Au-Si interface, electron energy loss and AES meas. 0-89096
 Au-Ti_{0.3}W_{0.7}, thermal annealing study of metallisation on Si 0-80134
 Au-W-GaAs Schottky barrier, elec. and chem. props., AES 0-96973
 Ba getter film, initial reaction probability with O₂, water, CO and CO₂, AES obs. 0-61153
 BaO, XPS valence bandstruct. 0-89117
 BaTiO₃, pure and doped crystals, surface and domain struct., AES and SEM expts. 0-71363
 BaTiO₃, surface study using AES and ion scatt. spectroscopy 0-65339
 Be, Auger spectra induced by 100 keV Ar⁺ impact 0-84820
 Be film, on W (110), growth mode, work function, thermal desorption, and struct. 0-75477
 Be, slowly oxidised, secondary electron yield changes, and AES characterisation 0-71524
 Be, thick film, amorphous, RF magnetron sputtering 0-80971
 Be thick film or Au substrate secondary electron emission 0-104022
 C:Ni, X-ray photoemission studies 0-76138
 CaO, XPS valence bandstruct. 0-89117
 n-Cd,Hg_{1-x}Te crystals, carrier recomb. in extrinsic conduction range 0-70722
 CdS:In(Cl) concentration quenching mechanism of luminescence 0-97336
 CdS:Li, pure and doped, green edge luminesc., complex nature of centres 0-60671
 CdSe film polycryst., thermal diffusion of Cr, 240-400°C 0-80001
 Cd₂SnO₄ and Cd₂SnO₄.CdO, thin film electrodes in H₂SO₄ electrolytes, reduction, AES and SEM 0-65674
 Co (0001), adsorption and reactivity of NO, LEED, AES, and thermal desorption study 0-80090
 Co, Auger spectrum, ab initio MO LCAO SCF CI calc. many electron contribs. 0-87169
 Co, radiative Auger effect, K-M² 0-71522
 Co-Si, surface physicochemical state, Auger electron spectroscopy study 0-100715
 Cr containing Cr₂O₃, film struct., oxide percentage determ. and temp. coeff. of resist. 0-103607
 Cr-Cr₂O₃, black, electrodeposited solar collector coatings, high temp. optical and struct. degradation 0-66995
 Cr-Cr₂O₃ black chrome, commercial, solar absorber coating characterisation 0-80111
 Cr(NO)₃, XPS and UV photoelectron spectra, compared to NO data 0-58317
 CsSn₃I₃, surface props., Auger study, elec. cond. meas., photochem. study 0-66339
 Cu, adsorption of O₂, N₂O on (100) surface, reaction with CO 0-103583
 Cu, chemisorption on low-index and stepped surfaces, LEED, AES and UPS obs. 0-84391
 Cu film, vacuum deposition on Pb (111), substrate diffusion effects, RHEED, LEED, AES 0-65410
 Cu, slip ring, spectroscopic obs. of elemental surface composition as function of temp. 0-66901
 Cu/Sn-Ni/Au tricomplexes, electrodeposited, interdiffusion obs. 0-84331
 Cu-Ag, surface segregation of S, Auger spectral study diffusion 0-76549
 Cu-Be, dynode surface, SEM and Auger microanalysis 0-100384
 Cu-Be(2 wt.%), tarnish surface films, formed in ammoniacal Cu(II) solns. 0-97624
 Cu-Co-Si (0.36, 0.11 wt.%), surface layer struct. on annealing, SIMS and AES exam. 0-88415
 Cu-Ni (110), adsorption of CO and H₂, UPS, thermal desorption, AES, and LEED study 0-80087
 Cu-Ni-Sn (9, 2 wt.%), surface comp., Auger electron spectroscopy study, manufacture and storage influence 0-65348
 Cu-Ni-Zn (18, 27 wt.%), surface comp., Auger electron spectroscopy study, manufacture and storage influence 0-65348
 Cu-Ni-Zn alloy, surface comp., outdoor exposure influence 0-59770
 Cu-Sn alloy, surface comp., outdoor exposure influence 0-59770
 Cu-Zn alloys, surface comp., outdoor exposure influence 0-59770
 CuO, on Cu, identification by electron spectroscopic methods 0-60747
 Cu₂O, on Cu, identification by electron spectroscopic methods 0-60747
 CuPd, chemical shift effects and origin of Pd 3d core level satellite 0-104039
 Cu₂S-CdS heterojunction interface, depth distribution profiles, Auger spectra 0-88622
 D, thermal desorption meas. of H-isotope retention in Alcator-A Tokamak 0-79588
 F K, X-ray satellite struct. and KLL Auger electron spectra, solid-state effects 0-89089
 Fe (110), coadsorption of K and O₂, XPS, UPS, AES, and LEED study 0-80084
 Fe desorption of H into ultrahigh vac. system, using permeation cell 0-86326
 Fe, free surface and grain boundary O₂ and S chemistry 0-75410
 Fe ions, Li-like Auger contribs. to electron impact ionisation 0-87231
 Fe, reaction with methane at 750 C micro Auger anal. 0-104020
 Fe surfaces, adsorption, segregation and reactions of non-metal atoms, LEED and AES obs. 0-59783
 Fe-Cr, high-temp. oxidation, borate inhibitors 0-66705
 Fe-Cr alloy, sputter etching oxide film, comp. profile, quantitative AES 0-81383

Auger effect continued

- Fe-M(1) (M=Ni, Cr, V, Ti, Mo; I=Sb, P), co-segregation at free surfaces studied by Auger spectroscopy 0-59767
 Fe-Ni (50 wt.%), surface comp. and oxide film thickness after various surface treatments, AES study 0-66693
 Fe-Ni-Cr (30.6, 21.3 wt.%), Alloy 800, high temp. oxidation at low O₂ press., SEM, AES and electron probe microanal. study 0-93688
 Fe-Si-Al, surface oxide layer struct., AES study 0-89396
 Fe_{1-x}O powder, wustite, AES study, ion and electron bombard. effects 0-76114
 α-Fe₂O₃ powder, hematite, AES study, ion and electron bombard. effects 0-76114
 Fe₃O₄ powder, magnetite, AES study, ion and electron bombard. effects 0-76114
 FeTi, surface and mag. props., heat treatment and hydrogenation effects 0-75447
 Ga, reson. photoemission shake-up and Auger processes at 3p photothreshold 0-100748
 GaAlAs-GaAs heteroepitaxial devices, interstitial impurities and degradation, Auger obs. 0-99730
 GaAlAs-GaAs heterostruc. lasers, interstitial impurities and degradation, Auger obs. 0-99730
 GaAs (100), Sb desorption props. 0-80074
 GaAs cleaved (110) face, interaction with O₂, influence of cleavage defects, AES study 0-66684
 GaAs, homoepitaxy and epitaxy, surface anal., using RHEED and Auger spectroscopy 0-66433
 GaAs, polycryst., wet and dry oxides, comparative study by AES, SIMS and XPS 0-80116
 GaAs solar cell, polycryst., grain boundary passivation by oxidation, AES, SIMS and XPS obs. 0-81467
 GaAs:Te(Cd)(Mg)(B), ion implant depth distribns., AES and glow discharge optical spectroscopy meas. 0-65028
 GaAs-Au(Ag) Schottky barrier solar cells, interface problems, AES, SIMS and XPS study 0-89627
 GaP, adsorption and desorption of Cs, LEED, AES, and photoemission meas. 0-70532
 GaP, reson. photoemission shake-up and Auger processes at 3p photothreshold 0-100748
 GaP:Cs-O simultaneous adsorption, oxidation interface chemical struct. 0-103584
 GaP-Pd contact system, low temp. alloyed contact formation 0-100519
 GaSb, adsorption and desorption of Cs, LEED, AES, and photoemission meas. 0-70532
 Gd, resonance recomb. lines in AES and photoelectron spectra 0-97390
 Gd₂(MoO₄)₃, surface study using AES and ion scatt. spectroscopy 0-65339
 Ge surface, (111), ion-bombarded and annealed, spectroscopic ellipsometry study 0-103543
 Hg_{1-x}Cd_xTe, recombination processes using impact ionization capture cross sections 0-75577
 In, K-fluorescence yield determ. from K-Auger electron emission rates 0-95569
 InAs and solid solutions, recombination mechanisms of excess carriers, luminesc. obs. 0-97337
 InGaAsP LPE heterostruc., interface grading, Auger depth profile 0-103585
 In₂O₃-InN film growth by reactive sputtering in N₂-O₂ discharge, mechanism 0-89108
 InP (110) surfaces, cleaved and polished-sputtered-annealed, LEED and AES study 0-103550
 InP/In_{0.4}As_{0.6}P_{1-y} interfaces, sputter-profiled, depth resolution degradation by cone form. 0-80094
 InP-Al interface struct., low temp. interaction, AES study 0-107661
 InP-Cu contact system, low temp. alloyed contact formation 0-100519
 InSb, Auger-governed decay of laser-induced plasma, optical probing 0-76105
 InSb, recombination processes using impact ionization capture cross sections 0-75577
 InSb-Au contact system, low temp. alloyed contact formation 0-100519
 Ir, Auger spectra, N_{4s}N_{6,7}N_{6,7} and N_{4s}N_{6,7}O_{4s} 0-89094
 K₂O-CaO-SiO₂ glasses, Auger analysis, alkali signal decrease 0-61189
 K₂O-SiO₂ glasses, Auger analysis, alkali signal decrease 0-61189
 K₂SO₄-Ag₂SO₄ mixtures, surface comp., AES and XPS obs. 0-81386
 Kr⁺, formed in 50 keV Kr⁺+Kr collisions, Auger transitions obs. by electron-scattered-ion coincidence method 0-74243
 LaB₆, direct recomb. and Auger deexcitation channels of La 4d to 4f reson. excitations, photoemission spectra 0-66395
 Li, 2s²2p double Auger rate 0-99489
 Li, valence band Auger spectra, surface effect 0-80915
 LiNdP₄O₁₂ laser, relaxation oscillations and mode spectra, high density pumping effect 0-69396
 Mg, Auger spectra, KLL and KLV, screening effects and plasmon gains 0-80913
 Mg, XPS, plasmon gains as monitor of incomplete relax., interference effects and sudden to adiabatic limits transition 0-66390
 Mg₂Cu polycrystals, surface study by AES, XPES and X-ray induced AES 0-65346
 MgO, XPS valence bandstruct. 0-89117
 Mn-Zn ferrites, grain boundary exam. using TEM and AES 0-107268
 Mo:C (110) surface, segregation, precip. and desorp. of C, AES and LEED study (French) 0-103480
 Mo-Si, film deposition by reactive sputtering, characteris. (Japanese) 0-93485
 Mo-Si, films, magnetron DC reactive sputtering, struct. and props. 0-80966
 N₁⁺ X₂Z₁⁺ state, vibr. states asymmetry parameter and photoelectron spectrum 0-95591
 Na, Auger electron emission due to ion collisions with solid targets (French) 0-104031
 Na, Auger spectra, KLL and KLV, screening effects and plasmon gains 0-80913
 Na K_α, X-ray satellite struct. and KLL Auger electron spectra, solid-state effects 0-89089
 Na, XPS, plasmon gains as monitor of incomplete relax., interference effects and sudden to adiabatic limits transition 0-66390
 Na₂O-CaO-SiO₂ glasses, Auger analysis, alkali signal decrease 0-61189
 Na₂O-SiO₂ glasses, Auger analysis, alkali signal decrease 0-61189
 Na₂WO₄, surface props., AES meas. 0-71767
 Nb-N, superconducting layers, sputtering in high vacuum apparatus (German) 0-89147

Auger effect continued

- Nb-Nb₂O₅-Pb(In) Josephson junctions, props. of Nb₂O₅ thermally grown tunnel barriers 0-100568
 NbN, supercond. RF reactively sputtered films, deposition parameter effects on props. 0-80972
 Ne, Auger electron emission due to ion collisions with solid targets (*French*) 0-104031
 Ni (001), adsorption of N₂, c(2×2) struct. form 0-80083
 Ni (001) surface, Ar ion bombarded, enhancement of oxidation, AES study 0-97644
 Ni (001) surface, electronic struct. of ordered S overlayers 0-84835
 Ni (100), adsorption of O₂ and reduction of surface oxide by H₂ 0-108741
 Ni (100), dissociative chemisorption and mol. adsorption of NO 0-65373
 Ni (100), kinetics of C deposition from adsorbed CO 0-76553
 Ni (100) surface, ang. resolved Auger emission and LEED Kikuchi intensities at 850 eV 0-66340
 Ni (100) surface, coadsorption of Sn on Pb, P or O contaminated surface, AES study 0-88437
 Ni film, interaction with O₂, AES, EELS, work function, and gravimetric meas. 0-75433
 Ni films, adhesion on graphite 0-80141
 Ni, M₁₁₁ spectrum, ab initio calculation 0-83276
 Ni, Medicus matrix cathode, surface characts. 0-66378
 Ni, oxide films, metal and O₂ transport, AES and inert marker, techniques 0-97641
 Ni passivation, S influence study by Auger and electron spectroscopy 0-65347
 Ni, stress corrosion susceptibility, S segregation effect, Auger spectrosc. study 0-61019
 Ni/GaAs film contact system, alloying reaction 0-96747
 Ni-Th (1 at.%), surface comp., temp. and O₂ exposure effects, AES study 0-80914
 β-NiAl, oxide films, metal and O₂ transport, AES and inert marker, techniques 0-97641
 NiO, (100) surface interaction with SO₂, electron diff. and Auger spectrosc. obs. (*French*) 0-97728
 NiO film, formed by Ni galvanic oxidation in borate buffer soln., struct. 0-100948
 Ni_{0.96}Sb_{0.04}, surface segregation, XPS and AES obs. 0-76135
 O ions, Li-like Auger contribs. to electron impact 0-87231
 Pb chalcogenides, Auger recomb., theory 0-65586
 Pb, deposition on Au, quantitative Auger electron spectroscopy, substrate and instrumental effects 0-71523
 Pb monolayer, double layer with Sn, growth on Al (111), struct. 0-70567
 Pb-In-(Au) base electrode film Josephson junctions, tunnel barrier oxide struct. 0-65750
 PbS-Si heterojunction, chem. struct., AES anal. 0-76115
 Pb_{1-x}Sn_xSe epitaxial layers, radiative and nonradiative recomb. processes 0-60670
 Pb_{0.78}Sn_{0.22}Te, Pb_{0.91}Sn_{0.09}Se, radiative and nonradiative recombination 0-80849
 PbTe-In contacts, fabrication and props. 0-60078
 Pd (110) surface, adsorption of S, characterised by LEED (*French*) 0-84422
 Pd (111), chemisorption of Cl₂, LEED, AES, thermal desorption, and work function meas. 0-75444
 Pd cluster, adsorption/desorption of CO, AES and thermal desorption meas. 0-75436
 Pd surface, segregated S state, AES, EELS, UPS and XPS study 0-93452
 Pd-Si structure, epitaxial silicide growth, LEED and AES study 0-103590
 Pt (111), adsorption of NO, EELS, thermal desorption, LEED, and AES study 0-80086
 Pt (111), chemisorption of Cl₂, LEED, AES, thermal desorption, and work function meas. 0-75444
 Pt (111) and Pt (S)-12(111)X(111)surfaces, adsorption of O, thermal desorption, AES, XPS, and LEED study 0-70534
 Pt, Auger spectra, N_{4s}N_{6s}N_{6p} and N_{4s}N_{6s}O_{4s} 0-89094
 Pt film, growth on amorphous Si:H, AES and LEED study 0-88447
 Pt₂Si, and PtSi, growth rate for form. by Pt film deposition under ultrahigh vac. and controlled impurity atm. 0-65388
 Pu, oxidation, binding energies, Auger and X-ray photoelectron spectra study 0-76550
 Re:C, work function, graphitic layer formation 0-96966
 Ru (001), chemisorption of O₂, uptake meas., thermal desorpt. spectroscopy and AES 0-108739
 Ru (110), kinetics of C deposition from adsorbed CO 0-76553
 Se compounds, LMM Auger spectra, relative intensity and relaxation energy 0-69115
 Se, LMM Auger spectra, relative intensity and relaxation energy 0-69115
 Si (111), ion bombard., struct. changes, AES obs. 0-79842
 Si (111), nitridation, AES and LEED results 0-80041
 Si (111) 7×7 clean surface and O chemisorbed stage valence band density of states from L₂₃VV Auger spectra 0-100717
 Si (111) surfaces, cleaved, electronic structure following Al adsorption 0-75610
 Si, Ar ion etching, carbide form. 0-81222
 Si, Auger electron emission, ion induced and secondary ion emission 0-71546
 Si, Auger spectra, KLL and KLV, screening effects and plasmon gains 0-80913
 Si, Auger spectra induced by 100 keV Ar⁺ impact 0-84820
 Si, CVD, surface anal. during growth, using RHEED and Auger spectroscopy 0-66433
 Si, chemisorption of XeF₂ and SiF₄, XPS and Auger spectra, surface chemistry 0-81358
 Si, epitaxial growth on sapphire by partially ionised vapour deposition, RHEED-AES obs. 0-80985
 Si, F-enhanced plasma growth of native layers, Auger profiles 0-93662
 Si, grain boundary elec. props./impurity correl. using surface anal. of multigrained samples by SIMS and AES 0-79816
 Si, hole-hole-electron Auger recombination 0-70720
 Si layer, on buried SiO₂ layer formed by high-dose, O ion implantation, TEM, AES, and XPS obs. 0-88172
 Si, multigrained, grain boundary elec. and compositional props., surface anal. 0-76575
 Si, multigrained, impurity segregation to grain boundaries, AES and SIMS obs. 0-65027

Auger effect continued

- Si p⁺-i-n⁺ field induced junction solar cells, conversion efficiency limit in concentrated sunlight 0-85282
 Si, phonon-assisted Auger recomb., direct calc. of overlap integrals 0-107808
 Si solar cells, fundamental efficiency limitations 0-93963
 Si solar cells, ion-implanted 0-81452
 Si solar cells, unified model of fundamental limitations 0-81448
 Si:Al, polycryst. film, grain boundary diffusion, Auger sputter profiling 0-75388
 Si:B diffusion at Si-SiO₂ interface, Auger spectra, Rutherford backscattering 0-70471
 Si:H, amorphous, Auger electron spectrosc. obs. 0-76112
 Si-refractory metal structures, interface modification by ion implantation 0-70475
 Si-SiO₂ (111) interface, H₂ effects, AES study 0-65688
 Si-SiO₂-Si₃N₄ MNOS structure, chem. comp. and electronic states, Auger and energy loss spectra obs. 0-92999
 Si_{1-x}C_xH glow discharge films, local atomic struct., XPS and AES study 0-93448
 SiH₄, L₂₃MM Auger spectrum, line width and intensities 0-58325
 Si₃N₄, Si(LVV) Auger spectra, ion bombardment, electron energy loss spectra 0-80911
 SiO₂ amorphous film, Si(LVV) Auger spectra, ion bombardment, electron energy loss spectra 0-80911
 SiO₂, Auger line shapes, final state correlation effects 0-89095
 SiO₂ coatings on SiO₂ substrate, cathodoluminescence spectra, electron irradi. 0-76085
 SiO₂ semi-insulating polycryst. films, AES and PES studies 0-107939
 SiO₂ thin films, deposition and characterisation study 0-80133
 Sn, (100) surface, clean and O₂ exposed, slow positron studies, positronium formation 0-93429
 Sn, internal conversion coeffs. for inner shells of atomic ions and relativistic ionic potentials 0-68600
 Sn, monolayer, double layer with Pb on Al (111), layer growth, struct. 0-70567
 Sn/Cu electroplated bimetallic films, interfacial reaction 0-96765
 SrO, XPS valence bandstruct. 0-89117
 Ti atoms sputtered from Ti, Ti oxides, photon emission, nonradiative transition effects 0-58208
 Ti:D, implanted, deuteride imaging using scanning Auger spectroscopy 0-89092
 Ti/Cu(Au) thin films thermocompression bonds degradation by thermal ageing 0-66546
 Ti-Mo alloy, thin anodic oxide, AES depth profile 0-71801
 Ti-W films, bias-sputtered, quantitative anal. 0-80114
 TiH₂ and TiD_{0.6}, surface characts., AES, EELS, SIMS, and XPS study 0-65343
 TiO₂, rutile, electron mean free path, four-step transition and Auger spectra investig. 0-97389
 TiO₂-Ni (100) interface, electronic props., struct., comp., chemical bonding 0-84499
 V₂O₅ and lower oxides, defect structures and related props. 0-59454
 W (100), condensation of Cu and Ag, early stage comparison with Mi(100) 0-80072
 W (110) surface, adsorbed Pd, growth, struct., stability, desorption 0-59794
 W surface, (100), photon and electron stimulated desorpt. of O 0-100397
 WC-Co DC and RF sputtered coatings, bias effect, struct., X-ray-Auger study 0-70565
 WSi₂, steam-oxidized, Auger sputter profiling studies 0-107663
 W(100), I adsorption at room temp., LEED and AES study 0-84389
 Xe adsorbed on Cu, NaCl, stepped and disordered surfaces, two-dimens. phase transformations 0-103580
 Zn, resonant two hole bound state at 3p core threshold 0-60750
 Zn, surface oxidation, Auger spectrosc. obs. 0-97388
 ZnTe clean and adsorbed O₂ (110) surfaces, UV photoemission spectra (*Japanese*) 0-93456
 Zr, adsorption and absorpt. of CO, NO, N₂, O₂, and D₂, dissoc. and diffusion 0-80085
- Auger electrons** *see Auger effect*
Auger showers *see cosmic ray showers and bursts*
Auger spectra *see Auger effect*
Auger spectroscopy *see Auger effect*
augmented plane wave calculations *see APW calculations*
- aurora**
see also airglow; atmospheric electron precipitation; atmospheric proton precipitation; atmospheric spectra
 acceleration region, altitudinal double-layer criterion 0-94656
 artificial aurora, conjugate to a Hawaiian launched electron accelerator 0-82124
 auroral arcs formation and V-potential double layers 0-103185
 Birkeland currents and auroral structure 0-77209
 current convective instability in auroral F-region 0-72680
 cyclotron soliton theory of Earth's kilometeric radiation 0-94657
 dayside aurora in F-region assoc. with magnetospheric cusp 0-90273
 dayside auroral morphology, from large scale obs. at 6300 Å, 5577 Å and 3914 Å 0-85786
 dayside auroral oval, elec. fields meas. 0-98501
 dayside auroral oval, evidence for parallel elec. field particle accel. 0-98503
 dayside cleft aurora and ionosphere effects, review 0-94633
 diffuse aurora, Birkeland current determ. from plasma line meas. of Chatanika 0-98507
 diffuse aurora, excitation by proton precip. due to magnetospheric proton-cyclotron instabilities 0-90286
 diffuse aurora equatorward boundary, 6300 Å obs. 0-72668
 discrete and diffuse aurorae, observed microstruct. 0-77188
 discrete auroral arcs and currents, review 0-77190
 discrete auroras near midnight, occurrence and lifetimes 0-67447
 double-layer criterion, trapped electrons and streaming speed 0-82123
 E₊-layer ionisation at high latitude, quiet and disturbed conditions 0-61941
 electric currents and potentials, generation by magnetosphere correction elec. field divergence 0-67453
 electric field, non-neutral field-aligned current sheet, theory 0-77196
 electric field of auroral arc, radar obs. 0-72692
 electrojet activity, rel. to LF/MF transmissions non-linear demodulation and ELF signals generation 0-94639

aurora continued

- electron accelerator expt. on POLAR-5 sounding rocket, for use within aurora 0-77170
 electron bunching near artificial electron beam 0-98511
 electron energy distrib. above aurora, secondary peaks driving instability 0-82135
 electron flux, rel. to field aligned elec. pot. difference 0-72684
 electron modulation at 2.2 Hz, geomagnetic equatorial origin 0-94632
 electron precipitation pulsating aurora 0-85794
 electrons acceleration mechanisms 0-77210
 equatorial latitude of auroral activity from DMSP satellite electron and visible obs. 0-98499
 field aligned current above auroral arc, e^- and H^+ precipitation obs. 0-77215
 field-aligned current closure and Joule heating near Harang discontinuity 0-72682
 global formation of auroral arcs, numerical simulation 0-67446
 historical aurorae, Latin terminology 0-62437
 history of auroral research, the less known contributors 0-73157
 infrasonic waves in substorm area, source regions (Japanese) 0-85788
 ion precipitation events in morning auroral oval, evidence for solar wind ion injections 0-98502
 ionosphere, auroral electron flux obs. 0-67466
 ionosphere electric field obs., comparative rocket obs. 0-85789
 ionosphere irregularities in auroral zone, simultaneous rocket probe, scintillation and incoherent scatter radar obs. 0-94640
 kilometer radio emission, obs. during JIKIKEN (EXOS-B) satellite initial phase (Japanese) 0-94675
 large scale structure observed by riometer radiowave absorpt. 0-72670
 latitudinal distribution, vars. during 18th and 19th centuries rel. to solar wind and sunspot activity long-term 0-98498
 location, visual and radio emission 0-82122
 luminosity rel. to geomag. field changes 0-77187
 meteoric aurora, review of historical obs. 0-94761
 microburst precipitation phenomena in auroral zone 0-77208
 neutral atmosphere interaction, obs. of neutral wind profiles in dayside auroral oval 0-98494
 nighttime auroral zone scintillation, struct. of localised enhancements 0-98506
 north-south movement of irregularities, 42 MHz obs. 0-67449
 palaeofield weak dipole epochs, nondipole component effect on auroral zone config. 0-105098
 particle dumping into ionosphere, Ariel 2 obs. 0-109313
 particle precipitation, high latit., relationship with auroral forms 0-77189
 particle precipitation, rel. to turbulence at 500 mb level 0-77218
 plasma parameters, incoherent scatt. of EM waves, EISCAT project (French) 0-82142
 polar luminance struct. depend. on plasma collective effects (Russian) 0-90274
 precipitating particle dynamics and auroral morphology, photometric data interpretation 0-82141
 pulsating aurora, the importance of the ionosphere 0-85787
 pulsating aurorae, evidence for limiting electron flux 0-72666
 pulsating auroral structures, implications of extreme vertical thinness 0-72667
 pulsations of electron and ion intensity 0-61934
 quiet auroral arc, electrostatic model 0-72669
 radio aurora (diffuse), rel. to field-aligned currents and particle precipitation 0-105119
 radio backscatter at 42 MHz, amplitude rel. to Doppler shift 0-61955
 radiowave absorption at mid-latitude coupled to auroral activity 0-61945
 rapid auroral fluctuations, obs., classification 0-77186
 SAR arc event, soft electron flux as excitation source 0-77217
 sky background elimination with stellar chopping photometer 0-72776
 spectroscopic observations, appl. of matched tandem etalon camera (MATEC) 0-101442
 time-dependent modelling 0-72672
 VHF radar aurora and strong HF backscatt. comparison 0-61960
 VLF hiss from auroral zone, direction find method and obs. 0-85777
 VUV global observations made by satellite, 110-290 nm region 0-90272
 N_2^+ I NG emissions from proton aurora, anomalous vibr. distrib. 0-67448
 $N(2D)$ emission and ion chemistry, satellite obs. 0-72673
 $N(2P)$, excitation and collisional deactivation processes in auroral arc 0-72658
 $N(2P)$ metastable atoms, UV spectra obs. 0-77185
 O I 6300 Å emission production efficiency by energetic electrons 0-72671
 O I forbidden emission, Fabry-Perot interferometer obs. for thermosphere wind and temp. meas. 0-101441
 O_2 ($^1\Delta_g$) emission, vibr. excitation process 0-82125

auroral ionisation see *aurora***austenitic stainless steel**

- ageing at high temp., effect on creep props. SEM 0-97516
 anodically polarised, Cl^- ion effect on passive film 0-97621
 bimetal with alloy steel, H permeability 0-107572
 cathodically charged, H, embrittlement, α' martensite effect 0-71725
 corrosion, and mass transfer in liq. Na of type 304, metallurgical factors influence (Japanese) 0-71804
 corrosion, crevice, rel. to surface comp., in type 316 0-93680
 corrosion, in molten SO_4 deposits of types AISI 316, 347 and Esstete 1250 0-97625
 corrosion behaviour in reducing environment of coal fired MHD generator 0-104322
 corrosion inhibition, of Li by AP additions 0-108646
 corrosion rate expressions, for type 304L in liq. Li, 600-100°C 0-93682
 corrosion resistance of cold deformed Cr-Ni austenitic stainless steel in N_2O_4 media at 433K (Russian) 0-76422
 corrosion resistance testing, urea plant applications (Czech) 0-61012
 corrosion testing, slow rate strain of type 55 23 33, under electrochem. control in high temp. water 0-97650
 crack growth behaviour, under creep and fatigue conditions, environment effects, on types 304 and 316 0-85035
 creep, cyclic, type 304, unbalanced tension-compression loading at elevated temp. 0-97545
 creep, effect of temp. and dose-rate variations on En58B, E, J, FV548 and type 316 in Dounreay fast reactor 0-93603
 creep, irradi. induced, 60 MeV alpha particles 0-92597
 creep, irradi. induced, deuteron bombarded type 316 0-93606
 creep, irradiation induced, type 316, climb induced glide model 0-89292

austenitic stainless steel continued

- creep crack growth, environmental sensitivity 0-85030
 creep deformation, under reversed cyclic stresses in type SUS 304 (Japanese) 0-81114
 creep dependence on electron irradi., in type SS316 steel, dislocation motion (Russian) 0-108495
 creep under irradi. of type 316 in HVEM 0-97523
 creep-fatigue crack propagation, in thermally aged type 316 0-89326
 diffusion coefficients of D, ion beam meas. technique 0-75382
 elastic constants, for N-alloyed steels, and low temp. sound vels. 0-108490
 embrittlement by He in 3H handling facilities 0-102285
 explosively welded, orientation relationship in martensitic transform. 0-104158
 fatigue behaviour, of soln. annealed and thermally aged type 304 0-100923
 fatigue crack growth and threshold measured at very high frequencies, for type 304 steel 0-71742
 fatigue crack propagation, effect of neutron irradiation 0-97583
 fatigue crack propagation, influence of neutron irradiation 0-97584
 fatigue mechanistic model, time-dependent, for type 304 0-100925
 fatigue properties, low cycle, in vac. of type 316 0-85021
 fatigue strength, low cycle, reduction factor for type SUS 304 (Japanese) 0-104259
 fatigue tests, low cycle, frequency effect on notch sensitivity at elevated temps. (Japanese) 0-104260
 fatigued, deform. substruct. and annealing stacking fault tetrahedra form 0-107282
 foil, in situ oxidation in HVEM 0-104354
 fracture-mechanisms, tensile specimens types 304 and 316 0-85039
 fretting corrosion of orthopaedic implant materials by bone cement 0-104813
 friction, wear and microstruct. of unlubricated 304, 316 and Nitronic 60 0-108589
 grain boundaries, interfacial structure effects on high temp. mechanical behaviour 0-59480
 grain boundary structure, during recrystn. and grain growth 0-76270
 induced martensites morphology 0-104153
 internal friction due to H_2 gas molecules 0-71682
 ion beam irradiation of type 316, effects study by HVEM 0-103396
 irradiation creep data, obtained in fast and thermal neutron spectra correlation with displacement cross-sections in types M316, FV548, 304 0-84993
 liquation cracking during welding, comp. influence 0-66645
 LWR piping, intergranular stress-corrosion cracking 0-81234
 martensite transformation of type 304, acoustic emission identification, opt. microscopy obs. 0-81062
 microarc studies in low temp. RF-plasma 0-96407
 nonsensitized, fatigue strength, intergranular corrosion effect (Japanese) 0-85027
 oxidation in CO_2 charged-particle nuclear techniques 0-61022
 phase identification, $2/3D$ imaging techniques 0-96424
 phosphide analysis using nonaqueous electrolyte potentiostatic etching method (Japanese) 0-89221
 pitting resistance, in low salinity brine 0-93681
 plastic deformation generalised constitutive rels. for type 304 0-104219
 plastic loosening and deform. defect healing during recovery annealing of 12Kh18N10T (Russian) 0-66530
 pool metal, solidification kinetics in welding with electromag. stirring 0-71636
 porous gauzes, hydraulic resist. in laminar filtration 0-100034
 precipitation behaviour under high temp. conditions, photoemission electron microscope obs. 0-108456
 precipitation of $M_{23}C_6$ type carbide on twin boundaries 0-89226
 radiational swelling of two-phase austenitic-ferritic stainless steels 0-65063
 repassivation kinetics study in Ct media 0-97614
 sensitisation assessment, Jominy bar technique 0-60887
 stacking fault energy, effect of N 0-107279
 steel, austenitic, type 316, in $MgCl_2$, acidity and applied potential effect on stress corrosion cracking 0-85076
 steel, austenitic stainless, stress corrosion crack growth, electrochem. aspects 0-97620
 steel, stainless, type 316, modelling effects of fast neutron irradiation in mech. behaviour 0-84234
 stress corrosion cracking, and K_{ISCC} in boiling $MgCl_2$ solns., effect of alloying elements on type 304 (Japanese) 0-93692
 stress corrosion cracking, classification in various environments (Japanese) 0-71805
 stress corrosion cracking, correl. between electrochem. and mech. parameters 0-97613
 stress corrosion cracking, factors influencing susceptibility 0-97617
 stress corrosion cracking, in $MgCl_2$ soln., temp. effect (Korean) 0-93694
 stress corrosion cracking, mechanisms (Japanese) 0-104336
 stress corrosion cracking, rel. between polarisation behaviour and susceptibility, in type 304 (Japanese) 0-93693
 stress corrosion cracking, role of H_2 , state of art review 0-61017
 stress corrosion cracking in $MgCl_2$ soln., cold working effect, in type 304 (Japanese) 0-104339
 stress corrosion cracking in various environments, fractography, of type SUS 304 (Japanese) 0-93690
 stress corrosion cracking inhibition, insensitized type 304 0-100939
 stress corrosion cracking susceptibility, effect of strain-induced α' -martensite (Japanese) 0-104335
 stress corrosion testing, slow strain rate, elevated temp. and high press. study 0-97615
 stress-strain relationships, uniaxial and biaxial, FBR containment 0-81122
 structural alloys for superconducting magnets in fusion energy systems, props. at 4K 0-86976
 surface, interaction with O_2 , AES and work function obs. 0-65364
 swelling in fission reactors, dose rate dependence 0-104233
 thermal fatigue, fractographic features of failure 0-76349
 thermal passivation of type AISI 316 steel in controlled vacuum 0-76276
 US examination, of type SIS 2343 butt welds 0-93710
 US wave velocity meas., rel. to cold working in type 304, 304L, 316L 0-99908
 viscoplastic behaviour, strain rate sensitivity, creep, relaxation, tensile tests 0-66727
 void volume, swelling, errors in determ. by TEM 0-84208
 weld, ferritic-austenitic solidification mode 0-89214

austenitic stainless steel continued

- welds, US inspection 0-71821
 X-ray stress meas., accuracy and method of data treatment (*Japanese*) 0-104365
 Cr-Ni, resist. damage rate during neutron irradiat. at 23K 0-96571
 Cr-Ni (18.22, 8.87 wt.%), welded joint, polarisation behaviour, boiling $MgCl_2$ soln. (*Japanese*) 0-93695
 Ni-Ni (20, 25 wt.%), Nb stabilized, oxidation behaviour in CO_2 , surface ion implantation effect 0-71791
 Cr-Ni-Ti (20,25,1.5 wt.%), dispersion-strengthened, threshold stress for creep 0-93626
 Cr-Ni (18.8 wt.%), X-ray stress meas., accuracy and method of data treatment (*Japanese*) 0-104365
 N-alloyed, room temp. elastic consts. and low temp. sound vels. 0-108490
 Ni-Cr, heat resist. and comp. of non-metallic inclusions, effect of La, Nd, Pr and Ce 0-76315
 Ni-Cr type, creep deformed, dislocation multipole obs. 0-107258
 Ti stabilised MC precipitate comp., APFIM study 0-104161

austenitic steel

- see also *austenitic stainless steel*
 10R6M5, atomised powders (*Russian*) 0-97446
 10R6M5K5, atomised powders (*Russian*) 0-97446
 ageing and plastic deform. effect on struct. and mech. props. of $Ni_{50}K_{50}G_{3}T_3$ (*Russian*) 0-71691
 carbide transformations on precipitation of C from austenite (*Russian*) 0-97487
 Charpy type bars of AISI 4340, varying notch root radii, fracture initiation and propag. at notch root 0-85050
 cold brittleness structural depend., fracture mechanisms in type 70 steel (*Russian*) 0-97571
 disc, biaxial fatigue testing under changing temps. (*German*) 0-71759
 electron beam welded, Charpy test expts. (*Hungarian*) 0-104252
 emissivity, integrated normal with low heat conductivity coeffs. of type $K_{23}Ni_{18}$ 0-103504
 explosive-thermal treatment, sulphide cracking decrease, hydrogen embrittlement (*Russian*) 0-108477
 friction in vacuum of type U8 steel under microshock loading (*Russian*) 0-108583
 heat resisting, creep rupture props., effect of grain- and grain boundary-strengths 0-97573
 high strength, treatment effect on ductility and strength 0-60880
 low-C, hot deform., austenite strengthening and weakening 0-76282
 metastable, fatigue testing machine and fatigue strength temp. dependence (*Japanese*) 0-71842
 plastic deformation influence on internal friction, relaxation processes (*Russian*) 0-100870
 precipitation behaviour under high temp. conditions, photoemission electron microscope obs. 0-108456
 quenched state, impact strength, influence of austenite stability (*Russian*) 0-81146
 rod, coupled flexural and torsional vibrs., energy dissipation 0-89281
 self diffusion of Fe, Cr and Ni (*Czech*) 0-107464
 steel, austenitic, ageing and plastic deform. effect on struct. and mech. props. of $Ni_{50}K_{50}G_{3}T_3$ (*Russian*) 0-71691
 steel, ferritic and austenitic, microstruct. study by means of replicas taken from components at 100°C 0-81256
 strength, ductility and fracture toughness, N and Cr effects 0-100878
 structure steels 4Kh4VMFSSh and 45Kh3V3MFSSh, grain size, hot deform. and austenitising effects 0-76286
 tensile strength, elec. current impulse effect down to 4.2K 0-81131
 thermal expansion, of heavily doped steels and alloys 0-103501
 white phases structure after heat treatment, steel 30KhGSA 0-76281
 Cr (2%), austenite decomp., phase diagrams and struct. form. kinetics 0-76223
 Cr, deform. on decomp. of austenite, carbide precipitation 0-84938
 Cr, post-hotforming recrystallisation condition, use of NEOPHOT 2 and EPIQUANT 0-84949
 Cr with metastable austenite, wear resist., temp. effect 0-76370
 Cr-Mn-B-N, phase composition and struct. transformations 0-104171
 Cr-Mo-V low-alloy, prior austenite grain boundary embrittlement by B 0-66657
 Cr-Mo-W, splat quenched, formation of metastable austenite 0-84974
 Cr-Mo(V), creep resist., high-temp. props. residuals effect 0-66600
 Cr-Ni, intergranular damage parameters in creep (*Czech*) 0-89342
 Cr-Ni, ion-implanted N, chem. state study by AES and XPS 0-79825
 Cr-Ni-Ti (08KH18Ni10T), heat treatment for fission reactor appls. 0-66454
 Fe-Mn-Cr-V-C, carbide strain hardened, strength and plasticity, effect of Mn content (*Russian*) 0-97500
 Fe-Mn-V-C, carbide strain hardened, strength and plasticity, effect of Mn content (*Russian*) 0-97500
 Fe-Mn-V-C type, ageing characts., discontinuous precip. nature 0-84940
 Mn (high), creep rupture, p addition and two-step soln. heat treatment effects (*Korean*) 0-93646
 Mn-Cr, austenitic struct. stability and low-temp. toughness (*Japanese*) 0-76356
 Ni (17 wt.%), martensitic deform. temp., cryst. struct. effect (*Russian*) 0-66576
 Ni-Cr-Fe base, radiation enhanced precip. and dissolution of precipitates, point defect kinetics and dislocation obs. 0-108467
 Ni-Cr-Mo, (En 24) deform. effect on decomp. of austenite, carbide precipitation 0-84938
 V, deform. effect on decomp. of austenite, carbide precipitation 0-84938

autoionisation

- see also *Auger effect*
 adsorbed layers, autoionisation bands due to one-centre resonances, theory 0-59790
 atomic photoionisation anal. using relativistic random phase approximation and multichannel quantum defect theory 0-63602
 atomic states, autoionising, electron impact ionisation obs., distortion effects calcs. 0-83491
 atoms, Rydberg states, autoionisation with large orbital angular momentum 0-87052
 azulene, multiphoton ionisation, mass spectra 0-63717
 decay state interactions, autoionisation bands (*Russian*) 0-75486
 electrons from autoionising states, angular distribution, fine and hyperfine struct. 0-58222
 excited atom thermal energy collisions, electron spectrometric studies 0-63788

autoionisation continued

- fast projectile electron loss forward peak oscill. struct. as autoionisation 0-69227
 ion+electron collision, resonant electron bremsstrahlung (*Russian*) 0-102580
 metastable autoionising states, ang. distrib. of electrons which decay via fine and hyperfine struct. interactions 0-102492
 multiply charged ion+atom, autoionisation, electron and photon emission 0-63813
 naphthalene, multiphoton ionisation, mass spectra 0-63717
 plasma dielectric satellite spectra, electron collisions, corona model theory 0-59188
 two step reson. photoionisation, multimode and level degeneracy effects 0-78583
 Ag, polarised photoelectron yields in VUV region 0-106307
 Al, autoionisation reson. determ. from photoelectron polarisation meas. 0-58221
 Ar, absorpt. spectra, field induced autoionisation near ionisation threshold 0-106301
 Ar, spin-polarised photoelectrons by circularly polarised synchrotron radiation 0-91516
 Ba I, two-step autoionisation 0-91513
 Be I like ions, resonant-scatt. contributions to excitation rates 0-58393
 CO, photoelectron ang. distributions, wavelength and vibr. state depend., reson. effects, asymmetry parameters 0-91602
 CO, $X^2\Sigma^+$, vibr. levels, UPS electron attachment obs. 0-95683
 CO₂, high resolution UV photoelectron spectra 0-91603
 COS, high resolution UV photoelectron spectra 0-91603
 CS₂, electronic autoionisation branching 0-91614
 CS₂, high resolution UV photoelectron spectra 0-91603
 Cd, $4d^{10}5p^1P$ autoionising state, electron impact ionisation obs., distortion effects calcs. 0-83491
 Cd, 5^1P_1 autoionising state, 150 eV electron impact excitation, (e, 2e) ang. distrib. study 0-83495
 He, metastable states, electron and proton impact ionisation, autoionisation 0-102573
 He, photoionisation cross sections up to $n=2$ excited state, evidence of autoionisation 0-91520
 He triplet states, doubly excited, spectrum and polarisation 0-99472
 He+Li⁺ autoionisation, electron spectra 0-91653
 He⁺+He, autoionisation electrons and scatt. ions, ang. correl. determ. 0-63792
 K₂, supersonic mol. beam, isotope selective two-step photoionisation study 0-74203
 Kr, absorpt. spectra, field induced autoionisation near ionisation threshold 0-106301
 Kr, spin-polarised photoelectrons by circularly polarised synchrotron radiation 0-91516
 Li core excited even parity 2P states, fluoresc. 0-69100
 Li⁺+Ne collisions, vel. dependence of Ne 2s and 2p, vacancy production, electron spectroscopy 0-58344
 Mg, 4snl autoionising states ejected electron spectra, low energy impact two electron excitation 0-83494
 N⁻ autoionisation from N₂ electron impact dissoci., EELS 0-106397
 N₂O, electronic autoionisation branching 0-91614
 N₂O, photoelectron spectrum, vibronic interaction and autoionis. effects 0-95680
 Na, overlapping autoionisation lines, interference effects 0-91677
 Ne⁻ scatt. electron spectra, distinction from neutral autoionising states 0-83482
 Ni, $M_{II,III}$ spectrum, ab initio calculation 0-83276
 O⁴⁺, resonant-scatt. contributions to excitation rates 0-58393
 O₂, I and I' resonance series, vibr. level populations in autoionisation, photoelectron spectra, bond length determ. 0-91612
 Ti, autoionisation reson. determ. from photoelectron polarisation meas. 0-58221
 Ti, ionisation limit and oscill. strength in VUV absorpt. spectra 0-74152
²⁰¹Tl β -decay, K-shell autoionisation accompanying internal bremsstrahlung 0-57745
 Xe, autoionising reson., Stark effect 0-58198
 Yb highly excited levels, reson., visible two photon absorpt. spectra obs. 0-58228

automatic control

- bubble chamber film analysis, semiautomatic measuring system 0-58105
 conductometer to record rapidly varying electrical conductivity 0-61184
 monochrome photographic print exposure control cct. (*Danish*) 0-62748
 photomicroscopes with automatic exposure control 0-86475
 plasma oscillations, stabilisation of spatial mode, algorithm 0-64721
 plastics sheet blowing and extruding, process identification for automatic process control (*German*) 0-81023
 quantum oscillator, phase automatic freq. control parameters, optimal values (*Russian*) 0-77814
 stereoscopic X-ray unit for medical diagnostic sets 0-85467
 X-ray spectrometer movements, automatic control system 0-69012
 H₂SO₄ mist monitor, semicontinuous 0-61495

automatic data processing see *data processing***automatic frequency control**

- IMPATT source, frequency-stabilised, 115 GHz 0-67573

automatic gain control

- double-beam single-detector wavelength-modulating spectrometer, appln. 0-86447

automatic test equipment

- blood cell leukocytes, automatic recognition and classification systems (*Italian*) 0-81780
 calculator-based instruments, meas. accel. due to gravity 0-73336
 channel separating system for multichannel radiometer (*Russian*) 0-58094
 dielectric loss of polymers determ., at 100 MHz to 300 MHz and 2°C to 40°C 0-68219
 digital equipment for recording acoustic emission signals 0-102948
 eddy current testing of wire and bar 0-71819
 fluctuating noise measurement system (*French*) 0-64316
 gel permeation chromatography, automated system using laboratory automation system 0-71961
 hardness testing apparatus display for time dependent hardness test on plastics (*German*) 0-66742
 impact machines, pendulum, energy meas. using optical system 0-69746
 Large Coil Test Facility, instrumentation system design 0-95446
 magnetic induction measuring device for superconducting solenoids, using NMR 0-57344

automatic test equipment continued

- material inspection techniques using lasers 0-66734
- measurement of thermoelectromotive force and resistance, study of kinetic phenomena of charge transfers 0-57330
- measuring-channel characteristics measurements, process control systems, compound and element-by-element methods 0-62612
- mechanical testing of materials automation, using 500 kN and 2.5 MN ATE (Czech) 0-66710
- microcomputer-based blood-pressure recorder (Japanese) 0-67139
- pacemaker testing in vivo, computerised system 0-94412
- PDP 11/40 minicomputer dynamic analysis system, noise analysis of fluid power equipment, graphical presentation of results 0-64327
- plastics testing, automation 0-76443
- resistance thermometer automatic calibration oven 0-98914
- reverberation time digital meas. instrum. for auditoria and studios (Japanese) 0-64321
- steel, ball bearing rods, inspection installation 0-81268
- submarine periscope optical test equipment 0-78943
- surface roughness meas., hand-held instrument with in-built data processor (German) 0-57255
- system to monitor effluent tank contents, HPLC analysis 0-71982
- tensile testing, control of test cycles, data logging and data processing (German) 0-97648
- tests control and evaluation, using 500 kN and 2.5 MN ATE, fracture toughness and fatigue strength determ. (Czech) 0-66710
- viscosimeter, high-temp. device for melt viscosity determ. 0-79418

automatic testing

- destructive examination of materials with data processing, microprocessor application (German) 0-93714
- digital voltmeters, pulse-counting, automatic checking method 0-57240
- ferrite materials and components, laboratory meas. automation (Polish) 0-101789
- fluorescence microscope photometry data processing and display (German) 0-86369
- hardness testing apparatus display for time dependent hardness test on plastics (German) 0-66742
- nuclear steam generator tubes testing and evaluation, using CIS/DASIO system (Czech) 0-63301
- piezoelectric transducer automatic setup, for continuous meas. of internal friction and elastic moduli of solids 0-108652
- pipes, hot-rolled, automatic mag. quality control on prod. line 0-108661
- plastics testing, automation 0-76443
- refractories, strength and thermal properties, automated test system 0-100986
- solar cell, automated electronic analysis system 0-93952
- weighing, automatic, application in ceramics industry 0-95074

automobile industry

- electron beam appl., to metal treatment (French) 0-66558
- motor-car corrosion protection improvement, primer paint appl. by electro-coating effect (Dutch) 0-71915
- polyurethane foam, processing machines and systems, motor car components appl. (German) 0-71955

autoresonant accelerators *see collective accelerators***avalanche diodes**

- see also avalanche photodiodes; IMPATT diodes*
- No entries

avalanche photodiodes

- laser low-level pulse meas. system at 1.064, transfer standards 0-86253
- for optical fibre communication (Japanese) 0-78977
- optical fibre sources and detectors (Italian) 0-69390
- optical fibre transmission system devices (Japanese) 0-58693
- SEM, electron beam induced cond. of defects, rel. to TEM 0-107027
- transmission system, semiconductor device reliability tests 0-58573
- Ge, ionisation rates, cryst. orientation depend. 0-103700
- $\text{In}_{0.51}\text{Ga}_{0.49}\text{As-InP}$ avalanche photodiode with guard-ring struct., characts. 0-96939
- $\text{In}_{0.51}\text{Ga}_{0.49}\text{As-InP}$ avalanche photodiode structure for 1 to 1.6 μm region 0-98978
- InGaAsP avalanche photodiode, 1.3 μm , noise performance, -190°C 0-57370
- InGaAsP avalanche photodiodes, breakdown mechanism, donor conc. effect 0-70710
- InP , microplasmas, investigation 0-60018
- InP-Cd(Zn) , avalanche photodiode characts., impurity diffusion effects 0-70709
- InP/InGaAsP , with guard ring structure 0-100506
- InP-InGaAsP p-n junction avalanche photodiodes, surface passivation techniques 0-100508
- $\text{n}^+\text{-n-pGe}$ avalanche photodiode, noise factors, internal quantum efficiency 0-70803
- Si, lightwave sources and detectors 0-64068
- Si p-n junctions, electron emission from depletion layers 0-100509
- Si photodiode, avalanche, n^+prp^+ -type, primary photocurrent anal. by noise measurements (French) 0-88624

avalanches, carrier *see impact ionisation***avalanches, electron** *see electron avalanches***avalanches, electron-hole** *see impact ionisation***avionic systems** *see aircraft instrumentation***avogadro's number** *see constants***axicons** *see lenses***axiomatic field theory**

- 1/N expansion in two-dimensional lattice gauge theory 0-86559
- θ^4 quantum fields, ground state energy per particle 0-68064
- $\lambda\phi^8$ field theory, 3 space-time dimensions, renormalisation, analytical continuation to imaginary time 0-86563
- $\lambda\phi^{(4,6)}$ field theory in curved spacetime 0-86556
- $\lambda\phi^4$ field theory at finite temp., Casimir effect and topological mass 0-57479
- $\lambda\phi^4$ self interaction theory, symmetry breaking and mass generation by space-time topology 0-82892
- $\lambda\phi^4$ theory, conformal symmetry breaking, cosmological particle creation 0-90998
- $\lambda\phi^4$ theory, dynamical mass generation in $\text{S}^1 \times \mathbb{R}^3$ 0-99046
- $\lambda\phi^4$ theory, renormalisation in nonsimply connected spacetime 0-90999
- $\text{LP}(\phi)_2$ model, bound states and irreducible kernels 0-73569
- $\text{LP}(\phi)$ lattice theory, coupling const., analyticity 0-99035
- ν -dimensional Yang-Mills and $(\nu-1)$ -dimens. nonlinear σ -model connection, quark confinement, dual strings 0-90978
- σ model, $\text{SU}(3)$ linear, renormalisation in one loop approx. 0-68368

axiomatic field theory continued

- σ model, two and four-dimens., classical solns., instantons and merons 0-86548
- σ models of nonlinear evolution equations 0-57487
- σ -model, classical solns., stability props. 0-77954
- σ -model, nonlinear, n-component, on lattice of arbitrary dimensions, 1/n expansion 0-73576
- σ -model, nonlinear, order-parameter relaxation from renormalisation group 0-57504
- ϕ_s^3 theory, anomalous dimension, Regge cut effect on structure function 0-62847
- Φ^{2k} theory in d-dimensions, strong coupling expansion 0-99054
- $(\phi^3)_1$ field theory, deep inelastic lepton-headron scatt., cut vertex theory and reciprocity relation 0-57466
- $(\phi^3)_6$ theory, composite particle form factor, asymptotic behaviour 0-86595
- $\phi^{4,6}$ self-interacting theory, three well potential, block spin renormalization 0-57490
- ϕ^4 lattice field theory, d-dimens., thermodynamic props. near Ising limit 0-82860
- ϕ^4 model, large order perturbation coeffs., asymptotic evaluation 0-82867
- ϕ^4 model, strong coupling and infrared struct., renormalisation 0-101921
- ϕ^4 theories, orthogonal transforms 0-82898
- ϕ^4 theory, bound states and irreducible kernels 0-73569
- Φ^4 theory, conformal-invariant, massive scalar, tadpole diagram, Ward identity 0-73593
- ϕ^4 theory, Euclidean, local existence of Borel transform of Schwinger functions 0-77932
- aesthetic field equations, behaviour of solutions, pulse and oscillatory solns. 0-68346
- bell's inequalities from the field concept in general relativity 0-105771
- confinement in $\text{SU}(N)$ lattice gauge theories 0-57493
- critical exponents to order ϵ^3 for ϕ^3 models of critical phenomena in $d-\epsilon$ dimensions 0-86547
- discrete lattice gauge theories with matter fields, 1/N expansions phase diagram 0-73603
- duality in field theory and statistical systems, review 0-73610
- elementary particle modeling in axiomatic relativistic field theories (German) 0-91009
- embedding lattice field theory in continuum field theory 0-77972
- Euclidean Dirac field, local structure, Green's function method 0-68347
- Euclidean fields, low momentum behaviour scale limit 0-62834
- Euclidean QED, on lattice, continuum limit, Schwinger functions, vacuum expectation values 0-73624
- Euclidean quantisation of gauge theories, Weinger integral and nonstandard analysis 0-68358
- Euclidean quantum field theory, 1/n expansion 0-82864
- Euclidean quantum field theory, n-point functions, renormalised G-convolution 0-68341
- Euclidean self-dual Yang-Mills field configurations, set of linear algebraic eqns. 0-73587
- Euclidean space, spherically symmetric self-dual eqns., representation theory and integration 0-77936
- evaluation functionals, products, convolutions, distribution integrals 0-57498
- Feynman amplitudes, zero-mass behaviour 0-68353
- free automorphic quantum field theory, gauge transformations and field algebras 0-86546
- ϕ^4 quantum field theory, clusterlike expansion based on static ultralocal approx. 0-62839
- $g\phi^4$ renormalised field theory in limit $g \rightarrow \infty$, effective potential 0-99058
- goldstone modes in vacuum decay and first-order phase transitions 0-77941
- gravitational instantons, self-dual soln. to Euclidean gravity 0-68118
- Green's functions, nonperturbative generating functionals 0-73588
- Haag-Ruelle formulation of scattering in hyperfunction quantum field theory 0-57497
- Hawking effect, temp. relativity, axiomatic field theory 0-109456
- holonomic fields, density matrix of impenetrable Bose gas 0-62576
- inclusive processes, analytic structure of the 3-3 forward amplitude 0-68376
- instanton system weakly interacting with anti-instanton system, external electric fields, structure and stability 0-77956
- instantons in the presence of a fixed density of massless fermions in two dimensions 0-62853
- lattice gauge theories, boxiton scatt. cross section 0-82890
- lattice gauge theories, chiral symmetry dynamical breaking 0-99061
- lattice gauge theories, vortex free energy, strong and intermediate coupling string tension 0-105786
- lattice gauge theories, $\text{Z}(N)$ system phase struct., dual variables 0-62848
- lattice Hamiltonian field theory, finite-size scaling 0-73580
- lattice massive dual fields for eqn. 0-105779
- lattice QCD, Wilson's loop eqn. soln. for large N limit 0-78030
- lattice QCD, hadron mass spectrum, effective Hamiltonians, degenerate perturbation theory 0-102003
- lattice regularised field theory, renormalised and bare coupling constants 0-77960
- lattice $\text{SU}(N)$ gauge theory, vacuum structure, large-scale 0-57470
- Luttinger-Thirring model on lattice, real space-time renormalisation 0-62590
- mass, physical, in ϕ^4 -model, renormalisation group and mass generation 0-77948
- massless $[g\phi^4]_4$ theory, functional integrals, complex instantons and asymptotic perturbation series 0-86571
- membrane models and generalized Z_2 gauge theories, renormalisation props. 0-86587
- Minkowski-space formulation of two-pseudoparticle processes 0-95220
- model $\text{U}(N)$ lattice gauge theories, exactly soluble, $N=\infty$ phase transition 0-86583
- model with anomalous dimensionalities in four-dimensional space 0-101934
- n-point functions, renormalised G-convolution, convergence in Euclidean case 0-77930
- nonAbelian lattice gauge theories, phase structure critical temp. 0-86592
- $\text{O}(N)$ invariant $(\phi^3)_1$ model, chiral field model and universality in 3-dimens. space 0-105796
- order, disorder and generalized statistics 0-99055
- propositional systems in local field theories 0-105799
- QCD, lattice and continuum, Λ parameters connections 0-82945
- random spin systems, gauge symm., phase transitions (Russian) 0-77929

axiomatic field theory continued

- scattering operator, analyticity in nonlinear relativistic classical and pre-quantised field theories 0-73611
- Schrodinger equation, nonlinear field equations, quantum inverse scattering transform method, 2-D ice and ferroelectric lattices 0-68348
- sequential events and objectivistic probabilities, quantum logic 0-94973
- sine-Gordon equation, discrete, on SU(2) lattice, group theory aspects 0-57486
- sine-Gordon equation, nonlinear field equations, quantum inverse scattering transform method, 2-D ice and ferroelectric lattices 0-68348
- spatial inversions in aesthetic field theory, complex fields, computer solns. 0-68350
- spin-statistics theorem, asymptotic, for composites containing electric and magnetic charges 0-68342
- SU(N) lattice gauge theories, weak to strong coupling crossover 0-95212
- thinning degrees of freedom in lattice field theories 0-57492
- transverse lattice QCD, hadron mass spectrum 0-57568
- tricritical behavior in a two-dimensional field theory 0-77726
- trilocal structures, expansions 0-57460
- twisted lattice gauge fields, local order parameter, phase transitions 0-77966
- U(1) lattice gauge model, phase transition in four-dimensional compact QED 0-105820
- U(1) lattice gauge theory, four dims., nonconfining phase, existence proof 0-73602
- U(N) lattice gauge theory as $N \rightarrow \infty$, planar diagram sums in terms of statistical ensembles 0-99052
- ultradistributions, Fourier-Laplace transforms, boundary values 0-57496
- Wightman function, two-point, asymptotic behaviour 0-73614
- Wightman theories, consequences of weakening positivity property 0-62833
- Wilson's lattice, local chiral symmetry for gauge theories 0-105774
- Wilson loop critical point behaviour in gauge and lattice gauge theories 0-90993
- Yukawa, quantum field theory, FKG correlation inequality 0-68357
- Yukawa field theory model, boson field fluctuations and FKG inequalities 0-77712
- Yukawa potentials, finite sum S-matrix 0-101940
- Z_2 lattice gauge Higgs theories, Monte-Carlo calcs. 0-86593
- Z_n four dimensional lattice gauge theories, series anal. 0-99050
- Z_n lattice gauge theory coupled to Higgs field, phase diagrams 0-57485
- Z_n symmetric models phase transitions 0-101922
- Z(2)(3) Ising spin systems, Hamiltonian formulation in 1+1 dims. 0-57491
- Z(2) gauge theories, hidden fermions 0-82899
- Z(2) gauge theory, phase transition, variational calcs. 0-99049
- Z(2) lattice gauge theory, variational approach, two phase struct., phase transition 0-68361
- Z(2) lattice gauge theory in 2+1 dims., fermion representation 0-82900
- Z(N) and U(1) lattice theories in three-dims., phase diagram 0-82901
- Z(N) strings and hadron structure 0-86572
- ϕ^4 model, free energy, spontaneous symmetry breaking 0-101925
- ϕ^4 -field model with image mass, spontaneous coherent state transition 0-99057
- $\pi\pi$ scatt. lengths, rigorous phenomenological anal. 0-102070

backscatter

see also particle backscattering

- acoustic backscatter in GATE, effect of wind shear and moisture fluctuations 0-85709
- acoustic backscattering cross-sections of live fish, probability density function and aspect 0-64260
- acoustic backscattering from a plate with a thickness discontinuity 0-96056
- acoustic backscattering measurements in laboratory waveguide 0-64259
- acoustic transducer, backscattering formula 0-96064
- active and passive remote sensing of Earth terrain, effects of scattering 0-101435
- broadband integrated backscatter approach to tissue characterization in vivo 0-74635
- cirrus clouds, lidar backscatter meas. rel. to visible and IR optical props. calc. 0-82060
- clouds, radar reflectivity rel. to cloud dynamics and microphysics 0-61877
- EM plane waves, scattering by metal cone, near its symmetry axis 0-106426
- heavy ion neutralization behaviour in the 30-130 keV energy regime 0-71542
- heterodyne optical radar S/N ratio in atmospheric turbulence 0-106558
- ionosphere, equatorial, backscatter data rel. to irregularity patch form., motion and decay 0-67456
- ionosphere, equatorial radar backscatter plumes spatial relationship with plasma bubbles 0-67457
- lidar target calibration, backscatter refl. for circularly polarised radiation 0-102750
- meteors, bright, radar backscatter meas. of ionisation columns initial radii 0-94762
- nonhomogeneous layer above reflecting surface, scattering of waves 0-58449
- optical fibre attenuation, bandwidth, and refractive index meas. methods compared 0-64190
- optical fibre attenuation charact. meas. by backscatter technique (Italian) 0-106600
- optical fibre attenuation meas. by backscattering method, effect of noise 0-102824
- optical fibre attenuation measurements performed by backscattering technique 0-64152
- optical fibre connector loss evaluation by backscattering 0-58721
- optical fibre loss estimation using backscatter technique, time domain reflectometry theoretical assumptions 0-74508
- optical fibre splice insertion loss meas., backscattering method 0-58720
- optical fibres, backscatter meas. theory (German) 0-91921
- optical fibres, backscattering method for attenuation and connection insertion loss meas. anal. 0-58675
- optical single-mode fibres, backscattering method analysis 0-106610
- optical time domain reflectometry by photon counting 0-95122
- optical waveguides, power decay eval. using backscattering technique 0-106599
- plasma, stimulated Raman and Brillouin backscattering along mag. field 0-69983

backscatter continued

- random media, active remote sensing, depolarisation effects 0-82090
- sea surface, microwave backscatter rel. to remote sensing using one and two freq. microwave techniques 0-94622
- single-mode optical fibres, backscattering signal anal. utilising wave optics approach 0-64151
- stimulated light scatt., wavefront reconstruction 0-64107
- stimulated Raman scatt., backscatter in an optical fibre 0-64109
- VHF radar aurora and strong HF backscatt. comparison 0-61960
- water, backscatter and absorption coeffs., simultaneous determ. 0-82074
- wave reflected from randomly inhomogeneous layer description, by series satisfying causality condition 0-106420
- CO₂-laser (long pulse)-plasma interaction, classical absorpt. and heat conduction in low-irradiance 0-75059
- H⁺, neutralisation in low energy surface scatt. by polycryst. graphite 0-71541
- He⁺ reflection from Pt surface, 10 to 35 keV 0-71543

backward wave oscillations *see backward wave tubes; electromagnetic oscillations*

backward wave tubes

see also carcinotrons

- BWO for 110 to 170 GHz, using Sm-Co using magnets, design and appl. (German) 0-105684
- EM waves generation and amplification based on Doppler effect 0-63902

bagging *see packaging*

balance (physiological) *see mechanoception*

balances

see also weighing

- beam microbalance for microweighing in vacuum and controlled environments, book 0-62401
- Faraday balance for teaching appl., strong mag. field rel. to react. rates 0-57043
- hydrostatic weighing, solid density standards 0-77758
- metal surface oxidation study, vacuum microbalance investigation 0-76552
- piezoelectric quartz cryst. microbalance for sorption studies under dynamic conditions 0-73323
- precision, electronic methods (French) 0-62660
- pressure, effective area at low press. 0-86332
- pressure, improved floating-element spinning mechanism 0-86331
- substance amount, precise meas. and dosage 0-90819
- vacuum microbalance, Cahn RG-2000, improvement in sensibility 0-77794
- vacuum microbalance, cryopump 0-77803
- vacuum microbalance, props., characts., applications 0-73322
- vacuum microbalance of physical adsorption studies 0-76551
- vibration isolation cantilevered bench 0-68183
- weight and cost read-out balances (Polish) 0-90820

ball lightning *see lightning*

ballistics

see also impact (mechanical); military equipment

- equivalence principle, monkey and hunter demonstration 0-67984
- Gurney's ballistics calc. 0-67946
- local inertial frame of reference, demonstration 0-67982
- spacecraft braking problem in Jupiter atmosphere, ballistic and navigation aspects 0-61981

balloons

see also aircraft

- air, buoyancy demonstration 0-67988
- astronomy and atmosphere programs, conf. Bournemouth, England (1980, Aug.) 0-105433
- atmosphere IR mosaic background obs. from balloon altitude expt. 0-90222
- double theodolite measurement of balloon height, control of inherent uncertainties 0-77160
- far IR calibration source for balloon-borne telescopes 0-62027
- magnetic measurement at high altitude, by high-sensitivity balloon-borne ring-core magnetometer (Japanese) 0-94608
- stratosphere superpress. balloon, used as radiometry sensor 0-85763

band gap *see energy gap*

band model of magnetism

see also Hubbard model

- amorphous alloys, Curie temp. comp. depend. 0-84597
- antiferromagnet, itinerant, paramag. impurity effects on Neel temp., calc. 0-60257
- electron-hole paired systems, ferromagnetic ordering phase diagram 0-97097
- Fermi surface, electronic props., book 0-105445
- ferromagnet, itinerant, mag. props., temp. depend., functional integral approach 0-60170
- ferromagnet, itinerant, spin waves, surface effects, RPA calc. 0-60226
- ferromagnet, itinerant electron, magnetoelastic contribs. to US vel., elastic consts., and susceptibility 0-75829
- ferromagnet, itinerant electron, magnetoresist. and anomalous Hall effect due to electron-phonon interactions 0-70680
- ferromagnet, itinerant electron, magnon spectrum just below T_c, theory 0-65833
- ferromagnet, itinerant electron, temp. depend. of angle-resolved photoemission 0-76142
- ferromagnetic conducting cryst., dynamics of s-d model in alternating mag. field (Russian) 0-65825
- ferromagnetic metal, exciton condensation effects on props., Hubbard model 0-60171
- ferromagnetic metal, uniaxial, anisotropic spin fluctuations and anisotropic band struct. effects on resist. near T_c 0-65543
- ferromagnetic s-d model, electronic spectrum struct., moments method 0-97052
- ferromagnetic semiconductor, two-band s-d model hybridization 0-65446
- ferromagnetic semiconductors, electronic quasiparticle spectrum 0-97051
- ferromagnetism, itinerant electron model, contrib. of Conyers Herring in 1930s 0-57056
- itinerant electron ferromagnets, elastic props. and electronic struct. 0-66001
- itinerant electron ferromagnets, magneto-volume effects 0-60397
- itinerant magnets, band struct., mag. props. and local moments 0-70929
- metal, electron-phonon interaction effects on spin susceptibility 0-93108
- metal, indirect coupling between localised mag. moments by narrow band electrons 0-70942

band model of magnetism continued

- metallic magnetic materials, high mag. field effects, interpretation of expt. results 0-60272
 narrow band electron systems, unified theory of magnetism 0-70928
 periodic Anderson Hamiltonian, alloy analogy treatment for mixed valence states 0-75527
 single-site spin fluctuation theory of itinerant-electron systems with narrow bands 0-97049
 susceptibility, local exchange approx. calc. in itinerant electron magnets 0-60169
 transition metal, chemisorption of H, effect of surface spin fluctuations 0-75613
 transition metal, ferromag., band theory of linear magnetostriction 0-71141
 transition metal 3d monoxides, specific vol. and mag. moment calcs. 0-65822
 transition metal alloys, dilute ferromagnetic, itinerant d-electron(hole) degenerate, spin stiffness constant 0-70930
 transition metal intermetallic cpds., H absorption and mag. props. 0-60224
 transition metals, 3d, ferromag. props., book contrib. 0-75724
 transition metals, paramagnetic state, itinerant electron model 0-65769
 CoS₂, itinerant ferromagnet, ferromag. reson. and EPR meas. 0-66044
 CoTi_{1-x}Al_x, mag. and electronic props., ferromag. and paramag. state 0-65814
 Cr, electronic struct., spin-density functional calcs. 0-88476
 Cr, spin density wave, Nambu-Eliashberg eqns. for k-state electron-hole pairing 0-97050
 Cr-V, itinerant electron antiferromag., spin fluctuations, low temp. specific heat 0-107439
 CrAs, high press. paramag. antiferromag. transitions, elec. props., band model development (*Russian*) 0-60277
 CrB₂, itinerant antiferromag., spin fluctuations, NMR study 0-108119
 Fe alloys, amorphous, mag. saturation, spin wave stiffness, temp. depend. 0-75741
 Fe alloys, amorphous, saturation magnetisation, Curie temp. and size effect 0-65815
 Fe, BCC, high field Knight shift and hyperfine anisotropy of ⁵⁷Fe 0-71205
 Fe, ferromag., dynamic susceptibility calc. 0-80488
 Fe, magnetic moments, local short range order, high temp. effects 0-65902
 Fe, magnetism at high temps., total electronic band struct. energy calc. 0-75721
 Fe-Ni Invar anomalies, explanation in terms of itinerant electron magnetism 0-75705
 Fe₃Al(Si), electronic structure, magnetic moments 0-107695
 (Fe_{0.9}Ni_{0.1})_{1-x}(SiO)_x, Permalloy material, magnetisation, temp. and impurity atom conc. depend., band model calcs. (*Russian*) 0-93088
 GdMg, noncollinear mag. struct., nonlinear band behaviour 0-75706
 LaMg, Pauli paramagnet, mag. susceptibility, nonlinear band behaviour 0-75706
 La_{1-x}Sr_xCoO₃, (0.5 ≤ x ≤ 0.9), ferromag., elec. props., itinerant electron model 0-107785
 τ -MnAl, estimated theoretical limit of mag. moment 0-97072
 MnSi, weak itinerant magnetic compound, paramagnetic response function, polarised neutron scattering 0-107982
 Ni, exchange splitting of 3d bands, angle-resolved photoemission meas. 0-71568
 Ni, ferromag., dynamic susceptibility calc. 0-80488
 Ni, paramagnetic, mag. form factors in Stoner-like model 0-97061
 Ni-Mn-H solid solutions, mag. props. 0-88753
 Ni-Ru (≤ 4 at.%), influence of alloying on mag. anisotropy, itinerant electron model 0-71010
 TiFe_{1-x}Co_x, electronic struct. and mag. moment calcs. 0-65821
 YMg, Pauli paramagnet, mag. susceptibility, nonlinear band behaviour 0-75706
 YNi₃, magnetism resurgence, neutron diffr. and mag. props. study 0-65819

band-pass filters

- see also crystal filters; vocoders
 image processing appl. of multiple bandpass filters 0-109002
 interference filters for 1-3 mm window, far IR astronomy 0-109368
 operation details, hearing analysis appl. (*Italian*) 0-94218
 SAW, combined bandpass and rejection filters, design and eval. (*Russian*) 0-83718
 SAW, use of charge distribution model 0-74678
 SAW, with three-transducer configuration 0-74610
 speech noise suppression filter for narrowband vocoder 0-91977
 surface skimming bulk wave filters using Y-rotated quartz 0-74583
 LiTaO₃ crystals for commercial SAW TV IF filters, fabrication 0-80961

band structure

- see also band structure of crystalline metals; band structure of crystalline semiconductors and insulators; band structure of semimetals; band theory models and calculation methods; Brillouin zones; conduction bands; degenerate semiconductors; electron energy states of amorphous solids; electron energy states of liquid metals; electron energy states of liquid semiconductors; energy gap; Fermi surface; many-valley semiconductors; valence bands
 binary alloys, random, quantum percolation 0-80156
 channelling in Kronig-Penney pot., band struct. and Bloch wavefunctions 0-65112
 conducting π -electron systems, electronic struct., one-electron band theory 0-65450
 diamagnetic band structure, first principles calc. 0-88470
 electron band structure, optically induced in external plane wave field 0-106432
 energy sub-bands in polar model of crystal (*Russian*) 0-80183
 graphite intercalated with AsF₆, quantum oscillatory phenomena 0-107823
 HEED atomic string approximation use in obtaining dispersion surfaces 0-100143
 metal-insulator transition region, narrow energy bands, electron correlation, Gutzwiller variational method 0-84426
 polyacetylene, electronic energy states and charge density contours studied muffin tin orbitals technique 0-80164
 polyacetylene, electronic struct., one-electron band theory 0-65450
 polyethylene, electronic energy states and charge density contours studied muffin tin orbitals technique 0-80164

band structure continued

- PTFE, electronic energy states and charge density contours studied muffin tin orbitals technique 0-80164
 solid state physics, book 0-101676
 TTF-TCNQ, elec. resist., electron-phonon scatt. 0-92884
 LiC₆, intercalation compound, electronic struct., XPS meas. 0-59850
 (SN)_x, electronic struct., one-electron band theory 0-65450
 ZrB₂, self-consistent band struct., XPS, reflectance, NQR, Hall effect and density of states meas. 0-107689

band structure of crystalline metals

- A-15 superconductors, transition temp., d band relative displacement (*Chinese*) 0-103770
 alkali metals, Fermi surface topological changes due to uniaxial stresses 0-92810
 alloys, CPA for props. 0-75493
 band structure, optical cond., Compton profile, self consistent calcs. 0-65435
 Fermi surface, electronic props., book 0-105445
 itinerant electron ferromagnets, elastic props. and electronic struct. 0-66001
 metals, electron-deformation interaction, lattice contraction, Hubbard model calcs. (*Russian*) 0-59592
 rare earth alloys, RBe₁₃, XPS, resist. and susceptibility study 0-71565
 TC, internal conversion, scattered-wave cluster technique 0-107696
 tight-binding metals, electronic struct. and kinetic props. at high temp. 0-59848
 transition, rare earth, and normal metals, electronic struct. and magnetism, review 0-70573
 transition metal alloys, binary, state density curves, relation between short-range order and Fermi level position, CPA calculations 0-107687
 transition metal alloys, cohesive properties and press.-vol. relation 0-92476
 transition metals, BCC, films, vac. evaporated, optical cond. 0-76100
 transition metals, universal LCAO parameters 0-75503
 Ag, Auger spectra, 4d bandwidth effect 0-89093
 Ag, thermomodulation spectra of high-energy interband transitions 0-108226
 Al, K X-ray absorption, K-emission spectrum, band struct. using APW method 0-97380
 Al, valence band Auger spectra, surface effect 0-80915
 AlAg, Auger spectra, 4d bandwidth effect 0-89093
 AlH₃, electronic struct. and electron-phonon interaction, hydrogenation effect, rel. to supercond. 0-107694
 Am, 5f-electron delocalisation 0-70595
 Au, energy band structure, X-ray N-emission spectra, relativistic APW calcs. 0-70596
 Au, energy band structure, X-ray emission spectra, APW calc. 0-92811
 Au, self-consistent relativistic band struct. 0-75501
 Au, thermomodulation spectra of high-energy interband transitions 0-108226
 Au(111), A-line valence bands, angle-resolved photoemission determ. 0-108323
 Be, electronic struct., NMR study 0-108085
 BeNi, dil., electronic struct., NMR study 0-108085
 Bi, deformation calculations, band struct. variation, electron phase transitions due to deform. (*Russian*) 0-65137
 Bi-Sb(-As), band struct., effects of Sb and As, mag. susceptibility meas. (*Russian*) 0-65775
 Bi_{1-x}Sb_x, deformation calculations, band struct. variation, electron phase transitions due to deform. (*Russian*) 0-65137
 Cd_{1-x}Mg_x, energy spectrum pseudopotential calcs., mag. props., impurity scatt. (*Russian*) 0-65430
 CeBe₃, intermediate valence state, XPS, resist. and susceptibility study 0-71565
 CeSn₃, mixed valence cpd., electronic struct. and mag. props. 0-70649
 Co, energy band dispersion and mag. exchange splitting, angle-resolved photoemission meas. 0-71567
 Co, energy band dispersions and mag. exchange splitting 0-76146
 Cr, electronic struct., spin-density functional calcs. 0-88476
 Cr, Neel temperature and Fermi energy, nonmag. impurity effects 0-65888
 Cr, spin density wave, Nambu-Eliashberg eqns. for k-state electron-hole pairing 0-97050
 Cs, supercond., elec. resist. and phase transforms. under high press. (*German*) 0-107763
 Cu (111), final state band gap effects in UPS 0-89120
 Cu (111) surface, PES and band struct. calcs. 0-89118
 Cu, bulk and (001) films, extended tight-binding calcs. 0-70592
 Cu, Fermi surface, electron mass enhancement, orthonormal function enhancement 0-96777
 Cu, thermomodulation spectra of high-energy interband transitions 0-108226
 Cu/Ni coherent modulated structures, electronic struct. and magnetism 0-103620
 Cu-phthalocyanine, photoemission multielectron effects from quasi atomic Cu 0-93458
 de Haas-van Alphen freq. and Fermi surface anisotropy press. depend. 0-59856
 Eu, electronic struct. investigation by electron spectroscopy method 0-92812
 Eu_{1-x}La_xS, electron struct., lattice const., X-ray spectral study (*Russian*) 0-100432
 Fe, energy band dispersion and mag. exchange splitting, angle-resolved photoemission meas. 0-71567
 Fe, magnetism at high temps., total electronic band struct. energy calc. 0-75721
 Fe₃Al(Si), electronic structure, magnetic moments 0-107695
 Fe_{1-x}(P,B)_x, amorphous and crystalline, photoemission and band structure 0-60754
 Fe₂Si(Al), electronic structure, X-ray spectra comparison with band struct. calcs. 0-97383
 H₂WO₃ bronzes, Anderson transition, XPS 0-107705
 In, lattice dynamics, pseudopot. computation (*Russian*) 0-92617
 Ir, (111) surface states, surface Umklapp effects, photoelectron spectra 0-93457
 Ir, energy band structure, X-ray emission spectra, APW calc. 0-92811
 LaAl₃, calc. of energy band-structure and Fermi surface by APW method 0-70590
 LaAl₃, electronic struct., APW method and local-spin-density approx. 0-65434

band structure of crystalline metals continued

- LaB₆, electronic struct., APW method and local-spin-density approx. 0-65434
 Li, cryst. wave function deter., muffin-tin method 0-65436
 Li, valence band Auger spectra, surface effect 0-80915
 MgAg, Auger spectra, 4d bandwidth effect 0-89093
 γ -Mn, antiferromagnetic, self-consistent bandstructure calcs. 0-88475
 δ -Mn, paramag., antiferromag. and ferromag., magnetic moment calcs. 0-60223
 MnP, spin polarised energy band struct., electronic specific heat, APW calcs. 0-65431
 MnSi, electronic energy band struct., self-consistent APW calc. 0-65433
 Mn₂Si, electronic structure, X-ray spectra comparison with band struct. calcs. 0-97383
 Na, equilibrium struct. and phys. props., pseudopot. method 0-96778
 Nb, electron-phonon interaction, relativistic, APW calc. 0-92837
 Nb, Fermi surface, electron mass enhancement, orthonormal function enhancement 0-96777
 Nb, thermoreflectance studies 0-76047
 NbC, electronic structure, PES study 0-70594
 Ni (100) films, spin density by self-consistent linear APW method 0-65710
 Ni (110) and (111), two-photon photoemission 0-76150
 Ni, band struct., angle-resolved photoemission meas. 0-71569
 Ni, band struct., cryst. pot. anisotropy effect (*Russian*) 0-88474
 Ni, band struct. and multielectron excitations, angle-resolved photoemission determ. 0-76147
 Ni, electronic structure, photoelectron spectra, theory 0-80168
 Ni, energy band dispersion and mag. exchange splitting, angle-resolved photoemission meas. 0-71567
 Ni, ferromagnetic, electronic struct. by real space approach 0-65432
 Ni, metallic particles, stability and electronic struct. (*French*) 0-80155
 Ni, quasi-particle energies, two-hole XPS satellite 0-66399
 Ni-Co(Fe)(V)(Ti), dil., optical absorpt., electronic struct. 0-108227
 Ni-Mn alloys, ferromagnetism-to-spin glass phase transition and strong mag. field effect 0-75773
 β -NiAl, electronic struct. and optical props. 0-97228
 Ni(001) surface states, surface magnetisation, electron spin polarisation 0-88612
 Os, electronic energy band struct. 0-107697
 Pb, ab initio band struct. calcs. 0-75502
 Pb, single and polytextured thin films, band struct., tunnelling spectroscopy 0-80169
 Pd, electronic band struct. and photoemission 0-97410
 Pd, thermomodulation spectra of high-energy interband transitions 0-108226
 Pd-Co, normal Hall effect (*Russian*) 0-103676
 Pd-Cu compound, KKR electronic struct. 0-59864
 Pd-Fe, normal Hall effect (*Russian*) 0-103676
 Pd-Ni, normal Hall effect (*Russian*) 0-103676
 Pt band-structure determ., angle-resolved photoemission 0-66398
 Pt, energy band structure, X-ray emission spectra, APW calc. 0-92811
 Pt, thermomodulation spectra of high-energy interband transitions 0-108226
 Pt(111), A-line valence bands, angle-resolved photoemission determ. 0-108323
 Rb, elec. resist. and phase transforms. under high press. (*German*) 0-107763
 Re, electronic struct. and CO adsorption characts., XPS, UPS, and thermal desorption study 0-71571
 Sc, band structure, density of states, absorpt. spectra, KKRZ calc. 0-70593
 Sm_{1-x}La_xS, electron struct., lattice const., X-ray spectral study (*Russian*) 0-100432
 Sn, white, band masses and deformation pots., OPW pseudopotential model 0-100430
 Ta, and α -TaH₃, thermoreflectance studies 0-76047
 Ta, electron-phonon interaction, relativistic, APW calc. 0-92837
 Te, rel. to superconductivity and Fermi surface calcs. 0-70873
 Th, photoelectron spectra study, core and valence levels 0-66394
 Th, valence and 5f states, XPS and bremsstrahlung isochromat spectroscopy 0-66393
 Ti alloys, Fermi sphere limiting electronic capacitance, Brillouin zones (*Russian*) 0-92808
 Ti, band struct., cryst. pot. anisotropy effect (*Russian*) 0-88474
 TiBe₂, de Haas-van Alphen effect, Fermi surface, theory 0-103614
 TiC, electronic structure, PES study 0-70594
 TiFe_{1-x}Co_x, electronic struct. and mag. moment calcs. 0-65821
 U, photoelectron spectra study, core and valence levels 0-66394
 U, valence and 5f states, XPS and bremsstrahlung isochromat spectroscopy 0-66393
 V, electronic structure, model potential calcs. (*Russian*) 0-100431
 V, thermoreflectance studies 0-76047
 Zr-Co, amorphous and crystalline, d-band struct., alloying effects 0-59862
 Zr-Ni, amorphous and crystalline, d-band struct., alloying effects 0-59862
 ZrZn₂, de Haas-van Alphen effect, Fermi surface, theory 0-103614

band structure of crystalline semiconductors and insulators

see also conduction bands; energy gap; valence bands

- 0-89016
 n-alkanes, conduction band struct., LEED, secondary electron emission and UPS study 0-70601
 diamond, quasiparticle states, quantitative calc. 0-88499
 education, forbidden energy gap meas. in Si and Ge p-n junctions 0-57027
 ferroelectric semiconductors, props., book 0-82590
 ferroelectrics, vibronic, band struct. temp. depend. 0-70598
 ferromagnetic semiconductor, doped, electron spin polarisation and conduction band struct. 0-65449
 ferromagnetic semiconductor, spectral density approach for s-f model quasiparticle concept 0-80173
 ferromagnetic semiconductor, two-band s-d model hybridization 0-65446
 four-photon transitions, perturbation theory calc. 0-96786
 graphite, electronic struct. exact exchange HF calcs. 0-65438
 graphite acceptor compounds, band struct. model and electrostatic effects 0-92814
 graphite intercalation compound, interaction between one or two s orbitals (*French*) 0-65440
 inert gas solids, collective excitations and EELS, calc. 0-92842

band structure of crystalline semiconductors and insulators continued

- Kane semiconductor films, thermomag. and thermolec. effects, theory 0-70864
 metal-dielectric transition, two-band model, Coulomb interactions, self consistent calcs. (*Russian*) 0-80185
 narrow band gap semiconductors, multiphoton absorption in crossed fields (*Russian*) 0-60553
 narrow-gap ferroelectric, phase transition due to strong mag. field 0-103924
 Peierls one dimensional model, exact solution, electron spectra, static lattice deformation (*Russian*) 0-70609
 perovskite oxides, point defects, elec. cond., and electron energy spectra 0-70706
 piezoelectric nondegenerate semicond., magnetoacoustic effects of nonparabolic band struct. 0-96948
 poly(p-phenylene), electronic struct., one-electron band theory 0-65450
 polyethylene, conduction band struct., LEED, secondary electron emission and UPS study 0-70601
 polypyrrole, electronic struct., one-electron band theory 0-65450
 α -quartz, electronic struct., local disorder influence 0-59870
 rare earths cpds., Fano-resonances, surface and bulk effects in photoemission 0-97405
 semiconductor, complex energy band under optical excitation, high-frequency negative cond. and population inversion 0-107858
 semiconductor, electron quantum states, nonequilibrium current fluctuations in quantised mag. fields (*Russian*) 0-107704
 semiconductor thin film, energy spectrum in mag. field, size effect, calc. 0-70865
 semiconductors, band states temp. depend., book contrib. 0-80182
 semiconductors, degenerate, energy band structure effect on transverse magnetoresistance 0-88580
 semiconductors, ferromagnetic multivalley anisotropic, electron autolocalisation (*Russian*) 0-92848
 semiconductors, free carrier optical props., book contrib. 0-80738
 semiconductors, optical props. above band edge, book contrib. 0-84425
 ternary system compound formation, comp. and props. w.r.t. component electronic struct., computer prediction 0-103444
 transition metal monoxides, 3d, ground state electronic struct., atomic sphere approx. 0-59855
 transition metal-metalloid band structure, nonorthogonality and tight-binding fit 0-59852
 variable gap semiconductors, carrier transport and fluctuation effects due to changes in gap width 0-107793
 AlN, luminesc. excitation spectrum and band struct. 0-84783
 Al₂O₃, corundum, calc. using semiempirical Mulliken-Rudenberg method 0-80177
 AlSb solar cell material, epitaxy, ionicity and bond struct. 0-61367
 Ar, solid, energy bands, depend. on choice of exchange-correlation pot. 0-70607
 As₂Se₃, monoclinic, chem. bonds rel. to electronic and vibr. states 0-64951
 As₂Se₃, single crystals, fine struct. of direct gap from electrolum. spectra 0-93280
 BN, electronic struct., exact exchange HF calcs. 0-65438
 BaTiO₃, band struct. calc., interpretation of XPS and UPS spectra 0-70597
 BaTiO₃, photoelectron and optical spectra derived from self-consistent charge MO and band calcs. 0-96785
 BeO, cryst., local centres, electronic struct. calcs. 0-100433
 Bi_{1-x}Sb_x, deformation calculations, band struct. variation, electron phase transitions due to deform. (*Russian*) 0-65137
 Bi_{1-x}Sb_x semiconducting alloy, band struct. study, Shubnikov-de Haas effect (*Russian*) 0-80181
 CaO, band struct. calc. rel. to high press. metallisation 0-84427
 Cd₃As₂, energy band structure calc. 0-75504
 Cd₃(As₂P_{1-x})₂, 0 $\leq x \leq 1.0$, band struct. calc. near Brillouin zone centre 0-107703
 CdCr₂S₄(Se₄), pure and Ag doped, electronic struct., mixed valence 0-70612
 CdCr₂Se₄, energy band struct. calc. by augmented plane wave method 0-103621
 CdCr₂Se₄, energy structure, magnetooptic effects 0-71394
 CdCr₂Se₄, modulated piezoreflection spectra 0-97237
 CdF₂, UPS and XPS spectra, rel. to optical props. 0-66386
 CdGa₂(S_{1-x}Se_x)₄ solid solns., band struct. behaviour w.r.t. comp. (*French*) 0-107699
 CdGa₂S₄(Se₄), band struct., pseudopot. method 0-92816
 Cd_{1-x}Hg_xGa₂S₄ solid solns., band struct. behaviour w.r.t. comp. (*French*) 0-107699
 CdS, XPS, secondary illumination effects, band bending, level shifts 0-108324
 CdTe, energy bands and optical props. calc., tight-binding model with spin-orbit interaction 0-65448
 CdTe-HgTe superlattice on CdTe layers, evanescent states, tight binding calcs. 0-70611
 CoCl₂, cryst., self-consistent band struct., intersecting spheres model 0-75505
 CoS₂(Se₂), electronic struct., UPS and XPS study 0-80935
 CrCl₃, electronic struct. and struct. phase transition 0-59644
 CsPbCl₃, electronic struct. and optical props. in fundamental absorpt. region 0-93367
 CuBr(I), reflectance and thermoreflectance spectra, electronic struct. 0-71444
 CuCl, band struct., OPW calc. and X-ray spectra meas. 0-75506
 CuCl, electronic struct. by LCAO and LMTO methods, direct gap semiconductor 0-59868
 CuCl, refl. spectra, 4.5-30 eV, vel. to band struct. 0-103969
 CuCr₂S₄(Se₄), electronic struct., mixed valence 0-70612
 CuCrSe₂, influence of excess Cu on physical props. 0-103836
 Cu₂O, self-consistent energy bands 0-59869
 Cu₂(Se₂), electronic struct., UPS and XPS study 0-80935
 Dy₂S₃, optical props. and electronic struct. in fund. absorpt. region 0-80817
 Eu chalcogenides, cond. band spin struct. 0-71577
 Eu solid solutions with lanthanides, monosulfides, and oxides, vacant d states, X-ray absorpt. 0-103623
 EuB₆, electronic struct., transport and mag. props. 0-96782
 EuMo₂S₈, Chevrel phase, mag. interactions, LMTO energy band studies 0-70606
 EuO, electronic struct. investigation by electron spectroscopy method 0-92812

band structure of crystalline semiconductors and insulators continued

- EuO magnetic semiconductor, quasiparticle lifetimes, CPA study 0-65443
 EuO(Se), complex elec. cond. anomalies 0-107812
 FeCl₂, cryst., self-consistent band struct., intersecting spheres model 0-75505
 FeCr₂S₄, ionic distrib. and band struct., Mossbauer study 0-80646
 (Ga, Al, As) heterostructures and compounds, electronic props., empirical pseudopot. calc. 0-80366
 Ga_{1-x}Al_xAs, band struct. from I-V, C-V meas. on Schottky diodes 0-96989
 n-Ga_{1-x}Al_xAs:Si, room-temp. cond. and band struct. 0-96869
 GaAs, (110) surface structure, rotational relaxation, cluster model (*Chinese*) 0-107621
 GaAs anodic oxide, states, electrochemical meas. 0-80176
 GaAs, XPS, secondary illumination effects, band bending, level shifts 0-108324
 GaAs:Se(Zn) polycrystalline film, Hall effect, resistivity meas. 0-96911
 Ga_{1-x}In_xAs_{1-y}P_{1-y}, electron effective mass, cyclotron reson. and magneto-phonon effect meas. 0-103618
 GaIn, electron struct., ESCA study 0-89116
 GaS₂Se_{1-x}, valence band states, composition depend., photoemission spectra study 0-100434
 GaTe, single cryst. prep. and electroabsorpt. spectra investig. 0-103968
 p-Ge, IR light free hole absorpt., nonvertical optical transitions (*Russian*) 0-80802
 Ge:Li, Cu p-n junctions, current stimulated LiCu complex formation, photocurrents 0-107897
 Ge-Si, electronic structure, short-range order effects, calc. 0-92861
 GeTe, bond orbital model of band struct. 0-59853
 GeTe, effective masses for cond., density of states 0-88472
 GeTe-Sb₂Te₃, solid solutions, cond., density of states 0-88472
 H₁(MoO₃), electronic props., mag. susceptibility and spectra 0-80266
 H₂WO₃ bronzes, Anderson transition, XPS 0-107705
 Hg_{1-x}Cd_xTe, optical absorpt., quasilocal acceptor level effects, theory 0-92853
 Hg_{1-x}Cd_xTe, recombination processes using impact ionization capture cross sections 0-75577
 HgSe, band struct. and spin splitting Shubnikov de Haas study 0-65445
 HgTe, energy bands and optical props. calcs., tight-binding model with spin-orbit interaction 0-65448
 In_{1-x}Ga_xP_{1-y}As_y, lattice matched to InP, electroluminescence obs. 0-93416
 n-InSb, cond. electron spectra in quantised mag. field, impurity resonance scatt. (*Russian*) 0-93178
 InSb, intensity depend. interband Faraday rot. obs., saturation and reson. enhancement effects 0-108186
 InSb, recombination processes using impact ionization capture cross sections 0-75577
 La₂S₃, optical props. and electronic struct. in fund. absorpt. region 0-80817
 LiC₆, and LiC₁₂, intercalation cpds., electronic struct. calcs. 0-70613
 LiNbO₃-Si, acoustoelectronic memory, effect of band-bending 0-70771
 MnBO₃, orthorhombic, electronic struct., SCF-MS-X α calc. 0-70600
 MnBO₃, tetragonal, electronic struct., optical anisotropy 0-70599
 MgO, bonding, pressure effects in lower mantle 0-72491
 MgZn_{1-x}Te, band struct. refl. spectra meas. 0-80813
 MnCl₂, cryst., self-consistent band struct., intersecting spheres model 0-75505
 MoS₂, molybdenite band structural props. rel. to supercond. and semicond. 0-96781
 MoS₂S₈ Chevrel phases with group IIIa metals, Nb, Hg, Pb and Cu, synthesis, stability and characts. 0-71608
 NaF, quasimolecular crystal. characts. of NaLi_{1/11} absorpt. edge 0-93436
 Na₆O₁₅ monocystal, electronic struct. and X-ray emission spectra anisotropy 0-84807
 Nb chalcogenides and chalcogenide halides, geometrical struct. and metal-metal bonding 0-80172
 NbC, band struct. and X-ray emission spectra, APW and X α calc. 0-70605
 NbN, band structure, nonorthogonality and tight-binding fit 0-59852
 Nd₂S₃, optical props. and electronic struct. in fund. absorpt. region 0-80817
 Ne, solid, energy bands, depend. on choice of exchange-correlation pot. 0-70607
 Ne, solid, hole band struct., Bratsev wave function calcs. (*Russian*) 0-65437
 NiCl₂, cryst., self-consistent band struct., intersecting spheres model 0-75505
 NiS₂(Se₂), electronic struct., UPS and XPS study 0-80935
 PbS, film, total current spectrum and energy struct. 0-100719
 PbS(Se)(Te), bond orbital model of band struct. 0-59853
 Pb_{1-x}Sn_xSe solid solns., photoluminesc. spectra, energy band parameter determ. 0-71484
 Pb_{0.82}Sn_{0.18}Te, film, effect of hydrostatic pressure on props. 0-70862
 Pb_{1-x}Sn_xTe, lattice and electronic props. and g-value 0-80161
 PbTe, far IR magnetorefl., band struct. 0-76010
 n-PbTe, noncubic (111) oriented epitaxial films, weak field magnetoresistance 0-75584
 SMS, band struct. and semicond. metal phase transition 0-80180
 Se, charge density, self-consistent OPW and pseudopot. calcs. 0-92813
 Se, electronic struct. of cryst. phases and hydrostatic press. effects 0-59865
 Se, trigonal and amorphous, electronic struct. and nonempirical calc. of struct. props. 0-59866
 Si, (001) (2 \times 1) reconstructed surface, dimer model self consistent calcs. 0-88613
 P-Si, conductivity and carrier lifetime, high injection effects 0-70719
 Si, defects, divacancy and split 100 interstitial, electronic structure calc. 0-65494
 n-Si, Faraday rot. temp. depend., effective mass determ. 0-71392
 p-Si, heavily doped, intra- and interband Raman scatt. by free carriers 0-108208
 Si, local pseudopotential, Gaussian band charge model 0-88477
 Si on sapphire, residual strain effect on elec. props. (*Japanese*) 0-84522
 Si, optical spectrum, many particle effects, band struct. 0-89024
 Si, semi-empirical APW calc. of band structure 0-84424
 Si:P, polycryst. films, elec. props., EPR, defect states, doping effects 0-75660
 n-Si:P(B), elec. cond. oscills., electron instability effects due to dislocations 0-103704
 SiO₂, Auger line shapes, final state correlation effects 0-89095

band structure of crystalline semiconductors and insulators continued

- SbB₆, mixed valent semicond., transport props. and electronic struct., review 0-96877
 Sn_{1-x}Mn_xTe, electronic struct., transport props., mag. ordering effects 0-65441
 SnMo₂S₈, Chevrel phase, mag. interactions, LMTO energy band studies 0-70606
 Sn(S₂Se_{1-x})₂, valence band states, composition depend., photoemission spectra study 0-100434
 SnTe, bond orbital model of band struct. 0-59853
 Sr, monochalcogenides, electronic energy band struct., APW calcs. 0-65439
 SrF₂, UPS and XPS spectra, rel. to optical props. 0-66386
 TCNQ, ab initio SCF LCAO band struct. calc. 0-70608
 TTF, ab initio SCF LCAO band struct. calc. 0-70608
 TaN, energy band struct. calc., symmetrised APW method 0-96784
 Te, cyclotron reson. in pulsed high mag. fields, cond. band struct. 0-59867
 Te, electronic struct. of cryst. phases and hydrostatic press. effects 0-59865
 Te, oriented films, semiconducting props., Hall coeff., band structure 0-70854
 Te, trigonal and amorphous, electronic struct. and nonempirical calc. of struct. props. 0-59866
 ThN, photoelectron spectra study, core and valence levels 0-66394
 TiC, N_{1-x}(O_{1-x}), electronic struct., KKR-ATA method 0-65447
 TiCl₃, electronic struct. and struct. phase transition 0-59644
 TiN, O_{1-x}, electronic struct., KKR-ATA method 0-65447
 TiO₂, rutile, optoelectronic props., band struct., theory 0-80175
 TiS₂, band struct., angle-resolved photoemission studies 0-70610
 Ti_{1-x}V_xC₂, electronic struct. and X-ray emission spectra, cluster MO calc. 0-65444
 TiCl, ground-state props., Wannier functions, and electronic struct., ab initio self-consistent calc. 0-80178
 U compounds, NaCl struct. type, relativistic energy bands, LMTO calcs. 0-65442
 UN, photoelectron spectra study, core and valence levels 0-66394
 UO₂, electronic distributions by X-ray spectroscopy 0-97407
 UO₂, electronic transitions, crystal field effects and phonons, phase transition 0-97303
 UO₂, photoelectron spectra study, core and valence levels 0-66394
 US(Se)(Te), electronic struct. and exchange band splitting, optical refl. meas. 0-66226
 U_{1-x}Th_xAs (Sb), electronic struct., relativistic KKR-averaged T-matrix approx. method 0-107702
 VCl₃, electronic struct. and struct. phase transition 0-59644
 VO₂, metal-insulator transition and electronic struct., ion bombard. effects 0-92948
 V₂O₅ and lower oxides, electronic, optical, structural and surface props., review 0-88120
 V₂O₅, energy band structure, tight-binding method 0-70602
 V₂O₅, energy band structure, bonding props., projected density of states anal. 0-70603
 YS, band struct. and X-ray emission spectra, APW and X α calc. 0-70605
 ZnGa₂S₄, band struct., pseudopot. method 0-92816
 ZnSe, band-edge photoluminesc., far-below band-gap excitation 0-76063
 ZnTe films, internal stress effect on fund. refl. spectra 0-60701
 ZrS, electronic struct., bonding effects, photoelectron spectroscopy and low temp. heat capacity cal. 0-96780

band structure of semimetals

- Bi, magnetoresistance, high temp. oscills., props. (*Russian*) 0-65606
 BiSb, alloys, semimetallic, camera, dispersion relations 0-59854
 EuB₆, ferromag., spin-polarised energy band struct., APW calc. 0-96779
 Hg_{1-x}Cd_xTe, optical absorpt., quasilocal acceptor level effects, theory 0-92853
 LiAl, transport props., rel. to semimetallic band struct. 0-88581
 TiSe₂, band struct., angle-resolved photoemission studies 0-70610

band theory models and calculation methods

- see also APW calculations; band model of magnetism; band structure; cellular method; free-electron approximation; Hubbard model; KKR calculations; k.p. calculations; Kronig-Penney model; muffin-tin potential; nearly-free-electron approximation; OPW calculations; pseudopotential methods; relativistic band structure calculations; tight-binding calculations
 Coulombic interaction summation in Gaussian basis 0-70575
 cubic crystals., perfect, nonBloch electron state density 0-75487
 disordered system electron energy system, calc. methods 0-75485
 energy bands, low-lying, Mathieu and Kronig-Penney potentials comparisons 0-70583
 intermediate valence, theory, electronic sp. ht. calc. 0-79956
 linear Brillouin zone integration method, generalised susceptibility calcs. 0-88462
 magnetic semiconductors, conference, Montpellier, France (Sept. 79) 0-94916
 metals, electron theory and cond. props., contrib. of Sir Rudolf Peierls, 1928-1935 0-57054
 molecular crystals, electronic excitation energy transfer, external elec. field effect 0-84431
 polymer, conjugated and saturated chain, electronic struct., review 0-59860
 pseudopotentials from self-consistent atomic calcs., appl. to band struct. determ. 0-59846
 semiconductors, temp. depend. electronic cond. 0-59975
 Slater-Koster integrals, general expressions in two-centre approx. 0-70585
 solid state physics, 1933-40, contrib. of Sir Nevill Mott 0-57055
 solid state physics, contrib. of Conyers Herring in 1930s 0-57056
 surface properties, two dimens. Brillouin zone and Wigner-Seitz cell integrations, special point formulae generation 0-70783
 CrAs, high press. paramag. antiferromag. transitions, elec. props., band model development (*Russian*) 0-60277
 GeTe, bond orbital model of band struct. 0-59853
 NiWO₄, AC elec. conductivity, thermoelec. power and dielec. const. 0-70736
 PbS(Se)(Te), bond orbital model of band struct. 0-59853
 SnTe, bond orbital model of band struct. 0-59853

bands (kink) *see* **kink bands**

bandwidth compression

see also **vocoders**

effect on military target observers' detection and recognition performance 0-106484

image bandwidth compression, scene analysis algorithms and rule-based controller 0-95819

Pioneer Venus occultation expt., bandwidth reduction for radio science data generation 0-67492

Bardeen-Cooper-Schrieffer theory *see* **BCS theory**

barium

see also **nuclei with**

adsorption, on (110), (121) and (111) faces of W 0-100411

atom, $4d^{10}$ shell, photoionisation cross sections, electron shell alterations determ. (Russian) 0-58144

atom, (5d⁶)²D_{3/2} state, lifetime meas. by dye laser spectrosc. 0-78577

atom, double ionisation, 20-25 eV photoionisation cross sections 0-83328

atom, electron impact step-wise excitation (Russian) 0-83497

atom, in shock heated Ar, absorpt. line broadening obs. (Japanese) 0-83464

atom, laser excited, ionisation studies 0-83330

atom, radioisotopes, at. beam laser spectroscopy, hyperfine struct., nucl. moments and radii 0-57678

atom, saturation spectroscopy with laser optical pumping 0-83324

atomic quasi-Landau spectrum, semiclassical strong field mixing models 0-63847

atoms, hyperfine splitting and isotope shift of high lying levels, Doppler-free 2-photon laser spectroscopy 0-58215

atoms, quantum defect param., ab initio calcs. 0-78525

atoms, X-ray spectra, high energy L γ satellites 0-102474

auroral oval, dayside, Ba plasma injection rel. to rocket-borne VLF and ELF waves meas. 0-98504

axons, giant, squid, interaction of Ba²⁺ with K⁺ channels 0-85379

coadsorption with Cu on W faces, work function changes 0-65378

film, semitransparent, opt. props. in 2-5.6 eV range, electronic transitions, thickness depend. (French) 0-108289

forced-flow chromatography, detection by photometric method 0-71965

getter film initial reaction probability with O₂, water, CO and CO₂, AES obs. 0-61153

ion polarisation and point defect resistivity in metals 0-103672

monoatomic film on W (110), characteristic electron energy loss 0-100720

phase transitions under high press. 0-96641

rail gun for plasma injection 0-59255

resonant photoemission, time-depend. density-functional technique 0-89114

vapour, level populations, laser pumping effects 0-91507

Ba, atomic beam and resonance spectroscopy 0-58180

Ba I, light shift induced zero-field level crossing 0-58220

Ba I, two-step autoionisation 0-91513

Ba II, 5d²D_{3/2,5/2} isotope shifts, hyperfine struct., collinear fast beam laser spectroscopy 0-83310

Ba II, 5p excitation, relativistic anal., multiconfig. Dirac-Fock calcs. 0-69240

Ba II lines in solar spectra, non-mag. polarisation, centre-to-limb var. 0-67678

Ba⁺ ions confined in cylindrical RF trap, lifetime meas., laser probing 0-95573

Ba²⁺ 3d⁴f config., collapse of 4f electron, X-ray spectra obs. (Russian) 0-58204

Ba-Tl laser optically pumped by pair-absorption transitions, 1.5 μ m emission obs. 0-58517

Ba+CO₂(O₂), crossed beam kinetics, BaO recoil velocity spectra 0-76500

Ba+Cl₂→BaCl⁺+Cl⁻, chemi-ionis. reaction, mol. beam obs. 0-104434

Ba+HBr, laser induced fluoresc. study at different collision energies 0-91632

Ba+HCl, laser induced fluoresc. study at different collision energies 0-91632

Ba+HF, product rot. and vibr. distributions and reaction cross sections depend. on reagent translational energy 0-93745

Ba+HF→BaF+H, dual mol. beam excitation difference spectroscopy, state-to-state vibr. resolved dynamics 0-89474

Ba+Ti, dipole-quadrupole radiative collisional fluoresc. 0-83315

Ba+Ti, radiative collisional fluoresc. obs. from thermally excited atoms 0-102480

Ba⁺+D₂→D+BaD⁺, sequential impulse model, prod. bond dissociation energy and cross section 0-81295

Ba²⁺, very long lived vibr. states, lifetimes, WKB calc. 0-78560

BaI resonance transitions, hyperfine struct. and isotope shifts, atomic beam laser spectroscopy 0-102141

¹³⁵Ba, γ -ray emission probabilities and half-life obs. 0-57723

KCl:Ba, symm. of elastic fields due to defect displacements, diffuse X-ray scatt. 0-70256

KCl:Ba²⁺, localised stress relaxation in excess vacancy system, prismatic loops (Russian) 0-88160

KCl:Br²⁺, solid solution periodic precipitation in inhomogeneous conc. field 0-103485

NaCl:Ba²⁺, dopant aggregation and precipitation 0-107306

Pb(Zr,Ti)O₃:Ba, paraelectric ceramic, electrostrictive effect 0-80701

ZnO:Ba varistors, microstructure-prop. relations 0-100249

barium alloys

see also **barium compounds**

BaCu, X-ray cryst. struct. determ. 0-92478

Ba₁₀Ga, cryst. struct. (French) 0-79749

BaPdSn₃, prep. and crystal structure (German) 0-84138

barium compounds

see also **barium alloys**

barium methylsulphonate, X-ray powder cryst. data 0-59451

barium stearate film, low energy electron range meas. using radioisotope Auger electrons 0-70257

baryta crystal gas-liquid inclusion meas. with microscope heating stage 0-76967

ferrite, FMR in uniaxial crystal plate with bubble domain lattice 0-93182

ferrite, hexagonal, with M, W and Y structures containing Fe²⁺ and Fe³⁺ mag. ions, saturation moment and anisotropy 0-71009

ferrite, plastic magnet appl., based on moulding ferromagnetic powder material with plastics (Japanese) 0-60829

barium compounds continued

perovskites, A₂²⁺B³⁺U₆⁶⁺₁₆O₆, struct., cation vacancies, X-ray diffr. study (German) 0-107147

perovskites, ordered cubic, cationic effect on intramolecular forces, stretching force const. 0-88979

stearate single-layer Langmuir films, elastic and inelastic tunnelling 0-80403

Al₂O₃:BaTiO₃, sintering temperature effect of titanate additions 0-60808

Al(PO₃)₃-BaF₂-Al₃ glasses, opt. props., group I-III fluorides effect 0-66143

(Ba,Sr)TiO₃, ferroelec. props., press. depend., anharmonic oscillator model 0-80716

Ba hexaferrite, irradiated by fast neutrons, mag. props. 0-97116

BaAl₁₂O₁₉, ref. index and optical absorpt. 0-66139

BaB₂O₄-R₂, R=Mg, Ca, Sr, Ba, glass form., struct. and props. 0-84077

BaBe(PO₃)₆F, babefphite, cryst. struct. determ. using P $\bar{1}$ automatic diffractometer 0-107179

BaCO₃, excited Ba emission by Ar⁺ impact 0-100727

BaCl₂ aq. soln., vel. correls., time integral calcs. 0-59360

BaCl₂, Sn-activated, luminescence studies 0-108246

BaCl₂, sp. ht. meas., Schottky-type diffuse phase transitions, defect form. energies and entropies 0-107441

BaCl₂:Eu²⁺, fluorescence lifetime and quantum efficiency for 5d→4f transitions 0-100681

BaCl₂:Pb crystal phosphor, emission spectra 0-66298

Ba₃Co_{1.65}Fe_{0.35}Fe₂₈⁴⁺O₄₆, temp.-mag. field phase diagram, torque method 0-60276

Ba₂CoS₃, linear chain antiferromag., mag. susceptibility meas. and Mossbauer spectra 0-107992

BaCrO₃, 27 layer polytype, struct. determ. 0-107162

BaF₂ crystal, selective etching and dissolution kinetics 0-71775

BaF₂, F⁻ interstitial and substitutional trivalent cations, phonon reson. and IR absorpt. 0-84752

BaF₂, ionic cond., activation vols., freq. depend. cond., press. effects 0-100354

BaF₂, planar channelling, minimum yields determ. 0-70280

BaF₂, sp. ht. meas., Schottky-type diffuse phase transitions, defect form. energies and entropies 0-107441

BaF₂, strain induced splitting and oscillator strength anisotropy of IR transverse optic phonon 0-92625

β -BaF₂, stress wave profiles 0-96593

BaF₂, thermal props. (German) 0-81355

BaF₂, ultralow loss optical fibre material, loss mechanism 0-78920

BaF₂:Eu²⁺, fluorescence lifetime and quantum efficiency for 5d→4f transitions 0-100681

BaF₂:Gd³⁺, spin-lattice coeffs., EPR study 0-66032

BaF₂:La³⁺, thermal depolarisation of La³⁺-F₂⁻ defect dipoles 0-75926

BaF₂:Pb²⁺, band struct., Jahn-Teller effect, UV luminesc. and optical absorpt. spectra 0-66243

BaFCl:Eu²⁺, fluorescence lifetime and quantum efficiency for 5d→4f transitions 0-100681

BaFe_{12-2x}M_xTi₂O₁₉ (M=Co, Ni, Zn), mag. props. determ. 0-75759

BaFe₂O₁₉, bubble and stripe lattice domain wall oscils. 0-97115

BaFe₂O₁₉, Ca²⁺ substitution effect on hexaferrite lattice and mag. props. 0-60243

BaFe₂O₁₉, ferrite, DC cond., dielec. props., lattice consts. 0-80272

BaFe₂O₁₉ particles, magnetic domain study by colloid-SEM method 0-97120

BaFe₂O₁₉ powder, hysteresis of microwave absorpt. and magnetisation reversal 0-75814

BaFe₂O₁₉, powder, milled and annealed, phase composition, lattice consts. and crystallite size 0-71677

BaFe₂O₁₉ powders, fast reaction presintering 0-97445

BaFe₂O₄ amorphous film, prep. by RF sputtering, crystallisation 0-76183

β -BaFe₂S₄, cryst. struct., X-ray diffr. obs. 0-84153

Ba_{1-x}Fe_{2-x}S₄, electron diffr. study, orientation anomaly 0-107152

Ba₂FeS₃, linear chain antiferromag., mag. susceptibility meas. and Mossbauer spectra 0-107992

Ba₂FeTa₂O₉, Mossbauer and X-ray diffr. studies 0-103905

BaGd₄X₂O₁₇ (X=Si,Ge), cell consts., luminesc. of various rare-earth activators 0-93376

BaHfO₃, high-density ceramics prep. and elec. props. 0-60812

Ba(IO₃)₂, complex salts, phase transitions, cryst. struct. (Chinese) 0-70171

Ba(IO₃)₂, cryst. struct. determ. by X-ray diffractometry 0-107139

BaIn₂Se₄, cryst. struct. (German) 0-79760

Ba_{1-x}La_xF_{2+x}, enhanced ionic motion in solid solutions 0-107491

BaLaMnRuO₆, (M=Mg, Fe, Co, Ni, Zn), cubic ordered perovskites, Mossbauer and mag. susceptibility meas. 0-75889

BaMgF₄:Mn²⁺ ferroelec., EPR and ENDOR study, cryst. field tensor 0-71162

BaMn_{0.99}Co_{0.01}F₄, magnetoec. phenomena, dielec. behaviour near Neel temp. 0-71151

BaMnF₄, anisotropic order parameter phase fluctuations, light scatt. and thermal diffusivity meas. 0-80807

BaMnF₄, magnetic neutron scatt. from structurally distorted cryst. 0-93086

BaMnF₄, magnetoec. phenomena, dielec. behaviour near Neel temp. 0-71151

BaMnF₄, pure and Co doped, ferroelec. antiferromag., dielec. anomalies 0-71288

BaMnF₄, spectroscopy near ferroelec. transition, dielec. anomalies near mag. ordering temp. 0-75965

BaMnF₄, struct. phase transition, optical parameters obs. 0-100328

Ba₂MnS₃, linear chain antiferromag., mag. susceptibility meas. and Mossbauer spectra 0-107992

BaMoO₄ crystals, growth in SiO₂ gel under influence of elec. field 0-93469

BaMoO₄, Davydov splitting of vibr. levels, short range interaction 0-71418

Ba₂Mo₂Se₁₀, superconducting chalcogenides containing Mo₆ and Mo₇ clusters 0-103804

Ba(NO₃)₂, isomorphous crystals, growth defects, X-ray topography 0-70188

Ba(NO₃)₂, Nd laser second harmonic stimulated Raman scatt., efficiency in calcite, nitrate crystals 0-95949

Ba(NO₃)₂·H₂O, crystal gyrotropy, meas. in IR region 0-88957

Ba(NO₃)₂·H₂O, pyroelec., room temp. cryst. struct. 0-96491

Ba₂NaNb₂O₁₅, cryst. comp. effect on low temp. phase transition 0-71346

Ba₂NaNb₂O₁₅ crystals, in Nd³⁺:YAG laser cavity, AM of optical second harmonic 0-78908

barium compounds continued

- Ba₂NbNb₂O₁₅, ferroelectric, local states, thermoluminesc. study 0-60690
 Ba₂NbNb₂O₁₅, growth layer form., crystallization conditions effect, light diff., Curie temp. 0-100778
 Ba₂NbNb₂O₁₅, high press. phase transitions, Raman scatt. studies 0-71402
 Ba₂NbNb₂O₁₅, incommensurate refls. near ferroelastic transition, neutron and X-ray precession obs. 0-70395
 Ba₂NbNb₂O₁₅, X-ray powder diffraction data determ. (*Chinese*) 0-70170
 Ba₂NbNb₂O₁₅:Fe,Mo, photorefractive mechanism and photoelec. props. 0-71381
 Ba₂NbRu₃O₁₂ (Ru₃O₁₂)¹³⁻ cluster obs. in presence of orbital degeneracy and spin-orbit coupling (*French*) 0-70655
 BaNd₂(MoO₄)₄, X-ray cryst. struct. determ. 0-88128
 Ba₂Ni₂F₁₀, cryst. struct. and antiferromag. props. 0-107153
 BaNi₂(PO₄)₂ and BaNi₂(AsO₄)₂, mag. props., neutron diff. and sp. ht. meas. 0-70948
 BaO, cohesive and thermophysical props., role of three-body interactions 0-92477
 BaO core glass/multicomponent clad glass optical fibres 0-78949
 BaO, excited electronic states, lifetimes and transition moments 0-87177
 BaO, film, emission props. in relation to struct. 0-100501
 BaO, meas. of time-resolved spectra of fluorescence using photon correlator 0-87250
 BaO, monolayer on W (110), film struct. and electron state 0-100498
 BaO optical waveguides, Fresnel lenses 0-96034
 BaO, recoil velocity spectra from form. in crossed beam system 0-76500
 BaO, reduction by C, kinetics and mechanism (*Russian*) 0-93743
 BaO solubility products in molten NaCl-KCl, potentiometric determ. 0-76488
 BaO, XPS valence bandstruct. 0-89117
 BaO-B₂O₃, glass, refraction, refractive index from 0.365 to 2.50 μ m 0-88953
 BaO-Fe₂O₃-B₂O₃(Na₂O) glasses, high Fe₂O₃ content, micromagnetic props. 0-65916
 BaO-Fe₂O₃-(Na₂O) glass, rapidly quenched, mag. and ferrimag. props. 0-75744
 BaO-GeO₂-Na₂O borosilicate core glasses for high numerical aperture fibres 0-69534
 BaO-La₂O₃-B₂O₃, glass, refraction, refractive index from 0.365 to 2.50 μ m 0-88953
 BaO-Mn₂O₃-B₂O₃, amorphous mag. oxide, field-cooling effect (*Japanese*) 0-84615
 BaO-Nd₂O₃-TiO₂-Bi₂O₃ system ceramics, high stability low loss dielectric preparation 0-81008
 BaO-P₂O₅, glass, US velocity rel. to elastic props. 0-103425
 BaO-P₂O₅, glass, ESR of VO²⁺ ions 0-100610
 BaO-P₂O₅-Mo⁵⁺ glass, EPR spectra, computer simulation 0-88872
 BaO-TiO₂-Al₂O₃ system, subsolidus equilibria, X-ray powder diff. 0-108413
 BaO-V₂O₅-CuO semiconducting glasses, impurity effects, elec. resist. and EPR study 0-103692
 BaO-WO₃-P₂O₅ glass, struct. and IR spectra 0-64914
 BaO+Ar(CO₂), in Ar flame, rot. and translational relax. by sub-Doppler optical-optical double reson. 0-95583
 BaOH, (BaCl), mol. dissoc. energies calc. by high temp. mass spectrometer 0-83514
 Ba(OH)₂+2K₂O.11TiO₂.3H₂O fibre hydrothermal reaction to form BaTiO₃ fibres (*Japanese*) 0-93527
 3BaO.5SiO₂ glass, nonisothermal devitrification kinetics 0-92465
 BaO.6Fe₂O₃, ferrite polycryst., depend. of domain width on sample thickness 0-108031
 BaO.6Fe₂O₃, solubility of CaO 0-100333
 Ba(PO₃)₂-AlF₃-CaF₂, glass, elec. cond. and IR spectra 0-89005
 Ba(PO₃)₂-AlF₃-MgF₂, glass, elec. cond. and IR spectra 0-89005
 Ba(PO₃)₂-fluoride glass, elec. cond., struct. 0-88056
 Ba(PO₃)₂-WO₃, electron-absorpt. spectra and structure of W centres 0-88873
 Ba(Pb,Bi)O₃ perovskites, resputtering effects 0-80969
 BaPb_{1-x}Bi_xO₃, superconducting thin films, RF sputtering prep. 0-76181
 BaPb_{1-x}Bi_xO₃, superconducting props., Hall coeff. and elec. resist. meas. 0-84531
 Ba₂RF₄ (R=Dy, Ho, Er, Tm, Yb, Lu, Y), superstructure phases, prep., thermal characterisation and X-ray powder diff. 0-96494
 BaR₂(MoO₄)₄, R=rare-earth, struct., optical, mech., spectral and physicochem. props. 0-84161
 Ba₂Ru₂Mo₂O₉ (M=Mg, Ca, Sr, Co, Ni, Cu, Zn, Ca), Mossbauer spectra 0-108136
 BaSO₄ tablet, reciprocity of reflection values for geometries 45/0 and 0/45 (*German*) 0-71370
 Ba₂Sb₂S₄, cryst. struct., selenoantimonate (III) anions (*German*) 0-103305
 (Ba,Sb_{1-x})TiO₃ 0-60514
 Ba₂Sc₂O₉, Ba₂Sc₂WO₉ and Ba₂ScTaO₉, elec. cond. nature, depend. on comp. and medium thermodynamic parameters 0-70773
 BaSi₂, trimorphic, transform. of three-connected Si nets, press.-temp. phase diagram, 40 kbar and 1000°C 0-75198
 BaSiO₃, solid state reactions, thermodynamics and kinetics (*German*) 0-76236
 Ba₂SiO₄, solid state reactions, thermodynamics and kinetics (*German*) 0-76236
 Ba₂SiO₅, solid state reactions, thermodynamics and kinetics (*German*) 0-76236
 Ba₂SiO₅Br₂Eu, blue emitting X-ray luminescent material for intensifying screens (*French*) 0-66260
 Ba_{1-x}Sm_xS, electron config. of Sm ions, X-ray L-absorpt. spectroscopy 0-60715
 BaSnO₃, high-density ceramics prep. and elec. props. 0-60812
 BaSn₂Ca_{1-x}Fe_xO₈, substituted hexagonal ferrites, mag. split Mossbauer spectra obs. and X-ray struct. data 0-71250
 Ba_{0.9}Sr_{0.5}Nb₂O₆, electronic props. and photoresponses 0-92925
 Ba₂Sr_{1-x}Nb₂O₆ crystals, defects and their characteristic features 0-88138
 Ba₂Sr_{1-x}Nb₂O₆, photoelectric states in real time spatial light modulators, photorefractive effect 0-80676
 Ba₂Sr_{1-x}Nb₂O₆Ce, pure and doped, photoelec. props. and photorefractive 0-60538
 Ba_{0.4}Sr_{0.6}TiO₃ films, DC conductivity, strong microwave field effect 0-65727
 Ba₂Sr_{1-x}TiO₃, ferroelec. film, heteroepitaxial growth in cathode sputtering 0-93486

barium compounds continued

- Ba_{2-x}Sr_xTiSi₂O₈, piezoelec. crystals, SAW characts. 0-84354
 BaTa₂O₆, structural study X-ray diff., IR absorpt. and Raman spectra (*French*) 0-107173
 Ba₄TaRu₃O₁₂ (Ru₃O₁₂)¹³⁻ cluster obs. in presence of orbital degeneracy and spin-orbit coupling (*French*) 0-70655
 BaTiO₃ (001), LEED and UPS studies 0-100747
 BaTiO₃, band struct. calc., interpretation of XPS and UPS spectra 0-70597
 BaTiO₃ ceramic, degradation under high AC elec. field 0-60499
 BaTiO₃ ceramic dielectric capacitor, processing prop. relations, hysteresis, permittivity 0-80730
 BaTiO₃ ceramic films, dielec. strength, statistical anal. 0-75935
 BaTiO₃ ceramic surface, neutralisation of bombarding ion beam 0-71528
 BaTiO₃ ceramics, PTC-type, grain boundary study using TEM 0-107267
 BaTiO₃, coupled acousto-optic modes 0-96093
 BaTiO₃, coupled electroacoustic eqns. 0-96092
 BaTiO₃, crystn. from melts, comparison of different prospective oxy-anion solvents 0-71583
 BaTiO₃, displacive ferroelectric, effective charge determ. 0-97212
 BaTiO₃, elastic props., singularities near tetragonal-cubic phase transition 0-70303
 BaTiO₃, elastooptic effect near ferroelec. transition, temp. depend. 0-97233
 BaTiO₃, electron exoemission unipolarity associated with phase transitions 0-97415
 BaTiO₃, electron microscopy investigs. of ferroelec. substances, review (*Japanese*) 0-71366
 BaTiO₃, ferroelec. cryst., IR and Raman spectra, mode coupling 0-66194
 BaTiO₃, ferroelectric ceramic, internal stress and strength, failure mechanism 0-66128
 BaTiO₃, ferroelectric mechanisms, anharmonic couplings by scanning IR interferometry 0-75978
 BaTiO₃, ferroelectric, polarisation reversal, electric field induced phase transform. 0-103925
 BaTiO₃, ferroic materials, fracture processes 0-79869
 BaTiO₃ fibres synthesised from Ba(OH)₂+2K₂O.11TiO₂.3H₂O fibre hydrothermal reaction (*Japanese*) 0-93527
 BaTiO₃ film, dielectric props. depend. on sinusoidal elec. field 0-71318
 BaTiO₃ film, struct. and dielec. props. 0-60514
 BaTiO₃, holographic storage props. 0-87354
 BaTiO₃, intrinsic luminesc. 0-71467
 BaTiO₃, K-edge X-ray absorpt., cond. band states 0-97382
 BaTiO₃, mean square atomic displacement temp. depend., sublattice vibration anharmonicity 0-79890
 BaTiO₃, Mossbauer spectroscopy, sample prep. and results 0-66078
 n-BaTiO₃, ohmic contact form. 0-92969
 BaTiO₃, paraelec. phase, stabilisation of soft mode 0-75985
 BaTiO₃, paraelectric crystal, nonlinear props. 0-84699
 BaTiO₃, periodic domain struct. and opalescence at tetragonal to orthorhombic transition 0-66131
 BaTiO₃, photoelectron and optical spectra derived from self-consistent charge MO and band calcs. 0-96785
 BaTiO₃ photorefractive material for real-time edge enhancement 0-99642
 BaTiO₃, polycryst., phase transition obs. in -170 to 220°C range (*Russian*) 0-103474
 BaTiO₃, polycrystalline ferroelectric, grain-size dependent props. 0-71352
 BaTiO₃, polydomain ferroelec. crystals, phys. consts., self consistent calcs. 0-88942
 BaTiO₃, polymorph, hexagonal, low temp. and surface CO₂ adsorption and desorption 0-80713
 BaTiO₃, powders, Bragg reflection integral intensities due to structural anomalies 0-107098
 BaTiO₃, pure and doped crystals, surface and domain struct., AES and SEM expts. 0-71363
 BaTiO₃, pure and Fe doped, ferroelec., switching and electrolum. 0-76079
 BaTiO₃ RF sputtered ferroelectric film on Si substrate, ferroelectric props. 0-80697
 BaTiO₃, reduction inhibition by impurity ions 0-101018
 BaTiO₃, soft mode spectroscopy IR refl. meas. 0-88982
 BaTiO₃, spontaneous polarisation, low temp. meas. 0-75921
 BaTiO₃, surface microrelief after ion irradi. 0-59774
 BaTiO₃, surface study using AES and ion scatt. spectroscopy 0-65339
 BaTiO₃ type crystal, thermodynamic analysis of struct. phase transitions (*Russian*) 0-103473
 BaTiO₃, valence band UPS and partial p and d density of states 0-71560
 BaTiO₃, vibronic theory and opt. props. 0-103939
 BaTiO₃, XPS and UPS from surface defects 0-76136
 BaTiO₃:BaTi₂O₇, dielec. props. and microstruct. 0-60481
 BaTiO₃:C, solubility of C at low O₂ potentials, 800°C 0-100334
 BaTiO₃:Co, tricritical point, X-ray diff. meas. 0-71341
 BaTiO₃:Co, voltaic current appearance on proton irradi. 0-104032
 BaTiO₃:Fe³⁺, local position determ. by EPR 0-108057
 BaTiO₃:La, Sb, second phase effect on elec. and mag. props. 0-60986
 BaTiO₃:Nb, elec. props., contact material influence 0-70848
 BaTiO₃:BiFeO₃ solid solns., ferroelec.-antiferromag., magnetoelectric effect at ferroelec. transition 0-100637
 Ba₂TiO₄, Ba₄Ti₂O₁₀, standard Gibbs free energy of formation, EMF meas. at 673K 0-85207
 Ba₂Ti₂O₂₀ single crystals, prep. and unit-cell parameters 0-103302
 BaTiO₃Fe₂O₃, photoacoustic effect, first order phase transitions at increasing and decreasing temp. 0-70320
 BaTi_{0.98}Sn_{0.02}O₃, ferroelec. film, switching process 0-60518
 Ba(Ti_{1-x}Sn_x)₂O₃ film, struct. and dielec. props. 0-60514
 Ba(Ti_{1-x}Sn_x)₂O₃ thick film, ferroelec., phase transitions and dielec. props. 0-97215
 BaV₂O₆:Cr, EPR spectra temp. depend., paramagnetic ion point symm. 0-71166
 BaVS₃, mag. transition and hyperfine interaction, neutron spin-flip scatt. obs. 0-97093
 BaVS₃, magnetisation and neutron study 0-84588
 BaVS₃:Fe, Mossbauer and mag. studies, electronic state of Fe 0-108130
 Ba(V_{1-x}Ti_x)S₂, synthesis and struct. phase transitions 0-107415
 Ba₃WFe₂O₉ and Ba₃WFe₂O_{8.42}, crystallographic and mag. props., comparative study 0-103303
 Ba₃WFe₂O₉-Ba₃WCo₂O₉-x system, struct. evolution (*French*) 0-88110
 BaWO₄, Davydov splitting of vibr. levels, short range interaction 0-71418
 BaWO₄, slow neutron inelastic scatt. spectra, Debye temp. calcs. (*Russian*) 0-59347

barium compounds continued

- Ba₂W₂O₉, X-ray powder struct., face shared octahedra with W(VI) 0-64974
 BaY₂X₂O₁₇ (X=Si,Ge), cell consts., luminesc. of various rare-earth activators 0-93376
 BaYbF₆:Ho³⁺, stimulated emission at 2 μm, Nd laser radiation freq. conversion 0-95902
 Ba₂YbF₇ single crystals, electron diff. cryst. struct. anal. (French) 0-92507
 Ba₂Zn_{1-x/2}(x+y)Cu_{2x}Cd_{2y}Fe₁₂O₂₂, mag. props. and Mossbauer spectrum 0-75765
 BaZn₂Fe_{16-x}M_xO₂₇ (M=Al, Ga, In, Sc), mag. props. and Mossbauer effect 0-75766
 Ba₂Zn₂Fe₂₄O₄₁, ferromag. reson., low power nonlinear effects 0-75861
 BaZnGeO₄, revised cryst. data 0-100210
 x-BaZrF₆, synthesis and characterisation (French) 0-92506
 α(β)-BaZr₂F₁₀, synthesis and characterisation (French) 0-92506
 Ba_{0.65}Zr_{0.35}F_{2.70}, synthesis and characterisation (French) 0-92506
 Ba₂ZrF₁₀, synthesis and characterisation (French) 0-92506
 Ba_{1-x}Zr_xF_{2+2x} (0≤x≤0.1), synthesis and characterisation (French) 0-92506
 Ba_{1-x}Zr_xF_{2+2x} (0.333≤x≤0.361), synthesis and characterisation (French) 0-92506
 BaZrO₃, high-density ceramics prep. and elec. props. 0-60812
 C₆Ba intercalation compounds, three dimensional continuous melting 0-59631
 Ca_{1-x}Sr_{x/2}Ba_{x/2}Zr_{1-x}Ti_xO₃, ceramic system, dielectric props., microwave resonator application 0-80674
 Fe₂O₃-BaO-B₂O₃, magnetic props. of Fe-rich amorphous oxide (French) 0-80511
 GdF₃-BaF₂-ZrF₄ glass fibres, IR transmission, losses, fabrication 0-87516
 HfF₄-BaF₂-LaF₃ glass system, IR transmitting, synthesis and props. 0-71623
 HfF₄-BaF₂-ThF₄ (ZrF₄) glass system, IR transmitting, synthesis and props. 0-71623
 K₂O-Al₂O₃-2SiO₂-BaO plasma emitter 0-96368
 K₂O-CaO-BaO-B₂O₃, glass, refraction, refractive index from 0.365 to 2.50 μm 0-88953
 Li₂Ba₂O₇ non-universality of TL-LET response, effect of high-temp. TL 0-99348
 Li₂O-BaO-SiO₂ glasses, elec. cond., room temp. to 450°C 0-107473
 NaBaZn glass, Eu³⁺ centre symm. 0-100447
 Na₂O-BaO-Al₂O₃-SiO₂, glass, nucleation, crystn., ceramic form. 0-84082
 Na₂O-BaO-SiO₂, glasses, elec. cond., room temp. to 450°C 0-107473
 (Na₂Ti₆O₁₃)_n(BaTi₄O₉)_m, tunnel struct. intergrowth, electron, microscopy investigations 0-100218
 (Pb,Ba)(Zr,Ti)O₃, diffuse phase transitions, Curie temp., dielectric props. 0-75979
 (Pb_{1-x}Ba_x)₂Ge₂O₁₁, ferroelec. phase transition, dielec. const. and quasi-elastic light scatt. 0-71289
 Pb_{0.94-x/2}Ba_{0.06}Nb_{0.5}Zr_{1-x/2}O₃, Nb dopant morphology effect on microstructure 0-81005
 Si, commercial, nitridation, effect of BaF₂ 0-81359
 SiO₂-Al₂O₃-CaO-BaO-SrO-ZnO-Na₂O-K₂O-B₂O₃, glaze effect of P₂O₅ additions 0-60824
 SiO₂-Al₂O₃-Na₂O-BaO-TiO₂, glass ceramic interaction with Pb borosilicate glaze 0-84398
 SiO₂-MgO-BaO ceramic, steatite, glass-ceramics technology appl. 0-104097
 SrBaNaNb₃O₁₂, X-ray powder diffraction data determ. (Chinese) 0-70170
 Sr_{0.5}Ba_{0.5}Nb₂O₇ piezoelectric transducer, SAW props. 0-79037
 Sr_{0.75}Ba_{0.25}Nb₂O₆, ceramic ageing, dielec. props. 0-88940
 Sr_{1-x}Ba_xNb₂O₆ crystals, defect-free growth 0-108346
 Sr_{1-x}Ba_xNb₂O₆, photorefractive in space charge field, phase transitions 0-97229
 Sr_{1-x}Ba_xNb₂O₆, appl. in sub-100 ps pyroelec. detectors, 10.6 μm damage threshold meas. 0-77859
 Sr_{1-x}Ba_xNb₂O₆, domain struct. influence on electrooptical props. 0-93283
 Sr_{1-x}Ba_xNb₂O₆, high press. phase transitions, Raman scatt. studies 0-71402
 U-Ba-C FBR nuclear fuels, phase anal., 1400°C 0-66487
 V₂O₅-As₂O₃-BaO, semicond., glass, electronic props. 0-88557
 V₂O₅-CuO-BaO glass, unpaired electron localisation, ESR study 0-66026
 V₂O₅-V₂O₄-BaZnO₂ glass, V ion states, mag. and elec. props. 0-88556
 ZrF₄-BaF₂-MF_n (M=Na, Ca, Ln, Th, n=1, 2, 3, 4), vitreous phases, network formers, modifiers and stabilisers (French) 0-64909
 ZrF₄-BaF₂-ThF₄(Rf₃) (R=rare-earth) glass system, anion cond. 0-70460
 ZrF₄-BaF₂-ThF₄(LaF₃)(NdF₃)(PrF₃), F⁻ ion cond. glasses, cond. process 0-107477

Barkhausen effect

- Bloch walls, history 0-86065
 ferromagnet, irreversible magnetising processes, random propag. 0-88818
 ferromagnetic rods, irreversible and reversible magnetising processes, impressed propag. 0-88819
 magnetizing device for inspection of products of ferromagnetic materials according to parameters of Barkhausen discontinuity 0-89457
 steel, mild, fatigue softening and hardening detected from Barkhausen noise 0-76428
 welds, residual stresses, evaluation by Barkhausen noise meas. 0-76436
 DyCu film, amorphous, asperomagnetic domains, Barkhausen jumps in hysteresis loop 0-75822
 Fe polycrystalline, two ferromag. methods for eval. of fatigue limit 0-89438
 Fe thin layers, vacuum coated on PMMA, mag. behaviour during mech. stress cycles (German) 0-80581
 Fe-Ci (3 wt.%), local magnetisation losses, grain orientation effect 0-88817
 Fe-Si (3 wt.%) laminations, grain oriented, plastically deformed, anomalous losses 0-88853
 Gd₂(MoO₄)₃, domain wall motion dynamics 0-108030
 NaH₂(SeO₃)₂, domain struct. realignment and Barkhausen effect 0-71361

Barnett effect *see gyromagnetic effect; magnetisation***barometers**

- demonstration model 0-73156
 microbarometer with capacitive detector, highly sensitive 0-109261

barometric pressure *see atmospheric pressure and density***barrages** *see dams***barrel distortion** *see aberrations***barretters** *see thermistors***baryon-baryon interactions**

- see also baryon-baryon scattering; hyperon-nucleon interactions; nucleon-nucleon interactions*
 SU(4), symmetry breaking effects on strong coupling const., charmed and uncharmed B F couplings calc. 0-105802
 p \bar{d} -e⁺e⁻+n_s, proton EM form factors, p \bar{p} annihilation (Russian) 0-68457

baryon-baryon scattering

- see also baryon-baryon interactions; hyperon-nucleon scattering; nucleon-nucleon scattering*
 No entries

baryon decay

- see also baryon hadronic decay; baryon leptonic decay; hyperon decay*
 asymptotically free SU(5) grand unification, proton stability, renormalisation group 0-82929
 baryon resonances, complex mixing, decays and mass splittings, Wigner-Weisskopf simultaneous treatment 0-62977
 neutron mean lifetime meas. using EM trap 0-73703
 nucleon decay, T violation possibility and consequences in superunified theories 0-82917
 nucleons, symmetry relations, effective Hamiltonian and inclusive decay rates, kinship hypothesis 0-78060
 O(10), SU(4) colour subgroup, fractional charged gauge boson, proton half-life 0-73644
 Q² dibaryon resonances, orbitally excited mass spectrum, decays 0-73670
 SU(5) and SO(10) grand unification, flavour mixing and proton instability (Russian) 0-68413
 SU(5) grand unification, p lifetime and branching ratio, bag model wavefunctions 0-78004
 SU(5) grand unification, superheavy fermions and proton lifetime (Russian) 0-91036
 SU(5) grand unified theory, proton lifetime estimate accuracy 0-101967
 subcomponent models of quarks and leptons in SU(3) subcolour, proton decay 0-78035
 ultracold neutron accumulation, above-barrier neutron effects, lifetime determ. 0-102227
 ultracold neutrons, lifetime in traps, film-substrate model calcs. 0-106098
 universe ultimate fate, effect of finite proton lifetime 0-82560
 n, decay, weak interaction meas., coincidence type ion electron converter detector obs. 0-58100
 n-H \bar{p} , atomic decay, scalar and tensor interaction effects (Russian) 0-68455
 p, baryon number nonconservation, expt. status 0-57594
 p decay, flavour geometry 0-99100
 π^+ p $\rightarrow\pi^+\pi^+$ N, 1.4-1.7 GeV, isobar model partial wave anal., baryon resonance decay 0-86750

baryon hadronic decay

- bottom hadrons, masses and allowed decays, SU(5) quark model 0-62954
 charmed baryon decays, noneleptonic, parity-violating, single-quark and two-quark transitions 0-68453
 charmed baryon decays, weak hadronic, SU(3) dynamical scheme 0-68454
 charmed baryons, weak decays, quark model framework 0-62976
 noneleptonic hyperon decays, final state interactions with inelastic effects, comments 0-99099
 noneleptonic hyperon decays, QCD corrections 0-91087
 penguins in Δ S=1 noneleptonic weak decays 0-91086
 QCD model for internal structure, pseudoscalar-meson and photon emission 0-68452
 radially excited states in baryon resonance pionic decays, relativistic quark model 0-95268
 Ω -AK, QCD and valence quark approx. 0-105893
 Ω - Ξ^* π (Ξ^{*0}), noneleptonic hyperon decays, QCD description, PCAC anal. 0-95269
 Ξ^+ -AK, QCD and valence quark approx. 0-105893
 $\Xi^+\rightarrow p\gamma$, 1/2⁻ resonance poles to parity-violating amplitude, two-quark weak transitions 0-78062
 Σ^+ lifetimes and longitudinal accel. 0-86709
 Σ_c^+ , production and decay obs. 0-105894

baryon interactions *see baryon-baryon interactions; lepton-hadron interactions; meson-baryon interactions; photon-hadron interactions***baryon leptonic decay**

- charmed baryons, weak decays, quark model framework 0-62976
 nonlocal quark model of leptonic decays and mag. moments (Russian) 0-86711

baryon mass

- see also hyperon mass*
 bottom hadrons, masses and allowed decays, SU(5) quark model 0-62954
 charmed baryon mass and F/D ratio, colour magnetic interaction 0-62957
 charmed baryons, mass spectrum from SU_{1,3} dynamical group theory 0-62956
 charmed hadrons, SU(4) mass-breaking, mass sum rules 0-62959
 meson and baryon mass formula, chromodynamics consideration (Russian) 0-91071
 naive quark model predictions for meson mass and baryon mass and mag. moment 0-78036
 QCD, hadron masses, behaviour of constituent quarks 0-57557
 s-wave baryon spectrum, phenomenological quark-quark interaction 0-101984
 SU(6) symmetry, mass relations for 1/2⁺-baryons 0-82962

baryon photoproduction

- see also hyperon production; neutron production; proton production*
 $\gamma d\rightarrow np$, 300 MeV, dibaryon resonance manifestation, pseudoindependent amplitude elimination (Russian) 0-57612
 $\gamma d\rightarrow pn$, proton polarisation energy depend., 400-700 MeV (Russian) 0-63000
 $\gamma p\rightarrow\pi^+p$, 450 to 800 MeV, proton polarisation, Walker-type anal., P₁₁(1470), D₁₃(1470), S₁₁(1535) resonances 0-73721
 $\gamma p\rightarrow K^+K^0(\Xi^0)$, π^+n , π^+p , $K^+\Lambda$, $K^+\Sigma^0$ final state comparisons above resonance region 0-105906

baryon production

- see also *baryon photoproduction; hyperon production; neutron production; proton production*
 grand unified theories, baryon production through primordial black holes 0-101970
 high-transverse-momentum symmetric-particle-pair spectra and correlations 0-95250
 primordial baryons, generation by black holes 0-98750
 resonance electro- and photoproduction, EM transitions, multipole moments in single quark transition model 0-62985
 superconducting early Universe, cosmological baryon prod., CP invariance grand unification 0-90592
 $\Delta(1232)$ production in deep inelastic electron-nucleus scatt. 0-57772
 $ed \rightarrow ed^*$, dibaryon resonance production 0-78070
 $e^+e^- \rightarrow$ charmed hadrons, quark mass effect on fragmentation functions 0-91098
 $e^+e^- \rightarrow \Delta X$, polarisation effects in nonperturbative parton model, scaling 0-105912
 $K^-p \rightarrow \Delta^{++}X$, 32 GeV, inclusive and total cross sections 0-105936
 K^+p , 147 GeV/c, inclusive Δ^{++} prod., cross section energy depend. 0-57651
 $Ld \rightarrow \Delta X$, deep inelastic scatt., isobar admixture possibility (Russian) 0-91095
 \bar{p} induced dimuon events, V^0 yield, possible beautiful baryon prod. 0-105882
 pp , 147 GeV/c, inclusive Δ^{++} prod., cross section energy depend. 0-57651
 pp , probabilistic quark-model approach to p fragmentation 0-63049
 pp -baryons by diquark-quark fusion model 0-102065
 $pp \rightarrow pX$, 6 GeV/c, π exchange, depolarisation parameter 0-78088
 pp -baryons by diquark-quark fusion model 0-102065
 $\pi N \rightarrow N(1360) \Gamma < 67$ resonance, dibaryon pp resonance systematics 0-68481
 π^-p , 2-14 GeV/c, total cross section, narrow baryon search 0-105922
 π^-p elastic scatt., 3.42-5.03 GeV, narrow baryon search in differential cross section 0-105921
 π^-p , 32 GeV/c, slow proton and $\Delta^{++}(1236)$ inclusive prod. (Russian) 0-63046
 $\pi^-p \rightarrow (\pi^+\pi^-\pi^0)\Delta^{++}$, 16 GeV/c, partial wave anal., ω^* and A_2^0 0-63033
 π^-p , 147 GeV/c, inclusive Δ^{++} prod., cross section energy depend. 0-57651

baryon resonances

- see also *hyperon resonances*
 baryon couplings and 'missing resonance' in quark model with chromodynamics 0-57558
 baryon spectroscopy and photoproduction couplings using new baryon wavefunctions 0-102016
 charm particle spectroscopy 0-73680
 complex mixing, decays and mass splittings, Wigner-Weisskopf simultaneous treatment 0-62977
 dispersion sum rules and exotic baryon resonances, reggeon scatt., E_{55} resonance (Russian) 0-101955
 EM transitions, multipole moments in single quark transition model 0-62985
 hadron induced multiparticle reactions, S-1500 GeV, resonance prod. correlations, jet model (German) 0-91118
 heavy meson exchange effect on 1D_2 and 3F_3 N-N partial waves, dibaryon resonances 0-105874
 Q^2 dibaryon resonances, orbitally excited mass spectrum, decays 0-73670
 radially excited states in baryon resonance pionic decays, relativistic quark model 0-95268
 s-channel resonance model based on peripheral resonances, exotic peaks 0-91069
 s-channel resonance prod. in πN scatt., amplitude zeros in Mandelstam plane 0-73686
 bb baryons, mag. moment sum rules, in $Su(8)$ 0-78065
 $\Delta(1232)$ from $NN \rightarrow N\Delta$, π production in $^{40}Ca(^{40}Ca,x)$, relativistic, compression and pion distrib., Monte Carlo calc. 0-73853
 $\Delta(1232)$ production in deep inelastic electron-nucleus scatt. 0-57772
 Δ - Δ resonance in nonrelativistic quark model 0-86692
 $\Delta^{++}(1232)$, effect on $\pi^+p \rightarrow \pi^+p\pi^+$, 165 MeV, spectrum 0-68476
 $\Delta_{33}(1925)$ baryonic degrees of freedom, nonrelativistic, harmonic oscillator quark model mass formula 0-91066
 $\Delta^0\Delta^{++}$ production from π^+p , partial wave anal., T-matrix poles and residues 0-63018
 $ed \rightarrow ed^*$, dibaryon resonance production 0-78070
 $e^-N \rightarrow e^-\Delta(3/2, 3/2)$, P-odd asymmetry, P nonconserving neutral current interaction 0-57611
 $\gamma d \rightarrow np$, 300 MeV, dibaryon resonance manifestation, pseudoindependent amplitude elimination (Russian) 0-57612
 $\gamma p \rightarrow \pi^+p$, 450 to 800 MeV, proton polarisation, Walker-type anal., $P_{11}(1470)$, $D_{13}(1470)$, $S_{11}(1535)$ resonances 0-73721
 $K^-d \rightarrow \Lambda p$, pole in 3S_1 hyperon-nucleon scattering amplitudes 0-102068
 $N(1360) \Gamma < 67$ resonance, πN channel, dibaryon pp resonance systematics 0-68481
 $N \rightarrow \Delta(1232)$ electromagnetic transition form factor and pion-nucleon dynamics at moderate energies 0-57598
 $N^*(1232)$ from pp inclusive process, π exchange, depolarisation parameter 0-78088
 N^* EM transition form factors 0-102049
 NN and πNN , $\pi\pi NN$ bound states from NN potentials 0-62951
 NN couplings, parity-violating, QCD and MIT bag model, $1/2^-$ resonance contribs., $SU(6)_v$ symmetry 0-57540
 $pp \rightarrow pppp$, 11.75 GeV/c, baryonium states, cross section and branching ratio 0-95288
 πN low energy scatt. from N, Δ poles, low energy theorems 0-86751
 πNN dynamics, Faddeev approach, 0-1200 MeV pp scatt. 0-57625
 π^-p , 2-14 GeV/c, total cross section, narrow baryon search 0-105922
 π^-p elastic scatt., 3.42-5.03 GeV, narrow baryon search in differential cross section 0-105921
 $\pi^-p \rightarrow \Delta^{++}\pi^0$, 9.8 GeV/c, narrow pp state search 0-57636
 $\pi^-p \rightarrow \pi^+N$, 1.4-1.7 GeV, isobar model partial wave anal., baryon resonance decay 0-86750

baryon scattering see *baryon-baryon scattering; lepton-hadron scattering; meson-baryon scattering; photon-hadron scattering*

baryon spin and parity

- see also *hyperon spin and parity*
 s-channel resonance prod. in πN scatt., amplitude zeros in Mandelstam plane 0-73686

baryons

- see also *baryon resonances; baryon spin and parity; hyperons; nucleons*
 charmed, hadronic props., superconvergence sum rules 0-78043
 early Universe, baryon number generation due to CP- and B-violating interactions 0-109571
 electric dipole moments in CP noninvariant Kobayashi-Maskawa theory (Russian) 0-105897
 exotic atoms, conf., Erice, Sicily, (1979) 0-67939
 field equation for baryons with arbitrary spin, generalisation of Dirac eqn., group scheme 0-73615
 heavy baryon spectroscopy in the QCD bag model 0-105866
 Higgs boson critical mass, baryon asymmetry from boson pair decay 0-90590
 isospin classification, same finite group for mesons and baryons (Chinese) 0-62887
 leptonic decays and mag. moments in nonlocal quark model (Russian) 0-86711
 magnetic moments, ground-state, $SU(6)$ symmetry 0-78064
 parton distrib. consistent with naive quark model and QCD 0-62937
 properties, review from particle data group 0-67944
 quark constituents, binding energy and rest mass of constituents, total symmetry effects (French) 0-63068
 $SU(5)$ grand unification, cosmological baryon asymmetry 0-86640
 b-quark baryons, magnetic moments, broken $SU(5)$ symmetry 0-95257

barysphere see *Earth core*

batteries see *cells (electric); primary cells; secondary cells; solar cells*

Bauschinger effect

- α -brass, polycrystals., deformed in tension or rolling, anneal hardening (Japanese) 0-93564
 β -brass, uniaxial tension and compression, cyclic stress-strain behaviour 0-97551
 β -brass bicrystals, shear-incompatible, grain boundary contrib. to Bauschinger effect 0-97550
 cell wall and lattice misorientation origin during deform. 0-71712
 steel, Fe-Si (3 wt.%), Bauschinger effect, computerised evaluation method 0-93625
 steel, Nb-Mn, Molytor 53, Bauschinger effect, computerised evaluation method 0-93625
 steels, high-strength low-alloy, Bauschinger effect, computerised evaluation method 0-93625
 Fe, Armo, Bauschinger effect, computerised evaluation method 0-93625

Bayard-Alpert gauges see *ionisation gauges*

bays (magnetic) see *geomagnetic variations*

BCS theory

- see also *many-body problems*
 helical order of spins in supercond. 0-70888
 nonequilibrium superconductor, high-freq. AC process dynamics 0-88674
 nuclear collective energy dissipation, into internal energy superfluid wall formula 0-63108
 superconducting transition critical temperature, BCS theory, phonon spectra, review (Spanish) 0-84535
 superconductor with magnetic impurities, coexistence of superconductivity and ferromagn., BCS and Zener models 0-88676
 Woods-Saxon potential spectrum, pairing force strength, Nilsson model comparison 0-57704
 Al film, crit. temp. enhancement (Russian) 0-93021
 3He , superfluid, transport parameters, Kubo formulae and BCS-Green's functions 0-88382
 In films, crit. temp. enhancement (Russian) 0-93021
 In-Bi(Tl)(Pb), small κ supercond., phase transitions higher than second order 0-88668
 Pb-formvar-Al tunnel junction, excitonic superconductivity, BCS theory, generalised jellium model 0-75684
 Sn film, crit. temp. enhancement (Russian) 0-93021
 Sn-Bi(Sb), small κ supercond., phase transitions higher than second order 0-88668

beam choppers

- electron, systems comparison and universal system development 0-68306

beam-foil spectra

- fast projectile electron loss forward peak oscill. struct. as autoionisation 0-69227
 ions emerging from C foils, mean charge, inner-shell vacancy effects 0-87219
 Al^{1+} foil-excited ion, X-ray spectra and satellite classification 0-95567
 Be III, doubly excited states, triplet spectra 0-87069
 He(2s-3p transitions), beam foil spectra, emitted light polarisation, depend. on foil tilt angle 0-63786
 Hg II, 6p 2 and 6p 2 D levels, radiative lifetimes meas. 0-78576
 Kr VII, beam-foil excitation, 4s4p $^1P^o$ level decay simulation 0-78578
 Kr VIII, excited state energies and lifetimes, beam foil spectra 0-63591
 Kr^+ , equilib. charge state distrib. and multiple scatt. angles in C foil 0-59532
 Li^+ , core excited bound states in beam foil expts., CI calcs. 0-78559
 Li^+ , optical transition between bound states, beam-foil spectrosc. obs. 0-91476
 Mg (Mg $^+$), lifetime meas., beam foil spectra, comparison with numerical coulomb approx. calc. 0-58367
 Mg III-V, beam-foil spectra, 100-450 Å 0-83308
 Mg $^{n+}$, foil-excited ion, X-ray spectra and satellite classification 0-95567
 Mo XIV to Mo XXIX, extreme UV spectra 0-87068
 Si(Si $^+$ (Si $^{2+}$)(Si $^{3+}$), excited levels, radiative lifetimes, beam foil spectra 0-58368
 Ti III, IV, V, radiative lifetime meas. using beam-foil technique, 700 to 1900 Å 0-78574

beam-foil spectroscopy

No entries

beam handling equipment

- see also *particle beam diagnostics*
 atomic O $_2$ supersonic nozzle beam source development 0-58016
 chromaticity correction in KEK main ring 0-74049
 coaxial diode electron beam system for excimer laser excitation 0-86509
 conference on nuclear spectroscopy of fission products, Grenoble, France (May 1979) 0-77546
 eight-magnet spin precession snakes, survey for new configurations 0-91352
 electron beam lithography, triple slit scheme for high current variable-shaped beam forming 0-68290
 electron gun system, pulsed, for use with superconducting accelerator and free-electron laser 0-68989

beam handling equipment continued

Fermilab Doubler warm Fe supercond. dipole, stress anal. 0-58012
 fusion reactor, ASDEX, neutral beam injection, beam line design 0-99395
 fusion reactor, Doublet III beamline, review, component relation and config., design constraints 0-99382
 fusion reactor, Doublet III beamline calorimeter, three dims. heat transfer anal. 0-99381
 fusion reactor, ISX-B, neutral beam system 0-99388
 fusion reactor, MFTF, ion and neutral beams dumps, design 0-102317
 fusion reactor, PDX, 6 MW Neutral Beam Project, overview 0-106223
 fusion reactor, TFTR, high energy heat sink, ion beam dump and calorimeter 0-99394
 fusion reactor, TFTR, neutral beam injector prototype, construction and performance 0-99390
 fusion reactor, TFTR, neutral beam line final design 0-99309
 fusion reactor, TFTR, neutral beam-torus connecting duct 0-99302
 fusion reactor, TMX, injector system mech. design and installation 0-99393
 fusion reactor PDX, ORNL prototype neutral beam injection system, ion source development 0-99391
 fusion reactors, TFTR neutral beam support system 0-102376
 ion beams, intense, production and postaccel. in magnetically insulated gaps 0-74041
 ion source fission product separators 0-78479
 ISOLDE as a source of neutron-rich nuclei 0-78480
 JET, extraction element design for long pulse multi-megawatt neutral beam 0-102373
 lenses, electrostatic, focusing of GeV particle beams 0-74061
 liquid jet vacuum seal, inflow, rel. to electron beam emergence into atmosphere 0-78469
 magnetic electron deflection system, high accuracy, shielding ferrite tube 0-102602
 neutron monochromator, curved Cu comb 0-63427
 normal incidence monochromator, 2m high throughput, for SURF II storage ring 0-90951
 proton accelerator beam scraper, photon dose rate calc. 0-99367
 proton beams, scattered, intensity distrib. monitor 0-74062
 RF contact for superconducting cavities 0-63429
 RF ion beam choppers, ion motion (*Chinese*) 0-99371
 SIN, pion beam line $\pi E3$ modifications 0-74054
 SIRIUS facility for neutron rich fission fragment studies 0-78484
 soft X-ray microscopy/lithography branch line at SSRL 0-91344
 superconducting magnets, high-energy physics appl. 0-68990
 synchrotron radiation, expt. enclosures and beam line safety components 0-91341
 tanked tube for open air accelerators 0-99356
 thermal neutron traps for nuclear pumped laser 0-64041
 thermomagnetic gates for ultracold neutrons, accumulation in closed vessels 0-87005
 transport of low energy divergent H_2 beam at 300 eV by permanent magnets 0-69001
 triple-focusing magnet for the collection of nuclear recoils 0-102363
 TRISTAN II mass separator, ion source, beam optics, computer system 0-78481
 TRISTAN II mass separator at Brookhaven HFBR, research programme for fission products 0-78482
 ultracold neutrons, multilayer ferromag. shutter 0-91354
 undulator design for ACO storage ring 0-91334
 undulator for the 700 MeV VUV-Ring of the National Synchrotron Light Source 0-91337
 unslowed fission product separators, gas filled JOSEF, parabola LOHENGRIN 0-78478
 UV beamlines for National Synchrotron Light Source 0-91342
 VUV beam line instrumentation for National Synchrotron Light Source storage ring 0-91343
 water trap, polarised-neutron beam shut-off 0-87004
 Wendelstein VII-A, neutral beam injectors, performance 0-99389
 wiggler magnets, use as synchrotron radiation source at SPEAR storage ring 0-91332
 wigglers and undulators, interaction with stored electron beam 0-91331
 X-ray monochromator development for synchrotron radiation facilities 0-91351
 Mo, extraction grid for high power ion source 0-102372

beam handling techniques

see also mass spectroscopy; particle beam diagnostics; particle optics
 bending of high energy beams using axial and planar channeling 0-88225
 betatron oscillation reduction, low-noise wide-band power amplifier system 0-58011
 charged particle beams, energy spread reduction, laser pulse technique 0-87279
 chromaticity correction in KEK main ring 0-74049
 cyclotron acceleration process and its influence on beam quality, theory 0-74051
 cyclotron resonance, Doppler effect, anomalous, amplification of slow waves in electron beam, obs. 0-78463
 cylindrical-mirror electrostatic analyser for beta spectroscopy of beams 0-63446
 Dee, bevelled, for beam centering in AVF cyclotron 0-63428
 electron beam guiding system including automatic capture circuitry 0-99005
 electron beam self-acceleration expts., regulation of magnetization of ferrite 0-63425
 electron beams, relativistic, intense, guiding with axial mag. field 0-87006
 electron cooling with magnetic field 0-58013
 electron probe forming systems, optimisation with respect to aberrations and vertical beam landing 0-68291
 electron-ion ring, stationary state 0-106217
 electrostatically focused ions, spherical potential profile, meas. 0-64762
 fusion reactor, TMX, neutral beam control systems 0-99323
 general orbit theory for accelerated particles in cyclotrons, appl. to synchrocyclotrons and omegatrons 0-74052
 ion beamlet steering by aperture displacement in 2-stage accelerator, experimental study 0-68998
 ion beamlet steering by aperture displacement in ion sources with large acceleration-deceleration ratio 0-63430
 ion transport in linear accelerators by electron neutralisation 0-58014
 ISX-B neutral beam injector expt. on prototype beam line 0-74039
 laser accelerator, phase-adjusted focusing 0-63434

beam handling techniques continued

laser-plasma ion source for ion implantation in solids 0-78474
 metal neutral beams, low energy (0.1 to 10 eV) prod. by laser vaporisation of metals 0-77910
 molecular beams, sources, gasdynamic, use of lasers, time-of-flight and detection techniques 0-69264
 neutral beam, increased divergence due to transverse mag. field 0-95494
 neutral beam divergence due to imperfect mag. shielding 0-91349
 neutron rich nuclei, beta decay half lives, expt. techniques 0-78224
 positrons, slow, time bunching for annihilation lifetime and pulsed laser photon absorpt. expts. 0-95492
 proton beam characs. control by laser-induced selective multistep processes 0-61122
 supersonic molecular beam source, simple calibration method 0-82845
 thermal particle motion effect on autoresonance acceleration process (*Russian*) 0-69007
 TRANSPORT, design program for charged particle beam transport systems 0-106220
 water trap, polarised-neutron beam shut-off 0-87004

beam-trapping *see self-trapping***bearings (machine) *see machine bearings*****bells**

see also musical instruments

forced damped harmonic oscillators, meas. separation and half-width of components of doublets, high-Q systems 0-74590

bending

see also bending strength; buckling; stress analysis; torsion
 alloys, shape memory effect, device for testing in bending 0-66723
 axisymmetric elastic bodies with arbitrary boundary conditions, semianalytical boundary integral 0-102969
 beam, slip line development 0-58928
 beam bending on Pasternak foundation, reciprocal variational inequalities 0-92091
 beam modelling, linear shape function for axial displacement approx., finite element anal. 0-69665
 beams, straight, homogeneous and isotropic, linear flexural theory (*French*) 0-74743
 beams in pure bending, distributed damage theory, cracks, fracture 0-64474
 circular membrane reflector made by surface bending due to electrostatic tension 0-91876
 circular plate of variable thickness, bending with symmetrical loading 0-69699
 circular plate on elastic foundation, bending and contact problems 0-96235
 composite beams, effects of fibre orientations on free vibrations 0-87734
 composite materials, fibre reinforced, rectangular rods, elastic wave propagation (*French*) 0-83749
 concrete reinforced rectangular membranes, torsional stiffness 0-65131
 continuous beams with concrete slabs under load, method for crack prevention in slab (*Japanese*) 0-83760
 coupled bending-torsion flutter in cascades, aeroelastic stability boundaries 0-64424
 crack, oblique edge, in semi-infinite plate, stress anal. 0-64463
 crack emanation, from circular hole in infinite sheet, Green's function methods 0-92084
 crack extension angle, influence of specimen's geometry 0-99965
 creep in circular specimen subject to pure bend, ultimate tensile and compressive strength (*Russian*) 0-74768
 cylindrical shells, stiffened, min. weight design for pure bending (*Japanese*) 0-64381
 deflection contour generation by white light projection speckle method 0-98881
 disc, axisymmetrically variable thickness, deflection by conc. lateral load (*Japanese*) 0-96194
 elastic plate, crack closure in bending, sixth order anal. 0-96231
 elastic plates and shells, bending, small parameter method 0-99930
 fibre reinforced plastics, bent thin-wall constructions, rupture 0-64472
 frame, two-bar, with tangential load, snap-through buckling 0-64406
 fusion reactor, toroidal field coil in-plane bending stress, struct. support design 0-106164
 graphitised viscose fibre, fluorination, change in struct. 0-88039
 hologram interference fringe bending analysis and expt. 0-106494
 holographic optical elements, third-order aberration theory and generalised aplanatic condition 0-74314
 ice, transverse flexure, refined Reissner anal. 0-88247
 infinite plate with doubly periodic hole array, transverse bending, Poisson-Kirchhoff theory 0-58920
 isotropic plane sandwich plates, constant shear theory 0-99943
 laminated plates, symmetric, specially orthotropic, thermoelastic anal. 0-92058
 laminates, multilayer, thick, hybrid-stress finite element formulation 0-92043
 linear elastic beams, shells and plates, elementary theories review 0-69677
 liquid crystals, piezoelectric effect use as light modulator 0-83679
 LMFBF fuel channels, measurement of irradiation creep in bending 0-104406
 matrix analysis of composed bar of open cross section 0-83736
 metal tubes, crushed between rigid plates, large deformation compression 0-66579
 metal-composite rods, compressed, delamination 0-64396
 metallic thin spring strip, bending test device 0-61052
 mortar specimens, repeated impact bending load study (*Japanese*) 0-93622
 optical fibre, microbending eqns., exact time-dependent, solns. 0-87530
 optical fibre, single mode, bending induced birefringence 0-87537
 optical fibre, single-mode, for current meas. system, birefr. induced by bends and twists 0-99832
 optical fibre bandwidth limitations and bend losses 0-87553
 optical fibre cables, single-mode and parabolic-index multimode, random-bend loss 0-78951
 optical fibre waveguides and cables, microbending losses, depend. on numerical aperture 0-96025
 piezoceramic plates, bending strains, electromechanical transformation, energetic method of calc. (*Ukrainian*) 0-71320
 pipe elbow element, linear anal., bending axial and torsional displacements, ovalisation 0-79177
 plane homogeneous curved beam 0-69697
 plate, annular, non-uniform thickness, partial arc loading effects 0-74774

bending continued

- plate, finite difference variational method 0-92045
 plate, rectangular, finite bending in creep conditions (*Russian*) 0-79169
 plate, rectangular with asymmetrically reinforcing beams, contact interaction 0-99975
 plate, variable thickness, on elastic foundation, bending, closed form soln. 0-79179
 plate, viscoelastic, heated, bending, Kelvin Voigt model 0-106731
 plates, annular, clamped edges, asymmetric bending, Ritz method 0-58907
 plates, circular, variable thickness, numerical solution for flexure 0-99951
 plates, laminated, cylindrical bending, random loading, dynamic response 0-58902
 plates, laminated anisotropic composite, penalty plate bending element 0-96200
 plates, rectangular, with internal rigid support, bending vibration 0-102981
 plates, rectangular and circular, bending, singularity function method 0-74740
 plates, rigidity matrix, triangular finite elements (*Russian*) 0-74739
 plates, thin and moderately thick, serendipity cubic displacement hybrid stress element 0-96202
 polyester polymer concrete, longitudinal deform. modulus study is creep conditions (*Bulgarian*) 0-71685
 porcelain-metal cermet, stress determ., meas. method (*German*) 0-76425
 rapidly rotating compressed rods, stability 0-79189
 rectangular plate, superpower degeneration of boundary layer of angular points (*Russian*) 0-74776
 rectangular plate with mixed fixing conditions on the outline 0-69696
 rod, elastoplastic, dynamic bending and residual deformation (*Russian*) 0-75293
 Saint Venant's solns. in rod and beam theories 0-69676
 sandwich composite beams, stress distrib. meas. under four-point bending, multilayer builtup theory 0-96190
 saturated elastic half-space with partially embedded elastic bar, quasi-static bending 0-79145
 semiinfinite strip with clamped sides, bending, Papkovitch-Fadle eigenfunction completeness 0-58929
 shallow shell bending, mixed variational eqn. 0-77618
 shell, cylindrical, isotropic, elastic stability, critical load analysis 0-83744
 shell, cylindrical, with spiral groove, Kirchhoff's boundary conditions deduced from energy principle 0-74741
 shells, axisymmetric, unsymmetrical bending, elastoplastic anal. 0-92065
 shells, long cylindrical, plastic buckling under pure bending 0-64409
 shells, oval cylinder, orthogonally stiffened, buckling under axial compression 0-74777
 shells, thin, doubly curved, numerical integration of triangular finite element 0-92044
 shells, toroidal, quasibending of surfaces (*Russian*) 0-79170
 single mode and graded-index multimode fibre cable random bend losses 0-58741
 sittal cylindrical shell reinforced with internal stiffening ribs, stress-strain state under external press. 0-71684
 smooth curved pipes, external bending, effect of thickness variations 0-69702
 steel, 4340, H₂ embrittlement, stress state, thickness and delayed failure in bending 0-71746
 steel, C, unnotched, fatigue life estimation, under combined torsion and bending (*Japanese*) 0-93647
 steel, high-strength, fatigue crack growth rate and crack tip shapes, cyclic bending (*Russian*) 0-71740
 steel, low-alloy, testing cracked specimens for impact bending, expt. planning method appl. 0-71831
 steel, plastic deform., density changes (*German*) 0-60908
 steel, stainless, 304, bend test ductility of irradiated specimens for LMFBR appls. 0-104235
 steel, stainless, global bending response analysis of elastic and viscoplastic nuclear shipping cask structures subjected to impact loading 0-76301
 steel, structural, type St 37, microstruct. rel. to fracture toughness and fracture load of bending specimens (*German*) 0-89352
 steel, type SAE 1008, finite fatigue life distrib., various load-time histories 0-97589
 steel 45G2, fracture resistance, from impact bending tests and oscillograms 0-61047
 steel sheet, hot and cold rolled, cold formability, notched tensile test and stretch bend test (*German*) 0-61031
 steels, wide plate and V-notch bending tests evaluation on basis of materials mechanics (*German*) 0-66571
 stiff bending plates, stress-strain states, finite element effectiveness, polynomial approx. (*Russian*) 0-58921
 surface crack in a clamped circular plate subjected to uniform lateral pressure, bending stress anal. 0-74811
 test apparatus for high press., high temp. 0-85126
 thermoelastic deformation, second order effects 0-92051
 thick plates, 3-dimens. refined elasticity theory, bending and torsion 0-64375
 thin plates, bending anal. hybrid stress finite element model 0-96201
 Timoshenko beam, shear coeff. (*German*) 0-106729
 trapezoid plate, freely rotating, mechanical effects, calc. method (*German*) 0-106728
 viscoplastic materials, elastic, rate-independent limit of constitutive eqns. 0-74753
 Zircaloy-4, stress-relieved and cold-worked, stress relaxation in bending at 673K 0-93609
 Ag film, intrinsic stress meas. 0-71696
 Al bicrystals, isoaxial, fatigue crack initiation in grain boundary affected regions (*Japanese*) 0-89338
 Al film, intrinsic stress meas. 0-71696
 Al₂O₃-SiO₂ (3 wt.%), J-integral meas. at high temps. (*German*) 0-93624
 Fe-Al-Si (6.22, 9.63 wt.%), bending test under high press., high temp. 0-85057
 Fe-Si (3 wt.%), magnetisation variation during bending oscills., rel. to ΔE effect (*Russian*) 0-65983
 Fe-Si-Al, Sendust, ribbon-form, prep. by rapid quenching, mech. and mag. props. 0-71611
 Fe₂₃Ni₃₆Cr₁₄P₁₂B₆ Metglas, bending deform., shear band form., high-speed cinematographic obs. 0-89322
 Fe₄₀Ni₄₀P₁₄B₆, metallic glass, bending tests, evidence of ideal elastoplastic deform. 0-97543
 LiF film, intrinsic stress meas. 0-71696

bending continued

- LiNbO₃, Fe diffused, single-mode waveguide, comparison of bending losses in integrated optical circuits 0-83684
 Nb₃Sn, composite superconducting wire, critical current-bend strain relationships 0-93063
 Ni_{0.5}Zn_{0.5}Fe₂O₄ coarse grain polycryst. ferrite, diffusional creep (*Japanese*) 0-104238
 Pd₂Si and PdSi films, on Si, stress obs. 0-80145
 PtSi films, on Si, stress obs. 0-80145
 Si, dislocation motion from indentation rosette 0-79798
 Si, single crystal, brittle fracture in axisymmetric bending, study at room temp. 0-81180
 ZnS film, intrinsic stress meas. 0-71696
 Zr, foil bending by in situ ion irradi., neutron damage simulation, room temp. oxide growth 0-107342
- bending of light** *see* gravitation; light
- bending strength**
 biaxial strength tests, finite element anal. 0-89431
 ceramics, bending test results processing 0-97672
 ceramics, mech. test apparatus for up to 2200°C (*French*) 0-104372
 ceramics containing metastable tetragonal ZrO₂, grinding induced tempering 0-89260
 concrete, high strength, made with a special cement admixture, mech. props. (*Japanese*) 0-89297
 concrete, impact bending capacity (*Japanese*) 0-89341
 ethylene propylene/polyolefin blends, radiation cross linking 0-66801
 glass, devitrified technical, bending strength, scale effect 0-89311
 glass, flat, strength and durability levels 0-66608
 glass components, life testing under flexing load (*French*) 0-89432
 glass fibre reinforced cement, durability in wet and dry conditions, fibre length and content effect 0-71726
 glass fibre reinforced plastics, ageing by boiling in water, effect on physico-mech. props. 0-60892
 glass fibre reinforced plastics, cylindrical shells, compressive and flexural strength (*Japanese*) 0-81115
 glass fibre reinforced plastics, damage summation in nonstationary cyclic loading 0-60969
 glass shell, built-up, local strengthening influence on supporting capacity 0-71714
 graphite, polygranular, flexural strength after heat treatment porosity correl. 0-84996
 graphite, pyrolytic commercial, high-temp. thermal and mech. props. 0-75372
 graphite fibre filled polyimide composite prepreg laminates, room-temp. ageing effect 0-81093
 illuminating fibre bundles, improved characts. due to glasses type VS 1637 and VO 720 0-102844
 kaolin bodies, effect of mineralizers on firing shrinkage, microstruct. and strength 0-97488
 mortar specimens, repeated impact bending load study (*Japanese*) 0-93622
 natural rubber vulcanisate, network changes during physical testing 0-60936
 optical waveguide fibre coating technology, overview 0-58828
 orthotropic laminates, torsion strength and shear modulus determ. 0-92587
 polyester resin, unsaturated, chalk filled, props. (*German*) 0-104228
 polyester resin concrete, effects of styrene-unsaturated polyester ratio on props. (*Japanese*) 0-89299
 Si₃N₄-Ce₂O₃-SiO₂ materials: phase relations and strength 0-97465
 steel, cast, SC49, rel. between rotating and flexural bending strengths (*Japanese*) 0-81117
 steel, Cr-Mo (2.25, 1.0 wt.%), temper embrittlement, effect of P, Sn, comp. and carbide precip. 0-85036
 steel, low C, impact strength and crit. brittleness temp., sample thickness and notch radius influence 0-85018
 steel, stainless, porous sheet, mech. strength, bend and reverse bend tests (*Russian*) 0-93595
 steel, types A533B and KAS, fracture toughness meas. using elect. potential method (*Japanese*) 0-93722
 steel fibre reinforced concrete, vibr. compaction, pressure compaction and curing (*Japanese*) 0-89179
 straight bar bending strength, brittle fracture energy conditions (*Russian*) 0-58974
 thermoplastic-based sheet materials, flexural anisotropy and stiffness assessment 0-76442
 Timoshenko rod, straight axis, free bending oscillations investigation (*Hungarian*) 0-89327
 Al-steel mixture, wear resistant, produced by compaction by discrete shock waves 0-84882
 AlN-Mo cermets, ZrO₂ and mullite whisker reinforced, strength var. with temp. 0-104232
 Al₂O₃ rod, damaged, mech. strength, surface defects effect, appl. as insulators (*German*) 0-76330
 Al₂O₃ substrates, tape-casted, fracture strength analysis 0-60948
 Al₂O₃-Mo cermets, ZrO₂ and mullite whisker reinforced, strength var. with temp. 0-104232
 Al₂O₃-TiC, composite, fracture behaviour in three-point bending 0-60951
 3Al₂O₃·2SiO₂-ZrO₂ composites, sintered, in situ-reacted, fracture props. 0-81158
 C fibre reinforced plastics, strength props., effect of SiC coating on fibre 0-104224
 C, polygranular, flexural strength after heat treatment porosity correl. 0-84996
 Fe-Ni-Al-Co-Cu-Ti YUNDK type, S effect on mech. props. 0-60927
 Fe-Si (3 to 5 wt.%) sinters, mag. props., Si and Fe-Si additions effect 0-71104
 Na₂O-B₂O₃-SiO₂ glass fibre, plastic-coated, liq. N₂, strength 0-58707
 Na₂O-B₂O₃-SiO₂ glass-Ni compact, indented, strength and fracture toughness 0-93636
 Na₂O-SiO₂ glass, OH⁻ content effect on mech. and other props. 0-89337
 Ni-Cr-Al sintered alloy, hot vac. pressure, fracture and mech. characts. 0-66667
 Ni-Cr-Ta-Ti-Si, EP557 precipitation hardening alloy, mech. props., heat treatment effect 0-60877
 SiC, controlled nucleation thermochemical deposition, charact. and props. 0-108355
 SiC, dense, joining by hot pressing, and bond strength 0-66458
 SiC fibre reinforced Al, synthesis by liquid pressing method 0-100816

bending strength continued

- SiC, pressureless-sintered, high temp. strength (*Japanese*) 0-104299
 Si₃N₄, bending strength, deformability, elastic moduli and brittleness 0-81191
 Si₃N₄, hot-pressed, strength anisotropy origins 0-89330
 Si₃N₄, reaction-bonded, strength, effect of Si purity in production 0-100902
 SiO₂ glass fibre, plastic-coated, liq. N₂ strength 0-58707
 Ti-Al-Mo-Cr (4.5, 5, 1.5 wt.%), weld metal, α/β interace sliding 0-108512
 Y₂O₃ ceramics, strength under mech. and thermal actions 0-97554
 ZrO₂, metastable, tetragonal, strengthening by surface grinding 0-71777
 ZrO₂, partially stabilised ceramics, strengthening, post-sintering heat treatment 0-97518
 ZrO₂, partially stabilized, props. and appl. to extrusion dies 0-97507
 ZrO₂, partially stabilized, processing defects 0-97558
 ZrSiO₄, zircon ceramic with glass-forming additives, sintering and mech. props. 0-60814

berkelium

see also nuclei with

No entries

berkelium compounds

No entries

beryllium

see also nuclei with

- atom, approximate relativistic Hartree-Fock eqns., soln. using Slater-type functions 0-58168
 atom, closed shell, Jastrow wave functions, var. calcs. 0-83249
 atom, correl. contribs. to dipole polarisability, coupled HF-perturbation theory 0-106269
 Auger spectra induced by 100 keV Ar⁺ impact 0-84820
 blisters due to He irradiat., proton backscatt. study 0-75273
 crystal, failure energy 0-81192
 electron microprobe local anal. of light elements, ultrasoft X-ray spectroscopy 0-99027
 electronic struct., NMR study 0-108085
 equation of state, solid-state models, comparison 0-75332
 Fermi surface, stress-induced changes 0-96770
 film, on W (110), growth mode, work function, thermal desorption, and struct. 0-75477
 foil, ion bombardment, secondary photon emission, ion energy depend. 0-97346
 fracture and strength properties, dynamic ageing effects 0-81202
 fusion reactor material, low energy ion erosion expts., Kaufman source appl. 0-68942
 fusion reactor material, range profiles of Li⁺, appl. of (n,p) and (n, α) reactions 0-61200
 ingot, high-purity, TEM obs. of BeO dispersion 0-104165
 ion-implanted, impurity lattice location, channelling meas., Monte Carlo calc. 0-107291
 isoelectronic sequence, electron impact excitation of reson. transitions 0-63825
 isoelectronic series, excited states, oscill. strengths calcs., influence of wave function determ. method 0-99478
 lattice site Be electric field gradients, gamma-spectral study 0-80224
 muonic X-ray transitions, nuclear charge radii 0-99589
 neutron forces in relativistic electron radiation field in crystal, channelling (*Russian*) 0-70287
 optical components, electroless Ni coated Be, comparison with glass 0-69473
 projected range distrib. of 5-25 keV ⁴He⁺ 0-65094
 proton stopping power, 20 to 120 keV 0-91411
 secondary photon emission following ion bombard. 0-71493
 sintered, physicochem. props. anisotropy, BeO inclusions effect 0-60804
 soft X-ray emission edge, temp. depend. 0-89090
 surface, slowly oxidised, secondary electron yield changes, and AES characterisation 0-71524
 surface damage, due to 20 keV He⁺ irradiation, gas trapping profile meas. (*French*) 0-84218
 thick film, amorphous, RF magnetron sputtering 0-80971
 thick film or Au substrate, secondary electron emission 0-104022
 X-ray scattering, Wannier function calcs. 0-87988
 Be I like ions, resonant-scatt. contributions to excitation rates 0-58393
 Be III, doubly excited states, triplet spectra 0-87069
 Be⁺, ²P shape resonances, shift potential calcs. 0-69089
 Be⁺, absolute cross sections and polarisation of electron-impact excitation of resonance multiplet 0-99577
 Be⁺+He(Ne), ns-np excitation, alignment and orientation, impact, parameter theory 0-91648
 Be⁺+He(Ne)(Ar), Be II 2²P excitation, alignment and orientation 0-91647
 Be⁺+Ne, 180 degree phase jumps for Be⁺(2s-2p) excitation amplitudes, coherence obs. 0-63793
 Be₂, ground state, multiple scatt. X α calcs. 0-58149
 Be₄(Be₄⁻), atomic clusters, electronic struct., LCAO-MO-SCF and HF calcs. 0-63880
 Be₂(² Σ _g⁺), binding energy, ab initio pot. curves, interacting correlated fragments method 0-63557
¹⁰Be geochemistry in North Pacific during Pliocene 0-101356
¹⁰Be/⁹Be ratio meas. using electrostatic tandem accelerator 0-76579
 (GaAl)As:Be implanted DH stripe geometry laser 0-64044
 GaAlAs/GaAs solar cells, Be and Zn behaviour 0-101111
 Ga_{1-x}Al_xAs low threshold stripe geometry DH laser, Be implanted, on semi-insulating substrate 0-69409
 GaAs-Ga₂Al_{0.8}As:Be, LPE, diffusion of Be into GaAs substrate 0-103517
 Ge:Be, P, absorption of radiation, 0.6-2.8 mm, 4.2 to 20K 0-66332
 Si:Be, ion implanted, correl. of atomic distrib. and implantation induced damage profiler 0-88199
 Si:Be ion implanted, channelling and random equivalent depth distrib. 0-100293
- beryllium alloys**
 see also beryllium compounds
 rare earth alloys, RBe₃, XPS, resist. and susceptibility study 0-71565
 superconducting high Debye temperature material, theoretical upper limit of crit. temp. 0-60129
 Al-Li-Mg-Be alloys, phase composition of surface films, oxidation protection mechanism (*Russian*) 0-65417
 Al₁₁Be_{0.6}B_{2.2}, metal distrib., X-ray diff. study 0-75204
 Be-Au, ohmic contact to p-InP, low contact resist. 0-65677

beryllium alloys continued

- Be-Cu, thermal expansion, vibr. characteristics at low temp., effect of substitution impurities (*Russian*) 0-103439
 Be-ir, dil., elec. field gradient, Mossbauer meas. 0-80665
 Be-Ni(Y)(Al), plastic deform., flow stresses, fracture (*Russian*) 0-108496
 Be_{1-x}Mn_x, Be-rich, NMR and paramag. susceptibility 0-71206
 BeNi, dil., electronic struct., NMR study 0-108085
 CeBe₁₃, intermediate valence state, XPS, resist. and susceptibility study 0-71565
 CeBe₁₃, lattice spacings and susceptibilities 0-65778
 Cu-Be, dynode surface, SEM and Auger microanalysis 0-100384
 Cu-Be, SCC in NH₃ 0-104326
 Cu-Be (1.8 wt.%), discontinuous precip. form. and growth, TEM, obs. 0-104169
 Cu-Be (2 at.%), plastic deform. and dislocation substruct. 0-76307
 Cu-Be (2 wt.%), precipitation sequence, TEM obs. 0-108450
 Cu-Be solid solutions, local oscill. conc. depend., impurity bands (*Russian*) 0-75318
 Cu-Be-Co, discontinuous reaction, analytical TEM 0-100842
 Cu-Be(2 wt.%), tarnish surface films, formed in ammoniacal Cu(II) solns. 0-97624
 Er_xLa_{1-x}Be₁₃, ESR studies 0-108064
 Er_xLa_{1-x}Be₁₃, mag. sp. ht. and ESR, cryst. field interactions 0-60290
 LaBe₁₃, lattice spacings and susceptibilities 0-65778
 LuBe₁₃, lattice spacings and susceptibilities 0-65778
 Mo-Be solid solutions, superconducting transition, temp. changing peculiarity due to press. (*Russian*) 0-70878
 (Tb₂La_{1-x})Be₁₃, mag. struct., cryst. field effects, neutron diff. study 0-65789
 ThBe₁₃, lattice spacings and susceptibilities 0-65778
 Ti-Al-V-Be-B, melt-extracted polycryst., mech. props. 0-76360
 TiBe₂, de Haas-van Alphen effect, Fermi surface, theory 0-103614
 TiBe_{1.8}Cu_{0.2}, ferromag., magnetisation density 0-103817
 TiBe_{2-x}Cu_x, high press. study of Curie temp. and mag. susceptibility 0-84600
 Ti₅₀Be₄₀Zr₁₀, amorphous, crystn. temp., press. and heating rate depend. 0-70132
 TiFe_{0.8}Be_{0.2} alloys for H₂ storage 0-97817
 VBe₂, fusion reactor material, low energy ion erosion expts., Kaufman source appl. 0-68942
 YBe₁₃, lattice spacings and susceptibilities 0-65778
 Zr-Ti-Be metallic glass, phase separation 0-97464

beryllium compounds

see also beryllium alloys

- beH₂, as a moderator in minimum critical mass systems 0-83151
 beryl, natural and synthetic, ion channelling transmission ratios 0-75277
 Al₂C₃-Be₂C-SiC system, phase analysis and TEM struct. obs. 0-108420
 AlN-Si₃N₄-Be₃N₂ system, phase equilibria 0-60844
 Be complexes, binding and orbital energies, biological systems ab initio calc. 0-102442
 Be-Si-Al-O-N ceramic, phase assemblages, relationships with props. 0-60848
 Be-Si-N system polytypes, struct. obs. using TEM 0-107192
 BeSi₂O₄ film on Al-Li-Mg-Be alloy, phase composition, oxidation protection mechanism (*Russian*) 0-65417
 Be₃Al₂(SiO₃)₆, beryls, optical absorpt. spectra in the near IR (900-2500 nm) 0-89004
 Be₃Al₂(Si₂O₁₃)₂Cr³⁺, artificial emerald, distrib. of Cr³⁺ impurity 0-59503
 BeAr⁺(X²⁺ Σ ⁺), spectrosc. determ., near-dissoc. expansions 0-83513
 BeBH₂, H bridged system, floating spherical Gaussian model 0-78518
 BeF, A ²I state config., ab initio MO calcs. 0-95532
 BeF, spin orbit coupling const., ab initio calcs. 0-63537
 BeF₂, aqueous solns., mag. and quadrupole relax. 0-71226
 BeF₂, glass, glass transition temp. and thermal expansion 0-64902
 BeF₂, glass, IR and UV transmission spectra 0-89019
 BeF₂, glass transition, Monte Carlo study 0-75343
 BeF₂, vitreous, ionic transport and defect struct. 0-107472
 BeF₂:Eu³⁺ glass, luminesc. of Eu³⁺, transition probabilities 0-80845
 BeF₂:Eu³⁺ glass, struct. and optical props. 0-84067
 BeF₂:Eu³⁺ glass, struct., Monte Carlo simulations 0-96448
 BeF₂-KF-CaF₂-AlF₃-EuF₃ fluoroberyllate glass, Eu³⁺ fluoresc. linewidth 0-66285
 BeH₂, ² Σ ⁺ states, spin-coupled valence bond theory of molecular electronic struct. 0-83285
 Be²⁺(H₂O)_n (n=1,2,3,4,6), FSGO-pair-pot. calcs. (*German*) 0-74277
 Be₂N₂-BeSiN₂ system, crystallography and phase relationships, TEM and electron diff. study 0-92502
 BeO, anodic film, trapping of ³He and ⁴He ions at room temp. 0-84221
 BeO black tarnish film, on Cu-Be alloy, Auger electron spectroscopy anal. 0-97624
 BeO, cryst., local centres, electronic struct. calcs. 0-100433
 BeO, field-assisted thermally stimulated exoelectron emission 0-100761
 BeO film, 5 keV D implantation 0-100268
 BeO, heated on W, thermal anal. using mass spectrometric, technique, vapourisation behaviour 0-79932
 BeO inclusions in sintered Be, effect on physicochem. props. anisotropy 0-60804
 BeO, MCSCF and CI calcs. 0-95526
 BeO, neutron wave propag., space and angle depend. study 0-106096
 BeO, photostimulated exoelectron emission under discontinuous stimulation 0-108329
 BeO, polycrystalline, stress-strain data up to 1.25 GPa 0-100899
 BeO, reduction by C, kinetics and mechanism (*Russian*) 0-93743
 BeO, TSEE, effect of surface SiO₂ 0-76159
 BeO, wurtzite-type crystals, lattice dynamics including the effect of electronic extension 0-59586
 BeO-P₂O₅ glass, ESR of VO²⁺ ions 0-100610
 Be(OH)₂, struct. and electronic props., ab initio calcs. 0-74113
 Be(OH)₂, black tarnish film, on Cu-Be alloy, Auger electron spectroscopy anal. 0-97624
 (Be(OH)(NH₃))₂⁺ model for biological active sites, ab initio calcs., comparison with Zn complex 0-104551
 Be₂SiO₄, phenakite, flux grown single crystals, twinning study by hydrothermal etching and X-ray diff. 0-107271
 K₂Zn₂Be₂(SiO₄)₂(Si₂O₇), cryst. struct. determ. 0-88121
 LiBe, ² Σ ⁺ and ²I states, mol. binding energy curves 0-58189
 MgAl₂O₄ crystals, flux grown, artificial spinel twin form. by BeAl₂O₄ addition 0-96542
 Si-Al-Be-C-N system, phase equilibria 0-60839

Bessel differential equation *see* Bessel functions

Bessel functions

education, spiral spring, (nonhelical) simple harmonic motion, Bessel functions, closed form solns. 0-57026
impulse response of Lorentz medium 0-59242
synchrotron radiation, angular and spectral distrib., modified Bessel functions of fractional order 0-91738
weakly absorbed particles, modified Austern-Blair theory, DWBA 0-86867

beta-decay

see also beta-decay theory; beta-ray spectra; nuclear electron capture
 β -active nuclei, neutrino exchange and long range interactions 0-73826
A=135-143, odd A fission products, delayed n, decay studies and Q_β meas. 0-78227
beta strength function, half life and delays, nuclear- and astro-physics consequences 0-102149
beta strength function structures, nuclear- and astro-physics consequences 0-99152
conference on nuclear physics, Mikolajki, Poland (2-14 Sept. 1979) 0-101662
conference on nuclear spectroscopy of fission products, Grenoble, France (May 1979) 0-77546
even-even neutron-rich fission products, de-excitation spectra, β -decay, deformation 0-78203
far unstable nuclei, beta delayed two neutron emission, nuclear structure 0-68606
neutron rich nuclei; β^- -emitters, deformation and spectroscopy 0-78223
neutron rich nuclei, beta decay half lives, expt. techniques 0-78224
nuclear far from β -stability, delayed neutron energy spectra, structure effects 0-78226
nuclei far from stability, β -decay energies, γ -rays, Q_β values and masses 0-78225
Q-values of β^- decay, rapid meas. from electron and gamma energy decays 0-78220
Rumanian primary standard (*Rumanian*) 0-68603
semileptonic weak and EM interactions, multipole operators, HO single particle matrix elements 0-73840
Z=37-43, neutron rich fission products, mass energy surface, decay props. 0-78228
(p,n), 120 MeV, 0° cross sections, Gamow-Teller matrix elements for A=7-90 0-86860
⁹⁴Rh isomers, beta decay, ⁹⁴Ru level structure, spin and parity 0-57747
²³⁸Ac decay, ²³⁸Ra levels, J^π and transitions, Nilsson assignments 0-68543
¹⁰⁰Ag^m decay, ¹⁰⁰Pd levels and γ -transitions 0-83077
¹⁰³Ag \rightarrow ¹⁰³Pd, β -ground state feedings and branchings 0-102147
²⁶Al, stellar weak interaction rates, supernova appl. 0-82336
 β β^+ -decay, β - α angular correlations, final state energy depend., current test 0-102151
¹²B, aligned, β -ang. distrib. asymmetry coeffs., pseudotensor interaction, T=1 isospin triplet decay 0-106021
⁸Br, A=89-91, delayed neutron emission probabilities, β -decay half-lives 0-83078
⁸⁴Br decay, ⁸⁴Kr levels, γ -cascades, J^π , mixing ratios and correlations 0-63134
¹²C(μ^+ , ν)¹²B, polarisation studies, muon capture, weak interaction aspects 0-68655
¹⁴C_{g.s.} β -decay, mesonic exchange currents, weak process microscopic treatment 0-57742
¹⁰³Cd \rightarrow ¹⁰³Ag, β -ground state feedings and branchings 0-102147
³⁵Cl, stellar weak interaction rates, supernova appl. 0-82336
⁵⁶Co β^+ -decay, ⁵⁶Fe low lying levels, J^π , γ - γ coincidences, internal conversion 0-86815
⁵⁶Co in Type II supernovae, decay rel. to supernova light curves 0-77427
⁶⁰Co polarised nuclei, β -ray emission, directional distrib. and asymmetry factor 0-95315
Cs, fission fragment, delayed neutron branches from γ -spectroscopy 0-78230
Cs, neutron rich isotopes, Q_β and direct mass meas. 0-78132
Cs decay, ¹³⁶Xe quasi-rotational bands, levels J^π and $T_{1/2}$ 0-83021
¹⁴²Cs decay, ¹⁴²Ba, γ ang. correlations, levels, spins and mixing ratios 0-57734
¹⁴³Cs, delayed neutrons, energy spectra 0-99153
¹⁶³Er decay, ¹⁵⁵Ho $L_{2,3}$ subshell X-ray fluorescence and Coster-Kronig yields 0-69102
Eu decay, ¹⁵², ¹⁵⁴Gd γ -transition energy and intensity meas. 0-73818
²²⁸Fr \rightarrow ²²⁸Ra, γ rays, internal conversion, $e\gamma$ coincidence spectra meas. 0-78216
¹⁵³Gd decay, EM transitions of ¹⁵³Eu, internal conversion coeffs. (*Russian*) 0-63121
³H β -decay spectrum, $\bar{\nu}_e$ mass (*Russian*) 0-91159
³H β -spectrum in valine molecule, $\bar{\nu}_e$ mass 0-91158
³H decay, electron spectra rel. to neutrino rest mass and astronomical consequences (*Russian*) 0-109575
¹⁵⁴Ho decay, ¹⁵⁴Dy N=88 nuclei quasirot. bands and J^π 0-83025
¹⁵⁷Ho \rightarrow ¹⁵⁷Dy decay, internal conversion electron spectra and $e\gamma$ coincidences (*Russian*) 0-68604
I β^+ decay force function resonance struct., level populations (*Russian*) 0-102154
¹Li, A=139-141, delayed neutron emission probabilities, β -decay half-lives 0-83078
¹³³I decay ¹³²Xe level struct., J^π , transitions and multipole mixing ratio 0-91134
¹³⁷I beta delayed neutrons, ¹³⁷Xe neutron unbound states, high energy X-rays 0-86856
³⁵K decay, ³⁵Ar levels, transitions and β -delayed protons 0-91156
³⁶K, beta delayed emission of protons and α -particles 0-83074
⁴⁵K β -decay, ⁴⁵Ca levels, excitation functions and J^π 0-105978
⁸⁵Kr^{m.s.} decay, ⁸⁵Rb levels, J^π and transitions 0-78162
⁸Li β^- -decay, β - α angular correlations, final state energy depend., current test 0-102151
¹¹Li beta decay, γ activity 0-106018
Lu β^+ decay force function resonance struct., level populations (*Russian*) 0-102154
¹⁶¹Lu, A=160-163, decay and $T_{1/2}$, ¹⁶⁰⁻¹⁶³Yb transitions 0-102146
¹⁶⁹Lu allowed hindered β^+ decay, ¹⁶⁹Yb $7/2^+ [404] \rightarrow 7/2^+ [633]$ transition ft value 0-102148
¹⁷²Lu decay, identification of γ -spectra unplaced energies by delayed coincidence meas. 0-78221

beta-decay continued

⁴⁹Mn, β^+ -decay superallowed branch, ⁴⁹Cr levels, transitions, and Gamow-Teller matrix elements 0-57746
¹⁰³Mo, A=103, 104, ²⁵²Cf fission fragment β -decay, X-ray- β particle coincidence technique 0-74094
¹⁰²Mo fission product decay, ¹⁰²Tc decay scheme and γ -intensities 0-78229
¹²N, aligned, β -ang. distrib. asymmetry coeffs., pseudotensor interaction, T=1 isospin triplet decay 0-106021
¹⁴N(γ , π^+), anomalous ¹⁴N_{g.s.} \rightarrow ¹⁴C_{g.s.} transition, Kroll Ruderman terms 0-63167
²⁴Na, A=30,31,32, beta-delayed two-neutron emission 0-95316
²⁴Na half-life determ., $T_{1/2}=(14.964\pm0.015)$ h 0-95311
²⁴Na^m, polarised, β -decay asymmetry and mag. moment from Na(n, γ) 0-91157
⁹⁰Nb giant particle hole resonances, Gamow-Teller strength from ⁹⁰Zr(p,n) 0-86877
Nd decay, ¹⁴⁶Pm, A=149,151, shape coexistence, deformed states 0-78135
¹⁴⁷Nd, β decay, ¹⁴⁷Pm level scheme 0-83073
¹⁴⁰N_{g.s.} β -decay, mesonic exchange currents, weak process microscopic treatment 0-57742
³⁰P, stellar weak interaction rates, supernova appl. 0-82336
Pb region, forbidden charge exchange collective modes, β - and γ -decay processes 0-86784
⁹Pd β^+ -decay, ⁹Rh levels and γ -transitions, 3QP model anal. 0-102120
²³⁹Pu, fission product beta decay, $\bar{\nu}_e$ spectra 0-102150
²³⁹Pu(n, γ), thermal, fission product $\bar{\nu}_e$ spectrum, β -decay characts. 0-78340
²³⁰Ra decay, ²³⁰Ac levels, J^π and transitions, Nilsson assignments 0-68543
Rb decay, ⁸⁶Sr, A=98, 100 rot. struct. sudden onset, gamma transitions 0-73777
Rb decay, ⁹⁴Se direct and skip cascades, $\gamma\gamma$ ang. correlations, levels, mixing ratios 0-86851
Rb, fission fragment, delayed neutron branches from γ -spectroscopy 0-78230
Rb, neutron rich isotopes, Q_β and direct mass meas. 0-78132
⁴Rb, A=93,94,95, delayed neutrons, energy spectra 0-99153
⁹²Rb decay, ⁹²Sr $\gamma\gamma$ ang. correlations, levels, J^π , mixing ratios 0-57725
⁹⁸Rb decay, ⁹⁸Sr very low lying 0^+ state, shape coexistence bands, $T_{1/2}$, transitions 0-78148
⁴Re, A=186,188, β -decay, weak magnetism effects, triaxial rotor model 0-91155
²⁰⁸Rn \rightarrow ²⁰⁸At, γ -ray, conversion electron spectra 0-83072
²²⁴Rn \rightarrow ²²⁴Fr \rightarrow ²²⁴Ra, γ -rays, internal conversion, $e\gamma$ coincidence spectra meas. 0-78216
⁴⁵Sc, A=31,32,33, stellar weak interaction rates, supernova appl. 0-82336
⁴⁸Sc spin-flip isovector giant resonance, T₁ Gamow-Teller strength from ⁴⁸Ca(p,n) 0-106019
⁴Se, A=71, 73 decay, ⁴As, A=71, 73, levels, J^π , transitions, $T_{1/2}$ 0-57684
³Si, half life determined from varved Gulf of California sediment core 0-91153
³²Si half life from tandem accelerator mass spectrometry 0-95313
³²Si half life via accelerator mass spectrometry 0-95314
¹²⁵Sn⁹, ¹²⁵Sb high spin levels, gamma transition energies and intensities 0-73819
¹⁸⁰Ta^m, β^- and EC branching ratios, K-internal conversion coeff., γ -intensities, $T_{1/2}$ 0-68601
¹⁴⁶Tb decay and $T_{1/2}$, ¹⁴⁶Gd lowest 2^+ state, J^π and transitions 0-105979
Tc decay, ¹⁰⁴, ¹⁰⁶, ¹⁰⁸Ru level scheme and transitions, collective model anal. 0-78166
Tc decay ¹⁰⁶, ¹⁰⁸Ru levels, transitions, J^π and shape 0-57744
⁹⁰Te, beta-decay and dose calcs. 0-91154
¹²⁹Te^{m.s.} decay, ¹²⁹I time depend. quadrupole interactions, γ - γ correlations 0-78145
¹³⁰Te double β -decay, lepton charge conservation (*Russian*) 0-102153
²⁰⁴Tl β -decay, K-shell autoionisation accompanying internal bremsstrahlung 0-57745
⁴U, A=235,238, fission product beta decay, $\bar{\nu}_e$ spectra 0-102150
²³⁵U(n, γ), thermal, fission product $\bar{\nu}_e$ spectrum, β -decay characts. 0-78340

beta-decay theory

see also beta-decay; beta-ray spectra
meson dominance model and second class currents 0-63132
³C(³Li,⁰He), 62 MeV, Gamow-Teller sum rules and ground state wave function 0-106073
⁴Nb, A=90,92,94, Gamow-Teller strength distrib., RPA calcs. 0-78218

beta-particles *see* beta-rays

beta-radiation *see* beta-rays

beta-ray absorption

see also electron absorption
energy distributions in homogeneous media 0-109033
inhomogeneous medium, density determ. by β -ray attenuation, calcs. and meas. 0-98182
lung, beta-emitting particles, fraction of energy absorbed, rat obs. 0-104641

beta-ray angular distribution

see also beta-ray spectra
¹²B, aligned, β -ang. distrib. asymmetry coeffs., pseudotensor interaction, T=1 isospin triplet decay 0-106021
¹²N, aligned, β -ang. distrib. asymmetry coeffs., pseudotensor interaction, T=1 isospin triplet decay 0-106021

beta-ray detection and measurement

see also beta-ray spectrometers; radioactivity measurement
air ionisation probe for α , β , γ hand and shoe monitor 0-58084
cameras, gas replacement monitor 0-95502
environmental samples, spectrometric method for meas. of hard β -emitters 0-94135
gas-chromatography, beta radio effluents, window flow counter 0-93824
highly stabilized hybrid spark chamber for β -ray imaging 0-102398
mixed β - γ dosimetry, ionisation and scintillation counters 0-57975
MWPC, beta-ray imaging device for radiochromatography 0-102387
needle counter, small size low-level 0-58075
particle detectors, microprocessor-controlled data acquisition system for temporal/angular correl. between β - and γ -ray emission (*Spanish*) 0-106238
particulate contamination monitoring, recent developments 0-57985

beta-ray detection and measurement continued

- Q-values of β^- decay, rapid meas. from electron and gamma energy decays 0-78220
 surface barrier detector for beta dosimetry 0-57973
 survey meter for meas. of absorbed dose rate independently of energy 0-106203
 TLD evaluation of internal beta-dose rate for archaeological dating 0-98478
 $\text{CaF}_2(\text{Eu})$ Phoswich detector, evaluation for ^{90}Sr in situ anal. 0-58067
 $\text{CaSO}_4:\text{Dy}$ Teflon TL dosimeters, thin, development for β -dosimetry in personnel monitoring 0-63399
 ^{252}Cf fission fragment β -decay, X-ray- β particle coincidence technique 0-74094
 ^3H -filled glass microspheres, assay by liquid scintillation counting 0-63481

beta-ray effects

see also *electron beam effects*

- beta-rays from ^{14}C , biological hazards, cell killing effects, E. coli expts. 0-89805
 death due to inhalation of β -emitters, probability estimation 0-89801
 E. coli, damage induced by T decay, secondary lethality under nongrowth conditions 0-104654
 lung tumorigenesis from particulate sources of ^{147}Pm β -radiation 0-72247
 skin, pig, response to ^{137}Cs -irrad. 0-67161
 skin, radiation fibrosis after β -irrad. and attempt at suppression, guinea pig expts. 0-72243
 skin, senescent, increased susceptibility to β -irrad., mouse obs. 0-104656
 ^{204}Tl β -particle excitation of external bremsstrahlung spectra from thick targets 0-84797

beta-ray polarisation

$\mu^+ \rightarrow e^+ \nu \nu$, pol. meas. 0-73760

beta-ray scattering see *beta-ray effects; collision processes; energy loss of particles; particle backscattering; potential scattering; transport processes*

beta-ray spectra

see also *beta-decay theory*

- cylindrical-mirror electrostatic analyser for electron spectroscopy of beams 0-63446
 ^{252}Cf spontaneous fission, fission product β spectra (Russian) 0-91204
 ^{76}Sr , mass excess values from beta and gamma spectra from $^{32}\text{S} + ^{54}\text{Fe}(^{58}\text{Ni})$ 0-63137
 ^{88}Y , A=82, 83, mass excess values from beta and gamma spectra from $^{32}\text{S} + ^{54}\text{Fe}(^{58}\text{Ni})$ 0-63137

beta-ray spectrometers

see also *beta-ray spectra; electron spectrometers*

- internal pair transition ion beam studies, combined mag. lens plus Si(Li) spectrometer 0-74073
 magnetic analysis of charged particles, α -, β - and mass spectrometers (Russian) 0-87011

beta-rays

see also *electrons*

No entries

beta spectrometers see *beta-ray spectrometers*

betatrons

- design and performance of 5 MeV betatron, X-ray prod. 0-63421
 gamma bremsstrahlung from thin target 0-86999
 magnetically excited, enhanced electron energies 0-86998
 NDT application in industrial products inspection 0-81267
 orbit expansion and beam extraction, simulation 0-91353
 stochastic beam cooling expts., low-noise wide-band power amplifier system 0-58011
 synchrotron radiation depend. on betatron oscillation linear coupling 0-91345

Bethe-Salpeter equation

- composite system, relativistic, light-front wave functions 0-73592
 dressed fermion bubble, real-space equivalent calcs. 0-101751
 mesons, bound state wave function, probability interpretation, form factors, Bethe-Salpeter eqn. (Chinese) 0-101930
 quasipotential eqn. derivation (Chinese) 0-68370
 relativistic harmonic oscillator for spin-1/2 particles in the Bethe-Salpeter formalism 0-91001
 scalar equation solns., self energy diagram effects 0-86590
 ν , charmonium and strangeonium, linear+Coulomb pot. study, high α_s regime 0-62935
 ^3H binding energy, relativistic calc., Bethe Salpeter eqn. 0-68519

Bethe-Uhlenbeck equations see *quantum statistical mechanics*

betatrons see *synchrotrons*

bicrystals

- α - β brass, interface segregation 0-89231
 brass, two phase α/β bicrystal, transgranular slip and fracture across an interface 0-81150
 α - β brass, two phase bicrystal, fatigue 0-108520
 β -brass bicrystals, shear-incompatible, grain boundary contrib. to Bauschinger effect 0-97550
 α/β -brass bicrystals, two-phase, with nearly uniform and thermodynamic equil. concs. 0-65383
 brass bicrystals, two-phase (α/β), interphase boundary sliding at high temperature 0-88164
 elastic incompatibility stresses (Japanese) 0-107361
 electrical conductivity versus interatomic bond character 0-59948
 electron diffraction theory 0-75122
 FCC polycrystals, under hydrostatic pressure 0-107356
 film/substrate interface, misfit dislocation obs. using electron microscopy 0-103605
 jimthompsonite and anthophyllite from Swiss Alps, disordered intermediate minerals imaging 0-72518
 oriented, sintering prod. technique 0-108371
 Ag, oriented bicrystal, sintering prod. technique 0-108371
 Ag, thin-film bicrystals, planar lattice defects and migrating grain boundaries interaction 0-79835
 AgMg two phase bicrystal growth, orientation, interface struct. 0-60773
 Al bicrystal, plastically deformed, slip heterogeneities 0-79858
 Al bicrystals, isoaxial, fatigue crack initiation in grain boundary affected regions (Japanese) 0-89338
 Al, high resolution electron microscopy obs. of dislocations 0-103347
 Au, bicrystalline thin films, faceting of [001] grain boundaries 0-70222
 Au bicrystals, struct. of grain boundaries using diffr. techniques 0-59478
 Au, epitaxially grown bicrystalline thin films, preferred inclinations of (100) grain boundaries 0-103367

bicrystals continued

- Au, thin film bicrystal, diffraction effects from inclined grain boundaries 0-103362
 Au/Cu, initial epitaxial growth at room temp. 0-59829
 Au-Ag, bicryst. thin film couples, interphase interfaces, TEM 0-70540
 Au-Pd, bicryst. thin film couples, interphase interfaces, TEM 0-70540
 Cu, bicrystalline thin films, characterisation of [001] tilt boundaries 0-75473
 Cu, oriented bicrystal, sintering prod. technique 0-108371
 Ge bicrystals, high angle tilt boundaries, TEM (French) 0-70224
 Ge, high resolution electron microscopy obs. of dislocations 0-103347
 LiF bicrystal, high-angle tilt boundary and edge dislocation intersection effects 0-79836
 NaCl:Ca crystals, surface recrystn., moisture effect 0-84950
 Ni, oriented bicrystal, sintering prod. technique 0-108371
 PbS-PbSe epitaxial bicrystals, direct scatt. of channelled He ions at dislocations 0-65110
 W bicrystals, crack propag. across grain boundaries, crack speed meas. technique appl. 0-108575
 Zn, crack form. at grain and twin boundaries at low temp. (Russian) 0-66620

biexcitons see *excitonic molecules*

big-bang theory see *cosmology*

bimetallic strips see *bimetals*

bimetallic wire see *bimetals*

bimetals

- contact unit, for liquid N_2 level monitor 0-57309
 diffraction gratings, theoretical study 0-87525
 steel, alloy with austenitic stainless, H permeability 0-107572
 Al/Cu thin film couples, TEM study of intermetallic nucleation at interface 0-65305
 Au-Al thermocompressional contacts, diffusional zones, phase growth during annealing (Russian) 0-75389

binaries (stellar) see *binary stars*

binary stars

see also *eclipsing binary stars*

- HR 1099, RS Canum Venaticorum type binary, light and colour curve meas. 0-73004
 2A 0311-227, AM Herculis type X-ray binary, optical counterpart, radial vel. obs. 0-94890
 2A 0311-227 optical counterpart, high speed photometry 0-82547
 2A 0311-227 optical counterpart, light curve Fourier anal. 0-82549
 2A 0526-328 optical counterpart, radial vel. meas. and orbital period 0-90579
 2A 0526-328 optical counterpart, spectroscopic obs. 0-77515
 absolute luminosity calibrations, consistency 0-62111
 accretion discs, steady, optically thick, convective vertical energy transport 0-62112
 accretion discs, viscosity determ. for Hercules X-1 and (SS 433) 0-62110
 accretion disks round neutron stars and white dwarfs, flux distrib. and colours 0-94778
 ADS 1833 and 6871 AB, visual binaries, orbital calc. (French) 0-98690
 Am-type, tidal interaction producing stable atm., evolution 0-67752
 CG Andromedae, Si star, spectrum variable, short period radial vel. variability determ. 0-72968
 Z Andromedae, symbiotic star, IUE obs. of UV spectrum 0-109450
 Ap stars in spectroscopic binary systems, chemical anomalies surface distrib. 0-62140
 AE Aquarii, cataclysmic variable, IUE satellite UV obs. 0-72985
 AE Aquarii, spectroscopic binary variable, X-ray source, orbital element determ. 0-105288
 R Aquarii, symbiotic long-period variable, spectrum of assoc. nebulosity 0-90450
 R Aquarii, UV, visible and 85 GHz continuum obs. 0-85946
 R Aquarii (M7+pec), late type variable star, IUE obs. of circumstellar emission 0-82370
 η Aquilae, classical Cepheid, companion star detect. and distance determ. 0-90443
 TT Arietis, nova-like cataclysmic variable, photoelectric photometry 0-82382
 BD+29°3805, K-type giant, spectroscopic binary orbit 0-67790
 BDS 1269, pulsation periods of metal-poor δ Scuti primary star 0-105247
 binaries, wide visual, spectral type, age and uvby β photometry 0-94833
 binding energy distrib. in cluster, homogeneous cluster model 0-62209
 blue supergiant+neutron star, evolution 0-98689
 ξ Bootis, late-type dwarf star, mag. field obs. in primary component 0-72949
 bright nearby stars, unseen companions discoveries from Sproul plates astrometric anal. 0-61991
 CC 1299 (BD+27°4120), unresolved astrometric binary, orbital anal., mass and parallax 0-109464
 Z Cameloparadisi, dwarf nova, spectrophotometry at standstill and in eruption 0-82366
 SV Cameloparadisi, RS Canum Venaticorum star, identification with X-ray source H0630+82, X-ray obs. 0-101654
 TX Canum Venaticorum, cataclysmic variable, P Cygni type, visible spectral obs. 0-105249
 RS Canum Venaticorum binary stars, mag. starspot model for photometric and spectroscopic behaviour 0-109488
 RS Canum Venaticorum stars, H α line variability, visible spectra obs. 0-105277
 RS Canum Venaticorum stars, HEAO 1 X-ray obs. of active coronae 0-72925
 RS Canum Venaticorum stars, out of eclipse light var. 0-109489
 RS Canum Venaticorum type binaries, H γ line vars., chromospheric diagnostics 0-62181
 ζ Capricorni, Ba star, white dwarf+giant, UV spectra obs. 0-105284
 cataclysmic binaries, circumstellar material geometrical and photometric parameters 0-109492
 cataclysmic binaries, role of white dwarf component 0-82356
 cataclysmic binary stars (CBS), critique of polarimetric evidence on physical parameters and orbital inclination 0-109486
 V810 Centauri (HD 101947), yellow variable supergiant near Cepheid instability strip, BLUW photometry 0-98672
 α Centauri binary system, spectroscopic chemical anal. 0-62128
 Centaurus X-4, spectroscopic obs. of visual counterpart, companion type 0-82545
 Centaurus X-4, transient X-ray burster, optical counterpart discovered 0-67906

binary stars continued

- Cepheid binary detection from U-V curve obs. 0-98667
 Cepheid variables, incidence of duplicity 0-90453
 δ Ceti, β Cephei variable, spectroscopic binary, radial vels. and period var. 0-82376
 Circinus X-1, binary model, orbital eccentricity from X-ray and radio obs. 0-98735
 Circinus X-1, binary model, radio emission 0-98736
 Circinus X-1, changes in optical, IR and radio emission 0-67910
 close binaries, energy release, flares and particle acceleration (*Russian*) 0-73005
 close binaries, intermediate mass, mass transfer for different stars within evolutionary scheme 0-109476
 close binaries, light scattering in extrastellar gaseous material, emission line profiles spectropolarimetry obs. 0-109471
 close binaries, period distrib. from secondary maxima 0-109467
 close binaries, synchronous systems devel. from tidal are rot. interactions 0-109468
 close binary stars, H I α and β line photometry 0-109470
 close binary stars, low mass, evolution, gravitational wave emission influence 0-82425
 close binary stars props. before and after mass transfer, obs. and theory comparison 0-62187
 close binary system with mass and ang. momentum loss, period changes 0-72998
 close binary systems in globular clusters, preliminary report 0-109505
 close detached, Ap components, chem. anomalies surface distrib. 0-109475
 conference on close binary stars, Toronto, USA (Aug. 1979) 0-105436
 contact binary star, idealised dynamical evolution (*French*) 0-62199
 Coronae Borealis, Hg-Mn star, spectroscopic binary, visible spectra obs. 0-72983
 σ Coronae Borealis (=ADS 9979), mass and orbital elements (*French*) 0-77449
 α Crucis, improved spectroscopic orbit 0-67792
 BI Crucis, new symbiotic star, spectrum 0-109442
 25 G Crucis (HD 108250), orbital elements from spectrograms 0-82432
 SS Cygni, dwarf nova, rapid optical oscils. phase variability 0-85947
 θ Cygni, F-type dwarf star, spectral type of faint distant companion 0-90481
 SS Cygni, spectroscopic binary variable, X-ray source, orbital element determ. 0-105288
 CH Cygni, symbiotic star, 1977 outburst, radial vel. and atm. struct. determ. 0-72969
 CH Cygni, symbiotic star, binary model 0-62158
 V1016 Cygni, symbiotic star, IR variability obs. from VJHKL photometry (*Russian*) 0-105263
 Cygnus X-1, critique of polarimetric evidence on physical parameters and orbital inclination 0-109486
 Cygnus X-1, neutron star model from bi-metric theory of gravitation 0-90466
 Cygnus X-1, obs. during high state (1980 June 11 to 27) 0-86017
 Cygnus X-1, transition from high X-ray state to low X-ray state, 1980 June to July 0-98738
 Cygnus X-1, X-ray binary, variable star, SHF obs. 0-73071
 Cygnus X-1 (V1357 Cygni), optical light curve vars. rel. to X-ray vars. 0-109560
 Cygnus X-1 (V1357 Cygni), optical photometry (1980 May 25 to July 7) 0-90578
 Cygnus X-1 (X-2), X-ray polarisation obs. from OSO 8 0-90571
 Cygnus X-2, radial vel. and orbital elements from visible spectra obs. 0-77519
 Cygnus X-3, 34.1 day period, 2-12 keV obs. by COS-B 0-94897
 Cygnus X-3, period derivative and asymmetric X-ray light curve from HEAO 2 obs. 0-105394
 degenerate star-red giant interacting binary stars, compressible fluid flow, accretion 0-67779
 HR Delphini (Nova 1967), simultaneous X-ray, UV and optical obs. 0-109440
 detached, evolution to contact binaries involving mass flow 0-109477
 double stars, focal grating photometer for magnitude difference determ. 0-67567
 double stars, position angles and separation, Venezuelan obs. (*French*) 0-77450
 double stars, separation and position angle obs. 0-98691
 double stars, visual, new spectral classification on MK system 0-109462
 CX Draconis, Be star, UVB obs. 0-82388
 BY Draconis stars, out of eclipse light var. and comparison with RS Canum Venaticorum stars 0-109489
 in E3 (ESO-037-SC 01), dying globular cluster, photometric evidence for binary systems 0-105291
 education, supernova explosion in binary system, classical mechanics appl. 0-62428
 evolution of close binary systems, collapse theory 0-77389
 formation, nonaxisymmetric collapse in rotating interstellar clouds 0-85927
 formation from rot. interstellar clouds fragmentation, three-dimensional hydrodynamical calcs. 0-62236
 G 208-44/45, possible double flare star, spectral obs. 0-67727
 gas accretion, thermodynamics and hydrodynamics 0-67696
 giant stars, G and K-type, Ca II H and K lines emission intensity 0-82420
 Gleise 490 AB (BD+36°2322), red dwarf binary, flares and starspots, rot. period determ. 0-77423
 gravitational radiation, relativistic corrections and spectrum fine structure 0-90479
 gravitational wave detection, astrophysical sources, resonant mass, laser interferometer and Doppler ranging methods 0-68122
 H 2252-035, cataclysmic variable, photometry and spectrum rel. to orbital and rot. periods 0-101651
 H 2252-035, spectrophotometry, no periodic linear polarization (1980 Sept.) 0-105401
 H 2252-035, X-ray flux modulation, compact star rotation 0-101652
 HD 102567, optical counterpart to 4U 1145-61, atm. model from UV obs. 0-105396
 HD 108078, spectroscopic binary orbit from photoelec. radial vel. meas. 0-77451
 HD 113001, photometric separation of visual binary (*French*) 0-105281
 HD 159378 (Tr 27-102), yellow variable supergiant near Cepheid instability strip, VBLUW photometry 0-98672

binary stars continued

- HD 166734, Of star, spectroscopic binary orbit determ. from visible obs. 0-82414
 HD 203631, spectroscopic binary orbit from photoelectric radial vels. 0-105285
 HD 22007 (primary of ADS 16681), spectroscopic binary, radial vel., orbit elements 0-67793
 HD 39937, 101379, 155555, 174429, southern RS Canum Venaticorum stars candidates, radial vel. study 0-98686
 HD 4174, symbiotic star, spectroscopic obs. 0-85945
 HD 4174 (=EG Andromedae), peculiar M giant, UV spectra obs. 0-94798
 HD 44179, 3.3 micron unidentified feature, high resolution spectra 0-82466
 HD 45088, BY Draconis binary, surface activity from high rot. vel., visible obs. 0-77425
 HD 45088, reticon obs. in red of dK3 spectroscopic binary 0-67778
 HD 50896, Wolf-Rayet star, linear polarisation periodic vars. rel. to binary star nature 0-72972
 HD 77581 (=Vela X-1), supergiant+neutron star, X-ray, UV and visible obs. 0-94892
 HD 77581 and 153919, polarimetric obs. of massive X-ray binaries 0-98688
 HDE 226868 (Cygnus X-1), X-ray and UV spectra from HEAO 2 and IUE 0-82543
 HDE 245770, optical counterpart to A 0535+26, dimens. spectral type and luminosity visible obs. 0-72976
 AH Herculis, dwarf nova outburst, rapid oscils. evolution 0-94805
 HR 1099, 10 GHz radio emission from RS Canum Venaticorum binary 0-82427
 HR 1099 (V711 Tauri), JHK photometry of noneclipsing RS Canum Venaticorum type star 0-72995
 HR 1099 (V711 Tauri), RS Canum Venaticorum star, H α line variability, visible spectra obs. 0-105277
 HR 2142 and 7084, mass loss from UV spectra obs. 0-109485
 HR 5110, RS Canum Venaticorum binary, V photometry near radio outburst time 0-90469
 HR 6659, spectroscopic binary, radial vel. obs. 0-82430
 HR 8752 emission feature variability, visible obs. 0-109463
 I-38, probable B-type binary in Norma OB1 assoc. 0-62129
 16 Lacertae, β Cephei star, light var. anal. and photoelec. photometry 0-77412
 19 Leonis Minoris, spectroscopic binary, orbital elements and mass ratio 0-62197
 LS 1+61°303, variable binary radio star (B1 Ib), X-ray emission detect. 0-105400
 lunar occultation obs. from University of Illinois Prairie Observatory (1977-1978) 0-105148
 lunar occultations of Hyades, photoelec. obs. 0-72921
 lunar occultations photoelec. obs. 0-72920
 main sequence, absolute dimens. determ., errors requirement review 0-109473
 mass-exchanging binary stars, XUV emission (*German*) 0-109372
 massive binaries, evolution review 0-82343
 massive close binaries with OB components, evolutionary calcs. comparison with obs. 0-90474
 massive close binary stars, effect of stellar evolution on components synchronous rot. 0-62192
 massive stars (M \geq 20 Mo), binary star mass transfer model rel. to evolutionary status (*Russian*) 0-109425
 MXB 1636-536, binary nature from simultaneous X-ray and optical obs. 0-82548
 neutron stars, electrodynamics of disk accretion, magnetic field structure 0-85973
 in NGC 6231, open cluster, double lined spectroscopic binaries discoveries 0-90492
 novae, effect of binary companion on outburst 0-82394
 novae, effects of white dwarf rot. on remnants shapes 0-105244
 O-type binaries, binary freq. and anomalous mass ratios 0-109478
 orbital eccentricity effect on polarimetric obs. 0-109472
 particle discs, infrequently colliding, in binary system, tidal torques and appl. to asteroid belt truncation 0-98596
 AG Pegasi, symbiotic binary system, UV and optical spectrum rel. to nature of components 0-109449
 II Pegasi (HD 224085), surface-active binary star, spectroscopic obs. 0-90480
 IW Persei, metallic-line close binary star, photometric and spectroscopic obs. 0-62186
 X Persei (4U 0352+30), Be star, evidence for 6-year photometric periodicity 0-109446
 UV Piscium, RS Canum Venaticorum star, identification with X-ray source H0118+067, X-ray obs. 0-101654
 planetary nebulae central stars, list of binary systems 0-109435
 planetary orbit stability, Hill's method appl. 0-94834
 polytropes in central orbits, Roche problem 0-82179
 PSR 1913+16, binary pulsar, nature from observational data 0-77435
 PSR 1913+16, binary pulsar, relativistic observable effects 0-77438
 PSR 1913+16, binary system, test of relativistic effects (*Dutch*) 0-62172
 PSR 1913+16, X-ray and timing meas. correlations, grav. radiation, gas cloud friction 0-62171
 radial velocity curves of close binary systems, anal. 0-90470
 radial velocity curves of close binary systems, anal. 0-94829
 HM Sagittae, symbiotic star, IR variability obs. from VJHKL photometry (*Russian*) 0-105263
 V818 Scorpii (Scorpius X-1), UV, visible, IR and X-ray obs. 0-82541
 Scorpius X-1, high energy X-ray and SHF radio obs. 0-73067
 Scorpius X-1, Prognoz-6 obs. of X-ray fluxes and energy spectra (*Russian*) 0-109562
 Scorpius X-1, rapid variability simultaneous X-ray and optical obs. 0-62322
 Scorpius X-1, X-ray obs. from 20 to 250 keV 0-94893
 Scorpius X-1, X-ray spectrum 20-75 keV, high sensitivity determ. 0-98741
 VY Sculptoris, novalike variable, precise position 0-101597
 VY Sculptoris, novalike variable, spectrum during faint state 0-98675
 Serpens X-1 (4U 1837+04), burster optical binary counterpart visible spectra and photometry 0-94891
 slow novae and symbiotic stars, late-type components spectral classifications 0-94813
 southern double stars, magnitude differences, focal grating photometer obs. 0-67785

binary stars continued

- speckle interferometric obs., with Haute-Provence 1.93 m telescope 0-90475
 speckle interferometric observations, of spectroscopic and visual binary stars 0-90477
 spectroscopic, in Seventh Catalogue of spectroscopic Binaries, orbital elements statistical anal. 0-82422
 spectroscopic, spectral obs. with solid state detector 0-109469
 spectroscopic, statistical investigation 0-109466
 spectroscopic binaries in young SMC cluster NGC 330, limits on frequency 0-67803
 spectroscopic binaries near southern open clusters, relative radial vel. obs. (German) 0-94724
 spectroscopic binary systems, apsidal motion 0-82413
 SS 433, accretion disc viscosity determ. using slaved disc model 0-62110
 SS 433, light curves, double peak and binary-like period, photometry 0-94804
 SS 433, magnetic X-ray binary model 0-109447
 SS 433, review of obs. and theories 0-72987
 SS 433, spectral features interpreted a precessing neutron star with jets, possible binary 0-90447
 statistical distrib. and evolution (Chinese) 0-85975
 surface nucl. reactions and origin of mag. fields 0-101616
 symbiotic star candidates in LMC, optical spectroscopy and IR photometry 0-62139
 symbiotic stars, evolutionary considerations 0-62144
 symbiotic stars and slow novae, late-type components spectral classifications 0-94813
 V711 Tauri (HR 1099), RS Canum Venaticorum star, BV light curve during (1978-79) 0-105279
 EK Trianguli Australis, SU Ursae Majoris dwarf nova, superhumps, light curve UVB obs. 0-105255
 4U 0115+634, X-ray binary, 1980 Aug. photometry and spectroscopy 0-101650
 4U 1223-62, X-ray pulsar, optical counterpart Wray 977, spectra 0-72984
 4U 1907+09, optical identification and OB supergiant binary hypothesis 0-82542
 SU Ursae Majoris, soft X-ray halo around dwarf nova 0-98677
 SU Ursae Majoris stars, important sub-group of dwarf novae, photometric props. 0-101596
 AH Velorum, classical cepheid, binary detect., UVB obs. 0-109443
 γ_2 Velorum, Wolf-Rayet binary, orbital element determ. from spectral obs. 0-85950
 γ_2 Velorum, Wolf-Rayet binary star, UV obs. from TD-1A satellite 0-77447
 vibrational stability of distorted stars, anal. using Clairaut coordinates 0-90408
 visual binaries, orbital elements and masses for 18 pairs 0-62180
 visual binaries with variable components, orbital elements, visible obs. (Russian) 0-77455
 white dwarf, outer layer C and O enrichment from companion 0-109465
 white dwarfs, rapid mass accretion and extended envelope form. 0-67723
 white dwarfs undergoing spherically symmetric steady-state accretion, stability 0-77402
 Wolf Rayet stars, binary freq., mass ratio, low mass companion evidence 0-109479
 Wolf-Rayet stars, CNO abundance var. in massive binaries 0-94802
 Wolf-Rayet stars, evolution and binary freq. distrib. 0-105250
 WRA 977 (4U 1223-62, GX 301-2) orbit determ. from X-ray obs. 0-90570
 X-ray, burst sources, thermonuclear flashes in envelope of accreting neutron star 0-109455
 X-ray binaries, accretion of plasma onto neutron stars 0-109452
 X-ray binaries, cyclotron emissivity in accreting neutron stars 0-90463
 X-ray binaries, Fe line emission from Alfvén shell 0-98737
 X-ray binaries, mass transfer rel. to radio emission 0-62317
 X-ray binaries, models of supercritical accretion discs around black holes 0-105272
 X-ray binaries, neutron stars accretion disc and rot. mag. full interaction 0-62173
 X-ray binaries, recurrent transients model 0-109565
 X-ray binary sources, pulsating, spin-up due to accretion from Keplerian disc 0-67904
 X-ray binary stars, review of types and props. 0-109564
 X-ray induced shocks in stellar winds of massive binaries 0-94784
 X-ray pulsar, polarized radiation transfer in analytical solns. 0-94894
 X-ray pulsars, cyclotron line formation in accretion column 0-67901
 X-ray sources, cyclotron line feature identification 0-90577
 X-ray sources, pulsating, accretion disc mag. field calc. for oblique mag. dipole configuration 0-94895
 X-ray sources, space distrib. and physical nature 0-62316
 X-ray transient sources, new class, cool dwarf+unseen companion with accretion disc 0-101653
 in young galaxies, role in contribution to X-ray background 0-82550
 Ba II giant stars binary nature from visible radial vel. obs. 0-82355
 CH stars in globular clusters, possible binary nature 0-82355
 Hg-Mn binary stars, inhibition of atmos. diffusion 0-62153

binding energy

- see also *lattice energy; nuclear binding energy; nuclear forces*
 absolute core-level binding energies for gaseous atoms and molecules 0-101670
 alkali chloride: Mn^{2+} , spin Hamiltonian parameters, binding energies for cation vacancy complexes 0-96461
 alkali halide: alkaline-earth cations, defect structs. examined by methods based on Mott-Littleton techniques 0-59487
 alkali halide: Eu^{2+} cation vacancy complexes, binding energies 0-96513
 alkali halides, crystal binding energy, long and short range forces 0-75200
 alkali hydride molecules, pot. energy function, rot. const., vibr. const., and binding energy 0-99532
 alkali hydrides, lattice props. from interaction pot. energy function 0-100199
 alkali metals, cohesive energy, teaching 0-90630
 alkaline earth fluorides, orbital binding energy and ionicity relations, XPS meas. 0-97399
 alkaline earth oxides, cohesive and thermophysical props., role of three-body interactions 0-92477
 alloy, cohesive energy, semiempirical model, heat of form. expressions 0-70160

binding energy continued

- amorphous surfaces, energy profile and binding energy, computer simulation 0-100381
 atomic binding energies, determ. from fund. theorems involving electron density, (r^{-1}) and Z^{-1} perturbation expansion 0-63521
 atomic radiative binding in slow collisions into molecules in a laser field (Russian) 0-93753
 composites, adhesion between two crystals, theory 0-104417
 Coulomb bound-state problem, semiquantal approx. 0-99435
 diatomic molecules, nucleus-nucleus interaction, Einstein relativistic correction, Born-Oppenheimer approx. 0-91463
 electron coincidence spectroscopy, binding energy charge density meas. 0-63817
 endothermic reaction rate enhancement in EM field 0-66852
 ESCA shifts and effective charges 0-78648
 exchange energy density functional, gradient expansion, rel. to at. energy functional 0-99441
 fast ion in solid, oscillatory wake, trapped electron binding energy, RPA calc. 0-96575
 first-row transition metal ions, core ionised states, Δ SCF MO calcs. 0-78523
 fluoride crystals, rutile-type, interionic pots., cohesive energy, bulk modulus, calc. 0-79741
 frozen core approx. and pseudopotential theory validity for cohesive energy calcs. 0-64949
 grain boundaries decohesion energy, solute adsorption influence 0-65009
 graphite intercalation cpds., electrostatic interactions and staging, non-linear Thomas-Fermi eqns. 0-107732
 insulators, XPS, binding energy, surface pot. and work function calcs. 0-89113
 jellium, chemisorption, effective-medium theory of chem. binding 0-65367
 metal, simple, non muffin-tin corrections to eqn. of state (French) 0-59906
 metallic elements, core-level binding-energy shifts 0-88502
 metals, atomic binding energy and surface energy rel. to prediction of physical props. 0-59434
 metals, Morse potential appl. in molecular-metallic framework 0-79742
 metals, simple, elastic moduli, chem. trends, pseudopot. method 0-107355
 metals, simple, static props., Thomas-Fermi-pseudopotential approach 0-75514
 methane, intermolecular interaction energies calcs. using minimal basis sets 0-78681
 methylamine, affinities for $H^+(Li^+)(K^+)(CH_3^+)$, ab initio SCF calculations 0-102443
 molecule, self-consistent charge calcs. of core-electron binding energy shifts 0-69084
 molecules containing 1st row atoms, K-shell binding energy shifts, NDDO MO calcs. 0-58413
 dimolybdenum tetraformate, metal-metal bond energy, SCF-X α -SW calcs. 0-78538
 neutral bound excitons, accurate binding energies, variational method calc. 0-107715
 oxide crystals, rutile-type, interionic pots., cohesive energy, bulk modulus, calc. 0-79741
 photoelectron spectrometer, calibration using binding energy scale 0-90930
 rare earth metals, 3d core electron XPS spectra, low-binding-energy satellites, exception of Eu 0-104040
 rutile-type compounds, crystal binding energies and electronic polarisabilities 0-75202
 semiconductors, deep defects, contrib. to binding energy 0-70634
 simple metals, compressibility, Harrison pot. calcs. 0-96460
 simple metals, model pseudopot. appl. to various props. 0-59845
 superheavy and intermediate atomic collision systems, UNILAC expts. 0-63751
 surface, adsorbed atoms thermal desorption, one dimens. microscopic model, weak binding case 0-96729
 surface bixcition in polar semicond., binding energy calc. 0-96796
 tetrafluoromethane, valence electron binding energies, molecular symmetry restrictions effect 0-63528
 total electronic energy, atoms and mols., SCF binding energy, Z^{-1} perturbation theory 0-83268
 transition metal oxides, second and third-row, XPES 0-87170
 transition metals, core levels between surface and bulk atoms, variation of binding energy shifts 0-88615
 [α]-SiC:H, prepared by reactive sputtering, layer props. (Japanese) 0-60695
 Ag-O-Cs surface, oxidation, role of Cs suboxides in low work function surface layers, XPS 0-76131
 AgI surface, adsorption of water, effective pair pot. model 0-100394
 Al, metallic, phonon freq., binding energy, compressibility, elastic const. and energy band gap calcs., linear pot. 0-88284
 $Al_2(Al_2^-)(Al_2^-)$ configurations, ab initio study, LCAO, STO, MO-SCF and CI calcs., binding energy (French) 0-91447
 Ar, solid, many-body contributions to OK binding energy 0-84135
 Au clusters on alkali halide surface, size depend. of valence bands, XPS study 0-65647
 Be complexes, binding and orbital energies, biological systems ab initio calc. 0-102442
 BeBH $_3$, H bridged system, floating spherical Gaussian model 0-78518
 Be $_2(\Sigma^+)$, binding energy, ab initio pot. curves, interacting correlated fragments method 0-63557
 C bonding to Tokamak walls, XPS studies 0-80942
 Cd, electron binding energy and shift, core level XPS 0-87088
 CdS, hydrogenlike donor negative ion, ground and excited states, obs. 0-70645
 CdS:D $^-$, binding energy of D $^-$ ion 0-92541
 Co II acetylacetonate, XPS 0-74196
 Cr, electronic struct., spin-density functional calcs. 0-88476
 CrN, antiferromagnetic EPR spectra, binding energy, isotropic exchange and ordering (German) 0-80604
 Cr(NO) $_3$, XPS and UV photoelectron spectra, compared to NO data 0-58317
 Cs, crystal struct., van der Waals and repulsive interaction 0-84137
 Cu, sputtering, binding energies 0-108312
 Cu $^{2+}$ -1,5-dimethyl-2,4-hexadiene, fluoresc. quenching method for determ. binding const. 0-89530
 CuO, on Cu, identification by electron spectroscopic methods 0-60747
 Cu $_2$ O, on Cu, identification by electron spectroscopic methods 0-60747
 Cu $_2$ Zn $_{1-x}$, sputtering, binding energies 0-108312

binding energy continued

- Fe₃₅Cr₃₂Ni₁₄B₁₃B₆, amorphous X-ray absorpt. spectra, effective co-ordination charges 0-84805
 Ga_{1-x}Al_xAs, epitaxial, radiative deep states 0-76061
 GeTe, bond orbital model of band struct. 0-59853
 H atoms, chemisorbed on cluster, indirect interactions, Grimley-Pisani model and tight-binding calc. 0-65370
 H₂O, intermolecular interaction energies calcs. using minimal basis sets 0-78681
³He, liq., binding energy, variational calcs. by Pandharipande's method 0-101752
³He, liq., binding energy and effective interactions, interactions, variational calcs. 0-107596
⁴He ground state binding energy, near threshold behaviour in 2 and 3 dims. 0-91716
⁴He, liq., binding energy, variational calcs. by Pandharipande's method 0-101752
⁴He₄, tetramer bound state binding energy, pot. model 0-63883
 HfC_{1-N_{1-x}}, X-ray valence photoelectron spectrum, 4f signal calc. 0-66391
 Hg, electron binding energy and shift, core level XPS 0-87088
 I₂Ar*, product state distrib. and binding energy 0-63857
 I₂He*, product state distrib. and binding energy 0-63857
 I₂Ne*, product state distrib. and binding energy 0-63857
 K, crystal struct., van der Waals and repulsive interaction 0-84137
 KBr(Cl):Mg²⁺, dopant aggregation and precipitation 0-107306
 KMgF₃, bond energy, equilb. distances and compressibility calcs. 0-70159
 Li complexes ((C₂H₅X)₂Li)ⁿ where X=S, O, binding and orbital energies, biological systems ab initio calc. 0-102442
 LiBH₄, H bridged system, floating spherical Gaussian model 0-78518
 LiBeH₃, H bridged system, floating spherical Gaussian model 0-78518
 LiBe(Mg)(Ca), 2⁺ and 11 states, mol. binding energy curves 0-58189
 LiCH₃, H bridged system, floating spherical Gaussian model 0-78518
 MnAg alloys, XPS meas. 0-60751
 Mo, N₂N₃N₄₅ super Coster Kronig processes 0-106303
 Mo-N, bond-strength bond-length relationships 0-91702
 Mo₂ metal-metal bond energy, SCF-X- α -SW calcs. 0-78538
 Mo₂Cl₈⁴⁻, metal-metal bond energy, SCF-X- α -SW calcs. 0-78538
 NH₃, affinities for H⁺(Li⁺)(K⁺)(CH₃⁺), ab initio SCF calculations 0-102443
 NH₄X, X=halogen, phonon dispersion, cohesive and dielec. props. in three body force shell model 0-79892
 Na, equilibrium struct. and phys. props., pseudopot. method 0-96778
 NaCl:Mg²⁺(Ba²⁺), dopant aggregation and precipitation 0-107306
 Na₂O-SiO₂-Fe₂O₃, glass, X-ray absorpt. spectra, effective co-ordination charges 0-84805
 Nb, N₂N₃N₄₅ super Coster Kronig processes 0-106303
 Nb-V system, H₂ absorpt. 0-59808
 Ni II acetylacetonate, XPS 0-74196
 Ni, L₁₁₁-binding energy, absolute determ. from self-absorpt. meas. 0-71519
 Ni surface, (111), chemisorbed CO, bond energies 0-100398
 Ni₉₈M₂, M=impurity metal, formation of MH(D)-complexes 0-65236
 O bonding to Tokamak walls, XPS studies 0-80942
 O²⁻ (n=0 to 2), core binding energy shifts, ASCF calcs. 0-95558
 O²⁻, electron coincidence spectrosc., valence electron momentum distrib. and binding energies 0-102583
 PbS(Se)(Te), bond orbital model of band struct. 0-59853
 Pd surface, segregated S state, AES, EELS, UPS and XPS study 0-93452
 Pd-H system containing d impurities, chem. binding energies of point defects 0-107214
 rare earth oxides, XPS 0-87170
 Rb, crystal struct., van der Waals and repulsive interaction 0-84137
 Re surface, interaction with N₂⁺ beam, reaction dynamics studied by XPS and thermal desorpt. spectrometry 0-93797
 Rh, N₂N₃N₄₅ super Coster Kronig processes 0-106303
 Ru, N₂N₃N₄₅ super Coster Kronig processes 0-106303
 Se compounds, LMM Auger spectra, relative intensity and relaxation energy 0-69115
 Se, LMM Auger spectra, relative intensity and relaxation energy 0-69115
 Si, total energy calcs. by r-space method, Wannier functions 0-88503
 Si:H, amorphous, 2p level shift, XPS obs. 0-97401
 Si_{1-x}C_xH glow discharge films, local atomic struct., XPS and AES study 0-93448
 SnTe, bond orbital model of band struct. 0-59853
 TiO₂-Ni (100) interface, electronic props., struct., comp., chemical bonding 0-84499
 Ti, core level binding energies, UPS obs. 0-66388
 TiCl₄ ground-state props., Wannier functions, and electronic struct., ab initio self-consistent calc. 0-80178
 Xe adsorbed on Pd (110), anomalous 5p photoemission, electron binding energies 0-100750
 Zn, electron binding energy and shift, core level XPS 0-87088
 Zn, sputtering, binding energies 0-108312
 ZnSe, exciton emission, halfwidths, thermal and optical activation energies obs. (French) 0-66268
 Zr-Co, amorphous and crystalline, d-band struct., alloying effects 0-59862
 Zr-Ni, amorphous and crystalline, d-band struct., alloying effects 0-59862

Bingham plastics and solids *see rheology***biocoustics**

- see also biological effects of acoustic radiation; biomedical ultrasonics; hearing; sonar*
 airway, collapsible, fluid-dynamic flapping, sound generation and flow limitation 0-94258
 blood pressure recording, simple method for fidelity improvement, Korotkoff sounds 0-76811
 bone, mammalian, acoustic emission testing 0-76783
 bone, US velocity meas. in temp. range of room temp. to 90°C 0-76787
 fish backscattering cross section, swimbladder effect in gadoid and macrkerel 0-89787
 frog entrainment to randomly generated calls, Hyla crucifer species 0-89789
 heart fourth sound studied by FFT 0-94397
 intravascular thrombus induction in vivo using localised hydrodynamic shear stresses 0-97997

biocoustics continued

- Korotkoff sounds, model expt. on generation 0-98207
 Korotkoff sounds possible origin from steady press. flow in compressed arteries 0-81639
 pulse echo waveform rel. to acoustic characteristics of continuous medium 0-67145
 respiratory sounds meas., laser vs. acoustical methods (German) 0-98058
 skeletal muscle, human, LF sounds from sustained contract. 0-61751
 skull bones, human, US flexural wave study 0-72277
 tissue absorption coeffs., automated meas. system using transient thermolec. technique 0-76817
 US absorpt. and vel. in mammalian tissue, dependence on constituent proteins 0-61621
 US effects on catalyse and malate dehydrogenase 0-76788
 US imaging, backscatter enhancement from collagen microspheres, dog liver, erythrocyte suspension 0-94281
 US props. of mammalian tissues, compilation of literature 0-98007
 US pulse propagation in dispersive media, human soft tissues 0-81644
 US shear velocity of muscle tissues, mech. props. determ. 0-108930
 US velocity meas. in liquids and small biological tissue specimens 0-76786
 valve vibrations, aortic and mitral, anal. and role in heart sound production 0-101214
 vertebrae, human, deflected US wave propag. tests 0-61617

biocommunications

- see also biocybernetics; hearing; learning systems; speech*
 bird song, species-specific coding 0-97950
 underwater, direction finding device for bearing determ. of whale sounds, real-time device 0-96079
 whales, southern right, sound playback expts. 0-89772

biocontrol

- see also biocommunications; biocybernetics*
 adaptive control mechanisms for complex motor systems 0-81573
 adaptive stiffness control in human movement 0-108947
 arm posture control, spring model and equivalent neural network 0-101196
 bipedal locomotion, inverted pendulums stabilisation algorithm (Japanese) 0-81630
 colonic electrical control activity, human, computer model 0-61537
 control signals and transducers for the control of upper extremities in plegic patients, computer controlled experiment (Slovak) 0-109061
 eye, accommodation and vergence state behaviour, computer simulation of interactive dual-feedback system 0-94205
 eye vergence control, role of spatial freq. tuned channels 0-101170
 firing rate control by inhibitory mechanism in tightly coupled two layer random nerve net 0-61533
 muscle, elec. stimulated, closed-loop control of force 0-76728
 myoelectrically controlled systems, five-state, error rate obs. 0-72376
 posture control system response to random accel. disturbances (Japanese) 0-72200
 posture-control system, responses to pseudorandom accel. disturbances 0-81640
 skin blood flow, reflex control by skin temp., role of core temp. 0-85427
 space suit cooling, automatic control of human thermal comfort 0-109046
 stochastic systems theory, appl. to blood pressure control 0-81522
 thermogenesis control in cold-exposed rabbits, variable open-loop gain 0-97868
 thermogenic control during exercise in a cold environment 0-72139
 vestibular control of oculomotor and postural mechanisms 0-72151
 walking, connections between different legs, quantitative model 0-101161
 walking, individual leg control, model 0-101160

biocybernetics

- see also artificial intelligence; brain models; learning systems; man-machine systems; neural nets*
 articular cartilage, viscoelastic properties (Japanese) 0-101215
 associative noise-like coding memory, algebraic model 0-76720
 auditory perception nonlinear model with autocorel. feedback 0-81615
 biological membrane, electrically excited, nonlinear dynamic models for simulation 0-94178
 blood flow in artery, stenosis effects on non-Newtonian flow 0-89775
 brain activities, synchronous, spatio-temporal filter approach 0-61503
 brain mechanism studies using evoked pots. (German) 0-61535
 cardiovascular system, mathematical models and identification problems 0-89780
 CECG waveform, statistical algorithm and struct. anal. 0-72341
 colour sensitive neural networks, reaction to intensity and colour steps (German) 0-76737
 dynamic models class, theoretical tools 0-94143
 EEG 0-85504
 eye and hand motor systems, optimal response in pointing at a visual target 0-61567
 human lung airways models, inhaled particle deposition appl. 0-89776
 kinetic depth effect, amplitude, freq. and phase determinants of perceived rotations and rigidity 0-76746
 Limulus ommatidia, resonant response of neural model to double freq. stimulation 0-76734
 macromolecules, biological, selection models, with time varying constraints 0-67029
 mammalian lung airways, aerosol deposition in anatomical models, theoretical evaluation 0-81627
 molecular self-organization, dynamics 0-67028
 multistate systems, freq. of cyclic processes 0-108834
 muscle, anatomical model, internal pressure effects 0-67103
 muscle system, contractile system, sliding motion anal. 0-67104
 neocognitron, self-organising neural network model, pattern recognition mechanism unaffected by shift in position 0-76745
 nerve excitation, gating currents and dipole transitions 0-67056
 nerve fields, topographic organisation 0-89742
 nerve signals, dipole theory of interactions 0-81574
 neural system, one-dimensional, numerical investigation of kinetic neuron equations 0-76725
 neural transformations of random signals, Wiener and of functionals of Markov chain 0-76727
 neuron model, two-terminal electronic circuit 0-61526
 neurons, electrical behaviour, general input-output relations 0-85378
 pattern separability in random neural net with inhibitory connections 0-76726
 peristaltic transport, asymptotic method 0-87805

biocybernetics continued

- photosensitive neuron, lateral inhibition, and optomotor function expts. (*French*) 0-89705
- physiology, flow problem, one tube 0-89703
- picture distortions compensation of moving patterns typical for time filters 0-76731
- pulmonary gas transport models, boundary conditions and geometry 0-85426
- pupillary light reflex system, modelling and identification 0-61554
- self-reproducing macromolecules, selection, controlled energy fluxes constraint 0-67027
- sensory neuron, second order, summation of excitation and inhibition by computer simulation 0-76769
- structural order and partial disorder 0-76695
- symmetry in systems 0-81519
- systems theory in biology and medicine, importance and motivations (*Spanish*) 0-104549
- tumours, fractionated irradi., math. derivation of optimal treatment schedules 0-98078
- variational principles, complementary with Michaelis-Menten kinetics 0-94142
- vision, human recognition system with thinking, model 0-76744
- visual information processing, multi-input system representation, polynomial algorithm properties 0-101145
- visual system, moving objects localisation, cats 0-76736
- visual systems, filter performance, inhomogeneous and anisotropic 0-76738
- visual-vestibular interaction during body rotation in man, nonlinear model 0-76735
- walking insect, *Carausius morosus*, coordination of force oscils. and leg movement 0-76775
- walking insect, *Carausius morosus*, oscillations of force in standing legs 0-76774

bioidiffusion

- acetylcholine, diffusion in synaptic cleft of normal and myasthenia gravis human endplates 0-94198
- alveolar gas exchange, effect of altered gas diffusivity 0-97970
- bacteriophages T4B and T7, determ. of rotational diffusion coeff. by depolarised dynamic light scattering 0-85549
- blood, shear-induced augmentation of O_2 transfer 0-94274
- cell surface anisotropic molecular motion 0-97883
- cell surface component rotational diffusion, time-resolved phosphoresc. anisotropy 0-97885
- cellular testing potential, membrane pot. rel. to ionic diffusion (*French*) 0-94184
- D-leucine, exchange diffusion in mouse Ehrlich ascites tumour cells, temp. reduction effect 0-67053
- DNA light induced diffusion in solutions due to laser cutting (*Russian*) 0-81646
- exhalation in lung model, effect of ventilation and diffusion nonuniformity 0-104603
- haemoglobin, mutual and tracer diffusion coeffs., photon correl. obs. 0-72123
- intravascular radioactive tracers, calc. of residence time distribns. in fields of external registration 0-72291
- isobaric counterdiffusion, middle ear gas exchange 0-81798
- macromolecular solution, rot. diffusion coeff. calc. method w.r.t. mol. struct., elec. birefringence relax. time data interpret. 0-85331
- membrane, water transport, NMR methods (*Rumanian*) 0-94435
- membrane diffusion measurement by fluorescence photobleaching recovery method, bleaching light effect 0-94434
- membrane integral proteins, mobility increase in spherocytic erythrocytes obs. 0-81569
- membranes, lateral diffusion on a spherical surface, normal mode anal. 0-61518
- membranes containing cholesterol, lateral diffusion calcs. 0-85356
- mesentery tissue, burn induced alterations of interstitial diffusion 0-104634
- oxymyoglobin, evidence for conformational and diffusional mean square displacements 0-89713
- plant fibre temperature stability investigation, rotary diffusion, spin label obs. 0-81529
- pulmonary gas transport and mixing, diffusivity effects 0-108927
- serum albumin, bovine, mutual and tracer diffusion coeffs., photon correl. obs. 0-72123
- substance diffusion in tissue with nonlinear consumption, math. model 0-67326
- tissue surrounding single capillaries, substrate concs. 0-97853
- variational principles, complementary with Michaelis-Menten kinetics 0-94142
- CO , single breath diffusing capacity, theoretical anal. 0-67328
- H_2O in biological samples, PMR, fast-exchange model interpretation via diffusional kinetics clarified 0-67033
- O_2 diffusion distance and necrosis development in multicell spheroids 0-81570

bioelectric phenomena

- see also *bioelectric potentials; biomagnetism*
- 60 Hz electric field, 240 kV/m, long-term effects on mice 0-89784
- 60 Hz high intensity electric fields, behavioural and biological effects in living organisms 0-89740
- action potential propagation, effects of cellular geometry on current flow 0-94196
- α -amino acids, naturally occurring, in aq. soln., Kerr constants 0-85353
- amputated finger tips, children, elec. current obs. during regeneration 0-72404
- antagonistic muscles, functional elec. stimulation optimisation, math. modelling, joint motion 0-61730
- auditory-nerve fibre encoding of 2-tone approximations to steady-state vowels 0-61582
- auditory-nerve fibre responses to bandlimited noise, nonlinearities 0-61583
- autorhythmicity and entrainment in excitable membranes 0-108866
- axonal membrane of mammals (myelinated fibres), K channel conduction 0-61538
- bacterial cell wall, surface charge and morphogenesis of regular arrays of macromols. 0-85366
- bacteriorhodopsin, elec. response of a back photoreaction 0-98008
- bacteriorhodopsin, photoelec. conversion in charged synthetic membranes 0-108954

bioelectric phenomena continued

- behaviour patterns in cod released by elec. stimulation of olfactory tract bundlets 0-97951
- bimolecular membranes, interaction with liposomes, elec. resistance obs. 0-81549
- biological effects of ELF electric fields: some US research results 0-94278
- biomembranes, excited, automatic meas. of ionic current electrophysiological characts. (*Russian*) 0-76865
- birefringence, transient, of macromol. solns. in reversing fields of arbitrary strength and duration 0-84719
- blink reflex, effects of elec. stimulus freq. during rest and a task 0-61547
- blood vessel coagulative commissures, influence of high amplitude elec. impulses on strength 0-104600
- bone, comparison of electromech. effects in wet and dry bone 0-97985
- bone piezoelectricity, role of stress-gradient effects 0-67113
- brain, elec. stimulation, awakening thresholds in 5 sleep-waking stages, cat expts. 0-85377
- cardiac cellular electrophysiologic-clinical correlations using a relational data base 0-89890
- cardiac fibrillation thresholds for 60 Hz currents and voltages directly applied to heart 0-101301
- cardiac tissue, pacemaker activity, phase resetting and annihilation 0-81565
- cartilage proteoglycan, association with hyaluronic acid, elec. birefringence obs. 0-85332
- cerebellar model, spatial freq. characts. (*Japanese*) 0-67068
- charge transfer reactions in biological systems, mech. of coupling 0-76889
- chlorophyll, colloidal solns., elec. charge of particles 0-94438
- collagen, polarisation, contribution of permanent and induced dipole moments, elec. birefringence 0-85351
- colon, turtle, active Na transport via an electrogenic Na-K exchange pump 0-108856
- colonic electrical control activity, human, computer model 0-61537
- complex mutual inductance concept for bioelectric impedance transformer bridge 0-63886
- conductivity distributions imaging, systems limitation 0-89901
- Coulter electrical sizing principle, appl. to new multiparameter system 0-89911
- current pulse-induced voltage variations in bilayer membranes, apparatus 0-94420
- cytochrome c_3 , anhydrous film, elec. cond., temp. and ambient press. depend. 0-85327
- dielectric meas. of biological liquids, reflection meas. of complex dielectric const. 0-101309
- dielectric properties meas. technique using an in vivo probe VHF to microwave freqs. 0-85542
- dielectric properties of biological substances, tabulation for freq. range 10 kHz to 10 GHz 0-108143
- dielectric props. of biological substances, physical meas. 0-94417
- DNA, calf-thymus Na-DNA aq. solns., dielec. behaviour in 5 kHz to 100 MHz range 0-85330
- DNA, dye labelled elec. dichroism and birefringence, comparison with mol. props. from polarised fluoresc. 0-84785
- DNA solution, elec. birefringence, stabilised induced dipole behaviour 0-85349
- double layer phenomena at particle surface (*Rumanian*) 0-94144
- E. coli* strains in aq. suspension, polarisability anisotropy and aminoglycoside antibiotic effects 0-85441
- E. coli* suspensions, dielec. anal., interfacial polarisation theory appl. 0-97876
- EEG, decision P350, waveform and neural mechanism, auditory click and elec. finger stimuli 0-61528
- egg cell membranes, starfish, inward rectification blocking model 0-61523
- electrets in biomaterials and biopolymers 0-80686
- electric fields, vertical, 45-Hz, influence on rats 0-76784
- electric shocks, 50/60-Hz AC, ventricular fibrillation tests on animals (*German*) 0-101154
- electrocoagulation, monoactive, controlled destruction and temp. distribns. 0-94176
- electromechanical model for human articular cartilage 0-104631
- electrophoresis of proteins in intercellular bridges 0-89734
- embryo primitive streak, chick, strong elec. currents obs. 0-72405
- ontogenetic experiments on teratogenic effects of EM fields 0-85446
- epidural neurostimulation, percutaneous, histological reaction, short and long term study results 0-67285
- erythrocytes, human, haemoglobin's suspending medium, dielec. props. obs. 0-76716
- eukaryotic cell cycle, long-range dielec. aspects 0-94182
- excitation properties of the squid axon membrane and model systems with current stimulation 0-67054
- excitation spread speed, 2D excitable medium 0-76717
- food, semi-solid, at low, intermediate and high-moisture contents, dielectric behaviour 0-101157
- forward problem of bioelectricity, numerical soln., implementation of a consistency criterion 0-76696
- gramicidin single-channel currents, rate theory calc. using NMR-derived rate consts. 0-94186
- high electric field biological effects on human nervous systems 0-89739
- high-pressure chamber for electrophysiological meas. 0-98185
- human body, dynamic voltage-current characts. 0-94443
- human body, elec. memory effects 0-94444
- HV lines to 800 kV, elec. and mag. field effects on human beings (*French, English*) 0-72209
- influx current of edible snail neurons, dependence on Ca^{2+} conc. and membrane pot. 0-108865
- intestinal myoelectrical models, pulse synchronisation expts. 0-67061
- intestinal tissue, electronic modelling of slow-waves and spike-activity 0-89737
- light scattering, dynamic, by flexible macromols. in fluctuating elec. field 0-84722
- light scattering from macromolecular soln. in alternating elec. field, low angle approx. 0-84721
- lipid bilayer, alkane solubility modified by elec. field 0-97874
- lipid bilayer electrical breakdown 0-81552
- lipid bilayers, elastic props. changes on exposure to different agents, elec. and chem. 0-81548
- lumbo-sacral motoneuron pools, human, response patterns to distant somatosensory stimuli 0-108924

bioelectric phenomena continued

- lysozyme, search for superconducting regions 0-101149
 magnetic fields produced by steady currents in human body 0-94248
 magnetocardiogram, PR segment theory rel. to current sources within heart 0-101191
 magnetoelectric dipole structure hypothesis, biological and cosmic appls. 0-91124
 mast cells, rat, electrophoretic mobility distrib. alteration after immunological activation 0-67047
 membrane, elec. excited, nonlinear dynamic models for simulation 0-94178
 membrane conductance channels, current-induced coupling, multi-channel interaction and mean field cond. 0-67063
 membrane electric properties measurement method using glass electrode impaled into single cell 0-89916
 membrane surface charge visualisation using SEM 0-85566
 micropipettes of very low resistance for intracellular meas., production method 0-61738
 Millipore-diethylphosphate model membrane, elec. current stimulus effects 0-67046
 motor neuron activity patterns of *Drosophila*, anal. with neural analogues 0-108870
 multi-enzyme complex carrying out electron transfer, asymptotic anal. of functioning 0-81523
 muscle, elec. stimulated, closed-loop control of force 0-76728
 muscle, multifibre preparation, intercellular clefts influence on pot. and current distrib. 0-72145
 muscle contraction elec. induced, meas. of suggestion effects (*Slovenian*) 0-81571
 muscle fatigue, electrophysiological pattern in healthy humans, effects of artificially induced ischemia 0-97890
 muscle fatigue in muscular dystrophy, electrophysiological pattern of development 0-97888
 muscle fibres, endogenous elec. field, dependency on Na⁺-K⁺ pump 0-108869
 myelinated nerve fibre, response to short duration biphasic stimulating currents 0-85373
 myocardial damage, induction by open-chest low energy countershock, rabbit expts. 0-72150
 myocardial damage from defibrillator discharges at various dosages 0-72368
 nerve excitation, gating currents and dipole transitions 0-67056
 nerve fibre membrane Na permeab. reversible blockage by increase in temp. of medium above 45°C 0-81576
 nerve signals derivation from contrast flash data 0-108885
 neural conduction times, central and peripheral, in multiple sclerosis, somatosensory obs. 0-89773
 neural single unit activity from foetal pig brains, recording method 0-67315
 neural unit activity rel. to movement, photographic technique for anal. 0-67310
 neuromuscular junction, frog, electrostatic screening of neurotransmitter release 0-89741
 neuromuscular unit discharge during muscle fatigue, structural model anal. 0-67066
 neuron membrane, design of a single electrode voltage clamp 0-72385
 neurons, cat eye, stereotaxic method for recording from single cells 0-89913
 nexus, evidence for fixed charge, permeability, obs. 0-94193
 nucleosomes and nucleosomal DNA, electro-optical props., relax. times and chain struct. 0-85350
 organic substances, electrochemiluminescence as possible source of coherent radiation, and role in biological processes (*Russian*) 0-76093
 pain control in man, medial thalamic permanent electrodes, electrophysiological and clinical study 0-67282
 paralysed muscle, treatment by elec. stimulation (*Slovenian*) 0-81771
 paralysed upper extremities rehabilitation systems, control signals (*Slovenian*) 0-81772
 Paramecium excitation, model anal. 0-61524
 paraplegic patient muscles, provision of functional use by elec. stimulation, review 0-101289
 paraplegic patients, functional elec. stimulation (*Croatian*) 0-109058
 phantom hand sensations elicited by afferent nerve stimulation, discrimination in below-elbow amputees 0-97892
 photosynthetic reaction centre functional reconstitution in planar lipid bilayers 0-97881
 placenta, human, detect. of pulsatile flow in situ by impedance meas. 0-104799
 plasmalemma of *Nitella flexilis*, selective centres of excitable channels of early ionic current 0-81568
 polymers, electro-optical changes, chem. and rotational contribs. 0-85352
 polynucleotide solution, elec. birefringence, stabilised induced dipole behaviour 0-85349
 polynucleotide solution, elec. field induced orientation and effects 0-85348
 polypeptide, conformational change induced by strong elec. field 0-85336
 polyribonucleotides, dye tagged, aqueous solns., elec. induced fluoresc. changes 0-85346
 protein kinases, cAMP-depend., membrane-localised, and regulation, of slow inward current, frog heart 0-81567
 proton transport across charged membrane and pH oscillations 0-61516
 purple membrane fragment suspensions, elec. dichroism obs., trimer model interpret. 0-89728
 R. sphaeroides, polarisation of photosynthetic membranes and reaction centres in elec. field 0-94277
 ratfish, electroreception, obs. 0-94442
 rats, lack of effect of elec. field exposure, data re-evaluation 0-72210
 retinal neuron firing rates, lack of predictability from interspike interval statistics 0-67075
 Rhodospirillum rubrum, chromatophores electron transport chain, functional organisation 0-81555
 serum albumin, bovine, hydrated, dielec. and elec. props. 0-97854
 serum low density lipoprotein, human, anomalous permittivity behaviour 0-81540
 skin resistance biofeedback, using frequency controlled oscillator detector 0-101156
 skin resistance measurements, collection and off-line processing (*German*) 0-67273
 somatosensory pathways, assessment of central conduction 0-97949
 spark discharges from body obs., nature and incendiary behaviour 0-72406

bioelectric phenomena continued

- spastic patients H-reflexes, factorial anal. of specific electrophysiological parameters 0-72148
 spinach chloroplasts, laser photoinduced changes in high freq. dielectric constant 0-85449
 spinal cord electrical stimulation, 2D finite element anal. 0-98054
 spinal cord to axilla, F-wave conduction vel. 0-97894
 stereodynamic interferential current, new electrotherapeutic technique 0-85458
 stereodynamic interferential current therapy, fundamentals and initial results 0-85459
 sympathetic ganglia stimulated in vitro, effect of temp. on coated vesicle form. in presynaptic terminals, cat 0-85380
 synaptic vesicles and synaptosomal membranes, electrokinetic props. 0-67055
 thymocytes, negative surface charge reduction and thymic phagocytosis after X-irrad. 0-81663
 tissues, excitable, dipole flip-flop theory for excitation and conduction 0-101153
 Vespa orientalis, photoelec. props. of 'yellow strips' on cuticle, math. model 0-104638
 vision, associative learning model, voltage-dependent Ca²⁺ and K⁺ conductances 0-72166
 vision, pattern recognition functional mechanisms in humans 0-81609
 vocal fundamental frequency measurement, comparison of contact microphone and electroglottograph 0-109056
 C-fibre microelectrodes, neurophysiology appl. 0-67314
 Na⁺ activity of epithelial cells, liquid-ion exchanger microelectrode estimates, resistive artifacts 0-89909
- bioelectric potentials**
see also contact potential; electrocardiography; electroencephalography
 40 Hz activity in sigmoid gyrus, nucleus accumbens and amygdala, cross correl. anal. 0-76730
 action potential propagation, effects of cellular geometry on current flow 0-94196
 action potentials from cultured neurons, recording by extracellular microcircuit electrodes 0-72382
 afferent nerves from muscle spindles, signal interpretation method 0-101188
 airway transepithelial elec. pot. in vivo, species and regional diffs. 0-98208
 arteries, small, isolated, perfused, method for simultaneous elec. and mech. recording 0-101300
 audition, compound PST histogram rel. to neural activity in cochlear 0-94148
 audition, freq. following pot., appl. of least-square-fit technique 0-94149
 audition, frequency following response and brainstem evoked response 0-94232
 auditory 0-94236
 auditory click evoked compound action pots., guinea pig obs. 0-94231
 auditory cortex unit response to synthesized formants, cat 0-67098
 auditory evoked brainstem response, age and sex diffs. 0-94234
 auditory evoked potentials, dependence of peripheral auditory adaptation on recording site 0-81613
 auditory evoked response, primary inhibited elements, review 0-94235
 auditory middle component AERs from neonates to low-level tonal stimuli 0-94220
 autoregressive model order selection applied to physiological signals 0-104780
 bacteriorhodopsin membrane preps. associated with lipid-water interface, form. of elec. pot. diff. 0-81551
 brainstem auditory evoked pot., human, sources 0-108919
 brainstem auditory on- and off-pots., latency determ. 0-94233
 brainstem-evoked response audiometry, combination with otometry 0-85417
 cellular testing potential, membrane pot. rel. to ionic diffusion (*French*) 0-94184
 checkerboard-evoked multichannel pot. fields, reference-free components identification 0-108887
 chromatophores of *R. rubrum*, induction of elec. pot. diff. by laser flash 0-81560
 click-evoked electric brainstem responses, use in audiological diagnosis 0-104689
 cochlear compound action pots., tuning curves and delay times 0-94230
 cochlear microphonic potentials rel. to cochlear injuries 0-94229
 cochlear microphonic responses, far-field, to continuous pure tones, cat scalp recordings 0-97924
 colon EMG, use of autoregressive-modelling techniques for anal. 0-101146
 compound PST histograms, deconvolution 0-94146
 contour map production for electrophysiology 0-72340
 control signals and transducers for the control of upper extremities in plegic patients, computer controlled experiment (*Slovak*) 0-109061
 convolution equation solution, problems arising, auditory appl. 0-94147
 cortex, human, no-stimulus, no-response, event-related pot., motosensory system obs. 0-108923
 cortical auditory evoked responses under hyperbaric conditions 0-94237
 decision making, split-second, electrophysiological signs, auditory stimuli 0-89771
 duodenal slow waves, human, anal. and modelling. 0-72146
 electrooculographic evaluation of eye movements in target tracking 0-109057
 EMG, filter bank analyser for automatic anal. 0-98162
 EMG, multichannel data acquisition system for the survey of intercostal muscle activity 0-81790
 EMG, pulsed integrator for anal. 0-61719
 EMG, rectified surface, time constant in low pass filtering 0-67266
 EMG, simultaneous recordings of parts of pectoralis major muscles during swimming 0-72147
 EMG, single motor unit action pots. identification by computerised anal. 0-72343
 EMG, single pots., anal. by means of multivariate methods 0-98170
 EMG, surface, dT-dL anal. during muscle fatigue, left hand obs. 0-104576
 EMG, surface, dT-dL anal. during muscle fatigue, right hand obs. 0-104575
 EMG, surface, system for meas., recording and digital anal. (*German*) 0-76848
 EMG biofeedback in hemiplegic patient treatment, comparison of actual and simulated treatment 0-104806

bioelectric potentials continued

- EMG investigations of gait in cerebral palsied children 0-72186
 EMG period-amplitude analysis, cat locomotion and jumping obs. 0-67057
 EMG processing for sleep research 0-67267
 EMG shimmer in patients with neuropathy and neurogenic atrophy 0-72149
 EMG silent period and muscle mechanics in human soleus muscle 0-67060
 EMG silent period measurement, automated system 0-89883
 endogenous and exogenous activity in molluscan neurone, identification by spike train anal. 0-89735
 ERG, human, nonlinear kernels 0-61545
 ERG, oscillatory pots., analogue circuit model and frog obs. 0-89750
 ERG and psychophysical obs. of cone spectral mechanisms 0-61565
 ERG recording, computer assisted standardised quantitative method 0-109048
 ERG studies on albino rats, mech. of formation of X-ray induced phosphenes 0-104675
 evoked potential and early studies of bioelectricity 0-101158
 evoked potential recordings, cancellation of coherent line-freq. noise 0-98161
 EVOQ: a system configurable for automatic simulation and recording of mean evoked potentials on a minicomputer (*French*) 0-85507
 extracellular potentials generated by curved fibres in a vol. conductor, modelling 0-97889
 ferrocyclochrome c_3 , anhydrous, ionisation pot., UV photoelectron spectrosc. obs. 0-85328
 filters as selective electrodes for synthetic penetrating ions 0-104821
 flash evoked potentials following unilateral electroconvulsive therapy 0-97906
 frequency following potential, 500 Hz, kangaroo rat, evaluation with noise masking 0-108905
 H. halobium, light-induced surface pot. changes in purple membranes and bacteriorhodopsin liposomes 0-98015
 heart Ca^{2+} transients during excitation-contraction coupling 0-97896
 intramembrane potential jump meas. by potentiodynamic method 0-81778
 maxillary gum trigeminal evoked pots. in humans 0-97948
 median nerve, transient responses to elec. stimulation, SQUID appl. to somatically evoked field meas. 0-104706
 motor unit activity and force gradation in human voluntary movements 0-97887
 multichannel analyser, microprocessor-controlled, transfer of blood pressures and neural activities for computer anal. 0-72356
 multipoint electrode for biological pot. recording 0-104784
 muscle, multifibre preparation, intercellular clefts influence on pot. and current distrib. 0-72145
 myoelectric signal processing, expt. demonstration of optimal myoprocessor performance 0-89882
 myoelectric signal processing, optimal myoprocessor derivation 0-89881
 myoelectric signals, improved processor 0-104800
 myoelectrically controlled systems, five-state, error rate obs. 0-72376
 nerve action pot., lipid bilayer local phase transition 0-89744
 nerve fibre membrane analogue-code conversion, ionic mechanisms 0-81575
 nerve impulse data treatment for comparison with theory 0-97893
 nerve impulse encoding, elec. processes 0-76718
 nerve spike trains, interleaved, in a noisy channel, separation system 0-94424
 nerve trunk multifibre activity quantitation 0-76853
 neural signal recording using implantable electrode and telemetry system, awake animals (*Japanese*) 0-94427
 neuromuscular block indicator, model INMB-1, EMG amplitude meas. 0-104785
 neuron input current, Helix pomatia, rel. to membrane pot. and extracellular Sr and Ca ion concs. 0-81577
 neuronal membrane process field potentials anal. and synthesis, computer system 0-85374
 neuronal spike train data, adaptive filtering 0-67265
 Nitella, fluctuation and instability in membrane pot. near threshold 0-89723
 oesophageal diaphragmatic EMG in humans, effects of electrode position 0-81753
 olfactory bulb, 55 counts/sec rhythm anal. and simulation 0-85422
 olfactory evoked brain pot., correl. anal. of recorded waveforms (*Japanese*) 0-97946
 oscillatory neural networks in the rabbit hippocampus 0-89743
 pancreatic islet cells, plateau pots. as voltage-dependent action pots. 0-94180
 pattern recognition of human brain electrical potentials 0-109051
 peripheral nerve, generation of unidirectionally propagated action pots. by brief stimuli 0-85546
 photoreceptor, invertebrate, basic mechanisms of excitation and adaptation 0-81593
 photoreceptor membrane interfacial pots., light-induced 0-72161
 retina, bovine, R2 component of early receptor pot. rel. to metarhodopsin II form. 0-97904
 somatosensory evoked potentials, review of acquisition and anal. 0-101281
 somatosensory evoked potentials, short latency, in man following median nerve stimulation 0-94243
 somatosensory potentials following electroconvulsive therapy 0-97947
 somatosensory short latency pots. in humans, mech. evoked 0-67099
 spinal field potential, rat, rel. to focal interictal epileptiform discharges 0-94191
 surface EMG, computer anal. during isometric exercise, muscle tension quantification 0-85505
 surface EMG and fatigue, muscle temp. and blood flow 0-94199
 vision, spectral sensitivity in goldfish, photochem. and neural correlates 0-81599
 visual 0-97905
 visual evoked potentials, latency and wave form obs. 0-97907
 visual evoked potentials to stimulus trains, normative data and photosensitive seizures appl. 0-94204
 visual evoked response, central visual field contribs. 0-108881
 visual evoked response in human albinos, brain abnormality 0-94208
 visual pattern-evoked cortical pots., human infants, spatial and temporal interaction 0-101169
 volume conducted potentials, averaged multiple unit activity as estimate of local neuronal activity changes 0-89917

biographical dictionaries *see biographies***biographies**

- Airy, G.B., Astronomer Royal 1835-81, contrib. to horology 0-86061
 Bardeen, John, contrib. to solid state physics 0-57057
 Bloch, Felix, electron theory of metals, contrib. 0-57053
 Brout, Vladimir L. (1924-1978), Russian physicist 0-82625
 Campbell, J.D., testing techniques and material behaviour at high strain rates, memorial lecture 0-82627
 Einstein, Albert, contrib. to cosmology 0-77530
 Einstein, Albert, relativity theory acceptance in Canada 0-68012
 Faraday and the concept of force 0-57048
 Frohlich, H., biographical notes rel. to solid state physics develop. 0-57059
 Gray, Stephen (1666-1736), astronomer 0-77601
 Hahn, Otto, discovery of nuclear fission 0-57063
 Herring, Conyers, contrib. to solid state physics in 1930s 0-57056
 J.J. Thomson, mechanical interpretation of nature 0-57049
 Judd's contributions to colour metrics and eval. of colour differences 0-94945
 Kukarkin, Boris Vasil'yevich (1909-77), Russian astronomer (*Russian*) 0-101701
 Lavoisier, du Pont families during French Revolution 0-57051
 Marquis de Charbert (1724-1805) and Louisbourg Observatory 0-68010
 Mayer, Tobias (1723-62), solar diameter obs. (1756-60) study 0-90389
 Mott, Sir Nevill, contrib. to solid state physics, 1933-40 0-57055
 Mouchot, A.B., solar power harnessing (*French*) 0-105484
 Peierls, Sir Rudolf Ernst, solid state physics, 1928-1935 0-57054
 Perutz, Max, molecular biology origins, autobiographical review 0-57052
 Planck, Max Karl Ernst Ludwig (1858-1947), quantum and relativity theories 0-68008
 Pohl, R., recollections of solid state physics 0-57060
 Seitz, Frederick, biographical notes on early solid state physics 0-57058
 Smyth, Charles Piazza (1819-1909) at Cape of Good Hope 0-68011
 Soddy, F., nuclear science, economics and social responsibility, holistic approach 0-90640
 Tobias Mayer, contrib. to observational astronomy 0-62438

biological cybernetics *see biocybernetics***biological effects of acoustic radiation**

- see also biomolecular effects of radiation; cellular effects of radiation*
 autonomic system activities 0-83700
 autonomic system activity and performance on a psychomotor task in noise 0-89790
 bean roots, non-thermal inhibition of growth and detect. of acoustic emissions, 1 MHz US 0-104643
 catalyse and malate dehydrogenase, effects of US waves 0-76788
 Chinese hamster V-79 cells, US lethality obs. 0-85443
 cochlear, struct. and functional changes following US irradi. 0-89791
 collagen synthesis stimulation, human fibroblasts, role of US-induced cavitation 0-85442
 Drosophila eggs, killing on exposure to traveling and standing US wave fields 0-101223
 E. coli, effect of US at 1.5 MHz 0-72212
 Elodea, cell death thresholds for 0.45-10 MHz US 0-67149
 erythrocyte membranes, US absorpt. in 12 to 68 MHz range 0-89727
 hyperthermia, deep local, induction by US and EM fields, problems and choices 0-94283
 hyperthermia in tissue-like substances, EM and US induction 0-98012
 infrasonic effects on man and construction of test chamber (*German*) 0-67147
 infrasound and pressure waveform generator, compact, for small cavity appls., animal research 0-104830
 intracellular temperature distribution produced by ultrasound 0-61623
 jet aeroplane noise, effects on facial expression, EEG and manual responses, human subjects 0-98006
 lymphocyte cell DNA damage by US diagnosis 0-67148
 mammalian cells, in vitro US irradi. at hyperthermic temps. 0-94282
 oedema experimentally induced in rats by $AgNO_3$, effect of US on response 0-104642
 pregnant mice, acute US exposure at different stages of gestation 0-94284
 thermistor probe use to meas. energy distrib. in US fields 0-109075
 thermocytes, rat, US-induced changes in rates of influx and efflux of K^+ in vitro 0-89793
 transkull transmission of an intense focused US beam, lesion production at 500 kHz 0-89792
 underwater noise spectra produced by fishing boats affecting albacore catch, comment 0-58844

biological effects of gamma-rays

- see also biomolecular effects of radiation; cellular effects of radiation*
 abdomen, pig, therapeutics of intense irrads. 0-67167
 absorbed dose estimates in prolonged ^{137}Cs γ -irrad facility for mice 0-101233
 acute radiation lethality, evidence for a decreased susceptibility in young lambs 0-108962
 adenovirus, decreased repair after γ -irrad. when infecting Xeroderma pigmentosum fibroblasts 0-61650
 amino acid transport in lymphoid cell lines, differences in ionising irrads. effects 0-72264
 Aspergillus nidulans, mutation induction by γ -irradiation in presence of O_2 or N_2 0-94297
 bacterial cells, heavy ion irrads., long range effects, comparison with γ -irrad 0-101236
 barley varietal differences in repair of induced lesions 0-104647
 bone marrow-engrafted mice, survival after irrads. 0-104681
 brain tumour, rat, RBE of cyclotron fast neutrons rel. to ^{60}Co γ -rays 0-76797
 breeding performance of female mice, comparative effects of ^{60}Co γ -rays and ^{239}Pu α -particles 0-72231
 broad bean, low dose effects on growth and yield of 2 cultivars 0-81653
 cells, human, multinucleate and micronucleus formation obs. 0-72219
 cells, human, radiosensitivity, comparative study with different statistical models 0-108967
 cells, lack of lethality threshold obs. 0-76810
 chromatin from cultured mammalian cells, radiolysis, DNA-protein cross-links formation 0-81655
 chromosomally aberrant cells, Japanese A-bomb survivors, dose-response relationship of neutrons and γ -rays 0-94295
 chromosome aberrations, dose-effect relationship, population exposed to increased natural radioactivity 0-72254

biological effects of gamma-rays continued

- Coastcross 1 bermudagrass, induced mutant with improved winterhardness 0-104645
 crypt system, mouse, alternating fractionation formula of cumulative radiation effect 0-104652
 DNA, calf-thymus and superhelical PM2 aq. solns., electro-optic obs. of γ -irrad. damage 0-85452
 DNA, properties changes caused by UV- and γ -irrad., electrochem. anal. 0-72271
 DNA, radiation-induced strand breaks in deoxygenated aq. solns. 0-61649
 Drosophila germ cells, decrease of γ -induced mutations by visible light 0-67159
 E. coli, photoreactivable component in the mutagenic action of ionising radiations 0-72225
 E. coli, photoreactivation following ionising irrad. rel. to Cherenkov emission 0-108969
 E. coli, UV-induced recovery of γ -irrad. bacteriophage DNA 0-72214
 E. coli, value of photoreactivable component after exposure to ionising radiation 0-72224
 E. coli, radiation killing, role of membrane fluidity, hypothermia and local anaesthetics 0-104653
 embryonic development and nucleic acids in trigeminal neurons, rats 0-72270
 emesis ED₅₀ determination, rhesus monkey obs. 0-104678
 energy metabolism of blood morphotic elements, ionising radiation effects 0-61645
 Fasciola gigantica infectivity to hamsters, effect of ⁶⁰Co γ -irrad. 0-85451
 fibrosarcoma cells, murine, separated by centrifugal elutriation, radiation sensitivity obs. 0-76808
 food preservation (Italian) 0-89799
 green alga, 2 species of Sirogonium with different chromosome types 0-81651
 HeLa cells, first postirrad. division obs. 0-72258
 intestinal stem cells and crypts of γ -irrad. mice, cell-survival characts. 0-72255
 leaves of Kalanchoe daigremontiana, organogenesis delay obs. 0-104650
 liver, RBE of cyclotron fast neutrons and γ -rays for late hepatic injury in rats 0-108975
 liver microsomes, γ -induced lipid peroxidation and membrane-bound enzymes 0-104660
 lymphocytes, human, effects of heat and radiation 0-97864
 lymphocytes, human, prediction of dose-rate effects for dicentric production by X- and γ -rays 0-72226
 lymphocytes, human peripheral blood grown in γ -irrad. medium, sister chromatid exchanges 0-104658
 lysosomal enzymes, pigeon tissue, effects of sub-lethal dose 0-98022
 melanoma, B16, in mice, effect of hyperthermia alone and in combination with ⁶⁰Co radiation 0-72138
 neoplastic disease development in mice, dose-rate effects 0-76803
 neoplastic disease development in mice, reticular tissue tumours 0-72259
 neoplastic disease development in mice, solid tumours 0-76802
 neoplastic transformation of 10T1/2 cells by ⁶⁰Co γ -rays 0-104659
 ovarian cortex effect of daily prenatal gamma irrad. in beagle pups 0-85453
 penicillamine-treated mice, survival following whole-body irrad. 0-98030
 prairie pepperweed, chronic irrad. effect on production and viability of seed 0-81649
 pyri pyriformis, \rightarrow pyriformis, 0-61648
 rice seeds, glucose metabolism effects 0-81650
 skin, pig, response to ¹³⁷Cs-irrad. 0-67161
 soft fruit cell walls, histochem. effects 0-81652
 testes, mice, comparative effects of various radiations on weight loss and spermatogenic stem-cell survival 0-108976
 testicles, mice, combined action of acute and chronic gamma irrad. 0-72241
 testicles, rat, comparison of acute and chronic gamma irrads. (Russian) 0-72240
 testis, house sparrow, effect of ⁶⁰Co external irrad. after testosterone propionate administration 0-101232
 Tetrahymena, γ -irrad., role of DNA damage and repair in eukaryotic gene function 0-104677
 Tetrahymena pyriformis, γ -irrad., release of thymine base damage from DNA 0-72268
 thymidine monophosphate, gamma irradiated, inorganic phosphate release, in presence and absence of O₂ 0-67168
 thymidine monophosphate aqueous solution, gamma irrad. effect on base damage, phosphate release 0-89806
 tumour incidence and longevity in neutron and γ -irrad. rabbits, RBE assess. 0-104661
 valyl-h-tRNA synthetase of chick embryo brain, ⁶⁰Co γ -irrad. obs. 0-72222
 yeast, diploid, radiation sensitive mutants, γ -ray response and recovery obs. 0-101227

biological effects of ionising particles

- see also biomolecular effects of radiation; cellular effects of radiation*
 bacterial cells, heavy ion irrad., long range effects, comparison with γ -irrad. 0-101236
 beta-rays from ¹⁴C, biological hazards, cell killing effects, E. coli expts. 0-89805
 brain, caudate nucleus, neurotransmitter activity transient alterations after electron irrad., rat expts. 0-72267
 brain, irradiation with C ions, recovery from pot. lethal damage, rat expts. 0-72234
 breeding performance of female mice, comparative effects of ⁶⁰Co γ -rays and ²³⁹Pu α -particles 0-72231
 catalase, glucose embedded, measurement and reduction of radiation damage in frozen hydrated crystalline specimens 0-89810
 cells, human, multinucleate and micronucleus formation obs. 0-72219
 cellular repair rates determined by split-dose and dose-rate methods, comparison 0-104680
 Chinese hamster cells, enhanced killing by ²³⁸Pu α -particles in the presence of cordycepin 0-72233
 Chinese hamster V79 cells, synchronised, inactivation with charged-particle track segments 0-108966
 chromosome aberrations, dose-effect relationship, population exposed to increased natural radioactivity 0-72254
 cosmic ray heavy ions, charge and LET distrib. meas., radiation damage in biological objects 0-94664
 death due to inhalation of β -emitters, probability estimation 0-89801

biological effects of ionising particles continued

- DNA, radiation induced mol. size change, electron irradiated, effect of p-nitroacetophenone 0-89807
 DNA, thymine damage production and excision, mammalian cells, high-LET irrad. obs. 0-72261
 DNA double strand breaks rel. to radiation dose, yeast cell obs. 0-72232
 E. coli, damage induced by T decay, secondary lethality under nongrowth conditions 0-104654
 E. coli, value of photoreactivable component after exposure to ionising radiation 0-72224
 electron radiation damage, knock-on process 0-79840
 embryo C3H10T1/2 cells, mouse, high-energy neon particle irrad., viral transformation enhancement 0-104668
 5-fluorocytosine, electron beam damage assessed by EELS 0-89809
 isocitrate dehydrogenase from Azotobacter vinelandii, essential amino-acid residues identification 0-76538
 kidney cells, inactivation by high-energy monoenergetic heavy-ion beams 0-72256
 low dose ionizing radiation, health hazard estimates 0-61646
 lung, carcinogenic effect of localised fission fragment irrad., rat expts. 0-81656
 lung parenchyma irradiated by inhaled ²³⁸PuO₂ particles, collagen localisation, Syrian hamsters 0-72252
 lung tumourigenesis from particulate sources of ¹⁴⁷Pm β -radiation 0-72247
 mammalian cells, cultured, interpretation of mutation and inactivation obs. 0-72229
 mammalian cells, lethally damaged, proliferation obs. after irrad. by various particles 0-108971
 protein, electron radiation damage on primary and secondary struct. level 0-89808
 rice, M₁ damage, RBE of thermal neutrons 0-104649
 skin, pig, response to ¹³⁷Cs-irrad. 0-67161
 skin, radiation fibrosis after β -irrad. and attempt at suppression, guinea pig expts. 0-72243
 skin, senescent, increased susceptibility to β -irrad., mouse obs. 0-104656
 testes, mice, comparative effects of various radiations on weight loss and spermatogenic stem-cell survival 0-108976
 5-trifluoromethylacetyl, electron beam damage assessed by EELS 0-89809
 uridine-5'-phosphate.2Na⁺ single crystals, radiation damage, ESR obs. 0-108964
 V79-spheroids, survival and kinetic response after heavy ion beam exposure 0-104651
 Vicia faba growth reduction, RBE of d(50)-Be neutrons and 650-MeV He²⁺ ion 0-98025
 yeast cells, dried, inactivation by accelerated heavy ions of very high LET 0-108965
 D⁺, dissociation on impact with mylar foil 0-67164
²³⁸Pu 4.4 MeV α -particles, mutagenicity and cytotoxicity rel. to X-rays 0-72265
²²²Rn, props. and behaviour of short lived daughter nuclides in the atmos. (Japanese) 0-72339

biological effects of microwaves

- see also biomolecular effects of radiation; cellular effects of radiation*
 anechoic chamber, miniature, for chronic exposure of small animals to plane-wave microwave fields 0-67304
 auditory responses induced by microwaves, guinea pig 0-61628
 auditory sensations evoked by pulsed microwave fields, some peculiarities 0-61636
 behaviour of rats, combined effects of microwaves and dextroamphetamine, expt. obs. 0-61635
 behavioural alterations of rats, interaction of ambient temp. and microwave irrad. 0-67153
 behavioural observations of microwave exposed rats and mice 0-61631
 blood-brain barrier, effects of microwave-induced hyperthermia, rat 0-61642
 blood-brain barrier, problems in quantifying effects, comparison of methods 0-61643
 blood-brain barrier, reversal of microwave-induced permeability 0-61641
 bone, granulocyte and macrophage precursor cells, mouse, microwave effects in vitro 0-76789
 cancer treatment appl. of microwave arrays for localised tumour heating 0-94308
 cancer treatment by controlled local heating, 915 MHz or 2450 MHz 0-76860
 cerebrovascular permeability, quantitative method for meas. of alterations 0-61748
 chronic exposure, physiological and behavioural effects, rat obs. 0-67152
 entomological experiments on teratogenic effects of EM fields 0-85446
 erythrocytes, rabbit, increased passive efflux of ²²Na and ⁸⁶Rb on irrad. 0-108957
 excitable cellular membranes, nonthermal interaction of RF and microwave fields, squid giant axon model 0-67150
 heart rate of embryonic quail, effect of 2450 MHz irrad. 0-89794
 heating effects of radiowaves and microwaves 0-98011
 heating patterns produced by 434 MHz Erbrotherm UHF⁶⁹ in tissue-equivalent medium 0-98013
 hyperthermia, rats, classical conditioning obs. 0-61629
 hyperthermia, rel. to visually evoked electrocortical response, guinea pig 0-61627
 hyperthermia to cancer treatment (Spanish) 0-89795
 labelled microspheres, localised embedding by microwave heating of tissues of hypothermic dogs 0-61640
 leg, human, elevated temps. induced by microwave diathermy with surface cooling 0-61638
 long-term irradiation, methodology and evaluation of ocular and physiological effects, rabbits 0-101225
 long-term irradiation, rabbits, evaluation of haematological and immunological effects 0-101226
 murine ocular lens in vitro, microwave and temp. effects 0-89798
 operant behaviour and rectal temp. during 2.45-GHz microwave irrad., squirrel monkey obs. 0-61630
 operant behaviour induced by microwave radiation, effect of psychoactive drugs 0-61632
 plasmonic absorpt. of RF energy, hypothesis 0-72215
 rat thermoregulatory behaviour when subject to microwave irrad. 0-81547
 Salmonella typhimurium LT2 mutants, effects of microwave radiation and heat 0-108958

biological effects of microwaves continued

- sciatic nerves, frog, isolated, effects on vitality 0-108959
 skin, pig, combined effects of X-irrad. and microwave heating 0-94290
 skin, pig, response to combined X-irrad. and microwave heating 0-61653
 Temebrio, developmental effects of microwave irrad., culturing protocol and carrier freq. influences 0-61626
 vasodilation, peripheral, induced in squirrel monkeys 0-104682
 visual-motor performance, skilled, by monkeys in a 1.2-GHz field 0-61634
 yeast cells, determ. of thermal equivalent to MM microwaves 0-67151

biological effects of radiation

- see also biological effects of acoustic radiation; biological effects of gamma-rays; biological effects of ionising particles; biological effects of microwaves; biological effects of ultraviolet radiation; biological effects of X-rays; biomolecular effects of radiation; cellular effects of radiation; dosimetry; radiation therapy*
 alpha emitters, health effects, man-made actinides compared with natural radionuclides 0-61647
 bacteriorhodopsin, elec. response of a back photoreaction 0-98008
 blood, extracorporeal irradiation method, for rats 0-72396
 bone lesions in CBA mice from nanocurie amounts of ²³⁹Pu 0-81657
 brain, quantitative assess. by computerised tomography scan anal. 0-72306
 breast carcinoma prognostic relevance of radiation induced immune suppression 0-72217
 bronchogenic carcinoma among former U mine workers at Port Radium, Canada 0-89802
 cancer, dose-effect relationship linearity 0-67157
 cancers and mutations, radiation levels and induced illnesses 0-76791
 cervical spinal cord, rhesus monkey, effects of 50 MeV (d-¹⁰Be) neutron irrad. 0-101228
 conference, Osaka, Japan (Nov. 1979) 0-98756
 corneal temperature range, implications in prediction of laser thermal damage 0-108848
 cranial structure exposed to RF radiation, thermal response model 0-94285
 cytogenetical indicator of radiation effect, chromosomal dosimeter (*Hungarian*) 0-94292
 2'-deoxyadenosine in aq. deaerated soln., new radiolysis mechanism 0-81350
 dose-effect relationship for quantifying health risks (*German*) 0-61644
 electric fields, vertical, 45-Hz, influence on rats 0-76784
 ELF electric fields as from EHV/UHV power transmission lines, US research results 0-94278
 EM energy irrad., research review 0-85444
 EM field of overhead power lines, rel. to suicide 0-94287
 EM irradiation, temp. distrib. in simulated living tissues 0-85354
 EM wave heating effects, radiowaves and microwaves 0-98011
 entomological experiments on teratogenic effects of EM fields 0-85446
 fast neutron facilities for radiobiological irrad. 0-109064
 FBR notional accidental releases, effect of duration on consequences 0-94296
 fusion reactor blanket material impurity hazardous activity and dose rates, biological hazard pot. 0-102315
 gliomas, malignant, anal. of dose-effect relationship 0-72331
 health of radiation workers 0-98038
 hereditary damage [review] after low-level radiation exposure 0-67165
 inhaled radioisotopes effects 0-94288
 ionising radiation, current research in Canada, review 0-104683
 ionising radiation effects (*Croatian*) 0-104644
 ionising radiation induced behavioural and physiological changes in rats, hormonal radioprotection 0-98026
 laser applications for discotheque light effects, safety considerations with respect to output power and exposure time, regulations and recommendations (*German*) 0-101224
 laser irradiated tissue, significance of blood flow in temp. calcs. 0-104563
 laser medicine in Japan, current status (*German*) 0-98059
 lasers, therapeutic appl. (*French*) 0-108996
 lethal diseases from ionising radiation, new index of risks 0-94294
 light, epileptic subjects, background illumination effect obs., intermittent stimulation 0-98009
 lung cancer rel. to Rn in dwellings 0-98970
 magnetic fields, cooperative phenomena 0-94247
 magnetic fields, magnetolectrets as possible mech. 0-93157
 magnetophosphenes, quantitative determ. of thresholds 0-61620
 man-made EM fields and georadiations, effect on man and protection from (*Polish*) 0-67258
 mandible, radiation necrosis, dental factors, radiotherapy complication 0-98021
 mandible, radiation necrosis, factors influencing onset, radiotherapy complication 0-98020
 nuclear waste ponds and streams, Hanford, ecological search for radiation effects 0-89804
 optical radiation composition and effects and usage in plant experiments (*Hungarian*) 0-109076
 orchids, photoperiodism effects on growth and flowering 0-89797
 pancreatic cancer, low-level radiation link 0-89803
 para-aortic irradiation, late effects in carcinoma of uterine cervix and endometrium 0-108979
 phase T7, inactivation by visible laser light (*German*) 0-98010
 plutonium, biologically important physicochemical props. and methods of human contamination (*French*) 0-98004
 radiation protection standards, quantitative risk 0-61708
 radiation sensitivity, conf., Rome, Italy (Sept. 1978) 0-62368
 radiolysis of heterogeneous inanimate systems, radiobiology appl. 0-66824
 retinal damage from a white-light laser, thresholds and mechanisms, rhesus monkey obs. 0-108955
 RF EM fields, review of effects and dosimetric data, safety standards development 0-67154
 RF EM fields (300 KHz-100 GHz), human exposure safety level 0-89869
 RF heating for solid tumour destruction, animal expts. 0-61637
 RF radiation exposed chicks, behavioural obs. 0-61633
 RF waves, effects of repeated exposure on growth and haematology of mice 0-61625
 safety estimation methods, problems (*French*) 0-98003
 small-bowel damage, prediction by dose-response curve anal. 0-98036

biological effects of radiation continued

- solar receiver radiative loss and eye hazard evaluation by Net-Radiometer 0-89673
 spinach chloroplasts, laser photoinduced changes in high freq. dielectric constant 0-85449
 thyroid tumours, human, radiation and host factors following thymus irrad. 0-89800
 transmission line AC EM fields, health effects regulation 0-94286
 vaginal mucosa, radiation tolerance obs. 0-104666
 whole-body irradiation, effects on different tissues, rat expts. 0-72216
 wound treatment by RF EM radiation, rabbit expts. 0-61639
¹⁴¹CeO₂, effects of repeated inhalation exposure, mouse obs. 0-104676
¹⁴¹CeO₂, inhalation exposed mice, toxicity, dosimetry and ¹⁴⁴Ce retention 0-98874
¹³⁷Cs-irradiation, response of pig skin, various schedules of irrad. 0-72237
¹³¹I, A=131-2, comparative effects in rat thyroid glands 0-104670
¹³¹I, age-related radiosensitivity obs. of guinea pig thyroid glands 0-104671
²³⁹PuO₂, inhaled by baboons and dogs, comparison of early mortality 0-108977
²³⁹PuO₂ inhaled by rhesus monkeys, cytogenetic and other biological effects 0-108968
- biological effects of ultraviolet radiation**
see also biomolecular effects of radiation; cellular effects of radiation
 bacteriophage T1, killing by irrad. in dry state with 122 nm and 254 nm light 0-101234
 biopolymers, deform. under uniaxial stretching during UV irrad. 0-108935
 coral reef epifauna, susceptibility to UV irrad. 0-98037
 corneal damage induced by near-UV laser, cumulative effects 0-85448
 cytochrome c, effects of UV and temp. on optical props. and enzymatic activity 0-81648
 DNA, properties changes caused by UV- and γ-irrad., electrochem. anal. 0-72271
 E. coli, UV-induced recovery of γ-irrad. bacteriophage DNA 0-72214
 E. coli B/r, UV sensitivity rel. to DNA content obs. 0-108960
 E. coli, lethality by 365 nm radiation under various conditions 0-61624
 E. coli, respiration cessation obs. after far UV irrad. 0-76799
 fibroblasts, human, UV-irrad., effects of radioactive labelled DNA on excision repair 0-94289
 lipids of membranes, free radical formation 0-81647
 nematode, Rhabditidae tokai, killing effects of UV light and X-rays 0-101235
 phosphatidyl choline, oxidised, free radical formation 0-76790
 potato virus S on Chenopodium quinoa 'Valdivia' leaves, local lesion development obs. 0-81654
 skin and UV radiation physics, review 0-81661
 solar UV radiation, changes at Earth surface due to stratospheric O₃ reductions 0-94577
 soybean suspension cultures, thymine dimer and glyceollin accumulation 0-104646
 VUV, broad-band synchrotron radiation, effects on wet yeast cells 0-108972
- biological effects of X-rays**
see also biomolecular effects of radiation; cellular effects of radiation
 N-acetylglycine, X-irrad., stable radical electronic and mol. struct., ENDOR and ESR 0-80637
 alveolar macrophages, mouse obs. 0-98024
 bacterial spores, breaking survival curves and O₂ removal times obs. 0-81658
 blood, gas valves, anal. in mice following pulmonary irrad. 0-104673
 bone, changes in ^{99m}Tc pyrophosphate imaging after X-irrad. 0-72239
 bone, radiation induced osteosarcomas, rabbits, scintigraphic and radiographic detect. 0-101231
 brain, late changes in biochem. and blood flow, rate expts. 0-72218
 brain, monkeys, delayed damage from therapeutic range irrad. 0-76801
 brain tumour cells, rat, anal. of interaction of 2 nitrosourea compounds and X-radiation 0-72230
 brain tumour cells, Z-ray-BCNU interactions in vitro, isobologram anal., rats 0-81662
 cell neoplastic transformation and dose fractionation, role of damage repair 0-72242
 cells, ¹²⁵IUdR-labelled and X-irrad., 4.2K and above 0-72211
 CHO cells, alterations in radiosensitivity by anisotonic treatments 0-72251
 CHO cells, asynchronous, fractionation of combined heat and radiation, cell-cycle redistrib. 0-76807
 chromosome aberrations, alteration in freqs. of different classes throughout first cell cycle after irrad. 0-104672
 chromosome aberrations induced by low doses of X-rays in human lymphocytes in vitro 0-72235
 computerised tomography, health risks due to radiation exposure 0-61654
 cytotoxicity of X-rays rel. to ²³⁸Pu 4.4 MeV α-particles 0-72265
 diploid cell populations, human, acute and late effects of single exposure 0-98029
 DNA, thymine damage production and excision, mammalian cells, high-LET irrad. obs. 0-72261
 E. coli, value of photoreactivable component after exposure to ionising radiation 0-72224
 ear skin, mouse, fractionation effects in response to combined heat and X-rays 0-76805
 embryo of 2 cells, mouse, cell cycle-dependent radiosensitivity obs. 0-104669
 erythrocyte membranes, fluidity change after X-irrad., pyrene excimer fluorescence obs. 0-72262
 haematopoiesis progenitor and effector cells, expt. murine system, whole body irrad. obs. 0-98034
 heart, dog expts. 0-104679
 in vitro transformation, conf., Toronto, Canada (May 78) 0-67931
 keratinocytes, dose-dependent vol. changes after X-irrad. 0-61652
 kidney, X-irradiation and induced autoallergic glomerulonephritis effects, rat obs. 0-76793
 lactate dehydrogenase, O₂ effect in radiolysis obs. 0-72223
 leukemias, nonlymphatic, rel. to adult exposure to diagnostic X-rays 0-67158
 liver membranes, mouse, dose-rate effects 0-94293
 lung, single dose, sequence of histological changes, mouse obs. 0-98019
 lung epithelial cells, type 2, proliferative response after X-rays and fission neutrons 0-108974

biological effects of X-rays continued

- lung tumour induction in RFM mice after localised X- or neutron irradiation 0-72260
 lymphocytes, acentric fragments formation, anal. of primary processes 0-72272
 Lymphocytes, human, effect of irradiation on hexose monophosphate shunt pathway 0-76798
 lymphocytes, human, prediction of dose-rate effects for dicentric production by X- and γ -rays 0-72226
 lymphocytes, human, variation in neutron RBE values compared to X-rays 0-101229
 lymphoma cells, mouse, of differential sensitivity to X-rays, expt. obs. 0-72221
 lymphoma cells, Murine L5178Y, production of radioresistant mutants 0-76809
 mammalian chromosomal DNA, single-strand breakage, sensitive detect. by sedimentation anomaly appl. 0-104825
 membranes, vitamin E deficiency and lipid peroxidation, mouse obs. 0-72263
 murine L5178Y cells, correl. of cell cycle parameters with radiation sensitivity 0-98016
 murine leukemic lymphoblasts, deficient repair and degradation of DNA after irradiation 0-72249
 murine leukemic lymphoblasts, deficient repair and degradation of DNA 0-72253
 mutagenicity of X-rays rel. to ^{238}Pu 4.4 MeV α -particles 0-72265
 nematode, Rhabditidae tokai, killing effects of UV light and X-rays 0-101235
 neuronal DNA damage accumulation rel. to death after whole-brain irradiation, rats 0-76804
 pelvic irradiation in gynaecological malignancy, effect on bile acids absorpt. 0-67160
 phosphenes, mech. of formation, electrophysiological obs. on albino rats 0-104675
 pollen mother cells, tradescantia, meiotic chromosomes, stage sensitivity and dose response 0-104648
 retina, albino rabbit SEM obs. 0-104674
 skin, pig, combined effects of X-irradiation and microwave heating 0-94290
 skin, pig, response to combined X-irradiation and microwave heating 0-61653
 skin, swine, response to single acute exposures, epidermal cell changes quantification 0-72245
 small-bowel adenocarcinoma, rat, circulating blocking factors of lymphoid cell cytotoxicity 0-72257
 somatic cell hybrid, intraspecific, radiation response obs. 0-72246
 sperm count reduction and abnormal sperm increase after X-irradiation or ^{22}Na injection, mouse 0-108961
 squamous-cell carcinoma, spontaneous, in mice, comparison of neutron- and X-irradiation effects 0-98033
 tail, rat, single dose radiation and hyperthermia rel. to growth 0-108963
 tail necrosis, mouse, multifraction X-irradiation, dose-incidence curve steepness anal. 0-98035
 testes, mice, comparative effects of various radiations on weight loss and spermatogenic stem-cell survival 0-108976
 testis mass loss obs., mouse 0-67156
 thymocytes, negative surface charge reduction and thymic phagocytosis 0-81663
 thymocytes, rat, reduction of interphase death by hyperthermia 0-108970
 thyroid hormone kinetic and serum levels, rats, effects of whole-body irradiation 0-104662
 tumour blood flow rel. to radiation and drug response 0-67114
 tumour cells, human, effect of irradiation. feeder cells on X-ray survival curve shape 0-98032
 tumour cells, human, X-ray sensitivity in vitro 0-104665
 visual phosphenes, mech. of formation, photochem. investigations 0-108877
 X-ray, cell survival at low O_2 tension and dose build-up in Ar 0-72220

biological fluid dynamics

- see also biorheology; haemodynamics*
 action potential correlates of pressure-induced changes in cardiac conduction 0-81572
 annual review of fluid dynamic, book 0-94927
 arterial collapse after subjection to an external pressure band 0-94271
 bio-fluid peristaltic transport, peripheral layer viscosity effects 0-61600
 bird flight, wake behind finch 0-81629
 cartilage, model for surface flow 0-85431
 catheter, multi-transducer, for intraluminal pressure recording in vivo 0-98979
 CHO fibroblast, press., inhibited thermal killing obs. 0-81564
 duodenum, fluid mechanics, review, book contrib. 0-97994
 high-pressure convolutions in rodents, associated heart rate changes 0-67124
 intra-articular pressures during joint use, changes with disease, pathological consequences 0-94252
 intracranial pressure measurement system 0-109084
 kidney, six-tube vasa recta model as test problem 0-104610
 kidney model, numerical soln. by multiple shooting 0-104609
 lung, zone I, transvascular fluid shifts, rabbit obs. 0-101198
 lung lymph transport increase without heart failure after coronary ligation in sheep 0-67122
 lymphatic vessel network, similarity anal. of design 0-101212
 macromolecules, rigid, modelling approaches of hydrodynamic props. 0-61613
 microorganisms, lack of intracellular bubble formation at very high gas supersaturations 0-81562
 oesophageal manometry by liquid-filled catheters 0-85514
 peribronchial fluid pressure rel. to vascular and airway pressure and interstitial oedema 0-97971
 peristaltic transport, asymptotic method 0-87805
 physiological compartment tracer flow modelling and digital imaging 0-101257
 pulmonary interstitial fluid space compliance, estimation in isolated perfused rabbit lung 0-104605
 semiconductor pressure transducer (*Japanese*) 0-94394
 squeeze forces in contact lenses with a steep base curve radius 0-108926
 thick layer above an active ciliated surface, fluid transport 0-85425
 urodynamics, mechs. and hydrodynamics of the lower urinary tract, book 0-98768

biological macromolecules *see macromolecules; molecular biophysics***biological sciences** *see biology***biological specimen preparation**

- acetylcholine receptor protein structure 0-85339
 aphid neurones, differential sensitivity to sucrose 0-98195
 autoradiograms of serial sections, preparation for electron microscopy 0-67312
 bacteriophages, freeze drying method for electron microscopy 0-104826
 critical point drying of hydrated specimens, principles and procedures 0-76882
 cryofixation of tissue specimens studied by cooling rate measurements and scanning electron microscopy 0-94430
 dispersion staining, in IR and UV 0-76874
 DNA, spreading of large associations, dark field electron microscopy 0-85563
 egg shells, electron microscope embedding medium for pore studies 0-98194
 electron microscopy, gentle bounce-free assembly for quick-freezing tissues 0-67316
 electron microscopy, quarter-micron serial sectioning and stereoscopy 0-72384
 epitaxially sandwiched macromolecules, contrast in TEM 0-85565
 fissured biological object prep. for SEM, vacuum deposition and cathode sputtering comparison 0-72390
 freeze drying technique for SEM 0-104828
 freeze-etching improvement using evaporated film 0-85558
 freeze-fracture technique, appl. to study of animal plasma membranes 0-104842
 freezer fracture autoradiography, red blood cell plasma membrane, electron microscopy 0-98192
 freezing, fracturing and coating system for low-temperature SEM 0-76883
 haematopoietic malignancy diagnosis, significance of SEM 0-85529
 histological and cytological reflection contrast microscopy 0-72389
 lipid bodies, saturated, in organ pipe cactus visualisation by cytochem. technique 0-76873
 liver sections, comparison of chemically prepared and freeze dried specimens for ion microscopy 0-95189
 membrane preparatory procedures, for electron microscopic anal., at mol. level resoln. 0-104843
 neurons, section embedding technique for sequential light and electron microscopic exam. 0-67317
 plant root transport studies using ion localisation, freeze substitution method 0-85569
 protein film method, basic, in electron microscopy of nucleic acids 0-104844
 red blood cell etching by ion beam sputtering for SEM 0-85554
 replication at -150°C with improved freeze-fracture apparatus 0-85560
 secretory granule membrane, particle clustering induced by centrifugation, freeze-fracture anal. 0-85559
 skeletal muscle preparation for SEM 0-94431
 soft specimens for electron microscopic analysis 0-98190
 spray freezing method, size determination of sonicated vesicles, freeze fracture electron microscopy 0-98188
 TEM specimen freeze drier, all-glass design 0-82854
 X-ray microanalysis 0-73566

biological techniques and instruments

- see also biological specimen preparation; biomedical equipment; biomedical measurement; microelectrodes; specimen preparation*
 40 Hz activity in sigmoid gyrus, nucleus accumbens and amygdala, cross correl. anal. 0-76730
 acoustic holographic in medicine and biology, state of art and future 0-67175
 agarose gel immunoelectrophoretic determination of molecular weights of tubulin antigens 0-67313
 algae sample analysis using coherent optical processing 0-98205
 Aiopex process: Visual receptive fields by response feedback 0-61546
 amplifier, special purpose, for insect taste cell spike train recording 0-72394
 anechoic chamber, miniature, for chronic exposure of small animals to plane-wave microwave fields 0-67304
 aortic valve study, by holographic interferometry and shadow Moire methods 0-104613
 apatite powder samples, peak positions determ. from step-scanned X-ray powder diffr. data 0-103217
 aquatic eyes, retinoscopy, refractive error considerations 0-61750
 arteries, small, isolated, perfused, method for simultaneous elec. and mech. recording 0-101300
 auditory cortex of unanaesthetised monkey, vertical stereotaxic approach to elec. recording 0-72383
 automatic identification equipment for cattle (*Czech*) 0-109073
 automatic parameterization of vocal cord motion from ultra high speed films 0-85419
 automatic sprayer with programmable dose for serial expts. (*Hungarian*) 0-104822
 autoradiographic visualisation of rat brain dopaminergic nerve endings, test of technique 0-61742
 averaged multiple unit activity as estimate of local neuronal activity changes, vol. conducted pots. 0-89917
 backscattered electron images of biological specimens 0-104827
 bacteria in H_2O , detection by resonance Raman spectra 0-94418
 beta-ray attenuation, inhomogeneous medium density determ., calcs. and meas. 0-98182
 bioelectrochemical sensor using immobilised enzyme electrodes (*Japanese*) 0-109071
 biomembranes, excited, automatic meas. of ionic current electrophysiological characts. (*Russian*) 0-76865
 blood cell leukocytes, automatic recognition and classification systems (*Italian*) 0-81780
 blood pressure automated control in dogs using microprocessor 0-81797
 blood pulse measuring by computer (*German*) 0-104823
 blood-brain barrier, problems in quantifying effects, comparison of methods 0-61643
 body joints, centres and angles of rotation meas., errors and optimisation study 0-61604
 bone strains of canine radius and ulna, in vivo meas. and anal. 0-67130
 brain reflectance, mapping technique using optical fibres 0-72381
 bremsstrahlung X-ray spectra, lightly filtered, generated at 200 to 300 kV 0-72397

biological techniques and instruments continued

- calorimetric instrumentation for studies of biopolymer model compounds 0-61746
 cardiac fibrillation thresholds for 60 Hz currents and voltages directly applied to heart 0-101301
 cartilage proteoglycan simultaneous localisation by light and electron microscopy 0-85571
 cathodoluminescence detection of Giemsa stain and its appls. 0-67323
 cattle feed utilisation exam., microscopic samples molecular analysis, with Raman microprobe 0-57391
 cell deposition system for deposition at predefined locations on microscopic slide 0-76876
 cell electrophoretic mobility meas. using new automatic method 0-67322
 cell element observations in same sections by light microscopy, TEM and/or SEM 0-85556
 cell membrane particle diameters meas. by computer from electron micrographs 0-101307
 cell size meas. by static light scatt. Fourier transform 0-81793
 cells growth research, non-thermal effects, BWO appl. (*German*) 0-105684
 cellular elastomer selection for use in biomechanical capacitive force transducers, measuring device (*German*) 0-85545
 cellular fluorescence polarisation measurements in flow systems, epillumination optical design 0-89908
 cellular mechanical and chemical analysis, recommendations of workshop on future of biomedical instrum. 0-81776
 cerebrovascular permeability, quantitative method for meas. of alterations 0-61748
 charged particle activation anal., determ. of Pb distrib. in human teeth 0-101303
 chromatography and mass spectrometry, conference, Carlsbad, Czechoslovakia (April 79) 0-73097
 chromosome classification system, banding technique 0-67320
 chromosome metaphase spread, automatic finding, prep. and eval. of object spectra 0-98168
 chronobiological movement transducer (*Spanish*) 0-89902
 cinematography, high-speed, appl. to laser damaged flagella of microscopic organisms 0-81785
 colonic contractile activity meas., pharmacological tests in dogs appl. 0-109068
 computer-assisted mapping with the light microscope 0-67308
 computerised technique for rapid eye movements detect. during paradoxical sleep 0-76870
 cone, computer-driven hardware model, response obs. 0-72402
 confinement device for determ. of whole-body radionuclide concs. in live ducks 0-67299
 confocal scanning light microscopy, imaging modes 0-86401
 confocal scanning light microscopy with high aperture optics 0-86400
 constant pressure reservoir for organ perfusion 0-94437
 contact microscope for medical laboratory use 0-85540
 continuous flow analysis, cell for use with O₂ membrane electrode, appls. 0-61736
 continuous relaxation spectra, direct anal. 0-10831
 Couette viscometer for short time shearing of blood 0-98179
 Coulter electrical sizing principle, appl. to new multiparameter system 0-89911
 cowpea chlorotic mottle virus packing in crystalline monolayers, electron microscopy 0-89922
 current pulse-induced voltage variations in bilayer membranes, apparatus 0-94420
 α -cyclodextrin and α,β -D-xylose, absorption mode spin-echo spectra appl. 0-78634
 cytofluorometric measurements by fluorescence extinction through a diaphragmed objective 0-67319
 cytological cell feature extraction using optical moments 0-98206
 cytophotometer, automatic 2-wave, with a calculator 0-104820
 cytospectrofluorometric installation, scanning attachment to dual-prism monochromator 0-101837
 data collection systems, rapid, for time resolved X-ray scatt. expts. in mol. biology 0-61740
 deconvolution nomogram for single exponential fluoresc. decays 0-67290
 deoxyhaemoglobin, proton NMR, modified DEFT technique for obs. hyperfine shifted line, T₁ values meas. 0-76871
 depolarised dynamic light scattering, determ. of rotational diffusion coeff. of bacteriophages T4B and T7 0-85549
 dextran T-10 and α -cyclodextrin, absorption mode spin-echo spectra appl. 0-78634
 diaphragm muscle, canine, in vivo stiffness props., obs. and meas. system 0-97988
 diathermy applicator for irradiation of rat brain 0-94425
 diatom recognition and counting, matched-filter and statistical method 0-101304
 dielectric meas. of biological liquids, reflection meas. of complex dielectric const. 0-101309
 dielectric properties meas. technique using an in vivo probe, VHF to microwave freqs. 0-85542
 dielectric props. meas. at RF and microwave freq. by coaxial line reflection methods 0-109065
 dielectric props. of biological substances, physical meas. 0-94417
 dielectric relaxation in biological model systems, time-range meas. method (*German*) 0-71308
 dielectrophoretic force, theory expt. 0-72403
 diffractometric method for meas. of cellular deformability 0-98187
 diving physiology research facility 0-82106
 DNA derivate melting curves, automatic recorder using real time processing (*French*) 0-104833
 DNA helix destabilising protein cryst., electron microscopy 0-85338
 Doppler flowmeters, directional, totally implantable, for animal research 0-67293
 double-barrel ion-sensitive microelectrodes, extra thin tip diameters, intracellular meas. appl. 0-101298
 education, Bernoulli's eqn. and Hagen-Poiseuille's law, capillary bed representation 0-57039
 electrical heart stimulator, versatile, wide-range, for animal expts. 0-89912
 electrodes, C-loaded teflon, for chronic EEG recordings in microwave research 0-67305
 electrofocusing, current major appls. 0-101306
 electron diffraction, low dose, of wet protein cryst. 0-85550
 electron microscope autoradiography, soln. of reverse problem 0-94419
 electron microscope autoradiography of isolated mols. 0-85564

biological techniques and instruments continued

- electron microscope imaging with superconducting lenses 0-73553
 electron microscopy, computer anal. of cell ultrastructure 0-85555
 electron microscopy, conf., Toronto, Canada (Aug. 1978) 0-82579
 electron microscopy, image reconstruction of low and high dose micrographs of neg. stained glutamine synthetase 0-85551
 electron microscopy, microdensitometer-computer correlation analysis of ultrastructural periodicity 0-85553
 electron microscopy, quarter-micron serial sectioning and stereoscopy 0-72384
 electron microscopy, three dimensional, minimal dose technique 0-86526
 electron microscopy of frozen hydrated crystalline specimens, meas. and reduction of damage 0-85552
 electron probe X-ray microanalysis, quantitative investigation of thin specimens 0-101068
 electron probe X-ray microanalysis for calcification studies of bone and cartilage 0-76885
 electronic method for determ. of footfall patterns of animals during treadmill locomotion 0-72386
 electronic metronome with luminous and audible signals (*Spanish*) 0-89885
 electronic speckle pattern interferometry in vivo 0-109083
 elemental analysis, quantitative, using energy-dispersive X-ray spectrometer 0-104840
 EM, electron exposure-dependent contrast transfer 0-104837
 EM control of cell functions 0-85535
 EM microelectrode holder for pulsating penetration of brain tissue 0-98199
 EMG, multichannel data acquisition system for the survey of intercostal muscle activity 0-81790
 endocardium motion during contraction, anal. method 0-109072
 environmental particulate exposure in humans, documentation using SEM and energy-dispersive X-ray analysis 0-76886
 enzyme-linked immunosorbent assay, apparatus for meas. light absorbance of small vols. of liquids 0-72387
 epiphyseal plate, method for evaluation and control of growth activity 0-81789
 ergometer for small-animal research 0-101295
 extracorporeal irradiation method for blood in rats 0-72396
 fast neutron facilities for radiobiological irradiation 0-109064
 fibre optic pH sensor, miniature, for physiological use 0-109074
 filters as selective electrodes for synthetic penetrating ions 0-104821
 flavins, meas. of sub ns fluoresc. decay by time-correl. photon counting and Ar laser 0-94429
 flow cytometric data, computerised display and anal., review, book contrib. 0-109082
 flow microcalorimetry, bioassay and enumeration, drug biopotency meas. 0-95100
 fluorescence microscopy of living cells, low level, appls. of image intensification 0-94432
 fluorescence photobleaching recovery method, bleaching light effect on membrane diffusion meas. 0-94434
 fluorescence spectroscopic investigations of the dynamic properties of proteins, membranes and nucleic acids 0-101148
 fluorescent excitation anal. of stable Rb, erythrocyte survival determ., rabbits 0-81788
 fluorescently labelled molecules as probes of living cells struct. and function, review 0-67321
 force plate, mech. design, construct. details and calibration 0-85544
 fossil dating by ESR technique 0-95209
 freeze fracture autoradiography, red blood cell plasma membrane, electron microscopy 0-98192
 glass electrode impaled into single cells, meas. of membrane and electrode elec. props. 0-89916
 glass micropipettes, comparative calibration by optical microscopy and SEM (*German*) 0-98201
 hair, human, PIXE analysis, correction factor, rel. to pollution monitoring 0-61743
 high resolution time lapse cinemicrography, use of improved air stream incubator 0-98196
 high-pressure chamber for electrophysiological meas. 0-98185
 histological and cytological reflection contrast microscopy 0-72389
 histological marking with multiple thin-film electrode probe for intracortical recording 0-67297
 hole-burning spectroscopy, electron phototransfer in reaction centres of Chlorella photosystem I 0-81561
 holocamera for 3-D micrography of the alert human eye 0-98057
 holographic interferometry set-up for seed studies 0-67325
 holographic interferometry with optical fibres, hearing mechanism obs. 0-76879
 holographic models of neural structs., optical system (*Russian*) 0-76878
 holography, autocorrelation of diatoms as a function of depth of focus [holography in biology] 0-67324
 holography, conf., Munster, Germany (Mar. 1979) 0-62390
 IC implantable systems for animal expts. 0-76887
 image converters, for HVEM 0-104839
 image processing applications at IBM Madrid Scientific Center 0-102657
 immunoelectronmicroscopy in detect. of antibodies to rabies virus 0-85567
 incubator, closed chambered, use in enzyme and immunoperoxidase histochemistry techniques 0-98191
 infrasonic test chamber for research into effects on man (*German*) 0-67147
 infrasound and pressure waveform generator, compact, for small cavity appls., animal research 0-104830
 integrated circuit approach to totally implantable telemetry systems 0-67291
 intelligent microscopes, recent and near-future advances 0-98166
 interactive image scanner, high resolution 0-94423
 intracellular pressure measurement system 0-109084
 intracortical recording of field pots., 16-fold semi-microelectrode 0-67298
 intramembrane potential jump meas. by potentiodynamic method 0-81778
 intravascular thrombus induction in vivo using localised hydrodynamic shear stresses 0-97997
 iontophoretic pipettes, theoretical physics of drug release 0-67311
 IR thermometry, appl. to remote detect. of biological stresses in plants 0-61749
 IR-ATR spectroscopy, appl. to struct. investigation of biological material in aq. environment 0-61735

biological techniques and instruments continued

- isopycnic centrifugation method for rapid separation of murine thymocytes 0-104832
- kinetic IR spectroscopy IR, appl. to biochem. systems 0-98178
- laser Doppler anemometer, directionally sensitive two-component, velocity meas. in artery casts 0-75004
- laser microprobe mass analyser, achievements and appls. 0-73536
- laser projection microscope, with brightness amplifier for biology and medicine 0-76875
- laser-Raman microprobe studies of mineralizing tissues 0-76884
- leukocytes of human blood, gravity sedimentation anal. 0-98197
- LF dielectric measurements using time-domain technique, 20 Hz to 10 kHz 0-57329
- lichen indicator appl. in PIXE and NRA environmental studies 0-61744
- liquid-crystal optical fibre temp. probe rel. to thermometry and dosimetry of heat 0-98204
- lithography, heavy ion, tool for object investigation and replication 0-90931
- lung degassing, evaluation of 2 methods 0-101294
- lung volume estimation method, constant inflation pressure 0-67306
- lysozyme, absorption mode spin-echo spectra appl. 0-78634
- macromolecule observation using CTEM and STEM with negative staining 0-85561
- macromolecules, nonlinear laser photomodification, radiation damage 0-61120
- magnetic circular dichroism of biological molecules, review, book contrib. 0-109080
- magnetic micro-rheometer evolution and theory 0-92099
- magnetic search coils for eye position meas., implantation method 0-85548
- magnetic susceptibility measurement, living rats 0-72391
- mammalian chromosomal DNA, single-strand breakage, sensitive detect. by sedimentation anomaly appl. 0-104825
- mean caliper diameter of lung nuclei determ. 0-98189
- membrane multilayer arrays, surface-induced lamellar orientation, theory and method 0-89724
- membrane surface charge visualisation using SEM 0-85566
- micro-object geometric feature determination, TV set 0-85538
- microcircuit electrodes, extracellular, recording of action pots. from cultured neurons 0-72382
- microdrive assembly, subminiature, for electrophysiological recording from freely moving rats 0-61737
- microelectrodes, open tip glass, influence of diffusion, double layer, and glass conduction on elec. resistance 0-67300
- microelectrodes, vibrating, excursion in tissue 0-104829
- microphotometry, compensation for fluctuations in illumination 0-73413
- micropipettes of very low resistance for intracellular meas., production method 0-61738
- microscope photometer/semiautomatic image anal. instrument system for morphometric and photometric value meas. 0-82815
- microscopic equipment, methods, appls. and related topics, bibliography 0-94941
- microscopic equipment, methods, appls. and related topics, bibliography 0-105450
- microscopic image processing (*Japanese*) 0-81784
- microscopy, argentaftin cells, correlative light microscopy, SEM and TEM 0-85557
- microstrip microwave biological exposure system 0-89924
- microwave imagery of isolated canine kidney, use of orthogonal polarisations 0-81783
- microwave irradiation, long-term, methodology and evaluation of ocular and physiologic effects, rabbits 0-101225
- microwave spot-size controlled Gaussian-beam launcher for microwave exposure studies 0-89920
- mineral fibre characterisation using energy dispersive X-ray spectrometry in TEM (*French*) 0-82857
- moire contourgraphy, computer-aided replication of human anatomy 0-67189
- morphometric cytology pictorial pattern recognition 0-81796
- moving cell microelectrode puller 0-67309
- multidimensional space and time signal processing in biology and medicine 0-85493
- multimode time-varying enclosures for exposure and dosimetry in bioelectromagnetic experiments 0-85497
- muscle contraction, single, high-time resolution X-ray investigation method 0-81777
- muscle contraction process, 10 ms time resolution X-ray diff. 0-61741
- mycoplasma contamination detect., SEM sensitivity 0-85568
- myelinated axon identification, SEM technique 0-85570
- nerve spike trains, interleaved, in a noisy channel, separation system 0-94424
- neural signal recording using implantable electrode and telemetry system, awake animals (*Japanese*) 0-94427
- neural single unit activity from foetal pig brains, recording method 0-67315
- neuron soma model with high reliability and low power consumption 0-72392
- neurons, single, rapid killing by irradiation of intracellularly injected dye 0-81795
- neurophysiological experiments, fast data acquisition and processing system, minicomputer appl. (*Japanese*) 0-85536
- neurostimulation automatic triggering as function of several EEG parameters, apparatus 0-98203
- neutron activation analysis, transportable system for determ. of P in sheep bone 0-109066
- neutron activation analysis of biological materials by the monostandard method 0-72398
- neutron activation analysis using coincidence counting, biological and soot samples (*Japanese*) 0-97750
- NMR applications to phosphoryl transfer enzymes and metal nuclei of metalloproteins, review, book contrib. 0-109081
- oesophageal geometry changes in swallowing, transduction, for animal grazing studies 0-76888
- optical confocal scanning microscope, image form, 0-68249
- optical microscope, focusing technique for digital image anal. system 0-68250
- optical radiation composition and effects and usage in plant experiments (*Hungarian*) 0-109076
- optical teaching microscope for investigation of transparent biological objects 0-82622

biological techniques and instruments continued

- capillary muscle selection and testing, some mech. considerations 0-89919
- particle etch track technique determ. of U trace content in normal human blood 0-89910
- pattern recognition, rotational matched spatial filter 0-76866
- peripheral nerve, generation of unidirectionally propagated action pots. by brief stimuli 0-85546
- phospholipid bilayers, use of nitroxide free radical spin label EPR spectra, determ. of rot. correl. time and HFS coupling 0-74260
- photoacoustic spectrometry of macroporous haemoglobin particles 0-85543
- photoacoustic spectroscopy, biological and medical appls., book contrib. 0-109078
- photoacoustic spectroscopy, blood and proflavine obs. (*French*) 0-101845
- photoelectrode for recording intracerebral cellular Ca^{2+} transients 0-67307
- photographic technique for anal. of neural unit activity rel. to movement 0-67310
- photometer, differential light scatt., for rapid analysis of particles in flow, appl. to biological cells 0-77834
- photoreceptor membranes, incorporation into a multilamellar film 0-89907
- photostimulator, LED fibre optic, for research on visual nervous integration 0-67302
- photosynthetic reaction centre functional reconstitution in planar lipid bilayers 0-97881
- PIXE, appl. to primate trace element retention 0-81792
- PIXE, biomedical and biophysical appls. 0-61691
- placental villi, human, average diameter estimation by stereologic method 0-67318
- plankton animal groupings pattern recognition, average similarities of Fourier spectra 0-104818
- positron camera system, ring detector, brain research, computed transaxial tomography 0-61739
- preparative scale thin-film dialysis apparatus 0-101296
- protein adsorbed layers on field-emitter tips, removal by UV radiation 0-104836
- protein molecular weight and ultrastruct. determ. in STEM 0-85562
- protein supramolecular structure, ordered, electron micrographs, image processing 0-89923
- proteins, mol. wt. determ. by monolayer surface press. meas. technique 0-89526
- pulmonary oedema of intact dogs, meas. by transthoracic γ -ray attenuation 0-81787
- radio-liquid chromatograph system, determ. of ^{14}C -labelled amino acids (*Japanese*) 0-104834
- radiochemical determination of short-lived radionuclides in neutron-activated biological samples 0-109067
- radioimmunoassay, fitting of general form of fundamental physical model 0-94150
- radioisotope counting techniques for analytical appls. in biology and medicine, review 0-81794
- radiolabelled microspheres, use in meas. of regional blood flows during +G, stress 0-81786
- radiotelemetry system for avian ECG meas. 0-98202
- refractometer laser detector for anal. of liquids 0-101830
- resistance strain gauge-meas. techniques in biomech. expts. (*German*) 0-104819
- respiratory process parameters determ., air flow consumption meas., using electric model (*Bulgarian*) 0-76867
- review of biophysics and bioengineering, book 0-105437
- RF-powered cage system for implant biotelemetry 0-94422
- rheometer, analytical, optical sliding contact, for flow visualisation at articular surface 0-104847
- ribosome subparticle fine struct. investigation by optical filtration of electron microscope images 0-81779
- scanning Auger microscopy for analysis of biological material 0-73535
- scanning electron microscopy at macromolecular resolution in low energy mode on biological specimens coated with ultra thin metal films 0-72401
- scanning microcalorimeters for studying macromolecules 0-61747
- SEM, reflected, viewing specimens in air 0-82853
- SEM cathodoluminescence appls. 0-72400
- semiconductor force transducer suitable for use with small muscles 0-72395
- silicone rubber substrata, appl. to study of cell locomotion 0-104835
- SIMS, histological section, high mass resolution by ionic analyser (*French*) 0-109069
- solution X-ray scattering, review of recent developments, book contrib. 0-109077
- spectrophotometer/fluorometer, dual-wavelength, high-performance 0-98198
- spermatozoa, human, motility evaluation, photon correlation meas. 0-61745
- spot scan TEM technique 0-82846
- SQUID instrumentation for biomagnetic meas. in unshielded and noisy environments 0-104710
- STEM, computer driven, image registration 0-104838
- STEM, obs. of single heavy atoms, in frozen biological specimens 0-89921
- STEM methods for mass measurement 0-73537
- stereophonic equalisation of artificial heads without exact replication of ear drum impedance 0-81614
- sterotaxic method for recording from single neurons in the cat eye 0-89913
- stimulating electrodes of different materials implanted in cat skeletal muscles, threshold meas. 0-101297
- Streptococcus mutans 10449, size determ. by laser light scatt. 0-109066
- substrate core sampler, lightweight low-friction, ecological survey appls. 0-95090
- sweep-freq. magnitude method for dielectric characterisation of chemical and biological systems 0-104824
- telemetry, totally implantable, integrated power controllers and RF data transmitters 0-67295
- telemetry system, implantable, multichannel, for physiological research 0-67292
- telemetry system, totally implantable, for dimensions meas., animal physiological research 0-67294
- telemetry systems, totally implantable, appls. to chronic medical research 0-67296

biological techniques and instruments continued

- TEM, digital image enhancement 0-82852
 temperature stabilisation of biological media, electronic device 0-85539
 temperature telemetry system with interference suppression, implantable, long-life, animal expts. appl. 0-101302
 temperature telemetry transmitter, crystal-controlled, surgically implantable, for animal expts. 0-72393
 tensile testing of small animal ligaments, gripping device 0-81791
 thermal blooming spectroscopy for enzymatic anal. 0-86441
 thermistor probe use to meas. energy distrib. in US fields 0-109075
 thermoelectric needle probe for medical and biological temp. meas. 0-101299
 tissues thin sections obs., Raman laser microprobe analysis appl. 0-57390
 tracheal ciliary beat, improved device for freq. recording 0-109070
 transponder dipole antennas in and near three-layered body 0-98181
 US meas. of larynx height and vocal fold vibratory pattern 0-98184
 US system for quantification of bubbles formed during decompression of animals and man 0-76869
 US velocity-of-propagation meter, based on interferometer 0-79084
 velocity sedimentation separation of mammalian cells 0-101293
 ventilators for animals, automatic sigh feature 0-8186
 vesicles, large, anal. of adhesion to surfaces, expt. procedure 0-109063
 vidicon Raman spectrometer, appl. to heme protein study 0-94428
 vision, Macular pigment, role in polarised light detect., meas. technique 0-61560
 visual adaptation, technique for estimating the contrib. of photomech. responses 0-85547
 visual system simulator, human (*Russian*) 0-76877
 vital microscopy, electronic thermostatic system 0-85537
 voltage clamp, single electrode, design for neuroresearch 0-72385
 whole body autoradiography of bumetanide-¹⁴C in dogs by round saw method 0-72399
 x-ray diffraction studies of the heart, review, book contrib. 0-109079
 X-ray films, selected, response to ¹⁴C-β-radiation 0-90937
 X-ray microtomography in SEM 0-101308
 zeugmatography of ³¹P metabolites 0-76872
 Al shielded room for biomag. meas. 0-104846
 Al, thick-walled conducting shield in biomag. expts. 0-104845
 C-fibre microelectrodes, neurophysiology appl. 0-67314
 Cu determination in serum/tissue specimens using flameless atomic absorption spectroscopy, effects of sample prep. and matrix 0-98200
¹⁸F, prep. with an electron linear accelerator, medical and biological appls. 0-98136
 Fe utilisation studies by stable tracer ⁵⁸Fe technique 0-61734
 HeNe laser light determ. of erythrocyte distrib. profiles during sedimentation 0-81563
³²P and ⁴⁵Ca determination by Cherenkov and liq. scintillation counting 0-98183
 Pb poisoning in human teeth, determ. using alpha-sensitive plastic track detector 0-94433
 Pb traces in human blood plasma, atomic absorbpt. anal., nonspecific absorbpt. correction using Zeeman effect 0-76881
 PdO-Pd miniature pH electrode description and use 0-89886
 Ta-Al₂O₃ microelectrode array, design and fabrication 0-76868
 U abundance in Himalayan plants, fission track determ. 0-101305
¹³³Xe clearance, meas. of pig cerebral blood flow 0-94421

biology

- see also biological fluid dynamics; biological techniques and instruments; biophysics; blood; cardiology; ecology; evolution (biological); medicine; physiology; zoology*
 S.Benguela Current, upwelling site nutrients, zooplankton and phytoplankton 0-104987
 biosatellite Cosmos-782, biological expts. 0-61710
 epidemic in discrete time, threshold theorem 0-61504
 Laccadive Sea, chemical oceanography and biological productivity 0-104995
 marine organisms around Marshall Islands nucl. test site, ¹¹³Cd^m conc. 0-109174
 multistable self-wave media 0-86094
 oceanic benthic communities, carbonate shells, ¹⁸O/¹⁶O vars. in East Pacific Rise hydrothermal field 0-109173
 E.Pacific Rise, benthic communities of hot springs areas 0-101360
 pollen record in N.America NW. coast region, appl. to Quaternary temps. and precip. determ. 0-98438
 tooth enamel crystallites, contrast effects in TEM 0-85572
 tropical rain forests, exploitation causing destruction (*German*) 0-101137

biology computing

- see also computerised instrumentation; computerised signal processing*
 40 Hz activity in sigmoid gyrus, nucleus accumbens and amygdala, cross correl. anal. 0-76730
 Alopec process: Visual receptive fields by response feedback, trigger features 0-61546
 blood flow, finite element soln. 0-94269
 blood pressure automated control in dogs using microprocessor 0-81797
 cardiograms, image processing, cardiac function meas. (*Japanese*) 0-94354
 colonic contractile activity meas., pharmacological tests in dogs appl. 0-109068
 dosimetry calculations due to radionuclides in aquatic food chains, NEP-TUN interactive code in FORTRAN 0-109039
 flow cytometric data, computerised display and anal., review, book contrib. 0-109082
 lumbar spine, human, dynamic 3D modelling, computer code 0-108948
 microscopic image processing (*Japanese*) 0-81784
 neuronal membrane process field potentials anal. and synthesis, computer system 0-85374
 neurophysiological experiments, fast data acquisition and processing system, minicomputer appl. (*Japanese*) 0-85536
 proteins, conform. anal., algorithms and data structs. for array processing 0-83530
 rapid eye movement analysis during sleep 0-76870
 sensory neuron, second order, summation of excitation and inhibition by computer simulation 0-76769
 weightlessness, haematological response, math. and exptl. simulation 0-61714

biomagnetism

- 60 Hz high intensity electric fields, behavioural and biological effects in living organisms 0-89740
 bacteria, magnetotactic, navigational compass 0-72183

biomagnetism continued

- behavioural sensitivity of a domestic bird to 60-Hz AC and to DC mag. fields 0-61622
 brain, human, mag. fields 0-72182
 brain, human, neural generator localisation underlying auditory evoked mag. fields 0-104703
 brain, mag. evoked field mapping 0-104705
 brain, magnetoencephalogram power spectrum estimation 0-104704
 cardiac mechanical activity, noninvasive mag. detect., instrumentation 0-89820
 cardiac mechanical activity, noninvasive mag. detect., theory 0-89819
 cardiomagnetism, high resolution 0-104698
 cellular current flow and biomag. fields 0-101192
 cooperative phenomena, rel. to biological effects of mag. fields 0-94247
 cytochrome c, haeme-haeme mag. interaction obs. 0-108836
 dipalmitoylphosphatidylcholine, changes in vol. mag. susceptibility at the phase transition 0-76770
 eye, retina injuries, magnetoretinographic meas. using SQUID magnetometer 0-104702
 frequency/depth-penetration considerations in hyperthermia by magnetically induced currents 0-63887
 geomagnetic field sensitivity in animals, ferromag. coupling to muscle receptors as basis 0-72185
 heart, human, elec. and mag. events, phase and amplitude relationship recording 0-104695
 heart vector components, simultaneous meas. with unipositional lead system 0-104697
 His-Purkinje conduction system, human, mag. study 0-89818
 HV lines to 800 kV, elec. and mag. field effects on human beings (*French, English*) 0-72209
 hyperthermia by magnetically induced currents, freq.-depth-penetration, comments and reply 0-108991
 LF biomag. meas. using thick-walled Al enclosure 0-62698
 lung, mag. field meas., comparison between two methods 0-104712
 lungs, freeze-dried, localised-field magnetopneumographic meas. 0-104714
 magnetocardiogram and cardiac output meas. with integrated system 0-104709
 magnetocardiogram enhancement by applied mag. field 0-104701
 magnetocardiogram meas. first order gradiometer and DC-thin film SQUID 0-89877
 magnetocardiograms of normal and abnormal subjects, anal. using 2D displaying method (*Japanese*) 0-67177
 magnetocardiography and ECG, R and T waves 0-104699
 magnetocardiography recording, props. of ideal system, appl. of ECG theory 0-104700
 magnetoelectrets, possible mech. of mag. field effects 0-93157
 magnetoelectric dipole structure hypothesis, biological and cosmic appls. 0-91124
 magnetoencephalography, distrib. of detector sensitivity, reciprocity appl. 0-72278
 magnetoencephalography, sensitivity distrib. 0-101246
 magnetophosphenes, quantitative anal. of thresholds 0-72184
 magnetophosphenes, quantitative determ. of thresholds 0-61620
 magnetopneumography, analytic methods 0-104713
 magnetopneumography, evaluation for assessing thoracic accumulation of welding fume particulate 0-101247
 MCG, PR segment theory rel. to current sources within heart 0-101191
 measurement facility installation in hospital environment, design criteria and procedure 0-104707
 measurements in unshielded and noisy environments 0-104710
 median nerve, transient responses to elec. stimulation, SQUID appl. to somatically evoked field meas. 0-104706
 molecules, mag. circular dichroism, review, book contrib. 0-109080
 neuromagnetic fields sources location, using SQUID system, comparison with electrical method 0-101190
 photosynthetic reaction centres, triplet population, mag. field and g-factor differences effect 0-97879
 physiological aqueous solution, possibility of hydromag. wave excitation 0-94246
 SQUID fluxgate magnetometers, magnetopneumographic meas. 0-104711
 SQUID gradiometer, second-derivative, magnetocardiogram meas. 0-104696
 steady current-produced fields in human body 0-94248
 superconductive helmet with SQUID for magnetoencephalography 0-104708
 susceptibility measurement, living rats 0-72391
 synovial fluid analysis by ferromagnetic 0-101242
 water mobility in blood plasma, NMR determ., viscosity correl. to 1/T₂ 0-67176
 Al shielded room for biomag. meas. 0-104846
 Al, thick-walled conducting shield in biomag. expts. 0-104845

biomechanics

- see also biological fluid dynamics; biorheology*
 actomyosin from a non-muscle system, tension generation 0-76781
 adaptive control mechanisms for complex motor systems 0-81573
 adaptive stiffness control in human movement 0-108947
 airway smooth muscle, contracted, hysteresis, dog expts. 0-81634
 antagonistic muscles, functional elec. stimulation optimisation, math. modelling, joint motion 0-61730
 aorta, canine, mech. props. following hypercholesterolemia 0-104620
 aorta, canine, mech. props. following hypercholesterolemia 0-108938
 aorta, root of, functional anatomy and deform. props. 0-67136
 aortic valve histology rel. to mechs., porcine expts. 0-85430
 aortic valve prostheses, hydrodynamic losses eval. 0-72378
 aortic valve study, by hydrodynamic interferometry and shadow Moire methods 0-104613
 aortic valve tissue, porcine, glutaraldehyde-treated, mech. fatigue study 0-67112
 arm posture control, spring model and equivalent neural network 0-101196
 arterial collapse after subjection to an external press. band 0-94271
 arterial vessels, small, critical changes in lumen 0-61615
 arteries, human, intracranial and extracranial, stiffness and elastic behaviour 0-85436
 arteries, small, pulmonary, elasticity in the cat 0-108942
 artificial heart valves, dynamics 0-72379
 ballistic walking, math. model of swing phase 0-67131
 binocular retinal image motion during active head rotation 0-72158

biomechanics continued

- biopolymers, deform. under uniaxial stretching during UV irradi. 0-108935
 bipedal hopping in small mammals, energetic cost obs. 0-108936
 blood vessel coagulative commissures, influence of high amplitude elec. impulses on strength 0-104600
 bone, attempts to stimulate longitudinal growth in dogs by mech. vibration 0-81638
 bone, compact, long-term torsional creep obs. 0-104619
 bone, comparison of electromech. effects in wet and dry bone 0-97985
 bone, crack velocity depend. of longitudinal fracture, bovine tibia 0-97965
 bone, demineralised dense human, strength props. nonuniformity 0-104611
 bone, mammalian, acoustic emission testing 0-76783
 bone fracture callus mech. props., intramedullary nailing rel. to plating 0-85438
 bone mechanical properties characterisation by dynamic response 0-76782
 bone remodelling, quantification of stresses 0-85437
 bone strains of canine radius and ulna, in vivo meas. and anal. 0-67130
 bone tissue, compact, destruction 0-67135
 brain, experimental oedema, serial meas. of specific gravity and computerised tomography attenuation 0-98005
 car accidents, correl. of field injuries and GM Hybrid III dummy responses 0-108939
 cardiac mechanical activity, noninvasive mag. detect., instrumentation 0-89820
 cardiac mechanical activity, noninvasive mag. detect., theory 0-89819
 cardiac muscle (*Japanese*) 0-72201
 cellular deformability, diffractometric method for meas. 0-98187
 cellular elastomer selection for use in biomechanical capacitive force transducers, measuring device (*German*) 0-85545
 centrifugation stress, effects on pituitary-gonadal function in male rats 0-98149
 chronobiological movement transducer (*Spanish*) 0-89902
 collagen, 3-dimens. struct., rel. to props. of connective tissue 0-67038
 collagen fibres, mech. props., role of struct. organisation 0-72207
 conference, Pennsylvania, USA (Oct.1979) 0-82567
 corneal pressures due to soft contact lenses and corneal asymmetry 0-104621
 cranial bone, fetal, elastic modulus obs., appl. to fetal head moulding biomechanics 0-67128
 critical light reflection at a plastic/glass interface and appl. to foot press. meas. 0-81681
 diaphragm muscle, canine, in vivo stiffness props., obs. and meas. system 0-97988
 dolphin swimming, leaping for efficiency at high speed 0-61619
 eardrum vibration meas. using electronic speckle pattern interferometry 0-67209
 ejection fraction rel. to ventricular vol., computer anal. 0-104599
 elbow joint, human, mech. anal. 0-104626
 electromechanical model for human articular cartilage 0-104631
 EMG period-amplitude analysis, cat locomotion and jumping obs. 0-67057
 EMG silent period and muscle mechanics in human soleus muscle 0-67060
 endocardium motion during contraction, anal. method 0-109072
 epiphyseal plate, method for evaluation and control of growth activity 0-81789
 ergometer for small-animal research 0-101295
 eye position measurement, method for implantation of mag. search coils 0-85548
 facial skeleton strain distrib. arising from orthodontic appliance activity, holographic interferometry 0-67143
 femoral fracture brace, biomech. study of function during stance 0-97990
 femoral necks, fracture fixation by Muller screws, mech. investigation 0-72377
 fetal head moulding, finite element model investigation 0-67129
 fibrosarcoma cells, buoyant density, effect of hypoxic growth conditions in vitro 0-104601
 fibula, direct meas. of load bearing function 0-104624
 foot load dynamic distrib., quantification system 0-94388
 foot load static distrib., quantification using the PET computer 0-94387
 foot pressure distributions, technique for display 0-85508
 foot-pressure measurements, static and dynamic, in clinical orthopaedics 0-98163
 footfall patterns of animals during treadmill locomotion, electronic method for determ. 0-72386
 force plate, mech. design, construct. details and calibration 0-85544
 forces exerted in walking and running, Fourier anal. 0-94266
 forces in animal joints 0-94251
 gait, automatic 3D anal. using a Selspot centred system 0-108998
 gait assessment using components of the ground reaction force, vector 0-101284
 gait measuring system for treatment evaluation, microprocessor controlled 0-61731
 gait of cerebral palsied children, EMG investigations 0-72186
 gait quality indication by temporal asymmetry 0-98164
 gait studies, planar control in multi-camera photogrammetric calibration for 3-D studies 0-67194
 gastropod locomotion, role of pedal mucus 0-76780
 geometric properties of paired human tibiae 0-67127
 glass-ceramic implants, loaded, expt. studies on anchoring in the femur (*German*) 0-81624
 ground reaction forces in distance running 0-97983
 head movements of mealworm beetle, props. and role 0-76772
 head movements of mealworm beetle, responses to rotating panoramas 0-76773
 heart, beating, kinematics theory 0-76777
 heart, ellipsoidal model, appl. to left ventricular contractions study 0-104608
 heart, isolated, grass-snake, motor reactivity obs. 0-67100
 heart contraction mechanism, modelling 0-72204
 heart valves, crescent-shaped aorta, deform. props. by holographic interferometry 0-61616
 Hill equation, fitting to expt. data 0-89777
 hip prosthesis stem loosening in human femur, biomechanical causes investigation 0-85435
 holographic interferometry, rigid body motion compensation 0-67213

biomechanics continued

- hyperbaric hyperflexia, tendon-jerk and Hoffman reflexes in Man, soleus muscle 0-61530
 intervertebral discs, statics and dynamics 0-104612
 intervertebral disk of Rhesus monkey, response to P-A shear stress 0-104617
 intracranial pressure meas. in newborns, new non-invasive technique 0-67272
 isopycnic centrifugation method for rapid separation of murine thymocytes 0-104832
 joint performance rel. to articular cartilage roughness 0-89782
 joints, centres and angles of rotation meas., errors and optimisation study 0-61604
 kinematic gait, system for simple meas. 0-85509
 knee, human, torsional characts. and passive elements, simulated anatomical conditions 0-104628
 knee biomechanics, review of some basic assumptions 0-94265
 knee ligaments, load transmission characts. during axial tibial rotations 0-104629
 lap-shoulder belt restraint, correl. of field injuries and GM Hybrid III dummy responses 0-108946
 left ventricle, math. model of mechs. 0-101195
 left ventricle, model study of isovolumic and non-isovolumic contracts 0-85428
 left ventricular diastole mechanics 0-94261
 leg, lower, external compression effect on venous blood vol. 0-97989
 leg loading in snow skiing, computer anal. 0-101208
 leg-foot, complex, in conditions of lesion and reconstruction, holography 0-67142
 lipid bilayers, elastic props. changes on exposure to different agents, elec. and chem. 0-81548
 locomotion dynamics, human, math. model 0-97981
 long bone mechanics study under microprocessor control 0-76851
 lumbar spine, human, dynamic 3D modelling, computer code 0-108948
 lumbar spine loads, anal. and meas. 0-104622
 lumbar spine loads during work at a table 0-101210
 lung, finite element model for macroscopic deform. 0-108945
 lung, macroscopic deformation, finite element model 0-89781
 lung parenchyma, math. model 0-108940
 mechanomyocardiography, left ventricular, technique for detect. of diseased myocardial elements and states 0-72363
 membrane flexural fluctuations and non-equilib. noise 0-76712
 motion studies and tissues and fluids characterisation (*French*) 0-89778
 motor output response to applied torque perturbations in man, nonlinearities evaluation 0-76771
 muscle, anatomical model, internal pressure effects 0-67103
 muscle, elec. stimulated, closed-loop control of force 0-76728
 muscle, upper extremity, eccentric-concentric contract. study 0-85432
 muscle actions, model for semi-quantitative studies 0-61605
 muscle fibre bundle tension development, action of regulatory light chains 0-94270
 muscle fibres of *Lethocerus maximus*, temp. dependance of cross bridge parameters 0-61598
 muscle force development, filament spacing effect on axial forces 0-61597
 muscle force development, geometrical factors influencing radial forces 0-67102
 muscle stiffness in hypertonic solns. 0-67140
 muscle stretch reflex system, math. model (*Japanese*) 0-67067
 muscle system, contractile system, sliding motion anal. 0-67104
 navicular bone, morphological features in functional adaptation of the foot (*Croatian*) 0-108944
 oesophageal accelerometer, cardiovascular function indication 0-104798
 oesophageal geometry changes in swallowing, transduction, for animal grazing studies 0-76888
 orofacial posture and movement, photo-elec. recording method 0-108995
 orthopaedic applications of holography 0-67196
 orthopaedic biomechanics (*Japanese*) 0-67133
 orthopaedics, exptl., quantitative eval. of holographic deform. investigations 0-67197
 osteosynthesis, internal, deform. of bone (*Croatian*) 0-108943
 papillary muscle selection and testing, some mech. considerations 0-89919
 patellofemoral joint, anal. model 0-104625
 periodonal ligament, in vitro rupture obs. 0-97982
 photographic technique for anal. of neural unit activity rel. to movement 0-67310
 posture control system response to random accel. disturbances (*Japanese*) 0-72200
 posture-control system, responses to pseudorandom accel. disturbances 0-81640
 pressure distribution under the foot during static activities 0-97964
 prosthetic, heart valves, load cell for meas. of dynamic forces 0-104815
 quadriceps femoris, function under maximal concentric and eccentric contractions 0-97963
 red blood cells, equilib. shapes in osmotic swelling 0-85368
 red blood cells, minimum energy anal. of membrane deform. 0-72141
 reflex stiffness of man's anti-gravity muscles during knee bends while carrying extra weights 0-61601
 regeneration of soft biological tissue, mech. conditions 0-104615
 regressive osteometric scaling appls. to mirror symmetry and statistical coordinate models 0-104627
 resistance strain gauge-meas. techniques in biomech. expts. (*German*) 0-104819
 rigid body motion calculated from spatial co-ordinates of markers 0-94267
 rigidity increase of material of bioconstructs. during morphogenesis 0-94249
 role of stress-gradient effects 0-67113
 runner's forward motion, effects of wind assistance and resistance 0-101204
 running, influence of track compliance, model and expts. 0-61602
 semiconductor force transducer suitable for use with small muscles 0-72395
 shearing forces on the sole of the foot, meas. system 0-72342
 skeletal muscle, frog, active tension changes during and after mech. stimulation 0-94262
 skeletal muscles, cat, force-vel. and fatigability obs. 0-81637
 skeletal muscles, contracting, simulation studies of mech. stretch 0-94263
 skull, macerated, human, orthodontic forces induced bone displacement obs. 0-61603

biomechanics continued

- skull and auditory ossicle vibr. anal., human preps., using holographic interferometry 0-67210
- soft tissues, elastic stress/strain relation based on a struct. model 0-101205
- soft tissues, human, rheological props. from local cyclic loading method 0-108932
- soft tissues, human, rheological props. investigation using elastography 0-108933
- spinal column, human, strength of construction 0-67137
- spine, human, finite element model for in vivo freq. response anal. 0-104623
- step length measurement apparatus 0-67271
- surface EMG, computer anal. during isometric exercise, muscle tension quantification 0-85505
- suture line stress in end-to-side anastomosis, math. assess. in pulsatile flow 0-97986
- suture line stress in the end-to-side anastomosis, math. assessment 0-61606
- synovial joints, immobility effects, pathomechs. of joint contracture 0-97954
- teeth and mandibles, deforms. due to occlusal forces, holographic interferometry 0-67205
- teleost fish, max. speed paradox resolution 0-67138
- tendon, rat tail, struct. and mech. props. 0-97953
- tendons preserved by different means, strength and morphological struct. 0-72208
- tensile testing of small animal ligaments, gripping device 0-81791
- thumb joints, mech. anal. 0-94264
- tibia, human, natural freq. anal. 0-85433
- tibia, human, simplified method of radiographic anal. of its cross-section, anthropometric correls. 0-89827
- tooth support, model of periodontal vasculature 0-85434
- trabecular bone from human vertebral body, elastomech. props. 0-67141
- trachealis muscle, dog, spontaneous mech. activities in vivo 0-101203
- tractor drivers, minimisation of vertical vibration responses 0-81626
- tractor vibrations, response of human body, vibration minimisation 0-101213
- tympenic membrane investigations in living man using holographic interferometry 0-67207
- tympenic membrane vibr. studies in living man using holographic interferometry 0-67208
- urethra, female, elastic length, initial obs. 0-81642
- urinary bladder interferometry, holography of bladder deforms. in vitro, rabbit expt. 0-67201
- urinary bladder interferometry, tumour and lesion detect. by holography 0-67202
- US shear velocity of muscle tissues, mech. props. determ. 0-108930
- valve vibrations, aortic and mitral, anal. and role in heart sound production 0-101214
- venous oscillations, ultrasonic Doppler study 0-108931
- vertebrae, human, deflected US wave propag. tests 0-61617
- vertebrae, human, mech. props. 0-72206
- vertebrae, human, strength under sagittal compression 0-61618
- voluntary movements in man, force gradation and motor unit activity 0-97887
- walking, 5 body-3D dynamic anal. 0-97987
- walking, normal, with different footwear, skeletal transients on heel strike 0-101207
- walking cycle stance phase, dynamic load line considerations (German) 0-81625
- walking insect, *Carausius morosus*, coordination of force oscills. and leg movement 0-76775
- walking insect, *Carausius morosus*, oscillations of force in standing legs 0-76774
- wheelchair locomotion, power output requirements for manual operation 0-94416
- work-effort ratio of a large muscle group, theoretical model 0-108949
- wrist position that facilitates max. power grip strength 0-101209

biomedical applications of computing *see medical computing***biomedical electronics**

- see also electrocardiography; electroencephalography; microelectrodes; patient monitoring; patient treatment; prosthetics; sensory aids*
- angiohaemodynamical catheterisation lab., electromedical devices 0-85515
- artificial eye for blind people, implementation through the optical nerve (Croatian) 0-109060
- calibrator for ECG/respiration monitor 0-98159
- cell deposition system for deposition at predefined locations on microscopic slide 0-76876
- cerebral activity monitor, using biofeedback rhythms inducing cct. (Spanish) 0-72359
- coherent line-frequency noise in evoked pot. recordings, cancellation 0-98161
- conference on medicine and techniques, Zagreb, Yugoslavia, 1979 0-101667
- deep-body pressure transducers, monolithic capacitive struct., pulse-period output 0-67274
- ECG multichannel recording using TDM 0-101283
- eEG transient detection by matched inverse digital filtering 0-85506
- electro-optics appl., 1980 development trends 0-85464
- electromyogram, muscle electrical impulses provide audible or visual indication using biofeedback 0-81782
- EMG, filter bank analyser for automatic anal. 0-98162
- galvanic skin response meter cct. using bipolar transistors 0-72380
- gamma-camera images of liver, improvement using physiological gating mechanism 0-98065
- heart, human, elec. and mag. events, phase and amplitude relationship recording 0-104695
- heart beat counter, versatile digital SAMI 0-85510
- HF current surgery, instruments and problems (Hungarian) 0-98172
- IC implantable systems for animal expts. 0-76887
- implantable multichannel neural stimulator, custom IC fabrication 0-85534
- instrumentation, review (French) 0-89884
- LED test checkerboard pattern reversal stimulator for visually evoked pots. study 0-61658
- moire topograms, real-time, video electronic generation 0-67198
- multichannel implantable stimulator (Slovenian) 0-81773
- nerve trunk multifibre activity quantitation 0-76853

biomedical electronics continued

- NMR whole-body imaging system design 0-98064
- noise generator for masking click stimuli 0-108980
- otology application of medical electronics (Japanese) 0-67268
- parylene (vacuum deposited polymeric coating) appl. 0-108607
- patient's surface contour measuring device 0-104717
- pattern rotation system for a visual stimulator 0-98061
- pressure sensor, monolithic, capacitive, with pulse-period output, microminiature and implantable 0-81752
- pulsed integrator for EMG analysis 0-61719
- reaction timer cct., using bipolar transistors and LEDs 0-81781
- safety on health care facilities, recommendations for Spanish hospitals (Spanish) 0-72350
- SQUID gradiometer, second-derivative, magnetocardiogram meas. 0-104696
- temperature stabilisation of biological media, electronic device 0-85539
- thermometer, electronic digital, for long-term patient monitoring 0-90849
- transducer, noncontact, for blood temp. monitoring during extracorporeal circulation 0-85513
- video radiographical images, enhancement 0-94353
- vital microscopy, electronic thermostatic system 0-85537
- X-ray image intensifier noise evaluation, digital method 0-98097

biomedical engineering

- see also biomedical electronics; biomedical equipment; orthotics; patient treatment; prosthetics; sensory aids*
- audiometric facility at West Middlesex Hospital, London for standardised hearing tests 0-76858
- biomagnetic measurement facility installation in hospital environment, design criteria and procedure 0-104707
- cardiac computing conf., Geneva, Switzerland, (Sept. 1979) 0-82582
- clinical physics, the lessons of history, review 0-62447
- clinical support surfaces, mech. compliance evaluation 0-92053
- conference, Jerusalem, Israel (Aug. 1979) 0-98758
- conference, New York, USA (Dec. 1979) 0-104561
- conference on medicine and techniques, Zagreb, Yugoslavia, 1979 0-101667
- cooperation requirement between countries at various stages of development 0-94382
- instrumentation, review (French) 0-89884
- materials for orthopaedic implants, review 0-76862
- photoacoustic spectroscopy, biological and medical appls., book contrib. 0-109078
- recent advances, conf., London, England (Mar. 1980) 0-94924
- review of biophysics and bioengineering, book 0-105437
- training biomedical engineers and technicians in developing countries 0-62408

biomedical equipment

- see also biomedical electronics; biomedical measurement; orthotics; prosthetics; radiography; radioisotope scanning and imaging; sensory aids*
- 21-channel EEG monitor with real-time result colour display 0-72364
- Aberdeen phased array, real-time US scanner with dynamic focus 0-72276
- accelerator leakage measurements 0-89839
- Anger camera/computer system using seven pinhole collimator for myocardial perfusion tomography 0-61663
- Anger-type bar cameras, positron imaging 0-61687
- arrhythmia ambulatory anal. in real-time with minicomputer 0-85523
- arrhythmia detection, edit and recall system, microprocessor-based 0-89891
- arrhythmia detection with a multi-microprocessor system for distributed and parallel processing 0-85524
- ATP-12M infrared imaging system (USSR), body temperature meas. 0-67280
- biofeedback training device for speech therapy, portable, microprocessor-based 0-104808
- biofoal diverging collimator for equilibrium radionuclide ventriculography 0-72310
- biomagnetic measurements in unshielded and noisy environments 0-104710
- blood flow detection in human heart, US pulsed Doppler flowmeter system, microcomputer based 0-104690
- blood gas catheter, fast-responding, flow-independent, for O₂ meas. 0-101277
- blood pressure ambulatory recordings, minicomputer processing 0-89887
- blood pressure automatic monitoring, long-term, minicomputer system 0-101276
- blood viscosity and red cell aggregation at zero and 1G, instrumentation for Space Lab 3 0-61716
- body surface potential mapping, microcomputer processing system (Japanese) 0-72347
- Brattle Physiological Synchroniser, simulator for testing respiratory gating function 0-109055
- bronchoscopic tumour localisation, small radiation detector probes, scintillation and semiconductor detectors 0-61676
- cameras, multi-, planar control in photogrammetric calibration for 3-D gait studies 0-67194
- canopy ventilation monitor for quantitative meas. of ventilation during sleep 0-104792
- cardiac mechanical activity, noninvasive mag. detect., instrumentation 0-89820
- cardiac monitor, heart rate meter and alarm eval., proposed standard test tapes 0-89899
- cardiac nuclear medicine instrumentation, review, book contrib. 0-101260
- cardiac scintigraphic image handling using microprocessor system 0-85489
- cardiovascular nuclear medicine, instrumentation and data processing, ventricular function evaluation 0-85481
- catheter, multi-transducer, for intraluminal press. recording in vivo 0-89879
- catheter tip pH electrodes for continuous intravascular recording 0-81755
- Cathetron, high intensity Co, gynaecological cancer therapy 0-72300
- cell electrophoretic mobility meas. using new automatic method 0-67322
- cerebral activity monitor, using biofeedback rhythms inducing cct. (Spanish) 0-72359
- colonic contractile activity meas., pharmacological tests in dogs appl. 0-109068
- combined microwave heating and radiometry methods 0-85465
- computerised tomography, expt. dual Xe detectors for quantitative CT and spectral artifact correct. 0-76825

biomedical equipment continued

- computerised tomography, positron emission, crystal size optimisation 0-61681
 computerised tomography, positron emission CT device with continuously rotating detector ring 0-81697
 computerised tomography, single-photon emission, imaging capabilities of Ge camera 0-61668
 computerised tomography 0-89832
 computerised tomography scanners, survey of noise, dose and contrast detectability and resolution 0-104750
 computerised tomography tilting unit, advantages in skull diagnosis (*German*) 0-94351
 conference, Denver, USA (Apr. 1979) 0-73100
 contact microscope for medical laboratory use 0-85540
 couch-cover, heatable, use in X-ray exams. (*German*) 0-104751
 data collection station, based on autonomous CAMAC crate 0-61689
 diagnostic X-ray tubes, meas. of focal spot size 0-89831
 diathermy indifferent electrodes, performance electrodes. 0-72367
 digital ECG systems testing 0-81756
 digital filtering and edge detection 0-58065
 ECG, ambulatory, computer processing system 0-89897
 ECG, EK1T Malyshev equipment, operational errors 0-61717
 ECG, QRS detector/delineator devel. and eval. 0-89892
 ECG 24 hr recording, anal. using operator-controlled computer system 0-89888
 ECG analysis system, long term recordings, quantitative evaluation of rhythm disturbances (*German*) 0-76847
 ECG automated monitoring, new electrode system 0-89898
 ECG signal-averaging system, flexible, computerised 0-67270
 echocardiogram, M-mode, automatic computer anal. (*Japanese*) 0-72274
 echocardiographic images, video recorded, interactive segmentation 0-89817
 Echosimulator, function generator for meas. of US diagnostic equipment characts. (*German*) 0-104685
 EEG period and amplitude anal. system, microcomputer-based 0-72353
 EEG potential measuring equipment (*French*) 0-85516
 EEG recording system, portable pulse-interval modulation telemetry/multiplexing system, home use 0-67261
 electric admittance blood flow monitor, clinical evaluation 0-81759
 electrochemical sensors for partial press. meas. in blood 0-67303
 electrocutaneous information transmission system using stimulus energy control device (*Japanese*) 0-101280
 electrode, C-fibre, elec. props. and EEG appls. 0-72355
 electromedical equipment, safety by monitoring leakage currents (*German*) 0-81749
 electron beam applicator, variable field, dosimetry evaluation 0-76839
 electron linear accelerator, radioactive and toxic gas production 0-94378
 electronic metronome with luminous and audible signals (*Spanish*) 0-89885
 electrooculographic system for detect. of oculomotor abnormalities in neurological disorders 0-108888
 electrosurgical dispersive electrodes metal-foil, dry thermal props., skin temp. rises 0-98171
 EM vibrator for denture prosthetics 0-104716
 EMG, surface, system for meas., recording and digital anal. (*German*) 0-76848
 EMG silent period measurement, automated system 0-89883
 endoholoscope, urinary bladder interferometry, holography of bladder deforms. in vitro, rabbit expt. 0-67201
 endoholoscope, urinary bladder interferometry, tumour and lesion detect. by holography 0-67202
 endoscopic carrier, design having complete directional control 0-101248
 endoscopic miniature camera with fibre-optic faceplate 0-77896
 epicardial mapping, computerised display system (*Japanese*) 0-101279
 epicardial mapping, DC, during exptl. coronary occlusion, digital data acquisition system 0-85527
 exercise body plethysmograph, head-out, for extrathoracic airways investigation 0-81754
 exercise therapy, walking simulator 0-81770
 extrasystole monitor using FIFO 0-72360
 fibrescopes using leached fibre image bundles, manufacture 0-83670
 films for nuclear medicine, sensitometry 0-72292
 fluorescein angiography of the ocular fundus 0-67185
 fluorescent decay thermometer for cancer treatment dosimetry 0-86306
 fluoroscopic examinations, multi-image camera for spot radiography 0-109020
 force measurements during operative correction of spinal deformities 0-76861
 frequency-time domain signal processing system 0-81760
 fundus photography in optometric practice 0-67183
 gait measuring system for treatment evaluation, microprocessor controlled 0-61731
 gamma camera, computer controlled, nuclear cardiology appl. 0-61682
 gamma camera systems, methods for MTF meas. 0-94324
 gamma camera visual outcome units comparison, use of MTF 0-94323
 gas analyzer, response time, incorporation in gas exchange computations 0-72344
 Gevamatc 240 developing machine, constancy testing by test film strips in a radiological practice (*German*) 0-95206
 Gipsplast-1, thermoelec. apparatus for local hypothermia 0-104807
 gonioscopy/holography in optometry 0-67182
 haemoglobin-O₂ equilibrium curve, instrument for determ. based on membrane diffusion 0-81761
 head holder for treatment of head and neck cancers 0-94333
 HF current surgery, instruments and problems (*Hungarian*) 0-98172
 holocamera for 3-D micrography of the alert human eye 0-98057
 holography applications in ophthalmology 0-67200
 hot-film shear probes, position sensitivity 0-101286
 hypodermic needle Po₂ electrode 0-98156
 image analyser, semiautomatic, use in investigation of muscle biopsies 0-85466
 imaging system evaluation using contrast-detail-dose anal. 0-98108
 imaging systems, information capacity considerations 0-98090
 imaging techniques implemented on pipeline minis and array processor, nerve fibre counting appl. 0-98165
 immunological reaction monitor using laser light scatt. 0-85463
 intelligent microscopes, recent and near-future advances 0-98166
 intravenous angiography, digital video subtraction system 0-98089
 IR back-scattered from vaginal tissue, self-stabilising meas. system 0-72281
 kinematic gait, system for simple meas. 0-85509

biomedical equipment continued

- laser image printer for X-ray tomographs (*French*) 0-72119
 laser medicine in Japan, current status (*German*) 0-98059
 laser microscope mass analyser 0-98060
 laser stethoscope for respiratory sounds meas., comparison with acoustical method (*German*) 0-98058
 linear accelerator, 4 MV, use for whole-body irradiat. 0-109001
 linear accelerator, field separation between lateral and anterior fields, dose distrib. 0-94336
 linear accelerator beam profile scanner 0-101267
 linear accelerator dosimetry control system, solid state 0-94371
 liquid-scintillation vial system, biphasic, for radiometry, modifications 0-101253
 load cell for meas. of prosthetic heart valves dynamic forces 0-104815
 long bone mechanics study under microprocessor control 0-76851
 Luer lock afterloading device for ¹⁹²Ir brachytherapy 0-104735
 lung, mag. field meas., comparison between two methods 0-104712
 lung volume, online calc. by digital computer 0-72351
 magnetic heart vector components, simultaneous meas. with unipositional lead system 0-104697
 magnetocardiogram and cardiac output meas. with integrated system 0-104709
 magnetocardiogram meas. first order gradiometer and DC-thin film SQUID 0-89877
 magnetocardiography recording, props. of ideal system, appl. of ECG theory 0-104700
 magnetometers, use to vol.-reference flow-vol. curves 0-104694
 mandibular movements diagnosis, system for meas. and processing (*Japanese*) 0-101249
 mechanical and chemical analysis at cellular level, recommendations of workshop on future of biomedical instrum. 0-81776
 median nerve, transient responses to elec. stimulation, SQUID appl. to somatically evoked field meas. 0-104706
 membrane hydrophone for 0.5 to 15 MHz range, press. meas. in US fields 0-108987
 micro-object geometric feature determination, TV set 0-85538
 microprocessor systems for data acquisition, image processing, RIA anal., patient data retrieval 0-61670
 microscope, scanning mirror, with optical sectioning characts., ophthalmology appls. 0-85461
 microstrip antenna for biomedical applications 0-89826
 microstrip slot radiator for medical appls. 0-108994
 microwave antenna, invasive, for locally-induced hyperthermia for cancer therapy 0-67193
 microwave apparatus for cancer treatment by controlled local heating, 915 MHz or 2450 MHz 0-76860
 microwave applicators, comparison of stray radiation patterns 0-61660
 microwave applicators for localised hyperthermia treatment of malignant tumours 0-89824
 microwave diathermy applicator with choke, 2450 MHz, slab-loaded, direct contact 0-89825
 microwave hyperthermia, localised, biomedical devices 0-104724
 microwave hyperthermia treatment and thermometry system 0-72280
 microwave system, dual mode, to enhance early detect. of cancer 0-89823
 mirror, new design for hemianopia detect. 0-108992
 motion phantom for ECG-gated cardiac computerised tomography 0-98115
 multichannel analyser, microprocessor-controlled, transfer of blood pressures and neural activities for computer anal. 0-72356
 multipoint electrode for biological pot. recording 0-104784
 nasal flowmeter for preterm infants, self-retaining 0-98158
 neonatal peripheral circulation, human, characterisation by US pulsed Doppler technique 0-76815
 neonate cardiorespiratory monitoring, automatic system with microprocessor 0-94399
 neural pulse wave analysis, microprocessor-based instrument 0-104791
 neuromuscular block indicator, model INMB-1, EMG amplitude meas. 0-104785
 neutron activation system for in vivo meas. of Cd 0-67224
 nuclear medical instrumentation, mobile, review 0-101262
 nuclear medicine, camera aperture for data collection optimisation 0-67221
 nuclear medicine, clinical and parametric evaluation of three large-field-of-view cameras 0-76823
 nuclear medicine, coded-aperture imaging of the heart, improved aperture 0-98072
 nuclear medicine imaging system for computerised longitudinal tomography 0-61666
 nuclear medicine instrumentation, recent developments 0-81692
 ocular cinema photography 0-67186
 ocular photodocumentation, conf., Birmingham, USA (Dec. 1977) 0-62362
 ocular photography, new instrumentation and techniques 0-67187
 oesophageal accelerometer, cardiovascular function indication 0-104798
 ophthalmic photography, external 0-67180
 ophthalmic photography instrumentation, survey of clinical impressions 0-67188
 optometer, IR, highly sensitive, for accommodation microfluctuation dynamics study 0-81580
 oscilloscope with digital storage for elec. signal obs. and storage 0-104786
 penetrometer cassette, multiple exposure, for meas. of effective kilovoltage of diagnostic X-ray beams 0-61662
 phantom for imaging biological fluids by US and computerised tomography scanning 0-104692
 photoluminescent thermometer probes, temp. meas. in microwave fields 0-104721
 piezoelectric earphones, usefulness in recording brain stem auditory evoked pots. 0-94389
 plethysmograph, body, vol.-displacement using large flowmeter without press. compensation 0-72345
 polarised polyvinylidene fluoride film, piezoelectric transducer 0-75993
 positron emission computed tomograph, POSITOLOGICA 0-104753
 positron emission transaxial tomography, ring detector, attenuation, scatt. radiation and random coincidences 0-61684
 positron emission-computed tomography, multi-slice, design criteria, shielding 0-61673
 preamplifier for muscle spindle afferents identification during in vivo recordings in man 0-98155
 pressure cuffs, hazards in single-stage regulation 0-98160

biomedical equipment continued

pressure recording apparatus for hydrostatic press. changes during
dowel-retained prostheses cementation 0-67287
pressure transducer, miniature implantable, biomedical appl. IC fabrication
techniques 0-76849
proportional chamber, multiwire, low energy radionuclide distrib.
0-61679
pumps for pulsed insulin delivery, modification 0-101290
radiation therapy, thin Pb sheets as tissue compensators for larger field
irrad. 0-104736
radioactivity checking instrument for shielded syringes 0-94325
radiographic equipment, computer-assisted quality assurance 0-89838
radiography, computed, low-dose X-ray imaging system 0-98092
radiography, holographic 3-D synthesis of X-ray pictures 0-67245
radiography, motor-tilted diagnostic examination device Model UV-5B
0-85479
radiography, scanning grid for novel and effective Bucky movement
0-104754
radiography, stereoscopic image evaluating device, Medcor Model SZRK
0-85478
radiology, diagnostic, analytical stereo system 0-67231
radiotherapy hard X-ray machine, RT 305, phys. aspects and appl.
0-81709
radiotherapy tissue compensators, use in improving dose uniformity in
total body irrad. 0-104767
rectilinear scanner, multichannel analyser interface 0-101254
red blood cell freezing, cryopreservation and refrigeration 0-67262
refractometer for eye refr. error meas. 0-81583
refractometers, IRF-454 and IRF-456 models 0-104715
respiration rate meter tester 0-81758
respiratory flowmeter, hot-wire, evaluation for clinical appls. 0-72346
respiratory gas monitoring instrument using microprocessor (*Japanese*)
0-72358
retinal image cinematographic recording, accommodation microfluctuation
appl. 0-81579
RF-powered cage system for implant biotelemetry 0-94422
rheocardiography, 4-electrode, in computer-aided cardiac output determ.
0-61718
rheograph linear-distortion estimation 0-85502
ring-core magnetometer sensor for articular movement meas. of jaw movements
0-101243
rotating disk device for slit radiography of the chest 0-98116
safety and technical service centres (*German*) 0-98151
safety standards for electromedical equipment and installations (*Croatian*)
0-104795
scattered radiation grids, method for testing 0-81717
scintigraphic TV displays, 4 standard types, comparative study 0-109005
scintillation camera collimator image form. 0-89844
scintillation camera field uniformity, global and local, statistical features
0-61677
semiconductor gamma-cameras in nuclear medicine 0-81693
shearing forces on the sole of the foot, meas. system 0-72342
slit lamp, hand-held, with lid opener for ocular exam. 0-67179
slit lamp photodocumentation of ocular structure 0-67181
smoking pattern recorder, portable 0-94385
SOLO monitor, microcomputer bedside monitor 0-94404
spectral reflectance photography of the ocular fundus 0-67184
spot scanning system for proton radiotherapy 0-89836
SQUID detection, low temp., NMR imaging improvement towards mol.
kinetic meas. 0-104723
SQUID fluxgate magnetometers, magnetopneumographic meas. 0-104711
SQUID gradiometer, second-derivative, magnetocardiogram meas.
0-104696
step length measurement apparatus 0-67271
stereopsis clinical test 0-61566
stereoscopic X-ray unit for medical diagnostic sets 0-85467
stereovision techniques for diagnosis (*Japanese*) 0-67279
stethophonendoscopes, design and production 0-104686
still-shade-temperature meter for use in assessing personnel cold stress
0-81764
stimulated Raman scatt. Dewar cell 0-99799
stress/duress automated detect. system 0-76852
strobe-sequenced device to facilitate 3D viewing of cross-sectional images
0-104720
superconductive helmet with SQUID for magnetoencephalography
0-104708
supraventricular arrhythmia rapid anal. from long-term oesophageal
recordings, drug assessment 0-89904
switch valve, lightweight, remotely actuated, for rebreathing exercise studies
0-101278
tape recorders, correction of timing errors due to tape speed variation
0-72354
telemetry device, chronically implanted, controlled transcutaneous power-
ing 0-98152
telemetry system synchronisation, with time division of channels 0-94386
temperature biotelemetry, modular, expandable, implantable 0-67191
tethered float radiometer for US therapy equipment output power meas.
0-104691
text-to-speech synthesizer for blind and handicapped 0-96142
TGM-1 multidirectional tomograph, operating characts. 0-104726
thermal entrainment device for cardiovascular investigation 0-104793
tissue-equivalent compensators for 4-MV X-rays, basic data 0-98069
tomography, single photon emission, camera configs., performance anal.
0-61686
tomography simulator, emission computed, design 0-61672
transducer for non-invasive intracranial pressure meas. in newborns
0-67272
transverse axial film tomography with a therapy simulator 0-81716
US B-scan imaging with automated water-delay system 0-98041
US dynamically focused electronic sector scanner based on CCDs
0-98042
US echolocating blind mobility aid, interpretation of stereophonic output
0-108989
US phantoms, water-based gels 0-81671
US probes, power meas. by use of semiconductor strain gauges 0-87679
US real-time scanner with pulsed Doppler and T-M facilities, obstetrical
appls. 0-67172
US system for blood press. anal. during treadmill stress testing 0-81674
US system for left ventricular function quantitative evaluation 0-85457
vectorcardiographic microprocessor system (*Bulgarian*) 0-61722

biomedical equipment continued

ventricular function monitor, ambulatory, CdTe detector, cardiac ejection
fraction meas. 0-61680
visual acuity screens, reflectance obs. 0-67178
whole-body NMR imaging machine 0-101285
Wisconsin mammographic kVp cassettes, evaluation of spectral response
0-81715
X-ray collimators, semi-automatic and automatic, manufactured by
Medcor Works 0-85475
X-ray equipment, state of the art 0-81688
X-ray image intensifier noise evaluation, digital method 0-98097
X-ray image storing equipment of Medcor Works 0-85476
X-ray intensifying screen, role of reflective layer 0-62816
X-ray spot-camera of Medcor Works 0-85477
X-ray tube, new type, Super Rotalix Ceramic 0-104749
X-ray XX 0-98091
CSF detector, positron emission tomography 0-61688
CdTe matrix γ -camera 0-76827
CsF scintillator, pot. advantages for a time-of-flight positron camera
0-81706
Hgl₂ detectors for X-ray 0-89837
NaI crystals, used in nuclear medicine, determ. of cause of breakage
0-98077
NaI(Tl) scintillation cameras, image artifacts and counting losses
0-94345
PdO-Pd miniature pH electrode for blood and extracellular fluid pH
meas. 0-89886
Si diaphragm pressure sensor, integrated signal conditioning 0-76859
¹³³Xe charcoal traps, simple leak tests, nuclear medicine appl. 0-104734

biomedical measurement

see also biological techniques and instruments; biomedical equipment;
electrocardiography; electroencephalography; radiography; X-ray appar-
atus
aortic valve replacement, computerised simultaneous press./vol. anal.
before and after 0-85531
biomagnetic measurement facility installation in hospital environment,
design criteria and procedure 0-104707
biomagnetic measurements in unshielded and noisy environments
0-104710
biostereometrics, automatic iconics meas. system 0-67214
blood, normal and pathologic, NMR T₂ relax. time studies 0-81682
blood flow, regional, assessment by intravenous injection of ^{99m}Tc pertech-
netate 0-104732
blood flow detection in human heart, US pulsed Doppler flowmeter
system, microcomputer based 0-104690
blood flow measurement, UDP-30 arterial US pulse Doppler flowmeter
0-104805
blood flow measurements by NMR of the intact body 0-81680
blood intravascular mean vel. meas. using crosscorrel. technique 0-81763
blood O₂, meas. by fast-responding flow-independent blood gas catheter
0-101277
blood perfusion rate estimation from diffusible indicator meas., sensitivity
anal. 0-104803
blood pressure, human, noninvasive meas. (*Japanese*) 0-94395
blood pressure, indirect meas., meaning of max. oscills. point in cuff press.
0-94396
blood pressure measurement with portable systems using Korotkov sounds,
meas. accuracy 0-76855
blood pressure recording, simple method for fidelity improvement, Korot-
koff sounds 0-76811
bone, mineral content, coherent scatt. of photons 0-67238
bone blood flow, meas. with a ¹³³Xe washout method 0-72288
bone mechanical properties characterisation by dynamic response
0-76782
brain, mag. evoked field mapping 0-104705
brain, magnetoencephalogram power spectrum estimation 0-104704
capillary blood flow, dual beam laser velocimeter anal. 0-75015
cardiac mechanical activity, noninvasive mag. detect., instrumentation
0-89820
cardiac mechanical activity, noninvasive mag. detect., theory 0-89819
cardiology, radioisotope sequential meas. of ventricular vols. and cardiac
output 0-94319
cardiomagnetism, high resolution 0-104698
carotid back pressures in conjunction with cerebral angiography 0-98119
catheter pressure meas., transducer smearing correction using microproces-
sor based discrete deconvolution 0-67275
cell membrane particle diameters meas. by computer from electron micro-
graphs 0-101307
chopping pyrometer for remote meas. below 200°C (*German*) 0-86313
chromoretinotomography and its instrumentation 0-94201
cineangiography, left ventricular contour segmentation from anatomical
landmark trajectories and its application to wall motion analysis
0-94363
coronary artery quantitation using digital image processing techniques
0-85517
critical light reflection at a plastic/glass interface and appl. to foot press.
meas. 0-81681
deep-body venous and arterial press. meas., monolithic capacitive trans-
ducers 0-67274
dielectric props. of biological substances, physical meas. 0-94417
drug radioreceptor analysis applications 0-94315
ear static acoustic-immittance measurements 0-76758
electrical conductivity and permittivity imaging, computed tomography
technique 0-98055
electromyogram, muscle electrical impulses provide audible or visual
indication using biofeedback 0-81782
electronic speckle pattern interferometry used to meas. eardrum vibrs. and
other biol. movements 0-67209
EMG silent period measurement, automated system 0-89883
eye, retina injuries, magnetoretiographic meas. using SQUID magne-
tometer 0-104702
eye chromatic aberration meas. with chromoretinotomography 0-81581
eye chromatic aberration rel. to accommodation, meas. using dynamic
laser speckle pattern 0-81582
eye movement evaluation in target tracking using EOG 0-109057
facial skeleton strain distrib. arising from orthodontic appliance activity,
holographic interferometry 0-67143
faecal samples, Ca determ. method using instrumental fast neutron activa-
tion anal. 0-104733

biomedical measurement continued

- femoral neck fractures, meas. of fissure, X-ray picture anal. (*Croatian*) 0-109023
- femur, human, pulse-echo technique for US vel. meas. in vivo 0-89812
- foot load dynamic distrib., quantification system 0-94388
- foot load static distrib., quantification using the PET computer 0-94387
- foot pressure distributions, technique for display 0-85508
- foot-pressure measurements, static and dynamic, in clinical orthopaedics 0-98163
- force measurements during operative correction of spinal deformities 0-76861
- gait, automatic 3D anal. using a Selspot centred system 0-108998
- gait assessment using components of the ground reaction force vector 0-101284
- gait measuring system for treatment evaluation, microprocessor controlled 0-61731
- galvanic skin response meter cct. using bipolar transistors 0-72380
- glomerular filtration rate meas., comparison of 4 commercial preps. of $^{99m}\text{Tc}(\text{Sn})\text{DTPA}$ 0-81704
- gonioscopic method for grading of the anterior chamber angle 0-108993
- haemoglobin- O_2 equilibrium curve, instrument for determ. based on membrane diffusion 0-81761
- hearing aid assessment and fitting by free field pure tone audiometry 0-108983
- holographic interferometry, rigid body motion compensation 0-67213
- holographic interferometry in dentistry 0-67203
- holography, conf., Munster, Germany (Mar. 1979) 0-62390
- human serum, definitive meas. of constituents 0-93818
- intracranial pressure and its epidural meas. 0-101282
- intracranial pressure meas. in newborns, new non-invasive technique 0-67272
- ion-selective electrodes for determination of urine-electrolytes (*German*) 0-94384
- IR back-scattered from vaginal tissue, self-stabilising meas. system 0-72281
- IR spectrometric method for meas. of slight heavy water enrichment in natural water (*French*) 0-104718
- kinematic gait, system for simple meas. 0-85509
- lactate dehydrogenase, H-forms, radioimmunoassay 0-67219
- laser applications, review (*Japanese*) 0-94311
- left ventricular wall motion determined by echocardiography in elderly subjects 0-98039
- light level measurement using photographic meters 0-94304
- lipid malabsorption, study by meas. of expired $^{14}\text{CO}_2$ (*French*) 0-94350
- liver functional reserve capacity meas. by organ-reflectance spectrometry (*Japanese*) 0-94313
- lung, mag. field meas., comparison between two methods 0-104712
- lung circulation, density dilution method appl. to obs. of fast osmotic fluid shifts 0-104781
- lung density, Compton scatt. meas., multiple photon interactions 0-67146
- lung nuclei, mean caliper diameter, method independent of shape assumptions 0-98189
- lung volume, online calc. by digital computer 0-72351
- lung volume measurement from supine portable chest radiographs 0-81703
- lungs, freeze-dried, localised-field magnetopneumographic meas. 0-104714
- magnetic heart vector components, simultaneous meas. with unipositional lead system 0-104697
- magnetocardiogram and cardiac output meas. with integrated system 0-104709
- magnetocardiogram enhancement by applied mag. field 0-104701
- magnetoencephalography, sensitivity distrib. 0-101246
- magnetopneumography, analytic methods 0-104713
- magnetopneumography, evaluation for assessing thoracic accumulation of welding fume particulate 0-101247
- mass spectroscopy, continuous in vivo meas. (*Japanese*) 0-94309
- median nerve, transient responses to elec. stimulation, SQUID appl. to somatically evoked field meas. 0-104706
- microwave measurements (*Japanese*) 0-94314
- moire contourgraphy, computer-aided replication of human anatomy 0-67189
- moire topography, devel. and present status 0-63960
- mucoiliary tracheal clearance vel., radiological method for determ. 0-104727
- neuromagnetic fields sources location, using SQUID system, comparison with electrical method 0-101190
- neutron activation anal., Cd conc. in kidney and liver, organ depth determ. 0-72321
- neutron capture γ -spectroscopy, medical appl., Cd and N meas. in living human subjects 0-67241
- NMR imaging, H tomography and pot. for imaging other body constituents 0-98062
- nystagmus, automatic on-line anal. (*German*) 0-76846
- ocular position determination for communications system, IR system 0-76821
- oesophageal manometry by liquid-filled catheters 0-85514
- organ blood flow measurements, effect of instantaneous partition coeff. of Xe 0-101256
- orofacial posture and movement, photo-elec. recording method 0-108995
- orthopaedic applications of holography 0-67196
- orthopaedics, exptl., quantitative eval. of holographic deform. investigations 0-67197
- orthopaedics, grating-TV method, image evaluation using moire figures 0-67199
- pacing, meas. of ohmic electrode-tissue contact resistance and voltage applied to myocardium 0-67284
- pathological samples, mol. microanal. in situ with laser-Raman microprobe 0-81683
- patient's surface contour measuring device 0-104717
- photoluminescent thermometer probes, temp. meas. in microwave fields 0-104721
- piezoelectric earphones, usefulness in recording brain stem auditory evoked pots. 0-94389
- PIXE, biomedical appls. 0-61691
- placenta, human, detect. of pulsatile flow in situ by impedance meas. 0-104799
- pneumodynamic MEFV curves, smoothing by digital filtering 0-98157
- pressure recording apparatus for hydrostatic press. changes during dowel-retained prostheses cementation 0-67287

biomedical measurement continued

- prostatic acid phosphatase, human, development of determ. by radioimmunoassay (*Japanese*) 0-98110
- prosthesis wear, holographic studies using optical contouring 0-67288
- pulmonary blood flow, method for noninvasive bedside determ. 0-81762
- pulmonary pressure-flow curves measured by a data-averaging circuit 0-61725
- pulse-wave velocity measurement in humans (*German*) 0-81751
- quantitation of infarct size using radionuclides 0-85492
- radiation meas. bibliography (1972-76) (*German*) 0-95510
- radioactive depositions, shallow, on body surfaces, meas. using M X-rays 0-67223
- radioisotope counting techniques for analytical appls. in biology and medicine, review 0-81794
- radioimmunoassay, review, book contrib. 0-109021
- reaction timer cct., using bipolar transistors and LEDs 0-81781
- renal uptake measurements using $^{197}\text{HgCl}_2$, single tracer method for background subtraction 0-67217
- respiratory process parameters determ., air flow consumption meas., using electric model (*Bulgarian*) 0-76867
- respiratory sounds meas., laser vs. acoustical methods (*German*) 0-98058
- respirometric open systems, error anal. (*German*) 0-104782
- rheoencephalographic curves, bipolar and tetrapolar techniques, comparison (*Croatian*) 0-104796
- rheograph linear-distortion estimation 0-85502
- ring-core magnetometer sensor for articulatory meas. of jaw movements 0-101243
- sandwich holography and applicability biomedical investigations 0-67211
- SEM cathodoluminescence appls. 0-72400
- serum, human, trace elements determ. by proton activation 0-81731
- serum thyroxine, radioimmunoassay by the antibody-coated test tube method (*Japanese*) 0-67237
- serum-electrophoresis, quantitative, by digital picture processing (*German*) 0-94306
- shearing forces on the sole of the foot, meas. system 0-72342
- SI units and legislation in medical measurements (*Croatian*) 0-104797
- skin perfusion, quantitative meas. with ^{133}Xe 0-81707
- skull and auditory ossicle vibr. anal., human preps., using holographic interferometry 0-67210
- soft tissues, human, rheological props. from local cyclic loading method 0-108932
- soft tissues, human, rheological props. investigation using elastography 0-108933
- speech analysis, children, improved spectrogram 0-94238
- speech reception threshold, reliability in the determ., psychometric function 0-61657
- SQUID fluxgate magnetometers, magnetopneumographic meas. 0-104711
- SQUID gradiometer, second-derivative, magnetocardiogram meas. 0-104696
- step length measurement apparatus 0-67271
- stereophotogrammetry, meas. of deforms. in human body (*Croatian*) 0-108997
- superconductive helmet with SQUID for magnetoencephalography 0-104708
- susceptometer, Fe stored in human tissue meas., in vivo 0-101245
- synovial fluid analysis by ferrography 0-101242
- teeth and mandibles, deforms. due to occlusal forces, holographic interferometry 0-67205
- temperature, human body-temp. sensor-environment system, analogue model of interaction 0-104783
- thermoelectric needle probe for medical and biological temp. meas. 0-101299
- thermometry, use of salt-hydrate transition temps. as fixed points 0-104801
- thyroid ^{131}I uptake determination (*Hungarian*) 0-94339
- thyroid function radioimmunoassay, quality control, computer program (*French*) 0-94348
- thyroxine, free, radioimmunoassay for quantitative meas. of serum conc. 0-94344
- tibia, human, simplified method of radiographic anal. of its cross-section, anthropometric correls. 0-89827
- topographical mapping of the human face by Moire photography 0-85462
- transducers and measurements, review (*Japanese*) 0-94393
- tumour blood flow, meas. by photon activation, ^{15}O decay technique 0-104755
- tympenic membrane investigations in living man using holographic interferometry 0-67207
- tympenic membrane vibr. studies in living man using holographic interferometry 0-67208
- urinary bladder interferometry, holography of bladder deforms. in vitro, rabbit expt. 0-67201
- urinary bladder interferometry, tumour and lesion detect. by holography 0-67202
- urinary tract infections, radiorespirometric testing of antibiotic sensitivity 0-81705
- US renal volumetry in children, accuracy and simplicity of the method 0-98044
- vibration waveform measurement using temporally modulated holography 0-67212
- visual evoked cortical potential meas., signal optimisation using Kalman filter (*Japanese*) 0-72348
- visually evoked response, simultaneous recording to flashes at different retinal locations. 0-72279
- vocal fundamental frequency measurement, comparison of contact microphone and electroglottograph 0-109056
- volume estimation algorithm based on polyhedral approx., using US or CT data 0-104790
- wheelchair locomotion, power output requirements for manual operation 0-94416
- Cd, organ tissue levels, in vivo meas. system using neutron activation 0-67224
- ^{125}I in the thyroid, 2-probe meas. method 0-81718

biomedical phenomena

- see also *biomagnetism*
- aerosols, biomedical influence, conf., Dusseldorf, Germany (Oct. 1979) 0-94915
- red cell membrane, Li transport in manic depressives 0-61525

biomedical ultrasonics

- A-mode ultrasonography and oculometry in retrolental fibroplasia 0-89816
 Aberdeen phased array, real-time US scanner with dynamic focus 0-72276
 acoustical imaging, US visualization and characterization, conf., vol.8, Key Biscayne, FL, USA (May-June 1978) 0-83720
 anatomical feature or lesion volume estimation algorithm 0-98080
 automated system for absorption coeff. meas. in tissue using transient thermoelectric techniques 0-76817
 B-mode images of human tissue, real-time speckle reduction 0-74634
 B-scan imaging, pancreas scans of cystic fibrosis sufferers, amplitude anal. 0-94302
 B-scan imaging, theory of image formation, technique for restoration 0-94300
 B-scan imaging with automated water-delay system 0-98041
 B-scan US, technical factors influencing the imaging of small anechoic cysts 0-98049
 B-scanning, computer simulation 0-81675
 bibliography from 1971 0-98769
 bibliography from Jan. 1971 0-86053
 bibliography of diagnostic uses of US in medicine and biology 0-62407
 blood, Doppler-shift waveforms, physiological interpretation 0-89814
 blood flow detection in human heart, US pulsed Doppler flowmeter system, microcomputer based 0-104690
 blood pressure analysis system for treadmill stress testing 0-81674
 bone, US velocity meas. in temp. range of room temp. to 90°C 0-76787
 broad-band echo characterization, unified method for diagnostic US 0-104687
 cardiac function and anatomy evaluation, complementary role of echocardiography and radionuclide imaging, book contrib. 0-101241
 cardiac US and nuclear medicine, complementary roles 0-98051
 cine display of numerous static US images 0-108984
 computer analysis of US signals in diffuse liver disease 0-67173
 CW measurement method for US velocity in small biological tissue specimens 0-76786
 cylindrical transducer scatter scanner for medical ultrasonographic imaging 0-96154
 data recording method using videotape (*German*) 0-81666
 diagnostic imaging, prospects and limitations 0-98040
 diagnostic imaging, transducer field intensity distribution meas., liquid-surface relief method for pulsed transducers 0-95073
 diagnostic pulse-echo US, inhomogeneous media model for determination of acoustic parameters in tissues 0-108981
 diffraction tomography, experimental results 0-76818
 Doppler diagnostic technique of carotid artery disease, objective feature extraction 0-72273
 dynamically focused electronic sector scanner based on CCDs 0-98042
 echo-tomographic imaging with SAW processing, ultrafast 0-74639
 echocardiogram, M-mode, automatic computer anal. (*Japanese*) 0-72274
 echocardiograms, 1D and 2D, computer processing (*German*) 0-81665
 echocardiograms, computer assisted left ventricular anal. (*German*) 0-81667
 echocardiograms, M-mode, microcomputer editing for semiautomatic anal. 0-94299
 echocardiograph signals, M-mode, analogue storage using video tape 0-94298
 echocardiographic images, video recorded, interactive segmentation 0-89817
 echocardiographic tracking system, microprocessor-controlled 0-67169
 echocardiography, clinical significance (*German*) 0-81664
 echocardiography, contrast cross-sectional (*Japanese*) 0-101237
 echocardiography, high-resolution, computerised US signal processing 0-76814
 echocardiography, pulsed Doppler, variable sample vol. dimension 0-76816
 echographic phased array for medical diagnostics, dynamically focused insonification 0-89813
 echolocating blind mobility aid, interpretation of stereophonic output 0-108989
 Echosimulator, function generator for meas. of US diagnostic equipment characts. (*German*) 0-104685
 femur, human, pulse-echo technique for US vel. meas. in vivo 0-89812
 fluid characterisation by US and computed tomography 0-98045
 foetal growth estimation from US image meas. 0-101239
 gallstones, acoustic shadow formation 0-98047
 heart diagnosis, using two dimensional real-time sector scanning facilities 0-81672
 hepatic metastases, γ -scan accuracy for detect., comparative study with grey scale ultrasonography (*French*) 0-104741
 holographic in medicine and biology, state of art and future 0-67175
 hyperthermia, localised, comparison of EM and US diathermy 0-104725
 hyperthermia, localised, design of heating protocols 0-104693
 image quality with US arrays for real-time diagnostics, artefacts (*German*) 0-61656
 imaging, conference, San Diego, USA (Aug. 1979) 0-94919
 imaging, piezoelectric micro-array technology for improved image quality (*German*) 0-98052
 imaging modalities for medical appls. 0-81669
 imaging overview 0-98082
 imaging system for chest and other body organs 0-67174
 imaging techniques including use of US scanner 0-72388
 implantable bidirectional pulsed Doppler US blood flowmeter, timing and signal processing ICs 0-76812
 Indian status in 1979, industry and medicine appl. 0-81668
 intracranial pathology in infants, US evaluation, new technique 0-98046
 intraoesophageal imaging, heart dynamics 0-94303
 larynx height and vocal fold vibratory pattern meas 0-98184
 left ventricular function quantitative evaluation by 2D ultrasonography system 0-85457
 left ventricular wall motion determined by echocardiography in elderly subjects 0-98039
 liver, human, scattering structure theoretical modelling 0-89785
 liver pathology characterisation, clinical appl. of a US attenuation coeff. estimation technique 0-76813
 lymphocyte cell DNA damage by US diagnosis 0-67148
 mammographic US image correlation with histopathologic sections 0-101240
 mammography, remote focus arc scanning 0-89815
 mastodynia and ultrasonography 0-85456
 measurement appls. (*Japanese*) 0-89811

biomedical ultrasonics continued

- membrane hydrophobe for 0.5 to 15 MHz range, press. meas. in US fields 0-108987
 multidimensional space and time signal processing in biology and medicine 0-85493
 multielement acoustic array characterisation by acousto-optic diffraction 0-99911
 neonatal peripheral circulation, human, characterisation by US pulsed Doppler technique 0-76815
 obstetric practice, the place of real-time and static B-mode scanning, educational syllabus 0-86057
 obstetrics and gynecology, safety and pot. hazards, review 0-67170
 ophthalmic diagnosis, use of US 0-81673
 organ-puncture needles, US wave propag. in needle and tissues 0-96052
 phantom for imaging biological fluids by US and computerised tomography scanning 0-104692
 phantoms, water-based gels 0-81671
 polarity estimation for reflected echo in ultrasonotomography 0-108986
 probe power meas. by use of semiconductor strain gauges 0-87679
 pulse echo system using interaural localization 0-89769
 pulse echo waveform rel. to acoustic characteristics of continuous medium 0-67145
 real-time scanner with pulsed Doppler and T-M facilities, obstetrical appls. 0-67172
 renal volumetry in children, accuracy and simplicity of the method 0-98044
 scattering by single objects 0-99892
 shadowing due to calculi and gas collections, differentiation 0-98048
 skull bones, human, US flexural wave study 0-72277
 spherically curved transducers, anal. of focusing action 0-64332
 spread energy method, use of time gain control 0-108988
 stochastic noise influence on perceived image 0-98053
 tethered float radiometer for US therapy equipment output power meas. 0-104691
 tissue characterization in vivo, broadband integrated backscatter 0-74635
 tissue identification, conf., London, England (Apr. 1980) 0-98757
 tissue quantitative characterisation, review 0-81670
 tissue structures characterisation, method of obtaining an acoustic impedance profile 0-67171
 tooth blood supply determination, US CW Doppler appl. 0-104684
 transmission media for ultrasonography 0-98050
 transmission tomography 0-94301
 transmitters and receivers for medical ultrasonics 0-76819
 two-dimensional echocardiographic images enhancement by lateral filtering 0-81677
 ultrasonographers, pot. hazard from previously administered radionuclides 0-98120
 ultrasonography, computer method for axisymmetric transducers with various boundary conditions 0-87591
 US Doppler returns from foetal heart, processing, valvular timing information extraction 0-101238
 US imaging, improvement of sensitivity or reduction of dose 0-74641
 venous flow, mech. oscills., ultrasonic Doppler study 0-108931
 ventricle, left, human, 3-D time-varying reconstruct error sources and magnitude estimation 0-85454
 volume estimation, computer algorithm 0-98043
 volume estimation algorithm based on polyhedral approx., using US or CT data 0-104790
 PVF₂ polymer probe for mapping pressure field from arrays 0-74669

biomembrane transport

- see also osmosis*
 albumin flux, differential permeability of endothelial and epithelial barriers, sheep expts. 0-81553
 amphipathic apolipoprotein ApoC-III bound to phosphatidylcholine bilayers, lateral mobility 0-97884
 artificial membranes, transport regulation by environmental H⁺ conc. 0-89725
 asymmetrically permeable membrane channels in cell junction 0-94187
 autorhythmicity and entrainment in excitable membranes 0-108866
 axonal membrane of mammals (myelinated fibres), K channel conduction 0-61538
 axons, giant, squid, interaction of Ba²⁺ with K⁺ channels 0-85379
 bladder, toad, temp. dependence of ADH-induced water flow and intramembranous particle aggregates 0-61520
 brown adipose tissue mitochondria, increased proton cond. pathway rel. to diet-induced thermogenesis 0-89722
 cellular testing potential, membrane pot. rel. to ionic diffusion (*French*) 0-94184
 colon, turtle, active Na transport via an electrogenic Na-K exchange pump 0-108856
 conductance channels, current-induced coupling, multi-channel interaction and mean field cond. 0-67063
 cone outer segments, light-induced changes in membrane current, tiger salamander and turtle 0-108899
 diffusion measurement by fluorescence photobleaching recovery method, bleaching light effect 0-94434
 egg cell membranes, starfish, inward rectification blocking model 0-61523
 electrogenic ion transport along oligomer channels capable of conformational transitions 0-108854
 electron and proton transport 0-67052
 erythrocytes, rabbit, increased passive efflux of ²²Na and ⁸⁶Rb on microwave irradiat. 0-108957
 flexural fluctuations and non-equilib. noise 0-76712
 glomerular permeability in foetal rabbit 0-85372
 gramicidin single-channel currents, rate theory calc. using NMR-derived rate consts. 0-94186
 integral proteins, mobility increase in spherocytic erythrocytes obs. 0-81569
 intestinal membrane transport of oligopeptides, intracellular study of underlying ionic events 0-104572
 ionic current in excited membrane, automated meas. of electrophysiological characts. (*Russian*) 0-76865
 lateral diffusion calcs. for membranes containing cholesterol 0-85356
 lateral diffusion on a spherical surface, normal mode anal. 0-61518
 lipid bilayer membranes, spectrophotometric and elec. correls. of cyanine-dye adsorpt. 0-85358
 lipid bilayer membranes, steady-state permeability behaviours induced by cyanine dyes 0-85357
 membrane charge transfer, possible role of α -helical proteins 0-81524

biomembrane transport continued

- nerve excitation, gating currents and dipole transitions 0-67056
- nerve fibre membrane analogue-code conversion, ionic mechanisms 0-81575
- nerve fibre membrane Na permeab. reversible blockage by increase in temp. of medium above 45°C 0-81576
- nerve membrane, excitability, genetic alteration, temp.-sensitive paralytic *Drosophila* mutants 0-97895
- nerve signals, dipole theory of interactions 0-81574
- neuron input current, *Helix pomatia*, rel. to membrane pot. and extracellular Sr and Ca ion concs. 0-81577
- neuron membrane, design of a single electrode voltage clamp 0-72385
- nexus, evidence for fixed charge, permeability, obs. 0-94193
- Paramesium excitation, model anal. 0-61524
- physiology, flow problem, one tube 0-89703
- plasmalemma of *Nitella flexilis*, selective centres of excitable channels of early ionic current 0-81568
- Porphyra osmoregulation, struct. aspects 0-85370
- protein kinases, cAMP-depend., membrane-localised, and regulation, of slow inward current, frog heart 0-81567
- proteins involved in active membrane transport, struct. review, book contrib. 0-108844
- proton transport across charged membrane and pH oscillations 0-61516
- purple membrane of *Halobacterium halobium*, quantum efficiency of proton pumping 0-72140
- pyrene, migration between lipid vesicles in aq. soln., fluoresc. stopped-flow obs. 0-85360
- red cell, human, increased passive permeability below 12°C 0-94185
- red cell membrane, Li transport in manic depressives 0-61525
- reptile epidermis, water permeability rel. to lipid content 0-97875
- sarcolemmal permeability changes during early myocardial anoxia 0-85371
- sarcoplasmic reticulum membranes, temp.-dependent functional changes 0-81550
- single-file model of ion transport, predicted current rel. to internal state transitions 0-85359
- substrate exchange between vascular and extravascular compartments, saturation kinetics 0-104571
- taste reception, physicochem. mechanism and chem. sensors development (*Japanese*) 0-85423
- tissues, excitable, dipole flip-flop theory for excitation and conduction 0-101153
- tracheal epithelium, dog, interdependence of Na⁺ and Cl⁻ transport 0-61519
- water transport, NMR methods (*Rumanian*) 0-94435
- Ca²⁺, passive and active fluxes across membranes, review 0-97886
- K⁺ currents in squid axons, single channel recordings 0-76721
- Na⁺ intracellular activity rel. to Na⁺ transport across a tight epithelium 0-67051
- Na⁺ saturation kinetics in frog skin, compartmental aspects 0-67050

biomembranes

- see also *biomembrane transport; lipid bilayers*
- n-alkanes, adsorption into bimolecular lipid layers 0-88435
- animal plasma membranes, study using freeze-fracture technique 0-104842
- ATPase, Ca²⁺-activated, of sarcoplasmic reticulum, rot. motion and evidence for oligomeric structs. 0-72124
- bacterial cell wall, surface charge and morphogenesis of regular arrays of macromols. 0-85366
- bacteriorhodopsin, photoelec. conversion in charged synthetic membranes 0-108954
- bacteriorhodopsin membrane preps. associated with lipid-water interface, form. of elec. pot. diff. 0-81551
- bilayers quasitwo dimens., theoretical models 0-76713
- bimolecular membranes, interaction with liposomes, elec. resistance obs. 0-81549
- cell membrane particle diameters meas. by computer from electron micrographs 0-101307
- cell membranes, at mol. resoln., introduction 0-104841
- chromophores in membrane suspensions, determ. of orientational order, intensity depend. of flash-induced anisotropy 0-94177
- current pulse-induced voltage variations in bilayer membranes, apparatus 0-94420
- cytoplasm spherical drop with effective surface tension influenced by oscillating enzymatic reactions 0-108862
- DECHEMA symposium, Tutzing, Germany, (Mar. 1978) 0-62373
- cardrum vibration meas. using electronic speckle pattern interferometry 0-67209
- E. coli*, radiation killing, role of membrane fluidity, hypothermia and local anaesthetics 0-104653
- electric properties measurement method using glass electrode impaled into single cell 0-89916
- electrically excited, nonlinear dynamic models for simulation 0-94178
- electron microscopic analysis at mol. level resolution, prep. procedures 0-104843
- energetics, conf., Bloomfields Hills, USA (Jul. 1979) 0-94923
- erythrocyte membrane alterations, rheological technique evaluation 0-61611
- erythrocyte membranes, fluidity change after X-irrad., pyrene excimer fluoresc. obs. 0-72262
- erythrocyte membranes, US absorpt. in 12 to 68 MHz range 0-89727
- fluidity modification, mechanism of hyperthermic cell killing and therapy appl. 0-104569
- fluorescence spectroscopic investigations of the dynamic properties of proteins, membranes and nucleic acids 0-101148
- H. halobium*, light-induced surface pot. changes in purple membranes and bacteriorhodopsin liposomes 0-98015
- hearing mechanism, tympanic membrane vibr. anal., holographic interferometry obs. 0-76879
- IR-ATR spectroscopy, appl. to struct. investigation of biological material in aq. environment 0-61735
- librational motion effects on fluoresc. depolarisation and NMR relax. in macromols. and membranes 0-85324
- lipid bilayer couple, cation-phospholipid-induced shape changes 0-108855
- lipid bilayers, elastic props. changes on exposure to different agents, elec. and chem. 0-81548
- lipid hydrocarbon chain, biomembrane, rot. motion and fluidity 0-76714
- lipid thermotropic clustering in *Tetrahymena* endoplasmic reticulum membranes 0-85363
- lipids, free radical formation on UV irrad. 0-81647

biomembranes continued

- liver membranes, mouse, X-irrad., dose-rate effects 0-94293
 - macromolecular systems, statistical thermodynamic analysis, heat capacity function 0-61514
 - mesomorphic monolayers, quasitwo dimens., theoretical models 0-76713
 - milk fat globule membrane, cryst. struct. 0-85364
 - mitochondrial complex III membranes preps., cryst. struct. 0-85365
 - multilayer arrays, surface-induced lamellar orientation, theory and method 0-89724
 - multiple steady states and solution of irreversible phase transitions with enzyme controlled membranes 0-108857
 - nerve cell membrane detection of HF EM fields, possibility discussion (*Russian*) 0-76785
 - nerve impulse encoding, elec. processes 0-76718
 - nerve membrane, electrostatic plasma probe physical analogue 0-79573
 - Nitella*, fluctuation and instability in membrane pot. near threshold 0-89723
 - nonpolar molecules, adsorption into lipid bilayer membranes 0-61517
 - otolith membrane, variable gravity model 0-85573
 - phosphatidylcholine bilayers, fluidity changes and phase transitions, intramol. excimer fluoresc. obs. 0-85342
 - phospholipid bilayers, carbonyl groups dynamics, ¹³C chem. shift anisotropy obs. 0-85326
 - photoreceptor membrane interfacial pots., light-induced 0-72161
 - photoreceptor membranes, incorporation into a multilamellar film 0-89907
 - photosynthetic membranes, functional processes, polarisation effects 0-67045
 - photosynthetic processes, electron conformation interactions 0-94183
 - protein membrane multilayers, thickness depend. of props. 0-89726
 - purple membrane, electron microscopy of frozen hydrated crystalline specimens, meas. and reduction of damage 0-85552
 - purple membrane, orthorhombic 2D crystal form 0-85362
 - purple membrane fragment suspensions, elec. dichroism obs., trimer model interpret. 0-89728
 - R. sphaeroides, polarisation of photosynthetic membranes and reaction centres in elec. field 0-94277
 - red blood cells, minimum energy anal. of membrane deform. 0-72141
 - red cell membrane, human, surface elasticity and viscosity 0-61608
 - reptile epidermis, water permeability rel. to lipid content 0-97875
 - rigidity increase of material of bioconstructs. during morphogenesis 0-94249
 - sarcoplasmic reticulum membranes, small angle X-ray data processing 0-81536
 - secretory granule membrane, particle clustering induced by centrifugation, freeze-fracture anal. 0-85559
 - structural order of lipids and proteins, fluoresc. anisotropy data eval. 0-97873
 - surface charge visualisation using SEM 0-85566
 - surface conditions simulation, relative compatibility of amino acid residues at interface 0-71951
 - synaptic vesicles and synaptosomal membranes, electrokinetic props. 0-67055
 - thylakoid membranes of wheat chloroplasts, proton spin-lattice relax. time, -8°C phase transition 0-108853
 - tympanic membrane investigations in living man using holographic interferometry 0-67207
 - tympanic membrane vibr. studies in living man using holographic interferometry 0-67208
 - vaginal mucosa, radiation tolerance obs., 0-104666
 - vesicles, large, anal. of adhesion to surfaces, expt. procedure 0-109063
 - X-irradiation, vitamin E deficiency and lipid peroxidation, mouse obs. 0-72263
- biomolecular effects of radiation**
 see also *biological effects of ... (type of radiation)*
 see also *photosynthesis*
- N-acetylglycine, X-irrad., stable radical electronic and mol. struct., ENDOR and ESR 0-80637
 - adenine, nucleic acid component, selective action by ps light pulses 0-72213
 - adenovirus, decreased repair after γ-irrad. when infecting Xeroderma pigmentosum fibroblasts 0-61650
 - allophycocyanin solutions from F-diplosiphon, photoreversible absorbance changes 0-97862
 - amphiphatic apolipoprotein ApoC-III bound to phosphatidylcholine bilayers, lateral mobility 0-97884
 - bacteriophage S13, lethal effect of ³²P transmutation, mech. of DNA double helix rupture (*French*) 0-98018
 - bacteriophage T1, killing by irrad. in dry state with 122 nm and 254 nm light 0-101234
 - bacteriorhodopsin chromophore, light-induced isomerisation 0-108956
 - catalase, glucose embedded, measurement and reduction of radiation damage in frozen hydrated crystalline specimens 0-89810
 - cell surface anisotropic molecular motion, photobleaching 0-97883
 - chlorophyllide fluorescence quantum yield during photochlorophyllide reduction in etiolated leaves 0-81542
 - chromatin from cultured mammalian cells, radiolysis, DNA-protein cross-links formation 0-81655
 - conference, Rotterdam, Netherlands (Aug. 1980) 0-105425
 - cytochrome c, effects of UV and temp. on optical props. and enzymatic activity 0-81648
 - deoxyribonuclease I in aq. soln., inactivation by thermal neutrons 0-104664
 - DNA, calf-thymus and superhelical PM2 aq. solns., electro-optic obs. of γ-irrad. damage 0-85452
 - DNA, properties changes caused by UV- and γ-irrad., electrochem. anal. 0-72271
 - DNA, radiation induced mol. size change, electron irradiated, effect of p-nitroacetophenone 0-89807
 - DNA, radiation-induced strand breaks in deoxygenated aq. solns. 0-61649
 - DNA, thymine base damage release, γ-irrad. *Tetrahymena pyriformis* 0-72268
 - DNA light induced diffusion in solutions due to laser cutting (*Russian*) 0-81646
 - dye proflavine bound to synthetic polynucleotides, selective laser photodamage 0-99525
 - electron microscopy of frozen hydrated crystalline specimens, meas. and reduction of damage 0-85552

biomolecular effects of radiation continued

- fibrinogen, bovine, high energy-induced aggregation, time resolved spectra 0-61655
 5-fluorocytosine, electron beam damage assessed by EELS 0-89809
 immunoglobulin, human, high energy-induced aggregation, time resolved spectra 0-61655
 o-iodotyrosine, intramol. effects of ^{125}I decay 0-108973
 lumirhodopsin, photoconversion at 77K, quantum efficiency estimation 0-67081
 photosensory retinal pigments in *Halobacterium halobium* 0-97860
 photosynthesis, energy and electron transfer speed, time resolution meas. (Russian) 0-94161
 photosynthetic reaction centre spectroscopy by tunable picosec. parametric oscillators 0-61513
 polynucleotide solution, elec. field induced orientation and effects 0-85348
 protein, electron radiation damage on primary and secondary struct. level 0-89808
 quinacrine mustard, 2-step laser-induced photodamage 0-85198
 radiolysis of DNA and other bipolymers 0-67163
 rhodopsin and thermal intermediates, fast struct. fluctuations in protein component 0-72137
 serum albumin, bovine, high energy-induced aggregation, time resolved spectra 0-61655
 thymidine monophosphate aqueous solution, gamma irradiat. effect on base damage, phosphate release 0-89806
 time effects in molecular radiation biology 0-72269
 5-trifluoromethyluracil, electron beam damage assessed by EELS 0-89809
 uracil, nucleic acid component, selective action by ps light pulses 0-72213
 uridine-5'-phosphate. 2Na^+ single crysts., radiation damage, ESR obs. 0-108964
 CO-haemoprotein photolysis, transient Raman study, quantum yield origin 0-67155

biomolecules see *macromolecules; molecular biophysics*

bionics see *bio cybernetics*

biophysics

- see also *biological fluid dynamics; biomechanics; cardiology; cellular biophysics; haemodynamics; hearing; molecular biophysics; speech; vision biochemistry and biotechnology, conf., Helsinki, Finland, 27-31 Aug. 1979* 0-57001
 bioluminescence of firefly larva, circular polarisation 0-94441
 bone density determination, effective attenuation coeff. of soft tissue, Compton scatt. 0-101220
 cardiac muscle, resting, activation monitored by intensity fluctuation spectroscopy 0-108953
 colloidal particles, in a flowing solution, SAXS 0-61163
 comb filter, use for describing time-varying biological rhythmicities 0-97852
 dissipative structures, formation and stability 0-108950
 EM energy deposition in inhomogeneous block model of man for near-field irradiation conditions 0-89788
 energy spectra of δ -rays produced due to high energy particles with biological systems 0-108951
 growth and patterns of spatial organisation 0-81287
 Hamiltonian content of biodynamics 0-89704
 lung, beta-emitting particles, fraction of energy absorbed, rat obs. 0-104641
 man's size in terms of fundamental constants 0-105489
 marine green alga, *Ulva fenestrata*, afterglow in the ms and ds intervals of attenuation 0-104636
 microwave power absorption differences between normal and malignant tissue 0-104640
 network structures of a system coded by groups 0-81286
 neutron cross-sections and kerma values for C, N and O from 20 to 50 MeV 0-101217
 plant leaves, microwave photoconductivity obs. 0-104637
 plasma in biological solids, resonant interactions with microwaves 0-101222
 prolate spheroidal models of humans in near field of short electric dipole, irradiat. 0-104639
 proteoglycans, swelling pressures at the concs. found in cartilaginous tissues 0-67327
 review of biophysics and bioengineering, book 0-105437
 skin, in vivo, light absorpt. and scatt., theoretical and expt. study 0-101219
 space motion sickness 0-61712
 tissue, rabbit, comparison of NMR water proton T_1 relax. times 0-101221
 tree-ring analysis in palaeoclimatology, preliminary survey and scope for Indian region 0-90212
 trees, use as local climatic wind indicator 0-82007
 weightlessness and man, sled programme, SpäcLab 0-94381
 $\text{Br}^{82\text{m}}$, 42 MeV, stopping power and radial dose distrib. obs. in tissue-equivalent gas 0-101218
 FeS_2 , acid bacterial leaching, lixiviant alteration by fungal absorpt. of Fe 0-108617
 ^{129}I in bovine thyroid glands, activation anal. obs. 0-94380

bioreology

- articular cartilage, drag-induced compression during a permeation expt. 0-97955
 articular cartilage, normal, quasi-linear viscoelastic props. 0-108937
 articular cartilage, viscoelastic properties (Japanese) 0-101215
 articular cartilage in compression, biphasic creep and stress relax., theory and expts. 0-94275
 articular cartilage single layer model, flow fields created by a sliding load 0-104630
 atherosclerosis, rheological aspects (Japanese) 0-94268
 blood, couple stress fluid flow through narrow tubes 0-67105
 blood, red cell flexibility, effect on blood flow through tubes of 30-500 μm 0-67111
 blood, red cells, rheological props. meas. by Couette viscometer 0-97992
 blood, rheological behaviour, viscoelastic model (French) 0-76779
 blood, rheological hysteresis at low shear rate 0-97962
 blood, viscoelastic properties, transient flow obs. 0-97980
 blood cells, stored, rheological behaviour obs. (French) 0-67110
 blood flow in artery, stenosis effects on non-Newtonian flow 0-89775
 blood flow mechanics 0-76778
 blood flow through narrow capillaries, rheological mechs. 0-97961

bioreology continued

- blood perfusion prediction from meas. of phase shift between heat flux and temp. 0-104804
 blood perfusion rate estimation from diffusible indicator meas., sensitivity anal. 0-104803
 blood plasma, normal and haemophilic, coagulation kinetics study 0-67107
 blood plasma viscosity in sickle-cell anaemia 0-94250
 blood rheology, erythrocyte rigidity effects on viscoelastic dilatancy 0-61610
 blood viscosity and red cell aggregation at zero and 1G, instrumentation for Space Lab 3 0-61716
 blood viscosity and red cell aggregation changes after haemodilution 0-97952
 blood viscosity at low shear rate, capillary viscometer and obs. 0-98180
 bone viscoelastic behaviour, anal. on basis of microstruct. 0-85429
 cardiac muscle, passive, viscoelastic theory and obs. 0-94273
 conference, Osaka, Japan (June-July 1979) 0-62364
 Couette viscometer for short time shearing of blood 0-98179
 epithelial mucus, rheology and mol. organisation 0-97959
 erythrocyte, flow resistance into pores 0-61609
 erythrocyte membrane alterations, rheological technique evaluation 0-61611
 erythrocyte membranes, fluidity change after X-irrad., pyrene excimer fluorescence obs. 0-72262
 fibrinolysis and coagulation, dynamic rheological studies 0-61614
 gelatin gels, in water and glycerol/water mixtures, dynamic viscoelastic props. 0-64508
 haemorheology, lecture (Japanese) 0-98752
 haemorheology and diseases, conf., Nancy, France (Oct. 1979) 0-56991
 haemorheology related to blood cells, conf., Hamburg, Germany (Aug. 1979) 0-62365
 lecithin-water system, lamellar phase, rheology 0-89779
 magnetic micro-rheometer evolution and theory 0-92099
 mesentery tissue, burn induced alterations of interstitial diffusion 0-104634
 micropolar fluid model for blood flow through narrow tubes 0-67109
 morphogenesis, growth, elastic and non-elastic deforms. 0-108928
 muco-ciliary transport mechs. 0-97956
 mucociliary flow mechanics, channel model obs. 0-97957
 phosphatidylcholine bilayers, fluidity changes and phase transitions, intramol. excimer fluoresc. obs. 0-85342
 platelet interaction with vessel surface, blood rheological factor influences 0-61612
 protein film, at liq. interfaces, shear rheologica props. 0-94256
 protein network formation dynamics, review, book contrib. 0-97995
 red blood cell ADP release at high shear stresses 0-98002
 red blood cell micromechanics in viscometric flow 0-98000
 red blood cells, viscoelastic study of aggregation 0-97960
 red cell membrane, human, surface elasticity and viscosity 0-61608
 rheoencephalographic curves, bipolar and tetrapolar techniques, comparison (Croatian) 0-104796
 rheometer, analytical, optical sliding contact, for flow visualisation at articular surface 0-104847
 soft tissues, human, rheological props. from local cyclic loading method 0-108932
 soft tissues, human, rheological props. investigation using elastography 0-108933
 sperm, human, flagellar propulsion in cervical mucus, interaction hydrodynamics model 0-97878
 sputum viscoelasticity, meas. using conventional dynamic and raised cosine pulse methods (Japanese) 0-67132
 tendon, viscoelastic deform. obs. 0-101211
 thrombosis, rheological aspects (Japanese) 0-94268
 tracheal muco-ciliary transport, theoretical and expt. study 0-97958
 uterine muscle, isotropy and anisotropy during labour contract. 0-94257
 viscoelastic tube, pulsatile flow, non-Newtonian effects (French) 0-59113
 water mobility in blood plasma, NMR determ., viscosity correl. to $1/T_2$ 0-67176

Biot-Savart law see *electromagnetism*

biothermics

- bee, thermoregulation by evaporative cooling of head (honeybee) 0-61515
 behavioural alterations of rats, interaction of ambient temp. and microwave irradiat. 0-67153
 biomedical thermal entrainment device for cardiovascular investigation 0-104793
 bladder, toad, temp. dependence of ADH-induced water flow and intramembranous particle aggregates 0-61520
 blood and its constituents, coeff. of thermal expansion, (German) 0-104556
 blood perfusion prediction from meas. of phase shift between heat flux and temp. 0-104804
 blood temperature monitoring during extracorporeal circulation, noncontact transducer 0-85513
 blood vessel heat transfer 0-108851
 blood-brain barrier, effects of microwave-induced hyperthermia, rat 0-61642
 brown adipose tissue, mitochondria implicated in diet-induced thermogenesis 0-89722
 calorimetric instrumentation for studies of biopolymer model compounds 0-61746
 cancer treatment appl. of microwave arrays for localised tumour heating 0-94308
 cells, mouse embryo, innocuous freezing during warming 0-94175
 cells, volumetric changes during freezing and thawing, thermodynamic model 0-108863
 cerebron, thermotropic and lyotropic mesomorphism 0-76703
 chloroplasts, isolated, effect of temp. on photo-induced pH gradient 0-81566
 CHO cells, asynchronous, fractionation of combined heat and radiation, radiation sensitivity obs. 0-76806
 CHO cells, asynchronous, fractionation of combined heat and radiation, cell-cycle redistrib. 0-76807
 CHO cells exposed to hyperthermia, radiosensitivity and recovery from radiation damage 0-72250
 CHO fibroblast, press., inhibited thermal killing obs. 0-81564
 chromatin, factors affecting the heat-induced increase in protein content 0-97882
 climatic stress on man, parameter recording and processing, math. method (German) 0-82047

biothermics continued

- cold exposure, mild, increased survival obs. in rats with medial preoptic lesions 0-101151
 conference, New York, USA (Dec. 1979) 0-104561
 corneal temperature range, implications in prediction of laser thermal damage 0-108848
 cortical evoked potentials, math. model for source localisation, somatosensory stimulation 0-89774
 cranial structure exposed to RF radiation, thermal response model 0-94285
 current field heating, localised, as an adjunct to radiation therapy 0-98056
 cytochrome c_3 , anhydrous film, elec. cond., temp. and ambient press. depend. 0-85327
 cytochrome c , effects of UV and temp. on optical props. and enzymatic activity 0-81648
 D-leucine, exchange diffusion in mouse Ehrlich ascites tumour cells, temp. reduction effect 0-67053
 diathermy applicator for irradi. of rat brain 0-94425
 1,2-dimyristoyl-sn-glycero-3-phosphoserine multilayers, phase transitions, temp. depend., ellipsometric study 0-108846
 1,2-dipalmitoyl-sn-glycero-3-phosphocholine multilayers, phase transitions, temp. depend., ellipsometric study 0-108846
 DNA derivative melting curves, automatic recorder using real time processing (*French*) 0-104833
 ear skin, mouse, fractionation effects in response to combined heat and X-rays 0-76805
 E.coli, radiation killing, role of membrane fluidity, hypothermia and local anaesthetics 0-104653
 education, human body, live, thermodynamics of cooling for treatment purposes 0-73128
 electrocoagulation, monoactive, controlled destruction and temp. distrib. 0-94176
 EM irradiation, temp. distrib. in simulated living tissues 0-85354
 EM wave heating effects, radiowaves and microwaves 0-98011
 enzyme-catalysed reactions, network thermodynamic modelling 0-89463
 erythrocyte nucleosomes, chicken, temp. dependence of ^{31}P -NMR spectra 0-94280
 evoked potentials, use in monitoring residual function of injured spinal cords 0-81747
 exercise thermoregulation after 14 days of bed rest 0-97865
 extravascular lung thermal vol., reappraisal as meas. of pulmonary oedema 0-97867
 fibrosarcoma, para-7, hamster, local thermal conductivity obs. 0-104562
 frequency/depth-penetration considerations in hyperthermia by magnetically induced currents 0-63887
 heat capacity function, of macromolecular systems, statistical thermodynamic analysis 0-61514
 hypercapnia, influence of aspects of heat exchange, rabbit obs. 0-97863
 hyperthermia, biological research, time-temp. conversions 0-104560
 hyperthermia, deep local, induction by US and EM fields, problems and choices 0-94283
 hyperthermia, local, theoretical and expt. study, nonperfused phantom (*French*) 0-104559
 hyperthermia, localised, comparison of EM and US diathermy 0-104725
 hyperthermia, localised, in the patient, clinical requirements 0-98173
 hyperthermia, role of thermal conduction 0-104558
 hyperthermia at 42°C, whole-body, temp. gradients in pigs 0-67043
 hyperthermia by magnetically induced currents, freq.-depth-penetration, comments and reply 0-108991
 hyperthermia due to exercise, effects on breathing pattern 0-72196
 hyperthermia in tissue-like substances, EM and US induction 0-98012
 hyperthermia-induced sensitisation of tumour cells to antibody-complement cytotoxicity 0-104570
 hypothermia, local, Gipospast-1, thermoelec. apparatus 0-104807
 IR thermometry, appl. to remote detect. of biological stresses in plants 0-61749
 kinetic proofreading in biosynthetic pathways, thermodynamic constraints 0-108861
 labelled microspheres, localised embedding by microwave heating of tissues of hypothermic dogs 0-61640
 laser irradiated tissue, significance of blood flow in temp. calcs. 0-104563
 leg, human, elevated temps. induced by microwave diathermy with surface cooling 0-61638
 leghaemoglobin, thermal denaturing in cryst. and soln. 0-108849
 lumbo-sacral motoneuron pools, human, response patterns to distant somatosensory stimuli 0-108924
 lymphocytes, human, effects of heat and radiation 0-97864
 lymphocytes exposed to temps. of 37-45°C, two types of interface death 0-104566
 macromolecules, conformation studied by calorimetry, review 0-97870
 mammalian cells, in vitro US irradi. at hyperthermic temps. 0-94282
 maxillary gum trigeminal evoked pots. in humans 0-97948
 median nerve, transient responses to elec. stimulation, SQUID appl. to somatically evoked field meas. 0-104706
 melanoma, B16, in mice, effect of hyperthermia alone and in combination with ^{60}Co radiation 0-72138
 membrane fluidity modification, mechanism of hyperthermic cell killing and therapy appl. 0-104569
 mesentery tissue, burn induced alterations of interstitial diffusion 0-104634
 microstrip slot radiator for medical appls. 0-108994
 microwave and temperature effects on the murine ocular lens in-vitro 0-89798
 microwave antenna, invasive, for locally-induced hyperthermia for cancer therapy 0-67193
 microwave applicators for localised hyperthermia treatment of malignant tumours 0-89824
 microwave diathermy direct-contact circular aperture applicator with corrugated flange, design 0-67190
 microwave heating combined with radiation therapy, skin and tumor thermal enhancement ratios 0-67192
 microwave hyperthermia, localised, biomedical devices 0-104724
 microwave hyperthermia, microwave leakage during treatment 0-76820
 microwave hyperthermia to cancer treatment (*Spanish*) 0-89795
 microwave hyperthermia treatment and thermometry system 0-72280
 microwave thermography, appl. in cancer diagnosis (*Spanish*) 0-67195
 microwave-induced hyperthermia, rats, classical conditioning obs. 0-61629

biothermics continued

- microwave-induced hyperthermia, rel. to visually evoked electrocortical response, guinea pig 0-61627
 muscle fibres of *Lethocerus maximus*, temp. dependence of cross bridge parameters 0-61598
 neck node metastases, effectiveness of microwave hyperthermia combined with ionising radiation 0-94307
 nerve membrane, excitability, genetic alteration, temp.-sensitive paralytic *Drosophila* mutants 0-97895
 neural conduction times, central and peripheral, in multiple sclerosis, somatosensory obs. 0-89773
 nonequilibrium linear behaviour, enzyme-mediated multidimensional inflection points 0-72122
 Peracarida, burrowing, temp. effects on emergence rhythms (*French*) 0-94174
 phospholipid bilayer, one- and two-component, main phase transition, Landau phenomenological theory 0-97872
 photoluminescent thermometer probes, temp. meas. in microwave fields 0-104721
 photosynthesis, electron transfer reactions in carrier mol. complexes, kinetics and thermodynamics 0-108859
 physiological thermoregulation, math. model 0-94173
 plant fibre temperature stability investigation, rotary diffusion, spin label obs. 0-81529
 plasma water shifts during thermal dehydration 0-67044
 rat thermoregulatory behaviour when subject to microwave irradi. 0-81547
 rectal temperature and operant behaviour during 2.45-GHz microwave irradi., squirrel monkey obs. 0-61630
 red cell, human, increased passive permeability below 12°C 0-94185
 RF EM fields, review of effects and dosimetric data, safety standards development 0-67154
Salmonella typhimurium LT2 mutants, effects of microwave radiation and heat 0-108958
 salt-hydrate transition temps., use as fixed pointed in biomedical thermometry 0-104801
 sarcoma, rate, temp. effect on microvascular haemodynamics during early growth 0-72188
 sarcoplasmic reticulum membranes, temp.-dependent functional changes 0-81550
 scanning microcalorimeters for studying macromolecules 0-61747
 serum low density lipoprotein, human, anomalous permittivity behaviour 0-81540
 skin, pig, combined effects of X-irrad. and microwave heating 0-94290
 skin, pig, response to combined X-irrad. and microwave heating 0-61653
 skin blood flow, reflex control by skin temp., role of core temp. 0-85427
 skin temperature rises, thermal props. of dry metal-foil dispersive electro-surgical electrodes 0-98171
 small intestine, mouse, transient heat-induced thermal resistance, crypt survival assay 0-108850
 somatosensory evoked potentials, reduction during movement, cat extralemniscal pathways recordings 0-85421
 somatosensory evoked potentials, review of acquisition and anal. 0-101281
 somatosensory evoked potentials, short latency, in man following median nerve stimulation 0-94243
 somatosensory pathways, assessment of central conduction 0-97949
 somatosensory potentials following electroconvulsive therapy 0-97947
 space suit cooling, automatic control of human thermal comfort 0-109046
 still-shade-temperature meter for use in assessing personnel cold stress 0-81764
 surface EMG and fatigue, muscle temp. and blood flow 0-94199
 surface tissue, two-phase theory for circulatory influence on heat transfer 0-104564
 surgical diathermy indifferent electrodes, performance electrodes. 0-72367
 tail, rat, single dose radiation and hyperthermia rel. to growth 0-108963
 telemetry system with interference suppression, implantable, long-life, animal expts. appl. 0-101302
 telemetry transmitter, crystal-controlled, surgically implantable, for animal expts. 0-72393
 temperature biotelement, modular, expandable, implantable 0-67191
 temperature measurement, human body-temp. sensor-environment system, analogue model of interaction 0-104783
 thermal sensation evaluation, comfort chart (*Japanese*) 0-81545
 thermoelectric needle probe for medical and biological temp. meas. 0-101299
 thermogenesis control in cold-exposed rabbits, variable open-loop gain 0-97868
 thermogenic control during exercise in a cold environment 0-72139
 thermometry and dosimetry of heat rel. to liquid-crystal optical fibre temp. probe 0-98204
 thermoregulation of rabbit head, facial vein myogenic mech. 0-97869
 thymocytes, rat, reduction of interphase death by hyperthermia 0-108970
 tissue heat balance, relationship between blood perfusion, metabolism and temp. 0-108852
 tissue perfusion measurements made with thermal diffusion probe, effect of probe geometry 0-104802
 tissue temperature simulation in cryosurgery 0-85355
 tissue-equivalent medium, heating patterns produced by 434 MHz Erbrother UHF[®] 0-98013
 tryptophan residue in horse liver alcohol dehydrogenase, room-temp. phosphoresc., temp. and enzymic complex form. effects 0-61512
 tumours, solid, destruction by RF heating 0-61637
 turtle, sex determination during embryo development, temp. depend. 0-81546
 US hyperthermia, localised, design of heating protocols 0-104693
 US irradiated cells, temp. distrib. calcs. 0-61623
 vasodilation, peripheral, induced in squirrel monkeys by microwaves 0-104682
 vasomotor thresholds, squirrel monkey, central and peripheral temp. effects 0-97866
 vegetation thermal IR emissivity, ecological variations 0-104557
 whole-body hyperthermia, core body temp. regulation by oesophageal temp. feedback 0-72371
 yeast cells, determ. of thermal equivalent to MM microwaves 0-67151

biotite *see mica*

biotransport

- see also* *biodiffusion; biological fluid dynamics; biomembrane transport; cellular transport and dynamics; neurophysiology*
- alveolar epithelium transport of albumin and sucrose, conc. diff. effect 0-67329
- blood-brain barrier, reversal of microwave-induced permeability 0-61641
- blood-organ transfer kinetics of radioisotopes 0-109044
- cerebrovascular permeability, quantitative method for meas. of alterations 0-61748
- epithelial mucus, rheology and mol. organisation 0-97959
- inert gas, exchange in living organs, stochastic description 0-81520
- mucociliary transport mechs. 0-97956
- mucociliary flow mechanics, channel model obs. 0-97957
- mucociliary tracheal clearance vel., radiological method for determ. 0-104727
- salivary gland electron transport, Lone Star tick 0-72144
- tracheal mucociliary transport, theoretical and expt. study 0-97958
- O₂, haemorrhagic shock, effect of anaemia 0-67330
- O₂, haemorrhagic shock, effect of increased blood-O₂ affinity on O₂ transport 0-67331
- O₂ transport system, functional state, math. model 0-104548

bipolar integrated circuits

- function testing with stroboscopic microcomputer-controlled SEM 0-68294
- temperature transducer, intrinsic bandgap voltage as reference, Fahrenheit, Celsius or arbitrary scale operation 0-82761
- BN glass transfer process appl. 0-107459
- GaAs-GaAlAs bipolar transistor and heterostruct. laser, monolithic integration 0-102858

bipolar transistor circuits

- Used for general papers and papers where use of bipolar transistors is significant*
- dynamic load line construction amplifiers, tutorial 0-67963
- photodetector with automatically adjustable threshold level, design considerations 0-62724
- reaction timer, using LEDs 0-81781
- thermometer, using Motorola MTS 102 transistor temperature transducer and LM 10 IC op amp (French) 0-86298

bipolar transistors

- see also* *bipolar integrated circuits*
- emitter-push effect, TEM analysis of isolated dislocation helices 0-70203
- noise figure, measurement by connecting source resistance between input and output (French) 0-68214
- GaAs-GaAlAs bipolar transistor and heterostruct. laser, monolithic integration 0-102858
- Si, heavily doped, excess intrinsic carrier density, deionisation of impurities as explanation, bipolar transistor/solar cell models 0-96864

bipoles *see network synthesis*

birefringence

- see also* *flow birefringence; Kerr electro-optical effect; light polarisation; magneto-optical effects; mechanical birefringence; optical constants; optical rotation*
- absorbing anisotropic and gyrotropic slab between crossed polarisers, transmitted intensity patterns 0-78762
- acousto-optical diffraction, multifrequency, in optically birefringent media 0-74300
- alkyl-cyanobiphenyl homologues, isotropic-nematic phase, optical Kerr effect 0-91866
- analogue birefringent element built from polarising wide field Michelson interferometer 0-91895
- benzene, quadrupole moments, elec. field-gradient birefringence method 0-95746
- birefringent plates, cracks, stress intensity factors, refl. caustics method 0-93718
- borosilicate glass, birefringent, X-ray small-angle scatt. study 0-103937
- borosilicate glass single-polarisation single-mode fibres 0-64205
- cartilage proteoglycan, association with hyaluronic acid, elec. birefringence obs. 0-85332
- chalcopyrite crystals, refractive index, temp. depend., appl. to nonlinear devices 0-60555
- chiral substances, electro-optical responses, Jones matrix, meas. system for rot. anisotropy 0-84723
- cholesteric liquid crystal coatings, superimposed left- and right-handed, peak refl. and colour gamut 0-74472
- coherent birefringent optical pulse compression 0-106437
- collagen, polarisation, contribution of permanent and induced dipole moments, elec. birefringence 0-85351
- colloids, rigid, size distributions, transient electric birefringence 0-85223
- Cotton-Mouton effect in Jupiter ionosphere and magnetosphere, rel. to decametre radio emission modulation 0-67643
- crystal faces, birefringent, meas. method of growth and dissoln. rates 0-79719
- crystalline optical material props., symmetries and tensorial relationships 0-108174
- p-cyanophenyl p-n-alkyloxybenzoates, nematic, birefringence, polarisability and order parameter 0-100642
- defect crystal structure determination, light interference, diffraction and scattering 0-103316
- disperse system, dilute, orientationally induced conservative dichroism 0-102623
- DNA, calf-thymus and superhelical PM2 aq. solns., electro-optic obs. of γ -irrad. damage 0-85452
- DNA, dye labelled elec. dichroism and birefringence, comparison with mol. props. from polarised fluoresc. 0-84785
- DNA solution, elec. birefringence, stabilised induced dipole behaviour 0-85349
- domain lattice of transparent crystal regular birefr. regions, optical wave diff. divergence 0-102616
- ethidium bromide E-DNA, intercalated birefringent fibres, microspectrophotometric investig. (German) 0-57392
- Faraday rotators in fibre Raman lasers 0-58775
- ferroelectric, large-gap type, vibronic theory and opt. props., anomalous bulk photovoltaic effect 0-103939
- ferromagnet, linear mag. birefr. (Russian) 0-93284
- fibre interferometric secondary light source 0-105702
- hexafluorobenzene, quadrupole moments, elec. field-gradient birefringence method 0-95746
- hexamethylbenzene, quadrupole moments, elec. field-gradient birefringence method 0-95746

birefringence continued

- hybrid field-effect liquid-crystal light valve, optical data processing performance 0-99860
- isopachies measurement of birefr. object, using immersion method polarisation holography 0-99672
- laser mirror birefringence, ellipsometric meas. using stabilised two-frequency laser 0-101820
- liquic crystals, orientational order parameter, optical birefr. meas., polarisation field problems 0-79688
- macromolecular solution, rot. diffusion coeff. calc. method w.r.t. mol. struct., elec. birefringence relax. time data interpret. 0-85331
- macromolecular solution, transient elec. birefringence in reversing fields of arbitrary strength and duration 0-84719
- magnetic colloids, birefringence and dichroism, magnetically-induced, sign inversion 0-60548
- magnetic fluids, mag., optical, and hydrodynamic props., expt. study, review 0-60376
- magnetic fluids, optical birefr. and dichroism in mag. field 0-60547
- MBBA, isotropic, surface-induced ordering 0-108176
- nematic crystals, of equimol. conc. with NaCl struct., piezo-optic birefringence theory 0-100643
- nematic liquid crystals, orientation fluctuations in high mag. field, quenching, birefringence effects 0-64892
- nematic liquid crystals, refractive index and birefringence by interference method 0-96440
- nonpolar molecule solutions, birefr. kinetics 0-100648
- nucleosomes and nucleosomal DNA, electro-optical props., relax. times and chain struct. 0-85350
- numerical calculation using optics 0-95832
- trans-p-n-octyloxy- α -methyl-p'-cyanophenyl cinnamate, mag. and elec. birefr. in isotropic phase 0-80744
- optical ceramics, dispersion, double refraction and storage effects, material appls. (German) 0-69471
- optical fibre, current measurement appl. 0-96015
- optical fibre, highly birefringent, Faraday rotation 0-58672
- optical fibre, single-mode, single-polarisation, with refractive-index pits on both sides of core 0-99846
- optical fibres, slightly elliptical 0-106602
- Oriental optical effects from above Rayleigh particles 0-106453
- orthorhombic crystal, birefr. and refr. index determ., refl. method 0-86380
- orthotropic composite model materials, photoelastic calibration 0-87715
- pentyl cyanobiphenyl, laser and electric field induced Kerr effect 0-84061
- 4-n-pentylbenzenethio-4'-n-alkoxybenzoates, birefr., crit. behaviour near smectic A-C transition 0-80745
- PET, amorphous, intrinsic birefringence calc. from wide angle X-ray scatt. 0-108178
- photographic emulsion coated on birefr. substrate, construction of multi-capacity matched filters 0-74478
- photomicrography of submicrometer birefringent contaminants in C black dispersions in polymer particles 0-62757
- PMMA, birefringence in elec. field 0-88962
- poly(vinylcarbazole), stress-induced crystn. from melt, optical studies 0-84113
- poly-4-vinylpyridine, electro-optic study of conformational changes induced by heavy metal ions 0-84725
- 1,4-polybutadiene, stress-induced crystn. from melt, optical studies 0-84113
- polycapromide, oriented filaments, mech. props. 0-66550
- polycarbonate, bisphenol A, birefringent plates, cracks, stress intensity factors, refl. caustics method 0-93718
- polydisperse dilute suspensions, of rod-like particles, anisotropy of electric polarisability 0-85224
- polyethylene, stretched, birefringence rel. to struct. changes 0-84714
- polymethacrylic acid, swollen networks, viscoelastic photoelastic behaviour 0-59366
- polynucleotide solution, elec. birefringence, stabilised induced dipole behaviour 0-85349
- polypeptide, conformational change induced by strong elec. field 0-85336
- polypeptides, ionic and non-ionic, electro-optical studies of conformation 0-71379
- prism cut from anisotropic media, ray refr., appl. to atm. optics haloes 0-63916
- quartz, cryst., birefringence, temp. depend., intracavity method meas. 0-78931
- quartz, electro-optical props. near phase transition 0-80756
- sepiolite, electric polarisability, anisotropy, length depend. of ionic contrib. 0-85224
- sepiolite, size distributions, transient electric birefringence 0-85223
- smectic A-nematic phase transform., liq. cryst. binary mixture, birefringence study 0-59638
- sodium bentonite, Wyoming suspension, comparison of optico-optical scattering and birefringence 0-85226
- squaric acid, antiferroelec., struct. phase transition mechanism 0-75969
- stress-induced crystn. from melt, optical studies 0-84113
- suspension of absorbing particles, simultaneous meas. of dichroism and birefringence in elec. field, photocurrent signal obs. 0-82801
- three-stage birefringent filter, tuning over visible region 0-58667
- 1,3,5-trifluorobenzene, quadrupole moments, elec. field-gradient birefringence method 0-95746
- 1,3,5-trimethylbenzene, quadrupole moments, elec. field-gradient birefringence method 0-95746
- triphenylphosphite, acoustically induced birefringence 0-93274
- uniaxial crystals, refl. ellipsometry nonlinear eqn. inversion 0-95120
- viologen films, on transparent oxide electrodes, morphology, electro-optical obs. 0-100703
- Ag halide thin-film optical recording medium 0-102786
- Au sols, acoustically induced birefringence 0-93274
- BaMnF₂, struct. phase transition, optical parameters obs. 0-100328
- Ba₂NbNb₂O₁₅, cryst. comp. effect on low temp. phase transition 0-71346
- BaTiO₃, vibronic theory and opt. props. 0-103939
- BiVO₄, ferroelastic phase transition, birefringence meas. using rotating-analyser method 0-80742
- BiVO₄, ferroelastic phase transition, birefringence meas. at simultaneous high pressure and temp. 0-80743
- CaCO₃, calcite linear polarizer, role in laser technology 0-64165
- CoCO₃, linear magneto-optical effect, birefr. 0-66155
- CoF₂, linear magneto-optical effect, birefr. 0-66155
- copper phthalocyanine, size distributions, transient electric birefringence 0-85223

birefringence continued

- DyVO₄, cooperative Jahn-Teller phase transition, linear birefr. meas. 0-88960
 Fe₃BO₆, Faraday rotation and birefringence 0-100650
 Fe₃BO₆, orthorhombic cryst., birefr. and refr. index determ., refl. method 0-86380
 Fe₂Zn_{1-x}F₂, Neel point and short range order, dilution effects, mag. birefr. obs. 0-71019
 GaAs, temp. coeff. of induced birefringence 0-93277
 GaP, temp. coeff. of induced birefringence 0-93277
 KAg₄I₃, superionic phase transition, dynamical and crit. pt. props. 0-107535
 KCN, multidomain birefr. solid, light scatt. and IR transmission spike 0-60587
 KCaF₃, struct. phase transitions, DSC, birefr., and neutron powder diff. obs. 0-70149
 KCl-KBr, with equimol. conc., piezo-optic birefringence theory 0-100643
 K₂CoF₆, two-dimens. Ising antiferromag., nearest neighbour correl. function, birefr. expts. 0-71386
 KCuF₂, linear chain Heisenberg antiferromag., nearest neighbour correl. function, birefr. expts. 0-71386
 KD₂PO₄, photo-spatial light modulator, optical data processing 0-102839
 KFe(MoO₄)₂, phase transitions at 312 and 139K 0-70396
 KMgF₃·Ni²⁺, acoustic Faraday and Cotton-Mouton effects, theory 0-65987
 LiGd₂(MoO₄)₅, single crystals, cryst. growth, optical props. 0-60763
 LiNbO₃:Fe, photoinduced refractive index discontinuities at surface 0-75999
 LiTaO₃, optical waveguide, Ag-Li ion exchange 0-91888
 Mn₂Zn_{1-x}F₂, Neel point and short range order, dilution effects, mag. birefr. obs. 0-71019
 NH₄Ag₄I₃, superionic phase transition, dynamical and crit. pt. props. 0-107535
 Na vapour, Zeeman coherence, transient and stationary, polarisation spectroscopy 0-58212
 NaCN, multidomain birefr. solid, light scatt. and IR transmission spike 0-60587
 Na₂CO₃, phys. props. related to phase transitions 0-96643
 Na₂O·B₂O₃·SiO₂, two-phase, stresses arising during leaching 0-81086
 Nd:glass laser rod, pumped, thermal relaxation 0-69397
 Nd³⁺:YAG laser, high repetition rate electrooptic Q-switching, birefringence 0-69430
 NiO, linear birefringence in S-domains near antiferromag. phase transition 0-60261
 PLZT slim-loop and linear ceramics, longit. electrooptic effects, display appl. 0-80751
 PbTiO₃, optical birefringence in low temp. region 0-93276
 PbTiO₃, vibronic theory and opt. props. 0-103939
 RbAg₄I₃, superionic phase transition, dynamical and crit. pt. props. 0-107535
 RbH₂PO₄, ferroelec. phase transition, birefringence studies 0-108162
 Rb₃MnCl₄, quasi-2D-antiferromag., linear birefr. and optical absorpt. spectra 0-71385
 SbSbBr, single crystals, birefringence meas., ferroelec. transition obs. 0-88933
 Sml, Zeeman coherence, transient and stationary, polarisation spectroscopy 0-58212
 Sr₂Ba_{1-x}Nb₂O₆, domain struct. influence on electrooptical props. 0-93283
 TbIG, [111] magnetoelastic props., rel. to Cotton-Mouton birefringence, 90-500K 0-103876
 TeO₂ shear wave acousto-optical device with polarisation filtering 0-106619
 YAG crystals, dislocations and inclusions, birefringence topography obs. 0-107248
 YAG:Nd crystal, orientation influence on thermally induced birefringence (Chinese) 0-88958

bismuth

see also nuclei with

- amorphous metal films, crystallisation with and without mag. field 0-70570
 anisotropic crystal, dislocation wall stress field and strain energy 0-100233
 anodic oxide film capacity in various soln. 0-104320
 atom, electron impact M-shell ionisation, 60-600 keV, absolute cross sections meas. 0-83493
 atom, Faraday effect and magnetic circular dichroism 0-83399
 charge carrier interaction with twinning planes in strong transverse mag. fields (Russian) 0-88577
 clusters, 2 to 500 atoms, nucleation, mass spectra 0-102596
 crystal growth from melt, impurity distrib. control by electrotransfer method (Russian) 0-66418
 deformation calculations, band struct. variation, electron phase transitions due to deform. (Russian) 0-65137
 degenerate electron liquid, skipping orbit cyclotron resonance, surface state transitions 0-103889
 ellipsoidal model of textured specimens with uniaxial symm. (Russian) 0-80100
 EM wave dispersion and damping, Voigt configuration, non-local calcs. 0-100475
 enstatite chondrite, Bi and Pb microdistribution obs. 0-62085
 film, adatom surface diffusion at low temps., elec. resist. study (French) 0-65376
 film, amorphous, temp. dependence of SAW attenuation 0-75679
 film, resistivity, rel. to thickness 0-107928
 film, single layer and multilayer systems, thickness determ. by X-ray fluoresc. 0-68180
 film, size effect of carrier heating, surface scatt. (Russian) 0-100474
 film, structure and electronic props. 0-70562
 films, resistance changes due to bombardment by N, C, or Ar ions 0-103670
 foil pressure transducer, determ. normal stress components in solid state high pressure test cell 0-73378
 fusion reactor molten-salt blanket, effect of Pb and Bi neutron multiplication zones on the fission rates of ²³³Th and ²³⁵U 0-99272
 gas-liquid type transform. and sound attenuation in strong mag. fields, electron-hole correl. effects 0-88598
 giant quantum attenuation anomalies of sound waves at high mag. field, temp. and freq. depend. 0-70587

bismuth continued

- giant quantum attenuation anomalies of sound waves at high mag. field, extra attenuation peaks 0-70588
 intervalley scattering processes, surface struct., transverse electron focusing study (Russian) 0-84352
 liquid, field ion source emission chars. 0-74059
 magnetoresistance, high temp. oscills, props. (Russian) 0-65606
 melting curve, effect by asymmetrical friction in piston-cylinder device 0-86292
 molecular clusters, laser fluoresc. spectrosc. 0-95755
 molecular laser, optically pumped, review 0-58519
 molecule, radiative lifetime and self-quenching cross sections meas. from laser induced fluorescence expt. 0-69189
 optical phonon anharmonicity and melting, light scatt. study 0-60621
 parity non-conservation effect 0-68395
 parity nonconservation effect (Russian) 0-77985
 phase transformation due to high press. and shear stress 0-75357
 phase transitions under high press. 0-96641
 photodetector, fast-response thin-film, employing charge carrier photon entrapment 0-73462
 quantum-EM excitations 0-88471
 quench-condensed films, superconducting transition temp., elastic stress and strain effects 0-70883
 slip systems, crit. resolved shear stress 0-59470
 solid and liquid, positron annihilation temp. depend. 0-108296
 strain hardening curve correlation with slip band nucleation stress spectra 0-70217
 superconducting amorphous film, Kosterlitz-Thouless transition 0-88699
 superconducting microbridge, high-resistance, with Bi crosspiece 0-93050
 superconducting modification obtained by impact compression (Russian) 0-93020
 superconducting film, critical temp., thermal equilibrium (Russian) 0-80438
 thermal EMF giant quantum oscills. (Russian) 0-59960
 thermoelectric power, electronic thermal cond., in mag. field 0-60015
 twin shape variation under long period loads (Russian) 0-65007
 whiskers, excess 1/f noise, 50 to 350K 0-92951
 whiskers, persistent metallic behaviour, elec. resist. meas. 0-75544
 X-ray absorption, discontinuities and limits, chem. combination effects 0-93435
 Young's modulus and internal friction, 20°C to melting point (Russian) 0-89278
 Bi II homologous ions series, Stark broadening trends 0-105157
 Bi-garnet thick layers, regular domain structure, magneto-optical diff. of light 0-108188
 Bi:Te(Sn,Sb,Pn), US attenuation meas. 0-92614
 Bi-BiO₃ black layer, on polyvinylidene fluoride film, thermal diffusivity pyroelec. camera tube for IR imaging 0-57369
 Bi-Te multilayer thin film struct. thermoelec. props. 0-92964
 Bi-Zn, light ion large angle scatt. in weakly screened Rutherford region 0-84823
 Bi₂, three photon excitation, Bi Rydberg series 0-106280
 Bi₂O₃/Bi³⁺/electrolyte system, field and temp. depend. of electronic current 0-66814
 CaO:Bi surface, O₂ chemisorpt., positive ion emission determ. 0-92785
 Cs₂NaYCl₆:Bi³⁺, luminescence props., emission and excitation spectra 0-108262
 GaP:Bi,N, photoluminesc., electroluminesc., 4.2 to 300K, excitons and hole traps 0-108275
 Ge:Bi, γ-irrad., carrier trapping and recomb. at point radiation defects 0-107810
 Si:Bi, dopant solubility limit, laser irrad. effects 0-84295
 Si:Bi, ion implanted, annealing of heavy ion cascade damage, channelling meas. 0-89255
 Si:Bi, ion implanted, channelling obs. of pulsed Q-switched ruby laser annealing 0-59542
 Si:Bi, ion-implanted, solid phase epitaxial growth during annealing, super-saturated solid soln. form. 0-103384
 Si:Mn,Bi, standard, doubly implanted, Rutherford backscattering meas. at MeV energies, screening corrections 0-88204
 Te:Bi, impurity spectroscopy 0-65499
 Te:Bi, photoconductivity in strong mag. fields, doping effects, impurity levels 0-75602
 Te-Bi, thin film system, stress-relief appearance conditions 0-65416
 ZnTe:Bi, laser annealing, channelling, reflectivity spectra 0-66215

bismuth alloys

see also bismuth compounds

- bounded semimetals, phonon two-stage drag of electrons, thermoelectric power, scatt. mechanism 0-92919
 Ag-Bi, liq. alloys, thermodynamic investigation 0-70428
 Al-Bi, rapid quenching, struct. and decomp. 0-76244
 Al-Bi(Cd)(Pb)-Ti, containing low-melting pt. inclusions, mech. props. 0-93632
 Bi-Cd(Sn), eutectic, contact melting kinetics (Russian) 0-70377
 Bi-Gd(Th) systems, heats of form. 0-89517
 Bi-MnBi eutectic region, of Bi-Mn phase diagram 0-81034
 Bi-Sb, crystallisation temp., overcooling temp. (Russian) 0-97472
 Bi-Sb, thermal EMF giant quantum oscills. (Russian) 0-59960
 Bi-Sb (1 at.%) alloy single cryst. growth solid-liq. interface study 0-107073
 Bi-Sb (12 at.%), cryst. growth from melt, impurity distrib. control by electrotransfer method (Russian) 0-66418
 Bi-Sb (6 at.%) whiskers, persistent metallic behaviour, elec. resist. meas. 0-75544
 Bi-Sb alloys, metal-semimetal point contacts, volt-ampere characteristics (Russian) 0-65683
 Bi-Sb-Te melt, Sb and Te distribution coeffs. during crystallisation (Russian) 0-93472
 Bi-Sb-(As), band struct., effects of Sb and As, mag. susceptibility meas. (Russian) 0-65775
 BiSb (>20 wt.%), electronic band struct. 0-107698
 BiSb alloys, semimetallic, camera, dispersion relations 0-59854
 Bi_{1-x}Sb_x, deformation calculations, band struct. variation, electron phase transitions due to deform. (Russian) 0-65137
 Bi_{1-x}Sb_x, semiconducting alloy, band struct. study, Shubnikov-de Haas effect (Russian) 0-80181
 Bi₂Te₃, alloy thermocouples for solar thermoelectric conversion 0-94095
 Cu-Bi, grain boundary struct. intergranular fracture, segregation role 0-66648

bismuth alloys continued

- Cu-Bi, grain boundary thickness obs. using electron diffr. techniques 0-79811
 Cu-Bi (0.02 wt.%), intergranular fracture, Kossel X-ray diffr. in SEM obs. 0-108579
 GdFeBi, amorphous ferrimag. films, magneto-optical props., optical spectra 0-76008
 In-Bi, mixed state, pinning centre distrib. statistics, I-V characts. (*Russian*) 0-100571
 In-Bi, small κ supercond., phase transitions higher than second order 0-88668
 In-Bi, pre-melting absorption of sound 0-88277
 Mn-Bi micromagnetic alloy, mag., elec. and elastic props. (*Russian*) 0-108028
 MnBi, domain boundary inertia during mag. reversals (*Russian*) 0-88776
 MnBi film, electrical props., in situ annealing effect 0-65708
 MnBi films, prep. by ionised-cluster beam deposition technique, magneto-optical props. 0-100790
 MnBi-Bi garnet film struct., thermomagnetic recording 0-100588
 Pb-Bi, creep, low-temp., thermal heating and quantum mechanisms, supercond. transition effects 0-79868
 Pb-Bi, strength loss in supercond. transition, nonmag. and paramag. impurities influence (*Russian*) 0-70875
 Pb-Bi, supercond., crit. mag. fields, influence of parameters 0-75691
 Pb-Bi, supercond., T_c evaluation, from ab initio band struct. calcs. on Pb 0-75502
 Pb-Bi, temp. regime of crystn. on rapid cooling (*Russian*) 0-66495
 Pb-Bi counterelectrode Pb alloy Josephson junctions 0-65743
 Pb-Bi liquid alloy, Pb and Bi diffusivities, temp. and conc. depend. (*German*) 0-84311
 Pb-Bi-Tl, supercond., crit. mag. fields, influence of parameters 0-75691
 Pb-Si superconducting solutions, effect of hydrostatic compression on tunnelling (*Russian*) 0-65746
 PbBi-Al superconducting tunnel junctions, optically illuminated, quasiparticle energy distribution 0-75688
 Pb_{1-x}Bi_x, liquid alloys, local fluctuations and quadrupolar relaxation 0-66060
 Pb, Bi_{1-x}, quench-condensed films, superconducting transition temp., elastic stress and strain effects 0-70883
 PtBi₂h₃, cryst. struct. (*German*) 0-107113
 PtPb₃Bi₃, crystal structure (*German*) 0-84139
 Pt₄PbBi₇, cryst. struct. (*German*) 0-107113
 Sn-Bi, crystallisation temp., overcooling temp. (*Russian*) 0-97472
 Sn-Bi, small κ supercond., phase transitions higher than second order 0-88668
 Sn-Bi, temp. regime of crystn. on rapid cooling (*Russian*) 0-66495
 Sn-Bi, thermal analysis in non-faceted/faceted eutectic systems 0-71637
 Sn-Pb-Bi-(Cd) infiltrated Ti base composite sintered bearing material, antifriction props. 0-60981
 TbBi, mag. transitions, quadrupolar interaction effects 0-80512
 Zn-Bi, liquid, inconsistent conjugated liquidus 0-76232
 Zn-Sn-Bi, ternary phase diagrams, interactive computer program 0-71629

bismuth compounds

- see also bismuth alloys
 electron spin echo envelope modulation, 2-dimens. Fourier transform 0-63680
 Fe₂O₃-Bi₂O₃ sintered material, elec. switching effects due to thermal ionic breakdown (*Korean*) 0-70776
 BaO-Nd₂O₃-TiO₂-Bi₂O₃ system ceramics, high stability low loss dielectric preparation 0-81008
 BaTiO₃-BiFeO₃ solid solns., ferroelec.-antiferromag., magnetoelectric effect at ferroelec. transition 0-100637
 (Bi,Sb)₂(Te,Se)₃, thermoelectric alloys, phase diagrams, and imperfection chemistry 0-108422
 Bi-BiO₂O₃ black layer, on polyvinylidene fluoride film, thermal diffusivity pyroelec. camera tube for IR imaging 0-57369
 Bi-S liquid soln., S activities meas. by EMF method (*Japanese*) 0-70425
 Bi³⁺-HCl solution, metal cation influence on spectra and luminescence kinetics (*Russian*) 0-78627
 Bi₂Al₂O₆, luminesc. expts. 0-60656
 Bi₂CaNa_{2-x}Nb₂O_{3n+3}, intergrowth, IMV high-resolution electron microscopy 0-107436
 BiFeO₃, ferroelec., antiferromag., cryst. and mag. struct., neutron diffr. study 0-65786
 BiFeO₃-LaFeO₃ solid solns., antiferroelec.-antiferromag., magnetoelectric effect at antiferroelec. transition 0-100637
 Bi_{1-x}FeO_{2x}, longitudinally vibrated bars, reson. freq., DC elec. field effects, elastic coupling polarising correction terms 0-60503
 BiGeO₂, photocurrent oscils. in pulsed illumination rel. to piezoelec. props. 0-80325
 Bi_{1-x}GeO_{2x}, crystal gyrotropy, meas. in IR region 0-88957
 Bi_{1-x}GeO_{2x} crystals, principal carriers obs., in dark and under laser illumination (*Russian*) 0-80312
 Bi_{1-x}GeO_{2x}, photoelectric states in real time spatial light modulators, photorefractive effect 0-80676
 Bi_{1-x}GeO_{2x}, thermal cond. and absorptivity 0-70480
 Bi_{1-x}GeO_{2x}, third-order elastic moduli determ. 0-65121
 Bi_{1-x}GeO_{2x}:Dy(Ho)(Er), luminesc., emission and excitation spectra 0-103975
 Bi₄Ge₂O₁₂, 38 mm scintillator, γ -ray response 0-58048
 Bi₃ film, exciton-phonon interaction, optical consts., Faraday effect., permitt. 0-59884
 Bi₃ photographic film, photochem. decomposition kinetics (*Russian*) 0-93782
 Bi₃ photosensitive layers, optical and thermal development (*Russian*) 0-73512
 Bi₃, structure, exciton states and physicochem. characteristics (*Russian*) 0-100435
 Bi₂In₂S₁₂, X-ray cryst. struct. determ. 0-107126
 Bi₂-La₂WO₆, synthesis and crystallography 0-66459
 BiLi, gas phase thermodynamics, Knudsen effusion mass spectrosc. 0-100057
 Bi₂MoO₆, superplasticity during phase transitions 0-108498
 Bi₂O₃, polymorphic transformation and elec. resistivity (*Japanese*) 0-93555
 δ -Bi₂O₃, thermoelectric power, heat of transport of O²⁻ ions 0-92713
 δ -Bi₂O₃, thermoelectric power rel. to fast ionic conduction 0-107549
 Bi₂O₃, thin film capacitor elec. props. under reduced press. 0-80397

bismuth compounds continued

- Bi₂O₃, X-ray absorption, discontinuities and limits, chem. combination effects 0-93435
 Bi₂O₃/Bi³⁺ electrolyte system, field and temp. depend. of electronic current 0-66814
 Bi₂O₃-PbO, glass, cond. meas. using complex impedance anal. (*French*) 0-92707
 BiOCl (BiCl₃), nuclear electric hexadecapole interactions 0-65513
 δ -(Bi₂O₃)_{1-x}(Y₂O₃)_x, thermoelectric power rel. to fast ionic conduction 0-107549
 Bi₂S₃, electrodeposition, using nonaqueous solvents 0-76200
 Bi₂S₃-Bi₂Se₃ and Bi₂Te₃-Bi₂Se₃ systems, thermal cond. change during phase transitions 0-100368
 Bi_{0.88}Sb_{0.12}, semiconducting transport props., 2 to 100K 0-59989
 Bi₂Sb₂O₁₂, magnetophonon effect on hot electrons (*Russian*) 0-107814
 Bi_{1-x}Sb_x, EM wave propag. for rot. of mag. field from Faraday to Voigt config. 0-84419
 Bi_{1-x}Sb_x, solid soln., temp. depend. of weak-field galvanomag. coeffs. (*Russian*) 0-70724
 Bi₂Sb₂Te₂, single crystal, dispersion of magnetoplasma waves (*Russian*) 0-70739
 Bi_{2-x}Sb_{2x}Te_{3-x}Se_x, elec. cond. and thermoelec. props., neutral defects influence 0-60017
 Bi₂SiO₂₀, electrooptic photorefractive crysts. for optical information processing 0-74313
 Bi₂SiO₂₀ film, photoelectric props. obs., UV illumination effects (*Russian*) 0-80313
 Bi₂SiO₂₀, growth of single cryst. thin plates by EFG method 0-97423
 Bi₂SiO₂₀, optical sensor for measurement of high electric field intensity 0-69509
 Bi_{1-x}SiO_{2x} PROM device, image recording and erasure mechanism 0-74490
 Bi₂SiO₂₀, photoelectric states in real time spatial light modulators, photorefractive effect 0-80676
 Bi₂SiO₂₀, photorefractive, vibr. struct. mode pattern visualisation, phase conjugation and dynamic holography 0-95938
 Bi₂SiO₂₀, photorefractive medium, real-time image processing via four-wave mixing 0-95944
 Bi₂SiO₂₀, third-order elastic moduli determ. 0-65121
 Bi₂SiO₂₀:Sn(Mo), Raman scatt. spectra, impurity effect 0-80795
 Bi₂Te₃, anodic film form., in situ ellipsometric study 0-104318
 Bi₂Te₃, surface prep. by etching for electroplating elec. contacts 0-108647
 Bi₂Te₃-Bi₂Se₃ solid solns., single cryst. growth and thermocouple construct. 0-104056
 Bi₂Te₃-Bi₂Se₃-Sb₂Te₃ solid solution, single crystal, elec. cond., thermoelectric props. 0-88550
 BiTel, melt and vapour grown, optical props. 0-84746
 (Bi₂Te₃)_{0.9}(Sb₂Te₃)_{0.1}(Sb₂Se₃)_{0.05} n-type alloy for thermogenerators, thermo-EMF, elec. cond. and thermoelec. efficiency factor, 300-600K 0-70735
 Bi₂Ti₂O₁₂, elec. characts., phase transition obs. 0-60517
 (BiTm)_{1-x}(FeGa)_xO₁₂ ion implanted epitaxial garnet film, bubble domains, cryst. struct. disorder 0-93150
 BiVO₄, ferroelastic domains, electron microscopy and electron diffr. obs. 0-100254
 BiVO₄, ferroelastic phase transition, birefringence meas. using rotating-analyser method 0-80742
 BiVO₄, ferroelastic phase transition, birefringence meas. at simultaneous high pressure and temp. 0-80743
 Bi₂WO₆, ferroelectric, dielectric props., elec. cond. and relaxation phenomena obs. 0-80692
 Bi₂WO₆, hydrothermal and flux growth 0-76166
 Bi₂WO₆ layered ferroelectric, anomalous photovoltaic effect, photovoltaic current 0-75603
 Bi₂WO₆, superplasticity during phase transitions 0-108498
 (Cu,Ag)₂Se/(Bi, Sb)₂Te₃, P type selenide segmented element fabrication, thermoelectric props. 0-107835
 Fe₂O₃-Bi₂O₃ sintered material, elec. switching effects for temp. range 700-850°C (*Korean*) 0-70775
 (Gd, Bi)₂ (Fe, Ga)₂O₁₂ magneto-optic LPE garnet films, high-energy heavy ion irradi., props. 0-71390
 N-Ge-Bi-Se glass, elec. and optical props. 0-65550
 Ge-Bi-Te system, thermal cond. change during phase transitions 0-100368
 K₂BiNb₂O₁₅ substrate for K₂Li₂Nb₂O₁₅ film for optical waveguide, cryst. struct., dielectric props. 0-79016
 (K₂/4)(Bi_{1-x})(Zn_{1-x}Nb₂O₁₀)O₃ cation disordered perovskite, elastic consts. and thermal expansion 0-96587
 Li₂O-Bi₂O₃, rapidly quenched glasses, Li⁺ ion cond., elec. cond. 0-100346
 Na₂O₂Bi₂O₃TiO₃, phase transition, hysteretic behaviour 0-71330
 Na₂O-B₂O₃-Bi₂O₃ glass with metallic Bi granules, elec. cond. 0-84493
 Pb_{1-x}Bi_xF_{2+x} solid soln., struct. and ionic cond. correl., neutron diffr. study (*French*) 0-84324
 PbO-B₂O₃-Bi₂O₃ glass with metallic Bi granules, elec. cond. 0-84493
 (Sb₂Se₃)_{0.7}(Bi₂Se₃)_{0.3} solid soln., prep. and elec. properties of layered crystals 0-70762
 Sb₂Te₃-Bi₂Te₃ solid solns., single cryst. growth and thermocouple construct. 0-104056
 Sb₂Te₃-Bi₂Te₃ system, thermal cond. change during phase transitions 0-100368
 Sr_{1-x}(Na_{0.5}Bi_{0.5})_x solid solutions, piezoelec. and ferroelec. props. (*French*) 0-108158
 Sr_{1-x}(Na_{0.5}Bi_{0.5})_x1-xTiO₃ ferroelec. ceramic, hot pressing, numerical simulation (*French*) 0-76220
 Te-(Bi,Sb)_{1-x}Te₃ eutectic, electrophys. props., directed crystn. conditions influence and comp. depend. 0-107827
 Te-Bi₂Te₃ and Te-(Bi_{1-x}Sb_x)₂Te₃ system eutectics, crystn. rate effect on electrophys. props. mutual solubility effect 0-60774
 Te₂Ge_{20-x}Bi_x, DSC studies of struct. phase transformation 0-66505
 Ti-Bi-Sb-Te system, peritectic reactions in TiBiTe₂-TiSbTe₂ cross section, crystn. character 0-108406
 (YGDyBiBi)(FeAl)₂O₁₂ ferrite-garnet films, effect of in-plane field on dynamics of domain walls 0-65979
 (YGDyBiBi)(FeAl)₂O₁₂ epitaxial garnet film, uniaxial ferromagnet domain struct., phase transition (*Russian*) 0-108044
 YIG, Bi-substituted, LPE, domain wall reson. 0-60387
 (YRbBi)(FeAl)₂O₁₂ films, R=Gd, Yb, Faraday effect in transverse mag. field, orientation depend. 0-88971

bistable multivibrators *see* flip-flops

Bitter patterns *see* magnetic domains

bitumen *see* materials

BL Lacertae-type objects

1308+32, rapid optical outburst, 1980 June to July 0-98733

1309-216, probable BL Lacertae object with absorpt. red shift 1.49, optical spectrum 0-67856

brightness rapid variability, search in eight quasars and BL Lacertae objects 0-90567

catalogue, optical revised 0-105177

distances, statistical upper limits determ. from absence of redshifted C IV absorpt. lines 0-62267

highly polarised objects detection device (*Japanese*) 0-82209

BL Lacertae, major radio outburst, (1980 April 17 to May 6) 0-73043

BL Lacertae, radiowave dispersion by plasma ejected from core 0-82516

MC2 1210+121 and 1620+103, radio-quiet objects 0-101641

MC5 1307+121, radio spectrum shape, VHF and SHF obs. 0-67866

millimetre wave emission, rapid variability obs. (*Russian*) 0-90559

O1 090.4, photometric history 0-77491

OJ-131, photometric history 0-77491

OJ 287, periodicity investigation at 21 cm 0-82529

OJ 287, radiowave dispersion by plasma ejected from core 0-82516

PKS 0735+178, flat radio spectrum as component synchrotron radiation 0-94880

PKS 2155-304, rapid X-ray variability obs. 0-73035

PKS 2155-304, spectral slope from far UV obs. 0-82509

polarisation, visual and IR photometry and polarimetry of 10 objects 0-77480

radio emission, variable, temporal characts. (*Russian*) 0-62307

radiowave dispersion by plasma ejected from core 0-82516

black holes

see also gravitational collapse

accretion discs, thick discs models rel. to supercritical luminosities 0-101614

accretion disk model, gas flow above alpha disk 0-62161

accretion process giving rise to X-ray emission 0-90459

adiabatic accretion onto Schwarzschild black hole 0-77445

charged black hole, motion in EM field, EM and gravitational perturb. of Reissner-Nordstrom space time 0-82407

collisions, time-asymmetric initial data from nonsingular vacuum Cauchy hypersurfaces 0-82408

cosmic censorship and test particles, black hole destruction 0-105552

Cygnus X-1, accretion disk round black hole, temp. var. 0-109561

Cygnus X-1 (V1357 Cygni), optical light curve vars. rel. to X-ray vars. 0-109560

electrodynamics in curved space, theory 0-90465

energy emission, Heisenberg's uncertainty principle 0-105454

evaporation back reaction problem, conserved energy flux 0-85972

formation, effect on radiation-matter flat universe 0-94900

galactic nucleus, tidally disrupted star gas debris accretion and radiation spectrum 0-90467

galaxies active nuclei, massive black hole binaries model 0-109546

galaxies active nuclei, massive black hole model and Monte Carlo simulation of relativistic Comptonisation 0-90566

geodesic equation, rel. to Hawking's black hole area theorem 0-90468

giant black holes mass-density diagram (*French*) 0-94828

Gibbs-Duhem relation from Weinholds geometric approach 0-57153

grand unified theories, baryon production through primordial black holes 0-101970

gravitational collapse, bimetric general relativity theory 0-85853

gravitational collapse of stellar core, secondary indications 0-62177

gravitational collapse with charge and small asymmetries, interacting EM and gravitational perturbation 0-105274

gravitational lens effect, EM wave diff. in Schwarzschild space-time 0-90750

gravitational lens effect, focusing by slowly rotating relativistic spherical mass 0-105155

gravitational radiation, collapsed objects and exact solns., Einstein Centenary Summer School, Perth, Australia, 1979 January 0-105434

gravitational wave detection, astrophysical sources, resonant mass, laser interferometer and Doppler ranging methods 0-68122

gravitational waves radiation, reson. freqs. of rotating black holes free oscills. 0-105271

growth in dense stellar systems with evaporation of stars 0-62178

Hawking effect, temp. relativity, axiomatic field theory 0-109456

inverted black holes, anisotropic collapse, static vacuum, electrovacuum field struct. 0-67776

Kerr black hole, low-freq. radiation from infalling particle 0-62176

Kerr black holes, stable circular orbits of test particles moving in equatorial plane 0-85970

Kerr metric effect on EM wave plane of polarization 0-94827

Kerr-Newman black-hole interior, quantised massless field, instability 0-82409

Kerr-type particle, uniformly accelerating and rotating, Schwarzschild, Rindler and Kerr surfaces 0-85855

Killing horizons around a uniformly accelerating and rotating particle emitting gravitational radiation 0-105557

M87, anisotropic stellar vels. distrib. rel. to supermassive black hole model 0-82500

M87, spectroscopic evidence for large central mass 0-94873

NGC 4151, Seyfert galaxy, massive collapsed object accretion model for repeated X-ray flaring 0-90534

NGC 741, 1316, 7626, radio galaxies, central dense star clusters luminosities rel. to accreting black holes 0-94871

observational traits of black holes in the optical band 0-67777

primordial black holes, baryons generation 0-98750

primordial black holes, evaporating, rel. to galactic positrons primary source and fates 0-109319

primordial black holes, influence on galactic radio spectrum 0-62179

primordial black holes, radiation accretion in early Universe 0-67918

primordial mini black holes explosion rate, upper limit from gamma-ray bursts search 0-67911

primordial singularity in uniform Friedmannian universe 0-101656

quantum evaporation, baryon asymmetry of the Universe (*Russian*) 0-109577

quasars, massive black hole model and Monte Carlo simulation of relativistic Comptonisation 0-90566

recoil velocities due to gravitational radiation reaction 0-85969

Reissner-Nordstrom, coupled gravitational and EM perturb., scatt. matrix, energy conversion, quasi-normal modes 0-67775

black holes continued

rotating black holes, superradiance, spin thermodynamic explanation 0-86179

rotation, spin-up by thick accretion discs 0-105273

Schwarzschild hole in radiation heat bath, stochastic evolution 0-85971

Schwarzschild space-time, vacuum polarisation induced by gravitation 0-82410

shear hell holes and anisotropic universes 0-95011

spherically symmetric, perturbations, linearised Einstein-Maxwell eqns. 0-72992

SS 433, accreting black hole model 0-85958

SS 433, emission regions and black hole accretion disk 0-67746

SS 433, massive black hole and pulsar models rel. to precessional motion origin of 164^d period 0-62138

stellar cluster around massive black hole, stationary state (*Russian*) 0-67806

superadditivity and concavity, black hole systems 0-98867

supercritical accretion discs around black holes, models 0-105272

thermally evaporating, Raychaudhuri eqn. 0-109457

vacuum, empty, fields and quanta, strong gravity, particle-antiparticle annihilations 0-68400

blast waves *see* shock waves

Bloch walls *see* magnetic domain walls

blood

see also haemodynamics

arterial vessels, small, critical changes in lumen 0-61615

atherosclerosis, rheological aspects (*Japanese*) 0-94268

body fluid volume changes induced by spaceflight 0-61715

brain-blood barrier, effects of microwave-induced hyperthermia, rat 0-61642

brain-blood barrier, problems in quantifying effects, comparison of methods 0-61643

brain-blood barrier, reversal of microwave-induced permeability 0-61641

Clq of human complement, neutron scatt. obs., conformational calcs. 0-81537

capillary tracer exchange, 4-phase model 0-101152

cardiac blood pool, ECG-gated emission computerised tomography 0-98117

cell electrophoretic mobility meas. using new automatic method 0-67322

cerebrovascular permeability, quantitative method for meas. of alterations 0-61748

characterisation by US and computed tomography 0-98045

chromosome aberrations, dose-effect relationship, population exposed to increased natural radioactivity 0-72254

chromosome aberrations induced by low doses of X-rays in human lymphocytes in vitro 0-72235

coagulation kinetics of normal and haemophilic plasma, rheological study 0-67107

Couette viscometer for short time shearing of blood 0-98179

couple stress fluid flow through narrow tubes 0-67105

criticality accidents, dosimetry using activations of blood and hair 0-89857

deoxyhaemoglobin, ferrous heme of high-spin type, MCD spectra in Soret, visible and near IR regions 0-94156

deoxyhaemoglobin, proton NMR, modified DEFT technique for obs. hyperfine shifted line, T₁ values meas. 0-76871

energy metabolism of blood morphotic elements, ionising radiation effects 0-61645

erythrocyte, flow resistance into pores 0-61609

erythrocyte distribution profiles during sedimentation as determ. by HeNe laser light 0-81563

erythrocyte membrane alterations, rheological technique evaluation 0-61611

erythrocyte membranes, fluidity change after X-irrad., pyrene excimer fluorescence obs. 0-72262

erythrocyte nucleosomes, chicken, temp. dependence of ³¹P-NMR spectra 0-94280

erythrocyte sedimentation rate in inclined tubes 0-67048

erythrocytes, ^{99m}Tc-labelled, spleen scanning in humans 0-67230

erythrocytes, human, haemoglobin's suspending medium, dielec. props. obs. 0-76716

erythrocytes, rabbit, increased passive efflux of ²²Na and ⁸⁶Rb on microwave irrad. 0-108957

erythrocytes labelled with stable Rb, survival determ. by fluorescence excitation anal. rabbits 0-81788

extracorporeal irradiation method for rats 0-72396

fibrinolysis and coagulation, dynamic rheological studies 0-61614

flow measurement, UDP-30 arterial US pulse Doppler flowmeter 0-104805

flow through narrow capillaries, rheological mechs. 0-97961

gas valves, anal. in mice following pulmonary irrad. 0-104673

gated blood pool scan, radioisotope evaluation of ventricular performance 0-85483

haematopoiesis progenitor and effector cells, expt. murine system, whole body irrad. obs. 0-98034

haematopoietic malignancy diagnosis, significance of SEM 0-85529

haemodilution effects on viscosity and red cell aggregation 0-97952

haemoglobin, human, maleimide spin labeled, proton ENDOR spectra obs. 0-89719

haemoglobin, quaternary struct., hydration and self-association, ¹H NMR obs. 0-67040

haemoglobin haem structure after photo-deligation, Raman spectra 0-61510

haemoglobin-O₂ equilibrium curve, instrument for determ. based on membrane diffusion 0-81761

haemorrhology, lecture (*Japanese*) 0-98752

haemorrhology and diseases, conf., Nancy, France (Oct. 1979) 0-56991

haemorrhology related to blood cells, conf., Hamburg, Germany (Aug. 1979) 0-62365

haemorrhagic shock, effect of anemia on O₂ transport 0-67330

haemorrhagic shock, effect of increased blood-O₂ affinity on O₂ transport 0-67331

leucocytes, radioactive-labelled, appl. for proof of inflammations 0-67218

leukocytes, automatic recognition and classification systems (*Italian*) 0-81780

leukocytes of human blood, gravity sedimentation anal. 0-98197

Lymphocytes, human, effect of irrad. on hexose monophosphate shunt pathway 0-76798

lymphocytes, human, effects of heat and radiation 0-97864

blood continued

- lymphocytes, human, effects of low-dose radiation on repair processes 0-98023
- lymphocytes, human, RBE for d(42 MeV)-Be neutrons based on chromosome-type aberrations 0-104663
- lymphocytes, human, variation in neutron RBE values compared to X-rays 0-101229
- lymphocytes, human peripheral blood grown in γ -irrad. medium, sister chromatid exchanges 0-104658
- lymphocytes, peripheral, population changes following radiation therapy to limited and extended fields 0-72236
- lymphocytes exposed to temps. of 37-45°C, two types of interface death 0-104566
- mechanics of blood flow 0-76778
- mesentery tissue, burn induced alterations of interstitial diffusion 0-104634
- micropolar fluid model for blood flow through narrow tubes 0-67109
- monocyte function rel. to irrad. in breast cancer patients 0-72238
- NMR T_2 relaxation time studies in normal and pathologic blood 0-81682
- organ transfer kinetics of radioisotopes 0-109044
- partial pressure of gases meas., in vitro electrochemical sensors 0-67303
- particle etch track technique determ. of U trace content in normal human blood 0-89910
- perfusion prediction from meas. of phase shift between heat flux and temp. 0-104804
- perfusion rate estimation from diffusible indicator meas., sensitivity anal. 0-104803
- plasma proteins, high energy-induced aggregation, time resolved spectra 0-61655
- plasma viscosity in sickle-cell anaemia 0-94250
- platelet interaction with vessel surface, blood rheological factor influences 0-61612
- red blood cell freezing, cryopreservation and refrigeration 0-67262
- red blood cells, equilib. shapes in osmotic swelling 0-85368
- red blood cells, minimum energy anal. of membrane deform. 0-72141
- red blood cells, rheological props. meas. by Couette viscometer 0-97992
- red blood cells, viscoelastic study of aggregation 0-97960
- red cell, human, increased passive permeability below 12°C 0-94185
- red cell etching by ion beam sputtering for SEM 0-85554
- red cell flexibility, effect on blood flow through tubes of 30-500 μ m 0-67111
- red cell membrane, human, surface elasticity and viscosity 0-61608
- red cell membrane, Li transport in manic depressives 0-61525
- RF waves, effects of repeated exposure on growth and haematology of mice 0-61625
- rheological behaviour, viscoelastic model (French) 0-76779
- rheological behaviour of stored blood cells (French) 0-67110
- rheological hysteresis at low shear rate 0-97962
- rheology, erythrocyte rigidity effects on viscoelastic dilatancy 0-61610
- rheology conference, Osaka, Japan (June-July 1979) 0-62364
- SCF-LCAO-ASMO and CI calcs. of low-lying multiplets and excited states 0-94155
- serum, human, trace elements determ. by proton activation 0-81731
- serum, rapid anal. by mass spectrometry/mass spectrometry 0-61173
- Shroud of Turin, blood presence identification, spectroscopic and chem. tests 0-102875
- stenosis effects on non-Newtonian flow in artery 0-89775
- temperature monitoring during extracorporeal circulation, noncontact transducer 0-85513
- thermal expansion coeff. of blood and its constituents (German) 0-104556
- thrombosis, rheological aspects (Japanese) 0-94268
- transport in biomembrane, NME determ. methods (Rumanian) 0-94435
- trauma in extracorporeal oxygenation, conf., Stolberg, Germany (Nov. 1978) 0-94922
- viscoelastic properties, transient flow obs. 0-97980
- viscoelastic tube, pulsatile flow, non-Newtonian effects (French) 0-59113
- viscosity and red cell aggregation at zero and 1G, instrumentation for Space Lab 3 0-61716
- viscosity at low shear rate, capillary viscometer and obs. 0-98180
- water mobility in blood plasma, NMR determ., viscosity correl. to $1/T_2$ 0-67176
- weightlessness, haematological response, math. and exptl. simulation 0-61714
- CO-haemoprotein photolysis, transient Raman study, quantum yield origin 0-67155
- 111 In labelled human platelets, dose obs. 0-94370
- O_2 , meas. by fast-responding flow independent blood gas catheter 0-101277

blood circulation see haemodynamics

blood dynamics see haemodynamics

blood flow see haemodynamics

blood platelets see blood

blue brittleness see brittleness

boilers

- 100 MW fluidised bed combustion district heating plant burning high S content residual oils 0-108777
- 200 MW atmospheric fluidised-bed combustion steam generator, comparison of three designs 0-108776
- atmospheric fluidised-bed combustion boiler development facility, first year of operation 0-108775
- drum boilers, working at 11.0 to 15.5 MPa, pH control by addition of caustic soda (Russian) 0-89420
- feedwater redox potential meas. by Pt thin-layer electrodes 0-89578
- fluidised-bed steam generating system to supply 100000 lb/h of saturated steam burning high S coal 0-108778
- heat transfer crisis location under conditions of nonuniform heat release 0-64534
- high pressure, in-service scavenging by intermittent dosing with chelating agent 0-89485
- inlet temps. and corrosion product deposits, water chemistry effects 0-89528
- LMFBR, Na-H₂O steam generators, safety problems and their solution in the USSR 0-63318
- multifuel fluidised bed combustion packaged boiler to supply 10000 lb/h saturated steam at 100 psig 0-108779
- nuclear steam generator tubes testing and evaluation, using CIS/DASIO system (Czech) 0-63301
- oil-fired, opacimeter use possibilities (Rumanian) 0-87483

boilers continued

- oil-fired boilers, noise reduction by casing (Hungarian) 0-106663
- once through steam generator, Na-heated, stability anal. nuclear reactor systems model 0-91218
- once-through high press. boiler feedwater solutes behaviour 0-63233
- once-through nuclear boiler at 14.5 MPa hydrothermal and chemical conditions 0-63232
- power plant dynamics and control, conf. Hyderabad, India (Feb. 1979) 0-91215
- PWR boiler tubes, denting type corrosion, control by use of neutralisers 0-106109
- PWR power station secondary water chemistry study, progress report 0-106108

boiling

- see also boiling point
- acetone, heat emission in crit. region, press. and heating surface temp. effects (Russian) 0-69634
- bubble growth on heating surfaces in pool boiling, conservation eqns. soln. (German) 0-74715
- bubbles, evaporating, of low-boiling liq., surface condensation of high-boiling mixture vapours 0-59021
- critical boiling heat fluxes to liquids at subatmospheric pressures 0-64345
- dielectric liquids, boiling process in narrow horizontal channels due to action of elec. field (Russian) 0-74707
- ethanol, boiling at subatmospheric press., heat transfer rate, heating surface effects 0-69630
- explosive flashing in pools of liquids 0-92024
- film- and transition-boiling heat transfer to cryogenic fluids 0-92026
- fission reactors, flow boiling dynamics in film region 0-83142
- flow film boiling, void fraction meas. 0-92207
- flow structure for critical discharge conditions of boiling water through cyl. channels 0-83145
- forced convection boiling, critical heat flux, Fe₂O₃ scale effects 0-64344
- Freon-113, boiling and heat transfer on horizontal pipes with annular fins 0-74855
- heat-emitted pipe, with surface boiling, temp. fluctuations (Russian) 0-102962
- heating element, heat exchange, effects of nonstationary liberation of power (Russian) 0-69636
- horizontal tubes, saturated flow boiling, non-uniform heat flux effects (German) 0-74716
- hydrothermal flows in permeable media, boiling rel. to two-phase flow struct. 0-85693
- laminar film boiling heat transfer, thermal conductivity and convection effects 0-74864
- liquid, underheated, boiling, sonic pulses generation, time and spectral characteristics 0-107373
- liquid metals, incipient boiling superheats, heat flux effects 0-74697
- LMFBR Na boiling, two-phase flow calculations in low-pressure systems 0-103068
- metastable flows of water, spontaneous boiling 0-106709
- mushroom shaped heating surface, computational errors and heat losses 0-64347
- nuclear reactor safety and performance, boiling crisis, state of the art review 0-63312
- partial nucleate boiling, eval. of Kutateladze's eqn. 0-79298
- power reactor, water cooled and moderated, tube film boiling heat transfer coeffs. 0-73877
- pure liquid and binary soln. superheat, convective heat transfer from thin wire 0-92139
- steam generating channel, nonuniform heat release, heat transfer crisis location 0-64534
- structured surfaces to liquid nitrogen, boiling heat transfer (German) 0-99919
- supercritical water, transient loads and flow, tube hot spots, nucleate boiling departure 0-64349
- superheated binary solns., flashing kinetics, nucleation and critical bubble 0-92035
- superheated water, flashing kinetics, γ -radiation effects 0-92025
- thin liquid film flows, boiling crisis models 0-74710
- tubes, nucleate pool boiling, critical heat flux, ferric oxide scale effects 0-64343
- tubes, straight and coiled, boiling heat transfer with low pressure water flows 0-74856
- tubes, temp. and heat transfer coeff. variation upon boiling mode changes 0-69629
- vapour bubble in saturated liq. free convection boiling, growth rate and detachment diameter 0-103057
- vertical tubes with zero inlet subcooling, forced convection boiling, critical heat flux 0-64549
- water, boiling and heat transfer on horizontal pipes with annular fins 0-74855
- water, boiling at subatmospheric press., heat transfer rate, heating surface effects 0-69630
- water, maximum boiling superheat, of drop submerged under immiscible liquid layer 0-79928
- water-fuel emulsion drop, microexplosive boiling of metastable overheated water, microblast (Russian) 0-74930
- water-in-oil emulsion, boiling, bubble formation, cinemicrophotography 0-74961
- Fe₂O₃, haematite, effect of boiling on the mass transfer of corrosion products in high temperature, high pressure water circuits 0-71766
- K channel flow, incipient boiling superheats 0-74709
- Na, liq., boiling hazard in LMFBRs (French) 0-78402
- UO₂, fuel-coolant interaction, film boiling and vapor explosion phenomena 0-95363

boiling point

- see also boiling: heat of vaporisation
- melting and boiling points vs. Coulomb pot., parabolic behaviour 0-70375
- vapour-liquid crit. props. for pure liqs. and mixtures 0-65213
- ⁴He, P- ρ -T data near vaporisation crit. point (Russian) 0-88373
- UF₆, vaporisation behaviour 0-84283

bolometers

- cone absorption calorimeter for pulsed laser meas. 0-98980
- laser calorimeter types and techniques 0-69441
- superconducting, high-speed, based on Ag-Sn double films 0-57368
- superconducting, space appl. 0-85836
- superconducting double multivibrator used as near- and medium-infrared radiation detector (German) 0-90892

bolometers continued

- superconductive FIR detectors, Josephson-junction direct devices and transition edge bolometers, review 0-77865
thin absorbing films, EM plane-wave interaction 0-95767
type BN (USSR), construction and characts. 0-57372
AI granular superconducting bolometer as mol. beam detector 0-73524
CO₂ rot. distrib. in supersonic beam, IR bolometry using tunable diode laser 0-63869
Ge and Ge-diamond bolometers operated at 4.2, 2.0, 1.2, 0.3, 0.1K, design and construction 0-77868
Ge film bolometer, radiation loss from JFT-2 Tokamak, meas. 0-95141

Boltzmann equation

- see also transport processes
Brownian fluid affected by potential, Maxwell-Boltzmann distrib. in infinite-time limit 0-105573
charge imbalance relaxation freq. depend. near superconducting T_c 0-93030
classical Boltzmann kinetic theory justification using Liouville theory 0-87838
clean superconductor, effect of impurity scatt. on thermally induced charge imbalance 0-60135
dilute gas, kinetic perturbation theory 0-100051
dipole relaxation in electric field, teaching 0-90625
early Universe, baryon number generation due to CP- and B-violating interactions 0-109571
elastic media, dissipative, relativistic electrodynamics 0-73219
electron backscattering transport theory, SEM and EPMA appl. 0-57439
electron-neutral collisions, calc. with respect to momentum transfer, new approach to Boltzmann collision integral 0-92255
electronic multiple-band systems, dielec. function in generalised relax.-time approx. 0-103637
electrons, field-accelerated, in dry air and pure O₂, macroscopic props. comparison (French) 0-59161
energy deposition, transport eqn. for point anisotropic source in infinite homogeneous medium 0-88228
equilibrium birefringence for weakly ionised molecular gas in strong mag. field 0-83881
Fokker-Planck model, transport equation renormalisation 0-82732
gas, electron and hole transport theory, free-path method, orders of approx. 0-62598
gas, moderately dense, Bhatnagar, Gross and Krook model from Chapman-Enskog equations 0-106864
gas, weakly ionised, electron distrib. function, isotropic component, collision source 0-62599
gas, weakly ionised, electron transport quantities, divergences 0-57222
gas dynamics eqn. boundary conditions in Chapman-Enskog Boltzmann eqn. soln. 0-96284
gas flows, entropy prod. determ. using Boltzmann's H-theorem, Knudsen effusion 0-106867
hard sphere gas mixture, vel. autocorrelation function calc. 0-75019
hard spheres in thermal eqn., time correlation functions in low-density limit 0-64859
heavy ions in light gases in electric field, limits of Kihara distrib. 0-87837
heterogeneous media, energy deposition of slowing down particles 0-88230
hot atom+mol. reaction, steady state vel. distrib., Boltzmann eqn. with BGK elastic collision model 0-66856
hot atom reactions, nonequilib. time-depend. theory, model calcs. 0-61125
initial boundary value problem of the linearized Boltzmann equation in an exterior domain 0-90797
internal state, similarity solutions 0-86231
ionised gas, macroscopic props. of field accelerated electrons, soln. of Boltzmann eqn. 0-61118
linear, spatial homogeneous eqn. with soft potential 0-77730
Liouville problem, quasi-particle dynamics from a given kinetic eqn., inverse 0-101749
many-valley semiconductors, conduct. in heating electromag. wave 0-84483
Maxwell models, similarity solutions 0-86231
metal, electron Boltzmann eqn. solns., energy depend. 0-88537
metal, linearized Boltzmann eqn. soln., resist. and deviation from Matthiessen's rule 0-65523
metals, surface positronium formation, stopping distance, positron-phonon interactions 0-96582
neutron Boltzmann eqn., P₁ and diffusion eqn. asymptotic equivalence 0-95334
neutron gas system in stationary power reactor with decoupling thermodynamics and distrib. function 0-86950
neutron transport theory, slabs and spheres, criticality problems 0-57817
nonequilibrium particle distrib., finite energy intervals (Russian) 0-77736
nonlinear, diffuse binary scattering in microcanonical ensemble, similarity solutions 0-86231
nonlinear, with soft potential, spatially periodic problems 0-77731
nonlinear Boltzmann equation, for internal state and Maxwell models 0-77733
nonlinear Boltzmann equation, solns. of Krook-Tjon-Wu model, Laguerre expansion of distrib. function 0-68157
plasma, relativistic Boltzmann theory, reduction of collision integrals 0-79560
reactor dynamics, localised, P, approx. to Boltzmann eqn. 0-78347
relativistic Boltzmann kinetic eqn. derivation 0-68161
semiconductor, ambipolar diffusion, electron-hole scatt. effect 0-59976
semiconductor, electron and hole transport theory, free-path method, orders of approx. 0-62598
semiconductor, homogeneous, nondegenerate, single-level Schockley-Read-Hall recomb. centres, flicker noise 0-70779
soluble-model Boltzmann equations for spatially uniform systems, written in form of stochastic equation 0-95046
spatially inhomogeneous Boltzmann eqn., soln. continuity from existence and uniqueness theories 0-105592
spinodal decomposition, phase separation kinetics, Boltzmann's transport eqn. calcs. 0-79952
stochastic Boltzmann equation, hydrodynamic fluctuations 0-68158
superconducting weak links, order parameter and quasiparticle dynamic props. 0-100555
swarm transport coefficients, iterative method calcs. 0-96336
Ar, electron avalanche development, exact Boltzmann eqn. anal. 0-59318

Boltzmann equation continued

- GaAs-Al_xGa_{1-x}As heterostructures, real-space electron transfer by thermionic emission, analytical model 0-100512
H₂, elec. discharge, non-equilib. ionisation rate calcs. 0-59319
HB rot. relaxation, diffusion theory 0-106313
HCl, rot. relaxation, diffusion theory 0-106313
He, superfluid B-phase, shear viscosity, s-p-d wave approximation 0-96715
He, electron localisation, mobility in dense low temp. gas 0-92247
He, liq., cyclotron reson. of hot electrons 0-88377
Hg positive column, electron energy distrib., numerical soln. of Boltzmann eqn. 0-87982
Li-Mg, Matthiessen's rule, elec. and thermal deviations, impurity scatt. 0-88536
N₂, weakly ionised, electron transport coeffs., Boltzmann eqn. anal. (Japanese) 0-59183
Na, Hall coefficient, quasiclassical Boltzmann eqn. calcs. 0-103678
Ne plasma, electron collision ionisation, electron kinetic behaviour during elec. field perturbation (German) 0-64676
O₂, weakly ionised, electron transport coeffs., Boltzmann eqn. anal. (Japanese) 0-59183
SF₆-N₂ mixture, electron swarm development, Boltzman eqn. anal. 0-87841

Boltzmann-Vlasov equation see Vlasov equation**bond angles**

- adamantane, derivatives in solution, mol. motion and methyl group rot. barriers from ¹³C NMR relax. times 0-74179
bond bending, bond orbitals rel. to nucl. motion 0-95513
covalent semiconductors, displacement correlations, adiabatic bond charge model 0-70350
cyclic 4-ring rotation-puckering, use of spherical coords. 0-58193
ethylene, molecular geometry optimisation, variable metric method, internal geometry 0-95744
metal surface, chemisorbed water molecule struct., interband angle 0-59787
methanol, molecular geometry optimisation, variable metric method, internal geometry 0-95744
molecules, bridge angle, vibr. behaviour, simplified and accurate calcs. 0-95735
norbornane, derivatives in solution, mol. motion and methyl group rot. barriers from ¹³C NMR relax. times 0-74179
oxirane cation, struct. rearrangement following vertical ionisation, ab initio CI calc. 0-58191
quartz, low, cell parameter variations between 94 and 298K 0-96497
quinazolines, enzyme inhibitory, structure-activity quantitative study 0-78540
spirohydrocarbons, strained, bond angles, interatomic distances, semiempirical and ab initio calcs. 0-95533
tetrafluoro-p-benzoquinone, mol. struct., gas phase electron diff. obs. 0-58386
1,1,1,2-tetrafluoroethane, mol. struct. studied by gas-phase electron diff., vibr. amplitudes, bond angles and lengths calc. 0-95740
toluene, mol. struct., ab initio calcs. 0-106262
triatomic dihydride molecules, Walsh's rules and small bond angle states 0-106255
BH₂, Walsh's rules and small bond angle states 0-106255
C₂A₂II₂ state, orbital angular momentum 0-78514
CH₂⁺, Walsh's rules and small bond angle states 0-106255
Cs₂Te₃, synthesis and cryst. struct. 0-88115
Cu complex, [Cu(1,4,7,10-tetrabenzyl-1,4,7,10-tetraazacyclododecane)Cl]NO₃, cryst. struct. 0-64966
Fe complex, nitrile nonacarbonyl, cryst., mol. struct. 0-64967
Fe complex, nitrile nonacarbonyl cryst., mol. struct. 0-64968
HCN⁺, ²Σ⁺ and ²Π states, SCF and CI calcs. for determ. optimum linear geometries, bond angles calc. 0-74114
HNC⁺, ²Σ⁺ and ²Π states, SCF and CI calcs. for determ. optimum linear geometries, bond angles calc. 0-74114
Os complexes, N-1-adamantylimido OsO₃, bis(N-tert-butylimido) OsO₂, cryst. struct., bonding, ligands π-donor capability 0-64969
Rb₂Te₃, synthesis and cryst. struct. 0-88115

bond lengths

- covalent semiconductors, displacement correlations, adiabatic bond charge model 0-70350
crystal structural fragment, automatic construction, taking account of attainable chem. bond lengths 0-92419
diatomic isovalent systems, pot. curves, ab initio MRD-CI method 0-83293
ethylene, diatomics-in-mols., semiempirical valence bond π-electron theory 0-99461
ethylene, molecular geometry optimisation, variable metric method, internal geometry 0-95744
graphite-Br₂ intercalation cpds., EXAFS study 0-71515
graphite-HSO₃F intercalation compound, Raman spectral study (French) 0-60581
graphitised viscose fibre, fluorination, change in struct. 0-88039
heterocyclic compounds, bond lengths, fifth overtone of C-H stretching vibr. obs. 0-91528
hydrocarbons, cyclic, non alternant, nonsingle instabilities of HF solns. 0-58164
methanol, molecular geometry optimisation, variable metric method, internal geometry 0-95744
naphtho[1,8-cd:4,5-c'd']bis[1,2,6]thiadiazine, mol., electronic, cryst. struct. 0-64984
quinazolines, enzyme inhibitory, structure-activity quantitative study 0-78540
spirohydrocarbons, strained, bond angles, interatomic distances, semiempirical and ab initio calcs. 0-95533
1,1,1,2-tetrafluoroethane, mol. struct. studied by gas-phase electron diff., vibr. amplitudes, bond angles and lengths calc. 0-95740
tetrafluoromethane, ν₂+ν₄ band, high resolution diode laser spectra 0-69138
toluene, mol. struct., ab initio calcs. 0-106262
trifluoromethyl bromide, microwave spectra, mol. rot., isotopic variation in bond lengths, Stark meas., dipole moments determ. 0-74165
trifluoromethyl iodide, microwave spectra; mol. rot., isotopic variation in bond lengths, Stark meas., dipole moments determ. 0-74165
uranyl complexes, IR spectra and bond distances 0-74167
urea molecule, bond-length corrections for external and internal vibr. 0-106402

bond lengths continued

BH₃, electronic wave function determ., genealogical technique using Clebsch-Gordan coeff. 0-95529
 Br₂ in Ar, solvent effects on equilibrium props. 0-61128
 C₂(C₂⁻)⁻ pot. energy curves calc. using SCF, MCSCF and CI methods, dissociation energies, bond lengths, electron affinity 0-95523
 CO, polarisability derivatives, bond length depend., SCF and CI calcs. 0-58162
 ClO, dissociation energy and bond length, CI calcs., bond function effects 0-102450
 Co-Al, X-ray K-absorption spectrum 0-97378
 Cs₂Te₃, synthesis and cryst. struct. 0-88115
 Cu complex, [Cu(1,4,7,10-tetrabenzyl-1,4,7,10-tetraazacyclododecane)Cl]NO₃, cryst. struct. 0-64966
 Fe complex, nitrile nonacarbonyl, cryst., mol. structs. 0-64967
 Fe complex, nitrile nonacarbonyl, cryst., mol. struct. 0-64968
 H+methane, abstraction and exchange reaction, barrier height calc. using POL-CI wave functions 0-81304
 H₂O⁺, spin and rot. fine struct., orbital angular momentum 0-83247
 LiBeF₄, pot. energy surface, struct., stability and internuclear distances, ab initio calc. 0-58147
 LiBr, pair pot., dipole moment, polarisability tensor, bond length depend., finite field SCF calcs. 0-58127
 Li₂F₂, struct., internuclear-distances and mean amplitude of vibr. determ. by electron diffraction 0-69252
 Mo-N, bond-strength bond-length relationships 0-91702
 NH₂, spin and rot. fine struct., orbital angular momentum 0-83247
 NO₂, gas phase equilib. geometry, force consts., vibr. freq., dipole moment function MCSCF/CI calcs. 0-78520
 O₂⁻, hypothetical, mol. self-consistent study, possible prep. method (French) 0-91717
 Os complexes, N-1-adamantylimido OsO₃, bis(N-tert-butylimido) OsO₂, cryst. struct., bonding, ligands π -donor capability 0-64969
 Rb₂Te₃, synthesis and cryst. struct. 0-88115
 Te₄²⁺, pseudopot. SCF-MO calcs., spectrum assignments 0-83269

bonds (adhesive) see adhesion

bonds (chemical)

see also binding energy; bond angles; bond lengths; crystal binding; hydrogen bonds; intermolecular forces; lattice energy
 acetonitrile, adsorption on MgO, IR and TPD study 0-70528
 acetylene, photoionisation cross section at distance from threshold, chemical bond influence 0-69196
 aliphatic ketones, freq.-topology-milieu relation, IR study, struct. and solvent effect (French) 0-95623
 alkali ionic conductors with sheet structures, ion mobility and influences 0-107522
 alkali metal chlorides, photofragment spectra, bond energies and excited state symmetries 0-87190
 alkali metal halides, zero point Compton profile anisotropies and bond polarities, correl. 0-78659
 alkyl halide+K potentially reactive collisions, electronic excitation 0-74239
 alkyl halides, conform. energy calcs., polar bonds and polarisability, polaris. model appl. 0-58188
 alkyl metal carbonyls, phosphine monosubstituted, LF vibr., IR and Raman spectra 0-95585
 allene-d₄, high resolution IR spectra 0-83365
 2-amino-4-chlorophenol in solutions, IR absorpt. spectra 0-69135
 2-amino-p-cresol in solutions, IR absorpt. spectra 0-69135
 aminoacetaldehyde, conformation calcs. rel. to protein struct. and bonding 0-74273
 benzene-1₂, π - σ charge-transfer complex, frozen soln., Mossbauer spectra obs. 0-91655
 binary crystals, electrical conductivity versus interatomic bond character 0-59948
 bond bending, bond orbitals rel. to nucl. motion 0-95513
 bonds in reactions, form and breaking, partitioning anal. of electron reorganisation 0-104419
 4-bromobenzoyloxymethyl-trifluorosilane, cryst. struct., X-ray study 0-70187
 α -bromofluoro alkyl π -radical, signs of hyperfine and quadrupole couplings, ESR determ. 0-97141
 carbenes, heterosubstituted, singlet-triplet splitting depend. on heteroatom electronegativity and conform. 0-63553
 chain mols., conformational transition kinetics 0-83339
 chemical bonding, antisymmetrised geminal power and simple correlated wave function 0-102423
 chemically-assisted fracture, atomic modelling at crack tips 0-106754
 chloroform-d in soln., vibr. and reorientational relax., Raman study 0-63636
 p-chloronitrobenzene, struct. determ. by electron diffraction, influence of NO₂ group on C-Cl bond 0-69251
 cobalt dimethyl glyoximate, molecular struct., cryst. structure 0-79769
 1,2-cyclononatriene, mol. struct. and conformation, gas phase electron diffraction 0-106400
 deoxyhaemoglobin, Fe(II)-N₂(His-F8) stretching freq. rel. to quaternary struct. 0-94160
 diatomic mols., electronegativity, bond charge and chemical pot. approach 0-91703
 dicyanoketene, and isomeric forms, heat of form., ab initio STO-3G calcs. 0-58190
 dithioferates (III), electronic struct. and hyperfine interactions, X α calcs. 0-100448
 effective atomic charge distribution in mols., multiple scatt. calcs. 0-83244
 electronic structure and solid props., rel. to chemical bonding, book 0-86044
 ethane, CH bond orbitals, internal rot. barriers, antisymmetrization effects 0-63529
 ethane, photoionisation cross section at distance from threshold, chemical bond influence 0-69196
 ethane gas, local mode overtone bands 0-83444
 ethidium bromide E-DNA, intercalated birefringent fibres, microspectrophotometric investig. (German) 0-57392
 ethyl radical, C-C bond barrier rot., IR spectra 0-76536
 ethylene, photoionisation cross section at distance from threshold, chemical bond influence 0-69196
 ferrous nitrosylhaemoglobin, NO binding, spin distrib., orbital model and mag. props. 0-81534

bonds (chemical) continued

2-fluoro ethanol, Ar matrix, induced conformational isomerisation by IR irradiation 0-101010
 formaldehyde, ³A" state, zero-field splitting param., ab initio CI calcs. 0-99454
 graphite, irradiation, lattice expansion, vacancies and interstitials contrib., bond order role 0-65042
 Group IV tetrabromides, intramol. force fields and mean vibr. amplitudes 0-106316
 Gruneisen parameters, bond anharmonicities and pressure induced freq. shifts 0-107397
 heavy elements, covalent bonding relativistic corrections, kappa valence method 0-91461
 hexamethylbenzene in tetrachloromethane soln., local mode overtone bands 0-83444
 hexaoxy ions, octahedral, mol. consts. calcs. 0-106317
 hydrazine adsorbed on Al, decomp., XPS obs. 0-92783
 hydrocarbons, liq., Compton profiles, bond additivity 0-93423
 hydrocarbons, non-alternant, reson. energies 0-106278
 ice, O-H and O-D bond stretching vibr., Raman spectra at atmospheric pressure 0-66166
 integrated spatial electron populations, evaluations for simple mols. 0-78524
 Kruszewski's rule, for stability of isomeric polycyclic conjugated cpds., proof 0-106249
 β -lactam antibiotics, ab initio SCF-MO-LCAO calcs., amidic bond breaking, methoxy substitution effect 0-78533
 lanthanide complex, struct. and equilib. by time resolved Eu(III) spectrosc. 0-78736
 lanthanide ion bound to macromol., struct. and equilib. by time resolved Eu(III) spectrosc. 0-78736
 linear mols., π orbital electron energy contrib. to reaction heat 0-76539
 liq., mag. susceptibility meas., electron localisation and chem. bonding 0-60178
 malonic acid, and α -alkyl derivatives, photoelectron spectra, lone-pair interactions 0-58315
 metal atom cluster compounds, bonding calc. using d-orbital overlap model, SCF-X α -SW calc. 0-102595
 metallic phase structures, dimensional analysis, bonding information from valency effects appearing as artefacts 0-96471
 methane, coord. bond calcs. 0-58129
 methanol, coord. bond calcs. 0-58129
 methotrexate-dihydrofolate reductase complex form., conform., laser Raman obs. 0-104553
 methyl fluoride, coord. bond calcs. 0-58129
 N-methyl m-fluoroaniline, conformational anal., microwave spectra obs. 0-58247
 methylamine, coord. bond calcs. 0-58129
 methylated benzene-1₂, π - σ charge transfer complex, frozen soln., Mossbauer spectra obs. 0-91655
 (+)-(3R)-methylcyclohexanone, vibr. optical activity, Raman obs. 0-102499
 modular cast Fe, probability prediction of spheroidisation by parametric diagram of chem. bond (Chinese) 0-66543
 molecular duplexes, graph construction yields 0-106245
 molecular structures, topological code, modified Morgan algorithm 0-58122
 molecules, chemical bonding studied using scattering theory concepts 0-103289
 molecules, direct CI calcs. with multiconfigurational reference state 0-63506
 molecules, Faraday effect measurement in pulsed mag. field 0-80758
 muscle chemomechanical energy transduction, mol. basis 0-72143
 myoglobins, Fe-, Co-substituted, O₂ binding, comparisons, thermodynamic investig. 0-67030
 neopentane liq., local mode overtone bands 0-83444
 nitrocyclopropane, vibr. spectra struct. and bonding 0-102520
 NQR, electronics appls. 0-63668
 nuclear spin-spin coupling constants, directly bonded C-C and C-H, CDOE/INDO LMO calcs. 0-95546
 organometallic compounds, EHT method calcs., parametrisation, population anal. (French) 0-58157
 oxyl fluoride ferroelectrics, chemical bonding, Curie temp., spontaneous polarisation 0-75981
 polar tensors, compact formulation on bond moment hypothesis 0-58108
 poly(p-phenylene), electronic struct., one-electron band theory 0-65450
 polyacetylene, electronic struct., one-electron band theory 0-65450
 polyacetylene film, anisotropy of dielec. const. 0-108146
 polyatomic molecules, bond distribution functions, anharmonicity effects of electron diffraction pattern 0-69234
 polyatomic molecules, cyclopropane, selective bond breaking by multiple IR photon absorption 0-66834
 polyethylene, nonoriented partially cryst., kinetic damage accumulation cure 0-71753
 polymers, breaking down of anharmonic chain, computer calc. 0-106410
 polypyrrole, electronic struct., one-electron band theory 0-65450
 polysiloxene, irradiation, linear, IR and solubility obs. 0-93775
 n-propanol, preferred conformers, PCILO study 0-95542
 propiyl chloride(-d), 357-333 nm absorpt. system 0-69161
 propiyl fluoride(-d), 290 nm absorpt. system 0-87142
 protein, structure and bonding, quantum theory, ab initio calcs. 0-61509
 proteins, structure and bonding, modelling using aminoacetaldehyde 0-74273
 pulsed opto-acoustic spectroscopy 0-62743
 pyramidal molecules and ions, bond polarisability and force constants 0-69260
 pyridine-1₂, π - σ charge-transfer complex, frozen soln., Mossbauer spectra obs. 0-91655
 quartz, low, CC Si-O bond characteristics 0-84132
 quartz, low, ionicity of Si-O bond 0-84133
 radical radiation formation in solid organic compounds 0-85201
 rare earth arsenides and bismuthides, chemical bonding and structural features, coherent alloying theory 0-107101
 rare earth-B, RB₂, thermochemistry and stability 0-97723
 9-cis retinal, visual pigment chromophore, twisting mechanism 0-58333
 11-cis retinal visual pigment chromophore, twisting mechanism 0-58333
 silane coupling agent deposited on E-glass fibre, hydrolysis and drying effect on siloxane bonds 0-85072
 small molecules, localised charge densities calcs., bond length effects 0-83256

bonds (chemical) continued

- sodium oxalate: Cu^{2+} , anhydrous spin Hamiltonian and bonding parameters and orbital-reduction factors 0-60408
- solids, chemical bonding studied using scattering theory concepts 0-103289
- spin polarisation analysis using intermolecular interactions theory, chemical polarisation, exchange repulsion 0-76510
- steel, H_2 embrittlement, effect on bond strength 0-104293
- surface theory, aims and recent accomplishments 0-75413
- tautomerism and alternating bonds, representation, Chemical Abstracts Systems 0-63851
- (TCNQ) $_2$, dimeric interactions, MO calcs., applicability to crystal struct. 0-75215
- tetracyanoplatinate, quasi 1d anion deficient, elec. and struct. props. 0-103683
- tetramethylbutane in hexachlorobutadiene soln., local mode overtone bands 0-83444
- thioureas, alkyl and phenyl groups trisubstituted, conformation, steric and stacking interaction 0-95587
- three-electron bonds, strengths, ab initio LCAO MO CI calcs. 0-87046
- transition metal cpds., rock salt struct., surface energy bands, Shockley surface states, bonding 0-92956
- transition metal-O bond energy in O_2 glow discharge, mass spectrometry obs. 0-64808
- trialkylthioureas, N-H stretching vibrs. and conformation 0-95586
- trichloroanilines in solutions, IR absorpt. spectra 0-69136
- triethylamine- I_2 , n- σ charge-transfer complex, frozen soln., Mossbauer spectra obs. 0-91655
- trigonal and triatomic molecules, orbital valency force field const. calcs. 0-78516
- trimethylbromosilane, microwave spectra, struct., chemical bonding 0-95602
- 1,3,5-trinitro 1,3,5-triazacyclohexane, shock-induced intramol. bond breaking, XPS and EPR study 0-76512
- trinitrotoluene, shock-induced intramol. bond breaking, XPS and EPR study 0-76512
- tris(trimethylstannyl)amine, gas phase electron diffraction 0-106401
- (TTF) $_2$, dimeric interactions, MO calcs., applicability to crystal struct. 0-75215
- TTF-TCNQ, dimeric interactions, MO calcs., applicability to crystal struct. 0-75215
- two and three-centre molecules, periodicity and internal torsional conformers around single bond, symmetry analysis 0-69250
- ureas, alkyl and phenyl groups trisubstituted, conformation, steric and stacking interaction 0-95587
- valence electron distribution, in crystals., diffraction data processing 0-92418
- $\text{AgF}(\text{AgI}, \text{AgBr}, \text{AgCl})$, NMR chemical shifts 0-74180
- AlBr_3 , thermochemistry and stability 0-97723
- $\beta\text{-Al}_2\text{O}_3\text{-D}_2\text{O}$, anhydrous, prep. and struct. of $\text{DAI}_2\text{O}_{17}$ 0-107187
- $\beta''\text{-Al}_2\text{O}_3\text{-H}_2\text{O}^+(\text{Na}_2\text{O})$, struct. basis for superionic cond. 0-107498
- As-Se-Sb, crystallised glasses, struct. from Mossbauer spectra 0-64917
- $\text{As}_{50}\text{S}_{100-x}$, amorphous films, optical props. and photoinduced changes 0-60700
- As_2Se_3 , monoclinic, chem. bonds rel. to electronic and vibr. states 0-64951
- As-O bond energy glow discharge, mass spectrometry obs. 0-64808
- Au_2C_2 , chem. bonding nature, static deform. densities and pictorial representation 0-92489
- BCl_2NCO , soln., force fields and normal modes, vibr. spectra, IR and Raman obs. (French) 0-58266
- BF_2 radical, thermomechanical studies by mass spectrometry, enthalpy of form. and ionisation pot. determ., chem. bonds 0-81382
- $\text{BX}_2^{14}\text{NCS}$ ($\text{X}=\text{Cl}, \text{Br}, \text{I}$), soln., force fields and normal modes, vibr. spectra, IR and Raman obs. (French) 0-58266
- $\text{BaO-B}_2\text{O}_3\text{-V}_2\text{O}_5$ glass, oxidation-reduction of V, thermodynamics 0-85169
- BaTiO_3 , displacive ferroelectric, effective charge determ. 0-97212
- C, amorphous film, spin resonance, IR spectra, microhardness 0-71157
- C polymeric chains, reduced from poly(tetrafluoroethylene), reactivity 0-89488
- C-N bond in methylamine, nucl. mag. isoscreening line diagrams 0-78555
- CH bond dipole calcs. 0-69067
- C_2H_2 species formed in chemisorption of ethylene on Pt, vibr. anal. 0-61150
- C_2N_2 , $2\nu_4$ band overtones, Raman intensities, bond polarisability theory 0-63639
- CO molecular adsorbed on Mo (110) surface, electronic states, photoemission spectra 0-65363
- CO-myoglobin, mol. tunnelling, isotope effect, time resolved IR Fourier transform obs. 0-72126
- CO_2 , stretch-stretch interaction force const., electron correlation influence, ab initio CI study 0-58161
- ^{13}C - ^{13}C spin-spin coupling const. and stretching force const., single and double bonds 0-63867
- CaCl_2 , X^{2+} pot. energy curves, polarisability and dissociation 0-91629
- CdAs_2 , cryst. struct. and vitrification capacity 0-88126
- Cd_3As_2 and CdAs_2 , molten, thermal expansion and atomic bond strength parameters 0-65257
- $\text{Cd}(\text{S}, \text{Se})$ film grown on InP substrate, mismatch dislocations and lattice distortion, dangling bond density 0-84406
- $\text{Cd-Si}(\text{Au})$ interfaces, bonding and interdiffusion, XPS obs. 0-80000
- CI overlayer on Cu (100), adatom bonding effects, photoemission study 0-104044
- Cl^- hydration complexes, gas phase, electrostatic calcs. 0-100055
- ClO_2^+ , ClO_2 and ClO_2^- ($n=1$ to 3), ab initio calcs., localised MO and nature of Cl-O bond 0-69070
- Co complex, $\text{Co}(\text{NO})_2^{4-}$, bond. props. and Jahn-Teller distortion, INDO-LCAO-MO calcs. 0-75532
- Co complex, O_2CoCl_4 and $\text{O}_2\text{CoCl}_4\text{NH}_3^{2-}$, struct. and bonding model, CNDO-UHF calcs. 0-95541
- CoIII salen complexes, O binding, reson. Raman obs. 0-58267
- Cr-Ge system, XPS, X-ray and neutron diffraction and mag. meas. to study chem. bonding and electronic struct. 0-60749
- $\text{Cr}(\text{NO})_4$, bonding, shake-up intensities and shake-up energies, SCF $\text{X}\alpha$ multiple scatt. calc. 0-74121
- $\text{Cr}(\text{NO})_4$, XPS and UV photoelectron spectra, compared to NO data 0-58317
- CSi crystals, relation of struct. and bond type to slip geometry 0-88165
- Cu complex, $\text{Cu}(\text{NO}_2)_6$, bond. props. and Jahn-Teller distortion, INDO-LCAO-MO calcs. 0-75532

bonds (chemical) continued

- Cu complex, $\text{N,N}'$ -ethylenebis(salicylaldiminato) copper (II)-thiourea, in solns., bond strength and hyperfine linewidth, EPR 0-74186
- Cu complex, $\text{N,N}'$ -o-phenylenebis(salicylaldiminato) copper (II)-thiourea, in solns., bond strength and hyperfine linewidth, EPR 0-74186
- Cu complexes, N ligands, X-ray K-absorpt. edge, expt. 0-89084
- $\text{Cu}(\text{II})$ -DL-proline complex, ESR, magnetic susceptibility and optical absorption 0-93167
- FeB and Fe $_2$ B, ESCA and mag. spin data, electronic struct., isomer shifts, valence bands and chemical bonding 0-75489
- FeCl_3 , intramolecular force fields, compliance const. and vibr. amplitudes 0-58234
- GaAs, (110) surface structure, rotational relaxation, cluster model (Chinese) 0-107621
- GaAs, lattice dynamics, phonon freq., bond bending force model calcs. 0-70335
- GaAs, modulation X-ray diffraction obs. 0-96464
- $\text{GaCl}_3(\text{Br}_3)(\text{I}_3)$, intramolecular force fields, compliance const. and vibr. amplitudes 0-58234
- GaI, rot. spectrum, EHF spectra obs. 0-58245
- GaSB, lattice dynamics, phonon freq., bond bending force model calcs. 0-70335
- Ge (100), dimer reconstruction, photoemission obs. 0-80939
- Ge, amorphous film, persistent photoconductivity, dangling bonds 0-84487
- N-Ge-Bi-Se glass, elec. and optical props. 0-65550
- GeP, thermodynamic characts. 10-300K, interatomic bond elasticity 0-59677
- H_2 , fluid, Raman meas., 0.2-630 kbar, at room temp. 0-58269
- H_2^+ , mol. electron density distrib., binding/antibinding anal. 0-95534
- HNO_3 , isomerism, low lying electronic states, ab initio MRD-CI calcs. 0-83291
- H_2O , affinity for $\text{Li}^+(\text{Na}^+)(\text{K}^+)$, ab initio SCF calcs. 0-58125
- H_2O , excited stretching vibrs., quantum mechanics. 0-91535
- H_2O , Raman and IR spectrum in overtone OH stretching region 0-58263
- He_2^+ , bond strength ab initio LCAO MO CI calcs. 0-87046
- HeH, bond strength ab initio LCAO MO CI calcs. 0-87046
- HfC, pressing regime influence on high-temp. creep (Russian) 0-100852
- I $^-$ hydration complexes, gas phase, electrostatic calcs. 0-100055
- In-Se(Te), liq., mag. susceptibility meas., electron localisation and chem. bonding 0-60178
- InCl_3 , intramolecular force fields, compliance const. and vibr. amplitudes 0-58234
- InSb (110) surface, LEED intensity dynamical anal. 0-88412
- KMgF_3 , bond energy, equilib. distances and compressibility calcs. 0-70159
- KNbO_3 , displacive ferroelectric, effective charge determ. 0-97212
- LaNi_4Al , solubility and sorption props. of H_2 , effect of Al 0-103482
- Li projectiles, electronic stopping cross section meas., intermolecular interactions 0-75279
- $\text{LiBe}(\text{Mg})(\text{Ca})$, $^2\Sigma^+$ and $^2\Pi$ states, mol. binding energy curves 0-58189
- LiF crystals, relation of struct. and bond type to slip geometry 0-88165
- LiH-NH_3 (ethylene)(acetylene), struct. and props., SCF ab initio calcs. 0-106250
- LiH_2PO_3 , P-H bond dipole direction, nonlinear optical coeffs. meas. 0-69253
- LiTaO_3 , displacive ferroelectric, effective charge determ. 0-97212
- MgO , bonding, pressure effects in lower mantle 0-72491
- Mn compounds, simple and complex, X-ray absorption near edge structs. 0-104013
- Mo-N, bond-strength bond-length relationships 0-91702
- Mo_2C_2 , pressing regime influence on high-temp. creep (Russian) 0-100852
- N-H bond in methylamine, nucl. mag. isoscreening line diagrams 0-78555
- N_2 adsorbed on W(100), vibr. spectra, bonding struct., LEED study 0-84387
- NH_3 , adsorption of Al surface, NH_3 decomp., XPS obs. 0-92783
- NH_3 , affinity for $\text{Li}^+(\text{Na}^+)(\text{K}^+)$, ab initio SCF calcs. 0-58125
- NH_3 , vibr. excitation in soft X-ray emission and core ESCA spectra 0-69163
- NH_4NO_3 , shock-induced intramol. bond breaking, XPS and EPR study 0-76512
- NOH isomerism, low lying electronic states, ab initio MRD-CI calcs. 0-83291
- Na-Co strip-chain silicates, structural-composition inhomogeneities 0-88122
- Nb chalcogenides and chalcogenide halides, geometrical struct. and metal-metal bonding 0-80172
- NbC, pressing regime influence on high-temp. creep (Russian) 0-100852
- NbC, rock salt struct., surface energy bands, Shockley surface states, bonding 0-92956
- Ni (001), chemisorption of CO, back donation in chemisorption bond, UPS study 0-107642
- Ni catalyst, chemisorption of ethylene-(d), Raman and vibr. spectra 0-108747
- Ni complex, nickel-bis-dithiolene, pseudopot. MCSCF and limited CI calcs. 0-83292
- NiCu molecule, electronic states determ. by ab initio HF and CI methods 0-69087
- O_2 , I and I' resonance series, vibr. level populations in autoionisation, photoelectron spectra, bond length determ. 0-91612
- $12\text{PbO} \cdot 6\text{SiO}_2 \cdot \text{PbSO}_4$, crystn. from $2\text{PbO} \cdot \text{SiO}_2 \cdot x\text{SO}_3$ melts, struct. and vibr. spectra 0-59400
- PbS, crystals, relation of struct. and bond type to slip geometry 0-88165
- Pd and Pt mixed valance complex, $[\text{Pd}(\text{ethylenediamine})_2]\text{Pt}(\text{ethylenediamine})_2(\text{ClO}_4)_4$, Raman spectra 0-84734
- (SN) $_n$, electronic struct., one-electron band theory 0-65450
- Se, bonding coordination defects 0-59927
- Se, electronic struct. of cryst. phases and hydrostatic press. effects 0-59865
- Se, mol. structure, local atomic arrangement at intrinsic bonding defects 0-59374
- Se, trigonal, Raman scatt. at very high press. 0-60566
- $\text{SeOCl}_2\text{-Pr}^{3+}(\text{Nd}^{3+})(\text{Er}^{3+})$, SbCl $_5$ acidified, Racah and Judd-Ofelt parameters in laser liqs. 0-106516
- Si (100), dimer reconstruction, photoemission obs. 0-80939
- Si (111), intermediate oxidation state, core photoelectron absorpt. vs. chemical shifts 0-81220

bonds (chemical) continued

- Si, amorphous film, RF plasma deposition from $\text{SiCl}_4\text{-H}_2$, characterisation 0-66435
Si, enhanced conductivity in plasma hydrogenated films, thermionic emission 0-70692
Si, impurity states, localised orbital approach 0-92851
Si, total energy calcs. by r-space method, Wannier functions 0-88503
Si:H, amorphous, 2p level shift, XPS obs. 0-97401
a-Si:H, electronic states and bonding config. 0-64900
Si:H amorphous films, ESR, optical gap and elec. cond. meas. 0-75842
Si:H amorphous films, reactively sputtered, prep. and characterisation 0-100785
Si-SiO₂-Si₃N₄ MNOS structure, chem. comp. and electronic states, Auger and energy loss spectra obs. 0-92999
Si₂, electronic struct. and bonding, atomic effective pot. appl. 0-95745
Si₃C_{1-x}H_x amorphous films, IR absorpt. bands 0-100705
SiH₂X (X=H, F, NH₂, OH), coord. bond calcs. 0-58129
SiO₂, fused, broken bond defect generation mechanisms 0-88044
SiO₂-Al₂O₃-CaO-Na₂O:Fe³⁺, optical absorpt. due to Fe³⁺ ligand field and charge transfer 0-89020
SiP, thermodynamic characts. 10-300K, interatomic bond elasticity 0-59677
α-Sn, ion implanted, defect struct., Mossbauer spectra 0-80214
Sn-Se(Te), liq., mag. susceptibility meas., electron localisation and chem. bonding 0-60178
SnCl₂·1.5H₂O single cryst., ³⁵Cl NQR, cryst. struct. 0-60449
¹¹⁹Sn, total mass absorpt. coeff. of gamma quanta, chem. binding influence, determ. using Mossbauer effect 0-99467
TaC, pressing regime influence on high-temp. creep (*Russian*) 0-100852
Te, electronic struct. of cryst. phases and hydrostatic press. effects 0-59865
Te, trigonal, Raman scatt. at very high press. 0-60566
UB₂, thermochemistry and stability 0-97723
V, and VD_{0.68}, anisotropic Compton profiles 0-97368
V₂O₅, energy band structure, bonding props., projected density of states anal. 0-70603
Zn₃As₂ and ZnAs₂, molten, thermal expansion and atomic bond strength parameters 0-65257
Zn₃P₂, evaporated metal contact barrier heights 0-80375
ZnS, lattice dynamics, phonon freq., bond bending force model calcs. 0-70335
ZrB₂, self-consistent band struct., XPS, reflectance, NQR, Hall effect and density of states meas. 0-107689
ZrF₄-BaF₂-MF_n (M=Na, Ca, Ln, Th, n=1, 2, 3, 4), vitreous phases, network formers, modifiers and stabilisers (*French*) 0-64909
ZrS, electronic struct., bonding effects, photoelectron spectroscopic and low temp. heat capacity cal. 0-96780

bone

- acoustic emission of fresh mammalian bones 0-76783
apatite crystal growth in skeletal tissues 0-94181
apatite powder samples, peak positions determ. from step-scanned X-ray powder diffr. data 0-103217
blood flow, meas. with a ¹³³Xe washout method 0-72288
calcification studies using electron probe X-ray microanalysis 0-76885
cement, fretting corrosion of orthopaedic implant materials 0-104813
cement used to grout hip prosthesis, stress distrib. obs. 0-104816
compact, long-term torsional creep obs. 0-104619
conduction mechanism rel. to hearing, holographic interferometry with optical fibres 0-76879
crack velocity depend. of longitudinal fracture, bovine tibia 0-97965
cranial bone, fetal, elastic modulus obs., appl. to fetal head moulding biomechanics 0-67128
demeralised dense human, strength props. nonuniformity 0-104611
density determination, effective attenuation coeff. of soft tissue, Compton scatt. 0-101220
destruction of compact tissue 0-67135
diseases, pot. use of stimulated positron emission in detect. and monitoring 0-81712
dose distribution calculation method for bone- and lung-equivalent material, diagnostic X-rays (*German*) 0-61704
dosimetry of bone-seeking radionuclides, comparative study in man, rhesus monkey, beagle and miniature pig 0-72338
electromechanical effects, comparison in wet and dry bone 0-97985
epiphyseal plate, method for evaluation and control of growth activity 0-81789
Ewing's sarcoma, place of bone scanning 0-72308
femoral neck fractures, meas. of fissure, X-ray picture anal. (*Croatian*) 0-109023
femoral necks, fracture fixation by Muller screws, mech. investigation 0-72377
femur, expt. studies on anchoring of loaded glass-ceramic implants (*German*) 0-81624
femur, human, pulse-echo technique for US vel. meas. in vivo 0-89812
fetal head moulding, finite element model investigation 0-67129
fibula, direct meas. of load bearing function 0-104624
fixing pins, stainless steel, strength, ultrasound effect 0-71710
fossil dating by ESR technique 0-95209
fracture callus mech. props., intramedullary nailing rel. to plating 0-85438
fracture healing, significance of scintigraphy (*German*) 0-76833
geometric properties of paired human tibiae 0-67127
growth stimulation attempts in dogs using mech. vibration 0-81638
healing fracture, blood flow rel. to ⁸⁵Sr uptake 0-72187
hip prosthesis stem loosening in human femur, biomechanical causes investigation 0-85435
lesions in CBA mice from nanocurie amounts of ²³⁹Pu 0-81657
long bone mechanics study under microprocessor control 0-76851
marrow colony-forming units, dose-dependence of the split-dose response 0-61701
marrow-engrafted mice, survival after γ-irrad. 0-104681
materials for orthopaedic implants, review 0-76862
mechanical properties characterisation by dynamic response 0-76782
microwave in vitro effects on granulocyte and macrophage precursor cells, mouse obs. 0-76789
mineral content, coherent scatt. of photons 0-67238
navicular bone, morphological features in functional adaptation of the foot (*Croatian*) 0-108944
orthopaedics, expl., quantitative eval. of holographic deform. investigations 0-67197

bone continued

- osteomyelitis, suspected, in children, value of radioisotope bone scanning 0-67216
osteosynthesis, internal, deform. of bone (*Croatian*) 0-108943
patellofemoral joint, anal. model 0-104625
piezoelectricity, role of stress-gradient effects 0-67113
PMMA bone cement, free radical EPR, feasibility study 0-94318
polychrome fluorescence labelling and photomicrography 0-89821
radiation biology conference, Rotterdam, Netherlands (Aug. 1980) 0-105425
radiography, skeletal diagnostics, direct magnification, exposure technique and timing 0-104747
radioisotope uptake of bone-seeking radioisotopes in normal bone rel. to blood flow 0-94320
remodelling, quantification of stresses 0-85437
revascularisation processes study method, local blood flow dynamic anal. using ⁸⁵Sr 0-81684
silicate glass bonding to bone rel. to Ca₃(PO₄)₂ surface film form. 0-85212
skeletal blood flow, implications for bone-scan interpretation 0-72199
skull, macerated, human, orthodontic forces induced bone displacement obs. 0-61603
skull, struct. changes due to Recklinghausen's disease, X-ray and nuclear medicine diagnosis (*German*) 0-76831
skull bones, human, US flexural wave study 0-72277
spinal column, human, strength of construction 0-67137
stimulation devices, anal. of sinusoidal EM fields 0-108990
strains of canine radius and ulna, in vivo meas. and anal. 0-67130
structure, anal. by X-ray pictures (*German*) 0-89828
tibia, human, natural freq. anal. 0-85433
tibia, human, simplified method of radiographic anal. of its cross-section, anthropometric correls. 0-89827
trabecular bone from human vertebral body, elastomech. props. 0-67141
US velocity meas. in temp. range of room temp. to 90°C 0-76787
vertebrae, abnormal accumulations found in the bone scintigram of cancer patients 0-67233
vertebrae, human, deflected US wave propag. tests 0-61617
vertebrae, human, mech. props. 0-72206
vertebrae, human, strength under sagittal compression 0-61618
viscoelastic behaviour, anal. on basis of microstruct. 0-85429
X-irradiated, changes in ^{99m}Tc pyrophosphate imaging 0-72239
X-ray induced osteosarcomas, rabbits, scintigraphic and radiographic detect. 0-101231
^{113m}In-tripolyphosphate, new radiopharmaceutical for bone scanning 0-67247
P, sheep, transportable system for neutron activation anal. determ. of P 0-109066
Pu dose to lung and bone from contaminated soils, statistical uncertainties 0-109028
⁹⁰Sr concentrations in pronghorn antelope bones near a nuclear fuel reprocessing plant 0-89875
^{99m}Tc-MDP scans in investigation of diffuse alterations, quantitative assessment 0-72287
- Boolean algebra**
see also *Boolean functions; formal logic*
formulae and transforms for automobile technicians (*French*) 0-94946
- Boolean functions**
formulae and transforms for automobile technicians (*French*) 0-94946
- Boolean lattices** see *Boolean algebra*
- bootstrap models** see *bootstrapping*
- bootstrap theory** see *bootstrapping*
- bootstrapping**
cluster expansion in the truncated bootstrap model and linear graphs theory 0-102029
cumulative hadron production, statistical bootstrap model with strangeness (*Russian*) 0-62948
Dual Topological Unitarisation scheme, flavour symmetry breaking 0-102030
internal quantum numbers for quarks and leptons in bootstrap approach 0-95254
leptons, geometrical approach 0-95258
leptons, topological bootstrap approach, rishon model 0-78046
pp collisions, high energy, fireball mass, rapidity, spin distrib. 0-57645
quarks and leptons, topological bootstrap approach, rishon model 0-78047
quarks and leptons in bootstrap topological approach 0-95253
topological bootstrap prediction for three coloured, eight flavoured quarks 0-86694
pp annihilations, multipion distrib., statistical bootstrap model 0-68472
- bootstraps** see *bootstrapping*
- borate glasses**
alkali borate glasses, Raman study at high temps. 0-93306
alkali borate glasses, single and mixed, viscosities 0-92701
alkali borosiluminosilicate system, self-focusing fibres with aperture of 0.18 0-87548
aluminoborate glass, Fe and Cr ion interaction, mag. and spectral props. 0-103883
B₂O₃-Li₂O-LiCl, ionic conductor, IR refl. Raman study 0-66173
BO₂-BO₂ 0-65252
borosilicate optical waveguide glass, B content determ. using nuclear track counting 0-95969
radioactive waste management, French research program for solidification and disposal in borosilicate glass 0-95377
Ag halide photochromic glasses, optical properties, effect of Cu ions 0-93364
(AgI)_x(Ag₂O B₂O₃)_{1-x}, amorphous superionic compound, ¹¹B lineshape and relaxation 0-108107
B₂O₃-PbO-GeO₂-Fe₂O₃ glasses, mag. props. and Mossbauer spectra, spero-mag. order at low temps. 0-80530
B₂O₃-V₂O₅-P₂O₅ glass, mech. and elec. props 0-84228
BaB₂O₇-RF₂, R=Mg, Ca, Sr, Ba, glass form., struct. and props. 0-84077
BaO-B₂O₃, refraction, refractive index from 0.365 to 2.50 μm 0-88953
BaO-B₂O₃-V₂O₅ glass, oxidation-reduction of V, thermodynamics 0-85169
BaO-Fe₂O₃-B₂O₃ glasses, high Fe₂O₃ content, micromagnetic props. 0-65916
BaO-La₂O₃-B₂O₃, refraction, refractive index from 0.365 to 2.50 μm 0-88953

borate glasses continued

- Cr complexes, ESR study of effect of glass composition on symmetry 0-88052
 $\text{Fe}_2\text{O}_3\text{-BaO-B}_2\text{O}_3$, magnetic props. of Fe-rich amorphous oxide (*French*) 0-80511
 $\text{K}_2\text{O-B}_2\text{O}_3\text{-Fe}_2\text{O}_3$, γ -irrad., Mossbauer spectroscopic study 0-108132
 $\text{K}_2\text{O-CaO-BaO-B}_2\text{O}_3$, refraction, refractive index from 0.365 to 2.50 μm 0-88953
 $\text{K}_2\text{O-MgO-B}_2\text{O}_3\text{:Cu}^{2+}$, micro-inhomogeneities, EPR and Raman study 0-84080
 Li^+ -rich borate glasses, ionic cond. and activation energy 0-107561
 $\text{Li}_2\text{B}_4\text{O}_7\text{-LiFeO}_4$, mag. props. of Fe^{3+} cations 0-100599
 $\text{Li}_2\text{B}_4\text{O}_7$, ferroelectric glass, phase transition, permittivity, electrochromism, photochromism 0-80719
 $(\text{Li}_2\text{B}_4\text{O}_7)_{1-x}(\text{WO}_3)_x$, dipolar glass, space charge injection, thermally stimulated depolarisation currents 0-66103
 $\text{Li}_2\text{O-B}_2\text{O}_3$, low Li_2O content, ^{11}B NMR study 0-84657
 $\text{Li}_2\text{O-B}_2\text{O}_3$ glass struct. study using ^{10}B NMR 0-84658
 $\text{Li}_2\text{O-B}_2\text{O}_3$ glasses, fast ion transport 0-107470
 $\text{Li}_2\text{O-B}_2\text{O}_3\text{:Cr}^{3+}$, absorpt. spectra, Fano antireson. and vibronic Lamb shift 0-71458
 $\text{Li}_2\text{O-B}_2\text{O}_3\text{-P}_2\text{O}_5$, glass, mech. and elec. props 0-84228
 $\text{Li}_2\text{O-LiF-B}_2\text{O}_3$ glasses, fast Li^+ conduction 0-79984
 $\text{Li}_2\text{O-LiF-B}_2\text{O}_3\text{-Li}_2\text{SO}_4$ glasses, DC cond. and secondary struct. relax. 0-107469
 $\text{Li}_2\text{O-LiX-B}_2\text{O}_3$ glass, X=halogen, high anionic cond. of new solid electrolytes 0-107546
 $\text{Na}_2\text{O-2B}_2\text{O}_3$ molten glass, reactions with conducting materials 0-85186
 $\text{Na}_2\text{O-Ag}_2\text{O-B}_2\text{O}_3$ glass, Ag^+ ion distrib., X-ray diffr. study 0-84076
 $\text{Na}_2\text{O-B}_2\text{O}_3$, enthalpy of form., calorimetric study 0-66861
 $\text{Na}_2\text{O-B}_2\text{O}_3$, ferroelectric glass, phase transition, permittivity, electrochromism, photochromism 0-80719
 $\text{Na}_2\text{O-B}_2\text{O}_3$ glass struct. study using ^{10}B NMR 0-84658
 $\text{Na}_2\text{O-B}_2\text{O}_3\text{:Cu}^{2+}$, Mn^{2+} glasses, $\text{Cu}^{2+}\text{-Mn}^{2+}$ interaction studied by ESR 0-93166
 $\text{Na}_2\text{O-B}_2\text{O}_3\text{-B}_2\text{O}_3$ glass with metallic Bi granules, elec. cond. 0-84493
 $\text{Na}_2\text{O-B}_2\text{O}_3\text{-CuO}$, γ -irrad., CuO effects on EPR 0-84645
 $\text{Na}_2\text{O-B}_2\text{O}_3\text{-GeO}_2$ glass-forming melts, thermodynamic props. and vapourisation processes, mass spectrometric study 0-79926
 $\text{Na}_2\text{O-B}_2\text{O}_3\text{-GeO}_2$ system glass-forming melts, mass spectrometry obs. of thermodynamic props. 0-97468
 $\text{Na}_2\text{O-B}_2\text{O}_3\text{-P}_2\text{O}_5$ glass, mech. and elec. props 0-84228
 $\text{Na}_2\text{O-B}_2\text{O}_3\text{-SiO}_2$, two-phase, stresses arising during leaching 0-81086
 $\text{Na}_2\text{O-MgO-B}_2\text{O}_3\text{:Cu}^{2+}$, micro-inhomogeneities, EPR and Raman study 0-84080
 $\text{PbO-B}_2\text{O}_3$, structure toughness-composition relationship 0-104257
 $\text{PbO-B}_2\text{O}_3$ glass-forming melt, specific volume and viscosity, temp. depend. 0-84073
 $\text{PbO-B}_2\text{O}_3$ glasses, microhardness 0-66612
 $\text{PbO-B}_2\text{O}_3$ phase-separated glass, fracture toughness, Vickers indentation method 0-85023
 $\text{PbO-B}_2\text{O}_3\text{-Bi}_2\text{O}_3$ glass with metallic Bi granules, elec. cond. 0-84493
 $\text{SiO}_2\text{-Al}_2\text{O}_3\text{-CaO-MgO-B}_2\text{O}_3$, E-glass, acid resist. studies 0-60991
 $\text{SiO}_2\text{-B}_2\text{O}_3$, Brillouin scattering meas. of attenuation and vel. of hypersounds 0-100309
 $\text{SiO}_2\text{-B}_2\text{O}_3$ glass system, gel hot pressing synthesis and characterisation (*French*) 0-66468
 $\text{SiO}_2\text{-B}_2\text{O}_3\text{-Na}_2\text{O-K}_2\text{O}$ glass, strengthening by partial leaching 0-60993
 $\text{SiO}_2\text{-BPO}_4$, glasses and devitrificates prep., IR spectra (*Polish*) 0-71624
 $\text{WO}_3\text{-B}_2\text{O}_3\text{-ZnO}$ semiconducting glasses, DC cond. and optical absorpt. 0-107783
 $\text{ZnB}_2\text{O}_4\text{-RF}_2$, R=Mg, Ca, Sr, Ba, glass form., struct. and props. 0-84077
 $\text{ZnO-B}_2\text{O}_3$, refraction, refractive index from 0.365 to 2.50 μm 0-88953
 $\text{ZnO-B}_2\text{O}_3$, structure toughness-composition relationship 0-104257
 $\text{ZnO-La}_2\text{O}_3\text{-B}_2\text{O}_3$, refraction, refractive index from 0.365 to 2.50 μm 0-88953

Bordoni effect

- FCC high purity metals, Double Kink Generation model 0-79873
 Al, Bordoni relaxation, microdeform. 0-104204
 Al dilute alloys, cold worked, internal friction peaks 0-97520
 Al, pure, cold worked, internal friction peaks 0-97520
 Cu single crystals., Bordoni peak, 10.2 and 30.6 MHz 0-66566

boron

- see also nuclei with
 amorphous, microimpurities determ. using hollow cathode discharge 0-85247
 boriding of high purity Fe with cryst. B powder 0-84951
 borosilicate optical waveguide glass, B content determ. using nuclear track counting 0-95969
 coadsorption with La on W, field emission and field ion microscopy 0-104049
 CVD, closed system, deposition rate, models for interpretation 0-97438
 CVD, closed system, deposition rate and rate-limiting steps 0-93492
 CVD, deposition rate, in closed system, influence of HCl 0-84855
 CVD, deposition rate and supersaturation relationship using combined flux model 0-84856
 CVD, morphologies, influencing factors, temp. range 1390-1640K 0-89154
 determination by activation anal. (α,n), (α,p) reacts. investig. 0-61206
 determination in optical waveguide glass by DC plasma emission spectroscopy 0-87446
 diffusion in SiC, elec. cond. meas. 0-96696
 diffusion in solids, double, gettering of impurities 0-75383
 diffusion into Si from CVD BN covered with Si_3N_4 , appl. to master slice p-MOS IC 0-107564
 electron microprobe local anal. of light elements, ultrasoft X-ray spectroscopy 0-99027
 evaporated, electronic struct., XPS, SXS and isochromat investig. 0-76143
 fibre, US inspection, immersion method 0-66757
 fibre reinforced Al, impact damage tolerance and reliability 0-81177
 fibre reinforced Al, thermophys. props. 0-59745
 fibre reinforced Al matrix, matrix-fibre interaction depend. on metallic dopants (*Russian*) 0-76479
 fibre reinforced epoxy composites, notched, tensile strength and failure modes 0-81205
 fumarole B isotope composition, Satsuma Iwo-Jima, Japan 0-67358
 impurity in Cr-Mo-V low-alloy steel, effect on prior austenite grain boundary embrittlement 0-66657

boron continued

- impurity migration from doped Si sources in epitaxial layers (*Russian*) 0-107570
 ion implantation in laminar Si-SiO₂ systems struct. change investig. by MSSI (*Russian*) 0-107918
 ion implanted MOS structure, radiation defects and impurity activation 0-103757
 microalloyed Cu, elec. cond. and strength props. (*Polish*) 0-89285
 muonic X-ray transitions, nuclear charge radii 0-99589
 plasma, efficient heating by superelastic laser energy conversion 0-96372
 quartz glass, Ge and B dopants, OH impurities, preform material and fibre optic waveguide struct. 0-64173
 β -rhombohedral, elec. props. at high temps. and in strong elec. fields, thermistor appls. 0-92903
 solid solution, in Si, equilib. with B_2H_6 0-97721
 steel, B concentration and solubility depend. on introduction of rare earth metals (*Russian*) 0-65226
 steel, hardenability, role of B and P segregation 0-97486
 transport and lattice parameter change during sintering of β -SiC 0-108370
 Al-B fibre-D16 alloy welded composites, structure, strength and fracture props. (*Russian*) 0-108524
 B:H amorphous films, optical band gap, thermal treatment effect 0-93415
 B-Ti composite material, for loudspeaker's diaphragm, preparation by physical vapour deposition (*Japanese*) 0-58883
 $\text{B}^{n+} + \text{H}$, charge transfer cross sections, oscillatory behaviour in low-energy collisions 0-63806
 ^{11}B , neutrino-induced prod. in stellar C layer 0-82337
 C:H:B film, amorphous elec. props., chem. modifications by doping with B 0-84523
 α -Fe:B, valency effect of interstitials 0-65502
 (FeNi)/PB amorphous wires, surface oxidation and annealing influence on induced anisotropy 0-100957
 GaAs:B, deep levels, optically stimulated transient current method (*French*) 0-59919
 GaAs:B, incorporation of B during growth 0-93471
 n-GaAs:Si, IR, IR absorpt. spectra, reson. and localised modes 0-66172
 Ge:B, shallow acceptor spectral line intensities 0-88517
 $\text{H} + \text{B}^{n+} (\text{C}^{n+}) (\text{N}^{n+}) (\text{O}^{n+})$, ($2 \leq n \leq 4, 5$), cross sections at keV energies 0-78705
 Si:B, amorphous, negative magnetoresist., localised mag. states 0-70731
 Si:B, anomalous B profiles prod. by BF_3 implantation 0-75252
 Si:B, bound many-exciton complexes, luminescence spectra, mag. props. 0-103994
 Si:B, dislocations under high stress, stacking fault energies, TEM study 0-70202
 n-Si:B, elec. cond. oscills., electron instability effects due to dislocations 0-103704
 Si:B, He^+ irradiation-induced diffusion, effect on impurity distrib. 0-70470
 Si:B, heavy-doping effects and impurity segregation during high-pressure oxidation 0-65014
 Si:B, high conc. effects in ion implantation 0-75245
 Si:B, implanted laser annealed, lattice strain, X-ray study 0-96554
 Si:B, impurity content characterisation, exciton luminesc. 0-60653
 Si:B, ion implantation, channelled, through metal silicide film 0-70231
 Si:B, ion implanted, doping profile, pulsed laser annealing effects 0-88197
 Si:B, ion implanted, structure defects formation and behaviour under annealing in various ambients 0-65033
 Si:B, ion implanted crystalline and amorphous, laser annealing 0-97509
 Si:B, layer resist. depend. on implanting and annealing conditions (*German*) 0-96551
 Si:B, nonequilibrium solid solutions obtained by heavy ion implantation and laser annealing 0-92544
 Si:B, P, long range enhancement of B diffusivity by P diffusion 0-103386
 Si:B, proton-irrad., impurity uphill diffusion, vacancy mechanism 0-92719
 Si:B, resonant scattering of phonons by bound holes in temp. range 1 to 5K 0-75393
 Si:B, spreading resist. calibration for Si:Al, Si:Ga 0-103690
 Si:B, use of BN source to achieve high surface concentration of B (*Russian*) 0-107639
 Si:B (0.2 wt.%) ion implanted, B atom displacement due to low temp. irradi. 0-88234
 Si:B diffusion at Si-SiO₂ interface, Auger spectra, Rutherford backscattering 0-70471
 Si:B implanted wafers, ionis. assisted annealing and effects 0-100257
 Si:B ion implanted, strain profiles from X-ray rocking curves 0-107290
 Si:B ion implanted grating-type solar cells, var. of junction depth, collection efficiencies 0-93934
 Si:B ion implanted layers, light refl. and transmission coeffs., computer program 0-66316
 Si:B ion ion implanted, channelling and random equivalent depth distrib. 0-100293
 Si:B material for space solar cell 0-94007
 Si:B photodiode front region collection efficiency models 0-96899
 Si:B radiation damage and minority carrier lifetime, SEM-EBIC obs. 0-96573
 Si:H,B, amorphous, field effect and thermolec. power 0-96924
 Si-Si₃N₄:B, ion-implanted, shallow trap energy spectra 0-80392
 SiO₂:Ge, B, P, optical fibre, radiation induced optical absorpt. spectra, 0.4 to 1.7 μm region 0-58761

boron alloys

see also boron compounds

- Colmonoy, self-weldability in high temp Na (*Japanese*) 0-89392
 Colmonoy hardfacing materials, friction characts. in high temp. Na (*Japanese*) 0-89356
 Hayes alloy no.716, Fe-Cr-Ni-Co-W-Mo-Si-C-B (26, 22, 12, 3.5, 3, 1.2, 1.1, 0.4 wt.%), hardfacing alloy 0-100802
 Metglas 2605 ribbon, saturation magnetostriiction meas. by small-angle magnetisation rot. 0-60391
 rare earth-B, RB₂, thermochemistry and stability 0-97723
 steel, B-Si, grain-oriented, high induction, Cu impurity effects 0-89366
 thermoelectric materials, B₄C_x and (B,Si)₄C_x-P-type LaS_x N-type alloys, fabrication and thermoelectric props. 0-107771
 AlB₂, thermochemistry and stability 0-97723
 Al_{1-x}Be_{0.6}B₂₂, metal distrib., X-ray diffr. study 0-75204

boron alloys continued

B-Si, (0 to 14.3 at.%), phase charact., regions of existence (*French*) 0-104117
B-Si alloys, B-rich, prep., anal. and cryst. growth (*French*) 0-104091
(Co,Fe)₈₀B₂₀ glass, induced anisotropy and time changes of permeability 0-75815
Co-B-Si amorphous alloy, liq. quenched, elec. resist. and cyclic deform. 0-59949
Co-(B-Cr) thin film glasses, mag. props. and corrosion resist. 0-80576
Co-Fe-B, amorphous, crystn. and thermal stability 0-107057
Co-Fe-Si-B, decomp. of amorphous state during annealing below recryst. temp., electron microscope study (*Russian*) 0-75164
Co-Fe-Si-B, ferromag., magneto-optical spectra in amorphous and cryst. states (*Russian*) 0-84749
Co-Mn-Ni-Fe-Si-B amorphous alloys, mag. props., low magnetostriction 0-75832
Co-Mo-B metallic glass ribbons, tensile strength, crystn. temp. 0-89173
Co-Si-B, amorphous ribbon, saturation magnetostriction meas. by small-angle magnetisation rot. 0-60391
Co_{100-x}B_x, amorphous, mag. struct., mag. susceptibility meas. 0-80485
Co₃B, glassy and cryst., hyperfine field distrib., ⁵⁹Co spin echo spectra 0-80635
(Co₉₃Fe₀₇)_{75-x}Cr_xSi₁₅B₁₀ amorphous alloy, thermal stability, Cr conc. effects, DTA expts. 0-59395
(Co₉₀Fe₁₀)₇₂Mo₂Si₁₃B₁₀, metallic glass, strain- and field-induced mag. anisotropy 0-108004
Co₇₂Fe₂₈Ni₁₀(Si₂B)₂₈, amorphous, soft mag. props., switched-mode power supply appls. 0-88850
Co₇₀Fe₃₀Si₁₅B₁₀, amorphous, crystn. and thermal stability 0-107057
Co₇₀Fe₃₀Si₁₅B₁₀, amorphous, mag. aftereffect spectra and annealing props. 0-88831
(Co_{1-x}Mn_x)_{75-x}B, magnetocrystalline anisotropy meas., 4.2-300K 0-71006
Co₇₀Mo₂Si₁₃B₁₀, metallic glass, strain- and field-induced mag. anisotropy 0-108004
Co₇₂Si₁₅B₁₀, amorphous, crystn. and thermal stability 0-107057
Cu-BN composite electromachining tools, dynamic hot pressing 0-84889
Er_{1-x}Ho_xRh₂B₄, mag. and supercond. transitions, cryst. field effects 0-107950
Er_{1-x}Tm_xRh₂B₄, mag. and supercond. transitions, cryst. field effects 0-107950
(Fe,Co,Ni)-B, amorphous alloys, magnetostriction rel. to soft mag. props. 0-84633
Fe, cast, white, high Cr, phase composition, B effect 0-104172
Fe-(Co)-B, amorphous, crystn. 0-79704
Fe-B, amorphous, anomalous thermal expansion, ΔE effect, Invar and Elinvar characts., delay time 0-80589
Fe-B, amorphous, crystn., metal or metalloid exchange influence 0-75172
Fe-B, amorphous, induced anisotropy, development by mag. annealing and under applied mech. stress 0-65868
Fe-B, amorphous, induced anisotropy by heat treatment in mag. field and under applied mech. stress 0-75758
Fe-B, amorphous, mag. aftereffect, initial susceptibility time depend. 0-88829
Fe-B, amorphous alloy, mag. props. 0-84618
Fe-B, amorphous alloys, compositional study on short-range struct. 0-84095
Fe-B, amorphous ferromag., temp. depend. of resist., appl. of extended Ziman theory 0-59950
Fe-B, for infiltration of Fe compacts 0-60806
Fe-B, liq., mag. susceptibility meas. 0-75740
Fe-B, metallic glasses and vapour deposited films, amorphous to cryst. transition 0-88048
Fe-B, rapidly quenched, metastable phases 0-76234
Fe-B amorphous alloy, annealed, microstruct. and mag. domain changes 0-75790
Fe-B amorphous alloy, fast neutron and ²³⁵U fission fragment irradi. 0-100288
Fe-B amorphous alloys, mag. aftereffect 0-65970
Fe-B amorphous ribbons formation, high-speed photography investigation 0-76216
Fe-B metallic glass, X-ray diffr. meas., semi-empirical struct. model 0-107059
Fe-B metallic glasses, diffusion coeffs. from primary crystn. data 0-100345
Fe-B metallic glasses, struct., stability and crystn. 0-75173
Fe-B metallic ribbons, correl. between quenching temp. and mech. and mag. props. 0-89373
Fe-B phase ferromag. amorphous alloys, stiffening below Curie temp., pole effect (*Japanese*) 0-84632
Fe-B ribbon, microhardness, and static coercive force, melt overheating effect 0-84978
Fe-B-C, amorphous, effects of replacement of B by C on mag. props. 0-84621
Fe-B-C amorphous alloy, formation, mag. props., thermal stability and density 0-75796
Fe-B-C amorphous alloys for use in power transformers 0-88808
Fe-B-C amorphous alloys with high saturation induction 0-84617
Fe-B-Cr(Mo), metallic glasses, mag. struct., and elec. props. 0-88751
Fe-B-Cr(Si) thin film glasses, mag. props. and corrosion resist. 0-80576
Fe-B-Si amorphous alloy, liq. quenched, elec. resist. and cyclic deform. 0-59949
Fe-B-Si-C amorphous alloys, prep. and props. 0-88748
Fe-B(Si), glassy, field-induced mag. anisotropy near eutectic comp. 0-93110
Fe-B(Si) alloy filaments produced by glass-coated melt spinning 0-76213
Fe-Co-Si-B, amorphous soft ferromagnet with high mag. induction 0-84619
Fe-Co-Si-B, zero magnetostrictive amorphous alloy with high saturation induction, mag. annealing 0-60362
Fe-Co-Si(B), amorphous ferromagnet, mag. after effect on soft mag. props. 0-84626
Fe-Mn-B, B effect on intergranular embrittlement 0-108555
Fe-Mo-B metallic glass ribbons, tensile strength, crystn. temp. 0-89173
Fe-Ni-B, amorphous, crystn. 0-79704
Fe-Ni-B and Fe-Ni-B metallic glasses, Curie pt. anomalies 0-60256
Fe-Ni-B glassy ribbons melt spinning, gas boundary layer effects 0-76217
Fe-Ni-B metallic glass, X-ray diffr. meas., semi-empirical struct. model 0-107059
Fe-Ni-B-Mo, crystn. temp. and elec. cond. correl., Mo effect 0-75179

boron alloys continued

Fe-Ni-B-Si, amorphous, mag. props., heat treatment effects 0-89370
Fe-Ni-B-(P), ferromag., magneto-optical spectra in amorphous and cryst. states (*Russian*) 0-84749
Fe-Ni-Cr (35, 15 wt.%) superalloy, stress rupture and tensile props., C and B additions effect (*Chinese*) 0-104244
Fe-Ni-P-B, amorphous, crystn. and struct. 0-75175
Fe-Ni-P-B, metallic glasses, struct. relax., annealing effects on mag. props. 0-89261
Fe-Ni-P-B amorphous ribbons, form. by melt spin technique 0-76215
Fe-Ni-P-B metallic glass, crystallisation temperature values from isothermal transformation times 0-59397
Fe-Si-B, high induction, hot rolling treatment 0-89266
Fe-Si-B, magnetic metallic glasses, mag. props. 0-84620
Fe-Si-B amorphous alloys, Mossbauer spectroscopy (*French*) 0-80653
Fe-Si-B glassy alloys, mag. props., comp. effects 0-88752
(Fe-Ni-Mo)₈₀(P-B)₂₀, amorphous, mag. aftereffects and struct. instabilities 0-88833
Fe_{1-x}B_x, amorphous, hyperfine fields and local mag. moments, Mossbauer study 0-75895
Fe_{100-x}B_x, amorphous, mag. saturation, spin wave stiffness, temp. depend. 0-75741
Fe_{100-x}B_x, amorphous, mag. struct., mag. susceptibility meas. 0-80485
Fe₇₂B₂₈, metallic glass, nonisothermal meas. evaluation, non-existence of dynamic correction term 0-107406
Fe₈₀B₂₀, amorphous, Brillouin scatt. from magnons, ferromag. reson. 0-65844
Fe₈₀B₂₀, amorphous, cold neutron scatt., local and extended defects 0-84089
Fe₈₀B₂₀, amorphous, crystn. 0-75187
Fe₈₀B₂₀, amorphous, mag. permeability aftereffect during annealing 0-88834
Fe₈₀B₂₀, amorphous ferromagnet, Mossbauer hyperfine fields, mag. struct. 0-75894
Fe₈₀B₂₀ amorphous ribbon, initial susceptibility time lag 0-100579
Fe₈₀B₂₀, amorphous struct., Mossbauer spectroscopy investigation 0-84677
Fe₈₀B₂₀ amorphous wire, crystn. by annealing at 780°C 0-100177
Fe₈₀B₂₀ film, amorphous metallic, standing spin waves, Brillouin scatt. obs. 0-97291
Fe₈₀B₂₀ glass, magnetisation reorientation, Mossbauer effect 0-66092
Fe₈₀B₂₀, metallic glass, Doppler broadening of positron annihilation γ-radiation and elec. resist. 0-66321
Fe₈₀B₂₀ metallic glass, crystn. and struct. relax., Mossbauer effect study 0-75182
Fe₈₀B₂₀ metallic glass, crystn. kinetics 0-84083
Fe₈₀B₂₀ metallic glasses, stability and transforms. 0-75174
Fe₈₀B₂₀, Metglas 2605, amorphous ribbon, power loss variation with freq. and applied stress 0-88849
Fe₈₀B₂₀, Metglas 2605, Young's modulus meas. using piezoelectric US composite oscillator technique 0-108656
Fe₈₃B_{16.6}, amorphous, mag. props. and microstruct., cooling rate and melt overheating effects 0-65965
Fe₈₃B_{16.6} amorphous, mag. props., melt overheating and cooling rate effects 0-89371
Fe₈₄B₁₆, metallic glass, electrical resistivity and crystallisation 0-88526
Fe₈₄B₁₆, metallic glass, ion implanted, UPS meas. 0-97411
Fe₈₄B_{16-x}C_x, amorphous, mag. saturation, spin wave stiffness, temp. depend. 0-75741
Fe₈₀B_{20-x}G_x, amorphous, mag. saturation, spin wave stiffness, temp. depend. 0-75741
Fe₄₀B₄₀P₁₄B₆, Metglas 2826, amorphous ribbon, power loss variation with freq. and applied stress 0-88849
Fe₈₀B_{20-x}Si_x, amorphous, mag. saturation, spin wave stiffness, temp. depend. 0-75741
Fe₈₄B₁₃Si₂, metallic glass, electrical resistivity and crystallisation 0-88526
Fe₈₀(C_{1-x}B_x)₂₀ amorphous alloy, α-Fe crystn., morphology 0-70129
(Fe_{0.5}Co_{0.5})_{1-x}B_x, amorphous, hyperfine fields and local mag. moments, Mossbauer study 0-75895
Fe_{0.7}Co_{0.3}B₂₀, amorphous, magnetisation reversal and domain boundary configs. 0-88809
Fe₃₅Co₃₂B₂₀Si₁₀Al₃, stress-induced variation in magnetisation and dynamic magnetostrictive charact. 0-88855
(Fe_{0.07}Co_{0.93})_{75-x}Cr_xSi₁₅B₁₀, amorphous, disaccommodation of mag. permeability and induced anisotropy 0-88741
(Fe_{0.05}Co_{0.95})₇₈Si₁₈B₄ amorphous ribbon, anomalous mag. aftereffect 0-100602
(Fe_{1-x}Co_x)₇₈Si₁₀B₁₂, amorphous, roll mag. anisotropy 0-75757
(Fe,Co)_{1-x}Fe_xSi₁₈B₁₄, amorphous, saturation magnetostriction, strain modulated FMR obs. 0-75863
Fe₃₆Cr₃₂Ni₁₄B₁₂B₆, amorphous X-ray absorpt. spectra, effective coordination charges 0-84805
Fe_{83-x}M_xB₁₇ and Fe_{78-x}M_xSi₁₀B₁₂ (M=refractory metal), glass form. and thermal stability 0-79703
Fe₇₈Mo₂B₂₀ amorphous ribbons, magnetoelastic effects in as-quenched and stress-relieved states 0-80588
Fe₇₈Mo₂B₂₀, metallic glass, Doppler broadening of positron annihilation γ-radiation and elec. resist. 0-66321
(Fe_{0.4}Ni_{0.4})_{100-x}B_x and (Fe_{100-x}Ni_x)₈₀B₂₀ amorphous alloys, X-ray diffr. struct. determ. 0-64906
(Fe_{1-x}Ni_x)₈₁B₁₉, amorphous alloys ferromagnetic resonance 0-108080
(Fe_{100-x}Ni_x)₈₃B₁₇, amorphous, crystn. 0-75176
Fe₄₀Ni₄₀B₂₀, amorphous, phase transforms., resistometric anal. 0-75538
Fe₄₀Ni₄₀B₂₀, amorphous, RF annealing effects 0-108037
Fe₄₀Ni₄₀B₂₀, amorphous ribbon, power loss variation with freq. and applied stress 0-88849
Fe₄₀Ni₄₀B₂₀ and Fe₄₀Ni₄₀P₁₄B₆, amorphous, mag. aftereffect spectra and annealing props. 0-88831
Fe_{80-x}Ni_xB₂₀ and Fe_{80-x}Ni_xP₁₄B₆ amorphous alloys, microhardness correl. with mag. props. 0-88826
Fe₈₀Ni_{80-x}B₂₀ and Fe₈₀Ni_{80-x}P₁₄B₆ metallic glasses, low temp. resist. and galvanomag. effects, mag. state influence 0-84461
Fe₈₀Ni_{80-x}B₂₀ glass, resist., magnetoresist., and thermolec. power 0-70681
(Fe_{1-x}Ni_x)_{0.8}B_{0.2-x}P_x, amorphous, hyperfine fields and local mag. moments, Mossbauer study 0-75895
Fe_{1.6}Ni_{7.8}B₁₀P₁₀ metallic glass, superparamag. behaviour, chem. inhomogeneities loc 0-84625
Fe₄₀Ni₄₀B_{20-x}P_x, amorphous, mag. saturation, spin wave stiffness, temp. depend. 0-75741

boron alloys continued

- Fe₄₀Ni₄₀B₂₀-P₂ metallic glasses, local struct. and dynamic disorder of Fe and Ni, EXAFS obs. 0-89088
- Fe_{80-x}Ni₁₀B_{20-y}P_y, amorphous, Rayleigh region and coercive force 0-88806
- (FeNi)₉₀B₁₀-Al₁₅Si₁₅, stress-induced variation in magnetisation and dynamic magnetostrictive charact. 0-88855
- Fe₂₃Ni₃₆Cr₁₄P₁₂B₆, metallic glass, Doppler broadening of positron annihilation γ -radiation and elec. resist. 0-66321
- Fe₂₃Ni₃₆Cr₁₄P₁₂B₆ metallic glass, crystn. kinetics by TEM 0-75186
- Fe₂₃Ni₃₆Cr₁₄P₁₂B₆, Metglas 2826A, EPR at 20 GHz 0-75848
- Fe₄₀Ni₄₀(Mo,Si)₂₀, amorphous, soft mag. props., switched-mode power supply appls. 0-88850
- Fe₄₀Ni₃₈Mo₄B₁₈ amorphous ribbons, magnetoelastic effects in as-quenched and stress-relieved states 0-80588
- Fe₄₀Ni₃₈Mo₄B₁₈, amorphous, mag. anisotropy, Mossbauer study 0-65864
- Fe₄₀Ni₃₈Mo₄B₁₈, amorphous, reversible enhancement of mag. directional ordering rate 0-103829
- Fe₄₀Ni₄₀P₁₄B₆, amorphous, resistometric study of short-range ordering rel. to heat treatment 0-70140
- Fe₄₀Ni₄₀P₁₄B₆, amorphous ferromagnet, Mossbauer hyperfine fields, mag. struct. 0-75894
- Fe₄₀Ni₄₀P₁₄B₆ amorphous alloy, temper embrittlement 0-76295
- Fe₄₀Ni₄₀P₁₄B₆, amorphous, mag. polarisation in approach to ferromag. saturation 0-80560
- Fe₄₀Ni₄₀P₁₄B₆, amorphous, steady-state creep rate, cryst. effect 0-81102
- Fe₄₀Ni₄₀P₁₄B₆, amorphous, mag. permeability aftereffect during annealing 0-88834
- Fe₄₀Ni₄₀P₁₄B₆, amorphous ferromag., spin wave excitations 0-97079
- Fe₄₀Ni₄₀P₁₄B₆ amorphous ribbon, mag. domains and anisotropy distrib. 0-108029
- Fe₄₀Ni₄₀P₁₄B₆ glass, viscosity near T_g, using rapid heating, and fusion characts. 0-70438
- Fe₄₀Ni₄₀P₁₄B₆ metallic glass, crystn. 0-70127
- Fe₄₀Ni₄₀P₁₄B₆, Metglas 2826, hot forming 0-84980
- Fe₄₀Ni₄₀P₁₄B₆, Metglas 2826, amorphous ribbon under tension, mag. domain walls and pulsed magnetisation reversal 0-88825
- (Fe_{1-x}Ni_x)₈₀P₁₀B₁₀, amorphous, magnetisation reversal and domain boundary configs. 0-88809
- Fe₂Ni_{80-x}P₁₄B₆ glass, resist., magnetoresist., and thermoelec. power 0-70681
- Fe₂Ni_{80-x}P₁₄B₆ metallic glass, low temp. sp. ht. for spin-glass and spin-cluster-glass regime 0-71071
- (Fe_{1-x}Ni_x)₇₀P₁₀B₁₀ metallic glass, low temp. sp. ht. for spin-glass and spin-cluster-glass regime 0-71071
- (Fe₆₅Ni₃₅)₇₅P₁₀B₁₀, amorphous, crystn. temp., press. and heating rate depend. 0-70132
- (Fe_{1-x}Ni_x)₇₇Si₁₀B₁₃, amorphous, Landau-Ginzburg theory, magnetisation and Curie temp. 0-75700
- (Fe_{1-x}Ni_x)₇₈Si₁₀B₁₂ amorphous alloys, cold rolled and as-quenched, mag. anisotropy 0-97089
- Fe_{1-x}(P,B)_x, amorphous and crystalline, photoemission and band structure 0-60754
- Fe₇₀P₁₀B₈ amorphous alloys, splat cooled, Mn, Cr and V substituted, mag. and transport props. 0-84593
- Fe₈₀(P₁₀C₇₀)_{20-y}B₆, density, microhardness, and crystn. temp., comp. depend. 0-84093
- Fe₈₀Si₁₀B₁₀, amorphous, soft mag. props. and potential uses 0-88807
- (Fe_{1-x}Si_x)₇₁-By, metallic glass, mag. props., crystallisation 0-65885
- Fe_{80-2x}Mo_{2x}C_x(Si₂)₂(Ge₂)₂, amorphous, size effect of metalloids on mag. props. 0-84594
- (Gd₆₅Fe₃₅)₉₀B₁₀, amorphous, mag. props., Mossbauer study 0-93093
- La-B, amorphous, B-rich, low freq. modes, Raman scatt. obs. 0-108202
- LaB₆-Cu, form. by wetting of LaB₆ with Cu 0-100813
- LaNi₄Al_{0.6}, H₂ absorpt. props. 0-88432
- Mo₇₀B₃₀, amorphous, local symmetry around glass-former sites, elec. quadrupole effects, NMR 0-80618
- Mo₄₀Ru₁₂B₂₀, amorphous, local symmetry around glass-former sites, elec. quadrupole effects, NMR 0-80618
- (Mo₆₀Ru₄₀)₈₀Si₁₀B₁₀, amorphous supercond. matrix, flux pinning by MoRu precip. 0-65756
- Mo₇₀Si₂₀B₁₀, amorphous alloys obtained by liq. quenching, superconductivity 0-75670
- Nb-Si-B, ductile amorphous, superconductivity 0-60131
- Nb₄₀Fe₄₀P₁₄B₆, metallic glass, explosive compaction, mech. props. 0-89176
- Ni-B, film crystallisation on C fibres and sapphire crystals (Russian) 0-75455
- Ni-B, grain boundary internal friction, B solid solubility as function of grain size 0-60903
- Ni-B electroless-plated amorphous films, anomalous mag. temp. characts. 0-96757
- Ni-B thin film glasses, mag. props. and corrosion resist. 0-80576
- Ni-Mo-B metallic glass ribbons, tensile strength, crystn. temp. 0-89173
- Ni-Si-B, amorphous, thermal stability of ductility 0-76327
- Ni_{100-x}B_x, amorphous, mag. struct., mag. susceptibility meas. 0-80485
- Ni₃₆Fe₃₂Cr₁₄P₁₂B₆ metallic glass, mech. props. and thermal stability 0-76362
- (Ni_{1-x}Fe_x)₈₀P₁₀B₁₀, amorphous, Curie temp., press. effect 0-75833
- Ni_{78-x}M_xSi₁₀B₁₂ (M=refractory metal), glass form. and thermal stability 0-79703
- Ni₇₈P₁₀B₈, amorphous, local symmetry around glass-former sites, elec. quadrupole effects, NMR 0-80618
- (Pd₄₅Si₄₅)₆₁/(Fe₄₅B₁₅)₃₉, compositionally modulated amorphous film, diffusion, struct. relax. 0-103518
- (Ti,Cr)B₂, sintering kinetics and props. 0-100811
- Ti-Al-V-B-B, melt-extracted polycryst., mech. props. 0-76360
- Ti₇₀Co₂₀B₁₀, amorphous alloys, crystn. behaviour, TEM study (Japanese) 0-84087
- Ti₇₀Fe₂₀B₁₀, amorphous alloys, crystn. behaviour, TEM study (Japanese) 0-84087
- Ti₇₀Ni₂₀B₁₀, amorphous alloys, crystn. behaviour, TEM study (Japanese) 0-84087
- UB₂, thermochemistry and stability 0-97723
- W₇₀Si₂₀B₁₀, amorphous alloys obtained by liq. quenching, superconductivity 0-75670
- Y-B, amorphous, B-rich, low freq. modes, Raman scatt. obs. 0-108202
- ZrB₂-Nb, reactions between components 0-100812

boron compounds

- see also boron alloys
- boracite, single cryst. prep. and phys. props. 0-100763
- borate inhibitors, for high-temp. oxidation of Fe-Cr alloys 0-66705
- borazines, substituted, Urey Bradley force field, pot. energy consts. 0-78588
- ceramic, B content by emission spectrosc. with high freq. plasma excitation (French) 0-76477
- ESCA shifts and effective charges 0-78648
- materials for thermoelectric conversion of solar energy (French) 0-89660
- molecules involving B and C atoms, self-consistent charge calcs. of core-electron binding energy shifts 0-69084
- optical fibres, GeO₂-B₂O₃-SiO₂, ageing effects of moisture on fatigue and tensile strength 0-66539
- optical fibres, ultraclean impurities determ., and behaviour during production by CVD process (Japanese) 0-87505
- steel, low C, electroboronising by superimposed cyclic current, Na₂CO₃, B₂C, NaCl, NaOH activator studies 0-85081
- AlB₂, α - and β -forms, elec. props. at high temps. and in strong elec. fields, thermistor appls. 0-92903
- B-C, B-C-Ti, B-C-Cr, paramagnetic centre struct. and defect form. 0-66034
- BC, sintered, struct. and props. 0-104181
- B₁₃C₂, chem. bonding nature, static deform. densities and pictorial representation 0-92489
- B₄C, densification kinetics during hot pressing, 1800-2200°C 0-60817
- B₄C, fusion reactor material, low energy ion erosion expts., Kaufman source appl. 0-68942
- B₄C neutron absorber for EBR-II, He release, in-reactor meas. 0-73951
- B₄C, reaction kinetics with liq. Al, Si, Ni and Fe 0-84344
- B₄C reflector-shield concept for fusion reactor designs 0-102293
- B₄C, sputtering, low energy, H, D and He ions 0-100734
- B₄C, TEM investigation using C replicas 0-61034
- B₄C, thermophysical props. and neutron absorpt. 0-103488
- B₄C-304 stainless steel cermet for nuclear shielding appls. 0-102352
- B₄C-Cu cermet fabrication for neutron shielding appls. 0-102354
- B₄C-phenolic fibre reinforced composite for nuclear shielding appls. 0-102353
- BCl₃, in solid Ar, Kr, high resolution IR absorpt. spectra, isotopic splitting 0-87109
- BCl₃, visible fluorescence dynamics due to IR laser irradi. (Chinese) 0-102534
- BCl₃-N₂ mixtures, thermodiffusion props., effect of resonant excitation of mol. vibr. by laser, isotope separation 0-100047
- BCl₃+N(CH₃)₃→BCl₂N(CH₃)₃, complex formation, reaction product isotopic composition change (Russian) 0-81316
- BCl₂F, in solid Ar, Kr, high resolution IR absorpt. spectra, isotopic splitting 0-87109
- BCl₂NCO, soln., force fields and normal modes, vibr. spectra, IR and Raman obs. (French) 0-58266
- BF, diagrammatic perturbation theory, using universal even-tempered basis set 0-58131
- BF, isoelectronic sequence, Rydberg transitions, term value-ionisation pot. correl. 0-58276
- BF₂, radical, thermomechanical studies by mass spectrometry, enthalpy of form. and ionisation pot. determ., chem. bonds 0-81382
- BF₂CH₃, nonrigid, symmetry group calcs. 0-106254
- BH₂, elec. polarisabilities and dipole moments, var. perturbation obs. 0-63527
- BH, one electron props., SCF-X α scattered wave method 0-83279
- BH₂, Walsh's rules and small bond angle states 0-106255
- BH₃, electronic wave function determ., genealogical technique using Clebsch-Gordan coeff. 0-95529
- BH₄⁻, electron momentum distribution and Compton profiles, FSGO calcs. 0-87032
- BH₄⁺, pot. energy surfaces and mol. deform. induced by external cation 0-106285
- B₂H₆, electron momentum distribution and Compton profiles, FSGO calcs. 0-87032
- B₂H₆, equilib. with solid soln. of B in Si 0-97721
- B₂H₆⁺, electron momentum distribution and Compton profiles, FSGO calcs. 0-87032
- B₂H₆⁰, electron momentum distribution and Compton profiles, FSGO calcs. 0-87032
- BN, ¹⁵N zero point vibr. energy from nuclear photon scattering 0-59593
- BN, contact reactions with Ti and WC-Co at high pressures 0-61029
- BN, conversion of wurtzite into cubic form, stress state effect 0-64943
- BN cutter contact plates, struct. and phase changes on working steel (Russian) 0-108433
- BN, electronic struct., exact exchange HF calcs. 0-65438
- BN films, humidity sensitive elec. props. and switching characts. 0-107938
- BN glass transfer process 0-107459
- BN, semicond. film, chemical deposition 0-71596
- BN, TEM investigation using C replicas 0-61034
- BN, use to obtain Si layers with high surface concentration of B (Russian) 0-107639
- BO₂, II vibronic states, laser induced fluoresc. obs. 0-58301
- B₂O₃, bipyramidal struct., stability, ab initio SCF-MO calcs. 0-99446
- B₂O₃ glasses, Raman study at high temps. 0-93306
- B₂O₃, laser-produced plasmas, isotopic enhancement 0-92349
- B₂O₃, vitreous, struct. study using small-angle X-ray scatt. 0-84071
- B₂O₃, vitreous, struct. study using ¹⁰B NMR 0-84658
- B₂O₃-containing ceramic glaze, neutron probe anal. for control of prep. process (Polish) 0-97751
- B₂O₃-Nb₂O₅ system, phase equil. and phase struct. obs. by high resolution TEM 0-108419
- B₂O₃-Fe₂O₃-nMO, (n=2 or 4, M=Mg, Co, Ni, Cu), mag. props., transitions 0-75763
- BP film, high temp. thermoelec. power, scattering processes 0-80305
- BP: Ni pillar crystal growth from vapour 0-60758
- BP: Zn(Se)(Cd), epitaxial layers, ion implantation, defects and lattice locations, channelling obs. 0-88179
- BX₂⁺, ¹⁴NCS (X=Cl, Br, I), soln., force fields and normal modes, vibr. spectra, IR and Raman obs. (French) 0-58266
- BaO-Mn₂O₃-B₂O₃, amorphous mag. oxide, field-cooling effect (Japanese) 0-84615
- 2,4-C₂H₂H₂, polyhedral, spin coupled ¹¹B-¹H systems, 2-dimens. correl. NMR 0-69166
- CaO-B₂O₃-SiO₂ glass-forming additive, effect on Al₂O₃ ceramics sintering 0-89187

boron compounds continued

CuB₂₄, elec. props. at high temps. and in strong elec. fields, thermistor appls. 0-92903
Na₂O-B₂O₃-GeO₂ vitreous melts, thermodynamic props. from mass spectra 0-65253
Na₂O-B₂O₃-NiO melts, NiO activity and solubility meas. by EMF method (*Japanese*) 0-92677
Na₂O-B₂O₃-SiO₂ glass, fracture toughness, effect of microheterogeneous struct. 0-104256
OBF, band strengths, shock tube IR spectrosc. meas. 0-106358
PbO-B₂O₃ glasses, microhardness 0-66612
Si:BF₃⁺, ion implantation appl. in semicond. device production 0-103383
Si-B system, DTA, X-ray diffr. and metallographic study (*German*) 0-66484
Si₃B₄-x films, anal. of H ratios and profiling using nucl. techniques and Rutherford backscatt. 0-61202
SiCl₄-GeCl₄-BCl₃ particulate layers consolidation, in fabrication of optical fibre preforms 0-60787
SiO₂:BF₃⁺, ion implanted, F influence on oxidation-induced stacking faults 0-65011
SiO₂-Al₂O₃-CaO-BaO-SrO-ZnO-Na₂O-K₂O-B₂O₃, glaze effect of P₂O₅ additions 0-60824
Sm_{1-x}B₂S, valence transition induced by alloying 0-96829

borosilicate glasses

alkali, phase separation, observation using SEM-EDX technique 0-76224
antireflection films, on alkali-borosilicate glasses produced by chem. treatment 0-66677
birefringent, X-ray small-angle scatt. study 0-103937
crack growth, phase separation effects 0-89336
electrical relax., Debye-Falkenhagen theory 0-108155
field-induced electron emission into ultra-high vacuum 0-104048
gamma irradiation effect on density, refractive index, thermal expansion 0-79838
liquids, viscosity meas. up to 1840°C (*French*) 0-79969
magnetic and spectral properties, Fe and Cr ion interaction 0-103883
optical fibres, GeO₂-B₂O₃-SiO₂, ageing effects of moisture on fatigue and tensile strength 0-66539
optical fibres, graded-index, manufacture, double-crucible method 0-83688
photochromic glass, darkening effect due to γ-irrad. 0-96566
powder, sintering, foaming by chemical reactions 0-81017
residual stresses, comparison of optical and fractographic meas. rods, compressively clad 0-108539
surface, adsorption of Au, AES study, electron bombardment effects 0-65380
vacuum-deposited intermediate layer, stable structure formation 0-80979
X-ray scattering at small angles study 0-84071
Al₂O₃-B₂O₃-SiO₂ sheet glass, solar energy appl., optical and mech. props. 0-87447
Al₂O₃-CaO-B₂O₃-SiO₂ (-Na₂O) composite glasses, high strength, prod. by overlaying 0-89193
Al₂O₃-glass seals, diffusion of Al, electron microprobe study 0-107577
B₂O₃-SiO₂-Na₂O phase-separated glass, creep fracture morphology 0-81151
BaO-GeO₂-Na₂O borosilicate core glasses for high numerical aperture fibres 0-69534
CaO-Al₂O₃-B₂O₃-SiO₂-FeO, glass, IR spectra at room and melt temp. 0-88986
GeO₂-Na₂O borosilicate glass fibre prod. by phase separation and leaching 0-69558
Li₂O-Na₂O-B₂O₃-Al₂O₃-SiO₂ glass, Young's modulus and density, ion exchange effects 0-84982
Na borosilicate glass microsphere material, sintering, struct., strength props. (*Russian*) 0-108383
20Na₂O-(80-x)B₂O₃-xSiO₂ system, structure toughness-composition relationship 0-104257
Na₂O-Al₂O₃-B₂O₃-SiO₂-AgCl(Br), photochromic glass, kinetics of thermal decolorisation 0-103931
Na₂O-B₂O₃-SiO₂, containing halogens glass formation 0-103254
Na₂O-B₂O₃-SiO₂, optical waveguide glass, molar absorptivity of water 0-80066
Na₂O-B₂O₃-SiO₂ glass fibre, plastic coating influence on strength 0-58697
Na₂O-B₂O₃-SiO₂ glass fibre, plastic-coated, liq. N₂ strength 0-58707
Na₂O-B₂O₃-SiO₂ glass, low-loss GRIN fibres, double-crucible prod., loss and bandwidth meas. 0-69559
Na₂O-B₂O₃-SiO₂ glass-Ni compact, indented, strength and fracture toughness 0-93636
Na₂O-B₂O₃-SiO₂ glasses, phase-separated, leaching rate 0-104131
Na₂O-B₂O₃-SiO₂ glass, fracture toughness, effect of microheterogeneous struct. 0-104256
Na₂O-B₂O₃-SiO₂-As₂O₃(As₂O₃) glasses, DC and AC resist., bipolaronic hopping cond. 0-88558
Na₂O-B₂O₃-SiO₂, mechanical strength and swelling in flow 0-85024
Na₂O-K₂O-B₂O₃-SiO₂, character of elec. cond. 0-103516
Si-Na-B-O-N glass, synthesis and characterisation 0-108381
SiO, fabric, prep. from E-glass, structural stability rel. to brittleness, X-ray diffr. and IR spectrosc. studies 0-96634
SiO₂-B₂O₃ glass, sintering kinetics 0-84898
SiO₂-Al₂O₃-B₂O₃ glass mech. strength increased by etching 0-97609
SiO₂-B₂O₃-GeO₂, optical fibres, UV radiation-induced losses 0-87517
SiO₂-B₂O₃-Li₂O-Al₂O₃ (28, 2, 1 wt.%) glass, dielec. const. at 3 GHz 0-93233
SiO₂-GeO₂-B₂O₃-P₂O₅, optical waveguide glass, comp. determ., plasma emission spectra 0-87446
SiO₂-PbO-B₂O₃-Al₂O₃-CaO-Na₂O-K₂O glaze, interaction with aluminosilicate glass-ceramics 0-84398

Borrmann effect see *X-ray crystallography; X-ray diffraction*

Bose-Einstein statistics see *quantum statistical mechanics*

Bose gas see *boson systems*

boson fluids see *boson systems*

boson systems

see also *liquid helium-4; quantum statistical mechanics*
binary mixtures, ground state configs. 0-105570
Bose gas, one dimensional, long wave asymptotic multi particle Green functions (*Russian*) 0-77700
charged boson interactions in random potential, extended states 0-86202
condensate, dynamic eqn. functional formulation, many body theory 0-84334
condensed phase of the imperfect Bose gas 0-86201

boson systems continued

core-hole processes, electronic Hamiltonian, many-body theory 0-91443
critical exponent, η and z to second order in ε=2-d at T=0 0-77696
damping superoperator eigenvalue problem, direct soln. for boson field 0-57180
density matrix of impenetrable Bose gas, Painleve-type eqn. 0-62576
density of states of the Tomonaga-Luttinger model 0-57182
density operator function space, boson fluid, uniform many particle system description 0-73260
dilute hard-sphere Bose-gas model, low-density atomic H gas property-calc. 0-87194
dynamical plane rotator model, dynamical correl. functions in mol. field approx. 0-88758
free boson gas in weak external pot. 0-86203
hypernetted chain generalised eqn. optimal solns. 0-75396
impenetrable Bose gas, density matrix, fifth Painleve transcendent 0-77701
interacting Bose gas, T=0K, self-consistent description 0-80015
Jahn-Teller systems as displaced para-Bose oscillators 0-77695
Josephson junctions, inelastic tunnelling, pair-quasiparticle interference current 0-84566
one particle distributions, entropy bounds 0-62607
para-Bose operators, simplified description 0-86200
polarons, energy eigenvalue, systematic calculation procedure 0-84439
polymer expansion for quantum many-body problem 0-57181
quadratic Hamiltonian diagonalisation 0-82719
quantum magnetic hamiltonians with remarkable spectral properties 0-82717
quantum vortices, dynamics 0-59758
SO(2N+1) algebra, time-dependent Hartree-Bogoliubov theory, quantisation 0-62575
stability and stratification of quantum liq. mixture 0-59754
superconducting systems, electrodynamics and quantum theory 0-60134
vacuum spontaneously broken symmetry of Higgs field and Bose condensation 0-82912
vortices in infinite free Bose systems in condensation region 0-73259
H, spin-polarised, Bose condensation, phenomenological description 0-77699
H, spin-polarised, Bose-Einstein condensation 0-77698
He superfluid, Bose spectrum nonphonon branches (*Russian*) 0-92750

bosons

see also *alpha particles; boson systems; deuterons; gravitons; intermediate bosons; meson resonances; mesons; photons*
X, X bosons evaporation by black holes, rel. to primordial baryon generation 0-98750

boundaries see *boundary layers; boundary value problems; grain boundaries; metal-insulator boundaries; semiconductor-insulator boundaries; semiconductor-metal boundaries*

boundary layer flow see *boundary layers*

boundary layer turbulence

see also *atmospheric boundary layer*
aeronautics, infinite swept attachment line boundary layer, turbulence 0-74840
air flow over rearward facing step, flow separation meas. 0-69885
air turbulent flow in heated channel, effect of gravitational field 0-64533
averaged velocity field from universal power law (*Russian*) 0-79276
axisymmetric afterbodies, separated turbulent flows, wakes, exhaust plume effects 0-74885
axisymmetric turbulent boundary layers, low-freq. pressure fluctuations 0-59014
blunt flat plates, air flow, 2-D, thermal boundary layer characteristics, nose shape effects 0-92121
bursting phenomenon in open channel flow, space-time correlations structure (*Japanese*) 0-96311
channel bottom, kinematic characts. of nonuniform flow, limiting stability, erosion 0-94547
channel flows, severe nonsymmetric constriction, curving or cornering, separation 0-92222
channel liquid flows, nonsteady convective heat transfer 0-59023
channels, constricted or dilated, pulsatile flow at high Reynolds number 0-74985
characteristics induced by two-dimens. bluff bodies 0-64525
circular cylinder, local heat transfer by turbulence of free-stream flow of viscous liquid, theoretical determ. of influence (*Russian*) 0-96252
circular cylinder flows, coherence function method 0-96068
circular cylinders, surface-roughness effects on mean flow, turbulent boundary layers 0-92128
circular impinging jet, heat transfer characts., stagnation point, boundary layers 0-79303
cohesionless bottom sediments, limiting stability in turbulent channel flow, erosion 0-94546
convection, nonlinear double-diffusive, low Prandtl number, boundary layer method 0-69816
cooling efficiency in flow around wall, initial turbulence effects 0-79315
corner interaction of boundary layer and shock wave, flow separation 0-96287
crossflow developing in boundary layer during longit. flow around right dihedral angle 0-59049
curved duct, boundary layer collision, entry and core flow 0-74984
cylinder, transverse curvature and turbulence effects on axisymmetric liquid flow (*Russian*) 0-59015
detonation wave, turbulent, boundary-layer treatment 0-106791
disc normal to wall, turbulence intensities and local mean vels., separated flow 0-64531
duct, variable density fluids, vel. profile axial development due to heat transfer 0-74987
duct flow, two-dimens., large and small scale motions 0-83847
duct flow near suction tube, turbulence intensities 0-64627
ducts, 3-dimens. viscous compressible flow, inviscid flow considerations for 90° elbow 0-64639
ducts, steady 2-dimens. axisymmetrical turbulent boundary layer, compressible fluid (*Chinese*) 0-59109
film flow down rough surface, kinematic features (*Russian*) 0-79277
finite amplitude wave propagation in nearly parallel flow 0-74899
flow acoustic interaction near a plane heat conducting compliant boundary 0-69809
freely flowing liquid film, cooling, heat transfer, turbulent transport model calcs. 0-64560
gas, turbulent boundary layer vel. distrib., probabilistic statistical approach, vortices 0-92123

boundary layer turbulence continued

gas jet blowing into supersonic flow without 3-dimens. boundary layer separation, nozzle shape 0-100009
 gas screen, subsonic turbulent boundary layer, friction behind permeable section 0-92127
 Gortler stability at rigid and elastic plane plates (*Russian*) 0-79261
 Gortler vortex type perturbation profiles in boundary layers problem on curved surface (*Russian*) 0-74834
 gradient sublayer turbulence of two dimensional boundary layers undergoing turbulence 0-87763
 heat source driven turbulent convection between 2 rigid plates at arbitrary Prandtl number 0-69829
 heated flat plate in water, critical Reynolds number, heat transfer 0-69766
 heated ponds, turbulent boundary layer of stratified airflow, surface waves 0-92133
 hot-wire measurements, wall proximity corrections 0-74841
 ice-water interface, wave formation, heat transfer in presence of turbulent flow 0-103015
 incompressible layer thickness change in presence of longitudinal pressure gradient 0-92126
 incompressible turbulence mixing length in diaphragm flow pipe region (*French*) 0-69775
 irrotational strain dissipation eqn. sensitisation 0-106794
 leading edge bubble formation, peaky airfoil (*French*) 0-64524
 liquid-metal-H₂O stratified flow, horizontal co-current, interface heat transfer, turbulence model 0-92131
 longitudinal blunt circular cylinder, axisymmetric separated and reattached flow, turbulence 0-79285
 low Mach number duct flows, combustion noise generation by chemical inhomogeneities 0-92237
 magnetic convection, nonlinear, mean field approx., boundary layer method 0-69930
 mass transfer in viscous sublayer, statistical method (*Russian*) 0-87764
 mean heat of emission and hydraulic resist. of banks of tubes (*Russian*) 0-96262
 mixing layer, free, axisymmetric, turbulent spot, data processing 0-79280
 mixing layer, free, axisymmetric, turbulent spot, vorticity and Reynolds stress 0-79281
 modelling of wavevector-frequency spectrum, turbulent boundary layer wall pressure 0-106793
 noise generation, role of tornado-like vortices 0-69811
 nonequilibrium turbulent flows near wall, matching problem 0-96250
 nonlinear interaction of two waves in boundary-layer flows 0-59016
 nonstationary layer with longitudinal press. gradient, friction law (*Russian*) 0-74842
 ocean surface layer, 2-parameter turbulence models (*Russian*) 0-79275
 perforated flat plate over porous medium, turbulence penetration, eddies, mass transfer 0-64528
 pipe, annular two-phase flow, downtake turbulent film and gas flows, pressure drop 0-92218
 pipe, asymmetrically heated, turbulent transport and thermal diffusivities 0-64636
 pipe, axially rot., turbulent flow patterns and hydraulic resistance 0-106850
 pipe, turbulent aerosol flows at high wall temps., heat transfer 0-74862
 pipe entrance region, mean vel. fluctuation 0-64526
 pipe flow with suction or injection, high Prandtl no. heat and mass transfer 0-74857
 pipe inlets, turbulent local mass and heat transfer, swirling effects 0-64542
 pipes, heat transfer to low Prandtl number turbulent fluids, numerical prediction 0-69833
 pipes and bends, structure-borne sound behind a jet nozzle (*German*) 0-87804
 plane channel with one or two rough walls, turbulent flow 0-79278
 plate, rotating, 3-D boundary layer turbulence, effects of rotating radial end-plates 0-69843
 plate surface with mass blowing and suction, heat transfer in turbulent boundary layer 0-64559
 plate to high turbulence air flow heat transfer 0-79292
 plate with cylinder in turbulent boundary layer, forced convection heat transfer 0-64540
 pressure correlation functions 0-83792
 pressure gradient velocity correlations 0-64530
 pulsating turbulent pipe flow, velocity field and press. gradients 0-64641
 rearward facing step, turbulent incompressible reattaching flow, adverse press. gradient effects 0-69773
 rectangular cavity with porous filling, steady convection and boundary layers 0-79309
 rectangular cylinders, 2-dimens., drag coeff., correction method comparison 0-64568
 rectangular elbow, 3-dimens. turbulent compressible duct flow, stagnation pressure losses, vortices 0-64640
 Reynolds stress tensor in curved duct expt., single rotating slanting hot wire technique 0-75006
 round tubes, non-Newtonian fluid transition and turbulent flow regions (*Russian*) 0-59077
 shear-stress transport, hyperbolic system of eqns., Keller-Cebeci 'box' scheme 0-79274
 shock tube driver gas flow with fluctuations 0-96282
 shock wave interaction with turbulent boundary layer disturbed by injection 0-74916
 short crested waves, boundary layer vels. and mass transport 0-92169
 simple law of wall formulation for Newtonian fluid, unified time mean velocity profile model 0-103017
 slot injection of He, Favre averages 0-83791
 square duct, developing turbulent flow and heat transfer, computational procedure 0-69926
 square duct, developing turbulent flow and heat transfer, numerical prediction 0-74986
 suction under nonisothermal conditions, heat and mass transfer 0-92125
 supercritical HeI, heat transfer to turbulent pipe flow 0-64348
 superimposed miscible liquids, dynamic stabilization, turbulent transport through diffuse boundary layer 0-74844
 supersonic boundary layers interacting with cooling wall jets, turbulent and optical characteristics 0-106792
 supersonic separation flow, 2- and 3-dimens., turbulent boundary layer and shock wave 0-100017
 surface friction in turbulent boundary layer, meas. using plane Pitot tube 0-79284

boundary layer turbulence continued

tensorial volume of turbulence 0-59012
 thick axisymmetric turbulent boundary layer on a circular cylinder, similarity laws 0-64529
 Tollmien-Schlichting waves, characteristic structures in timefunctions from turbulent wall pressure fluctuations 0-92130
 transonic flow, shock wave interaction with turbulent boundary layer, pressure distrib. 0-74918
 transonic flow, shock wave interaction with turbulent boundary layer, wall shear stress 0-74919
 transonic flow, unsteady, turbulence modelling, compression waves developing into shock wave 0-74909
 tube, cylindrical, sudden expansion, turbulent flow meas. by laser Doppler velocimeter 0-75003
 tube bundle in turbulent water crossflow, bent tube vibrations 0-92124
 tube bundles, high Re crossflow, hydraulic drag and flow patterns, boundary layers 0-92122
 tubes, viscous liquid turbulent unsteady flow, pressure drop in transition region 0-74978
 turbulent heat transfer from flat plates, facing curved wall effects (*Japanese*) 0-83799
 turbulent horseshoe vortex 0-103016
 turbulent Prandtl number behaviour near a wall 0-79279
 two circular discs in tandem, drag reduction, wakes 0-106795
 unsteady flow past semi-infinite porous flat plate with suction, velocity profiles 0-92129
 unsteady laminar boundary layers behind blast waves, num. soln. 0-69776
 upstream perturbation propagation, supersonic flow, self-induced press. boundary layer on moving surface 0-74914
 vaporisation channels, rough and smooth, heat transfer in post dry-out region 0-96255
 viscous drag of two-dimensional contours moving in a weak polymer solution 0-100014
 wall turbulence and bursts, surface rejuvenation model, u^+ and T^+ inner laws 0-96251
 wall-pressure spectrum in turbulent boundary layer, rel. to noise generation by boundary layer-surface interactions 0-69810
 wave generation on elastic surfaces, expt. study 0-74843
 wedges, high Reynolds number flow, base pressure in near wake 0-59038
 wind tunnels, turbulent boundary layers on rough surfaces, simple roughness elements, natural wind simulation 0-69774
 CO₂ absorption in H₂O, aq. solns. with interfacial turbulence due to microstirrers 0-64527
 CO₂ flow in heated tubes, with near critical parameters, turbulent flow, heat transfer 0-59022
 H₂O flow in heated tubes, with near critical parameters, turbulent flow, heat transfer 0-59022
 He, supercritical, turbulent pipe flow, heat transfer by Melik-Pashayev technique 0-74860
 N₂O₄, turbulent dissec. flow, along heated tubes, heat transfer 0-63225

boundary layer turbulent flow *see boundary layer turbulence*

boundary layers

see also atmospheric boundary layer; boundary layer turbulence
 acoustic impedance influence of a cylindrical wall cavity 0-69784
 aerosol particles in flow type chamber, coagulation, deposition 0-69908
 agitated vessels, heat transfer models, thermal boundary layer 0-79288
 Agulhas Current, topographically induced changes in struct. of inertial coastal jet 0-72545
 annual review of fluid dynamic, book 0-94927
 annuli, laminar flow, pressure drop and heat transfer with dissipation allowance 0-74858
 axisymmetric channel, laminar boundary layer in presence of external stream swirls 0-64631
 axisymmetric rotating round nosed bodies, flow and heat transfer, buoyancy effects 0-79306
 body of revolution with heating and cooling, boundary layer transition and separation 0-64518
 buoyancy driven flows originating from heated cylinders submerged in a finite water layer 0-59024
 carbon tetrachloride drops falling through H₂O, surfactants rel. to deform., oscill. (*French*) 0-66880
 cascade flow problem reduction of part channel of varying width to plane cascade problem 0-83844
 cascade flow problem reduction of part-channel of varying width 0-83843
 cavitation erosion, non-spherical bubble collapse near a solid wall, analytical soln. using matched asymptotic expansions 0-106824
 channel, constant depth, wave field from uniform movement bidimensional source (*French*) 0-79332
 channel, curved rectangular, secondary flow, Taylor-Gortler vortex pattern 0-106849
 channel, cylindrical, arbitrary cross section, nonlinearly viscous medium motion 0-69928
 channel, laminar boundary layer, Gortler vortices 0-64572
 channel, shock wave stationary motion for axial blowing and two-layer detonation 0-92177
 channel flow stability, influence of nonparallelism 0-83845
 channel laminar flow, thermal entrance zone, heat transfer, optically thin gas layer effects 0-74861
 channel with blocked branch, laminar flow, nonregular domain transformation into rectangular domain 0-64635
 channel with porous walls, convective diffusion and mass transfer (*French*) 0-79305
 channel with sloping bottom, heavy perfect fluid flow 0-96309
 channels with lengthwise nonuniform heat release, critical heat flux density 0-69824
 chemically reactive, nonequilibrium boundary layer flow, exact and approx. solns. 0-79409
 circular tube under centrifugal accel. field, condensation heat transfer 0-74713
 coiled tubes, laminar flow and heat transfer, efficient numerical procedure 0-64633
 combined convection flow along vertical surface, fluctuating boundary layers 0-96254
 compressible fluid flow past degenerate star-red giant interacting binary stars 0-67779
 compressible fluid flow through annular orifices, computer-aided numerical anal. 0-87806
 conduit with lateral outlet, two-dimens. flow past barrier 0-64642

boundary layers continued

conduit with variable gradient, rapidly flowing incompressible liquid, short waves 0-92219
 confined thermal convection driven by non-uniform heating from below, boundary layers 0-87769
 cooled pipe, droplets from vapour condensation, size distrib., laminar flow 0-79111
 Couette flow, plane, past permeable bed, buoyancy effect 0-92215
 crossflow developing in boundary layer during longit. flow around right dihedral angle 0-59049
 curved duct, boundary layer collision, entry and core flow 0-74984
 curved tubes, fully developed laminar flow and heat transfer 0-79308
 curved wall power fluidics characts. 0-103053
 CW supersonic chemical laser, porous nozzle, chemically reacting boundary layer 0-100022
 cylinder on β -plane, prograde and retrograde rot. flows, boundary layer separation 0-92189
 dielectric organic liquid, concentric annuli, heat and momentum transfer, electric field effects 0-96315
 disc in electrically conducting fluid, hydromagnetic flow due to torsional oscillations about non-zero mean 0-74992
 dissociated high enthalpy hypersonic laminar air flow, heat transfer to flat plate 0-69828
 divergent duct, vortex flow breakdown, group vel. criterion 0-87807
 drop formation hydrodynamics, macroencapsulation 0-64603
 duct, rectangular, laminar non-Newtonian flow, vel. profiles 0-92217
 duct, supersonic flow downstream oscillations from abrupt cross section increase, nozzles 0-74976
 duct entrance region, laminar heat transfer, finite element method 0-69836
 duct flow development, step-by-step anal. for laminar flow 0-64634
 duct with varying cross section and viscous mean flow, acoustic wave propag. 0-96267
 ducts, non-circular, forced convection heat transfer problems 0-64557
 ducts, one-dimensional models for transient gas-liquid flows 0-64614
 ducts, rapidly rot., variable area, rectangular, steady flow, inertial perturbations for small divergences 0-59112
 ducts, spanwise-periodic and corrugated, heat transfer and laminar flow 0-64547
 dusty fluid, laminar boundary layer flow, 2-D stagnation point near oscillating plate 0-64606
 elliptic flows calc., EMIT numerical procedure 0-79255
 ethane, flow continuity in arterial capillary systems in cryogenic heat pipes 0-64536
 extended Graetz problem with Dirichlet wall boundary conditions 0-74706
 film condensation of moving vapour on horizontal cylinder, exptl. dependences 0-58892
 finite difference methods, nonuniform grid generation 0-83780
 flat vertical plate, transient natural convection in air 0-64556
 flow from a channel with a flexible barrier 0-69922
 fluid layer between co-axial cylinders, instability of natural convection 0-64558
 free convection boundary layer flow and heat transfer, variational technique 0-106796
 free convection flow past vertical porous plate set in impulsive motion 0-69818
 free convection heat transfer from vertical thin wire to air, laminar-turbulent transitions (*Japanese*) 0-92152
 free interaction with supersonic flow, dispersion eqn. solutions 0-69867
 free laminar convection for liquid in ribbed slot 0-96261
 Freon-12, annular mist flow in tube, wall film mass flow rate 0-69905
 gas, perfect, vortex sheet, separation from smooth body at large Reynolds number (*French*) 0-74908
 gas carrying ducts in plate type heat exchangers, heat transfer and pressure drop 0-79291
 gaseous microbubble growth in laminar separation bubbles 0-106821
 geophysical fluid dynamics theory, book 0-105443
 heat transfer to laminar flow with internal heat source in channel 0-64532
 heated flat plate in water, critical Reynolds number, heat transfer 0-69766
 helically rib-roughened tubes, forced convection heat transfer and friction characts. 0-96258
 high loading ratio slurries, pressure flow, pressure drop calcs. in pipes 0-92202
 horizontal cylinder with different end temps., natural convection, jets 0-99996
 horizontal pipe subjected to external convection and radiation, laminar forced convection 0-79307
 horizontal wavy channels, heat transfer and flow 0-69921
 hydrodynamic lubrication, free boundary problem, variational inequalities 0-62475
 hydromagnetic flow, suction effect near accelerated plate 0-92232
 hypersonic laminar, nonequil. ionis. problem 0-59129
 impulsively started vertical plate, mass transfer and free convection currents 0-64567
 incompressible fluid laminar boundary layer, Gortler function existence problem (*German*) 0-64516
 incompressible laminar planar flow between parallel plates, ang. vorticity formulation 0-64643
 incompressible separated boundary layers including viscous-inviscid interaction, transition bubble 0-64515
 interaction with induced sound, flow past a square plate in a duct 0-69783
 ionising Ar flows, shock wave and laminar boundary layer coupled interaction 0-59071
 irregular wavy flow of a liquid film down a vertical plane 0-106808
 isothermal horizontal circular cylinder, laminar free convection, thick boundary layer 0-64566
 jet flow, appl. of Meksyn's method 0-96292
 laminar, heat transfer, mass transfer and friction coeffs. (*German*) 0-74881
 laminar, heat transfer along static and moving cylinders 0-79316
 laminar boundary layer, subsonic, strong slot injection, triple deck theory 0-74831
 laminar boundary layers, compressible, Prandtl=0.72, sharp pressure rise effect 0-83782
 laminar flow over porous flexible boundary, oscillatory flow 0-92107
 laminar heat transfer for boundary layers with mass injection and chemical reactions (*Chinese*) 0-59020

boundary layers continued

laminar liquid film, falling, O₂ adsorpt. with zero order react. in entrance region 0-64652
 laminar pipe flow heat transfer, simultaneous wall and fluid axial conduction 0-74870
 laminar tube flow, gravitational deposition of growing aerosol particles 0-59099
 liquid films, heated horizontal channel, heat transfer and dry patch formation 0-64554
 liquid layer flowing down inclined plane, heating and cooling effects on stability 0-79254
 liquid metals laminar flow in curved channels, transversely applied mag. field, flow anal. 0-59116
 LMFBF triangular rod array, flow resistance wall shear stress in interior subchannel 0-63244
 low Mach number duct flows, combustion noise generation by chemical inhomogeneities 0-92237
 low velocity vertical steam-water flow, void fraction in pipes 0-74964
 metastable flows of water, spontaneous boiling 0-106709
 MHD, sink flow with transverse mag. field, boundary layer thickness 0-69940
 MHD channels, voltage losses near electrodes 0-103079
 mHD flow past a semi-infinite flat plate with heat transfer, exact numerical solns. of boundary layer similarity eqns. 0-83861
 MHD forced convection in channel bounded by plate and permeable bed, Hall effects 0-69934
 micropolar fluid, heat transfer in stagnation point flow 0-79356
 moving horizontal flat plate, laminar boundary layer, buoyancy effects 0-74877
 narrow curved channels, vels. and flow rate, intrinsic coordinates formulation 0-79406
 natural convective wall plume, boundary layer eqns., higher order anal. 0-64550
 natural laminar convection about isothermal cylinder, Navier-Stokes eqn. soln. 0-92143
 Navier-Stokes equation, limiting form at high Reynolds number (*French*) 0-74823
 Navier-Stokes equations, linearised, numerical soln., effect of cell Reynolds number 0-106780
 non-Newtonian fluid, pseudoplastic, nonlinear singular boundary value problem 0-79362
 non-Newtonian fluid, viscoelastic boundary-layer flow past a parabola and a paraboloid 0-83817
 non-Newtonian fluids, boundary layer theory 0-83818
 nonuniform grids in finite difference approximations, application to fluid flow problems 0-105507
 nonuniform parallel stream, slender wing theory, flow and lift 0-74830
 nose separation for laminar boundary layers on body of revolution 0-59091
 nozzle in different jet regimes, internal and external flows, separation and wakes 0-100023
 ocean boundary current flow along continental margin, effect of localised topographic irregularity 0-72539
 ocean boundary-forced planetary waves, model mid-ocean response to strong current variability 0-72541
 ocean deep-water channel flow, rotating hydraulics theory 0-94539
 ocean gyre, boundary layer circulation effect on poleward heat flux 0-85668
 ocean surface currents mapping, HF radar system appl. 0-94626
 open pipe exits, flow during acoustic resonance, vortices and boundary layers 0-92224
 optically thick horizontal fluid layer heated below, heat transfer 0-99993
 oscillating source flow of ducting fluid between parallel discs 0-99986
 oscillatory flow in U-tube manometers, effect of drag reducing polymer additives 0-64584
 Pacific Ocean, barotropic and baroclinic tides over continental slope and shelf off Oregon 0-72543
 Pacific Ocean boundary flow forcing rel. to oceanic circulation around New Zealand 0-72538
 parallel plate channel, convective-radiative interaction, air-operated solar collectors appl. 0-96259
 periodic laminar boundary layers, theory 0-79257
 periodic wavy surface, laminar boundary layer, nonlinear anal. for long waves, separation 0-87759
 pipe flow, spatial cavitation-nuclei-measurements by means of laser velocimeter 0-64593
 pipe fluid flow, solid particle impurity propag. 0-64630
 plane jet, stability and autooscillations from channel anal. 0-100018
 plate, flat, normal to oncoming stream, 2-D boundary layer, extended series expansions 0-83781
 plate, heated, semiminfinite, vertical, with heat sources and sinks natural convection 0-59035
 plate, vertical, free convection boundary layers and heat transfer 0-59002
 plate and laminar slug flow with periodically changing temp., transient heat transfer 0-74872
 plate with nonsteady temp. on lower surface, laminar flow, conjugate heat transfer 0-74879
 plate with periodic suction and injections in supersonic region, boundary layers (*German*) 0-59069
 plates, vertical and inclined, mixed convection combined, heat and mass transfer 0-64552
 polymer solns., dilute, extensional and sink flow in channel 0-74925
 porous medium, saturated, mixed convection boundary layer flow on vertical surface 0-106798
 porous plate, gas injection, squeezing out of liq. 0-64622
 porous straight channel, MHD flow 0-69932
 pulsating stars asymptotic theory, boundary layer method 0-82389
 qualitative analysis of unsteady heat and mass transfer modes in a boundary layer with chemical reactions and intensive injections 0-69819
 Rayleigh-Benard convection, wave number selection, sidewalls effect 0-106799
 reacting particle in fluid, convective diffusion, nonlinear surface reaction kinetics 0-106854
 rectangular body, laminar flow, separation bubble and stagnation line 0-64514
 ripple and dune formation on erodible bed by low Froude number flow 0-106784
 rotating cylindrical annulus, transition to Taylor vortices, Ekman layers 0-87776
 rotating disc, heat exchange into unbounded rotating fluid, thermal and hydrodynamic boundary layers 0-59050

boundary layers continued

- rotating disc boundary layer transition regime, spiral vortices 0-59040
 rough interface between two fluids, coherent acoustic scatter 0-96074
 round tube flow, laminar dispersion 0-64638
 seawater during evaporation, optical interferometry (*Russian*) 0-61919
 shell deformation by supersonic gas flow, drag 0-96279
 shock wave interactions with boundary layers, review, book contrib. 0-96283
 short crested waves, boundary layer vels. and mass transport 0-92169
 sphere between plane parallel boundaries, creeping parallel motion, strong interaction theory 0-103075
 small channels, gas flow, graph and nomograph for anal. eval. 0-106848
 solid particle systems, high Reynolds number, momentum transfer. Karman-Pohlhausen method 0-74947
 solid reacting particles, ordered system at high Peclet numbers, mass transfer, convection 0-69830
 sphere between plane parallel boundaries, creeping perpendicular motion, strong interaction theory 0-100035
 spherical particle in circular tube flows, lateral migration 0-92221
 stagnation flow at a heated curved wall, ignition condition 0-96242
 stagnation point boundary layer flow with radiation 0-79258
 stagnation points on cycloidal boundary in flow with const. shear 0-87755
 steady rotating flow over topography, steady β -plane channel, quasi-linear theory 0-92159
 steady viscous flow past circular cylinder, numerical study, vortices and separation 0-92108
 steam generating channel, nonuniform heat release, heat transfer crisis location 0-64534
 steam generator tubes, forced and natural circulation, inception condition correlations 0-74868
 Stokes flow, slender body theory for viscous incompressible fluid 0-92160
 Stokes problem, effects of free convection on oscillatory flow past infinite porous vertical limiting surface 0-109348
 stratified fluid, duct, equilibrium breakdown, thermosphon work (*French*) 0-59114
 supercavity hydrofoil, wall effects, nose rounding 0-64594
 supersonic flow over compression ramp, laminar separation, second order asymptotic soln. 0-83828
 suspensions of charged particles, laminar tube flow, entrance deposition 0-59100
 swirling convective boundary layer, vorticity dynamics 0-59048
 T-junction laminar flow, partially elliptic flow numerical calcs., recirculation 0-64632
 thermal blooming in axial pipe flow: comment [and reply] 0-95966
 thermal boundary layer interactions in shock tube sampling for kinetic obs. 0-104420
 thermoelectric MHD, pipe end problem, boundary layers and rotation 0-69942
 three dimensional growing boundary layers, linear stability 0-74833
 three dimensional parallel shear flows, stability and transition for rot. disc 0-74887
 three-dimensional boundary layer eqns. 0-96241
 three-dimensional boundary-layer separation 0-92188
 three-dimensional flow over wings with leading-edge vortex separation 0-74927
 trench with radiative wall conditions, free convection 0-79324
 tube with variable boundary conditions, heat transfer, Laplace transform appl. 0-74859
 tubes, nonstationary thermal processes, heat transfer coeff. quasistationary value applicability 0-64562
 tubes, straight and coiled, boiling heat transfer with low pressure water flows 0-74856
 tunnels with continuous and perforated walls, cavity size 0-92193
 turbomachines, boundary layer charact., influence of external flow turbulence 0-87811
 two-dimensional viscous flow past circular cylinder, rapidly convergent series soln. 0-96244
 two-phase pressure driven stratified laminar pipe flow 0-64609
 unstable laminar boundary layers, nonlinear evolution and breakdown 0-92109
 unsteady, through pipes, modelling and simulation (*German*) 0-64637
 unsteady boundary layer on a two dimensional or axisymmetric body with higher order effects 0-92106
 unsteady boundary layer separation, mathematical criterion 0-69884
 unsteady compressible 3-D boundary layer flow, near axisymmetric stagnation point 0-103011
 unsteady hydromagnetic thermal boundary layer problem, numerical treatment 0-92227
 unsteady laminar boundary layer flows induced by impulsive accelerating motion (*Japanese*) 0-69765
 variable resistance boundary layers, frictional resist. effects on motion of bodies 0-96243
 velocity profile for boundary layer flow along a rectangular corner (*Japanese*) 0-74832
 vertical plate with uniform blowing, laminar combined forced and free convection 0-74876
 viscoelastic boundary layer flow, second order, at stagnation point, heat transfer 0-103025
 viscoelastic liquid, boundary-layer flow past symmetric wedge or right circular cone 0-64513
 viscoelastic pipes, press. transients 0-64644
 viscous flow through rough wall cracks, friction factor formula (*Rumanian*) 0-69925
 viscous fluid, plane squeezing flow, invariance group 0-79252
 viscous heat conducting fluid, acoustic boundary layer 0-107377
 walls, permeable, cooling characts., heat exchange, rad. emitter design 0-64535
 water, annular mist flow in tube, wall film mass flow rate 0-69905
 water, nondimensional heat transfer law for a slanted hot film 0-74853
 water boundary layer along heated cylinder, buoyancy and variable viscosity effects 0-79256
 water evaporative cooling, convection and mass transfer, fog formation in boundary layers 0-79293
 water evaporative cooling, heat and mass transfer coeffs., fog formation effects 0-79294
 Wedemeyer spin up model, Ekman compatibility conditions, Navier-Stokes eqns. 0-83802
 wedge impulsively set into motion, boundary layer development 0-79259
 wind flow over complex terrain, wind tunnel simulation 0-76596

boundary layers continued

- wire gauzes resistance coefficient measurement at low air velocity (*Japanese*) 0-106843
 Ar, shock-tube end-wall boundary layer 0-79348
 Fe-Ni-B glassy ribbons melt spinning, gas boundary layer effects 0-76217
 H, dissociated, heat transfer to catalytic surfaces, shock tube investigation 0-64551
 K channel flow, incipient boiling superheats 0-74709
 Li, liquid, transverse flow around tube bundle, heat transfer 0-64537
- boundary-value problems**
 see also initial value problems
 acoustic transmission, gas with porous medium obstacle, scalar Helmholtz eqn. 0-74552
 antenna-potential approx. of EM field 0-68060
 axisymmetric elastic problems, stress function solns. (*Japanese*) 0-64371
 axisymmetric transducers, with various boundary conditions, single integral computer method for Green's function 0-87591
 boundary layer flow past circular cylinder, rapidly convergent series soln. 0-96244
 Brownian motion with adsorbing boundary, joint position-vel. distribution determ. 0-62581
 concentric domains, two dimensional heat equation general solution (*German*) 0-99918
 coupled radiative plus conductive heat transfer, absorption coeff. temp. depend. allowance 0-74698
 cylinder, hollow with internal circular crack, axially symmetric torsion determ., numerical results for boundary value anal. 0-64456
 cylindrical pulse diff. by metallic half plane, boundary value problem, direct transform technique 0-69573
 cylindrical punch, three-dimensional stress field, photoelastic studies 0-93272
 dielectric ellipsoid or elliptic cylinder, Laplace eqn. soln. to electrostatic boundary value problem 0-63884
 diffusion equation, nonlinear, invariance props., Lie-Backlund groups 0-62596
 discontinuous deformation gradients near crack tip in finite anti-plane shear 0-58973
 disordered system, one-dimens., density of states and wavefunction shape, periodic boundary condition influence 0-80223
 elastic dielectrics with polarisation gradient, boundary value problem exact soln. 0-58898
 elastic plastic spherical body, instability under uniform loading 0-58946
 elastic strip, Griffith crack interactions, mixed boundary value problem 0-58969
 elastic-plastic damaged body, unknown boundary value problem explicit solution (*French*) 0-79166
 elastostatic theory, mixed periodic problems, quadrature solution 0-86088
 elastoplastic thin vertical columns, postbuckled, deflections 0-87728
 electric arc, steady-state, energy eqn. soln., boundary value problem 0-79601
 electrodynamic boundary problem solution for complex shape regions 0-69300
 electroelasticity for piezoelectric medium with cuts, 2-D boundary value problems 0-71319
 elliptic boundary-value problem asymptotic solutions, domain varied close to conical points 0-86075
 elliptic equations and systems, free-boundary problem solution method 0-69941
 EM field above two-dimensional inhomogeneous struct., boundary conditions 0-85595
 EM waves diffraction at surfaces with inhomogeneous admittance 0-69296
 EM waves scattering, in nonlinear medium with one-dimensional random nonuniformities, statistical analysis 0-106421
 filtration theory problem soln. (*Russian*) 0-74970
 finitely conducting cross grating theory 0-106635
 fluid dynamics, micropolar, potentials and Green's functions 0-96286
 fluid dynamics, pseudoplastic non-Newtonian fluid, nonlinear singular boundary value problem 0-79362
 fracture analysis, 2D linear, elastic, finite element anal. vs. the edge function method 0-99963
 gyrotropic absorbing crystals, nonorthogonal eigenwave refl. 0-99624
 heat and mass transfer, mixed and oblique derivative boundary conditions 0-69820
 heat conduction, inverse problem, integral eqns. calcs. 0-74695
 heat conduction, soln. 0-79106
 heat conduction explosive boundary condition problems, accuracy of approx. solutions (*Russian*) 0-99912
 heat transfer, nonstationary, finite element calcs. 0-83795
 inelastic deformation, stiff constitutive models, numerical integration 0-96208
 inhomogeneous elastic layer, torsion investigation by approx. methods 0-88799
 insulated water layer, combined heat transfer, stratified layer, energy eqn., boundary value problem 0-79290
 kidney model, numerical soln. by multiple shooting 0-104609
 Korteweg-de Vries eqn. and 2nd Painleve transcendent, boundary value problem in plasma theory 0-69971
 L-plasticity, boundary value problems for plane strain or stress 0-58926
 magnetic lens design, finite element program improvement 0-69316
 materials testing, strip with semicircular notches, tensile load conditions at end, interf. effects obs. 0-64455
 Maxwell equations, boundary value approx. using finite element anal. (*German*) 0-91718
 media with double diffusivity, diffusion theory, boundary value problems 0-75378
 MHD electrical potentials, uniqueness of solns. to extended class of elliptic boundary value problems 0-69937
 molar molecule heat and mass transfer phenomena, generalised variational principle 0-79104
 multidimensional diffusion equation, class of general boundary conditions 0-90796
 non-associated plasticity and elastoplasticity, rate boundary value problems, variational principles 0-87726
 nonlinear heat transfer on boundary, difference method of solving conjugate nonstationary convection problem 0-92020
 nonlinear shell theory, boundary value problem solutions 0-57094
 nonreflecting outflow boundary condition for subsonic Navier-Stokes calculations 0-74828

boundary-value problems continued

- parabolic equations, majorising solution boundary conditions, solution comparison 0-68023
- parabolic free boundary problem, numerical soln. via Newton's method 0-69632
- peristaltic transport, asymptotic method 0-87805
- physiology, flow problem, one tube 0-89703
- pile, numerical soln. of beam eqn. with nonuniform foundation coeff. 0-64361
- plane elastic wave diffraction by wedge, three dimensional nonstationary problem 0-69723
- plane elastostatic boundary value problems, Rizzo's integral and Kupradze's functional eqns. 0-57093
- plane elastostatics, integral equations for mixed boundary value problem 0-79143
- Poiseuille flow, compound matrix method 0-57096
- polycrystalline metals, effect of grain boundary sliding on steady creep 0-96590
- reinforcement material distrib. for specified stress field criteria, plane elasticity hybrid problem 0-64376
- rotating strings, elastic, heavy, nonlinear eigenvalue problems, bifurcating branches of solns. 0-73174
- simple body melting time with convection boundary condition 0-99914
- solar cell analysis, appl. of superposition principle 0-76631
- spatial dispersion exponential model, boundary conditions (*Russian*) 0-75994
- spherical nozzles of high-temperature heaters, heat transfer calcs. 0-103022
- stationary vibrations in 2-dimensional micropolar thermoelasticity 0-74793
- steady-state heat diffusion equation, alternate general solution 0-79103
- Stokes problem, second-order difference scheme 0-90678
- symmetrical branches at end of crack, effects on growth 0-103003
- thermal problems, nonhomogeneous, and Stefan single-phase problem in arbitrary domains 0-79102
- thermoelastic response of infinite flat slab 0-92052
- thermoelasticity, 2-D exterior boundary value problems (*French*) 0-79144
- traction problem, strain energy bound in finite elasticity with nonzero surface data 0-58909
- two-dimensional, conformal transformations combined with numerical techniques, with applications to coupled-bar problems 0-83538
- waves above level bottom, three-dimensional problem periodic solutions 0-57099
- wind-driven lake circulation models, boundary conditions 0-85688
- Yang-Mills equation, coupled solutions 0-105764

bowing see bending**brain**

- see also *neurophysiology*
- 40 Hz activity in sigmoid gyrus, nucleus accumbens and amygdala, cross correl. anal. 0-76730
- Alopec process: Visual receptive fields by response feedback 0-61546
- angioscintigraphy in posterior view, clinical value 0-72290
- associative noise-like coding memory, algebraic model 0-76720
- auditory cortex of unanaesthetised monkey, vertical stereotaxic approach to elec. recording 0-72383
- auditory cortex unit response to synthesized formants, cat 0-67098
- autoradiographic visualisation of rat brain dopaminergic nerve endings, test of technique 0-61742
- bifurcations geometry, human, effect of static distending press. 0-94259
- biomagnetic measurements in unshielded and noisy environments 0-104710
- blood flow, meas. in pig by ^{133}Xe clearance technique 0-94421
- blood flow, regional distrib. during exercise in dogs 0-101197
- blood flow, total and regional, effect of cerebral extracellular fluid acidity 0-67123
- blood-brain barrier, effects of microwave-induced hyperthermia, rat 0-61642
- blood-brain barrier, problems in quantifying effects, comparison of methods 0-61643
- blood-brain barrier, reversal of microwave-induced permeability 0-61641
- brainstem population responses, inhibitory influence 0-104595
- caudate nucleus, neurotransmitter activity transient alterations after electron irradiat., rat expts. 0-72267
- cerebrovascular permeability, quantitative method for meas. of alterations 0-61748
- circadian clock in Limulus brain, response increase and noise decrease of retinal photoreceptors 0-94210
- corpus callosum, cat, effect of sectioning on binocularity of vision 0-97922
- corpus callosum, effect of neonatal section on depth perception, young cats 0-61572
- cortical plasticity in monocularly deprived immobilized kittens, eye movement dependence 0-81588
- diagnostic technologies, comparative study of radionuclides and computerised tomography 0-72320
- diathermy applicator for irradiat. of rat brain 0-94425
- electric stimulation, awakening thresholds in 5 sleep-waking stages, cat expts. 0-85377
- EM microelectrode holder for pulsating penetration of brain tissue 0-98199
- external geniculate body, cat, geometric props. of space of description of images 0-94203
- gliomas, malignant, anal. of dose-effect relationship 0-72331
- gliomas, malignant, high dose radiation therapy 0-67254
- hippocampal burst-firing neurons, slow inward current, voltage clamp obs. 0-94194
- imaging, comparative study with γ -camera, single-photon emission CT, and transmission CT 0-109004
- infarction, abnormality of Xe brain/blood partition coeff. and blood flow 0-97993
- inferior colliculus neurons, cat, response to binaural beat stimuli obs. 0-72179
- intellectual activity, classification of normal and anomalous forms, quantised-wave theory of coherent brain appl. (*Russian*) 0-76722
- intellectual activity, psychoheuristic relationship of psychotom structs. and giftedness structs. introduction, quantised wave theory of coherent brain appl. (*Russian*) 0-76723
- irradiated, quantitative assess. by computerised tomography scan anal. 0-72306
- irradiation, low dose elective, in small cell lung carcinoma 0-67253

brain continued

- irradiation with C ions, recovery from pot. lethal damage, rat expts. 0-72234
- lateral geniculate cells, functional organisation after visual cortex removal in newborn kittens 0-81587
- lateralisation of function, detect. by alpha-contingent visual stimulation 0-94190
- locus coeruleus neurons, impulse activity in awake rats and monkeys 0-104581
- magnetic evoked field mapping 0-104705
- magnetic fields 0-72182
- magnetoencephalogram power spectrum estimation 0-104704
- magnetoencephalography, distrib. of detector sensitivity, reciprocity appl. 0-72278
- magnetoencephalography, sensitivity distrib. 0-101246
- magnetoencephalography, superconductive helmet with SQUID 0-104708
- mechanism studies using evoked pots. (*German*) 0-61535
- medial preoptic lesioned rats, increased survival in mild cold exposure 0-101151
- medullary respiratory neuron activity, rel. to tonic and phasic REM sleep 0-97891
- midbrain, similarities between overlapping visual and tactile maps in mammals and reptiles 0-61550
- neural generator localisation underlying auditory evoked mag. fields, human brain 0-104703
- neuronal DNA damage accumulation rel. to death after whole-brain irradiat., rats 0-76804
- neuronal membrane process field potentials anal. and synthesis, computer system 0-85374
- octopus, Eledone cirrhosa, electrophysiology of isolated central nervous system 0-104577
- oedema, experimental, serial meas. of specific gravity and 0-98005
- optic tectum, goldfish, fine struct. 0-85396
- optic tract fibres, physiologically characterised, projection patterns, cat obs. 0-101167
- pattern recognition of human brain electrical potentials 0-109051
- pattern separability in random neural net with inhibitory connections 0-76726
- photoelectrode for recording intracerebral cellular Ca^{2+} transients 0-67307
- reflectance, mapping technique using optical fibres 0-72381
- retinocortical projection abnormality of human albinos, vision defects 0-94208
- retinotectal projection in goldfish to an inappropriate region with a reversal in polarity 0-72153
- rheoencephalographic curves, bipolar and tetrapolar techniques, comparison (*Croatian*) 0-104796
- single unit activity from foetal pig brains, recording method 0-67315
- speech perception, hemispheric specialisation, acoustic change rate, expt. obs. 0-104594
- striate cortex, cat, differential responses of 'simple' and 'complex' cells during saccades 0-85394
- striate cortex, cat, inhibitory sidebands of complex receptive fields 0-67079
- striate cortex, cat, movement direction detect. and contrast reversal effects, cell response obs. 0-72155
- striate cortex, spatial mapping approach to perceptual coding 0-101168
- superior colliculus and frontal eye field ablations, effects on eye movement control 0-72154
- supraoptic neurons, rat hypothalamus, osmosensitivity obs. 0-104578
- tomography, transaxial, ring detector positron camera system for research 0-61739
- tumour, rat, RBE of cyclotron fast neutrons rel. to ^{60}Co γ -rays 0-76797
- tumour cells, rat, anal. of interaction of 2 nitrosourea compounds and X-radiation 0-72230
- tumour cells, Z-ray-BCNU interactions in vitro, isobologram anal., rats 0-81662
- US evaluation of intracranial pathology in infants, new technique 0-98046
- valyl-h-tRNA synthetase of chick embryo brain, ^{60}Co γ -irradiat. obs. 0-72222
- vision, human recognition system with thinking, model 0-76744
- vision binocularity affected by sectioning of corpus callosum, of cat 0-97922
- vision suppression by brain 0-97909
- visual cortical neurons, optimality of bar and grating stimuli 0-85391
- X-irradiation, late changes in biochem. and blood flow, rat expts. 0-72218
- X-irradiation in the therapeutic range, monkeys, delayed damage 0-76801
- Li, quantitative location in brain tissue using nuclear Track Etch techniques 0-98133
- ^{99m}Tc labelled DTPA and MDP, compensative value on brain lesion (*Japanese*) 0-67235
- Xe regional kinetics meas., imaging methods in transmission computerised tomography 0-98131

brain models

- see also *learning systems; neural nets*
- cerebellar model, spatial freq. characts. (*Japanese*) 0-67068
- distributed type associative memory model with quantised Hadamard transform 0-108867
- memory neuron, synapse microchem. for memory component of neurocognitive brain model 0-104579
- self-organising nerve nets, fundamental theory, developmental plasticity anal. 0-67062
- synchronous brain activities, spatio-temporal filter approach 0-61503
- synchronous oscillation in idealised neuronal circuit with recurrent inhibition (*Japanese*) 0-101164

brakes

- wheel temperature in railroad service, effect of brake shoes 0-93660

braking

- spacecraft braking problem in Jupiter atmosphere, ballistic and navigation aspects 0-61981

brass

- α - β phase transformation caused by friction 0-76378
- anneal hardening, of polycrysts. deformed in tension or rolling (*Japanese*) 0-93564
- bicrystal, two phase α/β , transgranular slip and fracture across an interface 0-81150

brass continued

- bicrystal, two-phase (α/β), interphase boundary sliding at high temps. 0-88164
 binding and cryst. struct., valence arguments 0-88081
 α - β brass, interface segregation 0-89231
 β -brass, uniaxial tension and compression, cyclic stress-strain behaviour 0-97551
 β -brass bicrystals, shear-incompatible, grain boundary contrib. to Bauschinger effect 0-97550
 α/β -brass bicrystals, two-phase, with nearly uniform and thermodynamic equilib. concs. 0-65383
 cold rolling, inhomogeneous texture 0-89251
 constitutional vacancies in brass like alloys 0-84168
 crack initiation at high strain rates, uniaxial and biaxial tests 0-85141
 creep, cyclic, constitutive eqn. under increasing stress condition 0-93593
 dislocation etchant, $(\text{NH}_4)_2\text{S}_2\text{O}_8\text{-HCl-H}_2\text{O}$ 0-65004
 electrode, electrical breakdown of water in μs region 0-103917
 electrode, in high repetition rate spark switches, surface ageing 0-106997
 fatigue crack growth micromechanisms at low stress intensities in α -phase 0-108570
 fatigue crack propag., role of dislocation substruct., for α -brass 0-60963
 fatigue of two phase bicrystal 0-108520
 in-depth profiles, non-destructive determ. 0-93836
 liquid, thermodynamic props. (German) 0-66482
 liquid impact erosion and cavitation erosion comparison 0-104302
 orientation distribution, texturised materials, Ghost effect demonstration 0-70080
 oxidation of α - and β -phases, prompt. nucl. reactions and reson. alpha scatt. study 0-66690
 plane stress ductile fracture, prestrain effects in α -phase 0-108532
 plastic deform., stress-strain relation of integral type 0-74754
 recrystallization during induction heating 0-97511
 rolling texture development and deform. struct., shear bands effect (Japanese) 0-84952
 rubbing of mild steel, magnetic field effect on diffusive wear of cutting tools 0-60985
 shape memory effect and martensitic transform. depend. on heating-cooling cycles (Russian) 0-97482
 spark gaps with brass, parallel plane electrodes, erosion characts. 0-70076
 spinodally decomposed, morphology and characts. 0-60863
 spring alloys, microplastic deform. and endurance limit 0-81197
 stress corrosion fracture surface anal. by AES 0-104321
 superstructures and defect obs. in alloys with γ -brass struct. 0-107284
 thermal conductivity, lattice component, 30 to 300K, microscopic mechanisms 0-107758
 thermal conductivity, lattice component, 4.2 to 30K, microscopic mechanisms 0-107757
 US velocity, meas. method for isotropic nondispersive solids 0-69616
 vacancy form., ordering effect, positron annihilation obs. 0-93427
 vacancy formation energies in mixed $\alpha+\beta$ phase 0-59456
 wear, rubbing on mild steel, mag. field influence 0-60982
 wire, US inspection, immersion method 0-66757
 workhardened thin specimens, fracture, anisotropy coeff. role (French) 0-104276
 yielding behaviour, rel. to low temp. annealing treatment (Japanese) 0-93582
 Al-brass tubes, passivation treatment for atmospheric corrosion protection during storage and transport 0-85079
 $\gamma\text{Cu}_2\text{Zn}_8$, high pressure effect on brass struct. 0-107108

Bravais lattice see crystal atomic structure

braz bonding see brazing

brazing

- see also soldering
 fusion reactor, TFR, large section water cooled Cu conductor, brazing joints 0-91260
 permanent joining techniques 0-82782

breakage see fracture

breakdown (electric) see electric breakdown

breakdown (mechanical) see manufacturing processes

breakdown diodes see avalanche diodes; Zener diodes

breeder reactors see fission reactors

bremsstrahlung

- see also electron radiation; gamma-ray spectra; gamma-rays; X-ray emission spectra; X-rays
 Brown-Goble soft photon approx. 0-95777
 channelled electrons, characteristic radiation, sharp lines obs. 0-65111
 channelling coherent radiation and bremsstrahlung 0-65079
 classical stimulated bremsstrahlung, electron beam bunching 0-69306
 Debye shielding corrections for 1- and 2-photon cross sections 0-106157
 electron bunching, scattering and bremsstrahlung in cryst. lattice in strong EM field 0-65113
 electron probe X-ray microanalysis, quantitative investigation of thin specimens 0-101068
 flare stars, fast electrons nonthermal bremsstrahlung rel. to flare emission spectrum 0-67731
 galactic disc gamma-ray emission, 80 keV to 8 MeV obs. rel. to bremsstrahlung contrib. 0-82540
 Galaxy gamma-ray emission, fluxes determ. from cosmic ray electron spectrum 0-62257
 gamma, from thin target of betatron 0-86999
 global structure of space-time, classical bremsstrahlung problem 0-105547
 internal bremsstrahlung in s-electron capture 0-63133
 ion+electron collision, resonant electron bremsstrahlung (Russian) 0-102580
 Langmuir waves, turbulent bremsstrahlung process 0-62009
 M87 halo, thermal bremsstrahlung contrib. to X-ray emission from Faraday rot. 0-67844
 neutral atoms, bremsstrahlung of low-energy electrons, polarisation effects 0-102577
 plasma, X-ray bremsstrahlung polarisation and anisotropy, evidence of suprathermal electron fluxes 0-103193
 plasma diagnostics, using multichannel X-ray spectrometer 0-57445
 polarisation-frequency characteristics for monoenergetic electron beam in Coulomb potential 0-95778
 polarised electrons, azimuthal asymmetry due to spin-orbit coupling 0-60705
 radiation absorption in magnetoplasma, rel. to laser fusion 0-92273

bremsstrahlung continued

- radiobiological experiments, lightly filtered X-ray spectra generated at 200 to 300 kV 0-72397
 rare earth metals, density of 4f states below and above Fermi level, XPS and bremsstrahlung isochromat spectroscopy 0-76140
 reflectivity and temp., scaling laws 0-87913
 scattered gamma ray spectra, bremsstrahlung contribution from low energy electrons 0-78192
 V818 Scorpii (Scorpii X-1), bremsstrahlung, model for UV continuum energy distrib. 0-82541
 solar flares, polarisation and directivity of hard X-ray bremsstrahlung from thermal source 0-90374
 4U 1700-37 (HD 153919), high-energy obs. rel. to thermal bremsstrahlung X-ray spectrum 0-86014
 X-ray intensity, microfocus source, non-linear rise studies 0-77927
 X-rays emitted from electron cyclotron reson. plasma, degree of polarisation 0-87944
 XPS Auger lines, generation by bremsstrahlung 0-87174
 γ circular polarisation, neutral current effect in bremsstrahlung and pair production 0-73655
 $^{16}\text{O}(\gamma, X)$, bremsstrahlung weighted cross section, two-body correlations effects, linked cluster expansion 0-106047
 Al laser plasma, high-Z, temp. meas. from bremsstrahlung emission 0-87914
 B, evaporated, electronic struct., XPS, SXS and isochromat investig. 0-76143
 $^{12}\text{C}(\text{p,p})$, bremsstrahlung near 1.7 MeV resonance 0-68670
 $^2\text{H}(\text{p,p})$, elastic cross sections, bremsstrahlung, threshold and Coulomb effects 0-91186
 ^7Li , photodisintegration, cluster model wave function, bremsstrahlung weighted cross section 0-63163
 Ni, X-ray intensity reson. near 2p threshold 0-60717
 Th, valence and 5f states, XPS and bremsstrahlung isochromat spectroscopy 0-66393
 ^{208}Tl β -decay, K-shell autoionisation accompanying internal bremsstrahlung 0-57745
 ^{208}Tl β -particle excitation of external bremsstrahlung spectra from thick targets 0-84797
 U, valence and 5f states, XPS and bremsstrahlung isochromat spectroscopy 0-66393

bridge circuits

see also bridge instruments

- temperature controller, use of ICs; at cryogenic temps. 0-90856
 thermistor, laboratory temp. control, modified window air conditioner 0-68192
 transformer, for meas. displacement (Russian) 0-98884

bridge instruments

see also bridge circuits

- automatic resistance thermometer bridge 0-98913
 capacitance detector for ion cyclotron resonance signals 0-62792
 capacitance meas. system for assessment of deep levels in semiconductors 0-105674
 complex mutual inductance concept for bioelectric impedance transformer bridge 0-63886
 dielectric const. meas. using automatic system (German) 0-90864
 digital Wheatstone bridge, automatically compensated, temperature transducer appl. (Rumanian) 0-57287
 four-probe AC bridge technique for ionic cond. meas. 0-57340
 Maxwell bridges for meas. of small complex impedances in RF range 0-98931
 pneumatic Wheatstone bridge for roughness measurement, improved version 0-62629
 porosimeter, continuous scan mercury type, pore pot. contrib. to hysteresis 0-77928
 semiconductor integrated bridge strain gauges with diffusion piezoresistors, strain sensitivity (Polish) 0-73341
 soil pressure meas., using capacitive sensor with polyurethane foam dielectrics (Slovak) 0-86281
 temperature check, linearisation of bridge measuring circuit (Russian) 0-90847
 tensometer, semicond., with parallel channel, operation principle (Russian) 0-73352
 thermometer, transistorised, with remote indication, up to 150°C (German) 0-73356
 unbalanced resistance bridge with linear charact., appl. to press. meas. using electroresistive gauges or extensometric transducers (Polish) 0-73385
 US transducer loading, effect of US field geometry 0-102950
 Wheatstone bridge fed from a bilateral constant current source 0-57338
 Wheatstone bridge formed by pressure sensor using Ge:Ga film strain gauges (Japanese) 0-105631
 wheatstone bridge technique for magnetostriction measurements 0-57348

Bridgman method see crystal growth from melt

brightness

see also sky brightness

- 0957+561A, B, double quasar, intervening galaxy IR obs. and holometric luminosity 0-73065
 1308+32, BL Lacertae object, rapid optical outburst, 1980 June to July 0-98733
 Abell 1060 galaxy cluster, X-ray surface brightness distrib. from HEAO-2 spectral obs. 0-82518
 asteroids, similarity of opposition effect 0-62064
 black hole, massive, radiation spectrum of gas debris from tidally disrupted star 0-90467
 black holes accretion discs, thick discs models rel. to supercritical luminosities 0-101614
 3C 120, radio galaxy, nucleus brightness changes rel. to vars. in optical spectrum (Russian) 0-90540
 3C 288, complex extragalactic radio source, radio brightness distrib. model 0-90558
 cataclysmic binaries, accretion disc surface brightness distrib. determ. 0-109492
 Centaurus galaxy cluster, X-ray surface brightness distrib. from HEAO-2 spectral obs. 0-82518
 clinical light level measurement using photographic meters 0-94304
 Comet Bennett (1970 II), CN (0-0) band brightness profile obs. rel. to CN prod. 0-82303
 comet tails, H_2O^+ surface brightness rel. to CO^+ 0-72880
 Comet West (1976 VI), CN (0-0) band brightness profile obs. rel. to CN prod. 0-82303

brightness continued

- Comet West (1976 VI) ionosphere CO^+ brightness profile 0-85896
 comets, magnitude distrib. 0-72886
 comets, neutral species brightness profiles, average random walk model for mol. photodissociation 0-77351
 cosmology, sources luminosity evolution from scale parameter for Friedmann models 0-77527
 Deimos, opposition brightness surge from Viking orbiter images 0-72838
 elliptical galaxies, U-R colours synthesis from chemical evolution model 0-67843
 fluorescent materials, reflective radiance factor meas. by two-monochromator method (*Japanese*) 0-68237
 Fornax cluster, luminosity function determ. by photographic photometry 0-82523
 galactic H I regions, brightness temp. from 21 cm obs. 0-85987
 galaxies, IR magnitude/H I vel. width relation rel. to distance scale and Universe expansion rate outside Local Supercluster 0-105325
 galaxies in compact groups, anomalous luminosity function 0-82520
 galaxy cluster X-ray sources, luminosity function evolution 0-62314
 galaxy clusters, luminosity dispersions of real and spurious clusters 0-101643
 general optical concentrator, max. radiant power density at receiver 0-102794
 geological IR multispectral aircraft scanner data, image processing 0-98454
 globular star clusters, brightness and density distrib., two parameter generalised isochronous models 0-67807
 hologram image reconstruction without using reference beam, brightness characts. (*Russian*) 0-69348
 holography, white light refl., developer compositions compared 0-102669
 illumination, relative, easy calc. 0-63920
 illumination and reflection edges, recognition by human visual system 0-94209
 imagery, 2-D sampled, aliasing and blurring effects 0-99635
 Jupiter, phase effect for disc features brightness coeff. 0-98602
 BL Lacertae objects, search for rapid brightness variability 0-90567
 LED, red, luminance-brightness discrepancy 0-91942
 light flux brightness meas., EM vacuum fluctuations, quantum noise 0-57361
 Magellanic Clouds, UV brightness maps and UV spectra 0-85994
 Mars, longit. var. of thermal inertia and 2.8 cm brightness temp. 0-105191
 MCG-6-30-15, type 1 Seyfert galaxy, X-ray luminosity and X-ray/optical luminosity ratio 0-82479
 measurement with LaB₆ cathodes 0-68296
 meteors, optical brightness rel. to ionised trail props. 0-77354
 Moon, disc brightness distrib. rel. to photometric props. and dimensional scatt. indicatrix 0-101538
 Neptune, albedo and brightness temp., 5 μm IR obs. 0-82300
 NGC 1275, Seyfert galaxy, nucleus, radio brightness distrib. rel. to mag. field struct. (*Russian*) 0-62288
 NGC 253, barred spiral galaxy, three component luminosity model from surface photometry 0-105327
 NGC 4565, edge-on spiral galaxy, halo luminosity from grid photography 0-62261
 NGC 5866, edge-on galaxy, luminosity obs., BV photometry 0-82511
 ocean underwater irradiances on horizontal surfaces, effects of clouds on diurnal var. 0-72549
 OI 090.4, BL Lacertae object, photometric history 0-77491
 OJ-131 BL Lacertae object, photometric history 0-77491
 optical fibre array, gradient-index, unevenness of illuminance 0-69482
 optical-TV velocity detector (*Russian*) 0-105695
 partially coherent source radiant intensity, theorems and expts. 0-78768
 Periodic Comet Stephan-Oterma (1980g), total visual magnitudes and coma diameters, (1980 September 7 to 11) 0-109397
 Phobos, opposition brightness surge from Viking orbiter images 0-72838
 TX Piscium, disc brightness distrib. and envelope obs. from lunar occultation meas. 0-67725
 PKS 2126-15, QSO ($z=3.27$), bolometric luminosity from JHK obs. 0-94888
 planetary nebulae, optically thin, radius/surface brightness relation rel. to distance scales 0-109521
 planetary nebulae spatial distrib. and luminosity function, evidence from obs. in (M31) 0-109520
 planets photometric properties, theory 0-67601
 psychometric measures for specifying colour appearance 0-76747
 Q0957+561, double quasar, components brightness ratio var. 0-77509
 Q 0420-388, QSO ($z=3.13$), bolometric luminosity from JHK obs. 0-94888
 QSOs, optically selected, intrinsic optical luminosity correl. with radio detectability 0-82536
 quasars, cyclic depend. of brightness on parameter $\ln(1+z)$ 0-105382
 quasars, luminosity and emission line intensity ratios 0-86011
 quasars, number-magnitude relation rel. to luminosity function and cosmological evolution 0-77507
 quasars, search for rapid brightness variability 0-90567
 quasars assoc. with compact radio sources, apparent magnitude-redshift relations for resolved and unresolved sources (*Chinese*) 0-105380
 radio brightness temp. of Earth from Kosmos 243 and Nimbus 5, SHF obs. 0-72521
 radio sources, extragalactic, study of emission variability in millimeter wave range (*Russian*) 0-90559
 retinal rivalry and brightness perception models in binocular vision 0-101180
 Saturn, IR brightness scans (1977 to 1978) 0-90363
 Saturn, limb darkening and brightness temp., 1.30 cm interferometry obs. 0-82279
 Saturn, phase effect for disc centre brightness coeff. 0-98602
 Saturn A and B rings, surface brightness obs. (*Russian*) 0-72872
 Saturn E-ring, obs. and brightness distrib. 0-67647
 Saturn ring system, brightness enhancements rel. to existence of supposed satellites (1980 S 7 and 23) 0-94749
 Sb-type galaxies, luminosity classification rel. to Hubble const. local value 0-62339
 Seyfert galaxies, nearby, discs radial surface brightness distrib. from photographic study 0-82478
 Seyfert galaxies, thermal IR emission vars. 0-67865
 shock waves brightness, in air with reduced density 0-86371
 small particles, brightness and contrast of holographic images 0-99675
 snow, microwave brightness temps. from 3 to 60 mm wavelength radiometry 0-72561

brightness continued

- solar 6 cm radio emission, peak brightness temps. of active region and burst sources 0-62096
 solar corona, 1973 June 30, polarised brightness distrib. rel. to N.polar hole density model 0-98627
 solar far IR brightness temp. minima rel. to sunspot activity 0-62035
 solar flares, radio brightness distrib. processing in one-dimensional synthesis (*Italian*) 0-98628
 specular sphere scatt. radiance matrix, refl. standard for polarised beam scatt. meas. 0-74299
 spiral galaxies, luminosity class correl. with number of comparison 0-77481
 spiral galaxies, types Sab to Sdd, luminosity, freq. distrib. 0-82482
 star image, true brightness distrib. 0-62034
 Sun, absolute brightness temp. meas. in far IR with balloon-borne interferometer 0-62095
 supernova remnants in LMC, SHF obs. 0-67864
 thermal source, use of optical parametric converter for brightness determ. 0-98979
 thick layers, refl., transmission and brightness coeffs. 0-63918
 Titan, light curve during eclipse by Saturn rel. to Saturn upper atmosphere struct. 0-90362
 TV colour films, usable range (*German*) 0-57408
 uneven interface of media with different refractive indices, statistical characts. of images 0-87331
 upper atmosphere, IR radiation flux meas. in 4 to 6 μm spectral range 0-61929
 Uranus, albedo and brightness temp., 5 μm IR obs. 0-82300
 Venus, IR brightness temp., daytime minima 0-77309
 visibility measurement, photometric contrast (*German*) 0-95118
 vision, asymmetry in the brightness and darkness Broca-Sulzer effects 0-101185
 vision, wavelength-specific brightness contrast as a function of surround luminance 0-61564
 visual flicker-induced asymmetries in border enhancement, brightness and darkness perception 0-67083
 volume-phase reflection hologram, recording medium thickness effect on image luminance 0-58479
 VUV spectral irradiance calibrations, method and appl. 0-87452
 zodiacal light, brightness depend. on heliocentric coords. 0-72878
 Au vapour brightness amplifier at 627.8 nm, for projection microscope 0-83616
 Cu, electrolytic coating, brightness and adsorption of surface-active additives 0-100963
 H I survey, brightness temp. contour maps, 21 cm obs. 0-85986
 H₂O maser source in Orion A, radio flux density and line width during outburst (*Russian*) 0-105320
 H α line brightness in solar prominences, radiation diffusion theory 0-67694
 KrF* laser, generation of high-spectral-brightness tunable XUV radiation at 83 nm 0-91846
 LaB₆ cathodes, mounting methods and operating characts. 0-57437
 LaB₆ cathodes, single crystal, of <100> and <110> orientations, brightness meas. from 1500 to 1950K 0-62808
 Nd:glass laser system, beam spatial profile optimization in amplifier channel 0-74407
 SnO₂-Cu₂S-ZnS:Mn, Cu-Al₂O₃-Al, light-emitting struct., cond. and electrolum., heat treatment 0-97345
 Y₂O₃ capillary discharge plasma, temp., radiation screening elimination 0-64682
- Brillouin scattering** *see Brillouin spectra*
- Brillouin spectra**
see also stimulated Brillouin scattering
 adsorbed monolayers, acoustic phonons, obs. method using Brillouin scatt. 0-59804
 Auger lineshape anal. of molecules and solids 0-76113
 biphenyl-d₁₀, Brillouin scatt. at room temp. 0-71433
 bisphenol A-phthalic anhydride epoxy resin, diglycidyl ether, Rayleigh scatt., Brillouin and IR spectra 0-66211
 carbon tetrachloride, polarized light scatt., relaxation processes 0-60615
 chlorobenzene, polarized light scatt., relaxation processes 0-60615
 cyclohexanol, orientationally disordered phase, Brillouin scatt. study 0-93351
 dichloromethane-cyclohexane, liq. mixture, intermol. vibrational energy transfer, US study 0-70313
 ferromagnet, surface, Brillouin light scatt. by spin waves 0-93359
 ferromagnetic thin films, Brillouin scattering from spin waves 0-65843
 fluorobenzene, polarized light scatt., relaxation processes 0-60615
 furan-cyclohexane, liq. mixture, intermol. vibrational energy transfer, US study 0-70313
 halobenzenes, liquid, vibr. relaxation, Brillouin spectra 0-108219
 intermolecular spectroscopy and dynamical properties of dense systems, conf. Varenna, Italy (1978) 0-82581
 light scattering in fluid far from equilibrium 0-103965
 Love waves, theory of Brillouin scatt. by 0-66212
 magnetised plasma, Brillouin and Raman scatt. by extraordinary mode 0-92269
 magnons, thermal and excited, Brillouin-Mandelstam scatt. 0-70980
 methane(-d₄), liq., Brillouin scatt. and refr. index measurements 0-76035
 nonlinear estimates of Brillouin scatt. in plasma 0-87895
 nonlocality effects on optical phenomena in bounded solids, developments 0-93328
 β -picoline-water solution, light scatt. spectra, ultra- and hypersonic absorpt. (*Russian*) 0-93353
 PMMA, Gruneisen const. and thermal props., temp. depend., 4-300K, Brillouin scatt. obs. 0-100662
 polydimethylsiloxanes, rubbery and liq., hypersonic sound vel., Brillouin spectra meas. 0-75308
 polymer films, Brillouin scatt. at transitions 0-70312
 polystyrene-cyclohexane mixture, Rayleigh and Brillouin scatt. and struct. relaxation 0-63640
 population-inverted semiconductors, resonant Brillouin scattering 0-76042
 resonant light scattering from magnetic excitations, review 0-97290
 scattering cell for liquids 0-106694
 semiconductor, resonant Brillouin scattering of exciton polaritons 0-93357
 semiconductors, optical props. due to phonons, book contrib. 0-80805
 semiconductors, population inverted, resonant Brillouin scatt., photoelastic consts. 0-89015
 short-pulse laser backscatter from gas target 0-79454

Brillouin spectra continued

- squaric acid, two dimensional antiferroelec., Brillouin scatt. at structural phase transition 0-71430
- Stoneley wave scatt., elasto-optic and surface ripple mechanisms 0-71435
- superheated water, Brillouin scatt., sound velocity meas. 0-95631
- p-terphenyl(d_{14}), Brillouin scatt. at room temp. 0-71433
- triiodomethane, polarized light scatt., relaxation processes 0-60615
- trissarcosine calcium chloride, ferroelec. phase transition, Raman and Brillouin scatt. studies 0-71340
- water, Brillouin light scatt., temp. gradient induced 0-100663
- water, supercooled, sound vel. dispersion, struct. relax. effect 0-107375
- Al, Brillouin spectra, light scatt. cross section for surface ripples 0-71434
- Ar, gas, compressed, Rayleigh-Brillouin spectrum, scaling 0-100062
- Ar, gas, compressed, Rayleigh-Brillouin spectrum, hydrodynamic region 0-100063
- BaMnF₄, spectroscopy near ferroelec. transition, dielec. anomalies near mag. ordering temp. 0-75965
- CdIn₂S₄, Brillouin scatt., elastic and photoelastic const. determ. 0-60619
- CdS, resonant Brillouin scatt., photoelastic const., imag. part contrib. 0-108218
- CdS, three-branch exciton-polariton dispersion, direct meas. by reson. Brillouin scatt. 0-60620
- CdSe:Li, pure and doped, reson. Raman and Brillouin scatt., elastic exciton-defect scatt. 0-80788
- CoCO₃, Brillouin-Mandelstam light scatt. obs. of spin wave spectra 0-93358
- CoCO₃, light scatt. from magnons and phonons excited by microwave pumping 0-66213
- Fe₈₀B₂₀, amorphous, Brillouin scatt. from magnons, ferromag. reson. 0-65844
- Fe₈₀B₂₀ film, amorphous metallic, standing spin waves, Brillouin scatt. obs. 0-97291
- GeAs, population inverted semicond., resonant Brillouin scatt., photoelastic const. 0-89016
- GaAs, Brillouin spectra, light scatt. cross section for surface ripples 0-71434
- GaS(Se), reson. Brillouin scatt. 0-89010
- Gal, Brillouin spectra, light scatt. cross section for surface ripples 0-71434
- He, gas, compressed, Rayleigh-Brillouin spectrum, scaling 0-100062
- He, gas, compressed, Rayleigh-Brillouin spectrum, hydrodynamic region 0-100063
- KD₂PO₄, acoustic phonon dispersion, elastic stiffness, light scatt. obs. 0-103966
- KFe(MoO₄)₂, phase transitions at 312 and 139K 0-70396
- K(H_{1/2}D_{1/2})₂P₄, polarised impurity cluster effects in light scatt. expts. 0-71431
- KH₂PO₄, Brillouin-Rayleigh scatt. studies near ferroelec. transition temp. 0-76036
- K₂ReCl₆, elastic constants, softening of acoustic modes, obs. by Brillouin scattering 0-71440
- K₂SeO₄, elastic props. at commensurate-incommensurate transition, Brillouin scatt. and US study 0-93248
- K₂SeO₄, hexagonal-orthorhombic transition, Brillouin scatt. study 0-97208
- K₂SnCl₆, elastic constants, softening of acoustic modes, obs. by Brillouin scattering 0-71440
- LaP₂O₁₄, continuous ferroelastic transition elastic and mechanical props. 0-92668
- LiCl, hypersonic relaxations studied by Brillouin light scatt. techniques, viscoelastic effects obs. 0-83375
- Li₂SO₄, fast ion conductors, X-ray diffr., neutron diffr., and Brillouin scatt. study 0-107170
- (NH₄)₂SiF₆, elastic constants, softening of acoustic modes, obs. by Brillouin scattering 0-71440
- (NH₄)₂SnCl₆, elastic constants, softening of acoustic modes, obs. by Brillouin scattering 0-71440
- NaNO₃, incommensurate antiferroelec. phase, Brillouin scatt. freq. shift 0-93349
- Ne, gas, compressed, Rayleigh-Brillouin spectrum, scaling 0-100062
- Ne, gas, compressed, Rayleigh-Brillouin spectrum, hydrodynamic region 0-100063
- Ni, Brillouin spectra, light scatt. cross section for surface ripples 0-71434
- Pb₃(P_{1-x}V_{1-x}O₄)₂, ferroelastic phase transition, DTA, dilatometric and Brillouin scatt. study 0-70398
- Si, amorphous, opaque, surface phonon attenuation, Brillouin scatt. 0-80808
- SiO₂, vitreous Brillouin scatt., 35 GHz phonon vel. and absorpt. below 1K 0-100664
- SiO₂-B₂O₃ glasses, Brillouin scattering meas. of attenuation and vel. of hypersounds 0-100309
- SnCl₂·2H₂O, Brillouin scatt. and thermal expansion 0-97289
- ZnP₂, Brillouin scattering and optical props. meas. 0-76041
- α -ZnP₂, resonant Brillouin scatt. near indirect band gap 0-93350
- ZnS, reson. Brillouin scatt. and piezobirefringence 0-93348

Brillouin zones

- see also band structure
- alloys, dil., of polyvalent and noble metals, deviations from Matthiessen rule 0-65525
- decay state interactions, autoionisation bands (Russian) 0-75486
- p-dibromo-tetrafluorobenzene mol. cryst., in commensurate phase, quasi-elastic neutron scatt. 0-107386
- extended unit cell-contracted Brillouin zone model, group-theoretical anal. 0-107093
- half space layered cryst., vibr. spectrum, Brillouin zone (Russian) 0-100313
- lattices, FCC and BCC, optical transitions, dipole selection rules 0-97409
- linear Brillouin zone integration method, generalised susceptibility calcs. 0-88462
- semiconductor, elec. field induced optical SHG theory, Brillouin zone integral 0-69457
- special point generation, large unit cell method (Russian) 0-88469
- special point generation by large unit cell approach 0-92806
- surface properties, two dims. Brillouin zone and Wigner-Seitz cell integrations, special point formulae generation 0-70783
- Al, K X-ray absorption, K-emission spectrum, band struct. using APW method 0-97380
- BiSb (>20 wt.%), electronic band struct. 0-107698
- Bi₈₆Sb₁₄Te, single crystal, dispersion of magnetoplasma waves (Russian) 0-70739

Brillouin zones continued

- Cs, Fermi-surface press. dependence 0-96772
- CsCrCl₃, α - β phase transition, dynamical aspects and thermodynamic theory 0-70404
- Cu (001), O₂ chemisorption, Cu3d-O2p interaction study by angular-resolved photoemission using synchrotron radiation 0-84836
- Cu₂Au, electrical resistivity and LRO, energy gap formation in Fermi surface 0-88533
- CuCl (100), obs. of p- and d-like surface states, angle resolved UPS study 0-104045
- EuTe, mag. 'Bragg' scatt. obs. through Raman scatt. 0-66179
- Fe₂Al, electrical resistivity and LRO, energy gap formation in Fermi surface 0-88533
- GaSe, lattice dynamics and elastic props., Born-von Karman model study 0-70337
- Hg₂Cl₂, neutron and Raman scatt. studies, ferroelastic transitions 0-76015
- InP, depend. of phonon spectrum on hydrostatic press., Raman spectra 0-93315
- LaB₆, de Haas-van Alphen effect, low-field 0-75497
- Mg(NH₃)₆(ClO₄)₂, phase transition, group theoretical anal. 0-65218
- Ni(NH₃)₆(BF₄)₂, phase transition, group theoretical anal. 0-65218
- Ni(NH₃)₆(ClO₄)₂, phase transition, group theoretical anal. 0-65218
- Ni(110), mag. exchange splitting of electronic surface states 0-88610
- Pb, single and polytextured thin films, band struct., tunnelling spectroscopy 0-80169
- Pb₃(P_{0.95}V_{0.05}O₄)₂, ferroelastic transition, soft mode, inelastic neutron scatt. study 0-70357
- Rb, Fermi-surface press. dependence 0-96772
- RbCrCl₃, α - β phase transition, dynamical aspects and thermodynamic theory 0-70404
- ReO₃, mag. breakdown above compressibility collapse transition 0-103617
- Sb, electronic struct., depend. on hydrostatic pressure 0-80158
- SmS, electron-phonon interaction, lattice dynamical model 0-96610
- Ti alloys, Fermi sphere limiting electronic capacitance, Brillouin zones (Russian) 0-92808
- TiCl₃, phonon difference band absorpt., far IR laser spectroscopy 0-93325
- VL₂, mag. 'Bragg' scatt. obs. through Raman scatt. 0-66179
- W (100) and (110) surface, theoretical Debye-Waller factors 0-92773
- W, XPS, angle-resolved, from valence bands, obs. of strong temp. depend. and direct-transition effects 0-60752
- W(001), surface states and surface resonances, self-consistent electronic struct. 0-96960

bristles see fibres**brittle fracture**

- see also ductile-brittle transition; notch brittleness
- body loading with cracks, energy conditions for brittle failure (Russian) 0-96234
- brittle fibre reinforced composite, static strength depend. on component separation boundaries (Russian) 0-76304
- ceramic filled with polymer, ZrO₂ stabilised, fracture mechanism (Russian) 0-100895
- ceramics, brittle, heat-transfer variables effect as thermal stress resist., meas. by quenching expts. 0-79871
- ceramics, fracture-mirror boundary formation, criteria 0-70297
- chemically assisted fracture, atomic models of crack growth 0-64466
- chemically assisted fracture, general reaction rate theory and thermodynamics 0-64465
- composites, single fibre-brittle zone model, fracture behaviour 0-97570
- concrete slab, explosive shock resist., tensile fracture 0-85065
- covalent crystals, nanosec. electron beam effects, size depend., Ioffe effect 0-88211
- crack propagation, computer simulation 0-59573
- dislocation theory, elastic energy momentum tensor and crack propagation 0-69741
- edge notched brittle plates, virgin waves and boundary reflections at fracture 0-79233
- elastic plane, stress-strain state at brittle crack vertex, geometric non-linearity effects (Russian) 0-79221
- energy release rate, equivalent to Rice integral (French) 0-64457
- epoxy-rubber particulate composite, toughness and fracture mech. 0-71727
- fibre reinforced composites, crack interactions 0-65149
- fluorite, use of proton irradi. to reveal growth and deform. features 0-84216
- grain boundary sliding and brittle crack extension failure mechanism 0-97557
- Hastelloy, H₂ embrittlement in H₂S environments, impurity segregation effects 0-71724
- ionic crystals, nanosec. electron beam effects, size depend., Ioffe effect 0-88211
- lightguide fibre, ensuring mechanical reliability 0-79001
- metals, brittle intercrystalline fracture, impurities effect 0-100915
- micromechanisms of crack extension, conf., Cambridge, England (March 1980) 0-105421
- plate with initial crack subject to extension, brittle fracture energy conditions (Russian) 0-103002
- PMMA, ductile glassy, notch brittleness under plane strain 0-100900
- PMMA based plastics, specific fracture energy depend. on crack growth rate, mol. struct. effect 0-66639
- polycarbonate, ductile glassy, notch brittleness under plane strain 0-100900
- polystyrene, glassy, crazing and brittle fracture on flat die indentation 0-60970
- polystyrene-polyethylene block copolymer, deformation ratios, Poisson ratio and adhesion, dilatometric obs. 0-60937
- PVC, ductile glassy, notch brittleness under plane strain 0-100900
- quasi-cleavage fracture, characteristic length parameter, correlation with fracture toughness (Chinese) 0-104246
- rock, fracture, role of crack inertia 0-109138
- rocks impulsive fracture, criteria 0-85646
- rupture of brittle bodies exposed to explosive action (Russian) 0-79223
- statistical theory, dislocation mechanism, crack propagation (Chinese) 0-106755
- steel, 15Cr1Mo1VL, susceptibility to brittle struct. and fracture, influence of props. 0-104298
- steel, austenitic, type 70, cold brittleness structural depend., fracture mechanisms (Russian) 0-97571

brittle fracture continued

steel, austenitic stainless, cathodically charged, H₂ embrittlement, α' martensite effect 0-71725
steel, C, tensile fracture surface in high press. H₂ at room temp. (Japanese) 0-108540
steel, Cr-Mo-Ni-V, dynamic stress intensity factor meas., possibilities and limits (German) 0-93719
steel, ferritic, cleavage fracture toughness, temp. and strain rate depend. 0-85028
steel, ferritic, crack extension, cleavage micromechanisms, review 0-108562
steel, grain boundary P segregation, effect after quenching and tempering (Russian) 0-81145
steel, high-strength, H distrib. and delayed brittle fracture 0-108577
steel, lamellar pearlite, containing proeutectoid cementite, brittle-fracture study (Japanese) 0-93648
steel, low C, dynamic stress intensity factor meas., possibilities and limits (German) 0-93719
steel, low-alloy, fracture toughness characts., loading rate effect 0-100897
steel, low-Mn low-C, susceptibility to brittle fracture 0-76340
steel, Mn-B-V, low alloy, transform. singularities (Russian) 0-104116
steel, Ni-Co-Mo, dynamic stress intensity factor meas., possibilities and limits (German) 0-93719
steel, Ni-Cr, Sb doped, solute segregation and brittle fracture 0-85033
steel, Ni-Cr, solute segregation and intergranular brittle fracture 0-108568
steel layer types St3+0Kh13, acoustic emission parameters, brittle fracture, crack propagation (Russian) 0-93633
steel layers, types St3+Kh18N9T, acoustic emission parameters, brittle fracture, crack propagation (Russian) 0-93633
steels, with yield pt. of about 420 to 720 N/mm², correlation between yield pt./tensile strength ratio and toughness (German) 0-66615
straight bar bending strength, brittle fracture energy conditions (Russian) 0-58974
strain driven thermoelastic instability toward brittle fracture 0-103415
strength of materials, empirical determ., cleavage fracture in plane waves 0-96225
styrene-acrylonitrile copolymer, crazing and brittle fracture on flat die indentation 0-60970
thin sheet impact strength study (Czech) 0-59571
viscoelastic strip, dynamic crack propagation due to antiplane loading 0-64464
Al₂O₃, polycrystalline, stress-strain data up to 1.25 GPa 0-100899
Be single crystal, failure energy 0-81192
Cu-Bi (0.02 wt.%) alloy, intergranular fracture, Kossel X-ray diffr. in SEM obs. 0-108579
Fe, cast, grey, fracture kinetics, surface hardening effect 0-76354
Fe-Al-Si (6.22, 9.63 wt.%), bending test under high press., high temp. 0-85057
InP single crystals, uniaxial compression deform. characts. 0-84991
 α -Li₂O₃, surface defect layer struct. due to mechanical working (Russian) 0-100238
MgO, fracture and crack tip plastic zones, in situ obs. 0-108686
Mo alloys, intercryst. fracture in ductile-brittle transition region, local internal stresses effect 0-81200
Na₂O-CaO-SiO₂ glass, hot erosion plastic flow and fracture 0-89354
Nb NbH_{0.82}, fracture, TEM obs. 0-108519
Si, single crystal, brittle fracture in axisymmetric bending, study at room temp. 0-81180
SiC, reaction-bonded, impact erosion by ang. Al₂O₃ particles 0-89362
Ti alloy, crack initiation on planar shear bands, H₂ assisted 0-71749
Ti alloys, delayed brittle fracture, H₂ effect 0-100912
 α -Ti sheet, texture dependent stress corrosion cracking in Br₂-methanol soln. 0-71803
Ti-Al, elec. spark Al doping of VT-18, surface struct. and props. (Russian) 0-76398
Ti-Al-Zr-Mo-Si (6, 5, 0.5, 0.25 wt.%), β -processed, fatigue props., hold time effect 0-60961
UO₂, surface energy, determ. by Hertzian indentation 0-93641
W wire, AKS-doped, second phase particle obs. by TEM, SEM and atom probe microanalysis 0-108457
Zr-Nb (2.5 wt.%), nuclear fuel channels, neutron effects on ultimate fracture strength, 293 to 573K 0-85054
ZrO₂ microsphere stabilised ceramic, fracture characts., thermal stability (Russian) 0-76335

brittle materials see brittleness

brittleness

see also brittle fracture; embrittlement; hydrogen embrittlement; liquid metal embrittlement; notch brittleness
atomically sharp cracks, TEM study 0-71729
body loading with cracks, energy conditions for brittle failure (Russian) 0-96234
brittle solids, microfracture resulting from anisotropic shape changes 0-88254
ceramics, brittle, heat-transfer variables effect as thermal stress resist., meas. by quenching expts. 0-79871
ceramics, brittle, partially absorbing, thermal stress anal. subjected to symmetric radiation heating 0-59570
ceramics, fracture-mirror boundary formation, criteria 0-70297
ceramics and brittle solids, abrasive wear, role of plastic deform. and fracture 0-108594
cracks in brittle solids, unstable growth 0-106756
critical temperatures, determ., impact toughness test results statistical processing 0-100980
engineering materials, intergranular fragility index 0-66637
glass rod, optimum sample shape for compression testing, failure 0-71756
impact damage thresholds in brittle materials impacted by water drops 0-81149
mirror/flaw-size relations, residual contact stresses effect 0-107363
optical fibre, strengthening by molecular stuffing 0-58830
PMMA, crack size and effective specific work for failure determ. 0-85108
polyacetylene films, tensile props. and partial alignment 0-104210
powders, brittle, shock wave disintegration test method 0-66744
silicate glass, mechanical stress field influence on structural mobility 0-103421
steel, cast, cold resistance determination, quick method 0-100997
steel, Cr-Mo and Ni-Cr-Mo-V low-alloy, additive remedy for temper brittleness 0-66659

brittleness continued

steel, low alloy, Mn-P, temper brittleness, rare earth mischmetal effect (Chinese) 0-104249
steel, low C, impact strength and crit. brittleness temp., sample thickness and notch radius influence 0-85018
steel, stainless, radiation damage by 1 MeV electrons, dislocation struct., brittleness (Russian) 0-75226
steel, type Kh12M, rel. between structural inhomogeneity and wear resist. (Russian) 0-66672
Al₂O₃, fracture toughness determ. using four-point-bend specimens 0-108536
Si₃N₄, bending strength, deformability, elastic moduli and brittleness 0-81191
Si₃N₄, hot-pressed, fracture toughness determ. using specimens with chevron and straight through notches 0-108538
SiO₂ fabric, structural stability rel. to brittleness, X-ray diffr. and IR spectrosc. studies 0-96634
Zn, internal friction anomalies in temp. initiated brittle-plastic transition (Russian) 0-96648
ZrO₂, porous, sintered stabilised microspheres, strength and fracture studies 0-85019

broadband amplifiers see wideband amplifiers

bromine

see also nuclei with
adsorbed on Si single cryst., X-ray standing waves obs. at cryst. surface 0-96417
adsorption, on Au electrode, anisotropy of optical props. 0-60534
atom, ESR study in N-bromosuccinimide, X-irrad. 0-66037
Br₂+As(III) reaction, flow coulometry, with ring-disk electrode 0-71966
chemisorbed on zeolites, Raman spectra 0-93301
chemisorption on V, layer struct., Na adsorption effects 0-101039
coadsorption with H₂O, on Cu(100), Helmholtz layer model system 0-92777
colour positive developer consumption, bromine ion extraction from over-flow using ion exchange resins (Russian) 0-105733
formaldehyde+Br reactions, rate consts. by EPR 0-93736
graphite-Br₂ intercalation cpds., EXAFS study 0-71515
impurity in Li aluminosilicate glasses, ESR spectra 0-66027
intercalation compounds with graphite, ¹³C NMR spectra 0-66048
molecular static polarisability, ab initio SCF wave functions 0-74106
molecule, B²II(Σ_u^+) predissoc. rates, analytical interpretation 0-91617
molecule, kinetics of excited states using laser excitation, radiative lifetimes and collisional deactivation 0-74237
molecule, Kr ion laser-excited fluorescence, predissoc. 0-83414
molecule, model potential SCF calcs. 0-95528
molecule, vac. UV absorpt. cross section 0-91574
molecule in -Z 0-58262
molecule in liq. Ar, effective intramol. pot. 0-69208
molecules, Q branches of $\Delta n=1$ profiles, calcs., rotation effect on scatt. amplitudes 0-63643
pionic, Auger electron emission (Russian) 0-69271
polyacetylene:Br, ion implantation effect on elec. props. 0-65026
polystyrene:Br₂, films, electron-beam induced carrier mobility and elec. breakdown 0-80429
polythylene:Br₂, films, electron-beam induced carrier mobility and elec. breakdown 0-80429
stratosphere chemistry of Br cpds., and O₃ depletion 0-98391
Br matrix isolation ESR 0-106336
Br⁺, 42 MeV, stopping power and radial dose distrib. obs. in tissue-equivalent gas 0-101218
Br+H₂, proximity induced electric dipole moment effect in laser field 0-83456
Br+H₂(HCl), relax. and chem. reaction, time resolved IR fluoresc. and mass spectrometry obs. 0-69177
Br+HCl, vibr. relaxation and reaction rates determ. 0-108698
Br+K₂(Cs₂), ionisation reactions, absolute cross sections 0-99565
Br + H₂(D₂), O₂(N₂)(CO)(CO₂)(methane), total electron detachment cross sections for energies around threshold 0-99550
Br₂ in Ar, solvent effects on equilibrium props. 0-61128
Br₂, long-lived A²II(Σ_u^+) state, quantum-resolved dynamics of excited states 0-69178
Br₂, single rot. states, lifetimes and collisional quenching cross sections determ. by obs. fluoresc. decay 0-91595
Br₂+Ar collisions, dissociation reaction, trajectory study by ensemble method 0-66765
Br₂+CO₂ mixture, Raman laser optical excitation, electron phototransition theory (Russian) 0-99711
Br₂+Cu(⁴D), beam-gas chemiluminesc. reactions 0-85151
Br₂+H reaction Br prod., matrix isolated ESR 0-106336
Br₂+OH, hydroxyl radicals reactive scatt. 0-85172
Br₂+Xe, excitation functions and rotational polarisation, chemiluminesc., crossed beam study 0-76491
⁷⁵Br, excitation functions for production, pot. nuclear medicine appls. 0-98135
CO₂-Br₂-He mixture, possible gas lasers with solar excitation 0-99695
H₂-Br₂ cell for energy storage appls. 0-72029
KCl:Br⁻, interstitial atomic H centres, formation kinetics and struct., MO calcs. and EPR studies 0-75854
Ni:Br, ferromagnetic, hyperfine field and relax. time obs. of impurity heavy nuclei 0-75533
RbCl:Br⁻, interstitial atomic H centres, formation kinetics and struct., MO calc. and EPR studies 0-75854
(SN)₂:Br, ion implantation effect on elec. props. 0-65026

bromine compounds

TTT⁺ Br⁻, cryst. and mol. struct., X-ray method 0-107202
Br+H₂, gas phase H-atom transfer reactions, struct.-reactivity correl., pot. energy surfaces 0-104433
BrCN, ¹⁴N quadrupole coupling consts., ab initio calcs. 0-58283
BrCl laser induced fluoresc., quantum resolved level dynamics in B²II(O⁺) state 0-74188
BrCl⁻ centre in alkali halides, analysis of spin-Hamiltonian parameters of heteronuclear XY⁻ defects 0-88509
BrF₃, electronic struct. and ionisation pot., SCF DV Xalpha method 0-69057
BrF₃, electronic struct. and ionisation pot., SCF DV Xalpha method 0-69057
BrF(Cl), rot. spectra in millimeter wave region, rot. transitions obs., equilib. const. determ. 0-78607
BrO, free radical, Ar matrix absorpt. spectra, mol. vibronic states obs., spectroscopic const. determ. 0-83387

Brownian motionsee also *colloids*

- absorbing boundary, joint position-velocity distribution function determ. for Brownian particle 0-62581
- aerosol particles in flow type chamber, coagulation, deposition 0-69908
- anthracene, electronic vibr. spectra, stochastic description, numerical modeling, comparison with expt. 0-63620
- bead-spring-type model in nonuniform vel. gradient, dil. soln. kinetic theory results 0-64628
- chemical reactions, Brownian dynamics simulation in soln. 0-104422
- colloidal dispersion dynamics, review 0-71956
- coloured noise approach, Smoluchowski eqn. corrections 0-101755
- complex diffusion processes, transforms., and nonrelativistic quantum mechanics 0-82670
- complex diffusion processes and nonrelativistic quantum mechanics 0-90707
- cylindrical surface, aerosol particle capture, thermophoresis forces 0-103060
- Debye generalised fluid model, dielectric relax., depolarised dynamic light scatt. 0-108156
- diffusion equation, hyperbolic, effect of finite correlation time 0-86214
- dispersive magnetisable media, hydrodynamics including Brownian motion 0-59120
- dynamics of colloidal systems: time-dependent structure factors 0-93803
- education, Brownian motion, melting, surface tension and rubber networks, thermodynamic anal. 0-73132
- Einstein's work and effect on atomic physics at the turn of the century (*German*) 0-90648
- Einstein and Brownian motion, student project 0-68000
- first-passage theory for Brownian motion with an absorbing boundary 0-86207
- flowing suspension, memory impairment, Brownian rotation of spheroids 0-79386
- Fokker-Planck approx. for n-dimensional nonMarkovian Langevin eqns. 0-57191
- generalised Brownian motion, scalar case, computer simulation 0-77704
- interacting Brownian particles, light multiple scatt. by correlation spectroscopy 0-87313
- ion trajectories in weak electrolytes, dissociation and recomb. of ions 0-85189
- kinetics of reacting solns., diffusional barrier crossing processes, trajectory simulation 0-81280
- Kramers equation, eigenvalues calc., Fokker-Planck eqn. for Brownian motion in a potential 0-86215
- last exit distributions for n-dimensional Brownian motion 0-82722
- macroparticles; charged spherical, dilute soln., Rayleigh scatt. 0-84748
- metals, liquid, structural micro-inhomogeneity, Brownian motion studies (*Russian*) 0-92426
- molecular liqs., Maxwell effect relax. time and light scatt. line broadening 0-76040
- moving acceptors, direct energy transfer, decay law 0-89045
- nonlinear filtering, conditional laws, smoothness, stochastic calculus of variations (*French*) 0-68128
- particle absorption rates at high cell concs., Monte Carlo simulation 0-94141
- particle escape over dynamic barrier, impurity diffusion in solid 0-107569
- periodic potential, bistability effects 0-68139
- polymer, spherical, in soln, long time tail in diffusion 0-88018
- polystyrene lattices, electro-flotation, collection efficiency 0-74946
- potential effect, Maxwell-Boltzmann distrib. in infinite-time limit 0-105573
- quantum theory, connection with Brownian motion 0-90786
- random motion and Brownian rotation, review 0-73266
- Schrodinger equation, Brownian motion interpretation challenged 0-94974
- stochastic particles, relativistic dynamics 0-82639
- superionic conductor, corrs. among mobile ions role, microscopic model 0-107534
- superionic conductor, interacting Brownian particles in periodic medium model 0-59712
- suspension, averaged size and polydispersity index meas. using laser light scatt. spectroscopy 0-77754
- suspensions, rheology, colloidal forces role, review 0-103063
- velocity autocorrelation function, direct meas. for Brownian test particle 0-57195
- viscous drop, almost spherical, Brownian motion and fluctuating hydrodynamics 0-87787
- ²³⁸U fission as multi-dimensional Brownian motion, Fokker-Planck soln. (*Chinese*) 0-99197

Brownian movement see *Brownian motion***brush discharges** see *discharges (electric)***bubble chambers**

- film analysis, semiautomatic measuring system 0-58105
- film processing using Hough-Powell digitizer, appl. to Mirabelle chamber in K⁺p expt. at 32 GeV/c 0-69040
- images, SNOOP module CAMAC interface to 168/E microprocessor 0-58103
- multiprocessor system for nucl. event picture anal. (*Italian*) 0-69047
- SKAT, electromagnet, main parameters and magnetic field meas. 0-69022
- SKAT, housing and main structural components of propane-Freon chamber 0-69019
- SKAT, photoregistration system for propane-Freon chamber 0-69020
- SKAT, pressure changing system for propane-Freon chamber 0-69021
- superconducting magnets appl. 0-68990
- track gap length distributions by PEPR 0-99420
- ZGS, 30" bubble chamber 0-91304
- ZGS, superconducting magnet bubble chambers, history 0-91368

bubble nuclei see *nuclear density***bubble point** see *boiling point***bubble points** see *bubbles***bubbles**see also *foams*

- acoustical meas. of gas bubble volumes and gas flow rates 0-62633
- acoustics, insertion loss of a layer on a plate 0-96072
- agarose gels, bubble prod., stabilisation by nonionic surfactants 0-76562
- air bubble entrainment in self-aerated flow, channel or pipe flow 0-106832
- air bubble growth meas. by rectified diffusion at 22.1 kHz 0-96155

bubbles continued

- blood, gas bubbles, behaviour when subjected to oscill. press. 0-97984
- blood, volume expansion effects, gas cavities 0-67134
- breakdown of liquid insulators 0-71313
- capillary waves, progressive, periodic, finite-amplitude 0-79339
- cavitating orifice under reattached flow conditions, noise and vibration characteristics 0-83829
- cavitation, acoustic field generated, review 0-74934
- cavitation bubbles, amplitude distrib. of pulses produced by shock waves 0-64252
- cavitation erosion, non-spherical bubble collapse near a solid wall, analytical soln. using matched asymptotic expansions 0-106824
- collapse in liquid, pressure wave, nonequilibrium vapour condensation effects 0-59060
- compressible liquid, bubble deformation in electric field 0-64618
- conical crossflow sonic line, flow patterns and bubble props. 0-69862
- critical two-phase flow, bubble nuclei 0-64615
- crystal growth, cylindrical pores growth, numerical calcs. 0-92471
- decompression of animals and man, quantification of bubbles formed, US system 0-76869
- detection in insulating liquid flow, using spiral delay line 0-79415
- distribution and size of intragranular fission gas bubbles in irradiated UO₂ nuclear fuels 0-57840
- ducts, one-dimensional models for transient gas-liquid flows 0-64614
- ethane, flow continuity in arterial capillary systems in cryogenic heat pipes 0-64536
- evaporating, surface condensation of vapours of high boiling substance 0-59021
- fibre reinforced polymer, soaking, wetting and compounding of materials during production (*German*) 0-93535
- fission gas bubble mobility in UO₂ 0-91222
- fission reactor carbide fuels, effect of burn-up and temp. on appearance of optically visible fission gas bubbles 0-63251
- fission reactor mixed oxide fuels, SEM obs. of gas bubble morphology 0-57843
- flow film boiling, void fraction meas. 0-92207
- fluidised bed bubble observation using probes and X-rays 0-79379
- fluidised beds, instability waves and bubble origin, two-fluid eqns. 0-92205
- fluidised beds, rise velocities of 2-D and 3-D gas bubbles 0-64610
- fluidised beds, theoretical bounding relations, for bubble void fraction 0-96296
- foam stability relation to structure, criteria derivation w.r.t. drainage stage 0-69904
- free motion transition criteria for single bubbles and drops 0-64605
- gas, free liquid surface oscils. 0-100025
- gas, in metals, light element implantation, radiation damage review 0-88219
- gas bubble, rise and cooling in viscous fluid (*Russian*) 0-74949
- gas bubble dissolution (growth), convective transport effect 0-87792
- gas bubble dynamics and acoustic props. of gas-bearing sediments 0-87630
- gas bubbles in low-viscosity liquids, US attenuation 0-58849
- gas injection into liquid through porous plate, squeezing out of liq. 0-64622
- gas-bubble entrapment in Czochralski-grown oxide crystals, fluid-flow effect 0-84121
- gas-liquid ascending flow, monodispersed, function stress on wall, bubble size effect 0-59098
- gas-liquid pipe flow, influence of return bends on velocity ratio 0-74962
- gaseous microbubble growth in laminar separation bubbles 0-106821
- glass, melt, bubble behaviour during refining, math. model 0-81277
- glass melt, multibubble dissolution 0-81371
- growth and decay, moment and Fokker-Planck eqns. 0-82709
- growth on heating surfaces in pool boiling, conservation eqns. soln. (*German*) 0-74715
- growth rate, during electrolysis in supersaturated liq. 0-61104
- icicle crystallisation phenomenon, growth mechanism, structure and shape 0-59423
- incompressible separated boundary layers including viscous-inviscid interaction, transition bubble 0-64515
- K₂O-PbO-SnO₂, glass, effect of DC on corrosion of SnO₂ electrodes 0-85075
- kinetic energy of particles in fluidised bed rel. to bubbling phenomena, theoretical anal. (*Russian*) 0-74965
- leading edge bubble formation, peaky airfoil (*French*) 0-64524
- liquid, positronium pick-off annihilation, improved bubble model 0-93424
- LMFBR advanced MX-type fuels, low-temp. microscopic swelling, phenomenological model 0-57851
- LMFBR HCDA, energetics of bubble expansions, potential attenuation mech. 0-83197
- low velocity vertical steam-water flow, void fraction in pipes 0-74964
- microorganisms, lack of intracellular bubble formation at very high gas supersaturations 0-81562
- molten metal cavitation bubble collapse and erosion intensity in constant mag. field (*Russian*) 0-60987
- Newton black film, line tension, determ. by cnt. bubble method 0-88406
- Newton black films, line tension determ. by diminishing bubble method 0-88407
- nonlinear acoustic disturbances in liquid containing gas bubbles 0-59104
- nuclear fuel, gas release and swelling, operational model, grain boundary gas 0-95346
- nuclear fuels, fission gas precipitation into intra- and intergranular porosity, theory 0-57849
- oscillating vessel with liquid containing compressible sphere, finely disperse inclusion motion 0-74963
- oscillations of large amplitude for bubbles in fluid of infinite extent 0-96298
- oxide nuclear fuel, fission gas release and swelling, simple operational model 0-92565
- polymer solutions, bubble behaviour in pulsating pressure, natural freqs. 0-64591
- polymeric liquid, viscoelastic, gas bubble pulsations and assoc. dissipation effects 0-59079
- polystyrene lattices, electro-flotation, collection efficiency 0-74946
- production, pulsation and damping, in dil. polymer solns. 0-69879
- radiolytic gas bubble growth in reactor irradiated PMMA 0-65058
- rectangular body, laminar flow, separation bubble and stagnation line 0-64514
- resonating gas, model used for deriving eqns. for sound speed and attenuation 0-87670

bubbles continued

- rupture between two solid walls, effect of drag-reducing polymers on cavitation 0-106822
- shape description in terms of dimensionless numbers 0-79382
- solitary gas bubble, growth from soln. 0-64617
- sound pulsation noise damping from small air bubbles in water 0-64253
- spherical, pressure waves produced by collapse (*Japanese*) 0-100027
- spherical cap bubble, mass transfer coeff. 0-79383
- spheroidal bubble, prolapse or oblate, collapse or expansion in incompressible perfect fluid (*French*) 0-74933
- in steel, carbon type, hydrogen press. effect on morphology of hydrogen attack 0-85052
- steel, high-strength low alloy, H₂ attack, 350-510°C 0-97636
- submerged gas injection into liquids, flow regimes 0-59101
- submerged jet cone angle from bubble theory 0-79372
- superheated binary solns., flashing kinetics, nucleation and critical bubble 0-92035
- superheated water at reduced pressures, bubble growth, finite difference anal. (*Japanese*) 0-92150
- suppression of finite-amplitude primary wave attenuation, parametric acoustic arrays, use of bubbles 0-74563
- Taylor bubble rise in circular vertical tube 0-64612
- translational motion in a viscoelastic liquid, retarded motion approx. 0-83777
- turbulent bubbly flow, drift velocity, analytical model of distrib. mechanisms 0-99992
- US wave in cavitating liquids, optical visualisation, nonlinear effects 0-106651
- vacuum bubble evaporation and thermodynamics, surface oscill. consideration 0-62608
- vapour bubble growth in US field 0-87608
- vapour bubble in saturated liq. free convection boiling, growth rate and detachment diameter 0-103057
- vapour bubbled through liquid pool, fractional vapour content 0-106831
- vapour-liquid mixture, propagation of acoustic disturbances, model 0-103058
- vertically vibrated liquid column, surface disintegration, bubbles and drops 0-74943
- water-in-oil emulsion, boiling, bubble formation, cinemicrophotography 0-74961
- Al film, deform. under He ion bombardment 0-65073
- Cu, formation of H₂O vapour bubbles, effect as intergranular creep fracture 0-71722
- H bubbles and Li colloids, formation and annihilation in LiH 0-107228
- H₂ evolution from H₂O electrolysis, nucleate boiling, vapour bubble behaviour, heat and mass diffusion 0-67013
- H₂ gas bubble struct. in proton irradiated Cu at 300K 0-92569
- He, cavity depth distribution in 20 and 500 keV ⁴He⁺ irradiat. Ni 0-107346
- He, in α -irrad. Al foils, bubble alignment during deform. 0-107345
- He ion irradiation of metals, blister form. and bubble growth 0-65072
- N₂ gas jet injection into Hg, interaction at submerged orifice 0-59102
- Na₂O-SiO₂ glass, bubble gas comp. change 0-79946
- Na₂O-SiO₂ glass melt, dissoln. of O₂ and CO₂ gas bubbles 0-79945
- O₂ evolution from H₂O electrolysis, nucleate boiling, vapour bubble behaviour, heat and mass diffusion 0-67013
- Y₃Al₅O₁₂ crystal growth from melt, gas bubble capture theory 0-64941

Buchholz relays *see relay protection***buckling**

- annular plates, nonsymmetric postbuckling behaviour, numerical analysis 0-102968
- beams, buckling loads and fundamental freqs. improved lower bounds 0-64416
- beams, uniform elastic, lateral buckling, perturbation methods 0-64417
- bifurcation and limit point instability of dual eigenvalue third order systems 0-87727
- circular annular plates of parabolically varying thickness, buckling and vibrs. 0-69698
- column on nonlinear elastic foundation, buckling imperfection sensitivity, Range-Domain implication (*German*) 0-74786
- column with nonlinear restraints and random initial displacement, buckling 0-79192
- columns, elastoplastic, thin and vertical, postbuckled, deflections 0-87728
- complex idealised bar, deformation processes, bifurcational elastic eqn. soln., pseudobifurcation (*Russian*) 0-58945
- cone cylinder jointed shell, ring stiffened, external hydrostatic pressure, elastic stability (*Chinese*) 0-64412
- conical shell, skew, truncated, external hydrostatic pressure, elastic stability (*Chinese*) 0-64413
- conical shell subjected to overall external pressure, postbuckling behaviour (*Chinese*) 0-64407
- cylinders, discretely stiffened, buckling under axial compression 0-64408
- cylindrical shells with various end conditions, buckling under normal pressure 0-69703
- elastic plastic spherical body, instability under uniform loading 0-58946
- elastic-plastic plates and shells, flow rule for lowering buckling stresses (*Japanese*) 0-99949
- fibre reinforced elastic slab subjected to axial loads, instability and buckling 0-64420
- frame, two-bar, with tangential load, snap-through buckling 0-64406
- glass fibre reinforced plastics, cylindrical shells, compressive and flexural strength (*Japanese*) 0-81115
- harmonic solid, crack parallel compression, crack plane strain buckling 0-64475
- honeycomb sandwich beams with laminated faces, flexural wrinkling 0-79183
- load-deflection curve, post-buckling behaviour of Hutchinson's plastic buckling model 0-64411
- nonsymmetric struts, static and dynamic imperfection sensitivity, buckling model modification 0-79190
- plane-strain buckling of cracks in incompressible elastic solids 0-79186
- plate, thin, elastoplastic, buckling model (*French*) 0-74778
- plate, thin, unilateral buckling, variational techniques (*French*) 0-74780
- plate on tridimensional elastic foundation (*French*) 0-79182
- plate with intermediate continuous elastic supports subjected to initial membrane forces 0-106744
- plates, annular, with variable thickness, critical buckling loads 0-106736
- plates, rectangular cross-ply laminated, with nonlinear stress-strain behaviour, buckling 0-64415
- plates, rectangular elastic, secondary buckling states 0-74782

buckling continued

- post-buckling behaviour of structures using a finite element-nonlinear eigenvalue technique 0-92078
- postbuckling analysis of elastic structures by the finite element method 0-96209
- shell, cylindrical, under external press., vibr. and buckling 0-102975
- shells, circular cylindrical, in axial compression, axisymmetric creep buckling, isotropic elasticity 0-69704
- shells, cylindrical, axially compressed, localised plastic buckling deformation 0-106735
- shells, cylindricals, composite, buckling and vibrational response to axial compression 0-64423
- shells, elastic-plastic circular cylindrical, under internal pressure, bifurcation 0-64421
- shells, imperfect circular cylindrical, under torsion, buckling, initial deflection effects 0-64414
- shells, long cylindrical, plastic buckling under pure bending 0-64409
- shells, oval cylindrical, orthogonally stiffened, buckling under axial compression 0-74777
- shells, shallow spherical, axisymmetric dynamic buckling 0-87729
- shells, shallow spherical, buckling, pole condition significance 0-64418
- shells with loaded free edges, pressure stiffness matrix symmetricability, buckling pressure 0-92079
- steel, stainless, type 304, plastic buckling of cylindrical shells under axial compression 0-74785
- structural member, dynamic loading and plastic response, review 0-83756
- strut creep buckling, damage effects 0-102976
- thin plate elastic-plastic buckling, Hencky effects, von Karman nonlinear strain (*French*) 0-58942
- three hinged circular arch, initial postbuckling 0-64422
- three-layer plates, circular, stability 0-79188
- webs, thin, under partial edge loading, stress state obs., influence of longitudinal stiffening determ. 0-79857
- Fe base superalloy, type A-286, elevated temp. fracture toughness testing of thin section irradiat. materials 0-61063
- Si thin ribbon grown at high speed, thermal stresses, reduced thermal buckling 0-107078

building*see also civil engineering: erection*

- air conditioning system using heat storage tank, energy saving control system (*Japanese*) 0-72087
- architectural acoustics of solid-borne sound, propagation characts., field and model expts. (*Japanese*) 0-64290
- broadcasting studio, 'Deutsche Welle' building construction and meas. (*German*) 0-106668
- domestic roofing sound insulation, test details, appl. to building industry 0-79058
- engineering design to resist earthquake loading 0-81844
- heating, solar, types, construction and thermal and environmental parameters (*French*) 0-85268

bulk density *see density***bulk diffusion** *see diffusion in solids***bundling** *see packaging***burning** *see combustion***burnout** *see combustion***burst noise** *see random noise***bus conductors (electric)** *see busbars***busbars**

- laser fusion reactor, NOVA, pulsed power control system, fibre-optic multi-tapped computer bus 0-95443

BWT *see backward-wave tubes***C invariance**

- baryon asymmetry of the Universe, quantum black hole evaporation (*Russian*) 0-109577
- conformal motions coupled to gauge transforms, charge conservation 0-62835
- hadron-hadron 3-jet collisions, charge conjugation asymmetries and trilinear gluon coupling 0-105934
- massive particles with any spin. consistent eqns., Klein-Gordon divisor, review 0-73577
- QED, renormalisation group equations, invariant charge function 0-57529
- quantum field theory, relativistic, discrete symmetries 0-68387
- SU(5), unification of weak, EM and strong interactions, review 0-105814
- superheavy boson decay, neutrino number and isotropy of Universe in grand unified theories 0-85852

cable insulation*see also insulating oils*

- high molecular weight polyethylene, characterisation using size exclusion chromatography 0-66897
- HV cable, PE-insulated, electron beam crosslinking process development 0-66846
- liquid dielectrics, thermal performance estimation 0-88582
- polymeric cable insulation, radiation modification using electron beams 0-66848
- polymeric insulating materials, water treeing initiation and growth, effects on cable service life 0-84698
- polyolefin, cross-linked, insulation system for wire and cable for locomotives 0-66851
- polyolefin, cross-linked, irradiation appl. to provide improved insulation props. to wires and cables 0-66850
- power cables, dry insulation, materials used and characteristics (*Spanish*) 0-81024
- PVC, cross-linked, irradiation appl. to provide improved insulation props. to wires and cables 0-66850
- PVC materials, cross-linkable, for wires and cable insulation 0-66849
- sheath and insulating materials for wire and cables, crosslinking by irradiation 0-66845

cable jointing

- fusion reactor, Large Coil Program, low temp. stability, joints, design method 0-106195
- fusion reactors, Torsatron T-1, demountable resistive joint for high current superconductors 0-106202
- optical fibre, in-the-field connections 0-69545
- optical fibre cable splice methods (*Japanese*) 0-58690
- optical fibre connectors, single- and multi-fibre, basic construction (*Japanese*) 0-87509
- optical fibre cutting tool and automatic splicing machine 0-87575

cable jointing continued

optical fibre jointing techniques and connections to communication equipment (*Norwegian*) 0-64179
optical fibre splicing, arc fusion, protection and reliability 0-69565

cable laying

telephone, underground, seismology appl., rocks location verification 0-72456

cable sheathing

HV, Rb coverings quality estimation using mechanical tests (*Polish*) 0-97525
insulating and sheath materials for wire and cable, crosslinking by irradiation 0-66845
optical fibre, jacketed and cabled, low-temp. attenuation increase 0-58732

cable sheaths see *cable sheathing***cables (electric)**

see also *coaxial cables; power cables; submarine cables; superconducting cables; telecommunication cables; underground cables*
flex lead, Ag-Cu corrosion study 0-76406
mineral insulated, radiation induced currents 0-65037
nuclear reactor power and control cable tests to IEEE standards 0-57884
thermocouple extension leads, universal, geometry of connection 0-57294
MgO insulated high voltage instrument cables for 650°C, in-vessel breeder reactor service 0-57878

CAD

see also *computer-aided analysis; interactive systems; power system CAD*
cooled epoxy resin vacuum mould computational simulation of design (*German*) 0-81020
ECG leads 0-85526
electronic systems, analog signal processing, book 0-86047
magnet design for high-current implanters or small isotope separators 0-68222
magnetic lens design, finite element program improvement 0-69316
measuring systems, systematic design 0-95094
MTF tolerancing computer program 0-78934
optical design, optimisation and interactive graphics improvements 0-78933
optical well-baffled axially symmetric system design program GOSBOP 0-78940
solar buildings, climatological design assessment interactive CAD techniques 0-61289
TRANSPORT, design program for charged particle beam transport systems 0-106220

cadmium

see also *nuclei with*
adsorption by Al_2O_3 , radioactive waste storage 0-99240
atom, $4d^{-1}5p^1$ P autoionising state, electron impact ionisation obs., distortion effects calcs. 0-83491
atom, 5^1P_1 autoionising state, 150 eV electron impact excitation, (e, 2e) ang. distrib. study 0-83495
atom, $5s5p^1P_1-5s^2^1S_0$ intercombination line, press. broadening and shift 0-95564
atom, 1S , 3P , 1P states, dipole polarisabilities from compact variational trial functions 0-63568
atom, n^1S_0 and n^1D_2 levels lifetimes, time-resolved spectrosc. obs. (*French*) 0-102456
atom, transition probabilities, 5^1P_1 level lifetime meas. 0-91500
atoms, electron binding energy and shift, core level XPS 0-87088
atoms, excited + molecules, collisions 0-58338
Cd + molecules collisions 0-58338
core level binding energies 0-71564
creep, low-temp., thermal heating and quantum mechanisms 0-79868
crystals, concentrated loads, 3-D anisotropic elasticity theory 0-83734
dimethylammonium manganese trichloride: Cd, impurities in quasi-one-dimens. Heisenberg systems, anisotropy effect 0-80502
evaporation rate, effect of inert gas 0-84285
Fermi surface, stress-induced changes 0-96770
film, dry lubrication on C steel, tribological behaviour 0-89364
film, surface RF impedance in strong mag. fields (*Russian*) 0-92920
films, struct. and props., X-ray diffr. spectra anal. 0-80119
hollow cathode laser, ion laser transitions 0-69366
ion polarisation and point defect resistivity in metals 0-103672
kidney, concentration of Cd, neutron activation anal., organ depth determ. 0-72321
laser, white light, hollow cathode, new design concept 0-87405
laser produced plasma recombination laser, power output enhancement by plasma confinement 0-63989
laser radiation absorption in craters on metal targets 0-97386
liquid, thermoelectric power, pseudopotential calc. 0-59959
liquid metal, electronic density of states, pseudopotential calcs. 0-70578
liver, concentration of Cd, neutron activation anal., organ depth determ. 0-72321
microplastic deformation, basal dislocation generation, glide and locking, X-ray topography study 0-88156
organ tissue levels, in vivo meas. system using neutron activation 0-67224
oxidation, chemisorption and oxide regimes, UPS and EELS study 0-81236
N.Pacific, trace metal vertical profiles 0-67381
passivity breakdown breakdown, of high purity metal 0-100947
photoelectric cross sections at 52.4, 60, 72.2 and 84.4 keV 0-69187
plasticity study during deformation by twisting (*Russian*) 0-93597
positron trapping at low temp. lifetime spectra 0-84799
proton-induced L-shell ionisation cross-sections 0-100707
sputtered excited states, secondary photon emission, role of transition probability 0-102483
tensile properties, texture and grain size depend. of warm-rolled specimens 0-71720
thermal expansion, temp. depend., vacancy effects 0-79962
vapour, RF discharge, isotope separation 0-79619
wear under reversed friction, temp. effect 0-108588
Young's modulus and internal friction, 20°C to melting point (*Russian*) 0-89278
AgCl: Cd $^{2+}$, heavily doped, free energy and point defect distrib., integral eqn. method 0-107219
AgI: Cd, polycrystalline, thermoelectric power meas. 0-59698
BP: Cd, epitaxial layers, ion implantation, defects and lattice locations, channelling obs. 0-88179
Cd IV, UV spectral analysis 0-83306
Cd-Cd $_{12}$ mixture, molten, nuclear spin relax. 0-88887

cadmium continued

Cd + H $_2$ → CdH + H, product initial rot. state distrib., pump and probe laser obs. 0-85158
Cd + He, Penning ionisation cross section of target atom, for He(2 1S_1) 0-63777
Cd + inert gas, broadening of 5^1P_1 level 0-83479
Cd + N $_2$, vap., creation of inverse population of atomic Cd 6 3S and 5 3P_2 levels 0-58219
Cd + O $_2$, matrix reactions, IR, Raman and visible spectra in Ar and N $_2$ matrices 0-87110
Cd($^1P_{0,1}$) + CO(CO $_2$)(NO), absolute quenching cross section, phase-shift method 0-58340
Cd(1P_1) radiation imprisonment lifetime, inert gas effect, phase-shift method 0-58213
 ^{111}Cd , nucl. orientation coeffs. with axially symm. elec. field gradient 0-97168
 $^{113}\text{Cd}^m$, in marine organisms and sediment around Marshall Island nucl. test site 0-109174
 $^{114}\text{Cd}/^{106}\text{Cd}$, isotope fractionation in fractions of H3 chondrites Tieschitz and Brownfield 0-94764
Cu-Cd thin film couples, room temperature interactions 0-96699
GaAs: Cd, ion implant depth distrib., AES and glow discharge optical spectroscopy meas. 0-65028
He-Cd vapour excitation in hollow cathode discharge 0-64815
He-Cd vapour laser, continuous wave, intensity fluctuations investig. 0-83593
InAs: Cd, Te, donor-acceptor interaction, elec. cond. and Hall coeff. meas. 0-59988
InP: Cd, avalanche photodiode characts., impurity diffusion effects 0-70709
InP: Cd, doping by UV laser photodeposition 0-84191
InP: Cd, p $^+$ -p $^-$ n $^-$ junction form, by diffusion doping 0-84504
p-InP: Cd, ohmic contact formation on InP by laser photochemical doping 0-80369
InSb: Cd, ion-irrad., p-n conversion during heat treatment 0-96558
InSb: Cd, thermal conductivity down to 0.38K 0-107582
Li $_2\text{O-Al}_2\text{O}_3\text{-SiO}_2\text{-Cd}^{2+}$, glass, ESR study 0-103879
Li $_2\text{O-Al}_2\text{O}_3\text{-SiO}_2\text{(P}_2\text{O}_5\text{):Cd}^{2+}$ glasses, γ -irrad., EPR study 0-84639
Li $_2\text{O-P}_2\text{O}_5\text{-Cd}^{2+}$ glass, γ -irrad., EPR study 0-84639
NaCl: Cd $^{2+}$, dielectric loss following plastic deform. 0-84690
Ni-Cd batteries, button and cylinder types, self discharge behaviour during storage (*German*) 0-66960
Ni-Cd sealed battery electrode performance meas. 0-66962
Pb-Cd-Pb, supercond. - normal-metal - supercond. junction, crit. currents 0-107965
Pb-Cd-Pb junctions, pair pot., mag. field depend., crit. currents meas. 0-84555
Pb $_{0.8}\text{Sn}_{0.2}\text{Te: Cd}$, influence of Cd doping on high field magnetoresist. and Hall effect 0-75590
Pb $_{1-x}\text{Sn}_x\text{Te: Cd}$, solid solutions, impurity states in photoluminescence spectra (*Russian*) 0-97333
Si/In-(Cd), Si/Cd Schottky contacts, electrochemically deposited 0-88633
Te-Se-Cd, sandwich structure, fabrication and characteristics 0-60089
Te-Se-Cd rectifying sandwich structs., elec. forming action, Schottky junction form. 0-80371

cadmium alloyssee also *cadmium compounds*

ion-selective membrane electrodes development, Ag ion conduction ceramic systems (*Japanese*) 0-61203
Ag-Cd peritectic system, separate crystallisation of phases (*Russian*) 0-66497
Ag-Cd-(Ni), internally oxidised, oxide particle size control (*Japanese*) 0-89480
Al-Bi(Cd)(Pb)-Ti, containing low-melting pt. inclusions, mech. props. 0-93632
Al-Ca, rapid quenching, struct. and decomp. 0-76244
Al-Ni(Cd)(Fe)(Si), cold worked, struct. and props. 0-71666
Bi-Cd, eutectic, contact melting kinetics (*Russian*) 0-70377
Cd-Ge broken lamellar eutectic composite, tensile and compressive props. 0-71694
Cd-Mg, selective dissolution, static samples 0-65228
Cd-Mg, selective dissolution, rotating ring disc electrode 0-65229
Cd-Sn alloy, superconductivity and microstructure 0-107949
Cd-Sn binary system, high press. study 0-93539
Cd-Tl binary alloy system at high press. 0-97461
Cd-Zn binary systems, melts, elec. resist., 0-700°C 0-65517
Cd-Zn eutectics, microstruct. after solidification, heat pipe influence 0-76243
CdHg, ω phase, mag. susceptibility anisotropy w.r.t. uniform compression (*Russian*) 0-71143
Cd $_{1-x}\text{Mg}_x$, energy spectrum pseudopotential calcs., mag. props., impurity scatt. (*Russian*) 0-65430
Cu-Cd (1.0 wt.%), yield stress and flow stress 0-97524
Li-Cd, phys. props. of liq. phase and LiCd solid cpd. 0-75537
MgCd wire, elongation during disorder-order transform. (*Russian*) 0-104148
Si/In-(Cd), Si/Cd Schottky contacts, electrochemically deposited 0-88633
Sn-Cd-Pb system, contacting layer struct. and phase composition (*Russian*) 0-66475
Sn-Pb-Bi-Cd infiltrated Ti base composite sintered bearing material, anti-friction props. 0-60981
Tb-Cd, elec. quadrupole interaction, temp. and press. depend., TDPAC meas. 0-60469
Zn-Cd alloys, liq. and solid, ultrasound speed and compressibility meas. 0-102941

cadmium compoundssee also *cadmium alloys*

alkylene di-ammonium cadmium tetrachlorides, sp. ht. anomalies at phase transitions 0-70421
cadmium formate, anhydrous, cryst. struct. 0-107195
CdS, single crystals, laser emission from surface diffraction grating 0-95900
CdTe thin film on ferroelectric TGS, influence of polarisation reversal on elec. cond. 0-65720
chalogenides, thin films, VPE, needle-like cryst. growth 0-80148
diethylammonium cadmium tetrachloride, dielec. props., phase transition 0-80675

cadmium compounds continued

- dimethylammonium cadmium tetrachloride, far IR refractive index, extinction coeff. and dichroism obs. 0-66144
- HgCdTe/CdTe, limited diffusion volume photodiode, characterisation 0-75627
- Langmuir multilayer films with and without dye-sensitisers, elec. props. 0-97006
- perovskite compound combination, Mossbauer spectroscopy study (*Russian*) 0-80666
- stearate based Langmuir films, deposition on p-CdTe, characts. and MIS struct. 0-92998
- Au-CdTe-Au structure, current transport props. 0-80408
- Ba₂Zn_{2-2x+y}Cu_{2x}Cd_{2y}Fe₁₂O₂₂, mag. props. and Mossbauer spectrum 0-75763
- (Cd,Hg)Te epitaxial structures, comp. profile depend. on deposition parameters 0-100795
- Cd complexes, dithiocyanato(diethylenetriamine) Cd(II) and dithiocyanato(pentamethyldiethylenetriamine) Cd(II), Cu²⁺ doped, ESR 0-108059
- Cd-P, p-T-x phase diagram, thermodynamic props. 0-88300
- CdAs₂, cryst. struct. and vitrification capacity 0-88126
- Cd₃As₂ and CdAs₂, molten, thermal expansion and atomic bond strength parameters 0-65257
- Cd₃As₂, energy band structure calc. 0-75504
- Cd₃As₂ film on NaCl substrate, vacuum deposition, growth morphology, microstructure 0-75479
- Cd₃AsCl₂, X-ray cryst. struct. anal. (*French*) 0-64957
- Cd₃AsCl₃, X-ray cryst. struct. determ. and refinement (*French*) 0-107119
- Cd₃(As₂P_{1-x})₂, 0 ≤ x ≤ 1.0, band struct. calc. near Brillouin zone centre 0-107703
- Cd₃B₂O₅, basalt atom coordinates isotropic temp. corrections, X-ray study 0-59449
- Cd₃B₂O₅Br(Cl)(I), boracite, single cryst. prep. and phys. props. 0-100763
- CdBr₂Co²⁺, exchange-coupled Co²⁺ pairs, optical absorpt. and Zeeman studies 0-66242
- CdCO₃Fe²⁺, Mossbauer spectra 0-108138
- Cd₂Ca_{1-x}MoO₄, growth and props. 0-71588
- Cd_{1-x}Ca_xS, solid soln., phase equilib. diagrams 0-108412
- CdCl₂ · 2.5H₂O, rel. between theoretical and obs. morphology (*French*) 0-70148
- Cd(ClO₄)₂ · 6H₂O and Cd(ClO₄)₂ · 6D₂O, single crystals, EPR study of phase transitions 0-66025
- CdCr₂S₄, ferromag. semicond., IR refl. spectra, phonon props. and dielec. function 0-66191
- CdCr₂S₄ magnetic semiconductor crystal growth, structural defects, physical properties 0-60759
- CdCr₂S₄, phototreshold changes below mag. ordering temp. 0-97406
- CdCr₂S₄, pure and Ag doped, electronic struct., mixed valence 0-70612
- CdCr₂S₄, thermorefectance, photoconductance, Raman scattering near magnetic phase transition 0-97298
- CdCr₂S₄(Se₄), spontaneous magnetisation temp. depend., nuclear resonance freq. depend. (*French*) 0-80483
- CdCr₂Se₄, Crit. relax. processes, mag. reson. expts. 0-60425
- CdCr₂Se₄, energy band struct. calc. by augmented plane wave method 0-103621
- CdCr₂Se₄, energy structure, magneto-optic effects 0-71394
- CdCr₂Se₄, ferromag. semicond., conc. anomalies rel. to red shift of absorpt. edge 0-70732
- CdCr₂Se₄ magnetic semiconductor, photoinduced centre kinetics 0-71110
- CdCr₂Se₄, magnetisation, study of photoinduced charges 0-80567
- CdCr₂Se₄, modulated piezoreflection spectra 0-97237
- CdCr₂Se₄, Mott ferromagnetic semiconductor, optical absorption edge, critical behaviour 0-97226
- CdCr₂Se₄, pure and Ag doped, electronic struct., mixed valence 0-70612
- CdCr₂Se₄, reactor radiation influence on ferromagnetic phase transform. (*Russian*) 0-75760
- CdCr₂Se₄, thermorefectance, photoconductance, Raman scattering near magnetic phase transition 0-97298
- CdCr₂Se₄Ag, magneto-optical effects in impurity spectral region 0-97313
- CdCr₂Se₄Ga(In), photoconductivity, photomagneto-resistance near Curie point (*Russian*) 0-100485
- CdCr₂Se₄In(Ga), elec. resist. and magneto-resist., 2 to 200K 0-96876
- CdCu₂Ru₂O₁₂, synthesis, cryst. struct., mag. and elec. props. (*French*) 0-107151
- CdF₂, colour centres, IR absorpt. and photocond. after UV irradiation 0-79784
- CdF₂, electrical transport limitation by electrodes, polarisation effects 0-96689
- CdF₂, high resolution NMR and chem. shifts of ¹¹¹Cd and ¹¹³Cd, double reson. expt. 0-60460
- CdF₂, ionic cond., activation vols., freq. depend. cond., press. effects 0-100354
- CdF₂, ionic conducting fluoride fluorite, US velocity meas. 0-107381
- CdF₂, UPS and XPS spectra, rel. to optical props. 0-66386
- CdF₂Er³⁺, Tm³⁺, evidence for Er³⁺ ↔ Tm³⁺ energy transfers, fluoresce. expts. 0-60655
- CdF₂Eu²⁺, EPR spectra, hydrostatic press. and temp. effects 0-84648
- CdF₂NaF thin films, electroluminescence obs. at 77K (*French*) 0-80866
- CdF₂NaF(AgF), colour centres, IR absorpt. and photocond. after UV irradiation 0-79784
- CdF₂Na(Nd), ionic cond. investigation by complex admittance method 0-100352
- CdF₂Sm³⁺, photoconverted, thermally stimulated relax. 0-84476
- CdF₂YF₃, thermal ionisation energy of monovalent centres 0-80207
- CdF₂(FCl)(FBr), matrix isolated IR and Raman spectra, assignments, force consts., isotope effects and thermodynamic props. 0-63631
- CdGa₂S₄, double surface-barrier diodes, current-voltage characts. 0-92972
- CdGa₂S₄, IR refl. spectra 0-60604
- CdGa₂(S_{1-x}Se_x)₄ solid solns., band struct. behaviour w.r.t. comp. (*French*) 0-107699
- CdGa₂S₄(Se₄), band struct., pseudopot. method 0-92816
- CdGeAs₂, vertical Bridgman growth with control of interface shape and orientation 0-66420
- CdGeAs₂, crystals, Bridgman grown, optical props. rel. to O₂ content of starting materials 0-81213
- Cd₂GeO₄, anode for H₂O photoelectrolysis 0-108716
- n-Cd₂GeO₄, electronic and cond. props. rel. to prep. conditions and defect struct. 0-107787
- CdGeP₂, thermo-optic coefficient, dispersion 0-71396
- Cd₂Hg_{1-x}Te, elec. characts., impurity effects 0-92890

cadmium compounds continued

- Cd_{1-x}Hg_xGa₂S₄ solid solns., band struct. behaviour w.r.t. comp. (*French*) 0-107699
- Cd₂Hg_{1-x}Se, phase transition and elastic consts., US vel. study 0-75354
- CdHgTe, anomalous avalanche breakdown 0-80284
- CdHgTe photoelectromagnetic detector for 10.6 μm radiation, non-cooled, performance 0-82818
- Cd_{0.15}Hg_{0.85}Te, photothermoelectric effect in mm range 0-92932
- Cd_{0.175}Hg_{0.825}Te-Au(In) contacts, photo-effect in the 77-300K range, barrier height estimation 0-107850
- Cd₂Hg_{0.8}Te, ion implantation doping for realisation of IR detectors, responsivity meas., ion range straggling 0-73452
- Cd₂Hg_{0.8}Te recrystallisation for supercooled IR detector production (*German*) 0-86403
- n-Cd_{0.21}Hg_{0.79}Te, excess generation-recombination noise 0-107880
- n-Cd_{0.3}Hg_{0.7}Te, photoelec. props. at 78K, relax. time, minority carrier extraction 0-107864
- Cd₂Hg_{1-x}Te, carrier lifetime, effect of comp. fluctuations and second-phase inclusions 0-80294
- n-Cd₂Hg_{1-x}Te crystals, carrier recomb. in extrinsic conduction range 0-70722
- Cd₂Hg_{1-x}Te crystals, donor compensation, low temp. cond. study 0-75571
- Cd₂Hg_{1-x}Te, dislocation motion, effect of lattice defects on microhardness (*Russian*) 0-70220
- Cd₂Hg_{1-x}Te epitaxial graded gap layers, plasma reflection and magnetoreflection 0-71391
- Cd₂Hg_{1-x}Te, epitaxial growth from stoichiometric melt, crystn. and diffusion 0-75475
- Cd₂Hg_{1-x}Te, epitaxial layer p-n junction, current-voltage characteristics of photovoltaic detectors, 1 to 15 μm 0-86407
- Cd₂Hg_{1-x}Te films, growth by cathodic sputtering in Hg vapour plasma 0-97431
- Cd₂Hg_{1-x}Te, graded gap epitaxial layers, spectral characts. of photoelectromagnetic effect 0-60022
- Cd₂Hg_{1-x}Te, graded-gap layers, galvanomag. props. at low temp. and in weak mag. field 0-75664
- Cd₂Hg_{1-x}Te layers, epitaxial graded-gap, nonlinear elec. effects 0-100468
- Cd₂Hg_{1-x}Te, long term stability at 300K, rel. to device appl. 0-59978
- n-Cd₂Hg_{1-x}Te, recombination due to surface excitation, photoconductivity, impurity states (*Russian*) 0-60042
- Cd₂Hg_{1-x}Te, tunnelling effect in p-n junctions 0-75630
- Cd₂Hg_{1-x}Te, vacancy electron states, acceptor behaviour, electron mobility 0-70193
- CdI₂, polytypes, vapour growth mechanism 0-84124
- CdI₂, polytypic crystals, dielectric loss behaviour 0-66108
- CdI₂-Cd(I) mixture, molten, nuclear spin relax. 0-88887
- Cd(IO₃)₂, complex salts, phase transitions, cryst. struct. (*Chinese*) 0-70171
- CdInGaS₄, crystal, Raman scattering spectra, polarisation meas. (*Russian*) 0-71410
- CdInGaS₄, layered structure crystals, refractive index meas. method 0-98966
- CdInGaS₄, pure and Cu-doped, electrophotography layers (*Russian*) 0-68282
- CdIn₂O₄, anode for H₂O photoelectrolysis 0-108716
- CdIn₂S₄, Brillouin scatt., elastic and photoelastic consts. determ. 0-60619
- CdIn₂S₄, partial inverse spinel struct., detection by Fourier transform spectroscopy 0-108197
- CdIn₂S₄ single crystals, recombination process and localised levels 0-93383
- CdIn₂Se₄, high resolution electron microscope study of polytypism 0-88119
- Cd₂M_{10-x}(PO₄)₆X₂(M=Ca, Sr, Ba, Pb; X=F, Cl) apatites, IR spectral study (*French*) 0-93316
- Cd₂Mg(Co)(Zn)(Mn)(Cd)(Ca)TeO₆, optical SHG study of acentricity, ferroelec. of low temp. phases 0-71324
- Cd_{1-x}Mg_xS, solid soln., phase equilib. diagrams 0-108412
- Cd_{1-x}Mn_xSe, fundamental optical props. 0-84751
- Cd_{1-x}Mn_xTe, exchange induced ionization of bound excitons, luminesc. meas. 0-97328
- Cd_{1-x}Mn_xTe, indirect exchange interaction 0-97087
- Cd_{1-x}Mn_xTe mixed crystals, Raman spectra 0-103961
- Cd_{1-x}Mn_xTe, semimagnetic, exchange interactions between localised and delocalised electrons 0-97245
- CdMoO₄Mn²⁺, zero-field splitting of Mn²⁺, EPR 0-75531
- Cd(NO₃)₂, phase transition, SHG, optical and dielec. meas. 0-71334
- CdNb₂O₆, force fields rel. to cryst. struct. (*French*) 0-107104
- Cd₂Nb₂O₇, photolum. and carrier drift mobility at ferroelec. transition 0-71469
- Cd_{1-x}Ni_xFe₂O₄, solid soln., mag. and structural characterisation 0-103906
- CdO, aqueous-deposited films, struct. and electronic props. for solar cell appls. 0-100797
- CdO-Al₂O₃-P₂O₅ glass, γ-irrad., EPR study 0-84639
- CdO-P₂O₅ glass, ESR of VO²⁺ ions 0-100610
- CdO-P₂O₅ glass, thin film, elec. cond., high and low fields 0-80427
- Cd-SnO₂, DC reactively sputtered films, elec. and optical props. 0-103763
- CdO-WO₃, phase rels. and cryst. struct. 0-108410
- CdP₂, 442 class gyrotropic crystals, self-induced rot. of light polarisation plane 0-99810
- CdP₂, cryst., tetragonal, 2-phonon IR absorpt. 0-66176
- CdP₂, resonance Raman scatt. singularities (*Russian*) 0-89007
- Cd₂P₁₃, X-ray cryst. struct. determ. and refinement (*French*) 0-107120
- Cd₁₀(RO₄)₆X₂(R=As, P, V; X=Cl, Br) apatites, IR spectral study (*French*) 0-93316
- Cd(S, Se) film grown on InP substrate, mismatch dislocations and lattice distortion, dangling bond density 0-84406
- CdS, acoustic wave attenuation, phonon viscosity and dislocation drag 0-70319
- CdS, acousto-voltaic effect, asymmetric electron ejection from trap levels (*Russian*) 0-65634
- CdS, additional waves and polariton dispersion, reflectivity, transmittivity spectra 0-71443
- CdS and CdSe, for thin film and ceramic solar energy convertors 0-93870
- CdS, aqueous-deposited films, struct. and electronic props. for solar cell appls. 0-100797

cadmium compounds continued

- CdS, charged dislocations, flow of charge with plastic deform. 0-85010
 CdS, charged impurity centres, drift during passage of photocurrent 0-70767
 CdS crystal growth from vapour, preferential deposition, elec. field effects 0-84122
 CdS crystals, electron-hole plasma, carrier optical orientation 0-100689
 CdS crystals, one-photon pumping, active layer structure, light amplification 0-78858
 CdS crystals, orientational depend. of photoacoustic effect (*Russian*) 0-65167
 CdS crystals, radiative recombination, high excitation rates 0-108269
 CdS, defect struct. and config. produced by irradi., elastic scatt. expts. 0-84178
 CdS, dislocation motion, TEM obs. 0-79799
 CdS, doped, amorphous antiferromagnet model, susceptibility and spin-flip Raman scatt. meas. 0-97057
 CdS, EPR of adsorbed oxygen radicals, temp. depend. 0-80612
 CdS, elastic, piezoelec. and dielec. props. 0-108157
 CdS, elastic, piezoelectric, and dielec. props., 4.2 to 300K 0-60508
 CdS, electro-acoustically active, AC impedance meas. 0-103726
 CdS, electron and hole trapped centres, EPR, photoluminescence, photoconductivity study 0-108071
 CdS, electron-hole pairs behaviour in energetic ion tracks 0-65457
 CdS, electron-hole plasma, gain and refl. spectra study 0-66227
 CdS, electronic two- and one-photon Raman scatt. via biexcitons, stimulated config. obs. mag. field shift 0-103963
 CdS, epitaxial growth and nucleation, on monocrystr. ZnS, substrate real struct. influence 0-88455
 CdS epitaxial layers on sapphire, exciton struct. of absorpt., photoluminesc. and photocond. spectra 0-89027
 CdS, exciton droplets, energy condensation (*Russian*) 0-107712
 CdS film, chemical bath deposited, solar energy conversion by photoelectrochem. cells 0-108804
 CdS film spray fabrication, physical props., Cu₂S-CdS solar cell applications (*French*) 0-60113
 CdS films, chem. deposited, growth kinetics and polymorphism 0-75463
 CdS films, prep. by reactive pulvisation, chemical, crystallographic and electronic props. (*French*) 0-60112
 CdS, flux exclusion, superconductivity at high temp. 0-97058
 CdS, generation of optical radiation in direction of propag. of streamer 0-69401
 CdS, green edge luminescence spectrum, temp. depend. 0-108274
 CdS γ -ray dosimeters with elevated stability under irradiation 0-86995
 CdS, highly excited, stimulated emission process at 80K 0-97307
 CdS, hydrogenlike donor negative ion, ground and excited states, obs. 0-70645
 CdS monocrystral petal lasers, single-photon excitation (*Russian*) 0-99736
 CdS, monodisperse particles form. from soln., light scatt. theory use in size estimation 0-76560
 CdS, multiphoton cross-section determination by means of luminescence experiments 0-93377
 CdS, nonlinear self-action effect and absolute two-photon absorption coeff. 0-83649
 CdS phosphor, powdered, in host material, solar cells wavelength shifting 0-85286
 CdS, photocond., spectral depend. at high excitation intensity, exciton effects 0-65619
 CdS photoconductivity, spatial homogeneities exam. using DC and microwave techniques 0-93895
 CdS, photoconductors, spectral sensitisation, role of local centres (*Russian*) 0-90924
 CdS, photophoretic spectroscopy, broadband 0-86469
 CdS, piezoelec. semicond., sound absorption 0-60051
 CdS plane parallel slab, optical const. determ. methods 0-60531
 CdS platelet laser, emission spectra, optical coupling between partial resonators 0-69400
 CdS platelet lasers, optically pumped, spatial and spectral distribution of laser emission 0-64032
 CdS, polaron cyclotron resonance freq. shifts, halfwidths, cumulant expansion method calcs. (*Russian*) 0-88880
 CdS polycrystalline films, high strain sensitivity 0-93017
 CdS, polytype relative stabilities, entropy contribs. 0-100197
 CdS, positron annihilation study 0-60713
 CdS, pure spin diffusion without charge transport, spin flip Raman scatt. obs. 0-93329
 CdS, quasimonopolar semicond., recombination in near surface space charge region (*Russian*) 0-88574
 CdS, resonant Brillouin scattering and photoelastic const. in population-inverted material 0-76042
 CdS, resonant Brillouin scatt., photoelastic const., imag. part contrib. 0-108218
 CdS, rock-salt type high-press. phase synthesis using metal sulphide additives 0-104084
 CdS single cryst., lasing action excited by ruby laser picosecond pulses 0-64035
 CdS single cryst., vaporization and form. of negative whiskers 0-92659
 CdS, single crystals, US luminesc. obs. 0-76092
 CdS, single-quantum radiative recomb. of biexcitons due to biexciton-exciton interactions 0-96793
 CdS solar cells, construction, solar photovoltaic systems for remote communications power supply 0-66980
 CdS, solar cells, polycrystalline and tandem, for high efficiencies, using compound semiconductors 0-72052
 CdS, spectra of refl. and transmission coeffs. near exciton absorpt. line 0-88951
 CdS, spectroscopic study of local centre interaction, change with external illumination 0-80323
 CdS, stimulated Mandelstam-Brillouin scatt. on acoustic phonon amplification (*Russian*) 0-71437
 CdS, subMM radiation excitation by N₂ laser pulse 0-60678
 CdS, surface energy struct. changes during ion cleaning and thermal annealing 0-92962
 CdS, surface photovoltage, characterisation 0-60033
 CdS thermo-optic coefficient, dispersion 0-71396
 CdS thin film solar cell fabrication, HCl etching 0-81474
 CdS thin films, growth and evaluation for fabrication of high performance photovoltaic solar cells 0-93501
 CdS thin films on brass substrates, nondestructive resistivity meas. tech. 0-93898

cadmium compounds continued

- CdS thin layers, recryst. from CdS-Cr₂O₃ mixtures, phys. and photoelec. props. 0-96935
 CdS, thin plates, piezosemiconductors, second harmonic acoustoelectric current obs. 0-80329
 CdS, three-branch exciton-polariton dispersion, direct meas. by reson. Brillouin scatt. 0-60620
 CdS, two-photon absorpt. effect on hyper-Raman scatt. 0-74441
 CdS, vacuum deposited film, orientation axis tilt rel. to vapour angle of incidence 0-88456
 CdS, XPS, secondary illumination effects, band bending, level shifts 0-108324
 CdS:Cu, C-V curves of MIS diode used to examine trapping levels 0-65697
 CdS:Cu, Cl films, photocond. growth and decay time 0-60041
 CdS:Cu, photocurrent, elec. field effect on recombination processes (*Russian*) 0-100484
 CdS:Cu, photosensitivity degradation mechanism 0-107851
 CdS:Cu sintered layers, relaxation photocurrent kinetics (*Russian*) 0-107852
 CdS:Cu(Ag), charge and transport mechanism of impurities, electrodiffusion doping 0-59725
 CdS:Cu(Cl) thin films, surface and bulk photocond. 0-88653
 CdS:D⁻, binding energy of D⁻ ion 0-92541
 CdS:Ga crystal cathodoluminescence, SEM analysis 0-97349
 CdS:In, impurity resist., Matsubara-Toyozawa theory extension 0-80264
 CdS:In(Cl) concentration quenching mechanism of luminescence 0-97336
 CdS:Li, complex luminescence centres, recombination-stimulated conversion 0-108268
 CdS:Li, luminescence bands, photocurrent spectra (*Russian*) 0-60677
 CdS:Li, pure and doped, green edge luminesc., complex nature of centres 0-60671
 CdS:Li, single crystals, anisotropic luminesc. centres 0-80857
 CdS:Li(Cu), pure and doped, electrodiffusion of shallow donors, photocurrent, TSC, and exciton luminesc. meas. 0-79992
 CdS:Mn, vacuum deposited film, Mn migration, EPR and X-ray study 0-65411
 CdS:Na, Hagemark theory, green edge emission line intensity 0-75517
 CdS:Ni, nonradiative recomb., photocond. spectra 0-70764
 CdS:Ni²⁺, Zeeman effect at Ni impurities 0-60633
 CdS:Te-based photoelectrochem. cell, luminesc., thermal manipulation of deactivation processes 0-81479
 CdS:Ti²⁺, superhyperfine interact., ENDOR study at 4.2K 0-80639
 CdS/Cu₂S heterojunction solar cells diffusion length determ. using minority carrier SEM 0-61359
 CdS/Cu₂S solar cells, polycryst. thin film photovoltaic materials, photon loss anal., expt. determ. 0-93888
 CdS/Cu₂S thin film heterojunctions, photocapacitance meas. of solar cell parameters 0-93897
 CdS/Cu₂S thin film solar cells, design and fabrication, 9.15% conversion efficiency 0-81438
 CdS/Cu₂S, sequential evap. for solar cell applic. 0-93902
 CdS/InP epitaxial thin films on NaCl, HEED and TEM study 0-88446
 n-CdS/n-InP/p-InP heteroface solar cell with ultrathin window layer, computer anal. 0-97788
 n-CdS/p-ZnIn₂Se₄ thin film solar cell, photovoltaic props. 0-89628
 CdS-Al(Au) interfaces, bonding and interdiffusion, XPS obs. 0-80000
 CdS-Au contacts, electronic states, vacuum UV photoelectron spectra 0-70827
 CdS-CdTe p-n junction screen printed thin film solar cells 0-72055
 CdS-Cu₂S ceramic solar cells, solar batteries operating characts. 0-93874
 CdS-Cu₂S heterojunction, energy-band struct., capacitance-voltage characts., illumination effects 0-96982
 CdS-Cu₂S heterophotocells based on CdS films of stoichiometric composition, elec. and photoelec. props. 0-93873
 CdS-Cu₂S junctions, carrier trap density, deep level defects 0-107801
 CdS-Cu₂S solar cells, design and fabrication, 8.5% conversion efficiency 0-72047
 CdS-Cu₂S solar cells, microstructural study of heterojunction materials 0-93978
 CdS-Cu₂S thin-film solar cells, low-cost manufacturing process outline, economic anal. 0-93930
 CdS-Cu₂S thin-film solar cells, high open-cct. voltage and low refl. losses 0-94088
 CdS-Cu₂S solar cell, prep. and characts. (*Croatian*) 0-93876
 CdS-Cu₂S solar cells, electron diffusion length determ. using spectral response meas. 0-81475
 CdS-CuInSe₂ solar cell, polycrystalline thin film, high photocurrent, characts. 0-61339
 CdS-glass layered system, characts. of phase-velocity dispersion and struct. of surface waves 0-59775
 CdS-InP(CdTe)(GaAs)(Ge), solar cell heterojunctions, CVD fabrication, photovoltaic response 0-93878
 CdS-LiNbO₃ system, expt. investigation of nonlinear Rayleigh wave interaction 0-102946
 CdS-O₂, photoactivated O desorption 0-100391
 CdS-SiO₂ layered system, characts. of phase-velocity dispersion and struct. of surface waves 0-59775
 CdS-SiO₂-Si solar cell, I-V characteristics 0-89621
 CdS(Se), electrodeposition, using nonaqueous solvents 0-76200
 CdS_{1-x}Se_x, chem. comp. and luminescence obs. 0-80869
 CdS_{1-x}Se_x, mixed crystals, deformation effects on free excitons 0-76073
 CdS_{1-x}Se_x monocrystral petal lasers, single-photon excitation (*Russian*) 0-99736
 CdS(Se)(Te), determ. of wurtzite, zincblende and rocksalt phases 0-100219
 CdS₂Te_{1-x}, recryst. from CdS₂Te_{1-x}-Cr₂O₃ mixtures, photocond. props. 0-96936
 CdSb:Al, p-n junction formation by laser emission, photoelectric effects (*Russian*) 0-70815
 CdSb:Al(In)(Ga)(Te), p-n junction formation by laser radiation 0-96983
 CdSb:Fe, self absorpt. edge, impurity effect (*Russian*) 0-97316
 CdSe 16 μ m parametric amplification with HF laser pumping 0-78910
 CdSe, charged dislocations, flow of charge with plastic deform. 0-85010
 CdSe, chemically sprayed thin films as photoanode in photoelectrochem. cells, power charact. meas. 0-85293
 CdSe down-conversion of LiNbO₃ broadly tunable picosecond IR source 0-74435
 CdSe film, soln. growth 0-66437

cadmium compounds continued

- CdSe film deposition, and reaction sequence of H_2SeO_3 reduction 0-71603
 CdSe film photoanodes for electrochem. photovoltaic cells, fabrication and evaluation 0-76641
 CdSe film polycryst., thermal diffusion of Cr, 240-400°C 0-80001
 CdSe films, oriented, epitaxial growth by epitaxial nucleation in submicroscopic holes method 0-59834
 CdSe films, solar energy conversion using electrodeposited films for photoelectrochemical cell 0-94093
 CdSe, fundamental absorpt. edge, influence of laser radiation intensity (*Russian*) 0-71445
 n-CdSe, laser excited stimulated emission, optical gain spectrum 0-76050
 CdSe photoanode improved efficiency by photoelectrochem. etching 0-104512
 CdSe photoanodes, S substitution during operation and mech. of surface protection 0-107906
 CdSe, piezoelec. semicond., sound absorption 0-60051
 CdSe, positron annihilation study 0-60713
 CdSe, recombination mechanism at dislocations, photoluminescence 0-103993
 CdSe, single crystals, luminesc. of electron-hole plasma 0-60675
 CdSe, temp. depend. phase-matched nonlinear optical devices 0-99794
 CdSe thermo-optic coefficient, dispersion 0-71396
 CdSe thin film transistor on Cr substrate, cryst. struct., substrate defect effects 0-70563
 CdSe thin-film solar cells 0-93970
 CdSe, undoped and Cr doped, far IR transmission and reflectance spectra 0-71429
 CdSe, vacuum deposited film, orientation axis tilt rel. to vapour angle of incidence 0-88456
 CdSe:Co, impurity luminescence no phonon line depend. on temp., Debye temp. 0-66273
 CdSe:Cu, impurity photocurrent, kinetics and oscils. 0-65624
 CdSe:Li, pure and doped, reson. Raman and Brillouin scatt., elastic exciton-defect scatt. 0-80788
 CdSe-Au contacts, electronic states, vacuum UV photoelectron spectra 0-70827
 CdSe-glass layered system, characts. of phase-velocity dispersion and struct. of surface waves 0-59775
 CdSe-O₂, photoactivated O desorption 0-100391
 CdSe-Sb₂Se₃ heterojunction, photoelec. props. 0-70816
 CdSe-SiO₂ layered system, characts. of phase-velocity dispersion and struct. of surface waves 0-59775
 CdSe(Te) and solid solns., optimal synthesis conditions for single cryst. growth 0-100776
 CdSe_{0.65}Te_{0.35}, polysulphide photoelectrochem. solar cell 0-72073
 p-CdSAs₂, electron irradi. elec. props. annealing, lattice defects 0-100465
 CdSiP₂, electronic struct., X-ray spectroscopic investigation 0-108300
 p-CdSnAs₂, Hall effect, thermo EMF, thermomagnetic effects 0-107822
 p-CdSnAs₂, heavily doped, elec. transport props. under elastic deformation 0-96915
 CdSnAs₂, solubility in Sn melt, temp. depend., enthalpy of melting 0-59658
 CdSnAs₂-Au(Al), surface barrier junction, elec. props., temp. depend. 0-65686
 CdSnAs₂-InP, n-p heterojunction, elec. props., electroluminesc., band struct. 0-75632
 CdSnO₂ films, transparent conducting, deposited by RF sputtering from CdO-SnO₂ target 0-76179
 Cd₂SnO₄ and Cd₂SnO₄:CdO, thin film electrodes in H₂SO₄ electrolytes, reduction, AES and SEM 0-65674
 Cd-SnO₄ anode for H₂O photoelectrolysis 0-108716
 Cd₂SnO₄ heat mirror on plastic sheet for radiation insulation of visible windows 0-95985
 Cd_{1-x}Sr_xS, solid soln., phase equilb. diagrams 0-108412
 CdTa₂O₆, force fields rel. to cryst. struct. (*French*) 0-107104
 CdTe AC Faraday rotation devices for far IR laser intracavity polarisation modulation 0-58613
 p-CdTe, barrier heights of metals on etched surface 0-80378
 CdTe, charged dislocations, flow of charge with plastic deform. 0-85010
 CdTe crystal Pockels modulator, PCM of CO₂ TEA laser pulse 0-102742
 CdTe, crystal size depend. of photopotential effect 0-92592
 CdTe crystals, exciton luminescence spectra rel. to shallow impurity conc. 0-97335
 CdTe, diffusion and solubility of Ge, 630-800°C, prep. conditions depend. 0-103519
 CdTe, elec. and photoelec. props. due to double injection, quenching spectra 0-70765
 CdTe electrode, redox reaction due to complex $\text{M}(\text{CN})_6^{3-/4-}$ (*French*) 0-89482
 CdTe, electron mean free path, 350-1450 eV 0-103707
 CdTe, energy bands and optical props. calc., tight-binding model with spin-orbit interaction 0-65448
 CdTe, exciton magnetoreflectance spectra, multicomponent polaritons, Zeeman splitting 0-88974
 CdTe film, exciton spectra, press. and temp. depend. 0-80886
 CdTe film, photogenerated carrier transport props. 0-88590
 CdTe films, oriented, epitaxial growth by epitaxial nucleation in submicroscopic holes method 0-59834
 CdTe, growth of epitaxial layers, activation by UV and IR radiation 0-71598
 CdTe, lattice dynamics and phonon parameters bond bending force model 0-59595
 n-CdTe layers, growth and characterisation, heterojunctions and Schottky barriers fabrication (*German*) 0-89151
 CdTe linear electro-optic translation of IR laser wavelengths 0-78878
 CdTe, low temp. thermal cond., growth parameter influence 0-92725
 CdTe matrix γ -camera, biomedical appl. 0-76827
 CdTe metal-semiconductor-metal γ -ray detector characts. 0-57451
 CdTe, minority carrier diffusion length from photocurrent meas. in semicond.-electrolyte boundary 0-65584
 p-CdTe, nondoped, heat treatment in vacuum, disloc. obs. effects on struct. and props. (*Japanese*) 0-60662
 p-CdTe, photocond., photoluminesc., spectral studies 0-88593
 CdTe, positron annihilation study 0-60713
 CdTe, recombination radiation due to high-density excitons 0-93392
 n-CdTe, semiconductor electrode, electrochem. behaviour in nonaqueous media (*French*) 0-66808
 CdTe single cryst., linear electro-optical props., temp. depend. 0-71376

cadmium compounds continued

- CdTe surface, sputter cleaning and dry oxidation, XPS and LEED study 0-108618
 CdTe thin film polycrystalline solar cells prepared by electrodeposition 0-93948
 CdTe thin films, oriented, VPE growth, infrared transmission, photovoltaic cells 0-59825
 CdTe, vacuum deposited film, orientation axis tilt rel. to vapour angle of incidence 0-88456
 CdTe, vapour-phase-grown, cathodoluminesc. study 0-76086
 CdTe:As(P), ion implanted, elec. props. 0-65021
 CdTe:Cl, semi-insulating, impurity photocond. spectra, local state distrib. in band gap 0-107865
 CdTe:Co, impurity luminescence no phonon line depend. on temp., Debye temp. 0-66273
 CdTe:Cu films, impurity behaviour, Hall mobility and hole density meas. 0-80420
 CdTe:Fe, Mn, Cr, introduction of elec. active defects 0-103647
 CdTe:Fe²⁺, reson. relax. time for impurity electrons and localised phonons interaction, appl. to thermal cond. 0-59590
 CdTe:In precipitation and out-diffusion of solute during cooling 0-100840
 CdTe:Li(Cl), acceptor states study by donor acceptor pair excitation luminesc. 0-100683
 CdTe:Mn, spin-lattice coeffs. of Mn²⁺ 0-84646
 CdTe:Mn²⁺, exciton refl. spectra and mag. susceptibility 0-66253
 CdTe:Mn²⁺, luminesc. and magnetooptic reson., mag. field effect 0-93390
 CdTe:Si(Cl), force variation due to charged defects 0-92634
 CdTe/Hg_{1-x}Cd_xTe multilayers, LPE growth 0-80104
 CdTe/SnCl₂/Pt, solar cell photoelectric props. (*Spanish*) 0-85290
 CdTe-Au contacts, electronic states, vacuum UV photoelectron spectra 0-70827
 CdTe-Au(In) contacts, photo-effect in the 77-300K range, barrier height estimation 0-107850
 CdTe-CdS heterojunctions, growth by closed-tube chem. transport, elec. props. 0-60070
 CdTe-CdS heterojunction, photocapacitance and photocond. 0-96978
 CdTe-CdS thin film p-n solar cells, spectral response temp. depend. 0-93871
 CdTe-HgTe superlattice on CdTe layers, evanescent states, tight binding calcs. 0-70611
 CdTe-In system, equilb. phase diagram and liq. phase epitaxial growth of CdTe from In soln. (*Japanese*) 0-71634
 CdTe-InAs quasi-binary system, temp.-comp. diagram, physicochem. and thermodynamic analysis 0-104127
 p-CdTe-Langmuir film interface, prep., characters. and MIS struct. 0-92998
 CdTe_{1-x}Se_x, multiband model of impurity complexes 0-65497
 CdTh(MoO₄)₃, X-ray cryst. struct. determ. (*French*) 0-64959
 CdTi₂Se₂:Au, solubility meas. by microhardness method 0-96650
 CdTi₂Se₂(Te₂):Au, elec. cond., density, dielectric const., changes on fusion 0-88553
 CdTi₂Te₂, single and polycryst. samples, linear expansion, heat capacity and thermodynamic props. 0-103489
 Cd(WO₄)₁₋₄(MoO₄)_x, growth and props. 0-71588
 CdZnS thin films, growth and evaluation for fabrication of high performance photovoltaic solar cells 0-93501
 Cd_{1-x}Zn_xS films, thermal evaporation prep., phys. props. 0-84410
 Cd_{1-x}Zn_xS heteroepitaxial single-cryst. layers, photoluminesc. props. 0-100692
 Cd_{1-x}Zn_xS solar cell thin films, microprobe characterisation (*French*) 0-61349
 Cd₂Zn_{1-x}S films, chem. sprayed, carrier density and mobility 0-60121
 CsCdBr₃, diamag. linear chain lattices, cryst. struct. 0-70172
 CuGa_{0.1}In_{0.9}Se₂/Zn_{0.29}Cd_{0.71}S heterojunction solar cell, preparation and props. 0-101110
 Cu₂S-CdS heterojunction solar cells, carrier transport, nonmonotonic band profiles 0-61361
 Cu₂S-CdS heterojunction interface, depth distribution profiles, Auger spectra 0-88622
 Cu₂S-CdS heterojunctions, role of deep levels in controlling photovoltaic props. 0-92941
 Cu₂S-CdS solar cell fabrication by magnetron reactive sputtering deposition 0-61363
 Cu₂S-CdS solar cells, Cu₂S film growth methods 0-80980
 Cu₂S-CdS solar cells, interface recombination phenomena and tunnel effect 0-66978
 Cu₂S-CdS solar cells, optical absorption coefficient changes in Cu₂S 0-93980
 Cu₂S-CdS solar cells, optimised grid patterns 0-108798
 Cu₂S-CdS solar cells with interdigitated grid, current-voltage analysis 0-93981
 Cu₂S-CdS sprayed solar cells, chemical spray deposition 0-93979
 Cu₂S-CdS thin film planar junction devices, quantitative photon loss anal. 0-61362
 Cu₂S-Zn_{1-x}Cd_xS and Cu₂S-CdS thin film solar cells by solid state reaction, comparison 0-101109
 Cu₂S-Zn-CdS p-n heterojunction, optical energy convertor, struct. and recomb. props. 0-72065
 Cu₂S-CdS p-n heterojunction, copper sulphide growth features during formation (*Russian*) 0-107898
 Cu₂S-CdS solar cells, Cu₂S growth kinetics and composition analysis by absorbance transient and galvanic electrochemical measurements 0-92797
 Cu₂S-CdS solar cells, SCL current 0-76634
 Cu₂S-CdS thin film solar cells, using all film vacuum deposited process 0-93977
 HgCdTe, ion implantation, junction form. 0-100260
 HgCdTe photodiodes formed by double-layer LPE 0-104078
 HgCdTe reverse-biased photodiodes for wideband apps., excess noise 0-107876
 HgCdTe solid solution photodiode for CO₂ laser active medium study 0-95868
 HgCdTe-CdTe photodiode, 1.33 μm , grown by LPE, phys. props. 0-107892
 Hg_{0.4}Cd_{0.6}Te LPE layer growth from Te-, Hg-, and HgTe-rich solns., comparison 0-76199
 (Hg_{0.4}Cd_{0.4})_{1-x}Te_x, defect anal., intrinsic material parameters 0-75519
 Hg_{0.4}Cd_{0.25}Te thin film deposition on Si substrates by RF triode-sputtering, large-area photodetector arrays 0-80965

cadmium compounds continued

- Hg_{0.77}Cd_{0.23}Te nonlinear optical IR generation 0-58642
 Hg_{0.8}Cd_{0.2}Te surface, sputter cleaning and dry oxidation, XPS and LEED study 0-108618
 Hg_{0.82}Cd_{0.18}Te, electronic anomalous mass near reson. acceptor level, Shubnikov-de Haas meas. 0-80163
 Hg_{1-x}Cd_xTe breakdown-limited MIS device, increased charge capacity using ramped gate voltage 0-103751
 Hg_{1-x}Cd_xTe, degenerate four-wave mixing of 10.6 μ m radiation 0-95943
 Hg_{1-x}Cd_xTe, Einstein relation for inversion layers 0-103706
 Hg_{1-x}Cd_xTe, epitaxial layers, elec. properties in the range 4.2 to 300K (French) 0-65721
 Hg_{1-x}Cd_xTe epitaxial layers, elec. props. 0-96910
 Hg_{1-x}Cd_xTe, grown from melt, Kirkendall and Frenkel effects 0-100365
 Hg_{1-x}Cd_xTe hot-electron photoconductive detection of near mm wave radiation 0-57377
 Hg_{1-x}Cd_xTe, implanted with Hg, Al, damage and lattice location study 0-103381
 Hg_{1-x}Cd_xTe, near band-gap photoluminesc., bound exciton luminesc. obs. 0-103973
 Hg_{1-x}Cd_xTe, optical absorpt., quasilocal acceptor level effects, theory 0-92853
 n-Hg_{1-x}Cd_xTe, optical phase conjugation 0-83644
 Hg_{1-x}Cd_xTe photodiodes, long cutoff wavelength, effect of trap tunnelling on IR detector performance 0-73451
 Hg_{1-x}Cd_xTe, recombination processes using impact ionization capture cross sections 0-75577
 Hg_{1-x}Cd_xTe, segregation, compositional characterisation 0-107434
 Hg_{1-x}Cd_xTe, semimetallic and semicond., Hall coeff., anomalous temp. depend., 4.2 to 70K 0-65604
 Hg_{1-x}Cd_xTe, theory of optical absorpt., contribution by quasilocal acceptor levels (Russian) 0-71451
 Hg_{1-x}Cd_xTe-In contact, diffusion of In 0-103520
 Hg_{1-x}Cd_xTe-type semimetals, kinetic props., local acceptor level effects 0-65557
 Hg_{1-x}Cd_xS binder layer photoreceptor, surface charge characts. thickness depend. 0-57409
 In₂O₃-SnO₂-CdTe:P, p-n homojunction solar cell, elec., photovoltaic props., photoluminescence 0-81463
 KCl-CdCl₂, elec. cond., role of electrode material, surface precipitation effects 0-59985
 LiNbO₃-CdSe layer structure, SAW absorpt., elec. field effects 0-65355
 Mg₂Cd_{1-x}Te, electroreflection spectra, comp. depend. 0-66230
 MgO-CdO interface, coincidence-site-lattice relations 0-103588
 Mn₂Cd_{1-x}Te single crystals, photoluminesc., composition depend. 0-80854
 Mn₂Cd_{1-x}Te, lattice vibrs., Raman and IR spectra meas. 0-93311
 Mn₂Cd_{1-x}Te, phonons, Raman scatt. and IR absorpt. meas. (French) 0-97275
 (NH₄)₂Cd₂(SO₄)₂, dielec. and spontaneous polarisation, -195 to -180°C, particle size depend. 0-97200
 Ni_{1-x}Cd_xFe₂O₄, mag. props. rel. to ionic struct. 0-75756
 xPbTiO₃ + (1-x)PbCd_{1/3}Nb_{2/3}O₃, phase transition spread, polarisation relaxation, dielectric susceptibility (Russian) 0-75922
 V-CdS-In preparation and behaviour obs. Josephson junctions 0-100559
 Zn_nCd_{1-n}S film, optimal synthesis conditions for single cryst. growth 0-100776
 Zn_nCd_{1-n}S films, spray pyrolysis, elec. props. 0-75657
 Zn_nCd_{1-n}S monocrystal petal lasers, single-photon excitation (Russian) 0-99736
 Zn_nCd_{1-n}S, thin solid soln. films, vapour deposited, elec. and optical characts. 0-60110
 Zn_nCd_{1-n}S-Cu₂S heterojunction solar cells, props., comp. meas. of interfacial region 0-81472
 Zn_nCd_{1-n}S_{1-y}Se_y, energy bandgap and lattice constant contours 0-103622
 Zn_nCd_{1-n}S_{1-y}Te_y, energy bandgap and lattice constant contours 0-103622
 p-Zn₀Cd_{0.9}Sb, thermoelec. anisotropic semicond., carrier kinetics at low temps. 0-92893
 Zn₀Cd_{0.9}Sb, thermoelectrically isotropic semicond., carrier kinetics in intrinsic cond. range 0-92894
 Zn_{1-x}Cd_xSe, mixed crystals, antireson. in phonon spectrum, Raman spectroscopy 0-88992
 Zn_nCd_{1-n}Se, exciton reflection spectra anomalies (Russian) 0-97304
 Zn_nCd_{1-n}Se_{1-y}Te_y, energy bandgap and lattice constant contours 0-103622
 ZnO/CdTe heterojunctions and ZnO films preparation using spray pyrolysis 0-96985
 ZnS-CdS:Ag(Cu), cathodoluminesc. investig., appl. to cathode ray tube screening 0-108282

caesium

see also nuclei with

- adsorbed on graphite, dissolution, lamellar cpd. form. (French) 0-100399
 adsorption and desorption on GaP and GaSb, LEED, AES, and photoemission meas. 0-70532
 adsorption by Al₂O₃, radioactive waste storage 0-99240
 adsorption on Mo covered with O₂, struct., emission props., thermal stability 0-66878
 atom, 4d¹⁰ shell, photoionisation cross sections, electron shell alterations determ. (Russian) 0-58144
 atom, 6s-electron photoionisation, ab initio calcs. 0-91523
 atom, HFS pressure effect determ. from absorption coeff. profiles 0-106299
 atom, hook spectra, evaluation limitations 0-90905
 atom, L-shell internal excitation accompanying L-capture 0-95726
 atom, n=15-17 f-g interval meas. 0-91477
 atom, orientation in CsI photodissociation by UV light (Russian) 0-69201
 atom, oscillator strength meas. by tunable laser interferometry 0-105697
 atom, radioisotopes, hyperfine spectroscopy, nucl. charge radius, ground and isomeric states 0-57677
 atom, Rydberg states, diatom, and collisional perturbations 0-58181
 atom, two photon ionisation, destructive interference effect 0-74153
 atom, two-photon ionisation, effective order nonlinearity var. 0-106304
 atomic, photoionisation cross sections determ. in vacuum UV using Xe excimer laser 0-102494
 atomic clock using laser optical pumping of Cs beam 0-101785
 atomic excited state, laser photoionisation theory, hyperfine coupling effect 0-102493

caesium continued

- atoms, 2-photon and 4-photon ionisation cross-sections, absolute determ. 0-83326
 atoms, laser beam excitation, multipass, optical pumping and weak neutral current parity violation 0-58207
 crystal struct., van der Waals and repulsive interaction 0-84137
 dense plasma, ionisation equilib. and cond., ion clusters effects 0-75032
 diffusion in Mo, W, divacancy mechanism (Russian) 0-70472
 entropy change on melting of simple substances, thermal expansion, configurational entropy 0-59630
 Fermi surface and quasiparticle props., density functional approx. 0-96771
 Fermi-surface press. dependence 0-96772
 field desorption and field ionisation on metal surface 0-104047
 getter development for radiocaesium, obs. of Cs-SiO₂-Al₂O₃ system interactions 0-83208
 heat of desorption from polycryst. W surfaces 0-75430
 heat pipe, H atom anal. appl. for plasma 0-70043
 ion source, CW monoenergetic, by photoionisation 0-63910
 ion source, thermionic emission in SF₆ mol. gas 0-71557
 low-level transuranic storage, radwaste Sr, Cs, Co sorption meas. on soil sediment 0-95482
 melting curve maximum at high press. 0-75337
 metal impurity effect on residual elec. resistance (Russian) 0-84457
 plasma, generation by adiabatic compression, elec. cond. and thermodynamic parameters meas. 0-59180
 positronium, formation in positron+alkali metal atom collisions, first Born approx. 0-83525
 positronium formation in positron+alkali metal atom collisions, pseudopot. calcs. 0-83524
 pulsed vapour source for ion sources in heavy ion accelerators 0-63423
 radioisotopes, liquid effluents, aquatic radiological impact anal., radiocaesium transport in sediment 0-95486
 sorption in Ba-impregnated nuclear graphite, thermodynamic modelling of multicomponent sorption behaviour 0-102243
 sorption in nuclear graphite, sorption kinetics modelling 0-102244
 superconductivity, elec. resist. and phase transforms. under high press. (German) 0-107763
 surface, caesiated negative ion emission (French) 0-108314
 surface, H(He) positive ions impact, backscattering, fraction reflected 0-60741
 trace identification in neutral-beam research 0-95401
 vapour, electrical cond. near saturation point 0-69967
 vapour, threshold for stimulated electronic Raman scatt. determ. using picosecond laser pulses 0-102768
 vapour source, thermionic energy converter with Cs-He gas controlled heat pipe 0-64791
 VPE on W emitter, FEM obs. 0-70552
 Ag-O-Cs surface, oxidation, role of Cs suboxides in low work function surface layers, XPS 0-76131
 Cs I, n²S_{1/2} and n²D_{3/2,5/2} states, energies 0-87066
 Cs, Knudsen arc, electron beam heating and ionisation 0-75114
 Cs, photoelectron spectra obs., comparison with mol. spectra of CsCl 0-83419
 Cs⁺, 3d⁴f⁴ config., collapse of 4f electron, X-ray spectra obs. (Russian) 0-58204
 Cs⁺ blocking of inward rectification of starfish egg cell membranes, model 0-61523
 Cs⁺ dipole and quadrupole polarisability fine struct. intervals and g-factor interval 0-91477
 Cs⁺ excited levels, hyperfine struct. and lifetimes 0-63590
 Cs²⁺, electron impact excitation studies by intersecting beam method 0-69239
 Cs/W, work function measurement in SEM 0-80918
 Cs-H₂ vapour, resonant character of laser induced formation of particles 0-89481
 Cs-O₂, desorption from W, activation energy 0-103562
 Cs-Sr(He) mixtures, photocond. at atm. press. 0-87844
 Cs-Xe solar-pumped MHD excimer laser, modelling 0-95873
 Cs+(AuF₅)_n, prod. of AuF₅⁺, ionisation cross section: energy depend. 0-81300
 Cs+(SbF₆)_n-Cs⁺+SbF₆⁻+SbF₄+(SbF₃)_{n-2}, ionisation cross section energy depend. 0-81300
 Cs+Cs, spin destruction, obs. 0-63781
 Cs+H⁺(H), single-electron capture total cross sections 0-91656
 Cs+H(ls), differential electron attachment and elastic scatt., 30-528 eV 0-63745
 Cs+He, interaction pot. and oscill. strength 0-91645
 Cs+inert gas, three body interaction, fluoresc. spectra principal series lines and secondary satellites 0-83313
 Cs+methyl cyanide, collisional ionisation obs. 0-95716
 Cs+O₂, collisional ionisation, energy spectra of forward and backward directed positive and negative ions 0-87200
 Cs+O₂, mol. target internal motion 0-78697
 Cs+Ti, Ti 6²P_{3/2}-state relax., NMR obs. 0-95653
 Cs+UF₆, ionisation reactions, absolute cross sections 0-99565
 Cs⁺+benzyl chloride, beam reactions for 5.8 eV collision energy, mechanism 0-66777
 Cs⁺+Dy charge exchange, isotope separation of laser excited Dy atoms 0-83512
 Cs₂, 4800 Å absorpt. band, classical method anal. 0-106330
 Cs₂, dimer and higher polymer IR absorpt. bands, triplet state 0-63629
 Cs₂, laser-induced fluoresc. spectrum, diffuse band anal. 0-106346
 Cs₂²⁺, interaction potential determ., comparison between all-electron frozen core and pseudo-potential results 0-69054
 Cs₂²⁺, low-lying states, MC SCF+CI 0-69053
 Cs₂+halogens(SnCl₄)(MoF₄)(UF₆), ionisation reactions, absolute cross sections 0-99565
 Cs(Ar-Cs) plasmas, electron momentum transfer cross section, cyclotron reson., temp. cond., and vel. meas. 0-106930
 Cs₂S₂O₆, piezoelectric, crystal struct. studied by X-ray diff. 0-100208
¹³³Cs, first excited D-level, hyperfine struct. meas. by cascade, fluoresc. spectrosc. 0-69101
¹³³Cs, freq. standard, optimum conditions for population inversion for 0-0 transition 0-78824
¹³⁴Cs and ¹³⁷Cs at Atlantic nuclear waste disposal site, radionuclide redistribution. 0-85309
¹³⁴Cs/¹³⁷Cs activity ratio for LWR fuel burn-up determ. (Russian) 0-68804
¹³⁷Cs, distrib. and behaviour in Urazoko Bay sediment 0-97825

caesium continued

- ¹³⁷Cs geologic insertions, expt. derived algorithm for computer calc. dose rates 0-101264
¹³⁷Cs, in molten alkali nitrates, diffusion coeffs. meas. 0-70437
¹³⁷Cs, intake by Bikini Island residents, model using bioassay data 0-109043
¹³⁷Cs sources, parametric definition 0-91346
¹³⁷Cs/¹³⁴Cs radioisotopes in seawater, Cs-selective resin determ. 0-94137
¹³⁷Cs-irradiation, response of pig skin, various schedules of irradiation 0-72237
GaP-Cs-O simultaneous adsorption, oxidation interface chemical study 0-103584
H⁰+Cs collisions, H⁻ production cross sections 0-78698
KCl:Cs⁺, low-temp. heat capacity enhancement due to impurities 0-107442
Sr-Cs mixture, laser induced collisional two-photon ionisation, fluorescence monitoring 0-91515
Tl-Cs vapour mixture, CO₂ CW laser radiation freq. conversion 0-74438
(U,Pu)O₂ fuel pins 0-102250

caesium alloys

- Cs-Au, liq., molar vol. meas. 0-59546
Cs-Au liq. alloy, formation of localised electronic states, NMR obs. 0-93201
Cs-K, thermal conductivity determ. 0-107760
CsAu, molten, equimolar, structural evidence of ionic nature 0-64882
K-Cs, extreme UV absorpt. spectra 0-97294
Na-Cs, internal energy, heat of mixing, entropy, dielectric function 0-88340
Na-Cs, liq., struct. factor, free energy of mixing, and electrochem. pot., thermodynamic calc. 0-96436

caesium clocks see atomic clocks

caesium compounds

see also caesium alloys

- halides, F-centre energy levels, ion-size effects, calc. 0-96519
halides, Gruneisen and Anderson-Gruneisen parameter determ. 0-59611
halides, luminesc. of interstitial atomic H 0-103986
halides, press. depend. of effective ionic charge 0-96462
perfluoro-octanoate/D₂O system, ²H NMR quantum orders, RF pulses 0-103892
salts, Raman and IR spectra of the dicyanoiodate (I) ion 0-60572
CaAl₂O₇, melilite struct., prep. and props. 0-93524
Cs-SiO₂-Al₂O₃ system interactions, getter development for radio-caesium 0-83208
(Cs-O)-Ag photocathode, operation mechanism involving Cs₂O₂ 0-66384
CsAlF₆, dissociation enthalpies, mass spectrometric determ., heat of form. 0-97720
CsAlF₆, single cryst., prep. and struct. (French) 0-79762
Cs₂Au₂Cl₆, electronic state of Au at high press., Mossbauer spectra 0-60467
CsBF₄, ionic radii and chem. shifts, correl. with electronegativity 0-66054
CsBO₂, vapour over heated solid, XPS, obs. 0-87171
CsBr, (110) surface, electronic struct. of valence bands calc. (Russian) 0-75621
CsBr, F-centre absorpt., uniaxial stress effects 0-60634
CsBr, gamma and additively coloured, dissolving in pure water, lyoluminesc. mechanism 0-100693
CsBr:Cu⁺, excitation and absorpt. spectra 0-108255
CsBr:Cu⁺, γ-irradiated, thermolum. emission 0-104001
CsBr:CN, Raman and IR vibr. spectra, struct. 0-102513
CsCN, inelastic neutron scatt. by coupled rotational and translational modes 0-70333
CsCaCl₃:Co(Mn), EPR, 4.2 to 450K, ferroelec. transition 0-60414
CsCdBr₃, diamag. linear chain lattices, cryst. struct. 0-70172
CsCdBr₃:Cr³⁺(Cr³⁺), EPR of impurities, charge compensation, X-ray effects 0-60407
Cs₂CdBr₄, struct. phase transitions, NQR study 0-71343
CsCl, (110) surface, electronic struct. of valence bands calc. (Russian) 0-75621
CsCl, activation coefficients and solvation numbers in mixed methanol solvents 0-81334
CsCl aqueous solutions, IR absorpt. ν₁ (CN) band parameter temp., conc. study (Russian) 0-80801
CsCl, gamma and additively coloured, dissolving in pure water, lyoluminesc. mechanism 0-100693
CsCl, luminesc. in vac. UV range above and below phase transition temp. 0-93399
CsCl, Madelung pot. determ. by Ewald method 0-92475
CsCl, photoelectron spectra obs., comparison with atomic spectra of Cs 0-83419
CsCl, photofragment spectra, bond energies and excited state symmetries 0-87190
CsCl, positron-trapping colour centre dynamics, positron annihilation study 0-108294
CsCl structure, evaluation of finite strain eqns. of state using lattice models 0-96620
CsCl:Cu⁺, γ-irradiated, thermolum. emission 0-104001
CsCl-type lattice, (111) superlattice screw dislocation motion, computer simulation 0-79793
CsCl-ZnCl₂, molten, US velocity, thermodynamic quantities and struct. (Japanese) 0-88270
CsCl-ZnCl₂, molten, US absorption coeffs. and bulk viscosity coeffs. (Japanese) 0-88271
CsCl:CN, Raman and IR vibr. spectra, struct. 0-102513
CsClO₄, AC elec. cond. temp. and freq. depend., obs. and unified defect struct. model 0-88554
CsClO₄, electrical conductivity, frequency dependence 0-65288
CsCoBr₃, ID Ising antiferromagnet, spin dependent Raman scattering from phonons and electronic excitations 0-103948
CsCoBr₃, quasi ID Ising antiferromag., polarised Raman scatt. from mag. excitations 0-66182
CsCoCl₃, spin dynamics, neutron scatt. study 0-80493
CsCrCl₃, α-β phase transition, dynamical aspects and thermodynamic theory 0-70404
CsCrCl₃, Jahn-Teller induced phase transitions 0-70391
CsCr₂, neutron diff. expts. at 300, 77 and 1.2K 0-107163
Cs₂CrO₄, mol. beam obs. of evap., saturated vapour press., 656.8 to 1151K 0-107411
CsCuCl₃, helical mag. struct., neutron diffraction study 0-107983
CsCuCl₃, Jahn-Teller induced phase transitions 0-70391

caesium compounds continued

- CsCuCl₃, phase transition, refr. index, electrooptic coeff., pyroelec. signal, and NQR meas. 0-70386
CsCuCl₃, phase transition obs., commensurate and incommensurate structural phase transitions in Jahn-Teller system 0-70403
CsCuCl₂·2H₂O, hyperfine and super-exchange interactions 0-103654
Cs₂AsO₄ crystals, SHG, temperature phase-matching curve hysteresis 0-81852
Cs₂PO₄, pseudo one-dimens. ferroelec. ordering dynamics, ³¹P NMR study 0-75971
Cs₂PO₄, pseudo-one-dimensional ferroelectric transition, ³¹P chemical shift and relaxation study 0-66123
Cs₂PO₄, pseudo-one-dimens. ferroelec. transition, DMR and relax. study 0-71223
Cs₂PO₄, pseudo-one-dimensional ferroelec. and antiferroelec. transitions, phase diagram obs., soft modes 0-93245
CsDy₂F₆ and Cs₃DyF₆, cryst. symm. and cell parameters (French) 0-81040
CsF scintillator, pot. advantages for a time-of-flight positron camera 0-81706
CsF:Li(Na), F-centres, saddle-point configuration, molecular model parameter 0-107234
CsF:AlF₃, ion-molecule equilibria studied by mass spectrometric method, heats of dissociation and form. calc. 0-104479
CsFeCl₃, pseudo-one-dimens. singlet ground state ferromag., mag. excitations, neutron scatt. study 0-97064
CsFeCl₃·2H₂O, rectangular Ising cpd., Mossbauer meas. 0-71252
Cs₂FeF₆, mag. struct. and one-dimens. antiferromagnetism 0-60209
CsGa_{1-x}Fe_xS₂, tetrahedrally coordinated Fe atoms in low spin state, mag. props. and neutron diff. study (German) 0-88714
CsH, structural transition from NaCl to CsCl type under high press. 0-96458
CsH₂AsO₄ crystals, dielectric radiation effects, γ-radiation 0-93234
CsH₂AsO₄, ferroelec., dielec. props., four-cluster approx. 0-97202
Cs(H₂-D₂)PO₄, dielec. props., temp. meas. 0-71335
CsH₂PO₄, ferroelec. transition, electrooptic 0-76005
CsH₂PO₄, ferroelec., X-ray struct. study at room temp. 0-88113
CsH₂PO₄, ferroelec. transition, neutron diff. study 0-93247
CsH₂PO₄, pseudo one-dimens. ferroelec. ordering dynamics, ³¹P NMR study 0-75971
CsHf(MoO₄), X-ray cryst. struct. determ. 0-107182
CsHg(CN)₃, CN and HgC stretching vibrations and HgCN bending vibration assignments 0-69140
CsI, (110) surface, electronic struct. of valence bands calc. (Russian) 0-75621
CsI crystals, relation of struct. and bond type to slip geometry 0-88165
CsI photocathodes, efficiency evaluation for soft X-ray diagnostics 0-57442
CsI, photodissoc., UV, Cs atom orientation (Russian) 0-69201
CsI, ultralow loss optical fibre material, loss mechanism 0-78920
CsI:Na, X-ray irradiated, optical and ESR studies in IR absorption band 0-80828
CsI:Na⁺(K⁺), luminesc. processes 0-103989
CsI:TI, precipitation of TI solid solns. 0-70419
CsI:TI(Na), light yield under charged-particle bombardment 0-93409
CsI:CN, Raman and IR vibr. spectra, struct. 0-102513
CsInCl₃, mixed-valence cpd., structural phase transition (German) 0-70406
CsLi_{0.5}(Al,Fe)_{0.5}F₆ pyrochlore, Mossbauer contrib. to exam. of cationic order (French) 0-93224
CsLi_{0.5}Fe_{0.5}F₆ pyrochlore, Mossbauer contrib. to exam. of cationic order (French) 0-93224
CsLiSO₄, crystal structures of I and III phases, twins 0-70181
CsMHoF₆, (M=Na, K, Rb), mag. behaviour (German) 0-65774
Cs₂MX₆ (M=Se, Te, X=Cl, Br), Γ₄ (³T_{1g}) state, Jahn-Teller effect, luminesc. obs. 0-60650
CsMgBr₃:Cr³⁺(Cr³⁺), EPR of impurities, charge compensation, X-ray effects 0-60407
CsMgBr₃(I₃), diamag. linear chain lattices, cryst. struct. 0-70172
CsMgCl₃:Cr³⁺(Cr³⁺), EPR of impurities, charge compensation, X-ray effects 0-60407
CsMnBr₃, EPR linewidth anisotropies 0-103878
CsMnCl₃, antiferromagnetic resonance, parametric spin wave excitation (Russian) 0-93183
CsMnCl₃·2H₂O, antiferromag. insulator, self-trapping of excitons 0-70619
CsMnCl₃·2H₂O, diagonal elastic const., thermal expansion coeffs., ultrasonic velocity meas. 0-79853
CsMnCl₃·2H₂O, mag. phase diagram near bicritical point 0-71021
CsMnCl₃·2H₂O, quasi one-dimensional mag. systems, impurity effects 0-71015
CsMnCl₃·2H₂O, subthreshold two-magnon absorpt., depend. on freq., temp. and mag. field, exchange coupling const. (Russian) 0-71184
CsMnCl₃·2H₂O, thermal cond. in mag. field 0-70481
CsMn_{1-x}Co_xCl₃·2H₂O, random mag. mixture, oblique-antiferromag. phase obs. 0-93142
CsMn_{1-x}Co_xCl₃·2H₂O, random mag. mixture, mag. torque and sp. ht. expts. 0-60323
CsMn_{1-x}Cu_xCl₃·2H₂O, impurities in quasi-one-dimens. Heisenberg systems, anisotropy effect 0-80502
CsMnF₃, antiferromag., variation of spin wave spectrum in interaction between magnons 0-65841
CsMnF₃, exciton migration, excitation and luminesc. study (Russian) 0-66264
CsMnF₃, exciton-magnon interactions in optical transition, absorpt. and emission spectra meas. 0-70981
CsMnF₃, mag. struct., phase transition, and magnon spectrum, random anisotropy effects 0-88722
CsMnF₃, parametric excitation of magnons, effect of RF modulation of mag. field 0-65842
CsMnF₃, parametric nuclear magnon excitation, mag. field modulation (Russian) 0-107999
CsMnF₄, planar ferromag., cryst. and mag. struct., Jahn-Teller effect 0-75715
Cs₂MoO₄F₃, ferroelec., transition obs. 0-75989
Cs₂NaErCl₆, mag. susceptibility and IR and Raman spectra meas., crystal field splitting determ. 0-100652
Cs₂NaM³⁺Cl₆ (M³⁺=Bi, Nd, Pr), ferroelastic phase transitions, thermal expansion, elasticity, and X-ray anal. 0-70393
Cs₂NaYCl₆:Bi³⁺, luminescence props., emission and excitation spectra 0-108262

caesium compounds continued

- α -CsNd(PO₃)₄, single cryst. struct. and spectral-luminescent props. 0-96490
 CsNiCl₃, noncollinear magnetic order and spin wave spectrum in presence of competing exchange interactions 0-65834
 CsNiF₃, 1D ferromag., optical absorption and spin dynamics 0-71417
 CsNiF₃, anisotropic Heisenberg chain, nonlinear excitations 0-70927
 CsNiF₃, longit. paramag. susceptibility, reaction field approx. 0-97059
 CsNiF₃, low frequency dynamics in external mag. field 0-108020
 CsNiF₃, nonlinear excitations, 1D-ferromag., neutron scatt. 0-70949
 CsNiF₃, one dimensional planar model with symm. breaking fields, thermodynamics, static props. 0-97111
 CsNiF₃, one-dimens. magnet, local magnon modes 0-65829
 CsNiF₃, quasi one dimensional planar ferromag., low temp. NMR study in mag. field 0-97157
 CsNiF₃, quasi-one-dimensional ferromagnet, subthreshold parallel pumping of magnons 0-75745
 CsNiF₃, quasielastic neutron scatt. around Neel-point 0-75768
 CsNiF₃, stochastic motion of Sine-Gordon-solitons, spin-correlation function 0-93105
 CsNiF₃, subthreshold parallel pumping of magnons and antiferromag. reson. 0-71185
 CsNiFeF₆ pyrochlore, Mossbauer contrib. to exam. of cationic order (*French*) 0-93224
 Cs₂NpCl₆, Mossbauer spectra and mag. susceptibility meas. 0-108140
 Cs₂O-P₂O₅, glass ESR of VO²⁺ ions 0-100610
 CsPbCl₃, electronic struct. and optical props. in fundamental absorpt. region 0-93367
 CsPbCl₃, nucl. smearing functions, multipole analysis 0-88097
 Cs₂PbCu(NO₂)₆, incommensurate Jahn-Teller transition, Huang scatt. 0-70401
 Cs₂PbCu(NO₂)₆, low-temp. γ -modification, struct., powder neutron diffr. study, 160K 0-84151
 CsR(MoO₄) R=Dy, Ho, Er, permittivity temp. depend., polymorphic transition 0-92670
 Cs₂RbMoO₄F₃, ferroelec., transition obs. 0-75989
 Cs₂RbWO₄F₃, ferroelec., transition obs. 0-75989
 CsReO₄, IR matrix-isolation spectra 0-87108
 Cs₂SO₄.Al₂(SO₄)₃.24H₂O, ⁵³Cr³⁺ ENDOR Lines, RF ENDOR power and modulation freq. effects 0-75884
 Cs₂Sb vacuum deposited photoemitter, XPS study 0-89122
 CsSbF₆, high press. phase relations, vibr. spectra, and cryst. chemistry 0-108200
 CsSbO₃, solid state synthesis (*French*) 0-104438
 CsSbO₃.1/6CsF, dielec. spectroscopy study, 100 Hz to 10 MHz, 238 to 417K (*German*) 0-108144
 Cs₂SiF₆.Mn²⁺, IR absorpt. band, electron-vibr. effect 0-108238
 CsSn₂, surface props., Auger study, elec. cond. meas., photochem. study 0-66339
 Cs₂Te₃, synthesis and cryst. struct. 0-88115
 Cs₂TiF₆.Mn²⁺, spin-orbit and field splitting, Jahn-Teller effect, Zeeman meas. 0-80234
 CsTi₂NbO₇, layer struct., X-ray and electron diffr. study 0-79753
 Cs_{1-x}(Ti_{1-x}Nb_{1+x})O₅, layer compound, cryst. struct., nonstoichiometry 0-64972
 CsTi(SeO₄)₂, Cs₂Tl(SeO₄)₃, and Cs₂Tl(SeO₄)₄, cryst. struct. (*French*) 0-84148
 Cs₂UO₂Cl₄ melts and mixtures, thermogravimetric determ. of uranyl cation state 0-101050
 Cs₂WO₄F₃, ferroelec., transition obs. 0-75989
 Cs₂ZnCl₂.Cu²⁺, electron spin echo envelope, Fourier transform ¹³³Cs modulation 0-58291
 Cs₂ZrBr₆.PtBr₆²⁻.PtBr₆²⁻ doped, mixed valence, absorpt. spectra, vibronic struct. 0-97308
 Cs₂ZrBr₆.Os⁴⁺, intraconfig. absorpt. and MCD spectra 0-80776
 Cs₂ZrCl₆.Os⁴⁺, intraconfig. absorpt. and MCD spectra 0-80776
 Cs₂[FeCl₂(H₂O)]₂, X-ray cryst. struct. determ. 0-107129
 Cs₂[U(GeW₁₁O₃₉)₂].13-14H₂O, X-ray cryst. struct. determ. (*French*) 0-107136
 (Cu,Zn)Cs₂(SO₄)₂.6(H₂D)₂O Tutton salt, proton spin-lattice relax. time, proton conc. depend. and spin diffusion rule 0-71221
 DyF₃-CsF, phase diagrams and ternary fluorides (*French*) 0-81040
 Na₂O-Cs₂O-SiO₂, glasses, thermal diffusivity, heat capacity and thermal cond., laser flash method study 0-65310
 SeCl₃-NaCl-CsCl ternary system, cpd. form., thermographic investig. (*Russian*) 0-66490
 V₂O₅-P₂O₅-Cs₂O glasses, enhanced secondary electron emission yield 0-93441

caesium generators *see plasma diodes***caesium plasma diodes** *see plasma diodes***calcium***see also nuclei with*

- 657.3 nm line saturated absorption spectroscopy, photon-recoil component resolution 0-86457
 atmosphere aerosols over tropica N.Atlantic Ocean, water-soluble K, Ca and Mg contents 0-72598
 atom, 4p² ¹S₀-4s4p ¹P₁-4s² ¹S₀ cascade rate, two photon coincidence meas. technique 0-95576
 atom, 4s4p ¹P₁ level Hanle effect density depend., lifetime 0-91494
 atom, in shock heated Ar, absorpt. line broadening obs. (*Japanese*) 0-83464
 atom, laser excited, ionisation studies 0-83330
 atom, stable and radioisotopes, hfs, isotope shifts, dye laser saturation spectroscopy, beam expt. 0-58169
 atoms, excitation series, potential barrier effects, single configuration HFC 0-78558
 atoms, fluoresc. excitation profile, laser saturation broadening in flames obs. 0-95568
 atoms, forbidden transitions, radiative lifetimes, MCSCF and CI calcs., time of flight spectra for metastable state 0-91498
 atoms, quantum defect param., ab initio calcs. 0-78525
 F-type supergiants in Magellanic Clouds, Ca abundances 0-98655
 faecal samples, Ca determ. method using instrumental fast neutron activation anal. 0-104733
 forced-flow chromatography, detection by photometric method 0-71965
 ion implantation in Al, defect structures obs. 0-59494
 isotopic anal. using double vaporizer 0-106398
 molecule, vibr.-rot. states, high accuracy wave functions and energies 0-74159
 ocean chemistry of N Pacific 0-90100

calcium continued

- photoelectric cross sections at 52.4, 60, 72.2 and 84.4 keV 0-69187
 photoelectrode for recording intracerebral cellular Ca²⁺ transients 0-67307
 solar quiescent prominence spectra, meas. of Ca⁺ 8542 and 8498 Å 0-90373
 spallogenic isotopes in Fe meteorites, radial distrib. 0-67488
 stars of solar neighbourhood, chromospheric Ca II H and K emission survey 0-109423
 vertebrate retinas, outer segment layer, light-induced Ca fluxes 0-94207
 Ca I, Ca II lines in solar spectra, non-mag. polarisation, centre-to-limb var. 0-67678
 Ca II, laser stimulation optimisation for intracranial spectroscopy 0-77881
 Ca II H and K-line, and abundance in globular star cluster giant stars 0-72940
 Ca II H and K-lines in binary star giants, emission intensity 0-82420
 Ca II H-K solar lines, non-mag. polarisation 0-63569
 Ca II IR triplet lines in sunspot umbrae 0-85918
 Ca II K-line in α Cygni, core asymmetry 0-85981
 Ca II K-line in quiescent solar prominence, influence of spatial resolution on line width and shift 0-77364
 Ca II lines in solar chromosphere, vel. and temp. disturbances, weighting functions 0-67679
 Ca II solar chromosphere lines, mech. flux determ. 0-67680
 Ca II solar K-line, centre-to-limb obs. of K₂ component (*French*) 0-82331
 Ca²⁺, passive and active fluxes across membranes, review 0-97886
 Ca+Ca(Mg)(inert gas), metastable ³P-state, quenching reactions, fluoresc. meas. 0-102477
 Ca+inert gas, ¹P₁-³P₁ excitation transfer 0-102559
 Ca+O₂ reaction, chemiluminesc. absolute cross sections, photon yields and CaO dissociation energy 0-97697
 Ca+Xe, collision-induced dipole transition due to long range interaction, absorpt. obs. 0-63779
 Ca₂, Λ ² Σ ⁺- Σ Σ ⁺ system, laser induced fluoresc., pot. energy curve and mol. consts. 0-58307
 Ca₂, ground state, multiple scatt. X α calcs. 0-58149
⁴³Ca, atomic beam and resonance spectroscopy 0-58180
⁴⁵Ca and ³²P determination in biological samples by Cherenkov and liq. scintillation counting 0-98183
 Ca*+HCl, reaction performed under high resolution, luminescence obs. 0-95662
 Cu II K-line in solar plage, peak separation due to microturbulence 0-109407
 KCl:Ca, Z₂ and Z₂⁺ centres, excited state, magneto-optical spectra 0-108233
 KCl:Ca²⁺, Z₂-centre thermolum. 0-80879
 NaCl:Ca crystals, surface recrystn., moisture effect 0-84950
 NaCl:Ca²⁺, dipole concs. determ. considering aggregation, expt. and theoretical comparison 0-59512
 NaI:Ca²⁺, ionic thermocurrents meas. 0-80677
 NaI:Ca²⁺, lattice defects, entropy and enthalpy of formation and migration 0-96687
 RbCl:Ca²⁺, thermolum. and optical absorption studies 0-104002
 YIG:Ca, oxidising effects of high temp. annealing in reducing atmosphere 0-66696

calcium alloys*see also calcium compounds*

- Al-Ca-Zn (5.5 wt.%) superplastic sheet alloy, mechanical properties, superplastic forming behaviour 0-60920
 CaCu₂, γ -phase in Ca-Cu system, calorimetric determ. of enthalpy of form. (*French*) 0-84915
 Ca_{0.6}Mn_{0.3}, glass transition temp., comp. depend. 0-79702
 CaNi₂, Hawke compounds, low temp. heat capacity, Debye temp. 0-96663
 CaSn₃, powdered, de Haas-van Alphen effect 0-59857
 CaZn₃, struct. with mixed BaLi₂ and CeCu₂-like ordering 0-107106
 Co-Ca, liq. alloy form. kinetics (*French*) 0-96652
 Gd_{1-x}Ca_xAl₂, mag. props. and phase relations 0-107991
 Ni-based superalloys, hot workability, effect of S, Ca, Mg, Y and Zr minor elements 0-66552
 Pr_{1-x}Ca_xAl₂, mag. props. and phase relations 0-107991

calcium compounds*see also calcium alloys*

- apatite crystal growth in skeletal tissues 0-94181
 behenate monomolecular layers between Al electrodes, nonlinear dielec. props. 0-80405
 bis-solycylato-diaquo calcium (II), cryst. struct. 0-100222
 Ca₃(PO₄)₂ film form. on silicate glass surface bonding to bone 0-85212
 calcite, luminescence spectral anal. of polycyclic aromatic hydrocarbon impurities 0-71483
 CaO-SiO₂-CO₂, subsolidus and liquidus phase relationships to 30 kbar 0-85643
 chalk filled unsaturated polyester resin, props. (*German*) 0-104228
 composite glasses, high strength, prod. by overlayering 0-89193
 dolomite, powders sintering, decarbonisation cycle effect 0-104102
 fluorapatites, carbonated, B-type, EPR of F[•]-centre after X-irrad. (*French*) 0-108065
 fluorite crystal gas-liquid inclusion meas. with microscope heating stage 0-76967
 gypsum, crystallisation 0-100766
 hydroxyapatites, dipolar reorientations, TSC study 0-60491
 hydroxylapatite, dense, fatigue and fracture strength from diametral tests, after various treatments 0-60953
 magnesite-dolomite refractories, tar bound, fracture and wear 0-104287
 oxalate hydrates, crystn. kinetics, comparison for mono-, di-, and trihydrates 0-81528
 perovskite compound combination, Mossbauer spectroscopy study (*Russian*) 0-80666
 polymer concretes, hydrothermally stable, hydraulic cement-type fillers 0-85144
 rustumite, crystal structure, X-ray anal. 0-79766
 rustumite, crystal structure determ. by X-ray diffr. method 0-70182
 tris-sarcosine calcium chloride:Mn²⁺ ferroelec. dynamics, EPR and ENDOR study 0-75972
 tris-sarcosine calcium chloride, phase transition, hydrostatic press. effect, dielec. const. meas. 0-71327
 trissarcosine calcium chloride, ferroelec. transition, press. effect 0-84681
 Al₂O₃:CaTiO₃, sintering temperature effect of titanate additions 0-60808

calcium compounds continued

- BaFe₂O₉-CaO, Ca²⁺ additives effect on hexaferrite lattice and mag. props. 0-60243
 Ba(PO₃)₂-AlF₃-CaF₂, glass, elec. cond. and IR spectra 0-89005
 BaSr_{1-x}Ca_xFe₂O₈, substituted hexagonal ferrites, mag. split Mossbauer spectra obs. and X-ray struct. data 0-71250
 BeF₂-KF-CaF₂-AlF₃-EuF₃ fluoroberyllate glass, Eu³⁺ fluoresc. linewidth 0-66285
 (Ca,Sr)₂(PO₄)₃Cl, partially substituted chlorapatite, cryst. struct. from X-ray data 0-96478
 Ca dichlorophosphate complexes, cryst. struct. ³⁵Cl NQR obs. 0-108108
 Ca ferrite, composition and mag. props., anisotropy field, magnetisation 0-71109
 Ca-Mg-Ni hydrides, water form. on O₂ exposure 0-97727
 Ca-Mg-Ni-B, hydriding behaviour 0-71942
 Ca-Mn-S-Se system, multicomponent solubilities 0-108416
 Ca₂Mn(PO₄)₂, hydrothermal synthesis and cryst. growth 0-60762
 Ca₂(Al,Fe,Cr)O₅ solid soln., planar interfaces, TEM obs. 0-65008
 CaAl₂O₄, high pressure modifications 0-104149
 Ca₂Al₂O₃, polar materials, appl. to SAW and other devices 0-66114
 CaBr₂, adsorption of NH₃ and ND₃, complex formation, IR and for IR spectra obs. 0-80063
 CaCO₃ accumulation, Ontong-Java Plateau box cores, radiometric investigation, 0-61793
 CaCO₃, calcite, Nd laser second harmonic stimulated Raman scatt., comparison with nitrates 0-95949
 CaCO₃, calcite, single-crystal, wave front reconstruction of light in stimulated Raman scatt. 0-93323
 CaCO₃, calcite linear polarizer, role in laser technology 0-64165
 CaCO₃, crystallisation from aqueous solutions, kinetic study 0-59419
 CaCO₃ decarbonation for solar energy thermochemical conversion 0-94097
 CaCO₃, luminesc. under N₂ laser excitation, and appl. to archaeological dating 0-60685
 CaCO₃ single crystals, positron annihilation, two photon angular correlation 0-108295
 CaCO₃:Fe²⁺, Mossbauer spectra 0-108138
 CaCO₃:Li, synthetic calcite, (CO₃Li)²⁻-Li⁺ defect after X-irrad., EPR study 0-75852
 CaCeAl₂O₇, melilite struct., prep. and props. 0-93524
 CaCl₂ B²⁺-X²⁺ transitions, rot. anal. by laser spectroscopy 0-91536
 CaCl₂ X²⁺ pot. energy curves, polarisability and dissociation 0-91629
 CaCl₂, adsorption of NH₃ and ND₃, complex formation, IR and for IR spectra obs. 0-80063
 CaCl₂ aq. soln., vel. corrs., time integral calcs. 0-59360
 CaCl₂:Eu²⁺, fluorescence lifetime and quantum efficiency for 5d-4f transitions 0-100681
 CaCl₂-NH₃, isothermal dissociation and regeneration, appl. to solar refrigeration (French) 0-61300
 CaCl₂-NH₃ dry absorption for solar refrigeration 0-61310
 CaCl₂(Br₂)₂, glassy aqueous soln., L₂ region Raman spectra 0-84729
 CaCl₂·2CH₃OH, solar heat pump and thermal storage system for space heating 0-85307
 CaCl₂·4NH₃-CaCl₂·2NH₃, solar energy storage system heating and cooling 0-81484
 CaCl₂·6H₂O, heat transfer props. for heat of fusion energy storage 0-76654
 CaCl₂·8NH₃-CaCl₂·4NH₃, solar energy storage system heating and cooling 0-81484
 CaCr₂O₄, β to α transform. temp., effect of partial O₂ press. 0-84292
 CaF₂, Σ ground state, laser-IR double reson. spectrosc. 0-69171
 CaF, A²⁺-X²⁺ transition, HFS and fine struct., intermodulated fluoresc. spectra obs. 0-63695
 CaF, B²⁺-X²⁺ system, rot. and vibr. anal. 0-74156
 CaF:Eu(Gd)(Dy)(Tb), dimer reorientation activation volume 0-107285
 CaF₂, anion motion at high temps., quasielastic neutron scatt. obs. 0-59715
 CaF₂, cathodoluminescence, SEM 0-100700
 CaF₂, cation jump freq., isotope effect, lattice dynamical calc. 0-88357
 CaF₂, cryst., (111) faces, selective etch rate and etch pit morphology, acid conc. and temp. effect 0-96524
 CaF₂ crystal active element for colour-centre laser, thermal strain anal. 0-91804
 CaF₂ crystal structure, stability compared with TiO₂ (Russian) 0-64945
 CaF₂, damage by UV laser radiation, avalanche ionization mechanism 0-76110
 CaF₂, doped with trivalent rare earths, migration entropy for bound fluorine motion 0-71303
 CaF₂, electron irradiation defect aggregates, ordering, U and Th impurity effects 0-75216
 CaF₂, fast ion transport, computer simulation 0-107485
 CaF₂, fluorite, use as standard specimen 0-96704
 CaF₂, fluorite, use of proton irradiation to reveal growth and deform. features 0-84216
 CaF₂, glass-coating apparatus for Na resistance 0-90874
 CaF₂, heteronuclear mag. spin system relaxation in many pulse NMR expts. 0-93203
 CaF₂, high-frequency phonon lifetimes 0-70338
 CaF₂, influence on melting of high ZrO₂ glass, surface crystallisation 0-84278
 CaF₂, ionic clusters, struct., thermodynamic functions, energy surfaces and SIMS 0-63881
 CaF₂, ionic cond., activation vols., freq. depend. cond., press. effects 0-100354
 CaF₂, melts, elec. cond., surface tension, viscosity, density (Russian) 0-92758
 CaF₂, mol. dynamics studies of superionic conductors 0-107547
 CaF₂, optical detection of acoustic phonons at THz freqs. 0-75320
 CaF₂, planar channelling, minimum yields determ. 0-70280
 CaF₂, slab with (110) free surfaces, lattice dynamics and thermodynamic functions 0-70519
 CaF₂ solid electrolyte use in galvanic cells for thermodynamic obs. on refractory double oxides (French) 0-85190
 CaF₂, strain induced splitting and oscillator strength anisotropy of IR transverse optic phonon 0-92625
 CaF₂, strength-controlling fracture energy depend. on flaw-size to grain-size ratio 0-81152
 CaF₂, thermal props. (German) 0-81355
 CaF₂ thin films, initial ionic thermocurrent meas. 0-97018
 CaF₂:Ni crystals, X-irradiated, EPR study of Ni²⁺ and Ni³⁺ 0-75849
 CaF₂:alkali metal cation, thermal depolarisation study 0-108147

calcium compounds continued

- CaF₂:Dy, TLD-200, thermolum. phosphor, photolum. and absorpt. spectra, thermolum. mechanisms 0-97321
 CaF₂:Er, defect structure, quenching effect, dielec. relax. and optical absorption 0-65031
 CaF₂:Er, near-Debye dielectric responses 0-71291
 CaF₂:Eu, CaF₂:Eu,Mn(Gd), single crystal predissociation phenomena, SEM cathodolum. obs. 0-59502
 CaF₂:Eu, Mn, cathodoluminescence SEM appl., stroboscopic 0-70088
 CaF₂:Eu, scintillation detector, in STEM 0-101897
 CaF₂:Eu²⁺, fluorescence lifetime and quantum efficiency for 5d-4f transitions 0-100681
 CaF₂:Eu²⁺, photoluminesc. mag. circ. polaris. 0-89056
 CaF₂:Eu²⁺, Sm²⁺, relaxed resonance acoustic phonons in vibronic anti-Stokes luminescence (Russian) 0-93404
 CaF₂:Eu³⁺(Sm³⁺), VUV absorpt. spectra, dopant clustering 0-108230
 CaF₂:La hologram recording medium, characteristic transfer curve description, using heuristic exponential model 0-78796
 CaF₂:La³⁺, thermal depolarisation of La³⁺-F_i⁻ defect dipoles 0-75926
 CaF₂:Li(Na)(K)(Rb), dielec. relax., activation energy, rel. to vacancy pair reorientation 0-88917
 CaF₂:M, M=Mn, Fe, Co, Ni, X-irrad., impurity effects on defect prod. 0-92525
 CaF₂:Mn, EPR and optical absorpt. spectra 0-93171
 CaF₂:Mn, low temp. X-irrad., Mn centres, optical absorpt. and emission props. 0-60635
 CaF₂:Mn(Co)(Ni), X-irrad., thermolum. 0-60686
 CaF₂:Nd³⁺(Eu³⁺)(Dy³⁺)(Ho³⁺)(Tm³⁺), ¹⁹F NMR studies 0-60429
 CaF₂:Ni, X-irrad., optical absorpt. spectra and dichroism meas. 0-108239
 CaF₂:Ni, X-irradiated, optical and EPR meas. 0-108235
 CaF₂:O²⁻, CaF₂:Na⁺, O²⁻ and CaF₂:Y³⁺, O²⁻, thermal depolarisation obs. of defect clusters 0-71299
 CaF₂:Pb²⁺, band struct., Jahn-Teller effect, UV luminesc. and optical absorpt. spectra 0-66243
 CaF₂:rare earth ion, elec. dipole-dipole interaction, ionic thermocurrent and EPR study 0-108060
 CaF₂:Sm²⁺, coherent population oscils. and hole burning observed using polarization spectroscopy 0-71457
 CaF₂:Tm²⁺, ultra-low nuclear spin temp., low field behaviour, EPR study 0-100614
 CaF₂:U³⁺, anomalous magnetooptic props., optical detection of ESR and cross-relax. resonances 0-93287
 CaF₂:Y³⁺, ionic cond. and thermal depolarisation obs. of defect clustering 0-71298
 CaF₂-AlF₃-Na₂AlF₆-(Al₂O₃), phase equilibria, X-ray diffraction and DTA meas. 0-108409
 CaF₂-CaO-Al₂O₃, phase diagram contribution (German) 0-100830
 CaF₂-MgO-SiO₂, melts, elec. cond., surface tension, viscosity, density (Russian) 0-92758
 CaF₂-MgO(SiO₂), melts, elec. cond., surface tension, viscosity, density (Russian) 0-92758
 CaF₂-H₂, ionic cond. determ. from admittance and dielec. loss meas. (French) 0-107479
 CaFe²⁺Fe²⁺(Si₂O₇)O(OH), ilvaite, electronic struct., press. and temp. depend. of ⁵⁷Fe Mossbauer spectrum 0-108129
 Ca₂Fe₂Ge₂O₁₂, garnet, light absorpt. spectral study 0-93322
 CaGa₂O₄ and CaGa₂O₃, cryst., thermodynamic parameters of reactions of form., thermodynamic stability 0-108726
 CaGa₂O₄, high pressure modifications 0-104149
 Ca₂Gd₂Sn₂-Sb₂O₇, pyrochlorate struct. form. 0-92504
 Ca₂Ge₂O₁₆, cryst. struct. interpretation by symmetrisation method 0-107180
 CaH method of metal powders manufacture, Ca(OH)₂ separation 0-84878
 CaH, spin doubling, SCF calcs. 0-95649
 CaH₂, simultaneous reduction of Nb₂O₅ and Al₂O₃, Nb₃Al prep. 0-100809
 CaHPO₄, powder and granules with starch mucilage binder, surface topography variation under compression 0-80998
 Ca(IO₃)₂, complex salts, phase transitions, cryst. struct. (Chinese) 0-70171
 CaLaFeO₄, two-dimens. mag. ordered, structural and mag. props. (French) 0-70173
 CaLaFeO₄, two-dimens. mag. props. rel. to cryst. struct. 0-75776
 Ca₁₈M₂H₂(PO₄)₄, (M²⁺=Mn, Co, Ni, and Cu), hydrothermal synthesis and cryst. growth 0-60762
 Ca₂(Mg,Fe)(Si₂O₇)₂·(OH)₂, amphibole nephrite, planar defects termination, high resoln. electron microscopy 0-79772
 Ca₂Mg(Co)(Zn)(Mn)(Cd)(Ca)TeO₆, optical SHG study of acentricity, ferroelec. of low temp. phases 0-71324
 Ca₃Mn₂Ge₂O₁₂, garnet, metamagnetic transition, high anisotropy peculiarities (Russian) 0-60274
 CaMoO₄, Davydov splitting of vibr. levels, short range interaction 0-71418
 CaMoO₄:Mn²⁺, of Mn²⁺, EPR zero-field splitting 0-75531
 α-CaNa₂P₂O₇·4H₂O, X-ray cryst. struct. determ. 0-64964
 CaNb₂O₆, force fields rel. to cryst. struct. (French) 0-107104
 Ca₂Nb₂O₇, ferroelectric phase transitions, dielec. constant and thermal expansion rel. to temp. 0-88934
 Ca₂Nb₂O₇, monoclinic modification, cryst. struct., X-ray diffraction method 0-64955
 Ca₂Ni_{1-x}Fe_xO₄, X-ray struct. anal., determ. of lattice constant and interplanar distances (French) 0-96487
 CaO, B¹⁺-X¹⁺ and C²⁺-X²⁺ electronic transition strengths meas. 0-78602
 CaO based refractory from industrial lime, with 5% added electrocorundum 0-89184
 CaO, cohesive and thermophysical props., role of three-body interactions 0-92477
 CaO dissociation energy from Ca+O₂ chemiluminesc. 0-97697
 CaO, EPR of colour centres, 295K (Russian) 0-84649
 CaO, eqn. of state at high press., appl. to Earth core and mantle 0-109122
 CaO, formation of surface O₂⁻ ion by O₂ adsorption, EPR 0-61155
 CaO, heated on W, thermal anal. using mass spectrometric technique, vapourisation behaviour 0-79932
 CaO high pressure metallisation, tentative evidence 0-84427
 CaO, obs. of dipolar induced spin depahsing, coherent optical-microwave spectroscopy 0-103900

calcium compounds continued

- CaO, photoionisation of F-centre, luminesc. and photocond. meas. 0-66270
 CaO, reduction by C, kinetics and mechanism (*Russian*) 0-93743
 CaO solubility in BaO.6Fe₂O₃ 0-100333
 CaO solubility products in molten NaCl-KCl, potentiometric determ. 0-76488
 CaO stabilised ZrO₂, preferred slip system 0-66585
 CaO, transition, Earth mantle implications 0-79876
 CaO, XPS valence bandstruct. 0-89117
 CaO:Bi surface, O₂ chemisorpt., positive ion emission determ. 0-92785
 CaO:Ce³⁺, Gd³⁺, sensitization of Ce³⁺ luminesc. by Gd³⁺ 0-97326
 CaO:Eu³⁺, influence of crystal field on luminesc. (*Russian*) 0-80834
 CaO-Al₂O₃-B₂O₃-SiO₂-FeO, glass, IR spectra at room and melt temp. 0-88986
 CaO-Al₂O₃-SiO₂ additive to zircon ceramic, sintering and mech. props. 0-60814
 CaO-Al₂O₃-SiO₂ glasses, density-of-states and structural forms, Raman spectra study 0-97255
 CaO-Al₂O₃(B₂O₃)-SiO₂ glass-forming additive, effect on Al₂O₃ ceramics sintering 0-89187
 CaO-Ca(OH)₂ reversible hydration-dehydration for solar energy storage 0-97810
 CaO-MgO-Cr₂O₃-Al₂O₃-ZrO₂-SiO₂ system, subsolidus region characts. 0-97466
 CaO-Na₂O-SiO₂ glass, leaching studies by sputter-induced photon spectrometry 0-80004
 CaO-Na₂O-SiO₂ glass, molten, metal ion diffusion and redox behaviour, electrochemical studies 0-81332
 CaO-P₂O₅, glass, US velocity rel. to elastic props. 0-103425
 CaO-P₂O₅ glass, ESR of VO²⁺ ions 0-100610
 CaO-P₂O₅:Cr³⁺ glass, absorpt. spectra, Fano antireson. and vibronic Lamb shift 0-71458
 CaO-SiO₂ glass, trimethylsilylation method for silicate ion anal. (*Japanese*) 0-71975
 CaO-SiO₂ glass prep. by gel method 0-100824
 CaO-SrO-Fe₂O₃ system, phase relations, Sr hexaferrite field occurrence 0-93545
 CaO-V₂O₅-SiO₂ system, compatibility triangles 0-81037
 Ca(OH)₂, dehydration, unsteady heat conduction, thermal conductivity change 0-76511
 Ca(OH)₂, separation in CaH method of metal powders manufacture 0-84878
 (CaO)₂SiO cement pastes, electron microsc. anal. 0-108761
 10CaO.15Na₂O.75SiO₂ glass, thermal cond., temp. depend. at low temps. 0-65322
 CaO.6Al₂O₃, thermodynamic stability, reaction with Ti, Cr and Zr oxides 0-92687
 12CaO.7Al₂O₃, composition of gases released on heating, crystallisation (*Russian*) 0-93820
 Ca₃(PO₄)₂ ceramic, material science, bone implant 0-93523
 Ca₃(PO₄)₂:Cu²⁺, ESR, high press. struct. transition 0-97134
 Ca₄P₂O₇ ceramic, material science, bone implant 0-93523
 Ca₁₀(PO₄)₆(OH)₂, dissolution kinetics, nucleation-controlled 0-59659
 Ca₃(PO₄)₂OH ceramic, material science, bone implant 0-93523
 CaS, atomic and mol. centres of O, ESR and luminesc. methods (*Russian*) 0-84764
 CaS, EPR of colour centres, 295K (*Russian*) 0-84649
 CaS:Ce, Na phosphor, photoluminescence and excitation spectra 0-89049
 CaS:Cu, colour centres, optical and thermal depths determ. 0-66275
 CaS:Nd phosphors, X-ray powder diff. anal. 0-100204
 CaS:Pd phosphors, trap and luminescent centre location, photo- and thermoluminescence studies 0-71482
 CaSO₄, body centered matrix basis 0-79765
 CaSO₄ crystallisation, from liq. solns. as heat-transfer surface 0-100772
 CaSO₄:Dy, phototransferred TL studies 0-80875
 CaSO₄:Dy, TLD-900, thermolum. stability at low radiation doses 0-101272
 CaSO₄:Dy, thermoluminescent glow peaks, post γ -irrad. annealing study 0-89077
 CaSO₄:Dy ribbon, dosimetric props. study 0-63395
 CaSO₄:Dy sintered pellets, thermolum. response 0-93411
 CaSO₄:Dy TLD phosphor, γ radiation changes in glow curve 0-60688
 CaSO₄:Dy Teflon TL dosimeters, thin, development for β -dosimetry in personnel monitoring 0-63399
 CaSO₄:Dy(Tm), thermolum. thermolum. phosphor, photolum. and absorpt. spectra, thermolum. mechanisms 0-97321
 CaSO₄:Sm phosphors, X-irrad., thermoluminesc., charge compensation effects 0-97351
 CaSO₄:Tm, sensitised TLD phosphor, photon energy dependence 0-78498
 CaSO₄.2H₂O, crystallisation 0-100766
 CaSO₄.2H₂O, gypsum, cryst. growth rates and nucleation (*French*) 0-80959
 CaSO₄.2H₂O-CaHPO₄.2H₂O system, solid solns., IR study (*French*) 0-66165
 CaSe:Sn³⁺, EPR study of octahedral Sn³⁺ centres, 4 to 290K (*Russian*) 0-84637
 CaSiO₃, fibrous, controlled crystallisation and anisotropy 0-59425
 β -Ca₂SiO₅, reaction kinetics with CO₂ and water vapour 0-76484
 γ -Ca₂SiO₅, polymorphic transformation scheme 0-71642
Ca₂SiO₅, structurally related phases, high-temp. X-ray powder diff. 0-81050
Ca₂SiO₅, reaction kinetics with CO₂ and water vapour 0-76484
Ca₂SiO₅, fracture surfaces, quantitative anal. using energy dispersive X-ray spectrometry (*French*) 0-89571
Ca₂Si₆O₁₇(OH)₂, xonotlite, polytype identification from electron diff. patterns 0-72519
Ca₁₀(SiO₄)₃(SO₄)₂(OH,Cl,F)₂, hydroxyllestadite, X-ray cryst. struct. determ. 0-96485
Ca_{1-x}Sm_xF_{2+x}, luminesc. exp. suggesting Sm³⁺ ion pairing 0-76065
Ca_{1-x}Sm_xS, electron config. of Sm ions, X-ray L-absorpt. spectroscopy 0-60715
CaSnO₃, high-density ceramics prep. and elec. props. 0-60812
Ca_{1-x}Sr_xY₂Ba_{7/2}Zr_{1-x}Ti_xO₃, ceramic system, dielectric props., microwave resonator application 0-80674
Ca_{1-x}Sr_xF₂:Er³⁺ mixed crystal, luminesc. transition, inhomogeneous line broadening calc. 0-97332
Ca_{10-x}Sr_x(PO₄)₆(OH)₂, continuous cation migration, IR spectra study 0-93297
CaTiO₃, prep. from film forming soln. 0-60811

calcium compounds continued

- CaV₂O₆:Cr, EPR spectra temp. depend., paramagnetic ion point symm. 0-71166
 CaWO₄:Mn²⁺, zero-field splitting of Mn²⁺, EPR 0-75531
 CaWO₄, body centered matrix basis 0-79765
 CaWO₄, centrosymmetric cryst., linear electrogyration study 0-60540
 CaWO₄, cryst. growth from solns. in melts, kinetics parameters and thermodynamic props. 0-59424
 CaWO₄, Davydov splitting of vibr. levels, short range interaction 0-71418
 CaWO₄, slow neutron inelastic scatt. spectra, Debye temp. calcs. (*Russian*) 0-59347
 CaWO₄, undyed X-ray intensifying screen, role of reflective layer 0-62816
 CaWO₄:Nd³⁺ absorpt. spectra, hypersensitivity of ⁴I_{9/2} to ⁴G_{5/2} ²G_{7/2} transition 0-97309
 CaWO₄:Pr³⁺, anomalous hypersensitive ³H₄→³P₂ transition 0-106296
 Ca₂YFe₂O₁₃, cryst. struct., electron microscopy and X-ray diff. study 0-88116
 CaZrO₃, high-density ceramics prep. and elec. props. 0-60812
 Ca₂(NH₄)H₇(PO₄)₄.2H₂O, X-ray cryst. struct., PO₄ ion with 3 symmetric H bonds 0-64956
 Ca₂[B₂O₃]Cl₂H₂O, hilgardite, PMR of water mol. 0-84655
 Ca₂Fe(CN)₆(NO)₂.4H₂O, X-ray cryst. struct. determ., heavy-atom method 0-92494
 Ca₂[SiO₄]₂(OH)₂, cryst. struct. refinement 0-107181
 Cd_{1-x}Ca_xS, solid soln., phase equil. diagrams 0-108412
 CeO₂:CaO, O ion cond. and defect struct. 0-107553
 Fe-Mo-CaF₂ sintered composite, struct. and mech. props., heat treatment effect 0-66526
 KCl-CaF₂-NaCl, ternary phase diagrams, interactive computer program 0-71629
 3KNO₃-2Ca(NO₃)₂, glass form. from liq., struct. transform., Raman spectrum obs. 0-64916
 K₂O-CaO-BaO-B₂O₃ glass, refraction, refractive index from 0.365 to 2.50 μ m 0-88953
 (La_{0.8}Ca_{0.2})MnO_{3+y}, mag. props., Faraday method meas. 0-103832
 (La_{0.8}Ca_{0.2})MnO_{3+y}, non-stoichiometry and lattice consts. 0-100212
 (LaTmCa₃)FeGe₂O₁₂, mag. loss and domain wall mobility 0-65980
 LiCa₂(CO₃)₂ and ⁴Li states, mol. binding energy curves 0-58189
 MgCa₂Si₂, dolomite, partial thermal decomp. into MgO and CaCO₃, product cryst. growth 0-108706
 MgO-CaO-FeO-Fe₂O₃-SiO₂-Cr₂O₃-Al₂O₃ spinel refractories, physicochem. prod. conditions 0-89185
 Na₂Ca₂SiO₅[Si₂O₇][PO₄]₃, synthesis conditions, cryst. struct. and IR spectra characts. 0-108335
 Na₂O-2CaO-3SiO₂ glass, cryst. nucleation and growth, viscosity, thermodynamic props. 0-84079
 Na₂O-CaO glass, (K₁V) diagram determ. (*French*) 0-108558
 Na₂O-CaO glass, wettability, effect of cleaning procedures 0-65336
 Na₂O-CaO glass phlogopite mica powders, composite fabrication, cellular struct. 0-84902
 Na₂O-CaO-Al₂O₃-SiO₂ glass, crystn. for the purpose of obtaining vitroceramics (*French*) 0-75163
 Na₂O-CaO-SiO₂ glass, formation of colour centres, linear absorption of UV radiation 0-103328
 Na₂O-CaO-SiO₂, proof testing 0-108654
 Na₂O-CaO-SiO₂ glass, grain-cleaning procedures effect on crushed glass chem. durability tests 0-66678
 Na₂O-CaO-SiO₂ glass, vol. relaxation and thermal history during forming process 0-70130
 Na₂O-CaO-SiO₂ glass, redox phenomena evaluation in melting-fining process, SO₂ evolution 0-84900
 Na₂O-CaO-SiO₂ glass, high-vel. liq. impact, oblique impact anomaly 0-89329
 Na₂O-CaO-SiO₂ glass, hot erosion plastic flow and fracture 0-89354
 Na₂O-CaO-SiO₂ glass foils, HVEM in-situ straining expts. 0-104216
 Na₂O-CaO-SiO₂ glasses, elec. cond., room temp. to 450°C 0-107473
 Na₂O-CaO-SiO₂, molten glass, electrolysis reactions 0-89496
 Na₂O-CaO-SiO₂:Cr³⁺ glass, absorpt. spectra, Fano antireson. and vibronic Lamb shift 0-71458
 Na₂O-CaO-SiO₂-Cr₂O₃ glass, redox equilibria of Cr ions, impurity effects 0-89477
 Na₂O-CaO-SiO₂-Fe₂O₃ molten glass, optical props., temp. depend. (*French*) 0-100667
 Na₂O-CaO-SiO₂-H₂O system gels, metastable nature 0-71952
 2Na₂O-CaO-3SiO₂ glass, cryst. nucleation rate, viscosity, heat treatment 0-84081
 Nd_{1-x}Ca_xVO₃, solid solutions, elec. props. 0-96866
 Pr_{1-x}Ca_xMnO₃, struct. and magnetisation study 0-65804
 3RbNO₃-2Ca(NO₃)₂, glass form. from liq., struct. transform., Raman spectrum obs. 0-64916
 SiO₂-Al₂O₃-CaO-BaO-SrO-ZnO-Na₂O-K₂O-B₂O₃, glaze effect of P₂O₅ additions 0-60824
 SiO₂-Al₂O₃-CaO-Na₂O:Fe³⁺, optical absorpt. due to Fe³⁺ ligand field and charge transfer 0-89020
 SiO₂-CaO-Na₂O glass, layers near surface, anal. using SIMS 0-88041
 SiO₂-Na₂O-CaO-MgO float glass, surface SnO₂ distrib., ellipsometry and XPS study 0-84346
 SiO₂-Na₂O-CaO-P₂O₅, BIOGLASS, surface, Ca₃(PO₄)₂ film form., bonding to bone 0-85212
 SiO₂-PbO-B₂O₃-Al₂O₃-CaO-Na₂O-K₂O glaze, interaction with aluminosilicate glass-ceramics 0-84398
 SrFe₂O₇:CaO, Ca²⁺ substitution effect on hexaferrite lattice and mag. props. 0-60243
 ThO₂-CaO, solid solns., defective oxides, ionic cond. 0-107548
 V₂O₅-As₂O₃-CaO, semicond. glass, electronic props. 0-88557
 (Y₂Sm₂Ca₂)(Fe₂Ge)₂O₁₂ epitaxial films, mag. props., growth condition effects 0-97124
 (YErCa₃)(Fe₂Ge)₂O₁₂, mag. loss and domain wall mobility 0-65980
 (YEuCa₃)(Fe₂Ge)₂O₁₂, mag. loss and domain wall mobility 0-65980
 (YLuSmCa₃)(Fe₂Ge)₂O₁₂ garnet film, bubble domain expansion, fuzzy wall struct. 0-71128
 (YLuSmCa₃)(GeFe)₂O₁₂ garnet films, bubble expansion saturation vel., sampling optical photography 0-75820
 (YSmLuCa₃)(Fe₂Ge)₂O₁₂, mag. loss and domain wall mobility 0-65980
 ZnF₂-BaF₂-CaF₂, vitreous phases, network formers, modifiers and stabilisers (*French*) 0-64909
 ZrO₂-CaO, solid solns., defective oxides, ionic cond. 0-107548
 ZrO₂-CaO, stabilised microspheres, structure, mechanical props. (*Russian*) 0-100379

calcium compounds continued

- ZrO₂-CaO ceramic with grainy structure, props., effect of heating to 2000°C 0-104194
ZrO₂-CaO solid electrolyte, for O₂ flow regulator 0-57301

calculating *see calculation***calculating apparatus**

- desk, calculator-based instruments, meas. accel. due to gravity 0-73336
programmable pocket calculator, short circuit current calc. (*German*) 0-68186

calculating machines *see calculating apparatus***calculation**

- see also graphs; nomograms*
No entries

calculators *see calculating apparatus***calculators (electronic)** *see electronic calculators***calculus**

- see also differentiation; integration; variational techniques*
ellipsometry, Mueller-Stokes calculus, conventions and formulas 0-102618

calibration

- see also measurement standards; standardisation*
600 MHz to 1 GHz coaxial thermal noise standard 0-98875
acceleration pick-ups, miniature vibrator for mechanical calibration (*German*) 0-95095
adiabatic calorimeter for continuous specific heat meas. 800 to 1800K, design and calibration 0-57299
AE transducer (*Czech*) 0-106697
aerosol counters, photoelectric, sedimentation method 0-99031
aerosol particle counter, optical, calibration by Doppler shift spectrometry 0-68173
biomedical calibrator for ECG/respiration monitor 0-98159
biomedical thermometry, use of salt-hydrate transition temps. as fixed points 0-104801
blackbody for energy calibration of infrared equipment 0-86377
cameras, multi-, planar control in photogrammetric calibration for 3-D gait studies 0-67194
chromatographic method of calibrating leaks 0-77800
circular scale calibration by reflection grating polygon (*German*) 0-86250
computerised analysis, collaboration collection report 0-73106
condensation nuclei counters at South Pole, calibration 0-98470
cone absorption calorimeter for pulsed laser meas. 0-98980
contactless thermal flowmeter, calibration characts. 0-103085
crop and soil bidirectional reflectance factor calibration, remote sensing field research 0-86382
cyclotron dee voltage calibration using an intrinsic Ge X-ray detector 0-99359
diamond turning precision machine tool system 0-69568
diffusion battery, screen type, theory 0-95208
dose meter calibration for radiation protection in European Community 0-58000
dosimeters, environmental and personal, calibration using ¹³³Xe 0-86992
dual-grating direct-reading spectrograph mirror system design and performance 0-81397
earphones, Telex 1470-A audiometric, calibration data 0-74685
electrical standardisation laboratory for developing countries 0-101774
extragalactic distance scale calibration, appl. to distance of giant spiral galaxy (M 101) 0-67852
far IR and near MM wave power energy meter calibration 0-57373
far IR calibration source for balloon-borne telescopes 0-62027
fast-response pyrometer 0-90852
fibre optics appl. in instrumentation 0-83665
flame temperature meas. using laser induced fluoresc. spectrosc. of OH 0-90839
flow meas., two-dimensional nonsteady, X-hot wire probe method (*Japanese*) 0-59134
flow measurement 0-92239
flowmeters, irrigation water mains 0-96325
force transducers, calibration by absolute impulsive method 0-105627
gas analyser, based on thermocouple vacuum gauge 0-61183
gas concentration meas. using Raman intensity depend. on giant pulse laser polarization 0-98986
gas mixtures preparation (1 to 10⁻³)% molar range 0-99030
gel permeation chromatography, calibration, appl. to polycarbonate 0-58424
glass micropipettes, comparative calibration by optical microscopy and SEM (*German*) 0-98201
global calibration of terrestrial reference cells and errors involved in using different irradiance monitoring techniques 0-93951
grazing incidence spectrometer, 1.0 m, photometric calibration for plasma fusion diagnostics 0-92386
hierarchical systems, calibration errors influence on end item performance 0-98788
high-pressure gas equation-of-state meas. interferometry 0-77810
hot-film probe, vel. meas. in liquid metal MHD duct flow 0-75009
hot-wire probes, very low velocity calibration 0-75008
impedance probe calibration, for vacuum meas. in single component two-phase mixture (*Italian*) 0-62677
incandescent lamp calibration for spectral irradiance by absolute radiometers 0-102788
interferometer, data handling in high vibration environment 0-95132
international calibration cycles of field intensity and power density, measurements 0-82752
international collaboration among calibration services 0-101773
ionisation chambers, calibration of dose to water for ⁶⁰Co γ -radiation 0-74032
IR and millimetric waves and applications, conf., Miami Beach, USA (Dec. 1979) 0-57009
IR and MM wave calibration standards requirements survey 0-57248
laboratory condenser microphones, note concerning the implementation of IEC 327:1971 for pressure calibration 0-74686
laser energy meters for calibrations at most principal laser wavelengths 0-99741
laser photoacoustic detector spectroscopy, calibration using HD 5-0 transition 0-77877
laser wavelength calibration using optogalvanic effect, atlas 0-62727
level gauge, linearisation of scale eqn. for resonance level gauges (*Russian*) 0-68176
lidar target calibration, backscatter refl. for circularly polarised radiation 0-102750

calibration continued

- low density supersonic gas flow, temp. meas. probe 0-74913
low-temperature blackbody source 0-73355
luxmeter, development in Yugoslavia (*Croatian*) 0-105616
magnetic circular dichroism recorder calibration at 10.6 μ m 0-90876
magnetic induction meters, electromagnet reference measure free from hysteresis effects 0-77817
magnetic spectrograph, calibration by electron capture reactions 0-63445
moisture meters, representation as two series transducers, total error estimation 0-77792
mosaic sensor test and calibration facility for focal plane arrays 0-86425
Mossbauer 14.4 keV gamma-ray source, design, calibration and polarimeter 0-86535
multiples of the unit of mass, systematic search for orthogonal systems 0-82747
neutron detector, calibration of zero-angle direction 0-91185
neutron detector calibration, simple recipes for ground scatt. 0-106231
neutron monitor calibration, standard fields at Physikalisches-Technische Bundesanstalt 0-57999
neutron rem counter, corrected calibration of Andersson and Braun type rem counter for divergently incident Am-Be neutrons 0-74031
nondestructive assay equipment, calibration using reference materials for fissile material assay 0-71880
nuclear materials accountability, tank volume calibration algorithm 0-83159
nuclear materials accountability tanks, automated calibrator 0-83158
optical fibre refracted near-field scanning, calibration technique 0-99823
optical fibre refractive index profile meas., near-field technique 0-91931
optical single-particle-size spectrometer calibration and testing, monofilament fibres as substitute particles 0-58819
orthotropic composite model materials, photoelastic calibration 0-87715
parameters, InSb and Ge magnetooptical rotation standards 0-60551
personnel neutron dosimeters, calibration for use in different neutron fields 0-58001
photodiode detector calibration using synchrotron radiation 0-90810
photoelectron spectrometer, calibration using binding energy scale 0-90930
photopic response sensor, calibration rel. to photopic handbook data 0-62732
photosensor spectral responsivity calibration microprocessor system 0-86409
piezoelectric transducers, absolute calibration 0-79099
Pirani gauges, performance reproducibility 0-77806
pohotometric calibrator, inverse fourth power, NBS optical density standards development and appl. 0-73412
pressure meas. in diamond anvil cell, improvement using ruby R₁ fluorescence 0-98928
probe, five-hole, for complex flow field meas. 0-69951
probe, spherical Pitot, for flow meas. (*Italian*) 0-69957
process gas chromatographs, microprocessor based, calibration and data reduction 0-81402
radiation irradiance scales intercomparison, 90 to 250 nm wavelength range 0-98963
Raman spectrometer calibration using Kr⁺ laser plasma lines 0-57394
Raman spin-flip laser, multiply pumped, coherence effects 0-87398
rapid-scan polarising Michelson interferometer and InSb detector calibration 0-59305
reference permeability meters, short cct. coaxial lines as inductance standards 0-77816
reference radiations for radiation protection dose meter calibration (*French*) 0-57998
resistance thermometer automatic calibration oven 0-98914
resistance thermometers, device for measurement of static characteristics 0-77784
satellite IR radiometer, calibration 0-101440
Seasat, scanning multichannel microwave radiometer, calibration algorithm development 0-94682
SEC Vidicon photometer, stellar photometry calibration and appl. to main sequence of ω Centauri 0-90491
secondary radiation dosimeters, prep., sensitivity anal. and calibration 0-74034
semiconductor packages, hermetically sealed, calibration and anal. of moisture by gas mass spectrometry 0-90928
spectrometer calibration chamber for SURF II storage ring 0-91339
specular gloss of paint, calibration of reference standards 0-95061
specular reflectometer-spectrophotometer, NBS reference, mirror refl. meas. 0-68236
spinning rotor gas friction gauge, calibration against fund. vac. press. standard 0-82787
standard stars, IUE photometric calibration, UV spectra 0-77383
steel, tool and high-speed, high freq. induction melting and centrifugal casting in instrumental anal. 0-84886
stellar absolute luminosity calibrations, consistency 0-62111
stellar IR airborne spectrophotometry, 1.2-5.5 μ m, spectra and absolute calibration 0-62117
stellar spectral energy distribution in 3500 to 7500 Å region, absolute calibration 0-67710
stylus tip instrums. for surface roughness meas. (*German*) 0-101782
subdwarf star 37-45 colour excess, calibration using Fe/H abundances 0-82363
superconductive temperature fixed point device, prep. and calibration 0-82770
supersonic molecular beam source 0-82845
SURF storage ring calibrations for NASA stratosphere and climate programs 0-94721
temperature calibration standards using graphite-halogens for TEM 0-86510
thermocouple, thermometers, voltage generation, calibration 0-57295
thermocouple calibrations, comparison, fixed point and melting wire methods 0-86252
thermocouple instrumentation, field calibration 0-90840
thermometers, surface contact, dynamic behaviour (*German*) 0-90843
thickness meter, eddy-current for thermal insulation meas. 0-73316
Tokamak diagnostic Fourier transform spectrometer calibration by liquid N₂ cooled microwave absorber 0-59304
track chamber slide processing, calibration programming problems (*Russian*) 0-73305
track etch detectors, neutron energy depend. and threshold energy 0-61703
transducer, with steady and pulsating flows, using computerised flowmeter system 0-79416

calibration continued

- transducers, alternating-voltage, analogue, Soviet methods development 0-98872
 triggered calibrated sweep for AC oscilloscope 0-67987
 US flowmeters, recal., of characts. and calibration 0-103086
 US immersion testing, effects of curved entry surfaces on calibration, steel sample expts. 0-71849
 vacuum gauge, mass spectrometer leak detector range extension 0-73375
 vacuum gauges, by expansion-reduction method 0-77807
 volume calibration of nuclear materials accountability tanks 0-68829
 VUV detectors absolute efficiency meas. using VEPP-2M storage ring synchrotron radiation 0-82824
 VUV spectral irradiance calibrations, method and appl. 0-87452
 X-ray radiometric analyser, appl. of expt. planning 0-61186
 X-ray source, industrial, use for electronic component radiation effects work 0-63402
 Ag-activated Geiger counter calibration for neutron yield determ. in Frascati plasma focus expt. 0-99409
 Cu-Mn alloy, manganin, hysteresis-corrected calibration under shock loading 0-74818
 Ge(Li) detectors, gamma-ray intensity standards for calibration 0-74083
 He, electron elastic scatt., 5 to 200 eV, cross-sections meas., calibration 0-63822
 He+H⁺, differential scatt., 1-12 eV, high resolution beam meas. 0-58348
 LiF-polytetrafluoroethane thermolumin. dosimeters, absorbed dose assessment 0-95470
 Pb glass counter, automated calibration system 0-106233
 Pt resistance thermometers, simple Cu holder for calibration 0-98911
 Si photodiode absolute spectral response self-calibration 0-73448
 Si, photovoltaic cell, absolute spectral sensitivity calibration, radiometry, photometry (*Chinese*) 0-86367
 Si ring photodiode reflectometer for cavity reflectance 0-86376
 W ribbon-filament temperature lamps, radiation error estimation 0-64128
 W-halogen quartz envelope lamp, polarization characteristics 0-95970
 Zr ribbon filament lamp, calibrated source for IR radiometer 0-83653

californium

- see also nuclei with
²⁵²Cf, medical appl., fast neutron therapy (*Japanese*) 0-98112

californium compounds

- No entries

calorimeters

- see also calorimetry
 adiabatic calorimeter for continuous specific heat meas. 800 to 1800K, design and calibration 0-57299
 air chamber isothermal calorimeters for calorimetric nondestructive assay for in-field meas. of Pu-bearing materials 0-71874
 automated high precision calorimeter, for 200K to 400K, temp. controller design 0-86310
 biopolymer model compounds, calorimetric instrumentation used for studies 0-61746
 broad-band dry calorimeter for mm and sub mm wave power meas. 0-105646
 calorimetry, applications of thermoelectric devices in various types of calorimeters 0-105648
 Calvet-type twin calorimeter, use of microcomputer-controlled integrator 0-77786
 cone absorption calorimeter for pulsed laser meas. 0-98980
 DSM-2 differential scanning microcalorimeter (USSR), capabilities 0-62671
 enthalpies of mixing of condensable vapours, calorimeter for meas. 0-93791
 fusion reactor, Doublet III beamline calorimeter, three dimens. heat transfer anal. 0-99381
 fusion reactor, TFTR, high energy heat sink, ion beam dump and calorimeter 0-99394
 graphite calorimeter in water phantom for absorbed dose meas. 0-74032
 high-pressure low-temp. differential scanning calorimeter 0-86311
 high-temperature, containerless, with sample heating by electron bombardment 0-73366
 laser calorimeter types and techniques 0-69441
 laser plasma recording system for plasma blowoff and scattered light distributions 0-59287
 liquid, 2-compartment bomb calorimeter for combustion in F 0-57300
 low temperature calorimetric investigations, simple off-line arrangement 0-90850
 low-inertia differential, for appl. from 20-250°C 0-57298
 low-temperature device for meas. heat capacity in 4 to 370K range 0-105647
 macromolecules, study by scanning microcalorimeters 0-61747
 mathematical simulation of calorimeters used for rapid nuclear fuel assay 0-95355
 micellar systems, aqueous, thermochemistry 0-61133
 polyamide-film calorimeter for measuring local electron-beam absorbed doses 0-83227
 relaxation calorimeter for temp. range 4-380K, automated 0-98915
 scanning ratio adiabatic calorimeter 0-62670
 segmented calorimeter, high energy performance, Monte Carlo simulation 0-58029
 unit power standard for 53.57 to 78.33 GHz 0-90808
 water calorimeter for absorbed dose meas. 0-76836
 Al plate calorimeter, meas. of local convective heat transfer coefft. by polarisation interferometry 0-82809
 Fe scintillator calorimeter, segmented, structure of hadronic and EM showers 0-74078

calorimetry

- see also calorimeters; specific heat; thermal analysis
 biological macromolecules, conformation studied by calorimetry, review 0-97870
 calibration standards requirements survey 0-57248
 compound glass rod absorption coeff. calorimetry 0-106631
 crystalline material optical absorption meas. 0-105718
 dialkylammonium zinc dichlorobromides, long chain cpds., phase transitions, calorimetric study 0-70390
 dielectric loss factors meas. at 1 kHz and 4.2K 0-98921
 flow microcalorimetry, bioassay and enumeration, drug biopotency meas. 0-95100
 instrumentation development for nuclear transportable instruments 0-77787

calorimetry continued

- laser beam heat flux and power profiling, using swept null point calorimetry 0-69439
 macromolecules, linear, heat capacities, scanning calorimetry meas. 0-61134
 optical material absorpt. meas., real time holographic interferometry 0-83569
 polymer glasses, enthalpy relax., scanning calorimetry technique 0-90851
 polymers, glassy, optical absorpt., visible region, determ. by laser calorimetry 0-66218
 radiation effects on material determ., thermal defect meas. using total-absorption calorimeters 0-99427
 refractories, integral radiant capacity, calorimetric meas. method 0-65259
 relaxation method using cryostat, 1.5 to 10K 0-68204
 rhodamine 6G solution, absolute fluoresc. quantum yield determ. by calorimetric method 0-78851
 surface emittance, calorimetric emissometer 0-86309
 thermoelectric devices application in various types of calorimeters 0-105648
 Van der Waals film adsorbed on graphite, two-dimensional phase transitions 0-107653
 Ag film, energy losses of electrons, microcalorimetric meas. 0-59543
 Ag halide crystals, relative dissolution rates meas. by flow calorimetry 0-85220
 Au film, energy losses of electrons, microcalorimetric meas. 0-59543
 D₂, sticking and accommodation on low-temp. substrate, mol. beam expts. 0-84368
 Fe₂Ni₃P₁₄B₂, metallic glass, glass transition, viscous flow and differential scanning calorimetry meas. 0-96635
 H₂, sticking and accommodation on low-temp. substrate, mol. beam expts. 0-84368
 HCl-Xe, liq., enthalpy of mixing, calorimetric meas. 0-59661
 Na₂O-B₂O₃, vitreous and cryst., enthalpy of form., calorimetric study 0-66861
 Nb, liq. and solid, enthalpy meas. by levitation calorimetry 0-103499
 Pu nondestructive analysis, calibration by calorimetric assay 0-71878

calorimeters see calorimeters**CAMAC**

- bubble chamber pictures, SNOOP module CAMAC interface to 168/E microprocessor 0-58103
 calorimetric system for recording plasma blowoff and scattered light distributions from laser plasmas 0-59287
 data collection station, based on autonomous CAMAC crate 0-61689
 Tokamak device, JT-60, microprocessor based distributed intelligence CAMAC system 0-59309
 universal branch driver, independent programmed control module 0-69046

camera lenses see photographic lenses**camera tubes, television see television camera tubes****cameras**

- see also coronagraphs; television cameras
 35 mm compact, with fully automatic exposure control 0-90916
 Anger camera/computer system using seven pinhole collimator for myocardial perfusion tomography 0-61663
 Arriflex 35BP-II motion picture camera mounted with 350PF-1A zoom lens for wide-screen filming (*Russian*) 0-95176
 astronomical cold camera, description 0-72779
 Auger camera, Lixiscope, X-ray and gamma-ray telescope system 0-62020
 beta-ray, gas replacement monitor 0-95502
 biomedical gamma camera systems, methods for MTF meas. 0-94324
 biomedical X-ray spot-camera of Medcor Works 0-85477
 Bonse-Hart X-ray diffractometer, asymmetrically cut, comparison with Kratky camera 0-77917
 C-CD camera, appl. to Einstein X-ray Observatory fields RI photometry 0-62315
 C-CD camera description performance and calibration 0-73499
 coded aperture imaging, review 0-101914
 compact solar camera, student project 0-67975
 Debye-Scherrer camera conversion to back reflection camera 0-99024
 Dicke camera, Lixiscope, X-ray and gamma-ray telescope system 0-62020
 EKTRAMAX camera lens design and performance 0-77894
 endoscopic miniature camera with fibre-optic faceplate 0-77896
 fast solid-state camera for high-speed event diagnostics 0-78985
 fluoroscopic examinations, multi-image camera for spot radiography 0-109020
 frame to hold 35 mm SLR to CRO, integral data display 0-68284
 gamma camera, appls. for three-dimensional emission tomography using scattered photon information 0-98134
 gamma camera, computer controlled, nuclear cardiology appl. 0-61682
 grainless focusing screen for light scatter reduction 0-101836
 high speed, with image commutation, calc. of reflex involute centre for image shift and defocussing (*Russian*) 0-90919
 high speed raster cameras, image dissection and mech. scanning for photographic recording (*Russian*) 0-95182
 holocamera for 3-D micrography of the alert human eye 0-98057
 holographic camera, automated thermoplastic for two-wavelength contouring 0-74318
 holographic movie camera and projection system 0-78808
 IR sky survey telescope, wide field photography 0-105167
 laser unequal path interferometer with electro-optical camera and mini-computer, fabrication/test appl. 0-77847
 Leitz Vario-Orthomat, a new camera system for automatic photomicrography 0-82841
 lens shutters, friction coefficient nonreproducibility evaluation 0-62765
 lens-array focusing system tests, commercial reflex cameras 0-86479
 Lyman α camera, for high resolution solar Lyman α filtergrams 0-82323
 manual movie camera, Kinor 35P (*Russian*) 0-90917
 MATEC (matched tandem etalon camera), appl. to auroral obs. 0-101442
 medicine, nuclear, digital filtering and edge detection 0-58065
 medicine, nuclear, microprocessor systems for data acquisition, image processing, RIA anal., patient data retrieval 0-61670
 motion picture camera gyroscopic stabilisation system, anal. of dynamics and accuracy (*Russian*) 0-95173
 nuclear medicine, camera aperture for data collection optimisation 0-67221

cameras continued

- nuclear medicine, clinical and parametric evaluation of three large-field-of-view cameras 0-76823
- photographic materials, MTF automatic evaluation 0-95170
- photorecorders, five-metre magnetic spark spectrometer, JINR (USSR) 0-87014
- pin bowing in AGR fuel elements, meas. by camera device 0-106146
- positron camera, computed tomography, 3-D image reconstruction, Fourier deconvolution method 0-61669
- positron camera system, ring detector, brain research, computed transaxial tomography 0-61739
- positron circular ring camera tomographic system, resolution improvement anal. (Korean) 0-72312
- scintillation camera collimator image form. 0-89844
- scintillation camera field uniformity, global and local, statistical features 0-61677
- semiconductor gamma-cameras in nuclear medicine 0-81693
- SFR-2M (USSR), synchronisation with LG-36A gas laser 0-73489
- streak, dynamic range measurements, picosecond time resolution 0-73490
- synchrotron radiation camera and data acquisition system for time resolved X-ray scattering studies 0-99023
- tomography, single-photon emission, imaging capabilities of Ge camera 0-61668
- topographic camera, high-sensitivity double-crystal, lattice parameter meas. 0-77915
- vacuum-cold camera, appl. to astronomical near IR photography 0-90341
- volume hologram superimposed information display 0-78807
- wafer exposure camera, optical, step-and-repeat, with dark field automatic alignment 0-68283
- X-ray, 5-frame, for charged particle, inertial confinement fusion studies 0-57453
- X-ray, attachment for aimed investigation of fractures 0-85102
- X-ray, topographic 0-84029
- X-ray camera, wide field for astronomy, design, sensitivity and performance 0-85863
- CdTe matrix γ -camera, biomedical appl. 0-76827
- CsF scintillator, pot. advantages for a time-of-flight positron camera 0-81706
- NaI(Tl) scintillation cameras, image artifacts and counting losses 0-94345
- Xe high pressure proportional, scintillation camera for X- and γ -ray imaging 0-99412

candoluminescence *see luminescence***canted spin arrangements**

- see also weak ferromagnetism*
- antiferromagnet, magnetic phases, spin configurations in external field 0-70955
- antiferromagnet, two-sublattice Neel-type, stable spin configurations, external mag. field and single-ion orthorhombic anisotropy effects 0-60249
- dialkylammonium iron tetrachloride, antiferromag., mag. susceptibility meas. 0-60220
- dimethylamine iron tetrachloride, antiferromag., mag. susceptibility meas. 0-60220
- exciton spectra, optical props. 0-70622
- Neel ferrimagnets, phase transitions, field-induced spin-orientational 0-75767
- Co(urea) $_2$ Cl $_2$ ·2H $_2$ O, two-dimens. mag. props., cryst. struct., specific heat 0-75777
- Fe complex, Fe(1,2,4-triazole) $_2$ (NCS) $_2$, quasi-2-dimens. S= $1/2$ antiferromag., mag. props., hidden canting 0-107986
- Fe $_{1.2}$ Mg $_{0.4}$ Ti $_{0.4}$ O $_4$, mag. ordering, Mossbauer effect in external mag. fields 0-71257
- GdAlO $_3$, canted antiferromagnetic, Mossbauer meas. 0-97171
- MnZn ferrous ferrites, mag. permeability stress depend. 0-88822
- Mn $_{1-x}$ Zn $_x$ Fe $_2$ O $_4$, prepared by wet method, neutron diff. and high field Mossbauer expts. 0-75719
- Ni $_{0.2}$ Zn $_{0.7}$ Fe $_2$ O $_4$, Mossbauer study, noncollinear spin struct. 0-60472
- RbFeCl $_3$ ·2H $_2$ O, pseudo-one-dimensional canted Ising antiferromag., spin-cluster excitations 0-70989
- RbFeCl $_3$ ·2H $_2$ O, spin cluster excitation expts. 0-66039
- Zn $_x$ Fe $_{3-x}$ O $_4$ ferrite, mag. struct., Mossbauer spectra and magnetisation study, 4.2K 0-103818

capacitance

- see also photocapacitance*
- calcium behenate monomolecular layers between Al electrodes, nonlinear dielec. props. 0-84045
- conformal transformations combined with numerical techniques, with applications to coupled-bar problems 0-83538
- cracks, capacitance, mech. loads effects 0-84242
- degenerate semiconductor-metal Schottky barriers, low temp. capacitance 0-60075
- electrode, impedance meas., accuracy 0-61108
- ferroelectrics, negative capacitances, comparison with negative viscosities 0-66118
- lead phthalocyanine:O $_2$ (l), Schottky barrier effect on AC current response 0-75623
- magnetite, electrode, polycrystn., differential capacitance 0-66136
- MIS structure, fast surface states density, photoelectric methods of determ. 0-70835
- MOS field-effect devices, mag. quantisation effect on surface capacitance 0-70834
- MOS structure, semiconductor conductance and capacitance, extended AC conductance-bias method 0-96995
- MOS structures, quasistatic and nonequilibrium phenomena with constant gate-current bias 0-80385
- MOS structures of small-gap semicond., capacitance, effect of quantising mag. field 0-84513
- p $^+$ -n junction diffusion capacitance calc., discrepancy problems 0-60068
- p-n junction, diffused, transition capacitance calc. methods, comparison (Rumanian) 0-88625
- semiconductor, bulk deep centres, continuous energy spectrum, isothermal capacitance relaxation method 0-107741
- solid electrolyte-metal interface adsorption layer capacitance calc. (Russian) 0-59697
- stearic acid films, evaporated, vac. effects 0-97435
- Al-anodised Ta $_2$ O $_5$ /native oxide-n-GaAs MOS structure evaluation 0-84514
- Al-stearic acid-Al, low-loss thin film capacitor 0-71317
- Al $_2$ O $_3$, anodic, passified, inhibition of reaction with water 0-89390

capacitance continued

- β -Al $_2$ O $_3$ -Na $_2$ O, single cryst., non-Debye capacitance 0-107497
- Cr-phthalocyanine-Cr sandwich, I-V and C-V characs. 0-60106
- D-T, liq., dielectric constant and elec. cond. 0-84680
- GaAs based MOS capacitors, scanning photovoltage investigation 0-80396
- GaAs oxide film form., ion implantation effects 0-100266
- GaAs:Cr, deep acceptor level, DLTS and optical DLTS study 0-92852
- n-GaAs:H(D), ion implanted, carrier removal, capacitance-voltage profiling 0-84195
- InSb MOS struct., capacitance of n-channel inversion layers, elec. field effects 0-80393
- Na $_2$ CO $_3$, phys. props. related to phase transitions 0-96643
- PLTZ ceramics, modified by Ca $^{2+}$ (Sr $^{2+}$)(Nd $^{3+}$)(Y $^{3+}$), dielec. behaviour 0-60519
- Pb-PbO $_2$ -Pb small supercond. tunnel junctions, effect of capacitance in I-V characs., high-freq. obs. 0-80448
- PbS-Si heterojunction, space charge capacitance, PbSn film thickness depend. 0-88630
- PbSnF $_4$, anionic conductor, thin films and ceramics 0-107556
- Pb(Zr,Ti)O $_3$, piezoelectric ceramics, low fluence neutron irradi. effects 0-92564
- Si based MOS capacitors, scanning photovoltage investigation 0-80396
- Si junction diode, diffused, with deep level traps, negative capacitance 0-96976
- Si MIS capacitors, C-V curves, outer oxide surface conditions effects 0-97000
- Si:F:H, amorphous, elec. and optical props. 0-60031
- Si-SiO $_2$, MOS interface states density, meas. techniques and model development 0-92988
- Si-SiO $_2$, MOS interface states density, transient capacitance meas. eval. 0-92989
- Si $_3$ N $_4$ thin film, reactively sputtered, struct. and elec. props. 0-88656
- SnO $_2$ -InP heterojunctions, elec. and photovoltaic characs. 0-75628
- TeO $_2$ thin films, dielec. props. rel. to fabrication conditions 0-97199
- ZnO non-ohmic ceramic, degradation props. under AC and DC bias 0-80262
- ZnTe:Cu, impurity identification and characterisation, capacitance, luminescence and IR absorption 0-60639

capacitance measurement

- bridge meas. system for assessment of deep levels in semiconductors 0-105674
- capacitor, stored energy meas. 0-77585
- CMOS ICM 7555 capacitance meter cct., using radio receiver indicator 0-62692
- digital capacitance meter, design and construction 0-57275
- DVM converted to capacitance meter, using diode pump cct. 0-62656
- high loss materials at high freqs. 0-62686
- Lampard-type electrostatic system, appl. of sensitivity criterion 0-98942
- liquids, guarded cylindrical capacitance cell 0-86268
- meters, new checking method for instruments having both uniform and non-uniform scales 0-62654
- precision thermostat and capacitor enclose, maintaining the unit of capacitance 0-95063
- small capacitances by comparison, digital cct. 0-57327
- small capacitances measurement by comparison, cct. 0-57327
- wide-range, on single scale of instrument, use of sinusoidal power generator 0-98935

capacitance meters *see capacitance measurement***capacitor storage**

- Antares laser fusion project, 300 kJ, 200 kA Marx energy storage module 0-68954

capacitor stores *see capacitor storage***capacitors**

- see also electrolytic capacitors; thin film capacitors; varactors*
- ceramic, nondestructive testing by scanning laser acoustic microscopes, comparison with SEM and optical microscopy results 0-58875
- ceramic multilayer capacitors, fracture mechanics approach to structural reliability assessment 0-89328
- charging polymer surfaces, injection times obs., with aid of computer 0-70796
- double layer capacitors, RF conduction in polar liqs., ion diffusion effect 0-107883
- electrometric fixed-capacitor and resistive methods compared 0-90866
- stored energy meas. 0-77585
- vibrating capacitor displacement transducer, eqn. of state 0-57281
- BaTiO $_3$ ceramic dielectric capacitor, processing prop. relations, hysteresis, permittivity 0-80730
- PLTZ modified high voltage dielectric, permittivity, Curie temp., loss meas. 0-80720
- Si-SiO $_2$ -Si capacitor, polycryst., capacitance voltage characterisation 0-70794

capillarity

- see also bubbles; contact angle; drops; foams; liquid films; surface tension*
- benzene adsorbent mesopores, capillary evaporation and struct. 0-107614
- condensation theory, adsorbates liq. or gaseous props. 0-80028
- constant pressure manometer with frequency read out, electrocapillary element appl. 0-73380
- crystallisation stability during capillary shaping, general theory of capillary and thermal stability 0-107076
- crystallisation stability during capillary shaping for arbitrary small perturbations 0-107077
- density measurement, using flexible capillary 0-98886
- drops, rotating, captive between co-rotating parallel faces, shapes and stability, capillarity eqns. 0-64592
- electrocapillary acceleration meters, electrolyte composition selection 0-73331
- electrocapillary acceleration meters with electrolyte in gel form 0-73330
- electrokinetic flow in a narrow cylindrical capillary 0-92233
- epoxy resin adhesives, capillary flow and bond strength 0-71883
- epoxy resin bond layer, prep. methods, ultimate thickness 0-71884
- ethane, flow continuity in arterial capillary systems in cryogenic heat pipes 0-64536
- flat plate streaming potential investigations: hydrodynamics and electrokinetic equivalency 0-106777
- flow analysis, initial state, relax. model 0-74977
- fluid bridges between solids in gravitational field, props. 0-88401
- fluid/fluid interfaces, capillary phenomena, review 0-70506

capillarity continued

- foam with high press. gradients, syneresis in Plateau-Gibbs channels, capillary press. 0-74948
 gravity-assist heat pipes with capillary flow, dry-out phenomena 0-79398
 HPAM dilute polymer solutions, elongational flow 0-103047
 hydromagnetic capillary instability of a liquid jet with an axial flow 0-74990
 jets, Newtonian, axisymmetric, die-swell, Galerkin finite element method 0-83830
 liquid rise in capillary tube, rate meas. demonstration 0-73147
 manometers, liq., sensitivity, wetting hysteresis effect 0-98926
 mass transfer to power law fluids in fluidised beds 0-100032
 McLeod gauge, capillary depression phenomena, Hg vapour drag effect 0-98923
 non-Newtonian fluid exit flow through capillaries, effect of vibrations 0-79358
 periodic capillary tube, two phase fluid flow and hysteresis 0-107615
 periodic capillary tube, two phase fluid flow and hysteresis 0-107616
 polyethylene melt, oscillatory flow through capillary 0-103046
 polyisobutylene in toluene solution, effect of capillary materials on drag reduction (*German*) 0-87785
 polymer additive effects on wall slip and viscosity in flow through capillaries (*German*) 0-59086
 polymer melts, laminar and melt fracture flow through successive capillaries 0-59085
 Pyrex glass capillary tubes, effect of adsorbed water vapour on liq. water flow 0-92759
 quartz, dynamic wetting angle of dry lyophilic surface 0-88405
 rivulets, static, moving contact lines and rivulet instabilities 0-79264
 surface tension temp. dependence from triple point to critical point (*German*) 0-100376
 thermally induced surface fluctuations on simple fluids 0-88403
 transient thermocapillary flow in thin liquid layers 0-92226
 variable pressure manometer, electrocapillary element appls. and properties 0-73379
 viscosity of liquids, capillarity method determ. 0-82619
 water impurity concentration in steam-generating channels with capillary-porous structure 0-103071
 CO₂, adsorption and capillary condensation on clays rel. to Mars volatile storage and atmospheric history 0-72833
³He-³He normal solution, size effect influence on capillary mass transport (*Russian*) 0-70497
 N₂ adsorbent mesopores, capillary evaporation and struct. 0-107614
 Na evaporation from slot type capillary structs., crit. heat fluxes 0-74854
 Na, liquid, evaporation from capillary-porous struct., capillary restriction in initial stages 0-107609
 W, molten drop break up in gas flow, surface drag, capillary excitation (*Russian*) 0-100024

capillary phenomena *see capillarity***capillary waves**

- capillary-gravity waves produced by moving press. distrib. 0-69859
 finite-amplitude periodic progressive capillary waves, enclosed bubbles 0-79339
 jets, capillary oscillations, meas. 0-96291
 propagation, experimental test of theories 0-69847
 short gravity-capillary waves modulation by longer-scale periodic flows 0-57106
 wind generated capillary waves, spectral characts. 0-59059

capture cross-sections, nuclear *see nuclear reactions and scattering***Caratheodory's principle** *see thermodynamics***carbon**

see also nuclei with

- see also carbon fibres; charcoal; diamond; graphite*
 abrasion against graphite, dusting wear regime 0-97595
 abundance anomalies in QSO Q0353-383, UV and visible spectral obs. 0-82532
 abundance in B-type stars in associations and general field 0-67702
 abundance in globular cluster NGC 6752 first giant branch 0-67719
 abundance in Orion Nebula and IC 418 from visible and IUE obs. 0-82451
 activated, adsorption in countercurrent flow 0-70524
 activated and impregnated, temp. depend. adsorption of HCN 0-89522
 adlayer effect on CO and H₂ adsorption and desorption on Fe(100) 0-71573
 adsorbed on Ni surface, location of adsorbed atoms, surface channelling meas. 0-84373
 adsorption on Fe(100), adsorbate coverage determ. by LEED, AES and XPS 0-103566
 amorphous, catalytic oxidation by Pd particles, TEM obs. 0-76555
 amorphous, Lifshitz constant for calc. of van der Waals force between two solids (*French*) 0-107658
 amorphous film, spin resonance, IR spectra, microhardness 0-71157
 amorphous grains, extinction coeffs., 0.21-340 μm, lab. meas., rel. to interstellar grains 0-73020
 atmosphere aerosol, C particles causing Denver Brown Cloud 0-81961
 atom, ³S-³P₂ and ³S₂-³P₁ transitions, ¹³C isotope shift 0-58201
 atom, electron excitation cross section calc., Born approx. with Slater wave functions 0-69243
 atom, ground state fine struct., laser mag. reson. obs. 0-87062
 atom, one-centre integrals of semiempirical theories of valence, ab initio calcs. 0-102441
 atom in molecule, K-shell fluoresc. yield, statistical scaling 0-78644
 black suspensions, simultaneous meas. of dichroism and birefringence in elec. field., photocurrent signal obs. 0-82801
 bonding to Tokamak walls, XPS studies 0-80942
 carbyne as possible constituent of interstellar dust 0-90514
 channel and thermal blacks, graphitisation at high press. and temp. for diamond synthesis, Ni influence 0-60795
 chaoite, a new allotropic form of carbon, produced by shock compression 0-80997
 chars, thermally activated paramagnetism, mag. susceptibility, meas. 0-75709
 clay, Al₂O₃ and SiC recovery by C reduction 0-108704
 coke, breakage behaviour rel. to struct. 0-85026
 coke, graphitisation at high press. and temp. for diamond synthesis, Ni influence 0-60795
 coke, metallurgical, industrial strength meas. methods, critique 0-85117
 coke, metallurgical, strength and struct. relationship 0-84997
 cokes, metallurgical, struct. and strength 0-93610
 carbon continued
 contaminant, effect on dissolution of quartz in liq. Si, rel. to melt growth of Si 0-70414
 contaminant, in EFG Si ribbon, conc. determ. by nuclear techniques and SIMS 0-59506
 contamination of metal surface, plasma etching and cleaning 0-97645
 determination by activation anal. (α,n), (α,p) reacts. investig. 0-61206
 diamondlike layers, RF plasma deposited, frictional props. 0-71762
 diffused C, influence on structure and oxidation of hot-pressed Zircaloy-2 0-61016
 diffusion from graphite to W coating prevention, in metal-graphite layer structure of X-ray tube (*German*) 0-105759
 dispersions of C black, in polymer particles, photomicrography of submicrometer birefringent contaminants 0-62757
 Earth upper mantle, C abundance rel. to plate tectonics 0-81845
 electrodes, used in emission spectrography, isotopic labelling study, plasma appl. (*Hungarian*) 0-106976
 electron microprobe local anal. of light elements, ultrasoft X-ray spectroscopy 0-90927
 electronic stopping power of heavy ions, empirical relation 0-92571
 enhancement in nova envelope on surface accretion at white dwarf 0-85936
 fabric reinforced plastic laminates, tensile and compressive strength determ., 20-1500°C 0-100880
 filamentous catalytic, rel. crystallographic orientations of C and metal 0-89240
 film, image contrast, rel. to inelastic scattering 0-100154
 films, diamond-like, on Si, colour chart 0-97366
 films with high conductivity, prep. and props. 0-80983
 foil, extreme UV induced forward photoemission 0-76137
 foil, H₂⁺ transmission field 0-100732
 foil, HeH⁺ impact, dissoci., emitted light polarisation meas. 0-58361
 foil, Kr⁺ incident, equilib. charge state distrib. and multiple scatt. angles 0-59532
 foils, He⁺ and HeH⁺ impact, quantum beat pattern depend. on foil thickness 0-58343
 fusion reactor material, low energy ion erosion expts., Kaufman source appl. 0-68942
 glassy, electrolytic durability 0-66809
 glassy C electrodes for photogalvanovoltaic and photovoltaic cells 0-89630
 glassy-C, irradiation induced dimensional changes 0-65052
 global C budget and CO₂ from fossil fuel burning 0-77080
 graphite, interstellar porous grains, free-space equilib. temps. calc., rel. to optical props. 0-62223
 graphitic overlayer on Ag electrode, pyridine adsorption, Raman spectra obs. 0-103954
 graphitisable, catalytic graphitisation by Cr, Mn and Mo oxides 0-89166
 hard, heat-treated under pressure, characterisation of carbon phases by electron microscope 0-60855
 hard, surface wear characts. 0-108596
 IC 418, planetary nebula, C abundance from UV spectra 0-67832
 impurity in Cr₂O₃, effect on sintering behaviour 0-66461
 induced amorphous surface layers in Ti-implanted Fe 0-107287
 interstellar C, 492 GHz line detection 0-90508
 ISSEC selection for fusion reactor 0-57950
 kaolinite-C, high temp. reduction reactions, thermodynamic anal. 0-104426
 KERMA values, consistent set for H, C, N, and O for neutrons from 10 to 80 MeV 0-68967
 laser, nuclear pumped, employing Ne(He)-CO(CO₂) mixtures, energy storage 0-63996
 muonic X-ray transitions, nuclear charge radii 0-99589
 Ni, adsorption residual C removal by electron beam irradi. and heat treatment (*Chinese*) 0-88421
 nongraphitizable, catalytic graphitization by Cr₂O₃, MnO₂ 0-97440
 Nova Serpentis 1978, C grains condensation in circumstellar dust shell 0-90430
 paint type coating layer with spherical pigment, radiative transfer theory 0-61405
 pionic, Auger electron emission (*Russian*) 0-69271
 plasma, spectral and absorpt. coeffs. 0-69985
 polycrystalline, flexural strength after heat treatment porosity correl. 0-84996
 potential in equilibrium with impure high temp. inert gases 0-104135
 pyrocarbon, irradiation-induced dimensional changes 0-65052
 pyrocarbon coating, isotropic, gas permeability, neutron irradiation effect (*French*) 0-63260
 pyrocarbon coating, isotropic, gas permeability meas. (*French*) 0-63259
 pyrocarbon coatings, refl. anisotropy and struct. determ. by perpendicular incidence microellipsometer 0-101824
 reduction of GeO₂-SiO₂ and 3Al₂O₃-GeO₂-SiO₂ in mixed diffusional kinetic regime (*Russian*) 0-66771
 reduction of MnO, surface reaction, CO regeneration (*Russian*) 0-66772
 reduction of rare earth metal oxides (*Russian*) 0-93743
 replicas, single-stage, detaching using glue films 0-61038
 smokes, vapour-condensed, 800 to 130 nm extinction and interstellar extinction curve 0-82180
 solar flares, O I 1355.6 Å and C I 1355.8 Å lines obs. 0-90381
 soot in urban atm., determ. by optical absorption technique 0-108824
 spark gaps with C parallel plane electrodes, erosion characts. 0-70076
 sputtering, low energy, H, D and He ions 0-100734
 steels thermodynamics, C-C interaction energy 0-93793
 strength and struct., conf., Bath, London, England (Apr. 1979) 0-82566
 support films for high-resolution STEM, prep. and observation 0-93496
 thin foil, irradiation with 1.2 MeV Ar⁺, electron diffraction study 0-103397
 vapour, Swan bands, oscillator strength 0-63712
 vitreous, directional O ion beam etching, compared with reactive ion etching 0-71781
 Au-C, light ion large angle scatt. in weakly screened Rutherford region 0-84823
 BaTiO₃:C, solubility of C at low O₂ potentials, 800°C 0-100334
 C and adsorbed acetylene on Fe, hydrogenation, C-1s XPS spectra obs. 0-84366
 C I 1101 Å absorpt. edge in A-type stars, effect of C+H⁺≡C⁺+H charge transfer 0-90423
 C II, UV line spectrum of active chromosphere star ε Eridani, models 0-77394
 C II, Zeeman splitting of high-n recomb. lines 0-58210
 C II homologous ions series, Stark broadening trends 0-105157

carbon continued

- C II line excitation by C I photoionisation 0-58223
 C IV, UV line identifications and lifetime meas. 0-106288
 C IV 1548 Å line profiles of impulsive EUV bursts, OSO-8 obs. 0-90401
 C IV interstellar column density towards early-type stars 0-73018
 C IV interstellar lines in Wolf-Rayet star spectra, IUE obs. 0-67748
 C ion+Au, L-shell X-ray production and subshell ionisation cross sections meas. 0-91637
 C polymeric chains, reduced from poly(tetrafluoroethylene), reactivity 0-89488
 C V, electron impact collision rates, reinterpretation of solar emission line ratios 0-98624
 C V, UV line identifications and lifetime meas. 0-106288
 C⁻ ion source for radiocarbon dating using tandem accelerators 0-94620
 C⁺, association reactions, isotopic exchange, SIFT study, review 0-58435
 C⁺, C²⁺ ion beams, intense, production and postaccel. in magnetically insulated gaps 0-74041
 C⁺ charge transfer in diffuse nebulae 0-77463
 C²⁺ ion energy loss spectra in Ti, Ni, Ge targets 0-65114
 C⁶⁺, microdosimetric measurements of pretherapeutic heavy ion beams 0-72337
 C:H films, amorphous, elec. props., chem. modifications 0-84523
 C:Ni, X-ray photoemission studies 0-76138
 C/Pt-W (8 wt.%), desorption of K from C film surfaces 0-59784
 C-graphite materials for HTR and fusion reactors 0-73928
 C-N bond in methylamine, nucl. mag. isoscreening line diagrams 0-78555
 C+Al(Sn), inner-shell multiple ionisation systematics, X-ray obs. 0-63790
 C+O⁺ ion-molecule reaction, 15 eV energy O⁺ production system 0-84817
 C+proton, charge transfer, target K-shell electron capture, impact parameter depend. 0-102552
 C⁺+H₂(N₂), reactant ion electronic states, effect on charge transfer cross sections 0-63809
 C²⁺+H₂, charge transfer cross sections, oscillatory behaviour in low-energy collisions 0-63806
 C²⁺+Ne, charge exchange contribution to K-vacancy production 0-102553
 C₂, (a¹Π_g), prod. from IR multiphoton dissoc. of acrylonitrile 0-63723
 C₂, interstellar, rot. fine-struct. lines obs. towards ζ Persei 0-67811
 C₂, laser stimulation optimisation for intracavity spectroscopy 0-77881
 C₂, rotational temp. and solar photospheric models 0-62099
 C₂, triplet ground state dissoc. continuum obs. is UV spectrum of C₂ white dwarf (LP 145-141) 0-67715
 C₂⁻, A¹Π_g-X²Σ_g⁺ lines, obs. in carbon stars 0-98661
 C₂⁻, dissociative recomb. cross section determ., merged beam obs. 0-78715
 C₂+acetylene, C₂ Swan band transition probabilities, collisional energy transfer effects 0-87214
 C₂+NO, laser-induced chemilum. reaction 0-61101
 C₂+O₂, C₂(X¹Σ_g⁺) and C₂(a¹Π_g) intersystem crossing and free radical kinetics 0-95668
 C₂+O₂(NO), IR laser photolysis of polyat. mols. photochem. appls. 0-66835
 C₃, A¹Π_g state, orbital angular momentum 0-78514
 C₃, ground state pot. surfaces, analytical functions 0-83304
 C₃ production by IR multiphoton allene photolysis, vibr. relax., chem. kinetics 0-66820
 C₂(C₂⁻) pot. energy curves calc. using SCF, MCSCF and CI methods, dissoc. energies, bond lengths, electron affinity 0-95523
 C-l-lactic acid, enzymatic synthesis 0-61695
 C-pyruvic acid, enzymatic synthesis 0-61695
 C and D labelled paeonol and urinary metabolites, synthesis and physicochem. props. 0-67250
 C natural abundance dipolar interaction in hexamethylethane, NMR longit. cross relax. 0-93196
 C¹³+¹²CO, isotopic exchange, interstellar implications 0-61087
 C β-rays, biological hazards, cell killing effects, E. coli expts. 0-89805
 C, cosmogenic conc. in Earth atm., diffusion distrib. 0-101510
 C dating, high energy mass spectrometer appls. 0-101917
 C dating of small samples via proportional counting 0-82102
 C in atmosphere, variability due to variable Sun 0-85730
 C in groundwater, possible subsurface prod. rel. to dating 0-85690
 C in wines, abundance vars. with 11-year solar cycle, (1909 to 1952) 0-109249
 C measurement in known age specimens, cosmic ray intensity determ. 0-101516
 C pollution of Atlantic from nucl. weapons tests 0-89683
 C, prod. of intense negative beam from graphite 0-102361
 C released to atmosphere, dynamic model for estimating radiation dose to world population 0-89852
 C-labelled bumetanide, whole body autoradiography in dogs by round saw method 0-72399
 C(2¹Σ_g⁺)+H₂(O₂)(ethylene) 0-74241
 Fe surface hardening, ion-carbo-nitriding in CO-N₂-H₂ gas mixtures, expt. (Japanese) 0-71670
 α-Fe:C, electron irradi., vacancy-C interaction, positron lifetime meas. 0-75264
 α-Fe:C, valency effect of interstitials 0-65502
 H+Bq⁺(C⁴⁺)(N^{q+})(O^{q+}), (2≤q≤4, 5), cross sections at keV energies 0-78705
 Mo:C (110) surface, segregation, precip. and desorpt. of C, AES and LEED study (French) 0-103480
 Pt-C replicas, for rapid aimed replica prep. 0-61037
 Re:C, work function, graphitic layer formation 0-96966
 Si:C, implant redistribution, annealing effects, SIMS meas. 0-96561
 Si:C, impurity determ. by IR absorpt. spectroscopy, room temp. and low temp. meas. comparison 0-108237
 Si:C wafers, impurity meas. by Fourier transform IR spectra 0-89030
 Si:C wafers, impurity meas. by Fourier transform IR spectra at low temp. 0-89031
 Zr-C composite system, negative magnetoresist. 0-60008

carbon compounds

see also organic compounds

- ¹³C/¹⁶O/¹²C¹⁸O double ratio, isotopic fractionation evidence in interstellar dark clouds 0-73017
 carbon tetrachloride, surface study, ellipticity coeff., ellipsometric method 0-84343

carbon compounds continued

- CO survey of mol. clouds, use as galaxy spiral struct. survey 0-105346
 ESCA shifts and effective charges 0-78648
 ethylene-CO copolymer, dielec. absorpt. meas., permittivity (French) 0-103916
 graphite fluorides, (CF)_n and (C₂F)_n, prep., struct., discharge characts., electrode props. 0-89502
 interstellar cloud gas phase chemistry 0-105319
 mixtures, marginal comp., thermal diffusion column performance evaluation (German) 0-59157
 molecule, pot. curves, ab initio MRD-CI method 0-83293
 molecules involving B and C atoms, self-consistent charge calcs. of core-electron binding energy shifts 0-69084
 rapid anal. by mass spectrometry/mass spectrometry 0-61173
 Ar-CO glow discharges, positive ion spectra, ion clusters obs. 0-64807
 Br₂+CO₂ mixture, Raman laser optical excitation, electron phototransition theory (Russian) 0-99711
 2,4-C₂B₂H₂, polyhedral, spin coupled ¹¹B-¹H systems, 2-dimens. correl. NMR 0-69166
 CCl, reaction rate const. determ. using laser-induced fluoresc. technique 0-97682
 CCl₂, reaction rate const. determ. using laser-induced fluoresc. technique 0-97682
 CClF, reaction rate const. determ. using laser-induced fluoresc. technique 0-97682
 CCl(X¹Π)+methylhalosilanes, reaction rate const. determ. by kinetic absorpt. spectroscopy 0-97683
 CD⁺+HD(H₂), isotopic exchange, interstellar implications 0-61087
 CF₂, excitation by Hg 253.7 nm line, reson. fluoresc.-spectra 0-63694
 CF₂+H, IR matrix isolation spectra 0-97706
 CF₂ laser, for 16 μm range, review (Rumanian) 0-87408
 CF₂, Nd laser excited stimulated Mendelstam-Brillouin scatt. phase fluctuations (Russian) 0-89014
 CF₄-UF₆ mixture, gas core fission reactor, fission based plasma engine 0-63366
 CH bond dipole calcs. 0-69067
 CH, formed by laser photolysis of methylamine fluoresc. obs. 0-97710
 CH⁺, photodissociation to C⁺ and H, wavelength depend. and photofragment kinetic energies, visible obs. 0-58275
 CH⁺+HD(D₂), isotopic exchange, interstellar implications 0-61087
 CN, (A²Π_g-X²Σ⁺) and (B²Σ⁺-X²Σ⁺) yields from HCN photodissoc. 0-87141
 CN, (X²Σ⁺), prod. from IR multiphoton dissoc. of acrylonitrile 0-63723
 CN, B²Σ⁺-A²Π 0-0 and 1-0 bands, laser excitation spectra 0-91588
 CN formed by laser photolysis of methylamine, fluoresc. obs. 0-97710
 CN free radical, A²Π-X²Σ⁺ Red system, perturbation analysis 0-87247
 CN in neutral cometary atmospheres, prod. 0-82303
 CN, internal energy distrib. following vinyl cyanide photodissoc., temp. depend. 0-78638
 CN, monolayer on Ag surface, vibr. spectra, picosec. Raman gain technique 0-91859
 CN variations among main-sequence 47 Tucanae stars 0-94794
 CN violet (0,0) spectrum of Comet Kohoutek (1973 XII) 0-82308
 CN⁻, adsorbed on Ag surface, Raman active librational modes 0-65359
 CN⁻, spectrosc. consts. for ground and excited states, ab initio, CI calcs. 0-78551
 CN⁺ ion, Σ⁺ and Π states, multi-reference CI study 0-83288
 CN⁺, pot. curves, ab initio MRD-CI method 0-83293
 CN+H, bimolecular exchange reactions, dynamical-statistical method calcs. 0-104435
 (CN)₂, ¹⁴N quadrupole coupling consts., ab initio calcs. 0-58283
 C₂N₂, 2_g band overtones, Raman intensities, bond polarisability theory 0-63639
 C₂N₂ gas, laser stimulation optimisation for intracavity spectroscopy 0-77881
 CN*, B²Σ⁺ state, fluoresc. decay dynamics, collisional quenching and radiative lifetimes 0-58306
 CO 2.7 mm line obs. of V645 Cygni 0-72956
 CO, (4+) system, electronic transition probability 0-106332
 CO, adsorbed c(2×2) layer on Ni, Cu(001), struct. 0-88428
 CO, adsorbed layer, electron impact, electron impulsive ionisation spectroscopy obs. 0-60720
 CO adsorbed layer on Si (111) surface, ion scatt. obs. 0-59810
 CO adsorbed on Ag, Au films, enhanced Raman scatt. mechanism in ultrahigh vacuum 0-107645
 CO, adsorbed on Cu (100), vibr. excitation cross-sections 0-75441
 CO adsorbed on graphite, fluid-registered solid transition 0-59796
 CO, adsorbed on jellium, surface plasmon relax. energies 0-70537
 CO adsorbed on Ni, valence band photoemission, SCF MO CNDO calc. 0-100754
 CO, adsorbed on Ni (111) and (110), laser induced charge transfer, photoemission expts. 0-59798
 CO adsorbed on Pd (111) surface, metastable He impact, electron emission, energy and ang. distrib. 0-60744
 CO adsorbed on Pd surface, Penning ionisation by metastable He beam, theory 0-60735
 CO, adsorbed on Pd/Al₂O₃, IR study 0-108193
 CO, adsorbed on Pt, internal optic modes, mol. dipole model 0-100395
 CO, adsorbed on Ru (001), temp. depend. ordering processes 0-80773
 CO adsorbed on W, electron-stimulated ion desorption 0-59797
 CO adsorbed on W, electron-stimulated desorption, photoemission, relax. energy 0-100401
 CO, adsorption, oxidation, and hydrogenation on Re, XPS, UPS, and thermal desorption study 0-71571
 CO, adsorption and catalytic reactions with H₂ and O₂ on Pt 0-81362
 CO, adsorption and desorption on Fe(100), C, O, S and K adlayer effects 0-71573
 CO, adsorption on Ag film, ellipsometric response 0-103571
 CO, adsorption on Cu-Ni (110), UPS, thermal desorption, AES, and LEED study 0-80087
 CO adsorption on evap. Au films, effect on opt. consts. (German) 0-89081
 CO, adsorption on Ni and Mo, effect on ion and photon yields from ion bombard. surfaces 0-89098
 CO, adsorption on Re(0001), XPS, UPS and temp. programmed desorption 0-71574
 CO, adsorption on Rh dispersed on Al₂O₃, ¹³C NMR obs. of adsorbed states 0-96733
 CO, adsorption on Ru (001), IR spectra, LEED, and thermal desorption meas. 0-70533
 CO, adsorption on Ru (1120), ellipsometry-LEED study 0-103570

carbon compounds continued

- CO, adsorption on SiO₂-supported Pt or Pt-Pd, IR spectrosc. obs. 0-92780
 CO, adsorption on Zr, dissociation and diffusion 0-80085
 CO, adsorption/desorption on Pd clusters, AES and thermal desorption meas. 0-75436
 CO and N₂ binary diffusion in chamber and formed coke (*German*) 0-100356
 CO, asymmetry parameter, angle resolved photoelectron spectra, multiple scatt. method 0-63708
 CO, c(2×2), adsorbed on Ni(001), struct. by LEED, self-consistent scatt. pot. 0-70536
 CO, catalytic interaction with H₂ on Ni (100), temp. programmed desorption study 0-66876
 CO, catalytic oxidation on ferrites, IR spectrosc. investig. 0-89524
 CO, centrifugal distortion calcs. by perturbed Morse oscillator model including Dunham parameters 0-63862
 CO chemisorption as Fe and Ni films surface demagnetisation, ferromagnetic reson. study 0-80616
 CO chemisorbed on Fe, low energy vibr. modes studied by tunnelling spectroscopy 0-78590
 CO, chemisorbed on Mo (100), surface kinetics, photoemission study method 0-80941
 CO, chemisorbed on Ni (111), bond energies 0-100398
 CO, chemisorbed on Pt, IR refl.-absorpt. spectra, adsorbate island struct. 0-84385
 CO chemisorpt. on evaporated Ni films, ellipsometric investig. (*German*) 0-61156
 CO chemisorption on Ni, Pd, Pt, Ir, mol. cluster calc. 0-100407
 CO, chemisorption on Ni (001), back donation in chemisorption bond, UPS study 0-107642
 CO chemisorption on Pd, Ag, PdAg, SIMS, XPS study 0-84382
 CO, chemisorption with O₂ on Pt, SCF-X α cluster calcs. 0-65365
 CO, co-adsorption with H₂ on Rh (111), segregation of co-adsorbed species 0-65361
 CO, coadsorption with H₂ on Rh (111) surface, 2-dimens. phase separation 0-107634
 CO concentration meas. in coal pulverising plant, IR gas analysers 0-89572
 CO, d¹ Δ state, low energy electron impact excitation and radiative decay 0-91691
 CO, determ. by portable IR tester 0-89569
 CO, Dunham vibration-rotation coefficients, isotope dependence 0-83518
 CO electric discharge lasers, vibr. kinetics, modelling and expts. 0-69374
 CO, electrochemical oxidation in fused alkali metal carbonates 0-72040
 CO, electron elastic scatt., low energy, static exchange approx. calcs. 0-69236
 CO, electron scatt., low energy, multichannel variational calcs., static exchange approx. 0-83483
 CO, electronic structure calcs., self-consistent, accelerating convergence of iterative process 0-87037
 CO emission from mol. clouds assoc. with refl. nebulae, EHF obs. 0-82447
 CO emission in W3 H II region, LF obs. 0-82446
 CO, energy levels for perturbed Morse oscillators 0-78676
 CO flame rise vel. meas. by particle track method 0-89489
 CO gasdynamic laser, elec. excited, with closed-cycle gas flow, operation 0-102732
 CO, heat capacity, calc. by modified Redlich-Kwong eqn. of state 0-69963
 CO, horizontal electric arc, in inhomogeneous mag. field, mass spectrometric anal. 0-79620
 CO, in circumstellar shell of 9 Cephei (B2 Ib), obs. 0-94795
 CO, in contracting interstellar clouds, influence on fragmentation 0-67838
 CO in evolved stars expanding envelopes, thermal and maser emission lines profiles 0-82334
 CO in IR spectra of III-106, CH star in M22 globular cluster 0-62131
 CO in nearby galaxies, survey 0-62276
 CO, in Venus atmos., O₂, Ar, CO abundances, error of Pioneer Venus chromatography obs. 0-105189
 CO in Venus upper atmosphere, dayglow spectrum obs., 1250 to 1430 Å 0-77311
 CO, initial reaction probability with Ba getter film, AES obs. 0-61153
 CO, interstellar, detect. in direction of supernova remnant (S147) 0-67836
 CO, interstellar, in Σ state, collisional excitation by H₂ 0-109508
 CO, interstellar, in W3/W4/W5 direction, correl. with heavy optical obscuration 0-62301
 CO, interstellar, obs. in galactic star-forming region (W58) 0-67810
 CO, interstellar, obs. in expanding mol. shell surrounding Pelican Nebula (IC 5070=W80) 0-105296
 CO, isoelectronic sequence, Rydberg transitions, term value-ionisation pot. correl. 0-58276
 CO J=1-0 and 2-1 obs. of Lynds 1551 dark interstellar cloud 0-105318
 CO, LCAO-X α method calcs., comparison with Hartree Fock and MS X α methods 0-95539
 CO laser, analytical theory, multilevel cascade emission (*Chinese*) 0-102702
 CO laser, CW, with RF excitation in supersonic flow 0-74375
 CO laser, cooled electroionisation type, in nucl. reactor active zone 0-64066
 CO laser, sealed-off, output power and efficiency meas. 0-99743
 CO laser, water-sealed, efficiency increase by reducing resonator losses 0-64081
 CO laser output power, active species and buffer He isotope effects (*Russian*) 0-63986
 CO lasers, scaling laws 0-95878
 CO, liq., pure vibr. Raman spectra 0-97262
 CO molecular adsorbed on Mo (110) surface, electronic states, photoemission spectra 0-65363
 CO, nucl. elec. shielding tensor calcs. 0-83296
 CO nuclear pumped lasers, electron impact cross section meas. 0-63985
 CO nuclear pumped laser, fission fragment excited with gas cooling, performance obs. 0-63997
 CO on Co surface, adsorption-desorption kinetics, surface carbide form. effects 0-103574
 CO, on CoO, catalytic oxidation 0-71945
 CO, one electron props., SCF-X α scattered wave method 0-83279
 CO, one-electron props., corrections, Moller-Plesset perturbation theory calc. 0-95519

carbon compounds continued

- CO, oriented molecule, photoelectron ang. distrib., energy depend. 0-76152
 CO oscillatory oxidation over Pt, theory 0-85215
 CO oscillatory oxidation over Pt, theory 0-85216
 CO, output spectra from CS₂-O₂-CO₂(N₂O) flame lasers 0-83601
 CO, oxidation on Ir films, IR absorpt. spectroscopy 0-71398
 CO, P(6) line absorpt. coeff. and halfwidth, temp. depend. 0-78618
 CO, photoelectric cross section and angular distribution calcs. 0-58323
 CO, photoelectron ang. distributions, wavelength and vibr. state depend., reson. effects, asymmetry parameters 0-91602
 CO, photoionisation cross sections and asymmetry parameters, SCF X α scatt. wave calcs. 0-63542
 CO, polarisability derivatives, bond length depend., SCF and CI calcs. 0-58162
 CO, pollution from road traffic, street level conc. 0-81500
 CO, pollution from vehicle emission in urban area cold engine startups 0-104527
 CO, prod. in Venus atmosphere by thunderstorms 0-98587
 CO production using fusion reactor heat, from 2CO₂→2CO+O₂, CO+steam→CO₂+H₂ 0-67014
 CO, reaction with adsorbed O₂, N₂O on Cu (100) surface 0-103583
 CO, reaction with H₂ on Ni(001), extended muffin-tin orbital theory 0-76557
 CO reduction in solar nebula, kinetic inhibition 0-85875
 CO, relative Raman scatt. cross section 0-100061
 CO, remote sensing using freq. doubled CO₂ laser radiation 0-67025
 CO room temperature nuclear pumped laser, parameter optimisation and spectral props. obs. 0-63995
 CO, rot. distrib. in supersonic beam, IR bolometry using tunable diode laser 0-63869
 CO, rotational Raman intensities and polarisability anisotropy change meas. with internuclear distance 0-63641
 CO, second virial coeffs. 0-83440
 CO, single breath diffusing capacity, theoretical anal. 0-67328
 CO, solid, CO laser excited, strong vibr. population inversion 0-58547
 CO supersonic lasers, CW double elec. discharge performance 0-69416
 CO, surface, (110), chemisorpt. effects on dielec. function, refl. spectra chemisorption on W(110) surface, effects on dielec. function, refl. spectra 0-75616
 CO, troposphere vertical profile, eastern USA in winter 0-77035
 CO, v=0→1 vibr. excitation, electron impact cross sections 0-83507
 CO, vibr. excitation via high-energy shape resonances 0-91693
 CO, vibrational transitions dipole matrix elements, numerical calc. 0-95594
 CO, X Σ^+ , vibr. levels, UPS electron attachment obs. 0-95683
 CO⁺ detection at outburst in Periodic Comet Schwassmann-Wachmann I (1974 II) 0-72881
 CO⁺, electron impact rot. excitation, Glauber approx. with Coulomb effect 0-63840
 CO⁺ in Comet West (1976 VI), brightness profiles of A² Π -X Σ^+ system (2-0) band 0-85896
 CO⁺ in cometary tails, surface brightness rel. to H₂O⁺ 0-72880
 CO⁺ in Periodic Comet Schwassmann-Wachmann I near minimum brightness 0-82305
¹³C¹⁶O⁺ (2,0) band, comet-tail system, rot. anal. 0-74157
 CO-³He nuclear pumped laser, optimisation with 2 MeV protons 0-64000
 CO-H₂O-NH₃-methanol, solid mixture vibr. modes, IR spectra 0-90504
 CO-HBr, weakly bound, rot. spectra 0-91544
 CO-HCN complex, charge transfer theory, Mulliken population, ab initio calc., multiconfiguration scheme 0-106392
 CO-HCl, weakly bound, rot. spectra 0-91544
 CO-HF, weakly bound, rot. spectra 0-91544
 CO-He glow discharge, positive column, ionisation processes 0-79618
 CO-He nuclear pumped laser, high energy beam deposition 0-63999
 CO-myoglobin, mol. tunnelling, isotope effect, time resolved IR Fourier transform obs. 0-72126
 CO-N₂, liq., N₂ Raman scatt. parameters, high resolution coherent active spectroscopy 0-66207
 CO-N₂ discharge, plasma characts. and vibr. kinetics anal. 0-59331
 CO-N₂O reacting gas mixture, gain due to CO₂ 0⁰₀1-10⁰₀ transition 0-74337
 CO+¹²C⁺(HCO⁺), isotopic exchange, interstellar implications 0-61087
 CO+¹⁴N₂, vibr.-vibr. energy transfer, long and short range pot. effect 0-99556
 CO+¹⁴N₂, vibr.-vibr. energy transfer, long and short range pot. effect 0-99556
 CO+¹⁵N₂, vibr.-vibr. energy transfer, long and short range pot. effect 0-99556
 CO+Ar, molecular fluid mixtures, equilibrium props. 0-64867
 CO+Br⁺, total electron detachment cross sections for energies around threshold 0-99550
 CO+Cd(P₀), absolute quenching cross section, phase-shift method 0-58340
 CO+Cl⁺, total electron detachment cross sections for energies around threshold 0-99550
 CO+DCI, V-V energy transfer 0-78695
 CO+F in Ar matrix, vibr. and electronic spectra, valence force potential determ., mol. photodissoc. obs. 0-85170
 CO+H₂, rot. excitation, rel. between tensorial cross sections 0-83454
 CO+H₂O⁺, rate constants determ. as function of relative kinetic energy 0-81292
 CO+H⁺, computed cross section vibr. threshold effects 0-63759
 CO+H⁺, ground state pot. energy surface, ab initio SCF calc., protonated equilib. geometry 0-83301
 CO+H⁺, vibr. excitation calc., close coupling and sudden approx. 0-78561
 CO+HBr, rate consts. for vibr. energy transfer meas. using laser. induced fluorescence technique 0-87206
 CO+HF, HF(v=3) relax. and rate consts. 0-61069
 CO+Hg(P₁), quenching rate constants determ. with nanosecond light pulser with Hg vapour 0-100111
 CO+Kr²⁺, charge transfer reactions, rate coeffs. and product-ion distributions meas. 0-104431
 CO+NO, NO γ (0,0) band, oscillator strength and line broadening 0-106356
 CO+Ne²⁺, charge transfer reactions, rate coeffs. and product-ion distributions meas. 0-104431
 CO+U⁺(UO⁺), reaction cross-sections, ion beam apparatus study 0-97691

carbon compounds continued

- CO⁺+D₂, state selected reaction cross-sections, coincidence technique obs. 0-66797
 CO⁺+NO₂→CO₂⁺+N, crossed beam study 0-104436
¹²C¹⁶O+¹³C¹⁶C, vibr. energy transfer, laser-induced fluoresc. obs. 0-78690
 CO₂, 00⁰1-10⁰ transition in CO-N₂O reacting gas mixture, gain 0-74337
 CO₂, 4.3 μm band absorpt. in atmosphere, solar occultation sounding for temp. and press. profiles meas. 0-98452
 CO₂, absorption in H₂O, aq. solns. with interfacial turbulence due to microstirrers 0-64527
 CO₂, adsorbed on Al₂O₃, Raman spectroscopy study 0-65358
 CO₂, adsorption and capillary condensation on clays rel. to Mars volatile storage and atmospheric history 0-72833
 CO₂, air composition at Barrow, Alaska, wind direction depend. 0-85704
 CO₂, amplifier, pulsed, large-vol., small-signal gain meas. 0-91772
 CO₂, and CO binary diffusion in chamber and formed coke (*German*) 0-100356
 CO₂, and climate, model of geographically nonuniform effects 0-90143
 CO₂, asymmetry parameter, angle resolved photoelectron spectra, multiple scatt. method 0-63708
 CO₂, atmospheric, climatological significance of doubling of conc. 0-101426
 CO₂, atmospheric content, climatological consequences (*Dutch*) 0-98411
 CO₂, atmospheric environmental control technology 0-104529
 CO₂, bond distribution functions, anharmonicity effects on electron diffraction 0-69234
 CO₂, CW laser, axial gain distribution 0-58502
 CO₂, CW laser, vibr. temp., dissociation and gain limitation determ., new technique 0-87369
 CO₂, CW laser radiation, freq. conversion in Ti-Cs vapour mixture 0-74438
 CO₂, collision-induced Raman spectrum, theoretical studies 0-63646
 CO₂, compact repetitively pulsed superatm. press. laser with high output power density 0-102731
 CO₂, content of polar ice, 20000 yr BP 0-61891
 CO₂, continuously tunable laser, optical pumping of NH₃ laser 0-83596
 CO₂, corrosion of graphite, CO production, radiolytically induced gas pressure effects 0-106115
 CO₂, determ. in rocks and minerals by inorganic gas chromatography 0-85767
 CO₂, diagrammatic perturbation theory, using universal even-tempered basis set 0-58131
 CO₂, diffusion rate in Au thin layers 0-100359
 CO₂, dipole moment functions 0-87094
 CO₂, dissociation in a nonequilibrium plasma 0-87851
 CO₂, dissociation into CO and O₂, H₂ production from CO+steam, fusion reactor heat 0-67014
 CO₂, electric-discharge mixing laser, 30 kW output, 9% efficiency 0-87410
 CO₂, electron elastic scatt. and vibr. excitation by 4, 10, 20 and 50 eV electrons 0-83484
 CO₂, enriched in ¹⁷, ¹⁸O, diode laser spectroscopy of Q branches 0-78621
 CO₂, from fossil fuel burning and global C budget 0-77080
 CO₂, fundamental condensation cycles in steam and nucl. power plants, performance characts. 0-63368
 CO₂, gas, electron impact ionisation, electronic fluoresc. spectra 0-95664
 CO₂, gas transport laser, discharge and power extraction characts. (*Rumanian*) 0-95869
 CO₂, gasdynamic laser, 16 μm radiation, modified Anderson's time-depend. anal. 0-106505
 CO₂, gasdynamic laser, depopulation of lower active level by CO₂+NO collisions 0-74336
 CO₂, gasdynamic laser, energy characts. calcs. 0-95866
 CO₂, gasdynamic laser, operating on combustion products, gain coeffs. of complex working media 0-58506
 CO₂, gasdynamic laser, population inversion, press. effect 0-102692
 CO₂, gasdynamic laser with partial inversion at 16 μm, gain calcs. 0-78833
 CO₂, gasdynamic lasers, combustion driven, effect of residual CO on small signal gain 0-63973
 CO₂, gasdynamic lasers, multicomponent working media, energy characts. calcs. 0-95867
 CO₂, harmonic force const., vibr. freqs., integrated intensities, MINDO/3 method 0-58411
 CO₂, high density behaviour, extrapolated P-T surfaces and critical density 0-78734
 CO₂, high resolution UV photoelectron spectra 0-91603
 CO₂, high-power pulsed laser, wave-optical resonator modelling, gain saturation law 0-99693
 CO₂, high-power pump laser, direct narrow-line tuning 0-58579
 CO₂, high-pressure reinjection oscillator design and performance 0-78867
 CO₂, horizontal electric arc, in inhomogeneous mag. field, mass spectrometric anal. 0-79620
 CO₂, IR band intensity 0-83425
 CO₂, IR bands transmission functions 0-106324
 CO₂, ice clouds on Mars, brightness temp. and radiative props. 0-105192
 CO₂, ice on Mars surface, evidence from reflectance spectroscopy 0-72834
 CO₂, ice spheres, IR scatt. and absorpt. props. 0-97269
 CO₂, in atmosphere, ¹³C/¹²C vars. in last 22 yrs. 0-104530
 CO₂, in atmosphere, climate-C budget model 0-98381
 CO₂, in climate feedback systems, involving sea-ice, ocean temp. and CO₂ 0-98443
 CO₂, in comet comae, effect of solar photodissociative ionisation 0-90370
 CO₂, induced absorpt. spectral moment, mol. calcs. 0-63737
 CO₂, induced atmospheric temp. rise, Arctic sea ice decay 0-61802
 CO₂, initial reaction probability with Ba getter film, AES obs. 0-61153
 CO₂, inverted, wavefront reversal, high efficiency 0-74436
 CO₂ laser, atmospheric pulsed photoionisation, active medium optical homogeneity 0-58508
 CO₂ laser, detuning effects of FM mode-locking 0-69434
 CO₂ laser, for 16 μm range, review (*Rumanian*) 0-87408
 CO₂ laser, frequency stabilisation method, phase-locking 0-74401
 CO₂ laser, high-pressure CW, output power fluctuations 0-74333
 CO₂ laser, mode locking obs. by intracavity plasma injection 0-83624
 CO₂ laser, output characts. at high pump levels 0-58509
 CO₂ laser, pulsed, elec. field distrib. in vol. discharge controlled by electron beam 0-58505
 CO₂ laser, pulsed, high repetition rate, average power limitations at 10.6 and 16 μm 0-58503

carbon compounds continued

- CO₂ laser, pulsed, high-pressure, high-power, electron-beam-controlled, continuously tunable 0-64065
 CO₂ laser, selected two-colour operation for length meas. scheme 0-99747
 CO₂ laser, TEA, double helical, computer simulation study of dynamics (*Chinese*) 0-74390
 CO₂ laser, TEA, single longit. mode, various prod. techniques 0-106547
 CO₂ laser, transitions, linewidth, temp. depend. 0-69360
 CO₂ laser active medium study using heterodyne photoreceiver 0-95868
 CO₂ laser amplifier multipulse energy extraction 0-78832
 CO₂ laser Antares fusion system power amplifier optics 0-74394
 CO₂ laser Antares fusion system beam alignment 0-74422
 CO₂ laser Antares fusion system optical diffraction computation 0-74424
 CO₂ laser cavity and Ge phase-conjugate 10 μm reflection expts. 0-78894
 CO₂ laser discharge tube, phase distortions due to heating differential 0-95865
 CO₂ laser fusion system optical design and analysis 0-74391
 CO₂ laser fusion system alignment by IR Smart interferometer 0-74425
 CO₂ laser fusion system wavefront correction, deformable mirror design 0-74427
 CO₂ laser fusion system, optical design considerations 0-78868
 CO₂ laser gain switch, pulse characts., approx. evaluation 0-58504
 CO₂ laser gas mixture, vol. photo-preionisation by VUV radiation 0-87966
 CO₂ laser gas mixture seeded with tripropylamine, photoionisation meas. 0-78829
 CO₂ laser Gemini fusion system optical performance 0-74392
 CO₂ laser Gemini fusion system, wavefront error correction by deformable mirror 0-74426
 CO₂ laser Helios fusion system, multicomponent gaseous saturable absorber optimisation 0-74393
 CO₂ laser Helios fusion system, beam simultaneity system 0-74419
 CO₂ laser Helios fusion system alignment 0-74420
 CO₂ laser Helios fusion target positioning with orthogonal telescopes 0-74421
 CO₂ laser Helios fusion system beam diagnostics 0-78882
 CO₂ laser irradiation of air, breakdown plasma prod., elec. field meas. by probes (*Russian*) 0-59334
 CO₂ laser modulation, plasma injection into cavity 0-83626
 CO₂ laser power variation detection via plasma tube impedance changes 0-69437
 CO₂ laser prod. microballoon plasma, fast ion emission 0-103172
 CO₂ laser produced plasma, nonlinear scattering of laser radiation by fast ion waves in plasma 0-106916
 CO₂ laser pulse, nonlinear propagation, computer simulation (*Japanese*) 0-95963
 CO₂ laser pulse, nonlinear propagation characts., computer simulation 0-106575
 CO₂ laser short pulse propagation and energy extraction 0-74335
 CO₂ laser small-signal gain coefficient calc. 0-78831
 CO₂ lasers, IR saturable absorpt. in benzene, chlorobenzene and bromobenzene 0-69465
 CO₂ lasers, optically pumped, use of crystalline reflector in cavity 0-64080
 CO₂, light scattering, multiple scattering contribs. to depolarisation 0-87842
 CO₂ long-pulse 2 GW single longit. mode source for laser-matter expts. 0-78860
 CO₂ lowest triplet state, Ar matrix isolation spectra 0-91569
 CO₂, mantle related thermodynamic props. and reactions at high press. and temp. 0-81874
 CO₂, molecular fluid, Rayleigh and Raman light scatt. props., orientational and collision induced effect 0-63644
 CO₂ multi-rotational line TEA laser, theoretical model 0-69361
 CO₂ multiatmosphere laser tuning for methyl fluoride laser pumping 0-69421
 CO₂, near critical point Rayleigh and Raman scatt., Fermi diad 0-80765
 CO₂, new impurity analysis method 0-66908
 CO₂, photoacoustic Raman spectroscopy under pulsed laser excitation 0-82825
 CO₂, photoionisation, nuclear motion effects 0-58324
 CO₂, photoionisation TEA laser, characteristics calculation using computer model (*Russian*) 0-83589
 CO₂, pressure, end-tidal and arterial diff. obs. 0-72193
 CO₂ pressures in dogs during acute hypercapnia, arterial-expired differences 0-72198
 CO₂ pulse-periodic TEA laser freq. stabilisation by low press. CW laser signal injection 0-74408
 CO₂ pulsed electroionisation laser with controllable emission parameters 0-78865
 CO₂, pulsed gas-discharge laser, skimming discharges for preionisation 0-99740
 CO₂ pulsed laser system, acoustic suppression 0-74378
 CO₂, pure gas, enthalpy, Carlson-Thodos van der Waals eqn. calcs. 0-83878
 CO₂, quenching of laser-excited O₂ 0-99515
 CO₂ R-branch line intensities and press.-broadened line widths at 15 μm 0-102508
 CO₂, ratio of lateral diffusion to mobility for electrons at moderate E/N 0-59160
 CO₂, relative Raman scatt. cross section 0-100061
 CO₂, rotating-mirror Q-switched TEA laser, mode sweeping effects 0-99769
 CO₂, seabed gas seep, Norton Sound, Alaska 0-67361
 CO₂, sealed high-pressure pulsed laser, gas equilibrium chemical comp. 0-63972
 CO₂, self-pumping on pulsed periodic energy input (*Russian*) 0-106506
 CO₂ self-sustained laser system, electron avalanche and electron-ion recomb. coeffs. meas. 0-102694
 CO₂ single-discharge self-sustained laser, 5 cm gap distance, high power output 0-102735
 CO₂, solid, Fermi reson. press. tuning, Raman spectra 0-93293
 CO₂, solid, high press. mol. libration calc. with Kihara core pots., Gruneisen parameter and lattice 0-65173
 CO₂, solid, IR spectra and refr. index, Martian implications 0-72821
 CO₂, solid, melting curves, Lennard-Jones Devonshire theory 0-65201
 CO₂, stability of parallel pin electrode laser discharges, theoretical investigation 0-83588

carbon compounds continued

- CO₂, stretch-stretch interaction force const., electron correlation influence, ab initio CI study 0-58161
 CO₂, supercritical, vertical plate, laminar natural convection heat transfer 0-64544
 CO₂, TEA laser, injection tuning and mode locking on low gain rot. lines 0-95928
 CO₂, TEA laser, isolation between amplifiers using absorbing gases 0-95911
 CO₂, TEA laser, mode-locked, cavity-dumping 0-87415
 CO₂, TEA laser, sequence band effect on 10.4 μm band multiline oscillation 0-74334
 CO₂, TEA laser, tri-n-propylamine doped, parametric meas. 0-78830
 CO₂, TEA laser, UV preionisation, parametric studies 0-64040
 CO₂, TEA laser, UV preionised, characts. 0-69414
 CO₂, TEA Laser pulse, PCM with CdTe crystal Pockels modulator 0-102742
 CO₂, TEA laser system, 20-J nanosecond pulse, based on injection-mode-locked oscillator 0-99752
 CO₂, TEA pulsed, UV preionized, high power laser, development and performance 0-106539
 CO₂, TEA waveguide laser, high power 0-91814
 CO₂, tectonic processes causing emission from crust, seismicity prediction possibility 0-94470
 CO₂, thermal conductivity, corresponding states model 0-69964
 CO₂, thermochem. reduction using solar energy to provide C-based fuels 0-76610
 CO₂, total scatt. cross sections for intermediate-energy positrons 0-91692
 CO₂, UV preionised TEA laser, parametric study 0-102738
 CO₂, VV processes, estimation of almost resonant molecular energy transfer due to multipolar pot. 0-91642
 CO₂, waveguide laser, CW, optical pumping of far-IR molecular lasers 0-83615
 CO₂, waveguide laser, multibeam, excited by AC discharge 0-99754
 CO₂, waveguide laser, saturation parameter meas. method 0-87372
 CO₂, waveguide laser, tunability calc. (*Rumanian*) 0-87371
 CO₂, waveguide laser amplifier with strong discharge tube 0-74398
 CO₂, waveguide laser with pulsed high-freq. discharge 0-99755
 CO₂⁺, electron impact ionisation, cross section obs. 0-58397
¹²C¹⁶O₂, ν₃ band, IR single line strength 0-83370
¹³C¹⁶O₂, IR line strength 0-83371
¹³C¹⁶O₂ laser, isotopically enriched, appl. in optically pumping far IR laser 0-58507
 CO₂-2,2-dimethylpropane, liquid, -vapour equil., 220 to 300K and 6.7 MPa 0-62821
 CO₂-Ar mixture, Ar* prod. by electron excitation, transfer reaction kinetic study 0-63824
 CO₂-Br₂-He mixture, possible gas lasers with solar excitation 0-99695
 CO₂-He-N₂, absorpt. coeff. for 10.6 μm CO₂ laser radiation, 295 to 650 K 0-92252
 CO₂-methane reforming-methanation cycle for Solchem thermochemical solar energy transport 0-94096
 CO₂-N₂ electroionisation laser mixture, ionisation instability of semi self maintaining discharge 0-63971
 CO₂-N₂ fast-flow laser with unstable resonator, self-oscillation instability 0-58780
 CO₂-N₂ mixture, strongly excited, vibr. relax. 0-102555
 CO₂-N₂ mixture, temperature measurement by spectrum line reversal 0-73358
 CO₂-N₂ mixture gasdynamic laser, energy characts. 0-69362
 CO₂-N₂-H₂O fast flow discharge laser, output power time depend. 0-99697
 CO₂-N₂-He, pulse-periodic operation of electron-beam-controlled discharges, energy characts. changes 0-102695
 CO₂-N₂-He electroionisation laser, freq. mode, lasing conditions 0-63970
 CO₂-N₂-He laser media excitation by electron beams admitted through gasdynamic windows 0-99694
 CO₂-N₂-He-O₂ discharge mixture, three body electron attachment to O₂ 0-64779
 CO₂-O₂ coupling in CI free stratosphere, photochemical-radiative column model 0-85723
 CO₂-O₂ stratosphere coupling, photochemical radiative column model with CI chemistry 0-85724
 CO₂-water, saturated two phase flow system, non-equilib. state transient process 0-59096
 CO₂+Ar, short-range intermol. pots., combined interatomic pots. calcs. 0-87198
 CO₂+Ba, crossed beam kinetics, BaO recoil velocity spectra 0-76500
 CO₂+BaO, in Ar flame, rot. and translational relax. by sub-Doppler optical-optical double reson. 0-95583
 CO₂+Br⁻, total electron detachment cross sections for energies around threshold 0-99550
 CO₂+COS mixture, Raman laser optical excitation, electron phototransition theory (*Russian*) 0-99711
 CO₂+Cd(P_{0,1}), absolute quenching cross section, phase-shift method 0-58340
 CO₂+Cl⁻, total electron detachment cross sections for energies around threshold 0-99550
 CO₂+H₂, exponential gap relation, rot. inelasticity 0-78693
 CO₂+H₂, rot. transfer, ab initio intermol. pot. energy surface 0-58354
 CO₂+H⁺(D⁺), vibr. excitation, 10-30 meV 0-58358
 CO₂+H⁺(D⁺), vibr. excitation, isotope and time effects 0-63773
 CO₂+HBr, rate consts. for vibr. energy transfer meas. using laser induced fluorescence technique 0-87206
 CO₂+HF, HF(v=3) relax. and rate consts. 0-61069
 CO₂+He, collinear atom-triatom transition probabilities for anharmonic triatom pots., quantum mech. calcs. 0-83455
 CO₂+He, rot. inelastic collision, ab initio SCF, electron gas and pot. energy surfaces 0-83468
 CO₂+He, translational-vibrational energy transfer, quantum dynamical study 0-63746
 CO₂+He⁺, 0.7-2 MeV, charge-changing collisions, electron capture 0-58372
 CO₂+Kr 0-83455
 CO₂+Li⁺, collisional excitation, quasiclassical trajectory calcs. 0-83467
 CO₂+monobromomethane mixture, Raman laser optical excitation, electron phototransition theory (*Russian*) 0-99711
 CO₂+N₂+He, glow discharge positive ion species identification (*Russian*) 0-84014
 CO₂+N₂+benzene, electronically excited, mol. fluoresc., vibr. relax. cross sections and equilibration rates determ. 0-87205

carbon compounds continued

- CO₂+NH₃, collisional broadening of NH₃ inversion spectrum lines 0-99521
 CO₂+NO, NO γ(0,0) band, oscillator strength and line broadening 0-106356
 CO₂+Ne, energy transfer rate consts., semiclassical method 0-91640
 CO₂+Ne, intermol. pot. in repulsive short-range region, ab initio 0-69204
 CO₂+Ne²⁺, charge transfer reactions, rate coeffs. and product-ion distributions meas. 0-104431
 CO₂+polyatomic molecule, (00⁰) mode deactivation, laser induced fluoresc. obs. 0-83453
 CO₂+U⁺(UO⁺), reaction cross-sections, ion beam apparatus study 0-97691
 CO₂⁺+ethylene, rate coeffs. and product distribution determ. 0-97693
 CO₂⁺, laser photodissociation, tandem quadrupole study 0-81343
 C₂O+NO(O₂)(isobutene), absolute reaction rate consts. meas. by laser induced fluoresc. 0-93738
 C₂O₂, semirigid bender, rot.-vibr. energy level separations obs., struct. and pot. functions determ. 0-83446
 COF₂, dipole moment from compact formulation of polar tensors on bond moment hypothesis 0-58108
 COS, asymmetry parameter, angle resolved photoelectron spectra, multiple scatt. method 0-63708
 COS, high resolution UV photoelectron spectra 0-91603
 COS, in stratosphere, effects on sulphate aerosol layer 0-109212
 COS+Cl⁺, reactions at room temp. 0-93749
 COS+U⁺(UO⁺), reaction cross-sections, ion beam apparatus study 0-97691
 CO* prod. from Ar*+CO₂, use in laser systems 0-63824
 CO₂⁺+SO₂, near-reson. energy transfer, fluoresc. obs. 0-106348
 CO₂⁺(ν₃) fluoresc. obs. of N₂⁺+H₂O(H₂S)(methane) deactivation 0-63776
 CO₂⁺(ν₃)+H₂O(H₂S)(methane), deactivation 0-63776
 CO(1)+CO(ν)-CO(0)+CO(ν+1), vibr. energy accumulation, reaction rate anal. 0-78692
 CO₂, CO₂⁺+ethylene, rate coeffs. and product distribution determ., dissoc. energy and heat of form. 0-97693
 CP⁺, pot. curves, ab initio MRD-CI method 0-83293
 CS emission in W3 H II region, LF obs. 0-82446
 CS, heat of form calc. 0-102581
 CS, prompt emission and internal energy distrib. of X¹Σ⁺ state 0-106364
 CS, rotation analysis of d³Δ_g-a¹Π_g transition, IR spectra 0-78591
 CS, S isotopic composition, spectroscopic meas. (*Russian*) 0-91696
 CS₂, 193 nm laser dissoc., prompt emission and internal energy distrib. of CS 0-106364
 CS₂, asymmetry parameter, angle resolved photoelectron spectra, multiple scatt. method 0-63708
 CS₂ bond distribution functions, anharmonicity effects on electron diffr. pattern 0-69234
 CS₂, electron impact excitation and ionisation 0-63837
 CS₂, electronic autoionisation branching 0-91614
 CS₂, high resolution UV photoelectron spectra 0-91603
 CS₂ in cooled supersonic expansion, electronic absorpt. spectra obs. 0-78629
 CS₂, ionisation and fragmentation by monoenergetic electron impact, mass spectrometric study 0-102581
 CS₂ laser, for 16 μm range, review (*Rumanian*) 0-87408
 CS₂, liq., diamagnetism, mass mag. suscept. meas., temp. depend. 0-97054
 CS₂, liq., time-reversed replica generation of image-bearing optical beam 0-69459
 CS₂, liquid, light field reconstruction accuracy after stimulated scatt. 0-78911
 CS₂ liquid, Rayleigh and Raman bands, intensities of interaction induced components 0-63645
 CS₂, ν₂ bending fundamental, high resolution IR spectrum 0-91559
 CS₂, photodissoc., fragment energy distrib. 0-69200
 CS₂, radiation self synchronisation on Rayleigh edge time stimulated scatt. in external resonator (*Russian*) 0-69461
 CS₂, second order Raman spectrum in condensed phase 0-93299
 CS₂, shock heated, visible emission 0-58274
¹²C³⁴S₂, ¹³C³⁴S₂, high resolution IR spectra (*French*) 0-58249
 CS₂-O₂ additive flame laser, design and performance 0-78870
 CS₂+fluoromethane, fluoromethane laser, buffer gases collisional narrowing 0-99710
 CS₂+He⁺, dissoc. charge-transfer, CS⁺(B²Σ⁺-A²Π_g) emission prod., Morse pot. Franck-Condon factors calc., vibr. anal. 0-99539
 CS₂+OH, lower atmosphere chem. 0-61870
 CS₂+O-CS+SO, vibrational distribution of CS, laser-induced fluorescence meas. 0-71895
 CS₂+S, electronically excited atom, reson. fluoresc. 0-99476
 CS₂+U⁺(UO⁺), reaction cross-sections, ion beam apparatus study 0-97691
 C₂S, influence of polymorphic transform. on sinter stability (*Russian*) 0-66503
 CS₂⁺+CS₂-CS₂⁺+CS+e⁻, chemiionisation, mol. beam photoionisation 0-76495
 CSe₂, liq., partial struct. factor, neutron diffraction meas. 0-79672
¹²C¹⁶O and ¹²C¹⁸O J=2-1 transitions obs. towards galactic H II regions 0-73022
¹³C-¹³C spin-spin coupling const. and stretching force consts., single and double bonds 0-63867
¹³CO self-absorption in the ρ Ophiuchi dark cloud 0-90500
 CICO radical, struct. and props. calcs. 0-74112
 CO, Auger spectrum, ab initio MO LCAO SCF CI calc. many electron contribs. 0-87169
 Co, chemisorbed on Al₂O₃-supported Rh-Cu catalysts, IR spectra (*French*) 0-60559
 CO₂, electrooptical consts., 2ν₃ band induced component 0-78626
 CO₂ flow in heated tubes, with near critical parameters, turbulent flow, heat transfer 0-59022
 CS₂, a²A_g-state detect. by reson. enhanced multiphoton ionis. spectrosc. 0-95551
 Cu, liq., deoxidation rates by CO₂-CO gas mixture (*Japanese*) 0-89394
 DF-CO₂ chemical laser, photon branching in chain reactions, IR radiation initiation 0-91785
 DF-CO₂ chemical laser, amplification of long and short pulses 0-95883
 FCO, radical, struct. and props. calcs. 0-74112
 FCP, microwave spectrum, struct., dipole moment and vibr.-rot. props. obs. 0-91549

carbon compounds continued

H₂+CO, coadsorption on Cu-Ni (110) single cryst. surface, TDS and UPS obs. 0-80052
HCP, force fields and force consts. of electronically excited states 0-69116
He-CO glow discharges, positive ion spectra, ion clusters obs. 0-64807
He+OCS, emission spectra in He afterglow 0-87139
K+CO, rotational inelastic scatt., uniform semiclassical sudden approx. 0-99544
KBr:CN⁻, neutron scatt. studies of (CN)⁻ defects 0-92620
Mn-Al-C, metallic magnets investigations, present state (*Polish*) 0-107987
N₂-CO, liquid, high resolution CW CARS spectra 0-63635
Ne+CS₂, metastable atoms, energy transfer processes 0-83466
O₂-CO₂ mixture, temp. difference of molecular vibr. relaxation freq. from 300 to 675K 0-74238
OCS, electron impact excitation and ionisation 0-63837
OCS, IR spectra, diode laser calibration 0-83363
OCS, microwave spectra, Ku-band Fourier transform spectrometer appl. 0-68265
OCS, millimeter wave rot. spectra, isotope shifts, freqs. and mol. consts. 0-78611
OCS, optically pumped CW subMM emission lines 0-95876
OCS, T₂ relax. meas. using budge-type superhet. microwave spectrometer 0-91551
OCS, vibr. energy transfer map 0-99560
¹⁶O<sub>12C³⁴S and ¹⁶O<sub>13C³⁴S, IR spectra, ν₁ band anal. 0-95620
OCS+benzene, microwave line width and quadrupole moments, perturbation theory 0-69190
OCS+He, translational-vibrational energy transfer, quantum dynamical study 0-63746
OCS+He⁺, dissociation charge-transfer, CS⁺(B²+A²Π_g) emission prod., Morse pot. Franck-Condon factors calc., vibr. anal. 0-99539
OCS+S, electronically excited atom, reson. fluoresc. 0-99476
OCS₂, quantum yields for Se, ⁷⁶Se, ¹²⁷I₂ and ¹³¹I₂ atoms determ. in photolysis, lifetime and quenching rate meas. 0-97741
QCS, static polarisability, ab initio SCF wave functions 0-74106
SeO₂+CO₂, radiative lifetime and quenching rates 0-95685</sub></sub>

carbon fibre reinforced composites

aligned, prep. and theoretical strength agreement 0-84906
graphite fibre epoxy composites, exposed to high temp., degradation of tensile and shear props. 0-81113
graphite fibre reinforced epoxy, US attenuation as an indicator of fatigue life 0-85118
graphite/epoxy composite, high elec. cond., engineering appl. 0-70780
graphite/epoxy composite, single ply, elec. cond. meas. 0-92953
graphite/epoxy laminates, statistical fatigue, high load effect 0-93642
graphite/epoxy laminates, stress wave damage 0-93611
high work of fracture composites, prep. and mech. tests 0-81029
hybrid glass fibre/C fibre reinforced epoxy-phenolic, elastic characts. prediction 0-108491
nylon matrix, design parameters, fibre orientation effect 0-81141
plastic matrix, degraded, study of strain, 20 to 1000°C 0-71680
plastic matrix, props., implications for structural design 0-81174
plastics, strength props., effect of SiC coating on fibre 0-104224
polycarbonate matrix, design parameters, fibre orientation effect 0-81141
preparation, properties and structure for spacecraft use 0-71625
resin matrices and their contribution to composite properties 0-81028
stress/strain behaviour, split Hopkinson press. bar test, opt. and strain gauge methods comparison 0-85132
testing, using burn test apparatus with metal grid and indicator lamp 0-76441
Al matrix, matrix-fibre interaction depend. on metallic dopants (*Russian*) 0-76479
C-fibre reinforced plastic insert molding strength (*Japanese*) 0-66588
Si-Al C fibre composite technological coatings, liquid phase method preparation (*Russian*) 0-108375

carbon fibres

see also carbon fibre reinforced composites
biomedical electrode, elec. props. and EEG appls. 0-72355
coating with SiC, effect on strength props. of C fibre reinforced plastics 0-104224
engineering applications, production requirements and mech. props. 0-89168
graphite, surface anal. by XPS and polar/dispersive free energy anal. 0-65340
graphitised viscose fibre, fluorination, change in struct. 0-88039
irradiation-induced dimensional changes 0-65052
mechanical properties, thermal stability up to 2000°C 0-60929
mesophase-pitch-derived, Young's modulus and tensile strength, struct. flow elimination 0-80995
metal-coated with Cu, Co or Ni, coating struct., SEM study 0-97605
microelectrodes, neurophysiology appl. 0-67314
structure, recent advances 0-81069
structure obs., Raman microprobe-microscope appl. 0-62737
substrate for crystallisation of Ni, Ni-B films, struct. evolution (*Russian*) 0-75455
technology advancements, Indian developments 0-93562
tensile strength, heat treatment and flaw effects 0-81173
thermal expansion coeff. meas. using TEM fitted with furnace 0-102966
SiC-coated C fibre, compatibility with Al (*Japanese*) 0-71700

carbon microphones see microphones

carbon steel

adhesive bonds with polymers, shear resist., polymer crystn. effect 0-89462
boride coatings, spectroscopic thickness determ. 0-85099
built-up edge form., direct SEM obs. 0-104303
carburising kinetics, in endothermal atm. 0-76410
channelling contrast, to investigate fatigue crack propag. 0-66609
chemicothermal treatment, diffusional basis 0-104343
coated with TiC, prep. and props. 0-76414
cold worked, original struct. effect on softening during heating 0-60882
corrosion behaviour in reducing environment of coal fired MHD generator 0-104322
corrosion by aq. H₂S solns. 0-100946
crack growth in high-temp. water 0-108636
crack initiation and propagation life under repeated impact tensile loads (*Japanese*) 0-104264
creep, expt. investigation above 900°C 0-81134

carbon steel continued

creep deformation, under reversed cyclic stresses in type S15C (*Japanese*) 0-81114
deformation ageing, of medium and high C steel, entropy, free energy, dislocations (*Russian*) 0-66581
density and thermal expansion in liq. and solid states 0-96668
dissolution of Cr₇C₃ in austenite (*Russian*) 0-103479
dry lubrication by Cd film, tribological behaviour 0-89364
electroheated, thermal cycling and corrosion behaviour 0-61006
electrophoretic Cr₇C₃ alloy coatings on C steel, sintered, struct. form., Ni-P undercoat effect 0-61027
eutectoid, mech. behaviour, thermomech. treatment effects 0-84970
eutectoid, Si partitioning during pearlite transform., analytical electron microscopy appl. 0-108458
fatigue crack propagation in sheet, influence of struct. of ferrite-pearlite bands (*French*) 0-76338
fatigue life estimation, under combined torsion and bending (*Japanese*) 0-93647
fatigue strength, low cycle, reduction factor for type SFV1 (*Japanese*) 0-104259
fatigue strength, small defect effect 0-104255
ferrite, transform. kinetics, grain size, alloying element effect, carbide precip. 0-93560
ferrite-martensite microstructure, microstructural parameters effect on fatigue strength (*Japanese*) 0-71735
ferritic, fatigue crack growth micromechanisms at low stress intensities 0-108570
hardened by HF current, mech. testing method 0-61053
heat exchanger, gas-flame spray deposited Fe-Si protective coating 0-61025
high C, 0.7% C, welded zone, fatigue strength and microstruct. (*Japanese*) 0-89339
high C, investigation of transformations during tempering by nuclear gamma resonance method (*Russian*) 0-76256
high C, type 7KhFNSh, plastic deform. influence of X-ray interference line breadth (*Russian*) 0-93599
hot plastic deform., vac. colour etching investigation 0-61036
hydrogen attack morphology, effect of hydrogen press. 0-85052
lamellar pearlite, containing proeutectoid cementite, brittle fracture study (*Japanese*) 0-93648
law-C, hot deform., austenite strengthening and weakening 0-76282
low C, cold rolled, graphite precip. and S segregation, AES investigation (*Japanese*) 0-89222
low C, crack initiation at root of circumferential notch of round bar specimens (*Japanese*) 0-60947
low C, cyclic loading, change in mech. props. rel. to heat treatment 0-104282
low C, dual-phase, law of mixtures, applicability 0-89346
low C, dynamic and static strength, strain rate and temp. depend. of flow stress 0-85139
low C, electroboronising by superimposed cyclic current, Na₂CO₃, B₄C, NaCl, NaOH activator studies 0-85081
low C, etchant for revealing austenite grain boundaries 0-85098
low C, fatigue life, variable strain ranges (*Czech*) 0-60956
low C, HF oscillations during electron beam welding (*Russian*) 0-76273
low C, highcycle fatigue, crack initiation model (*Japanese*) 0-104258
low C, impact strength and crit. brittleness temp., sample thickness and notch radius influence 0-85018
low C, initial stages of plastic deform. (*Japanese*) 0-93618
low C, low-cycle failure investigation, elec. resist. meas. appl. 0-85109
low C, mech. characts., specimen size and shape effects 0-66715
low C, nil ductility transition temp. 0-100896
low C, spheroidization of pearlite, global microstruct. evolution 0-108482
low C, stress ageing embrittlement under short term thermally stressed cycle (*Russian*) 0-60885
low C, surface damage produced by pulsating impact contact load (*Japanese*) 0-104263
low C, type 38NCD4, fatigue life improvement by N ion implantation, dose depend. 0-76328
low C, type En3, high strain deform., struct. and props. 0-89301
low C, type KAS, fracture toughness meas. using elect. potential method (*Japanese*) 0-93722
low C, type SAE 1008, finite fatigue life distrib., various load-time histories 0-97589
low C steel, explosive-thermal treatment, sulphide cracking decrease, hydrogen embrittlement (*Russian*) 0-108477
low C structural, fracture toughness and X-ray diffr. obs. of surface (*Japanese*) 0-66634
low C type 08KP, plastic deform. depend. on grain size (*Russian*) 0-66580
low temperature strength, preliminary plastic deform. effect 0-81128
low-C, 510 C and 520 C, tensile fracture at low temps. (*Japanese*) 0-81163
low-C, aged after quenching, rel. between micro-cracks and coarsening effect (*Japanese*) 0-81159
low-C, cast, SC49, rel. between rotating and flexural bending strengths (*Japanese*) 0-81117
low-C, crack growth rate and crack tip shapes, fatigue, cyclic bending (*Russian*) 0-71740
low-C, fatigue strength and crack prop. behaviour under impact program loading conditions (*Japanese*) 0-66635
low-C, high-strength low alloy, Nb(CN) precipitation and coarsening during hot compression 0-97514
low-C, HSLA, austenite recrystn. 0-97512
low-C, kinetics of void development in fracturing A533B tensile bars 0-76357
low-C, Nb microalloyed, interaction between deform., recrystn. and precip. 0-97515
low-C, pitting resist. in low salinity geothermal brines 0-93681
low-C, type dynamic stress intensity factor meas., possibilities and limits Ni-Cr-Mo 37, dynamic stress intensity factor meas., possibilities and limits (*German*) 0-93719
low-C, types 535C, SB 42-B, fatigue crack prop. and crack closure behaviour under plain strain conditions (*Japanese*) 0-81160
low-C, types SS41, SB42, SM50A, STK55, liq. Zn embrittlement (*Japanese*) 0-81164
low-C containing Ti, sheets, recrystn. texture effects on plastic strain ratio and deep-drawing (*Chinese*) 0-66527
machining theory, for chip geometry, cutting forces etc. 0-93629
magnetomechanical acoustic emission for residual stress NDT 0-71149
massive martensitic transformation kinetics 0-81060

carbon steel continued

- medium, C, US attenuation, mag. field effect 0-89428
 medium C, Cr-Mn-Mo, austenising temp. effect on microstruct. and fracture toughness (*Chinese*) 0-66542
 medium C, dynamic and static strength, strain rate and temp. depend. of flow stress 0-85139
 medium C, electrolytic Fe coated, distrib. of bounded fatigue limits 0-81198
 medium C, etchant for revealing austenite grain boundaries 0-85098
 medium C, ground, residual stresses, X-ray evaluation 0-79863
 medium C, S45C notched specimens, Charpy impact tests, notch angle effects (*Japanese*) 0-85124
 medium C, thermomechanical working influence on mech. props. (*Russian*) 0-93578
 medium C, type 45, Cr galvanic coating thickness determ. by profilography 0-85095
 medium C, type 45, fatigue strength improvement after glow discharge treatment 0-108573
 microflow and strain hardening under cyclic loading 0-104182
 mild, 1019 AISI, acoustic emission generated during deform. 0-60921
 mild, anodic polarisation behaviour in hot alkaline sulphide solns. 0-100949
 mild, cold rolled, texture and plastic anisotropy rel. to alloying and precipitation (*French*) 0-108475
 mild, constitutive eqn. covering wide range of strain rates (*Japanese*) 0-79862
 mild, corrosion rate meas. in H_2SO_4 using microprocessor controlled potentiostat 0-71798
 mild, cyclic strain enhanced dissolution in NH_4NO_3 , corrosion fatigue props. 0-85083
 mild, descaling by HCl (*French*) 0-108642
 mild, electrodes, in H_2SO_4 , H evolution reaction kinetics 0-97630
 mild, eval. of cold rolling oils and boundary lubrication characts. by SEM 0-85068
 mild, fatigue crack arrest and retardation, load stepdown effect 0-108527
 mild, fatigue crack growth and threshold measured at very high frequencies 0-71742
 mild, fatigue crack propag. study using servohydraulic test system 0-76431
 mild, fatigue crack propagation, stress ratio effect 0-71733
 mild, fatigue softening and hardening detected from Barkhausen noise 0-76428
 mild, fractography study of shear mode fatigue crack growth by etch pits (*Japanese*) 0-108545
 mild, laser microspectral anal., Si and Cr trace element identification 0-108769
 mild, plastic flow localisation under dynamic torsional loading, crit. variables 0-85015
 mild, solderability, annealing effect (*Japanese*) 0-89244
 mild, surface hardness improvement by dynamic recoil implantation 0-61008
 mild, transgranular stress corrosion cracking in H_2SO_4 -KI soln. 0-71797
 mild, tubes, crushed between rigid plates, large deformation compression 0-66579
 mild, US detect. of H embrittlement 0-71822
 mild steel pipe corrosion, mass transfer coeffs. under isothermal flow conditions 0-97628
 nonmetallic inclusion segregation during cooling (*Russian*) 0-100330
 pearlite, deform. and fracture mechanisms, HV SEM obs. 0-104243
 pearlitic, struct. variations under plastic strain and subsequent heating, cementite decomp. (*Russian*) 0-84954
 phosphide analysis using nonaqueous electrolyte potentiostatic etching method (*Japanese*) 0-89221
 pipes, welded branch, stresses calc. 0-108493
 plain C, Nb microalloyed, interaction between deform., recrystn. and precip. 0-97515
 plates, residual elements effect on through-thickness props. 0-66660
 plating with Ni, Zn and Cu, barrel plating efficiency 0-100964
 powder forged, fatigue, surface treatment effect 0-85048
 quenched, restoration of austenite grains during rapid heating (*Russian*) 0-76272
 recrystallization annealing, grain growth, effect of type of deform. 0-100847
 residual elements, effect on props. 0-66643
 rolling contact fatigue, tuffriding effect on 0.2% C cylindrical specimen 0-100954
 rolling wear study of misaligned cylindrical contacts 0-108590
 steel, medium C, 40MnB, dissoln. and precipitation of $M_{23}(C,B)_6$ (*Chinese*) 0-66511
 steel, medium C, Ni-Cr-Mo, overheated, fractographic study (*Chinese*) 0-66616
 sulphide cracking resistance 0-108640
 sulphides, obs. and anal. using non-aqueous electrolyte-potentiostatic etching method (*Japanese*) 0-89433
 surface damage produced by pulsating impact contact load (*Japanese*) 0-104263
 tempered, with different Ni contents, scaling behaviour obs. 0-71817
 tensile fracture surface in high press. H_2 at room temp. (*Japanese*) 0-108540
 tensile props. in high press. H_2 at room temp. (*Japanese*) 0-108501
 tensile strength, working and heat treatment effects (*Japanese*) 0-104209
 trapping mechanism, detection, positron meas. 0-84798
 tuffrided steel, type S15CK, fatigue strength, estimation of size effect (*Japanese*) 0-81166
 US wave velocity meas., rel. to cold working in type 38NiCrMo₄ 0-99908
 welds, residual stresses, evaluation by Barkhausen noise meas. 0-76436
 C-Mn, stress corrosion cracking failure, predictive approaches 0-97611
 Cu-mild steel explosively welded interface, SEM examination (*German, English*) 0-96746
 H permeation, and trapping meas. in plain C type 1045, rel. to cryst. microstruct. 0-84328
 low-C, Nb, microalloyed, hot rolled, Nb(CN) precip. and austenite recrystn. 0-97513

carbon tetrachloride, CCl_4 see *organic compounds*

carcinotrons

No entries

cardiology

see also *blood; electrocardiography; haemodynamics*
 angiocardiology, digital multiprocessor system 0-94362

cardiology continued

- aorta, root of, functional anatomy and deform. props. 0-67136
 aorta valves, crescent-shaped, deform. props. by holographic interferometry 0-61616
 aortic valve prostheses, hydrodynamic losses eval. 0-72378
 aortic valve replacement, computerised simultaneous press./vol. anal. before and after 0-85531
 aortic valve study, by holographic interferometry and shadow Moire methods 0-104613
 artificial heart, microcomputer based automatic controls 0-67289
 artificial heart, transfer function governing ventricular ejection in assisted circulation 0-104817
 artificial heart valves, dynamics 0-72379
 atrial contraction, model anal. of contrib. to ventricular filling 0-85424
 biofoal diverging collimator for equilibrium radionuclide ventriculography 0-72310
 blood flow detection in human heart, US pulsed Doppler flowmeter system, microcomputer based 0-104690
 blood flow through heart valves, vortex method calcs. 0-72189
 cardiac mechanical activity, noninvasive mag. detect., instrumentation 0-89820
 cardiograms, image processing, cardiac function meas. (*Japanese*) 0-94354
 cardiomagnetism, high resolution 0-104698
 cardiopulmonary resuscitator, programmable, for evaluation of standards 0-72374
 cardiovascular nuclear medicine, an overview 0-85480
 cardiovascular nuclear medicine, instrumentation and data processing, ventricular function evaluation 0-85481
 cardiovascular shunts, detection and quantitation with commonly available radioisotopes 0-94356
 cardiovascular system, haemodynamic obs. in awake rabbits during hyperbaric $He-O_2$ exposure 0-101200
 cardiovascular system, mathematical models and identification problems 0-89780
 cellular electrophysiologic-clinical correlations using a relational data base 0-89890
 cineangiocardiology, accuracy of ventricular models and localisation of contraction anomalies 0-89845
 cineangiograms, computerised anal. system 0-72284
 cineangiography, automatic detect. of apex of heart 0-89847
 cineangiography, left ventricular contour segmentation from anatomical landmark trajectories and its application to wall motion analysis 0-94363
 cineangiocardiology of left ventricle, automatic processing and cardiac function display techniques (*Japanese*) 0-72311
 computed tomography 0-98088
 computerised tomography, ECG-gated, motion phantom 0-98115
 computing conf., Geneva, Switzerland, (Sept. 1979) 0-82582
 conference on cardiac defibrillation and cardiopulmonary resuscitation, Lafayette, USA (Sept. 1979) 0-67929
 contraction mechanism modelling 0-72204
 coronary artery bypass graft patient recovery trajectory classification algorithm 0-94411
 coronary artery quantitation using digital image processing techniques 0-85517
 data collection station, based on autonomous CAMAC crate 0-61689
 defibrillator, automatic, implantable, cardiac pumping detect., optimal electrode spacing 0-72373
 defibrillator electrodes, recovery curves for different materials 0-67283
 echocardiogram, M-mode, automatic computer anal. (*Japanese*) 0-72274
 echocardiograms, 1D and 2D, computer processing (*German*) 0-81665
 echocardiograms, computer assisted left ventricular anal. (*German*) 0-81667
 echocardiograms, M-mode, microcomputer editing for semiautomatic anal. 0-94299
 echocardiograph signals, M-mode, analogue storage using video tape 0-94298
 echocardiographic images, video recorded, interactive segmentation 0-89817
 echocardiographic tracking system, microprocessor-controlled 0-67169
 echocardiography, clinical significance (*German*) 0-81664
 echocardiography, contrast cross-sectional (*Japanese*) 0-101237
 echocardiography, pulsed Doppler, variable sample vol. dimension 0-76816
 ejection fraction rel. to ventricular vol., computer anal. 0-104599
 electric shocks, 50/60-Hz AC, ventricular fibrillation tests on animals (*German*) 0-10154
 electrical heart stimulator, versatile, wide-range, for animal expts. 0-89912
 electromedical devices of the angiohaemodynamical catheterisation laboratory 0-85515
 ellipsoidal model, appl. to left ventricular contractions study 0-104608
 emission computerised tomography, ECG-gated, cardiac blood pool 0-98117
 endocardium motion during contraction, anal. method 0-109072
 epicardial mapping, DC, during exptl. coronary occlusion, digital data acquisition system 0-85527
 equilibrium left ventricular ejection fraction determ., background noise estimation 0-94365
 fibrillation thresholds for 60 Hz currents and voltages directly applied to heart 0-101301
 fourth sound studied by FFT 0-94397
 gamma camera, computer controlled 0-61682
 gated blood pool scan, radioisotope evaluation of ventricular performance 0-85483
 gated cardiac scintigram anal., digital boundary detect. techniques 0-98106
 gated cardiac scintigram analysis, digital boundary detection techniques 0-98081
 haemofol mitral valve, results of flow visualisation expts. 0-104632
 high-pressure convolutions in rodents, associated heart rate changes 0-67124
 His-Purkinje conduction system, human, mag. study 0-89818
 imaging with ^{11}C -palmitate and PETT IV system 0-89849
 intracoronary radiolabelled particulate imaging 0-94360
 kinematics of the beating heart 0-76777
 left ventricle, 3D image expression, nuclear medicine 0-104731
 left ventricle, math. model of mechs. 0-101195
 left ventricle, model study of isovolumic and non-isovolumic contracts 0-85428

cardiology continued

- left ventricle dynamic geometry in intact unanaesthetised man, midwall motion 0-85491
- left ventricular ejecting beats, estimation of hydromotive source press. 0-76776
- left ventricular diastole mechanics 0-94261
- left ventricular diastolic press.-area curves, shifting with positive end-expiratory press. 0-104604
- left ventricular function, radioisotope evaluation with nonimaging probes 0-85484
- left ventricular function assessment using radionuclide techniques, technical considerations, review, book contrib. 0-101261
- left ventricular function evaluation by myocardial scintigraphy and radionuclide angiocardiology (*Japanese*) 0-81724
- left ventricular function quantitative evaluation by 2D ultrasonography system 0-85457
- left ventricular haemodynamics during respiration, dog expts. 0-81635
- left ventricular localised wall motion abnormality assessment, usefulness of quantitative parameters 0-89848
- left ventricular performance characteristics in trained and sedentary dogs 0-97969
- left ventricular performance parameters rel. to max. dZ/dt 0-101159
- left ventricular wall motion anal., externally referenced polar coord. system 0-89846
- left ventricular wall motion determined by echocardiography in elderly subjects 0-98039
- magnetic heart vector components, simultaneous meas. with unipositional lead system 0-104697
- magnetocardiogram, PR segment theory rel. to current sources within heart 0-101191
- magnetocardiogram and cardiac output meas. with integrated system 0-104709
- magnetocardiogram enhancement by applied mag. field 0-104701
- magnetocardiogram meas. first order gradiometer and DC-thin film SQUID 0-89877
- magnetocardiograms of normal and abnormal subjects, anal. using 2D displaying method (*Japanese*) 0-61777
- magnetocardiography and ECG, R and T waves 0-104699
- mechanical activity, noninvasive mag. detect., theory 0-89819
- mechanomyocardiography, left ventricular, technique for detect. of diseased myocardial elements and states 0-72363
- mechanopressography, left-ventricular, noninvasive intrinsic assessment of pumping efficiency 0-72203
- medical evaluation of function and anatomy, echocardiography and radionuclide imaging, book contrib. 0-101241
- microwave irradiation effect on embryonic quail heart rate, 2450 MHz irr. 0-89794
- mitral valve, conditions of closure 0-85439
- motor reactivity of isolated heart of the grass-snake 0-67100
- muscle, passive, viscoelastic theory and obs. 0-94273
- muscle, resting, activation monitored by intensity fluctuation spectroscopy 0-108953
- muscle biomechanics (*Japanese*) 0-72201
- myocardial ²⁰¹Tl scintigram anal., nonredundant coded aperture tomographic method 0-94364
- myocardial blood flow, ¹³³Xe studies, theoretical, technical and practical aspects 0-94355
- myocardial damage, induction by open-chest low energy countershock, rabbit expts. 0-72150
- myocardial damage from defibrillator discharges at various dosages 0-72368
- myocardial imaging with ²⁰¹Tl, subtraction imaging using ²⁰¹TlCl and ^{99m}TcO₄ 0-72318
- myocardial infarction, acute, comparison of ^{99m}Tc pyrophosphate with ^{99m}Tc hydroxymethylene diphosphate 0-94342
- myocardial infarcts, acute modified ^{99m}Tc heparin for imaging, dog expts. 0-81733
- myocardial perfusion imaging, quantitative aspects, review 0-94358
- myocardial perfusion imaging with ²⁰¹Tl, single photon emission computerised tomography (*Japanese*) 0-98114
- myocardial uptake of ²⁰¹Tl, correl. with local perfusion, dog expts. (*French*) 0-104740
- neonate cardiorespiratory monitoring, automatic system with microprocessor 0-94399
- nuclear, beat-by-beat validation of ECG gating [nuclear medicine] 0-98071
- nuclear cardiology, automated chest parsing algorithm 0-61678
- nuclear medical instrumentation, mobile, review 0-101262
- nuclear medicine, coded-aperture imaging of the heart, improved aperture 0-98072
- nuclear medicine, left ventricular edges detect. methods 0-98132
- nuclear medicine for clinicians, book 0-98765
- nuclear medicine instrumentation, review, book contrib. 0-101260
- nuclear performance characts. of a commercial ECG gate 0-98073
- oesophageal accelerometer, cardiovascular function indication 0-104798
- output estimation from isotope dilution and residue detect., time-varying flow and vol. effects 0-101194
- pacemaker activity, phase resetting and annihilation 0-81565
- pacing, meas. of ohmic electrode-tissue contact resistance and voltage applied to myocardium 0-67284
- papillary muscle selection and testing, some mech. considerations 0-89919
- physiological compartment tracer flow modelling and digital imaging 0-101257
- prosthetic, heart valves, load cell for meas. of dynamic forces 0-104815
- prosthetic disk valves, max. opening rel. to aortic blood flow characts. 0-108941
- prosthetic heart valve, trileaflet, design, fabrication and evaluation 0-94415
- protein kinases, cAMP-depend., membrane-localised, and regulation, of slow inward current, frog heart 0-81567
- proton spin-lattice relaxation times prolongation, regionally ischemic dog heart tissue 0-101216
- pulse-wave velocity measurement in humans (*German*) 0-81751
- Purkinje fibres, canine, activity-dependent extracellular K⁺ fluctuations 0-89733
- pyrophosphate myocardial imaging, review 0-94359
- quantitation of infarct size using radionuclides 0-85492
- radioisotope angiocardiology, image enhancement and left ventricular contour extraction techniques appl. 0-72283

cardiology continued

- radioisotope sequential meas. of ventricular vols. and cardiac output 0-94319
- radionuclide angiography, gated, use of computer-generated functional images to define ventricular boundaries 0-85487
- radionuclide angiography of the left ventricle using the first-pass technique (*German*) 0-109019
- radionuclide angiography technique for assessment of regional wall motion abnormalities 0-85488
- radionuclide evaluation of cardiac trauma 0-94361
- radionuclide ventriculography, computerised, assessment of LV wall motion and regional kinetics 0-89850
- regional left ventricular wall motion in coronary heart disease 0-85490
- relaxation parameters, digital anal. of isovolumic press. fall, dogs 0-94276
- rheocardiography, 4-electrode, in computer-aided cardiac output determ. 0-61718
- rotation coronary angiography 0-104744
- sarcolemmal permeability changes during early myocardial anoxia 0-85371
- scintigraphic image handling using microprocessor system 0-85489
- shunt detection with the short-lived radioactive gases 0-94357
- SOLO monitor, microcomputer bedside monitor 0-94404
- SQUID gradiometer, second-derivative, magnetocardiogram meas. 0-104696
- stress ²⁰¹Tl scintigram anal. methods comparison 0-89851
- synchronised diagnostic and treatment techniques 0-61727
- thermal entrainment device for cardiovascular investigation 0-104793
- tomography, myocardial perfusion, Anger camera/computer system using seven pinhole collimator 0-61663
- two-dimensional echocardiographic images enhancement by lateral filtering 0-81677
- US and nuclear medicine, complementary roles 0-98051
- US Doppler returns from foetal heart, processing, valvular timing information extraction 0-101238
- US intraoesophageal dynamic imaging 0-94303
- valve vibrations, aortic and mitral, anal. and role in heart sound production 0-101214
- valves, appraisal of power loads on elements 0-104811
- ventricle, left, human, 3-D time-varying reconstruct error sources and magnitude estimation 0-85454
- ventricular defibrillation with myocardial electrodes in the dog, calf pony, and pig 0-72369
- ventricular fibrillation and defibrillation 0-81769
- ventricular function monitor, ambulatory, CdTe detector, cardiac ejection fraction meas. 0-61680
- ventricular performance, 1st pass radioisotope assess. 0-85482
- ventricular wall motion assessment, terminology 0-85528
- weightlessness, bedrest analogue studies of exercise response 0-61713
- X-irradiation effects, dog expts. 0-104679
- x-ray diffraction studies of the heart, review, book contrib. 0-109079
- Ca²⁺ transients during excitation-contraction coupling 0-97896
- ³¹P NMR of the perfused heart 0-77534

carrier avalanches see impact ionisation

carrier density

- see also current density; electron density; electron density (metals)
- benzophenone, cryst., charge carrier generation by exciton-exciton collisions 0-88568
- C-CD, signal charge and surface pot., steady-state distrib. calc. 0-100525
- degenerate semiconductors, heterogeneous state, first-order phase transition, Ginzberg-Landau method analogue 0-70372
- dielectric, free charge carrier density calc., error in quasistationary approx. (*Russian*) 0-65544
- dielectric breakdown with picosecond laser pulses, large carrier conc. prod., SHG increase 0-102769
- dielectrics containing impurities, carrier distrib. and currents, numerical simulation (*French*) 0-70718
- electron-hole paired systems, ferromagnetic ordering phase diagram 0-97097
- EPR line shape, magnetoresist. effect 0-84638
- films, elec. and galvanomag. props., microstruct. 0-70859
- hopping in two-dimensional impurity bands, activation energy depend. 0-88561
- insulator-semicond. interface, impurity-band hopping conduction in surface layers 0-75649
- Kapton, pyrolysed, cond. polymer, transport and mag. props. 0-96887
- magnetodiode and magnetocapacitance effects, influence of field effect 0-107903
- MISIM struct. inversion layer, symmetrical/ carrier conc. calc. 0-75651
- n-n homojunction, calc. of free carrier density profile in a semicond. near ohmic contact 0-70810
- nematic liquid crystal, elect. conduct. based on injection-contact phenomena theory (*Russian*) 0-107807
- nonuniform band structure materials, Shockley like equations for current density and carrier density 0-60001
- photoconductivity, short-pulse, transit time effects 0-70754
- polyacetylene conductivity mechanism, Peierls phase one dimensional cond. (*Russian*) 0-88546
- polystyrene atactic carrier transport and photogeneration 0-80318
- rare earth chalcobismuthites, RBiTe₃, prep., elec. props., and crystallographic date 0-59981
- semiconductor, electron-hole plasma and elec. field, stratification at low temp. 0-60020
- semiconductor, free carrier density profile near ohmic contact calc. 0-70810
- semiconductor, graded-gap, internal photo-effects, excess carrier distrib. 0-107847
- semiconductor, large-band-gap, self-compensation, role of impurities 0-92850
- semiconductor, nonlinear conductivity, vortex waves, carrier mobility and lifetime 0-96893
- semiconductor, optical heating, coupled diffusion eqns. for heat and excess carrier density 0-60718
- semiconductor Fabry-Perot interferometer retuning by optical excitation (*Russian*) 0-98970
- semiconductor heating, thermal domain investigation, current voltage characts. 0-70711
- semiconductor isotype heterojunction barriers, cond. band discontinuity, C-V profiling meas. method 0-70801

carrier density continued

- semiconductors, determ. using calibrated polarimeters and the Faraday magneto-optical effect 0-60551
- semiconductors, heterogeneous, anisotropic, Hall coeffs., Hall mobility, carrier density (*Russian*) 0-70734
- semiconductors, photocarrier distrib. and photomagnetolectric effect near stimulated emission threshold 0-80320
- semiconductors, van Hove critical point region, electron-phonon interactions, dispersion law 0-70344
- Si, on sapphire, Schottky magnetodiode, integrated mag. sensor 0-68223
- surface magnetoplasmon type polaritons, LF, existence criterion in Faraday config. 0-96961
- AlGaAs buried heterostructure lasers, gain and absorpt. spectra meas. 0-91792
- AlGaAs DH laser, self-pulsations due to proton bombarded region self-annealing during ageing 0-99728
- AlGaAs p-n diodes, I-V characs., tunnelling 0-100510
- α -Al₂O₃, energy levels of donor and acceptor dopants and electron and hole mobilities 0-59911
- As chalcogenides, deep levels, photoluminesc. and photocond. 0-70641
- As₂Se₃ glassy films, current-voltage characs., temp. depend., SCL current 0-92902
- Au, thin film, discontinuous, high resist., Hall effect meas. 0-65716
- Bi_{1-x}Ge_xO₂₀ crystals, principal carriers obs., in dark and under laser illumination (*Russian*) 0-80312
- Bi_{0.88}Sb_{0.12}, semiconducting transport props., 2 to 100K 0-59989
- Bi_{1-x}Te_xBi_{1-x}Se_xSb_{1-x}Te_x, solid solution, single crystal, elec. cond., thermoelectric props. 0-88550
- n-Cd₂GeO₄, electronic and cond. props. rel. to prep. conditions and defect struct. 0-107787
- Cd_{1-x}Hg_xTe, elec. characs., impurity effects 0-92890
- n-Cd_{1-x}Hg_xTe crystals, carrier recomb. in intrinsic conduction range 0-70722
- Cd_{1-x}Hg_xTe epitaxial graded gap layers, plasma reflection and magnetoreflection 0-71391
- CdS, surface photovoltage, characterisation 0-60033
- CdS:Cu, photocurrent, elec. field effect on recombination processes (*Russian*) 0-100484
- p-CdTe, nondoped, heat treatment in vacuum, dissociation obs. effects on struct. and props. (*Japanese*) 0-60662
- Cd_{1-x}Zn_xS films, chem. sprayed, carrier density and mobility 0-60121
- Co₂RhS₄, mag. semicond., mag. and elec. props. 0-93121
- Cu₂Au, electrical resistivity and LRO, energy gap formation in Fermi surface 0-88533
- CuInTe₂ epitaxial layers, on GaAs, growth and props. 0-108359
- Cu₂O:Mn, photomemory mobility components, charged centre conc. 0-103725
- EuO nonstoichiometric film, ESR spectra and exchange interaction 0-93176
- EuO:Gd, elec. cond. under hydrostatic press., Curie temp. 0-96881
- EuO(Se), complex elec. cond. anomalies 0-107812
- Fe₂Al, electrical resistivity and LRO, energy gap formation in Fermi surface 0-88533
- α -Fe₂O₃ electrode, carrier density determ. by optical absorpt. and photoelectrolysis spectra 0-71462
- FeRh₂S₄, mag. semicond., mag. and elec. props. 0-93121
- GaAlAs DH laser, narrow stripe geometry, spontaneous carrier lifetime 0-87392
- Ga_{1-x}Al_xAs:Zn, acceptor energy level and elec. props. 0-65482
- GaAs, carrier conc. and compensation microprofiles 0-80820
- n-GaAs, crystal growth by Czochralski method kinetics, total emittance determ. 0-75193
- GaAs, electrical conductivity and thermoelectric power charge due to melting 0-100490
- p-GaAs, impurity band Hall mobility 0-70730
- n-GaAs, LPE, deep trapping centre characterisation by Hall and photo-Hall meas. 0-88578
- GaAs LPE from Ga soln., carrier conc., growth condition depend. 0-71584
- GaAs, n⁺-n-n⁺ and n⁺-p-n⁺ structs., ballistic electron motion at room temp. 0-80360
- GaAs, surface wetting with Hg, doping degree influence 0-92762
- p-GaAs:Cr, semi-insulating, mobilities and carrier concentrations, temp. depend. 0-70702
- GaAs:Ge film, MBE grown, heavily doped, elec. props. rel. to growth parameters 0-100537
- GaAs:Se, Ga, dual species ion implantation, elec. characs. 0-103377
- GaAs:Se ohmic contacts, pulsed electron beam annealing donor density, mobility 0-65678
- GaAs:Se(Zn) polycrystalline film, Hall effect, resistivity meas. 0-96911
- GaAs:Si, Li, IR absorpt., microstruct., charge compensation 0-107565
- GaAs:Si(Sn), ion implanted, laser annealed, high doping levels 0-88181
- GaAs:Zn, sign inversion of the linear photogalvanic effect (*Russian*) 0-80321
- GaAs-AlGa_{1-x}As heterojunction interface, two-dimensional hole gas obs., Shubnikov-de Haas meas. 0-80357
- GaSb, bulk and epitaxial, IR reflect. meas., carrier conc. and mobility determ. 0-80769
- GdN, and GdN_{1-x}O_x, mag. interactions 0-60218
- GdN, mag. interaction and carrier conc. 0-71005
- GdN_{1-x}O_x, magnetic interaction and carrier conc. 0-71005
- Ge, electron-hole drop drag by ultrasound (*Russian*) 0-100437
- Ge epitaxial film, ion implantation and electron beam anneal effects on carrier conc. 0-75255
- Ge, exciton condensation, electron-hole drop investigation in UHF field, nucleation (*Russian*) 0-80193
- p-Ge, IR light free hole absorpt., nonvertical optical transitions (*Russian*) 0-80802
- n-Ge, laser irradi., accumulation of defects, effect on elec. props. 0-107317
- Ge, oscillatory exciton breakdown, microwave cond. 0-103716
- Ge, uniformly deformed, free carrier cyclotron resonance, electron-hole drops (*Russian*) 0-71182
- p-Ge:As,Sb,Hg(Zn), radiation-defect form., Au influence 0-92911
- Ge:Mn, Sb, recombination waves, convective instability development 0-70721
- n-Ge:Ni⁺ p⁺-n-n⁺ structs., double-injection current-voltage characs. 0-60074
- Ge-SbCu, photoelec. props., fast electron irradi. effects 0-60036
- Ge-InAs based MIS struct., avalanche carrier multiplication 0-88566

carrier density continued

- Ge-Si alloys, n-type, phosphorous doped, precipitation effects due to heat treatment 0-107833
- (H_{0.6}Cd_{0.4})_{1-x}Te_x, defect anal., intrinsic material parameters 0-75519
- Hg_{1-x}Cd_xTe epitaxial layers, elec. props. 0-96910
- HgCr₂Se₄, electronic props. rel. to departure from stoichiometry 0-100472
- InAs, electrical conductivity and thermoelectric power charge due to melting 0-100490
- InAs:Cd, Te, donor-acceptor interaction, elec. cond. and Hall coeff. meas. 0-59988
- InAs:Sn, single crystals, defect formation 0-88606
- p-In_{0.53}Ga_{0.47}As:Zn on InP, elec. and optical props. 0-75662
- In_{1-x}Ga_xAs:P_{1-y}, Hall mobility, comp. depend. 0-75587
- In_{1-x}Ga_{1-x}P_{1-y}As_{1-y}, electron effective mass and Dingle temp., Shubnikov-de Haas oscils. 0-59859
- In₂O₃ films, reactively evaporated, elec. props. 0-84521
- In₂O₃:Sn films; vac. deposited, elec. props. 0-100542
- In₂O₃:SnO₂ thin film, Hall mobility, temp. depend., grain boundary effects 0-75658
- InP, Zn diffused single-crystal, substitutional dopant and hole conc. meas. 0-75260
- n-InSb based MIS struct., carrier generation under nonequilibrium conditions 0-88640
- InSb, high-resistivity p-type or crystals of n-type, recombination processes, photocond. and photomag. effect meas. (*Russian*) 0-88567
- InSb lattice, static dielec. const. and carrier conc. meas. via gyrotropic sphere reson. 0-97143
- n-InSb, microwave helicon resonances, carrier density, mobility, dielectric const. 0-96930
- n-InSb, negative longit. magnetoresist., carrier conc. and mobility depend., 77K 0-60007
- n-InSb, proton irradi. defects energy level scheme, transport props. meas. 0-96576
- InSb:Cd (Zn) (Ge), ion-irradiated, p-n conversion during heat treatment 0-96558
- p-InSb:Ge, proton irradi. defects energy level scheme, transport props. meas. 0-96576
- In₂SnO₃ film, effect of ambient atmosphere during annealing, elec. props. 0-97510
- Li-Pb liquid alloys, elec. resistivity, negative temp. coeff. 0-88527
- MnAs₂P₂, mixed crystals, metallic magnetically ordered, Hall effect 0-65536
- PbS:TL self-compensation of acceptors by vacancies, Hall coeff. meas. 0-92913
- PbSe:TL self-compensation of acceptors by vacancies, Hall coeff. meas. 0-92913
- PbSnTe, optical dielectric const. variation with carrier conc. 0-84709
- Pb_{0.8}Sn_{0.2}Te: Cd, influence of Cd doping on high field magnetoresist. and Hall effect 0-75590
- Pb_{0.8}Sn_{0.2}Te:La, evaporated thin films, low carrier conc. 0-65414
- Pb_{0.8}Sn_{0.15}Te homostructure diode laser, LPE growth, with controlled carrier conc. 0-95903
- Pb_{1-x}Sn_xTe epitaxial films, adsorption-induced accumulation layer formation on surface 0-60117
- Pb_{1-x}Sn_xTe-PbTe heterostructures, MBE produced on mica and LiNbO₃, elec. props. study 0-88629
- n-PbTe, noncubic (111) oriented epitaxial films, weak field magnetoresistance 0-75584
- SbSe, amorphous thin film high field charge transport and quasi-Fermi level location 0-70863
- Si, amorphous and crystalline, heating by Q-switched laser radiation 0-84963
- n-Si channel (100) inversion layer MOSFET, valley splitting, conductivity 0-70840
- n-Si, deformed, thermal treatment effect on elec. cond. and dislocation mobility 0-107265
- Si, dense plasma dynamics during pulsed laser annealing, carrier density, recombination 0-84479
- Si, diffusion coefficient determ. from carrier conc. depth profile 0-107566
- Si, heavily doped, excess intrinsic carrier density, deionisation of impurities as explanation 0-96864
- Si, laser induced dense plasma, dynamics 0-65612
- p-Si, laser irradi., accumulation of defects, effect on elec. props. 0-107317
- Si, local pseudopotential, Gaussian band charge model 0-88477
- n-Si, relaxation of electron energy, carrier-density dependence 0-107809
- Si:As, heavily As-diffused, Hall mobility and resist. rel. to carrier conc. 0-107815
- Si:As, shallow junctions by high-dose implants 0-96694
- Si:Li, electron-phonon scatt., in intermediate conc. region 0-65180
- Si:P, implanted low temp. annealed, elec. activation, damage depend. 0-88182
- Si:P, incoherent light flash annealing, elec. props., backscattering spectra 0-97504
- Si:P, neutron transmutation doping, elec. props. rel. to neutron fluence 0-96555
- Si:P film, polycryst., heavily doped, mobility and carrier conc., optical determ. 0-66314
- Si:P implanted, multicasting electron beam annealing 0-75242
- SnO₂:P, CVD films, elec. props., cryst. to amorphous transition effects 0-107933
- SnO₂-InP heterojunctions, elec. and photovoltaic characs. 0-75628
- SnTe, annealed, iodide method of prep., props. meas. 0-71591
- TiO₂ electrode, carrier density determ. by optical absorpt. and photoelectrolysis spectra 0-71462
- TiO₂, rutile, optoelectronic props., band struct., theory 0-80175
- V₂O₅, ferroelec. semicond., dielec. and elec. meas. 0-60516
- Zn,Cd_{1-x}S films, spray pyrolysis, elec. props. 0-75657
- ZnO films, RF sputtered single-cryst., on sapphire, struct. and SAW props. 0-80105
- ZnO sputtered films, undoped and Ga doped, props. rel. to deposition conditions 0-107935
- Zn₃P₂, elec. cond., Hall effect, P interstitial effects 0-84465
- ZnSe, self-compensation, role of impurities 0-92850

carrier diffusion length see carrier lifetime

carrier lifetime

- alkali metal halides, hole self-localization and capture, temp. depend. 0-92526
- diffusion length and lifetime meas. and assessment by SEM 0-96902

carrier lifetime continued

electron-beam-induced current, minority carrier generation vol. influence 0-84475
 generation lifetime, surface generation velocity determ., linear sweep MOS-CV method (*Chinese*) 0-107916
 homojunction solar cells, superposition principle 0-81449
 III-V semiconductor epitaxial structures as wide-gap substrates, minority carrier diffusion length determ. by photoluminesc. 0-103992
 measurements from transient elect. photoresponses in solar cells 0-61346
 minority carrier lifetime mapping by SEM 0-96903
 minority carrier lifetime-meas. technique using SEM-electron beam induced current 0-59999
 MIS structure, hysteresis pulsed C-V method for minority-carrier lifetime and surface generation velocity determ. 0-70839
 molecular crystals, electronic transport theory, local linear electron phonon coupling 0-65545
 MOS pulsed capacitor, minority carrier lifetime meas. influence of Si-wafer surface state density 0-60098
 narrow gap semiconductors, recombination mechanisms, review 0-96905
 optical beam size effects on diffusion length meas. by surface photovoltage method 0-60002
 $p^+-n^-n^+$ pulsed diodes, forward pulsed case, voltage transient response 0-60071
 $p-n$ junction solar cells, determ. of lifetime and recombination currents 0-89637
 photoconductor carrier lifetime, nonequilibrium, phase method for determ. 0-65629
 poly-N-vinyl carbazole, trap-free lifetime, neutral traps, hopping systems 0-65566
 Schottky barrier solar cell, doping density effect on efficiency 0-101100
 semiconducting photocathodes, carrier transport simulation, Monte Carlo method 0-71575
 semiconductor, homogeneous, nondegenerate, single-level Schockley-Read-Hall recomb. centres, flicker noise 0-70779
 semiconductor, n -type, inhomogeneous, nonequib. carrier diffusion and lifetime 0-60005
 semiconductor, nonlinear conductivity, vortex waves, carrier mobility and lifetime 0-96893
 semiconductor, optical absorpt. coeff. and minority-carrier diffusion length, differential photocurrent method of meas. 0-96896
 semiconductor, photomagnetolectric effect, injection-level dependent lifetime 0-80319
 semiconductor, SEM electron beam induced current images of dislocations and stacking faults, computer simulation 0-70198
 semiconductor, spin-dependent recomb. and scatt. in presence of optical orientation of electrons 0-96908
 semiconductor depth profiling by electron beam induced junction current meas. 0-96977
 semiconductor laser, photopumped, III-V semiconductor, book contrib. 0-99732
 semiconductor layers, double injection in transverse mag. field, theory 0-80421
 semiconductor layers, thin, theory of lifetime meas. with SEM, transient anal. 0-88573
 semiconductor surface eval. using SAW convolver 0-97677
 semiconductors, photoconductivity measurement at UHF and at high excitation levels 0-65627
 n -Si, recombination centres and carrier lifetimes after γ -irrad. 0-60004
 solar cell, diffusion equation, surface boundary condition 0-66975
 solar cells, output monitoring, design and utilization of a microprocessor-controlled absolute spectral response system 0-81476
 solar cells, polycryst., recomb. at grain boundaries, effect on photoresponse 0-108796
 solar cells, surface recombination velocity and diffusion length meas. 0-93965
 Teflon FEP, N implanted, TSC spectra 0-88912
 AgBr, photoexcited electrons and holes in latest image form., review 0-73496
 AlGaAs-GaAs proton irradiated solar cells, deep level defects and recombination parameters 0-94032
 $Al_{0.5}Ga_{0.5}As$:Cu, variable-gap semicond., impurity props., carrier recomb. 0-96907
 BN glass transfer process 0-107459
 Cd, positron trapping at low temp. lifetime spectra 0-84799
 $Cd_{0.9}Hg_{0.1}Te$, carrier lifetime, effect of comp. fluctuations and second-phase inclusions 0-80294
 n - $Cd_{0.9}Hg_{0.1}Te$ crystals, carrier recomb. in extrinsic conduction range 0-70722
 n - $Cd_{0.9}Hg_{0.1}Te$, recombination due to surface excitation, photoconductivity, impurity states (*Russian*) 0-60042
 CdS crystals, electron-hole plasma, carrier optical orientation 0-100689
 CdS:Cu(Cl) thin films, surface and bulk photoconc. 0-88653
 CdS-Cu₂S solar cells, electron diffusion length determ. using spectral response meas. 0-81475
 CdTe, minority carrier diffusion length from photocurrent meas. in semicond.-electrolyte boundary 0-65584
 CdTe-CdS thin film $p-n$ solar cells, spectral response temp. depend. 0-93871
 Cr-SiO₂-Si MIS solar cells, photovoltaic performance and interface states, nucl. radiation effects 0-94004
 CuInSe₂ thin films for solar cells, radiofrequency sputtering technique, elec. props. 0-93487
 Cu₂O-Cu diode junction, Schottky barrier, electronic structure and minority carrier diffusion length (*French*) 0-65682
 Cu₂S, diffusion length meas. using scanned laser beam tech. 0-93886
 Cu₂S/CdS heterojunction solar cells, diffusion length determ. using minority carrier SEM 0-61359
 Cu₂-S-CdS $p-n$ heterojunction, optical energy convertor, struct. and recomb. props. 0-72065
 α -Fe₂O₃ electrode, carrier density determ. by optical absorpt. and photoelectrolysis spectra 0-71462
 GaAlAs DH laser, narrow stripe geometry, spontaneous carrier lifetime 0-87392
 Ga_{1-x}Al_xAs- $p-n$ and $p-p-n$ heterojunction solar cells, high efficiency, prep., eval. and characters (*Japanese*) 0-61342
 GaAs, diffusion and power spectral density and correl. function of vel. fluctuation for electrons 0-65576
 n -GaAs, electron irrad. defects, carrier removal rate, annealing effects 0-75269
 GaAs, laser heating of lightly damaged material, carrier diffusion effect 0-84809

carrier lifetime continued

GaAs, polycrystalline films, meas. of effective diffusion length by SEM 0-80424
 GaAs, proton irradiated, low energy, deep level defects and hole diffusion length meas. 0-60000
 GaAs solar cell polycrystalline conducting substrate, minority carrier diffusion length spatially-resolved meas. 0-94084
 GaAs, valence-band dispersions, electron and hole lifetimes, angle-resolved photoemission 0-80947
 GaAs:Se cathodoluminescence decay obs. with SEM and streak camera, 90 to 300K 0-97348
 GaAs:Te Schottky barrier solar cells, diffusion length determ. using minority carrier SEM 0-61359
 GaAs-Ga_{1-x}Al_xAs DH lasers, electron beam induced current microscopy 0-95899
 GaInAsP/InP lasers, LPE grown, effect of p -doping on carrier lifetime and threshold current density 0-99726
 n -Ga_{1-x}In_xP photoelectrochemical cells, bandgap energy, electronic transition mode, and diffusion length 0-72070
 p -GaSe, back wall Schottky barrier cells, diffusion length, RT spectral response meas. 0-107806
 Ge, compensated by thermal defects, recomb. and optical props. 0-64989
 Ge, photomagnetic effect, space inhomogeneous nonequilibrium carrier lifetimes (*Russian*) 0-71152
 n -Ge, proton and γ irrad., minority carrier recombination 0-65591
 n -Ge:Ni $p^+-n^-n^+$ structs., double-injection current-voltage characts. 0-60074
 Ge:P(Sb)(Bi), γ -irrad., carrier trapping and recomb. at point radiation defects 0-107810
 Ge:Zn photoresistor, current responsivity rel. to nonequib. hole lifetime 0-60035
 Ge:Zn^{II} carrier lifetime, nonequilibrium, phase method for determ. 0-65629
 Ge-metal Schottky barrier photodetectors, near IR interband transitions and optical parameters 0-73449
 Hg_{1-x}Cd_xTe, Einstein relation for inversion layers 0-103706
 InAs and solid solutions, recombination mechanisms of excess carriers, luminesc. obs. 0-97337
 InGaAsP-InP DH laser, threshold current, temp. depend. 0-106521
 In_{0.5}Ga_{0.5}As_{1-y}P_y epitaxial layers, characterisation and relation to lattice matching 0-100540
 InP, impact ionisation by electrons and holes 0-100467
 InSb, Auger-governed decay of laser-induced plasma, optical probing 0-76105
 InSb, carrier heating by microwave field, inertia effects 0-65580
 InSb, Einstein relation for inversion layers 0-103706
 InSb, high-resistivity p -type or crystals of n -type, recombination processes, photocond. and photomag. effect meas. (*Russian*) 0-88567
 p -InSb, magnetoconcentration effect in extrinsic cond. range 0-65593
 n -InSb, proton irrad. defects energy level scheme, transport props. meas. 0-96576
 p -InSb:Ge, proton irrad. defects energy level scheme, transport props. meas. 0-96576
 Si, carrier capture at amphoteric deep level defects 0-88569
 Si, carrier lifetime depth distrib. due to Ar ion implantation 0-70232
 Si, compensated by thermal defects, recomb. and optical props. 0-64989
 p -Si, conductivity and carrier lifetime, high injection effects 0-70719
 n -Si, defect charge states, complex form., gamma-ray effects 0-96564
 Si, deformed, annealed and recrystallized, struct., implications for solar cells 0-60922
 Si, diffusion and power spectral density and correl. function of vel. fluctuation for electrons 0-65576
 Si, float zone, process-induced effects on carrier lifetime and defects 0-81216
 Si, gettering by ion damage, minority carrier lifetime and backscatt. study 0-100286
 Si junction diodes, fabrication by LPE on Si:B substrates, and characts. 0-80363
 Si, laser heating of lightly damaged material, carrier diffusion effect 0-84809
 Si, lifetime in Ar^+ ion implant damage getterted, MOS voltage ramping 0-75247
 Si, MOS diode, dependence of minority carrier bulk generation on HCl concentration 0-88639
 Si, minority carrier lifetime improvement through laser damage getterting 0-65589
 Si, n^+-p diode, γ -radiation defects, annealing and recomb. props. 0-65045
 Si, neutron and electron bombard., radiation defect recomb., photoelec. props. meas. 0-60039
 Si $p^+-n^-n^+$ back-surface-field solar cells, physics underlying performance 0-85283
 Si $p-n$ junction diodes and solar cells, minority carrier diffusion length 0-107894
 Si, polycrystalline films, meas. of effective diffusion length, by surface photovoltage meas. 0-80424
 Si ribbon solar cells, var. of minority-carrier diffusion length with light intensity, heavy metal doping effects 0-93937
 Si solar cell parameters, grain size dependence 0-94049
 Si solar cells, effect of Ti, Cu, and Fe 0-72064
 Si solar cells, inhomogeneities and their influence on cell performance 0-93967
 Si solar cells, ion-implanted, expt. study of efficiency controlling factor 0-93997
 Si solar cells, radiation damaged, origin of reverse annealing 0-76630
 Si:B photodiode front region collection efficiency models 0-96899
 Si:B radiation damage and minority carrier lifetime, SEM-EBIC obs. 0-96573
 p -Si:B(Al), radiation defect form. and annealing study using Hall effect, cond. and carrier diffusion length 0-84214
 Si:Co, minority carrier lifetime investigation 0-80292
 Si:Fe(Al), compensated substrates for solar cells, effects of Fe and Al 0-94009
 n -Si:H, amorphous, photoelectromagnetic effect 0-107845
 Si:H, amorphous, solar-cells, charge collection and spectral response 0-85275
 SiO, carrier recomb. processes, role of vacancy-O complexes 0-65592
 SiO, heat treated, excess carrier recomb. rate, defect levels 0-75579
 Si:Zn, minority carrier lifetime investigation 0-80292
 Si-Ge, amorphous, solar cells, tandem multiple gap 0-94029
 Si-metal contact, transport theory of Schottky barriers 0-80372

carrier lifetime continued

- Si-SiO₂ MOS interface, surface-state density and minority carrier generation rate, meas. by DLTS, hot hole effect 0-100527
 TiO₂ electrode, carrier density determ. by optical absorpt. and photoelectrolysis spectra 0-71462
 ZnO, single crysts., photocond. lifetimes, Zn⁺ hole traps 0-75581
 Zn₃P₂ thin polycrystalline films for solar photovoltaic cells 0-97797
 ZnSe, minority carriers diffusion length by surface photovoltage method 0-60003

carrier mean free path

- see also *electron mean free path (metals)*
 Bloembergen-Rowland approximation, indirect exchange interaction, mean free path effects 0-60238
 exchange interactions in semiconductors and insulators, mean free path and energy gap effects 0-88522
 heterojunction multilayered structs., effective impact ionisation rates 0-88621
 indirect exchange in Bloembergen-Rowland approx., ellipsoidal Fermi surface and relax. process effects 0-107754
 magnetic semiconductor, indirect exchange interaction, mean free path effects 0-97088
 Bi thin film, structure and electronic props. 0-70562
 CdTe, electron mean free path, 350-1450 eV 0-103707
 InP, impact ionisation by electrons and holes 0-100467
 Si:F,H, amorphous efficient carrier generation for solar photovoltaic energy conversion 0-92906
 TiO₂, rutile, electron mean free path, four-step transition and Auger spectra investig. 0-97389

carrier mobility

- see also *carrier mean free path; carrier relaxation time; current density; electron-hole recombination; electron mobility (metals)*
 alkali halide, dynamics of nonrelaxed and self-trapped holes (Russian) 0-80607
 amorphous, high field transport, impact ionisation, carrier mobility 0-80286
 compensated semiconductors, low temp. mobility, unscreened charged impurities effects calcs. 0-75562
 trans-decaline-cyclohexane liq. mixtures, hole mobility, percolation model 0-65551
 diamond, ion-doped with Li electron transport 0-92917
 EPR line shape, magnetoresist. effect 0-84638
 films, elec. and galvanomag. props., microstruct. 0-70859
 glass, electron migration and spectral relax., random-walk model 0-80280
 graphite, resistivity and magnetoresistance, 4.2 to 293K 0-100459
 Hall effect, 1/f noise, mobility fluctuations 0-92950
 heavily doped semiconductor, with Gaussian band tails, modification of Einstein relation 0-80270
 hexafluorobenzene liq., electron mobility, percolation model 0-65551
 hexafluorobenzene-benzene liq. mixture, electron mobility, percolation model 0-65551
 n-hexane-ethanol liq. mixtures, electron mobility, percolation model 0-65551
 homojunction solar cells, superposition principle 0-81449
 hopping transport kinetic theory, localised state separation, Pauli master eqn. 0-80276
 IGFT, velocity-field curves for surface-free carrier in Si 0-60095
 inflowing structure, Anderson localisation, elec. cond. temp. depend. (Russian) 0-103639
 Kapton, pyrolysed, cond. polymer, transport and mag. props. 0-96887
 measurement, contactless measurement of sheet conductivity and mobility of semiconductor wafer by using eddy current 0-62693
 molecular crystals, electronic transport theory, local linear electron phonon coupling 0-65545
 molecular crystals, exciton-phonon coupling and exciton transport 0-84430
 naphthalene, charge carrier drift mobility, semi empirical anal. 0-65553
 naphthalene, electron and hole off-diagonal mobility component determ. 0-65552
 narrow gap semiconductor, modification of Einstein relation for inversion layers in strong elec. field 0-96959
 nematic liquid crystal, elect. conduct. based on injection-contact phenomena theory (Russian) 0-107807
 NLC, effective ion mass and mobility calcs. (Russian) 0-79694
 organic semiconductor films, Schrieffer effect 0-60118
 phenothiazine derivatives, semicond. elec. props., optical spectra, and EPR 0-103693
 piezosemiconductors, second harmonics of acoustoelectric current 0-80329
 poly(p-phenylene), AsF₃ doped, highly cond. charge transfer complexes, elec. and optical props. 0-70778
 poly-N-vinyl carbazole, hole hopping mobility, transit pulse dispersion 0-65565
 poly-N-vinylcarbazole thin amorphous film, hole drift mobility, mol. mass. depend. 0-75663
 polyacetylene, doped, elec. cond. and thermopower 0-96951
 polyethylene:Br₂(I₂), films, electron-beam induced carrier mobility and elec. breakdown 0-80429
 polyethylene, elec. cond. of high and low density samples, oxidation effects 0-107784
 polyethylene, halogen-doped, carrier transport and breakdown characteristics (Japanese) 0-96889
 polyethylene, space-charge storage under high DC voltage condition, TSC meas. (German) 0-75576
 polyethylene terephthalate films, current peaks obs. with linearly increasing voltage 0-88654
 polystyrene:Br₂(I₂), films, electron-beam induced carrier mobility and elec. breakdown 0-80429
 polystyrene, halogen-doped, carrier transport and breakdown characteristics (Japanese) 0-96889
 polystyrene atactic carrier transport and photogeneration 0-80318
 polystyrene thin films, TSC and surface charge meas. 0-103769
 proton semiconductors, with H-bonds, quantum theory of proton cond. 0-65641
 quasi-two dimensional conductor, galvanomagnetic props., optical analogy (Russian) 0-60108
 quinolinium (TCNQ)₂, charge transport, proton spin-lattice relaxation 0-88545
 rare earth chalcobismuthites, RBiTe₃, prep., elec. props., and crystallographic date 0-59981
 Schottky barrier solar cell, doping density effect on efficiency 0-101100

carrier mobility continued

- semiconductor, ambipolar diffusion, electron-hole scatt. effect 0-59976
 semiconductor, elec. cond., hopping model, semi-classical, effective mass and carrier mobility calc. 0-96872
 semiconductor, electron quantum states, nonequilibrium current fluctuations in quantised mag. fields (Russian) 0-107704
 semiconductor, nonlinear conductivity, vortex waves, carrier mobility and lifetime 0-96893
 semiconductor, two-valley, carrier vel.-field characts. under high elec. field 0-70713
 semiconductor epitaxial layers, varizional, parameter determ. by photoluminescence method (Russian) 0-108291
 semiconductor heating, thermal domain investigation, current voltage characts. 0-70711
 semiconductor junction lasers, transport phenomena, junction effects and devices, book 0-98766
 semiconductor thin films, fabrication for device appls. 0-100418
 semiconductors, drift velocity relation to low-field mobility and high-field saturation velocity 0-75563
 semiconductors, electron-phonon interactions, combined phonon resonance (Russian) 0-75321
 semiconductors, exciton-impurity state with low binding energy 0-103646
 semiconductors, heterogeneous, anisotropic, Hall coeffs., Hall mobility, carrier density (Russian) 0-70734
 semiconductors, impurity electron scatt., resonance scatt., Hall and drift mobility 0-65487
 semiconductors, light induced electron drift, two-photon transitions (Russian) 0-107853
 semiconductors, mobility-fluctuation description of 1/f noise 0-84496
 semiconductors, temp. depend. electronic cond. 0-59975
 semiconductors, variable gap, carrier transport and fluctuation effects due to changes in gap width 0-107793
 semiconductors with impurities, electron cond. temp. and freq. depend., two band model (Russian) 0-75564
 silicone oil, ionic behaviour, carrier mobility and viscosity 0-107453
 solar cell, diffusion equation, surface boundary condition 0-66975
 solar cell, low resistivity, rel. to open cct. voltage improvement 0-93910
 solar cells, Cu₂S-CdS, collection coefficient theoretical anal. at conjunction 0-101094
 spatially inhomogeneous magnetic field effect on semiconductor carriers 0-92916
 TCNE, hole drift mobility, temp. depend. and anisotropy, photocond. meas. 0-80314
 Teflon FEP, N implanted, TSC spectra 0-88912
 p-terphenyl, hopping cond. among localised states 0-70861
 p-terphenyl film, polycryst., charge carrier transport and DC cond. 0-70858
 tetracene, hopping cond. among localised states 0-70861
 thermal conductivity, electronic contribution, mobility threshold effects 0-65570
 TTT film, Schrieffer effect 0-60118
 AgBr, photoexcited electrons and holes in latest image form., review 0-73496
 AgCNS, mixed conductor, elec. cond. props. 0-65639
 AgInS₂, and AgInS₈, spray pyrolysis, film struct., elec. and optical props. 0-71592
 AgN₃, high-resist. explosive cpd., elec. and galvanomag. props., temp. depend. 0-103728
 Ag₂Se, electronic and electrogalvanic props. in α -phase region (French) 0-107820
 Al_{0.5}Ga_{0.5}As, compensated, electron mobility temp. depend. 0-96868
 Al_{0.5}Ga_{0.5}As, electron mobility illumination, compensation, space charge regions, carrier scatt. 0-70691
 p-Al_{0.5}Ga_{0.5}As film, variable-gap photo-EMF 0-65626
 α -Al₂O₃, energy levels of donor and acceptor dopants and electron and hole mobilities 0-59911
 Al₂O₃ polycrystalline, effects of space charge, grain-boundary segregation and mobility differences on conductivity 0-79979
 Ar, condensed, electron drift, Davydov electron energy distribution function, diffusion (Russian) 0-80339
 Bi₂GeO₂₀ crystals, principal carriers obs., in dark and under laser illumination (Russian) 0-80312
 BiSb (>20 wt.%), electronic band struct. 0-107698
 Bi_{0.8}Sb_{0.2}, semiconducting transport props., 2 to 100K 0-59989
 Bi_{1-x}Sb_x, solid soln., temp. depend. of weak-field galvanomag. coeffs. (Russian) 0-70724
 n-Cd₂GeO₄, electronic and cond. props. rel. to prep. conditions and defect struct. 0-107787
 Cd_{0.5}Hg_{0.5}Te, graded-gap layers, galvanomag. props. at low temp. and in weak mag. field 0-75664
 Cd_{0.5}Hg_{0.5}Te, vacancy electron states, acceptor behaviour, electron mobility 0-70193
 Cd₂Nb₂O₇, photolum. and carrier drift mobility at ferroelec. transition 0-71469
 p-CdSnAs₃, heavily doped, elec. transport props. under elastic deformation 0-96915
 CdTe metal-semiconductor-metal γ -ray detector characts. 0-57451
 p-CdTe, photocond., photoluminesc., spectral studies 0-88593
 CdTe:Cu films, impurity behaviour, Hall mobility and hole density meas. 0-80420
 Cd₂Zn_{1-x}S_x films, chem. sprayed, carrier density and mobility 0-60121
 Cu₂O:Mn, photomemory mobility components, charged centre conc. 0-103725
 Cu₂S-CdS heterojunction solar cells, carrier transport, nonmonotonic band profiles 0-61361
 EuO(Se), complex elec. cond. anomalies 0-107812
 α -Fe₂O₃ electrode, carrier density determ. by optical absorpt. and photoelectrolysis spectra 0-71462
 GaAs, semi-insulating and n-type, doping by neutron transmutation 0-96553
 Ga_{1-x}Al_xAs, LPE layers, electron mobility, scatt. processes 0-84519
 GaAs, ballistic and near ballistic transport 0-96867
 GaAs, carrier diffusion in transient response regime 0-103688
 GaAs, circuit effects in time-of-flight diffusivity meas., Monte Carlo method 0-88563
 GaAs, compensated, electron mobility temp. depend. 0-96868
 GaAs compensated VPE thin film, electron Hall mobilities 0-107932
 GaAs, electron mobility illumination, compensation, space charge regions, carrier scatt. 0-70691
 n-GaAs, epitaxial, high temp. carrier transport 0-65725

carrier mobility continued

GaAs epitaxial films on strongly doped substrate, basic parameter meas. utilising magnetoresist. and SEM techniques under cathodoluminesc. conditions 0-65728
n-GaAs, heavily-doped, with Gaussian band tails, modification of Einstein relation 0-80270
p-GaAs, impurity band Hall mobility 0-70730
n-GaAs, LPE, deep trapping centre characterisation by Hall and photo-Hall meas. 0-88578
GaAs, organometallic VPE, with varying As/Ga ratios, deep states 0-65480
GaAs, self-scattering in Monte Carlo calcs. of transient dynamic response 0-103687
GaAs, semi-insulating, undoped and Cr-doped, compensation mechanisms, Hall effect and optical absorpt. meas. 0-84477
GaAs:Cr, FET, influence of Cr on mobility of electrons 0-92910
p-GaAs:Cr, semi-insulating, mobilities and carrier concentrations, temp. depend. 0-70702
GaAs:Se ohmic contacts, pulsed electron beam annealing donor density, mobility 0-65678
GaAs:Se(Zn) polycrystalline film, Hall effect, resistivity meas. 0-96911
n-GaAs-Ga_{1-x}Al_xAs, heavily doped superlattice, electronic props., perpendicular low temp. mobility 0-65660
GaAs-Si ion implanted, impurity profiles elec. props. 0-96550
GaInAs-InP, growth by low-pressure metalorganic CVD 0-71595
Ga_{0.47}In_{0.53}As, HF carrier mobility, temp. depend., theory 0-75593
Ga_{1-x}In_xAs, IR reflectivity, cluster effect on optical phonons 0-97259
Ga_{1-x}In_xAs, on (111)B InP, LPE growth, characterisation of high purity lattice 0-104082
GaSb, bulk and epitaxial, IR reflect. meas., carrier conc. and mobility determ. 0-80769
GaSb LEC single crystal growth, novel encapsulant material 0-93475
p-Sb:Ga, majority carrier drift mobility meas. 0-92895
Ge, effective masses of heavy and light holes, from ohmic mobility data 0-80160
Ge epitaxial film, vac. deposited on GaAs, doping effect of annealed GaAs surface 0-65718
Ge, exciton condensation, electron-hole drop investigation in UHF field, nucleation (*Russian*) 0-80193
Ge, nonequilibrium charge carrier-mag. field interaction electron-hole drops, recombination (*Russian*) 0-75511
Ge, surface, Hall effect study, channel cond. (*Russian*) 0-92909
Ge:Mn, Sb, recombination waves, convective instability development 0-70721
⁴He, electron localisation, mobility in dense low temp. gas 0-92247
Hg_{1-x}Cd_xTe, Einstein relation for inversion layers 0-103706
Hg_{1-x}Cd_xTe, epitaxial layers, elec. properties in the range 4.2 to 300K (*French*) 0-65721
Hg_{1-x}Cd_xTe epitaxial layers, elec. props. 0-96910
HgCr₂Se₄, electronic props. rel. to departure from stoichiometry 0-100472
HgTe, mobility of electrons and holes, 4 to 100K 0-107821
HgTe, vacancy electron states, acceptor behaviour, electron mobility 0-70193
InAs films, MBE grown on GaAs, electron mobilities, lattice mismatch effect 0-80419
InAs:Cd, Te, donor-acceptor interaction, elec. cond. and Hall coeff. meas. 0-59988
InAs:Sn, single crystals, defect formation 0-88606
p-In_{0.53}Ga_{0.47}As:Zn on InP, elec. and optical props. 0-75662
In_{1-x}Ga_xP_{1-y}As_y, evidence for alloy scatt. from press. induced changes of electron mobility 0-88548
In_{1-x}Ga_xAs_{1-y}P_y, Hall mobility, comp. depend. 0-75587
In_{1-x}Ga_xAs_{1-y}P_y, hole mobility over temp. range 77 to 300K 0-60111
In_{1-x}Ga_xP_{1-y}As_y, electron effective mass and Dingle temp., Shubnikov-de Haas oscills. 0-59859
In₂O₃ films, reactively evaporated, elec. props. 0-84521
In₂O₃, thermally evaporated film, struct. and elec. props. 0-104066
In₂O₃:Sn films, vac. deposited, elec. props. 0-100542
In₂O₃:SnO₂ thin film, Hall mobility, temp. depend., grain boundary effects 0-75658
n-InP, compensated, elec. props., space-charge effects 0-65569
InP, compensation ratio, electron mobility and free-carrier absorpt. 0-80261
InP epitaxial films, grown on heavily doped substrates, carrier mobility study, magnetoresist. meas. 0-60116
InP films, organometallic VPE grown, props. 0-96753
InSb, carrier heating by microwave field, inertia effects 0-65580
InSb, current-voltage characteristics at room temperature and high hydrostatic pressure 0-88560
InSb, Einstein relation for inversion layers 0-103706
InSb, electron-hole plasma instabilities, impact ionisation conditions, microwave emission 0-107840
InSb, extrinsic and intrinsic, interaction of transverse magnetoresist. effects 0-65596
InSb, galvanomagnetic props. of annealed single crystals 0-96909
p-InSb, influence of plastic deform. on elec. props. 0-103711
n-InSb, ionized impurity scatt. limited mobility, expt. 0-80274
p-InSb, magnetococoncentration effect, negative differential conductance 0-70729
n-InSb, microwave helicon resonances, carrier density, mobility, dielectric const. 0-96930
n-InSb, negative longit. magnetoresist., carrier conc. and mobility depend., 77K 0-60007
InSb, neutron irradi., defect cluster form., effect on elec. props. 0-65062
n-InSb, proton irradi. defects energy level scheme, transport props. meas. 0-96576
InSb recrystallised thin films on mica substrate, elec. props. 0-70867
n-InSb, spin polarisation, anisotropic size effect, effect on CESR signal 0-70743
p-InSb:Ge, proton irradi. defects energy level scheme, transport props. meas. 0-96576
InSb_{1-x}Bi_x, multitarget RF sputtering, metastable phase, conductivity transition 0-76178
In₂SnO₃ film, effect of ambient atmosphere during annealing, elec. props. 0-97510
KInbO₃ reduced, phase hologram recording sensitivity, energy transfer, photovoltaic effects 0-78799
LiNbO₃:Cu(Fe), light induced charge transport, photovoltaic effects, impurity states 0-80317

carrier mobility continued

LiNbO₃:Fe, electro-optic cryst., light induced charge transport, holographic obs. 0-70747
LiTaO₃:Cu(Fe), light induced charge transport, photovoltaic effects, impurity states 0-80317
LiTaO₃:Fe, electro-optic cryst., light induced charge transport, holographic obs. 0-70747
LuRhO₃, elec., mag. and photoelectrochemical props. 0-96925
NbSe₂(2H), low field magnetoresist. and anomalous transport props. 0-65602
Ni film, evaporated, elec. resist. and galvanomagnetic props. 0-80411
PbMg_{1/3}Nb_{2/3}O₃, photolum. and carrier drift mobility at ferroelec. transition 0-71469
Pb_{0.8}Sn_{0.2}Te:Cd, influence of Cd doping on high field magnetoresist. and Hall effect 0-75590
Pb_{1-x}Sn_xTe-PbTe heterostructures, MBE produced on mica and LiNbO₃, elec. props. study 0-88629
PbTe, effect of pressing and sintering, study of induced defects by SEM 0-59983
n-PbTe, low temperature electrical transport, Hall effect 0-84478
n-PbTe, noncubic (111) oriented epitaxial films, weak field magnetoresistance 0-75584
PbTe:In, electron mobility, temp.-independent part, Hall effect and elec. cond. meas. 0-92914
n-PbTe:In(Cu) epitaxial films, elec. transport props. 0-75659
PbTiO₃, photolum. and carrier drift mobility at ferroelec. transition 0-71469
Se, trigonal, acoustoelectric current saturation 0-60053
Se₂Te_{1-x}, acoustoelectric current saturation 0-60053
Se₁₂Te₄₉As₂₉Ge₁₀ semiconductor amorphous films, field effect, trapping 0-84472
Si, (100) inversion layer, electromigration in two dimensional electron gas, driving force 0-84441
Si, amorphous, hydrogenated, electron drift mobility meas. 0-75565
Si, amorphous, transport results, interpretation 0-80260
Si, amorphous film, RF plasma deposition from SiCl₄-H₂, characterisation 0-66435
n-Si, deformed, thermal treatment effect on elec. cond. and dislocation mobility 0-107265
Si, effective masses of heavy and light holes, from ohmic mobility data 0-80160
Si, electron drift in high elec. fields, long-time tail of autocorrelation function 0-103702
n-Si, electron heating by static elec. field 0-96894
Si, epitaxial layer deposition by ion beam methods 0-100417
Si epitaxial thin film growth on sapphire and spinel by MBE 0-76186
Si inversion layers, mobility temp. depend., Coulomb and surface roughness scatt. 0-80390
n-Si inversion layers, resist. temp. depend. at liq. He temps. 0-80391
Si on sapphire, residual strain effect on elec. props. (*Japanese*) 0-84522
Si on sapphire thin film, Hall effect, magnetoresistance (*French*) 0-65601
Si p-channel MOS structure, stress effects on elec. props., press. transducer props. 0-100526
n⁺⁺Si planar device, hot electron flicker noise at 78K 0-103732
Si, polycrystalline, Hall mobility 0-60006
Si, polycrystalline, phenomenological model for mobility 0-65564
Si, radiation defects, influence of dislocations on accumulation, elec. props. 0-92558
Si ribbons for solar cells, ultra high speed growth, elec. props. 0-89162
Si, thermally oxidised surfaces, electron mobility in inversion and accumulation layers, MOS devices 0-103753
Si:As, polycrystalline, As segregation at grain boundaries, elec. props. meas. 0-75259
Si:H, amorphous, geminate recombination model for photoluminescence decay 0-71481
n-Si:H, amorphous, photoelectromagnetic effect 0-107845
Si:H, amorphous, solar-cells, charge collection and spectral response 0-85275
Si:P, incoherent light flash annealing, elec. props., backscattering spectra 0-97504
Si:P, neutron transmutation doping, elec. props. rel. to neutron fluence 0-96555
Si:P film, polycryst., heavily doped, mobility and carrier conc., optical determ. 0-66314
Si-SiO₂ boundary, surface charge transport in valence band of Si 0-70789
Si-SiO₂ in MOSFETs, inversion layer carrier mobility, theory 0-60094
Si-SiO₂ interface, remote polar phonon scatt. in Si inversion layers 0-80095
SiO₂, mobility and trapping of ions, Si-SiO₂ interface states 0-92985
SnO₂:P, CVD films, elec. props., cryst. to amorphous transition effects 0-107933
SrTiO₃, photolum. and carrier drift mobility at ferroelec. transition 0-71469
Te, a-edge dislocated crystals, mobility anisotropy 0-107781
Te, two types of carriers 0-60013
Te:Cu films, elec. transport props. 0-60120
TiO₂, electrode, carrier density determ. by optical absorpt. and photoelectrolysis spectra 0-71462
V₂O₅, ferroelec. semicond., dielec. and elec. meas. 0-60516
Zn,Cd_{1-x}S films, spray pyrolysis, elec. props. 0-75657
Zn,Hg_{1-x}Se, current carrier scattering mechanism 0-65546
Zn,Hg_{1-x}Te, vacancy electron states, acceptor behaviour, electron mobility 0-70193
ZnO films, RF sputtered single-cryst., on sapphire, struct. and SAW props. 0-80105
ZnO sputtered films, undoped and Ga doped, props. rel. to deposition conditions 0-107935
ZrS₃, quasi one-dimens. semicond., elec. transport props. 0-107790

carrier relaxation time

see also electron relaxation time (metals)

ferromagnetic semiconductors, hot electron relax. time 0-59996
metallic films, grain boundary scatt., Hall coeff., theory 0-88649
semiconductor, carrier relaxation time anisotropy effect on free carrier dispersion studies 0-84474
semiconductor, IR absorpt. and optical relax. time of free carriers 0-66206
semiconductor, phonon conduction and relaxation times 0-107585
semiconductors, thermoelectrically anisotropic, carrier kinetics at low temp. 0-92893

carrier relaxation time continued

- semiconductors, thermoelectrically anisotropic 0-92894
 Au/oxide/n-GaAs struct., photocurrent relax. 0-92978
 Bi_{0.85}Sb_{0.15}, semiconductor transport props., 2 to 100K 0-59989
 n-Cd_{0.9}Hg_{0.1}Te, photoelec. props. at 78K, relax. time, minority carrier extraction 0-107864
 Ge, carrier relaxation rate temp. depend. and pair density in large electron-hole drop 0-75509
 Ge, compensated, impurity photocond. relax times 0-88592
 n-InAs, photoelectric props., inhomogeneous impurity distrib. 0-107867
 Si, amorphous evaporated, picosecond optoelectronic detect., sampling and correlation meas. 0-100478
 Si, electrical conductivity, inertia of electron heating, expt. and theory 0-65613
 Si on sapphire thin film, Hall effect, magnetoresistance (French) 0-65601
 n-Si, relaxation of electron energy, carrier-density dependence 0-107809

carrier scattering at surfaces see *surface scattering***carrier scattering by dislocations** see *dislocation scattering***carrier scattering by impurities** see *impurity scattering***carrier scattering by point defects** see *point defect scattering***carrier traps** see *electron traps; hole traps***CARS** see *coherent antiStokes Raman scattering***cartography**

- Africa CITHARE project, soil thermal inertia and humidity cartography by geostationary satellite 0-76980
 Brazil Patanal, drainage network mapping from Landsat-2 imagery 0-81944
 Canada, vertical crustal movements, map 0-109130
 coastal photogrammetric mapping 0-104960
 colour maps from black and white photographs in remote sensing 0-109270
 contour maps, structural description, weather map appls. 0-101419
 Dakota landforms and drainage patterns, IR thermal imagery remote sensing 0-81892
 densification of ground control networks, computer program package (German) 0-94452
 geophysical mapping and remote sensing by optical filtering 0-101458
 image scanner technology for digital mapping systems 0-85773
 Japanese Islands region, geophysical data compilation and maps (Japanese) 0-67332
 land-use mapping, evaluation of LANDSAT image data 0-101443
 land-use maps extraction, from satellite data 0-76899
 Landsat imagery geometrical correction (French) 0-81889
 magnetic anomaly map of Republic of Djibouti, reduction techniques 0-61753
 seismic velocity anomaly mapping by graphical method 0-77146
 Venus radar mapping, Pioneer Venus Orbiter mapper design and operation 0-76495

cascade showers see *cosmic ray showers and bursts***Cassegrain antennas** see *reflector antennas***casting**

- continuous ingots, two phase zone critical parameters during casting (Russian) 0-93549
 fluorophosphate optical glass development 0-106588
 melt extraction technology, advances 0-76207
 molten metal binary mixtures with wide immiscibility range, gravitational layering of components (Russian) 0-104092
 Nylon-12 film, casting conditions effect on polymorphism 0-84903
 pyrometer, radiation, for molten cast Fe, design and field test (Japanese) 0-98917
 steel, Mn-Nb-Al-C, crack prop. and hot ductility during straightening concast strand 0-66646
 steel, solidification during continuous casting, cooling regime comparison (Russian) 0-93548
 steel, tool and high-speed, high freq. induction melting and centrifugal casting in instrumental anal. 0-84886
 steel casting, calc. method of thermal and thermo-visco-elasto-plastic processes (German) 0-79859
 steel continuous casting, thermal, thermo-visco-elasto-plastic processes (German) 0-81044
 Al alloy-mica particle composite, cast prep. and mech. props., bearing appl. 0-71613
 Al alloys, columnar struct. of alloys solidified in flowing melt in centrifugal casting 0-71640
 Al-CuAl₃ eutectics, microstruct. after solidification, heat pipe influence 0-76243
 α-Al₂O₃ fibre FP reinforced Al and Mg composites, fabrication and props. 0-81004
 Al₂O₃ substrates, tape-casted, fracture strength analysis 0-60948
 Cd-Zn eutectics, microstruct. after solidification, heat pipe influence 0-76243
 Cu-Nb alloy, chill casting, consumable arc melting, ingot prep. techniques 0-84879
 Fe-B amorphous ribbons formation, high-speed photography investigation 0-76216
 Fe-Cr-Mo alloy castings, thick-section, factors affecting 0-108374
 Fe-Ni-B glassy ribbons melt spinning, gas boundary layer effects 0-76217
 NiTaC eutectic superalloy, casting, furnace atm. effects 0-84880
 Si multicrystalline solar cell material prep., fast-pulled float zone, CZ and cast ingot and foil methods 0-93483
 Si sheet casting for solar cells 0-89139
 ZrSiO₄-Al₂O₃ (SiO₂) suspensions for slip casting, prep. and props. 0-104103

castings

- epoxy resins, AC breakdown-voltage characts. (Japanese) 0-88927
 flexible scanning industrial X-ray/fluoroscopy inspection 0-89459
 steel, radiography with the 25000 R/min Linac 0-97656
 white cast Fe, abrasive wear 0-108587
 Al-Mg-Si alloys, precip.-rich zones on grain boundaries, soln. heat treatment conditions effect on mech. props. 0-104176
 Be ingot, high-purity, TEM obs. of BeO dispersion 0-104165
 Fe nodular castings, comparison of sonic-resonance and US velocity techniques for quality control 0-97654
 Fe-Cr-Mo alloy castings, thick-section, factors affecting 0-108374
 Fe-Mn, as cast, pseudo-composite struct. resulting from interdendritic segregation, cryogenic materials appl. (French) 0-93556

catalysissee also *catalysts; reaction kinetics*

- acetylene, reaction with Ni (100) and (110), room temp., UPS expts. 0-61151
 autocatalytic deposition of Sn 0-100965
 chemical rectifiers, one-way catalysis 0-71901
 chemisorption kinetics, determ. from substrate current fluctuations 0-84383
 cluster systems, program for calc. electronic struct. with double self-consistency-Bersuker's method 0-69289
 diamond synthesis by graphitisation of carbon materials at high press. and temp., Ni influence 0-60795
 diffusion-controlled reactions on a two-dimensional lattice 0-71940
 electrocatalysis, radiotracer method investig. appls. 0-70525
 electrocatalysis, surfaces modified by metal adatoms, review 0-61110
 enzyme-catalysed reactions, network thermodynamic modelling 0-89463
 ethylene-Co copolymers and -SO₂ copolymers prep. by catalysis and ⁶⁰Co γ-radiation, mech. props. 0-66841
 graphite, Fe-catalysed gasification, electron, microscopy 0-104358
 heterogeneous catalysis, conference, Varna, Bulgaria (Oct. 1979) 0-82578
 heterogeneously catalyzed oscillatory reactions 0-108732
 historical review, rel. to stochastic models of chem. kinetics 0-105483
 metal cluster growth and props., appl. to catalysis, conf., Villeurbanne, France (Sep. '79) 0-105431
 metallic surface, catalysed thermal desorption and dissoc. processes, microscopic theory 0-75439
 microreactor assembly to study heterogeneous catalyst system, IR emission spectra anal. 0-98988
 propylene, oxidation on MgO:Mo catalyst, surface structs., IR absorpt spectra obs. 0-66868
 PVC thermal degradation, reinitiation mechanism of HCl catalysis 0-71944
 rare earth manganites, catalytic activity 0-71941
 rare-earth compounds, catalytic props. 0-66875
 semiconductor catalytic kinetics, complex mech. of excitation, constant state problems 0-85213
 sodium 10-undecanoate, γ-ray induced polymerisation in aq. micelle solns. 0-61093
 solid surface, mol. dynamic processes interaction with laser radiation 0-71943
 solid surfaces, surface processes, and solid/gas interactions 0-73125
 TEM, advances, catalytic chem. appls. 0-85214
 thermal desorption and dissociation catalyzed by a solid surface 0-108734
 C, amorphous, catalytic oxidation by Pd particles, TEM obs. 0-76555
 C, graphitisable, catalytic graphitisation by Cr, Mn and Mo oxides 0-89166
 CO, catalytic oxidation on ferrites, IR spectrosc. investig. 0-89524
 Ca-Mg-Ni hydrides, water form. on O₂ exposure 0-97727
 Co/Na zeolite, -A and -Y type, local coordination of Co(II) ions studied by X-ray absorpt. fine struct. spectroscopy 0-93434
 Cr carbides, catalytic oxidation of H₂, 0-104462
 Fe₃C, catalytic oxidation of H₂, 0-104462
 H, dissociated, heat transfer to catalytic surfaces, shock tube investigation 0-64551
 H₂, ortho-para conversion, magneto-catalytic reaction, quantum formulation 0-108750
 H₂, photocatalytic production by carbohydrate conversion using RuO₂/TiO₂/Pt photocatalyst powder 0-94120
 H₂+N₂O, HO radical form. on Pt surface, laser-induced fluoresc. obs. 0-108738
 H₂O, gaseous, photodecomposition over TiO₂ and TiO₂-RuO₂ surfaces 0-85194
 H₂O, photoelectrolysis with TiO₂ catalyst 0-60755
 H₂O photolysis using biological and artificial catalysts for H prod. 0-61444
 Mg₂Cu polycrystals, surface study by AES, XPES and X-ray induced AES 0-65346
 N atom recom. on Fe, vibr. energy of desorbing N₂, electron beam induced fluoresc. 0-61149
 N₂+methane, N₂ fixation, catalytic processes in non-equilibrium plasma chemical reactors (French) 0-89483
 N₂+O₂, N₂ fixation, catalytic processes in non-equilibrium plasma chemical reactors (French) 0-89484
 NH₃, chemisorption on Ni (111) and reaction, LEED, desorption and photoemission expts. 0-59799
 NO, electrocatalytic decomp. on electrochem. reduced zirconia surface 0-61113
 Ni (100), interaction of adsorbed H₂, CO, and methanol, temp. programmed desorption study 0-66876
 Ni (111), chemisorption and reaction of NH₃, LEED, desorption and photoemission expts. 0-59799
 Ni-Co-Cr/Al₂O₃ catalyst, IR spectra of adsorption and interaction with pyridine 0-71946
 Ni(CO)₄, form. reaction rate, substrate mag. phase depend. 0-108737
 Pd film, work function changes due to adsorbed H₂, surface and interface dipoles 0-96972
 Pt, adsorption and catalytic reactions of H₂, CO, and O₂ 0-81362
 Pt/Al₂O₃, electron accepting sites by pyridine absorpt. 0-71947
 Si, oxidation, solubility and transport behaviour of water, dissolution 0-93801
 p-Si:P(P⁺) photolytic props. in HF 0-89504
 Sm_{0.8}M_{0.2}CoO₃ (M=Ca, Sr, Ba), catalytic props. 0-66875
 SrTiO₃ photocatalyst for H₂O decomp. 0-85202
 TiO₂, nonstoichiometric anodic films, O incorporation kinetics 0-97733
 TiO₂-Ni, electronic props., struct., comp., chemical bonding 0-84499
 ZnO powder, effect of dry grinding in EPR and catalytic activity (Japanese) 0-84640
 Zr(BH₄)₃, catalytic reactions on Al₂O₃, inelastic electron tunnelling spectra 0-75425

catalystssee also *catalysis*

- catalyst for water photolysis, I-V model 0-108721
 chlorophyll a dihydride, photocatalysis of H₂O photolysis for H₂ prod. 0-61458
 heterogeneous catalysis, conference, Varna, Bulgaria (Oct. 1979) 0-82578
 laser Raman spectroscopy in controlled atm. rot. cell 0-86437
 metal oxide, convergent beam electron microscopy obs. 0-108689

catalysts continued

- metal particles, small, characterisation and props., book contrib. 0-84417
PIXE appl. to design and evaluation of catalysts 0-61201
STEM, atomic number contrast, supported catalyst particles 0-79651
transition metal oxide catalysts, reduction, cryst. defects influence, in-situ electron microscopy 0-81322
Ag, for oxidation of rubber, prep. of diene oligomers with hydroxyl groups (German) 0-85175
 δ -Al₂O₃, isomerisation of adsorbed 1-butene, IR study 0-76554
 Γ -Al₂O₃, with Pt on, STEM, atomic number contrast, supported catalyst particles 0-79651
C, graphitisable, catalytic graphitisation by Cr, Mn and Mo oxides 0-89166
CoO, for catalytic oxidation of CO 0-71945
CuAl₂O₄, pure and NiO promoted catalysts, surface oxidation state and comp., XPS study 0-76134
Fe, gasification of graphite, electron microscopy 0-104358
LaPO₄ catalyst crystals, high resolution electron microscopy, morphological charact. rel. to catalytic activity 0-107193
MgO:Mo catalyst, adsorpt. of propylene, oxidation reactions, surface structs., IR absorpt. spectra obs. 0-66868
MgTeMoO₆, prep., cryst. struct., and catalytic props. 0-108709
MnO₂ dispersion mode on Al₂O₃ and SiO₂ powder supports, N adsorption obs. 0-81363
MoO₃ + Ni²⁺ interaction on Al₂O₃, Raman spectrum 0-108742
Na₂WO₃ bronzes, reaction with Fe powder, reaction mechanism and reactivity 0-108712
Ni (100), kinetics of C deposition from adsorbed CO 0-76553
Ni catalyst, chemisorption of benzene, Raman and vibr. spectra 0-108747
Ni, diamond synthesis by graphitisation of carbon materials at high press. and temp. 0-60795
Ni/Al₂O₃ catalysts, coprecipitated methanation type, metal-support interaction, XPS obs. 0-80936
Ni-Th (1 at.%), surface comp., temp. and O₂ exposure effects, AES study 0-80914
NiO-Cr₂O₃-MgSiO₃ methanation catalyst, S-resistant, IR and Raman spectra 0-93290
Pd, for oxidant impurities elimination, in viologens electrochromic solutions 0-78922
Pt and Pt/Ru electrocatalysts for methanol oxidation in acid electrolyte with improved steady state activity for fuel cell apps. 0-76629
Pt, on C electrode, surface area loss in H₃PO₄ 0-101091
Pt/TiO₂ catalysts, photodecomp. of water 0-81337
Rh-Cu catalyst, Al₂O₃ supported, chemisorbed CO, IR spectra (French) 0-60559
Rh-TiO₂ catalyst, adsorpt. of H₂, surface states, NMR spectrosc. investig. 0-103891
Ru (110), kinetics of C deposition from adsorbed CO 0-76553
Ru-Cu clusters, EXAFS study 0-84804
SiO₂-Al₂O₃ porous catalysts, EPMA quantitative anal., new correction calc. method, modified ZAF method (Japanese) 0-93822
SiO₂-MgO porous catalysts, EPMA quantitative anal., new correction calc. method, modified ZAF method (Japanese) 0-93822
V₂O₅ and lower oxides, defect structures and related props., review 0-59454
 α -VOPO, VPO₄, V₄(P₂O₇)₃ and (VO)₂P₂O₇, IR absorpt. spectra, bond freqs. 0-108192
WCs, preparation method effects on catalytic activity for H₂ evolution 0-101024
ZrO₂ solid electrolyte, electrochem. reduced, electrocatalytic decomp. of NO 0-61113

cataphoresis *see electrophoresis***catastrophe theory**

- butterfly catastrophe in high density behaviour of real fluids 0-87834
discontinuous transitions into chaos after single bifurcation, hysteresis existence 0-73264
electrochemistry, steady-state conversion rate rel. to surface reaction process, catastrophe theory 0-108717
phonon Focusing catastrophes 0-59591
plastics, crack growth stability anal. using catastrophe theory 0-74810
reaction-diffusion systems, bifurcation theory, classification 0-108713

cathode-ray oscilloscopes

- see also oscillographs*
biomedical oscilloscope with digital storage for elec. signal obs. and storage 0-104786
camera frame, integral data display 0-68284
digital storage oscilloscope principles and applications (Danish) 0-62647
high-speed oscillographic investigation, subnanosecond Nd glass pulse oscillator 0-74411
high-speed storage oscilloscope, Tektronix 7104 (Danish) 0-62646
low repetition trigger cct., for high speed pulse observation (Spanish) 0-62657
sampling stroboscopic transformation of pulsed photocurrent from electron beam multiplier ELUFT-01 (USSR) 0-73471
stereo vector CRO 0-90833
triggered calibrated sweep for AC oscilloscope 0-67987

cathode-ray tube displays

- see also cathode-ray oscilloscopes*
half-tone image displays using MIR-2 computer 0-62641
PLZT electro-optic shutter stereoscopic display applications 0-90826

cathode-ray tube screens *see cathode-ray tubes; fluorescent screens***cathode-ray tubes**

- see also image converters; image intensifiers; image storage tubes; television camera tubes; television picture tubes*
alternative scanned light sources 0-69477
phosphors, cathodoluminesc. investig., appl. to cathode ray tube screening 0-108282
semiconductor laser screens, scanning optical microscopy appl. 0-86398
vidicon, Si-intensified-target, low intensities meas., astronomy appl. (German) 0-98545

cathode rays

No entries

cathodes

- see also electron emission; oxide coated cathodes; photocathodes; thermionic cathodes*
disc LaB₆ cathode for plasma production in magnetic field 0-106951
field at the surface of a field-emission cathode 0-100757
fuel cell, voltage losses 0-104503

cathodes continued

- high current discharge from cold LaB₆ cathode 0-107011
hollow cathode, glow discharge, current balance and secondary electron emission 0-75108
hollow cathode discharge, Al spectral line, pulse feeding 0-64797
laser tube design, cathode fall theory studies 0-58560
metal cathodes, oxidised and clean, basic erosion processes in electric arcs 0-103211
metal cathodes subjected to pulsed electric fields, electron field emission charact. 0-71580
metallic heated cathodes, physics of electron emission (French) 0-104033
MIM, LF noise sources and reduction 0-108328
MIM cathode, local electron emission and electroluminescence patterns obs. 0-108327
nanosecond discharge in vac., cathode polishing effect 0-79599
Penning discharge, cathode sheath, RF impedance study 0-106935
porous metal cathodes, emission props., work function 0-100502
positive ion source, hollow cathode design 0-99399
pulsed desorption slot, operating stability 0-87002
sheaths in K₂CO₃ seeded petroleum MHD combustion plasma 0-87870
Al-Si₃N₄-O₂-Al thin film cathode, physical model from expt. study 0-100535
Al-Ti alloy spark alloying, cathode weight change and hardened layer obs. (Russian) 0-61005
Cu, broad area type, electrolum. regions, current-voltage charact. 0-84019
LaB₆ cathodes for Kohler illum. and brightness meas. 0-68296
LaB₆, hollow cathode mag. multipole ion source 0-102369
Li-(CF₃)_n high energy density battery, cathode materials evaluation 0-77780
Li₂MO₃ (M=transition metal), thermodynamic investigations 0-89210
Mo fine tip cathode, field emission stability, rel. to passivation 0-100760
Mo-Cu cathode, spot motion and nature in UHV 0-79597
W fine tip cathode, field emission stability, rel. to passivation 0-100760

cathodes, electrochemical *see electrochemical electrodes***cathodochromism**

- Na₂Al₂Si₂O₈·2Cl(Br)(I), cathodochromic sodalites, coloured crystals, tunnel and recomb. luminesc., temp. depend. (Russian) 0-66261
Na₂Al₂Si₂O₈·2NaX₂(γ), (X=Cl, Br, I), X-ray irradi., thermal-erase cathodochromism and dihalide mol. centres (Russian) 0-66236

cathodoluminescence

- biomedical apps. of SEM cathodoluminescence method 0-72400
diamond, industrial, anal. cathodoluminesc. studies in SEM 0-81410
diamond, natural type-IIb, single dislocations, cathodoluminescence obs. by STEM 0-80871
diamonds, synthetic, polarised infra-red cathodoluminescence 0-89073
Giemsa stain, detection of cathodoluminescence and its apps. 0-67323
growth-layering effect on optical symmetry in cubic crystals, rel. to cathodolum. data 0-88072
III-V multilayer structure, as-grown, assessment of defects by differentiated cathodolum. topography 0-59819
microprobe analyser, scanning cathodolum. 0-81409
minerals, ionisation enhanced diffusion effect obs. 0-71497
minority carrier lifetime mapping by SEM 0-96903
phosphors, cathodoluminesc. investig., appl. to cathode ray tube screening 0-108282
photon counter design for low light detection systems, spectroscopy, cathodolum. materials appl. 0-105711
rare earth double orthophosphates with alkali metals, conc. depend. of luminesc. props. 0-100673
rare earth double orthophosphates with alkali metals, spectroscopic obs., struct. and chem. nature 0-100674
SEM, detector system 0-101898
SEM, stroboscopic cathodolum., apps. 0-70088
semiconductor, STEM spectroscopic techniques for simultaneous electronic and defect obs. 0-100145
semiconductor defects, spectroscopic techniques to study of electronic props. 0-84446
semiconductors, quasi-equilib. approx. 0-84779
CaF₂, SEM 0-100700
CaF₂:Eu, CaF₂:Eu,Mn(Gd), single crystal predisintegration phenomena, SEM cathodolum. obs. 0-59502
CaF₂:Mn, CaF₂:Eu,Mn, single crystal predisintegration phenomena, SEM cathodolum. obs. 0-59502
CdS:Ga crystal cathodoluminescence, SEM analysis 0-97349
CdS_{1-x}Se_x, chem. comp. and luminescence obs. 0-80869
CdTe, vapour-phase-grown, cathodoluminesc. study 0-76086
Cu, hot cathodoluminescence study, electron-hole recombination 0-93410
CuI, single crystals, growth and optical props. 0-93470
(Ga,Al)As:Si(Ge), epitaxial layers, radiative recomb., compensation, cathodolum. study 0-66307
Ga_{1-x}Al_xAs structures, STEM and scanning deep level transient spectroscopy in defect centre anal. cathodoluminesc. techniques 0-103642
Ga_{1-x}Al_xN heteroepitaxial films, photoluminesc., cathodoluminesc. 0-66292
Ga_{1-x}Al_xP:N epitaxial films, ion implanted, cathodoluminescence study 0-60684
GaAs epitaxial films on strongly doped substrate, basic parameter meas. utilising magnetoresist. and SEM techniques under cathodoluminesc. conditions 0-65728
GaAs film, electron scatt., cathodoluminesc. meas., energy depend. of electron deposition depth determ. 0-104023
GaAs:Se cathodoluminescence decay obs. with SEM and streak camera, 90 to 300K 0-97348
GaAs:Si defect density before and after Zn diffusion, SEM and TEM obs. 0-96529
GaAs-Cu:Ti, cathode luminescence spectra, Hall effect, cryst. defects 0-76087
GaAs-Ga_{1-x}As DH laser material crystal cathodoluminescence, SEM analysis 0-97349
GaAs-GaAlAs wafers, defects and degradation, transmission cathodolum. evaluation 0-65395
GaN epitaxial films, cathodoluminesc. spectra 0-71496
GaN, VPE growth rate influence on elec. and luminesc. props. 0-100702
GaP, green cathodolum. from cryst. defects, SEM, TEM study 0-80870
GaP LED, SEM study of charge collection and cathodoluminesc. 0-65661
GaP:N LED structures, local dopant conc. determ. using SEM cathodolum. spectra 0-101057

cathodoluminescence continued

- GaSe, exciton-phonon quasibound states, photocond. and luminesc. study 0-96800
 InAs and solid solutions, recombination mechanisms of excess carriers, luminesc. obs. 0-97337
 n-In_{1-x}Ga_xP, direct-gap semiconductor, cathodoluminesc., electron irradiation effects 0-108283
 KCl:Ti, temp. depend. of cathodolum. (*Russian*) 0-80868
 KI, self trapped exciton form. time at Σ_u^+ state under pulsed electron beam in ps range 0-97347
 LaGaS₃:Ce³⁺, phosphor, luminesc. props. 0-103979
 LiF crystal, contact damage obs. by cathodoluminesc. 0-71728
 MgO crystal, contact damage obs. by cathodoluminesc. 0-71728
 MgO crystal cathodoluminescence, SEM analysis 0-97349
 MgO, deformed, cathodolum. obs. by STEM 0-76088
 N₂ film, on metal or sapphire substrates, luminescence and nonradiative energy transfer to surfaces 0-97350
 RbBr, self trapped exciton form. time at Σ_u^+ state under pulsed electron beam in ps range 0-97347
 RbI, luminesc. spectra induced by pulsed Ne⁺ and electron beams and X-rays 0-80851
 SiO₂ coatings on SiO₂ substrate, cathodoluminescence spectra, electron irradiation 0-76085
 SiO₂ layers in LSI cct. device, cathodoluminesc. obs. 0-80867
 W, surface adsorption processes following electron excitation, cathodoluminescence studies 0-100390
 Xe, liq., α -particle and electron excited luminesc., time depend., specific ionisation density effect 0-71495
 (Zn,Mg)₃(PO₄)₂:Mn²⁺, cathodoluminescence obs. 0-71492
 ZnS, cathodolum. emission spectra, exciton lines 0-76084
 ZnS, single electron excitation study, cathodoluminescence image contrast using STEM 0-89072
 ZnS,Se_{1-x}, VPE on CaF₂ substrate, in flowing H₂, growth and characterisation (*French*) 0-107678
 ZnTe, edge luminesc. excited by electron bombard. 0-66308
 ZnTe, ion implantation defect introduction, cathodolum. studies 0-75250
 ZnTe, low voltage green LED, struct. double diffusion procedure 0-100697
 ZnTe:P(As), ion implanted, cathodoluminescence emission spectrum 0-108281

cathodophosphorescence *see* cathodoluminescence

cathodothermoluminescence *see* cathodoluminescence

catholytes *see* electrolytes

causality *see* physics fundamentals

causticity *see* pH

cavitation

see also bubbles; vortices

- acoustic field generated cavitation, review 0-74934
 acoustic wave reflection from fluid-solid boundary, bubble collapse, US cleaning and cavitation erosion 0-65158
 air bubble growth meas. by rectified diffusion at 22.1 kHz 0-96155
 alloys, creep cavitation control, intergranular precipitates role 0-66664
 AMTE/QUEL underwater jet noise rig, working report for 1977/78 0-79286
 approximate analysis with allowance for surface tension and gravity 0-92191
 blood, volume expansion effects, gas cavities 0-67134
 brass, comparison of liquid impact erosion and cavitation erosion 0-104302
 bubble rupture between two solid walls, effect of drag-reducing polymers on cavitation 0-106822
 bubbles, amplitude distrib. of pulses produced by shock waves 0-64252
 conf., New Orleans, LA, USA, March 1980 0-105430
 creep crack propag. by cavitation near crack tips 0-107364
 cylinders, elliptic 2-D, cavitation shock-noise measurement for different eccentricities 0-79368
 diffusional growth of intergranular cavities in uniform stress field and ahead of crack-like stress concentrator 0-107366
 disc wake, cavitating flows with perturbations 0-92190
 driven, Navier-Stokes eqn. soln. numerical stability 0-92147
 erosion, non-spherical bubble collapse near a solid wall, analytical soln. using matched asymptotic expansions 0-106824
 erosion of alloys in venturi 0-108602
 film cleaning by ultrasonic liquid cavitation and acceptable solvents 0-62769
 flow visualization of cavitation in water jets and nuclei distribution measurement by holography 0-106862
 fluid, radio band pulse radiation due to spark initiated cavity dynamics, sonoluminescence (*Russian*) 0-66313
 gaseous microbubble growth in laminar separation bubbles 0-106821
 hydraulic liquids, cavitation-erosion props. assessment using ultrasonic dispersator 0-71832
 hydrodynamic cavitation in viscous liquid, investigation using HF US probing method 0-87676
 incompressible perfect fluid, collapse or expansion of prolate and oblate spheroidal bubbles (*French*) 0-74933
 liquid cavity collapse, accompanied by RF emission 0-87790
 molten metal cavitation bubble collapse and erosion intensity in constant mag. field (*Russian*) 0-60987
 n-octane fluid, spontaneous cavitation 0-69886
 orifice, cavitating, under reattached flow conditions, noise and vibration characteristics 0-83829
 pipe flow, spatial cavitation-nuclei-measurements by means of laser velocimeter 0-64593
 pressure transient analysis in piping systems including the effects of plastic deformation and cavitation 0-74775
 propeller cavitation tunnel hydroacoustic transfer function, meas. and anal. (*Croatian*) 0-92002
 pulsed radiolysis, nonlinear radiation-acoustic phenomena 0-79029
 spherical cavity in compressible liquid in sound field, eqns. for dynamics 0-87612
 steel, austenitic Cr-Ni, intergranular damage parameters in creep (*Czech*) 0-89342
 steel, Cr-Mo-V low-alloy with high residual element content, cavitation control 0-66663
 supercavity hydrofoil, wall effects, nose rounding 0-64594
 superplasticity, cavity growth anal. 0-60923
 threshold meas. for polyalkylene glycol and castor oil, underwater sound transducer appl. 0-107374
 tunnels with continuous and perforated walls, cavity size 0-92193

cavitation continued

- turbulent jets, influence of drag reducing polymers on cavitation inception 0-106823
 US and laser cavitation in liquid crystals 0-87633
 US cavitation intensity in liquids, organic comparisons 0-106820
 US wave in cavitating liquids, optical visualisation, nonlinear effects 0-106651
 vapour bubble growth in US field 0-87608
 vertical axisymmetric cavitating flow around a body, independ. cavity expansion method 0-92192
 void swelling, nucleation theory 0-65038
 water, cavitation expts. in steel Berthelot tube 0-87788
 water, cavitation expts. using shock tube 0-87789
 wing-tip vortex cavitation, vapour core characteristics eval. by asymptotic expansion 0-106825
 Al and Al-Cu(Mg), comparison of liquid impact erosion and cavitation erosion 0-104302
 Al-Zn-Mg superplastic alloy, cavity growth under creep conditions 0-60940
 Co, single crystal, cavitation erosion, role of twinning 0-107272
 Cu and alloys, intergranular damage parameters in creep (*Czech*) 0-89342
 Cu, high purity, creep cavitation topology, high temperature region (*Czech*) 0-65138
 Fe, comparison of liquid impact erosion and cavitation erosion 0-104302
 Ni, oxidation, high temp., effect of C on cavity form., SEM study 0-97638

cavity resonators

see also acoustic resonators; laser cavity resonators

- 2.148 GHz SAW oscillator using AlN/Al₂O₃ delay line 0-74680
 absorptive optical bistability, two-level atom system, photon antibunching 0-58486
 bistable nonlinear Fabry-Perot resonator switching speed and energy calc. 0-64095
 coaxial, with lumped capacitance, appl. to complex permittivity determ. for wide range of materials (*Polish*) 0-73382
 coaxial microwave cavity for improved EPR sensitivity with loss solvents 0-62705
 cylindrical, H_{010} mode, accurate complex permittivity, meas. for wide range of materials (*Polish*) 0-73383
 cylindrical cavity resonator in H_{010} mode, for complex permittivity meas., approx. method (*Polish*) 0-73384
 DC permeameter for ring specimens 0-98954
 Earth-ionosphere cavity, Schumann resonances, book 0-86050
 electron cyclotron maser, fundamental mode, linear theory 0-58496
 electron cyclotron maser device theory 0-58494
 electron cyclotron maser in overmoded cavity, nonlinear multimode formulation 0-58495
 EPR high-temp. cavity for easily oxidised fluorides 0-77831
 Fabry-Perot cavity, absorptive bistability, mean-field approx., truncated Bloch hierarchy 0-83631
 Fabry-Perot cavity, optical bistability, spatial effects 0-83632
 Fabry-Perot cavity, optical bistability, standing wave effects 0-91837
 fusion reactor, ELMO Bumpy Torus, microwave coupling 0-99328
 gyromonotron, operating characteristics at 35 GHz 0-58497
 gyromonotron design, 240 GHz, using supercond. magnet system 0-58498
 HF field distrib. meas. 0-98930
 linear accelerators, resonator sensor for the parameter of charged-particle beams 0-68991
 multicavity IR electro-optical tunable filter 0-102831
 optical bare resonator eigenvalue analysis, matrix methods 0-78927
 optical bistability, absorptive and dispersive, in Fabry-Perot and ring-cavity geometries 0-95942
 optical bistability, exact semiclassical treatment of ring cavity 0-58627
 optical bistability in bad cavity limit, Fokker Planck eqn. approach 0-64116
 optical bistability of a homogeneously broadened medium with dispersion 0-83630
 optical cavity filled with Kerr dielectric, nonlinear effect of powerful laser radiation field 0-99787
 optical dispersive resonators with system of reflective gratings (*Russian*) 0-96029
 Q-factor meas. by analytic method using reflection coeff. vs. freq. 0-98937
 ring cavity, chaotic behaviour of transmitted light, optical turbulence 0-102760
 Stark microwave, for continuous NH₃ monitoring 0-61500
 tubular dielectric, complex permittivity and loss angle meas. in X-band using H_{011} cavity resonator method (*German*) 0-62690
 two-resonator CRM oscillator with external feedback 0-87362
 X-ray resonator based on successive refls. of surface wave 0-99021
 H masers, with automatic tuning 0-95859

c.c.d. circuits *see* charge-coupled device circuits

CCTV *see* closed circuit television

celestial mechanics

see also N-body problems; stellar motion

- 1980 LB, improved orbital elements rel to 2:1 Jupiter libration hypothesis 0-94744
 2101 Adonis, orbital problem soln. 0-72842
 analytical satellite theory in extended phase space 0-67524
 artificial Earth satellites, second order perturbation soln. (*Chinese*) 0-77270
 artificial satellites, anomalistic period, solar radiation press. effects 0-77255
 artificial satellites, critical inclination problem with small eccentricity 0-67525
 artificial satellites, orbits, short periodic drag perturbations 0-67522
 asteroids, regular proximities concept and approximate perturbation methods 0-72843
 asteroid belt truncation, theory of tidal torques on infrequently colliding particle discs in binary systems of tidal torques on infrequently colliding particle discs in binary systems 0-98596
 asteroid family detection by new criterion, orbital data 0-82256
 asteroids, Munich meridian obs. (1941-61), orbital elements determ. (*German*) 0-77306
 Babylonian lunar theory 0-94729
 Castor satellite, accel. below 10^{-9} g meas. by Cactus accelerometer, flight results synthesis 0-77251
 central configurations, families (*Russian*) 0-90327

celestial mechanics continued

Charon (1978 P 1), satellite of Pluto, positions and dynamical parameters 0-62069
collisions in Keplerian systems, numerical analysis 0-109342
comet belt beyond Neptune, orbital diffusion rel. to short-period comets origin 0-94759
comet dynamics, exact solns. of diffusion eqn. 0-82304
comet orbital elements distrib., effect of galactic forces (*Russian*) 0-77353
comet orbits, evolution under perturbing influence of giant planets and nearby stars 0-98613
cometary equations of motion, recurrent power series integration 0-72882
cometary orbits, reciprocal semimajor axes accuracy 0-62074
comets, ancient and medieval, orbits 0-62077
comets, long-period, distrib. of inclination of perihelion dynamical implications 0-101563
comets, nearly parabolic orbits, distrib. of nodes and perihelia 0-67661
comets, orbital evolution of short-period objects, Monte Carlo simulations 0-62073
comets, original, orbital inclinations distrib. anomalies rel. to origin of comets 0-98615
comets origin, celestial mechanical aspects of planetary ejection hypothesis 0-62080
comets perihelia longitudes concentration, reality from discovery probability anal. 0-67660
commensurabilities in solar system 0-109418
conference, Washington, DC, USA (Nov.-Dec. 1978) 0-90605
c Coroneae Borealis (=ADS 9979), binary, mass and orbital elements (*French*) 0-77449
Earth, cyclical orbital variations detect in S.Australian beach ridges chronology rel. to Milankovitch ice age theory 0-98307
Earth, orbit determination on basis of radar and visible observations 0-90323
Earth grazing fireball, eqns. of motion, vel., orbit and mass determ. 0-67663
Earth motion from self consistent FORTRAN subroutines 0-85845
Earth orbit variations as cause of climatic fluctuations, geological support 0-72509
Earth satellite orbits with resonance lunisolar perturbations, dependent on inclination 0-90326
elliptic motion, mean anomaly as random variable 0-67523
FK5, equinox and equator of new fundamental reference coord. system 0-109341
flight trajectory between satellite orbits of Earth and Moon, variational problem 0-72754
four-body systems, statistical theory for disruption 0-101531
Galilean satellites motion, new theory and improved ephemerides 0-62066
geostationary satellite, orbit determ. by single ground station tracking 0-109329
gravitational potential of a body of revolution, representation by finite system of mass points (*Russian*) 0-72757
gyrostatic satellite in Kepler orbit, rot. motions 0-86080
Hill's equation, new exact method (*Chinese*) 0-105152
hyper-periods and Kirkwood Gaps 0-105153
inner planets, second order perturbation theory (*French*) 0-72801
inner planets orbits, discrepancies in motions of perihelia 0-67531
Jupiter close encounter with planet crossing objects, orbit changes 0-77329
Jupiter close encounters with minor bodies, importance of nearly tangent orbits 0-82248
Jupiter ring, orbit changes depend. on dust charge 0-82273
Kepler's equation, generalisation using Banach's contraction principle 0-105151
Keplerian motion, isochronous derivatives and uniform formulae of Langrange multipliers (*Russian*) 0-72756
non-Keplerian orbit, Keplerian representation 0-90324
LAGEOS orbit, long-term evolution 0-94676
Lagrangian points L_4 and L_5 , positions rel. to radiation and gravity forces ratio 0-85843
lunar theories, main problem, comparison between ELP and SALE (*French*) 0-85844
luni-solar nutation tables, Earth liquid core effects 0-98210
Mars, orbit determination on basis of radar and visible observations 0-90323
meteor trajectories and orbits, visible obs. 0-72887
meteoroid flight trajectory azimuth from Sikhote-Alin field craters 0-72893
meteoroids and dust, orbits from radio and photographic meteor obs. 0-101555
minor planet orbit determ. using Chebyshev's approx. (*French*) 0-94720
minor planet satellites, occultations of stars 0-94741
modified conservation laws in the classical Kepler problem 0-72755
Monte Carlo orbit evolution simulations for comets becoming asteroids 0-82261
Moon, peculiarities of translatory-rotatory motion caused by force function third and higher harmonics (*Russian*) 0-90349
Moon main problem, ELP soln. (*French*) 0-62044
N-body problem, translational-rotational motion of six bodies (*Russian*) 0-67528
New South Wales fireball, 7 April 1978, trajectory and ground track 0-82313
one-dimensional self-gravitating isothermal systems, stability 0-73008
orbit determination for cosmic object, Green's functions appl. 0-61992
orbital dynamics and rigid body dynamics, analogy 0-98537
orbital motion on an interactive-graphics terminal, teaching appl. 0-73152
peculiar direct motions, loops made by objects in strange orbits 0-109346
perihelion displacement, gravitational wave effects 0-61998
Periodic Comet Boethin (1975 I), libration around 1/1 resonance with Jupiter 0-72883
Periodic Comet Chernykh (1977I), definitive orbit at first apparition (1977 to 1978) 0-62079
perturbed motion rel. to KS transformation osculating variables 0-109344
perturbing planet coordinates, expression through perturbed planet eccentric anomaly 0-67530
Phobos, orbital inclination evolution 0-67628
planar magnetic-binary problem, equilib. points 0-82178
plane motion with two-fold vel. field, eqns. for potentials (*Russian*) 0-67527

celestial mechanics continued

planetary, solar and lunar positions, low-precision formulae 0-61990
planetary orbits computation using Chebyshev polynomials, appl. to minor planets (*French*) 0-61997
planetary satellite ejecta, effect of proximity to Roche limit on dynamics 0-98592
planetary satellite orbits, third and fourth-order perturbations rel. to flattening of planet 0-67529
planets, Munich meridian obs. (1941-61), orbital elements determ. (*German*) 0-77306
planets, orbit stability in binary systems, Hill's method appl. 0-94834
Pluto, orbital motion, long term librational character 0-94753
resonance problems, regularising function 0-94693
restricted three-body problem, Sun-Jupiter-satellite system, three dimens. orbit determ. 0-67526
rigid bodies under mutual gravitational attraction, motion 0-61996
rigid body, regular motions in gravit. field of sphere 0-62000
Roche problem, for polytropes in central orbits 0-82179
solar system, Titius-Bode law for planet distances from Sun 0-82236
stellar aberration, classical rel. to relativistic theory 0-67517
stellar reson. orbits comparison, 2/1 reson. 0-67796
three-body problem, restricted case secular post-Newtonian effects, Tredar dynamics 0-72753
three body problem, planar circular restricted case, stochastic behaviour, reson. overlap criterion 0-105150
three rigid bodies problem, particular solns. for translational motion (*Russian*) 0-61999
three-body problem, classical restricted, Coriolis asymm. and Jacobian integral 0-61994
three-body problem, conditionally periodic solns., KAMo method 0-109343
three-body problem, elliptical restricted case, Lagrangian soln. stability (*Russian*) 0-94695
three-body problem, general, three-dimens., biparametric family of symm. periodic orbits 0-61995
three-body problem, photogravitational restricted circular case, triangular libration points stability (*Russian*) 0-72772
three-body problem, plane averaged restricted case, qualitative analysis 0-109345
three-body problem, restricted, in resisting medium, particular solution (*Italian*) 0-90325
three-body problem, restricted case, Sun-Jupiter case, doubly symm. periodic orbit determ. 0-77269
three-body problem, restricted case, u-type families of periodic orbits 0-101530
three-body problem, spatial periodic orbit families 0-77271
three-body problem, triple collision and tri-parabolic escape 0-67521
115 Thyra, astrometry and orbit improvement (*German*) 0-85881
Titan-Hyperion resonances and close approaches, restricted three-body problem anal. 0-77347
Trojan asteroids with large orbital inclination, dynamics 0-77323
two body problem in invariant mechanics (*French*) 0-94696
Venus orbit determ. using radar obs., appl. to spacecraft navigation 0-109386

cell model (liquids) *see liquid theory*

cell motility
erythrocyte tank-treading motion in a shear flow, model 0-104568
flagella, laser damage, high speed cinematography 0-81785
silicone rubber substrata, appl. to study of cell locomotion 0-104835
sperm, human, flagellar propulsion in cervical mucus, interaction hydrodynamics model 0-97878
spermatozoa, human, motility evaluation, photon correlation meas. 0-61745

cells (electric)
see also fuel cells; photoelectric cells; photoelectrochemical cells; primary cells; secondary cells
catecholamines, HPLC and continuous flow anal. using flow cell based on rotating disk electrode 0-66894
cylindrical, for making standard samples of metal coatings 0-85106
materials needs, in energy conservation and storage 0-66958
multicomponent impedance diagrams, resolution technique 0-66959
prosthetics, energy sources for long-term implantable devices 0-98175
reverse electroanalysis of brine solns., elec. cell design and cost 0-85271
standard cells with low temp. coeff., characts. 0-101090
 $\text{Ag(s)/Ag}_2\text{SO}_4\text{+Na}_2\text{SO}_4\text{(l)}$ high temp. ref. electrode, study 0-76622
 CaF_2 solid electrolyte use in galvanic cells for thermodynamic obs. on refractory double oxides (*French*) 0-85190
 $\text{Cu}_x\text{Mo}_{1-x-y}$, mixed conductor, equilb. partial thermodynamic props. 0-85270
 Li-Si , electrode pot., Li utilisation determ. 0-81427
 ^{147}Pm small-size nuclear battery, characts. of luminophores and photoelements (*Bulgarian*) 0-72084
WCs, preparation method effects on catalytic activity for H_2 evolution 0-101024

cellular automata *see finite automata*

cellular biophysics
see also biomembrane transport; biomembranes; cellular effects of radiation; cellular transport and dynamics; lipid bilayers
action potentials from cultured neurons, recording by extracellular microcircuit electrodes 0-72382
algae, living electrode for biophotolysis of water, long-lived photoconverter 0-104510
apatite crystal growth in skeletal tissues 0-94181
bacteria in H_2O , detection by resonance Raman spectra 0-94418
bacterial cell wall, surface charge and morphogenesis of regular arrays of macromols. 0-85366
bacterial single cells, bioluminesc. obs. 0-108860
blood, red cell flexibility, effect on blood flow through tubes of 30-500 μm 0-67111
blood cell leukocytes, automatic recognition and classification systems (*Italian*) 0-81780
blood rheology, erythrocyte rigidity effects on viscoelastic dilatancy 0-61610
blue-green algae, absorpt. spectrum, struct. resolution 0-76715
cardiac tissue, pacemaker activity, phase resetting and annihilation 0-81565
cell size meas. by static light scatt. Fourier transform 0-81793
CHO cells exposed to hyperthermia, radiosensitivity and recovery from radiation damage 0-72250
CHO fibroblast, press., inhibited thermal killing obs. 0-81564

cellular biophysics continued

- chromatin, factors affecting the heat-induced increase in protein content 0-97882
- chromosome classification system, banding technique 0-67320
- chromosome metaphase spread, automatic finding, prep. and eval. of object spectra 0-98168
- compound eye of worker honey bee, cell junctions, electron microscopy 0-85383
- Coulter electrical sizing principle, appl. to new multiparameter system 0-89911
- cytoplasm spherical drop with effective surface tension influenced by oscillating enzymatic reactions 0-108862
- diatom recognition and counting, matched-filter and statistical method 0-101304
- diffraction method for meas. of cellular deformability 0-98187
- DNA kinetoplast, ultrastruct., interpretation of dark field electron microscopy images of isolated purified networks 0-85369
- double-barrel ion-sensitive microelectrodes, extra thin tip diameters, intracellular meas. appl. 0-101298
- E. coli* strains in aq. suspension, polarisability anisotropy and aminoglycoside antibiotic effects 0-85441
- E. coli* suspensions, dielec. anal., interfacial polarisation theory appl. 0-97876
- electron microscopy, characterisation of cell membranes 0-104841
- electron microscopy symposium, Toledo, Ohio, USA (Aug. 1979) 0-82571
- embryo, mouse, innocuous freezing during warming 0-94175
- EPR of ¹²⁵I-UdR-labelled and X-irrad. cells at 4.2K and above 0-72211
- erythrocyte distribution profiles during sedimentation as determ. by HeNe laser light 0-81563
- erythrocyte membrane alterations, rheological technique evaluation 0-61611
- erythrocyte nucleosomes, chicken, temp. dependence of ³¹P-NMR spectra 0-94280
- erythrocytes, human, haemoglobin's suspending medium, dielec. props. obs. 0-76716
- erythrocytes labelled with stable Rb, survival determ. by fluoresc. excitation anal., rabbits 0-81788
- eukaryotic cell cycle, long-range dielec. aspects 0-94182
- extracellular potentials generated by curved fibres in a vol. conductor, modelling 0-97889
- fibrosarcoma cells, buoyant density, effect of hypoxic growth conditions in vitro 0-104601
- fluorescence polarisation measurements in flow systems, epi-illumination optical design 0-89908
- fluorescently labelled molecules as probes of living cells struct. and function, review 0-67321
- freeze-fracture technique, appl. to study of animal plasma membranes 0-104842
- ganglion cells, adjacent, serial reconstruct. in the retina 0-89749
- histological and cytological reflection contrast microscopy 0-72389
- human retinal image processing, two-channel model 0-94215
- hyperthermia-induced sensitisation of tumour cells to antibody-complement cytotoxicity 0-104570
- intracellular pressure measurement system 0-109084
- ionic balance during cultivation of cell populations in a spatially homogeneous medium 0-81557
- isopycnic centrifugation method for rapid separation of murine thymocytes 0-104832
- kinetic proofreading in biosynthetic pathways, thermodynamic constraints 0-108861
- Krebs II ascites cells, subcellular localisation and paramag. props. of observed signals 0-108952
- leucocytes, radioactive-labelled, appl. for proof of inflammations 0-67218
- lipid bodies, saturated, in organ pipe cactus visualisation by cytochem. technique 0-76873
- lymphocytes exposed to temps. of 37-45°C, two types of interface death 0-104566
- mammographic US image correlation with histopathologic sections 0-101240
- membrane electric properties measurement method using glass electrode impaled into single cell 0-89916
- membrane energetics, conf., Bloomfields Hills, USA (Jul. 1979) 0-94923
- membrane fluidity modification, mechanism of hyperthermic cell killing and therapy appl. 0-104569
- membrane particle diameters meas. by computer from electron micrographs 0-101307
- metabolism intensity relation with embryonic cell determ. process 0-85367
- microdosimetry, role in radiobiology 0-61705
- microorganisms, lack of intracellular bubble formation at very high gas supersaturations 0-81562
- micropipettes of very low resistance for intracellular meas., production method 0-61738
- muscle, multifibre preparation, intercellular clefts influence on pot. and current distrib. 0-72145
- muscle, tryptophan fluorescence polarisation 0-97877
- muscle chemomechanical energy transduction, mol. basis 0-72143
- muscle cross bridge rotation during contraction, fluctuations in polarised fluoresc. 0-97856
- nerve cell membrane detection of HF EM fields, possibility discussion (Russian) 0-76785
- neuron soma model with high reliability and low power consumption 0-72392
- neurons, cat eye, stereotaxic method for recording from single cells 0-89913
- neurons, section embedding technique for sequential light and electron microscopic exam. 0-67317
- Nitella, fluctuation and instability in membrane pot. near threshold 0-89723
- oocyte paracrystalline structs., mouse, *Mus cervicolor* poppaues 0-89731
- optical microscopy, cell deposition system for deposition at predefined locations on microscopical slide 0-76876
- pancreatic islet cells, plateau pots. as voltage-dependent action pots. 0-94180
- plant cell walls, viscoelastic props. 0-67106
- red blood cells, equilib. shapes in osmotic swelling 0-85368
- red blood cells, minimum energy anal. of membrane deform. 0-72141
- red cell membrane, human, surface elasticity and viscosity 0-61608
- retina, frog, morphometric anal. of internal horizontal cells 0-108892

cellular biophysics continued

- ribosome subparticle fine struct. investigation by optical filtration of electron microscope images 0-81779
- rigidity increase of material of bioconstructs. during morphogenesis 0-94249
- size analysis of single particles in flow, appl. of differential light scatt. photometer 0-77834
- small intestine, mouse, transient heat-induced thermal resistance, crypt survival assay 0-108850
- spermatozoa, bull, laser light-scatt. studies, orientational effects 0-89786
- Streptococcus mutans* 10449, size determ. by laser light scatt. 0-109062
- Streptococcus mutans* aggregation, dextran-induced, laser light scatt. meas. 0-89729
- stress-strain meas. on living cells using cell poker 0-76880
- taste cells, insect, special purpose amplifier for spike train recording 0-72394
- thylakoid membranes of wheat chloroplasts, proton spin-lattice relax. time, -8°C phase transition 0-108853
- urinary tract infections, radiorespirometric testing of antibiotic sensitivity 0-81705
- vertebrate retina modelling and simulation, extended networks 0-108884
- volumetric changes during freezing and thawing, thermodynamic model 0-108863
- Xeroderma pigmentosum fibroblasts infected with γ -irrad. adenovirus, decreased viral rep. obs. 0-61650
- T distribution in cells exposed to HTO 0-72142

cellular effects of radiation

see also biological effects of (type of radiation)

see also photosynthesis

- alveolar macrophages, effect of X-irrad. in mice 0-98024
- Aspergillus nidulans*, mutation induction by γ -irradiation in presence of O₂ or N₂ 0-94297
- bacterial cells, heavy ion irrad., long range effects, comparison with γ -irrad 0-101236
- bacterial spores, breaking survival curves and O₂ removal times obs. 0-81658
- bacteriophage λ superinfecting *E. coli*, induction and repair of DNA strand breaks 0-72228
- bacteriorhodopsin, photoelec. conversion in charged synthetic membranes 0-108954
- beta-rays from ¹⁴C, biological hazards, cell killing effects, *E. coli* expts. 0-89805
- bone, granulocyte and macrophage precursor cells, mouse, microwave effects in vitro 0-76789
- brain tumour cells, rat, anal. of interaction of 2 nitrosourea compounds and X-radiation 0-72230
- brain tumour cells, Z-ray-BCNU interactions in vitro, isobologram anal., rats 0-81662
- carcinogenic action of fluoresc. light on mice cells 0-98014
- Chinese hamster cells, enhanced killing by ²³⁸Pu α -particles in the presence of cordycepin 0-72233
- Chinese hamster V79 cells, synchronised, inactivation with charged-particle track segments 0-108966
- Chinese hamster V-79 cells, US lethality obs. 0-85443
- CHO cells, alterations in radiosensitivity by anisotonic treatments 0-72251
- CHO cells, asynchronous, fractionation of combined heat and radiation, radiation sensitivity obs. 0-76806
- CHO cells, asynchronous, fractionation of combined heat and radiation, cell-cycle redistrib. 0-76807
- CHO cells exposed to hyperthermia, radiosensitivity and recovery from radiation damage 0-72250
- CHO synchronous cells, ionising radiation induced 6-thioguanine-resistant clones 0-98027
- chromatin from cultured mammalian cells, radiolysis, DNA-protein cross-links formation 0-81655
- chromatophores of *R. rubrum*, induction of elec. pot. diff. by laser flash 0-81560
- chromosomally aberrant cells, Japanese A-bomb survivors, dose-response relationship of neutrons and γ -rays 0-94295
- chromosome aberrations, alteration in freqs. of different classes throughout first cell cycle after irrad. 0-104672
- chromosome aberrations, dose-effect relationship, population exposed to increased natural radioactivity 0-72254
- chromosome aberrations induced by low doses of X-rays in human lymphocytes in vitro 0-72235
- cochlear, struct. and functional changes following US irrad. 0-89791
- collagen synthesis stimulation, human fibroblasts, role of US-induced cavitation 0-85442
- conference, Brussels, Belgium (Oct. 79) 0-105416
- conference, Osaka, Japan (Nov. 1979) 0-98756
- conference, Rotterdam, Netherlands (Aug. 1980) 0-105425
- crypt system, mouse, alternating fractionation formula of cumulative radiation effect 0-104652
- cytotoxicity of X-rays rel. to ²³⁸Pu 4.4 MeV α -particles 0-72265
- diploid populations, human, acute and late effects of single exposure of X-rays 0-98029
- DNA, thymine base damage release, γ -irrad. *Tetrahymena pyriformis* 0-72268
- DNA, thymine damage production and excision, mammalian cells, high-LET irrad. obs. 0-72261
- DNA double strand breaks rel. to radiation-dose, yeast cell obs. 0-72232
- DNA double-strand breaks, repair in isolated nuclei of *Physarum polycephalum* 0-72248
- dose-rate effects in plateau-phase cultures of S3 HeLa and V79 cells 0-76796
- Drosophila* germ cells, decrease of γ -induced mutations by visible light 0-67159
- E. coli*, damage induced by T decay, secondary lethality under nongrowth conditions 0-104654
- E. coli*, effect of US at 1.5 MHz 0-72212
- E. coli*, photoreactive component in the mutagenic action of ionising radiations 0-72225
- E. coli*, photoreactivation following ionising irrad. rel. to Cherenkov emission 0-108969
- E. coli*, value of photoreactive component after exposure to ionising radiation 0-72224
- E. coli* B/r, UV sensitivity rel. to DNA content obs. 0-108960
- E. coli* strains differing in DNA repair capability, survival after fission-spectrum neutrons irrad. 0-98031

cellular effects of radiation continued

E.coli, lethality by 365 nm radiation under various conditions 0-61624
E.coli, radiation killing, role of membrane fluidity, hypothermia and local anaesthetics 0-104653
E.coli, respiration cessation obs. after far UV irradi. 0-76799
Elodea, cell death thresholds for 0.45-10 MHz US 0-67149
EM control of cell functions 0-85535
embryo C3H10T1/2 cells, mouse, high-energy neon particle irradi., viral transformation enhancement 0-104668
embryo of 2 cells, mouse, cell cycle-dependent radiosensitivity obs. 0-104669
energy metabolism of blood morphotic elements, ionising radiation effects 0-61645
EPR of ¹²⁵IUDR-labelled and X-irrad. cells at 4.2K and above 0-72211
erythrocyte membranes, fluidity change after X-irrad., pyrene excimer fluorescence obs. 0-72262
erythrocytes, rabbit, increased passive efflux of ²²Na and ⁸⁶Rb on microwave irradi. 0-108957
excitable cellular membranes, nonthermal interaction of RF and microwave fields, squid giant axon model 0-67150
fast neutron induced DNA strand breaks and repair obs., cultured mammalian cells 0-61651
fibroblasts, human, UV-irrad., effects of radioactive labelled DNA on excision repair 0-94289
fibrosarcoma cells, murine, separated by centrifugal elutriation, radiation sensitivity obs. 0-76808
flagella, laser damage, high speed cinematography 0-81785
gamma rays, lack of lethality threshold obs. 0-76810
green alga, 2 species of *Sirogonium* with different chromosome types, γ -irrad. effects 0-81651
H. halobium, light-induced surface pot. changes in purple membranes and bacteriorhodopsin liposomes 0-98015
haematopoiesis progenitor and effector cells, expt. murine system, whole body irradi. obs. 0-98034
HeLa cells, first postirrad. division obs. 0-72258
HeLa cells, S3, dose-rate effects on cell cycle and survival 0-76794
Hiroshima A-bomb survivors, whole-body doses estimation by chromosome aberrations 0-109035
human, multinucleate and micronucleus formation obs. 0-72219
immunological effects of irradi., review 0-81660
in vitro transformation, conf., Toronto, Canada (May 78) 0-67931
intestinal stem cells and crypts of γ -irrad. mice, cell-survival characts. 0-72255
keratinocytes, dose-dependent vol. changes after X-irrad. 0-61652
kidney cells, inactivation by high-energy monoenergetic heavy-ion beams 0-72256
liver membranes, mouse, X-irrad., dose-rate effects 0-94293
liver microsomes, γ -induced lipid peroxidation and membrane-bound enzymes 0-104660
lung cells, mouse, radiosensitivity, in vitro colony method obs. 0-101230
lung epithelial cells, type 2, proliferative response after X-rays and fission neutrons 0-108974
lymphocyte cell DNA damage by US diagnosis 0-67148
lymphocytes, acentric fragments formation, anal. of primary processes, X-irrad. 0-72272
Lymphocytes, human, effect of irradi. on hexose monophosphate shunt pathway 0-76798
lymphocytes, human, effects of heat and radiation 0-97864
lymphocytes, human, effects of low-dose radiation on repair processes 0-98023
lymphocytes, human, prediction of dose-rate effects for dicentric production by X- and γ -rays 0-72226
lymphocytes, human, RBE for d(42 MeV)-Be neutrons based on chromosome-type aberrations 0-104663
lymphocytes, human, variation in neutron RBE values compared to X-rays 0-101229
lymphocytes, human peripheral blood grown in γ -irrad. medium, sister chromatid exchanges 0-104658
lymphocytes, peripheral, population changes following radiation therapy to limited and extended fields 0-72236
lymphoma, murine, effect of synchrony on survival of L5178Y cells after neutron irradi. 0-72227
lymphoma cells, mouse, of differential sensitivity to X-rays, expt. obs. 0-72221
lymphoma cells, Murine L5178Y, production of radioresistant mutants 0-76809
malignant melanoma, thermal neutron capture therapy, in vitro radiobiological anal. 0-104657
mammalian cells, cultured, dose-rate effects obs. 0-76795
mammalian cells, cultured, interpretation of mutation and inactivation obs. 0-72229
mammalian cells, in vitro US irradi. at hyperthermic temps. 0-94282
mammalian cells, lethally damaged, proliferation obs. after irradi. by various particles 0-108971
mammalian chromosomal DNA, single-strand breakage, sensitive detect. by sedimentation anomaly appl. 0-104825
marrow colony-forming units, dose-dependence of the split-dose response 0-61701
melanoma and radiation, mouse tumour cells and clonal lines obs. 0-76800
membrane diffusion measurement by fluorescence photobleaching recovery method, bleaching light effect 0-94434
monocyte function rel. to irradi. in breast cancer patients 0-72238
murine L5178Y cells, correl. of cell cycle parameters with radiation sensitivity 0-98016
murine leukemic lymphoblasts, deficient repair and degradation of DNA after X-irrad. 0-72249
murine leukemic lymphoblasts, deficient repair and degradation of DNA after X-irrad. 0-72253
mutagenicity of X-rays rel. to ²³⁸Pu 4.4 MeV α -particles 0-72265
neoplastic transformation and dose fractionation, role of damage repair 0-72242
neoplastic transformation of 10T1/2 cells by ⁶⁰Co γ -rays 0-104659
neuronal DNA damage accumulation rel. to death after whole-brain irradi., rats 0-76804
neurons, single, rapid killing by irradi. of intracellularly injected dye 0-81795
Nitellopsis obtusa, photo-induced H⁺ transport 0-81645
nucleic acids in trigeminal neurons, γ -irrad. expts., rats 0-72270
nucleus, radiotoxicity of ¹²⁵I atoms not bound to DNA 0-104655

cellular effects of radiation continued

ovarian cortex effect of daily prenatal gamma irradi. in beagle pups 0-85453
photosensory retinal pigments in Halobacterium halobium 0-97860
pion⁺, radiobiological evaluation of suitability for tumour therapy 0-67166
pollen mother cells, tridescantia, meiotic chromosomes, stage sensitivity and dose response to X-ray 0-104648
pyri pyriformis, -pyriformis, 0-61648
R. sphaeroides, polarisation of photosynthetic membranes and reaction centres in elec. field 0-94277
radiosensitivity of 6 human cell lines, comparative study with different statistical models 0-108967
repair rates determined by split-dose and dose-rate methods, comparison 0-104680
Salmonella typhimurium LT2 mutants, effects of microwave radiation and heat 0-108958
sensitivity to radiation, physical aspects 0-67162
skin, swine, response to single acute X-ray exposures, epidermal cell changes quantification 0-72245
soft fruit cell walls, histochem. effects of γ -irrad. 0-81652
somatic cell hybrid, intraspecific, radiation response obs. 0-72246
sperm count reduction and abnormal sperm increase after X-irrad. or ²²Na injection, mouse 0-108961
spermatogonial stem cells, mouse, survival after split-dose irradi. with fission neutrons 0-72244
spheroids grown in different O₂ concs., survival obs. 0-76792
spheroids of V79 Chinese hamster cells, variable radiobiological responses 0-98028
spinach chloroplasts, laser photoinduced changes in high freq. dielectric constant 0-85449
spore radiobiology, conf., Tokyo, Japan (May 1979) 0-101660
squamous-cell carcinoma, spontaneous, in mice, comparison of neutron- and X-irrad. effects 0-98033
surfactant early release following lung irradi. of alveolar type II cells 0-94291
survival curves, biological variability model 0-108978
survival formulation, nature and limitations of approx. 0-98017
testes, mice, comparative effects of various radiations on weight loss and spermatogenic stem-cell survival 0-108976
Tetrahymena, γ -irrad., role of DNA damage and repair in eukaryotic gene function 0-104677
thermocycles, rat, US-induced changes in rates of influx and efflux of K⁺ in vitro 0-89793
thymocytes, negative surface charge reduction and thymic phagocytosis after X-irrad. 0-81663
thymocytes, rat, reduction of interphase death by hyperthermia 0-108970
total body irradiation, radiobiological bases 0-104667
Tridescantia, somatic mutations induction by low-dose irradi. from ¹³¹I 0-72266
tumour cells, human, effect of irradi. feeder cells on X-ray survival curve shape 0-98032
tumour cells, human, X-ray sensitivity in vitro 0-104665
tumours, fractionated irradi., math. derivation of optimal treatment schedules 0-98078
US irradiated cells, temp. distrib. calcs. 0-61623
V79 cells, dose-rate effects on cell cycle and survival 0-76794
V79-spheroids, survival and kinetic response after heavy ion beam exposure 0-104651
VUV, broad-band synchrotron radiation, effects on wet yeast cells 0-108972
X-irradiation, vitamin E deficiency and lipid peroxidation, mouse obs. 0-72263
X-ray, cell survival at low O₂ tension and dose build-up in Ar 0-72220
yeast, diploid, radiation sensitive mutants, γ -ray response and recovery obs. 0-101227
yeast, sensitivity to ionising radiations and damage repair 0-81659
yeast cells, determ. of thermal equivalent to MM microwaves 0-67151
yeast cells, dried, inactivation by accelerated heavy ions of very high LET 0-108965

cellular method

No entries

cellular transport and dynamics

see also cell motility
action potential propagation, effects of cellular geometry on current flow 0-94196
amino acid transport in lymphoid cell lines, differences in ionising irradi. effects 0-72264
asymmetrically permeable membrane channels in cell junction 0-94187
autorhythmicity and entrainment in excitable membranes 0-108866
axonal membrane of mammals (myelinated fibres), K channel conduction 0-61538
axonal transport, theoretical approach to anal. 0-67064
biomagnetic fields and cellular current flow 0-101192
blood flow through narrow capillaries, rheological mechs. 0-97961
blood viscosity and red cell aggregation changes after haemodilution 0-97952
cameral liquid transport rel. to buoyancy control in chambered nautilus 0-89732
capillary permeability evaluation from multiple indicator data, effects of red cell and tissue exchange 0-101193
capillary tracer exchange, 4-phase model 0-101152
chloroplasts, isolated, effect of temp. on photo-induced pH gradient 0-81566
cone outer segments, light-induced changes in membrane current, tiger salamander and turtle 0-108899
D-leucine, exchange diffusion in mouse Ehrlich ascites tumour cells, temp. reduction effect 0-67053
drug radioreceptor analysis applications 0-94315
egg cell membranes, starfish, inward rectification blocking model 0-61523
electron and proton transport in membranes 0-67052
electrophoresis of proteins in intercellular bridges 0-89734
erythrocyte, flow resistance into pores 0-61609
erythrocyte sedimentation rate in inclined tubes 0-67048
erythrocytes, rabbit, increased passive efflux of ²²Na and ⁸⁶Rb on microwave irradi. 0-108957
flow cytometric data, computerised display and anal., review book contrib. 0-109082
gland cells, stimulus-response coupling, review, book contrib. 0-108864

cellular transport and dynamics continued

- glial smooth endoplasmic reticulum acid phosphatase transport into damaged axons, role of microtubules 0-85381
glomerular permeability in foetal rabbit 0-85372
glycoproteins, fast axonal transport in guinea pig auditory neurons 0-104573
haemorrhology related to blood cells, conf., Hamburg, Germany (Aug. 1979) 0-62365
hippocampal burst-firing neurons, slow inward current, voltage clamp obs. 0-94194
intestinal membrane transport of oligopeptides, intracellular study of underlying ionic events 0-104572
Lymphocytes, human, effect of irradiation on hexose monophosphate shunt pathway 0-76798
mast cells, rat, electrophoretic mobility distrib. alteration after immunological activation 0-67047
membrane charge transfer, possible role of α -helical proteins 0-81524
membrane diffusion measurement by fluorescence photobleaching recovery method, bleaching light effect 0-94434
membrane integral proteins, mobility increase in spherocytic erythrocytes obs. 0-81569
microtubules in optic nerves of temperature acclimated goldfish, electron microscopy 0-85395
nerve fibre membrane analogue-code conversion, ionic mechanisms 0-81575
nerve fibre membrane Na permeab. reversible blockage by increase in temp. of medium above 45°C 0-81576
neuron input current, *Helix pomatia*, rel. to membrane pot. and extracellular Sr and Ca ion concs. 0-81577
neuron membrane, electrostatic plasma probe physical analogue 0-79573
neurons, transport of substances 0-89745
Nitellopsis obtusa, photo-induced H⁺ transport 0-81645
osmotic behaviour of unperfused tissues 0-104574
Paramesium excitation, model anal. 0-61524
particle absorption rates at high cell concs., Monte Carlo simulation 0-94141
photoelectrode for recording intracerebral cellular Ca²⁺ transients 0-67307
plant root transport studies using ion localisation, freeze substitution method 0-85569
plasmalemma of *Nitella flexilis*, selective centres of excitable channels of early ionic current 0-81568
platelet interaction with vessel surface, blood rheological factor influences 0-61612
Porphyra osmoregulation, struct. aspects 0-85370
protein kinases, cAMP-depend., membrane-localised, and regulation, of slow inward current, frog heart 0-81567
Purkinje fibres, canine, activity-dependent extracellular K⁺ fluctuations 0-89733
red blood cells, rheological props. meas. by Couette viscometer 0-97992
red blood cells, viscoelastic study of aggregation 0-97960
red cell, human, increased passive permeability below 12°C 0-94185
red cell membrane, Li transport in manic depressives 0-61525
rheological behaviour of stored blood cells (French) 0-67110
sarcolemmal permeability changes during early myocardial anoxia 0-85371
supraoptic neurons, rat hypothalamus, osmosensitivity obs. 0-104578
surface anisotropic molecular motion 0-97883
surface component rotational diffusion, time-resolved phosphoresc. anisotropy 0-97885
synaptic vesicles and synaptosomal membranes, electrokinetic props. 0-67055
testing potential, membrane pot. rel. to ionic diffusion (French) 0-94184
thermocytes, rat, US-induced changes in rates of influx and efflux of K⁺ in vitro 0-89793
tracheal ciliary beat, improved device for freq. recording 0-109070
transport in biomembrane, NME determ. methods (Rumanian) 0-94435
Ca²⁺, passive and active fluxes across membranes, review 0-97886
Na⁺ activity of epithelial cells, liquid-ion exchanger microelectrode estimates, resistive artifacts 0-89909
Na⁺ intracellular activity rel. to Na⁺ transport across a tight epithelium 0-67051
Na⁺ saturation kinetics in frog skin, compartmental aspects 0-67050
O₂ diffusion distance and necrosis development in multicell spheroids 0-81570

cement industry

- IR pyrometer performance parameters and applications (German) 0-86315

cements (building materials)

- used only for those materials which bind together particulate matter so as to form a coherent mass of considerable strength. For cements that cause two or more separate masses to adhere see adhesion
admixture, for making high strength concrete (Japanese) 0-89297
asbestos fibre reinforced cement, strength and fracture props. 0-108533
basalt fibres, alkali resist. in cement soln. 0-89377
grog bodies, high Al₂O₃ cement, creep characts. obs. 0-66578
jute fibres, alkali resist. in cement soln. 0-89377
mortar, impact bending capacity (Japanese) 0-89341
mortar bars, aggregate particle size influence as expansion caused by alkali-SiO₂ reaction 0-66762
paste, elasticity modulus and strength, aggregate conc. effect 0-66591
pastes, flow behaviour, specific surface and conc. of solids influence 0-65132
polypropylene fibrillated film reinforced cement matrix for low cost sheeting 0-80996
Portland cement, absorbed H₂O, pulsed NMR study 0-84665
portland cement, doped with ZnO, struct. and props. 0-60914
wood fibre reinforced Portland cement composite, strength 0-100822
(CaO)₂SiO cement pastes, electron microsc. anal. 0-108761

centrifuges

- interference optics of analytical ultracentrifuges, background suppression of multiplexer-gated modulatable laser 0-73430
mechanical strength obs. of low-density fibrous struct. using centrifugal method 0-71823
polymer systems, sedimentation field-flow fractionation in macromolecule characterization 0-66879
velocity sedimentation, separation of mammalian cells 0-101293
U enrichment, centrifuge process, LWR fuel (German) 0-68905

ceramics see cermets**ceramic industry**

- weighing, automatic, application in ceramics industry 0-95074

ceramics

- see also ceramic industry; refractories
abrasive wear, role of plastic deform. and fracture 0-108594
acoustic wave attenuation mechanisms for ceramics containing volatiles 0-74560
annular crack at spherical voids, stress intensity factor estimates 0-106757
bending test results processing 0-97672
brittle, heat-transfer variables effect as thermal stress resist., meas. by quenching expts. 0-79871
brittle ceramics, partially absorbing, thermal stress anal. subjected to symmetric radiation heating 0-59570
building materials, breakdown kinetics by X-ray diffr. 0-108526
building materials, high-temp. microscopy interpretation (Polish) 0-66743
bulk defects and surface cracks determ. by US means 0-76473
cement grog bodies, high Al₂O₃ content, creep characts. obs. 0-66578
ceramic-glass composites, crack growth, elec.-mech. analogue 0-85022
ceramics, photovoltaic effect application to information storage 0-80316
characterisation with analytical electron microscope 0-84068
clays, heat treatment, effect on rheological props. of enamel slips 0-60809
crack extension micromechanisms, review 0-108567
cracking characterisation by double torsion test (French) 0-104369
creep, porosity depend. 0-97530
density measurement, true and apparent, specimen liquid saturation cell 0-62636
development from organosilicon polymers by heat treatment 0-81014
diffusion constants, melting pt. diffusivity activation energy and volume correls. 0-96679
disilicate, piezoelectric glass ceramic, recrystallisation, pyroelectric response, permittivity 0-80703
electrodes, high dielectric constant materials for ultraminiature high power N₂ discharge lasers 0-58572
electron diffraction and imaging, at high resolu., characterisation of alloys and ceramics 0-104050
fatigue, subcrit. crack extension charact. (German) 0-100888
fatigue testing, subcrit. crack extension meas. with double-torsion specimens (German) 0-104359
ferrites, soft, production and props. 0-88801
ferroelectric, mech. and elec. losses, correl., theory and expt. 0-66133
ferroelectric, tetragonal, 90° domain-rot. fraction after polarisation, X-ray determ. 0-75992
ferroelectric ceramic, polycryst., elasticity props., neutron bombardment effects 0-79856
ferroelectric ceramics, materials and dielec. props., review 0-75957
fine-grained, cyclic plastic deform. as cause for thermal expansion hysteresis 0-89290
fracture mech., probability, micromech. models of crack growth 0-108571
fracture mechanics, and mech. props., fragile materials (French) 0-104274
fracture strength, dimensional anal. of grain size depend. 0-70299
fracture-mirror boundary formation, criterion 0-70297
gas turbine engine, substitution of ceramics for high temp. alloys 0-97678
glass ceramic mineralogy 0-60826
glass-ceramic, machinable, elastic const. temp. depend. 0-79852
glass-ceramics, transient heterogeneous nucleation of glass-forming systems 0-88042
glassy, struct. and electron beam sensitivity 0-79841
glazing with gaseous P₂O₅ 0-108609
grinding induced tempering, in ceramics containing ZrO₂ 0-89260
growth micromechanism in corrosive environment 0-108616
Humicram-III, multifunctional sensor to detect humidity and gases (Japanese) 0-105659
ion-selective membrane electrodes development, Ag⁺ and F⁻ based materials appl. (Japanese) 0-61203
kaolin bodies, effect of mineralizers on firing shrinkage, microstruct. and strength 0-97488
kaolin grog particles, shape and density 0-97450
layers on metallic substrates, mech. props. meas. (French) 0-104375
leading in glazed ceramics, colorimetric method (Spanish) 0-73414
lifetimes and slow crack growth prediction (German) 0-104250
local in depth anal. by neutral beam SIMS 0-89565
lyophilisation parameters of ceramic compounds, freeze-drying synthesis 0-97453
mechanical properties measurement, apparatus for up to 1700°C (French) 0-104374
mechanical properties measurement, using disc-shaped specimens (French) 0-104367
mechanical test apparatus for up to 2200°C (French) 0-104372
membrane, chalcogenide ceramic, Cu-selective electrode (Chinese) 0-81357
metal layer/crystalline ceramic adhesion mechanism for metallization of electronic ceramics, elec. props. (German) 0-76381
microcracks, and thin intergranular films obs. by TEM 0-68295
mullite-corundum, thread-like crystals reinforced, props. 0-108525
mullite-corundum ceramics, electron microscopy of damaged surface 0-88413
multilayer capacitors, fracture mechanics approach to structural reliability assessment 0-89328
NASICON solid electrolyte, processing and phys. props. 0-60820
nondestructive testing, scanning laser acoustic microscopy, appl., comparison with SEM and optical microscopy results 0-58875
optical ceramic, KOI, homogeneity in terms of refr. index 0-64125
optical ceramics, dispersion, double refraction and storage effects, material appls. (German) 0-69471
phosphate containing materials, technological prod. processes, review 0-97452
phosphate glass-Al alloys seals, elec. and mech. props., glass transition 0-81018
photoacoustic effect in piezoelectric ceramics 0-84252
piezoceramic aperiodic transducer, mech. load study 0-87700
piezoceramic plates, bending strains, electromechanical transformation, energetic method of calc. (Ukrainian) 0-71320

ceramics continued

- piezoceramics, converters of shock wave mech. energy into elec. power 0-61429
- piezoelectric, filters for HF appl., using $\text{Pb}(\text{Zn}_{1/3}\text{Nb}_{2/3})\text{O}_3\text{-PbTiO}_3\text{-PbZrO}_3$ and $\text{Pb}(\text{Mg}_{1/3}\text{Nb}_{2/3})\text{O}_3\text{-PbTiO}_3\text{-PbZrO}_3$ (Japanese) 0-60507
- piezoelectric, nonlinear charge release before uniaxial press. 0-80706
- piezoelectric, reflection and transmission of elastic waves at boundary with water 0-87588
- piezoelectric, US instrument for determ. characts. 0-66752
- piezoelectric acoustic Lamb wave focusing devices 0-79093
- piezoelectric buzzers for high sound levels 0-92005
- piezoelectric material for electrostatic voltage sensor (Japanese) 0-105632
- piezoelectric transducer, anomalous radiation pattern due to parasitic Lamb wave generation 0-96170
- piezoelectric transducers, broadband, production 0-61044
- PLTZ coarse-grained solid solutions, electro-optical processes induced by longitudinal electric field (Russian) 0-80750
- polymer filled ceramic, ZrO_2 stabilised, fracture mechanism (Russian) 0-100895
- porcelain, crack prop. data applicability to failure prediction 0-81154
- porcelain, electrotechnical, compressive strength 0-100882
- porcelain, neutron-ratardation behaviour for continual moisture determ. (German) 0-105660
- portland cement, doped with ZnO , struct. and props. 0-60914
- powder synthesis from laser-heated gas phase reactants 0-93525
- proof testing 0-104207
- proof testing 0-108654
- pyroceramic lightweight mirror blank fabrication using standard metal-working equip. 0-102871
- PZT, ferroelec. energy conversion under shock loading 0-108163
- rare earth elements, use in glass and ceramics (Polish) 0-97455
- raw kaolin, acoustical investigations of the effect of additives on elastic props. 0-66559
- recycling, residual and additive elements control by specifications 0-66522
- refractory coatings, for high temp. use, current status (Japanese) 0-71619
- relaxor ferroelectrics, electrostrictive effects 0-66112
- ruthenates, $\text{ACu}_3\text{Ru}_2\text{O}_{12}$, $\text{A}=\text{Na}, \text{Ca}, \text{Sr}, \text{Cd}, \text{La}, \text{Pr}, \text{Nd}$, synthesis, cryst. struct., mag. and elec. props. (French) 0-107151
- $\text{Si}_3\text{N}_4\text{-Ce}_2\text{O}_3\text{-SiO}_2$ materials: phase relations and strength 0-97465
- spinel single crystals, mech. props., 1350-1650°C (French) 0-104374
- steatite, glass-ceramics technology appl. 0-104097
- surface cracks, acoustic surface wave meas. 0-61055
- surface metrology using peak counting, quality control 0-95065
- SYNROC-B ceramic for radwaste disposal, feasibility of subsolidus sintering 0-83198
- SYNROC-B sintered ceramics for high-level radwaste fixation, comp. and phase charact. 0-106126
- thermal expansion hysteresis, cyclic plastic deform. explanation 0-89290
- thermal stress failure mode, effect of data scatter, brittle ceramics 0-60949
- thermoluminesc. dating, comparison of results 0-84791
- transformation toughening, martensitic transforms. in crack-tip stress fields 0-104154
- translucent systems, absorption and scatt. coeffs. for visble light, Kubelka-Munk theory 0-60627
- transparent ferroelectric, composition selection for appl. in light modulators (Russian) 0-91869
- US transducers array, transducer elements tuning 0-87684
- vitreous ceramics, slow neutron irradiation effect (Spanish) 0-57816
- Weibull distribution, adding static and dynamic fatigue effects 0-70298
- X-ray analysis of inhomogeneities, using STEM with field emission gun 0-59354
- Al-Si-N-O system, comps. corresponding to β' -sialon phase reaction hot-pressing 0-84891
- $\text{Al}_2\text{C}_3\text{-Be}_2\text{C-SiC}$ system, phase analysis and TEM struct. obs. 0-108420
- AlN filamentary crystal reinforced mullite-corundum ceramics, filaments strength, eval. 0-104230
- AlN, polycrystalline, stress-strain data up to 1.25 GPa 0-100899
- AlN-Si₃N₄-Be₂N₃ system, phase equilibria 0-60844
- Al_2O_3 (96 wt.%), fractographic criteria for subcritical crack growth boundaries 0-81155
- Al_2O_3 , alumina, deformed by prismatic slip, HV TEM obs. of dislocations 0-108517
- Al_2O_3 , bioceramic synthesis, for orthopedic purposes, props. (Polish) 0-66465
- $\alpha\text{-Al}_2\text{O}_3$, ceramic, prod. from etching wastes of Al foils 0-108376
- $\beta\text{-Al}_2\text{O}_3$, conduction and dielec. loss mechanisms, paired interstitially model 0-107468
- Al_2O_3 dispersion in polycryst. NaCl, diffusive creep 0-97531
- $\alpha\text{-Al}_2\text{O}_3$, energy levels of donor and acceptor dopants and electron and hole mobilities 0-59911
- $\alpha\text{-Al}_2\text{O}_3$ fibre FP, manufacture, strength and modulus 0-81013
- $\alpha\text{-Al}_2\text{O}_3$ filamentary crystal reinforced mullite-corundum ceramics, filaments strength, eval. 0-104230
- Al_2O_3 , fine grained, basal slip and nonaccommodated grain boundary sliding 0-60916
- Al_2O_3 , fine grained, interface-controlled diffusional creep 0-60915
- Al_2O_3 fracture toughness determ. using four-point-bend specimens 0-108536
- $\beta\text{-Al}_2\text{O}_3$, hot isostatic press. 0-108377
- Al_2O_3 , hot pressed, fracture stress-reflecting spot relations 0-71731
- Al_2O_3 humidity sensor, ageing improvement (Japanese) 0-100863
- $\beta\text{-Al}_2\text{O}_3$, internal friction and Na transport 0-59578
- $\beta\text{-Al}_2\text{O}_3$, long-period struts., electron microscope obs. 0-92501
- Al_2O_3 polycrystalline, effects of space charge, grain-boundary segregation and mobility differences on conductivity 0-79979
- Al_2O_3 , polycrystalline, stress-strain data up to 1.25 GPa 0-100899
- Al_2O_3 , polycryst., high-temp. fatigue and strength 0-60954
- Al_2O_3 rod, damaged, mech. strength, surface defects effect, appl. as insulators (German) 0-76330
- Al_2O_3 single cryst., O self diffusion, ion-probe meas. 0-59701
- Al_2O_3 sintering, effect of SrO , MgO and Y_2O_3 additives on $\alpha\text{-Al}_2\text{O}_3$ mineralisation 0-89186
- Al_2O_3 sintering, role of MgO 0-81010
- Al_2O_3 sintering mechanism and kinetics, glass-forming additives effect 0-89187
- Al_2O_3 thin film used in inelastic electron tunnelling spectroscopy, X-ray photoelectron spectrum 0-108319

ceramics continued

- Al_2O_3 , transparent hot-pressed, transparent and translucent properties 0-60533
- $\text{Al}_2\text{O}_3\text{-MgO}$, grain boundary segregation of Ca and Mg X-ray spectrosc. and STEM study 0-107269
- $\text{Al}_2\text{O}_3\text{-Zr}$ ceramic, elec. props., additives effect, and interaction with steel melt 0-104305
- Al_2O_3 -based ceramics, high rate reactive ion etching 0-85070
- $\beta\text{-Al}_2\text{O}_3\text{-Li}_2\text{O-Na}_2\text{O}$, spin-lattice relaxation and Li motion 0-70451
- $\beta\text{-Al}_2\text{O}_3\text{-Na}_2\text{O}$, AC impedance, microstruct. and strength 0-100349
- $\beta\text{-Al}_2\text{O}_3\text{-Na}_2\text{O}$, development for Na/S battery 0-71615
- $\beta\text{-Al}_2\text{O}_3\text{-Na}_2\text{O}$, solid electrolyte, behaviour at high current density, sodium heat engine mode 0-61330
- $\beta\text{-Al}_2\text{O}_3\text{-Na}_2\text{O}$ solid electrolyte, tube fabrication from cast ceramic tape 0-60819
- $\beta\text{-Al}_2\text{O}_3\text{-Na}_2\text{O}$ solid electrolyte, processing and phys. props. 0-60820
- $\beta\text{-Al}_2\text{O}_3\text{-Na}_2\text{O}$ solid electrolyte, strength degradation under electrolytic conditions 0-61329
- $\beta\text{-Al}_2\text{O}_3\text{-Na}_2\text{O}$ solid electrolyte, heat treatment effects on ionic cond. and microstruct. 0-65293
- $\text{Al}_2\text{O}_3\text{-SiO}_2$ (3 wt.%), J-integral meas. at high temps. (German) 0-93624
- $\text{Al}_2\text{O}_3\text{-SiO}_2$ glass ceramic, surface streaks and blisters, UV fluoresc. study 0-84347
- $\text{Al}_2\text{O}_3\text{-SiO}_2$ system, evidence for metastable miscibility gap 0-71632
- $\text{Al}_2\text{O}_3\text{-TiO}_2$ powder, plasma-prepared, morphology and phase constitution 0-100833
- $3.5\text{Al}_2\text{O}_3\cdot 2\text{SiO}_2$, mullite, decomposition by SiO_2 volatilisation 0-61082
- $3\text{Al}_2\text{O}_3\cdot 2\text{SiO}_2\text{-ZrO}_2$ composites, sintered, in situ-reacted, fracture props. 0-81158
- B content by emission spectrosc. with high freq. plasma excitation (French) 0-76477
- BN films, humidity sensitive elec. props. and switching characts. 0-107938
- B_2O_3 -containing ceramic glaze, neutron probe anal. for control of prep. process (Polish) 0-97751
- $\text{B}_2\text{O}_3\text{-Nb}_2\text{O}_5$ system, phase equil. and phase struct. obs. by high resolution TEM 0-108419
- BaHfO_3 , BaSnO_3 and BaZrO_3 , high-density ceramics prep. and elec. props. 0-60812
- $\text{Ba}_2\text{NaNb}_2\text{O}_{15}$, X-ray powder diffraction data determ. (Chinese) 0-70170
- $\text{BaO-Nd}_2\text{O}_3\text{-TiO}_2\text{-Bi}_2\text{O}_3$ system ceramics, high stability low loss dielectric preparation 0-81008
- BaTiO_3 ceramic, degradation under high AC elec. field 0-60499
- BaTiO_3 ceramic dielectric capacitor, processing prop. relations, hysteresis, permittivity 0-80730
- BaTiO_3 ceramic films, dielec. strength, statistical anal. 0-75935
- BaTiO_3 ceramic surface, neutralisation of bombarding ion beam 0-71528
- BaTiO_3 , crystn. from melts, comparison of different prospective oxy-anion solvents 0-71583
- BaTiO_3 , ferroelectric, internal stress and strength, failure mechanism 0-66128
- BaTiO_3 fibres synthesised from $\text{Ba}(\text{OH})_2\cdot 2\text{K}_2\text{O}\cdot 11\text{TiO}_2\cdot 3\text{H}_2\text{O}$ fibre hydrothermal reaction (Japanese) 0-93527
- BaTiO_3 , Mossbauer spectroscopy, sample prep. and results 0-66078
- BaTiO_3 , PTC-type, grain boundary study using TEM 0-107267
- $\text{BaTiO}_3\text{:BaTiO}_3$, dielec. props. and microstruct. 0-60481
- $\text{BaTiO}_3\text{:La}$, Sb, second phase effect on elec. and mag. props. 0-60986
- BaTiO_3 single crystals, prep. and unit-cell parameters 0-103302
- Be-Si-Al-O-N ceramic, phase assemblages, relationships with props. 0-60848
- Be-Si-N system polytypes, struct. obs. using TEM 0-107192
- BeO, polycrystalline, stress-strain data up to 1.25 GPa 0-100899
- BeO, TSEE, effect of surface SiO_2 0-76159
- $\text{Bi}_{2-x}\text{La}_x\text{WO}_6$, synthesis and crystallography 0-66459
- Bi_2MoO_6 , superplasticity during phase transitions 0-108498
- Bi_2WO_6 , superplasticity during phase transitions 0-108498
- $\text{CaCeAl}_3\text{O}_7$, meltite struct., prep. and props. 0-93524
- CaF_2 , strength-controlling fracture energy depend. on flaw-size to grain-size ratio 0-81152
- $\text{Ca}_2\text{Mg}(\text{Co})(\text{Zn})(\text{Mn})(\text{Cd})(\text{Ca})\text{TeO}_6$, optical SHG study of acentricity, ferroelec. of low temp. phases 0-71324
- $\text{Ca}_3(\text{PO}_4)_2$ ceramic, material science, bone implant 0-93523
- $\text{Ca}_3\text{P}_2\text{O}_9$ ceramic, material science, bone implant 0-93523
- $\text{Ca}_3(\text{PO}_4)_2\text{OH}$ ceramic, material science, bone implant 0-93523
- CaSiO_3 , fibrous, controlled crystallisation and anisotropy 0-59425
- CaSnO_3 and CaZrO_3 , high-density ceramics prep. and elec. props. 0-60812
- $\text{Ca}_{1-x}\text{Sr}_x\text{Ba}_{1-x}\text{Zr}_{1-x}\text{Ti}_x\text{O}_3$, ceramic system, dielectric props., microwave resonator application 0-80674
- CaTiO_3 , prep. from film forming soln. 0-60811
- $\text{Cd}_2\text{Mg}(\text{Co})(\text{Zn})(\text{Mn})(\text{Cd})(\text{Ca})\text{TeO}_6$, optical SHG study of acentricity, ferroelec. of low temp. phases 0-71324
- Ce-Si-Al-O-N ceramic, phase assemblages, relationships with props. 0-60848
- $\text{CeO}_2\text{:Y}$, slow transient phenomenon 0-107550
- CoAl_2O_3 , prep. from film forming soln. 0-60811
- CoTiO_3 , prep. from film forming soln. 0-60811
- CrNbO_4 , elec. cond. meas. 0-100463
- $\text{Cr}_2\text{O}_3\text{-Al}_2\text{O}_3$ solid soln., Vickers micro-hardness 0-66629
- CrVO_4 , elec. cond. meas. 0-100463
- Cu-coated TiO_2 particles, prep. for composites 0-89159
- $\alpha\text{-Fe}_2\text{O}_3$, semiconducting, gas sensor for city gas appl. (Japanese) 0-61498
- $\text{Gd}_2\text{Zr}_{1-x}\text{O}_{2-x/2}$, elec. cond. of ceramic solid solutions 0-107554
- $\text{Gd}_2\text{Zr}_{1-x}\text{O}_{2-x/2}$, fluorite and pyrochlore solid solutions, electrical conductivity meas. 0-65287
- HF adsorption, by smelter-grade aluminas, during Al smelting 0-80075
- $\text{LaCrO}_3\text{-Cr}$ ceramic, prep., phase comp. and elec. cond. (Polish) 0-71621
- $\text{LaCrO}_3\text{-MgO}$, LC20M electrode material in open cycle MHD systems, thermionic emission characts. 0-97394
- La_2NbO_7 , synthesis and cryst. growth 0-71590
- $\text{La}_2\text{SiO}_5\text{-N}_2$ single cryst. growth by floating zone method with $\text{SiO}_2\text{-Si}_3\text{N}_4$ additions 0-93481
- $\text{La}_{1-x}\text{Sr}_x\text{CoO}_3$, ($0.5\leq x\leq 0.9$), ferromag., elec. props., itinerant electron model 0-107785
- $\text{Li}_2\text{O-Fe}_2\text{O}_4$ milled ferrite powder, substruct. and sinterability 0-84894
- Li_2GeO_3 piezoelectric glass ceramic, recrystallisation, pyroelectric response, permittivity 0-80703
- $\text{Li}_2\text{O-Al}_2\text{O}_3\text{-Cr}_2\text{O}_3$ system, subsolidus equilibria 0-60843
- $\text{Li}_2\text{O-Al}_2\text{O}_3\text{-SiO}_2$ glass-ceramic, near-zero thermal-expansion heat treatment effect in fracture behaviour 0-66537

ceramics continued

- Li₂O-Al₂O₃-SiO₂-TiO₂ system glasses, Raman spectra obs. of glass-ceramics form. 0-60825
 Li₂O-MgO-Al₂O₃ system, subsolidus phase equilibria 0-81036
 Li₂O-SiO₂-P₂O₅ glass ceramic fibres, heat treatment, crystn., tensile strength 0-84995
 Li₂O.2SiO₂, prep. from film forming soln. 0-60811
 Li₂O.2SiO₂, prep. of oriented microstructure by unidirectional solidification of melts 0-71614
 Li₂SiO₄, piezoelectric glass ceramic, recrystallisation, pyroelectric response, permittivity 0-80703
 Li₂Si₂O₅, pyroelectric glass-ceramics 0-75950
 Li_{1+y}Ta_{1-y/2}W_{1/2}O₃ (0≤y≤0.028), non-stoichiometric phase, crystallographic and dielec. props. 0-75212
 Li_{1-x}Zn(GeO₄)_x, LISICON, AC meas. of ionic cond., 298 to 573K 0-107526
 Mg-Si-Al-O-N ceramic, phase assemblages, relationships with props. 0-60848
 MgAl₂O₄, pure and Fe-doped spinel, elec. cond. 0-59702
 MgAl₂O₄, strength-controlling fracture energy depend. on flaw-size to grain-size ratio 0-81152
 Mg_{1.86}Al_{0.67}Si_{2.47}O_{3.19}N_{3.81}, 12H polytype, intergranular phases and compositional variations 0-79645
 MgCr₂O₄-TiO₂, porous ceramics, humidity-sensitive electrical conduction 0-107782
 MgCr₂O₄-TiO₂, porous ceramic humidity sensors 0-86325
 MgF, polycryst., quartz particle impacts no. effect on erosion in elastic-plastic response regime 0-81209
 MgO polycrystals, mech. props., 900-1150°C (French) 0-104374
 MgO single cryst., impact wear characts. 0-76374
 MgO single cryst., impact wear damage 0-76375
 MgO sintered-ceramic separator plate development, Li-Al/LiCl-KCl/FeS battery applications 0-61321
 MgO:(Li), polycrystn., internal friction (German) 0-59577
 MgO-Al₂O₃-SiO₂, sintered, cordierite, mineralogy and props. 0-60827
 MgO-NiO, STEM microanal., absorpt. effects 0-80902
 (Mn,Zn)Fe₂O₄:Si, Ca, Ti, second phase effect on elec. and mag. props. 0-60986
 MnO₂ porous powders, Al₂O₃ and SiO₂ coated, changes in surface free energy for N adsorption 0-84363
 MnZn ferrite powder prep., wet method 0-89180
 (NH₄)₂Cd₂(SO₄)₂, dielec. and spontaneous polarisation, -195 to -180°C, particle size depend. 0-97200
 Na₂O-Al₂O₃-SiO₂, glass, nucleation, crystn., ceramic form. 0-84082
 Na₂O-BaO-Al₂O₃-SiO₂, glass, nucleation, crystn., ceramic form. 0-84082
 Na₂O-Li₂O-Al₂O₃, local electrode current density and flow decoration 0-100935
 Na₂O-MgO-Al₂O₃, β"-alumina, high-resolution electron microscopy 0-75208
 Na₂O-PbO-SiO₂ glass-ceramic composite, directionally crystallised 0-107058
 Na₂O-SiO₂, prep. from film forming soln. 0-60811
 Na₂O.11Al₂O₃, polycrystalline with preferably orientated grains, preparation (Japanese) 0-81012
 Nb₂O₅-V₂O₅-P₂O₅, glasses and glass ceramics, elec. cond., struct. 0-84466
 Nd₂Zr_{1-x/2}O_{2-x/2}, elec. cond. of ceramic solid solutions 0-107554
 Nd₂Zr_{1-x/2}O_{2-x/2}, fluorite and pyrochlore solid solutions, electrical conductivity meas. 0-65287
 Ni-ceramic coating structure, influence of micropowder inclusion (Russian) 0-59820
 NiFe₂O₄ milled ferrite powder, substruct. and sinterability 0-84894
 NiTaC, eutectic alloys, chem. incompatibility of ceramic nitrides for directionally solidifying 0-81046
 NiZn ferrite, ZrO₂ additions influence on sintering and physicochem. props. 0-108369
 PLZT ceramic, ageing, dielec. props. 0-88940
 PLZT ceramic, bonded lens assembly manufacture 0-79018
 PLZT ceramic, modulator for optical communication 0-78964
 PLZT ceramic, proton implanted, photoferroelectric effect for image storage and display devices 0-80315
 PLZT ceramic, thin wafer electrode slotting process 0-79017
 PLZT ceramic, thin wafer production polishing process 0-81214
 PLZT ceramic, visible light scatt. depend. on photoferroelectric space charge fields 0-80806
 PLZT ceramics, elastooptic effect, stress induced birefr. 0-60543
 PLZT ceramics, modified by Ca²⁺(Sr²⁺)(Nd³⁺)(Y³⁺), dielec. behaviour 0-60519
 PLZT ceramics photosensitivity enhancement by H- and He-ion implantation 0-96934
 PLZT, mech. and elec. losses, correl., theory and expt. 0-66133
 PLZT, photoferroelectric image storage in antiferroelectric-phase PLZT ceramics 0-71353
 PLZT powder preparation, hydrolysis ball mixing 0-81006
 PLZT slim-loop and linear ceramics, longit. electrooptic effects, display appl. 0-80751
 PLZT slugs, powder hot pressing technique 0-81007
 PLZT thermal, flash, ferroelectric protective goggles 0-81746
 PLZT/TFPD thermal/flash protective lens assembly, polarised delamination investigation 0-78929
 Pb_{0.94-x/2}Ba_{0.6}Nb_xZr_{1-x/2}O₃, Nb dopant morphology effect on microstructure 0-81005
 Pb(Mg_{1/3}Nb_{2/3}O₃)₂PbTiO₃, ceramic dielectric, electrostriction, relaxation, polarisation 0-80700
 Pb₂MgNb₂O₉-PbTiO₃, relaxor ferroelectrics, electrostrictive effects 0-66112
 PbSnF₆, anionic conductor, thin films and ceramics 0-107556
 Pb_{0.94}Sr_{0.06}Ti_{0.47}Zr_{0.53}O₃, piezoelectric ceramic, stress relax., time depend. deformation 0-60899
 Pb,Sr_{1-x}(Zr,Ti,Nb)_xO₃, hydrophobic ceramic, effect of one-dimensional uniaxial stress 0-80705
 Pb(Ti,Zr)O₃ solid solutions, phase coexistence discrepancies 0-96662
 xPbTiO₃+(1-x)PbCd_{1-x/2}Nb_{x/2}O₃, phase transition spread, polarisation relaxation, dielectric susceptibility (Russian) 0-75922
 Pb(Z,Ti,Mg,W)O₃, low-Q ceramics, props. and transducer appl. 0-75944
 Pb(Zn,Ti)O₃ piezoelectric electrically deformable diffraction grating 0-78963
 Pb(Zr,Ri)O₃:Ni-silicon surface flexible composite pyroelectric, dielectric props. 0-80704
 Pb(Zr,Ti)O₃ ceramic, surface barrier electroreflectance, hysteresis, ageing 0-80752

ceramics continued

- Pb(Zr,Ti)O₃ ceramics, low temp. sintering, elec. and mech. props. 0-71616
 Pb(Zr,Ti)O₃ ceramics with ladder type struct., prep. and props. 0-75945
 Pb(Zr,Ti)O₃ ceramics, DC field sintering preparation, piezoelectric props., ageing behaviour 0-81211
 Pb(Zr,Ti)O₃ fibre arrays in epoxy cement, ferroelectric ceramic-plastic composites 0-81015
 Pb(Zr,Ti)O₃, fracture and deform. 0-79870
 Pb(Zr,Ti)O₃, internally electroded with Pt, resonance behaviour 0-84701
 Pb(Zr,Ti)O₃, PCD ceramic, pyroelectric props. 0-100635
 Pb(Zr,Ti)O₃, piezoelectric ceramics, low fluence neutron irradi. effects 0-92564
 Pb(Zr,Ti)O₃, porosity-permittivity relations, depolarising factors determ. and pore effects (Japanese) 0-97189
 Pb(Zr,Ti)O₃, research grade, hydrophobic ceramic, effect of one-dimensional uniaxial stress 0-80705
 Pb(Zr,Ti)O₃, shock depoled ferroelec. ceramic, anal. of ideal response 0-60511
 Pb(Zr,Ti)O₃, tetragonal ferroelec. ceramic, 90° domain-rot. fraction after polarisation, X-ray determ. 0-75992
 Pb(Zr,Ti)O₃ type 1 ceramic, appl. in Langevin type sonar transducer, performance characts. 0-79095
 Pb(Zr,Ti)O₃:Ba, paraelectric ceramic, electrostrictive effect 0-80701
 Pb(Zr,Ti)O₃:Cr₂O₃ ceramics, reson. freq. comp. and temp. depend. 0-70413
 Pb(Zr,Ti)O₃:Fe(Nb) ceramic, elec. and electromechanical props., depend. on dopants 0-81212
 Pb(Zr_{1-x}Ti_x)O₃ solid solution, piezoelectric ceramic, prop. improvement by multiple substitution 0-80702
 PbZr_{1-x}Ti_xO₃:Nb₂O₅ ceramic, ferroelec. transitions, polarisation meas. (French) 0-66124
 PbZr_{1-x}Ti_xO₃ ceramics, morphotropic phase boundary 0-81035
 PbZr_{1-x}Ti_xO₃, meas. of Hugoniot curve with commercial manganin stress gauges 0-70362
 Si on ceramics, coating with inverted meniscus (SCIM) technique, solar cell appl. 0-89163
 Si-Al-O-N ceramic, grain boundary desegregation and intergranular cohesion 0-100872
 Si-Al-O-N system, phase analysis and TEM struct. obs. 0-108420
 Si-Na-B-O-N glass, synthesis and characterisation 0-108381
 Si-Ti-O-N system, formation of TiN and SiO₂ 0-71617
 SiAlON, prepared from siliceous sand and Al powder, hot pressing, steatite contamination effects (Japanese) 0-93528
 SiC fibre, development from organosilicon polymers by heat treatment 0-81014
 SiC, nondestructive evaluation, scanning photoacoustic microscopy 0-85115
 Si₃N₄ ceramic inclusions meas. and characterisation using US 0-76474
 Si₃N₄, cracking characterisation by double torsion test (French) 0-104369
 Si₃N₄, high-speed rolling bearings, fatigue strength 0-93655
 Si₃N₄, nondestructive evaluation, scanning photoacoustic microscopy 0-85115
 Si₃N₄:MgO, hot-pressed, linear thermal expansion rel. to MgO content 0-70430
 Si₃N₄/ZrO₂, hot-pressed, compressive surface stresses developed by oxidation induced phase change 0-60992
 Si₃N₄-Al₂O₃-SiO₂ systems, glass forming regions 0-84070
 Si₃N₄-SiO₂-Y₂O₃, subsolidus phase relations 0-60845
 Si₃N₄-Y₂O₃-Al₂O₃ (4-17, 4 wt.%), sintering 0-81009
 Si₃N₂O, thermal decomp. 0-81311
 SiO₂, fused, surface crystn. by Li⁺ ion implantation and annealing 0-89383
 SiO₂ phase equilibrium and microstructure interpretation 0-60847
 SiO₂-Al₂O₃ (8 mol.%) glass, heat treated, devitrified phases 0-66469
 SiO₂-Al₂O₃-CaO-MgO-B₂O₃, E-glass, acid resist. studies 0-60991
 SiO₂-Al₂O₃-K₂O glass ceramic interaction with Pb borosilicate glaze 0-84398
 SiO₂-Al₂O₃-Na₂O-BaO-TiO₂, glass ceramic interaction with Pb borosilicate glaze 0-84398
 SiO₂-MgO porous catalysts, EPMA quantitative anal., norm correction calc. method, modified ZAF method (Japanese) 0-93822
 SiO₂-MgO-BaO, steatite, glass-ceramics technology appl. 0-104097
 SnO₂-NiO(ZnO)(Nb₂O₅), activated sintering mechanism 0-60810
 SrBaNaNb₅O₁₂, X-ray powder diffraction data determ. (Chinese) 0-70170
 Sr_{0.75}Ba_{0.25}Nb₂O₆, ceramic ageing dielec. props. 0-88940
 SrFe₂O₉:Si, Sr, second phase effect on elec. and mag. props. 0-60986
 Sr₂Mg(Co)(Zn)(Mn)(Cd)(Ca)(Sr)TeO₆, optical SHG study of acentricity, ferroelec. of low temp. phases 0-71324
 SrMnO_{3-x}, O-deficiency induced polymorphs and elec. cond. 0-71643
 Sr₂(Na_{0.5}Bi_{0.5})_{2-x}TiO₃ ferroelec. ceramic, hot pressing, numerical simulation (French) 0-76220
 Sr_{2.05}Na_{0.95}Nb₅O₁₅, X-ray powder diffraction data determ. (Chinese) 0-70170
 SrSnO₃ and SrZrO₃, high-density ceramics prep. and elec. props. 0-60812
 SrTiO₃ ceramic, electrocaloric effects for refrigeration at cryogenic temp. 0-77789
 SrTiO₃, Mossbauer spectroscopy, sample prep. and results 0-66078
 SrTiO₃, prep. from film forming soln. 0-60811
 TiO₃ brookite synthesis from Ti in NaF or Ti compounds, form. mechanism (Japanese) 0-93529
 TiO₃, porosity-permittivity relations, depolarising factors determ. and pore effects (Japanese) 0-97189
 UO₂, crystn., specific heat anomaly 0-84299
 UO₂, pellets, sinterability, particle size effect 0-104098
 UO₂ powder compaction, friction between particles and die walls 0-71620
 UO₂-PuO₂, fuel pin, hyperstoichiometric, post irradiation examination 0-63258
 Y-Si-Al-O-N ceramic, phase assemblages, relationships with props. 0-60848
 Y₂O₃ sintered-ceramic separator plate development, LiAl/LiCl-KCl/FeS battery applications 0-61321
 Y₂O₃, strength under mech. and thermal actions 0-97554
 Y₂O₃, strength-controlling fracture energy depend. on flaw-size to grain-size ratio 0-81152
 (Zn_{0.2}Co_{0.8}(Ni_{0.8}))O-Al₂O₃, ZnO evaporation in vac. 0-59640
 ZnO, fully dense, grain growth 0-93526

ceramics continued

- ZnO non-ohmic ceramic, degradation props. under AC and DC bias 0-80262
 ZnO nonohmic ceramic, formation mechanism 0-60813
 ZnO varistor ceramics, current-voltage characts., inhomogeneities and single barriers 0-80273
 ZnO:Bi, Sb, Co, second phase effect on elec. and mag. props. 0-60986
 ZrO₂ ceramic, dense nonstabilized, fabrication by hydrothermal reaction sintering 0-97451
 ZrO₂, metastable, tetragonal, strengthening by surface grinding 0-71777
 ZrO₂ microsphere stabilised ceramic, fracture characts., thermal stability (*Russian*) 0-76335
 ZrO₂, partially stabilised ceramics, strengthening, post-sintering heat treatment 0-97518
 ZrO₂, partially stabilized, processing defects 0-97558
 ZrO₂ particles in ceramics, grinding induced tempering 0-89260
 ZrO₂, porous, sintered stabilised microspheres, strength and fracture studies 0-85019
 ZrO₂, synthesis by solid state reaction 0-100821
 ZrO₂-CaO (15 mol.%), precipitation and ordering 0-100837
 ZrO₂-CaO(Y₂O₃) ceramics with grainy structure, props., effect of heating to 2000°C 0-104194
 ZrO₂-Y₂O₃ (9 mol.%), precipitation and ordering 0-100837
 6.14ZrO₂-Nb₂O₅, elec. cond. meas. 0-100463
 6.14ZrO₂-Ta₂O₅, elec. cond. meas. 0-100463
 ZrSiO₄ zircon ceramic with glass-forming additives, sintering and mech. props. 0-60814
 ZrSiO₄, zircon yellow pigment, synthesis (*Polish*) 0-66466

Cherenkov counters see Cherenkov counters

Cherenkov radiation see Cherenkov radiation

cerium

see also nuclei with

- addition to Cr-Mo and Ni-Cr-Mo-V low-alloy steels, remedy for temper brittleness 0-66659
 addition to Ni-Cr austenitic stainless steel, effect on heat resist. and comp. of non-metallic inclusions 0-76315
 Compton scattering study of γ - α phase transition 0-59650
 depletion in Melrose-b howardite 0-101566
 gettering of H, mass spectrometry and microgravimetry study, rel. to HTGR gas purification 0-73374
 high pressure phase transition, anomalous Gruneisen parameter behaviour 0-79934
 implantation on Cr-Ni Nb stabilized austenitic stainless steel surface, effect on oxidation behaviour 0-71791
 isostructural solid-solid phase transitions, core collapse, cell theory 0-59620
 Kondo-like anomaly in FCC phase 0-96857
 localised vibration of interstitial H impurities in FCC γ -Ce 0-75322
 marine sediment Ce composition, determination method 0-104543
 oxidation agent for Fe-Armco, grain size and strength depend. on non-metallic inclusions (*Russian*) 0-100894
 resonant photoemission, time-depend. density-functional technique 0-89114
 surface and volume props., flow props., surface layer thickness (*Russian*) 0-59760
 Ba,Sr_{1-x}Nb₂O₆:Ce, photoelec. props. and photorefraction 0-60538
 CaO:Ce³⁺, Gd³⁺, sensitization of Ce³⁺ luminesc. by Gd³⁺ 0-97326
 CaS:Ce, Na phosphor, photoluminescence and excitation spectra 0-89049
 α -Ce, exchange-enhanced, elec. resist. T² depend., press. effect 0-96845
 Ce III, 3d and 4f energy level parametrisation, Slater parameters and correl. corrections 0-87041
 Ce³⁺ impurities in cubic crystals, 5d-4f radiative transition probability calc. 0-71474
 Ce:LaF₃ 286 nm laser, optically pumped 0-99738
 Ce-S-O equilibrium in molten Fe (*Chinese*) 0-104423
¹⁴⁴Ce, inhalation exposed mice, toxicity, dosimetry and ¹⁴⁴Ce retention 0-89874
 GaP:Ce epitaxial films, photoluminesc. spectra 0-66294
 LaGa₂S₄:Ce³⁺, phosphor, luminesc. props. 0-103979
 MgS:Ce³⁺ phosphors, emission and excitation spectra (*French*) 0-93380
 SiO₂-MgO-CaO-Al₂O₃:Ce,Fe, redox equilib., expt. 0-85171
 SrF₂:Ce³⁺, cryst. field energies 0-59941
 ThO₂:Ce³⁺ (Ce⁴⁺), mixed ionic and electronic transport 0-107875
 YAlO₃:Ce, fast decay UV phosphor 0-71471
 Y₂SiO₅:Ce³⁺, EPR and spin-lattice relax. 0-108063
 ZnO:Ce phosphor, electrolum. brightness, voltage and freq. depend. 0-60681

cerium alloys

- mischmetal-Co system, phase relations, microstruct., mag. props. 0-104118
 steel, low alloy, Mn-P, temper brittleness, rare earth mischmetal effect (*Chinese*) 0-104249
 (Ce,Lu)Al₂, collective phenomena 0-65933
 (Ce,Lu)In₃, heat capacity and elec. resist. 0-71049
 (Ce,Y)Al₂, collective phenomena 0-65933
 Ce-Cu, liquid, normal spectral emissivity 0-103506
 Ce-In, phase equilibrium and cryst. struct. 0-66483
 Ce-M intermetallic cpds., M=3d transition metal, sorption of H₂, structural charges 0-88429
 Ce-Mg-Fe master-alloy inoculated cast Fe, struct. and props. 0-100843
 Ce-Tl, phase equilibrium and cryst. struct. 0-66483
 CeAl₃, antiferromag. ordering and Kondo behaviour, ²⁷Al NQR study 0-71231
 CeAl₃, collective phenomena 0-65933
 CeAl₃, magnetic ordering, 24 component Ginzburg-Landau model 0-97095
 CeAl₃, multiple-q structure or coexistence of different mag. phases, neutron diff. study 0-107985
 CeAl₃, resistivity and volumetric meas., phase diagrams, comparison with CeS 0-107789
 CeAl₃, sp. ht., Kondo effect and ferromag. order coexistence 0-65927
 Ce₂Al₁₁, competition between ferro- and antiferromag. interactions 0-60258
 Ce₃Al₁₁, sp. ht., Kondo effect and ferromag. order coexistence 0-65927
 Ce₉₀Al₁₀, metallic glass, mag. ordering and cryst. field effects, speromagnetism 0-80531
 CeBe₃, intermediate valence state, XPS, resist. and susceptibility study 0-71565
 CeBe₃, lattice spacings and susceptibilities 0-65778
 CeCo₃ and ternary hydride, mag. props. 0-108007

cerium alloys continued

- CeCo₃, sorption at press. up to 1500 atm. 0-97819
 Ce₂Co₃ and ternary hydride, mag. props. 0-108007
 CeCo_{3-x}Cu_x, 0≤x≤ internal oxidation kinetics, oxide struct., X-ray study 0-104329
 CeCu₂Si₂, collective phenomena 0-65933
 Ce(In,Sn)₃, heat capacity and elec. resist. 0-71049
 Ce(In,Sn)₃, mag. susceptibility, temp. depend., intermediate valence 0-65779
 CeIn₃, mag. struct., neutron diff. study 0-80481
 CeIn₃-Sn, mixed valence system, low-temp. susceptibility, paramagnon study 0-97077
 Ce_{1-x}La_x, dil., γ - α transition temp. and press., elec. resist. meas. up to 10 kbar 0-59643
 Ce_{0.9-x}La_xTh_{0.1}, mixed valence state, static and dynamic mag. response 0-103816
 CeNi₂-CePt₃ system, structural and mag. studies on valence behaviour of Ce 0-103809
 CeNi₃, and ternary hydride, mag. props. 0-108007
 CeNi₃, sorption at press. up to 1500 atm. 0-97819
 CeNiAl₄, mag. susceptibility, H adsorption-desorption cycle effects 0-107990
 CeNi₃Si₄, X-ray cryst. struct. determ. 0-88089
 CePd₃, fluctuating-valence compound, anomalous far IR absorption 0-66210
 CePd₃, mixed-valence, 3d and 4d core levels, XPS study 0-89111
 CePd₃-Er, dil., low field mag. susceptibility, electro-nuclear effects 0-60189
 CePd₃-MPd₃ mixed valent systems, nonlinear conc. depend. of resist. 0-65528
 Ce₂Sc₂Si₄, X-ray cryst. struct. determ. 0-92480
 CeSn₃, intermediate valence cpd., search for phonon anomalies, inelastic neutron scatt. 0-100317
 CeSn₃, mixed valence cpd., electronic struct. and mag. props. 0-70649
 CeSn₃, mode softening and elastic const., acoustic vel. meas. 0-88242
 CeTi₃, mag. susceptibility, magnetisation, neutron diff., elec. resist., and sp. ht. meas. 0-75733
 (Ce₂Y_{1-x})Fe₂, mag. susceptibility and Mossbauer meas., lattice parameters 0-97068
 Fe, cast hypoeutectic, Ce distrib. in graphite grains 0-100279
 Gd-Ce, magnetocrystalline anisotropy, magnetisation and torque curve meas. 0-65859
 (La,Y)Ce, dil., Kondo supercond., transition temp., susceptibility and resist. 0-65733
 Mg-Ce, appl. to H₂ storage 0-72093
 Mg-Mn-Ce (1.5, 0.3 wt%), superplasticity role of diffusional creep (*Russian*) 0-97528
 Sb-Ce system, heats of form. 0-89517
 Sn-Ce system, heats of form. 0-89517

cerium compounds

see also cerium alloys

- monochalcogenides, mag. ordering, expt. test for ϵ -expansions with n=4 0-60259
 mononitrides, anomalous mag. props., planar coupling theory 0-60245
 Si₃N₄-Ce₂O₃-SiO₂ materials: phase relations and strength 0-97465
 Ce-Si-Al-O-N ceramic, phase assemblages, relationships with props. 0-60848
 CeB₆, anomalous sp. ht. intrinsic mag. phase transitions obs. 0-108027
 CeB₆, crystal preparation, elec. resistance, phase transitions 0-97427
 CeB₆, mag. and electronic props. 0-71048
 CeB₆, magnetostriiction, US absorpt. and thermal expansion 0-66004
 CeBi, unusual anisotropy mechanism due to virtual valence fluctuation 0-96828
 CeBi₂Sb_{1-x}, mag. props. and press. effects 0-71026
 CeC₂, mag. props. 0-108008
 CeCrO₂, X-ray cryst. struct. determ. (*French*) 0-92485
 CeD₂, phonon dispersion relations 0-88287
 Ce₂Dy_{1-x}C₂, mag. props. 0-108008
 CeFe₂As₂, synthesis and cryst. struct. 0-84154
 CeFe₂Sb₂, prep. and cryst. struct. 0-100211
 CeH₃, phonon features in IR and Raman spectra 0-93310
 CeIr₃(Al₂)₃, cryst. struct. determ. 0-64960
 (Ce₂La_{1-x})₂Mg₂(NO₃)₁₂·24H₂O, adiabatic demagnetisation temp., mag. entropy (*Russian*) 0-65892
 Ce₂Mg₂(NO₃)₁₂, spin-lattice relax., dynamic susceptibility meas., liq. He contact effects 0-66011
 Ce₂Mg₂(NO₃)₁₂·24H₂O, ground state with dipole-dipole and exchange interactions in external mag. field 0-84582
 CeN, miscibility with UC (*German*) 0-96654
 CeNH₄P₂O₇ and Ce(NH₄)₂(PO₃)₃, synthesis by solid-phase reaction, characts. 0-60778
 CeO, dissoci. energy, rel. band strengths of a₂-X₂ and b₂-X₂ systems 0-99495
 CeO₂:CaO(Y₂O₃), oxygen ion cond. and defect struct. 0-107553
 CeO₂:Y, slow transient phenomenon 0-107550
 CeO₂-Y₂O₃ solid soln. phases, synthesis 0-104132
 CeO₂As₂, synthesis and cryst. struct. 0-84154
 CeO₂Sb₂, prep. and cryst. struct. 0-100211
 CePd₃ single crystal Czeochralski growth and characterisation 0-60767
 CeRu₄As₂, synthesis and cryst. struct. 0-84154
 CeRu₂Sb₂, prep. and cryst. struct. 0-100211
 CeS, resistivity and volumetric meas., phase diagrams, comparison with CeAl 0-107789
 Ce₂(SO₄)₃·8H₂O:Gd³⁺, single cryst., EPR study, spin Hamiltonians 0-80606
 Ce₂(SO₄)₃·9H₂O(D₂O), polarised Raman spectra, vibr. props. and role of lattice H₂O 0-66201
 CeSb, antiferromag., first-order transitions, mag. phase diagram 0-60252
 CeSb, unusual anisotropy mechanism due to virtual valence fluctuation 0-96828
 CeSb₂As₂-x, mag. props. and press. effects 0-71026
 Ce₂-Se₂Pd₂, intermediate valence of Ce, susceptibility, lattice const., ESR meas. 0-103648
 CeSe, mag. ordering, expt. test for ϵ -expansions with n=4 0-60259
 Ce₂Sn₂Mo₂Se₈, supercond. props. 0-97023
 CeTe, mag. ordering, expt. test for ϵ -expansions with n=4 0-60259
 Ce₂Ti₂O₇, ferroelec., layer type struct., cryst. growth 0-108348
 Ce_{0.08}Y_{0.92}Sb₂, dilute f-electron system in cluster regime, crystal field and exchange splittings 0-97062
¹⁴⁴CeO₂, effects of repeated inhalation exposure, mouse obs. 0-104676

cerium compounds continued

- $^{144}\text{CeO}_2$, repeated inhalation exposure of mice, retention and dosimetry 0-109034
 $(\text{La}_x\text{O}_{3-x})(\text{CeO}_2)_x$:Mn, valence state of Mn, effect of annealing in H_2 atm., ESR obs. (*French*) 0-71164
 $(\text{La}_2\text{O}_3)_{0.95}(\text{CeO}_2)_{0.05}:\text{Mn}^{2+}$, X-band EPR study 0-60409
 $\text{Na}_3\text{La}_{1-x-y}\text{Ce}_x\text{Ti}_y(\text{PO}_4)_2$, optical props. (*French*) 0-103991
 $\text{Na}_2\text{O}-\text{SiO}_2-\text{Au}+\text{CeO}_2$, Au particle nucleation 0-81066
 $\text{Si}_3\text{N}_4-\text{CeO}_2$ additive, hot-pressing and oxidation behaviour 0-71618
 (U,Ce) , U self-diffusion 0-92711

cermets

- adhesion mechanism for metallization of electronic ceramics, elec. props. (*German*) 0-76381
 cemented carbides, physical and chem. nature 0-76265
 effective medium theory: mathematical determination of the physical solution for the dielectric constant 0-93230
 gas turbine engine, substitution of ceramics for high temp. alloys 0-97678
 granular media, dielectric function theory, permittivity, percolation transport props. 0-88498
 porcelain-metal cermet, stress determ., meas. method (*German*) 0-76425
 porous cermet, heat transfer and stability for moving evaporating coolant 0-64563
 rare earth chromite based electrode material development for MHD generators 0-84893
 solar selective absorber design, optimal comp. profiles for max. solar absorptance 0-101129
 Al-SiC cermet elasticity, porosity meas. by US means 0-81101
 AlN-Mo cermets, ZrO_2 and mullite whisker reinforced, strength var. with temp. 0-104232
 Al_2O_3 -Mo cermets, ZrO_2 and mullite whisker reinforced, strength var. with temp. 0-104232
 Al_2O_3 -Pt metal-ceramic reaction, micro/macro obs. 0-66467
 B_4C -304 stainless steel cermet for nuclear shielding appls. 0-102352
 B_4C -Cu cermet fabrication for neutron shielding appls. 0-102354
 $\text{Cr-Al}_2\text{O}_3$ powder targets for plasma-ion spray deposition of resistance films 0-84897
 MgO-Pd metal-ceramic reaction, micro/macro obs. 0-66467
 Mn-SiO_2 annealed cermet films, elec. resist., composition depend. 0-97007
 Mn-SiO_2 cermet thin film, DC resist., activation energy, thickness depend. 0-84518
 $\text{Ni-Cr-Al}_2\text{O}_3$ powder targets for plasma-ion spray deposition of resistance films 0-84897
 Pt-SiO_2 cermet films, struct. and props. 0-96956
 $(\text{Ti,Cr})\text{B}_2$, sintering kinetics and props. 0-100811
 ZrB_2 -Nb, reactions between components 0-100812

CESR

- degenerate semiconductor, conduction electron acoustic spin resonance, oscillations of absorbed power 0-108075
 metal CESR, mm waves, surface effects 0-66036
 metal colloids in ionic cryst., preparation, optical, mag. resonance, elec. props. 0-59459
 metals, cond. electron and spin scatt. due to dislocations 0-75856
 semimetal, degenerate, conduction electron acoustic spin resonance, oscillations of absorbed power 0-108075
 superconductors, zero-gap dirty, cond. electron spin resonance theory 0-103888
 tetramethylammonium(0), $\text{Li}(\text{CH}_3\text{NH}_2)_4$, existence, conduction- and localised-electron spin reson. 0-66035
 $(\text{TMTSF})_2\text{PF}_6$, ESR g-factor, linewidth, spin susceptibility, metal-insulator transition 0-103887
 $(\text{TMTSF})_2\text{PF}_6(\text{AsF}_6)$, linear-chain conductor, semicond.-metal transition in small elec. field 0-103730
 Ag foil, or film, conduction electron spin disorientation at surface 0-75855
 Ag, resonant and nonresonant conduction-electron-spin transmission 0-75857
 Au, resonant and nonresonant conduction-electron-spin transmission 0-75857
 Cu foil, conduction electron spin disorientation at surface 0-75855
 Cu, resonant and nonresonant conduction-electron-spin transmission 0-75857
 GaAs, electron-spin relaxation and recomb. kinetics, time-resolved luminesc. study 0-108074
 InSb, CESR at high mag. fields, scatt. mechanisms 0-93177
 n-InSb, cond. electron spectra in quantised mag. field, impurity resonance scatt. (*Russian*) 0-93178
 n-InSb, spin polarisation, anisotropic size effect, effect on CESR signal 0-70743
 Li particle size distrib. meas. by SEM 0-101775
 Nb₃Ge film, superconductivity, relevance of mag. interactions, EPR study 0-100545
 Si p-i-n structure, ESR of conduction electrons 0-93179
 W, resonant and nonresonant conduction-electron-spin transmission 0-75857

chalcogenide glasses

- defect model, neutral diamagnetic quasimolecules, excess orbital bonds (*Russian*) 0-70647
 defect models, optical, versus transport processes. 0-84449
 defect reactions, ionicity dependence, negative-U states 0-88510
 defects, band gap states 0-80215
 electronic transport mechanisms and coeffs. 0-80282
 filament waveguides for signal transmission in far IR region (*Czech*) 0-96017
 films, threshold switching 0-96950
 inhomogeneous thin amorphous chalcogenide films, reversible switching, thermal stability criteria 0-70856
 ionicity dependence of defect reactions and negative-U states in glasses 0-88511
 Luminescence, temp. depend. rel. to nonradiative transitions 0-71485
 memory effect, local doping, switching 0-107873
 optical constants, cooling rate influence, O₂-free glasses in crit. annealing region 0-88952
 Poole-Frenkel effect, charged dangling bonds model 0-59994
 review of structural and electronic props. 0-64901
 short-range order, theory and probes 0-79698
 $\text{Ag}_x\text{Sb}_{1-x}\text{Se}_2$, single-phase, thermoelectric efficiency 0-107826
 As chalcogenides, deep levels, photoluminesc. and photocond. 0-70641
 As-Ge-Te, chalcogenide glass, elec. cond. and dielec. const. 0-75567

chalcogenide glasses continued

- As-S amorphous chalcogenide thin film, transient photoinduced phenomena 0-80884
 As-S-Tl, viscosity and elastic props. 0-100180
 As-Se amorphous system, photocond. props. 0-88587
 As-Se amorphous system, Raman scatt. 0-88984
 As-Se glasses, elec. transport studies 0-103695
 As-Se-Ge(-S), photostructural change in Urbach tail 0-76021
 As-Se-S-Ge chalcogenide amorphous film, computer-generated holograms using electron beam irradiation 0-95846
 As-Se-Sb, crystallised glasses, struct. from Mossbauer spectra 0-64917
 As-Te-Ge/n-Si, film on cryst., heterojunction, elec. and photovolt. props. 0-100514
 As-Te-In, glass-forming, density and microhardness 0-103257
 As-Te-Si-Ge amorphous chalcogenide semiconductor, thin film interface, electrical charact. (*Korean*) 0-97014
 $\text{As}_{10}\text{Ge}_5\text{Te}_5\text{Ag}_5$, elec. and dielec. props., Ag additions effect 0-65558
 As_2S_3 , amorphous, time resolved luminesc. 0-66288
 As_2S_3 and As_2S_4 vapour-deposited films, valence states, thermal and photo-induced changes UPS study 0-93459
 $\alpha\text{-As}_2\text{S}_3$, energy gap meas., by Faraday rotation 0-66161
 As_2S_3 film, amorphous, photo-induced dynamical changes 0-66142
 As_2S_3 films, photographic Ag photodoping to produce negative relief image 0-59490
 As_2S_3 glasses, DC elec. cond. and thermo-elec. power 0-96865
 As_2S_3 , glassy, photoinduced defects, EPR and absorpt. spectra 0-59398
 As_2S_3 , luminescence 0-80862
 As_2S_3 , photosensitive etching in nonoxidising etchants 0-78813
 As_2S_3 , thermal capacity, 300 to 600K 0-103492
 $\alpha\text{-As}_2\text{S}_3$, time-resolved photoluminescence study 0-89057
 As_2S_3 , two photon light absorpt. dispersion, induced linear light absorpt. (*Russian*) 0-66231
 $\text{As}_2\text{S}_3\text{Ag}$ glassy films, optical transmission spectra, photodoping effect 0-66317
 As_2S_3 , amorphous, struct., vibr. and electronic spectra 0-64908
 $\text{As}_x\text{Si}_{100-x}$ amorphous films, optical props. and photoinduced changes 0-60700
 $\text{As}_x\text{Si}_{100-x}$ glasses, Raman spectrum and structure 0-60593
 $(\text{As}_2\text{S}_3)_{100-x}(\text{Cu}_2\text{S})_x$, glassy, struct. and elec. cond. study 0-59399
 $\text{As}_2\text{S}_3-\text{Se}_2$, amorphous, picosecond relax. of optically induced absorption 0-97302
 $\text{As}_2\text{S}_3(\text{Se}_2)$, photoconductivity dependences applied elec. field 0-107857
 $\text{As}_x\text{Si}_{100-x}(\text{Se}_{100-x})$, localised states density near valence band edge (*Russian*) 0-103638
 $\text{As}_2\text{Sb}_2\text{Se}_3$ glassy semiconductors, electronic props. 0-103712
 As_2Se_3 , amorphous radiative interband recombination 0-66286
 As_2Se_3 glass, mol. struct. model 0-100179
 As_2Se_3 , glassy defect electron states, tight binding calc. 0-96818
 As_2Se_3 glassy films, current-voltage characts., temp. depend., SCL current 0-92902
 As_2Se_3 , luminescence 0-80862
 As_2Se_3 , modulated photocurrent, analysed for trap-limited case (*Japanese*) 0-60030
 As_2Se_3 , thermal capacity, 300 to 600K 0-103492
 As_2Se_3 , thermally reversible photodarkening effects obs. 0-103970
 As_2Se_3 , transient electrical transport, general and unified treatment 0-59977
 $\text{As}_2\text{Se}_3\text{Ag}$ amorphous, freq. depend. cond. 0-88565
 $\text{As}_2\text{Se}_3\text{Pt}$, glass, effect of impurities on elec. props. 0-103699
 $\text{As}_2\text{Se}_3\text{Ge}$ glassy thin films, flash photoresponse 0-107863
 $\text{As}_2\text{Se}_3\text{GeSe}_2$ glass, bulk and impurity IR absorpt. 0-71455
 As_2Se_3 and As_2Se_4 semicond. glasses, densified, photoluminesc., inelastic deform. effect 0-66293
 $\text{As}_2\text{Se}_3\text{Ag}$, glassy semicond. film, prep. by photodiffusion of Ag, negative photocond. 0-92934
 As_2Se_3 , between Al and Sb electrodes, rectifying effects 0-75654
 $\text{As}_2\text{Se}_3\text{Te}_3$, thermally reversible photodarkening effects obs. 0-103970
 As_2Te_3 and $\text{As}_2\text{Te}_2\text{Ge}$, amorphous, AC cond. at low temps. 0-80269
 As_2Te_3 , thermal capacity, 300 to 600K 0-103492
 $\text{EuS-Ga}_2\text{S}_3\text{-GeS}_2$, chalcogenide glasses, conditions of form. of glassy prod. (*French*) 0-100325
 Ga-Ge-Se chalcogenide glasses, rare earth element doped, elec. props. 0-96885
 Ge-As-Se IR transmitting glass composition, prep. and props. 0-69474
 Ge-As-Se-Te glasses for 8-12 μm IR optics 0-69475
 N-Ge-Bi-Se glass, elec. and optical props. 0-65550
 Ge-P-S glass system, EPR of intrinsic and Mn^{2+} impurity centres 0-88870
 Ge-Pb-S, glassy, photoconductivity dependences applied elec. field 0-107857
 Ge-S, melt-quenched photoinduced ESR, annealing behaviour and glass comp. depend. 0-71156
 Ge-S-Ga amorphous thin film, memory switching effects 0-88605
 Ge-S-Se, glass formation 0-103251
 Ge-Sb-Se glass, elec. props. comp. depend. 0-70697
 Ge-Si-S system, glass formation, transition temp., crystallisation and melting 0-100178
 $\text{Ge}_3\text{As}_2\text{S}_7\text{S}_5\text{Te}_{25}$, chalcogenide thin films, coupled carrier theory test, high field conditions 0-100466
 $\text{Ge}_{30}\text{As}_{17}\text{Te}_{30}\text{Se}_{23}\text{As}_2\text{S}_3$, two-layer antirefl. coating, error considerations in design 0-74477
 $\text{Ge}_{20}\text{Bi}_8\text{Se}_{80-x}$, semicond. glass, resist., thermoelec. power, optical absorpt. 0-88555
 $\text{Ge}_{20}\text{Bi}_8\text{Se}_{70-x}\text{Te}_{10}$, semicond. glass, resist., thermoelec. power, optical absorpt. 0-88555
 Ge_2S_3 , glass form. and characterisation (*German*) 0-64913
 $\text{Ge}_2\text{S}_7\text{Mn}$, bond struct. and character in Ge-S system, EPR obs. 0-66014
 $\text{Ge}_{40}\text{S}_{60}:\text{Mn}(\text{Ag})(\text{Cu})$, bond struct. and character in Ge-S system, EPR obs. 0-66014
 $\text{Ge}_{40}\text{S}_{60}$, amorphous, bulk and film forms, elec. props. and ESR study 0-103691
 GeSe, amorphous, film, thermally induced effects, UPS study 0-104042
 GeSe, amorphous, film, thermally induced effects, UPS study 0-104042
 GeSe, amorphous layers, photoconduction meas. 0-65632
 GeSe, glassy, powdered and bulk, fatigue of photolum. 0-80855
 GeSe-As₂Se₃-Sb₂Se₃, elec. cond. over wide range of temp. 0-88564
 Ge₂Se₃, glass form. and characterisation (*German*) 0-64913
 Ge₂Se₃, vitreous, evaporation kinetics and amorphous film deposition 0-97434
 Ge₂Se₃Te amorphous layers, prep. and elec. props. 0-97436

chalcogenide glasses continued

- Ge₂Si₂As₂Te₃Ga₁₀, chalcogenide thin films, coupled carrier theory test, high field conditions 0-100466
 Ge_{1-x}Sn_xTe film, amorphous, elec. cond. 0-93016
 Li₂S-GeS₂, glass forming region, struct. and ionic cond. 0-88358
 Mo-chalcogenide glass-Mo-Al struct., strong elec. field effects 0-97004
 Na₂S-P₂S₅, glass forming region, struct. and ionic cond. 0-88358
 Na₂S-SiS₂(GeS₂)(P₂S₅), synthesis, structure and ionic conduction (*French*) 0-65291
 Na₂S-XS₂, X=Si, Ge, glass forming region, struct. and ionic cond. 0-88358
 Sb-S-I, activation energy of crystn. 0-64920
 Sb₂S₃ (Se₂), photoconductivity dependences applied elec. field 0-107857
 SbSe, amorphous thin film high field charge transport and quasi-Fermi level location 0-70863
 Se, bonding coordination defects 0-59927
 Se, photoelectronic behaviour, in glass transition region 0-60045
 Se, transient electrical transport, general and unified treatment 0-59977
 Se-As, photoelectronic behaviour, in glass transition region 0-60045
 Se-Ge amorphous films, obliquely deposited, photoinduced chem. changes 0-76385
 Se-Ge-Te, chalcogenide glass, elec. cond. and dielec. const. 0-75567
 Se-Te-Sb glasses, electronic transport 0-88579
 Se_{0.09}Te_{0.08}, crystallisation, effect of an alternating electric field 0-88054
 Se_{1-x}Te_x, film, photo-crystallisation 0-59839
 Se_{1-x}Te_x, optical and elec. props. 0-84506
 Se_{1-x}Te_x amorphous, structural relaxation and crystallisation kinetics study by DTA 0-59394
 Se_{1-x}Te_{0.09}As_{0.25}Ge_{0.10} semiconductor amorphous films, field effect, trapping 0-84472
 Te₆₀Ge_{20-x}As_x glasses, rapid melt cooled, glass transition and stability range 0-75170
 Te₆₀Ge₁₅Pb₅, DSC sensitivity to controlled ageing in glass transition region 0-71673
 Te₆₀Ge_{20-x}Sb_x(Bi_x), DSC studies of struct. phase transformation 0-66505
 Te_{50-x}Se₅₀Sn_x, thin films, elec. cond. and thermoelectric power meas. (*French*) 0-80335
 Te₆₀Si_{20-x}Pb_x glasses, phase separation, double T_g presence 0-88306
 Ti-Ge-Te, glass formation 0-103255
 TlAsS₂, crystallisation, effect of an alternating electric field 0-88054
 TlAsS₂(Se₂)(Te₂), vitreous, crystn. kinetics 0-64918

change of state see phase transformations**channelling**

see also energy loss of particles

- accelerator irradiation, heavy ion irradiation damage 0-100291
 bending of high energy beams using axial and planar channelling 0-88225
 beryl, natural and synthetic, ion channelling transmission ratios 0-75277
 charged particle energy loss in cryst., theory 0-79847
 coherent and magneto-blocking effects of relativistic particle radiation in crystal (*Russian*) 0-92577
 coherent radiation and bremsstrahlung 0-65079
 conference, atomic collisions in solids, Hamilton, Canada (Aug. 1979) 0-62375
 crystal, channelled particle γ -quanta generation in external ultrasonic field 0-70282
 crystal, charged particle energy loss (*Russian*) 0-75280
 crystal orientation determ. from selected area channelling patterns 0-70092
 crystals, EM rapid cascades (*Russian*) 0-107348
 crystals, relativistic electron channelling, overbarrier states (*Russian*) 0-92576
 dechannelling mechanism due to dislocations, anal. 0-59538
 diamond/Sb, implanted, radiation damage and annealing study 0-100263
 diamond, accelerator irradiation, heavy ion irradiation damage 0-100291
 diamond, electron channelling radiation comparison with coherent stopping radiation (*Russian*) 0-103403
 diamond, half wavelength and stopping power of planar channelled protons 0-65087
 diamond, ion channelling and dechannelling meas. 0-65090
 diamond, light ion damage, channelling investigation 0-65068
 diamond, proton channelling, transverse energy evolution in planar channels, computer simulation 0-79849
 diamond, sound excitation orientational effect due to channelled electrons 0-84254
 dislocation imaging, electron channelling appl. with SEM 0-70214
 electron, axial channelling, quantum mechanical treatment 0-65091
 electron bunching, scattering and bremsstrahlung in cryst. lattice in strong EM field 0-65113
 electron channelling pattern, large angle, generation and appl. 0-100296
 electron channelling pattern, indexing method (*Chinese*) 0-103402
 electron diffraction symmetries 0-100138
 electrons, characteristic radiation, sharp lines obs. 0-65111
 electrons, relativistic, quantum beats 0-88226
 electrons in crystals, quasi-synchrotron radiation characts. 0-92572
 EM, Schwinger scattering of fast neutrons in crystals (*Russian*) 0-70286
 fast charged particle, dechannelling from planar channel, stochastic theory 0-96579
 fission nuclei lifetimes from ²³⁵U(d,f) study using blocking technique 0-63216
 GeV region, density effect 0-65085
 heavy ions, channelled, stopping power Z₁ oscillation vel. depend. 0-65101
 heavy ions, electron pick-up from free electron gas in thin solid film 0-107349
 heavy ions, low vel., channelling stopping power oscils. 0-103404
 ion beam surface crystallography, channelling and blocking effects, double alignment backscattering 0-65350
 ion implantation by laser annealing, characterisation, solar cell applications 0-70247
 ion motion in crystal, effect of polarisation field 0-103406
 ion scattering, 180°, on solid targets, evidence for yield enhancement, channelling case 0-70281
 Kronig-Penney potential, charged particle motion, band struct. and Bloch wavefunctions 0-65112
 lattice vibration correlations in computer simulations 0-65086
 leptons, coherent radiation emission 0-65080
 metal, ion implanted H(D), interstitial positions and vibr. amplitudes, fast ion channelling study, review 0-79848

channelling continued

- metal target preparation for stopping power meas. of channelled ions in low energy region 0-63431
 metals, mixed dumbbells, ion channelling studies 0-70277
 monocrystals, EM radiation of relativistic positrons and electrons during axial and planar channelling 0-79845
 neutron beam channelling and focusing in ferromagnets (*Russian*) 0-107351
 particle radiation spectra, emitted quanta angular distrib. 0-96578
 photon production by channelled electrons 0-79846
 planar dislocation channelling in modified continuum model 0-65089
 positrons, relativistic, radiation at channelling 0-70279
 protons, relativistic, channelling in bent crystals, theory 0-96581
 γ -quanta channelling effect in periodic struct. (*Russian*) 0-96584
 quantum channelling theory, channelled particle multiple scatt. by electrons, contrib. to dechannelling rate 0-107350
 rapid-scan polarising Michelson interferometer and InSb detector calibration 0-59305
 relativistic channelled nuclei, effects of Coulomb excitation and electrodisintegration 0-59539
 relativistic charged particle in electric field, spin rot., curved crystal p.e.⁺ channelling (*Russian*) 0-63907
 relativistic electrons, self-acceleration in single cryst. planar channelling 0-65084
 relativistic particles emission spectrum, rel. to interplanar pot. 0-65115
 resonance acceleration of channelled particles in intense laser field 0-88236
 resonance dechannelling under axial-to-planar transition conditions 0-59540
 resonant coherent excitation in planar channelling 0-65081
 resonant coherent excitation of channelled ions 0-65082
 semiconductor materials, channelling-blocking measurements, (n, α) method for B-depth profiling 0-70276
 semiconductor microstructure fabrication, ion channelling effects 0-70230
 semiconductors, ion-implanted, laser pulse annealing, TEM and channelling study 0-100264
 spontaneous radiation higher harmonics of ultrarelativistic channelled particles (*Russian*) 0-75281
 steel, low C, channelling contrast to investigate fatigue crack propag. 0-66609
 stratified crystal structs., strongly bound γ -rays 0-80895
 surface semichannel effects on fast ion recoil energy distrib. 0-65092
 ultrarelativistic channelled particles, spontaneous radiation, theory 0-92573
 ultrarelativistic electron and positron radiation in planar channelling 0-65083
 pN, 2-15 GeV/c, in Ge, Si, influence of channelling on scattering 0-73729
 π^+ N, 2-15 GeV/c, in Ge, Si, influence of channelling on scattering 0-73729
 Ag, electron channelling pattern, large angle, generation and appl. 0-100296
 Al, defect structures depend. on Ca and Ga implanted species 0-59494
 Al, single crystal, ¹⁸O⁺ ion implantation in channelling directions, expt. conditions and range profile obs. 0-65022
 Al single crystal, ¹⁸O⁺ ions implantation in channelling directions, stopping power meas. from max. range 0-65078
 Al-Ge (0.1 wt.%), channelling meas. of Al interstitial atom trapping by Ge atoms 0-59537
 Au cryst., ion bombarded, Ar⁺ ions, time-of-flight spectra of sputtered atoms 0-89103
 Au, electron channelling pattern, large angle, generation and appl. 0-100296
 Au-Ag (35 at.%), dechannelling of energetic He ions at dislocations 0-70275
 BP:Zn(Se)(Cd), epitaxial layers, ion implantation, defects and lattice locations, channelling obs. 0-88179
 BaF₂, planar channelling, minimum yields determ. 0-70280
 BaTiO₃:Co, voltaic current appearance on proton irradi. 0-104032
 Be, ion-implanted, impurity lattice location, channelling meas., Monte Carlo calc. 0-107291
 Be, neutron forces in relativistic electron radiation field in crystal, channelling (*Russian*) 0-70287
 CaF₂, planar channelling, minimum yields determ. 0-70280
 CdS, defect struct. and config. produced by irradi., elastic scatt. expts. 0-84178
 Cu, implanted with Cu⁺, effect on cryst. orientation, Kr penetration, meas. 0-88174
 Cu single crystals Au ion implanted, pulsed electron beam irradi. 0-65019
 Cu, vacuum deposited layer, ion bombardment induced preferential orientation 0-100290
 Cu-O single crystal, ¹⁸O⁺ ion implantation in channelling directions, expt. conditions and range profile obs. 0-65022
 Cu-O single crystal, ¹⁸O⁺ ions implantation in channelling directions, stopping power meas. from max. range 0-65078
 GaAs, amorphous layers, ion-implanted, low-temp. epitaxial regrowth 0-92790
 GaAs, ion beam induced annealing effects 0-59530
 Hg electric field gradients at different Be lattice sites, gamma-spectral study 0-80224
 Hg, quadrupole interactions in Zn, lattice location, gamma spectral study 0-80227
 Hg_{1-x}Cd_xTe, implanted with Hg, Al, damage and lattice location study 0-103381
 InP, Zn diffused single-crystal, substitutional dopant and hole conc. meas. 0-75260
 KCl(l), electron range-energy relation, thermally created lattice vacancies effect 0-92574
 Mo, electron irradi. in HVEM, channelling effect on damage prod. 0-107322
 NaCl, Ne⁺, Ar⁺, Kr⁺ bombard., sputtering and ionoluminescence 0-96583
 Ni, ion-implanted and virgin, laser irradi. effect, Rutherford backscatt. and channelling obs. 0-108306
 Ni surface, location of adsorbed atoms, surface channelling meas. 0-84373
 Ni-O, single crystal, ¹⁸O⁺ ion implantation in channelling directions, expt. conditions and range profile obs. 0-65022
 Ni-O single crystal, ¹⁸O⁺ ions implantation in channelling directions, stopping power meas. from max. range 0-65078

channelling continued

- Ni-Si(111), interface, reactivity and struct., ion channelling meas. 0-92788
- NiSi₃, epitaxial film on (111) Si substrate, interfacial order, backscatter, channelling study 0-65390
- PbS-PbSe epitaxial bicrystals, direct scatt. of channelled He ions at dislocations 0-65110
- Pt, (111) surface, backscattering, channelling spectra, H adsorption, surface relaxation 0-71552
- Si (100), H adsorption, MeV ion scatt. study 0-80071
- Si, (110) plane, quantum state observation during fast electron channelling (*Russian*) 0-59541
- Si, (111) surface, proton dechannelling under channelling, blocking and double alignment conditions 0-88235
- Si, amorphous, substrate orientation effect on regrowth by laser pulses, channelling, backscatter 0-84409
- Si, bent crystal, γ -radiation beam deflection due to 900 MeV channelled electrons 0-84223
- Si, diffracted X-ray channelling by special deform. fields 0-100295
- Si, epitaxial layers, stacking defect distrib. anal. using ion channelling tech. 0-100294
- Si, half wavelength and stopping power of planar channelled protons 0-65087
- Si, heavy ion induced disorder in surface and at shallow depths 0-59535
- Si, impurity solubility limit after laser induced melting, Rutherford backscatt. spectrum 0-107426
- Si, ion bombardment, anomalous surface damage from channelling-backscatt. meas. 0-84222
- Si, ion implantation, channelled, through metal silicide film 0-70231
- Si, ion implantation, channelling, alignment effects 0-88183
- Si, ion implantation, high dose, solid phase epitaxial regrowth 0-103380
- Si, ion implanted, annealing of heavy ion cascade damage, channelling meas. 0-89255
- Si, ion implanted, damage profiles, Rutherford backscattering 0-100733
- Si, ion-implanted layers, epitaxial regrowth by laser beam and flash annealing 0-100420
- Si:As(Pb), high-dose ion implanted and annealed, implant redistribution 0-107309
- Si:Ar, As, ion implanted, laser annealing, doping profiles, channelling 0-97506
- Si:As, CW CO₂-laser annealing, comparison with thermal annealing 0-84193
- Si:As, scanning electron beam annealing, spreading resistance, junction depth 0-75267
- Si:As, solid solubility and thermal behaviour of metastable 0-75359
- Si:B (0.2 wt.%), ion implanted, B atom displacement due to low temp. irradi. 0-88234
- Si:BF₃⁺, ion implantation appl. in semicond. device production 0-103383
- Si:B(Be)(Li) ion implanted, channelling and random equivalent depth distrib. 0-100293
- Si:Bi, ion implanted, channelling obs. of pulsed Q-switched ruby laser annealing 0-59542
- Si:Co, ion implanted, Co lattice location, channelling meas. 0-88201
- Si:Ga(As), laser-doped, impurity distrib., Rutherford backscatt. and channelling anal. 0-59507
- Si:P, ion implanted, subsurface damage, TEM and channelled Rutherford backscatt. study 0-107337
- Si:P, polycryst., channelling of implanted P during MOS device processing 0-65017
- Si:Sb, ion implanted, annealed, dislocation generation, channelling and Rutherford backscatt. meas. 0-88158
- Si:Sb, ion implanted, annealing, Sb behaviour above solid solubility, channelling meas. 0-88200
- Si:Sb(Ga)(Bi)(In), dopant solubility limit, laser irradi. effects 0-84295
- Si/Pd system, solid phase epitaxial growth control by C ion implantation 0-75466
- Si-CoSi₃Si, double heteroepitaxy, solid phase and MBE 0-104063
- Si-epitaxial film, ionised-cluster-beam deposited, cryst. and elec. chars. 0-70553
- Si-SiO₂, two layer system, P⁺-ion penetration tails, expt. and computer anal. 0-75249
- Ti-Al-Sn-Zr (6.19, 1.92, 1.43 wt.%), fatigue fracture facet investigation by selected area electron channelling 0-89344
- Ti-Al-Zr-Mo-Si (5.97, 4.73, 0.49, 0.34 wt.%), fatigue fracture facet investigation by selected area electron channelling 0-89344
- W, atomic density, effect on proton energy loss and dechannelling 0-65088
- W, electron-channelling patterns, crit. voltage effects 0-79647
- W, enhanced penetration of low energy He along (100) channel 0-65093
- ZnTe:As, impurity identification and characterisation, capacitance, luminescence and IR absorption 0-60639
- ZnTe:Bi, laser annealing, channelling, reflectivity spectra 0-66215

characteristic temperature *see Debye temperature***characteristics measurement**

- see also headings for specific characteristics, e.g. gain measurement; viscosity measurement*
- jet displacement transducers, relation between dynamic and precision chars. 0-64660
- pressure transducers, amplitude-frequency and phase-frequency chars. 0-62650
- recording systems, determination of complete dynamic chars. 0-62651
- Si solar cell, I-V charact. meas., effect of voltage ramp, theoretical anal. using linear model 0-61354

charcoal

- see also carbon*
- cryosorption pumping of He by charcoal, cryopump design for fusion reactor 0-105654
- filters, NDT of residual adsorption capacity 0-89523
- polymer charcoal, adsorpt. isotherms of organic vapours 0-96731

charge (electric) *see electric charge***charge compensation**

- see also crystallography*
- alkaline earth fluoride, doped with trivalent rare earths, migration entropy for bound fluorine motion 0-71303
- compensated semiconductor, low temp. mobility, unscreened charged impurities effects calcs. 0-75562
- phthalocyanines, elec. cond., compensation effect 0-100455
- semiconductor, cluster scattering, DC resist., energy-loss method 0-96862
- semiconductor, electron-hole plasma and elec. field, stratification at low temp. 0-60020

charge compensation continued

- semiconductor, impurity characterisation from thermal carrier meas. 0-65595
- semiconductor, large-band-gap, self-compensation, role of impurities 0-92850
- semiconductor, lightly doped, compensated, percolation level, Monte Carlo calc. 0-59923
- Al_{0.5}Ga_{0.5}As, compensated, electron mobility temp. depend. 0-96868
- B-Al_{0.5}O_{1.5}K_{0.5}MgO, cryst. struct., nonstoichiometry, ion-ion correlations 0-88129
- CaF₂:O²⁻, CaF₂:Na⁺, O²⁻ and CaF₂:Y³⁺, O²⁻, thermal depolarisation obs. of defect clusters 0-71299
- CaF₂:Y³⁺, ionic cond. and thermal depolarisation obs. of defect clustering 0-71298
- CaSO₄:Sm phosphors, X-irrad., thermoluminesc., charge compensation effects 0-97351
- Cd_{0.9}Hg_{0.1}Te crystals, donor compensation, low temp. cond. study 0-75571
- CsCdBr₃:Cr³⁺(Cr⁺), EPR of impurities, charge compensation, X-ray effects 0-60407
- CsMgCl₂(Br₃):Cr³⁺(Cr⁺), EPR of impurities, charge compensation, X-ray effects 0-60407
- Fe_{10.92}K_{1.55}O₁₇, ferrite, cryst. struct., nonstoichiometry, ion-ion correlations 0-88130
- GaAs, carrier conc. and compensation microprofiles 0-80820
- GaAs, compensated, electron mobility temp. depend. 0-96868
- GaAs, semi-insulating, undoped and Cr-doped, compensation mechanisms, Hall effect and optical absorpt. meas. 0-84477
- GaAs:Si, Li, IR absorpt., microstruct., charge compensation 0-107565
- Ge, compensated by thermal defects, recomb. and optical props. 0-64989
- Ge:In(Hg), impurity characterisation from thermal carrier meas. 0-65595
- Ge:Sn(Cu), photoelec. props., fast electron irradi. effects 0-60036
- n-InAs, photoelectric props., inhomogeneous impurity distrib. 0-107867
- n-InP, compensated, elec. props., space-charge effects 0-65569
- PbS:Ti, self-compensation of acceptors by vacancies, Hall coeff. meas. 0-92913
- PbSe:Ti, self-compensation of acceptors by vacancies, Hall coeff. meas. 0-92913
- Si, compensated by thermal defects, recomb. and optical props. 0-64989
- Si:P, ion implanted with small doses, defect annealing by nanosecond laser pulses 0-107297
- Si:P, neutron transmutation doping, elec. props. rel. to neutron fluence 0-96555
- Si:P, neutron transmutation doping, resist. homogeneity rel. to compensation ratio 0-96556
- SrF₂:La, type-I, dipole reorientation, activation vol. determ. from dielec. const. 0-88916
- SrF₂:rare earth ion, elec. dipole-dipole interaction, ionic thermocurrent and EPR study 0-108060
- TiO₂:Cr(Ta), slightly doped, elec. cond. and defect struct., charge compensation and point defect model 0-75568
- ZnS, ion implantation effects on luminesc., thermo-EMF 0-88178
- ZnSe, self-compensation, role of impurities 0-92850

charge-coupled device arrays *see charge-coupled device circuits***charge-coupled device circuits**

- automatic measuring machine for star images (*Japanese*) 0-82212
- camera, description performance and calibration, astronomical appl. 0-73499
- charge injection device as stellar tracking sensor 0-85861
- CTEM image recording apps. 0-68329
- digital images from 800X800 detector arrays on Space Telescope 0-109370
- dynamically focused electronic sector scanner based on CCDs 0-98042
- electron spectrometer using new multidetector based on charge-coupled imaging device 0-86502
- electronic detectors to enhance optical information from telescopes, image intensifiers and CCDs (*French*) 0-67569
- Galileo Jupiter Orbiter Mission CCD camera 0-85859
- imager, edge enhancement using 3X3 pixel neighbourhood operator functions 0-102644
- integrated optical channel waveguide-CCD transversal filter 0-58797
- low-background astronomical integrated IR detector array development 0-85860
- optical channel waveguide array coupled to integrated C-CD, appl. 0-102860
- photodetector for optical information processing 0-91753
- thinned back-illuminated CCD, for extreme UV direct detect. 0-77852
- LiTaO₃/CCD hybrid focal plane, IR imaging and detection, crosstalk 0-77856
- PtSi Schottky-barrier monolithic IRCCD focal plane 0-86427
- Si, phase transformation, lattice dynamics, microscopic theory 0-107387

charge-coupled devices*see also charge-coupled device circuits*

- astronomical CCD spectrometer for 500 to 900 nm range 0-82207
- MOS inversion layers, freq. response of charge transfer 0-88638
- MOS structures, inversion layer near electrode edge, pot. and charge density distribution 0-88642
- signal charge and surface pot., steady-state distrib. calc. 0-100525
- Al-anodised Ta₂O₃/native oxide-n-GaAs MOS structure evaluation 0-84514
- GaAlAsSb-GaSb p-n heterojunction CCD, charge transfer, charge exchange 0-65658

charge density waves

- commensurate-incommensurate transition in the quasi-one-dimensional Frohlich model with a nearly half-filled band 0-80199
- coupled incommensurate charge density waves, 3D ordering, mean field theory calcs. 0-107719
- electron gas, dielectric function, dynamical exchange decoupling, plasmon dispersion, SDW and CDW 0-59900
- electron gas, one-dimens., interacting, ground-state energy in mean field approx. and instabilities 0-88493
- ferromagnet, magnetic susceptibility, spin and charge density waves, Curie temp. (*Russian*) 0-100581
- incommensurate Peierls systems, amplitude solitons, implications for TTF-TCNQ 0-92841
- Israel Physical Society 1980 annual meeting, Rehovot, Israel (April 1980) 0-94909
- jellium, two- and three-dimens., CDW, appl. to liq. He surface and semiconductors 0-65476

charge density waves continued

- layer structures, intercalation with N_2H_4 , charge density waves or artefacts 0-100221
 linear conductor, CDWs and impurity effects 0-59967
 magnetic order coexistence with charge density waves 0-97096
 nonlinear amplitude-phase interaction 0-88490
 Peierls transition, Frohlich model, one-dimens., CDW stability, electron-phonon coupling 0-65452
 phase transition between commensurate and incommensurate charge-density wave states, nearly half-filled Frohlich model 0-107723
 phase transition to incommensurate excitonic phase 0-75510
 polyacetylene, continuum model for solitons 0-65472
 polyenes, long chain, electronic struct. in Peierls-PPP model 0-84423
 quasi one-dimensional conductor, CDW onset and pinning 0-70690
 quasi two dimensional, phason and sound wave coupling 0-92839
 quasi-one-dimensional CDW distorted solid, charge density fluctuations and dielec. matrix 0-107726
 quasi-one-dimensional CDW systems, commensurability pinning of fluctuation cond. 0-75555
 scattering effects on CDW transition temperature 0-107720
 thallium hexanoate, soliton conduction, elec. cond. field and temp. depend. anomaly (*Russian*) 0-103703
 transition metal chalcogenides, quasi-one-dimens., elec. mag., and supercond. props., review (*Russian*) 0-93022
 transition metal dichalcogenides, trigonal-prismatically coordinated layers, phenomenological theory of CDW state 0-80200
 TiF_4 , $TiSeF_6$ -TCNQ, $2k_F$ and $4k_F$ CDWs, X-ray study 0-65474
 $(TiF)_Cl_3$, disorder transition, cond. decrease and commensurate charge density waves 0-70153
 TTF-TCNQ, CDW transition with tripling of period along chains 0-96805
 TTF-TCNQ, implications of amplitude solitons in incommensurate Peierls systems 0-92841
 TTF-TCNQ, Landau theory of phase transitions 0-92666
 de Haas-van Alphen freq. and Fermi surface anisotropy press. depend. 0-59856
 Fe_3O_4 , Verwey transition, charge density-phonon condensation 0-65217
 Ga ultrathin metallic filaments, appearance of dielec. instability, coexistence with supercond. 0-103784
 GaAs-Al_xGa_{1-x}As multilayers, two-dimens. transport at high mag. fields 0-65724
 Hg ultrathin metallic filaments, appearance of dielec. instability, coexistence with supercond. 0-103784
 In ultrathin metallic filaments, appearance of dielec. instability, coexistence with supercond. 0-103784
 K, phasons, transverse, freq. dispersion relation in CDW state 0-96804
 $K_2Pt(CN)_3Br_{0.3} \cdot 3H_2O$, CDW system, nonlinear amplitude-phase interaction 0-88490
 $NbSe_2$ (2H), Raman scatt. from supercond. gap excitations 0-93340
 $NbSe_2$ (2H), Raman scatt. by supercond. gap excitations, coupling to CDWs 0-103956
 $NbSe_3$, CDW form., supercond. and Fermi surface determ., press. study 0-70891
 $NbSe_3$, CDW noise, temp. and freq. depend. 0-103681
 $NbSe_3$, depinning props. of lower CDW, weak pinning model (*French*) 0-70630
 $NbSe_3$, freq. depend. conductivity 0-107838
 $NbSe_3$, interference effects of CDW motions 0-88544
 $NbSe_3$, mag. susceptibility, CDW effect 0-88716
 $Nb_{1-x}V_xSe_2$, elec. and mag. anomalies at CDW transition 0-107722
 Sn ultrathin metallic filaments, appearance of dielec. instability, coexistence with supercond. 0-103784
 TaS_3 , 1T and 1H polytypes, fast neutron irradi., defect prod., effects on resist. and charge density waves 0-65060
 TaS_3 (1T) electron irradiated, lattice contraction 0-59520
 $TaSe_2$ (2H), broken hexagonal symm., incommensurate charge-density wave struct. 0-96646
 $TaSe_2$ (2H), CDW and discommensurations, ^{77}Se NMR study 0-88883
 $TaSe_2$ (2H), Raman scatt. from CDW 0-93340
 $TaSe_2$ (2H) CDW, reentrant lock in transition at high press. 0-88320
 $Ta_{1-x}Ti_xS_2$ (1T), magnetoresist. near metal-nonmetal transition at ultra low temps. 0-88600
 α -U, CDW at 43K 0-80198
 VSe_2 (1T), incommensurate periodic lattice distortion, X-ray diffraction study 0-107414

charge exchange

- for charge exchange in particle and nuclear physics see elementary particle interactions and nuclear reactions and scattering
 see also charge transfer states; ionisation
 acceptors, randomly distributed, direct energy transfer via exchange from excited donor 0-65483
 alkali metal atoms, charge exchange, exciplex or excimer form. in plasma 0-75026
 alkali metal vapour-H plasma, charge exchange role in optical props. 0-59284
 anthracene-amine cation radicals, electron transfer with heterocyclic and carbonyl anion radicals, triplet state electrogeneration 0-63803
 ascorbic acid adduct model systems, SCF calc., rel. to protein internal charge transfer 0-69072
 atom+ion multielectron collisions, charge transfer at intermediate energy, atomic model 0-91652
 biomembrane charge transfer, possible role of α -helical proteins 0-81524
 biomolecules+chloranil, charge transfer interaction, equilb. const., enthalpy and entropy determ., mol. polarisability 0-89708
 carbonyl anion radicals, electron transfer with anthracene-amine cation radicals, triplet state electrogeneration 0-63803
 clusters, small, formation, struct. and props. 0-58437
 contact charge transfer complexes of organic molecules with O_2 , CNDO/S calcs., absorpt. spectra obs. 0-69076
 Coulomb centres with different charges, asymptotic expansions 0-69211
 diatomic molecules, diatom, susceptibility and second moments, intramol. charge transfer effects 0-78702
 double well damped motion, proton tunnelling, transfer rate temp. depend. (*German*) 0-87058
 electron attachment to mol. and mol. clusters, electron-mol. collision, Rydberg electron exchange 0-63843
 electronic and at. collisions, conference, Kyoto, Japan (Aug.-Sept. 1979) 0-62394
 ethylene, twisted, intervalence charge transfer and reson., sudden polarisation effect 0-69230

charge exchange continued

- exciplexes and excited aromatic molecules, donor-acceptor props., comparison of fluorescence quenching 0-69174
 excited states, interpretation charge-transfer numbers 0-78530
 fast molecular ions, break-up on collision with solids 0-66533
 fixed-bed electrodes, three-dimensional, mass and charge transfer (*French*) 0-71920
 formamide-glyoxal, charge transfer theory, Mulliken population, ab initio calc., multiconfiguration scheme 0-106392
 glyoxal, electron affinity at centrosymm. trans geometry 0-87225
 graphite-Br₂, intercalation cpds., EXAFS study 0-71515
 graphite-K intercalation compounds, electronic props., de Haas-van Alphen effects and Fermi surfaces 0-75498
 graphite-K intercalation compounds, electronic props., resistivity, Hall effect and magnetoresistance 0-75585
 heavy-ion collisions, charge transfer, target K-shell electron capture, impact parameter depend. 0-102552
 heterocyclic anion radicals, electron transfer with anthracene-amine cation radicals, triplet state electrogeneration 0-63803
 hole-burning spectroscopy, electron phototransfer in reaction centres of *Chlorella* photosystem I 0-81561
 inert gas atom+ $Ne^{2+}(A_2^{2+})(Kr^{2+})(Xe^{2+})$, low energy reactions, SIFT and drift tube obs. 0-97705
 inert gas halides, exciplex mol. form., rel. to laser operation 0-81318
 integrated spatial electron populations, evaluations for simple mols. 0-78524
 iodide, charge transfer to solvent spectra, spectral shift data, Madelung const. determ. 0-85204
 ion+ion collisions, charge exchange Coulomb scatt. 0-69232
 ion+ion mutual neutralisation rate coefficient parametrisation 0-81301
 ion kinetics in high-pressure laser plasmas 0-64002
 ionic crystals, coupling of interfacial charge transfer and bulk transport 0-79986
 ions emerging from C foils, mean charge, inner-shell vacancy effects 0-87219
 laser pumping, quasi-reson. energy and charge exchange processes, new transitions 0-58526
 lysine, aq. solns., $H^+(D^+)$ exchange rates, ^{17}O NMR linewidths, pH depend. 0-91661
 Mattauch-Herzog mass spectrometer, charge exchange 0-86486
 metal atoms, investig. in ion source for twin mass spectrometer 0-106215
 metal polymer contact, charge transfer and contact charge spectroscopy 0-65680
 metal polymer contact, charge transfer and contact charge spectroscopy 0-65681
 methyl glyoxal, electron affinity at centrosymm. trans geometry 0-87225
 MIN, negative ion injector, Na charge exchange cell 0-99386
 multicharged ion thermal charge exchange reaction, rel. to astrophysics 0-63815
 NGC 7662, planetary nebula, photoionisation model with charge transfer reactions rel. to emission-line spectrum 0-62233
 p-nitroanilines, intramol. charge transfer satellites, XPS 0-78650
 NMP-TCNQ, partial charge transfer effect, one dimensional disordered Hubbard model study 0-70687
 outer-sphere electron transfer in polar solvents, Debye theory 0-93762
 2-oxyphenylbenzoxazol, proton intramolecular transfer, light absorpt. and emission, dichroism, polarised fluoresc. 0-87166
 photoactive pigment electrophotographic imaging system, dark charge exchange process 0-62758
 photoconductor image charge transfer to electrographic film 0-101864
 phthalocyanine compounds, XPS and charge transfer 0-95681
 phthalocyanine-alkane interface, charge transfer, rel. to photoelectrophoretic image form. 0-65616
 planetary nebulae, charge transfer and He II Ly α photons absorpt. rel. to forbidden lines intensities 0-67833
 plasmas, laser-produced, expansion, ion energy distrib., charge transfer effects 0-106953
 polar mol.+ion, statistical and thermodynamic theory 0-99562
 poly(p-phenylene), AsF_5 doped, highly cond. charge transfer complexes, elec. and optical props. 0-70778
 polymer film, proton intramolecular transfer, light absorpt. and emission, dichroism, polarised fluoresc. 0-87166
 positive ion formation energetics by negative ion charge stripping 0-78700
 protein internal charge transfer, ascorbic acid adduct model systems, SCF calc. 0-69072
 quantum mechanical and impact parameter capture amplitude 0-87226
 rare-earth ions, charge transfer and crystal field theory 0-70654
 shake-up and UV charge transfer transitions, comparison 0-102567
 small molecules, diatom, susceptibility and second moments, intramol. charge transfer effects 0-78702
 TCNE-benzene, charge transfer theory, Mulliken population, ab initio calc., multiconfiguration scheme 0-106392
 two-centre charge distrib., Fourier transform, STO general expression derivation 0-58119
 $Ar+Ar^+$, charge exchange, Σ oscill. and spin change 0-74247
 $Ar+H_2^+$, endothermic charge transfer reaction, low energy crossed beam study 0-95720
 Ar^+ +proton, charge transfer, target K-shell electron capture, impact parameter depend. 0-102552
 Ar^+ + Ar , charge transfer, fine-structure transitions 0-63808
 $Ar^{6+}+H_2$, collisions, ionisation and excitation resulting from electron capture 0-78683
 Ar^+O_2 , ion pair form. explained by charge transfer model 0-99546
 C^+ charge transfer in diffuse nebulae 0-77463
 $C+H^+$ collision, electron capture cross section 0-63804
 $C+H^+=C^++H$, effect on C I 1101 Å absorpt. edge in A-type stars 0-90423
 C +proton, charge transfer, target K-shell electron capture, impact parameter depend. 0-102552
 CdTe electrode, redox reaction due to complex $M(CN)_6^{3-/4-}$ (*French*) 0-89482
 n-CdTe, semiconductor electrode, electrochem. behaviour in nonaqueous media (*French*) 0-66808
 $Cr(CO)_6$, MCD spectra, charge transfer transitions 0-95658
 $Cs+(AuF_3)_n$, prod. of AuF_3^- , ionisation cross section energy depend. 0-81300
 $Cs+(SbF_5)_n \rightarrow Cs^++SbF_6^-+SbF_4^+(SbF_5)_{n-2}$, ionisation cross section energy depend. 0-81300
 D_2O , $H^+(D^+)$ exchange rates, ^{17}O NMR linewidths, pH depend. 0-91661

charge exchange continued

- Dy atom isotope separation, laser excitation, charge exchange with Cs⁺ ions 0-83512
- ¹⁵¹Eu (¹⁵¹Eu) excitation transfer, effect on selective photoionisation 0-99538
- ¹⁹F, nuclear dealignment of multiply ionised 3 and 6 MeV atoms recoiling in gases 0-78267
- Fe group elements, singly ionised, charge transfer, rel. to laser action 0-74246
- Fe XXII, XXIV, XXV, charge exchange recomb. in Princeton large torus during beam heating 0-100067
- Fe²⁺ and Fe³⁺ hydrate clusters, aq. electron exchange reaction, ab initio RHF MO calc. of inner shell reorganisations, vibr. freq. 0-102564
- H, inverted, optical gain at Lyman- α spectral line 0-95880
- H species, on C foil, 800 keV amu⁻¹, electron loss and capture cross-sections 0-65066
- H⁻ form. by surface and vol. processes, neg. ion source appl., review 0-58375
- H+O⁺(Nⁿ⁺)(Cⁿ⁺)(Bⁿ⁺), charge transfer cross sections, oscillatory behaviour in low-energy collisions 0-63806
- H⁺+alkali metal, charge exchange, eikonal approx. calcs. 0-78703
- H⁺+Ar, charge exchange excitation, alignment tensor components, coincidence method 0-63795
- H⁺+Li, charge exchange, eikonal approx. calcs. 0-78703
- H⁺+Li⁺, charge transfer and ionisation, total cross sections for production of Li²⁺ determ. 0-91657
- H₂⁺ differential cross section rel. to charge exchange cross sections of fragments 0-78704
- H₂+C⁺(N⁺)(O⁺), reactant ion electronic states, effect on charge transfer cross sections 0-63809
- H₂⁺+Ar, low energy proton transfer reactions, crossed beam studies 0-108697
- HCN-CO complex, charge transfer theory, Mulliken population, ab initio calc., multiconfiguration scheme 0-106392
- H₃⁺(D₃⁺)+H₂(D₂) collisions, slow ion production, charge transfer cross sections 0-106378
- H₂O, H⁺(D⁺) exchange rates, ¹⁷O NMR linewidths, pH depend. 0-91661
- ³H(p,n)³He charge exchange reaction, multifold diff. scatt. theory (*Russian*) 0-78303
- He I 2³P-3¹D intercombination line, collision-induced, obs. by laser absorpt. spectroscopy 0-58194
- He species, on C foil, 800 keV amu⁻¹, electron loss and capture cross-sections 0-65066
- He-Hg nuclear pumped laser, charge exchange pumping 0-63996
- He+He⁺, double collision spectroscopy 0-58378
- He+OCS, emission spectra in He afterglow 0-87139
- He⁺+CS₂, dissoci. charge-transfer, CS⁺(B² Σ^+ -A² Π) emission prod., Morse pot. Franck-Condon factors calc., vibr. anal. 0-99539
- He⁺+H₂(D₂), dissociative charge transfer, 78-330K 0-61079
- He⁺+N₂, collisional excitation processes, visible emission, cross-sections 0-99571
- He⁺+O₂, charge transfer product state distrib., time of flight obs. 0-87223
- He⁺+OCS, dissoci. charge-transfer, CS⁺(B² Σ^+ -A² Π) emission prod., Morse pot. Franck-Condon factors calc., vibr. anal. 0-99539
- He⁺+SO₂, dissoci. charge transfer reaction, SO⁺(A¹ Π -X² Π) emission 0-95659
- He⁺+Xe, internal energy distrib. at 100 eV 0-99564
- He²⁺+Li collisions, soft X-ray emission obs. 0-83591
- (HeH)⁺, breakup in single dissociative collision, fragment charge states 0-74226
- ¹²⁹I₂, frozen soln. in o- or p-xylene, Mossbauer effect obs. 0-78637
- IBr-benzene in n-decane soln., IR line broadening by chemical exchange 0-87111
- K+K⁺ collisions, charge exchange cross section 0-58374
- K⁺+molecule, ²P_{3/2}(²P_{1/2}) doublet ground state reactions at 300K 0-108702
- Kr²⁺+H₂(N₂)(O₂)(CO)(CO₂)(methane), charge transfer reactions, rate coeffs. and product-ion distributions meas. 0-104431
- Li⁺-H₂O complex, charge transfer theory, Mulliken population, ab initio calc., multiconfiguration scheme 0-106392
- Mo(CO)₆, MCD spectra, charge transfer transitions 0-95658
- N⁺+H₂, electron capture and ion-loss cross-section, 2.4-24.3 keV 0-58373
- N⁺+O₂, branching ratio kinetic energy depend. 0-97703
- N⁺+O₂, electron capture and ion-loss cross-section, 2.4-24.3 keV 0-58373
- N₂⁺+He, ion loss cross-section, 2.4-24.3 keV 0-58373
- N₂⁺+O₂, electron capture and ion loss cross-section, 2.4-24.3 keV 0-58373
- Ne+C^{N+}(Nⁿ⁺)(Oⁿ⁺), charge exchange contribution to K-vacancy production 0-102553
- Ne+proton, charge transfer, target K-shell electron capture, impact parameter depend. 0-102552
- Ne²⁺+H₂(N₂)(O₂)(CO)(CO₂)(methane), charge transfer reactions, rate coeffs. and product-ion distributions meas. 0-104431
- O ions, non-equilibrium charge state distrib. charge exchange cross-sections in solid targets 0-65109
- O⁺+O₂→O₂⁺+O, cross section kinetic energy depend., rate consts. meas. and Monte Carlo calcs. 0-78701
- O⁺+N₂, charge exchange collision, rate coeff. and ionosphere implications 0-87224
- O⁺+N₂(O₂), excited ion reactions, charge transfer coeffs. at thermal energy 0-95721
- O⁺+O₂, charge exchange collision, rate coeff. and ionosphere implications 0-87224
- O₂⁺+inert gas, electron transfer meas., 60-200 keV 0-83480
- O⁺(²D)+N₂, charge exchange, rate coeff. temp. depend. 0-77179
- O⁺+O₂(N₂), metastable ion reactions, rate consts. and ion mobility at 300K 0-95722
- ²¹⁰Po, nucl. alpha decay, electron inner shell vacancy creation, semi-quantal approach 0-68607
- S⁺ charge transfer in diffuse nebulae 0-77463
- Ta surface, nonstationary heating and oxidation in low temp. plasma flow, heat and charge transfer obs. (*Russian*) 0-104341
- Ti XX 0-100067
- UO₆⁶⁻, octahedral uranate group, charge transfer transition and luminesc. 0-97324
- W(CO)₆, MCD spectra, charge transfer transitions 0-95658

charge exchange continued

- Xe⁺+molecules, ²P_{3/2}(²P_{1/2}) doublet ground state reactions at 300K 0-108702
- Xe⁺+Xe⁺, charge transfer and ionisation Xe²⁺ prod. 0-91659
- ZnTe electrode, redox reaction due to complex M(CN)₆^{3-/4-} (*French*) 0-89482
- charge measurement**
see also *electrometers*
electrolyte timing cell and coulometer 0-68216
electrostatic charges meas. and localisation, neutralised during lightning flashes 0-77097
electrostatic precipitation, charge measurement, positive and negative corona 0-96403
rotating sector type instrument, edge effect (*Japanese*) 0-86269
Hg-polymer interface, contact potential and charge exchange determ. 0-75642
- charge-ordered states**
CsAu, molten, equimolar, structural evidence of ionic nature 0-64882
Fe₂O₄, Verwey transition, charge density-phonon condensation 0-65217
Fe₂O₄, Verwey transition, cond. processes 0-96787
- charge storage diodes**
No entries
- charge transfer** see *charge exchange*
- charge transfer states**
acceptor-donor-acceptor complex, Frenkel excitons and ionic excited states 0-92824
acceptors, randomly distributed, direct energy transfer via exchange from excited donor 0-65483
anthracene-tetracyanobenzene charge transfer complex, cryst. struct., temp. effects 0-96508
anthracene-phenanthrene-TCNB, exciton transport obs. 0-65461
anthracene-phenanthrene-tetracyanobenzene, CT-cryst., mini-excitons and lattice dynamics, ESR, optical and Raman spectra 0-60406
anthracene-pyrometallic dianhydride cryst., refl. and absorpt. spectra of singlet charge transfer excitons 0-71442
benzyl radicals, monomethyl- and dimethyl-substituted, electronic spectra and electron affinity 0-63618
binary compounds, energy gap trends, correl. with electron transfer parameters from optical spectroscopy 0-80174
6-cyanobenzquinoclidine, intramol. electron-transfer excited state 0-58295
DNA, Hg (II) and Ag (I) complexes in soln., theoret. interpret. of elec. dichroism obs. 0-85347
exciton transport, low-dimensional in mixed charge transfer crystals, statistical model and expts. 0-65461
haematoporphyrin, complexed with chloranil and tryptophane, energy spectra, transition moments and intermolecular distances 0-72127
hydronaphthal radicals embedded in naphthalene cryst., optical transition energies and ionisation energies 0-78595
insulators, charge transfer processes influence on cryst. field 0-92865
lanthanide-porphyrin complexes, upper $\pi\pi^*$ electronic states, fluoresc. 0-83410
phenothiazine derivatives, semicond. elec. props., optical spectra, and EPR 0-103693
rare gas adsorbates on simple metals, optical excitation, configurational switching, charge transfer 0-107643
(TCNQ)₂, dimeric interactions, MO calcs., applicability to crystal struct. 0-75215
p-tricyanovinylphenyldicyanomethide ion, donor props., cyclic voltammetry and π -complex form. 0-88520
(TTF)₂, dimeric interactions, MO calcs., applicability to crystal struct. 0-75215
TTF-TCNQ, dimeric interactions, MO calcs., applicability to crystal struct. 0-75215
TTF-TCNQ complex, trans-diethyl-dimethyl TTF-TCNQ, one-dimens. cond. 0-96853
 α -Al₂O₃.V³⁺(V⁴⁺)(Co³⁺)(Co²⁺), optically and thermally stimulated reactions, absorpt. spectra 0-80825
Ba_{1-x}Sm_x, electron config. of Sm ions, X-ray L-absorpt. spectroscopy 0-60715
Ca_{1-x}Sm_x, electron config. of Sm ions, X-ray L-absorpt. spectroscopy 0-60715
Cu complex, bis(triphenylphosphine) phenanthroline copper (I), luminesc. spectra, decay times 0-60648
Eu_{1-x}Sm_x, electron config. of Sm ions, X-ray L-absorpt. spectroscopy 0-60715
La₂O₃:Eu, high press. effect on luminesc. efficiency and lifetime, charge transfer absorpt. 0-66266
Ni (111) and (110), laser-induced charge transfer to adsorbed CO, photoemission expts. 0-59798
Ru complexes, [Ru(bipy)₃(pq)_{3-n}]²⁺ mixed-ligand, electronic absorpt. and emission spectra meas. 0-71441
S₂N₂, gas phase and solid state core level XPS 0-66401
S₂N₄, solid state core level XPS 0-66401
(SbBr_{0.04})_x and (SbBr_{0.32})_x, solid state core level XPS 0-66401
(SbI₃)_x crystals, reson. Raman scatt. meas. 0-66203
SiO₂-Al₂O₃-CaO-Na₂O-Fe³⁺, optical absorpt. due to Fe³⁺ ligand field and charge transfer 0-89020
Sr_{1-x}Sm_x, electron config. of Sm ions, X-ray L-absorpt. spectroscopy 0-60715
TiO₂-Ni, electronic props., struct., comp., chemical bonding 0-84499
Yb_{1-x}Sm_x, electron config. of Sm ions, X-ray L-absorpt. spectroscopy 0-60715
- charge transfer transitions** see *charge transfer states*
- charged dislocations** see *dislocation dipoles*
- charm particles**
see also *D mesons; psi mesons*
baryon decays, noneptonic, parity-violating, single-quark and two-quark transitions 0-68453
baryon decays, weak hadronic, SU(3) dynamical scheme 0-68454
baryon mass and F/D ratio, colour magnetic interaction 0-62957
baryons, mass spectrum from SU₃ dynamical group theory 0-62956
baryons, weak decays, quark model framework 0-62976
charm photoprod. with linearly pol. photons, QCD calcs., gluons 0-68464
charmonium, hyperfine interaction, nonperturbative treatment 0-62944
charmonium decay, effective strong coupling constant for timelike Q² 0-99091
charmonium electromagnetic decay, relativistic eval. 0-68459

charm particles continued

charmonium resonances above open charm threshold, nonrelativistic quark model 0-78039
dilepton charge production cross section for ν and $\bar{\nu}$, parton model 0-62966
elementary particle theories, properties (*Spanish*) 0-73681
flavour changing weak radiative decays, short and long distance effects 0-73712
hadron-hadron inclusive interactions, charmed particle production, η_c , ψ and other $c\bar{c}$ bound states 0-63036
hadronic props., superconvergence sum rules 0-78043
hadrons, charmed, SU(4) mass-breaking, mass sum rules 0-62959
heavy baryon spectroscopy in the QCD bag model 0-105866
hierarchical fermion masses from grand unification 0-105832
lifetime measurement 0-73693
 $M_b - M_{\psi(c)}$ and $M_T - M_{\eta(b)}$ lower bounds, concave and convex pots. 0-91057
meson decays, soft hadron interaction effects on nonleptonic weak decays 0-86705
meson radiative decay, quark loop model, SU(3) splitting of quark masses 0-62990
mesons, production in e^+e^- annihilation 0-91106
mesons, semileptonic decays, charged weak current struct. 0-102042
MIT bag model, charmed and b-flavoured hadron mag. moments 0-95271
perturbative QCD, renormalisation improvement, charmonium decay and scaling violations 0-101993
production of charm-pairs in νN , $\mu^- N$ and pN 0-73748
QCD, lifetime of QQ states, pseudoscalar charmonium and upilon states 0-68429
 $B^0 \rightarrow D^+ X(F^+ X)$, W-exchange dominance, decay rates 0-86706
 $c\bar{c}$, fine-hyperfine splittings and Lorentz structure of confining potential with vacuum polarisation corrections 0-78041
 $c\bar{c}$ qq states, decay, hadronic and photo-prod., e^+e^- annihilation prod. 0-99092
 $c\bar{c}$ spectrum, equaltime relativistic wave eqn. with confining potential 0-7977
 $c\bar{c}g(c\bar{c}q)$, exotic mesons, masses, decay widths, mixing matrix elements 0-62943
 $\chi \rightarrow \psi\gamma$, charmonium E1 radiative transitions and quark mag. moments 0-86721
DD molecular charmonium from dual diagram and Schrodinger eqn. 0-86660
 $e^+e^- \rightarrow FF(B\bar{B})$, $\tau\nu$ decay signature for F^\pm and B^\pm detection 0-91099
 η_c , candidate evidence from SPEAR, crystal ball detector, recent results 0-74046
 η_c , mass and other props, review from theoretical models 0-102025
 η_c associated with gluon, hadronic prod. 0-105846
F, nonleptonic decay rates and branching ratios, lifetimes 0-102047
F parity violating nonleptonic decays, vector meson dominance model 0-78058
F-meson decay, hadronic, role of free-quark pairs 0-78059
 F^+ nonleptonic decay, quark annihilation hypothesis test 0-102044
 $F^+ \rightarrow p\pi$, decay mode meas. for PCAC test 0-91018
 $F^+ \rightarrow \pi^+\nu$, gluon enhancements in charmed-meson decays 0-95265
 F^{**} weak decay constant from bag model extension 0-62967
 F^{**} , charmed tensor meson, strong and EM decay modes 0-68451
 Λ_c , charmed baryon mass in SU(1,4) dynamical group theory 0-62882
 Λ_c , structure of hadrons containing heavy quark, MIT bag model 0-86672
 ν , charmonium and strangeonium, linear+Coulomb pot. study, high α_s regime 0-62935
 $\nu D \rightarrow \Lambda_c^+ X$, high energy charmed baryon prod. obs. 0-105881
 νN , charmed particle prod. due to neutral weak currents (*Russian*) 0-68447
 νN , F^+ (2030) prod. and hadronic decay $F^+ \rightarrow \pi^+\pi^+\pi^-\pi^0$, mass 0-91085
 $\nu p \rightarrow \mu^- p K^+\pi^+\pi^0$, Σ_c^+ prod. and decay 0-86710
p, intrinsic charm from non-negligible udc \bar{c} Fock component 0-86691
pN-charm particles, obs. in high resolution streamer chamber 0-73742
pp, ISR energies, p fragmentation, D^+ prod. from Λ_c^* and Λ_b decay 0-102080
pp resonant annihilation, η_c charmonium state prod. cross section 0-82991
 $\pi^- p$, 340 GeV, associated charm prod. evidence, D^+ prod. 0-86767
 $\pi^- p$, 70 GeV/c, direct electron prod. from charm particle pair decay, e/π ratio 0-105928
 ψ (4.03), isospin and G-parity, model independent prediction 0-86689
 $\psi \rightarrow \chi\gamma$, charmonium E1 radiative transitions and quark mag. moments 0-86721
 Σ_c , charmed baryon mass in SU(1,4) dynamical group theory 0-62882
 Σ_c , structure of hadrons containing heavy quark, MIT bag model 0-86672
 Σ_c^+ , mass and mean life from high energy cosmic ray data (*Chinese*) 0-102045
 Σ_c^+ , production and decay obs. 0-105894
T and charmonium spectra, common pot. fit, $T^{**}-T$ mass difference 0-86712

charring see combustion

Chebyshev approximation

celestial mechanics, planetary orbits computation using Chebyshev polynomials (*French*) 0-61997
minor planet orbit determ. using Chebyshev's approx. (*French*) 0-94720
planets rectangular coordinates, approximation via Chebyshev polynomials (*Russian*) 0-62033
rare earth elements, atomic partition functions, Chebyshev approximations 0-67544
satellite navigation, Chebyshev approximations for compression of Ephemerides 0-61993
ternary system compound formation, comp. and props. w.r.t. component electron struct., computer prediction 0-103444

chelates see coordination complexes

chemical analysis

see also chemical analysis by nuclear reactions and scattering; chromatography; electrochemical analysis; electron probe analysis; ion microanalysis; mass spectroscopic chemical analysis; polarimetry; pollution detection and control; radioactive chemical analysis; spectrochemical analysis; thermal analysis; X-ray chemical analysis
adhesion, surface chemistry studies, anal. appls. 0-88440
ambient air analysis, area survey and sampling mobile laboratory 0-104528

chemical analysis continued

amino acid analyser, LKB 400 automatic ninhydrin, new sampler loader 0-101916
asbestos fibres concentration meas., in air and liquid, analytical methods review 0-72120
atmospheric pollutants, gaseous, analytical control, review 0-101140
cellular mechanical and chemical analysis, recommendations of workshop on future of biomedical instrum. 0-81776
coal analysis, Cl_2 content determ. using British Standard high temp. method 0-85252
coal gasification reactor atmospheres, industrial gaseous environment characterisation, Brinkley method 0-93817
combustion system atmospheres, industrial gaseous environment characterisation, Brinkley method 0-93817
compound conductors, impulse heating, Cu vapour conc. determ. 0-75346
crystalline solids, electronic industry, chem. anal. instrumental methods progress 0-66903
cyclobutanone, absorpt. of pulsed IR radiation and decomp., joulemeter and opto-acoustic obs. 0-58328
determination of minor impurities and alloying constituents in steel, appl. of inductively coupled plasma spectrometry 0-90903
EELS, filtered images 0-101062
EELS, in STEM, multi-channel averaging 0-101061
EELS, microanalysis, quantitative approach to inner shell losses 0-101059
EELS, standard for TEM, implanted Si 0-99017
electric insulating oils, composition, physical and chemical props. and determ. of free radicals (*Rumanian*) 0-97745
electron energy loss spectroscopy for direct elemental analysis 0-71998
electronic gas detection, Pellistor, VQ and TGS sensors (*Spanish*) 0-93832
ELISA and immunofluorescence, comparison 0-97749
environmental chemistry, anal. techniques, conf., Barcelona, Spain, (Nov. 1978) 0-88038
environmental radioactive pollution by U industry, monitoring using analytical chemistry 0-95488
ethylene furnace atmospheres, industrial gaseous environment characterisation, Brinkley method 0-93817
Fisher moisture content determ., using titrimetric analyser with ammeter pick-up (*Russian*) 0-71984
fission reactor safety, role of analytical chemistry in accident control, assessment and recovery 0-95389
fossil fuels, appl. of cross-polarisation ^{13}C NMR with magic angle spinning 0-77819
gas analyser, based on thermocouple vacuum gauge 0-61183
gas analyser with acoustooptic detector and semiconducting generator based on Gunn diode (*Russian*) 0-101141
gas mixtures preparation, $(1 \text{ to } 10^{-3})\%$ molar range, installation for testing and calibration 0-99030
gas purity under measuring conditions, W-value determ. (*German*) 0-104489
geometrical and chemical knowledge at high resolution, electron microscopy and inner shell excitations 0-79646
graphite-AsF $_5$ intercalated species, fractional ionisation and identification 0-97397
high pressure pressure-jump apparatus for fast reactions in solution 0-62681
high-volume preparation of air to standard quality for zeroing analyzers 0-90829
III-V semiconductor, and related cpds., low energy ion scattering spectrometry (*French*) 0-71551
industrial gaseous environment characterisation, Brinkley method 0-93817
iodobenzene, soln., non-linear dielec. effect, comparison with fluoro, chloro and bromobenzene 0-60478
ion-selective membrane electrodes development, Ag ion conduction ceramic systems (*Japanese*) 0-61203
laser interferometry in analytical ultracentrifuges, background suppression of multiplexer-gated modulatable laser 0-73430
low-atomic-mass solids, high precision depth profiling of light isotopes 0-66902
mixtures, multicomponent, by method of additions 0-61187
natural and industrial objects, quality control, future programme, computer appls. 0-104484
NMR and EPR appls., conf., Denver, CO, USA (Aug. 1979) 0-90598
nuclear materials safeguards, LASL analytical chemistry program 0-78380
nuclear materials safeguards and materials control, meas. tech. conf. Charleston, SC, USA (November 1979) 0-77544
nuclear reactor atmosphere, helium cooled, industrial gaseous environment characterisation, Brinkley method 0-93817
oil immersed transformers, dissolved gas causes and phenomena, anal. (*German*) 0-76570
optical fibres, ultraclean impurities determ., and behaviour during production by CVD process (*Japanese*) 0-87505
physical adsorption, vacuum microbalance studies 0-76551
plating line Co concentration monitoring, by automatic colorimeter 0-105691
polarizing microscope components and applications 0-98973
polycyclic aromatic hydrocarbons sorbed on fly ash, recovery for quantitative determ. 0-61177
polymer systems, sedimentation field-flow fractionation in macromolecular characterization 0-66879
polymers, appl. of cross-polarisation ^{13}C NMR with magic angle spinning 0-77819
power transformers, electromagnetic testing of partial discharges for failure and breakdown prevention (*Russian*) 0-97743
sea and beach persistent oil spill identification methods 0-90101
secondary ion yield, linear variation, quantitative anal. of mineral silicates (*French*) 0-108763
SEM microanalysis techniques, review 0-71995
semiconductor impurities, trace element anal. 0-81399
solid surface, microgravimetric-IR study 0-76577
solid-solid interface chemistry, characterisation, theory 0-75448
standard sample homogeneity evaluation, optimal obs. planning 0-93721
steam reformer atmospheres, industrial gaseous environment characterisation, Brinkley method 0-93817
steel, industrial, surface, chem. characterisation by SIMS, glow discharge spectrometry and other techniques 0-66907
steel powder, high speed, S and O reduction in a H_2 gas stream 0-61015

chemical analysis continued

- steels, nuclear reactor pressure vessel steels, optimum chem. comp. rel. to props. 0-93517
 surface analysis techniques and appls., symposium, Dayton, USA (Jun. 1979) 0-62363
 surface analysis techniques appl., electrification phenomena 0-80354
 surface potential changes meas. upon adsorption of gases using static capacitor method 0-62691
 techniques for archaeological artefacts 0-89575
 TEM, quantitative elemental analysis 0-101060
 thin films, chem. anal. by energy loss spectroscopy 0-104493
 thin films and interfaces, analytical techniques, review 0-80120
 tinplate surfaces, Auger depth profiling and anal. 0-59768
 trace element profile of a California Redwood tree for environmental monitoring 0-97850
 transformer testing, preventive, by analysis of gases dissolved in transformer oil (*German*) 0-71969
 transition metal ferrocyanide selective sorbents for alkali metals, sorptive props. w.r.t. struct. 0-101051
 AgGaS₂-AgGaSe₂ system, phase diagram, lattice consts., and IR spectra 0-60841
 Al sheet surfaces, chem. characterisation by SIMS, glow discharge spectrometry and other techniques 0-66907
 Al-Al₃Ni eutectic, Al₃Ni distribution along temp. gradient 0-84971
 Al-Mg (2.5wt.%) sheet, surface oxide state and weldability 0-59769
 BN, in steel, extraction, identification by IR anal. 0-85254
 CO₂, new impurity analysis method 0-66908
 CaO-SiO₂ glass, trimethylsilylation method for silicate ion anal. (*Japanese*) 0-71975
 CsSn₂I₃, surface props., Auger study, elec. cond. meas., photochem. study 0-66339
 Cu slip ring, Auger spectrosc. obs. of elemental surface composition as function of temp. 0-66901
 Cu(I) complex, oxidation, fast reactions meas. by pulsed-flow instrument 0-66890
 β -FeOOH, Mossbauer spectra obs., chemical and thermal anal., X-ray diffr., saturation magnetisation 0-88896
 Fe, cast, white, high Cr, phase composition, B effect 0-104172
 Fe determinations, effect of surface changes in Pt crucibles 0-61192
 Fe ore, reduction degree, chemical anal. calcs. (*Russian*) 0-66769
 Fe(OH), thin films, Mossbauer spectra obs., chemical and thermal anal., X-ray diffr., saturation magnetisation 0-88896
 Fe₂O(OH)₄, Mossbauer spectra obs., chemical and thermal anal., X-ray diffr., saturation magnetisation 0-88896
 InSe thin film, sputter growth and chem. anal. by XPS/ESCA 0-80976
 KCl crystal, Sr and Na impurities radial distrib., influence of form of crystn. front 0-107312
 Li, surface characterization of film growth 0-81240
 LiI UV photodissoc. cross section, reson. ionis. Li detection 0-63719
 NO measurement, photometric process analyser 0-57360
 NbN single crystal preparation, zone melting and nitriding techniques 0-60776
 Ni-Cd sealed battery electrode performance meas. 0-66962
 organohalogen analyser system, drinking water total organic halogen anal. 0-93830
 Pb salts, inorganic 0-77081
 PbO-SiO₂ glass, trimethylsilylation method for silicate ion anal. (*Japanese*) 0-71975
 Pu safeguarding, automated ion-exchange system for rapid Pu separation from impurities 0-78383
 Si, EFG ribbon, characterisation by ion beam tech. 0-79833
 Si, multigrained, grain boundary elec. and compositional props., surface anal. 0-76575

chemical analysis by mass spectrometry *see mass spectroscopic chemical analysis*

chemical analysis by nuclear reactions and scattering

- see also chemical effects of nuclear reactions and scattering; neutron activation analysis*
 activation analysis, (α,n), (α,p) reacts. on B, C, N, Mg, Al, P 0-61206
 activation analysis, new irradiat. head design, electronic control system 0-66896
 air pollution monitoring, PIXE and NRA studies using lichen indicator 0-61744
 borosilicate optical waveguide glass, B content determ. using nuclear track counting 0-95969
 brass, α - and β -phase, oxidation, prompt. nucl. reactions and reson. alpha scatt. study 0-66690
 charged particle activation anal., determ. of Pb distrib. in human teeth 0-101303
 coal calorific value determ., by neutron inelastic scattering (*Czech*) 0-101048
 gamma counting, pulse pileup, random summing losses 0-58023
 gamma spectrometry, Ge(Li) and HPGe detectors, coincident sum peaks 0-63447
 glass, float, low-Fe, weathered, surface, characterisation 0-93666
 in situ capture gamma analysis of large mineral samples 0-61215
 metals, airborne, in industrial districts, conc. rels., nuclear anal. technique 0-72107
 metals, analysis of H ratios and profiling using nucl. techniques and Rutherford backscatt. 0-61202
 meteoritic and lunar samples 0-62089
 neutron capture γ -spectroscopy, medical appl., Cd and N meas. in living human subjects 0-67241
 phosphosilicate glasses, P content determ. by Rutherford backscatt., PIXE, and activation anal. (*Hungarian*) 0-85233
 semiconductor materials, channelling-blocking measurements, (n,α) method for B-depth profiling 0-70276
 serum, human, trace elements determ. by proton activation 0-81731
 stable isotope tracer analysis by proton scattering 0-104487
 steel, N determ. by track autoradiography 0-100979
 water pollution, arsenic in freshwater fish traced to fly ash leachate using neutron activation analysis 0-97827
 zircaloy, nuclear microprobe methods for investigating oxidative corrosion 0-71787
 (n,p) and (n,α) reactions, and backscatt., appl. to fusion reactor materials, archeometry and nuclear spectroscopy 0-61200
 Al-Nb superimposed metallic layers, ionic movements during anodization, Rutherford backscatt. and nuclear microanal. 0-71913
 Al₂O₃ anodic films, H conc. profiles meas. 0-75261

chemical analysis by nuclear reactions and scattering continued

- ¹¹B(p,n)¹¹C, steel B depth distrib. meas. using time of flight method 0-71986
 CdSe film polycryst., thermal diffusion of Cr, 240-400°C 0-80001
 Cr-Ni-Nb steel, oxidation in CO₂, charged-particle nuclear techniques 0-61022
 Cs, trace identification in neutral-beam research 0-95401
 Fe-Cr (9 wt.%), oxidation studied using C¹⁸O₂ and D₂O tracers 0-71784
 Fe-Ni-Cr (44, 17 wt.%), nuclear microprobe methods for investigating oxidative corrosion 0-71787
 Ge, single cryst., ¹⁸F penetration, charged particle activation anal. 0-93828
¹²⁹I in bovine thyroid glands, activation anal. obs. 0-94380
 Li, quantitative location in brain tissue using nuclear Track Etch techniques 0-98133
 MgO, atomic C anal. by ¹²C(d,p)¹³C method 0-108766
 Mo, activation anal., charged particle prod. cross sections by 14 MeV neutrons 0-93829
 Mo, D and ³He trapping and mutual replacement 0-59493
 N determination by track autoradiography 0-100979
 Na, trace identification in neutral-beam research 0-95401
 Nb, activation anal., charged particle prod. cross sections by 14 MeV neutrons 0-93829
 Nb-Al superimposed metallic layers, ionic movements during anodization, Rutherford backscatt. and nuclear microanal. 0-71913
 Nb-Ta superimposed metallic layers, ionic movements during anodization, Rutherford backscatt. and nuclear microanal. 0-71913
²²⁹Pu, alpha spectrometric determ. 0-81404
 Si, impurities of O, N, C, trace anal. by proton activation (*Chinese*) 0-81403
 Si ribbon, EFG, C contaminant conc. determ. by nuclear techniques and SIMS 0-59506
 Si:Al epitaxial layers, nuclear microanalysis of Al impurities ²⁷Al(d, α)²⁵Mg 0-61193
 Si₃B₄ films, anal. of H ratios and profiling using nucl. techniques and Rutherford backscatt. 0-61202
 Si₃C₂H₂ amorphous film, H content determ. by nuclear reaction analysis 0-59821
 SiH₄ amorphous film, H content determ. by nuclear reaction analysis 0-59821
 Si₃N₄ films on Si wafers, O determ. by ³He activation anal. 0-71981
 Si₃O₄ films, anal. of H ratios and profiling using nucl. techniques and Rutherford backscatt. 0-61202
 Ta-Nb superimposed-metallic layers, ionic movements during anodization, Rutherford backscatt. and nuclear microanal. 0-71913
 Ti:Pd, ion implanted, corrosion behaviour and Rutherford backscatt. anal. 0-71792
 U prospecting using microdistrib. anal. of Siwalik vertebrate fossils by nuclear Track Etch tech. 0-98489
 Zr, ion-implanted polycryst., thermal oxidation 0-71786
- chemical association** *see association*
chemical batteries *see cells (electric)*
chemical bonding *see bonds (chemical)*
chemical bonds *see bonds (chemical)*
chemical composition *see chemical analysis*
chemical diffusion *see diffusion*
chemical effects of nuclear reactions and scattering
see also chemical analysis by nuclear reactions and scattering; radiation chemistry
 No entries
- chemical effects of radiation** *see radiation chemistry*
chemical elements *see elements (chemical)*
chemical engineering *see chemical technology*
chemical engineering computing
see also computerised control; computerised instrumentation
 bipolar cell stacks, leakage currents 0-76526
 pharmaceutical dissolution testing, microprocessor controlled sampling system 0-86273
 turbulent friction factor, calc. by TI-57, binary-search method 0-83788
- chemical equilibrium**
see also chemical reactions; reaction kinetics
 Belousov-Zhabotinsky reaction, chem. turbulence, strange attractor representation 0-85148
 biomolecules+chloranil, charge transfer interaction, equilb. const., enthalpy and entropy determ., mol. polarisability 0-89708
 Coordination equilibria in non-aqueous solvents. I 0-66860
 divalent transition metal halides, Coordination equilibria in non-aqueous solvents. I 0-66860
 Field-Koros-Noyes chemical wave equation, asymptotic solutions 0-66857
 fluctuation on dissipative structs., external constraints 0-71894
 glasses, dielectric relax., order parameter model appl. 0-108151
 isotropic solid soln. cryst. surfaces, surface stress and chem. equilb. 0-107628
 lanthanide complex, struct. and equilb. by time resolved Eu(III) spectrosc. 0-78736
 lanthanide ion bound to macromol., struct. and equilb. by time resolved Eu(III) spectrosc. 0-78736
 liquids, dielectric relax., order parameter model appl. 0-108151
 maser equation near nonequilibrium transition, stationary solns. 0-89466
 methylene glycol(-d₄)=formaldehyde(-d₂)+H₂O(D₂O) Raman spectra and normal vibr. 0-58271
 micelle formation model, relaxation spectra 0-71934
 multivariate master equation for reaction-diffusion system 0-95045
 oscillators responding frequency switch 0-108837
 oscillatory chemical reaction systems, weak coupling 0-66775
 phase transitions, nonequilibrium transient behaviour 0-93732
 potentiometric titration apparatus, microprocessor controlled, for equilb. studies 0-89579
 primitive solar nebula, equilb. chemistry thermodynamics calcs. 0-82231
 rare earth (III) complexes, cysteinates, thermodynamics of form. 0-89515
 Schlogl model, transition time statistics 0-89467
 thymopoeitin active fragment in H₂O, soln. conformation by DNMR spectroscopy 0-89710
 unsaturated two-component associated vapour, press., comp., thermodynamic calcs. (*Russian*) 0-64671
 Ar+Br₂ collisions, dissociation reaction, trajectory study by ensemble method 0-66765
 Ar+N₂(O₂, CO), molecular fluid mixtures, equilibrium props. 0-64867

chemical equilibrium continued

- Ar+Xe⁺, XeAr⁺ form., dissoc. energy, reaction equil. and rate consts. 0-61071
 B₂H₆, equil. with solid soln. of B in Si 0-97721
 Br₂ in Ar, solvent effects on equilibrium props. 0-61128
 BrF(CI), rot. spectra in millimeter wave region, rot. transitions obs., equil. const. determ. 0-78607
 ClF, rot. spectra in millimeter wave region, rot. transitions obs., equil. const. determ. 0-78607
 Fe³⁺ solutions, UV absorption spectrosc. obs. of equil. 0-93812
 HF molecules, infinite linear chain, equilibrium structure and stabilisation energy 0-63856
 ICl(Br), rot. spectra in millimeter wave region, rot. transitions obs., equil. const. determ. 0-78607
 N₂+H₂+N₂H₄, mixtures with nonthermal vibr. excitation of mol. N₂ 0-76545
 N₂+O₂, molecular fluid mixtures, equilibrium props. 0-64867
 N₂+O₂+NO, mixtures with nonthermal vibr. excitation of mol. N₂, formula for calc. equil. const. 0-76545
 Na₂O-CaO-SiO₂-Cr₂O₃ glass, redox equilibria of Cr ions, impurity effects 0-89477
¹⁷O+¹⁶O, fractionation by chemical equil. 0-89513
¹⁸O+¹⁶O, fractionation by chemical equil. 0-89513
 PbTe homogeneity region investig. in Pb-Te system, equil. consts. of quasi-chem. reactions 0-108405
 SeCl₄-SbCl₃ systems, Raman spectra (*German*) 0-93324
 Si, solid soln. of B, equil. with B₂H₆ 0-97721
 Si₃N₄, low pressure CVD, thermochemical calcs. 0-108356
 SiO₂, low pressure CVD, thermochemical calcs. 0-108356
 SiO₂-MgO-CaO-Al₂O₃-Ce₂Fe, redox equil., expt. 0-85171
 SnSe₂, sublimation, temp. depend. of equil. constants 0-88312

chemical exchanges

- see also ion exchange; isotope exchanges*
 atom+diatom, collinear quantum mech. reactive scatt., hyperspherical coords. 0-108694
 bimolecular exchange reactions, dynamical-statistical method calcs. 0-104435
 boronising, powder, physicochem. characts. 0-61024
 fast nucleus+molecule, atom capture, quantum calcs. 0-71911
 light atom exchange reactions quantum dynamics 0-101011
 Mars, Viking gas exchange reaction simulation on UV irradiated MnO₂ substrate 0-72831
 minimum energy reaction paths, virial theory implications 0-97686
 steel melt, interaction with Al₂O₃-Zr ceramic 0-104305
 sudden rotational approximation, reactive and inelastic, body-fixed frame, light-heavy-light systems 0-61073
 Al₂O₃-Zr ceramic, elec. props., additives effect, and interaction with steel melt 0-104305
 BaF₂ crystal, selective etching and dissolution kinetics 0-71775
 D+HX(H=Cl,I), HX dissociative ionisation, H⁺ signal origin, mol. beam obs. 0-66778
 H+CN(NSi), bimolecular exchange reactions, dynamical-statistical method calcs. 0-104435
 H+H₂, collinear quantum mech. reactive scatt., hyperspherical coords. 0-108694
 H+H₂(v₁=1), exchange reaction, integral and differential cross sections determ. 0-85153
 H⁺+methane→H₃⁺+methyl radical, quantum 0-71911
 HD(v=5)+HD(v=0)→H₂+D₂, mol. H₂ exchange, reaction mechanism 0-85167
 IBr-benzene in n-decane soln., IR line broadening by chemical exchange 0-87111

chemical industry

- electrochemical processes, energy use analysis (*Dutch*) 0-72019
 electrochemical processes, energy use optimisation (*Dutch*) 0-72020
 lasers for industrial chemistry 0-87427
 reaction kinetics measurement and control using laser technology, free electron laser appl. 0-81349

chemical kinetics *see reaction kinetics***chemical lasers**

- atomic and molecular lasers appl. to collision physics 0-63596
 chemically reacting flow heterogeneous mixing, energy level population inversion 0-78848
 DF, pulsed, beam attenuation for spatial profiling of small focal spots 0-99780
 HF laser, CW, with unstable telescopic resonator, radiation field structure 0-91786
 low pressure, line-shape flattening resulting from hypersonic nozzle wedge flow 0-91783
 metal-atom resonance-line lasers using UV photodissoc. of alkali and group IIIA metal halides 0-58529
 molecular laser, optical excitation by photodissoc. wave propag. in dense gas 0-74352
 photodissociation, switched, for inversion of atomic and molecular species 0-74206
 power-per-line analyser for real-time display of laser spectra on oscilloscope 0-58552
 review of lasers oscillating on rot., vibr. and electronic transitions 0-102716
 CO, output spectra from CS₂-O₂-CO₂(N₂O) flame lasers 0-83601
 CO₂ 00¹-10⁰ transition in CO-N₂O reacting gas mixture, gain 0-74337
 ClF-H₂ chem. laser, HCl vibr. emission 0-97709
 DF chemical laser, small-scale CW, operation 0-58528
 DF chemical lasers, high-performance dichroic beam splitters 0-95932
 DF laser, phase conjugation of 4 μm for single line and multiline radiation in Ge 0-83641
 DF TEA laser, He-free, with MW output 0-64060
 DF-CO₂ chemical laser, photon branching in chain reactions, IR radiation initiation 0-91785
 DF-CO₂ chemical laser, amplification of long and short pulses 0-95883
 DF-HBr CW optical resonance transfer laser 0-64003
 F+H₂(D₂)ZZ 0-81303
 GeF, use in chemical lasers 0-64004
 H₂/F₂ laser, initiation using surface spark discharge UV light source 0-78923
 HF, CW, longit. and transverse mode competition in stable, unstable resonators 0-95917
 HF CW chemical laser, spatial homogeneity of radiation improvement using telescopic resonator 0-106549
 HF chemical laser initiation by relativistic electron beam 0-64005

chemical lasers continued

- HF chemical TE laser, 16 μm emission 0-83600
 HF in absorption, anomalous dispersion meas. 0-95881
 HF laser with resistive Ge electrodes, for optical studies of semiconductors 0-64061
 HF premixed chain reaction CW laser, spectral output 0-95882
 HF, pulsed, H₁/SF₆ system 0-106514
 HF, pulsed, H₁/SF₆ system 0-106515
 HF pulsed laser, appl. of CW X-ray preioniser 0-64037
 HF pulsed laser, Xe flashlamp efficiency for photoinitiation 0-69403
 HF, pulsed laser numerical modelling, rot. relax. 0-87388
 HF TEA laser, He-free, with MW output 0-64060
 HF, with flow-through chem. active medium, pulsed-periodic regime realisation 0-106513
 HF/UF₆-H₂ nuclear pumped laser, characts. 0-78847
 HF-DF simultaneous laser excited by ferroelec. ceramic capacitatively coupled discharge 0-69413
 HgCl₂(Br₂), low lying excited state electronic struct. and photodissoc., appl. to lasers 0-63560
 I, direct solar-pumped 0-74353
 I laser radiation, 2nd, 3rd and 4th harmonic generation 0-91844
 I, methyl iodide photodissoc. laser, kinetic model, cross-section calcs. 0-58530
 I, organic compounds usable as solvents in saturable absorber, nonlinear refr. index meas. 0-102758
 I, photodissociated by nucl. induced excimer fluoresc. 0-78846
 I photodissociation laser, characts. of new dye comps. for passive switches 0-91826
 O₂-I₂ chemical laser, quenching of laser-excited O₂ by I₂ 0-99515
 Pb atomic photodissociation laser, 405.8, 368.3, 364.0 nm emission lines 0-87387
 SF₆+H₂ chemical laser, electron beam pumping 0-91784
 SiF, use in chemical lasers 0-64004
 SnF, use in chemical lasers 0-64004

chemical reactions

- see also association; atom-atom collisions; atom-ion collisions; atom-molecule reactions; atomic inelastic collisions; catalysis; charge exchange; chemical exchanges; chemically reactive flow; chemiluminescence; chemisorption; CIDEF; CIDNP; corrosion; dissociation; electrolysis; free radical reactions; heat of reaction; ion-molecule reactions; isomerisation; molecule-molecule reactions; oxidation; photochemistry; polymerisation; pyrolysis; radiolysis; reaction kinetics; reduction (chemical); solvation*
 absorption, atmospheric NO_x removal, using MARTZCLEAN reagents based on NaClO₂ and K₂CO₃ (*Japanese*) 0-61147
 acetic acid, vapour, chem. reaction effect on speed of sound 0-103100
 activated complexes, exp. obs., bonding MO LCAO states 0-76506
 atoms, general adiabatic-diabatic transformation matrix, electronic non-adiabatic transitions 0-93751
 atoms, laser excited, reactive collisions 0-66793
 Belousov-Zhabotinsky reaction, chem. turbulence, strange attractor representation 0-85148
 benzene/cyclohexane reversible chemical reaction systems for thermal energy transport 0-67009
 bipolar trickle reactors, electric current versus potential plots 0-76521
 bipolar trickle reactors, flow models for hydrodynamic characts. and reaction rate constants, 0-76522
 bipolar trickle reactors, study using electrochemical tracer method 0-76523
 bonds in reactions, form, and breaking, partitioning anal. of electron reorganisation 0-104419
 Brownian dynamics simulation in soln. 0-104422
 chelotropic reaction, intrinsic single and dual mol. orbital symmetry conservation 0-102419
 clay, Al₂O₃ and SiC recovery by C reduction 0-108704
 collinear asymmetric model reaction probabilities quantum and quasiclassical calcs. 0-85145
 coupled multistep chemical reactions, rate const. determ., relax. spectroscopy 0-66766
 decomposition driven convection of dissociating Navier Stokes fluid, instabilities 0-59128
 dihydroxyanthraquinone, light-induced proton transfer, photochem. hole-burning obs. 0-76535
 electrochemical reactor characterisation, marker pulse method improvements 0-76524
 electrochemical reactors with three-dimensional electrodes, characterisation using electrochemical tracer method 0-76520
 electrostatic interactions in liquid state, effect on frontier orbitals and chem. reactivity 0-84046
 endoergic reactions, reagent internal excitation effects on rates 0-93731
 endothermic solid reaction, unsteady heat conduction, thermal conductivity change 0-76511
 ethylene, rearrangement to ethylene, barriers, ab initio MO calcs. 0-104424
 fast reactions in soln. under high pressure, investigation using stopped-flow apparatus 0-86335
 Field-Koros-Noyes chemical wave equation, asymptotic solutions 0-66857
 fracture, chemically-assisted, atomic modelling at crack tips 0-106754
 gas phase chemical reactions in IR laser field, collision-induced absorpt. spectra 0-76499
 gas-phase reactions, anal. using computer interfaced time-of-flight mass spectrometer 0-71967
 glass reactions with aq. solns., influence of surface pot. on kinetics 0-108612
 heat engines, chemically driven, finite time thermodynamics 0-76541
 heterogeneous nonideal chemically reacting system, comp., thermodynamic props. calcs. 0-76492
 hexafluoroethane, chemical conversion and uniformity of etching SiO₂ in radial flow plasma reactor 0-76391
 hexafluoroethane, RF discharge chem., added acetylene effect, mechanistic model for fluorocarbon plasmas 0-84017
 high pressure boiler in-service scavenging by intermittent dosing with chelating agent 0-89485
 interstellar cloud gas phase chemistry for C, N and O compounds 0-105319
 interstellar clouds gas phase chemistry, nonequilibrium processes and temp. and activation energies effects 0-105298
 interstellar plasmas, ion chemistry 0-62254
 intramolecular interactions effect on transferability props. of localised description of chemical groups 0-102424

chemical reactions continued

- ion reactivity arising from different region of translational energy release distribution, need for ang. collimation 0-104483
 laser-chemical reaction kinetic mechanism (*Russian*) 0-101007
 liquid membranes, separation and reaction appls. 0-66871
 melt reacting with gas jet, heat and mass transfer, mathematical modeling 0-87819
 metal gas reactions in arc plasma spraying 0-66427
 micelle formation model, relaxation spectra 0-71934
 minimum energy reaction paths, reactive domains of energy hypersurfaces and stability 0-71893
 molten alloys, compound-forming, vol. of mixing, conc. depend. 0-103484
 naphthylamines, abnormal fluorimetric titration behaviour, kinetic anal., fluoresc. quantum yields and lifetime meas. 0-89560
 nonadiabatic cage reactions, relaxation hindrance 0-93740
 nonequilibrium reacting systems, critical bifurcations, scaling and Ginzburg criteria 0-81290
 nonlinear eqns. for reacting system with physical interactions 0-81288
 oscillatory chemical reaction systems, weak coupling 0-66775
 oxoniomethylene cation, rearrangement to hydroxymethyl cation, barriers, ab initio MO calcs. 0-104424
 petroleum spills on water, control using gellants 0-61496
 photochromic glass, thermochemical effects 0-87448
 prochiral, gravitational field effects 0-71899
 product initial rot. state distrib., pump and probe laser obs. 0-85158
 PVC, thermal stabilisation by triazine dithiols (*Japanese*) 0-108386
 pyrimidine, bi-exponential decay, methylation and vibr. excitation, proximity effects 0-78641
 quantum chemical methods appls. 0-93752
 quantum chemistry, conf., Kyoto, Japan, 29 Oct.-3 Nov. 1979 0-101659
 rare earth metal+H₂O vapour, hydride form. 0-76504
 reaction-diffusion systems, bifurcation theory, classification 0-108713
 reaction-diffusion systems, dissipative struct., sphere bifurcation numerical determ. 0-76483
 reactivity, reliability of quantum mechanical predictions, config. of reaction prod., H-bonded species 0-108691
 recombination probability, reactivity depend., scavenger effects 0-76494
 refractory metals and oxides, reactions of liq. alkali metals, relevance to reactor technology 0-85173
 reversible reactions, first order, time depend. behaviour 0-97699
 ruthenium tris-bipyridyl, excited state electron transfer quenching, H₂O photoreduction mediators effects 0-102536
 1,3-sigmatropic rearrangements, ab initio calcs., basis set and electron correl. effects 0-104428
 silicate glass, hydration thermodynamics 0-81313
 solar thermochemical electric power generation, reversible chemical reactions 0-61394
 solid phase chemical reactions, low temp. and fast, mol. motion effect 0-97681
 solid-state reaction, photoacoustic photocalorimetric obs. 0-61089
 solvated electron+phenanthrene, diffusion controlled reactions in polar solvents, reaction parameters 0-97687
 solvated electrons, diffusion controlled reactions in polar solvents, reaction parameters 0-97687
 spin polarisation analysis using intermolecular interactions theory, chemical polarisation, exchange repulsion 0-76510
 stationary states, pumped, model for mixing 0-71887
 steam plant, chemical washing, aqueous effluent neutralisation by use of ash 0-89486
 stopped-flow apparatus for rapid mixing and study of two fluids under high hydrostatic pressures 0-98929
 superposition of reactive and nonreactive scattering amplitudes in the presence of a conical intersection 0-63733
 supra-antarafacial cycloaddition intrinsic single and dual mol. orbital symmetry conservation 0-102419
 symmetry correl. and perturbation calcs. methods 0-104427
 thermal electrocyclic reactions, anal. using topological model 0-78512
 topological model and orbital mapping for chemical systems 0-78512
 travelling waves for a model non-linear reaction-diffusion system 0-89476
 unimolecular dynamics, classical trajectory calcs. 0-108692
 unimolecular reaction, thermal, expressions for deriving rate const. 0-85164
 Venus, S chemistry of atmosphere/lithosphere system rel. to oxidation state of atmosphere and crust 0-95856
 wave propagation, coherent probe light pulse 0-61190
 Al₂O₃(H₂O)_n, uniform colloidal dispersion, prep. by chem. reactions in aerosols 0-97735
 Ar+H₂⁺ endothermic charge transfer reaction, low energy crossed beam study 0-95720
 BCl₃+N(CH₃)₃→BCl₃N(CH₃)₃, complex formation, reaction product isotopic composition change (*Russian*) 0-81316
 Ba, silicates, solid state reactions, thermodynamics and kinetics (*German*) 0-76236
 BaTiO₃ fibres synthesised from Ba(OH)₂+2K₂O.11TiO₂.3H₂O fibre hydrothermal reaction (*Japanese*) 0-93527
 BeO, heated on W, thermal anal. using mass spectrometric, technique, vaporisation behaviour 0-79932
 CN₂, electron propagator theory, mol. electron affinities calcs. 0-83521
 CO₂-methane reforming-methanation cycle for Solchem thermochemical solar energy transport 0-94096
 CaO, heated on W, thermal anal. using mass spectrometric, technique, vaporisation behaviour 0-79932
 Ca(OH)₂, dehydration, unsteady heat conduction, thermal conductivity change 0-76511
 CeNH₄P₂O₁₂ and Ce(NH₄)₂(PO₃)₃, synthesis by solid-phase reaction, characts. 0-60778
 Cl₂⁺, electron propagator theory, mol. electron affinities calcs. 0-83521
 Cs-H₂ vapour, resonant character of laser induced formation of particles 0-89481
 CsSbO₃, solid state synthesis (*French*) 0-104438
 Cu(I) complex, oxidation, fast reactions meas. by pulsed-flow instrument 0-66890
¹⁹F+hexafluoropropylene nonequilibrium effects in moderated nuclear recoil experiments 0-89509
¹⁹F+methane, nonequilibrium effects in moderated nuclear recoil experiments 0-89509
 FeH and FeH₂ formation in interstellar clouds 0-98704
 FeMoO₄+TeO₂, solid state reaction 0-108709
 Fe(NH₄)₂(SO₄)₂.4H₂O, rehydration kinetics, Mossbauer effect study 0-61081
 H₂, field ionisation under nonequilibrium conditions 0-74244

chemical reactions continued

- InVO₄, synthesis and thermal props. (*French*) 0-97443
 K₄Sb₂O₇, solid state synthesis (*French*) 0-104438
 Li/SO₂ cells, safety studies, kinetics of Li-organic solvent exothermic reactions 0-72030
 Li(2P_{1/2,3/2}), laser induced flame chemistry, saturated mode fluoresc. meas. 0-89491
 Mg hydriding, Kirkendall marker movement 0-75385
 Mg(NO₃)₂.RNO₃ (R=Li, Na, K), thermogravimetric anal. of dehydration processes (*Japanese*) 0-66791
 MgO, heated on W, thermal anal. using mass spectrometric, technique, vaporisation behaviour 0-79932
 Mn²⁺-oxalacetic acid-H₂SO₄-KBrO₃, chaos type reactions anal. 0-85165
 N₂+H₂+N₂H₄, mixtures with nonthermal vibr. excitation of mol. N₂ 0-76545
 N₂+O₂+NO, mixtures with nonthermal vibr. excitation of mol. N₂, formula for calc. equil. const. 0-76545
 Na₂O-SiO₂ glasses, water reactions at elevated temps. and press. 0-81312
 Na(3P_{1/2,3/2}), laser induced flame chemistry, saturated mode fluoresc. meas. 0-89491
 Ni(CO)₄, form. reaction rate, substrate mag. phase depend. 0-108737
 NiMoO₄+TeO₂, solid state reaction 0-108709
 O₂ b¹Σ_g⁺ state prod. and deactivation following O(¹D₂) quenching 0-76493
 Rb₂Sb₂O₇, solid state synthesis (*French*) 0-104438
 SeCl₃-NaCl-CsCl ternary system, cpd. form., thermographic investig. (*Russian*) 0-66490
 Si, commercial, nitridation, effect of BaF₂ 0-81359
 Si-Ti-O-N system, formation of TiN and SiO₂ 0-71617
 Si₃N₄, reaction-bonded, theoretical model of manufacture, effect of ambient reaction temp. and compact size 0-108379
^{99m}TcBr₂⁺, preparation problems, decay const. 0-106020
^{99m}TcI₆²⁻, preparation problems, decay const. 0-106020
 Tl₂CO₃+8-hydroxyquinoline, solid state reaction 0-108708
 U extraction by transfer between liq. phases, laser radiation effect 0-66795
 WO₃+CuO- solid state reaction kinetics, CuWO_{4-x} formation study 0-66796
 ZnO nonohmic ceramic, formation mechanism 0-60813
 ZrSiO₄, zircon yellow pigment, synthesis (*Polish*) 0-66466
- chemical reactivity** see *chemical reactions*
- chemical relaxation**
 activated processes in condensed phases, general kinetic models 0-81281
 coupled multistep chemical reactions, rate const. determ., relax. spectroscopy 0-66766
 high pressure pressure-jump apparatus for fast reactions in solution 0-62681
 nonadiabatic cage reactions, relaxation hindrance 0-93740
 Zn-nucleotide, triphosphate complexes, ³⁵Cl NMR obs. 0-63661
- chemical shift**
 see also *isomer shift*
 acetone, ¹³C chemical shift and NMR linewidth meas., self-association equil. const. determ., mol. reorientations obs. 0-87148
 acetophenones, spectrosc. characts. using PPP SCF CI calcs. 0-102448
 L-alanine, ¹⁵N NMR chemical shifts and linewidths, pH dependence 0-80625
 alkanes, H⁺ chemical shifts, extended Huckel calcs. with gauge in variant atomic orbitals 0-102449
 amorphous materials, X-ray K-absorption edge chemical shifts 0-80904
 benzene, H⁺ chemical shifts, extended Huckel calcs. with gauge in variant atomic orbitals 0-102449
 bis-methylidgermyl chalcogenide, ¹H and ¹³C NMR study, chemical shifts 0-71201
 bis-methyldisilyl chalcogenide, ¹H and ¹³C NMR study, chemical shifts 0-71201
 n,t-butanol in alkanes, molecular relaxation processes studied by ¹³C NMR 0-63654
 CO₂ ferrite, crystal structure, X-ray absorpt. spectra, chemical shifts 0-88118
 cytochrome c, PMR, eight-ring current model heme ring, conformation depend. shifts 0-74185
 dipole NMR line width red. under magic angle conditions 0-60435
 DOBAMBC, smectic A and ferroelec. smectic phases, ¹³C NMR study 0-75153
 ESCA shifts and effective charges 0-78648
 ethylenic compounds, H⁺ chemical shifts, extended Huckel calcs. with gauge in variant atomic orbitals 0-102449
 glycine, ¹⁷O NMR chemical shifts and linewidths, pH dependence 0-80625
 hard X-ray lines, chemical shifts, applicability of Koopmans' theorem, HF calcs. 0-74145
 hormonal steroids, ¹³C NMR spectra 0-81543
 hydrocarbons, ¹³C chem. shifts, simplex optimized INDO calcs. 0-83284
 macromolecule, microconformation by fast exchange NMR spectra 0-102593
 methyl group, ¹³C chemical shifts, H/H, H/Me and Me/Me interactions 0-95652
 molecules, diamagnetic susceptibilities and NMR chemical shifts in terms of localised MO's 0-106256
 molecules containing 1st row atoms, K-shell binding energy shifts, NDDO MO calcs. 0-58413
 neopentane adsorbed on graphite, quasi two-dimens. fluid, NMR 0-102525
 NMR, double-quantum, cross-polarization, in solids, theory 0-100623
 NMR, high resolution, automated anal., principles and computational strategy 0-58287
 nuclear magnetic shielding density 0-63559
 octahedral paramagnetic complex ions, isotropic chem. shift, pseudocontact contrib. 0-91577
 phenylphosphines, and derivatives, ¹H, ¹³C and ³¹P NMR studies 0-87152
 phospholipid bilayers, carbonyl groups dynamics, ¹³C chem. shift anisotropy obs. 0-85326
 poly-L-ornithine solution, ¹⁵N NMR, coil-helix transition, solvent effects and pH depend. 0-74275
 polypropylene, isomeric, microconformation from slow exchange ¹³C-NMR spectra of low mol. wt. cmpds. 0-102592
 potassium hydrogen malonate, carboxylic proton chem. shift tensor 0-58280

chemical shift continued

- propionitriles (-O, NH, S), conformational investig., NMR, IR and semiempirical MO methods 0-95650
propylene-butene copolymers, PB centred tetrad ^{13}C NMR spectra assignment 0-58428
tetramethylammonium zinc tetrachloride, incommensurate phase transitions, ^{13}C NMR study 0-75968
titanocene, alkyl-substituted ^{13}C and ^1H NMR, chemical shifts prediction 0-63671
transition metal tetrahedral complex ions, F NMR chem. shifts, outer sphere cation effects 0-102527
two-dimensional systems, order parameter from chemical shift anisotropy patterns 0-80624
zirconocene dichlorides, alkyl-substituted, ^{13}C and ^1H NMR, chemical shifts prediction 0-63671
Ag and Ag_2O , X-ray absorption, discontinuities and limits, chem. combination effects 0-93435
 AgBF_4 , ionic radii and chem. shifts, correl. with electronegativity 0-66054
 $\text{AgF}(\text{AgI}, \text{AgBr}, \text{AgCl})$, NMR chemical shifts 0-74180
Au and Au_2O_3 , X-ray absorption, discontinuities and limits, chem. combination effects 0-93435
Bi and Bi_2O_3 , X-ray absorption, discontinuities and limits, chem. combination effects 0-93435
 $2,4\text{-C}_6\text{H}_3$, polyhedral, spin coupled ^{11}B - ^1H systems, 2-dimens. correl. NMR 0-69166
 ^{13}C , 2D NMR spectra, off-resonance decoupling 0-74182
 CdF_2 , high resolution NMR and chem. shifts of ^{111}Cd and ^{113}Cd , double reson. expt. 0-60460
 CdSe photoanodes, S substitution during operation and mech. of surface protection XPS study 0-107906
Co complexes, Co(III) mixed complexes, orbital angular momentum reduction, ^{59}Co NMR chemical shift 0-58137
Cr complexes, NMR study ^{31}P chemical shift, substituents electronegativity steric hindrance and π -bonding effect 0-95651
 CsBF_4 , ionic radii and chem. shifts, correl. with electronegativity 0-66054
 CsD_3PO_4 , pseudo-one-dimensional ferroelectric transition, ^{31}P chemical shift and relaxation study 0-66123
Cu and Cu oxides, X-ray absorption, discontinuities and limits, chem. combination effects 0-93435
Cu-phthalocyanine, photoemission multielectron effects from quasi atomic Cu 0-93458
 CuO , on Cu, identification by electron spectroscopic methods 0-60747
 Cu_2O , on Cu, identification by electron spectroscopic methods 0-60747
 CuPd , chemical shift effects and origin of Pd 3d core level satellite 0-104039
 Cu_2S - CdS heterojunction interface, depth distribution profiles, Auger spectra 0-88622
Fe and compounds, X-ray absorpt. spectra, effective co-ordination charges, chem. shift 0-84805
 H_2MoO_3 bronze, proton shift tensors PMR meas. 0-71202
 H_2O , liquid, diamagnetism, temp. dependence, NMR chemical shift calcs., molecular interactions data 0-75707
 $^{138,139}\text{La}$, Fourier transform NMR 0-57354
 Li^+ -ligand complexes, NMR appl. ^7Li chemical shifts, expt. and ab initio studies 0-63670
 MoO_3 , X-ray absorption, discontinuities and limits, chem. combination effects 0-93435
 NF_3 , nuclear resonance, effects of intermolecular interactions and intramolecular dynamics 0-63658
 NH_4BF_4 , ionic radii and chem. shifts, correl. with electronegativity 0-66054
 $\text{NH}_4\text{H}_2(\text{SeO}_3)_2$, single crystal, ^{77}Se magnetic shielding, chemical shift tensors 0-71207
 Na_2O - TiO_2 - SiO_2 glass, co-ordination of Ti, X-ray emission spectra study 0-84072
Nb films, oxidation, XPS study 0-80944
 PF_3 , nuclear resonance, effects of intermolecular interactions and intramolecular dynamics 0-63658
 PF_5 , nuclear resonance, effects of intermolecular interactions and intramolecular dynamics 0-63658
 POF_3 , nuclear resonance, effects of intermolecular interactions and intramolecular dynamics 0-63658
Pb and Pb oxides, X-ray absorption, discontinuities and limits, chem. combination effects 0-93435
 $\text{Ru}(\text{NH}_3)_6^{3+}$, isotropic chem. shift, pseudocontact contrib. 0-91577
Se, solid, chemical shift and nucl. spin-lattice relax., high temp behaviour 0-60445
Si (111), intermediate oxidation state, core photoelectron absorpt. vs. chemical shifts 0-81220
Si, chemisorption of XeF_2 and SiF_4 , XPS and Auger spectra, surface chemistry 0-81358
 SiH_4 , amorphous, 2p level shift, XPS obs. 0-97401
TGS, ferroelectric phase transition, high resolution NMR study 0-97214
Te, photoconductivity in strong mag. fields, doping effects, impurity levels 0-75602
 TiO_2 -Ni, electronic props., struct., comp., chemical bonding 0-84499
Ti complex of lasalocid (X-537A), ^{205}Ti NMR study 0-58288
VB, nuclear quadrupole parameters 0-103896
 ^{59}V spin-relaxation times, pH depend. 0-66059
 ZnS , ^{67}Zn and ^{35}S nuclear magnetic shielding, chemical shifts and linewidths 0-60434
 ZnSe , ^{67}Zn nuclear magnetic shielding, chemical shifts and linewidths 0-60434
 ZnTe , ^{67}Zn nuclear magnetic shielding, chemical shifts and linewidths 0-60434

chemical structure

- see also bonds (chemical); crystal atomic structure; crystal chemistry; molecular configurations*
computer representation, block-cutpoint tree method 0-63522
crown ether-containing polymers, in alkali salt solns., complexation, viscosity obs. 0-64877
ethidium bromide E-DNA, intercalated birefringent fibres, microspectrophotometric investig. (German) 0-57392
hydrocarbon ions, mass spectra, H atom scrambling, delocalisation 0-58135
lithium oligopentadienyl and complexes, IR spectra (Russian) 0-71424
NMR spectra, computer-aided interpretation, minicomputer based file search system 0-62702

chemical structure continued

- NMR spectra, computer-aided interpretation using artificial intelligence system 0-62701
novolac and novolac allyl ether electrets, thermal depolarisation, chem. struct. effect 0-71297
polymer crosslinking, rel. to azide photooxidation in polymer matrix 0-66832
polymer structure and optical behaviour 0-106583
rare earth double orthophosphates with alkali metals, spectroscopic obs., struct. and chem. nature 0-100674
ring characterisation method 0-63853
tautomerism and alternating bonds, representation, Chemical Abstracts Systems 0-63851
thiourea, struct., hydration, ab initio SCF calcs. 0-58142
Al chalcogenate and chalcogenite double salts, form. laws and acid-base props. 0-101070
Au, Co-hardened, characterisation by Mossbauer spectroscopy, Co precip. formation 0-80108
Ga chalcogenate and chalcogenite double salts, form. laws and acid-base props. 0-101070
In chalcogenate and chalcogenite double salts, form. laws and acid-base props. 0-101070
 NbSe_3 , electronic struct., chem. interpret. of geom. deform., oxidation state formalism 0-107690
 ^{18}O isotope shift in ^{13}C NMR, struct. depend. 0-69165
 PbS-Si heterojunction, chem. struct., AES anal. 0-76115
 $\text{Si}_{1-x}\text{C}_x\text{H}_x$, amorphous film, H content determ. by nuclear reaction analysis 0-59821
 SiH_4 , amorphous film, H content determ. by nuclear reaction analysis 0-59821
(Th,U) O_2 , burnup simulated, high O_2 pot., chem. state 0-91220

chemical technology

- see also chemical industry; chemical variables control; chemical variables measurement*
atoms, laser excited, reactive collisions 0-66793
bipolar trickle reactors, electric current versus potential plots 0-76521
bipolar trickle reactors, flow models for hydrodynamic characts. and reaction rate constants, 0-76522
bipolar trickle reactors, study using electrochemical tracer method 0-76523
CHISA international conference, Prague, Czechoslovakia (Aug. 1978) 0-62372
electrochemical processes, energy use analysis (Dutch) 0-72019
electrochemical reactor characterisation, marker pulse method improvements 0-76524
electrochemical reactors with three-dimensional electrodes, characterisation using electrochemical tracer method 0-76520
ethanol, industrial, production from municipal cellulosic waste 0-61502
fluidised system, heterogeneous, aerodynamic aspects of transfer processes, crit. state 0-79394
gas trace monitor, control of toxic gases 0-61499
industrial gaseous environment characterisation, Brinkley method 0-93817
methanol derivation from lignite, fuel appl. 0-61223
phosphate containing materials, technological prod. processes, review 0-97452
plasma chemistry, history, diagnostics, production, organic compd. synthesis 0-61099
plasma chemistry of heterogeneous systems 0-61100
NO measurement, photometric process analyser 0-57360
NbC production and superconductive props. (Bulgarian) 0-80467
NbN production and superconductive props. (Bulgarian) 0-80467

chemical vapour deposited coatings *see CVD coatings***chemical vapour deposition**

- see also vapour phase epitaxial growth*
boundary layer theory application, introduction 0-66431
III-V semiconductor thin film prep. by low temp. CVD 0-60789
laser applications in materials processing, seminar, San Diego, CA, USA (Aug. 79) 0-90609
lightguide fibre preform manufacture using modified CVD process 0-64228
low-loss graded-index fibre, 3 km and 10 km preform design and modified CVD method 0-58746
LPCVD-type plasma-enhanced deposition system [for semiconductor wafer processing] 0-60791
magnetic bubble materials, props. and preparation models, review (Rumanian) 0-93149
mass transport model, deposition rates 0-103599
metal silicides, fabrication technique/ and characterisation, review (Japanese) 0-60779
optical fibre, modified CVD prep., optical and mechanical props. reproducibility 0-69535
optical fibre, PCVD, dispersion measurement by mode-locked synchronously-pumped dye laser 0-64191
optical fibres, SiO_2 , manufacture using modified CVD method (Japanese) 0-99864
optical graded-index fibre vapour-phase axial deposition method, fibre characteristics 0-58824
optical single mode CVD fibre, bend-induced birefringence obs. 0-58723
optical single mode fibres, homogeneous CVD fabrication and characterisation 0-69562
quartz glass, Ge and B dopants, OH impurities, preform material and fibre optic waveguide struct. 0-64173
reactor, containing SiO_2 , dispersed particulates, correlations with film characts. 0-76192
reactor improved design, with horizontally stacked quartz slabs 0-76195
refractory ceramic coatings, for high temp. use, current status (Japanese) 0-71619
rod-in-tube fabricated optical fibre characteristics 0-87574
semiconductor film growth, multilayer systems, spectroscopic ellipsometry, review 0-103603
thin films, deposition techniques, review 0-80964
vacuum creation problems (French) 0-101803
 $\text{Al-Al}_2\text{O}_3\text{-SiO}_2$ -Si capacitors, physical and elec. props. of RF plasma grown Al_2O_3 0-100530
 Al-AlN-SiO_2 -Si capacitors, physical and elec. props. of RF plasma grown AlN 0-100530
 $\text{Al}_2\text{Ga}_{1-x}\text{As}_{1-x}$, $\text{Al}_2\text{Ga}_{1-x}\text{As}_{1-x}$ DH lasers grown by metalorganic CVD, CW operation in wavelength range 760-780 nm 0-64053

chemical vapour deposition continued

- Al_{0.7}Ga_{0.3}As-GaAs, quantum-well heterostructure laser diode, temp. depend. of threshold current 0-87395
 AlN film, thermodynamics and kinetics of CVD 0-108354
 Al₂O₃, CVD film on III-V semicond. substrate, ion beam etching, defect detection 0-89155
 B, closed system CVD, deposition rate and rate-limiting steps 0-93492
 B, closed system CVD, deposition rate, models for interpretation 0-97438
 B, deposition rate and supersaturation relationship using combined flux model 0-84856
 B, deposition rate in closed systems, influence of HCl 0-84855
 B, morphologies, influencing factors, temp. range 1390-1640K 0-89154
 B-Si alloys, B-rich, prep., anal. and cryst. growth (*French*) 0-104091
 BN, semicond. film, chemical deposition 0-71596
 BPi:Ni pillar crystal growth from vapour 0-60758
 CdCr₂S₄ magnetic semiconductor crystal growth, structural defects, physical properties 0-60759
 Co_{3-x}Mo_xO₄ films, prep., struct. and elec. characteris. 0-108353
 Cr, preparation by decomp. of bis-arene cpds., struct. and phys. props. 0-60785
 (GaAl)As low-beam-divergence CW DH laser, grown by low press. metal-organic CVD 0-74376
 GaAs homojunction solar cells, large-grained, passivation method to improve open-circuit voltage 0-94070
 GaAs:Se(Zn) polycrystalline film, Hall effect, resistivity meas. 0-96911
 GaInAs-InP, growth by low-pressure metalorganic CVD 0-71595
 Ga_{0.9}In_{0.1}As_{0.9}P_{0.1}/InP DH laser emitting at 1.15 micron grown by low-pressure CVD 0-64052
 GaN preparation in sealed fused silica ampoules 0-80982
 GaN, VPE growth rate influence on elec. and luminesc. props. 0-100702
 GeO₂-P₂O₅-SiO₂ graded-index fibres, effect of deposition rate on spectral loss 0-87485
 InP-SiO₂ interface, CVD problems, ESCA profiles 0-93497
 MnS(Se)(Te), CVD crystal growth, role of Mn-Al-Cl complexes 0-84840
 Mo, film, formation by reduction of MoCl₅, influence of electric field 0-93491
 Nb-Ga, A15 phase, chem. deposition on Hastelloy substrate, for superconducting tape (*German*) 0-104071
 Nb-Ge, compounds with A15 structure, films, TEM study (*French*) 0-80135
 Nb-Ge-Si, compounds with A15 structure, films, TEM study (*French*) 0-80135
 Nb-Si, compounds with A15 structure, films, TEM study (*French*) 0-80135
 Nb₃Nb_{1-x}Si_x(Ge)_x, impurity stabilised A15 supercond., transition temp., lattice const., specific heat 0-93026
 P₂O₅-SiO₂ glass, flow for integrated optical cct. fabrication 0-79005
 Sc, CVD, open-tube technique 0-89128
 Si amorphous film preparation, by SiH₄ decomposition 0-80956
 Si, CVD, surface anal. during growth using RHEED and Auger spectroscopy 0-66433
 Si, CVD from SiH₂-HCl-H₂ system, rate-determining reactions and surface species 0-84405
 Si, deposition on rotating disc, one-dimens. model 0-75461
 Si film, polycryst., laser-induced CVD growth from SiCl₄ 0-84852
 Si optical fibres, advances in fabrication using MCVD process 0-99875
 Si, polycryst., deposition as example of pyrolytic CVD process 0-84407
 Si, prod. of polySi vapour deposited coatings for solar cells, cost anal. 0-93495
 Si ribbons for solar cells, ultra high speed growth, elec. props. 0-89162
 Si rich SiO₂-SiO₂-Si rich SiO₂ layers for dual electron injector struct. 0-96991
 Si:As, CVD, doping using SiH₄-H₂-AsH₃ system 0-79823
 Si-SiO₂ interface in IGFETs, anal. of CVD SiO₂ on (100) and (111) surfaces, near-ideal structs. 0-100528
 SiC, controlled nucleation thermochemical deposition, charact. and props. 0-108355
 SiCl₄-GeCl₄-BCl₃ particulate layers consolidation, in fabrication of optical fibre preforms 0-60787
 SiN_x films, plasma enhanced CVD, props., meas. and interpretations 0-80987
 Si₃N₄, dielectric films made by NH₃-silane reaction, TEM study 0-84413
 Si₃N₄ layers deposition, high-temperature, in resistance furnace, temperature gradient and nitrogen flow influence obs. (*Bulgarian*) 0-80981
 Si₃N₄, low pressure CVD, thermochemical calcs. 0-108356
 Si₃N₄, room temp. CVD on InSb 0-71597
 SiO₂ glass, high rate MCVD of optical fibres 0-83671
 SiO₂, low pressure CVD, thermochemical calcs. 0-108356
 SiO₂ separation below 500°C, state and tendency of chemical gas phase separation (*German*) 0-100794
 SiO₂-P₂O₅-GeO₂ optical fibres, CVD, losses, reactant impurity effects 0-87522
 SnO₂/n⁺-pSi heterojunction solar cells, fabrication by paint-on-diffusant method 0-94048
 TiB₂, thick film on low C steel substrate, CVD in US field, crystallite size 0-84854
 TiC, deposition rate meas., rel. to mass transport model 0-103599
 TiC, laser CVD, coating characterisation 0-93494
 TiN(C) whisker growth in CVD 0-59843
 VO₂, V₂O₃ and V₂O₅, film prep. under equil. conditions, struct. and elec. props. 0-108352
 W needle crystal growth, discharge-induced decomp. of hexacarbonyltungsten mols. 0-84414
 WC, sinterability of ultrafine powders obtained by CVD method 0-108378
 ZrN(C) whisker growth in CVD 0-59843

chemical variables control

- see also *pollution detection and control*
 gas trace monitor, control of toxic gases 0-61499
 industrial gaseous environment characterisation, Brinkley method 0-93817

chemical variables measurement

- see also *chemical analysis; moisture measurement; pollution detection and control*
 cloud chamber, thermal diffusion, unsteady state, supersaturation profile 0-63449
 equipment for the measurement of ions in solution, review 0-71983
 gas trace monitor, control of toxic gases 0-61499
 human serum, definitive meas. of constituents 0-93818

chemical variables measurement continued

- plating line Co concentration monitoring, by automatic colorimeter 0-105691
 salinity of seawater, microprocessor-based instrument 0-67440
 stearic acid homogeneous vapour phase nucleation, diffusion cloud chamber obs. 0-79923
 steel, mild, corrosion rate meas. in H₂SO₄ using microprocessor controlled potentiostat 0-71798
 supersaturated vapour, equilb. press. depend. on nucleating drop radius 0-69960
 Cl monitoring, TAGA 3000 mobile test unit 0-72114
 NO measurement, photometric process analyser 0-57360
 O₂ analysis, electrochemical sensors 0-93816
 O₂ determination in flue gas of 200 MW plant, trial operation with Westinghouse probe (*Czech*) 0-89562
- chemically reactive flow**
 air suspension homobaric flow in presence of physicochemical transform. 0-87820
 bipolar trickle reactors, flow models for hydrodynamic characts. and reaction rate constants, 0-76522
 burning rate in engine cylinder, swirl and turbulence effects 0-89492
 convective diffusion, nonlinear surface reaction kinetics 0-106854
 convective diffusion to a particle in a fluid with linear kinetics 0-69943
 CW supersonic chemical laser, porous, nozzle, chemically reacting boundary layer 0-100022
 drop formation hydrodynamics, macroencapsulation 0-64603
 EHD flow, nonstationary, with charge diffusion, nonlinear and linear wave processes 0-59124
 electrolyte, ionic mass transfer in narrow rectangular conduits 0-61105
 flames, local turbulence props., Raman spectroscopy meas. 0-64648
 gas injected into shock layer flow, aerodynamic heating of blunt bodies 0-74998
 gas mixtures, detonating, symmetric piston motion 0-59073
 gas-liquid interaction in turbulent reacting flows, mathematical model 0-83862
 gasdynamic disturbance in chem. reacting gas mixture, shock wave formation 0-74999
 heat engines, chemically driven, finite time thermodynamics 0-76541
 heterogeneous mixing, energy level population inversion 0-78848
 laminar heat transfer for boundary layers with mass injection and chemical reactions (*Chinese*) 0-59020
 laminar liquid film, falling, O₂ adsorpt. with zero order react. in entrance region 0-64652
 localized patterns in reaction-diffusion systems 0-59130
 low Mach number duct flows, combustion noise generation by chemical inhomogeneities 0-92237
 mass transfer, ionic, in open channels, electrolyte probe determ. 0-59110
 melt reacting with gas jet, heat and mass transfer, mathematical modeling 0-87819
 nonequilibrium boundary layer flow, exact and approx. solns. 0-79409
 nonequilibrium isobaric chemically reactive flow, parameters for heating (cooling) (*Russian*) 0-59131
 nonuniform grids in finite difference approximations, application to fluid flow problems 0-105507
 parallel flows of unmixed reactants, temp. and conc. distrib. in reaction region 0-92236
 partial chemical equilibrium in fluid dynamics 0-69946
 polyethylene oxide, dilute aqueous solution, effect of chemical additives on flow 0-83823
 polymerisation in flow-through reactor, low-temp. conditions 0-61092
 qualitative analysis of unsteady heat and mass transfer modes in a boundary layer with chemical reactions and intensive injections 0-69819
 Rayleigh-Benard instability, n-component reactive fluids 0-69945
 Rayleigh-Benard instability, reactive binary fluids 0-69944
 shock waves, completely dispersed, in relaxing mixtures, struct. obs. 0-59072
 stagnation flow at a heated curved wall, ignition condition 0-96242
 stationary system, diffusion mixing model, approx. soln. 0-79410
 stopped-flow apparatus for rapid mixing and study of two fluids under high hydrostatic pressures 0-98929
 supersonic stream of chemically reacting gas mixture, thermal crisis suppression by laser radiation 0-75000
 thermal diffusion flame, two dimens. cellular struct. formation 0-69947
 thermal kinetics meas. using modified commercial stopped flow apparatus 0-86291
 turbulent boundary layer with suction under nonisothermal conditions, heat and mass transfer 0-92125
 turbulent flames, laser Doppler vel. meas., using spark discharge particle generator 0-59139
 turbulent mixing with react. of miscible reactant streams, simulation 0-64651
 wavefronts in reaction-diffusion systems, instability and turbulence 0-106855
 CO-N₂O reacting gas mixture, gain due to CO₂ 0⁰1-10⁰0 transition 0-74337
 H supersonic flames, chemical kinetics and unmixedness effects on burning 0-64649
 N₂O₄, fission reactor coolant, heat transfer on condensation (*Russian*) 0-57860
 N₂O₄, turbulent dissoc. flow, along heated tubes, heat transfer 0-63225
 TiO₂:TeCl₄ system, chem. vapour transport, matrix isolation IR studies 0-93755
- chemiluminescence**
 aromatic compounds in benzene polycrystalline host, active N₂ induced chemilum., 77K 0-60691
 earthquake lights, proposed for study by chemiluminesc. NO air pollution apparatus 0-61906
 fluorocarbon solutions, dye-sensitized, spectroscopic obs. of 1.27 μm and 1.58 μm emission of single (¹Δ_g) mol. O₂ 0-85178
 gas chromatography, selective detection by N₂ induced chemiluminesc. 0-89495
 IR laser photolysis of polyat. mols. photochem. appls. 0-66835
 methyl radical+O(F), infrared chemiluminescence obs. 0-61080
 organic substances, electrochemiluminescence as possible source of coherent radiation, and role in biological processes (*Russian*) 0-76093
 rubrene, electrochemilum. by DC, highly organised EHD convection obs. 0-71499
 Ar*+Fe(CO)₅, chemiionisation and chemiluminescence reactions, Penning ionisation and fluoresc. obs. 0-97689
 C₂+NO, laser-induced chemilum. reaction 0-61101

chemiluminescence continued

- C₂+NO(O₂), IR laser photolysis of polyat. mols. photochem. appls. 0-66835
 Ca+O₂ reaction, chemiluminesc. absolute cross sections, photon yields and CaO dissociation energy 0-97697
 Cl+vinyl bromide-d₃ reaction, IR chemiluminesc. 0-102506
 Cl+HBr(HI)—HCl+Br (I⁻), vibr. product state distrib., IR chemiluminesc. obs. 0-81309
 Cu+Cl₂(Br₂)(I₂), beam-gas chemiluminesc. reactions 0-85151
 Cu+F₂, chemiluminesc. reactions, mol. beam study 0-97702
 F+ethylene (benzene) derivatives, deuterated, IR chemiluminesc. 0-102506
 F+H₂(D₂), rate consts., temp. depend. 0-81302
 F+HCl—HF+Cl, time resolved vibr. chemiluminesc. and rate consts. 0-61069
 Ge+N₂O, chemiluminesc. reaction, HTFFR kinetics study 0-76496
 H+Cl—HCl+e, associative reaction, product vibr. state distrib. 0-66794
 HCl, vibr. emission from ClF-H₂ chem. laser 0-97709
 HNO, low-lying states, pot. energy surfaces calcs. 0-102460
 He⁺+SO₂, dissociation charge transfer reaction, SO⁺ (A²Π-X²Π_g) emission 0-95659
 LiCa, laser chemiluminesc. 0-93759
 NO+O₃, fs-states and rot. states, effect on reactivity 0-89473
 Ne⁺+Fe(CO)₅, chemiionisation and chemiluminescence reactions, Penning ionisation and fluoresc. obs. 0-97689
 O source with improved long term stability for chemiluminescence reaction, mol. dissociation and recombination 0-93758
 O₂(¹Σ_g⁺—³Σ_g⁻), in O-COS-O₂(¹Δ_g)/O₂ system, chemiluminescence 0-66806
 SO(²Σ⁺—³Σ⁻), in O-COS-O₂(¹Δ_g)/O₂ system, chemiluminescence 0-66806
 Se+NO₂, chemiluminesc., nonequilibrium product distrib. 0-101014
 SiF, use in chemical lasers 0-64004
 SiS, chemiluminescent flame spectra, electronic states and rot. struct. obs., vibr. assignments, Franck-Condon factors determ. 0-85179
 SnF, use in chemical lasers 0-64004
 Xe+Br(CCl₄), excitation functions and rotational polarisation, chemiluminesc., crossed beam study 0-76491

chemioception

- afferents from aortic and carotid bodies, relative latency of responses 0-101189
 behaviour patterns in cod released by elec. stimulation of olfactory tract bundles 0-97951
 evoked brain potentials, correl. anal. (*Japanese*) 0-97946
 olfactory bulb, 55 counts/sec rhythm anal. and simulation 0-85422
 taste cells, insect, special purpose amplifier for spike train recording 0-72394
 taste reception, physicochem. mechanism and chem. sensors development (*Japanese*) 0-85423

chemisorption

- Ag clusters, of I, UPS obs. 0-84830
 atoms on semi-infinite linear chain, chemisorption theory and superoperator formalism 0-93800
 catalysis, chemisorption kinetics, determ. from substrate current fluctuations 0-84383
 cellulose char, O₂ chemisorpt. kinetics 0-96730
 cluster chemisorption, book contrib. 0-107650
 conference, New York, USA (Oct. 79) 0-73093
 ellipsometry of clean surfaces, submonolayer and monolayer films, review 0-103546
 gelatin layer, dry, aqueous soln. penetration 0-85221
 graphite, of O₂, influence of Fe as impurity 0-96732
 graphite intercalation compound, interaction between one or two s orbitals (*French*) 0-65440
 image charge effects, surface plasmons 0-84381
 image charge effects on adsorbate valence spectra, perturbational study 0-84380
 ion electrostatic interaction at electrode surface, ion field penetration 0-81333
 jellium, effective-medium theory of chem. binding 0-65367
 laser irradiation effects 0-84812
 metal particles, small, characterisation and props., book contrib. 0-84417
 metal surface chemisorption theory, electron localisation, surface interactions 0-84376
 metallic surface, self-consistent electron theory, review 0-88616
 multiphoton processes, chemisorbed species on solid surfaces, desorption dynamics, quantum-stochastic approach 0-66864
 neutron scattering from adsorbed mols., surfaces and intercalates, review, book contrib. 0-84394
 pair interaction energies between chemisorbed atoms on metallic surface (*French*) 0-80076
 perovskites, d-band, concepts of surface states and chemisorption, book contrib. 0-107651
 phase transitions in chemisorbed systems 0-107656
 photoelectron spectroscopy, solid-state, with synchrotron radiation, review 0-71570
 Pt surface, chemisorbed CO, IR refl.-absorpt. spectra, adsorbate island struct. 0-84385
 semiconductor, surface and adsorbate states, charge injection into space charge layers 0-100496
 semiconductor surface, of mol. complexes, bond orbital model (*German*) 0-59807
 semiconductor surfaces, review, book contrib. 0-107648
 simple metals, density functional calcs. 0-108733
 simple metals, density functional theory of chemisorption, book contrib. 0-107647
 solid surfaces, surface processes, and solid/gas interactions 0-73125
 solid-liquid metallic binary alloy, interfacial tension, chem. adsorption and temp. depend. 0-59777
 solid/liquid adsorption equilib., kinetic studies using isotopic mol. exchange method 0-84427
 stainless steel, austenitic, surface, interaction with O₂, and work function obs. 0-65364
 theoretical issues, book contrib. 0-107652
 theory, book 0-105440
 transition and noble metals, d-band metals, chemisorption, book contrib. 0-107649
 transition metal, chemisorption of H, effect of surface spin fluctuations 0-75613

chemisorption continued

- transition metal compound surfaces, review 0-84349
 transition metals, core levels between surface and bulk atoms, variation of binding energy shifts, chemisorption effects 0-88615
 transition metals, of H₂ and O₂, chemisorpt. energy trends 0-107631
 water on metal surface, molecule struct., interband angle 0-59787
 zeolites, of Br₂ and I₂, Raman spectra 0-93301
 Ag surface, CO chemisorption, SIMS, XPS study 0-84382
 Al (111), bonding of O, electronic struct. calcs., rel. to UPS data 0-59801
 Al (111), oxidation, initial stages, LEED anal. 0-80082
 Al, initial interaction of O with single cryst. faces, LEED, AES and work function study 0-84392
 Al surface, hydrazine and NH₃ adsorption and decomp., XPS obs. 0-92783
 Al₂O₃, of ethylene glycol, inelastic electron tunnelling spectroscopic study rel. to lubrication 0-70302
 Al(111), oxide layer amorphous to cryst. surface transition, slow positron obs. 0-75417
 Au, chemisorption of I, AES and LEED study 0-100405
 C, activated and impregnated, temp. depend. adsorption of HCN 0-89522
 CaCl₂(Br₂), adsorption of NH₃ and ND₃, complex formation, IR and for IR spectra obs. 0-80063
 CaO:Bi surface, O₂ chemisorpt., positive ion emission determ. 0-92785
 Cd, oxidation, chemisorption and oxide regimes, UPS and EELS study 0-81236
 Co (0001) of NO, surface reactivity, LEED, AES, and thermal desorption study 0-80090
 Cu (001), O₂ chemisorption, Cu3d-O2p interaction study by angular-resolved photoemission using synchrotron radiation 0-84836
 Cu adsorption of O₂, N₂O on (100) surface, reaction with CO 0-103583
 Cu, chemisorption on low-index and stepped surfaces, LEED, AES and UPS obs. 0-84391
 Cu, oxidation, EXAFS obs. 0-71808
 Cu surface, (100), O chemisorption, angle-resolved UPS study 0-84384
 Cu-O (0.05 to 0.1 wt.%) liquid alloy, deoxidation kinetics by rotating graphite cylinders 0-61084
 Cu(110), of O₂, enhancement during Ne⁺ bombard. 0-65070
 Fe, H₂ embrittlement and H₂ adsorption 0-89401
 Fe thin films, surface demagnetisation due to chemisorption, ferromagnetic reson. study 0-80616
 GaAs (100), of O and Al, ab initio theory 0-75612
 GaAs (110), order-disorder interaction with O₂, LEED anal. 0-75445
 GaAs, chemisorption of Li, charge injection into space charge layers 0-100496
 In, chemisorption of O₂, XPS and static SIM spectral study 0-80055
 Ir (111), of NH₃, mol. adsorbate structs. from angular-resolved photoemission 0-76141
 Ir, of H₂, adsorption and desorption kinetics, struct. of overlayer 0-84367
 Ir surface, of CO, mol. cluster calc. 0-100407
 LaB₆ (210) surface, work function, struct. and chemisorpt. stability, XPS, UPS and LEED 0-65344
 Mo(001), of H, atomic displacements, LEED obs. 0-70514
 N₂+methane, N₂ fixation, catalytic processes in non-equilibrium plasma chemical reactors (*French*) 0-89483
 N₂+O₂, N₂ fixation, catalytic processes in non-equilibrium plasma chemical reactors (*French*) 0-89484
 Nb, of H, photoemission studies 0-76145
 Nb, of H, two-state model kinetics 0-75438
 Ni (001), of CO, back donation in chemisorption bond, UPS study 0-107642
 Ni (100), dissociative chemisorption and mol. adsorption of NO 0-65373
 Ni (100) and (110), reaction of acetylene, room temp., UPS expts. 0-61151
 Ni (110), adsorbed H, adatom configuration, He diff. study 0-103569
 Ni (111), chemisorption and reaction of NH₃, LEED, desorption and photoemission expts. 0-59799
 Ni, Al₂O₃-supported, of S, thermodynamic parameters meas. 0-88424
 Ni catalyst, chemisorption of ethylene(d), Raman and vibr. spectra 0-108747
 Ni catalysts, of H₂(H₂O), dynamics, neutron spectrosc. obs. 0-59778
 Ni film, evaporated, of CO, ellipsometric investg. (*German*) 0-61156
 Ni films, electronic struct. calcs., effects of chemisorption; contact pot. and surface magnetisation 0-103734
 Ni, of O, effect on surface vibrs. 0-84361
 Ni, Raney, chemisorbed benzene struct., neutron inelastic spectroscopy study 0-101038
 Ni surface, (001), H₂ dissociative adsorption, calc. 0-101036
 Ni surface, (111), chemisorbed CO, bond energies 0-100398
 Ni surface, of CO, mol. cluster calc. 0-100407
 Ni, thin films, surface demagnetisation due to chemisorption, ferromagnetic reson. study 0-80616
 Ni-Co-Cr/Al₂O₃ catalyst, IR spectra of adsorption and interaction with pyridine 0-71946
 Ni-Fe, electronic struct. calcs., effects of chemisorption; contact pot. and surface magnetisation 0-103734
 Ni-Th (1 at.%), surface comp., temp. and O₂ exposure effects, AES study 0-80914
 NiO (001) surface, chemisorption of H, surface and second-layer defect effects 0-65369
 NiO, prepared by thermal decomp. of Ni(OH)₂, microporosity and irreversible water vapour adsorption 0-80060
 Pd surface, CO chemisorption, SIMS, XPS study 0-84382
 Pd surface, of CO, mol. cluster calc. 0-100407
 PdAg surface, CO chemisorption, SIMS, XPS study 0-84382
 Pt 6(111)×(100), of O₂, UPS studies 0-76151
 Pt (111), of Cl₂, LEED, AES, thermal desorption, and work function meas. 0-75444
 Pt (111), of mol. O₂, XPS, UPS, EELS, and work function meas. 0-76139
 Pt (111) surface, chemisorption of ethylene, vibr. anal. of C₂H₂ species 0-61150
 Pt, of O₂ and CO, SCF-X α cluster calcs. 0-65365
 Pt surface, of CO, mol. cluster calc. 0-100407
 Pt(111) plane and stepped surfaces, of H₂, bond breaking activity, model potential 0-108744
 Re surface, long range and temp.-depend. interaction with alkali metal atom, theory 0-59802
 Rh (111), of acetylene and ethylene, EELS, LEED and thermal desorption mass spectrometry 0-80057

chemisorption continued

- Rh (111), of water, effect of adsorbed O, H, or CO, LEED and thermal desorption meas. 0-75435
 Rh-Cu catalyst, Al_2O_3 supported, chemisorbed CO, IR spectra (French) 0-60559
 Ru (001), of O_2 , uptake meas., thermal desorpt. spectroscopy and AES 0-108739
 Sd (111), of Cl_2 , LEED, AES, thermal desorption, and work function meas. 0-75444
 Si (111) 7×7 clean surface and O chemisorbed stage valence band density of states from L_{23}VV Auger spectra 0-100717
 Si, chemisorption of XeF_2 and SiF_4 , XPS and Auger spectra, surface chemistry 0-81358
 SnO_2 , O chemisorption, elec. cond. and EPR meas. correlation 0-84369
 SrTiO_3 (111), O_2 , H_2 and H_2O chemisorption, UPS and XPS studies, illum. effects 0-71572
 SrTiO_3 surface, oxidation and reduction by D_2O , H_2^{18}O , D_2 , isotope exchange study 0-104461
 V surface, chemisorption of Br_2 , struct., Na adsorption effects 0-101039
 W (001), displacive transition, H adsorpt. effects, theoretical model 0-65352
 W (100), of H, H_2 , vibrational mode, IR study 0-60582
 W, chemisorbed H_2 , vibr. spectra characts., adsorption sites 0-70535
 W, direct inelastic and trapping-desorpt. scatt. of N_2 , elementary steps in N_2 chemisorpt. 0-60737
 W, of cyclic hydrocarbons, on (100) surface 0-59782
 W surface, (110), chemisorpt. effects on dielec. function, refl. spectra 0-75616
 ZnO epitaxial film, nonuniform cond. due to H chemisorption (Russian) 0-65723
 Zr, adsorption and absorpt. of CO, NO, N_2 , O_2 , and D_2 , dissoci. and diffusion 0-80085

chemistry

- see also atmospheric chemistry
 carbohydrate nomenclature, digital representation, chemistry education 0-62435
 relativistic corrections, anomalous chemical properties of elements due to high speeds of inner electrons (French) 0-93839

chemistry, physical see physical chemistry**chemistry computing**

- see also computerised instrumentation; spectroscopy computing
 block-outpoint tree representation of chemical structures for use in computers 0-63522
 characterisation of rings of a molecule 0-63853
 coal chemical analysis, SEM images evaluation 0-71994
 electrochemical system, LF impedance meas. technique using on-line computer 0-57339
 interactive molecular analysis system, MOLY 0-63852
 molecular structures, topological code, modified Morgan algorithm 0-58122
 neutron activation anal., cyclic instrumental, optimum timing parameters for determ. of short-lived nuclides, computer program 0-61211
 nuclear materials safeguards, computerised chemical modelling of deviations, from mass transfer equilib. 0-83171
 pulse polarography, microcomputer-controlled polarograph appls. 0-66895
 quality control and chemical analysis of natural and industrial objects, future programme 0-104484
 staircase voltammetry, microcomputer-controlled polarography appls. 0-66895

Cherenkov counters

- biological sample ^{32}P and ^{45}Ca determ. by Cherenkov and liq. scintillation counting 0-98183
 eight-channel wide aperture, secondary particle identification 0-91371
 fibre-optic data transmission systems for plasma diagnostics 0-79571
 gas Cherenkov counter with ionisation spectrometer, appl. to cosmic ray studies 0-94662
 imaging Cherenkov detector using gas-filled MWPC, photoionisation of triethylamine 0-91400
 multineedle counter with cathodic focusing (French) 0-102392
 multistep avalanche chamber, far UV Cherenkov photon detection appl. 0-58042
 ninety channel, mass spectrometer, high energy electrons and gamma photons 0-91362
 ring imaging Cherenkov detection using multi-needle cathodic focusing detector 0-58040
 ring imaging counter, single photon detectors 0-58036
 SF₆ lead glass Cherenkov counter, high energy photon position determ. 0-58032
 silica aerogel Cherenkov detector development 0-58037
 Tyan Shan Cherenkov detector with conical reflector, electronics 0-102403
 water Cherenkov neutrino detector, construction and performance 0-91397
 Pb glass counter, automated calibration system 0-106233

Cherenkov detectors see Cherenkov counters**Cherenkov radiation**

- see also Cherenkov counters; electron radiation
 charged particles internal forces, moving faster than light in a medium 0-78751
 Cherenkov type parametric optical oscillator, optical saturation 0-102771
 cosmic ray photons, effect on IR interferometric search for non-solar planets 0-98523
 E. coli, photoreactivation following ionising irradi. rel. to Cherenkov emission 0-108969
 generation and transition in cylinder 0-82653
 heavy ion Z^2 depend. of Cherenkov emission, expt. limits 0-78495
 mica, 210 keV electrons, Vavilov-Cherenkov radiation, ang. distrib. half width, spectral depend. (Russian) 0-71505
 optical SHG by guided radiation mode coupling in thin film optical waveguide, aspects 0-106567
 photographic sensitive material, short time exposure, expt. technique 0-86477
 quasar emission-like spectra, H atom L_{α} line (Chinese) 0-105378
 reactor core monitoring of boiling water and of steam content using Cherenkov radiation 0-73957
 rectangular waveguide, Cherenkov radiation source 0-99373
 spatially dispersive media, Cherenkov effect 0-105516
 spent nuclear fuel inventory confirmation technique using Cherenkov light intensity meas. 0-78419
 Tokamak, enhanced plasma-frequency radiation (Chinese) 0-59185

Cherenkov radiation continued

- transition Cherenkov radiation in a dielectric slab 0-86099
 waveguide, superluminal radiator theory (Russian) 0-64156
 K, atomic vapour, resonant interaction with laser, Vavilov-Cherenkov effect (Russian) 0-106573
 ^{32}P radiation, counting efficiency improvement, wavelength-shifting compounds investigation 0-90893

chilling see cooling**chiral symmetries**

- see also SU_n theory
 σ model, SU(3) linear, renormalisation in one loop approx. 0-68368
 σ -model supersymmetric extensions, dynamical conservation laws, symmetric space valued fields 0-95227
 σ -models, non-linear, and universality in 3-D, scaling limit, and critical behaviour, chirality 0-62824
 Abelian gauge theories with dynamical symmetry breaking, effective pot., scale and chiral invariance (Russian) 0-57503
 chiral rotations and the fermion-boson equivalence in the Schwinger model 0-101919
 confining theories, chiral symmetry breaking in gauge theories 0-95244
 conformal and chiral anomalies, anomalous Ward-Takahashi identities 0-86612
 CP(N) ($N \geq 2$) chiral theory, 2-dimens., non-selfdual instantons 0-86585
 gauge theory, renormalisation of ghost and Goldstone fields and ghost symmetries 0-90987
 Gross-Neveu model, chiral invariant, S-matrix direct calc. 0-68362
 Gross-Neveu model embedded in U(1) gauge theory, fractional winding 0-86569
 large-N chromodynamics, chiral symmetry breakdown 0-91052
 meson decay, tensor, current algebra approach, symmetry-breaking Hamiltonian, chiral SU(3) \times SU(3) or SU(4) \times SU(4) 0-68450
 meson dipion cascade decays, current algebra techniques, pole plus remainder model, chiral symmetry breaking and QCD 0-62972
 neutral pseudoscalar meson radiative decays, K_{14} decay in chiral quark model (Russian) 0-105900
 O(N) \times O(N) and SU(N) \times SU(N) 2-dimens. models, conservation laws and S-matrices 0-68389
 O(N) invariant $(\phi^2)^2$ model, chiral field model and universality in 3-dimens. space 0-105796
 principle chiral fields, Backlund transformations and local conservation laws 0-68388
 QCD, large N limit, pseudoscalar noget chiral dynamics and low energy spectrum 0-101988
 QCD vacuum in strong external gauge fields, spontaneously, broken chiral symmetries 0-57555
 QED, Ward identity, axial vector current divergence, chiral invariant regulator field 0-57526
 quantum contour field equations, renormalisation and string like eqn. 0-86581
 Schwinger model, equivalent boson theory, anomaly-free Ward-Takahashi identities 0-82873
 Schwinger model, Ward identity, fermion axial vector current divergence, chiral invariant regulator field 0-57524
 spin $\pm 1/2$ polarised neutrons, differential scatt. by chiral systems, coupled oscill. model 0-102177
 spinor models, integrability in two-dimens. space-time 0-77935
 SU, grand unification model, two (V-A) and one (V+A) generations of quarks and leptons 0-57538
 SU(2)_L \times U(1) \times U(1)_R model, chiral symmetry and weak neutral currents 0-101980
 SU(2) \times U(1) gauge model, chiral SU(2) \times SU(2) symmetry and electron mass 0-57542
 SU(2) supergroups, Yang-Mills, Lie groups, chiral coeffs., Baker-Campbell-Hausdorff formula 0-68355
 SU(N $>$ 5) chiral grand unification 0-91028
 SU(N) \times SU(N) symmetry breaking with extremum constraints 0-68385
 superspace geometry and N=1 non-minimal supergravity 0-57155
 supersymmetric chiral field, 1/N perturbation theory and quantum conservation laws 0-68373
 supersymmetry, OSp(1,4), superfield formulation in anti-de Sitter space 0-57508
 Thirring model, chiral, CP^{n-1} and SU_n , exact S-matrix 0-90985
 tumbling gauge theories with chiral fermion fields, symmetry breaking 0-99042
 U(1) chiral symmetry breaking from SU(1) gauge theory 0-86617
 Wilson's lattice, local chiral symmetry for gauge theories 0-105774
 (π, π) , Weinberg chiral Lagrangian nonlinear terms, nuclear binding, optical pot. 0-78329
 π condensed phase, σ -model, alternating-layer- π struct. 0-83057
 $\pi \rightarrow e \nu \gamma$, isospin-breaking, chiral limit, conserved-vector-current violation, σ model 0-62988
 $\pi \rightarrow e \nu \gamma$ and SU(3) \times SU(3) σ -model 0-78054
 π K scattering amplitude, analytic continuation, chiral symmetry breaking 0-63027
 π N scattering, sigma term related to scatt. length, Altarelli-Cabibbo-Maiani relation derivation 0-57632
 π N σ term in hybrid chiral bag model, PCAC and SU(3) \times SU(3) symmetry violation 0-78096
 $\pi\pi$, p -meson contrib. in broken chiral symmetry model, phase shifts and lengths (Russian) 0-86756
 $^2\text{H}(\pi, \pi)$, scatt. length, exchange current contrib. 0-78328

chlorine

- see also nuclei with
 adsorption in Al-Al₂O₃-Au device rel. to press. depend. of current-voltage characts. 0-65704
 atom, K-shell ionisation by ultrarelativistic electrons, density effect 0-99576
 atom, photoionisation cross section and reson. theory, many body perturbation theory, 3p and 3s subshells 0-69114
 atoms, photorecombination, rate constants determ., identification of spectral distribution of recombinative emission intensity 0-85195
 chemisorption on Pd (111) and Pt (111), LEED, AES, thermal desorption, and work function meas. 0-75444
 determination, in coal, British Standard high temp. method 0-85252
 impurity in Li aluminosilicate glasses, ESR spectra 0-66027
 molecular static polarisability, ab initio SCF wave functions 0-74106
 molecule, inner shell excited states, X-ray absorpt. spectra, HF calcs. 0-78536
 molecule, model potential SCF calcs. 0-95528

chlorine continued

- molecule, one electron props. and polarisability, SCF and CI calcs. 0-58159
 molecule, pseudopot. calcs. 0-91446
 molecule, quadrupole moment determ. by refr. index anisotropy meas. method 0-78722
 molecule, vac. UV absorpt. cross section 0-91574
 monitoring of leaks using TAGA 3000 mobile test unit 0-72114
 Orion Nebula, Cl and Fe abundances from forbidden Cl II and Fe II near IR mapping 0-62217
 overlayer on Cu (100), adatom bonding effects, photoemission study 0-104044
 planetary nebulae, abundances of He, Ne, Ar, N, and Cl 0-109532
 saline cooling waters, free and total residual Cl determ. via modified amperometric membrane probes 0-82112
 simultaneous interactions with O₂ on Ta under low press. and high temp. 0-71938
 stratosphere O₃-CO₂ coupling, photochemical radiative column model with CI chemistry 0-85724
 X-ray emission spectra, detect. from Alcator-A Tokamak 0-92389
 Ar-Hg-Cl₂, elec. discharge, electron inelastic collision props. 0-79617
 CdS:Cl, photoluminesc., conc. quenching mechanism 0-97336
 CdS:Cl thin films, surface and bulk photoconc. 0-88653
 CdS:Cu, Cl films, photocond. growth and decay time 0-60041
 CdTe:Cl, acceptor states study by donor acceptor pair excitation luminesc. 0-100683
 CdTe:Cl, force variation due to charged defects 0-92634
 CdTe:Cl, semi-insulating, impurity photocond. spectra, local state distrib. in band gap 0-107865
 Cl⁻ and Na⁺, interdependence of transport in dog tracheal epithelium 0-61519
 Cl⁻, atomic core states, antishielding effects calcs. 0-83299
 Cl⁻, contracted Gaussian basis sets for mol. calcs. 0-83264
 Cl⁻, formation by HCl dissociative electron attachment, differential cross section, Feshbach resons. 0-83508
 Cl⁻ ions in nuclear reactor water coolant, determination by flow-type porous metallic Ag electrode 0-89577
 Cl²⁺, static dipole quadrupole polarisabilities and shielding factors calc. using HF scheme 0-99450
 Cl+fluoromethane, photochlorination electron and oscill. energy 0-81320
 Cl+H₂(HCl), relax. and chem. reaction, time resolved IR fluoresc. and mass spectrometry obs. 0-69177
 Cl+HCl, vibr. relaxation and reaction rates determ. 0-108698
 Cl+vinyl bromide-d₂ reaction, IR chemiluminesc. 0-102506
 Cl+H₂(D₂)(O₂)(N₂)(CO)(CO₂)(methane), total electron detachment cross sections for energies around threshold 0-99550
 Cl+HBr(HI)-HCl+Br⁻(I⁻), vibr. product state distrib., IR chemiluminesc. obs. 0-81309
 Cl+H-HCl+e, associative reaction, product vibr. state distrib. 0-66794
 Cl+Xe+Ne, three body ion-ion recombination probability, Monte Carlo simulation 0-85160
 Cl¹⁴⁺+Cu, K X-ray production and radiative electron capture, fluoresc. yield determ. 0-99553
 Cl₂, molecular fluid, Rayleigh and Raman light scatt. props., orientational and collision induced effect 0-63644
 Cl₂, electron propagator theory, mol. electron affinities calcs. 0-83521
 Cl₂+Ba-BaCl⁺+Cl⁻, chemi-ionis. reaction, mol. beam obs. 0-104434
 Cl₂+Cu(²D), beam-gas chemiluminesc. reactions 0-85151
 Cl₂+H, reactivity-selectivity, bounds derivation 0-66763
 Cl₂+H, stoichiastic-collision complex model theory 0-108696
 Cl₂+Hg+h ω -HgCl⁺+Cl, laser-induced harpooning reactions 0-83458
 Cl₂+K₂(Cs₂), ionisation reactions, absolute cross sections 0-99565
 Cl₂+muonium (H)(D), pot. energy surfaces, inversion calcs. 0-93734
 Cl₂+N₂ mixture, Raman laser optical excitation, electron phototransition theory (Russian) 0-99711
 Cl₂+Xe, classical trajectory calcs., energy threshold for collision-induced dissociation, determ. 0-95709
 Cl₂+Xe, XeCl form., relax. and quenching 0-81314
 Fe-Cl thermochem. cycle for H₂ prod. by H₂O pyrolysis 0-97811
³He-Cl, nucl. lasing, population inversion mechanism 0-63980
³He-Cl volume pumped nuclear laser survey of lasing 0-63979
 Re-O-Cl system, gas-transition metal interaction, kinetic model (French) 0-108740
 Si, thermal oxidation, role and effects of Cl 0-108622
 Si-SiO₂:Cl⁻, physics, electron and ion motion (Dutch) 0-60093
 ZnS:Cu, Cl, Mn film, AC electrolum. 0-60680
 ZnS:Mn, Cu, Cl films, AC electrolum. 0-60679

chlorine compounds

- hydration complexes, gas phase, electrostatic calcs. 0-100055
 [Cl₃PNPCL₃][PCl₆], X-ray cryst. struct. determ. 0-88095
 Cl+H₂, gas phase H-atom transfer reactions, struct.-reactivity correl., pot. energy surfaces 0-104433
 ClO radical, struct. and props. calcs. 0-74112
 ClF, rot. spectra in millimeter wave region, rot. transitions obs., equilib. const. determ. 0-78607
 ClF UV laser system 0-83597
 ClF-H, chem. laser, HCl vibr. emission 0-97709
 ClF+SF₆ (perfluoroethane) (Xe), thermal and photochem. reactions invest. 0-61117
 ClH-dimethyl ether, vibr.-rot. IR spectra, quantum and classical mechanics 0-91561
 ClNSO, ground state geometry, ab initio calcs. 0-106259
 ClO composition of stratosphere, balloon borne in situ reson. fluoresc. obs. 0-90167
 ClO, dissociation energy and bond length, CI calcs., bond function effects 0-102450
 ClO, free radical, Ar matrix absorpt. spectra, mol. vibronic states obs., spectroscopic const. determ. 0-83387
 ClO, in stratosphere, conc. vars. at twilight rel. to interpretation of solar occultation meas. 0-85756
 ClO+HO₂, free radical reaction rate consts. and products at 298K, discharge flow mass spectra 0-67391
 ClO+HO₂, reaction product distrib. 0-72586
 ClO₂, CW for IR mol. laser, optical pumping with ¹⁶CO₂ and ¹⁸CO₂ lasers 0-74343
³⁷ClO₂, ν_2 =1 state, laser-microwave double reson. obs. 0-95657
 ClO₄⁻, dummy spheres in SCF Xalpha calcs. 0-69056
 ClO₄⁻, ionisation energies, SCF-X α transition state calcs. 0-74115

chlorine compounds continued

- ClO₄⁻, ClO₃⁻ and ClO₂⁻ (n=1 to 3), ab initio calcs., localised MO and nature of Cl-O bond 0-69070
 ClOO radical, struct. and props. calcs. 0-74112
 ClO₂ in stratosphere, possible existence and chemistry 0-77066
 ClPF₆, nonrigid mol., tunnelling mechanisms, spectrosc. theory 0-78605
 Cl₃Si(CH₃)_{4-n}-n³⁵Cl NQR, geminal and vicinal interactions on substituents electronic effect 0-63663
 Cl₃Si(OCH₃)_{4-n}-n³⁵Cl NQR, geminal and vicinal interactions on substituents electronic effect 0-63663
cholesteric liquid crystals
 acceleration wave propag., theory 0-75154
 3-arylcholest-2-enes and 3-arylcholest-3,5-dienes, synthesis and liq. cryst. props. 0-79689
 biphenyl mixtures with cholesteryl chloride, static and dynamic electro-optical props., cholesteric-nematic transition 0-100646
 biphenyls, cholesteric blue phases, struct. and props. 0-103243
 blue phase, BCC struct., theory 0-59380
 blue phase, struct., Bragg diffraction of visible and UV light 0-59385
 capronate, proton spin-lattice relaxation in various phases (Russian) 0-97163
 cholesterol derivatives, mol. packing coeffs. and thermal stabilities 0-100201
 cholesteryl chloride+cholesteryl laurate, binary compensated, rhodamine 6G guest, electro-optical colour effect 0-71378
 cholesteryl decanoate, optical activity in blue phase 0-100641
 cholesteryl esters, blue phase, model 0-88030
 cholesteryl ethyl carbonate, long periods in sol. state, X-ray diffraction study 0-96503
 cholesteryl laurate-cholesteryl caprylate (75 wt.%), polymorphic behaviour, optical, elec. and dielec. meas. 0-65208
 cholesteryl myristate, cholesterogenic, blue phase, D NMR obs. 0-97151
 cholesteryl myristate, smectic A-cholesteric transition, tricritical behaviour, DTA and DSC study 0-65206
 cholesteryl nonanoate, cholesterogenic, blue phase, D NMR obs. 0-97151
 cholesteryl nonanoate, cyclohexanone admixture effect on mesophase order parameter, refr. index meas. 0-100165
 cholesteryl nonanoate-MBBA, liq. cryst. mixture, two colour display device 0-70116
 coatings, superimposed left- and right-handed, peak refl. and colour gamut 0-74472
 COC, cholesteric liq. cryst., positron lifetimes and phase transitions 0-59383
 colour temperature characts. obs., using temperature wedge method 0-57359
 COOB-cholesteric liq. cryst. mixtures, helix pitch, temp. depend. 0-64895
 crystallisation, quasithermal, of cholesteric mixtures 0-92652
 cyanobiphenyl E-7 mixture, bistable cholesteric liquid crystal display 0-96437
 disclinations, rotation defects, topology (French) 0-79679
 dye activated CLC, distributed feedback, tunable radiation generation (Russian) 0-102720
 EM radiation in media with spatial dispersion, spatial coherence formation and polarisation increase 0-106442
 ferrofluid/lyotropic liq. cryst. combination, ferronematics and ferrocholesterics 0-59378
 fibreglass laminates, thermal NDT using liq. crystals 0-93709
 films, absorpt. and contrast in dichroic liq. cryst. displays 0-75155
 flow normal to helical axis, steady, low shear rate 0-96443
 fluorescence of guest mols. in scatt. state 0-63698
 formate, proton spin-lattice relaxation in various phases (Russian) 0-97163
 gamma-ray radiation effects, dosimetry, thermography appl. (Spanish) 0-92457
 isotropic phase, pretransitional viscosity 0-84312
 Keating-Bottcher theory, of cholesteric systems with nonmesogenic additives 0-84057
 long pitch type, with homeotropic boundary alignment, elongated and spherulitic domain struct. 0-107047
 macroscopic helical structure origin 0-107043
 microwave thermophotodiodes, analysis of diffuse light spectra 0-73457
 molecular-optical, and structural anisotropy 0-84056
 multiplexed liquid cryst. display, use of cholesteric-nematic phase change 0-107408
 nematic-chiral-dye mixture, circular dichroism, selective light scatt. (Russian) 0-103944
 4-nitrophenyl-4-octyloxybenzoate/cholesteric liq. cryst. mixtures, helix pitch, temp. depend. 0-64895
 nonlinear reversible hydrodynamics, external mag. field influence 0-75156
 nonyloxybenzoic acid/cholesteric liq. cryst. mixtures, helix pitch, temp. depend. 0-64895
 optical properties, diffraction nature, review 0-70123
 oscillatory convective instabilities, caused by heating from below 0-103239
 poly- γ -benzyl-L(D)-glutamate, soln., liq. cryst. and pretransitional regions, optical rot. 0-66145
 poly- γ -benzyl-L-glutamate, soln., liquid crystal transitions anal. 0-65207
 polymer liquid-crystalline solns., struct. 0-103235
 radiation effect on cholesteric liquid crystals, gamma-ray dosimetry, thermography appl. (Spanish) 0-92457
 screw sense determ. by Grandjean-Cano wedge method, theory 0-84058
 shear flow induced propagating domains in cholesterics 0-64887
 stearate, proton spin-lattice relaxation in various phases (Russian) 0-97163
 surface and bulk configurations, topology 0-59381
 thermotropic polymers, cholesteric with mesogenic moieties and flexible spacers in main chain, synthesis and light reflection 0-88028
 MBBA+optically active substance, pretransitional optical rotation in isotropic phase (Russian) 0-92657
chondrites see meteorites
choppers (circuits)
 fusion reactor, Doublet III, plasma shape control, 1.5 Megawatt DC chopper power supply 0-102333
chopping see cutting
chromatic aberration see aberrations
chromatography
 azo dyes, UV-visible spectrophotometric 0-61207

chromatography continued

capillary column gas chromatography at nanogram resolution using dual beam Fourier transform IR spectroscopy 0-89554
 catecholamines, HPLC and continuous flow anal. using flow cell based on rotating disk electrode 0-66894
 cellulose acetate butyrate, in soln., hydrodynamic behaviour 0-64876
 chromatographic method of calibrating leaks 0-77800
 composition determination, cc $\text{LaS}_{1.500}\text{-LaS}_{1.333}$, solid soln. region, density meas. 0-95075
 conference, Carlsbad, Czechoslovakia (April 79) 0-73097
 dual-phase column, gas chromatography, two GC columns arranged coaxially are inside the other 0-71962
 fluoromethane, deuterium separation at high press. by ns CO_2 laser multiple-photon dissociation 0-91616
 forced-flow, alkaline earth ions detected by photometric method 0-71965
 gas, automatic purge and concentrator, volatile organic compounds in water determ. 0-97739
 gas, conc. device 0-85235
 gas, unit employing integral photoionisation detector 0-71963
 gas chromatograph element-specific detection systems (*German*) 0-93837
 gas chromatographic air analyser fabricated on Si wafer 0-73343
 gas chromatographic bipolar pulse differential electrolytic cond. detector 0-93814
 gas chromatographic purge-and-trap concentrator with microprocessor control 0-93815
 gas chromatography, selective detection by N_2 induced chemiluminescence 0-89495
 gas chromatography-IR spectroscopy using Sadtler CIRA 101 analyser, vapour phase spectra of liqs. and solids 0-93809
 gas chromatography-mass spectrometry, computerised, data-blocking cross-correlation peak detection 0-62725
 gas-chromatography, beta radio effluents, window flow counter 0-93824
 GC/MS integrated systems, review of current techniques 0-68289
 gel permeation, automated system using laboratory automation system 0-71961
 gel permeation chromatography, calibration, appl. to polycarbonate 0-58424
 gel permeation chromatography anal., data acquisition, computer control 0-97746
 graphite, Fe-catalysed gasification, electron, microscopy 0-104358
 high molecular weight polyethylene for HV cables, characterisation using size exclusion chromatography 0-66897
 high performance liquid, automatic system to monitor effluent tank contents 0-71982
 high performance liquid, sample introduction, syringe injection 0-66906
 information processing by computer 0-71970
 inorganic gas chromatography for determ. of H_2O and CO_2 in rocks and minerals 0-85767
 interferometric data from GC Fourier transform IR spectroscopy, functional group anal. 0-89548
 ion, equipment for the measurement of ions in solution 0-71983
 light pipe gas cell, Au coated internally, for gas chromatography/Fourier transform IR spectroscopy 0-89555
 liquid, radial compression separation system for improved column performance 0-76568
 liquid, UV detector suitable for preparative work, effluent flow over angled quartz plate 0-71960
 liquid chromatography, organic compound ionisation under atm. press. 0-86488
 liquid chromatography effluents on line anal., micro liq. chromatograph-interfaced Fourier transform IR spectrophotometer 0-73483
 liquid phase elution chromatography for determining solubilities of organic liqs. in H_2O 0-71958
 Micronova computer interfacing scheme 0-93813
 Microprobe Mole/plasma chromatograph system, for anal. of compounds on micron scale 0-101049
 microprocessor based chromatographic system 0-71999
 microprocessor based process gas chromatograph, System 9010 0-61205
 multidimensional gas chromatography, pressure balancing techniques 0-89576
 nonlinear, nonideal, computer simulation models 0-62639
 Pioneer Venus Sounder Probe gas chromatograph 0-67507
 plasma chromatography and electron capture detector, comparison between two techniques 0-61176
 plastics testing, automation 0-76443
 polybutadienes, radiation chemically cross-linked, charact. by pyrolysis gas chromatography (*German*) 0-81348
 polycarbonate, bisphenol-A, mol. wt. determ. using gel permeation chromatography 0-58424
 polyphenylacetylene cis-trans isomers, rel. mol. wt. distrib., heating effect 0-106409
 process gas chromatographs, microprocessor based, calibration and data reduction 0-81402
 proteins on diol-bonded SiO_2 gel stationary phase, high performance liquid chromatography 0-61174
 pyrolysis gas chromatography for polymer quantitative anal., internal standard choice 0-61180
 radio-liquid chromatograph system, determ. of ^{14}C -labelled amino acids (*Japanese*) 0-104834
 radiochromatography, beta-ray imaging using a multiwire proportional counter 0-102387
 Raman spectroscopy, chemical species anal. in conjunction with liq. phase chromatography (*French*) 0-93823
 shape variation detection, two-component chromatographic peaks resolution 0-71971
 technique and applications (*Dutch*) 0-93819
 tetrachlorodibenzo-p-dioxin determ. by low resolution gas chromatography-mass spectrometry 0-66893
 trans-Pu solvent extraction recovery and purification by trioctylphosphine oxide chromatography 0-93826
 transformer oil diagnosis, computerised evaluation of results (*Czech*) 0-97744
 waterborne oil fractional analysis by high-performance liquid chromatography (*Japanese*) 0-81936
 Ba, detection by photometric method 0-71965
 Ca, detection by photometric method 0-71965
 Mg, detection by photometric method 0-71965
 N_2O , determ. in water using electron capture detection gas chromatography, multiple equilib. 0-76566

chromatography continued

SF₆ with gaseous contaminants, arc decomposition kinetics investigation by combined gas chromatography-mass spectrometry methods 0-92250
 Sr, detection by photometric method 0-71965

chromium

see also nuclei with
 alkali halide:Cr³⁺, Szegedi charge and correl. with hyperfine coupling const. 0-96831
 antiferromagnetic, mag. struct., phase transition, and magnon spectrum, random anisotropy effects 0-88722
 antiferromagnetic, muon diffusion, spin relax. and coherent motion 0-71281
 antiferromagnetic, transverse magnetoresist., electron interference oscills. 0-65534
 antiferromagnetic, US attenuation and phase diagram 0-103831
 antiferromagnetic structure, mag. field effect, spin density wave model (*Russian*) 0-70953
 atom, $^3\text{P}_0$ state, radiative lifetime in matrices, meas. using laser ablation and selective excitation 0-71959
 atom, multiphoton ionisation and absorpt. 0-95575
 atom, X-ray transitions in laser produced plasma 0-100093
 black, electrodeposited solar collector coatings, high temp. optical and struct. degradation 0-66995
 black solar selective absorbers, thermal degradation 0-61417
 cathodic alloying on surface, for increased passivation and corrosion resist. 0-100940
 condensates, lattice const., internal stresses (*Russian*) 0-107141
 corrosion due to V_2O_5 melts (*Japanese*) 0-93691
 corrosion in SO_2 , 700-1000°C 0-97642
 corundum, Cr influence as impurity on thermochem. etching 0-88190
 Debye-Waller factors, extended De Launay model calcs. 0-70352
 determination in urine by electrothermal atomic absorpt. spectrophotometry 0-61175
 diffuse electron scatt. (*Russian*) 0-103438
 diffusion through Au films at low temp., Co effect 0-100361
 electrochemical behaviour, in molten V_2O_5 (*Japanese*) 0-92683
 electrode reactions with molten glass 0-85186
 electronic struct., spin-density functional calcs. 0-88476
 electroplating, prod. experience with trivalent plating solns. 0-71606
 enthalpy and specific heat, empirical eqn. (*Russian*) 0-92683
 Fermi surface under press., de Haas-van Alphen effect meas. 0-75499
 film, 3p-3d intershell interaction, photoemission 0-80934
 film, EELS, anomalous L_3/L_2 white-line ratios 0-93444
 film, evaporated, concurrent ion bombard. effects 0-80142
 film, obtained by thermo ionic precipitation, phase composition, lattice parameters (*Russian*) 0-96756
 film, on polycryst. CdS, thermal diffusion, 240-400°C 0-80001
 film, pattern generation by laser-induced oxidation 0-61009
 film, prep. by decomp. of bis-arene cpds., struct. and elec. props. 0-60785
 film, thickness meas., using nondestructive radioisotopic technique 0-68179
 film, trivalent, cathodic deposition, as bonding interface between Cu and polyethylene 0-76201
 film containing Cr_2O_3 , struct., oxide percentage determ. and elec. props. 0-103607
 film on steel, type AISI 316, thermal passivation in controlled vacuum 0-76276
 films, photoresist film on reverse gas plasma etching 0-97634
 films, vac. evaporated, optical cond. 0-76100
 foil, laser irradiated, low-angle X-ray scatt., angular block misalignment and hardness (*Russian*) 0-103413
 galvanic coating on steel 45, thickness determ. by profilography 0-85095
 glass:Cr³⁺, absorpt. spectra, Fano antireson. and vibronic Lamb shift 0-71458
 guanidine aluminium sulphate hexahydrate:Cr³⁺, ESR spectra fine struct. 0-93169
 hardfacing materials, friction characts. in high temp. Na (*Japanese*) 0-89356
 hyperfine interactions on ^{111}Cd -probe nuclei, TDPAC meas. 0-75904
 implantation into Cu for corrosion protection 0-71789
 ion beam milling, amomalous sputter yield behaviour 0-108624
 K-shell X-ray prod. by $^{14}\text{N}^+$ bombardment 0-91482
 laser, near IR transitions in Cr vapour 0-99704
 lattice dynamics, improved Fiekle model 0-59598
 magnetic phase diagram, near spin-flip temp. 0-60267
 magnetic superspace-group symmetry 0-79726
 methylammonium aluminium sulphate dodecahydrate, single crystals, high-order EPR transitions of Cr³⁺ 0-108052
 n=2-2 transitions in XUV spectra, anal. 0-102472
 Neel temperature and Fermi energy, nonmag. impurity effects 0-65888
 oxidation resistance, rare earth impurities effect 0-66703
 particle formation, ultrafine, via pulsed laser breakdown of $\text{Cr}(\text{CO})_6$ 0-84881
 phonon dispersion relations, modified tensor force model 0-103428
 photon emission due to Ar⁺ ion bombard., adsorbed and recoil-implanted O effect 0-80872
 plated on steel, factors influencing durability 0-108643
 Q-vector locking, press. induced hardening 0-103870
 ruby:Cr, relaxation behaviour, EPR study, environmental effects 0-66021
 self-weldability in high temp. Na (*Japanese*) 0-89392
 spallogenic isotopes in Fe meteorites, radial distrib. 0-67488
 spin density wave, Nambu-Eliashberg eqns. for k-state electron-hole pairing 0-97050
 spin density wave phases, domains 0-103871
 spin density wave state, phenomenological free energy density description 0-75720
 spin-flip transition temperature, press. depend. from elastic const. meas. 0-65944
 substrate for CdSe, thin film transistor, cryst. struct., substrate defect effects 0-70563
 volt ampere characteristics during electron melting process (*Russian*) 0-75336
 X-ray K-emission satellites, quasi-stationary states and origin 0-80903
 Al-Cr, thin film metal contact, sheet resistance changes 0-80356
 Al_2O_3 :Cr, electron irradi. induced cond., TSC and EPR study 0-80277
 Al_2O_3 :Cr photoexcited crystals, cooperative thermoluminescence quenching (*Russian*) 0-80881
 Al_2O_3 :Cr³⁺, HF phonon spectroscopy using supercond. tunnel junctions 0-65178

chromium continued

Al₂O₃:Cr³⁺, inhomogeneous spin system, time evolution towards saturated state 0-88869
 Al₂O₃:Cr³⁺, Jahn-Teller system, zero-phonon line broadening due to non-radiative transitions 0-108258
 Al₂O₃:Cr³⁺, ruby, reson. scatt. and trapping of 29 cm⁻¹ acoustic phonons 0-93403
 Al₂(WO₄)₃:Cr, and undoped crystals, luminesc. obs. 0-89047
 BaV₂O₆:Cr, EPR spectra temp. depend., paramagnetic ion point symm. 0-71166
 Be₃Al₂(Si₂O₇)₂:Cr³⁺, artificial emerald, distrib. of Cr³⁺ impurity 0-59503
 Bi₂Al₂O₆:Cr³⁺, luminesc. expts. 0-60656
 CaV₂O₆:Cr, EPR spectra temp. depend., paramagnetic ion point symm. 0-71166
 CdSe:Cr far IR transmission and reflectance spectra 0-71429
 CdTe:Cr, introduction of elec. active defects 0-103647
 Cr IV, 3d and 4f energy level parametrisation, Slater parameters and correl. corrections 0-87041
 Cr⁺ bombardment of stainless steels, effect on stress corrosion cracking and microhardness 0-85087
 Cr²⁺/Cr³⁺ colloidal SiO₂ surface films on Al, TEM/XPS study 0-85090
 Cr-Al₂O₃ powder targets for plasma-ion spray deposition of resistance films 0-84897
 Cr-Cr₂O₃ black chrome, commercial, solar absorber coating characterisation 0-80111
 Cr-Cr₂O₃ black solar absorber surfaces, microstruct. rel. to electroplating parameters 0-61418
 Cr-MIS solar cells, on polycryst. Si, grain boundary effect and conduction mech. 0-93894
 Cr-phthalocyanine-Cr sandwich, I-V and C-V characts. 0-60106
 Cr-Si interfaces, metallurgical and electrical props. 0-60081
 Cr-SiO₂-Si MIS solar cells, photovoltaic performance and interface states, nucl. radiation effects 0-94004
 Cr(II) lines, oscill. strengths in 2413-2718 Å wavelength range 0-106294
 Cr³⁺ production for life sciences appls. 0-94367
 CsCdBr₃:Cr³⁺(Cr⁺), EPR of impurities, charge compensation, X-ray effects 0-60407
 CsMgCl₂(Br₂):Cr³⁺(Cr⁺), EPR of impurities, charge compensation, X-ray effects 0-60407
 Fe-Ni-C martensite morphology, butterfly-lenticular transition temp., Cr addition effect (Japanese) 0-81053
 GaAs:Cr, impurity levels charact., using dark capacitance and photocapacitance transient techniques 0-59920
 GaAs:Cr, 0.84 eV no-phonon luminesc., fine struct. and origin 0-103980
 GaAs:Cr, carrier equilibrium effects, impurity states, elec. resistivity 0-65488
 GaAs:Cr, Cr distrib. and heat-treatment migration studies by SIMS 0-107305
 GaAs:Cr, Cr⁺ and Cr²⁺ centres, thermal treatment effects, EPR 0-65492
 GaAs:Cr, deep acceptor level, DLTS and optical DLTS study 0-92852
 GaAs:Cr, deep levels, wavelength-modulated photocapacitance spectroscopy 0-76055
 GaAs:Cr, dislocation-free single crystals, point defects and rad. damage 0-88141
 GaAs:Cr, FET, influence of Cr on mobility of electrons 0-92910
 GaAs:Cr, hole traps, ESR studies 0-75843
 GaAs:Cr, ion implanted, implantation damage profiles, laser annealing, ellipsometry study 0-79819
 GaAs:Cr, low temp. gettering 0-96549
 GaAs:Cr, photoionisation transition Cr²⁺→Cr³⁺, EPR studies 0-60638
 GaAs:Cr, photoluminescence, YAG laser or krypton laser 0-60668
 GaAs:Cr, photoluminescence in strong electric fields 0-108270
 GaAs:Cr, redistrib. of Cr during laser annealing 0-88192
 p-GaAs:Cr, semi-insulating, mobilities and carrier concentrations, temp. depend. 0-70702
 GaAs:Cr, semi-insulating, Cr redistrib. during thermal annealing as function of encapsulant and implant fluence 0-84199
 GaAs:Cr, semi-insulating, compensation mechanisms, Hall effect and optical absorpt. meas. 0-84477
 GaAs:Cr, semi-insulating, Zeeman studies of 0.839 eV emission 0-103987
 GaAs:Cr, semi-insulating, damage gettering of Cr during annealing of Cr and S implants 0-107304
 GaAs:Cr, thermally grown, DLTS study of Cr trap density 0-96815
 GaAs:Cr, zero-phonon struct. in Cr²⁺ (3d⁴) optical absorption 0-60640
 GaAs:Cr₂O₃ semi-insulating monocrystal development and four-level model 0-88191
 GaAs:Cr₂Se₃, ion-implanted, semi-insulating effects of Cr redistrib. on elec. characts. 0-59982
 GaAs:Cr capless annealed, under As press., Cr redistrib., SIMS obs. 0-59503
 GaAs:Cr semi-insulating wafer, heat treatment technique for no thermal conversion 0-100857
 GaAs:Cr²⁺, Jahn-Teller effect for ion impurities 0-107753
 GaP³¹:Cr, paramag. centres, identification from ESR and ENDOR spectra 0-80600
 p-GaP:Cr, hole traps, ESR studies 0-75843
 GaP:Cr epitaxial layers, Cr conc. profile determ. 0-65029
 n-InP:Cr, press. depend. of elec. resist. and Cr ionisation energy 0-80281
 InP:Cr²⁺, Jahn-Teller effect for ion impurities 0-107753
 n-InSb:Cr, deep impurities, elec. cond. and Hall coeff. meas., 4.2 to 120K 0-107791
 InSb:Cr, Zn impurity centre behaviour, impurity conc. and Hall coeff. meas. 0-65490
 KMgF₃:Cr²⁺, HF phonon spectroscopy using supercond. tunnel junctions 0-65178
 K₂NaGaF₆:Cr³⁺, magneto-optical study of ²T_{1g}, ⁴T_{2g}, ²E_g-⁴A_{2g} transitions 0-71384
 KVO₃:Cr³⁺, study of ESR spectra 0-80601
 LaCrO₃:Cr ceramic, prep. phase comp. and elec. cond. (Polish) 0-71621
 LiVO₃:Cr³⁺, study of ESR spectra 0-80601
 Lu₂(WO₄)₃:Cr, and undoped crystals, luminesc. obs. 0-89047
 MgO:Cr, high resolution far IR spectroscopy of lower energy levels of Cr²⁺ 0-80822
 MgO:Cr²⁺, HF phonon spectroscopy using supercond. tunnel junctions 0-65178
 MgO:Cr²⁺, reson. relax. time for impurity electrons and localised phonons interaction, appl. to thermal cond. 0-59590
 MgO:Cr³⁺, EPR spectra obtained at room temp. and 1200°C 0-68233

chromium continued

MgO:Cr²⁺, emission and excitation spectra 0-93387
 MgO:Cr³⁺, ODMR, octahedral and orthorhombic site symm. 0-71243
 MgO:Cr³⁺, ODMR study, Cr³⁺ ions in tetragonal symm. sites 0-88892
 MgO:Cr³⁺, optical excitation transfer 0-97325
 NaVO₃:Cr³⁺, study of ESR spectra 0-80601
 Nd-Cr:Li-La phosphate glass, Nd luminesc. quantum efficiency meas., Nd-Cr nonradiative transfer 0-66296
 Pt-Cr interface, low-temp. diffusion, ambient effects 0-100355
 RbVO₃:Cr³⁺, study of ESR spectra 0-80601
 Sc₂(WO₄)₃:Cr, and undoped crystals, luminesc. obs. 0-89047
 Si:Cr, impurity states, localised orbital approach 0-92851
 Si:Cr⁺, spin-lattice relax. of Jahn-Teller centres, coexistence of minima with different symmetries 0-80602
 TiO₂:Cr, slightly doped, elec. cond. and defect struct., charge compensation, point defect model 0-75568
 YAG:Cr, optical detection of phonons 0-92630
 ZnGa₂O₄:Cr³⁺, weak exchange interaction determ., ESR study 0-93107
 (ZrO₂)_{0.9}(Y₂O₃)_{0.1}:Cr, Mn, stabilised single crystal, EPR of Mn²⁺ and Cr³⁺ obs. 0-66024

chromium alloys

see also chromium compounds

Carpenter 20 Cb-3 alloy, pitting resist. in low salinity geothermal brines 0-93681
 Colmonoy, self-weldability in high temp Na (Japanese) 0-89392
 Colmonoy hardfacing materials, friction characts. in high temp. Na (Japanese) 0-89356
 dilute alloys, amorphous, exhibiting Mossbauer effect, mean mag. props. (French) 0-80489
 Hastelloy, C-276, H transport rel. to ageing treatment 0-75384
 Hastelloy, C-276, H-induced crack growth 0-71747
 Hastelloy-X, low cycle fatigue crack propagation at 25°C and 760°C 0-104270
 Hastelloy-X, Ni-Cr-Fe-Mo, cyclic oxidation resist. improvement by high temp. etching treatment 0-97627
 Hayes alloy no.716, Fe-Cr-Ni-Co-W-Mo-Si-C-B (26, 22, 12, 3.5, 3, 1.2, 1.1, 0.4 wt.%), hardfacing alloy 0-100802
 Haynes alloy 20 Mod, pitting resist. in low salinity geothermal brines 0-93681
 Incoloy 800, clean and steam oxidised, T₂ permeation 0-88364
 Incoloy 800, steam oxidised, oxide coating anal. 0-89399
 Incoloy 800, stress corrosion cracking in NaOH solns., electrochem. aspects, peening treatment 0-97618
 Inconel, caustic stress corrosion cracking resistance, processing variables effect 0-71796
 Inconel, steam generator tubing, mag. probe inspection 0-85119
 Inconel, type 600, Li corrosion inhibitions by Al additions 0-108646
 Inconel 600, small bore tubing, crevice corrosion 0-60999
 Inconel 600, stress corrosion cracking in NaOH solns., electrochem. aspects, peening treatment 0-97618
 Inconel 600, thermal treatment, grain boundary microstruct. and SCC resistance 0-71675
 Inconel 600 alloys, stress corrosion cracking, prediction in 10% NaOH soln. at 315°C 0-97616
 Inconel 600 safe-end cracking failure at Duane Arnold reactor 0-104295
 Inconel 617, creep, morphological changes of carbides, affect on creep props. 0-108509
 Inconel 625, electron yields under ion bombardment for clean and oxidised surfaces 0-66368
 Inconel 625, organic contamination removal by plasma cleaning and etching 0-97645
 Inconel 718, grain growth during sintering 0-97449
 Inconel 800, simulated, steam oxidation 0-76405
 Inconel hardfacing materials, friction characts. in high temp. Na (Japanese) 0-89356
 Inconel X-750, deprim. and fracture characts., 24-816°C 0-108551
 Neel temperature of one dimens. electron gas in spin density wave state 0-65884
 Nimonic, irradiated, void nucleation, numerical evaluation 0-70252
 Nimonic 80A, order hardening, comparison between revised theory and expt. 0-93565
 Nimonic PE16, irradiation creep data obtained in fast and thermal neutron spectra correlation with displacement cross-sections 0-84993
 Nimonic PE-16, electron irradi. in HVEM, void growth, vacuum environment influence 0-107323
 nuclear microprobe methods for investigating oxidative corrosion 0-71787
 p 0-88364
 rare earth ternary alloys, RT₆Al₆, T=Cr, Mn, Fe, Cu, cryst. struct. 0-107110
 steel, austenitic (03KH18N10T), heat treatment for fission reactor appls. 0-66454
 steel, austenitic stainless Ni-Cr, heat resist. and comp. of non-metallic inclusions, effect of La, Nd, Pr and Ce 0-76315
 steel, C-Cr (1.0, 1.5 wt.%), 52100 bearing steel, control of surface residual stress by heat treatment 0-97501
 steel, Cr, carburising kinetics, in endothermal atm. 0-76410
 steel, Cr, carburising with high-activity carburiser 0-76412
 steel, Cr, coated with TiC, prep. and props. 0-76414
 steel, Cr (2%), austenite decomp., phase diagrams and struct. form. kinet. 0-76223
 steel, Cr with metastable austenite, wear resist., temp. effect 0-76370
 steel, Cr-C (1, 1 wt.%), hot ductility and S segregation 0-66594
 steel, Cr-Mn (13, 19 wt.%), elastic const. behaviour, anomalous, low temp. 0-97521
 steel, Cr-Mo, ferritic, grain boundary segregation, X-ray microanal. by STEM 0-66740
 steel, Cr-Mo, H embrittlement in H₂S environment, Mo effect 0-76415
 steel, Cr-Mo and Ni-Cr-Mo-V low-alloy, additive remedy for temper brittleness 0-66659
 steel, Cr-Mo weld metal, reheat cracking, residual elements and microstruct. influence 0-66553
 steel, Cr-Mo weld metal, trace element embrittlement suppression by creep strength effects 0-66656
 steel, Cr-Mo-(V) austenitic, creep resist., high-temp. props. residuals effect 0-66600
 steel, Cr-Mo-V, strength and ductility in creep, purity influence 0-66598
 steel, Cr-Mo-V low-alloy, high-temp. ductility and crack growth, impurities effect 0-66652
 steel, Cr-Mo-V low-alloy, mech. props. and stress relief cracking, effects of impurities and deoxidation practice 0-66599

chromium alloys continued

- steel, Cr-Mo-V low-alloy, prior austenite grain boundary embrittlement by B 0-66657
- steel, Cr-Mo-V low-alloy, stress relief cracking, impurity and alloy content effects 0-66654
- steel, Cr-Mo-V low-alloy with high residual element content, cavitation control 0-66663
- steel, Cr-Mu-W, carbide form., W effect 0-76259
- steel, Cr-Ni, pendulum drop melt extracted, struct. and props. 0-76242
- steel, Cr-Ni-Mo-Mn, wetting of TiC, expt. planning investigation 0-60822
- steel, Cr-Si, oxidation resist. in high pressure CO₂, Si effect 0-66704
- steel, Cr-W-Mo-Co, high-speed, from atomised powders, mech. and cutting props. 0-66556
- steel, high-strength, fatigue, interaction effects between trace impurities and environment 0-66651
- steel, martensitic, alloying element effect on coarsening behaviour of cementite particles in ferrite 0-66518
- steel, martensitic 12% Cr, temper embrittlement 0-66650
- steel, Ni-Co-Cr, high-strength medium C, Cr effect on props. 0-76339
- steel, Ni-Cr, anodic dissoln. in NaCl solns. at high current densities (*Russian*) 0-76396
- steel, Ni-Mo-Cr, embrittling effects of residual elements 0-66655
- steel, stainless, 20Kh13, prep. by diffusion impregnation 0-60803
- steel, stainless, Cr-Ni-Ti, metallographic detection of (Ti,Ni)₆C 0-66721
- steel, stainless, FeCrAl, creep-rupture props., 650-800°C 0-97535
- steel, W-Mo-Cr-V tool, laser surface melted, struct., heat treatment effect 0-76424
- steel turbine casings, residual life determ. 0-93585
- Stellite, self-weldability in high temp Na (*Japanese*) 0-89392
- stellite hardfacing materials, friction characts. in high temp. Na (*Japanese*) 0-89356
- Stellite-6, XPS obs. of aqueous oxidation, surface comp. and gaseous oxidation effect 0-81238
- stress corrosion cracking test machine, design and construction, appl. to Fe-Cr-Ni alloys 0-97649
- Ag-Cr, dil., specific heat, impurity contrib. Kondo temp. 0-65903
- Al-Cr, dil., supercond., nucl. spin relax. and quasiparticle excitations 0-88680
- Al₂O₃-NiCr composite, plasma sputtering of electroheating coatings, elec. props. (*Russian*) 0-108350
- Au-Cr, conc. spin glasses, thermopower 0-65538
- Au-Cr, dil., elec. resist., generalised phase shift anal. of Kondo effect 0-75556
- Au-Cr, dil. alloys., elec. resist., deviations fro Matthiessen's rule 0-75541
- Au-Cr, UPS study, localised states 0-93449
- CC Fe-Ni-Cr (35, 15 wt.%): Nb(Ti)(Mo), corrosion in HTGR He environment 0-61021
- Co-Cr mag. film, crystallographic texture formation effects on props. (*Russian*) 0-108471
- Co-Cr-C eutectic alloy, thermal conductivity and electric resist. at high temp. 0-103668
- Co-Ni-Cr-Mo (35, 20, 10 wt.%), MP35N, TEM study of phase transformations 0-81054
- Co-Ni-Cr-Nb (40, 18, 1.8 wt.%), precipitation behaviour of NbC, effect of ageing temp. on morphology 0-89227
- (Co_{100-x}B_x)_{1-x}Cr_x thin film glasses, mag. props. and corrosion resist. 0-80576
- CoCr, dil., low temp. specific heat and magnetisation 0-65925
- (Co₉₃Fe₀₇)_{75-x}Cr₂₅B₁₀ amorphous alloy, thermal stability, Cr conc. effects, DTA expts. 0-59395
- 25Cr-20Ni stainless steel dendritic solidification, growth morphology and solute redistrib. (*Japanese*) 0-81045
- Cr-(Cr,Co)₃ eutectic, oxidation effect on toughness and strength 0-89404
- Cr-Al-C, ternary system, phase relationships 0-76230
- Cr-Co, dil., antiferromag., elec. resist. min., press. and impurity effects 0-59970
- Cr-Co, magnetic transformations, triple point (*Russian*) 0-88747
- Cr-Co, phase transformations and magnetostriction (*Russian*) 0-103869
- Cr-Co-Fe, low Co, phase separation, TEM and Mossbauer spectra obs. 0-71269
- Cr-Fe, dil., antiferromag., elec. resist. min., press. and impurity effects 0-59970
- Cr-Fe, dil., magnetisation, Fe local moments 0-60215
- Cr-Fe, dil., spin correlations and neutron scatt. near crit. conc., theory 0-60327
- Cr-Fe, elastic moduli, electron conc., pulse echo overlap meas. 0-59550
- Cr-Fe (6.5 wt.%), atomic clustering and mag. defects, mag. moments 0-60246
- Cr-Fe-C (28.4, 9.1 wt.%) prep. from FeCr₂O₄ chromite 0-100804
- Cr-Fe-Ni, γ -solid soln., thermodynamic activity determ. at 1500K 0-108397
- Cr-Fe-Ni alloys, claddings, chemical compatibility with UC nuclear fuels, thermodynamic model 0-63263
- Cr-Fe-Ni-Si, ternary phase equilibria for Cr-Fe-Ni rich portion, lattice stabilities 0-71628
- Cr-Ge system, phase diagram, thermal anal., X-ray diffr., microhardness, and electron probe anal. (*French*) 0-97462
- Cr-Ge system, XPS, X-ray and neutron diffr. and mag. meas. to study chem. bonding and electronic struct. 0-60749
- Cr-Ir, magnetic transformations, triple point (*Russian*) 0-88747
- Cr-Mo, elec. resist. and thermo-EMF, conc. depend., 4.2 to 1500K (*Russian*) 0-80247
- Cr-Mo, electrical resistivity, spin density wave gap, Neel temp. 0-88534
- Cr-Mo steel types JIS SCMV 2, SCMV 3 and SCMV 4, high-temp. high-cycle fatigue props., press. vessel appls. (*Japanese*) 0-93650
- Cr-Mo-V-Nb, supercooled austenite isothermal decomp., struct., strength and fracture characts. 0-60966
- Cr-Nb-Mo system, comp. and temp. depend. alterations in mech. props., phase diagram interpret. (*Russian*) 0-85045
- Cr-Ni compressor disk, surface plastic deform., optimal method 0-60924
- Cr-Ni-Fe, ternary phase diagrams, interactive computer program 0-71629
- Cr-Ni-Nb steel, oxidation in CO₂, charged-particle nuclear techniques 0-61022
- Cr-Os, magnetic transformations, triple point (*Russian*) 0-88747
- Cr-Re, phase transformations and magnetostriction (*Russian*) 0-103869
- Cr-Re (0.18 wt.%), mag. excitations in longitudinal and transverse SDW phases 0-70946
- Cr-Rh, magnetic transformations, triple point (*Russian*) 0-88747

chromium alloys continued

- Cr-Ru, magnetic transformations, triple point (*Russian*) 0-88747
- Cr-Si, dilute alloy, mag. susceptibility and Neel temp. meas. 0-71017
- Cr-Si-V, (2, 0.1 at.%), paramag. to commensurate spin density wave transition 0-65875
- Cr-V, itinerant electron antiferromag., spin fluctuations, low temp. specific heat 0-107439
- Cr-W, anodic dissoln. at high current densities (*Russian*) 0-76395
- Cr-W-O, phase relations, thermodynamic props. of CrWO₄ and Cr₂WO₆ 0-104120
- Cr-Zr evaporation source improvement, diffusion barrier layer deposition for IC metallurgy 0-76163
- Cr₂C₃ electrophoretic alloy coatings on C steel, sintered, struct. form., Ni-P undercoat effect 0-61027
- Cr₂C₃/Ni-Cr, self-weldability in high temp Na (*Japanese*) 0-89392
- Cr₂C₃/Ni-Cr hardfacing materials, friction characts. in high temp. Na (*Japanese*) 0-89356
- CrCo, dil., low temp. specific heat meas., 1.5 to 4K 0-60328
- 10CrNiCuP, suitability for power station chimney flue structural material, corrosion testing 0-108681
- Cr₂Os, σ phases, ordering, X-ray cryst. struct. determ. 0-107107
- Cr_{99.995}Fe_{0.005} alloy, mag. struct., neutron diffr. study 0-60198
- Cr₂Ru, σ phases, ordering, X-ray cryst. struct. determ. 0-107107
- Cr₂Si, mag. susceptibility, 2 to 300K, rel. to electron energy spectrum 0-60185
- Cr_{2.8}V_{0.2}Fe_{3.4}C₃, stacking fault study, morphology, comp. and struct. 0-84196
- Cu-Cr, dil., spin-density magnetisation near Cr atoms, NMR study 0-80626
- Cu-Cr, Kondo alloy, Josephson tunnelling effect 0-60145
- Cu-Cr (0.75 wt.%), deformation characts., fully reversed cyclic strain with fatigue cracks and dislocation struct. 0-81148
- Cu-Cr alloy, laser irradi., structural changes (*Russian*) 0-100247
- Cu-Cr-SiO₂ system, age and dispersion strengthened, dislocation struct. around SiO₂ particles 0-108468
- Cu-Cr(SiO₂), single crystals, yield and pre-yield behaviour rel. to aging time 0-81103
- CuCr, dil., anisotropic hyperfine coupling, NMR study 0-65784
- CuCr, dil., specific heat, impurity contrib. Kondo temp. 0-65903
- Fe, cast, white, high Cr, phase composition, B effect 0-104172
- Fe-B-Cr, metallic glasses, mag., struct., and elec. props. 0-88751
- Fe-Cr, BCC, local moments in Mossbauer study 0-108125
- Fe-Cr, crystallisation temp., overcooling temp. (*Russian*) 0-97472
- Fe-Cr, dil., spin density wave under high press., neutron diffr. study 0-65798
- Fe-Cr, high-temp. oxidation, borate inhibitors 0-66705
- Fe-Cr, hyperfine magnetic fields, Mossbauer spectra 0-97165
- Fe-Cr, influence of annealing on hyperfine interaction parameters, Mossbauer effect 0-71263
- Fe-Cr, random ferromag. alloys, local mag. moment calc. 0-70974
- Fe-Cr, specific heat enhancement and electron-phonon interaction 0-65242
- Fe-Cr (12 wt.%), corrosion in o-phosphoric acid 0-97622
- Fe-Cr (9 wt.%), extrinsic grain boundary dislocations, low C content influence 0-107273
- Fe-Cr (9 wt.%), oxidation studied using C¹⁸O₂ and D₂O tracers 0-71784
- Fe-Cr alloy, N solubility investigation (*Russian*) 0-92675
- Fe-Cr alloy, sputter etching oxide film, comp. profile, quantitative AES 0-81383
- Fe-Cr alloys, cold worked, internal friction due to H (*Japanese*) 0-70305
- Fe-Cr alloys, in acid and neutral solns., thickness and optical constants of passive and transpassive films 0-66698
- Fe-Cr-Al, HOS 875, oxidation, cyclic, role of thermal shock 0-97640
- Fe-Cr-Al, Kanthal films, vac. deposited, evaporation characts., comp., struct. and elec. props. 0-88646
- Fe-Cr-Al, scales, α -Al₂O₃, early stages development at high temp. 0-89413
- Fe-Cr-Al (12, 3 wt.%), internal friction and rigidity modulus, strain amplitude depend. (*Japanese*) 0-92606
- Fe-Cr-Al (7, 5 wt.%), expt. stainless alloys, phys. and mech. props. 0-97637
- Fe-Cr-Al-Y, oxidation resistance, heat treatment and Al³⁺ ion implantation 0-71785
- Fe-Cr-Al-Y, scales, α -Al₂O₃, early stages development at high temp. 0-89413
- Fe-Cr-Co, ductile magnet alloys, mech. props. 0-85001
- Fe-Cr-Co, elastic props. anisotropy at room temp. (*Russian*) 0-89279
- Fe-Cr-Co, magnetic domain walls, Lorentz microscopy 0-103854
- Fe-Cr-Co, metallic magnets investigation, present state (*Polish*) 0-107987
- Fe-Cr-Co (28, 10.5 wt.%) ductile magnet alloy, humidity-induced H₂ embrittlement 0-89406
- Fe-Cr-Co alloy, coercive force mechanism 0-71103
- Fe-Cr-Co alloy, spinodally decomposed, micro-twinning 0-92537
- Fe-Cr-Co alloys, (5-9 wt.% Co), obtained by slow cooling under mag. field, permanent magnet props. 0-75797
- Fe-Cr-Co permanent magnet system, miscibility gap, microstruct. and mag. props. obs. 0-76228
- Fe-Cr-Co-Mo high energy permanent magnets, mag. props. 0-97119
- Fe-Cr-Mo, white cast, optimising fracture toughness and abrasion resist. 0-85042
- Fe-Cr-Mo alloy castings, thick-section, factors affecting 0-108374
- Fe-Cr-Mo and Fe-Cr-Mo-Si, amorphous films, corrosion resist. and ion plating use 0-89423
- Fe-Cr-Ni, corrosion behaviour in hot conc. NaOH soln. (*Japanese*) 0-85082
- Fe-Cr-Ni, foil, in situ oxidation in HVEM 0-104354
- Fe-Cr-Ni (12, 15 wt.%) austenitic alloy, Ni⁶⁺ irradiated, void swelling and phase stability, Si and Ti effects 0-65055
- Fe-Cr-Ni (18, 14 wt.%), γ to ϵ to α martensitic transform., external stress effect, double tensile deform. exam. 0-108438
- Fe-Cr-Ni (19, 13 wt.%), austenitic, Ni⁺ ion irradiated, multiple dislocation loops (*French*) 0-65064
- Fe-Cr-Ni based alloys, surface oxides at high temps., backscattering Raman spectroscopy 0-93291
- Fe-Cr-O system, phase relations at 1200°C using diffusion couple technique 0-89205
- Fe-Cr-Si, heat resistive films prepared by sputtering, lifetime meas. 0-80132
- Fe-Cr-Si, oxidation resist. in high pressure CO₂, Si effect 0-66704
- Fe-Cr-Ti (18, 0.1-0.9 wt.%), high temp. oxidation (*Japanese*) 0-71806

chromium alloys continued

Fe-Cr-Ti-Mo-TiO₂ (13, 3.5, 1.5, 2 wt.%) dispersion hardened, void swelling 0-65046
Fe-Cr-Ti(Al) liquid alloy, thermodynamical anal. of O₂ solubility (*Russian*) 0-92676
Fe-Ni-Cr, carbide form. by C diffusion, precip. distrib. and morphology 0-104164
Fe-Ni-Cr, heavy ion irradiat., defect cluster obs. 0-107341
Fe-Ni-Cr, mag. props. in weak mag. fields (*Russian*) 0-75771
Fe-Ni-Cr (30.6, 21.3 wt.%), Alloy 800, high temp. oxidation at low O₂ press., SEM, AES and electron probe microanal. study 0-93688
Fe-Ni-Cr (35, 15 wt.%) superalloy, stress rupture and tensile props., C and B additions effect (*Chinese*) 0-104244
Fe-Ni-Cr based alloy, KhN35VTYu, temp. depend. of energy of fracture, influence of γ' phase (*Russian*) 0-81147
Fe-Ni-Cr-Al-Ti-W-Mo (35, 15, 2.4, 2.3, 2.2 wt.%) wrought superalloy, freckles (*Chinese*) 0-104137
Fe-Ni-Cr-Al-Y, oxidation mechanism, Y addition effect on kinetics and oxide adherence 0-97623
Fe-Ni-Cr-Ti-Al, with thermoelastic control coeff., comp. and heat treatment influence on props. (*French*) 0-81074
Fe-Ni-Cr-Y, Y addition effect on selective oxidation/diffusion phenomena relationship (*French*) 0-108623
Fe-Sb-Cr, dil., short range order, NMR study 0-71237
Fe-Sb-Cr, interactions and segregations, Mossbauer and X-ray diffr. study 0-70415
Fe-Si-Cr magnetic films, sputtered, corrosion reduction, effect of Cr obs. 0-80573
Fe-W-Cr-Mo system, mag. and mech. props. rel. to production methods (*Japanese*) 0-71107
(Fe_{100-x}B_y)_{1-x}Cr_x thin film glasses, mag. props. and corrosion resist. 0-80576
Fe_{0.5}Co_{0.5-x}Cr_x films, vacuum-deposited cryst. and mag. struct. (*Russian*) 0-93081
(Fe_{0.07}Co_{0.93})_{75-x}Cr_xSi₁₅B₁₀, amorphous, disaccommodation of mag. permeability and induced anisotropy 0-88741
Fe,Cr_{1-x} spin-wave evolution crossing from ferromag. to spin-glass regime 0-97080
Fe₃Cr₃Ni₄B₁₂B₆, amorphous X-ray absorpt. spectra, effective co-ordination charges 0-84805
(Fe_{100-x}Cr_x)₇₉P₁B₈ amorphous alloys, sput cooled mag. and transport props. 0-84593
(Fe₉₈Cr₂)₇₉P₁B₈ and (Fe₉₆Cr₄)₇₉P₁B₈, amorphous, low temp. sp. ht., mag. contribs. 0-80552
Fe₇₃Ni₁₆Cr₄P₇B₆, metallic glass, Doppler broadening of positron annihilation γ -radiation and elec. resist. 0-66321
Fe₇₃Ni₁₆Cr₄P₇B₆ metallic glass, crystn. kinetics by TEM 0-75186
Fe₇₃Ni₁₆Cr₄P₇B₆, Metglas 2826A, EPR at 20 GHz 0-75848
Fe₇₃Ni₁₆Cr₄P₇B₆ Metglas, bending deform., shear band form., high-speed cinematographic obs. 0-89322
Fe₇₃Ni₁₆Cr₄P₇B₆, Metglas amorphous films, corrosion resist. and ion plating use 0-89423
Fe₇₃Ni₁₆Cr₄P₇B₆ metallic glass, effect of pre-ageing on glass transition temp. 0-100326
Gd-Cr amorphous films, spontaneous Hall effect and elec. resist. 0-80251
Hg_{1-x}Zn_xCr₂Se₄, magnetic struct., neutronographic and mag. investigation (*Russian*) 0-88726
Mn-Cr-Ti layers on low C steel, composite, residual stresses rel. to arc-spraying parameters (*German*) 0-104077
Mn_{1.86}Cr_{0.12}Sb, antiferromag.-ferrimag. transition, neutron crit. scatt. and crossover effect 0-71023
Mo-Cr-V-P, load curves, structure states boundaries and strain hardening (*Russian*) 0-89241
Ni-(Co)-Cr, aluminide coating, microstruct. and chem. 0-76189
Ni-Al-Cr₂Cr₂, eutectic alloy, directionally solidified, oxidation resistance, influence of Y 0-89409
Ni-based TaC eutectic, directionally solidified, elastic moduli 0-84984
Ni-Co-Cr TEM foils, white band contrast 0-75134
Ni-Co-Cr/Al₂O₃ catalyst, IR spectra of adsorption and interaction with pyridine 0-71946
Ni-Co-Cr-Mo-Al-Ti (17.5, 15.1, 4.9, 4.15, 3.25 wt.%), creep and stress rupture behaviour in air and vacuum 0-60918
Ni-Cr (30 wt.%), collective dislocation movements, in situ study 0-100243
Ni-Cr, anodic dissoln. in NaCl solns. at high current densities (*Russian*) 0-76396
Ni-Cr, degradation after exposure to 1% H₂S/H₂ gas mixture at 1000°C 0-89408
Ni-Cr, heat-resist., high-temp. ductility and embrittlement 0-76314
Ni-Cr, heavy ion irradiat., defect cluster obs. 0-107341
Ni-Cr, high temp. thermomech. treatment effect on tensile diagrams of KhN77TYuR (*Russian*) 0-60884
Ni-Cr, low short-term creep resist. at 700°C 0-76313
Ni-Cr, matrix effect in SIMS anal. using O₂⁺ primary beam 0-76576
Ni-Cr, partial dislocation, stacking fault TEM study (*Chinese*) 0-84174
Ni-Cr, self-weldability in high temp Na (*Japanese*) 0-89392
Ni-Cr (33 at.%), plastic deformation, HVM study (*French*) 0-66605
Ni-Cr (70 wt.%), oxidation behaviour, 1073-1473K 0-89416
Ni-Cr alloy KhN70MYYu wire, recrystn., optimum heat treatment 0-76278
Ni-Cr alloys, creep crack growth, environmental sensitivity 0-85030
Ni-Cr austenitic alloy, oxidation mechanism, intergranular diffusion effect (*French*) 0-81229
Ni-Cr films implanted with N ions, electric properties (*Russian*) 0-107927
Ni-Cr Nimonic alloys, mech. props., high-temp. irradiat. effects 0-100885
Ni-Cr superalloy, interactions between creep and low cycle fatigue (*Chinese*) 0-66572
Ni-Cr/Au films, interdiffusion processes and oxidation phenomena 0-59735
Ni-Cr-Al (20, 4 wt.%), tensile stress effect on high temp. oxidation (*Japanese*) 0-89393
Ni-Cr-Al sintered alloy, hot vac. pressure, fracture and mech. characts. 0-66667
Ni-Cr-Al₂O₃ powder targets for plasma-ion spray deposition of resistance films 0-84897
Ni-Cr-Al-TaC, eutectic composite, microstructure, fatigue props. 0-85038
Ni-Cr-Al-Ti, stress corrosion cracking, factors influencing susceptibility 0-97617

chromium alloys continued

Ni-Cr-Co based alloy, IN-738 turbine blades, hot isostatically pressed investment castings, effect of heat treatment on grain boundary struct. 0-89270
Ni-Cr-Co superalloy, combined TEM, FIM, atom probe microanalysis of precipitates and carbide phase comp. 0-100844
Ni-Cr-Co-Al-W-Mo-Ti-Ta, heat resist. and struct., Ta effect 0-76312
Ni-Cr-Co-Ti-Mo-W-Al (14, 9.8, 5, 4, 3.9, 3 wt.%), low cycle fatigue, prior heat treatment effect 0-60962
Ni-Cr-Fe, radiation enhanced precip. and dissolution of precipitates, point defect kinetics and dislocation obs. 0-108467
Ni-Cr-Fe, stress corrosion cracking, factors influencing susceptibility 0-97617
Ni-Cr-Mo-W-Al-Ti, heat-resist., phase comp. 0-76250
Ni-Cr-NbC eutectic composite, unidirectional solidification, thermal cycling, temp. range effect on microstructural degradation 0-89272
Ni-Cr-P, amorphous, corrosion behaviour, immersion tests and electrochem. meas. (*Japanese*) 0-85085
Ni-Cr-Ta system, phase equilib. of Ni rich region at 1523 and 1273K 0-93541
Ni-Cr-Ta-Ti-Si, EP557 precipitation hardening alloy, mech. props., heat treatment effect 0-60877
Ni-Cr-Ti rapidly solidified superalloys, surface segregation 0-76263
Ni-Cr-W, oxidation behaviour in air at 1000-1250°C 0-89407
Ni-Cr-W-Co granules type ZhS6U, EP741, hot hydrostatic pressing 0-60796
Ni-Cr-W-Co-Ti, thermal fatigue, effects of inclusions 0-81183
Ni-Cr-W-Co-(Al)(Ti)(Mo), high-temp. sulphide corrosion 0-76408
Ni-Cr-W-Mo-Ti-Al, heat-resist., recovery and recrystn. 0-76268
Ni-Cr-Zr, degradation after exposure to 1% H₂S/H₂ gas mixture at 1000°C 0-89408
Ni-Fe-Cr superalloy type 718, heat treatment effect on room temp. and elevated temp. fracture toughness response 0-100922
Ni-Fe-Cr-Mo-Ti-Al, PE 16, thermally activated domain wall motion 0-88777
Ni_{0.89}Cr_{0.11}, phonons with disorder caused by force consts., neutron diffr. obs. and CPA calc. 0-96602
Ni(Fe,Cr), electron states density model and mag. characts. calcs. (*Russian*) 0-92804
Ni₂(Fe,Cr), electron states density model and mag. characts. calc. (*Russian*) 0-92804
Ni₃₆Fe₃₂Cr₄P₁₂B₆ metallic glass, mech. props. and thermal stability 0-76362
Pd-Cr, dil., temp. dependent scatt. 0-59973
Pd_{1-x}Cr_xH_x, resistive Kondo behaviour as function of Cr and H conc. 0-59971
Pt-Cr, disordered, atomic order-disorder transform. effect on resist. min. 0-65911
Pt-Cr, shallow silicide contact 0-70819
Pt-Cr, AC susceptibility near percolation limit, ordered and disordered alloy 0-65900
Pt-Cr, ferrimag., magnetisation density, polarised neutron diffr. meas. 0-60204
Pt-Cr, L₁ ordered alloy, positive temp. depend. on strength, phase destabilization 0-81203
Pt_{0.75}(Cr_{1-x}Mn_x)_{0.25}, pseudobinary, magnon energy derivation 0-107996
Si-Cr, dil., spin density wave under high press., neutron diffr. study 0-65798
steels, Cr-C-Mn(Ni), struct. prop. rel., design of struct. steels for high strength and toughness 0-97491
Ta-Cr-Si-Al, heat resistive films, prepared by sputtering, lifetime meas. 0-80132
Th-Cr, supercond., press. meas. to 20 kbar 0-88667
(Ti,Cr)B₂, sintering kinetics and props. 0-100811
Ti-Al-Cr-Mo-V, VT22 alloy, metastable β -phase decay under continuous heating, plastic strain effect (*Russian*) 0-71656
Ti-Al-Mo-Cr, weldment containing orthorhombic martensite, auto-tempering behaviour and alpha precip. strengthening 0-84976
Ti-Al-Mo-Cr (4.5, 5, 1.5 wt.%), weld metal, α/β interface sliding 0-108512
Ti-Cr, diffuse electron scatt. (*Russian*) 0-103438
Ti-Mo-V-Al-Cr-Fe (4.8, 4.7, 5.2, 1.1, 1.0 wt.%), structural changes during heating up to 1000°C, DTA study (*Russian*) 0-93552
Ti-V-Cr-Mo, fracture resistance at low temps. 0-104284
TiC-(Mo-Cr-Ni-Mn) steel alloy, optimum comp. and manufacture conditions, Mn effect 0-84896
TiCr_{0.8}, H and D soln., enthalpy, solubility and mol. vibr. determ., comparison with soln. in metals and binary alloys 0-79951
Ti_{1-x}Zr_xMn_{2-y-z}Cr_yV_z, hydrogen storage appl. (*Japanese*) 0-61443
U-Cr metallic glasses, glass form. and thermal stability 0-75183
(V_{1-x}Cr_x)₃Si, elastic moduli, 4.2 to 290K, softening near supercond. transition (*Russian*) 0-92582
Zircaloy-4, deformation behaviour between 77 and 900K 0-71686
ZrCr₂, Zr(Cr₁Fe_{1-x})₂ and Zr(Cr₁Co_{1-x})₂, mag. props. H absorpt. effect 0-88821
ZrCr₂D_x, site occupation modes and cryst. struct., neutron diffr. study 0-59440
Zr(Cr₁M_{1-x})₂ (M=Fe, Co), H₂ absorpt. capacity 0-88433

chromium compounds

see also chromium alloys
carbides, oxidation of H₂ 0-104462
complex in borate glass, ESR study of effect of glass composition on symmetry 0-88052
complexes, NMR study ³¹P chemical shift, substituents electronegativity steric hindrance and π -bonding effect 0-95651
(iron, chromium) carboxylates, heteronuclear trimer exchange clusters, ESR spectra 0-80603
methylammonium alums, dielec. relax. near transition point 0-71301
mol. consts. and mean vibr. amplitudes calcs. 0-106318
oxide, catalysis of graphitisable C graphitisation 0-89166
3p photoelectron spectra, light-induced changed in multiplet satellites 0-80946
B-C-Cr, paramagnetic centre struct. and defect form. 0-66034
CaO-MgO-Cr₂O₃-Al₂O₃-ZrO₂-SiO₂ system, subsolidus region characts. 0-97466
CdCr₂Se₄(Se₄), spontaneous magnetisation temp. depend., nuclear resonance freq. depend. (*French*) 0-80483
CdCr₂Se₄, energy band struct. calcs. by augmented plane wave method 0-103621
CdCr₂Se₄, energy structure, magneto-optic effects 0-71394

chromium compounds continued

- CdCr₂Se₄, magnetic semiconductor, photoinduced centre kinetics 0-71110
 CdCr₂Se₄, modulated piezoreflection spectra 0-97237
 CdCr₂Se₄, reactor radiation influence on ferromagnetic phase transform. (Russian) 0-75760
 CdCr₂Se₄-Ga(In), photoconductivity, photomagnetoresistance near Curie point (Russian) 0-100485
 CdCr₂Se₄-In(Ga), elec. resist. and magnetoresist., 2 to 200K 0-96876
 (Co,Cr,Fe)₂O₄ film magneto-optical switch for synchronization of CO₂ and red laser beams 0-58615
 Cr complex, (-)-tris(ethylenediamine) chromium (III), solid-state circular dichroism spectra, phase modulation spectrosc. obs. 0-93271
 Cr complex, tris(2,2'-bipyridine)Cr(III), excited states, Raman spectra 0-97263
 Cr-Cr₂O₃, black chrome, solar absorptance of high temp. selective absorbers 0-101131
 Cr-Cr₂O₃, black chrome electrolytic coatings for solar collectors 0-94100
 Cr-Cr₂O₃ black, electrodeposited solar collector coatings, high temp. optical and struct. degradation 0-66995
 Cr-Cr₂O₃ black chrome, commercial, solar absorber coating characterisation 0-80111
 Cr-Cr₂O₃ black solar absorber surfaces, microstruct. rel. to electroplating parameters 0-61418
 Cr-Ge, thermophysical props., at elevated temp. 0-103493
 CrAs, high press. paramag. antiferromag. transitions, elec. props., band model development (Russian) 0-60277
 CrB₂, itinerant antiferromag., spin fluctuations, NMR study 0-108119
 Cr₃B₂O₃Cl, cubic, approx. nonlinear optical susceptibility 0-78904
 Cr₃B₂O₃Cl, ferroelec. 43m-mm2 phase transition, molar heat capacity meas. 0-93249
 CrBr₂, ferromag. domains, using liq. He mag. specimen stage 0-103855
 CrBr₃, Brillouin-Mandelstam scattering from thermal and excited magnons 0-70980
 CrBr₃, HF spectra, susceptibility, spin waves in domain walls (Russian) 0-80909
 CrC, precipitates in Ni-base superalloy, STEM microanal. 0-81067
 Cr₂C₃, reactively sputtered solar selective absorbers for all-glass tubular evacuated collectors, absorptance and emittance 0-101132
 Cr₂C₃ fibre reinforced Ni-based composite, oxidation and creep, Y additions effect 0-66685
 Cr₂C₃/Ni-Cr hardfacing materials, friction characts. in high temp. Na (Japanese) 0-89356
 Cr₂C₃ dissolution in high and medium C steels (Russian) 0-103479
 Cr₂C₃ electrophoretic coatings on steel, sintering 0-66707
 Cr₂C, cathodic needle growth, at lower electric fields from Cr(CO)₆ vapour 0-76161
 Cr₂C₃-(Ni-Cr), self-weldability in high temp Na (Japanese) 0-89392
 Cr(CO)₆, MCD spectra, charge transfer transitions 0-95658
 Cr(CO)₆, photodissoc., Cr prod. 0-95575
 CrCl₃, electronic struct. and struct. phase transition 0-59644
 CrCl₄, mol. const. and mean vibr. amplitudes calcs. 0-106318
 Cr₂Er₂S₁₁, X-ray cryst. struct. determ. and refinement (French) 0-103298
 (CrF₃)₃ 6a AR-AT complexes, electron densities, local orbital populations, polarised neutron diffraction 0-88725
 Cr_{1-x}Fe_xOOH, 0 ≤ x ≤ 10, prep., Mossbauer effect, Neel temp. 0-108134
 Cr₂H₂(SO₄)₇·24H₂O, X-ray cryst. struct. determ., H bond study 0-92491
 Cr, Mn_{1-x}As, mag. susceptibility anomaly at displacive phase transition 0-93091
 Cr_{1-x}Mn_xO₂, hyperfine mag. fields at ¹¹⁹Sn, Mossbauer study 0-71260
 Cr₂Mo_{1-x}O₂ (x ≤ 0.5), solid soln., trivalent Cr, X-ray powder diff. anal. 0-70177
 CrN, antiferromagnetic EPR spectra, binding energy, isotropic exchange and ordering (German) 0-80604
 Cr(NO₃)₃, Cr ⁷P₀ state, radiative lifetime in matrices, meas. using laser ablation and selective excitation 0-71959
 Cr(NO)₄, bonding, shake-up intensities and shake-up energies, SCF Xα multiple scatt. calc. 0-74121
 Cr(NO)₄, XPS and UV photoelectron spectra, compared to NO data 0-58317
 CrNbO₄, elec. cond. meas. 0-100463
 CrO, A¹¹X²II transition, rot. anal. laser induced fluoresc. and discharge emission spectra 0-69173
 CrO₂ and Cr(OH)₃, fine particle obs. of cryst. morphology and topotaxy 0-65969
 CrO₂, particulate, proton donor adsorption effect on mag. moment, XPS anal. 0-71117
 CrO₂, semidry refractory, struct. and mech. props., surface-active agents effect 0-89304
 CrO₂-PbO, acoustooptic props. from comp. and density 0-76000
 Cr₂O₃ additive for Pb(Mg_{1/3}Nb_{2/3})O₃-PbTiO₃-PbZrO₃ ceramics, HF filters appl. (Japanese) 0-60507
 Cr₂O₃, catalytic graphitization of nongraphitizable C 0-97440
 Cr₂O₃ crystals, flux growth from K₂Cr₂O₇-K₂CrO₄-K₂B₄O₇ mixture (Japanese) 0-108339
 Cr₂O₃ crystals, growth by decomposition of K₂Cr₂O₇ melt (Japanese) 0-108338
 Cr₂O₃, decomp. of CaO-6Al₂O₃ 0-92687
 Cr₂O₃, dielec. const. in mag. field, nonlinear magnetoelec. effect in Neel pt. region 0-66006
 Cr₂O₃ in Cr film, struct., oxide percentage determ. and elec. props. 0-103607
 Cr₂O₃, muon spin rotation expts. 0-71282
 Cr₂O₃, muon states, local mag. fields 0-75911
 Cr₂O₃, sintering behaviour, effect of TiO₂, C additions 0-66461
 Cr₂O₃-Al₂O₃ solid soln., Vickers micro-hardness 0-66629
 Cr₂O₃-doped Ca₂(Al,Fe)O₃, planar interfaces, TEM obs. 0-65008
 Cr₂O₃-ZrO₂ granules, from spray drying of suspensions 0-104100
 CrOCl₃, electronic structure and valence ionisation energies, obs. by ab initio and SW-Xα methods 0-69073
 CrO₂Cl₂, multiphoton induced inverse electronic relax. 0-66836
 CrO₂Cl₂+carbon tetrachloride+acetone, intermediate complex form., electronic spectra 0-61075
 Cr₄(OH)₄(NH₃)₂Cl₄·4H₂O, exchange coupled mol. Cr³⁺ tetramers, inelastic neutron scatt. 0-65792
 CrOOH(D), barrier to proton or deuteron tunnelling 0-70156
 CrSb_{1-x}As_x, struct., elec. and mag. props. 0-107160
 Cr₃Se₄, struct., elec. and mag. props. 0-107160
 Cr₃Si phase structure, rel. between phase diagrams and superconductivity 0-88330
 CrVO₄, elec. cond. meas. 0-100463
 (Cr₂V_{1-x})₂O₃, impurity doping effects, elec. props. obs. 0-75609

chromium compounds continued

- CuCrSe₂, influence of excess Cu on physical props. 0-103836
 Cu_{1-x}Cr_xSe₂, influence of excess Cu on physical props. 0-103836
 CuCr₂Se₄-Br₂, ferromagnetic semicond., Hall effect 0-60012
 FeC₂-Cr₂C-NiC₂, stainless steel carbide, solar selective surface, fabrication, magnetron sputtering system description 0-80967
 FeC₂-Cr₂C-NiC₂, stainless steel carbide, graded solar selective surface, magnetron sputtered 0-81485
 FeC₂-Cr₂C-NiC₂, stainless steel carbide, sputtered solar selective surface, grading profile 0-81486
 (Fe₂Cr₄-Al₃)O₉, IR spectra, lacunar γ-phase to corundum α-phase transform. 0-108199
 (Fe_{1-x}Cr_x)₂O₃, yH₂O crystal growth, characterisation by Mossbauer spectroscopy, mag. meas. and electron microscopy (French) 0-80655
 (Fe_{4-x}Cr_x)O₉, IR spectra, lacunar γ-phase to corundum α-phase transform. 0-108199
 (Fe,Cr_{1-x})₂O₃ corundum-type solid solution single crystal growth, chem. vapour transport 0-93465
 Fe_{0.5}Cu_{0.5}Cr₂Se₄, ESR spectra, elec. and mag. props., Curie temp. 0-97137
 α-Fe₂O₃-Cr₂O₃ solid solution, Mossbauer effect studies 0-71249
 HgCr_{2-x}Al_xSe₄ and HgCr_{2-x}Ga_xSe₄, temp. depend. of ESR linewidth, 105-300K 0-71161
 HgCr₂Se₄, electronic props. rel. to departure from stoichiometry 0-100472
 HgCr₂Se₄, spontaneous magnetisation temp. depend., nuclear resonance freq. depend. (French) 0-80483
 KClO₄-CrO₄²⁻ AC elec. cond. and dielec. loss meas. 0-59699
 KCr alum., relaxation behaviour, EPR study, environmental effects 0-66021
 KCrAl_{1-x}(SO₄)₂·12H₂O, EPR of single crystals, zero-field splitting of Cr³⁺ 0-66015
 LaCrO₃-Cr eutectics, prep. and microstruct. 0-108380
 Li₂O-Al₂O₃-Cr₂O₃ system, subsolidus equilibria 0-60843
 MgO-CaO-FeO-Fe₂O₃-SiO₂-Cr₂O₃-Al₂O₃ spinel refractories, physicochem. prod. conditions 0-89185
 MgO-NaCl refractory clinkers, Cr containing, densification, thermal treatment and phase composition effect (French) 0-76219
 Mn_{1-x}Cr_xAs, double exchange ferromag. coupling, magnetisation meas. 0-75751
 MnSb-CrSb, NiAs-type system, single crystals, neutron diff. studies 0-60200
 Na₃Cr₂(PO₄)₃, crystallographic data, ionic conductivity (French) 0-88077
 Na₃Cr₂(PO₄)₃, crystallographic data, ionic conductivity (French) 0-88077
 NaF-SrF₂-CrF₃, glass transition, crystn. and melting temps., optical transmission (French) 0-64910
 Na₂O-CaO-SiO₂-Cr₂O₃ glass, redox equilibria of Cr ions, impurity effects 0-89477
 NaOH·CrO₄²⁻, electron tunnelling, pulse radiolysis 0-108722
 Ni_{1-x}Cr_xS, elec. transport, mag. susceptibility and DTA meas. 0-96954
 NiO-Cr₂O₃-MgSiO₃, methanation catalyst, S-resistant, IR and Raman spectra 0-93290
 Pb(Zr,Ti)O₃-Cr₂O₃ ceramics, reson. freq. comp. and temp. depend. 0-70413
 Si-Cr₂O₃Al, current-voltage characts., oxide film effects 0-70841
 (V_{1-x}Cr_x)₂O₃, Raman scatt. and phase transitions 0-71420
 (V_{1-x}Cr_x)₂O₃, elec. props. and struct. 0-84494
 YCrO₃-Cr eutectics, prep. and microstruct. 0-108380
 ZnCr₂Se₄-In, magnetoresist. and elec. resist. above and below Neel temp. (Russian) 0-88576
- chromosphere**
 active regions, bidimensional spectroscopy obs. with birefringent filter (Italian) 0-98568
 active regions, coronal and transition region temp. struct. 0-67692
 activity from moving mag. feature in McMath region 12417 0-98642
 chromosphere-corona transition region, thickness rel. to plasma flow along chromosphere sheared mag. arches 0-62092
 continuum radiative losses, comparison with mechanical energy supply 0-72924
 corona transition zone of solar active regions, non-thermal velocities (French) 0-77371
 five-minute oscillations, horizontal energy flows struct. 0-62103
 flares, initial phase parameters determ. method 0-62104
 flares, O I 1355.6 Å and C I 1355.8 Å lines obs. 0-90381
 flash spectrum, obs. at 1979 February 26 eclipse 0-67687
 limb flare, 1959 July 25, spectrum rel. to physical conditions 0-105227
 line profiles from OSO-8 spectrometer meas. 0-67690
 Lyman α filtergrams, high resolution, new transition region structs. obs. 0-82323
 magnetic field above flocculus, determ. from radio obs. 0-98635
 mechanical flux determ. from Ca II lines 0-67680
 peak separation due to microturbulence 0-109407
 plage fragments, characts. assoc. with photosphere network props. 0-98634
 plasma ejection during solar transients, rel. to He⁺ obs. in interplanetary shock wave 0-72735
 spectra, optically thick line formation, atmospheric dynamics 0-94767
 temperature minimum, absolute brightness temp. meas. in far IR with balloon-borne interferometer 0-62095
 transition region, C V and O VII emission line ratios interpretation 0-98624
 transition region, Ni IX to Ni XII lines identifications from laboratory wavelengths 0-99474
 transition region, origin for UV and radio fluctuations 0-90398
 transition region, theoretical network structure for coronal holes 0-85917
 transition region, theoretical network structure for quiet Sun 0-85916
 transition region and inner corona, energy balance 0-90379
 transition zone, EUV lines from limb brightening data in coronal hole 0-82333
 transition zone, nonresonant heating mechanism (Chinese) 0-85921
 Ca II lines, vel. and temp. disturbances, weighting functions 0-67679
 Hg spicules, dynamics at various heights, spectral obs. 0-90392
 Mg I and II, line profiles calc., comparison with expt. results 0-82320
- chronographs** see **chronometers**
- chronometers**
 horological microprocessor, design and circuit architecture, functions (French) 0-90822
- CIDEP**
 chemically induced dynamic spin polarisation, orientation depend. 0-63656

CIDEP continued

photosystem I, of green plants and algae, CIDEP obs. 0-63679
 quinones, triplet quenching by organometal cpds., time resolved CIDEP and ESR obs. 0-95654
 surface diffusion and spin polarisation, 2-D CIDEP, asymptotic Green's function method appl. 0-91584

CIDNP

chemically induced dynamic spin polarisation, orientation depend. 0-63656
 free radical reaction, chemically induced dynamic polarisation in strong mag. field, radical rotation influence 0-76509
 nuclear spin isotope effects 0-69167
 trifluoroacetophenone+dimethoxy benzene. in acetonitrile photoreaction, nuclear spin polarisation, criterion for triplet-Overhauser mechanism 0-69168
¹³C, CIDNP, obs. in reactions of organic and inorganic radicals during pulse radiolysis 0-63660

cinefilming *see cinematography***cinematography**

see also cameras

35 mm projectors, new projection lenses 0-87469
 animated cartoons, computer appl. (Russian) 0-105739
 Arriflex 35BP-II motion picture camera mounted with 350PF-1A zoom lens for wide-screen filming (Russian) 0-95176
 biomedical US images, cine display 0-108984
 camera development, interdisciplinary and international approach 0-81342
 cell flagella, laser damage, high speed cinematography 0-81785
 chemical photographic processing of colour positive motion picture films (Russian) 0-93780
 cinefilm copying equipment using interference light filters, additive printing appl. (Russian) 0-62774
 colour film copying techniques, lighting control (German) 0-62751
 colour negative film Gevacolor type 682, 35 mm, 16 mm professional film making appl. 0-82838
 continuous film copying equipment (German) 0-68281
 densitometer measurement transformation into spectral density distrib. and colour coordinates (Russian) 0-77902
 equipment designs, Moscow design office (Russian) 0-62772
 equipment designs from Odessa design office over 25 years (Russian) 0-62771
 exposure measurements, quantitative study of additional measured exposure, continuous processing appl. (Russian) 0-62775
 external synchronization of electric drive SA-120 when shooting combine pictures with TV images (Russian) 0-86484
 film production, use of different computer techniques 0-77887
 films, 16 mm Fujicolor reversal film RT 500 and RT125 0-106585
 films, new Gevacolor negative film type 682 0-106586
 flow measurement, plane mixing layer vortex digital image processing 0-103095
 high resolution time lapse cinemicrography, use of improved air stream incubator 0-98196
 high speed camera CKC-1M modifications and control (Russian) 0-105740
 holographic movie camera and projection system 0-78808
 illumination control of cine projectors, foreign equipment (Russian) 0-105741
 image quality transfer 0-68279
 instant high-speed colour, Polaroid system, scientific and engineering appls. 0-98993
 laser based, operation and applications 0-57405
 lens-array photographic system, depth of sharp focusing, resolution 0-62763
 light sources for Super 8 film projectors, short-arc lamp filled with rare earth halogens 0-62747
 lip synchronised recording technique for speech translation in cinefilms (Russian) 0-105737
 Loch Ness and Morar Photographic Expedition (1979) 0-68280
 magnetic sound records release print KMP-23 (Russian) 0-90918
 manual movie camera, Kinor 35P (Russian) 0-90917
 mixing boxes for motion picture studios (Russian) 0-62773
 mixing complex at motion picture studio (Russian) 0-86483
 motion picture camera gyroscopic stabilisation system, anal. of dynamics and accuracy (Russian) 0-95173
 motion picture rerecording, warning system devices and electronic digital counter utilisation (Russian) 0-95177
 motion picture sound track, freq. distortion and two dimens. sound record scatt. (Russian) 0-95175
 neural unit activity rel. to movement, photographic technique for anal. 0-67310
 object-related colour reproduction in film scanning [TV broadcasting], TV broadcasting appl. (German) 0-105726
 ocular cinema photography 0-67186
 production association Ecran, 25 years of achievement (Russian) 0-62770
 projection equipment for 16 mm films, perspectives (Russian) 0-77903
 recording equipment KZM-24, post-synchronization (Russian) 0-86482
 recording of fast processes, extension of meas. parameter ranges 0-57413
 retinal image cinematographic recording, accommodation microfluctuation appl. 0-81579
 reversal cinefilm development, effect of temperature, concentration factors on speed of process (Russian) 0-105735
 rotating lens system for cine projection with continuous film transport 0-62766
 sound negative film, Eastman sound recording II film, 5373/7373 0-62768
 sound track films, appl. of computer program simulation of recording and reproducing system 0-62767
 sound-track cinefilms 3T-8, 3T-7, comparison (Russian) 0-105738
 stepper motor drives for use in synchronous interlock systems for cinematographic special effects 0-98991
 time control system, Q-Lock, for editing, dubbing 0-68278
 TV colour films, usable subject contrast range (German) 0-57408
 zoom lens system design and manufacture 0-68288

circuit analysis computing

fusion reactor, PHIBEX, poloidal field power supply for ignition, computer based oct. anal. 0-102329

circuit breakers

see also circuit breaking arcs; gas blast circuit breakers
 arcs, HV, AC, switching, spectroscopic measurement of temp. distribution in constant pressure axial air flow (Czech) 0-86296

circuit breakers continued

fusion reactor, Doublet III, ohmic heating E-coil vacuum breaker system, function and operation 0-102323
 interrupter and hybrid-switch testing for fusion devices 0-99289
 plasma sheath breakdown to glow transition in plasma filled gap 0-100105

circuit-breaking arcs

see also circuit breakers; sparks

HV, AC, switching, spectroscopic measurement of temp. distribution in constant pressure axial air flow (Czech) 0-86296
 HV gas blast circuit breakers, arc mechanism and control 0-92409
 SF₆ plasma thermodynamic props. at arc extinction temp. and pressures 0-79435

circuit design *see network synthesis***circuit oscillations**

see also circuit resonance

No entries

circuit resonance

see also circuit oscillations

No entries

circuit synthesis *see network synthesis***circuit theory**

see also filters; network parameters; network synthesis

dual representation with field theory, Poynting's theorem 0-94963
 mesh analysis using graph theory, generalised procedure, teaching 0-101681
 simple DC circuits, student concepts 0-77569

circuits *see networks (circuits)***circular polarisation** *see polarisation***circular waveguides**

cylindrical waveguide filled with uniaxial, collisional, hot and moving plasma, dispersion for TE and TM modes 0-106934
 optical inhomogeneous circular waveguide, asymptotic eigenvalues of vector waves 0-96010
 optical strip type, fabrication by Ag ion migration 0-96042
 radially inhomogeneous waveguide modes, vector wave characts. 0-78960

citation analysis *see information analysis***civil engineering**

see also building; dams

aseismic bearing foundation system for power station earthquake protection 0-83206
 bridges, dynamic interaction of moving vehicles and structures 0-64357
 design to resist earthquake loading 0-81844
 nuclear reactor containment structure design and service loads 0-106138
 PWR containment vessel optimisation 0-106137

cladding techniques

No entries

claddings

alkali lime germanosilicate GRIN fibre prep., losses and geometrical props. 0-69560
 austenite cladding layers, damping of ultrasound 0-104390
 BWR fuel preconditioning, initial pressurisation, fuel temps., fission product release 0-63357
 Caramel fuel cladding rupture, development and detection at OSIRIS experimental reactor (French) 0-95371
 EBR II, metallic driver fuel, irradi. perform. at high burn-up, fuel-cladding interactions 0-95348
 FBR cladding dilatation, effect of radial temp. gradient 0-68776
 FBR fuel development, international development programs 0-102248
 FBR fuel pin failure, fuel porosity and crack effects on transient over-power analysis 0-71760
 fission reactor fuel performance modelling, pellet-cladding interaction 0-63264
 fission reactor materials, clad failure prediction during FBR overpower transiency, JANE code 0-78363
 fuel pins, fast breeder, fuel-cladding mech. interaction, obs. and anal. 0-86959
 GCFR advanced alloy cladding, oxidation behaviour in the environment 0-104350
 glass fibres, clad, thermal stresses 0-107360
 glass rods, compressively clad, residual stresses, comparison of optical and fractographic meas. 0-108539
 laser, double-current-confinement channelled-substrate struct., near-field and beam-waist position 0-106553
 lightweight fibre preform manufacture using modified CVD process 0-64228
 nuclear fuel element cladding, corrosion product deposition, heat transfer model (Bulgarian) 0-71818
 nuclear fuel element codes, structural anal. 0-78362
 optical compound glass fibres, silicone and glass clad, medium loss 0-69533
 optical fibre, single-polarisation single-mode, exposed cladding fabrication 0-58725
 optical fibre refractive index profile distortion due to thermal stresses 0-58726
 optical single mode fibres, homogeneous CVD fabrication and characterisation 0-69562
 optical waveguide, semiconductor clad, attenuation and propagation coeffs. 0-79004
 PCI-induced cladding strain, effect of fuel density and fuel relocation, in-reactor meas. 0-104408
 polymer cladding/glass core optical fibre waveguides, high numerical aperture 0-96024
 PWR core power manoeuvres, fuel duties and fuel preconditioning, FLAIR-CENSOR 0-63337
 PWR LOCA reflow, effect of low containment press. on peak cladding temp. 0-57897
 rod-in-tube fabricated optical fibre characteristics 0-87574
 steel, stainless, 316, oxidation behaviour in the environment, appl. to GCFR fuel claddings 0-104350
 steel, stainless, cladding dimensional changes in FBR (U,Pu)O₂ fuel pins due to swelling and inelastic strain 0-104296
 steel, stainless, LWR fuel cladding material evaluation 0-99213
 steel, stainless, type 316 20% cold worked fission reactor fuel cladding, axial stress effects on transient mech. response 0-71743
 steel, stainless type 316, irradi. induced nuclear cladding swelling, empirical development of design equation 0-59527
 steel plates, explosively clad, fatigue crack propagation behaviour (Japanese) 0-104262

claddings continued

- thermomechanical transient anal., strain-rate dependent plasticity 0-79864
- thin-film waveguide laser amplifier with lossy cladding 0-64074
- Zircaloy, LWR fuel rod cladding, damage accumulation during I₂-induced stress corrosion cracking 0-71810
- Zircaloy, PWR fuel induced cladding deformation, creep correl., in-pile meas. 0-97547
- Zircaloy cladding, stress corrosion cracking, inner surface texture effect 0-66695
- Zircaloy cladding stress corrosion cracking due to I (*Japanese*) 0-78361
- Zircaloy fuel cladding, irradiation-induced in-reactor corrosion in CANDU reactors 0-104352
- Zircaloy-2, hot-pressed, influence of diffused C on structure and oxidation 0-61016
- Zircaloy-4, creep rupture at superimposed non-stationary stress and temp. loading 0-66630
- Zircaloy-4, elastic props., O additions effect 0-66565
- Zircaloy-4 cladding deformation under LOCA transient heating conditions, analytical modelling 0-104236
- BaO-GeO₂-Na₂O borosilicate core glasses for high numerical aperture fibres 0-69534
- Cr-Fe-Ni alloys, claddings, chemical compatibility with UC nuclear fuels, thermodynamic model 0-63263
- GeO₂-Na₂O borosilicate glass fibre prod. by phase separation and leaching 0-69558
- UO₂-PuO₂ fuel pin, hyperstoichiometric, post irradiation examination 0-63258
- Zircaloy-2, effect of simulated fission products on mech. props. 0-73922

classical algebra *see algebra***classical field theory**

- see also classical mechanics; electromagnetic field theory; gravitation; special relativity*
- acceleration through random classical radiation, thermal effects 0-73191
- charged particle system, virial theorem 0-86101
- education, classical mechanics gauge invariance, derivation of Maxwell's eqns. 0-73131
- electron acceleration in EM field, new field theory appl. (*Chinese*) 0-62494
- extended phase space, classical fields 0-86550
- ferromagnetic systems, crit. experiments, field theory, Borel transform. 0-80541
- field analysis computers, colloquium, London, England (March 1980) 0-94964
- gravitation, electromagnetic interpretation, contribution to classical theory (*Rumanian*) 0-68109
- gravitation, electrothermodynamical theory, gravitational field shielding (*Rumanian*) 0-68107
- gravitational field and force derivation using Faraday's and Maxwell's ideas of electromagnetic waves (*French*) 0-68106
- multi-terminal representations appl., graph theoretical field model 0-90689
- orbital angular momentum of 'lumps' 0-86098
- pre- and post-processing techniques for complex analysis 0-94965
- time dependent constraints in classical dynamics 0-57111

classical mechanics

- see also classical mechanics of continuous media; classical mechanics of discrete systems; classical theories of fluid structure*
- conserved densities, Hamiltonian systems 0-90682
- education, classical mechanics operator formulation, wave packets in conf. space 0-73137
- education, harmonic plane waves, particle displacement 0-73138
- Lagrange's equations, invariance in form 0-82630
- Lie-Backlund operators, exam. of isomorphic correspondence between classical and quantum-mech. invariants 0-90700
- nonlinear oscillators, 1-D, intramolecular vibr. energy transfer, quantal, classical and statistical behaviour 0-91641
- quadratic and cubic invariants in classical mechanics 0-90663

classical mechanics of continuous media

- see also elasticity; fluid mechanics; mechanical contact; plasticity*
- anisotropic media, natural oscils., partial differential eqn. system 0-57091
- atmosphere dynamics in quasistatic approximation, characterisation of approximation (*German*) 0-98383
- averaging in nonlinear mechanics 0-98796
- beams flexural-torsional problem by series expansion in eigenfunctions 0-83732
- cable-band membrane, axisymmetric, interdependence between geometry and forces 0-96185
- circular plate cantilever, calc. method (*German*) 0-83731
- cylindrical shells, inverse problems 0-99925
- cylindrical shells, stiffened, min. weight design for pure bending (*Japanese*) 0-64381
- dielectrics, hyperelastic, with saturated polarisation, variational and invariance principles 0-74730
- differential type media with internal variables, thermodynamic theory 0-99923
- Duffing's equation, steady and chaotic motions 0-77616
- Duffing's equation, strange attractors, explosion, chaotic behaviour 0-76717
- effective implicit time integration in analysis of fluid-structure problems 0-92040
- elastic medium, surface concentrated loading, axisymmetric problem for homogeneous medium (*French*) 0-92041
- elastic shells, cylindrical, and of revolution, path independent integrals 0-87711
- geometrical theory of structural defects (*German*) 0-88136
- gross variables, microdynamics and nonlinear stochastic processes 0-101754
- instability, post-, in class of smooth functions, mathematical model 0-69649
- intrinsic parameters schematising shape and stress, Lagrangian formulation (*French*) 0-73173
- loaded construction, randomly loaded, crossing probabilities, numerical anal. (*German*) 0-96186
- Maxwell's initial boundary value problem, horizontal line (Rothe) method, convergence and error estimates 0-94957
- nondissipative medium, boundary problem soln. with surface discontinuity (*Russian*) 0-101716

classical mechanics of continuous media continued

- nonisothermal rigid shell theory using fundamental laws of thermodynamics 0-87712
- nonlinear second order system, eigenfunction expansion solutions of Fokker Planck eqn. 0-73172
- objective and regular differentiation and integration, constitutive law and transport (*French*) 0-57090
- pile, numerical soln. of beam eqn. with nonuniform foundation coeff. 0-64361
- plate, circular, with rigid inclusions, antisymmetrical carrying capacity 0-69650
- plate, cylinder, sphere, temperature (one-dimensional) and thermal stress fields, inverse problems 0-79134
- plate, reinforced strip, 2-dimens. nonsteady temperature stresses 0-74734
- plate, rib reinforced and supported, lying on a linearly deformable base flexure 0-69651
- plates, orthotropic circular, nonlinear dynamic anal. 0-64360
- porous media models using thermodynamics of mixtures 0-96184
- rectangular vibrating plates separated by liquid filled gaps, viscosity friction calc. (*German*) 0-105504
- rheometric structure theory, convective differentiation and continuum electrodynamics 0-86087
- ribbed-shell theory, inhomogeneous nonlinear problems 0-99924
- rods, prismatic, torsion with internal constraints (*Russian*) 0-69647
- rods, prismatic, torsion with internal constraints (*Russian*) 0-69648
- semiclassical Green's function, energy-representation 0-90692
- shell, cylindrical, thin, circular, supercritical forms during axial compression (*Russian*) 0-74733
- shell, ring-stiffened, cylindrical and skew conical, under hydrostatic pressure, minimum-weight design (*Chinese*) 0-79135
- shell, spherical, with rigid inclusions, antisymmetrical carrying capacity 0-69650
- shell, three-layer orthotropic cylindrical, with stiffening ribs, stability 0-74784
- shells, cylindrical, layered, rotationally symmetric problems, isothermic solutions 0-77619
- shells, flexible, self checking stepping calc. process 0-68044
- shells, Kirchhoff-Love, structural stability, mixed variational principles and non holonomous constraints (*French*) 0-74779
- shells, thin, stressed in axial compression, mass reduction, stress anal. 0-106716
- stiffness, exact straight line element calc. 0-79138
- stresses in mixtures 0-62469
- string, vibrating, motion above a concave obstacle, second order hyperbolic problem with unilateral constraints 0-57101
- summed progressing wave formalism for initial value problem calcs. 0-92039
- symmetry groups in crystals and elastic media 0-70147
- thermodynamic functions, relations for irreversible processes 0-101715
- thin shell theory, stress boundary conditions 0-79137
- thin walled cylinder, minimum weight design, flexural and torsional stiffness constraints 0-79136
- virtual work and differentiable manifolds, global and local model of material body 0-68043
- wave fronts defined by eikonal equations, structural stability, elementary catastrophes 0-73187

classical mechanics of discrete systems

- see also N-body problems*
- acceleration dependent lagrangians, eqns. of motion 0-98795
- anharmonic oscil., classical versus quantum case (*Spanish*) 0-73210
- asymptotic stability of resonance systems 0-68031
- averaging in nonlinear mechanics 0-98796
- axially moving string on cylindrical guide surface, lateral motion 0-64358
- ball and spring, elliptical motion 0-82613
- damped oscillator motion, expansion in normal modes 0-67951
- differentiable dynamical systems, transformation frequency spectrum 0-77608
- dynamical system, compactness of bounded trajectories in infinite dimensional Banach space 0-82636
- dynamical system, limit cycles and symmetries 0-62462
- dynamical systems, dissipative, intermittent transition to turbulence 0-79132
- dynamical systems, homoclinic and heteroclinic points in Hemon mapping, analyticity 0-82634
- education, circular motion with friction, numerical and analytical solns 0-57029
- education, multiple scatt., elastic and inelastic, two particle system with fixed wall, air track expt. 0-73135
- education, spiral spring, (nonhelical) simple harmonic motion, Bessel functions, closed form solns. 0-57026
- education, supernovae in binary systems: an application of classical mechanics 0-62428
- electric power systems, interconnected, large-scale, derivability from Lagrangian 0-101707
- follower load type systems, time invariant functionals 0-77609
- forced oscillations, averaging and chaotic motions 0-73166
- gross variables, microdynamics and nonlinear stochastic processes 0-101754
- Gurney's ballistics calc. 0-67946
- gyro-stabilisation platform, nonlinear loss of stability and trembling (*Chinese*) 0-62457
- Hamilton's principle for canonical equations of motion, teaching 0-105464
- Hamiltonian classical mechanics, gauge theory for long range fields 0-86077
- Hamiltonian mechanics 0-82631
- Hamiltonian with ergodic behaviour, classical quantisation 0-86148
- hyperbolic systems, high-order methods, dynamic problems 0-68033
- infinite crystal, classical statistical mechanics 0-107067
- Kepler ellipse, symmetry prop. of vel. 0-101694
- linear oscillator, nonstationary narrow band response and first passage probability, stochastic process 0-62465
- linear system mean square response to nonstationary random excitation 0-57085
- marginal local instability of quasi-periodic motion, separation distance effects 0-82633
- modified conservation laws in the classical Kepler problem 0-72755
- nondissipative system, universal properties, bifurcation phenomena and universal numbers 0-68035
- nonlinear mechanical systems, constraint simulation 0-62461

classical mechanics of discrete systems continued

nonlinear oscillators, turning point approx. and appl. 0-67952
orbiting trajectories in noncentral fields 0-98794
oscillators, weakly nonlinear, system with slowly varying parameters, resonance 0-62463
particle in selfgravitating spherical dust shell, adiabatic invariance, education 0-105459
particles with spin, Hamiltonian and Lagrangian formulation 0-86079
physical pendula, reconstructed 19th century expt. 0-82612
point particle in viscous medium, Lagrangian for eqn. of motion 0-77610
principles of least action, minimal interpretation, variational calcs. 0-68039
Ray-Reid generalised systems, invariants derivation 0-101710
rigid body, regular motions in gravit. field of sphere 0-62000
rigid shaft rotating in antifriction bearings, motion stability 0-68038
solid body with partly filled cavity, joint motion under total weightlessness 0-94952
sphere on imperfectly rough sloping plane 0-62464
stationary motion, stability, Lagrangian eqns. and Liapunov's direct method 0-69645
structural resonance, mechanical impedance and complex elasticity models, coupled systems (*German*) 0-99953
symmetric structures, group representation theory appl. 0-74727
symmetries of time-dependent Hamiltonians 0-101709
turbulent systems, transition to aperiodic behavior, recursive method 0-105493
v=gt expression, origins of derivation 0-77593
vector laws of physics, reformulation 0-68036
vibrating systems, nonlinear, multi-degree-of-freedom, harmonic excitation, instability 0-73162
work hardening adaptation of discrete structures under dynamic loading 0-74726

classical theories of fluid structure

see also kinetic theory; liquid theory
charged hard sphere dense classical fluid, equation of state and crit. point 0-64849
Coulombic systems, charged hard sphere system, rel. to restricted primitive model 0-64854
critical viscosity of classical fluid, dynamic scaling 0-59689
electric double layer, primitive models, pot. difference and charge density 0-76515
equation of state, hard core fluid with two-Yukawa tail, appl. to Ar 0-59618
hard core fluids, asymptotic behaviour of virial expansions 0-88010
hard disc fluid, infinite dilution solute chemical pot. by Monte Carlo simulation 0-88009
hard ion mixtures, Ornstein-Zernike eqn. and Yukawa closure 0-107031
hard sphere fluid, role of structure factor poles in prop. determ. 0-88011
hard sphere fluid near hard wall, diffusion coefficient, mol. dynamics simulation 0-64858
hard spheres in Percus-Yevick approximation used to derive sedimentation equilibrium eqns. 0-66884
hard spherocylinder fluid, Monte Carlo simulation, ang. correl. functions 0-75140
hard-particle fluids, general scaled-particle-like descriptions 0-103231
hard-particle fluids, general y-expansion-like descriptions 0-107032
hard-sphere liquid, pair pot. softness effect on liq. struct. factor 0-88012
inert gas mixture, dipole autocorrelation function, Lennard-Jones and exponential dipole pots., classical calcs. 0-64665
light scattering in fluid far from equilibrium 0-103965
modified cell theory, eqn. of state for hard spheres 0-103445
molecular dynamics simulations at constant pressure and/or temperature 0-64852
molecular fluids at equilibrium, integral equation derivation 0-64861
nonuniform one dimensional classical fluids, Lennard-Jones pot. interactions, Percus Yevick approx. and density functional calcs. 0-64864
Ornstein-Zernike and Percus-Yevick temperature dependent fluids, solvation forces 0-64862
particle distrib. function, theoretical method 0-64856
real fluids, short range repulsions and long range attractions, simple pair pot. model 0-64850
simple classical fluids theory, universality in short range struct. 0-75141
simple fluids, hard and soft-core eqns. of state, termination temps., Kihara pot. 0-70360
solvent-rod mixture, two phase, interfacial free energies, quartic van der Waals theory 0-59377
H₂, states velocity auto-correl. function, relax time, neutron scatt. obs. 0-58401
H₂-Ar, states velocity auto-correl. function, relax time, neutron scatt. obs. 0-58401

classification

see also indexing
failure micromechanisms, classification according to failure type (*Russian*) 0-108557
galaxies of Magellanic type, classification system and struct. (*German*) 0-105348
materials science, concept of system 0-101003
molecular structures, topological code, modified Morgan algorithm 0-58122
NGC 3928 C (Markarian 190), identification as miniature spiral galaxy 0-105347
Sb-type galaxies, luminosity classification rel. to Hubble const. local value 0-62339

classification, pattern *see pattern recognition*

clathrates *see molecules; organic compounds*

clay

brown clay from North Pacific, ¹⁰Be geochemistry and sedimentation 0-101356
deep-lake clays from pluvial Lake Lahontan, palaeomagnetic record 0-101321
heat treatment, effect on rheological props. of enamel slips 0-60809
kaolin bodies, effect of mineralizers on firing shrinkage, microstruct. and strength 0-97488
kaolin grog particles, shape and density 0-97450
mechanical properties at high-pressure. 0-76966
nontronite, CO₂ adsorpt. and capillary condensation rel. to Mars volatile storage and atmospheric history 0-72833
rectorite, stacking and ordered interstratification, high-resolution TEM obs. 0-109140

clay continued

sample preparation for X-ray diffr. anal. 0-97647
Al₂O₃ and SiC recovery by C reduction 0-108704
cleaning see surface treatment
cleanliness see hygiene
cleavage, crystal see crystal cleavage
Clebsch-Gordan coefficients
see also elementary particle theory
caesium perfluoro-octanoate/D₂O system, ²H NMR quantum orders, RF pulses 0-103892
constellations and projective classical groups, PO(n+1, C) and PSp(n+1, C), Lorentz and rotation subgroups 0-62869
Kronecker products, decomposition into corepresentations of type I only 0-62517
Kronecker products, decomposition into corepresentations of type I and II 0-62518
Kronecker products, decomposition into corepresentations of type II 0-62519
Kronecker products, decomposition into corepresentations of type III 0-62520
Kronecker products, decomposition into corepresentations of type I and III 0-68066
Kronecker products, decomposition into corepresentations of type II and III 0-68067
magnetic space groups, Clebsch-Gordan coeff. calcs. 0-79731
molecules, isolated, intersystem crossing, rot. motion effect 0-95669
selection rules for Pn³n 0-98820
selection rules for type II Shubnikov space groups 0-98819
Shubnikov point groups, corepresentations 0-86121
spl(2,1) superalgebra, irreducible representations, tensor product 0-82909
SU(2), Clebsch-Gordan coeffs., bilinear relns., based on anal. of Poincare, Lorentz and rotation group SO(3) 0-57509
symmetries of 3j and 6j coeffs. 0-86621
BH₃, electronic wave function determ., genealogical technique using Clebsch-Gordan coeff. 0-95529
MnF₂, antiferromag., mag. space groups, Clebsch-Gordan coeff. calcs. 0-79731

climatology

see also atmospheric humidity; atmospheric precipitation; sunlight; wind
Aberdeenshire, mesoclimate of Upper Don Basin 0-61889
aerosols affecting temperature, zonal average climate model 0-77102
Alaska, climate reconstruction from modern climate-tree ring relations 0-101425
albedo changes of land surface affecting climate 0-98434
N.America, Quaternary temps. and precip. for NW. coast region 0-98438
NW.America albedo increase following Pleistocene explosive eruptions, climatic effects 0-61789
Antarctic Peninsula area, climatic vars. rel. to W. Antarctic ice sheet fluctuations 0-94549
Antarctica, climatic record down to last ice age from ice cryst. size 0-94544
Arctic, warm season affected by rainfall and temp. anomalies 0-98433
astroclimate, influence on precision of photographic star positions obtained with wide-angle astrophotographs (*Russian*) 0-72748
astronomical theory of climatic fluctuations geographical support 0-72509
N.Atlantic easterly gales, 1881-1970 period 0-77101
Birmingham, England, heat island synoptic climatology (1965-74) 0-85740
Bombay (1848-1967), annual mean values rel. to sunspot nos. 0-81811
Britain, water balance, 50000 yr BP to present day 0-72566
British spring weather, survey (1950 to 1979) 0-98427
British winters (1659 to 1979), study of temp. correl. with precipitation 0-98444
China, agricultural growing season vars. in historical time (*Chinese*) 0-109246
China, effect of planetary motion on climatic changes 0-85741
NE.China, persistently low summer temp., causative circulation pattern (*Chinese*) 0-109235
climate change, study of upper air data 0-105045
cloud cover influence on atmos. top radiation budget 0-98398
clouds, stratiform, modelling and effect on radiation balance (*French*) 0-82017
conference, on climatology, hydrology, atmospheric research and meteorology from space, Ajaccio, Corsica (1979 November 12 to 16) 0-62397
continental ice sheet, stochastically driven with planetary wave feedback, model 0-77025
data archiving and quality control by computer 0-61907
drought definitions 0-105010
drought in streamflow series, statistical characts. 0-105009
Earth albedo, anthropogenic changes and effects on climate 0-81893
Earth orbit and climate change relationship (*Chinese*) 0-67406
Earth surface temperature, climatological significance of doubling of atmospheric CO₂ conc. 0-101426
Earth surface temperatures, implications of stratospheric aerosol modification by supersonic transports and space shuttle 0-98408
energy balance climate models tests 0-77098
energy balance models, global and one dims., stability comparison 0-94596
England, air temp. variability (1660-1977) 0-98437
England, summer index (1971-78) 0-85742
Eocene terminal event, formation of ring system around Earth 0-76890
feedback mechanisms in climate models, new modeling approach 0-98435
feedback systems, involving sea-ice, ocean temp. and CO₂ 0-98443
Florida, USA, increased aridity since 1960 rel. to atmos. cooling 0-90214
glacial sediments of English Lake District, pre-Devensian till 0-94523
global climate, rel. of stratospheric sulphate aerosol layer 0-109212
global solar radiation in California, interpolation technique based on orthogonal functions 0-67402
greenhouse effect rel. to trace gas transport and photochemistry (*Russian*) 0-81989
W.Greenland, glacier response to climate change 0-61820
Greenland Sea area, climatic normals 0-77100
growing season length as climatic indicator, fluctuations 0-61887
NE. Gulf of Alaska, development of synoptic climatology 0-98405
heat from anthropogenic sources, affecting climate and general circulation 0-89694
heat stress on man, parameter recording and processing, math. method (*German*) 0-82047

climatology continued

- Himalaya, summer weather and climate 0-72620
 hurricane season activity analysis, N. Atlantic (1886-1974) 0-101427
 ice age, CO₂ content of atmos. by polar ice core 0-61891
 ice age beginning, instantaneous glacierisation, albedo rate change and feedback effects 0-105006
 ice albedo feedback on global sensitivity 0-109245
 ice cap-albedo feedback, effects on global climate, 2-D energy balance model 0-67407
 SW Iceland, glacial chronology from palaeomagnetism of Esja, Eyrafljall and Akrafljall mountains 0-89950
 Illinoian glaciation sea-level lowering, Bahama 'blue hole' 0-72557
 Illinois climate centre, review 0-77118
 Lake Naivasha, Kenya, level changes rel. to equatorial westerlies over E. Africa 0-61819
 Liege, Belgium, sixteenth century weather record (*French*) 0-82029
 Little Ice Age, N. Hemisphere average temp. obs. rel. to model calcs. 0-82050
 man's influence on climate, conference, Manlo Park, California (1979 February 21 to 22) 0-62381
 methane greenhouse effect in climate model 0-90211
 Milankovitch theory of ice ages, evidence from palaeomag. chronology of S. Australian beach ridges 0-98307
 model with ice-sheet dynamics, stable periodic solns. 0-90210
 models, sensitivity to external forcing 0-82049
 Mohliner Feld (east of Basle), topoclimate investigations (*German*) 0-61890
 New York State, local climate trends in four cities 0-105044
 New Zealand, temp. record, historical data and agricultural implications 0-61886
 Nile, climate variation affecting discharge 0-81946
 orbital changes of Earth in climate variation models 0-98441
 palaeoclimate of S. Hemisphere since 80 Myr BP, causes for change (*Russian*) 0-98440
 palaeoclimatology, role of tree-ring anal. in Indian region from preliminary survey 0-90212
 potential evapotranspiration, continental maps based on Penman concept calcs. (*German*) 0-98368
 Late Precambrian glaciation in Adelaide Geosyncline, palaeomag. evidence for low-latitude glaciation 0-101325
 quasi-cycles in meteorology, anal. of evidence 0-109239
 radiation budget means by satellite, climate appls. 0-109283
 rapid glaciation in N. Hemisphere climatological conditions from oceanic evidence 0-90213
 regional anomalies assoc. with hemisphere averaged temp. variation 0-77099
 Scotland, summers index (1881-1978) 0-85742
 sediment climate record, diatomaceous sediments of Gulf of California 0-98351
 seismic activity triggered by rapid climate change 0-81858
 Sierra Leone, climatic regime rel. to surface and soil temps. seasonal vars. 0-109242
 solar variability and climate change, 1000-1980 AD, ¹⁴C tree ring study 0-101424
 SURF storage ring calibrations for NASA stratosphere and climate programs 0-94721
 tornado activity rel. to precipitation, assessment 0-61882
 tree ring width climatic interpretation, South Africa Widdingtonia cedar-bergensis anal. 0-98439
 United Kingdom, cloud freq. distrib. analysis 0-61892
 United States, 1896-1975 interannual temp. variability 0-61888
 urban microclimate of Alma-Ata, significant factors 0-101418
 Utah, Colorado, climatic/hydrologic regime rel. to rapids in canyon rivers 0-72564
 variation throughout Earth's history, causal mechanisms 0-82048
 volcanic activity causing climate change, ¹⁴C and historical records 0-98442
 volcanic activity triggered by rapid climate change 0-81858
 Wales, summer index (1971-78) 0-85742
 Late Weichselian ice sheet of N. Eurasia 0-90109
 wind, use of trees as local climatic indicator 0-82007
 wind speed at sea, climatic comparisons of estimated and measured winds from ships 0-105020
 windchill maps of lowland Britain, calc. from instantaneous data 0-61893
 zonal climate models, inclusion of meridional motion and large eddies 0-90138
 C flux between biosphere and atmosphere, biomass burning 0-97838
 CO₂ and climate, model of geographically nonuniform effects 0-90143
 CO₂, atmospheric content, climatological consequences (*Dutch*) 0-98411
 CO₂ induced atmospheric temp. rise, Arctic sea ice decay 0-61802
 CO₂ model run in tandem with climate model, 1800-2100 AD 0-98381
 N₂O causing atmos. warming, fertilizer pollution 0-94579
 N₂O greenhouse effect in climate model 0-90211
 O₃ depletion by halocarbons, climate effects 0-98436

climb, dislocation *see* **dislocation climb****clock paradox** *see* **special relativity****clocks**

- see also* **atomic clocks**; **chronometers**; **time measurement**
 automated time keeping system of Van Swinden Lab. 0-98891
 LASSO experiment on Spiro-2 spacecraft laser synchronisation from stationary orbit 0-82211
 portable quartz, accuracy in comparing time scales 0-101786
 quartz clock, accuracy, radio signal control (*French*) 0-95079
 synchronisation experiment using Symphonie satellite 0-68184
 Cs clocks made by Oscilloquartz Company, investigation of metrological characts. 0-101787

closed circuit television

- holocamera for 3-D micrography of the alert human eye 0-98057

closed loop control systems *see* **closed loop systems****closed loop systems***see also* **feedback**

- Shuttle Orbiter re-entry, remote IR imagery and tracking 0-82171
 stochastic systems theory, appl. to blood pressure control 0-81522

cloud chambers

- low-pressure, anal. of ionisation distribts. 0-106236
 supersaturation profile in thermal diffusion cloud chamber in unsteady state 0-63449
 time expansion chamber, relativistic rise meas. by cluster counting method 0-58030

cloud physics *see* **clouds****clouds**

- see also* **atmospheric precipitation**; **sky**
 aerosol, scavenging of particles by cloud drops and small rain drops, elec. field effect 0-82001
 aerosols of marine air, submicron size distrib. and CCN supersaturation 0-77041
 altocumulus billows, example of large amplitude Kelvin-Helmholtz wave 0-72621
 atmosphere, fixed cloud-top temp. and fixed cloud-top altitude approximations for temp. profile 0-72616
 California coast, marine fog form and fog-stratus systems development 0-77060
 charge separation, rel. to secondary ice crystal prod. 0-81998
 cirrostratus clouds, IR emissivity meas. by remote sounding 0-82061
 cirrus, radiative transfer model for IR region 0-98397
 cirrus sunpillar form, from ice crystals, theory 0-85747
 cold front of midlatitude cyclone, cloud and precipitation struct. 0-109192
 condensation equations for turbulent cloud (*Russian*) 0-77039
 condensation initiation by gravity waves 0-90159
 condensation nuclei, meas. using horizontal thermal gradient spectrometer 0-77158
 condensation nuclei, obs. over N. Atlantic 0-77074
 condensation nucleus spectrometer, new design 0-85765
 conductivity charges in cloud due to lightning 0-61867
 convective clouds, models of thermals 0-109228
 convective day precipitation, correl. with atmos. parameters observed by radar 0-109205
 convective flux estimation over tropical ocean, sensitivity to model assumptions 0-90155
 convective systems during Phase III of GATE 0-90153
 cumuli, droplet size distrib. spectra (*Russian*) 0-81991
 cumulonimbus, updraft-downdraft interaction, numerical model 0-98377
 cumulus, air entrainment mech., obs. in Colorado, USA 0-90133
 cumulus, convection model response to radiative heating change 0-98396
 cumulus cloud, vertical air vel. determ. using airborne meas. system 0-77159
 cumulus cloud vorticity, determ. from GATE A/B scale pot. vorticity budget 0-90157
 cumulus clouds, satellite tracking and derived mesoscale wind fields covariance analys. 0-82013
 cumulus clouds, warm rain and salt seeding, numerical simulation 0-90201
 cumulus congestus in Colorado, ice initiation 0-81997
 cumulus convection, vorticity horizontal transport parameterisation 0-90158
 cumulus convection in tropical depression, synoptic scale kinetic energy source 0-77088
 drop coalescence, collection efficiency of 81 μ m drop falling in 20 μ m drop cloud 0-90134
 droplet collision efficiency enhanced by elec. field 0-61863
 droplet nucleation, expts. with monodisperse NaCl aerosols 0-82003
 dry air entrainment into cloud top, theory 0-90145
 electric charge separation in thunderstorm, model 0-77076
 explosion influencing development of convective cloud (*Chinese*) 0-82042
 extinction coefficient, estimation from multiwavelength lidar backscatter meas. 0-98446
 formation and development, numerical convection model (*Russian*) 0-81987
 Fuego volcano eruption, aerosol emission, density temp. and particle content 0-90050
 GATE aircraft measurements, their value 0-82071
 GATE cloud-subcloud layer interactions, 3-dimens. cumulus model 0-101400
 general circulation by GLAS model, cumulus friction and Jan. Hadly circulation 0-72588
 glory formation, diff. model 0-82053
 hail cell detection, for cloud seeding criteria, radar method 0-90170
 hail growth in supercell cloud, theory 0-98419
 hailstone formation within cloud, microphysics, recycling 0-90146
 hailstorms, finger radar echoes form. mechanism (*Chinese*) 0-109234
 high ice clouds, visible and LR optical props. from lidar and radiometer meas. 0-82060
 hurricane formation, tropical storm control by cloud seeding (*German*) 0-90207
 ice crystal production, secondary, charge separation laboratory meas., thunderstorm electrification exam. 0-72623
 ice nucleation by aerosol particles 0-61864
 ice splinter production during riming, NH₃ addition expts. 0-72585
 intense tropical convective system, mesoscale motion contrib. to convective fluxes 0-90156
 IR long-wave (8 to 13 μ m) radiation fluxes in free atmosphere, effects of clouds (*Russian*) 0-94598
 IR radiative transfer in finite cloud layer 0-72629
 lee wave clouds, S.W. airflow over Bank's Peninsula, New Zealand 0-85739
 light pulse propagation through thick clouds, pulse width expression for scatt. slab 0-82059
 light pulse reflection, height meas. (*Russian*) 0-82056
 liquid content measurement with ground based microwave instrument 0-94623
 liquid water content, retrieval from scanning multichannel microwave radiometer obs. 0-90261
 mass and heat flux determ. in GATE over tropical ocean 0-90154
 mesoscale convergence affecting cloud convection, model 0-109201
 mesoscale rainbands in extratropical cyclones, assoc. cloud microphysics and dynamics 0-82030
 meteorological parameters, feasibility of determination by microwave radiometric method 0-67435
 microphysical model, sensitivity to urban environment 0-82004
 microwave absorption, rel. to pollutant gases monitoring from space using passive sensing techniques 0-76690
 Mohliner Feld (east of Basle), cloud layer effects on topoclimate (*German*) 0-61890
 moisture excess, long distance meas. by radiometry 0-90196
 monsoon airstream at metres height, temp. fluctuations 0-61845
 Mount Kenya, condensation nuclei and weather obs. 0-82012
 multiple light scattering, theory for dispersive media with spherical particles (*Russian*) 0-94599

clouds continued

- noctilucous clouds, advances in space era, review 0-105095
 noctilucous clouds over W. Europe (during 1979) 0-109289
 ocean, effects of clouds on diurnal var. of underwater irradiances on horizontal surfaces 0-72549
 optical props., similarity criteria (*Russian*) 0-85745
 orographic clouds leeward of the Lesser Antilles (*French*) 0-94575
 overcast sky, ang. distrib. of diffuse solar radiation 0-85719
 Pacific, equatorial waves in cloud vel. field 0-67395
 NE. Pacific Ocean, clouds liq. water data rel. to United States west coast rainfall 0-82005
 particle size spectra evolution by condensation and coalescence, analytical soln. 0-109194
 planetary boundary layer, topped with cumulus, numerical model (*French*) 0-94574
 pyrocumulus cloud over North Canterbury, New Zealand, 1878 April 10, obs. 0-109240
 radar reflectivity rel. to cloud dynamics and microphysics 0-61877
 radiation budget at top of atmos., influence of cloud cover 0-98398
 radiative transfer, cloud shape and mutual shading effects 0-101430
 radiative transfer, mathematical modelling 0-90215
 rain systems, large scale, vertical vels. and precipitation patterns, model 0-85727
 remove sensing in 0.35-3 μ m range 0-77085
 seeding, anal. of Florida Area Cumulus Expt. (FACE) rainfall results, natural variability effects 0-82002
 seeding, Climax and Wolf Creek Pass expts. 0-82094
 seeding studies application of lidar remote sensing 0-109203
 seeding with AgI, studies of ice-forming activity, verification of theory 0-101406
 silver clouds, visible spectroscopic investig. from Salyut-4 orbit 0-82014
 Skylab conical multispectral scanner IR data statistics 0-90223
 smoke/dust cloud temporal analysis algorithm 0-98484
 solar radiation absorption, vertical and horiz. distrib. 0-72596
 storm clouds, elec. field obs. (*French*) 0-85712
 stratiform, modelling and effect on radiation balance (*French*) 0-82017
 stratocumulus, cloud top entrainment of dry air and cloud breakup 0-90145
 stratocumulus layer, entrainment affected by radiative cooling 0-94573
 stratocumulus layer, entrainment leading to turbulence kinetic energy 0-90144
 stratus cloud, temp. profiles meas. using low-level atmospheric thermograph 0-105073
 temperature and humidity changes and overcloud inversion 0-77083
 three-dimensional cloud model, storm and boundary condition simulations 0-77049
 thundercloud, positive streamer velocities meas., in quasi-uniform electric fields 0-72625
 thunderstorm top, ascent rate obs. 0-61861
 topographic wave clouds in central and northern Urals, characts. 0-101413
 trace constituents in Indian west coast SW monsoon clouds 0-81967
 two-dimensional model, incorporating eddy viscosity parameterisation 0-85708
 United Kingdom, cloud freq. distrib. analysis 0-61892
 vorticity transport eqn. solns. for Atmospheric Cloud Physics Laboratory 0-94690
 warm cloud electricity, shallow axisymmetric cloud model 0-81999
 warm frontal clouds in midlatitude cyclones, air motion and precipitation 0-109193
 wind derivation from cloud motion fully automated method, Meteosat data comparison with gradient winds 0-109244
 wind velocity indicated by cumulus motion across sky 0-98418
 winds in ocean regions, satellite obs. technique 0-85764

Clusius-Dickel columns see *isotope separation*

cluster analysis see *pattern recognition*

cluster approximation

- alloys, disordered, residual resistivity due to clustering, ageing effects 0-65521
 chemisorption, appl. of cluster techniques, book contrib. 0-107650
 disordered system, low-freq. cond. due to variable range hopping, cluster approx. 0-92886
 Hubbard model, single band, magnetic phase diagram, cluster variational calc. 0-60340
 insulators, charge transfer processes influence on cryst. field 0-92865
 Ising model, quenched-bond disorder, cluster extension of effective-interaction approximation 0-93130
 metal particles, small, characterisation and props., book contrib. 0-84417
 α -quartz, CNDO/2 calcs., electronic props. of perfect cluster, EPR parameters of O⁻ vacancy 0-107701
 rare gas clusters, small, structure, thermodynamic properties 0-88341
 semiconductor, deep transition metal impurity states, SCF CNDO cluster calcs. 0-100442
 semiconductor, with defects or impurities, local density of electron states 0-92857
 semiconductors, doped, shallow impurity states, Hubbard bands and donor excitonic states, HF calc. 0-100443
 Si (111), surface relax., EHT and cluster calcs. (*Chinese*) 0-59762
 solid electrolyte, mobility paths for M_{14}^{-3} clusters, ab initio electronic struct. calcs. 0-70458
 strongly coupled Jahn-Teller system, cluster model for optical absorption spectrum 0-89034
 AlZn, disordered, residual resistivity due to clustering, ageing effects 0-65521
 CO chemisorption on Ni, Pd, Pt, Ir, mol. cluster calc. 0-100407
 Cu₄ clusters, electronic structures, SCF-X α -SW method 0-88468
 Cu₂Zn clusters, electronic structures, SCF-X α -SW method 0-88468
 GaAs (110), surface electronic struct. calcs. 0-80343
 GaAs, (110) surface structure, rotational relaxation, cluster model (*Chinese*) 0-107621
 NaV₆O₁₅ monocrystal, electronic struct. and X-ray emission spectra anisotropy 0-84807
 Ni, adsorption of N₂, photoemission and electronic struct., cluster calcs. 0-97403
 Ni clusters local densities of states 0-88466
 Ni-Cu, ferromag., mag. moment, local environment effects, HF CPA cluster calc. 0-65817
 NiO (001) surface, chemisorption of H, surface and second-layer defect effects 0-65369

cluster approximation continued

- NiO, bulk props., initial state MO Ni₄O₄ and Ni₁₃O₁₄, cluster model, lattice and force consts., photoemission and CT absorpt. spectra 0-84828
 Si, deep level defects, struct. bonding, amphoteric centres 0-88506
 Ti₄V₁₋₃-C, electronic struct. and X-ray emission spectra, cluster MO calc. 0-65444
 Zn₆ clusters, electronic structures, SCF-X α -SW method 0-88468
cluster model (nuclear) see *nuclear cluster model*
clustering, impurity see *segregation*
clustering, solute see *segregation*
clusters, atomic see *atomic clusters*
clusters, globular (stellar) see *globular star clusters*
clusters, metal see *metal clusters*
clusters, molecular see *molecular clusters*
clusters, stellar see *stellar clusters and associations*
clusters of galaxies
 see also *galaxies; intergalactic matter*
 Abel 1060 cluster, X-ray spectrum obs. by (HEAO A-2) 0-82518
 Abell 194, dynamical anal. using Multi Mass Model 0-98726
 Abell 2029, radio and SAS 3 X-ray obs. 0-82519
 Abell 2197 and 2199, Westerbork survey at 610 MHz, 18W catalogue 0-67883
 Abell 2199, 3.5 and 4.0 mm obs. of central regions (*Russian*) 0-82525
 Abell 399/Abell 401, X-ray binary galaxy cluster, mass 0-90546
 Abell 401, X-ray cluster of galaxies, radio emission distrib. 0-98731
 Abell cluster, lunar occultation obs. at 327 MHz, survey 0-73052
 Abell cluster radio sources, spectra and optical identification, SHF obs. 0-98729
 Abell clusters, 3-D nearest neighbours test 0-90545
 Abell clusters, evidence against real existence 0-101643
 AWM 7, X-ray source identification by HEAO 1 0-90573
 Cancer cluster, Westerbork survey at 610 MHz 0-67884
 catalogue inhomogeneity, cluster props. distortion, statistical anal. method 0-67888
 Centaurus cluster, X-ray spectrum obs. by (HEAO A-2) 0-82518
 Centaurus I cluster, resolution into two velocity systems using new redshift data 0-77499
 clustering, statistical studies 0-105363
 clustering on large scale rel. to matter-radiation decoupling epoch of early Universe 0-62355
 collapse, disk galaxy gas envelopes ejection 0-82483
 colour distribution of E and S0 galaxy clusters rel. to redshift 0-105361
 Coma cluster, 3.5 and 4.0 mm obs. of central regions (*Russian*) 0-82525
 Coma cluster, mass segregation and missing mass 0-98730
 compact groups, galaxies anomalous luminosity function 0-82520
 compact groups, X-ray emission obs. 0-90574
 deep sample analysis 0-105362
 distant clusters, brightest galaxies pseudo-pairs in Turner's (1976) sample 0-67849
 distribution of galaxies round cluster from cluster-galaxy-galaxy three-point correlation function 0-94875
 dynamical age determ., appl. to Virgo cluster 0-77498
 Emden sphere model embedded in background supercluster, dynamical theory 0-62296
 emission line galaxies, spatial distrib. rel. to clusters, visible spectra obs. 0-73046
 evolution of galaxies and intergalactic matter in clusters, model 0-85992
 evolution of galaxy clustering, anal. from galaxy fields stochastic simulation 0-90530
 faint blue objects, distrib., clustering props. and nature 0-82476
 formation, tenacious myths about cosmological perturbations larger than horizon size 0-105408
 Fornax cluster, membership determ. by photographic photometry 0-82523
 galaxy correlation function evolution, N-body Monte Carlo model 0-62292
 galaxy number density, radial number density and radial cumulative galaxy distrib. 0-73050
 Hercules cluster, 3.5 and 4.0 mm obs. of central regions (*Russian*) 0-82525
 hierarchical clusters as opposed to continuous clusters, determ. 0-73051
 Indus Supercluster galaxies, UVB photoelectric photometry and photometric parameters 0-67855
 interacting galaxy pair, zero relative vel. surfaces in gravit. field 0-67881
 intergalactic matter, effects on evolution of galaxies 0-109543
 intracluster medium, mass and metal abundance from elliptical galaxies chemical evolution 0-67843
 ionised gas in clusters of galaxies, microwave search 0-82477
 linear clustering in low-density universes 0-85993
 linear clusters, member galaxy alignment, visible obs. 0-90516
 Local Group, motion towards Virgo from galaxies distance scale and expansion rate outside Local Supercluster 0-105325
 Local Group, peculiar vel. rel. to Virgo cluster, deceleration parameter determ. 0-62351
 Local Group, peculiar vels. 0-62284
 Local Supercluster, non-linear collapse in high density Universe 0-62330
 inner M101 galaxy group, H I obs. 0-67885
 M 101 group, reality questioned rel. to M 101 distance 0-67852
 mass to light ratio using negative energy concept 0-86002
 member galaxies, morphology rel. to spiral galaxy evolution 0-90543
 MFJG 18 and 19, dynamics of superclusters 0-105365
 microwave background, cluster effects (*Russian*) 0-94899
 missing mass problem, implication of neutrino rest mass (*Russian*) 0-105414
 MKW 11, identification with X-ray source 4U 1326+11 using HEAO 1 data 0-90574
 MKW-AWM poor clusters, optical props. 0-94878
 Morgan's poor clusters, optical props. 0-94878
 morphology, positioned and photometric data anal. 0-67887
 MR 2251-178, nearby QSO in cluster of galaxies 0-67900
 N-body simulations of galaxy clustering, fraction in groups as function of density enhancement 0-67879
 nearby Abell clusters, associated bright galaxies position and magnitudes 0-67880
 nests, origin, geometrical colour and morphological props. 0-67889
 NGC 1023 galaxy group, H I obs. and possible intergalactic H I cloud discovery 0-67886

clusters of galaxies continued

- NGC 1023 galaxy group, H I radial vels. rel. to group membership and mass/light ratio 0-82521
 NGC 3686 galaxy quartet, surface photometry, mass distrib. and group stability 0-62297
 orientations of member galaxies, Monte-Carlo simulation 0-90528
 origin, spontaneous prod. of cosmological fluctuations 0-94902
 Perseus X-ray cluster, form. of optical filaments in cooling gas round NGC 1275 galaxy 0-67862
 photometry of remote clusters 0-105364
 poor clusters, 1400 MHz pencil beam obs. in direction of cD galaxies 0-62263
 poor clusters containing cD and related galaxies, pencil beam obs. of radio emission at 6 cm 0-62293
 protocluster, gaseous, vortex generation in protogalactic medium 0-62360
 QSO-galaxy group assoc., 3C 273 field obs. 0-105385
 redshift determination using Image Dissector Scanner, visible spectra 0-90544
 rich clusters, catalogue of galaxy morphological types 0-85872
 rich clusters, galaxy morphology and implications for galaxies form. and evolution 0-62255
 rich X-ray emitting clusters, VHF obs. 0-62294
 rotation as opposed to transverse vel. 0-94876
 scaling law for clustering 0-82522
 scattering of microwave background, 9 mm obs. 0-105366
 scattering of microwave background radiation 0-105367
 secondary peak rel. to formation 0-77497
 separations, effects of neutrino rest mass on Universe density perturbations spectrum (*Russian*) 0-109576
 Shahbazian 1 group of galaxies, dynamics from spectroscopic, obs. 0-67878
 spiral galaxies, membership of sparse groups rel. to number of companions 0-77481
 Stephan's Quintet, redshifted H I associations 0-67882
 Stephen's Quintet, broadband 21 cm H I emission 0-109554
 stochastic simulation of fields of galaxies 0-62295
 supercluster dynamics 0-105365
 superclusters and density profile secondary max. 0-98727
 tidal forces, in inhomogeneous cosmological models 0-62338
 tidal interactions in rich clusters, stochastic phenomena 0-105161
 Ursa Major Cloud, probable membership of miniature spiral galaxy NGC 3928 (Markarian 190) 0-105347
 Virgo cluster, 3.5 and 4.0 mm obs. of central regions (*Russian*) 0-82525
 Virgo cluster, dynamical age determ. 0-77498
 Virgo cluster, evidence for confining environment for Virgo A (M87) from 610 MHz map 0-62302
 Virgo cluster, intracluster gas interaction with hot interstellar gas in elliptical galaxy (M86) 0-90535
 Virgo cluster, luminosity-vel. width relation, distance and recession vel. 0-90542
 Virgo cluster, perturbation to Hubble flow rel. to elliptical galaxies mass to light ratios 0-98707
 Virgo cluster, possible supernova discovery 0-90460
 Virgo cluster, total mass-energy density in open Universe 0-62351
 Virgo cluster galaxies, 1.4 GHz continuum survey 0-98721
 Virgo cluster spiral galaxies, H I deficiency from 21 cm obs. 0-62277
 Virgo supercluster and mean mass density of Universe 0-94877
 virial masses, scale covariant gravitation 0-98728
 VV 150, galaxy chain, photoelectric and spectroscopic study 0-98724
 VV 493 (UGC 07910), possible galaxy chain, morphology and spectrum 0-98718
 VV 644, compact 'nest' of galaxies (*Russian*) 0-94879
 X-ray cluster found by Einstein Observatory, CCD camera study and redshift 0-62315
 X-ray clusters of galaxies, large-scale struct. 0-82524
 X-ray observations of objects at cosmological distances from the 'Einstein' observatory 0-105171
 X-ray sources, luminosity function evolution 0-62314
 Zw 0335.1+0956, identification with X-ray source 2A 0335+096 using HEAO data 0-90574

clutter

- quasi-staring IR sensor clutter rejection processor design 0-86417

CNDO calculations

- adenine, hydroxy and methoxy derivatives, absorption UV spectroscopy and electronic struct. of ionic and tautomeric forms 0-74177
 alcohol H-complexes interactions, H-bond vibr. freq., anharmonic calcs. 0-99453
 contact charge transfer complexes of organic molecules with O₂, CNDO/S calcs., absorpt. spectra obs. 0-69076
 cyanine dyes, excited electronic states, CNDO/S CI calc., visual pigment spectra appl. 0-85333
 cytosine, hydroxy and methoxy, derivatives, absorption UV spectroscopy and electronic struct. of ionic and tautomeric forms 0-74177
 electrostatic interactions in liquid state, effect on frontier orbitals and chem. reactivity 0-84046
 excited states, variable metric optimisation of mol. geometry 0-58178
 formic acid dimer, vibr. spectra, CNDO/2 interpretation (*French*) 0-58155
 formic acid-d₀(d₁)-(d₁)-(d₂), vibr. spectra, CNDO/2 interpretation (*French*) 0-58155
 haloalkane-aromatic complexes, ground and excited states, CNDO calcs. 0-69082
 invariance of CNDO/S method rel. to basis functions 0-74125
 liver alcohol dehydrogenase, proton relay system, SCRF PCE theory, CNDO/2 calcs. 0-85325
 methyl fluoroformate, isomer conformation, CNDO and ab initio STO calcs. 0-58151
 monochloroacetic acid, isolated molecules, internal rotation, CNDO/2 calcs., IR spectra 0-69254
 n- π^* singlet-singlet transition probabilities 0-95689
 nucleic acids bases, excited state dipole moments and geometries 0-95738
 organic compounds, excitation energies, CNDO/S-CI method calc. appls. (*German*) 0-106275
 organic mols., relative Raman intensities, CNDO/2 INDO param. effect 0-95633
 phthalic acid derivatives, excitation energies, CNDO/S-CI method calc. appls. (*German*) 0-106275
 porphyrin, hypersurface of adiabatic pot. calc. by CNDO/2 method, vibr. freqs., absorpt. spectra calc. 0-95543
 n-propanol, preferred conformers, PCIO study 0-95542

CNDO calculations continued

- propyne-d₀(d₁), absolute and integrated IR intensities of fundamental modes 0-87179
 pyridine(-d), force consts. and vibr. spectra by CNDO/2 force method 0-95540
 pyrimidines, substituted analogues, absorption UV spectroscopy and electronic struct. of ionic and tautomeric forms 0-74177
 α -quartz, CNDO/2 calcs., electronic props. of perfect cluster, EPR parameters of O²⁻ vacancy 0-107701
 quinoxalines, enzyme inhibitory, structure-activity quantitative study 0-78540
 radical doublet states, positive ion potential anal. in CNDO/BW calc. 0-91452
 semiconductor, deep transition metal impurity states, SCF CNDO cluster calcs. 0-100442
 semiempirical theory for ground and excited states, Fock operator expansion, STO-3G and CNDO/S calcs. 0-58154
 spin-spin coupling constant calculations in mol. by CNDO/SP methods 0-74126
 thioformaldehyde, $\bar{a}^3A_2-\bar{X}^1A_1$ IR absorpt. spectra 0-83362
 bis-triazolopyridazines, conformation calcs. by mol. mechanics and CNDO/2 method 0-69079
 bis-triazolyls, conformation calcs. by mol. mechanics and CNDO/2 method 0-69079
 two photon absorptivities, CNDO/S-CI calc. with second order time depend. perturbation eqns. 0-74122
 two photon absorptivity, ion cyclotron reson. photodissoc. spectra, CNDO/S-CI-perturbation theory 0-74123
 two-photon spectroscopy, dipole-forbidden transitions, double excited configurations, CNDO-CI methods 0-58332
 vibrational intensity calcs., CNDO/2 method with extended basis set 0-91445
 Ag latent image particles, electronic effects 0-82840
 CH₃, CH₂ and CH deformation vibration group frequencies and MO electron densities, interaction force const. 0-87101
 Cl₂Si(CH₃)₂-n, ³⁵Cl NQR, geminal and vicinal interactions on substituents electronic effect 0-63663
 Cl₂Si(OCH₃)₂-n, ³⁵Cl NQR, geminal and vicinal interactions on substituents electronic effect 0-63663
 Co complex, O₂CoCl₂ and O₂CoCl₂NH₃²⁺, struct. and bonding model, CNDO-UHF calcs. 0-95541
 Cu complex, Cu(NH₃)₂(NCX)₂, X=O, S, electronic struct., stereochem. 0-58156
 H₂O, semiempirical CNDO/2 wave functions, pair density anal., environmental effects 0-91451
 (H₂O)₂, struct. studied by CNDO/2 method 0-69081
 Na zeolites, electronic struct., quantum chemical study 0-69058
 NaCl crystals, electronic and hole centres and surface, quantum-chemical calcs. 0-65489
 Ni surface, adsorbed CO, N₂, valence band photoemission, SCF MO CNDO calc. 0-100754
 S-N system, inorganic, electronic struct. obs. by photoemission XPS and UPS, CNDO calcs. 0-78653
 Se, amorphous film, highly disordered, UPS study 0-76148
- coagulation**
 aerosol, high Knudsen number, coagulation rate measurement 0-71954
 aerosol particles in flow type chamber, coagulation, deposition 0-69908
 aerosols, coagulation, initial size distrib. effect 0-104698
 colloidal particles, Poiseuille flow, total particle conc. axial change 0-108752
 fibrinogen, bovine, high energy-induced aggregation, time resolved spectra 0-61655
 fibrinolysis and coagulation, dynamic rheological studies 0-61614
 immunoglobulin, human, high energy-induced aggregation, time resolved spectra 0-61655
 interstellar dust, grain growth by radiation pressure induced coagulation 0-94851
 molten metal binary mixtures with wide immiscibility range, gravitational layering of components (*Russian*) 0-104092
 monomer externally controlled coagulation, exactly solvable model 0-81368
 Schulze-Hardy rule, theory 0-89540
 serum albumin, bovine, high energy-induced aggregation, time resolved spectra 0-61655
 Re hydrosols under action of US irradiation 0-58853

coal

- see also mining
 aerosol particle size classifier, parallel plate electrostatic device 0-95070
 Bonnet Plume Basin, Yukon Territory, Canada, gravity profile anal. as aid to coal basin evaluation 0-76898
 calorific value determ., by neutron inelastic scattering (*Czech*) 0-101048
 chemical analysis, computer evaluation of SEM images 0-71994
 cleaved surface, photoacoustic IR spectra 0-87104
 coke, shrinkage kinetics during calcination 0-93572
 combustion, radiological aspects 0-61485
 conversion technologies, health and environmental effects 0-81493
 dispersion, solvent refined, elec. props., surface characts. 0-80333
 dust mass flow meas. methods (*German*) 0-92242
 fault location in underground coal seams 0-94613
 fluidised-bed steam generating system to supply 100000 lb/h of saturated steam burning high S coal 0-108778
 gasification, potential fuel source 0-93842
 gasification environment simulation 0-100831
 gasification for industrial scale H₂ production 0-61438
 hydraulic coal trunk pipeline transport systems, methods of improving economic effectiveness 0-106837
 liquefaction, potential for synthetic crude oil production, Canada 0-93841
 magnetic susceptibility and Mossbauer meas. 0-60464
 MHD power systems, coal-fired, retrofitting to existing non-coal power stations 0-66983
 mineral content characterisation by Fourier transform IR spectroscopy 0-104474
 review of developments for efficient energy use (*Swedish*) 0-93845
 Rosebud coal ash, elec. cond. 0-107476
 seismic imaging of faults in multi-modal coal seams 0-85778
 seismic prospecting for coal, approx. diff. theory for transparent half-planes 0-89974
 solar coal gasification reactors, tech. and economic feasibility 0-76613
 CO concentration meas. in coal pulverising plant, IR gas analysers 0-89572

coal continued
Cl₂ content determ. using British Standard high temp. method 0-85252
H₂ production from coal by centrifugal separation from gasification products 0-76643

coating processes *see* **coating techniques**

coating techniques
see also anodisation; cladding techniques; coatings; electrodeposition; electrophoretic coating techniques; encapsulation; epitaxial growth; metallisation; spray coating techniques; vapour deposition
laser applications in materials processing, seminar, San Diego, CA, USA (Aug. 79) 0-90609
metallurgical coatings, fabrication, struct., and appls., review 0-80121
multilayer beamsplitter coatings, accelerated fabrication method 0-102873
optical fibre coating with conical shape applicator 0-58820
photoresist, negative, spin-coating technique for producing multilayer IR optical medium 0-74451
thin films, deposition techniques, review 0-80964
vacuum deposition, of graded-thickness film 0-76164
Au deposition at high rates from organic plating baths (*French*) 0-66441
CaF₂ on glass, Na-resistant cell, coating apparatus 0-90874
Cu-coated TiO₂ particles, prep. for composites 0-89159
Cu-n-Si diodes, fabrication by electroless deposition method, characts. 0-100520
Na₂O-B₂O₃-SiO₂ glass fibre, plastic coating influence on strength 0-58697
Ni electroless plating on Zn-Al alloys, baths and activating solns. (*Japanese*) 0-71604
Ni-B electroless-plated amorphous films, anomalous mag. temp. characts. 0-96757
Si on ceramics, coating with inverted meniscus (SCIM) technique, solar cell appl. 0-89163
Si, SOC (Si on ceramic) continuous coating for solar cells 0-93904
Si thick-film growth using contiguous capillary coating on porous C substrates 0-93507

coatings
see also anodised layers; antireflection coatings; claddings; decorative coatings; electrodeposits; electrophoretic coatings; epitaxial layers; insulating coatings; protective coatings; spray coatings; sputtered coatings; vapour deposited coatings; varnish
fusion reactor, low Z coating development program 0-106182
fusion reactors Doublet III neutral beam injector system, outgassing rate meas. and residual gas anal., coating props. 0-95457
metallurgical coatings, fabrication, struct., and appls., review 0-80121
metals, coated, IR surface wave interferometry 0-63913
phosphate containing materials, technological prod. processes, review 0-97452
porosity determination by hydrostatic weighing 0-66714
powder coatings, in metal finishing, review 0-104330
pyrocarbon coating, isotropic, gas permeability, neutron irradiation effect (*French*) 0-63260
pyrocarbon coating, isotropic, gas permeability meas. (*French*) 0-63259
refractory ceramic coatings, for high temp. use, current status (*Japanese*) 0-71619
semiconductor laser, electron beam pumping efficiency, coating effect 0-91795
solar collector glazings, effective beam rad. incidence angles for determ. of diffuse rad. transmittance 0-94112
solar energy collectors, black Ni electrochemical coatings, characts. investigation 0-95975
solar flat plate collector coatings, perf. comparison of flat black and selective coatings 0-61426
textured, crystallites faces determ. 0-64846
thickness inspection, correct. of errors of mounted eddy-current transducers 0-7775
thickness measurement, metrological provisions 0-77749
Al coating reflectivity in vacuum UV, heating effect 0-95981
C fibre, metal-coated with Cu, Co or Ni, coating struct., SEM study 0-97605
C, paint type coating layer with spherical pigment, radiative transfer theory 0-61405
Cr black solar selective absorbers, thermal degradation 0-61417
Cr³⁺/Cr²⁺ colloidal SiO₂ surface films on Al, TEM/XPS study 0-85090
Cr-Cr₂O₃ black chrome, commercial, solar absorber coating characterisation 0-80111
Cu-coated TiO₂ particles, prep. for composites 0-89159
CuO, black Zn-dust pigmented solar selective coatings for solar photothermal conversion 0-66997
CuS, black Zn-dust pigmented solar selective coatings for solar photothermal conversion 0-66997
CuS-PbS, black Zn-dust pigmented solar selective coatings for solar photothermal conversion 0-66997
Fe-Si (3 wt.%), domain wall spacing and core loss, forsterite and stress coatings effect 0-88780
Fe₂O₃, paint type coating layer with spherical pigment, radiative transfer theory 0-61405
Mo coated diamond powders, X-ray diffr. study 0-100936
Ni-ceramic coating structure, influence of micropowder inclusion (*Russian*) 0-59820
Ni-SiC coating adhesion to Al alloy, metal interdiffusion (*Russian*) 0-66697
PbS-CuS, black Zn-dust pigmented solar selective coatings for solar photothermal conversion 0-66997
SiC coated C fibres, effect on strength props. of C fibre reinforced plastics 0-104224
ThO₂ microspheres, coated, coating permeability meas. 0-95343
TiO₂, paint type coating layer with spherical pigment, radiative transfer theory 0-61405
UO₂-UC microspheres, coated, coating permeability meas. 0-95343
ZrO₂ coating on Zircaloy-2, thermal cond. meas. 0-80009

coatings, protective *see* **protective coatings**

coaxial cables
biological substances, dielectric props. meas. at RF and microwave freq. by coaxial line reflection methods 0-109065
ionisation chamber cables, exp. investigation 0-78489
pulse forming network as rare gas halide laser pump 0-69424

coaxial lines *see* **coaxial cables**

cobalt
see also nuclei with
adsorption and reactivity of NO on (0001) face, LEED, AES, and thermal desorption study 0-80090
adsorption by Al₂O₃, radioactive waste storage 0-99240
atom, X-ray transitions in laser produced plasma 0-100093
atom + H⁺ (D⁺), K shell ionisation, nuclear Coulomb effect 0-91650
cavitation erosion, role of twinning in single crystal 0-107272
coated C fibre, coating struct., SEM study 0-97605
corrosion, indoor, rate meas. 0-76404
Debye-Waller factor and Lindemann parameter, temp. depend., lattice dynamical model calcs. 0-59610
dissolution kinetics and diffusion coefficients in molten Al 0-59666
electrode reactions with molten glass 0-85186
electrodeposited, influence of soln. pH on microstruct. 0-65399
energy band dispersion and mag. exchange splitting, angle-resolved photoemission meas. 0-71567
energy band dispersions and mag. exchange splitting 0-76146
epitaxial films, even magneto-optical effects 0-76007
Fermi surface under press., de Haas-van Alphen effect meas. 0-75499
ferromagnetic film, mag. anisotropy study using NMR spin echo method 0-60384
ferromagnetic metals, spin fluctuation theory, Curie temp., mag. susceptibility 0-65937
ferromagnetic micropowder, cryst. struct., coercivity, remanence, saturation 0-65967
ferromagnetic properties, book contrib. 0-75724
film, mag. domain wall obs. by electron holography 0-80582
fine particles in Cu, interface magnetisation 0-88858
glide ahead of terminating {1012} twins 0-96545
HCP film, uniaxial, mag. domain struct. 0-60385
implantation in Al, replacement collision probability at 4.2K 0-70237
impurity, in Pd-H, Mossbauer study of local environment of substitutional impurities 0-60475
interstitial site determ., μ SR technique 0-71287
itinerant electron ferromagnet, magnetovolume effects 0-60397
K-shell X-ray prod. by ¹⁴N⁺ bombardment 0-91482
liquid, Hall effect, band struct. and exchange scatt. 0-80250
liquid, N solubility depend. on added elements, mechanism (*Russian*) 0-65223
low-level transuranic storage, radwaste Sr, Cs, Co sorption meas. on soil sediment 0-95482
n=2-2 transitions in XUV spectra, anal. 0-102472
oxidation, XPS obs. of epitaxial CoO form. 0-66396
particle formation by evap., electron microscopy obs. of interaction processes 0-104053
particles, single domain, randomly oriented easy axes and particle size distrib., coercivity 0-71119
particles, vibrations associated with twins 0-100253
passivation films in neutral and alkaline borate soln., modulation spectroscopic anal. (*Japanese*) 0-108628
permanent magnet material savings (*German*) 0-103851
plating line Co concentration monitoring, by automatic colorimeter 0-105691
radiative Auger effect, K-M² 0-71522
surface, CO adsorption-desorption kinetics, surface carbide form. effects 0-103574
thin film, nuclear spin echo excitation on subharmonics, and multiple freq. (*Russian*) 0-60454
thin films, optical and magneto-optical permittivities 0-66163
twins, {1121}, in single crystals, accommodation and form. 0-96540
vacuum deposited coatings on metal substrates, cryst. struct. and stability 0-75481
X-ray K-absorption spectrum 0-97378
X-ray K-emission satellites, quasi-stationary states and origin 0-80903
X-ray reflectivity, L_{2,3} absorpt. edge 0-71513
 α -Al₂O₃:Co³⁺ (Co²⁺), optically and thermally stimulated reactions, absorpt. spectra 0-80825
BaTiO₃:Co, tricritical point, X-ray diffr. meas. 0-71341
BaTiO₃:Co, voltaic current appearance on proton irradi. 0-104032
CaF₂:Co, X-irrad., impurity effects on defect prod. 0-92525
CaF₂:Co, X-irrad., thermolum. 0-60686
CdBr₂:Co²⁺, exchange-coupled Co²⁺ pairs, optical absorpt. and Zeeman studies 0-66242
CdTe(Se):Co, impurity luminescence no phonon line depend. on temp., Debye temp. 0-66273
Co II, unidentified lines in spectrum of HR 5049, southern Ap-star 0-82384
Co XI-XVII solar 3s²3pⁿ-3s3pⁿ⁺¹ transition arrays, UV spectra classification 0-63570
Co²⁺, doped ion in divalent metal cpds., correl. between Szigei charge and hyperfine coupling consts. 0-96832
Co:MgF₂, tunable transition-metal-doped solid state lasers 0-58549
Co-CoO films, evaporated, exchange anisotropy 0-88841
Co-Si interface, glassy layer, ellipsometric charact. 0-103589
CoCO₃, mag. props., microscopic level calcs. (*Russian*) 0-97078
⁵⁷Co labelled bleomycin, Bayer map evaluation in lung scintigraphy (*Japanese*) 0-72319
⁵⁷Co, Mossbauer absorpt. and emission spectra, hyperfine struct. and relax. effects 0-71279
⁶⁰Co, distrib. and behaviour in Urazoko Bay sediment 0-97825
⁶⁰Co gamma rays effects obs., on polyethylene loss tangent variation (*German*) 0-75266
⁶⁰Co source for radiographic inspection method 0-71861
⁶⁰Co sources for total body irradi., uniformity and standardisation 0-94338
CsCaCl₂:Co, EPR, 4.2 to 450K, ferroelec. transition 0-60414
Cu:Co precipitates, mag. anisotropy, precipitate shape, coercive force 0-80500
GaAs:Co, intra d-shell excitations of acceptors 0-84757
GaAs:Co, substitutional impurity elec. struct. 0-88513
GaP:Co, optical spectra and Zeeman anal. of Co 3d⁷ state 0-66247
GaP:Co, photolum. excitation spectroscopy 0-80841
GaP:Co, positron annihilation meas. rel. to deep levels study 0-60712
KMgF₃:Co²⁺, ⁴T₁-⁴T₂ transition, zero-phonon lines intensities 0-75529
Li-Co ferrite, mag. anisotropy induced by thermomag. treatment, ionic order effect, magnetostriction meas. 0-103830
LiF:Co, flow stress changes during precipitation 0-92594

cobalt continued

- LiNbO₃:Co²⁺, Zr⁴⁺ film, improvement in temp. stability and SAW device appls. 0-75939
 MgO:Co²⁺ ESR linewidths of Co²⁺ 0-80596
 MgO:Co²⁺, electronic and impurity-induced Raman scatt. 0-100659
 MgO:Co²⁺, weak dynamic Jahn-Teller coupling, neutron inelastic scatt. obs. 0-59934
 in Ni, paramag. region, impurity effects on susceptibility, Faraday obs. (Russian) 0-88731
 PdH₂:Co²⁺, diffusion-induced reduction, Mossbauer study 0-108131
 Si³¹:Co, implanted, Mossbauer spectra, study of dose dependence 0-75900
 Si:Co, ion implanted, Co lattice location, channelling meas. 0-88201
 Si:Co, minority carrier lifetime investigation 0-80292
 SrO:Co, noncentral and interstitial ion complexes, ESR obs. 0-71169
 WC-Co DC and RF sputtered coatings, bias effect, struct., X-ray-Auger study 0-70565
 YIG-Co film, influence of stress induced anisotropy on domain struct. 0-100605
 ZnO:Co varistors, microstructure-prop. relations 0-100249
 ZnS:Co Mossbauer sources, Fe³⁺ transient charge state 0-108128
 ZnS₂Co electrolytes containing Ge and Co, polarisation charact., exam. by cyclic voltammetry 0-104444
 ZnS(Se)(Te):Co, impurity luminescence no phonon line depend. on temp., Debye temp. 0-66273

cobalt alloys*see also cobalt compounds*

- adhesive wear under unlubricated conditions 0-108593
 Alnico 5 alloy, S and Ti additions effect rel. to non-metallic inclusions, coercive force and grindability 0-89375
 Alnico type YuNDK25DA alloy permanent magnets, thermal mag. hysteresis 0-75818
 amorphous, alloying elements influence on corrosion behaviour, XPS obs. 0-89422
 amorphous, effects of metalloids on mag. props. 0-75738
 creep-fatigue interaction in aligned eutectic and solid soln. 0-108554
 dilute alloys, amorphous, exhibiting Mossbauer effect, mean mag. props. (French) 0-80489
 Hayes alloy no.716, Fe-Cr-Ni-Co-W-Mo-Si-C-B (26, 22, 12, 3.5, 3, 1.2, 1.1, 0.4 wt.%), hardfacing alloy 0-100802
 Incoloy 800, nuclear grade boiling tubing superalloy, Co and C content anal. 0-78397
 Inconel 600, nuclear grade boiling tubing superalloy, Co and C content anal. 0-78397
 Inconel 617, creep, morphological changes of carbides, affect on creep props. 0-108509
 Kovar-silicon oxynitride-aluminium cathode, local electron emission and electroluminesc. patterns obs. 0-108327
 magnetic susceptibility and Knight shift meas., d-metal alloys 0-66055
 mischmetal-Co system, thermomagnetic analysis of intermediate phases 0-93115
 Ni-Co, H₂ embrittlement, heat treatment and impurities effect 0-76331
 rare earth Co compounds, RCo₂, metamagnetic transitions in internal fields 0-60272
 rare earth cobaltes, RCo₂ type, hydride phase synthesis, thermal stability and struct. 0-59438
 rare earth-Co, plastic magnet appl., anisotropic, based on moulding ferro-magnetic powder material with plastics (Japanese) 0-60829
 rare earth-Co, R₆₉Co₃₁, amorphous, mag. props. 0-84590
 rare earth-Sn-X, X=Rh, Ir, Ru, Co, cryst. growth and cryst.-chem. invest, supercond./mag. ternary cpds. 0-100777
 rare-earth intermetallics, R₂Co₂, polymorphism of Ce subgroup alloys, eutectic decomposition (Russian) 0-66504
 steel, Cr-W-Mo-Co, high-speed, from atomised powders, mech. and cutting props. 0-66556
 steel, Ni-Co-Cr, high-strength medium C, Cr effect on props. 0-76339
 steel, W-Mo-Co, high-speed tool, struct. and props., cooling rate effect at primary crystn. temp. 0-76241
 Stellite, self-weldability in high temp Na (Japanese) 0-89392
 stellite hardfacing materials, friction characts. in high temp. Na (Japanese) 0-89356
 Stellite-6, XPS obs. of aqueous oxidation, surface comp. and gaseous oxidation effect 0-81238
 AlCu-NiCo (5 at.%), θ' hardened, creep mechanism 0-85013
 Al₄(Ni, Co)₃ ternary phase in Al-Ni-Co system, cryst. struct., vacancy controlled phase (Chinese) 0-70164
 Au-Co, dil., valence and core level spectra, XPS study 0-84838
 Au-Co, electron scatt., spin-orbit effects 0-65533
 Au-Co, liquidus line determ. by mag. meas. 0-60250
 Au-Co, UPS study, localised states 0-93449
 Au-Co electrodeposit, Co-hardened, characterisation by Mossbauer spectroscopy, Co precip. formation 0-80108
 CeCo₃, and ternary hydride, mag. props. 0-108007
 CeCo₃, sorption at press. up to 1500 atm. 0-79819
 Ce₂Co₃, and ternary hydride, mag. props. 0-108007
 CeCo_{3-x}Cu_x, 0≤x≤ internal oxidation kinetics, oxide struct., X-ray study 0-104329
 (Co,Fe)₈₀B₂₀ glass, induced anisotropy and time changes of permeability 0-75815
 Co-⁴⁸V, nucl. orientation of ⁴⁸V, γ -ray anisotropy obs. 0-97169
 Co-(Cr,Co)₂C₃ eutectic, oxidation effect on toughness and strength 0-89404
 Co-Al, multilayer martensite phases, illustration of polypolyte structures 0-84932
 Co-Al, X-ray K-absorption spectrum 0-97378
 Co-B-Si amorphous alloy, liq. quenched, elec. resist. and cyclic deform. 0-59949
 Co-B-(Cr) thin film glasses, mag. props. and corrosion resist. 0-80576
 Co-Ca, liq. alloy form. kinetics (French) 0-96652
 Co-CoAl, two phase, interaction between deform., fracture initiation and propag. 0-85006
 Co-Cr mag. film, crystallographic texture formation effects on props. (Russian) 0-108471
 Co-Cr-C eutectic alloy, thermal conductivity and electric resist. at high temp. 0-103668
 Co-Fe, dil., hyperfine mag. fields, press. effect, Mossbauer meas. 0-71277
 Co-Fe, dil., magnetocrystalline anisotropy anomalous temp. depend. 0-71007
 Co-Fe, soft mag. props. rel. to metallurgical aspects 0-88810

cobalt alloys continued

- Co-Fe amorphous alloys, worked, permivar type mag. hysteresis loop, longit. Kerr effect obs. 0-65958
 Co-Fe-B, amorphous, crystn. and thermal stability 0-107057
 Co-Fe-Si-B, decomp. of amorphous state during annealing below recryst. temp., electron microscope study (Russian) 0-75164
 Co-Fe-Si-B, ferromag., magneto-optical spectra in amorphous and cryst. states (Russian) 0-84749
 Co-Fe-V-Ni, mag. and mech. props., heat treatment and stress effects 0-60363
 Co-Ga, spin glass materials, mag. field dependence of susceptibility peak 0-103840
 Co-Ga binary system, lattice const., phase transform (Chinese) 0-88108
 Co-Gd film, magneto-optic coeff. and refr. index, ellipsometric determ. 0-71501
 Co-Gd-Mo amorphous films, resist. and extraordinary Hall effect, thermal annealing effect 0-70852
 Co-Gd-Mo films, sputtered, O effects on mag. props. during annealing 0-89374
 Co-Ge binary system, phase diagram rel. to that of Ni-Ge (French) 0-97463
 Co-mischmetall system, phase relations, microstruct., mag. props. 0-104118
 Co-Mn, FCC, micromagnetism, magnetisation and mag. susceptibility meas. 0-60310
 Co-Mn alloys, ferromagnetic, high field mag. susceptibility meas. 0-75729
 Co-Mn-Ni-Fe-Si-B amorphous alloys, mag. props., low magnetostriction 0-75832
 Co-Mo-B metallic glass ribbons, tensile strength, crystn. temp. 0-89173
 Co-Nb-C, obtained by liq. quenching, superconductivity 0-75699
 Co-Ni, Hall effect, anomalous, residual coeff. calcs. using coherent pot. method (Russian) 0-80249
 Co-Ni-Cr-Mo (35, 20, 10 wt.%), MP35N, TEM study of phase transformations 0-81054
 Co-Ni-Cr-Nb (40, 18, 1.8 wt.%), precipitation behaviour of NbC, effect of ageing temp. on morphology 0-89227
 Co-Ni-Mo-C, amorphous alloys, med. props. and thermal stability (Japanese) 0-85049
 Co-Ni-Zn, diagram of state, crystalline lattice const., microhardness (Russian) 0-66479
 Co-P, amorphous, domain struct., mag. anisotropy origin 0-80554
 Co-P, electrodeposited alloys, heat-induced structural changes (Japanese) 0-89263
 Co-P, electrodeposited amorphous alloys with high permeability, thermal treatment with and without field 0-89372
 Co-P alloys, geometric struct. models and diffraction exam. techniques 0-79700
 Co-P films with various preferred orientations, mag. props. 0-100604
 Co-Pt, mag. annealing, form. of ordered phase, study using X-ray scatt. (Russian) 0-81052
 Co-Pt ferromagnetic alloy, 6 T ultrasonic study of magnetoelastic coupling 0-93154
 Co-Si, surface physicochemical state, Auger electron spectroscopy study 0-100715
 Co-Si-B, amorphous ribbon, saturation magnetostriction meas. by small-angle magnetisation rot. 0-60391
 Co-Sm film, magneto-optic coeff. and refr. index, ellipsometric determ. 0-71501
 Co-Sn system, phase Co₂Sn obtained by splat cooling (German) 0-104147
 Co-Sn-M, n=Mg, Ca, Sr, Sc, Y, Zn, Cd, In or Th, cryst. growth and cryst.-chem. invest, supercond./mag. ternary cpds. 0-100777
 Co-Tb film, magneto-optic coeff. and refr. index, ellipsometric determ. 0-71501
 Co-Ti-C, secondary precipitation and allotropic transform., TEM obs. 0-108453
 Co-Ti-Fe (3, 1 to 2 wt.%), spinodal decomposition 0-100839
 Co-Ti(Hf)(Ta)(Mo)(Zr)(Al)(Fe)(Ni), dendritic segregation 0-76260
 Co-V, Co rich, ferromag. behaviour, mag. moments, Curie temp., and NMR spectrum 0-70964
 Co-V, ferromag. struct. in nucl. spin echoes 0-60453
 Co-W alloy electrodeposition, influence of MgSO₄ and gum arabic additives (Russian) 0-80991
 Co-W alloy electrolytic coatings, heat treatment effects on coercivity, hysteresis and structure (Russian) 0-60381
 Co-WC hard alloys, rapidly quenched struct. 0-76233
 Co-Zn, physical-chemical metallurgy (German) 0-108390
 Co-Zr, amorphous phase form. in Zr-poor region, hardness and fracture strength (Japanese) 0-84914
 Co_{1-x}Al_x, ordered β -phase, enthalpy of formation are defect struct. descript. 0-89519
 Co_{100-x}B_x, amorphous, mag. struct., mag. susceptibility meas. 0-80485
 Co₂B, glassy and cryst., hyperfine field distrib., ⁵⁹Co spin echo spectra 0-80635
 CoCr, dil., low temp. specific heat and magnetisation 0-65925
 Co₆₇Er₃₃, amorphous alloy, sputtered, local order and amorphous struct. 0-88061
 Co, Fe_{2-x}, ferromagnetism and spatial long-range order 0-60159
 (Co₉₃Fe₀₇)_{75-x}Cr₂₅Si₁₀B₁₀ amorphous alloy, thermal stability, Cr conc. effects, DTA expts. 0-59395
 (Co₈₉Fe₁₀)₇₂Mo₅Si₁₃B₁₀, metallic glass, strain- and field-induced mag. anisotropy 0-108004
 Co₅₇Fe₂Ni₁₀(Si,B)₂₃, amorphous, soft mag. props., switched-mode power supply appls. 0-88850
 Co₇₀Fe₅Si₁₀B₁₀, amorphous, crystn. and thermal stability 0-107057
 Co₇₀Fe₄Co₅Si₁₀B₁₀, amorphous, mag. aftereffect spectra and annealing props. 0-88831
 Co_{0.54}Ga_{0.46}, frequency depend. magnetisation, superparamagnetic behaviour 0-84624
 β -Co₂Ga₄₈, negative TCR obs. 0-75543
 CoGa_{1-x} alloys, cluster spin glass, host and impurity NMR and AC susceptibility 0-71194
 CoGa_{1-x}, NMR expts. interpretation 0-75870
 CoGa_{2-x}Fe_x, elec. resist., temp. and mag. field depend., mag. contrib. 0-96846
 CoGa_{2-x}Fe_x, mag. field depend. of resist., 5.80K 0-70676
 Co(GaTiV) alloys, ferromag. onset, electron conc. depend. 0-60203
 Co-HfAl, hyperfine fields of Fe impurities, Mossbauer spectra 0-71255
 CoMn, dil., low temp. specific heat and magnetisation 0-65925
 (Co_{1-x}Mn_x)₂B, magnetocrystalline anisotropy meas., 4.2-300K 0-71006

cobalt alloys continued

Co₃₀Mn₇₀Ga_{50-x} ordering and disordering phenomena, mag. study 0-70154
CoMnP, cryst. mag. struct., neutron diffr. study (French) 0-59439
CoMnSi_{1-x}Ge_x, amg. props. 0-60270
Co₇₂Mo₂₈Si₁₅B₁₀, metallic glass, strain- and field-induced mag. anisotropy 0-108004
CoNiP, cylindrical amorphous electrodeposited layers, mag. props., torsion influence 0-88848
CoP amorphous alloy, heat treatments influence on opt. props., struct. and DC resist. obs. 0-80892
CoP, cylindrical amorphous electrodeposited layers, mag. props., torsion influence 0-88848
Co_{1-x}P_x amorphous alloy film, elec. resistance, temp. depend. (Russian) 0-103660
Co₂P, struct. comparison with Co₂Si, PbCl₂, and SbSI (French) 0-84155
Co₅₇P₁₈, amorphous alloys, electronic struct., γ-ray Compton scatt. study (Japanese) 0-84422
CoPd, single crystals, domain struct., temp. and field depend. 0-71085
CoPd film, ordered, stacking fault obs. by TEM and interpret. using many-beam theory 0-107680
Co_{80-x}Si₂₀, amorphous, structural and mag. heterogeneities 0-80484
Co₂Si, struct. comparison with Co₂P, PbCl₂, and SbSI (French) 0-84155
Co₇₂Si₁₅B₁₀, amorphous, crystn. and thermal stability 0-107057
Co₂Sm crystals, microstruct., homogeneous precip. and nucleation 0-104160
Co₂Sn, intermetallic phase, obtained by splat cooling (German) 0-104147
CoTi, dil., low temp. specific heat and magnetisation 0-65925
CoTi_{1-x}Al_x, mag. and electronic props., ferromag. and paramag. state 0-65814
Co₂TiAl, hyperfine fields of Fe impurities, Mossbauer spectra 0-71255
CoV, dil., low temp. specific heat and magnetisation 0-65925
CoV, phase dependent MNR spectra 0-108114
Co₂VAl, hyperfine fields of Fe impurities, Mossbauer spectra 0-71255
Co₉₀Ti₁₀, ferromag. amorphous alloy, crystn. and domain struct. study 0-107056
Cr-Co, dil., antiferromag., elec. resist. min., press. and impurity effects 0-59970
Cr-Co, magnetic transformations, triple point (Russian) 0-88747
Cr-Co, phase transformations and magnetostriction (Russian) 0-103869
Cr-Co-Fe, low Co, phase separation, TEM and Mossbauer spectra obs. 0-71269
Cr-Co, dil., low temp. specific heat meas., 1.5 to 4K 0-60328
Cu-Al-Co liquid alloys, constant Co-content of 5 wt.%, mag. props. (German) 0-88720
Cu-Be-Co, discontinuous reaction, analytical TEM 0-100842
Cu-Co, dil., valence and core level spectra, XPS study 0-84838
Cu-Co, time of flight atom probe, quantitative microanal., metallurgical appl. 0-86498
Cu-Co (1.5 and 4 wt.%), coherent Co-rich separations obs. by positron annihilation (Russian) 0-89082
Cu-Co single cryst., precip. hardening (German) 0-84946
Cu-Co-Si (0.36, 0.11 wt.%), surface layer struct. on annealing, SIMS and AES exam. 0-88415
Cu-Ni-Co, mag. props. of system of disperse ferromag. particles, 73 to 673K (Russian) 0-65968
(Cu-Au)-Co, single crystals, solid soln. and particle strengthening, superposition 0-97495
Cu₃Au-Co single cryst., precip. hardening (German) 0-84946
Dy(Co,Ni)₂, intrinsic mag. aftereffect meas., domain wall motion 0-71121
DyCo₂-DyAl₂ system, mag. and structural studies 0-108006
DyCo₃, noncollinear mag. struct. appearance in mag. fields, magnetostriction meas. (Russian) 0-100607
ErCo₂, mag. excitations, RPA theory 0-65830
ErCo₂, sorption at press. up to 1500 atm. 0-97819
(Fe,Co,Ni)-Si(B), amorphous mag. alloy, magnetostriction rel. to soft mag. props. 0-84633
Fe-Co, 3d ferromagnet nuclear spin-lattice relaxation 0-80627
Fe-Co, ferromagnetic micropowder, cryst. struct., coercivity, remanence, saturation 0-65967
Fe-Co, Hall effect, anomalous, residual coeff. calcs. using coherent pot. method (Russian) 0-80249
Fe-Co-Al-Cu-Ti (40, 14, 7.5, 4.5 wt.%), metastable equilibrium, high coercive state (Russian) 0-66476
Fe-Co-B, amorphous, crystn. 0-79704
Fe-Co-Mo, phase relations in system at 1100°C 0-108392
Fe-Co-Mo-C, amorphous alloys, med. props. and thermal stability (Japanese) 0-85049
Fe-Co-Mo-Nb(Ta) semihard mag. alloy, mag. props., thermal expansion, elec. resistivity and hardness (Japanese) 0-88789
Fe-Co-Ni Perminvar, mag. props. singularities in region of mag. anisotropy (Russian) 0-84614
Fe-Co-Ni-C, activity coeff. of C at 1273K 0-96667
Fe-Co-Si-B, amorphous soft ferromagnet-with high mag. induction 0-84619
Fe-Co-Si-B, zero magnetostrictive amorphous alloy with high saturation induction, mag. annealing 0-60362
Fe-Co-Si(B), amorphous ferromagnet, mag. after effect on soft mag. props. 0-84626
Fe-Co-Ti-Al alloy type YuNDK magnets, metallographic method of distinguishing cracks 0-85096
Fe-Co-Ti(V)(Cr)(Mn), sp. ht. in ordered and disordered phases 0-71061
Fe-Co-V(Ni), annealing effect on microstruct. rel. to mag. and mech. props. 0-89267
Fe-Co-2 V, (49, 2 wt.%), solid soln., rheological study of crystallographic order on creep (French) 0-97548
Fe-Cr-Co, ductile magnet alloys, mech. props. 0-85001
Fe-Cr-Co, elastic props. anisotropy at room temp. (Russian) 0-89279
Fe-Cr-Co, magnetic domain walls, Lorentz microscopy 0-103854
Fe-Cr-Co, metallic magnets investigation, present state (Polish) 0-107987
Fe-Cr-Co alloy, coercive force mechanism 0-71103
Fe-Cr-Co alloy, spinodally decomposed, micro-twinning 0-92537
Fe-Cr-Co alloys, (5-9 wt.% Co), obtained by slow cooling under mag. field, permanent magnet props. 0-75797
Fe-Cr-Co permanent magnet system, miscibility gap, microstruct. and mag. props. obs. 0-76228
Fe-Cr-Co-Mo high energy permanent magnets, mag. props. 0-97119
Fe-Ni-Al-Co-Cu-Ti YuNDK type, S effect on mech. props. 0-60927
Fe-Ni-Co-Cu-Ti YuNDK alloys, impaired mag. props. with C and S additions 0-60368

cobalt alloys continued

Fe-Ni-Co-Ti, coherent particles effect inherited by martensite on α-γ transformation (Russian) 0-108443
Fe-Ni-Co-W(Mo) (18.65, 8.99, 4.87 wt.%), ageing charact., 380-530°C 0-60876
Fe-Sb-Co, interactions and segregations, Mossbauer and X-ray diffr. study 0-70415
FeCo, ferromag., surface spin waves, cluster Bethe lattice approach 0-70983
FeCo, planar faults, faint electron microscopic image contrast obs. 0-107283
Fe_{3-x}Co_xAl, site preference and local environment effects, Mossbauer and NMR meas. 0-71264
(Fe_{0.5}Co_{0.5})_{1-x}B_x, amorphous, hyperfine fields and local mag. moments, Mossbauer study 0-75895
Fe₂Co₇₅B₂₀, amorphous, magnetisation reversal and domain boundary config. 0-88809
Fe₃Co₇₅B₂₀Si₁₀Al₃, stress-induced variation in magnetisation and dynamic magnetostrictive charact. 0-88855
Fe_{0.5}Co_{0.5-x}Cr_x films, vacuum-deposited cryst. and mag. struct. (Russian) 0-93081
(Fe_{0.05}Co_{0.95})_{75-x}Cr_xSi₁₅B₁₀, amorphous, disaccommodation of mag. permeability and induced anisotropy 0-88741
(Fe_{0.05}Co_{0.95})₇₅Si₁₅B₁₄ amorphous ribbon, anomalous mag. aftereffect 0-100602
(Fe_{1-x}Co_x)₇₅Si₁₅B₁₂, amorphous, roll mag. anisotropy 0-75757
(Fe_{0.1}Co_{0.9})₇₅Si₁₅B₁₄, amorphous, saturation magnetostriction, strain modulated FMR obs. 0-75863
Gd-Co, amorphous, mag. props. and ferromag. reson. 0-75862
Gd-Co, amorphous films, mag. props. ferromag. reson. meas., 20-520°C (Russian) 0-97144
Gd-Co alloy film, sputter yield ratio, combined ion deposition and etching 0-71594
Gd-Co amorphous films, mag. struct., mag. bubbles, electron diffr. study (Chinese) 0-71126
Gd-Co based amorphous sputtered films, microstruct. variability and mag. anisotropy, implanted ion effects 0-88459
GdCo₂, dilute ferromagnets, press. effect on Curie temp. 0-65873
Gd₂Co₇, NMR spin echo meas., dipolar field anisotropy 0-71236
(Gd_{1-x}Co_x)_{1-x}Ar, amorphous films, effective anisotropy field, ferromag. reson. obs. 0-71123
Gd(Co_{1-x}Ni_x)₂ compounds, NMR and thermal expansion 0-66070
GdCo₅Ni₅₋₅₀, intrinsic coercivity, anisotropy, exchange and cryst. field interactions 0-75806
(Gd_{1-x}Y_x)₄Co₃, Curie temp. and resist.-temp. curves, comp. depend. 0-71020
HoCo₂, mag. excitations, neutron inelastic scatt. meas. 0-60231
Ho₂Co₇, spin wave excitations, 4.8 and 78K 0-60230
HoCo_{5-x}Mn_x(Fe_{1-x}Ni_x)₄(Cu)₃, cryst. struct. and mag. props. 0-75800
Ho₂Tb_{1-x}Co_x, lath phase compounds, elastic props., temp. and magnetic field dependence 0-60393
LaCo₂, sorption at press. up to 1500 atm. 0-97819
La₂Co₂, mag. props. changes upon H₂ absorpt. 0-71270
La(Co_{1-x}Ni_x)₂, distrib. of Co and Ni atoms, neutron diffr. obs. (Russian) 0-64954
La₂Co₂Sn₇, prep. and crystal structure (German) 0-84138
Mo-Co Kondo alloy, Co impurity susceptibilities, Knight shift 0-88721
NdCo₂, magnetocrystalline anisotropic props., torque meas. 0-108003
Ni based Rene 80 superalloy, initial stages of pack aluminisation 0-76188
Ni-(Co)-Cr, aluminide coating, microstruct. and chem. 0-76189
Ni-based TaC eutectic, directionally solidified, elastic moduli 0-84984
Ni-Co, dil., optical absorpt., electronic struct. 0-108227
Ni-Co, high-field susceptibility, spin-wave spectrum, CPA calc. 0-65818
Ni-Co (25 wt.%), single crystals, mag. annealing effect on magnetostriction and magnetisation at high temps. 0-108047
Ni-Co-Al alloys, continuous precip., SEM, TEM, X-ray diffr. study 0-89220
Ni-Co-C solid solution, C precipitation, Ni₃Co ordering, Ni-Co lattice parameter meas. (Czech) 0-60867
Ni-Co-Cr TEM foils, white band contrast 0-75134
Ni-Co-Cr/Al₂O₃ catalyst, IR spectra of adsorption and interaction with pyridine 0-71946
Ni-Co-Cr-Mo-Al-Ti (17.5, 15.1, 4.9, 4.15, 3.25 wt.%), creep and stress rupture behaviour in air and vacuum 0-60918
Ni-Co-H, hydride formation in high press. range 0-65235
Ni-Co-Mo, phase relations in system at 1100°C 0-108392
Ni-Co-W, electrodeposition, surface morphology and cryst. struct. 0-71602
Ni-Cr-Co based alloy, IN-738 turbine blades, hot isostatically pressed investment castings, effect of heat treatment on grain boundary struct. 0-89270
Ni-Cr-Co superalloy, combined TEM, FIM, atom probe microanalysis of precipitates and carbide phase comp. 0-100844
Ni-Cr-Co-Al-W-Mo-Ti-Ta, heat resist. and struct., Ta effect 0-76312
Ni-Cr-Co-Ti-Mo-W-Al (14, 9.8, 5, 4, 3.9, 3 wt.%), low cycle fatigue, prior heat treatment effect 0-60962
Ni-Cr-W-Co granules type ZhS6U, EP741, hot hydrostatic pressing 0-60796
Ni-Cr-W-Co-Ti, thermal fatigue, effects of inclusions 0-81183
Ni-Cr-W-Co-(Al)(Ti)(Mo), high-temp. sulphide corrosion 0-76408
Ni-Fe-Co-Ti, electron microscopy and mag. meas. 0-71097
NpCo₂Si₂, mag. struct., neutron diffr. determ. 0-93084
Pd-Co, dil., breakdown of ferromag. order, magnetoresist. obs. 0-71046
Pd-Co, dilute ferromagnets, press. effect on Curie temp. 0-65873
Pd-Co, normal Hall effect (Russian) 0-103676
Pd-Co (0.1-45.7 at %), thermo EMF at 4.2-300K (Russian) 0-92881
PrCo₂, strongly exchange-enhanced paramagnetism, susceptibility 0-60179
PrCo_{2-x}, high field first order transitions, role of K₂ anisotropy const. 0-65879
PrCo₂, sorption at press. up to 1500 atm. 0-97819
Pt-Co, dil., skew scatt. Hall effect, magnetoresist. and mag. anisotropy, orbital magnetism of impurity 0-70678
Pt-Co, dilute ferromagnets, press. effect on Curie temp. 0-65873
Pt-Co system, low temp. susceptibility 0-65920
Pt₂Co, radiation damage profiles from low energy Ne⁺, bombard. 0-70268
R_{1-x}Co_x, rare earth amorphous alloys, thermal stability, elec. cond. enthalpy 0-100172
Si-CoSi₂Si, double heteroepitaxy, solid phase and MBE 0-104063

cobalt alloys continued

- Sm-Co, amorphous, plasma-sprayed, role of Ar or H₂ atm. in mag. props. and crystal., rel. to H₂ storage 0-64898
 Sm-Co ring magnets for BWO, 110 to 170 GHz, design and appl. (*German*) 0-105684
 SmCo₅, amorphous, supermag.-ferromag. transition and directional crystallisation 0-65891
 SmCo₅, H₂ absorption in thin film hydriding alloys 0-65238
 SmCo₅, high coercivity isotropic plasma-sprayed magnet, eutectoid decomp. 0-80568
 SmCo₅, isotropic plasma-sprayed high coercivity magnet, eutectoid decomp. 0-75810
 SmCo₅, nucleation of reversed domains at Co₂Sm₂ precip. 0-75791
 SmCo₅, permanent magnets, crystal texture effects on props. 0-100600
 SmCo₅, sintered, hard mag. material, magnetisation behaviour 0-75805
 SmCo₅, sintered, mag. after-effect, expt. and model 0-75816
 SmCo₅ sintered magnets, eutectoid decomp. 0-89219
 Sm₂Co₁₇, coercive force depend. on annealing temp. 0-65964
 Sm₂Co₁₇ sintered magnets, coercive force and constitution, annealing temp. depend. (*Russian*) 0-88786
 Sm_{0.91}Zr_{0.09}(Co_{0.68}Cu_{0.10}Fe_{0.22})_{6.7}, alloy permanent magnet, coercive force (*Russian*) 0-65966
 Sr₂(Co_{1-x}M_x)₁₇, M=Mn, Ti, Zr, powders, influence of substitutes on mag. props. 0-100601
 TbCo₂, magnetocrystalline anisotropy and spontaneous magnetostriction 0-75831
 TbCo₃, sublattice magnetisation, temp. depend., neutron diff. anal. (*Russian*) 0-103815
 (Tb_{1-x}Gd_x)Co, intermetallic cpd. mag. props., phase transform, and mag. hysteresis (*Russian*) 0-93113
 Th-Co, effect of absorbed H₂ on mag. behaviour 0-60184
 Ti-Ni-Co, constitution diagram, isothermal section, interdiffusion coeffs. (*Russian*) 0-89200
 TiC coated WC-Co cemented carbides, fracture toughness 0-85046
 Ti₇₀Co₃₀B₁₀, amorphous alloys, crystn. behaviour, TEM study (*Japanese*) 0-84087
 TiCo_{1-x}Mn_x, H absorption-desorption characteristics 0-96735
 Ti(Fe, Co), off-stoichiometric alloy, inverse mag. susceptibility rel. to defect conc. 0-60216
 Ti(Fe,Co)H₂, mag. and ⁵⁷Fe Mossbauer studies 0-71272
 Ti(Fe,Co)₂, itinerant electron ferromagnet, magnetovolume effects 0-60397
 TiFe_{1-x}Co_x, electronic struct. and mag. moment calcs. 0-65821
 TiFeCo_{1.69}, thermal expansion and magnetoelastic effects 0-80585
 TmCo₂, Tm Mossbauer effect 0-71261
 U-Co metallic glasses, glass form. and thermal stability 0-75183
 UCo₂, surface comp. and electronic struct., photoemission study 0-66382
 U(Co_{1-x}Fe_x)₂, ferromag. onset, susceptibility and resist. meas. 0-70967
 U₁₀Co₅Si₃, crystal struct., dimensions, space group and coord. (*Russian*) 0-88085
 U₂Co₉Si₁₀, X-ray cryst. struct. determ. 0-107111
 V-Co sigma phase alloys, NMR and electric-field gradients 0-108109
 W-Ni(Co) point-contact diodes as harmonic generators and mixers, DC bias dependence 0-75653
 WC-Co, contact reaction with BN at high pressures 0-61029
 WC-Co, STEM anal. of grain boundaries 0-79644
 WC-Co alloys, fracture toughness model 0-84243
 WC-Co hard alloys, hot-pressed, wear resist. under abrasive friction, heat treatment effect 0-66555
 WC-Co sphere, erosion of Al by solid particle impingement at normal incidence 0-104304
 Y-Co, amorphous, thermal stability, crystn., DSC and elec. resist. study 0-107060
 YCo₃ amorphous films, ⁵⁹Co spin echo study 0-80636
 YCo₃, hydride phase synthesis, thermal stability and struct. 0-59438
 YCo₅, uniaxial intermetallic, large magnetisation anisotropy 0-71011
 Y_{1-x}Co_x, amorphous, mag. props. 0-84590
 Y₂Co₁₇, NMR spin echo meas., dipolar field anisotropy 0-71236
 Y(Co_{1-x}Ni_x)₅, distrib. of Co and Ni atoms, neutron diff. obs. (*Russian*) 0-64954
 Y(Fe_{1-x}Co_x)₂, NMR study 0-75882
 Y(Fe,Co_{1-x})₂, x=0.2, mag. props. and Mossbauer meas. 0-75798
 Y_{1-x}R_xCo₅, R=Gd,Tb,Nd, ferrimag., magnetisation, exchange interactions, mag. anisotropy 0-80565
 Zr-Co, amorphous and crystalline, d-band struct., alloying effects 0-59862
 Zr-Co metallic glasses, glass form. and thermal stability 0-75177
 Zr₇₀Co₃₀ amorphous alloys, struct. factors and radial distrib. functions 0-84096
 Zr(Cr,Co_{1-x})₂, mag. props. H absorpt. effect 0-88821
 Zr(Fe,Co)₂, itinerant electron ferromagnet, magnetovolume effects 0-60397
 Zr(Fe_{1-x}Co_x)₂, ferromag. and mictomag., thermal expansion and forced volume magnetostriction 0-75830
 Zr(Fe_{1-x}Co_x)₂, NMR study 0-75882
 Zr(M_{1-x}Co_x)₂ (M=V, Cr, Mn), H₂ absorpt. capacity 0-88433
 Zr(V_{1-x}Co_x)₂, relation between electronic struct. and H₂ storing props. 0-76662

cobalt compounds

see also cobalt alloys

- aluminosilicate glass:Co (14.3 wt.%), AC susceptibility meas. 0-88771
 Co₃Sb₂(CO)₁₂, electronic struct. calc. (*Russian*) 0-58136
 dimethyl glyoximate, molecular struct., cryst. structure 0-79769
 ferrite, crystal structure, X-ray absorpt. spectra, chemical shifts 0-88118
 ferrites, magnetostriction due to Co²⁺ ions, effect of excited states 0-65990
 intercalation, electron microscopy 0-84164
 myoglobins, Co-substituted, O₂ binding, thermodynamic investig. 0-67030
 phthalocyanine, electrochromism and oxidation 0-93768
 polyphosphinate, bulk compressibility meas. to 30 kbar 0-76306
 rare earth cobalt silicides, RCo₂Si₂, mag. props. 0-107988
 stearate, monomolecular multilayers, XPS escape length depend. on emission angle, elastic scatt. role (*Japanese*) 0-84833
 tetramethylammonium cobalt tetrachloride, Raman spectra near incommensurate phase transitions 0-76013
 trimethylammonium cobalt trichloride, metamagnet, AC susceptibility and exchange consts. 0-70961
 tris (3-mercaptop-1, 3-diphenyl-2-propen-1-onato) Co(III), multiple twinning 0-100250

cobalt compounds continued

- Ba₂Co_{1.65}Fe_{0.35}²⁺Fe_{0.35}³⁺O₄₆, temp.-mag. field phase diagram, torque method 0-60276
 BaMn_{0.99}Co_{0.01}F₄, ferroelec. antiferromag., dielec. anomalies 0-71288
 BaMn_{0.99}Co_{0.01}F₄, magnetoelec. phenomena, dielec. behaviour near Neel temp. 0-71151
 CO III-EDTA solution, radiolysis by charged particles through ⁶Li(n,α)³H reaction 0-93788
 (Co,Cr,Fe)₂O₄ (Co,Rh,Fe)₂O₄ film magnetooptical switches, for laser beam synchronisation 0-58615
 Co complex, 2,6-N,N-diacetyldiaminopyridine-Co(II) elec. cond., γ dose and temp. (303-363K) effects 0-103696
 Co complex, 2,6-N,N-dibenzoyldiaminopyridine-Co(II) elec. cond., γ dose and temp. (303-363K) effects 0-103696
 Co complex, [Co(NH₃)₆]³⁺, enantiotropic phase transition obs. 0-107412
 Co complex, Co(II)(1,2,4-triazole)₂(NCS)₂ quasi two-dimens. canted S=1/2 antiferromag. 0-70976
 Co complex, Co(NO₂)₆⁴⁻, bond. props. and Jahn-Teller distortion, INDO-LCAO-MO calcs. 0-75532
 Co complex, O₂CoCl₄ and O₂CoCl₄NH₂²⁻, struct. and bonding model, CNDO-UHF calcs. 0-95541
 Co complex, triazene-1-oxide complexes, EPR spectra in frozen nematic liq. cryst. glass 0-88871
 Co complexes, Co II tetraphenylporphyrins, constraint, ESR and optical detect. 0-83394
 Co complexes, Co(III) mixed complexes, orbital angular momentum reduction, ⁵⁹Co NMR chemical shift 0-58137
 Co complexes, Co(en)₂Cl₂·Cl·HCl·2H₂O, temp. dependence of NQR frequencies 0-66068
 Co II acetylacetonate, XPS 0-74196
 Co II complexes, with tetradentate Schiff bases, synthesis, struct. and ESR obs. 0-80598
 Co/Na zeolite, -A and -Y type, local coordination of Co(II) ions studied by X-ray absorpt. fine struct. spectroscopy 0-93434
 Co-CoO films, evaporated, exchange anisotropy 0-88841
 Co₃(AsO₄)₂, polymorph, cryst. struct., closest packing 0-70174
 Co₃(AsO₄)₂Cl, temp. depend. of mag. susceptibility 0-70962
 Co₃B₂O₇Cl(II), boracite, single cryst. prep. and phys. props. 0-100763
 CoBr₂·6(0.48D₂O, 0.52H₂O) spin-flop system, intermediate phase existence, sublattice magnetisation reorientation 0-80510
 CoBr₂·6[(1-x)H₂O·xD₂O], mag. intermediate phase, magnetisation and neutron scatt. meas. 0-60195
 Co(C₂H₃NO)₂(ClO₄)₂ [(BF₄)₂], X-Y antiferromagnet, Neel temp., spin correlation functions 0-60345
 Co(CN)₆^{3-/4-}, redox reaction on CdTe and ZnTe electrodes (*French*) 0-89482
 CoCO₃, Brillouin-Mandelstam scattering from thermal and excited magnons 0-70980
 CoCO₃, Brillouin-Mandelstam light scatt. obs. of spin wave spectra 0-93358
 CoCO₃, LF exciton and Raman spectra, one-magnon and two-magnon scatt. 0-93333
 CoCO₃, light scatt. from magnons and phonons excited by microwave pumping 0-66213
 CoCO₃, linear magneto-optical effect, birefr. 0-66155
 CoCO₃, spin excitation energies, quantum theory (*Russian*) 0-88735
 CoCO₃, two-sublattice noncollinear antiferromag., exciton-magnon light absorpt. mechanisms (*Russian*) 0-89017
 CoCO₃, weakly ferromag., light absorpt. dichroism and mag. config. 0-66223
 CoCl₂, antiferromag., phase diagram, heat capacity meas. 0-93126
 CoCl₂, cryst., self-consistent band struct., intersecting spheres model 0-75505
 CoCl₂, EXAFS amplitudes, many-body effects 0-97379
 CoCl₂·2H₂O, Ising antiferromag., high field transverse magnetisation meas. 0-93143
 CoCl₂·6H₂O solution in ethanol, thin absorbing film, nonlinear optical props., Q-switch appl. 0-91836
 CoCr₂S₄, ferrimag. semicond., magnetocrystalline anisotropy 0-71012
 CoF₂, antiferromag. crit. props., neutron scatt. obs. 0-88749
 CoF₂, linear magneto-optical effect, birefr. 0-66155
 CoFe₂O₄ mag. fluid particles, comp., struct., and mag. props. 0-60374
 CoFe₂O₄ mag. hyperfine fields, Mossbauer spectra 0-108139
 CoFe₂O₄ ultrafine particles, prep. and mag. props. 0-71116
 CoGa₂-Fe₂O₄, x=0.1-0.4, mag. susceptibility temp. depend. (*Russian*) 0-70957
 Co(H₂O)₆[SnF₃]₂, crystal structure (*French*) 0-59441
 CoIII salen complexes, O binding, reson. Raman obs. 0-58267
 Co₂Mg_{1-x}O system, thermodynamic investigation, 1100 to 1300K (*German*) 0-107430
 Co²⁺Mo⁴⁺O₃, defect spinel struct., elec. and mag. props. 0-70176
 Co₃Mo₂O₄ films, prep., struct. and elec. characteris. 0-108353
 Co₂Mo₂S₂O₄, O-containing Chevrel phases, synthesis and props. 0-108368
 Co₂(Ni_{0.5}Cu_{0.5})₂Fe₂O₄ ferrite, relation between elec. cond. and mag. anisotropy 0-75548
 Co₂Ni_{1-x}Fe₂O₄, induced mag. anisotropy consts., conc. and temp. depend. 0-108001
 CoO epitaxial layers, XPS obs. of formation on Co (0001) 0-66396
 CoO, for catalytic oxidation of CO 0-71945
 CoO, isotope effects in CoO diffusion rel. to vacancies 0-84319
 CoO single crystals, strain rate deform. characts., yield stresses and work hardening 77 to 1400K 0-60939
 CoO-Al₂O₃, isoelectric point meas. 0-88609
 CoO-Al₂O₃-SiO₂, amorphous, remanent magnetisation short time depend. 0-65919
 CoO-Fe₂O₃, isoelectric point meas. 0-88609
 CoO-ZnO-MgO ternary systems, solid solns., struct. charact. 0-60629
 Co₂O₃, black cobalt, solar absorptance of high temp. selective absorbers 0-101131
 Co_{1-x}O, single cryst. growth by skull melting 0-84844
 Co₃O₄, isoelectric point meas. 0-88609
 CoO-Al₂O₃, prep. from film forming soln. 0-60811
 CoRhS₄, mag. semicond., mag. and elec. props. 0-93121
 Co(S, Se)₂, metamagnetic transitions in external fields 0-60272
 CoS, electrodeposition, using nonaqueous solvents 0-76200
 CoS₂, core-level and valence-band XPS 0-93450
 CoS₂, galvanomagnetic effect of single cryst. 0-96912
 CoS₂, itinerant ferromagnet, ferromag. reson. and EPR meas. 0-66044
 CoS₂, narrow-band ferromag., high press. effect on anomalous elec. resist. 0-70698

cobalt compounds continued

- CoS₂(s), black cobalt, solar absorbance of high temp. selective absorbers 0-101131
- CoS₂(Se₂), electronic struct., UPS and XPS study 0-80935
- Co(S₂Se₂)₂, galvanomag. effects, obs. and interpretation 0-70726
- CoSb₂O₆, force fields rel. to cryst. struct. (*French*) 0-107104
- CoSe₂, core-level and valence-band XPS 0-93450
- Co₂SiO₄, local in depth anal. by neutral beam SIMS 0-89565
- CoTa₂O₆, force fields rel. to cryst. struct. (*French*) 0-107104
- Co_{1-x}Te, fluctuating localised mag. moments, d band motion, Mossbauer study 0-65768
- CoTiO₃, antiferromag., mag. anisotropy, magnetisation meas. 0-65856
- CoTiO₃, prep. from film forming soln. 0-60811
- Co₂Z ferroxplana form. process peculiarities 0-89368
- Co_{1-x}Zn_xF₂, antiferromag. crit. props., neutron scatt. obs. 0-88749
- Co₂Zn_{1-x}Fe₂O₄, ferrite, DC cond., dielec. props., lattice consts. 0-80272
- Co₂Zn_{1-x}Rh_xO₄, mag. props., EPR spectra, antiferromag. order 0-75736
- Co(urea)₂Cl₂·2H₂O, two-dimens. mag. props., cryst. struct., specific heat 0-75777
- CsMn_{1-x}Co_xCl₂·2H₂O, random mag. mixture, oblique-antiferromag. phase obs. 0-93142
- Fe₂Co_{1-x}Cl₂, metamagnet, mag. phase diagram by mag. induced light scatt. 0-65883
- Fe_{1-x}Co_xCl₂·2H₂O, random mixture with competing spin anisotropies, tetracrit. behaviour 0-60324
- Fe₂Co_{0.8}S₂, narrow-band ferromag., high press. effect on anomalous elec. resist. 0-70698
- Fe_{1-x}Co_xSi solid solution, semiconductor-metal transition 0-103627
- (Gd_{1-x}Co_x)_{1-y}Ar_y, amorphous mag. film, elec. and mag. prop. depend. on Ar 0-80410
- La₂Li_{0.5}Co_{0.5}O₄, phase, intermediate electronic configuration 0-80226
- Na-Co strip-chain silicates, structural-composition inhomogeneities 0-88122
- NaCo(CO)₄, soln., ion sites, cryptand C221 doping effects 0-70102
- Na₂SO₄·CoSO₄·H₂O, phase equilib., activities, Pitzer eqn. calcs. (*Russian*) 0-65190
- Ni-Zn-Co ferrites, synthesis from solid solns. of schoenite-type salts 0-93511
- Ni_{1-x}Co_xCl₂·6H₂O, mixed uniaxial planar antiferromag., magnetisation process 0-88788
- Ni₂Co_{1-x}O, composition depend antiferromagnetic-ferrimagnetic ordering, mag. susceptibility meas. 0-70973
- Ni_{1-x}Co_xS₂, elec. cond., thermolec. power and optical meas. 0-59986
- NiZnCo ferrites, switching time and coeff., hydrostatic press. effect 0-88802
- NiZnCo ferrites, voltage response under sinusoidal and pulse magnetisation effected by hydrostatic press. 0-88846
- RbCl:CoCl₂ system, precipitate form., ionic cond. meas. 0-96653

cochlea see ear

code converters

- see also codes; information theory
- noise-tolerant continuously variable slope DM to linear predictive coding conversion 0-96141

codes

- see also encoding; error correction codes
- radio time-signal codes in Italy (*Italian*) 0-98888

coding see encoding

coefficient of thermal expansion see thermal expansion

coercive force

- see also magnetic hysteresis
- Alnico 5 alloy, S and Ti additions effect rel. to non-metallic inclusions, coercive force and grindability 0-89375
- Alnico type YuNDK25DA alloy permanent magnets, thermal mag. hysteresis 0-75818
- amorphous ribbons, twisted, magnetisation process, domain theory 0-71101
- amorphous thin films, struct. and mag. props., review 0-93148
- coercimeter KIFM-1 with automatic measurement of the demagnetizing current 0-68229
- domain boundaries, pinning on defects with finite radius of interaction, random pot. form effect on mag. hysteresis (*Russian*) 0-84611
- domain boundary interacting with strongly localised pinning centres, influence on hysteresis (*Russian*) 0-65961
- ferrimagnetic magnetisation theoretical models, for uniparametric materials 0-65960
- high-coercivity, magnetisation characteristic linearity determ. using flux controlling technique (*Russian*) 0-100597
- magnetic, bubbly dynamics and jump probability 0-65977
- magnetic domain boundary, interacting with localised defects, unidimensional flow of configs. (*Russian*) 0-65954
- metallic glass, micromag. calcs. and props. 0-80501
- metallic glasses, production and properties, technological appl. 0-71105
- orthoferrite cryst. films, local coercivity of domains boundaries (*Russian*) 0-80578
- Permalloy, 50NP, and 79NM, magnetic properties and structure, environment effect during annealing 0-60366
- Permalloy films, RF sputtered on Au, coercivity 0-80575
- Permalloy RF sputtered films, O effects in mag. and elec. props. 0-100603
- rare earth alloys, R₂Ni₃, amorphous, Curie temp., mag. susceptibility and coercive force, 4.2 to 300K 0-93092
- rare earth-Co, R₆₀Co₃₁, amorphous, mag. props. 0-84590
- ring specimens, computer controlled mag. meas. system 0-86346
- steel case depth after quench hardening, inspection using coercimeters 0-104377
- BaTiO₃ film, dielectric props. depend. on sinusoidal elec. field 0-71318
- Co alloys, amorphous, effects of metalloids on mag. props. 0-75738
- Co, ferromagnetic micropowder, cryst. struct., coercivity, remanence, saturation 0-65967
- Co single domain particles, randomly oriented easy axes and particle size distrib., coercivity 0-71119
- Co-Cr mag. film, crystallographic texture formation effects on props. (*Russian*) 0-108471
- Co-Fe, soft mag. props. rel. to metallurgical aspects 0-88810
- Co-Fe-V-Ni, mag. and mech. props., heat treatment and stress effects 0-60363
- Co-P films with various preferred orientations, mag. props. 0-100604
- Co-W alloy electrodeposition, influence of MgSO₄ and gum arabic additives (*Russian*) 0-80991

coercive force continued

- Co-W alloy electrolytic coatings, heat treatment effects on coercivity, hysteresis and structure (*Russian*) 0-60381
- Co₃Fe₂Ni₁₀(Si₂B)₂₈, amorphous, soft mag. props., switched-mode power supply appls. 0-88850
- CoP, and CoNiP, cylindrical amorphous electrodeposited layers, mag. props., torsion influence 0-88848
- Co₂Sm crystals, microstruct., homogeneous precip. and nucleation 0-104160
- Cu-Co precipitates, mag. anisotropy, precipitate shape, coercive force 0-80500
- Cu-Mn-Al alloys, displaced hysteresis loop and microstructure obs. 0-84613
- Cu-Ni-Co, mag. props. of system of disperse ferromag. particles, 73 to 673K (*Russian*) 0-65968
- Cu-Ni-Fe, magnetic properties, heat treatment and compressive stress effects 0-60367
- EuS films, mag. and elec. props. rel. to stoichiometry and defects 0-97122
- (Fe₂Co₂Ni)-Si(B), amorphous mag. alloy, magnetostriction rel. to soft mag. props. 0-84633
- Fe alloys, amorphous, effects of metalloids on mag. props. 0-75738
- Fe, ferromagnetic micropowder, cryst. struct., coercivity, remanence, saturation 0-65967
- Fe-B, amorphous alloy, mag. props. 0-84618
- Fe-B metallic ribbons, correl. between quenching temp. and mech. and mag. props. 0-89373
- Fe-B ribbon, microhardness, and static coercive force, melt overheating effect 0-84978
- Fe-B-C amorphous alloy, formation, mag. props., thermal stability and density 0-75796
- Fe-B-C amorphous alloys for use in power transformers 0-88808
- Fe-B-C amorphous alloys with high saturation induction 0-84617
- Fe-B-Cr(Mo), metallic glasses, mag., struct., and elec. props. 0-88751
- Fe-Co, ferromagnetic micropowder, cryst. struct., coercivity, remanence, saturation 0-65967
- Fe-Co-Al-Cu-Ti (40, 14, 7.5, 4.5 wt.%), metastable equilibrium, high coercive state (*Russian*) 0-66476
- Fe-Co-Mo-Nb(Ta) semihard mag. alloy, mag. props., thermal expansion, elec. resistivity and hardness (*Japanese*) 0-88789
- Fe-Co-Si-B, zero magnetostrictive amorphous alloy with high saturation induction, mag. annealing 0-60362
- Fe-Cr-Co alloy, coercive force mechanism 0-71103
- Fe-Cr-Co permanent magnet system, miscibility gap, microstruct. and mag. props. obs. 0-76228
- Fe-Cr-Co-Mo high energy permanent magnets, mag. props. 0-97119
- Fe-Ni-B-Si, amorphous, mag. props., heat treatment effects 0-89370
- Fe-Ni-Co-Cu-Ti YuNDKT alloys, impaired mag. props. with C and S additions 0-60368
- Fe-Si (3 to 5 wt.%) sinters, mag. props., Si and Fe-Si additions effect 0-71104
- Fe-Si (6.5 wt.%) filament, formation by modified Taylor technique, and mag. props. 0-75795
- Fe-Si (6.5 wt.%) ribbon, splat-cooled, mag. props. 0-88805
- Fe-Si-B, magnetic metallic glasses, mag. props. 0-84620
- Fe-Zn alloys, coercive force anisotropy after cold plastic deform. (*Bulgarian*) 0-75809
- Fe_{31.4}B_{6.6}, amorphous, mag. props. and microstruct., cooling rate and melt overheating effects 0-65965
- Fe_{31.4}B_{6.6}, amorphous, mag. props., melt overheating and cooling rate effects 0-89371
- Fe_{80-x}Ni_{20-y}P_y, amorphous, Rayleigh region and coercive force 0-88806
- Fe₄₀Ni₄₀(Mo₂Si₂B)₂₀, amorphous, soft mag. props., switched-mode power supply appls. 0-88850
- FeSi picture frame single cryst., domain wall motion and magnetisation reversal, time-depend. neutron depolarisation study 0-88782
- (Fe_{1-x}Si_x)_{1-y}By, metallic glass, mag. props., crystallisation 0-65885
- Fe_{3-x}Ti_xO₄, 0.5 ≤ x ≤ 1, mag. props. of antiferromag. phase 0-70960
- Gd-Al(Cu)(Ga)(Ni)(Pd)(Rh) alloys, amorphous, mag. and elec. props. 0-80499
- (Gd_{1-x}Co_x)_{1-y}Ar_y, amorphous mag. film, elec. and mag. prop. depend. on Ar 0-80410
- GdCo₅Ni₅-Sc, intrinsic coercivity, anisotropy, exchange and cryst. field interactions 0-75806
- Li matrix ferrites, coercivity, synthesis, thermostability control 0-80569
- Mn-Al-C, fine-grained cast struct., remanence and coercive force 0-60365
- Ni-Fe, soft mag. props. rel. to metallurgical aspects 0-88810
- Ni-Fe-Nb-Mo-Al, head material for mag. recording, DC and AC mag. props. 0-88812
- NiFe, single and multilayer thin films, strip domains, inplane magnetisation 0-103866
- Si₂Fe_{100-x} polycryst. ribbon, prep. by rapid quenching, and props. 0-75803
- Sm-Co, amorphous, plasma-sprayed, role of Ar or H₂ atm. in mag. props. and crystn., rel. to H₂ storage 0-64898
- SmCo₅, high coercivity isotropic plasma-sprayed magnet, eutectoid decomp. 0-80568
- SmCo₅, isotropic plasma-sprayed high coercivity magnet, eutectoid decomp. 0-75810
- SmCo₅, nucleation of reversed domains at Co₂Sm₂ precip. 0-75791
- SmCo₅, sintered, hard mag. material, magnetisation behaviour 0-75805
- Sm₂Co₇, coercive force depend. on annealing temp. 0-65964
- Sm₂Co₇, sintered magnets, coercive force and constitution, annealing temp. depend. (*Russian*) 0-88786
- Sm₉₀Y₁₀(Co₆₈Cu₁₈Fe₁₄)_{6.7}, alloy permanent magnet, coercive force (*Russian*) 0-65966
- Sr₂(Co_{1-x}M_x)₇, M=Mn, Ti, Zr, powders, influence of substitutes on mag. props. 0-100601
- (Ti_{1-x}Gd_x)₂Co, intermetallic cpd. mag. props., phase transform, and mag. hysteresis (*Russian*) 0-93113
- (Y_{1-x}Sm_x)₂(Fe₂Ge)₅O₁₂ epitaxial films, mag. props., growth condition effects 0-97124
- Y_{1-x}Co_x, amorphous, mag. props. 0-84590
- YIG, domain wall mobility and mass meas. method (*Russian*) 0-108033

coercivity *see* **coercive force**

cognitive systems

see also **adaptive systems**; **artificial intelligence**

EEG patterns during cognitive tasks, controlled tasks anal. 0-67059

EEG patterns during cognitive tasks, methodology and complex behaviours anal. 0-61531

coherence

see also **light coherence**

atomic systems, coherent transients theorem 0-99808

concert hall problem, coherence length and diffuse reflection formulation 0-91962

cyclic X-ray monochromators, with perpendicular dispersion planes, emission coherence 0-90974

EEG coherence estimates, significance in determ. of central α and μ activities 0-61720

EM radiation in media with spatial dispersion, spatial coherence formation and polarisation increase 0-106442

frictional quantum mechanical system, one-dimens. scatt. model for coherence in stopping power problem 0-101736

impurity trapping of quasifree excitons and electrons, finite coherence effects 0-59880

ocean acoustics, two-point coherence function models with inhomogeneous background and anisotropy 0-81922

radio waves, transionospheric, scintillation coherence time struct. 0-90281

relativistic electrons, channelling radiation, quantum beats 0-88226

RF superradiance optical pulse generated under photon-echo conditions 0-95858

underwater acoustic time delay estimation, cross-correl. and smoothed coherence transform methods compared 0-96086

coherence distance *see* **coherence length**

coherence length

granular microcylinder, flux quantisation phenomena above T_c (Russian) 0-70899

superconducting layered cpds., upper crit. fields and reduced dimensionality 0-70910

superconductor resistive state, coherence length, penetration depth 0-97030

Nb₃Sn, coherence parameter, nonlinear high temp. supercond. elements with A-15 lattice (Russian) 0-60127

Ta₂Nb₃O, Abrikosov vortex formation kinetics (Russian) 0-93055

TaS₂ intercalated with methylamine, supercond. layer cpd., crit. field enhancement and reduced dimensionality 0-60152

V₃Si(Ga), coherence parameter, nonlinear high temp. supercond. elements with A-15 lattice (Russian) 0-60127

coherent accelerators *see* **collective accelerators**

coherent antiStokes Raman scattering

air, atmospheric, pure rot. CARS obs. 0-99511

anthracene, single cryst., CARS and CSRS, two-photon reson. effect 0-59946

chrysene, excited singlet and triplet state, CARS obs. 0-83374

four-photon spectroscopy of condensed media, nonlinear spectroscopy developments 0-91860

four-wave mixing spectroscopy in crystals, nonlinear spectroscopy developments 0-91861

methane-d₀(-d₁) vibrational state rotational struct., CARS spectra (Russian) 0-99513

naphthalene, vibr. relax. studied by four wave mixing (CARS), spectral lineshapes obs. 0-80762

nickel-octaethylporphyrin, in benzene soln., reson. CARS and CSRS line shapes 0-74432

phase matching, three-dimensional, in four-wave mixing 0-83635

quasiequilibrium sample, light scatt. and thermal radiation, phenomenological approach 0-91840

resonant coherent Raman scatt. spectra of excited molecules 0-87129

rotational Raman studies, folded BOXCARs 0-101846

spectrometer for gases and flames 0-95154

s-tetrazine, vapour, reson. CARS spectrosc., radiationless relax. rate 0-78614

water, coherent Raman ellipsometry, vibr. stretching region and liq. struct. obs. 0-93341

GeH₄, vibrational state rotational struct., CARS spectra (Russian) 0-99513

⁷⁴GeH₄ mol. vibr., IR and CARS spectra (Russian) 0-102509

H₂, CARS, optical Stark effect on vibr., and rot. transitions 0-99512

p-H₂, solid, time-resolved CARS, disorder effects on coherent vibr. states 0-93342

N₂, CARS, optical Stark effect on vibr., and rot. transitions 0-99512

N₂ in nonequilibrium gas-dynamic current, vibr.-level populations determ. by Raman scatt. 0-99509

N₂, pure rot. CARS obs. 0-99511

α -N₂ solid, time-resolved CARS, disorder effects on coherent vibr. states 0-93342

N₂-Ar(Kr)(O₂)(CO)(CH₄), liquid, high resolution CW CARS spectra 0-63635

NO₂, discrete reson. CARS emission, temporal and spectral props. 0-95630

Nd:YAG pumped tunable sources, appl. to spectroscopy 0-58576

O₂, pure rot. CARS obs. 0-99511

Si-O fibres, parametric excitation of anti-Stokes coherent stimulated scatt. (Russian) 0-58637

coherent optical transients *see* **optical coherent transients**

coherent potential approximation *see* **CPA calculations**

cohesive energy *see* **binding energy**

coils

see also **solenoids**

air coils, FFT calc. of mag. fields 0-74280

circumferential stress in large high field magnet coils, thick-thin cylinder approach 0-95761

cryogenic rings, current induction and decay 0-106972

fusion, toroidal field superconducting coil cryogenic stability and field anal., design parameter 0-106200

fusion reactor, CC NbTi, pool cooling superconducting test coil, Japanese design 0-99340

fusion reactor, cluster test facility, design 0-90835

fusion reactor, DITE Tokamak bundle divertor, Mk.II design 0-91268

fusion reactor, Doublet III, neutral beam injection system, two-gap magnet design and performance 0-92379

fusion reactor, Doublet III, ohmic heating E-coil vacuum breaker system, function and operation 0-102323

coils continued

fusion reactor, Doublet III, toroidal field coils, Cu alloy plate defect size restrictions 0-91257

fusion reactor, FTR, equilib. field coils, electrical supply system, optimisation and computer aided performance anal. 0-91288

fusion reactor, Heliotron E, helical coil design, mag. field perturbations 0-99300

fusion reactor, high current density superconducting coils, cryostability 0-106201

fusion reactor, induction heating coils, 50 kA prototype superconducting cable, critical current 0-106196

fusion reactor, ISX-B, with bundle divertor, structural anal. 0-91254

fusion reactor, ISX-B toroidal field coil finger joints, fatigue life, structural evaluation 0-91253

fusion reactor, Large Coil Program, coil winding development support 0-106190

fusion reactor, Large Coil Program, General Dynamics Convair/IGC manufacturing engineering 0-106169

fusion reactor, Large Coil Program, Nb₃Sn forced flow superconducting test coil, Westinghouse design 0-99337

fusion reactor, Large Coil Program, NbTi superconducting test coil, General Electric design and manufacture program 0-102319

fusion reactor, Large Coil Program, test heater conceptual designs 0-91251

fusion reactor, Large Coil Program, Westinghouse superconducting mag. elec. design 0-91250

fusion reactor, Large Coil Task, CC NbTi forced flow superconducting test coil, Swiss design 0-99341

fusion reactor, Large Coil Test Facility test stand design description 0-102320

fusion reactor, large superconducting toroidal field coil program, progress report 0-99335

fusion reactor, maximum toroidal mag. field value by core constraint 0-102349

fusion reactor, MFTF, mag. cryostability 0-106198

fusion reactor, MFTF, superconducting mag. quench vent rate 0-106197

fusion reactor, multiple mirror, coil design and economic optimisation 0-99284

fusion reactor, multipole fusion confinement with 2 MA levitated superconducting coil 0-106191

fusion reactor, non-circular Tokamak field shaping coils, current optimisation 0-95426

fusion reactor, PDX, toroidal field coil and frame struct., anal., finite element anal. 0-106165

fusion reactor, PDX toroidal field coil joint fatigue testing 0-91252

fusion reactor, press. induced flow cooling, highly stable superconducting mag. systems 0-106192

fusion reactor, safety of superconducting fusion magnets: twelve problem areas 0-102348

fusion reactor, SLPX TF coil, stress anal. using COSMIC-NASTRAN 0-106168

fusion reactor, STARFIRE project, superconducting poloidal coils design study 0-106185

fusion reactor, STARFIRE project, toroidal field coil system preliminary assessment 0-106186

fusion reactor, superconducting toroidal system, force anal. for all fault conditions 0-91258

fusion reactor, superconductor optimisation for 12 Tesla toroidal field coils from Nb-Ti and Nb-Ti-Ta alloys 0-91272

fusion reactor, TEXT, toroidal field coil fabrication 0-91267

fusion reactor, TEXT, toroidal field coil power supply, thyristor controlled 0-91289

fusion reactor, TFTR, eddy current theory for structural materials 0-95427

fusion reactor, TFTR, large section water cooled Cu conductor, brazing joints 0-91260

fusion reactor, TFTR outer poloidal field coil insulation and mould design 0-91261

fusion reactor, TFTR poloidal field coils, tooling and manufacture 0-91262

fusion reactor, TFTR toroidal field coil support restraint struct. 0-95428

fusion reactor, toroidal field coil in-plane bending stress, struct. support design 0-106164

fusion reactor Large Coil Program, NbTi, superconducting test coil, General Dynamics Convair Division, Intermagnetics General Corp. design 0-99338

fusion reactor toroidal field coil finite element stress anal. 0-91256

fusion reactors, Large Coil Program, low temp. stability, joints, design method 0-106195

fusion reactors, Large Coil Program, pool boiling mag. quench press. calc. 0-106199

fusion reactors, Large Coil Program, superconducting mag. coil struct. design status 0-106189

fusion reactors, large Coil Program, Westinghouse coil cooldown and warmup 0-106193

fusion reactors, Large Coil Program, Westinghouse coil stability testing, pulsed induction heating 0-106194

fusion reactors, Large Coil Task, NbTi, forced flow superconducting test coil, EURATOM design 0-99339

fusion reactors, Large Coil Test Facility, liq. He cooling system 0-102321

fusion reactors, steady state resistive toroidal field coils 0-91264

fusion reactors, TFTR mag. field coil electrical insulation system and test results 0-95429

fusion reactors, TFTR poloidal field coil system, characts. 0-95430

Large Coil Program, insulation system cryogenic elec. test 0-91263

Large Coil Program, research and development activity 0-99336

Large Coil Test Facility, instrumentation system design 0-95446

magnetic defectoscopes, nonsinusoidal periodic currents meas. 0-104386

magnetic search coils for eye position meas., implantation method 0-85548

miniature coil wound systems protection, parylene (vacuum deposited polymeric coating) appl. 0-108607

Mirror Fusion Test Facility, superconductor core manufacturing and quality 0-93521

mutual inductance on infinite cylinder 0-58443

STEM zone-axis pattern formation using four sets of coils 0-70091

TEXT Tokamak, contacts for pulsed high currents 0-70029

toroidal field coils, EM parameters calcs. of current paths in homogeneous media (Japanese) 0-106155

coils continued

winding turns counting, using moire system 0-73428
 Nb₃Sn, multifilamentary coils for Lawrence Livermore Laboratory superconducting High Field Test Facility 0-90834

coincidence circuits

see also counters
 active well coincidence counters, expt. comparison with random drivers for U assay 0-78503
 Euratom variable dead-time neutron counter, use for Pu passive assay 0-69042
 ion electron converter device, neutron decay weak interaction obs. 0-58100
 megachannel pulse height analyser for gamma-ray coincidence analysis 0-99430
 nuclear materials accountability, U and P NDA of crated waste by gamma-ray and neutron coincidence counting 0-83166
 portable neutron coincidence counter for assaying large Pu samples 0-69041
 thermal neutron coincidence counting, correction for variable moderation and multiplication 0-69045
 X-ray- β particle coincidence technique to exam. β -decay of ²⁵²Cf fission fragments 0-74094

coincidence counters *see coincidence circuits; counters***cold-cathode tubes**

see also counting tubes; photomultipliers; phototubes
 Antares CO₂ laser power amplifier, design 0-69423
 compact cold cathode electron beam gun, appl. CO₂ laser (German) 0-86501
 ion gun for sputter-etching, discharge characts. and improvements 0-105748
 large-area cold-cathode grid-controlled electron gun for Antares CO₂ laser amplifier 0-68955

cold rolling

brass, cold rolling, inhomogeneous texture 0-89251
 ferromagnetic single crystal, mag. anisotropy induced by cold rolling (Russian) 0-84955
 metallic glass, current exptl. data on struct., review 0-88058
 moments, calc. for longit. rolling periodically changing sections (Polish) 0-89239
 steel, cold-rolled sheet, surface chemistry 0-61146
 steel, eutectoid, mech. behaviour, thermomech. treatment effects 0-84970
 steel, low C, type EN3, high strain deform., struct. and props. 0-89301
 steel, mild, cold rolled, texture and plastic anisotropy rel. to alloying and precipitation (French) 0-108475
 steel, mild and type EN31, eval. of cold rolling oils and boundary lubrication characts. by SEM 0-85068
 steel, P, deep-drawing, spatial orientation distrib. of crystallites in cold-rolled and in annealed sheets 0-81079
 steel, Si, nonoriented sheet prod. with texture of {100} (ovw) 0-89246
 steel, Si (3 wt.%), textured, secondary recrystn., precip. annealing effect (Japanese) 0-71662
 steel, stainless, Cr-Cu (17, 0.6 to 1.1 wt.%), texture 0-84957
 steel sheet, hot and cold rolled, cold formability, notched tensile test and stretch bend test (German) 0-61031
 thin-wall cylinder cold rolling method 0-66535
 Zircaloy-4, stress-relieved and cold-worked, stress relaxation in bending at 673K 0-93609
 Ag, cold rolling, inhomogeneous texture 0-89251
 Al, 1100 plates, substruct. development 0-108476
 Al, cold rolling, inhomogeneous texture 0-89251
 Al-Cu (4 wt.%), supersaturated and aged conditions, high strain deform. 0-60907
 Al-Cu-Mg, type D16T, thin-wall cylinder cold rolling method 0-66535
 Al-Mn (1 wt.%), single crysts., rolled to (123)[412], recrystn. textures 0-104183
 Al-Ni (6 wt.%) alloy, misorientation between subgrains, second-phase particles role, STEM microdiff. obs. 0-104415
 Co-Fe, soft mag. props. rel. to metallurgical aspects 0-88810
 Cu, cold rolled sheet, anisotropy of elastic and strength props. 0-81077
 Cu crystals, two-phase, recrystn. retardation, particle size, spacing effects 0-89242
 Fe, creep at 77, 295K, formation of five struct. 0-60926
 Fe, high purity, boring with cryst. B powder 0-84951
 Fe, texture, recryst. annealing effect (Czech) 0-89249
 Fe-Cr-Co (28, 10.5 wt.%) ductile magnet alloy, humidity-induced H₂ embrittlement 0-89406
 Fe-Ni-C (25, 0.2 wt.%), strain-induced martensite (Korean) 0-71646
 Fe-Si (3 wt.%) high-permeability grain-oriented steel, quenching effect on primary recrystn. texture development 0-84956
 (Fe_{1-x}Co_x)₇₈Si₁₂B₁₀ amorphous, roll mag. anisotropy 0-75757
 (Fe_{1-x}Ni_x)₇₈Si₁₂B₁₀ amorphous alloys, cold rolled and as-quenched, mag. anisotropy 0-97089
 Ni, cold-rolled, anomalous effects during X-ray stress meas. (German) 0-104184
 Ni, creep at 77, 295K, formation of five struct. 0-60926
 Ni-Fe, soft mag. props. rel. to metallurgical aspects 0-88810
 Ni, commercial, texture depend. stress corrosion cracking 0-104334
 α -Ti, primary recrystn., in situ invest. in HVEM 0-104185
 α -Ti sheet, texture dependent stress corrosion cracking in Br₂-methanol soln. 0-71803
 Ti-Al-V (6, 4 wt.%), texture depend. stress corrosion cracking 0-104334
 β -Ti-Mo, thermal instability, hardness and tensile deform. (Japanese) 0-71703
 Ti-Mo-Zr-Sn (11.5, 6.0, 4.5 wt.%) alloy, struct. as affected by processing history 0-84972
 Zn-Al (22 wt.%), alloy sheet, superplastic, cold-rolling effects on mech. props. and microstructure (Japanese) 0-71671

cold shortness *see brittleness***cold working**

see also bending; cold rolling; plastic deformation; slip; work hardening
 α -brass, polycryst., deformed in tension or rolling, annual hardening (Japanese) 0-93564
 Incoloy 800, steam oxidised, oxide coating anal. 0-89399
 internal friction meas. of thin wire U-shape specimens, electric circuitry modifications 0-59579
 metals, tension methods in X-ray diffraction (Italian) 0-87984
 steel, austenitic stainless, types 304 and 316, environment effect on crack growth, under creep and fatigue conditions 0-85035
 steel, austenitic stainless 304, stress corrosion cracking in MgCl₂ soln., cold working effect (Japanese) 0-104339

cold working continued

steel, C, magnetomechanical acoustic emission for residual stress NDT 0-71149
 steel, cold strained, defects interaction with carbide strengthening phases, carbide decomp. degree (Russian) 0-84955
 steel, cold worked, original struct. effect on softening during heating 0-60882
 steel, ferritic, magnetomechanical acoustic emission for residual stress NDT 0-71149
 steel, high strength, treatment effect on ductility and strength 0-60880
 steel, stainless, surface chem. rel. to metallurgical props., SIMS, XPS and AES (French) 0-80045
 steel, stainless 304, metallurgical factors on the corrosion and mass transfer in liq. Na (Japanese) 0-71804
 steel, US wave velocity meas. rel. to cold working 0-99908
 steel, wear characts. of burnished machined surfaces 0-108595
 steels, low alloy, particle coarsening reactions, effect of cold deform. 0-71664
 Al alloys, thermomech. treatments, effects on microstruct. 0-100858
 Al, deformed in uniaxial and equibiaxial tension, dislocation arrangements 0-108516
 Al dilute alloys, cold worked, internal friction peaks 0-97520
 Al, pure, cold worked, internal friction peaks 0-97520
 Al-Cu (4.6 wt.%), cold work and ageing influence on ductility and fracture behaviour (Japanese) 0-89295
 Al-Ni(Cd)(Fe)(Si), cold worked, struct. and props. 0-71666
 Al-Zn, type 7075-T6, coldworked hole specimens, residual stresses, fracture mech. anal. 0-97587
 Co-Ni-Cr-Mo (35, 20, 10 wt.%), MP35N, TEM study of phase transformations 0-81054
 Cu-Ag (0.1 wt.%), cold-worked, internal friction peaks in kHz range 0-89276
 Cu-Al(Au)(Ga)(Ni)(Pd)(Rh)(Zn) (4 at.%), anneal hardening mechanism 0-60879
 Cu-Fe system, ageing and reversion phenomena study 0-89274
 Cu-Ni (30-90 wt.%), elect. resist. rel. to cold working and heat treatment 0-71765
 Cu-Ni-Sn (15, 8 wt.%), prior deform. effect on spinodal age hardening 0-108465
 α -Fe, cold work aftereffects 0-88830
 Fe, magnetomechanical acoustic emission for residual stress NDT 0-71149
 Fe-Cr alloys, cold worked, internal friction due to H (Japanese) 0-70305
 Fe-Ni-Cr (30.6, 21.3 wt.%), Alloy 800, high temp. oxidation at low O₂ press., SEM, AES and electron probe microanal. study 0-93688
 Fe-W-Cr-Mo system, mag. and mech. props. rel. to production methods (Japanese) 0-71107
 Mo, single and polycryst., struct. change during work softening, HVEM 0-103336
 Nb, dislocation damping, amplitude depend. 0-59469
 Nb-Ti multifilaments, effect of mech. and thermal treatments of supercond. props. 0-104197
 Nb₃Al, A-15 struct., converted from cold worked BCC struct., crit. currents 0-75697
 Ni-Cr-W-Mo-Ti-Al, heat-resist., recovery and recrystn. 0-76268
 β -Ti-Mo-Zr-Sn (11.5, 6, 4.5 wt.%), metastable phase III, microstruct. and age hardening response 0-84945
 Zr-Nb (2.5 wt.%), cold-worked, pressure tubing, metallography and mech. props. 0-89269

collections of physical data

A=112, experimental nuclear structure data to January 1979 0-98763
 A=123, experimental nuclear structure data to June 1979 0-94931
 A=145, experimental nuclear structure data to August 1979 0-94932
 A=163, nuclear data sheets to April 1979 0-98762
 absolute core-level binding energies for gaseous atoms and molecules 0-101670
 absorption line lists for quasars, visible obs. 0-67899
 alkaline earth halides, refractive index, wavelength and temp. derivatives 0-88948
 bright galaxies associated with nearby Abell clusters, position and magnitude 0-67880
 Copernicus UV spectral atlas for B3 IV type star ϵ Herculis 0-67583
 crystal sources, geometrical coeffs. for interpretation of γ -ray perturbed angular correl. with quadrupole interactions 0-73109
 differential polarisation coefficients for (γ ,X) reactions 0-73838
 earthquakes in Japan, 1885 to 1925, catalogue of M \geq 6 earthquakes and smaller, damaging, earthquakes (Japanese) 0-67341
 elementary particle properties, leptons, mesons, baryons 0-67944
 EM depth sounding interpretation, master tables, book 0-86043
 ES type galaxies, UVB photometry obs. 0-73053
 formic acid (-d), microwave spectra and rot. const., astrophysical appl. 0-91550
 gamma reactions initiated by polarised particles, Legendre polynomial coeffs. 0-73107
 hydrocarbons, 30.4 nm He(I) photoelectron spectra 0-82589
 interstellar molecular transitions, rest freqs. 0-62218
 Japanese Islands region, geophysical data compilation (Japanese) 0-67332
 linear polarisation mixing coeffs. for mixed dipole and quadrupole γ -radiations, Compton polarimeter 0-73110
 metal monolayers, on metal cryst. surfaces, surface struct., review 0-80067
 Mossbauer atoms, electron densities at nuclear centre and surface, calcs. using Dirac-Fock eqn. 0-74100
 neutron effective resonance energy values for 96 isotopes 0-71978
 noctilucent clouds over W.Europe (during 1979) 0-109289
 nuclear data sheets, levels, J^π and transitions for A=73 0-101673
 nuclear data sheets, levels, J^π and transitions for A=77 0-105439
 nuclear structure data sheets, 1979 recent references, cumulation 0-94930
 nuclear structure data sheets (July 1979) for A=213 0-67942
 nuclear structure data sheets (July 1979) for A=217 0-67943
 nuclear structure data sheets for A=63 (July 1979) 0-67941
 optical glass, refr. index tables and calcs. for optical designer 0-83650
 palaeomagnetic pole positions and palaeomag. directions, pole numbers (16/1 to 16/296) 0-72415
 photochemical data and kinetics of gas phase chemical reaction in atmosphere 0-101671
 photoelectric photometry obs. of globular star clusters 0-67800

collections of physical data continued

- pulsar radiation at 430 MHz, statistical summary of polarization 0-67760
 radioactive nuclides, quantum radiation, data handbook 0-94933
 radioisotope dosimetric data tables 0-105438
 rare earth intermetallic compounds, ferromag. props., book contrib. 0-75726
 semileptonic weak and EM interactions, multipole operators, HO single particle matrix elements 0-73840
 spectral classification of early type stars using UV line features 0-72927
 thermonuclear reaction rates, thick target meas. 0-73108
 thermophysical process ambiguous data gathering and processing optimisation (*Russian*) 0-73335
 As VI, VII, spectra 100 to 300 and 500 to 1200 Å ranges 0-83307
 FeVIII-XXVI energy level tables and Grotrian diagrams 0-74142
 H I 21 cm line survey of M31, contour maps, vel. profiles 0-73038
 Mg, I-XII, energy levels and optical spectra 0-87065
 O₃, in lower atmos., Uccle, Belgium, April-June 1979 obs. (*French, Flemish*) 0-98385
 O₃, in lower atmos. Jan.-March 1979, obs. over Uccle, Belgium (*French, Flemish*) 0-94571
 Sc I to Sc XXI, energy level tables derived from atomic spectra anal. 0-101672

collective accelerators

- accel. of projectiles to hypervelocities using series of imploded annular plasma discharges 0-74042
 cyclotron resonance, Doppler effect, anomalous, amplification of slow waves in electron beam, obs. 0-78463
 electron-ion ring, stationary state 0-106217
 future technologies in high-energy physics, collective accelerators, laser accelerators, single-pass collectors 0-78466
 heavy ion acceleration, time-depend. study, fusion ignition appl. 0-86997
 ion beam production, high current in triode 0-99372
 metallic ion collective accel. 0-74040
 rectangular waveguide, Cherenkov radiation source 0-99373
 relativistic electron beams, collective acceleration, beamfront velocity effects 0-75063
 relativistic electron beams with finite energy spread and improved emission, development and investigation 0-91741
 waveguide containing relativistic electron beam, slow cyclotron wave 0-106983
 X-ray diagnostics on collective heavy ion electron ring accelerators 0-102358

collective states, nuclear *see nuclear collective states and giant resonances***collimators (optical)** *see optical collimators***collision processes**

- see also atom-surface impact; atomic inelastic collisions; charge exchange; chemical reactions; elastic scattering of atoms and molecules; elastic scattering of electrons by atoms and molecules; electron attachment; electron impact; elementary particle interactions; intermolecular mechanics; ion-surface impact; molecular inelastic collisions; molecular-surface impact; negative ions; Penning ionisation; plasma collision processes; potential energy surfaces for collision processes; quantum field theory; quasimolecules; radiation quenching*
 anharmonically coupled oscillators, semiclassical calcs. of eigenvalues 0-95514
 galaxies, collisions with intergalactic neutral clouds rel. to interstellar super 0-98717
 galaxies, tidal encounters rel. to Arp QSO-galaxy associations 0-90564
 galaxy mergers, stellar populations mixing processes 0-67860
 gas, electron and hole drift velocity 0-57223
 gas, weakly ionised, electron distrib. function, isotropic component, collision source 0-62599
 gas, weakly ionised, electron distribution function, steady-state conditions and elastic collisions 0-57224
 gas, weakly ionised, electron drift velocity and distrib. function 0-57225
 gas, weakly ionised, electron transport quantities, divergences 0-57222
 impact craters, diameter to depth ratio dependence 0-94765
 interstellar clouds collision and star form., suppression by interstellar gas heating 0-105349
 interstellar grains, collisions in turbulent gas 0-77470
 ion cyclotron resonance spectrometry, collisionally damped ion motion 0-57419
 Keplerian systems, numerical simulations of collisional evolution 0-109342
 novae, nonuniform stellar wind collision with main shell filaments rel. to light curves 0-62160
 particle collisions, conservation of energy and conservation of vector momentum 0-101693
 particle passage through thin layers, Monte Carlo calc. 0-100708
 reduced phase space approach calcs. 0-83438
 relativistic Boltzmann kinetic eqn. derivation 0-68161
 scattering resonances, tunnelling decay, absorbing boundary layer 0-57121
 semiconductor, electron and hole drift velocity 0-57223
 semiconductor, intrinsic, electron distribution function, steady-state conditions and elastic collisions 0-57224
 semiconductor, intrinsic, electron drift velocity and distrib. function 0-57225
 spiral galaxies merging hypothesis for elliptical galaxies form., refutation 0-98723
 spiral galaxies of Virgo cluster, collisions rel. to H I deficiencies 0-62277

collision sequences, focused *see sputtering***colloid chemistry** *see colloids***colloids**

- see also Brownian motion; coagulation; electrophoresis; electroviscous effect; emulsions; gels; magnetic fluids; thixotropy*
 aerosol OT-n-heptane-water, reversed micellar solution; addition of electrolyte, neutron small angle scattering 0-104468
 Agave cantala natural fibre, small-angle X-ray scatt. of densely packed colloidal system, scatt. inhomogeneities 0-76565
 amino acid residues, form. of mixed micelles and relative compatibility at interface 0-71951
 benzophenone ketyl radical, in micelle, decay rate in mag. field, photolysis meas. 0-85154
 cetyltrimethylammonium bromide-1-butanol system, micellar conc. meas. using fluoresce, probe study 0-85217
 chlorophyll, colloidal sols., elec. charge of particles 0-94438
 coal dispersions, solvent refined, elec. props., surface characts. 0-80333

colloids continued

- decylammonium chloride micelles, ¹³C longitudinal relax. times and nuclear Overhauser enhancement anal. 0-83390
 depletion stabilisation and depletion flocculation, theory 0-89534
 dibenzylketone, photolysis in micellar soln., quantum yield and ¹³C enrichment 0-97711
 3,3'-diethyldithiocarbocyanine iodine-rhodamine 6G, energy transfer with increased local conc., Förster mechanism 0-69220
 diphenylanthracene in 2,2,4-trimethylpentane, light scatt. and fluoresc. standard by monochromator 0-57247
 dynamics of colloidal dispersions, review 0-71956
 dynamics of colloidal systems: time-dependent structure factors 0-93803
 electro-optic studies, electric polarisability, stability 0-85222
 electro-optics and dielectrics, conf., Uxbridge, England (Apr. 1978) 0-82577
 electrolyte solution containing spherical particles, appln. of hypernetted chain approximation to particle interaction 0-85185
 flow alignment, transition from isotropic to nematic phase 0-84060
 fluoroanthene in micelles soln., fluoresc., halide ion induced quenching and enhancement 0-95672
 hydrophobic particle interactions, stability, dynamic theory 0-89544
 interfacial electric polarisability, and interactions 0-108751
 intermicellar kinetics theory, stochastic approach, master equation for, irreversible reactions 0-76561
 latex, shear waves, elastic modulus determ., light scatt. 0-58956
 materials with ionisable surface groups, colloidal behaviour 0-89543
 Maxwell-Wagner dielectric dispersions, vol. ion polarisations 0-97188
 metal, annealing, irradiation-induced defects in alkali halide crystals 0-107316
 metal colloids in ionic cryst., preparation, optical, mag. resonance, elec. props. 0-59459
 metal-filled epoxy polyester, PE-933, elec. cond., theory and expt. 0-60057
 metal-filled polymer, elec. cond., theory and expt. 0-60057
 metals and alloys, corrosion, colloid chem. appls. 0-89541
 micellar solutions, cluster size distribution for the Ornstein-Zernike correlation 0-97734
 micellar solutions, crit. behaviour 0-105601
 micellar systems, aqueous, thermochemistry 0-61133
 micellar systems, solubilisation 0-89546
 micelle formation model, relaxation spectra 0-71934
 microemulsions, quasi-elastic light scatt. 0-108755
 model, elastic moduli, Monte Carlo methods 0-108754
 molecular attraction forces between solids, effect of EM lag 0-71949
 particles, in a flowing solution, SAXS 0-61163
 photochromic dyes, quasi-crystals produced in applied electric field 0-85225
 Poiseuille flow, total particle conc. axial change 0-108752
 polymer spheres colloidal suspension, steady state shear flow coupled to conc. fluctuations 0-61170
 polystyrene interfacial colloidal crystals, microscopic obs. 0-97737
 polystyrene latex particles, swollen, aggregation studied by photon correlation spectrosc. 0-66886
 polystyrene latexes, monodisperse, model colloid systems 0-89545
 polystyrene-polyethylene/propylene block copolymer, micelle form. in lubricating oil 0-61171
 preparation 0-71953
 pyrene derivatives, micelle-embedded, rot. relax., time-resolved fluoresc. depolaris. obs. 0-58300
 sedimentation, rapid, under gravity, basic theory and experimental demonstrations 0-66885
 sedimentation equilibrium eqns. derivation using hard spheres in Percus-Yevick approximation 0-66884
 sepiolite, electric polarisability, anisotropy, length depend. of ionic contrib. 0-85224
 sepiolite, size distributions, transient electric birefringence 0-85223
 size distributions, transient electric birefringence 0-85223
 sodium 10-undecanoate, γ-ray induced polymerisation in aq. micelle solns. 0-61093
 sodium dodecyl sulphate: Gd³⁺, micellar system, chain folding, ¹³C NMR obs. 0-61158
 sodium dodecyl sulphate, polydisperse micellar solns., light scatt., size, shape and aggregation number calcs. 0-89531
 sodium dodecyl sulphate micelles-ω-(α-naphthyl) dodecanoic acid soln. fluoresc. decay obs. 0-61158
 spherical particles, colloidal dispersions, refractive index 0-106454
 stability, dynamic theory 0-89544
 surface and colloid science, conf., Stockholm, Sweden (Aug. 1979) 0-86035
 surface forces, direct meas., elastic deform. effect 0-93805
 surfactant micelles, hydration 0-89518
 surfactant solutions, aggregation, micelle and microemulsion form. 0-89547
 suspensions, rheology, colloidal forces role, review 0-103063
 thermodynamic stabilisation, theory 0-81369
 thionine in sodium lauryl sulphate micellar solns., absorpt. spectra and fluoresc. yield, local dye conc. depend. 0-106343
 Ag, adsorpt. of acetonitrile, surface enhanced Raman spectra obs. 0-97251
 Ag, adsorpt. of benzene (deutero benzene), surface enhanced Raman spectra obs. 0-97251
 Ag, adsorpt. of N,N-dimethyl aniline, adsorpt. on Ag colloids, surface enhanced Raman spectra obs. 0-97251
 Ag, adsorpt. of pyridine, surface enhanced Raman spectra obs. 0-97251
 AgCl, luminescence fatigue, adsorbed Ag atoms 0-66281
 AgI hydrosols, kinetics and mechanics of colloid systems formation 0-101045
 AgI, stability, dynamic theory 0-89544
 Al₂O₃(H₂O)_n, uniform colloidal dispersion, prep. by chem. reactions in aerosols 0-97735
 Au sols, solutions of large colloidal particles acoustically induced birefringence 0-93274
 copper phthalocyanine, size distributions, transient electric birefringence 0-85223
 Cr⁶⁺/Cr³⁺ colloidal SiO₂ surface films on Al, TEM/XPS study 0-85090
 Cu²⁺-1,5-dimethyl-2,4-hexadiene, fluoresc. quenching method for determ. binding conc. 0-89530
 Fe₂O₃, prep., thermal decomposition of metal chelates 0-71953
 NH₃-AlCl₃ solution, Al₂O₃ ultrafine gel particle form. 0-93807

colloids continued

²³Na in heterogeneous system, nuclear mag. relaxation time determ., rel. with dimensions of colloidal particles 0-75876
V₂O₅, amorphous semicond., solubility and fibrous texture 0-75162

colorimeters

see also colorimetry
automatic, plating line Co concentration monitoring 0-105691
photocolorimeter, automation of measurements (Russian) 0-68238

colorimetry

see also colorimeters; spectrochemical analysis; spectrophotometry
cholesteric liquid crystals, investigation of colour-temp. characts. 0-75359
colour image evaluation from tristimulus values transfer functions measurements 0-87333
colour scicence contributions, collection of papers by D.B. Judd 0-98761
consumer product quality assurance, colorimetric theory and equipment (German) 0-86372
diacetylenes, photopolymerisation, solid-state reaction, photoacoustic photocalorimetric obs. 0-61089
fluorescent materials, reflective radiance factor meas. by two-monochromator method (Japanese) 0-68237
grating type monochromators, errors caused by polarisation of meas. system (Japanese) 0-101815
Judd's contributions to colour metrics and eval. of colour differences 0-94945
leading in glazed ceramics, colorimetric method (Spanish) 0-73414
matrix techniques in colorimetry 0-105690
metrics, facts and formulae 0-97900
microprocessor controlled spectrophotometric colorimeters (Hungarian) 0-101851
optimum colour appearance anal using spectrophotometers in quality assurance laboratories 0-90877
photographic materials, colour component triads, colorimetric determ. for positive materials (Russian) 0-95178
reflective glass colour standards 0-90878
reproductions, colorimetric comparison 0-95119
retroreflecting material metrology, errors in luminous refl., chromaticity meas. 0-68235
retroreflective material chromaticity meas. under nighttime geometry 0-73411
sensitometry characteristic curves corresponding to visual impression 0-82803
sensitometry system based on spectral densitometer 0-82804
sensitometry using densitometer with more than 3 channels, dye specific densities 0-82802
solid-state reaction, photoacoustic photocalorimetric obs. 0-61089
spectrocolorimeter, SPEKOL, meas. of diffuse reflectance spectra, of differently matted polyamide fibres 0-77836
ultramarine pigments, instrum. for colour measurement and control 0-62711
whiteness, visual impression and colorimetric definition 0-81597
Al film, energy losses of electrons, microcalorimetric meas. 0-59543

colour

see also colour vision
alloy colour and colour stability as alloy design criteria 0-101005
cholesteric liquid crystal coatings, superimposed left- and right-handed, peak refl. and colour gamut 0-74472
colour scicence contributions, collection of papers by D.B. Judd 0-98761
fluorite, use of proton irradi. to reveal growth and deform. features 0-84216
luminous colour control methods in pulsed arc discharges in Ne-Hg lamps (Japanese) 0-103214
photographic materials, colour component triads, colorimetric determ. for positive materials (Russian) 0-95178
psychometric measures for specifying colour appearance 0-76747
C films, diamond-like, on Si, colour chart 0-97366
NiO samples, colour difference, X-ray line broadening study 0-100206

colour blindness see colour vision

colour cameras, television see colour television cameras

colour centres

see also F-centres; OH⁻-centres; paramagnetic resonance of colour centres; U-centres; V-centres
alkali halides, polarization, photoinduced, rel. to exchange between vacancy and impurity 0-59914
metal colloids in ionic cryst., preparation, optical, mag. resonance, elec. props. 0-59459
mixed fluoride crystals, nucl. radiation effects 0-80831
optical fibres, UV radiation-induced losses rel. to colour centre form. 0-87517
optical glass, coloured, laser damage threshold, optical absorpt. influence 0-91830
photographic emulsions, ultra-fine grained, nature of produced colour centres during photolysis (Russian) 0-73517
quartz, electron irradiation effects on optical, dielec. elastic props. 0-59521
radiation damage, mechanisms, in semiconductors and insulators, review 0-107315
review, fifty years of colour centre physics 0-105487
ruby, radiation-induced optical processes, impurity effects 0-66310
Ag halide, glass, kinetics of photochromic processes 0-103930
Ag halide photochromic glasses, colour centres struct. 0-66254
β-Al₂O₃-Na₂O, ENDOR meas. of defects 0-66074
CaS:Cu, colour centres, optical and thermal depths determ. 0-66275
CdF₂, colour centres, IR absorpt. and photocond. after UV irradi. 0-79784
CdF₂:NaF(AgF), colour centres, IR absorpt. and photocond. after UV irradi. 0-79784
GaP crystals, radiation defects, TSC obs. 0-65588
KBr, defect accumulation under electron irradi. at 4K 0-107233
KBr:Au⁺, optical absorpt. bands and MCD, electron-lattice interaction 0-108236
LiF, γ-irrad. induced defects, positron capture and annealing obs. 0-60707
LiF, γ-irrad. pure and Mg-doped, phonon scatt. and interstitial clusters 0-70254
LiF:Mg cryst., Mg electron colour centers 0-100229
LiNbO₃, optical absorption of hole centres, polaron model 0-97314
MgO:Li, mech. deformed crystals, imprinting of slip bands using Li impurities 0-59473
Na₂Al₂Si₂O₁₀(NaX)₂, X=Cl, Br or I, sodalites, thermal destruction of colour centres (Russian) 0-84169

colour centres continued

Na₂O-Al₂O₃-B₂O₃-SiO₂-AgCl(Br), photochromic glass, kinetics of thermal decolourisation 0-103931
Na₂O-CaO-SiO₂, glass, formation of colour centres, linear absorption of UV radiation 0-103328
Na₂O-SiO₂ glasses, elementary electronic excitations, refl., luminesc., and photoemission meas. 0-84778
PbMoO₄, optical absorption of hole centres, polaron model 0-97314
RbCl:Au⁺, optical absorpt. bands and MCD, electron-lattice interaction 0-108236
V₂O₅ amorphous film, photochromism and thermochromism 0-93254
WO₃-electrolyte electrochromic cells, proton injection phenomena 0-71448
YAG, optical absorption of hole centres, polaron model 0-97314

colour display tubes, television see colour television picture tubes

colour filters see optical filters

colour model

θ-vacua and confinement in two-dimensional models 0-77990
asymptotic freedom infrared instability 0-73678
baryon couplings and 'missing resonance' in quark model with chromodynamics 0-57558
baryon decay, QCD model for internal structure, pseudoscalar-meson and photon emission 0-68452
baryon spectroscopy and photoproduction couplings using new baryon wavefunctions 0-102016
baryonium states in QCD, review 0-102001
baryons and mesons, parton distrib. consistent with naive quark model and QCD 0-62937
Bjorken scaling violation, QCD and models of quarks with substructure 0-105851
charge confinement, Schwinger model compared with (QED)₄ 0-62902
charge invariance, QCD, renormalisation group, confining and asymptotically free soln. 0-62881
charm, elementary particle theories, properties (Spanish) 0-73681
charm photoprod. with linearly pol. photons, QCD calcs., gluons 0-68464
charmed baryon mass and F/D ratio, colour magnetic interaction 0-62957
charmonium, mass in QCD 0-105867
composite quarks and leptons, mag. moments 0-91056
conference, lepton-hadron physics, Karlsruhe, Germany (Sep. 1978) 0-73098
CPN⁻¹ model, instanton and large-N methods, QCD similarity 0-77963
CP invariance, QCD confinement of colour, modification of axion scheme 0-73663
deep inelastic lepton-hadron scatt., seminclusive hadron prod., quark fragmentation function corrections, QCD 0-63013
deep inelastic leptonproduction, normalising the renormalisation group anal., QCD twist effects 0-86690
deep inelastic scatt., inclusive observables and hard gluon emission 0-99094
deep inelastic struct. function behaviour near physical region endpoints, QCD anal. 0-99101
deep inelastic structure functions, QCD tests, Bernstein moments 0-101983
Dirac particle+two Klein-Gordon particles, relativistic three-body wave equation, preon model 0-73574
direct lepton generation in strong interactions, unified model, colour quark state (Russian) 0-82933
double-logarithmic quark and form factors and the evolution of parton jets 0-68421
Drell-Yan model at measured Q_T: asymptotic smallness of the one-loop corrections 0-105847
Drell-Yan muon prod., QCD correction uniqueness 0-78032
Drell-Yan process higher order corrections, QCD and parton model sum rules 0-95251
Drell-Yan processes, asymptotic freedom corrections, Q²-dependence 0-62933
dynamical preon model from primordial QCD 0-105840
effective hamiltonian for ΔC=1 nonleptonic interactions in the Kobayashi-Maskawa model 0-86667
effective Lagrangian due to heavy quarks in quantum chromodynamics 0-90900
effective Lagrangian with two color-singlet gluon fields 0-86680
energy momentum sum rule beyond the leading order in QCD 0-78024
exotic new quarks and dynamical symmetry breaking 0-73669
flavour changing weak radiative decays, short and long distance effects 0-73712
gauge field propagator and the number of fermion fields 0-62928
gauge theory aspects 0-91011
geometrodynamics, eightfold way, review 0-95243
glueball pomeron singularity cancellation 0-73687
glueball spectra, prod. and decay for QCD and SU(n) gauge theories 0-62941
gluon and quark jets in a recursive model motivated by quantum chromodynamics, T decay 0-62936
gluon and quark population evolution in QCD jets, numerical estimates 0-101987
gluon condensation and QCD 0-102007
gravitationally induced CP effects, quantum gravidynamics, QCD quark sector 0-86616
hadron+hadron inclusive cross section of symmetric hadron pairs produced, hard scatt., parton model and QCD 0-63052
hadron calorimeter expts., asymptotic power laws, QCD and parton model predictions 0-57560
hadron inelastic scatt., secondary hadron multiplicity distribution, Regge like parton model (Russian) 0-78100
hadron interactions, inclusive, large momentum transfer, quark counting, EM form factors 0-68498
hadron jets, rapid parton and hadron distribution 0-86693
hadron masses, behaviour of constituent quarks 0-57557
hadron scatt. mediated by qg→qg and gg→gg 0-82988
hadron-hadron, in H, AL, inclusive particle distrib., QCD predictions 0-99112
hadron-hadron 3-jet collisions, charge conjugation asymmetries and tri-linear gluon coupling 0-105934
hadron-hadron inclusive interactions, charmed particle production, η_c, ψ and other cc bound states 0-63036
hadronic form factor asymptotics in QCD (Russian) 0-62983
hadronic lepton pair production, QCD jets 0-62994

colour model continued

hadronic wave functions at short distances and the operator product expansion, QCD tests 0-57564
 hadrons, QCD model, asymptotically free field theory, anomalous dimensions of composite particles 0-73665
 heavy baryon spectroscopy in the QCD bag model 0-105866
 heavy meson weak decays, heavy quark decay, QCD corrections, real gluon role 0-57586
 heavy quark bound states of top quark and antiquark pairs, QCD test 0-68430
 heavy quark prod., nonperturbative gluoprod. versus perturbative QCD fusion models, B and ψ 0-91058
 heavy quarkonium states, hadronic transitions, QCD anomalies for T^* and ψ 0-105888
 heavy quarks in QCD (French) 0-78017
 hidden colour and the isobar content of the deuteron 0-102024
 Higgs boson decay, QED and QCD radiative corrections 0-95275
 high-transverse-momentum symmetric-particle-pair spectra and correlations 0-95250
 higher order QCD jets in photoproduction 0-99087
 higher-twist effects in QCD, deep inelastic scattering and the Drell-Yan process 0-102020
 instanton statistical mechanics in QCD 0-57567
 instanton system weakly interacting with anti-instanton system, external electric fields, structure and stability 0-77956
 instanton-anti-instanton interaction effects on current correlation functions in QCD 0-102010
 instantons, gravitational, flavour currents of QCD, Green's functions, foam-like structure of space-time 0-62825
 instantons in nonAbelian gauge theories and QCD mesons 0-105777
 interacting instanton-antiinstanton system under external colour mag. fields in SU(2) gauge 0-101920
 interaction potentials for multi-quark states from instantons and other background gauge field configurations 0-101995
 intermediate vector boson decay, QED and QCD radiative corrections, hadronic jets 0-73759
 jet structures of leptons, quarks and gluons, perturbative QCD, process dependence 0-68470
 jets of quarks and gluons, leading logarithmic approx., parton interpretation 0-68433
 Klein-Gordon particles + Dirac particle, relativistic three-body wave equation, preon model 0-73574
 large p_T hadronic collisions, QCD sensitive test, quark and gluon jets 0-57647
 large-N chromodynamics, chiral symmetry breakdown 0-91052
 lattice gauge theories, chiral symmetry dynamical breaking 0-99061
 lattice QCD₂, Wilson's loop eqn. soln. for large N limit 0-78030
 lattice QCD, hadron mass spectrum, effective Hamiltonians, degenerate perturbation theory 0-102003
 lattice SU(N) gauge theory, vacuum structure, large-scale 0-57470
 lepton + nucleon, quark and gluon jets, Breit frame, QCD 0-62995
 lepton pair prod. struct. functions, QCD improved quark-parton model 0-73671
 lepton pair production, QCD and hard-scatt. model, spin-spin asymmetries 0-63014
 lepton structure model 0-91063
 light-cone gauge, QCD calcs., non-singlet quark struct. function 0-57464
 mass differences of up and down quarks, grand unification 0-62978
 masses in scalar dynamics, gluon theories compared with QCD 0-57553
 massless QCD₂, non-Abelian travelling wave solns., SU(2) subalgebra 0-57563
 meson and baryon mass formula, chromodynamics consideration (Russian) 0-91071
 meson dipion cascade decays, current algebra techniques, pole plus remainder model, chiral symmetry breaking and QCD 0-62972
 multiparticle production in chromoelectric flux tube model in 1+1 dims. field theory 0-73666
 Nachtmann moments of $F_2^{N(x,Q^2)}$ and energy momentum sum rule 0-57580
 neutron matter-quark matter phase transition, QCD and extended Higgs model, instantons 0-91062
 non-Abelian Block-Nordsieck conjecture, counter-example 0-78021
 non-Abelian gauge theories, high energy behaviour, reggeon field theory, QCD 0-62822
 nonleptonic hyperon decays, QCD corrections 0-91087
 nonperturbative QCD, large N_c , QCD bag model, instantons and η' mass 0-57559
 nucleon-nucleon interaction as derived from the De Rujula, Georgi, Glashow phenomenological quark-quark potential 0-78172
 O(10), SU(4) colour subgroup, fractional charged gauge boson, proton half-life 0-73644
 off-shell particle scattering, total cross sections, QCD 0-68418
 OZI rule, justification in QCD 0-62924
 parton distribution functions, Q^2 depend., QCD parameterisation 0-82937
 perturbative QCD, renormalisation improvement, charmonium decay and scaling violations 0-101993
 photon distribution functions, QCD predictions using Altarelli-Parisi eqns. 0-78019
 polarised deep inelastic scatt., parton transverse momenta role, struct. function, QCD evolution 0-78034
 polarised electroproduction, target mass effects 0-78072
 power corrections at short distances, hadronisation, smearing, higher twist 0-105844
 Q^2 dependence for quark and gluon fragmentation functions, QCD predictions, Altarelli-Parisi eqns. 0-78018
 QCD₂, qq bound state spectrum in leading 1/N approx. 0-78031
 QCD, 1+1 dims., dynamical symmetry breakdown 0-82949
 QCD, 2-dimens. multicolour, local colour symmetry breakdown, massive gluons and quarks 0-82942
 QCD, anomalous dimensions of gauge-invariant three-fermion local operators of twist three 0-86662
 QCD, colour ferromag. vacuum states, two loop energy densities, MIT bag constant 0-99085
 QCD, confinement and long range gauge fields 0-73668
 QCD, direct γ prod. beyond leading order, qq \rightarrow q γ process 0-86664
 QCD, effective Lagrangian, possible σ -model 0-86679
 QCD, equations of motion for n-loop averages 0-82935
 QCD, gauge indep. approach to hard processes, structure functions, gluons 0-86665
 QCD, Gell-Mann-Low function in 3 loop approx., nonAbelian gauge theory with fermions 0-86675

colour model continued

QCD, ghost gluon bound state and pseudoscalar mixing 0-86685
 QCD, high p_T hadron prod. in pionisation region and vacuum singularity (Russian) 0-86772
 QCD, improved evolution eqns. based on probabilistic interpretation 0-86673
 QCD, large N limit, pseudoscalar nonet chiral dynamics and low energy spectrum 0-101988
 QCD, lattice and continuum, Λ parameters connections 0-82945
 QCD, lifetime of QQ states, pseudoscalar charmonium and upslon states 0-68429
 QCD, long range parton correlations at large Q^2 (Russian) 0-68428
 QCD, Migdal approx. and 1/N expansion, string tension 0-101992
 QCD, parton jet and shower model 0-86663
 QCD, renormalisation group calcs., cancellation of ambiguities (Russian) 0-62930
 QCD, stagnant gauge for gluon propagator 0-57554
 QCD, string constant, Regge slope and Λ parameter, empirical quarkonium approach 0-91053
 QCD, two-dimens. with massless fermions in 1-1 dimensions 0-62926
 QCD and short range nuclear phenomena 0-91060
 QCD approx. for nucl.-quark matter phase transition in neutron star cores 0-67771
 QCD at low Q^2 , structure function moments, correspondence relation 0-73673
 QCD axial gauge, $O(\alpha_s)$ infra-red divergences, deep inelastic quark struct. function 0-86676
 QCD black body radiation, big bang universe hadron era 0-62341
 QCD contributions to vacuum polarization 0-91059
 QCD contributions to vacuum polarization 0-105834
 QCD corrections at Z_0 for hadron initiated lepton pair prod., renormalisation appl. 0-86678
 QCD corrections for Higgs-boson production 0-68419
 QCD expansion parameter choice 0-78025
 QCD ground state wave function, model 0-73662
 QCD hadron jets, branching processes, multiplicity distrib., KNO scaling (Russian) 0-101998
 QCD higher order effects of structure function moments 0-62979
 QCD jet fragmentation functions in leading log approx. 0-101981
 QCD jet simulation, cutoff choice effects 0-102015
 QCD low energy tests, gluon non-zero effective mass, ψ decays 0-91054
 QCD phenomenology of deep-inelastic scattering 0-73660
 QCD polarisation operator at finite temps. and densities, one loop approx., gluons (Russian) 0-68427
 QCD processes, large IR corrections, soft gluon emission 0-78028
 QCD renormalisation in two loop approx. in arbitrary gauge 0-102002
 qCD scattering processes with hard gluon emission, jet prod. 0-62939
 QCD spectral function sum rules, EM current flavour components 0-99084
 QCD tests and singlet struct. function moments 0-82941
 QCD tests in τ -lepton decay and e^+e^- annihilation 0-102006
 QCD vacuum, asymptotic freedom, quark confinement, Yang-Mills theory for strong interactions 0-73638
 QCD vacuum in strong external gauge fields, spontaneously, broken chiral symmetries 0-57555
 QCD with N colours, approx. solns. 0-91051
 QDD, quantum dath dynamics, SU(3) model for composite quarks and leptons 0-91055
 quark fragmentation jets in QCD, cascade model 0-78045
 quark gas at finite temp. and density, QCD effects 0-95248
 quark mass, electroweak contrib. 0-101990
 quark structure model 0-91063
 quark-gluon field coupling const., meson mass differences (Russian) 0-105898
 quark-nucleon phase diagram and quantum chromodynamics 0-105855
 quasiconfinement in colour gauge symmetry, unconfined quarks and gluons 0-86686
 random colour magnetic quantum liquid formation in QCD 0-99088
 restricted theory as subset of nonAbelian gauge theory 0-62851
 saturation of colour confining forces and effects 0-73672
 soft gluon resummation formulae for hard parton processes in QCD 0-105842
 strong coupling QCD, variational approach, Schrodinger eqn. and effective Hamiltonian 0-95245
 structure function in deep inelastic scatt., QCD predictions for singlet case 0-73707
 structure functions, bounds for the ratio of anomalous dimensions, scalar gluon theories 0-57595
 structure functions, nonsinglet, parton distributions, QCD parameterisation, leading and next-to-leading order corrections 0-68456
 SU(2)_c \times U(1)_c, strong CP-violating phase, one-loop corrections, Higgs particles 0-62910
 SU(3)_{colour} \times SU(2)_c \times U(1)_c gauge, full operator structure of the non-leptonic $|\Delta S|=1$ weak Hamiltonian 0-99089
 SU(3)_c \times U(1)_c electroweak model, strong extension, flavour and colour gauge exchange symmetries (Chinese) 0-101975
 SU(3) colour gauge group, coloured monopoles 0-68360
 SU(5), unification of weak, EM and strong interactions, review 0-105814
 SU(5) electroweak-strong interaction model, broken colour symmetry and gluon mass 0-73650
 SU(5) grand unification, heavy coloured Higgs scalars, b-quark mass 0-57543
 subcomponent models of quarks and leptons in SU(3) subcolour, proton decay 0-78035
 superdense matter, quark and gluon plasma, hadronic structure, neutron stars, hadron collisions, review 0-73683
 three gluon integral equation and odd \bar{C} singlet Regge singularities in QCD 0-101991
 three quark Hamiltonian from qq interaction, pairwise interactions in colour hypothesis 0-86670
 topological bootstrap prediction for three coloured, eight flavoured quarks 0-86694
 totally inclusive leptonprod., scaling anal., target mass corrections in QCD parton model 0-102052
 transverse lattice QCD, hadron mass spectrum 0-57568
 unconfined colour quark models, weak interactions and neutral currents (Russian) 0-105841
 unconfined quarks and gluons, quasiconfinement model, confining and nonconfining phase transition 0-86687
 unified gauge theories, grand, asymptotic freedom constraints 0-62914
 unified theory of elementary-particle forces 0-105827

colour model continued

universal Regge slope α' from the QCD gluon propagator 0-78026
 unpolarised lepton-lepton collisions, photon 3rd struct. function, QCD implications 0-73708
 vacuum, QCD, colour mag. permeability 0-78023
 vacuum behaviour in QCD 0-62923
 valence quark clusters in nucleon structure functions from neutrino scatt. 0-95252
 vector meson leptonic width, duality between vector mesons and perturbative QCD 0-57589
 Yang-Mills theory, covariant canonical formalism, quark confinement, absence of localised coloured/charged physical states 0-57573
 $\psi\bar{\psi}$ ($\psi\bar{\psi}$), exotic mesons, masses, decay widths, mixing matrix elements 0-62943
 D-meson decay, hadronic, six-quark model, quark-mass dependence, final state interactions, mixing angle effects 0-62973
 e^+e^- 0-63010
 $e^+e^- \rightarrow$ jets, on-shell QCD quark form factor from two particle correlations 0-86740
 $e^+e^- \rightarrow$ 3 jets, three gluon coupling in perturbative QCD 0-105913
 $e^+e^- \rightarrow$ 4 jets, differential 4-jet acoplanarity distrib., QCD predictions, heavy quark prod. 0-78083
 e^+e^- annihilation, charge current asymmetry as QCD test, neutral gluons 0-57616
 e^+e^- annihilation, gluon jets, multiplicity and ang. distrib. asymmetries 0-91105
 e^+e^- annihilation, hadron multiplicity distribution, Regge like parton model (Russian) 0-78100
 e^+e^- annihilation, jets, colour-singlet subsystems, large rapidity gaps 0-68469
 e^+e^- annihilation, opposite side quantum number correlations 0-105863
 e^+e^- annihilation, QCD and semilocal duality (hadrons/ $\mu^+\mu^-$) cross section ratio 0-78085
 e^+e^- annihilation, QCD and jet acollinearity, quark-gluon coupling 0-105914
 e^+e^- annihilation, quark fragmentation in field-theoretic model of composite hadrons 0-82986
 e^+e^- annihilation cross section, fourth-order QCD contribs. 0-82987
 $e^+e^- \rightarrow e^+e^- + 2$ jets, $\gamma\gamma \rightarrow q\bar{q}$ contrib. to cross section, QCD corrections 0-78106
 $e^+e^- \rightarrow e^+e^- q\bar{q}(q\bar{q}) +$ jet, $\gamma\gamma$ initiated 3 jet events in QCD 0-102057
 e^+e^- final states, $q\bar{q}$ decay, semiclassical model, vacuum polarisation by colour field 0-63011
 $e^+e^- \rightarrow \gamma^* \rightarrow \gamma +$ hadrons, QCD predictions 0-63009
 $e^+e^- \rightarrow \gamma^* \rightarrow$ hadrons, hadron calorimetric meas., QCD predictions, gluon emission 0-91102
 $e^+e^- \rightarrow$ hadrons, 12, 30 GeV, jets, quark fragmentation and coupling constant, QCD comparison 0-105915
 $e^+e^- \rightarrow$ hadrons, higher order QCD corrections 0-95280
 $e^+e^- \rightarrow$ hadrons, jets from heavy quarks, QCD perturbation theory 0-63012
 $e^+e^- \rightarrow$ hadrons, non-perturbative QCD vacuum, total cross section corrections 0-86735
 $e^+e^- \rightarrow$ hadrons, parton model and QCD 0-105860
 $e^+e^- \rightarrow$ hadrons, R problem, QED and QCD corrections, quarks and leptons 0-95281
 $e^+e^- \rightarrow$ hadrons, semiinclusive hadron prod., quark fragmentation function corrections, QCD 0-63013
 $e^+e^- \rightarrow$ hadrons, two and three point energy correlations, QCD struct. 0-102019
 e^+e^- high energy data from PETRA, QCD anal., QCD coupling constants 0-82985
 $e^+e^- \rightarrow$ jets, energy cone distrib. around jet axis, QCD anal. 0-86732
 $e^+e^- \rightarrow$ jets, exclusive calcs. for QCD jets, Monte Carlo approach 0-105911
 $e^+e^- \rightarrow$ jets, jet ang. momentum, ang. distrib., oblateness and invariant mass, QCD calcs. 0-73722
 $e^+e^- \rightarrow$ jets, two-particle distrib. from single-particle fragmentation functions, effects of heavy quark flavours 0-68468
 $e^+e^- \rightarrow q\bar{q}g$, (3g), jet-mass spectra, perturbative QCD 0-63006
 $e^+e^- \rightarrow q\bar{q}g$, gluon fragmentation, polarised 0-82988
 $e^+e^- \rightarrow q\bar{q}g$, long. polarised beams, beam-event asymmetry, massless QCD null result 0-91104
 $e^+e^- \rightarrow$ quark jet, dimensionally regularised box graphs, zero mass case 0-102005
 $e^+e^- \rightarrow$ quark jet, two particle correlations in QCD 0-105858
 eN , deep inelastic scattering and asymptotic freedom, Q^2 dependence of moments 0-82978
 eN deep inelastic scatt., QCD anal. 0-95276
 ep , deep inelastic scatt., higher order asymptotic freedom corrections 0-105903
 $eq \rightarrow eqg$, gluon fragmentation, polarised 0-82988
 $\gamma +$ hadron \rightarrow lepton pair, perturbative QCD, twist-2 photon operator, parton subprocesses 0-73716
 $\gamma^* \rightarrow 2$ jets in e^+e^- , parton model QCD corrections for doubly deep processes 0-73758
 $\gamma N \rightarrow$ jet + X, QCD cross sections 0-73715
 $\gamma N \rightarrow \pi^+ X$, QCD cross sections 0-73715
 γp , heavy quark particle photoprod., QCD model, vector dominance implications 0-86730
 $\gamma p \rightarrow \pi X$, large p_T , perturbative QCD 0-86723
 $\gamma p \rightarrow q\bar{q}p$, quark-antiquark jet diffractive photoprod. in perturbative QCD 0-73714
 in deep inelastic scattering, quark jet as trigger for gluon jet 0-62996
 K charge radius, coloured quark field theory 0-62945
 $K^0\bar{K}^0$ mixing, strong interaction corrections in six quark model, QCD calcs. 0-82957
 K^+n scatt., QCD, one-gluon-exchange, resonating group method, soft-core approx. 0-63025
 K^+p scatt., QCD, one-gluon-exchange, resonating group method, soft-core approx. 0-63025
 K^+p , 130, 200 GeV, jet prod. cross sections, QCD anal. and scale breaking 0-99111
 $K^+\pi$ scatt., QCD, one-gluon-exchange, resonating group method, soft-core approx. 0-63025
 lh deep inelastic processes, QCD predictions 0-73677
 μN , deep inelastic scattering and asymptotic freedom, Q^2 dependence of moments 0-82978
 μp , deep inelastic scatt., higher order asymptotic freedom corrections 0-105903

colour model continued

μp , hadron prod. ang. distrib. and transverse momentum, QCD test 0-82980
 n , structure function nonsinglet moments from deep inelastic lepton scatt., QCD 0-62980
 N form factors, weak, asymptotic behaviour within QCD dipole and tri-pole formulae 0-62987
 NN_p couplings, parity-violating, QCD and MIT bag model, $1/2^-$ resonance contribs., $SU(6)$, symmetry 0-57540
 νN , deep inelastic scattering and asymptotic freedom, Q^2 dependence of moments 0-82978
 νN , structure functions of deep inelastic scatt., QCD test, high-twist contribs. 0-57579
 νN , two gluon mechanisms, quarkonia, glueballs and Higgs scalars 0-78077
 $\Omega \rightarrow \Delta K$, QCD and valence quark approx. 0-105893
 $\Omega \rightarrow \Xi^* \pi$ ($\Xi^* \pi$), nonleptonic hyperon decays, QCD description, PCAC anal. 0-95269
 p , structure function nonsinglet moments from deep inelastic lepton scatt., QCD 0-62980
 pd , 70 GeV, π^+ , K^+ , p , \bar{p} prod. with 0.5-2.2 GeV/c transverse momenta, yield ratio, QCD (Russian) 0-83012
 pp , 70 GeV, π^+ , K^+ , p , \bar{p} prod. cross sections, QCD-parton model anal. (Russian) 0-63044
 pp , D, B, K prod., QCD model for heavy flavour prod., two gluon annihilation 0-86744
 pp , pp, 130, 200 GeV, jet prod. cross sections, QCD anal. and scale breaking 0-99111
 pp , pol. and unpol. beams, hadronic jets, vector bosons, QCD and weak interference 0-57648
 $pp \rightarrow \gamma X$, perturbative QCD anal. 0-63042
 $pp \rightarrow pp$, large momentum transfer, multiple-scattering model, three-quark proton 0-63031
 $pp \rightarrow \pi X$, intermediate p_\perp distribution through a QCD resummation mechanism 0-83010
 $pp \rightarrow \pi X$, large- p_T reactions in broken color gauge theory 0-95292
 π charge radius, coloured quark field theory 0-62945
 π EM form factor asymptotics in QCD perturbation theory, partonic interpretation (Russian) 0-62984
 π EM form factor factorisation and asymptotic behaviour in QCD 0-91090
 $\pi^0\pi^0$ EM polarisabilities, sum rules, coloured quark field theory 0-57561
 $\pi^- N$, 16, 22 GeV, dimuon prod. parton intrinsic transverse momentum, QCD perturbation 0-63037
 $\pi p \rightarrow \pi X$, high p_T π^0 prod., leading particle contrib., QCD calcs. 0-73746
 $\pi p \rightarrow \pi p$, large momentum transfer, multiple-scattering model, three-quark proton 0-63031
 $\pi^2 p$, 130, 200 GeV, jet prod. cross sections, QCD anal. and scale breaking 0-99111
 $\pi^+\pi^-$ scatt., QCD, one-gluon-exchange, resonating group method, soft-core approx. 0-63025
 $\Psi \rightarrow \eta \gamma$, QCD, width, exclusive OZI violating radiative decay 0-68458
 $(q\bar{q}) \rightarrow (q'\bar{q}') \gamma$, width, exclusive OZI violating radiative decay 0-68458
 $q\bar{q}$ systems, nonperturbative potential model 0-78040
 $\Sigma \rightarrow \Delta K$, QCD and valence quark approx. 0-105893
 $\Sigma^+ \rightarrow p \gamma$, $1/2^-$ resonance poles to parity-violating amplitude, two-quark weak transitions 0-78062
 $T(9.46) \rightarrow$ hadrons, gluon spin and colour, QCD nontrivial test 0-82971
 $\gamma N \rightarrow \mu\mu X$, QCD cross sections 0-73715
 2H nucleus wave function momentum contribution from QCD diagrams (Russian) 0-68562
 $Y \rightarrow 3g$, angular patterns and front-back moments, QCD 0-73702

colour perception see colour vision

colour photography

aerial photography maps, colour maps made from B & W negative 0-109270
 camera and instant film development, interdisciplinary and international approach 0-81342
 colorimetric comparison of colour reproductions 0-95119
 exposure meter errors during colour photographic printing 0-101818
 film archival storage, white light processing technique 0-99637
 image archival storage using Fourier multicolour holograms 0-102674
 image stability and dye fading mechanisms 0-62754
 optical printers, electronically controlled additive lamp house 0-105732
 opto-electronic device for aerial colour photograph interpretation (Russian) 0-61920
 polychromatic processing technique for colour image transparencies 0-86473
 subtractive photographic colour printing, correcting light filter selection 0-62764

colour picture tubes, television see colour television picture tubes

colour television

microscopy, applications 0-98972
 underwater TV, wide angle correcting lens 0-91883

colour television cameras

underwater TV, wide angle correcting lens 0-91883

colour television picture tubes

large-screen colour projection TV system, using electron-beam-scanned semicond. laser quantoscope 0-99783

colour tv see colour television

colour vision

see also eye

acuity with short exposure times 0-81603
 adaption, additive effect, unambiguous evidence 0-89760
 adaption curiosity, expt. obs. 0-89757
 Bezold-Brücke hue shifts, short-flash obs. 0-72170
 Bezold-Brücke phenomenon for purple colours 0-108898
 binocular colour fusion, wavelength difference limit 0-101182
 chromatic aberration meas. with chromotomography 0-81581
 chromatic aberration rel. to accommodation, meas. using dynamic laser speckle pattern 0-81582
 chromatic temporal freq. response in humans 0-108902
 chromotomography and its instrumentation 0-94201
 colour science contributions, collection of papers by D.B. Judd 0-98761
 cone outer segments, light-induced changes in membrane current, tiger salamander and turtle 0-108899
 cone spectral mechanisms, ERG and psychophysical obs. 0-61565

colour vision continued

- cyanine dyes, excited electronic states, CNDO/S CI calc., visual pigment spectra appl. 0-85333
 dichromats, large-field substitution Rayleigh matches 0-101173
 evoked potentials, luminosity and chromatic responses in man, subjective hue estimates 0-97903
 far peripheral retina, spectral sensitivity 0-104586
 field-additive pathway detection of brief-duration, long-wavelength incremental flashes 0-89758
 flashes, incremental, long-duration, long-wavelength, detect. by chromatically coded pathway 0-89759
 focus on retina, best value for various fixation distances, phakic and aphakic eyes 0-108882
 hummingbird, near UV light perception 0-97914
 inductive colour contrast, expt. investigation of model (*Russian*) 0-76739
 infant, search for short-wavelength-sensitive mechs. by chromatic adaption obs. 0-85397
 insect colour vision, effected by one visual pigment and filters 0-94212
 Judd's contributions to colour metrics and eval. of colour differences 0-94945
 large-aperture holographic visual simulator 0-102679
 luminance flicker enhancement by colour-opponent mechanisms, monkey obs. 0-61549
 luminous efficiency in the red-green region of the spectrum 0-61563
 macular pigmentation density and short-wave cone sensitivity variations with eccentricity 0-97912
 metrics, facts and formulae 0-97900
 model simulating luminous-signal processing 0-81604
 movement aftereffect, colour-contingent, interocular transfer obs. 0-61578
 movement detection mechanism spatial characts., abnormal visual pathways 0-89756
 movement detection mechanism spatial characts., chromatic stimuli 0-89755
 neural networks, colour sensitive, reaction to intensity and colour steps (*German*) 0-76737
 night myopia, night presbyopia and colour discrimination 0-81602
 physiological models and line elements 0-97910
 pineal organ, frog, change of threshold after light-adaptation of chromatic response 0-72164
 psychometric measures for specifying colour appearance 0-76747
 pupil responses to foveal exchange of monochromatic lights 0-97911
 quality control and appearance, CIE Standard Observer colour specification 0-61539
 retinal suprathreshold time integrative props. studied using pairs of pulses of different hues 0-81600
 retinex systems' role 0-81598
 saturation enhancement in coloured Hermann grids varying only in chroma 0-72168
 scaling data analysis 0-97901
 senile macular degeneration, colour discrimination rel. to visual acuity 0-108897
 sensitivity, resolution and Rayleigh matches following monocular occlusion for one week 0-104585
 signal transmission by visual pathways, distortions of retinal images 0-85400
 spatial adaptation of short-wavelength pathways in humans 0-97913
 spectral sensitivity in goldfish, photochem. and neural correlates 0-81599
 spectral sensitivity of human eye, colour coordinates number triple (*Russian*) 0-76741
 spectral sensitivity of human eye, deductive derivation of mathematical model (*Russian*) 0-76740
 vector magnitude operation in colour vision models, derivation from signal detect. theory 0-101174
 wavelength-specific brightness contrast as a function of surround luminance 0-61564
 whiteness, visual impression and colorimetric definition 0-81597
 zone fluctuation model, nonlinear processing at receptor level 0-81601

columbium *see niobium***coma** *see aberrations***combination scattering spectra** *see Raman spectra***combustion**

- see also explosions; flames; heat of combustion; reaction kinetics*
 100 MW fluidised bed combustion district heating plant burning high S content residual oils 0-108777
 200 MW atmospheric fluidised-bed combustion steam generator, comparison of three designs 0-108776
 air, plasma, slow burning gasdynamics, due to Nd laser beam (*Russian*) 0-108715
 air suspension homobaric flow in presence of physicochemical transform. 0-87820
 atmospheric fluidised-bed combustion boiler development facility, first year of operation 0-108775
 burning rate in engine cylinder, swirl and turbulence effects 0-89492
 coal, radiological aspects 0-61485
 complex systems, pyrolysis and combustion charact., Fourier transform IR spectroscopy 0-86462
 deflagration waves, heterogeneous, flame model for gas phase, nonlinear differential eqn. 0-81326
 deflagration waves, heterogeneous, flame model for gas phase, partial differential eqn. 0-85177
 detonation wave magnification by pulsation energy 0-59075
 driven acoustic oscillators, plane wave theory anal. 0-102951
 EHD flow, nonstationary, with charge diffusion, nonlinear and linear wave processes 0-59124
 ethylene-O₂-N₂-Ar particle mixture, two-phase detonation and combustion (*French*) 0-61097
 fluidised beds, combustion facility, radiation heat transfer, particle size and flow parameter effects 0-69641
 fluidised-bed steam generating system to supply 100000 lb/h of saturated steam burning high S coal 0-108778
 fuel drop, surface eqn., burning rate vs. Damkohler number 0-81327
 gas turbine chamber flow three-dimens. calc. 0-79405
 industrial gaseous environment characterisation, Brinkley method 0-93817
 internal combustion engine, conc. fluctuation meas. 0-71973
 laminar flames, premixed, non-adiabatic, nonlinear theory 0-93757
 liquefied petroleum gas, burning velocity, gas comp. and air/fuel ratio effects 0-66804
 liquid scintillation wastings, combustion system (*Japanese*) 0-63503

combustion continued

- monopropellant drop, surface eqn., burning rate vs. Damkohler number 0-81327
 multifuel fluidised bed combustion packaged boiler to supply 10000 lb/h saturated steam at 100 psig 0-108779
 photographic recording of combustion processes, thermograms of flames (*Russian*) 0-62779
 process admittance measurement, acoustic impedance tube technique 0-64320
 propane flame, wake stabilized, response to sudden accel. or deceleration of free stream 0-61096
 Raman spectroscopy, remote spontaneous, new trends in recording of signals 0-73485
 reaction zone propagation, combustion wave structure inversion in porous media 0-89494
 simulated MHD combustion chamber working on natural gas and O₂ enriched air, NO formation, investigation 0-106984
 supersonic flow, nonequilibrium physicochemical processes, open-cycle MHD generator 0-103196
 technology, IR applications 0-86431
 wood energy in W. Virginia 0-72006
 CO₂ gasdynamic laser, operating on combustion products, gain coeffs. of complex working media 0-58506
 F₂-compartment bomb calorimeter 0-57300
 H₂+O₂, combustion, kinetic modeling and sensitivity anal. 0-89490

comets

- Bennett (1970 II), CN (0-0) band brightness profile obs. rel. to CN prod. 0-82303
 P/Boethin (1975 I), libration around 1/1 resonance with Jupiter 0-72883
 P/Borrelly (1980i), recovery and approximate positions, (1980 July 9 and 21) 0-94755
 Bowell (1980b), precise positions, elements and ephemeris (1980 March-July) 0-62075
 Bradfield (1979i), spectroscopic and photographic obs. in near IR 0-105205
 Bradfield (1979i), UV spectrum, IUE obs. 0-90371
 P/Brooks 2 (1980f), recovery, positions and perihelion passage correction 0-85899
 catalogue of ancient and naked-eye objects (2314 BC-AD 1970) 0-105181
 Cernis-Petruska (1980k), antitail, precise posns., parabolic elements and ephemeris 0-105206
 Cernis-Petruska (1980k), positions, (1980 August 10 and 17) 0-101556
 Cernis-Petruska (1980k), positions, parabolic orbital elements and ephemeris 0-98614
 Cernis-Petruska (1980k), total visual mag. and coma dia. (1980 Aug.-Sept.) 0-101561
 P/Chernykh (1977i), definitive orbit at first apparition (1977 to 1978) 0-62079
 Chernykh-Petruska, discovery posn. (1980 July) 0-94756
 close encounters with Jupiter, mass distrib. throughout Solar System implications 0-77329
 comae, effect of solar photodissociative ionisation 0-90370
 Cretaceous species extinction explained by cometary impact 0-76977
 discovery probability, vel. to reality of concentration of perihelia 0-67660
 dust and cold-cloud aggregates theory 0-105210
 dynamics, exact solns. of diffusion eqn. 0-82304
 dynamics and evolution, review 0-82260
 P/Encke, changes in orbital period due to rotation of nucleus 0-62078
 P/Encke, ephemeris (1980 Oct.-Dec.) 0-105209
 P/Encke, precise posn. for 1980 Oct. 8 and perihelion passage correction 0-109398
 P/Encke, semiaaccurate posn. and appearance (1980 August 8) 0-94758
 equations of motion, recurrent power series integration 0-72882
 evolution to asteroids, Monte Carlo orbit evolution simulations 0-82261
 P/Halley, joint NASA-ESA mission 0-82168
 P/Halley, orbit parameters and ephemeris, 1759-2024 period 0-62076
 P/Halley, space mission (*Polish*) 0-67516
 P/Harrington (1980m), recovery and precise positions (1980 September 4 to 9) 0-101558
 historical comets, Latin terminology 0-62437
 P/Honda-Mrkos-Pajusakova (1980c), independent recovery 0-67658
 P/Honda-Mrkos-Pajusakova (1980c), recovery and positions (1980 May 1 and 6) 0-67656
 International Comet Mission, proposed fast flyby of P/Halley P/Tempel 2 rendezvous 0-82166
 interstellar medium interaction, effects of solar system encounters with dense interstellar clouds (*German*) 0-109500
 isophotometric atlas, pt. II 0-109377
 Kohler (1977m), precise positions, (1977 October 5 to 19) 0-105203
 Kohoutek (1972 XII), Swan Cloud, 1974 January 11, rel. to cometary plasma tails general morphology 0-98612
 Kohoutek (1973 XII), CN violet (0,0) spectra 0-82308
 Kohoutek (1973 XII), ion tail dynamical response to solar wind interaction 0-85899
 P/Kohoutek (1980j), recovery and approximate positions (1980 August 6 and 7) 0-94757
 long-period comets, distrib. of inclination of perihelion dynamical implications 0-101563
 loss of long-period objects, planetary collisions 0-77358
 magnitude distrib. 0-72886
 Meier (1978 XXI), position from 1979 April 21 to 30, meas. and reduction (*French*) 0-72884
 Meier (1978f), precise positions meas. at ESO, La Silla, in (April 1979) 0-105204
 neutral cometary atmospheres, average random walk model for mol. phot. dissociation 0-77351
 neutral cometary atmospheres, CN production 0-82303
 nuclei, dust layer models 0-77350
 P/Olbers, orbit parameters and ephemeris, 1759-2024 period 0-62076
 orbital elements distrib., effect of galactic forces (*Russian*) 0-77353
 orbital evolution of short-period objects, Monte Carlo simulations 0-62073
 orbital inclinations distrib. of original comets, anomalies rel. to origin of comets 0-98615
 orbits, evolution under perturbing influence of giant planets and nearby stars 0-98613
 orbits, of ancient and medieval comets 0-62077
 orbits, reciprocal semimajor axes accuracy 0-62074
 orbits of nearly parabolic comets, distrib. of nodes and perihelia 0-67661

- comets continued**
 origin, celestial mechanical aspects of planetary ejection hypothesis 0-62080
 Palomar Sky Survey comet, discovery and semi-accurate position 0-77352
 periodic comets, major semi-axis less than 30 AU, catalogue 0-72791
 plasma, acceleration in solar wind, rel. to ion-acoustic turbulence (*Russian*) 0-106923
 precise posns. on Minor Planet Circular 5333-5390 for eight objects 0-77325
 precise posns. on Minor Planet Circulars 5189-5248 for 13 objects 0-67631
 precise posns. on Minor Planet Circulars 5249-5286 for six objects 0-67632
 precise posns. on Minor Planet Circulars 5287-5332 for eight objects 0-67633
 precise posns. on Minor Planet Circulars 5391-5422 for eight objects 0-85884
 precise posns. on Minor Planet Circulars 5423-5454 for seven objects 0-98599
 primordial comets, interiors radiogenic melting 0-67659
 P/Reinmuth 2 (1980n), recovery posns. and appearance (1980 Sept.) 0-101560
 Russell (1980l), discovery posns. and ephemeris (1980 September) 0-101557
 Russell (1980l), ephemeris (1980 Sept.-Dec.) 0-105207
 Russell (1980l), precise positions, parabolic orbital elements and ephemeris 0-101559
 P/Schwassmann-Wachmann 1, CO⁺ obs. near minimum brightness 0-82305
 P/Schwassmann-Wachmann 1, rotation and outbursts 0-67655
 P/Schwassmann-Wachmann 1 (1974 II), outburst and CO⁺ detect. spectrophotometric obs. 0-72881
 short-period comets origin, comet belt beyond Neptune model 0-94759
 P/Stephan-Oterma (1980g), recovery positions, elements and ephemeris 0-82307
 P/Stephan-Oterma (1980g), total visual magnitudes and coma diameters, (1980 September 7 to 11) 0-109397
 tails, H₂O⁺ surface brightness rel. to CO⁺ 0-72880
 P/Tempel 2, joint NASA-ESA mission 0-82168
 Torres, discovery and positions, 1980 June 13 and 14 0-82306
 Torres (1980e), 1980 June 17 semi-accurate posn. 0-85898
 Torres (1980e), precise posns., elements and ephemeris (1980 June-July) 0-85900
 P/Tuttle (1980h), ephemeris (1980 Oct.-1981 Feb.) 0-105208
 P/Tuttle (1980h), recovery and precise position (1980 July 14) 0-85901
 volatile gases rel. to solar nebula NH₃ synthesis, kinetic model 0-62041
 West (1976 VI), CN (0-0) band brightness profile obs. rel. to CN prod. 0-82303
 West (1976 VI), coma mols. and dust distrib., visible emission profiles 0-101562
 West (1976 VI), ionosphere CO⁺ brightness profile 0-85896
 P/Wild 3 (1980d), discovery posns., orbital elements and ephemeris (1980 April-June) 0-67657
 P/Wild 3 (1980d), precise positions, improved orbital elements and ephemeris 0-72885
 C II line excitation by C I photoionisation 0-58223
¹³C¹⁶O⁺ (2,0) band, comet-tail system, rot. anal. 0-74157
- communication channels**
 supervisory/service channel for fibre optic transmission systems 0-95803
- communication theory** *see information theory*
- communications applications of computing** *see communications computing*
- communications applications of control**
see also telephony
 light beams propagation, thermal self-action and compensation methods 0-106579
- communications computing**
 acoustic radar systems, microcomputer appl. 0-106685
 acoustic transmission system, impulse response meas. with digital computer processing (*German*) 0-91999
 nuclear reactor accident management, automated notification of reactor data to off-site personnel 0-95388
 speaker verification device, microprocessor based 0-102936
 speech coding, parametric coding of speech spectra, computer studies 0-96137
- computators**
 electric machines, volts-per-bar and flashover, causal mechanisms and preventive measures 0-92408
 explosive-magnetic generators, energy take-off to inductive load using circuit breaking 0-59323
- compacting** *see densification*
- comparators (circuits)**
 timer, touch controlled, photography appls. (*Spanish*) 0-86478
- compasses**
see also navigation
 No entries
- compensation**
see also error compensation
 anemometers using thermally compensated thermistors, math. models (*French*) 0-90227
 chromatic-aberration-free microscope optics 0-86395
 IC temperature sensors used in thermocouple cold junction compensation circuits 0-77777
 load cell design and development for materials testing 0-105628
 noise in Fourier spectrometer, improved InSb photodiode preamplifier circuit 0-73474
 optical systems, high-precision compensated levels, geodetic appl. 0-101813
 optotransducers, electronic compensation for dirty lenses 0-68189
 pressure transducer, miniature implantable, biomedical appl. IC fabrication techniques 0-76849
 resistance thermometer thermal inertia (*Russian*) 0-62667
 step-stare spaceborne optical system image motion compensation 0-90322
 step-stare spaceborne optical system smear compensation by focal plane manipulation 0-82172
 temperature, pure water electrical conductivity meas. (*Czech*) 0-62684
 temperature compensation techniques for SAW devices 0-74614
 temperature compensation with metallic overlay films on quartz 0-79043
- compensation, charge** *see charge compensation*
- compilers (program)** *see program compilers*
- compiling programs** *see program compilers*
- complementarity**
 No entries
- complete computer programs**
see also subroutines
 atmospheric sound absorpt., personal computer program 0-96065
 dosimetry calculations due to radionuclides in aquatic food chains, NEP-TUN interactive code in FORTRAN 0-109039
 Easter date determ. for any year, program for HP 29C 0-77268
 equation of state variables calculation using TI-59 0-77738
 FORTRAN, for analysis of variance and means 0-98792
 geomagnetic anomaly of thin dike, curve fit by calculator program 0-98228
 landform erosion simulation program in FORTRAN 0-85650
 linear prediction in least-squares scheme for max. entropy spectra, Fortran subroutines 0-98465
 mathematics teaching by computer, long-division practice program in BASIC 0-98775
 nuclear power stations, accumulation ponds cooling possibility analysis (*Slovenian*) 0-91208
 physics teaching using SWTP 6800 system in BASIC 0-98776
 radioactivity, decay product radioactive accumulation, FORTRAN program 0-68611
 seismic refr. survey depth determination, program for pocket calculator 0-82088
 selenide thermoelectrics, analytical model for performance and degradation predictions 0-108805
 self consistent FORTRAN subroutines for Earth motion determ. 0-85845
 single crystals, growth simulation in FORTRAN 0-88069
 speed and displacement relations for tire skids for PET in BASIC 0-57038
 traverse point location in stack sampling, for HP calculator program 0-94139
- complex angular momentum plane**
see also angular momentum theory; Pomeranchuk poles and trajectories; Regge poles and trajectories
 operator addition 0-86622
 scattering amplitude, quasipotential, analytic props. in complex planes of rapidity and angular momentum 0-68399
- compliance constants** *see elastic constants*
- composite insulating materials**
 epoxy resin insulation, adapted models selection problems for electric ageing (*German*) 0-89365
 fatigue behaviour, influence of superposition of elec., mech. and environmental stresses 0-97590
 fatigue damage monitoring of processes damaging elec. insulating materials 0-97673
- composite materials**
see also cermets; composite insulating materials; composite superconductors; concrete; eutectic alloys; fibre reinforced composites; fibres; filled polymers; laminates
 adhesion between two crystals, theory 0-104417
 advanced, design, applications and test methods 0-77550
 bitumen-silica composites, dynamical mechanical props. 0-58996
 bone tissue, compact, destruction 0-67135
 ceramic filled with polymer, ZrO₂ stabilised, fracture mechanism (*Russian*) 0-100895
 ceramic-glass-glass composites, crack growth, elec.-mech. analogue 0-85022
 complex dielectric const., bounds 0-108170
 complex dielectric constant, exactly solvable microscopic geometries and rigorous bounds, for two-component dielec. material 0-75918
 composite glasses, high strength, prod. by overlayering 0-89193
 constrained viscoelastic damping composites, noise and vibration insulation 0-83743
 crack emanating from circular hole, mixed-mode crack anal. using conservation laws of elasticity 0-84239
 crack extension micromechanism 0-108566
 crack growth, conc. criterion 0-65146
 cylinder, circular, transversely isotropic, concentrated loads, 3-D anisotropic elasticity theory 0-83734
 cylindrical rod, periodic structure, torsional vibrations, interfacial elastic parameters 0-96215
 damage studying by NDT 0-66735
 diaphragm for loudspeaker, B-Ti, preparation by physical vapour deposition (*Japanese*) 0-58883
 epoxy-rubber particulate composite, toughness and fracture mech. 0-71727
 epoxy/graphite composite and cured epoxy resin, thermal expansion and swelling 0-92450
 failure criteria, for complex loading 0-81206
 fibrous composites, stationary transfer, effective heat conduction coeffs. 0-64337
 flow through porous medium, Rayleigh-Taylor instability 0-69912
 flywheels, filament wound composite materials, characterisation 0-81097
 friction and bearing materials, development, friction and wear theory, review 0-60979
 glass-sintered metal, fracture energy, direct meas. (*French*) 0-104376
 graphite dispersed Al-Si, wear characts. (*Korean*) 0-93658
 IR segmented composite window design 0-106621
 layered composites, heat conduction eigenvalue problems 0-74702
 matrix impurity distrib. in melt crystallisation (*Russian*) 0-100277
 mechanical behaviour, book 0-94935
 mechanical properties, theory, review 0-64392
 metal wire reinforcing rolled glass 0-104107
 metallic, thermal fatigue, effects of inclusions 0-81183
 molten metal binary mixtures with wide immiscibility range, gravitational layering of components (*Russian*) 0-104092
 mortar specimens, repeated impact bending load study (*Japanese*) 0-93622
 orthotropic composite model materials, photoelastic calibration 0-87715
 overall elastic moduli prediction 0-75285
 phosphate containing materials, technological prod. processes, review 0-79452
 plasticity, field theory, integral presentations of second-rank tensors 0-69690

composite materials continued

- plate like inclusions, plastic props., sintered Al-Al₂O₃ results (*Russian*) 0-58923
 Plexiglas 0-66592
 plexiglass composite, long term strength and durability 0-75294
 Poisson coefficients, allowable values 0-64370
 polyester polymer concrete, longitudinal deform. modulus study is creep conditions (*Bulgarian*) 0-71685
 polyester resin concrete, effects of styrene-unsaturated polyester ratio on props. (*Japanese*) 0-89299
 polymer latex film composite, glass transition temp. determ. using thermomech. curves 0-75342
 polymer-containing metal-filled lubricant, tribological study on steel 0-104301
 polymeric, thin-wall tubes, rupture time determ. 0-64473
 PVC-Cu composites with chemically deposited ultrafine copper particles 0-93534
 quartz dental composites, acrylic acid grafted on particles by gamma-radiation 0-66840
 random elastic sphere distrib. in elastic matrix, effective bulk and shear moduli 0-99927
 random particulate composite, US wave propagation, velocity as function of frequency and volume fraction of inclusions 0-59583
 reinforced plastic cylindrical shells, optimal design under dynamic constraints 0-102996
 reinforced plastics, load-bearing capacity, effect of one-sided heating 0-81135
 rib stiffened constructions, design criteria 0-102977
 ribbed multilayer cylindrical shells, stability and optimal design 0-58949
 sandwich composite beams, stress distrib. meas. under four-point bonding, multilayer builtup theory 0-96190
 shell, thick walled, composite radial bonding efficiency 0-99926
 shells, cylindricals, composite, buckling and vibrational response to axial compression 0-64423
 shock compression at 30 kbar, expansion adiabats 0-66592
 slab, spatially reinforced, optimisation in stability problem 0-102978
 small-particle metal-insulator composites, anomalous far IR absorption 0-71427
 spacecraft polymer composite matrix materials, space radiation effects evaluation 0-70263
 spatially reinforced, viscoelastic props. determ. using averaging methods 0-102973
 stability of multilayer composites under inelastic deformations 0-99944
 stability of viscoelastic rods and shells under loads that decrease with time 0-69700
 steel, martensitic, welded composite vessels, glass fibre reinforced plastic wound, struct. strength 0-97552
 steel (alloy)-TiC (70, 30 wt.%) composite, sintered, wear resist. 0-100815
 steel-based, corrosion behaviour of composite materials in N₂O₄ oxidising atmospheres (*Russian*) 0-76421
 stochastic fracture models, and strength test results statistical anal. 0-64470
 stretching, stress distrib. 0-58931
 thermal conduction processes, nonstationary, numerical simulation (*Russian*) 0-92016
 three-layer cylindrical shells, initial stressed and deformed state 0-102974
 unidirectional, three-dimens. fracture 0-64471
 urea-formaldehyde resin/wood materials, book 0-73114
 US inspection system for aircraft materials 0-81274
 viscoelastic layered composites, wave propag., dispersion and dissipation effects 0-102982
 wear of water-lubricated composite materials 0-60984
 wedge, plane composite, singular eigenfunctions for plane harmonic problems 0-79206
 Ag particles embedded in dielec. KCl medium, search for maximum metallic resist. 0-107756
 Al-Cu-Mg/mica particulate composite mech. props. 0-100919
 Al-SiC cermet elasticity, porosity meas. by US means 0-81101
 Al-Si(9.3, 12) with graphite particles seizure resistance study using Hohman wear tester 0-89360
 AlN thread-like crystals reinforced mullite-corundum ceramics, props. 0-108525
 α-Al₂O₃ thread-like crystals reinforced mullite-corundum ceramics, props. 0-108525
 Al₂O₃-NiCr composite, plasma sputtering of electroheating coatings, elec props. (*Russian*) 0-108350
 Al₂O₃-TiC, composite, fracture behaviour in three-point bending 0-60951
 3Al₂O₃-2SiO₂-ZrO₂ composites, sintered, in situ-reacted, fracture props. 0-81158
 Cu/graphite-SbF₅ wire composites, synthesis and elec. props. 0-70781
 Cu-BN composite electromachining tools, dynamic hot pressing 0-84889
 Cu-coated TiO₂ particles, prep. for composites 0-89159
 Cu-Nb multifilamentary composite, dislocation resistivity 0-70671
 Cu-SiO₂, low-temp. recovery creep, Orowan loop accumulation 0-81126
 Fe powder-plastic composite, soft mag. material, mag. and mech. props. 0-75812
 Fe-Al₂O₃ granular films, superparamagnetism and relax. effects 0-71118
 Fe-Mo-CaF₂ sintered composite, struct. and mech. props., heat treatment effect 0-66526
 Fe-TiC pseudofused composite magnetoabrasive powders, props. 0-100926
 H₂ production from coal by centrifugal separation from gasification products, high strength composite materials appl. 0-76643
 NaCl polycryst. containing Al₂O₃ dispersion, diffusive creep 0-97531
 Na₂O-B₂O₃-SiO₂ glass-Ni compact, indented, strength and fracture toughness 0-93636
 Na₂O-CaO glass phlogopite mica powders, composite fabrication, cellular struct. 0-84902
 Na₂O-PbO-SiO₂ glass-ceramic composite, directionally crystallised 0-107058
 Ni-Cr-Al-TaC, eutectic composite, microstructure, fatigue props. 0-85038
 Ni-Ti/Cu composite, plastic deform. influence on internal friction (*Russian*) 0-100871
 Pb(Zr,Ri)O₃-Ni-silicon rubber flexible composite pyroelectric, dielectric props. 0-80704
 Sb₂O₃-nH₂O acid membranes, synthesis and characterisation 0-81027
 SiC thread-like crystals reinforced mullite-corundum ceramics, props. 0-108525
 SiC-Si, wear resist., props. under abrasion and corrosion 0-100927

composite materials continued

- Ti base sintered bearing materials, metallic solid lubricant infiltrated, antifriction props. 0-60981
 TiC-(Mo-Cr-Ni-Mn) steel alloy, optimum comp. and manufacture conditions, Mn effect 0-84896
 TiC-C composites, hot pressed, thermophys. props. at high temps. 0-59675
 W-PVC material, fabrication and performance, acoustic properties 0-76218
 WC-Ni hard alloy composite, sintered, void healing 0-60821
 ZrC-C composite system, negative magnetoresist. 0-60008
 ZrC-C composites, hot pressed, thermophys. props. at high temps. 0-59675
 ZrN-Al₂O₃ composites, strength rel. to solid-, liquid-phase sintering 0-100823
- composite models of hadrons**
see also parton model; quark models
 1/N expansion and the theory of composite particles 0-73604
 dyons, spatial volume integral of Tr F(tilde) F, Yang-Mills theory 0-77943
 extended technicolour scalarless theories 0-78001
 magnetic monopole model, partial wave dispersion relations, strong van der Waals force 0-105849
 magnetically bound monopole pair, possible fermion struct. 0-86661
 nonrelativistic many-body theory, foundations and statistical mechanics 0-82947
 number operators for composite particles in nonrelativistic many-body theory 0-94982
 relativistic composite system, light-front wave functions 0-73592
 SU(5) model, dyons and monopoles 0-82931
 Yang-Mills dyons, mag. charge and Pontryagin index equality in SU(2) 0-57562
 π compositeness from wave function renormalisation constant 0-10197
- composite particles**
see also alpha-particles; deuterons; nuclei with mass number 1 to 5; tritons
 No entries
- composite superconductors**
 flux jumps and training 0-70911
 granular, Ginzburg-Landau theory, props. 0-88673
 inhomogeneous combined superconductor, normal zone equilibrium 0-75675
 inhomogeneous superconductivity, Ginzburg-Landau theory 0-88672
 magnetoresistance and Hall coeff., classical theory 0-84547
 multifilament superconductors, effect of local heat dissipation on stability 0-60156
 multifilamentary, carrying DC transport currents, transient field losses 0-84551
 multifilamentary, mag. props. effect on losses in variable mag. field 0-60136
 multifilamentary, voids growth obs., via hot stage SEM 0-70089
 multifilamentary wire, transverse resistance effect on volt-ampere characts. 0-70897
 propagation velocity expressions 0-60155
 Cu-Nb alloy, prep. for multifilamentary Nb₃Sn supercond. wire 0-84879
 Cu-Nb₃Sn multifilamentary tapes, in situ formed, crit. current density anisotropy 0-84576
 Cu-NbTi, composite conductor, acoustic emission 0-97032
 Cu-V₃Ga, supercond. in situ composites, stress effects on crit. props. 0-65757
 Mo₃PbS₃ embedded in resin, composite supercond., high transition temp. 0-88660
 Nb/In composite superconductor, transport props. 0-88658
 Nb-Ti, multifilamentary, Mirror Fusion Test Facility, superconductor core manufacturing and quality 0-93521
 Nb-Ti, pinning curves, high field J_c and scaling behaviour 0-93064
 Nb-Ti-Ta, pinning curves, high field J_c and scaling behaviour 0-93064
 Nb₃Sn/Cu composites, in situ processed, supercond. props. 0-75698
 NbN embedded in resin, composite supercond., high transition temp. 0-88660
 Nb₃Sn Al₁₅ composite superconductors, hydrostatic extrusion (*French*) 0-104090
 Nb₃Sn, composite superconducting wire, critical current-bend strain relationships 0-93063
 Nb₃Sn, filaments in Cu matrix, thermal strain effects on superconducting critical temp. 0-93032
 Nb₃Sn monofilamentary composite conductors, tensile stress influence on critical current 0-97046
 Nb₃Sn, monofilaments, radiation-enhanced diffusion growth, crit. current density 0-65758
 Nb₃Sn, multifilamentary coils for Lawrence Livermore Laboratory superconducting High Field Test Facility 0-90834
 Nb₃Sn multifilamentary composite supercond. wires, transverse sections prep., ion milling, TEM obs. of grain size 0-101000
 Nb₃Sn multifilamentary supercond. composites, crystallographic texturing 0-71669
 Nb₃Sn, multifilamentary superconductor preparation by 'in situ' and cold powder methods, review 0-93522
 Nb₃Sn, supercond. composite, residual stress state, crit. currents 0-80468
 Nb₃Sn-Cu multifilamentary composite wire, Nb₃Sn filament morphology and grain size 0-100855
 NbTi/In composite superconductor, transport props. 0-88658
 NbTi-Cu, acoustic emission 0-84546
 NbTi-Cu, supercond. composite, use in temp. and heat transfer coeff. meas. 0-77780
 NbTi-In granular supercond. composites, mag. field-induced dissipation 0-84545
 Pb-Cd-Pb junctions, pair pot., mag. field depend., crit. currents meas. 0-84555
 Sn-KCl granular superconductors, far IR absorpt. 0-84548
 V/Cu-Ga, V₃Ga phase form., TEM obs. (*Russian*) 0-84933
 V₃Si embedded in resin, composite supercond., high transition temp. 0-88660
- composition measurement** *see chemical analysis*
- compressibility**
see also compressibility of gases; compressibility of liquids; compressive strength
 alkali hydrides, lattice props. from interaction pot. energy function 0-100199

compressibility continued

- alkali metal alloys, dil., binary, equilib. at. vol. and compressibility 0-70295
 alkali metals, contrib. of John Bardeen 0-57057
 alkali metals, effective ion-ion potential, compressibility and force consts. 0-70158
 alkali metals, phonon dispersion binding energy, compressibility, elastic consts. electron screening and Ashcroft pot. calcs. 0-65174
 Born model, electrostriction rel. to dielec. and thermoelastic props. 0-71322
 diamond, compressibility, appl. of Murnaghan eqn. of state, Morse pot. 0-79861
 dielectric function, degenerate electron gas at metallic densities, nonlocal interactions, compressibility and dispersion 0-107730
 Earth mantle elements compounds and modifications, high press. and temp. thermodynamics 0-81874
 electron-hole liquids, relation between bulk compressibility and surface energy 0-65465
 fatty acid monolayers, light scatt. meas. 0-89011
 fibre reinforced plastic, props., implications for structural design 0-81174
 interfaces separating compressible bulk phases, stability 0-107610
 ionic crystals, migration volumes calc. 0-103324
 itinerant electron ferromagnets, magneto-volume effects 0-60397
 metal polyphosphates, bulk compressibility meas. to 30 kbar 0-76306
 metal-composite rods, compressed, delamination 0-64396
 metals, ground state of solids, spin density functional method, binding energy, compressibility 0-65477
 metals, local pseudopot. approach 0-65129
 natural rubber vulcanisate, network changes during physical testing 0-60936
 nuclear matter, incompressibility rel. to superdense celestial bodies theory 0-67773
 polyacetylene, pristine and doped, press. effects on resist. 0-103698
 polydimethylsiloxane, crosslinked, stress/strain relations from large compression to high elongation 0-66589
 polyethylene terephthalate, solid and molten, press. effects on compressibility and crystn., thermodynamic interpret. 0-84102
 PTFE and filled PTFE, nonlinear creep, compression bulk modulus 0-66595
 Rayleigh-Taylor instability, thermal cond. and compressibility effects 0-79262
 simple metals, compressibility, Harrison pot. calcs. 0-96460
 simple metals, model pseudopot. appl. to various props. 0-59845
 spherical laser target hydrodynamic compression stability (*Russian*) 0-106159
 Al alloy with different props. in tension and compression, creep 0-81129
 Al, metallic, phonon freq., binding energy, compressibility, elastic const. and energy band gap calcs., linear pot. 0-88284
 Al, shock compression at high press. (*Russian*) 0-92608
 CdTe, δ , single and polycryst. samples, linear expansion, heat capacity and thermodynamic props. 0-103489
 Cu-Ni-Fe, magnetic properties, heat treatment and compressive stress effects 0-60367
 CuCl, pressure depend. of structural, chemical, elec. and mag. props. 0-96596
 CuCl₂·2D₂O, cryst. struct., mag. and reson. props. 0-60424
 Fe-Ag (50 wt.%), plastic behaviour in compression, deform. rate effect (*French*) 0-71711
 Fe-Ni Invar, magnetovolume coupling enhancement factor, temp. depend. 0-88851
 GaS, elastic prop. anisotropy, Debye temp. (*Russian*) 0-88244
 Ge, carrier relaxation rate temp. depend. and pair density in large electron-hole drop 0-75509
 H₂, solid, metallic, high density, thermodynamic props. 0-88337
³He, solid, ordering obs. at melting press. in high mag. fields 0-84341
 Ho,Tb_{1-x}Co_x rare earth compounds, elastic props., temp. and magnetic field dependence 0-60393
 KM₂F₃, bond energy, equilib. distances and compressibility calcs. 0-70159
 (Mg,Fe)₂SiO₄, shock deform. expts., Hugoniot data implications 0-94497
 Mn₂Si₃, elastic moduli, phase transitions, ultrasonic velocity 0-92589
 NaF, isothermal compression at 673K, up to 10 GPa, X-ray diff. study 0-59565
 Pb, shock compression at high press. (*Russian*) 0-92608
 SiO₂, shock compression at high press. (*Russian*) 0-92608
 α -Sn, lattice dynamics 0-107389
 SrF₂:La, type-I dipole reorientation, activation vol. determ. from dielec. const. 0-88916
 TiC, deform. at high temps. 0-104239
 TiO₂, rutile phase, shock induced phase transition anisotropic behaviour 0-103475
 TiCl, ground-state props., Wannier functions, and electronic struct., ab initio self-consistent calc. 0-80178
 W (110) mobility and two-dimensions. compressibility of adsorbed Xe, field emission current fluctuation method 0-80089
 Zn-Cd alloys, liq. and solid, ultrasound speed and compressibility meas. 0-102941
 ZnS, cubic, compression 0-107358

compressibility of gases

- see also high pressure phenomena and effects*
 large-volume gas mixture preparation, compressibility ratio 0-59165
 Ar, compressed gas, PVT meas. at high press. 0-98927

compressibility of liquids

- acrylamide aqueous solution, ultrasonic investigation (*Chinese*) 0-107371
 binary mixtures near critical state, gravitational distrib. of thermodynamic props. (*Russian*) 0-88241
 t-butyl alcohol, aq. soln. 0-88237
 o-chlorophenol-acetone (ethyl methyl ketone), thermodynamic and transport props. 0-92686
 hard sphere, surface tension, compressibility, bulk modulus press. coeffs. and Rao's acoustical parameter 0-80027
 metals, isothermal compressibility and eqn. of state at m.p. 0-79673
 micellar solutions, crit. behaviour 0-105601
 organic ternary liq. mixtures, intermolecular interaction study, US vel. meas. 0-79879
 polyacrylamide aqueous solution, ultrasonic investigation (*Chinese*) 0-107371
 polyethylene terephthalate, solid and molten, press. effects on compressibility and crystn., thermodynamic interpret. 0-84102
 quantum liquid mixture, stability and stratification 0-59754

compressibility of liquids continued

- solutions in alcohols, ultrasonic vel. and density meas. used to calc. compressibility, intermol. free length and salivation no. 0-96150
 thermally induced surface fluctuations on simple fluids 0-88403
 water, determ. of adiabatic compressibility on basis of Schaaffs' molecular kinetic theory, 25 to 80°C 0-88265
 water, physical props., two-state model approach 0-75144
 water, relax. compressibility and heat capacity 0-92580
 water, shock compression at press. approaching 1 Mbar (*Russian*) 0-79851
 Ar, hole theory, compressional viscosity and vibrational relaxation 0-70311
 F, hard sphere model with attractive interactions 0-96434
 H₂O, shock compression at high press. (*Russian*) 0-92608
 Pb, thermodynamic characterisation, by isobaric expansion meas. 0-103494
 Te-Se liquid mixtures, sound vel. meas., adiabatic compressibility determ. 0-65161
 Zn-Cd alloys, liq. and solid, ultrasound speed and compressibility meas. 0-102941
 ZnCl₂-LiCl(NaCl)(KCl)(CsCl), molten, US velocity, thermodynamic quantities and struct. (*Japanese*) 0-88270

compressible flow

- see also compressibility*
 air, damp, working characteristics of vortex tubes (*Russian*) 0-74903
 approximate solution in gasdynamics 0-92174
 boundary layer flow, unsteady, compressible, 3-D, near axisymmetric stagnation point 0-103011
 boundary layers, laminar, compressible, Prandtl=0.72, sharp pressure rise effect 0-83782
 conservation equations, characteristic method of lines soln. 0-59064
 dispersive compressible fluid, steady two-dimens. jet flow 0-64598
 dispersive compressible fluid, transonic nozzle flows 0-69895
 ducts, 3-dimens. viscous compressible flow, inviscid flow considerations for 90° elbow 0-64639
 ducts, steady 2-dimens. axisymmetrical turbulent boundary layer, compressible fluid (*Chinese*) 0-59109
 gas, dissociating, relativistic flows, growth and decay of weak waves, shock wave formation 0-69949
 gas, perfect, vortex sheet, separation from smooth body at large Reynolds number (*French*) 0-74908
 gas compression in heavy piston, hypersonic speed, shock waves 0-69869
 gas flow past surface, interaction of radiation with convection (*Russian*) 0-99994
 gas flow through cracks, surface roughness influence 0-69929
 gas flow through exhaust valve, analytical calc. using flux analysis method (*Japanese*) 0-69896
 gas-particle flow in shock tube, finite difference calc. (*Japanese*) 0-79390
 gases with molecular viscosity, flow calc. in large particles method (*Russian*) 0-74826
 ideal gas, polytropic soln. to problem of spherically symmetric flow 0-106810
 inviscid, rotating, compressible fluid, linear stability 0-92161
 inviscid linearly-sheared parallel flow, characterisation of acoustic disturbances 0-69848
 meridional flow of compressible fluid in a rapidly rotating short cylinder 0-106812
 Navier-Stokes equation, limiting form at high Reynolds number (*French*) 0-74823
 nonthermally conducting gas, monotonic difference scheme of open calculation (*Russian*) 0-103039
 nonuniform grids in finite difference approximations, application to fluid flow problems 0-105507
 numerical integration of the gasdynamic equations 0-92175
 orifice flow, computer-aided numerical anal. 0-87806
 plane periodic waves, nonlinear propagation in relaxing gas, numerical anal. 0-92170
 plane steady flow, variational anal. 0-92173
 polytropic medium layer on linear elastic substrate, mass-impact generated shock waves 0-69870
 porous medium, laminar isothermal flow of two immiscible compressible fluid phases 0-69919
 radiating gases, sonic wave propag., wave front curvature effects, shocks 0-87784
 radiative gas dynamics, radiation transfer eqn. (*Russian*) 0-64653
 rectangular elbow, 3-dimens. turbulent compressible duct flow, stagnation pressure losses, vortices 0-64640
 relativistic gas dynamics in two dimensions. 0-83863
 Reynolds equation at very low spacing, compressible, numerical soln., factored implicit scheme, mag. recording appl. 0-92183
 rotating gas, perfectly conducting compressible in mag field under gravity, wave dispersion relations (*Chinese*) 0-77276
 semibounded compressible stream, optimal suction at heat-cond. porous surface (*Russian*) 0-79346
 shell, cylindrical, impact on surface of compressible fluid, numerical method (*Russian*) 0-87746
 shell, spherical, impact on surface of compressible fluid, numerical method (*Russian*) 0-87747
 shock wave interaction with turbulent boundary layer disturbed by injection 0-74916
 solid particle suspension in compressible fluid, wave propag. 0-69858
 sound wave transmission through nonuniform circular ducts 0-74900
 steady homenergetic compressible flow with finite shocks, variational principle 0-69874
 subsonic plane pot. flows, least squares finite element anal. (*Chinese*) 0-59063
 thermal pipes, sonic restriction on power at high temp. 0-103023
 transonic flow, shock wave interaction with turbulent boundary layer, pressure distrib. 0-74918
 transonic flow, shock wave interaction with turbulent boundary layer, wall shear stress 0-74919
 transonic flow, unsteady, turbulence modelling, compression waves developing into shock wave 0-74909
 transonic flow problems, modified FLIC method, finite element anal. 0-74911
 variable density turbulent subsonic flow, pressure pulsation and vel. divergence correlations 0-100008
 velocity measurements inside a rotating cylindrical cavity with a radial outflow of fluid 0-96275

compressible flow continued

- viscous compressible flow, hybrid integration scheme, shock tube problem 0-69868
- viscous compressible fluid motion in unbounded domain, weight function approach 0-79345
- viscous drop, almost spherical, in arbitrary flow of compressible fluid, Faxen's theorem 0-87786
- viscous fluid, eqns. of motion, initial value problem 0-62477
- wave linear propagation in rotating fluid, critical level absorption and valve effects 0-106805
- weak nonlinear waves in compressible fluid, higher order approx. 0-92165

compression, bandwidth *see bandwidth compression***compressive strength**

- see also compressibility*
- centering device for specimens in compression tests 0-61033
- ceramics, mech. props. meas., apparatus for up to 1700°C (French) 0-104374
- ceramics, mech. test apparatus for up to 2200°C (French) 0-104372
- chamotte concretes, phosphate binder based, strength props. 0-89305
- concrete, elasticity modulus and strength, aggregate conc. effect 0-66591
- concrete, flowing, expt. studies (Japanese) 0-89298
- concrete, high strength, made with a special cement admixture, mech. props. (Japanese) 0-89297
- concrete, relayed addition of admixture and flowing concrete, props. (Japanese) 0-89461
- concrete, strain rate effect on strength and deform. during hardening process (Japanese) 0-93616
- concrete, strength, shrinkage strain and deterioration down to -160°C (Japanese) 0-100886
- creep in circular specimen subject to pure bend, ultimate tensile and compressive strength (Russian) 0-74768
- fibrous structure, low-density, centrifugal method for mech. prop. obs. 0-71823
- glass fibre reinforced plastics, cylindrical shells, compressive and flexural strength (Japanese) 0-81115
- glass rod, optimum sample shape for compression testing, failure 0-71756
- glass shell, built-up, local strengthening influence on supporting capacity 0-71714
- glass shell, cylindrical, bearing capacity under axial compression 0-76323
- graphite, pyrolytic commercial, high-temp. thermal and mech. props. 0-75372
- graphite fibre filled polyimide composite laminates, space environment, phys. and mech. response 0-81140
- HTGR graphites, irradiation effect on thermal shock resist. and mech. props. (Japanese) 0-66622
- laminates, damage zone failure analysis 0-85059
- LI, ordered alloys, positive temp. depend. of strength, phase destabilization 0-81203
- magnesian refractory concretes, cast. props. 0-89306
- magnesite artifacts, roasted, props., filler porosity effect 0-104099
- metallurgical coke, mech. behaviour charact. (French) 0-104371
- organoplastics, fracture characts., effect on strength 0-66642
- Plexiglas 0-66592
- polyester resin concrete, effects of styrene-unsaturated polyester ratio on props. (Japanese) 0-89299
- polyethylene-glass fibre composites, gamma-irradiated filler 0-66840
- polymer concretes, hydrothermally stable, hydraulic cement-type fillers 0-85144
- porcelain, electrotechnical, compressive strength 0-100882
- portland cement, doped with ZnO, struct. and props. 0-60914
- PVC, fatigue life, influence of cyclic loading conditions 0-76350
- quartz dental composites, acrylic acid grafted on particles by gamma-radiation 0-66840
- rock half-space, impact of steel cylinder and effects 0-85649
- spheroplastic, spherical shells, supporting capacity 0-87723
- steel, fatigue life, influence of cyclic loading conditions 0-76350
- Textolite 0-66592
- Al alloy with different props. in tension and compression, creep 0-81129
- Al alloy-mica particle composite, cast prep. and mech. props., bearing appl. 0-71613
- Al, fatigue life, influence of cyclic loading conditions 0-76350
- Al-Cu-Mg/mica particulate composite mech. props. 0-100919
- AlN, polycrystalline, stress-strain data up to 1.25 GPa 0-100899
- AlN-Mo cermets, ZnO₂ and mullite whisker reinforced, strength var. with temp. 0-104232
- α-Al₂O₃ fibre FP reinforced Al and Mg composites, fabrication and props. 0-81004
- Al₂O₃, polycrystalline, stress-strain data up to 1.25 GPa 0-100899
- Al₂O₃-Mo cermets, ZnO₂ and mullite whisker reinforced, strength var. with temp. 0-104232
- BeO, polycrystalline, stress-strain data up to 1.25 GPa 0-100899
- C fabric reinforced plastic laminates, tensile and compressive strength determ., 20-1500°C 0-100880
- C fibre reinforced plastics, strength props., effect of SiC coating on fibre 0-104224
- Ca₃(PO₄)₂OH bioceramic, material props. 0-93523
- Cd-Ge broken lamellar eutectic composite, tensile and compressive props. 0-71694
- Cr-Ni compressor disk, surface plastic deform., optimal method 0-60924
- Cu powder compacts, yield curve comparison, different loading paths (Japanese) 0-93621
- Li₂O.2SiO₂, ceramic, prep. of oriented microstructure by unidirectional solidification of melts 0-71614
- Mo-TiC lamellar eutectic composite, deformation and strength, room temp. to 2073K (Japanese) 0-71702
- Na₂O-CaO glass phlogopite mica powders, composite fabrication, cellular struct. 0-84902
- Nb₃Sn, hot isostatically pressed, plastic deform. 0-108510
- Ni alloy, heat resistant, fatigue limit comparison in torsion and tension-compression 0-81181
- Ni single crystal, compressed, strengthening and dislocation cells (German) 0-66536
- 239PuO₂, stoichiometric, high-temp. deformation 0-81111
- (Ti,Cr)B₂, sintering kinetics and props. 0-100811
- Ti-Al-Mo-Zr, compressor disk, surface plastic deform., optimal method 0-60924
- TiO₂-Al₂O₃-SiO₂ system, ternary glass-forming region and phys. props. 0-84919
- ZrV₂, anomalous softening at martensitic transform. 0-93630

compressors

- air compressor, reciprocating, capacity control system 0-90859
- axial flow, stator blade wake guidevane mean velocity and decay characts. anal. 0-95085
- boundary layer charact., influence of external flow turbulence 0-87811
- cryogenics of Sulzer, Switzerland 0-82769
- supercritical, transonic flow computation 0-96276
- three-dimension transonic flow prediction, characteristic method appl. 0-96277

Compton effect

- alkali metal halide molecules, zero point Compton profile anisotropies and bond polarities, correl. 0-78659
- astrophysical sources, Compton emission models, constraints from gamma-ray data 0-67902
- astrophysics, relativistic electron spectra inference from meas. of inverse Compton radiation 0-90339
- band structure, optical cond., Compton profile, self consistent calcs. 0-65435
- bone density determination, effective attenuation coeff. of soft tissue 0-101220
- cosmic microwave background, inverse Compton scatt. by ionised gas in clusters of galaxies, microwave search 0-82477
- critical angles in total reflection of, Compton, X-ray and fluoresc. scatt. 0-59343
- electron gas-radiation field interactions, instability development, interstellar case 0-77274
- flare stars, fast electrons inverse Compton effect rel. to flare emission spectrum 0-67731
- galactic cosmic rays, contrib. to diffuse X-ray flux in 2 to 7 keV range 0-98745
- hadronic targets, spin-1/2, Compton scatt., optimal sum-rule inequalities 0-105815
- Hercules X-1, Compton scatt. rel. to X-ray continuum and Fe line emission during X-ray low state 0-105393
- hydrocarbons, liq., Compton profiles, bond additivity 0-93423
- inverse Compton reflection, steady-state theory 0-67533
- lung density, Compton scatt. meas., multiple photon interactions 0-67146
- M87 halo, 3K background photons Compton scatt. contrib. to X-ray emission from Faraday rot. 0-67844
- multiple scattering effects in Compton profile meas., correction using semi-empirical methods 0-91093
- quasars, Comptonised spectrum, Monte Carlo simulation 0-90566
- radio sources, form. of universal and diffusion regions of relativistic electrons non-linear spectra 0-109555
- superconducting thin films Cooper pairs, photon scatt. on plasmons, Landau-Ginzburg theory 0-65738
- synchrotron reabsorption sources, Compton scatt., rel. to quasars 0-72761
- tomography, emission computed, Compton scatter correction, integral transport method 0-61683
- vacuum polarisation effects on Compton scatt., unmagnetised electrons, ambient mag. field, astron. appls. 0-86631
- water irradiated by photons up to 2 MeV, initial energies of Compton electrons and photoelectrons 0-108320
- wave and particle descriptions of light, equivalence, rel. to radar freq. shift 0-101692
- X-ray sources, time-dependent Comptonisation and X-ray reverberations rel. to rapid time variability 0-86013
- XX Ce, γ-α phase transition, study by Compton scattering 0-59650
- py, Compton scattering, 375 to 1150 MeV, differential cross section 0-57604
- Al, incoherent scatt. factors calc. by direct integration over impulse approx. Compton profiles 0-102475
- Ar, Compton profiles, Xalpha wavefunctions 0-106265
- Ar electron energy loss spectra, Compton defect characterised by shift and asymmetry parameters 0-95723
- Ar, incoherent scatt. factors calc. by direct integration over impulse approx. Compton profiles 0-102475
- BH₄⁻, electron momentum distribution and Compton profiles, FSGO calcs. 0-87032
- B₂H₆, electron momentum distribution and Compton profiles, FSGO calcs. 0-87032
- B₃H₈, electron momentum distribution and Compton profiles, FSGO calcs. 0-87032
- B₄H₁₀, electron momentum distribution and Compton profiles, FSGO calcs. 0-87032
- Co₃P₁₈, amorphous alloys, electronic struct., γ-ray Compton scatt. study (Japanese) 0-84422
- HeH⁺, electronic momentum distribution, Coulomb shift and correl. coeffs. 0-83266
- inert gases, solid, Compton profiles, APW-Xα calc. 0-80894
- Kr, incoherent scatt. factors calc. by direct integration over impulse approx. Compton profiles 0-102475
- LiF, anisotropic Compton scattering using synchrotron radiation 0-60703
- Li₂N, electron density study using Compton scattering 0-79750
- NH₃, electron impact, 35 keV, Bethe surface and Compton profile 0-87235
- NH₃, expt. electron Compton profile beyond impulse approx. 0-87083
- Na, incoherent scatt. factors calc. by direct integration over impulse approx. Compton profiles 0-102475
- Ne, Compton profiles, Xalpha wavefunctions 0-106265
- Ne, electron energy loss spectra, Compton defect characterised by shift and asymmetry parameters 0-95723
- Ne, expt. electron Compton profile beyond impulse approx. 0-87083
- Ni-P amorphous alloys, electrodeposited and melt-quenched atomic and electronic structures 0-88062
- Ni₃P₁₀, amorphous alloys, electronic struct., γ-ray Compton scatt. study (Japanese) 0-84422
- V, and VD_{0.68}, anisotropic Compton profiles 0-97368

Compton profile *see Compton effect***Compton scattering** *see Compton effect***computation** *see calculation***computational complexity**

- image generation system for nonplanar projection modelling 0-99667

computer-aided analysis

- see also analogue simulation; CAD; circuit analysis computing; digital simulation; hybrid simulation; power system analysis computing*
- axisymmetric transducers, with various boundary conditions, single integral computer method for Green's function 0-87591
- crystal structural fragment, automatic construction, taking account of attainable chem. bond lengths 0-92419

computer-aided analysis continued

- echocardiograms, left ventricular anal. (*German*) 0-81667
- EEG sleep state analysis, automatic real-time practical method 0-67263
- EMG, single motor unit action pots. identification by computerised anal. 0-72343
- field analysis computers, colloquium, London, England (March 1980) 0-94964
- flow cytometric data, computerised display and anal., review, book contrib. 0-109082
- Frevel ZRD-SEARCH-MATCH program, for powder diffr. anal., generalisation 0-59341
- interactive graphics system developed for NDT 0-66729
- nuclear tracks, etched, statistical distrib. using computer image anal. 0-83235
- nystagmus, automatic on-line anal. (*German*) 0-76846
- pre- and post-processing techniques for complex analysis 0-94965
- river pollution distribution determination by remote sensing, computer aided analysis 0-81512
- semiconductor-insulator interface, microcomputer-aided interface-state analysis 0-80383
- steel, Fe-Si (3 wt.%), Bauschinger effect, computerised evaluation method 0-93625
- steel, Nb-Mn, Molytor 53, Bauschinger effect, computerised evaluation method 0-93625
- steels, high-strength low-alloy, Bauschinger effect, computerised evaluation method 0-93625
- two-phase cryst. structures, orientational electron microdiffr. anal. with aid of OMEGA program 0-103218
- US test procedure, for detection of fatigue damage 0-71848
- wind turbines variable pitch vertical axis 0-61265
- X-ray stress meas., computer-aided system (*Japanese*) 0-104366
- Fe, Armcro, Bauschinger effect, computerised evaluation method 0-93625
- Na₂XO₄, (X=S, Cr, Mo, W), anal. and calc. of binary and ternary phase diagrams 0-88299

computer-aided circuit analysis *see circuit analysis computing***computer-aided design** *see CAD***computer-aided instruction***see also education*

- chemistry, CAI using microcomputer, systems, appls. 0-57042
- chemistry education, binary system for carbohydrate nomenclature 0-62435
- mathematics teaching by computer, long-division practice program in BASIC 0-98775
- microcomputer use at University of Michigan 0-62431
- microcomputers in schools, software and equipment choice 0-98772
- numerical analysis, interactive teaching package 0-86058
- PET 2001, multidisciplinary summer course for schoolchildren 0-98774
- physical pendulum, computer-aided laboratory exercise 0-67985
- physics computer-aided teaching, hinted finding scheme, simulation appls. (*French*) 0-98777
- physics teaching using SWTP 6800 system in BASIC 0-98776
- SEM Plato IV network teaching 0-68003
- speed and displacement relations for tire skids, program for PET 0-57038
- TRS-80, teaching at Keene High School 0-98773

computer applications*see also CAD; complete computer programs; computer-aided analysis; computerised control; computerised instrumentation; computerised signal processing; engineering computing; information science; military computing; subroutines*

- saturated steam parameters in reactor containments with escape of coolant, equations of state, integration by computer 0-68764

computer evaluation *see computer selection and evaluation***computer-generated holography**

- aberrated diffraction pattern obs. 0-102681
- aspheric, testing in reflected light using blazed synthetic holograms 0-91881
- aspheric testing, in-line and carrier freq. holograms, comparison 0-87349
- binary Fresnel zone plate construction 0-78809
- digital holography applied to borehole electromagnetic wave exploration (*Chinese*) 0-82080
- hologram construction from X-ray views or acoustic views, using iterative technique 0-69339
- incoherent polychromatic imaging with holographic optical elements 0-69349
- IR optical components and aspherics, 10.6 μ m interferometric testing 0-74523
- lens recording techniques for IR wavelengths 0-95847
- mapping and remote sensing by optical filtering 0-101458
- polarisation holography system and reconstructed image quality 0-102677
- scale and rotation invariant optical pattern recognition and classification 0-99655
- spectrum shaping, iterative computer method 0-102634
- spectrum shaping and image reconstruction, iterative method 0-106475
- As-Se-S-Ge chalcogenide amorphous film, computer-generated holograms using electron beam irradi. 0-95846

computer graphic equipment*see also interactive terminals; plotters*

- astronomy, graphic processor for pseudo-colour images representation (*Italian*) 0-98562
- colour plotter system for computer graphics output, appls. in geoscience 0-98467
- STEM image analysis techniques 0-73539

computer graphics*see also curve fitting; interactive systems*

- 21-channel EEG monitor with real-time result colour display 0-72364
- astronomy, graphic processor for pseudo-colour images representation (*Italian*) 0-98562
- contour map production for electrophysiology 0-72340
- fusion reactor, PDX Tokamak, finite element anal. using computer graphics 0-95424
- image generation system for nonplanar projection modelling 0-99667
- image processing microprogrammed video display 0-72366
- interactive graphics system developed for NDT 0-66729
- Landsat imagery geometrical correction (*French*) 0-81889
- optical design, optimisation and interactive graphics improvements 0-78933
- orbital motion on an interactive-graphics terminal, teaching appl. 0-73152

computer graphics continued

- physics laboratory experiments, graphic computer simulations 0-105470
- US imaging system appl. 0-99905
- video interferogram analysis by TV camera-microprocessor system 0-73440
- video monitor, large screen, for computer output display 0-77597
- PLTZ electro-optic shutter stereoscopic display applications 0-90826

computer interfaces*see also CAMAC; data communication equipment; program processors**chromatographic Micronova computer interfacing scheme 0-93813**echocardiogram, M-mode, automatic computer anal. (Japanese) 0-72274**High Density Connector Interface, fibre optic link 0-91901**IEEE-488 bus compatible DVM variations and advanced features 0-86279**interface for serial computer terminals plotter 0-98904**IR spectrophotometer data processing system applications 0-90912**laboratory interface system for general purposes, appl. to LSI-11 minicomputer 0-77763**microprocessor multichannel analyzer laboratory project 0-101685**repeater gyrocompass angular digitiser construction principle (Russian) 0-73311**SNOOP module CAMAC interface to 168/E microprocessor, bubble chamber pictures 0-58103**terminal to audiovisual device interface 0-67986**weather forecaster console for satellite data handling system 0-90205***computer networks***distributed, solar thermal test facility control 0-72075**hierarchical computer networks for processing data base generated by X-ray CT scanner 0-81732***computer operator training** *see training***computer printers** *see printers***computer programs, complete** *see complete computer programs***computer programs (listings)** *see complete computer programs***computer selection** *see computer selection and evaluation***computer selection and evaluation***METEOSAT data processing system (Italian) 0-109275***computer software***not used for applications software for which see specific applications'**see also systems software**microprocessor-controlled pulse sequencer for pulsed NMR experiments 0-68231***computer storage devices** *see storage devices***computer subroutines** *see subroutines***computerised control***see also chemical engineering computing; electrical engineering computing; industrial computer control; mechanical engineering computing; nuclear engineering computing; power system computer control**21-channel EEG monitor with real-time result colour display 0-72364**computer-based instrument using SK.2 cylindrical coordinator (Russian) 0-76856**fusion reactor, Doublet III, computer control system 0-99321**fusion reactor, Doublet III, neutral beam injector system, instrumentation and control 0-99322**fusion reactor, MFTF, supervisory control and diagnostics system software 0-99324**fusion reactor, MFTF, supervisory control and diagnostics system, database management system 0-99326**fusion reactor, MFTF, supervisory control and diagnostics system, database management system, data structs. 0-99327**fusion reactor, TFTR, energy conversion and storage systems, fault detection and protection 0-95431**heart, artificial, microcomputer based automatic controls 0-67289**JET, control system, communications, diagnostics, data storage and anal., NORD computers 0-68943**laser fusion reactor, NOVA, pulsed power control system, fibre-optic multi-tapped computer bus 0-95443**microcomputer-based blood-pressure recorder (Japanese) 0-67139**nuclear steam generator tubes testing and evaluation using CIS/DASIO system (Czech) 0-63301**reactor neutron density microprocessor-based flux wire evaluation and anal. system 0-63353**solar energy management system 0-66951**solar thermal, test facility, 5 MW, real-time computer control 0-72075**thyroid function radioimmunoassay, quality control, computer program (French) 0-94348**US flaw detector, microprocessor controlled, for flaw classification in welded plates 0-100992**US plate testing equipment, computer controlled, working experience (German) 0-93720**H₂O vapour under point corona discharge, microprocessor control for vapour generator and EHD phenomena 0-106852**TeO₂ acousto-optical tunable filter with microcomputer control 0-102833***computerised industrial control** *see industrial computer control***computerised instrumentation***see also astronomy computing; astrophysics computing; automatic test equipment; biology computing; chemical engineering computing; chemistry computing; computerised monitoring; computerised spectroscopy; computerised tomography; electrical engineering computing; electronic engineering computing; geophysics computing; nuclear engineering computing; physics computing**8450A spectrophotometer, microcomputer system based on MCS SOS processor 0-68272**absorption spectrometer for gas phase samples, computer controlled 0-86459**acoustic coupling between rooms, meas. system using decrease in sound level method (French) 0-69611**Anger camera/computer system using seven pinhole collimator for myocardial perfusion tomography 0-61663**APD 3600 automatic X-ray powder diffractometer, sophisticated derivative method appls., JCPDS data base 0-107017**asbestos fibre counting by automatic image analysis 0-73538**Auger microprobe, scanning, with advanced image processing 0-68304**automatic sprayer with programmable dose for serial expts. (Hungarian) 0-104822**biofeedback training device for speech therapy, portable, microprocessor-based 0-104808**biological research, computer-assisted mapping with the light microscope 0-67308*

computerised instrumentation continued

blood flow detection in human heart, US pulsed Doppler flowmeter system, microcomputer based 0-104690
 blood pulse measuring by computer (*German*) 0-104823
 body surface potential mapping, microcomputer processing system (*Japanese*) 0-72347
 bubble chamber film analysis, semiautomatic measuring system 0-58105
 BWR systems 0-83211
 calligraphic projection display resolution and contrast photometer and X-Y plotter 0-86373
 calorimeter, low temperature investigations, simple off-line arrangement 0-90850
 calorimeter for temp. range 4-380K 0-98915
 calorimetric system for recording plasma blowoff and scattered light distributions from laser plasmas 0-59287
 capillary column gas chromatography at nanogram resolution using dual beam Fourier transform IR spectroscopy 0-89554
 cardiopulmonary resuscitator, programmable, for evaluation of standards 0-72374
 catheter pressure meas., transducer smearing correction using microprocessor based discrete deconvolution 0-67275
 charge injection device as stellar tracking sensor 0-85861
 chromatographic Micronova computer interfacing scheme 0-93813
 computer-based instrument using SK.2 cylindrical coordinator (*Russian*) 0-76856
 cone, computer-driven hardware model, response obs. 0-72402
 control of Joyce-Loebl microdensitometer for objective-prism spectra meas. 0-105173
 coordinate meas., uncertainty computation program (*German*) 0-86256
 cryoelectronics appls. 0-98920
 data loggers 0-73337
 data recording system for KSC 60 cm reflecting telescope, microcomputer control (*Japanese*) 0-94717
 digitizer and image analyzer, microcomputer-controlled 0-86270
 dosimeter for pulsed neutron dose rate meas., portable, microcomputer-based 0-86991
 drift chamber data acquisition, microprocessor based system 0-58066
 dynamically focused electronic sector scanner based on CCDs 0-98042
 echocardiographic tracking system, microprocessor-controlled 0-67169
 EEG period and amplitude anal. system, microcomputer-based 0-72353
 electromanometer, appl. for nuclear materials safeguarding 0-99211
 electron microscopy, image processing system for micrographs based on minicomputer 0-73549
 elementary particle interaction event recording and analysis by computer (*French*) 0-63496
 epicardial mapping, computerised display system (*Japanese*) 0-101279
 film thickness measurement, microprocessor based instrumentation (*German*) 0-57260
 flowmeter reference installations, development prospects for meas. computer complexes 0-96320
 flowmeter system for calibrating transducers, with steady and pulsating flows 0-79416
 fluctuating noise measurement system (*French*) 0-64316
 foot load dynamic distrib., quantification system 0-94388
 foot load static distrib., quantification using the PET computer 0-94387
 fracture surface SEM analysis, microtopography 0-68312
 gait measuring system for treatment evaluation, microprocessor controlled 0-61731
 gamma camera, computer controlled, nuclear cardiology appl. 0-61682
 gas chromatographic purge-and-trap concentrator with microprocessor control 0-93815
 gas flow meas. with vortex meter and microcomputer (*German*) 0-92241
 gel permeation chromatography, automated system using laboratory automation system 0-71961
 gel permeation chromatography anal., data acquisition, computer control 0-97746
 general purpose automated meas. system based on synchronous waveform digitisation under computer control (*Portuguese*) 0-82753
 GenRad 2512 portable digital spectrum analyser, simplicity of operation due to interactive display, technical specifications 0-64326
 gravity sedimentation anal. of human blood leukocytes 0-98197
 Hewlett-Packard 8450A UV/Vis spectrophotometer, user interface 0-68268
 hysteresisgraph with discontinuous sweep mode 0-86351
 instantaneous frequency measurement system for microwave signals (*Japanese*) 0-73327
 intelligent microscopes, recent and near-future advances 0-98166
 interferometry seminar, San Diego, CA, USA (Aug. 1979) 0-73096
 Large Coil Test Facility, instrumentation system design 0-95446
 large-aperture interferometer with low-resolution holographic corrector plate 0-74315
 laser unequal path interferometer with electro-optical camera and minicomputer, fabrication/test appl. 0-77847
 long bone mechanics study under microprocessor control 0-76851
 lung volume, online calc. by digital computer 0-72351
 machine tool industry, angle measurement, automatic testing of precision dividing heads (*German*) 0-82740
 magnetic meas. system for ring specimens 0-86346
 mandibular movements diagnosis, system for meas. and processing (*Japanese*) 0-101249
 medical microscopy, advent of intelligent microscopes 0-81678
 Meteosat sea-surface temperature DP, analysis of first results 0-76985
 MHD combustor and channel temp. meas. 0-73364
 microcomputer based laser interferometer for angular displacement in instrument graduation (*Polish*) 0-90816
 microcomputer based nuclear data acquisition system 0-63500
 microprocessor based chromatographic system 0-71999
 microprocessor multichannel analyzer laboratory project 0-101685
 microprocessor-based, characts. 0-67440
 microprocessor-based diffractometer 0-70082
 microprocessor-based interferometric data reduction system versatility 0-73439
 minority carrier lifetime mapping by SEM 0-96903
 mirror electron microscope, microprocessor system 0-62798
 monochromator, high-intensity, automation using wavelength-scan and intensity-control system 0-86366
 mosaic sensor test and calibration facility for focal plane arrays 0-86425
 multiaxis neutron diffractometer automation 0-102417
 multichannel analyser, microprocessor-controlled, transfer of blood pressures and neural activities for computer anal. 0-72356

computerised instrumentation continued

multichannel polarimeter, data acquisition and control system (*Japanese*) 0-77842
 multichannel radiometer, programmable, for Earth remote sensing 0-77253
 neural pulse wave analysis, microprocessor-based instrument 0-104791
 NMR zeugmatographic imaging, gradient control device using microprocessor 0-89822
 nuclear energy level lifetime measurement using on-line computer and registration time shift compensation 0-68577
 nuclear medicine, precision computer display techniques 0-109011
 nuclear reactor, microprocessor appl. 0-83147
 online topographical analysis in SEM 0-68310
 optical shop computer-controlled interferometry, in-process production tool 0-74531
 paralysis treatment, microprocessor based stimulator (*Slovenian*) 0-104809
 particle detectors, microprocessor-controlled data acquisition system for temporal/angular correl. between β - and γ -ray emission (*Spanish*) 0-106238
 PDP 11/40 minicomputer dynamic analysis system, noise analysis of fluid power equipment, graphical presentation of results 0-64327
 permittivity meas. apparatus for VLF high-field meas. on insulating materials (*French*) 0-98933
 photometer for rapid stellar light variation, microprocessor controlled (*Spanish*) 0-82222
 photometry for astronomical appl., data collection with aid of microcomputer (*Czech*) 0-67570
 polymer contact electrification measuring apparatus, computer-controlled 0-86341
 potentiometric titration apparatus, microprocessor controlled, for equilib. studies 0-89579
 precision optical element testing by phase meas. interferometry 0-74520
 process gas chromatograph, System 9010, microprocessor based 0-61205
 process gas chromatographs, microprocessor based, calibration and data reduction 0-81402
 radiation monitoring, multi-channel analyser, portable microprocessor controlled, accessories, data acquisition 0-63474
 radioheliograph control system, 8 cm instrument at Toyokawa, Japan 0-98549
 radiotelescope RT-22, automatic obs. by computer 0-109359
 remote multiplexing for nuclear reactor instrumentation and control circuits 0-57885
 repeater gyrocompass angular digitiser construction principle (*Russian*) 0-73311
 resistance thermometer automatic calibration oven 0-98914
 respiratory gas monitoring instrument using microprocessor (*Japanese*) 0-72358
 Rome road traffic noise, 24-hour obs. and statistical analysis (*Italian*) 0-87651
 SEM, ultra high resolution, with electron optical system and microprocessor control 0-99002
 SEM computer-aided topographical analysis 0-70094
 SEM diffractogram online computation 0-70095
 SEM images evaluation, coal chemical analysis 0-71994
 semiconductor-insulator interface, microcomputer-aided interface-state analysis 0-80383
 spectrophotometric colorimeters (*Hungarian*) 0-101851
 speech trainer for multihandicapped children, display method and control program (*Japanese*) 0-108922
 SQUID fluxgate magnetometers, magnetopneumographic meas. 0-104711
 STEM, computer graphics analysis of images 0-73539
 STEM, data recording and replay with aid of minicomputer 0-57440
 STEM, image registration 0-104838
 strain meas. speckle photography with hybrid optical/electronic image processing 0-106768
 terminal to audiovisual device interface 0-67986
 time keeping system of Van Swinden Lab. 0-98891
 Tokamak data processing, no. of computers required 0-59252
 US system for left ventricular function quantitative evaluation 0-85457
 vapour pressure computer-automated meas. by simultaneous Knudsen torsion-effusion method 0-73334
 video interferogram analysis by TV camera-microprocessor system 0-73440
 water quality monitoring, portable laboratory 0-61472
 NaCl 46 cm window optical evaluation facility 0-74526

computerised manufacturing control *see manufacturing computer control***computerised monitoring**

arrhythmia ambulatory anal. in real-time with minicomputer 0-85523
 arrhythmia detection, edit and recall system, microprocessor-based 0-89891
 arrhythmia detection with a multi-microprocessor system for distributed and parallel processing 0-85524
 arrhythmia identification and verification by 3-channel eval. of long-term ECG records 0-85518
 arrhythmia monitoring, single scan algorithm for QRS-detect. and feature extraction 0-85520
 arrhythmia quantification, template matching algorithm evaluation 0-85519
 biomembranes, excited, automatic meas. of ionic current electrophysiological characts. (*Russian*) 0-76865
 blood pressure ambulatory recordings, minicomputer processing 0-89887
 blood pressure automatic monitoring, long-term, minicomputer system 0-101276
 clinical vectorcardiographic microprocessor system (*Bulgarian*) 0-61722
 ECG, 24 hr, automatic analysis on minicomputer-based system 0-89889
 ECG, ambulatory, computer processing system 0-89897
 ECG, Frank xyz signal interpretation by unmodified 12-lead computer system 0-94400
 ECG, Holter recordings, low cost arrhythmia analyser, GRETA 0-94403
 ECG, Holter tape high speed digital anal. with full editing capability 0-89896
 ECG, QRS detector/delineator devel. and eval. 0-89892
 ECG 24 hr recording, anal. using operator-controlled computer system 0-89888
 ECG automated monitoring, new electrode system 0-89898
 ECG frequency-domain analysis 0-85521
 EEG, automated monitoring of long-term implanted electrodes (*Russian*) 0-76857

computerised monitoring continued

ethylene, air pollution monitoring, computer controlled CO₂ laser absorpt. system 0-89699
fast solid-state camera for high-speed event diagnostics 0-78985
in situ coal gasification using EM remote sensing, reconstruction algorithms for geophysical applications in noisy environments 0-77168
myocardial ischaemia and necrosis monitoring in acute myocardial infarction 0-85525
neonate cardiorespiratory monitoring, automatic system with microprocessor 0-94399
neurosurgical intensive care, non-invasive monitoring techniques 0-81757
nuclear materials safeguards, nondestructive, energy-dispersive, X-ray fluorescence analysis of product-stream concentrations from reprocessed nuclear fuels 0-83163
rheocardiography, 4-electrode, in computer-aided cardiac output determ. 0-61718
seismic recording network at Campotosto reservoir (*Italian*) 0-101446
solar cells, output monitoring, design and utilization of a microprocessor-controlled absolute spectral response system 0-81476
SOLO monitor, microcomputer bedside monitor 0-94404
supraventricular arrhythmia rapid anal. from long-term oesophageal recordings, drug assessment 0-89904
ventricular arrhythmia model 0-89893
vinyl chloride, air pollution monitoring, computer controlled CO₂ laser absorpt. system 0-89699
water monitoring system, Finland 0-67026

computerised pattern recognition

adenocarcinoma cell clump feature extraction methods in automated uterine cancer cytology (*Japanese*) 0-72362
arrhythmia ambulatory anal. in real-time with minicomputer 0-85523
arrhythmia detection, edit and recall system, microprocessor-based 0-89891
arrhythmia detection with a multi-microprocessor system for distributed and parallel processing 0-85524
arrhythmia identification and verification by 3-channel eval. of long-term ECG records 0-85518
arrhythmia monitoring, single scan algorithm for QRS-detect. and feature extraction 0-85520
arrhythmia quantification, template matching algorithm evaluation 0-85519
astronomical digitized images, use of interactive structural instruments (*Italian*) 0-98554
chest X-ray automated anal. 0-98098
coronary artery bypass graft patient recovery trajectory classification algorithm 0-94411
ECG, Holter recordings, low cost arrhythmia analyser, GRETA 0-94403
ECG, QRS detector/delineator devel. and eval. 0-89892
ECG 24 hr recording, anal. using operator-controlled computer system 0-89888
ECG diagnosis improvement by nonlinear feature extraction methods 0-85530
ECG frequency-domain analysis 0-85521
ECG rhythm analysis, syntactic approach 0-89900
HG ECG, computer methods for anal. 0-72352
line detection algorithm, for Landsat data 0-77150
medical imaging techniques implemented on pipeline minis and array processor, nerve fibre counting appl. 0-98165
morphometric cytology pictorial pattern recognition 0-81796
myocardial ischaemia and necrosis monitoring in acute myocardial infarction 0-85525
nerve fibre counting by pipeline multimicrocomputer image processing 0-109013
rapid eye movement analysis during sleep 0-76870
scale and rotation invariant optical pattern recognition and classification 0-99655
speech trainer for multihandicapped children, display method and control program (*Japanese*) 0-108922
textural pattern recognition, comparison of optical-digital and all-digital techniques 0-99638
two-dimensional random field model for image structural analysis (*Russian*) 0-63932
ventricular arrhythmia model 0-89893

computerised picture processing

see also computer-generated holography
adenocarcinoma cell clump feature extraction methods in automated uterine cancer cytology (*Japanese*) 0-72362
angiocardiology, digital multiprocessor system 0-94362
astronomical images, interactive program for digital display (*Italian*) 0-98559
astronomy, digitised images anal. via interactive data processing system (CIPS) (*Italian*) 0-98560
Auger microprobe, scanning 0-68304
cardiac nuclear medicine, left ventricular edges detect. methods 0-98132
cardiac scintigrams, time gated, analysis by digital boundary detect. techniques 0-98081
cardiac scintigraphic image handling using microprocessor system 0-85489
cardiograms, image processing, cardiac function meas. (*Japanese*) 0-94354
cardiology, nuclear, automated chest parsing algorithm 0-61678
cell membrane particle diameters meas. by computer from electron micrographs 0-101307
chest photofluorograms, computer anal. and appl. to automated screening 0-72282
chest X-ray automated anal. 0-98098
chromosome metaphase spread, automatic finding, prep. and eval. of object spectra 0-98168
cineangiocardiology, accuracy of ventricular models and localisation of contraction anomalies 0-89845
cineangiograms, anal. system 0-72284
cineangiography, automatic detect. of apex of heart 0-89847
cineangiography, left ventricular contour segmentation from anatomical landmark trajectories and its application to wall motion analysis 0-94363
cineangiocardigram of left ventricle, automatic processing and cardiac function display techniques (*Japanese*) 0-72311
coronary artery quantitation using digital image processing techniques 0-85517
CRT half-tone image display system using MIR-2 computer 0-62641
dark-field imaging, computer simulation 0-100151

computerised picture processing continued

digital data composition for satellite and radar imagery 0-67413
digital image enhancement by median masking technique 0-106483
digital image processing, architectural breakthroughs 0-63939
digital image processing applications, seminar, San Diego, CA, USA (Aug. 79) 0-105424
digital image-enhancement, used for human anatomy scanning 0-94408
digital system for image processing (*Italian*) 0-98558
echocardiogram, M-mode, automatic computer anal. (*Japanese*) 0-72274
echocardiograms, 1D and 2D (*German*) 0-81665
echocardiographic images, video recorded, interactive segmentation 0-89817
electron micrograph, 500 kV, atomic resolution 0-100149
electron microscope images, automatic investigation 0-92425
electron microscopy, bright field images, signal-to-noise enhancement in incoherent superposition 0-101906
electron microscopy, cell ultrastructure anal. 0-85555
electron microscopy, image reconstruction of low and high dose micrographs of neg. stained glutamine synthetase 0-85551
electron microscopy, imaging and diffraction from localised defects and disorder 0-100152
electron microscopy, many-beam structure images, optimal comput. techniques 0-95203
electron microscopy, microdensitometer-computer correlation analysis of ultrastructural periodicity 0-85553
electron microscopy, phase contrast simulation, of Au cluster atoms on W support film 0-100150
environmental change detection in digitally registered aerial photographs 0-106477
enzymes, molecular struct. reconstruction from electron microscopy images 0-89715
flow measurement, plane mixing layer vortex digital image processing 0-103095
gated cardiac scintigram anal., digital boundary detect. techniques 0-98106
high-temperature reactor structural displacement and strain analysis (*Japanese*) 0-78352
image analysis by LEITZ-TAS with process computer 0-68773
image generation system for nonplanar projection modelling 0-99667
image processing applications at IBM Madrid Scientific Center 0-102657
image reconstruction, computerized, fragment size choice 0-78785
intravenous angiography, digital video subtraction system 0-98089
IR staring mosaic sensor background suppression and tracking 0-86415
Jovian centre location in Voyager image transformation 0-101534
land-use mapping, evaluation of LANDSAT image data 0-101443
LANDSAT data anal. for geological structure research (*Italian*) 0-109281
LANDSAT georexploration, digital mosaicking and lineament enhancement (*Japanese*) 0-82169
Landsat imagery laser film recorder and processor 0-105084
laser spatial profile meas. by pyroelectric vidicon camera 0-87425
left ventricular localised wall motion abnormality assessment, usefulness of quantitative parameters 0-89848
linearly degraded images, iterative image restoration 0-95807
linearly degraded images, iterative restoration, reblurring procedure 0-99640
medical computerised tomography, streak artifact reduction method 0-98067
medical image processing in diagnostic radiology 0-81690
medical images, edge coincidence segmentation 0-109012
medical imaging system evaluation by contrast-detail-dose analysis 0-98140
medical imaging techniques implemented on pipeline minis and array processor, nerve fibre counting appl. 0-98165
medicine, nuclear, digital filtering and edge detection 0-58065
medicine, nuclear, microprocessor systems for data acquisition, image processing, RIA anal., patient data retrieval 0-61670
METEOSAT project, interactive image system 0-109330
microprogrammed video display 0-72366
molecule images, simulation by point models and kinematical struct. amplitudes 0-103223
multiple analysis at JPL's Image Processing Laboratory 0-82219
nerve fibre counting by pipeline multimicrocomputer image processing 0-109013
nuclear events picture anal. multiprocessor system (*Italian*) 0-69047
nuclear medicine, coded aperture imaging, qualitative and quantitative 0-89843
nuclear medicine, precision computer display techniques 0-98100
optical microscopy, automatic image analyzer appls., densitometric and geometric studies 0-98974
particle size distribution meas., online stroboscopic microscope apparatus 0-101783
phosphorylase A crystals, automated struct. determ., from micrographs 0-92425
photographic plate digitalised image, object detect. using FINDER program (*Italian*) 0-98575
precision image isocan X-ray TV camera 0-101263
precision SEM image analysis system with full-feature EDXA characterization 0-68311
radiocardiography, equilibrium left ventricular ejection fraction determ., background noise estimation 0-94365
radiographic image computer-controlled subtraction procedures 0-109014
radiographic image smoothing and edge enhancement 0-109015
radiography, computed, low-dose X-ray imaging system 0-98092
radiography, digital processing appls. 0-98103
radiography, video subtraction procedures 0-98102
radioisotope angiocardiology, image enhancement and left ventricular contour extraction techniques appl. 0-72283
radioisotope imaging, digital images, math. models and physiological parameters 0-98107
radionuclide angiography, gated, use of computer-generated functional images to define ventricular boundaries 0-85487
radionuclide angiography technique for assessment of regional wall motion abnormalities 0-85488
radionuclide tomographic section, synthesis, and enhancement 0-109003
radionuclide ventriculography, computerised, assessment of LV wall motion and regional kinetics 0-89850
review of methods 0-83562
SEM diffractogram online computation 0-70095
SEM images evaluation, coal chemical analysis 0-71994
smoke/dust cloud temporal analysis algorithm 0-98484

computerised picture processing continued

- square-field scanned image construction time optimisation (*Russian*) 0-63933
 - stereo image digitiser for automatic feature extraction 0-106614
 - stress ²⁰¹Tl scintigram anal. methods comparison 0-89851
 - submarine periscope optical test equipment 0-78943
 - TEM 0-82852
 - texture analysis by hybrid optical/digital system 0-78787
 - tomographic image boundary finding and complex object localisation 0-109016
 - tomographic image correction, with simulation 0-85470
 - tomographic image reconstruction using two-dimens. kernels formed by simple back-projection., ramp filter realisation (*Korean*) 0-72275
 - tomographic scan edge position uncertainty reduction by density derivative processing 0-109017
 - tomography, boundary-finding scheme and complex object location 0-98104
 - tomography, dynamic and ECG-gated, reflection technique for improved temporal resolution 0-98094
 - tomography, edge position uncertainty reduction 0-98105
 - tomography, global local edge coincidence segmentation 0-98101
 - tomography, limited data, image reconstruction using polar pixel Kalman filter 0-98095
 - tomography, multiple window display techniques 0-98099
 - tomosynthesis, flashing system, using simultaneously 25 X-ray tubes 0-81768
 - two-dimensional random field model for image structural analysis (*Russian*) 0-63932
 - vectorcardiography, 3-dimens. 0-94405
 - ventriculography, left ventricular wall motion anal., externally referenced polar coord. system 0-89846
 - weather maps, structural description of contour maps 0-101419
 - weighted line-finding algorithm for digitised picture 0-99660
- computerised power station control** *see power station computer control*
- computerised power system control** *see power system computer control*
- computerised process control** *see process computer control*
- computerised signal processing**
see also biology computing; computerised pattern recognition; computerised picture processing; medical diagnostic computing
- arrhythmia detection with a multi-microprocessor system for distributed and parallel processing 0-85524
 - atmosphere radar signal processing, for SOUSY-VHF-radar, using preprocessor 0-85774
 - biomedical frequency-time domain signal processing system 0-81760
 - biomedical US signals in diffuse liver disease 0-67173
 - digital correlator signal preprocessing 0-83556
 - ECG, 24 hr, automatic analysis in minicomputer-based system 0-89889
 - ECG, ambulatory, computer processing system 0-89897
 - ECG, flexible signal-averaging system 0-67270
 - ECG, measurement error determ. 0-94401
 - ECG, microprocessor-based evaluation system for conventional leads 0-89894
 - ECG, T-wave location by computer, R-T interval 0-76854
 - ECG, time-selective filtering 0-89895
 - ECG artifact in referential EEG recordings, minimisation by computer subtract 0-94390
 - ECG contour analysis system utilising decision tables, real-time, microprocessor-based 0-89880
 - ECG processing optimisation, conf., Halifax, Nova Scotia, Canada (Jan. '79) 0-76850
 - echocardiography, high-resolution 0-76814
 - EEG, microcomputer-based period and amplitude anal. system 0-72353
 - EMG, filter bank analyser for automatic anal. 0-98162
 - gamma emitting organs, 2 and 3-dimens. digital Fourier reconstruction 0-101705
 - heart block computer detect. by correl. of surface and endocardial ECG 0-94410
 - long-term spectra, computerised meas. method, English and Finnish data comparative study 0-104688
 - microwave radiometers, microprocessor-based unit 0-77874
 - multichannel analyser, microprocessor-controlled, transfer of blood pressures and neural activities for computer anal. 0-72356
 - myocardial ischaemia and necrosis monitoring in acute myocardial infarction 0-85525
 - neural pulse wave analysis, microprocessor-based instrument 0-104791
 - polygraphic sleep recordings, computerised scoring method 0-109049
 - real-time speech high-performance processor design 0-96144
 - tomography, focal-plane, image reconstruction using digital computer 0-61674
 - tomography simulator, emission computed, design 0-61672
 - vectorcardiogram information enhancement, automatic pre-processing 0-94402
 - ventricular fibrillation signal anal. 0-85522

computerised spectroscopy

- see also spectroscopy computing*
- acousto-optical tunable filter spectrometer development 0-101848
- Auger microprobe, microprocessor controlled 0-81414
- Brillouin spectrometer with high contrast and resolution, fully stabilized 0-57386
- digitised EPR system, appln. to saturation transfer 0-77825
- diver-operable multiwavelength spectroradiometer 0-90251
- dual-grating direct-reading spectrograph mirror system design and performance 0-81397
- dye laser spectrometer, computer controlled, time averaging to improve sensitivity 0-101850
- Fabry-Perot spectrograph, self-scanned photodiode array for image detect. (*French*) 0-73465
- Fourier NMR spectroscopy, computer programmable digital pulse generator 0-98959
- Fourier transform spectrometer, rapid scanning, very high resolution, data processing aspects 0-95150
- gamma spectrometer system for meas. isotopic and total Pu conc. in solns. 0-63363
- gas chromatography-mass spectrometry, computerised, data-blocking cross-correlation peak detection 0-62725
- GC/MS integrated systems, review of current techniques 0-68289
- IR microscopy coupled with scanning photoluminescence spectrophotometry 0-73447
- IR spectrophotometer, digital data acquisition/analysis system 0-73482
- IR spectrophotometer data processing system applications 0-90912

computerised spectroscopy continued

- IR spectroscopy, computerised, noise props. 0-86466
 - magnetic double focusing mass spectrometer, microprocessor controller for linked scans 0-101870
 - mass spectrometry, technical aspects including data reduction and analysis 0-57417
 - Michelson Fourier transform stellar spectrometer 0-98552
 - microcomputer interfaced spectrophotometer for kinetic studies 0-62726
 - microcomputer-controlled microwave-optical spectrometer 0-86448
 - microprocessor-controlled apparatus for pulsed spectra meas. 0-68261
 - microprocessor-controlled pulse sequencer for pulsed NMR experiments 0-68231
 - monochromator scanning control system using microprocessor, spectral line shift correction (*Japanese*) 0-57384
 - multichannel apparatus for material analysis using atomic spectra 0-76586
 - NMR spectrometer, FT, multipurpose, design and computer interfaces 0-86362
 - NQR, electronics appls. 0-63668
 - Omega spectrometer, CERN, modular trigger basic techniques 0-58104
 - phosphate and alkaline phosphate activity determ. by dual microcomputer-controlled stopped-flow spectrometer 0-57379
 - photoionisation mass spectrometer 0-77905
 - photosensor spectral responsivity calibration microprocessor system 0-86409
 - pulsed FT NQR, automation for Zeeman studies of single crystals 0-66066
 - reaction products, weak excitation spectra, automatic recording of laser-induced fluorescence signal 0-76574
 - SHG, computer controlled intracavity, in CW ring dye laser 0-91841
 - Spectronic 2000 spectrophotometer, interactive microprocessor-controlled instrument 0-105716
 - steelworks computerised spectrometric analysis and management information system 0-89574
 - thermal desorption mass spectroscopy, computer control, data acquisition, appls. 0-61181
 - thermal ionisation spectrometry with automatic data eval. for isotopic comp. determ. of U and Pu 0-66913
 - time-of-flight mass spectrometer, computer interfaced, gas-phase reactions anal. 0-71967
 - tunable diode laser spectrometer, rapid-scanning computer-controlled 0-101854
 - CO₂ laser Helios fusion system beam diagnostics 0-78882
 - Cl monitoring using TAGA mass spectrometer-based instrumentation and minicomputer system 0-72114
 - NaI(Tl) scintillation detectors, microprocessor-based multichannel analyser 0-91378
 - X-ray fluorescence analysis energy-dispersive, for nondestructive assay of nuclear materials 0-83163
- computerised test equipment** *see automatic test equipment*
- computerised tomography**
see also tomography
- acoustical imaging, US visualization and characterization, conf., vol.8, Key Biscayne, FL, USA (May-June 1978) 0-83720
 - analogue optical method of information processing (*French*) 0-94349
 - anatomical cross-sectional geometry and density distribution data base 0-101287
 - anatomical feature or lesion volume estimation algorithm 0-98080
 - artifacts, nonlinear, partial vol., correct. algorithms 0-76829
 - body tomography, single photon emission, nuclear medicine computer interfaced to Anger multplane scanner 0-61665
 - boundary-finding scheme and complex object location 0-98104
 - brain, experimental oedema, serial meas. of specific gravity and CT attenuation 0-98005
 - brain, imaging, comparative study with γ -camera, single-photon emission CT, and transmission CT 0-109004
 - brain, irradi. quantitative assess. by CT scan anal. 0-72306
 - brain, Xe regional kinetics meas., imaging methods in transmission CT 0-98131
 - brain diagnosis, comparative study of radionuclides and CT 0-72320
 - Buddha sculpture survey using X-ray computed tomography (*Japanese*) 0-101915
 - cardiac blood pool, ECG-gated emission CT 0-98117
 - cardiac imaging, ECG-gated, motion phantom 0-98115
 - cardiac imaging with ¹¹C-palmitate and PETT IV system 0-89849
 - cardiac studies 0-98088
 - cerebral angiography, simultaneous multisection method 0-98127
 - coded aperture imaging, qualitative and quantitative 0-89843
 - digital image processing applications, seminar, San Diego, CA, USA (Aug. 79) 0-105424
 - digital image-enhancement, used for human anatomy scanning 0-94408
 - digital processing appls. 0-98103
 - distortion problems in secondary-scan reconstruction in CAT 0-104729
 - divergent beams, reconstruction, comparison of algorithms with and without rebinning 0-98066
 - edge coincidence segmentation for medical images 0-109012
 - edge position uncertainty reduction 0-98105
 - electrical conductivity and permittivity imaging 0-98055
 - electronic file for X-ray pictures 0-101288
 - emission, double-tracer, multiple-organ, transaxial, radiotracer distrib. localisation and characterisation 0-98128
 - emission axial CT from multiple γ -camera views using freq. filtering 0-94321
 - emission computed tomography, Compton scatter correction, integral transport method 0-61683
 - emission computed tomography stimulator, design 0-61672
 - emission tomography, single-photon, physical attributes 0-109007
 - fan-beam to parallel-beam conversion by rubber sheet transformation 0-109009
 - field measurement utilising the partial vol. effect 0-89865
 - filter function technique for tomographic reconstruction 0-61729
 - filtered neutron-beam computed axial tomography 0-101258
 - flashing tomosynthesis system, using simultaneously 25 X-ray tubes 0-81768
 - fluid characterisation by US and CT 0-98045
 - focal-plane tomography, image reconstruction using digital computer 0-61674
 - gamma camera, computer controlled 0-61682
 - gantry geometry rel. to aliasing and other geometry dependent errors 0-81695
 - generalized image synthesis from projections 0-67579

computerised tomography continued

geophysical EM remote sensing, appl. 0-77169
 geophysical techniques 0-82114
 global local edge coincidence segmentation 0-98101
 health risks due to radiation exposure 0-61654
 heavy ion therapy, treatment planning programme 0-72295
 hierarchical computer networks for processing data base generated by X-ray CT scanner 0-81732
 history, early 2D reconstruction and recent topics stemming from it 0-86029
 Hounsfield, G.N., Nobel Award Address 0-86030
 image boundary finding and complex object localisation 0-109016
 image correction with simulation 0-85470
 image formation using fan-beam scanning and noncircular source motion 0-101913
 image function reconstruction from noisy data in low-dose case, algorithm based on Wiener filter (*Korean*) 0-76824
 image processing appl. of multiple bandpass filters 0-109002
 image quality in photon imaging 0-81687
 image reconstruction filters, Fourier convolution algorithm for three-dimensional density function, critical review of previous filters (*Korean*) 0-72313
 image reconstruction from projections, blurring due to object movement 0-78784
 image reconstruction using two-dimens. kernels formed by simple back-projection, ramp filter realisation (*Korean*) 0-72275
 image statistics, information and artifact 0-81713
 image understanding systems, seminar, San Diego, CA, USA (Aug. 79) 0-94918
 industrial NDT computed transverse axial tomography system 0-89430
 interstitial dosimetry, utilisation of the CT scanner 0-104770
 intrathoracic space demands, CT representation (*German*) 0-109018
 iodinated contrast studies, optimum energy study 0-81685
 kidney diseases, value of CT (*German*) 0-76832
 limited data, image reconstruction using polar pixel Kalman filter 0-98095
 liver carcinoma, VX2, improved detectability in the rabbit with contrast enhancement 0-98118
 longitudinal, bilateral collimator, gamma camera and minicomputer 0-61666
 lung dose in half body radiotherapy, determ. by CT 0-104763
 mediastinum diseases diagnosis appl. (*French*) 0-85473
 medical imaging, conference, San Diego, USA (Aug. 1979) 0-94919
 medical imaging overview 0-98082
 medical imaging systems, information capacity considerations 0-98090
 microwave CT, 10.5 GHz 0-104719
 motion blur recovery technique, system resolution recovery, appl. to X-ray computerised tomography 0-105756
 multichannel semiconductor detectors for X-ray transmission computed tomography 0-58058
 multidimensional space and time signal processing in biology and medicine 0-85493
 multiple window display techniques 0-98099
 multiple window display techniques 0-109010
 multiple-energy scans, increased tissue differentiation using colour display 0-98125
 myocardial ^{201}Tl scintigram anal., nonredundant coded aperture tomographic method 0-94364
 myocardial perfusion imaging with ^{201}Tl , single photon emission CT (*Japanese*) 0-98114
 myocardial perfusion tomography, Anger camera/computer system using seven pinhole collimator 0-61663
 myocardium, transverse CAT with ^{201}Tl 0-67222
 NDT applications (*German*) 0-76439
 nerve fibre counting by pipeline minicomputer image processing 0-109013
 nuclear fuel element inspection 0-73927
 nuclear reactor 0-99268
 performance and applications 0-98085
 phantom for imaging biological fluids by US and CT scanning 0-104692
 physiologic tomography, noninvasive meas. of myocardial metabolism, blood flow and function 0-104730
 positron camera, 3-D image reconstruction, Fourier deconvolution method 0-61669
 positron camera system, ring detector, brain research, computed transaxial tomography 0-61739
 positron circular ring camera tomographic system, resolution improvement anal. (*Korean*) 0-72312
 positron CT, data acquisition and processing electronics 0-61690
 positron emission computed tomograph, POSITOLOGICA 0-104753
 positron emission CT crystal size optimisation 0-61681
 positron emission CT device with continuously rotating detector ring 0-81697
 positron emission transaxial tomography, ring detector, attenuation, scatt. radiation and random coincidences 0-61684
 positron emission-computed tomography, multi-slice, design criteria, shielding 0-61673
 positron imaging (*Japanese*) 0-94347
 positron tomograph, Donner 280-crystal, data acquisition, image reconstruct. and display 0-61671
 positron tomography, $^{52\text{m}}\text{Mn}$, new short-lived, generator produced radionuclide 0-109006
 precision image isocan X-ray TV camera 0-101263
 projection reconstruction (*Japanese*) 0-81700
 quantitative CT, progress toward 0-81696
 radiation therapy, utility of CT, estimate of outcome 0-67229
 radiation therapy treatment planning, value of CT scanning 0-72294
 radiation therapy treatment planning and the distortion of CT images 0-76830
 radiographic imaging, 3-dimens. 0-85486
 radionuclide tomographic section, synthesis, and enhancement 0-109003
 radiotherapy planning appl. 0-94334
 radiotherapy program development by means of CT (*French*) 0-85472
 reconstruction, three-dimensional, from planar projections 0-99639
 reconstruction algorithm, smoothed, clinical and expt. investigation 0-98122
 reflection technique for improved temporal resolution with dynamic and ECG-gated imaging 0-98094
 region-of-interest X-ray tomography 0-98093
 resolution, comparative studies with spiral and elliptical blurring patterns 0-104728

computerised tomography continued

review and comparison with classical X-ray diagnostic technique (*German*) 0-67239
 review of state of the art and introduction to CT (*German*) 0-101251
 scan edge position uncertainty reduction by density derivative processing 0-109017
 scanners, specification and evaluation of performance 0-89832
 scanners, survey of noise, dose and contrast detectability and resolution 0-104750
 scanogram, technique and appls. 0-104748
 secondary sections for radiotherapy plane section (*German*) 0-89841
 section images, three-dimensional display (*Japanese*) 0-81701
 short-scan fan-beam algorithms for CT 0-85469
 simulated neutron tomography for nondestructive assays 0-99218
 single photon emission CT, review 0-81698
 single photon emission tomography, camera configs., performance anal. 0-61686
 single-photon emission tomography, imaging capabilities of Ge camera 0-61668
 skull, diagnostic advantages of tilting investigation unit (*German*) 0-94351
 skull, struct. changes due to Recklinghausen's disease, X-ray and nuclear medicine diagnosis (*German*) 0-76831
 spinal cord, X-ray reconstruct. using bone suppression 0-76822
 streak artifact reduction, computational method 0-98067
 streaking artifacts, edge-induced evaluation 0-81711
 strobe-sequenced device to facilitate 3D viewing of cross-sectional images 0-104720
 structural material analysis 0-101001
 TGM-1 multidirectional tomograph, operating characts. 0-104726
 three-dimensional emission tomography using scattered photon information 0-98134
 tomosynthesis and computer tomography: a continuous description with examples 0-99020
 transaxial scanners for reconstructing objects from their X-ray projections, review 0-102632
 two phase flow, computerised tomography meas. technique 0-59135
 two-phase flow, isotopic computerised tomography meas. 0-59136
 volume estimation, computer algorithm 0-98043
 volume estimation algorithm based on polyhedral approx., using US or CT data 0-104790
 whole-body NMR imaging machine 0-101285
 X-ray tube, heavy-duty rotating anode type 0-73568
 Hgl₁ detectors for X-ray CT, evaluation 0-89837
 Xe detectors, dual, experimental, for quantitative CT and spectral artifact correct. 0-76825

computing applications to aerospace engineering *see aerospace computing*
computing applications to art *see art*
computing applications to astronomy *see astronomy computing*
computing applications to astrophysics *see astrophysics computing*
computing applications to biology *see biology computing*
computing applications to biomedical engineering *see medical computing*
computing applications to chemical engineering *see chemical engineering computing*
computing applications to chemistry *see chemistry computing*
computing applications to circuit analysis *see circuit analysis computing*
computing applications to communications engineering *see communications computing*
computing applications to education *see educational computing*
computing applications to electrical engineering *see electrical engineering computing*
computing applications to electronic engineering *see electronic engineering computing*
computing applications to engineering *see engineering computing*
computing applications to geophysics *see geophysics computing*
computing applications to history *see history*
computing applications to information science *see information science computing*
computing applications to literature *see literature*
computing applications to manufacturing *see manufacturing data processing*
computing applications to mathematics *see numerical analysis*
computing applications to mechanical engineering *see mechanical engineering computing*
computing applications to medical administration *see medical administrative data processing*
computing applications to medical diagnostics *see medical diagnostic computing*
computing applications to medicine *see medical computing*
computing applications to music *see music*
computing applications to nuclear engineering *see nuclear engineering computing*
computing applications to physics *see physics computing*
computing applications to power system analysis *see power system analysis computing*
computing applications to power system design *see power system CAD*
computing applications to psychology *see psychology*
computing military applications *see military computing*
concrete
see also cement industry
 BWR containment vessels of prestressed concrete, pressure tests 0-81254
 chamotte concretes, phosphate binder based, strength props. 0-89305
 compression tests, device for centering specimens 0-61033
 concrete, fresh, behaviour under a vibr. action, large particle segregation (*Japanese*) 0-88329
 concrete, impact bending capacity (*Japanese*) 0-89341
 concretes, further development of 2 point test for workability and extension of its range 0-66728
 elasticity modulus and strength, aggregate conc. effect 0-66591
 flowing concrete, expt. studies (*Japanese*) 0-89298
 fresh concrete, props., relayed addition of admixture and flowing concrete (*Japanese*) 0-89461
 high strength, made with special cement admixture, mech. props. (*Japanese*) 0-89297
 LMFBR, liquid Na-limestone concrete interaction following HCDA, US meas. 0-78412
 magnesial refractory concretes, cast. props. 0-89306
 membranes, rectangular reinforced, torsional stiffness 0-65131

concrete continued

- polyester resin concrete, effects of styrene-unsaturated polyester ratio on props. (Japanese) 0-89299
- polymer concrete, longitudinal deformation modulus investigation in creep conditions (Bulgarian) 0-71685
- polymer concretes, hydrothermally stable, hydraulic cement-type fillers 0-85144
- quality assessment, US pulse vel. meas. practical use 0-100991
- quartzite, vitrified, and quartzite based refractory concretes, prep. and props. 0-89188
- refractory, fracture strength meas., test apparatus simulating usage conditions 0-71824
- reinforced beams, shear strength calc. 0-99942
- reinforced slabs, punching shear strength under in-plane biaxial tension 0-100876
- slab, explosive shock resist., tensile fracture 0-85065
- steel fibre reinforced concrete, vibr. compaction, pressure compaction and curing (Japanese) 0-89179
- strain rate effect, on strength and deform. during hardening process (Japanese) 0-93616
- strength, shrinkage strain and deterioration down to -160°C (Japanese) 0-100886
- stress-strain relationships, applicable to biaxial tension and compression 0-65133
- tensile testing device, axial 0-61054
- $\text{Al}_2\text{O}_3\text{-SiO}_2$ refractory concrete, elastic props. 0-89280

concurrency (computers) see multiprocessing systems**condensation**

- see also clouds; drops; fog*
- bubble collapse in liquid, pressure wave, nonequilib. vapour condensation effects 0-59060
- capillary condensation theory, adsorbates liq. or gaseous props. 0-80028
- circular tube under centrifugal accel. field, condensation heat transfer 0-74713
- cloud condensation nuclei, meas. using horizontal thermal gradient spectrometer 0-77158
- condensation on AgI aerosol particles, implications for ice-forming activity 0-101406
- condensation-driven fluid motions, nuclear reactor safety 0-63228
- cooled pipe, droplets from vapour condensation, size distrib., laminar flow 0-79111
- crystal rough surface smoothing, during evaporation or condensation 0-103470
- electron irradiation effects on surface prop. of solids 0-70261
- ethane, flow continuity in arterial capillary systems in cryogenic heat pipes 0-64536
- film, condensation of moving vapour on horizontal cylinder, exptl. dependences 0-58892
- forced convection condensation in the presence of noncondensables, boundary values (Japanese) 0-92151
- heat transfer, nonequilib. temp. profiles, mass transfer engineering calc. 0-63227
- heterogeneous photocondensation process initiation by laser radiation 0-67410
- interaction force between droplet and condensing vapour 0-79113
- interstellar volatiles condensation on dust grains, role of grain growth by radiation pressure induced coagulation 0-94851
- LWR safety, condensation heat transfer in stably stratified systems 0-63311
- metal films, nucleation on alkali halide crystals, effect of ionisation of condensing flux 0-107675
- non-condensing gas on flat plate and horizontal tube, forced convection condensation 0-64553
- p 0-80072
- parallel-flow and counter-flow condensation on an internally cooled vertical tube 0-64555
- perturbed flow, moisture form. kinetics 0-79387
- physical clusters, modified Mayer theory for homogeneous condensation from small nuclei 0-79924
- rate of formation of condensation nuclei in two component metastable media 0-79930
- spherical droplet, evaporation and condensational growth, mass transport calcs. 0-97736
- statistical mechanical theory of the kinetics of phase transitions, review, book contrib. 0-73270
- steam, dropwise condensation, moving picture study 0-74863
- stearic acid homogeneous vapour phase nucleation, diffusion cloud chamber obs. 0-79923
- sulphate aerosol, stratospheric, kinetics of growth by condensation in homogeneous medium (Russian) 0-94566
- supersonic two-phase flow, nonequilib. condensation, boundary condition numerical anal. 0-64565
- thin films, kinetics under complete condensation conditions 0-88453
- thin films, precipitation and nuclei form. in presence of condensation centres, thermodynamic model 0-103594
- two dimensional system, melting and condensation theory 0-57231
- two-phase countercurrent flow, turbulent steam condensation in a horizontal channel 0-106800
- vapour of high-boiling mixture, condensation on evaporating bubbles of low-boiling liq. 0-59021
- vapour-liquid-solid growth mechanism (Russian) 0-107074
- vertical flat plate, generalised soln. 0-59028
- water vapour expansion with condensation, nozzle flow at high pressure 0-106828
- Ar, cluster formation and homogeneous nucleation, comparison of expt. and theory 0-79925
- Ar, nonequilibrium condensation and surface tension in supersonic jet flow (Russian) 0-65210
- CO_2 , adsorption and capillary condensation on clays rel. to Mars volatile storage and atmospheric history 0-72833
- Cu on Mo and steel, substrate limiting temp. during vaporisation and condensation coating in vacuum (Russian) 0-100787
- Hg, two-dimensional, on W 0-107666
- N_2O_4 , fission reactor coolant, heat transfer on condensation (Russian) 0-57860
- Ti-N_2 , condensate formed by plasma flow precipitation in vacuum, cryst. and surface props. (Russian) 0-100788
- U enrichment by photochemical laser, two-phase flow with condensation, mathematical model (French) 0-74029

condensation continued

- W (100), condensation of Cu and Ag, early stage comparison with $\text{Ni}(100)$ 0-80072
- Zr-N_2 , condensate formed by plasma flow precipitation in vacuum, cryst. and surface props. (Russian) 0-100788
- condensers (electric) *see capacitors*
- condensers (steam plant)
 - steam turbine condensates, ion-exchange polishing analysis (Russian) 0-89487
- condensing *see condensation*
- conductance, electric *see electric admittance*
- conductance, electric, measurement *see electric admittance measurement*
- conductance measurement, electric *see electrical conductivity measurement*
- conducting materials
 - see also bimetals; electrolytes; metals; semiconductor materials; superconducting materials*
 - No entries
- conduction, heat *see heat conduction*
- conduction bands
 - see also Fermi level; semiconductor materials*
 - n-alkanes, conduction band struct., LEED, secondary electron emission and UPS study 0-70601
 - ethylene, conduction band struct., LEED, secondary electron emission and UPS study 0-70601
 - ferromagnetic semiconductor, doped, electron spin polarisation and conduction band struct. 0-65449
 - ferromagnetic semiconductor, spectral density approach for s-f model quasiparticle concept 0-80173
 - ferromagnetic semiconductors, electronic quasiparticle spectrum 0-97051
 - ferromagnetic semiconductors, s-f interaction on conduction band, red shift effect theory 0-59872
 - graphite, diamagnetism with quasilinear dispersion law, orbital susceptibility, valence bands (Russian) 0-80475
 - graphite intercalation compound, interaction between one or two s orbitals (French) 0-65440
 - metal, antiferromag., thermoelec. power in mag. field 0-70686
 - metals, conduction band widths 0-103619
 - p-n heterojunctions, forward-biased, charge accumulation 0-107902
 - polypeptide chains, struct. of conduction and valence band 0-76700
 - polypeptides, electronic struct., side-chain disorder effect 0-76706
 - rare earth compounds, mixed valence state, conduction band struct. 0-103624
 - semiconductor isotype heterojunction barriers, cond. band discontinuity, C-V profiling meas. method 0-70801
 - substitutional alloys of intermediate valence systems, static mag. susceptibility con. and temp. depend. 0-84586
 - tunnelling MIS structures photovoltaic energy conversion, band struct. 0-92995
 - AlGaAs p-n diodes, I-V charact., tunnelling 0-100510
 - $\text{Al}_{0.35}\text{Ga}_{0.65}\text{As-GaAs}$ N-p heterojunction diodes, current suppression by cond. band discontinuity 0-80362
 - Au, core-electron excitation edges 0-66345
 - B, evaporated, electronic struct., XPS, SXS and isochromat investig. 0-76143
 - BaTiO_3 , K-edge X-ray absorpt., cond. band states 0-97382
 - $\text{CdGa}_2\text{S}_4(\text{Se}_4)$, band struct., pseudopot. method 0-92816
 - Cu, core-electron excitation edges 0-66345
 - Eu chalcogenides, cond. band spin struct. 0-71577
 - GaAs anodic oxide, states, electrochemical meas. 0-80176
 - GaAs, conduction band effective mass, influence of high uniaxial stress 0-80162
 - GaAs, DC biased, filamentation of laser radiation 0-74428
 - GaAs:Cr, carrier equilibrium effects, impurity states, elec. resistivity 0-65488
 - GaAs- $\text{Al}_{0.3}\text{Ga}_{0.7}\text{As}$ n-N heterojunction, LPE grown, cond. band discontinuity, C-V profiling meas. 0-70801
 - GaP, electron-hole drops, self-consistent surface calculation 0-65464
 - GaSb, solid solns., impact ionisation, cond. and valence band effects 0-65583
 - Ge, electron-hole drop freq. depend. damping 0-88482
 - H_2WO_3 bronzes, Anderson transition, XPS 0-107705
 - $\text{n-Hg}_{1-x}\text{Cd}_x\text{Te}$, optical phase conjugation 0-83644
 - NbSe_3 , electronic struct., chem. interpret. of geom. deform., oxidation state formalism 0-107690
 - Ni, core-electron excitation edges 0-66345
 - $\text{Pb}_{1-x}\text{Sn}_x\text{Te:In}$, Hall effect and photoconductivity (Russian) 0-103720
 - Pt, core-electron excitation edges 0-66345
 - ReO_3 , cubic lattice stability, screening effect on vibrs. 0-75356
 - Si on sapphire, residual strain effect on elec. props. (Japanese) 0-84522
 - Si:Se, impurity states, A- and B-centres, electron, hole thermionic emission rates 0-96813
 - SmZn , ferromag., cond. band antiparallel polarisation exceeding 4f moment 0-60207
 - SrTiO_3 , K-edge X-ray absorpt., cond. band states 0-97382
 - Te, cyclotron reson. in pulsed high mag. fields, cond. band struct. 0-59867
 - TiO_2 , rutile, K-edge X-ray absorpt., cond. band states 0-97382
 - V_2O_5 , energy band structure, tight-binding method 0-70602
 - ZnGa_2S_4 , band struct., pseudopot. method 0-92816
- conduction electron spin resonance *see CESR*
- conduction in solids, ionic *see ionic conduction in solids*
- conductivity, electrical *see electrical conductivity*
- conductivity, thermal *see thermal conductivity*
- conductors (electric)
 - see also bimetals; overhead line conductors*
 - 1/f noise in electrical conductors, survey 0-107878
 - hollow conductors for force-cooled superconducting magnets, fabrication and properties (Japanese) 0-90868
 - multiparallel system of conductors losses in thin nonmagnetic plate calc. 0-78743
- confinement, plasma *see plasma confinement*
- connecting *see joining processes*
- connectors (electric) *see electric connectors*
- conservation laws
 - see also C invariance; CP invariance; CPT invariance; elementary particle symmetry; P invariance; T invariance*
 - σ -model supersymmetric extensions, dynamical conservation laws, symmetric space valued fields 0-95227

conservation laws continued

σ -models, conservation laws, infinite series, differential geometric content 0-62841
anomalous muon capture and lepton number conservation 0-68654
baryon asymmetry of the Universe, quantum black hole evaporation (*Russian*) 0-109577
chiral field, supersymmetric, 1/N perturbation theory and quantum conservation laws 0-68373
chiral $O(N) \times O(N)$ and $SU(N) \times SU(N)$ 2-dimens. models, conservation laws and S-matrices 0-68389
classical systems with infinite set of conservation laws 0-86102
 CP^N σ -models, 2-dimens., local conserved currents, conservation laws 0-86579
dielectrics, hyperelastic, with saturated polarisation, variational and invariance principles 0-74730
early Universe, baryon number generation due to CP- and B-violating interactions 0-109571
evolution equations, nonlinear, and their conservation laws, spectral transform method 0-62488
general reactivity weak conservation law covariant formulation 0-73224
Goldstone theorem generalisation, scalar fields, conserved current and mass spectra struct. 0-68339
grand unification, neutron oscillations and massive neutral Majorana leptons, baryon number 0-91033
group theoretical construction of two-dimensional models with infinite sets of conservation laws 0-99056
hydrodynamics, quantum relativistic, nonlinear generalised equations 0-68380
Korteweg-de Vries eqn., generalised, conserved quantities 0-68054
Korteweg-de Vries system, Lax representation, conservation laws 0-82893
mechanical systems, follower load type, time invariant functionals 0-77609
neutron-antineutron oscills., proton instability (*Russian*) 0-101948
nonlinear evolution eqns., conservation laws, group theoretical derivation 0-57520
nonlinear evolution eqns., inverse scatt. method, conservation laws (*Russian*) 0-105804
particle collisions, conservation of energy and conservation of vector momentum 0-101693
physical system, model of space-time from set theory concepts 0-82660
principle chiral fields, Backlund transformations and local conservation laws 0-68388
quantum field theory, Lagrangian formulation, conservation laws, relativistic gravitation (*Russian*) 0-68337
relativistic quantum theory with correct conservation laws 0-82677
Schmurs, combinatorial hierarchy, spin dichotomy and conservation of quantum numbers 0-68383
sine-Gordon system, Lax representation, conservation laws 0-82893
 $SU(2n)$ principle models for integrable nonlinear systems, current constraints, conservation laws 0-86619
 $SU(5)$ invariant theory, B-L nonconservation and neutron oscillation 0-78005
 $SU(5)$ without symmetry constraints, unified model of quarks and leptons, conservation laws 0-101968
unified models of quarks and leptons, B-L conservation and B nonconservation 0-95229
Yang equations, invariance props. 0-62836
Yang-Mills field, conservation-law violation at high energy by anomalies 0-62855
 $\bar{\nu}_e \rightarrow \nu_\mu$, exotic lepton number violation and neutrino Majorana masses, Higgs sector 0-86615

constant current modulation *see amplitude modulation*

constant current sources

GaAs laser diode power supply control oct. (*German*) 0-78852
mass spectrometer magnetic analyser constant current solid-state power unit 0-86499
Wheatstone bridge fed from a bilateral constant current source 0-57338

constant voltage diodes *see avalanche diodes; Zener diodes*

constants

see also elastic constants; gravitational constant; lattice constants; optical constants
conference on metrology and fundamental constants, Varenna, Italy (July 1976) 0-105603
man's size in terms of fundamental constants 0-105489
H, Rydberg consts., saturated absorpt., spectroscopy meas. 0-105604

constitution diagrams *see phase diagrams*

constraint theory

nuclear power stations, optimal size and location in energy parks 0-95489

construction *see building*

constructional engineering *see civil engineering*

contact (mechanical) *see mechanical contact*

contact angle

see also capillarity; surface tension; wetting
albumin, adsorbed layers on polystyrene 0-61508
capillary flow, initial stage analysis, relax. model 0-74977
drop spreading on solid surface, initial stage charact. 0-59761
emulsion, creamed, vol. fraction, effect of film thickness and contact angle 0-81370
fibrinogen, adsorbed layers on polystyrene 0-61508
hysteresis, mol. interpretations 0-88400
Newton black film, line tension, determ. by cnt. bubble method 0-88406
Newton black films, line tension determ. by diminishing bubble method 0-88407
poly(dihydroxypropyl methacrylate), surface charact. 0-61140
poly(hydroxyethyl methacrylate), surface charact. 0-61140
poly(methoxyethyl methacrylate), surface charact. 0-61140
quartz, dynamic wetting angle of dry lyophilic surface 0-88405
solid/melt interfacial tension and contact angles of small particles, determ. from crit. vel. of engulfing 0-79915
thin liquid films in emulsions, contact angles 0-92761
wet particulate systems, pendular band strength between unequal-sized spherical particles 0-104418
Au surface, clean, hydrophilic nature 0-80029
Cu-Sn binary system, wettability and interaction between solids and liqs. (*Japanese*) 0-92760
 SiO_2 thin films, deposition and characterisation study 0-80133

contact e.m.f. *see contact potential*

contact lenses

back surface aspheric, inspection 0-66711
corneal pressures due to soft contact lenses and corneal asymmetry 0-104621
corneal sensitivity and thickness after wearing PMMA and gas-permeable contact lenses 0-61544
hydrogel lens power changes due to flexure 0-67286
longitudinal spherical aberration and its effect on visual acuity 0-99816
peripheral curve design, specifying for reproducible performance 0-61733
refractive error stability of contact lens wearers 0-108879
soft, back radius changes on flexure 0-61732
squeeze forces in contact lenses with a steep base curve radius 0-108926

contact potential

see also contact resistance

eye, retina injuries, magnetoretinographic meas. using SQUID magnetometer 0-104702
multilayer thin film struct. thermoelec. props. 0-92964
GaAs-GaSe n-p heterojunction, elec. props., interface states 0-65670
Hg-polymer interface, contact potential and charge exchange meas. 0-75642
Ir, chemisorption of H_2 , adsorption and desorption kinetics, struct. of overlayer 0-84367
Mo, coadsorption of O_2 and Cs, struct., emission props., thermal stability 0-66878
Re/C, work function, graphitic layer formation 0-96966
Si-GaSe n-p heterojunction, elec. characts., interface states 0-70812

contact resistance

see also contact potential

insulating mechanical supports, appl. to meas. thermal conductance 0-82772
metal-semiconductor interface, meas. method 0-105672
metal-semiconductor ohmic contact props., factors affecting contact resistance of semiconductors, theoretical model 0-60076
metal-semiconductor thermoelectric coolers, effects of contact resist. and dopant conc. 0-81481
ohmic contacts to semiconductor, meas. of contact resistance using transmission line model 0-70826
Ag-Zn, internally oxidized, elec. contact characts., alloying additions effect (*Japanese*) 0-88619
Al-Au couple, electroformed, nonohmic characts. and electron emission 0-60066
Al-Cr, thin film metal contact, sheet resistance changes 0-80356
Au surface, lubrication by plasma-deposited thin films of fluorocarbon polymer 0-89157
 $CdGa_2S_4$ double surface-barrier diodes, current-voltage characts. 0-92972
 $CdSnAs_2$ -Au(Al), surface barrier junction, elec. props., temp. depend. 0-65686
GaAs, circuit effects in time-of-flight diffusivity meas., Monte Carlo method 0-88563
n-GaAs, study of ohmic contacts 0-60083
 $GaNAsP$, rectifying and ohmic contacts 0-80376
p-Ga, $In_{1-x}PyAs_x$ - $/Au-Zn$, specific contact resist. 0-84509
GaP, comparison of contact resistances of Au-Zn, Au-Zn-Sb, Au-Ge-Ni and Au-Ge-Ni-Sb alloyed contacts 0-70825
p-InP, ohmic contact using Be-Au metallisation, low contact resist. 0-65677
p-InP-Cd(Zn), ohmic contact formation on InP by laser photochemical doping 0-80369
Mo-Si sputtered contacts, contact resistance 0-92970
 $PbS_{1-x}Se_x$ diode laser, contact degradation due to diffusion 0-102734
 $Pb_{1-x}Sn_x$ Te diode laser, contact degradation due to diffusion 0-102734
Ti metal-metal interface, adhesion energy, surface treatment and ion implantation effects 0-107660

contacts, electrical *see electrical contacts*

continuous creation hypothesis *see cosmology*

continuum hypothesis *see set theory*

continuum mechanics *see classical mechanics of continuous media*

contours, surface *see surface contours*

contrast transfer function *see optical transfer function*

control facilities

nuclear power stations, control rooms, human factors design approaches, improvement of man-machine interface, error reduction 0-63327

control gear, electric *see electric control equipment*

control rooms, radio *see radio studios*

control system analysis

see also correlation methods; frequency response; perturbation techniques; phase space methods; poles and zeros; sensitivity analysis; stability; transfer functions
differential games, control systems with aftereffect 0-68025

control systems

see also adaptive systems; closed loop systems; discrete time systems; distributed parameter systems; multidimensional systems; multivariable control systems; optimal control; physical instrumentation control
prosthesis, sensory feedback system for above knee prosthesis (*Japanese*) 0-72372
USSR State Bureau of Standards, metrological resource programmes 0-90809

control theory

see also control system analysis; optimal control; stability
differential encounter-evasion game, nonstationary, theorem on the alternative 0-68026

controllability

see also stability

pendulum inverted, design and stabilisation control (*Japanese*) 0-73167

controllers

see also cryostats; instruments; servomechanisms; thermostats
heart, artificial, microcomputer based automatic controls 0-67289
solar energy management system 0-66951
temperature, at cryogenic temps. 0-90856
thyristor temp. regulator for pulsed NMR spectrometer 0-105687
voltammetric analysis, automatic controller, design 0-71968
 O_2 flow regulator, solid-state, high-temperature 0-57301
SiC thin-film thermistors with high thermal response (*Japanese*) 0-105629

convection

- see also convection in liquids
- air suspension homobaric flow in presence of physicochemical transform. 0-87820
- alloy melt, temperature distribution during cryst. growth by Czochralski method (*Russian*) 0-75192
- annulus, tall, vertical, conduction regime of natural convection stability 0-99987
- aquifer, temp. field due to hydrothermal convection, numerical calcs. 0-90105
- Archaean crust, geothermal heating rel. to vertical tectonism in greenstone belts 0-81861
- atmosphere, African wave disturbances, convection role, linear primitive eqn. model 0-77043
- atmosphere, forward air flow effect on evolution of convection 0-90116
- atmosphere, meas. of heat flux and struct. functions of temp. fluctuations with acoustic Doppler sodar 0-105023
- atmosphere, models of thermals 0-109228
- atmosphere boundary layer, boundary layer, appl. of mixed-layer similarity scaling to observed dispersion from ground-level source 0-105021
- atmosphere convection dynamics equations, non-Archimedean approach 0-77048
- atmosphere surface layer, convection speed of features of organised motion 0-72602
- atmospheric, fixed cloud-top temp. and fixed cloud-top altitude approximations for temp. profile 0-72616
- atmospheric transport problems, contaminant movement, Galerkin finite element method 0-74902
- axisymmetric convection in shallow rotating cylinder, centrifugal acceleration effects 0-96260
- axisymmetric jets, coherent structs. using optical technique, convection vel. 0-69888
- baroclinic atmosphere, two dimensional, zonal flows convective instability (*Russian*) 0-94564
- Benard convection, mean field equations 0-83798
- Benard problem, R^2 class of mappings, invariant Cantor sets and strange attractors 0-59037
- bounded coaxial jets, convective heat transfer in turbulent mixing, swirling 0-64541
- Boussinesq fluids, viscosity, conductivity and power spectrum of turbulent convection 0-98543
- buoyancy-thermocapillary convection layers with free surface, energy stability theory 0-87768
- cellular convection in a stratified atmosphere 0-98652
- β Cephei stars, effects of convection and mass loss on instability strip 0-90436
- channel with porous walls, convective diffusion and mass transfer (*French*) 0-79305
- chemically driven convection of dissociating Navier Stokes fluid, instabilities 0-59128
- closed gas centrifuge, eigenvector soln. of linearised eqns. of thermal convection 0-83797
- cloud development, effects of explosion (*Chinese*) 0-82042
- coaxial radiative and convective heat transfer in gray and nongray gases 0-102963
- combined convection flow along vertical surface, fluctuating boundary layers 0-96254
- combined free and forced convection, periodic vortex formation 0-74878
- combined heat transfer, state of the art review 0-79119
- compressible fluid layer through porous medium, thermal instability 0-92114
- conduction-convection problems, error growth for explicit difference schemes 0-92017
- confined thermal convection driven by non-uniform heating from below, boundary layers 0-87769
- cooling efficiency in flow around wall, initial turbulence effects 0-79315
- cosmic rays, radially outward convection rel. to large amplitude wave-trains of neutron intensity 0-94660
- cylinders, vertical and coaxial, theory of convection, velocity profile and heat transfer 0-59036
- cylinders in crossflow, forced convection heat transfer, aspect ratio effects 0-64546
- cylindrical porous medium, free convection boundary conditions, mean heat transfer 0-79302
- Czochralski crystal growth, heat, mass and fluid flow, computer simulation 0-104055
- diffusion and convection in parallelogram cross-section pipe with plug flow (*German*) 0-100000
- diffusion-convection equation, stability of finite difference approximations 0-82730
- ducts, non-circular, forced convection heat transfer problems 0-64557
- Earth mantle, convection and subcrustal stresses under Australia 0-72484
- Earth mantle, radiogenic heating in convecting mantle rel. to oceanic bathymetry flattening 0-85642
- Earth mantle, solid-state convection rel. to Earth thermal evolution 0-89988
- Earth mantle convection, countercurrent accompanying descending Pacific lithosphere beneath Japan (*Japanese*) 0-94514
- Earth plasma sheet, magnetised plasma slow convection theory 0-109312
- EHD, convective instability in dielectric fluid between two coaxial cylinders 0-74994
- electrostatically assisted, steel plate cooling meas. 0-69628
- evolution systems and convection-diffusion, stiffness and stability, Gershgorin theory 0-77626
- external noise effect on transition to turbulent convection 0-96263
- extrudate swell, thermally induced, Galerkin method 0-79312
- F-type star, main sequence, convection and photospheric granulation 0-90417
- finite-amplitude thermal convection and geostrophic flow in a rotating magnetic system 0-87813
- finned assemblies, dimensions effects on heat flowrate, free convection to condensation 0-74714
- flms, nonlinear problems, 1-D conduction, initial value problem 0-83726
- flat vertical plate, transient natural convection in air 0-64556
- fluid heated from below, Benard problem with perturbed lower wall 0-79320
- fluid layer between co-axial cylinders, instability of natural convection 0-64558
- fluidised bed, rate of heat transfer from freely-rising slug of hot gas 0-96307

convection continued

- free convection boundary layer flow and heat transfer, variational technique 0-106796
- free convection flow between heated vertical parallel plates, quasilinearization 0-92148
- free convection flow past vertical porous plate set in impulsive motion 0-69818
- free convection heat transfer from vertical thin wire to air, laminar-turbulent transitions (*Japanese*) 0-92152
- free convection in rectangular enclosures filled with fluid and with porous media, review 0-79115
- free convection loop embedded in heat conducting solid, heat transfer 0-96257
- free thermal convection in a vibrational field under conditions of weightlessness 0-87773
- free-convection flow past an accelerated vertical infinite plate 0-92154
- gas, circulating, forced convection through porous cavity, solar heating (*French*) 0-69626
- gas bubble dissolution (growth), convective transport effect 0-87792
- gas flow past surface, interaction of radiation with convection (*Russian*) 0-99994
- glass, melting in fire-heated tanks, modelling (*Polish*) 0-96633
- granitic magma of Bushveld Complex, convective mixing rel. to crystallisation history and trace element abundances 0-109145
- heat pipe, spectroscopic, operation 0-106708
- heat source driven turbulent convection between 2 rigid plates at arbitrary Prandtl number 0-69829
- heat transfer in laminar region, horizontal and inclined cylinders 0-99915
- heated curved wire, free convective heat transfer, numerical study 0-69835
- helically rib-roughened tubes, forced convection heat transfer and friction characs. 0-96258
- homogeneous isotropic turbulence, inertial convective region, scalar fluctuation spectrum (*German*) 0-92120
- horizontal cylinder with different end temps., natural convection, jets 0-99996
- horizontal fluid layer in porous medium, convective instability, critical Rayleigh number 0-64564
- horizontal pipe subjected to external convection and radiation, laminar forced convection 0-79307
- horizontal ribbon growth from melt, forced convection heat flow effects 0-107079
- hydrodynamic instabilities and turbulence, flow states, examples and meas. methods 0-92116
- hydromagnetic free convection flow in Stokes problem, for porous vertical limiting surface with const. suction 0-90328
- hydrothermal flows, two-phase, in permeable media, struct. 0-85693
- impulsively started vertical plate, mass transfer and free convection currents 0-64567
- inclined fluid layer, double diffusive instability, secondary convecting layers 0-92112
- inclined surfaces, wave instability of laminar mixed convection flow 0-69837
- infinite Prandtl number thermal convection in a spherical shell, Earth mantle 0-59033
- interstellar medium, absolute and convective instabilities 0-98539
- ionosphere, auroral convection over $60^\circ \leq A \leq 75^\circ$ from Millstone Hill incoherent scatter 0-67454
- ionosphere, elec. fields and plasma convection in dayside auroral oval 0-98501
- isothermal concentric spheres, natural convective heat exchange 0-64340
- isothermal horizontal circular cylinder, laminar free convection, thick boundary layer 0-64566
- Jharia Gondwana sedimentary basin, India, groundwater movement rel. to geothermal meas. 0-98276
- kinetic theory, convective diffusion to a particle in a fluid with linear kinetics 0-69943
- laminar film boiling heat transfer, thermal conductivity and convection effects 0-74864
- linear convective stability, Soret effect, horizontal quiescent layer of two-component fluid 0-92144
- Lorenz model dynamics for convective instability 0-59007
- low Prandtl number fluid, nearly insulating boundaries, two-dimensional convection rolls 0-74883
- magnetic fluids, heat and mass transfer 0-59123
- magnetic fluids, instabilities, leading to rupture of continuity 0-59003
- magneto-active plasma convection, two velocity hydrodynamic eqn. solution (*Russian*) 0-79459
- magnetosphere, polar cap convection after interplanetary mag. field becomes northward 0-94658
- magnetosphere convection, role in global scale electrodynamic coupling of ionosphere high and low latit. regions 0-77194
- magnetosphere convection electric field, divergence rel. to auroral currents and elec. pots. and precip. generation 0-67453
- Marangoni convection 0-66425
- mesoscale convective systems, inertial instability 0-90131
- metals, unidirectional solidification, heat flow model 0-79914
- MHD convective flow through porous channel with Hall and wall conductance effects 0-74993
- mist formation in turbulent convection field, critical supersaturation model 0-64611
- molten materials with internal heat sources and consolidated boundaries, free convection (*German*) 0-59019
- moving horizontal flat plate, laminar boundary layer, buoyancy effects 0-74877
- natural, Navier-Stokes eqn. soln. numerical stability 0-92147
- natural convection in a shallow annular cavity with differential heated walls 0-79295
- natural convection in a vertical cylindrical well filled with porous medium 0-79297
- natural convective wall plume, boundary layer eqns., higher order anal. 0-64550
- natural laminar convection about isothermal cylinder, Navier-Stokes eqn. soln. 0-92143
- Neptune, convective vortices rel. to equatorial flow 0-67653
- non-condensing gas on flat plate and horizontal tube, forced convection condensation 0-64553
- non-Newtonian liquid mixture separation by thermal diffusion in parasitic convection 0-64587
- nonisothermal magnetisable fluid, thermal convective stability, modulated mag. field effects 0-64646

convection continued

nonlinear heat transfer on boundary, difference method of solving conjugate nonstationary convection problem 0-92020
 ocean gyre, poleward heat flux 0-85668
 mid-ocean ridges, convective heat transport by ridge crest hot springs 0-98304
 oceanic crust, topographically driven subcritical hydrothermal convection 0-101345
 open systems, definitions of heat, internal energy transfer by convection 0-69644
 optimisation of convective annular/circular fin of minimum mass 0-79109
 parallel plate channel, convective-radiative interaction, air-operated solar collectors appl. 0-96259
 plane parallel flow, free convection in Couette and Poiseuille flows, numerical simulation 0-99995
 plasma convective cells, nonlinear excitation by interchange modes and spectrum cascade processes 0-69997
 plate, flat, transparent, non-absorbing, natural convection due to solar radiation, buoyancy-driven flow 0-69826
 plate, heated, semiinfinite, vertical, with heat sources and sinks natural convection 0-59035
 plate, vertical, free convection boundary layers and heat transfer 0-59002
 plate and laminar slug flow with periodically changing temp., transient heat transfer 0-74872
 plate with cylinder in turbulent boundary layer, forced convection heat transfer 0-64540
 plate with impinging hot gas jet with low Re, convective heat transfer 0-96256
 plates, vertical and inclined, mixed convection combined, heat and mass transfer 0-64552
 porous medium, saturated, mixed convection boundary layer flow on vertical surface 0-106798
 positive surface tension gradients, Rayleigh-Benard convection (*French*) 0-75404
 Puna geothermal area, Hawaii, thermally driven ground gas convection system discovery from Rn survey 0-85657
 pyroclumulus cloud over North Canterbury, New Zealand, 1878 April 10, obs. 0-109240
 radiative convective heat transfer of thermally thin body 0-79110
 Rayleigh-Benard convection, wave number selection, sidewalls effect 0-106799
 Rayleigh-Bernard convection, forced phase diffusion 0-103019
 reaction zone propagation, combustion wave structure inversion in porous media 0-89494
 rectangular body in forced convection, heat transfer study, flow separation 0-74874
 rectangular cavity with porous filling, steady convection and boundary layers 0-79309
 refrigeration, heat transfer by natural convection with simultaneous frosting on horizontal cylinders in a vertical array (*Japanese*) 0-58890
 rotating fluid, layer heated, turbulent convection 0-100003
 rubrene, electrochemilum. by DC, highly organised EHD convection obs. 0-71499
 saturated porous layer, sudden temp. rise, stability, linear and energy methods, convection 0-74972
 second order fluid, natural convection flow from porous plate, suction and injection effects 0-59029
 semi-infinite porous medium bounded by horizontal surface, mixed convective flow, vortex instability 0-79304
 semicircular cross section tube, nonsteady convective heat transfer 0-99999
 simple body melting time with convection boundary condition 0-99914
 small particles suspended in turbulent fluid, convection, mass transfer 0-87793
 solar atmosphere, penetrative instabilities theory in presence of thermal dissipation 0-109406
 solar convection zone, struct. adjustments rel. to solar luminosity short term fluctuations 0-82321
 solar energy collection, double glass, convection in vertical rectangular channels (*French*) 0-85300
 solar energy collection and storage, latent heat diode walls, space heating (*French*) 0-61298
 solar granular convection, effects in response of C I 5380 Å response to solar luminosity vars. 0-85910
 solar granulation motions, effects on photosphere mag. fields fine struct. 0-98646
 solar granulation structure, vertical motion models 0-90375
 solar granulation structure, vertical motions spatial and temporal behaviour obs. 0-85912
 solar heating, air movement control 0-66946
 solar nebula, primordial, influence of convection on struct. and evolution 0-62042
 solar photosphere, waves and convective motions determ. from spectral lines asymmetry (*Russian*) 0-72901
 solid reacting particles, ordered system at high Peclet numbers, mass transfer, convection 0-69830
 solidifying melt, two phase zone formation, convection (*Russian*) 0-93547
 spherical laser target hydrodynamic compression stability (*Russian*) 0-106159
 stably stratified medium, plane free convection from local heat source 0-96253
 stars, magnetic, convective stability 0-94781
 stars, main sequence intermediate and late differential rot. models 0-105238
 stars, massive, convective and semiconvective mixing 0-90405
 steady state convection-diffusion eqn., quadratic finite element solns. 0-92019
 steady State stefan problem with convection 0-69625
 stellar accretion discs, steady, optically thick, convective vertical energy transport 0-62112
 stellar convection, value of mixing length 0-77379
 stellar convective envelopes, non-local convection, statistical theory (*Chinese*) 0-85933
 stellar interiors, core He flash models with two-dimensional convection 0-105230
 stellar interiors, degenerate C burning front convective propag. rel. to core implosion 0-77390
 stellar turbulence, conference, London, Ontario, Canada (1979 August 27 to 30) 0-73102
 stellar turbulent convection equations, ensemble averaging 0-67698

convection continued

stochastic perturbation of convective motion, truncated spectral model 0-92146
 Stokes' problem, mass transfer effects of MHD free convective flow 0-62003
 Stokes problem, effects of free convection on oscillatory flow past infinite porous vertical limiting surface 0-109348
 stratified fluid, duct, equilibrium breakdown, thermosiphon work (*French*) 0-59114
 Sun, convective element intrinsic mag. field 0-101583
 Sun, differential rot. effect on convection struct., Maunder minimum nature 0-101573
 supernova core, Rayleigh-Taylor convective overturn rel. to explosion 0-77429
 supernovae, explosive core overturn and mass ejection 0-72988
 swirling convective boundary layer, vorticity dynamics 0-59048
 thermal convection at high Rayleigh number, variation of Nusselt number 0-79300
 thermal convection in porous media, dispersion effects 0-103027
 thermal perturbations in moving nonlinear media, convective spatial localisation, cond. coeff. depend. 0-106706
 thermal-convective instability of partially ionized plasma, radiative transfer, medium porosity and collisional effects 0-67538
 transient free convection flow around two-dimensional or axisymmetric bodies 0-69817
 trench with radiative wall conditions, free convection 0-79324
 tropical depression, synoptic scale kinetic energy source, cumulus cloud convection 0-77088
 turbulent free convection in mag. field, statistical characts., vortices 0-79310
 uniformly heated horizontal circular cylinder banks, natural convection heat transfer 0-64538
 Uranus, convective vortices rel. to equatorial flow 0-67653
 vertical cylinder, combined heat and mass transfer in natural convection 0-59027
 vertical plate, laminar natural convection heat transfer, supercritical CO₂ and He 0-64544
 vertical plate with uniform blowing, laminar combined forced and free convection 0-74876
 vertical surface melting, heat transfer interferometric meas., convection effects 0-64339
 vertical tubes with zero inlet subcooling, forced convection boiling, critical heat flux 0-64549
 viscous fluid, stability of steady vertical flow 0-64520
 volumetrically heated fluid layer, combined natural turbulent convection and radiation 0-74871
 walls, permeable, cooling characts., heat exchange, rad. emitter design 0-64535
 H₂-He gas mixtures, 1000-25000K, transport property correlations 0-75029
 He, sound transmission at liq. solid interface, probe of melting kinetics 0-92734
⁴He gas lasers, horizontal, heated from below, Nusselt and Rayleigh numbers 0-79311

convection in liquids
 Benard convection, stability of horizontal layer of fluid heated from below 0-87767
 Bernard convection, and linear fluctuation theory, Markovian processes and irreversibility 0-87766
 binary alloy indirectional solidification, convective and interfacial instabilities 0-60851
 binary fluid system, Onsager coeffs., steady state soln. for Benard convection 0-64851
 binary liq. layer, microgravity, thermoconvective stability 0-74866
 buoyancy induced flow adjacent to vertical uniform flux surface in cold water 0-69834
 cholesteric liquid crystals, oscillatory convective instabilities, caused by heating from below 0-103239
 combined convective heat transfer along vertical plate with uniform blowing (*Japanese*) 0-74867
 combined convective heat transfer with opposing flow around an isothermal wedge (*Japanese*) 0-69838
 convective cells, stochastic oscil. spatial-time spectra (*Russian*) 0-103029
 crystal growth from melts, hydrodynamic behaviour under large interfacial accelerations 0-66421
 crystal growth from solution, convection effects, holographic interferometric obs. 0-77565
 crystal rotation in crucible, melt forced convection, computational results 0-84116
 dielectric organic liquid, concentric annuli, heat and momentum transfer, electric field effects 0-96315
 diffusive convection, fluids with gradients of two properties, low Prandtl number, boundary layer method 0-69816
 elastoviscous liquid, combined free and forced convection flow through porous channel 0-103073
 electrodes, sheet, mass transfer to continuous moving surface 0-69821
 electrolyte, ionic mass transfer in narrow rectangular conduits 0-61105
 electroviscous effect, AC characteristics, pressure-drop fluctuations 0-107457
 energy stability of the Eulerian-mean motion in the upper ocean to three-dimensional perturbations 0-92149
 filtration, plane, of underground waters, convective mass transfer, boundary problems (*Russian*) 0-83793
 flat-plate solar collectors, laminar mixed convection in fully developed flow (*French*) 0-61411
 flow in porous media, diphasic incompressible, diffusion-convection eqn., mixed finite element method, water flooding 0-74969
 forced convection boiling, critical heat flux, Fe₂O₃ scale effects 0-64344
 forced convection condensation in the presence of noncondensables, boundary values (*Japanese*) 0-92151
 forced heat convection of linear flow of non-Newtonian fluids through rectangular channels 0-92141
 free convection heat transfer on a magnetic cylinder in a uniform magnetic field 0-83852
 free laminar convection for liquid in ribbed slot 0-96261
 free turbulent heat exchange surface, free convection liquid flow 0-64543
 Gorter-Mellink convection in He II, axial heat slw eqn. and dims. anal. 0-64545
 hydromagnetic flow, stability in temp. field 0-92231

convection in liquids continued

- immiscible incompressible fluids, interfacial convective instability, diffusional exchanges, adsorption-desorption processes 0-70504
 insulants, elec. stressed, bulk electroconvection 0-87814
 magnetic convection, nonlinear, mean field approx., boundary layer method 0-69930
 MHD forced convection in channel bounded by plate and permeable bed, Hall effects 0-69934
 Newtonian fluid, recirculating flow in rectangular cavity, free convective flow in enclosed container 0-74852
 non-stationary heat and mass transfer, coupled, with convective motion and relaxation, variational principle 0-106797
 Parowax, thermal energy storage, phase change material, time variation of storage and release 0-67008
 pure liquid and binary soln. superheat, convective heat transfer from thin wire 0-92139
 Rayleigh-Benard convection, randomly forced, initial value problem 0-79314
 Rayleigh-Benard convection, turbulence and intermittency, expt. 0-99998
 reacting particle in fluid, convective diffusion, nonlinear surface reaction kinetics 0-106854
 smectic-A liq. crystals, sub-Rayleigh oscill. convection 0-87774
 smectic-A liquid crystals, oscillatory convective instabilities, caused by heating from below 0-103239
 solar absorbers, heat transfer by natural convection in an isothermal rectangular cavity open on one side (*French*) 0-61412
 solid spheres, reacting, in periodic array, convective mass transfer in liq. laminar flow 0-96176
 sphere in current carrying liq., convection mass transfer, num. anal. 0-83851
 stratified liquid, convective free flow struct. above heated cylinder 0-79322
 stratified liquid, free convective flow struct. over point heat source 0-79323
 thin film, viscous, between two nearly parallel walls, temp. distrib., convection effects 0-83801
 transient natural convection in a liquid during cooling 0-87770
 turbulent channel liquid flows, nonsteady convective heat transfer 0-59023
 two-component liquid layer heated from below, convective instability, analogy with laser with saturable absorber 0-79319
 vertical natural laminar convection flows in cold water, buoyancy force reversals 0-59034
 viscous convective flow, mixed finite element soln., discrete least squares approach 0-74851
 viscous fluid, incompressible, hydromagnetic free convective flow past vertical porous wall, mass transfer 0-64645
 water at 4°C, unsteady free convection past infinite vertical plate 0-69822
 water evaporative cooling, convection and mass transfer, fog formation in boundary layers 0-79293
 water evaporative cooling, heat and mass transfer coeffs., fog formation effects 0-79294
 water near 4°C, plane-parallel convective flow instability 0-92137
 CuSO₄ soln., electrochemical analogue of Benard instability, isothermal and potentiostatic conditions 0-76530
³He superfluid ³He mixture, dil. soln. of ³He convection 0-107600
 InSb, convection in melts, and cryst. growth under large inertial accelerations 0-66421
 NH₄Cl-H₂O, solidification microstructs., effect of reduced gravity 0-96632
 NaK, liquid metal natural convection under transverse magnetic field 0-69827

convergence

- see also *convergence of numerical methods*
 adaptive beam forming processor formulation 0-91967
 Maxwell's initial boundary value problem, horizontal line (Rothe) method, convergence and error estimates 0-94957
 nonstatistical parameter estimation adaptive algorithms 0-91995

convergence of numerical methods

- electronic structure calcs., self-consistent, accelerating convergence of iterative process 0-87037
 MHD equilibrium equations, convergence of iterative schemes 0-59115
 three-dimensional neutron transport, discrete ordinate solution 0-63222
 Cu, Fermi surface, electron mass enhancement, orthonormal function enhancement 0-96777
 Nb, Fermi surface, electron mass enhancement, orthonormal function enhancement 0-96777

conversion electron spectra

- Mossbauer spectroscopy, cryogenic proportional He counter 0-69010
¹²³Cs(^{123m}Cs), gamma and conversion electron radiation 0-106017
²²⁴Fr-²²⁴Ra, γ rays, internal conversion, $\epsilon\gamma$ coincidence spectra meas. 0-78216
¹⁵⁵Gd, vibr. state, level scheme, γ and conversion electron spectra from ¹⁵⁴Gd(n,γ) 0-57696
¹⁵⁷Ho-¹⁵⁷Dy decay, internal conversion electron spectra and $\epsilon\gamma$ coincidences (*Russian*) 0-68604
²⁰⁴Po, γ -rays, conversion electron spectra, $\gamma\gamma$ coincidences 0-83061
²⁰⁸Rn-²⁰⁸At, γ -ray, conversion electron spectra 0-83072
²²⁴Rn-²²⁴Fr-²²⁴Ra, γ -rays, internal conversion, $\epsilon\gamma$ coincidence spectra meas. 0-78216
 UF₄, inner conversion electron spectra, electron orbit hybridisation (*Russian*) 0-87227
 γ -UO₃, inner conversion electron spectra, electron orbit hybridisation (*Russian*) 0-87227

convertors

- see also *analogue-digital conversion; code convertors; digital-analogue conversion; direct energy conversion; frequency convertors; image convertors; magnetohydrodynamic convertors; power convertors; solar absorber-convertors*
 air flow consumption meas., respiratory process parameters determ. using electric model (*Bulgarian*) 0-76867
 Hough-Powell digitizer for processing film from bubble chamber Mirabelle in K⁺p expt. at 32 GeV/c 0-69040
 O/E and E/O, connected to both ends of optical fibre giving low-loss, broad band, non-inductive line (*Japanese*) 0-87510
 readout conversion, mechanical to electrical, of differential oil flowmeter 0-75013
 readout conversion, mechanical to electrical 0-75012

convertors continued

- time to amplitude, performance tests at high conversion rates 0-62648
 LiNbO₃:Ti electro-optic TE-TM mode convertor structure 0-64215
- cooling**
 see also *Joule-Thomson effect; low-temperature production; magnetic cooling; refrigeration; supercooling*
 absorption chillers, solar-fired, capacity modulation 0-66952
 absorption refrigeration machine driven by solar heat for air conditioning, math. modelling 0-76651
 alkylbenzenes, jet-cooled, vibr. relax., absorpt. spectra 0-74236
 alkylbenzenes, jet-cooled, vibr. relax., fluoresc. spectra 0-78694
 alloys, apparatus for rapid hardening from liquid state 0-76275
 atomisation of water drops on hot metal wall (*French*) 0-79112
 boundary value problems, mixed and oblique derivative boundary conditions 0-69820
 trans-butadiene, ¹B₁₀-state dynamics in cooled supersonic expansion, electronic absorpt. spectra obs. 0-78629
 chalcogenide glasses, O-free, cooling rate influence on optical consts. 0-88952
 conduction cooling device for low temp. phosphorimetry 0-90855
 cryorefrigerator, double-stage for cooling to 10K on a 4-circle diffractometer 0-98919
 cylinder in still air, DC corona cooling obs. 0-70071
 Earth, interior cooling contrib. to surface heat flow rel. to Earth thermal evolution 0-89988
 efficiency in flow around wall, initial turbulence effects 0-79315
 electron microscope, 1.2 MV, high-resolution double-tilt cooling stage 0-68322
 electrostatically assisted, steel plate at 500°C 0-69628
 ethyl acetate, gas, radiatively heated by CO₂ laser, cooling mechanism investig. 0-75021
 Ettingshausen device, transient cooling effects, theory 0-80304
 fission product decay heat removal with fusion-fission hybrid mobile blanket 0-99282
 freely flowing liquid film, cooling, heat transfer, turbulent transport model calcs. 0-64560
 fusion reactor, long pulse high current ion source electrode cooling 0-91360
 fusion reactor, press. induced flow cooling, highly stable superconducting mag. systems 0-106192
 fusion reactor, TFTR, field coils cooling water system 0-106160
 fusion reactors, large Coil Program, Westinghouse coil cooldown and warmup 0-106193
 fusion reactors, Large Coil Test Facility, liq. He cooling system 0-102321
 gas atmosphere quantitative analysis adsorption chamber 0-85234
 gases, radiatively heated by CO₂ laser, cooling mechanism investig. 0-75021
 generators, H₂ production, on-site, electrolysis of H₂O 0-72097
 generators, H₂ technology, solid polymer electrolyte H₂O electrolysis 0-67012
 glass, isobaric thermal behaviour during heating and cooling, rate of recovery, one-parameter model 0-75165
 glass, viscous deformation during heating and cooling 0-89314
 heat pump, chemical, hydride conversion and storage system 0-72077
 heat transfer and evaporation from cooled surfaces, nonlinear eqns. numerical soln. (*German*) 0-58893
 heated cylinder in still air, cooling by corona wind expt. 0-84023
 heated pounds, turbulent boundary layer of stratified airflow, surface waves 0-92133
 III-V compounds, Stefan problem, exact soln. describing growth rate with linear cooling 0-59411
 ingots, cooling regime in conditions of minimal thermal stress, modelling (*Russian*) 0-65194
 ion, electromagnetically confined, laser cooled, double resonance and optical pumping 0-87155
 Jupiter cooling time, effect of dense cores on evolutionary models 0-98603
 line-focus parabolic-trough photovoltaic arrays, active and passive cooling 0-93988
 liquid, transient natural convection during cooling 0-87770
 liquid-glass transition, glass transition depend. on heating and cooling rates 0-79920
 low temp. melt spinning device 0-100825
 meltspinning, theoretical anal. of ribbon thickness formation 0-104143
 metal cryostat, evacuation of ³He vapour by an absorpt. pump 0-73369
 metal-semiconductor thermoelectric coolers, effects of contact resist. and dopant conc. 0-81481
 mineral cooling rates, implications of antiphase domains exptl. coarsening in pigeonite 0-81886
 N₂O refrigerator, thermodynamics and thermoelectric condenser design 0-108809
 negative ion source, nucleated boiling water cooled cathode, design and testing 0-102370
 neutral beam, continuously operating, convectively cooled ion accelerator, mech. design and fabrication 0-102374
 neutral beam injector, continuous operation, water cooled U-tube extraction grid 0-99392
 neutron stars, cooling 0-77443
 nuclear power stations, accumulation ponds cooling possibility analysis (*Slovenian*) 0-91208
 optical fibres, cooling rates during drawing 0-66538
 orbiting IR detector cooling by multimission solid cryogen cooler 0-86423
 phosphorimetry, low-temp., conduction cooling system for sample introduction 0-87158
 phthalocyanine, free base, fluoresc. excitation spectrum, cooling in supersonic free jet 0-95670
 plasma sources, cooling pattern of acceleration grids meas. by IR scanning 0-86303
 plate, vertical, unsteady free convection of water at 4°C 0-69822
 point-focus Fresnel lens photovoltaic arrays, active and passive cooling 0-93988
 polarised target in high energy physics, horizontal dilution refrigerator with high cooling power 0-73372
 polyethylene terephthalate, low temp. sp. ht., effect of cooling rate 0-100336
 porous structures for cooling laser reflectors, theoretical study 0-91809
 Saturn cooling time, effect of dense cores on evolutionary models 0-98603

cooling continued

- silicate melts, cooling rate rel. to chondrules textures experimental reproduction 0-94763
 solar absorption and vapour compression, residential cooling systems 0-72017
 solar air conditioning with solid absorbents, earth and underground water cooling 0-72018
 solar assisted thermoelec. air conditioner humidifier (SATEACH) 0-108802
 solar cell modules, high-efficiency with improved glass, adhesives and heat dissipation 0-76636
 solar collector wall, bi-coolant, heating cycle, thermosiphoning, building heating and cooling 0-72083
 solar energy cooling, operating systems and current developments, review 0-85265
 solar energy storage system, ammoniated salt heat pump using MgCl_2 , CaCl_2 , NH_4Cl 0-81484
 solar evaporation and refrigeration units, assurance of specified energy parameter values, statistical analysis 0-93848
 solid state energy conversion, appl. of solid state cooling to spaceborne IR focal planes 0-107772
 spent nuclear fuel cooling time determ. utilising gamma-ray meas. 0-63268
 steel, Cr-Ni-C (3, 1, 0.6 wt.%), grain boundary sulphide precip. and hot ductility (Japanese) 0-71654
 steel, low C, low alloy, ferritic-pearlitic, high temp. mech. treatment, cooling effect 0-104193
 steel, Mn-Si-Cr-Mo, dual phase, as-rolled, continuous cooling transformation diagram to optimize composition 0-100829
 steel, W-Mo-Co, high-speed tool, struct. and props., cooling rate effect at primary crystn. temp. 0-76241
 superconductor, hard, critical state stability and oscillations 0-107959
 TEM liquid He cooled environmental cell 0-68323
 thermoelectric devices, maximum refrigerating capacity determ. 0-86318
 thermoelectric heat pumps, two-stage, design criteria anal. for cool-down speed maximisation 0-108812
 trapped ion, laser cooling, theory 0-58414
 turbogenerators, high capacity, heating reduction measures for enhanced reliability and interval between maintenance (Russian) 0-96175
 turbulent channel liquid flows, nonsteady convective heat transfer 0-59023
 vacuum chamber-bell jar with built-in cooling body 0-90860
 vertical surface, cooling by liquid spray, heat transfer 0-74711
 walls, permeable, cooling characts., heat exchange, rad. emitter design 0-64535
 water evaporative cooling, convection and mass transfer, fog formation in boundary layers 0-79293
 water evaporative cooling, heat and mass transfer coeffs., fog formation effects 0-79294
 water films, subcooled, flowing down vertical tube, heat transfer 0-79318
 C-O white dwarfs, effect of C-O eutectic form. on cooling time 0-77405
 Co-Sn system, phase Co_3Sn obtained by splat cooling (German) 0-104147
 Fe-Ti-C, rapidly quenched by splat-cooling 0-84923
 GaAs, cryst. growth from large GaAs solns., critical cooling rate 0-64938
 He, forced flow cooling system for superconducting magnet, numerical anal. of heat-induced transients 0-82773
 O_2 , attachment cooling, press. depend. 0-91663
 O_2 - N_2 mixture, attachment cooling, press. depend. 0-91663
 Pb-Bi, temp. regime of crystn. on rapid cooling (Russian) 0-66495
 $2\text{PbO} \cdot \text{SiO}_2$ melt, coding rate influence on constitution of silicate anions, crystn. kinetics 0-103248
 Sn-Bi(Pb)(Ga), temp. regime of crystn. on rapid cooling (Russian) 0-66495
 $\text{Te}_{50}\text{Ge}_{15}\text{Pb}_{35}$, DSC sensitivity to controlled ageing in glass transition region 0-71673
 Xe arc lamp, air-water cooling system, DKsSh-1000 high pressure lamp (USSR) 0-74452
 Zn-Ga, temp. regime of crystn. on rapid cooling (Russian) 0-66495

cooling towers

- see also water supply
 dry cooling, feasibility study, for industrial applications 0-87705
 plumes, interaction with atm., numerical model simulation (French) 0-94126
 plumes simulation, model calibration at Meppen power station (German) 0-94130

Cooper Hewitt lamps see mercury vapour lamps

Cooper pairing see Cooper pairs

Cooper pairs

- see also BCS theory; Josephson effect
 critical pair-breaking current density, temp. depend. (Russian) 0-70887
 ferromagnetic superconductor, paramagnetic fluctuations, influence on superconductivity 0-70900
 formation, and nature of supercond. currents 0-65736
 Josephson junction, pair transfer, quantum-mechanical description, commutator and anticommutator of collective operators 0-60146
 metal-insulator transition, electron pairing, effect on optical props. of supercond. 0-60139
 semimetal, simultaneous Cooper and insulating pairing, physical states 0-93036
 superconducting thin films Cooper pairs, photon scatt. on plasmons, Landau-Ginzburg theory 0-65738
 superconductivity and phonons, review 0-84543
 Al granular films, inhomogeneous supercond. transitions, microwave meas. 0-103789
 ^3He , superfluid A-phase, mass current, intrinsic orbital angular momentum 0-84338
 Pb-Cd-Pb junctions, pair pot., mag. field depend., crit. currents meas. 0-84555
 Sn superconducting films, Ge-covered, effect on excess elec. cond. 0-65741

coordination complexes

- inorganic complexes are indexed under the appropriate metal compound headings
 No entries

copolymerisation see polymerisation

copper

- see also nuclei with
 (111) surface, PES and band struct. calcs. 0-89118

copper continued

- acoustic losses due to strong ultrasonic and static stress fields 0-79886
 adsorbed CO on (100), vibr. excitation cross-sections 0-75441
 adsorbed formate and acetate species on (100), EELS study 0-76120
 adsorbed NO_2 , ultrahigh vacuum ESR studies 0-97729
 adsorbed Xe on stepped and disordered surfaces, two-dimens. phase transformations 0-103580
 adsorption of O_2 , N_2O on (100) surface, reaction with CO 0-103583
 annealed OFHC Cu, plastic behaviour 0-59559
 annealed polycryst., torsional vibrations decrement, deformed vol. effect 0-76326
 anode, passivating behaviour and illum. effects in alkaline soln. 0-104449
 anodic oxidation, photoelectrochemical effects (French) 0-93701
 atom, orbital energies and X-ray K-absorb. spectra 0-69060
 atom + $\text{H}^+(\text{D}^+)$, K shell ionisation, nuclear Coulomb effect 0-91650
 band structure, optical cond., Compton profile, self consistent calcs. 0-65435
 bicrystalline thin films, characterisation of [001] tilt boundaries 0-75473
 biological specimen Cu content determ. using flameless atomic absorption spectroscopy, effects of sample prep. and matrix 0-98200
 blisters due to He irradiat., proton backscatt. study 0-75273
 Bordoni effect in single crystals, 10.2 and 30.6 MHz 0-66566
 cathode vacuum arc, cathode spot and cell areas, meas. 0-96405
 cathodes, broad area type, electrolum. regions, current-voltage characts. 0-84019
 cell structures, in deformed single crystals, TEM 0-70209
 cementation, electrochem. nucleation and growth on Fe and Al, TEM 0-104451
 cementation, on Fe, deposit struct., reaction rates, SEM 0-104421
 chemisorption, of O_2 , enhancement during Ne^+ bombard. 0-65070
 chemisorption on low-index and stepped surfaces, LEED, AES and UPS obs. 0-84391
 coadsorption of H_2O and Br, on (100) face, Helmholtz layer model system 0-92777
 coadsorption with Ba on W faces, work function changes 0-65378
 coated C fibre, coating struct., SEM study 0-97605
 cold rolled sheet, anisotropy of elastic and strength props. 0-81077
 compressed powder, thermal cond. meas. (German) 0-70669
 condensation on Mo(100) and W(100), early stage comparison 0-80072
 constant junctions with solder, shock-induced elec. response 0-75626
 core-electron excitation edges 0-66345
 corrosion, indoor, rate meas. 0-76404
 corrosion/protection by ion implantation of Al and Cr 0-71789
 creep cavitation topology in high purity Cu, high temperature region (Czech) 0-65138
 creep damage and cavity growth, assessment using density meas. 0-104217
 creep data, comparison with dislocation creep theory 0-71708
 cyclic loading, change in mech. props. rel. to heat treatment 0-104282
 differential ranges of fission products by a coulometric method 0-65097
 diffusion and oxidation of Cu^+ in glass 0-79980
 diffusion in Ag, SIMS investigations 0-59717
 diffusion layer cathodic deposition and anodic dissolution rates 0-93503
 diffusion of H_2 , isotope depend. 0-59727
 diffusion of H and trapping 0-70447
 dimethylammonium manganese trichloride:Cu, impurities in quasi-one-dimens. Heisenberg systems, anisotropy effect 0-80502
 dislocation cell form. during plastic deform., TEM obs. 0-60935
 dislocation pinning rate, neutron and electron irradiat., meas. by internal friction method 0-96570
 dislocation structure, evolution at heating 0-103337
 dislocation velocity, thermal activation exam. of applied stress and temp. depend., expt. methods (French) 0-59474
 dislocations gliding on (001) planes, bright field and weak-beam images 0-107266
 dynamic uniaxial tension and compression curves 0-100884
 electrical resistance of edge dislocations (German) 0-96859
 electrochemical nucleation, and growth on Fe and Al, TEM 0-104451
 electrocrystallisation on graphite electrodes, nucleation 0-93504
 electrode, electrical breakdown of water in μs region 0-103917
 electrode, ionic mass transfer coeffs. determ. in open channels 0-59110
 electrodeposition, on a Cu single cryst. (110) face in presence of sulphauranidine 0-76203
 electrodeposition, on Cu single cryst. (111) plane in presence of sulphauranidine 0-76204
 electrodeposition in cylindrical pores by pulse plating 0-81330
 electrodes, breakdown voltage, prebreakdown current in vacuum, crossed elec. mag. fields depend. 0-79604
 electroless bath, electrochem. control system 0-71601
 electrolytic coating, brightness and adsorption of surface-active additives 0-100963
 electrolytic epitaxial nucleation and growth, on (111) Ag 0-104081
 electron backscattering by bulk target, theoretical model (French) 0-60722
 electron diffraction study, ECP contrast, Bloch wave model 0-96419
 electron emission depend. on surface mechanical treatment (Russian) 0-100945
 electron irradiated, elastic point defect-dislocation interactions, defect dragging model extension 0-65050
 electron irradiated, migration and thermal conversion of defects, 100 to 330K 0-59519
 electron irradiated, selfinterstitial atomic defect interaction radii, recovery expts. and error sources 0-65049
 electron-irradiated, monovacancy migration during stage III annealing, NQR study 0-107576
 electron-irradiated, point defect agglomerates, HVEM invest. during in-situ annealing 0-84213
 electronic structure, bulk and (001) film, extended tight-binding calcs. 0-70592
 electroplating method for sensitizing stress meas. (Japanese) 0-68197
 electroplating of Ni alloy, protection against hydrogen embrittlement, aerospace engine appl. 0-76416
 energy losses and straggling for H^+ and He^+ beams (Russian) 0-84226
 epitaxially grown film, on Au (111), twin form., LEED detection 0-88442
 erosive wear mechanisms, combined TEM and SEM obs. 0-108601
 EXAFS amplitudes, many-body effects 0-97379
 EXAFS analysis of interatomic distances, coord. numbers, and mean relative displacements 0-89087
 extended screw dislocation, (110) misfit defect elastic interactions 0-100232

copper continued

extended X-ray fine struct., lattice consts. 0-89085
 fatigue crack growth and threshold measured at very high frequencies 0-71742
 fatigue crack propag., influence of specimen thickness (*German*) 0-66669
 fatigue crack propag., role of dislocation substruct. 0-60963
 FCC, twist boundaries, struct. invest. using computer simulation technique 0-84185
 FCC(111) substrate, orientation relationship with Fe vac. deposits 0-59836
 Fermi surface, electron mass enhancement, orthornormal function enhancement 0-96777
 film, diffuse optical scattering from variable roughness surfaces 0-100704
 film, EELS, anomalous L_3/L_2 white-line ratios 0-93444
 film, electron transmission, calc. 0-60724
 film, Gorsky effect, internal friction maxima, atom diffusional mobility (*Russian*) 0-70446
 film, interlaser glow induced by picosecond laser pulses (*Russian*) 0-100714
 film, interaction with adsorbed dye mols., absorpt. and luminesc. 0-103981
 film, on amorphous C and Si substrates, dispersion force contrib. to adhesion (*French*) 0-59842
 film, on Au substrate, oxidation and interfacial behaviour, ion scatt. spectroscopy study 0-66691
 film, optical consts. deduced from surface EM wave propag. 0-60697
 film, partially oxidised, EXAFS studies on superficial regions 0-75474
 film, photoelectron emission, intershell interaction influence on 3d and 5d branching ratio 0-104038
 film, single layer and multilayer systems, thickness determ. by X-ray fluorescence. 0-68180
 film, vacuum deposition on Pb (111), substrate diffusion effects, RHEED, LEED, AES 0-65410
 film deposition, thermal effects, influence on internal stress meas. 0-96767
 films, resistance changes due to bombardment by N, C, or Ar ions 0-103670
 films, vac. condensed at oblique vapour incidence, oriented cryst. growth, electron diffr. study 0-97432
 foil, conduction electron spin disorientation at surface 0-75855
 foil, high purity, identification of imperfections by thermal resistivity meas. 0-59951
 foil, laser irradiated, low-angle X-ray scatt., angular block misalignment and hardness (*Russian*) 0-103413
 foils, faulted defect formation by moving boundaries 0-107281
 foils, near $\Sigma 9$ grain boundary properties, boundary dissociation 0-100251
 fracture speed during phase explosion due to electron beam irradi. (*Russian*) 0-76336
 friction surface structural investigation, O_2 surface diffusion (*Russian*) 0-96726
 fusion reactor material, low energy ion erosion expts., Kaufman source appl. 0-68942
 grain boundaries, intrinsic struct., electron diffr. anal. 0-84186
 grain boundaries, near $\Sigma 9$, structure and dislocation interactions 0-79808
 grain boundary, near $\Sigma 9$, props., identification by image matching of Burgers vectors 0-79810
 grain boundary intrinsic structure, boundary mobility 0-103368
 grain boundary migration, TEM obs. on mechanism 0-79812
 Grueneisen number and nonlinearity const., elastic moduli data, US attenuation 0-65165
 Hall coefficient, relaxation times, Fermi surface 0-84460
 high strain rate behaviour, incremental elastic-viscoplastic constitutive eqns. integration 0-85138
 high-purity, grain size and strain rate influence on mech. behaviour, precursors existence 0-85016
 hollow cathode laser, ion laser transitions 0-69366
 hot cathodoluminescence study, electron-hole recombination 0-93410
 human serum Cu, EPR spectrum obs. 0-91582
 impact welding to steel, fundamental parameters 0-97679
 impact welding to steel, wavy interface characts. and formation 0-97680
 implantation in Fe, effect on corrosion by H_2SO_4 soln. 0-71793
 implanted with Cu^{+} , effect on cryst. orientation, Kr penetration meas. 0-88174
 impurity diffusion of V^{th} period elements and self-diffusion 0-65301
 impurity in Cr-Mo-V low-alloy steel, effect on high-temp. ductility and crack growth 0-66652
 impurity in Li aluminosilicate glasses, ESR spectra 0-66027
 impurity in Mn steel, effect on mech. props. 0-66596
 intergranular creep fracture surfaces, with slip band spacing, dimple spacing 0-76345
 intergranular damage parameters in creep (*Czech*) 0-89342
 ion bombard, by 5 keV Ar^{+} , sub-surface damage 0-103399
 ion bombardment, development of pyramidal structures on surfaces 0-84177
 ion bombardment induced preferential orientation of vacuum deposited layer 0-100290
 ion bombardment-induced photon emission as function of target temp. 0-100698
 ion implanted in Al, doping after laser pulse irradiation 0-88194
 ion selectivity, chalcogenide ceramic membrane as Cu-selective electrode (*Chinese*) 0-81357
 irradiated with 20 keV He^{+} , surface damage and gas trapping profile meas. (*French*) 0-84219
 irradiation with O_2 ions, defect production and annealing 0-88214
 K-shell ionisation cross sections, slow electron impact 0-83498
 K-shell X-ray prod. by $^{14}N^{+}$ bombardment 0-91482
 Langmuir films on Cu surface, surface EM wave absorpt. study 0-97359
 laser, atomic, finely dispersed metal particle active medium 0-91777
 laser, energy conversion efficiency, reson. levels excitation 0-99715
 laser light absorpt. by plasma with very steep density gradient 0-96348
 laser pulse irradi. of Cu targets, absorpt. studies 0-79455
 laser radiation absorption in craters on metal targets 0-97386
 Lifshitz constant for calc. of van der Waals force between two solids (*French*) 0-107658
 liq., thermal cond. and elec. resistivity 0-103661
 liquid, deoxidation rates by CO_2 -CO gas mixture (*Japanese*) 0-89394
 liquid, dissolved O below 0.02 wt.% effect on surface tension 0-107618
 liquid, electronic structure, structured medium approx. 0-84421
 liquid, impurity diffusion, shear cell assembly meas. (*French*) 0-75375
 liquid, thermodynamic study of O_2 0-88342

copper continued

magnetic susceptibility, Animalu transition metal model pot. invest. 0-75711
 magnetic susceptibility, model pot. theory 0-75710
 magnetoresistance, temp. depend., impurity effects 0-70682
 matrix for filamentary Nb_3Sn superconductor, thermal strain effects of superconducting critical temp. 0-93032
 membrane, lifetime prediction and design 0-71752
 metal cathodes, oxidised and clean, basic erosion processes in electric arcs 0-103211
 metallised coating on polyethylene terephthalate film, fracture under laser irradi. (*Russian*) 0-76333
 metallization of glass fibre reinforced epoxy laminate (*German*) 0-93670
 microalloyed with B, elec. cond. and strength props. (*Polish*) 0-89285
 microcrack propagation and plastic strain 0-81187
 muon diffusion data anal., theory of incoherent direct and indirect multiphonon transitions 0-70448
 neutron and electron irradi., interstitial formation, dislocation pinning, internal friction meas. 0-100284
 NMR study on nuclear ordering below $1 \mu K$ 0-93187
 nonstationary temperature fields due to moving heat sources, heat capacity, thermal cond. (*Russian*) 0-107448
 nuclear antiferromagnetism, low temp. NMR study 0-66049
 oriented bicrystal, sintering prod. technique 0-108371
 oxidation, secondary ion energy spectra 0-71788
 oxidation kinetics, influence of intermediate annealing treatment 0-89412
 oxidation processes, EXAFS investigation 0-71808
 N.Pacific, trace metal vertical profiles 0-67381
 pickling in HCl waste free system 0-71795
 pin against steel ring, dry sliding wear, role of dynamic recrystallisation 0-108599
 pin-on-disc friction and wear under boundary lubrication, dissolved O_2 effect 0-76365
 plane coalescence, at grain boundaries 0-70221
 plasma arc sputtering, chem. reaction with plasma gases 0-66427
 plasma EM macroparticle acceleration, high press. gas temp. density 0-79583
 plastic deformation thermal activation parameters from creep kinetics and stress relaxation 0-71717
 plastic strain, during non-proportional loading 0-89291
 plastically deformed, lattice strain distrib. (*German*) 0-85012
 plating C steel nails, barrel plating efficiency 0-100964
 point and planar defects, computer simulation 0-59455
 polycryst., creep and fracture behaviour, effects of prestrain and O 0-97544
 polycrystalline, recovery and recrystn. kinetics 0-81081
 polycrystalline target, X-ray intensity, microfocus source, non-linear rise studies 0-77927
 powder, sp. ht. cond. and sp. elec. cond. meas., Wiedemann Franz Lorenz law (*German*) 0-92872
 powder compacts, yield curve comparison, different loading paths (*Japanese*) 0-93621
 prevacancy temperature depend. of positron annihilation, Doppler broadening lineshape parameters 0-60709
 projected range distrib. of 5-25 keV He^{+} 0-65094
 proton-induced L-shell ionisation cross-sections 0-100707
 proton-irradiated, H_2 gas-bubble struct., study at 300K 0-92569
 pure, vacuum environment and grain size effects on creep rupture props. at elevated temps. (*Japanese*) 0-81162
 PVC, Cu evaporated film, electron-induced metallochromic reaction for metal image formation 0-86476
 PVC-Cu composites with chemically deposited ultrafine copper particles 0-93534
 recovery from secondary sources, recent development 0-100800
 recrystallisation centre growth kinetics, impurity effects (*Russian*) 0-89253
 recrystallisation retardation, two-phase Cu crystals, particle size, spacing effects 0-89242
 recrystallisation texture, of deformed single crystals, HVEM study 0-104179
 recrystallised state, of single crystals, (110) oriented, tensile deformed, HVEM of recrystn. 0-89256
 recrystallization annealing, grain growth, effect of type of deform. 0-100847
 recycling, effect on comp. 0-66455
 reorientation following ion bombard. 0-70269
 resistivity and thermoelec. ratio, electron-electron scatt. contrib. 0-70670
 resonant and nonresonant conduction-electron-spin transmission 0-75857
 rod, dynamic bending and residual deformation (*Russian*) 0-75293
 screening charge density round $\Delta Z = -1$ impurities, vacancies, NQR study 0-103897
 secondary electron low energy distrib. meas. using double-pass cylindrical mirror analyser 0-68293
 secondary slip, in neutron irradiated crystals 0-88161
 secondary slip, in neutron irradiated monocrystals, secondary slip between overlapping dislocation arrays 0-88162
 shell, explosive expansion, deform. and rupture modes and mechanisms 0-85064
 shock wave data, 'solid Hugoniot' rel. to 'fluid Hugoniot' 0-65155
 SIMS depth profiling, surface roughening, by low energy ion irradi. 0-60727
 single cryst., latent hardening in tension 0-60878
 single crystals Au ion implanted, pulsed electron beam irradi. 0-65019
 single particle lifetime 0-103612
 sliding behaviour, against polymers laminates and coated surfaces at cryogenic temps. 0-66671
 slip ring elemental surface composition as function of temp. 0-66901
 sodium oxalate Cu^{2+} , anhydrous spin Hamiltonian and bonding parameters and orbital-reduction factors 0-60408
 solderability, annealing effect (*Japanese*) 0-89244
 spatial electron beam-matter interaction, model calcs. for Cu (*German*) 0-84815
 sputter deposit PIXE expt. 0-61196
 sputtered Cu^{+} ion energies by low energy inert gas ion bombard. 0-71555
 sputtering, binding energies 0-108312
 strain localisation, during hot deform. 0-104195
 strained, interpolation functions for Fermi surface 0-65425
 stray X-rays from Cu components in transmission electron microscope, reduction 0-73550

copper continued

- substrate, (001), Ni electrodeposition, three-dimens. epitaxial crystallites, TEM image contrast 0-88457
 substrate, electrodeposition of Au film 0-81329
 substrate, Sn autocatalytic deposition 0-100965
 substrate for SiO₂ film, surface EM wave absorpt. optical const. (*Russian*) 0-108216
 surface, ⁴He backscatt., Rutherford scatt. cross section correction test 0-66369
 surface, (001), adsorbed c(2×2)CO layer, struct. 0-88428
 surface, (001), O₂ adsorption effect on surface barrier, LEED study 0-84378
 surface, (100), electronic struct., self-consistent local-orbital calc. 0-80348
 surface, (100), O chemisorption, angle-resolved UPS study 0-84384
 surface, (100), ordered Cl overlayer, adatom bonding effects, photoemission study 0-104044
 surface, (100) and (111), high resolution normal and near-normal UPS 0-80933
 surface, (100) coherent elastic scatt. of He, Ne, thermal attenuation 0-89105
 surface, (110), adsorbed pyridine, photoemission selection rules 0-100751
 surface, (110), methanol adsorption, XPS, UPS and thermal desorpt. study 0-84388
 surface, (111), final state band gap effects in UPS 0-89120
 surface, (111), positronium form. due to slow positron trapping 0-107748
 surface, Ar ion bombardment, fast ionized recoils, thermal lattice vibr. effects 0-100737
 surface, fast D₂ desorpt. mechanism, time-of-flight spectra 0-84379
 surface, inert gas ion irradiat., fast ionized recoils, blocking effect 0-71550
 surface, luminesc. accompanied by ion implantation 0-60683
 surface, negative affinity, narrow beam emission of slow positrons 0-89091
 surface, obs. of positron Bragg refl. 0-103221
 surface, plasma cleaning and etching, removal of C 0-97645
 surface, positronium emission 0-80897
 surface (001), barrier struct., LEED study 0-65354
 surface (001), M-point surface state, high-resolution angle resolved photoemission study 0-108322
 surface (001), O chemisorption, Cu3d-O2p interaction study by angular-resolved photoemission using synchrotron radiation 0-84836
 surface (100), adsorption of O₂, LEED study 0-100408
 surface (100) crystallography, LEED I-V profile anal. 0-75415
 surface (110), electronreflectance, surface state contrib. 0-80755
 surface (111), low-energy positron diff. 0-70511
 surface layer hardening by multiple impact 0-108469
 surface layer of Ge, heterodiffusion due to H atom surface recombination stimulation (*Russian*) 0-59726
 surface morphology influence on sputtered yield angular distribution 0-65338
 surface phenomena, electron microscopy 0-103556
 surface states, (100) and (111), polarisation depend. photoemission 0-100495
 surface topographical features formed by ion bombard., crystallographic depend. 0-70266
 surface treatment by the low-energy ions of plasma accelerators 0-97608
 surfaces, with Langmuir films, surface EM wave absorpt. using CO₂ laser excitation 0-97365
 swaged, inhomogeneous work hardening (*German*) 0-76267
 tensile deformed (110) orientated single cryst., recrystn., high voltage electron microscopy study 0-84958
 theoretical strength 0-104229
 thermal expansion reference data: 1-1000K 0-96669
 thermomodulation spectra of high-energy interband transitions 0-108226
 thick probes, subthermal neutron transmission curves for grain size and texture eval. (*German*) 0-71667
 thin film, elec. resist., effect of annealing In electrodes 0-80416
 thin film, electromigration, adhesion layer effects 0-96685
 thin film, oxidation, RMEED/SEM studies 0-100968
 thin targets, electron transmission below 3 keV (*French*) 0-60725
 triglycine calcium bromide: Cu²⁺, ESR studies 0-97136
 two-photon photoemission near single-photon photoelec. effect threshold 0-89121
 US torsional vibrations in metals, measurement of absorpt. 0-58856
 US velocity, temp. depend., stress effects 0-75307
 vacancy form. enthalpy, positron annihilation meas. 0-97371
 vacuum deposited epitaxial layer on Fe (001) substrate, orientation relationship 0-65415
 vaporisation and condensation coating on Mo and steel, substrate limiting temp. (*Russian*) 0-100787
 vapour laser, characts. comparison with 0-102711
 vapour laser, induced emission, spectral comp., time evolution 0-74344
 vapour laser, preionisation effect 0-87377
 vapour laser, rate processes, computer simulation 0-69371
 vapour laser discharge, power deposited, pump pulse repetition freq. influence 0-74350
 vapour laser excited by single elec. pulse, lasing characts. 0-87386
 vapour pulsed laser, spectral comp. of superradiance, stimulated and spontaneous radiation 0-102713
 vicinal surfaces, LEED study, S, O and Pb adsorption effects 0-103575
 wear under reversed friction, temp. effect 0-108588
 wire, axial texture after electroplastic drawing, X-ray struct. investigation (*Russian*) 0-104177
 wire, negative longitudinal magnetoresist. size effect 0-80252
 wire, tough-pitch, cupping fracture, Cu₂O particle size effect 0-66668
 X-ray absorption, discontinuities and limits, chem. combination effects 0-93435
 X-ray K-emission satellites, quasi-stationary states and origin 0-80903
 yield and flow behaviour, effect of cold drawing under combined stress 0-60912
 Young's modulus depend. on temp. and mech. action (*Russian*) 0-92584
 Z dependence of thick target β -ray backscattering 0-76118
 Ag-Cu flex leads, microstruct. study of corrosion 0-76406
 Al-Cu thin film couples, TEM study of intermetallic nucleation at interface 0-65305
 Al₁Ga_{1-x}As:Cu, variable-gap semicond., impurity props., carrier recomb. 0-96907
 Au/Cu, double layer film, oxidation (*Japanese*) 0-61010
 Ca₃(PO₄)₂:Cu²⁺, ESR, high press. struct. transition 0-97134
 CaS:Cu, colour centres, optical and thermal depths determ. 0-66275

copper continued

- CdCr₂S₄:Cu magnetic semiconductor growth, structural defects, physical properties 0-60759
 CdCr₂Se₄:Cu, ferromag. reson. and ESR line widths 0-60413
 CdS:Cu, C-V curves of MIS diode used to examine trapping levels 0-65697
 CdS:Cu, charge and transport mechanism of impurities, electrodiffusion doping 0-59725
 CdS:Cu, Cl films, photocond. growth and decay time 0-60041
 CdS:Cu, electrodiffusion of shallow donors, photocurrent, TSC, and exciton luminesc. meas. 0-79992
 CdS:Cu, photocurrent, elec. field effect on recombination processes (*Russian*) 0-100484
 CdS:Cu, photosensitivity degradation mechanism 0-107851
 CdS:Cu sintered layers, relaxation photocurrent kinetics (*Russian*) 0-107852
 CdS:Cu thin films, surface and bulk photocond. 0-88653
 CdSe:Cu, impurity photocurrent, kinetics and oscils. 0-65624
 CdTe:Cu films, impurity behaviour, Hall mobility and hole density meas. 0-80420
 Co-Cu interface, Co fine particles in Cu, interface magnetisation 0-88858
 CsBr:Cu⁺, excitation and absorpt. spectra 0-108255
 CsBr(Cl):Cu⁺, γ -irradiated, thermolum. emission 0-104001
 Cs₂ZnCl₄:Cu²⁺, electron spin echo envelope, Fourier transform ¹³³Cs modulation 0-58291
 Cu (111)/Na interface, UPS study of surface electronic struct. 0-80350
 Cu Cu²⁺ doped Cd complexes, ESR study 0-108059
 Cu, electrolytic epitaxial nucleation and growth, on (111) Ag 0-104081
 Cu, electronic and mag. structure calcs. of mag. impurities 0-80213
 Cu I, high-dispersion absorpt. spectrum obs. 1570 to 2500 Å 0-78564
 Cu II laser, UV, operating period extension by Ar admixture 0-74342
 Cu II laser with cylindrical hollow cathodes, UV performance 0-102709
 Cu IV, wavelength region 700-1200 Å, extended analysis 0-99473
 Cu polycrystal, fatigued, interior dislocation struct. 0-88147
 Cu single crystals, [100]- and [111], dislocation density meas. using TEM 0-79803
 Cu, single crystals, cyclically and unidirectionally deform. X-ray diff. study 0-89319
 Cu⁺, approximate relativistic Hartree-Fock eqns., soln. using Slater-type functions 0-58168
 Cu²⁺ containing Ag halide photochromic glasses, optical props. 0-93364
 Cu²⁺ ion, ground state wavefunctions and ESR parameters 0-88868
 Cu:Co precipitates, mag. anisotropy, precipitate shape, coercive force 0-80500
 Cu:In, He, lattice defect struct., PAC meas. 0-70190
 Cu:O single crystal, ¹⁸O⁺ ion implantation in channelling directions, expt. conditions and range profile obs. 0-65022
 Cu:O single crystal, ¹⁸O⁺ ions implantation in channelling directions, stopping power meas. from max. range 0-65078
 Cu/Au, bilayers, interdiffusion phenomena, lattice dislocations, TEM obs. 0-59736
 Cu/Au, initial epitaxial growth at room temp. 0-59829
 Cu/CuCl double pulse laser, pumping pulse and output pulse characts. 0-87380
 Cu/CuCl double pulse laser, dissoc. pulse, afterglow, and laser pulse model 0-91775
 Cu/graphite-SbF₆ wire composites, synthesis and elec. props. 0-70781
 Cu/Nb layered ultrathin coherent struct. 0-80122
 Cu/Ni coherent modulated structures, electronic struct. and magnetism 0-103620
 Cu/Sn-Ni/Au tricouples, electrodeposited, interdiffusion obs. 0-84331
 Cu-Al thin film multistucture, Xe⁺ ion beam cratering 0-66708
 Cu-Cu₂O diode junction, Schottky barrier, electronic struct. and minority carrier diffusion length (*French*) 0-65682
 Cu-Ge Schottky barrier photodetectors, near IR interband transitions and optical parameters 0-73449
 Cu-like ions, 4s-4p reson. lines and transitions obs. by means of laser prod. plasma, appl. to Tokamaks 0-99468
 Cu-metal thin film couples, room temperature interactions 0-96699
 Cu-mild steel explosively welded interface, SEM examination (*German, English*) 0-96746
 Cu-n-Si diodes, fabrication by electroless deposition method, characts. 0-100520
 Cu-Nb/Sn multifilamentary tapes, in situ formed, crit. current density anisotropy 0-84576
 Cu-NbTi, composite conductor, acoustic emission 0-97032
 Cu-Permalloy two-layer films, mag. anisotropy, grain boundary diffusion (*Russian*) 0-71122
 Cu-phthalocyanine, photoemission multielectron effects from quasi atomic Cu 0-93458
 Cu-SiO₂, low-temp. recovery creep, Orowan loop accumulation 0-81126
 Cu²⁺-1,5-dimethyl-2,4-hexadiene, fluoresc. quenching method for determ. binding const. 0-89530
 Cu+Cl₂(Br₂)(I₂), beam-gas chemiluminesc. reactions 0-85151
 Cu+Cl⁺, K X-ray production and radiative electron capture, fluoresc. yield determ. 0-99553
 Cu+Cu collisions, K α X-ray energy shifts, target thickness depend. 0-83311
 Cu+F₂, chemiluminesc. reactions, mol. beam study 0-97702
 Cu+H⁺, K-shell ionisation 0.5 to 40 MeV, meas. and PWBA-BEA calcs. 0-78699
 Cu+H⁺(He ions), K-shell ionisation cross-section, 85 to 790 keV 0-106390
 Cu₂, Harris-Pohl selected valence electron split-shell MO calcs. 0-91439
 Cu₄ clusters, electronic structures, SCF-X α -SW method 0-88468
 Cu⁺ ion cluster yield intensity from Cu target bombard. by H⁺, Ne⁺, Xe⁺, Kr⁺ 0-100728
⁶³Cu, A'₁u-X'₁⁺ transition, Franck-Condon factors and r-centroids 0-95690
 GaAs:Cu, substitutional impurity elec. struct. 0-88513
 GaAs:Cu, Te, photoelec. props. 0-92936
 GaAs:Cu:Ti, cathode luminescence spectra, Hall effect, cryst. defects 0-76087
 Ge:Cu, solubility and behaviour of Cu, internal friction investigations 0-92678
 Ge:Cu, surface waves at static domain boundaries (*Russian*) 0-80288
 Ge:O, Cu, amorphous thin film, impurity effects on struct. 0-107054
 Ge:Sb, Cu, high resist. compensated, impurity of photocond., pulsed unipolar injection carriers 0-92935
 Ge:Sb, Cu, photoelec. props., fast electron irradiat. effects 0-60036

copper continued

- Ge₄₀S₆₀:Cu, bond struct. and character in Ge-S system, EPR obs. 0-66014
 H₂O vapour bubble formation, along grain boundaries, effect on intergranular creep fracture 0-71722
 In-Pb-Cu contact system, low temp. alloyed contact formation 0-100519
 KBr(Cl):Sr²⁺, Cu²⁺, thermolum. response, extension of two-step reaction model 0-89075
 KCl:Cu⁺, excitation and absorpt. spectra 0-108255
 KCl:Cu⁺, exciton bands, optical absorpt. and MCD spectra 0-80821
 K₂Cl:Cu⁺, exciton bands, optical absorpt. and MCD spectra 0-80821
 K₂O-MgO-B₂O₃:Cu²⁺, micro-inhomogeneities, EPR and Raman study 0-84080
 LiAlSiO₄:Cu, β -eucryptite solid electrolyte, Cu²⁺ EPR obs. of ion exchange props. 0-108056
 LiNbO₃:Cu(Fe), light induced charge transport, photovoltaic effects, impurity states 0-80317
 LiTaO₃:Cu(Fe), light induced charge transport, photovoltaic effects, impurity states 0-80317
 Mg₂TiO₄:Cu ESR of Cu²⁺ 0-97131
 Mo fibre reinforced Cu, rule of mixtures of deform. parameters in stage III 0-97532
 Mo fibre reinforced Cu with weak interfaces, stability of tensile deform. 0-97533
 Mo-Cu cathode, spot motion and nature in UHV 0-79597
 N₂-Cu arc plasma, transport coeffs. 0-96344
 ND₂Br:Cu²⁺, pseudo-Jahn-Teller effect manifestation in ESR spectrum 0-71168
 NH₂Br:Cu⁺, luminesc., orientation phase transition 0-100687
 NaCl:Cu⁺, electrolytically coloured, electron trapping, optical absorpt. 0-100672
 Na₂O-B₂O₃:Cu²⁺, Mn²⁺ glasses, Cu²⁺-Mn²⁺ interaction studied by ESR 0-93166
 Na₂O-MgO-B₂O₃:Cu²⁺, micro-inhomogeneities, EPR and Raman study 0-84080
 Nb/Cu, layered ultrathin coherent structs., supercond. props. 0-84525
 Nb-Cu-Nb junctions, Josephson effect meas., critical current, temp. depend. 0-93041
 Nb₃Sn-Cu multifilamentary composite wire, Nb₃Sn filament morphology and grain size 0-100855
 NbTi-Cu, composite superconductor, acoustic emission 0-84546
 NbTi-Cu, supercond. composite, use in temp. and heat transfer coeff. meas. 0-77780
 Ni-Cu conductor system for Si solar cells 0-93991
 Ni-Ti/Cu composite, plastic deform. influence on internal friction (*Russian*) 0-100871
 Pb-Cu(Ag) double layers, intermetallic boundary effects, tunnelling 0-88692
 Pb_{1-x}Cu_x, light sensitive, internal photoelectric emission 0-107910
 n-PbTe:Cu epitaxial films, elec. transport props. 0-75659
 Si-Cu, ion implanted, doping profile, pulsed laser annealing effects 0-88197
 Si-Cu, precipitate morphology, IR microscopy study (*Chinese*) 0-103539
 n-Si-Cu Schottky contacts, electrochem. deposition, barrier height and ideality factor 0-75641
 Si-SiO₂-Mg-Cu powder compact, nitridation to form Si₃N₄ whiskers (*Japanese*) 0-93674
 SiO₂:Cu, XPS line broadening and extra-atomic relax. energies 0-71561
 Sn/Cu electroplated bimetallic films, interfacial reaction 0-96765
 SnO₂-Cu₂S-ZnS:Mn₂O₃-Al₂O₃-Al, light-emitting struct., cond. and electrolum., heat treatment 0-97345
 SrCl₂:Cu⁺, exciton bands, optical absorpt. and MCD spectra 0-80821
 Te:Cu films, elec. transport props. 0-60120
 TiO₂ particle, Cu-coated prep., ceramic composites 0-89159
 W fibre reinforced Cu composites, correl. between thermal cycling-induced microstructural changes at interphase boundaries and tensile behaviour (*Japanese*) 0-71674
 W/Cu, Stoneley waves at (001) interface between cubic symm. cryst. 0-100388
 ZnS:Cu, Cl, Mn film, AC electrolum. 0-60680
 ZnS:Cu, deep transition metal impurity states, SCF CNDO cluster calcs. 0-100442
 ZnS:Cu, Mn DC electroluminescent powder panels, bulk and junction effects 0-89068
 ZnS:Cu, spectral distrib., rise and decay behaviour (*German*) 0-60625
 ZnS:Cu, Tb phosphors, luminesc. props. 0-100690
 ZnS:Cu crystal, powder, epitaxial film, luminescence anomalous thermal 0-76077
 ZnS:Mn, Cu, Cl films, AC electrolum. 0-60679
 ZnS:CdS:Cu, cathodoluminesc. investig., appl. to cathode ray tube screening 0-108282
 ZnTe:Cu, elec. field and impurity conc. effect on ionisation energy 0-88514
 ZnTe:Cu films, high cond., elec. and optical props. 0-88651
⁶³Zn/⁶²Zn generator, source of ⁶²Zn for radiopharmaceuticals 0-67248

copper alloys

- see also brass; copper compounds
 Admiralty Metal, transgranular stress corrosion crack propag. 0-89402
 Alnico 5 alloy, S and Ti additions effect rel. to non-metallic inclusions, coercive force and grindability 0-89375
 bronze, diffusion of Ga in V₂Ge layer, grain boundaries (*Russian*) 0-65297
 bronze, low-cycle fatigue, NH₃ effect 0-104348
 bronze, powders, electric-pressure sintering onto cylindrical parts in fluidised bed 0-100960
 Cu-Zn-Mn, de-alloying props. 0-104332
 dilute binary solid solutions, enthalpies of mixing and excess free enthalpies (*French*) 0-107427
 FCC, climb of extended dislocations due to irradiation HVEM 0-103343
 intergranular damage parameters in creep (*Czech*) 0-89342
 ion-selective membrane electrodes development, Ag ion conduction ceramic systems (*Japanese*) 0-61203
 liquid, thermal cond. and elec. resistivity 0-103661
 low-cycle fatigue and cyclic creep, -196-20°C 0-100913
 manganin foil like gauge calibration in planar shock wave expts. 0-95091
 microcrystalline, rapidly quenched particulates, appl. 0-84887
 molten, gas content meas., reduced pressure test (*Chinese*) 0-81390
 rare earth ternary alloys, RT₂Al₆, T=Cr, Mn, Fe, Cu, cryst. struct. 0-107110

copper alloys continued

- recrystallisation retardation, Al₂O₃ dispersion effect on kinetics 0-89242
 stacking faults, weak-beam contrast in TEM 0-75132
 steel, Cu-Ni-Mo (2, 2, 0.25 wt.%), sintering, kinetic characts. 0-60805
 STEM imaging of alloy containing Cr and SiO₂ particles 0-108685
 Ag-Au-Cu, surface composition change on sputtering with 2 keV Ar ions 0-66365
 Ag-Cu metastable solid soln., form. by ion-beam mixing 0-75244
 Ag-Cu surface alloyed films, laser melt quenched, microstruct. 0-76423
 Ag₃Au_{1-x}-Cu_x, phase relations, X-ray diffr. and differential thermal anal. 0-108395
 Al-Cu, comparison of liquid impact erosion and cavitation erosion 0-104302
 Al-Cu, dil., core and valence band spectra, XPS study 0-84837
 Al-Cu, dil. binary alloy, planar interface stability during solidification (*Slovak*) 0-108424
 Al-Cu, high strength, type 2024-T3, crack growth, fatigue induced surface deform., holographic detect. 0-85120
 Al-Cu, liq. alloys, with zero superheat, fluidity 0-70289
 Al-Cu, liquid impact erosion 0-108598
 Al-Cu, low freq. internal friction during plastic deform. (*Chinese*) 0-103420
 Al-Cu, molten, showering cryst. form. in mould cooled from top (*Japanese*) 0-66498
 Al-Cu, rapid quenching, struct. and decomp. 0-76244
 Al-Cu, solidification, solid-liq. interface, solute conc. effects 0-59632
 Al-Cu, superconducting amorphous films of high stability 0-70889
 Al-Cu, type 1100, synchrotron radiation microradiography 0-85121
 Al-Cu, type 2036-T4, plane-strain work hardening, meas. and anal. 0-81073
 Al-Cu, type 2219-T851, fracture mechanics and surface chemistry of fatigue crack growth 0-81168
 Al-Cu (0.5 wt.%), evaporated layers, electromigration, linewidth depend. 0-65277
 Al-Cu (1 wt.%), electron irradiated, dislocation damage, HVEM study 0-103389
 Al-Cu (1.9 at.%), solute fluctuations, EXAFS study 0-79949
 Al-Cu (2-5 wt.%), precipitation total surface influence on resistivity (*French*) 0-71650
 Al-Cu (3 wt.%), stress aged, GP zone struct. by X-ray diffuse scatt. meas. (*Japanese*) 0-71653
 Al-Cu (3 wt.%) single cryst., stress aging, oriented precipitation (*Japanese*) 0-71652
 Al-Cu (33 wt.%) eutectic, solidification under reduced gravity, behaviour of suspended Al₂O₃ particles (*German*) 0-60853
 Al-Cu (3.97 wt.%), containing Guinier-Preston zones, high resolution lattice images 0-107114
 Al-Cu (4 wt.%), high temp. cyclic deform., θ' particle dissolution obs. 0-108515
 Al-Cu (4 wt.%), neutron irradiat., weak-beam dark-field obs. of dislocations near θ' precipitates 0-107333
 Al-Cu (4 wt.%), reversion process of Guinier-Preston zones, ⁶³Cu NMR obs. 0-60871
 Al-Cu (4 wt.%), supersaturated and aged conditions, high strain deform. 0-60907
 Al-Cu (4.3 wt.%), containing Guinier-Preston zones, high resolution lattice images 0-107115
 Al-Cu (4.6 wt.%), cold work and ageing influence on ductility and fracture behaviour (*Japanese*) 0-89295
 Al-Cu alloy dendritic solidification kinetics 0-81041
 Al-Cu alloys, coarsening mechanisms of secondary dendrite arm, and organic analogue 0-81049
 Al-Cu dilute alloys, vein closing mechanism in fluidity tests 0-84924
 Al-Cu films, DC sputtered, Cu distrib. 0-80113
 Al-Cu type 2024 alloy, erosion in cavitating venturi 0-108602
 Al-Cu-Mg, type RR55, high strength, creep behaviour, effect rel. to anodic coatings, SEM study 0-97542
 Al-Cu-Mg, type D16T, thin-wall cylinder cold rolling method 0-66535
 Al-Cu-Mg (4, 1.5 wt.%), mica dispersed, wear characts. and bearing performance 0-108591
 Al-Cu-Mg/mica particulate composite mech. props. 0-100919
 Al-Cu-Mg-Li alloy extrusions, microstruct., embrittlement and fracture props. 0-60965
 Al-Cu-Mg-Mn-Si-Fe, torsional vibrations decrement, deformed vol. effect 0-76326
 Al-Cu-Mn, long term strength and creep 0-60925
 Al-Cu-Mn, type 2219, synchrotron radiation microradiography 0-85121
 Al-Cu-Mn (1-5, 0-6 wt.%), N alloying and comp. effect on mech. props. (*Bulgarian*) 0-71719
 Al-Cu-Si-Mg, deform. simulation using torsional test, elastoplastic constitutive eqn. 0-93594
 Al-Cu-Si-Mn, type 2017S-T4, crack initiation at root of circumferential notch of round bar specimens (*Japanese*) 0-60947
 Al-CuAl, eutectics, microstruct. after solidification, heat pipe influence 0-76243
 Al-Cu(-Mg), dimensional changes in heat treatment. 0-89271
 Al-Cu(0-10 wt.%) sintered alloys using composite powder 0-76210
 Al-Cv (0.3 wt.%), moving solid-liq. interface, diffusion in liq. 0-107456
 Al-Mg, dynamic uniaxial tension and compression curves 0-100884
 Al-Mg-Zn-Cu, type 7050, calorimetric study of fatigue induced microstructural changes 0-85034
 Al-Mg(Cu)(Si), (5.0(4.5)(11.8) wt.%), ingots, vibr. effect during solidification on porosity formation 0-108426
 Al-Si-Cu, fracture resistance at low temps. 0-104284
 Al-Si-Cu-Zr, ageing kinetics (*Russian*) 0-76274
 Al-Zn-Mg-Cu (6, 2.5, 1.5 wt.%), deform. simulation using torsional test, elastoplastic constitutive eqn. 0-93594
 Al-Zn-Mg-Cu (6.2, xwt.%) type alloy, fatigue crack propag., Cu content and recryst. effect 0-60960
 Al-Zn-Mg-Cu type 7075, heat treatment optimisation 0-60888
 (Al-Cu)/Si system, Si regrowth minimisation through overlying Al or Al alloy film 0-70569
 AlCu-NiCo (5 at.%), θ' hardened, creep mechanism 0-85013
 Al₂₀Cu₃₅Zr₅₅ metallic glass, inelastic deform., free energy spectra 0-71699
 Au-Cu, Ising FCC and antiferromag., mag. phase diagram, ordering, Monte Carlo calc. 0-103833
 Au-Cu, surface conc. profile and surface energy 0-84350
 Au-Cu-Fe spin glass alloys, impurity mag. resist. meas. 0-59972
 Au-Pt-Pd-Ag-Cu, commercial dental alloy, age-hardening characts. 0-89235

copper alloys continued

- Au-Cu-Al thin film bilayer system, phase formation, backscattering spectra 0-96728
- Au₂Cu_{1-x}Ag_x, phase relations, X-ray diffr. and differential thermal anal. 0-108395
- BaCu, X-ray cryst. struct. determ. 0-92478
- Be-Cu, thermal expansion, vibr. characteristics at low temp., effect of substitution impurities (*Russian*) 0-103439
- CaCu₂, γ -phase in Ca-Cu system, calorimetric determ. of enthalpy of form. (*French*) 0-84915
- Ce-Cu, liquid, normal spectral emissivity 0-103506
- CeCo_{5-x}Cu_x, 0 ≤ x ≤ 1, internal oxidation kinetics, oxide struct., X-ray study 0-104329
- CeCu₂Si₂, collective phenomena 0-65933
- Cu binary alloy, polarisation studies, electrode design 0-93761
- Cu-Ag, surface segregation of S, Auger spectral study diffusion 0-76549
- Cu-Ag (0.1 wt.%), cold-worked, internal friction peaks in kHz range 0-89276
- Cu-Ag (3 at.%), plastically deformed, lattice strain distrib. (*German*) 0-85012
- Cu-Ag-Au, coherent phase diagram, theoretical calc. 0-70373
- Cu-Ag-Ge, Hume-Rothery glass form. 0-96449
- Cu-Ag-O alloys, dil., O-metal interactions, activity coeff. meas. at 1423K 0-93792
- Cu-Ag-P(6-14, 11-14 wt.%) amorphous, crystn. and elec. props., X-ray diffr., elec. resist. and DTA meas. (*Japanese*) 0-84088
- Cu-Al, dislocation core cut-off parameter, estimation from stacking fault nodes 0-103370
- Cu-Al, dislocations, dissociated, climb mechanism, nucleated loops, Burgers vectors 0-65002
- Cu-Al, disordered alloys, interatomic distances, coord. numbers, and mean relative displacements, EXAFS anal. 0-89087
- Cu-Al, HV electron microscopy, crit. voltages depend. on comp., temp. and short-range order 0-100146
- Cu-Al, irradi. in HVEM, climb of dissociated dislocations and point defect absorpt. 0-107257
- Cu-Al, linear dislocation multipoles, weak-beam TEM 0-75233
- Cu-Al, liq., elec. cond., temp. and conc. depend., model interpret. and alloy struct. (*Russian*) 0-88528
- Cu-Al, ordered, superlattice fringe images, computer simulation 0-103296
- Cu-Al, planar faults, faint electron microscopic image contrast obs. 0-107283
- Cu-Al, short range order and static distortion contribution to residual elec. resistivity (*Russian*) 0-70672
- Cu-Al (10, 16 at.%), dislocation interactions, influence of jogs on extension of dislocation nodes 0-84176
- Cu-Al (11 at.%) single cryst., dislocation reactions during deform. twinning 0-79795
- Cu-Al (14.3 wt.%), ¹¹⁰Ag diffusion in β/γ_2 interphase boundary 0-79989
- Cu-Al (5 wt.%), subjected to tension-compression fatigue, deform. and fracture strength (*Japanese*) 0-93644
- α -Cu-Al (6 to 17 at.%), short-range order investigated by diffuse X-ray scatt. (*Russian*) 0-104187
- α -Cu-Al (9.13, 13.56, 14.76, wt.%) short-range ordered, characterisation of locally ordered regions 0-79747
- Cu-Al bulk and thin-film forms, reflecting surface absorpt. coeffs. at 10.6 μ m 0-95984
- Cu-Al films, elec. cond. of vacuum condensates depend. on composition, annealing (*Russian*) 0-65709
- Cu-Al spherical crystals, grown from drop of melt, topography 0-84353
- Cu-Al₂O₃(SiO₂)(TiO₂) alloys, internally oxidised, plastically deformed, influence of particle form on primary loop nature (*French*) 0-103344
- Cu-Al-Co liquid alloys, constant Co-content of 5 wt.%, mag. props. (*German*) 0-88720
- Cu-Al-Mn liq. alloys, susceptibility behaviour 0-93077
- β -Cu-Al-Ni (14, 3 wt.%), single cryst., thermal effect due to stress induced martensite formation 0-81059
- Cu-Al-Ni (14.1, 3 wt.%), autooscillations and nonlinear anelasticity 0-70307
- Cu-Al-Ni Marmen alloys, rapid solidification and ageing 0-76245
- Cu-Al-Sn system, coexistence of different and brass like phases 0-89206
- Cu-Al(Au)(Ga)(Ni)(Pd)(Rh)(Zn) (4 at.%), anneal hardening mechanism 0-60879
- Cu-Au, corrosion in HNO₃ 0-85091
- Cu-Au, dil., magnetostrict., temp. depend. 0-70682
- Cu-Au, HV electron microscopy, crit. voltages depend. on comp., temp. and short-range order 0-100146
- Cu-Au alloys, vacancy and divacancy migration activation energies, elec. cond. meas. 0-88140
- Cu-Au system, two-phase mixtures, long-period superlattices 0-84140
- Cu-Au-Fe, ferromag. ordering in FCC γ -Fe precipitates, Mossbauer study 0-71267
- Cu-Au-O alloys, dil., O-metal interactions, activity coeff. meas. at 1423K 0-93792
- Cu-BN composite electromachining tools, dynamic hot pressing 0-84889
- Cu-Be, dynode surface, SEM and Auger microanalysis 0-100384
- Cu-Be, SCC in NH₃ 0-104326
- Cu-Be (1.8 wt.%), discontinuous precip. form. and growth, TEM, obs. 0-104169
- Cu-Be (2 at.%), plastic deform. and dislocation substruct. 0-76307
- Cu-Be (2 wt.%), precipitation sequence, TEM obs. 0-108450
- Cu-Be solid solutions, local oscill. conc. depend., impurity bands (*Russian*) 0-75318
- Cu-Be-Co, discontinuous reaction, analytical TEM 0-100842
- Cu-Be(2 wt.%), tarnish surface films, formed in ammoniacal Cu(II) solns. 0-97624
- Cu-Bi, grain boundary struct. intergranular fracture, segregation role 0-66648
- Cu-Bi, grain boundary thickness obs. using electron diffr. techniques 0-79811
- Cu-Bi (0.02 wt.%), intergranular fracture, Kossel X-ray diffr. in SEM obs. 0-108579
- Cu-Cd (1.0 wt.%), yield stress and flow stress 0-97524
- Cu-Co, dil., valence and core level spectra, XPS study 0-84838
- Cu-Co, time of flight atom probe, quantitative microanal., metallurgical appl. 0-86498
- Cu-Co (1.5 and 4 wt.%), coherent Co-rich separations obs. by positron annihilation (*Russian*) 0-89082
- Cu-Co single cryst., precip. hardening (*German*) 0-84946

copper alloys continued

- Cu-Co-Si (0.36, 0.11 wt.%), surface layer struct. on annealing, SIMS and AES exam. 0-88415
- Cu-Cr, dil., spin-density magnetisation near Cr atoms, NMR study 0-80626
- Cu-Cr, Kondo alloy, Josephson tunnelling effect 0-60145
- Cu-Cr (0.75 wt.%), deformation characts., fully reversed cyclic strain with fatigue cracks and dislocation struct. 0-81148
- Cu-Cr alloy, laser irradi., structural changes (*Russian*) 0-100247
- Cu-Cr-SiO₂ system, age and dispersion strengthened, dislocation struct. around SiO₂ particles 0-108468
- Cu-Cr-(SiO₂), single crystals, yield and pre-yield behaviour rel. to aging time 0-81103
- Cu-Cu₂Y eutectic alloy, cast and directionally solidified, struct. and props. (*Russian*) 0-104138
- Cu-Fe, dil., valence and core level spectra, XPS study 0-84838
- Cu-Fe, explosive plasma sputtered coatings, struct. and props. (*Russian*) 0-100783
- Cu-Fe (1.5 wt.%), precipitation-effect on void formation during electron irradiation 0-84211
- Cu-Fe (1.5 wt.%), void form. during irradi. in HVEM, reactor irradi. simulation and ageing effects 0-107327
- Cu-Fe group, dil., NMR satellite data calc., struct. of mag. impurities 0-103894
- Cu-Fe system, ageing and reversion phenomena study 0-89274
- Cu-Ga, binary alloy constituent EDS anal., secondary fluorescence, SEM study (*Chinese*) 0-85231
- Cu-Ga, liq., elec. cond., temp. and conc. depend., model interpret. and alloy struct. (*Russian*) 0-88528
- Cu-Ga (17 wt.%), elec. resist. and TEM studies 0-108604
- Cu-Ga bulk and thin-film forms, reflecting surface absorpt. coeffs. at 10.6 μ m 0-95984
- Cu-In, liq., elec. cond., temp. and conc. depend., model interpret. and alloy struct. (*Russian*) 0-88528
- Cu-M-O ternary liquid alloys, thermochem. calcs. 0-85209
- Cu-Mn, de-alloying props. 0-104332
- Cu-Mn, exchange-coupled localised moments, Korringa relaxation rate 0-75851
- Cu-Mn, mag. viscosity below freezing temp. 0-65910
- Cu-Mn, spin glass, transition temp., freq. depend. 0-97113
- Cu-Mn, spin glass materials, mag. field dependence of susceptibility peak 0-103840
- Cu-Mn, spin glasses, alternating susceptibility 0-65912
- Cu-Mn, zero field ESR in spin glass state 0-66017
- Cu-Mn (8 to 75 at.%), spin correl., neutron polarisation anal. study 0-65905
- Cu-Mn alloy, manganin, hysteresis-corrected calibration under shock loading 0-74818
- Cu-Mn spin glass, spin freezing and exchange narrowing of mag. reson. 0-60411
- Cu-Mn-Al, Heusler alloys, ferromag. inclusions, mag. props. and struct. study (*Russian*) 0-80570
- Cu-Mn-Al alloys, displaced hysteresis loop and microstructure obs. 0-84613
- Cu-Mn-Au(Pt) spin glasses, anisotropic exchange interactions, effect of nonmag. impurities 0-80534
- Cu-Nb alloy, chill casting, consumable arc melting, ingot prep. techniques 0-84879
- Cu-Nb multifilamentary composite, dislocation resistivity 0-70671
- Cu-Ni, adsorption of H₂-CO on (110) surface, TDS and UPS obs. 0-80052
- Cu-Ni, cast, strength and hot ductility, alloying and residual elements effect 0-66595
- Cu-Ni, crystallisation temp., overcooling temp. (*Russian*) 0-97472
- Cu-Ni, density of states of d-electrons, tight binding approx. calcs. 0-59863
- Cu-Ni, dil., screening charge density round $\Delta Z = -1$ impurities, vacancies, NQR study 0-103897
- Cu-Ni, dil., valence and core level spectra, XPS study 0-84838
- Cu-Ni, evaporation limited segregation 0-70513
- Cu-Ni, galvanic corrosion in sulphide modified seawater 0-100953
- Cu-Ni, liq., surface conc. profile and surface energy 0-84350
- Cu-Ni, random ferromag. alloy, local mag. moment calc. 0-70974
- Cu-Ni, rubbing contact with cast Fe, surface temperature effect on dry sliding wear 0-60983
- Cu-Ni, sintering, Kirkendall effect 0-93518
- Cu-Ni (10 at.%), creep, substruct. and internal stresses (*Russian*) 0-97527
- Cu-Ni (10 at.%), hardening, recovery, and struct. changes during high temp. creep (*Russian*) 0-89288
- Cu-Ni (110), adsorption of CO and H₂, UPS, thermal desorption, AES, and LEED study 0-80087
- Cu-Ni (30-90 wt.%), elect. resist. rel. to cold working and heat treatment 0-71765
- Cu-Ni alloys, chemical interdiffusion under uniaxial stress 0-65307
- Cu-Ni films, compositionally modulated, magnetic anisotropy, magnetisation curves 0-88840
- Cu-Ni thin films, ferromag., Hall effect meas. 0-80428
- Cu-Ni/Au-Ni multilayer films, ohmic behaviour, use as strain gauge 0-65713
- Cu-Ni-Al (5, 2.5 at.%), precip. hardening (*Japanese*) 0-71663
- Cu-Ni-Co, mag. props. of system of disperse ferromag. particles, 73 to 673K (*Russian*) 0-65968
- Cu-Ni-Fe, magnetic properties, heat treatment and compressive stress effects 0-60367
- Cu-Ni-Nb (30, 0.9 at.%), precipitate free zones, X-ray microanal. 0-108768
- Cu-Ni-S, molten, thermodynamic props. 0-104122
- Cu-Ni-Sn (10, 6 wt.%), spinodal decomposition, X-ray and electron diffr. study 0-81063
- Cu-Ni-Sn (15, 8 wt.%), prior deform. effect on spinodal age hardening 0-108465
- Cu-Ni-Sn (9, 2 wt.%), surface comp., Auger electron spectroscopy study, manufacture and storage influence 0-65348
- Cu-Ni-Ti, ordering within precipitates, TEM obs. 0-108461
- Cu-Ni-Ti system, phase equilibria in Cu rich region and Cu-T quaternary constitution (*Japanese*) 0-89203
- Cu-Ni-Ti system, reactions with melt in Cu-rich region (*Japanese*) 0-89202
- Cu-Ni-Zn (18, 27 wt.%), surface comp., Auger electron spectroscopy study, manufacture and storage influence 0-65348

copper alloys continued

- Cu-Ni-Zn alloy, surface comp., outdoor exposure influence 0-59770
 Cu-Ni-Zn-Mn fine grained precipitation-hardenable alloy, high strength and ductility 0-100805
 Cu-O (0.05 to 0.1 wt.%) liquid alloy, deoxidation kinetics by rotating graphite cylinders 0-61084
 Cu-Pb (Fe), liq., thermodynamic props. (Polish) 0-89199
 Cu-Pd, dil., screening charge density round $\Delta Z = -1$ impurities, vacancies, NQR study 0-103897
 Cu-Pt, dil., screening charge density round $\Delta Z = -1$ impurities, vacancies, NQR study 0-103897
 Cu-Pt system, phonon dispersion relations, force constant disorder effect 0-84263
 Cu-Pt-O alloys, dil., O-metal interactions, activity coeff. meas. at 1423K 0-93792
 Cu-Si (6.5 at.%), plastic deformation, HVEM study (French) 0-66605
 Cu-Si (7 at.%), dislocation interactions, influence of jogs on extension of dislocation nodes 0-84176
 Cu-Si (8 wt.%), intrinsic struct. in grain boundaries and boundary mobility 0-103368
 Cu-Sn, thermodynamics of Cu and Sn solns. using copper β -alumina solid electrolyte, 800-1100K 0-107502
 Cu-Sn, vacuum condensed, reflecting surface absorpt. coeffs. at 10.6 μm 0-95984
 Cu-Sn (4.9 wt.%), role of mech. twinning on stress/strain behaviour 0-85004
 Cu-Sn alloy, surface comp., outdoor exposure influence 0-59770
 Cu-Sn binary system, wettability and interaction between solids and liqs. (Japanese) 0-92760
 Cu-Sn industrial bronzes, Sn diffusion in deform. zone influence on wear resistance, friction (Russian) 0-108582
 Cu-Sn liquid, optical reflectivity spectra of virtual bound states 0-89021
 Cu-Sn system, long period superlattice obs. and impurity effects 0-103297
 Cu-Sn-Al, deform at high temps. (Polish) 0-89284
 Cu-Ti, strengthened by modulated structs., anomalous age hardening effects 0-97497
 Cu-Ti-Al(Ga)(Au)(In)(Ag)(Ni), wetting of Al_2O_3 , alloying effects 0-107617
 Cu-transition metal, dil., mag. impurities, electronic struct., KKR-Green's function calc. 0-65783
 Cu-V₆Si, supercond. in situ composites, stress effects on crit. props. 0-65757
 Cu-V-Si, supercond. props. 0-107945
 Cu-Zn, de-alloying props. 0-104332
 Cu-Zn, interface sliding of FCC and BCC boundaries 0-104240
 Cu-Zn, solid soln., rheological study of crystallographic order on creep (French) 0-97548
 Cu-Zn (30 wt.%), single crystals., quantitative anal. of stress relax., obstacle strength and thermal stress variation 0-89277
 Cu-Zn alloys, surface comp., outdoor exposure influence 0-59770
 Cu-Zn-Al, β' martensite crystal crossing rel. to reversible shape memory effect (Japanese) 0-108499
 Cu-Zn-Al, reversible shape memory effect (Japanese) 0-108500
 Cu-Zn-Al martensite, lattice dynamics, neutron scatt. meas. 0-88286
 Cu-Zn-Mn, steady-state diffusion of Zn and Mn 0-70445
 Cu-Zn(Ge)(Ni)(Ga), α -phase alloys, lattice sp. ht. calcs. 0-65246
 Cu-Zr amorphous alloy, sputter cooled, local order and amorphous struct. 0-88061
 Cu₂Zn_{1-x}, sputtering, binding energies 0-108312
 (Cu-Au)-Co, single crystals., solid soln. and particle strengthening, superposition 0-97495
 Cu₃Ag_{1-x}Au_x, phase relations, X-ray diffr. and differential thermal anal. 0-108395
 CuAu, ordered, vacuum deposited epitaxial films, orientation control by external stress 0-100426
 Cu₃Au alloys, superlattice-fringe imaging theory, images formed from two beams 0-79649
 Cu₃Au, disordered [001]-orientated single crystals., plastic deform., TEM and slip line studies 0-97541
 Cu₃Au, electrical resistivity and LRO, energy gap formation in Fermi surface 0-88533
 Cu₃Au, neutron irradi., displacement cascades, direct obs. method 0-107335
 Cu₃Au thin films, fine-grained and disordered, low temp. ordering 0-97433
 Cu₃Au-Co single cryst., precip. hardening (German) 0-84946
 Cu₃Au-Ni, antiphase domains morphology 0-108460
 CuCr, dil., anisotropic hyperfine coupling, NMR study 0-65784
 CuCr, dil., specific heat, impurity contrib. Kondo temp. 0-65903
 CuFe, dil., anisotropic hyperfine coupling, NMR study 0-65784
 CuFe solid solns., quenched from vap. phase, mag. props. 0-60307
 CuH dilute alloy, Hall coefficient, relaxation times, Fermi surface 0-84460
 CuLa_{1-x}, sputter-cooled, phase diagram and supercond. props. 0-70881
 r-CuMn, annealing ordered phase study by neutron diffr. 0-89265
 CuMn, dil., anisotropic hyperfine coupling, NMR study 0-65784
 CuMn, hysteresis, spin orbit scattering effect on anisotropy in spin glass state 0-71095
 CuMn spin glass, AC susceptibility 0-60305
 CuMn spin glass, μ^+ zero-field spin relax. probe for spin dynamics 0-97177
 CuMn, spin glass, random moments time correl., zero field muon spin relax. meas. 0-60335
 CuMn spin glass, specific heat and entropy 0-60354
 Cu_{0.86}Mn_{0.14}, hysteresis loop development 0-65922
 Cu_{0.98}Mn_{0.02}, spin glass, Heisenberg model, RPA approx. 0-65904
 Cu₃MnAl-Pd, MnAl mixed Heusler alloys, mag. props. 0-60269
 Cu_{3-x}Mn_xAl, and Cu₂Mn_{2-x}Al_x, Heusler alloys, order-disorder transitions 0-59619
 Cu₂MnAl_{1-x}Sn_x, Mossbauer effect study 0-60473
 Cu₂MnIn_{1-x}Sn_x alloy, compositional SRO, hyperfine interactions 0-71065
 Cu₄₀Nb₃₀X₃₀ (X=Ti, Zr, Hf), superconductors with metastable ordered structs. 0-108484
 CuNi molecule, electronic states determ. by ab initio HF and CI methods 0-69087
 Cu₂NiSn, Heusler alloy, elec. resist., 4.2 to 300K 0-75547
 Cu₂NiZn, comparison between different theories predicting stacking fault energy from extended nodes 0-75240
 Cu₂NiZn, stacking fault energy determ. from extended nodes 0-107280

copper alloys continued

- CuPd, chemical shift effects and origin of Pd 3d core level satellite 0-104039
 Cu₃Pd, periodic antiphase boundaries, electron microscopy study (French) 0-59481
 Cu_{1-x}Pd_xMnSb, mag. phase transition 0-60268
 Cu₃Pt, antiphase domains morphology 0-108460
 Cu₄₆Zr₅₄, Cu₅₂Zr₄₈, and Cu₆₀Zr₄₀ metallic glass, inelastic deform., free energy spectra 0-71699
 β -CuZn, acoustic emission rel. to stress induced martensitic transformation 0-81061
 CuZn, planar faults, faint electron microscopic image contrast obs. 0-107283
 Cu₃Zn clusters, electronic structures, SCF-X α -SW method 0-88468
 CuZr, photoemission study 0-104046
 Cu₃₅Zr₆₅ amorphous alloy, neutron diffr. obs. of struct. 0-88060
 Cu₄₆Zr₅₄ amorphous alloys, supercond. transition temp., press. depend. 0-84524
 Cu₅₇Zr₄₃, amorphous alloy, computer simulation of atomic structure 0-70125
 Cu₆₀Zr₄₀, amorphous, ductility and stress relief, low-temp. annealing effects 0-76296
 Cu₄₆Zr₅₄, amorphous metallic glass, differences caused by preparation technique (French) 0-103247
 Dy-Cu, amorphous, mag. phase diagram, magnetisation and sp. ht. meas. 0-80532
 DyCu film, amorphous, asperomagnetic domains, Barkhausen jumps in hysteresis loop 0-75822
 EuCu₂Si₂, interconfiguration fluctuation, NMR expts. 0-66069
 Fe-Co-Al-Cu-Ti (40, 14, 7.5, 4.5 wt.%), metastable equilibrium, high coercive state (Russian) 0-66476
 Fe-Cu, lath martensite habit planes, TEM study 0-84942
 Fe-Cu (4.54 wt.%) alloy, scaling behaviour, 700-1000°C, 1 atm. O₂ 0-93679
 Fe-Cu liquid alloy, heats of mixing, mixing entropies (Russian) 0-65224
 Fe-Cu-C, phase equilibria, 950 to 1500°C 0-60836
 Fe-Cu-C sintered porous materials, machinability 0-66457
 Fe-Cu-Zn, high-temperature phase diagrams (German) 0-108390
 Fe-Ni-Al-Co-Cu-Ti Y₂NdK type, S effect on mech. props. 0-60927
 Fe-Ni-Al-(Cu) (12, 0.5, 0.5 to 3 wt.%), Cu addition strengthening at 77K, mech. props. 0-60875
 Fe-Ni-Co-Cu-Ti Y₂NdKT alloys, impaired mag. props. with C and S additions 0-60368
 Fe-Ni-Ti-(Cu) (12, 0.25, 2 wt.%), Cu addition strengthening at 77K, mech. props. 0-60875
 Fe-Ni-V-(Cu) (12, 2, 2 wt.%), Cu addition strengthening at 77K, mech. props. 0-60875
 Fe-Ni-(Cu) (12, 0.5 to 3 wt.%), Cu addition strengthening at 77K, mech. props. 0-60875
 Gd-Cu, amorphous, mag. and elec. props. 0-80499
 Gd-Cu, amorphous, mag. props. and ferromag. reson. 0-75862
 GdCu, electrical resistivity and length changes with temp., hysteretic behaviour 0-97600
 Hf-Cu, amorphous, thermal stability, crystn., DSC and elec. resist. study 0-107060
 Ho-Cu intermetallics, resist. and magnetoresist., mag. ordering obs. 0-70677
 HoCu_{0.5-1}, Cu_x, cryst. struct. and mag. props. 0-75800
 HoCu₂, mag. struct. and elec. resist., neutron diffr. obs. 0-60206
 LaB₆-Cu, form. by wetting of LaB₆ with Cu 0-100813
 La₂₀Cu₈₀, disordered ribbons, production of quenched samples using arc furnace 0-71612
 Mg₂Cu polycrystals, surface study by AES, XPES and X-ray induced AES 0-65346
 Mn-Cu, micromagnetic props., neutron diffr. obs. 0-65906
 γ -Mn-Cu (10 at.%), spin wave studies using neutron diffraction 0-70991
 Mn-Cu (25, 62 wt.%), elast. consts., temp. depend., 170-300K (Russian) 0-81095
 Mn-Cu (25 wt.%) rod, transverse vibrations, energy dissipation, static longitudinal load effect 0-81099
 Mn-Cu (75, 25 wt.%), rod, coupled flexural and torsional vibr., energy dissipation 0-89281
 γ -MnCu crystals, antiferromag. Czochralski growth 0-97420
 γ -MnCu, Mn-rich, inclined spin axis, neutron diffr. study 0-75723
 Nb-Al-Ge-Cu, rapidly quenched, comp. and phase equilib. 0-76235
 Nb-Al(Ga, Si, Ge, Sn)-Cu, rapidly quenched, comp. and phase equilib. 0-76235
 Nb₃/Sn-Cu composites, in situ processed, supercond. props. 0-75698
 Ni alloy, precipitation strengthened compositions with oxide particles, condensed, struct. criteria and thin layer possibilities (Russian) 0-89236
 Ni-Cu, dil., ferromagnetic, hyperfine field and relax. time obs. of impurity heavy nuclei 0-75533
 Ni-Cu, electron-irrad., neutron-scatt. studies 0-75268
 Ni-Cu, ferromag., mag. moment, local environment effects, HF CPA cluster calc. 0-65817
 Ni-Cu, high-field susceptibility, spin-wave spectrum, CPA calc. 0-65818
 Ni-Cu, implantation damaged, crit. behaviour, perturbed ang. distrib. meas. anal. 0-60476
 Ni-Cu, itinerant electron ferromagnet, magnetovolume effects 0-60397
 Ni-Cu, magnetoresistivity anisotropy, spin mixing 0-88538
 Ni-Cu, matrix effect in SIMS anal. using O₂⁺ primary beam 0-76576
 Ni-Cu, surface segregation, computerised atom-probe FIM study 0-75412
 Ni-Cu-H systems, Curie temp. during phase transitions under high press. H₂ 0-71029
 Ni-Cu-X (X=Sn, Nb, Ti), spinodal decomp. alloys, linear expansion coeff. influence on morphological anisotropy (Japanese) 0-70431
 NpCu₂Si₂, mag. struct., neutron diffr. determ. 0-93084
 Pd-Cu, alloys-H solid solutions, superconducting transition temp. behaviour (Russian) 0-70879
 Pd-Cu compound, KKR electronic struct. 0-59864
 Pd-Cu-Si, glass form., crit. cooling rate 0-75169
 Pd-Si-Cu, amorphous, Hall effect meas. and electronic struct. 0-75551
 Pd-Si-Cu amorphous ribbons, low temp. sp. ht., density of states trends 0-79957
 Pd₇₅Cu₂₅Si_{16.5}, heat of crystn. and viscous behaviour 0-75166
 Pd₇₅Cu₂₅Si_{16.5} metallic glass, glass transition temp., cooling rate depend. 0-75181
 PdSiCu, amorphous, US attenuation and vel. studies at low temps. 0-88278

copper alloys continued

- Rh-Cu catalyst, Al_2O_3 supported, chemisorbed CO, IR spectra (*French*) 0-60559
- Ru-Cu clusters, EXAFS study 0-84804
- $\text{Sm}_{0.91}\text{Zr}_{0.09}(\text{Co}_{0.68}\text{Cu}_{0.16}\text{Fe}_{0.22})_{6.7}$, alloy permanent magnet, coercive force (*Russian*) 0-65966
- Sn-Cu film, metastable supercond. alloys produced by low temp. ion implantation 0-88670
- $\text{Sn}_{90}\text{Cu}_{10}$, quench-condensed films, superconducting transition temp., elastic stress and strain effects 0-70883
- SrCu, X-ray cryst. struct. determ. 0-92478
- Th-Cu, amorphous, thermal stability, crystn., DSC and elec. resist. study 0-107060
- Ti-Al-V-Fe-Cu, melt-extracted polycryst., mech. props. 0-76360
- $\text{TiBe}_{18}\text{Cu}_{0.2}$, ferromag., magnetisation density 0-103817
- $\text{TiBe}_{18}\text{Cu}_{0.2}$, high press. study of Curie temp. and mag. susceptibility 0-84600
- V/Cu-Ga, composite superconductor, V_3Ga phase form., TEM obs. (*Russian*) 0-84933
- W-Cu (92.8, 7.2 wt.%), liq.-phase sintered, embrittlement and interfacial impurity segregation 0-66647
- W-Cu pseudoalloy, porous, chromising 0-100959
- YbCuAl , mixed valence cpd., dynamic susceptibility, neutron inelastic scatt. 0-65807
- YbCuAl , mixed-valent cpd., thermal expansion and magneto-volume effects 0-66005
- YbCu_2Si_2 , interconfiguration fluctuation, NMR expts. 0-66069
- $\text{Yb}_{1-x}\text{Y}_x\text{CuAl}$, disordered extended Anderson model, CPA-alloy analogue treatment 0-65506
- Zn-Al-Cu, mech. and technological props. (*Polish*) 0-89286
- Zn-Al-Cu casting alloys, mech. props. and dendritic morphology, Al content effect (*Korean*) 0-93612
- Zr-Cu amorphous alloys, glass transition and ductility, O additions effect 0-75168
- Zr-Cu metallic glasses, glass form. and thermal stability 0-75177
- Zr-Cu, constitutional and struct. studies, by mag. susceptibility, metallography and X-ray diff. 0-70166
- $\text{Zr}_{0.475}\text{Cu}_{0.475}\text{Mn}_{0.05}$, glass transition temp., comp. depend. 0-79702

copper compounds

- see also copper alloys
- $\beta\text{-Al}_2\text{O}_3\text{-Cu}_2\text{O}$, phys. and chem. props., use in determ. of thermodynamics of Cu-Sn alloys 0-107502
- aluminium copper tetrahalides, exchange, mag. anisotropy, and spin diffusion contribs. to EPR linewidth 0-80597
- benzoate, one-dimens. antiferromag., heat capacity, field-induced crossover of spin-dimensionality 0-97099
- benzoate low-dimensional Heisenberg antiferromag., high field magnetisation 0-80558
- complexes, N ligands, X-ray K-absorpt. edge, expt. 0-89084
- copper phthalocyanine, chlorinated, radiation damage mechanism 0-88000
- cyclo-hexyl-ammonium-copper-trichloride, specific heat, ferromagnetic chain system 0-103491
- diethylammonium copper tetrabromide, mag. struct., NMR meas. 0-71192
- diisopropylammonium copper chloride, mag. interactions, susceptibility, 2-230K 0-60237
- dimethylammonium copper manganese chloride, two-dimens. mixed magnet, EPR 0-66030
- dimethylammonium copper tetrachloride, crit. slowing down and anomalous relax. near Curie temp. 0-71053
- dimethylammonium copper tetrachloride-tetrabromide mixed cryst., mag. transition 0-65874
- ferrite films, Mn-, Ni- and Al-substituted, LPE growth 0-96752
- formate anhydrate, cryst. struct. and mag. props. 0-79768
- formate tetrahydrate, antiferromag. phase, neutron diff. study 0-93085
- formate tetrahydrate, ice rule ferroelectric, polarisation correlations 0-97190
- halide laser driving ccts., parametric study 0-83610
- hexadecachlorophthalocyanato-copper discrimination of individual atoms in mol. images 0-100226
- oxide reduction by electron cyclotron reson. plasma of H, model study on discharge cleaning 0-76548
- oxides, X-ray absorption, discontinuities and limits, chem. combination effects 0-93435
- phthalocyanine, simulated mol. images, point models and kinematical struct. amplitudes 0-103223
- phthalocyanine, size distrib., transient elec. birefr. 0-85223
- α' phthalocyanine and chlorinated derivative mol. crystals, radiation damage in electron microscope 0-107328
- phthalocyanine-iodine, amorphous cpd. prep. by I_2 diffusion in polycryst., triplet EPR signals obs. (*Russian*) 0-66016
- polyphosphinate, bulk compressibility meas. to 30 kbar 0-76306
- polyvinyl alcohol film containing Cu^{2+} complexes, photoconductivity 0-107849
- porphyrins mag. susceptibility and EPR, sample grinding effects 0-60420
- tetraamine sulphate two-dimensional Heisenberg antiferromag., high field magnetisation 0-80558
- thiophenols, quaternary, mag. and elec. props. (*French*) 0-65771
- TMNC, Cu-substituted, spin dynamics, neutron scatt. cross section 0-60312
- $(\text{As}_{0.4}\text{S}_{0.6})_{100-x}\text{Cu}_x$, glassy, struct. and elec. cond. study 0-59399
- $\text{B}_2\text{C-Cu}$ cermet fabrication for neutron shielding appls. 0-102354
- $\text{BaO-V}_2\text{O}_5\text{-CuO}$ semiconducting glasses, impurity effects, elec. resist. and EPR study 0-103692
- $\text{Ba}_2\text{Zn}_{1-2(x+y)}\text{Cu}_{2x}\text{Cd}_{2y}\text{Fe}_{12}\text{O}_{22}$, mag. props. and Mossbauer spectrum 0-75765
- CdS/Cu-S solar cells, polycryst. thin film photovoltaic materials, photon loss anal., expt. determ. 0-93888
- $\text{CdS/Cu}_2\text{S}$ thin film heterojunctions, photocapacitance meas. of solar cell parameters 0-93897
- CdS/Cu-S thin film solar cells, design and fabrication, 9.15% conversion efficiency 0-81438
- $\text{CdS/Cu}_2\text{S}$ heterojunction, energy-band struct., capacitance-voltage characts., illumination effects 0-96982
- $\text{CdS/Cu}_2\text{S}$ junctions, carrier trap density, deep level defects 0-107801
- $\text{CdS-Cu}_2\text{S}$ solar cells, design and fabrication, 8.5% conversion efficiency 0-72047
- $\text{CdS-Cu}_2\text{S}$ solar cells, microstructural study of heterojunction materials 0-93978

copper compounds continued

- $\text{CdS-Cu}_2\text{S}$ solar cells, electron diffusion length determ. using spectral response meas. 0-81475
- $\text{Co}_2(\text{Ni}_{0.5}\text{Cu}_{0.5})_{1-x}\text{Fe}_x\text{O}_4$ ferrite, relation between elec. cond. and mag. anisotropy 0-75548
- $(\text{Cu}_2\text{Ag})_2\text{Se}/(\text{Bi}, \text{Sb})_2\text{Te}_3$, P type selenide segmented element fabrication, thermoelectric props. 0-107835
- $(\text{Cu}_2\text{Zn})\text{C}_2(\text{SO}_4)_2 \cdot 6(\text{H}_2\text{D}_2)\text{O}$ Tutton salt, proton spin-lattice relax. time, proton conc. depend. and spin diffusion role 0-71221
- Cu complex, (4,4'-bipy H_2) CuCl_6 , with infinite linear chains of dimeric units, struct. and mag. susceptibility 0-96498
- Cu complex, $[\text{Cu}(1,4,7,10\text{-tetraabenzyl-1,4,7,10-tetraazacyclododecane})\text{Cl}]\text{NO}_3$, cryst., struct. 0-64966
- Cu complex, bis(triphenylphosphine) phenanthroline copper (I), luminesc. spectra, decay times 0-60648
- Cu complex, copper (II) [2,5-diphenylazoxole] $_2$ $(\text{ClO}_4)_2 \cdot 4\text{H}_2\text{O}$, ESR studies 0-88867
- Cu complex, $\text{Cu}_2\text{Cl}_6(\text{H}_2\text{O})_2 \cdot 2$ tetramethylsulphone, mag. interactions, susceptibility, 2-230K 0-60237
- Cu complex, $\text{Cu}(\text{H}_2\text{O})_6^{2+}$, ligand hyperfine interactions, orbital angular momentum contrib. 0-96833
- Cu complex, Cu(II) bis(dithiocarbamate), ^1H ENDOR 0-87154
- Cu complex, $\text{Cu}(\text{NH}_3)_2(\text{NCX})_2$, X=O, S, electronic struct., stereochem. 0-58156
- Cu complex, $\text{Cu}(\text{NO}_2)_4^{4-}$, bond. props. and Jahn-Teller distortion, INDO-LCAO-MO calcs. 0-75532
- Cu complex, hexadecachlorophthalocyanatocopper (II), atomic resolution by computer image processing from electron micrographs 0-100149
- Cu complex, N,N'-ethylenebis (salicylaldehyde) copper (II)-thiourea, in solns., bond strength and hyperfine linewidth, EPR 0-74186
- Cu complex, N,N'-o-phenylenebis (salicylaldehyde) copper (II)-thiourea, in solns., bond strength and hyperfine linewidth, EPR 0-74186
- Cu complex, polyvinylimidazole-Cu(II) complex, ESR studies on dimer form. between copper ions 0-100613
- Cu complex, triazene-1-oxide complexes, EPR spectra in frozen nematic liq. cryst. glass 0-88871
- Cu complexes of 2-amino-5-methyl-1,3,4-thiadiazole and 2,5-dimethyl-1,3,4-thiadiazole, conductometric and IR meas. 0-87121
- Cu II acetylacetonate, XPS 0-74196
- Cu II complex, extended X-ray absorpt. fine struct. study 0-104011
- Cu phthalocyanine, grain boundary struct., crystallographic planes 0-103366
- Cu^{2+} systems, magnetic, nuclear spin Hamiltonians (*Japanese*) 0-60430
- Cu/CuCl double pulse laser, pumping pulse and output pulse characts. 0-87380
- Cu/CuCl double pulse laser, dissoc. pulse, afterglow, and laser pulse model 0-91775
- Cu-Cl boracite, pyroelec. coeff. meas. 0-75951
- Cu-CuI-graphite secondary cell, transient ionic current obs. 0-108790
- Cu-CuI-graphite secondary cell, steady state hole current obs. 0-108791
- Cu-Sb-I system, glass form., struct. and IR spectra 0-64915
- Cu-SiO $_2$, in-situ deform. in HVEM 0-103338
- $\text{Cu}_2\text{Ag}_{1-x}\text{I}_x$ crystals, layer structs., X-ray diff. studies 0-96457
- CuAl_2O_4 , pure and NiO promoted catalysts, surface oxidation state and comp., XPS study 0-76134
- $\text{Cu}_2(\text{AsO}_4)\text{Cl}$, temp. depend. of mag. susceptibility 0-70962
- Cu_2B_2 , elec. props. at high temps. and in strong elec. fields, thermistor appls. 0-92903
- $\text{Cu}_2\text{B}_2\text{O}_7\text{Cl}$, cubic, approx. nonlinear optical susceptibility 0-78904
- $\text{Cu}_2\text{B}_2\text{O}_7\text{Cl}$, ferroelec. 43m-mm2 phase transition, molar heat capacity meas. 0-93249
- CuBr, biexciton dispersion, two-photon absorpt. 0-76045
- CuBr, EXAFS amplitudes, many-body effects 0-97379
- CuBr, electronic dielec. const., vol. depend., Clausius-Mossotti model 0-100630
- CuBr, LF light scatt. spectra in superionic cond. phases, ion motion obs. 0-108217
- CuBr, lattice dynamics of binary superionic conductors 0-107393
- CuBr, polariton Raman spectra, oscillator strengths, temp. depend. 0-66197
- CuBr, reflectance and thermorefectance spectra, electronic struct. 0-71444
- CuBr, superionic behaviour at high temp., EXAFS study 0-107496
- CuBr vapour laser, characts. comparison with Cu, CuCl lasers 0-102711
- CuBr_2 , aq. soln., structural transition, neutron diff. study 0-64872
- CuBr_2 , aq. solns., EXAFS meas. 0-60714
- CuCl (100), obs. of p- and d-like surface states, angle resolved UPS study 0-104045
- CuCl, band struct., OPW calc. and X-ray spectra meas. 0-75506
- CuCl crystal resonant Raman scatt., and luminescence competition (*Japanese*) 0-80770
- CuCl, dielectric function for semiconductors with high exciton conc. 0-84443
- CuCl, electron-hole pairs behaviour in energetic ion tracks 0-65457
- CuCl, electronic dielec. const., vol. depend., Clausius-Mossotti model 0-100630
- CuCl, electronic struct. by LCAO and LMTO methods, direct gap semiconductor 0-59868
- CuCl, excitation spatial dispersion determ., two-photon Raman scatt. via excitonic mol. state 0-60595
- CuCl, four-wave mixing spectroscopy in crystals, nonlinear spectroscopy developments 0-91861
- CuCl, interface supercond., piezoelec. hypothesis 0-60128
- CuCl, LF light scatt. spectra in superionic cond. phases, ion motion obs. 0-108217
- CuCl, lattice dynamics of binary superionic conductors 0-107393
- CuCl, mech. vibrs. in piezoelec. solid, excitation by light pulses 0-75305
- CuCl, mol. emission spectrum, 5900-6800 angstrom, rot. anal. of A-X system 0-58273
- CuCl, nonrelativistic calcs., rel. to Ag halide photoelectron spectra 0-95679
- CuCl, optical absorpt. meas., evidence against intrinsic electron-hole supercond. 0-108172
- CuCl, polariton Raman spectra, oscillator strengths, temp. depend. 0-66197
- CuCl powder compacts, DC voltage depend. resist. under press. 0-80334
- CuCl, pressure depend. of structural, chemical, elec. and mag. props. 0-96596
- CuCl, refl. spectra, 4.5-30 eV, vel. to band struct. 0-103969
- CuCl, superionic behaviour at high temp., EXAFS study 0-107496

copper compounds continued

- CuCl₃, three-branch polariton dispersion curve, two-oscillator model 0-92832
- CuCl vapour laser, characts. comparison with Cu, CuBr lasers 0-102711
- CuCl vapour laser, output power limiting processes 0-91776
- CuCl₂, anhydrous, mag. phase transition 0-80506
- CuCl₂, aq. soln., structural transition, neutron diff. study 0-64872
- CuCl₂, aq. solns., EXAFS meas. 0-60714
- CuCl₂, ESCA satellite intensity, ab initio SCF calcs. 0-74103
- Cu₂Cl₂, cyclic, nonrelativistic calcs., rel. to Ag halide photoelectron spectra 0-95679
- CuCl₂(Cl₂²⁻)(Cl₆⁴⁻), electronic struct. studies by SCF, MSX α and INDO method 0-74119
- CuClO₄, neutron activated, radiation annealing 0-93569
- CuCl₂·2D₂O, cryst. struct., mag. and reson. props. 0-60424
- CuCrS₄, domain struct. and superstructure, TEM obs. 0-79779
- CuCr₂S₄, electronic struct., mixed valence 0-70612
- CuCr₂S₄-Se, spinels, NMR spin echo study 0-71238
- CuCrSe₂, influence of excess Cu on physical props. 0-103836
- CuCr₂Se₄, Crit. relax. processes, mag. reson. expts. 0-60425
- CuCr₂Se₄, electronic struct., mixed valence 0-70612
- CuCr₂Se₄, mag. moment distrib. by neutron diff., Goodenough model 0-70945
- CuCr₂Se₄, mag. reson. and valence state of Cu and Cr ions 0-60413
- Cu_{1-x}Cr₂Se₄, influence of excess Cu on physical props. 0-103836
- Cu₂Cr₂Se₄-Br₂, ferromagnetic semicond., Hall effect 0-60012
- CuF from Cu + F₂, chemiluminesc. reactions, mol. beam study 0-97702
- Cu²⁺F⁻ and Cu²⁺F²⁺, transferred hyperfine interactions 0-70659
- CuF₂, high temp. polymorphism and thermal props. 0-75199
- CuF₂(F₂²⁻), electronic struct. studies by SCF, MSX α and INDO method 0-74119
- CuF₂·2H₂O, synthesis, appl. for carrier-distillation emission spectroscopy 0-89164
- CuFe₂O₄, Jahn-Teller type crystal distortions 0-103904
- Cu_{0.9}Fe_{2.1}O₄-ZnFe₂O₄, cation distrib., mag. moment, Mossbauer spectra, chem. anal. 0-75210
- CuFeS₂, antiferromag., NQR local mag. field effects 0-71234
- CuFeS₂, chalcopyrite, ionic diffusion obs., use of cathodolum. and AES 0-71497
- CuFeS₂, superficial degradation in air and water, XPS obs. (French) 0-89110
- Cu₂FeS₄, bornite, cathodolum. and AES, ionic diffusion obs. 0-71497
- CuGa_{0.5}In_{0.5}Se₂/Zn_{0.25}Cd_{0.75}S heterojunction solar cell, preparation and props. 0-101110
- CuGa_{1-x}In_xSe₂, X-ray diff. cryst. data 0-84147
- CuGaS₂, thermo-optic coefficient, dispersion 0-71396
- CuGaSe₂, evidence of donor-acceptor type transition 0-93375
- CuGaSe₂, single crystals, electrical and photovoltaic props. 0-92940
- CuGaTe₂, refr. indices meas. 0-93259
- CuH, UV absorpt. spectra 0-87143
- Cu(I) complex, oxidation, fast reactions meas. by pulsed-flow instrument 0-66890
- CuI, EXAFS investigation of struct. and ion motion 0-108302
- CuI, ionic motions nature, mol. dynamics calcs., sp. ht. anomaly due to order-disorder transform. 0-107533
- CuI, LF light scatt. spectra in superionic cond. phases, ion motion obs. 0-108217
- CuI, lattice dynamics of binary superionic conductors 0-107393
- CuI photocathodes, efficiency evaluation for soft X-ray diagnostics 0-57442
- CuI, polariton Raman spectra, oscillator strengths, temp. depend. 0-66197
- CuI, reflectance and thermoreflectance spectra, electronic struct. 0-71444
- CuI single cryst., linear electro-optical props., temp. depend. 0-71376
- CuI, single crystals, growth and optical props. 0-93470
- Cu(II) complex, 2,2',2''-tri-aminotriethylamine, EPR and optical absorpt. obs. 0-108055
- Cu(II) complex, hexamethyltri-aminotriethylamine, EPR and optical absorpt. obs. 0-108055
- Cu(II) complexes, reversible excited-state electron transfer reactions for solar energy conversion 0-89655
- Cu(II)-DL-proline complex, ESR, magnetic susceptibility and optical absorption 0-93167
- CuIn_{0.7}Ga_{0.3}Se₂, epitaxial layers, on GaAs substrates, struct. and elec. props. 0-107670
- CuIn_{1-x}Ga_xSe₂(1-x)Te_{2x} pentenary alloy compounds for photovoltaic solar energy conversion 0-93971
- CuInS₂, films, RF sputtered, growth and props. 0-80124
- n-CuInS₂, mag. props., obs. 0-70939
- CuInS₂, single phase thin film prep. by flash evaporation 0-100796
- CuInS₂, sulphoselenite electron diff. and electron microscopy study, order-disorder transform obs. 0-88080
- CuInSe₂, amorphous thin film, flash evaporation, struct., stoichiometry 0-89150
- CuInSe₂, heteroepitaxy on {111} oriented Ge by flash evaporation, struct. 0-108333
- CuInSe₂, influence of impurities and free carriers on optical props. 0-108225
- CuInSe₂, refr. indices meas. 0-93259
- p-CuInSe₂, thermal props. 0-96705
- CuInSe₂, thin film fabrication by RF-sputtering for solar cell apps. 0-100786
- CuInSe₂, thin films, prep. by spray pyrolysis, struct., elect. and optical props. for solar cell apps. 0-100781
- CuInSe₂, thin films for solar cells, radiofrequency sputtering technique, elec. props. 0-93487
- CuInSe₂-CdS solar cell, polycrystalline thin film, high photocurrent, characts. 0-61339
- CuInTe₂, epitaxial layers, on GaAs, growth and props. 0-108359
- CuInTe₂, refr. indices meas. 0-93259
- CuInTe₂, single crystals, directional freezng growth and doping, resist. changes on annealing 0-60768
- Cu₂In₂Zr_{1-x}S₂ system, struct. and cond. meas. (French) 0-88354
- Cu_{1.5}Mo_{0.5}S₈, supercond. Chevrel phase, electron tunnelling spectroscopy expts. (German) 0-107966
- Cu₂Mo₂S₈, Chevrel phase, synthesis, stability and characts. 0-71608
- Cu₂Mo₂S₈, constitution diagram, 11-2000K 0-108407
- Cu₂Mo₂S_{8-y}, electrodes, thermodynamic and transport props. 0-66963
- Cu₂Mo₂S_{8-y}, mixed conductor, partial Cu ion cond. and chem. diffusion 0-84323

copper compounds continued

- Cu₂Mo₂S_{8-y}, mixed conductor, equilib. partial thermodynamic props. 0-85270
- Cu₂Mo₂S₈O₂, O-containing Chevrel phases, synthesis and props. 0-108368
- Cu₂NiSi₂S₃, X-ray cryst. struct. determ., mag. props. 0-107172
- CuO aggregates, solid, aerosols, dynamic shape factors meas. 0-61165
- CuO, black Zn-dust pigmented solar selective coatings for solar photothermal conversion 0-66997
- CuO, desorpt. of ions by low power laser beam 0-80092
- CuO formed anodically in phosphorus medium, photoelectrochemical effects (French) 0-93701
- CuO, isoelectric point meas. 0-88609
- CuO, mol. orbital energies and X-ray K-absorpt. spectra 0-69060
- CuO, on Al or Cu, solar selective coating, figure of merit 0-72082
- CuO, on Cu, identification by electron spectroscopic methods 0-60747
- CuO powder, surface area determ. by adsorpt. of stearic acid and pyridine 0-107636
- CuO-Fe₂O₃, isoelectric point meas. 0-88609
- CuO + WO₃ solid state reaction kinetics, CuWO_{4-x} formation study 0-66796
- Cu₂O, Cu inclusions and annealing, optical and IR absorpt. obs. 0-60630
- Cu₂O, exciton luminesc. spectra, mag. field influence 0-80860
- Cu₂O formed anodically in phosphoric medium, photoelectrochemical effects (French) 0-93701
- Cu₂O MIS solar cell with SiO₂ interfacial layers, semi-transparent layers of Au, Cu, Ag and Al 0-93946
- Cu₂O, mol. orbital energies and X-ray K-absorpt. spectra 0-69060
- Cu₂O, on Cu, identification by electron spectroscopic methods 0-60747
- Cu₂O, photosensitive etching in nonoxidising etchants 0-78813
- Cu₂O polycryst., dislocation obs. by electron microscope (Spanish) 0-75230
- Cu₂O, reson. Raman scatt. from stress-split forbidden excitons 0-93332
- Cu₂O, self-consistent energy bands 0-59869
- Cu₂O solar cells, electrical and optical props., photocurrent anal. 0-101116
- Cu₂O, standard free energy of formation, by EMF method with solid oxide electrolyte at low temps. (Japanese) 0-88338
- Cu₂O, uniaxial stress effects on excitons 0-60589
- Cu₂O:Ag⁺, exciton-neutral and exciton-charged impurity scatt. cross sections 0-70618
- Cu₂O:Mn, photomemory mobility components, charged centre conc. 0-103725
- Cu₂O-Cu diode junction, Schottky barrier, electronic structure and minority carrier diffusion length (French) 0-65682
- Cu₂O formation on Cu oxidation, EXAFS obs. 0-71808
- Cu₂PS₄Br, cryst. struct. at 293 and 473K, thermal parameters, neutron diff. obs. 0-59450
- Cu(Rh)_{1-x}Cr_xS₄, spinel system, susceptibility and metallic resistivity, anomalies due to s-d interaction 0-70958
- CuS, black Zn-dust pigmented solar selective coatings for solar photothermal conversion 0-66997
- CuS-PbS, black Zn-dust pigmented solar selective coatings for solar photothermal conversion 0-66997
- Cu₂S, Cu_{1.5}S, α - β transition, thermographic investigation of heats, entropies and activation energies 0-88314
- Cu₂S, diffusion length meas. using scanned laser beam tech. 0-93886
- Cu₂S, electrodeposition, using nonaqueous solvents 0-76200
- Cu₂S films, prpe. methods, appl. to Cu₂S-CdS solar cells 0-80980
- Cu₂S, on Cu, solar selective coating, figure of merit 0-72082
- Cu₂S/CdS heterojunction solar cells, diffusion length determ. using minority carrier SEM 0-61359
- Cu₂S-CdS heterojunction solar cells, carrier transport, nonmonotonic band profiles 0-61361
- Cu₂S-CdS heterojunction interface, depth distribution profiles, Auger spectra 0-88622
- Cu₂S-CdS heterojunctions, role of deep levels in controlling photovoltaic props. 0-92941
- Cu₂S-CdS heterophotocells based on CdS films of stoichiometric composition, elec. and photoelec. props. 0-93873
- Cu₂S-CdS solar cell applications, CdS film spray fabrication, physical props. (French) 0-60113
- Cu₂S-CdS solar cell fabrication by magnetron reactive sputtering deposition 0-61363
- Cu₂S-CdS solar cells, interface recombination phenomena and tunnel effect 0-66978
- Cu₂S-CdS solar cells, optical absorption coefficient changes in Cu₂S 0-93980
- Cu₂S-CdS solar cells, optimised grid patterns 0-108798
- Cu₂S-CdS solar cells with interdigitated grid, current-voltage analysis 0-93981
- Cu₂S-CdS sprayed solar cells, chemical spray deposition 0-93979
- Cu₂S-CdS thin film planar junction devices, quantitative photon loss anal. 0-61362
- Cu₂S-CdS thin-film solar cells, low-cost manufacturing process outline, economic anal. 0-93930
- Cu₂S-CdS thin-film solar cells, high open-cct. voltage and low refl. losses 0-94088
- Cu₂S-Zn_{0.5}Cd_{0.5}S and Cu₂S-CdS thin film solar cells by solid state reaction, comparison 0-101109
- Cu₂S-Zn_{0.5}Cd_{0.5}S heterojunction, improved model of electro-optic behaviour 0-94023
- Cu₂S + Ln₂S₃, powdered mixtures, reaction rate, production of ionic semiconductors 0-93741
- Cu₂-S, and related disordered crystals, diff. pattern, cluster theory 0-75123
- Cu₂-S, digenite, X-ray determ. of structural transitions 0-92474
- Cu₂-S-CdS ceramic solar cells, solar batteries operating characts. 0-93874
- Cu₂-S-CdS p-n heterojunction, optical energy convertor, struct. and recomb. props. 0-72065
- Cu₂-S-CdS p-n heterojunction, copper sulphide growth features during formation (Russian) 0-107898
- Cu₂S, 1 \leq x \leq 2, quantum temp. size effect and magnetism (Russian) 0-103764
- Cu₂S evaporated layer growth in vacuum, compositional and optical characterisation, solar cell apps. 0-97437
- Cu₂S/CdS, sequential evaporation, for solar cell applic. 0-93902
- Cu₂S-CdS solar cell, prep. and characts. (Croatian) 0-93876

copper compounds continued

Cu₂S-CdS solar cells, Cu₂S growth kinetics and composition analysis by absorbance transient and galvanic electrochemical measurements 0-92797
 Cu₂S-CdS solar cells, SCL current 0-76634
 Cu₂S-CdS thin film solar cells, using all film vacuum deposited process 0-93977
 Cu(SCN)_{1/2}, synthesis and high elec. cond., activated and metallic cond. obs. 0-96957
 CuSO₄ aq. solns., densities, viscosities, elec. cond. meas., 20 to 70°C 0-59688
 CuSO₄ soln., electrochemical analogue of Benard instability, isothermal and potentiostatic conditions 0-76530
 CuSO₄ solution, thermooptical excitation of sound by ns. laser pulses 0-79884
 CuSO₄/H₂SO₄ electrolytes, densities, elec. cond., viscosities 0-107455
 CuSO₄·5H₂O, dehydration into trihydrate obs. using monocryst. platelets, product domains shape 0-71905
 CuSO₄·5H₂O, EXAFS, rel. between Debye-Waller factor and thermal parameters meas. by neutron diff. 0-84803
 CuSO₄·5H₂O, low freq. spin dynamics, proton relax. study 0-71218
 CuSO₄·5H₂O monocryst. platelets, dehydration into trihydrate, displacement rate modulation of reaction front 0-108711
 CuS₂(Se₂), electronic struct., UPS and XPS study 0-80935
 CuSbS₃ crystals, growth and characterisation 0-60770
 Cu₂Se, kinetics of polymorphic $\alpha \rightarrow \beta$ transformation (Russian) 0-70152
 Cu₂-Se, nonstoichiometric, diamag. and paramag. props., susceptibility meas. 0-70936
 CuSe₂O₅, strongly antiferromag. coupled Cu linear chain, orbital props. 0-100580
 Cu₂-Te₂, non-stoichiometric phases, electron microscopic and electron diffraction studies 0-64977
 CuTiS, melting heat and melting entropy (Russian) 0-70374
 Cu₂U₂S₁₃, cryst. struct. and magnetic props. (French) 0-96496
 Cu₂U₂Se₁₃, cryst. struct. and magnetic props. (French) 0-96496
 p-Cu₂VS₄, mixed conduction due to cationic interstials 0-70772
 Cu₂VS₄, out of equil. mixed cond., electronic cond. decrease in ionic soln. 0-107874
 Cu₂VS₄, out of equil. mixed cond., off-centre positions and order-disorder transition, ultrafast nucl. relax. obs. 0-108103
 Cu₂VS₄, out of equil. mixed cond., chem. origin of mobile ions, spin-lattice relax. and NQR obs. 0-108104
 Cu₂VS₄, Raman linewidth of A₁ mode under high press., reson. effects 0-108210
 CuWO₄, elec. cond., thermoelectric power and dielectric constant temp. depend. 0-96886
 CuWO_{4-x} prod. from CuO+WO₃ solid state reaction 0-66796
 EuCu₂Si₂, mixed valence system, X-ray absorption spectroscopic study 0-80906
 Fe_{0.5}Cu_{0.5}Cr₂S₄, ESR spectra, elec. and mag. props., Curie temp. 0-97137
 (Fe_{1-x}Cu_x)O₃, yH₂O crystal growth, characterisation by Mossbauer spectroscopy, mag. meas. and electron microscopy (French) 0-80655
 (Fe_{0.45}²⁺Mn_{0.32}²⁺Mn_{0.03}²⁺Cu_{0.10}²⁺)[(Fe_{1.74}³⁺Al_{0.26}³⁺)O₄]²⁻, influence of Fe²⁺ ion substitution on electron hopping, Mossbauer study 0-71247
 Ge:Li, Cu p-n junctions, current stimulated LiCu complex formation, photocurrents 0-107897
 KCl-CuCl eutectic fused salt, potential as intermediate temp. solar heat transfer and storage medium 0-101135
 K₂CuF₄, layered spin system, planar rotator symmetry, phase transition 0-65951
 K₂CuZn_{1-x}F₄, Curie temp., Cu conc. depend. 0-60255
 NH₄Cu₂Cl₃(I₂-Cl₂), highly conducting solid electrolyte 0-65280
 Na₂O-B₂O₃-CuO, γ -irrad., CuO effects on EPR 0-84645
 Na₂O-P₂O₅-CuO, γ -irrad., CuO effects on EPR 0-84645
 Na₂O-SiO₂-CuO glass, gamma-irradiated, EPR and optical spectra 0-103885
 Na₂O-SiO₂-CuO, γ -irrad., CuO effects on EPR 0-84645
 RbCu₂Cl₃I₂, development of Cu⁺ ion cond. 0-107532
 SbCu₂Si₂, mixed valence system, X-ray absorption spectroscopic study 0-80906
 SiO₂-Al₂O₃-Cu₂O glass alkaline durability, corrosion rate, heat capacity and elastic moduli 0-93673
 SnO₂-copper phthalocyanine-Ag systems, elec. and electroluminescent behaviour 0-80864
 SnO₂-Cu₂S-ZnS:Mn-Cu-Al₂O₃-Al, light-emitting struct., cond. and electrolum., heat treatment 0-97345
 V₂O₅-CuO-BaO glass, unpaired electron localisation, ESR study 0-66026
 Zn₂Cd_{1-x}S-Cu₂S heterojunction solar cells, props., comp. meas. of interfacial region 0-81472
 Zn₂Cu_{0.1}Fe_{2.9-x}O₄, ferromag. reson., g-factors, Jahn-Teller ion effects 0-66043
 Zn₂Cu_{0.1}Fe_{2.9-x}O₄, ferromag. relax. 0-60422
 ZnO-Cu₂O heterojunction solar cells, prop. by RF sputtering 0-93945

copper zinc alloys see brass

copying see reproduction (copying)

Corbino effect

see also Hall effect
 n-InSb Corbino disc, acoustic noise effect on I-V characts. (Russian) 0-100492
 n-Si inversion layers, electronic g-factor, spin-split Landau levels 0-80346

Coriolis force

see also rotation
 atmosphere, E.African jet dynamics, July mean conditions simulation 0-77045
 atmospheric movements, spatial problem on influence of orography with Coriolis force included (Russian) 0-94565
 deformed nuclei, effect on Coriolis interaction, Nilsson model and Woods-Saxon pot. calcs. 0-63071
 ethyl iodide, microwave spectra and internal rot. anal. 0-69130
 ethylene, IR absorpt. spectra of ν_1 , ν_{10} and ν_4 interacting band 0-83369
 Group IIIA metal tetrahalide ions, vibr. anal. 0-63608
 Group IV tetrabromides, intramol. force fields and mean vibr. amplitudes 0-106316
 hexahalo ions, octahedral, mol. consts. calcs. 0-106317
 hexaoxy ions, octahedral, mol. consts. calcs. 0-106317
 ion cyclotron motion, Coriolis coupling of ion internal degrees of freedom 0-87246
 mass flow meter using Coriolis principle, electro-optical force sensing techniques 0-103094

Coriolis force continued

mass flowmeter, meas. Coriolis effect on mols., electro-optical sensing 0-96327
 mol. consts. and mean vibr. amplitudes calcs. 0-106318
 molecules, isolated, intersystem crossing, rot. motion effect 0-95669
 phosphine, IR spectrum, ν_1 and ν_2 band analysis 0-83366
 rotational alignment in nuclei and planets 0-90636
 tetrafluoromethane, $\nu_2 + \nu_4$ band, high resolution diode laser spectra 0-69138
 tetrafluoromethane, mol. consts. and mean vibr. amplitudes calcs. 0-106318
 XY₂ bent symmetrical molecules, Coriolis coupling consts., centrifugal distortion consts. 0-58236
 CF₃S, mol. consts., kinetic consts. method calcs. 0-58235
 CF₂Se, mol. consts., kinetics consts. method calcs. 0-58235
 CO₂, IR band intensity 0-83425
 CrCl₄, mol. consts. and mean vibr. amplitudes calcs. 0-106318
 Ga trihalides, vibr. anal., pot. const. determ., mol., compliance and Coriolis coupling const. calc. 0-95579
 In trihalides, vibr. anal., pot. const. determ., mol., compliance and Coriolis coupling const. calc. 0-95579
 NH₄⁺, mol. consts. and mean vibr. amplitudes calcs. 0-106318
 O₃, line position and intensities of $2\nu_3$, $\nu_1 + \nu_3$ bands 0-87181
 SO₂, IR spectra, Coriolis intensity perturbations 0-95617
 Se+NO₂, chemiluminesc., nonequilib. product distrib. 0-101014

cornea see eye

corona

see also electric breakdown; flashover; solar corona
 AC, at 50 Hz, DC electric field influence obs. (German) 0-70052
 AC, point-plate arrangement, behaviour near threshold voltage obs. (German) 0-70051
 cylinder in still air, DC corona cooling obs. 0-70071
 electro-gas dynamic technologies, corona discharge industrial applications, qualitative analysis (Rumanian) 0-70061
 electrostatic deposition of thin particulate layer, resistivity meas. under ionic bombardment 0-68218
 electrostatic precipitation, charge measurement, positive and negative corona 0-96403
 electrostatic precipitators, corona discharge theory analytic developments (Rumanian) 0-70062
 electrostatically assisted heat transfer 0-69628
 heated cylinder in still air, cooling by corona wind expt. 0-84023
 impulsive discharges around conductors, phys. aspects consideration (French) 0-92406
 laser induced microscope, electron density profile, interaction and transport profile 0-107008
 long spark form. mechanism 0-59326
 optical component protection in dusty environments, electrostatic techniques 0-58657
 optoelectronics, appl. in measuring gas discharge phenomena 0-107007
 polyethylene films, corona charged, charge trapping 0-88571
 polyvinylidene fluoride, corona-charged, surface effects 0-66102
 pulse character in strongly heterogeneous field formed by electrodes point-plate arrangement (Czech) 0-70048
 rod-to-plate system, initial corona voltage calculated according to Townsend's Theory (Czech) 0-87961
 transition region and inner corona, energy balance 0-90379
 transmission lines, high voltage, depend. of coronal discharge power loss on instantaneous rainfall rate 0-98471
 H₂O vapour under point corona discharge, microprocessor control for vapour generator and EHD phenomena 0-106852
 N glow discharges surface coronas and photopreionisation stability, demonstration 0-105475
 N-O mixtures, positive glow corona in quasi-uniform fields 0-100104
 SF₆ and SF₆-air mixture gas under impulse voltage, discharge phenomena (Japanese) 0-96409
 SF₆ corona-stabilised breakdown, computations and obs. 0-64804

coronagraphs

see also solar corona
 diffraction limit problems and design approaches 0-82200
 Norikura Observatory equipment for polarimetry (Japanese) 0-82223
 objective component surface scatt. angular distrib. obs. 0-74463
 Solwind, NRL coronagraph, initial obs. 0-82325
 white light coronagraph and X-ray XUV solar telescope, CCD camera systems and support electronics 0-62023
 white light coronagraph/XUV telescope expt., quadratic A/D converter 0-62024

corpuscular streams see cosmic rays; solar wind

correlation methods

see also correlators
 acoustic correlation measurement method for rotating sources of noise 0-64279
 acoustic wave reflection from ocean bottom and surface, correlation measurement of coeff. 0-58848
 automatic speaker recognition, cepstral/spectral and linear prediction techniques compared 0-91993
 brain, 40 Hz activity in sigmoid gyrus, nucleus accumbens and amygdala, cross correl. anal. 0-76730
 complex plates, anal. non-stationary random vibrations 0-102991
 coupled-core nuclear reactor, distributed parameters identification, pseudorandom perturbation and correlation anal. 0-86966
 creep rupture data analysis, development of correlation and extrapolation methods 0-58975
 diffusing surface optical autocorrelation 0-99646
 dislocations and microplasma sites, STEBIC/STEM/EELS correlation 0-96528
 distributed type associative memory model with quantised Hadamard transform 0-108867
 errors, signal parameter meas. 0-57241
 fast image recognition by generalised harmonic analysis (Russian) 0-63930
 fluctuations of intensity at two wavelengths in turbulent medium 0-87318
 galaxy correlation function evolution, N-body Monte Carlo model 0-62292
 identification of acoustic pathways through barriers 0-102880
 image alignment errors due to aliasing 0-106480
 image correlation based on extracted edges 0-99658
 image registration and differencing by coherent optical pattern recognition 0-99648

correlation methods continued

- image registration using material information 0-99664
- implicit sampling for noncoherent optical data processing 0-99652
- incoherent optical correlation operations 0-99650
- jet turbulence, laser velocimeter correlation meas. 0-106785
- laser surface speed measurement by correlation, industrial paper machine test (*French*) 0-95082
- linear predictive coded speech digitisers, background noise spectral subtraction 0-96140
- liquid mixture, surface tension theory 0-88404
- mammographic US image correlation with histopathologic sections 0-101240
- multisensor image pattern recognition, statistical and deterministic aspects 0-99647
- multisignal time difference estimator for transient sound source location 0-96127
- multispeaker phoneme classification by canonical correlation analysis 0-91988
- natural terrain scenes, segmentation-based boundary-modelling processor 0-99661
- nonperiodic objects, reconstruction from electron micrographs using correlation methods 0-86527
- optical pattern recognition, discriminant hypersurface prod. by average filters 0-99649
- optical pattern recognition by thermoplastic complex filter 0-99656
- optical signal and image processing, US Air Force research programme 0-78791
- outputs of acoustic arrays, crossarray beamforming with a parametric receiving array and a line array 0-79078
- PARCOR anal. lattice, inverse filter reflection coeff. calc. (*German*) 0-96114
- passive time-delay estimation with moving source or receivers, correlator compensation requirements 0-58843
- periodic sampling in periodic fluid flow measurement by laser anemometry 0-64657
- photon correlator, near ideal, with SAW device 0-68252
- propeller cavitation tunnel hydroacoustic transfer function, meas. and anal. (*Croatian*) 0-92002
- pseudonoise signals reflected from ocean bottom, correlation with transmitted signal 0-58846
- PWR components vibrations meas. (*German*) 0-79247
- quantum chemistry, matching model calcs. with experiment through linear regression 0-58243
- quasar redshifts distributions, periodicity from correl. and power-spectrum anal. 0-62313
- radiographs, industrial, discontinuous registration using profile analysis and piecewise correlation techniques 0-102645
- reflected-beam laser anemometry using photon correlator 0-106861
- scale and rotation invariant optical pattern recognition and classification 0-99655
- signal processing, time-integrating, acousto-optic 0-102641
- solar wind velocity recurrence period, depend. on heliographic latit. 0-62106
- spatial coherence meas. by correlated diffusers 0-74296
- spatial pattern recognition by spectral feature classification and coherent optical correlation 0-99644
- speckle pattern time-space cross-correlation for in-plane vel. meas. 0-105623
- Sun glitter on sea, correl. function appl. to sea surface slope distrib. function determ. (*Russian*) 0-94611
- synoptic climatology development for NE Gulf of Alaska, automated correl. technique appl. 0-98405
- two-tone image analysis using one-dimensional autocorrelation function (*Russian*) 0-63931
- underwater acoustic source location and motion estimation, joint reduction of bias and variance 0-96087
- underwater acoustic time delay estimation, cross-correl. and smoothed coherence transform methods compared 0-96086
- underwater sunlight fluctuations in sea spatial and temporal correlation 0-94533
- US-optical correlator for spatial freq. meas. 0-95995
- Venera 9 televised pictures of Venus cloud layer, geometrical correl. methods 0-67604
- water waves, wind-generated, spatial correls. rel. to freq. independent phase vels. 0-98333

correlation theory

- see also correlators; information theory
- atmosphere optics, phase correlation scale effects rel. to atmospheric imaging characts. 0-94604
- Fresnel plane interference fringe generation by correlated speckle patterns 0-106462
- IR staring mosaic sensor performance, effect of spacecraft-induced line-of-sight jitter 0-86416
- non-gaussian field, clipped time autocorrelation function of intensity fluctuations 0-106472
- ring laser mode competition and anticorrelation calc. and expt. 0-102740
- space-time optics, speckle phenomena and white light correlations 0-106460
- speech quality and intelligibility measures and their correlations 0-91978
- speech quality parametric objective measures correlated with subjective results 0-91980
- speech quality subjective and objective measures and their correlations 0-91979
- stereo-pair images, correlation error prediction 0-102636

correlators

- see also correlation methods; correlation theory; information theory
- acousto-optical, with two-dimensional reference transparency, testing 0-106485
- active optical devices, seminar, San Diego, CA, USA (August 1979) 0-101664
- ambiguity processing by joint Fourier transform holography 0-58468
- digital correlator signal preprocessing 0-83556
- integrated optics coherent correlator for real-time signal processing 0-79007
- joint transform correlator performance rel. to wavefront modulator characteristics 0-102651
- laser diode lensless MSF holographic optical element correlator, optical pattern recognition 0-102663
- liquid crystal image transducer, performance effects of liquid crystal thickness 0-102838

correlators continued

- matched filter, multicapacity, for correlator appl., using birefr. object film 0-74478
- matched filtering using band-limited illumination 0-69531
- optical, nonlinear t-E curve effects for matched spatial filter material 0-95812
- optical coherent correlator operation in image segment identification, aerial photograph anal. 0-102654
- optical diffraction correlators invariant to optical element shifts 0-106471
- optical matched filter correlator memory techniques and storage capacity 0-102643
- OTF measurement using autocorrelation method 0-58469
- photodichroic spatial light modulator for joint Fourier transform correlation 0-106617
- photon correlator for meas. transient waveforms of very weak fluorescence 0-87250
- plasma line correlator and filter bank, appl. to plasma line meas. at Chatanika 0-98507
- radio antenna arrays, incoherent optical 1-bit cross-correlators, radioastron. appls. 0-98555
- SAW acousto-optic time integrating correlator 0-64295
- semiconductor injection lasers in correlative data processing systems 0-74307
- surface-wave acousto-optic signal processors 0-102640
- time-integrating acousto-optical correlator design and performance 0-106618
- unclipped digital correlator for quasielastic light scattering 0-57387
- US return signals, correlation with bipolar digital representation of broadcast waveform 0-99897
- TeO₂ time-integrating acousto-optical correlator for chirp spectrum analyses 0-106474

correspondence principle

- indeterminacy, classical tests without corresponding quantum tests 0-62527
- stochastic action integral interpretation of quantum mechanical transformation function 0-77644

corrosion

- see also corrosion protection; corrosion testing; electrochemistry; stress corrosion cracking; surface chemistry
- alloy, HTR material, oxidation and carburization in He 0-108645
- alloy colour and colour stability as alloy design criteria 0-101005
- alternating current electrode processes, review 0-61107
- basalt fibres, alkali resist. in cement soln. 0-89377
- BWR, calc. of shutdown dose rate around recirculation pipes, radioactive corrosion products in primary cooling water 0-68734
- Carpenter 20 Cb-3 alloy, pitting resist. in low salinity geothermal brines 0-93681
- cavitation corrosion of materials in molten metals on const. mag. field appl. (*Russian*) 0-60987
- Cu-Zn-Mn, de-alloying props. 0-104332
- electrochemistry, steady-state conversion rate rel. to surface reaction process, catastrophe theory 0-108717
- field-ion microscope specimens caused by polymer gaskets 0-57425
- fluoride mixture, molten, resist. of materials to corrosion by 0-60797
- n-GaAs, stabilisation against photodecomposition, surface damage influence 0-76390
- glass, excavation type, layers and profiles of SiOH, CaOH, and KOH polyatomic ion groups special corrosion effect 0-81387
- glass, float, low-Fe, weathered, surface, characterisation 0-93666
- glass, stained, deterioration by atmospheric corrosion and micro-organisms 0-93664
- glass fibre, preparation, appl. in Portland cement reinforcement, alkali resistance 0-81019
- glass fibre reinforced plastics, ageing by boiling in water, effect on physicochem. props. 0-60892
- glass reactions with aq. solns., influence of surface pot. on kinetics 0-108612
- graphite, corrosion by CO₂, CO production radiolytically induced gas pressure effects 0-106115
- graphite, from reactor, quantitative microanalysis by laser emission spectroscopy 0-81384
- graphite, synergistic effect of electrons on atomic H activity 0-106112
- graphite corrosion in PBHTGR process heat reactor following massive air ingress (*German*) 0-83181
- Hastelloy G, and C-276, pitting resist. in low salinity geothermal brines 0-93681
- Hayes alloy no.716, Fe-Cr-Ni-Co-W-Mo-Si-C-B (26, 22, 12, 3.5, 3, 1.2, 1.1, 0.4 wt.%), hardfacing alloy 0-100802
- Haynes alloy 20 Mod, pitting resist. in low salinity geothermal brines 0-93681
- implantation in Al and Al-Zn-Mg-Cu, effect on corrosion behaviour 0-71794
- implanted prosthesis failure analysis techniques and results 0-89906
- Inconel 600, nuclear reactor boiler corrosion, XPS 0-66709
- Inconel 600, nuclear reactor boiler corrosion, XPS 0-71816
- Inconel 625, pitting resist. in low salinity geothermal brines 0-93681
- ion-implanted alloys, surface props. effects and appls. 0-79824
- jute, cement reinforcing fibre, alkali resist. 0-89377
- marine corrosion, and its prevention 0-104333
- metallic glass, corrosion behaviour, metalloid elements influence, review 0-89421
- metallisation, IR microscopy failure anal. 0-98976
- metals, colloid chem. appls. 0-89541
- metals, indoor corrosion rates meas. 0-76404
- metals, pure, corrosion due to V₂O₅ melts (*Japanese*) 0-93691
- metals, rapidly quenched, conf., Brighton, England (July 1978) 0-67934
- nuclear fuel element cladding, corrosion product deposition, heat transfer model (*Bulgarian*) 0-71818
- nuclear steam generator tubes testing and evaluation, using CIS/DASIO system (*Czech*) 0-63301
- optical glass, chem., durability, pragmatic view 0-78921
- periclase refractories, props. after testing at over 2000°C 0-104317
- phosphate glass-Al alloy seals, elec. and mech. props., glass transition 0-81018
- plastic encapsulated and hermetic modules, permeation properties 0-100937
- polymers, atmospheric resistance, distrib. function determ. and anal. (*German*) 0-81225
- power line equipment, field work investigating corrosive effects (*Norwegian*) 0-97631

corrosion continued

rate measurement, with dual electrodes 0-85180
rates, error anal. in using 2 and 3 electrode polarisation resist. meas. 0-100930
refractory metals and oxides, reactions of liq. alkali metals, relevance to reactor technology 0-85173
resistant alloys, metastable microcrystalline, appl. 0-84887
scanning electron microscopy, appl. to surface anal. 0-99004
silicate glass, hydration in steam atmosphere 0-85211
stainless steel, in MgCl₂ solutions, Cl distrib. in oxide films, SIMS (French) 0-108765
steel, austenitic stainless, corrosion resistance of cold deformed Cr-Ni austenitic stainless steel in N₂O₄ media at 433K (Russian) 0-76422
steel, austenitic stainless, corrosion resistance testing, urea plant applications (Czech) 0-61012
steel, austenitic stainless, fretting corrosion of orthopaedic implant materials by bone cement 0-104813
steel, austenitic stainless, nonsensitized, fatigue strength, intergranular corrosion effect (Japanese) 0-85027
steel, austenitic types AISI 316, 347 and Eshete 1250, corrosion in molten SO₄ deposits 0-97625
steel, C, corrosion by aq. H₂S solns. 0-100946
steel, C, Cr-Mo ferritic and austenitic stainless, corrosion behaviour in reducing environment of coal fired MHD generator 0-104322
steel, Cr-Mn(Ni), Mn and Ni additions, effect on corrosion resistance and hardness 0-104342
steel, Cr-Ni-Mo, resist. to corrosion and corrosion-fatigue in seawater 0-104346
steel, ferritic, Cr-Mo-Nb, intergranular corrosion resistance 0-104319
steel, ferritic stainless, Cr-Mo (12.1wt.%) microstructure influence on localised corrosion behaviour 0-61018
steel, high and low C, wires, electroheated, thermal cycling and corrosion behaviour 0-61006
steel, high-strength, fatigue, interaction effects between trace impurities and environment 0-66651
steel, high-strength low alloy, H₂ attack, 350-510°C 0-97636
steel, hydrogen absorption, anilines surfactants effectiveness, HCl conc. effect 0-108638
steel, low-C, pitting resist. in low salinity geothermal brines 0-93681
steel, martensitic cutlery, pitting corrosion 0-100962
steel, mild, corrosion rate meas. in H₂SO₄ using microprocessor controlled potentiostat 0-71798
steel, notched specimens in sea water, endurance limit enhancement, specimen size, freq. effects 0-93678
steel, stainless, 18Cr-2Mo-Ti, atmospheric corrosion 0-85078
steel, stainless, amorphous films, corrosion resist. and ion plating use 0-89423
steel, stainless, corrosion and grain boundary penetration on exposure to coal gasification environment 0-61003
steel, stainless, corrosion behaviour of composite materials in N₂O₄ oxidising atmospheres (Russian) 0-76421
steel, stainless, duplex, STEM obs. of localized corrosion 0-104324
steel, stainless, E-brite 26-1, pitting resist. in low salinity geothermal brines 0-93681
steel, stainless, heat treated, oxide comp. and corrosion susceptibility of grades 410 and 430, AES study 0-66692
steel, stainless, liq. Li corrosion rate expressions, 600-1000°C 0-93682
steel, stainless, pitting corrosion in chloride media, electrochem. aspects 0-61007
steel, stainless, sensitization, C content and ferrite morphology effect 0-89400
steel, stainless, type 316, corrosion behaviour in high temp. impure He gas 0-76402
steel, stainless, type 316, surface comp. rel. to crevice corrosion initiation 0-93680
steel, stainless, type 316L, pitting resist. in low salinity geothermal brines 0-93681
steel, stainless 304, metallurgical factors on the corrosion and mass transfer in liq. Na (Japanese) 0-71804
steel, structural types St. 3PS, 10CrNiCuP, corrosion rates 0-108681
steel, type 12X18H10T, defect development in contact area with coolant (Russian) 0-57859
steel, volatile products from reaction with H₂O-CO₂, high temp. 0-81233
steel, wear resistance of low temp. nitriding treatment 0-89357
steel electrodes, pitting corrosion currents rel. to conc. of inhibitive and corrosive anions under corrosion conditions 0-85181
steel pipe corrosion, mass transfer coeffs. under isothermal flow conditions 0-97628
X-ray diffraction apparatus, for in-situ high temp. water corrosion 0-90936
Zircaloy, breakaway mechanism, corrosion kinetics in steam 0-61030
zircaloy, nuclear microprobe methods for investigating oxidative corrosion 0-71787
Zircaloy fuel cladding, irradiation-induced in-reactor corrosion in CANDU reactors 0-104352
Zircaloy-2, hot-pressed, influence of diffused C on structure and oxidation 0-61016
Zircaloy-4 BWR channels, corrosion resistance 0-104351
Ag-Au, corrosion in HNO₃ 0-85091
Ag-Cu flex leads, microstruct. study of corrosion 0-76406
Ag-Sn alloys and amalgams, electrochem. considerations, corrosion in physiological soln. 0-93760
Al alloy electrode, corroding, acoustic emission 0-60997
Al, corrosion, general and pitting, Mo and Ar ion implantation effects 0-71794
Al, corrosion by carbon tetrachloride, IETS obs. 0-81230
Al-(Mn), effects of Mn on electrode or free corrosion potentials 0-100942
Al-Ca-Zn (5.5 wt.%) superplastic sheet alloy, mechanical properties, superplastic forming behaviour 0-60920
Al-Mg (7 wt.%), bare surface reaction rates in aq. solns. 0-101022
Al₂O₃-SiO₂-ZrO₂ refractories, corrosion behaviour in glassmelting furnaces (Polish) 0-71783
C, glassy, electrolytic durability 0-66809
CC Fe-Ni-Cr (35, 15 wt.%) Nb(Ti)(Mo), corrosion in HTGR He environment 0-61021
Ca₂(PO₄)₂OH bioceramic, material props. 0-93523
Co base amorphous alloys, alloying elements influence on corrosion behaviour, XPS obs. 0-89422
Co-B(-Cr) thin film glasses, mag. props. and corrosion resist. 0-80576
Cr, corrosion in SO₂, 700-1000°C 0-97642

corrosion continued

Cr, electrochemical behaviour, in molten V₂O₅ (Japanese) 0-89498
Cr, pure, corrosion due to V₂O₅ melts (Japanese) 0-93691
Cu-Au, corrosion in HNO₃ 0-85091
Cu-Cu₂Y eutectic alloy, cast and directionally solidified, struct. and props. (Russian) 0-104138
Cu-Mn, de-alloying props. 0-104332
Cu-Ni, galvanic corrosion in sulphide modified seawater 0-100953
Cu-Ni-Zn-Mn fine grained precipitation-hardenable alloy, high strength and ductility 0-100805
Cu-Zn, de-alloying props. 0-104332
Fe, colloid chem. appls. 0-89541
Fe commercial piping, corrosion under flow conditions, SO₄ ion effect 0-97629
Fe, corrosion and passivation in LiCl soln., peripheral velocity effect 0-61000
Fe, corrosion behaviour in H₂SO₄ soln., ion implantation effect 0-71793
Fe corrosion in aq. H₂S, FeS polymorph form. 0-81231
Fe, dissolution and passivation kinetics in solns. containing O 0-76547
Fe, electrochemical behaviour, in molten V₂O₅ (Japanese) 0-89498
Fe, pure, corrosion due to V₂O₅ melts (Japanese) 0-93691
Fe-B-Cr(Si) thin film glasses, mag. props. and corrosion resist. 0-80576
Fe-Cr (12 wt.%), corrosion in o-phosphoric acid 0-97622
Fe-Cr-Al (7, 5 wt.%), expt. stainless alloys, phys. and mech. props. 0-97637
Fe-Cr-Mo and Fe-Cr-Mo-Si alloys, amorphous films, corrosion resist. and ion plating use 0-89423
Fe-Cr-Ni, corrosion behaviour in hot conc. NaOH soln. (Japanese) 0-85082
Fe-Cu (4.54 wt.%) alloy, scaling behaviour, 700-1000°C, 1 atm. O₂ 0-93679
Fe-Ni-Cr (44, 17 wt.%), nuclear microprobe methods for investigating oxidative corrosion 0-71787
Fe₂Ni₃Cr₁₄P₁₂B₆, Metglas amorphous films, corrosion resist. and ion plating use 0-89423
Fe₂O₃, haematite, effect of boiling on the mass transfer of corrosion products in high temperature, high pressure water circuits 0-71766
HF electrode, surface oxide film, impedance and pot. behaviour 0-61001
Li₂O-GeO₂-Ga₂O₃ glass, electrode props., dissolution kinetics 0-89387
Li₂O-SiO₂, corrosion behaviour in aq. solns. of Al compounds 0-66679
MgO, sintered, refractories, props. after testing at over 2000°C 0-104317
Mo, corrosion behaviour in high temp. impure He gas 0-76402
Mo-Ti-Zr, TZM, corrosion behaviour in high temp. impure He gas 0-76402
NaCl:Ca crystals, surface recrystn., moisture effect 0-84950
Na₂O-(CaO)-SiO₂, diffusion controlled attack by aq. solns. 0-81218
Nb-Zr (1 wt.%), corrosion behaviour in high temp. impure He gas 0-76402
Ni alloys, corrosion behaviour in reducing environment of coal fired MHD generator 0-104322
Ni alloys, Nimonic PE 16, corrosion behaviour in high temp. impure He gas 0-76402
Ni, atmospheric corrosion, moisture adsorption and indoor corrosion rates 0-71799
Ni, corrosion and passivation in phosphate soln., pH depend., ellipsometric study 0-104448
Ni, electrochemical behaviour, in molten V₂O₅ (Japanese) 0-89498
Ni, high temp., SO₄ induced, studied at 900°C in O₂+4.2% SO₂ 0-97639
Ni, pure, corrosion due to V₂O₅ melts (Japanese) 0-93691
Ni-B thin film glasses, mag. props. and corrosion resist. 0-80576
Ni-Cr, degradation after exposure to 1% H₂S/H₂ gas mixture at 1000°C 0-89408
Ni-Cr-P, amorphous, corrosion behaviour, immersion tests and electrochem. meas. (Japanese) 0-85085
Ni-Cr-W-Co-(Al)(Ti)(Mo), high-temp. sulphide corrosion 0-76408
Ni-Cr-Zr, degradation after exposure to 1% H₂S/H₂ gas mixture at 1000°C 0-89408
Ni-Ti-P, amorphous, corrosion behaviour, immersion tests and electrochem. meas. (Japanese) 0-85085
Ni₂ coating corrosion by fission product Pd in HTGR coated particle fuels 0-102237
SiC-Si, wear resist., props. under abrasion and corrosion 0-100927
SiO₂-Al₂O₃-CaO-MgO-B₂O₃-E-glass, acid resist. studies 0-60991
SiO₂-Al₂O₃-Cu₂O glass alkaline durability, corrosion rate, heat capacity and elastic moduli 0-93673
SiO₂-Al₂O₃-Y₂O₃-La₂O₃-TiO₂ glasses with high elastic moduli, alkaline durability 0-85071
Sn, pitting corrosion in aq. solns., influence of Cl⁻, ClO₄⁻, SO₄²⁻, and NO₃ (French) 0-89389
SnO₂, electrodes, effect of DC on corrosion in lead glass melt 0-85075
Te film, stability in moist air, rel. to information storage capability, atmospheric corrosion model 0-71774
Ti corrosion by a hot perfluoropolyether 0-93684
Ti, corrosion in H₂SO₄, estimated from weight loss meas. at 270°C and 56 bar (French) 0-85080
Ti electrodes, RuO₂ coated, corrosion during O evolution rel. to electrode prep. (French) 0-76420
Ti, pit nucleation in bromide media, ion beam anal. 0-93683
Ti:Pd, ion implanted, corrosion behaviour and Rutherford backscatt. anal. 0-71792
Ti-Al-V (6, 4 wt.%), fretting corrosion of orthopaedic implant materials by bone cement 0-104813
Ti-Fe-C, type 50A, pitting resist. in low salinity geothermal brines 0-93681
Ti-Ni-Mo, Ticon 12, pitting resist. in low salinity geothermal brines 0-93681
UO₂-PuO₂ fuel pin, hyperstoichiometric, post irradiation examination 0-63258
V-Mo (25 wt.%), corrosion behaviour in high temp. impure He gas 0-76402
ZrO₂-SiO₂-(Na₂O) glass fibres, prep. from metal alkoxides, resistance to NaOH soln. 0-97454

corrosion control see corrosion protection

corrosion fatigue see stress corrosion cracking

corrosion fatigue testing *see* corrosion testing

corrosion prevention *see* corrosion protection

corrosion protection

see also anodisation; corrosion; corrosion protective coatings; packaging;

pH control

boiler feedwater redox potential meas. by Pt thin-layer electrodes 0-89578

cathodic protection for small plant, economic method (*German*) 0-100943

drum boilers, working at 11.0 to 15.5 MPa, pH control by addition of caustic soda (*Russian*) 0-89420

fracture preservation and cleaning, for fractography 0-71866

fusion reactor, Li cooling system, corrosion inhibition by Al additions 0-108646

Incoloy 800, stress corrosion cracking in NaOH solns., electrochem. aspects, peening treatment 0-97618

Inconel, type 600, Li corrosion inhibitions by Al additions 0-108646

Inconel 600, stress corrosion cracking in NaOH solns., electrochem. aspects, peening treatment 0-97618

magnetic thin films, Fe-Sr-Cr, produced by sputtering process 0-80573

marine corrosion, and its prevention 0-104333

motor-car corrosion protection improvement, primer paint appl. by electrocoating effect (*Dutch*) 0-71915

multilayer Ni deposits, simultaneous thickness and electrochemical potential determination for individual layers 0-71813

PWR boiler tubes, denting type corrosion, control by use of neutralisers 0-106109

stainless steel, laser surface melting 0-93698

steel, austenitic type 304, sensitised, intergranular stress corrosion cracking inhibition study 0-100939

steel, high-strength, type 4340, new inhibitors for crack arrestment in corrosion fatigue 0-100941

steel, stainless, highly protective film development by surface treatment 0-66699

steel, stainless, surface cathodic alloying, for increased passivation and corrosion resist. 0-100940

steel, stainless type 316, Li corrosion inhibition by Al additions 0-108646

steel surface, ellipsometric obs. of corrosion inhibitor action, propargyl alcohol film growth (*Rumanian*) 0-60996

Al-brass tubes, passivation treatment for atmospheric corrosion protection during storage and transport 0-85079

Al₂O₃, anodic, passified, inhibition of reaction with water 0-89390

Cr, surface cathodic alloying, for increased passivation and corrosion resist. 0-100940

Cu, corrosion protection by ion implantation of Al and Cr 0-71789

Fe, effect of anion and organic corrosion inhibitors on H₂ penetration rate 0-100938

Fe, film growth under organic coatings, qualitative ellipsometric-electrochem. approach 0-104344

Ti, surface cathodic alloying, for increased passivation and corrosion resist. 0-100940

corrosion protective coatings

dip-applied coating for water-immersed wedge-gate valve of cast Fe with stainless steel trim 0-93677

Ioncote coating process, using field emission systems for corrosion and abrasion protection (*German*) 0-76205

metal barrier-layer protective deposits, inorganic finish selection and appl. 0-71812

plasma sprayed coating consolidation by laser remelting 0-93697

steel, stainless, type 316, surface comp. rel. to crevice corrosion initiation 0-93680

steel, stainless type 304, anodically polarised, Cl⁻ ion effect on passive film 0-97621

Zircaloy, breakaway mechanism, corrosion kinetics in steam 0-61030

Cr plated steel, factors influencing durability 0-108643

Cr(Ni) films on steel, type AISI 316, thermal passivation in controlled vacuum 0-76276

Ni based Rene 80 superalloy, initial stages of pack aluminisation 0-76188

Ni-(Co)-Cr, aluminide coating, microstruct. and chem. 0-76189

Sn, autocatalytic deposition on steel, Ni, Cu, polypropylene and ABS 0-100965

Ti, coatings, electrolytically deposited, texture, anti-corrosional props. (*Russian*) 0-66532

Zn bright coating, rack parts or bulk goods, in GTL-barrel units (*German*) 0-84862

corrosion testing

conference on electrochem. test methods for stress corrosion cracking, Firminy, France (Sep. 78) 0-94910

field testing, NBS program 0-76427

holographic interferometry of corrosion 0-71853

Inconel 600 alloys, stress corrosion cracking, prediction in 10% NaOH soln. at 315°C 0-97616

machine with asymmetric loading 0-100983

optical glass, chem., durability, pragmatic view 0-78921

polarisation resistance method, using 2 and 3 electrodes, error anal. in corrosion rates 0-100930

potentiostat, P-04, for electrochem. meas. 0-61185

sheet materials, failure kinetics, method for investigating under long-term static loading in corrosive medium 0-85110

steel, austenitic stainless, of type 55 23 33, slow strain rate testing under electrochem. control in high temp. water 0-97650

steel, martensitic stainless, in SO₂ solns., activation pH and susceptibility to H₂ assisted stress corrosion cracking 0-97619

steel, mild, cyclic strain enhanced dissolution in NH₄NO₃, corrosion fatigue props. 0-85083

steel, stainless, stress corrosion testing, slow strain rate, elevated temp. and high press. study 0-97615

steel, stainless type 10CrNiCuP, and St. 3PS, suitability for power station chimney flue structural material 0-108681

steels, austenitic stainless, stress corrosion cracking, correl. between electrochem. and mech. parameters 0-97613

stress corrosion cracking test machine, design and construction, appl. to Fe-Cr-Ni alloys 0-97649

Al alloy V95T1 sheets, failure kinetics, method for investigating under long-term static loading in corrosive medium 0-85110

Al alloys, types Indal 3S and 6061-T6, corrosion behaviour evaluation, for heat exchanger appls. 0-85092

Cu-Ni-Zn alloy, surface comp., outdoor exposure influence 0-59770

Cu-Sn alloy, surface comp., outdoor exposure influence 0-59770

corrosion testing continued

Cu-Zn alloys, surface comp., outdoor exposure influence 0-59770

Mo electrode, corrosion rate in molten glass (*Chinese*) 0-66687

corundum

see also ruby; sapphire

additive for CaO based refractory from industrial lime 0-89184

attachment energy as habit controlling factor 0-59422

band structure, calc. using semiempirical Mulliken-Rudenberg method 0-80177

ceramic, prod. from etching wastes of Al foils 0-108376

CVD film on III-V semicond. substrate, ion beam etching, defect detection 0-89155

defect crystal structure 0-103316

energy levels of donor and acceptor and electron and hole mobilities 0-59911

fibre FP, manufacture, strength and modulus 0-81013

fibre FP reinforced Al and Mg composites, fabrication and props. 0-81004

filamentary crystal reinforced mullite-corundum ceramics, filaments strength, eval. 0-104230

Fourier transform IR spectroscopy of vibr. states at high temp. 0-97256

mantle related, thermodynamic props. at high press. and temp. 0-81874

mullite-corundum ceramics, electron microscopy of damaged surface 0-88413

mullite-corundum ceramics, thread-like crystals reinforced, props. 0-108525

polishing of single cryst. corundum, dispersion medium formulation 0-102870

single crystal transmission and reflectance IR phonon spectra, polariton dispersion 0-66170

surface microstructural changes due to reduction by C (*Russian*) 0-100378

thread-like crystals reinforced mullite-corundum ceramics, props. 0-108525

Ag:Al₂O₃:Al tunnel-junction struct., surface polariton mean free path, roughness 0-93008

α-Al₂O₃, charge distribution determ., SCF calc., Slater-type orbitals, Madelung type const. 0-107100

Al₂O₃-ZrSiO₄, granular corundum-zircon refractory, development 0-66462

Li₂O-Al₂O₃, rapidly quenched glasses, Li ion cond., elec. cond. 0-100346

Si-Al₂O₃ system, solid phase Si regrowth on sapphire 0-100413

SiAlON, prepared from siliceous sand and Al powder, hot pressing, steatite contamination effects (*Japanese*) 0-93528

cosmic dust

see also meteoroids

V1301 Aquilae (Nova Aquilae 1975), dust grain IR emission model 0-105254

ε Aurigae, extinction by circumstellar matter rel. to wavelength-depend. fluctuations 0-62190

3C 120, radio galaxy, dust rel. to vars. in optical spectrum (*Russian*) 0-90540

TX Canum Venaticorum, cataclysmic variable shell and dust emission, visible spectra obs. 0-105249

carbyne as possible constituent 0-90514

charged spherical dust shell, gravitational collapse, maximal time slicing condition 0-67554

chromite grains in Fe formation from Early Precambrian Isua supracrustal belt, W. Greenland, probable cosmic origin 0-72508

circumstellar dust cloud, inner F-corona, model and composition 0-82162

circumstellar dust shells, polarisation by Mie scatt., Monte Carlo anal. 0-98650

circumstellar matter round OB3 type stars in young clusters, 2200 Å hump interpretation 0-82351

collisional growth to planetesimals, relative vel. 0-82247

comet nuclei, dust layer models 0-77350

Comet West (1976 VI), coma mols. and dust distrib., visible emission profiles 0-101562

R Coronae Austrinae interstellar molecular cloud, for IR study and dust temp. profiles 0-62237

V1668 Cygni (Nova 1978) envelope, dust form. rel. to multifilter photometry and polarimetry 0-90454

dark nebulae in M31, catalogue 0-72787

distribution from obs. of OB stars near Carina arm, UVB photometry 0-85941

distribution from UVB photometry of OB stars in Puppis 0-85937

galactic dust emission rel. to microwave background anisotropy 0-77524

in galaxies, effect on optical surface brightness 0-90518

galaxies, nearby, interstellar reddening law and dust content (*German*) 0-67850

grain growth, by radiation pressure induced coagulation 0-94851

grain growth in interstellar clouds, theory and obs. 0-67834

grain surface ion reactions, S interstellar molecule formation 0-101632

grains in IR sources, possible origin for unidentified IR features 0-82452

grains surrounding variable source of heating radiation, IR flow development 0-105324

graphite, hydrocarbon formation on interstellar grain surfaces 0-82458

IC 1396 interstellar molecular cloud, for IR study and dust temp. profiles 0-62237

IC 342, Scd galaxy dust thermal IR emission obs. rel. to star form. in central regions 0-62256

insulating dust grains, photoelectric yield 0-90507

intergalactic pyrolytic graphite whiskers, absorpt. effects rel. to cosmic microwave background 0-94866

interplanetary, origin and evolution 0-101555

interplanetary dust, light scatt. intensity, theory 0-109324

interplanetary dust complex, azimuthal asymmetry mechanism from restricted three-body problem 0-85843

interplanetary dust components in inner Solar System 0-85914

interplanetary dust in stratosphere, visible absorpt. spectra 0-101554

interplanetary dust particles, Mg isotopic composition 0-72879

interstellar bacterial grains, prod. of 3μ spectral feature in galactic IR sources 0-62227

interstellar clouds, grain absorption rel. to UV radiation field (*Russian*) 0-73026

interstellar dust, cloudlike distrib. rel. to integrated starlight synthetic spectrum between 3000 and 10000 Å 0-62200

interstellar dust, far IR emission from galactic plane at longit. (l^{II}=27.5°) 0-62231

interstellar dust distrib. within 3 kpc in galactic plane 0-109512

cosmic dust continued

interstellar dust distribution perpendicular to galactic plane, fine struct. study (*Russian*) 0-73036
 interstellar dust grains, photoelectric effect rel. to gas heating by galactic UV radiation 0-67839
 interstellar dust temperature statistical distrib. resulting from star random distrib. 0-98700
 interstellar dusty H II blisters, appearance at radio and IR wavelengths 0-85979
 interstellar extinction curve, comparison with visible and UV extinction of silicate, C and SiC smokes 0-82180
 interstellar gas-dust clouds assoc. with open star clusters, effect on cluster dynamics 0-101622
 interstellar grain composition constraints from 10 μ m data 0-82471
 interstellar grains, chemical role 0-82470
 interstellar grains, collisions in turbulent gas 0-77470
 interstellar grains, effects on gravit. instability of rotating plasma 0-109347
 interstellar grains, organic composition, IR obs. 0-77460
 interstellar grains causing IR polarisation of mol. clouds 0-82469
 interstellar grains comprised of organic cpds., 3.4 microns absorpt. obs. 0-109514
 interstellar grains in SNRs, effect on X-ray spectra 0-94849
 interstellar porous grains, free-space equil. temps. calc., rel. to optical props. 0-62223
 IRC +10216, C star, circumstellar dust cloud size from far IR obs. 0-82539
 irregular absorbing particles, new scatt. model rel. to zodiacal light 0-67543
 Jupiter ring, dust EM scatt. lifetimes 0-82273
 L 183 (L 134 N) dust cloud, NH₃ and cyanoacetylene mapping at 23 GHz 0-105307
 CW Leonis (IRC+10216), IR C star, circumstellar dust orientation by paramag. relaxation rel. to intrinsic polarisation 0-67730
 lunar rock surfaces, accretionary grain populations development under meteoroid and solar wind bombardment 0-94731
 lunar rock surfaces, accretionary grain populations development obs. from Apollo samples 0-94732
 Markarian 3, 231, Seyfert galaxies, evidence for asymmetric dust envelopes from optical polarisation 0-90533
 Mars, dust storms, opacity from Viking IR thermal mapping 0-82253
 Mars, global dust storms effects on pressure vars. meas. by Viking landers 1 and 2 0-72812
 Mars atmosphere, dust content rel. to longit. var. of 2.8 cm brightness temp. 0-105191
 Mars atmosphere, general circulation model, including dust and topography 0-90354
 Mars dust storm of 1971, cloud form., multicolour TV photometry obs. 0-101546
 in molecular clouds NGC 2264, ρ Ophiuchi, B335 and S140, dust/gas ratio and mass 0-94842
 NGC 3227, 3516, Seyfert galaxies, evidence for asymmetric dust envelopes from optical polarisation 0-90533
 in NGC 4314, barred spiral galaxy, distrib. from UB_V surface photometry of central region 0-77482
 NGC 604, 5471, giant extragalactic H II regions, internal dust extinction from UV spectra 0-77467
 NGC 604, H II region in M 33, dust densities in nebula core and halo 0-85984
 NGC 7000 (North America Nebula), dust scatt. of stellar continua rel. to rocket UV imagery 0-82440
 in NGC 7023, refl. nebula, optical and UV extinction of HD 200775 by dust 0-109515
 NGC 7027, planetary nebula, interstellar, local and internal dust extinction from UV spectrum 0-82459
 nova envelopes, dust form. and ionisation theory 0-98678
 Nova Serpentis 1978, evolution of dust shell 0-90430
 Orion Nebula, evidence for scatt. by dust from long-slit spectroscopy in rocket UV 0-105297
 Orion Nebula, stellar radiation scatt. by dust, contrib. to nebula UV continuous spectrum 0-90499
 in planetary nebulae, dust continuous IR emission 0-109525
 planetary nebulae, dust temp. and mass, IR photometry obs. 0-94850
 planetary nebulae, theoretical data review 0-109536
 planetary nebulae dust, observational review 0-109535
 pregalactic dust, distortion of cosmological microwave black body radiation spectrum 0-67915
 pregalactic dust and distortions of the cosmic-background spectrum 0-67916
 presolar interstellar grains in Allende meteorite, evidence from ⁴⁰Ar-³⁹Ar ages 0-98621
 protosolar nebula, dust grain motion time evolution 0-82234
 relativistic and non-relativistic dust grains, rel. to high energy particles in EAS 0-61975
 S140 interstellar molecular cloud, for IR study and dust temp. profiles 0-62237
 FH Serpentis (Nova Serpentis 1970), dust grain IR emission model 0-105254
 Seyfert galaxies, interstellar dust heating rel. to thermal IR emission vars. 0-67865
 solid particles growth in contracting interstellar clouds, influence of turbulence 0-62251
 spherical dust shell around central star, two-shell moment method for radiative transfer 0-62001
 spiral and elliptical, optical surface brightness, dust effects 0-90518
 in spiral galaxies, galaxy classification from dust lane strength 0-82484
 in spiral galaxies, late type, optical anal. method, visible obs. 0-101638
 SU Tauri, R Coronae Borealis star, circumstellar dust shell discovery from optical and IR photometry 0-101601
 UV opacity effects on stellar spectra 0-90505
 Venus, surface dust detected by Venera 9 and 10 radiant flux obs. 0-72803
 W3/W4/W5 region, heavy optical obscuration obs. 0-62301
 Wolf Rayet stars, late type with circumstellar dust shell, 8-13 micron spectral obs. 0-101599
 zodiacal dust cloud, thermal emission at 11 and 20 microns 0-90367

cosmic radiation *see cosmic rays***cosmic radiations, radiofrequency** *see radiofrequency cosmic radiation***cosmic radio waves** *see radiofrequency cosmic radiation***cosmic ray absorption**

heavy ions, charge and LET distrib. meas., radiation damage in biological objects 0-94664

cosmic ray alpha-particles and helium nuclei

solar cosmic rays, obs. of events with high relative ³He abundances during 1976 November to December 0-61972
 solar heavy-ion-rich particle events, ³He/⁴He ratios energy depend. and temporal evolution, ³He/⁴He in heavy-ion-rich solar energetic particle events, energy depend. and temporal evolution 0-90299
³He in lunar rocks, method for solar flare cosmic ray proton flux determ. 0-98576
³He/⁴He isotopic composition of solar cosmic rays 0-72725

cosmic ray apparatus

see also particle detectors
 gas Cherenkov counter with ionisation spectrometer, appl. to cosmic ray studies 0-94662
 high resolution gas scintillation proportional counter for studying low energy cosmic X-ray sources 0-58052
 TLD system for meas. of cosmic dose on board a spacecraft 0-109047
 undersea detection system, located in deep ocean 0-98522
 Si(Li)-emulsion shower counter for cosmic ray electron obs. 0-58033

cosmic ray composition

see also cosmic ray alpha-particles and helium nuclei; cosmic ray deuterons; cosmic ray electrons; cosmic ray mesons; cosmic ray muons; cosmic ray neutrinos; cosmic ray nuclei; cosmic ray photons
 Biobloc II expt. results for high-LET particles 0-94663
 galactic cosmic nuclei abundance, time averaged for Z \geq 50, tracks in meteorite minerals 0-101513
 galactic cosmic rays, Fe nuclei isotopic comp. 0-72729
 hadron flux composition at mountain altitudes (*Russian*) 0-61973
 hadronic component and momentum spectrum at 2 km altitude in 70-350 GeV/c range (*Russian*) 0-67486
 heavy long lived cosmic ray particles 0-90300
 horizontal cosmic ray penetrating particles identification, fractional charge search (*Chinese*) 0-101514
 near-Earth cosmic rays, short-term fluctuations in electron and γ quanta components 0-67483
 nuclei with Z \geq 50 in olivine from meteorites 0-105139
 proton nucleon component, rel. to galactic cosmic ray origin models with halo 0-61971
 solar cosmic rays, obs. of events with high relative ³He abundances during 1976 November to December 0-61972
 solar flare energetic particle abundances in range 2 \leq Z \leq 28, Voyager obs. 0-90382
 solar particles, isotope composition form., effect of ion-sonic turbulence 0-101574
¹⁰Be nuclei, rel. to galactic cosmic ray origin models with halo 0-61971
¹⁴C measurement in known age specimens, cosmic ray intensity determ. 0-101516
 He isotope composition of solar cosmic rays from Venera 9 obs. 0-72725
³He/⁴He in heavy-ion-rich solar energetic particle events, energy depend. and temporal evolution 0-90299
 Me to Fe nuclei, primary, 200 to 650 MeV/ nucleon, relative abundances 0-77246

cosmic ray deuterons

No entries

cosmic ray effects and interactions

see also high-energy cosmic ray interactions
 Dhajale meteorite, India, cosmic radiation effects, fossil track studies 0-72733
 Earth atmosphere, effects of energetic particle precip. on middle atmosphere chemical comp. 0-109213
 electrons, relativistic, form. of regions of nonlinear electron spectrum rel. to synchrotron spectrum generation 0-109555
 Fabry-Perot etalon, optically contacted, stability to cosmic radiation 0-98544
 galactic cosmic rays, effect on solar wind vel. 0-101506
 gamma-ray spectrometers; calc. of radioactivity induced during spaceflight 0-102382
 interstellar medium, electrons contrib. to diffuse X-ray flux in 2 to 7 keV range 0-98745
 lunar soil samples from Luna-24, radioactivity and cosmic ray dose rate, thermolum. obs. 0-67596
 Marjalahti pallasite, cosmic ray induced ⁵⁵Mn production 0-72891
 meteorites, secondary cosmic ray interactions rel. to isotopically anomalous Ag in Santa Clara and Pinon Fe meteorites 0-85902
 positrons, galactic, primary source, interactions and fates 0-109319
 solar flare tracks in Luna 24 core samples, thermolum. obs. 0-82246
 solar wind particles trapping and accel. at Earth 0-98532
 St. Severin chondrite, ⁵⁵Mn production due to nucl. spallation, depth-depend. 0-82316
¹⁴C form. in atm., diffusion distrib. 0-101510
 Fe meteorites, radial distrib. of spallogenic K, Ca, Cr, Ti, V and Mn isotopes 0-67488

cosmic ray electrons

black holes, primordial, electron-positron radiation, spectrum rel. to galactic radio spectrum 0-62179
 EAS, lateral age parameter and radial electron distrib. 0-85828
 energy spectrum and propag. 0-67485
 energy spectrum of galactic cosmic rays, fundamental props. (*Chinese*) 0-105138
 galactic disc, primary electron component estimate from gamma-ray emission obs. 0-82540
 galactic electrons, contrib. to diffuse X-ray flux in 2 to 7 keV range 0-98745
 galactic electrons, spectrum determ. from radio emission rel. to Galaxy gamma-rays prod. 0-62257
 galactic primary cosmic-ray electrons, 30-1000 GeV, emulsion chamber obs. 0-85827
 Jupiter origin for energetic electrons, study of 1972-7 intensity variations 0-72726
 near-Earth cosmic rays, short-term fluctuations in electron and γ quanta components 0-67483
 positrons, galactic, primary source, prod. rate, and escape probability 0-109319

cosmic ray electrons continued

- positrons in primary cosmic radiation and collisions in interstellar medium 0-77241
- radio sources, compact, extragalactic, synchrotron and relativistic Maxwellian source models rel. to spectra 0-62299
- radio sources, extragalactic, relativistic electron clouds rel. to variable radio emission temporal characts. (*Russian*) 0-62307
- in radio sources, form. of universal and diffusion regions of relativistic electrons non-linear spectra 0-109555
- relativistic electron spectra, inference from meas. of inverse Compton radiation 0-90339
- solar electrons, Prognoz-6 fluxes and spectra meas. during large scale interplanetary disturbances 0-90315
- solar flare particle accel. and generation 0-101575
- solar impulsive electron events not assoc. with flares, ISEE 3 obs. 0-67683

cosmic ray energy spectra

- air shower muons lateral distrib. and spatial separation of distrib. 0-109320
- atmospheric neutrinos, 10^{-10} GeV, energy spectra and ang. distrib. (*Russian*) 0-85830
- EeV cosmic rays, energy spectrum and arrival direction 0-67480
- electron spectra in cosmic extragalactic radio sources, rel. to radio spectra 0-62299
- electron-positron radiation from primordial black holes, spectrum rel. to galactic radio spectrum 0-62179
- electrons, energy spectrum and propag. 0-67485
- electrons, energy spectrum of galactic cosmic rays and fundamental props. (*Chinese*) 0-105138
- electrons, relativistic, in radio sources, form. of universal and diffusion regions of non-linear spectra 0-109555
- extragalactic cosmic rays, 10^{20} eV, energy spectrum and arrival direction 0-82157
- galactic electrons, spectrum determ. from radio emission rel. to Galaxy gamma-rays prod. 0-62257
- galactic primary cosmic-ray electrons, 30-1000 GeV, emulsion chamber obs. 0-85827
- gamma ray spectroscopy, review 0-67582
- hadronic component and momentum spectrum at 2 km altitude in 70-350 GeV/c range (*Russian*) 0-67486
- heavy ions, charge and LET distrib. meas., radiation damage in biological objects 0-94664
- horizontal muon intensity and momentum spectrum at 3220m above sea level (*Chinese*) 0-101515
- interplanetary cosmic ray protons, 1-4.5 MeV, spectral anal. and correl. study 0-77243
- muon charge ratio, sea level, phenomenological model, review 0-67487
- muons, parent nucleons, energy distrib., at sea level and underground, phenomenological model 0-61974
- nuclei, energy spectra determ. by gas Cherenkov counter with ionisation spectrometer 0-94662
- power type spectrum for particle accel. at spherical shock wave (*Russian*) 0-72730
- relativistic and non-relativistic dust grains, rel. to high energy particles in EAS 0-61975
- relativistic electron spectra, inference from meas. of inverse Compton radiation 0-90339
- solar ^3He rich cosmic ray events, ^3He and ^4He nuclei energy spectra 0-61972
- solar active region protons at 1 AU, energy spectra from Prognoz-3 0-101512
- solar cosmic rays, spectra rel. to particles shock accel. in solar wind corotating interaction regions 0-82159
- solar energetic particles, Prognoz-6 fluxes and spectra meas. during large scale interplanetary disturbance 0-90315

cosmic ray geophysical effects *see geophysical aspects of cosmic rays***cosmic ray jets** *see cosmic ray showers and bursts***cosmic ray mesons**

- pions, cosmic ray composition at 2 km altitude in 70-350 GeV/c range (*Russian*) 0-67486

cosmic ray muons

- charge ratio, sea level, phenomenological model review 0-67487
- horizontal muon intensity and momentum spectrum at 3220m above sea level (*Chinese*) 0-101515
- pair generation, nucleon cascade role 0-91120
- parent nucleons, energy distrib., at sea level and underground, phenomenological model 0-61974
- sea level charge ratio, energy depend. 0-94665
- sea-level spectrum 0-98527
- time distribution, random and nonrandom components of arrival times 0-72732
- underground muons, response functions for different depths 0-82160

cosmic ray neutrinos

- atmospheric neutrinos, 10^{-10} GeV, energy spectra and ang. distrib. (*Russian*) 0-85830
- galactic neutrinos and decay to UV photons 0-109566
- solar flux calcs., neutrino oscills. constraint 0-109410
- undersea detection system, located in deep ocean 0-98522

cosmic ray neutrons

- altitude variation, Feynman scaling hypothesis calcs. 0-77245
- diurnal anisotropy, anal. of 0-94660
- intensity variations in interplanetary space, 1972-7 period 0-72726
- variations during September 1977, Mirny and Moscow obs. 0-105137

cosmic ray nuclei

- see also cosmic ray alpha-particles and helium nuclei; cosmic ray neutrons; cosmic ray protons*
- detection of heavy cosmic rays aboard Cosmos-936 using plastic nuclear track detectors 0-94663
- Earth atmosphere penetration by energetic heavy nuclei 0-85826
- energy spectra, determ. by gas Cherenkov counter with ionisation spectrometer 0-94662
- galactic abundance, time averaged for $Z \geq 50$, tracks in meteorite minerals 0-101513
- galactic cosmic rays, energy dependent diffusion in dynamic halo model 0-82156
- heavy ions, charge and LET distrib. meas., radiation damage in biological objects 0-94664
- proton generation in solar flares 0-101575

cosmic ray nuclei continued

- solar active region protons at 1 AU, energy spectra from Prognoz-3 0-101512
- solar flare energetic particle abundances in range $2 \leq Z \leq 28$, Voyager obs. 0-90382
- VVH nuclei in meteorite olivines, fossil track studies 0-105139
- ^{10}Be nuclei, rel. to galactic cosmic ray origin models with halo 0-61971
- (Fe,X), 1.9 GeV/N, in emulsion, mean free paths, and fragmentation parameters 0-102197
- Ne to Fe nuclei, 200 to 650 MeV/nucleon, relative abundances 0-77246

cosmic ray-nucleus reactions

- for inelastic cosmic ray-nucleus scattering, see "cosmic ray-nucleus scattering"*
- galactic centre, cosmic ray flux, predicted from high energy γ ray observations 0-72731
- gamma ray spectroscopy, review 0-67582
- muon charge ratio, sea level, phenomenological model, review 0-67487
- ultra-high energy nuclear interaction event with large transverse momentum at 445 TeV (*Chinese*) 0-105140

cosmic ray-nucleus scattering

- No entries

cosmic ray origin

- see also cosmology; element origin*
- acceleration by shock waves in astrophysical plasma, implications for origin 0-82192
- electrons, galactic, evidence for continuous ejection model from energy spectrum (*Chinese*) 0-105138
- extragalactic cosmic rays, 10^{20} eV, energy spectrum and arrival direction 0-82157
- galactic cosmic ray Fe nuclei source, neutron excess from isotopic comp. 0-72729
- gamma-ray origin in protogalaxy formation, model 0-62325
- gamma-ray transient event of 1979 March 5, location 0-73074
- Gould belt OB type stars 0-77512
- interplanetary cosmic ray protons, 1-4.5 MeV, spectral anal. and correl. study 0-77243
- interstellar medium interaction with stellar wind, cosmic ray accel. 0-77512
- Jupiter origin for energetic electrons, study of 1972-7 intensity variations 0-72726
- 3K microwave background, in Universe expansion model 0-98746
- positrons, galactic, primary source, prod. rate, and escape probability 0-109319
- Ne to Fe nuclei, primary, 200 to 650 MeV/nucleon, relative abundances 0-77246

cosmic ray photons

- see also cosmic ray X-rays; solar cosmic ray photons*
- Cherenkov photons, effect on IR interferometric search for non-solar planets 0-98523
- conference, non-solar gamma-rays (Bangalore, India, May-June 1979) 0-77548
- EUV background, point source contribs. 0-62324
- galactic 0.511 MeV annihilation radiation, theory of positrons primary source, prod. rate, and escape probability 0-109319
- Galaxy gamma-ray emission, fluxes determ. from cosmic ray electron spectrum 0-62257
- gamma burst detector on Pioneer Venus Orbiter 0-67505
- gamma rays from galactic disc, obs. between $-45^\circ < l < 45^\circ$ in 80 keV to 8 MeV energy range 0-82540
- gamma-ray background and protogalaxy formation model 0-62325
- gamma-ray bursts, ultra high energy, from celestial sources, unsuccessful search 0-67911
- gamma-ray fast intense transient (1979 March 5), detect. 0-73073
- gamma-ray transient event of 1979 March 5, location 0-73074
- gamma-rays, quasi-periodic intensity variations in stratosphere (*Russian*) 0-90177
- 3K microwave background, in Universe expansion model 0-98746
- near-Earth cosmic rays, short-term fluctuations in electron and γ quanta components 0-67483

cosmic ray propagation

- accel. in expanding coronal mag. bottle 0-77244
- acceleration by shock waves in astrophysical plasma 0-82192
- electrons, energy spectrum and propag. 0-67485
- electrons, relativistic, in radio sources, form. of universal and diffusion regions of non-linear spectra 0-109555
- energy variation in interplanetary space of solar and galactic cosmic rays 0-101505
- equivalent diffusion coefficients of solar cosmic rays 0-85825
- Fermi-accelerated cosmic rays mediation of shock front 0-85829
- galactic cosmic ray acceleration by supernova shock waves 0-82154
- galactic cosmic rays, effect on solar wind vel. 0-101506
- galactic cosmic rays, energy dependent diffusion in dynamic halo model 0-82156
- galactic cosmic rays, equilb. configs. stability, hydromagnetic energy principle 0-82448
- galactic cosmic rays, interplanetary modulation allowing for generalised anisotropic diffusion tensor 0-101504
- galactic electrons, propag. rel. to energy spectrum and fundamental props. (*Chinese*) 0-105138
- galactic primary cosmic-ray electrons, 30-1000 GeV, emulsion chamber obs. 0-85827
- interplanetary magnetic field sector structure and anisotropy of 50-1000 GV cosmic rays 0-62072
- interplanetary modulation processes, evidence from stratosphere obs. 0-101508
- interplanetary propagation, anal. of large amplitude wave-trains of cosmic-ray intensity 0-94660
- interplanetary propagation, cosmic ray flow lines and energy changes 0-82158
- interstellar cosmic ray acceleration models, inconsistencies 0-82155
- interstellar diffusion in galactic models with halo, appl. to proton nucleon component 0-61971
- interstellar medium interaction with stellar wind, cosmic ray accel. 0-77512
- interstellar propagation of primary Ne to Fe nuclei, 200 to 650 MeV/nucleon, relative abundance 0-77246
- magnetospheres, effect on cosmic ray propag. 0-101517
- mean free path of low-rigidity cosmic rays, weak turbulence diffusion theory 0-98524
- ρ Ophiuchi cloud, cosmic ray accel. by stellar winds 0-77512

cosmic ray propagation continued

- particle accel. at spherical shock wave front, power spectrum (*Russian*) 0-72730
- positrons, galactic, prod. rate and probability of escape from Galaxy 0-109319
- proton generation in solar flares 0-101575
- Saturn magnetic field, cosmic ray cutoff rigidities 0-72873
- solar cosmic ray propagation in interplanetary medium, solns. to Fokker-Planck eqn. 0-77242
- solar flare particle accel., injection energy concept 0-101509
- solar flare protons, flux limit due to accel. mechanism saturation effects 0-98645
- solar particle events with high relative ^3He abundances, interplanetary propag. conditions 0-61972
- solar wind particles trapping and accel. at Earth 0-98532
- Sun's inner heliosphere, longit. modulation of galactic cosmic rays 0-90298

cosmic ray protons

- altitude variation, Feynman scaling hypothesis calcs. 0-77245
- antiprotons in primary cosmic radiation and collisions in interstellar medium 0-77241
- galactic cosmic ray intensity out to 18 AU, Pioneer 10 and 11 obs. 0-90297
- galactic cosmic rays origin, galactic models with halo 0-61971
- generation in solar flares 0-101575
- interplanetary, 1-4.5 MeV, spectral anal. and correl. study 0-77243
- interplanetary, use in galactic modulation parameter determ. 0-82156
- solar active region protons at 1 AU, energy spectra from Prognos-3 0-101512
- solar flare flux determ. from ^3He meas. in lunar rocks 0-98576
- solar flare protons, flux limit due to accel. mechanism saturation effects 0-98645
- solar flare protons near-Earth radiation hazard, dosage estimation technique 0-67482
- solar proton event of 1978 May 7, neutron monitor obs. 0-67686
- solar protons, Prognos-6 fluxes and spectra meas. during large scale interplanetary disturbance 0-90315
- solar wind protons vel., effect of galactic cosmic rays 0-101506
- sun, flare proton generation 0-109413

cosmic ray showers and bursts

- see also cosmic ray electrons; cosmic ray X-rays*
- development repudiation of putative primary mass composition change 0-61976
- direct cosmic ray muon pair generation, nuclear cascade role 0-91120
- EAS, array density spectrum 0-90301
- EAS, lateral area parameter and radial electron distrib. 0-85828
- muons, lateral distrib. and spatial separation of distrib. 0-109320
- proportional counter for air shower observation, counter prod. characts. and lifetime determ. 0-98526
- relativistic and non-relativistic dust grains, rel. to high energy particles in EAS 0-61975

cosmic ray solar modulation

- corona holes correlated to cosmic ray intensity, during solar cycle 0-94661
- coronal holes modulation effects 0-77370
- galactic cosmic ray intensity out to 18 AU, Pioneer 10 and 11 obs. 0-90297
- galactic cosmic rays, spatial vars., meteorite radioactivity record (*Bulgarian*) 0-72728
- intensity variations in interplanetary space, 1972-7 period 0-72726
- longitudinal intensity modulation of galactic cosmic rays, models 0-90298
- relativistic galactic cosmic rays, anisotropies assoc. with solar rotation 0-67481
- short-term fluctuations, evidence for solar origin 0-67483
- solar flare of 1976 April 30, modulation region 0-67484
- solar wind, high speed stream effects on solar cycle 20 cosmic ray modulation 0-72914

cosmic ray variations

- see also geomagnetism*
- diurnal anisotropy, anal. of 0-94660
- energy variation in interplanetary space of solar and galactic cosmic rays 0-101505
- Forbush decrease in model of solar wind shock wave (*Chinese*) 0-90302
- Forbush effect in solar wind particles 0-98532
- galactic cosmic ray intensity out to 18 AU, Pioneer 10 and 11 obs. 0-90297
- galactic cosmic rays, solar latitude variations from chondrite cosmogenic isotope radioactivity 0-101507
- galactic cosmic rays affected by Sun's inner heliosphere, models 0-90298
- intensity, long term, ^{14}C obs. in known age specimens 0-101516
- intensity at Earth of supernovae cosmic rays, cosmogenic isotope obs. 0-101503
- intensity variations in interplanetary space, 1972-7 period 0-72726
- neutron component vars. during September 1977, Mirny and Moscow obs. 0-105137
- short-term cosmic ray fluctuations, time anal. 0-67483
- solar flare particle intensity variations, depend on interplanetary mag. field and solar wind 0-77372
- solar modulation, climate record from tree ring ^{14}C link with solar variability 0-101424
- stratosphere obs., evidence for interplanetary modulation processes 0-101508
- two year variations in Earth atm., sonde obs. 0-101511
- He isotope composition of solar cosmic rays from Venera 9 obs. 0-72725

cosmic ray X-rays

- background radiation, possible origin 0-94898
- diffuse 0-82551
- diffuse X-ray background, rel. to intergalactic matter 0-109543
- diffuse X-ray background intensity, implications of uniformity of quasars radial distrib. in chronometric cosmology 0-105409
- diffuse X-ray flux in 2 to 7 keV range, galactic component obs. 0-98745

cosmic rays

- see also cosmic ray absorption; cosmic ray apparatus; cosmic ray composition; cosmic ray effects and interactions; cosmic ray energy spectra; cosmic ray origin; cosmic ray propagation; cosmic ray showers and bursts; cosmic ray solar modulation; cosmic ray variations; galactic cosmic rays; geophysical aspects of cosmic rays; high-energy cosmic ray interactions; primary cosmic rays; radiofrequency cosmic radiation; solar cosmic ray particles; solar radiation*

cosmic rays continued

- conference on nuclear cosmic physics, Leningrad, USSR (Oct. 1978) 0-98755
- magnetoelectric dipole structure hypothesis, biological and cosmic appls. 0-91124
- Salyut-6 orbital station, cosmic radiation dose field meas. 0-89876

cosmic X-rays *see cosmic ray X-rays***cosmogony *see cosmology*****cosmology**

- see also black holes; element origin; general relativity; red shift*
- Λ^4 theory, conformal symmetry breaking, cosmological particle creation 0-90998
- Abell clusters, 3-D nearest neighbours test 0-90545
- acoustic wave spontaneous birth in early Universe (*Russian*) 0-90593
- adiabatic cosmological perturbations, propag. through matter-radiation decoupling era rel. to galaxies form. 0-62337
- Ambartsumian's proto-matter hadronic nature from ang. momentum-mass relation 0-77528
- anisotropic universe, relict radiation polarisation and anisotropy 0-67917
- anisotropy dissipation by scalar particle prod. in early universe 0-86025
- antimatter, origin, whereabouts 0-62340
- background isotropic radiation excess at 1 MeV, possible origin from Seyfert galaxies 0-77522
- background radiation spectrum, early energy release distortion in Rayleigh-Jeans region 0-73077
- baryon annihilation 0-90590
- baryon synthesis from unconfined primordial quarks 0-57566
- baryon/photon ratio bounds due to human existence, grand unification 0-62345
- Bianchi model universes, hypersurfaces of transitivity, Riemann curvature 0-67922
- Bianchi type I space-time gravitational field, particles eqn. of state 0-77664
- Bianchi type II exact cosmological model with matter and EM field 0-105560
- Bianchi type-I cosmologies and spinor fields 0-62347
- Bianchi universes, magnetic fields and fluids with conductivity 0-83864
- Bianchi V type universe, red shift and anisotropic microwave background 0-98744
- Bianchi-V cosmological space-time, Einstein-Weyl equations, neutrino currents 0-86023
- big bang, helium synthesis, neutrino flavors, and cosmological implications 0-73084
- black hole quantum evaporation, baryon asymmetry of the Universe (*Russian*) 0-109577
- Brans-Dicke cosmology, nonhomogeneous space-time 0-86024
- chaotic Universe, Friedmannian expansion, degree of chaos and He abundance 0-67920
- chaotic Universe, Friedmannian expansion 0-67919
- chronometric cosmology, uniformity of quasars radial distrib. rel. to X-ray background 0-105409
- chronometric predictions, tests using galaxy and quasar samples 0-86022
- closed Universe, elliptical de Sitter metric 0-109570
- clusters of galaxies, tidal forces in inhomogeneous cosmological models 0-62338
- cold dense universes, photoionisation by quasars, QSO spectral indices and cut off energy determ. 0-77526
- conference on Universe at large redshifts, Copenhagen (June 1979) 0-57000
- cosmic censorship and test particles, black hole destruction 0-105552
- cosmic microwave background spectrum, G-varying cosmology 0-86020
- cylindrical general relativistic systems, numerical codes 0-67549
- decay of fluctuations in the early universe and high energy particle interaction 0-109573
- deceleration parameter, comparison of various cosmological tests, static Euclidean model 0-73081
- deceleration parameter determ. using local data 0-62351
- density irregularities on large scale, X-ray background evidence 0-105405
- density parameter, lower limit from NGC 1023 galaxy group dynamics 0-82521
- dynamical eqns., variation of parameters 0-109568
- early nucleosynthesis and He and D abundances 0-62356
- early Universe, baryon asymmetry development in big bang 0-62346
- early Universe, baryon number generation due to CP- and B-violating interactions 0-109571
- early Universe, gauge theories, grav. constant time depend. and antigravity 0-90591
- early Universe, horizon problem and the broken-symmetric theory of gravity 0-62344
- early Universe, inhomogeneity and origin of entropy 0-62350
- early universe density-temp. fluctuations, present observability 0-82554
- Einstein's contribution 1905 to 1915 0-77530
- Einstein's theory of relativity, acceptance in Canada 0-68012
- Einstein equations, general cosmological solution, singularity problems 0-82686
- Einstein-de Sitter universe, classical predictive electrodynamics 0-86175
- Einstein-Maxwell equations, inhomogeneous stationary cosmological solns. 0-62556
- Einstein-Maxwell theory, cosmological model with gravitational, electromagnetic, and scalar waves 0-86188
- element origin rel. to cosmology, review 0-62359
- elementary particle physics, cosmological approach, review, book contrib. 0-68440
- evolution of large-scale structure from relict radiation temp. fluctuations 0-105360
- evolving hierarchical cosmologies, cosmic background radiation fluctuations 0-101655
- fermion asymmetry of the Universe and the W condensate, Weinberg Salam model (*Russian*) 0-73087
- fluid drops as cosmological models, stellar evolution, solar system origin, planetary geology 0-73086
- formation of clusters of galaxies and secondary peak 0-77497
- Friedmann model, expanding Universe, nonlinear acoustic effects (*French*) 0-67921
- Friedmann model universes with decoupled radiation field, density perturbations growth 0-109567
- Friedmann models, scale parameter 0-77527
- Friedmann universes, cosmological principle appl. to variational methods (*French*) 0-77529

cosmology continued

- Friedmannian universe, cosmological fluctuations produced near a singularity 0-101656
 galaxies, deep samples, cosmological implications 0-62285
 galaxies, luminosity evolution from 2.2 μ m of giant ellipticals 0-105358
 galaxies evolution, evidence from redshift distrib. in extragalactic objects 0-90527
 galaxies evolution, state of fundamental knowledge inferred from study of globular clusters 0-90488
 galaxies fields stochastic simulation 0-62295
 galaxies formation by gravit. instability, role of ang. momentum 0-98722
 galaxy cluster interaction with supercluster, model of Emden sphere embedded in background 0-62296
 galaxy cluster X-ray sources, luminosity function evolution rel. to source counts 0-62314
 galaxy clustering, search for evolutionary effects from galaxy fields stochastic simulation 0-90530
 galaxy clustering N-body simulations, fraction in groups as function of density enhancement 0-67879
 galaxy correlation function evolution, N-body Monte Carlo model 0-62292
 galaxy counts and colours for faint objects 0-105351
 galaxy counts in $21 < B < 25$ apparent mag. range 0-105352
 galaxy covariance function, technique for shape determ. at small scales 0-82506
 galaxy distribution evolution 0-62287
 galaxy evolution and automated faint galaxy counts 0-105350
 general relativity, caustics and singularities, gravitational converging effects 0-77654
 general relativity, vacuum field equations, fifth dimension, ratio of EM to gravitational force 0-77679
 globular clusters ages, effects of He settling in low mass stars 0-73013
 grand unified theories, compatibility with big bang cosmology, superheavy monopoles 0-86647
 grand unified theories, mag. monopoles and cosmological implications 0-86643
 gravitation and dynamical space, geometrical framework, Mach's principle 0-95001
 gravitation bimetric theory, flat metric election 0-62004
 gravitational const. var. cosmological light element abundance constraint, comment on errors 0-72767
 gravitational constant, cosmological var. rel. to solar luminosity 0-82182
 gravitational constant variations, effect on stellar evolutionary tracks 0-82186
 gravitational force and cosmic matter-antimatter asymmetry 0-90586
 gravitational theory, cosmological soln, with matter 0-86021
 gravitational waves, origin and consequences for Universe 0-109569
 H_0 and q_0 determ. from Baade's distance method 0-73082
 Hagedorn temperature and Dirac's large numbers hypothesis 0-105410
 heavy Majorana particles, cosmological and astrophysical implications 0-90331
 high-energy gravity and the very early universe 0-98847
 homogeneous cosmologies, dipole and quadrupole anisotropies 0-109572
 homogeneous universes, qualitative behaviour 0-94904
 hot Universe, entropy perturbations and cosmogenic processes 0-105411
 Hubble constant, determ. outside Local Supercluster from new galaxy distance scale 0-105325
 Hubble constant, local value from Sb galaxies luminosity classification 0-62339
 Hubble flow, Virgo-centric perturbation rel. to elliptical galaxies mass to light ratios 0-98707
 inhomogeneous Universe, gravitational wave effects, on orbital motions 0-61998
 intergalactic C model abundance, X-ray absorpt. effects 0-62270
 intergalactic clouds rel. to origin of universe (French) 0-67874
 IR Hubble diagram for giant elliptical galaxies 0-105359
 isotropic cosmological models, vacuum stress energy tensor and particle creation (German) 0-94901
 isotropic universe, particle creation and vacuum polarisation, cosmological models 0-90582
 isotropic Universe, quantum gravitational effects, spontaneous particle production (Russian) 0-94711
 isotropy, vacuum polarisation contrib. to energy content of Universe 0-73083
 Lagrangian or Hamiltonian formulations, shift vector field restrictions, symmetry group 0-67923
 low-density universes, linear clustering, of galaxies 0-85993
 mass/light ratio of Universe from mean overdensity toward Virgo supercluster 0-94877
 massive particle production in anisotropic space-times 0-90583
 mathematical theories and philosophical insights in cosmology 0-90650
 matter and radiation fluctuations after decoupling epoch 0-62354
 matter distrib. now and at matter-radiation decoupling epoch 0-62355
 MHD cosmological models, plane symmetry 0-82556
 microwave background, residual fluctuations, gravitational effects 0-62332
 microwave background, review 0-62336
 microwave background angular distrib., large scale fluctuations 0-62328
 microwave background angular distrib., small scale fluctuations 0-62329
 microwave background dipole anisotropy, dynamical inferences 0-62330
 microwave background fluctuations, recombination epoch effects 0-62333
 microwave background longward of 3 mm, spectral distortions 0-62326
 microwave background small-scale fluctuations, consequences of neutrino rest mass (Russian) 0-109576
 microwave background spectrum, distortion by pregalactic dust 0-67916
 microwave black body radiation spectrum, implications for Population III stars 0-67915
 millimetre region cosmic background radiation, large scale anisotropy meas. 0-82553
 missing mass in massive, slow-moving neutrinos, decay 0-109566
 net baryon number and CP nonconservation with unified fields 0-62349
 neutrino number and isotropy of Universe in grand unified theories 0-85852
 neutrino systems, relativistic kinetic theory of transport processes 0-73283
 nuclear astrophysics, introduction to form. and evolution of matter in Universe, book 0-105447
 observational test of cosmological particle production theories 0-109574
 observational tests of the cosmic turbulence theory 0-98747
 one-electron atom in curved space-time 0-78509

cosmology continued

- open Universe geometrical struct., deceleration parameter and spatial curvature 0-62343
 origin of galaxies in expanding Universe, plasma cond. and instabilities, MHD soln. 0-62283
 particle pair creation, canonical quantisation for Chitre-Hartle model 0-62342
 perfect fluid cosmology with geodesic world lines 0-67924
 perturbations larger than horizon size in big-bang cosmology, tenacious myths 0-105408
 philosophical relevance (German) 0-90652
 photon parametric creation in model cosmological problems, nonlinear optics equivalence 0-73085
 photon splitting into 3, cosmological limits, spectral broadening, frequency-dependent and multiple red-shifts 0-77284
 physical laws large-scale uniformity, evidence from QSO absorpt. redshifts 0-73079
 physics of microwave background, conference Jodlowy Dwor, Poland, 1978 September 0-62389
 Poincare and cosmic evolution 0-57073
 polarisation effects in cosmological models with anisotropic curvature 0-94903
 primeval cosmic microwave background radiation, polarisation in anisotropic universe 0-82552
 primordial baryons, generation by black holes 0-98750
 primordial black holes, evaporating, rel. to galactic positrons primary source and fates 0-109319
 primordial black holes, influence on galactic radio spectrum 0-62179
 primordial black holes, radiation accretion in early Universe 0-67918
 primordial cosmic turbulence, spectrum evolution 0-90589
 primordial mini black holes explosion rate, upper limit from gamma-ray bursts search 0-67911
 protogalactic medium, vortex generation 0-62360
 protogalaxy formation age and γ -ray background 0-62325
 QCD and superdense matter, quark and gluon plasma, hadronic structure, neutron stars, hadron collisions, review 0-73683
 QCD black body radiation, big bang universe hadron era 0-62341
 QSO resonance lines as luminosity calibrators 0-105388
 quantum many-particle systems in curved spacetime 0-98751
 quantum processes at large redshifts 0-62357
 quark confinement, relevant cosmological f-g fields 0-86659
 quasars, evidence for nature of redshifts from brightness cyclic depend. on parameter $\ln(1+z)$ 0-105382
 quasars, number-magnitude relation rel. to luminosity function and cosmological evolution 0-77507
 radiation-matter flat universe, small perturbations and black hole form. effects 0-94900
 radio galaxies, red shift dependence of proper densities and colours 0-62286
 radio sources, extragalactic, ang. distrib., no evidence for anisotropy from deep survey at 4.85 GHz 0-77502
 radio sources, faint, evidence for cosmological evolution from statistical study at 81.5 MHz 0-90554
 radiosource counts and isotropy of faint sources in B2 survey 0-105374
 radiosource counts and spectral index distrib. 0-98732
 radiosources, space distrib. from short wavelength surveys 0-62305
 recombination epoch and microwave background, spectrum distortions 0-62334
 relativistic hierarchical cosmology, mathematical formalism and Einstein eqns. 0-82555
 relic θ particle concentration in the Universe (Russian) 0-86026
 relic monopoles from big bang, cosmological problem for standard unified theories 0-77532
 Riemannian manifolds, symmetric vectors and algebraic classification 0-68094
 rigidly rotating relativistic dust cylinder, Riemann tensor, ultrarelativistic case 0-86158
 rotating metrics, scalar perturbations 0-62348
 scale covariant cosmology, primordial He prod. 0-105412
 scale covariant gravity theories, astrophysical tests 0-73216
 self-consistent variational theory, Machian model 0-67558
 solar system motion rel. to diffuse X-ray background, evidence from Compton-Getting anisotropy 0-98745
 space-time metric, quantised field influence, external grav. field (Russian) 0-86027
 space-time metrical fluctuations induced by cosmic turbulence 0-82557
 spatially homogeneous neutrino cosmologies 0-90585
 spiral structures, geophysical and astrophysical 0-77287
 stable method heavy leptons, astrophysical mass constraint, condensation in stars and galaxies (Russian) 0-72768
 standard candle location, giant elliptical galaxy selection 0-105353
 strong gravitational field and general relativity 0-67548
 structure of early Universe 0-90594
 SU(5) grand unification, cosmological baryon asymmetry 0-86640
 SU(5) theories with both proton stability and cosmological baryon-number generation 0-86642
 superconducting early Universe, cosmological baryon prod., CP invariance grand unification 0-90592
 supernovae at great distance, luminosity and temporal var. as cosmological probes 0-94821
 symmetries and metrics of homogeneous cosmologies 0-90584
 universal evolution, steady-state and big-bang theories (Italian) 0-98748
 universal expansion and big-bang theory rel. to stellar cluster formation (Dutch) 0-62212
 universal fragmentation model, appl. to spiral galaxies form. 0-90529
 universal large scale shearing, Ariel V X-ray background data 0-62352
 Universe, closed or open, Fornax system density profile, strong gravitational interactions 0-90587
 Universe, very massive unstable particles, prop. bounds 0-82558
 Universe baryon asymmetry, left-right symmetric grand unified models 0-82559
 Universe before nucleosynthesis, first three minutes 0-62358
 Universe density perturbations, consequences for evolution nonlinear stage of neutrino rest mass (Russian) 0-105414
 Universe density perturbations spectrum, consequences of neutrino rest mass (Russian) 0-109576
 Universe expansion and time variation of atomic mass 0-90588
 Universe expansion model, explanation of 3K background 0-98746
 Universe fluctuations, spontaneous prod. 0-94902
 Universe large-scale struct. form., two-dimensional simulation of gravit. system dynamics 0-98749

cosmology continued

Universe mass density and age, implications of neutrino rest mass (*Russian*) 0-109575
Universe mean density, implications of intergalactic matter obs. 0-109543
Universe model, homogeneous, isotropic, close to cosmological singularity, long-wave disturbances 0-73078
Universe preferred frame optical test, Earthbound ring laser interferometry 0-77531
universe ultimate fate, effect of finite proton lifetime 0-82560
vacuum structure in gauge theories, strong CP violation and cosmology 0-86578
vacuum superfluidity near anisotropic singularity, phase transitions (*Russian*) 0-94905
variable rest mass field theory and the cosmological singularity models 0-77525
Vlasov-Einstein eqns. in spherical symmetry, self-similar analysis 0-67535
Weinberg-Salam model, vacuum instability, cosmology and particle mass constraints 0-78007
Wheeler's 'rule of unanimity' in quantum cosmology 0-98846
X-ray background, contrib. of discrete evolving sources 0-82551
X-ray background, contribution from young galaxies 0-82550
X-ray background irregularities 0-62331
X-ray background sources 0-94898
Zeldovich spectrum of cosmological fluctuations from spontaneous symmetry breaking 0-62353
 ν sea, cosmological, EM wave propagation, torsionic background 0-77283
 ^4He production, nonzero neutrino rest mass effects 0-105413

cosmotrons

No entries

Costa Ribeiro effect *see dielectric phenomena; phase transformations*

Cotton-Mouton effect *see birefringence; magneto-optical effects*

Cottrell atmospheres

diffusion length and lifetime meas. and assessment by SEM 0-96902
metals, research at Birmingham, (1945-55) 0-62444
Fe-Al(Ti), O containing, mag. aftereffect and disaccommodation meas., time depend., activation energy, and ageing props. 0-88836
LiF:Ni, dislocation behaviour in diffusion zone, Cottrell clouds (*Russian*) 0-70212

Cottrell locking *see Cottrell atmospheres*

Couette flow

see also jets
anemometry, hot-wire, in very low velocity flow, calibration of probes 0-75008
anisotropic liquid, axially symmetric flow 0-103050
bead-spring-type model in nonuniform vel. gradient, dil. soln. kinetic theory results 0-64628
blood suspension aggregation in Couette flow (*French*) 0-97991
buoyancy effect on plane Couette flow past permeable bed 0-92215
convective cells, stochastic oscill. spatial-time spectra (*Russian*) 0-103029
Couette-Taylor flow, laser Doppler velocimetry obs. of transition to turbulence 0-92163
early nonperiodic transitions in Couette flow 0-59056
hydrodynamic instabilities and turbulence, flow states, examples and meas. methods 0-92116
laminar to turbulent transition spectrum evolution 0-103034
MHD, unsteady, between two plates when one subjected to random pulses 0-69938
MHD Couette flow, Hall effect in rot. system 0-74991
nematic liquid crystals, Couette flow, orientation instability for finite anchoring energies 0-74923
nonlinearity viscoplastic liquid, convective dissipative heat exchange 0-87772
plane parallel flow, free convection in Couette and Poiseuille flows, numerical simulation 0-99995
resonance mechanism, small 3-D disturbances 0-79269
sphere between plane parallel boundaries, creeping parallel motion, strong interaction theory 0-103075
Taylor cells hydrodynamics instability and vortex currents in Couette flow 0-64571
transition regime, Couette flow between cylinders (*Chinese*) 0-59042
vortex flows, between rotating cylinders, axisymmetric Navier-Stokes equations 0-59044

counter accessories

see also counting circuits
No entries

counters

see also Cherenkov counters; counting tubes; fission counters; Geiger counters; proportional counters; scintillation counters; semiconductor counters; spark counters
active well coincidence counters, expt. comparison with random drivers for U assay 0-78503
aerosol, photoelectric, calibration by sedimentation method 0-99031
coincidence type ion electron converter device, neutron decay weak interaction obs. 0-58100
Euratom variable dead-time neutron counter, use for Pu passive assay 0-69042
gamma counting and self-shielding efficiency, activated thick foil 0-69043
heart beat counter, versatile digital SAMI 0-85510
megachannel pulse height analyser for gamma-ray coincidence analysis 0-99430
multistage time averaging filters for timing measurements with large counters 0-99425
nuclear materials accountability, U and P NDA of crated waste by gamma-ray and neutron coincidence counting 0-83166
nuclear radiation pulse counter control cct. (*Spanish*) 0-95508
optical single-particle-size spectrometer calibration and testing, monofilament fibres as substitute particles 0-58819
portable neutron coincidence counter for assaying large Pu samples 0-69041
submicron particulates size determ. by sideway light scattering method 0-98883
thermal neutron coincidence counting, correction for variable moderation and multiplication 0-69045
whole body counters, international intercomparison 0-78504

counters (circuits) *see counting circuits*

counting circuits

see also coincidence circuits; pulse height analysers; scaling circuits
amplifier, fast DC coupled linear pulse, gain and phase response design 0-58088
digitisers of time and pulse height, monolithic flash A/D convertor 0-63475
dissector pickup tube operating as a counter 0-95153
Geiger-Mueller survey meter, portable, compensated count rate cct. 0-99426
multistage parallel-serial time averaging filters to reduce time jitter in scintillation counter time meas. 0-102405
multistage time averaging filters for timing measurements with large counters 0-99425
multiwire proportional counter, linear read out electronics, hybrid preamplifier realisation 0-58091
MWPC, cylindrical, event triggers, correlation of wire addresses 0-58092
nuclear reactor instrumentation, microprocessor controlled, digital period meter, hardware and software 0-63473
pile-up rejection system for high threshold experiments 0-95509
preamplifier, charge sensitive, loop phase shift and delays 0-58089
proportional counter, position-sensitive, direct position and time digitizer 0-58090
radiation counting rate meter output at threshold, fluctuation and arrival shift by computer simulation 0-106240
scintillation counters, time-of-flight, electronics system for Mark II Detector 0-58093
solar gamma ray emissions study, Solar maximum mission, detector assembly and electronic assembly 0-63476
very fast time pick-off for low intensity pulsed particle beams 0-63478
wire spark chambers, capacitive read-out system 0-102407

counting tubes

see also dekatrons
No entries

coupled circuits

planar waveguide structure for integrated optics, props. (*Czech*) 0-96018

coupled networks *see coupled circuits*

coupled superconductor devices *see superconducting junction devices*

couplers (electric connectors) *see electric connectors*

couplers (waveguide) *see waveguide couplers*

coupling (process) *see joining processes*

coupling circuits *see coupled circuits*

CP invariance

baryon asymmetry of the Universe, quantum black hole evaporation (*Russian*) 0-109577
baryon electric dipole moments in CP noninvariant Kobayashi-Maskawa theory (*Russian*) 0-105897
cosmic matter-antimatter asymmetry and gravitational force 0-90586
CPⁿ⁻¹ model, embeddings of classical solns. of O(2p+1) nonlinear σ -models, instantons 0-86562
early Universe, baryon number generation due to CP- and B-violating interactions 0-109571
electroweak interactions, dynamically broken gauge theories, CP nonconservation without elementary scalar fields 0-86613
gravitationally induced CP effects, quantum gravodynamics, QCD quark sector 0-86616
high energy lepton pair prod. with pol. hadrons, P and C violations 0-99068
 $K^0 \rightarrow \bar{K}^0$ transition in the standard SU(3) \otimes SU(2) \otimes U(1) scheme (*Russian*) 0-82951
left-right symmetric model from general horizontal symmetry, Cabibbo angle, CP violation 0-101972
milliweak gauge models of CP violation 0-73633
mixing matrix and CP violation for n quark generations 0-101986
net baryon number and CP nonconservation with unified fields 0-62349
Poincare group, irreducible representations of groups containing subgroup of finite index 0-68384
Pontecorvo neutrino oscillations for Dirac and Majorana masses, CP nonconservation 0-105829
QCD confinement of colour, modification of axion scheme 0-73663
Reggeization of elementary fermions in arbitrary renormalizable gauge theories 0-68367
relativistic two fermion equations, Lorentz, parity and charge conjugation invariance 0-90976
SU₁₀, soft CP violation and complex Majorana mass relations 0-78010
SU(2)_c \times U(1)_c, strong CP-violating phase, one-loop corrections, Higgs particles 0-62910
SU(2)_c \times U(1)_c gauge model, mixing angles and CP violation 0-73648
SU(5), unification of weak, EM and strong interactions, review 0-105814
SU(5) gauge model, masses, mixing angles, CP violation and b-quark decay 0-78006
SU(5) grand unification, cosmological baryon asymmetry 0-86640
SU(N) \times SU(N) symmetry breaking with extremum constraints 0-68385
superconducting early Universe, cosmological baryon prod., CP invariance grand unification 0-90592
superheavy boson decay, neutrino number and isotropy of Universe in grand unified theories 0-85852
supersymmetry, OSp(1,4), superfield formulation in anti-de Sitter space 0-57508
vacuum structure in gauge theories, strong CP violation and cosmology 0-86578
weak interactions, lepton-hadron symmetry, CP violation and $\Delta I = 1/2$ rule 0-82934
B meson, cascade decays, CP nonconservation 0-105811
D $\rightarrow K^*\mu\nu$, in e^+e^- annihilation, T-odd asymmetry in CP violation model (*Russian*) 0-105885
 $K^- \rightarrow \pi\mu\nu$, μ polarisation and T-odd correlations, Weinberg model of CP violation (*Russian*) 0-62969
 $K_L \rightarrow \pi^+\pi^-\pi^0$, CP violation parameters in six quark model (*Russian*) 0-62974
 μ decay correlations and lifetime meas. 0-77996
 n electric dipole moment, CP violation in gauge theories 0-91041
 $\tau \rightarrow K^*\nu$, in e^+e^- annihilation, T-odd asymmetry in CP violation model (*Russian*) 0-105885
Cs cell, laser beam excitation, multipass, optical pumping and weak neutral current parity violation 0-58207
 $K \rightarrow \pi e^+\pi^-$, six-quark model, CP violation 0-78055

CPA calculations

alloy, pseudobinary, ferromag., magnon energy derivation 0-107996

CPA calculations continued

- alloy thin film, thickness depend. of CPA electronic densities of states 0-65644
 alloys, binary, 50-50, singularities at metal-insulator transition, CPA calc. 0-84428
 alloys, CPA for props. 0-75493
 alloys, random, equilib. and transport props., single-site approx. 0-92801
 alloys, substitutionally disordered, optical cond., intraband transitions 0-103933
 binary alloys, acoustic modes in random and correlated alloys, order-disorder transform. 0-65189
 dilute systems, donor fluorescence at high trap concentration 0-71479
 disordered alloys, electronic density of states in muffin tin model 0-88467
 disordered crystal, biphonon spectra, light absorpt. coeff. and density of states, CPA calc. 0-84271
 disordered crystals, biphonon spectra, CPA calc. 0-70341
 disordered extended Anderson model, CPA-alloy analogue treatment 0-65506
 EM wave multiple scatt. by random distrib. of discrete scatterers with coherent pot. and quantum mech. formalism 0-95768
 ferromagnetic metals, spin fluctuation theory, Curie temp., mag. susceptibility 0-65937
 fundamental Korringa-Kohn-Rostoker eqn. version of coherent potential approx. 0-59847
 Heisenberg amorphous ferromagnet, magnetisation and Curie temp., CPA calc. 0-75703
 Heisenberg ferromagnet, disordered two-dimens., CPA theory of bond model 0-60163
 insulator-to-metal transition for half-filled Hubbard band in paramagnetic state 0-92817
 Lloyd formula and muffin-tin CPA local density of states 0-70577
 phonons in disordered shell models 0-70347
 quasi-one-dimensional conductors, alloys, Peierls distortion 0-59965
 random lattice, atom site diagonal perturbation, functional integral approach 0-57218
 substitutional alloys of intermediate valence systems, static mag. susceptibility con. and temp. depend. 0-84586
 thin film, 11-layered, CPA calc. of local density of electronic states 0-65643
 transition metal alloys, binary, state density curves, relation between short-range order and Fermi level position, CPA calculations 0-107687
 transition metal alloys, cohesive properties and press.-vol. relation 0-92476
 Co-Ni, Hall effect, anomalous, residual coeff. calcs. using coherent pot. method (*Russian*) 0-80249
 Cu-Ni, random ferromag. alloy, local mag. moment calc. 0-70974
 Cu-Pt system, phonon dispersion relations, force constant disorder effect 0-84263
 EuO magnetic semiconductor, quasiparticle lifetimes, CPA study 0-65443
 Fe-Co, Hall effect, anomalous, residual coeff. calcs. using coherent pot. method (*Russian*) 0-80249
 Fe-Cr, random ferromag. alloys, local mag. moment calc. 0-70974
 Fe-Ni, Hall effect, anomalous, residual coeff. calcs. using coherent pot. method (*Russian*) 0-80249
 Fe₂Al(Si), electronic structure, magnetic moments 0-107695
 GaP, As_{1-x}N_x, luminesc. of N bound state excitons, local-environment effects 0-100691
 N₂, vertical valence ionis. pot. calc., by perturbation, CI and CPA techniques 0-69263
 Ne, vertical valence ionis. pot. calc. by perturbation, CI and CPA techniques 0-69263
 Ni-Co, high-field susceptibility, spin-wave spectrum, CPA calc. 0-65818
 Ni-Cu, ferromag., mag. moment, local environment effects, HF CPA cluster calc. 0-65817
 Ni-Cu, high-field susceptibility, spin-wave spectrum, CPA calc. 0-65818
 Ni-Fe, high-field susceptibility, spin-wave spectrum, CPA calc. 0-65818
 Ni-Mn alloys, ferromagnetism-to-spin glass phase transition and strong mag. field effect 0-75773
 Ni_{0.89}Cr_{0.11}, phonons with disorder caused by force consts., neutron diff. obs. and CPA calc. 0-96602
 Sm_{1-x}B_xS, valence transition induced by alloying 0-96829
 TiN_{1-x}, stoichiometric, electronic density of states, CPA method calcs. 0-88464
 U, Th, _xAs (Sb), electronic struct., relativistic KKR-averaged T-matrix approx. method 0-107702
 Yb_{1-x}Y_xCuAl, disordered extended Anderson model, CPA-alloy analogue treatment 0-65506

CPT invariance

- causality, macroscopic, Einstein correlation, CPT symmetry, decreasing probabilities, advanced waves, antiparticles 0-68073
 Poincare group, irreducible representations of groups containing subgroup of finite index 0-68384
 quantum gravity and time reversibility 0-82704
 quantum mechanical interpretation 0-105805
 K₂⁰→Kπ, k=2 or 3, Racah time reversal, a C,P,T scheme 0-78056
 μ decay correlations and lifetime meas. 0-77996

crack detection

see also cracks

- acoustic emission appl. to materials testing plastic strain and growing cracks identification 0-81252
 acoustic emission method and development of equipment for monitoring crack formation during welding 0-89451
 automatic mechanical scanning, TV signal form. on basis of digital memory 0-71864
 brass wire, US inspection, immersion method 0-66757
 ceramics, surface cracks, acoustic surface wave meas. 0-61055
 depth measurement by US techniques 0-71859
 dielectric waveguide, flow detection using UHF EM field pattern display 0-104378
 dimensions of flaws in direction of irradiation determ. from radiographs with aid of defectometer 0-71863
 eddy current imaging flow detection system 0-89426
 eddy-current flow detect., suppression of interf. parameters 0-89442
 eddy-current flow detection of long ferromag. products, magnetizing device parameters 0-89447
 eddy-current transducers, double-ended, signal calc. for nonferromag. cylindrical products 0-89443

crack detection continued

- fatigue cracks, US visualization, advantages over pulse-echo methods 0-66738
 fatigue detection and rating by acoustic emission, review 0-104380
 ferromagnetic material, flaw detected by high freq. magnetization, harmonic content in mag. field 0-71857
 fibre composite structure, thermal field techniques for NDT 0-66737
 fibreglass laminates, thermal NDT using liq. crystals 0-93709
 flaw-detection apparatus, noise immunity, sounding signal freq. modulation 0-89441
 flaws in solids, low-frequency props. from scattering meas. 0-76475
 holographic interferometry, using He in test chamber 0-93723
 industrial NDT computed transverse axial tomography system 0-89430
 inspection penetrants, evaluation 0-61056
 insulation, foam, spray-on, using dye solution or X-ray opaque solution 0-76440
 internal flaw, transverse dimension determ. by thermal control 0-104400
 IR non-destructive testing of bonded materials, theory and practice 0-93708
 magnetographic method, depending on coordinates in weld seam 0-108668
 metal fatigue crack detection using nondestructive evaluation (NDE) methods 0-71826
 metals, ultrasonic inspection, echo-mirror method with transform. of elastic waves 0-108663
 microtrons, appl. in nondestructive inspection of industrial products 0-81267
 near-surface defects, US detection and analysis (*German*) 0-93728
 noise immunity of flow detection system 0-104385
 physical optics farfield inverse scatt., mathematical inversion technique for nondestructive eval. 0-69580
 piezoelectric transducer, composite, of low freq. acoustic flow detector, natural freq. calc. 0-89450
 plate, flaw reconstruction by automatic US testing (*German*) 0-61059
 pressure vessel crack detection by magnetic crack detection and dye-penetrant inspection 0-100994
 pressure vessels, AE during fatigue crack expansion 0-108675
 radiation flaw detection, correction of shadow images 0-89456
 radiographic image quality, effect of inadequate screen-film contact (*German*) 0-61057
 radiographic inspection algorithm speedup by array processor 0-108659
 rolled sheet, artificial surface cracks, reflection of normal shear waves 0-89448
 rubber, thermal defectoscopy study 0-89445
 servo-hydraulic test system, for fatigue crack propagation studies under biaxial loading 0-76431
 sputter target cracking, acoustic emission testing 0-81248
 steam generator tubes, EM acoustic transducer 0-76464
 steel, austenitic stainless, butt welds, US exam. 0-93710
 steel, ball bearing rods, inspection installation 0-81268
 steel, Co-Cr-Mo, type HY 180 correl. between advanced NDT evaluation methods and fracture mech. parameters 0-97675
 steel, Cr-Ni-Mn, AISI 4340, correl. between advanced NDT evaluation methods and fracture mech. parameters 0-97675
 steel, types A533B and KAS, fracture toughness meas. using elect. potential method (*Japanese*) 0-93722
 steel, US inspection to 1000°C, hot-metal defectoscopy 0-66750
 steel pipe, flaw detection by US pulse-echo method 0-66756
 steel wire, US inspection, immersion method 0-66757
 Temp-1 system for the ultrasonic inspection of bulky aluminium alloy plates 0-66755
 thermal detection of delamination and inclusion flaws, ID anal. 0-71820
 thermovision flaw detector 'Stator-1', meas. channel 0-76449
 turbine rotor shaft, US testing, sensitivity multiplication factor 0-85125
 US flaw detection, diffraction of normal modes by a compliant disk 0-87603
 US flaw detection, focusing probes 0-104383
 US flaw detector, microprocessor controlled, for flaw classification in welded plates 0-100992
 US flow detectors, tuning methods for time depend. sensitivity control unit 0-108667
 US methods, progress in theory and principles 0-81262
 US resonance method, appl. in inspection of symmetrical products 0-89449
 US shadow flaw detectors, metrological peculiarities when inspecting thick rolled steel sheet 0-81263
 US sonoprobe for Si crystal microcracks detection 0-76462
 US test procedure for early detect. and remaining life prediction 0-71848
 welded joint, radiographic inspection, standardization of sensitivity and flaw size 0-89455
 welded joint, US reflection from irregularities 0-104389
 welded joints, radiographic inspection, real flaws detectability evaluation 0-81266
 welded plates, flaw classification using microprocessor controlled flaw detector 0-100992
 width investigation by inclined scanner with regulated directivity diagram 0-89452
 wood, standing trees, US pulse echo method for flaw detection 0-66731
 Al alloy sheets, type 7075-T6 used in aircraft, early detection of fatigue cracks 0-66730
 Al, subsurface flaw detection by photoacoustic microscopy 0-66725
 Al-Cu, high strength, type 2024-T3, crack growth, fatigue induced surface deform., holographic detect. 0-85120
 Al-Cu, type 1100, synchrotron radiation microradiography 0-85121
 Al-Cu-Mn, type 2219, synchrotron radiation microradiography 0-85121
 B fibre, US inspection, immersion method 0-66757
 Fe, cast, US flaw detection by boxcar integration 0-89437
 Fe-Co-Ti-Al alloy type YuNDK magnets, metallographic method of distinguishing cracks 0-85096
 Mo wire, US inspection, immersion method 0-66757
 Na₂O-Li₂O-Al₂O₃, local electrode current density and flow decoration 0-100935
 Si crystal microcrack detection by ultrasonoprobe 0-66733
 W wire, US inspection, immersion method 0-66757

crack-edge stress field analysis

see also penny-shaped cracks

- annular crack at spherical voids, stress intensity factor estimates 0-106757
 bar, rectangular, torsion crack problem, harmonic function continuation technique soln. 0-99969

crack-edge stress field analysis continued

birefringent plates, cracks, stress intensity factors, refl. caustics method 0-93718
 body loading with cracks, energy conditions for brittle failure (*Russian*) 0-96234
 brittle materials, water drop impacted, damage thresholds 0-81149
 ceramics, transformation toughening, martensitic transforms. in crack-tip stress fields 0-104154
 composite structural elements, stress intensity factors determ. 0-99973
 crack extension angle, influence of specimen's geometry 0-99965
 creep deform., stress field and modified J-integral near crack tip. (*Japanese*) 0-103411
 creep fracture, failure mechanism involving grain boundary sliding and brittle crack extension 0-97557
 cylinder with oblate spheroidal cavity or internal penny shaped crack under tension, stresses 0-69736
 disc, with crack, stress and strain calcs. (*German*) 0-106760
 discontinuous deformation gradients near crack tip in finite anti-plane shear 0-58973
 dislocation theory, elastic energy momentum tensor and crack propagation 0-69741
 ductile materials, crack extension rates 0-96230
 Dugdale crack, dynamic effects in propagation, Hankel and Laplace transform methods 0-87741
 dynamic crack-tip fields according to deformation theory 0-64481
 dynamic finite element analysis of cracked bodies subjected to impact loading 0-69742
 dynamic propagation in anti-plane shear, anal. by finite differences 0-84240
 edge crack, oblique, in semi-infinite plate, stress anal. 0-64463
 edge cracked sheets with mixed boundary conditions, stress intensity factors, displacements, stresses 0-64477
 edge notched brittle plates, virgin waves and boundary reflections at fracture 0-79233
 elastic crack tip enclave model, fracture stress 0-71730
 elastic plane, stress-strain state at brittle crack vertex, geometric non-linearity effects (*Russian*) 0-79221
 elastic plate, crack closure in bending, sixth order anal. 0-96231
 elastic-plastic plane-strain crack growth, comparison of theory and experiment 0-108560
 elastic-plastic stress field, plane stress and plane strain, blunting of tip (*Chinese*) 0-64469
 embedded semicircular surface crack, stress intensity factors, superposition methods 0-79217
 exterior interface cracks, shear and tensile tractions, stress anal. 0-58971
 fatigue crack propagation, crack closure, effective stress range factors 0-100924
 ferromagnetic elastic solid, two coplanar Griffith cracks, singular stresses 0-65985
 fibre reinforced composites, angle ply, delamination mechanics and failure mode 0-79236
 fibre reinforced composites, unidirectional, anal. of cracks emanating from circular hole 0-103001
 finite plate, propag. mode III crack, dynamic stress intensity factor, reflected stress waves 0-103001
 glass, fracture and fatigue, crack tip radii influence 0-89335
 granular solids, cracks, stress concentrations and shapes, Fourier transform methods 0-83761
 Green's function analysis, crack emanation from circular hole in infinite sheet 0-92084
 Griffith crack opened by rigid inclusion, stress distrib. 0-79228
 Griffith crack-antiplane shear wave interaction at interface of two bonded elastic half-spaces, geophys., seismological appl. 0-92087
 half space, elastic, edge cracks, dynamic growth 0-58972
 harmonic solid, crack parallel compression, crack plane strain buckling 0-64475
 high-temperature reactor structural displacement and strain analysis by picture processing (*Japanese*) 0-78352
 Homalite-100 plates, modified compact-tension specimens, dynamic anal. 0-97561
 infinite cracked isotropic sheet, under symmetric loads, Green's functions for stresses, stress intensity factors and displacements 0-99967
 infinite elastic medium, diffraction of torsional waves by flat annular crack 0-64447
 infinite elastic medium with cylindrical inclusion, external crack in torsion, stress distrib. 0-79216
 infinite power law viscoelastic body, crack propag. by rigid wedge, stress intensity 0-64476
 infinite transversely isotropic solid, containing penny-shaped crack, stress intensity factor 0-69738
 interface edge cracks, energy release rate calc. based on M-integral 0-87742
 penny-shaped crack problem, deformed incompressible elastic solid 0-92085
 penny-shaped cracks, in elastic sphere embedding in infinite elastic space, thermal stresses 0-64460
 penny-shaped cracks, transverse tension, stresses, micropolar elasticity 0-64459
 perfectly plastic medium, elastic-plastic field at tip of steadily growing crack (*Chinese*) 0-58968
 plane elastic crack, dynamics under variable loading (*Russian*) 0-79222
 plane elasticity, curvilinear crack edges concentrated forces and edge dislocations, numerical soln. 0-58970
 plastic blunting at tip, relationship with J-integral (*Japanese*) 0-103414
 plastic deformation at the tip of an edge crack 0-69734
 plate, elastic, containing through crack, skew symmetric loading, transverse shear effects 0-64478
 plate structure, crack simulation computer program (*Japanese*) 0-79218
 plate with initial crack subject to extension, brittle fracture energy conditions (*Russian*) 0-103002
 plates under uniaxial load, optimum hole shapes, cracks and fracture appl. 0-64479
 PMMA, craze zones at crack tips, validity of Dugdale model, comment 0-108535
 PMMA, craze zones at crack tips, validity of Dugdale model 0-108534
 polycarbonate, bisphenol A, birefringent plates, cracks, stress intensity factors, refl. caustics method 0-93718
 polycarbonate plates, modified compact-tension specimens, dynamic anal. 0-97561
 power-law hardening material, pre-cracked plate, unstable fracture criterion 0-84238

crack-edge stress field analysis continued

rectilinear anisotropic solids, mixed-mode crack anal. using conservation laws of elasticity 0-84239
 semi-elliptical surface crack in semi-infinite solid, stress intensity factors 0-84241
 semi-infinite crack tips, practical evaluation of stress intensity factors 0-99962
 shear loaded interface crack, friction effects, contact zones, stress fields 0-79225
 shear wave scattering by cracks in elastic medium, stress intensity factors 0-74787
 slab containing annular crack, thermal stresses, integral transform techniques 0-96229
 state of stress, role in crack tip failure 0-106758
 steel, alloy A533B1, neutron irradi., flow growth characs. by acoustic monitoring 0-100918
 steel, austenitic stainless type SUS 316, low cycle fatigue tests, freq. effect on notch sensitivity at elevated temps. (*Japanese*) 0-104260
 steel, C, crack initiation and propagation life under repeated impact tensile loads (*Japanese*) 0-104264
 steel, effect of H₂ on phys. and mech. props. 0-101657
 steel, ferritic, cleavage fracture toughness, temp. and strain rate depend. 0-85028
 steel plates, explosively clad, fatigue crack propagation behaviour (*Japanese*) 0-104262
 stress corrosion cracking failure, predictive approaches 0-97611
 stress intensity factors, modified Lobatto-Chebyshev method 0-99972
 strip, elastic, Griffith crack interactions, mixed boundary value problem 0-58969
 surface crack in a clamped circular plate subjected to uniform lateral pressure, bending stress anal. 0-74811
 thermoelastic cracks in plane, boundary integral eqn. method (*German*) 0-106761
 trajectory, unstable crack extension 0-64462
 transversely isotropic solid, penny shaped crack, stress anal. 0-92083
 two bonded elastic solids interface, penny shaped crack, torsional wave interaction 0-64484
 wearing half-space, determ. of stress intensification factors 0-99964
 wedge, symmetric cracking by transverse displacements, stress intensity factors 0-79226
 wedge shaped crack, apex singularities under all modes 0-64480
 Al alloy, type 7175 T 651 (*French*) 0-65145
 Zr-Nb (2.5 wt.%) pressure type rel. between stress intensity factor, crack opening displacement and J-integral 0-100920
 ZrO₂ microsphere stabilised ceramic, fracture characs., thermal stability (*Russian*) 0-76335

crack inspection see *crack detection*
crack-tip stress field analysis see *crack-edge stress field analysis*
cracking see *fracture*
cracks
 see also *crack detection; crack-edge stress field analysis; crazing; fatigue cracks; penny-shaped cracks; stress corrosion cracking; thermal stress cracking*
 antiplane strain, crack at boundary between two materials with branch into one of them 0-79231
 Araldite B specimens, dynamic fracture toughness, influence on dynamic crack propag. 0-99966
 bar, rectangular, torsion crack problem, harmonic function continuation technique soln. 0-99969
 beam, cracked, dynamic weight function from finite element soln. 0-79234
 beams in pure bending, distributed damage theory, cracks, fracture 0-64474
 birefringent plates, cracks, stress intensity factors, refl. caustics method 0-93718
 body loading with cracks, energy conditions for brittle failure (*Russian*) 0-96234
 α -brass, plane stress ductile fracture, prestrain effects 0-108532
 brittle fracture, statistical theory, dislocation mechanism, crack propagation (*Chinese*) 0-106755
 brittle solids, unstable growth of tension cracks 0-106756
 built-up edge form, direct SEM obs. 0-104303
 bulk crack propag., use of partial props. in coarse two-phase materials 0-108531
 BWR fuel rod relocation, gap conductance anal. 0-83192
 capacitance, mech. loads effects 0-84242
 ceramic multilayer capacitors, fracture mechanics approach to structural reliability assessment 0-89328
 ceramics, coarse-grained, dimensional anal. of grain size depend. of fracture strength 0-70299
 ceramics, crack extension micromechanisms, review 0-108567
 ceramics, fracture mech., probability, micromech. models of crack growth 0-108571
 ceramics, microcracks, and thin intergranular films obs. by TEM 0-68295
 chemically assisted fracture, atomic models of crack growth 0-64466
 chemically assisted fracture, general reaction rate theory and thermodynamics 0-64465
 chevron notched short bar specimens, compliance and stress intensity coefficients 0-96232
 circular crack under general asymmetric loads, related integral eqns. 0-64483
 cleavage crack tip lattice trapping, relation between macroscopic and microscopic thermodynamic surface energies 0-59572
 cokes, metallurgical, struct. and strength 0-93610
 composite, crack extension micromechanism 0-108566
 continuous beams with concrete slabs under load, method for crack prevention in slab (*Japanese*) 0-83760
 covalent crystals, nanosec. electron beam effects, size depend., Ioffe effect 0-88211
 creep crack growth, diffusion and deformation controlled 0-79867
 creep crack propag. by cavitation near crack tips 0-107364
 cropping and blanking, plastic flow, fracture, crack propagation 0-74761
 defect dimension determination by acoustic emission 0-104381
 deformation and fracture of materials in creep range, effects of nonlinear stress-strain rate relations 0-58938
 diffraction by a crack of a cylindrical longitudinal pulse 0-92082
 diffusional growth of intergranular cavities in uniform stress field and ahead of crack-like stress concentrator 0-107366
 discrete dislocation analysis 0-84236

cracks continued

dislocation distrib., fracture relation, plastic flow at crack tip, slip line theory 0-64482
 dislocation theory for stress intensity factors around a crack tip 0-69741
 dissolved species, advection-diffusion eqn. in pulsating crack 0-96312
 dynamic finite element analysis of cracked bodies subjected to impact loading 0-69742
 dynamic fracture toughness, influence on dynamic crack propag. 0-99966
 elastic body with plane cracks of normal fracture, 3D problems (*Russian*) 0-79219
 elastic equilibrium of a wedge with a crack 0-69733
 elastic plane, stress-strain state at brittle crack vertex, geometric non-linearity effects (*Russian*) 0-79221
 elastic plate, crack closure in bending, sixth order anal. 0-96231
 elastostatic problems, three-dimens., Mode I loading, soln. method 0-92086
 epoxide resin, low temp. crack propag. 0-85020
 epoxy materials, crack blunting mechanisms 0-66624
 extension angle, influence of specimen's geometry 0-99965
 exterior interface cracks, shear and tensile tractions, stress anal. 0-58971
 ferromagnetic solids, magnetomechanical effects, magnetostriction, hysteresis, stress, yielding, fatigue damage, crack growth (*Polish*) 0-71150
 fibre reinforced composites, micro- and macrocracks 0-65148
 fibre reinforced composites, unidirectional, anal. of cracks emanating from circular hole 0-100301
 flaw size measurement, nondestructive evaluation 0-71855
 flaws, 2D, irregularly shaped, fracture mechanics transfer function 0-99970
 fracture, chemically-assisted, atomic modelling at crack tips 0-106754
 gas flow through cracks, surface roughness influence 0-69929
 glass fibre reinforced plastic, acoustic emission 0-104294
 glass fibre reinforced plastic, fracture dynamics 0-100906
 glass fibres, flaw generation by indentation fracture technique 0-81156
 glass-glass-ceramic composites, crack growth, elec.-mech. analogue 0-85022
 Green's function analysis, crack emanation from circular hole in infinite sheet 0-92084
 Griffith crack opened by rigid inclusion, stress distrib. 0-79228
 Griffith crack-antiplane shear wave interaction at interface of two bonded elastic half-spaces, geophys., seismological appl. 0-92087
 haematite, degree of reduction, potential relaxation due to cracks (*Russian*) 0-66770
 half space, elastic, edge cracks, dynamic growth 0-58972
 harmonic solid, crack parallel compression, crack plane strain buckling 0-64475
 Hastelloy, C-276, H-induced crack growth 0-71747
 Homalite-100 plates, modified compact-tension specimens, dynamic anal. 0-97561
 hydrogen embrittlement, adsorpt. model and equilibrium crack growth meas. 0-108574
 Inconel 600 safe-end cracking failure at Duane Arnold reactor 0-104295
 infinite elastic medium, diffraction of torsional waves by flat annular crack 0-64447
 infinite power law viscoelastic body, crack propag. by rigid wedge, stress intensity 0-64476
 inorganic glass, effect of liq. medium on process of mechanical destruction 0-89283
 interacting cracks, in a cruciform pattern, spontaneous growth 0-99961
 interface edge cracks, energy release rate calc. based on M-integral 0-87742
 interfacial crack between dissimilar media, biaxial load effects 0-99968
 ionic crystals, nanosec. electron beam effects, size depend., Ioffe effect 0-88211
 Joule heat concentrators, metal foil expts. max. heat release, cracks in conductors 0-92022
 Lamb wave diffraction by finite crack in elastic layer 0-64244
 longitudinal-shear crack refraction, Wiener-Hopf method calcs. 0-87743
 magnetic tapes, calcs. of field reflections due to extensive flaws 0-104387
 measurement, recording instrument 0-100984
 medium with large no. of cracks, direct elec. current calcs. 0-96233
 nitrated layer, fracture toughness determ. from hardness impressions (*German, English*) 0-97575
 nonlinear materials, Mode I fracture behaviour, finite element anal. 0-84237
 nuclear reactor materials, crack-front tunnelling, investigated by single specimen compliance technique 0-70300
 nuclear reactor piping system, crack initiation and propagation, fracture mechanics 0-83193
 photoelastic prediction of crack propag. angle 0-87748
 plane cracks, occupying two-connected domain, elasticity theory problems (*Ukrainian*) 0-74804
 plane elastic crack, dynamics under variable loading (*Russian*) 0-79222
 plane elasticity, curvilinear crack edges concentrated forces and edge dislocations, numerical soln. 0-58970
 plane-strain buckling of cracks in incompressible elastic solids 0-79186
 plastic deformation at the tip of an edge crack 0-69734
 plastics, crack growth stability anal. using catastrophe theory 0-74810
 plate, elastic, containing through crack, skew symmetric loading, transverse shear effects 0-64478
 plate structure, crack simulation computer program (*Japanese*) 0-79218
 plate weakened by equal-armed cross-shaped crack, plastic strain and fracture 0-69740
 Plexiglas, fast cracks propag. and interaction 0-100905
 PMMA, instantaneous crack resist. during stable crack propag. 0-85058
 PMMA plates with flawed faster holes, static fracture testing 0-97651
 polished glass surface, reflected light phase rotation 0-66147
 polycarbonate, bisphenol A, birefringent plates, cracks, stress intensity factors, refl. caustics method 0-93718
 polycarbonate plates, modified compact-tension specimens, dynamic anal. 0-97561
 polymer, crack extension micromechanisms, review 0-108561
 polymer, crack tip failure mechanism modelling 0-108565
 polymer multilayer composite, wire-reinforced, dynamically loaded, crack propagation and arrest 0-97567
 polymers, glassy, craze surface displacements, model 0-93651
 porcelain, crack propag. data applicability to failure prediction 0-81154
 power-law hardening material, pre-cracked plate, unstable fracture criterion 0-84238
 propagation, computer simulation 0-59573
 PVC, rigid, internal struct. of diamond shaped cavities 0-66628

cracks continued

PWR piping, circumferential cracks, opening and extension, MARC finite element program 0-78364
 quasi-static crack propagation in single cells of fibre reinforced materials under tension (*German*) 0-106759
 reactor technology, conference, Berlin, Germany (Aug. 1979) 0-77539
 rectilinear anisotropic solids, mixed-mode crack anal. using conservation laws of elasticity 0-84239
 rolled sheet, artificial surface cracks, reflection of normal shear waves 0-89448
 ruby, structural defects due to laser irradi. (*Russian*) 0-100303
 semi-elliptical surface crack in semi-infinite solid, stress intensity factors 0-84241
 semi-infinite crack tips, practical evaluation of stress intensity factors 0-99962
 shear loaded interface crack, friction effects, contact zones, stress fields 0-79225
 shear microcrack propag. in triaxially-compressed brittle rocks 0-90080
 shell, cylindrical, closed, laminated, longitudinal crack, elastic eqn., energy approach (*Russian*) 0-87740
 solar cells, faulty, scanning light spot anal. 0-89625
 solid popellant, delayed fracture and crack propagation (*French*) 0-108521
 steel, carbon type, hydrogen press. effect on morphology of hydrogen attack 0-85052
 steel, continuously cast, segregation at half-way cracks 0-60869
 steel, Cr-Mo, oxidised, mechanism of crack decoration of oxides by electrodeposition 0-97560
 steel, fibrous crack extension, micromechanisms 0-108563
 steel, H embrittlement mechanism, microcrack formation, dislocation model (*Russian*) 0-65143
 steel, lamellar pearlite, containing proeutectoid cementite, brittle-fracture study (*Japanese*) 0-93648
 steel, low alloy-high strength, deforms. during cold crack developments in welded joints 0-81142
 steel, low-C, S10C and 520C, tensile fracture at low temps. (*Japanese*) 0-81163
 steel, structural, impurity effect on crack initiation, dynamical loading (*Czech*) 0-60955
 steel, type 4140, elastic-plastic plane-strain crack growth, comparison of theory and experiment 0-108560
 steel, type Kh13N9D2MT martensitic aged, struct. and mech. props. (*Russian*) 0-93600
 steel, types A533B and KAS, fracture toughness meas. using elect. potential method (*Japanese*) 0-93722
 steel, types S25C and S45C surface damage produced by pulsating impact contact load (*Japanese*) 0-104263
 steel, welded-joints, H₂ induced cracking, S content effect 0-97562
 steel layer types St3+Kh13, acoustic emission parameters, brittle fracture, crack propagation (*Russian*) 0-93633
 steel layers, types St3+Kh18N9T, acoustic emission parameters, brittle fracture, crack propagation (*Russian*) 0-93633
 steels, low-C, aged after quenching, rel. between micro-cracks and coxing effect (*Japanese*) 0-81159
 stress intensity factor determ. along crack path., numerical method 0-74808
 stress-intensity factor determ. by strain-gauge method 0-76445
 strip, elastic, Griffith crack interactions, mixed boundary value problem 0-58969
 surface crack in a clamped circular plate subjected to uniform lateral pressure, bending stress anal. 0-74811
 symmetrical branches at end of crack, effects on growth 0-103003
 thermoelastic cracks in plane, boundary integral eqn. method (*German*) 0-106761
 thin sheet impact strength study (*Czech*) 0-59571
 tip strain meas. by electron micrograph stereoscopy 0-69752
 viscoelastic bodies, crack growth kinetics under cyclic loads (*Russian*) 0-87739
 viscoelastic body containing cracks, durability calcs. 0-79227
 viscoelastic solids, linear, crack growth law derivation, fracture process zone concept 0-92088
 viscoelastic strip, dynamic crack propagation due to antiplane loading 0-64464
 wearing half-space, determ. of stress intensification factors 0-99964
 wedge shaped crack, apex singularities under all modes 0-64480
 Weibull distribution, adding static and dynamic fatigue effects 0-70298
 Zircaloy-2, hydride precipitation and growth at crack tips, electron optical obs. 0-108449
 Al alloy type 7010-T7651, high toughness, cyclic and monotonic crack propag. 0-108528
 Al-Ag (7.27 wt.%), peculiarities exhibited during fatigue loading (*Chinese*) 0-71723
 Al-Cu, type 1100, synchrotron radiation microradiography 0-85121
 Al-Cu-Mn, type 2219, synchrotron radiation microradiography 0-85121
 Al₂O₃, fracture toughness determ. using four-point-bend specimens 0-108536
 Al₂O₃, hot pressed, fracture stress-reflecting spot relations 0-71731
 Al₂O₃ substrates, tape-casted, fracture strength analysis 0-60948
 Al₂O₃-SiO₂ (3 wt.%), J-integral meas. at high temps. (*German*) 0-93624
 B₂O₃-SiO₂ glass, crack growth, phase separation effects 0-89336
 CaF₂, strength-controlling fracture energy depend. on flaw-size to grain-size ratio 0-81152
 Cu-Be (2 at.%), plastic deformation and dislocation substruct. 0-76307
 Fe, pure, hydrogen-charged, initial cracking obs. 0-108580
 Fe, volume changes and defect healing due to plastic deform. (*Russian*) 0-81139
 Fe-Al-Si (6.22, 9.63 wt.%), bending test under high press., high temp. 0-85057
 InBi single crystal, deform. mode under dynamic indentation 0-88163
 LiF bicrystal, high-angle tilt boundary and edge dislocation intersection effects 0-79836
 MgAl₂O₄, strength-controlling fracture energy depend. on flaw-size to grain-size ratio 0-81152
 MgO, crack tip dislocations and dislocation-free zones 0-96533
 MgO single cryst., impact wear damage 0-76375
 Na₂O-CaO glass, shear deform. under pyramidal indentations 0-84989
 Na₂O-CaO-SiO₂ glass, high-vel. liq. impact, oblique impact anomaly 0-89329
 Na₂O-CaO-SiO₂ glass foils, HVEM in-situ straining expts. 0-104216
 Na₂O-SiO₂ glass, microcracking about NiS inclusions, fracture mech. description 0-89333

cracks continued

- Na₂O-SiO₂ glass, OH⁻ content effect on mech. and other props. 0-89337
- Na₂O-SiO₂ glass, scoring, deform. and fracture mech. approach 0-89332
- Ni, volume changes and defect healing due to plastic deform. (*Russian*) 0-81139
- Ni-base superalloys, powder metallurgical, creep-rupture at intermediate temps. 0-97568
- Ni-base wrought superalloy, creep and stress rupture behaviour in air and vacuum 0-60918
- Ni-Cr-Al-Ta-C, eutectic composite, microstructure, fatigue props. 0-85038
- Pb(Zr,Ti)O₃, fracture and deform. 0-79870
- Si, crack-tip dislocation pattern, X-ray topography (*French*) 0-107253
- Si, near (111), fracture by painted indenter, SEM study 0-71734
- SiC, fracture toughness and high-temp. slow crack growth 0-81153
- Si₃N₄, hot-pressed, fracture mech. parameters, indentation-precracking and double-torsion methods 0-104364
- Si₃N₄, hot-pressed, fracture toughness determ. using specimens with chevron and straight through notches 0-108538
- Si₃N₄, hot-pressed, strength anisotropy origins 0-89330
- SiO₂ films sputtered in H-Ar mixed gas, enhanced step coverage 0-75470
- Ti, oxidation behaviour under pure O₂ atmos., temp. range 600-800°C 0-89415
- Ti, volume changes and defect healing due to plastic deform. (*Russian*) 0-81139
- Ti-Al-Mo-Cr (4.5, 5, 1.5 wt.%), weld metal, α/β interface sliding 0-108512
- UO₂, surface energy, determ. by Hertzian indentation 0-93641
- W bicrystals, crack propag. across grain boundaries, crack speed meas. technique appl. 0-108575
- Y₂O₃, strength-controlling fracture energy depend. on flaw-size to grain-size ratio 0-81152
- Zr, hydride precipitation and growth at crack tips, electron optical obs. 0-108449
- Zr-Nb (2.5 wt.%), hydride precipitation and growth at crack tips, electron optical obs. 0-108449
- Zr-Nb (2.5 wt.%) pressure type rel. between stress intensity factor, crack opening displacement and J-integral 0-100920

cranes

- bridge, vibration damping calc. 0-101711

cranking model, nuclear see nuclear cranking model**crazing**

- see also stress corrosion cracking
- micromechanisms of crack extension, conf., Cambridge, England (March 1980) 0-105421
- PMMA, craze zones at crack tips, validity of Dugdale model, comment 0-108535
- PMMA, craze zones at crack tips, validity of Dugdale model 0-108534
- PMMA, crazing, deform. kinetics 0-84990
- PMMA, fatigue life enhancement, prior crazing 0-89331
- PMMA, large deforms. at tip of running crack, opt. interference obs. 0-85062
- PMMA, plastic deform. by crazing (*Japanese*) 0-93619
- polycarbonate, glassy, fatigue crack initiation in high strain fatigue tests 0-97564
- polycarbonate, neck propag., rel. to dry craze growth mechanism 0-59563
- polymer, crack extension micromechanisms, review 0-108561
- polymer, crack tip failure mechanism modelling 0-108565
- polymer materials, characterisation 0-103270
- polymers, glassy, craze surface displacements, model 0-93651
- polymers, HVEM in-situ deform. 0-104215
- polypropylene, microstruct. changes during large strain cyclic deform. 0-66627
- polystyrene, glassy, crazing and brittle fracture on flat die indentation 0-60970
- polystyrene-polyethylene block copolymer, deformation ratios, Poisson ratio and adhesion, dilatometric obs. 0-60937
- PVC, crazing, deform. kinetics 0-84990
- PVC, glassy, fatigue crack initiation in high strain fatigue tests 0-97564
- steel, Cr-Mo, oxidised, mechanism of crack decoration of oxides by electrodeposition 0-97560
- styrene-acrylonitrile copolymer, crazing and brittle fracture on flat die indentation 0-60970
- B₂O₃-SiO₂-Na₂O phase-separated glass, creep fracture morphology 0-81151

creation hypothesis, continuous see cosmology**creation of electron pairs see electron pair production****creep**

- see also creep fracture; creep testing; diffusion creep; elastic aftereffect; irradiation induced creep; recovery-creep; stress relaxation
- alkali silicate glasses, secondary relax. transitions 0-88261
- alloy, cryogenic, creep, review 0-104222
- articular cartilage in compression, biphasic creep and stress relax., theory and expts. 0-94275
- Bakor 33, refractory, stress relaxation capacity determ. 0-60910
- bone, compact, long-term torsional creep obs. 0-104619
- brass, cyclic creep under increasing stress condition, constitutive eqn. 0-93593
- brass bicrystals, two-phase (α/β), interphase boundary sliding at high temperature 0-88164
- cavity growth anal. during superplasticity 0-60923
- cavity growth diagram, for high temp. creep 0-65140
- cement grog bodies, high Al₂O₃ content, creep characts. obs. 0-66578
- ceramic, porosity depend. 0-97530
- circular specimen subject to pure bend, ultimate tensile and compressive strength (*Russian*) 0-74768
- concrete, high strength, made with a special cement admixture, mech. props. (*Japanese*) 0-89297
- constructional materials, creep, viscosity, resist. to inelastic deform. 0-89309
- cracktip under incipient creep deform., stress field and modified J-integral (*Japanese*) 0-103411
- crystals, quantum effects in plasticity 0-59561
- cyclic creep under increasing stress condition, constitutive eqn. 0-93593
- cylindrical punch, three-dimensional stress field, photoelastic studies 0-93272
- damage analysis under nonproportional cycling 0-97556

creep continued

- deformation, and diffusion controlled creep crack growth 0-79867
- deformation and fracture of materials in creep range, effects of nonlinear stress-strain rate relations 0-58938
- discs, circularly symmetric, rupture, ductile-brittle creep 0-69735
- elastic-viscoplastic materials, uniaxial cyclic loading, stresses, relaxation, creep 0-64402
- epoxy composites, with different degrees of hardening, bulk-creep prediction 0-104223
- epoxy resin, filled and unfilled, subjected to extensional creep, dynamic props. 0-71697
- epoxy resin composites, cooldown residual thermal stresses, viscoelastic response 0-60941
- failure, high temp., life fraction rule and probabilistic approach 0-93608
- fibre glass laminate in tension, creep 0-71718
- filled polymer mechanical properties, particle shape effect, review 0-100864
- glassy state and highly viscous liq., rheology 0-70130
- high temperature plant design methods, reference stresses and bounding theorems 0-58937
- Inconel 617, morphological changes of carbides, effect on creep props. 0-108509
- internal stress, stochastic model for dip test in steady-state creep 0-58915
- internal stress measurement, in creep, anelasticity influence 0-70306
- isotropic stable media, stress tensors and creep-strain rates correl. 0-87722
- life prediction modelling for creep damage 0-59574
- metals, creep limit and long-term strength, parametric eval. method 0-100996
- metals, engineering, multi-axial creep characts. 0-64398
- metals, polycrystn., creep damage and cavity growth, assessment using density meas. 0-104217
- metals under combined stresses, review of creep behaviour 0-59567
- metals under creep loading, cumulative damage, engineering approach 0-58935
- methacrylic polymers, multiple dielectric relaxations, investigation by thermally stimulated creep method 0-93238
- modelling of creep incorporating initial strain and ageing 0-58939
- naphthalene single crystals, steady creep obs. 0-75296
- Nimonic 105, creep and stress rupture props., trace elements influence 0-66602
- Nimonic 80A, creep rupture under non-proportional loading 0-108518
- nonisothermal creep, reference stress and temp. 0-64401
- parametric data handling method development, creep and creep-rupture data 0-58934
- plastics under combined stresses, review of creep behaviour 0-59567
- plate, rectangular, finite bending in creep conditions (*Russian*) 0-79169
- PMMA, crazing, deform. kinetics 0-84990
- PMMA, creep compliance calc. from short-term creep expts. 0-89303
- PMMA organic glass, stress relax. calc. from creep curves 0-71709
- polycrystalline metals, effect of grain boundary sliding on steady creep 0-96590
- polyethylene, creep during shear deform. with applied hydrostatic press. 0-76324
- polyethylene, high-density unorientated, damage buildup kinetics under creep conditions, during prolonged loading 0-60932
- polyethylene, nonorientated partially cryst., kinetic damage accumulation cure 0-71753
- polymer concrete, longitudinal deformation modulus investigation in creep conditions (*Bulgarian*) 0-71685
- polymers, amorphous, glass-rubber transition, time-temp. superposition, shear creep compliance meas. 0-88309
- polymers, creep under plane stress, nonlinear viscoelasticity models appl. 0-89308
- polymers, cross-linked, with different degrees of hardening, bulk-creep prediction 0-104223
- polymers, long-term strength prediction, review 0-104226
- polystyrene-tricresyl phosphate solns., viscoelastic props., conc. depend. 0-76299
- polyurethane solid foams, creep laws (*German*) 0-65139
- POM, creep compliance calc. from short-term creep expts. 0-89303
- pressure sintering, inhomogeneous flow and effective press. 0-93512
- PTFE, stress-time analogy under shear and hydrostatic pressure in creep regime 0-104227
- PTFE and filled PTFE, nonlinear creep, compression bulk modulus 0-66593
- PVC, crazing, deform. kinetics 0-84990
- quartz, naturally deformed, dynamic recrystn. during creep, dislocation substruct., Mg alloy comparison 0-109142
- rate equations for elevated temperature creep 0-65141
- remaining creep life for components under stress at elevated temperatures 0-59566
- rheonomic shell, cylindrical, local stability in creep conditions (*Russian*) 0-92069
- screw subboundaries as dislocation sources, creep 0-100234
- SEM of bulk specimens using imaging of subgrains 0-66609
- shells, circular cylindrical, in axial compression, axisymmetric creep buckling, isotropic elasticity 0-69704
- statistical methods for creep, fatigue and fracture data analysis 0-58936
- steel, alloy X8CrNiNb1613, creep limit and long-term strength, parametric eval. method 0-100996
- steel, austenitic stainless, ageing at high temp., effect on creep props. SEM 0-97516
- steel, austenitic stainless, type 304, cyclic creep during unbalanced tension-compression loading at elevated temp. 0-97545
- steel, austenitic stainless, types 304 and 316, environment effect on crack growth, under creep and fatigue conditions 0-85035
- steel, austenitic stainless Ni-Cr, heat resist. and comp. of non-metallic inclusions, effect of La, Nd, Pr and Ce 0-76315
- steel, austenitic stainless type 304, time-depend. fatigue, mechanistic model 0-100925
- steel, C expt. investigation above 900°C 0-81134
- steel, Cr-Mo (2.25, 1 wt.%), creep and high temp. low-cycle fatigue tests 0-85061
- steel, Cr-Mo (2.25, 1 wt.%) pipe, high temp. fatigue and creep strength 0-85060
- steel, Cr-Mo-(V), microstruct. effect on high-temp. props. (*Czech*) 0-89300
- steel, Cr-Mo-(V) austenitic, creep resist., high-temp. props. residuals effect 0-66600
- steel, Cr-Mo-V, strength and ductility in creep, purity influence 0-66598

creep continued

- steel, Cr-Mo-V low-alloy, mech. props. and stress relief cracking, effects of impurities and deoxidation practice 0-66599
- steel, cryogenic, creep, review 0-104222
- steel, ferritic, creep resist., high-temp. props. residuals effect 0-66600
- steel, heat resistance, thermal stability, stress-rupture strength, and creep 0-81194
- steel, heat resistant, tensile strain and endurance, normal and radiation conditions, linear load variation 0-81189
- steel, low and high-alloy, expt. investigation above 900°C 0-81134
- steel, low-alloy, impurities, segregation and creep embrittlement 0-66653
- steel, Ni-Cr-Mo, cyclic creep under increasing stress condition, constitutive eqn. 0-93593
- steel, pearlitic, creep-induced microcreep healing kinetics of 12MKh and 15Kh1M1F, TEM obs. (Russian) 0-71690
- steel, plastic deform., density changes (German) 0-60908
- steel, stainless, AISI 316, high-temp. mech. props. 0-66601
- steel, stainless, austenitic Ni-Cr type, creep deformed, dislocation multipole obs. 0-107258
- steel, stainless, creep limit, cyclic load component effect at high temps. 0-104231
- steel, stainless, FeCrAlloy, creep-rupture props., 650-800°C 0-97535
- steel, stainless, type 304, viscoplastic model, uniaxial, based on total strain and overstress 0-64387
- steel, stainless type 316, thermally aged, accelerated creep-fatigue crack propag. 0-89326
- steel, steam pipes, 12Cr1MoV, selection of allowable stresses based on minimum possible strength data 0-104237
- steel, SUS 304 and S15C, creep deform. under reversed cyclic stresses (Japanese) 0-81114
- steel E1736, creep, viscosity, resist. to inelastic deform. 0-89309
- steels, austenitic stainless, stress corrosion cracking, correl. between electrochem. and mech. parameters 0-97613
- stiff constitutive models, numerical integration, inelastic deform. 0-96208
- stress clock function in viscoelasticity 0-99941
- structural elements, creep limit eval. by method of charact. parameters 0-79174
- strut creep buckling, damage effects 0-102976
- superplastic alloys, cavity growth 0-93627
- textolite glass, stress relax. calc. from creep curves 0-71709
- theory problems for ageing bodies with growing slits and cavities 0-69678
- threshold stress, importance in anal. of creep data 0-64389
- tubes, thick-walled, thermoelastoplastic creep stress anal. 0-58922
- variational principles, generalised, Lagrange multiplier method applied to flow theory (Chinese) 0-79171
- viscoelastic-plastic tube, successive deformation under cyclic, temp. variation 0-92074
- Zircaloy PWR fuel cladding deformation tests under mainly convective cooling conditions 0-57862
- Zircaloy-4, failure strain prediction under non-stationary loading conditions 0-93640
- Ag-Mg (18.5 wt.%), rheological study of crystallographic order on creep (French) 0-97548
- Al, 2618, creep under step stress changes, viscous viscoelastic model 0-81138
- Al alloy, 2618-T61, creep behaviour prediction, physically consistent method 0-66610
- Al alloy, creep crack growth 0-60976
- Al alloy AK4-1, crack growth rate prediction under creep conditions 0-85107
- Al alloy with different props. in tension and compression, creep 0-81129
- Al, plastic deformation thermal activation parameters from creep kinetics and stress relaxation 0-71717
- Al, polycrystalline, movement of 3-fold nodes of boundaries in high temp. creep 0-89317
- Al, polycrystn., HVEM in-situ investigation of creep mechanism 0-104214
- Al, stationary creep in HVEM, cell struct. evolution 0-104242
- Al, superpure, rate-controlling processes 0-85009
- Al, threshold stress, importance in anal. of creep data 0-64389
- Al-Al₂O₃, dispersion hardened, creep (Czech) 0-108463
- Al-Ca-Zn (5.5 wt.%) superplastic sheet alloy, mechanical properties, superplastic forming behaviour 0-60920
- Al-Cu-Mg, type RM55, high strength, creep behaviour, effect rel. to anodic coatings, SEM study 0-97542
- Al-Cu-Mn, long term strength and creep 0-60925
- Al-Mg(Zn-Mg), long term strength and creep 0-60925
- Al-Si alloy, eutectic, quasiisotropic 0-79165
- Al-Si-N-O system, comps. corresponding to β' -sialon phase reaction hot-pressing 0-84891
- Al-Zn-Mg superplastic alloy, cavity growth under creep conditions 0-60940
- AlCu-NiCo (5 at.%), θ' hardened, creep mechanism 0-85013
- Al₂O₃, vacuum condensate, struct. and mech. props., second phase effect (Russian) 0-71705
- Al₂O₃-SiO₂ refractory, creep, viscosity, resist. to inelastic deform. 0-89309
- Ar, solid, diffusion processes in plastic deform. (Russian) 0-92591
- Be-Si-Al-O-N ceramic, phase assemblages, relationships with props. 0-60848
- Cd, creep, low-temp., thermal heating and quantum mechanisms 0-79868
- Ce-Si-Al-O-N ceramic, phase assemblages, relationships with props. 0-60848
- Co base alloy, creep-fatigue interaction in aligned eutectic and solid soln. 0-108554
- Cr₂C₃ fibre reinforced Ni-based composite, oxidation and creep, Y additions effect 0-66685
- Cu alloys, low-cycle fatigue and cyclic creep, -196-20°C 0-100913
- Cu, creep damage and cavity growth, assessment using density meas. 0-104217
- Cu, high purity, creep cavitation topology, high temperature region (Czech) 0-65138
- Cu, OFHC effect of cold drawing under combined stress 0-60912
- Cu, plastic deformation thermal activation parameters from creep kinetics and stress relaxation 0-71717
- Cu, polycryst., creep and fracture behaviour, effects of prestrain and O 0-97544
- Cu-Ni (10 at.%), creep, substruct. and internal stresses (Russian) 0-97527
- Cu-Zn, interface sliding of FCC and BCC boundaries 0-104240

creep continued

- Cu-Zn, rheological study of crystallographic order on creep (French) 0-97548
- Fe, creep at 77, 295K, formation of five struct. 0-60926
- Fe, polycryst., influence of α - γ transform. on creep (Russian) 0-89289
- Fe, pure, cathodic charging effect on creep and tensile deformation 0-76320
- Fe-Mo(4.1 wt.%), steady state creep at high temps. 0-89316
- Fe₂-Al, solid soln., rheological study of crystallographic order on creep (French) 0-97548
- Fe₈₀Ni₁₀P₁₀B₁₀, amorphous, steady-state creep rate, cryst. effect 0-81102
- Ge, heavily doped, microcreep breakdown 0-97549
- Ge, plastically deformed under high temp. creep conditions, elec. props. 0-92915
- Ge, stationary creep depend. on deform. stabilisation of material struct. (Russian) 0-100300
- HfC, pressing regime influence on high-temp. creep (Russian) 0-100852
- Mg alloy, dil., dynamic recrystn. during creep, dislocation substruct., quartz comparison 0-109142
- Mg-Si-Al-O-N ceramic, phase assemblages, relationships with props. 0-60848
- MgO, single cryst., tensile creep, stress induced dislocation structs. 0-96539
- MgO.1.1 Al₂O₃ spinel, high temp. deform., cryst. orientation effect 0-107263
- Mo alloy TSM-6, creep rate in vacuum, grain size effect 0-108514
- Mo, creep deformed single crystals, subboundary struct. obs., dislocation sets 0-103348
- Mo wire, struct. and high-temp. creep, dopant elements influence 0-66603
- Mo₂C₃, pressing regime influence on high-temp. creep (Russian) 0-100852
- Nb, creep rate in vacuum, grain size effect 0-108514
- Nb:He, mech. props. and microstruct. 0-85003
- Nb-W-Mo-Zr (5, 2.1, 0.92 wt.%), creep resist., high temp. ageing in vacuum 0-71716
- Nb-W-Zr-Ta (90, 4.5, 3.5, 2 wt.%) creep and creep limit in super vac. at 1100°C, heat treatment effect 0-81133
- NbC, pressing regime influence on high-temp. creep (Russian) 0-100852
- NbC, vacuum condensate, struct. and mech. props., second phase effect (Russian) 0-71705
- Nb₂Sn, hot isostatically pressed, plastic deform. 0-108510
- Ni alloy KhN56VMKYu, creep, viscosity, resist. to inelastic deform. 0-89309
- Ni, creep, substruct. and internal stresses (Russian) 0-97527
- Ni, creep at 77, 295K, formation of five struct. 0-60926
- Ni, creep rates, stress depend., and activation energies, constant stress tests, comparison with dislocation creep theory 0-71708
- Ni, oxidation, high temp., effect of C on cavity form., SEM study 0-97638
- Ni, structural changes, creep mechanism, multiple dislocation cross slip (Russian) 0-59476
- Ni, variation in dislocation density during creep, determ. by X-ray diffraction analysis (Russian) 0-76302
- Ni-Al, rheological study of crystallographic order on creep (French) 0-97548
- Ni-base wrought superalloy, creep and stress rupture behaviour in air and vacuum 0-60918
- Ni-Cr, low short-term creep resist. at 700°C 0-76313
- Ni-Cr superalloy, interactions between creep and low cycle fatigue (Chinese) 0-66572
- Ni-Cr-Al-Ta-C, eutectic composite, microstructure, fatigue props. 0-85038
- Ni-Cr-Co-Ti-Mo-W-Al (14, 9.8, 5, 4, 3.9, 3 wt.%), low cycle fatigue, prior heat treatment effect 0-60962
- Ni-Cr-Ta-Ti-Si, EP557 precipitation hardening alloy, mech. props., heat treatment effect 0-60877
- NiO, stress relief and plastic flow in temp. range 1323-1473K 0-89302
- Pb creep, low-temp., thermal heating and quantum mechanisms, supercond. transition effects 0-79868
- Pb-Bi(Ni), creep, low-temp., thermal heating and quantum mechanisms, supercond. transition effects 0-79868
- Pb-Sn(Bi)(Ni), strength loss in supercond. transition, nonmag. and paramag. impurities influence (Russian) 0-70875
- Pt alloys, influence of Rh, Au, Mo, W, Zr, Hf alloying elements on creep activation energy at high temp. (Chinese) 0-66573
- Si, heavily doped, microcreep breakdown 0-97549
- Si, stationary creep depend. on deform. stabilisation of material struct. (Russian) 0-100300
- TaC, pressing regime influence on high-temp. creep (Russian) 0-100852
- Ti alloy, crack initiation on planar shear bands, H₂ assisted 0-71749
- Ti alloy, heat resistance, thermal stability, stress-rupture strength, and creep 0-81194
- Ti-Al-Cr-Mo-V(Fe), low cycle fatigue in repeated tension 0-76348
- Ti-Al-Mo-Zr, type VT-9, creep eqns. rel. to extension and compression props. 0-100875
- Ti-Al-V (6.4 wt.%), cyclic temp. creep, transition effect 0-97539
- Ti-Al-Zr-Mo-Si (6, 5, 0.5, 0.25 wt.%), β -processed, fatigue props., hold time effect 0-60961
- TiB₂, TiC, vacuum condensate, struct. and mech. props., second phase effect (Russian) 0-71705
- V₂Si single cryst., creep deform. 0-71695
- V₂Si, supercond. structure and properties (German) 0-93631
- Va, creep rate in vacuum, grain size effect 0-108514
- W single cryst., high temp. creep and dislocation struct. 0-71715
- W wire, struct. and high-temp. creep, dopant elements influence 0-66603
- Y-Si-Al-O-N ceramic, phase assemblages, relationships with props. 0-60848
- Zn alloys, rolled and press. die-cast, creep and deformation behaviour (German) 0-66611
- Zn, creep, low-temp., thermal heating and quantum mechanisms 0-79868
- Zn-Al (22 wt.%), eutectoid, low stress and superplastic creep behaviour 0-81120
- α -Zr-Sn(Mo), creep charact., influence of Sn and Mo (Czech) 0-81119
- ZrO₂, ZrB₂, vacuum condensate, struct. and mech. props., second phase effect (Russian) 0-71705

creep fracture

- ageing at high temp., effect on creep props. SEM 0-97516
- alloys, creep cavitation control, intergranular precipitates role 0-66664
- alloys, high temperature, creep failure criteria 0-65150

creep fracture continued

correlation and extrapolation methods; creep rupture data analysis 0-58975
 crack propag. by cavitation near crack tips 0-107364
 deformation and fracture of materials in creep range, effects of nonlinear stress-strain rate relations 0-58938
 failure mechanism involving grain boundary sliding and brittle crack extension 0-97557
 geofracture creep, meas. using interference of light with equal optical paths (*Chinese*) 0-82113
 high temperature plant design methods, reference stresses and bounding theorems 0-58937
 intergranular fracture during power-law creep under multiaxial stresses 0-107365
 life prediction modelling for creep damage 0-59574
 metals, engineering, multi-axial creep characts. 0-64398
 metals under creep loading, cumulative damage, engineering approach 0-58935
 micromechanisms of crack extension, conf., Cambridge, England (March 1980) 0-105421
 Nimonic 80A, creep rupture under non-proportional loading 0-108518
 parametric data handling method development, creep and creep-rupture data 0-58934
 plate weakened by equal-armed cross-shaped crack, plastic strain and fracture 0-69740
 PMMA, plastic deform. by crazing (*Japanese*) 0-93619
 polycrystalline body, rupture curves, isochronous, in plane stress 0-69739
 polyethylene, environmental stress cracking correl. with liq. sorption for low-swelling liqs. 0-81165
 remaining creep life for components under stress at elevated temperatures 0-59566
 steel, 12Cr1MoV, thermal fatigue and creep effect in fracture 0-104297
 steel, austenitic Cr-Ni, intergranular damage parameters in creep (*Czech*) 0-89342
 steel, austenitic heat resisting, creep rupture props., effect of grain- and grain boundary-strengths 0-97573
 steel, austenitic stainless type 304, time-depend. fatigue, mechanistic model 0-100925
 steel, austenitic stainless, creep crack growth, environmental sensitivity 0-85030
 steel, Cr-Mo, effect of Mo on high-temp. props. 0-85005
 steel, Cr-Mo (10-14, 2-6 wt.%), heat-resist., creep-rupture strengths 0-104271
 steel, Cr-Mo (2.25, 1 wt.%), creep and high temp. low-cycle fatigue tests 0-85061
 steel, Cr-Mo weld metal, trace element embrittlement suppression by creep strength effects 0-66656
 steel, Cr-Mo-V, stress rupture, notch influence, temp. depend. (*German*) 0-60945
 steel, creep rate mismatch interaction in stress relief cracking 0-97578
 steel, high Mn austenitic, creep rupture, p addition and two-step soln. heat treatment effects (*Korean*) 0-93646
 steel, stainless, FeCrAlloy, creep-rupture props., 650-800°C 0-97535
 steel, stainless 304, crack propagation under fatigue-creep conditions and fractography (*Japanese*) 0-104267
 steel, stainless casts, creep ductility, Auger spectroscopy study 0-60917
 superimposed non-stationary stress and temp. loading, creep rupture 0-66630
 Zircaloy-4, creep rupture at superimposed non-stationary stress and temp. loading 0-66630
 Ag, microcrack propagation and plastic strain 0-81187
 Al alloys, types 1100 and 5454, long-time rupture tests 0-76434
 Al, microcrack propagation and plastic strain 0-81187
 B₂O₃-SiO₂-Na₂O phase-separated glass, creep fracture morphology 0-81151
 Cu and alloys, intergranular damage parameters in creep (*Czech*) 0-89342
 Cu, commercial, pure, vacuum environment end grain size effects on creep rupture props. at elevated temps. (*Japanese*) 0-81162
 Cu, dimple spacing on intergranular creep fracture surfaces with slip band spacing 0-76345
 Cu, formation of H₂O vapour bubbles, effect as intergranular creep fracture 0-71722
 Cu, microcrack propagation and plastic strain 0-81187
 Cu, polycryst., creep and fracture behaviour, effects of prestrain and O 0-97544
 KCl, microcrack propagation and plastic strain 0-81187
 LiF, microcrack propagation and plastic strain 0-81187
 NaCl, microcrack propagation and plastic strain 0-81187
 Ni, microcrack propagation and plastic strain 0-81187
 Ni-base superalloys, powder metallurgical, creep-rupture at intermediate temps. 0-97568
 Ni-Cr alloys, creep crack growth, environmental sensitivity 0-85030
 Pt alloys, influence of Rh, Au, Mo, W, Zr, Hf alloying elements on creep activation energy at high temp. (*Chinese*) 0-66573
 Si-Al-O-N ceramic, grain boundary desegregation and intergranular cohesion 0-100872
 Ti-Al-V-Sn (5.5, 5.5, 2 wt%), crack growth, slow, H-induced 0-104272
 Zn, microcrack propagation and plastic strain 0-81187
 α -Zr-Sn(Mo), creep characts., influence of Sn and Mo (*Czech*) 0-81119

creep-recovery see recovery-creep

creep testing

apparatus for creep and long-term strength tests, with cyclic temp. var. 0-61046
 constant tensile stress with elastic compressibility, creep test (*Bulgarian*) 0-108680
 device for producing constant stress 0-71835
 extensometric method, for inside nuclear reactor channels 0-100998
 fatigue and creep testing installation for wide range of strain rates 0-76447
 LMFBR structure materials in liquid Na, capsule type creep tester (*Japanese*) 0-108653
 nuclear steam generator tubes testing and evaluation, using CIS/DASIO system (*Czech*) 0-63301
 plastic deformation, creep test method (*Hungarian*) 0-97660
 plastics testing, automation 0-76443
 steel, stainless, type 304, viscoplastic behaviour, strain rate sensitivity, creep, relaxation, tensile tests 0-66727
 strain range partitioning method for anal. of material creep fatigue behaviour 0-104361

crestatrons see travelling-wave-tubes

crimping

collagen with planar crimp, tensile deformation 0-84235
 filaments, slender, with planar crimp, tensile deformation 0-84235
 textiles with planar crimp, tensile deformation 0-84235

critical constants, thermal see critical points

critical current density (superconductivity)

Al₅-type compounds, review of superconducting props. and structure 0-70909
 composite superconductor, propagation velocity expressions 0-60155
 granular films, percolation threshold and crit. current, theory 0-88706
 molybdenum chalcogenides, multicomponent, physical props. 0-84577
 pair-breaking current density, temp. depend. (*Russian*) 0-70887
 percolating two-dimens. square lattice, normal-state cond. and crit. current density, crit. exponents 0-84541
 proximity effect weak links, steady-state and RF props. 0-84563
 two-band superconductors, external mag. field depend. (*Russian*) 0-88707
 type II superconductors, order parameter change near H_{c2}, influence of transport current 0-75690
 type II wires, general crit. state model in two dimens. and zero applied field, uniqueness theorem 0-93062
 Cu-Nb₃Sn multifilamentary tapes, in situ formed, crit. current density anisotropy 0-84576
 Cu-V₃Ge, supercond. in situ composites, stress effects on crit. props. 0-65757
 (Mo_{0.4}Ru_{0.4})₈₀Si₁₀B₁₀, amorphous supercond. matrix, flux pinning by MoRu precip. 0-65756
 Nb₃Si₂B₁₀, amorphous alloys obtained by liq. quenching, superconductivity 0-75670
 Nb, critical current density, deviation from critical state model 0-84578
 Nb, single crystals, fluxoid pinning by small nitride precip. 0-70913
 Nb-Si-(V)(Zr)(Mo)(Ta)(W)(C)(B)(Ge), ductile amorphous, superconductivity 0-60131
 Nb-Ti-Zr ternary system, high-field supercond. 0-97045
 Nb₃(Al,Ge) and Nb₃(Al,Si), liq. quenched, supercond. props. 0-84580
 Nb₃Sn bronze process, flux pinning scaling law depend. on strain 0-75696
 Nb₃Sn, flux density gradient determ. by Faraday effect 0-107969
 Nb₃Sn microfilamentary superconducting composite, critical currents, fracture props. 0-107970
 Nb₃Sn monofilamentary composite conductors, tensile stress influence on critical current 0-97046
 Nb₃Sn, monofilaments, radiation-enhanced diffusion growth, crit. current density 0-65758
 Nb₃Sn, multifilamentary superconductor preparation by 'in situ' and cold powder methods, review 0-93522
 Pb foil, crit. current density, pinning force density, shadow electron microscopy obs. 0-88696
 PbMo₃S₈ wire, powder processed, crit. current density and field 0-80466
 V-(Ti), supercond., rotating discs, hysteresis losses and mag. phenomena 0-75695
 V₃Si, neutron irradiat., grain boundary pinning, field-depend. change of crit. current density 0-65759
 W₇₀Si₃₀B₁₀, amorphous alloys obtained by liq. quenching, superconductivity 0-75670

critical currents

see also critical current density (superconductivity); flux creep; flux flow; flux pinning
 granular microbridges, fluctuations and crit. current determ. 0-84562
 granular superconductors, coherence transition, structural disorder effects 0-88657
 granular superconductors, percolation theory, crit. props. 0-84575
 Josephson FET, hybrid, feasibility 0-80451
 Josephson junctions, inelastic tunnelling, pair-quasiparticle interference current 0-84566
 point contacts, three-dimens. assembly, crit. currents and penetration depth 0-84560
 superconducting film, critical electric fields and currents in two dimensional systems (*Russian*) 0-107972
 superconducting film, inhomogeneous, pair-breaking current, Ginzburg-Landau theory 0-97029
 superconductor, long thin-film, paradox in crossover of mech. causing hysteresis 0-107971
 superconductors, critical parameters during field emission of electrons 0-88682
 superconductors, type I, surface impedance, anomalous skin effect, surface supercond. regime (*Russian*) 0-80459
 tokamak induction heating coils, 50 kA prototype superconducting cable, critical current 0-106196
 transport current effects on superconducting thin-walled cylinder in mag. field (*Russian*) 0-100573
 tunnel junction, paramag. impurities effect on Josephson current (*Russian*) 0-70903
 type-II superconductor with flux pinning, max. possible loss-free current 0-84579
 Al granular bridges, with different thicknesses and widths, crit. current, temp. depend. 0-88688
³He, superflow, gap functions, critical currents, susceptibilities 0-103531
³He, superfluid B-phase, anisotropic gap distortion due to superflow and depairing crit. current 0-88383
 Nb, film, critical mag. fields and currents, temp. depend. (*Russian*) 0-103798
 Nb film, struct. and electrophys. props. at 4.2K 0-80436
 Nb, granulated film, critical current temp. depend. (*Russian*) 0-103803
 Nb microbridges, vertical type, fabrication and DC characts. 0-103788
 Nb/In composite superconductor, transport props. 0-88658
 Nb-Cu-Nb junctions, Josephson effect meas., critical current, temp. depend. 0-93041
 Nb-NbO₂-Pb Josephson junctions with high current densities, critical current 0-100552
 Nb-Ti, pinning curves, high field J_c and scaling behaviour 0-93064
 Nb-Ti-Ta, pinning curves, high field J_c and scaling behaviour 0-93064
 Nb-Zr, crit. current, flow-flow resist. depend., allowance for superheating (*Russian*) 0-93061
 Nb₃/Sn-Cu composites, in situ processed, supercond. props. 0-75698
 Nb₃Al, A-15 struct., converted from cold worked BCC struct., crit. currents 0-75697
 Nb₃Ge, bridge contact, Josephson effect 0-70906
 NbN granular films, supercond., crit. props. 0-88661
 NbN granular microbridges, Josephson effects 0-84556

critical currents continued

- NbN, granulated film, critical current temp. depend. (*Russian*) 0-103803
 Nb₃Sn, composite superconducting wire, critical current-bend strain relationships 0-93063
 Nb₃Sn, supercond. composite, residual stress state, crit. currents 0-80468
 NbTi/In composite superconductor, transport props. 0-88658
 Pb film, monocryst., heteroepitaxial growth, struct. defects, and elec. props. (*Russian*) 0-84403
 Pb-Cd-Pb, supercond. - normal-metal - supercond. junction, crit. currents 0-107965
 Pb-Cd-Pb junctions, pair pot., mag. field depend., crit. currents meas. 0-84555
 Sn film, limitation in microwave stimulation of supercond., crit. current meas. (*Russian*) 0-88695
 Sn, long film, crit. currents in microwave EM fields 0-70898
 Ti-Nb-Si, amorphous alloy, supercond. props. and crystn. behaviour, TEM and DTA study (*Japanese*) 0-84536
 Ti-Nb-Zr-Ta, superconducting props. comp. depend., stress effects and precipitation behaviour, X-ray scatt. 0-93059
 TiN, low-energy ion-stimulated deposited, supercond. props. 0-88664
 V₃Si, supercond. structure and properties (*German*) 0-93631

critical field, superconducting *see superconducting critical field***critical fluctuations**

- see also fluctuations in superconductors*
 chemical model, Schlogli's, critical fluctuations near non-equilib. critical point 0-85150
 classical fluids, laminar flow critical phenomena in mean field approx. 0-59001
 dielectric fluid, Debye absorption at crit. liq.-vapour transition 0-100322
 dimethylammonium copper tetrachloride, crit. slowing down and anomalous relax. near Curie temp. 0-71053
 elastic phase transitions, order parameter and mode softening 0-75325
 fluid, Stokes-Einstein diffusion coeff. determ. 0-90783
 light generation at impurity atoms in ferroelectrics and LC, fluctuation effects (*Russian*) 0-91767
 limit cycle fluctuations near bifurcation point, Fokker Planck, Langevin eqn. calcs. 0-77709
 2,6-lutidine-water critical mixture, spinodal decomposition, Rayleigh scatt. 0-70416
 MBBA, proton spin-lattice relax. in crit. regime 0-80631
 micellar solutions, crit. behaviour 0-105601
 nematic liquid crystals, orientation fluctuations in high mag. field, quenching, birefringence effects 0-64892
 nematic-isotropic phase transition character, molecular bending fluctuations critical growth (*Russian*) 0-79919
 NLC inelastic light scattering by order parameter biaxial and longitudinal fluctuations (*Russian*) 0-75160
 non equilibrium systems, stochastic model, master eqns. (*Chinese*) 0-68126
 PAA, nonlinear soft mode at Rayleigh-Benard instability, neutron cond. spectrosc. obs. 0-79266
 PAA-di, nematic liquid crystal, NMR data, appl. of Landau-de Gennes theory 0-64893
 4-n-pentylbenzenethio-4'-n-alkoxybenzoates, birefr., crit. behaviour near smectic A-C transition 0-80745
 polyacrylamide gel and single chain in soln., laser light scatt. obs. near phase transitions 0-93808
 polystyrene networks swollen in cyclohexane, swelling equil. and light scatt. at theta conditions 0-107036
 random ferromagnets, Ginzburg criterion, critical fluctuations 0-71032
 roughness fluctuation in layer between two phases 0-85147
 zero-point fluctuations in direct-action electrodynamics 0-57528
 CoF₂, antiferromag. crit. props., neutron scatt. obs. 0-88749
 Co_{1-x}Zn_xF₂, antiferromag. crit. props., neutron scatt. obs. 0-88749
 Fe-Ni (33-38 at.%), low-angle neutron diffr., anomalous crit. scatt. (*Russian*) 0-60193
 Fe-Ni Invar alloys of crit. conc., mag. props., flow theory methods (*Russian*) 0-65894
³He fluid-superfluid transition phase diagram, thermodynamic stability, fluctuations (*Russian*) 0-80023
³He, spin flow density fluctuations, superfluidity (*Russian*) 0-65328
 KD₂PO₄, polarisation fluctuations, wavevector depend. 0-71295
 K₂FeO₄, crit. slowing down of spin fluctuations, Mossbauer spectra and relax. theory 0-65882
 KMn_{1-x}Ni_xF₂, antiferromag. crit. props., neutron scatt. obs. 0-88749
 Mn_{1.88}Cr_{0.12}Sb, antiferromag.-ferrimag. transition, neutron crit. scatt. and crossover effect 0-71023
 Ni-Mn (17-27 at.%), low-angle neutron diffr., anomalous crit. scatt. (*Russian*) 0-60193
 Rb₂CoF₄, critical fluctuations near Neel temp., US attenuation study 0-108013

critical mixtures

- aniline-cyclohexane, hypersound velocity, absorption temp. depend. (*Russian*) 0-75303
 benzonitrile-isooctane mixture, dielec. const. near consolute point, temp. and freq. depend. meas. 0-71292
 binary mixtures, near critical, metastable, phase separation and nucleation and drop growth, rate eqns. 0-65232
 binary mixtures, sound propag., mode coupling theory, validity breakdown 0-65159
 cyclohexane-aniline critical mixture, shear and critical fluctuations, instantaneous mapping of velocity gradients 0-79420
 isobutyric acid-water, US and hypersonic study 0-88268
 2,6-lutidine-water, anomalous supercooling near critical point 0-70384
 2,6-lutidine-water critical mixture, spinodal decomposition, Rayleigh scatt. 0-70416
 2,6-lutidine-water thick films, interferometric obs. of crit. behaviour 0-93266
 nitrobenzene and n-heptane, US and hypersonic acoustical props. 0-65170
 nitrobenzol-n-hexane, hypersound velocity, absorption temp. depend. (*Russian*) 0-75303
 phase separation kinetics, percolation effects 0-65233
 3-phenylpropanol-hexane, nonlinear dielectric effect, critical exponent 0-93227
 polystyrene-diethyl malonate, strongly opalescent critical isochore, scattered light intensity 0-71436
 propionitrile-hydrocarbon systems, critical solns., Kerr electrooptical Kerr effect meas. 0-100645

critical mixtures continued

- Ne-H₂ liq. mixtures, phase equilib. effects, thermodynamic perturb. theory (*Russian*) 0-92663
 SO₂-tetrachloromethane, solns., near critical point, ultrasound absorpt. obs. 0-65160

critical opalescence

- density fluctuations and critical opalescence in a gravitational field 0-66137
 polystyrene-diethyl malonate, strongly opalescent critical isochore, scattered light intensity 0-71436
 propionitrile-hydrocarbon systems, critical solns., Kerr electrooptical Kerr effect meas. 0-100645
 BaTiO₃, periodic domain struct. and opalescence at tetragonal to orthorhombic transition 0-66131

critical path analysis

- see also systems analysis*
 fission reactors, BWR, Enrico Fermi-2, system turnover, test and startup program 0-63338
 nuclear power plant, Virgil C., startup, conduct of operations, organisation and personnel 0-63340

critical path scheduling *see critical path analysis***critical phenomena**

- see also critical fluctuations; critical mixtures; magnetic transitions; phase equilibrium; phase transformations; renormalisation*
e-expansion technique, appl. to integral evaluation in critical dynamics 0-57187
 acetone, heat emission in crit. region, press. and heating surface temp. effects (*Russian*) 0-69634
 antiferromagnetic Fermi liquid, critical phenomena, neutron scatt., Neel point (*Russian*) 0-71077
 Bose systems, critical exponents, η and z to second order in $\epsilon=2-d$ at $T=0$ 0-77696
 compressible dilute Ising systems, critical behaviour 0-108017
 correction-to-scaling amplitudes on coexistence curve 0-57234
 critical exponents to order ϵ^3 for ϕ^4 models of critical phenomena in 6- ϵ dimensions 0-86547
 diffusion in the one-dimensional Ising model 0-77719
 dynamic critical exponents, inequalities 0-79662
 dynamical systems, critical transition to stochasticity 0-73265
 elastically coupled systems at marginal dimensionalities, crit. dynamics and stability 0-101769
 Fisher-Domb cluster model, pseudospinodals in first order transitions 0-57213
 ionic mixtures phase separation, critical parameters 0-77279
 Ising model, duality relations and replica method 0-77722
 Ising model, two-dimensional kinetic, dynamic correlation functions, real space renormalisation group approach 0-62589
 lattice animals, critical dimension 0-57208
 local equilibrium theory for steady states with heat flow near critical points 0-105599
 long-range site percolation, crossover from mean-field to crit. behaviour 0-82728
 low temperature critical phenomena, review 0-73297
 magnets, randomly distributed point defects, critical exponents, renormalisation theory 0-60346
 metastable states close to instability, phase transition parameter eqn. of motion 0-57230
 nonuniform external force field effects 0-73296
 percolation, universal critical amplitude ratios 0-101765
 percolation theory, review 0-98868
 Potts model, critical dynamics 0-101766
 Potts model, dilute random bond, critical curve 0-80518
 q-state Potts model multicritical point, singularities and scaling functions 0-57215
 quadratic lattice, correlated percolation 0-68149
 quantum spin model, appl. of projective renormalisation group 0-84607
 recurrence technique for confluent singularity analysis of power series 0-73277
 relaxational dynamics, renormalisation group anal., scaling fields and variables 0-105602
 relaxational dynamics in systems with many-component order-parameter, scaling fields and variables 0-101772
 second-order expansion of indices in the generalised Villain model 0-90801
 self-consistent screening approximation, long range interactions and the critical exponent η 0-101761
 spherical limit of coupled time depend. n-vector models, relaxation phenomena 0-86238
 spherical model with layered impurities, critical behaviour 0-93124
 spherical random field model, low dimensionality for transition 0-68150
 structural phase transformations, static critical behaviour 0-92640
 structural phase transitions, crit. dynamics and quasi-elastic scatt. 0-92641
 structure of the BBGKY hierarchy near phase transition 0-88013
 superconductors, critical slowing down, dynamic-exponents, Ginzburg-Landau theory 0-103783
 surface percolation processes, scaling theory and real space renormalisation group 0-86223
 thermodynamic properties, crit. behaviour, correction-to-scaling amplitudes, crit. exponents 0-57233
 two-spin correlation function, dipolar crossover 0-80516
 Universe, spontaneous prod. of cosmological fluctuations 0-94902
 XY model, $S=1/2$, in transverse field in two and three dimensions, zero temp. renormalisation group method 0-108025
 Gd, thermal conductivity critical behaviour near Curie point 0-75540
 Ni-H system, phase diagram and thermodynamic properties calcs. 0-66480
 Pd-H system, phase diagram and thermodynamic properties calcs. 0-66480
 SF₆, critical isochore, dielectric const. critical anomaly upper bound 0-84679
 SrTiO₃, critical elastic compliance, acoustic resonance meas. 0-65118
- critical points**
see also boiling point; melting point
 alloys, binary, elec. resist. near crit. point 0-96847
 antiferroelectrics, multicritical points in structural phase transitions, renormalisation 0-75982
 antiferromagnets, disordered spin flop, bicritical behaviour, critical experiments 0-65899
 binary fluid, molecular dynamics 0-88014

critical points continued

bimodal decomposition near crit. point, scaling hypothesis 0-79912
 boson systems, dynamical plane rotator model, dynamical correl. functions in mol. field approx. 0-88758
 charged hard sphere dense classical fluid, equation of state and crit. point 0-64849
 Coulomb gas 2-D, interaction potential, screening length, critical temp. 0-62571
 crystal lattice stability and deform. phase transitions under press. 0-59624
 degenerate semiconductors, heterogeneous state, first-order phase transition, Ginzburg-Landau method analogue 0-70372
 β,β' -dichloroethyl ether-isooctane, critical indices, allowance for light double scatt. (Russian) 0-60624
 ethane, gas, liq., and crit., electron mobility, density and temp. effects 0-92246
 ethylene, high density behaviour, extrapolated PpT surfaces and critical density 0-87834
 FCC Blume-Capel model, Monte Carlo study 0-103453
 ferromagnetic metals, resist. anisotropy, crit. behaviour and temp. depend. 0-96858
 fluid near critical point, spin-lattice relaxation time 0-80630
 fluids, dynamical scaling and crit. point universality 0-88297
 Fokker-Planck eqn. expansion, weak diffusion, critical point 0-57228
 fractal lattices, crit. phenomena 0-105587
 heat flux at flow boiling of N₂ in horizontal tube up to critical press. (German) 0-99921
 Ising model, spin-one, bilinear and biquadratic interactions, phase diagram 0-75772
 Ising model correlation quadratic identities, discrete-time Toda eqn. 0-105582
 Ising model strips, scaling theory, wall effects in crit. systems 0-80539
 light scattering near phase transition pts. in pure and defect containing crystals, review 0-93361
 liquid crystal, binary mixtures, phase transition, entropy, relation to smectic plane tilt angle 0-65203
 liquid-gas critical point, quantum mechanical effects, theory 0-103452
 liquid-vapour transition, non-Ising-like effects, eqn. of state, renormalisation group calc. 0-84286
 liquids, simple, corresponding states correl. and triple point solid vol. 0-92649
 2-6-lutidine-water, anomalous supercooling near critical point 0-70384
 metals and alloys, critical temperatures determination, elec. resist. method, IMASH-5S-69 installation 0-71827
 metamagnet, two-dimens., tricritical spinodal decomp., Monte Carlo study 0-93117
 methane triple point sealed cells using stainless steel envelope 0-95099
 micellar solutions, crit. behaviour 0-105601
 nitrobenzene/n-hexane (n-heptane), critical exponent β , phase coexistence curve anal., viscosity coeff. meas. 0-100327
 nonpolar fluid, excessive electrons near crit. points 0-92836
 nucleation theory and first order phase transition dynamics near critical points 0-84284
 ordering alloys, nonlinear critical relaxation of the Ginzburg Landau field coupled to a conserved density 0-90803
 oriented bond percolation, threshold probability and correlation length exponent calc. 0-68146
 pentane-benzene solution, vapour-liquid equilibrium study, vaporisation critical state (Russian) 0-79931
 phase diagram with first-order transition close to second-order transition 0-59625
 3-phenylpropanol-hexane, nonlinear dielectric effect, critical exponent 0-93227
 polymer chains, θ -domain, tricrit. props. in poor solvent 0-103450
 Potts lattice gas, crit. and tricrit. exponents using Kadanoff transform. 0-101768
 Potts model, three-state, effects of symmetry-breaking perturbations 0-105579
 Potts model, two dimensional three state, critical exponents 0-105583
 propylene, high density behaviour, extrapolated PpT surfaces and critical density 0-87834
 PTFE, γ -ray effects on 19 and 30°C phase transitions, Fourier transform IR spectroscopy 0-103387
 quasielastic light scattering near phase transitions 0-93362
 rarefied shock wave existence near thermodynamic critical point of a substance (Russian) 0-88263
 relaxational dynamics in systems with many-component order-parameter, scaling fields and variables 0-101772
 single component system near critical point, equilibrium achievement delay 0-90799
 spin systems, dynamical plane rotator model, dynamical correl. functions in mol. field approx. 0-88758
 square lattice, critical dynamics and potential moving approx., renormalisation group approach 0-57209
 star-triangle transformation, phase boundary for planar site-bond percolation problems 0-95042
 superheated binary solns., flashing kinetics, nucleation and critical bubble 0-92035
 surface polariton scattering by order, parameter fluctuations near crit. pts. 0-92835
 surface tension temp. dependence from triple point to critical point (German) 0-100376
 transition metal dichalcogenides, trigonal-prismatically coordinated layers, phenomenological theory of CDW state 0-80200
 two dimensional system, melting and condensation theory 0-57231
 universality class of asymmetric fluid critical points 0-57098
 US velocity in crit. region water 0-59582
 water, triple point as temp. fixed point 0-59626
 Ar, liq., critical exponent, γ , X-ray scatt. 0-92660
 Ar, liquid, depolarized Rayleigh scatt. at triple point, mol. dynamics simulation 0-60617
 Ar triple point sealed cells using stainless steel envelope 0-95099
 BaTiO₃/Co, tricritical point, X-ray diff. meas. 0-71341
 CO₂, high density behaviour, extrapolated PpT surfaces and critical density 0-87834
 CO₂, near critical point Rayleigh and Raman scatt., Fermi diad 0-80765
 CsMnCl₂·2H₂O, mag. phase diagram near bicritical point 0-71021
³He-⁴He tricritical mixture, universality under press. 0-103533
 K, liq., density, at near critical temp. 0-103407
 KAgI₃, superionic phase transition, dynamical and crit. pt. props. 0-107535

critical points continued

KBr, molten, solutions of K, conc. fluctuations, small angle neutron scatt. study 0-92448
 N₂, high density behaviour, extrapolated PpT surfaces and critical density 0-87834
 NH₄AgI₃, superionic phase transition, dynamical and crit. pt. props. 0-107535
 Nb-V system, H₂ absorpt. 0-59808
 Pb₃(P₂V₁₀O₄₀)₂, ferroelastic phase transition, DTA, dilatometric and Brillouin scatt. study 0-70398
 RBAgI₃, superionic phase transition, dynamical and crit. pt. props. 0-107535
 S-benzene systems, liq.-liq. phase separation 0-96658
 Xe, fluid, near crit. point, correl. range and Rayleigh linewidth 0-93352
 Xe, high density behaviour, extrapolated PpT surfaces and critical density 0-87834
critical temperature, superconducting see *superconducting transition temperature*
CRO see *cathode-ray oscilloscopes*
crocidolite see *asbestos*
crops see *farming*
cross-sections (nuclear) see *nuclear reactions and scattering*
crosstalk
 optical waveguides, multichannel, cross-talk noise anal. 0-91922
 polarisation-independent optical switch using weighted directional coupler 0-58798
 LiTaO₃ monolithic pyroelectric array, IR detectors 0-77857
 LiTaO₃/CCD hybrid focal plane, IR imaging and detection, crosstalk 0-77856
crowdions
 KBr, defect accumulation under electron irradi. at 4K 0-107233
 Ni₃Fe, disaccommodation meas. after low temp. electron and neutron irradi. 0-88832
 Pt, ion irradi. damage, temp. depend., electron microscopy obs. of defect kinetics 0-107339
CRT see *cathode-ray tubes*
crushing
 kaolin grog particles, shape and density 0-97450
 metal tubes, crushed between rigid plates, large deformation compression 0-66579
 powder, dry ball milling, breakage parameters variation with ball and powder loading 0-80999
 CaHPO₄, powder and granules with starch mucilage binder, surface topography variation under compression 0-80998
crushing strength see *compressive strength*
cryogenic pumps see *cryopumping*
cryogenics
 see also *cryopumping; cryoscopy; cryostats; cryotrons; Joule-Thomson effect; low-temperature production; low-temperature techniques; magnetic cooling; refrigeration*
 acoustic microscopy, scanning 0-79080
 alkanes, light, solubility in liq. N₂, IR spectroscopy obs. 0-59654
 alloy, cryogenic, creep, review 0-104222
 alloys, FCC base hard materials, low temp. toughness (Japanese) 0-100916
 calorimetric determ. of dielectric loss factors at 1 kHz and 4.2K 0-98921
 displacement transducer optimisation 0-86323
 double-stage cryorefrigerator, for cooling to 10K on a 4-circle diffractometer 0-98919
 electric lines, physical parameters anal. 0-82768
 ethane, flow continuity in arterial capillary systems in cryogenic heat pipes 0-64536
 film- and transition-boiling heat transfer to cryogenic fluids 0-92026
 fusion, toroidal field superconducting coil cryogenic stability and field anal., design parameter 0-106200
 fusion reactor, high current density superconducting coils, cryostability 0-106201
 fusion reactor, MFTF, cryogenic system 0-106163
 fusion reactor, MFTF, mag. cryostability 0-106198
 fusion reactor, press. induced flow cooling, highly stable superconducting mag. systems 0-106192
 fusion reactor, TMX, config., liq. N₂ supply and operation of vacuum system 0-95448
 fusion reactors, Large Coil Program, pool boiling mag. quench press. calc. 0-106199
 fusion reactors, Large Coil Program, Westinghouse coil cooldown and warmup 0-106193
 fusion reactors, Large Coil Test Facility, liq. He cooling system 0-102321
 fusion reactors, TMX, installation and operation of cryoliner in vacuum system 0-95449
 high-pressure apparatus, appl. of sintered diamond tipped, opposed piston apparatus 0-86322
 high-pressure cell for gas-mixture expts. 0-86334
 IR detector balanced common module coolers 0-95142
 IR detector-preamplifier for cryogenic spectrometer, optimization 0-95164
 laser beam waveguide propag. in frozen gaseous layers at 4.2K 0-64168
 laser fusion cryogenic target characterisation by wavefront shearing interferometer 0-74008
 laser fusion targets, cryogenic technology 0-68939
 low and ultralow temp. cryogenic coolers for space missions 0-77790
 magnetic field, weak, meas. of absolute intensity, use of RF biased SQUID 0-82794
 magnetic flux-free environment creation 0-101797
 metal-insulator pairs, frictional heating at cryogenic temps., rel. to supercond. magnet technology 0-66671
 Michelson interferometer, cryogenic, rocket-borne, for EXCEDE II expt. 0-95133
 NMR meas. at ultra-low tapes, S/N ratio, appl. to thermometry 0-73400
 nonisothermal pumping lines, conductance calcs. (Spanish) 0-82776
 nuclear magnetism, review (Japanese) 0-86806
 orbiting IR detector cooling by multimission solid cryogen cooler 0-86423
 rocket-borne cryogenically cooled field-widened interferometer for the 2 to 8 μ m spectral region 0-95163
 solar cooling, Rankine-cycle systems, selection of working fluids 0-104515

cryogenics continued

- solid insulating materials, dielectric properties at cryogenic temps. 0-90867
 spacecraft, cryogenic instrumentation 0-86319
 Speer carbon resistors as pressure gauges 0-95108
 SQUID appl. to nuclear gyros and magnetometers, high stability and sensitivity 0-98949
 steel, cryogenic, creep, review 0-104222
 superconducting lens, electron microscope appl. 0-86530
 superconducting temperature sensor, NbTi monofilamentary wire in current sharing state 0-57288
 superconductivity, computerised measurement instrumentation 0-98920
 temperature controller, use of ICs 0-90856
 vapour pressure meas. gauge of ^3He for use up to 0.3K 0-68207
 Fe-Ni-Al-(Cu) (12, 0.5, 0.5 to 3 wt.%), Cu addition strengthening at 77K, mech. props. 0-60875
 Fe-Ni-Ti-(Cu) (12, 0.25, 2 wt.%), Cu addition strengthening at 77K, mech. props. 0-60875
 Fe-Ni-V-(Cu) (12, 2, 2 wt.%), Cu addition strengthening at 77K, mech. props. 0-60875
 Fe-Ni-(Cu) (12, 0.5 to 3 wt.%), Cu addition strengthening at 77K, mech. props. 0-60875
 He cycles, minimal losses due to thermodynamic irreversibility 0-86320

cryopumping

- bakeable ion-cryopumped ultrahigh vac. system 0-77802
 cryosorption pumping of He by charcoal, cryopump design for fusion reactor 0-105654
 fusion reactor, neutral beam inject cryogenic pumping panel chevron baffles, black coating materials, selection 0-95456
 fusion reactor, STARFIRE project, T handling and vacuum requirements 0-106187
 fusion reactor vacuum pumping using compound cryopumps, performance 0-95452
 Helios Laser Facility, cryopump high-vac. system for 25000-l. target chamber, design and operational characts. 0-77801
 microbalance, vac. type, cryopump 0-77803
 neutral beam source, cryopumping and mag. shielding, fabrication and operating cost 0-106229
 neutral injector modular cryopumping system 0-105656
 quartz crystal production, cryopump appls. 0-90861
 H^+ , energetic beam direct cryosorption pumping 0-105655

cryoscopes see *cryoscopy*

cryoscopy

No entries

cryosorption see *sorption*

cryostats

- EPR study 0-86321
 flowthrough opt. cryostat for operation with superconducting solenoid, for magnetoopt. investigations 0-105651
 heat capacity cryostat for small specimens in 1.5 to 10K range 0-68204
 magneto-optical, optical meas. at 0.4K, cooling by evacuation of ^3He vapour by an absorpt. pump optical meas. at 0.4K, cooling 0-73369
 SQUID magnetometer with temp. control, spontaneous magnetisation and mag. susceptibility meas. 0-68221
 SQUID magnetometers, geophysical dewar systems design 0-101462
 student demonstration He cryostat for superfluidity and superconductivity obs. (Polish) 0-86059
 superconducting lens system for 500 kV electron microscope 0-68321
 TEM liquid He cooled environmental cell 0-68323
 throat, with coaxial extension elements, heat exchange efficiency 0-77769
 twin-chamber flexible vacuum connection 0-73368
 vacuumless, optical investigations of semiconductors 0-73370
 X-irradiation of solids at low temps. 0-86321
 *He cryostat design, superconductive tunnelling study (Spanish) 0-73347
 Nb-Ti (50%), supercond., cryostat design for magnetisation study (Spanish) 0-75673

cryotrons

No entries

crystal atomic structure

- see also *crystal atomic structure of alloys; crystal atomic structure of elements; crystal atomic structure of inorganic compounds; crystal atomic structure of organic compounds; electron diffraction crystallography; lattice constants; neutron diffraction crystallography; space groups; superlattices; X-ray crystallography*
 Bragg reflections, ratio of integral intensities, determ. struct. perfection of single crystals 0-87987
 coordination numbers in solids, Pearson diagrams 0-107103
 dislocation core, symmetry of dynamical electron microdiffraction patterns 0-100140
 KKR method, structure constants, electronic struct. 0-80152
 Patterson method, multiple solutions for low symm. systems (Chinese) 0-87986
 periodic structure homometric set, search algorithm 0-75118
 polyhedral cavity field tensors 0-100182
 quasi-symmetry and double point groups C_4 and D_3 0-92472
 Racah coefficients for point groups, chemical space groups and mag. group symmetry 0-57214
 solids, evaluation of finite strain eqns. of state using lattice models 0-96620
 structural fragment, automatic construction, taking account of attainable chem. bond lengths 0-92419
 substitutionally disordered binary systems, existency domain 0-88068
 triclinic lattices, planewise summation method 0-107069
 triplet phase invariants, formula for acentric case 0-84115
 two-phase cryst. structures, orientational electron microdiff. anal. with aid of OMEGA program 0-103218

crystal atomic structure of alloys

- brass-like alloy phases, binding and cryst. struct., valence arguments 0-88081
 $\gamma\text{-Cu}_2\text{Zn}_8$, high pressure effect on brass struct. 0-107108
 dimensional analysis, bonding information from valency effects appearing as artefacts 0-96471
 disordered alloys, interatomic distances, coord. numbers, and mean relative displacements, EXAFS anal. 0-89087
 intermetallic phases, struct. description (German) 0-88090
 nonstoichiometric compounds, physicochem. props. depend. on short-range order struct. 0-100227
 rare earth alloys, RBe_{13} , XPS, resist. and susceptibility study 0-71565

crystal atomic structure of alloys continued

- rare earth cobaltides, RCO_3 type, hydride phase synthesis, thermal stability and struct. 0-59438
 rare earth intermetallic cpds., R_3Os , cryst. struct. 0-96475
 rare earth phase structure, dimens. anal. 0-96470
 rare earth-transition metal-aluminum intermetallics, RT_6Al_6 , $\text{T}=\text{Cr, Mn, Fe, Cu}$, cryst. struct. 0-107110
 X-ray diffraction powder patterns, standard, for 87 substances 0-64839
 $\gamma\text{-Ag}_2\text{Zn}_8$, high pressure effect on brass struct. 0-107108
 Al-Cu (1.9 at.%), solute fluctuations, EXAFS study 0-79949
 Al-Cu (3.97 wt.%), containing Guinier-Preston zones, high resolution lattice images 0-107114
 Al-Cu (4.3 wt.%), containing Guinier-Preston zones, high resolution lattice images 0-107115
 Al-Fe (49 at.%) quenched alloy, neutron diffuse scatt., diffuse ω phase obs. 0-84141
 Al-Fe-X-Si (X=transition metal), struct. and comp. by electron microscopy 0-88093
 Al-Mg-Li alloy, metastable S'-phase, struct. (Russian) 0-103291
 $\text{Al}_3\text{B}_2\text{Co}_2$, metal distrib., X-ray diff. study 0-75204
 $\text{Al}_4(\text{Ni, Co})_3$ ternary phase in Al-Ni-Co system, cryst. struct., vacancy controlled phase (Chinese) 0-70164
 Au_3Mn , ordered phase formation, electron diff. and microscopy study 0-107418
 Au_4Mn , heat treated, short-range order, diffuse X-ray diff. study (German) 0-88092
 $\text{Au}_{15}\text{Ni}_{15}$, vapour quenched amorphous alloy, atomic arrangements 0-100173
 BaCu, X-ray cryst. struct. determ. 0-92478
 Ba_2Ga , cryst. struct. (French) 0-79749
 BaPdSn_3 , prep. and crystal structure (German) 0-84138
 CaZn_3 , struct. with mixed BaLi_4 and CeCu_2 -like ordering 0-107106
 Ce-In, phase equilibrium and cryst. struct. 0-66483
 Ce-Ti, phase equilibrium and cryst. struct. 0-66483
 CeBe_3 , intermediate valence state, XPS, resist. and susceptibility study 0-71565
 CeNi_8Si_4 , X-ray cryst. struct. determ. 0-88089
 $\text{Ce}_2\text{Se}_3\text{Si}_4$, X-ray cryst. struct. determ. 0-92480
 Co-Al alloy, multilayer martensite phases, illustration of polytype structures 0-84932
 Co-mischmetall system, phase relations, microstruct., mag. props. 0-104118
 CoMnP , cryst. mag. struct., neutron diff. study (French) 0-59439
 Co_2P , struct. comparison with Co_3Si , PbCl_2 , and SbSi (French) 0-84155
 Co_3Si , struct. comparison with Co_2P , PbCl_2 , and SbSi (French) 0-84155
 Cr_2Os , σ phases, ordering, X-ray cryst. struct. determ. 0-107107
 Cr_2Ru , σ phases, ordering, X-ray cryst. struct. determ. 0-107107
 Cu-Al, disordered alloys, interatomic distances, coord. numbers, and mean relative displacements, EXAFS anal. 0-89087
 $\alpha\text{-Cu-Al}$ (9.13, 13.56, 14.76, wt.%) short-range ordered, characterisation of locally ordered regions 0-79747
 Cu-Al alloy, ordered, superlattice fringe images, computer simulation 0-103296
 Cu-Ni-Sn (10, 6 wt.%), spinodal decomposition, X-ray and electron diff. study 0-81063
 $\text{DyCo}_2\text{-DyAl}_3$ system, mag. and structural studies 0-108006
 EuPt_3 compounds, partial valence change, ^{151}Eu Mossbauer and magnetisation obs. 0-70167
 Fe cast with spheroidal graphite, fine cryst. struct. on tempering (Russian) 0-96476
 Fe-Al alloy, ordered, superlattice fringe images, computer simulation 0-103296
 Fe-Co, ferromagnetic micropowder, cryst. struct., coercivity, remanence, saturation 0-65967
 Fe-Ni (25 to 50%), FCC, meteorites and thermodynamic equilib., Mossbauer and X-ray diff. study 0-88087
 $\text{Fe}_{1-x}\text{Mn}_x\text{Al}$, ordering of Fe atoms, X-ray diff. meas. and mid gamma reson. anal. (Russian) 0-96469
 FePC molten and amorphous alloys, struct. factors 0-79674
 FeTi-D(H), γ -phase, neutron and electron diff. 0-84156
 FeTiD, ($0 \leq x \leq 1.9$), neutron diff. struct. anal. 0-75447
 $\text{Gd}_{1-x}\text{Dy}_x\text{Ni}$, FeB-CrB type stacking variations, cryst. struct. 0-64952
 $\text{GdMn}_2\text{-GdAl}$, system, mag. and structural studies 0-108006
 GdRh_2H_2 , GdRu_2H_2 , struct. and mag. props., Mossbauer and magnetisation meas. 0-71271
 $\text{Gd}_{1-x}\text{Y}_x\text{Ni}$, FeB-CrB type stacking variations, cryst. struct. 0-64952
 $\text{HoCo}_5\text{-Mn}_2(\text{Fe}_2)(\text{Ni}_2)(\text{Cu}_2)$, cryst. struct. and mag. props. 0-75800
 In-Sb, cryst. struct. after appl. of high press., supercond. transition temp. 0-70169
 Ir alloys, Ir_2R ($\text{R}=\text{Pr, Nd, Sm, Gd, Tb, Dy, Ho, Er, Tm, Lu, Y}$), cryst. struct. 0-96473
 K_3Ga_{13} , X-ray cryst. struct. determ. 0-92479
 $\text{La}(\text{Co}_{1-x}\text{Ni}_x)_3$, distrib. of Co and Ni atoms, neutron diff. obs. (Russian) 0-64954
 $\text{La}_2\text{Co}_2\text{Sn}_7$, prep. and crystal structure (German) 0-84138
 7LiAl , cryst. growth, Stockbarger method, struct. and homogeneity 0-89137
 Mg-Nd-Zn dilute alloy, metallography and precip. kinetics 0-71655
 MgNi_2 , four-layer, Friauf-Laves phases, stacking variants 0-96468
 MgZn_2 , two-layer, Friauf-Laves phases, stacking variants 0-96468
 $\text{MgZn}_2\text{-MgAg}_2$ system, Friauf-Laves phases, stacking variants 0-96468
 Mn-Ga system, X-ray struct. investigation, solubility (Chinese) 0-88084
 $\gamma\text{-MnAu}$, antiferromag., phase diagram, X-ray diff. and Young's modulus meas. 0-71024
 MnSi-Si system, striations and cryst. struct. of matrix 0-103292
 Mo-Al-Ge, X-ray phase and microstructural anal. 0-93536
 Mo-Sn-Se system, supercond. crit. temp. and cryst. struct. (Russian) 0-107947
 Nb-H system, phase diagram and transforms., struct. obs. of various phases 0-104125
 Os intermetallic cpds., R_3Os ($\text{R}=\text{La, Pr, Nd, Gd, Tb, Dy, Ho, Er, Y}$), cryst. struct. 0-96474
 $\text{PdD}_{0.73}$, (1, 1/2, 0)-superlattice reflection splitting near 50K, neutron diff. studies 0-70168
 $\text{Pd}_2\text{Mn}_2\text{V}_{1-x}\text{Sn}$, Heusler alloy, structural disorder, Mossbauer study 0-80650
 PdPb_3 , crystal structure (German) 0-96472
 Pd_3Pb_3 , r. cryst. struct., X-ray study 0-103293
 $\text{Pd}_{30}\text{Si}_{20}$, vapour quenched amorphous alloy, atomic arrangements 0-100173
 PrRh_3 , Sny, crystallography X-ray powder diff. study 0-100217

crystal atomic structure of alloys continued

PtBi₂H₃, cryst. struct. (*German*) 0-107113
PtPb_{0.7}Bi_{1.3}, crystal structure (*German*) 0-84139
Sn₂PbBi₃, cryst. struct. (*German*) 0-107113
Re₂Si₃, X-ray cryst. struct. determ., microhardness rel. to Re content 0-84142
SeGa₄, atomic structure determ. using single crystal method (*Ukrainian*) 0-70165
SeH₂, electron diffr. investigation 0-107112
Sn-Ni electrodeposited eutectic alloy, cryst. struct., X-ray, electron diffr. anal. 0-79748
SrCu, X-ray cryst. struct. determ. 0-92478
SrPdSn₃, prep. and crystal structure (*German*) 0-84138
Ta-H system, phase diagram and transforms., struct. obs. of various phases 0-104125
TbRh₂Sn₃, crystallography X-ray powder diffr. study 0-100217
ThC_{0.063}, cryst. struct. and lattice dynamics 0-88088
Ti alloys, Fermi sphere limiting electronic capacitance, Brillouin zones (*Russian*) 0-92808
 α -Ti alloys VT1 and VT5, struct. and phys. props., H₂ effect 0-108576
Ti-Mo (20 at.%), incommensurate struct., stacking soliton 0-107109
Ti₆C₅, X-ray order struct. determ. 0-103295
U₁₀Co₅Si₃₃, crystal struct., dimensions, space group and coord. (*Russian*) 0-88085
U₆Co₁₀Si₁₉, X-ray cryst. struct. determ. 0-107111
V₁₆Ni₁₅ solid solution, quenched, ordered structure (*Russian*) 0-88086
Y₆Co₃, hydride phase synthesis, thermal stability and struct. 0-59438
Y(Co_{1-x}Ni_x)₅, distrib. of Co and Ni atoms, neutron diffr. obs. (*Russian*) 0-64954
Y₂O₃, cryst. struct. 0-96475
Y₂Ru(Pd), cryst. struct. 0-96474
ZrCr₂D₃, site occupation modes and cryst. struct., neutron diffr. study 0-59440
ZrCu, constitutional and struct. studies, by mag. susceptibility, metallography and X-ray diffr. 0-70166
Zr(Fe_{1-x}Al_x)₂, Curie temp., magnetisation, and cryst. struct., conc. depend. 0-75730
ZrV₂D₂(H₂), site occupation modes and cryst. struct., neutron diffr. study 0-59440
ZrX₂ alloy, Laves phases with MgZn₂, MgCu₂ structs., X-ray emission Zr spectra (*Russian*) 0-71517

crystal atomic structure of elements

diamond, dislocation growth degree of supersaturation determ. 0-88145
graphitised viscose fibre, fluorination, change in struct. 0-88039
Al, low-order Fourier coeff. of pot., modified thickness fringe method 0-75130
Al, proton irradiation, Al atomic displacement position study 0-103401
Am, phase transformation at high press., X-ray diffr. obs. 0-107422
Ar, solid, vacancy conc., X-ray study at const. vol. 0-64991
Au, atomic struct. of large angle [001] twist boundary, determ. by computer modelling and X-ray diffr. study 0-70162
Co, ferromagnetic micropowder, cryst. struct., coercivity, remanence, saturation 0-65967
Cs, crystal struct., van der Waals and repulsive interaction 0-84137
Cu, cementation, on Fe, deposit struct., reaction rates, SEM 0-104421
Cu, interatomic distances, coord. numbers, and mean relative displacements, EXAFS anal. 0-89087
Fe, ferromagnetic micropowder, cryst. struct., coercivity, remanence, saturation 0-65967
Fe, high-purity single crystals, X-ray topography and double-crystal diffraction 0-92534
K, crystal struct., van der Waals and repulsive interaction 0-84137
Kr, solid, vacancy conc., X-ray study at const. vol. 0-64991
Li, anharmonicity and low temp. phase struct., neutron diffr. study 0-107105
Li₂N₂, solid struct., and thermodynamic props. (*Russian*) 0-88083
 γ -O₂, mol.-dynamic study of struct., dynamics 0-96467
Rb, crystal struct., van der Waals and repulsive interaction 0-84137
 α -S₈, attachment energy as habit controlling factor 0-59421
Se, habit variation of crystals of the C₃,2-C₃,2 space group 0-107090
Se, trigonal and amorphous, electronic struct. and nonempirical calc. of struct. props. 0-59866
Si, (110) oriented, electron optical conditions for struct. image form. 0-75131
Ta BCC lattice, strain ordering in interstitial solutions 0-107420
Te, habit variation of crystals of the C₃,2-C₃,2 space group 0-107090
Te, Kikuchi patterns, of non-centrosymmetrical crystal 0-100202
Te, trigonal and amorphous, electronic struct. and nonempirical calc. of struct. props. 0-59866
Th, atomic struct. by field ion microscopy 0-59437
V, small particles, crystal structure, magnetic and superconducting props. 0-97121
W, atom, high resolution phase contrast electron microscopy imaging 0-103224

crystal atomic structure of inorganic compounds

β -Al₂O₃-Cu₂O, phys. and chem. props., use in determ. of thermodynamics of Cu-Sn alloys 0-107502
alkali chloride:Mn²⁺, spin Hamiltonian parameters, binding energies for cation vacancy complexes 0-96461
alkali germanate crystals and glasses, struct. and stability, IR spectra meas. 0-64911
alkali ionic conductors with sheet structures, ion mobility and influences 0-107522
boracite, single cryst. prep. and phys. props. 0-100763
calcite, luminescence spectral anal. of polycyclic aromatic hydrocarbon impurities 0-71483
cemented carbides, physical and chem. nature 0-76265
CO₂ ferrite, crystal structure, X-ray absorpt. spectra, chemical shifts 0-88118
conference, Crystal XII, Canberra, Australia (Jan.-Feb. 1980) 0-62388
corundum, attachment energy as habit controlling factor 0-59422
divalent Sr, Ba, Ca, Zn, Cd iodates, complex salts, phase transitions, cryst. struct. (*Chinese*) 0-70171
ferroactive thin films, physical prop. optimisation 0-80698
graphite fluorides, (CF₂)_n and (C₂F_n)_n, prep., struct., discharge characts., electrode props. 0-89502
graphite salts, C₈MF₆, (M=Os,Ir,As), struct. and elec. props. 0-70183
graphite-Rb, intercalation cpd., superlattice struct., electron diffr. study 0-75214

crystal atomic structure of inorganic compounds continued

group IIIa dihydrides, structs. and stabilities 0-107146
ice, Ih, elastic diffuse neutron scattering due to D-D correlation functions 0-96493
layer structures, intercalation with N₂H₄, charge density waves or artefacts 0-100221
metal silicides, fabrication technique and characterisation, review (*Japanese*) 0-60779
4,4'-methylenebis(1,3,5-trimethyl-4-imidazolin-2-one), cryst. and mol. struct. 0-107201
Na₂Zn[SiO₄], X-ray cryst. struct. determ., thermal vibration anisotropy allowance 0-92510
oxides, ABO₄ type, high press. phase transforms. and struct. types, cryst. chem. aspects 0-79940
oxides, RCu₃Mn₄O₁₂, R=La to Lu, Y, synthesis and mag. props. 0-75717
penninite, one-layer triclinic chlorite, neutron diffraction study 0-84144
perovskite compound combination, Mossbauer spectroscopy study (*Russian*) 0-80666
perovskites, A²⁺B³⁺U_{1/2}⁶⁺Y_{1/6}O₆, struct., cation vacancies, X-ray diffr. study (*German*) 0-107147
pyrophosphatase, inorganic, of yeast, cryst. growth, derivatives formation, heavy atoms positions 0-108842
quartz, crystal structure rearrangement due to neutron irradiation 0-64981
quartz, habit variation of crystals of the C₃,2-C₃,2 space group 0-107090
quartz, low, cell parameter variations between 94 and 298K 0-96497
 α -quartz, Renninger effect, forbidden X-ray reflections 0-64980
rare earth arsenides and bismuthides, chemical bonding and structural features, coherent alloying theory 0-107101
rare earth chalcobismuthites, RBiTe₃, prep., elec. props., and crystallographic date 0-59981
rare earth cpds., RM₂Sb₂ (R=La, Ce, Pr, Nd, Sm, Eu; M=Fe, Ru, Os), prep. and cryst. struct. 0-100211
rare earth double orthophosphates with alkali metals, spectroscopic obs., struct. and chem. nature 0-100674
rare earth germanates, R₂O₃-GeO₂ system cpds., physicochem. characts. 0-97469
rare earth oxides, perovskite-like, synthesis, struct., elec. props. 0-65554
rare earth oxyorthotitanates, crystallochem. classification 0-107142
rare earth oxyphosphates, IR and Raman spectra, vibr. assignments, cryst. struct. characts. 0-97258
rare earth substituted lead apatites, Pb_{10-2x}R_x(PO₄)₆Z₂, M=Na or K and Z=F or Cl, cryst. struct. and IR spectra 0-107167
rare earth titanium oxides, RTiO₃ type, bulk mag. and struct. props., ferrimag. order 0-107993
rustumite, crystal structure, X-ray anal. 0-79766
rustumite, crystal structure determ. by X-ray diffr. method 0-70182
ruthenates, ACu₃Ru₄O₁₂, A=Na,Ca,Sr,Cd,La,Pr,Nd, synthesis, cryst. struct., mag. and elec. props. (*French*) 0-107151
silicate HV high-resolution electron microscopy 0-70096
titanomagnetites, temp. depend. cation distrib., mag. prop. obs. 0-85647
transition metal chalcogenide layer compounds, convergent beam electron microscopy obs. 0-108689
wustites, X-ray diffr. and electron microscopy study (*French*) 0-64973
X-ray diffraction powder patterns, standard, for 87 substances 0-64839
[Cl₂PNPCL]₂[PCl₄], X-ray cryst. struct. determ. 0-88095
Ag complex, dioxane perchlorate, cryst. struct., phase transitions, X-ray study 0-59646
Ag orthophosphates and sulphates, anhydrous, struct. relationships w.r.t. fast ion cond. 0-107188
AgBi(Cr₂O₇), cryst. struct. determ. by X-ray and neutron diffr. (*French*) 0-92492
AgGa₂In_{1-x}Se₂, X-ray diffr. cryst. data 0-84147
AgI, EXAFS investigation of struct. and ion motion 0-108302
 α -AgI, ionic motions nature, mol. dynamics calcs. 0-107533
 α -AgI, structural and dynamical behaviour 0-107544
AgIO₃, chem. prep. and cryst. struct. 0-75207
Ag₂Na_{2-x}Te_{2-x}VO₁₄, (x=0.4), mixed tellurate, cryst. chem. and elec. cond. (*French*) 0-107150
Ag₂O-Al₂O₃-MgO-Na₂O, β'' -alumina, structure, X-ray determ. 0-107148
Ag₃SbR, superionic conductor, phase transition, struct. 0-107144
 β -Ag₃Si, anharmonic thermal vibr. of cations 0-65214
Ag₂SO₃N₂, X-ray cryst. struct. determ. 0-88101
Ag₂TeO₃, chem. prep. and cryst. struct. (*French*) 0-79755
Ag₂TiTe(S)(Se), cryst. struct. 0-107156
Al oxides and hydroxides, electro-erosional prep. (*Russian*) 0-81297
Al₂C₃-Be₂C-SiC system, phase analysis and TEM struct. obs. 0-108420
Al(IO₃)₃.8H₂O, crystal structure, thermal vibr. parameters, X-ray study 0-64979
 β -Al_{1-x}γ-Mg_{0.16}, X-ray diffuse scatt. obs. of struct. 0-107186
 β -Al₂O₃, long-period structs., electron microscope obs. 0-92501
 β -Al₂O₃-(Na,K)₂O, equil. distrib. of ionic species 0-107511
 β -Al₂O₃-Ag₂O, stoichiometric A phase, X-ray diffuse scatt. obs., sublattice phase transition 0-64944
 β -Al₂O₃-Ag₂O(D₂O)(NH₄⁺) 0-107512
 β'' -Al₂O₃-Ag₂O(K₂O)(Li₂O)(Na₂O)(Rb₂O), single cryst. Raman scatt., cond. mechanism and cryst. struct. 0-66209
 β -Al₂O₃-D₂O, anhydrous, prep. and struct. of DA1₁O₁₇ 0-107187
 β'' -Al₂O₃-H₂O⁺(Na₂O), struct. basis for superionic cond. 0-107498
 β -Al₂O₃-K₂O-MgO, cryst. struct., nonstoichiometry, ion-ion correlations 0-88129
 β -Al₂O₃-NH₄⁺, single cryst. characts. and AC cond. obs. 0-107514
 β -Al₂O₃-Na₂O, cond. plane struct. and energetics 0-92715
Al₂O₃-NiCr composite, plasma sputtering of electroheating coatings, elec. props. (*Russian*) 0-108350
 γ -AlOOH and γ -AlOOD, IR and Raman spectra obs., struct. and D₂¹⁷ space group anal. 0-89000
 γ -AlOOH, boehmite, proton pair obs. from NMR absorpt. spectra 0-75866
AlOOH, diaspor, cryst. struct. refinement and electron density distrib. 0-79758
AsF₅-graphite intercalation compound nature 0-103308
AsI₃, X-ray cryst. struct. refinement 0-64961
AsSbO₄, X-ray cryst. struct. determ. 0-107127
As₂Se₃, monoclinic, chem. bonds rel. to electronic and vibr. states 0-64951
B₁₃C₂, chem. bonding nature, static deform. densities and pictorial representation 0-92489
BaBe(PO₄)F, bafephite, cryst. struct. determ. using P1 automatic diffractometer 0-107179

crystal atomic structure of inorganic compounds continued

- BaCrO₃, 27 layer polytype, struct. determ. 0-107162
 BaFe₂O₁₉, ferrite, DC cond., dielec. props., lattice const. 0-80272
 β-BaFe₂S₄, cryst. struct., X-ray diff. obs. 0-84153
 Ba₂+₂Fe₂S₄, electron diff. study, orientation anomaly 0-107152
 Ba(IO₃)₂, cryst. struct. determ. by X-ray diffractometry 0-107139
 BaIn₂Se₄, cryst. struct. (*German*) 0-79760
 Ba(NO₃)₂·H₂O, pyroelec., room temp. cryst. struct. 0-96491
 Ba₂NaNbO₅, X-ray powder diffraction data determ. (*Chinese*) 0-70170
 BaNd₂(MoO₄)₄, X-ray cryst. struct. determ. 0-88128
 Ba₂Ni₂F₁₀, cryst. struct. and antiferromag. props. 0-107153
 Ba₂Rf₇, (R=Dy, Ho, Er, Tm, Yb, Lu, Y), superstructure phases, prep., thermal characterisation and X-ray powder diff. 0-96494
 Ba₂Sb₃, cryst. struct., selenoantimonate (III) anions (*German*) 0-103305
 BaTa₂O₆, structural study X-ray diff., IR absorpt. and Raman spectra (*French*) 0-107173
 BaTiO₃, mean square atomic displacement temp. depend., sublattice vibration anharmonicity 0-79890
 Ba₃WFe₂O₉ and Ba₃WFe₂O_{8.42}, crystallographic and mag. props., comparative study 0-103303
 Ba₃WFe₂O₉-Ba₃WCo₂O_{9-x} system, struct. evolution (*French*) 0-88110
 Ba₃W₂O₉, X-ray powder struct., face shared octahedra with W(VI) 0-64974
 Ba₂YbF₇, single crystals, electron diff. cryst. struct. anal. (*French*) 0-92507
 BaZnGeO₄, revised cryst. data 0-100210
 Be-Si-N system polytypes, struct. obs. using TEM 0-107192
 Be₃N₂-BeSiN₂ system, crystallography and phase relationships, TEM and electron diff. study 0-92502
 BiFeO₃, ferroelec., antiferromag., cryst. and mag. struct., neutron diff. study 0-65786
 BiI₃, structure, exciton states and physicochem. characteristics (*Russian*) 0-100435
 Bi₂In₂S₂, X-ray cryst. struct. determ. 0-107126
 Bi₂-xLa_xWO₆, synthesis and crystallography 0-66459
 C₂Br₂Cl₂-x intercalate, crystallographic, elec. mag. props. 0-107184
 C₁₂+PtF₆, struct. and elec. props. 0-70183
 C₂Rb, intercalated graphite, order struct. determ. by neutron scatt. 0-107143
 (Ca,Sr)₂(PO₄)₂Cl, partially substituted chlorapatite, cryst. struct. from X-ray data 0-96478
 Ca dichlorophosphate complexes, cryst. struct. ³⁵Cl NQR obs. 0-108108
 CaCeAl₃O₇, mellite struct., prep. and props. 0-93524
 CaF₂, crystal structure, stability compared with TiO₂ (*Russian*) 0-64945
 Ca₂Ge₂O₁₀, cryst. struct. interpretation by symmetrisation method 0-107180
 CaLaFeO₄, two-dimens. mag. ordered, structural and mag. props. (*French*) 0-70173
 CaLaFeO₄, two-dimens. mag. props. rel. to cryst. struct. 0-75776
 α-CaNa₂P₂O₇·4H₂O, X-ray cryst. struct. determ. 0-64964
 Ca₂Nb₂O₇, monoclinic modification, cryst. struct., X-ray diff. method 0-64955
 Ca₂Ni_{1-x}Fe_xO₄, X-ray struct. anal., determ. of lattice constant and interplanar distances (*French*) 0-96487
 CaS:Nd phosphors, X-ray powder diff. anal. 0-100204
 CaSO₄, body centered matrix basis 0-79765
 Ca₁₀(SiO₄)₃(SO₄)₂(OH,Cl,F)₂, hydroxyllestadite, X-ray cryst. struct. determ. 0-96485
 CaWO₄, body centered matrix basis 0-79765
 Ca₂YFe₂O₁₃, cryst. struct., electron microscopy and X-ray diff. study 0-88116
 Ca₂(NH₄)₂(PO₄)₂·2H₂O, X-ray cryst. struct., PO₄ ion with 3 symmetric H bonds 0-64956
 Ca₂[B₂O₃][C₂H₃O], hilgardite, PMR of water mol. 0-84655
 Ca[Fe(CN)₅(NO)]·4H₂O, X-ray cryst. struct. determ., heavy-atom method 0-92494
 Ca₂(SiO₄)₂(OH)₂, cryst. struct. refinement 0-107181
 CdAs₂, cryst. struct. and verification capacity 0-88126
 Cd₂AsCl₂, X-ray cryst. struct. anal. (*French*) 0-64957
 Cd₃AsCl₃, X-ray cryst. struct. determ. and refinement (*French*) 0-107119
 Cd₂B₂O₅, basal atom coordinates isotropic temp. corrections, X-ray study 0-59449
 CdCl₂ · 2.5H₂O, rel. between cryst. struct. and morphology, PBC theory of Hartman and Perdok (*French*) 0-70148
 Cd₂P₂I₂, X-ray cryst. struct. determ. and refinement (*French*) 0-107120
 CdS(Se)(Te), determ. of wurtzite, zincblende and rocksalt phases 0-100219
 CdTh(MoO₄)₃, X-ray cryst. struct. determ. (*French*) 0-64959
 CdWO₄, X-ray cryst. struct. determ. 0-108410
 CeCo_{2-x}Cu_x, 0 ≤ x ≤ internal oxidation kinetics, oxide struct., X-ray study 0-104329
 CeCrO₃, X-ray cryst. struct. determ. (*French*) 0-92485
 Ce₂Ir₃(₄), cryst. struct. determ. 0-64960
 Co intercalation compound, electron microscopy 0-84164
 Co Na zeolite, -A and -Y type, local coordination of Co(II) ions studied by X-ray absorpt. fine struct. spectroscopy 0-93434
 Co₂(AsO₄)₂, polymorph, closest packing 0-70174
 Co₂(H₂O)₆(F₂), crystal structure (*French*) 0-59441
 Co²⁺Mo⁴⁺O₃, defect spinel struct., elec. and mag. props. 0-70176
 Co₂Zn_{1-x}Fe_xO₄, ferrite, DC cond., dielec. props., lattice const. 0-80272
 Co(urea)₂Cl₂·2H₂O, two-dimens. mag. props., cryst. struct., specific heat 0-75777
 Cr₂Er₂S₁₁, X-ray cryst. struct. determ. and refinement (*French*) 0-103298
 Cr₄H₂(SO₄)₇·24H₂O, X-ray cryst. struct. determ., H bond study 0-92491
 Cr₂Mo_{2-x}O₇ (x≤0.5), solid soln., trivalent Cr, X-ray powder diff. anal. 0-70177
 Cr₃Se₄, struct., elec. and mag. props. 0-107160
 CsAlF₄, single crystal, prep. and struct. (*French*) 0-79762
 CsCdB₃, CsMgBr₃ and CsMgI₃, diatom. linear chain lattices 0-70172
 CsCl structure, evaluation of finite strain eqns. of state using lattice models 0-96620
 CsCrI₃, neutron diff. expts. at 300, 77 and 1.2K 0-107163
 CsGa_{1-x}Fe_xS₂, tetrahedrally coordinated Fe atoms in low spin state, mag. props. and neutron diff. study (*German*) 0-88714
 Cs₂H₂PO₄, ferroelec., X-ray struct. study at room temp. 0-88113
 Cs₂Hf(MoO₄)₃, X-ray cryst. struct. determ. 0-107182
 CsInCl₃, mixed-valence cpd., structural phase transition (*German*) 0-70406
 CsLiSO₄, crystal structures of I and III phases, twins 0-70181

crystal atomic structure of inorganic compounds continued

- CsMnF₄, planar ferromag., cryst. and mag. struct., Jahn-Teller effect 0-75715
 α-CsNd(PO₃)₄, single cryst. struct. and spectral-luminescent props. 0-96490
 CsPbCl₃, nucl. smearing functions, multipole analysis 0-88097
 Cs₂PbCu(NO₂)₆, low-temp. γ-modification, struct., powder neutron diff. study, 160K 0-84151
 Cs₂S₂O₆, piezoelectric, crystal struct. studied by X-ray diff. 0-100208
 CsSn₂I₅, surface props., Auger study, elec. cond. meas., photochem. study 0-66339
 Cs₂Te₃, synthesis and cryst. struct. 0-88115
 CsTi₂NbO₆, layer struct., X-ray and electron diff. study 0-79753
 Cs₂-(Ti_{1-x}Nb_{1+x})O₅, layer compound, cryst. struct., nonstoichiometry 0-64972
 CsTi(SeO₄)₂, Cs₂Ti(SeO₄)₃, and Cs₂Ti(SeO₄)₄, cryst. struct. (*French*) 0-84148
 Cs₂[FeCl₂(H₂O)]₂, X-ray cryst. struct. determ. 0-107129
 Cs₁₂[U(GeW₁₁O₃₉)₂]₁₃₋₁₄H₂O, X-ray cryst. struct. determ. (*French*) 0-107136
 Cu complex, (4,4'-bipy H₂)CuCl₆, with infinite linear chains of dimeric units, struct. and mag. susceptibility 0-96498
 Cu complex, [Cu(1,4,7,10-tetrabenzyl-1,4,7,10-tetraazacyclododecane)Cl]NO₃, cryst. struct. 0-64966
 CuBr, superionic behaviour at high temp., EXAFS study 0-107496
 CuCl, superionic behaviour at high temp., EXAFS study 0-107496
 CuCl₂·2D₂O, cryst. struct., mag. and reson. props. 0-60424
 CuCrS₂, domain struct. and superstructure, TEM obs. 0-79779
 Cu_{0.9}Fe_{2.1}O₄-ZnFe₂O₄, cation distrib., mag. moment, Mossbauer spectra, chem. anal. 0-75210
 CuGa₂In₂-Se₂, X-ray diff. cryst. data 0-84147
 CuI, EXAFS investigation of struct. and ion motion 0-108302
 CuI, ionic motions nature, mol. dynamics calcs., sp. ht. anomaly due to order-disorder transform. 0-107533
 Cu₂In₂Zr_{1-x}S₂ system, struct. and cond. meas. (*French*) 0-88354
 Cu₂NiS₂S₇, X-ray cryst. struct. determ., mag. props. 0-107172
 Cu₂PS₂Br, cryst. struct. at 293 and 473K, thermal parameters, neutron diff. obs. 0-59450
 Cu_{3-x}Te₂, non-stoichiometric phases, electron microscopic and electron diffraction studies 0-64977
 Cu₂U₂Si₃(Se₃)₂, cryst. struct. and magnetic props. (*French*) 0-96496
 D₂O·ClO₄, solid, neutron powder-diff. study 0-107176
 Dy₂Ru₂, Mn₂C₂-type struct., X-ray cryst. struct. determ. 0-96483
 ErCl₃·6H₂O, single cryst., H⁺ coords., NMR 0-97152
 ErP₂O₄, X-ray cryst. struct. determ. 0-96486
 EuB₂O₇, X-ray cryst. struct. determ. 0-107135
 Eu₂IrH₃, prep., cryst. struct., mag. and elec. props. 0-88117
 F_{1-x}O_x, wustite, X-ray struct. anal. (*French*) 0-70175
 Fe complex, nitrile nonacarbonyl, cryst., mol. struct. 0-64967
 Fe complex, nitrile nonacarbonyl cryst., mol. struct. 0-64968
 Fe intercalation compound, electron microscopy 0-84164
 α-FeGa₂S₄, 1T polytype, cryst. struct. refinement (*French*) 0-103304
 Fe_{10.92}K_{1.55}O₁₇, ferrite, cryst. struct., nonstoichiometry, ion-ion correlations 0-88130
 FeLu₂S₄, structural study, X-ray diff., Mossbauer spectroscopy 0-107159
 (Fe_{0.45}Nb_{0.55})O₂, rutile, cation distrib. and mag. ordering (*German*) 0-107116
 Fe_{1-x}O_x, wustite, defect struct. 0-107216
 α-Fe₂O₃, asymmetric line shapes of Mossbauer spectra (*Chinese*) 0-103902
 β-FeOOH, dehydration 0-79767
 β-FeOOH, lattice imaging and pore struct., high resolution electron microscopy obs. 0-103310
 FeSO₃, anhydrous, X-ray cryst. struct. determ. (*French*) 0-92486
 FeSO₃·2¹/₂H₂O, X-ray cryst. struct. determ. 0-88107
 Fe(Sb_{1-x}Te_x)₃ system cpds., prep., cryst. struct., elec. and mag. characteristics 0-108349
 Fe₂SiO₄, fayalite, Czochralski growth under controlled O₂ fugacity conditions 0-84843
 (Fe_{0.2}Ta_{0.5})O₂, rutile, cation distrib. and mag. ordering (*German*) 0-107116
 Fe₂TiO₅, spin glass system, cation distrib. Mossbauer spectra 0-71248
 FeYb₂S₄, structural study, X-ray diff., Mossbauer spectroscopy 0-107159
 Ga-Se system, phase diagram and cryst. struct. of phases (*French*) 0-93544
 GaTe, cryst. struct., TEM and X-ray diff. study 0-79757
 Gd₂SiO₅, atomic positions, high resolution electron microscopy 0-100220
 GeO₂, particles used for optical fibre fabrication, struct. props. 0-89167
 GeS, anisotropic EXAFS, cryst. struct. determ. 0-66323
 HSB₂Cl₆·3H₂O, cryst. struct., cation H₃AsO₄²⁺ (*German*) 0-107133
 HUO₂AsO₄·4H₂O and HUO₂PO₄·4H₂O layered cpds., struct. invests. below antiferroc. transition temps., H bond ordered structs. 0-107416
 HgBi₂S₄, X-ray cryst. struct. determ., rel. with pavonite homologous series 0-92487
 HgCl₂, X-ray cryst. struct. redeterm. and refinement 0-107140
 HgS, habit variation of crystals of the C₃2-C₃2 space group 0-107090
 HoCo₂Ge₂, crystal and magnetic structure obs. 0-64976
 InCuAlO₄, rhombohedral oxides, symmetry group (*French*) 0-84157
 InFe_{1-x}Si_{0.2x}O₄, rhombohedral oxides, symmetry group (*French*) 0-84157
 InMo₂Se₈, X-ray cryst. struct. determ. 0-103299
 InMo₂Se₉, X-ray cryst. struct. determ. 0-103299
 InMo₂Se₉(Te₃), synthesis and struct. 0-92498
 γ-InSe, 3R struct. type refinement 0-64962
 InSeI, X-ray cryst. struct. determ. (*German*) 0-100214
 InTa_{1-x}Nb_xO₄ system, structural and luminescent props. 0-84769
 InTeBr, intermediate phase, cryst. struct. 0-100834
 InTeI, X-ray cryst. struct. determ. (*German*) 0-100214
 KAlF₄, single crystal, prep. and struct. (*French*) 0-79762
 K₂As₂O₁₀, X-ray single-cryst. struct. determ., Patterson method 0-96484
 K₂K₂B₄O₇(OH)₄·8H₂O, synthetic, X-ray cryst. struct. study, H bond geometry 0-92509
 KCoCr₂(VO₄)₃, synthesis and cryst. struct. 0-88114
 KCrO₂, two-dimens. mag. props. rel. to cryst. struct. 0-75776
 KCoCr₂(VO₄)₃, synthesis and cryst. struct. 0-88114
 K₂PO₄, phase transitions study, role of cryst. struct. determ. 0-75197
 β-K₂FeF₇, crystal struct. (*French*) 0-107164
 KF-FeF₃, phase diagram 0-92645
 KH₂PO₄, phase transitions study, role of cryst. struct. determ. 0-75197

crystal atomic structure of inorganic compounds continued

KH_2PO_4 , single crystal neutron diffraction study at high pressure 0-92497
 $\text{KHSO}_4 \cdot \text{KH}_2\text{PO}_4$, cryst. struct. 0-75211
 $\text{K}_2\text{InCl}_5 \cdot \text{H}_2\text{O}$, crystal structure and H-bonding 0-64978
 KMgF_3 , bond energy, equilib. distances and compressibility calcs. 0-70159
 $\text{K}_x(\text{M}_{1-x}\text{Ti}_{1-x})\text{O}_4$, ($\text{M} = \text{Mg}, \text{Zn}, \text{Ni}, \text{Cu}, \text{Fe}^{\text{III}}, \text{Mn}^{\text{III}}$), ($0.7 \leq x \leq 0.9$), new layer struct. (French) 0-84149
 $\text{KMgCr}_2(\text{VO}_4)_3$, synthesis and cryst. struct. 0-88114
 $\text{K}_2\text{Mg}_2\text{LiSi}_2\text{O}_{30}$, cryst. struct., X-ray diffr. and IR spectra (French) 0-107158
 $\text{K}_2\text{Mg}_2\text{M}_2\text{Si}_2\text{O}_{30}$ ($\text{M} = \text{Cu}, \text{Fe}, \text{Zn}, \text{Mg}$), cryst. struct., X-ray diffr. and IR spectra (French) 0-107158
 $\text{K}_2\text{Mo}_2\text{S}_4$, prep. and struct., Mo_2 cluster in Mo_2S_4 unit 0-107168
 $\text{K}_2\text{Mo}_2\text{V}_2\text{O}_{40} \cdot 8\text{H}_2\text{O}$, containing structurally new K-coordinated octamolybdopentavanadate anion, cryst. struct. 0-96479
 $\text{K}_2\text{Na}(\text{Fe}, \text{Cu}, \text{Ni})_{24} \cdot \text{S}_{26}\text{Cl}$, jeffersite, X-ray cryst. struct. determ. 0-92512
 KNaSO_4 , X-ray cryst. struct. determ. 0-64963
 $\text{K}_2\text{Na}(\text{SO}_4)_2$, X-ray cryst. struct. determ. 0-64963
 $\text{K}_2\text{Nb}_{15}\text{O}_{35} \cdot \text{F}_{18.5}$, cryst. struct. determ. (French) 0-96489
 $\text{K}_2\text{Nb}_{15}\text{O}_{35} \cdot \text{F}_{18.5}$, cryst. struct. determ. (French) 0-96489
 KNiCl_3 , disorder as observed by electron diffr. 0-75213
 $\text{KNiCr}_2(\text{VO}_4)_3$, synthesis and cryst. struct. 0-88114
 $\text{KPhl}_2 \cdot 2\text{H}_2\text{O}$, X-ray cryst. struct. determ. 0-64958
 $\text{K}_2\text{Pb}[\text{Co}(\text{NO}_2)_6]$, X-ray cryst. struct. determ. 0-88106
 K_2SO_4 , anhydrous, struct. relationships w.r.t. fast ion cond. 0-107188
 $\text{K}_2\text{Se}(\text{OH})_2\text{Si}_2\text{O}_{12}$, crystal struct., X-ray diffr. study 0-79763
 K_2SeBr_6 , rotational phase transitions, cryst. struct., X-ray diffr. study 0-70400
 K_2TeCl_6 , cryst. data from Guinier powder diagrams (German) 0-79751
 $\text{K}_2\text{Te}^{10}\text{O}_{12}$, mixed tellurate, cryst. chem. and elec. cond. (French) 0-107150
 $\text{K}_{1-x}(\text{Ti}_{1-x}\text{M}_{1+x})\text{O}_5$, $\text{M} = \text{Nb}, \text{Ta}$, layer compound, cryst. struct., nonstoichiometry 0-64972
 KTi_2SbO_6 , X-ray cryst. struct. determ. (French) 0-107178
 KTi_2TaO_6 , chemically twinned rutile struct., X-ray study 0-107149
 $\text{K}_2\text{Ba}_2\text{Ti}_2\text{Fe}_2\text{O}_{10}(\text{SO}_4)_2 \cdot 5\text{H}_2\text{O}$, X-ray cryst. struct. determ. 0-92483
 $\text{K}_2\text{Ti}(\text{SeO}_4)_2$, $\text{K}_2\text{Ti}(\text{SeO}_4)_3$, and $\text{K}_2\text{Ti}(\text{SeO}_4)_4$, cryst. struct. (French) 0-84148
 $\text{K}_2(\text{V}_2\text{Mo}_6)\text{VO}_{10} \cdot 13\text{H}_2\text{O}$, X-ray cryst. struct., electron spin resonance spectrum 0-88096
 $\text{K}_2\text{Zn}_2\text{Be}_2(\text{SiO}_4)(\text{Si}_2\text{O}_7)$, cryst. struct. determ. 0-88121
 $\text{K}_2(\text{ZnCl}_4)$, modulated struct. in ferroelec. phase, X-ray obs. 0-64970
 $\text{K}[(\text{OH})_{0.42}(\text{O})_{0.58}]$, cubic solid soln., structural and mag. study (French) 0-107177
 $\text{K}_2[\text{Pt}(\text{CN})_4]\text{Br}_{0.3} \cdot 3\text{H}_2\text{O}$, high press. structs. and phase transitions 0-107423
 Li_2UO_4 , energy transfer, cryst. struct. and chemical composition effect 0-108248
 La-H(D) , lattice parameters 0-64982
 $\text{La}_{2-x}\text{A}_{1+x}\text{Cu}_2\text{O}_{6-x/2}$ ($\text{A} = \text{Ca}, \text{Sr}$), synthesis and characterisation (French) 0-104085
 LaB_2C_2 , ordering of B and C atoms in struct. 0-96481
 LaCrOS_2 , X-ray cryst. struct. anal. (French) 0-92484
 LaFeP_{12} -type structure ternary arsenides, synthesis and cryst. struct. 0-84154
 La_2MoO_6 , paramag. resonance and struct. 0-84162
 La_2O_3 , cryst. struct., X-ray powder diffr. and electron diffr. study 0-107161
 La_2RuO_6 , perovskite-type cryst. struct., X-ray determ. (French) 0-75206
 $\text{La}_2\text{Si}_2\text{O}_7\text{N}_2$ single cryst. growth by floating zone method with $\text{SiO}_2\text{-Si}_3\text{N}_4$ additions 0-93481
 Li solid electrolyte materials, review of crystal and electrochem. props. 0-107524
 LiAlSiO_4 , β -eucryptite one-dimens. fast ion cond., temp. depend. of cryst. struct. 0-107191
 LiCrO_2 , two-dimens. mag. props. rel. to cryst. struct. 0-75776
 $\text{Li}_2\text{Fe}_2\text{O}_4$ milled ferrite powder, substruct. and sinterability 0-84894
 $\text{Li}_2\text{Fe}_2\text{O}_4$ Ru substitution effect on struct. and mag. props., and max. solubility determ. 0-75364
 $\text{LiH}_2(\text{SeO}_4)_2$, ferroelec., absolute atomic arrangement and spontaneous polarisation, neutron diffr. study 0-59442
 $\alpha\text{-LiIn}(\text{MoO}_4)_2$, high-temp. form., X-ray cryst. struct. determ. 0-107183
 Li_2N , electron density study using Compton scattering 0-79750
 Li_2N , interstitial sites and anharmonic thermal vibrs. in cryst. struct., ionic cond. mechanism 0-107190
 $\text{LiNO}_3 \cdot 3\text{H}_2\text{O}$, neutron diffr. studies at 120 and 295K, H bond studies 0-88099
 LiNbO_3 :Na structure field stability limits, LPE film growth, SAW velocity 0-80102
 Li_2SO_4 , high temp. fast ion cond. phases, neutron diffr. obs. of struct. 0-107512
 $\text{Li}_2\text{Si}_2\text{O}_7$, cryst. struct. and electrochem. anal. (German) 0-88132
 Li_2TiS_2 , alkali ion ordering, X-ray study 0-107165
 Li_2VSe_2 , intercalation cpds., electron chem., ionicity 0-89501
 Li_2WO_3 , electrochem. and chem. Li incorporation, cryst. struct. 0-88131
 $\text{Li}_2\text{WO}_4(\text{IV})$, cryst. struct. rel. to wolframite-type struct. 0-92505
 $\text{LiY}(\text{MoO}_4)_2$, X-ray cryst. struct. determ. 0-107124
 $\text{Li}_2\text{Zr}(\text{MoO}_4)_3$, X-ray cryst. struct. determ. 0-88125
 $\text{Li}_2\text{Zr}_2\text{UO}_{10}$, energy transfer, cryst. struct. and chemical composition effect 0-108248
 Mg dichlorophosphate complexes, cryst. struct. ^{35}Cl NQR obs. 0-108108
 $\text{Mg}_{10}\text{An}_{0.04}\text{Mn}_{1.39}(\text{SO}_4)_2(\text{OH})_{26} \cdot 8\text{H}_2\text{O}$, moorite, X-ray cryst. struct. determ. and refinement 0-92488
 MgCl_2 -alkali metal chloride system, solid and molten states, struct. props., Raman spectra 0-76011
 $\text{Mg}_2\text{GeO}_4 \cdot \text{Mg}_2\text{SiO}_4$ system, struct. similar solid soln. obs. and characts. 0-108403
 $\text{MgHPO}_4 \cdot 3\text{H}_2\text{O}$ and $\text{MgDPO}_4 \cdot 3\text{D}_2\text{O}$, IR absorpt. and Raman spectra, vibr. assignments 0-97257
 $\text{Mg}(\text{IO}_3)_2 \cdot 4\text{H}_2\text{O}$, crystal struct., unit cell, X-ray study 0-59447
 $\text{Mg}(\text{NH}_3)_6(\text{ClO}_4)_2$, phase transition, group theoretical anal. 0-65218
 MgTeMoO_6 , prep., cryst. struct., and catalytic props. 0-108709
 MgUO_4 , energy transfer, cryst. struct. and chemical composition effect 0-108248
 $\text{Mg}_{0.25}\text{Zn}_{0.75}\text{Fe}_2\text{O}_4$, ferrite, DC cond., dielec. props., lattice consts. 0-80272
 Mn dichlorophosphate complexes, cryst. struct. ^{35}Cl NQR obs. 0-108108

crystal atomic structure of inorganic compounds continued

$\text{MnHPO}_4 \cdot 3\text{H}_2\text{O}$ and $\text{MnDPO}_4 \cdot 3\text{D}_2\text{O}$, IR absorpt. and Raman spectra, vibr. assignments 0-97257
 $\text{Mn}^{2+}\text{Mo}^{6+}\text{O}_3$, defect spinel struct., elec. and mag. props. 0-70176
 Mn_2SnS_4 , cryst. struct. refinement and mag. struct. determ. (French) 0-107131
 Mo-Si , film deposition by reactive sputtering, characteris. (Japanese) 0-93485
 MoO_3 , topotactic transform into MoO_2 , electron microscopy, X-ray anal. 0-107417
 MoS_2 , molybdenite crystal, direct imaging of atom configuration projected onto the basal plane 0-64847
 Mo_2S_8 , Chevrel phases with group IIIa metals, Nb, Hg, Pb and Cu, synthesis, stability and characts. 0-71608
 $(\text{ND}_2)_2\text{D}_2\text{IO}_6$, neutron diffr. study 0-88098
 ND_2DSeO_4 , crystals, struct., IR spectra, dielec. props. 0-75919
 NH_4AlF_6 , single cryst., prep. and struct. (French) 0-79762
 $(\text{NH}_4)_2\text{BeF}_4$, paratelec. phase, X-ray and neutron diffr. cryst. struct. anal. 0-84159
 NH_4Br , NH_4^+ rot. motion, quasielastic neutron scatt. obs. 0-96492
 NH_4ClO_4 , polymorphous phase transition mechanism 0-79737
 $(\text{NH}_4)_2\text{H}_2\text{IO}_6$, neutron diffr. study 0-88098
 NH_4HSeO_4 , cryst. struct., dielec. and ferroelec. props. 0-60528
 NH_4HSeO_4 , ferroelec. props. rel. to struct. 0-71345
 NH_4NO_3 , phase III, cryst. struct., neutron powder diffractometer study 0-107134
 $(\text{NH}_4)_2\text{Ni}(\text{BeF}_4)_2 \cdot 6\text{H}_2\text{O}$, X-ray cryst. struct. determ. 0-107137
 $(\text{NH}_4)_2\text{PCr}_2\text{O}_6$, cryst. struct., $(\text{PCr}_2\text{O}_6)^{3-}$ anion geometry 0-107157
 $\text{NH}_4\text{PbI}_2 \cdot 2\text{H}_2\text{O}$, X-ray cryst. struct. determ. 0-64958
 $(\text{NH}_4)_2\text{PtF}_6$, X-ray cryst. struct. determ. 0-107125
 $\text{NH}_4\text{Ti}(\text{SeO}_4)_2$, $(\text{NH}_4)_3\text{Ti}(\text{SeO}_4)_3$, and $(\text{NH}_4)_5\text{Ti}(\text{SeO}_4)_4$, cryst. struct. (French) 0-84148
 $(\text{NH}_4)_2[\text{VF}_6]$, X-ray cryst. struct. determ. 0-107128
 $(\text{NH}_4)_2[\text{ZnCl}_4]$, X-ray cryst. struct. determ. 0-107138
 Na orthophosphates and sulphates, anhydrous, struct. relationships w.r.t. fast ion cond. 0-107188
 Na-Co strip-chain silicates, structural-composition inhomogeneities 0-88122
 Na-Co-O system, synthesis and cryst. struct. determ. 0-107185
 Na-graphite intercalates, preparation, struct. 0-103307
 NaAlCl_4 , Raman spectra, cryst. struct. (French) 0-60578
 $\text{NaBe}(\text{SiO}_4)_2$, X-ray cryst. struct. determ., thermal vibration anisotropy allowance 0-92510
 $\text{Na}_2\text{Ca}_2\text{SiO}_5[\text{Si}_2\text{O}_7][\text{PO}_4]_3$, synthesis conditions, cryst. struct. and IR spectra characts. 0-108335
 NaCl structure, evaluation of finite strain eqns. of state using lattice models 0-96620
 $\text{NaClO}_4 \cdot \text{H}_2\text{O}$, cryst. struct. determ. refinement 0-107123
 NaCrO_2 , two-dimens. mag. props. rel. to cryst. struct. 0-75776
 $\text{Na}_2\text{Cr}_2(\text{PO}_4)_3$, crystallographic data, ionic conductivity (French) 0-88077
 $\text{Na}_2\text{Cr}_3(\text{PO}_4)_4$, crystallographic data, ionic conductivity (French) 0-88077
 NaFeF_2 , Mossbauer and low-temp. dilatometry study (French) 0-80662
 $\text{Na}_2\text{Fe}_2(\text{PO}_4)_3$, crystallographic data, ionic conductivity (French) 0-88077
 $\text{Na}_{0.70}\text{Ga}_{0.72}\text{Ti}_{0.28}\text{O}_8$, one-dimens. Na^+ ion cond., cryst. struct. and cond. meas. 0-107521
 NaGdSiO_4 , single cryst. data and ionic cond. 0-84158
 NaIO_3 , crystal struct. determ., anisotropic thermal vibr. parameters 0-88123
 $\text{NaIn}(\text{SeO}_4)_2 \cdot 6\text{H}_2\text{O}$, X-ray cryst. struct. determ., H bond system 0-92511
 $\text{NaKMg}_2\text{M}_2\text{Si}_2\text{O}_{30}$ ($\text{M} = \text{Cu}, \text{Mg}$), cryst. struct., X-ray diffr. and IR spectra (French) 0-107158
 $(\text{Na}, \text{K})_2\text{CO}_3$, non-stoichiometric, cryst. struct. (French) 0-79761
 $\text{Na}_2\text{-Li-ErSiO}_4$, solid electrolytes for Na/TiS_2 cells, synthesis, characts. and utilisation 0-107518
 $\text{Na}_3\text{Mg}_2\text{LiSi}_2\text{O}_{30}$, cryst. struct., X-ray diffr. and IR spectra (French) 0-107158
 $\text{Na}_2\text{Mg}_2\text{M}_2\text{Si}_2\text{O}_{30}$ ($\text{M} = \text{Cu}, \text{Fe}, \text{Zn}, \text{Mg}$), cryst. struct., X-ray diffr. and IR spectra (French) 0-107158
 NaNO_3 , electron density distrib. (German) 0-92481
 $\text{Na}_2\text{-MgO-Al}_2\text{O}_3$, β'' -alumina, high-resolution electron microscopy 0-75208
 $\text{Na}_2\text{PCr}_2\text{O}_6 \cdot 3\text{H}_2\text{O}$, cryst. struct. 0-107154
 Na_2PO_4 , high temp. fast ion cond. phases, neutron diffr. obs. of struct. 0-107512
 $\text{Na}_2\text{Se}_2\text{P}_2\text{O}_{12}$, superionic cond. synthesis, cryst. struct. and ionic cond. 0-107519
 NaTaO_3 , high temp. structs. neutron powder diffr., comparison with SrZrO_3 and NaNbO_3 0-88094
 Na_2TeO_3 , chem. prep. and cryst. struct. (French) 0-79755
 $\text{Na}_2\text{Ti}_2\text{Fe}_2\text{O}_4$, short period β -alumina type cpds., cryst. struct. and superionic cond. 0-107499
 Na_2TiO_9 , orthorhombic, unit-cell twinning of monoclinic $\text{Na}_2\text{Ti}_6\text{O}_{19}$, cryst. struct. 0-107155
 $\text{Na}_2\text{Ti}_6\text{O}_{19}$ bronze, hydrothermal prep., Na ion arrangement 0-75209
 $(\text{Na}_2\text{Ti}_6\text{O}_{19})_n(\text{BaTi}_4\text{O}_{13})_m$, tunnel struct. intergrowth, electron, microscopy investigations 0-100218
 Na_2TiS_2 , alkali ion ordering, X-ray study 0-107165
 Na_2WO_3 , $0.22 < x < 0.84$, low temp. struct., press. effects, NMR study 0-59443
 $\text{Na}_4\text{YSi}(\text{SiO}_7)_2$, crystal struct., atom coordinates, X-ray study 0-59446
 Na_2SiO_4 , crystal structure refinement, X-ray anal. 0-79764
 Na_2YSiO_4 , $\text{Na}_2\text{YSi}_2\text{O}_7$, $\text{Na}_2\text{YSi}_4\text{O}_9$ and $\text{Na}_2\text{YSi}_4\text{O}_{12}$, single cryst. data and ionic cond. 0-84158
 $\text{Na}_2\text{Zr}_2\text{Si}_2\text{O}_{12}$, struct. analysis at 300 and 600°C, rel. to ionic cond. 0-107189
 $\text{Na}_2[\text{Ti}(\text{Ti}_{0.9}\text{Nb}_{0.1})_4(\text{Si}_6\text{O}_{17})_2(\text{O}, \text{OH})_5] \cdot 11\text{H}_2\text{O}$, zorite, X-ray cryst. struct. determ. 0-92513
 $(\text{Nb}, \text{Ta})_2\text{N}_6$, cryst. struct. determ. (German) 0-107145
 Nb chalcogenides and chalcogenide halides, geometrical struct. and metal-metal bonding 0-80172
 Nb-Ta family minerals, cryst. struct., X-ray powder diffr. study 0-107169
 NbGa_2O_6 , O stabilised cpd., struct. determ. 0-103301
 NbH_3 , structural transform. rel. to order-disorder transform. 0-60858
 $4\text{NbO}_{0.76}$, thin film, FCC cell struct. investigation 0-92796
 $\text{Nb}_2\text{O}_5\text{-WO}_3$ system complex cpds. with TTB type subcells, HV superhigh resolution electron microscopy obs. of struct. 0-103311
 $\text{Nb}_2\text{Pt}_2\text{O}_8$, R phase of Nb-Pt/O system, cryst. struct. 0-96495
 NbS_2 , intercalate with tetraalkylammonium hydroxide, prep. and struct. 0-79752

crystal atomic structure of inorganic compounds continued

- NbS₂-(pyridine)_{1/2} intercalation complex, superlattice struct., NMR meas. 0-70180
- Nd-H(D), lattice parameters 0-64982
- Nd_{1-x}Ca_xVO₃, solid solutions, elec. props. 0-96866
- Nd₂O₃, cryst. struct., X-ray powder diffr. and electron diffr. study 0-107161
- Ni complex, diaquo-bis-(acetylacetonate) nickel (II), cryst. struct. 0-100205
- Ni intercalation compound, electron microscopy 0-84164
- Ni_{1-x}Cd_xFe₂O₄, mag. props. rel. to ionic struct. 0-75756
- NiFe₂O₄ milled ferrite powder, substruct. and sinterability 0-84894
- Ni(NH₃)₈(BF₄)₂, phase transition, group theoretical anal. 0-65218
- Ni(NH₃)₆(ClO₄)₂, phase transition, group theoretical anal. 0-65218
- NiO-Cr₂O₃-MgSiO₃ methanation catalyst, S-resistant, IR and Raman spectra 0-93290
- Ni₂S₃, hazelwoodite, X-ray cryst. struct. determ. 0-88105
- Ni₂Zn ferrite, ZnO₂ additions influence on sintering and physicochem. props. 0-108369
- Os complexes, N-1-adamantylimido OsO₃, bis(N-tert-butylimido) OsO₂, cryst. struct., bonding, ligands π-donor capability 0-64969
- PCl₃, structural study at 123K (French) 0-88111
- (Pb, Sr)₂Ge₂O₁₁, single crystals, growth and X-ray and dielec. investigations 0-88127
- PbAl₂Se₄, X-ray cryst. struct. determ. (German) 0-107174
- Pb_{1-x}Bi_xFe_{2+x}, solid soln., struct. and ionic cond. correl., neutron diffr. study (French) 0-84324
- PbCl₂, struct. comparison with Co₂Si, Co₂P, and SbSi (French) 0-84155
- Pb₂Ga₂S₆, X-ray cryst. struct. determ. and refinement (French) 0-107130
- PbGa₂Se₄, X-ray cryst. struct. determ. (German) 0-107174
- Pb_{1-x}Ge_xO₁₇, X-ray powder cryst. data, struct. rel. to Pb₆GeO₈ and PbO 0-84146
- Pb₂GeO₈, X-ray powder cryst. data, struct. rel. to Pb₁₁Ge₃O₁₇ and PbO 0-84146
- PbHPO₄, phase transitions study, role of cryst. struct. determ. 0-75197
- PbI₂-PbBr₂ mixed systems, cryst. growth, struct. and optical props. (German) 0-96499
- PbIn₂S₄, X-ray powder cryst. struct. determ. 0-66488
- PbIn₁₀S₂₁, X-ray powder cryst. struct. determ. 0-66488
- PbO, X-ray powder cryst. data, struct. rel. to Pb₂GeO₈ and Pb₁₁Ge₃O₁₇ 0-84146
- PbO-MoO₃-MO and PbO-WO₃-MO systems, M=Ca, Ba, Mg, Sr, perovskite type cpds. detection 0-108404
- PbO-Nb₂O₅ system, pyrochlore block structs., cryst. struct. determ. (German) 0-70178
- Pb₃(PO₄)₆, X-ray cryst. struct. determ. and refinement 0-103300
- Pb₃Rh₂O₅, struct. study, X-ray diffr. (French) 0-88100
- Pb₂Sn_{1-x}F_{2+x}, solid soln., struct. evolutions (French) 0-96488
- Pb_{1-x}Sn_xTe_{1-x}Se_x, quaternary solid solns. with const. lattice parameter, cryst. growth and characts. 0-108332
- Pb₃(VO₄)₃, ferroelastic, phase transitions, boundary walls 0-107419
- Pb(Zr, Ti)O₃ ceramics, low temp. sintering, elec. and mech. props. 0-71616
- Pb₂[As₂O₅], paulmooreite, crystal struct., dimeric arsenite groups 0-84143
- PdD_{0.73}, (1, 1/2, 0)-superlattice reflection splitting near 50K, neutron diffr. studies 0-70168
- Pd₃P₈, pure and deuterated, cryst. struct., neutron diffr. study 0-84152
- Pr-H(D), lattice parameters 0-64982
- PrCo₂Ge₂, crystal and magnetic structure obs. 0-64976
- Pt intercalation compound, electron microscopy 0-84164
- RbAlF₄, single cryst., prep. and struct. (French) 0-79762
- β-RbAlF₄, struct. and irreversible and topotactic phase transition β→α mechanism 0-107132
- RbCoCr₂(VO₄)₃, synthesis and cryst. struct. 0-88114
- RbCuCr₂(VO₄)₃, synthesis and cryst. struct. 0-88114
- Rb₂Fe₂(SO₄)₆·5H₂O, cryst. struct. determ. 0-92482
- RbH₂PO₄, phase transitions study, role of cryst. struct. determ. 0-75197
- RbHSO₄, ferroelec. props. rel. to struct. 0-71345
- RbIn(SO₄)₂·4H₂O, refinement of cryst. struct., interatomic distances, bonds 0-59448
- RbMgCr₂(VO₄)₃, synthesis and cryst. struct. 0-88114
- RbNO₃, struct., high temp. phases, neutron diffr. study 0-79756
- RbNaMg₂M₂Si₂O₁₀ (M=Cu, Fe, Mg), cryst. struct., X-ray diffr. and IR spectra (French) 0-107158
- Rb₂Nb₂O₁₇·3H₂O, cryst. struct. by X-ray diffr. (French) 0-92503
- RbNiCr₂(VO₄)₃, synthesis and cryst. struct. 0-88114
- RbPb_{1-x}2H₂O, X-ray cryst. struct. determ. 0-64958
- Rb₂Pb[Co(NO₂)₆], struct. study 0-88106
- Rb₁₀Ta₂₉O₇₈, tunnel struct. 0-107166
- Rb₂Ta₂, synthesis and cryst. struct. 0-88115
- Rb_{1-x}(Ti_{1-x}M_{1+x})O₅, M=Nb, Ta, layer compound, cryst. struct., nonstoichiometry 0-64972
- RbTi(SeO₄)₂, Rb₂Ti(SeO₄)₃, and Rb₃Ti(SeO₄)₄, cryst. struct. (French) 0-84148
- Rb₂[C₂O₄].D₂O, neutron profile refinement at 5K 0-88103
- Sb₂₀(2.04)MoO₃, synthesis, struct. and oxidation state (French) 0-64971
- SbSi₃, struct. comparison with Co₂Si, Co₂P, and PbCl₂ (French) 0-84155
- SeCl₃-NaCl-CsCl ternary system, cpd. form., thermographic invstg. (Russian) 0-66490
- Si-Al-O-N system, phase analysis and TEM struct. obs. 0-108420
- SiC polytypes, lattice imaging studies on intergrowth structs. 0-107025
- α-Si₃N₄, stable phase in Si-Al-O-N system, cryst. struct. obs. using TEM 0-108421
- SnCl₄, X-ray cryst. struct. determ., Patterson synthesis (French) 0-96480
- SnCl₂·1.5H₂O single cryst., ¹¹⁹Sn NQR, cryst. struct. 0-60449
- SnF₂, cryst. struct. of β- and γ-phases 0-92500
- SnI₄, attachment energy as habit controlling factor 0-59421
- Sn₂Mo₆S₈, struct. anal. supercond. props. 0-97023
- Sn₂P₂Se₆, ferroelec. semicond., phase transition and lattice dynamics 0-60526
- Sr Nb₂O₆, crystallography, polymorphism and isomerism, X-ray diffr. and DTA study 0-100216
- SrBaNaNb₃O₁₂, X-ray powder diffraction data determ. (Chinese) 0-70170
- SrIn₂Se₄, cryst. struct. (German) 0-79760
- SrLaFeO₄, two-dimens. mag. props. rel. to cryst. struct. 0-75776
- Sr_{2.05}Na_{0.90}Nb₂O₁₅, X-ray powder diffraction data determ. (Chinese) 0-70170
- SrTa₂O₆, structural study X-ray diffr., IR absorpt. and Raman spectra (French) 0-107173

crystal atomic structure of inorganic compounds continued

- SrTiO₃, mean square atomic displacement temp. depend., sublattice vibration anharmonicity 0-79890
- Ta-Ga, at high press. polymorphism 0-88112
- 2Ta₂O₃ thin film, FCC cell struct. investigation 0-92796
- Ta₂O₅, with hexagonal lattice in thin layers, atomic struct., electron diffr. 0-84160
- Ta₂S₃ (1T) electron irradiated, lattice contraction 0-59520
- Ta₂S₃ intercalate with tetraalkylammonium hydroxide, prep. and struct. 0-79752
- Ta₂S₃, monoclinic form, cryst. struct. determ., Peierls type transition obs. (French) 0-88109
- Ta₂(NH₄)₃ and Ta₂(NH₄)_{1/3}(H₂O)_{2/3}, incoherent inelastic neutron spectra 0-84163
- Tb(MoO₄)₃, cryst. struct. in ferroelec., ferroelastic, antiferroelec. and paraelectric phases 0-75205
- Te(OH)₆.Cs₂HPO₄, cryst. struct. 0-64975
- Te(OH)₆.Cs₂HPO₄.2Cs₂H₂PO₄, cryst. struct. 0-64975
- Th-C-N system, existence of new β'ThCN' phase, struct. and thermodynamic study (French) 0-92499
- Ti-N₂, condensate formed by plasma flow precipitation in vacuum, cryst. and surface props. (Russian) 0-100788
- TiN_{0.32}H_{0.19}, cryst. struct., neutron diffr. anal. (Russian) 0-64965
- TiO₂, crystal structure, stability compared with CaF₂ (Russian) 0-64945
- TiO_{2-x}, reduced, crystallographic shear planes, dislocation struct. 0-107175
- Ti₂O₃, electron density distrib., deform. density at 295K, X-ray anal. 0-107117
- TiAlF₆, single cryst., prep. and struct. (French) 0-79762
- TiCoCr₂(VO₄)₃, synthesis and cryst. struct. 0-88114
- TiCuCr₂(VO₄)₃, synthesis and cryst. struct. 0-88114
- Ti₄(M₂)₂(L₄)₂, (M=Pb, Ag, Au, (Bi_{0.5}Tl_{0.5})), struct., rel. to phonon spectra 0-71425
- TiMgCr₂(VO₄)₃, synthesis and cryst. struct. 0-88114
- Tl₂Mo₂Si₁₁, X-ray cryst. struct. determ., Mo₁₂ and Mo₆ isolated clusters (French) 0-92490
- Tl₂Mo₂Si₁₁, prep. and struct., Mo₁₂ cluster in Mo₁₂Si₁₄ unit 0-107168
- Tl₂Mo₂Se₆, X-ray cryst. struct. determ., monodimensional clusters (Mo₆)₂∞ (French) 0-96482
- TlMo₂Se₆(Te₂), synthesis and struct. 0-92498
- TiNiCr₂(VO₄)₃, synthesis and cryst. struct. 0-88114
- Ti₂SnGeO₂ system, structure of thallium I germanates (French) 0-79754
- Tl₂SnSe₃, X-ray cryst. struct. determ. (French) 0-107171
- Tl_{1-x}(Ti_{1-x}Nb_{1+x})O₅, layer compound, cryst. struct., nonstoichiometry 0-64972
- Tl^{III}(SeO₄)₂, Tl^{III}(SeO₄)₃, and Tl^{III}(SeO₄)₄, cryst. struct. (French) 0-84148
- TiVO₄, synthesis and thermal props. (French) 0-97443
- Tl₂[Fe(CN)₅(NO)], X-ray cryst. struct. determ., heavy atom method 0-92495
- UO₂, single-cryst. neutron diffr. data, reanal. using third cumulants 0-100130
- U₂O₇Cl₃, prep. and cryst. struct. (French) 0-84150
- U₂Zr₂FO₄, X-ray cryst. struct. determ. and refinement (French) 0-107122
- (V_{1-x}Cr_x)₂O_{3+x}, elec. props. and struct. 0-84494
- V₂O₃, electron-density studies, deform. density at 295K, metal-metal bonds 0-107118
- V₂O₅ and lower oxides, electronic, optical, structural and surface props., review 0-88120
- V₂O₅, low-temp. modification, cryst. struct. and valency distrib., importance of very weak reflections 0-92493
- β-VOSO₄·5H₂O, X-ray cryst. struct. determ. and refinement (French) 0-107121
- V₂Si, supercond. structure and properties (German) 0-93631
- VO₂ polymorph, hexagonal, cryst. struct. imaging by high-resolution electron microscopy 0-103309
- Y oxides, perovskite-like, synthesis, struct., elec. props. 0-65554
- YAG, as substrate for Er₃Al_{5-x}Ga_xO₁₂ LPE film for solid laser 0-93419
- YAG, simulated mol. images, point models and kinematical struct. amplitudes 0-103223
- YD_{1.96}, cryst. struct. by neutron diffr. 0-70179
- YH_{9.98}, cryst. struct. by neutron diffr. 0-70179
- YH₂, location of H, PMR rigid-lattice second moment meas. 0-71198
- Y_{1-x}La_xFe₂O₁₂, mag. props. rel. to ionic struct. 0-75756
- Y₂Ru₂, Mn₂C₂ type struct., X-ray cryst. struct. determ. 0-96483
- YSeF₃, orthorhombic polytype 140, struct. study (French) 0-88102
- Y₂UO₁₂, energy transfer, cryst. struct. and chemical composition effect 0-108248
- Yb_{0.5}Eu_{0.5}Fe₂O₄, rhombohedral oxides, symmetry group (French) 0-84157
- YbFe₂O₄, rhombohedral oxides, symmetry group (French) 0-84157
- Zn₂(AsO₄)(OH), paramadite, crystal struct., anisotropic temp. factors 0-84145
- ZnF₂, X-ray absorpt. spectrum polarisation depend. 0-104012
- Zn²⁺Mo⁴⁺O₄, defect spinel struct., elec. and mag. props. 0-70176
- ZnNH₄H₃(PO₄)₂·H₂O, X-ray cryst. struct. determ. (French) 0-88104
- ZnS structure, evaluation of finite strain eqns. of state using lattice models 0-96620
- ZnY₂O₄, cryst. struct. 0-100207
- Zr-N₂, condensate formed by plasma flow precipitation in vacuum, cryst. and surface props. (Russian) 0-100788
- Zr(Ca,Y)O_{2-x}, local ionic arrangement, X-ray diffr. study 0-100203
- ZrF₄-BaF₂ system solid phases, synthesis and characterisation (French) 0-92506
- Zr(KPO₄)₂, cryst., ionic cond., layered struct. 0-92710
- Zr(LiPO₄)₂, cryst., ionic cond., layered struct. 0-92710
- Zr(NbO₄)₂, cryst., ionic cond., layered struct. 0-92710
- ZrO₂ thin film, optical props. rel. to cryst. struct. 0-97357
- ZrSiO₄, body centered matrix basis 0-79765

crystal atomic structure of organic compounds

- acetate-ferrileghemoglobin, X-ray struct. anal., 3D refinement at resoln. of 2.0 Å 0-104554
- 2-Adamantanone, cryst. struct. in plastic phase 0-88065
- aluminium copper tetrahalides, exchange, mag. anisotropy, and spin diffusion contribs. to EPR linewidth 0-80597
- alkylammonium compounds, intercalation of ions in (TiNbO₅)⁻ layers 0-64985
- anthanthrene, mol. cryst. images in electron diffr. patterns 0-103315

crystal atomic structure of organic compounds continued

anthracene:tetracyanobenzene charge transfer complex, *cryst. struct.*, temp. effects 0-96508
 anthracene, attachment energy as habit controlling factor 0-59421
 anthracene, metastable triclinic phase 0-59452
 anthracene-phenanthrene-tetracyanobenzene, CT-cryst., mini-excitons and lattice dynamics, ESR, optical and Raman spectra 0-60406
 9-anthraldehyde, *struct.* by TEM 0-79771
 9-anthronitrile, *struct.* by TEM 0-79771
 barium methylsulphonate, X-ray powder *cryst. data* 0-59451
 benzoic acid, *struct.* refinement at room temp. 0-96502
 benzyl mercury chloride, *cryst. struct.* and absorpt. calcs. 0-84166
 2-benzyl-5-benzilydene-cyclopentanone, and substituted form, topochem. single-cryst.-to-single-cryst. photodimerisation 0-66819
 bie-solycylato-diaquo calcium (II), *cryst. struct.* 0-100222
 4-bromobenzyloxymethyl-trifluorosilane, *cryst. struct.*, X-ray study 0-70187
 cadmium formate, anhydrous, *cryst. struct.* 0-107195
 calcium dipicolate trihydrate, IR and Raman spectra, isotopic frequency shift, mol. vibr. obs., point groups determ. 0-89001
 ceruloplasmin, human, calc. of rotation function for tetragonal *cryst.* at 10 Å resoln. 0-108843
 cholesteryl ethyl carbonate, long periods in sol. state, X-ray diff. study 0-96503
 cobalt dimethyl glyoximate, molecular *struct.*, *cryst. structure* 0-79769
 conference, Crystal XII, Canberra, Australia (Jan.-Feb. 1980) 0-62388
 copper formate anhydride, *cryst. struct.* and mag. props. 0-79768
 copper phthalocyanine, molecule images, simulation by point models and kinematical *struct.* amplitudes 0-103223
 cordycepin, X-ray *cryst. struct.* determ. 0-107198
 coriol, crystal *struct.* determ. using NQUEST(x) function 0-64986
 deuteromethane, crystalline, X-ray powder diff. study 0-96500
 di(tert. butylperoxy)triphenylantimony, X-ray *cryst. struct.* determ. 0-92517
 5,7-dimethoxyindane-1-one, *cryst.* and mol. *struct.* 0-100223
 m-dinitrobenzene, oriented film, intermol. vibr. coupling, polarised IR spectra 0-97264
 dipicolinic acid, IR and Raman spectra, isotopic frequency shift, mol. vibr. obs., point groups determ. 0-89001
 EBBA, mol. and *cryst. struct.*, X-ray diff. study 0-88134
 erbium triethyl sulphate, *cryst. struct.*, H⁺ coords., NMR 0-97152
 p-(p'-ethoxybenzylidene)amino-benzonitrile, *cryst. struct.* rel. to liq. crystallinity 0-100225
 F 0-92515
 ferrocene, orthorhombic low-temp. *cryst. phase*, characterisation 0-96507
 hexadeca-chlorophthalocyanato-copper discrimination of individual atoms in mol. images 0-100226
 p-hydroxy-trans-cinnamic acid, *cryst. struct.* basis for absence of thermal mesomorphism 0-96509
 lanthanum nicotinate dihydrate, *cryst.*, nucl. quadrupole interactions, D atom coords., ENDOR obs. 0-97161
 manganese adipate dihydrate, *cryst. struct.*, H-bonding and O atom coordination 0-96506
 manganese carboxylate, dodecanuclear mixed-valence, prep., *struct.*, and mag. props. 0-107196
 methane, crystalline, *struct.* and compression at high press., room temp. 0-107199
 α-methane-d₄, crystalline, X-ray powder diff. study 0-96500
 p-(p'-methoxybenzylidene)amino-phenyl acetate, *cryst. struct.* rel. to liq. crystallinity 0-100225
 p-methoxybenzylidene-cyanoaniline, mol. and *cryst. struct.*, X-ray diff. study 0-88134
 methylzinc methoxide, tetrameric, X-ray *cryst. struct.* determ. 0-107197
 molecular crystals, use of atom-atom pots. in interpreting behaviour, book contrib. 0-84136
 monoadipate-tetraquo-cobalt (II), *cryst. struct.*, H-bonding scheme 0-96504
 naphtho[1,8-cd:4,5-c'd']bis[1,2,6]thiadiazine, mol., electronic, *cryst. struct.* 0-64984
 palmitic acid-choleic acid complex, *cryst. struct.* and van der Waals energy 0-64983
 phosphorylase A crystals, automated *struct.* determ., from micrographs 0-92425
 phthalocyanines, metal free, mol. *cryst. images* in electron diff. patterns 0-103315
 polyacetylene:I, NMR *struct.* investigation 0-108082
 trans-polyacetylene, bulk crystallinity, small-angle X-ray diff. study 0-103263
 polyamides containing 1,3-cyclohexane rings, *cryst. struct.* 0-103262
 polyamine iodide-AgI solid electrolytes, elec. cond. and *cryst. struct.* 0-107537
 potassium formate, X-ray *cryst. struct.* determ. 0-107194
 praseodymium tricarbamide acetate hydrate, *cryst. struct.*, Patterson function anal. 0-79770
 protein, *struct.* analysis by electron diff., single scatt. approx., domains of validity 0-101150
 pyrene picrate, crystal *struct.* oscill. and Weissenberg photographs 0-107200
 ribonuclease A, bovine, *cryst. struct.* determ. by X-ray and neutron diff. 0-108841
 ribosomal component, *cryst. struct.* at 2.6 Å resolution 0-97859
 satellite tobacco necrosis virus *struct.*, detect. and idealisation procedures of non-crystallographic symmetry with phase refinement appl. 0-108840
 strontium maleate tetrahydrate, *cryst. struct.*, H-bonding scheme 0-96505 (TCNQ)₂, dimeric interactions, MO calcs., applicability to crystal *struct.* 0-75215
 TCNQ salt, Ag.TCNQ, *cryst. struct.* 0-70186
 tetra-isoamyl phosphonium bromide hydrate, clathrate, *cryst. struct.*, X-ray study 0-64987
 2,3,4,5-tetraacetoxymercurithiophene, dark-field imaging, computer simulation 0-100151
 1,2,4,5-tetrachlorobenzene, exciton states in crystals and dimers 0-70620
 tetracyanoplatinates, quasi 1d anion deficient, elec. and *struct.* props. 0-103683
 2,2,5,5-tetramethyl-4-phenyl-3-imidazalin-3-oxide-1-oxyl, deform. electron density determ., X-ray diff. 0-88135
 2,2,6,6-tetramethyl-piperidino-oxyl, *cryst. growth* and polymorphism 0-96645
 tetramethylammonium hexafluorophosphate, X-ray *cryst. struct.* determ., full-matrix least-squares refinement 0-92514

crystal atomic structure of organic compounds continued

tetramethylammonium tetrachlorozincate, incommensurate *phase study*, ferroelectric-paraelectric phases (*French*) 0-88318
 tetraphenyldithiopyranilidene mixed valence polyiodides, crystalline *struct.* and optical props. 0-92516
 tetraselenotetracene iodides, *struct.* and physical props., DC electrical cond. and EPR linewidth meas. 0-103312
 thiourea, incommensurate *phase*, soft modes, condensation of even-order harmonics 0-103313
 thorium phthalocyanine, *phase-contrast* characteristics in STEM 0-100153
 thulium phthalocyanine, mol. image in high resolution electron microscopy, radiation damage effect 0-107203
 2-(2-tosylaminophenyl)-4H-3,1-benzoxazine-4-one, *cryst.* and mol. *struct.* 0-84167
 bis-triazolopyridazines, conformation calcs. by mol. mechanics and CNDO/2 method 0-69079
 bis-triazolyls, conformation calcs. by mol. mechanics and CNDO/2 method 0-69079
 p-tricyanovinylphenyldicyanomethide ion, donor props., cyclic voltammetry and π-complex form. 0-88520
 tris(hydroxymethyl)aminomethane, crystalline and plastic *structs.* *phase transforms.* studied by X-ray diff. 0-84130
 (TTF)₂, dimeric interactions, MO calcs., applicability to crystal *struct.* 0-75215
 TTF-TCNQ, dimeric interactions, MO calcs., applicability to crystal *struct.* 0-75215
 TTF-TCNQ complex, trans-diethyl-dimethyl TTF-TCNQ, one-dimens. cond. 0-96853
 TTT⁺Br⁻, *cryst.* and mol. *struct.*, X-ray method 0-107202
 TTT, donor-acceptor system, physico-chemical studies (*Hungarian*) 0-75554
 urea, electron density distrib., multipolar expansion 0-96501
 X-ray diffraction powder patterns, standard, for 87 substances 0-64839
 Co II complexes, with tetradentate Schiff bases, synthesis, *struct.* and ESR obs. 0-80598
 CsDNA of T2 *phase*, in classical *crystn. B form*; *struct.*, amplitudes, synchrotron radiation diffraction 0-85335
 Pt complex, [2, 2', 2"-terpyridine PtCl]⁺, motion of Pt atoms, electron microscopy obs. 0-103314
 (TMCHDT)₂ClO₄, organic conductor, *struct.* study (*French*) 0-88133

crystal binding

see also binding energy; lattice energy

acetylene, *cryst.*, semiempirical atom-atom pots. appls. 0-100200
 alkali chalcogenides, electronic polarizabilities and ion sizes 0-59432
 alkali halide solid solns., lattice parameter and heat of form. 0-79739
 alkali halides, repulsive softness parameter anal. 0-107102
 alkali metal halides, interionic repulsive short-range interaction pot., lattice energy calc. 0-96466
 alkali metals, effective ion-ion potential, compressibility and force consts. 0-70158
 alkali metals, partial pressure contributions to equation of state 0-107401
 alkali metals, phonon dispersion binding energy, compressibility, elastic consts. electron screening and Ashcroft pot. calcs. 0-65174
 alkaline earth chalcogenides, electronic polarizabilities and ionic radii of metal and chalcogenide ions in *cryst. state* 0-100198
 alkaline earth chalcogenides, interionic repulsive short-range interaction pot., lattice energy calc. 0-96466
 alkaline earth halides, electronic polarizabilities and ion sizes 0-59432
 anthracene, attachment energy as habit controlling factor 0-59421
 antimonates, columbite or trirutile *struct.*, force fields rel. to *cryst. struct.* (*French*) 0-107104
 atoms as structural components in metallurgy (*Dutch*) 0-96465
 bonding charge densities, determ. by electron diff. 0-75125
 brass-like alloy phases, binding and *cryst. struct.*, valence arguments 0-88081
 caesium halides press. depend. of effective ionic charge 0-96462
 cholesterol derivatives, mol. packing coeffs. and thermal stabilities 0-100201
 coordination numbers in solids, Pearson diagrams 0-107103
 corundum, attachment energy as habit controlling factor 0-59422
 Coulomb systems, absence of long-range order with long-range potentials 0-70157
 electronic structure and solid props., rel. to chemical bonding, book 0-86044
 electrostatic potential of point charge lattice having lamina geometry 0-59433
 EM field in crystalline slab 0-96463
 ethanol-d₁(d₂)(d₃), glassy state, solvated electron geometry, electron spin echo modulation obs. 0-66009
 fluoride crystals, rutile-type, interionic pots., cohesive energy, bulk modulus, calc. 0-79741
 graphite, electronic *struct.* exact exchange HF calcs. 0-65438
 group IIIa dihydrides, *structs.* and stabilities 0-107146
 growth models, attachment energy as habit controlling factor 0-59420
 Hartree-Fock theory, ab initio effective potentials 0-103290
 ionic crystals, binding forces and eqns. of state, inner electron contrib., calc. 0-64950
 ionic crystals, interatomic forces, Gruneisen and Anderson-Gruneisen parameters 0-79904
 lattice oscillations and molecular oscillation, change in bond length and angles as coordinates 0-107385
 melting and boiling points vs. Coulomb pot., parabolic behaviour 0-70375
 metal oxides, ESCA, Madelung pot. effects 0-104036
 metals, ground state of solids, spin density functional method, binding energy, compressibility 0-65477
 molecular *crysts.*, symmetrised valence and relative motion coords. 0-84134
 niobates, columbite or trirutile *struct.*, force fields rel. to *cryst. struct.* (*French*) 0-107104
 oxide crystals, rutile-type, interionic pots., cohesive energy, bulk modulus, calc. 0-79741
 penninite, one-layer triclinic chlorite, neutron diffraction study 0-84144
 polyhedra coordination, identification in *cryst. struct.* 0-59431
 quartz, crystal *structure rearrangement* due to neutron irradi. 0-64981
 quartz, low, CC Si-O bond characteristics 0-84132
 quartz, low, ionicity of Si-O bond 0-84133
 radical radiation formation in solid organic compounds 0-85201
 rare earth cobaltides, RCo₃ type, hydride *phase synthesis*, thermal stability and *struct.* 0-59438

crystal binding continued

- rare earth compounds, Curie constant rel. to valence bond strength 0-60251
 repulsive short-range interaction pot., lattice energy calc. 0-96466
 rutile-type compounds, crystal binding energies and electronic polarisabilities 0-75202
 stability and three-body interactions 0-79740
 tantalates, columbite or tri-rutile struct., force fields rel. to cryst. struct. (French) 0-107104
 tetragonal crystals, unstressed, for arbitrary interatomic interactions, simple proof for existence 0-79746
 transition metal 3d monoxides, specific vol. and mag. moment calcs. 0-65822
 transition metal alloys, cohesive properties and press.-vol. relation 0-92476
 transition metal cpds., rock salt struct., surface energy bands, Shockley surface states, bonding 0-92956
 transition metals silicides, atomic volume deviations and supercond. T_c 0-75203
 TTF-TCNQ, nonbonding intermolecular forces 0-83443
 water-water, pair pot. near H bonded equilib. config., amorphous and crystalline solid and liq. 0-64946
 Ag halides, cryst., van der Waals coeffs. calcs. 0-96459
 AgBF₄, ionic radii and chem. shifts, correl. with electronegativity 0-66054
 Al, low-order Fourier coeff. of pot., modified thickness fringe method 0-75130
 α -Al₂O₃, charge distribution determ., SCF calc., Slater-type orbitals, Madelung type const. 0-107100
 BN, electronic struct., exact exchange HF calcs. 0-65438
 CaF₂ crystal structure, stability compared with TiO₂ (Russian) 0-64945
 Co₂(AsO₄)₂, polymorph, cryst. struct., closest packing 0-70174
 CsBF₄, ionic radii and chem. shifts, correl. with electronegativity 0-66054
 Fe, X-ray absorpt. spectra, effective co-ordination charges 0-84805
 Fe₂O₃, X-ray absorpt. spectra, effective co-ordination charges 0-84805
 Fe₃O₄, X-ray absorpt. spectra, effective co-ordination charges 0-84805
 Fe₂O, X-ray absorpt. spectra, effective co-ordination charges 0-84805
 H₂, metallic, ground-state energies of liq. and solid phases, variational and Monte Carlo methods 0-70502
 KBr crystals, binding forces and eqns. of state, inner electron contrib., calc. 0-64950
 Li intercalated atoms, host lattice strain effects 0-88082
 NH₄BF₄, ionic radii and chem. shifts, correl. with electronegativity 0-66054
 NbC, rock salt struct., surface energy bands, Shockley surface states, bonding 0-92956
 Ni, band struct., cryst. pot. anisotropy effect (Russian) 0-88474
 PdPb₃, crystal structure (German) 0-96472
 Pu, oxidation, binding energies, Auger and X-ray photoelectron spectra study 0-76550
 α -S, attachment energy as habit controlling factor 0-59421
 Si noncrystalline film, struct., interatomic distances, SRO 0-107053
 Si, phase transformation, lattice dynamics, microscopic theory 0-107387
 Si-Ge system, phase diagram, lattice const. var. effects 0-97470
 Si₃-H₂, noncrystalline film, struct., interatomic distances, SRO 0-107053
 SnI₄, attachment energy as habit controlling factor 0-59421
 Ti, band struct., cryst. pot. anisotropy effect (Russian) 0-88474
 TiO₂ crystal structure, stability compared with CaF₂ (Russian) 0-64945
 TiO₂, interionic repulsive short-range interaction pot., lattice energy calc. 0-96466
 TI halides, cryst., van der Waals coeffs. calcs. 0-96459
 TmSe, Curie constant rel. to valence bond strength 0-60251
 V₂O₅ and lower oxides, electronic, optical, structural and surface props., review 0-88120
 YCo₃, hydride phase synthesis, thermal stability and struct. 0-59438

crystal chemistry*see also crystallography*

- alloys, criteria of chemical inhomogeneity 0-59670
 chromite natural samples of Brazilian, Philippine origin, chem. comp., Mossbauer spectroscopy 0-103901
 intermetallic phases, struct. description (German) 0-88090
 nontransition metals, electron density, bulk and surface props. relation 0-103609
 oxides, ABO₄ type, high press. phase transforms. and struct. types, cryst. chem. aspects 0-79940
 pyrochlorides of charge-coupled type, form. in comps. A²⁺A⁴⁺Ti₂O₇ and A³⁺A³⁺B⁴⁺B⁶⁺O₇ 0-92504
 rare earth cobaltides, RCo₃ type, hydride phase synthesis, thermal stability and struct. 0-59438
 rare earth compound properties, periodicity at atom props. 0-96586
 rare earth oxyorthotitanates, crystallochem. classification 0-107142
 semiconducting alloys, comp. profile, second derivative wavelength modulation 0-103967
 solid electrolyte materials chemistry problems 0-96680
 steel, inclusion chemistry control for machinability enhancement 0-85067
 Ag₂(Na_{2-x}Te₂)_{1-x}Te₂VO₁₄ (x=0,4), mixed tellurate, cryst. chem. and elec. cond. (French) 0-107150
 Ba₂WFe₂O₉ and Ba₂WFe₂O_{8.42}, crystallographic and mag. props., comparative study 0-103303
 Ca₂Gd_{2-x}Sn_{2-x}Sb₂O₇, pyrochlorate struct. form. 0-92504
 CaS:Nd phosphors, X-ray powder diffr. anal. 0-100204
 Cd₂Hg_{1-x}Te, carrier lifetime, effect of comp. fluctuations and second-phase inclusions 0-80294
 CdS, rock-salt type high-press. phase synthesis using metal sulphide additives 0-104084
 CsSbF₆, high press. phase relations, vibr. spectra, and cryst. chemistry 0-108200
 Cs_{1-x}(Ti_{1-x}Nb_{1+x})O₅, layer compound, cryst. struct., nonstoichiometry 0-64972
 Fe_{1-x}Sb, nonstoichiometry influence on mag. props. (Russian) 0-65813
 HuO₃P(As)O₄·4H₂O, water deficiency, enthalpy of dehydration, thermogravimetric anal. 0-65251
 K₂Te^{IV}Te^{VI}O₁₂, mixed tellurate, cryst. chem. and elec. cond. (French) 0-107150
 K_{1-x}(Ti_{1-x}M_{1+x})O₅, M=Nb, Ta, layer compound, cryst. struct., nonstoichiometry 0-64972
 Li₂UO₄, energy transfer, cryst. struct. and chemical composition effect 0-108248

crystal chemistry continued

- (La_{0.8}Ca_{0.2})MnO_{3+x}, non-stoichiometry and lattice consts. 0-100212
 La₂O₃, cryst. struct., X-ray powder diffr. and electron diffr. study 0-107161
 Li₂d₄UO₅, energy transfer, cryst. struct. and chemical composition effect 0-108248
 MgUO₄, energy transfer, cryst. struct. and chemical composition effect 0-108248
 MnZn ferrites, form. of comp. heterogeneity during high-temp. sintering 0-60818
 (Na₂Ky)₂CO₃, non-stoichiometric, cryst. struct. (French) 0-79761
 Na₄R(WNb₃)O₉F₃ (R=Y, Nd, Eu, Gd, Dy, Lu), synthesis, cryst.-chem. and dielec. study (French) 0-108164
 Nb-Pd constitution diagram, metallographic and X-ray diffr. anal. 0-89204
 Nd₂O₃, cryst. struct., X-ray powder diffr. and electron diffr. study 0-107161
 Rb_{1-x}(Ti_{1-x}M_{1+x})O₅, M=Nb, Ta, layer compound, cryst. struct., nonstoichiometry 0-64972
 Si₂O₃⁶⁻, double chain anion containing anhydrous silicates, synthesis, cryst. chem. 0-59444
 Sr Nb₂O₆, crystallography, polymorphism and isomerism, X-ray diffr. and DTA study 0-100216
 Ti-Ni (48 to 53 at.%), heat treatment and deviation from stoichiometry 0-104192
 Ti_{1-x}(Ti_{1-x}Nb_{1+x})O₅, layer compound, cryst. struct., nonstoichiometry 0-64972
 Tm_{1-x}Eu_xSe, semicond. with valence instabilities, cryst. chem. considerations 0-100213
 TmSe and its mixed crystals, valence instabilities, phase diagram 0-70651
 TmSe_{1-x}Te_x, semicond. with valence instabilities, cryst. chem. considerations 0-100213
 YCo₃, hydride phase synthesis, thermal stability and struct. 0-59438
 Y₂UO₁₂, energy transfer, cryst. struct. and chemical composition effect 0-108248

crystal classes *see crystal symmetry***crystal cleavage**

- Admiralty Metal, transgranular stress corrosion crack propag. 0-89402
 graphite, ion bombarded, light gases, structural study using TEM 0-92570
 guanidinium aluminium sulphate hydrate, ferroelec., decoration patterns on cleavage surface, domain obs. 0-97218
 guanidinium uranyl sulphate hydrate, ferroelec., decoration patterns on cleavage surface, domain obs. 0-97218
 quartz, habit variation of crystals of the C₃2-C₃2 space group 0-107090
 steel, structural, second phase particle effects on impact strength 0-108581
 TGS, ferroelec., vacuum cleaved, charge compensation 0-60510
 triglycine sulphate, ferroelec., decoration patterns on cleavage surface, domain obs. 0-97218
 Fe-Si (2.6 wt.%) single cryst., crack propag., controlled plastic crack tip opening rate 0-60943
 Gd₂SiO₅, atomic positions, high resolution electron microscopy 0-100220
 HgS, habit variation of crystals of the C₃2-C₃2 space group 0-107090
 InP (110) surfaces, cleaved and polished-sputtered-annealed, LEED and AES study 0-103550
 LiNbO₃, cleaved, crystallographic and electrooptic props. 0-59575
 Mg₂SiO₄ crystals, dislocations configuration and cleavage steps dissoln. 0-107250
 NaCl, cleavage faces, evaporation pattern determ. by decoration method in electron microscopy (German) 0-107626
 NaCl:Ca crystals, surface recrystn., moisture effect 0-84950
 NaI crystals, used in nuclear medicine, determ. of cause of breakage 0-98077
 Sb, cleavage faces, evaporation pattern determ. by decoration method in electron microscopy (German) 0-107626
 Sb₂Te₃, cleavage faces, evaporation pattern determ. by decoration method in electron microscopy (German) 0-107626
 Se, habit variation of crystals of the C₃2-C₃2 space group 0-107090
 Si, near (111), fracture by painted indenter, SEM study 0-71734
 Te, habit variation of crystals of the C₃2-C₃2 space group 0-107090
 W bicrystals, crack propag. across grain boundaries, crack speed meas. technique appl. 0-108575

crystal defects

- see also Cottrell atmospheres; crowdions; crystal inclusions; crystal microstructure; defect electron energy states; disclinations; dislocations; grain boundaries; impurity-defect interactions; phonon-defect interactions; point defects; stacking faults; twinning*
 accelerator irradiation, heavy ion irradiation damage 0-100291
 adsorbed layers, commensurate-incommensurate transitions, substrate defects effect 0-75437
 alkali halide:alkaline-earth cations, defect structs. examined by methods based on Mott-Littleton techniques 0-59487
 anthracene, orientationally disordered cryst., lattice relax. effect 0-107278
 brass wire, US inspection, immersion method 0-66757
 chalcogenide glass-like semiconductors, defect model, neutral diamagnetic quasimolecules, excess orbital bonds (Russian) 0-70647
 classification according to influence on radiative diffraction (Russian) 0-70189
 α' copper phthalocyanine and chlorinated derivative mol. crystals, radiation damage in electron microscope 0-107328
 corundum, defect cryst. struct. study 0-103316
 dating method with digital ESR 0-86542
 diamond, accelerator irradiation, heavy ion irradiation damage 0-100291
 diamond, ultradisperse, ESR, particle size and lattice microdistortions 0-97140
 dickite, unusual crystal habit, structural disorder 0-59445
 diffraction contrast and defect symm. 0-79778
 dimension determination by acoustic emission 0-104381
 early work on imperfections in crystals, and forerunners of dislocation theory 0-62450
 elastic interaction of defects in crystal under high hydrostatic press. 0-96512
 electron diffraction contrast and defect symmetry, theory 0-96418
 electron diffraction contrast for lattice defects, analytical calcs. in two-beam case 0-100134
 electron microscope imaging 0-88006

crystal defects continued

- electron microscopy, imaging and diffraction from localised defects and disorder 0-100152
- elemental semiconductors, group IV, Mossbauer spectroscopy of defects, radiation damage and deep levels 0-59533
- entropy of formation, of defects or inhomogeneities, validity of eqn. 0-79960
- extended defect system, phase transform., critical props. 0-103455
- ferromagnet, domain wall motion, pinning by lattice defects, magnetisation 0-71079
- film defect growth and nucleation, electron microscopy and diffraction exam. (French) 0-59824
- geometrical theory of structural defects (German) 0-88136
- III-V multilayer structure, as-grown, assessment of defects by differentiated cathodolum. topography 0-59819
- III-V semiconductors, radiative recomb., optical evaluation review 0-60647
- ill-condensed matter, summer school, Les Houches, France (July-Aug. 1978) 0-82561
- insulator, wide-gap, damage by UV laser radiation 0-76110
- intermetallic phases, B2 struct., substitutional and triple defects, enthalpies of formation 0-96520
- ionic crystals, defects, computer modelling, review 0-107205
- ionic crystals, influence of defect interaction upon their recomb. 0-84206
- ionic crystals, lattice defects, conference, Canterbury, England (Sept. 1979) 0-105420
- IR crystals, optical imaging of growth defects 0-64988
- lattice defect information from diffusion studies (Dutch) 0-96681
- lattice defects and diffusion processes in solids, book 0-107207
- lattice fringe imaging theory 0-103225
- lattice image calculations for imperfect crystals, superlattice approach 0-107030
- lattice images of defects, computer simulation of high resolution images 0-107208
- Laue reflections splitting and defects image contrast form. (Russian) 0-64833
- macroscopic defects, ordered regions and percolation phase transform. (Russian) 0-92665
- magnetic field, technical-saturation approx. 0-87262
- many-beam lattice images from thicker crystals 0-88004
- metal, blister formation due to the ion irradi. 0-65072
- metal, induced elastic interaction of dilatation centres with grain boundaries (Russian) 0-84205
- metal, pure, with max. of cryst. lattice distortion, struct. and strength props. (Russian) 0-89234
- metals, positron trapping by defects influence of positron-phonon and electron-phonon interactions (Russian) 0-93425
- metals, radiation defect treatment at annealing stages V and VI (Russian) 0-71676
- minerals, high-resolution TEM obs. 0-72517
- minority carrier recombination 0-65591
- muon spin rotation method, review (Polish) 0-88901
- negative activation volumes calc. 0-92518
- phase transitions, defect influence on solid props. 0-75334
- α -quartz, synthetic, growth, defects induced by seed orientation 0-96454
- radiation damage, mechanisms, in semiconductors and insulators, review 0-107315
- SEM observation of single defects using electron channel imaging 0-64848
- semiconductor, defect electronic structure and lattice config., MO approaches 0-65495
- semiconductor, kinetics of defect cluster annealing 0-84209
- semiconductor, SEM charge-collection images, contrast formation 0-70087
- semiconductor injection lasers, defect-induced pulsations, theory 0-91793
- p-Si, anodic etching for discriminating between elec. active and inactive defects 0-108605
- n-Si, recombination centres and carrier lifetimes after γ -irrad. 0-60004
- stationary lattice defects as sources of elastic singularities in micropolar media 0-107206
- steel, stainless, Type 316, neutron irradi. effects on tensile props. and microstruct. 0-65059
- steel wire, US inspection, immersion method 0-66757
- STEM, structural and chemical analysis, apps. 0-88003
- structural phase transitions, crit. dynamics and quasi-elastic scatt. 0-92641
- structure determination, light interference, diffraction and scattering 0-103316
- TGS, static crit. phenomena, lattice defect influence 0-71336
- thermoelectric alloys, phase diagrams, and imperfection chemistry 0-108422
- transparent solid optical materials, laser damage statistics rel. to structural defect statistics 0-91829
- TTF-TCNQ crystals, X-ray topographic study of cryst. perfection 0-96525
- X-ray diffraction by close-packed crystals, chaotic subtraction packing defects, general soln. 0-92422
- X-ray topography, developments, review 0-64836
- AgGaS₂/Fe, EPR of Fe-associated defect 0-60412
- Al-Ag, type-II superconductor, torque oscillations in mag. field (Russian) 0-103800
- Al-Ta₂O₃-Al, healing of defects in dielec. film by anodisation 0-65406
- Al₂O₃, β - and β' -phases, defect struct. obs. by high resolution TEM, battery ageing relevance 0-107501
- B fibre, US inspection, immersion method 0-66757
- BP:Zn(Se)(Cd), epitaxial layers, ion implantation, defects and lattice locations, channelling obs. 0-88179
- BaF₂:La³⁺, thermal depolarisation of La³⁺-F_i⁻ defect dipoles 0-75926
- Ba₂Sr_{1-x}Nb₂O₆ crystals, defects and their characteristic features 0-88138
- Be, blisters due to He irradi., proton backscatt. study 0-75273
- δ -Bi₂O₃, thermoelectric power rel. to fast ionic conduction 0-107549
- δ -(Bi₂O₃)_{1-x}(Y₂O₃)_x, thermoelectric power rel. to fast ionic conduction 0-107549
- CaCO₃:Li, synthetic calcite, (CO₃Li)²⁻-Li⁺ defect after X-irrad., EPR study 0-75852
- CaF₂:Er, defect structure, quenching effect, dielec. relax. and optical absorption 0-65031
- CaF₂:Eu, Mn, cathodoluminescence SEM appl., stroboscopic 0-70088
- CaF₂:La³⁺, thermal depolarisation of La³⁺-F_i⁻ defect dipoles 0-75926

crystal defects continued

- Ca₂(Mg,Fe)₂(Si₄O₁₁)₂(OH)₂, amphibole nephrite, planar defects termination, high resoln. electron microscopy 0-79772
- Cd,Hg_{1-x}Te, elec. characts., impurity effects 0-92890
- CdSe:Li, pure and doped, reson. Raman and Brillouin scatt., elastic excitation-defect scatt. 0-80788
- p-CdSiAs₂, electron irradi. elec. props. annealing, lattice defects 0-100465
- CdTe:As(P), ion implanted, elec. props. 0-65021
- CeO₂:CaO(Y₂O₃), oxygen ion cond. and defect struct. 0-107553
- Cu, blisters due to He irradi., proton backscatt. study 0-75273
- Cu, irradiation with O₂ ions, defect production and annealing 0-88214
- Cu₃Au, neutron irradi., displacement cascades, direct obs. method 0-107335
- CuWO_{4-x} prod. from CuO+WO₃ solid state reaction 0-66796
- EuS films, mag. and elec. props. rel. to stoichiometry and defects 0-97122
- Fe-Si (2-8 wt.%), single crystals, growth striations, X-ray studies 0-79774
- Fe₈₀B₂₀, amorphous, cold neutron scatt., local and extended defects 0-84089
- Ga_{1-x}Al_xAs visible diode lasers, degradation mechanisms 0-64026
- GaAs cleaved (110) face, interaction with O₂, influence of cleavage defects, AES study 0-66684
- GaAs, defect cluster annealing, pot. barrier height determ. 0-84209
- GaAs, epitaxy by metallorganic and chloride depositions, defect characterisation at growth interface 0-59817
- GaAs, gas-phase epitaxy, step stopping centre form. kinetics 0-65407
- GaAs single crystals, laser damage statistics rel. to structural defect statistics 0-91829
- GaAs:Si, IR absorpt. bands, localised modes, Si-related defects 0-76054
- GaInAsP diode lasers, self-sustained pulsations in light output 0-64012
- Ge, compensated by thermal defects, recomb. and optical props. 0-64989
- Ge foil, [110] oriented, seven-beam lattice images of defects 0-107209
- Ge, lattice images of defects and radiation damage appls. 0-107210
- InGaAsP-InP DH LED, high temp. aged, dark-spot defects, TEM obs. 0-66300
- In₂O₃, thin film, sputter deposition form., optical and elec. props. 0-60123
- n-InP, heat treatment in controlled P vapour 0-88137
- In₂O₃, thin film, sputter deposition form., optical and elec. props. 0-60123
- KCl, pure and Ba doped, symm. of elastic fields due to defect displacements, diffuse X-ray scatt. 0-70256
- KClO₄:CrO₄²⁻(SO₄²⁻), AC electrical conductivity meas. between temp. range 25-325°C, automated technique 0-59699
- K₂Pt(CN₅)Br_{0.1}3H₂O, anisotropic radiation damage in electron microscopy, diff. spot fading rate obs. 0-107329
- LaB₆ crystals, zone refined, chem. characterisation 0-93821
- LaPO₄, catalyst crystals, high resolution electron microscopy, morphological characts. rel. to catalytic activity 0-107193
- α -LiIO₃, defects decorated by space charge, X-ray topography study (Chinese) 0-107204
- α -LiIO₃, surface defect layer struct. due to mechanical working (Russian) 0-100238
- Li₂O, neutron irradi. effects, optical absorpt. spectra 0-75271
- Mo crystals, joined by compression during heating, structural changes (Russian) 0-108513
- Mo wire, US inspection, immersion method 0-66757
- MoS₂, lattice images of defects and radiation damage appls. 0-107210
- N₂ matrix N-N stretching vibr., IR activation, guest mol. depend. 0-60570
- Na-Co strip-chain silicates, structural-composition inhomogeneities 0-88122
- Nb, blisters due to He irradi., proton backscatt. study 0-75273
- Nd_{1-x}Ca_xVO₃, solid solutions, elec. props. 0-96866
- Ni-NbC (10 wt.%) eutectic alloy, directional solidification and struct. (Russian) 0-84922
- Pb film, monocryst., heteroepitaxial growth, struct. defects, and elec. props. (Russian) 0-84403
- PbTe, effect of pressing and sintering, study of induced defects by SEM 0-59983
- Si, annealed, photoluminesc. anal. of defects 0-80836
- Si, annealing during Czochralski growth, influence on defect density 0-60769
- Si, blistering due to 400 to 1800 keV ⁴He⁺ ions, modal range determ. 0-100289
- Si, compensated by thermal defects, recomb. and optical props. 0-64989
- Si, crucible grown, virgin and implanted, laser irradiation effects on surface structure 0-92768
- Si crystal, Czochralski grown, enhanced Borrmann effect 0-70191
- Si crystal growth, for electronic devices 0-66419
- Si, defect crystal structure 0-103316
- Si dislocation free, quantitative determ. of microdefect density by preferential chem. etching 0-65001
- Si, float zone, process-induced effects on carrier lifetime and defects 0-81216
- Si, heavy ion induced disorder in surface and at shallow depths 0-59535
- Si, high-dose Ar implantation, X-ray topographic obs. of strains and damage 0-59496
- Si, ion bombardment induced defect distrib., IR and electron diff. study 0-65074
- Si, lattice images of defects and radiation damage appls. 0-107210
- Si, n⁺-p diode, γ -radiation defects, annealing and recomb. props. 0-65045
- Si p-n junctions, avalanche breakdown anisotropy 0-70811
- Si polycrystalline film, effect of defects/grain boundaries on photovoltaic mech. 0-93883
- Si, residual stress and defects induced by scribing 0-60990
- Si single crystals, laser damage statistics rel. to structural defect statistics 0-91829
- Si solar cells, capacitance transient spectra of processing- and radiation-induced defects 0-61340
- Si surface, thermal oxidation induced defects, origin and growth (Chinese) 0-66681
- Si wafers, floating-zone, etch struct. on microdefects as affected by dopants and surface treatment 0-79773
- Si:B, ion implanted, structure defects formation and behaviour under annealing in various ambients 0-65033
- Si:B implanted wafers, ionis. assisted annealing and effects 0-100257
- Si:H, Li, amorphous, photoluminescence obs. 0-66280
- SiO, Czochralski crystal, oxygen striation and thermally induced microdefects 0-100275

crystal defects continued

- Si:P polycrystalline layer, role in lattice defect reduction assoc. with P predeposition 0-70229
 Si:Sb, high dose Sb ion implantation, buried layer appls. 0-88186
 Si-SiO₂, ion implantation through SiO₂ film, recoil implantation of O, EPR study 0-88180
 Si-SiO₂ interface in MIS strucs., effects of crystal defects on generation process 0-65702
 SiO₂ films, growth on Si, role of defect structure 0-65403
 (SiTe)_{1-x}(ATe)_x, A=Ge, Sn, Pb, solid soln. with small substitution, mag. susceptibility (*Russian*) 0-70933
 SrF₂:La³⁺, thermal depolarisation of La³⁺-F⁻ defect dipoles 0-75926
 TMMC, antiferromagnetic chain, 3-D ordering temp. controlled by solitons and defects, mag. field depend. 0-60275
 TaS₂, 1T and 1H polytypes, fast neutron irradi., defect prod., effects on resist. and charge density waves 0-65060
 V₂O₅, wedge shaped cryst., electron lattice image interpret. 0-103319
 W (110) stepped surface, electron stimulated desorption of O, atomic steps and defects influence 0-80091
 W wire, US inspection, immersion method 0-66757
 WO₃, reduction, defect role, in situ HVEM obs. 0-81323
 Y₃Al₂O₁₂ crystal growth from melt, gas bubble capture theory 0-64941
 Y₃Fe_{5-x}Ga_xO₁₂, mag. domains and cryst. defects 0-75789
 ZnS film, defect form. and development 0-96759
 p-ZnSAs₂, electron irradi. elec. props. annealing, lattice defects 0-100465
 Zr, H(D) implanted, superconductivity enhancement obs. 0-70884
 ZrO₂, doped, ionic cond., theoretical model 0-107552

crystal dislocations see dislocations

crystal electron states see electron energy states (condensed matter)

crystal energy see lattice energy

crystal etching see etching

crystal faces

- birefringent crystal faces, meas. method of growth and dissoln. rates 0-79719
 coatings, textured, crystallites faces determ. 0-64846
 cubic crystals, growth-layering effect on optical symmetry 0-88072
 growth models, attachment energy as habit controlling factor 0-59420
 ice disc growth from vapour, cryst. habit change mechanism 0-84117
 Mg (0001) face, incipient oxidation, EELS and LEED studies 0-81237
 sapphire, growth angle determ. from cryst. lateral face shape and solidified separation drops 0-103282
 Ag, electrodeposit, on (111) face, habit modification caused by Cl⁻ 0-71600
 Au particles, small single cryst., habit plane characterisation 0-79733
 InSb, crystal growth from melt, facets and twin formation obs. (*Chinese*) 0-59409
 InSb, growth angle determ. from cryst. lateral face shape and solidified separation drops 0-103282
 KH₂PO₄ single crystal evidence for spiral growth on pyramidal faces 0-84120
 NH₄H₂PO₄ single crystal evidence for spiral growth on pyramidal faces 0-84120

crystal field interactions

see also crystal hyperfine field interactions

- A-15 superconductors, transition temp., d band relative displacement (*Chinese*) 0-103770
 alkali halide:Eu²⁺, spin-Hamiltonian parameters, superposition model calcs. 0-96830
 alkali halides: cation with s² ground-state configuration, absorption bands assignment 0-97310
 alloys, magnetic anisotropy, influence of local symmetry (*Russian*) 0-93109
 aniline, in p-xylene host cryst., phosphoresc. triplet state, ESR and MIDP obs. 0-66077
 aniline-chlorophenol complexes, ³⁵Cl NQR, inter- and intramol. interactions 0-63666
 anthracene:tetracene, electronic absorpt. spectrum, host-cryst. field effect 0-100669
 biphenyl:tetracene, electronic absorpt. spectrum, host-cryst. field effect 0-100669
 boracite, single cryst. prep. and phys. props. 0-100763
 carbazole:tetracene, electronic absorpt. spectrum, host-cryst. field effect 0-100669
 chloroanisoles, ³⁵Cl NQR, inter- and intramol. interactions 0-63666
 chlorophenols, ³⁵Cl NQR, inter- and intramol. interactions 0-63666
 cubic complexes, weak-field coupling scheme 0-92866
 cubic crystals, pseudo-tetragonal AFR spectra 0-88861
 diatomic molecule, electron correlations, cryst. field interactions, Hubbard calc. 0-75530
 displacive phase transition, S ion spin Hamiltonian parameter dependence on order parameter 0-70356
 ferromagnet, easy-plane, magnetic anisotropy, temp. and field depend., classical model 0-71008
 garnets, superexchange operator and cryst. field interactions 0-59931
 guanidine aluminium sulphate, lattice charge contribution to coordination polyhedron cryst. potential 0-103651
 guanidine aluminium sulphate hexahydrate:Cr³⁺, ESR spectra fine struct. 0-93169
 insulators, charge transfer processes influence on cryst. field 0-92865
 Ising spin glass, glass, Edwards-Anderson order parameter instability 0-71043
 lanthanum ethylsulphate:Gd³⁺, zero-field splitting, contributory mechanism 0-80231
 magnetism, conference, Munich, Germany (Sep. 1979) 0-56997
 metals, Kondo effect, Anderson hamiltonian 0-60187
 metamagnetic tricritical point, effective exponent β 0-71045
 Mossbauer ⁵⁷Fe spectra, ferrous charact., cryst. field interactions 0-108133
 naphthalene:tetracene, electronic absorpt. spectrum, host-cryst. field effect 0-100669
 radiative transitions, proximity effects, role of vibronic coupling and static crystal field interactions model 0-69126
 rare earth compounds, multipolar interactions, evidence and origins 0-59935
 rare earth impurity, ESR, exchange induced broadening in low lying crystalline field system 0-108062
 rare earth intermetallic cpds., cryst. field effects rel. to mag. props. 0-59933
 rare earth ion spectra, crystal field integral parameters, spin-orbit interaction 0-100447
 rare earth orthoferrites, mag. anisotropy in cryst. field approx. 0-60241
 rare earth oxyhalides: Eu³⁺, fluorescence spectra obs. (*French*) 0-89042
 rare earth pseudobinary intermetallic compounds, ESR studies 0-108064
 rare earth-Ag alloy, amorphous, model calcs., of mag. props. 0-84616
 rare-earth ions, charge transfer and crystal field theory 0-70654
 reduction symmetry method in crystal field theory 0-70656
 solid state theory, 1926-33 0-57067
 TGS crystals, effects of radiation induced defects on internal bias field 0-88941
 transition metal compound, superexchange interaction, effective spin-orbital Hamiltonian 0-70998
 transition metal compound, superexchange interaction, multielectron theory 0-70997
 transition metal halides and oxides, cryst. field stabilisation and lattice energy 0-75201
 3d-transition metal ions, s-doublet struct., appl. of exchange correlation mass operator approx. 0-106266
 Al/AlO₃/La-rare earth metal tunnel junctions, cond. meas., cryst. field effects 0-88694
 Au(111), A-line valence bands, angle-resolved photoemission determ. 0-108323
 BaMgF₂:Mn²⁺ ferroelec., EPR and ENDOR study, cryst. field tensor 0-71162
 Ba₂NbRu₃O₁₂ and Ba₄TaRu₃O₁₂, (Ru₃O₁₂)¹³⁻ cluster obs. in presence of orbital degeneracy and spin-orbit coupling (*French*) 0-70655
 CaO:Eu²⁺, influence of crystal field on luminesc. (*Russian*) 0-80834
 Cd complexes, dithiocyanato(diethylenetriamine) Cd(II) and dithiocyanato(pentamethyldiethylenetriamine) Cd(II), Cu²⁺ doped, ESR 0-108059
 CdCr₂Se₄, energy structure, magnetooptic effects 0-71394
 (Ce, La)Ni₃, heat capacity and elec. resist. 0-71049
 CeAl₃, resistivity and volumetric meas., phase diagrams, comparison with CeS 0-107789
 CeBiSb_{1-x}, mag. props. and press. effects 0-71026
 Ce(In, Sn)₃, heat capacity and elec. resist. 0-71049
 Ce_{0.9}-La_{0.1}Th_{0.1}, mixed valence state, static and dynamic mag. response 0-103816
 CeS, resistivity and volumetric meas., phase diagrams, comparison with CeAl₂ 0-107789
 CeSb₂As_{1-x}, mag. props. and press. effects 0-71026
 CeTi₃, mag. susceptibility, magnetisation, neutron diff., elec. resist., and sp. ht. meas. 0-75733
 Ce_{0.08}O_{0.92}Sb, dilute F-electron system in cluster regime, crystal field and exchange splittings 0-97062
 CrAs, high press. paramag. antiferromag. transitions, elec. props., band model development (*Russian*) 0-60277
 CsCoBr₃, ID Ising antiferromagnet, spin dependent Raman scattering from phonons and electronic excitations 0-103948
 CsMHoF₆, (M=Na, K, Rb), mag. behaviour (*German*) 0-65774
 Cs₂NaErCl₆, mag. susceptibility and IR and Raman spectra meas., crystal field splitting determ. 0-100652
 DyNi₃, crystal, basal plane anisotropy, torque meas. 0-65857
 Er_{1-x}La_xRh₂B₄, mag. and supercond. transitions, cryst. field effects 0-107950
 Er_{1-x}La_xBe₁₃, mag. sp. ht. and ESR, cryst. field interactions 0-60290
 ErMo₆Se₆, mag. supercond., neutron scatt. obs. 0-70952
 Er_{1-x}Tm_xRh₂B₄, mag. and supercond. transitions, cryst. field effects 0-107950
 Eu double metaphosphates with alkali metals or H, luminesc. props. 0-100675
 Eu²⁺ impurities in cubic crystals, 5d-4f radiative transition probability calc. 0-71474
 Eu_{1-x}La_xAl₂, cryst. fields and exchange parameters, ESR meas. 0-71175
 EuO, cryst. field parameters due to 4f⁷-5D configs. 0-80230
 Fe³⁺, zero-field splittings, correl. with axial site distortions, superposition model 0-93168
 FeCl₂, reorientation of mag. moments under mech. stresses at 0K 0-93153
 Fe₃O₄, polar Kerr effect invisible and near IR spectral regions 0-108187
 Fe³⁺(S) paramagnetisations, spin lattice relaxation Mossbauer study, dynamic spin Hamiltonian formalism 0-97173
 Fe_{1-x}Zn_xF₂, dil. antiferromag., electronic and mag. props., Raman scatt. and optical absorpt. study 0-108207
 GaAs:V, ion implanted, luminesc., level splitting 0-97338
 GaP:Co, optical spectra and Zeeman anal. of Co 3d⁷ state 0-66247
 GdCo₅Ni_{1-x}, intrinsic coercivity, anisotropy, exchange and cryst. field interactions 0-75806
 Gd₂La_{1-x}Al₃, cryst. fields and exchange parameters, ESR meas. 0-71175
 H₂, molecular, interact. with solid matrix. 0-80229
 HoCo₅, mag. excitations, neutron inelastic scatt. meas. 0-60231
 HoMo₆Se₆(Se₈), mag. supercond., neutron scatt. obs. 0-70952
 HoRh₂B₄, low temperature magnetic properties 0-88728
 KCr₂Al_{1-x}(SO₄)₂·12H₂O, EPR of single crystals, zero-field splitting of Cr³⁺ 0-66015
 K₂FeF₄, two-dimensional antiferromag., cryst. field effects, Mossbauer spectroscopy 0-71254
 K₂FeF₇, two-dimensional antiferromag., cryst. field effects, Mossbauer spectroscopy 0-71254
 K₂NaGaF₆:Cr³⁺, magneto-optical study of ²T_{1g}, ⁴T_{2g}, ²E_g-A_{2g} transitions 0-71384
 KY₃F₁₀:Eu³⁺, cryst. field parameters and intensity parameters, J-mixing effects 0-59932
 (La,Nd)Sn₃, reverse Kondo effect in presence of crystalline elec. field splitting 0-103684
 LaAl₂, doped with Tb, Nd, or Pr, crystal field effects, tunnelling within mK range 0-70907
 LaBe₁₃:Er, ESR, appl. of exchange induced broadening in low lying crystalline field system 0-108062
 La₂Be₂O₇:Nd³⁺(Pr³⁺), cryst. growth, spectral and laser properties in ⁴F_{3/2}-⁴I_{11/2} and ⁴F_{3/2}-⁴I_{13/2} transitions 0-80853
 LaBr₃:Nd³⁺, energy level anal., polarised absorpt. and fluoresc. spectra 0-76056
 LaCl₃:Nd³⁺, energy level anal., polarised absorpt. and fluoresc. spectra 0-76056
 LaCl₃:U³⁺, cryst. spectrum anal., cryst. field parameters 0-76057
 LaF₃:Pr³⁺, ultraslow optical depahing 0-58648
 LaF₃:Pr³⁺, R=rare earths, crystal field anal., intensity calcs. 0-100670
 La₂Li_{0.5}Co_{0.5}O₃ phase, intermediate electronic configuration 0-80226
 (La₂O₃)_{0.95}(CeO₂)_{0.05}:Mn²⁺, X-band EPR study 0-60409
 LaPb₃, doped with Tb, Nd, or Pr, crystal field effects, tunnelling within mK range 0-70907

crystal field interactions continued

- LaSn₃, doped with Tb, Nd, or Pr, crystal field effects, tunnelling within mK range 0-70907
 Li_{0.5}Fe_{2.5-x}Cr_xO₄ press. depend. of anisotropy consts. 0-65865
 LiR₂F₄ (R=Th, Ho, Er), cryst. field parameters, mag. susceptibility meas., 0.3 to 100K 0-60214
 LiTmF₄:rare earth, EPR spectra, elec. field effects, cryst. field interactions 0-71176
 LiYF₄:rare earth, EPR spectra, elec. field effects, cryst. field interactions 0-71176
 Mg-Tb(Dy)(Ho)(Tm), dil., macroscopic shape effect due to quadrupole orientation, magnetostriction and thermal expansion meas. 0-60396
 MgO:Cr³⁺, ODMR study, Cr³⁺ ions in tetragonal symm. sites 0-88892
 MgS:Ce³⁺ phosphors, emission and excitation spectra (French) 0-93380
 Mg₂TiO₄:Cu(Ni), ESR of Cu²⁺ and Ni²⁺ 0-97131
 Mn²⁺, zero-field splittings, correl. with axial site distortions, superposition model 0-93168
 N₂ complex, Ni(C₆H₅NO)₆(NO₃)₂, singlet ground-state systems, field induced mag. long range order 0-60266
 Na₃Pr(C₆H₄O₃)₃·2NaClO₄·6H₂O, absorpt., circular dichroism, and mag. circular dichroism spectra 0-97243
 Nb, isotope effects for H₂ diffusion, crystal field stabilisation 0-59728
 Nd₂O₃ and Nd₂O₂S, electrostatic cryst. field parameters including induced dipole contribs. 0-80233
 Nd(OH)₃, heat capacity from 10 to 350K, lattice and Schottky contribs. 0-84300
 NdSn₃, elec. cond., cryst. field effect, spin disorder contrib. 0-65540
 Ni complexes hexamethylamine nickel halides, Ni²⁺ EPR in high pulsed mag. field, zero field splitting parameters 0-71160
 Ni Tulton salts, cryst. field spectra in visible and near IR regions, solid diffusion effect 0-100666
 Ni-Cu, ferromag., mag. moment, local environment effects, HF CPA cluster calc. 0-65817
 NiPtCl₆·6H₂O, singlet-ground-state magnets, ESR at low temps. 0-97132
 NiSiF₆, dilute, single-spin cross-relax. calcs. 0-97129
 NiSnCl₆·6H₂O, singlet-ground-state magnets, ESR at low temps. 0-97132
 NpO₂, mag. transition at 25K, Kramers doublet as cryst. field ground state 0-59936
 PbMoO₄, doped and undoped single crystals, polarisation of luminesc. and assignments 0-76069
 PbWO₄, doped and undoped single crystals, polarisation of luminesc. and assignments 0-76069
 Pd-Co, dil., breakdown of ferromag. order, magnetoresist. obs. 0-71046
 PrIn₃, nucl. orientation of ¹⁴¹Pm in singlet ground state, exchange interaction and cryst. field splitting obs. 0-71275
 Pr₂La₂₀-Au₂₀, amorphous, low temp. excitations, specific heat 0-100337
 PrMg₃, cryst. field study, inelastic neutron scatt. and sp. ht. meas. 0-59939
 PrNi₂-Gd, dil., single crystal, ESR study 0-75850
 Pr₂Se₄(S₄), induced ferromagnet, mag. props. under hydrostatic press. 0-60395
 Pt porphyrin in n-alkane single cryst. ³E_u-¹A_{1g} transition, Zeeman expts. at 4.2K 0-78645
 Pt-Fe, dil., breakdown of ferromag. order, magnetoresist. obs. 0-71046
 Pt(III), A-line valence bands, angle-resolved photoemission determ. 0-108323
 SmO, cryst. field parameters due to 4f^{N-1}5D configs. 0-80230
 SrF₂:Ce³⁺, cryst. field energies 0-59941
 (Tb₂La_{1-x})Be₁₃, mag. struct., cryst. field effects, neutron diff. study 0-65789
 TbPO₄, zircon struct., cryst. field analysis 0-80232
 TbZn, mag. excitations meas. 0-70979
 TiO₂, core levels, cryst.-field splitting, X-ray emission study 0-66328
 TiO₂:Ru⁴⁺, rutile, EPR and cryst. field const. 0-60415
 Tm_{1-x}Eu_xSe, semicond. with valence instabilities, cryst. chem. considerations 0-100213
 TmSe, first obs. of negative elastic const. 0-103409
 TmSe, intermediate valence cpd., susceptibility, single-ion approach 0-70935
 TmSe_{1-x}Te_x, semicond. with valence instabilities, cryst. chem. considerations 0-100213
 U₂As₄, ferromag., mag. field induced phase transitions 0-65887
 U₂As₄, heat capacity, 5-300K, ferromag. transition obs. 0-88769
 U(BH₄)₄ in Hf(BH₄)₄, excited state assignments and E-symmetry ground state, near IR MCD obs. 0-66153
 UBr₃, cryst. field levels, neutron scatt. determ. 0-65509
 UF₆, matrix isolated, vibronic fine struct. in fluorenc. spectrum 0-83406
 UO₂, electronic transitions, crystal field effects and phonons, phase transition 0-97303
 V, isotope effects for H₂ diffusion, crystal field stabilisation 0-59728
 V₂O₅, core levels, cryst.-field splitting, X-ray emission study 0-66328
 α-W₂V₂O₈, paramag. defect study by ESR 0-103881
 YFeO₃, mag. anisotropy in cryst.-field approx. 0-60241
 Y_{1-x}Tb_xPd₃, magnetisation, magnetostriction, and inelastic neutron spectra 0-65998
 YVO₄:Nd³⁺, zircon struct., cryst. field analysis 0-80232
 YbFe₃, cryst. elec. field and exchange interac., ¹⁷⁰Yb Mossbauer obs., magnetostriction contrib. 0-108124
 YbGa₃, mag. props. between 44-600 mK 0-80517
 YbO, cryst. field parameters due to 4f^{N-1}5D configs. 0-80230
 Y-Yb₂Se₃, mag. susceptibility and cryst. field parameters 0-65510
 Zn, core levels, cryst.-field splitting, X-ray emission study 0-66328
 Zn(BF₄)₂·6H₂O:Ni, phase transition study, EPR of diluted Ni²⁺, 98-298K 0-75846
 ZnCr₂O₄, antiferromag. spinel, absorpt. and luminesc. spectra 0-66225
 (Zr_{0.2}Y_{0.8})₂O₃:Cr, Mn, stabilised single crystal, EPR of Mn²⁺ and Cr³⁺ obs. 0-66024

crystal field splitting see crystal field interactions

crystal field theory see crystal field interactions

crystal fields see crystal field interactions

crystal filters

- band stop using periodically corrugated piezoelec. cryst., Bleustein-Gulyaev waves behaviour 0-96115
 HF, using Pb(Zn_{1/3}Nb_{2/3})O₃-PbTiO₃-PbZrO₃ and Pb(Mg_{1/3}Nb_{2/3})O₃-PbTiO₃-PbZrO₃ (Japanese) 0-60507
 LiTaO₃ crystals for commercial SAW TV IF filters, fabrication 0-80961

crystal growth

- see also crystal growth from melt; crystal growth from solution; crystal growth from vapour; crystal purification; crystallisation; dendrites; epitaxial growth; nucleation
 apatite crystal growth in skeletal tissues 0-94181
 conference, 3rd international summer school on cryst. growth, New Hampshire, USA (July 1977) 0-57008
 conference, Lancaster, England, Sept. 1979 0-62369
 crystal face, growth behaviour in presence of screw dislocations 0-103276
 cubic crystals, growth-layering effect on optical symmetry 0-88072
 dynamic computer models 0-103284
 electron microscopy, decoration method, rel. to crystal growth (German) 0-103222
 electronic materials 0-66405
 face effect, with paraboloidal or ellipsoidal isotherm effect 0-107085
 graphitisation and crystal growth, review 0-89165
 ice, Antarctic, cryst. size and climatic record down to last ice age 0-94544
 III-V semiconductors, point defects and deep traps, thermodynamic history, model 0-59908
 kinetic coefficient of two-phase transitional region between A+B melt and crystalline bulk phase A 0-96455
 kinetic theory equation, binary system crystallisation 0-88071
 melt crystallisation in self-excited vibr. regime 0-103275
 one-dimensional Stefan problem, expansions in time 0-64354
 phase boundaries in first-order phase transitions, dynamics stability 0-107403
 phase diagrams and crystal growth 0-66407
 polar materials, appl. to SAW and other devices 0-66114
 sealed ampoule of fused SiO₂ for cryst. growth, thermal transmission function 0-84731
 semiconductors, appl. of analytical techniques for observation 0-73546
 single crystals, growth simulation 0-88069
 stress, and dislocations, creation during crystal growth (Russian) 0-103277
 topological modelling of crystal growth 0-59418
 transients in cryst. growth rate 0-84118
 transition metal silicides, growth and characterisation 0-66408
 TTF-TCNQ crystals, X-ray topographic study of cryst. perfection 0-96525
 α-Ag₂Se, single cryst. growth through capillary tube 0-108331
 Fe(Sb_{1-x}Te_x)₃ system cpds., prep., cryst. struct., elec. and mag. characteris. 0-108349
 K₂Mo₂S₁₁, prep. and struct., Mo₁₂ cluster in Mo₁₂S₁₄ unit 0-107168
 LiNbO₃ single crystals grown by automatic diameter control, power striations (Chinese) 0-81080
 Mo₂Si₃, layer electrotransfer of Si 0-92708
 Pb_{1-x}Pb_x mixed systems, cryst. growth, struct. and optical props. (German) 0-96499
 Ti₂Mo₂S₁₁, prep. and struct., Mo₁₂ cluster in Mo₁₂S₁₄ unit 0-107168

crystal growth from gel

- modified gel technique improved design to grow larger more perfect single crystals 0-84842
 AgCl crystal growth in gelatin soln. 0-64942
 BaMoO₄ crystals, growth in SiO₂ gel under influence of elec. field 0-93469
 CsSn₃I₃, surface props., Auger study, elec. cond. meas., photochem. study 0-66339
 PbI₂ single crystal growth, modified gel technique improved design 0-84842

crystal growth from melt

- see also liquid phase epitaxial growth; zone melting
 accelerated crucible (and crystal) rotation technique, for cryst. pulling 0-64935
 alkaline earth fluorides, cryst. growth in reactive atmosphere 0-80962
 n-alkanes purification and single cryst. growth 0-71589
 alloy melt, impurity conc. field model, growth by Czochralski method (Russian) 0-75191
 alloy melt, temperature distribution during cryst. growth by Czochralski method (Russian) 0-75192
 benzil cored fibres, void-free cryst. growth, X-ray diff. and optical microscopy study 0-71586
 binary alloys, directional solidification, theory of dendritic growth 0-70145
 binary alloys, initial transient segregation during unidirectional solidification in a furnace with thermal damping 0-70146
 Bridgman-Stockbarger technique, influence of insulation on stability of interface shape and position 0-59412
 chondrules, experimental reproduction of textures 0-94763
 composite material, matrix impurity distrib. in melt crystallisation (Russian) 0-100277
 convection caused by cryst. rotation in crucible, computational results 0-84116
 convection in melts, and cryst. growth under large inertial accelerations 0-66421
 countercurrent melt crystallisation, ultra-pure substance prep. 0-100779
 crystallising bar, oscillations, EM excitation 0-84845
 cylindrical pores growth, numerical calcs. 0-92471
 Czochralski crystal growth, heat, mass and fluid flow, computer simulation 0-104055
 Czochralski growth model, transient phenomena 0-84125
 Czochralski method, modified, variations of impurity distrib. 0-88193
 m-dinitrobenzene cored fibres, void-free cryst. growth, X-ray diff. and optical microscopy study 0-71586
 docosane, purification and single cryst. growth 0-71589
 edge-defined film-fed growth process, invention and appl. to sapphire 0-104057
 eicosane, purification and single cryst. growth 0-71589
 flow method, simple and economical apparatus (Italian) 0-80960
 glass forming melts, crystn. kinetics processes 0-64905
 heat resistant monocrystal growth apparatus, heat regimes, crystallisation (Russian) 0-107071
 horizontal crystal ribbon growth, meniscus stability 0-103281
 horizontal ribbon growth from melt, forced convection heat flow effects 0-107079
 II-VI and IV-VI semiconductors, optimal synthesis conditions for single cryst. growth 0-100776
 II-VI semiconductors, optimal synthesis methods for single cryst. growth 0-100764
 III-V semiconductors, methods (Czech) 0-89131

crystal growth from melt continued

- kinetic equation theory of multi-component crystal growth 0-75194
magnetic bubble materials, props. and preparation models, review (Rumanian) 0-93149
microsegregation in crystals, anal. 0-59410
mirror furnace at Czochralski growth 0-60766
multi-component growth, kinetic equation theory 0-79721
nondecane, purification and single cryst. growth 0-71589
rare earth-Sn-X, X=Rh, Ir, Ru, Co, cryst. growth and cryst.-chem. invest, supercond./mag. ternary cpds. 0-100777
refractories, single crystal growth, techniques 0-108341
ribbon growth by EFG method, dynamics and control of meniscus height 0-107081
ribbon growth using scanned focused CO₂ laser beams 0-66417
rotating container melt growth, crystallisation parameters calcs. 0-103285
sapphire, edge-defined film-fed growth process 0-104057
sapphire, growth angle determ. from cryst. lateral face shape and solidified separation drops 0-103282
sapphire, Stepanov's growth method, axial temp. distrib. 0-103280
sapphire ribbon crystals, EFG growth and charact., voids, grain boundaries and dislocations 0-103283
sapphire ribbon EFG prod., substrate for heteroepitaxial Si 0-108342
segregation, fluctuating growth rates effect, backmelting 0-59413
shaped crystal growth from melt, meniscus-controlled process 0-107075
Si:In growth by Czochralski crystal pulling, characterisation for extrinsic IR detectors, focal-plane arrays 0-76168
single crystal, techniques 0-108341
solute redistribution during crystallisation, interface field effects 0-84119
stability during capillary shaping, general theory of capillary and thermal stability 0-107076
stability during capillary shaping for arbitrary small perturbations 0-107077
Stepanov method, physical problems in shaped cryst. growth 0-103279
trivalent metal phosphates, condensed, synthesis in polyphosphoric acid melts, physicochem. equil. considerations 0-97419
vapour-liquid-solid growth mechanism (Russian) 0-107074
AgMg two phase bicrystal, growth by solid state diffusion couple method 0-60773
Al bicrystals, isoaxial, fatigue crack initiation in grain boundary affected regions (Japanese) 0-89338
Al single crystals, relation between axial orientation rotating and deform. banding 0-104206
B-Si alloys, B-rich, prep., anal. and cryst. growth (French) 0-104091
Ba₂NaNb₂O₁₅, growth layer form., crystallization conditions effect, light diff., Curie temp. 0-100778
Ba₂Ti₂O₇ single crystals, prep. and unit-cell parameters 0-103302
Bi and Bi-Sb (12 at.%), impurity distrib. control by electrotransfer method (Russian) 0-66418
Bi₂SiO₂₀, growth of single cryst. thin plates by EFG method 0-97423
Bi₂Te₃Bi₂Se₃ solid solns., single cryst. growth and thermocouple construct. 0-104056
BiTeI, melt and vapour growth, optical props. 0-84746
CaSiO₃, fibrous, controlled crystallisation and anisotropy 0-59425
Cd₂Ca_{1-x}MoO₄, growth and props. 0-71588
CdGeAs₂, vertical Bridgman growth with control of interface shape and orientation 0-66420
CdGeAs₂ crystals, Bridgman grown, optical props. rel. to O₂ content of starting materials 0-81213
Cd₂Hg_{1-x}Te, elec. characts., impurity effects 0-92890
CdTe, low temp. thermal cond., growth parameter influence 0-92725
Cd(WO₄)_{1-x}(MoO₄)_x, growth and props. 0-71588
CeB₆, crystal preparation, elec. resistance, phase transitions 0-97427
CePd₃ single crystal Czochralski growth and characterisation 0-60767
Co_{1-x}O, single cryst. growth by skull melting 0-84844
CsR(MoO₄) R=Dy, Ho, Er, permittivity temp. depend., polymorphic transition 0-92670
Cu-Al spherical crystals, grown from drop of melt, topography 0-84353
CuInTe₂ single crystals, directional freezing growth and doping, resist. changes on annealing 0-60768
CuSbS₂ crystals, growth and characterisation 0-60770
Er₃Al_{1-x}Ga₃O₁₂, LPE, spectroscopic props. 0-93419
Fe_{1-x}O, single cryst. growth by skull melting 0-84844
Fe₂SiO₄, fayalite, Czochralski growth under controlled O₂ fugacity conditions 0-84843
GaAs crystal growth, thermal and elastic const. evaluation 0-92586
n-GaAs, crystal growth by Czochralski method kinetics, total emittance determ. 0-75193
GaAs:B, incorporation of B during growth 0-93471
GaBO₃:Fe³⁺, ESR spectra, lattice parameters 0-93170
Ga_{1-x}In_xSb, Ga-rich, prep. by Czochralski technique 0-60771
GaP electroluminescent diode struct. prep. by SSD and Czochralski methods, dynamic props. (Czech) 0-97425
GaP, growth conditions rel. to dislocation structure 0-88151
GaSb, LEC growth, Hall coeff. 0-89133
GaSb LEC single crystal growth, novel encapsulant material 0-93475
α(β)-Ga₂Se₃, cryst. growth, optical, X-ray diff. and SEM study 0-71587
GaTe, single cryst. prep. and electroabsorp. spectra investig. 0-103968
GdBr₃, crystal preparation, elec. resistance, phase transitions 0-97427
Ge ribbon single crystals, grown from melt, dislocation struct. form. under thermal stress 0-107082
Ge single crystals, constitutional supercooling growth conditions, structural and chem. inhomogeneities 0-93473
Ge:O, IR absorpt. at low temp. (Chinese) 0-108228
Hg_{1-x}Cd_xTe, grown from melt, Kirkendall and Frenkel effects 0-100365
InBO₃:Fe³⁺, ESR spectra, lattice parameters 0-93170
InP, LEC growth of dislocation free crystals 0-89134
InP:S, SSD growth of low dislocation density crystals 0-89135
InSb, convection in melts, and cryst. growth under large inertial accelerations 0-66421
InSb, facets and twin formation obs. (Chinese) 0-59409
InSb, growth angle determ. from cryst. lateral face shape and solidified separation drops 0-103282
InSb:Te, cryst. growth from melt, pulling method, US effects on facet growth 0-76169
KMn_{1-x}Me_xF₃ (Me=Mg²⁺, Fe²⁺, Co²⁺ and Ni²⁺) Bridgman growth, 0-60764
KZnF₃ single crystal growth, Czochralski method 0-97421
La₂Be₂O₇:Nd³⁺ (Pr³⁺), cryst. growth, spectral and laser properties in ⁴F_{3/2}→⁴I_{11/2} and ⁴F_{3/2}→⁴I_{13/2} transitions 0-80853
La₃NbO₇, synthesis and cryst. growth 0-71590

crystal growth from melt continued

- 7LiAl, cryst. growth, Stockbarger method, struct. and homogeneity 0-89137
LiAl single crystals, growth by Tamman technique 0-66422
LiGd₂(MoO₄)₃, single crystals, cryst. growth, optical props. 0-60763
LiHfO₄ crystal melt growth, comparison of Czochralski and Bridgman-Stockbarger methods 0-60765
LiNbO₃ Czochralski grown single crystals, faceted and nonfaceted growth sections, growth striae (Chinese) 0-64940
LiNbO₃ single crystals, growth from melt, Czochralski method (Chinese) 0-76171
LiNbO₃ single crystals, wetted-die technique 0-97426
LiNbO₃:Rh, Czochralski-grown oxide crystals, fluid-flow effect on gas-bubble entrapment 0-84121
Li₂O, single crystal synthesis using vacuum fusion technique 0-71585
LiTaO₃ crystals for commercial SAW TV IF filters, fabrication 0-80961
LiTaO₃, Czochralski-grown oxide crystals, fluid-flow effect on gas-bubble entrapment 0-84121
LiTaO₃, single crystal. prep. for surface acoustic wave device appls. (Japanese) 0-60772
LuBO₃:Fe³⁺, ESR spectra, lattice parameters 0-93170
γ-MnCu crystals, antiferromag. Czochralski growth 0-97420
Mn_{1-x}O, single cryst. growth by skull melting 0-84844
MnSi_{1-1.73} crystal growth and characterisation 0-93474
MnSi₃, elastic moduli, phase transitions, ultrasonic velocity 0-92589
NaCl Czochralski crystal growth for large CO₂ laser windows 0-74525
NaCl-KCl novel encapsulant for LEC growth of GaSb single crystals 0-93475
Na₂O-Ga₂O₃ system β and β' phases, fast ion cond., prep. and phase comp. 0-59716
(Pb, Sr)₂Ge₂O₁₁, single crystals, growth and X-ray and dielec. investigations 0-88127
Pb, Ca_{1-x}MoO₄, growth and props. 0-71588
Pb₂Ge₂O₁₁, Czochralski-grown oxide crystals, fluid-flow effect on gas-bubble entrapment 0-84121
Pb_{0.97}Hg_{0.03}Te photovoltaic detector produced by Sb⁺ ion implantation 0-82821
Pb_{1-x}Sn_xTe_{1-x}Se_x, quaternary solid solns. with const. lattice parameter, cryst. growth and characts. 0-108332
Pb(WO₄)_{1-x}(MoO₄)_x, growth and props. 0-71588
(Sb₂Se₃)_{0.7}(Bi₂Se₃)_{0.3}, solid soln., prep. and elec. properties of layered crystals 0-70762
Sb₂Te₃Bi₂Te₃ solid solns., single cryst. growth and thermocouple construct. 0-104056
SeBO₃:Fe³⁺, ESR spectra, lattice parameters 0-93170
Se₂Te_{1-x}, growth of single crystals by Czochralski method 0-66423
Si, annealing during Czochralski growth, influence on defect density 0-60769
Si, as-grown Czochralski crystal, multiple p-n junction structure obtained by heat treatment, appl. to solar cells 0-101099
Si crystal growth, for electronic devices 0-66419
Si, Czochralski grown, dislocation free, swirl defect form., doping effect 0-92519
Si, Czochralski grown crystal, O precip., nucleation behaviour and dislocation loop form. (Japanese) 0-59664
Si, Czochralski grown crystals, swirl-type defect obs. 0-100236
Si, doping impurity distrib., during cryst. growth by Czochralski method (Russian) 0-100276
Si, EFG ribbon, characterisation by ion beam tech. 0-79833
Si, effect of C on dissolution of quartz in liq. Si, rel. to melt growth 0-70414
Si, liquid, interaction with die material during edge defined film fed growth 0-104060
Si, melt grown crystals, impurity incorporation, calcs. 0-79718
Si, metallurgical-grade, fabrication by epitaxial growth or direct diffusion 0-101104
Si monocrystalline sheet fabrication for solar cells, CLF Czochralski furnace and enhanced slicing technology 0-93476
Si multicrystalline solar cell material prep., fast-pulled float zone, CZ and cast ingot and foil methods 0-93483
Si on ceramic, coating with inverted meniscus (SCIM) technique, solar cell appl. 0-89163
Si polycrystalline, low cost conversion into sheet by heat exchange method and fixed abrasive slicing technique 0-93479
Si ribbon, dendritic web growth from melt, solar cell module fabrication 0-93478
Si ribbon, low angle sheet growth technique, direct shaping characts. 0-93480
Si ribbon crystal growth, 10 cm wide, temp. distrib. meas. in die 0-104059
Si ribbon crystals, edge-defined film-fed growth technique for solar cells 0-89633
Si ribbon growth by EFG, thermal sensitivity and stability 0-107080
Si ribbons, dendritic web for solar cells 0-89634
Si ribbons, edge-defined film-fed growth technique for solar cells 0-89138
Si ribbons grown by capillary action shaping technique, surface quality and impurity distrib. 0-108343
Si sheet casting for solar cells 0-89139
Si single crystal, improved horizontal ribbon growth technique 0-108345
Si single crystal growth, Czochralski method, small-angle dislocation boundary form. anal. 0-89136
Si single crystal ingot growth from metallurgical grade Si, inhomogeneities 0-59416
Si solar cell fabrication from multiple ingots using melt replenishment Czochralski method, cell anal. 0-93477
Si solar cells, capacitance transient spectra of processing- and radiation-induced defects 0-61340
Si, square single crystals, Czochralski growth 0-97422
Si thin ribbon grown at high speed, thermal stresses, reduced thermal buckling 0-107078
Si tube growth by EFG process 0-108344
Si wide ribbon, high speed edge-defined film-fed growth 0-104058
Si:O, IR absorpt. at low temp. (Chinese) 0-108228
SiAs, cryst. growth from melt, elec. props. 0-76170
α/β-Si₃N₄, phase yields during form., influencing factors 0-108408
SbBr₃, crystal preparation, elec. resistance, phase transitions 0-97427
SnTe, annealed, iodide method of prep., props. meas. 0-71591
Sr_{1-x}Ba_xNb₂O₆ crystals, defect-free growth 0-108346
SrWO₄ cryst. growth, from Na₂WO₄ melts, thermodynamic props. 0-107084

crystal growth from melt continued

Te, growth of single crystals by Czochralski method 0-66423
TeO₂, Czochralski-grown oxide crystals, fluid-flow effect on gas-bubble entrapment 0-84121
Ti₂V₂S₆ single crystal growth, Bridgman-Stockbarger technique 0-89132
YAG:Ho³⁺, spectroscopy, stimulated emission 0-93374
Y₂Al₂O₁₂ crystal growth from melt, gas bubble capture theory 0-64941
Zn, growth from melt, conditions influencing dislocation struct. (*Russian*) 0-97424

crystal growth from solution

see also crystal growth from gel; liquid phase epitaxial growth
birefringent crystal faces, meas. method of growth and dissoln. rates 0-79719
Burton-Cabrera-Frank surface diffusion model, 0-59415
convection effects, holographic interferometric obs. 0-77565
crystal frequency distribution, simulation taking nuclei distrib. into account 0-100184
crystallisation systems, and their mathematical models 0-100186
cubic crystal growth, from soln., numerical soln. 0-88074
growth, and dissoln. of crystals in suspension, kinetic expts. anal. 0-59414
growth rate studies 0-100188
growth rates determination, in batch fluidized beds 0-100187
hexachloroparaxylene, crystn. from heptane, optimising purification 0-100774
high compression crystal growth system 0-66415
hollandites, cryst. growth and structural props. 0-89129
impurity incorporation into vicinal faces, interface model 0-84127
magnetic bubble materials, props. and preparation models, review (*Rumanian*) 0-93149
manganese carboxylate, dodecanuclear mixed-valence, prep., struct., and mag. props. 0-107196
mechanism, equil. props. of crystallising systems, theoret. interpret. (*Rumanian*) 0-88073
monostearine crystals, spiral growth from organic soln. 0-93467
nosean identification, in sodalite and conversion of nosean sodalite 0-84907
pyrophosphatase, inorganic, of yeast, cryst. growth, derivatives formation, heavy atoms positions 0-108842
 α -quartz, synthetic, growth, defects induced by seed orientation 0-96454
rare earth germanates, flux-grown, X-ray topography 0-64939
(rare-earth) Fe₃(BO₃)₄ cryst. growth from soln.-melt, props. 0-108337
silicate gardens, growth morphology, mechanisms 0-100765
solution concentration, interconversion during crystn. 0-100773
stearic acid crystals grown from solution, spatial correlation between growth spirals and inclusions 0-96527
sucrose crystal formation, and growth, effect of same metallic impurities 0-100768
supersaturated soln., shape stability of growing cylindrical particle due to diffusion and interface kinetics 0-79720
theory, review (*Chinese*) 0-66414
transition metal oxides cryst. growth, using K₂S₂O₇ as flux material 0-71582
triglycine fluoborillate, deuterated, dislocation line defect X-ray topographic analysis 0-59465
two-step mechanism, anal. and identification 0-100190
uric acid occurrence, growth morphology of C₃H₄N₄O₃ anhydrous monoclinic modification 0-84123
viscosity, rel. to temp. 0-100189
zinc oxalate, isothermal crystallisation from soln. 0-108336
Al₂(SO₄)₃·(NH₄)₂SO₄·24H₂O, crystn. kinetics in an MSMPR crystalliser 0-100185
Ba(NO₃)₂, isomorphous crystals, growth defects, X-ray topography 0-70188
BaTiO₃, crystn. from melts, comparison of different prospective oxy-anion solvents 0-71583
Bi₂WO₆, hydrothermal and flux growth 0-76166
Ca₂Mn(PO₄)₂, hydrothermal synthesis and cryst. growth 0-60762
CaCO₃ crystallisation from aqueous solutions, kinetic study 0-59419
Ca₃(M₂H₂(PO₄)₄)₄ (M²⁺=Mn, Co, Ni, and Cu), hydrothermal synthesis and cryst. growth 0-60762
CaSO₄ crystallisation, from liq. solns. as heat-transfer surface 0-100772
CaSO₄·2H₂O, gypsum, cryst. growth rates and nucleation (*French*) 0-80959
CaWO₄, cryst. growth from solns. in melts, kinetics parameters and thermodynamic props. 0-59424
Cr₂O₃ crystals, flux growth from K₂Cr₂O₇-K₂CrO₄-K₂B₄O₇ mixture (*Japanese*) 0-108339
Cr₂O₃ crystals, growth by decomposition of K₂Cr₂O₇ melt (*Japanese*) 0-108338
Cu, electrochem. nucleation and growth on Te and Al, TEM 0-104451
CuI, single crystals, growth and optical props. 0-93470
(Fe_{1-x}M_x)₂O₃, yH₂O, M=Cr,Cu,Ni, characterisation by Mossbauer spectroscopy, mag. meas. and electron microscopy (*French*) 0-80655
 α -Fe₂O₃ crystal flux growth, solubility and relative supersaturation in Fe₂O₃-PbO-V₂O₅ fluxed melt system 0-64934
Fe₃O₄, magnetite, hydrothermal crystal growth 0-66411
FeO₂H, growth in alkaline solution, phase composition (*Chinese*) 0-108334
GaAs, cryst. growth from large Ga:As solns., critical cooling rate 0-64938
Gd₃Ga₂O₁₂, flux growth and nucleation temp. determ. (*Chinese*) 0-60761
HgI₂, soln. grown crystals, low-energy gamma-ray cond. type detectors 0-97418
KH₂PO₄, growth and dissolution kinetics, temp. and pH effect 0-88070
KH₂PO₄ single crystal evidence for spiral growth on pyramidal faces 0-84120
MgAl₂O₄ crystals, flux grown, artificial spinel twin form. by BeAl₂O₄ addition 0-96542
NH₄H₂PO₄, cryst. growth in presence of Mn ions 0-93468
NH₄H₂PO₄, crystal growth kinetics, in situ X-ray topography study 0-76167
NH₄H₂PO₄, single crystal evidence for spiral growth on pyramidal faces 0-84120
Na₂Ca₂SiO₃[Si₂O₇][PO₄]₃, synthesis conditions, cryst. struct. and IR spectra characts. 0-108335
NaCl-NH₃-CO₂-H₂O system, NaHCO₃ crystn. 0-100771
NaClO₃, dislocations rel. to growth mechanism from aq. soln., X-ray topography 0-59464
Na₂Sc₂P₂O₁₂, superionic cond. synthesis, cryst. struct. and ionic cond. 0-107519

crystal growth from solution continued

Nd₃R_{1-x}P₂O₁₄ (R=La, Y; 0.1<x<1), laser quality cryst. growth, morphology 0-66412
RbNbW₂O₉ crystals, growth and props. 0-104054
Sr(NO₃)₂, isomorphous crystals, growth defects, X-ray topography 0-70188
Tb₂Ge₂O₇, flux-grown, X-ray topography 0-64939
Y₂(CO₃)₃·nH₂O, tengerite, single cryst. hydrothermal growth 0-97417
YIG crystals, bulk growth from high temp. solns., props. 0-66413
YIG single crystals, liq. flux growth, obs. 0-66416
YIG:Si single crystals, liq. flux growth, obs. 0-66416
Y(OH)CO₃, ancyllite like phase, hydrothermal cryst. growth (*French*) 0-108340
ZnSe, near band edge photoluminescence, electron-hole recombination 0-80835

crystal growth from vapour
see also vapour phase epitaxial growth
boracite, single cryst. prep. and phys. props. 0-100763
diamond, homogeneous formation in gas phase, laser beam effects (*Russian*) 0-104052
ice crystal morphology, vapour growth, influence of vapour diffusion and heat diffusion 0-64933
ice disc growth from vapour, cryst. habit change mechanism 0-84117
II-VI semiconductors, optimal synthesis methods for single cryst. growth 0-100764
metallic multi-point field emission source, prep. by cathodic growth 0-100758
nucleation kinetics, at high supersaturations on (111) faces of crystals with diamond struct. 0-84128
2,2,6,6-tetramethyl-piperidino-oxy, cryst. growth and polymorphism 0-96645
whisker crystal growth, radial periodic instability mechanism (*Russian*) 0-107682
Ag on Si and W substrates, UHV-SEM studies of Stranski-Krastanov growth 0-79722
BP:Ni pillar crystal growth from vapour 0-60758
BiTeI, melt and vapour grown, optical props. 0-84746
CdCr₂S₄ magnetic semiconductor crystal growth, structural defects, physical properties 0-60759
CdI₂ polytypes, vapour growth mechanism 0-84124
CdS crystal growth from vapour, preferential deposition, elec. field effects 0-84122
Cr₂C₃, cathodic needle growth, at lower electric fields from Cr(CO)₆ vapour 0-76161
(Cu,Ag)₂Se/(Bi, Sb)₂Te₃, P type selenide segmented element fabrication, thermoelectric props. 0-107835
CuGaSe₂ single crystals, electrical and photovoltaic props. 0-92940
Fe₂B₂O₇·3H₂O, boracite single cryst., nucleation control density growth 0-80955
(Fe,Cr_{1-x})₂O₃ corundum-type solid solution single crystal growth, chem. vapour transport 0-93465
FeI boracite single crystals, dielectric, pyroelectric props., vapour phase transport growth 0-80673
Gd₂Se₃/PbTe, N type selenide segmented element fabrication, thermoelectric props. 0-107835
HfO₂ crystallite growth from oxide plasmas, growth morphology 0-59417
Hg, condensation, two-dimensional, on W 0-107666
In₂O₃ smoke particles prepared by gas evap., morphology and coalescence growth 0-97738
MnS(Se)(Te), CVD crystal growth, role of Mn-Al-Cl complexes 0-84840
Mo, film, formation by reduction of MoCl₅, influence of electric field 0-93491
Mo₂C, cathodic needle growth, at lower electric fields from Mo(CO)₆ vapour 0-76161
MoO₃ smoke particles prepared by gas evap., morphology and coalescence growth 0-97738
Mo_{0.5}W_{0.5}Se₂ single cryst. vapour growth, characterisation 0-93466
Ni₂B₂O₇·Br, boracite single cryst., nucleation control density growth 0-80955
NiBr boracite single crystals, dielectric, pyroelectric props., vapour phase transport growth 0-80673
NiFe ferrite, prep. of single crystal by chem. transport with TeCl₄ 0-104051
NiZn ferrite, prep. of single crystal by chem. transport with TeCl₄ 0-104051
NbO₂ single crystal growth, gas phase chemical transport method (*French*) 0-60760
Pb_{1-x}Sn_xTe_{1-y}Se_y, quaternary solid solns. with const. lattice parameter, cryst. growth and characts. 0-108332
PbTe single crystals, growth from vapour phase under micro-gravity conditions 0-80957
Sc, CVD, open-tube technique 0-89128
Si crystal growth, for electronic devices 0-66419
Si:P, doping during growth from gas phase, thermodynamic analysis 0-59489
Te film, vacuum deposited, growth and morphology of crystals 0-96766
Te-Se-Cd, sandwich structure, fabrication and characteristics 0-60089
ThO₂ crystallite growth from oxide plasmas, growth morphology 0-59417
TiN(C) whisker growth in CVD 0-59843
UO₂ crystallite growth from oxide plasmas, growth morphology 0-59417
V₁, single crystals, growth from vapour phase 0-66410
W needle crystal growth, discharge-induced decomp. of hexacarbonyltungsten mols. 0-84414
W needles, mechanism of cathodic growth, decomp. of W(CO)₆ under high field conditions 0-76162
WO₃ smoke particles prepared by gas evap., morphology and coalescence growth 0-97738
WSe₂, chem. vapour transport growth, microstruct. develop. 0-103278
ZnO, single cryst., photo- and thermoluminescence 0-66311
Zn₃P₂ large crystal growth, vapour transport perforated capsule technique, prototype solar cell appls. 0-93464
ZnTe growth from vapour, growth interruption 0-97416
ZrN(C) whisker growth in CVD 0-59843
ZrO₂ crystallite growth from oxide plasmas, growth morphology 0-59417

crystal hyperfine field interactions
alkali dithioferates (III), electronic struct. and hyperfine interactions, X α calcs. 0-100448
alkali metal halides, analysis of spin-Hamiltonian parameters of heteronuclear XY defects 0-88509
alkali metavanadates:Cr³⁺, study of ESR spectra 0-80601

crystal hyperfine field interactions continued

- alloys and semiconductors, Mossbauer spectrometry (*French*) 0-80660
 amidinium salts, ^{14}N NQR spectra, H^+ relax. times 0-60448
 α -bromofluoro alkyl pi-radical, signs of hyperfine and quadrupole couplings, ESR determ. 0-97141
 N-bromosuccinimide, X-irrad., ESR study of Br and σ^* radical 0-66037
 dibenzenechromium-dibenzenevanadium, proton HFS data, ENDOR obs. 0-66073
 dichloromethane- d_2 , spectral densities determ. from spin-lattice relax. and spin-echo decay rates 0-75877
 dimethylbenzaldehydes, in durene single cryst., zero-field splitting, guest and host isotope effects 0-107752
 electric quadrupole interactions measured by nuclear orientation and NMR on oriented nuclei, review 0-92868
 ferromagnet, nuclear magnetisation motion, hyperfine field microscopic inhomogeneity, NMR freq. shift (*Russian*) 0-80623
 ferromagnet, one-dimensional localised nuclear magnon modes 0-93098
 fluorene crystal, doped, photochemical hydrogen abstraction, proton hyperfine structure via optical nuclear polarisation 0-63659
 fluorides, electric field gradient, time-differential-angular-distrib. method 0-0463
 $\text{GaAl}_{1-x}\text{As}$, optically oriented electron, nuclei spin instability (*Russian*) 0-70660
 gamma-ray perturbed ang. correls. with quadrupole interactions, geometrical coeffs. 0-73109
 hexaquo-magnesium dihydrogen EDTA: VO^{2+} , single cryst., ESR spectra and spin Hamiltonian parameters 0-75845
 high speed rot., spin diffusion, NMR spin lattice relax. obs. of D 0-66056
 hippuric acid, X-irrad. single cryst., ^{14}N and ^1H ENDOR study; 0-71240
 interdoublet EPR spectrum ang. depend. for ions with arbitrary electron and nuclear spins in strong axial cryst. field 0-93164
 intermediate state perturbation in low temperature nuclear orientation 0-97168
 ionic compounds, amorphous, Mossbauer study, frozen mag. state and hyperfine interaction (*French*) 0-80661
 ionic crystals, Sternheimer quadrupole shielding-antishielding function for F^- , Cl^- , Br^- and I^- 0-80236
 lanthanum nicotinate dihydrate, cryst., nucl. quadrupole interactions, D atom coords., ENDOR obs. 0-97161
 magnetic metals, hyperfine mag. fields at ^{119}Sn nuclei 0-60248
 magnetic semiconductor, helicon wave propag., hyperfine interaction effect 0-80307
 magnetically ordered cryst., indirect nuclear spin interactions 0-103847
 methyl-d groups, reorienting or tunnelling spin-lattice relax. 0-97156
 monochloroacetic acid single crystal, Zeeman and ^{35}Cl NQR investig. 0-66066
 Mossbauer ^{57}Fe spectra, ferrous charact., cryst. field interactions 0-108133
 nuclear electric hexadecapole interactions, in solids 0-65513
 α -quartz: ^{57}Fe , anomalous hyperfine splitting 0-103650
 rare earth intermetallic compounds, NMR anal. of indirect mag. interactions 0-71193
 rare earth nonmetallic compounds, indirect spin-spin coupling, models 0-80238
 rare earth orthoferrites, hyperfine interaction anisotropy, NMR study (*Russian*) 0-66052
 rare earth-transition metal alloys, $\text{RM}_2\text{Si}_{2-x}\text{Ge}_x$ and $\text{RM}_{4-x}\text{Al}_{8-x}$, magnetism and hyperfine interactions, magnetisation and Mossbauer effect studies 0-75892
 relaxation phenomena and magnetic hyperfine fields of isolated Ce ions in liquid and solid metals 0-108137
 scheelites, zero-field splitting of Mn^{2+} ions 0-75531
 semiconductor with transition metal impurity states, EPR linewidth calc. 0-80599
 sodium oxalate: Cu^{2+} , anhydrous spin Hamiltonian and bonding parameters and orbital-reduction factors 0-60408
 spin correlated crystalline elec. field effective operators 0-59938
 tetraethylammonium neptunium hexachloride, Mossbauer spectra and mag. susceptibility meas. 0-108140
 tetramethylammonium neptunium hexachloride, Mossbauer spectra and mag. susceptibility meas. 0-108140
 triglycine calcium bromide: Cu^{2+} , ESR studies 0-97136
 trinuclear exchange clusters, Dzyaloshinsky coupling effects in Mossbauer spectra (*Russian*) 0-108142
 ytterbium ethyl sulphate, crystal field effects on mag. and hyperfine props. of Yb^{3+} 0-97101
 $3d^3$ -ions, variation of hyperfine splitting const. with interatomic distance 0-97133
 $\text{AgNa}(\text{NO}_2)_2$, ^{23}Na elec. field gradient tensor from NMR satellite lines near phase transition 0-71191
 Al_2O_3 : $\text{V}^{3+}(\text{Fe}^{3+})$, hyperfine splitting and magnetoelastic const., freq. crossing spectroscopy 0-107392
 $\beta\text{-Al}_2\text{O}_3$ -(Na,Li) O , first-order quadrupole NMR obs. of cation distrib. and ion motion 0-108113
 $\beta\text{-Al}_2\text{O}_3$ - Na_2O , anomalous Na behaviour obs. using pulsed and CW NMR 0-108095
 $\beta\text{-Al}_2\text{O}_3$ - Na_2O , ENDOR meas. of defects 0-66074
 $\beta''\text{-Al}_2\text{O}_3$ - Na_2O , NMR of ^{23}Na , elec. quad. interaction, 185 to 419K, ion motion obs. 0-108110
 Au lattice location in Zn, gamma-spectral study 0-80227
 Au-Dy, dil., hyperfine interaction, Mossbauer study, Kramers quartets 0-66083
 Au-Fe ion implanted alloy, Mossbauer conversion electron scatt. 0-88898
 $\text{BaSr}_{1-x}\text{Ca}_x\text{Fe}_2\text{O}_8$, substituted hexagonal ferrites, mag. split Mossbauer spectra obs. and X-ray struct. data 0-71250
 BaV_2O_6 :Cr, EPR spectra temp. depend., paramagnetic ion point symm. 0-71166
 BaVS_3 , mag. transition and hyperfine interaction, neutron spin-flip scatt. obs. 0-97093
 BaVS_3 :Fe, Mossbauer and mag. studies, electronic state of Fe 0-108130
 Be, electronic struct., NMR study 0-108085
 Be-Ir, dil., elec. field gradient, Mossbauer meas. 0-80665
 BeNi, dil., electronic struct., NMR study 0-108085
 CaF_2 : Ni crystals, X-irradiated, EPR study of Ni^+ and Ni^{3+} 0-75849
 CaF_2 : Mn^{2+} , ultra-low nuclear spin temp., low field behaviour, EPR study 0-100614
 $\text{CaFe}^{3+}\text{Fe}^{2+}(\text{Si}_2\text{O}_7)\text{O}(\text{OH})$, ilvaite, electronic struct., press. and temp. depend. of ^{57}Fe Mossbauer spectrum 0-108129

crystal hyperfine field interactions continued

- $\text{CaSe}:\text{Sn}^{2+}$, EPR study of octahedral Sn^{3+} centres, 4 to 290K (*Russian*) 0-84637
 CaV_2O_6 :Cr, EPR spectra temp. depend., paramagnetic ion point symm. 0-71166
 $\text{CdS}:\text{Ti}^{2+}$, superhyperfine interact., ENDOR study at 4.2K 0-80639
 ^{111}Cd , nucl. orientation coeffs. with axially symm. elec. field gradient 0-97168
 $(\text{Ce},\text{Y}_{1-x})\text{Fe}_2$, mag. susceptibility and Mossbauer meas., lattice parameters 0-97068
 Co^{2+} , doped ion in divalent metal cpds., correl. between Szegedi charge and hyperfine coupling const. 0-96832
 Co^{48}V , nucl. orientation of ^{48}V , γ -ray anisotropy obs. 0-97169
 CoFe_2O_4 , mag. hyperfine fields, Mossbauer spectra 0-108139
 Co_2HfAl , hyperfine fields of Fe impurities, Mossbauer spectra 0-71255
 Co_2TiAl , hyperfine fields of Fe impurities, Mossbauer spectra 0-71255
 CoV alloys, phase dependent MNR spectra 0-108114
 Co_2VAl , hyperfine fields of Fe impurities, Mossbauer spectra 0-71255
 ^{57}Co , Mossbauer absorpt. and emission spectra, hyperfine struct. and relax. effects 0-71279
 Cr, hyperfine interactions on ^{111}Cd -probe nuclei, TDPAC meas. 0-75904
 $\text{Cr}_{1-x}\text{Mn}_x\text{O}_2$, hyperfine mag. fields at ^{119}Sn , Mossbauer study 0-71260
 $\text{CsCuCl}_4 \cdot 2\text{H}_2\text{O}$, hyperfine and super-exchange interactions 0-103654
 $\text{CsFeCl}_3 \cdot 2\text{H}_2\text{O}$, rectangular Ising cpd., Mossbauer meas. 0-71252
 Cs_2NpCl_6 , Mossbauer spectra and mag. susceptibility meas. 0-108140
 Cu complex, $\text{Cu}(\text{H}_2\text{O})_6^{2+}$, ligand hyperfine interactions, orbital angular momentum contrib. 0-96833
 Cu, screening charge density round $\Delta Z = -1$ impurities, vacancies, NQR study 0-103897
 Cu^{2+} ion, ground state wavefunctions and ESR parameters 0-88868
 Cu/Ni coherent modulated structures, electronic struct. and magnetism 0-103620
 $\text{Ni}(\text{Pd})(\text{Pt})$, dil., screening charge density round $\Delta Z = -1$ impurities, vacancies, NQR study 0-103897
 $\text{CuCr}(\text{Fe})(\text{Mn})$, dil., anisotropic hyperfine coupling, NMR study 0-65784
 Cu^{2+}F and Cu^{2+}Te , transferred hyperfine interactions 0-70659
 CuFe_2O_4 , Jahn-Teller type crystal distortions 0-103904
 CuFeS_2 , antiferromag., NQR local mag. field effects 0-71234
 $\text{Cu}_2\text{MnAl}_{1-x}\text{Sn}_x$, Mossbauer effect study 0-60473
 $\text{Cu}_2\text{MnIn}_{1-x}\text{Sn}_x$ alloy, compositional SRO, hyperfine interactions 0-71065
 DyAG, electrostatic model of cryst. field 0-59945
 $\text{Dy}_{1-x}\text{Gd}_x\text{Al}_2$, ordered alloys, hyperfine field, anomalous con. depend. NMR 0-75868
 $\text{Er}_{1-x}\text{Gd}_x\text{Al}_2$, effective mol. field at ^{167}Er , NMR meas. 0-71197
 ErRh_2Si_6 , superconducting, magnetic dilemma 0-75680
 $\text{Eu}_2\text{La}_{1-x}\text{Al}_2$, dil. EPR, cryst. fields and effective exchange interaction 0-66029
 EuLiH_3 , transferred hyperfine fields at Eu nuclei, NMR meas. 0-71195
 $\text{EuO}:\text{Sm}^{2+}$, hyperfine field at Sm, TDPAC meas. 0-93215
 $\text{EuSe}_{1-x}\text{Te}_x$, transferred hyperfine fields at Eu nuclei, NMR meas. 0-71195
 $(\text{Eu},\text{Sr}_{1-x})\text{S}$, transferred hyperfine fields, NMR 0-71196
 Fe, BCC, high field Knight shift and hyperfine anisotropy of ^{57}Fe 0-71205
 Fe complex (2, 9-dimethylphenanthroline) sulphate, mag. props., Mossbauer spectra 0-66081
 Fe dicyclopentadienyl-dibenzenevanadium, coalescence temps., full proton HFS tensor, ENDOR obs. 0-66073
 Fe, hyperfine fields for transition metal impurities 0-80237
 Fe, mag. hyperfine field at ^{121}I , press. depend., nucl. gamma reson. 0-71256
 Fe, transient magnetic low velocity field 0-80642
 α -Fe, uniaxial stress effect on Mossbauer spectrum 0-71244
 Fe^{48}V , nucl. orientation of ^{48}V , γ -ray anisotropy obs. and NMR meas. 0-97169
 Fe-Cr, hyperfine magnetic fields, Mossbauer spectra 0-97165
 Fe-Cr, influence of annealing on hyperfine interaction parameters, Mossbauer effect 0-71263
 Fe-Ni-Mn, Invar, RF collapse and thermal effects, Mossbauer study 0-100624
 Fe-Ta, nuclear mag. moment of ^{182}Ta NMR-ON study 0-78139
 $\text{Fe}_{30}\text{B}_{70}$, amorphous ferromagnet, Mossbauer hyperfine fields, mag. struct. 0-75894
 FeBO_3 , parametric echo, magnetoelastic NMR excitation (*Russian*) 0-66072
 FeCr_2S_4 , ionic distrib. and band struct., Mossbauer study 0-80646
 $\text{Fe}_2\text{Mg}_{1-x}\text{Ti}_x\text{O}_4$, mag. ordering, Mossbauer effect in external mag. fields 0-71257
 $\text{Fe}_{0.33}\text{NbS}_2$, lattice dynamics and hyperfine interactions, Mossbauer spectra study 0-108135
 $\text{Fe}_{40}\text{Ni}_{40}\text{P}_{14}\text{B}_6$, amorphous ferromagnet, Mossbauer hyperfine fields, mag. struct. 0-75894
 $\text{Fe},\text{Sn}_{1-x}$, amorphous film, struct. and mag. props. 0-65972
 Fe_2TiO_5 , spin glass system, cation distrib. Mossbauer spectra 0-71248
 Fe_2TiS_2 , lattice dynamics and hyperfine interactions, Mossbauer spectra study 0-108135
 ^{57}Fe , hyperfine interactions in implanted metals, Mossbauer spectra 0-108141
 ^{57}Fe , Mossbauer absorpt. and emission spectra, hyperfine struct. and relax. effects 0-71279
 GaAs-AlAs mixed crystals, valence charge distrib. and elec. field gradients 0-80239
 $\text{GaP}:\text{Ge}$, ENDOR study, superhyperfine interactions 0-93210
 GdAG, electrostatic model of cryst. field 0-59945
 $\text{Gd}(\text{Al},\text{Fe}_{1-x})_2$, intermetallic compounds, pseudobinary, Mossbauer studies 0-75887
 GdAlO_3 , canted antiferromagnetic, Mossbauer meas. 0-97171
 GdRh_2H_6 , GdRu_2H_6 , struct. and mag. props., Mossbauer and magnetisation meas. 0-71271
 GdZrFe_2 , hyperfine field at Gd, TDPAC meas. 0-93214
 Ge, spin Hamiltonian and anomalous muonium states 0-71286
 Hf-Ir , dil., elec. field gradient at ^{193}Ir , Mossbauer meas. 0-66090
 $\text{Hf}(\text{SO}_4)_2$, elec. quadrupole interaction, TDPAC technique, coincidence system 0-93216
 Hg electric field gradients at different Be lattice sites, gamma-spectral study 0-80224
 Hg, quadrupole interactions in Zn, lattice location, gamma spectral study 0-80227
 $\text{HgSe}:\text{Mn}^{2+}$, temp. depend. of EPR of ^6S state ions 0-80593
 HoAlO_3 , electronic and nucl. mag. ordering, mol. field approx. 0-60157

crystal hyperfine field interactions continued

¹¹³In, nucl. orientation coeffs., nucl. mag. moment 0-97168
 KCl:H, ENDOR and ESR study of anion sites 0-108118
 K₂CuCl₄·2H₂O, hyperfine and super-exchange interactions 0-103654
 K₂FeF₆, one-dimensional antiferromag. systems, Mossbauer studies 0-71266
 KMgF₃, F-centre ENDOR study 0-108117
 KMgF₃:Yb³⁺, perovskite type cryst., ENDOR meas. 0-80638
 KMg₃[AlSi₃O₁₀]F₂ with excess Al, synthetic fluorophlogopite, radiation-induced paramag. O⁻ centres 0-60417
 KZnF₃, exchange interactions of transition metal ions in orbitally degenerated excited states 0-65512
 KZnF₃:Yb³⁺, perovskite type cryst., ENDOR meas. 0-80638
 LaAlO₃, exchange interactions of transition metal ions in orbitally degenerated excited states 0-65512
 LaNi_{1-x}Fe_xO₃, magnetisation meas. and ⁵⁷Fe Mossbauer studies 0-93217
 La_{1-x}Tb_xAl₃, competing paramag. anisotropy from cryst. field and indirect quadrupolar coupling 0-60180
 Li-Zn ferrites (Li, Zn, Ti, Cr substituted), Mossbauer spectrometry, effect of supertransferred hyperfine fields and relaxation (*French*) 0-80654
 LiBaF₃:Mn²⁺, having inverse periodic struct., ENDOR study 0-97162
 LiF:OH, neutron irradi., interstitial H-centres, ESR obs. 0-93175
 LiYF₄:Pr, NMR meas. of hyperfine const. of Pr³⁺ excited state 0-88895
 Lu-ir, dil., elec. field gradient at ¹⁹³Ir, Mossbauer meas. 0-66090
 LuAG, electrostatic model of cryst. field 0-59945
 LuPO₄:Pb³⁺, EPR, hyperfine interactions 0-108050
 Mg, quadrupole interaction of ¹⁸¹Ta, gamma-spectral study 0-80228
 Mg(NH₄)₂(SO₄)₆H₂O·VO(H₂O)₂²⁺, proton ENDOR meas. used to determine hyperfine coupling tensors 0-66075
 Mn²⁺, doped ion in divalent metal cpds., Szigeti charge and correl. with hyperfine coupling const. 0-96831
 Mn²⁺F⁻ and Mn²⁺F⁻Mn²⁺ systems, transferred hyperfine interaction at F⁻ site 0-70657
 Mo-Co Kondo alloy, Co impurity susceptibilities, Knight shift 0-88721
 N₂, solid, exciton-phonon coupling in strong coupling limit, temp. depend. 0-92616
 (NH₄)₂CuBr₄·2H₂O, hyperfine and super-exchange interactions 0-103654
 (NH₄)₂CuCl₄·2H₂O, hyperfine and super-exchange interactions 0-103654
 (NH₄)₂FeF₆, one-dimensional antiferromag. systems, Mossbauer studies 0-71266
 N₂H₂FeF₆, one-dimensional antiferromagnetism, Mossbauer study 0-65872
 (NH₄)₂SO₄, paraelectric, N-quadrupole coupling meas. by proton-N double resonance 0-60459
 NaCl, electric field gradients near dislocations, resulting NMR lineshapes 0-75225
 Na₂(Fe,Mg)₂Si₈O₂₂(OH)₂, riebeckite, low temp. Mossbauer obs. of oriented single cryst. behaviour and mag. props. 0-84674
 NaFeF₃, Mossbauer and low-temp. dilatometry study (*French*) 0-80662
 NaNO₂, ²³Na elec. field gradient tensor from NMR satellite lines near phase transition 0-71191
 Nd³⁺:LaCl₃, laser-induced fluoresc., hyperfine struts. 0-100677
 Nd³⁺:LaCl₃, laser-induced fluoresc. energy transfer effects 0-100678
 NdFe₃, high field Mossbauer study 0-75893
 Ni alloys, dil., hyperfine field distrib., DPAC meas. 0-93222
 Ni, ferromagnetic, electronic struct. and hyperfine field of nonmag. impurities, calc. 0-70658
 Ni, self implantation damaged, crit. behaviour, perturbed ang. distrib. meas. anal. 0-60476
 Ni-Cu(Zn)(Ga)(Ge)(As)(Se)(Br)(Kr), dil., ferromagnetic, hyperfine field and relax. time obs. of impurity heavy nuclei 0-75533
 Ni-Cu(Zn)(In), implantation damaged, crit. behaviour, perturbed ang. distrib. meas. anal. 0-60476
 NiSe₂, paramag. props., NMR, mag. susceptibility 0-60175
 Pd-Fe, very dil., Mossbauer emission spectra, relax. effects 0-66084
 PdH, Fe_{0.003}, Kondo system, local moments, hyperfine fields, Mossbauer study 0-80478
 Pd_{1-x}MnSb Heusler alloys, magnetic hyperfine fields on ¹¹¹Cd, TDAPAC and magnetisation meas. 0-93219
 PrFe₂, high field Mossbauer study 0-75893
 PrFe₂, Laves phase, mag. props., Mossbauer spectra, crystalline field mag. anisotropy 0-65851
 PrIr₂(Pt₂)(Rh₂)(Ru₂), hyperfine sp. ht. and magnetisation meas. at 4.2K 0-75775
 Pt-Fe, very dil., Mossbauer emission spectra, relax. effects 0-66084
 RbAl(SO₄)₂·12H₂O, spin-Hamiltonian with trigonal S¹I terms for describing ⁵⁷Fe³⁺ ENDOR spectra 0-75885
 (Rb)₂CuBr₄·2H₂O, hyperfine and super-exchange interactions 0-103654
 Rb₂CuCl₄·2H₂O, hyperfine and super-exchange interactions 0-103654
 RbFeCl₃·2H₂O, rectangular Ising cpd., Mossbauer meas. 0-71252
 Rb₂FeF₆, one-dimensional antiferromag. systems, Mossbauer studies 0-71266
 RbGa(SO₄)₂·12H₂O, spin-Hamiltonian with trigonal S¹I terms for describing ⁵⁷Fe³⁺ ENDOR spectra 0-75885
 Re-ir, electric quadrupole orientation of ^{186,188-190}Ir 0-78140
 Rh₂Mn₂Pb, hyperfine fields, ferromag., NMR and Mossbauer effect studies 0-71259
 Rh₂MnSb, hyperfine fields, ferromag., NMR and Mossbauer effect studies 0-71259
 Ru-FeSn, ferromag. Heusler alloys, hyperfine fields at nonmagnetic atoms in various sites, Mossbauer effect and NMR meas. 0-66089
 Sc-Fe(ru)(Au), dil., elec. field gradient, Mossbauer meas. 0-80665
 Sc-ir, dil., elec. field gradient at ¹⁹³Ir, Mossbauer meas. 0-66090
 Sc-Ru, elec. field gradient and temp. depend. TDAPAC meas. 0-60477
 ScFe₂, Mossbauer effect of ⁵⁷Fe 0-75903
 ScFe₂H₂, Mossbauer effect of ⁵⁷Fe 0-75903
 Si, ^μSr, spin Hamiltonian and anomalous muonium states 0-71286
 Si:Au, EPR spectrum, strong nucl. quadrupole effect 0-93172
 Si:Sn, Mossbauer study of defects due to ¹¹⁹In implantation 0-80641
 Sm-Eu alloy, dil., mag. and elec. hyperfine interac., TDAPAC obs., paramag. behaviour, exchange integral 0-103908
 Sn_{1-x}Pb_xSe(Te) films, Mossbauer effect of ¹¹⁹Sn, spectral characts., conc. depend. 0-103903
 SrCl₂:Gd³⁺, hyperfine interaction, X-band ENDOR 0-60457
 SrFe_{2-x}Cr_xO₉, hexagonal ferrite series, Mossbauer study 0-71258
 Tb-Ta(Cd), elec. quadrupole interaction, temp. and press. depend., TDAPAC meas. 0-60469
 Tb_{1-x}Gd_xAl₂, effective mol. field at ¹⁵⁹Tb, NMR meas. 0-71197
 Ti²⁺, doped ion in divalent metal cpds., correl. between Szigeti charge and hyperfine coupling consts. 0-96832

crystal hyperfine field interactions continued

Ti-ir, dil., elec. field gradient at ¹⁹³Ir, Mossbauer meas. 0-66090
 TiO₂:Mo³⁺, interstitial EPR, g-tensor and hyperfine tensor 0-84647
 Tm-3d transition metal intermetallics, ¹⁶⁹Tm Mossbauer effect 0-71261
 TmAG, Mossbauer study of crystal field props. 0-66082
 Tm₂Ga₂O₁₇, Mossbauer study of crystal field props. 0-66082
 TmZn₂, Mossbauer effect meas. in antiferromag. and paramag. states 0-71265
 V²⁺, doped ion in divalent metal cpds., correl. between Szigeti charge and hyperfine coupling consts. 0-96832
 V₂S₃:Fe, Mossbauer and mag. studies, electronic state of Fe 0-108130
 Y-ir, dil., elec. field gradient at ¹⁹³Ir, Mossbauer meas. 0-66090
 Y-Ru, elec. field gradient and temp. depend. TDAPAC meas. 0-60477
 YAG, electrostatic model of cryst. field 0-59945
 YIG, electrostatic model of cryst. field 0-59945
 YIG:Si(Ge), effects of nontrigonal cryst. field on spectroscopic props. of Fe²⁺ ions 0-92864
 YPO₄:Pb³⁺, EPR, hyperfine interactions 0-108050
 YbAG, electrostatic model of cryst. field 0-59945
 YbFe₂, high field Mossbauer study 0-75893
 ZnF₂:Co²⁺, Raman tensor calcs. of isolated impurity in diamagnetic matrix 0-76025
 ZnSe:Ti²⁺, EPR meas. 0-80594
 ZnTe:Mn²⁺, forbidden transitions of Mn²⁺ induced by hyperfine interactions 0-60458
 Zr-ir, dil., elec. field gradient at ¹⁹³Ir, Mossbauer meas. 0-66090
 ZrSiO₄, natural, radiation defect centre, EPR obs. 0-75853

crystal imperfections see crystal defects

crystal inclusions

Allende mineral grain inclusion, excess ¹²⁹Xe meas., chronological information 0-67675
 Alnico 5 alloy, S and Ti additions effect rel. to non-metallic inclusions, coercive force and grindability 0-89375
 baryta crystal gas-liquid inclusion meas. with microscope heating stage 0-76967
 cleanliness assessment by US (*French*) 0-104411
 diamond, polycryst. sintered under ultra high press., binary inclusion content effect on thermal stability (*Chinese*) 0-66453
 diamond, synthetic monocrystals, inclusions phase comp., radiographic method 0-100978
 diffusion motions of macroscopic inclusions in nonuniform compressive stress fields (*Russian*) 0-88351
 elastic wave scatt. by thin inclusions 0-65151
 eutectics, single grained, directionally solidified, anisotropic yielding behaviour 0-103412
 fluorite crystal gas-liquid inclusion meas. with microscope heating stage 0-76967
 graphite, from reactor, quantitative microanalysis by laser emission spectroscopy 0-81384
 guanidine aluminium sulphate, lattice charge contribution to coordination polyhedron cryst. potential 0-103651
 impurity incorporation into vicinal faces grown from dil. solutions 0-84127
 macroscopic defects, ordered regions and percolation phase transform. (*Russian*) 0-92665
 metal-C system, spheroidal graphite formation, role of high angle boundaries (*Russian*) 0-81065
 metals and alloys, BCC lattice, crit. embrittlement temp., struct. parameters effect (*Russian*) 0-66618
 motion, equation of 0-75387
 nuclear fuel shell inspection, mag. method for detecting ferromag. particles 0-66746
 parastic force on homogeneous cryst. inclusion, theory 0-79777
 Permalloy, 50NP, and 79NM, magnetic properties and structure, environment effect during annealing 0-60366
 α-quartz, synthetic, growth, defects induced by seed orientation 0-96454
 radiographic detection, eval. of detectability in welded joints 0-81266
 second phase particle, diffusional relaxation 0-60898
 semiconductor, enhanced electrodiffusion purification in mag. field, GaAs epitaxial film appl. 0-66409
 spherical strain fields, caused by inclusions, S-matrix theory calcs. 0-100133
 stearic acid crystals grown from solution, spatial correlation between growth spirals and inclusions 0-96527
 steel, Al semikilled, (Fe,Mn_{1-x})O₂ inclusions, deoxidation, thermodynamic conditions 0-60830
 steel, Al-Cr, FeO(Al,Cr_{1-x})₂O₃ inclusions, thermodynamics 0-60831
 steel, austenitic stainless Ni-Cr, heat resist. and comp. of non-metallic inclusions, effect of La, Nd, Pr and Ce 0-76315
 steel, ball bearing, fatigue damage, influence of dispersed phases in martensitic matrix 0-108549
 steel, BN extraction, and identification, IR anal. 0-85254
 steel, carbon type, hydrogen press. effect on morphology of hydrogen attack 0-85052
 steel, Cr-Mo-P (2.25, 1 wt.%), stress relief cracking, effect of P segregation 0-89324
 steel, inclusion chemistry control for machinability enhancement 0-85067
 steel, non-metallic inclusions 0-84839
 steel, nonmetallic inclusion segregation during cooling (*Russian*) 0-100330
 steel, powder forged, fatigue, surface treatment effect 0-85048
 steel, railway, oxidation by Fe-Si-Ca-V complex alloy, nonmetallic inclusions (*Russian*) 0-93685
 steel, rolled, anisotropic, fatigue fracture surface obs. (*Japanese*) 0-108546
 steel, structural, impurity effect on crack initiation, dynamical loading (*Czech*) 0-60955
 steel, structural, second phase particle effects on impact strength 0-108581
 steel, thermal fatigue, effects of inclusions 0-81183
 steel, types 60G, ShKh15, structural changes near holes and inclusions due to pulsed currents (*Russian*) 0-108459
 steel sheet, hot and cold rolled, cold formability, notched tensile test and stretch bend test (*German*) 0-61031
 steel wire, US inspection, immersion method 0-66757
 superconductor, type II, with normal inclusions, current density distrib., theory 0-80461
 surfaces and interfaces, elastic energy of point defects and inclusions 0-73272

crystal inclusions continued

- triglycine fluoberyllate, deuterated, dislocation line defect X-ray topographic analysis 0-59465
 Al-Bi(Cd)(Pb)-Ti, containing low-melting pt. inclusions, mech. props. 0-93632
 Al-Zn-Mg alloy, TEM characteris. of precipitates 0-104166
 B fibre, US inspection, immersion method 0-66757
 Be, fracture and strength properties, dynamic ageing effects 0-81202
 Be ingot, high-purity, TEM obs. of BeO dispersion 0-104165
 Be, sintered, physicomech. props. anisotropy, BeO inclusions effect 0-60804
 Cd,Hg_{1-x}Te, carrier lifetime, effect of comp. fluctuations and second-phase inclusions 0-80294
 CuCrS₂, domain struct. and superstructure, TEM obs. 0-79779
 Cu₂O, Cu inclusions and annealing, optical and IR absorpt. obs. 0-60630
 Fe, Arcco, grain size and strength depend. on nonmetallic inclusions (Russian) 0-100894
 Fe, cast, inoculated with Ce-Mg-Fe master alloy, struct. and props. 0-100843
 Fe, cast, US study of sections undergoing deform. or thermal cycling 0-104285
 Fe-Si (3 wt.%), behaviour of disperse inclusions, influence of recrystn. processes (Russian) 0-66519
 Mg, inclusions, types and size distrib. (German, English) 0-97492
 Mo wire, US inspection, immersion method 0-66757
 NaCl single crystals, thermomigration of brine inclusions, eval. of radioactive waste repositories 0-99251
 Nb-Zr-C welding solid solutions, ageing kinetics, influence of inclusion elements (Russian) 0-100853
 Ni, ductility and fracture, nonmetallic inclusions effect 0-104221
 Ni-ceramic coating structure, influence of micropowder inclusion (Russian) 0-59820
 Ni-Cr-W-Co-Ti, thermal fatigue, effects of inclusions 0-81183
 Ni-Fe (36 to 50 wt.%), initial permeability, domain struct. model 0-88811
 NiO, Hall effect anomaly, sign reversal at 600K 0-100471
 Si, amorphous, scanning TEM studies of cryst. inclusions 0-79699
 Si single crystal ingot growth from metallurgical grade Si, inhomogeneities 0-59416
 Tb₂Ge₂O₇, flux-grown, X-ray topography 0-64939
 α -U, strain rate effect on flow and fracture 0-100887
 W, elastic wave scatt. from oblate spheroidal WC inclusion 0-65151
 W wire, US inspection, immersion method 0-66757
 YAG crystals, dislocations and inclusions, birefringence topography obs. 0-107248
 Zn-In alloy, solid-liq. equil. roughening transition 0-96630

crystal internal fields see crystal field interactions

crystal interstitials see interstitials

crystal lattice structures see crystal atomic structure

crystal microphones see microphones

crystal microstructure

- for microstructural changes, see also phase transformations, hardening, heat treatment, metalworking
 see also crystal defects; crystal inclusions; crystallites; dendritic structure; domain boundaries; domains; electron microscope examination of materials; eutectic structure; grain boundaries; grain size; Guinier-Preston zones; mosaic structure (microstructure); noncrystalline state structure; precipitation; segregation; subboundary structure; superlattices; texture; X-ray diffraction examination of microstructure
 acoustic wave analysis of material structure 0-65163
 Alnico 5 alloy, S and Ti additions effect rel. to non-metallic inclusions, coercive force and grindability 0-89375
 anthracene, ultrathin films on fused quartz and sapphire 0-59812
 [CC] Ag-(100)InP, metal-semicond. cathode contact, metallurgical, physical, chemical processes 0-107911
 coke, metallurgical, microstruct., using refl. light microscopy and image anal. 0-66732
 creep and growth, radiation induced, fundamental mechanisms 0-92596
 electron microscopy, developments in high resolution imaging 0-99001
 eutectic alloy, dendrite growth—the coupled zone 0-97489
 fatigue resistance, in metals 0-94907
 ferrite, orientation in pearlite, rel. to austenite (Russian) 0-81072
 ferrite, transform. kinetics, grain size, alloying element effect, carbide precip. 0-93560
 film, evaporated at oblique incidence, columnar grains inclination angle 0-75468
 films, elec. and galvanomag. props., microstruct. 0-70859
 fine fragmented crystals, complex struct. analysis by electron microscopy 0-104416
 graphites, strength and struct., conf., Bath, London, England (Apr. 1979) 0-82566
 metal, pure, with max. of cryst. lattice distortion, struct. and strength props. (Russian) 0-89234
 metal powder, method for TEM study 0-84038
 metals, cubic, heavily deformed, development of lattice curvature 0-81136
 NASICON solid electrolyte, processing and phys. props. 0-60820
 quartz grains in Moine thrust zone, deformation-induced microstructs. rel. to differential stress 0-85652
 Raman microprobe-microscope appl., molecular optical laser examiner 0-62737
 rectorite, stacking and ordered interstratification, high-resolution TEM obs. 0-109140
 steel, 0.7% C, welded zone, fatigue strength and microstruct. (Japanese) 0-89339
 steel, 12Cr1MoV, thermal fatigue and creep effect in fracture 0-104297
 steel, austenitic stainless, unlubricated, friction, wear and microstruct. of types 304, 316 and Nitronic 60 0-108589
 steel, austenitic stainless, welded explosively, induced martensites morphology 0-104153
 steel, austenitic stainless type 304, time-depend. fatigue, mechanistic model 0-100925
 steel, C, fatigue crack propagation in sheet, influence of struct. of ferrite-pearlite bands (French) 0-76338
 steel, C, quenched, restoration of austenite grains during rapid heating (Russian) 0-76272
 steel, Cr, post-hotforming recrystallisation condition, use of NEOPHOT 2 and EPIQUANT 0-84949
 steel, Cr plated, factors influencing durability 0-108643
 steel, Cr-Mo-(V), microstruct. effect on high-temp. props. (Czech) 0-89300

crystal microstructure continued

- steel, Cr-Mo-V pressure vessel, microstruct. parameters and yielding rel. to plastic deform. 0-89318
 steel, CrMoV, creep resistant, quantitative struct. parameter use in props. prediction (Czech) 0-108481
 steel, ferritic and austenitic, microstruct. study by means of replicas taken from components at 100°C 0-81256
 steel, ferritic stainless, Cr-Mo (12,1wt.%) microstructure influence on localised corrosion behaviour 0-61018
 steel, ferritic stainless, embrittlement 0-85041
 steel, heating effect on phase composition, microstruct. and mech. props. 0-100859
 steel, high Mn-Cr, austenitic struct. stability and low-temp. toughness (Japanese) 0-76356
 steel, high strength weld metal, fractography, microstructure and reheated zone toughness effects (Japanese) 0-108543
 steel, high-speed, fracture toughness, carbides influence (French) 0-108559
 steel, low-alloy, bearing, mech. props., carbide behaviour effect (Korean) 0-93615
 steel, low-alloy structural 16G2 and 16GFR, struct. and props. after quenching and tempering 0-76280
 steel, microstructure of 0Kh16N15M3B after creep tests in BR-10 reactor, electron, microscope invest. (Russian) 0-92531
 steel, Mn-Sn-(Nb), extra low C, shear transformation struct. (German) 0-60873
 steel, pearlitic, wear behaviour rel. to basic material props. 0-108592
 steel, plain C having ferrite-martensite mixed struct., microstructural parameters effect on fatigue strength (Japanese) 0-71735
 steel, railway, oxidation by Fe-Si-Ca-V complex alloy, nonmetallic inclusions (Russian) 0-93685
 steel, SAE 1045, permeation meas. of H trapping, rel. to cryst. microstruct. 0-84328
 steel, Si (3 wt.%), struct. and preferred orientation, annealing parameters influence (Czech) 0-89248
 steel, stainless, austenitic, explosively welded, orientation relationship in martensitic transform. 0-104158
 steel, stainless, ferrite to austenite decomp. 0-93554
 steel, stainless, stress corrosion testing, slow strain rate, elevated temp. and high press. study 0-97615
 steel, stainless, Type 316, neutron irradi. effects on tensile props. and microstruct. 0-65059
 steel, stainless 304, metallurgical factors on the corrosion and mass transfer in liq. Na (Japanese) 0-71804
 steel, surface Si reinforced type U8, metastable phase, composition, struct. (Russian) 0-92599
 steel, tempered martensitic, type AISI 410, role of C in embrittlement phenomena 0-93652
 steel, type Kh13N9D2MT martensitic aged, struct. and mech. props. (Russian) 0-93600
 steel, W alloy, microstruct. and hardness, splat quenching effect 0-76293
 steels 60, 18Kh2N4MA, 17GSDN, and 12Kh21NST structure after high-speed cold plastic deformation 0-76316
 subgrain imaging, in bulk specimens to study localised plasticity using SEM 0-66609
 surface microstructure determ. and microanalysis by ultrahigh vacuum field emission gun SEM 0-96423
 thin films and interfaces, analytical techniques, review 0-80120
 white Fe castings, morphology of eutectic M₂C and M₇C₃ 0-108427
 Zircaloy-4, resistance-welded, microstruct. of weld region 0-66549
 Ag-Cu flex leads, microstruct. study of corrosion 0-76406
 Ag-Cu surface alloyed films, laser melt quenched, microstruct. 0-76423
 AgCdO, powder metallurgy production, for switchgear in power engineering 0-104094
 Ag₂S+Ln₂S₃, powdered mixtures, reaction rate, production of ionic semiconductors 0-93741
 Al, deformed in uniaxial and equibiaxial tension, dislocation arrangements 0-108516
 Al, solidification, high press. effects 0-66499
 Al-Al₃Ni eutectic, temp. gradients, microstructural changes 0-84971
 Al-Bi(Cd)(Pb)-Ti, containing low-melting pt. inclusions, mech. props. 0-93632
 Al-Cu (4 wt.%) alloy, high temp. cyclic deform., θ' particle dissolution obs. 0-108515
 Al-CuAl₃ eutectics, microstruct. after solidification, heat pipe influence 0-76243
 Al-Cu(0-10 wt.%) sintered compacts, mech. props. rel. to sintering 0-76210
 Al-Mg-Li alloy, metastable S'-phase, struct. (Russian) 0-103291
 τ -Al-Mn-C, permanent magnetism and microstruct. 0-75811
 Al-Ni (3-18wt.%) gun-quenched from melt, struct. 0-76225
 Al-Ni(Cd)(Fe)(Si), cold worked, struct. and props. 0-71666
 Al-Ni(Pt)(Zn), rapidly solidified, twinned dendrites 0-70572
 Al-Si (25.4 wt.%), solidification, high press. effects 0-66499
 Al-Zn (38 at.%), TEM study of precipitation processes or different microstructures during ageing 0-93561
 Al-Zn-Mg type 7N01-T4, weld, SCC in NaCl-H₂O soln. (Japanese) 0-108631
 Al₄C₃-Be₂C-SiC system, phase analysis and TEM struct. obs. 0-108420
 Al₃Ga_{1-x}As epitaxial film, microstruct., effect on elect. characts. of Schottky diode (Russian) 0-107671
 AlN film, oriented c-axis, low temp. deposition by reactive magnetron sputtering 0-76180
 Al₂O₃, derived from boehmite, phase transformations and microstruct. 0-60857
 β -Al₂O₃-Na₂O, AC impedance, microstruct. and strength 0-100349
 β'' -Al₂O₃-Na₂O solid electrolyte, processing and phys. props. 0-60820
 B fibre, US inspection, immersion method 0-66757
 BC, sintered, struct. and props. 0-104181
 B₂O₃-SiO₂, optical waveguide glass, sintering kinetics 0-84898
 BaO-Nd₂O₃-TiO₂-Bi₂O₃ system ceramics, high stability low loss dielectric preparation 0-81008
 BaTiO₃:BaTi₃O₉, dielec. props. and microstruct. 0-60481
 Bi₂CaNa_{2-x}Nb₂O_{3+3x}, intergrowth, IMV high-resolution electron microscopy 0-107436
 C, strength and struct., conf., Bath, London, England (Apr. 1979) 0-82566
 Ca₂(Al,Fe,Cr)₂O₇ solid soln., planar interfaces, TEM obs. 0-65008
 Cd-Sn alloy, superconductivity and microstructure 0-107949
 Cd-Zn eutectics, microstruct. after solidification, heat pipe influence 0-76243

crystal microstructure continued

Co-Sm crystals, microstruct., homogeneous precip. and nucleation 0-104160
 Cr foil, laser irradiated, low-angle X-ray scatt., angular block misalignment and hardness (*Russian*) 0-103413
 Cu foil, laser irradiated, low-angle X-ray scatt., angular block misalignment and hardness (*Russian*) 0-103413
 Cu, polycrystn., strain localisation during hot deform. 0-104195
 Cu-Al-Sn system, coexistence of different and brass like phases 0-89206
 Cu-Be-Co, discontinuous reaction, analytical TEM 0-100842
 Cu-Fe system, ageing and reversion phenomena study 0-89274
 Cu-mild steel explosively welded interface, SEM examination (*German, English*) 0-96746
 Cu-Nb-Al alloys, displaced hysteresis loop and microstructure obs. 0-84613
 Cu-Nb alloy, chill casting, consumable are melting, ingot prep. techniques 0-84879
 Cu-Zn, interface sliding of FCC and BCC boundaries 0-104240
 Cu-S+Ln₂S₃, powdered mixtures, reaction rate, production of ionic semiconductors 0-93741
 Fe, cast, grey, solidified in oscillatory and rotating moulds, metallographic study 0-89213
 Fe, cast, inoculated with Ce-Mg-Fe master alloy, struct. and props. 0-100843
 Fe oxides, phase equilibrium and microstructure interpretation 0-60847
 Fe-Al(24.3 at.%) C alloy, magnetic permeability disaccommodation, 260-400K 0-93144
 Fe-Cr-Co, magnetic domain walls, Lorentz microscopy 0-103854
 Fe-Cr-Co permanent magnet system, miscibility gap, microstruct. and mag. props. obs. 0-76228
 Fe-Cr-Co-Mo high energy permanent magnets, mag. props. 0-97119
 Fe-Cr-Mo alloy castings, thick-section, factors affecting 0-108374
 Fe-Cr(W)-M, (M=Si,Mo,Ni,Mn,P,Cr), cellular growth of S-pearlite formed by carburisation 0-108486
 Fe-Cu, lath martensite habit planes, TEM study 0-84942
 Fe-M, (M=Cr,W,Mo,V,Ti), morphology and growth kinetics of δ -pearlite formed by carburisation 0-108485
 Fe-Ni, secondary recrystn. and mag. props. 0-89247
 α -Fe-Ni (3-12 wt.%), structure and γ - α polymorphic transform. kinetics 0-71645
 Fe-Ni-C (31.9, 0.02 wt.%) alloy, hardness of martensite-austenite mixtures 0-60959
 Fe-Ni-C (31.9, 0.02 wt.%), determ. of number and size distrib. of martensitic plates 0-76255
 Fe-Ni-Cr (35, 15 wt.%) superalloy, stress rupture and tensile props., C and B additions effect (*Chinese*) 0-102444
 Fe-Ni-Cr-Al-Y, oxidation mechanism, Y addition effect on kinetics and oxide adherence 0-97623
 Fe-Ni-Mn (20, 5 wt.%), rel. orientation between adjacent martensite laths 0-76254
 Fe-Si, grain oriented sheet, grain struct. by computer mapping 0-88168
 Fe-Ti, ion implanted, with C impurity, microstruct. of TiC precip. 0-66513
 Fe-Ti-C, rapidly quenched by splat-cooling 0-84923
 Fe-X-C (X=Cr, Mo, W), quenched rapidly from melts, nonequilibrium phases (*Japanese*) 0-71630
 Fe-Zn, quenched, martensite struct. and hardness, electron microscope exam. (*Russian*) 0-66619
 Fe₂Co_{0.5}-Cr_x films, vacuum-deposited cryst. and mag. struct. (*Russian*) 0-93081
 β -FeOOH, lattice imaging and pore struct., high resolution electron microscopy obs. 0-103310
 GaAs epitaxial film, microstruct., effect on elect. characts. of Schottky diode (*Russian*) 0-107671
 GaAs:Si, Li, IR absorpt., microstruct., charge compensation 0-107565
 Gd films, electrical props. correlation with microstructure 0-97009
 HfC, etchant for revealing microstructure 0-85097
 InAs-CdTe quasi-binary system, temp.-comp. diagram, physicochem. and thermodynamic analysis 0-104127
 Li₂O.2SiO₂, ceramic, prep. of oriented microstructure by unidirectional solidification of melts 0-71614
 Mg_{1.86}Al_{0.75}Si_{2.47}O_{3.19}N_{3.81}, 12H polytype, intergranular phases and compositional variations 0-79645
 MnSi-Si system, striations and cryst. struct. of matrix 0-103292
 MnZn ferrite, microstructure and initial permeability, presintering process effect 0-89367
 MnZn ferrite powders, reactive, mag. materials obtained by compaction 0-89182
 Mo-Al-Ge, phase equilibria, X-ray and microstructural anal. 0-93536
 NH₄Br, dislocation influence on phase transition and light scatt. (*Russian*) 0-59648
 Na-rich plagioclase microstructure and exsolution 0-72501
 Nb-Ge, compounds with A15 structure, films, TEM study (*French*) 0-80135
 Nb-Ge-Si, compounds with A15 structure, films, TEM study (*French*) 0-80135
 Nb-Si, compounds with A15 structure, films, TEM study (*French*) 0-80135
 NbC, etchant for revealing microstructure 0-85097
 Nb₂O₅-V₂O₅-P₂O₅, glasses and glass ceramics, elec. cond., struct. 0-84466
 Nb₃Sn film formation, solubility, precipitating processes (*Russian*) 0-92792
 Nb₃Sn-Cu multifilamentary composite wire, Nb₃Sn filament morphology and grain size 0-100855
 Ni base superalloy Nimonic 80A, microstruct. anal. by high-resolution electron microscopy 0-76459
 Ni, dislocation structure evolution after hydroextrusion (*Russian*) 0-96530
 Ni-Al (2 and 6 wt.%), oxidation, α -Al₂O₃ growth, microstruct., precip. 0-108626
 Ni-ceramic coating structure, influence of micropowder inclusion (*Russian*) 0-59820
 Ni-Co-Al alloys, continuous precip., SEM, TEM, X-ray diffr. study 0-89220
 Ni-Cr-Al-TaC, eutectic composite, microstructure, fatigue props. 0-85038
 Ni-Cr-Ta-Ti-Si, EP557 precipitation hardening alloy, mech. props., heat treatment effect 0-60877
 Ni-Cu-X (X=Sn, Nb, Ti), spinodal decomp. alloys, linear expansion coeff. influence on morphological anisotropy (*Japanese*) 0-70431

crystal microstructure continued

Ni-Fe-Cr superalloy type 718, heat treatment effect on room temp. and elevated temp. fracture toughness response 0-100922
 Ni-ferrite powders, form. in presence of Li₂SO₄-Na₂SO₄ molten salts, prep. and characts. 0-84869
 Ni-NbC (10 wt.%) eutectic alloy, directional solidification and struct. (*Russian*) 0-84922
 Ni-Ni₃Mo system, deformation microstruct. 0-93591
 β -NiAl, oxidation, α -Al₂O₃ growth and microstruct. 0-108627
 NiFe, single and multilayer thin films, strip domains, inplane magnetisation 0-103866
 Ni₃Fe_{1-x}O₄, DC and low freq. cond. and influence of microstruct. 0-70699
 NiTaC eutectic superalloy, casting, furnace atm. effects 0-84880
 NiZn ferrites, nonstoichiometric, initial susceptibility and microstruct. 0-84591
 PbO, thin film, microstruct. and thermal stress, doping effects 0-88458
 Pb_{0.94-x/2}Ba_{0.5}Nb_{0.5}Zr_{1-x}O₃, Nb dopant morphology effect on microstructure 0-81005
 PbTe thermoelectric materials, microstructure anal. using SEM X-ray microanalysis 0-107211
 Pb(Zr,Ri)O₃:Ni-silicon rubber flexible composite pyroelectric, dielectric props. 0-80704
 PbZrTi_{1-x}O₃, ceramics, morphotropic phase boundary 0-81035
 239PuO₂, stoichiometric, high-temp. deformation 0-81111
 Si film, polycryst., grain struct. and surface roughness, TEM study 0-70556
 Si, polycrystalline structure stability, stacking defects, twins grain struct. (*Russian*) 0-100248
 Si solar cells, polycrystalline, from recrystallized plasma deposited thin films 0-104509
 Si:Ar, ion-implanted, epitaxial regrowth by laser annealing, microstruct. 0-84404
 SiO₂, Czochralski crystal, oxygen striation and thermally induced microdefects 0-100275
 Si-Al-O-N system, phase analysis and TEM struct. obs. 0-108420
 SiC, reaction-bonded, 'REFEL', microstruct. characterization 0-97490
 SiC-AlB₂ (0.61 to 1.2 wt.%), hot pressed, microstruct. 0-93563
 SiFe sheets, grain-oriented, stray field meas. 0-88775
 Si₃Fe_{0.5}, polycryst. ribbon, prep. by rapid quenching, and props. 0-75803
 SiO₂ phase equilibrium and microstructure interpretation 0-60847
 SnO₂ CVD coating on glass, elec. resist. rel. to cryst. microstruct. 0-84520
 Sn_{1-x}Pb_xSe(Te) films, oxidation rel. to annealing temp. and time, Mossbauer spectra, X-ray and microstruct. obs. 0-104311
 TaC, etchant for revealing microstructure 0-85097
 Tb_{0.27}Dy_{0.73}Fe₂, vertically zoned, magnetomechanical coupling and magnetstriction 0-65999
 Te film, microstructure 0-103598
 Ti-Mo-Zr-Sn (11.5, 6.0, 4.5 wt.%) alloy, struct. as affected by processing history 0-84972
 Ti-Bi-Sb-Te system, peritectic reactions in TiBiTe₂-TiSbTe₂ cross section, crystn. character 0-108406
 U-Mo (2 wt.%), depleted, effect of microstruct. on mech. props. 0-108497
 (W,Mo)C, hard-facing applications, effect of Mo on struct. and hardness of WC 0-108474
 W, SEM expts., anomalous patterns (*Chinese*) 0-59349
 W-Co, STEM anal. of grain boundaries 0-79644
 WSe₂, chem. vapour transport growth, microstruct. develop. 0-103278
 Zn-Al(22 wt.%), alloy sheet, superplastic, cold-rolling effects on mech. props. and microstructure (*Japanese*) 0-71671
 Zr alloys, irradiation growth, influence of microstructure and test conditions 0-92561
 Zr₂, irradiation growth, influence of microstructure and test conditions 0-92561
 Zr-Nb (2.5 wt.%), cold-worked, pressure tubing, metallography and mech. props. 0-89269
 Zr-Ru, alloy Zr rich, Ru solubility, eutectic decay, α - β transform., struct. (*Russian*) 0-65227

crystal morphology
 boracite, single cryst. prep. and phys. props. 0-100763
 β -brass, spinodally decomposed, morphology and characts. 0-60863
 crystal face, growth behaviour in presence of screw dislocations 0-103276
 crystal surface morphology development during sputter erosion 0-88414
 dickite, unusual crystal habit, structural disorder 0-59445
 ice crystal morphology, vapour growth, influence of vapour diffusion and heat diffusion 0-64933
 icicle crystallisation phenomenon, growth mechanism, structure and shape 0-59423
 monostearine crystals, spiral growth from organic soln. 0-93467
 trans-polyacetylene, bulk crystallinity, small-angle X-ray diffr. study 0-103263
 polyethylene, single crystal, electron microscopy study 0-103273
 polyethylene fibre, high-strength high-modulus, morphology and tensile prop. relations 0-103264
 polyvinylidene fluoride, melt-solidified, crystn. and morphology 0-103461
 (rare-earth) Fe₃(BO₃)₄, cryst. growth from soln.-melt, props. 0-108337
 silicate minerals Raman spectra, microscopic samples molecular analysis 0-57391
 solid-solid interface chemistry, characterisation, theory 0-75448
 sputtering induced topography on solids, energetics and kinetics 0-88220
 triglycine fluoborillate, deuterated, dislocation line defect X-ray topographic analysis 0-59465
 tris (3-mercaptop-1, 3-diphenyl-2-propen-1-onato) Co(III), multiple twinning 0-100250
 uric acid occurrence, growth morphology of C₃H₄N₄O₃ anhydrous monoclinic modification 0-84123
 Ag, electrodeposit, on (111) face, habit modification caused by Cl⁻ 0-71600
 Ag electrodeposition, on (100) face of single crystal Ag in presence of sulphadiazine 0-89161
 AgMg two phase bicrystal growth, orientation, interface struct. 0-60773
 AgNO₃, centre of symmetry and cryst. perfection (*French*) 0-107089
 AlGaAsSb LPE growth, lattice-matched to GaSb, characterisation 0-60794
 Al₃Ni, cryst., theoretical morphology and comparison with observed habits (*French*) 0-79732

crystal morphology continued

- Al₂O₃-TiO₂ powder, plasma-prepared, morphology and phase constitution 0-100833
 BP-Ni pillar crystal growth from vapour 0-60758
 BaMoO₄ crystals, growth in SiO₂ gel under influence of elec. field 0-93469
 CdCl₂ · 2.5H₂O, rel. between theoretical and obs. morphology (*French*) 0-70148
 CdS/Cu₂S solar cells, polycryst. thin film photovoltaic materials, photon loss anal., expt. determ. 0-93888
 25Cr-20Ni stainless steel dendritic solidification, growth morphology and solute redistrib. (*Japanese*) 0-81045
 CrO₂ and CrO(OH), fine particle obs. of cryst. morphology and topotaxy 0-65969
 Cr_{2.8}V_{0.7}Fe_{3.4}C₃, stacking fault study, morphology, comp. and struct. 0-84190
 Cu, cementation, on Fe, deposit struct., reaction rates, SEM 0-104421
 CuSO₄·5H₂O, dehydration into trihydrate obs. using monocryst. platelets, product domains shape 0-71905
 α-Fe crystals, growing in Fe₈₀(C_{1-x}B_x)₂₀ glass, morphology 0-70129
 Fe, high purity, boriding with cryst. B powder 0-84951
 α-Fe-Ni (3-12 wt.%), structure and γ-α polymorphic transform. kinetics 0-71645
 HfO₂ crystallite growth from oxide plasmas, growth morphology 0-59417
 In₂O₃ smoke particles prepared by gas evap., morphology and coalescence growth 0-97738
 InP, SSD growth of low dislocation density crystals 0-89135
 LaPO₄ catalyst crystals, high resolution electron microscopy, morphological charact. rel. to catalytic activity 0-107193
 LiNbO₃ Czochralski grown single crystals, faceted and nonfaceted growth sections, growth striae (*Chinese*) 0-64940
 MoO₃ smoke particles prepared by gas evap., morphology and coalescence growth 0-97738
 NH₄ClO₄, polymorphous phase transition mechanism 0-79737
 (NH₄)₂Cr₂O₇, crystal hypomorphism and hypermorphism 0-59427
 NH₄H₂PO₄ cryst. growth in presence of Mn ions 0-93468
 NH₄H₂PO₄·⁵⁷Fe, Mossbauer study, Fe³⁺ effect in habit 0-100627
 NaCl:Ca crystals, surface recrystn., moisture effect 0-84950
 Nd,R_{1-x}P₃O₁₄ (R=La, Y: 0.1<x<1), laser quality cryst. growth, morphology 0-66412
 Ni, electrocrystallisation, reaction mechanism, appl. of impedance meas. (*French*) 0-103597
 Pb, underpotential adsorption, cathodic deposition, on Ag(111) and (100) (*German*) 0-108363
 Pb_{0.94-x/2}Ba_{0.6}Nb_{0.5}Zr_{1-x}O₃, Nb dopant morphology effect on microstructure 0-81005
 PbS, chem. deposited thin film, effect of morphological struct. on photosensitivity 0-70760
 Si epitaxial thin film growth on sapphire and spinel by MBE 0-76186
 Si-Cu, precipitate morphology, IR microscopy study (*Chinese*) 0-103539
 Si-SiO₂ interface, thermal SiO₂ sputter induced roughness, Auger sputter profiling study 0-75424
 Te film, vacuum deposited, growth and morphology of crystals 0-96766
 Te, vacuum deposited on NaCl, crystallite growth and morphology, electron microscopy 0-65401
 ThO₂ crystallite growth from oxide plasmas, growth morphology 0-59417
 Ti-Mo-Zr-(Al) (15, 5 (3) wt.%), quenched and aged metastable β-phase, crystallography, morphology and decomposition 0-76262
 TiN(C) whisker growth in CVD 0-59843
 Tl, underpotential adsorption, cathodic deposition, on Ag(111) and (100) (*German*) 0-108363
 UO₂ crystallite growth from oxide plasmas, growth morphology 0-59417
 WO₃ smoke particles prepared by gas evap., morphology and coalescence growth 0-97738
 Zn, electrocrystallisation, reaction mechanism, appl. of impedance meas. (*French*) 0-103597
 ZrN(C) whisker growth in CVD 0-59843
 ZrO₂ crystallite growth from oxide plasmas, growth morphology 0-59417

crystal orientation

- channelling patterns, selected area, cryst. orientation determ. method 0-70092
 FCC crystal-melt interfaces, mol. dynamics simulation 0-79913
 films, orientation effects in quantitative X-ray microanal. 0-85259
 ice, c-axis alignment, Arctic Alasca coast 0-67375
 ice crystals at base of Ross Ice Shelf, alignment rel. to subglacial ocean currents 0-101393
 Kossel technique in SEM for crystallographic orientation 0-75133
 lattice images of defect, misorientation effects 0-107210
 Laue photograph indexing and monocrystal orientation determination by computer, new approach (*Chinese*) 0-79636
 metals and alloys, HCP struct., relative orientation of cryst. lattices 0-84181
 mica solid state particle track detectors, fission fragment ranges rel. to cryst. orientation 0-91408
 polypropylene, isotactic, uniaxially oriented, Raman spectra (*French*) 0-60557
 quartz, c-axis fabrics anal. via photometric method 0-101456
 solid-solid interface chemistry, characterisation, theory 0-75448
 steel, Cr-W(Mo), quenched, carbide reactions during tempering 0-89229
 steel, P, deep-drawing, spatial orientation distrib. of crystallites in cold-rolled and in annealed sheets 0-81079
 vacuum deposited film, orientation axis tilt rel. to vapour angle of incidence 0-88456
 zone axis method, appl. to grain boundaries, TEM 0-103226
 AgMg two phase bicrystal growth, orientation, interface struct. 0-60773
 AlN films on glass substrate, prep. by reactive DC magnetron sputtering technique, c-axis orientation 0-89146
 AuMn alloy, ordered, vacuum deposited epitaxial films, orientation control by external stress 0-100426
 Co-P films with various preferred orientations, mag. props. 0-100604
 Cu, crystalline reorientation following ion bombard. 0-70269
 Cu, electrolytic epitaxial nucleation and growth, on (111) Ag 0-104081
 Cu, implanted with Cu⁺, effect on cryst. orientation, Kr penetration meas. 0-88174
 CuAu alloy, ordered, vacuum deposited epitaxial films, orientation control by external stress 0-100426
 Fe zone refined crystals, cryst. orientation and distrib. of stray grains 0-70509
 Fe₂O₃/Fe₃O₄ transformation matrices, higher-order orientation relationships 0-100846

crystal orientation continued

- GaP, growth conditions rel. to dislocation struct. 0-88151
 Ge, ionisation rates, cryst. orientation depend. 0-103700
 Ge, volume plasmon, cryst. orientation influence 0-80921
⁴He crystals, nucleation and orientation 0-84339
 KNO₃ calcite-type crystals, topotaxial decomp. TEM obs. 0-108710
 LaB₆ cathodes, single crystal, of <100> and <110> orientations, brightness meas. from 1500 to 1950K 0-62808
 MgO-CdO, interface, coincidence-site-lattice relations 0-103588
 MgO.1.1 Al₂O₃ spinel, high temp. deform., cryst. orientation effect 0-107263
 Mo single crystals, orientation and alloying effect on mech. props. (*Russian*) 0-71706
 Mo-Nb-C, mech. props., effect of alloying and Mo cryst. orientation (*Russian*) 0-71706
 Na₂(Fe,Mg)₂Si₈O₂₂(OH)₂, riebeckite, low temp. Mossbauer obs. of oriented single cryst. behaviour and mag. props. 0-84674
 V-Ti-C, high temp. carbide form., electron microscopy study 0-89228
 Y₂Fe₂O₁₂ LPE growth on Gd₂Ga₂O₁₂ substrates, substrate orientation effect 0-66438
 ZnO RF sputtered films, post deposition annealing behaviour 0-100416
 ZnS, single electron excitation study, cathodoluminescence image contrast using STEM 0-89072
- crystal oscillators** *see* **crystal resonators**
- crystal properties**
see also **crystal chemistry**
 No entries
- crystal purification**
see also **zone refining**
 semiconductor, doping reduction using zone recrystn. with temp. gradient 0-104062
 semiconductor, enhanced electrodiffusion purification in mag. field, GaAs epitaxial film appl. 0-66409
 Fe, purification, recrystn. temp. and elec. resistivity (*Japanese*) 0-100780
 HgI₂, soln. grown crystals, low-energy gamma-ray cond. type detectors 0-97418
 KBr(Cl), prep. of crystals containing impurities of specified amounts (*Russian*) 0-66424
 Si, metallurgical grade, impurity gettering of polycrystalline solar cells 0-81441
 Si purification, plasma melting zone technique (*French*) 0-89141
 Si purification, plasma melting zone technique, optimisation (*French*) 0-89142
- crystal resonant gamma-ray interactions** *see* **Mossbauer effect**
- crystal resonators**
see also **piezoelectric oscillations**
 immunity to acceleration fields in any shock/vibration environment 0-91953
 orientation of industrially cut alpha quartz AT plates 0-92008
 quartz, SEM surface patterns obs., energy trapping appl. 0-71323
 quartz plates, surface irregularities due to mechanical, chemical treatment (*Polish*) 0-89380
 quartz wafer surface contaminant estimation methods, cleaning processes appl. (*Polish*) 0-89381
 SAW, 1.56 GHz operating freq. 0-87687
 temperature stable oscillators employing parallel-connected SAW resonators 0-74615
 thickness-extensional trapped energy resonators, mode coupling 0-74655
 tuning fork for HF operation, second-mode, finite element anal. and expts. 0-102980
- crystal structure**
see also **crystal atomic structure; crystal microstructure; crystal morphology; crystal orientation; crystal symmetry; crystallography; granular structure; polymorphism**
 electron microscope imaging 0-88006
 α-Fe, nitrided, aging at room temp. 0-71679
- crystal surface and interface vibrations**
 adatom-surface interaction potential, vibr. spectrum 0-103581
 adsorbate vibrations, large-angle inelastic electron scatt., theory 0-75427
 adsorbed molecule, angle-resolved and variable impact energy electron vibr. excitation spectroscopy 0-76119
 adsorbed molecules, electron-impact vibr. excitation, specular selection rule 0-80051
 benzene, deuterated and chemisorbed on glass, vibr. bands, Raman scatt. study 0-84737
 Brillouin scattering by Stoneley waves, elasto-optic and surface ripple mechanisms 0-71435
 cubic crystals, anisotropic, surface Green function matching anal. 0-70518
 desorption, multiphonon processes, quantum-statistical theory 0-107641
 elastic surface waves in crystals, special surfaces, directions 0-92604
 electrons in surface phonon field 0-107885
 exceptional surface waves in triclinic crystals, existence problems, general props. 0-92603
 finite harmonic oscillator chain with surface impurity, dynamics 0-59776
 metal surface, rough, anomalous low-freq. Raman scatt. from localised acoustic vibrs. 0-93307
 metal surface, sticking rate, transmission problem, model Hamiltonian 0-107640
 molecular monolayers, IR absorpt. enhancement by thin metal overlayers, ATR technique 0-88995
 naphthalene, surface dynamics, calc. 0-92772
 piezoelectric crystal, surface polaron states, polaron-phonon interactions 0-70790
 plasmarons, effect of finite thickness of accumulation layer, theory 0-103636
 polar semiconductor crystalline thin films, surface vibr. states, IR absorpt. spectra obs. (*Russian*) 0-60606
 sapphire-Pb interface, heat transfer coeff. meas., 2-80K 0-88419
 semiconductor, degenerate, surface optical phonons 0-70520
 Stoneley waves at (001) interface between cubic symm. cryst. 0-100388
 transition metal, tight-binding model, surface atom vibrations, self-consistent calc. 0-103560
 water, chemisorbed on Pt (111), EELS spectra, vibr. freqs. 0-80920
 Ag (111) surface phonon dispersion, He atom scatt. meas. 0-75426
 Ag, adsorbed CN monolayer, vibr. spectra, picosec. Raman gain technique 0-91859
 Al, Brillouin spectra, light scatt. cross section for surface ripples 0-71434
 CO chemisorbed on Fe, low energy vibr. modes studied by tunnelling spectroscopy 0-78590

crystal surface and interface vibrations continued

- CaCl₂(Br₂), adsorption of NH₃ and ND₃, complex formation, IR and for IR spectra obs. 0-80063
 CaF₂, slab with (110) free surfaces, lattice dynamics and thermodynamic functions 0-70519
 Cu (100), adsorbed formate and acetate species, EELS study 0-76120
 Ga_{1-x}Al_xSb, surface oxidation, Raman spectra, residual Sb layers 0-71419
 GaAs, Brillouin spectra, light scatt. cross section for surface ripples 0-71434
 GaSe, lattice dynamics and elastic props., Born-von Karman model study 0-70337
 Gal, Brillouin spectra, light scatt. cross section for surface ripples 0-71434
 InP, surface phonon polariton dispersion and damping, frustrated total internal refl. meas. 0-80792
 LiF (001), surface phonon obs. in He atom inelastic scatt. 0-80927
 LiF film, surface phonons and thickness variation, EELS meas. 0-92774
 LiF surface, diffractive scatt. of H atoms, meas., Debye temp. and Morse pot. determ. 0-76124
 LiF surface, He atom inelastic scatt., phonon coupling 0-71554
 Nb₂Sn, softening of surface phonons in (100) plane 0-107627
 Ni (111), adsorbed H, angle-resolved and variable impact energy electron vibr. excitation spectroscopy 0-76119
 Ni, Brillouin spectra, light scatt. cross section for surface ripples 0-71434
 Ni catalysts, chemisorption of H₂(H₂O), dynamics, neutron spectrosc. obs. 0-59778
 Ni, chemisorbed O influence 0-84361
 Pt (111), adsorption of NO, EELS, thermal desorption, LEED, and AES study 0-80086
 Ru (001), CO adsorbed, temp. depend. ordering processes 0-80773
 Si, amorphous, opaque, surface phonon attenuation, Brillouin scatt. 0-80808
 Si-SiO₂ interface, remote polar phonon scatt. in Si inversion layers 0-80095
 Si-SiO₂ interface, thermal SiO₂ sputter induced roughness, Auger sputter profiling study 0-75424
 SiO₂, hydroxylated amorphous, small-particle dynamics, neutron scatt. 0-79899
 Sn film-quartz substrate interface, anomalous transmittance for thermally radiated phonons of thin metal films (*Russian*) 0-103664
 W (100), adsorbed H, angle-resolved and variable impact energy electron vibr. excitation spectroscopy 0-76119
 W (100), chemisorbed H, ν , vibrational mode IR study 0-60582
 W (100) and (110) surface, theoretical Debye-Waller factors 0-92773
 W, chemisorbed H₂, vibr. spectra characts., adsorption sites 0-70535
 W(100) surface, instability, distortion and dynamics 0-84360
 Zr(BH₄)₂ catalytic reactions on Al₂O₃, inelastic electron tunnelling spectra 0-75425

crystal symmetry

- see also crystallography; group theory*
 43m symmetry geometric units, cryst. structs. 0-107087
 alkali chloride:Mn²⁺, spin Hamiltonian parameters, binding energies for cation vacancy complexes 0-96461
 anisotropic materials, class D_{6h}, constitutive relations 0-59426
 anthracene, attachment energy as habit controlling factor 0-59421
 anthracene, metastable triclinic phase 0-59452
 continuous crystalline transitions, counterexample to maximal subgroup rule 0-59428
 corundum, attachment energy as habit controlling factor 0-59422
 cubic and non-cubic, distinguished by weak field galvanomagnetic meas. 0-60009
 cubic structures, symmetry of coincidence site lattices (*Russian*) 0-79807
 D_{2d} crystals, structural phase transitions, soft modes, group theory 0-92638
 dislocation core, symmetry of dynamical electron microdiffraction patterns 0-100140
 elastic media and crystal, groups of materials symmetry 0-70147
 elastic surface waves in crystals, special surfaces, directions 0-92604
 electron microscope imaging 0-88006
 EPR, low symmetry effects, review 0-71159
 ferroelectrics, unit cell multiplication during phase transform., spontaneous polarisation 0-75983
 ferroic phase transitions, non-mag., unified classification 0-70387
 grain orientation, of neighbours, disorientation description 0-79725
 growth models, attachment energy as habit controlling factor 0-59420
 growth-layering effect on optical symmetry in cubic crystals, rel. to cathodolum. data 0-88072
 icosahedral multishell clusters, stability and formation modes (*French*) 0-79728
 incommensurate crystal phases, symmetry, superspace-group approach, commensurate basic structs. 0-79726
 incommensurate crystal phases symmetry, incommensurate basic struct., superspace group approach 0-79727
 Jahn-Teller crystals., ferroelec. transitions, elastic and dielec. anomalies, microscopic model 0-71332
 magnetic structure, neutron diff. study, symm. anal., polarisation effects 0-93083
 magnetostriiction in terms of hexagonal and cubic harmonics up to degree 6 0-88856
 methane, phase II, nuclear spin-lattice relax. and site symm. 0-97155
 molecular crystals, dipolar coupling and phonon symm. (*Chinese*) 0-103437
 molecular crystals., symmetrised valence and relative motion coords. 0-84134
 molecular low dimensional system, spontaneous symm. distortion 0-96456
 multivector analysis, comparison with tensor algebra 0-100195
 multivector analysis, comparison with vector anal. 0-100196
 optical material props., symmetries and tensorial relationships 0-108174
 organic crystals, macroscopic prop. observation forbidden by point group symm. (*Russian*) 0-88075
 periodic structure homometric set, search algorithm 0-75118
 plastic crystal, orientational disorder, group theory method 0-107091
 plastic crystal, orientational dynamics, neutron scatt. data interpret. using functions derived from group theory 0-107092
 polyhedral cavity field tensors 0-100182
 polymeric series of coverings, symmetry, comparison with layers of real structs., Belov subclass development 0-84129
 pseudosymmetric crystals, isovector struct. theory, Cochran struct. 0-88076

crystal symmetry continued

- quartz, habit variation of crystals of the C₃2-C₃2 space group 0-107090
 quasi-symmetry and double point groups C₄ and D₃ 0-92472
 reduction symmetry method in crystal field theory 0-70656
 rhombohedral oxides, symmetry group (*French*) 0-84157
 rotational symmetry, and tensor props., 1-, 2- and 4-fold principal symmetry, trigonal, and hexagonal groups 0-100193
 rotational symmetry, and tensor props., method for group 3(2) 0-100192
 Stoney waves at (001) interface between cubic symm. cryst. 0-100388
 structure semi-invariants, representations method 0-79724
 triclinic lattices, planewise summation method 0-107069
 wreath groups, symm. of crystals with struct. distortions 0-75196
 AgCl-AgBr mixed crystals., elastic const. and cryst. symm. 0-70290
 AgNO₃, centre of symmetry and cryst. perfection (*French*) 0-107089
 Au, pentagonal symmetry, icosahedral struct. (*French*) 0-79729
 BaCl₂, Sn-activated, luminescence studies 0-108246
 CsAlF₄, single cryst., prep. and struct. (*French*) 0-79762
 CsDyF₇ and Cs₂DyF₆, cryst. symm. and cell parameters (*French*) 0-81040
 HgS, habit variation of crystals of the C₃2-C₃2 space group 0-107090
 KAlF₄, single cryst., prep. and struct. (*French*) 0-79762
 LaNbO₄, room temp. form., symmetry determ. by convergent beam electron diff. 0-79723
 La₂S₄(Se₄), structural transitions, symm. anal. 0-92671
 NH₄AlF₄, single cryst., prep. and struct. (*French*) 0-79762
 (NH₄)₂Cr₂O₇, crystal hypomorphism and hypermorphism 0-59427
 NH₄LiSO₄, point group symm. at high press. phase 0-70150
 NdNbO₄, room temp. form., symmetry determ. by convergent beam electron diff. 0-79723
 RbAlF₄, single cryst., prep. and struct. (*French*) 0-79762
 RbDyF₇, RbDyF₇ and Rb₂DyF₆, cryst. symm. and cell parameters (*French*) 0-81040
 α -S, attachment energy as habit controlling factor 0-59421
 Se, habit variation of crystals of the C₃2-C₃2 space group 0-107090
 SnI₄, attachment energy as habit controlling factor 0-59421
 SrCl₂, in-activated, luminescence studies at 77 and 300K 0-108247
 TaSe₂ (2H), broken hexagonal symm., incommensurate charge-density wave struct. 0-96646
 Te, habit variation of crystals of the C₃2-C₃2 space group 0-107090
 TlAlF₄, single cryst., prep. and struct. (*French*) 0-79762
 TiSe type crystals, possible second-order phase transitions, group-theoretical anal. 0-92672
- crystal whiskers** *see whiskers (crystal)*
- crystallisation**
see also crystal growth; dendrites; heat of crystallisation; nucleation
 alkali metals, crystalline and alkaline, eqns. of state, zero compression isotherms (*Russian*) 0-103446
 alloy melt, impurity conc. field model, growth by Czochralski method (*Russian*) 0-75191
 amorphous alloys, thermal stability, crystn., DSC and elec. resist. study 0-107060
 amorphous materials, laser irradi., electronic struct., one-electron approx. 0-70576
 amorphous solid, rapid quenching, techniques for determ. very short room temp. lifetimes 0-84981
 anthraquinone, UV light effect on nucleation during crystallisation on anthracene surface 0-75478
 anthrone, UV light effect on nucleation during crystallisation on anthracene surface 0-75478
 p-azoxyanisole, directed crystn. in elec. and mag. fields 0-107052
 benzil core fibres, void-free cryst. growth, X-ray diff. and optical microscopy study 0-71586
 borosilicate glass, powder, sintering, foaming by chemical reactions 0-81017
 bounded domain undergoing sequential crystallisation, stress and strain investigation 0-100183
 calcium oxalate hydrates, crystn. kinetics, comparison for mono-, di-, and trihydrates 0-81528
 cellulose, fibrous crystn., from flowing solns. 0-84106
 cholesteric mixtures, quasithermal crystn. 0-92652
 composite material, matrix impurity distrib. in melt crystallisation (*Russian*) 0-100277
 conference, Lancaster, England, Sept. 1979 0-62369
 countercurrent melt crystallisation, ultra-pure substance prep. 0-100779
 crystal frequency distribution, simulation taking nuclei distrib. into account 0-100184
 crystal growth, modified Czochralski method, variations of impurity distrib. 0-88193
 demonstration, teaching aids, convention of secondary school physics teachers (*Hungarian*) 0-67957
 dendrite development and growth in very small crystals, Monte Carlo study 0-107683
 diamond, homogeneous formation in gas phase, laser beam effects (*Russian*) 0-104052
 diamond synthesis by graphitisation of carbon materials at high press. and temp., Ni influence 0-60795
 m-dinitrobenzene core fibres, void-free cryst. growth, X-ray diff. and optical microscopy study 0-71586
 equilibrium properties of crystallising systems, theoret. interpret. of cryst. growth mechanism (*Rumanian*) 0-88073
 ethylene-vinyl alcohol copolymer, drawn samples, annealing effect around T_g temps. on shrinkage and mol. orientation 0-79712
 face effect, with paraboloidal or ellipsoidal isotherm effect 0-107085
 fractional crystallisation, applying very high pressure 0-100775
 front interaction with turbulent alloy melt stream, heat exchange (*Russian*) 0-74708
 glass, crystallisation and nucleation of reheating 0-84078
 glass, electrothermal props. in structural transform. zones (*French*) 0-88047
 glass ceramic mineralogy 0-60826
 glass ceramics, transient heterogeneous nucleation 0-88042
 glass forming melts, crystn. kinetics processes 0-64905
 glass forming systems, induced crystallisation, transient heterogeneous nucleation 0-64903
 granitic magma of Bushveld Complex, crystallisation history as revealed by trace element abundances 0-109145
 graphite, from C melt, review 0-89165
 growth models, attachment energy as habit controlling factor 0-59420
 gypsum, crystallisation 0-100766

crystallisation continued

- heat resistant monocrystal growth apparatus, heat regimes, crystallisation (*Russian*) 0-107071
- Helmholtz free energy, crystn. of phase A from A+B melt 0-79911
- hexachloroparaxylene, crystn. from heptane, optimising purification 0-100774
- ice, crystallisation and melting rate in laminar stream of liquid 0-100770
- ice crystal morphology, vapour growth, influence of vapour diffusion and heat diffusion 0-64933
- icicles, growth mechanism, structure and shape 0-59423
- kinetic coefficients, of crystn. process 0-100188
- lithium polyisoprene, struct. regularity and crystn. 0-103269
- melt crystallisation in self-excited vibr. regime 0-103275
- metallic glasses, annealing behaviour, thermal stability and crystn. 0-75167
- metallic glasses, crystn., thermosonimetric investigation 0-75180
- metals, glassy, structure, transport props., magnetic behaviour, review 0-70138
- Metglas 2826 ribbon, voids formation during crystallisation 0-108428
- n-nitroaniline, UV light effect on nucleation during crystallisation on anthracene surface 0-75478
- nonisothermal devitrification kinetics 0-92465
- optical glass, melting, fining, surface tension, diffusion, nucleation in microgravity 0-81016
- periodic density patterns as uniform fluid crystallizes 0-107404
- periodic structure homometric set, search algorithm 0-75118
- PET, crystallization, lamellar growth kinetics and thickness 0-103266
- polyethylene-polypropylene blend, extruded, thermal swelling and mech. characterisation 0-81110
- poly(ethylene terephthalate), stress-induced crystn. from melt, optical studies 0-84113
- poly(vinylcarbazole), stress-induced crystn. from melt, optical studies 0-84113
- polyalkane imides, crystallisability, supermol. and crystalline structures 0-84100
- 1,4-polybutadiene, stress-induced crystn. from melt, optical studies 0-84113
- polybutylene terephthalate, melt crystallised, solvent crystallised films and moulded bars, morphological obs. 0-84101
- polycrystal, linear, E and G moduli, crystallisation effect (*German*) 0-59556
- polydioxolan, crystn. kinetics, dilatometric analysis and microscopy obs. 0-79706
- polydiphenylgermylene, crystn. from chem. transport reaction 0-104439
- polyether-polyester elastomers, differential scanning calorimetry, crit. points (*Japanese*) 0-75344
- polyethylene, linear, melt-crystallised sharp fraction, lamellar morphology, electron microscopy obs. 0-84099
- polyethylene, low density, melting and crystallisation, DSC characterisation 0-64927
- polyethylene, low density, morphology and props. 0-64926
- polyethylene flow crystallisation, in extensional flow developed by convergent capillaries, props. 0-84111
- polyethylene fractions, quasi-binary systems, solidification and crystn. 0-84108
- polyethylene melt, cryst. kinetics during cooling, nucleation density effect 0-100181
- polyethylene ribbons, flow-induced crystn. from melt, in dies fed by single screw extruder 0-84110
- polyethylene surface-growth fibres, hot drawing 0-97517
- polyethylene terephthalate, oriented, amorphous, stress-induced crystn., shrinkage meas. 0-92466
- polyethylene-polystyrene blends, crystn. characts. 0-103261
- polyethylene/polypropylene blends, surface growth of fibres and films 0-66470
- trans-1,4-polyisoprene crystals, press. effect on growth rate 0-88064
- trans-1,4-polyisoprene crystals, press. effect on melting temp. and lamellar thickness, press. crystn. 0-88302
- polymer crystallisation, review 0-64925
- polymer melting, theoretical aspects 0-59633
- polymer melts, crystallisation from melt 0-84107
- polymer systems, crystallisation from solution 0-84105
- polymer systems, crystallisation kinetic data, status of anal. 0-84104
- polymer systems, flow-induced crystallisation, conference, Midland, MI, USA (Aug. 1977) 0-82576
- polymer-metal adhesive bonds, shear resist., polymer crystn. effect 0-89462
- polymers, crystn. under mol. orientation, formation of stacked lamellar structs. 0-84109
- polymers, stressed, thermodynamically controlled cryst. orientation 0-84112
- polypropylene, flow-induced crystn. from melt, in dies fed by single screw extruder 0-84110
- polypropylene, isotactic, low temp. annealing, differential scanning calorimetry obs. 0-60895
- polypropylene, isothermal crystn., effect of contact with fibrous substrates 0-79708
- polystyrene, isotactic, spherulite radial growth retardation by SiO₂ nucleation 0-107066
- polystyrene-b-isoprene-b-styrene, struct. regularity and crystn. 0-103269
- polyvinylidene fluoride, melt-solidified, crystn. and morphology 0-103461
- purification optimisation, by crystn. 0-100774
- quartz, synthetic, Al centres conc. and anomalous pleochroism depend. on crystn. parameters 0-107311
- rare earth chromite based electrode material development for MHD generators 0-84893
- rotating container melt growth, crystallisation parameters calcs. 0-103285
- single crystal growth, techniques 0-108341
- solute redistribution during crystallisation, interface field effects 0-84119
- solution concentration, interconversion during crystn. 0-100773
- solution crystallisation, US viscosities 0-100189
- stability during capillary shaping, general theory of capillary and thermal stability 0-107076
- stability during capillary shaping for arbitrary small perturbations 0-107077
- steel, nonmetallic inclusion segregation during cooling (*Russian*) 0-100330
- steel, W-Mo-Co, high-speed tool, struct. and props., cooling rate effect at primary crystn. temp. 0-76241

crystallisation continued

- stress, and dislocations, creation during crystal growth (*Russian*) 0-103277
- sucrose, crystn. rate in impure solns., influence of non-sugar and colouring substance quantity 0-100767
- sucrose crystal formation, and growth, effect of same metallic impurities 0-100768
- suspensions, crystallisation, aggregate stability and effect on purity of product 0-100769
- systems, and their mathematical models 0-100186
- TCNQ salts, crystallisation versus electrical conductivity 0-92885
- technical crystallisation, modern trends, computer modelling 0-66406
- tetrabenz[a, cd, j, lm]perylene evaporated film, crystn., time depend. as function of purity 0-88449
- tetraphenylsilane, crystn. from chem. transport reaction 0-104439
- thermally induced structural changes, specimen surface influence 0-103559
- topological modelling of crystal growth 0-59418
- trivalent metal phosphates, condensed, synthesis in polyphosphoric acid melts, physicochem. equil. considerations 0-97419
- vapour-liquid-solid growth mechanism (*Russian*) 0-107074
- zinc oxalate, isothermal crystallisation from soln. 0-108336
- Ag-Cd peritectic system, separate crystallisation of phases (*Russian*) 0-66497
- AgBr-AgI emulsion sensitivity improved by AgCl shell crystallisation (*German*) 0-104453
- Al, molten, showering cryst. form. in mould cooled from top (*Japanese*) 0-66498
- Al-Cu, molten, showering cryst. form. in mould cooled from top (*Japanese*) 0-66498
- Al-Cv (0.3 wt.%), moving solid-liq. interface, diffusion in liq. 0-107456
- Al-Ti, molten, showering cryst. form. in mould cooled from top (*Japanese*) 0-66498
- Al₂O₃-Y₂O₃, melting behaviour and metastability determ. by optical DTA 0-92648
- Al₂(SO₄)₂·(NH₄)₂SO₄·24H₂O, crystn. kinetics in an MSMR crystalliser 0-100185
- AlSb, laser pulse annealing, induced nucleation, crystal growth 0-84966
- Al(111), oxide layer amorphous to cryst. surface transition, slow positron obs. 0-75417
- Au₃Si₆₅, amorphous vacuum-deposited and liquid-quenched films, diffusion and crystn. 0-84094
- Au₃Si_{1-x} amorphous alloy, crystallisation, elec. cond. study 0-103246
- Au₃Si_{1-x} amorphous films, phys. studies 0-75476
- BaFe₂O₄ amorphous film, prep. by RF sputtering, crystallisation 0-76183
- BaTiO₃, crystn. from melts, comparison of different prospective oxy-anion solvents 0-71583
- Ba₂TiO₂₀ single crystals, prep. and unit-cell parameters 0-103302
- Bi, amorphous metal films, crystallisation with and without mag. field 0-70570
- Bi-Sb, crystallisation temp., overcooling temp. (*Russian*) 0-97472
- Bi-Sb-Te melt, Sb and Te distribution coeffs. during crystallisation (*Russian*) 0-93472
- CaCO₃ crystallisation from aqueous solutions, kinetic study 0-59419
- CaO-SiO₂ glass prep. by gel method 0-100824
- 12CaO.7Al₂O₃, composition of gases released on heating, crystallisation (*Russian*) 0-93820
- CaSO₄ crystallisation, from liq. solns. as heat-transfer surface 0-100772
- CaSO₄·2H₂O, crystallisation 0-100766
- CaSiO₃, fibrous, controlled crystallisation and anisotropy 0-59425
- CaWO₄, cryst. growth from solns. in melts, kinetics parameters and thermodynamic props. 0-59424
- CeNH₄P₂O₇ and Ce(NH₄)₂(PO₃)₃, synthesis by solid-phase reaction, characts. 0-60778
- Co-Fe-B, amorphous, crystn. and thermal stability 0-107057
- Co-Fe-Si-B, decomp. of amorphous state during annealing below recryst. temp., electron microscope study (*Russian*) 0-75164
- Co-Mo-B metallic glass ribbons, tensile strength, crystn. temp. 0-89173
- Co-Ni-Mo-C, amorphous alloys, med. props. and thermal stability (*Japanese*) 0-85049
- Co-Zr, amorphous phase form. in Zr-poor region, hardness and fracture strength (*Japanese*) 0-84914
- (Co₉₃Fe_{0.07})_{75-x}-Cr₂Si₃B₁₀ amorphous alloy, thermal stability, Cr conc. effects, DTA expts. 0-59395
- Co₇₀Fe₃Si₃B₁₀, amorphous, crystn. and thermal stability 0-107057
- Co₇₂Si₃B₁₀, amorphous, crystn. and thermal stability 0-107057
- Co₉₀Zr₁₀, ferromag. amorphous alloy, crystn. and domain struct. study 0-107056
- Cu electrocrystallisation on graphite electrodes, nucleation 0-93504
- Cu-Ni, crystallisation temp., overcooling temp. (*Russian*) 0-97472
- EuS-Ga₂S₃-GeS₃, chalcogenide glasses, conditions of form. of glassy prod. (*French*) 0-100325
- Fe, cast, with spherical graphite, crystn. (*German, English*) 0-97473
- Fe, pure and alloyed, density and thermal expansion in liq. and solid states 0-96668
- Fe-(Co)-B and Fe-Ni-B(P), amorphous, crystn. 0-79704
- Fe-B, amorphous, crystn., metal or metalloidal exchange influence 0-75172
- Fe-B, metallic glasses and vapour deposited films, amorphous to cryst. transition 0-88048
- Fe-B amorphous alloy, annealed, microstruct. and mag. domain changes 0-75790
- Fe-B metallic glasses, diffusion coeffs. from primary crystn. data 0-100345
- Fe-B metallic glasses, struct., stability and crystn. 0-75173
- Fe-B-Cr(Mo), metallic glasses, mag., struct., and elec. props. 0-88751
- Fe-B-Si-C amorphous alloys, prep. and props. 0-88748
- Fe-Co-Mo-C, amorphous alloys, med. props. and thermal stability (*Japanese*) 0-85049
- Fe-Cr, crystallisation temp., overcooling temp. (*Russian*) 0-97472
- Fe-Mo-B metallic glass ribbons, tensile strength, crystn. temp. 0-89173
- Fe-Ni, crystallisation temp., overcooling temp. (*Russian*) 0-97472
- Fe-Ni film, amorphous, martensite form. time and struct. 0-104159
- Fe-Ni-B-Mo, crystn. temp. and elec. cond. correl., Mo effect 0-75179
- Fe-Ni-B-Si, amorphous, mag. props., heat treatment effects 0-89370
- Fe-Ni-Mo-C, amorphous alloys, med. props. and thermal stability (*Japanese*) 0-85049
- Fe-Ni-P-B, amorphous, crystn. and struct. 0-75175
- Fe-Ni-P-B metallic glass, crystallisation temperature values from isothermal transformation times 0-59397
- Fe-P-C, amorphous, crystn. and struct. 0-75175
- Fe-Si-B amorphous alloys, Mossbauer spectroscopy (*French*) 0-80653

crystallisation continued

- Fe-Si-B glassy alloys, mag. props., comp. effects 0-88752
 Fe-Zr, amorphous phase form. in Zr-poor region, hardness and fracture strength (*Japanese*) 0-84914
 Fe₇₅B₂₅ metallic glass, nonisothermal meas. evaluation, non-existence of dynamic correction term 0-107406
 Fe₈₀B₂₀, amorphous, crystn. 0-75187
 Fe₈₀B₂₀ amorphous wire, crystn. by annealing at 780°C 0-100177
 Fe₈₀B₂₀ metallic glass, crystn. and struct. relax., Mossbauer effect study 0-75182
 Fe₈₀B₂₀ metallic glass, crystn. kinetics 0-84083
 Fe₈₀B₂₀ metallic glasses, stability and transforms. 0-75174
 Fe₈₃B_{16.6}, amorphous, mag. props. and microstruct., cooling rate and melt overheating effects 0-65965
 Fe₈₃B_{16.6} amorphous, mag. props., melt overheating and cooling rate effects 0-89371
 Fe₈₄B₁₅Si₁, metallic glass, electrical resistivity and crystallisation 0-88526
 Fe₈₄B₁₆, metallic glass, electrical resistivity and crystallisation 0-88526
 Fe₈₀(C_{1-x}B_x)₂₀ amorphous alloy, α -Fe crystn., morphology 0-70129
 Fe_{83-x}M_xB₁₇ and Fe_{78-x}M_xSi₁₀B₁₂ (M=refractory metal), glass form. and thermal stability 0-79703
 FeNi amorphous films, fast phase transition investigation by TEM method 0-107029
 (Fe_{100-x}Ni_x)₈₃B₁₇, amorphous, crystn. 0-75176
 Fe₄₀Ni₄₀B₂₀, amorphous, RF annealing effects 0-108037
 Fe₃₂Ni₃₆Cr₁₄P₁₂B₂ metallic glass, crystn. kinetics by TEM 0-75186
 Fe₃₂Ni₃₆Cr₁₄P₁₂B₂ metallic glass, effect of pre-ageing on glass transition temp. 0-100326
 Fe₄₀Ni₄₀P₁₄B₆, amorphous, steady-state creep rate, cryst. effect 0-81102
 Fe₄₀Ni₄₀P₁₄B₆ metallic glass, crystn. 0-70127
 Fe₄₀Ni₄₀P₁₄B₆, Metglas 2826, hot forming 0-84980
 (Fe₆₅Ni₃₅)₇₅P₁₅B₁₀Al₃, amorphous, crystn. temp., press. and heating rate depend. 0-70132
 α -Fe₂O₃ crystal flux growth, solubility and relative supersaturation in Fe₂O₃-PbO-V₂O₅ fluxed melt system 0-64934
 Fe₄₀(P_{1-x}C_x)_{20-x}B₁₀(Si_y), density, microhardness, and crystn. temp., comp. depend. 0-84093
 (Fe_{1-x}Si_x)_{1-y}By, metallic glass, mag. props., crystallisation 0-65885
 Ga, amorphous metal films, crystallisation with and without mag. field 0-70570
 Ga-In-Sb system, phase diagram calcs. in Ga+In rich region 0-60842
 Ga_{1-x}Al_xP varigap struct., crystallisation 0-80993
 GaP films on Si, epitaxial crystallisation by nanosecond laser pulses 0-107674
 Gd-Co(Ni)(Cu)(Rh)(Ru)(Pd)(Ga), amorphous, mag. props. and ferromag. reson. 0-75862
 Ge amorphous film, crystn. front velocity during scanned laser crystn. 0-107662
 Ge, amorphous film, DC sputter deposited, effect of trapped Ar on minimum temp. for impulse stimulated explosive crystallisation 0-100422
 Ge amorphous films, structural relaxation and crystallisation 0-100170
 Ge, laser pulse annealing, induced nucleation, crystal growth 0-84966
 Ge single crystals, constitutional supercooling growth conditions, structural and chem. inhomogeneities 0-93473
 Ge-Si-S system, glass formation, transition temp., crystallisation and melting 0-100178
 GeO₂ glass, nonisothermal devitrification kinetics 0-92465
 GeO₂-K₂O(Na₂O)(Li₂O), glass, Raman spectra, struct. and crystn. 0-92463
 He, liquid, surface liquid-crystal transition in two dimensional electronic system 0-88303
⁴He crystals, nucleation and orientation 0-84339
 Hf_{1-x}Fe_x amorphous alloys, formation, crystallisation and electrical resistivity 0-96838
 In_{1-x}Ga_xP, compositional inhomogeneity 0-88444
 In-SnO₃ film, effect of ambient atmosphere during annealing, elec. props. 0-97510
 insular metal films, influence on crystn. of continuous films 0-88454
 KCl cryst., Sr and Na impurities radial distrib., influence of form of crystn. front 0-107312
 KLa(MoO₄)₂, solubility in aq. K₂MoO₄ solns., hydrothermal conditions 0-96651
 KMg₂LiSi₄O₁₀F₂-NaMg₂LiSi₄O₁₀F₂, solid soln., solid solubility and swelling characts. 0-59660
 LiO₂-Al₂O₃-SiO₂ glass containing ZrO₂, cryst. process 0-103253
 Li₂O-2SiO₂ glass, DTA study, Kissinger plot 0-84084
 Li₂O-Al₂O₃-SiO₂, phase separation of initial stages of sitalisation 0-88053
 Li₂O-Al₂O₃-SiO₂-TiO₂ system glasses, Raman spectra obs. of glass-ceramics form. 0-60825
 Li₂O-SiO₂-P₂O₅ glass ceramic fibres, heat treatment, crystn., tensile strength 0-84995
 Li_{1+x}P₂O_{3+x}, polyphosphate, melting and crystallisation 0-70376
 Mg-MgNi₂-Zn, diagram of state, Zn solubility, initial phase precipitation (*Russian*) 0-66478
 MnAlGe film, mag. domains and amorphous to cryst. phase transition, electron microscopy obs. 0-71129
 MnGaGe film, mag. domains and amorphous to cryst. phase transition, electron microscopy obs. 0-71129
 Mo-Mo₂C(HfC)(TiC)(ZrC), eutectic formation of regular struct., crystn. (*Russian*) 0-66496
 Mo-W alloy type MW25N, crystallisation form, globular dendrites, grain boundaries (*Russian*) 0-66494
 NH₄Cl-H₂O solidification model for showering cryst. form. in molten metal cooling (*Japanese*) 0-66498
 NH₄H₂PO₄, crystal growth kinetics, in situ X-ray topography study 0-76167
 Na₃Ca₂SiO₄[Si₂O₇][PO₄]₃, synthesis conditions, cryst. struct. and IR spectra characts. 0-108335
 NaCl-NH₃-CO₂-H₂O system, NaHCO₃ crystn. 0-100771
 Na₂Cr₂(PO₄)₃, crystallographic data, ionic conductivity (*French*) 0-88077
 NaF-SrF₂-CrF₃, glass transition, crystn. and melting temps., optical transmission (*French*) 0-64910
 Na₃Fe₂(PO₄)₃, crystallographic data, ionic conductivity (*French*) 0-88077
 NaNO₃(₂), precipitation from mixed aq. solns. 0-100191
 Na₂O-Al₂O₃-SiO₂, glass, nucleation, crystn., ceramic form. 0-84082
 Na₂O-BaO-Al₂O₃-SiO₂, glass, nucleation, crystn., ceramic form. 0-84082
 Na₂O-CaO-Al₂O₃-SiO₂ glass, crystn. for the purpose of obtaining vitreoceramics (*French*) 0-75163
 2Na₂O-CaO-3SiO₂ glass, cryst. nucleation rate, viscosity, heat treatment 0-84081

crystallisation continued

- Na₂O-P₂O₅-SiO₂ glass, substitution of Li⁺, Mg²⁺, Sr²⁺, Ba²⁺, Zn²⁺ for Na⁺ 0-100332
 Na₂O-PbO-SiO₂ glass-ceramic composite, directionally crystallised 0-107058
 5Na₂O.Fe₂O₃.8SiO₂, glass crystallisation study by Fe³⁺ EPR and Mossbauer spectra 0-64904
 Nb-Ir(Rh) system glasses, form., crystn. and microhardness, resist. obs. 0-89178
 Nb-Si(-V)(Zr)(Mo)(Ta)(W)(C)(B)(Ge), ductile amorphous, superconductivity 0-60131
 Nb₄₀Fe₄₀P₁₄B₆, metallic glass, explosive compaction, mech. props. 0-89176
 Ni, electrocrystallisation, reaction mechanism, appl. of impedance meas. (*French*) 0-103597
 Ni film crystallisation on C fibres and sapphire crystals (*Russian*) 0-75455
 Ni-B, film crystallisation on C fibres and sapphire crystals (*Russian*) 0-75455
 Ni-Cr-P, amorphous, corrosion behaviour, immersion tests and electrochem. meas. (*Japanese*) 0-85085
 Ni-Mo-B metallic glass ribbons, tensile strength, crystn. temp. 0-89173
 Ni-Si-B, amorphous, thermal stability of ductility 0-76327
 Ni-Ta (70, 30 wt.%) metallic glass, struct. and crystn. (*Russian*) 0-70136
 Ni-Ti-P, amorphous, corrosion behaviour, immersion tests and electrochem. meas. (*Japanese*) 0-85085
 Ni-Zn amorphous phase form. in Zr-poor region, hardness and fracture strength (*Japanese*) 0-84914
 Ni_{78-x}M_xSi₁₀B₁₂ (M=refractory metal), glass form. and thermal stability 0-79703
 (Ni₃₅Pd₆₅)₈₂P₁₈ amorphous alloy, liquid-quenched, crystn. kinetics, effect of thermal history 0-100175
 (Ni₃₅Pd₆₅)₈₂P₁₈ amorphous alloy, liquid-quenched, crystn. kinetics, nucleation 0-100176
 Ni₂Zr_{1-x} metallic glass, crystallisation kinetics, elec. resist. and mag. susceptibility meas. 0-103659
 Pb-Bi, temp. regime of crystn. on rapid cooling (*Russian*) 0-66495
 2PbO-SiO₂-xSO₃ melts, crystn. 0-59400
 2PbO-SiO₂ melt, coding rate influence on constitution of silicate anions, crystn. kinetics 0-103248
 12PbO.6SiO₂.PbSO₄, crystn. from 2PbO-SiO₂-xSO₃ melts, struct. and vibr. spectra 0-59400
 PbTiO₃, amorphous, crystallisation process, DTA and Raman spectroscopy meas. 0-75161
 Pd-Ni-Si amorphous alloys, crystn. process during isothermal ageing 0-89275
 Pd-Si, amorphous, struct., crystn. and Hall effect meas. 0-75178
 Pd-Si amorphous alloy, heat treated, low temp. lattice sp. ht. 0-75368
 R_{1-x}Co_x, rare earth amorphous alloys, thermal stability, elec. cond. enthalpy 0-100172
 Sb-S-I glasses, activation energy of crystn. 0-64920
 Se, amorphous and liquid state, Raman spectra, crystn. processes 0-60608
 Se, amorphous film, photocond., dark cond., rel. to crystn. 0-88596
 Se, amorphous films, evaporated, ageing and crystn., DTA 0-65413
 Se-I, vitreous, crystn. kinetics determ. (*German*) 0-79936
 Se_{0.09}Te_{0.91}, glass, effect of an alternating electric field 0-88054
 Se_{1-x}Te_x, amorphous film, photo-crystallisation 0-59839
 Se, Te_{1-x}, amorphous, structural relaxation and crystallisation kinetics study by DTA 0-59394
 Si amorphous layers, glow-discharge, laser-annealed, elec. props. 0-75661
 Si, amorphous layers, RF-sputtered on sapphire, crystallisation by CW ion laser annealing 0-80109
 Si, graphoeptitaxy on fused SiO₂ using surface micropatterns and laser crystn. 0-70554
 Si, laser annealing mechanisms, disordered overlayers, crystalln. 0-84967
 Si single crystal growth, Czochralski method, small-angle dislocation boundary form. anal. 0-89136
 Si wafer, thin surface layers, amorphous to cryst. transform., obs. technique 0-107288
 SiO₂, fused, surface crystn. by Li⁺ ion implantation and annealing 0-89383
 SiO₂-Al₂O₃ (8 mol.%) glass, heat treated, devitrified phases 0-66469
 SiO₂-Al₂O₃-MgO-TiO₂ devitrificates, microstruct. and props. (*Polish*) 0-70141
 SiO₂-BPO₄, glasses and devitrificates prep., IR spectra (*Polish*) 0-71624
 SiO₂-water system, inorg. polymer struct. form., globular crystn. 0-101042
 Sm-Co, amorphous, plasma-sprayed, role of Ar or H₂ atm. in mag. props. and crystn., rel. to H₂ storage 0-64898
 SmCo₅, amorphous, supermag.-ferromag. transition and directional crystallisation 0-65891
 Sm₂O₃-Ga₂O₃ system, garnet-perovskite transform., phase diagram relationships 0-97460
 Sn-Bi, crystallisation temp., overcooling temp. (*Russian*) 0-97472
 Sn-Bi(Pb)(Ga), temp. regime of crystn. on rapid cooling (*Russian*) 0-66495
 SrWO₄ cryst. growth, from Na₂WO₄ melts, thermodynamic props. 0-107084
 Ta-Ir(Rh) system glasses, form., crystn. and microhardness, resist. obs. 0-89178
 Te, Raman spectra, crystn. processes 0-60608
 Te-based eutectics, crystn. rate effect on electrophys. props. mutual solubility effect 0-60774
 Te₆₀Ge_{40-x}As_x glasses, rapid melt cooled, glass transition and stability range 0-75170
 Te₆₀Ge_{40-x}Sb_x(Bi_x), DSC studies of struct. phase transformation 0-66505
 Te_{60-x}Se_{40-x}Sn_x, thin films, elec. cond. and thermoelectric power meas. (*French*) 0-80335
 Ti-Nb-Si, amorphous alloy, supercond. props. and crystn. behaviour, TEM and DTA study (*Japanese*) 0-84536
 Ti₅₀Be₄₀Zr₁₀, amorphous, crystn. temp., press. and heating rate depend. 0-70132
 Ti₇₀Co₂₀B₁₀, amorphous alloys, crystn. behaviour, TEM study (*Japanese*) 0-84087
 Ti₇₀Fe₂₀B₁₀, amorphous alloys, crystn. behaviour, TEM study (*Japanese*) 0-84087
 Ti₇₀Ni₂₀B₁₀, amorphous alloys, crystn. behaviour, TEM study (*Japanese*) 0-84087

crystallisation continued

- TiO₂ brookite synthesis from Ti in NaF or Ti compounds, form. mechan. (Japanese) 0-93529
 Ti-Bi-Sb-Te system, peritectic reactions in TiBiTe₂-TiSbTe₂ cross section, crystn. character 0-108406
 TiAsS₂, glass, effect of an alternating electric field 0-88054
 TiAsS₂(Se₂)(Te₂), vitreous, crystn. kinetics 0-64918
 WO₃ film, amorphous, struct. and crystn., TEM obs. 0-103606
 Y₃Al₂O₇ crystal growth from melt, gas bubble capture theory 0-64941
 Yb, amorphous metal films, crystallisation with and without mag. field 0-70570
 Zn, electrocrystallisation, reaction mechanism, appl. of impedance meas. (French) 0-103597
 Zn-Ga, temp. regime of crystn. on rapid cooling (Russian) 0-66495
 ZnSb, oriented crystn. conditions during reaction diffusion (Russian) 0-70558
 Zr-ZrC, eutectic formation of regular struct., crystn. (Russian) 0-66496
 ZrO₂ glass, melting depend. on minute components, surface crystallisation 0-84278
 ZrO₂, glaze, liq. phase separation rel. to cryst. in glassy phase 0-103252

crystallite texture *see texture***crystallites**

- see also crystal microstructure*
 coatings, textured, crystallites faces determ. 0-64846
 island film growth, cluster size distrib. 0-107665
 metal, characterisation by selected-zone and weak-beam dark field TEM 0-79654
 polyethylene, γ -irrad., asymmetric 002 X-ray line profiles, analysis 0-96567
 polyethylene, flow-induced fibril form. from soln. 0-59402
 polyoxymethylene, nascent, morphology, optical and electron microscopic obs. 0-59403
 steel, P, deep-drawing, spatial orientation distrib. of crystallites in cold-rolled and in annealed sheets 0-81079
 tooth enamel crystallites, contrast effects in TEM 0-85572
 topological modelling of crystal growth 0-59418
 X-ray powder reflection profiles calc., principles 0-100124
 Ag-Sn, splat-quenched, X-ray diff. study 0-81094
 Au particles, small single cryst., habit plane characterisation 0-79733
 BaFe₂O₉, powder, milled and annealed, phase composition, lattice const. and crystallite size 0-71677
 BaTiO₃ polymorph, hexagonal, low temp. and surface CO₂ adsorption and desorption 0-80713
 CdI₂ polytypes, vapour growth mechanism 0-84124
 CrO₂ and CrO(OH), fine particle obs. of cryst. morphology and topotaxy 0-65969
 Cu, electrolytic epitaxial nucleation and growth, on (111) Ag 0-104081
 HfO₂ crystallite growth from oxide plasmas, growth morphology 0-59417
 MgCa(CO₃)₂, dolomite, partial thermal decomp. into MgO and CaCO₃, product cryst. growth 0-108706
 Ni electrodeposition, structure-internal stress relationship 0-70561
 NiZn ferrite, ZrO₂ additions influence on sintering and physicochem. props. 0-108369
 PbO layer vapour deposition, structure, and props. 0-65408
 Pd-D, crystallite size effects, simultaneous sorption and X-ray study 0-65237
 Pt, on C electrode, surface area loss in H₃PO₄ 0-101091
 Sn polycrystalline films, elec. props. and crystallite size, 4.2K to room temp. (Russian) 0-93011
 T-metal, thin film contact, time evolution of photovoltaic effect 0-65687
 Te film, vacuum deposited, growth and morphology of crystals 0-96766
 Te, vacuum deposited on NaCl, crystallite growth and morphology, electron microscopy 0-65401
 Te-Ag, thin film system, stress-relief appearance conditions 0-65416
 Te-Bi thin film system, stress-relief appearance conditions 0-65416
 ThO₂ crystallite growth from oxide plasmas, growth morphology 0-59417
 α -Ti, plastic deform., anharmonicity, and Gruneisen parameter 0-88246
 TiB₂ thick film on low C steel substrate, CVD in US field, crystallite size 0-84854
 UO₂ crystallite growth from oxide plasmas, growth morphology 0-59417
 WO₃ film, amorphous, struct. and crystn., TEM obs. 0-103606
 ZrO₂ crystallite growth from oxide plasmas, growth morphology 0-59417

crystallographic shear

- Admiralty Metal, transgranular stress corrosion crack propag. 0-89402
 brass, rolling texture development and deform. struct., shear bands effect (Japanese) 0-84952
 metallic shell, explosive expansion, deform. and rupture modes and mechanisms 0-85064
 metals, dislocations and shock compression, thermodynamics 0-100235
 minerals, dislocations and shock compression, thermodynamics 0-100235
 PbO-Nb₂O₅ system, X-ray and electron microscopic phase and struct. determ. (French) 0-92508
 polyethylene terephthalate, shear compliances meas. of oriented sheet 0-104363
 steel, Cr, lower bainite transform., significance of carbide precip. 0-97476
 steel, Cr-Ni-Mn, adiabatic shear band determ. by surface obs. 0-97579
 steel, mild, plastic flow localisation under dynamic torsional loading, crit. variables 0-85015
 steel, pearlite, deform. and fracture mechanisms, HV SEM obs. 0-104243
 steel fracture mode, determ. from shear lip width 0-60968
 transition metal oxide catalysts, reduction, cryst. defects influence, in-situ electron microscopy 0-81322
 Cu-Co single cryst., precip. hardening (German) 0-84946
 Cu₂Au-Co single cryst., precip. hardening (German) 0-84946
 Fe₃Ni₃₆Cr₁₄P₁₂B₈ Metglas, bending deformation, shear band form., high-speed cinematographic obs. 0-89322
 PbZrO₃, ferroelec., crystallographic shear planes as nonstoichiometric defects 0-59484
 Pd₃Si₂₀ metallic glass, tensile deform., shear band form., high-speed cinematographic obs. 0-89322
 Ti alloy, crack initiation on planar shear bands, H₂ assisted 0-71749
 α - β Ti Widmanstätten alloy interfaces, elastic interact. stresses, effect on plastic flow onset 0-104218
 V₂O₅ and lower oxides, defect structures and related props., review 0-59454
 WO₃, reduced, elastic strain energy in cryst. shear planes 0-75239
 WO₃, reduction, defect role, in situ HVEM obs. 0-81323
 Zr-H alloy, precip. of γ -ZrH, shear mechanism 0-104170

crystallography

- see also crystal atomic structure; electron diffraction crystallography; gamma-ray diffraction; isomorphism; lattice constants; neutron diffraction crystallography; space groups; X-ray crystallography*
 crystallograms, cryst. struct. determ. method 0-103286
 derivative lattices, determ. of relationships 0-107012
 disordered structures, two-dimensional, computer program for modelling (French) 0-59337
 electron and magnetisation densities in molecules and crystals, Arles, France (Aug. 1978) 0-105428
 fragile lattice packings of spheres in 4D space 0-100194
 incommensurate crystal phases, symmetry, superspace-group approach, commensurate basic structs. 0-79726
 incommensurate crystal phases symmetry, incommensurate basic struct., superspace group approach 0-79727
 infinite crystal, classical statistical mechanics 0-107067
 one-phase semiinvariants, practical aspects and appls. of probabilistic formulae 0-100119
 one-phase structure semiinvariants, of first rank, estimation by generalised second representations 0-107013
 polymeric series of coverings, symmetry, comparison with layers of real structs., Belov subclass development 0-84129
 RE-1306 radiospectrometer improvement, use of LF modulation of magnetic field 0-57350
 rotational symmetry, and tensor props., 1-, 2- and 4-fold principal symmetry, trigonal, and hexagonal groups 0-100193
 rotational symmetry, and tensor props., method for group 3(3)₂ 0-100192
 six-membered rings, conformation, nomenclature 0-78721
 spheres, fragile lattice packings in 4D space 0-100194
 stereodiagrams, 3D coordinates of mol. structs. 0-64824
 structure semi-invariants, representations method 0-79724
 surface crystallography, ion beam, channelling and blocking effects, double alignment backscattering 0-65350
- crystals**
see also bicrystals; crystal structure; crystallography; dendrites; epitaxial layers; liquid crystals; plastic crystals; whiskers (crystal)
 No entries
- Curie point** *see Curie temperature*
- Curie point writing** *see thermomagnetic recording*
- Curie temperature**
see also ferroelectric Curie temperature
 actinide elements and compounds, mag. props., book contrib. 0-75727
 alloys, binary, ferromagnetism and spatial long-range order 0-60159
 amorphous alloys, Curie temp. comp. depend. 0-84597
 amorphous alloys, indirect exchange interaction and paramag. Curie temp. 0-75752
 amorphous ferromagnet, Landau-Ginzburg theory, magnetisation and Curie temp. 0-75700
 amorphous ferromagnets, book contrib. 0-75743
 (CaO₆Fe₂O₃)_{2/3}(La₂O₃)_{1/3} compounds, effects of Nd₂O₃ substitution on magnetic props. (Japanese) 0-108010
 copper formate anhydride, cryst. struct. and mag. props. 0-79768
 dimethylammonium copper tetrachloride, crit. slowing down and anomalous relax. near Curie temp. 0-71053
 dimethylammonium copper tetrachloride, ferromag., quasi. two-dimensional, ordering temp., press. depend. 0-84601
 electron-hole paired systems, ferromagnetic ordering phase diagram 0-97097
 extended defect system, phase transform., critical props. 0-103455
 ferrites, determination for toroidal samples as function of temp. 0-57346
 ferromagnet, determ. using magnetic pendulum (Japanese) 0-82797
 ferromagnet, disordered, phase transitions, mol. field and Landau-Ginzburg theories 0-93118
 ferromagnet, effects of biquadratic exchange and uniaxial anisotropy 0-60329
 ferromagnet, magnetic susceptibility, spin and charge density waves, Curie temp. (Russian) 0-100581
 ferromagnetic metal, uniaxial, anisotropic spin fluctuations and anisotropic band struct. effects on resist. near T_c 0-65543
 ferromagnetic metals, spin fluctuation theory, Curie temp., mag. susceptibility 0-65937
 ferromagnetic metals, transport props., crit. behaviour 0-65522
 ferromagnetic plate, domain struct. near first-order phase transition resembling second-order transition 0-93139
 ferromagnetic semiconductors, s-f interaction on conduction band, red shift effect theory 0-59872
 Heisenberg amorphous ferromagnet, magnetisation and Curie temp., CPA calc. 0-75703
 Heisenberg ferromagnet, correlation functions in ferromagnetic and paramagnetic regions, RPA 0-71075
 Heisenberg ferromagnet, magnon renormalisation 0-65849
 inhomogeneous ferromagnets, phase transitions, micromagnetic theory 0-65942
 Ising ferromagnet, one-dimens., with phase transition, thermodynamic props. calc. 0-80536
 itinerant electron ferromagnet, magnon spectrum just below T_c, theory 0-65833
 itinerant electron ferromagnets, magneto-volume effects 0-60397
 lattice parameters, mag. and elec. props. 0-100578
 metal, indirect coupling between localised mag. moments by narrow band electrons 0-70942
 metal particles, form. by evap., Curie temp. depend. 0-104053
 metallic glass, splat cooled, mag. props. 0-80491
 metals and alloys, amorphous, exhibiting Mossbauer spectra, mean magnetic props. (French) 0-80489
 mischmetal-Co system, thermomagnetic analysis of intermediate phases 0-83115
 order parameter spatial variation near Kondo impurity 0-103813
 oxides, RCu₂Mn₂O₁₂, R=La to Lu, Y, synthesis and mag. props. 0-75717
 planar Ising ferromagnet solvable model with roughening transitions 0-71069
 random binary Ising system with transverse field, Curie temp., paramagnetic susceptibility 0-65938
 random ferromagnets, Ginzburg criterion, critical fluctuations 0-71032
 rare earth alloys, R₂Ni₁₃, amorphous, Curie temp., mag. susceptibility and coercive force, 4.2 to 300K 0-93092
 rare earth compounds, pressure effect on mag. ordering temp. 0-100584
 rare earth intermetallic compounds, ferromag. props., book contrib. 0-75726

Curie temperature continued

semiconductor, ferromag., red shift effect, optical absorpt. edge calc. 0-66140
semiconductors, ferromagnetic multivalley anisotropic, electron autolocalisation (Russian) 0-92848
simple ferromagnets, crit. behaviour 0-60331
singlet-triplet system in paramag. phase, low-freq. response 0-60172
steel, stainless, Feccralloy, creep-rupture props., 650-800°C 0-97535
superconductivity-ferromagnetism coexistence in two-band model (Russian) 0-84539
superconductor with magnetic impurities, coexistence of superconductivity and ferromag., BCS and Zener models 0-88676
temperature measurement, using magnetically controlled reed switches (French) 0-75291
thin film alloys, surface magnetism props., Curie temp., Ising model 0-108039
titanomagnetites, temp. depend. cation distrib., mag. prop. obs. 0-85647
transition metal alloys, amorphous, mag. props., chem. short-range order 0-75739
transition metal alloys, amorphous, mag. props., structure and preparation 0-75737
transition metals, 3d, ferromag. props., book contrib. 0-75724
uniaxial ferromagnet, domain struct. in mag. field 0-103853
X-Y model, biquadratic, spin one, variation of Curie temp. 0-97102
BaFe₂O₉, Ca²⁺ substitution effect on hexaferrite lattice and mag. props. 0-60243
Ba₃NaNb₃O₁₅, growth layer form., crystallization conditions effect, light diff., Curie temp. 0-100778
Ba₂Zn_{1-x}(x+y)Cu_{2x}Cd_{2y}Fe₁₂O₂₂, mag. props. and Mossbauer spectrum 0-75765
BaZnFe_{16-x}M_xO₂₇ (M=Al, Ga, In, Sc), mag. props. and Mossbauer effect 0-75766
C chars, thermally activated paramagnetism, mag. susceptibility meas. 0-75709
CH₃NH₂Ga(SeO₄)₂·12H₂O, dielec. relax. near transition temp. 0-60493
CdCr₂Se₄, Mott ferromagnetic semiconductor, optical absorption edge, critical behaviour 0-97226
CdCr₂Se₄, reactor radiation influence on ferromagnetic phase transform. (Russian) 0-75760
CdCr₂Se₄Ga(In), photoconductivity, photomagnetoresistance near Curie point (Russian) 0-100485
CeC₂, mag. props. 0-108008
Ce₂Co₇, and ternary hydride, mag. props. 0-108007
Ce₂Dy_{1-x}C₂, solid solns., mag. props. 0-108008
(Ce₂Y_{1-x})Fe₂, mag. susceptibility and Mossbauer meas., lattice parameters 0-97068
Co alloys, amorphous, effects of metalloids on mag. props. 0-75738
Co-Fe, soft mag. props. rel. to metallurgical aspects 0-88810
Co-V, Co rich, ferromag. behaviour, mag. moments, Curie temp., and NMR spectrum 0-70964
CoGa_{2-x}Fe_xO₄, x=0.1-0.4, mag. susceptibility temp. depend. (Russian) 0-70957
Co(GaTiV) alloys, ferromag. onset, electron conc. depend. 0-60203
Co₃₀Mn₄₀Ga_{50-x}, ordering and disordering phenomena, mag. study 0-70154
CoMnSi_{1-x}Ge_x, amg. props. 0-60270
Co₂RhS₄, mag. semicond., mag. and elec. props. 0-93121
CsMnF₄, planar ferromag., cryst. and mag. struct., Jahn-Teller effect 0-75715
Cu_{1-x}Cr₂Se₄, influence of excess Cu on physical props. 0-103836
CuFe solid solns., quenched from vap. phase, mag. props. 0-60307
Cu₂MnIn_{1-x}Sn_x alloy, compositional SRO, hyperfine interactions 0-71065
Dy, domain effects near order-disorder and order-order ferromagnetic transitions 0-65886
Dy_{1-x}Sm_x, magneto resist. of polycryst. specimens in fields up to 44 kOe (Russian) 0-92880
EuB₆, Hall effect and resistivity data, ferromagnetic ordering temp., pressure depend. 0-60010
Eu_{1-x}Gd_xO, mag. props., transport meas. 0-97117
EuO nonstoichiometric film, ESR spectra and exchange interaction 0-93176
EuO, physical and physicochem. props., review 0-96875
EuO, transmission and resistivity, stress modulation effect near Curie temperature 0-96874
EuO:Gd, elec. cond. under hydrostatic press., Curie temp. 0-96881
EuS films, mag. and elec. props. rel. to stoichiometry and defects 0-97122
(Fe,Co,Ni)-Si(B), amorphous mag. alloy, magnetostriction rel. to soft mag. props. 0-84633
Fe alloys, amorphous, effects of metalloids on mag. props. 0-75738
Fe alloys, amorphous, mag. saturation, spin wave stiffness, temp. depend. 0-75741
Fe alloys, amorphous, saturation magnetisation, Curie temp. and size effect 0-65815
Fe and Fe-Ni Metglas alloys, ohmic and Hall resist. 100-700K, mag. behaviour 0-80254
Fe-B, amorphous alloy, mag. props. 0-84618
Fe-B-C, amorphous, effects of replacement of B by C on mag. props. 0-84621
Fe-B-C amorphous alloy, formation, mag. props., thermal stability and density 0-75796
Fe-B-Cr(Mo), metallic glasses, mag., struct., and elec. props. 0-88751
Fe-B-Si-C amorphous alloys, prep. and props. 0-88748
Fe-Cr-Co alloys, (5-9 wt.% Co), obtained by slow cooling under mag. field, permanent magnet props. 0-75797
Fe-Ni, Invar, Curie point, annealing effects and time depend. 0-80508
Fe-Ni Invar alloys, splat quenched, mag. props. 0-75799
Fe-Ni Invar alloys of crit. conc., mag. props., flow theory methods (Russian) 0-65894
Fe-Ni-B-Si, amorphous, mag. props., heat treatment effects 0-89370
Fe-Ni-P-B, metallic glasses, struct. relax., annealing effects on mag. props. 0-89261
Fe-Pd Invar alloy, Young's modulus, magnetostriction, Curie temp. 0-65988
Fe-Pd Invar alloys, elec. and mag. props. and thermal expansion 0-75732
Fe-Pt, Invar alloy, paramag. susceptibility 0-70940
Fe-Si-B glassy alloys, mag. props., comp. effects 0-88752
Fe₄₀P₂₀ metallic glasses, stability and transforms. 0-75174
Fe_{0.5}Cu_{0.5}Cr₂S₄, ESR spectra, elec. and mag. props., Curie temp. 0-97137

Curie temperature continued

(Fe_{1-x}Mn_x)₂Y(B), Mn effect on Fe mag. moments, Mossbauer and mag. meas. 0-71016
(Fe_{1-x}Ni_x)₂P, Curie temp., press. depend. meas. 0-97091
(Fe_{1-x}Ni_x)₇₇Si₂₃B₁₃, amorphous, Landau-Ginzburg theory, magnetisation and Curie temp. 0-75700
(Fe_{0.2}Ni_{0.8})_{1-x}(SiO₂), Permalloy material, magnetisation, temp. and impurity atom conc. depend., band model calcs. (Russian) 0-93088
Fe₇₀P₁₀B₂₀ amorphous alloys, splat cooled, Mn, Cr and V substituted, mag. and transport props. 0-84593
Fe₈₀P_{20-x}C_x(Si₃(Ge_x), amorphous, size effect of metalloids on mag. props. 0-84594
Fe₃Pt, atomic thermal vibr. anisotropy, martensitic transform. model (French) 0-70355
Fe₃Pt Invar alloy, anomalous Curie const., susceptibility meas. 0-75731
FeRh₂S₄, mag. semicond., mag. and elec. props. 0-93121
(Fe_{1-x}Si_x)_{1-x}By, metallic glass, mag. props., crystallisation 0-65885
Fe₈₀P_{20-x}C_x(Si₃(Ge_x), amorphous, size effect of metalloids on mag. props. 0-84594
Ga_{1-x}Mn_xSb, elec. cond., mag. susceptibility, Hall const., and thermo-EMF, 80 to 1000K (Russian) 0-88549
Gd, coil noise due to permeability fluctuations at phase transition temp. 0-84598
Gd, domain effects near order-disorder and order-order ferromagnetic transitions 0-65886
Gd, ferromagnetic, crit. sp. ht. and thermal expansion 0-60343
Gd, mag. domain struct., 230-293K 0-88783
Gd, thermal conductivity critical behaviour near Curie point 0-75540
Gd-Al(Cu)(Ga)(Ni)(Pd)(Rh) alloys, amorphous, mag. and elec. props. 0-84019
Gd-Co(Ni)(Cu)(Rh)(Ru)(Pd)(Ga), amorphous, mag. props. and ferromag. reson. 0-75862
Gd-Ni, ferromag., elec. resist. temp. depend. 0-96843
Gd-Y alloys, mag. crit. temp. gap 0-60260
Gd_{1-x}Ca_xAl₂, mag. props. and phase relations 0-107991
GdCo₃, dilute ferromagnets, press. effect on Curie temp. 0-65873
Gd₂Nd_{1-x}Zn_x, ferromag., mag. susceptibility and magnetisation, temp. depend. 0-70975
Gd₂Si₃, ferromag., elec. props. near Curie temp. 0-107788
GdTb, ferromag., magnetisation and microwave absorpt. 0-65816
Gd₇₀Tb₃₀, magnetisation, AC susceptibility and microwave absorption meas. 0-60221
(Gd_{1-x}Y_{1-x})Al₂, ferromag. and spin glass like behaviour, magnetisation meas. 0-75734
(Gd_{1-x}Y_{1-x})Co₃, Curie temp. and resist.-temp. curves, comp. depend. 0-71020
Gd₂Y_{1-x}Zn_x, ferromag., mag. susceptibility and magnetisation, temp. depend. 0-70975
HgCr₂Si_{4-x}Te_x, ferromag. semicond., zero bandgap transition 0-96783
HgCr₂Se₄, n-type ferromag. semicond., galvanomagnetic props. 0-70727
Hg_{1-x}Mn_xTe, non-parabolic zero-gap semicond., indirect exchange interaction 0-80498
HoCo₂Si₂, mag. props. 0-107988
Ho₂Tb_{1-x}Co_x lath phase compounds, elastic props., temp. and magnetic field dependence 0-60393
K₂Cu₂Zn_{1-x}F_x, Cu conc. depend. 0-60255
La-Fe alloy, amorphous, sputtered at high rate, mag. props. 0-75753
(La_{0.8}Ca_{0.2})MnO_{3+y}, mag. props., Faraday method meas. 0-103832
La_{1-x}Sr_xCoO₃, (0.5≤x≤0.9), ferromag., elec. props., itinerant electron model 0-107785
Li₂B₂O₄-LiFeF₆, borate glass, mag. props. of Fe³⁺ cations 0-100599
MnAs_{1-x}P_x mixed crystals, metallic magnetically ordered, Hall effect 0-65536
Mn(CN)₃(H₂O)_{0.57}, mag. interactions, theory 0-97085
MnSb_{1-x}Sn_x films, Faraday rotation, optical absorpt. coeffs. 0-97242
Ni, ferromag. props., teaching expt. 0-82608
Ni, stress induced cross-over effect near Curie point (German) 0-103873
Ni, stress induced crossover effect near Curie point (German) 0-103874
Ni-Cu-H systems, Curie temp. during phase transitions under high press. 0-71029
Ni-Fe, soft mag. props. rel. to metallurgical aspects 0-88810
Ni-Fe based metallic glasses, Curie pt. anomalies 0-60256
Ni-Fe-Nb-Mo-Al, head material for mag. recording, DC and AC mag. props. 0-88812
Ni-Mn, ordered and disordered, press. effect on Curie temp. 0-71148
Ni-Mn-H solid solutions, mag. props. 0-88753
Ni-Pd, high mag. field effects, mag. isotherms near Curie point, exchange splitting energies 0-60272
Ni-Pd-Mn ternary alloys, mag. characts., use for thermoseed 0-107995
Ni_{1-x}Cd_xFe₂O₄, mag. props. rel. to ionic struct. 0-75756
Ni(Fe,Cr) and Ni₂(Fe,Cr), electron states density model and mag. characts. calcs. (Russian) 0-92804
Ni₃₆Fe₂₇Cr₁₄P₁₂B₆ metallic glass, mech. props. and thermal stability 0-76362
Ni₂Fe_{1-x}O₄, spinels, fine particles, magnetic properties obs. 0-71031
(Ni₂Fe_{1-x})₈₀P₁₀B₁₀, amorphous, Curie temp., press. effect 0-75833
NiZn ferrite, ZrO₂ additions influence on sintering and physicochem. props. 0-108369
PbSe_{2/3}Te_{1/3}O₃-PbS_{2/3}W_{1/3}O₃(PbFe_{2/3}Te_{1/3}O₃) ferroelec. props. and lattice consts. 0-60520
Pd, sd hybridisation, paramagnetic Curie temp. and susceptibility (Russian) 0-103808
Pd-Fe, magnetic anisotropy near Curie point, quasi domain struct. (Russian) 0-65867
Pd-Fe(Co)(Ni), dilute ferromagnets, press. effect on Curie temp. 0-65873
Pd-Mn, ferromagnetism to spin glass behaviour transition 0-71062
Pd_{1+x}MnSb Heusler alloys, magnetic hyperfine fields on ¹¹¹Cd, TDPAC and magnetisation meas. 0-93219
Pd_{2-x}MnSb, struct., appl. as improved neutron polariser 0-60199
PrAg₃, low temp. mag. meas. 0-107989
Pr_{1-x}Ca_xAl₂, mag. props. and phase relations 0-107991
PrCo₂, strongly exchange-enhanced paramagnetism, susceptibility 0-60179
Pt-Fe(Co), dilute ferromagnets, press. effect on Curie temp. 0-65873
R₂In, R₂In, R=Gd, Tb, Dy, Ho, Nd, mag. props. 0-108009
Sm₂Mn_{2-x}Fe_x, magnetic behaviour, temp. and comp. depend. 0-93090
SrCoO_{3-δ} (0<δ<0.5), ferromag., metallic elec. props. 0-70668
SrFe₂O₁₉, Ca²⁺ additives effect on hexaferrite lattice and mag. props. 0-60243

Curie temperature continued

- Tb, magnetisation, AC susceptibility and microwave absorption meas. 0-60221
 TbCo₂Si₂, mag. props. 0-107988
 TbZn, ferromag., thermoelec. power, temp. depend. and crit. behaviour 0-96852
 TiBe_{2-x}Cu_x, high press. study of Curie temp. and mag. susceptibility 0-84600
 Ti(Fe,Co)H₂, mag. and ⁵⁷Fe Mossbauer studies 0-71272
 U(Co_{1-x}Fe_x)₂, ferromag. onset, susceptibility and resist. meas. 0-70967
 UFe₂, giant magnetoelastic deform. of cryst. struct. mag. props. (Russian) 0-93159
 UFe₂B₂(B₂), Mossbauer effect of ⁵⁷Fe nuclei, mag. props. 0-103907
 U(Fe_{1-x}Mn_x)₂, Curie temp. and saturation moment at 4.2K 0-70966
 U₃P₄, press. effects on elec. resist. and Curie temp. 0-75559
 UTe₃, crit. exponents, neutron and magnetisation meas. 0-88823
 U₂Fe_{1-x}Fe_x, Curie temp. and saturation moment at 4.2K 0-70966
 V, small particles, crystal structure, magnetic and superconducting props. 0-97121
 VTe, mag. and elec. transport props. 0-92897
 Y(Fe_{1-x}Co_x)₂, x≤0.2, mag. props. and Mossbauer meas. 0-75798
 YIG: Si single crystals, mag. props. 0-107981
 Y_{3-x}La_xFe₂O₁₂, mag. props. rel. to ionic struct. 0-75756
 YMn_{2-x}Fe_xH₂, mag. props., ordering temps. 0-71028
 ZnGa₂O₄:Cr³⁺, weak exchange interaction determ., ESR study 0-93107
 Zr(Fe_{1-x}Al_x)₂, Curie temp., magnetisation, and cryst. struct., conc. depend. 0-75730
 ZrZn₂, high press. study of Curie temp. and mag. susceptibility 0-84600

curium

- see also nuclei with
 oxalate precipitation for separation of Am, Cm, and trivalent lanthanides 0-83202
 Cm+Pb, 1s₀ excitation probability, scaling law, breakdown at very small internuclear distances 0-58365
²⁴⁷Cm in early Solar System, Allende ²³⁸U/²³⁵U ratio evidence 0-90347

curium compounds

No entries

current (electric) see electric current**current algebra**

- see also elementary particle theory; hadron current; light cones; quantum field theory
 σ -models, nonlinear, supersymmetric, nonlocal conserved currents and instanton-like solutions 0-86544
 charmed baryon decays, nonelectronic, parity-violating, single-quark and two-quark transitions 0-68453
 charmed baryon decays, weak hadronic, SU(3) dynamical scheme 0-68454
 charmed baryons, weak decays, quark model framework 0-62976
 charmed mesons, semileptonic decays, charged weak current struct. 0-102042
 conserved axial second class current, sum rule, dispersion calc. 0-77986
 CP^N σ -models, 2-dimens., local conserved currents, conservation laws 0-86579
 dimensional reduction and axial anomalies 0-86561
 Goldstone theorem, struct. of conserved currents and mass spectra 0-82920
 Goldstone theorem generalisation, scalar fields, conserved current and mass spectra struct. 0-68339
 gravitino, axial current anomaly, Faddeev-Popov ghosts 0-68120
 instantons, generation of meson mass spectrum, current algebra, mixing angles 0-86567
 meson decay, tensor, current algebra approach, symmetry-breaking Hamiltonian, chiral SU(3)×SU(3) or SU(4)×SU(4) 0-68450
 meson dipion cascade decays, current algebra techniques, pole plus remainder model, chiral symmetry breaking and QCD 0-62972
 muon-electron mass ratio in a semi-classical model 0-91072
 neutrino oscillations, Majorana and Dirac mass mixing 0-101969
 nonelectronic hyperon decays, final state interactions with inelastic effects, comments 0-99099
 nuclear matter, S-wave π N interactions and PCAC 0-78185
 parton model interpretation of cut vertex formalism 0-86566
 pseudoscalar mesons, charge radii and PCAC without soft current limit 0-99070
 QCD spectral function sum rules, EM current flavour components 0-99084
 QED, supersymmetric, renormalised supercurrents and scale anomaly 0-105818
 QED, Ward identity, axial vector current divergence, chiral invariant regulator field 0-57526
 radiative muon capture, transition amplitude, PCAC test 0-83076
 Schwinger model, Ward identity, fermion axial vector current divergence, chiral invariant regulator field 0-57524
 SU(2n) principle models for integrable nonlinear systems, current constraints, conservation laws 0-86619
 subquark model of leptons and quarks, unification, currents and exotic states 0-86683
 supersymmetric QED, supercurrent gauge invariance, α -independ. 0-95233
 supersymmetric Yang-Mills field theory, point splitting regularisation, superformal anomaly 0-91014
 supersymmetric Yang-Mills theory in Wess-Zumino gauge, supersymmetric regulators and supercurrent anomalies 0-86614
 unification of EM, weak and strong interactions, massless fermions coupling to vector mesons 0-73637
 vector meson leptonic width, duality between vector mesons and perturbative QCD 0-57589
 D→K π lv, charm-changing weak hadronic current, models 0-57585
 D⁰ Cabibbo suppressed hadronic decays, Cabibbo universality fake violation, RH currents 0-73699
 e⁺e⁻ annihilation, charge current asymmetry as QCD test, neutral gluons 0-57616
 e⁺e⁻ annihilation, superheavy flavour prod., weak current effects, Z⁰ effects 0-57614
 F⁺→p π , decay mode meas. for PCAC test 0-91018
 γ p→W⁺n, current algebra and sum rules high energy W⁺ prod. 0-102039
 μ p→ μ nW⁺, current algebra and sum rules high energy W⁺ prod. 0-102039
 N form factors, weak, asymptotic behaviour within QCD dipole and tri-pole formulae 0-62987

current algebra continued

- $\nu(\bar{\nu})$ N→N' γ e(E), current algebras and high energy γ -prod., sum rules 0-102039
 $\nu(\bar{\nu})_p$, 2 GeV elastic scatt., charged current/neutral current event ratio 0-57582
 ν N, charged and neutral current interactions, cross sections and scaling variable distrib. 0-57581
 $\bar{\nu}$ N deep inelastic scatt., net charge in current fragmentation region, quark fragmentation 0-62964
 $\bar{\nu}$ p, 1.1 GeV, charged and neutral current events, strangeness changing currents, charm prod. 0-57583
 $\bar{\nu}$ p charged current interaction, inclusive ρ^0 prod. 0-62963
 Ω^- → Ξ^0 π^+ (Ξ^0 → Λ^0), nonelectronic hyperon decays, QCD description, PCAC anal. 0-95269
 π →e ν γ , isospin-breaking, chiral limit, conserved-vector-current violation, σ model 0-62988
 π K scattering amplitude, analytic continuation, chiral symmetry breaking 0-63027
 π N σ term in hybrid chiral bag model, PCAC and SU(3)×SU(3) symmetry violation 0-78096
 π NN vertex function and off-mass-shell π N scatt. 0-73739
 π^+ p→ π^+ p γ , 165 MeV, monotonically decreasing photon energy spectrum, no Δ^{++} (1232) bump 0-68476
 ψ , ψ decay branching ratios, isospin and flavour symmetry breaking 0-95264
 τ → ρ π ν , quark model, current algebra model, divergence of axial vector current 0-76555
³He(μ , γ ν), transition amplitude, PCAC tests 0-102152

current collection, traction see traction current collection**current density**

- see also critical current density (superconductivity); electron density
 EM scatterer surface current density, calc. using numerical technique 0-78747
 Joule heat concentrators, metal foil expts. max. heat release, cracks in conductors 0-92022
 MHD channel, anisotropically conducting plasma in inhomogeneous elec. and mag. fields, current calc. (Russian) 0-74995
 nonuniform band structure materials, Shockley like equations for current density and carrier density 0-60001
 pulsed electron beams, measurement of current density distrib. 0-63426
 superconductor, type II, with normal inclusions, current density distrib., theory 0-80461
 Al_{0.1}Ga_{0.9}As-GaAs, quantum-well heterostructure laser diode, temp. depend. of threshold current 0-87395
 AlGaAsSb-GaSb heterojunction injection laser, radiative props. 1.4 to 1.8 μ m range 0-91798
 β^0 -Al₂O₃-Na₂O, solid electrolyte, behaviour at high current density, sodium heat engine mode 0-61330
 (GaAl)As DH laser, threshold current density, growth terraces effect 0-99723
 InGaAsP DH lasers with etched reflectors, fabrication, current density 0-64050
 Li₂CoO₂, cathode material for batteries of high energy density 0-101089
 Na₂O-Li₂O-Al₂O₃, local electrode current density and flow decoration 0-100935
 Si, high electronic current density in anodic oxidation 0-89386
 Si-on-ceramic solar cells, short-circuit current density meas. using light-beam-induced-current tech. 0-93887
 SnO₂, electrodes, effect of DC on corrosion in lead glass melt 0-85075

current distribution

- see also current density
 AC distribution in solid turns with skin effect, calc. (German) 0-69319
 antennas, horizontal, above infinite plane Earth, input impedance and current distrib. 0-90259
 current distribution cell for qualitatively predicting differences in barrel plating performance of electroplating solutions 0-71917
 AgBr evaporated layer response in ionisation semiconductor photographic system (German) 0-101859

current fluctuations

- see also noise
 isotropic media, current fluctuation anisotropy, electron diffusion, quasi-elastic scatt. (Russian) 0-107882
 MIM cathodes, LF noise sources and reduction 0-108328
 semiconductor, electron quantum states, nonequilibrium current fluctuations in quantised mag. fields (Russian) 0-107704
 Al thin conducting film, electromigration under superimposed DC and noise powers 0-107879

current measurement, electric see electric current measurement**current transformers**

- see also electric current measurement
 electric current measurement, AC, using magneto-optical methods, principles and advantages (Polish) 0-105676
 magnetisation curve, piece-wise linear, design method (Russian) 0-100598
 MV, constructional principles and production technology (Hungarian) 0-100118
 oil immersed transformers, dissolved gas causes and phenomena, anal. (German) 0-76570
 oil insulated, parameters influencing heating assessment using sensibility matrix (Hungarian) 0-87708

current transients see transients**currents algebra see current algebra****curvature measurement**

- component profile inspection equipment 0-105608
 concentric round parts, profile determ., concentricity errors (German) 0-57249
 gear tooth profile, portable meas. instrum. for large gears, interchangeable standard profiles 0-57259
 long-radius concave optical surface curvature meas., differential technique 0-74534
 optical surfaces, concave and convex, radii of curvature meas. 0-83654
 pin bowing in AGR fuel elements, meas. by camera device 0-106146
 profile multi-axis meas. with vector drive 0-105609
 roundness, reference criteria 0-62628
 spherical surfaces shape deviation determ., using sphero-interferometer (Czech) 0-58821
 Zygo interferometer system 0-73437

curvature of field *see aberrations*

curve fitting

allyl ether, dielectric relaxation obs. at millimetric wavelengths 0-71311
TEM, quantitative elemental analysis 0-101060

cutting

see also machine tools; machining

adhesion in metal cutting, direct SEM obs. of frictional sliding 0-104412
fluid, hydrolysed polyacrylonitrile based, operational characteristics 0-89359
goniometer for cutting single crystals 0-86275
instrumentation engineering, laser beam apps. in drilling, welding, cutting, definite abrasion and surface treatment (*German*) 0-108608
machine tools, chip geometry and cutting forces 0-93629
machine tools, diffusive wear, mag. field effect 0-60985
metals, deformation structure during cutting, investigation by TEM (*Japanese*) 0-70086
optical fibre cutting tool and automatic splicing machine 0-87575
porous materials, effects of different methods of prep. on reproducing surface 0-60995
steel, Cr-W-Mo-Co, high-speed, from atomised powders, mech. and cutting props. 0-66556
steel, stainless, smoothing for plastic pre-straining of material cut by turning (*Russian*) 0-60911
Al-Mg, type A5083P-0 effects of anisotropy in cutting mechanism (*Japanese*) 0-89232

CVD *see chemical vapour deposition*

CVD coatings

epitaxial films, model for autodoping lateral variation 0-103595
III-V semiconductor thin film prep. by low temp. CVD 0-60789
laser CVD, film physical props. and applications 0-93493
materials for thermoelectric conversion of solar energy (*French*) 0-89660
phosphosilicate glass, bridge struct. across V-groove formed by etching in Si 0-104312
phosphosilicate glass coatings, measurement of P content using SEM and energy-dispersive X-ray analyser 0-76588
plastic resins, secondary coating of optical fibres, effect on transmission props. 0-58704
spectrally selective surfaces for photothermal conversion of solar energy 0-101125
Al_{0.5}Ga_{0.5}-As-GaAs DH laser operation, phonon contrib. 0-102724
AlSb solar cell materials, epitaxy of metalorganic-CVD layers 0-61367
AlSb, thin film growth on insulating substrates, by metal organics CVD 0-60786
BN films, humidity sensitive elec. props. and switching characts. 0-107938
C film on substrates for STEM specimen support, prep. and observation 0-93496
GaAs shallow-homojunction solar cells on single crystal GaAs and Ge substrates, CVD fabrication and conversion efficiency 0-61364
Ga_{0.5}N_{0.5} VPE growth rate influence on elec. and luminesc. props. 0-100702
P₂O₅-SiO₂ glass film, thickness and IR spectrum changes on heat treatment in H₂ 0-70549
PbS, effect of morphological struct. on photosensitivity 0-70760
Si, CVD amorphous films, effect of surface characts. on visible and UV optical props. 0-60698
Si film, low press. CVD prep., struct., elec. and optical props. 0-70548
Si, polycryst., CVD, recrystn. on heating 0-80107
Si, polycryst., layer structure dependence on carrier gas moisture and O₂ content (*Bulgarian*) 0-59811
Si, polycrystalline, As segregation at grain boundaries, elec. props. meas. 0-75259
Si thin film, polycryst., CVD, elec. props. 0-107934
Si₃B_{1-x} films, anal. of H ratios and profiling using nucl. techniques and Rutherford backscatt. 0-61202
SiC (6H), blue-emitting diodes by CVD 0-97439
SiC-coated C fibre, compatibility with Al (*Japanese*) 0-71700
SiCl₄-GeCl₄-BCl₃ particulate layers consolidation, in fabrication of optical fibre preforms 0-60787
Si₃N₄ film, elastic stiffness and thermal expansion coeffs. 0-107451
Si₃N₄ films, CVD in MNOS and MNS structs., elec. resist. 0-97019
SiO₂ CVD layer, high current injection from Si rich SiO₂ film 0-80430
SiO₂ coatings on SiO₂ substrate, cathodoluminescence spectra, electron irradi. 0-76085
SiO₂ films, Si-rich, amorphous Si region obs. 0-84400
SiO₂ on Si producing near-ideal Si-SiO₂ interfaces, props. 0-80382
SiO₂-P₂O₅ glass film, CVD, P conc. profile by etch rate technique 0-96450
SiO₂ semi-insulating polycryst. films, AES and PES studies 0-107939
Si₃O₅ films, anal. of H ratios and profiling using nucl. techniques and Rutherford backscatt. 0-61202
SnO₂ CVD coating on glass, elec. resist. rel. to cryst. microstruct. 0-84520
SnO₂-P, CVD films, elec. props., cryst. to amorphous transition effects 0-107933
SnO₂-P, CVD growth and etching characts., doping effects 0-107667
TiB₂ thick film on low C steel substrate, CVD in US field, crystallite size 0-84854
TiC coated WC-Co cemented carbides, fracture toughness 0-85046
TiC coatings, on cemented carbides, struct. and hardness 0-59771
TiC, laser CVD, coating characterisation 0-93494
VO₂, V₂O₅, and V₂O₃, film prep. under equil. conditions, struct. and elec. props. 0-108352
W, dislocation struct., rel. to texture (*Russian*) 0-65394
ZnS CVD IR window, optical and physical characteristics 0-106620
ZrC-C composite system, negative magnetoresist. 0-60008

CVD epitaxial growth *see vapour phase epitaxial growth*

CVD thin films *see CVD coatings*

cyanogen, C₂N₂ *see carbon compounds*

cyclopentadienylides *see organometallic compounds*

cyclotron resonance

for ion cyclotron resonance spectroscopy *see mass spectroscopy*; for ion cyclotron resonance heating *see plasma heating*
see also diamagnetism; dopplers
degenerate electron liquid, skipping orbit cyclotron resonance, surface state transitions 0-103889
Doppler effect, anomalous, amplification of slow waves in electron beam, obs. 0-78463
EBT heating, electron-cyclotron absorption and microwave propagation 0-64749

cyclotron resonance continued

electron cyclotron heating, superthermal electrons 0-64753
electron cyclotron reson. ion source with permanent mag., plasma-wall interaction expts. 0-99378
electron-phonon system, cyclotron reson. lineshape 0-97142
glow discharge tube, EM MM-wave detection properties in mag. field 0-70059
ionic semiconductors, cyclotron resonance, elec. cond., electron-phonon interactions 0-93180
magnetised semiconductor plasma, EM wave amplitude modulation and demodulation 0-84482
metal, cyclotron reson. on open electron orbits (*Russian*) 0-88878
metals, cyclotron resonance depend. on surface, anomalous skin effect (*Russian*) 0-75860
metals, longitudinal weakly damped EM waves near cyclotron resonance 0-103890
metals, sound pulse spike like transport near acoustic cyclotron resonance (*Russian*) 0-100617
semiconductor, complex energy band under optical excitation, high-frequency negative cond. and population inversion 0-107858
semiconductor surface, cyclotron reson., projection operator formalism 0-88524
semiconductors with superlattices, Stark-cyclotron resonance, Larmour freq. (*Russian*) 0-60421
small-radius scatterers, cyclotron resonance harmonics 0-71183
Takamak plasma density profiles from electron cyclotron radiation spectra 0-103179
two-resonator CRM oscillator with external feedback 0-87362
AgBr, cyclotron reson. of polarons at high density excitation 0-75859
Bi, magnetoresistance, high temp. oscils., props. (*Russian*) 0-65606
Bi_{1-x}Sb_x, EM wave propag. for rot. of mag. field from Faraday to Voigt config. 0-84419
CdS, polaron cyclotron resonance freq. shifts, halfwidths, cumulant expansion method calcs. (*Russian*) 0-88880
Cs(Ar-Cs) plasmas, electron momentum transfer cross section, cyclotron reson., temp., cond., and vel. meas. 0-106930
Ga_{0.5}In_{0.5}As_{0.5}P_{0.5}, electron effective mass, cyclotron reson. and magneto-phonon effect meas. 0-103618
Ge, pure, electron hole size distribution at pulse optical excitation 0-59883
Ge, uniformly deformed, free carrier cyclotron resonance, electron-hole drops (*Russian*) 0-71182
He liq. surface, cyclotron reson. of two-dimens. electrons (*Russian*) 0-88374
⁴He, liq., cyclotron reson. of hot electrons 0-88377
n-InSb, anomalous three LO phonon assisted cyclotron resonance 0-108078
InSb lattice, static dielec. const. and carrier conc. meas. via gyrotropic sphere reson. 0-97143
n-InSb, microwave helicon resonances, carrier density, mobility, dielectric const. 0-96930
n-InSb, phonon-assisted cyclotron reson. strongly depend. on surface condition 0-70755
Mo, effective mass meas. and electron velocities 0-96773
Mo, longwave dopplers, nonlocal Hall effect, surface impedance, size effect (*Russian*) 0-80253
p-Pb_{1-x}Ge_xTe film, cyclotron reson. above and below struct. phase transition 0-88879
PbTe, far IR magnetorefl., band struct. 0-76010
Te, in pulsed high mag. fields, cond. band struct. 0-59867
W, longwave dopplers, nonlocal Hall effect, surface impedance, size effect (*Russian*) 0-80253

cyclotrons

see also microtrons; synchrocyclotrons

120-centimeter cyclotron, modernisation 0-99358
acceleration process and its influence on beam quality, theory 0-74051
AVF cyclotron, central region, changes of puller shape, axial focusing 0-74050
Dee, bevelled, for beam centering in AVF cyclotron 0-63428
de voltage calibration using an intrinsic Ge X-ray detector 0-99359
fast neutron facilities for radiobiological irradi. 0-109064
general orbit theory for accelerated particles in cyclotrons, appl. to synchrocyclotrons and omegatrons 0-74052
heavy ion, current trends (*Hungarian*) 0-57786
medical application of a compact cyclotron, isotope production (*Japanese*) 0-104757
Princeton Cyclotron data acquisition system 0-102415
remotely controlled target transport system for cyclotron irradiations 0-69005
SIN, π E3 channel, cloud and surface μ on studies 0-74055
SIN, pion beam line π E3 modifications 0-74054
SIN π E3 channel, pion prod. meas. 0-74056
SIN accelerator system, operation and new projects 0-74053
synchrocyclotron, Orsay, experimental programs and results (*French*) 0-78464
Texas A&M polarised proton beam meas. 0-102360
TRIUMF, 500 MeV, 100 μ A isotope production facility 0-68985
 π production and properties, SIN and TRIUMF cyclotrons (*French*) 0-63417

Czochralski method *see crystal growth from melt*

D-layer *see D-region*

D mesons

Cabibbo suppressed hadronic decays, Cabibbo universality fake violation, RH currents 0-73699
decay, charged Higgs boson couplings 0-62917
decay, current algebra approach, symmetry-breaking Hamiltonian, chiral SU(3)×SU(3) or SU(4)×SU(4) 0-68450
decay, hadronic, role of free-quark pairs 0-78059
decay, hadronic, six-quark model, quark-mass dependence, final state interactions, mixing angle effects 0-62973
mass and mean life from high energy cosmic ray data (*Chinese*) 0-102045
nonleptonic decay rates and branching ratios, lifetimes 0-102047
parity violating nonleptonic decays, vector meson dominance model 0-78058
structure of hadrons containing heavy quark, MIT bag model 0-86672
B⁰-D⁺X(F⁺X), W-exchange dominance, decay rates 0-86706
D-K⁰ μ ν , in e⁺e⁻ annihilation, T-odd asymmetry in CP violation model (*Russian*) 0-105885
D-K π , effective Hamiltonian in Kobayashi-Maskawa model 0-105887

D mesons continued

- D \rightarrow K π (K π), nonleptonic decay rates, quark diagrams and pole approx. 0-86707
- D \rightarrow K π (π), current algebra relations and dual model amplitudes 0-82969
- D \rightarrow K π ν , charm-changing weak hadronic current, models 0-57585
- D 0 lifetime difference from D $^+$ 0-91084
- D 0 D $^+$ decays, gluon enhancements in charmed-meson decays 0-95265
- D 0 decay enhancement mechanism, quark diagram with gluon prod. 0-105891
- D 0 hadronic decay modes, W boson exchange model clean test 0-57592
- D $^0\rightarrow$ K 0 π^+ , quark total number conservation, D $^+$ lifetime longer than D 0 0-57590
- D $^0\rightarrow$ K 0 π^0 , $\Delta T=1$ constraints and final state interactions 0-95267
- D $^0\rightarrow$ K 0 π^0 , quark total number conservation, D $^+$ lifetime longer than D 0 0-57590
- D $^0\rightarrow$ K 0 π^0 (K 0 π^+), weak interaction effects, K π scatt. phase shifts 0-57591
- D $^0\rightarrow$ K 0 π^0 ($\pi^+\pi^-$)(K 0 K 0), phenomenological model for inclusive and exclusive decays 0-99098
- D 0 lifetime from ν and $\bar{\nu}$ interactions 0-105890
- D 0 nonleptonic decay, quark annihilation hypothesis test 0-102044
- D 0 D 0 mixing, flavour-changing Higgs bosons 0-62915
- D $^+$ \rightarrow K 0 π^+ , quark total number conservation, D $^+$ lifetime longer than D 0 0-57590
- D $^+$, weak decay constant from bag model extension 0-62967
- D $^+$ nonleptonic and semileptonic decays, isospin selection rule tests 0-73700
- D $^{*+}$, photoprod., D 0 mass difference 0-73720
- D $^{*+}$, charmed tensor meson, strong and EM decay modes 0-68451
- DD, DD*, D 0 D*, charm molecules, dynamical model, light meson exchange 0-57572
- DD molecular charmonium from dual diagram and Schrodinger eqn. 0-86660
- e $^+e^-$ \rightarrow DD, above charm threshold at energy corresponding to ψ' (3770) 0-73723
- e $^+e^-$ inclusive hadron prod., polarisation and p nonconservation asymmetries, π , K $^+$, D $^+$ prod. 0-78084
- γ p, 40-70 GeV, inclusive D 0 photoprod. cross sections, pair and associated prod. 0-91097
- ν production, prompt sources, and axion decays and interactions, pN beam-dump experiment 0-63028
- pp, D, B, K prod., QCD model for heavy flavour prod., two gluon annihilation 0-86744
- pp, ISR energies, p fragmentation, D $^+$ prod. from Λ_c^* and Λ_b decay 0-102080
- π^- p, 340 GeV, associated charm prod. evidence, D $^+$ prod. 0-86767
- π^- p, 70 GeV/c, directly produced electrons from charmed D particle decay, cross sections 0-73755
- $\psi(4.03)\rightarrow$ DD(D 0 D*, DD*, D 0 D*), vector state strong decay 0-78057
- D $^0\Rightarrow$ D 0 , weak neutral current diagonality, mixing amplitude, multi-quark gauge model (Russian) 0-68414
- pN, 350 GeV in Ne, D $^+$ prod. cross section and lifetime 0-68494

D-region

- electron density profiles, statistical model 0-61964
- EM wave partial reflection, ang. variation obs. at 1.98 MHz 0-101487
- enhanced electron conc. at mid-latitude, positive-ion model 0-105115
- geomag. storm effects at low and mid latitudes, electron density vars. 0-101474
- ion chemistry during intense radiowave heating 0-61952
- ion composition at midlatitude in quiet conditions, model 0-109307
- ionisation enhancements in lower D-region, rel. to radio waves winter absorpt. anomaly at middle latits. 0-67459
- MF wave absorpt. after HF wave heating 0-94646
- radiowave absorption at mid-latitude coupled to auroral activity 0-61945
- solar X-ray control of ionisation 0-77198
- NO density enhancement on winter anomalous day at S. Uist 0-82130
- NO $^+$ cluster ion formation, temp. control 0-61931

D/A conversion *see digital-analogue conversion***damage, radiation** *see radiation effects***damming** *see dams***damping***see also dislocation damping; internal friction*

- acoustic steady-state response of internally damped circular plates 0-106658
- air bubbles, production, pulsation and damping, in dil. polymer solns. 0-69879
- airborne sound by laminated building components (German) 0-102877
- austenite cladding layers, damping of ultrasound 0-104390
- boson field, damping superoperator eigenvalue problem, direct soln. 0-57180
- Brownian motion, bistability effects in periodic potentials 0-68139
- capacitive parametric transducer for displacements under dynamic damping 0-105626
- constrained viscoelastic, FEM of composite systems 0-83743
- dielectric waveguide hybrid and transverse mode dispersion calc. (Russian) 0-99857
- drives, rotational, damping of torsional vibrations, experimental determ. (Russian) 0-74816
- effect on impact response, two degrees of freedom system 0-74587
- elastic mechanical systems, vibr. damping by dampers with filled voids (Russian) 0-58954
- electric traction units, driving axle oscillations damping using seismic dampers (German) 0-62458
- floating rod with loaded end, damping during transverse vibr. 0-79205
- free damped mech. vibration logarithmic decrement, optoelectronic meas. 0-92095
- liquid oscillations, hydraulic torsional vibration damper (Russian) 0-92164
- materials, hinged-hinged beam, in terms of mode of vibration (Japanese) 0-91954
- Mathieu equation with damping, variational anal. 0-57079
- mesosphere, effect of Rayleigh frictional damping on mean meridional circulation 0-109219
- modal damping bounds by component modes method using Lagrange multipliers, natural freqs. 0-79213
- nonlinear, parametrically excited oscill. of coupled second order systems 0-86078
- open dynamical system, equations with fluctuating parameters 0-62584
- oscillation rods in viscous fluids, added mass and damping, finite element anal. 0-58967
- damping continued
 - oscillator motion, expansion in normal modes 0-67951
 - overhead crane, method 0-101711
 - piezoelectric solids, shape-dependent damping 0-93242
 - pneumatic floor vibration isolators, with two-chamber damping systems, isolation of very sensitive meas. apparatus (German) 0-69590
 - polymers filled with agglomerated particles, dynamic mech. props. 0-66569
 - radiation damping force, 1-D, new mechanics 0-82632
 - semiconductors, heat pulse absorpt. in nonquantising mag. fields 0-60054
 - sound pulsation noise damping from small air bubbles in water 0-64253
 - spring-loaded mass system vibration analysis (German) 0-96224
 - steel, austenitic, rod, coupled flexural and torsional vibrs., energy dissipation 0-89281
 - steel, ferromag., rod, coupled flexural and torsional vibrs., energy dissipation 0-89281
 - vibrating plates, unconstrained layer damping treated, response to random acoustic excitation 0-74798
 - vibrating plates, unconstrained layer damping treated, response to random acoustic radiation 0-74799
 - Cu-Ag (0.1 wt.%), cold-worked, internal friction peaks in kHz range 0-89276
 - CuCl crystal resonant Raman scatt. and luminescence competition (Japanese) 0-80770
 - 4 He, superfluid, fourth sound attenuation 0-100370
 - Mn-Cu (75, 25 wt.%), rod, coupled flexural and torsional vibrs., energy dissipation 0-89281
- dams
 - see also civil engineering; hydroelectric power stations*
 - Campotosto reservoir, seismic recording network (Italian) 0-101446
 - Kama Reservoir, USSR, forecasting spring inflow 0-105008
 - Lake Jocassee, S.Carolina, seismicity rel. to Rn content of groundwater 0-94466
 - Spain, induced seismicity of dams and reservoirs 0-61776
 - Tsengwen reservoir, Taiwan, seismicity due to fault and lake filling 0-81930
- dark space *see discharges (electric)*
- data acquisition
 - see also CAMAC; data handling; data processing; indicators; recorders*
 - accuracy determ. based on risk for arbitrary volume of a priori data 0-95054
 - acoustic emission signal processing and recording system, on-line 0-57266
 - airflow rate meas., with electrical indication and automatic data logging system 0-75014
 - APODAS ocean profiling automatic data acquisition system (Japanese) 0-85769
 - astronomy, data recording system for KSC 60 cm reflecting telescope (Japanese) 0-94717
 - autoguiders and acquisition systems for optical telescopes 0-82206
 - computerised tomography, positron emission, data acquisition and processing electronics 0-61690
 - COSMOS machine for automatic photographic plate image meas. 0-77293
 - diver-operable multiwavelength spectroradiometer 0-90251
 - drift chamber data acquisition, microprocessor based system 0-58066
 - EMG, multichannel data acquisition system for the survey of intercostal muscle activity 0-81790
 - epicardial mapping, DC, during exptl. coronary occlusion, digital data acquisition system 0-85527
 - error definition, for steady and unsteady states 0-95056
 - Fabry-Perot interferometer, piezoelectrically scanned, microcomputer-based data acquisition and stabilization system 0-62719
 - fusion reactor, mFTF plasma diagnostics Data Acquisition System 0-99319
 - fusion reactor, TEXTOR, mag. diagnostics and monitoring systems data acquisition 0-99320
 - fusion reactors, PLT and PDX data acquisition systems, networking and distrib. processing improvements 0-99318
 - gel permeation chromatography anal., data acquisition, computer control 0-97746
 - general purpose automated meas. system based on synchronous waveform digitisation under computer control (Portuguese) 0-82753
 - general purpose laboratory microprocessor system, design and construction 0-82754
 - geophysical, Fourier series and Markov processes (Italian) 0-109254
 - IR spectrophotometer, digital data acquisition/analysis system 0-73482
 - medicine, nuclear, microprocessor systems for data acquisition, image processing, RIA anal., patient data retrieval 0-61670
 - microclimatology, process computer appl. thermal balance recording methods 0-82044
 - microcomputer based nuclear system 0-63500
 - molecular biology, time resolved X-ray scatt. expts., rapid data collection systems 0-61740
 - multiaxis neutron diffractometer automation 0-102417
 - multiband radiometer for field research 0-90250
 - multichannel polarimeter, data acquisition and control system (Japanese) 0-77842
 - MWPC, flat area detector data acquisition system for X-ray crystallography 0-91381
 - neurophysiological experiments, fast data acquisition and processing system, minicomputer appl. (Japanese) 0-85536
 - nuclear steam generator tubes testing and evaluation, using CIS/DASIO system (Czech) 0-63301
 - oceanographic information, automation of collection, processing and anal. on small-computer base 0-101439
 - particle detectors, microprocessor-controlled data acquisition system for temporal/angular correl. between β - and γ -ray emission (Spanish) 0-106238
 - photometry for astronomical appl., data collection with aid of microcomputer (Czech) 0-67570
 - Pioneer Venus Differential Long Baseline Interferometry expt. 0-67578
 - Pioneer Venus Multiprobe entry phase, telemetry recovery 0-67493
 - Princeton Cyclotron data acquisition system 0-102415
 - prototype autoresonant, accelerator, computer system, data acquisition and processing 0-99433
 - raingauges, tipping bucket type, digital recording system description and field testing 0-77161
 - remote sensing of Earth from space, role of 'smart sensors', book 0-62402
 - seismic, Tasmania University seismic net, electronic development 0-82073

data acquisition continued

- solar collector-heat pump installations, meas. of efficiency under operational conditions (*German*) 0-101077
- SOLIS system 0-74030
- speccraft, manned, data acquisition and logging system incl. speech 0-61979
- striated muscle diffraction patterns, use of direct memory access microprocessor system 0-89918
- synchrotron radiation camera and data acquisition system for time resolved X-ray scattering studies 0-99023
- thermal desorption mass spectroscopy, computer control, data acquisition, appls. 0-61181
- thermophysical process ambiguous data gathering and processing optimisation (*Russian*) 0-73335
- Tokamak far IR Fourier transform spectroscopic Michelson interferometer 0-59294
- tomography, Donner 280-crystal positron tomograph, data acquisition, image reconstruct. and display 0-61671
- US imaging system appl. 0-99905
- vapour pressure computer-automated meas. by simultaneous Knudsen torsion-effusion method 0-73334
- Venus Pioneer Orbiter, electron temp. probe data acquisition and handling 0-67500

data communication equipment

- see also data transmission equipment*
- optical data bus single mode fibre, with star couplers 0-64199

data communication systems

- buoy for oceanographic and atmos. data acquisition, using Meteosat data transmission (*German*) 0-90224
- digital data composition for satellite and radar imagery 0-67413
- fibre-optic data transmission systems for plasma diagnostics 0-79571
- parallel transmission system using high density optical fibres (*Japanese*) 0-87507
- Pioneer Venus, Unified Abstract Data Library and Quick Look Data Delivery System 0-67494

data compression

- see also information theory*
- digital image processing applications, seminar, San Diego, CA, USA (Aug. 79) 0-105424
- EEG signals hierarchical modelling 0-109052
- time-varying images, object displacement estimation adaptive algorithm 0-99668

data description

- see also computer software; data processing*
- uniform data description for a generalized real-time nuclear materials control system 0-63498

data dictionaries *see database management systems***data handling**

- digital data composition for satellite and radar imagery 0-67413
- fusion reactor, magnetic confinement, structural anal., combined interactive/batch computer environment 0-91255
- interferometer, data handling in high vibration environment 0-95132
- multiband radiometer for field research 0-90250
- oceanographic information, automation of collection, processing and anal. on small-computer base 0-101439
- particle accelerators, future, LEP colliding beam machine, data handling and standard practices 0-58009
- particle detectors, high speed data processing, histogram and tape writing 0-58101
- Pioneer Venus occultation experiment, radio science data generation 0-67492
- seismic, Tasmania University seismic net, electronic development 0-82073
- spectrometers, off-line data anal., 168/E microprocessor 0-58102
- spectroscopy, multiplex and high-throughput 0-95145

data loggers

- automatic, airflow rate meas., with electrical indication 0-75014
- review of developments and systems available 0-73337
- speccraft, manned, data acquisition and logging system incl. speech 0-61979
- weighing, automatic, application in ceramics industry 0-95074

data processing

- for computer applications see under relevant applications e.g. administrative data processing; computerised instrumentation; natural sciences computing*
- see also computer applications; data handling; data reduction and analysis; management information systems*
- interferometer, data handling in high vibration environment 0-95132
- nuclear materials safeguards within Euratom framework, NUMSAS data processing system for statistical accountability 0-73926

data reduction and analysis

- see also data acquisition*
- air pollution, factor of safety calc. method 0-94140
- atmosphere parameters, retrieval from scanning multichannel microwave radiometer obs. 0-90261
- atmosphere radiances meas. from TIROS-N processing for temp. sounding 0-77133
- binary stars, radial vel. curves anal. 0-90470
- biomedical volume estimation, computer algorithm 0-98043
- blood pressure ambulatory recordings, minicomputer processing 0-89887
- body surface potential mapping, microcomputer processing system (*Japanese*) 0-72347
- bubble chamber film analysis, semiautomatic measuring system 0-58105
- chromatographic information processing by computer 0-71970
- collocation method compared to traditional adjustment 0-77130
- crystal setting, and data reduction, on a PW 1100 diffractometer, program using simple method based on real space 0-59342
- destructive examination of materials with data processing, microprocessor application (*German*) 0-93714
- ECG, Holter tape high speed digital anal. with full editing capability 0-89896
- electron image recording system, detection quantum efficiency 0-99009
- gamma ray spectra anal., fast Fourier transform (*Chinese*) 0-77762
- geodetic measurements, parameters estimation models for crustal deformation anal. (*German*) 0-101319
- geomagnetic and gravity anomaly data, curve-matching optimisation method (*Chinese*) 0-89935
- geomagnetic data obtained from satellite magnetometer 0-77141
- geoscience, data graphical output, colour plotter system appl. 0-98467
- gradiometer data integration in geomagnetic surveying 0-105064

data reduction and analysis continued

- gravity anomaly from masses distributed over infinite regions, interpretation theory 0-82103
 - HVEM, image converters 0-104839
 - least squares method, generalisation 0-62028
 - line detection algorithm, for Landsat data 0-77150
 - linear prediction in least-squares scheme, algorithms 0-98464
 - linear prediction in least-squares scheme for max. entropy spectra, Fortran subroutines 0-98465
 - machine processing of remotely sensed data, conference, West Lafayette, Indiana (1980 June 3 to 6) 0-82586
 - magnetic anomalies interpretation, estimation of cover thickness above magnetised mass (*Russian*) 0-105069
 - mass spectrometry, computerised 0-57417
 - meteorology, interpretation of asynchronous data 0-109271
 - microclimatology, process computer appl. thermal balance recording methods 0-82044
 - microcomputer based system for automatic reduction of astronomical spectra 0-77296
 - microprocessor-based interferometric data reduction system versatility 0-73439
 - multivariate data set, directed canonical analysis 0-73333
 - noise pollution, factor of safety calc. method 0-94140
 - nuclear steam generator tubes testing and evaluation, using CIS/DASIO system (*Czech*) 0-63301
 - ocean surface parameters, retrieval from scanning multichannel microwave radiometer obs. 0-90261
 - oceanographic information, automation of collection, processing and anal. on small-computer base 0-101439
 - oceanographic research, data processing and anal. 0-94605
 - palaeomagnetic data analysis, elimination of secular variation 0-61755
 - palaeomagnetic inclination data analysis by statistical method 0-109101
 - palaeomagnetic records, running means calc. for Holocene short period secular geomag. vars. determ. 0-98221
 - photographic images, quantitative anal. of autoradiographic image intensification using Thiourea-³⁵S 0-90343
 - potential field data, constrained inversion, use of pseudohyperellipsoids 0-85752
 - process gas chromatographs, microprocessor based, calibration and data reduction 0-81402
 - random data, detrending and smoothing techniques 0-67425
 - reflectivity meas., total, using specular-reflectance and diffuse reflectance references 0-73421
 - remote sensing data (multispectral), contextual classification 0-77149
 - seismic recording network at Campotosto reservoir (*Italian*) 0-101446
 - seismic refr. survey depth determination, program for pocket calculator 0-82088
 - seismic signals deconvolution, adaptive filter structs. 0-98451
 - solar spectrum, automatic processing by digital double-pass monochromator (*Russian*) 0-72777
 - space domain filter method (*Chinese*) 0-89933
 - stellar spectra, line profiles anal. using linear filtering theory (*Italian*) 0-90340
 - stellar uvby δ photometric data, appl. to MK spectral classification prediction 0-67700
 - STEM, computer driven, image registration 0-104838
 - stress/duress automated detect. system 0-76852
 - TEM, quantitative elemental analysis 0-101060
 - truncated real sinusoids, frequency estimator methods 0-73161
 - weather data, asynchronous, method for reduction to a common time 0-85735
 - weather forecasting processing of radar and satellite imagery data 0-109252
- data structures**
- array processing, algorithms and data structs. for conformational analysis of proteins 0-83530
- data tables *see collections of physical data***
- data transmission equipment**
- see also data communication equipment; telemetering equipment*
 - telemetry, totally implantable, integrated power controllers and RF data transmitters 0-67295
- data transmission systems *see data communication systems***
- database management systems**
- continuous speech recognition system for data base consultation 0-91990
 - fusion reactor materials, experience at the International Atomic Energy Agency in processing safeguards information 0-63497
 - fusion reactor, MFTF, supervisory control and diagnostics system, database management system 0-99326
 - fusion reactor, MFTF, supervisory control and diagnostics system, database management system, data structs. 0-99327
 - hydrogeological, characts. (*Italian*) 0-109255
 - Pioneer Venus, Unified Abstract Data Library and Quick Look Data Delivery System 0-67494
- dating, Earth *see geochronology***
- dating, radioactive *see radioactive dating***
- Davydov splitting**
- dicarboxylic acids, IR spectra Davydov splitting, methylene chain pendular vibrs. (*Russian*) 0-89008
 - phenanthrene, two-photon excitation spectra, exciton-phonon and intramol. vibronic coupling 0-84774
 - pyrene, triplet state, excitonic energy transfer, phosphoresc. and delayed fluoresc., 2 to 300K 0-84776
 - scheelite crystals, Davydov splitting of vibr. levels, short range interaction 0-71418
 - 1,2,4,5-tetrachlorobenzene, exciton states in crystals and dimers 0-70620
 - CdP₂, cryst., tetragonal, 2-phonon IR absorpt. 0-66176
 - ZnP₂, cryst., tetragonal, 2-phonon IR absorpt. 0-66176
- Davydov states *see Davydov splitting***
- dawn *see twilight***
- dawn chorus *see atmospheric***
- dayglow *see airglow***
- d.c. amplifiers**
- linear pulse amplifier, fast DC coupled, gain and phase response design 0-58088
 - photoamplifier circuit, dynamic compensation of photodetector DC component temp. drift 0-73460
- d.c. motors**
- angular velocity meas., contactless method (*Russian*) 0-73329

d.c. sputtering

- cylindrical magnetron sputtering system for coating solar selective surfaces onto batches of tubes 0-80967
 Langmuir probe technique, plasma characts. in sputtering 0-80929
 magnetic bubble materials, props. and preparation models, review (Rumanian) 0-93149
 Al, magnetron sputtering in Ar and Ar/O₂ mixtures, discharge characts. 0-89145
 Al, planar magnetron sputtering, H₂ effect on Ar discharge 0-80970
 AlN film, oriented c-axis, low temp. deposition by reactive magnetron sputtering 0-76180
 AlN films on glass substrate, prep. by reactive DC magnetron sputtering technique, c-axis orientation 0-89146
 CdO-SnO₂ DC reactively sputtered films, elec. and optical props. 0-103763
 Fe-Cr-Si, heat resistive films prepared by sputtering, lifetime meas. 0-80132
 Fe_x-Cr_x-NiC_x, stainless steel carbide, solar selective surface, fabrication, magnetron sputtering system description 0-80967
 Fe_x-Cr_x-NiC_x, stainless steel carbide, graded solar selective surface, magnetron sputtered 0-81485
 Fe_x-Cr_x-NiC_x, stainless steel carbide, sputtered solar selective surface, grading profile 0-81486
 In, reactive sputtering in Ar-N₂, N₂-O₂ discharges, mechanism, model 0-89109
 InN film growth by reactive sputtering in Ar-N₂ discharge, mechanism 0-89107
 In₂O₃-InN film growth by reactive sputtering in N₂-O₂ discharge, mechanism 0-89108
 Mo₃Si₃ films, magnetron DC reactive sputtering, struct. and props. 0-80966
 Si₃N₄ amorphous film deposition by high rate DC reactive sputtering, passivation appl. 0-100784
 Ta-Cr-Si-Al, heat resistive films, prepared by sputtering, lifetime meas. 0-80132
 Ta₂Cr-Si-Al, heat resistive films prepared by sputtering, lifetime meas. 0-80132
 W₄₀Fe₆₀ glassy alloy, refractory, triode sputtered 0-75185
 ZnO film on glass substrate, high-rate deposition using DC reactive magnetron sputtering 0-80978
 ZnO low-loss optical waveguides on amorphous substrates 0-58793

d.c. to a.c. invertors *see invertors***de Haas-van Alphen effect**

- see also diamagnetic properties of substances; diamagnetism*
 antiferromagnets, field depend. spin-splitting zero 0-84450
 electron fluid, adiabatic de Haas-van Alphen effect at low temp., Fermi fluid interaction and chem. pot. effects (Russian) 0-84442
 graphite intercalated with AsF₅, quantum oscillatory phenomena 0-107823
 graphite intercalation cpds., Fermi surface and transport props., LCAO model 0-80159
 graphite-K intercalation compounds, electronic props., de Haas-van Alphen effects and Fermi surfaces 0-75498
 metals and alloys, electrons at Fermi surface, book 0-105445
 Ag, virtual bound states due to 4d- and 5d-transition metal impurities 0-70667
 Au, virtual bound states due to 4d- and 5d-transition metal impurities 0-70667
 CaSn₃, powdered, de Haas-van Alphen effect 0-59857
 Co, Fermi surface under press., de Haas-van Alphen effect meas. 0-75499
 Cr, Fermi surface under press., de Haas-van Alphen effect meas. 0-75499
 Cu, quenched, Hall coefficient, relaxation times, Fermi surface 0-84460
 CuH dilute alloy, Hall coefficient, relaxation times, Fermi surface 0-84460
 Fe, Fermi surface under press., de Haas-van Alphen effect meas. 0-75499
 FeGe₂, antiferromag., Fermi surface, stress effects, oscillatory magnetotri-
 ction and torque meas. 0-103616
 K, de Haas-van Alphen freq., and Fermi surface anisotropy, press. depend. 0-59856
 LaB₆, de Haas-van Alphen effect, low-field 0-75497
 Mo, effective mass meas. and electron velocities 0-96773
 Mo, vol. depend. of extremal cross sectional areas of Fermi surface from de Haas-van Alphen meas. 0-70589
 Ni, Fermi surface under press., de Haas-van Alphen effect meas. 0-75499
 Sn, white, Fermi surface, dilational strain depend., OPW calcs. 0-84418
 TiBe₂, de Haas-van Alphen effect, Fermi surface, theory 0-103614
 α-U, Fermi surface and effective masses, de Haas-van Alphen meas. 0-65426
 YbSn₃, powdered, de Haas-van Alphen effect 0-59857
 ZrZn₂, de Haas-van Alphen effect, Fermi surface, theory 0-103614

Debye-Huckel theory

- alkali metals, condensed phase, free energy, Debye-Huckel theory calcs. 0-79958
 electric double layer, primitive models, pot. difference and charge density 0-76515
 glass, electrical relax., Debye-Falkenhagen theory 0-108155
 macroparticles; charged spherical, dilute soln., Rayleigh scatt. 0-84748
 plasma, two-component, structure and thermodynamics, mean spherical approx. 0-64683
 polymer, low conc., complex coacervation occurrence condition 0-79944
 H plasma, thermal emission and Debye shielding 0-64692

Debye-Scherrer cameras *see cameras; X-ray crystallography apparatus***Debye temperature**

- see also specific heat*
 alkali hydrides, lattice props. from interaction pot. energy function 0-100199
 alkali metals, rel. to elec. and thermal cond. in weak mag. fields 0-65535
 alkaline earth oxides, cohesive and thermophysical props., role of three-body interactions 0-92477
 covalent semiconductors, displacement correlations, adiabatic bond charge model 0-70350
 crystals, quantum effects in plasticity 0-59561
 insulator, thermal expansion, empirical determ. with no exptl. input 0-107450
 liquid mixtures, US propag. parameters, effective Debye temp. 0-79882
 resistivity strain coeff. calcs. 0-100449

Debye temperature continued

- solid lattice thermodynamics, two-temp. Debye approx. (Russian) 0-77728
 superconducting high Debye temperature material, theoretical upper limit of crit. temp. 0-60129
 tetragonal crystals with TII Laue symmetry, series expansion method 0-96615
 Ag, Debye temp., X-ray diffr. determ., anharmonic parameters of pot. function 0-100320
 Ag surface, scatt. of He, H₂, Debye-Waller factors, expt. 0-60736
 Al, Debye temp., X-ray diffr. determ., anharmonic parameters of pot. function 0-100320
 Au, fine particles, gas evaporation technique of prep., X-ray diffr. study, charact. temp. 0-75328
 Au thin films, electron diffr. investigation of Debye temp. 0-88420
 BaO-P₂O₅, glass, US velocity rel. to elastic props. 0-103425
 BaWO₄, slow neutron inelastic scatt. spectra, Debye temp. calcs. (Russian) 0-59347
 Be intermetallics, MB_{Be}, (M=Y, La, Ce, Lu, Th), lattice spacings and susceptibilities 0-65778
 CaNi₂, Hauke compounds, low temp. heat capacity, Debye temp. 0-96663
 CaO-P₂O₅, glass, US velocity rel. to elastic props. 0-103425
 CaWO₄, slow neutron inelastic scatt. spectra, Debye temp. calcs. (Russian) 0-59347
 Cd₃As₂ and CdAs₂, molten, thermal expansion and atomic bond strength parameters 0-65257
 CdTe(Se):Co, impurity luminescence no phonon line depend. on temp., Debye temp. 0-66273
 CdTi₂Te₄, single and polycryst. samples, linear expansion, heat capacity and thermodynamic props. 0-103489
 Cr, lattice dynamics, improved Fiekle model 0-59598
 DyAsO₄, phase transitions obs. 0-70412
 DyVO₄, phase transitions obs. 0-70412
 Eu₂Ir₂O₇, pyrochlore, sp. ht. below 20K, Debye temp. 0-65241
 Fe-Pd Invar, low temp. FCT phase obs. 0-93538
 Fe_{0.9}Mn_{0.1}Ti_{0.9}H_{0.1}, localised vibrs, sp. ht. obs., room temp. 0-65248
 Fe₂Pt-Sn Invar alloy, Mossbauer shift temp. depend. 0-100626
 Ga II, superconducting high pressure phase, sp. ht. 0-70894
 GaAs, lattice dynamics, phonon freq., bond bending force model calcs. 0-70335
 GaS, elastic prop. anisotropy, Debye temp. (Russian) 0-88244
 GaS(Te)(Se), elastic characteristics, Debye temp., ultrasonic study (Russian) 0-79872
 GaSb, lattice dynamics, phonon freq., bond bending force model calcs. 0-70335
 Ge-^{119m}Sn, impurity lattice dynamics, Mossbauer spectra, Debye temp. 0-84262
 GeP, thermodynamic characts. 10-300K, interatomic bond elasticity 0-59677
⁴He, solid-fluid, eqn. of state, melting props. under press. 0-96721
 HgTe, 1.5 to 30K, thermal expansion and heat capacity meas. 0-59681
 Ir, phonon/wave vector dispersion relations, Debye temp., modified axial symmetric model 0-70339
 Ir-Y eutectic alloy, supercond. transition enhancement due to lattice softening 0-103775
 KCl(F)(Br)(I), elastic constants, temp. derivatives at constant volume 0-59549
 LaNi₂, Hauke compounds, low temp. heat capacity, Debye temp. 0-96663
 LiCl(F)(Br)(I), elastic constants, temp. derivatives at constant volume 0-59549
 LiF, (001) surface, diffractive scatt. of H atoms, 78K 0-76124
 LiH, cryst., specific heat at const. vol., isotopic modifications effects 0-103490
 Lu₂Ir₂O₇, pyrochlore, sp. ht. below 20K, Debye temp. 0-65241
 MgO-P₂O₅, glass, US velocity rel. to elastic props. 0-103425
 Mo, lattice dynamics, improved Fiekle model 0-59598
 N₂, solid, exciton-phonon coupling in strong coupling limit, temp. depend. 0-92616
 NaBrO₃, X-ray Debye temp. 0-103440
 NaCl(F)(Br)(I), elastic constants, temp. derivatives at constant volume 0-59549
 Nb_{0.75}Ga_{0.25}, A 15 phase high transition temp., sp. ht. determ. 0-60140
 Ni₂Fe alloys, low-temperature specific heat, long and short range order effects 0-100339
 Pd-Si amorphous alloy, heat treated, low temp. lattice sp. ht. 0-75368
 Rb halides, role of quantum effects in lattice dynamics, Debye temp., shell model calcs. 0-70336
 RbCl(F)(Br)(I), elastic constants, temp. derivatives at constant volume 0-59549
 Se-Zr(Mg), low-temp. heat capacity 0-75370
 Si-^{119m}Sn, impurity lattice dynamics, Mossbauer spectra, Debye temp. 0-84262
 Si:Sb, Mossbauer spectra of ¹¹⁹Sn defect struct. 0-97174
 Si:Sn, Mossbauer study of defects due to ¹¹⁹In implantation 0-80641
 Si:Te, Mossbauer spectra of ¹¹⁹Sn defect struct. 0-97175
 SiP, thermodynamic characts. 10-300K, interatomic bond elasticity 0-59677
 α-Sn, ion implanted, defect struct., Mossbauer spectra 0-80214
 α-Sn, lattice dynamics 0-107389
 α-Sn-^{119m}Sn, impurity lattice dynamics, Mossbauer spectra, Debye temp. 0-84262
 SrO-P₂O₅, glass, US velocity rel. to elastic props. 0-103425
 SrWO₄, slow neutron inelastic scatt. spectra, Debye temp. calcs. (Russian) 0-59347
 ThNi₂, Hauke compounds, low temp. heat capacity, Debye temp. 0-96663
 YNi₂, Hauke compounds, low temp. heat capacity, Debye temp. 0-96663
 Zn, mean square displacement of atoms in cryst. lattice, rel. to sp. ht. (German) 0-79902
 Zn₃As₂ and ZnAs₂, molten, thermal expansion and atomic bond strength parameters 0-65257
 ZnCr₂Fe_{2-x}O₄, Mossbauer spectra, quadrupole splitting, Debye temp. 0-93218
 ZnP₂, Brillouin scattering and optical props. meas. 0-76041
 ZnS, lattice dynamics, phonon freq., bond bending force model calcs. 0-70335
 ZnS(Se)(Te):Co, impurity luminescence no phonon line depend. on temp., Debye temp. 0-66273

Debye-Waller factors

- see also lattice dynamics*
 amorphous solids, Raman intensities, connection with EXAFS Debye-Waller factors 0-108214
 anharmonic, temp. dependence 0-79903
 impurity atom in solid, reson. fluoresc., transient spectrum, intensity, and intensity correl. 0-84777
 incommensurate structure, Debye-Waller factors, modulation wave thermal fluctuations 0-84274
 n-octane-3,4,6,7-dibenzopyrene impurity, fluorescence impurity spectra, phonon free line broadening (*Russian*) 0-108279
 solid phase chemical reactions, low temp. and fast, mol. motion effect 0-97681
 X-ray diffraction and lattice dynamics, early work by I. Waller 0-62439
 Ag surface, scatt. of He, H₂, Debye-Waller factors, expt. 0-60736
 Al-Fe, dil. solid soln., vacancy-trapped Mossbauer impurity Debye Waller factor 0-60468
 Au, fine particles, gas evaporation technique for prep., X-ray diffr. study 0-75327
 Au, fine particles, gas evaporation technique of prep., X-ray diffr. study, charact. temp. 0-75328
 Co, Debye-Waller factor and Lindemann parameter, temp. depend., lattice dynamical model calcs. 0-59610
 Cr, Debye-Waller factors, extended de Launay model calcs. 0-70352
 Cr, lattice dynamics, improved Fiekle model 0-59598
 Cu surface, (100) coherent elastic scatt. of He, Ne, thermal attenuation 0-89105
 CuSO₄·5H₂O, EXAFS, rel. between Debye-Waller factor and thermal parameters meas. by neutron diffr. 0-84803
 Er, Debye-Waller factor and Lindemann parameter, temp. depend., lattice dynamical model calcs. 0-59610
 α-Fe, Debye-Waller factors, extended de Launay model calcs. 0-70352
 FeSiF₆, isotropy of Lamb-Mossbauer factor, Debye model 0-60465
 He, liq. surface, electron solid, self-consistent Debye-Waller factors 0-84337
³He, solid, valence band struct., zero-point motion effect 0-65333
 Li, anharmonicity and low temp. phase struct., neutron diffr. study 0-107105
 LiF (001), multiple Debye-Waller effects at selective adsorption in atom-surface scattering 0-76126
 Mo, lattice dynamics, improved Fiekle model 0-59598
 Na, Debye-Waller factors, extended de Launay model calcs. 0-70352
 PbF₂, anion disorder at high temps., neutron diffr. obs. 0-59614
 Ru, Debye-Waller factor and Lindemann parameter, temp. depend., lattice dynamical model calcs. 0-59610
 Sc, Debye-Waller factor and Lindemann parameter, temp. depend., lattice dynamical model calcs. 0-59610
 Si:Sb, Mossbauer spectra of ¹¹⁹Sn defect struct. 0-97174
 Si:Te, Mossbauer spectra of ¹¹⁹Sn defect struct. 0-97175
 SrCl₂, anion disorder at high temps., neutron diffr. obs. 0-59614
 W (100) and (110) surface, theoretical Debye-Waller factors 0-92773

decay periods (radioactive) *see radioactive decay periods*

decay schemes (radioactive) *see radioactive decay schemes*

decay theory (nuclear) *see nuclear decay theory*

decision theory *see decision theory and analysis*

decision theory and analysis

- see also dynamic programming*
 EEG automatic classification, decision rules comparison 0-109054
 Markov decision processes, infinite-horizon, denumerable-state, finite-state approx. 0-68130
 radioactive waste, management alternatives for low-level waste 0-99259

decoding

- see also demodulation*
 coded aperture imaging, review 0-101914
 optical processor, time- and space-integrating, for spread spectrum appl. 0-78777
 PCM encoding and decoding for optical memories 0-102658
 picture direct transmission via single optical fibre 0-106628
 radiography, flashing tomosynthesis 0-67243

decomposition

- microstructure features and processes only; for other aspects see dissolution and pyrolysis*
see also spinodal decomposition
 alkali borosilicate glasses, observation of phase separation using SEM-EDX technique 0-76224
 alloys, resistivity evolution during decomposition, theory (*French*) 0-75546
 binodal decomposition near crit. point, scaling hypothesis 0-79912
 di(alkylammonium)CdCl₂Br₂, solid-solid phase transitions 0-84290
 n-GaAs, stabilisation against photodecomposition, surface damage influence 0-76390
 Guinier-Preston zones, X-ray small angle scattering, for extra-resist. calcs. 0-92873
 mischmetal-Co system, thermomagnetic analysis of intermediate phases 0-93115
 ordered alloys with periodic struct., decomp. invest. (*Russian*) 0-93558
 oversaturated solid solution, directed decomposition (*Russian*) 0-97458
 quasi binary eutectic systems, with inclusive phases, hardness, transform., decomposition (*Russian*) 0-97572
 rare-earth intermetallics, R₂Co₃, polymorphism of Ce subgroup alloys, eutectic decomposition (*Russian*) 0-66504
 solid solution, supersaturated, cellular precip. features, review (*Russian*) 0-84937
 solid solutions, diffusion equation, during a decomp. process, role of non-linearised terms (*Japanese*) 0-92723
 steel, cold strained, defects interaction with carbide strengthening phases, carbide decomp. degree (*Russian*) 0-84955
 steel, Cr (0.5 wt.%), austenite-pearlite transformation 0-97480
 steel, Cr (10 wt.%), precip. free ferrite form., STEM 0-84941
 steel, Cr (2%), austenite decomp., phase diagrams and struct. form. kinetics 0-76223
 steel, Cr-Mn(Ni), Mn and Ni additions, effect on corrosion resistance and hardness 0-104342
 steel, Cr-Mo-Mn-Si-W (3, 1.95, 1.55, 1.45, 0.95 wt.%), struct. and props. 0-104175
 steel, maraging, Fe-Cr-Co-Mo, phase transforms. during high temp. austenitisation and solid soln. decomp. (*Russian*) 0-66524
 steel, pearlitic, struct. variations under plastic strain and subsequent heating, cementite decomp. (*Russian*) 0-84954
 steel, stainless, ferrite to austenite decomp. 0-93554

decomposition continued

- steel, structural, supercooled austenite, structural charact. of decomposition 0-60870
 steel, V, precip. and transform. kinetics, effect of N 0-97485
 steel, V-Nb and Cr-Mo-V-Nb, supercooled austenite isothermal decomp., struct., strength and fracture charact. 0-60966
 Al-Zn (70, 30 wt.%), decomp. study, 25-160°C (*Czech*) 0-89225
 Ce-In, phase equilibrium and cryst. struct. 0-66483
 Ce-Tl, phase equilibrium and cryst. struct. 0-66483
 Fe, sintered, austenitic nitriding and austenitic hardening 0-85084
 Fe-B, rapidly quenched, metastable phases 0-76234
 Fe-Mn-Ni-V-C (0.5, 3.0, 1.0, 0.2 wt.%), austenite decomp., isothermal transform. charact. 0-97477
 Fe-Mn-V-C (0.5, 1.0, 0.2 wt.%), austenite decomp., isothermal transform. charact. 0-97477
 Fe-N alloys, secondary ion emission, phase transforms. effect (*Russian*) 0-66347
 Fe-Ni (25 to 50%), FCC, meteorites and thermodynamic equilb., Mossbauer and X-ray diffr. study 0-88087
 Fe-Si cast alloy with spheroidal graphite, transform. investigation during tempering (*Russian*) 0-97479
 Fe-Zn, physical-chemical metallurgy (*German*) 0-108390
 FeTi, surface and mag. props., heat treatment and hydrogenation effects 0-75447
 InP surface decomposition prevention in LPE growth 0-96749
 β-In₃Sn, decomposition, X-ray powder diffr. study 0-89196
 (La_{0.8}Ca_{0.2})MnO_{3+x}, non-stoichiometry and lattice consts. 0-100212
 Li_{1+x}Ti_{2-x}O₄, high temp. spinel-Ramsdellite transform. 0-70407
 NaCl-Eu, secondary Eu phase dissolution, EPR and optical absorpt. study 0-96655
 Na₂S₂O₄·2H₂O hydrogenase-catalysed decomposition for biologically-assisted H₂ prod. 0-61460
 Ni-Ti (12 wt.%), early stages of transformation 0-76251
 NiH₂, formation and decomp. studies 0-71626
 Pb-As (~0.01 wt.%), enhanced precip. phenomena, invest. of mechanism by elec. resist. meas. 0-104162
 Pb-Sb-As (1.1-1.8, ~0.01 wt.%), enhanced precip. phenomena, invest. of mechanism by elec. resist. meas. 0-104162
 Pb(Zr_{1-x}Ti_x)O₃, solid solution, piezoelectric ceramic, prop. improvement by multiple substitution 0-80702
 Pd-H system, solvus hysteresis 0-71659
 β-SiC, polycryst., ³⁰Si self-diffusion 0-100350
 SmCo₅, high coercivity isotropic plasma-sprayed magnet, eutectoid decomp. 0-80568
 SmCo₅, isotropic plasma-sprayed high coercivity magnet, eutectoid decomp. 0-75810
 SmCo₅ sintered magnets, eutectoid decomp. 0-89219
 steels, Cr-C-Mn(Ni), struct. prop. rel., design of struct. steels for high strength and toughness 0-97491
 Te-In system, enthalpies of fusion, peritectic decomp. and allotropic transition, DTA (*French*) 0-76226
 Ti-Mo-Zr-(Al) (15, 5 (3) wt.%), quenched and aged metastable β-phase, crystallography, morphology and decomposition 0-76262
 Ti-Si amorphous alloy, melt-quenched, transform. studies and mech. props. 0-100838
 Zr₃Al, ordered, oxidation, weight gain and metallography 0-89398

decomposition, spinodal *see spinodal decomposition*

decomposition, thermal *see pyrolysis*

decorative coatings

- guanidinium aluminium sulphate hydrate, ferroelec., decoration patterns on cleavage surface, domain obs. 0-97218
 guanidinium uranyl sulphate hydrate, ferroelec., decoration patterns on cleavage surface, domain obs. 0-97218
 triglycine sulphate, ferroelec., decoration patterns on cleavage surface, domain obs. 0-97218

deep levels

- bridge meas. system for assessment of deep levels in semiconductors 0-105674
 DLTS, photo-excited, minority carrier trap meas. 0-96816
 electronic structure and lattice distortion, Green's function methods (*French*) 0-59917
 elemental semiconductors, group IV, Mossbauer spectroscopy of defects, radiation damage and deep levels 0-59533
 high field conduction in solids, effect of collision ionisation space charge 0-84469
 III-V semiconductors, point defects and deep traps, thermodynamic history, model 0-59908
 impurity levels, spectroscopic determ. by compensation method 0-108229
 many-valley semiconductors, donor impurity levels and excitons, shallow-deep instabilities 0-75520
 MOS capacitor, interface state parameter determ. by DLTS 0-65642
 MOS interface states density, photoemission obs. using photocurrent and photocapacitance meas. 0-92990
 MOS structure implanted with B ions, radiation defects and impurity activation 0-103757
 naphthalene, pure and doped, exciton-phonon luminesc. 0-84773
 ODMR, review (*French*) 0-60461
 poly-N-vinyl carbazole, trap-free lifetime, neutral traps, hopping systems 0-65566
 polyacetylene films, AsF₆ doped, photocond. and junction props. 0-70770
 polyethylene, elec. cond. of high and low density samples, oxidation effects 0-107784
 Schottky-barrier diodes, resonant tunnelling spectroscopy, deep centre detection 0-96968
 semiconductor, continuous energy spectrum, isothermal capacitance relaxation method 0-107741
 semiconductor, deep impurity centres, elastic light scattering 0-97315
 semiconductor, deep levels, review 0-103640
 semiconductor, space charge region thickness, deep level props., determ. by γ-ray absorpt. 0-59995
 semiconductor, STEM spectroscopic techniques for simultaneous electronic and defect obs. 0-100145
 semiconductor deep transition metal impurity states, SCF CNDO cluster calcs. 0-100442
 semiconductor junction barrier depletion region, capture from free-carrier tails 0-78082
 semiconductor lasers, triggerable, light-coupled logic appl. 0-74360
 semiconductors, deep defects, contrib. to binding energy 0-70634
 semiconductors, deep level carrier trapping and emission, transient spectroscopy, book contribution 0-80216

deep levels continued

semiconductors, deep level impurity photoionisation cross-section 0-65485
 semiconductors, impact ionisation, Auger recombination involving traps 0-80912
 semiconductors, impurity photoionisation, quantum-defect, billiard-ball model comparison 0-65486
 semiconductors, isothermal and non-isothermal C-V deep level meas. using Schottky contacts 0-88515
 sucrose, single cryst., absorption spectrum of electron traps, pulse radiolysis obs. 0-93369
 AgCl, luminescence fatigue, adsorbed Ag atoms 0-66281
 AgGaS₂, deep level obs. by TSC meas. 0-65590
 (Al,Ga)As double-heterostructure lasers degraded, deep-level changes during accelerated ageing at high temps. 0-74356
 AlGaAs semiconductor lasers, single-mode stabilisation by traps 0-95893
 AlGaAs-GaAs proton irradiated solar cells, deep-level defects, recombination mechanisms, performance characts. 0-81459
 AlGaAs-GaAs proton irradiated solar cells, deep level defects and recombination parameters 0-94032
 Al,Ga_{1-x}Sb-Pd contacts, band gap depend. of barrier height 0-65685
 As chalcogenides, deep levels, photoluminesc. and photocond. 0-70641
 CdS:Li, pure and doped, green edge luminesc., complex nature of centres 0-60671
 n-CdTe layers, growth and characterisation, heterojunctions and Schottky barriers fabrication (*German*) 0-89151
 CdTe_{1-x}Se_x, multiband model of impurity complexes 0-65497
 Cu₂S-CdS heterojunctions, role of deep levels in controlling photovoltaic props. 0-92941
 Fe:Y, ion implanted, deep D traps due to Y-vacancy complex 0-103372
 Ga_{1-x}Al_xAs, epitaxial, radiative deep states 0-76061
 Ga_{1-x}Al_xAs structures, STEM and scanning deep level transient spectroscopy in defect centre anal, cathodoluminesc. techniques 0-103642
 GaAs, deep centre free energy level determ. by transient capacitance technique 0-103641
 GaAs, deep impurity levels, activation energy 0-107742
 GaAs, deep levels, optical and thermal spectroscopy, lattice relaxation (*French*) 0-66248
 GaAs, epitaxy by metallorganic and chloride depositions, defect characterisation at growth interface 0-59817
 GaAs, grain boundaries investigation using DLTS techniques, photovoltaic material appls. 0-92539
 n-GaAs, LPE, deep trapping centre characterisation by Hall and photo-Hall meas. 0-88578
 GaAs, luminescence emitted from deep centres, plastic deform. effect on internal quantum efficiency 0-60672
 n-GaAs, MBE, correl. between electron traps and growth processes 0-65387
 GaAs, organometallic VPE, with varying As/Ga ratios, deep states 0-65480
 GaAs, photoionisation of impurities with deep levels 0-65484
 GaAs, proton irradiated, low energy, deep level defects and hole diffusion length meas. 0-60000
 GaAs, semi-insulating, undoped and Cr-doped, compensation mechanisms, Hall effect and optical absorpt. meas. 0-84477
 GaAs solar cells, electron and proton radiation damage 0-94034
 n-GaAs surface barrier diodes for nuclear radiation detection, deep trapping centres 0-92849
 GaAs:B, deep levels, optically stimulated transient current method (*French*) 0-59919
 GaAs:Cr, deep acceptor level, DLTS and optical DLTS study 0-92852
 GaAs:Cr, deep levels, wavelength-modulated photocapacitance spectroscopy 0-76055
 GaAs:Cr, thermally grown, DLTS study of Cr trap density 0-96815
 GaAs:Fe p⁺n junction minority carrier trap meas. by photo-excited DLTS 0-96816
 GaAs:O, deep level, Franck-Condon shift, photocond. and Hall effect study 0-70642
 GaAs:O, junction barrier depletion region, capture from free-carrier tails 0-70802
 GaAs:O, semi-insulating, excitation temp. effect on TSC 0-70717
 GaAs:O p-n struts., injection current and negative photocond., saturation mechanism 0-92967
 GaAs:Se, low dose Se⁺ ions implanted, DLTS study of laser annealing 0-80204
 GaAs-Si heterojunction, IR quenching of photocapacitance 0-92968
 GaP, IR absorpt. spectra depend. on compensating defects and thermal treatment (*Russian*) 0-71465
 GaP:Fe, optical absorption spectrum and Faraday effect 0-108245
 GaP:Ti(Co)(Ni), positron annihilation meas. rel. to deep levels study 0-60712
 Ge, compensated, impurity photocond. relax times 0-88592
 Ge, deep impurity levels, activation energy 0-107742
 Ge:Be, P, absorption of radiation, 0.6-2.8 mm, 4.2 to 20K 0-66332
 n-Ge:Sb, high-field Hall effect spectroscopy 0-65600
 Ge:Sb, Ni(Mn), recombination wave spectrum, two-level traps 0-96906
 n-InSb:Cr, deep impurities, elec. cond. and Hall coeff. meas., 4.2 to 120K 0-107791
 InSb:Cr, Zn impurity centre behaviour, impurity conc. and Hall coeff. meas. 0-65490
 Si, carrier capture at amphoteric deep level defects 0-88569
 Si, deep impurity levels, activation energy 0-107742
 Si, deep level defects, struct. bonding, amphoteric centres 0-88506
 Si, deep-level point defects, effective-mass nature 0-59922
 Si, dislocation-free, deep centres formed after high temp. treatment 0-96824
 Si, electron beam scan annealed, deep levels 0-65481
 Si, float zone, meas. of deep levels by photovoltage spectroscopy 0-103723
 Si junction diode, diffused, with deep level traps, negative capacitance 0-96976
 Si n⁺-p junction solar cells, electron irradi., DLTS spectra and defect effects 0-93999
 Si n⁺-p solar cells, degradation mechanisms associated with Ti impurities 0-81465
 Si n⁺p solar cells, effect of elec. bus during 1 MeV electron irradi. and isochronal annealing, elec. characts. and deep level pop. 0-94086
 Si single crystal ingot growth from metallurgical grade Si, inhomogeneities 0-59416
 Si solar cells, effect of Ti, Cu, and Fe 0-72064
 Si solar cells, POCl₃ gettering of Ti, Mo and Fe-contaminated cells 0-94010

deep levels continued

n-Si wafer, trap centres of self-interstitials 0-75516
 Si, with dislocations, noise spectrum 0-107881
 Si:Al, electron irradi. induced defects, transient capacitance study 0-59516
 Si:Au, amphoteric centre, struct. bonding of deep level defects 0-88506
 Si:Au, P-induced point defects influence on Au gettering mechanism 0-65030
 Si:Au deep level parameter determ. by isothermal capacitance transient spectroscopy 0-88507
 Si:Co, minority carrier lifetime investigation 0-80292
 Si:Cr²⁺(Mn²⁺), spin-lattice relax. of Jahn-Teller centres, coexistence of minima with different symmetries 0-80602
 n-Si:H, amorphous, bulk density of deep states, DLTS meas. 0-88518
 Si:H, amorphous, discharge prod., optically induced cond. changes 0-96937
 Si:H, amorphous, solar cells, trap spectroscopy using transient current techniques 0-104508
 Si:N, laser-annealed, Jahn-Teller distorted donor, EPR meas. 0-84642
 Si:S, deep level characterisation, implantation predeposition technique 0-100444
 Si:V p-n junctions, thermal emission rates and capture cross sections of majority carriers at V centres 0-96980
 Si:Y, photoelectric props. 0-107860
 Si:Zn, minority carrier lifetime investigation 0-80292
 Si-SiO₂, MOS interface states density, meas. techniques and model development 0-92988
 Si-SiO₂, interface in MOS struts., low-energy electron beam irradi., charge accumulation process anal. 0-65701
 Si-SiO₂, MOS interface, surface state density and minority carrier generation rate, meas. by DLTS, hot hole effect 0-100527
 Si-SiO₂, MOS interface states density, transient capacitance meas. eval. 0-92989
 α-SiC, afterglow stimulated by IR radiation (*Russian*) 0-89066
 ZnO, single crystals, photocond. lifetimes, Zn⁺ hole traps 0-75581
 ZnP₂In(Ga)(Ge)(S)(Se), doped and undoped, optical absorpt. spectra in range 0.5 to 2.2 eV 0-66250
 ZnS_{1-x}Se_x, electron trap associated with anion vacancy, DLTS study 0-80210
 ZnSe, band-edge photoluminesc., far-below band-gap excitation 0-76063
 ZnSe, donor-acceptor pair emissions characts. (*French*) 0-108249
 ZnSe, electron trap associated with anion vacancy, DLTS study 0-80210
 ZnSe-Si heterojunctions, IR quenching of photocapacitance 0-92968
 ZnTe, edge luminesc. excited by electron bombard. 0-66308
 ZnTe, elec. field and impurity conc. effects on ionisation energy of impurities, appl. to acceptors 0-88514

defect electron energy states
 see also colour centres; deep levels
 acceptor-donor-acceptor complex, Frenkel excitons and ionic excited states 0-92824
 alkali halides, thermally stimulated depolarisation of NCO⁻ centres 0-80678
 alkali halides, U-centre electronic struct. cluster-Bethe lattice calc. 0-107737
 alkali metal chloride crystal, F centre energy level shift and splitting in O⁻ field 0-70640
 chalcogenide glass-like semiconductors, defect model, neutral diamagnetic quasimolecules, excess orbital bonds (*Russian*) 0-70647
 chalcogenide glasses, ionicity depend. of defect reactions and negative-U states 0-88511
 covalent semiconductors, electronic interface states in intrinsic stacking-faults 0-75522
 energetical trap distrib., first principles model, linear finite defect chain 0-59912
 EuSe, photocond. and photodiffusive voltage spectra 0-96940
 functional eqn., Tamm Dancoff procedure, canonical transformation (*German*) 0-84448
 glasses, defect reactions, ionicity dependence, negative-U states 0-88510
 grain boundaries, electronic structure, development of analytical electron microscope 0-86521
 II-VI compounds, charged dislocations and plastic deform. 0-107264
 III-V semiconductor-oxide interface states, photoemission obs. of energy levels induced by adsorpt. 0-93000
 ionic crystals, dislocations, review 0-107236
 Ising model, two-dimens., ferromagnet-spin glass transition, Monte Carlo calc. 0-60287
 non-metallic crystals, electric field influence on defect creation mechanism 0-70251
 one-dimensional periodic system, energy spectrum of defects, pseudopot. approach (*Russian*) 0-59909
 p-n tunnel junctions, photoinduced transitions, theory 0-65669
 perovskite oxides, point defects, elec. cond., and electron energy spectra 0-70706
 plastically deformed compound semiconductors, electronic transport and opt. props. of dislocations 0-80212
 polyacetylene, intrinsic conformational defect states 0-65500
 polydiacetylene, intrinsic conformational defect states 0-65500
 semiconductor, deep centre, electronic structure and lattice distortion, Green's function methods (*French*) 0-59917
 semiconductor, defect electronic struct., SCF method 0-80208
 semiconductor, defect electronic structure and lattice config., MO approaches 0-65495
 semiconductor, dislocation struct. and elec. props. 0-70201
 semiconductor, localised states near dislative transition 0-70644
 semiconductor, STEM spectroscopic techniques for simultaneous electronic and defect obs. 0-100145
 semiconductor, with defects or impurities, local density of electron states 0-92857
 semiconductor defects, electronic props. study by spectroscopic techniques 0-84446
 semiconductors, amorphous, defects, band gap states 0-80215
 semiconductors, thermally stimulated conductivity luminescence, defect levels, traps, book contribution 0-80296
 semiconductors, thermally stimulated relaxation processes, book contribution 0-80295
 solar cells, polycryst., influence of grain boundaries electronic structure on diode characts. 0-94068
 surface and interface defects, electronic struct., scatt. theory 0-84498
 surface bands, lattice and symmetrical description 0-70785
 trap depth, determ. from TSC, theory 0-70716

defect electron energy states continued

- trap effects on exciton bands, masking by exciton-phonon coupling 0-80186
- As₂S₃, glassy, photoinduced defects, EPR and absorpt. spectra 0-59398
- As₂Se₃, glassy defect electron states, tight binding calc. 0-96818
- Au discontinuous film, electroluminescence obs. 0-103998
- BaTiO₃, XPS and UPS from surface defects 0-76136
- CaCO₃:Li, synthetic calcite, (CO₃Li)²⁻-Li⁺ defect after X-irrad., EPR study 0-75852
- Cd_{0.9}Hg_{0.1}Te, vacancy electron states, acceptor behaviour, electron mobility 0-70193
- CdS-Cu₂S junctions, carrier trap density, deep level defects 0-107801
- CoCr₂S₄, ferrimag. semicond., magnetocrystalline anisotropy 0-71012
- Cu, screening charge density round AZ=-1 impurities, vacancies, NQR study 0-103897
- GaAlAs, surface vacancies, bound state energy levels calc. 0-80340
- n-GaAs, electron irrad. defects, carrier removal rate, annealing effects 0-75269
- GaAs, electron irrad. induced defect levels, hydrostatic press. effect 0-92858
- GaAs, epitaxial layers, electron irrad. deep level trap energy depend. 0-80205
- GaAs Schottky barrier structure, defects from proton irradiation, thermal transients and optical capacity (*French*) 0-59534
- GaAs:Cr, Cr³⁺ and Cr²⁺ centres, thermal treatment effects, EPR 0-65492
- GaAs:Cr, hole traps, ESR studies 0-75843
- GaAs:Cr, photoionisation transition Cr³⁺→Cr²⁺, EPR studies 0-60638
- p-GaP:Cr, hole traps, ESR studies 0-75843
- GaP:Fe, double Fe-thermal acceptor centre, energy states 0-96823
- Ge, dislocation electron states, from press. depend. of photocond. 0-96819
- Ge, energy spectra of dislocations 0-70637
- (Hg_{0.6}Cd_{0.4})_{1-x}Te, defect anal., intrinsic material parameters 0-75519
- Hg_{0.8}Cd_{0.2}Te, optical absorpt., quasilocal acceptor level effects, theory 0-92853
- HgTe, vacancy electron states, acceptor behaviour, electron mobility 0-70193
- InP, surface vacancies, bound state energy levels calc. 0-80340
- n-InSb, proton irrad. defects energy level scheme, transport props. meas. 0-96576
- p-InSb:Ge, proton irrad. defects energy level scheme, transport props. meas. 0-96576
- KCl:Br⁻(I⁻), interstitial atomic H centres, formation kinetics and struct. MO calc. and EPR studies 0-75854
- KCl:Ca(Yb), Z₂ and Z₂⁺ centres, excited state, magneto-optical spectra 0-108233
- KCl:Na, F₀ centre energy levels 0-107738
- LiF, F-centres, defect electron struct., extended-ion model calcs. 0-59907
- LiF:Mg,Ti, defect states, ESR and ionic cond. study 0-108058
- LiNbO₃, surfaces, ion and electron bombard., photoelectron spectroscopy and electronic props. 0-71559
- LiNbO₃, XPS and UPS from surface defects 0-76136
- PbS:Ti, self-compensation of acceptors by vacancies, Hall coeff. meas. 0-92913
- PbSe:Ti, self-compensation of acceptors by vacancies, Hall coeff. meas. 0-92913
- RbCl:Br⁻(I⁻), interstitial atomic H centres, formation kinetics and struct. MO calc. and EPR studies 0-75854
- Se, bonding coordination defects 0-59927
- Se, glassy, structural excitation energies of defects, pseudopot. approach 0-107061
- Si, core structure of glide-set 90° and 30° partial dislocations 0-96523
- Si, deep-level point defects effective-mass nature 0-59922
- Si, defects, divacancy and split 100 interstitial, electronic structure calc. 0-65494
- Si, energy spectra of dislocations 0-70637
- Si, high-resistivity layer form. during electron irrad. 0-80352
- Si, isolated vacancy, electronic struct., SCF method 0-80208
- Si, point defects, H passivation 0-75515
- Si, poly crystalline, electronic behaviour of grain boundaries, solar cell appl. 0-92859
- Si, polycryst., energy distrib. of trapping states, from impedance of MOSS struct. 0-65691
- Si, polycrystalline barrier heights and passivation of grain boundaries 0-93890
- Si solar cells, radiation damaged, origin of reverse annealing 0-76630
- Si solar cells, radiation damage annealing mechanisms and low temp. annealing 0-94003
- p-Si, vacancy, charge states, Jahn-Teller stabilisation energy 0-80209
- Si vacancy, electron states, Anderson negative-U system 0-96820
- Si:B implanted wafers, ionis. assisted annealing and effects 0-100257
- p-Si:B(Al), radiation defect form. and annealing study using Hall effect, cond. and carrier diffusion length 0-84214
- Si:H, amorphous, defect states, luminesc. and ESR obs. 0-76075
- Si:Li, defect electronic struct. and config., semi-empirical calc. 0-107739
- Si:O, heat treated, excess carrier recomb. rate, defect levels 0-75579
- Si:P, polycryst. films, elec. props., EPR, defect states, doping effects 0-75660
- Si-SiO₂, interface states, deposition of H containing layers and annealing 0-92991
- Si-SiO₂ structures, B ions implanted, energy spectra of shallow traps at various implantation energies 0-80392
- SiC (6H), IR absorpt., UV illumination effects, defect levels 0-66251
- SiO₂, fused, broken bond defect generation mechanisms 0-88044
- SiO₂, vitreous, charged defect centres 0-107745
- SiO₂, vitreous, paramag. centres associated with bonding defects 0-80609
- Sms type semiconductors, electronic struct., influence of point defects 0-70650
- α-Sn, ion implanted, defect struct., Mossbauer spectra 0-80214
- Ti, oriented films, semiconducting props., Hall coeff., band structure 0-70854
- Zn_{0.9}Hg_{0.1}Te, vacancy electron states, acceptor behaviour, electron mobility 0-70193
- ZnO, defect struct. calc., doping effects 0-107218
- ZnTe, doping and intrinsic stoichiometric defects, self-compensation 0-59918
- ZnTe, edge luminesc. excited by electron bombard. 0-66308
- ZrSiO₄, X-irrad., trapping and emission centres, OH⁻ ion contribution 0-80876

defects, crystal *see crystal defects*

defibrillators

- see also patient treatment*
- automatic, implantable, cardiac pumping detect., optimal electrode spacing 0-72373
- conference on cardiac defibrillation and cardiopulmonary resuscitation, Lafayette, USA (Sept. 1979) 0-67929
- electrodes, recovery curves for different materials 0-67283
- myocardial damage from defibrillator discharges at various dosages 0-72368
- trapezoidal waveform defibrillators, operating internal resistance and capacitance 0-72375
- trapezoidal waveforms, haemodynamic responses 0-72370
- ventricular defibrillation with myocardial electrodes in the dog, calf pony, and pig 0-72369
- deformation**
- see also bending; cold working; creep; drawing (mechanical); elastic deformation; elongation; ferroelasticity; plastic deformation; shape memory effects; thermomechanical treatment*
- alkali metal halides, ionic crysts., impulse compression temps. 0-100307
- bone strains of canine radius and ulna, in vivo meas. and anal. 0-67130
- brittle solids, shock deform., review of theory 0-72493
- BWR containment vessels of prestressed concrete, pressure tests 0-81254
- cellular deformability, diffractometric method for meas. 0-98187
- composite materials, mech. props., theory, review 0-64392
- concrete, strain rate effect on strength and deform. during hardening process (*Japanese*) 0-93616
- contact structure, deformation of Lie algebra, of infinitesimal automorphisms (*French*) 0-62867
- crystal rotations, under constrained deform. (*Japanese*) 0-92593
- crystalline materials, in situ deform. by high voltage electron microscopy 0-103352
- cubic crystals, tensile deform. induced transitions 0-59653
- curved crystal-monochromator, influence of elastic element area on reflecting surface relief (*Russian*) 0-64157
- cylinder, hollow thick-walled, having axial holes and varying section thickness, stress state anal. 0-100879
- drawing, of continuous round ultrasonically perturbed profiles, stressed states at centre of deformation (*Russian*) 0-59557
- drop deformation and orientation in shear and extensional flow fields, dynamic interfacial props. 0-107611
- Earth crust, model for vertical displacements during rifting in Afar triangle 0-98295
- Earth crust, tectonic deform. characts. from seismological data in China (*Chinese*) 0-76951
- Earth crust anal. of Turgen' Geophysical Observatory data 0-76935
- Earth crust deformation analysis, models for estimation of parameters (*German*) 0-101319
- Earth deformation, mag. field effects 0-109085
- elastic plate, impact load impulse form determination by the displacements and strains of a circular plate (*Russian*) 0-74751
- elastoplastic bodies, asymptotic behaviour under periodic loading 0-83740
- ethylene propylene/polyolefin blends, radiation cross linking 0-66801
- fibre reinforced composite bodies, structure optimisation in stability problems 0-58947
- glass, photoelastic const. for chem. strengthening, circular plate compression method (*Japanese*) 0-93279
- granular media, density measurement, plane strain conditions, acoustic method (*Polish*) 0-62635
- ice, transverse flexure, refined Reissner anal. 0-88247
- Indo-Australian plate, evidence for internal deformation 0-109134
- liquid surface, free, charged, isolated, exptl. study of deform. (*French*) 0-88240
- lung, finite element model for macroscopic deform. 0-108945
- lung, macroscopic deformation, finite element model 0-89781
- measurement, in-plane, by video-electronic hologram interferometry 0-106488
- metal strips, welded, aged, reduction of deformations (*Russian*) 0-97508
- metallic membrane, lifetime prediction and design 0-71752
- mobile load on ideally packed material layer 0-99952
- morphogenesis, growth, elastic and non-elastic deforms. 0-108928
- osteosynthesis, internal, deform. of bone (*Croatian*) 0-108943
- out-of-plane, measurement using holographic interferometry and speckle photography, comparative accuracy 0-78804
- periodically layered composites in plane strain, dispersion eqn. for waves 0-79212
- plate, loaded cantilevered, exact eqns. for inextensional deformation 0-64399
- plates, arbitrary, quadrilateral and triangular, inextensional deformation, alternate exact eqns. 0-69694
- plates, large deformation anal., variational formulations 0-92067
- 1,2-polybutadiene, crosslinked in states of strain, entanglement networks, swelling anisotropy obs. 0-79666
- polyethylene terephthalate, oriented, amorphous, stress-induced crystn., shrinkage meas. 0-92466
- poroelastic cylinder, twisted pore effect on fluid flow, solid deformation and stress 0-64377
- powder, deforming, self-diffusion coeffs. in failure zones and percolation 0-76209
- quartz, torsional vibration frequency temp. depend. 0-70294
- quartz grains in Moine thrust zone, deformation-induced microstructs. rel. to differential stress 0-85652
- reactor fuel cladding strain, effect of fuel density and fuel relocation, in-reactor meas. 0-104408
- red cell membrane, human, surface elasticity and viscosity 0-61608
- Rzhanitsyn-Koltunov nucleus, anal. determ., relax. function for shear and stretching 0-58932
- shell design by finite element method, deformation and elasticity theory 0-74747
- shell formed by truncated cones, stability and deformation 0-69691
- spherical pore in solid body, physicochemical processes 0-100364
- steel, low C, low alloy, ferritic-pearlitic, high temp. mech. treatment, cooling effect 0-104193
- steel, stainless, cladding dimensional changes in FBR (U,Pu)₂ fuel pins due to swelling and inelastic strain 0-104296
- strain driven thermoelastic instability toward brittle fracture 0-103415
- teeth and mandibles, deforms. due to occlusal forces, holographic interferometry 0-67205
- telescope, altazimuth mounted, primary mirror deflection and stress anal. 0-58659

deformation continued

- thermal, interference 0-78806
transversely isotropic half space, indentation anal. 0-92090
viscoelastic rod, standard linear body, free torsional ascills. 0-99940
viscoelasticity, time reversal and symmetry relations 0-102970
X-ray integration method, extension of $\sin^2\psi$ method (*German*) 0-92420
Zircaloy cladding, enhanced steam oxidation by deformation under LWR
LOCA 0-73917
Al film, deform. under He ion bombardment 0-65073
As₂₀Se₈₀ and As₂₀Se₈₀ semicond. glasses, densified, photoluminesc., inelastic deform. effect 0-66293
(Mg,Fe)₂SiO₄, shock deform. expts., Hugoniot data implications 0-94497
Mo crystals, joined by compression during heating, structural changes (*Russian*) 0-108513
Nb₃Sn, filaments in Cu matrix, thermal strain effects on superconducting critical temp. 0-93032
Ni perfect crystal, stability under various stresses 0-104208
Pb_{0.94}Se_{0.06}Ti_{0.47}Zr_{0.53}O₃, piezoelectric ceramic, stress relax., time depend. deformation 0-60899
Pb(Zr,Ti)O₃, fracture and deform. 0-79870
Re, Fermi surface, Landau quantum oscill. meas. in magnetostriction, stress and strain derivatives 0-107691
Si, polycrystalline multilayer support struct., control of deform. in dielec. isolated substrates 0-107681
Sn, white, Fermi surface, dilational strain depend., OPW calcs. 0-84418
 α -Ti, strain driven thermoelastic instability toward brittle fracture 0-103415

deformation lines *see* **Luder's bands****degenerate semiconductor materials** *see* **degenerate semiconductors****degenerate semiconductors**

- see also heavily doped semiconductors; superconducting semiconductors*
acoustodielectric effect, permissivity modulation by acoustic wave in resonance conditions 0-92944
conduction electron acoustic spin resonance, oscillations of absorbed power 0-108075
energy band structure effect on transverse magnetoresistance 0-88580
heterogeneous state, first-order phase transition, Ginzberg-Landau method analogue 0-70372
piezoelectric, transverse magnetoresist. in strong field, quantum effect 0-80299
resonance Raman scatt., Green's function approach 0-80781
Schottky barrier, low temp. capacitance 0-60075
surface optical phonons 0-70520
 θ -Al_{0.35}V₂O₅, NMR of ⁵¹V 0-71232
EuB₆, Hall effect and resistivity data, ferromagnetic ordering temp., pressure depend. 0-60010
 θ -Fe_{0.35}V₂O₅, NMR of ⁵¹V 0-71232
Mo₆S₈ Chevrel phases with group IIIa metals, Nb, Hg, Pb and Cu, synthesis, stability and characts. 0-71608
Pb_{1-x}Sn_xO₂:Sb films, DC sputtered, elec. props. 0-80426
SnTe:Mn, NMR shift meas. 0-97154

dekstrons

- No entries

delay circuits

- see also delay lines; phase shifters*
slave triggers for photographic flash 0-95168
sound triggered electronic photo flash unit, using variable time delay 0-57407

delay elements (circuits) *see* **delay circuits****delay lines**

- see also acoustic delay lines*
capacitively coupled distributed parameter delay lines, development for use in a multiparameter focal plane detector 0-78491
differentiator for meas. of electron energy distrib. function in plasma (*Japanese*) 0-84002
metal-magnetodielectric layered delay lines, dispersion eqn. (*Russian*) 0-88736
optical, to control solid state laser output characts. 0-99758
plasma waves, delay line simulation, wave propag. in dispersive and attenuating media 0-82606
spiral, bubbles detection in insulating liquid flow 0-79415
(Tb,Dy)-Fe amorphous films prep. by cosputtering, magnetostrictive characts. 0-97429

delayed neutrons

- A=135-143, odd A fission products, delayed n, decay studies and Q _{β} meas. 0-78227
beta strength function, half life and delays, nuclear- and astro-physics consequences 0-102149
beta strength function structures, nuclear- and astro-physics consequences 0-99152
conference on nuclear spectroscopy of fission products, Grenoble, France (May 1979) 0-77546
far unstable nuclei, beta delayed two neutron emission, nuclear structure 0-68606
fission product mass region, delayed neutrons and P_n values 0-78339
nuclear far from β -stability, delayed neutron energy spectra, structure effects 0-78226
subcritical cyclostationary nuclear reactor, neutron counting statistics, sinusoidally modulated neutron source 0-99203
Z=37-43, neutron rich fission products, mass energy surface, decay props. 0-78228
⁸¹Br, A=89-91, delayed neutron emission probabilities, β -decay half-lives 0-83078
Cs, fission fragment, delayed neutron branches from γ -spectroscopy 0-78230
¹⁴³Cs, delayed neutrons, energy spectra 0-99153
¹⁴¹I, A=139-141, delayed neutron emission probabilities, β -decay half-lives 0-83078
¹³⁷I beta delayed neutrons, ¹³⁷Xe neutron unbound states, high energy X-rays 0-86856
¹¹Li beta decay, γ activity 0-106018
²⁴Na, A=30,31,32, beta-delayed two-neutron emission 0-95316
Rb, fission fragment, delayed neutron branches from γ -spectroscopy 0-78230
⁸⁶Rb, A=93,94,95, delayed neutrons, energy spectra 0-99153
⁹⁰Sr neutron binding energy from transitions and β -delayed neutron defined level correspondences 0-63070

delayed protons

- beta strength function, half life and delays, nuclear- and astro-physics consequences 0-102149
beta strength function structures, nuclear- and astro-physics consequences 0-99152
³⁵Ar levels, transitions and β -delayed protons from ³⁵K decay 0-91156

delays

- see also delay circuits; distributed parameter systems*
loudspeaker system group and phase delay requirements 0-92014
sonar array paired element delay meas. with sequential state estimation 0-96128
speech intelligibility, time delay effect experiment 0-91996
underwater acoustic source location and motion estimation, joint reduction of bias and variance 0-96087
underwater acoustic time delay estimation, cross-correl. and smoothed coherence transform methods compared 0-96086

delta modulation

- noise-tolerant continuously variable slope DM to linear predictive coding conversion 0-96141

demagnetisation

- see also magnetisation*
automatic demagnetisation and measurement system for time decreasing permeability meas. 0-62696
ferromagnets, cyclically remagnetised, discrete spectra of induction calcs., demagnetising factor 0-103859
hard material demagnetisation curve evaluation 0-90869
steel, Si, permeability change due to stress variation after demagnetization in Rayleigh region 0-88854
type II superconductors, anisotropic, demagnetisation effects on lower critical field 0-97043
Au₃Fe₁₅, and Au₃Fe₁₈, mag. props. 0-84592
Ba ferrite, FMR in uniaxial crystal plate with bubble domain lattice 0-93182
Fe thin films, surface demagnetisation due to chemisorption, ferromagnetic reson. study 0-80616
Fe-Si (3 wt.%), losses, demagnetisation freq. and grain orientation depend. 0-88796
Fe-Si (3 wt.%), nonoriented sheets, magnetisation, tensile stress effects 0-88845
Fe₈₀B₂₀ amorphous ribbon, initial susceptibility time lag 0-100579
Nb-Ti superconducting single layered multifilamentary coil, eddy current loss depend. on demagnetisation 0-97040
Ni, thin films, surface demagnetisation due to chemisorption, ferromagnetic reson. study 0-80616

demagnetisation, adiabatic *see* **magnetic cooling****Demer effect**

- InSb-NiSb, photovolt. effects rel. to theory of semicond. with internal elec. short circuits 0-65620

demodulation

- see also demodulators; modulation*
acousto-optic modulator for CO₂ laser rangefinder using heterodyne detect. 0-102825
flaw-detection apparatus, noise immunity, sounding signal freq. modulation 0-89441
Fourier transform spectrosc., new developments—passive heterodyne spectrosc. and diode laser absorpt. spectrosc. 0-95148
laser heterodyne spectroscopy for stratospheric trace constituents meas. 0-109257
LF/MF radio transmissions, non-linear demodulation in auroral ionosphere rel. to ELF signals generation 0-94639
magnetised semiconductor plasma, EM wave amplitude modulation and demodulation 0-84482
nerve trunk multifibre activity quantitation 0-76853
partially coherent radiation, optical heterodyne detection 0-77871
RF SQUID magnetometer, synchronous demodulation, amplitude- and phase-sensitive detection 0-105679
Rydberg atom maser emission, heterodyne detection 0-78822

demodulators

- see also demodulation; discriminators*
heterodyne receivers for atmospheric optical communications 0-58663

demography

- education, radioactive dating and population growth by dice game 0-57030
effect on subjective road traffic noise investigations, a socioeconomic study 0-67022
nuclear power station, operation, socio-economic effects on demography, finance and local activities of region (*French*) 0-74038

demonstrations

- includes student experiments*
see also student laboratory apparatus
AC rectification 0-77598
air, buoyancy demonstration 0-67988
appearance pot. spectrometer design 0-105477
atoms in solids, focusing and defocusing collisions model 0-82618
barometer, capillary tube type 0-73156
Bernoulli's eqn. and Hagen-Poiseuille's law, capillary bed representation 0-57039
Bernoulli's principle, spin of balls and coins 0-77592
blackbody radiation and Planck function, derivative spectroscopy expt. 0-77563
capacitor, stored energy meas. 0-77585
Cartesian diver, minimal buoyancy effects 0-67989
castor oil dielectric fluid, microwave propag., permittivity effect 0-105468
crystal growth from solution, convection effects, holographic interferometric obs. 0-77565
Doppler effect, ripple-tank demonstration 0-82621
education, advanced undergraduate expts. in vacuum physics and mass spectrometry 0-73153
electromagnetic wave propagation in Al 0-73149
electrostatic imaging problems with plane boundaries 0-90629
equivalence principle, monkey and hunter demonstration 0-67984
ferromagnetic material props., teaching expt. 0-82608
forbidden energy gap meas. in Si and Ge p-n junctions 0-57027
Foucault pendulum, continuously operating 0-73151
Fraunhofer diffraction patterns, phase reversal effect 0-101691
Gassiot's cascade, 19th century discharge tube demonstration 0-77586
glasses, prescription meas. 0-67981
gyroscope precession 0-73155

demonstrations continued

- holograms, rainbow, demonstration of diffraction and interference of light (*Polish*) 0-68001
- holographic plates, rear refl. elimination technique 0-73145
- impulse recorder for small rocket engines 0-77595
- Joule heat engine and pump 0-105480
- laser beam UHF and audio freq. difference heats 0-73139
- LED point source emitter 0-73150
- light polarisation classical model 0-77576
- light velocity measurement using two dollar rotators 0-77578
- liquid rise in capillary tube, rate meas. demonstration 0-73147
- local inertial frame of reference 0-67982
- magnetic induction, large-scale demonstration 0-101699
- mode conversion, shear, Lamb and Rayleigh waves 0-101687
- multiple lens experiment 0-82596
- multiple scatt., elastic and inelastic, two particle system with fixed wall, air track expt. 0-73135
- NMR-ESR spectroscopy, miniature magnetic assembly 0-105467
- one beam transmission holography, practical hints 0-57046
- parametric instability, demonstration and discussion 0-57032
- partially coherent light, lecture demonstrations 0-101700
- physical pendula, reconstructed 19th century expt. 0-82612
- physical pendulum, computer-aided laboratory exercise 0-67985
- physics teaching aids, convention of secondary school physics teachers (*Hungarian*) 0-67957
- plasmon surface polariton dispersion curve, optical obs. 0-101690
- Poisson statistics demonstration using X-ray tube, electronic 'shot noise' 0-73129
- reduced eye, expts. in life science labs. 0-82617
- refractive index, spatially varying, demonstration and theory 0-62425
- refractive index measurements 0-77577
- rotating objects, centre of mass rel. to centre of rotation 0-77579
- rotational motion phenomena, turntable accessories 0-77571
- sound analyser, undergraduate lab. expts. 0-82600
- spark chamber 0-77596
- speed of sound, meas. by clapping technique 0-82620
- structural instability critical behaviour and broken symm. 0-105476
- superfluidity and superconductivity phenomena demonstrated with He cryostat. (*Polish*) 0-86059
- thermal conductivity of gases 0-82614
- vibrating plate reson. characts., quality factor and nonlinearity 0-73133
- vibrating string, tuning guitar by television 0-73134
- virtual image position determ., demonstration using TV camera 0-67992
- viscosity of liquids, capillarity method determ. 0-82619
- N high pressure discharge and associated lasing phenomena 0-105475
- Na arc lamp, light-induced ignition method 0-77599

dendrites

- see also crystal growth*
- dendrite development and growth in very small crystals, Monte Carlo study 0-107683
- steel, 10R6M5 and 10R6M5K5, atomised powders (*Russian*) 0-97446
- web dendrites, dislocations, stacking faults, X-ray topographic study (*Chinese*) 0-88148
- Al-Ni(Pt)(Zn), rapidly solidified, twinned dendrites 0-70572
- CaSiO₃, fibrous, controlled crystallisation and anisotropy 0-59425
- Cd chalcogenides, thin films, VPE, needle-like cryst. growth 0-80148
- Cr₂C₃, cathodic needle growth, at lower electric fields from Cr(CO)₆ vapour 0-76161
- Fe₂O₃, haematite, dendrite formation from high temp. soln. (*Japanese*) 0-107684
- Mo₂C, cathodic needle growth, at lower electric fields from Mo(CO)₆ vapour 0-76161
- PbTiO₃, optical birefringence in low temp. region 0-93276
- Si materials, advanced, preliminary evaluation for space solar cells 0-94006
- Si ribbon, dendritic web growth from melt, solar cell module fabrication 0-93478
- W needle crystal growth, discharge-induced decomp. of hexacarbonyltungsten mols. 0-84414
- W needles, mechanism of cathodic growth, decomp. of W(CO)₆ under high field conditions 0-76162
- Zn chalcogenides, thin films, VPE, needle-like cryst. growth 0-80148

dendritic crystals *see dendrites***dendritic structure**

- binary alloys, directional solidification, theory of dendritic growth 0-70145
- cellular and cellular dendritic growth, general microsegregation eqn. 0-84921
- dendrite development and growth in very small crystals, Monte Carlo study 0-107683
- eutectic alloy, dendrite growth—the coupled zone 0-97489
- metal powder, method for TEM study 0-84038
- steel, alloy type, photoemission electron microscope obs. of high temp. precip. behaviour 0-108456
- steel, austenitic stainless, weld, ferritic-austenitic solidification mode 0-89214
- steel, continuously cast, segregation at halfway cracks 0-60869
- steel, low impurity, peritectic transformations, influence on initial struct., solidification, grain boundaries (*Russian*) 0-66621
- Al, molten, showering cryst. form. in mould cooled from top (*Japanese*) 0-66498
- Al-Cu, molten, showering cryst. form. in mould cooled from top (*Japanese*) 0-66498
- Al-Cu alloy dendritic solidification kinetics 0-81041
- Al-Cu alloys, coarsening mechanisms of secondary dendrite arm, and organic analogue 0-81049
- Al-Si (2.4 wt.%), liq. fluidity in solid-liq. zone 0-108429
- Al-Ti, molten, showering cryst. form. in mould cooled from top (*Japanese*) 0-66498
- Au-Ge contacts on GaAs, SEM and TEM obs. of struct. 0-100522
- Cd-Ge broken lamellar eutectic composite, tensile and compressive props. 0-71694
- Co-Ti(Hf)(Ta)(Mo)(Zr)(Al)(Fe)(Ni), dendritic segregation 0-76260
- 25Cr-20Ni stainless steel dendritic solidification, growth morphology and solute redistrib. (*Japanese*) 0-81045
- Cu-Al spherical crystals, grown from drop of melt, topography 0-84353
- Cu-Nb alloy, chill casting, consumable arc melting, ingot prep. techniques 0-84879
- Fe, cast, with spheroidal graphite, crystn. (*German, English*) 0-97473

dendritic structure continued

- Fe-Mn, as cast, pseudo-composite struct. resulting from interdendritic segregation, cryogenic materials appl. (*French*) 0-93556
- Fe-Ni film, amorphous, martensite form. time and struct. 0-104159
- Fe-Ni-Cr-Al-Ti-W-Mo (35, 15, 2.4, 2.3, 2.2 wt.%) wrought superalloy, freckles (*Chinese*) 0-104137
- Mo-W alloy type MW25N, crystallisation form, globular dendrites, grain boundaries (*Russian*) 0-66494
- NH₄Cl-H₂O solidification model for showering cryst. form. in molten metal cooling (*Japanese*) 0-66498
- Nb fibre glass composites, new technique for producing fine metal fibres 0-108384
- Ni-Al-Ta dendritic monocrysts., directionally solidified, coarsening kinetics 0-108425
- Zn-Al-Cu casting alloys, mech. props. and dendritic morphology, Al content effect (*Korean*) 0-93612
- ZrO₂-SiO₂, liquid immiscibility, microstruct. of plasma dissociated ZrSiO₄ 0-107429

dense fluids, theory *see liquid theory***densification**

- see also density; powders; sintering*
- borosilicate glasses, gamma irradiation effect on density, refractive index, thermal expansion 0-79838
- ceramic powder synthesis from laser-heated gas phase reactants 0-93525
- chaotite, a new allotropic form of carbon, produced by shock compression 0-80997
- diamond powder, consolidation by thermal decomposition of methane and benzene 0-66448
- granular materials, random packing, statistical mech. considerations 0-104088
- plasma sprayed coating consolidation by laser remelting 0-93697
- porous materials, density variation during plastic shaping 0-84873
- powder metallurgy, electrohydraulic effect appl. 0-60798
- powders, during isostatic compression 0-66449
- performing using high-voltage electrical discharge 0-84872
- pressure sintering, inhomogeneous flow and effective press. 0-93512
- SEM stereoscopic quantitative analysis 0-57433
- steel, Mn, sintered, production, effect of initial Fe powder struct. on mech. props. 0-104095
- steel fibre reinforced concrete, vibr. compaction, pressure compaction and curing (*Japanese*) 0-89179
- surface redistribution by grain boundary diffusion 0-84871
- TCNQ salts, crystallisation versus electrical conductivity 0-92885
- Zircaloy-2, hot-pressed, influence of diffused C on structure and oxidation 0-61016
- Al-Si-N-O system, comps. corresponding to β -sialon phase reaction hot-pressing 0-84891
- Al-steel mixture, wear resistant, produced by compaction by discrete shock waves 0-84882
- As₂Se₃₀ and As₂Se₂₀ semicond. glasses, densified, photoluminesc., inelastic deform. effect 0-66293
- BC, sintered, struct. and props. 0-104181
- B₂C, densification kinetics during hot pressing, 1800-2200°C 0-60817
- BaTiO₃:La, Sb, second phase effect on elec. and mag. props. 0-60986
- Be-Si-Al-O-N ceramic, phase assemblages, relationships with props. 0-60848
- CaHPO₄, powder and granules with starch mucilage binder, surface topography variation under compression 0-80998
- Ce-Si-Al-O-N ceramic, phase assemblages, relationships with props. 0-60848
- Fe powders, cold-pressed, props., effect of air 0-100810
- β -Fe₂Ge₃ formation in isothermal sintering, phase transition kinetics 0-89197
- Mg-Si-Al-O-N ceramic, phase assemblages, relationships with props. 0-60848
- MgO-NaCl refractory clinkers, Cr containing, densification, thermal treatment and phase composition effect (*French*) 0-76219
- (Mn,Zn)Fe₂O₄:Si, Ca, Ti, second phase effect on elec. and mag. props. 0-60986
- MnZn ferrite powders, reactive, mag. materials obtained by compaction 0-89182
- Mo powder, influence of powder reduction processes on props. 0-89175
- Na₂O-CaO glass phlogopite mica powders, composite fabrication, cellular struct. 0-84902
- Nb₆Fe₄₀P₁₄B₆, metallic glass, explosive compaction, mech. props. 0-89176
- Ni-Zn-Co ferrites, synthesis from solid solns. of schoenite-type salts 0-93511
- Pb_{0.94-x/2}Ba_{0.06}Nb₂Zr_{1-x/2}O₃, Nb dopant morphology effect on microstructure 0-81005
- Re film, prep. by laser melting 0-84859
- Si-SiO₂-Mg-Cu powder compact, nitridation to form Si₂ON₂ whiskers (*Japanese*) 0-93674
- SiAlON, prepared from siliceous sand and Al powder, hot pressing, steatite contamination effects (*Japanese*) 0-93528
- β -SiC, sintering, B transport and lattice parameter change 0-108370
- Si₃N₄, reaction bonded, post-sintering, injection moulding applications 0-60807
- Si₃N₄, reaction-bonded, theoretical model of manufacture, effect of ambient reaction temp. and compact size 0-108379
- SiO₂, vitreous, X-ray compaction efficiency 0-65044
- SrFe₂O₁₉:Si, Sr, second phase effect on elec. and mag. props. 0-60986
- TiC_x, nonstoichiometric, densification during sintering 0-84895
- UO₂ powder compaction, force transmission and friction 0-71620
- Y-Si-Al-O-N ceramic, phase assemblages, relationships with props. 0-60848
- ZnO:Bi, Sb, Co, second phase effect on elec. and mag. props. 0-60986

densimeters *see densitometry***densitometers *see densitometry*****densitometry**

- see also photometry*
- accuracy of optical density meas. by means of optical wedge 0-73416
- air/water mixture mass flow meas. by drag devices and γ densitometer 0-79385
- colour densitometry characteristic curves corresponding to visual impression 0-82803
- colour densitometry system based on spectral densitometer 0-82804
- colour densitometry using densitometer with more than 3 channels, dye specific densities 0-82802
- combined scanning microdensitometer and diffractometer 0-73529

densitometry continued

- computerised tomographic scan edge position uncertainty reduction by density derivative processing 0-109017
- electron microdensitometer system for use in TEM 0-95197
- flaw dimensions in direction of irradiation determ. from radiographs with aid of defectometer 0-71863
- heavy charged particle specific energy losses meas. using densitometric method (*Russian*) 0-63482
- high-speed automatic microdensitometer 0-101817
- image weak modulation detection in film grain noise with partially coherent illumination 0-77897
- K-edge densitometer, appl. to Pu nuclear fuel reprocessing product soln. accounting 0-95352
- liquid, extinction coefficient meas. using coaxial dual channel laser system 0-73425
- microdensitometer performance, effective incoherence and flare tradeoff 0-77851
- microdensitometry, linear, sensor optics design 0-62710
- microphotometry, compensation for fluctuations in illumination 0-73413
- optical fibre refractive index profile microdensitometry 0-106632
- photographic materials, MTF automatic evaluation 0-95170
- photography, densitometer measurement transformation into spectral density distrib. and colour coordinates (*Russian*) 0-77902
- photometric calibrator development and appl., inverse fourth power 0-73412
- single beam microdensitometer, liquid electron diffraction pattern evaluation 0-86370
- US, two-phase flow density meas. in pressurised water reactor 0-77759
- X-ray microphotodensitometry in traumatology and orthopaedic surgery (*Croatian*) 0-109022
- Pu safeguards, product soln. gamma-ray NDA using K-absorption edge densitometer 0-83162
- U/Pu fuel reprocessing solutions, NDA using X-ray L-edge densitometer for materials safeguards 0-83167

density

- see also *atmospheric pressure and density; density measurement; density of gases; density of liquids; density of solids*
- brain, experimental oedema, serial meas. of specific gravity and computerised tomography attenuation 0-98005
- Coulomb systems, equilib. distrib. functions expansion in power of density 0-64681
- critical opalescence and density fluctuations in gravitational field 0-66137
- 30 Doradus nebula, density struct. and chemical comp. 0-62226
- early universe, density-temp. fluctuations present observability 0-82554
- fibrosarcoma cells, buoyant density, effect of hypoxic growth conditions in vitro 0-104601
- interstellar large globules, density radial distrib. rel. to dynamics 0-62246
- ocean, buoyancy flux effects on density field and continental shelf circulation 0-72540
- spiral galaxies, surface mass density distrib. in galaxy form. model 0-90529
- universe, Friedmann model, with decoupled radiation field, density perturbations growth 0-109567
- Venus, density rel. to tectonics and comp. 0-72805
- H II regions density fluctuations, statistical approach 0-77468
- NH₄Cl, submicron particles, density, morphology 0-61166
- SiO₂-Al₂O₃-CaO-BaO-SrO-ZnO-Na₂O-K₂O-B₂O₃, glaze effect of P₂O₅ additions 0-60824

density, atmospheric see *atmospheric pressure and density*

density, vapour see *density of gases*

density measurement

- see also *hydrometers*
- benzene, using flexible capillary 0-98886
- ceramic density measurement, true and apparent, specimen liquid saturation cell 0-62636
- coal dust mass flow meas. methods (*German*) 0-92242
- electrolyte solutions in glycerol, investigation by US shear strains 0-88266
- fluid, laser interferometry appl. 0-75018
- fluid, using gamma radiation, theory, practices and appl. 0-73325
- fluid meas. in mechanical engineering, conf., Johannesburg, South Africa, (Feb. 1979) 0-75016
- granular materials, particle density measurement by pycnometry 0-69903
- granular media, density measurement, plane strain conditions, acoustic method (*Polish*) 0-62635
- imaging space-time-density contours in gas, overlapping pulse technique 0-73320
- inhomogeneous medium, density determ. by β -ray attenuation, calcs. and meas. 0-98182
- laser Doppler velocimeter for particle size and density simultaneous determ. 0-98880
- liquid, 25 to 100 C, up to 500 MPa, falling body instrument 0-103510
- liquid metals, errors from pycnometers 0-73321
- liquids, using flexible capillary 0-98886
- lung density, Compton scatt. meas., multiple photon interactions 0-67146
- measurement methods in Yugoslavia (*Croatian*) 0-105616
- metals, using X-ray total external reflect. and double crystal spectrometer 0-64831
- mineral microcrystals, mag. fluid technique for density determ. 0-85751
- particles in dilute suspension in general flow, mass flow and density meas. 0-101784
- polyester film 3-dimens. network, using chloroform sorption (*Russian*) 0-59405
- radioactive waste density measuring meter, digital, remotely operated 0-68927
- solution density, in-tank based of differential press. meas. 0-78391
- standards, in solid density meas., hydrostatic weighing 0-77758
- US densitometer for two-phase flow density meas. in pressurised water reactor 0-77759
- Cs-Au, liq., molar vol. meas. 0-59546
- LaS_{1.500}-LaS_{1.333}, solid soln. region 0-95075

density of gases

- Bose-gas model, dil. hard sphere, calc. of low density atomic H gas props. 0-87194
- dense gases, vel. autocorrelation function, memory function 0-59154
- ethylene, high density behaviour, extrapolated PpT surfaces and critical density 0-87834
- high-pressure gas equation-of-state meas. interferometry 0-77810

density of gases continued

- propylene, high density behaviour, extrapolated PpT surfaces and critical density 0-87834
- tetrachloromethane, fluid, collision induced light scatt. intensity 0-103955
- Ar, gas, liquid, solid, refractive index, density and dielectric const. 0-66138
- CO₂, high density behaviour, extrapolated PpT surfaces and critical density 0-87834
- Kr, gas, liquid, solid, refractive index, density and dielectric const. 0-66138
- N₂, high density behaviour, extrapolated PpT surfaces and critical density 0-87834
- Xe, gas, liquid, solid, refractive index, density and dielectric const. 0-66138
- Xe, high density behaviour, extrapolated PpT surfaces and critical density 0-87834

density of liquids

- see also *hydrometers*
- benzene, density meas. using flexible capillary 0-98886
- binary mixtures near critical state, gravitational distrib. of thermodynamic props. (*Russian*) 0-88241
- changes during melting by X-ray absorption 0-103462
- o-chlorophenol-acetone (ethyl methyl ketone), thermodynamic and transport props. 0-92686
- cyan compounds, liq. cryst. phases, incommensurate coexistent density fluctuations 0-79691
- cyclohexane, liquid, density effect on transport properties 0-65264
- dense fluids, solvation forces between two solids, density profile calc. 0-64855
- elastohydrodynamic traction, granular behaviour 0-103008
- p-p'-n-heptyl-cyanobiphenyl-isotropic solute systems, nematic-isotropic phase transformation, volumetric study 0-92653
- hexafluorobenzene, liq., self-diffusion and density as functions of press. and temp. 0-92696
- n-hexane-cyclohexane mixture, 25 to 100 C, up to 500 MPa 0-103510
- liquid crystals, thermodynamic props. calc. 0-103464
- measurement, using flexible capillary 0-98886
- polar solvents, solvated electron absorpt. spectra, intrasolvent and intersolvent correls. 0-93840
- polyesterimides, solns., ultrasonic vel. and Rao formulism 0-103422
- polymethylsiloxane-2, liq., thermodynamic props. at high press., US prog. meas. (*Russian*) 0-65157
- seawater, density, dependence on temp., salinity and press., math. expressions 0-94540
- surface tension theory for liquid mixtures 0-88404
- tetrachloromethane, fluid, collision induced light scatt. intensity 0-103955
- tetrahedral mol. fluids, collision induced light scatt. intensity 0-103955
- trifluoropropylmethylsiloxane fluids, viscoelastic props., mechanical impedance, viscosity and density meas. 0-79249
- water, compressed, thermodynamic props., evaluation by statistical error anal. 0-92685
- Al, density fluctuations, neutron scatt. anal. 0-70349
- Ar, gas, liquid, solid, refractive index, density and dielectric const. 0-66138
- Ar-H₂(Ne) liquid solution, dielectric props., intermolecular interactions (*Russian*) 0-88904
- As-S, melt struct., orientation birefr., viscosity, refr. index, and density 0-84713
- CaF₂, melts, elec. cond., surface tension, viscosity, density (*Russian*) 0-92758
- CaF₂-MgO-SiO₂, melts, elec. cond., surface tension, viscosity, density (*Russian*) 0-92758
- CaF₂-MgO(SiO₂), melts, elec. cond., surface tension, viscosity, density (*Russian*) 0-92758
- Cd₃As₂ and CdAs₂, molten, thermal expansion and atomic bond strength parameters 0-65257
- CdTe_{1-x}Se_x(Te₄):Au, elec. cond., density, dielectric const., changes on fusion 0-88553
- Ce, surface and volume props., flow props., surface layer thickness (*Russian*) 0-59760
- Cs-Au, liq., molar vol. meas. 0-59546
- CuSO₄, aq. solns., densities, viscosities, elec. cond. meas., 20 to 70°C 0-59688
- CuSO₄/H₂SO₄ electrolytes, densities, elec. cond., viscosities 0-107455
- D₂O, liquid, volumetric and derived thermal characteristics at low temp. and high pressure 0-107352
- Fe, pure and alloyed, density and thermal expansion in liq. and solid states 0-96668
- Fe-As melts, surface tension, density, adsorption (*Russian*) 0-92757
- He II, superfluid flow hydrodynamics, normal density component velocity depend. (*Russian*) 0-65326
- He liquid, plane surface layer, density profiles and pair correlation asymptotics (*Russian*) 0-88371
- ³He, sound propag. at elevated densities, 0.35 to 1.4K (*Russian*) 0-92741
- ³He, superfluid, Barnett effect 0-88388
- ³He, superfluid, size effect influence on fluid density and transition temp., fourth sound meas. 0-80022
- ³He, superfluid B phase, gap distortion, depairing critical currents, all temperatures 0-92743
- Ir, thermophysical props. at temps. up to 7000K 0-103497
- K, density, at near critical temp. 0-103407
- KCl-CuCl eutectic fused salt, potential as intermediate temp. solar heat transfer and storage medium 0-101135
- Kr, gas, liquid, solid, refractive index, density and dielectric const. 0-66138
- La, surface and volume props., flow props., surface layer thickness (*Russian*) 0-59760
- LiH, liq., density and surface tension, 982-1280K 0-59548
- Nd, surface and volume props., flow props., surface layer thickness (*Russian*) 0-59760
- Pr, surface and volume props., flow props., surface layer thickness (*Russian*) 0-59760
- Rn, calc. of critical density 0-59547
- Se, electronic transport props., equation of state, to 1900K and 1800 bars 0-65574
- V, thermophysical props. at temps. up to 7000K 0-103497
- Xe, gas, liquid, solid, refractive index, density and dielectric const. 0-66138
- Zn₃As₂ and ZnAs₂, molten, thermal expansion and atomic bond strength parameters 0-65257

density of solids

alkali hydrides, structural transition from NaCl to CsCl type under high press. 0-96458
borosilicate glasses, gamma irradiation effect on density, refractive index, thermal expansion 0-79838
ceramic density measurement, true and apparent, specimen liquid saturation cell 0-62636
changes during melting by X-ray absorption 0-103462
elastic waves in crystals, invariance relations 0-84250
graphite, polygranular, flexural strength after heat treatment porosity correl. 0-84996
kaolin grog particles, shape and density 0-97450
metals, polycryst., creep damage and cavity growth, assessment using density meas. 0-104217
Nafion, densities and expansion coeffs. as function of various parameters 0-79711
NASICON solid electrolyte, processing and phys. props. 0-60820
Nylon 6 film, prior high-press. treatment effects, weight swelling, density, IR crystallinity, X-ray and viscosity obs. 0-81025
photographic positive film density, depend. on conc. of stabilizers and antifoggants added to developer (German) 0-73497
Polimal 109, polymer resin laminate, density porosity, water vapour diffusion sorption and permeation (Polish) 0-59665
polycarbonate, glassy state, enthalpy relax., thermal density fluctuations 0-59678
rare earth germanates, R_2O_3 - GeO_2 system cpds., physicochem. characts. 0-97469
rare earth oxyorthotitanates, crystallochem. classification 0-107142
steel, plastic deform., density changes (German) 0-60908
thermoelectric materials, B_2C_x and $(B,Si)_x$ -C_x-P-type LaS_x N-type alloys, fabrication and thermoelectric props. 0-107771
titanomagnetite sand from New Zealand, density, elec. and mag. prop 0-98311
transition metals, thermophysical data at high temps., submicrosecond-pulse-heating method 0-103459
Zircaloy-2, irradiation growth, shape and volume changes 0-92562
 β'' - Al_2O_3 - Na_2O solid electrolyte, processing and phys. props. 0-60820
Ar, gas, liquid, solid, refractive index, density, and dielectric const. 0-66138
As-Te-In, glass-forming, density and microhardness 0-103257
Au, Si_{1-x} amorphous films, phys. studies 0-75476
Au₂Si₃m, metastable phase, substruct. unit cell (German) 0-88091
B₂C, thermophysical props. and neutron absorpt. 0-103488
B₂O₃-V₂O₅-P₂O₅ glass, mech. and elec. props 0-84228
Ba(PO₃)₂-AlF₃-CaF₂ glass, elec. cond. and IR spectra 0-89005
Ba(PO₃)₂-AlF₃-MgF₂ glass, elec. cond. and IR spectra 0-89005
C, polygranular, flexural strength after heat treatment porosity correl. 0-84996
C reinforced plastic, degraded, study of strain, 20 to 1000°C 0-71680
CaAl₂O₇, mellilite struct., prep. and props. 0-93524
CaO, density above 100 GPa rel. to high press. metallisation 0-84427
Ca₃(PO₄)₂OH bioceramic, material props. 0-93523
CdTi₂Se₄(Te₄)₂Au, elec. cond., density, dielectric const., changes on fusion 0-88553
Co₂Z ferroxplana form. process peculiarities 0-89368
CsMnCl₃·2H₂O, diagonal elastic const., thermal expansion coeffs., ultrasonic velocity meas. 0-79853
Cu, creep damage and cavity growth, assessment using density meas. 0-104217
Cu₂Mo₂S₈, constitution diagram, 11-2000K 0-108407
Eu₂O₃, thermophysical props. and neutron absorpt. 0-103488
Fe, Armco, dyamic $\alpha \rightarrow \epsilon$ transform., stress gauge meas. 0-96594
Fe, powder-forged, elastic const., density depend. 0-84987
Fe, pure and alloyed, density and thermal expansion in liq. and solid states 0-96668
Fe-B-C amorphous alloy, formation, mag. props., thermal stability and density 0-75796
Fe-B-Si-C amorphous alloys, prep. and props. 0-88748
Fe-C (graphite, 0.3 wt.%), powder-forged, elastic const., density depend. 0-84987
Fe-Si (3 to 5 wt.%) sinters, mag. props., Si and Fe-Si additions effect 0-71104
(Fe_{0.9}Ni_{0.1})_{100-x}B₂ and (Fe_{100-x}Ni_x)_{80B₂₀} amorphous alloys, X-ray diffr. struct. determ. 0-64906
Fe₈₀(P₁C₇)_{20-y}B₂(Si₁)₂, density, microhardness, and crystn. temp., comp. depend. 0-84093
Fe₅₄Sb, temperature effect on lattice const., Mossbauer spectra and density 0-88124
 $\alpha(\beta)$ -Ga₂Se₃, cryst. growth, optical, X-ray diffr. and SEM study 0-71587
HfF₂-BaF₂-LaF₃ glass system, IR transmitting, synthesis and props. 0-71623
HfF₂-BaF₂-ThF₄-(ZrF₄) glass system, IR transmitting, synthesis and props. 0-71623
Ir, thermophysical props. at temps. up to 7000K 0-103497
KCl-CuCl eutectic fused salt, potential as intermediate temp. solar heat transfer and storage medium 0-101135
Kr, gas, liquid, solid, refractive index, density and dielectric const. 0-66138
LaB₆ crystals, zone refined, chem. characterisation 0-93821
LaS_{1.500}-LaS_{1.333}, solid soln. region, density meas. 0-95075
Li₂O-Al₂O₃-SiO₂ glass, study of elastic props. 0-104205
Li₂O-B₂O₃-P₂O₅ glass, mech. and elec. props 0-84228
Li₂O-Na₂O-B₂O₃-Al₂O₃-SiO₂ glass, Young's modulus and density, ion exchange effects 0-84982
Mg₂GeO₄-Mg₂SiO₄ system, struct. similar solid soln. obs. and characts. 0-108403
¹⁵¹Nb, solid struct., and thermodynamic props. (Russian) 0-88083
NaCl with divalent impurities, lattice relax. from density meas. 0-70226
Na₂O-B₂O₃-P₂O₅ glass, mech. and elec. props 0-84228
Na₂O-CaO glass phlogopite mica powders, composite fabrication, cellular struct. 0-84902
Na₂O-SiO₂ glass, bridging to non-bridging ratio and correl. to glass density and refr. index, ESCA study 0-84832
Na₂O-SiO₂ glass, OH⁻ content effect on mech. and other props. 0-89337
Na₂O-SiO₂ glass drops, quenched from liq. state, thermally treated, density profile 0-81085
Nb₄₀Fe₄₀P₁₄B₆, metallic glass, explosive compaction, mech. props. 0-89176
Ni₁₁Sb, temperature effect on lattice const., Mossbauer spectra and density 0-88124

density of solids continued

Ni₂Zn ferrite, ZrO₂ additions influence on sintering and physicochem. props. 0-108369
Ni₂Zn ferrites, density and mag. props., isostatic pressure effect 0-60816
PbO-containing binary systems, acoustooptic props. from comp. and density 0-76000
Pb_{1-x}Sn_xTe_{1-y}Se_y, quaternary solid solns. with const. lattice parameter, cryst. growth and characts. 0-108332
Pb(Zr, Ti)O₃ ceramics, low temp. sintering, elec. and mech. props. 0-71616
Se, amorphous, elec. cond., activation energy, density, cryst. Se effect 0-65548
SiC:H amorphous reactively sputtered film, H content effect on film props. 0-75459
SiO₂ film, prep. using high press. O₂, residual stress, chemical etch rate, refr. index and density meas. 0-71768
SiO₂ glass, formation by hydrolysis of Si(O₂C₂H₅)₄ with NH₄OH and HCl soln., and characterisation 0-71622
SiO₂-B₂O₃ glass system, gel hot pressing synthesis and characterisation (French) 0-66468
Ta, thermophysical props. and neutron absorpt. 0-103488
TeO₂-MoO₃-V₂C₅, phase comp. determ. using X-ray diffr., electron microscopy and DTA (German) 0-88046
 α -Ti alloys VT1 and VT5, struct. and phys. props., H₂ effect 0-108576
Ti base alloys, melt-extracted polycryst., mech. props. 0-76360
TiO₂-Al₂O₃-SiO₂ system, ternary glass-forming region and phys. props. 0-84919
V, thermophysical props. at temps. up to 7000K 0-103497
Xe, gas, liquid, solid, refractive index, density and dielectric const. 0-66138
ZnAs₂, homogeneity region and electrophys. props. 0-60833
Zr-Al (8.6 wt.%), dimensional stability struct. and mech. props, effects of neutron irradi. 0-92563
ZrO₂-CaO(Y₂O₃) ceramics with grainy structure, props., effect of heating to 2000°C 0-104194

density of states, electron *see electronic density of states*
deoxyribonucleic acids *see DNA*
deperming *see demagnetisation*
desalination
25 kW solar photovoltaic flat panel power supply for electro dialysis water desalination unit 0-89643
desert pastures irrigation using solar desalination plants 0-89594
evaporator, falling-film, with vertically finned surface, hydrodynamics and heat transfer 0-58891
reverse osmosis using solar and wind powered plant 0-61282
seawater desalination by wind power, anal. 0-108781
solar desalination unit with evaporation chamber, test results 0-96178
solar distillation plant, 5000 lit/day, drinking water production in India 0-61280
solar energy appl., multistage flash evaporation process, demonstration project 0-61283
solar energy powered plant, MSF, technical and economic evaluation 0-61281
thermal power plant, antiscaling forming effectiveness of seeding crystals 0-89527

desalting *see desalination*
design aids
see also design engineering; nomograms
No entries
design engineering
see also systems engineering
60 m diameter wind turbine generator, design concept 0-61262
200 MW atmospheric fluidised-bed combustion steam generator, comparison of three designs 0-108776
crowbar transformer, low leakage and high current for ZT-40 toroidal pinch power supply 0-102322
electrical and electronic engineering undergraduate courses, engineering design importance 0-67972
engineering education, importance of research and design for satisfying industrial needs 0-67974
epicyclic gears for wind power plants 0-61252
fusion, toroidal field superconducting coil cryogenic stability and field anal., design parameter 0-106200
fusion reactor, ASDEX, neutral beam injection, beam line design 0-99395
fusion reactor, commercial Tokamak hybrid reactor, blanket and shield design 0-106179
fusion reactor, commercial Tokamak Hybrid Reactor, reference design 0-106171
fusion reactor, compact ignition test reactor, engineering design using Bitter type magnet 0-102310
fusion reactor, Doublet III, neutral beam test tank design 0-99301
fusion reactor, ETF, design considerations 0-95438
fusion reactor, first wall blanket, cylindrical module, reference design 0-106181
fusion reactor, Heliotron E, helical coil design, mag. field perturbations 0-99300
fusion reactor, HFCTR, demonstration reactor conceptual design, high force density magnets and modularisation 0-95439
fusion reactor, ISX-B tokamak, design of bundle divertor expt. 0-102341
fusion reactor, JXFR, superconducting mag. system conceptual design 0-99295
fusion reactor, Large Coil Program, low temp. stability, joints, design method 0-106195
fusion reactor, LARTS, extended burn operation, physics, engineering and economics 0-95440
fusion reactor, LINUS, imploding liq. liner system, engineering anal. 0-99315
fusion reactor, low power Tokamak experimental fusion power plant, scoping studies with empirical scaling, SiSYFUS code 0-102309
fusion reactor, LPTT, engineering design 0-102308
fusion reactor, MFTF, intense neutron environment, test cell side wall design, shielding materials 0-102318
fusion reactor, MFTF, ion and neutral beams dumps, design 0-102317
fusion reactor, neutral beam ion source, core snubber network design, fabrication and testing 0-102378
fusion reactor, PDX, flexible work platform and balcony design 0-106161
fusion reactor, STARFIRE project, design parameters 0-106184

design engineering continued

- fusion reactor, STARFIRE project, first wall and blanket design 0-106188
- fusion reactor, STARFIRE project, superconducting poloidal coils design study 0-106185
- fusion reactor, TEXT, assembly plan 0-99305
- fusion reactor, TEXT, poloidal field power systems, design and anal. 0-102328
- fusion reactor, TFTR, blanket module expts., engineering test station design 0-102338
- fusion reactor, TFTR, electrical power blanket module, conceptual design 0-102339
- fusion reactor, TFTR, high energy heat sink, ion beam dump and calorimeter 0-99394
- fusion reactor, TFTR, neutral beam injector prototype, construction and performance 0-99390
- fusion reactor, TFTR, neutral beam source, arc current modulator design 0-102379
- fusion reactor, TMX, injector system mech. design and installation 0-99393
- fusion reactor, TNS, electron cyclotron heating startup system, design 0-99330
- fusion reactor, toroidal field coil in-plane bending stress, struct. support design 0-106164
- fusion reactor, torsatron, superconducting mag. engineering design 0-99297
- fusion reactor vacuum vessel, large, ultra high vacuum, design and manufacturing problems 0-99276
- fusion reactors, Large Coil Program, superconducting mag. coil struct. design status 0-106189
- fusion reactors, Tokamaks, maintenance design requirements and economics 0-99285
- fusion reactors, ZT-40, reverse field pinch engineering prototype 0-102316
- high temperature plant design methods, reference stresses and bounding theorems 0-58937
- instrumentation, innovation and business opportunity 0-98909
- metals, engineering, multi-axial creep characts. 0-64398
- neutral beam, continuously operating, convectively cooled ion accelerator, mech. design and fabrication 0-102374
- nuclear reactor containment structure design and service loads 0-106138
- reversed field pinch, RFX constructional details 0-91277
- shrouded wind turbine, pilot plant design 0-66931
- solar stills, inclined-stage type, basic parameters determ. 0-89595
- structural stress distrib. determ. by remote IR thermometry 0-87749
- university engineering education courses economics 0-67973
- vertical axis wind turbines 0-66929
- wind generator design, atmospheric turbulence structural influences 0-61247

desk calculators see *calculating apparatus; electronic calculators*

desk-top computers see *minicomputers*

desorption

- chemical desorption theory, rates of reaction 0-71939
- chemisorbed species on solid surfaces, quantum-stochastic approach to desorption dynamics 0-66864
- chlorophyll-a, hydration, field desorpt. mass spectral obs. 0-71936
- cyclic hydrocarbons, chemisorpt. on W(100) surface, decomp., UPS and thermal desorpt. obs. 0-59782
- diffusion controlled processes, nonequilibrium decay effects 0-66764
- electron and photon stimulated, from metal surfaces 0-75440
- electron-stimulated desorption ion imaging of adsorbate distrib. 0-103572
- ferrite, 350 NN1, for use in superhigh vacuum systems 0-108478
- flash desorption meas. from single cryst. surfaces, simple improvements 0-81360
- gas desorption from solid, two diffusion mechanisms 0-92784
- glass, gas content determ. by dynamic extraction method 0-61219
- glow curves and desorption spectra anal. method 0-80053
- heavy-ion induced desorption of organic cpds. from solid surfaces 0-100739
- immiscible incompressible fluids, interfacial convective instability, diffusional exchanges, adsorption-desorption processes 0-70504
- LEP, electron positron storage ring, vac. chamber, glow discharge surface cleaning 0-58010
- metal, ion beam induced desorption of overlayers 0-59786
- metal surface, field desorption and field ionisation of Cs, H, and He 0-104047
- metal-H system, hydride formation in high press. range 0-65235
- metallic surface, catalysed thermal desorption and dissoc. processes, microscopic theory 0-75439
- metals, defect chemistry, He desorption spectrometry (*Dutch*) 0-96737
- metals and alloys, segregation studies by imaging atom probe microscopy 0-66911
- molecule desorption and surface diffusion from critical deposition rate 0-92786
- multilayer insulation materials, ambient temp. outgassing rate 0-84370
- multiphonon processes, quantum-statistical theory 0-107641
- p 0-80072
- porous material, outgassing, area/vol. config. influence 0-84371
- precursor intermediates in adsorption, desorption and reaction 0-108731
- proteins, on polymer surfaces, structural changes 0-89712
- pulsed surface flashover mechanism involving electron-stimulated desorption 0-70055
- refractory metals, heat of desorption of alkali metals 0-75430
- relaxation time approach limitations 0-93795
- solid surface, mol. dynamic processes interaction with laser radiation 0-71943
- solid surfaces, surface processes, and solid/gas interactions 0-73125
- steel, stainless, O₂ desorpt. during laser irradi., etching, AES study 0-66338
- steel, stainless, vacuum components, pre-vacuum surface finish influence on electron stimulated desorption in ultrahigh vacuum 0-57320
- surface, adsorbed atoms thermal desorption, one dimens. microscopic model, weak binding case 0-96729
- surface layers, photon induced ion desorption, surface atom core ionisation, Auger decay 0-59809
- surface processes, interatomic forces, theories 0-107632
- thermal desorption and dissociation catalyzed by a solid surface 0-108734
- thermal desorption mass spectroscopy, computer control, data acquisition, appls. 0-61181

desorption continued

- vacuum system construction material selection and degassing 0-82783
- valine surface, heavy-ion induced desorption of organic cpds. 0-100739
- Ag (110) surface, adsorption of mol. O₂ species 0-103578
- Ag, adsorption of pyridine, UPS, AES and flash desorption meas. 0-92776
- Al, thermal desorption of oxide film, influence of grain boundaries and recrystn. 0-61023
- Au film growth on Mo (110) surface, AES, LEED, thermal desorption study 0-80130
- BaTiO₃ polymorph, hexagonal, low temp. and surface CO₂ adsorption and desorption 0-80713
- Be film, on W (110), growth mode, work function, thermal desorption, and struct. 0-75477
- C/Pt-W (8 wt.%), desorption of K from C film surfaces 0-59784
- CdS-O₂, photoactivated O desorption 0-100391
- CdSe-O₂, photoactivated O desorption 0-100391
- CeNi₄Al, mag. susceptibility, H adsorption-desorption cycle effects 0-107990
- Co (0001), adsorption and reactivity of NO, LEED, AES, and thermal desorption study 0-80090
- Co, adsorption-desorption kinetics of CO, surface carbide form. effects 0-103574
- Cu surface, (110), methanol adsorption, XPS, UPS and thermal desorpt. study 0-84388
- Cu surface, fast D₂ desorpt. mechanism, time-of-flight spectra 0-84379
- Cu-Ni (110), adsorption of CO and H₂, UPS, thermal desorption, AES, and LEED study 0-80087
- CuO, desorpt. of ions by low power laser beam 0-80092
- D, thermal desorption meas. of H-isotope retention in Alcatraz-A Tokamak 0-79588
- DyFe₂ hydrides, desorption isotherms 0-103565
- DyFe₂H_x, thermodynamic props., H₂ desorption isotherm meas. 0-89516
- ErFe₂H_x, thermodynamic props., H₂ desorption isotherm meas. 0-89516
- Fe desorption of H into ultrahigh vac. system, using permeation cell 0-86326
- Fe surface, N atom recomb., vibr. energy of desorbing N₂, electron beam induced fluoresc. 0-61149
- Fe(100), of CO and H₂, C, O, S and K adlayer effects 0-71573
- GaAs (100), of Sb, AES obs. 0-80074
- GaP, adsorption and desorption of Cs, LEED, AES, and photoemission meas. 0-70532
- GaSb, adsorption and desorption of Cs, LEED, AES, and photoemission meas. 0-70532
- Ge (111) surface, clean, O₂ adsorption rate and electron work function 0-59779
- H from metal hydride beds, hydride conversion and storage system chemical heat pump 0-72077
- He desorption spectrometer, clustering of Kr in W (100) obs. 0-77908
- Ir, (111) surface, decomp. of hydrazine, N₂ emission, ang. depend. 0-97731
- Ir, adsorbed gases, field desorption from field ion tips 0-59793
- Ir, chemisorption of H₂, adsorption and desorption kinetics, struct. of overlayer 0-84367
- La_{0.5}Eu_{0.5}Ni_{4.6}Mn_{0.4}, absorption-desorption props. of H₂, degradation mechanism, Mossbauer study 0-88431
- LaNi₅ hydrides, of H₂, 4.2K paramag. susceptibility 0-70934
- MnO₂ coated Al₂O₃ and SiO₂ supports, N adsorption obs. of dispersion modes 0-81363
- Mo:C (110) surface, segregation, precip. and desorpt. of C, AES and LEED study (*French*) 0-103480
- Na atoms, desorbed, ang. and velocity distrib. 0-75428
- Nb, adsorbed H distrib., electron-stimulated desorption ion imaging 0-103572
- Ni (100), dissociative chemisorption and mol. adsorption of NO 0-65373
- Ni (100), interaction of adsorbed H₂, CO, and methanol, temp. programmed desorption study 0-66876
- Ni (100) and (110), reaction of acetylene, room temp., UPS expts. 0-61151
- Ni (111), chemisorption and reaction of NH₃, LEED, desorption and photoemission expts. 0-59799
- Pd (111), chemisorption of Cl₂, LEED, AES, thermal desorption, and work function meas. 0-75444
- Pd cluster, adsorption/desorption of CO, AES and thermal desorption meas. 0-75436
- Pd ribbon, of H₂, thermal desorption and work function meas. 0-70538
- Pd surface, fast D₂ desorpt. mechanism, time-of-flight spectra 0-84379
- Pt (100) (5×20) and (1×1) surfaces, stability and reactivity, adsorption of H 0-75434
- Pt (111), adsorption of NO, EELS, thermal desorption, LEED, and AES study 0-80086
- Pt (111), chemisorption of Cl₂, LEED, AES, thermal desorption, and work function meas. 0-75444
- Pt (111), interaction with water, thermal desorption, UPS, and XPS study 0-80088
- Pt (111) and Pt (S)-12(111)X(111) surfaces, adsorption of O, thermal desorption, AES, XPS, and LEED study 0-70534
- Pt, of Ar, gas surface interactions, 3-D generalised Langevin model appl. 0-107637
- Pt, of Xe, gas surface interactions, 3-D generalised Langevin model appl. 0-107637
- Pt, surface, (111), O₂ interactions, UPS, EELS and thermal desorption study 0-100409
- Pt surface, chemisorbed CO, IR refl.-absorpt. spectra, adsorbate island struct. 0-84385
- ²²⁶Ra desorption from sediments of Pee-Dee River-Winyah Bay estuary, effects on dissolved ²²⁶Ra 0-98360
- Re, adsorption, oxidation, and hydrogenation of CO, XPS, UPS, and thermal desorption study 0-71571
- Re surface, interaction with N₂⁺ beam, reaction dynamics studied by XPS and thermal desorpt. spectrometry 0-93797
- Re(0001), of O₂, CO, NO, and H₂O, XPS, UPS and temp. programmed desorption 0-71574
- Rh (111), chemisorption of water, effect of adsorbed O, H, or CO, LEED and thermal desorption meas. 0-75435
- Rh (111), co-adsorption of H₂ and CO segregation of co-adsorbed species 0-65361
- Ru (001), adsorption of CO, IR spectra, LEED, and thermal desorption meas. 0-70533
- Si, CVD from SiH₄-HCl-H₂ system, rate-determining reactions and surface species 0-84405

desorption continued

- SiO₂ films, desorption from Si single cryst., ellipsometric obs. 0-100410
 SrTiO₃ surface, oxidation and reduction by D₂O, H₂¹⁸O, D₂, isotope exchange study 0-104461
 Ti thin films, H absorption and desorption, Tokamak gettering, Auger electron spectrosc. 0-75092
 TiCo_{1-x}Mn_x, H absorption-desorption characteristics 0-96735
 TiO₂ suspension, adsorption-desorption of IO₃⁻ 0-93804
 V, dehydrogenation by annealing with Zr foils, internal friction meas. 0-96736
 W (100), condensation of Cu and Ag, early stage comparison with Mo(100) 0-80072
 W (100) and (111), O₂ electron stimulated desorption patterns, computer simulations 0-75443
 W (110) and (111) surfaces, KCl adsorption-desorption behaviour 0-75442
 W (110) stepped surface, electron stimulated desorption of O, atomic steps and defects influence 0-80091
 W (110) surface, adsorbed Pd, growth, struct., stability, desorption 0-59794
 W (111), angle-resolved photon-stimulated desorption of O⁺ 0-88434
 W, adsorbed gases, field desorption from field ion tips 0-59793
 W, adsorbed Hg, thermal desorption kinetics, theory 0-59792
 W, direct inelastic and trapping-desorpt. scatt. of N₂, elementary steps in N₂ chemisorpt. 0-60737
 W, of Cs-O₂ 0-103562
 W, polycryst. surface, heat of desorption of Cs 0-75430
 W, powder, gas adsorption and desorption (*Russian*) 0-75429
 W surface, (100), photon and electron stimulated desorpt. of O 0-100397
 W surface, adsorbed CO, electron-stimulated desorption, photoemission, relax. energy 0-100401
 W surface, electron-stimulated ion desorption of CO 0-59797
 W surface, polycryst., N₂ adsorption states 0-100404
 W(001), photon and electron stimulated desorption energy and angular distributions for O⁺ 0-96734

detection (demodulation) see demodulation**detector circuits**

- see also demodulation; demodulators
 ion cyclotron resonance signal, broadband detection 0-62792

detectors

- see also electric sensing devices; hydrophones; infrared detectors; micro-wave detectors; nonelectric sensing devices; particle detectors; photodetectors; ultraviolet detectors
 Brillouin ring laser, fibre-optic, use for inertial sensing 0-87411
 flaw detection system, noise immunity 0-104385
 gas chromatograph element-specific detection systems (*German*) 0-93837
 low-level gated oscillator, ion cyclotron resonance 0-86492
 optical radiation detector laboratory, graduate-level, expts. 0-62432
 position-sensitive detector, appl. to high pressure X-ray diff. using diamond-anvil cell 0-79632
 sensing techniques (*Japanese*) 0-73345
 shock wave, detonation wave propagation in shock tube, investigations on suitability of piezoelectric and magnetoelastic detectors (*Polish*) 0-79351
 O₂ analysis, electrochemical sensors 0-93816
 Si diode radiation detector, stabilisation of radiation damage 0-91377
 SnO₂-based gas sensors, resist. temp. depend. on exposure to CO, H₂, and propane 0-103694

determinants

- see also matrix algebra
 elastic shear waves propagation in fibrous composites 0-58963

detonation

- see also explosions; shock waves
 blast wave initiation and propagation of cylindrical heterogeneous detonation waves 0-74915
 deposition of coatings, monitoring method 0-60780
 ethylene-O₂-N₂-Al particle mixture, two-phase detonation and combustion (*French*) 0-61097
 gas mixtures, detonating, symmetric piston motion 0-59073
 nitromethane, DETA sensitized, steady state detonation vel., chemical inhomogeneity effect 0-89493
 slurry explosives, layered medium with liquid-polytropic gas structure, pressure pulse propagation 0-69872
 underwater charge, reflection of detonation wave from water surface 0-87628
 water, cavitation expts. using shock tube 0-87789
 wave magnification by pulsation energy 0-59075
 wave propagation investigations on suitability of piezoelectric and magnetoelastic detectors (*Polish*) 0-79351
 Ni coatings, detonation powder spray deposition 0-61028

deuterium

- adsorption and absorpt. on Zr, dissoci. and diffusion 0-80085
 alkali halide:D⁺, local modes and colour centre absorpt. bands, analogy 0-60632
 atom, 1S Lamb shift and 1S-2S isotope shift 0-91464
 atom, adsorption, on graphite (0001) surface, vibr. spectrum, at. beam scatt. obs. 0-92779
 atomic, Fermi fluid, stabilisation 0-100374
 atoms, ionisation by Nd laser radiation 0-70015
 backscattering from solid surfaces, positive charge fractions 0-66375
 chemisorption on SrTiO₃, oxidation and reduction, isotope exchange study 0-104461
 diffusion and permeation in stainless steel, ion beam meas. 0-59492
 diffusion coefficients in austenitic stainless steel, ion beam meas. technique 0-75382
 diffusion in BCC metals, phonon-assisted quantum-mechanical tunnelling of interstitials 0-59730
 diffusion in glassy and rubbery polymer films, isotope effect 0-84327
 diffusion in ion implanted Fe:Y, deep D traps 0-103372
 diffusion in Nb(V)(Pd), role of tunnelling, reson./nonreson. approaches 0-59718
 discharge lamps, influence of Ne and Ar on spectral parameters 0-86460
 dissolution of interstitial atoms in metals, diffusion coeffs., reverse isotope effect (*Russian*) 0-88368
 double quantum NMR in solids, magic angle spinning 0-108120
 gas, thermal cond. meas., 2-36 MPa 0-64668
 implantation of 5 keV D in BeO film 0-100268
 ion implanted in metal, interstitial positions and vibr. amplitudes, fast ion channelling study, review 0-79848

deuterium continued

- KBr(1):D, inelastic light scattering of localised vibration of interstitial H atom in alkali halides 0-88998
 laser isotope separation, large-scale, generalised concepts 0-68958
 metallic, ground-state energies of liq. and solid phases, variational and Monte Carlo methods 0-70502
 molecule, electron impact dissociation 0-83510
 molecule, IR spectra, mol. rot. and vibr. const. determ. 0-78617
 molecule, sticking and accommodation on low-temp. substrate, mol. beam expts. 0-84368
 muonic atom+Y, muon transfer mechanism from free muonic deuterium 0-69218
 NQR, Robinson scheme, electronics appls. 0-63668
 overbarrier states in metals, subsystem heat capacity, equilibrium props. (*Russian*) 0-79998
 oxidation on Pt, matrix isolation and laser fluoresc. obs. of prods. 0-66865
 paeonol and urinary metabolites labelled with ¹³C and D, synthesis and physicochem. props. 0-67250
 physisorbed monolayer on graphite, neutron scatt. studies 0-107655
 plasma, in ring cusp type mag. bottle, width meas. 0-87927
 in powders, high speed rot., spin diffusion, NMR spin lattice relax. obs. of D 0-66056
 pressure effect on width and shift of atomic fluorescence of TII 0-99475
 probe for investigating ultraslow rot. in solids 0-88890
 scattering from and selective adsorption on graphite (0001) surface 0-71553
 solid, room temp. melting point, press. depend. calcs. 0-103463
 solubility, in nonstoichiometric Pd₃P_{1-x} 0-59662
 solution in TiCr_{1.8}, enthalpy, solubility and mol. vibr. determ., comparison with soln. in metals and binary alloys 0-79951
 sorption at press. up to 1500 atm. on rare earth alloys, RM_x (M=Co, Ni) 0-97819
 thermal desorption meas. of H-isotope retention in Alcator-A Tokamak 0-79588
 universal abundance 0-62356
 uptake kinetics and energetics by Mn vacuum evaporated films 0-88430
 VUV radiation, narrowband tunable, at Lyman- α wavelength 0-78907
 β radiative atomic recombination, antiprotonic atoms 0-83527
 Ar⁺(²P_{1/2})+D₂, Ar⁺ two spin orbit state, reaction cross section, direct determ. 0-93748
 Ba⁺+D₂ \rightarrow D+BaD⁺, sequential impulse model, prod. bond dissoci. energy and cross section 0-81295
 Cds:D⁻, binding energy of D⁻ ion 0-92541
 D⁻ ion source for high voltage neutral beams for fusion reactors 0-99379
 D-T, liq., dielectric constant and elec. cond. 0-84680
 D+Ar(Kr)(Xe), ion pair formation, curve crossing model 0-87216
 D+Cl₂ 0-93734
 D+FD(FM), low barrier quantum model, vibr. deactivation on chemically reactive potential surfaces 0-69216
 D+H, close coupling calc., resonant spin-flip process, Ramsauer-Townsend effects 0-99547
 D+H₂, reaction, transition state theory calculations, kinetic isotope effect explanation 0-66784
 D+H₂, reactions, accurate pot. energy surface, isotope effects, quasiclassical trajectory study 0-97698
 D+H₂, rearrangement collision, vibr. excitation effects 0-71910
 D+H₂(HCl), relax. and chem. reaction, time resolved IR fluoresc. and mass spectrometry obs. 0-69177
 D+HX(H=Cl,I), HX dissociative ionisation, H⁺ signal origin, mol. beam obs. 0-66778
 D+PTFE, DF⁺ prod., Fourier transform IR spectroscopy 0-87105
 D+T₂, H-exchange studied by crossed molecular beam experiments 0-93747
 D+toluene(1,3,5-trimethylbenzene), vibrational and rotational energy effect 0-76497
 D⁺+atoms (Z=27 to 34), K shell ionisation, nuclear Coulomb effect 0-91650
 D⁺+CO₂, vibr. excitation, isotope and time effects 0-63773
 D₂, electron scattering, total cross section meas. at very low energies 0-58398
 D₂, rotational Raman intensities and polarisability anisotropy change meas. with internuclear distance 0-63641
 D₂⁺ implantation in Mo, radiation induced vacancies 0-65076
 D₂-Ne capillary-arc lamp, optimum parameters 0-95971
 D₂+Br⁺, total electron detachment cross sections for energies around threshold 0-99550
 D₂+CH₄⁺, isotopic exchange, interstellar implications 0-61087
 D₂+CO⁺, state selected reaction cross-sections, coincidence technique obs. 0-66797
 D₂+Cl⁺, total electron detachment cross sections for energies around threshold 0-99550
 D₂+D₂, ladder operators in vibr.-vibr. and vibr.-translational transitions at high collisional energies 0-106382
 D₂+F, absolute rate coeffs. at 295 to 765K 0-81303
 D₂+F, rate consts., temp. depend. 0-81302
 D₂+H reaction, transition state theory calculations, kinetic isotope effect explanation 0-66784
 D₂+H reactions, accurate pot. energy surface, isotope effects, quasiclassical trajectory study 0-97698
 D₂+H₂⁺ \rightarrow D₂H⁺+H, product angular and vel. vector distributions meas. by crossed beam expt. 0-101012
 D₂+H⁺, collisional complex form. 0-58339
 D₂+HCl, HCl ν_2 - ν_1 band perturbations, linewidth and shifts calcs., IR spectra obs. (*French*) 0-58251
 D₂+HD(De)(Ar), state-resolved $\Delta j=2$ rot. transitions 0-63772
 D₂+Li⁺(²P_{1/2}), collision induced quenching and transition rate coefficients meas. 0-74221
 D₂+Ne, anisotropic potentials, direct inversion methods calcs. 0-69090
 D₂+Ne(Ne⁺), energy-loss scaling in 0.5-3.5 keV 0-63768
 D₂+Ni⁺, endothermic reactions, investig. 0-97692
 D₂+Y, high temp. equilb. meas. 0-66780
 D₂, emission spectra, rot. struct. obs. mol. const. determ., predissociation 0-106331
 D₂, Rydberg states, spectroscopic B₀ consts. 0-74109
 D₂⁺, IR spectrum, vibr.-rot. assignment 0-95627
 D₂⁺, rot.-vibr. spectrum, ab initio calcs. 0-95595
²D₂, compressed fluid, vibrational population relaxation time obs. 0-69219
 D⁺⁺+N₂ fast collisions, impulse approx. 0-106281

deuteron continued

- n-GaAs:D, ion implanted, carrier removal, capacitance-voltage profiling 0-84195
 H+D₂, collinear motion, energy transfer and dissociation, collision dynamics 0-99563
 H₂-D₂ gas, thermal cond. meas., 2-36 MPa 0-64668
 H₂-D₂ isotope separation by permeation through Pd membrane 0-68959
 HF+H₂(D₂)(N₂), 200K and 295K vibr. relax. rates 0-63766
²H-³H fuel pellet electrostatic injection (*Japanese*) 0-78434
²H-³H ionised plasma, fast α particle energy deposition, transport eqn. 0-100071
 Li-D equation of state under extreme conditions, solid state to plasma region 0-69976
 Mo-D, trapping of D and mutual replacement 0-59493
 Ne+D₂, anisotropic inversion pot., rot. inelastic cross sections 0-78696
 Ne+H⁺(D⁺), electron detachment, dynamical phenomenon 0-106305
 O₂+He(D₂)(H₂), vibr. relax. rate consts. 0-74231
 p-D₂, solid, slow neutron scatt. into external radiation field (*Russian*) 0-59348
 Ti:D, implanted, deuteride imaging using scanning Auger spectroscopy 0-89092
 Ti:D, implanted, nucleation and growth of TiD₂ 0-97717
 Ti:D, ion implanted, depth profiles, temp. depend. 0-100270
 Zr-He, implanted, superconductivity enhancement obs. 0-70884

deuteron compounds

- see also heavy water
 β -Al₂O₃·D₂O, anhydrous, prep. and struct. of DA₁₁O₁₇ 0-107187
 β -Al₂O₃·D₂O, neutron diff. obs. of struct. 0-107512
 DBF₂, harmonic force field and ground-state average struct. determ. 0-83342
 DBR+F, H abstraction reactions, temp. depend., laser photolysis IR fluores. obs. 0-93744
 DCN waveguide lasers, optimised 190/195 μ m, amplifying medium characts. 0-99709
 DCl, plastic cryst. phase, struct. and dynamics 0-92469
 DCl+CO, V-V energy transfer 0-78695
 DF chemical laser, small-scale CW, operation 0-58528
 DF chemical lasers, high-performance dichroic beam splitters 0-95932
 DF laser, phase conjugation of 4 μ m for single line and multiline radiation in Ge 0-83641
 DF TEA laser, He-free, with MW output 0-64060
 DF, vibr. relax., isotope effect, quantum model 0-91460
 DF-CO₂ chemical laser, photon branching in chain reactions, IR radiation initiation 0-91785
 DF-CO₂ chemical laser, amplification of long and short pulses 0-95883
 DF-HBr CW optical resonance transfer laser 0-64003
 DF* prod. from D+PTFE, Fourier transform IR spectroscopy 0-87105
 DNF₂, photoelectron spectra, vibr. struct. obs, ionisation pot. determ., ab initio calcs. of ionic geometry 0-83418
 DNSO, IR spectra obs., mole. vibr., anharmonicity constant determ. 0-83357
 D₂O laser, 66 μ m, with unstable reststrahlen resonator 0-83619
 D₂O, models of bond distribution functions, anharmonicity effects on electron diff. pattern 0-69234
 D₂O, vibr. relax. rates 0-95717
 D₂O+H₂O⁺(H₂O)_n, binary reactions, rate coeffs. and product ion distributions determ. 0-81305
 D₂O+U⁺(UO⁺), reaction cross-sections, ion beam apparatus study 0-97691
 DOD, vibr. intensities, ab initio and empirical calcs. 0-78592
 DOD, vibr. intensities, ab initio and empirical calcs., band strengths 0-78593
 D₂O⁺(D₂O)_n+H₂O(NH₃), binary reactions, rate coeffs. and product ion distributions determ. 0-81305
 D₂O⁺(H₂O)_{0.1-1}+H₂O reactions, SIFT studies, review 0-58435
 D₂O·ClO₄, solid, neutron powder diff. study 0-107176
 D₂S, photodissoc., SH internal energy distribution 0-95697
 D₂S+K, collisional ionisation, positive and negative ion energy spectra obs. 0-63775
 DT, vibr. rot. Raman anal. 0-87126
 HCl-DCI mixed crystals, ferroelec. transition, ³⁵Cl NQR study 0-71233
 HF-DF simultaneous laser excited by ferroelec. ceramic capacitatively coupled discharge 0-69413
 TiD₂PO₄, antiferroelectricity, permittivity, electric field double hysteresis loops 0-60512

deuteron effects

- steel, austenitic stainless, type 316, irradi. induced creep 0-93606
 steel, stainless, retention and re-emission of 0.125-1 keV D⁺ ions 0-66349
 CdCr₂Se₄Ag, magneto-optical effects in impurity spectral region 0-97313
 GaAs device isolation with deuteron bombardment 0-75248
 Ni, creep, irradi. induced with 17 MeV deuterons 0-93607

deuteron interactions see deuteron-nucleus reactions; hadron-deuteron interactions; lepton-deuteron interactions; meson-deuteron interactions; photon-deuteron interactions; proton-deuteron interactions

deuteron-nucleus reactions

- for inelastic deuteron-nucleus scattering, see 'deuteron-nucleus scattering'
 see also nuclear fusion
⁵⁶Co particle-hole states, T=1, zero DWBA anal. 0-78308
 deformed tensor interactions, folding model 0-57783
 emulsion nucleus+deuteron, 9.38 GeV/c, nucleon stripping probability and charged particle multiplicity 0-78306
 light relativistic ion-target interactions, particle emission 0-102193
 nucleus-nucleus total cross section energy depend. 0-106071
 (d,⁶Li), A=144-238, alpha-cluster transfer from alpha-decaying nuclei 0-91166
 (d,⁶Li), A~60,116, L=0 transitions, cross sections, microscopic anal. 0-78189
 (d,p), composite particle scatt. breakup mechanism 0-83105
 (d,p), role of $\Delta N=2$ interaction, differential cross sections, DWBA anal. 0-91189
 (d,t), deep hole states observed in particle transfer reactions 0-68511
 (d,t), role of $\Delta N=2$ interaction, differential cross sections, DWBA anal. 0-91189
 n-p potential form, influence on differential cross-section of d break-up (*Russian*) 0-78173
[^]Si(d,X), A=112, 124, 7.6 GeV/c, isotopic cross section ratios, He, Li fragments isotopic effects (*Russian*) 0-63154

deuteron-nucleus reactions continued

- ²Al(d, α)²⁵Mg, nuclear microanalysis of Al impurities in Si epitaxial layers 0-61193
²Al(d,pX) 80 MeV, inclusive proton spectra, d break-up, DWBA anal. 0-91190
¹⁹⁷Au(d,f), 80 MeV, post neutron emission fission products 0-83136
¹⁹⁷Au(d,pX), 80 MeV, inclusive proton spectra, d break-up, DWBA anal. 0-91190
¹⁰B(d,p)¹¹B, 2.5 to 21.0 MeV, angular distrib., DWBA analysis 0-68675
⁹Be(d,n)¹⁰B use of neutrons for meas. of full cross sections (*Russian*) 0-69008
²¹⁰Bi^m(d,t), 17 MeV, ²⁰⁹Bi levels and spectroscopic factors, ²¹⁰Bi(9⁻) parentage 0-78158
¹C(d,X), 4.2 GeV/c, multitudes of secondary negative particles, momentum distrib. ratios (*Russian*) 0-63178
¹²C(d,p)¹³C, 0.5 to 2.5 MeV, excitation functions and angular distrib., possible doorway state (*Chinese*) 0-68679
¹³C(d,³He), isospin violating direct reaction, Coulomb interaction role 0-102170
¹³C(d,t), isospin violating direct reaction, Coulomb interaction role 0-102170
¹³C(d,p), 2.7 MeV, ¹⁴C first excited 0⁺ state, lifetime and E⁰ decay 0-102145
⁴⁰Ca(d,p), 4.5-5.4 MeV, ⁴¹Ca excited states, excitation functions and ang. distrib., statistical anal. 0-57686
⁴⁰Ca(d,p_γ), 2.01 MeV, ⁴¹Ca parity doublet gamma lifetimes, 3/2 levels, parity mixing 0-78209
⁴Ca(d, α), pol.d, 7.5-9.0 MeV, ⁴⁶K levels, J^π and tensor anal. powers 0-102113
⁴⁸Ca(d,n), 20 MeV, ⁴⁹Sc proton single particle states, spectroscopic factors, DWBA anal. 0-99118
⁶³Cu(d,X), 247 MeV, ⁶⁶Zn* composite particle emission, ang.-distrib., exciton-coalescence model 0-78265
 (d,X), neutron excess isotope prod. in fragmentation, ^{6,8}He, ^{7,8,9,11}Li (*Russian*) 0-86888
 DY(d,t), [^]Dy, A=161, 163, Nilsson state $\Delta N=2$ mixing, rot. bands 0-95295
[^]Dy(d,t), A=162, 164, coupled-channels Born approx. anal. 0-83104
 Dy(d,p), [^]Dy, A=161, 163, Nilsson state $\Delta N=2$ mixing, rot. bands 0-95295
[^]Er(d,t), A=166, 168, coupled-channels Born approx. anal. 0-83104
¹⁵²Eu(d,p), 20 MeV, ¹⁵³Eu 5/2⁺ ground state rot. band, J^π, shape coexistence 0-86799
¹⁵²Eu(d,t), 20 MeV, ¹⁵¹Eu narrow band and pickup strength shape coexistence 0-86799
⁵⁶Fe(d, α), pol.d, 7.5-9.0 MeV, ⁵⁴Mn low lying 2p-4h states, J^π from tensor anal. powers 0-99124
¹⁶⁰Gd(d,t), ¹⁵⁹Gd, coupled-channels Born approx. anal. 0-83104
 H(d,X), x=p,n, ⁴He continuum microscopic calcs. cross sections and levels 0-57702
²H(d,n), 18-26 MeV, differential cross sections, ang. distrib., ⁴He broad level search 0-102117
²H(d,n), pol.d, anal. power and polarisations in R-matrix methodology, comparison with (d,p) 0-78273
²H(d,p), pol.d, anal. power and polarisations in R-matrix methodology, comparison with (d,n) 0-78273
³H(²H,n)⁴He, chain carriers in fusion reaction kinetics 0-86969
³H(d,n)⁴He, neutron fluence and energy transfer standard 0-102194
⁶Li(d,X) system, resonating group method, single channel approx., cluster states 0-57782
⁶Li(d, α), 1.2-8 MeV, ⁸Be high spatial symmetry excited states, resonances, rot. band 0-86780
⁷Li(d,t), 12 MeV, ⁷Li- α virtual decay vertex constant 0-78231
[^]Mg(d,⁶Li), 80 MeV, A=24,26, α -spectroscopic factors and ang. distrib., DWBA anal. 0-99126
¹⁴N(d, α), pol.d, 1.5-3 MeV, vector anal. capacity for two α -particle groups 0-78266
⁹⁹Nb(d,pX), 80 MeV, inclusive proton spectra, d break-up, DWBA anal. 0-91190
¹⁴⁴Nd(d,p), 12.1 MeV, ¹⁴⁵Nd energy levels, DWBA calcs. 0-68533
¹⁴⁶Nd(d,p_γ), 10 MeV, ¹⁴⁷Nd low spin states ns lifetimes, particle rotor model interpretation 0-78207
¹⁴⁶Nd(d,t), 12.1 MeV, ¹⁴⁵Nd energy levels, DWBA calcs. 0-68533
 Nd(d,t), 17 MeV, [^]Nd, A=145, 147, 149, single neutron hole states spectroscopic factors, DWBA anal. 0-78109
²⁰Ne(d,pol.p), 10 MeV, ²¹Ne deduced spectroscopic factors, levels and anal. powers 0-83087
[^]Ni(d,X), A=58, 64, 7.6 GeV/c, isotopic cross section ratios, He, Li fragments isotopic effects (*Russian*) 0-63154
¹⁶O(d,X), X=d or n, elastic scatt. and stripping, three body calc. 0-91165
²⁰⁸Pb(d,p), tensor analyzing power, deuteron wave functions 0-99137
²⁸Si(d,p), ²⁹Si rot.-vibr. coupling effects, excitation spectrum and ang. distrib. 0-57661
²⁸Si(d,p), ²⁹Si 3/2⁺ and 5/2⁺ states population, (p, π^+) comparison 0-95307
²⁸Si(d,pn), ²⁹P and ²⁹Si nucleon unbound states, spin, parity, partial width 0-102118
²⁸Si(d,pol.p_γ), ²⁹Si, low lying energy level structure, multi-step reaction calcs. 0-68537
²⁸Si(d,p), 1.1-2.1 MeV, excitation functions, statistical fluctuations anal. 0-95322
¹⁴⁴Sm(d,p), ¹⁴⁵Sm primary γ -rays, direct capture and neutron separation energy, (n, γ) correlation 0-57738
 Sn(d,⁶Li), Cd 2₁⁺ excitation, α -spectroscopic factors in IBA model 0-105967
¹⁸¹Ta(d,X), 4.2 GeV/c, multitudes of secondary negative particles, momentum distrib. ratios (*Russian*) 0-63178
¹²⁶Te(d,t), 17 MeV, ¹²⁵Te low lying negative parity high spin states multistep induced population 0-57657
 Te(d,⁶Li), Sn 2₁⁺ excitation, α -spectroscopic factors in IBA model 0-105967
²³⁵U(d,f), ²³⁵Np fission lifetime meas. 0-63216
²³⁵U(d,p), 11 MeV, ²³⁶U shape isomer, γ branch upper limit, γ -yields 0-99145
²³⁵U(d,pf), ²³⁶U isomeric and prompt fission, nuclear superfluidity evidence 0-68711
²³⁵U(d,pf), 17-25 MeV, ²³⁶U^m isomeric to prompt fission ratios; fission fragments 0-86940
 U(d,pnf), 17-25 MeV, ^{236,238}U^m isomeric to prompt fission ratios; fission fragments 0-86940

deuteron-nucleus reactions continued

- ⁹¹Zr(d,³He), 24.3 MeV, ⁹⁰Y low lying multiplets, DWBA anal. for spectroscopic factors 0-57685
⁹¹Zr(d,p), pol. d, 12 MeV, ⁹²Zr levels, J^π, cross sections, vector anal. power, optical parameters 0-78268

deuteron-nucleus scattering

- deformed tensor interactions, folding model 0-57783
 optical model analyses (*German*) 0-68676
 (d,d), A=27-238, 12-90 MeV, global optical model pot. 0-78305
 (d,d), pol. d, 56 MeV, A=16-208, cross sections, optical parameters, anal. powers 0-78270
 (d,d), pol.d, 52 MeV, A=12-197, vector anal. power and optical parameters 0-57764
 (d,d) medium heavy nuclei, optical model anal., cross sections, anal. powers 0-73839
 (d,d'), A=40 to 208, 108 MeV, giant monopole resonance excitation and ang. distrib. 0-102164
⁷H(d,d), 5-45 MeV deuteron wave function asymptotic D- to S-state normalisation, anal. power 0-78304
¹²C(d,d'), isospin violating direct reaction, Coulomb interaction role 0-102170
¹²C(d,d), 1.69 GeV/c, Coulomb interference region, Glauber theory anal. 0-99178
⁴⁰Ca(d,d), 4.5-5.4 MeV, excited states, excitation functions and ang. distrib., statistical anal. 0-57686
 (d,d), A=24-54, pol.d, 20 MeV, quadrupole transition amplitudes 0-99148
²H(d,d), ⁴He continuum microscopic calcs. cross sections and levels 0-57702
⁴He(d,d), distortion effects, orthogonality condition model 0-63190
⁵⁸Ni(d,d'), 10 MeV, diff. cross sections and d-γ ang. correlations, multi-shell coupled channel calcs. 0-83064
 Ni(d,d'), 13-80 MeV, second order breakup corrections in DWBA 0-86910
¹⁶O(d,X), X=d or N, elastic scatt. and stripping, three body calc. 0-91165
²⁰⁸Pb(d,d'), 86 MeV, giant monopole and quadrupole resonances, multipole excitations 0-106031
⁸⁴Se(d,d'), A=76,78,80,82, 12 MeV, two-step scatt. process via J^π=2₁⁺ excited states 0-57781
⁹¹Zr(d,d), pol. d, 12 MeV, ⁹²Zr levels, J^π, cross sections, vector anal. power, optical parameters 0-78268

deuteron photodisintegration

- γd→np, 300 MeV, dibaryon resonance manifestation, pseudoindependent amplitude elimination (*Russian*) 0-57612
 γd→np, 400-650 MeV, proton polarisation and possible dibaryon resonances 0-105908
 γd→pn, proton polarisation energy depend., 400-700 MeV (*Russian*) 0-63000
²H(γ,n), 20.3 MeV, linearly pol. γ, neutron yield and cross section 0-91171
²H(γ,n)¹H, 400-700 MeV, p polarisation (*Russian*) 0-106046
²H(γ,n)p, 375-650 MeV, proton polarisation energy depend. at CMS angle 90° (*Russian*) 0-63159
²H(γ,n)p, parity violation expts. review, weak NN interaction 0-73792

deuteron polarisation

No entries

deuteron scattering see *deuteron-nucleus scattering; hadron-deuteron scattering; lepton-deuteron scattering; meson-deuteron scattering; photon-deuteron scattering; proton-deuteron scattering*

deuterons

- see also *cosmic ray deuterons*
 D-state probability, three lower bounds 0-102129
 form factors and spectroscopic factors in heavy spherical nuclei, shell model (*Russian*) 0-63078
 gluon distribution from elastic dd scatt. 0-82939
 hidden colour and the isobar content of the deuteron 0-102024
 relativistic heavy ion collisions, d prod. mechanism, three models, fireball rate eqns. 0-63198
 relativistic nuclear collisions, p, d, and t inclusive energy spectra 0-63199
 wave functions from ²⁰⁸Pb(d,p) tensor analyzing powers 0-99137
⁷H(d,d), 5-45 MeV deuteron wave function asymptotic D- to S-state normalisation, anal. power 0-78304
²H D-state probability lower bound, binding energy, quadrupole moment 0-91137
²H(p,2p)n, 22.7 MeV, proton analysing power 0-78302

developers (photographic) see *photographic materials*

development, photographic see *photographic process*

development management see *research and development management*

diagnosis, patient see *patient diagnosis*

diagnostics, particle beam see *particle beam diagnostics*

diagnostics, plasma see *plasma diagnostics*

diagrams

see also *Feynman diagrams; nomograms; phase diagrams*

multicomponent impedance diagrams for electrochem. cells, resolution technique 0-66959

dialogue systems see *interactive systems*

diamagnetic properties of substances

- see also *de Haas-van Alphen effect; diamagnetism*
 4-cyanobenzoyloxy-4'-pentylstilbene, nematic, smectic A, and orthogonal smectic B phases 0-64890
 diamagnetism with quasilinear dispersion law, orbital susceptibility, valence bands (*Russian*) 0-80475
 mesophase pitch, magnetically-oriented, phys. props., mol. struct. 0-64885
 organic liquids, diamagnetism, mass mag. suscept. meas., temp. depend. 0-97054
 semiconductor, tetrahedrally coordinated, temp. depend. of diamagnetic susceptibility (*Rumanian*) 0-88717
 semiconductors, glassy, diamag., photostructural changes, mechanism 0-92557
 thermoelectret and magnetoelectret states, diamag. anisotropy 0-97053
 (TMTSF)₂PF₆, quasi-dimens. cond., diamagnetic AC susceptibility 0-103781
 Ag, mag. susceptibility, Animalu model pot. calc. 0-75711
 Ag-S(Se)(Te), liq., mag. susceptibility meas., electron localisation and chem. bonding 0-60178
 Al, dynamic susceptibility, model pot. theory 0-75710
 Au, mag. susceptibility, Animalu model pot. calc. 0-75711

diamagnetic properties of substances continued

- CS₂, liq., diamagnetism, mass mag. suscept. meas., temp. depend. 0-97054
 CdS, flux exclusion, superconductivity at high temp. 0-97058
 Cu, dynamic susceptibility, model pot. theory 0-75710
 Cu, mag. susceptibility, Animalu model pot. calc. 0-75711
 CuCl, interface supercond., piezoelec. hypothesis 0-60128
 n-CuInS₂, mag. props., obs. 0-70939
 Cu_{2-x}Se, nonstoichiometric, diamag. and paramag. props., susceptibility meas. 0-70936
 Fe(Sb_{1-x}Te_x), system cpds., prep., cryst. struct., elec. and mag. characteristics 0-108349
 In-Se(Te), liq., mag. susceptibility meas., electron localisation and chem. bonding 0-60178
 Li₂₃Si, cryst. struct. and electrochem. anal. (*German*) 0-88132
 NbSe₃, superconducting transitions and diamagnetism 0-84526
 PbTe:In, mag. susceptibility, temp. depend., 4.2 to 200K 0-65773
 Ru₂Ge_{3-x}Sn_x, and Ru₂Ge_{3-x}Si_x, diffusionless phase transitions, elec. and mag. props. 0-96871
 Sn-Se(Te), liq., mag. susceptibility meas., electron localisation and chem. bonding 0-60178
 TaSe₃, superconducting transitions and diamagnetism 0-84526
 ZnF₂:Co²⁺, Raman tensor calcs. of isolated impurity in diamagnetic matrix 0-76025

diamagnetic resonance see *cyclotron resonance*

diamagnetism

- see also *cyclotron resonance; de Haas-van Alphen effect; diamagnetic properties of substances*
 band structure diamag., first principles calc. 0-88470
 Bloch electrons, nonlinear orbital magnetisation in weak mag. fields (*Russian*) 0-70931
 domains, diamag., study by positive muon method 0-60174
 electron gas, diamagnetism and surface currents 0-88496
 exciton, Bose condensation and superdiamag. current prod. possibility 0-65456
 graphite, diamagnetism with quasilinear dispersion law, orbital susceptibility, valence bands (*Russian*) 0-80475
 metal film, size effect in Landau diamagnetism, surface pot. effect (*Russian*) 0-93012
 polarisation and magnetisation of electronic matter 0-75929
 sphere, strongly magnetised, interaction with weakly magnetised particles carried by fluid flow 0-69320

diameter measurement

- bubbles, acoustical meas. of gas bubble volumes and gas flow rates 0-62633
 cell membrane particle diameters meas. by computer from electron micrographs 0-101307
 cylindrical products, interfering factors elimination 0-77755
 cylindrical surface two-wavelength speckle pattern intensity distrib. at optical transform plane 0-106487
 electro-optical instrument for hole-diameter meas. 0-98882
 glass micropipettes, comparative calibration by optical microscopy and SEM (*German*) 0-98201
 glass tubing dia. and wall thickness meas., P-329M instrum. 0-86262
 isolated surface circular defect diameter determ. based on Fraunhofer diffr. 0-73307
 laser bar gauge for diameter measurement of hot or cold objects 0-105605
 laser beam diameter meas. using a grating 0-102745
 laser scanned gauge (*Chinese*) 0-77756
 optical fibre diameter measurement using fast Fourier transform 0-91894
 optical fibre preform core diameter and Ge doping profile meas., X-ray nondestructive method 0-64231
 pore size measurement, comparison of methods 0-62622
 projected inertial confinement fusion reactor target evaluation by buoyancy analysis 0-78442
 small holes, optomechanical instrum. 0-77750

diamond

- accelerator irradiation, heavy ion irradiation damage 0-100291
 bolometer, Ge-diamond, operated at 4.2, 2.0, 1.2, 0.3, 0.1K, design and construction 0-77868
 coatings, for increased wear resist. 0-76371
 compressibility, appl. of Murnaghan eqn. of state, Morse pot. 0-79861
 Cosserat continuum model, elastic props., lattice dynamics 0-59552
 defect electronic struct. and lattice config., MO approaches 0-65495
 diamond:Li, electron transport character 0-92917
 diamond:Sb, implanted, radiation damage and annealing study 0-100263
 diamond, vacancy enhanced N aggregation, electron irradiation effects IR spectra 0-70245
 diamond-anvil press, cell for photoluminescence meas. 0-108256
 diffuse reflectance Fourier transform IR spectroscopy using diamond anvil cell 0-101855
 dislocation growth degree of supersaturation determ. 0-88145
 effective ion interaction and force const., model of Si point defect 0-65185
 electron channelling radiation comparison with coherent stopping radiation (*Russian*) 0-103403
 electron irradiated, photochromism 0-71454
 etch-pit formation on cube faces, electron microscopy obs. 0-75232
 four-wave mixing spectroscopy in crystals, nonlinear spectroscopy developments 0-91861
 GRI band, anal. of satellite lines by quadratic Jahn-Teller coupling 0-97295
 graphite-diamond, shock induced transform. anal., post shock graphitisation 0-79933
 half wavelength and stopping power of planar channelled protons 0-65087
 homogeneous formation in gas phase, laser beam effects (*Russian*) 0-104052
 industrial, anal. cathodoluminesc. studies in SEM 0-81410
 ion channelling and dechannelling meas. 0-65090
 Jahn-Teller coupling at neutral vacancy 0-71453
 lattice dynamics, valence force field, rel. to tensor force const. 0-79888
 light coupling prism, Raman spectra for thin film props. study 0-88978
 light ion damage, channelling investigation 0-65068
 Mossbauer spectroscopy of defects, radiation damage and deep levels 0-59533
 origin, role of C in Earth upper mantle 0-81845
 polycrystal, sintered under ultra high press., binary inclusion content effect on thermal stability (*Chinese*) 0-66453

diamond continued

- powder, consolidation by thermal decomposition of methane and benzene 0-66448
 powders, Mo coated, X-ray diffr. study 0-100936
 proton channelling, transverse energy evolution in planar channels, computer simulation 0-79849
 quasiparticle states, quantitative calc. 0-88499
 radiation dosimeters, evaluation 0-78456
 section topograph technique, high resolution, applicable to synchrotron radiation sources 0-57449
 sintering of a polycryst. diamond with Ni additives under ultrahigh pressures 0-84870
 solid thermal cond. and interface resistance meas. by radiation thermometry 0-86289
 sound excitation orientational effect due to channelled electrons 0-84254
 structure transformation from graphite probability under high temp. and press. (*Chinese*) 0-65220
 surface, polished, RHEED pattern 0-65345
 synthesis (*Japanese*) 0-80994
 synthesis by graphitisation of carbon materials at high press. and temp., Ni influences 0-60795
 synthetic, oxidized in fused salts, etch features 0-97604
 synthetic, polarised IR cathodolum. 0-89073
 synthetic diamond drills, improved durability 0-87573
 synthetic high strength material structures, mechanical strength, microstress levels (*Russian*) 0-76334
 synthetic monocrystals, inclusions phase comp., radiographic method 0-100978
 synthetic powder, thermal cond. 0-96702
 thermal conductivity, high temp., electron irradi. effects 0-65318
 three-body abrasive wear with small size diamond abrasives 0-76373
 tool bit machining, comparison with conventional optical process 0-69569
 turned surface production, interferometric test repeatability 0-74538
 turning precision machine tool system 0-69568
 two-phonon bound state, Raman freq. 0-65179
 Type I from Arkansas, Ar isotopic composition 0-94493
 ultradisperse, ESR, particle size and lattice microdistortions 0-97140
 uniaxial stress splitting of E to E transitions at trigonal centres in cubic crystals 0-97312
 van Hove singularities, absorpt. and luminesc. electronic-vibr. spectra 0-70639

diaphragms

- see also valves*
 laser cavity diffraction experiment with 1-D diaphragm 0-95920
 loudspeaker's, composite, B-Ti, preparation by physical vapour deposition (*Japanese*) 0-58883
 Si diaphragm pressure sensor, integrated signal conditioning 0-76859

dichroism

- see also magnetic circular dichroism; pleochroism*
 absorbing anisotropic and gyrotropic slab between crossed polarisers, transmitted intensity patterns 0-78762
 acetaldehyde, dichroic effects, computational expts. 0-83424
 p-alkoxybenzylidene-p-n-butylanilines, IR absorpt. spectra, elec. field effects, orientational order parameter determ. by IR dichroism 0-80778
 p-alkoxybenzylidene-p-aminocyananilines, IR absorpt. spectra, elec. field effect, orientational order parameter determ. by IR dichroism 0-80777
 ATPase, Ca^{2+} -activated, of sarcoplasmic reticulum, rot. motion and evidence for oligomeric struts. 0-72124
 trans-1,4-chlorobromocyclohexane, liq. crystalline and amorphous state, conformation and vibr. spectra, IR obs. 0-60568
 trans-1,4-chloriodocyclohexane, liquid, crystalline and amorphous state, conformation and vibr. spectra, IR obs. 0-60568
 cholesteric films, absorpt. and contrast in dichroic liq. cryst. displays 0-75155
 chromophore aggregates in Frenkel exciton model, dynamic perturbation effects on circular dichroism intensity 0-93273
 cyclic ketones, electrochromism and electric dichroism for studying transitions to second excited singlet 0-63692
 differential absorption at high modulation frequencies using a Fourier transform infrared spectrometer 0-95160
 dimethylammonium cadmium tetrachloride, far IR refractive index, extinction coeff. and dichroism obs. 0-66144
 disperse system, dilute, orientationally induced conservative dichroism 0-102623
 DNA, dye labelled elec. dichroism and birefringence, comparison with mol. props. from polarised fluoresc. 0-84785
 DNA, Hg (II) and Ag (I) complexes in soln., theoret. interpret. of elec. dichroism obs. 0-85347
 DNA, linear dichroism in pulsed elec. field, meas. apparatus 0-90875
 EBBA, IR absorpt. spectra, elec. field effects, orientational order parameter determ. by IR dichroism, bend elastic consts. 0-80778
 EBBA, orientational order in glassy and nematic phases, IR dichroism meas. 0-64891
 electric dichroism measurement instrument with digital processing 0-82800
 electronic spectra of molecules, pure elec. quadrupole transition polaris. 0-63691
 ethylenediamine sulfate, cryst., induced gyrotropy of CrO_4^{2-} ion 0-108175
 ferroelectric, large-gap type, vibronic theory and opt. props., anomalous bulk photovoltaic effect 0-103939
 free particle on helix, light circular dichroism and optical rotation, theoretical anal. 0-66146
 graphite, suspensions, particle shape influence on light absorpt. in mag. field 0-60549
 isotropic medium, moments of optical rotary power and circular dichroism 0-88956
 linear dichroism in pulsed elec. field, meas. apparatus 0-90875
 linear dichroism meas. over large wavelength ranges 0-98962
 liquid crystal matrix, orientational distrib. coeffs. from UV and circular dichroism meas. 0-92452
 magnetic colloids, birefringence and dichroism, magnetically-induced, sign inversion 0-60548
 magnetic fluids, optical birefr. and dichroism in mag. field 0-60547
 MBBA, IR absorpt. spectra, elec. field effects, orientational order parameter determ. by IR dichroism, bend elastic consts. 0-80778
 MBBA, orientational order in glassy and nematic phases, IR dichroism meas. 0-64891
 Orientational optic effects from above Rayleigh particles 0-106453

dichroism continued

- 2-oxiphenylbenzoxazol, proton intramolecular transfer, light absorpt. and emission, dichroism, polarised fluoresc. 0-87166
 partially oriented molecules, uniaxial, two-photon processes, polarised spectrosc. 0-74209
 photodichroic spatial light modulator for joint Fourier transform correlation 0-106617
 polymer film, proton intramolecular transfer, light absorpt. and emission, dichroism, polarised fluoresc. 0-87166
 polynucleotide solution, elec. field induced orientation and effects 0-85348
 N-p-propoxybenzylidene-p-pentylaniline, orientational order in glassy and nematic phases, IR dichroism meas. 0-64891
 purple membrane fragment suspensions, elec. dichroism obs., trimer model interpret. 0-89728
 silicate glass surface, photodichroic for laser recording 0-102785
 solid-state circular dichroism spectra, phase modulation spectrosc. obs. 0-93271
 solute orientation in stretched polymer matrix, dichroism anal. 0-75998
 solutes in stretched polymers, linear dichroism methods for analysis 0-63693
 suspension of absorbing particles, simultaneous meas. of dichroism and birefringence in elec. field, photocurrent signal obs. 0-82801
 vacuum UV circular dichroism spectroscopy using synchrotron radiation 0-91575
 vibrational circular dichroism in the mid-infrared 0-87157
 X-irrad., optical absorpt. spectra and dichroism meas. 0-108239
 Ag halide photochromic glasses, optical absorpt. of Ag, optically induced dichroism 0-108177
 Ag halide thin-film optical recording medium 0-102786
 BaMnF_6 , struct. phase transition, optical parameters obs. 0-100328
 BaTiO_3 , vibronic theory and opt. props. 0-103939
 CaF_2 :Ni, X-irrad., optical absorpt. spectra and dichroism meas. 0-108239
 CoCO_3 , weakly ferromag., light absorpt. dichroism and mag. config. 0-66223
 Cr complex, $(-\text{D})$ -tris(ethylenediamine) chromium (III), solid-state circular dichroism spectra, phase modulation spectrosc. obs. 0-93271
 $\text{CsBr}:\text{Cu}^{+}$, excitation and absorpt. spectra 0-108255
 $\text{CsI}:\text{Na}$, X-ray irradiated, optical and ESR studies in IR absorption band 0-80828
 FeBO_3 , mag. linear dichroism and absorpt. spectra, exciton-magnon absorpt. mechanism 0-66160
 Fe_2BO_6 , Faraday rotation and birefringence 0-100650
 KBr, cation defects creation mechanism 0-75224
 KBr, colour centre form. under polarised UV irradi., dichroism in absorpt. spectra 0-107232
 KCl and $\text{KCl}:\text{NO}_2$, X-irrad. crystals, Cl_3^- centres photodissoc., optical anisotropy and creation mechanisms (*Russian*) 0-66235
 $\text{KCl}:\text{Cu}^{+}$ excitation and absorpt. spectra 0-108255
 $\text{KCl}:\text{Li}$, $(\text{F}_2^-)_A$ centres, optical props. 0-89026
 KH_2PO_4 crystal, optical activity 0-71373
 Na vapour, Zeeman coherence, transient and stationary, polarisation spectroscopy 0-58212
 $\text{NaCl}(\text{Br})$, X-ray or UV irradiated, cation defects creation mechanism 0-75224
 $\text{Na}_3\text{Pr}(\text{C}_4\text{H}_9\text{O}_2)_2 \cdot 2\text{NaClO}_4 \cdot 6\text{H}_2\text{O}$, absorpt., circular dichroism, and mag. circular dichroism spectra 0-97243
 PbF_2 -ZnSe multilayer 16 μm dichroic mirror, 16 μm region, mech. stress compensation 0-74465
 Pr tinted glasses, transparency, dichroism and colour effects (*Polish*) 0-71371
 $\text{RbCl}(\text{Br})$, cation defects creation mechanism 0-75224
 Sml, Zeeman coherence, transient and stationary, polarisation spectroscopy 0-58212

dictionaries *see glossaries***dielectric breakdown** *see electric breakdown***dielectric constant** *see permittivity***dielectric depolarisation**

- apatites, dipolar reorientations, TSD study 0-107068
 ferroelectrics, photoelectric states in real time spatial light modulators, photorefractive effect 0-80676
 field induced thermally stimulated polarisation-depolarisation currents, relaxation, book contribution 0-80687
 poly- α -naphthol, semicond., isothermal depolarisation currents, electron trap parameters 0-60492
 polycarbonate films, high temp. relaxations 0-97187
 TGS, internal field prod. in layer periodical domain struct. by X-ray irradi. 0-71359
 urethane polyester elastomers, dielectric relax., spatial network density (*Russian*) 0-71310
 $\text{BaF}_2:\text{La}^{3+}$, thermal depolarisation of $\text{La}^{3+}-\text{F}^-$ defect dipoles 0-75926
 $\text{CaF}_2:\text{La}^{3+}$, thermal depolarisation of $\text{La}^{3+}-\text{F}^-$ defect dipoles 0-75926
 $\text{Li}_2\text{B}_4\text{O}_7$, ferroelectric glass, phase transition, permittivity, electrochromism, photochromism 0-80719
 $\alpha\text{-LiIO}_3$, depolarisation current, dielectric const. relaxation behaviour (*Chinese*) 0-88905
 $\text{Pb}(\text{Zr,Ti})\text{O}_3$, porosity-permittivity relations, depolarising factors determ. and pore effects (*Japanese*) 0-97189
 S, polycryst., photoelectric state following X-irrad. 0-60485
 $\text{SrF}_2:\text{La}^{3+}$, thermal depolarisation of $\text{La}^{3+}-\text{F}^-$ defect dipoles 0-75926
 SrTiO_3 ceramic, electrocaloric effects for refrigeration at cryogenic temp. 0-77789
 TeO_2 , ferroelectric glass, phase transition, permittivity, electrochromism, photochromism 0-80719
 TiO_2 , porosity-permittivity relations, depolarising factors determ. and pore effects (*Japanese*) 0-97189

dielectric devices

- see also capacitors; ferroelectric devices; insulators; piezoelectric devices; pyroelectric devices; space-charge limited devices*
 No entries

dielectric function

- alkali halide elastic dielectrics, Gruneisen parameter, effective ionic charge volume derivative 0-84273
 anisotropic continuum, with anisotropic surface layer, coeff. of attenuated total reflection 0-60535
 anthracene-pyrometallitic dianhydride cryst., refl. and absorpt. spectra of single charge transfer excitons 0-71442
 aqueous media, ion-pairing, hard sphere model 0-96428

dielectric function continued

CDW distorted solid, quasi-one-dimens., charge density fluctuations and dielec. matrix 0-107726
cermet film granular media, dielectric function theory, permittivity, percolation transport props. 0-88498
Clausius-Mosotti relations in dielec. matrix calcs. 0-59898
cubic symmetry cryst., quadrupole exciton theory 0-103632
degenerate electron gas at metallic densities, nonlocal interactions, compressibility and dispersion 0-107730
disordered conduction, dielectric function, phenomenological derivation 0-77692
dynamical local field corrections 0-88500
electron gas, dynamical exchange decoupling, plasmon dispersion, SDW and CDW 0-59900
electron scattering, inelastic, dynamical diffraction and generalised dielec. response function 0-75120
electron-ion system, effective ion interaction and force consts. 0-65185
ellipsometric function, Kramers-Kronig relations and sum rules, Lorentz oscillator model 0-102617
ellipsometry, metallic films and surfaces, nonlocal effects, theory 0-104006
fast ion in solid, oscillatory wake, trapped electron binding energy, RPA calc. 0-96575
inert gas solids, collective excitations and EELS, calc. 0-92842
inverse dielectric matrix calc. via recursion method 0-88495
jellium, two- and three-dimens., CDW, appl. to liq. He surface and semiconductors 0-65476
Kohn singularities near gapless state 0-59904
metal, non-simple, dielectric matrix, analytic model 0-75512
metal, work function, pseudopot. calc. 0-96970
metal particles, small, dielectric function and IR absorption 0-60607
metal surface, force on moving charge, spatial dispersion effects 0-65646
metal-dielectric interface, static point charge in dielec., pot. distrib. (*Russian*) 0-60088
metals, classical plasma frequency in long-wavelength limit, quantum correction 0-107728
metals, ground state energy, structural expansion, HF approx. 0-65420
molecular crystals, microscopic dielec. theory 0-97186
multiple-band systems, dielec. function in generalised relax-time approx. 0-103637
perovskites, matrix element effects in freq. dependent dielectric function 0-70632
plane-parallel absorbing layer, nonlinear optical props. 0-58631
plasma, one dimens. screening 0-65478
polar semiconductors, highly excited, optical dielec. function of electron-hole plasma 0-92847
polaritons, LT mixed mode, dispersion relation 0-65470
semiconductor, impurity ion pot., approx. equivalence of Csavinsky and Resta models 0-59901
semiconductor, Moss formula, refr. index rel. to energy gap 0-108173
semiconductor, shielding by electron gas in magnetic field 0-107727
semiconductors, dielec. function, modulation spectroscopy and elec. field effects book contrib. 0-80201
semiconductors, optical props. above band edge, book contrib. 0-84425
simple metals, model pseudopot. appl. to various props. 0-59845
smectic liquid crystal, chiral, optics and electro-optics, kinematical diffraction theory 0-92461
spinach chloroplasts, laser photoinduced changes in high freq. dielectric constant 0-85449
stimulated acoustooptical effects due to nonlinear photoelasticity 0-103941
surface plasmon dispersion relation at short wavelengths 0-96962
thermally stimulated depolarisation, many-body model of universal dielec. response 0-75927
zero gap semiconductor, thin layer, dielec. response 0-103635
anthracene, polycrystalline, optical props., 3.2-9.3 eV 0-76097
Au, optical props., dielec. function, void model, sample effects 0-76048
BaO-B₂O₃, glass, refraction, refractive index from 0.365 to 2.50 μ m 0-88953
BaO-La₂O₃-B₂O₃, glass, refraction, refractive index from 0.365 to 2.50 μ m 0-88953
BaTiO₃, ferroelec. cryst., IR and Raman spectra, mode coupling 0-66194
BaTiO₃, soft mode spectroscopy IR refl. meas. 0-88982
BiTeI, melt and vapour grown, optical props. 0-84746
CdCr₂S₄, ferromag. semicond., IR refl. spectra, phonon props. and dielec. function 0-66191
CdSe, undoped and Cr doped, far IR transmission and reflectance spectra 0-71429
CdTe, energy bands and optical props. calc., tight-binding model with spin-orbit interaction 0-65448
CuCl, dielectric function for semiconductors with high exciton conc. 0-84443
Dy₂S₃, optical props. and electronic struct. in fund. absorpt. region 0-80817
FeCl₃ intercalated with graphite, stage 1, dielec. response and intraband plasmon dispersion 0-59902
Fe₂O₄, dielec. function and polar Kerr rotation, 0.5-3.6 eV 0-66221
Fe₂O₄, polar Kerr effect visible and near IR spectral regions 0-108187
Ge surface, (111), ion-bombarded and annealed, spectroscopic ellipsometry study 0-103543
HgSe, two-phonon resonant effect, far-infrared reflectivity 0-108203
HgTe, energy bands and optical props. calcs., tight-binding model with spin-orbit interaction 0-65448
K-Rb, internal energy, heat of mixing, entropy, dielectric function 0-88340
KNbO₃, ferroelec. cryst., IR and Raman spectra, mode coupling 0-66194
K₂O-CaO-BaO-B₂O₃, glass, refraction, refractive index from 0.365 to 2.50 μ m 0-88953
La₂S₃, optical props. and electronic struct. in fund. absorpt. region 0-80817
Mn₂Fe_{1-x}O₄, dielec. function and polar Kerr rotation, 0.5-3.6 eV 0-66221
Na, IR and optical props., surface-plasmon-mediated absorpt. mechanism 0-93308
Na-Cs, internal energy, heat of mixing, entropy, dielectric function 0-88340
Na-K, internal energy, heat of mixing, entropy, dielectric function 0-88340
Nd₂S₃, optical props. and electronic struct. in fund. absorpt. region 0-80817
Ni, dielectric matrix, analytic model 0-75512

dielectric function continued

β -NiAl, electronic struct. and optical props. 0-97228
Pb, liq., elec. resist. calcs., pseudopot. depend. 0-96840
PbSnTe, optical dielectric const. variation with carrier conc. 0-84709
Pb_{1-x}Sn_xTe, lattice and electronic props. and g-value 0-80161
PbTe, far IR magnetorefl., band struct. 0-76010
SbSBr glass, IR reflectivity spectra 0-71403
Se, amorphous, bulk, reson. Raman scatt. 0-60597
Se, amorphous, electronic struct. and optical props., pseudopot. calc. 0-65428
Se, electronic struct. of cryst. phases and hydrostatic press. effects 0-59865
Si, dielectric function spectra, ellipsometric determ., many-particle effects at E₁-transition 0-93363
Si, laser induced dense plasma, dynamics 0-65612
Si, local pseudopotential, Gaussian band charge model 0-88477
Si, optical spectrum, many particle effects, band struct. 0-89024
Si₃N₄, electronic struct., LCAO calc. 0-96776
SiO₂, dielec. and optical props., chemical disorder effects 0-80815
SrTiO₃, calc. of matrix element effects in freq. dependent dielectric function 0-70632
Te, amorphous, electronic struct. and optical props., pseudopot. calc. 0-65428
Te, electronic struct. of cryst. phases and hydrostatic press. effects 0-59865
TiO₂, rutile, optoelectronic props., band struct., theory 0-80175
V₂O₅, energy band struct. rel. to expt. studies 0-70603
W surface, (110), chemisorpt. effects on dielec. function, refl. spectra 0-75616
ZnO-B₂O₃, glass, refraction, refractive index from 0.365 to 2.50 μ m 0-88953
ZnO-La₂O₃-B₂O₃, glass, refraction, refractive index from 0.365 to 2.50 μ m 0-88953

dielectric hysteresis
ceramics, transparent ferroelectric, composition selection for appl. in light modulators (*Russian*) 0-91869
DOBAMBC, ferroelec. liq. crystals, elec. and optical props., appls. (*Japanese*) 0-88943
ferroelectric materials for dielectric power conversion, dielectric prop. anal. 0-80712
ferroelectricity, hysteresis loops and butterfly loops, macroscopic theory 0-66132
ferroelectrics hysteresis loop sensing (*Czech*) 0-82792
piezoelectric ceramic, nonlinear charge release under uniaxial press. 0-80706
PLZT coarse-grained solid solutions, electro-optical processes induced by longitudinal electric field (*Russian*) 0-80750
polyvinylidene fluoride, hysteresis phenomena under high elec. field 0-66134
polyvinylidene fluoride film, hysteresis and dipolar orientation 0-97217
pyroelectric high power density heat engine, dielectric losses, polarisation 0-80689
rare earth arsenates, RAsO₄, ferroelectricity, dielec. meas. 0-60515
RNA, solid hydrated samples, hysteresis loops, nonlinear dielectric properties 0-71294
tetramethylammonium cobalt tetrachloride, ferroelectricity, triple 60 Hz D-E hysteresis loops 0-71365
tetramethylammonium tetrachloroferrate, press. induced ferroelectricity, dielec. and DTA meas. 0-80722
tetramethylammonium zinc tetrachloride, ferroelectricity, triple 60 Hz D-E hysteresis loops 0-71365
TGS, ferroelectric hysteresis, dielectric and pyroelectric props. (*Chinese*) 0-88938
TGS, internal bias field, hysteresis loops (*Chinese*) 0-84705
TGS, L-alanine disordered regions, dielec. prop. changes in transition region 0-108159
BaTiO₃ ceramic dielectric capacitor, processing prop. relations, hysteresis, permittivity 0-80730
BaTiO₃ RF sputtered ferroelectric film on Si substrate, ferroelectric props. 0-80697
Ba(Ti_{1-x}Sn_x)₂O₇ thick film, ferroelec., phase transitions and dielec. props. 0-97215
Bi₂Ti₂O₇, elec. characts., phase transition obs. 0-60517
KD₂PO₄, X-irradiated, hysteresis effects obs. by ESR 0-103928
KH₂PO₄, X-irradiated, hysteresis effects obs. by ESR 0-103928
K₂SeO₄, ferroelectricity, triple 60 Hz D-E hysteresis loops 0-71364
K₂ZnCl₄, ferroelectricity, triple 60 Hz D-E hysteresis loops 0-71365
(NH₄)₂SO₄, ferroelectricity, triple 60 Hz D-E hysteresis loops 0-71364
(NH₄)₂BeF₄, ferroelectricity, triple 60 Hz D-E hysteresis loops 0-71364
NH₄HSeO₄, cryst. struct., dielec. and ferroelec. props. 0-60528
Na_{0.5}Bi_{0.5}TiO₃, phase transition, hysteretic behaviour 0-71330
NaNbO₃, hydrostatic press. effect on permittivity, phase transition, hysteresis 0-80670
PLZT ceramic, ageing, dielec. props. 0-88940
PLZT ceramic, visible light scatt. depend. on photoferroelectric space charge fields 0-80806
Pb₂(Ge_{1-x}Si_x)₃O₁₁, electrogyration, phase transition and dielectric props. 0-93269
PbIn_{0.5}Nb_{0.5}O₃, ferroelectric, dielectric props. 0-103923
Pb(Zr,Ti)₂O₇ ceramic, surface barrier electroreflectance, hysteresis, ageing 0-80752
RbH₂PO₄, X-irradiated, hysteresis effects obs. by ESR 0-103928
Rb₂ZnBr₄, ferroelectricity, triple 60 Hz D-E hysteresis loops 0-71365
Rb₂ZnCl₄, ferroelectricity, triple 60 Hz D-E hysteresis loops 0-71365
Sr_{0.75}Ba_{0.25}Nb₂O₆, ceramic ageing dielec. props. 0-88940
V₂O₅, ferroelec. semicond., dielec. and elec. meas. 0-60516

dielectric-loaded antennas

far IR antennas for 0.1 to 3.0 mm range, review 0-69553
microstrip slot radiator for medical appls. 0-108994

dielectric-loaded waveguides

inhomogeneous dielectric filled uniform waveguides, EM wave propag. 0-83666
strip lines meas., small standing wave ratio and losses meas. 0-77811
VHF waveguide dielectric scatt. model for pulse-probe data interpretation (*Russian*) 0-62682

dielectric loss angle *see dielectric losses*

dielectric loss-angle measurement *see dielectric loss measurement*

dielectric loss measurement

see also dielectric losses

automatic, high resolution, at 100 MHz to 300 MHz and 2°C to 40°C 0-68219
calorimetric determ. of dielectric loss factors at 1 kHz and 4.2K 0-98921
polyethylene, loss tangent variation obs., under long term irradiation by ^{60}Co rays (German) 0-75266
strip lines, dielectric, use of tuned reflectometer 0-77811
time domain spectroscopy for low loss dielectric meas. 0-98983
tubular dielectric, complex permittivity and loss angle meas. in X-band using H_{011} cavity resonator method (German) 0-62690

dielectric losses

see also loss angle

anisotropic artificial dielectrics, dispersion props, investigation, electrodynamic method 0-88903
apatites, dipolar reorientations, TSD study 0-107068
biological substances, tabulation for freq. range 10 kHz to 10 GHz 0-108143
calcium behenate monomolecular layers between Al electrodes, nonlinear dielec. props. 0-80405
chloranil pellets, thermally stimulated discharge current and dielectric studies 0-93236
chlorobenzene-cis-decalin, mixtures, dielec. const. and loss tangent in liq. and solid phases 0-100628
coal dispersions, solvent refined, elec. props., surface characts. 0-80333
defect-free crystals, dielec. losses due to phonon system perturb. in elec. field 0-80693
defective dielectrics, EM heating with time depend. param., WKB calcs. 0-71367
dielectric surface, charge accumulation, losses, electron-beam treatment (Russian) 0-75931
dihydroxy benzenes in ethyl alcohol, dielec. dispersion charact. 0-75932
dihydroxy toluene in ethyl alcohol, dielec. dispersion charact. 0-75932
dipolar materials, temp. depend. of loss peak freq. 0-88922
ethanol solution in benzene, dielec. relax. time by RF cond. meas. 0-71302
ferrites, microwave, dielectric constants and permeability (Chinese) 0-66096
ferroelectric ceramic, mech. and elec. losses, correl., theory and expt. 0-66133
ferroelectric ceramics, materials and dielec. props., review 0-75957
glass, dielectric relax. loss, two level Anderson Halperin Varma model 0-66106
n-heptyl-4-cyanobiphenyl, nematic phase, diffusion equation 0-71305
hexafluoropropylene-tetrafluoroethylene copolymer, surface component of vac. absorpt. and resorpt. currents, source of dielec. loss 0-70792
kaolinite rare-earth complexes, relax., molar free energy of activation for dipole relax. 0-88919
lead phthalocyanine- $\text{O}_2(\text{I})$, Schottky barrier effect on AC current response 0-75623
MBBA, dielec. relax. in metastable modification of solid phase 0-84689
methanol solution in benzene, dielec. relax. time by RF cond. meas. 0-71302
microwave freqs., two coupled method modification 0-100632
phenolic Mannich bases, dielec. relax. study 0-97196
piezoelectric solids, shape-dependent damping 0-93242
polar liquids in double layer capacitors, RF conduction, ion diffusion effect 0-107883
poly- γ -benzyl-L-glutamate, synthetic polypeptide, nonlinear dielectric effect in nonpolar medium 0-84682
poly-p-xylylene films, carrier traps, X-ray induced TSC, thermolum. and dielec. loss study 0-88570
polycarbonate, γ -irradiated, dielec. behaviour and glass transition 0-97182
polychlorotrifluoroethylene, crystalline and amorphous peaks, dielectric props. 0-93237
polyethylene, alcohol infused, loss peaks due to secondary groups 0-84688
polyethylene, low-density natural, at elevated temps. 0-97185
polyethylene terephthalate, TSC and thermolum. due to electron detrapping by local mol. motions 0-96898
polypropylene films, dielec. props., impurity effects 0-71304
polypropylene glycol melt, mol. motion, dielectric and Kerr effect relax. obs. 0-60498
polystyrenes, anionic, TSC obs. of T_g and T_{β} transitions 0-84686
1,2-propane diol-dipropylene glycol, dielec. dispersion charact. 0-75932
propyl acetate-propyl alcohol, dielec. dispersion charact. 0-75932
pyroelectric high power density heat engine, dielectric losses, polarisation 0-80689
quartz, electron irradiation effects on optical, dielec., elastic props. 0-59521
rare earth aluminate, scandate and zirconate film coatings, electrophys. props. w.r.t. prep. technology 0-60781
rare earth oxides, dielec. const. and loss at low temp. 0-93229
stearic acid films, evaporated, vac. effects 0-97435
thermal charge carrier movement in lossy dielects. 0-88920
vitreous systems, local motions, dielec. losses and relax. phenomena 0-108154
Al-stearic acid-Al, low-loss thin film capacitor 0-71317
AlF₃ in Al-AlF₃-Al MIM thin film structures, dielec. and elec. props. (Slovak) 0-100536
 β -Al₂O₃, conduction and dielec. loss mechanisms, paired interstitially model 0-107468
 β -Al₂O₃-Na₂O, AC ionic cond., dielec. and NMR relax. 0-59713
BaFe₂O₉, ferrite, DC cond., dielec. props., lattice consts. 0-80272
BaO-Nd₂O₃-TiO₂-Bi₂O₃ system ceramics, high stability low loss dielectric preparation 0-81008
(Ba,Sb)_{1-x} TiO₃ 0-60514
BaTiO₃ film, dielectric props. depend. on sinusoidal elec. field 0-71318
BaTiO₃ film, struct. and dielec. props. 0-60514
BaTiO₃:BaTi₂O₇, dielec. props. and microstruct. 0-60481
BaTi₂(Sn_{1-x})₂O₇ film, struct. and dielec. props. 0-60514
Bi₂WO₆, ferroelectric, dielectric props., elec. cond. and relaxation phenomena obs. 0-80692
CH₃NH₂/Ga(SeO₂)₂·12H₂O, dielec. relax. near transition temp. 0-60493
CaF₂-H₂, ionic cond. determ. from admittance and dielec. loss meas. (French) 0-107479
CdI₂ polytypic crystals, dielectric loss behaviour 0-66108

dielectric losses continued

Co₂Zn_{1-x}Fe_xO₄, ferrite, DC cond., dielec. props., lattice consts. 0-80272
CsH₂AsO₄ crystals, dielectric radiation effects, γ -radiation 0-93234
KClO₄:CrO₄²⁻(SO₄²⁻), AC electrical conductivity meas. between temp. range 25-325°C, automated technique 0-59699
K₂Fe(CN)₆·3H₂O, ferroelec. and paraelec. phases, dielec. props. meas. 0-60494
Li ferrites, MW dielectric losses, causes and reduction (Chinese) 0-75930
Mg_{0.25}Zn_{0.75}Fe₂O₄, ferrite, DC cond., dielec. props., lattice consts. 0-80272
NaCl:Ca²⁺, dipole concs. determ. considering aggregation, expt. and theoretical comparison 0-59512
NaCl:Cd²⁺, dielectric loss following plastic deform. 0-84690
Na₂O-SiO₂ glass, conduction and dielec. loss mechanisms, paired interstitially model 0-107468
Na₂Sc₂P₂O₁₂, fast-ion conductor, struct. phase transition 0-88362
PLZT ceramic, ageing, dielec. props. 0-88940
PLZT, mech. and elec. losses, correl., theory and expt. 0-66133
PLZT modified high voltage dielectric, permittivity, Curie temp., loss meas. 0-80720
(Pb, Sr)₂Ge₂O₁₁, single crysts., growth and X-ray and dielec. investigations 0-88127
PbI₂, dielectric props., elec. cond., space charge polarisation 0-100631
Pb(Zr, Ti)O₃ ceramics, low temp. sintering, elec. and mech. props. 0-71616
Se, amorphous film, dielec. activity obs. near glass transition temp. 0-75933
Se film, amorphous, empirical formula for temp. depend. of dielec. loss peak 0-97197
Se:As, amorphous film, dielec. activity obs. near glass transition temp. 0-75933
Sr_{0.75}Ba_{0.25}Nb₂O₆, ceramic ageing dielec. props. 0-88940
Ta₂O₅ film, reactively sputtered on Si, dielectric and optical props. obs. (Bulgarian) 0-89144
TeO₂ thin films, dielec. props. rel. to fabrication conditions 0-97199
WO₃-P₂O₅ glass, AC cond. and dielec. props. 0-92717
YIG, MW dielectric losses, causes and reduction (Chinese) 0-75930
Y₂O₃-AlN-SiO₂ oxynitride glasses, elec. props. 0-80267
ZnO non-ohmic ceramic, degradation props. under AC and DC bias 0-80262

dielectric materials

see also antiferroelectric materials; dielectric thin films; electrets; ferroelectric materials; glass; insulating materials; insulation; piezoelectric materials

capacitors, power, dielectric liquids flammability and degradation 0-88944
moistening diffusion kinetics, forecasting (Hungarian) 0-96692
NDT using Kirlian effect, high freq. technique 0-66749
raw material acceptance testing for dielectric applications 0-97646

dielectric measurement

see also dielectric loss measurement; permittivity measurement

biological liquids, reflection meas. of complex dielectric const. 0-101309
biological substances, dielectric props. meas. at RF and microwave freq. by coaxial line reflection methods 0-109065
conducting solutions, bridge method for meas. dielectric relaxation 0-82793
dielectric constant, laser photoinduced changes, of chloroplasts and dyes 0-85449
ice containing ionic impurities, relax. meas. by blocking layer method 0-103914
in vivo probe measurement technique for determining dielectric properties at VHF through microwave frequencies 0-85542
insulating gases and gas mixtures, maximum electric strength and vapour pressure relationships 0-92249
LF measurements using time-domain technique, 20 Hz to 10 kHz 0-57329
liquids, coaxial transmission line terminated by shielded open circuit 0-82789
liquids, meas. methods comparison in freq. range 1 GHz to 4 THz 0-100639
solid insulating materials, dielectric properties at cryogenic temps. 0-90867
time domain spectroscopy, survey 0-68212
VHF waveguide dielectric scatt. model for pulse-probe data interpretation (Russian) 0-62682
water pollution, dielectric props. and determ. of microwave emissivity 0-101142
CCl₄-F₂-CO₂ gas mixture, field breakdown gradients calc. method 0-92248
CCl₄-F₂-N₂ gas mixture, field breakdown gradients calc. method 0-92248

dielectric phenomena

see also dielectric hysteresis; dielectric losses; dielectric properties of substances; dielectric relaxation; dielectric resonance; electric strength; ferroelectricity; photoinduced effect; piezoelectricity; solvated electrons; dielectrophoretic force, theory expt. 0-72403

dielectric polarisation

see also Barkhausen effect

air-dielectric interface, EM wave reflection and transmission in terms of polarisation, education 0-105458
alkali halides, polarization, photoinduced, rel. to exchange between vacancy and impurity 0-59914
alkyl halide, amorphous, depolarisation thermocurrents and dielectric relaxation time distrib. (French) 0-60490
ammonium Rochelle salt, thermodynamics of ferroelec. transition 0-84702
amorphous solid, constitutive relation derivation 0-84684
calcium behenate monomolecular layers between Al electrodes, nonlinear dielec. props. 0-80405
chloranil pellets, thermally stimulated discharge current and dielectric studies 0-93236
coal dispersions, solvent refined, elec. props., surface characts. 0-80333
copper formate tetrahydrate, ice rule ferroelectric, polarisation correlations 0-97190
crystalline dielectric, local electric fields near surface 0-80733
crystalline slab of point molecules, dielec. theory 0-97222
cubic lattice of polarisable spheres, dielectric constant 0-60483
dipolar liquid time-variation of dispersion and absorption of third-order electric polarisation, mol. relax. times 0-60487
electrets, prepolarised, meas. microphones appl. 0-74649

dielectric polarisation continued

- electrets, radiation-induced charge storage and polarisation effects 0-80684
- electric dielectric, hyper-, with saturated polarisation, variational and invariance principles 0-74730
- electronic matter, polarisation and magnetisation 0-75929
- esters, SLC, ferroelectric behaviour, specific heat, spontaneous polarisation 0-75958
- extrinsic ferroelectrics, transition, polarisation, dielectric divergence 0-80718
- ferroelectric, uniaxial, Urbach rule and polarisation fluctuations, optical absorpt. edge 0-88910
- ferroelectric ceramic, rel. to mech. and elec. losses, correl., theory and expt. 0-66133
- ferroelectric liquid crystals., chiral smectic C phase, phys. props., review 0-75150
- ferroelectric materials for dielectric power conversion, dielectric prop. anal. 0-80712
- ferroelectric semiconductor, band bending in surface layer 0-60061
- ferroelectric semiconductors, props., book 0-82590
- ferroelectrics, unit cell multiplication during phase transform., spontaneous polarisation 0-75983
- ferroelectrics hysteresis loop sensing (*Czech*) 0-82792
- field induced thermally stimulated polarisation-depolarisation currents, relaxation, book contribution 0-80687
- liquid dielectrics, local field, two-parameter mean field approach 0-93232
- liquid-vapour interface, non-polar fluid, variation of local field 0-80734
- lossy dielectrics, thermal charge carriers movement 0-88920
- Maxwell-Wagner dielectric dispersions, vol. ion polarisations 0-97188
- molecular crystals, microscopic dielec. theory 0-97186
- Mott transition in Hubbard long range model, isostructural instability, thermodynamic props. (*Russian*) 0-65454
- non polar fluid dielectrics, mechanical forces 0-60529
- oxyfluoride ferroelectrics, chemical bonding, Curie temp., spontaneous polarisation 0-75981
- p-alkoxybenzylidene-p'-amino-2-chloropropyl-cinnamate, chiral smectic, dielec. props. 0-96441
- paraelectric-ferroelectric-antiferroelectric phase transitions, electrostrictive effects 0-97209
- piezoelectric ceramics, photovoltaic effect application to information storage 0-80316
- piezoelectric powder, memory echo, dipolar field contrib. 0-84700
- piezoelectricity, mechano-electric coupled fields, polarisation gradient 0-75940
- PMMA moist surface mech. strength reduced by electric charge (*Russian*) 0-60486
- poly- γ -benzyl-L-glutamate, synthetic polypeptide, nonlinear dielectric effect in nonpolar medium 0-84682
- polyacetylene:I, dc microwave cond., permittivity 0-107843
- polystyrene:I films, thermally stimulated discharge, I conc. and polarisation temp. depend. 0-107937
- polystyrene film, thermally stimulated discharge currents 0-71300
- polystyrene thin films, TSC and surface charge meas. 0-103769
- polyvinylidene fluoride, corona-charged, surface effects 0-66102
- polyvinylidene fluoride, electro-optic and elasto-optic effects 0-80754
- polyvinylidene fluoride, hysteresis phenomena under high elec. field 0-66134
- polyvinylidene fluoride, piezoelec. props., polarisation and appls. 0-75947
- polyvinylidene fluoride, plasma poling, piezoelec. and pyroelec. responses 0-71296
- polyvinylidene fluoride, poled, dielec. relax. spectra 0-80690
- polyvinylidene fluoride, poling process, kink propag. model 0-80679
- polyvinylidene fluoride film, hysteresis and dipolar orientation 0-97217
- PVC films, soln. grown, DC cond. mechanisms, field and temp. depend. 0-97021
- pyroelectric high power density heat engine, dielectric losses, polarisation 0-80689
- RNA, solid hydrated samples, hysteresis loops, nonlinear dielectric properties 0-71294
- saclicidenanilines, SLC, ferroelectric behaviour, specific heat, spontaneous polarisation 0-75958
- semi-infinite cubic lattice, response to static point charge 0-75928
- SLC, chiral structure in electric field, dielectric permeability, spontaneous polarisation (*Russian*) 0-75159
- solid dielectrics, molecular optics model, macroscopic theory 0-84683
- Stockmayer fluids, static dielec. props. 0-93231
- tetramethylammonium tetrachlorobaltate, ferroelec., pressure-temp. phase diagrams 0-97205
- tetramethylammonium tetrachlorozincate, ferroelec., pressure-temp. phase diagrams 0-97205
- tetramethyldiaminodiphenyl ketone, binder layer, photoinduced polarisation and voltage 0-75923
- TGS- α -alanine, single crystals., dielec. spectrum in RF range (*Russian*) 0-66097
- TGS: nitroaniline, dielec. and pyroelec. props. 0-75916
- TGS, L- α -alanine disordered regions, dielec. prop. changes in transition region 0-108159
- TGS, spontaneous polarisation, low temp. meas. 0-75921
- TGS crystals., effects of radiation induced defects on internal bias field 0-88941
- uniaxial dielectric crystals, wave propag., polarisation relations and dispersion eqns. 0-64723
- vinylidene-fluoride-trifluoroethylene copolymer, piezoelectricity 0-88930
- AgNa(NO₂)₂, order-disorder ferroelec., influence of hydrostatic press. on polarisation dynamics 0-103913
- (Ba,Sr)₂TiO₃, ferroelec. props., press. depend., anharmonic oscillator model 0-80716
- BaTiO₃ film, dielectric props. depend. on sinusoidal elec. field 0-71318
- BaTiO₃ RF sputtered ferroelectric film on Si substrate, ferroelectric props. 0-80697
- BaTiO₃, spontaneous polarisation, low temp. meas. 0-75921
- Ba(Ti_{1-x}Sn_x)O₃ thick film, ferroelec., phase transitions and dielec. props. 0-7515
- Bi_{1/2}FeO₂₀, longitudinally vibrated bars, reson. freq., DC elec. field effects, elastic coupling polarising correction terms 0-60503
- CaF₂:alkali metal cation, thermal depolarisation study 0-108147
- CaF₂:Er, near-Debye dielectric responses 0-71291
- CaF₂:rare earth ion, elec. dipole-dipole interaction, ionic thermocurrent and EPR study 0-108060
- CdF₂, electrical transport limitation by electrodes, polarisation effects 0-96689

dielectric polarisation continued

- Cs(H_{1-x}D_x)₂PO₄, dielec. props., temp. meas. 0-71335
- FeF₃ thin film, polarisation mechanism, AC and TSC study 0-66104
- Gd₂O₃, B-type monoclinic, DC(AC) elec. cond., thermoelectric power, dielectric const., temp. depends. 0-59980
- KD₂PO₄, polarisation fluctuations, wavevector depend. 0-71295
- K₂FeF₄, charge transport and polarisation 0-80681
- KH₂PO₄, ferroelectric transition, order-disorder character of hydrogen bond 0-93251
- KH₂PO₄, spontaneous polarisation, low temp. meas. 0-75921
- KH₂PO₄-type ferroelectrics, dielec. props., four-cluster approx. 0-97202
- K₂ZnF₄, charge transport and polarisation 0-80681
- LiH₃(SeO₃)₂, ferroelec., absolute atomic arrangement and spontaneous polarisation, neutron diff. study 0-59442
- LiNbO₃, spontaneous polarisation, low temp. meas. 0-75921
- MnNbO₃, orthorhombic, electronic struct., SCF-MS-X α calc. 0-70600
- MnNbO₃, tetragonal, electronic struct., optical anisotropy 0-70599
- (NH₄)₂Cd₂(SO₄)₃, dielec. and spontaneous polarisation, -195 to -180°C, particle size depend. 0-97200
- NH₄HSeO₄, cryst. struct., dielec. and ferroelec. props. 0-60528
- NH₄HSeO₄, ferroelec. phase transition, pyroelec. props. 0-60513
- NH₄HSeO₄, ferroelec. props. rel. to struct. 0-71345
- ((NH₄)_{1-x}Rb_x)₂SO₄, isomorphous impurity effect on dielec. and nonlinear optical props. 0-88911
- NaNO₂, ²³Na elec. field gradient tensor from NMR satellite lines near phase transition 0-71191
- NaNO₂, ferroelec., dielec. and thermal behaviour 0-80680
- MnNbO₃, ferroelec. nuclear quadrupole coupling const. and spontaneous polarisation 0-71229
- NaNbO₃, hydrostatic press. effect on permittivity, phase transition, hysteresis 0-80670
- Ni-I single crystals, mag. and dielectric props. 0-93095
- NiZn ferrite, dielec. props., Jahn-Teller ion effects 0-97181
- PLZT ceramic, visible light scatt. depend. on photoferroelectric space charge fields 0-80806
- (Pb,Sr)TiO₃, ferroelec. props., press. depend., anharmonic oscillator model 0-80716
- Pb_{0.94-x/2}Ba_{0.06}Nb_xZr_{1-x}O₃, Nb dopant morphology effect on microstructure 0-81005
- Pb₂Ge₂O₁₁, pulsed polarisation switching process depend. on illumination 0-93253
- Pb₂Ge₂O₁₁:Gd³⁺, ferroelec. transition, temp. depend., EPR study 0-66127
- PbI₂, dielectric props., elec. cond., space charge polarisation 0-100631
- Pb(Mg_{1/3}Nb_{2/3})O₃, electrostrictive effect 0-66113
- Pb(Mg_{1/3}Nb_{2/3})O₃:PbTiO₃, ceramic dielectric, electrostriction, relaxation, polarisation 0-80700
- Pb₃(PO₄)₂, ferroelastic, dielectric anomalies, phase transitions, permittivity, relaxation (*Russian*) 0-71293
- xPbTiO₃ + (1-x)PbCd_{1/3}Nb_{2/3}O₃, phase transition spread, polarisation relaxation, dielectric susceptibility (*Russian*) 0-75922
- Pb(Zr,Ti)O₃ ceramic, surface barrier electroreflectance, hysteresis, ageing 0-80752
- PbZr_{1-x}Ti_xO₃:Nb₂O₃ ceramic, ferroelec. transitions, polarisation meas. (*French*) 0-66124
- RbHSeO₄, ferroelec. props. rel. to struct. 0-71345
- RbH₂(SeO₃)₂ crystal, incommensurable phase, quadrupole moment study 0-97213
- Rb₂ZnBr₄, ferroelec., photovoltaic and photorefractive phenomena 0-75598
- SbSI, absorption edge, elec. field effect rel. to ferroelec. props. 0-97240
- SbSI, ferroelectric, dark current and spontaneous polarisation, ferro-paraelectric transitions obs. 0-60521
- Si:P, dielec. susceptibility meas., polarisation catastrophe at metal-insulator transition 0-59873
- SiO₂ thin film dielec., in MIM struct., interfacial props. rel. to non-stoichiometry 0-80399
- Sm₂O₃, B-type monoclinic, DC(AC) elec. cond., thermoelectric power, dielectric const., temp. depends. 0-59980
- Sr_{1-x}Ba_xNb₂O₆, photorefraction in space charge field, phase transitions 0-97229
- SrF₂:rare earth ion, elec. dipole-dipole interaction, ionic thermocurrent and EPR study 0-108060
- SrO:Ni²⁺, ionic thermocurrent meas. 0-108148
- Tb₂O₃, B-type monoclinic, DC(AC) elec. cond., thermoelectric power, dielectric const., temp. depends. 0-59980
- TiD₂PO₄, antiferroelectricity, permittivity, electric field double hysteresis loops 0-60512

dielectric power factor see power factor**dielectric properties of gases**

- polar mol. rot. relax., dielectric friction, Onsager cavity model 0-64664
- SF₆ with gaseous contaminants, arc decomposition kinetics investigation by combined gas chromatograph-mass spectrometry methods 0-92250

dielectric properties of liquids and solutions

- allyl ether, dielectric relaxation obs. at millimetric wavelengths 0-71311
- benzonitrile-isooctane mixture, dielec. const. near consolute point, temp. and freq. depend. meas. 0-71292
- t-butyl acetate, rot. isomerism, dielect. and Raman spectra 0-106328
- t-butyl alcohol, self-assoc., linear and nonlinear dielec. effects obs. 0-60484
- t-butyl formate, rot. isomerism, dielect. and Raman spectra 0-106328
- capacitance cell, guarded cylindrical 0-86268
- castor oil dielectric fluid, microwave propag., permittivity effect, demonstration 0-105468
- cholesteryl laurate-cholesteryl caprylate (75 wt.%), polymorphic behaviour, optical, elec. and dielec. meas. 0-65208
- conducting solutions, bridge method for meas. dielectric relaxation 0-82793
- 4-cyano-4'-octylbiphenyl, dielectric relax. anal. in nematic and smectic phases 0-108153
- Debye absorption at crit. liq.-vapour transition in dielec. fluid 0-100322
- Debye generalised fluid model, dielectric relax., depolarised dynamic light scatt. 0-108156
- dihydroxy benzenes in ethyl alcohol, dielec. dispersion charact. 0-75932
- dihydroxy toluene in ethyl alcohol, dielec. dispersion charact. 0-75932
- N,N-dimethylacetamide in tetrachloromethane, dielectric relax. and complex permittivity 0-108149
- dimuristoyl-1-3-lecithin aqueous soln., pulse relaxation method for dielec. const. determ. (*German*) 0-71308

dielectric properties of liquids and solutions continued

- dipolar liquid time-variation of dispersion and absorption of third-order electric polarisation, mol. relax. times 0-60487
 dipolar molecules in dil. soln., nonlinear dielec. relax., effective relax. time 0-97195
 DNA, calf-thymus Na-DNA aq. solns., dielec. behaviour in 5 kHz to 100 MHz range 0-85330
 electroviscous effect, AC characteristics, pressure-drop fluctuations 0-107457
 erythrocytes, human, haemoglobin's suspending medium, dielec. props. obs. 0-76716
 ferroelectric liquid crysts., chiral smectic C phase, phys. props., review 0-75150
 fluid mixtures, dil., spherical mols., struct. and permittivity 0-92433
 glycerol, highly viscous state, static and dynamic Kerr effect obs. 0-60545
 heavy water dielectric constant meas. over temp. range 473K to 643K 0-103912
 n-heptyl-4-cyanobiphenyl, nematic phase, dielec. loss, diffusion equations 0-71305
 iodobenzene, soln., non-linear dielec. effect, comparison with fluoro, chloro and bromobenzene 0-60478
 liquid crystals, prep. and phys. props., book 0-105444
 liquids, meas. methods comparison in freq. range 1 GHz to 4 THz 0-100639
 local field, two-parameter mean field approach 0-93232
 macromolecules and colloids, conf., Uxbridge, England (Apr. 1978) 0-82577
 Maxwell-Wagner dielectric dispersions, vol. ion polarisations 0-97188
 methyl alcohol, dielec. relaxation spectroscopy in microwave region, double-beam interferometry (*German*) 0-71309
 methyl iodide, liq., mol. reorientation, dielec. and viscosity meas. 0-100157
 mixed salt solution approximating seawater composition, dielec. and radiation characts. 0-97184
 nematic liquid crystal mixtures, dielec. permittivity dispersion 0-88921
 non polar fluid dielectrics, mechanical forces 0-60529
 organic liquid systems, dielectric and dynamic Kerr-effect studies 0-60496
 organic liquids in freq. range 400 MHz to 285 GHz, internat. comparison of meas. methods (*German*) 0-68168
 p-alkoxybenzylidene-p'-amino-2-chloropropyl-cinnamate, chiral smectic, dielec. props. 0-96441
 4-n-pentyloxy-phenyl-4'-n-octyloxybenzoate, nematic, dielec. relax. and freq. depend. of threshold voltage 0-60497
 perfluorinated polymer, Krytox 143-AB, viscous, viscoelastic and dielectric properties 0-70440
 3-phenylpropanol-hexane, nonlinear dielectric effect, critical exponent 0-93227
 polar fluid, molecular pair effects, Onsager dielec. theory breakdown 0-75917
 polar liqs. permittivity, computer simulation with hard sphere point dipole pot. 0-103911
 polar liquids, binary mixtures, Sarma and Rao's rel. for dielectric relax. time 0-88914
 polar liquids in double layer capacitors, RF conduction, ion diffusion effect 0-107883
 polar molecules, viscosity activation energy and relax. time, RF cond. meas. 0-96677
 polar molecules in nonpolar solvent, far IR spectra and dielec. relax. 0-71312
 polar solvents, solvated electron absorpt. spectra, intrasolvent and intersolvent correls. 0-93840
 poly-4-chlorostyrene, undiluted, dielec. relax. spectrum above Tg 0-97194
 polyethylene, alcohol infused, loss peaks due to secondary groups 0-84688
 polymer chains with rigid bonds, local relax. times, mol. dynamics study (*Russian*) 0-59373
 polypropylene glycol melt, mol. motion, dielectric and Kerr effect relax. obs. 0-60498
 polystyrene, bridge method for meas. dielectric relaxation 0-82793
 1,2-propane diol-dipropylene glycol, dielec. dispersion charact. 0-75932
 propyl acetate-propyl alcohol, dielec. dispersion charact. 0-75932
 relaxation time rel. to single particle correl. time 0-97193
 smectic phases, long mol. axis reorientation, LF dielec. dispersion 0-70124
 trans-stilbene, soln., lifetime and anisotropic fluoresc., viscosity effects (*German*) 0-106352
 Stockmayer fluids, static dielec. props. 0-93231
 Stockmayer fluids with dipoles and quadrupoles, spherical harmonic coeffs., dielec. const. and Kerr factor calcs. 0-84678
 Stockmayer molecular fluid, 2-dimens., permittivity and dynamic props. 0-103910
 Sumoto effect under transient conditions 0-97198
 tetraphenylboron sodium aqueous soln., dielec. relaxation spectroscopy in microwave region, double-beam interferometry (*German*) 0-71309
 water, complex permittivity meas. and microwave heating for specific purities and salt soln. 0-60480
 water, dielec. relaxation of compressed liquid at 17.613 GHz using microwave refl. meas. method (*German*) 0-71306
 water, dielec. relaxation spectroscopy in microwave region, double-beam interferometry (*German*) 0-71309
 water, permittivity at mm wavelengths 0-66098
 water pollution, dielectric props. and determ. of microwave emissivity 0-101142
 water-oil microemulsions, optical matching 0-61157
 D-T, liq., dielectric constant and elec. cond. 0-84680
 ethanol-water system, complex dielec. permitt. in UHF region and NMR spectra (*Japanese*) 0-100620
 NaCl, monoelectrolyte, highly mineralised salt soln., dielec. and radiation characts. 0-97184
 SF₆, critical isochore, dielectric const. critical anomaly upper bound 0-84679
 Se₂(SO₄)₃ aqueous soln., dielec. relaxation spectroscopy in microwave region, double-beam interferometry (*German*) 0-71309
 Se, liq., dielectric relax. and elec. cond. 0-108150
 Se-Ti-S alloys, liq., dielectric relax. and elec. cond. 0-108150

dielectric properties of solids

- alkali metal compounds, ASbO₃.1/6AF, dielec. spectroscopy study, 100 Hz to 10 MHz, 238 to 417K (*German*) 0-108144

dielectric properties of solids continued

- alkaline earth fluoride, doped with trivalent rare earths, migration entropy for bound fluorine motion 0-71303
 amorphous solid, constitutive relation derivation 0-84684
 anisotropic artificial dielectrics, dispersion props, investigation, electrodynamic method 0-88903
 calcium benenate monomolecular layers between Al electrodes, nonlinear dielec. props. 0-80405
 cellulose fibres, elec. anisotropy 0-97220
 chloranil pellets, thermally stimulated discharge current and dielectric studies 0-93236
 composite material, two-component, complex dielectric constant, exactly solvable microscopic geometries and rigorous bounds 0-75918
 crystalline dielectric, local electric fields near surface 0-80733
 defect-free crystals, dielec. losses due to phonon system perturb. in elec. field 0-80693
 dimensional effects in ultrasonic wave absorpt. coeff. (*Russian*) 0-70321
 electric breakdown in dielectric solids 0-66111
 Estrudur 31s, polyester moulding material (*Polish*) 0-66523
 eukaryotic cell cycle, long-range dielec. aspects 0-94182
 ferrites, microwave, dielectric constants and permeability (*Chinese*) 0-66096
 fluctuation theorems for dielectrics with periodic boundary conditions 0-80735
 food, semi-solid, at low, intermediate and high moisture contents 0-101157
 glass, electrical relax., Debye-Falkenhagen theory 0-108155
 glass characteristics, electromagnetic, mechanical and thermal props. 0-106587
 ice, dielectric relaxation in presence of ionic impurities, block layer meas. tech. 0-103914
 ice, permittivity at mm wavelengths 0-66098
 ionic crystals, lattice defects, conference, Canterbury, England (Sept. 1979) 0-105420
 lead phthalocyanine:O₂(I), Schottky barrier effect on AC current response 0-75623
 lossy dielectrics, thermal charge carriers movement 0-88920
 MBBA, dielec. relax. in metastable modification of solid phase 0-84689
 metal-dielectric interface, static point charge in dielec., pot. distrib. (*Russian*) 0-60088
 methylammonium alums, dielec. relax. near transition point 0-71301
 mica, pulse electric breakdown under pressure, lamination effects 0-66110
 molecular optics model, macroscopic theory 0-84683
 noncrystalline model systems, local elec. field, embedding-field method 0-108169
 perspex, electric conduction and isothermal dielectric relax. 0-80285
 poly- α -naphthol, semicond., isothermal depolarisation currents, electron trap parameters 0-60492
 polyacetylene film, anisotropy of dielec. const. 0-108146
 polycarbonate, γ -irradiated, dielec. behaviour and glass transition 0-97182
 polychlorotrifluoroethylene, crystalline and amorphous peaks, dielectric props. 0-93237
 polyethylene, loss tangent variation obs., under long term irradiation by ⁶⁰Co rays (*German*) 0-75266
 polyethylene, low-density natural, at elevated temps. 0-97185
 polymer films, dielectric constant meas. parallel to film surface 0-97183
 polystyrene atactic carrier transport and photogeneration 0-80318
 polyvinylidene fluoride, cryst. form II, anisotropy of dielec. relax. 0-103915
 polyvinylidene fluoride, poled, dielec. relax. spectra 0-80690
 polyvinylidene fluoride film, biaxially oriented, charact. for transducer appl. 0-88931
 rare earth aluminate, scandate and zirconate film coatings, electrophys. props. w.r.t. prep. technology 0-60781
 rare earth arsenates, RAsO₄, ferroelectricity, dielec. meas. 0-60515
 rare earth oxides, dielec. const. and loss at low temp. 0-93229
 (rare-earth), Ti₂O₃, (RE=La-Nd, Sm, Gd, Y), ferroelec., layer type struct., cryst. growth 0-108348
 RNA, solid hydrated samples, hysteresis loops, nonlinear dielectric properties 0-71294
 serum albumin, bovine, hydrated, dielec. and elec. props. 0-97854
 spacecraft dielectrics, charging and discharging 0-71315
 spacecraft materials, surface discharge arc propag. and damage 0-71314
 specimen holder for transmission dispersive far IR Fourier transform spectrometry 0-84648
 stearic acid multilayers, dielec. props. 0-80404
 TCNQ salt, MEM(TCNQ)₂, dielec. const. obs., DC and microwave cond. obs. 0-59963
 tetramethylammonium tetrachloroferrate, press. induced ferroelectricity, dielec. and DTA meas. 0-80722
 TGS: α -alanine, single crystals, dielec. spectrum in RF range (*Russian*) 0-66097
 TGS: nitroaniline, dielec. and pyroelec. props. 0-75916
 TGS, deuterated, ferroelec., dielec. nonlinearity 0-75959
 TGS, effect of Fe³⁺ admixture on phys. props. 0-76052
 TGS, electrostrictive and dielec. coeffs., neutron diff. study 0-75943
 TGS, L- α -alanine disordered regions, dielec. prop. changes in transition region 0-108159
 TGS, spontaneous polarisation, low temp. meas. 0-75921
 TGS powders, dielec. dispersion 0-97180
 TGSe, ferroelec., dielec. nonlinearity 0-75959
 thermal breakdown, theory 0-75938
 thermally stimulated characts., dipolar relaxation time, trap levels and ionic space charge polarisation 0-84685
 TSC with two trapping levels, calc. 0-60489
 urethane polyester elastomers, dielectric relax., spatial network density (*Russian*) 0-71310
 vitreous systems, local motions, dielec. losses and relax. phenomena 0-108154
 X-zeolites, dielectric relax. anal. 0-108153
 Ag halides, static dielec. constant, strain derivatives 0-100629
 AgCl(Br), electronic dielec. const., vol. depend., Clausius-Mossotti model 0-100630
 AgNO₃, single crystal, dielec. const., low temp. meas. 0-71290
 AgNa(NO₃)₂, crit. dynamics, hydrostatic press. effect, dielec. props. meas. 0-71328
 AgNa(NO₃)₂, order-disorder ferroelec., influence of hydrostatic press. on polarisation dynamics 0-103913
 Al/Al₂O₃/Al, dielec. props. 0-80404

dielectric properties of solids continued

β -Al₂O₃, conduction and dielec. loss mechanisms, paired interstitialty model 0-107468
 β -Al₂O₃-Na₂O, AC ionic cond., dielec. and NMR relax. 0-59713
 As₁₀Ge₅Te₇Ag, glass, elec. and dielec. props., Ag additions effect 0-65558
 BaFe₂O₉, ferrite, DC cond., dielec. props., lattice consts. 0-80272
 Ba₂NaNb₆O₁₅, cryst. comp. effect on low temp. phase transition 0-71346
 (Ba,Sb)_{1-x}TiO₃ 0-60514
 BaTiO₃ film, struct. and dielec. props. 0-60514
 BaTiO₃, paraelectric crystal, nonlinear props. 0-84699
 BaTiO₃, spontaneous polarisation, low temp. meas. 0-75921
 BaTiO₃:BaTiO₃, dielec. props. and microstruct. 0-60481
 Ba(Ti_{1-x}Sn_x)O₃ film, struct. and dielec. props. 0-60514
 Ba(Ti_{1-x}Sn_x)O₃ thick film, ferroelec., phase transitions and dielec. props. 0-97215
 Bi₂Ti₂O₁₂, elec. charact., phase transition obs. 0-60517
 Bi₂WO₆, ferroelectric, dielectric props., elec. cond. and relaxation phenomena obs. 0-80692
 CH₃NH₃Ga(SeO₄)₂·12H₂O, dielec. relax. near transition temp. 0-60493
 CaF₂:Er, defect structure, quenching effect, dielec. relax. and optical absorption 0-65031
 CaF₂:Er, near-Debye dielectric responses 0-71291
 CaF₂:Li(Na)(K)(Rb), dielec. relax., activation energy, rel. to vacancy pair reorientation 0-88917
 CaF_{2-x}H_x, ionic cond. determ. from admittance and dielec. loss meas. (French) 0-107479
 Cd₂ polytypic crystals, dielectric loss behaviour 0-66108
 Cd(NO₃)₂, phase transition, SHG, optical and dielec. meas. 0-71334
 CdS, elastic, piezoelec. and dielec. props. 0-108157
 CdS, elastic, piezoelectric, and dielec. props., 4.2 to 300K 0-60508
 Co, Zn_{1-x}Fe_xO₄, ferrite, DC cond., dielec. props., lattice consts. 0-80272
 Cs(H_{1-x}D_x)₂PO₄, dielec. props., temp. meas. 0-71335
 CuCl(Br), electronic dielec. const., vol. depend., Clausius-Mossotti model 0-100630
 Fe borate single crystals, dielectric, pyroelectric props., vapour phase transport growth 0-80673
 Ga ultrathin metallic filaments, appearance of dielec. instability, coexistence with supercond. 0-103784
 GaAs, semi-insulating, microwave permitt. meas. 0-60479
 Hg ultrathin metallic filaments, appearance of dielec. instability, coexistence with supercond. 0-103784
 HgI₂, IR lattice vibr. and dielec. dispersion 0-76018
 In ultrathin metallic filaments, appearance of dielec. instability, coexistence with supercond. 0-103784
 KClBr_{1-x}, dielectric const. determ. 0-108145
 K₂F(CN)₆·3H₂O, ferroelec. and paraelec. phases, dielec. props. meas. 0-60494
 KH₂PO₄, critical and tricritical phenomena, susceptibility, exponents 0-75976
 KH₂PO₄ family of crystals, proton modes, dielec. spectroscopy 0-75915
 KH₂PO₄, spontaneous polarisation, low temp. meas. 0-75921
 KH₂PO₄-type ferroelectrics, dielec. props., four-cluster approx. 0-97202
 K₂H(SO₄)₂ and K₂D(SO₄)₂, dielec. props. and phase transitions 0-60482
 K_{1-x}Na_xTaO₃, quantum ferroelectric, dielec. susceptibility 0-103922
 K₂O₂Cl₂, single cryst. with H⁺ interstitials, protonic cond. from dielec. meas. 0-107515
 K₂SO₄, phase transform., mech. of thermal hysteresis, DTA, dilatometry and dielec. meas. 0-75353
 K₂SnCl₆, phase-transition-induced dipolar relax. 0-66107
 KTa_{1-x}Nb_xO₃, quantum ferroelectric, dielec. susceptibility 0-103922
 LiNH₄SO₄ and LiND₄SO₄, dielec. pyroelec., and thermal props. 0-60509
 LiNbO₃, spontaneous polarisation, low temp. meas. 0-75921
 Mg₂SiO₄:SiO₂, elec. and dielec. props. 400-900°C 0-104953
 Mg_{0.25}Zn_{0.75}Fe₂O₄, ferrite, DC cond., dielec. props., lattice consts. 0-80272
 ND₂D₂PO₄, cryst., transverse and longit. elec. susceptibilities, modified Ising model calcs. 0-97203
 (NH₄)₂BeF₄, far-infrared and submillimetre dielectric response 0-80782
 (NH₄)₂Cd₂(SO₄)₃, dielec. and spontaneous polarisation, -195 to -180°C, particle size depend. 0-97200
 NH₄H₂PO₄, cryst., transverse and longit. elec. susceptibilities, modified Ising model calcs. 0-97203
 NH₄HSeO₄, cryst. struct., dielec. and ferroelec. props. 0-60528
 NH₄HSeO₄, ferroelec., phase transitions, permittivity and pyroelectricity meas. 0-71350
 (NH₄)₂SO₄, static and dynamic dielec. behaviour 0-71337
 NH₄X, X=halogen, phonon dispersion, cohesive and dielec. props. in three body force shell model 0-79892
 NaCl:Ca²⁺, dipole concs. determ. considering aggregation, expt. and theoretical comparison 0-59512
 NaCl:Cd²⁺, dielectric loss following plastic deform. 0-84690
 NaCl-type crystals, ionic polarisabilities, pseudopot. calc. 0-88913
 Na_{1-x}Li_xNbO₃ mixture, ferroelec.-paraelec. transitions, dielec. props. meas. 0-66125
 NaNO₂, ferroelec., dielec. and thermal behaviour 0-80680
 Na₂O-SiO₂ glass, conduction and dielec. loss mechanisms, paired interstitialty model 0-107468
 Na₂Sc₂P₂O₇, fast-ion conductor, struct. phase transition 0-88362
 NbSe₃, freq. depend. conductivity 0-107838
 NiBr borate single crystals, dielectric, pyroelectric props., vapour phase transport growth 0-80673
 NiZn ferrite, dielec. props., Jahn-Teller ion effects 0-97181
 PLZT ceramic, ageing, dielec. props. 0-88940
 PLZT ceramics, modified by Ca²⁺(Sr²⁺)(Nd³⁺)(Y³⁺), dielec. behaviour 0-60519
 PLZT, diffuse phase transitions, Curie temp., dielectric props. 0-75979
 (Pb,Ba)(Zr,Ti)O₃, diffuse phase transitions, Curie temp., dielectric props. 0-75979
 (Pb_{1-x}Ba_x)₂GeO₁₁, ferroelec. phase transition, dielec. const. and quasi-elastic light scatt. 0-71289
 PbHPO₄, crystals, ferroelec. phase transition, hydrostatic press. influence, dielec. meas. 0-88936
 Pb(Mg_{1/3}Nb_{2/3})O₃:PbTiO₃, ceramic dielectric, electrostriction, relaxation, polarisation 0-80700
 PbS(Se)(Te), energy gap and dielec. props., 77 to 373K 0-66100
 PbSc_{0.5}Nb_{0.5}O₃, single cryst., dielec. props. 0-66126
 Pb(Zr,Ti)O₃, ceramics with ladder type struct., prep. and props. 0-75945
 Pb(Zr,Ti)O₃, porosity-permittivity relations, depolarising factors determ. and pore effects (Japanese) 0-97189

dielectric properties of solids continued

RbH₂PO₄, critical and tricritical phenomena, susceptibility, exponents 0-75976
 Rb₃H(SO₄)₂ and Rb₃D(SO₄)₂, dielec. props. and phase transitions 0-60482
 Se film, amorphous, empirical formula for temp. depend. of dielec. loss peak 0-97197
 Si-SiO₂-polySi thin film structures, dielectric props. (Slovak) 0-75934
 SiO₂, dielec. and optical props., chemical disorder effects 0-80815
 Sn ultrathin metallic filaments, appearance of dielec. instability, coexistence with supercond. 0-103784
 Sr_{0.75}Ba_{0.25}Nb₂O₆, ceramic ageing dielec. props. 0-88940
 SrF₂:La, type-I dipole reorientation, activation vol. determ. from dielec. const. 0-88916
 TiO₂, porosity-permittivity relations, depolarising factors determ. and pore effects (Japanese) 0-97189
 Tl halides, static dielec. constant, strain derivatives 0-100629
 V₂O₅, ferroelec. semicond., dielec. and elec. meas. 0-60516
 WO₃-P₂O₅ glass, AC cond. and dielec. props. 0-92717
 Y₂O₃-AlN-SiO₂ oxynitride glasses, elec. props. 0-80267
 ZnO, elastic, piezoelec. and dielec. props. 0-108157
 ZnO non-ohmic ceramic, degradation props. under AC and DC bias 0-80262

dielectric properties of substances

see also antiferroelectricity; dielectric depolarisation; dielectric function; dielectric materials; dielectric measurement; dielectric phenomena; dielectric polarisation; dielectric properties of gases; dielectric properties of liquids and solutions; dielectric properties of solids; electric strength; optical susceptibility; permittivity; piezoelectricity; pyroelectricity
 biological, dielectric constant meas. 0-94417
 biological substances, tabulation for freq. range 10 kHz to 10 GHz 0-108143
 E.coli suspensions, dielec. anal., interfacial polarisation theory appl. 0-97876

dielectric relaxation

see also dielectric resonance
 alkali halides, thermally stimulated depolarisation of NCO⁻ centres 0-80678
 alkaline earth fluoride, doped with trivalent rare earths, migration entropy for bound fluorine motion 0-71303
 alkyl halide, amorphous, depolarisation thermocurrents and dielectric relaxation time distrib. (French) 0-60490
 allyl ether, dielectric relaxation obs. at millimetric wavelengths 0-71311
 apatites, dipolar reorientations, TSD study 0-107068
 aromatic butadienes, dipole moment and dielectric relax. meas. 0-83516
 aromatic ethylenes, dipole moment and dielectric relax. meas. 0-83516
 cellulose, dielec. relax. studies, TSD meas. 0-88907
 conducting solutions, bridge method for meas. dielectric relaxation 0-82793
 4-cyano-4'-octylbiphenyl, dielectric relax. anal. in nematic and smectic phases 0-108153
 t-cyanobutane, dielectric relaxation study, complex permittivity 0-80688
 Debye generalised fluid model, dielectric relax., depolarised dynamic light scatt. 0-108156
 N,N-dimethylacetamide in tetrachloromethane, dielectric relax. and complex permittivity 0-108149
 dimurstoyl-1-3-lecithin aqueous soln., pulse relaxation method for dielec. const. determ. (German) 0-71308
 p-dioxane-H₂O at 11 and 25°C, US absorption 0-65171
 dipolar liquid time-variation of dispersion and absorption of third-order electric polarisation, mol. relax. times 0-60487
 dipolar molecules in dil. soln., nonlinear dielec. relax., effective relax. time 0-97195
 dipoles in asymmetric potentials 0-88915
 distribution function of relax. times, first order moments from permittivity data (French) 0-88918
 epoxides, dielectric relax. and deform props., cross-link density effect (Russian) 0-60942
 ethanol, electron solvation, ps laser study 0-101032
 ethanol solution in benzene, dielec. relax. time by RF cond. meas. 0-71302
 ethylene-CO copolymer, dielec. absorpt. meas., permittivity (French) 0-103916
 ferroelectric bodies, deformable, coupled electroacoustic eqns. 0-96092
 field induced thermally stimulated polarisation-depolarisation currents, relaxation, book contribution 0-80687
 glass, dielectric relax. loss, two level Anderson Halperin Varma model 0-66106
 glass, electrical relax., Debye-Falkenhagen theory 0-108155
 glass, high-field ionic and polaronic cond., dielec. relax., Poole-Frenkel theory 0-100351
 glasses, dielectric relax., order parameter model appl. 0-108151
 glycerol, highly viscous state, static and dynamic Kerr effect obs. 0-60545
 hydroxyapatites, dipolar reorientations, TSC study 0-60491
 ice, dielectric relaxation in presence of ionic impurities, block layer meas. tech. 0-103914
 kaolinite rare-earth complexes, relax., molar free energy of activation for dipole relax. 0-88919
 LF fluctuation, dissipation and relaxation properties, universality 0-84687
 liquid, dielectric relax. time rel. to single particle correl. time 0-97193
 liquids, associated, mechanism of structural dielectric relaxation 0-107034
 liquids, dielectric relax., order parameter model appl. 0-108151
 MBBA, dielec. relax. in metastable modification of solid phase 0-84689
 methacrylic polymers, multiple dielectric relaxations, investigation by thermally stimulated current and creep methods 0-93238
 methanol, electron solvation, ps laser study 0-101032
 methanol solution in benzene, dielec. relax. time by RF cond. meas. 0-71302
 methyl iodide, liq., mol. reorientation, dielec. and viscosity meas. 0-100157
 methylammonium alums, dielec. relax. near transition point 0-71301
 nematic liquid crystal mixtures, dielec. permittivity dispersion 0-88921
 4-n-octyloxyphenyl 4-n-pentylxybenzoate, permittivity, microwave dielectric relaxation 0-80671
 organic liquid systems, dielectric and dynamic Kerr-effect studies 0-60496
 4-n-pentylxy-phenyl 4'-n-octyloxybenzoate, nematic, dielec. relax. and freq. depend. of threshold voltage 0-60497

dielectric relaxation continued

- perfluorinated polymer, Krytox 143-AB, viscous, viscoelastic and dielectric properties 0-70440
- perspex, electric conduction and isothermal dielectric relax. 0-80285
- phenolic Mannich bases, dielec. relax. study 0-97196
- piezoelectric solids, shape-dependent damping 0-93242
- PMMA, effect of fillers on molecular motions, dielectric relax. meas. 0-80691
- polar fluids, dielec. relaxation spectroscopy in microwave region, double-beam interferometry (*German*) 0-71309
- polar fluids, rigid, dielectric relaxation theory 0-60495
- polar liquids, binary mixtures, Sarma and Rao's rel. for dielectric relax. time 0-88914
- polar liquids, HF conductivity and relaxation time 0-96929
- polar liquids in double layer capacitors, RF conduction, ion diffusion effect 0-107883
- polar molecules, viscosity activation energy and relax. time, RF cond. meas. 0-96677
- polar molecules in nonpolar solvent, far IR spectra and dielec. relax. 0-71312
- poly-4-chlorostyrene, undiluted, dielec. relax. spectrum above T_g 0-97194
- polycarbonate films, high temp. relaxations 0-97187
- polyethylene, alcohol infused, loss peaks due to secondary groups 0-84688
- polyimide films, transient current in time range 10⁻⁴ to 10 s at temps. 180 to 280°C 0-65729
- polymer chains with rigid bonds, local relax. times, mol. dynamics study (*Russian*) 0-59373
- polyoxymethylenes, dielectric property relaxation, unidentical relaxator system activation model (*Russian*) 0-80694
- polyoxymethylenes, dielectric relaxation, molecular mechanism (*Russian*) 0-88923
- polypropylene film, dielectric relaxation, β -mode investigation 0-93239
- polypropylene glycol melt, mol. motion, dielectric and Kerr effect relax. obs. 0-60498
- polystyrene, particles in dil. soln., bridge method for meas. dielectric relaxation 0-82793
- polyvinylidene fluoride, cryst. form II, anisotropy of dielec. relax. 0-103915
- polyvinylidene fluoride, poled, dielec. relax. spectra 0-80690
- serum albumin, bovine, hydrated, dielec. and elec. props. 0-97854
- smectic phases, long mol. axis reorientation, LF dielec. dispersion 0-70124
- trans-stilbene, soln., lifetime and anisotropic fluoresc., viscosity effects (*German*) 0-106352
- tartrate, Na[K_{1-x}(NH₄)_x].C₄H₄O₆.4H₂O, dielec. relaxation 0-108152
- TGS powders, dielec. dispersion 0-97180
- thermally stimulated depolarisation, many-body model of universal dielec. response 0-75927
- time range spectroscopy with real-time evaluation for nanosecond range (*German*) 0-71307
- urethane polyester elastomers, dielectric relax., spatial network density (*Russian*) 0-71310
- vitreous systems, local motions, dielec. losses and relax. phenomena 0-108154
- water, dielec. relaxation of compressed liquid at 17.613 GHz using microwave refl. meas. method (*German*) 0-71306
- X-zeolites, dielectric relax. anal. 0-108153
- AgNa(NbO₃)₂, crit. dynamics, hydrostatic press. effect, dielec. props. meas. 0-71328
- Al₂O₃, anodic film, trapped O₂ and effect on dielec. stability 0-100634
- β -Al₂O₃-Na₂O, AC ionic cond., dielec. and NMR relax. 0-59713
- As₁₀Ge₅Te₇₅Ag_x glass, elec. and dielec. props., Ag additions effect 0-65558
- Au/n-TiO₂ Schottky diodes, I-V and C-V characts. 0-96988
- BaF₂:La³⁺, thermal depolarisation of La³⁺-F⁻ defect dipoles 0-75926
- Bi₂WO₆, ferroelectric, dielectric props., elec. cond. and relaxation phenomena obs. 0-80692
- CH₃NH₂Ga(SeO₄)₂.12H₂O, dielec. relax. near transition temp. 0-60493
- CaF₂:alkali metal cation, thermal depolarisation study 0-108147
- CaF₂:Er, defect structure, quenching effect, dielec. relax. and optical absorption 0-65031
- CaF₂:La³⁺, thermal depolarisation of La³⁺-F⁻ defect dipoles 0-75926
- CaF₂:Li(Na)(K)(Rb), dielec. relax., activation energy, rel. to vacancy pair reorientation 0-88917
- CaF₂:O²⁻, CaF₂:Na⁺, O²⁻ and CaF₂:Y³⁺, O²⁻, thermal depolarisation obs. of defect clusters 0-71299
- CaF₂:Y³⁺, ionic cond. and thermal depolarisation obs. of defect clustering 0-71298
- KClO₄:CrO₂²⁻(SO₄²⁻), AC electrical conductivity meas. between temp. range 25-325°C, automated technique 0-59699
- K₂Fe(CN)₆.3H₂O, ferroelec. and paraelec. phases, dielec. props. meas. 0-60494
- K₂SeO₄, dielec. dispersion, 5-900 MHz, near incommensurate-commensurate transition 0-60522
- K₂SnCl₆, phase-transition-induced dipolar relax. 0-66107
- α -LiIO₃, depolarisation current, dielectric const. relaxation behaviour (*Chinese*) 0-88905
- (NH₄)₂SO₄, static and dynamic dielec. behaviour 0-71337
- PLZT ceramic, ageing, dielec. props. 0-88940
- Pb(Mg_{1/3}Nb_{2/3})O₃:PbTiO₃, ceramic dielectric, electrostriction, relaxation, polarisation 0-80700
- Pb₃(PO₄)₂, ferroelastic, dielectric anomalies, phase transitions, permittivity, relaxation (*Russian*) 0-71293
- xPbTiO₃+(1-x)PbCd_{1/3}Nb_{2/3}O₃, phase transition spread, polarisation relaxation, dielectric susceptibility (*Russian*) 0-75922
- RbHSO₄, ferroelec., dielec. dispersion 0-97179
- RbH₂(SeO₃)₂, dielec. relax. near ferroelec. Curie temp. 0-97207
- Rb₂ZnCl₄, dielec. dispersion, 5-900 MHz, near incommensurate-commensurate transition 0-60522
- Se, amorphous film, dielec. activity obs. near glass transition temp. 0-75933
- Se, liq., dielectric relax. and elec. cond. 0-108150
- Se:As, amorphous film, dielec. activity obs. near glass transition temp. 0-75933
- Se-Tl-S alloys, liq., dielectric relax. and elec. cond. 0-108150
- Si-SiO₂-polySi thin film structures, dielectric props. (*Slovak*) 0-75934
- Sr_{0.75}Ba_{0.25}Nb₂O₆, ceramic ageing dielec. props. 0-88940
- SrF₂:La, type-I dipole reorientation, activation vol. determ. from dielec. const. 0-88916

dielectric relaxation continued

- SrF₂:La³⁺, thermal depolarisation of La³⁺-F⁻ defect dipoles 0-75926
- WO₃-P₂O₅ glass, AC cond. and dielec. props. 0-92717
- dielectric resonance**
see also *dielectric relaxation; paraelectric resonance*
No entries
- dielectric strength** see *electric strength*
- dielectric susceptibility** see *optical susceptibility*
- dielectric thin films**
see also *ferroelectric thin films; insulating thin films; optical films; piezoelectric thin films*
electron microscopy, dielectric support film screening effects 0-86504
hexamethyldisiloxane plasma polymerised thin film, charge trapping characts. 0-96895
polymer films, dielectric constant meas. parallel to film surface 0-97183
polyphenylene oxide thin films, electrochem. prep., impurity effects on cond., electroforming 0-88655
polypropylene films, dielec. props., impurity effects 0-71304
polystyrene film, thermally stimulated discharge currents 0-71300
polystyrene films, soln. grown, elec. cond. meas. 0-97020
PVC films, soln. grown, DC cond. mechanisms, field and temp. depend. 0-97021
silicate: Yb₂O₃ glassy film, Yb laser spectral microanalysis 0-76585
stearic acid, vacuum evaporated film, for low-loss capacitors 0-71317
stearic acid films, evaporated, vac. effects 0-97435
thickness and refractive index meas. by photoelectric scanning 0-105606
thin island films, statistical theory for dielectric props. 0-80699
Al-Ta₂O₅-Al, healing of defects in dielec. film by anodisation 0-65406
AlF₃ in Al-AlF₃-Al MIM thin film structures, dielec. and elec. props. (*Slovak*) 0-100536
AlN films, RF reactive ion-plating, struct. and morphology 0-104074
BaTiO₃ ceramic films, dielec. strength, statistical anal. 0-75935
BaTiO₃ film, dielectric props. depend. on sinusoidal elec. field 0-71318
FeF₃ thin film, polarisation mechanism, AC and TSC study 0-66104
GaAs oxide film form., ion implantation effects 0-100266
MoSi₃ oxide film, dielec. props. and growth kinetics 0-81215
NiFeF₃, form. on Fe-Ni alloys by fluorination 0-101035
Si-SiO₂ interface, barrier height in MOS tunnelling structures 0-88644
Si₃N₄ thin film, reactively sputtered, struct. and elec. props. 0-88656
SiO deposition using solar furnace 0-89148
SiO_x on YZ-LiNbO₃, SAW props. 0-84356
SiO₂ thin film dielec., in MIM struct., interfacial props. rel. to non-stoichiometry 0-80399
Ta₂O₅ film capacitive humidity sensor Panahume (*Japanese*) 0-105658
Ta₂O₅, reactively sputtered on Si, dielectric and optical props. obs. (*Bulgarian*) 0-89144
TeO₂ thin films, dielec. props. rel. to fabrication conditions 0-97199
TiO₂ film, ion plated, DC cond. study 0-100457
TiO₂-SiO₂ mirror, dielectric, Rayleigh scatt. at 441.6 nm 0-97367
ZnS-MgF₂ mirror, dielectric, Rayleigh scatt. at 441.6 nm 0-97367
- dielectric triodes** see *space-charge limited devices*
- dielectric waveguides**
see also *optical waveguides*
far IR antenna appls., reviews 0-69553
flow detection using UHF EM field pattern display 0-104378
low-loss dielectric tube leaky waveguide, transmission characts. 0-95999
weakly anisotropic rectangular dielec. optical waveguides, wave propag. anal. using coupled modes 0-64154
- dielectrics** see *dielectric materials*
- diesel-electric power stations**
hybrid solar-diesel power stations for optimum energy utilisation 0-89598
present net value anal., cost reduction factor 0-94027
- diesel engines** see *internal combustion engines*
- diesel power stations** see *diesel-electric power stations*
- difference equations**
bubble growth in superheated water at reduced pressures, finite difference anal. (*Japanese*) 0-92150
conduction-convection problems, error growth for explicit difference schemes 0-92017
container subjected to forced pitching oscillation, liquid motion, nonlinear anal. 0-96270
cracks dynamic propagation in anti-plane shear, anal. by finite differences 0-84240
dielectric gratings, arbitrary profiles, scatt. and guiding of EM waves 0-96005
electric fields, intensity, numerical calculation methods (*French*) 0-106413
ferromagnetic optical inspection, method of higher harmonics, difference schemes 0-89444
flow, supersonic, parabolic Navier-Stokes equations, implicit finite-difference method using fractional steps technique 0-69866
furnaces, walking-beam, numerical soln. of two-dimens. temp. field, boundary condition modification (*Polish*) 0-87706
gas-particle flow in shock tube, finite difference calc. (*Japanese*) 0-79390
generalised random walks, transform. of recursion relations 0-101757
inelastic power-law fluid, unsteady flow in circular tube; implicit finite difference anal. 0-83821
inverse method for solving differential-difference and difference-difference eqns. 0-105513
lossy corrugated structures, plane wave scatt., quantitative results 0-96005
mechanics, mountain massif, pre-face zone, stressed state, finite difference method (*Ukrainian*) 0-74735
multiparameter splitting schemes for solution of spatially three-dimensional nonstationary problems 0-68047
Navier-Stokes equations, two dimensional, numerical soln. methods (*Russian*) 0-101718
nonlinear heat transfer on boundary, difference method of solving conjugate nonstationary convection problem 0-92020
nonthermally conducting gas, monotonic difference scheme of open calculation (*Russian*) 0-103039
nonuniform grids in finite difference approximations, application to fluid flow problems 0-105507
optical waveguide calc., finite difference methods (*Russian*) 0-64189
otolith membrane, variable gravity model 0-85573
point-defect clustering during irradiation 0-92521
seismic depth migration after stack, finite-difference method 0-98254
seismic depth migration before stack, finite-difference method 0-98255

difference equations continued

stability of difference schemes for multidimensional equations of acoustics 0-105512
steady flow about blunt bodies, finite difference methods 0-96280
steady-state recirculating flows, finite difference schemes, practical evaluation 0-106776
Stokes problem, second-order difference scheme 0-90678
thermal characteristics of finite element and finite difference calcs. for transient problems, comments 0-69633
triangular gratings, surface wave guiding, quantitative results 0-96005
two dimensional, nonlinear partial difference eqns., two point function 0-101762

differential calculus see differentiation

differential equations

see also boundary-value problems; difference equations; Green's function methods; integro-differential equations; linear differential equations; Navier-Stokes equations; nonlinear differential equations; partial differential equations
atom+ molecule, rotational rainbow maxima: a time dependent study 0-58353
atoms, general adiabatic-diabatic transformation matrix, electronic non-adiabatic transitions 0-93751
bifurcation and transition toward stochasticity for dissipative dynamical systems 0-57201
Brillouin theorem, proof 0-91415
determination from experimental curves 0-77604
dynamical system, limit cycles and symmetries 0-62462
eigenvalues, coupled second-order differential eqns., numerical solution 0-94976
evolution equations, connection to P-type differential eqns. 0-57078
fission reactor digital simulator software development, kinetic equations integration, numerical solution method 0-68901
graphite arc, in Ar flow, meas. of anode voltage drop 0-84022
Gurney's ballistics calc. 0-67946
holographic gratings, 4-port Bragg device anal. 0-83564
Lagrange eqn. symmetries and equivalent Lagrangians 0-86071
Mathieu equation with damping, variational anal. 0-57079
nonlinear field eqn. and differential Schrodinger eqn. correction (French) 0-77637
nonlinear optical amplifier, coherent radiation statistical props. 0-99691
nonlinear sonic wave, excitation by quasi-monochromatic Alfven pumping 0-106649
nonmonotone stochastic integrals and stochastic differential calculus (French) 0-90779
oil-bearing layer with input parameter correction, discrete dynamic model 0-83778
one-component plasma in two and three dims., static props., semi-analytic theory 0-87853
optically thin phase grating, comparison of optical path and differential eqn. methods 0-102823
optimal control, differential eqn., canonical, functional relation expressed by Volterra series (French) 0-73159
perturbed motion rel. to KS transformation osculating variables 0-109344
physical parameter reduction and similarity anal., mathematical theory 0-98785
polymer diffusion equation with hydrodynamic interaction, equiv. normal coord. 0-79966
pulmonary gas transport models, boundary conditions and geometry 0-85426
quantum scattering theory, variable interval variable step method for soln. of linear second order coupled differential eqn. 0-105527
quantum three particle system, action-angle variables 0-95708
radiative plus conductive heat transfer, differential anal. method 0-74699
saturated steam parameters in reactor containments with escape of coolant, equations of state 0-68764
second order, without first derivatives, fourth-order numerical method 0-86107
second order differential equations, symmetries and invariants 0-82915
second order equation invariants, auxiliary, eqn. struct. 0-68021
stationary system, diffusion mixing model, approx. soln. 0-79410
Sturm Liouville eqns., numerical anal. and eigenvalue problems 0-90655
supernovae, type II, light curves analytic solns. 0-77427
symmetries and differential equations 0-105807
symmetry, non-pointlike transformations 0-98786
viscoelastic body containing cracks, durability calcs. 0-79227
viscous incompressible liquid, heat conductivity problem (Russian) 0-69897
volume phase gratings at higher Bragg angle incidence, coupled wave differential eqns. 0-102666
³He-⁴He dilution refrigeration system, choice of tube lengths and diameters 0-57308

differential scanning calorimetry see thermal analysis

differential thermal analysis see thermal analysis

differentiation

see also differential equations
education, exterior algebra and exterior differential forms for electromagnetic problems 0-57037
objective and regular differentiation and integration, constitutive law and transport (French) 0-57090
spectra, filtering props. of polynomial methods 0-66900

diffraction

see also acoustic wave diffraction; diffraction gratings; diffractometers; electromagnetic wave diffraction; electron diffraction; neutron diffraction
corner diffraction, Albertsen's coeff. testing via spectral domain approach 0-87304
cylindrical longitudinal pulse, diffracted by crack 0-92082
elastic wave front excitation and diffr., by point source with semi-infinite shield 0-79202
forward diffraction of Stokes waves by a thin wedge 0-92167
plane elastic wave diffraction by wedge, three dimensional nonstationary problem 0-69723
plane pulse diffracted by plane screen 0-82652
seismic wave diffraction at coal seams, approx. diffr. theory for transparent half-planes 0-89974
solitary wave, diffraction by circular island in ocean, shallow-water theory (French) 0-83803
spherical wave diffracted by plane screen 0-82652

diffraction gratings

see also holographic gratings
absolute efficiency meas. device 0-87540
anastigmatic mounting for ellipsoidal concave grating 0-106634
angle measurement between edges of distant objects using diffr. grating 0-86259
bi-metallic diffraction grating study 0-87525
binary phase gratings for fibre-optic communications 0-64201
blazed dielectric gratings for integrated-optics applications, microwave models 0-87564
blazed dielectric gratings with high beam coupling efficiencies 0-64211
CdS, single crystals, laser emission from surface diffraction grating 0-95900
circular scale calibration by reflection grating polygon (German) 0-86250
concave, efficiency changes across the ruled area 0-91896
concave grating, polarisation anomalies 0-69519
coupler, chirped and curved, for focusing beam 0-78979
crossed-beam volume gratings, three dimens., diffr. characts. 0-78975
curved, coupled mode theory 0-83668
Czerny-Turner grating monochromator, Cary principle dynamic dispersion determ. 0-58666
deep dielectric gratings, light diffr., transform. props. 0-99835
dielectric gratings, arbitrary profiles, scatt. and guiding of EM waves 0-96005
dielectric waveguide, energy diffraction input induced power depend. on impact parameter 0-64170
diffractive logic elements for optical computers 0-78993
double-grating monochromator, theory 0-58708
dual-grating direct-reading spectrograph mirror system design and performance 0-81397
dye DFB laser with integrated Si and polyurethane channel waveguide 0-74373
echelle efficiencies, theory and expt. 0-102802
electrooptic deflector of blazed grating type, multistage system 0-106625
EM theoretical developments 0-106633
EM wave props., theoretical model 0-91732
evanescent wave holography using Gaussian beam, recording geometry and colour sensitivity 0-58473
finitely conducting cross grating theory 0-106635
finitely conducting crossed grating applications 0-106636
fixed groove depth lamellar grating Fourier transform spectrometer 0-77885
four-layer waveguide diffractive injection efficiency optimisation (Russian) 0-64206
Fourier hologram recording in optical system with synthetic aperture 0-95852
grazing incidence grating techniques to tune flash lamp pumped dye lasers 0-95914
Hadamard spectrometer, curved slits used to increase throughput 0-95149
harmonic phase grating with inclined layers, Bragg peak angular widths 0-58712
holographic platform, optical path stabilisation with magnetooptic periodic grating 0-99678
image, dissector tubes, echelle spectrographs, design considerations 0-91918
image transmission through monomode fibres, restoration using grating 0-69512
integrated grating circuit for guided-beam multiple division fabricated by electron-beam direct writing 0-91934
integrated optical grating circuit fabrication by electron beam direct writing 0-64214
integrated programmable planar waveguide components formed by optically writing Bragg diffraction gratings into photochromic structs. 0-79011
laser beam diameter meas. using a grating 0-102745
laser produced gratings, review (Rumanian) 0-87542
lossy corrugated structures, plane wave scatt., quantitative results 0-96005
magnetic domain gratings, and appl. 0-88970
masters, manufacture using radial metrological pattern generating engine 0-57282
mechanically ruled and holographic concave diffr. grating parameter relationships 0-87543
microgratings for guided-beam deflection, electron-beam direct-writing fabrication 0-102856
modelling of planar transmission-type diffraction gratings compatible with synchrotron radiation sources 0-90964
monochromator mounting with ruled diffr. grating at 45° off-plane 0-87479
multichannel apparatus for material analysis using atomic spectra 0-76586
optical dispersive resonators with system of reflective gratings (Russian) 0-96029
optical processor, incoherent, for making 'spectrogram' of 1-D function 0-87528
parallel plane, periodic structure, diffr. of plane wave 0-102620
periodic grating, mixed diffraction problem (Ukrainian) 0-69323
periodic object single sideband Fresnel diffr. pattern studies 0-106440
periodic structure generation by coherent beam interference 0-69570
phase grating, optically thin, comparison of optical path and differential eqn. methods 0-102823
planar optical waveguide concentric-arc grating for thin-film spectrograph 0-58778
planar waveguide blazed dielectric diffraction gratings, anal. and design 0-58779
predisperser for large plane-grating spectrograph 0-73477
prism-grating, prism-prism and grating-grating compounds for deflection angle compensation 0-95990
radial grating lateral shear heterodyne interferometer, adaptive optics appl. 0-77843
radiation generators, echelle use, electron flow (Russian) 0-69314
reflective, high efficiency, scattering types 0-99619
Rowland circle, corrected, least-squares method derivation 0-64161
ruled, lamellar and holographic, equivalence in const. deviation mountings 0-87474
Schlieren apparatus with multiple slit grating, optical inhomogeneity study (Hungarian) 0-69515
soft X-ray performance of toric gratings fabricated with plane waves 0-90967
soft X-ray spectra, meas. by photoelectron anal. 0-73557

diffraction gratings continued

- spatial gratings, transient light-induced, by successive optical coherent pulses 0-64115
- spectrophotometer for measuring small sharp absorption bands in solids at low temps. 0-86456
- telescope-spectrometer combination, optical props. 0-87455
- theoretical model and numerical apps. 0-95786
- thick planar grating, Bragg diffraction of finite beams, coupled-wave theory 0-63917
- thin film electrooptic deflector using induced grating with variable blaze angle 0-99862
- transmission gratings for meas. of optical constants of Au , 100 to 1000 eV 0-93258
- triangular gratings, surface wave guiding, quantitative results 0-96005
- unpolarised monochromatic light, total absorption by crossed grating 0-106448
- volume reflecting grating parameters determ. for freq. selective optical elements (*Russian*) 0-74492
- VUV concave gratings, holographic and conventionally ruled, efficiency meas. 0-91910
- waveguide grating, diffraction efficiency, Brewster's law 0-91935
- white light processing using diffraction grating method 0-106470
- Woods anomaly angular alignment gratings 0-69503
- X-ray grating optical blazing configuration calc. 0-105762
- X-ray gratings, diffraction efficiency and radiation resistant substrate materials 0-90960
- X-ray lithography, spatial period division, submicrometre linewidth grating prod. 0-69556
- X-ray spectrometer-telescope system for solar corona studies 0-105168
- X-ray spectroscopy, ultrashort, electron microprobe local anal. of light elements 0-99027
- X-ray transmission gratings for 7-304 Å operation, efficiency and resolution 0-82195
- GaInPAs/InP heterostructure DFB laser under optical pumping, lasing characts. 0-87396
- Ge surface reflectivity changes and moving diffraction grating efficiency 0-58662
- LiNbO_3 grating-tuned picosecond IR source with CdSe down-conversion 0-74435
- LiNbO_3/Ti optical waveguide, SiO_2 thin film grating, surface wave mode conversion, static strain-optic effect 0-87561
- $\text{Pb}(\text{Zn},\text{Ti})\text{O}_3$ piezoelectric electrically deformable diffraction grating 0-78963
- SiO_2 thin film grating for LiNbO_3/Ti waveguide mode convertor and reflector 0-64216

diffraction instruments *see* **diffractometers****diffraction model**

- coherent production on nuclei and measurements of total cross sections for unstable particles 0-102034
- diffraction dissociation processes and quark-antiquark jets 0-95246
- diffraction hadronic reactions, statistical description of multipion prod. 0-95260
- elastic hadron-hadron diffraction scatt. processes, scaling, conformal mapping without spurious cut 0-82992
- elastic scattering, small and large momentum transfer relations (*Russian*) 0-86698
- hadronic diffraction, elastic scatt. as tunnelling phenomenon, dual model relation 0-57575
- inelastic diffraction cross section, quark model and three reggeon limit 0-102035
- P+f diffraction model, two component duality and flavouring, Regge fits and pomerons 0-95261
- d inelastic screening, form factor at $t \neq 0$ 0-91070
- $\gamma p \rightarrow \pi^+ \pi^- \pi^+ \pi^- p$, diffractive production, jet-like structure 0-57606
- $\gamma p \rightarrow q\bar{q}p$, quark-antiquark jet diffractive photoprod. in perturbative QCD 0-73714
- K^+n , inelastic charge exchange scatt., diffraction approach, convergent polynomial expansion, scaling 0-78095
- K^+p , 32 GeV/c, exclusive reactions, diffractive dissociation processes, $\pi^+ \pi^-$ and K^+K^- prod. 0-86760
- $K^+p \rightarrow K^+ \pi^+ \pi^- p$, 2.7 to 32 GeV/c, impact parameter bounds, energy and effective mass dependence 0-57640
- K^+p , elastic scatt. and diffractive dissociation, Regge model with $\alpha_p(0) > 1$ (*Russian*) 0-57630
- K^+p , inelastic charge exchange scatt., diffraction approach, convergent polynomial expansion, scaling 0-78095
- μN , 209 GeV, ψ diffractive prod. cross section, $\psi \rightarrow \mu^+ \mu^-$ decays 0-102054
- pp, diffraction dissociation, dip and kink structs., differential cross sections 0-95284
- pp, pp, elastic scatt. and diffractive dissociation, Regge model with $\alpha_p(0) > 1$ (*Russian*) 0-57630
- pp annihilation cross sections, corrected differences, fireball model, diffraction cross sections 0-91108
- pp $\rightarrow p\pi\pi\pi$, 12 GeV/c, final state diffraction dissociation, cross section 0-99109
- pp scatt. at higher energies, differential cross section ratio. scaling 0-73741
- πN collisions, $N \rightarrow N\pi^-$ diffractive dissociation, Deck mechanism (*Russian*) 0-86699
- πN in nucleus, diffraction dissociation, dip and kink structs., differential cross sections 0-95284
- πp , inelastic charge exchange scatt., diffraction approach, convergent polynomial expansion, scaling 0-78095
- π^-p , 150 GeV/c, leading particles and diffraction dissociation, 2-, 4- and 6-prong events 0-68486
- $\pi^-p \rightarrow \rho^- \pi^+ X$, diffractive contrib. in multi-Regge factorisation 0-73753
- π^-p , elastic scatt. and diffractive dissociation, Regge model with $\alpha_p(0) > 1$ (*Russian*) 0-57630

diffractometers

- see also* X-ray diffractometers
- combined scanning microdensitometer and diffractometer 0-73529
- light, on-line electron-optical correlation computing, in CTEM 0-99008
- light optical, for electron microscope images operating on line 0-101900
- multiaxis neutron diffractometer automation 0-102417
- neutron, transit-time, for structural investigations of monocrystals 0-64840
- neutron time of flight single crystal diffractometer using a position sensitive detector 0-99404
- optical diffractometer analogue of electron microscope 0-69494

diffusion

- see also* biotransport; diffusion in gases; diffusion in liquids; diffusion in solids; electromigration; membranes; osmosis; permeability; self-diffusion; surface diffusion; thermal diffusion; turbulent diffusion
- adsorbates, surface diffusion calcs. 0-107633
- advective diffusion in branching channels 0-92223
- air pollutants long distant transport, analytical diffusion model 0-94125
- air pollution transport, air quality models development for limited wind fetch 0-104533
- Allende meteorite, tracer elements high-temp. diffusion rel. to primitive meteorites thermal metamorphism 0-109401
- atmosphere, advection diffusion model for real-time forecasting of air pollution episodes in Venetian region 0-77096
- atmosphere, eddy diffusion models for mesosphere and lower thermosphere 0-109198
- atmosphere lowest layers, diffusive character rel. to solar modulation of lunar tide 0-94593
- atmosphere pollutants diffusion, field meas. of benefits of increased stack height 0-76676
- Brownian moving particle, hyperbolic diffusion eqn., effect of finite correlation time 0-86214
- butane, flexible chain molecules, momentum space diffusion eqns. 0-75142
- chemical reaction, diffusion equation, nearly degenerate bifurcations, mode interactions 0-85149
- chemical reaction diffusion systems, Chapman-Enskog development of multivariable master eqn. 0-81283
- chemical reaction diffusion systems, quantum statistical theory, multi-channel reactive scatt. 0-81284
- chemical system, two chemical species reacting at boundary 0-93733
- chemically induced dynamic spin polarisation, orientation depend. 0-63656
- chemically reacting system, coupled heat and mass transfer, finite element soln. 0-68153
- comet belt beyond Neptune, orbital diffusion rel. to short-period comets origin 0-94759
- complex diffusion processes and nonrelativistic quantum mechanics 0-90707
- constrained systems, Hamiltonian construction and diffusion eqns. derivation 0-73258
- controlled processes, nonequilibrium decay effects 0-66764
- controlled reactions, passage time approach 0-71903
- convection-diffusion equation, stability of finite difference approximations 0-82730
- convolutional diffusion in parallelogram cross-section pipe with plug flow (*German*) 0-100000
- convective diffusion to a particle in a fluid with linear kinetics 0-69943
- cosmic ray interstellar diffusion in galactic models with halo appl. to proton nucleon component 0-61971
- cosmic rays, field-aligned inward diffusion rel. to large amplitude wave-trains of neutron intensity 0-94660
- cosmic rays, low-rigidity, weak turbulence diffusion theory rel. to mean free paths 0-98524
- disordered system, donor-acceptor energy transfer, diffusion modulated 0-71888
- dissipative structures, nonlinear reaction-diffusion model, stability of secondary multiple steady states 0-76485
- dissolved species, advection-diffusion eqn. in pulsating crack 0-96312
- electrodes, sheet, mass transfer to continuous moving surface 0-69821
- evolution systems and convection-diffusion, stiffness and stability, Gershgorin theory 0-77626
- fluid, crit. fluctuations, Stokes-Einstein diffusion coeff. determ. 0-90783
- Fokker-Planck eqn. expansion, weak diffusion, critical point 0-57228
- fractured medium, transient 2-D diffusion 0-106841
- globular cluster stars, He settling and effect on inferred ages 0-73013
- growth and patterns of spatial organisation 0-81287
- heat transfer, nonstationary, finite element calcs. 0-83795
- impact parameter for given diffraction angle (*French*) 0-68155
- inhomogeneous Boltzmann gas, lumped phase space, non-linear diffusion approx., stochastic hydrodynamic theory 0-64666
- intermicellar kinetics theory, stochastic approach, master equation for, irreversible reactions 0-76561
- kinetics of reacting solns., diffusional barrier crossing processes, trajectory simulation 0-81280
- layered porous medium transient 2-D diffusion 0-106841
- leaching from model porous bodies by reflection spectroscopy 0-100031
- linear non-stationary diffusion models, non-parametric estimation by Grenander's method of sieves (*French*) 0-57219
- localized patterns in reaction-diffusion systems 0-59130
- macromolecule rotational diffusion props., validity of general ellipsoid model 0-95751
- mass transfer coefficients, concentration dependent diffusivities effect 0-98864
- middle atmosphere (mesosphere), eddy diffusion coeff. determ. from energetics and thermal struct. 0-98412
- multicomponent fluid systems, symmetry of transport matrix for diffusion and heat flow 0-99997
- multidimensional bistable potential, diffusion, WKB calc. 0-101770
- multidimensional diffusion equation, class of general boundary conditions 0-90796
- multiplicative functionals on diffusion processes 0-73286
- multivariate master equation for reaction-diffusion system 0-95045
- neutrino systems, relativistic kinetic theory of transport processes 0-73283
- nonlinear diffusion equation, invariance props., Lie-Backlund groups 0-62596
- nonlinear diffusion equation, stable profile evolution 0-82731
- nonlinear filtering, conditional laws, smoothness, stochastic calculus of variations (*French*) 0-68128
- nonlinear systems, dynamics, heavy damping limit 0-86199
- nonspherical molecules, rot. diffusion tensors determ. from rot. friction tensor calcs. 0-63861
- optically thick horizontal fluid layer heated below, heat transfer 0-99993
- particle motion delocalisation in non-uniform HF field with finite correl. time 0-58450
- periodic wind-tree model 0-86230
- plasma transport, anomalous, electron temp. gradient instability 0-75034
- pollutant, Gaussian plume model parameters for ground-level and elevated sources 0-82010
- protons of inner radiation belt, radial diffusion rel. to energy and pitch angle distrib. 0-67471

diffusion continued

- radiatively driven diffusion in upper main-sequence peculiar stars, rel. to chemical and physical props. 0-82374
 random media, anisotropic, Fourier transformation of space-time transport equation 0-62595
 random networks near percolation threshold, ant in labyrinth problem 0-77732
 reaction rates, diffusion theory, rate const. and transmission coeffs. calcs. 0-89464
 reaction-diffusion systems, bifurcation theory, classification 0-108713
 recombination probability, reactivity depend., scavenger effects 0-76494
 solid particle systems, high Reynolds numbers, mass transfer, Karman-Pohlhausen method 0-79378
 solutes in aqueous fissures in porous rocks, effects of diffusion into rock on transport 0-94553
 stationary system, diffusion mixing model, approx. soln. 0-79410
 steady-state recirculating flows, finite difference schemes, practical evaluation 0-106776
 stellar interiors, astrophysical context of diffusion 0-77381
 travelling waves for a model non-linear reaction-diffusion system 0-89476
 two-way diffusion equations, separation of variables, decaying and growing eigenfunctions 0-62594
 variables separation in diffusion eqn. 0-73285
 H₂, through Pd membrane, diffusion-cell for separation H₂ containing mixtures, solar furnace appl. 0-92245
 Hg discharge, high-pressure, NaI and TlI additives, line broadening and radiative transport 0-74199
 HgMn stars, diffusion model rel. to obs. of Hg in thin atmospheric layer 0-105243

diffusion coefficient *see diffusion***diffusion creep**

- deformation, and diffusion controlled creep crack growth 0-79867
 dislocation and diffusion creep transition 0-88253
 forsterite, ¹⁸O self-diffusion expts., high-temp. creep implications 0-81870
 grain boundaries, interfacial structure effects on high temp. mechanical behaviour 0-59480
 high temperature mechanical behaviour of crystalline solids 0-59568
 Al, creep behaviour, at high temp., influence of oxidation 0-97538
 Al, grain boundary migration, TEM obs. on mechanism 0-79812
 Al₂O₃, fine grained, interface-controlled diffusional creep 0-60915
 Cu, grain boundary migration, TEM obs. on mechanism 0-79812
 Mg-Mn-Ce (1.5, 0.3 wt%), superplasticity role of diffusional creep (*Russian*) 0-97528
 Mg₂SiO₄, ¹⁸O self-diffusion expts., high-temp. creep implications 0-81870
 NaCl polycryst. containing Al₂O₃ dispersion, diffusive creep 0-97531
 Ni, creep rate at low stresses, effect of grain size 0-71707
 Ni_{0.5}Zn_{0.5}Fe₂O₄ coarse grain polycryst. ferrite, diffusional creep (*Japanese*) 0-104238
 Pb, film, thermal strain, strain relax. above room temp. 0-59841
 Si-Al-O-N ceramic, grain boundary desegregation and intergranular cohesion 0-100872
 Zn-Al (22 wt.%) superplastic alloy, grain growth texture 0-81075

diffusion in gases

- see also self-diffusion in gases; thermal diffusion in gases*
 atmospheric transport problems, contaminant movement, Galerkin finite element method 0-74902
 ellipsoidal aerosol particles in binar binary gas mixture, diffusophoresis under hydrodynamic conditions 0-66888
 Fick's law modification 0-96333
 ice crystal morphology, vapour growth, influence of vapour diffusion and heat diffusion 0-64933
 light induced diffusion of gases, isomer, isotope separation (*Russian*) 0-79430
 pollutant transport eqn., 3-D, numerical algorithm 0-106811
 F⁻ ions in Kr and Xe; mobilities and diffusion coeffs. determ. 0-100048
 H, diffusion coeff., in H₂, luminesc. intensity meas. 0-103098
 He-Kr mixture, diffusion coeff. meas. by diffusion in flowing gas 0-83876
 He-Kr mixture, diffusion coeff. meas. by diffusion in flowing gas 0-83877
 N₂O₄, turbulent dissoc. flow, along heated tubes, heat transfer 0-63225
 Na⁺, mobility and longit. diffusion coeffs. in Kr and Xe 0-106866
 Ne discharge in high press. narrow tube, Kadomtsev-Nedospasov instability 0-107004

diffusion in liquids

- see also electromigration; self-diffusion in liquids; thermal diffusion in liquids*
 alkali chlorides, molten, Ag⁺ impurity diffusion 0-59685
 alkali nitrates, molten, Rb⁺ and Cs⁺ ion tracer diffusion coeffs. meas. 0-70437
 anthracene dianions in dimethyl ether, rotational diffusion meas. 0-65262
 binary homogeneous mixtures, motion in infinite rot. cylinder, generalised diffusion theory 0-79328
 binary liquid mixtures, spinodal decomposition, review 0-96657
 carboxymethyl cellulose, aqueous soln., diffusion and mass transfer from rotating disc 0-83827
 cluster diffusion in non-ideal liquids 0-65260
 coefficient meas. and refractive index depend. on concentration at different wavelengths 0-88346
 colloidal dispersion dynamics, review 0-71956
 Fick's law modification 0-96333
 flow in porous media, diphasic incompressible, diffusion-convection eqn., mixed finite element method, water flooding 0-74969
 glass, melt, bubble behaviour during refining, math. model 0-81277
 hard sphere fluid near hard wall, diffusion coefficient, mol. dynamics simulation 0-64858
 n-heptyl-4-cyanobiphenyl, nematic phase, dielec. loss, diffusion equations 0-71305
 Kramer's chemical reaction model, barrier mediated diffusion, generalisation to include viscosity term 0-71890
 laminal flowing liquids, concurrent, in horizontal cylindrical channel 0-79397
 macromolecular solution, rot. diffusion coeff. calc. method w.r.t. mol. struct., elec. birefringence relax. time data interpret. 0-85331
 macroparticles; charged spherical, dilute soln., Rayleigh scatt. 0-84748
 metal, of oxygen, electrochem. obs. using solid oxide electrolytes 0-59669
 9-methylanthracene, solubilisation in water by hypercoiled polymethacrylic acid 0-91591
 microemulsions, quasi-elastic light scatt. 0-108755

diffusion in liquids continued

- migration mechanism of approaching particles, energy transfer, luminesc. quenching study 0-100343
 multicomponent systems, rel. to electroepitaxy, theoretical model 0-65396
 organic molecules, long-chain, diffusion through polymer matrix, hydrostatic press. effect on diffusion coeff. 0-92697
 pentacene dianions in dimethyl ether, rotational diffusion meas. 0-65262
 polar liquids in double layer capacitors, RF conduction, ion diffusion effect 0-107883
 polar solvent mixtures, solvated electron diffusion, 2-absorber model 0-85206
 poly(2-vinyl pyridine), dil. solns., translational diffusion, chain conformation influence 0-103508
 polymer, entangled, phenomenological consequences of Doi-Edwards viscoelasticity theory 0-79250
 polymer diffusion equation with hydrodynamic interaction, equiv. normal coord. 0-79966
 polymer solns., dynamic scaling theories at nonzero concs., tagged chain translational diffusion coeffs. 0-75143
 polymer solution, diffusion of a chain, conc. effects 0-70103
 polymer solutions, aqueous, diffusion and mass transfer from rotating disc 0-83827
 polymer solutions, diffusion of ionic species, meas. by diffusion controlled electrolysis 0-74920
 polystyrene, sulphonated, polyelectrolyte solution, correlations and dynamics 0-104446
 pyrene dodecanoic acid, lateral diffusion at air-water interface, monomer excimer dynamics 0-92693
 reacting particle in fluid, convective diffusion, nonlinear surface reaction kinetics 0-106854
 rod-shaped molecules, restricted rot. diffusion, time correl. functions 0-79655
 solid spheres, reacting, in periodic array, convective mass transfer in liq. laminal flow 0-96176
 solvated electron + phenanthrene, diffusion controlled reactions in polar solvents, reaction parameters 0-97687
 solvated electrons, diffusion controlled reactions in polar solvents, reaction parameters 0-97687
 tetracene dianions in dimethyl ether, rotational diffusion meas. 0-65262
 viscosity measurement method at high press. 0-69955
 water-toluene-sodium dodecyl sulphate-butanol 1 mixture, interface light scatt., interface tension meas. 0-76039
 Ag-In melt system, conc. depend. of component and impurity diffusion coeffs., radioactive isotope method (*Russian*) 0-107454
 Al, molten, dissoln. kinetics and diffusion coeffs. of Fe, Co and Ni 0-59666
 Al, molten, impurity diffusion of fourth period solutes and homovalent solutes (*Japanese*) 0-70436
 Al-Cv (0.3 wt.%), moving solid-liq. interface, diffusion in liq. 0-107456
 Al-Ni solid, liquid mixture, diffusion processes (*Russian*) 0-107563
 Cu diffusion layer cathodic deposition and anodic dissolution rates 0-93503
 Cu, liquid, impurity diffusion, shear cell assembly meas. (*French*) 0-75375
 H₂O in biological samples, PMR, fast-exchange model interpretation via differential kinetics clarified 0-67033
³He-³He normal solution, size effect influence on capillary mass transport (*Russian*) 0-70497
 NaCl, water-HMPT soln., ionic diffusion coeffs. meas. (*French*) 0-65265
 Na₂O-SiO₂(-CaO) glass, molten, metal ion diffusion and redox behaviour, electrochemical studies 0-81332
 Sb, liquid, diffusion of O₂, activity coeff. 0-65267
 SiO₂, fused, He solubility and diffusion above transform. range 0-79965
 Sn, diffusion coeff. of ¹¹³Sn, ¹²⁴Sb, ¹¹⁰Ag, and ¹⁹⁵Au 0-96676
 Sn, liquid, impurity diffusion, shear cell assembly meas. (*French*) 0-75375

diffusion in plasma *see plasma transport processes***diffusion in solids**

- see also electromigration; ionic conduction in solids; self-diffusion in solids; surface diffusion*
 ? 0-100817
 A15 compounds, disordered, reordering kinetics 0-96678
 alkali borosilicates, disordered, self-focusing fibres with aperture of 0.18 0-87548
 alkali chlorides, positron-trapping colour centre dynamics, positron annihilation study 0-108294
 alkali halide:alkaline-earth cations, defect structs. examined by methods based on Mott-Littleton techniques 0-59487
 alloys, binary, marker displacements as result of diffusion 0-92724
 alloys, spinodal decomposition, review 0-96657
 barrier layers, against diffusion 0-66444
 BCC metals, of H₂ and its isotopes, phonon-assisted quantum-mechanical tunnelling of interstitials 0-59730
 binary alloy, solidification chemical inhomogeneity (*Russian*) 0-75335
 binary and multicomponent solids, chem. diffusion coeff., Darken's expressions modification 0-59738
 binary multiphase system, interdiffusion coeffs. determ. 0-70477
 α/β-brass bicrystals, two-phase, with nearly uniform and thermodynamic equilib. concs. 0-65383
 brass bicrystals, two-phase (α/β), interphase boundary sliding at high temperature 0-88164
 cavity growth, by surface diffusion in polycrystn. metals 0-104217
 ceramic nuclear fuels, irradi. induced rare gas diffusion 0-59524
 ceramics, lattice and grain boundary diffusion const., cor. 0-96679
 coarsening, time depend. of average particle size 0-79994
 coherent quantum diffusion in a single band, theory 0-107463
 coke, chamber and formed, binary diffusion of CO₂ with CO and CO with N₂ (*German*) 0-100356
 contact film absorption on plastic deform. of contacting bodies (*Russian*) 0-93596
 copper phthalocyanine-iodine, amorphous cpd. prep. by I₂ diffusion in polycrystn., triplet EPR signals obs. (*Russian*) 0-66016
 correlated particle migration in cryst. struct. (*Russian*) 0-96683
 crystal lattice sites, many-particle random motion 0-92703
 defect annealing, diffusion controlled, generalised theory 0-92520
 defect diffusion coeffs., site blocking, correlated defect motion 0-84315
 defective solids, Haven ratio in athermal lattice gas, Monte Carlo method 0-84313
 dielectric moistening diffusion kinetics, forecasting (*Hungarian*) 0-96692
 disordered one-dimensional lattice systems, diffusion and hopping conductivity 0-59991

diffusion in solids continued

- double diffusion, gettering of impurities 0-75383
- double diffusivity media, discrete random walk model 0-92702
- elastic amorphous medium, relax. by defect diffusion 0-58925
- energy spike development and quenching depend. on thermal diffusion 0-88367
- exotic atoms, conf., Erice, Sicily, (1979) 0-67939
- Fick's equations solutions for impurity diffusion, dislocations, interstitials, vacancies 0-70469
- fission fuel grain boundary loss terms, use in fission gas release and swelling models 0-63257
- float glass, Sn penetration in bottom surface, synthesis 0-79993
- Fourier transform, of diffusion eqn. with non-linear terms 0-103514
- Frenkel defects, form. and collapse, defect migration, electron irradiation effects, computer simulation 0-92523
- gas diffusion in linear elastic solid, stress-assisted 0-65294
- gelatin layers, permeation of photographic developer, potentiometric exam. (Russian) 0-73500
- glass, diffusion coefficient equation 0-103521
- glass, float, low-Fe, weathered, surface, characterisation 0-93666
- glass, refractive index gradients, form. using ion exchange diffusion 0-64227
- glasses, spinodal decomposition, review 0-96657
- glaze/glass-ceramic, interface reactions, electron microprobe anal. 0-84398
- grain boundary migration kinetics, atom diffusion across boundary, theory 0-79809
- graphite fibre reinforced composites, damage by moisture, diffusion anal. 0-81227
- hard spheres permeation through hard disc monolayers, interfacial mass transfer 0-107460
- Hastelloy, C-276, H transport rel. to ageing treatment 0-75384
- heat conduction and diffusion localisation in const. property media 0-58888
- III-V semiconductors, point defects and deep traps, thermodynamic history, model 0-59908
- inclusions, equations of motion 0-75387
- inclusions, macroscopic, diffusion motions in nonuniform compressive stress fields (Russian) 0-88351
- Incoloy 800, clean and steam oxidised, T_2 permeation 0-88364
- Inconel 617, creep, morphological changes of carbides, affect on creep props. 0-108509
- intercalation and substitution-intercalation cpds. in dichalcogenide hosts, factors affecting ion mobility 0-59707
- intercalation compound electrodes, thermodynamic and transport props. 0-66963
- interdiffusion coefficients, determ. in growing multiphase layer 0-70477
- intergranular cavity growth in uniform stress field ahead of crack-like stress concentrator 0-107366
- interstitial alloys, interstitial atomic arrangement and mobility at high degrees of interstice filling (Russian) 0-107223
- interstitial defects, migration kinetics and thermodynamics 0-107461
- ion beam induced atomic transport and conc. profiles 0-59723
- ion plating, interface broadening 0-65405
- ionic, in natural materials, cathodolum. and AES obs. 0-71497
- ionic solids, diffusion routes and thermal vibr., calc. method 0-107462
- island film growth, cluster size distrib. 0-107665
- isotropic media, current fluctuation anisotropy, electron diffusion, quasi-elastic scatt. (Russian) 0-107882
- kinetics of diffusion limited reactions (Dutch) 0-96682
- lattice defect information from diffusion studies (Dutch) 0-96681
- lattice defects and diffusion processes in solids, book 0-107207
- lattice gas, phys. correl. factor in Nernst-Einstein relation 0-105591
- long-range, anelasticity, review 0-60904
- media with double diffusivity, diffusion theory, boundary value problems 0-75378
- media with double diffusivity, diffusion theory, mathematical results 0-75377
- metal, diffusion welding, migration of oriented intergranular boundary with pores (Russian) 0-84943
- metal, H(D) diffusion, role of tunnelling, reson./nonreson. approaches 0-59718
- metal silicide formation, induced by scanning CW laser, reaction rates, analytical model 0-66334
- metal-H system, hydride formation in high press. range 0-65235
- metal-semiconductor interfacial reaction, AES study (Japanese) 0-96701
- metals, μ^+ diffusion, LAMPF results 0-71285
- metals, atomic binding energy and surface energy rel. to prediction of physical props. 0-59434
- metals, BCC and FCC, H-diffusion and trapping 0-70447
- metals, dissolution of interstitial H_2 and D_2 , diffusion coeffs., reverse isotope effect (Russian) 0-88368
- metals, FCC, H_2 diffusion, isotope depend. 0-59727
- metals, lattice and grain boundary diffusion consts., corrs. 0-96679
- metals, overbarrier states of H and D, subsystem heat capacity, equilibrium props. (Russian) 0-79998
- metals, point defect diffusion controlled reaction theory, book contrib. 0-103318
- metals, point defect dynamic props. and diffusion controlled reactions, book 0-101674
- metals, polycrystn., creep damage and cavity growth, assessment using density meas. 0-104217
- metals and alloys, FCC, interstitial diffusion, theory (Russian) 0-65296
- MIS solar cells, interface problems, AES, SIMS and XPS study 0-89627
- muon diffusion and trapping in solids 0-71283
- nitriding in glow discharges, influence on phase comp. and plasticity of diffusion layer (Russian) 0-76400
- noninteracting particle diffusion between semipermeable cell walls 0-70442
- nuclear fuels, radiation enhanced kinetics in the fuel lattice 0-59522
- Nylon 6 film, prior high-press. treatment effects, weight swelling, density, IR crystallinity, X-ray and viscosity obs. 0-81025
- one dimensional diffusion, iterative solns. with time varying surface comp. and comp. depend. diffusion coeff. 0-84314
- oxide films, passivating, transient growth kinetics 0-93672
- oxides, impurity diffusion and self-diffusion, review and bibliography 0-59719
- particle escape over dynamic barrier, impurity diffusion in solid 0-107569
- Permalloy-Cu(Al) two-layer films, mag. anisotropy, grain boundary diffusion (Russian) 0-71122

diffusion in solids continued

- photographic layer, homogeneous solid, diffusion, one-dimensional case (German) 0-73495
- photovoltaics and absorber/reflectors, diffusion, chemical reactions, contamination, AES and SIMS 0-72066
- PMMA, reactor irradiation, growth of macroscopic radiolytic gas bubbles, diffusion model 0-65058
- point traps, effect on diffusion and diffusing element distrib. function in crystals. (Russian) 0-59692
- Polimal 109, polymer resin laminate, density porosity, water vapour diffusion sorption and permeation (Polish) 0-59665
- polyester-E glass composites, types SMC-25, SMC-65 and SMC-30EA, moisture absorpt. 0-93799
- polymer film, glassy and rubbery, isotope effect in H_2 and D_2 diffusion, T_2 region behaviour 0-84327
- polymer films, permeation, diffusional time lags determ. 0-65272
- polyurethane foams, elastic, stability against organic solvents (German) 0-85074
- porous media, laminar flow, velocity and longitudinal dispersion, deterministic model 0-83842
- porous solids, diffusion of gases, Monte Carlo simulation 0-65299
- PTFE grafted membranes, struct.-properties relationships for poly-N-vinylpyrrolidone-containing membranes (French) 0-61138
- Pyrex glass, cation exchange and interdiffusion 0-80002
- quartz, synthetic, deuteration, EPR and IR absorpt. characterisation 0-92721
- quinolinium (TCNQ) $_2$, charge transport, proton spin-lattice relaxation 0-88545
- refractory metals, group V, diffusions of O and N, statistical calculations on Arrhenius lines 0-59722
- rubber, blooming by waxes 0-104109
- Sanicro 31, T_2 permeation 0-88364
- second phase particle, diffusional relaxation 0-60898
- semiconductor, polycrystalline, grain boundary effects, doping tech. for study and control 0-79815
- semiconductors, charge neutrality produced by impurity diffusion 0-59724
- semiconductors, doped and amorphous, ionised centre diffusion accel. by electrostatic fields 0-70473
- silicate glass, hydration thermodynamics 0-81313
- sintering, ohmic, temp. distrib. influence 0-92704
- solar cells, polycryst., influence of grain boundaries electronic structure on diode characts. 0-94068
- solid electrolytes and mixed conductors, materials stability and chem. diffusion 0-65292
- solid solutions, diffusion equation, during a decomp. process, role of non-linearised terms (Japanese) 0-92723
- solid solutions, Fourier transform, of diffusion eqn. with non-linear terms 0-103514
- solid-state diffusion from a limited source 0-70444
- spherical pore in solid body, physicochemical processes 0-100364
- spherical precipitate isotropic diffusion controlled growth 0-100344
- steel, aluminising, thermodynamic anal. of phase transforms. 0-76413
- steel, austenitic stainless, creep dependence on electron irradiation, in type SS316 steel, dislocation motion (Russian) 0-108495
- steel, austenitic stainless, D diffusion coeffs., ion beam meas. technique 0-75382
- steel, austenitic stainless, internal friction due to H_2 gas molecules 0-71682
- steel, C, dissolution of Cr_2C_3 in austenite (Russian) 0-103479
- steel, carburizing, vacuum, case depth 0-100956
- steel, chemicothermal treatment, diffusional basis 0-104343
- steel, Cr-Mn, high temp. oxidation, sub-cinder layer formation, protective coating role (Russian) 0-93686
- steel, CrMoV, low alloy, coarsening rate and activation energy of M_4C_3 and M_7C_3 carbides (Czech) 0-108480
- steel, high-strength, H distrib. and delayed brittle fracture 0-108577
- steel, high-strength low alloy, H_2 attack, 350-510°C 0-97636
- steel, Ni-Cr-Mo-V, corrosion fatigue crack growth in NaOH soln., cathodic pot. effect 0-89403
- steel, SAE 1045, permeation meas. of H trapping, rel. to cryst. microstruct. 0-84328
- steel, stainless, D_2^+ diffusion and permeation, ion beam meas. 0-59492
- steel, stainless, Ferralloy, creep-rupture props., 650-800°C 0-97535
- steel, stainless, retention and re-emission of 0.125-1 keV D^+ ions 0-66349
- steel, stainless, type 4301, radiation enhanced permeation of H_2 0-59732
- steel welds, bead-on-plate, H_2 diffusion and trapping 0-96697
- superconductors, multifilamentary, bronze process fabrication, voids growth obs., via hot stage SEM 0-70089
- superionic fluorites, structure and transport 0-84318
- superplasticity, region I characteristics 0-107357
- surfaces and interfaces, elastic energy of point defects and inclusions 0-73272
- thin film, influence of grain boundary migration on diffusion behaviour 0-88460
- thin polycrystalline films, rate of mixing depend. on grain boundary struct. 0-107578
- transition metal, BCC, neutron spectroscopy of fast H diffusion 0-59731
- waveguide fabrication in glass, optical, by low-temperature diffusion process 0-102867
- Ag film, Ge coated, electrical resistance and ageing (Russian) 0-103759
- Ag film growth on Pd substrate, interface cpd. form., AES study (French) 0-80131
- Ag, of Cu, SIMS investigations 0-59717
- Ag-Cd(-Ni), internally oxidised, oxide particle size control (Japanese) 0-89480
- Ag-In-Sn, internal oxidation, solute element and O_2 behaviour (Japanese) 0-89479
- Ag-InP interface, AgP_2 formation during sintering 0-65309
- Ag-Zn-Te(-Sn)(-In), internally oxidised, oxide particle size control (Japanese) 0-89480
- AgBr:Na $^+$ (Li $^+$), correlated diffusion of impurities, nuclear spin relax. meas. 0-108094
- AgI/RbI quasibinary system, solid state reactions and transport props. 0-96700
- AgMg two phase bicrystal, growth by solid state diffusion couple method 0-60773
- (Al,Ga)As:Zn planar stripe lasers with deep Zn diffusion, guiding mechanisms controlled by impurity concs. 0-78853
- Al, grain boundary migration, TEM obs. on mechanism 0-79812

diffusion in solids continued

Al, pipe diffusion along segment of faulted dislocation loops during annealing 0-107256
Al/Cu thin film couples, TEM study of intermetallic nucleation at interface 0-65305
Al-Ni multiphase system, simultaneous diffusion in cylindrical symm. (Russian) 0-100357
Al-Ni solid, liquid mixture, diffusion processes (Russian) 0-107563
Al-Ti system, interdiffusion coeffs. determ. 0-70477
 β -Al₂O₃, internal friction and Na transport 0-59578
Al₂O₃-glass seals, diffusion of Al, electron microprobe study 0-107577
Au film, Cr and Si low temp. diffusion, CO effect 0-100361
Au thin layers, diffusion rate of H₂, N₂, Ar, CO₂, air, and O₂ 0-100359
Au/Al thin film, Al diffusion studied by attenuated total reflection method 0-92722
Au/Cu, bilayers, interdiffusion phenomena, lattice dislocations, TEM obs. 0-59736
Au/Ni(Ni-P), interdiffusion, backscatt. study 0-79991
Au-Al thermocompressional contacts, diffusional zones, phase growth during annealing (Russian) 0-75389
Au-Al/GaAs interfaces, atomic interdiffusion, soft XPS studies 0-65302
Au-refractory thin film systems, interdiffusion obs. by combination of scattering techniques 0-65308
Au-Si interface, critical Au-film thickness obs. for room temp. interfacial reaction 0-75390
Au-Si thin film double layer, silicide form., electron diff. study 0-80005
Au₃Si₅, amorphous vacuum-deposited and liquid-quenched films, diffusion and crystn. 0-84094
BN glass transfer process 0-107459
C diffusion from graphite to W coating prevention, in metal-graphite layer structure of X-ray tube (German) 0-105759
CdS:Mn, vacuum deposited film, Mn migration, EPR and X-ray study 0-65411
CdS:Al(Au) interfaces, bonding and interdiffusion, XPS obs. 0-80000
CdSe film polycryst., thermal diffusion of Cr, 240-400°C 0-80001
CdTe, of Ge, 630-800°C, prep. conditions depend. 0-103519
CdTe:As(P), ion implanted, elec. props. 0-65021
CdTe:In precipitation and out-diffusion of solute during cooling 0-100840
CeCo₅-Cu_x, 0≤x≤ internal oxidation kinetics, oxide struct., X-ray study 0-104329
Cr substrate for CdSe, thin film transistor, cryst. struct., substrate defect effects 0-70563
CsI:Ti, precipitation of Ti solid solns. 0-70419
Cu, electron-irradiated, monovacancy migration during stage III annealing, NQR study 0-107576
Cu film, on Au substrate, oxidation and interfacial behaviour, ion scatt. spectroscopy study 0-66691
Cu, grain boundary migration, TEM obs. on mechanism 0-79812
Cu, H₂ diffusion, isotope depend. 0-59727
Cu, impurity diffusion of Vth period elements and self-diffusion 0-65301
Cu, oxidation kinetics, influence of intermediate annealing treatment 0-89412
Cu/Sn-Ni/Au tricouples, electrodeposited, interdiffusion obs. 0-84331
Cu-Ag, surface segregation of S, Auger spectral study diffusion 0-76549
Cu-Al (14.3 wt.%), ¹¹⁰Ag diffusion in β/γ_2 interphase boundary 0-79989
Cu-metal thin film couples, room temperature interactions 0-96699
Cu-Ni, evaporation limited segregation 0-70513
Cu-Ni, sintering, Kirkendall effect 0-93518
Cu-Ni alloys, chemical interdiffusion under uniaxial stress 0-65307
Cu-Sn industrial bronzes, Sn diffusion in deform. zone influence on wear resistance, friction (Russian) 0-108582
CuWO_{4-x} prod. from CuO+WO₃ solid state reaction 0-66796
Fe desorption of H into ultrahigh vac. system, using permeation cell 0-86326
Fe film, coated, interface magnetism by Mossbauer spectroscopy 0-75890
Fe, irradiated with electrons then annealed, magnetoresistance at 20K (French) 0-103677
Fe, muon diffusion and relaxation studies 0-75913
Fe powder based sintered porous permeable materials, diffusion chromising 0-100958
Fe, quantum diffusion of positive muons, 3 to 300K 0-75909
Fe, trapping of H, average trapping depth and trapping sites density 0-84297
Fe, white cast, migration of C to the surface, solubility (Russian) 0-92720
Fe:Y, ion implanted diffusion of D, deep traps 0-103372
Fe-Cr-Al, scales, α -Al₂O₃, early stages development at high temp. 0-89413
Fe-Cr-Al-Y, scales, α -Al₂O₃, early stages development at high temp. 0-89413
Fe-Cr-O system, phase relations at 1200°C using diffusion couple technique 0-89205
Fe-N system, Fe₂N growth kinetics (Korean) 0-93540
Fe-Ni-Cr (30.6, 21.3 wt.%), Alloy 800, high temp. oxidation at low O₂ press., SEM, AES and electron probe microanal. study 0-93688
Fe-Ni-Cr alloy, carbide form. by C diffusion, precip. distrib. and morphology 0-104164
Fe-Ni-Cr-Y, Y addition effect on selective oxidation/diffusion phenomena relationship (French) 0-108623
Fe-Ti, solubility and diffusivity of H and D in mixed crystal phase, elec. cond. meas. (German) 0-107575
Fe₃O₄-FeAl₂O₄ spinels, Fe⁵⁹ diffusion 0-59721
GaAlAs-GaAs heteroepitaxial devices, interstitial impurities and degradation, Auger obs. 0-99730
GaAlAs-GaAs heterostruc. lasers, interstitial impurities and degradation, Auger obs. 0-99730
GaAs, carrier diffusion in transient response regime 0-103688
GaAs, ion implanted, capless annealed and dielectrically annealed, comparison of doping profiles 0-100278
GaAs, open tube diffusion of Zn 0-84326
GaAs thin film polycrystalline solar cells, grain boundary edge passivated 0-94069
GaAs:Cr, Cr distrib. and heat-treatment migration studies by SIMS 0-107305
GaAs:Cr, semi-insulating, damage gettering of Cr during annealing of Cr and S implants 0-107304
GaAs:Si, Li, IR absorpt., microstruct., charge compensation 0-107565
GaAs:Sn thermal diffusion from spin-on SnO₂/SiO₂ source 0-96691
GaAs-Au(Ag) Schottky barrier solar cells, interface problems, AES, SIMS and XPS study 0-89627

diffusion in solids continued

GaAs-Cu:Ti, cathode luminescence spectra, Hall effect, cryst. defects 0-76087
GaAs-Ga₂Al_{0.8}As:Be, LPE, diffusion of Be into GaAs substrate 0-103517
(GaAs)_n(AlAs)_m multilayers, MBE, interdiffusion, X-ray diff. study 0-70474
GaSb, diffusion of In, 520 to 712°C 0-79995
GaSe, ¹¹⁰Ag diffusion, temp. depend. and solution (Russian) 0-70467
GaSe:Sn, ¹¹³Sn diffusion, temp. depend. and Sn solubility (Russian) 0-70466
GaTe, ¹¹⁰Ag diffusion, temp. depend. and solution (Russian) 0-70467
Ge, heterodiffusion due to H atom surface recombination stimulation, Cu, Zn, In coated (Russian) 0-59726
Ge, single cryst., ¹⁸F penetration, charged particle activation anal. 0-93828
H embrittlement, trap theory 0-89325
H thermal diffusion, apparatus 0-100358
H₂ embrittlement cracking and impurity atom migration (Chinese) 0-104247
H₂ permeation through HTGR heat exchanger tubes, reduction using calorising method (Japanese) 0-100360
H₂, single crystals, NMR, dynamic effects 0-107608
O-H₂, solid, quantum diffusion of p-H₂ impurities 0-88398
H₂, solid, quantum diffusion 0-107607
³He, phase separation of dil. ⁴He impurities 0-88393
Hg_{1-x}Cd_xTe, grown from melt, Kirkendall and Frenkel effects 0-100365
Hg_{1-x}Cd_xTe-In contact, diffusion of In 0-103520
p-H₂, quantum diffusion of O-H₂ impurities 0-96719
InP, Zn diffused single-crystal, substitutional dopant and hole conc. meas. 0-75260
InP:Cd, p⁺-n⁻ junction form. by diffusion doping 0-84504
InP:Cd(Zn), avalanche photodiode charact., impurity diffusion effects 0-70709
InSb:F, acceptor props. and diffusion coeff. of F 0-70643
InSe, ¹¹⁰Ag diffusion, temp. depend. and solution (Russian) 0-70467
Ir-Fe, spin fluctuation alloy, thermopower peak diffusion origin 0-88542
KCl, Born-Mayer parameters of He and Ar, interstitial interaction with neighbouring ions 0-100228
KCl:Ba²⁺, localised stress relaxation in excess vacancy system, prismatic loops (Russian) 0-88160
K₂O₈Cl₆, single cryst. with H⁺ interstitials, protonic cond. from dielec. meas. 0-107515
LaNi₅, H₂ absorpt. kinetics (Chinese) 0-103561
Li-Al system, Li solubility and chem. diffusion in Al, electrochem. study 0-107432
LiF, alkali ion implantation, migration, segregation, effect on optical props. 0-100269
LiF:Ni, dislocation behaviour in diffusion zone, Cottrell clouds (Russian) 0-70212
Li₃N thin film, vacuum evaporation on WO₃, retarded deposition 0-108351
LiNbO₃ layers, Li out-diffused, SHG phase matching temp. variation 0-69455
LiNbO₃:Ti, planar and channel optical waveguides, anisotropic diffusion expts. 0-64200
LiNbO₃:Ti diffused optical waveguide, guided light scatt. sources 0-78966
LiNbO₃:Ti Z-cut crystals, Ti diffusion process parameters 0-102849
Li₂O-Al₂O₃-GeO₂ glass, interdiffusion coeffs. of Li and Na 0-88369
Li₂Ta₂S₇ and Li₂Ti₂S₇, chem. diffusivity of Li at 30°C 0-59737
Mg hydriding, Kirkendall marker movement 0-75385
MgF₂:Li⁺, atom transport, diffusion and ionic cond. meas. 0-107492
Mn-H, hydride formation in high press. range 0-65235
Mo, diffusion of Li, Cs, vacancy and divacancy mechanisms (Russian) 0-70472
Mo, H₂ diffusion enhanced by self-interstitial atoms, surface reaction const. determ. 0-75386
Mo:C (110) surface, segregation, precip. and desorpt. of C, AES and LEED study (French) 0-103480
Mo-Si film-substrate interface, reaction on heat treatment, silicide formation 0-79999
NaCl, Born-Mayer parameters of He and Ar, interstitial interaction with neighbouring ions 0-100228
NaCl, impurity precipitation and grain boundary diffusion 0-107567
NaCl polycryst. containing Al₂O₃ dispersion, diffusive creep 0-97531
NaCl-KCl system, interdiffusion, miscibility, Kirkendall effect 0-107568
Na₂O-Al₂O₃-SiO₂-(K₂O) glasses, ion exchange kinetics and interdiffusion mechanisms 0-80003
Na₂O-CaO-SiO₂ glass, leaching studies by sputter-induced photon spectrometry 0-80004
Na₂O-SiO₂ glasses, water reactions at elevated temps. and press. 0-81312
Nb, electron irradiated, muon diffusion 0-80668
Nb, isotope effects for H₂ diffusion, crystal field stabilisation 0-59728
Nb-H system, local frequency spectrum, mean thermal displacement of H 0-59604
Nb-Ta alloys, H diffusion at 296K 0-84329
NbC single cryst., Vickers microhardness, slip mechanism 0-71732
Nb₂Sn, monofilaments, radiation-enhanced diffusion growth, crit. current density 0-65758
Ni alloys, aluminium, thermodynamic anal. of phase transforms. 0-76413
Ni, diffusion and solubility of S (Russian) 0-70465
Ni, diffusion welding, migration of oriented intergranular boundary with pores (Russian) 0-84943
Ni, H-charged cold-worked, internal friction peak 0-107368
Ni, oxidation kinetics, influence of intermediate annealing treatment 0-89412
Ni-Al (2 and 6 wt.%), oxidation, α -Al₂O₃ growth, microstruct., precip. 0-108626
§ Ni-Al system, solid soln., interdiffusion (Japanese) 0-70476
Ni-Cr/Au films, interdiffusion processes and oxidation phenomena 0-59735
Ni-Cr-W, oxidation behaviour in air at 1000-1250°C 0-89407
Ni-Cr(Fe)/Cu alloy, matrix effect in SIMS anal. using O₂⁺ primary beam 0-76576
Ni-Fe-H and Ni-Co-H, hydride formation in high press. range 0-65235
Ni-Mn, permeability, diffusion and solubility of H 0-107573
Ni-Mn (10-40 wt.%), γ solid soln., interdiffusion 0-100366

diffusion in solids continued

- Ni-SiC coating adhesion to Al alloy, metal interdiffusion (*Russian*) 0-66697
- Ni-V, solid soln., diffusion and thermodynamic props. 0-65278
- β -NiAl, oxidation, α -Al₂O₃ growth and microstruct. 0-108627
- Ni₃Fe, change of H₂ diffusivity with order-disorder transformation 0-59729
- Ni₈₈M₂, M=impurity metal, formation of MH(D)-complexes 0-65236
- Ni₃Mn, change of H₂ diffusivity with order-disorder transformation 0-59729
- NiO, diffusion of ³⁵S by two different modes 0-59720
- NiO-Al₂O₃ reaction at film-substrate interface, Rutherford backscatt. obs. 0-59733
- Ni₃Pt, change of H₂ diffusivity with order-disorder transformation 0-59729
- Pb and Pb alloys, interstitial substitutional model for anomalous diffusion 0-84330
- Pb, diffusion and saturation solubility of Pt, melting curve, conc. profiles 0-88365
- PbF₂:Mn, mag. tagging of ion diffusion, ¹⁹F NMR meas. 0-108106
- PbS_{1-x}Se_x diode laser, contact degradation due to diffusion 0-102734
- Pb_{1-x}Sn_xTe diode laser, contact degradation due to diffusion 0-102734
- PbTe, diffusion of Ag, effect of gamma irradiation 0-59515
- Pd alloys, effect of alloying on activation energy of H₂ diffusion 0-107571
- Pd, of H₂, elastic energy dissipation peak 0-60905
- Pd-Ag, of H₂, elastic energy dissipation peak 0-60905
- Pd-H, of H₂, Mossbauer study of local environment of substitutional Co and Fe impurities 0-60475
- Pd-H system, local frequency spectrum, mean thermal displacement of H 0-59604
- Pd-Ni, spin fluctuation alloy, thermopower peak diffusion origin 0-88542
- Pd-Ni-H, hydride formation in high press. range 0-65235
- Pd-Pt, of H₂, elastic energy dissipation peak 0-60905
- Pd-Rh-H and Pd-Ni-H, hydride formation in high press. range 0-65235
- (Pd₈₀Au₂₀Si₁₀)/Fe₃₀, compositionally modulated amorphous film, diffusion, struct. relax. 0-103518
- β -PdH, diffusion-induced reduction of ⁵⁷Fe Mossbauer fraction 0-108131
- (Pd₈₅Si₁₅)₆₁/(Fe₈₅B₁₅)₃₉, compositionally modulated amorphous film, diffusion, struct. relax. 0-103518
- Pt-Cr(Si) interface, low-temp. diffusion, ambient effects 0-100355
- Pt-Ni vacuum condensates on Si and SiO₂, thermally treated, X-ray anal. (*Russian*) 0-70559
- PtSi film, form. problems, diffusion coeff. of Si 0-100782
- Pt-Si, and PtSi, growth rate for form. by Pt film deposition under ultrahigh vac. and controlled impurity atm. 0-65388
- ²²²Rn diffusion through U mill tailings covers, coeff. meas., lab. techniques 0-95387
- Se films, Ag diffusion, effect on interferometric thickness meas. 0-96695
- Si, amorphous, hydrogenation using DC and HF plasma treatment 0-59497
- Si, amorphous layer prod. by ion implantation, diffusion broadening, ESR study 0-92552
- Si, Czochralski grown, oxide precipitates, diffusion-limited growth 0-97484
- Si device metallisation, TiN and TaN as diffusion barriers 0-65304
- Si, diffusion coefficient determ. from carrier conc. depth profile 0-107566
- Si, doping impurity distrib., during cryst. growth by Czochralski method (*Russian*) 0-100276
- Si epitaxial layers, vacuum deposited, conditions for impurity migration from B, P, Sb doped sources (*Russian*) 0-107570
- Si, etching by CF₄, plasma deposition reactor gas phase characts., mass spectra 0-70566
- Si, implanted crystal, laser induced annealing and diffusion behaviour 0-88202
- Si, migration of Au, electron bombardment effects 0-100362
- Si, of B, from CVD BN covered with Si₃N₄, appl. to master slice p-MOS IC 0-107564
- Si, of P, elastic deform. relax. and dislocation generation 0-79997
- Si, of P, mechanism, migration channels along vacancies and interstices 0-79996
- Si, oxide scale microstruct. of oxidised single cryst. 0-108613
- Si, polycrystalline, solar cells, grain-boundary hydrogenation technique for improvement 0-85273
- Si solar cells, realisation by laser induced diffusion of deposited Sb 0-93998
- Si solar cells, solid source diffusion process for fabrication 0-93994
- Si solubility and transport behaviour of water, dissolution 0-93801
- Si surface electron beam deposited silicide formation using scanning CW laser beam 0-66862
- Si wafer stacking faults, preoxidation gettering by reverse side P diffusion-induced misfit dislocations 0-60988
- Si:Al, polycryst. film, grain boundary diffusion, Auger sputter profiling 0-75388
- Si:Al(Ga), O₂ diffusion, conc. profile meas. 0-79990
- Si:As, diffusion model, degeneracy and partial ionisation effects 0-96693
- Si:As, heavily As-diffused, Hall mobility and resist. rel. to carrier conc. 0-107815
- Si:As, shallow junctions by high-dose implants 0-96694
- Si:As laser annealing, heat and mass transport model 0-92546
- Si:B, He⁺ irradiation-induced diffuion, effect on impurity distrib. 0-70470
- Si:B, high conc. effects in ion implantation 0-75245
- Si:B, ion implanted, structure defects formation and behaviour under annealing in various ambients 0-65033
- Si:B, P, long range enhancement of B diffusivity by P diffusion 0-103386
- Si:B diffusion at Si-SiO₂ interface, Auger spectra, Rutherford backscattering 0-70471
- Si:B(P), proton-irrad., impurity epitaxial diffusion, vacancy mechanism 0-92719
- Si:Bi, ion-implanted, solid phase epitaxial growth during annealing, supersaturated solid soln. form. 0-103384
- Si:Fe, solubility study by EPR and neutron activation anal. 0-75361
- Si:H, amorphous, geminate recombination model for photoluminescence decay 0-71481
- Si:P bipolar transistors, interstitial supersaturation and misfit dislocation climb, TEM study 0-70203
- Si:Sb, ion implanted, Sb diffusion during oxidation, snow-plough effect 0-88366

diffusion in solids continued

- Si:Sb, laser doping, evaporation loss and diffusion of Sb, under pulsed laser irradi. 0-59508
- Si:Sb vacuum deposited coating, p-n junction, pulsed electron beam annealing doping, diffusion 0-75480
- Si/Al and Si/Al-Si(Cu), Si regrowth minimisation through overlying Al or Al alloy film 0-70569
- Si/refractory metal-Ni(Pd)(Pt) interactions, phase separation 0-65303
- Si-metal interface, silicide formation, interface marker technique obs. 0-59734
- Si-Pd-Ti, silicide form. in evaporated films 0-80006
- Si-refractory metal structs., interface modification by ion implantation 0-70475
- Si-SiO₂ interface in MOS capacitors, lateral diffusion of Na⁺, neutralisation 0-92986
- Si-SiO₂ structure, alkali metal ion migration and accumulation, interface struct. 0-107574
- SiAlON, prepared from siliceous sand and Al powder, hot pressing, steatite contamination effects (*Japanese*) 0-93528
- SiC, diffusion of B, elec. cond. meas. 0-96696
- SiC, oxide scale microstruct. of oxidised single cryst. 0-108613
- β -SiC, sintering, B transport and lattice parameter change 0-108370
- SiO₂, mobility and trapping of ions, Si-SiO₂ interface states 0-92985
- SiO₂, vitreous, hydroxyl free, reaction with H₂, diffusion, absorpt. spectra 0-85210
- Si(111):Pb ion implanted amorphous layers, recrystallisation, impurity out-diffusion model (*Chinese*) 0-88363
- Sn/Au thin film diffusion couples, Kirkendall void form. 0-96698
- Sn/Cu electroplated bimetallic films, interfacial reaction 0-96765
- SnO₂/n⁺-pSi heterojunction solar cells, fabrication by paint-on-diffusant method 0-94048
- Ta-H system, local frequency spectrum, mean thermal displacement of H 0-59604
- Ta-H(D), anelasticity due to long-range diffusion 0-60904
- Ti, oxidation, linear, O diffusion coeff. depend. on rutile layer struct. (*French*) 0-104328
- Ti, oxidation behaviour under pure O₂ atmos., temp. range 600-800°C 0-89415
- Ti:D, ion implanted, depth profiles, temp. depend. 0-100270
- Ti-Al-V (6.4 wt.%), microstruct. effect of base metals on diffusion welding (*Japanese*) 0-89296
- Ti-Nb (4.32 wt%), high temp. oxidation kinetics under 1 bar pressure, 1255-1471K 0-89410
- Ti-Ta (4.37 wt%), oxidation kinetics, 1258-1473K, and at pressure of 0.013, 0.133 and 1.0 bar 0-89411
- UC, nuclear fuels, irradi. induced kinetics, diffusion and fission gas resolu. 0-59523
- UO₂, high burnup nuclear fuels, relation between fission product release and fuel microstruct. 0-57845
- UO₂ nuclear fuels, irradi. induced kinetics, diffusion and fission gas resolu. 0-59523
- V, isotope effects for H₂ diffusion, crystal field stabilisation 0-59728
- V-H system, local frequency spectrum, mean thermal displacement of H 0-59604
- V-H(D), anelasticity due to long-range diffusion 0-60904
- VC single cryst., Vickers microhardness, slip mechanism 0-71732
- V₂Ga layer on bronze, diffusion of Ga (*Russian*) 0-65297
- W, diffusion of Li, Cs, vacancy and divacancy mechanisms (*Russian*) 0-70472
- W, porous, chromising 0-100959
- W-Cu pseudoalloy, porous, chromising 0-100959
- WO₃ thin film, Li diffusion, appl. of AC techniques 0-70468
- WSi₂, steam-oxidized, Auger sputter profiling studies 0-107663
- ¹³³Xe in a plastic catheter, diffusion dynamics obs. 0-79973
- Yb-Al mixed valent film form., XPS study 0-80943
- ZnSb, orientated crystn. conditions during reaction diffusion (*Russian*) 0-70558
- ZnTe, low voltage green LED, struct. double diffusion procedure 0-100697
- Zr and its alloys, H diffusion, NMR study 0-108088
- diffusion pumps**
review, advantages over other types, newest devices 0-57321
- diffusivity** *see* **diffusion**
- diffusivity, thermal** *see* **thermal diffusivity**
- digital-analogue conversion**
see also **analogue-digital conversion**
analog signal processing, book 0-86047
- digital circuits**
see also **pulse circuits; switching circuits**
decade counter for measuring thickness of multilayer electrodeposits (*Czech*) 0-95071
small capacitances measurement by comparison, oct. 0-57327
timer with memory, appl. to dynamics experiments, principles of electronic circuitry 0-67994
- digital communication systems**
800 Mbit/s optical transmission experiments with dispersion-free fibres at 1.5 μ m 0-58680
Gaussian signals in Gaussian noise transmitted over digital channel, degradation of S/N ratio 0-64298
high-speed optical systems at 0.85 μ m, modal noise, and optical feedback 0-87323
multimode digital system wavelength multiplexing constraints in 850 nm region 0-63942
noise-tolerant continuously variable slope DM to linear predictive coding conversion 0-96141
optical fibre, intermode phase scanning for recovering phase-modulated signals on multimode optical fibres 0-58682
optical fibre cables, graded-index, transmission expts., 1.2-1.6 μ m wavelength range 0-102813
optical fibre transmission expts. at 34 Mb/s with HDB3 line code 0-64198
optical long-span single-mode fibre transmission characts. in long wavelength regions 0-99850
perceptual coding in the cosing transform domain 0-102635
SAW compensated filter used in wide spread MSK waveform generator 0-74670
speech interpolation system called adaptive DPCM with time assignment
speech interpolation 0-99903
speech transmission, forward and backward prediction in adaptive differential PCM over nonideal channels 0-99902

digital communication systems continued

voice multiplex systems, acquisition performance of frame synchronisation system 0-99901
(GaAl)As-GaAs narrow stripe laser, improved optical communication system performance 0-102733

digital control

see also numerical control
H₂O vapour under point corona discharge, microprocessor control for vapour generator and EHD phenomena 0-106852

digital filters

see also signal processing; wave digital filters
catheter pressure meas., transducer smearing correction using microprocessor based discrete deconvolution 0-67275
edge detection, numerical, optical and hybrid methods compared 0-102662
frequency instability meas. (Russian) 0-57264
Kalman, phasemeter appl., synthesis with a priori uncertainty of data 0-98934
medicine, nuclear, digital filtering and edge detection 0-58065
mosaic IR image differencing for track assembly 0-86420
multimicroprocessor implementation of all-digital speech synthesizer 0-96143
noise-reduction filter for resolution enhancement in Fourier transform NMR 0-73403
quasi-staring IR sensor clutter rejection processor design 0-86417
speech signal pitch determ. using nonlinear digital filter (German) 0-91972

digital instrumentation

see also digital readout; digital voltmeters
A/D converter with special appl. to medium precision Pt resist. thermometry 0-86297
analogue digital double integration joulemeter, AC loss meas. in superconducting magnets 0-57325
anemograph, for wind direction and average speed meas. (Czech) 0-77174
balances, precision, electronic methods (French) 0-62660
Calvet-type twin calorimeter using digital calculating integrator 0-77786
capacitance meter, design and construction 0-57275
Coanda fluidic gas flowmeter 0-59138
drive system displacement meas., features (Polish) 0-86260
ECG systems testing 0-81756
events analyser of low-cost construction 0-57267
filter for frequency instability meas. (Russian) 0-57264
frequency meter, Heathkit IM-4100 multi-function, circuit diagrams and performance data (French) 0-73348
frequency synthesizers, low-freq. signals, performance data for LEA GSN 20 and GSN 80 series (French) 0-73393
heart beat counter, versatile digital SAMI 0-85510
high pressure piston flowmeter with digital readout (Polish) 0-64661
isotope ratio meas. system, using programmable calculator with double collector mass spectrometer 0-63845
klirr-factor unit dimension meas., errors evaluation 0-98873
multimeter, Avo DA117, overview of field servicing appls. 0-68210
nuclear reactor instrumentation, microprocessor controlled, digital period meter, hardware and software 0-63473
panel meters, characts. and appls. 0-68190
phase meter, Dranetz model 314, comparison with analogue techniques and significant advantages (Italian) 0-68211
PWR control rod digital position indicating system (Japanese) 0-63314
radioactive waste density measuring meter, digital, remotely operated 0-68927
rangauges, tipping bucket type, digital recording system description and field testing 0-77161
reverberation time digital meas. instrum. for auditoria and studios (Japanese) 0-64321
SIMS, depth profiling, automatic sequential mass analysis 0-108764
solar double-pass monochromator, with digital device for obs. and spectrum processing automation (Russian) 0-72777
submarine quantum irradiance and photoperiod meter, with digital recording 0-98474
tachometers, error analysis 0-90832
temperature determ. of molten metal (Russian) 0-90846
temperature transducer, solid-state, using automatically balanced Wheatstone bridge (Rumanian) 0-57287
time-domain reflectometer for dynamic shock position measurements 0-79248
timer with memory, appl. to dynamics experiments, principles of electronic circuitry 0-67994
tomography, focal-plane, image reconstruction using digital computer 0-61674
treatment voltage and current, fast technique (Polish) 0-86340
unsteady pressure coefficients digital measuring unit for wind tunnel tests (French) 0-68169
UV radiometer, Spectroline DM series 0-77854
velocity meas. device, error calc. (Russian) 0-86266
video-electronic hologram interferometry for in-plane displacement measurement 0-106488
Watford Electronics 0-050 MHz digital frequency meter measures frequency and time intervals 0-68191
waveform recorder functions and appls. 0-57278

digital instruments see digital instrumentation

digital readout
see also digital instrumentation
astronomical images, interactive program for digital display (Italian) 0-98559
automatic linear expansion coefficient meter with digital readout 0-106713
automatic thermal conductivity meter with digital readout 0-106714
electric dichroism measurement instrument with digital processing 0-82800
panel meters, characts. and appls. 0-68190
weighing system, electronic, digital transducer instruments 0-95076

digital signals
atmosphere radar signal processing, for SOUSY-VHF-radar, using preprocessor 0-85774
generator for rapid scan differential pulse voltammetry 0-61182
image enhancement by median masking technique 0-106483
image improvement, thermal imager pictures delining 0-106466
image processing applications, seminar, San Diego, CA, USA (Aug. 79) 0-105424

digital signals continued

radio antenna arrays, incoherent optical 1-bit cross-correlators, radioastron. appls. 0-98555
time-integrating acousto-optical correlator design and performance 0-106618

digital simulation

alloy, binary, order-disorder transition kinetics, computer simulation 0-92643
alloy melt, temperature distribution during cryst. growth by Czochralski method (Russian) 0-75192
amorphous solid, structural defects, computer simulation study 0-88040
amorphous surface, energy profile and binding energy, computer simulation 0-100381
atom ejection studies by classical trajectory simulation 0-108311
atom-atom collision cascades localisation, impurity and thermal vibr. influence, computer simulation method 0-88227
axisymmetric field problem soln. by Gaussian surface charge simulation 0-95758
bulk trap energetic distribution props., space charge limited current meas. use 0-80293
chaotic branched macromolecules, struct. simulation, parameters calcs. (Russian) 0-69283
chemical system, equilibrium fluctuations, deviations from Poisson behaviour, molecular dynamics 0-86211
chromatography, nonlinear, nonideal, computer simulation models 0-62639
cooled epoxy resin vacuum mould computational simulation of design (German) 0-81020
crack propagation, computer simulation 0-59573
crack simulation computer program for plate structures (Japanese) 0-79218
crystal defects, simulation of high resolution images 0-107208
diffuse light scattering, mathematical modelling 0-106450
direct radiator loudspeaker model, finite element approach 0-69622
dislocation motion, lattice resist. effect of impurity interstitials 0-84170
dislocation percolation through absolute obstacles in impurity crystals (Russian) 0-70196
disordered crystals, optical transforms 0-78783
distortive phase transitions, order-disorder and displacive regimes, mol. dynamics study 0-75324
ECG signals, diagonal functions, effect of random noise (Croatian) 0-98169
ECG simulation using a microprocessor 0-61726
electric field computation by charge simulation and finite element methods 0-95759
epitaxial films, condensed from vapour or molecular ion beams, impurity distrib. 0-65032
excitons, diffusive and percolative lattice migration 0-59879
explosive forming, computer numerical simulation 0-59560
fatigue behaviour of fibre reinforced plastics, under random loadings (Japanese) 0-85032
FCC crystal-melt interfaces, mol. dynamics simulation 0-79913
ferromagnetic alloys, disordered cryst. and amorphous, mag. dipolar field distrib., computer simulation 0-65790
fission reactor digital simulator software development, kinetic equations integration, numerical solution method 0-68901
flexible structures, dynamic simulation by substructure synthesis 0-87733
fluid, cavity-biased (T,V, μ) Monte Carlo method, computer simulation 0-92434
formic acid, cryst., H bonded, IR spectrum computer simulation 0-97253
free electron lasers, energy transfer, computer simulation 0-83578
fusion reactor, low power Tokamak experimental fusion power plant, scoping studies with empirical scaling, SISYFUS code 0-102309
fusion reactor, MFTF, power supply system, digital simulation using EMTP code 0-91286
fusion reactor, TFTR energy conversion system simulation 0-99303
fusion reactors, JT-60, poloidal field power supply system, AC voltage behaviour, simulation 0-91287
gas-filled microballoons, radiation effects MEDUSA code calcs. 0-83220
grain boundary migration, effect on thin film diffusion behaviour 0-88460
hard sphere fluid near hard wall, diffusion coefficient, mol. dynamics simulation 0-64858
hopping conduction, random one-dimens. system, Monte Carlo computer simulation 0-80278
image formation, partially coherent, two dimens., computer simulation 0-106434
ion beam trajectory focusing effects on total reflection coeff., computer studies 0-89102
island films, statistical model 0-92795
landform erosion simulation program 0-85650
laser fusion, parameter study of exploding pusher target (Japanese) 0-96376
laser fusion system beam quality, Laser Optical Train Simulation code 0-78886
Lennard-Jones fluid, nonequilibrium molecular dynamics, $t^{-3/2}$ long-time tail for stress-stress time correlation 0-70100
liquid structure, S-D periodic particle-particle/particle-mesh program P3M3DP 0-84041
liquids, monoatomic, quasi-crystalline structure, role of vacancies in dynamics 0-92438
low-temperature plasma production by electron beam ionisation of gas mixture 0-87908
magnetic alloys, binary, spinodal decomp., computer simulation study of interface behaviour 0-84913
magnetic moment spatial distribution in single ground state systems with impurities 0-97074
metals, constitutive model at high strain-rate, shear modulus, yield strength 0-75292
metals, FCC, twist boundaries, struct. invest. using computer simulation technique 0-84185
MHD converter, supersonic flow of combustion products, nonequilibrium physicochemical processes, open-cycle MHD generator 0-103196
molecule images, simulation by point models and kinematical struct. amplitudes 0-103223
Mori theory evaluation, molecular dynamics simulation 0-92443
multicomponent percolation, conduction 0-92871
nanosecond beam dynamics in linear electron accelerator 0-86996
nuclear accidents, loss-of-coolant, data analysis using computer-aided models (Czech) 0-73949

digital simulation continued

- nucleic acids, bases and base pairs, water struct. in soln., Monte Carlo simulation 0-76709
 optical multilayer filters, non normal incidence, optical monitoring, allowable tolerances (*French*) 0-87526
 particle physics, relativistic discrete unified field theories, computer field interaction simulation system 0-68412
 photochemical air pollution formation simulation 0-81504
 physics computer-aided teaching, hinted finding scheme, appls. (*French*) 0-98777
 physics laboratory experiments, graphic computer simulations 0-105470
 plane coalescence, at grain boundaries 0-70221
 planetary and satellite systems evolution 0-77308
 plasma, pressure, virial kinetic definition, spherical geometry calcs. (*French*) 0-69973
 polymer chain, linked rigid body, Brownian dynamics 0-74267
 polymeric macromolecule containing mesogroups, phase diagrams (*Russian*) 0-58433
 polymorphic transformations kinetics model, computer modelling (*Russian*) 0-97478
 polytypes, computer simulation 0-79734
 radiation counting rate meter output at threshold, fluctuation and arrival shift by computer simulation 0-106240
 random packing of spheres modelling 0-77705
 road traffic noise, traffic passing through road intersections controlled by roundabouts, model 0-64280
 semiconductor, amorphous, field effect and capacitance-voltage meas. anal., localised density of states 0-103686
 semiconductor, ion implanted, pulsed laser and electron beam annealing comparison 0-92547
 semiconductor, SEM electron beam induced current images of dislocations and stacking faults, computer simulation 0-70198
 sensory neuron, second order, summation of excitation and inhibition 0-76769
 shells, plastic, explosive forming, computer numerical simulation 0-59560
 single crystals, growth simulation 0-88069
 sound-absorbing wedge design, reflection characts., materials and dimens. (*Japanese*) 0-64322
 spin wave parametric excitation, stochastic auto-oscill., Kolmogorov entropy (*Russian*) 0-75749
 square-well fluid, viscosity below critical density, molecular dynamical calcs. 0-79661
 steel, type SAE 1008, finite fatigue life distrib., various load-time histories 0-97589
 superionic conductors, theoretical models, review 0-107465
 TEM crystal atomic structure imaging technique and applications 0-105752
 texture transformations, 'brass to copper' in FCC metals 0-76246
 thin film condensates coalescence, influence on morphological changes, modelling 0-107676
 thin film deposition process, line-edge profile simulation appl. 0-104068
 three-dimensional thin pyroelectric IR detector simulation 0-57375
 tomographic image correction, with simulation 0-85470
 traffic flows, car following theory, intersections having traffic lights 0-72109
 ventricular arrhythmia model 0-89893
 water, Monte Carlo simulation of struct. and thermodynamic props. 0-88017
 windmill arrays, wake interaction, theory and preliminary results 0-61246
 Al alloys, fatigue crack initiation, computer simulation 0-100893
 Ar liquid, quasi-crystalline structure, role of vacancies in dynamics 0-92438
 Au, atomic struct. of large angle [001] twist boundary, determ. by computer modelling and X-ray diff. study 0-70162
 Au, polycrystn., deformed, computer simulation of vacancy annihilation to dislocations (*Japanese*) 0-88205
 BaO-P₂O₅-Mo³⁺ glass, EPR spectra, computer simulation 0-88872
 CO₂ laser Antares fusion system optical diffraction computation 0-74424
 CO₂ laser pulse, nonlinear propagation, computer simulation (*Japanese*) 0-95963
 CaF₂, fast ion transport, computer simulation 0-107485
 n-CdS/n-InP/p-InP heteroface solar cell with ultrathin window layer, computer anal. 0-97788
 CsCl-type lattice, (111) superlattice screw dislocation motion, computer simulation 0-79793
 Cu₅₇Zr₄₃, amorphous alloy, computer simulation of atomic structure 0-70125
 Fe₃Pt Invar alloy, thermal expansion and spontaneous magnetisation, Invar anomalies, low spin model 0-71001
 HCL, fluid states, mol. dynamics simulation 0-79671
 Kr submonolayer films on graphite, mol. dynamics simulation 0-88425
 Kr VII, beam-foil excitation, 4s4p ¹P^o level decay simulation 0-78578
 Mg, HCP, vacancy clusters and interstitials, computer simulation study 0-64992
 Mg SiO₃ melt, instantaneous struct. simulated by mol. dynamics 0-84049
 Ni-Fe Invar, thermal expansion and spontaneous magnetisation, Invar anomalies, low spin model 0-71001
 Si wafer, ion implanted, electron beam annealing, computer simulation 0-96569
 Si:Au deep level parameter determ. by isothermal capacitance transient spectroscopy 0-88507
 Ta BCC lattice, strain ordering in interstitial solutions 0-107420
 VB, nuclear quadrupole parameters 0-103896
 WO₃ electrodes, electrochromic processes, digital simulation model 0-76518
 Zr(Ca,Y)O_{2-x}, local ionic arrangement, X-ray diff. study 0-100203

digital storage

- see also *cryotrons; optical stores; read-only storage*
 electron image recording system, detection quantum efficiency 0-99009
 EM image accumulation, digital storage and processing system 0-101901
 flaw detector with automatic mechanical scanning, TV signal form. on basis of digital memory 0-71864
 holographic storage of TV signals 0-87353
 oscilloscope principles and applications (*Danish*) 0-62647

digital systems

- see also *computer networks; multiprocessing systems; real-time systems*
 holography appl. to borehole EM wave exploration (*Chinese*) 0-82080

digital voltmeters

- automatic test method for pulse-counting digital voltmeters 0-57240

digital voltmeters continued

- capacitance meter, using DVM and diode pump cct. 0-62656
 IEEE-488 bus compatible DVM variations and advanced features 0-86279
 instrumental error estimation 0-57239
 sound level meter output level measurement 0-79077
- digitisers** see *analogue-digital conversion*
- dilatometers** see *extensometers*
- dilute alloys**
 see also *impurity electron states; Kondo effect; magnetic properties of dilute systems*
 alkali metal alloys, dil., binary, equilib. at vol. and compressibility 0-70295
 binary alloy, unidirectional growth, morphological stability of planar interface 0-84920
 elec. resist. for non-orthogonal Anderson model 0-59947
 electrical transport and deviations from Matthiessen's rule 0-65524
 electron sound absorpt., disordered mag. impurities, spin glasses (*Russian*) 0-80503
 Kondo alloys, DC Josephson effect 0-88690
 perturbation expansion for the asymmetric Anderson Hamiltonian 0-80202
 Seebeck coefficient, electron-phonon enhancement 0-70685
 transport properties in magnetic field, impurity-electron scatt. 0-65541
 AgNi, dil., mag. susceptibility of isolated Ni atoms 0-65777
 Al-Cu, dil., diffusion thermopower, inelastic electron-phonon interaction 0-96851
 Al, cold worked, internal friction peaks 0-97520
 Al-(Mg)(Fe), pure (dilute), large wire drawing plastic deform. 0-108508
 Al-Cu (0.5 wt.%), evaporated layers, electromigration, linewidth depend. 0-65277
 Al-Cu dilute alloys, vein closing mechanism in fluidity tests 0-84924
 Al-Cu(Mg), dil. binary alloy, planar interface stability during solidification (*Slovak*) 0-108424
 Al-Ge, magnetoresist., temp. depend. 0-70682
 Al-Mg, dil., ang. correlation of annihilation radiation from impurity trapped positrons 0-104010
 Al-Mg, dilute, dislocation loops, interstitial, size distrib. for metal irradiated in high voltage electron microscope (*Russian*) 0-103335
 Al-Mg, foil, oxidation in O₂ atm., TEM study 0-104356
 Al-Zn, magnetoresist., temp. depend. 0-70682
 Au-Cr, dil., elec. resist., generalised phase shift anal. of Kondo effect 0-75556
 Au-Cr, dil. alloys, elec. resist., deviations fro Matthiessen's rule 0-75541
 Au-Dy, dil., hyperfine interaction, Mossbauer study, Kramers quartets 0-66083
 Au-Ni, surface segregation, strain effects 0-80042
 BeNi, dil., electronic struct., NMR study 0-108085
 Ce_{1-x}La_x dil., γ-α transition temp. and press., elec. resist. meas. up to 10 kbar 0-59643
 Cu dilute binary solid solutions, enthalpies of mixing and excess free enthalpies (*French*) 0-107427
 Cu-Ag-O alloys, dil., O-metal interactions, activity coeff. meas. at 1423K 0-93792
 Cu-Al spherical crystals, grown from drop of melt, topography 0-84353
 Cu-Au, magnetoresist., temp. depend. 0-70682
 Cu-Au-O alloys, dil., O-metal interactions, activity coeff. meas. at 1423K 0-93792
 Cu-Bi (0.02 wt.%), intergranular fracture, Kossel X-ray diff. in SEM obs. 0-108579
 Cu-Cd (1.0 wt.%), yield stress and flow stress 0-97524
 Cu-Fe group, dil., NMR satellite data calc., struct. of mag. impurities 0-103894
 Cu-Ni(Pd)(Pt), dil., screening charge density round ΔZ=-1 impurities, vacancies, NQR study 0-103897
 Cu-Pt-O alloys, dil., O-metal interactions, activity coeff. meas. at 1423K 0-93792
 Eu,La_{1-x}Al_x, dil. EPR, cryst. fields and effective exchange interaction 0-66029
 Fe-M, M=transition metal, impurity electronic struct., multiple scatt. approach 0-92856
 Fe-Ni, impurity electronic struct., multiple scatt. approach 0-92856
 Fe-Ti (V)(W), dil., thermophysical props. and elec. cond., temp. depend. 0-96842
 Fe-Ti (0.15 wt.%), Ti distrib., segregation, FIM anal. 0-84200
 Hf-Ir, dil., elec. field gradient at ¹⁹¹Ir, Mossbauer meas. 0-66090
 Lu-Ir, dil., elec. field gradient at ¹⁹¹Ir, Mossbauer meas. 0-66090
 Mg, dynamic recrystn. during creep, dislocation substruct., quartz comparison 0-109142
 Mg-Nd-Zn dilute alloy, metallography and precip. kinetics 0-71655
 Mg-Tb(Dy)(Ho)(Tm), dil., macroscopic shape effect due to quadrupole orientation, magnetostriction and thermal expansion meas. 0-60396
 Mo, HVEM bombarded, neutron damage simulation, defect cluster and dislocation obs. 0-107330
 Ni alloys, dil., hyperfine field distrib., DPAC meas. 0-93222
 Ni dilute alloys, implant profiles modification by radiation enhanced diffusion and segregation 0-88217
 Ni-Co(Fe)(V)(Ti), dil., optical absorpt., electronic struct. 0-108227
 Ni-Cu(Zn)(Ga)(Ge)(As)(Se)(Br)(Kr), dil., ferromagnetic, hyperfine field and relax. time obs. of impurity heavy nuclei 0-75533
 Ni₉₅M₅, M=impurity metal, formation of MH(D)-complexes 0-65236
 P+Nb, dil. alloy, NMR obs. of ⁹³Nb 0-71203
 Pb alloys, dil., diffusion thermopower, inelastic electron-phonon interaction 0-96851
 Pd-Co (0.1-45.4 at.%), thermo EMF at 4.2-300K (*Russian*) 0-92881
 Pd-Cr, dil., temp. dependent scatt. 0-59973
 Pd-Fe, very dil., Mossbauer emission spectra, relax. effects 0-66084
 Pd-Fe (0.54-8.0 at.%), thermo EMF at 4.2-300K (*Russian*) 0-92881
 Pd-H dilute alloy, impurity elec. struct. 0-103643
 Pd-Ni (15-90 at.%), thermo EMF at 4.2-300K (*Russian*) 0-92881
 Pd-Sn_y (x=0.95, y=0.05; x=3, y=1), Mossbauer spectra, high press. effects, force consts. 0-84669
 Pt-Au, recovery spectrum after thermal neutron irr., Au effect and defect conc. depend. 0-65057
 Pt-Fe, very dil., Mossbauer emission spectra, relax. effects 0-66084
 PtV, dil. alloys, NMR obs. of ⁵¹V 0-71203
 Sc-Ir, dil., elec. field gradient at ¹⁹¹Ir, Mossbauer meas. 0-66090
 Si-Fe-W, dil. alloy, compositional changes on sputtering, projectile energy depend. 0-66362

dilute alloys continued

- Tb-Ta(Cd), elec. quadrupole interaction, temp., and press. depend., TDPAC meas. 0-60469
Th-Gd(Tb)(Dy)(Ho)(Er)(Tm)(Lu) (1. at.%), Heisenberg exchange, residual resist. meas. 0-75558
Ti-Fe-C-N, ion irradiated, microstruct. study using TEM 0-96572
Ti-Ir, dil., elec. field gradient at ¹⁹³Ir, Mossbauer meas. 0-66090
Y-Ir, dil., elec. field gradient at ¹⁹³Ir, Mossbauer meas. 0-66090
ZnMn, dil., magnetoresist. meas., temp. depend. anisotropy 0-65532
Zr-Ir, dil., elec. field gradient at ¹⁹³Ir, Mossbauer meas. 0-66090

dimensions

- analysis, modification and generalisation in physics teaching 0-105481
klirr-factor unit dimension meas., digital, errors evaluation 0-98873
measurement units, historical review and current systems in use (*German*) 0-68166
physical quantities, use in metrology 0-77740
wet steam, high speed flows, drop dimensions meas. method 0-90817

dimers see molecules

dineutrons see neutrons

Dingle temperature

- In_{1-x}Ga_xP, As_{1-y}, electron effective mass and Dingle temp., Shubnikov-de Haas oscills. 0-59859

diode lasers see semiconductor junction lasers

diode sputtering

- closed anode bias sputtering method for film deposition (*Japanese*) 0-93484
Al, planar magnetron sputtering, H₂ effect on Ar discharge 0-80970
Fe-Cr-Si, heat resistive films prepared by sputtering, lifetime meas. 0-80132
Ta-Cr-Si-Al, heat resistive films, prepared by sputtering, lifetime meas. 0-80132
TaB₂-Cr-Si-Al, heat resistive films prepared by sputtering, lifetime meas. 0-80132
Ta₂N, thin film deposition by closed anode bias sputtering (*Japanese*) 0-93484

diode tubes see diodes

diodes

- see also plasma diodes; rectifier tubes; rectifiers; semiconductor diodes
cylindrical relativistic diode, space charge limited, voltage distrib. and current calc. 0-63437
intense relativistic electron beam generation by foillless diodes, simulation 0-63438
optical diode to enforce one-direction travelling wave operation 0-69427
vacuum beam diodes, repetitively pulsed, lifetime and stability 0-63386
Si diode radiation detector, stabilisation of radiation damage 0-91377

dipole antennas

- magnetoactive plasma surrounding dipole antenna, radiation pattern 0-100079
moving collisional plasma and moving plasma with intrinsic spatial dispersion, emission of longit. waves 0-87848
transponder dipole antennas in and near three-layered body 0-98181
vertical magnetic dipole on two-layer Earth 0-76906

dipole moment, electric see electric moments

dipole moments, magnetic see magnetic moments

Dirac electron theory see Dirac equation; electron theory

Dirac equation

- see also electron theory
APW method, linearised relativistic using approx. pure spin basis functions 0-70581
atoms, analytical relativistic SCF calcs. 0-83248
baryons with arbitrary spin, generalisation of Dirac eqn., group scheme 0-73615
Dirac's monopoles and action-at-a-distance theory: classical dynamics 0-95210
Dirac-Coulomb waves in electron theory, involuntal transforms 0-99037
electron spin, Dirac equation, mechanical sphere, magnetic momentum and lines of force (*Hungarian*) 0-68344
Euclidean Yukawa₂ quantum field theory, FKG correlation inequality 0-68357
free EM field quantisation, gauge invariant fields 0-105817
gravitational field and arbitrary gauge field, equations of motion, Heisenberg and classical, force term, spin-curvature coupling 0-57158
invariance algebras of Schrödinger and Dirac eqns. (*Russian*) 0-68081
Lorentz's equations, relativistic and nonrelativistic, maximally extensive local group of invariance 0-77946
Lorentz basis of quantum fields 0-86565
M₄ factorisation, spinor algebra, Dirac equation geometrical, interpretation 0-62838
magnetic resonances between massive and massless spin-1/2 particles with magnetic moments 0-62895
monopole+electron, scatt. through small angles, Dirac-Schwinger monopole 0-68398
motion of charged particle in uniform magnetic field motion of charged particle 0-90690
nonlinear spinor field, charged Coulomb-like potential, localised solns. 0-68351
one-electron atom in curved space-time, energy shifts 0-78509
one-electron polynuclear systems, Dirac eqn., variational soln. 0-83242
plane waves in Dirac electron theory, involuntal transforms 0-99036
potential interaction using a metric space 0-82879
QED tests of electron propagator, vacuum polarisation 0-77994
radiating particles of finite size, Dirac's subtraction formalism (*German*) 0-91740
relativistic electron wave equation 0-101702
self-adjointness of Dirac operators, maximum principle 0-68352
solutions using a quadratic scalar potential 0-86564
spin 1/2 massive and massless particles, invariance algebra, Maxwell eqn. extension 0-82923
spinor and scalar fields in 4-D non-Euclidean momentum space, eqns. of motion, vacuum momentum 0-68379
spinor electrodynamics, conformed invariance 0-99074
zero-energy eigenstates for the Dirac boundary problem 0-101961
gyromagnetic ratio in Coulomb field 0-82870
H atom, Dirac and Klein-Gordon relativistic eqns., energy level splitting 0-77938

direct coupled amplifiers see d.c. amplifiers

direct current amplifiers see d.c. amplifiers

direct current motors see d.c. motors

direct energy conversion

- see also cells (electric); magnetohydrodynamic conversion; photothermal conversion; plasma diodes; solar energy conversion; thermionic conversion; thermoelectric conversion
chemical to electrical conversion using semiconductors 0-66984
fusion reactor, TFTR, high power direct energy converters for beams and plasma 0-99334
ion beam deceleration across mag. fields, expt. 0-99384
ion-exchange membrane, electroosmotic energy conversion efficiency 0-61430
large-scale elec. energy storage, review 0-89676
shock wave mechanical energy conv. to electrical energy using ferroelectrics 0-61429
synthetic and fissile fuel prod. by Cat-D fueled SAFFIRE reactors 0-99280
thermodynamic energy conversion efficiencies 0-101081
Cu_{2-x}S-CdS p-n heterojunction, optical energy convertor, struct. and recomb. props. 0-72065

direct nuclear reactions and scattering

- see also pick-up reactions; stripping reactions
cool compound nucleus formation with oriented heavy ions, ²⁵⁸104 and ²⁶⁰106 prod. 0-99179
DWBA integrals, evaluating strategies for computation 0-86863
elastic two fragment collisions, Pauli principle and optical pot. 0-63153
heavy ion deep inelastic and high energy reactions, fragmentation cross section 0-78259
heavy ion inelastic scatt., coupled channels calcs. for direct reactions, long range Coulomb coupling 0-83117
heavy ion inelastic scatt., direct reactions, coupled channel calcs., coupled radial eqns. 0-83118
high energy heavy ion collisions, single nucleon knockout, DWIA formalism 0-99165
radiative nucleon capture, pure resonance model, direct-semidirect model, pure semidirect model 0-78257
relativistic heavy ion collisions, fragmentation cross sections, abrasion-ablation model, factorisation 0-78261
(α,2α), A=9, 12, 16, 20, 22 0-68629
(α, ³HeX), 1 GeV/N, momentum distrib. after high energy fragmentation, spectator peak 0-99164
(α,X), relativistic collisions, slow and fast fragment correlations, multiplicity association 0-86886
(γ,n), 45-160 MeV, cross sections in quasi-deuteron model for direct reactions 0-63170
(n,n'), 14 MeV, continuous spectra, multi-step direct reaction anal. 0-78258
(p,p'), 800 MeV, cross sections, quasifree knockout mechanisms, PWIA calcs. 0-78294
(p,X), neutron excess isotope prod. in fragmentation reactions ^{6,8}He, ^{7,8,9,10}Li (*Russian*) 0-86888
(p,X), relativistic collisions, slow and fast fragment correlations, multiplicity association 0-86886
(π⁻X), n and charged particle emission following π⁻ capture 0-73867
^ΛSi(d,X), A=112, 124, 7.6 GeV/c, isotopic cross section ratios, He, Li fragments isotopic effects (*Russian*) 0-63154
Al(He,X), proton inclusive spectra, direct plus thermal model 0-57799
¹¹B(p,⁶Li)⁶Li, 51.9 MeV, five nucleon transfer mechanisms, DWBA calcs. 0-73845
⁷Be(p,γ), low energy cross section from direct, capture potential model 0-102184
⁹Be(π⁺,πN), 1 GeV/c, heavy fragment knockout process, ⁸Li ang. distrib. 0-106036
²⁰⁹Bi(¹⁶O,X), 940 MeV bombarding energy depend., fragment deformation, sequential fision 0-86938
¹²C(⁶Li,d)¹⁶O-¹²C+α, reaction mechanism from ang. correlations, direct transfer 0-78319
¹²C(d, d'), isospin violating direct reaction, Coulomb interaction role 0-102170
¹²C(p,X), reaction and scatt. dynamics, optical and coupled channel anal. 0-78297
¹²C(π⁺, π⁺p), 100, 180 MeV, knock out reaction, cross section and pion distortion in DWIA 0-91167
⁴⁰Ca(n,γ), direct-semidirect and compound nucleus contribs. to cross sections 0-68662
¹⁴¹Ce collective M1 excitation effects on γ-ang. distrib., direct semidirect model of ¹⁴⁰Ce(n,γ) 0-57733
Cl(Ar,X), 800 MeV/N, single particle spectra from high multiplicity events 0-99184
Cl(Ar,X), proton inclusive spectra, direct plus thermal model 0-57799
C(π⁺, π⁺X), X=He or d, 170 MeV, cross sections and ang. distrib., direct knockout mechanism (*Russian*) 0-86887
C(π,πp), 170 MeV, two stage and knock out contribs., π⁺,π⁻ spallation differences (*Russian*) 0-68632
(d,X), neutron excess isotope prod. in fragmentation, ^{6,8}He, ^{7,8,9,11}Li (*Russian*) 0-86888
^ΛFe(p,γ)Co, A=54.56, giant dipole resonance splitting, direct-semidirect capture model anal. 0-106055
(⁵⁶Fe,X), 2 GeV/N, anomalous nuclei among relativistic projectile fragments 0-106034
¹⁶⁰Gd(¹²C, αxn)¹⁶⁸Xr, particle fragmentation accompanied by incomplete fusion, two step model 0-86947
³He(γ,2p)n, 80-120 MeV, proton energy distrib., diff. cross sections, direct breakup 0-86897
H(p,x), direct and charge transfer scattering processes, second quantisation 0-78289
K(Ar,X), 800 MeV/N, single particle spectra from high multiplicity events 0-99184
K(Ar,X), proton inclusive spectra, direct plus thermal model 0-57799
(⁶Li,X), 156 MeV, projectile break up in continuous particle spectra, cross section, fragmentation 0-86889
⁶Li(⁶Li,αα), 36 to 46 MeV, reaction mechanism 0-83113
⁶Li(n,γ), cross section and spectroscopic factors from direct capture pot. model 0-99171
⁶Li(p,γ), cross section and spectroscopic factors from direct capture pot. model 0-99171
²⁴Mg ground and γ-bands, direct and multistep processes from (α,⁶He), (p,t), (¹⁶O, ¹⁶O) 0-102094

direct nuclear reactions and scattering continued

- ²⁰Ne(X), relativistic collisions, slow and fast fragment correlations, multiplicity association 0-86886
^ANi(d,X), A=58, 64, 7.6 GeV/c, isotopic cross section ratios, He, Li fragments isotopic effects (*Russian*) 0-63154
^ANi(p,X), A=58, 64, 7.6 GeV/c, isotopic cross section ratios, He, Li fragments isotopic effects (*Russian*) 0-63154
^ANi(p_{pol}, α), A=58, 60, 62, 22 MeV, analysing power and cross sections, Co proton-hole states 0-68663
N(π,πp), 170 MeV, two stage and knock out contribs., π⁺, π⁻ spallation differences (*Russian*) 0-68632
N(π[±], π[±] X), X=He or d, 170 MeV, cross sections and ang. distrib., direct knockout mechanism (*Russian*) 0-68687
¹⁶O(X), 2 GeV/N, anomalous nuclei among relativistic projectile fragments 0-106034
¹⁶O(X), A=54-208, direct transfer to discrete and continuum states, DWBA diffraction model 0-78262
¹⁶O α-cluster states, widths and resonances, optical model, direct transfer in ¹²C(¹⁶O,d) 0-105975
¹⁶O fragmentation at intermediate energies, statistical fluctuation, fragment momentum distributions 0-78263
¹⁶O(p,¹²Li)¹²C, 51.9 MeV, five nucleon transfer mechanisms, DWBA calcs. 0-73845
O(π[±], π[±] X), X=He or d, 170 MeV, cross sections and ang. distrib., direct knockout mechanism (*Russian*) 0-68687
O(π,πp), 170 MeV, two stage and knock out contribs., π⁺, π⁻ spallation differences (*Russian*) 0-68632
Pb(Ar,X), 800 MeV/N, single particle spectra from high multiplicity events 0-99184
²⁰⁶Pb(n,γ), direct-semidirect and compound nucleus contribs. to cross sections 0-68662
²⁰⁶Pb(¹²C,¹¹B), 77 MeV, bound and continuum state excitation, direct and two step processes 0-63205
²⁰⁶Pb(¹⁶O,X), 140-315 MeV, projectile fragmentation, ¹⁵N, ¹²C transfer spectra, direct contrib. 0-63155
²⁸Si(³²S,X), 135 MeV, multi-particle prod., two fragment reactions, kinematical anal. 0-83111
¹⁴S primary γ-rays, direct capture and neutron separation energy, (d,p),(n,γ) correlation 0-57738
¹⁵²Sm ground and γ-bands, direct and multistep processes from (α,⁴He), (p,t), (¹⁶O,¹⁶O) 0-102094
^ASn(p,X), A=112, 124, 7.6, 10 GeV/c, isotopic cross section ratios, He, Li fragments isotopic effects (*Russian*) 0-63154
¹²⁰Sn(p,n), statistical multistep direct emission, p-h and DWBA calcs. 0-106035
¹⁸¹Ta(p,n)¹⁸¹W, multi-step compound and direct reactions, statistical theory 0-57761
U(Ne,X), proton inclusive spectra, direct plus thermal model 0-57799
²³⁸U(⁸⁴Kr,X), mass fragmentation, dynamical theory, two centre shell model, binary decay process 0-68628
²³⁸U(p,X), 0.8-400 GeV 0-83099
²³⁸U(p,X), 400 GeV, ^ASc, A=44m,46,47,48, fragment emission, two-step model applicability 0-99177
¹⁸¹W level density, n spectra and ang. correls., direct and nonequilib. processes from ¹⁸¹Ta(p,n) (*Russian*) 0-68631
⁸⁹Y(n,γ), direct-semidirect and compound nucleus contribs. to cross sections 0-68662

directional antennas *see* **directive antennas****directional couplers**

- GAAs homojunction rib waveguide directional coupler switch 0-69554
integrated optics sub-ps gate 0-58809
interference filter all-fibre for wavelength division multiplexing 0-91900
optical directional couplers with graded index profile, variational analysis 0-96037
optical fact directional coupler switch/modulators, novel ps optical pulse sampling method 0-58784
optical slab-type directional coupler with activated rhodamine 6G top layer, amplified oscill. 0-99718
optical subpicosecond gate, velocity-matched directional coupler 0-74512
optical waveguide tap with infinitesimal insertion loss 0-99883
polarisation-independent optical switch using weighted directional coupler 0-58798
rotation-splice tapered fibre star coupler directivity and mode dependence 0-58748
single-mode fibre optic directional coupler 0-58683
travelling wave optical modulator using a directional coupler LiNbO₃ waveguide 0-96035
LiNbO₃ waveguide modulators and switches, Ti-diffused, fabrication on directional coupler principle 0-83678
LiNbO₃/Ti optical waveguide electrooptic devices, polarisation independ. directional coupler switch 0-58783

directional patterns *see* **antenna radiation patterns****directive antennas**

- meteor recording freq., influence of form and orientation of antenna directivity diagram (*Russian*) 0-67665

dirty superconductors

- ferromagnetic superconductor, paramagnetic fluctuations, influence on superconductivity 0-70900
Ginzburg-Landau equations, time-depend., near supercond. transition temp. 0-70886
microbridges, with paramag. impurities, Josephson steady-state effect (*Russian*) 0-93042
nonequilibrium superconductor, normal component drag by condensate, tunnelling (*Russian*) 0-93051
periodic structures, crit. fields (*Russian*) 0-88700
quasi-two-dimensional dirty superconductor, nonstationary Josephson effect (*Russian*) 0-100556
supercond. cylinder, order parameter enhancement by microwave irradiation 0-70896
zero-gap dirty, cond. electron spin resonance theory 0-103888
Nb, effect of changes in α²(Ω)F(Ω) on the zero-temp. energy gap 0-97025
Nb₃Sn, effect of changes in α²(Ω)F(Ω) on the zero-temp. energy gap 0-97025
Pb, effect of changes in α²(Ω)F(Ω) on the zero-temp. energy gap 0-97025
Ta, effect of changes in α²(Ω)F(Ω) on the zero-temp. energy gap 0-97025

discharge lamps

- see also* arc lamps; flash lamps; fluorescent lamps; metal vapour lamps
glow, alternative scanned light sources 0-69477

discharge lamps continued

- microwave, VUV resonance radiation source for photochemical work 0-59330
photoreceiver time resolution meas. using gas-discharge lamps 0-73461
radio-frequency excited pulsed hollow-cathode lamp, absorpt. and emission characteristics 0-89550
spherical integrating photometers, luminous flux meas. accuracy, expt. anal. of group discharge lamps (*Polish*) 0-73407
sunlight simulation, review of various light sources 0-87454
D₂ lamps, influence of Ne and Ar on spectral parameters 0-86460
D₂, magnesium fluoride windowed, radiance transfer standards from 115 nm to 370 nm 0-87451
Hg discharge, high-pressure, NaI and TlI additives, line broadening and radiative transport 0-74199

discharge lasers *see* **gas lasers****discharge tubes** *see* **gas discharge tubes****discharges (electric)**

- see also* arcs (electric); electric breakdown; exploding wires and foils; flashover; glow discharges; high-frequency discharges; lightning; partial discharges; positive column; sparks; surface discharges; Townsend discharge
AC electrodeless narrow gap discharge, anal. and plasma display design 0-70063
beam plasma discharge, electron beam energy distrib., in E-region approximated plasma 0-103163
book, gaseous electronics and gas lasers 0-73120
breakdown wave propagation in ionised gas in nanosecond discharges 0-87890
cathode discharge, hollow, Al spectral line, pulse feeding 0-64797
charged microparticles productions under high electric field intensity in ultra high vacuum, measurement (*Japanese*) 0-96411
cold-cathode ion gun for sputter-etching, discharge characts. and improvements 0-105748
columns, electron density distrib. for electron prod. and loss rates linear and quadratic in electron density 0-96400
condensed media, electrodynamics problems, theoretical investigation (*Russian*) 0-75116
conference, general congress, Societe Francaise de Physique, Toulouse, France (June 1979) 0-77536
crossed field plasma discharges characts. 0-100116
current carrying double layer production in focus device 0-83953
dielectric materials, spacecraft, charging and discharging 0-71315
diffuse discharge, current constriction near anode in combustion product plasma 0-103201
disc cathode in He flow, spectrosc. investig. 0-64809
DITE, low Q discharges 0-92374
electrodes, screening, discharge phenomena with UHV positive and negative lightning and switching pulses for dimensioning (*German*) 0-87963
electron cloud in equilib., mag. field effect, pot. and space charge distrib. 0-92410
electrostatically deposited films obs., using image intensifier and laser Doppler anemometer 0-71593
fission reactor, gas-discharge, fuel element component conc., plasma temp. profile instabilities 0-63253
fluid, radio band pulse radiation due to spark initiated cavity dynamics, sonoluminescence (*Russian*) 0-66313
FT-1 Tokamak, discharges in low density plasma (*Russian*) 0-106958
gas, low density, space charge limited current flow 0-79605
gas discharge instability near electrode 0-70064
Gassiot's cascade, 19th century discharge tube demonstration 0-77586
HF discharge, ionisation overheat instability in EM wave field (*Russian*) 0-106990
high current discharge from cold LaB₆ cathode 0-107011
high voltage opening switch using spoiled electrostatic confinement 0-103205
high-current, gas superluminesc. polarisation due to Zeeman level splitting 0-100060
hollow cathode discharge, for spectrochem. anal. of microimpurities in amorphous B 0-85247
hollow cathode discharge with variable voltage 0-59336
impulsive corona discharge around conductors, phys. aspects consideration (*French*) 0-92406
inert gas, electroionisation discharge, negative cathode pot. drop 0-79615
inert gas ion laser, high voltage-low press. discharges, stationary props. 0-92400
inert gas mixture, electrophotoionization discharge, laser pumping 0-91781
inert gases, atomic alignment in positive column (*Russian*) 0-87981
inert gases, self-sustained discharge possibility with bulk photoionisation impurities 0-75113
insulators, HV, influence of air pollution on dielectric rigidity (*Slovenian*) 0-64801
laser, elec. discharge-pumped excimer type, model 0-58516
laser discharge, high-power, stabilisation with mag. field 0-99739
laser wavelength calibration using optogalvanic effect, atlas 0-62727
laser-triggered discharge gap characts., influence of discharge medium, electrooptic switch control appls. 0-64818
light source, electrodeless, slab-line cavity design 0-83652
liquid cavity collapse, accompanied by RF emission 0-87790
low pressure gas, electron energy distribution meas. 0-96412
low pressure plasma arc, energy parameters experimental study 0-75117
magnetic dipole transitions in TiXIV, TiXV, TiXVII ground state terms in Tokamak discharge 0-63575
metal oxide reduction by electron cyclotron reson. plasma of H, model study on discharge cleaning 0-76548
metal vapour laser, hollow cathode, review (*Rumanian*) 0-87409
metal-vapour recombination lasers using segmented plasma excitation 0-74370
MHD accelerators, electrodynamic characts. 0-64788
microsecond stratified pulsed discharge 0-87975
molecular mixture, strongly excited, vibr. relax. 0-102555
moving striations, conditions for self-excitation 0-69358
multicharged ion heating in Z-pinch, column compression, temp. and density (*Russian*) 0-64754
nanosecond discharge in vac., cathode polishing effect 0-79599
optoelectronics, appl. in measuring gas discharge phenomena 0-107007
ORMAK Tokamak, runaway-electron-dominated discharges 0-87971
plasma beam discharge, electron kinetics, charge particle finite lifetime effect 0-92404

discharges (electric) continued
plasma beam discharge, electron kinetics, deexcitation processes effect 0-92405
plasma compression between parallel plates, recomb. press., phase transition 0-64799
plasma decay under constant voltage (*Russian*) 0-106988
plasma shell, cylindrical, apparatus for production 0-106948
positive, propag. in transformer oil and silicone fluids, variations 0-88926
positive gas-discharge column with allowance for metastable atom effect, excitation of strata 0-96410
positive streamer velocities meas. in quasi-uniform electric fields 0-72625
preforming using high-voltage electrical discharge 0-84872
pressure wave generation and propagation by spark discharges in liquids (*Japanese*) 0-70060
probe cct. used in pulsed plasma diagnostics 0-87947
pulse character in strongly heterogeneous field formed by electrodes point-plate arrangement (*Czech*) 0-70048
pulsed discharge of inductive storage element into fluid gap, electrohydraulic effect (*Russian*) 0-100117
pulsed discharges in gases, theoretical and expt. study 0-92416
pulsed transversally excited discharge, appl. to N₂ laser (*French*) 0-107009
reflex discharge, plasma quiescence 0-64806
RF discharge, inert gas isotope separation in travelling magnetic field 0-78719
RF sputtering systems, discharge suppression within piezoelectric gas admission valves 0-100110
SF₆ discharge inception voltage affected by avalanche growth space charge (*German*) 0-75109
skimming discharges for pulsed gas-discharge laser preionisation, spectral characts. 0-99740
spark gaps, HV switching surges, influencing factors (*German*) 0-87958
spark gaps, long air, disruptive voltage calc. with positive switch voltages (*German*) 0-87964
spectroscopic electron density meas., hot point low induction vacuum spark gas (*Russian*) 0-92390
stratified pulsed discharge with limited surface area 0-87974
sustained optical discharges in molecular gases 0-100085
testing, Voyager spacecraft, JPL, Pasadena, USA 0-92415
thermionic triode, oscills. in low press. inert gas discharge 0-79590
Tokamak plasma, very-low-q discharges in DIVA 0-64765
Tokamak Thor, discharge, electron distribution function, laser Thomson scatt. 0-59327
two-temperature discharge, transport eqns., transient phenomena 0-96402
unipolar pulsed LCD discharge, spectrum, time scanning 0-64774
vacuum breakdown, Trump-Van de Graaff condition anal. 0-79613
volumetric discharge, semi-self-maintaining, excited by electron beam, current maintenance in cathode layer 0-59322
water vapour, electron energy distrib. function, electron sink and plasma resist. effect (*Russian*) 0-106987
Ar, CW optical discharge in laser plasmatron mode 0-75078
Ar decaying pulsed discharge plasma, acoustic waves density modulation 0-103143
Ar discharge, ion density profile, reson. laser light meas. 0-92401
Ar, excitation by pulsed electric discharge, luminescence obs., time resolved spectra meas. 0-102482
Ar-air, transformer plasmatron, LF discharge, electrical and energy props. 0-103200
Ar-Hg-Cl₂, elec. discharge, electron inelastic collision props. 0-79617
CO electric discharge lasers, vibr. kinetics, modelling and expts. 0-69374
CO supersonic lasers, CW double elec. discharge performance 0-69416
CO-N₂ discharge, plasma characts. and vibr. kinetics anal. 0-59331
CO₂ dissociation in a nonequilibrium plasma 0-87851
CO₂ gas transport laser, discharge and power extraction characts. (*Rumanian*) 0-95869
CO₂ laser, pulsed, elec. field distrib. in vol. discharge controlled by electron beam 0-58505
CO₂ TEA laser, UV preionised, characts. 0-69414
CO₂ waveguide laser, multibeam, excited by AC discharge 0-99754
CO₂ waveguide laser with pulsed high-freq. discharge 0-99755
CO₂-N₂ mixture, strongly excited, vibr. relax. 0-102555
CO₂-N₂-He, pulse-periodic operation of electron-beam-controlled discharges, energy characts. changes 0-102695
CO₂-N₂-He-O₂ discharge mixture, three body electron attachment to O₂ 0-64779
Cn, vapour laser excited by single elec. pulse, lasing characts. 0-87386
Cu electrodes, breakdown voltage, prebreakdown current in vacuum, crossed elec. mag. fields depend. 0-79604
F₂, stationary vol. discharge, reduced power meas. 0-75115
H, Rydberg consts., saturated absorpt., spectroscopy meas. 0-105604
H₂ beam discharge, electron kinetics in collisionless non-equilibrium plasma 0-92402
H₂ hot-iron plasma, ion temp. and electron density depend. studied by laser light scatt. and emission spectroscopy 0-96342
H₂, non-equilib. ionisation rate calcs. 0-59319
H₂+He, N₂, Ne, Ar, Kr, Xe admixtures for increased proton yield in HF ion source 0-57422
HCl, vibr. excitation in electric discharge 0-87978
HF-DF simultaneous laser excited by ferroelec. ceramic capacitatively coupled discharge 0-69413
H₂O vapour under point corona discharge, microprocessor control for vapour generator and EHD phenomena 0-106852
He, hollow-cathode type, spectroscopic obs., laser light source appl. 0-95335
He, low press. discharge, electron free streaming waves expansion 0-79595
He, positive column plasmas, metastable atom density meas. by improved self absorpt. method 0-87968
He, self-oscillating props. of discharge in mag. field 0-64814
He-Kr hollow cathode CW laser, Kr II 4584 Å generation 0-58510
He-Ne laser, 6328 Å power fluctuations due to striation noise 0-78834
He-Ne laser, compact, transverse microwave discharge, energy characts. 0-64064
He-O₂ DC discharge, electron distrib. function 0-92407
Hg vapour line splitting on Tonks-Dattner reson. 0-59317
Hg-Tl-I discharges, 50 Hz, axial segregation effect on elec. field strength 0-59320
⁸⁶Kr, discharge, metastability-exchange cross section 0-99464
⁸⁶Kr-⁷⁸Kr, discharge, metastability-exchange cross section 0-99464
Mg-Xe discharge and MgXe excimer band, emission intensities and excited-state densities meas. 0-92413

discharges (electric) continued
Mo, dislocation structure evolution near electro-eroded crater (*Russian*) 0-100237
N₂-methane, rapidly developing discharge, streak camera records interpretation 0-59280
Na-Hg high-press. discharge, Na reson. radiation, self-reversed maxima shifts 0-92411
Ne discharge in high press. narrow tube, Kadomtsev-Nedospasov instability 0-107004
Ne, isotope separation by cataphoresis in DC gas discharge 0-103213
Ne, low press. discharge, electron free streaming waves expansion 0-79595
Ne positive column plasmas, metastable atom density meas. by improved self absorpt. method 0-87968
Ne pulsed transverse discharge, spectrosc. absorpt. investig with nanosec. time resolution (*Russian*) 0-64782
Ne-N₂ AC discharge, pulse to continuous mode transition, Ne metastable effects (*German*) 0-84011
Ni-Cd batteries, button and cylinder types, self discharge behaviour during storage (*German*) 0-66960
O₂, A³Δ_g state, inversion, presence in nightglow and discharges 0-63616
O₂, electron energy distrib. function, electron sink and plasma resist. effect (*Russian*) 0-106987
S (S-He) discharges, stability, emission spectra 0-107003
SF₆ high-current discharge plasma column, radiation charact. and struct. (*Russian*) 0-106989
SF₆ insulation, under impulse voltage stress, effects of pressure and vol. on firing delay (*German*) 0-87959
SF₆-inert gas mixture, high power cylindrical spark discharge, dynamic and visible charact. 0-64816
Xe-F two module discharge laser, gain and temporal characts. 0-87385
Y₂O₃ capillary discharge plasma, temp., radiation screening elimination 0-64682
discharges (partial) *see partial discharges*
disclinations
amorphous magnets, disclinations and solitons 0-75786
cholesteric, liquid crystals, disclinations, rotation defects, topology (*French*) 0-79679
disclinations and melting in two and three dimensions 0-103454
dynamics, field equations, four dimensional space-time setting 0-96521
fragmented structures, dislocation and disclination kinetics (*Russian*) 0-79788
hexagonal liquid crystals, developable domains 0-92453
melting, two-dimens., dislocation-mediated theory predictions, light scatt. use as probe 0-92651
orientational bistability, nematic storage effects 0-70112
straight wedge disclination near a free surface 0-96511
surface dislocations, universal concept, rel. to disclinations and grain boundaries 0-100231
two-face dislocation boundary, energy and induced stresses (*Russian*) 0-103331
discontinuous metallic thin films
conductivity, appl. of percolation theory 0-65712
island films, coalescence kinetics, ageing rate, Kahlweit approx. (*Russian*) 0-59838
nucleation on alkali halide crystals, effect of ionisation of condensing flux 0-107675
optical properties of rough surfaces, discontinuous films, heterogeneous materials, review 0-103935
Ag film growth on Si (111), nucleation and growth modes, SEM study 0-100423
Al, granular, transition to localisation, elec. resist. 0-70877
Al granular films, inhomogeneous supercond. transitions, microwave meas. 0-103789
Au discontinuous film, electroluminescence obs. 0-103998
Au film, discontinuous, centre-to-centre particle distrib. determ. 0-96761
Au, thin film, discontinuous, high resist., Hall effect meas. 0-65716
Mo islet films, effect of external elec. field on electron emission 0-80952
Pb granular film, Josephson coupled, resistive transition 0-88683
Sb, discontinuous thin films, cluster shape models 0-100419
W epitaxy on W(110) substrate, work function meas., LEED investigation 0-80103
discrete symmetries
see also C invariance; CP invariance; CPT invariance; P invariance; parity; T invariance
integrable system concealed symm. (*Russian*) 0-91016
quantum field theory, relativistic, discrete symmetries 0-68387
discrete time systems
blood pressure automated control in dogs using microprocessor 0-81797
discriminators
see also demodulators
US, automatic noise-blanking, pulse-timing discriminator for production inspection of parts 0-76472
disinclinations *see disclinations*
disintegration (radioactive) *see radioactivity*
disintegration energies *see radioactivity*
dislocation anchoring *see dislocation pinning*
dislocation arrays
α-brass, fatigue crack propag., role of dislocation substruct. 0-60963
crack dislocation model 0-69741
cracks, discrete dislocation analysis 0-84236
grain boundary dislocations, effects on grain boundary processes of the steps in boundary plane 0-79785
Incoloy 901, foil prep. for TEM exam. 0-88001
α-quartz, synthetic, growth, defects induced by seed orientation 0-96454
Al, surface deformation and wear track obs. using analytical electron microscope 0-108687
Cu, fatigue crack propag., role of dislocation substruct. 0-60963
Cu, single crystals, neutron irradiated, stresses and secondary slip between overlapping and dislocation arrays 0-88162
Cu-Ni-Al (5, 2.5 at.%), precip. hardening (*Japanese*) 0-71663
Fe, epitaxial growth on Au platelets, dislocations 0-96760
Ge single crystals, constitutional supercooling growth conditions, structural and chem. inhomogeneities 0-93473
PbFe_{1/2}O₃, dislocation etch pit morphology study (*Chinese*) 0-88150
Si, dislocation motion from indentation rosette 0-79798
dislocation breakaway, pinned *see dislocation damping*
dislocation climb
ceramic, creep, porosity depend. 0-97530

dislocation climb continued

- creep, irradi, induced in transient irradi. environments 0-92598
 creep, irradiation induced, dislocation glide enabled by preferred absorption of point defects 0-88250
 creep, swelling and growth, radiation induced, bias factors estimated from self-consistent model 0-88249
 creep, transition between dislocation and diffusion 0-88253
 creep and growth, radiation induced, fundamental mechanisms 0-92596
 dispersion-strengthened alloys, threshold stress for creep 0-93626
 double jog side-motion, elastic theory 0-84171
 faulted dislocation loops induced by elastic interaction, climbing motion 0-75227
 FCC material, irradiation induced creep, climb induced glide model 0-89292
 grain boundary dislocations, effects on grain boundary processes of the steps in boundary plane 0-79785
 metals, submicroscopic defects, influence on HVEM in-situ expts. 0-103392
 modulated structures, dislocation climb under irradiation conditions 0-70195
 oxides, dislocation climb model 0-100230
 Zircaloy-2, electron irradiation damage, direct obs. 0-84212
 Al, creep behaviour, at high temp., influence of oxidation 0-97538
 Cu alloys, FCC, climb of extended dislocations due to irradiation in HVEM 0-103343
 Cu-Al, dislocations, dissociated, climb mechanism, nucleated loops, Burgers vectors 0-65002
 Cu-Al (10, 16 at.%), influence of jogs on extension of dislocation nodes 0-84176
 Cu-Al alloy, irradi, in HVEM, climb of dissociated dislocations and point defect absorpt. 0-107257
 Cu-Ni alloys, chemical interdiffusion under uniaxial stress 0-65307
 Cu-Si (7 at.%), influence of jogs on extension of dislocation nodes 0-84176
 GaAs degraded lasers, climb asymmetry, TEM obs. 0-79802
 GaAs-(GaP) single cryst., defect distrib. near abraded surface 0-92533
 GaP single cryst., defect distrib. near abraded surface 0-92533
 Ge, dissociated dislocations, constriction correlation with jogs 0-79801
 MgO, single cryst., tensile creep, stress induced dislocation structs. 0-96539
 MgO.1.1 Al₂O₃ spinel, high temp. deform., cryst. orientation effect 0-107263
 NbC single cryst., Vickers microhardness, slip mechanism 0-71732
 Ni, creep, irradi. induced with 17 MeV deuterons 0-93607
 Ni_{0.5}Zn_{0.5}Fe₂O₄ coarse grain polycryst. ferrite, diffusional creep (*Japanese*) 0-104238
 Pb, film, hillock formation by grain boundary sliding 0-107673
 Sb, electron microscope irradiation effects, agglomeration of point defects, dislocation climb and loops (*French*) 0-59518
 Si, epitaxial wafer, saucer pit microdefects reduction by intrinsic gettering 0-75450
 Si:As, ion implanted, laser annealed, lattice defects, epitaxial regrowth 0-103334
 Si:P bipolar transistors, interstitial supersaturation and misfit dislocation climb, TEM study 0-70203
 VC single cryst., Vickers microhardness, slip mechanism 0-71732
 V₂Si single cryst., creep deform. 0-71695
 Y₂O₃, dislocation and plasticity dissociation 0-107247
 Zr alloys, creep and growth, irradiation induced, microstruct. depend. 0-93602
 Zr, electron irradiation damage, direct obs. 0-84212
 Zr-Sn(Fe)(Ni) (0.15 wt.%), electron irradiation damage, direct obs. 0-84212

dislocation damping

- see also *Bordoni effect*
 ferromagnet, pinned domain wall motion, magnetic damping studies 0-65956
 unified theory, point defect dragging 0-88144
 Fe-Al(Ti), O containing, mag. aftereffect and disaccommodation meas., time depend., activation energy, and ageing props. 0-88836
 Nb, dislocation damping, amplitude depend. 0-59469
 Ni, cold-worked, rel. between dislocation and ferromag. damping 0-107369

dislocation density

- collective behaviour, velocity of slip band and mobile dislocation densities, HVEM study (*French*) 0-65006
 discrete obstacle model, dislocation and stress field distrib. 0-79794
 film/substrate interface, misfit dislocation obs. using electron microscopy 0-103605
 grain boundary sliding model 0-75237
 metal, FCC, dislocation behaviour at high strain rates, US detection method, data analysis basis 0-85136
 metals, dislocations and shock compression, thermodynamics 0-100235
 minerals, dislocations and shock compression, thermodynamics 0-100235
 monocrystal surface layer damage depend. on abrasive working parameters (*Russian*) 0-76368
 Rene 80, dislocation behaviour during plastic deform. (*Japanese*) 0-108504
 ruby, structural defects due to laser irradi. (*Russian*) 0-100303
 sapphire ribbon crystals, EFG growth and charact., voids, grain boundaries and dislocations 0-103283
 steel, Mn-Sn(-Nb), extra low C, shear transformation struct. (*German*) 0-60873
 steel, stainless, austenitic, deform. substruct. and annealing, stacking fault tetrahedra form 0-107282
 steel, stainless, fracture and crack tip plastic zones, in situ obs. 0-108686
 steel, stainless, martensite nucleation mechanisms, HVEM obs. 0-104157
 steel, stainless, radiation damage by 1 MeV electrons, dislocation struct., brittleness (*Russian*) 0-75226
 steels, low alloy, particle coarsening reactions, effect of cold deform. 0-71664
 strain rate, dislocation density, dislocation motion and dislocation constitutive eqns. 0-103329
 straining experiments, in situ, strong frictional force, quantitative anal. 0-100244
 Zircaloy-2, pressure tubes, irradi. creep and growth, anisotropy factors 0-97536
 Al, polycrystalline, movement of 3-fold nodes of boundaries in high temp. creep 0-89317
 Al single cryst., latent hardening in tension 0-60878

dislocation density continued

- Al wire, grain boundary internal friction after recrystn. annealing (*Russian*) 0-66561
 Al-Cu (4 wt.%), supersaturated and aged conditions, high strain deform. 0-60907
 AlCu-NiCo (5 at.%), θ' hardened, creep mechanism 0-85013
 Au, deformed, annealing kinetics of vacancies (*Japanese*) 0-88139
 Au/Cu, bilayers, interdiffusion phenomena, lattice dislocations, TEM obs. 0-59736
 Au/Cu, initial epitaxial growth at room temp. 0-59829
 CdS-Cu₂S solar cells, microstructural study of heterojunction materials 0-93978
 Cu, high-purity, grain size and strain rate influence on mech. behaviour, precursors existence 0-85016
 Cu, polycryst., surface layer hardening by multiple impact 0-108469
 Cu single cryst., latent hardening in tension 0-60878
 Cu single crystals, [100]- and [111], dislocation density meas. using TEM 0-79803
 Cu-Fe (1.5 wt.%), precipitation-effect on void formation during electron irradiation 0-84211
 Cu-Nb multifilamentary composite, dislocation resistivity 0-70671
 Cu-Ni (10 at.%), creep, substruct. and internal stresses (*Russian*) 0-97527
 Cu-Ni (10 at.%), hardening, recovery, and struct. changes during high temp. creep (*Russian*) 0-89288
 Fe-Mo(4.1 wt.%), steady state creep at high temps. 0-89316
 Fe-Ni-C, intercrystalline embrittlement in tempered martensite, elimination by re-austenitization (*Slovak*) 0-108548
 GaAs crystal growth, thermal and elastic const. evaluation 0-92586
 n-GaAs, crystal growth by Czochralski method kinetics, total emittance determ. 0-75193
 GaAs epitaxial multilayer photocathode structures, TEM obs. of dislocations generated 0-100241
 GaAs, luminescence emitted from deep centres, plastic deform. effect on internal quantum efficiency 0-60672
 GaAs, pulled, dislocation generation, thermoelastic anal. 0-79787
 GaAs:Si defect density before and after Zn diffusion, SEM and TEM obs. 0-96529
 GaAs-(GaP) single cryst., defect distrib. near abraded surface 0-92533
 GaAs-, Sb, layer on GaAs, dislocation density reduction by improved LPE growth method 0-76202
 GaP, crystal, growth conditions rel. to dislocation struct. 0-88151
 GaP single cryst., defect distrib. near abraded surface 0-92533
 GaP, VPE layer structures for LEDs, SEM, and TEM obs. of dislocation density reduction expt. 0-100425
 GaP:Si, defect struct. and tetrahedral precipitates, TEM study 0-107246
 Ge ribbon single crystals, grown from melt, dislocation struct. form. under thermal stress 0-107082
 Ge single crystals, constitutional supercooling growth conditions, structural and chem. inhomogeneities 0-93473
⁴He, solid, thermal cond., 0.4 to 1.8K (*Russian*) 0-103535
 InAs films, MBE grown on GaAs, electron mobilities, lattice mismatch effect 0-80419
 InP:SSD growth of low dislocation density crystals 0-89135
 InSb, galvanomagnetic props. of annealed single crystals 0-96909
 p-InSb, influence of plastic deform. on elec. props. 0-103711
 KCl:Br⁺, solid solution periodic precipitation in inhomogeneous conc. field 0-103485
 LiF, dislocation structure, influence of variable deform. temp. 0-70211
 LiF:Ni, dislocation behaviour in diffusion zone, Cottrell clouds (*Russian*) 0-70212
 α -LiIO₃, surface defect layer struct. due to mechanical working (*Russian*) 0-100238
 MgO, fracture and crack tip plastic zones, in situ obs. 0-108686
 MgO, single cryst., tensile creep, stress induced dislocation structs. 0-96539
 MgO:Li, mech. deformed crystals, imprinting of slip bands using Li impurities 0-59473
 MgO.1.1 Al₂O₃ spinel, high temp. deform., cryst. orientation effect 0-107263
 Mo alloys, dil., HVEM bombarded, neutron damage simulation, defect cluster and dislocation obs. 0-107330
 Mo, fracture and crack tip plastic zones, in situ obs. 0-108686
 Mo, plastically deformed single cryst., mag. susceptibility (*Russian*) 0-93074
 Mo polycrystn., cyclically deformed, dislocation arrangements 0-108506
 NaCl, dislocation density in monocrystal deformed under high hydrostatic press. 0-70216
 NaCl, dislocation ordering influence on integrated X-ray coeff. 0-103357
 NaCl, high resolution TEM and radiation sensitivity, dislocation obs. on deformed crystals. 0-107260
 Ni, carbonyl powder, dislocation density sintering 0-108372
 Ni, creep, substruct. and internal stresses (*Russian*) 0-97527
 Ni, dislocation structure evolution after hydroextrusion (*Russian*) 0-96530
 Ni, ion irradi. with 20 and 500 keV ⁴He⁺, depth distrib. of cavities and dislocation damage 0-107346
 Ni, polycrystalline, strain hardening, dislocation link length model 0-84953
 Ni precipitates, isothermal annealing influence on structural state, X-ray diff. anal. (*Russian*) 0-100849
 Ni, push-pull fatigued polycrystals, point defects, elec. excess resist. meas. 0-100910
 Ni, structural changes, creep mechanism, multiple dislocation cross slip (*Russian*) 0-59476
 Ni, variation in dislocation density during creep, determ. by X-ray diff. analysis (*Russian*) 0-76302
 Pd-H system, solvus hysteresis 0-71659
 Si, controlled dislocation formation, struct. density (*Russian*) 0-107244
 Si crystals, photoelectret state investigation 0-97191
 Si, diffusion of P, elastic deform. relax. and dislocation generation 0-79997
 Si film, MBE, cryst. defect props., substrate treatment effects 0-70551
 Si:B, ion implanted, structure defects formation and behaviour under annealing in various ambients 0-65033
 n-Si:P(B), elec. cond. oscils., electron instability effects due to dislocations 0-103704
 α -Ti, plastic deform., anharmonicity, and Gruneisen parameter 0-88246
 Ti-Mo-Zr-Sn (11.5, 6.0, 4.5 wt.%) alloy, struct. as affected by processing history 0-84972

dislocation density continued

- W, plastically deformed single cryst., mag. susceptibility (*Russian*) 0-93074
- W, vapour deposited, dislocation struct., rel. to texture (*Russian*) 0-65394
- Y₂O₃(Nd) single crystal growth, floating zone method with Xe arc lamp imaging furnace 0-60777
- Zn crystal, {1122}{1123} slip system, deform. stress, dislocation density depend. (*Russian*) 0-103353
- Zn, single cryst., contribution of basal dislocations to residual elec. resist. (*Russian*) 0-75539
- Zr alloys, creep and growth, irradiation induced, microstruct. depend. 0-93602
- Zr-Nb (2.5 wt.%), pressure tubes, irradi. creep and growth, anisotropy factors 0-97536

dislocation dipoles

- electron microscopy, calc. of weak-beam images 0-75231
- II-VI compounds, charged dislocations and plastic deform. 0-107264
- melting and dislocations in two and three dimensions 0-103454
- steel, stainless, austenitic, deform. substruct. and annealing, stacking fault tetrahedra form 0-107282
- steel, stainless, austenitic Ni-Cr type, creep deformed, dislocation multipole obs. 0-107258
- CdI₂ polytypic crystals, dielectric loss behaviour 0-66108
- Co, single crystals, {1121} twins, accommodation and form. 0-96540
- Cu-Al, linear dislocation multipoles, weak-beam TEM 0-75233
- Cu-Cr-SiO₂ system, age and dispersion strengthened, dislocation struct. around SiO₂ particles 0-108468
- LiF, dislocation structure, influence of variable deform. temp. 0-70211
- NaCl, γ -irrad., F-stimulated inversion of sign of dislocation charge 0-59475
- NaCl, high resolution TEM and radiation sensitivity, dislocation obs. on deformed crystals. 0-107260
- Si, Czochralski grown crystals, swirl-type defect obs. 0-100236
- ZnS crystals, structural change under plastic deform., partial dislocation movement 0-79736

dislocation drag

- magnetically ordered cryst., dislocation drag, magnetoelastic waves 0-103332
- point defect dragging, unified theory of dislocation damping 0-88144
- steel, low-alloy, plastic deform. mechanisms under dynamic loading 0-100883
- Al-Mg (0.3 wt.%) single cryst., dislocations obs. by high voltage electron microsc. 0-79796
- Zn, twinning, influence of dislocation drag. mag. field effects 0-59472

dislocation energy

- displacement energy determ. by electron beam induced conductivity 0-70097
- grain boundary energy-misorientation relationship use in modelling grain boundary defects and props. 0-84188
- two-face dislocation boundary, energy and induced stresses (*Russian*) 0-103331
- two-phase anisotropic medium, interfacial dislocation, stresses, displacements and energy calc. 0-79786
- AgMg, B2 intermediate phase, slip system, ordering energy and atomic size ratio depend. 0-59471
- AgZn, B2 intermediate phase, slip system, ordering energy and atomic size ratio depend. 0-59471
- AuMg, B2 intermediate phase, slip system, ordering energy and atomic size ratio depend. 0-59471
- NaCl, edge dislocation, core struct. and props., theory 0-70194

dislocation etching

- β -brass, dislocation etchant, (NH₄)₂S₂O₈-HCl-H₂O 0-65004
- monostearine crystals, spiral growth from organic soln. 0-93467
- stearic acid crystals grown from solution, spatial correlation between growth spirals and inclusions 0-96527
- steel, mild, fractography study of shear mode fatigue crack growth by etch pits (*Japanese*) 0-108545
- velocity, thermal activation exam. of applied stress and temp. depend., expt. methods (*French*) 0-59474
- Be-SiO₂, phenakite, flux grown single crystals, twinning study by hydrothermal etching and X-ray diff. 0-107271
- CaF₂, cryst., {111} faces, selective etch rate and etch pit morphology, acid conc. and temp. effect 0-96524
- n-GaAs, current-voltage charact., dislocation etch pits and perfect cryst. 0-70695
- GaAs, epitaxial layer, nondislocation etch pits 0-92535
- KH₂PO₄ single crystal evidence for spiral growth on pyramidal faces 0-84120
- LiF, dislocation structure, influence of variable deform. temp. 0-70211
- Mg-SiO₂ crystals, dislocations configuration and cleavage steps dissoln. 0-107250
- NH₄H₂PO₄ single crystal evidence for spiral growth on pyramidal faces 0-84120
- (NH₄)₂S₂O₈-HCl-H₂O dislocation etchant for β -brass crystals. 0-65004
- PbFe₂O₁₉, dislocation etch pit morphology study (*Chinese*) 0-88150
- Se-Te single crystals, chem. etching 0-96526
- Si, crystal defects and impurities interaction obs. by electron microscopic methods 0-65003
- Si, Czochralski grown crystals, swirl-type defect obs. 0-100236
- Si, dislocation generation in local oxidation 0-107245
- Si, isolated dislocation motion, velocity determ. (*Chinese*) 0-107243
- Te, a-edge dislocated crystals, mobility anisotropy 0-107781
- Te crystals, thermal etch pits shape on cleavage faces 0-107251
- W, vapour deposited, dislocation struct., rel. to texture (*Russian*) 0-65394

dislocation glide see slip

dislocation interactions

- see also impurity-dislocation interactions; vacancy-dislocation interactions
- collective behaviour, velocity of slip band and mobile dislocation densities, HVEM study (*French*) 0-65006
- crack propagation effect of 2- or 3-dimensional macrodefect (*Japanese*) 0-104261
- creep, swelling and growth, radiation induced, bias factors estimated from self-consistent model 0-88249
- dechanneling mechanism due to dislocations, anal. 0-59538
- F-centre, dislocation influence on optical props. 0-108234
- ferroelastic, dislocation-phonon interactions, phase transition effects 0-59600

dislocation interactions continued

- ice, plastic deformation, ultrasonic wave attenuation by dislocations (*French*) 0-59564
- ionic crystals, dislocations, review 0-107236
- magnetic domain boundary, interacting with localised defects, unidimensional flow of configs. (*Russian*) 0-65954
- mass flux, irradiation enhanced, dislocation interactions 0-88206
- metal, electron irradi., elastic point defect-dislocation interactions, defect dragging model extension 0-65050
- metals, FCC, dislocation barriers at coherent twin boundaries, anisotropic elasticity solns. 0-96522
- metals, FCC, misfit defect and extended screw dislocation anisotropic elastic interaction 0-96563
- metals, point defect diffusion controlled reaction theory, book contrib. 0-103318
- parelastic force on homogeneous cryst. inclusion, theory 0-79777
- phonon-dislocation interactions, drag of phonon gas by moving dislocations 0-70218
- point defect-edge dislocation interaction near solid surface 0-79834
- steel, austenitic, ageing and plastic deform. effect on struct. and mech. props. of N15Kh5G3T3 (*Russian*) 0-71691
- steel, high-speed, low temp. mag. cycling effects, dislocation interactions with mag. domain walls. 0-100928
- steel, medium and high C, deformation ageing, entropy, free energy, dislocations (*Russian*) 0-66581
- steel, pearlitic, struct. variations under plastic strain and subsequent heating, cementite decomp. (*Russian*) 0-84954
- steel, stainless, in-situ obs. of deform. in HVEM 0-103338
- steel, stainless, radiation damage by 1 MeV electrons, dislocation struct., brittleness (*Russian*) 0-75226
- strain ageing, dynamic, and serrated yielding, mechanism 0-88245
- transition metals, BCC, interaction energy between self-interstitial and screw dislocation, calc. 0-70248
- Al, polycrystn., HVEM in-situ investigation of creep mechanism 0-104214
- Cd crystals, X-ray topographic examination of basal dislocation glide, generation and locking 0-88156
- Cu, electron irradi., elastic point defect-dislocation interactions, defect dragging model extension 0-65050
- Cu, near Σ 9 grain boundary, structure and dislocation interactions 0-79808
- Cu-Al (10, 16 at.%), influence of jogs on extension of dislocation nodes 0-84176
- Cu-Al (11 at.%) single cryst., dislocation reactions during deform. twinning 0-79795
- Cu-Ni-Al (5, 2.5 at.%), precip. hardening (*Japanese*) 0-71663
- Cu-Si (7 at.%), influence of jogs on extension of dislocation nodes 0-84176
- Cu-SiO₂, in-situ deform. in HVEM 0-103338
- LiF bicrystal, high-angle tilt boundary and edge dislocation intersection effects 0-79836
- MgO crystals, geometrical-statistical parameters of dislocation interactions with point obstacles 0-103341
- MgO:Fe³⁺, point defect complex-edge dislocation interaction energies, atomistic calc. 0-107314
- NH₄Br, dislocation influence on phase transition and light scatt. (*Russian*) 0-59648
- NaCl, γ -irrad., F-stimulated inversion of sign of dislocation charge 0-59475
- Ni, H-charged cold-worked, internal friction peak 0-107368
- Ni, plastically deformed, positron trapping rate, temp. depend. 0-71507
- Ni, rel. to alloying influence on recrystn. and grain growth (*Russian*) 0-81071
- Ni, Fe, domain struct. after tensile deform., dislocation effects 0-71083
- PbS-PbSe epitaxial bicrystals, direct scatt. of channelled He ions at dislocations 0-65110
- Pd, solubility of H, lattice defects influence, extended core model 0-88326
- Si, near (111), fracture by painted indenter, SEM study 0-71734
- Zn crystals X-ray topographic examination of basal dislocations 0-88156
- ZnSe, electric charge transport by dislocations 0-103709

dislocation jog motion see dislocation jogs

dislocation jogs

- double jog side-motion, elastic theory 0-84171
- Cu alloys, FCC, climb of extended dislocations due to irradiation in HVEM 0-103343
- Cu-Al (10, 16 at.%), influence of jogs on extension of dislocation nodes 0-84176
- Cu-Al alloy, irradi. in HVEM, climb of dissociated dislocations and point defect absorpt. 0-107257
- Cu-Si (7 at.%), influence of jogs on extension of dislocation nodes 0-84176
- Ge, dissociated dislocations, constriction correlation with jogs 0-79801
- MgO, electron irradiation damage, cryst. defects 0-107320
- Ni, electron irradi. in HVEM, interstitial loop growth 0-107326

dislocation locking

- see also Cottrell atmospheres
- Cd crystals, X-ray topographic examination of basal dislocations during microplastic deformation 0-88156
- Zn crystals X-ray topographic examination of basal dislocations 0-88156

dislocation loops

- see also vacancy condensation loops
- alkali halide, crystal, irradiation-induced defects 0-107316
- alloy, dispersion hardened, work hardening due to Orowan loops, temp. depend. (*Japanese*) 0-66534
- capture efficiency of dislocation loops, effect of nonlinear elasticity 0-59461
- creep, irradiation induced, correlation of theory with expt. evidence 0-88255
- creep and growth, radiation induced, fundamental mechanisms 0-92596
- crystalline materials, in situ deform. by high voltage electron microscopy 0-103352
- cubic crystal, image contrast of dislocation loops, elastic anisotropy depend. 0-103349
- cubic media, electron microscopy, black-white contrast 0-75234
- deformation due to stress induced preferred adsorption induced dislocation anisotropy 0-75265
- deformed crystal, theory of X-ray scatt. (*Russian*) 0-70077
- double jog side-motion, elastic theory 0-84171

dislocation loops continued

forest dislocations, motion of train through forest modelling methods 0-107238
 metal, FCC, dislocation behaviour at high strain rates, US detection method, data analysis basis 0-85136
 metal, irradi., containing pre-existing dislocations, interstitial loop form. kinetics 0-65040
 metal, polycrystalline, strain hardening, dislocation link length model 0-84953
 metal, single crystal, dislocation loop formation, during deformation in quantising mag. fields (*Russian*) 0-103354
 metals, interstitial loop growth, pulsed irradi. effects 0-88210
 mobile pinning points on dislocations, equilibrium distrib. 0-79792
 neutron-bombarded, diffuse X-ray scattering (*Russian*) 0-92560
 oxides, dislocation climb model 0-100230
 precipitate and dislocation loop strain and stress field calcs. using affine transformations 0-106722
 semiconductor, STEM spectroscopic techniques for simultaneous electronic and defect obs. 0-100145
 steel, austenitic stainless, irradi. creep of type 316 in HVEM 0-97523
 steel, microstructure of 0Kh16N15M3B after creep tests in BR-10 reactor, electron, microscope invest. (*Russian*) 0-92531
 steel, stainless, radiation damage by 1 MeV electrons, dislocation struct., brittleness (*Russian*) 0-75226
 steels, stainless, electron irradiated, dislocation damage, HVEM study 0-103389
 TEM black-white contrast images, loop analysis and identification 0-103350
 triglycine fluoborillate, deuterated, dislocation line defect X-ray topographic analysis 0-59465
 Zircaloy-2, irradiation growth, shape and volume changes 0-92562
 Zircaloy-2, neutron irradi. damage, TEM characts. 0-107332
 Ag halide crystals, dislocations, survey of post-war research 0-62449
 Al {111}, X-ray Huang diffuse scatt. from dislocation loops 0-79797
 Al, deformed in uniaxial and equibiaxial tension, dislocation arrangements 0-108516
 Al, dislocation loops, interstitial, size distrib. for metal irradiated in high voltage electron microscope (*Russian*) 0-103335
 Al, foil, influence of O₂-pressure on oxidation rate, TEM study 0-104355
 Al, laser strengthening, struct., hardness and dislocation density (*Russian*) 0-76399
 Al, pipe diffusion along segment of faulted dislocation loops during annealing 0-107256
 Al-Cu (1 wt.%), electron irradiated, dislocation damage, HVEM study 0-103389
 Al-Cu (4 wt.%) alloy, neutron irradi., weak-beam dark-field obs. of dislocations near θ' precipitates 0-107333
 Al-Mg, dilute, dislocation loops, interstitial, size distrib. for metal irradiated in high voltage electron microscope (*Russian*) 0-103335
 Al-Mg, foil, oxidation in O₂ atm., TEM study 0-104356
 Al-Si (1.2 wt.%), dispersion hardened, work hardening due to Orowan loops, temp. depend. (*Japanese*) 0-66534
 Al₂O₃, alumina, deformed by prismatic slip, HV TEM obs. of dislocations 0-108517
 Al₂O₃, sapphire, edge dislocation loop obs. by high resolution lattice imaging 0-103346
 Cu alloys, FCC, climb of extended dislocations due to irradiation in HVEM 0-103343
 Cu foils, electron-irradiated, point defect agglomerates, HVEM invest. during in-situ annealing 0-84213
 Cu, foils, faulted defect formation by moving boundaries 0-107281
 Cu-Al, dislocations, dissociated, climb mechanism, nucleated loops, Burgers vectors 0-65002
 Cu-Al alloy, irradi. in HVEM, climb of dissociated dislocations and point defect absorpt. 0-107257
 Cu-Al₂O₃(SiO₂) alloys, internally oxidised, plastically deformed, influence of particle form on primary loop nature (*French*) 0-103344
 Cu-Cr-SiO₂ system, age and dispersion strengthened, dislocation struct. around SiO₂ particles 0-108468
 Cu-Fe (1.5 wt.%), precipitation-effect on void formation during electron irradiation 0-84211
 Cu-SiO₂, low-temp. recovery creep, Orowan loop accumulation 0-81126
 Fe-Cr-Ni (19, 13 wt.%), austenitic, Ni⁺ ion irradiated, multiple dislocation loops (*French*) 0-65064
 GaAs:Si, ion implantation, thermal annealing, Hall meas., SIMS atomic profile meas. 0-75243
 GaAs:Si, Li, IR absorpt., microstruct., charge compensation 0-107565
 GaP:S, defect struct. and tetrahedral precipitates, TEM study 0-107246
 Ge crystals, electron beam induced changes of real struct., HVEM 0-103390
 Ge, ion beam irradi., defects prod. by individual displacement cascades, TEM study 0-70265
 InSb, X-ray topographic evidence of asymmetrical pre-yield behaviour 0-75229
 KCl, cryst. isolated pore healing under press., dislocation struct. evolution (*Russian*) 0-100245
 MgAl₂O₄, faulted defect aggregates prod. by neutron-irrad. 0-107331
 MgO, crack tip dislocations and dislocation-free zones 0-96533
 MgO, electron irradiation damage, cryst. defects 0-107320
 Mo alloys, dil., HVEM bombarded, neutron damage simulation, defect cluster and dislocation obs. 0-107330
 Mo, ion irradi., defect anal., electron microscopy, appl. of theory of non-edge loop image contrast 0-70200
 MoSe₂, imperfections from TEM study 0-79800
 NaCl, high resolution TEM and radiation sensitivity, dislocation obs. on deformed crystals. 0-107260
 Nb-H system, accommodation effects during hydride precipitation, TEM 0-89218
 Ni, electron irradi. in HVEM, interstitial loop growth 0-107326
 Ni-Cr-Fe alloys, radiation enhanced precip. and dissolution of precipitates, point defect kinetics and dislocation obs. 0-108467
 NiAl, nonstoichiometric, interstitial defect cluster obs. 0-107226
 Sb, electron microscope irradiation effects, agglomeration of point defects, dislocation climb and loops (*French*) 0-59518
 Si, ambient effect of O precipitation, self interstitial mechanisms, IR spectra, TEM study 0-66510
 Si, crack-tip dislocation pattern, X-ray topography (*French*) 0-107253
 Si crystals, dynamic processes associated with stacking faults and deform. twins, HVEM in-situ obs. 0-103369
 Si, Czochralski grown, dislocation free, swirl defect form., doping effect 0-92519

dislocation loops continued

Si, Czochralski grown crystal, O precip., nucleation behaviour and dislocation loop form. (*Japanese*) 0-59664
 Si, ion beam irradi., defects prod. by individual displacement cascades, TEM study 0-70265
 Si, ion implanted, complex annealing behaviour of amorphous layers, TEM obs. of defect struct. 0-107299
 Si, ion implanted, damage struct. obs. using TEM and cross section specimens 0-107298
 Si, ion implanted, defect struct., dislocation loops and elongated defects 0-107300
 Si, ion implanted, interstitial generation and loop form. during annealing in oxidising medium 0-107225
 Si ion-implanted laser-annealed solar cells 0-93881
 Si, oxidation-induced Frank sessile dislocation loops, struct. change 0-75228
 Si, slip, room temp., TEM obs. 0-79804
 Si:As, ion implanted, laser annealed, lattice defects, epitaxial regrowth 0-103334
 Si:B, ion implanted, structure defects formation and behaviour under annealing in various ambients 0-65033
 Si:P, incoherent light flash annealing, elec. props., backscattering spectra 0-97504
 Si:P, ion implanted, regrowth of damage structs. by laser annealing 0-107289
 Si:Sb, ion implanted and annealed, influence of implantation temp. on dislocation generation 0-88158
 Ti, neutron irradiated, characterization of dislocation loops 0-88155
 Ti-Al-V (6.4 wt.%), ion irradiated, microstruct. study using TEM 0-96572
 Ti-Fe-C-N, ion irradiated, microstruct. study using TEM 0-96572
 V₂Si, neutron irradi., grain boundary pinning, field-depend. change of crit. current density 0-65759
 ZnO, irradiation in high voltage electron microscope dislocation loops study 0-88157
 Zr alloys, creep and growth, irradiation induced, rate theory approach 0-89294
 Zr and alloys, neutron irradi. at 573 to 923K, damage struct. 0-107334
 Zr, foil, dislocation loop nucleation and growth during 1 MeV electron irradi. 0-88152
 Zr-Al (8.6 wt.%), dimensional stability struct. and mech. props, effects of neutron irradi. 0-92563
 Zr-Nb (0.1, 2.5 wt.%), foil, dislocation loop nucleation and growth during 1 MeV electron irradi. 0-88152

dislocation motion

for dislocation relaxation see dislocation damping
 see also dislocation climb; slip
 alkali halides, dislocation dynamics studied by nucl. spin relax. meas. 0-108091
 alloys, with ordered domains and disordered regions, critical shear stress (*Russian*) 0-107237
 Bergers, W.G., and J.M., work on dislocation theory 0-62440
 binary, ternary oxides, dislocation motion and high temp. plasticity 0-59468
 book on effects of many dislocations 0-105441
 brass bicrystals, two-phase (α/β), interphase boundary sliding at high temperature 0-88164
 charged impurity influence on dislocation motion in cryst. 0-103333
 collective behaviour, velocity of slip band and mobile dislocation densities, HVEM study (*French*) 0-65006
 contact film absorption on plastic deform. of contacting bodies (*Russian*) 0-93596
 creep, transition between dislocation and diffusion 0-88253
 discrete obstacle model, dislocation and stress field distrib. 0-79794
 dislocation motion, lattice resist., effect of impurity interstitials 0-84170
 dislocation-soft mode interaction in displacive transitions (*Russian*) 0-84172
 elastoplastic relaxing media, shock waves struct., distribution model 0-58961
 electron microscopy, HV, in situ obs. techniques and applics., review (*Japanese*) 0-59351
 field equations, four dimensional space-time setting 0-96521
 forest dislocations, motion of train through forest modelling methods 0-107238
 ionic crystal defects, mag. reson. studies 0-108066
 ionic crystals, dislocations, review 0-107236
 magnetically ordered cryst., dislocation drag, magnetoelastic waves 0-103332
 metals, atomic mobility under pulsed loading conditions (*Russian*) 0-96684
 metals, BCC, plastic deform., review 0-104213
 metals, dislocation-core movement and frictional stress 0-92529
 metals, inductional dislocation braking in mag. field (*Russian*) 0-79791
 metals, research at Birmingham, (1945-55) 0-62444
 mobile pinning points on dislocations, equilibrium distrib. 0-79792
 mobility in inhomogeneous stress field, hardening effects 0-70219
 Nabarro, F.R.N., dislocation physics research 0-62441
 percolation through absolute obstacles in impurity crystals (*Russian*) 0-70196
 phonon-dislocation interactions, drag of phonon gas by moving dislocations 0-70218
 resistance fluctuations, anal. independ. of thermal voltage noise 0-84495
 solid solutions, dislocation-core movement and frictional stress 0-92529
 solid-state turbulence 0-92528
 start stresses of ensemble leading dislocations 0-92530
 steel, acoustic emission sources and dislocation patterns 0-61040
 steel, austenitic stainless, creep dependence on electron irradi., in type SS316 steel, dislocation motion (*Russian*) 0-108495
 steel, Cr-Mo-V pressure vessel, microstruct. parameters and yielding rel. to plastic deform. 0-89318
 steel, high strength, dislocation sweeping model for hydrogen assisted subcritical crack growth 0-97577
 strain rate, dislocation density, dislocation motion and dislocation constitutive eqns. 0-103329
 straining experiments, in situ, strong frictional force, quantitative anal. 0-100244
 TEM, work of Hirsch et al., (1946-56) 0-62445
 theory, book contrib. 0-107240
 theory, development, inc. work of C. Crussard 0-62443

dislocation motion continued

- thermal activation analysis, of plastic deformation and dislocation motion using stress and temp. jumps 0-74771
 unbounded elastically isotropic medium, fields generated by moving dislocations, multipole-moment expansion (*Russian*) 0-103330
 velocity, thermal activation exam. of applied stress and temp. depend., expt. methods (*French*) 0-59474
 Ag halide crystals, dislocations, survey of post-war research 0-62449
 Al foil, α -particle irradi. under fusion reactor conditions, He bubble alignment during deform. 0-107345
 Al, grain boundary migration, TEM obs. on mechanism 0-79812
 Al, pipe diffusion along segment of faulted dislocation loops during annealing 0-107256
 Al-Al₂O₃, dispersion hardened, creep (*Czech*) 0-108463
 Al-Cu-Mg, type RR55, high strength, creep behaviour, effect rel. to anodic coatings, SEM study 0-97542
 Al-Mg (0.3 wt.%) single cryst., dislocations obs. by high voltage electron microsc. 0-79796
 Cd, Hg, -, Te, dislocation motion, effect of lattice defects on microhardness (*Russian*) 0-70220
 CdS, acoustic wave attenuation, phonon viscosity and dislocation drag 0-70319
 CdS, dislocation motion, TEM obs. 0-79799
 CdTe, crystal size depend. of photoplastic effect 0-92592
 Cu, grain boundary migration, TEM obs. on mechanism 0-79812
 Cu, high-purity, grain size and strain rate influence on mech. behaviour, precursors existence 0-85016
 GaSb, acoustic wave attenuation, phonon viscosity and dislocation drag 0-70319
 KCl:Br²⁺, solid solution periodic precipitation in inhomogeneous conc. field 0-103485
 KCl-KBr, solution hardening and softening at low temp. 0-108462
 MgO crystal, yield strength and dislocation mobility 0-93601
 MgO crystals, radiation damage influence on deform. in HVEM 0-103391
 MgO single crystals, dislocation processes, obs. by HVEM in-situ deform. 0-103340
 Mo fibre reinforced Cu, rule of mixtures of deform. parameters in stage III 0-97532
 NH₄Cl, acoustic absorption by soft modes of defects 0-59584
 NaCl, dislocation mobility under high press., temp. depend. 0-75235
 NaCl, γ -irrad., F-stimulated inversion of sign of dislocation charge 0-59475
 NaCl, polarisation caused by charged dislocation motion 0-59463
 Nb, deformed polycryst., γ -peak obs. and interpret. in internal friction, 300-500K 0-81098
 Nb, superconducting state influence on dislocation motion (*Russian*) 0-70208
 Nb-H system, accommodation effects during hydride precipitation, TEM 0-89218
 Ni, creep rates, stress depend., and activation energies, constant stress tests, comparison with dislocation creep theory 0-71708
 Ni, single cryst., cyclically deformed, HVEM in-situ deform. study 0-103339
 Ni-Cr, (30 wt.%), collective dislocation movements, in situ study 0-100243
 PbTiO₃, phase transform., different kinetic types 0-71347
 Si crystals, in-situ HVEM obs. of dislocation processes during high temp. deform. 0-103342
 Si, dislocation motion from indentation rosette 0-79798
 Si, isolated dislocation motion, velocity determ. (*Chinese*) 0-107243
 Y, polycrystn., plastic deform. at different deform. speeds, dislocation glide (*Russian*) 0-93598
 Zn single cryst., dislocation velocity and plastic deform. 0-64998
 Zn, twinning, influence of dislocation drag, mag. field effects 0-59472
 ZnS crystals, structural change under plastic deform., partial dislocation movement 0-79736
 ZnSe, electric charge transport by dislocations 0-103709
 Zr-H alloy, precip. of γ -ZrH, shear mechanism 0-104170

dislocation motion, nonconservative see *dislocation climb***dislocation motion hindrance** see *dislocation drag***dislocation multiplication**

- crystalline materials, in situ deform. by high voltage electron microscopy 0-103352
 Al, polycrystn., HVEM in-situ investigation of creep mechanism 0-104214
 Al-Mg (0.3 wt.%) single cryst., dislocations obs. by high voltage electron microsc. 0-79796
 Cu, single crystals, neutron irradiated, stresses and secondary slip between overlapping and dislocation arrays 0-88162
 Fe-Cr-Ni (19, 13 wt.%), austenitic, Ni⁺ ion irradiated, multiple dislocation loops (*French*) 0-65064
 MgO single crystals, dislocation processes, obs. by HVEM in-situ deform. 0-103340
 Si crystals, in-situ HVEM obs. of dislocation processes during high temp. deform. 0-103342
 Si, diffusion of P, elastic deform. relax. and dislocation generation 0-79997
 α -Ti, plastic deform., anharmonicity, and Gruneisen parameter 0-88246

dislocation nucleation

- Bi, strain hardening curve correlation with slip band nucleation stress spectra 0-70217
 Cd crystals, X-ray topographic examination of basal dislocation glide, generation and locking 0-88156
 Cu-Al alloy, irradi. in HVEM, climb of dissociated dislocations and point defect absorpt. 0-107257
 LiF, strain hardening curve correlation with slip band nucleation stress spectra 0-70217
 MgO, crack tip dislocations and dislocation-free zones 0-96533
 Zn crystals X-ray topographic examination of basal dislocations 0-88156
 ZnO, irradiation in high voltage electron microscope dislocation loops study 0-88157

dislocation pile-ups

- discrete obstacle model, dislocation and stress field distrib. 0-79794
 Incoloy 901, foil prep. for TEM exam. 0-88001
 steel, low C, high cycle fatigue, crack initiation model (*Japanese*) 0-104258
 steel, stainless, in-situ obs. of deform. in HVEM 0-103338
 Al-Li-Mn (2.8, 0.3 wt.%), recrystallised sheet, fracture behaviour, SEM and TEM study 0-97566

dislocation pile-ups continued

- Al-Mg (0.3 wt.%) single cryst., dislocations obs. by high voltage electron microsc. 0-79796
 Cu-Bi, grain boundary struct. intergranular fracture, segregation role 0-66648
 Cu-Ni-Al (5, 2.5 at.%), precip. hardening (*Japanese*) 0-71663
 Cu-SiO₂, in-situ deform. in HVEM 0-103338
 LiF bicrystal, high-angle tilt boundary and edge dislocation intersection effects 0-79836
 Mo, dislocation structure evolution near electro-eroded crater (*Russian*) 0-100237
 NaCl, dislocation ordering influence on integrated X-ray coeff. 0-103357
 Si crystals, in-situ HVEM obs. of dislocation processes during high temp. deform. 0-103342

dislocation pinning

- see also *dislocation damping*
 creep and growth, irradiation induced, solute effects on defect precip. rate 0-88252
 edge dislocation screening in metals and superconductors, metal softening (*Russian*) 0-64997
 metal, electron irradi., elastic point defect-dislocation interactions, defect dragging model extension 0-65050
 mobile pinning points on dislocations, equilibrium distrib. 0-79792
 oxides, dislocation climb model 0-100230
 solid-state turbulence 0-92528
 Cu, dislocation pinning rate, neutron and electron irradi., meas. by internal friction method 0-96570
 Cu, electron irradi., elastic point defect-dislocation interactions, defect dragging model extension 0-65050
 Cu, electron irradi., migration and thermal conversion of defects, 100 to 330K 0-59519
 Cu, neutron and electron irradi., interstitial formation, dislocation pinning, internal friction meas. 0-100284
 Cu-Cd (1.0 wt.%), yield stress and flow stress 0-97524
 Nb-O(N), dislocation pinning, impurity interactions, strengthening (*Russian*) 0-92532
 Ta-O(N), dislocation pinning, impurity interactions, strengthening (*Russian*) 0-92532
 V-O, dislocation pinning, impurity interactions, strengthening (*Russian*) 0-92532
 Zn, line energy of basal screw dislocation, exptl. determ. 0-88154

dislocation relaxation see *dislocation damping***dislocation scattering**

- used for carrier scattering by dislocations
 metal, electron-dislocation scattering and negative deviations from Matthiessen's rule 0-80248
 metals, cond. electron and spin scatt. due to dislocations 0-75856
 Al, with linear lattice defects, temp. depend. of magnetoresist. and Matthiessen's rule departure (*Russian*) 0-84456
 Cu, electrical resistance of edge dislocations (*German*) 0-96859
 Cu-Nb multifilamentary composite, dislocation resistivity 0-70671
 InSb, galvanomagnetic props. of annealed single crystals 0-96909
 n-PbTe:In(Cu) epitaxial films, elec. transport props. 0-75659

dislocation sources

- see also *Frank-Read sources*
 screw subboundaries as dislocation sources, creep 0-100234
 Cu, single crystals, neutron irradiated, stresses and secondary slip between overlapping and dislocation arrays 0-88162
 Ge-GaAs, heteroepitaxial systems, misfit dislocations obs. using HV electron microscopy 0-100242
 Si single crystal growth, Czochralski method, small-angle dislocation boundary form. anal. 0-89136

dislocation structure

- α -brass, fatigue crack propag., role of dislocation substruct. 0-60963
 γ - brass type alloys, superstructures and defect obs. 0-107284
 cell wall and lattice misorientation origin during deform. 0-71712
 creep, irradiation induced, correlation of theory with expt. evidence 0-88255
 crystal growth, creation of stress and dislocations (*Russian*) 0-103277
 crystalline materials, in situ deform. by high voltage electron microscopy 0-103352
 deformed crystal, theory of X-ray scatt. (*Russian*) 0-70077
 dislocation structure, high press. effects, plastic deform. (*Russian*) 0-88159
 electron microdiffraction patterns, point group symmetry from dislocation cores 0-100140
 electron microscopy, high resolution, dislocation core studies, image calc. methods 0-96535
 film defect growth and nucleation, electron microscopy and diffraction exam. (*French*) 0-59824
 film/substrate interface, misfit dislocation obs. using electron microscopy 0-103605
 fine fragmented crystals, complex struct. analysis by electron microscopy 0-104416
 fluorite, use of proton irradi. to reveal growth and deform. features 0-84216
 fracture surfaces in fatigue, and dislocation structs. (*Japanese*) 0-65144
 grain boundaries, high angle, plane matching secondary relaxations, electron microscopy 0-103363
 intrinsic structure, in grain boundaries and boundary mobility 0-103368
 ionic crystals, dislocations, review 0-107236
 martensitic transformation, crystallography, describable by nonuniform lattice strain (*Russian*) 0-81056
 martensitic transformations, electron microscope study of cryst. geometry (*Russian*) 0-108441
 metal, single crystal, dislocation loop formation, during deformation in quantising mag. fields (*Russian*) 0-103354
 metals, FCC, deformed single crystals, struct. evolution at heating 0-103337
 quartz, fine structure under electron irradi. 0-70213
 quartz, naturally deformed, dynamic recrystn. during creep, dislocation substruct., Mg alloy comparison 0-109142
 semiconductor, structures and elec. props. 0-70201
 sputtering induced topography on solids, energetics and kinetics 0-88220
 steel, austenitic stainless, stacking fault energy, effect of N 0-107279
 steel, cold worked, original struct. effect on softening during heating 0-60882
 steel, Cr-Mo-V pressure vessel, microstruct. parameters and yielding rel. to plastic deform. 0-89318

dislocation structure continued

- steel, microstructure of 0Kh16N15M3B after creep tests in BR-10 reactor, electron, microscope invest. (*Russian*) 0-92531
- steel, stainless, radiation damage by 1 MeV electrons, dislocation struct., brittleness (*Russian*) 0-75226
- steel, type 12Kh1MF, dislocation struct. changes after thermomechanical treatment (*Russian*) 0-66545
- TEM images of dislocation core, optical filtering for noise removal 0-107254
- thinned semiconductor device, SEM, electron beam induced cond. of defects, rel. to TEM 0-107027
- web dendrites, dislocations, stacking faults, X-ray topographic study (*Chinese*) 0-88148
- Ag halide crystals, dislocations, survey of post-war research 0-62449
- Ag, multiply twinned particles, internal and surface struct. by electron microscopy 0-84189
- Al bicrystal, high resolution electron microscopy obs. of dislocations 0-103347
- Al, cold rolling of 1100 plates, substruct. development 0-108476
- Al, deformed in uniaxial and equibiaxial tension, dislocation arrangements 0-108516
- Al foil, α -particle irradi. under fusion reactor conditions, He bubble alignment during deform. 0-107345
- Al, stationary creep in HVEM, cell struct. evolution 0-104242
- Al, superpure, creep rate-controlling processes 0-85009
- Al, surface deformation and wear track obs. using analytical electron microscope 0-108687
- Al-(Mg)(Fe), pure (dilute), large wire drawing plastic deform. 0-108508
- Al-Cu (4 wt.%) alloy, neutron irradi., weak-beam dark-field obs. of dislocations near θ' precipitates 0-107333
- Al-Ni (6 wt.%), fine-grained, deform. in tension and torsion 0-85008
- Al-Ni(Cd)(Fe)(Si), cold worked, struct. and props. 0-71666
- AlCu-NiCo (5 at.%), θ' hardened, creep mechanism 0-85013
- Al₂O₃, alumina, deformed by prismatic slip, HV TEM obs. of dislocations 0-108517
- Au, multiply twinned particles, internal and surface struct. by electron microscopy 0-84189
- Au, thin film bicrystal, diffraction effects from inclined grain boundaries 0-103362
- Au-Pd, bicryst. thin film couples, interphase interfaces, TEM 0-70540
- Cd-(S, Se) film grown on InP substrate, mismatch dislocations and lattice distortion, dangling bond density 0-84406
- Cu, acoustic losses due to strong ultrasonic and static stress fields 0-79886
- Cu, erosive wear mechanisms, combined TEM and SEM obs. 0-108601
- Cu, fatigue crack propag., role of dislocation substruct. 0-60963
- Cu phthalocyanine, grain boundary struct., crystallographic planes 0-103366
- Cu polycrystal, fatigued, interior dislocation struct. 0-88147
- Cu, single crystals, deformed in [001] and [111] axes, cell structs., TEM 0-70209
- Cu, single crystals, dislocation cell form. during plastic deform., TEM obs. 0-60935
- Cu-Be (2 at.%), plastic deform. and dislocation substruct. 0-76307
- Cu-Cr (0.75 wt.%), deformation charact., fully reversed cyclic strain with fatigue cracks and dislocation struct. 0-81148
- Cu-Cr-SiO₂ system, age and dispersion strengthened, dislocation struct. around SiO₂ particles 0-108468
- Cu-Fe (1.5 wt.%), precipitation-effect on void formation during electron irradiation 0-84211
- Cu₂Au, disordered [001]-orientated single crystals, plastic deform., TEM and slip line studies 0-97541
- α -Fe whiskers, pure, ductile fracture, microscopic obs. of initiation mechanism 0-85044
- Fe-Al, single crystals, deform. at high temps. 0-81125
- Fe-Mo (4.1 wt.%), steady state creep at high temps. 0-89316
- Fe-Si (3 at.%), deformation and electron bombardment, influence on dislocation struct., 20-500°C (*Russian*) 0-92536
- Fe₄₀Ni₄₀C₁₀P₆ amorphous film, dislocation and mag. struct., neutron diffr. study 0-70956
- GaAs crystals, IR light scattering and absorpt. microscopy study of dislocations 0-107249
- GaAs degraded lasers, climb asymmetry, TEM obs. 0-79802
- GaAs epitaxial multilayer photocathode structures, TEM obs. of dislocations generated 0-100241
- GaAs:Sn(Te), epitaxial film, influence of impurities on stacking fault energy 0-103371
- GaAs-GaAlAs wafers, defects and degradation, transmission cathodolum. evaluation 0-65395
- GaAs-GaInAs structure, dislocation struct., TEM anal., appl. as IR LED 0-70206
- GaP, crystal, growth conditions rel. to dislocation struct. 0-88151
- Ge bicrystal, high resolution electron microscopy obs. of dislocations 0-103347
- Ge ribbon single crystals, grown from melt, dislocation struct. form. under thermal stress 0-107082
- Ge single crystals, constitutional supercooling growth conditions, structural and chem. inhomogeneities 0-93473
- Ge-GaAs, heteroepitaxial systems, misfit dislocations obs. using HV electron microscopy 0-100242
- InSb, X-ray topographic evidence of asymmetrical pre-yield behaviour 0-75229
- KCl, cryst. isolated pore healing under press., dislocation struct. evolution (*Russian*) 0-100245
- KCl:Ba²⁺, localised stress relaxation in excess vacancy system, prismatic loops (*Russian*) 0-88160
- KCl:Br⁻, solid solution periodic precipitation in inhomogeneous conc. field 0-103485
- Li, temp. depend. of dislocation behaviour between 90 and 300K 0-88146
- LiF bicrystal, high-angle tilt boundary and edge dislocation intersection effects 0-79836
- LiF, dislocation structure, influence of variable deform. temp. 0-70211
- LiF:Ni, dislocation behaviour in diffusion zone, Cottrell clouds (*Russian*) 0-70212
- Li₂Fe₂O₄ milled ferrite powder, substruct. and sinterability 0-84894
- Mg alloy, dil., dynamic recrystn. during creep, dislocation substruct., quartz comparison 0-109142
- MgO, high temperature prestrain effect on plastic props., dislocation struct. 0-79866

dislocation structure continued

- MgO, subgrain boundaries form. obs. by TEM, diffusion coeff. determ. 0-79817
- MgO:Ni, heavily doped, defect characterisation, rel. to use as laser material 0-65000
- MgO:1.1 Al₂O₃ spinel, high temp. deform., cryst. orientation effect 0-107263
- Mg₂SiO₄ crystals, dislocations configuration and cleavage steps dissoln. 0-107250
- Mo, creep deformed single crystals, subboundary struct. obs., dislocation sets 0-103348
- Mo, dislocation structure evolution near electro-eroded crater (*Russian*) 0-100237
- Mo, dislocation structure of diffusional welding zone (*Russian*) 0-96531
- Mo, fatigue of single crystals, dislocation struct. and strain localisation (*Russian*) 0-71741
- Mo polycrystn., cyclically deformed, dislocation arrangements 0-108506
- Mo, single and polycrystals, struct. change during work softening, HVEM 0-103336
- Mo single crystal, laser induced dislocation struct. 0-70210
- NaCl, dislocation ordering influence on integrated X-ray coeff. 0-103357
- NaCl, edge dislocation, core struct. and props., theory 0-70194
- Ni alloys, creep transients, friction stress and recovery, dislocation substruct. 0-60933
- Ni, dislocation structure evolution after hydroextrusion (*Russian*) 0-96530
- Ni, erosive wear mechanisms, combined TEM and SEM obs. 0-108601
- Ni, ion irradi. with 20 and 500 keV ⁴He⁺, depth distrib. of cavities and dislocation damage 0-107346
- Ni, slip character, H effect 0-89287
- Ni, structural changes, creep mechanism, multiple dislocation cross slip (*Russian*) 0-59476
- Ni-base superalloys, powder metallurgical, creep-rupture at intermediate temps. 0-97568
- Ni-Cr-Co-Ti-Mo-W-Al (14, 9.8, 5, 4, 3.9, 3 wt.%), low cycle fatigue, prior heat treatment effect 0-60962
- NiFe₂O₄ milled ferrite powder, substruct. and sinterability 0-84894
- Pd₂Si films on Si, lattice imaging obs. of structural details 0-103604
- Sb₂S₃ spherulite crystals, direct lattice resolution obs. of defect struct. 0-107255
- Si, controlled dislocation formation, struct. density (*Russian*) 0-107244
- Si, core structure of glide-set 90° and 30° partial dislocations 0-96523
- Si, crack-tip dislocation pattern, X-ray topography (*French*) 0-107253
- Si, HVEM struct. images of extended 60° and screw dislocations 0-59466
- Si, ion implanted, complex annealing behaviour of amorphous layers, TEM obs. of defect struct. 0-107299
- Si, ion implanted, defect struct., dislocation loops and elongated defects 0-107300
- Si, plastically deformed, dislocation structure with different sample orientation 0-70207
- Si, screw dislocation networks, TEM study 0-70204
- Si single crystal growth, Czochralski method, small-angle dislocation boundary form. anal. 0-89136
- Si:P, dislocation dissoc. mode obs. by weak-beam TEM 0-107259
- SmCo₅, mag. domains structure rel. to crystal defects, electron microscopy 0-103856
- TiO_{2-x} reduced, crystallographic shear planes, dislocation struct. 0-107175
- W single crystal, dislocation effects on thermionic emission and work function 0-76129
- W single crystal, high temp. creep and dislocation struct. 0-71715
- W, vapour deposited, dislocation struct., rel. to texture (*Russian*) 0-65394
- Y₂O₃, dislocation and plasticity dissociation 0-107247
- Zn crystal, {1122}{1123} slip system, deform. stress, dislocation density depend. (*Russian*) 0-103353
- Zn, growth from melt, conditions influencing dislocation struct. (*Russian*) 0-97424
- Zn-Al (0.4 wt.%), intergranular slip during in situ superplastic deform. 0-96538
- Zr₃Al, deformed and irradi., lattice defects obs., superlattice dislocations and defect clusters 0-107261

dislocation translation see slip**dislocations**

- For pipe diffusion, see diffusion in solids. See also dislocation see also Bordon effect; Cottrell atmospheres; disclinations; edge dislocations; grain boundaries; screw dislocations
- alloy, cryogenic, creep, review 0-104222
- anisotropic crystals, long-wave vibr. localised near dislocations 0-59603
- brittle fracture, elastic energy momentum tensor and crack propagation 0-69741
- brittle fracture, statistical theory, dislocation mechanism, crack propagation (*Chinese*) 0-106755
- brittle solid, atomically sharp cracks, TEM study 0-71729
- Burgers vector, determ. by weak-beam image in HVEM (*Japanese*) 0-70199
- chemical potentials of structural elements of compounds and face or dislocation specificity, thermodynamic parameters 0-96514
- cholesteric mixtures, quasithermal crystn. 0-92652
- collective vibrations of a dislocation wall 0-70346
- composites, adhesion between two crystals, theory 0-104417
- conference, Masnuy-St-Jean, Mons, Belgium, Oct. 1979 0-82570
- covalent or ionic-covalent crystals, dislocation-free contact 0-80096
- crack propagation, computer simulation 0-59573
- crystal growth, dynamic computer models 0-103284
- diamond, dislocation growth degree of supersaturation determ. 0-88145
- diffusion length and lifetime meas. and assessment by SEM 0-96902
- early work on imperfections in crystals, and forerunners of dislocation theory 0-62450
- epitaxial film, interfacial boundaries and transition regions (*Russian*) 0-103596
- FCC alloy, hardening by spinodal modulated structure 0-60874
- ferrite, transform. kinetics, grain size, alloying element effect, carbide precip. 0-93560
- ferromagnetic domain theory, quasi-dislocation theory appl. (*Japanese*) 0-60358
- ferromagnets, spin wave excitation due to parallel pumping, mag. impurity interactions (*Russian*) 0-80497

dislocations continued

Fick's equations solutions for impurity diffusion, dislocations, interstitials, vacancies 0-70469
fragmented structures, dislocation and disclination kinetics (*Russian*) 0-79788
grain boundary dislocations, effects on grain boundary processes of the steps in boundary plane 0-79785
isotropic medium, elastic vibrations localised near dislocation 0-79897
lattice defects, characterisation 0-103320
lattice transformations and dislocations, book contrib. 0-107242
melting, dislocation theory 0-65198
melting, two-dimens., dislocation-mediated theory predictions, light scatt. use as probe 0-92651
metal, US attenuation, quantum oscills. with dislocations under press. (*Russian*) 0-88273
metal powder, method for TEM study 0-84038
metals, FCC, twist boundaries, struct. invest. using computer simulation technique 0-84185
metals, research at Birmingham, (1945-55) 0-62444
mineral, Burgers vector characterisation method using electron microscope contrast simulations 0-109141
NaCl, dislocation charge photostimulated variation kinetics (*Russian*) 0-79806
Nimonic 80A, order hardening, comparison between revised theory and expt. 0-93565
olivine in Japanese peridotites, dislocation densities rel. to uppermost mantle differential stress lateral var. 0-98275
ordered regions near macroscopic defects and percolation phase transform. in crystals (*Russian*) 0-92665
plastically deformed compound semiconductors, electronic transport and opt. props. of dislocations 0-80212
PMMA, plastic deform. by crazing (*Japanese*) 0-93619
quartz, dislocations, electron irradi. induced vitrification 0-107252
quartz grains in Moine thrust zone, deformation-induced microstructs. rel. to differential stress 0-85652
seismology, use of dislocation theory, book contrib. 0-109119
SEM dislocation imaging, electron channelling appl. 0-70214
semiconductor, SEM electron beam induced current images of dislocations and stacking faults, computer simulation 0-70198
semiconductor devices dislocations and microplasma sites, STEBIC/STEM/EELS correlation 0-96528
semiconductors, appl. of analytical techniques for observation 0-73546
shift-type packing defects, involving dislocation representations, influence on diffraction pattern 0-107239
solid state physics, 1933-40, contrib. of Sir Nevill Mott 0-57055
solid state physics, historical aspects, symposium, London, England (Apr.-May 1979) 0-56999
steel; low alloy, high strength, hot compression dynamic precip. and coarsening of Nb(CN) 0-97514
steel, cryogenic, creep, review 0-104222
steel, H embrittlement mechanism, microcrack formation, dislocation model (*Russian*) 0-65143
steel, V, precip. and transform. kinetics, effect of N 0-97485
superconductors near critical temperature at acoustic frequencies, internal friction 0-100305
TGS, autostabilised state, elec. second harmonic generation 0-103921
TGSSe, autostabilised state, elec. second harmonic generation 0-103921
thermodynamics and thermal activation of dislocations, book contrib. 0-107241
thin crystals and films, nondestructive microhardness testing of near-surface layers 0-71829
TTF-TCNQ crystals, X-ray topographic study of cryst. perfection 0-96525
vacancy formation energy and vibr. freq. of atom in dislocation core region 0-103322
Wigner solid, two-dimens., melting temp., quantum effects 0-88491
Wigner solid, two-dimens., melting temp. in strong mag. fields, quantum effects 0-88492
X-ray interferometer, LLL type, interfering beam phase rels. 0-90973
Al alloys, thermomech. treatments, effects on microstruct. 0-100858
Al film, dislocation observation by electron microscope using convergent beam (*French*) 0-96532
Al-Cu-Mg type 2036, thermomech. treatment, flow stress anal., effect in mech. props. 0-93584
Al-Cu(Mg), low freq. internal friction during plastic deform. (*Chinese*) 0-103420
Al-Zn-Mg, oriented growth of precipitates on dislocations, model 0-108448
Al₃Ga_{1-x}P, LPE, crystallographic obs. and electrolum. 0-88445
Al₂O₃, surface microstructural changes due to reduction by C (*Russian*) 0-100378
Au-Ag (35 at.%), dechannelling of energetic He ions at dislocations 0-70275
CdS(Se)(Te), charged dislocations, flow of charge with plastic deform. 0-85010
CdSe, recombination mechanism at dislocations, photoluminescence 0-103993
CdTe-In precipitation and out-diffusion of solute during cooling 0-100840
CsI crystals, relation of struct. and bond type to slip geometry 0-88165
Cu, grain boundaries, intrinsic struct., electron diffraction anal. 0-84186
Cu single crystals, neutron irradiated, secondary slip 0-88161
Cu-Al, dislocation core cut-off parameter, estimation from stacking fault nodes 0-103370
Cu-Al(Au)(Ga)(Ni)(Pd)(Rh)(Zn) (4 at.%), anneal hardening mechanism 0-60879
Cu-Si (6.5 at.%), plastic deformation, HVEM study (*French*) 0-66605
Cu₂O polycrystals, dislocation obs. by electron microscope (*Spanish*) 0-75230
EuS, single cryst., high-field susceptibility meas., temp. range 2.5 to 16.5K 0-84589
Fe, high-purity single crystals, X-ray topography and double-crystal diffraction 0-92534
Fe, internal friction in plastic deformation process (*Chinese*) 0-88259
Fe, thin foil, extrinsic grain boundary dislocations, low C content influence 0-107273
Fe, volume changes and defect healing due to plastic deform. (*Russian*) 0-81139
Fe-Au bimetal epitaxial films, examination of interaction at temps. $\geq 600^{\circ}\text{C}$ 0-75482

dislocations continued

Fe-Cr (9 wt.%), extrinsic grain boundary dislocations, low C content influence 0-107273
Fe-Mn (0.5 wt.%) alloy, Burgers vector of dislocation determ. by weak-beam image in HVEM 0-103351
Fe-Ni (4 wt.%), extrinsic grain boundary dislocations, low C content influence 0-107273
GaAs, grain boundaries, extended Read model 0-96543
GaAs, semi-insulating, optical and electron microscopy exam., line dislocation precipitates 0-70205
GaAs:Zn(Cr), As precipitation at dislocations, TEM study 0-79820
GaP, green cathodolum. from cryst. defects, SEM, TEM study 0-80870
GdIG, local mag. anisotropy in stress field of single dislocation 0-88744
Ge, dislocation electron image filtering in electron microscopy 0-75129
Ge, dislocation electron states, from press. depend. of photocond. 0-96819
Ge, faulted dipoles, high-resolution TEM study 0-103345
Ge, high-doped single crystals, impurity atom distrib. changes around growth dislocations in thermocyclic treatment (*Russian*) 0-107307
Ge-GaAs heterojunction, elec. and recomb. props., interface defect effects 0-80365
H embrittlement, trap theory 0-89325
In₂Bi, pre-melting absorption of sound 0-88277
InP, LEC growth of dislocation free crystals 0-89134
InP photodiodes, dark current and breakdown characts. 0-70806
KMg₂AlSi₂O₁₀F₂, dislocations, subgrain boundaries, X-ray diffraction topography study (*Chinese*) 0-88149
LiF crystals, relation of struct. and bond type to slip geometry 0-88165
LiF:Co, flow stress changes during precipitation 0-92594
LiNbO₃, crystal defects, X-ray diffraction topographic study (*Chinese*) 0-84173
(Mg,Fe):SiO₂, dislocation recovery rate affected by high-pressure 0-94515
Mg-Al-Zn (94.3, 3.9, 1.8 wt.%), precip. on dislocations, weak-beam TEM 0-76264
MgO, deformed, cathodolum. obs. by STEM 0-76088
Na-A zeolite, struct. obs. by high-resolution electron microscopy 0-84175
NaCl, high-temp. deformed, dislocation grain subboundaries (*Russian*) 0-96534
NaCl:Ca²⁺, dielectric loss following plastic deform. 0-84690
NaClO₃, dislocations rel. to growth mechanism from aq. soln., X-ray topography 0-59464
Ni, magnetic neutron scattering by dislocations, temp. depend. 0-103820
Ni single crystal, compressed, strengthening and dislocation cells (*German*) 0-66536
Ni, stress induced crossover effect near Curie point (*German*) 0-103874
Ni, volume changes and defect healing due to plastic deform. (*Russian*) 0-81139
Ni-Al, order hardening, comparison between revised theory and expt. 0-93565
Ni-Cr, partial dislocation, stacking fault TEM study (*Chinese*) 0-84174
Ni-Cr (33 at.%), plastic deformation, HVEM study (*French*) 0-66605
Ni-Ni₃Mo system, deformation microstruct. 0-93591
PbIn films strengthening, by preventing formation of misfit dislocations 0-84858
PbS, crystals, relation of struct. and bond type to slip geometry 0-88165
Pb(Zr,Ti)O₃, fracture and deform. 0-79870
Si, crucible grown, virgin and implanted laser irradiation effects on surface struct. 0-92768
Si, epitaxial (111) surface, etching observation of stacking faults, dislocations, S-pits, etch pits (*Chinese*) 0-70197
Si, float zone crystal, dislocation creation and elimination 0-107072
Si, high dose self-irrad., spatial correl. between primary and secondary defect profiles 0-59536
Si laser annealing of SiO₂ layers 0-97505
Si, p-n junction, current-voltage characts., misfit dislocations, high pressure effects 0-65671
Si, surface, pulsed electron beam processing, doping, annealing 0-75254
Si wafer stacking faults, preoxidation gettering by reverse side P diffusion-induced misfit dislocations 0-60988
Si, with dislocations, noise spectrum 0-107881
Si:P(As)(B), nonequilibrium solid solutions obtained by heavy ion implantation and laser annealing 0-92544
Si:Sb,P, double implants, residual defect reduction after damage anneal 0-88170
SiC ion implanted, laser induced ordering and defects 0-84754
p⁺-Si_{1-x}Ge_x-nSi junction diodes, lattice misfit effects on I-V characts. 0-70804
Si, Ge_{1-x}Ga_x, heterojunction, elec. and recomb. props., interface defect effects 0-80365
Te, negative photoconductivity, intraband absorpt. (*Russian*) 0-107854
Te, strained and unstrained, SHG and propag. of CO₂ laser radiation 0-58641
Ti, volume changes and defect healing due to plastic deform. (*Russian*) 0-81139
Ti-Mo-Zr-Sn (11.5, 6, 4.5 wt.%), β III, mech. props. rel. to heat treatment 0-84961
YIG, domain wall mobility and mass meas. method (*Russian*) 0-108033
ZnO(S)(Se)(Te), charged dislocations, flow of charge with plastic deform. 0-85010
ZnS:Cu crystal, powder, epitaxial film, luminescence anomalous thermal 0-76077
ZnSe, multiphonon ionisation of deep point centres in a charged dislocation field (*Russian*) 0-100281
Zr, void swelling during electron irradi., HVEM study 0-92559

disordered systems, vibrational states see vibrational states in disordered systems

disperse systems

see also aerosols; Brownian motion; colloids; dust; emulsions; foams; fog; gels; powders; smoke; sols; suspensions
biphase liquid cylindrical vortex, mass force effect on dispersion phase distrib. (*Russian*) 0-79388
cement pastes, flow behaviour, specific surface and conc. of solids influence 0-65132
ceramics containing metastable tetragonal ZrO₂, grinding induced tempering 0-89260
dense scattering media, anisotropy factor 0-87307
dilute system, orientationally induced conservative dichroism 0-102623
disperse powder interaction in high temp. gas flow (*Russian*) 0-106830
dispersed materials, effective thermal conductivity meas. (*Japanese*) 0-70485

disperse systems continued

- dispersion resulting from flow through spatially periodic porous media 0-92216
- drop dynamics in mixture with uniform temp., thermal diffusion effects 0-103097
- dust-gas flows, steady and oscill., mean heat transfer 0-89536
- dusts, electrostatic precipitation (*German*) 0-89532
- effective viscosity and heat cond. coeffs. 0-89537
- electric conductivity of dispersed mixtures containing high-conductivity components 0-92954
- electrostatic deposition of thin particulate layer, resistivity meas. under ionic bombardment 0-68218
- ferroactive fluids, advanced appls. 0-80714
- fine particles aggregation, mechanism and rate at uniform shear field 0-101046
- flow, cooperative phenomenon, theory 0-69878
- gas-electrolyte dispersions, void fraction meas. using conductivity method 0-76525
- glass melt, multibubble dissolution 0-81371
- glass-metal composite, heat conduction, memory switching 0-96703
- graphite-air mixture steady and oscill., mean heat transfer 0-89536
- horizontal gas-liquid stream, flow vel. meas. 0-96301
- inclusions in gas-liquid mixture, effect on interphase heat and mass exchange 0-103059
- latex spheres in H_2O , photon correlation spectroscopy, diffusion coeffs. determ. 0-93802
- lecithin-water system, lamellar phase, rheology 0-89779
- liquid films, dynamic behaviour, surface mobility effects 0-88409
- liquid-liquid dispersion, phase inversion characteristics 0-69898
- macroparticles; charged spherical, dilute soln., Rayleigh scatt. 0-84748
- microemulsion, sound velocity and absorption 0-81374
- mist formation in turbulent convection field, critical supersaturation model 0-64611
- mists, electrostatic precipitation (*German*) 0-89532
- ore in a gas flow, mixing stage calcs. (*Russian*) 0-106829
- Oriental optical effects from above Rayleigh particles 0-106453
- particle diameter spectrum determ. by light scatt. 0-61169
- perturbed flow, moisture form. kinetics 0-79387
- plastic disperse systems, laminar flow in circular tubes 0-87798
- plastoviscous, cone plastometer for strength props. determ. 0-76426
- polyamide-polyurethane copolymer dispersions, structuration and relax. props., coating from props. 0-76559
- polydisperse media, optical characts., approx. representation 0-63922
- polydisperse particle size distrib. function determ. from angularly scatt. light intensity profile 0-98879
- polydisperse systems, photon correlation spectroscopy, diffusion coeffs. determ. 0-93802
- polydispersed flows, Doppler signal spectrum 0-103081
- polymeric particles obtained by suspension polymerisation, particle size distrib. eval. using Coulter Counter data 0-76564
- polystyrene lattices, electro-floitation, collection efficiency 0-74946
- polystyrene particles, monodisperse, dil. and conc. aqueous dispersions, elec. cond., surface cond. and double-layer polarisation 0-89533
- polystyrene-benzene, dil. solns., polymer excluded volume exponent, experimental verification of n vector model for $n=0$ 0-70104
- protein dispersions, viscoelastic effects, shear viscosity and primary normal stress difference 0-87754
- ruthenium trisbipyridyl ions in surfactant solns., excited state decay kinetics 0-83407
- Schulze-Hardy rule, theory 0-89540
- solid, electro-osmotic mass transfer, surface cond. influence (*Russian*) 0-76546
- solid particle systems, high Reynolds number, momentum transfer. Karman-Pohlhausen method 0-74947
- solid particle systems, high Reynolds numbers, mass transfer, Karman-Pohlhausen method 0-79378
- solubility increase, phase composition, size effect calcs. 0-70418
- spectral transparency approx. by Legendre polynomials, distrib. density of particle size 0-95800
- spherical droplet, evaporation and condensational growth, mass transport calcs. 0-97736
- surfactant solutions, aggregation, micelle and microemulsion form. 0-89547
- surfactant solutions, review of concepts 0-89542
- thermoplastic/unsaturated polyester resins, moulding materials (*Polish*) 0-66523
- two-phase dispersed flow, relationship between radiation transmissivity and void fraction (*Japanese*) 0-100026
- vapour-liquid mixtures, acoustic velocity, damping decrement 0-66881
- AgBr dispersion in gelatin, adsorbed S and Au, transient absorpt. spectra, latent image form. and decay 0-66837
- Al-Cu-Mg/mica particulate composite mech. props. 0-100919
- Al₂O₃ dispersion in polycryst. NaCl, diffusive creep 0-97531
- C black, in polymer particles, photomicrography of submicrometer birefringent contaminants 0-62757
- Cr black selective absorbers, thermal degradation 0-61417
- Cr-Cr₂O₃ black, electroplated solar collector coatings, high temp. optical and struct. degradation 0-66995
- Cr-Cr₂O₃ black solar absorber surfaces, microstruct. rel. to electroplating parameters 0-61418
- Cu crystals, two-phase, recrystn. retardation, particle size, spacing effects 0-89242
- Cu-SiO₂, in-situ deform. in HVEM 0-103338
- (Cu-Au)-Co, single crystals, solid soln. and particle strengthening, superposition 0-97495
- Fe-Cu: graphite-BaSO₄-CuSO₄, friction material, solid state sintering kinetics 0-104096
- Mn II-lecithin lipid-water system, NMR and EPR obs. 0-61168
- NaA neolyte, Hg cluster transition to paramagnetic state due to mag. field (*Russian*) 0-60183
- SiO₂ dispersed particulate in CVD reactor, correlations with film characts. 0-76192
- Ti-Er(Y), effects of Er and Y additives on deformation behaviour 0-81121
- UAl₃ dispersion nuclear fuels, development and irradi. performance 0-78368

dispersion (wave)

- see also acoustic dispersion; optical dispersion
- dissipative and nonequilibrium media, pulse spreading 0-94961

dispersion (wave) continued

- Earth surface layer, EM wave refl. and transmission coeffs., linear ramp model 0-61759
- elastic shear waves propagation in fibrous composites 0-58963
- EM waves dispersion equations in moving media, relativistic electrodynamics 0-57089
- HF wave dispersion for complex wave numbers, ordinary waves 0-70740
- M87, highly dispersed millisecond radio bursts discovery 0-73034
- modulated electron beams, instability, spatially separated in plasma 0-70012
- nonlinear dispersive waves, bifurcation and symmetry breaking, four wave interactions 0-69855
- ocean trench waves, dispersion curves and eigenfunctions 0-72547
- plasma waves propagating along mag. field in strongly anisotropic relativistic plasma, dispersion props. 0-67542
- pressure-scanning millimetric-wave dispersion spectrometer expt. 0-61904
- pulsar dispersion data anal., scale height determ. 0-85965
- pulsar radio emission scintillation, decorrelation bandwidth rel. to dispersion measure 0-85964
- pulsars, low-latit., dispersion measures and distances rel. to interstellar electron density 0-101606
- rotating gas, perfectly conducting compressible in mag. field under gravity, wave dispersion relations (*Chinese*) 0-77276
- surface wave propagation over liquid and crystalline layers, dispersion eqns. 0-76925
- surface waves propagation over liquid and crystalline layers, dispersion eqns. 0-76924
- YIG sandwiched between grounded dielectric layers, magnetostatic bulk wave propagation 0-60380
- dispersion hardening**
see also precipitation hardening
dispersion-strengthened alloys, threshold stress for creep 0-93626
steel, low alloy, ferritic-pearlitic, carbonitride hardening 0-104174
strengthening theories for dispersion hardened alloys 0-97498
Al-Al₂O₃, dispersion hardened, creep (*Czech*) 0-108463
Al-Cu-Mg (4, 1.5 wt%), mica dispersed, wear characts. and bearing performance 0-108591
Al-Mg-Si alloy, Mg₂Si dispersion hardened US waveguides, concentrators (*Polish*) 0-89237
Fe-Ni-Cr based alloy, KhN35VTYu, temp. depend. of energy of fracture, influence of γ phase (*Russian*) 0-81147
Ni-Mo-W, diagram of state; W solubility, dispersion hardening (*Russian*) 0-66477
- dispersion power, rotatory** see optical rotation
- dispersion relations**
see also dispersion (wave); Kramers-Kronig relations; Mandelstam representation; N/D method; phonon dispersion relations; phonons;
plasma instability; plasma waves; S-matrix theory
cubic symmetry cryst., quadrupole exciton theory 0-103632
decay state interactions, autoionisation bands (*Russian*) 0-75486
electronic localised state at edge dislocations, parabolic dispersion law (*Russian*) 0-65479
EM oscill. spectrum, toroidal plasma-containing system 0-79471
ghost-pole subtraction and the σ -exchange NN potential 0-86819
graphite, diamagnetism with quasilinear dispersion law, orbital susceptibility, valence bands (*Russian*) 0-80475
HF wave dispersion for complex wave numbers, ordinary waves 0-70740
holographic unslanted transmission and reflection gratings, modal theory, EM wave propag. 0-83673
magnetised plasma, parametric instabilities with well separated freq. (*Chinese*) 0-106887
magnetised plasma stability in large amplitude circularly polarised wave, dispersion relations 0-59223
massless $[g\phi^4]_4$ theory, functional integrals, complex instantons and asymptotic perturbation series 0-86571
medium beta plasma with velocity gradients, dispersion relation for drift waves 0-64719
metallic ferromagnet, antiresonance region, EM wave propag., Maxwells' eqns. soln. 0-66038
MHD pulses in Sun, dispersion relations rel. to use as diagnostic technique 0-109405
mixed valence compounds, dynamic susceptibility, RPA study of Anderson lattice 0-97075
plasma, Bernstein dispersion relation for oblique propagation 0-75052
plasma, dispersion relation for EM instability 0-64725
plasma, drift and Alfvén modes, current driven, electron-ion collisions and full dispersion function, numerical anal. 0-64726
plasma, instability hindrance in a magnetically confined plasma with finite press. 0-59221
plasma, ion-acoustic waves freq. and damping from dispersion relations 0-69991
plasma, moving weakly nonsteady, plasma wave propag. 0-106918
plasma, self-gravitating, isotropic pressure, wave propag. and dispersion relation 0-72763
plasma, turbulent, parametric instabilities, anomalous energy absorpt., dispersion eqn. 0-92291
plasma electrostatic shear flow instability linear dispersion relation 0-96359
plasma interaction with strong EM wave, efficient transformation of radiation frequency 0-106931
plasmon surface polariton dispersion curve, optical obs., demonstration 0-101690
polytypes, one-dimens. Kronig-Penney model and calcs. 0-75494
relativistic plasma, nonlinear dispersion relation for transverse wave 0-87939
s-channel resonance prod. in πN scatt., amplitude zeros in Mandelstam plane 0-73686
semiconductors, EM wave interaction in weakly nonlinear medium with superlattice 0-93257
semiconductors, two-dimensional, Mott exciton formation in high mag. fields (*Russian*) 0-65467
soliton nonlinear refraction and self-focusing effects (*Russian*) 0-98805
surface plasmon dispersion relation in presence of surface roughness 0-65650
tunnelling MIS structures photovoltaic energy conversion, band struct. 0-92995
two dimensional dispersion relations, phase problem appl. 0-102631
 $\gamma p \rightarrow \pi^0 p$, high energies, semiempirical amplitude anal. dispersion relations and Regge poles 0-86726

dispersion relations continued

- N- Δ (1232) electromagnetic transition form factor and pion-nucleon dynamics at moderate energies 0-57598
 pp, 1 GeV, elastic scatt. amplitude, phase shift anal. (*Russian*) 0-86746
 π photoproduction amplitudes, Padé approximants and dispersion relation solns. 0-91096
 π K scattering amplitude, analytic continuation, chiral symmetry breaking 0-63027
 π K scattering length, dispersion relation anal. of phase-shift 0-63026
 π NN vertex function and off-mass-shell π N scatt. 0-73739
 Ag, surface plasmon dispersion relation in presence of surface roughness 0-65650
 Au, energy band structure, X-ray N-emission spectra, relativistic APW calcs. 0-70596
 Bi, EM wave dispersion and damping, Voigt configuration, non-local calcs. 0-100475
 BiSb, alloys, semimetallic, camera, dispersion relations 0-59854
 CdCr₂Se₄, reactor radiation influence on ferromagnetic phase transform. (*Russian*) 0-75760
 CdTe, exciton magnetoreflexance spectra, multicomponent polaritons, Zeeman splitting 0-88974
 GaAs, field ionisation speed of shallow impurity levels, quantum-mechanical estimates 0-97412
³He, liquid, electrostatic image force depend. on spatial dispersion, energy spectrum (*Russian*) 0-107593
³He, superfluid, magnetic relaxation and high amplitude spin waves (*Russian*) 0-92749
⁴He, liquid, electrostatic image force depend. on spatial dispersion, energy spectrum (*Russian*) 0-107593
 n-InSb, cond. electron spectrum in quantised mag. field, impurity resonance scatt. (*Russian*) 0-93178
 K, phasons, transverse, freq. dispersion relation in CDW state 0-96804
 KN(\bar{K} N) scattering amplitudes, resonance region, t-channel couplings, hyperbolic dispersion relations 0-57643
 PbI₂, photoexciton interaction, luminescence spectra, polariton dispersion diagram 0-93397
 SiC, dielectric coating effect on surface polaritons, optical consts. (*Russian*) 0-88489
 Tm-Zn, paramagnetism, mag. excitations, exchanges interactions 0-88718
 YGaIG, magnetoelastic wave propagation time dispersion reduction 0-75836
 YIG, magnetoelastic wave propagation time dispersion reduction 0-75836

dispersions *see* **disperse systems****dispersoids** *see* **disperse systems****displacement measurement**

- cryogenics, linear variable differential transformer displacement transducer optimisation 0-86323
 deformation measurement, in-plane, by video-electronic hologram interferometry 0-106488
 deformation measurement, out-of-plane, using holographic interferometry and speckle photography, comparative accuracy 0-78804
 derived holographic interferometric methods (*German*) 0-91758
 diffusely reflecting objects with time-varying surface microrelief, holographic interf. deform. recording 0-74322
 double exposure interferometry through speckle photography (*French*) 0-83568
 drive system, digital method (*Polish*) 0-86260
 fast precision capacitance transducer, design procedure (*Russian*) 0-98884
 general object deformation decomposition by speckle displacement 0-106486
 high-temperature reactor structural displacement and strain analysis by picture processing (*Japanese*) 0-78352
 holographic interferometric evaluation of rigid body displacement 0-105610
 in-plane motion measurements with Fourier lensless holography 0-77746
 interferometry, multimode fibre optic, applications 0-86387
 interior displacement and strain measurement using white light speckles 0-95064
 laser appl., three-mode, geodesic problems solution 0-77748
 laser interferometers, AM and FM operation and applications (*German*) 0-86389
 linear displacement meas. accuracy meas. accuracy improvement under vibration 0-90815
 mechanical displacement of specimens using laser 0-73309
 noncontact material testing using laser energy deposition and interferometry 0-71846
 optical system, trihedron, for linear displacement meas., accuracy estimation 0-101780
 real-time measurement of in-plane translation and tilt by electronic speckle correlation 0-57252
 sliding bodies, friction apparatus for meas. normal displacement 0-99977
 speckle interferometric analysis of transient phenomena 0-105701
 speckle photographic technique, hybrid optical and electronic image processing 0-99976
 speckle photographs, displacement measurement using electro-optical readout system 0-62708
 strain meas. by holographic interferometry, mathematical formulation (*German*) 0-78815
 time-varying images, object displacement estimation adaptive algorithm 0-99668
 vibrating capacitor displacement transducer, eqn. of state 0-57281

displacive transformations

- see also* martensitic transformations; polymorphic transformations; soft modes
 alloys, phase transition premonitory phenomena, exam. by electron diffr. and microscopy (*French*) 0-59651
 antiferroelectrics, multicritical points in structural phase transitions, renormalisation 0-75982
 continuum ϕ^4 equation, kink-phonon and kink-kink interactions 0-70354
 cubic antiferroelectric struts., halogen NQR spectra, struct. information for R₂MX₆ compounds 0-71228
 D_{2d} crystals, structural phase transitions, soft modes, group theory 0-92638
 defect-containing crystals, US absorpt. near displacive phase transitions, anomalous temp. depend. 0-92612
 dislocation-soft mode interaction in displacive transitions (*Russian*) 0-84172
 distortive phase transitions, order-disorder and displacive regimes, mol. dynamics study 0-75324

displacive transformations continued

- F 0-100329
 ferroelectrics, order-disorder, displacive transformations, tunnelling, phonons 0-75975
 incommensurate crystal phases, symm. props., superspace groups 0-75195
 semiconductor, localised states near displacive transition 0-70644
 semiconductor thin films, ferroelectric properties, quantum size effect 0-97201
 spin Hamiltonian of S ions, depend. on order parameter 0-70356
 steel, bainite formation mechanism 0-108431
 superconductor, metal-insulator transition, electron pairing, effect on optical props. 0-60139
 transition metal pnictides, displacive and mag. transitions 0-59616
 transitions metal sulphides, displacive transitions, theory 0-59616
 Ag₂AsS₃, and Ag₂SbS₃, Raman spectra obs. of low-temp. phases 0-93327
 BaMnF₄, magnetic neutron scatt. from structurally distorted cryst. 0-93086
 BaTiO₃, displacive ferroelectric, effective charge determ. 0-97212
 Cr₂Mn_{1-x}As, mag. susceptibility anomaly at displacive phase transition 0-93091
 GeTe, Hall coeff., temp. depend. rel. to order parameter 0-96921
 HfO₂AsO₄·4H₂O and HfO₂PO₄·4H₂O layered cpds., struct. investigs. below antiferroelec. transition temps., H bond ordered struts. 0-107416
 HfO₂AsO₄·4H₂O and HfO₂PO₄·4H₂O layered cpds., single and polycryst., proton cond. behaviour w.r.t. antiferroelec. transition temps. 0-107481
 KMnF₃, Mossbauer gamma quanta scattering near 186K transition 0-108126
 KMnF₃, second-order displacive transition region, static and dynamic charact. determ. 0-70409
 KNbO₃, displacive ferroelectric, effective charge determ. 0-97212
 K₂OCl₆, Cl NQR spectra by Fourier transform methods 0-75879
 La₂S₃(Se₄), structural transitions, symm. anal. 0-92671
 LiNbO₃, ferroelec., displacive type phase transition, far IR reflection spectra 0-71339
 LiTaO₃, displacive ferroelectric, effective charge determ. 0-97212
 LiTaO₃, ferroelec., displacive type phase transition, far IR reflection spectra 0-71339
 MnAs_{1-x}P_x, mag. susceptibility anomaly at displacive phase transition 0-93091
 Ni_{0.25}Zn_{0.75}Fe₂O₄, structural phase transition, X-ray and neutron diffr. study 0-79735
 SF₆, matrix isolated, IR spectrosc., temp. reversible site structural changes 0-95613
 SnF₂, second order $\beta \leftrightarrow \gamma$ transition, neutron diffr. and NMR obs. 0-107095
 SnTe, displacive transform., interband electron-phonon interactions, phase diagram 0-93252
 W (001), displacive transition, H adsorpt. effects, theoretical model 0-65352
 W(100) surface, instability, distortion and dynamics 0-84360

display devices

- AC electrodeless narrow gap discharge, anal. and plasma display design 0-70063
 anthraquinone pleochroic dyes in liq. cryst. soln., photostability, appl. to liq. cryst. displays 0-88961
 cholesteric films, absorpt. and contrast in dichroic liq. cryst. displays 0-75155
 cholesteryl nonanoate-MBBA, liq. cryst. mixture, two colour display device 0-70116
 cyanobiphenyl E-7 mixture, bistable cholesteric liquid crystal display 0-96437
 graphic processor for pseudo-colour images representation (*Italian*) 0-98562
 hologram electronic heterodyne recording and self-interference term rejection 0-91756
 liquid crystal display elements, principles and applications (*German*) 0-86277
 liquid crystal for UHF EM field pattern display, flow detection 0-104378
 multiplexed liquid cryst. display, use of cholesteric-nematic phase change 0-107408
 nematic liquid crystal display, twisted, ang. and voltage depend. of light transmission, two-layer model 0-76006
 numeric, effect of vibration on reading 0-104582
 orientational bistability, nematic storage effects 0-70112
 4-n-pentyloxy-phenyl-4'-n-octyloxybenzoate, nematic, dielec. relax. and freq. depend. of threshold voltage 0-60497
 short circuit memory in electrochromic displays 0-97238
 twisted nematic display with cholesteric dopant, transmission characteristic temp. depend. compensation 0-103934
 vacuum-deposited layers formation, use of borosilicate glass intermediate layer 0-80979
 volume hologram superimposed information display 0-78807
 X-ray image receptor, large area, with electrophoretic display 0-98091
 p-GaAs/heptyl viologen system, appl. in photoelectrochemical cells and photoelectrochromic displays 0-76640
 IrO_x, anodic film electrochromic cell, fabrication and display device use 0-61320
 IrO_x, anodic films, electrochromic props. and device uses 0-61319
 PLZT slim-loop and linear ceramics, longit. electrooptic effects, display appl. 0-80751

display equipment *see* **display instrumentation****display instrumentation**

- see also* cathode-ray tube displays; display devices; screens (display)
 analogue digital double integration joulemeter, AC loss meas. in superconducting magnets 0-57325
 automatic fluorescence microscope photometry data processing and display (*German*) 0-86369
 biomedical US images, cine display 0-108984
 calligraphic projection display resolution and contrast photometer and X-Y plotter 0-86373
 computerised tomography, multiple window display techniques 0-109010
 digital image display, interactive program (*Italian*) 0-98559
 electro-optical readout system for analysis of speckle photographs 0-62708
 epicardial mapping, computerised display system (*Japanese*) 0-101279
 interferometric examination of lenses, mirrors and optical systems, 3D display 0-69497

display instrumentation continued

- large-aperture holographic visual simulator 0-102679
 METEOSAT interactive image system 0-109330
 nuclear medicine, precision computer display techniques 0-98100
 nuclear medicine, precision computer display techniques 0-109011
 radial metrological pattern generating engine for manufacture of masters including scales and gratings 0-57282
 speech trainer for multihandicapped children, display method and control program (*Japanese*) 0-108922
 UV polymer-film dosimeters, automatic read-out device 0-78455
 weighing system, electronic, digital transducer instruments 0-95076
 SiC thin-film thermistors with high thermal response (*Japanese*) 0-105629

display instruments *see display instrumentation***display systems** *see display instrumentation***display tubes, television** *see television picture tubes***disruptive voltage** *see electric breakdown***dissemination of information** *see information dissemination***dissipation (heat)** *see cooling***dissociation**

- see also electrolytic dissociation; heat of dissociation; ionisation; molecular dissociation; molecular dissociation energies; photodissociation*
 CaO-SiO₂-CO₂, subsolidus and liquidus phase relationships to 30 kbar 0-85643
 chemically driven convection of dissociating Navier Stokes fluid, instabilities 0-59128
 E-glass fibre, silane coupling agent deposited on surface, hydrolysis and drying effect on siloxane bonds 0-85072
 metal chelates, prep. of colloidal particles 0-71953
 polymers, solid interaction with SF₆ plasma, in glow discharge, emission spectrum 0-87960
 reverse pulsed polarography, reversibility characterisation, electrode reaction product determ. 0-66889
 transformer oil diagnosis, computerised evaluation of results (*Czech*) 0-97744
 Ag/RbAg₄I₃/I₂ solid state battery, low temp. degradation 0-61331
 p-CdTe, nondoped, heat treatment in vacuum, dissoc. obs. effects on struct. and props. (*Japanese*) 0-60662
 Cu₂S, Cu₂S, α - β transition, thermographic investigation of heats, entropies and activation energies 0-88314
 CuSO₄·5H₂O monocryst. platelets, dehydration into trihydrate, displacement rate modulation of reaction front 0-108711
 Fe chelates, prep. of Fe₂O₃ colloid particles 0-71953
 KNO₃ calcite-type crystals, topotaxial decomp. TEM obs. 0-108710
 K₂O-Al₂O₃-P₂O₅-TiO₂, structural role of Ti, kinetic study of chem. destruction 0-88055
 La₂S₃, unsaturated and saturated vapour press., 673-1173K, thermal dissoc. pattern 0-104457
 N₂O, turbulent dissoc. flow, along heated tubes, heat transfer 0-63225
 NaCl-KCl, molten, alkaline earth oxides solubility products, potentiometric determ. 0-76488
 TiCo_{1-x}Mn_x, H absorption-desorption characteristics 0-96735
 W(CO)₆, decomp. under high field conditions, cathodic growth of W needles 0-76162

dissolution *see dissolving***dissolving**

- see also solubility; solutions; solvation*
 benzoic acid, dissolution, mass transfer at vibr. spheres 0-57220
 birefringent crystal faces, meas. method of growth and dissoln. rates 0-79719
 ceramic compounds, lyophilisation parameters, freeze-drying synthesis 0-97453
 crystal growth, and dissoln. in suspension, kinetic expts. anal. 0-59414
 electron microscopy, decoration method, rel. to crystal growth (*German*) 0-103222
 GaAs wafer, dissolution kinetics in undersaturated isothermal solns. in Ga-Al-As systems 0-80106
 glass melt, multibubble dissolution 0-81371
 graphite surface, adsorbed Cs, dissolution, lamellar cpd. form. (*French*) 0-100399
 metals, dissolution of interstitial H₂ and D₂, diffusion coeffs., reverse isotope effect (*Russian*) 0-88368
 pharmaceutical dissolution testing, microprocessor controlled sampling system 0-86273
 sand, during glass melting, kinetic equation for interaction between grain material and liq. 0-84901
 steel, C, dissolution of Cr₇C₃ in austenite (*Russian*) 0-103479
 steel, mild, cyclic strain enhanced dissolution in NH₄NO₃, corrosion fatigue props. 0-85083
 steel, Ni-Cr, anodic dissoln. in NaCl solns. at high current densities (*Russian*) 0-76396
 steel, Si, grain-oriented, high permeability, dissoln. and precip. of AlN and MnS 0-89223
 Ag halide crystals, relative dissolution rates meas. by flow calorimetry 0-85220
 AgCl, ionic space charge and dissolution 0-107431
 Al alloys, age-hardenable, precipitation and dissolution processes, positron annihilation and X-ray small-angle scattering comparison 0-89238
 Al, molten, dissoln. kinetics and diffusion coeffs. of Fe, Co and Ni 0-59666
 Al-Mg (2 wt.%), hardening and fracture characts., β -phase dissolution role 0-81178
 Al-Mg (7 wt.%), bare surface reaction rates in aq. solns. 0-101022
 Al-Si (0.57 at.%), Si precipitate dissolution kinetics 0-84935
 BaF₂ crystal, selective etching and dissolution kinetics 0-71775
 CaF₂, cryst., (111) faces, selective etch rate and etch pit morphology, acid conc. and temp. effect 0-96524
 Ca₁₀(PO₄)₆(OH)₂, dissolution kinetics, nucleation-controlled 0-59659
 Ca₃(PO₄)₂·OH bioceramic, material props. 0-93523
 Cd-Mg, selective dissolution, static samples 0-65228
 Cd-Mg, selective dissolution, rotating ring disc electrode 0-65229
 CdTe:Cu films, impurity behaviour, Hall mobility and hole density meas. 0-80420
 Co-Ca, liq. alloy form. kinetics (*French*) 0-96652
 Cr-W, anodic dissoln. at high current densities (*Russian*) 0-76395
 CsI:Ti, precipitation of Ti solid solns. 0-70419
 Cu diffusion layer cathodic deposition and anodic dissolution rates 0-93503

dissolving continued

- Fe, corrosion and passivation in LiCl soln., peripheral velocity effect 0-61000
 Fe, dissolution and passivation kinetics in solns. containing O 0-76547
 Fe dissolution kinetics, and passivation depend. on temp. and ionic strength 0-97626
 Fe-Cr-Ni, corrosion behaviour in hot conc. NaOH soln. (*Japanese*) 0-85082
 Ga_{1-x}Al_xAs heterostructure, LPE prep., growth and dissolution kinetics, thermodynamic and kinetic models 0-75456
 GaAs anodic oxide films, optical studies using rot. light-pipe reflectometer 0-76096
 GaAs_{1-x}P_x heterostructure, LPE prep., growth and dissolution kinetics, thermodynamic and kinetic models 0-75456
 GeO₂-Na₂O borosilicate glass fibre prod. by phase separation and leaching 0-69558
 HF electrode, surface oxide film, impedance and pot. behaviour 0-61001
 InGaAsP-InP DH lasers, perturbed InP growth, photoluminesc. study 0-106518
 KH₂PO₄, growth and dissolution kinetics, temp. and pH effect 0-88070
 Li₂O-GeO₂-Ga₂O₃, glass, electrode props., dissolution kinetics 0-89387
 Mg, H₂ dissolution, resistometric study under press. 0-70417
 Mg₂SiO₄ crystals, dislocations configuration and cleavage steps dissoln. 0-107250
 Mo oxides, low-grade, soda roasting study (*Korean*) 0-93508
 NaCl:Eu, secondary Eu phase dissolution, EPR and optical absorpt. study 0-96655
 Na₂O-SiO₂, glass melt, dissoln. of O₂ and CO₂, gas bubbles 0-79945
 Ni-Cr, anodic dissoln. in NaCl solns. at high current densities (*Russian*) 0-76396
 Si, liq., dissolution of quartz, effect of C, rel. to melt growth 0-70414
 Si solubility and transport behaviour of water, dissolution 0-93801
 p-Si-Al, ohmic contacts, Si dissoln. and recrystn. effects, computer calc. 0-103749
 SiO₂, dissolution rate in molten Si 0-103481
 Ti:Pd, ion implanted, corrosion behaviour and Rutherford backscatt. anal. 0-71792
 W monocrystals in alkaline electrolyte, surface orientation, effect on anode current (*Russian*) 0-75360

distance measurement

- automatic differential variometer type equipment feasibility and preliminary design for big structure displacements remote measurements (*Italian*) 0-62623
 extragalactic distance scale calibration, appl. to distance of giant spiral galaxy (M 101) 0-67852
 galaxies distance scale, determ. from IR magnitude/H I vel. width rel. to expansion rate outside Local Supercluster 0-105325
 geodesic interference distance meas. using semicond. lasers 0-77175
 gyromagnetic ratio of proton and fine-structure constant redemter., by meas. distance between wires, with aid of laser interferometer 0-74253
 IR, optocoupler system, precision measurements non involving contact (*German*) 0-82823
 laser rangefinder and 3D object recognition algorithm 0-96016
 light rangefinder and profilometer, high-resolution gas laser 0-102754
 optical surface contact interaction zone, thickness calc. and distance meas. methodology (*Russian*) 0-99889
 planetary nebulae, distance scale 0-109521
 planetary nebulae, distances determ. through nebular ionised mass/nebula radius relation 0-101625
 planetary nebulae, new distance scale and galactic distrib. 0-67819
 point-surface distance meas. adjustment, geometrical aspects (*German*) 0-86255
 projector, development and use of special mirror, examination of recording heads 0-83657
 pulsars, low-latit., distances from H I absorpt. meas. 0-101606
 quasars, distances from transverse vels. obtained from redshifts relativistic Doppler formula (*Chinese*) 0-105379
 SHF light rangefinder, optical elements, orientation errors effects (*Russian*) 0-64158
 throwing distance, for the Olympic Games, Moscow 0-82743

distillation

- see also isotope separation*
 solar, drinking water production in India, 5000 lit/day plant 0-61280
 solar still, double basin, performance and periodic anal. 0-89671
 vaporizer which induces vapour flow pattern producing centrifugal field 0-86274

distortive transformations *see solid-state phase transformations***distributed Bragg reflector lasers**

- beam divergence reduction by corner-reflector type Bragg mirrors 0-91822
 AlGaAs transverse junction stripe laser 0-106535
 GaInAsP/InP 1.5-1.6 micron integrated twin-guide lasers with distributed Bragg reflectors 0-74380
 GaInAsP/InP integrated twin-guide lasers with first order distrib. Bragg reflector, room temp. operation at 1.3 μ m 0-64077
 GaInAsP/InP integrated twin-guide lasers with distributed Bragg reflector, spectral behaviour 0-74381
 GaInAsP/InP integrated twin-guide lasers with first-order distributed Bragg reflectors, 1.3 μ m 0-58567

distributed feedback lasers

- corrugated waveguides, effective index approach to distrib. feedback, TE polarisation 0-102859
 dye activated CLC, distributed feedback, tunable radiation generation (*Russian*) 0-102720
 dye laser, DFB, single-mode operation 0-74409
 dye laser, N₂ laser pumped, self Q-switched, tunable picosecond pulse generation 0-69432
 dye laser, noncollinear wave interaction 0-99722
 dye laser, optically induced distributed feedback prod. of single ultrashort pulse 0-64067
 dye laser, ultrashort pulse generation, self Q-switching mechanism 0-58612
 dye laser with integrated Si and polyurethane channel waveguide 0-74373
 gas laser waveguide precision calc. and pulse energy obs. 0-58577
 heterojunction laser diodes, book contrib. 0-99733
 self-induced distributed feedback, stability, in system without resonator 0-87368
 semiconductor, population-inverted, resonant Brillouin scattering and photoelastic consts. 0-76042

distributed feedback lasers continued

- semiconductor diode lasers, book contrib. 0-106525
 semiconductor laser diodes, present status and technology (*German*) 0-58561
 semiconductor super-DFB single-mode laser with periodic stripe width variations 0-58574
 semiconductors, population inverted, resonant Brillouin scatt., photoelastic consts. 0-89015
 two-mode operation, index and gain grating configurations 0-69357
 GaInPAs/InP heterostructure DFB laser under optical pumping, lasing chars. 0-87396
 $\text{Ga}_{1-x}\text{In}_x\text{P}_y\text{As}_{1-y}$ /InP DFB injection laser, one-step LPE 0-58575

distributed parameter systems

- coupled-core nuclear reactor, distributed parameters identification, pseudorandom perturbation and correlation anal. 0-86966
 LMFBR fuel rod subassembly, thermal-hydraulic anal. as distrib. parameter system (*Japanese*) 0-68736
 one dimensional distributed parameter system parameter and state estimation, heat conduction experimental result (*Japanese*) 0-83727

distribution networks

- classical systems, particle distrib. function, theoretical method 0-64856
 fusion reactor, TEXTOR, poloidal coil system power distrib. system 0-102327

distributions, statistical *see statistical analysis; statistics***district heating**

- 100 MW fluidised bed combustion district heating plant burning high S content residual oils 0-108777
 geothermal district heating system, planning assessment, financing and design optimisation 0-61279
 solar heating system, annual cycle thermal energy storage, sensitivity anal. 0-67007
 steam turbine district heating plant, condensing and regenerating equipment 0-92029

DNA

- B form conformations, double-helix and side-by-side models, X-ray diffraction 0-78735
 B-form, closer definition of struct. from X-ray diffr. and energetic criteria 0-81533
 bacteriophage λ superinfecting *E. coli*, induction and repair of DNA strand breaks 0-72228
 bacteriophage S13, lethal effect of ^{32}P transmutation, mech. of DNA double helix rupture (*French*) 0-98018
 chromatin-DNA cross-links formation, radiolysis of extracts from cultured mammalian cells 0-81655
 compact form, tertiary struct., small angle X-ray scatt. 0-72129
 complexes with Hg (II) and Ag (I) in soln., theoret. interpret. of elec. dichroism obs. 0-85347
 conformational fluctuations, internal motion correl. times, ^{31}P NMR obs. 0-72135
 conformational transitions of DNA in conc. solns. of neutral salts 0-81531
 conformations, possible, calcs. 0-76705
 cyclophosphazene-DNA complex, spectrofluorometric and spectrophotometric invest. 0-95643
 dielectric properties of low-mol. wt. DNA in aq. solns. at low ionic strength 0-85330
 DNA(Cu^{2+}) ^{11}In bound, rot. correl. times, from γ -ray perturbed angular correl. 0-94152
 double strand breaks rel. to radiation dose, yeast cell obs. 0-72232
 double-stranded, ^{13}C NMR obs. 0-69281
 dye labelled, elec. dichroism and birefringence, comparison with mol. props. from polarised fluoresc. 0-84785
E. coli, UV-induced recovery of γ -irrad. bacteriophage DNA 0-72214
E. coli B/r, UV sensitivity rel. to DNA content obs. 0-108960
E. coli strains differing in DNA repair capability, survival after fission-spectrum neutrons irradi. 0-98031
 electronic interaction with N-methyl-N-nitrosourea, ESR obs. and INDO calcs. 0-94154
 erythrocyte nucleosomes, chicken, temp. dependence of ^{31}P -NMR spectra 0-94280
 ethidium bromide E-DNA, intercalated birefringent fibres, microspectrophotometric invest. (*German*) 0-57392
 fast neutron induced DNA strand breaks and repair obs., cultured mammalian cells 0-61651
 gamma-ray induced damage, electro-optic meas. 0-85452
 hydrate, struct. conversions of sugar phosphate chain and nitrogenous bases, IR spectra 0-81530
 hypochromism of natural DNAs, dependence on content and sequence of nucleotides 0-76711
 in vitro transformation, conf., Toronto, Canada (May 78) 0-67931
 interactions with cations, UV difference spectrosc. and Marcus theory 0-94153
 internal motions, ^{31}P NMR and PMR 0-97855
 kinetoplast, ultrastruct., interpretation of dark field electron microscopy images of isolated purified networks 0-85369
 laser multiplet selective excitation of DNA and RNA fragments, uses 0-61122
 light induced diffusion in solutions due to laser cutting (*Russian*) 0-81646
 linear dichroism in pulsed elec. field, meas. apparatus 0-90875
 lipid interaction, IR spectroscopic obs., DNA compactisation on disperse particles 0-104550
 lymphocyte cell DNA damage by US diagnosis 0-67148
 lymphocytes, human, effects of low-dose radiation on repair processes 0-98023
 mammalian chromosomal DNA, single-strand breakage, sensitive detect. by sedimentation anomaly appl. 0-104825
 melting curves, automatic recorder using real time processing, DNA derivative (*French*) 0-104833
 molecular motions, investigated by ^{31}P and ^{13}C NMR relaxation 0-63657
 murine leukemic lymphoblasts, deficient repair and degradation of DNA after X-irrad. 0-72249
 murine leukemic lymphoblasts, deficient repair and degradation of DNA after X-irrad. 0-72253
 neuronal DNA damage accumulation rel. to death after whole-brain irradi., rats 0-76804
 nucleic acids, electron microscopy using basic protein film method 0-104844
 nucleosomal, electro-optical props., relax. times and chain struct. 0-85350
 oriented DNA, hydration, neutron scatt. obs. 0-89714

DNA continued

- phase transitions in water-ethanol solns. (*Japanese*) 0-89709
 proton radiationless transitions for hydrogen bonds (*Russian*) 0-97857
 radiation biology conference, Rotterdam, Netherlands (Aug. 1980) 0-105425
 radiation induced mol. size change, electron irradiated, effect of p-nitroacetophenone 0-89807
 radiation induced properties changes caused by UV- and γ -irrad., electrochem. anal. 0-72271
 radiation sensitivity, physical aspects 0-67162
 radiation-induced double-strand breaks, repair in isolated nuclei of *Phy-sarum polycephalum* 0-72248
 radioactive labelled, effect on excision repair in UV-irrad. human fibroblasts 0-94289
 radiolysis of DNA and other bipolymers 0-67163
 RNA, molecular motions investigated by ^{31}P and ^{13}C NMR relaxation 0-63657
 solution, elec. birefringence, stabilised induced dipole behaviour 0-85349
 spreading of large associations, dark field electron microscopy 0-85563
 strand breaks induced by γ -irrad. of deoxygenated aq. solns. 0-61649
 supercoiled torsional stress and local denaturation 0-72131
 Tetrahymena, γ -irrad., role of DNA damage and repair in eukaryotic gene function 0-104677
 thymine base damage release, γ -irrad. *Tetrahymena pyriformis* 0-72268
 thymine damage production and excision, mammalian cells, high-LET irradi. obs. 0-72261
 torsionally stressed, equilibrium statistical mechanics of helix coil transition 0-67032
 torsionally stressed, transitions between B- and Z-conformations, theoretical anal. 0-94166
 trigeminal neurons, rat, effects of γ -irrad. 0-72270
 water localisation in a DNA mol. by differential Fourier synthesis 0-94164
 CsDNA of T2 phage, in classical crystn. B form, struct., amplitudes, synchrotron radiation diffraction 0-85335
 ^{11}In bound, rot. correl. times, from γ -ray perturbed angular correl. 0-94152

documentation *see information science***Doherty amplifiers** *see power amplifiers***domain boundaries**

- for boundaries between magnetic domains and electric domains *see magnetic domain walls and electric domains walls respectively*
see also antiphase boundaries
 adsorbed layer, commensurate-incommensurate transition and domain walls 0-107654
 kinks, solitons, and nonlinear transport in solids 0-65421
 BiVO_4 , ferroelastic domains, electron microscopy and electron diffr. obs. 0-100254
 Ge/Cu, surface waves at static domain boundaries (*Russian*) 0-80288
 ^3He , superfluid, domain wall energy and spatial conformation in parallel plate geometry 0-96716
 Nb-H system, phase diagram and transforms., struct. obs. of various phases 0-104125
 $\text{Ni}_3\text{Ti}_{0.5}\text{Ta}_{0.5}$, conservative domain struct., TEM study 0-79776
 ZrV_2 , anomalous softening at martensitic transform. 0-93630

domains

- see also antiphase domains; crystal microstructure; domain boundaries; electric domains; magnetic domains*
 adsorbed layers, commensurate-incommensurate transitions, substrate defects effect 0-75437
 bounded domain undergoing sequential crystallisation, stress and strain investigation 0-100183
 cholesterics, shear flow induced propagating domains 0-64887
 J-ferroics, rotational-invariant classification of structural phase transitions 0-70369
 liquid crystal, cholesteric, long pitch type, with homeotropic boundary alignment, elongated and spherulitic domain struct. 0-107047
 MBBA, positive space charge influence on texture, domain form. factor, polarised light study 0-88037
 polyurethane, segmented, domain struct., deform. effect 0-93623
 transition metal oxide catalysts, reduction, cryst. defects influence, in-situ electron microscopy 0-81322
 Co-Pt, mag. annealing, form. of ordered phase, study using X-ray scatt. (*Russian*) 0-81052
 $\text{CuSO}_4 \cdot 5\text{H}_2\text{O}$, dehydration into trihydrate obs. using monocryst. platelets, product domains shape 0-71905
 ^3He , superfluid, domain wall energy and spatial conformation in parallel plate geometry 0-96716
 $\text{Nb}_2\text{O}_5\text{-WO}_3$ system complex cpds. with TTB type subcells, HV superhigh resolution electron microscopy obs. of struct. 0-103311
 NiPt, quenched, ordering kinetics and domain struct. form. during isothermal tempering (*Russian*) 0-66502
 RbMnCl₃, twinning struct., cryst. domains, orientation mag. transition (*Russian*) 0-107275
 WO_3 , reduction, defect role, in situ HVEM obs. 0-81323

domestic appliances*see also ovens; refrigerators*

- heat pumps for space heating appls. (*German*) 0-94099
 temperature measurement, using A/D converters TL505/507 and TMS 1000 microprocessor (*French*) 0-57290

doping, semiconductors *see semiconductor doping***doping profiles**

- algorithm for calc. of impurity concentration from sheet resistivity and sheet Hall coefficient data 0-70246
 anomalous avalanche breakdown, effects 0-80284
 C-V measurement interpretation, determ. of doping profile in semiconductors 0-59510
 depth distrib., secondary ion mass spectra 0-79829
 high-resolution photoacoustic spectroscopy for dopant depth profiling 0-77883
 ion implantation, depth distrib., analytical calcs. using inhomogeneous equations 0-84203
 metal-semiconductor thermoelectric coolers, effects of contact resist. and dopant conc. 0-81481
 optical fibre preform core diameter and Ge doping profile meas., X-ray nondestructive method 0-64231
 optical fibre refractive index profile distortion due to thermal stresses 0-58726
 optical multimode fibres with index profiles varying along length, pulse propag. 0-87534

doping profiles continued

- Pearson IV distrib., appl. to ion implanted depth profiles 0-88195
 quartz glass, Ge and B dopants, OH impurities, preform material and fibre optic waveguide struct. 0-64173
 semiconductor, surface depletion and inversion, arbitrary doping profile, theory 0-107912
 semiconductor depth profiling by electron beam induced junction current meas. 0-96977
 semiconductor materials, channelling-blocking measurements, (n,α) method for B-depth profiling 0-70276
 semiconductor microstructure fabrication, ion channeling effects 0-70230
 semiconductor spreading-resistance meas. for doping profile determ., pre-processing of data for resistivity calcs. 0-57265
 shallow-level concentration, instrum. for automatic meas. 0-105673
 steel, austenitic, Cr-Ni, ion-implanted N, chem. state study by AES and XPS 0-79825
 (Al,Ga)As:Zn planar stripe lasers with deep Zn diffusion, guiding mechanisms controlled by impurity concs. 0-78853
 Al, polycrystalline, high dose implanted with Cu and Pb, doping profile after laser pulse irradiation 0-88194
 BP:Zn(Se)(Cd), epitaxial layers, ion implantation, defects and lattice locations, channelling obs. 0-88179
 CdTe crystals, exciton luminescence spectra rel. to shallow impurity conc. 0-97335
 Cu single crystals Au ion implanted, pulsed electron beam irradi. 0-65019
 Cu₂S-CdS heterojunction interface, depth distribution profiles, Auger spectra 0-88622
 GaAs epitaxial layers, meas. of doping profiles (*Hungarian*) 0-70545
 GaAs epitaxial layers, doping profile degradation due to ion implantation 0-84194
 GaAs, ion implanted, capless annealed and dielectrically annealed, comparison of doping profiles 0-100278
 GaAs:Cr, ion implanted, implantation damage profiles, laser annealing, ellipsometry study 0-79819
 GaAs:Cr, low temp. gettering 0-96549
 GaAs:Cr capless annealed, under As press., Cr redistrib., SIMS obs. 0-59503
 GaAs:Ge MBE power FETs with Sn surface impurities 0-80374
 GaAs:Si, ion implantation, thermal annealing, Hall meas., SIMS atomic profile meas. 0-75243
 GaAs:Sn(Te), epitaxial film, influence of impurities on stacking fault energy 0-103371
 GaAs:Te(Cd)(Mg)(B), ion implant depth distrib., AES and glow discharge optical spectroscopy meas. 0-65028
 GaAs-Si heterojunction, IR quenching of photocapacitance 0-92968
 GaAs-Si ion implanted, impurity profiles elec. props. 0-96550
 GaP:Cr epitaxial layers, Cr conc. profile determ. 0-65029
 GaP-N LED structures, local dopant conc. determ. using SEM cathodolum. spectra 0-101057
 Ni dilute alloys, implant profiles modification by radiation enhanced diffusion and segregation 0-88217
 Si amorphous p-n junctions, high current, characts. 0-70807
 Si, carrier lifetime depth distrib. due to Ar ion implantation 0-70232
 Si, determ. by DC MOSFET dopant profile method 0-70244
 Si, doping impurity distrib., during cryst. growth by Czochralski method (*Russian*) 0-100276
 Si epitaxial layers, meas. of doping profiles (*Hungarian*) 0-70545
 Si, implanted crystal, laser induced annealing and diffusion behaviour 0-88202
 Si, ion implantation, channelling, alignment effects 0-88183
 a-Si, laser induced crystallisation mechanism, epitaxial regrowth 0-84962
 Si layers amorphized by molecular ions, laser annealing 0-103379
 Si, melt grown crystals, impurity incorporation, calcs. 0-79718
 Si, polycrystalline, As segregation at grain boundaries, elec. props. meas. 0-75259
 Si solar cells, ion implanted grating type 0-101102
 Si, surface, pulsed electron beam processing, doping, annealing 0-75254
 Si: As(Pb), high-dose ion implanted and annealed, implant redistribution 0-107309
 Si:Al(Ga), spreading resist. calibration using Si:B 0-103690
 Si:Ar, As, ion implanted, laser annealing, doping profiles, channelling 0-97506
 Si:As, ion implanted, formation of As complexes 0-59511
 Si:As high-dose implanted single crystals, pulsed electron-beam annealing 0-103373
 Si:As ion implanted layers, annealing by CO₂ laser, doping profile shift 0-84965
 Si:As(B), heavy-doping effects and impurity segregation during high-pressure oxidation 0-65014
 Si:As(Pb), ion-implanted, impurity redistrib. during laser irradi. 0-100280
 Si:As(Sb), ion implanted, lattice location of impurities after pulsed laser annealing 0-88196
 Si:B, anomalous B profiles prod. by BF₃ implantation 0-75252
 Si:B, He⁺ irradiation-induced diffusion, effect on impurity distrib. 0-70470
 Si:B, P, long range enhancement of B diffusivity by P diffusion 0-103386
 Si:B diffusion at Si-SiO₂ interface, Auger spectra, Rutherford backscattering 0-70471
 Si:B photodiode front region collection efficiency models 0-96899
 Si:B(Be)(Li) ion implanted, channelling and random equivalent depth distrib. 0-100293
 Si:B(P), proton-irrad., impurity uphill diffusion, vacancy mechanism 0-92719
 Si:B(P)(As)(Sb)(Cu)(Fe), ion implanted, doping profile, pulsed laser annealing effects 0-88197
 Si:Be, ion implanted, correl. of atomic distrib. and implantation induced damage profiler 0-88199
 Si:Co, ion implanted, Co lattice location, channelling meas. 0-88201
 Si:Ga(As), laser-doped, impurity distrib., Rutherford backscatt. and channelling anal. 0-59507
 a-Si:H film, glow discharge deposited, H profiles, doping level 0-84202
 p-Si:In, ion implanted, doping profiles from capacitance-voltage characts. 0-88203
 Si:O, incorporation of O during pulsed-laser irradi. 0-96557
 Si:O(C), implant redistribution, annealing effects, SIMS meas. 0-96561
 Si:P, incoherent light flash annealing, elec. props., backscattering spectra 0-97504
 Si:P, measurement techniques for determining P densities 0-75262
 Si:Sb, ion implanted, annealed, dislocation generation, channelling and Rutherford backscatt. meas. 0-88158

doping profiles continued

- Si:Sb, laser doping, evaporation loss and diffusion of Sb, under pulsed laser irradi. 0-59508
 Si:Sb, low energy ion implantation, profile determ. 0-88176
 Si:Sb, low energy ion implantation Schottky barrier diodes and resistors 0-88177
 Si:Sb, MBE film, doping technique 0-79821
 Si:Sb, produced by ion implantation and laser annealing, Sb behaviour above solid solubility 0-88200
 Si:Te, laser melting, surface Te atom accumulation, profiles 0-100258
 SiO₂ coatings on SiO₂ substrate, cathodoluminescence spectra, electron irradi. 0-76085
 SiO₂:BF₃, ion implanted, F influence on oxidation-induced stacking faults 0-65011
 Zn:Al, ion implantation, temp. and time depend. 0-65013
 ZnSe-Si heterojunctions, IR quenching of photocapacitance 0-92968
- Doppler broadening** *see Doppler effect*
- Doppler effect**
see also atomic spectra; red shift; spectral line breadth
 aerosol particle size meas., optical particle counter calibration by Doppler shift spectrometry 0-68173
 animal research, totally implantable directional Doppler flowmeters 0-67293
 anomalous, amplification of slow waves in electron beam, obs. 0-78463
 aperture synthesis by object rotation in coherent imaging 0-69336
 atom, two-photon resonance in coherent fields 0-63606
 auroral forbidden O I emission, Fabry-Perot interferometer obs. for thermosphere wind and temp. meas. 0-101441
 beam-plasma instability singularities, anomalous Doppler effect 0-75040
 biomedical US diagnostic technique of carotid artery disease, objective feature extraction 0-72273
 biomedical US real-time scanner with pulsed Doppler and T-M facilities, obstetrical appls. 0-67172
 blood, US, Doppler-shift waveforms, physiological interpretation 0-89814
 carbon tetrafluoride ¹²CF₄ laser, Doppler-limited absorption spectroscopy 0-74347
 conference on satellite Doppler tracking and geodetic appl., London, England (Oct. 1978) 0-77264
 deflection effect of light reflected from moving mirror in ether theory 0-91749
 differential measurements, continuous-wave transmitting projectile, passive array tracking 0-94955
 diode laser, appl. of Doppler line convolution by Gaussian instrument function 0-82830
 electron waves, Doppler shift illustration using electron mirror interference microscope 0-95783
 electrostatic precipitator, particle velocity, laser Doppler anemometry study 0-59144
 EM waves generation and amplification based on Doppler effect 0-63902
 emission line shapes from a rotating ring radiator 0-83998
 energy level transitions, excitation by monochromatic laser radiation, Doppler-broadened transitions 0-78582
 ether theory, relativistic formula for Doppler effect (*French*) 0-105494
 falling objects accel. due to gravity, Doppler effect, student microwave expt. 0-105472
 fluid mechanics, photon correlation techniques, conf., Cambridge, England (March 1979) 0-56998
 gas, inhomogeneous layer, transmission calc. for spectral line with Voigt profile 0-59164
 gas, resonance four-photon shift, optimal focusing of high-power pumping 0-95574
 gravitational Doppler effect explored using geostationary satellite 0-109351
 Hertzian waves, reflection and diffraction by moving layers (*German*) 0-87266
 interplanetary H I, λ emission Doppler shifts anal. rel. to local interstellar gas temp. and vel. 0-105141
 ionosphere, HF radio waves Doppler shifts rel. to bottomside mid-latit. trough 0-109300
 ionosphere plasma line, Doppler shift detect. rel. to auroral Birkeland current meas. 0-98507
 IR spectrum deconvolution beyond the Doppler limit 0-86467
 laser based on coupled transitions with arbitrary polarization of radiation 0-78827
 laser Doppler blood velocimetry (*Japanese*) 0-94310
 laser Doppler microscope, vel. measuring device 0-68251
 metallic glasses, Doppler broadening of positron annihilation γ-radiation and elec. resist. 0-66321
 molecular energy level transitions, excitation by monochromatic laser radiation, Doppler-broadened transitions 0-78582
 Mossbauer effect, second order Doppler shift, press. depend. 0-66088
 nonlinear spectroscopy, recoil effects on Doppler-free lineshapes 0-82829
 plasma, Brillouin and dielec. side-scatt. of 10 μm laser light 0-103156
 plasmas, Tormac, Gaussian HeII 4686 Å spectral lines, Doppler and Stark broadening effect, turbulence 0-106980
 polydispersed flows, Doppler signal spectrum 0-103081
 positron annihilation radiation spectra measured with Ge(Li) detectors, iterative unfolding method 0-97373
 positronium formation inhibition by solvated electron precursor scavenging, line shape Doppler broadening, lifetime spectroscopy 0-93784
 quasars redshifts, relativistic Doppler formula rel. to transverse vels. and distances (*Chinese*) 0-105379
 radar echoes, type 1, from equatorial electrojet, with double-peaked Doppler spectra 0-67458
 radio galaxies components, radio continuum spectra rel. to fly away velocities (*Russian*) 0-62306
 real-time optical processing using the liquid crystal light valve 0-63936
 relativity, special, Doppler effect 0-82637
 research in the nineteenth century 0-86070
 RF target simulator using acousto-optical device 0-102843
 ripple-tank demonstration 0-82621
 sea waves, height, length and velocity, radar and Doppler effect, OREME project (*French*) 0-94625
 six-dimensional space, hidden variables 0-82666
 solar photosphere, vel. gradients retrieval from line asymmetries, linearised approach 0-62093
 solar rotation induced Doppler spectral shift meas. by scanning Fabry-Perot interferometer 0-77298
 solar spectrum, Doppler shift meas. rel. to solar oscillations and Sun internal struct. 0-105226

Doppler effect continued

- spectral line broadening, elimination problem, parametric soln. 0-62730
 steel, positron meas., for trapping mechanism detection 0-84798
 three-level spectra, lineshapes in intense laser field, theory 0-69109
 trapped ion, laser cooling, theory 0-58414
 two-level atom, radiation by intense laser beam, resonance fluorescence, photon antibunching, Doppler shift 0-74146
 US Doppler returns from foetal heart, processing, valvular timing information extraction 0-101238
 vanless diffuser of centrifugal compressor, flow velocity meas. using laser Doppler anemometer 0-59147
 venous flow, mech. oscills., ultrasonic Doppler study 0-108931
 VLF signals in magnetosphere, Doppler shift meas. by JIKIKEN (EXOS-B) satellite (Japanese) 0-94651
 wave and particle descriptions of light, equivalence, rel. to radar freq. shift 0-101692
 Ag, positron annihilation spectra, Doppler-broadened, temp. depend., 9 to 1098K 0-71510
 Ar plasma arc, wall-confined, nonequilibrium effects 0-70058
¹²C gamma line Doppler broadening in ¹²C(n,n' γ)¹²C and ⁹Be(α ,n' γ)¹²C, 4438 keV 0-91147
 Ca 657.3 nm line saturated absorption spectroscopy, photon-recoil component resolution 0-86457
 Fe,Pt:Sn Invar alloy, Mossbauer shift temp. depend. 0-100626
 H, photon emission, Bohr theory covariant eqns, teaching 0-105482
 H α and H β , Stark profiles, ion-motion effect 0-63592
 He-Ne ring laser, unidirectional, modes 0-91818
 NH₃, phase conjugation in an inhomogeneously broadened medium 0-83642
 Ne(³P₂) elastically scattered, metastable, ang. distrib., conventional rel. to Doppler shift methods 0-58418

Doppler shift see Doppler effect**dopplers**

- Mo, longwave dopplers, nonlocal Hall effect, surface impedance, size effect (Russian) 0-80253
 W, longwave dopplers, nonlocal Hall effect, surface impedance, size effect (Russian) 0-80253

dosimeters

- see also dosimetry; thermoluminescent dosimeters
 A-150 plastic-equivalent gas for ionisation chambers 0-81745
 air monitoring systems for radioiodine and inert gases, evaluation 0-95480
 beta-ray survey meter for meas. of absorbed dose rate independently of energy 0-106203
 bremsstrahlung dose measurement using convertor-detector system, electron dose determ. 0-91294
 calibration of environmental and personal dosimeters using ¹³³Xe 0-86992
 corrected calibration of Andersson and Braun type rem counter for divergently incident Am-Be neutrons 0-74031
 diamond, radiation dosimeters, evaluation 0-78456
 electronic, compromise between accuracy and sensitivity (Italian) 0-63394
 film badge dosimeter for UVA radiation 0-61702
 film photon and electron absorbed-dose detector 0-91379
 gamma, reference material based on silicate glass 0-78454
 graphite calorimeter in water phantom for absorbed dose meas. 0-74032
 ion chambers, photon dosimetry in phantoms, effective meas. point 0-78453
 ionisation chamber, parallel plate, thin-walled, for use with photon and electron beam dosimetry 0-78490
 ionising chambers with electrostatic relays, investigation of stability, reproducibility, and orientation characts. 0-57966
 laser light, dosimeter for health physics evaluation of operating conditions at laser installations 0-76835
 lignocellulose polymer composites as γ -dosimeters in the kilorad range 0-95465
 linear accelerator beam profile scanner, medical appls. 0-101267
 luminescent detector efficiency for 600 MeV protons, mass stopping power calc. 0-99346
 medical X- and γ -ray dosimeter with digital display, portable and versatile 0-81744
 mica, for visualisation of electron isodose curves in a medium 0-99349
 microdosimetric measurements with spherical proportional counters and solid-state detectors, comparative study 0-109038
 parallel plate ionisation chamber, absorbed dose meas. in polystyrene phantoms 0-72335
 polyamide-film calorimeter for measuring local electron-beam absorbed doses 0-83227
 polycarbonate fast neutron dosimeter, development and comparison with conventional emulsion dosimeter 0-86990
 pulsed neutron dose rate meas. instrument, portable, microcomputer-based 0-86991
 secondary radiation dosimeters, prep., sensitivity anal. and calibration 0-74034
 solid dielectric detectors with breakdown phenomena and their applications in radioprotection 0-91388
 solid state dosimetry, tissue-equivalent systems, review (Hungarian) 0-91291
 surface barrier detector for beta dosimetry 0-57973
 track etch detectors, neutron energy depend. and threshold energy 0-61703
 ultra-thin dosimeter for skin dose assessment, development 0-57974
 UV polymer-film dosimeters, automatic read-out device 0-78455
 water calorimeter for absorbed dose meas. 0-76836
 wrist watch dosimeter for ionising radiations, practicality tests 0-57972
 CdS γ -ray dosimeters with elevated stability under irradiation 0-86995

dosimetry

- see also dosimeters; radiation detection and measurement; radiation monitoring
 A₀₁ and A₀₂ meaning of 0-89867
 absorbed dose determination, fund. principles for radiation technology 0-95467
 absorbed dose estimates in prolonged ¹³⁷Cs γ -irrad facility for mice 0-101233
 absorbed dose measurements using parallel plate ionisation chambers in polystyrene phantoms 0-72335
 albedo neutron dosimetry, advances 0-57982
 alpha emitters, health effects, man-made actinides compared with natural radionuclides 0-61647

dosimetry continued

- aquatic food chains appl., dosimetry calculations due to radionuclides, NEPTUN interactive code in FORTRAN 0-109039
 beta radiation, absorbed energy distribns. in homogeneous media 0-109033
 Bikini population, dosimetric results for man-made radiation 0-85498
 biological effects of radiation, methods of safety estimation and problems encountered (French) 0-98003
 bladder wall dose after ^{99m}Tc-microspheres administration 0-109030
 bleomycin, effect of dose loading and double labelling with ⁵⁷Co and ¹²⁵I on animal tissue distrib. 0-67220
 bone-seeking radionuclides, comparative study in man, rhesus monkey, beagle and miniature pig 0-72338
 brachytherapy program used with the Philips Treatment Planning System 0-81738
 brain low dose elective, in small cell lung carcinoma 0-67253
 build-up curves of scanned high energy electron beams, Sagittaire linear accelerator 0-89864
 calibration for radiation protection in European community 0-58000
 cancer induced by radiation, dose-effect relationship linearity 0-67157
 cell neoplastic transformation and dose fractionation, role of damage repair 0-72242
 cellular repair rates determined by split-dose and dose-rate methods, comparison 0-104680
 centralized TLD service and record keeping in Canada 0-58003
 ceric/thallous dosimetry at less than 1000 rad 0-63400
 chest wall irradiation, technique to improve electron dose distrib. homogeneity 0-72332
 chromosomally aberrant cells, Japanese A-bomb survivors, dose-response relationship of neutrons and γ -rays 0-94295
 chromosome aberrations, dose-effect relationship, population exposed to increased natural radioactivity 0-72254
 committed effective dose equivalent conversion factors for intake of selected radionuclides 0-67256
 computerized operation of a dosimetric service 0-58004
 computerized tomography field measurement utilising the partial vol. effect 0-89865
 conference, radiation protection monitoring advances, Vienna, Austria (June 1978) 0-57007
 cosmic radiation dose field, meas. aboard Salyut-6 orbital station 0-89876
 criticality accidents, dosimetry using activations of blood and hair 0-89857
 cytogenetical indicator of radiation effect, chromosomal dosimeter (Hungarian) 0-94292
 dental patients, X-ray exposure obs. 0-104761
 depth dose distributions in water phantom irradiated by teleisotope photon beam 0-81741
 diagnostic X-rays, dose distrib. calc. method for bone- and lung-equivalent material (German) 0-61704
 dose-rate conversion factors, radiation from nuclear fuel cycle facilities routine releases 0-86993
 dose-rate conversion factors for external exposure to photons and electrons, modifications to DOSFACTER code 0-104775
 drinking water, Finland, internal radiation doses due to radioactivity 0-109029
 electrets, radiation-induced charge storage and polarisation effects 0-80684
 electron beam applicator, variable field, dosimetry evaluation 0-76839
 electron beam dose distribns., model for calculating effects of small inhomogeneities 0-76837
 electron dosimetry, scatter effects, plane ⁹⁰Sr-⁹⁰Y medical applicator 0-61699
 electron irradiated solid, dynamic and dosimetric characts., laser and holographic interferometry obs. (Rumanian) 0-90886
 embryo, radiation absorbed dose estimates from some nuclear medicine procedures 0-104760
 emitted radiation, clarification of concept, brachytherapy dosimetry appl. 0-76843
 environmental radioactivity, determ. for dose assess. 0-85321
 environmental radioactivity, radiation dosimetry control, exposure rate monitoring of natural radiation reference field 0-67017
 environmental thermoluminescent dosimetry, regulation compliance, data interpretation 0-57995
 fast neutron beams, linear regression anal. of γ -dose 0-89866
 fast neutron facilities for radiobiological irradiation 0-109064
 film dosimetry of multiple electron beam ports with wedges 0-98138
 finger doses received by radiologists during Chiba needle percutaneous cholangiography 0-81737
 fission counters, high sensitivity, neutron spectroscopy and dosimetry appl. (French) 0-58078
 fission neutron spectra, light water-moderated, depth-dose characts. 0-106205
 fusion reactors, TFTR test cell, calc. dose rates from induced activity, Monte Carlo methods 0-57967
 gamma and X-ray, phys. quantities used in radiation safety monitoring 0-99344
 gamma dose to gastric wall, estimation after administration of ¹³¹I (Japanese) 0-98141
 geometric factors, relation for different media 0-109036
 glass dosimeter reader, design improvements (French) 0-57970
 gliomas, malignant, anal. of dose-effect relationship in radiotherapy 0-72331
 gliomas, malignant, high dose radiation therapy 0-67254
 glottic cancer, T3, anal. of dose time-vol. factors 0-104764
 head and neck cancer, advanced and recurrent, short course high fractional dose irradiation 0-72297
 Hiroshima A-bomb survivors, whole-body doses estimation by chromosome aberrations 0-109035
 Hiroshima mass radiologic gastric surveys, examinees' doses 0-89858
 Howe Caverns, USA, doses to employees and public from Rn and Rn daughters 0-89859
 human exposure due to environmental radiation (Japanese) 0-72336
 impulsive and continuous noise, combined dose meas. 0-102929
 interstitial dosimetry, utilisation of the computerised tomography scanner 0-104770
 intracavity implant therapy, appl. of linear programming to dose optimisation 0-72329
 ionisation chamber dose meter unit for emergency operations (French) 0-57977
 ionising radiation, detection device, electret based (French) 0-57971

dosimetry continued

- ionising radiation, dose-effect relationship for quantifying health risks (*German*) 0-61644
 ionising radiation, personnel exposures, dose limits 0-99350
 KERMA values, consistent set for H, C, N, and O for neutrons from 10 to 80 MeV 0-68967
 linear accelerator, field separation between lateral and anterior fields, dose distrib. 0-94336
 linear accelerator dosimetry control system, solid state 0-94371
 linear accelerator X-ray beam energy at off-axis points, calc. technique for correct. 0-81742
 Lipowitz metal shielding thickness for dose reduction of 6-20 MeV electrons 0-76842
 liver membranes, mouse, X-irrad., dose-rate effects 0-94293
 LR115 cellulose nitrate detector system for personal dosimetry near high energy accelerators 0-58081
 lung, nuclear medical imaging, estimates of radiation absorbed doses from radioxenons 0-101269
 lung dose in half body radiotherapy, determ. by computerised tomography 0-104763
 LWPR, radiological emergency monitoring and instrumentation, Federal guidance 0-57961
 lymphocytes, human, prediction of dose-rate effects for dicentric production by X- and γ -rays 0-72226
 malignant melanoma, radiation treatment 0-94372
 mammography, absorbed dose evaluation, Monte Carlo simulation studies 0-98143
 management of an automated dosimetry and dose record keeping service 0-58006
 marrow colony-forming units, dose-dependence of the split-dose response 0-61701
 medical imaging system evaluation by contrast-detail-dose analysis 0-98140
 methane-based tissue equivalent gas, W_n and neutron kerma 0-104769
 method for calculating the dose commitment from bioassay data 0-109031
 microdosimetric measurements of pretherapeutic heavy ion beams 0-72337
 microdosimetry, role in radiobiology 0-61705
 microdosimetry of the pion beam at TRIUMF 0-109037
 microwave far-field, dosimetric meas. of full-scale man model 0-67255
 mixed β - γ dosimetry, ionisation and scintillation counters 0-57975
 mixed radiations, device for dose-equivalent index determ. (*Russian*) 0-57976
 MPD reduction suggestion to meet requirements of higher safety 0-85499
 multimode time-varying enclosures for exposure and dosimetry in bioelectromagnetic experiments 0-85497
 neutron cross-sections and kerma values for C, N and O from 20 to 50 MeV 0-101217
 neutron dose and quality factor meas. by tissue equivalent proportional counters 0-58079
 neutron dosimetry, dose distrib. depend. on linear energy transfer (*Czech*) 0-68965
 neutron dosimetry, photointerference corrections for reactor pressure vessel lifetime studies 0-99345
 neutron dosimetry, problems rel. to incorrect composition of tissue-equivalent gas 0-81743
 neutron dosimetry at JINR synchrocyclotron 0-57983
 neutron dosimetry system, based on fission counter for fuel processing plant 0-57981
 neutron irradiation facilities, dosimetric meas. 0-104762
 neutron monitor calibration, standard fields at Physikalisches Technische Bundesanstalt 0-57999
 neutron personnel dosimeters, European comparisons 0-57980
 neutrons, $p(90)+(Be+Ta)$ and $p(101)+(Be+Al)$, dosimetric props. 0-89861
 NRPB thermoluminescent dosimetry and dose record keeping service 0-91293
 nuclear accident dosimetry, blood-Na meas. 0-57979
 nuclear accident dosimetry system, Czechoslovakia 0-57978
 nuclear industry, health risks from various power sources 0-57899
 nuclear medicine, computer software package for internal dose calc. 0-98139
 oral mucosa, determ. of dose from, and content of, U in dental porcelains 0-89830
 organ doses from isotropic γ -ray fields, review 0-109026
 personal dosimetry and dose equivalent index 0-109027
 personal dosimetry instrument for airborne radon daughter meas. (*French*) 0-57989
 personal monitoring, effect of environmental radiation, thermoluminescent dosimeter (*Japanese*) 0-61707
 personal sampling devices for atmospheric contamination monitoring (*French*) 0-57986
 personnel dosimetry, data processing system, mini-computer appl. 0-58005
 personnel dosimetry methods introduced in the Czechoslovak national laboratories 0-57969
 personnel neutron dosimeters, calibration for use in different neutron fields 0-58001
 prosthetic silicone breast, dose obs. 0-98144
 Q-factor for charged particle recoils rel. to neutron energy 0-63397
 radiation biology conference, Rotterdam, Netherlands (Aug. 1980) 0-105425
 radiation meas. bibliography (1972-76) (*German*) 0-95510
 radiation therapy, algorithm for calc. of central ray TAR and TMR values 0-76844
 radiation therapy, dosage calculation and compensation, basic data 0-104765
 radiation therapy, dose response curves, methods of extraction 0-94374
 radiation therapy, dosimetric considerations of very large ^{60}Co fields 0-104766
 radiation therapy, estimate of risk due to unwanted neutrons by dose calcs. 0-81714
 radiation therapy, high-energy proton beam, physical meas. using tissue substitutes 0-81720
 radiation therapy, procedures with electron and photon beams 0-101266
 radiation therapy, squamous cell carcinoma of head and neck, time-dose factors anal. 0-72333
 radiation therapy, total body techniques for bone marrow transplantation, review 0-104738

dosimetry continued

- radiation therapy planning, revision of tissue-max. ratio and scatter-max. ratio concepts 0-76840
 radiation treatment of obstruction of superior vena cava, optimum schedule importance of ^{99m}Tc scintiangiograms 0-72334
 radiation treatment planning, computerised, accuracy 0-72328
 radioactive pollution consequences from liquid pathways due to reactor core meltdown accident 0-104778
 radioactive pollution from nuclear facilities, T population dose in the Northern Hemisphere 0-104779
 radioactive seed implants, computation of dose distrib. 0-101265
 radiographic dose reduction 0-98087
 radiography, free-focus, using conventional films, exposures in a simulated clinical study 0-89835
 radioisotope dosimetric data tables 0-105438
 radioisotope transport in terrestrial food chains, dynamic modelling using RAGTIME code 0-104776
 radioisotopes manipulated in syringes, radiation exposure obs. 0-67252
 radiological implications of Pu recycling in HTGR fuels 0-68777
 radiotherapy, ^{60}Co total body irradiat. at 220 cm source axis distance 0-104768
 radiotherapy, linear accelerator, SL 75-20, neutron and gamma doses in entrance mazes of treatment rooms 0-85500
 radiotherapy hard X-ray machine, RT 305, phys. aspects and appl. 0-81709
 radiotherapy tissue compensators, use in improving dose uniformity in total body irradiat. 0-104767
 radiotherapy treatment planning, FORTRAN program for optimisation using complication probability factor 0-81686
 radiotherapy treatment planning, inhomogeneity correction methods compared with Monte Carlo data 0-61698
 radiotherapy treatment planning for irregular fields 0-81739
 radiotherapy with electrons, up to 20 MeV, phys. aspects 0-85474
 radiotherapy with fast electrons, computerised treatment planning, dose distrib. calc. 0-81740
 reactor core gamma dosimetry, solid state nucl. track detector appl. 0-95466
 REBEL-3, code for dose calcs., phantom standing in dwelling room 0-94377
 reference radiations for radiation protection dose meter calibration (*French*) 0-57998
 RF EM fields, review of effects and dosimetric data, safety standards development 0-67154
 Rossi counter equivalent dose meas. in high-energy radiation fields 0-94376
 scanning electron beam, semi-empirical model for dose distrib. generation 0-94373
 solar flares near-Earth radiation hazard, dosage estimation technique 0-67482
 solid state nuclear track detectors, reactor neutron fluence meas. using Au and In foils 0-69035
 stainless steel, neutron dose determ., from isotope abundance ratio, mass spectra obs. 0-61220
 tail necrosis, mouse, multifraction X-irrad., dose-incidence curve steepness anal. 0-98035
 terrestrial sources, possibility of estimating population exposure 0-89855
 therapy, source motion, calc. in intracavity moving-beam and multipositional irradiat. 0-104759
 thermally stimulated luminescence application, radiation dosimetry, book contribution 0-80882
 thermoluminescence dosimetry in patients (*German*) 0-104758
 thermoluminescent dosimetry system for high energy bremsstrahlung dosimetry 0-106209
 thyroid, absorbed fractions of photons of ^{125}I and ^{129}I 0-109032
 tissue equivalent phantom, dose distrib. calc. using Monte Carlo programme 0-78457
 tissue equivalent torso phantom for transuranic nuclide counting facility calibration 0-67257
 tissue-equivalent compensators for 4-MV X-rays, basic data 0-98069
 TLD evaluation of internal beta-dose rate for archaeological dating 0-98478
 US imaging system for chest and other body organs 0-67174
 workers in isotope diagnostics and nuclear therapy, annual dose distrib. anal. 0-61706
 X-ray source, industrial, use for electronic component radiation effects work, calibration 0-63402
 X-ray units used outside radiology, dose obs. 0-89856
 n radiation, meas. standard for equivalent dose 0-102351
 Br^{61} , 42 MeV, stopping power and radial dose distrib. obs. in tissue-equivalent gas 0-101218
 ^{14}C released to atmosphere, dynamic model for estimating radiation dose to world population 0-89852
 $CaSO_4:Dy$ ribbon, dosimetric props. study 0-63395
 $CaSO_4:Dy$ sintered pellets, thermolum. response 0-93411
 $^{144}CeO_2$, repeated inhalation exposure of mice, retention and dosimetry 0-109034
 ^{60}Co photon beam dose distrib., oblique incidence correct., comparison of shift factors 0-76838
 ^{137}Cs gynecologic insertions, expt. derived algorithm for computer calc. dose rates 0-101264
 ^{137}Cs -irradiation, response of pig skin, various schedules of irradiat. 0-72237
 $FeSO_4$ dosimetry for electrons, a re-evaluation 0-68963
 ^{125}I , determ. of exposure rate constant using a scintillation detector 0-89863
 ^{131}I -ortho-iodohippurate absorbed kidney dose calc., literature review 0-76841
 ^{111}In labelled human platelets, dose obs. 0-94370
 $^{13}NH_3$, intravenous injection, absorbed radiation dose calcs. 0-94375
 Pu dose to lung and bone from contaminated soils, statistical uncertainties 0-109028
 Rn water spas, TLD and solid state track detector direct dosage approach 0-68966
 ^{99m}Tc , beta-decay and dose calcs. 0-91154
 ^{99m}Tc -hepatobiliary agents, absorbed dose estimation 0-72330
 ^{123m}Te -labelled adrenal-imaging agents, radiation dosimetry 0-101268
 (Th,U)C advanced FBR fuels, radiological assessment of reprocessing 0-73983
 Xe whole-body counting and dose determs. 0-89853
 ^{129}Xe , health physics, dose calcs. 0-98142

double nuclear magnetic resonance

see also *INDOR*
benzene, solid, double-quantum cross-polarization in solids 0-100623
cross-polarization double-quantum NMR in solids, theory 0-100623
double spin flips, in nucl. double reson., theory 0-66076
glassy polymers double NMR, appl. of cross relaxation dynamics in modulated systems 0-71242
low-temperature double electron-nuclear resonance obs. using 3 cm rectangular resonator 0-98956
solids, selective double quantum NMR 0-97164
thymopoietin active fragment in H₂O, soln. conformation by DNMR spectroscopy 0-89710
CdF₂, high resolution NMR and chem. shifts of ¹¹¹Cd and ¹¹³Cd, double reson. expt. 0-60460
D double-quantum NMR with magic angle spinning in solids 0-108120
(NH₄)₂SO₄, paraelectric, N-quadrupole coupling meas. 0-60459
NaNO₃, double quantum nuclear magnetic resonance of ²³Na by double resonance, line shape 0-75886
³¹P, obs. using RYa-2308 radiospectrometer with attachment 0-98957

double refraction see *birefringence*

double refraction, electric see *electro-optical effects*

double refraction, magnetic see *magneto-optical effects*

double resonance, electron nuclear see *ENDOR*

doublet antennas see *dipole antennas*

DPPH, diphenylpicrylhydrazyl see *organic compounds*

drag reduction

bubble rupture between two solid walls, effect of drag-reducing polymers on cavitation 0-106822
electrochemical mass transfer, drag-reducing polymers, effects, comparative study 0-76528
fluidised bed, effect of particle proximity on drag force 0-96306
laws of motion of solid particles in laminar flow 0-83779
oscillatory flow in U-tube manometers, effect of drag reducing polymer additives 0-64584
polyisobutylene in toluene solution, effect of capillary materials on drag reduction (*German*) 0-87785
polymers in liquid stream, Toms effect mechanism, turbulent drag decrease 0-79270
Polyox, drag reduction meas. in square duct, anomalous effects due to polymer degradation 0-83824
turbulent jets, influence of drag reducing polymers on cavitation inception 0-106823
turbulent pipe flow, use of eddy viscosity expressions for vel. profiles in Newtonian, non-Newtonian and drag-reducing flows 0-83789
two circular discs in tandem, drag reduction, wakes 0-106795
weak polymer solutions, flow props. in narrow channel between rotating and stationary discs (*Russian*) 0-59089

drawability see *ductility*

drawing (mechanical)

continuous drawing of liquids to form fibers, review, book contrib. 0-97444
CVD optical fibre, long length strength 0-58752
deep drawing, energy saving, and role of friction in metalworking 0-76271
ethylene-vinyl alcohol copolymer, drawn samples, annealing effect around T_g temps. on shrinkage and mol. orientation 0-79712
explosive forming, computer numerical simulation 0-59560
glass fibre, forming process, characts., anal. techniques 0-58827
glass fibre drawing process, characterization and control 0-58826
glass fibre drawing process, extensional instabilities 0-89258
lightguide fibre, prototype drawing facility 0-64229
metals, residual stress on drawing calcs. by stress state changes variational principle (*Russian*) 0-65125
Nylon 6 gut yarn, fine struct. change in twisting, annealing and untwisting, microbeam X-ray obs. 0-81026
Nylon 6 gut yarn, fine struct. change in twisting, annealing and untwisting, X-ray and electron microscopy obs. 0-84904
optical fibre, furnace drawn, tensile strength 0-58751
optical fibre coating with conical shape applicator 0-58820
optical fibre crystals floating zone growth, for IR optical waveguides 0-79019
optical fibre preparation methods and performance factors 0-69557
optical fibres, cooling rates during drawing 0-66538
optical fibres, high temp. resistance oven 0-74491
optical single mode fibres, homogeneous CVD fabrication and characterisation 0-69562
PET films, one-way drawn, constant strain effects, IR meas. 0-60584
polyacetylene films, stretch-aligned, prep. and morphology 0-66471
polyethylene, dielectric props., investigation for morphology changes created by mechanical drawing and annealing 0-84697
polyethylene, high density, solid state coextrusion, technique for ultradrawing thermoplastics 0-84979
polyethylene, high mol. wt., porous, hot drawing 0-60894
polyethylene, linear, draw temp. and mol. wt. effect on draw ratio and Young's modulus 0-84998
polyethylene fibre, high-strength high-modulus, morphology and tensile prop. relations 0-103264
polyethylene film, minimum running thickness, biaxial extensional flow study 0-100993
polyethylene surface-growth fibres, hot drawing 0-97517
polyethylenes, ultra-high modulus, manufacture by drawing through conical die 0-66583
polyolefins, ultra-high modulus, production by tensile drawing and hydrostatic extrusion 0-81022
polypropylene, ultrahigh modulus, tensile drawing, mol. wt. effect 0-104211
polypropylene sheet, deep drawing (*German*) 0-104114
PVC, oriented mouldings, struct. order 0-60896
quartz glass, Ge and B dopants, OH impurities, preform material and fibre optic waveguide struct. 0-64173
round profiles, US perturbed, stresses during drawing (*Russian*) 0-59557
shells, plastic, explosive forming, computer numerical simulation 0-9560
steel, cold worked, original struct. effect on softening during heating 0-60882
steel, high strength, treatment effect on ductility and strength 0-60880
steel, low-C containing Ti, sheets, recrystn. texture effects on plastic strain ratio and deep-drawing (*Chinese*) 0-66527
steel, pearlitic, struct. variations under plastic strain and subsequent heating, cementite decomp. (*Russian*) 0-84954

drawing (mechanical) continued

steel, stainless, wire, axial texture after electroplastic drawing, X-ray struct. investigation (*Russian*) 0-104177
thermoplastic sheet, deep drawing (*German*) 0-104114
Al single crystals, relation between axial orientation rotating and deform. banding 0-104206
Al-(Mg)(Fe), pure (dilute), large wire drawing plastic deform. 0-108508
Al-Ni(Cd)(Fe)(Si), cold worked, struct. and props. 0-71666
Cu, OFHC effect of cold drawing under combined stress 0-60912
Cu, wire, axial texture after electroplastic drawing, X-ray struct. investigation (*Russian*) 0-104177
Fe ore super-concentrate, deep drawing props. by integrated powder technology route 0-100806
Fe-Si (6.5 wt%) filament, formation by modified Taylor technique, and mag. props. 0-75795
MgCd wire, elongation during disorder-order transform. (*Russian*) 0-104148
Nb-Ti, multifilamentary, Mirror Fusion Test Facility, superconductor core manufacturing and quality 0-93521
Ni-Ti/Cu composite, plastic deform. influence on internal friction (*Russian*) 0-100871
SiO₂ fibres, fused, drawn from rods, oxy-H₂ flame, prep., strength, dia. var. 0-102868

drives

see also *electric drives*

displacement digital method (*Polish*) 0-86260

drop model (nuclear) see *nuclear liquid drop model*

droplets see *drops*

drops

air bubble entrainment in self-aerated flow, channel or pipe flow 0-106832
almost spherical viscous drops, time-depend., shear induced deformation 0-87794
aqueous film, plane-parallel symmetrical, stability, non-spreading oil droplet effect 0-107620
binary mixtures, near critical, metastable, phase separation and nucleation and drop growth, rate eqns. 0-65232
capillary phenomena for fluid/liquid interface, review 0-70506
carbon tetrachloride drops falling through H₂O, surfactants rel. to deform., oscill. (*French*) 0-66880
charged liquid drops, dynamics, symmetric and asymmetric stabilities 0-79366
chlorobenzene drops falling freely through water, breakup 0-69899
cloud droplet nucleation, expts. with monodisperse NaCl aerosols 0-82003
cloud droplets concentration, microphysical model sensitivity to urban environment 0-82004
cooled pipe, droplets from vapour condensation, size distrib., laminar flow 0-79111
deformation, shear and vorticity effects 0-87795
deformation and orientation in shear and extensional flow fields, dynamic interfacial props. 0-107611
dichloroethane drops falling freely through water, breakup 0-69899
direct contact heat transfer with intermittent electric field 0-74869
disintegration mechanisms of liquid droplets due to air stream 0-74959
dispersed droplet past-dryout regime, nonequilib. heat transfer model 0-64548
dispersed supersonic two-phase flow, shock characts., droplet size depend. at nozzle 0-106815
droplet transport in gases and liquids, gravitational and thermophoretic contribs. 0-100052
ducts, one-dimensional models for transient gas-liquid flows 0-64614
dynamics in mixture with uniform temp., thermal diffusion effects 0-103097
dynamics in shear fields, role of dynamic interfacial effects 0-107612
EHD flow, with small Reynolds number, resulting deformation 0-59126
electric field enhancement of collision efficiency 0-61863
electrolyte, on heated metal surface, charge separation 0-88617
emulsified fuel drop, microexplosive boiling of metastable overheated water, microblast (*Russian*) 0-74930
emulsion, dilute, straining motion, effect of inertia on dynamic viscosity 0-87797
fast flowing wet steam, electrical meas. of droplet size 0-64659
flame spectroscopy, droplet size distrib., impact beads, mixer paddle and oxidant effects 0-93810
free motion transition criteria for single bubbles and drops 0-64605
growth and decay, moment and Fokker-Planck eqns. 0-82709
grotzstic liquid drops, captive between co-rotating parallel faces, shapes and stability, capillarity eqns. 0-64592
heterogeneous photocondensation process initiation by laser radiation 0-67410
ice splinter production from accreting drop 0-72585
incompressible fluid, equilib. and stability analysis 0-59092
interaction force between droplet and condensating vapour 0-79113
laminar gas flow, transverse migration of individual particles 0-96240
long slender drops in a simple shear flow, slow viscous motion 0-79365
macroencapsulation, composite drop form., hydrodynamics 0-64603
quiescent liquid-liquid systems, low vel. drop formation 0-79364
rainbow phenomena and the detection of nonsphericity in drops 0-58456
Raman scattering by forced surface oscills. in liquid drop 0-92763
rotating liquid drops, asymmetric shapes and stability 0-87796
rotating liquid drops, held together by surface tension, equilibrium shapes and stability 0-79367
size and falling velocity meas. using laser Doppler velocimeter 0-68185
size distribution in liquid phase of two-phase flow effect on characts. 0-103070
spherical droplet, evaporation and condensational growth, mass transport calcs. 0-97736
spherical drops in Stokesian field, interfacial boundary conditions 0-74931
spherical solids melting in turbulent carrier fluid, deformation and breakup 0-92646
spreading on solid surface, initial stage characts. 0-59761
steam, dropwise condensation, moving picture study 0-74863
steam, wet, drop coagulation in cross-over pipe flows 0-74982
vertically vibrated liquid column, surface disintegration, bubbles and drops 0-74943
viscoelastic droplet break-up, in nonuniform shear flow 0-64588
viscous drop, almost spherical, Brownian motion and fluctuating hydrodynamics 0-87787

drops continued

- viscous drop, almost spherical, in arbitrary flow of compressible fluid, Faxen's theorem 0-87786
viscous liquid drop in immiscible liquid, normal-mode anal. of oscillations 0-74932
water drop impacted brittle materials, damage thresholds 0-81149
water droplet freezing process under supercooled conditions 0-65192
water droplet size distrib. spectra in cumulus clouds (*Russian*) 0-81991
water droplets, ebullition under steady-state superheated conditions 0-74928
water droplets, ebullition under transient superheated conditions 0-74929
water drops in stratosphere, size distrib. rel. to sulphate aerosol growth by condensation (*Russian*) 0-94566
water vapour expansion with condensation, nozzle flow at high pressure 0-106828
H₂O droplets, subcooled, nucleation in Ar-H₂O vapour mixture, rate const. 0-61131
H₂O-H₂SO₄ ion aerosol particles, ultrafine, stratospheric form., ion-induced nucleation 0-72608
Na₂O-SiO₂ glass drops, quenched from liq. state, thermally treated, density profile 0-81085
W, molten drop break up in gas flow, surface drag, capillary excitation (*Russian*) 0-100024

drying

- boiling point drying by volumetric abs. of RF and MW EM energy, heat and mass transfer characts. 0-79130
disperse materials, conductive drying kinetics and dynamics 0-81278
E-glass fibre, silane coupling agent deposited on surface, hydrolysis and drying effect on siloxane bonds 0-85072
latex solids, agglomerating and dewatering 0-104470
porous media, heat transfer and moisture flow (*Hungarian*) 0-83839
solar powered installation for drying tobacco 0-93850
timber drying process, detection of acoustic emission 0-102940

dual resonance model *see* **duality and dual models****duality (mathematics)**

- Ising model, duality relations and replica method 0-77722

duality and dual models

- see also* **Veneziano model**
 ν -dimensional Yang-Mills and (ν)-dimens. nonlinear σ -model connection, quark confinement, dual strings 0-90978
baryonium, geometrical approach 0-91065
bound-state/free-state duality, JWKB connection with radial wave functions 0-62950
classical interacting strings, dimensional reduction, Abelian gauge fields 0-73685
cylindrical mixing phenomena in dual topological unitarisation, pomerons, reggeons and gluonic states 0-86696
dual topological expansion, Reggeon and Pomeron slopes 0-102032
Dual Topological Unitarisation scheme, flavour symmetry breaking 0-102030
duality in field theory and statistical systems, review 0-73610
hadronic collisions, jet structure, two-jet events, glueball-Pomeron identity, dual field theory 0-63051
hadronic diffraction, elastic scatt. as tunnelling phenomenon, dual model relation 0-57575
hadrons and baryonium, geometrical approach 0-91065
Hamilton-Jacobi formalism for strings, string-gauge theory link 0-78048
hard processes, large rapidity separation of baryonic number, partons, and dual topology 0-95255
lattice gauge theories, vortex free energy, strong and intermediate coupling string tension 0-105786
lattice massive dual fields for gravity 0-105779
Lorentz force in loop space, duality functional equations 0-78049
Nambu string model, scatt. amplitude (*Russian*) 0-86695
non-Abelian theories, dual formulation 0-82902
P+ \bar{p} diffraction model, two component duality and flavouring, Regge fits and pomerons 0-95261
QCD, Migdal approx. and 1/N expansion, string tension 0-101992
QCD, string constant, Regge slope and Λ parameter, empirical quarkonium approach 0-91053
quantum relativistic strings and the multiplicative dual model (*Russian*) 0-82958
quark confinement without van der Waals forces, link operator formulation and string breaking 0-101994
relativistic string model in differential form 0-105870
s-channel resonance prod. in πN scatt., amplitude zeros in Mandelstam plane 0-73686
Schwinger model, equivalent boson theory, anomaly-free Ward-Takahashi identities 0-82873
self dual SU(2) fields in multicentre spaces 0-73600
space-time anomalous dimension in Veneziano and Neveu-Schwarz models (*Russian*) 0-68434
U(N) gauge theory, Nambu-Gato string like equation 0-105785
vector meson leptonic width, duality between vector mesons and perturbative QCD 0-57589
d inelastic screening, form factor at $t \neq 0$ 0-91070
D-K(π), current algebra relations and dual model amplitudes 0-82969
DD molecular charmonium from dual diagram and Schrödinger eqn. 0-86660
 e^+e^- annihilation, Q² duality test with nonrelativistic potentials 0-102011
 e^+e^- annihilation, QCD and semilocal duality (hadrons/ $\mu^+\mu^-$) cross section ratio 0-78085
np elastic scatt. at high energies and dual absorptive model 0-102072
pp, smooth interpolation between Orear- and fixed angle scaling behaviour of the scattering amplitude 0-105873
 $\pi N \rightarrow \pi N$, finite-energy sum rules, three component duality 0-82996
 πN scattering, amplitudes, singularities of zero trajectories, dual model predictions 0-63021
T, vibrational states in string picture, mass and leptonic width 0-62949
pp annihilations, studied using topological cross-section differences between pp and pp at 48.9 GeV/c 0-83011

ductile-brittle transition*see also* **embrittlement**

- discs, circularly symmetric, rupture, ductile-brittle creep 0-69735
epoxide resin, low temp. crack propag. 0-85020
metals and alloys, BCC lattice, crit. embrittlement temp., struct. parameters effect (*Russian*) 0-66618
power-law hardening material, pre-cracked plate, unstable fracture criterion 0-84238

ductile-brittle transition continued

- steel, cast automatic couplings, yield strength, crack propag. resistance and ductile-brittle transition temp. 0-104281
steel, Cr-Mo, impact fatigue crack growth at low temps. (*Japanese*) 0-104266
steel, Cr-Mo (2.25, 1.0 wt.%), temper embrittlement, effect of P, Sn, comp. and carbide precip. 0-85036
steel, Cr-Mo and Ni-Cr-Mo-V low-alloy, additive remedy for temper brittleness 0-66659
steel, ferritic stainless welds, type 444, ductility loss rel. to ductile-brittle transition temp. 0-85002
steel, low alloy, ferritic-pearlitic, carbonitride hardening 0-104174
steel, low C, impact strength and crit. brittleness temp., sample thickness and notch radius influence 0-85018
steel, low C, nil ductility transition temp. 0-100896
steel, Mn-Mo-Ni (A533 B), ductile-brittle transition, material fracture temp. depend., Gauss distrib. function 0-97574
steel, S45C notched specimens, Charpy impact tests, notch angle effects (*Japanese*) 0-85124
steel, structural 15KhNMFA, resist. to weakening during tempering, high purity effect 0-76279
AlN, polycrystalline, stress-strain data up to 1.25 GPa 0-100899
BeO, polycrystalline, stress-strain data up to 1.25 GPa 0-100899
Co-Zr, amorphous phase form. in Zr-poor region, hardness and fracture strength (*Japanese*) 0-84914
Fe-Al-Si (6.22, 9.63 wt.%), bending test under high press., high temp. 0-85057
Fe-Zr, amorphous phase form. in Zr-poor region, hardness and fracture strength (*Japanese*) 0-84914
GeTe, stoichiometry deviations influence on mech. props., 25-500°C 0-103410
InP single crystals, uniaxial compression deform. characts. 0-84991
Mo alloys, intercryst. fracture in ductile-brittle transition region, local internal stresses effect 0-81200
Mo-Nb-Ti-N alloy, with dispersed second phase, ductile-brittle transition 0-93653
Mo-Ti-N alloy, with dispersed second phase, ductile-brittle transition 0-93653
Nb-W-Zr-N alloy, with dispersed second phase, ductile-brittle transition 0-93653
Nb₃Sn, hot isostatically pressed, plastic deform. 0-108510
Ni-Zr, amorphous phase form. in Zr-poor region, hardness and fracture strength (*Japanese*) 0-84914
V-Nb-Ti-N alloy, with dispersed second phase, ductile-brittle transition 0-93653

ductile fracture*see also* **ductile-brittle transition; notch ductility**

- alloys, two-phase, void growth, finite element anal. 0-64383
 α -brass, plane stress ductile fracture, prestrain effects 0-108532
metallic shell, explosive expansion, deform. and rupture modes and mechanisms 0-85064
metallic shell, explosive expansion, rupture behaviour 0-85063
micromechanisms of crack extension, conf., Cambridge, England (March 1980) 0-105421
plastic instabilities and uniaxial tensile ductilities 0-79180
polyethylene film, minimum running thickness, biaxial extensional flow study 0-100993
steel, C, tensile fracture surface in high press. H₂ at room temp. (*Japanese*) 0-108540
steel, C, tensile props. in high press. H₂ at room temp. (*Japanese*) 0-108501
steel, crack-resistance limit and stress analysis in the ductile state 0-81188
steel, effect of H₂ on phys. and mech. props. 0-101657
steel, low alloy, isothermal tempering effect on acoustic emission during ductile fracture 0-85047
steel, low C, crack initiation at root of circumferential notch of round bar specimens (*Japanese*) 0-60947
steel, low C, type En3, high strain deform., struct. and props. 0-89301
steel, low-C, S10C and 520C, tensile fracture at low temps. (*Japanese*) 0-81163
steel, Mn-B-V, low alloy, transform. singularities (*Russian*) 0-104116
steel, Ni-Cr-Mo and Cr-Cu-Mo and sintered, ductile fracture, microvoid effects (*Japanese*) 0-108542
steel, pearlite, deform. and fracture mechanisms, HV SEM obs. 0-104243
steel, stainless, fracture and crack tip plastic zones, in situ obs. 0-108686
strain hardening and damage relationship 0-108564
Al alloy 2024-T4, ductile fracture, microvoid effects (*Japanese*) 0-108542
Al-Cu-Si-Mn, type 2017S-T4, crack initiation at root of circumferential notch of round bar specimens (*Japanese*) 0-60947
Al-Mg-Si alloys, ductile intergranular fracture mechanisms, void formation and nucleation 0-108578
Be-Ni(Y)(Al), plastic deform., flow stresses, fracture (*Russian*) 0-108496
 α -Fe whiskers, pure, ductile fracture initiation, macroscopic obs. of deform. history and failure 0-85043
 α -Fe whiskers, pure, ductile fracture, microscopic obs. of initiation mechanism 0-85044
Mo-Nb-Ti-N alloy, with dispersed second phase, ductile-brittle transition 0-93653
Mo-Ti-N alloy, with dispersed second phase, ductile-brittle transition 0-93653
Nb-W-Zr-N alloy, with dispersed second phase, ductile-brittle transition 0-93653
V-Nb-Ti-N alloy, with dispersed second phase, ductile-brittle transition 0-93653
Zn, pure single cryst., fracture stress 0-104269
Zr-Nb (2.5 wt.%), nuclear fuel channels, neutron effects on ultimate fracture strength, 293 to 573K 0-85054

ductility*see also* **ductile fracture; notch ductility**

- austempered reinforcing wire, tempering under stress, effect on mech. props. and relaxation resistance 0-100861
crack extension rates in ductile materials 0-96230
metal, ductile, jet-impingement solid-particle erosion testing, halo effect 0-76376
metallic fibre knitted gauze permeable materials, mech. props. 0-66607
microcrystalline alloys, metastable, rapidly quenched particulates, props. appl. and production 0-84887

ductility continued

Nimonic 105, creep and stress rupture props., trace elements influence 0-66602
 nonferrous metal, semi-brittle, high-speed backward extrusion using superimposed hydrostatic press. 0-84865
 plastic instabilities and uniaxial tensile ductilities 0-79180
 PMMA, ductile glassy, notch brittleness under plane strain 0-100900
 polycarbonate, ductile glassy, notch brittleness under plane strain 0-100900
 polyethylene surface-growth fibres, hot drawing 0-97517
 PVC, ductile glassy, notch brittleness under plane strain 0-100900
 steel, alloy, deformation, rapid dynamic, at -196°C 0-104220
 steel, alloy high-C, amorphous, mech. props. and thermal stability 0-76361
 steel, austenitic, ageing and plastic deform. effect on struct. and mech. props. of N15Kh5G3T3 (*Russian*) 0-71691
 steel, austenitic, strength, ductility and fracture toughness, N and Cr effects 0-100878
 steel, austenitic stainless Ni-Cr, heat resist. and comp. of non-metallic inclusions, effect of La, Nd, Pr and Ce 0-76315
 steel, C, plates, residual elements effect on through-thickness props. 0-66660
 steel, cast automatic couplings, yield strength, crack propag. resistance and ductile-brittle transition temp. 0-104281
 steel, Cr-C (1, 1 wt.%), hot ductility and S segregation 0-66594
 steel, Cr-Mo-(V) austenitic, creep resist., high-temp. props. residuals effect 0-66600
 steel, Cr-Mo-V, strength and ductility in creep, purity influence 0-66598
 steel, Cr-Mo-V low-alloy, high-temp. ductility and crack growth, impurities effect 0-66652
 steel, Cr-Mo-V low-alloy, mech. props. and stress relief cracking, effects of impurities and deoxidation practice 0-66599
 steel, Cr-Mo-V low-alloy with high residual element content, cavitation control 0-66663
 steel, Cr-Ni-C (3, 1, 0.6 wt.%), grain boundary sulphide precip. and hot ductility (*Japanese*) 0-71654
 steel, ductile structural, fatigue crack propag. rate and striation spacing 0-93635
 steel, eutectoid, mech. behaviour, thermomech. treatment effects 0-84970
 steel, ferritic, creep resist., high-temp. props. residuals effect 0-66600
 steel, ferritic stainless, type 444 welds, ductility loss mechanism 0-85002
 steel, high strength, failure stress, structural relationships 0-81190
 steel, high strength, treatment effect on ductility and strength 0-60880
 steel, high-strength tool steel D7KhFN, remelting effect on mech. props. 0-76284
 steel, low alloy, S and Mn influence on high temp. strength and ductility after solidification from melt (*German*) 0-81106
 steel, low-alloy, bearing, mech. props., carbide behaviour effect (*Korean*) 0-93615
 steel, low-alloyed, C-content influence on high temp. strength and ductility after solidification from melt (*German*) 0-81105
 steel, maraging, ductility and resist. to deform., -196 - 1000°C 0-89313
 steel, martensitic stainless, in SO_4 solns., activation pH and susceptibility to H_2 assisted stress corrosion cracking 0-97619
 steel, Mn-B-V, low alloy, transform. singularities (*Russian*) 0-104116
 steel, Mn-Mo, castings, mech. props., Cu and Sn trace elements effect 0-66596
 steel, Mn-Nb-Al-C, crack propag. and hot ductility during straightening concast strand 0-66646
 steel, Mn-Sn-(Nb), extra low C, shear transformation struct. (*German*) 0-60873
 steel, stainless, 304, bend test ductility of irradiated specimens for LMFBR appls. 0-104235
 steel, stainless, creep limit, cyclic load component effect at high temps. 0-104231
 steel, stainless, deformation, rapid dynamic, at -196°C 0-104220
 steel, stainless, stress corrosion testing, slow strain rate, elevated temp. and high press. study 0-97615
 steel, stainless casts, creep ductility, Auger spectroscopy study 0-60917
 steel, structural 15KhNMF, resist. to weakening during tempering, high purity effect 0-76279
 steel, type IN-787, for use in Arctic, low temp. effects on mech. props. 0-76310
 steel, welded-joints, H_2 induced cracking, S content effect 0-97562
 TZM-Mo alloy, mech. props., effect of exposure to high temp. He containing O_2 , room temp. study 0-93639
 Zircaloy-2, mech. props. after exposure to I_2 -methanol solutions, SEM study 0-93689
 Al foils, high strength, vapour deposited on curved surfaces, quantitative characterisation 0-80144
 Al, strain rate sensitivity and ductility, trace element conc. effect 0-66597
 Al-Cu (4.6 wt.%), cold work and ageing influence on ductility and fracture behaviour (*Japanese*) 0-89295
 Al-Cu-Mg/mica particulate composite mech. props. 0-100919
 Co-Ni-Mo-C, amorphous alloys, med. props. and thermal stability (*Japanese*) 0-85049
 Cu, polycryst., creep and fracture behaviour, effects of prestrain and O 0-97544
 Cu-Ni, cast, strength and hot ductility, alloying and residual elements effect 0-66595
 Cu-Ni-Zn-Mn fine grained precipitation-hardenable alloy, high strength and ductility 0-100805
 $\text{Cu}_{60}\text{Zr}_{40}$, amorphous, ductility and stress relief, low-temp. annealing effects 0-76296
 Fe, ductile, influence of crack tip sharpness and morphology of graphite on K_{IC} (*Chinese*) 0-81144
 Fe-Al-Si (6.22, 9.63 wt.%), bending test under high press., high temp. 0-85057
 Fe-Co-Mo-C, amorphous alloys, med. props. and thermal stability (*Japanese*) 0-85049
 Fe-Cr-Al, HOS 875, oxidation, cyclic, role of thermal shock 0-97640
 Fe-Cr-Co, ductile magnet alloys, mech. props. 0-85001
 Fe-Cr-Co (28, 10.5 wt.%) ductile magnet alloy, humidity-induced H_2 embrittlement 0-89406
 Fe-Mo-CaF₂ sintered composite, struct. and mech. props., heat treatment effect 0-66526
 Fe-Ni-Al-Co-Cu-Ti YuNDK type, S effect on mech. props. 0-60927
 Fe-Ni-Al-(Cu) (12, 0.5, 0.5 to 3 wt.%), Cu addition strengthening at 77K, mech. props. 0-60875

ductility continued

Fe-Ni-Mo-C, amorphous alloys, med. props. and thermal stability (*Japanese*) 0-85049
 Fe-Ni-Ti-(Cu) (12, 0.25, 2 wt.%), Cu addition strengthening at 77K, mech. props. 0-60875
 Fe-Ni-V-(Cu) (12, 2, 2 wt.%), Cu addition strengthening at 77K, mech. props. 0-60875
 Fe-Ni-(Cu) (12, 0.5 to 3 wt.%), Cu addition strengthening at 77K, mech. props. 0-60875
 ($\text{Fe}_{100-x}\text{Ni}_x$)_{83B17}, amorphous, crystn. 0-75176
 Ir-W (0.3%), grain boundary comp., trace element additions effect 0-66661
 Mo fibre reinforced Cu, rule of mixtures of deform. parameters in stage III 0-97532
 Mo fibre reinforced Cu with weak interfaces, stability of tensile deform. 0-97533
 Mo, mech. props., effect of exposure to high temp. He containing O_2 , room temp. study 0-93639
 Mo powder, influence of powder reduction processes on props. 0-89175
 Nb-He, mech. props. and microstruct. 0-85003
 Nb-Ni amorphous alloys, glass transition and ductility, O additions effect 0-75168
 Nb-Si(-V)(Zr)(Mo)(Ta)(W)(C)(B)(Ge), ductile amorphous, superconductivity 0-60131
 Ni base alloys, IN-702, IN-601, TD-Ni-Cr-Al, B-1900+Hf, oxidation, cyclic, role of thermal shock 0-97640
 Ni, ductility and fracture, nonmetallic inclusions effect 0-104221
 Ni-base superalloys, powder metallurgical, creep-rupture at intermediate temps. 0-97568
 Ni-based superalloys, hot workability, effect of S, Ca, Mg, Y and Zr minor elements 0-66552
 Ni-Cr, heat-resist., high-temp. ductility and embrittlement 0-76314
 Ni-Cr Nimonic alloys, mech. props., high-temp. irradiation effects 0-100885
 Ni-Cr superalloy, interactions between creep and low cycle fatigue (*Chinese*) 0-66572
 Ni-Cr-Al sintered alloy, hot vac. pressure, fracture and mech. characts. 0-66667
 Ni-Si-B, amorphous, thermal stability of ductility 0-76327
 Ni-ThO₂, oxidation, cyclic, role of thermal shock 0-97640
 Pd-H, mech. props., influence of dissolved H_2 (*Russian*) 0-81109
 239PuO₂, stoichiometric, high-temp. deformation 0-81111
 Ta single crystal, H_2 embrittlement (*Japanese*) 0-66636
 Ti-Al-V (6.4 wt.%) superplastic alloy, maximum attainable ductility 0-60919
 Ti-Mo-Zr-Sn (11.5, 6, 4.5 wt.%), β III, mech. props. rel. to heat treatment 0-84961
 Ti-Ni amorphous alloys, glass transition and ductility, O additions effect 0-75168
 α -U, strain rate effect on tensile flow and fracture 0-84992
 U-Mo (2 wt.%), depleted, effect of microstruct. on mech. props. 0-108497
 Zn-Al(22 wt.%), alloy sheet, superplastic, cold-rolling effects on mech. props. and microstructure (*Japanese*) 0-71671
 Zr-Al (8.6 wt.%), fast neutron irradiated, tensile props. and fracture toughness 0-84994
 Zr-Cu amorphous alloys, glass transition and ductility, O additions effect 0-75168

duplicating see reproduction (copying)

dusk see twilight

dust

see also cosmic dust
 airborne, dust fallout in Kuwait, summer 1978 obs. 0-81966
 airborne, Nigeria during dry dusty season 0-81960
 airborne, Saharan dust affecting radiative transfer rates, model 0-90149
 atmosphere, dust grains mean radius rel. to transparency meas. on Maidanak mountain (*Russian*) 0-72627
 atmosphere, dust haze of African Harmattan wind, 1962-1973 visibility obs. 0-61900
 atmosphere, Harmattan dust deposition rel. to visibility, wind and solar rad. 0-94578
 atmosphere, near IR absorpt. due to soot particles (*Russian*) 0-82055
 atmosphere soil-derived dust, Christiansen effect in IR spectra, Rayleigh limit 0-105046
 atmospheric, airborne metal conc. rels. in industrial district, nuclear anal. technique 0-72107
 charged, rotating, cylindrically symmetric interior soln of Einstein-Maxwell eqns. 0-82688
 contaminant particle microanalytical methods 0-86397
 destruction degree, determ. in mech. screening 0-66882
 dielectric constant at X-band, effect of moisture content 0-72578
 explosion, flame propag. vel., uniform dispersion of single sized particles 0-66803
 fluid containing dust particles, laminar boundary layer flow, 2-D stagnation point near oscillating plate 0-64606
 fly ash particles, water accretion, refract. index and accreted layer thickness 0-58462
 IR Test-1 lidar obs., transmission meas. 0-99625
 optical component protection in dusty environments, electrostatic techniques 0-58657
 pulmonary fibrosis disease diagnosis, histological section SEM and energy-dispersive X-ray microanalysis 0-72314
 retention effect on pressure drop, in high vel. pulse-jet fabric filter 0-103072
 Sharav (Khamisin) dust storm, optical depth and particle size distrib. 0-90162
 smoke/dust cloud temporal analysis algorithm 0-98484
 soil-derived atmospheric dusts, particle absorption contributions to mass extinction coefficients 0-61896
 sphere, slowly rotating, maximal slicing condition, initial value equations 0-73246
 stratosphere, dust collected from interplanetary space, visible absorpt. spectra 0-101554
 velocity measurement of charged dust particles using laser Doppler velocimeter 0-95083
 volcanic dust in atmosphere, correl. with N.Hemisphere average temps. during Little Ice Age 0-82050
 volcanic dust in stratosphere, effect on radiation reaching Earth surface 0-82035

dust storms *see storms*

dwarf stars

see also white dwarfs

- AE Aquarii, cataclysmic variable, IUE satellite UV obs. 0-72985
late B dwarf in circumstellar dust cloud, IR source coincident with OH 205.1-14.1 0-101630
ξ Bootis A, late-type dwarf star, mag. field obs. 0-72949
α Centauri binary system, spectroscopic chemical anal. 0-62128
UV Ceti stars, photometric features near flare initial phase 0-105252
EM Cygni, cataclysmic variable, red and white dwarf binary, period change, B photometry 0-90434
θ Cygni, F-type dwarf star, spectral type of faint distant companion 0-90481
degenerate star, accretion process giving rise to X-ray emission 0-90459
BY Draconis stars, angular momentum initial distrib. and evolution 0-85954
F, G, K-type stars, chromospheres, wave dissipation of mechanical energy 0-82340
F, G and K-type stars, chromospheric radiative losses in continuum 0-72924
flare stars, flare emission spectrum rel. to fast electron hypothesis 0-67731
flare stars, multichannel spectrophotometry 0-105256
flare stars in Pleiades, spatial distrib. using recovery method (*Russian*) 0-94722
flare stars in Scorpius-Ophiuchus region, discoveries (*Chinese*) 0-77418
flare stars in Taurus Cloud, comparison with ρ Ophiuchi flare stars, visible obs. (*Chinese*) 0-85957
G 208-44/45, possible double flare star, spectral obs. 0-67727
YY Geminorum, eclipsing binary, photometry and orbital period study 0-105287
Gleise 490 AB (BD+36°2322), red dwarf binary, flares and starspots, rot. period determ. 0-77423
HD 25329, subdwarf, metal deficiency from spectroscopic anal. 0-62122
HD 45088, BY Draconis binary, surface activity from high rot. vel., visible obs. 0-77425
HD 45088, reticon obs. in red of dK3 spectroscopic binary 0-67778
AM Herculis, M-type component detect. from spectrophotometry at min. light 0-98692
DQ Herculis, red and white dwarf eclipsing binary, emission line eclipse phenomena 0-94800
high galactic latitude stars, division into giants and dwarfs by proper motion (*Russian*) 0-109431
hot subdwarfs in Carochan and Wilson catalogue, UV spectra 0-82354
Hyades metal content and distance rel. to solar colour 0-101569
e Indi, late type dwarf star, model atmosphere 0-90425
K dwarfs assoc. with X-ray transients A060-00 to A1742-28, visible and IR obs. 0-101653
EV Lacertae, flare star, photometry and spectrum rel. to starspots and rot. period 0-98665
late type temp. minima, chromosphere models 0-67717
LB 3479, subdwarf eclipsing binary, evolutionary model comment 0-90426
M-type dwarf stars in galaxy cluster Abell 2029, coronal X-ray emission rel. to SAS 3 obs. 0-82519
M-type dwarfs, space densities derivation via new matrix method 0-85932
M-type stars in halo of galaxy NGC 4565, identification from grid photography 0-62261
metal abundances of F- and G-dwarfs from CORAVEL radial vel. scanner 0-94791
novae, effect of red dwarf companion on outburst 0-82394
old dwarf stars, kinematics rel. to Galaxy initial contraction 0-62204
70 Ophiuchi A, late-type dwarf star, mag. field obs. 0-72949
parallax and proper motion meas. for seven stars 0-62109
planetary nebulae central stars, temps. determ. rel. to nebulae evolution 0-67724
proper motion stars in direction of galactic centre (*French*) 0-77404
VV Puppis, polar, evidence for M-type companion from IR photometric obs. 0-98687
red dwarfs, nature of flares optical continuum (*Russian*) 0-109445
red dwarfs in southern hemisphere, absolute magnitude and distance, BVRI photometry 0-90419
red nearby star suspects selection from Luyten proper motion catalogues, use of Luyten's magnitude estimates 0-82353
WZ Sagittae, image-tube spectroscopic obs. of 1978 Dec. outburst 0-72958
Stepanyan's star, obs. of G8 V absorpt. spectrum and emission spectrum 0-67788
subdwarf ionization equilibrium 0-90421
subdwarfs, 37-45 excess calibration using Fe/H abundances 0-82363
subdwarfs, masses and metal abundances from spectroscopic anal. 0-62122
subdwarfs, photometry rel. to compositions and kinematics 0-82364
subdwarfs, Population II, luminosity functions in SA 51, SA 57 and (SA 68) 0-98648
subdwarfs in 47 Tucanae, CN vars. 0-94794
thermonuclear bursts assoc. with chromosphere flares 0-98684

dye lasers

- aerosols of dye solutions as active media 0-95887
4-amino-N-methylphthalimide in n-propanol, nanosecond laser fluorometry 0-102721
amplifier, DC elec. field effects 0-64006
amplified spontaneous emission in dye solutions, effect of O₂ 0-95885
anisotropy of amplifying props., dye laser oscillator and amplifier in liq. cryst. matrix 0-74355
anthracene derivatives in solution, polarisability and dipole moments, emission and absorpt. spectra obs. 0-69256
beam expander for short cavity dye laser 0-87532
benzoxazole, aromatic derivatives, spectral luminesc. and lasing props. rel. to electronic struct. 0-99519
book, quantum electronics 0-105442
carbazine 720, single freq. CW dye laser operation in 690-700 nm gap 0-99719
conference, laser and electro-optical systems, San Diego, CA, USA (Feb. 1980) 0-62392
CW dye laser, cavity configuration anal. (*Chinese*) 0-64010
CW dye laser single mode, tunable 0-106534
cylindrical active element with sheath, radiation intensity distrib. calc. 0-58531

dye lasers continued

- deterioration of dye, effect on performance 0-83602
DFB, single-mode operation 0-74409
DFB laser, N₂ laser pumped, self Q-switched, tunable picosecond pulse generation 0-69432
DFB laser, noncollinear wave interaction 0-99722
DFB laser with integrated Si and polyurethane channel waveguide 0-74373
9,10-dichloroanthracene with iso-amyl acetate or esters as solvents, dye laser material 0-74354
3,3-diethyl thiadibocyanine iodide dye, stimulated fluoresc. and stimulated reson. Raman scatt. relationship 0-91853
DODCI in ethanol, DQOCI added, electronic energy transfer, real-time ps meas. 0-58311
DODCI in ethanol, malachite green added, electronic energy transfer, real-time ps meas. 0-58311
double grazing-incidence single-mode dye laser 0-95906
double mode-locked CW, pulse cross-correlation studies 0-69389
dye activated CLC, distributed feedback, tunable radiation generation (*Russian*) 0-102720
emission locking onto wavelength of I₂ mol. fluoresc. 0-99721
fast mode-locking dyes, IR fluoresc. and laser action obs. 0-102717
flash lamp pumped, tuning by grazing incidence grating technique 0-95914
flashlamp-pumped, pump source for colour centre laser 0-102737
flashlamps, coaxial and preionised linear, comparison as pumping sources for high power dye lasers 0-102730
frequency locking by injection, CW and delta pulse regime anal. 0-87389
internally pumped mode-locked CW, theory 0-91787
intracavity absorber effect on laser characts. with forced mode synchronisation 0-78873
metastable state relaxation time determ. 0-102719
β-methylumbelliferone in ethanol solns., spontaneous luminesc. kinetics 0-74192
mode self-synchronisation in dye laser with continuous pumping 0-83605
mode-locked, synchronously pumped, pulse-width stabilization 0-83622
nanosecond laser fluorometry, spontaneous and stimulated emission kinetics 0-102721
nonlinear transmission including stimulated emission influence 0-99720
optically induced distributed feedback prod. of single ultrashort pulse 0-64067
organic scintillators, vap. phase dye laser media, photophysical parameters 0-95884
organic solutions, lasing, excitation by excimer laser radiation 0-64007
output coupling, optimisation by consideration of spatial gain distrib. 0-83603
oxazine 720, single freq. CW dye laser operation in 690-700 nm gap 0-99719
phenyloxazolyl pyridinium salt dye lasers, flashlamp pumped, blue-greenlasing 0-95886
picosecond pulse emission, stable, multifreq., phase-locked radiation pumped CW dye laser 0-91789
picosecond pulse generation, excitation by passively mode locked Ar laser 0-95930
polymethine dye lasers, optical absorpt. 0-64009
polymethine dye nonequilibrium, protolytic forms, lasing, fluoresc. and nonradiative transitions 0-102722
polyphenyl 1 laser dye for pulsed and CW operation in UV 0-78850
POPOP solution dye lasers, multiplate reflectors 0-83606
POPOP vapour lasing, buffer gases influence, theory 0-91790
pulse structure and cavity length determ., synchronously pumped picosecond laser 0-95935
pulsed, transient behaviour 0-69388
pulsed and CW laser comparison for reaction product excitation spectra meas. 0-76574
pulsed opto-acoustic spectroscopy 0-62743
pulsed oscillator-amplifier system, high power narrowband, design and operation 0-58570
pumped by Nd:YAG, stimulated Raman scattering appl. 0-69451
resonant Rayleigh-type mixing spectroscopy using ps light pulses, ultrafast relax. study 0-91834
review of dye laser devices, book contrib. 0-106517
rhodamine, activated 6G top layer in slab-type directional coupler, amplified oscill. 0-99718
rhodamine 6G dye in ethylene glycol, broadband optical diode, one directional traveling wave operation of ring laser 0-58606
rhodamine 6G dye in quartz glass microcomp. matrix, as tunable solid laser 0-99734
rhodamine 6G dye laser, induced radiation spectral characts., effect of vibr. relax. 0-64008
rhodamine 6G ethanol soln., absorpt. and luminesc. spectra using picosecond excitation 0-106351
rhodamine 6G laser radiation interaction with Al 0-97387
rhodamine 6G solution, absolute fluoresc. quantum yield determ. by calorimetric method 0-78851
rhodamine 6G-safranin-T mixed dye laser energy transfer, 31 nm tuning range 0-58532
rhodamine G solutions, LiCl and NaClO₄ electrolyte influence on its lasing props. 0-91788
rhodamine-6G mode locked dye laser pulse width monitoring by rapid scan autocorrelator 0-87421
ring, optical bistability and first order phase transition 0-95918
ring laser, CW, optical diode to enforce one-direction travelling wave operation 0-69427
SHG, computer controlled intracavity, in CW ring dye laser 0-91841
single-frequency pulsed dye laser with injection of low-power radiation 0-99756
single-mode and multimode CW, as sources for obtaining power-squared corrected two-photon spectra 0-78849
spectral properties, hole-burning effects 0-102718
subnanosecond pulse generation with N₂ laser pumping, laser design 0-87403
synchronously mode-locked CW laser, intracavity SHG in thin NH₄H₂PO₄ cryst. 0-95945
thin film waveguide evanescent type, gain meas. 0-95908
thin-film waveguide laser amplifier with lossy cladding 0-64074
three-stage birefringent filter, tuning over visible region 0-58667
TOPOP vapour dye lasers with multiplate reflectors 0-83606
tricarboyanine near IR dyes, flashlamp-pumped, photochemical stability 0-83604

dye lasers continued

- tunable, 545-680 nm radiation efficient conversion to 360-415 nm UV range 0-74439
- tunable dye laser, N₂-laser pumped, using single prism beam expander (*Chinese*) 0-74389
- tunable laser interferometry, oscillator strength meas. 0-105697
- tunable ultrashort pulse generation 0-95931
- tuning by multistage interference polarisation filter 0-64091
- ultrashort pulse generation 0-58612
- unstable resonator calculation, laser operating on organic compound solution 0-58600
- VUV radiation, narrowband tunable, at Lyman- α wavelength 0-78907

dynamic braking *see braking***dynamic nuclear polarisation**

- see also CIDNP; Overhauser effect; solid effect*
- ⁶LiD, polarised target material, DNP 0-87007
- ZnTe:Mn²⁺, forbidden transitions of Mn²⁺ induced by hyperfine interactions 0-60458

dynamic programming

- see also integer programming*
- Attached Processor for Speech 0-96145
- automatic speaker verification by cepstral analysis 0-91998
- continuous speech recognition system for data base consultation 0-91990
- syllable-based recogniser for continuous speech 0-91986

dynamic response

- bone mechanical properties characterisation by dynamic response 0-76782
- elastodynamic equation on sphere, tensor spherical harmonics appl. 0-98296

dynamic stability *see stability***dynamic testing**

- see also fatigue testing*
- alloys, shape memory effect, device for testing in bending 0-66723
- bar-to-block based testing method for materials characteris. in high-vel. tension 0-85133
- biaxial loading techniques and apparatus, cruciform specimen, elec. motor and hydropneumatic based devices 0-85129
- brass, crack initiation at high strain rates, uniaxial and biaxial tests 0-85141
- coke, metallurgical, industrial strength meas. methods, critique 0-85117
- cyclic strain diagrams recording under nonisothermal conditions, review 0-71830
- fatigue crack growth testing, computer-controlled stress intensity gradient technique 0-76432
- glass fibre reinforced plastics, exposed to liq. media, dynamic high-speed Young's modulus determ. (*German*) 0-85123
- hermetically sealed box, dynamic testing system, vacuum or controlled environment (*French*) 0-61060
- high strain rate behaviour, incremental elastic-viscoplastic constitutive eqns. integration 0-85138
- Homalite-100 plates, modified compact-tension specimens, dynamic anal. 0-97561
- hot metal, dynamic yield characts. during multistage deform., plastometer design 0-85135
- laminates, exposed to liq. media, dynamic high-speed Young's modulus determ. (*German*) 0-85123
- limestone tubes, dynamic torsional failure obs. 0-85648
- metal, FCC, dislocation behaviour at high strain rates, US detection method, data analysis basis 0-85136
- metal, strong, compressive stress/strain props. meas. at very high strain rates, modified Hopkinson bar system 0-85128
- metallic thin spring strip, bending test device 0-61052
- plastics testing, automation 0-76443
- poly(di-n-heptyl itaconate), alkyl side chain independent relax., double glass transition 0-59636
- polycarbonate plates, modified compact-tension specimens, dynamic anal. 0-97561
- polyethylene, high-density, impact fracture behaviour, adiabatic heating at crack tip 0-85142
- polyethylene, linear, draw temp. and mol. wt. effect on draw ratio and Young's modulus 0-84998
- polyethylene, rheological behaviour at high shear strain rates (*French*) 0-66574
- polymer multilayer composite, wire-reinforced, dynamically loaded, crack propagation and arrest 0-97567
- porcelain-metal cermet, stress determ., meas. method (*German*) 0-76425
- radial expansion technique for fracture strain meas. at high strain rates 0-85134
- split Hopkinson pressure bar application to fracture dynamics 0-85140
- steel, low alloy, S and Mn influence on high temp. strength and ductility after solidification from melt (*German*) 0-81106
- steel, low and medium C, dynamic and static strength, strain rate and temp. depend. of flow stress 0-85139
- steel, low-alloyed, C-content influence on high temp. strength and ductility after solidification from melt (*German*) 0-81105
- steel, mild, plastic flow localisation under dynamic torsional loading, crit. variables 0-85015
- steel, stainless, austenitic, dynamic uniaxial and biaxial stress-strain relationships 0-81122
- steel, types S25C and S45C surface damage produced by pulsating impact contact load (*Japanese*) 0-104263
- steel (*German*) 0-100869
- stress corrosion cracking test machine, design and construction, appl. to Fe-Cr-Ni alloys 0-97649
- structural deformation under dynamic loading, state variable description of material behaviour 0-85137
- superplastic flow, activation enthalpy determ. from strain rate changes in tensile tests 0-81127
- tensile testing of small animal ligaments, gripping device 0-81791
- torsion bomb machine for dynamic stress/strain measurements under superimposed high press. 0-85130
- Al alloy, crack initiation at high strain rates, uniaxial and biaxial tests 0-85141
- C fibre reinforced composite, split Hopkinson press. bar test, opt. and strain gauge methods comparison 0-85132
- Cu, high-purity, grain size and strain rate influence on mech. behaviour, precursors existence 0-85016

dynamic testing continued

- Si₃N₄, hot-pressed, fracture mech. parameters, indentation-precracking and double-torsion methods 0-104364
- α -U, mech. props. at very high strain rates, double-notch shear test use 0-85131

dynamical symmetry

- δ -function regularisation, symmetric spaces of rank 1, physical instabilities 0-57519
- cosmology, Lagrangian or Hamiltonian formulations, shift vector field restrictions, symmetry group 0-67923
- first integrals and differential forms of dynamical systems 0-77983
- free particle, Hamiltonian mechanics, Lie theory of extended groups 0-77982
- Hamiltonian mechanics, Lie theory of extended groups 0-77982
- invariant sets of dynamical system 0-57518
- lattice gauge theories, chiral symmetry dynamical breaking 0-99061
- left-right symmetry breaking and fermion masses 0-105810
- models of dynamically broken gauge theories 0-77974
- nonlinear dissipative classical systems, time-depend. canonical transforms. 0-62885
- pseudosymmetries and first integrals of dynamical systems 0-57517
- QCD, 1+1 dimens., dynamical symmetry breakdown 0-82949
- Schrodinger equations, 3-D, rotationally invariant time-dependent potentials, degeneracy and dynamical algebras 0-62510
- second order differential equations, symmetries and invariants 0-82915
- SL(2,R) dynamical Lie group, hyperbolic transforms 0-57515
- Sp(3,R) matrix elements, recursion formula 0-62878
- SU(N) symmetric quantum dynamical systems, N $\rightarrow\infty$, energy spectrum for singlet and adjoint states 0-62880
- H, n-dimensional atom, Kepler problem, dynamical symmetries 0-58121

dynamics

- see also ballistics; fluid dynamics; force; friction; haemodynamics; impact (mechanical); kinematics; resonance; rotating bodies; rotation; vibrating bodies; vibrations*
 - chain of flexible bodies, appl. to NASA Space Shuttle remote manipulator arm 0-94953
 - clusters of galaxies, tidal forces in inhomogeneous cosmological models 0-62338
 - Coma galaxy cluster, dynamics rel. to mass segregation and missing mass 0-98730
 - deterministic dynamics to probabilistic descriptions 0-68029
 - education, circular motion with friction, numerical and analytical solns. 0-57029
 - galaxy cluster interaction with supercluster, model of Emden sphere embedded in background 0-62296
 - galaxy clusters, struct. and dynamics distortion by inclusion of spurious clusters 0-101643
 - Galaxy disc, local K₂-force field rel. to interstellar matter z-distrib. 0-62271
 - gravitational system dynamics, two-dimensional simulation rel. to Universe large-scale struct. form. 0-98749
 - homoclinic and heteroclinic points in Hemon mapping, analyticity 0-82634
 - interstellar large globules, struct. and dynamics 0-62246
 - Lagrangian-Hamiltonian systems, partial quantisation (*Portuguese*) 0-77653
 - LMC, kinematics and dynamics compared to galaxies of Magellanic type (*German*) 0-105348
 - MHD generator channel, liquid metal piston dynamics, math. model (*Russian*) 0-74996
 - N70, giant filamentary shell in LMC, dynamics 0-90511
 - NGC 1023 galaxy group, H I radial vels. rel. to group membership and mass/light ratio 0-82521
 - NGC 3686 galaxy quartet, crossing time from galaxies surface photometry 0-62297
 - NGC 741, 1316, 7626, radio galaxies, dynamics 0-94871
 - nondissipative system, universal properties, bifurcation phenomena and universal numbers 0-68035
 - one-dimensional self-gravitating isothermal systems, stability 0-73008
 - open star clusters assoc. with interstellar gas-dust clouds, dynamics 0-101622
 - orbital dynamics and rigid body dynamics, analogy 0-98537
 - planetary satellite ejecta, effect of proximity to Roche limit on dynamics 0-98592
 - rotationally periodic large space structures, finite element transfer matrix dynamic analysis, 100 m parabolic dish 0-74731
 - Shahbazian 1 group of galaxies, dynamics from spectroscopic. obs. 0-67878
 - solar surges, dynamics of descending stage (*Chinese*) 0-105221
 - spring-mass systems, transfer props. of nonlinear resonators (*German*) 0-98793
 - star clusters dynamics, higher order fluid eqns. for multicomponent nonequilib. systems 0-105156
 - stellar system dynamics, field of directions of motion in Contopoulos potential (*Russian*) 0-62205
- dynamometers**
- see also force measurement*
 - electrodynamometer modification for realization of ampere at NBS 0-98938
 - hydraulic universal testing machine, K value determ. (*German*) 0-90836
 - strain gauge system, body of rotation form, non axially symm. load 0-73350
- dysprosium**
- see also nuclei with*
 - adsorption on W, field emission electron study 0-100393
 - atom, isotope separation, laser excitation, charge exchange with Cs⁺ ions 0-83512
 - atoms, prod. in nucl. reaction, K-shell ionisation cross-sections meas. 0-78687
 - atoms, visible spectra obs., hyperfine struct., mag. dipole and electric quadrupole interaction const. anal. 0-91698
 - domain effects near order-disorder and order-order ferromagnetic transitions 0-65886
 - interstitial site determ., μ SR technique 0-71287
 - magnetic domain structure, hysteresis, thermal modulation study 0-71082
 - magnetocaloric effect and mag. phase transitions, 80 to 300K 0-60279
 - neutron radiographic film imaging systems, MTFs and resolution capabilities 0-66758
 - Al-Al₂O₃-Dy thin junctions, Poole-Frenkel effect obs. and cause 0-80398
 - Bi₁₂GeO₂₀:Dy, luminesc., emission and excitation spectra 0-103975

dysprosium continued

- CaF₂:Dy, dimer reorientation activation volume 0-107285
 CaF₂:Dy, TLD-200, thermolum. phosphor, photolum. and absorpt. spectra, thermolum. mechanisms 0-97321
 CaF₂:Dy³⁺, ¹⁹F NMR studies 0-60429
 CaSO₄:Dy, phototransferred TL studies 0-80875
 CaSO₄:Dy, TLD-900, thermolum. stability at low radiation doses 0-101272
 CaSO₄:Dy, thermolum. phosphor, photolum. and absorpt. spectra, thermolum. mechanisms 0-97321
 CaSO₄:Dy, thermoluminescent glow peaks, post γ -irrad. annealing study 0-89077
 CaSO₄:Dy ribbon, dosimetric props. study 0-63395
 CaSO₄:Dy sintered pellets, thermolum. response 0-93411
 CaSO₄:Dy TLD phosphor, γ radiation changes in glow curve 0-60688
 CaSO₄:Dy Teflon TL dosimeters, thin, development for β -dosimetry in personnel monitoring 0-63399
 Dy, isotope shift meas. using laser atomic beam technique specific mass shift determ. 0-91497
 GaP:Dy epitaxial films, photoluminesc. spectra 0-66294
 SrF₂:Dy³⁺, cluster form., IR absorption study (*French*) 0-108240
 ZnO:Dy, electrolum. brightness, field strength and freq. depend. 0-100696

dysprosium alloys

- Au-Dy, dil., hyperfine interaction, Mossbauer study, Kramers quartets 0-66083
 Dy-Cu, amorphous, mag. phase diagram, magnetisation and sp. ht. meas. 0-80532
 DyAg_{1-x}In_x, elec. and Hall resist. 0-96844
 Dy(Co,Ni)₂, intrinsic mag. aftereffect meas., domain wall motion 0-71121
 DyCo₂-DyAl₃ system, mag. and structural studies 0-108006
 DyCo₃ noncollinear mag. struct. appearance in mag. fields, magnetostriction meas. (*Russian*) 0-100607
 DyCu film, amorphous, asperomagnetic domains, Barkhausen jumps in hysteresis loop 0-75822
 DyFe₂ and Dy₂Fe₁₇, magnetostriction, room temp. to 80K 0-65993
 DyFe₂ hydrides, desorption isotherms 0-103565
 DyFe₁₇, domain structures and anisotropy constant. 0-93136
 DyFe₂H₂, thermodynamic props., H₂ desorption isotherm meas. 0-89516
 Dy_{1-x}Gd_xAl₃, ordered alloys, hyperfine field, anomalous con. depend. NMR 0-75868
 Dy₂In, mag. props. 0-108009
 Dy₃In, mag. props. 0-108009
 Dy₃Ir₂, cryst. struct. 0-96473
 DyNi, crystal, basal plane anisotropy, torque meas. 0-65857
 Dy₆₉Ni₃₁, amorphous, Curie temp., mag. susceptibility and coercive force, 4.2 to 300K 0-93092
 Dy₂Os, cryst. struct. 0-96474
 DyPt₃, low temp. mag. susceptibility 0-93075
 Dy₂Pt, mag. susceptibility meas., mag. transitions obs. 0-60222
 DyRh_{1-x}Sn_{3x/4}, new supercond./mag. cpds., X-ray powder diff. data 0-100215
 Dy_{1-x}Sm_x, magnetoresist. of polycryst. specimens in fields up to 44 kOe (*Russian*) 0-92880
 Dy₂Tb_{1-x}Fe₂, single cryst., torque meas. 0-65877
 Gd_{1-x}Dy_xNi, FeB-CrB type stacking variations, cryst. struct. 0-64952
 (Ho_{0.98}Tb_{0.02}Dy_{0.22})Fe₂, microwave mag. props. 0-65860
 Mg-Dy, dil., macroscopic shape effect due to quadrupole orientation, magnetostriction and thermal expansion meas. 0-60396
 (Tb,Dy)-Fe amorphous films prep. by cosputtering, magnetoelastic props. 0-97429
 Tb_{0.27}Dy_{0.73}Fe₂, vertically zoned, magnetomechanical coupling and magnetostriction 0-65999
 Tb_{0.3}Dy_{0.7}Fe₂, prep. by powder metallurgy, magnetostrictive props. 0-75826
 Th-Dy, dil., type I superconductor, paramag. Dy moment relax., Mossbauer spectra study 0-65755
 Th-Dy (1 at.%), Heisenberg exchange, residual resist. meas. 0-75558

dysprosium compounds

- see also dysprosium alloys*
 Ce₂Dy_{1-x}C₂, mag. props. 0-108008
 CsDy(MoO₄), permittivity temp. depend., polymorphic transition 0-92670
 DyAG, antiferromag., induced staggered mag. fields 0-65810
 DyAG, antiferromag., induced staggered magnetic fields, microscop. mech. 0-80527
 DyAG, electrostatic model of cryst. field 0-59945
 DyAsO₄, ferroelectricity, dielec. meas. 0-60515
 DyAsO₄, first order Jahn-Teller phase transition, sp. ht. and refr. index meas. 0-59645
 DyAsO₄, phase transitions obs. 0-70412
 DyBi, mag. behaviour 0-71025
 DyCl₃, vapour press. and sublimation thermodynamics, mass loss effusion meas. 0-88313
 DyCo₂Si₂, mag. props. 0-107988
 DyF₃-CsF, phase diagrams and ternary fluorides (*French*) 0-81040
 DyF₃-RbF, phase diagrams and ternary fluorides (*French*) 0-81040
 DyFeO₃, field induced spin reorientation, Mossbauer spectroscopy 0-65878
 DyFeO₃, Raman scatt. from magnons, anisotropy consts. determ. 0-66178
 DyFeO₃, spin reorientation transitions induced by magnetic fields, Mossbauer study 0-71246
 DyFeO₃, weak ferromagnet, μ SR study 0-93226
 Dy₂Ga₂O₇, dipolar magnet, sp. ht. and magnetisation meas. 0-60344
 Dy₂Ga₂O₇, induced staggered mag. fields, neutron diff. study 0-60196
 Dy_{0.8}Ho_{0.2}FeO₃ orthoferrite, domain struct., temp. depend. 0-71086
 DyLG, spontaneous Faraday rot. rel. to sublattice magnetisation 0-66159
 DyN, miscibility with UC (*German*) 0-96654
 DyNi₂Si₂, mag. props., 4.2-200K 0-84602
 DyO, UV emission spectrum, high resolution, band systems and isotopic shifts 0-87146
 Dy₂O₃-ZrO₂ phase diagram and long range ordering 0-93542
 Dy₂O₃SO₄, mag. ordering, magnetisation, AC susceptibility and Zeeman effect meas. 0-60205
 DyPO₄, mag. transitions under hydrostatic press., neutron diff. study 0-71030
 Dy₂Ru₂, Mn₂C₂-type struct., X-ray cryst. struct. determ. 0-96483

dysprosium compounds continued

- Dy₂S₃, optical props. and electronic struct. in fund. absorpt. region 0-80817
 Dy₂S₃, vibr. spectra, factor-group anal. 0-80793
 DyTiO₃, bulk mag. and struct. props., ferrimag. order 0-107993
 DyVO₄, cooperative Jahn-Teller phase transition, linear birefr. meas. 0-88960
 DyVO₄ Jahn-Teller crystal, deform. induced transitions, elastic and dielectric characts. (*Russian*) 0-80726
 DyVO₄, phase transitions obs. 0-70412
 K₂Dy(MoO₄)₂, polarised IR and Raman struct., ⁹²Mo/¹⁰⁰Mo isotope effect 0-108198

E-layer *see E-region***E-region**

- see also sporadic-E layer*
 auroral E-region, enhanced plasma line spectra meas. 0-98507
 cosmic radio noise 'absorbed' by E-region plasma waves 0-82139
 discrete auroral arcs and currents, review 0-77190
 drift variability above Tiruchirappalli, rel. to electrojet strength 0-82129
 electrojet, equatorial, plasma instability and electron density irregularities, HF radar obs. 0-105112
 electron density profile, distortion meas. using group and phase height meas. 0-109299
 electron temp. compared to neutral temp., 100-120 km altitude 0-77211
 fading records over Tiruchirappalli (1973-5), cross spectral anal. 0-101478
 fading records over Tiruchirappalli (1973-5), full correl. anal. 0-101473
 gravity waves at E-region heights, obs. of Es 0-72657
 plasma interaction with electron beam, beam energy distrib. appl. to ionosphere 0-103163
 polar slant-E condition, rel. to polar cap plasma flow entry region longit. position 0-67472
 temperature and wind measurement Fabry-Perot-interferometer imaging system appl. 0-101441
 temperatures and collision freq. in polar regions, incoherent scatter meas. 0-72688
 VHF radar aurora and strong HF backscatt. comparison 0-61960
 whistlers at low latitude, banded struct. origin on refl. from E-region 0-101476

ear

- see also hearing*
 acceleration effects, +Gz influence on semicircular canal function, aircraft appl. 0-94245
 acoustic nerve paths, hearing analysis appl. (*Italian*) 0-94218
 acoustical research into life sciences, review 0-97925
 actin in the inner ear, struct. of the stereocilium 0-108918
 auditory physics, hearing theory physical principles 0-85410
 aural reflex, influence on sound transmission in the inner ear (*Japanese*) 0-81620
 basilar membrane motion in alligator lizard, relation to tonotopic organization and freq. selectivity 0-76753
 cochlea model, acoustic wave reflection and resonance 0-61581
 cochlear, evoked mech. response and the auditory microstruct. 0-94223
 cochlear, struct. and functional changes following US irradi. 0-89791
 cochlear compound action pots., tuning curves and delay times 0-94230
 cochlear fibre responses in guinea pigs with well defined cochlear lesions 0-94226
 cochlear injuries rel. to CM pots. 0-94229
 cochlear mechanics, 5 decade or research 0-76749
 cochlear mechanics, nonlinear behaviour in 2-tone responses 0-76751
 cochlear micromechanics and anatomy, review 0-76750
 cochlear models, 2-tone suppression and second filter 0-76752
 cochlear models-1978 0-94221
 cochlear nonlinear phenomena in two-tone responses 0-94225
 cochlear partition vibration, recent views 0-81617
 cochlear temperature depression in guinea pig caused by anaesthesia and ventral ear surgery 0-97938
 compound PST histogram rel. to neural activity in cochlear 0-94148
 differential electrical excitation of auditory nerve 0-67092
 eardrum vibration meas. using electronic speckle pattern interferometry 0-67209
 hair cells, mechanism of production of summing potential, elec. cct. model 0-72176
 HF audiometry and stapedius muscle reflex thresholds in juvenile diabetics 0-85411
 holography in otology 0-67206
 human, ipsilateral stimulus intensity, tympanometry 0-104592
 implantable middle ear, development prospects (*Japanese*) 0-81775
 inner, sound-induced resistance changes 0-81618
 intracochlear acoustic pressure measurements in guinea pigs 0-94228
 ipsilateral acoustic reflex artefacts measured in cadavers 0-85414
 isobaric counterdiffusion, middle ear gas exchange 0-81798
 lateral line microphonic response to high-level stimuli, analytical model 0-61580
 microwave auditory perception, contrib. of middle-ear structs. 0-67097
 middle, and sinuses, ventilation and clearance using ¹³³Xe 0-98075
 models and signal processing, conf., Munster, Germany (Sep. 1978) 0-90610
 movement of human ear, electronic speckle pattern interferometry in vivo 0-109083
 neonatal acoustic reflex, static and dynamic impedance obs. 0-104597
 nerve fibre model 0-94227
 peripheral auditory adaptation, dependence on recording site 0-81613
 physical principles of audiology, book 0-82592
 primary neurons, comparative physiology 0-94224
 protection systems, attenuation produced at each normal freq., Noise Reduction Rating calc. (*Spanish*) 0-109041
 protectors, relation of attenuation to noise spectra 0-96100
 review of sound anal. by the ear 0-104593
 skin, mouse, fractionation effects in response to combined heat and X-rays 0-76805
 static acoustic-immittance measurements 0-76758
 stereophonic equalisation of artificial heads without exact replication of eardrum impedance 0-81614
 travelling waves and cochlear resonance 0-94222
 tympanic membrane investigations in living man using holographic interferometry 0-67207
 tympanic membrane vibr. studies in living man using holographic interferometry 0-67208
 tympanometric screenings of 2-year-old children, repetitive obs. 0-85412

ear continued
 tympanometry in 3-year-old children, correl. with findings at paracentesis 0-85416
 vestibular control of oculomotor and postural mechanisms 0-72151
 vibration waveform measurement using temporally modulated holography 0-67212

ear microphones *see microphones*

earphones

see also hearing aids

Telex 1470-A audiometric, calibration data 0-74685

Earth

see also Earth composition; Earth rotation; Earth structure; earth-quakes; geochemistry; geochronology; geodesy; geomagnetic variations; geomagnetism; terrestrial atmosphere; terrestrial electricity; terrestrial heat

albedo, anthropogenic changes and effects on climate 0-81893
 astronomical theory of climatic fluctuations geographical support 0-72509

comet impact, explanation of Cretaceous species extinction 0-76977

free oscillation, radial mode Q-value using 1977 Indonesia earthquake data 0-67346

geocentre position variation determ. using geostationary satellite obs. 0-82083

geoid, longitude-averaged meridional profile of pear-shaped section 0-94450

gravity anomalies and tectonics, review 0-98593

ice cover and climatic models, sensitivity to external forcing 0-82049

IR radiation pressure on Castor satellite, meas. from Cactus accelerometer results 0-77251

Jupiter as source of electrons 0-90357

libration points of Earth-Moon system, search for assoc. natural or artificial objects 0-98647

Moon, fission theory origin and geosynchronous release 0-101536

Moon origin from Earth mantle, geosynchronous phase, consequences for Moon 0-101537

normal mode oscillations, tensor spherical harmonics appl. to anisotropic Earth model 0-98296

orbit determination on basis of radar and visible observations 0-90323

orbital motion from self consistent FORTAN subroutines 0-85845

orbital variations, cyclic, detect in S.Australian beach ridges chronology rel. to Milankovitch ice age theory 0-98307

oscillations, split normal modes, theoretical amplitude and Green's dyadics 0-101341

protoplanetary nebula formation of inhomogeneous Earth 0-90348

radiance meas. from Miranda (X4) satellite, IR expt. design and performance 0-72745

research programme of ESA 0-109251

solar-lunar tidal force calc. accuracy (*Russian*) 0-61813

surface albedo, vars. during recent Sahel drought (1967 to 1974) 0-76981

surface thermal radiation interpretation, emissivity correction 0-82092

tidal evolution of Earth-Moon system 0-82240

tidal friction with Moon changing Earth moment of inertia 0-81803

tidal-friction theory of the Earth-Moon system 0-81802

viscoelastic model, appl. to Earth tides theoretical study 0-67333

earth (electric) *see earthing*

earth (soil) *see soil*

Earth age *see geochronology*

Earth atmosphere *see terrestrial atmosphere*

Earth composition

see also Earth structure

Archean metasedimentary rocks from Kambalda, Western Australia, rare earth element geochemistry 0-109143

Archean rocks of E.Lac Seul region, English River subprovince, NW.Ontario, Rb-Sr isotopic study 0-94486

N.Atlantic mantle, chemistry and Pb, Nd, Sr isotopic correl. 0-90023
 basalt, $^{238}\text{U}/^{235}\text{U}$ ratio and comparison with chondritic meteorites 0-85903

basalt glasses from Mid-Cayman Rise spreading centre, geochemical var. and petrogenesis 0-101364

Bay of Islands ophiolite complex Nd and Sr isotopic study rel. to midocean ridge basalts source evolution 0-85651

biotites, Alpine, excess Ar evolution from ^{40}Ar - ^{39}Ar anal. 0-94521

Caledonian granites of Scotland, Nd and Sr isotope study rel. to provenance 0-109146

continental crust, constraints on comp. and nature of lower crust from mantle Nd-Sr isotope correl. 0-94498

core, comp. rel. to dynamics of fluid core with inward growing boundaries 0-76934

core, monosulphide solid soln. in Fe-Ni-S system 0-90038

Cretaceous mid-ocean ridge basalt (MORB), Nd and Sr isotopic comps. and rare earth element abundances 0-94520

crustal rocks, isotopic ratios rel. to rel. to mantle chemical evolution 0-90043

Duxbury massif (2.5 Ga), Quebec, initial $^{87}\text{Sr}/^{86}\text{Sr}$ rel. to remobilised pre 3.0 Ga gabbro basement hypothesis 0-76970

fumarole B isotope composition, Satsuma Iwo-Jima, Japan 0-67358

granites of E.United States, radioactive elements concs. rel. to low-temp. geothermal resources 0-85264

granitic magma of Bushveld Complex, trace element abundances rel. to crystallisation history 0-109145

granitoid rocks, Nd-Sr isotopic relationship and continental crust development, chemical approach to orogenesis 0-94522

groundwater ^{14}C content, possible subsurface prod. rel. to dating 0-85690

halogen content of ultramafic nodules, determ. by gamma-ray spectroscopy and radioactivity meas. 0-76945

hyperthemic magmas, water contents 0-72507

SE.Indian Ridge, seafloor mag. anomalies rel. to chem. of mid-ocean ridge basalt 0-109102

inert gas composition, Earth's origin from solar nebula 0-61785

inorganic gas chromatography for determ. of H_2O and CO_2 in rocks and minerals 0-85767

interior shells, chemical composition, analogous to components of highly reduced enstatite chondrite meteorites 0-85624

lithosphere, present struct. and struct. evolution (*Russian*) 0-81857

lower crust, O isotope study of xenoliths showing heterogeneity 0-89992

mantle, $^3\text{He}/^4\text{He}$ ratio in injected volatiles in Gulf of California, meas. in Guaymas Basin 0-85640

Earth composition continued

mantle, equilibrated Nd and unequilibrated Sr isotopes in xenoliths 0-98321

mantle, sub-Andean, $^{87}\text{Sr}/^{86}\text{Sr}$ ratio from Sr isotope anal. of Cerro Galan

Calc-alkaline volcanic rocks 0-98318

mantle chemical heterogeneity, evidence, conf., Nov. 1978, London 0-85623

mantle composition, derivation from comp. of lherzolites 0-76940

mantle Nd and Sr isotopes, differentiation occurring in episodes 0-67352

Mid-Atlantic Ridge basalts, geochem. variation along length of ridge 0-90027

mid-ocean ridge basalt, composition restrictions, fluid dynamical model 0-90025

Norwegian eclogites, Nd and Sr isotopic comps. rel. to crustal origin 0-76978

oceanic mantle, evidence for enriched mantle sources from Nd isotopic study of Kerguelen Islands igneous rocks 0-98319

oceanic upper mantle, comp. from petrology of ultramafics from Owen fracture zone, NW Indian Ocean 0-94519

primitive mantle structure, Pb isotope study of layered intrusions 0-81847

E.Scotia Sea, back-arc basin, volatiles in submarine volcanic rock 0-67353

sedimentary rocks, Th and U abundances rel. to crustal evolution and sedimentary recycling 0-85654

Troodos ophiolite complex, major oxide geochemistry and origin 0-98317

ultramafic xenolith petrology and upper mantle processes, Kapfenstein, Austria 0-76973

ultramafic xenolith suite from Tahiti, petrology and genetic significance 0-90086

^{27}Al , use as probe nucleus in NQR techniques appl. to geosciences 0-67426

^{36}Ar in primordial mantle from Arkansas diamond comp. 0-94493

C in upper mantle, implications for plate tectonics 0-81845

CO_2 gas seep from seabed, Norton Sound, Alaska 0-67361

He in Earth interior, incorporated from immature Sun (*Russian*) 0-81856

K depletion inferred from mantle heat loss estimate 0-76943

$^{187}\text{Re}/^{186}\text{Os}$ in Earth mantle, rel. to use of Os isotopes as petrogenetic and geological tracers 0-89989

$^{87}\text{Sr}/^{86}\text{Sr}$ initial ratios and Rb-Sr ages, from Oxford Lake-Knee Lake greenstone belt, N.Manitoba 0-94485

U, conc. in mantle rel. to Earth thermal evolution 0-89988

U in sandstone-type ore from Pakistan, assessment by charged particle track analysis 0-91405

U prospecting by γ -ray logging of borehole, factors affecting resolution 0-98463

Earth core

chemical composition, analogous to components of highly reduced enstatite chondrite meteorites 0-85624

composition, monosulphide solid soln. in Fe-N-S system 0-90038

conference, Potsdam, Germany (Oct 1979) 0-86034

discovery, historical aspects 0-105486

dynamo model of magnetic field, self-consistent treatment 0-81808

equation of state (thermal), calc. method 0-90029

fluid core with inward growing boundaries, dynamics 0-76934

fluid motion, thermal and mag. instabilities 0-81850

fluid oscillation of core, effect of Earth rot. 0-89965

formation simulation for originally homogeneous planets 0-90041

free oscillation of Earth, radial mode, damping by bulk attenuation 0-76928

geomagnetic dynamo action in rotating shell 0-81807

geomagnetic field of crust and core, spherical harmonic spatial power spectra 0-104882

Gruneisen parameter, generalisation of Vashchenko-Zubarev formula 0-90030

Gruneisen parameter, melting curve and adiabatic gradient 0-90028

liquid core, dynamical effects and luni-solar nutation tables 0-98210

lower mantle convection requiring core heat supply 0-76944

magnetic waves in fluid core and torsional oscils. 0-89993

mantle interface friction effect on geomag. secular variation 0-98218

mantle-core boundary, magnetic contour map 0-104880

material properties by dynamic compression expts. 0-98315

minerals, thermodynamic functions from eqns. of state for end members 0-90084

oxides (FeO and CaO), eqn. of state at high press. 0-109122

paradox of thermal convection, Gruneisen's parameter vol. depend. theory from melting point curves 0-90033

PKIKIKP wave detect. and damping in inner core 0-104925

seismic waves, attenuation coeff. distrib. 0-90035

stratification in early history, heat generation and heat-mass transfer 0-90040

synthetic seismograms, full wave theory and reflectivity method 0-61777

temperature distribution of outer core, Gruneisen's parameter vol. depend. theory 0-90033

Fe melting under core conditions in shock wave expt. 0-104931

Earth crust

see also geology; oceanic crust

Aburatsubo Crustal Movement Observatory obs. of tidal gravity 0-101316

abyssal fracture detection in Mountain Crimea region using Rayleigh wave amplitude spectra 0-89969

Adirondacks, geomag. fluctuations gradient anal. 0-89947

Adirondak mountains, deep crustal elec. cond. obs. 0-89946

Afar triangle, geodetic evidence for rifting, model for vertical displacements 0-98295

Afghanistan, geology and tectonics of Himalayas 0-72513

E.Afghanistan, Logar ultrabasic massif, geology and geomag. 0-72512

Pan-African fracture system, expansive brittle deformation 0-61788

E.African Rift, cross-cut by volcanic chain in N.Tanzania, gravity survey 0-98301

E.African Rift valley, seismic wave travel times 0-98238

after shock region of Off-Izu Peninsula earthquake, 1974 May 9, seismic waves attenuation 0-76926

Alpine region, tectonic stress directions, correl. with joint orientations 0-105052

Alps, Longitudinal profile (Judenburg to Hozzuperszeg), refr. seismic meas. (*German*) 0-76916

S.Alps, Permian volcanics palaeomag. props. rel. to S.Alpine block plate tectonics 0-89948

Earth crust continued

- N.America, effect of craton on distrib. of seismicity and intraplate stresses 0-98248
 N.Anatolian fault zone, Plio-Pleistocene reversal of displacement 0-94512
 anisotropic dynamic elasticity, tensor spherical harmonics appl. 0-98296
 anomalous strain before 1923 Kanto earthquake, Japan 0-85616
 Antarctica, subglacially erupted rocks of Early Miocene 0-98287
 Anti-Atlas, Morocco, Pan-African province geodynamic interpretation from geology and geochronology (*French*) 0-76952
 N Apennines, obs. rel. to lithospheric split in descending plate 0-85639
 Appalachians, structural trends NE of Newfoundland and Trans-Atlantic correlation 0-85656
 aquifer water extraction leading to land deformation 0-105003
 Archaean crust, geothermal heating rel. to vertical tectonism in greenstone belts 0-81861
 Archaean greenstone belts, tectonic hypothesis rel. to Agnew belt, Australia 0-94507
 Archaean rocks of Limpopo Mobile Belt, crustal thickness ~3, 100 Myr B.P. 0-94502
 Archaean greenstone belt, NW. Ontario, Zr-U-Pb geochronology 0-98272
 Arctic Ocean Basin, plate tectonic evolution 0-76953
 astrobles on Earth's surface, review 0-98324
 Atotsugawa Fault, Japan, seismicity and focal mechanism of local earthquakes (*Japanese*) 0-94482
 Australia, geophysical profile along 29°S 0-72460
 Australia, isostatic compensation of topography 0-72479
 Australia, tectonic, igneous and metallogenic provinces rel. to mantle convection and subcrustal stresses 0-72484
 back-arc basin basalt, compositional evolution of mantle source 0-72471
 NE.Baikar region, regional gravity anomalies and seismicity 0-98217
 Baikar region hot springs (*Russian*) 0-94551
 SW Baikar Rift, crust and upper mantle struct. according to seismic data 0-94503
 Balei gold region (E.Transbaikalia), structural features and tectonics 0-98300
 Basque Provinces, Pyrenean folding, deep geomagnetic sounding (*French*) 0-67351
 Bay of Islands ophiolite complex Nd and Sr isotopic study rel. to midocean ridge basalts source evolution 0-85651
 Beijing, China, crust and upper mantle three dimens. P-wave vel. struct. (*Chinese*) 0-104894
 Beijing area, earthquake stress field direction, composite nodal plane solns. (*Chinese*) 0-76910
 Bering Island, tectonic struct. of mountainous region 0-90045
 Black Sea NW shallow and nearby land areas, appl. of seismic multi-dimensional vel. generalisation (*Russian*) 0-105068
 Blue Mountains, Oregon, Jurassic plutons tectonic rot., palaeomagnetic obs. 0-109099
 Bonnet Plume Basin, Yukon Territory, Canada, gravity profile anal. as aid to coal basin evaluation 0-76898
 borehole γ -ray logging, exact inverse filters 0-94609
 Brazilian Highlands, crustal heat flow obs. 0-109124
 British Columbia, north-central, northward displacement during late Cretaceous/early Tertiary 0-76955
 British Isles 0-109086
 brown coal basins of Hungary, Eocene, geophys. exploration (*Hungarian*) 0-104938
 buried conducting dykes, resistivity anomalies, model tank expts. 0-85582
 Burma and S China, seismicity and tectonics 0-89983
 Bushveld Complex, geology, eastern compartment emplacement model 0-94505
 Bushveld Complex Main Granite, magma crystallisation history from trace element abundances 0-109145
 calc-alkaline volcanic rocks of Cerro Galan, NW.Argentina, Sr isotope evidence for crustal contamination 0-98318
 Caledonian granites, isotopic evidence for continental crust provenance 0-109146
 California, crust tectonic tilt rate, lake level obs. 0-90065
 central California, seismic vel. structure of metamorphic belt 0-98270
 California Coast Range, seismic vel. struct. model 0-61783
 Canada, lithospheric features correl. with long-wavelength mag. anomalies 0-85594
 E. Canada, sedimentary cover thickness meas. by aeromag. survey 0-77138
 Canada, vertical crustal movements, map 0-109130
 Canary Islands, palaeomagnetism and early magnetic history 0-72431
 Carpathian Mountains, disjunctive dislocations revealed by interpretation of space television photographs (*Russian*) 0-104958
 Carpathian region and Ukrainian shield adjacent slope, basic crustal surfaces, seismic obs. 0-89995
 Carpathian region sedimentary cover, elec. conduction 0-89940
 Carpathian regional lithosphere, geoelectric model from data along deep seismic sounding profile (*Russian*) 0-104934
 W.Carpathians, Czech Massif and Saxon Turing zone, crustal model 0-89994
 central Alps, Infrahelvetic complex, fold strain analysis 0-61787
 Cerro Prieto geothermal field, conf. at San Diego, (Sept. 1978) 0-94911
 Cesano geothermal field, Italy, geological study 0-76975
 chelonian cycles in continental crust evolution (*Chinese*) 0-89984
 chemical evolution and sedimentary recycling, evidence from Th and U abundances in sedimentary rocks 0-85654
 Chibougamau pluton, Quebec, Precambrian Rb/Sr geochronology 0-98273
 Chilkat Peninsula, Alaska Upper Triassic rocks, regional implications 0-98271
 China, seismic surface wave study of crust and mantle 0-104916
 China, tectonic deform. characts. from seismological data (*Chinese*) 0-76951
 S China and Burma, seismicity and tectonics 0-89983
 China region, plate tectonic stress field, numerical simulation (*Chinese*) 0-90055
 Columbia Plateau, basalt flow, contact zone remanent magnetisation 0-81881
 contemporary structural and structural evolution of lithosphere (*Russian*) 0-81857
 continent formation due to geosynchronous revolution of Moon 0-101348
 continental crust, constraints on comp. and nature of lower crust from mantle Nd-Sr isotope correl. 0-94498
 continental crust development, implications of Nd-Sr isotopic relationship in granitoid rocks 0-94522

Earth crust continued

- continental crust development, use of Os isotopes as petrogenetic and geological tracers 0-89989
 continental crust transformation to oceanic type 0-89997
 Coral Sea, crustal struct. from seismic data 0-72459
 Coso geothermal area, underlying low-vel. body, teleseismic evidence 0-90005
 Coso Range, California, structure, tectonics and stress field 0-90003
 creep deformation model, deformation due to geologic load 0-104939
 E.Crimea, new evidence for deep crustal struct. (*Russian*) 0-104933
 Dahomeyide orogenic belt, geology and struct. correl. with Volta Basin 0-109121
 Dead Sea Rift and N.Israel, mag. and gravity obs. and interpretation 0-98233
 deep seismic zone, Tohoku, Japan, freq.-magnitude obs. rel. to geochem. changes 0-72447
 deformation analysis, models for estimation of parameters (*German*) 0-101319
 deformation from Turgen' Geophysical Observatory data 0-76935
 density, rigidity and incompressibility rel. to seismic vel., model 0-89990
 Diablo Plateau region, W.Texas, new evidence for tectonic uplift 0-72481
 dike burial depth estimation by mag. palaeogeobarometric method 0-98220
 Djibouti Republic, magnetic anomaly map and tectonic interpretation 0-61753
 Duxbury massif (2.5 Ga), Quebec, remobilised piece of pre 3.0 Ga sialic basement 0-76970
 elastic characteristics of rocks at high-pressure and temp. (*Russian*) 0-76933
 Elberton pluton, Georgia, USA, palaeomag. of granite 0-72423
 electrical sounding, elec. fields in random cond. layered Earth 0-77171
 EM wave refl. and transmission coeffs., linear ramp model 0-61759
 NE.England, granite plutons effecting surface heat flow 0-94490
 Eurasian and North American plates, relative rot. pole determ. 0-85637
 fault strain field, included rectangular fault in semi-infinite media 0-98261
 fault termination deformation, normal fault in shade 0-90048
 faulting model of earthquake 0-109114
 faulting rupture process, plane shear faulting model of earthquake (*Chinese*) 0-104893
 faults and other linear features, detect. from LANDSAT images 0-77177
 faults and shear zones, assoc. deep focus earthquakes 0-61786
 Foreddobrogen area, USSR abyssal elec. cond. 0-90000
 France, heat flow rel. to deep struct. and mantle convection 0-98291
 Franciscan formation, California, pedestrians guide to rock exposures 0-81849
 Friuli, Italy, tectonic stress revealed by aftershocks 0-85597
 Fuji river, active faults anal. by track etch method (*Japanese*) 0-109127
 Garm region, temporal changes in elastic wave vel. 0-104914
 Garon Lake Archaean geothermal system, Matagami rock-water interaction 0-98283
 geomagnetic field of crust and core, spherical harmonic spatial power spectra 0-104882
 geothermal energy resources in Oregon, USA, elec. and EM sounding obs. 0-97761
 Geotraverse Rhenohertzynikum, fault zones investigation by seismic refl. and refr. studies 0-90046
 glacial deposits of Brecon Beacons, S.Wales, Loch Lomond Stadial 0-105005
 Gondwana configuration in Early Palaeozoic, palaeomag. study of Argentina 0-89938
 gravimetric and seismic methods combination for initial seismic data crustal vel. sections 0-105070
 gravity anomaly due to geologic contact, Fourier transform method for horiz. profile 0-94447
 gravity gliding tectonics, orogenic wave simulation, model 0-94506
 gravity sounding, calc. of gravity field of three-dimensional masses 0-94451
 E Greenland, southern Caledonian fold belt polyorogenic nature from isotopic age study 0-76938
 Grenville Front Zone, Precambrian geological struct. of Labrador 0-98274
 Guadeloupe, seismic profiles of superficial struts. (*French*) 0-76932
 Gulf of Aqaba, sinistral movement rel. to Red Sea opening 0-76954
 Gulf of Papua, crustal struct. from seismic data 0-72459
 heat flow, global scale pattern (*Russian*) 0-98284
 heat flow in continent, tectonic age and thermal evolution effects 0-72472
 heat flow in Malaysia offshore areas, estimation in exploration wells 0-67349
 heat flow of continental crust affected by erosion 0-89991
 heat loss of Earth, review 0-98286
 N. Hida region, Japan, seismicity and focal mechanism of local earthquakes (*Japanese*) 0-94482
 Hidaka mountain region, Hokkaido, Japan, unusual seismic waves from shallow quakes (*Japanese*) 0-94477
 W.Himalaya, Central Crystallines, geology and tectonics 0-72516
 Himalaya, Tethyan and Higher, geological description 0-72515
 Himalaya, two intracrustal boundary thrusts 0-104948
 Himalaya, uplift and cooling rates from geochronological data 0-85627
 Himalaya and Indo-Gangetic Plains, geology and pre-Mesozoic orogeny 0-72514
 Himalaya and Tibet Plateau region, tectonic history 0-72486
 Himalayan Suture Zone, Landsat picture obs. 0-76948
 Himalayas region, conf., Mar. 1978, Katmandu, Nepal 0-72523
 Hindu Kush region, microearthquake seismicity and fault plane solns. 0-72446
 NE.Honshu, Japan, crust vel. struct. from earthquake data 0-76937
 hot spots, sublithospheric upwelling distrib. 0-109126
 Iberian margin ocean-continent boundary struct., discovery of serpentinite diapir W. of Galicia Bank 0-94489
 SW. Iceland, axial rift zone, seismic crustal study 0-90014
 Iceland, continuum model of crustal generation, kinematic aspects 0-90059
 NE.Iceland, elec. resist. model from magnetotelluric obs., correl. with temp. 0-89954
 N. Iceland, gravity and height vars. during present rifting episode 0-90060
 NE Iceland, mag. anomalies (ΔZ) and interpretation based on rock magnetic investigations 0-89951

Earth crust continued

- Iceland, seismic structure along RRISP-Profile I 0-90018
 N Iceland, vertical crustal movements from height meas., (1965 to 1977) 0-89931
 Iceland crust above layer three, seismic structure 0-90015
 N.Iceland fissures, relative movements and tile changes 0-90062
 NE Iceland rift zone, geodetic meas. and horizontal crustal movements 0-89930
 N.Iceland rift zone, seismic study of crust struct. 0-90013
 Icelandic thermal area rock stress implication for oceanic lithosphere 0-90012
 impact craters, modification by fallback ejecta 0-82317
 India, Bouguer gravity anomaly map and tectonics 0-61791
 India, peninsular, fan faults rel. to origin of Himalayas 0-85630
 S.Indian craton, tectonic-framework deduced by LANDSAT imagery 0-82920
 Indo-Australian plate, evidence for internal deform. 0-109134
 Indo-Gangetic Plains and Himalaya, geology and pre-Mesozoic orogeny 0-72514
 intra-plate volcanism during Cainozoic, rel. to mantle convection 0-98293
 intracratonic basin, formation model involving deep metamorphism 0-85618
 island arc development, obs. expts. and speculations 0-98298
 isostatic compensation and viscosity differences between crust and asthenosphere 0-104947
 isotopic ratios of trace elements, rel. to mantle chemical evolution 0-90043
 Israel, Mesozoic palaeomag. results and inferences for microplate struct. in Lebanon 0-61760
 Itapicuru greenstone belt, Bahia, Brazil, mag. survey for ore bodies 0-81879
 Izu Peninsula, active faults anal. by track etch method (*Japanese*) 0-109127
 Japanese Islands, compilation of eleven new heat flow meas. 0-67350
 Japanese Islands region, geophysical data compilation (*Japanese*) 0-67332
 Jharra coalfield of India, survey of struct. and geol. 0-76972
 Jharra Gondwana sedimentary basin, India, heat flow meas. and basement rocks heat prod. 0-98276
 Jurassic rock in N.Armenia, palaeomagnetic directions rel. to remanent magnetisation 0-104870
 S.Kanto area, seismic waves vel. change meas. from Tateyama explosions (*Japanese*) 0-67338
 S. Kanto Region, Japan, crustal struct. from body wave propag. derived from earthquakes initial motion (*Japanese*) 0-94481
 Kharkov-Yalta profile, crustal structure (*Russian*) 0-85622
 Krafla Caldera, NE Iceland, gravity and elevation changes caused by magma movement 0-90052
 Krafla fissure swarm, Iceland, surface deform. in rifting events 0-90061
 Krafla volcano area, N. Iceland, horizontal magma flow rel. to subsidence events, (1975 to 1979) 0-90053
 E.Lac Seul region, English River subprovince, NW.Ontario, crust form. history from Rb-Sr isotopic study 0-94486
 Laramide orogeny, seismic profiles in Wyoming, USA 0-85626
 lava flow terrain, radar imaged by satellite 0-98285
 Lepontine Alps, temporal changes in heat flow distrib. assoc. with metamorphism 0-101347
 liquid-filled vertical crack propagating due to hydrostatic press. 0-72505
 magma chamber, fluid dynamics model of differentiation and layering 0-76939
 magmatic arcs, arc-trench gap accretion and episodic plutonism 0-76956
 magmatic diapires evolution, influence of temp. and heat exchange with crustal rocks (*Russian*) 0-104957
 magnetic anomalies, estimation of cover thickness above magnetised mass (*Russian*) 0-105069
 magnetic anomalies of long-wavelength for deep struct. 0-72430
 magnetic anomaly due to 2-D assym. triangular prism, expression for total field 0-94457
 magnetic depth sounding by induction arrow representation, review 0-98486
 magneto-telluric response dispersion relations, inversion problem theory 0-104861
 magnetostatic anomaly field problem, soln. in high susceptibility case via method of subsections 0-105065
 Messina Layered Intrusion, Limpopo Mobile Belt, S.Africa, tectonic setting, geology and age 0-76969
 metallic mineral deposits of Australia mag. induced polarisation survey results 0-98223
 meteorite impact structure, Gosses Bluff, Australia 0-72520
 Michoacan, Mexico, seismic gap, length of earthquake-free period 0-76919
 mining tectonical forecast maps, geoelectric bed sounding method (*Hungarian*) 0-105075
 Moho P-wave velocity depth, regional distrib. from Rumania earthquake (1977 March 4) (*German*) 0-98256
 Mongolo-Okhotsk mobile belt, rift formation and tectonic history 0-90066
 movement, measured by geodesic networks, design (*German*) 0-76897
 Nepal, basic intrusions of volcanic origin 0-72477
 Nepal Himalaya, body waves from earthquakes, focal mechanism and tectonics 0-72455
 Nepal Himalaya, struct. geology of Kusma-Sirkang section 0-72478
 N-central Nevada, faulting patterns and crustal strength 0-72467
 New Zealand (N.Island), plate boundary microearthquake study 0-109131
 Newfoundland, Early Palaeozoic plate tectonic model 0-94509
 Nias Island, Indonesia, sedimentology and palaeobathymetry of Neogene trench-slope deposits 0-104950
 Nias Island, Indonesia, structural geology implications for subduction zone tectonics 0-109120
 N.Nigeria, pipe in schist belt, geophys. anomaly study 0-76971
 Norris Geyser, Yellowstone Park, USA, microseisms of geothermal area 0-104909
 North Sea basin, subsidence in post-mid-Cretaceous 0-109133
 Norwegian eclogites, Caledonian Sm-Nd ages and crustal origin 0-76978
 olivine, shock deform. expts., Hugoniot data implications 0-94497
 NW.Ontario, Canada, trondhjemitic basement enclave near Archaean Favourable Lake volcanic complex 0-94518
 ophiolite complex of Point Sal, California, seismic vel. struct. 0-109110
 ophiolitic melange of Late Precambrian, Egyptian desert, formation process 0-81884

Earth crust continued

- orogenic volcanism caused by thermal runaways? 0-90057
 Oxford Lake-Knee Lake greenstone belt, N.Manitoba, Rb-Sr ages 0-94485
 P-wave vel. struct to depth of 150 km, Kanto District, Japan (*Japanese*) 0-94475
 SW.Pacific, Eocene subduction zone, disruptive ophiolitic belt evidence 0-104949
 Pacific plate subduction (*Japanese*) 0-94514
 Pamir-Hindu Kush region, seismicity and fault plane solns. 0-72445
 passive continental margin, evolution in light of drilling results 0-76942
 Philippine Islands, tectonic struct. revealed by seismicity and volcanicity 0-94511
 Philippines, microearthquake survey of tectonic features 0-81827
 plate tectonic explanation of Earth struct. 0-81855
 plutonic environment, contrasted magmas commingling in Nain anorthositic complex, Labrador 0-104959
 plutons, thermal evolution, parameterised approach 0-90042
 post glacial uplift mechanism, phase boundary reaction to medium press. changes 0-90058
 postglacial uplift of crust, mechanism 0-104943
 postseismic surface stress, viscoelastic model 0-98278
 postseismic viscoelastic surface deform. and stress, theory 0-94496
 Precambrian shield of Liberia, heat flow 0-98279
 pretercynian continental configuration, palaeomag. data from NW.France 0-72414
 Proterozoic anorthositic massif of Labrador's Nain complex, magma origin 0-94500
 Middle Proterozoic continental arrangement, based on palaeomag. of Coronation Geosyncline 0-94456
 Proterozoic crust, gravit. instability inferred from mantled gneiss dome pattern 0-81848
 Pyrenean mountains, explosion seismic sounding of continental Moho throws and dips 0-85620
 N.Queensland, Australia, crust struct. from gravity survey 0-72458
 radiogenic heat generation in old platform crusts 0-89996
 radiogenic heat production, depth depend. modelling by variational approach 0-72464
 radiogenic heat production, vertical distrib. 0-85619
 Reykjanes Ridge Iceland Seismic Experiment (RRISP 77), for crust struct. 0-90017
 Rhinegraben area, gravity anomalies and geothermal implications 0-104852
 Rhinegraben geothermal anomaly at Landau oil-field, model 0-98281
 rhyolitic ignimbrites origin, Batopilas area, Mexico, Sr isotope study 0-94501
 Rio Grande rift, USA, deep crust struct., magnetotelluric interpretation 0-104878
 rock crack mapping by obs. of seismic velocity anisotropy 0-98253
 rockfall from cliff face, seasonal variation obs. in N.Ireland 0-105001
 salt glaciers of Iran, seasonal movement obs. 0-104942
 San Andreas fault, fault creep obs. rel. to local mag. field meas. 0-85629
 San Andreas fault, geodetic tilt obs. 0-81800
 San Andreas fault, shear stress meas. profile at shallow depth 0-76947
 San Andreas Fault, wire strainmeter data subject to meteorological noise 0-81831
 San Andreas transform, geometry of subducted slab 0-98297
 Scotland, electrical model of crust and upper mantle 0-98234
 SW. Scottish Highlands, temporal changes in heat flow distrib. assoc. with metamorphism 0-101347
 sedimentary basins, development in Archaean rel. to lithosphere thickness 0-89986
 sedimentary basins, form. with finite crustal extension rates 0-89987
 sedimentary rock faulting and folding, strain hardening theory 0-85628
 seismic fracture zones, effects of groundwater hydrostatic press. vars. on seismicity (*Russian*) 0-104913
 seismic ground response near Long Beach, California 0-61775
 seismic shear-wave travel time for Earth struct. 0-81817
 seismic strong motion attenuation, regions of USA 0-81834
 seismic velocity inversion in upper crust (*Japanese*) 0-94478
 seismic wave diffraction, using Earth crust models 0-98239
 seismology, implications of dilatancy-fluid diffusion theory for aftershock sequences 0-85604
 Senegal, telluric current variation obs. (*French*) 0-76903
 shallow earthquakes, seismic efficiency, radiated seismic energy, fault motion energy balance 0-76927
 Shikoku district, Japan, upper crustal struct. from seismic anal. (*Japanese*) 0-94508
 SE Siberia, crust struct. and role of Archean folded ovals 0-101349
 Sicily, Mesozoic continental margin, palaeomagnetism and deformation 0-61761
 Siebengebirge, Germany, K-Ar age of Tertiary volcanics 0-98280
 Sierra Nevada batholith, elec. conductivity of crust 0-72411
 E.Sierran Front, shallow crustal conductors under Coso Range, DC conc. 0-89942
 Souss Basin, S.W. Morocco, mag. survey and crustal struct. 0-89958
 St. Vincent's Gulf, South Australia, Island and coast effect in geomag. vars. 0-72426
 stress determ., statistical anal. 0-81852
 stress fields, plume generated, expressed in Hawaiian rifts and recent Icelandic volcanism 0-90051
 structural geology, conf. (1978), Toronto, Canada 0-101666
 subducted lithosphere, correl. with positive geoid height anomalies 0-90056
 subducting lithosphere, heat transfer with continental asthenosphere 0-94510
 subducting slab undergoing upper surface melting, thermal field 0-85638
 subduction zones, material transport within accretionary prisms and 'knocker' problem 0-101353
 subsurface electrically excited conductors, pot. field mathematical model 0-98230
 Sulawesi (E Indonesia) western arc, palaeomag. studies and fission-track dating rel. to tectonic history 0-89957
 sulphide prospect in California copper belt, broadband EM study 0-72503
 Superior-Churchill provinces boundary zone, S.Canada, cooperative seismic surveys 0-89985
 surface deformation due to volcanic eruptions, piezomag. field assoc. with Mogi model 0-67334
 Surkhob fault zone, USSR, tidal deform. determ. for crustal movement anal. 0-104944

Earth crust continued

- Tabas-e-Golshan earthquake, Iran, Sept. 1978, faulting and bedding thrust 0-81826
 Tataria, USSR, lithological data from seismic refl. of longit. and transverse waves (*French*) 0-101335
 tidal forces deforming crust, causing orogeny 0-85625
 tidal tilt obs. in N.Wales mine, strain-tilt coupling and Earth model 0-89926
 Triassic Hound Island Volcanics, Alaska, crustal movement from palaeo-magnetic obs. 0-89945
 Troodos ophiolitic complex, major oxide geochemistry and origin 0-98317
 Turkey-Iran, crustal thickness and uppermost mantle P-wave vels. 0-72462
 Ukrainian Carpathians, crustal interface, phase substance transformation contrib. 0-89999
 Ukrainian Shield, geothermal survey peculiarities rel. to search for fracture waters (*Russian*) 0-104935
 United States Atlantic continental shelf, US Geological Survey core drilling 0-72511
 W.USA, vertical crustal movement, anal. of levelling survey 0-72409
 Vancouver Island, 1946 earthquake mechanism, geodetic study 0-61770
 Vancouver Island region, terrestrial EM induction 0-104879
 visco-elastic modelling of tectonic systems, by finite element anal. 0-104930
 Volta Basin, geology and struct. correl. with Dahomeyide orogenic belt 0-109121
 Voronezh Crystalline Massif, seismic vels. significance of mineral substance inhomogeneous compression 0-94504
 Western Cordillera, Colombia, upper crust seismic vel. 0-81819
 Wyoming, Wind River Mountains stress system 0-94492
 S.Yamanashi Prefecture, Central Japan, crustal movements changes rel. to microearthquake activity (*Japanese*) 0-67343
 Yellowknife supergroup, Northwest Territories, volcanic rock density determ. from gravity obs. 0-98320
 Zendan Fault region, Iran, struct. lineaments, interpretation of Landsat 1 obs. 0-104941
 CO₂ gas seep from seabed, Norton Sound, Alaska 0-67361
 CO₂ production associated with tectonic processes 0-94470
 O isotope study of lower crust xenoliths 0-89992

Earth electricity see terrestrial electricity**Earth heat see terrestrial heat****Earth interior**

- see also Earth core; Earth crust; Earth mantle; tectonics; volcanology*
 convective models and radiogenic heat production constraints 0-90006
 cooling rate of Earth, reappraisal 0-76943
 core fluid motion, thermal and mag. instabilities 0-81850
 core-mantle coupling rel. to Earth rot. due to zonal tides 0-104850
 crystalline layers, elastic consts. rel. to surface waves propag. 0-76924
 degassing and thermal history, simple calcs. 0-98282
 differentiation processes of interior, trace elements as probes, review 0-98584
 elastic characteristics of rocks at high-press. and temp. (*Russian*) 0-76933
 elastic wave velocity at high-press., using Debye theory of sp. ht. 0-89979
 EM sounding, iterative ray tracing between boreholes for underground image reconstruction 0-98466
 equation of state (thermal), calc. method 0-90029
 evolution of Earth's interior, heat generation and heat-mass transfer 0-90040
 formation of core and mantle, simulation 0-90041
 free oscill. spectra, coupling and attenuation of near reson. multiplets 0-61778
 free oscillation of Earth, attenuation of radial modes 0-89966
 free oscillation of Earth, radial mode, damping by bulk attenuation 0-76928
 geomagnetic dynamo action in rotating shell 0-81807
 Gruneisen function evaluated in harmonic approx. 0-72474
 inertia and gravity in deep interior, effects of convection 0-98269
 magma, solubility and saturation of apatite, laboratory expts. 0-72504
 magnetic secular variation, modelled on mantle elec. cond. inhomogeneity (*German*) 0-81806
 mantle, seismic vel. variations, origins 0-81854
 mantle convection driven by radioactive energy, model for decaying source 0-72461
 mantle solidus curve beneath mid-ocean ridge, double partial melt zone 0-104940
 mantle viscosity, derived in convective plate tectonic model 0-85634
 material properties by dynamic compression expts. 0-98315
 mineral composition of rocks at great depths, prediction from longit. elastic wave vels. (*Russian*) 0-104956
 ocean EM induction affecting Sq during IGY 0-72428
 olivine, dislocation recovery rate affected by high-press. 0-94515
 olivine, shock deform. expts., Hugoniot data implications 0-94497
 P- and S-waves of deep interior, max. vel. amplitudes 0-98262
 Q-factor, freq. depend. rel. to seismic pulse propag. 0-72438
 radial overtone eigenfrequencies, prediction for specified Earth model 0-104889
 radioactive heat generation in crust, model 0-85619
 rock melts, prediction of major element mineral/melt equilibria 0-109125
 seismic body-wave inversion method for Earth struct., using travel time and amplitude data 0-109108
 seismic refl. and refr. of magnetoviscoelastic waves at welded contact 0-89967
 seismic sounding, iterative ray tracing between boreholes for underground image reconstruction 0-98466
 seismic velocity changes in deep interior, press. and temp. induced phase transitions 0-90034
 seismic wave propagation and damping coeff. in electrically charged water-saturated rock 0-76921
 structure for seismic wave source antipodal region obs. 0-89972
 tidal tilt obs. in N.Wales mine, strain-tilt coupling and Earth model 0-89926
 tides in solid Earth, dynamic shear modulus influence 0-76901
 tides in solid Earth, review (*Chinese*) 0-89925
 upper mantle physical conditions, Walsh's model 0-90047
 Vashchenko Zubarev formula for Gruneisen parameter, generalisation 0-90030
 viscoelastic model, appl. to Earth tides theoretical study 0-67333
 viscoelastic response to deglaciation, causing Earth rot. change 0-85576

Earth interior continued

- CaO, eqn. of phase at high press., appl. to core and mantle 0-109122
 CaO, solid, phase transition at high-press., lower mantle implications 0-79876
 FeO, eqn. of state at high press., appl. to core and mantle 0-109122
- Earth lower mantle see Earth mantle**
- Earth magnetic field see geomagnetism**
- Earth magnetic field variations see geomagnetic variations**
- Earth mantle**
- Alpine orogeny, Europe, upper mantle horizontal inhomogeneities, P-wave obs. 0-98268
 sub-Andean mantle, partial melting as source of Cerro Galan calc-alkaline volcanic rocks 0-98318
 anorthite, thermal eqn. of state up to 120 GPa 0-109136
 asthenosphere, kinematic viscosity rel. to median valley of Mid-Atlantic Ridge 0-90071
 N.Atlantic, chemistry and Pb, Nd, Sr isotopic correl. 0-90023
 equatorial Atlantic (7 to 10°N), fracture zones lithospheric struct. (*Russian*) 0-104932
 Atlantic fracture zones in equator region, gravimetric model 0-72483
 central Australia, elec. con. profile from geomag. induction meas. 0-72424
 Australia, mantle convection and subcrustal stresses 0-72484
 SW Baikal Rift, crust and upper mantle struct. according to seismic data 0-94503
 Beijing, China, crust and upper mantle three dimens. P-wave vel. struct. (*Chinese*) 0-104894
 S California, upper mantle seismic velocity, regional variations 0-109111
 Carpathian regional lithosphere, geoelectric model from data along deep seismic sounding profile (*Russian*) 0-104934
 chemical composition, analogous to components of highly reduced enstatite chondrite meteorites 0-85624
 chemical evolution, nature and timing of mantle's differentiation 0-90043
 chemical heterogeneity, evidence, conf., Nov. 1978, London 0-85623
 China, seismic surface wave study of crust and mantle 0-104916
 composition, derivation from comp. of lherzolites 0-76940
 conductivity rel. to geomagnetic secular variation impulse 0-98236
 conference, Potsdam, Germany (Oct 1979) 0-86034
 convection, countercurrent accompanying descending Pacific lithosphere beneath Japan (*Japanese*) 0-94514
 convection, rel. to inertia and gravity asymmetry 0-98269
 convection, solid-state, rel. to Earth thermal evolution 0-89988
 convection currents influenced by subduction zone heat balance 0-94510
 convection driven by radioactive energy, model for decaying source 0-72461
 convection model, finite element method 0-67354
 convection model entailing moving surface plates 0-85634
 convection rolls, stability anal. 0-76957
 convective instability of upper mantle, thermomechanical model 0-90063
 cooling rate of Earth, reappraisal 0-76943
 core interface friction effect on geomag. secular variation 0-98218
 core-mantle boundary, magnetic contour map 0-104880
 crust hot spots, and sublithospheric upwelling distrib. 0-109126
 degassing and thermal history, simple calcs. 0-98282
 density, rigidity and incompressibility rel. to seismic vel., model 0-89990
 density anomalies of lower mantle, derived from geophys. data 0-89927
 differential stress in uppermost mantle, lateral var. across SW Japan island arc 0-98275
 differentiation occurring in episodes, Nd and Sr isotope evidence 0-67352
 double partial melt zone beneath ocean ridge 0-104940
 earthquakes in mantle, spatial distrib. in Japan and Aleutian arcs 0-81820
 electrical conductivity model, effect of partial melting 0-76936
 equation of state (thermal), calc. method 0-90029
 equation of state of lower mantle 0-90032
 W.Europe, upper mantle P-wave vel., large scale variations 0-109112
 Europe and Eurasia, inferences from higher mode seismic data 0-72436
 European upper mantle struct. from Vrancea earthquake seismic wave travel-time curves 0-89998
 Fennoscandia, subcrustal lithosphere seismic investigations 0-90009
 flow and convection, inference from obs. of meteorite high-press. minerals 0-85909
 Foredobrogen area, USSR abyssal elec. cond. 0-90000
 formation simulation for originally homogeneous planets 0-90041
 France, heat flow rel. to deep crust. and mantle convection 0-98291
 geomagnetic secular variations, constraints on elec. cond. 0-61754
 Gruneisen parameter, generalisation of Vashchenko-Zubarev formula 0-90030
 Gruneisen parameter, melting curve and adiabatic gradient 0-90028
 Gruneisen parameter and eqn. of state determ. at press. induced phase transition 0-90031
 heat flow from old platform mantle 0-89996
 high-pressure phase transformations of fluorite-type dioxides 0-101363
 Himalaya and Tibet Plateau region, tectonic history 0-72486
 hotspots, correl. with positive geoid height anomalies 0-90056
 NE.Iceland, elec. resist. model from magnetotelluric obs., correl. with temp. 0-89954
 Iceland, seismic structure along RRISP-Profile I 0-90018
 Iceland plume, rel. to sea floor morphology and mag. anomalies N of Iceland 0-89953
 Indian geopotential anomaly, seismic and gravity data anal. 0-90037
 induced electrical currents below ocean bottom with vertical water flow 0-104863
 isotostic compensation and viscosity differences between crust and asthenosphere 0-104947
 Japan-Bonin trench, crustal and upper mantle changes 0-72466
 jointed blocks of peridotite xenoliths in basalts and mantle dynamics 0-61796
 lithosphere subduction beneath active margins, implications of earthquake foci three-dimensional projection 0-72453
 lithospheric split in descending plate, obs. from N Apennines 0-85639
 lower mantle convection, inferred from low Q zone 0-76944
 lower mantle minerals, evaluation of finite strain eqns. of state using lattice models 0-96620
 magnetic secular variation, modelled on mantle elec. cond. inhomogeneity (*German*) 0-81806
 material properties by dynamic compression expts. 0-98315
 melt production in mantle, by viscous dissipation 0-72463
 Mid-Atlantic Ridge basalts, geochem. variation along length of ridge 0-90027

Earth mantle continued

- mid-ocean ridge basalt, mantle origin, composition restrictions 0-90025
 mid-ocean ridge basalt (MORB) sources, heterogeneous sources mixing rel. to Nd and Sr isotopic comps. 0-94520
 midocean ridge basalts, source evolution from Bay of Islands ophiolite complex Nd and Sr isotopic study 0-85651
 minerals, thermodynamic functions from eqns. of state for end members 0-90084
 Moho P-wave velocity depth, regional distrib. from Rumania earthquake (1977 March 4) (*German*) 0-98256
 Moon origin from Earth mantle, geosynchronous phase, consequences for Moon 0-101537
 North America, S and P station anomalies 0-94460
 oceanic mantle, evidence for enriched mantle sources from Nd isotopic study of Kerguelen Islands igneous rocks 0-98319
 oceanic upper mantle, comp. from petrology of ultramafics from Owen fracture zone, NW Indian Ocean 0-94519
 olivine, shock deform. expts., Hugoniot data implications 0-94497
 oxides (FeO and CaO), eqn. of state at high press. 0-109122
 P-wave refraction, hydrophone recordings of underground nuclear explosions 0-98257
 P-wave travel time anomalies rel. to epicentral distance to African stations 0-98237
 P-wave vel. struct. to depth of 150 km, Kanto District, Japan (*Japanese*) 0-94475
 P-wave velocities, in uppermost mantle beneath Turkey and Iran 0-72462
 W. Pacific, multiple ScS travel time implications on mantle heterogeneity 0-72443
 Pamir-Hindu Kush region, seismicity and fault plane solns. 0-72445
 Pamirs-Hindu-Kush upper mantle, vel. inhomogeneity, mapping by graphical method 0-77146
 partial melts liquid distrib., effect of gravity field 0-81851
 phase separation surfaces shapes, material parameters effects 0-90036
 plate tectonic explanation of Earth struct. 0-81855
 plumes, crustal radial stress fields rel. to Hawaiian rifts and recent Icelandic volcanism 0-90051
 postseismic viscoelastic surface deform. and stress, theory 0-94496
 primitive mantle structure, Pb isotope study of layered intrusions 0-81847
 Pyrenean mountains, explosion seismic sounding of continental Moho throws and dips 0-85620
 radiative transfer of lower mantle, spectral obs. of shock compressed MgO-Fe²⁺ 0-90039
 radiogenic heating in convecting mantle, rel. to oceanic bathymetry flattening 0-85642
 Rayleigh waves higher modes to determine upper mantle struct. 0-104890
 Reykjanes Ridge, lithosphere lower boundary temp. from heat flow obs. 0-90011
 Reykjanes Ridge, Profile I on SE. flank, seismic struct., RRISP 0-90019
 Reykjanes Ridge Iceland Seismic Experiment (RRISP 77), for mantle struct. 0-90017
 rheological behaviour from creep eqns. of olivine, steady state flow 0-104924
 Rhinegraben area, gravity anomalies and geothermal implications 0-104852
 Rhinegraben area, heat and matter transfer in upper mantle 0-104927
 S-wave velocity model, based on great circle Rayleigh waves 0-109107
 Scotland, electrical model of crust and upper mantle 0-98234
 seismic shear-wave travel time for Earth struct. 0-81817
 seismic vel. anomalies below Colorado Rocky Mountains 0-81853
 seismic vel. variations, origins 0-81854
 seismic velocity of lower mantle, meas. using wide aperture array 0-105071
 Sp. waves, from upper-lower mantle transition cone, seismogram calcs. 0-104901
 stratification in early history, heat generation and heat-mass transfer 0-90040
 structure models from flood basalt isotopic abundances of Nd and Sr 0-72475
 Sunda trench and forearc basin, seismic study 0-72470
 Takayama volcanic area, Japan, upper mantle S-wave anisotropy 0-90024
 thermal convection, time dependent simulation 0-101352
 thermal evolution of differentiated upper mantle 0-98288
 thermoconvective waves, propag. without attenuation 0-90064
 thermodynamic properties of relevant substances at high press. and temp. 0-81874
 tidal tilt obs. in N.Wales mine, strain-tilt coupling and Earth model 0-89926
 tide of solid Earth, mantle anelasticity influence 0-76900
 N.Tonga region, Wadati-Benioff zone morphology and complicated subduction closure model 0-90010
 Ukrainian Carpathians, crustal interface, phase substance transformation contrib. 0-89999
 ultramafic xenolith petrology and upper mantle processes, Kapfenstein, Austria 0-76973
 ultramafic xenoliths, mantle-derived, from Tahiti, petrology and genetic significance 0-90086
 W.United States, 3-D mantle struct., P vel. study 0-85621
 upper mantle physical conditions, Walsh's model 0-90047
 E.USA, seismic vel. profile of upper mantle 0-81818
 visco-elastic modelling of tectonic systems, by finite element anal. 0-104930
 viscosity, rel. to Earth tides theory assuming Earth as viscoelastic body 0-67333
 viscosity deduced from deglaciation Earth rot. effects 0-85576
 Voronezh Crystalline Massif, seismic vels. significance of mineral substance inhomogeneous compression 0-94504
 xenoliths, equilibrated Nd and unequilibrated Sr isotopic comp. meas. 0-98321
³⁶Ar in primordial mantle from Arkansas diamond comp. 0-94493
 C in upper mantle, implications for plate tectonics 0-81845
 CaO, solid, phase transition at high-press., lower mantle implications 0-79876
³He injection in Gulf of California, meas. in Guaymas Basin 0-85640
 MgO, bonding, pressure effects in lower mantle 0-72491
 Nd-Sr isotope correlation, constraints on continental crust comp. and nature of lower crust 0-94498
¹⁸⁷Re/¹⁸⁶Os ratio, rel. to use of Os isotopes as petrogenetic and geological tracers 0-89989

Earth rotation

see also time and latitude

- angular momentum correl. with geomag. field, theory 0-67337
 annual polar motion, many-year var. rel. to atmospheric circulation many-year fluctuation (*Chinese*) 0-104848
 atmosphere, middle, superrotation rel. to damped planetary wave interaction with zonally averaged circulation 0-109217
 atmosphere, solar modulation of lunar tide 0-94593
 BIH data (1962-79) 0-101314
 core fluid oscillations, transverse motion, Earth rot. effects 0-89965
 Coriolis force, rel. to spatial problem of influence of orography on air motion (*Russian*) 0-94565
 day duration rel. to solar activity 0-104853
 day length and zonal tides, effect of core-mantle coupling 0-104850
 day length changes rel. to atmospheric angular momentum fluctuations 0-85715
 deglaciation effects, viscoelastic response to unloading 0-85576
 geophysical causes and consequences, book 0-76902
 gravitational field, local vanishing due to left turning motion (*Japanese*) 0-98798
 Greenwich Obs. Time and Latitude Service, Time Report (January to March 1979) 0-72749
 Greenwich Obs. Time and Latitude Service Time Report (April-June 1979) 0-72750
 latitude variation, polar motion and declination, effects of Oppolzer terms (*Chinese*) 0-76891
 liquid core effects, luni-solar nutation tables 0-98210
 moment of inertia change due to Earth-Moon tidal friction 0-81803
 Moon, fission theory origin and geosynchronous release 0-101536
 polar motion, International Latitude Service Observations (1899-1977) anal. 0-104851
 polar motion determ., satellite Doppler tracking, MEDOC 0-101445
 pole posn. and rotation from lunar laser range-differencing 0-101312
 secular polar motion, low frequency spectrum anal. (*Chinese*) 0-104849
 spin axis location, control by subducted lithosphere and hotspots mass anomalies 0-90056
 Tokyo Astronomical Obs., Time and Latitude Bulletins (April/June 1979) 0-72752
 Tokyo Astronomical Obs., Time and Latitude Bulletins (Jul-Sep 1979) 0-82177
 Tokyo Astronomical Observatory Time and Latitude Service, Bulletin (January to March 1979) 0-72751
 variations due to continental drift of islands 0-94445
 variations due to upper stratosphere zonal winds 0-81804

Earth satellites see artificial satellites; Moon

Earth structure

see also Earth composition; Earth interior

- circum-Arctic Ocean region, tectonic plates struct. rel. to Arctic Basin form. 0-98294
 Azov-Kuban' oil-gas basin structure from seismic data (*Russian*) 0-85601
 Balei gold region (E.Transbaikalia), structural features and tectonics 0-98300
 Basque Provinces, Pyrenean folding, deep geomagnetic sounding (*French*) 0-67351
 Black Sea NW shallow and nearby land areas, appl. of seismic multi-dimensional vel. generalisation (*Russian*) 0-105068
 central California, seismic vel. structure metamorphic belt 0-98270
 conference on plateau uplifts, Flagstaff, Arizona (August 1978) 0-57004
 conference on satellite Doppler tracking and geodetic appl., London, England (Oct. 1978) 0-77264
 continent formation due to geosynchronous revolution of Moon 0-101348
 Coso geothermal area, underlying low-vel. body, teleseismic evidence 0-90005
 Coso Hot Springs, Known Geothermal Resource Area, model 0-90004
 Coso Range, California 0-90003
 Coso Range, California 0-90049
 deep crustal struct. inferred from mag. anomalies of long-wavelength 0-72430
 density structure, max. entropy inversion 0-67602
 earthquake foci beneath active continental margins, three-dimensional projection 0-72453
 European upper mantle struct. from Vrancea earthquake seismic wave travel-time curves 0-89998
 fission theory for Moon origin 0-101536
 free oscillation of Earth, attenuation of radial modes 0-89966
 Gondwana configuration in Early Palaeozoic, palaeomag. study of Argentina 0-89938
 gravity anomalies, surface harmonic expansion coeffs. from orthogonal collocation calcs. 0-81801
 gravity anomaly from masses distributed over infinite regions, interpretation theory 0-82103
 interior structure from seismic wave source antipodal region obs. 0-89972
 Kharkov-Yalta profile, crustal structure (*Russian*) 0-85622
 Kurile trench-Hokkaido rise system, flexure profile by plate model 0-72482
 layered Earth model for resistivity sounding 0-85583
 layered transitional Earth, resistivity sounding 0-85584
 mantle, seismic vel. variations, origins 0-81854
 model based on torsional oscill. eigenperiods 0-90044
 Moho, continental, throws and dips sounding by explosion seismology 0-85620
 Moho P-wave velocity depth, regional distrib. from Rumania earthquake (1977 March 4) (*German*) 0-98256
 New Hebrides arc-trench system, structure 0-72465
 Pacific sea-floor topography and isostatic compensation mechanism (Hawaii region) 0-104945
 Pamirs-Hindu-Kush upper mantle, vel. inhomogeneity, mapping by graphical method 0-77146
 plate tectonic explanation of Earth struct. 0-81855
 primitive mantle structure, Pb isotope study of layered intrusions 0-81847
 seismic body-wave inversion method for Earth struct., using travel time and amplitude data 0-109108
 seismic shear-wave travel time for Earth struct. 0-81817
 subduction zones, three-dimensional struct. from stereoviews of seismicity 0-72452
 Sunda trench and forearc basin, seismic study 0-72470
 surface deformation detect., 500-m base laser interferometer 0-105087
 tidal tilt obs. in N.Wales mine, strain-tilt coupling and Earth model 0-89926

Earth structure continued

- N.Tonga region, Wadati-Benioff zone morphology and complicated subduction closure model 0-90010
 SW.Tunguska syncline, platform structure from gravity surveys 0-98289
 velocity-depth structure, using waveform inversion method 0-105060
 Wyoming, Wind River Mountains stress system 0-94492

Earth third layer *see Earth mantle***Earth upper layer** *see Earth mantle***earthling**

- checking instrument, meas. of resist. of ground at various levels and of earthing connections (*German*) 0-98936
 fusion reactor, JT-60, fault current anal. in grounding system 0-99307
 fusion reactor, JT-60, grounding system design 0-102313
 fusion reactor, JT-60, grounding system pot. rise during lightning strike, anal. 0-102314

earthquake recorders *see seismometers***earthquakes***see also seismology*

- active continental margins, earthquake foci three-dimensional projection 0-72453
 E.Afghanistan, shallow earthquakes and tectonic activity 0-72444
 aftershock sequences, implications of dilatancy-fluid diffusion theory 0-85604
 aftershocks, stochastic modelling of earthquake freqs. (*Japanese*) 0-94480
 aftershocks with different focal mechanism to main quake, causes (*Chinese*) 0-89960
 Alaska, Saint Elias earthquake within seismic gap (Feb. 1979) 0-109116
 E. Alpine region, seismicity and earthquakes assoc. with Bohemian Massif-Carpathians contact zone 0-104888
 Alpine region, tectonic stress directions, correl. with joint orientations 0-105052
 S.America, earthquake migration, spectral anal. 0-85614
 N.America, effect of craton on distrib. of seismicity and intraplate stresses 0-98248
 N.W.America, peak acceleration, velocity, and displacement from strong-motion records 0-98246
 N.Anatolian fault zone, earthquake migration and seismic gaps 0-85613
 animal behaviour before quakes, alternative explanations 0-85599
 Asama Volcano, spectral studies of explosion earthquakes assoc. with 1973 eruptions (*Japanese*) 0-67340
 Atotsugawa Fault, Japan, seismicity and focal mechanism of local earthquakes (*Japanese*) 0-94482
 Azores (1980 January 1), aftershock sequence and present day tectonics 0-104911
 Baltic earthquake, October 1976, source mech., surface wave study 0-81830
 Beijing area, earthquake stress field direction, composite nodal plane solns. (*Chinese*) 0-76910
 Burma and S. China, seismicity and tectonics 0-89983
 California 1857 earthquake, body-wave magnitude estimate 0-81840
 California earthquake parameters, statistics and model 0-104891
 Carlisle, 1979 December 26, fault plane soln., aftershock study 0-89977
 catalogues, geographical distrib. of detectability of ISC data 0-109117
 S. China and Burma, seismicity and tectonics 0-89983
 Chinese earthquake history, point process anal. 0-85612
 circular sources, source dimension, stress drop and radiated energy 0-98240
 Colima earthquake, Mexico, Jan. 1973, source mech. and aftershocks 0-81823
 Conference, New Delhi, India (March 1978), prediction 0-85602
 Coyote Lake, California (1979 August 6), local magnitude and seismic moment determ. 0-104904
 descending slab stress state, anal. of seismic source parameters 0-104946
 dip slip fault, ground motion 0-72440
 dislocation source in heterogeneous crust, propag. study using dislocation model 0-101340
 epicentre determ. using P-wave arrival-time differences 0-101328
 Fairbanks, Alaska seismic zone, earthquake migration 0-101330
 fault model (stochastic) 0-109114
 fault model for strong motion short period accel., vel. and displacement 0-104918
 fault rupture propagation, theory 0-104910
 fault unstable slippage, facing media of different elastic consts. 0-72506
 faulting rupture process, plane shear faulting model of earthquake (*Chinese*) 0-104893
 focal mechanisms, classical seismological study techniques 0-76918
 foreshocks, differentiation from earthquake swarms via seismic waveform variability (*Japanese*) 0-67342
 Fort Ross, California, earthquake sequence, March-April 1978 0-81824
 Fort Tejon, California (1857), tree ring growth and seismic disturb. 0-98259
 frequency-magnitude distribns., universal shape regularity obs. 0-101333
 frequency-magnitude relations, in NGSCD earthquake data file 0-81838
 Friuli, 1976 May 6, focal mechanism 0-85603
 Friuli, Italy, May 6, 1976, earthquake sequence 0-81822
 Friuli aftershocks of 1977, fault-plane solns. and hypocentral distrib. 0-85597
 geodesy, artificial satellite laser ranging, high precision, earthquake anal. 0-98215
 geological faults and shear zones, assoc. deep focus earthquakes 0-61786
 granite microfracture, source process rel. to earthquake prediction 0-104919
 great earthquake occurrence, chaos theory of fault block behaviour 0-72448
 great earthquakes, chaotic behaviour, coupled relax. oscillator model, billiard model and electronic circuit model 0-94462
 great shallow earthquakes, 1953 to 1977, magnitudes 0-85617
 Haicheng, 1975, February 4, rupture analysis method (*Chinese*) 0-76911
 Haicheng, China, source processes of Feb. 1975 event 0-81828
 Hawaii, 1975 November 29, tsunami numerical anal. by finite-element method 0-72449
 Hawaii, Honoumuli, April 26, 1973, subcrustal quake 0-81821
 Hengill-Hellisheidi area, SW. Iceland, seismicity obs. 0-89976
 N. Hida region, Japan, seismicity and focal mechanism of local earthquakes (*Japanese*) 0-94482
 Hidaka mountain region, Hokkaido, Japan, unusual seismic waves from shallow quakes (*Japanese*) 0-94477
 Hindu Kush region, microearthquake seismicity and fault plane solns. 0-72446
 earthquakes continued
 Hindukush, Baluchistan arc, seismotectonics and struct. (1890-1970) 0-104922
 Hollister, California (1974, November 28), localised geomag. field vars. as precursors 0-104912
 NE.Honshu, Japan, crust vel. struct. from earthquake data 0-76937
 hypocentre parameters in Kanto District, Japan (*Japanese*) 0-94475
 Iceland, statistical anal. of damaging earthquakes and volcanic eruptions, (1550 to 1978) 0-89975
 imminent earthquake precursors, anomalies and errors statistical anal. (*Chinese*) 0-104895
 NE.India, teleseismic P-wave residual anal. at Shillong, rel. to earthquake prediction 0-104921
 Indonesia, 1977 August 19, Earth free oscill. Q-value 0-67346
 Indonesia earthquake exciting free modes, 19th Aug. 1977 gravimeter obs. 0-61767
 induced versus natural earthquakes in geothermal area, discrimination 0-101332
 Iran, seismic waves from Iranian quakes, excitation and attenuation 0-104900
 Iran and Turkey, focal and seismicity depth determ. errors 0-61779
 Italy, precursory seismicity to strong earthquakes 0-104884
 Off-Izu Peninsula, 1974 May 9, seismic waves attenuation in aftershock region 0-76926
 Izu-Oshima earthquake, Japan, Jan. 14 1978, quake parameters 0-61763
 Izu-Oshima-kinkai earthquake (1978), precursory Rn changes 0-94472
 Japan, statistics of earthquakes energy release (1915 to 1978) 0-94471
 Japan arcs, time-predictable recurrence model for large earthquakes 0-85598
 Japan seismicity, 1885 to 1925, catalogue of M \geq 6 earthquakes and smaller, damaging, earthquakes (*Japanese*) 0-67341
 Japanese earthquakes, 1901 to 1925, instrumental magnitudes (*Japanese*) 0-94484
 Japanese Islands region, earthquakes and mechanisms data compilation (*Japanese*) 0-67332
 Kanto, Japan, 1923, Sept. 1, anomalous crustal strain before quake 0-85616
 Kanto District, Japan, earthquakes rel. to countercurrent accompanying descending Pacific plate (*Japanese*) 0-94514
 Kern County, California, (1952, July 20) precursory seismicity and small quakes 0-104902
 Kurile Island earthquake, seismic quiescence precursory 0-85610
 La Malbaie, Quebec (1924-1978), epicentre relocation 0-104903
 Lacq, France, petroleum exploitation rel. to non-natural earthquakes (*French*) 0-104892
 Lake Jocassee, S.Carolina, seismicity rel. to Rn content of groundwater 0-94466
 light emission by atmosphere, explained by chemiluminesc. of gas released from rocks 0-61906
 local earthquakes coda, Q-estimates 0-104899
 magnitude correl. with focal parameters, theoretical basis 0-101338
 magnitude rel. to rupture length, regional variations 0-81837
 magnitude rel. to tsunami height, empirical relation 0-94461
 magnitude scale based on strong-motion horizontal particle vel. 0-81836
 Makran region, seismicity var. rel. to large earthquakes 0-85611
 Malibu earthquake, Jan. 1979, precursory Rn changes 0-94464
 mantle earthquakes, spatial distrib. in Japan and Aleutian arcs 0-81820
 maximum ground acceleration determ. for large earthquakes (*Japanese*) 0-101453
 mechanism leading to P-wave first arrival sign distrib. 0-94474
 meizoseismal shaking of long-period, for strike-slip event 0-81814
 Mexico, 1911 June 7, epicentre relocation rel. to Michoacan seismic gap 0-76919
 Miyagi-Oki, Japan, 1978 June 12, rupture process 0-98263
 Miyagiken-oki (1978, June 12), aftershock spectral anal. 0-109118
 Nankaido earthquakes correl. with Shikoku seismicity characts. 0-101339
 Nepal Himalaya, body waves from earthquakes, focal mechanism and tectonics 0-72455
 nuclear power stations, seismic safety margins research program of the US Nuclear Regulatory Commission 0-99229
 Oaxaca, Mexico, prediction using seismic gap obs. 0-85609
 Oaxaca earthquake, Mexico, aftershocks in former seismic gap 0-98265
 ocean bottom hydrophone array obs. of P and S waves, wave train characts. 0-104898
 Oita, Japan, 1975, maximum ground acceleration determ. using overturned gravestones (*Japanese*) 0-101453
 Onikobe earthquake, Japan, ground motion deduced from damage, source model (*Japanese*) 0-94479
 Oroville, California, 1975 August 6, strong-motion accelerograms of aftershocks 0-101331
 P-wave travel time anomalies rel. to epicentral distance to African stations 0-98237
 Pamir-Hindu Kush region, seismicity and fault plane solns. 0-72445
 Parkfield, California, 1966, strong-motion accelerograms, statistical analysis 0-98245
 Peru, seismic gaps and source zones 0-85607
 Petatlan (Guerrero, Mexico), 1979 March 14, first report 0-76920
 Philippine Islands, tectonic struct. revealed by seismicity and volcanicity 0-94511
 Philippines, microearthquake survey of tectonic features 0-81827
 plate boundary seismic pot., major boundaries 0-85606
 Pocatello Valley 1975 March 28, source model 0-104896
 postseismic surface stress, viscoelastic model 0-98278
 postseismic viscoelastic surface deform. and stress, theory 0-94496
 precursory acoustic emission, sound source direction formula (*Chinese*) 0-89961
 precursory changes of groundwater Rn content 0-94467
 precursory CO₂ changes, tectonic processes causing release from rocks 0-94470
 precursory He changes of soil, limitations imposed on method by daily variations 0-94469
 precursory rainfall to San Andreas fault quakes 0-85615
 precursory Rn changes in California Transverse Ranges 0-94464
 precursory Rn changes in shallow subsurface of New York State 0-94463
 precursory Rn changes in soil before San Jacinto Fault, California 0-94468
 precursory Rn episodic outgassing, active faults of California 0-94465
 precursory rock cracking, size estimation of preparation zone 0-76930
 precursory seismicity burst, long-term prediction of strong quake 0-72441
 prediction, appl. of geodetic research (*German*) 0-101317

earthquakes continued

- prediction, based on geochem. meas., conf., San Francisco, USA (Dec. 1980) 0-90606
 prediction, workshop, Strasbourg, France, (1980 January 31 to February 1) 0-62396
 prediction (*German*) 0-98267
 prediction based on dilatancy induced seismogram polarisation anomalies 0-101342
 prediction based on tilt anomaly 0-104917
 prediction from pseudo-periodicity of strong aftershocks (*Chinese*) 0-76913
 prediction of large earthquakes on San Andreas fault, shear stress meas. profile at shallow depth 0-76947
 Rayleigh-wave radiation pattern, for small earthquake mechanism 0-61764
 recurrence of large events, semi-Markov model 0-98247
 regional focal mechanism solns., probability models 0-98244
 Reykjanes Ridge at 59°N, microearthquake epicentres and seismic vel. 0-89964
 Reykjanes Ridge crest studied by surface waves with an earthquake-pair technique 0-90021
 Rumania, 1977 March 4, P-waves obs. rel. to Moho vel. depth distrib. (*German*) 0-98256
 San Andreas Fault, 1973 January 15, section seismicity and failure 0-101329
 San Fernando earthquake, California (1971), dislocation fault model, tectonic significance (*Japanese*) 0-104923
 San Fernando earthquake, strong ground motion, ray models 0-61762
 scientific and economical aspect of earthquake engineering 0-81844
 seismic energy dissipation during propag., by solid friction 0-109106
 seismic gaps, two types of definition 0-85608
 seismic moment, method of determination from seismological bulletin data 0-89980
 seismic moment tensor elucidation from teleseismic data 0-104915
 seismic radiation pattern theory 0-61780
 seismicity associated with subduction zones, stereoviews 0-72452
 shallow earthquakes, seismic efficiency, radiated seismic energy, fault motion energy balance 0-76927
 Shikoku, Japan, shallow earthquakes focal distrib. rel. to upper crustal struct. (*Japanese*) 0-94508
 Sitka, Alaska, 1972 July 30, changes in direction of mag. vector of short-period geomag. vars. 0-76923
 small earthquakes, detailed spatial distrib. of foreshock and aftershock activities (*Japanese*) 0-94483
 source mechanism model, for pre-stressed self-gravitating, thermo-visco-elastic Earth 0-104886
 spatial distribution of earthquakes, two-point correl. function 0-89963
 St. Elias, Alaska, 28 Feb. 1979, 1974-9 tilt obs. 0-81841
 St. Elias, Alaska (1978 February 28), body wave anal. 0-104897
 strike slip fault, ground motion 0-72439
 strong ground motions at short epicentral distance, simulation 0-104906
 strong motion prediction for pot. earthquake fault, barrier model 0-105053
 surface seismic Rayleigh waves, amplitude spectra in Mountain Crimea region 0-89969
 Swabian Jura earthquake of Sept. 1978, macroseismic field obs. 0-72451
 swarm earthquakes, differentiation from foreshocks via similarity of seismic waveform (*Japanese*) 0-67342
 swarms, stochastic modelling of earthquake freqs. (*Japanese*) 0-94480
 Sweden (1951-76), error anal. of source parameters 0-104920
 Tabas-e-Golshan earthquake, Iran, Sept. 1978, faulting and bedding thrust 0-81826
 Tabas-e-Golshan earthquake, Iran, Sept. 1978, mechanism and aftershocks 0-81825
 Taft, California, 1952, strong-motion accelerograms, statistical analysis 0-98245
 technique for parameter determ. by computer (*Chinese*) 0-77126
 teleseismic magnitude relations, extension of Zurich magnitude recommendations (1967) 0-109105
 Tibet and Himalaya, long-term premonitory seismicity 0-72442
 Tonankai (Japan), 1944, source model for accompanying tsunami (*Japanese*) 0-67344
 N.Tonga region, earthquake distrib. geometry and complicated subduction closure model 0-90010
 travel-time inversion method, for earthquake location and vel. struct. 0-109109
 tree ring growth, affected by Fort Tejon 'quake, California 0-98259
 tsunamis in Kanto, 1677 and 1703, behaviour along Kujukuri-hama coast from old monuments (*Japanese*) 0-67339
 W.United States, horizontal ground accel. attenuation rel. to magnitude 0-104905
 Upper Amur region USSR, seismicity, tectonic features and earthquake epicentre confinement 0-101343
 USSR, correl. between seismicity and underground water regime (*Russian*) 0-104913
 Vancouver Island, 1946 earthquake mechanism, geodetic study 0-61770
 Virgin Islands, tectonic struct. and earthquake swarms, seismic network obs. 0-89973
 Vrancea Rumania (1977 March 4), precursors to S and SKS waves, seismogram calcs. 0-104901
 Vrancea earthquake seismic wave travel-time curves giving European upper mantle struct. 0-89998
 Xingtai, 1966, March aftershock freq., rel. to subsequent N.China strong earthquakes (*Chinese*) 0-76912
 Yakataga Gap, Alaska, seismic history and earthquake pot. 0-109115
 S.Yamanashi Prefecture, Central Japan, microearthquake activity (*Japanese*) 0-67343
 NWSyria, seismic risk to large quakes 0-72454

EAS see *cosmic ray showers and bursts***Eberhard effect** see *photographic materials***ebullition** see *boiling***e.c.g.** see *electrocardiography***echelons** see *diffraction gratings***echo**

- see also *anechoic chambers; architectural acoustics; clutter; reverberation; sonar*
 acoustic imaging, phased array for medical diagnostics, dynamically focused insonification 0-89813
 air pollution meteorology, use of sodar acoustic echo sounder, low level stability and wind velocity monitors 0-108828

echo continued

- bat detection instruments 0-69609
 Demey metro station, noise level increase due to echoes from passing vehicles (*French*) 0-69600
 Hertzian waves, reflection and diffraction by moving layers (*German*) 0-87266
 radar echoes, type 1, from equatorial electrojet, with double-peaked Doppler spectra 0-67458
 speech intelligibility, time delay effect experiment 0-91996

eclipsessee also *solar eclipses*

- Galilean satellites, eclipses rel. to improved ephemerides 0-62066
 Titan by Saturn, light curve obs. rel. to Saturn upper atmosphere struct. 0-90362

eclipsing binary stars

- 2A 0311-227, AM Herculis type binary star, IR photometry and polarimetry 0-77517
 2A 0311-227, optical counterpart, AM Herculis type eclipsing binary, V-band obs. 0-101617
 2A 0311-227 optical counterpart, simultaneous photometric and spectroscopic obs. 0-90572
 2A 0526-328, optical counterpart, eclipsing binary, visible emission line variability 0-73075
 Abell 46, planetary nebula, nucleus, hot component UV continuum obs. by IUE 0-98693
 Algol, orbit, lightcurve and struct. review 0-109460
 Algol, X-ray spectral obs., description and interpretation 0-105283
 Algol type star, accretion and chem. struct., evolutionary calcs. 0-109481
 Algol type stars, H I α obs. 0-109484
 Algol type stars, mass loss and transfer 0-109480
 apsidal motion, discrepancy with main-sequence homogeneous stellar models 0-82413
 V342 Aquilae, period and light curve changes, (1966 to 1976) 0-67791
 KO Aquilae, UVB photoelectric study 0-62198
 T Aquilae (Nova 1891), spectrophotometry of shell 0-72955
 V603 Aquilae (Nova 1918), IUE obs. of periodic light vars. 0-105251
 V603 Aquilae (Nova 1918), old nova, eclipses obs. 0-90476
 V603 Aquilae (Nova 1918), periodic light vars. detect. 0-82391
 ϵ Aurigae, dual aspect of wavelength depend. fluctuations 0-62190
 AO Aurigae, Hg star, peculiar spectral var. during eclipse 0-98679
 EO Aurigae, revised elements from light curve anal. 0-90471
 ζ Aurigae, UV obs. of supergiant atmos. 0-94836
 T Aurigae (Nova 1891), old nova, photometric and spectroscopic obs. 0-90446
 TZ Bootis, W Ursae Majoris type system, photoelec. obs. 0-73001
 SZ Camolopardalis, semi-detached eclipsing binary, UVB lightcurves 0-85974
 UW Canis Majoris, mass flow anal. and circumstellar component from UV spectrum 0-109429
 UW Canis Majoris, O7f supergiant, mass loss rate meas. 0-67736
 R Canis Majoris type, struct. and dims. 0-82423
 RS Canum Venaticorum, out of eclipse light var. and comparison with similar stars 0-109489
 RS Canum Venaticorum type binaries, H γ line vars., chromospheric diagnostics 0-62181
 OY Carinae, white dwarf cataclysmic, eclipsing binary, parameter determ. 0-82385
 QZ Carinae (HD 93206), O-type quadruple eclipsing system, spectroscopic and radial vel. study 0-105275
 AB Cassiopeiae, light vars. preliminary study 0-94831
 AR Cassiopeiae rel. to supernova remnant Cassiopeiae A 0-72792
 cataclysmic binaries, disc and hot spot eclipses anal. for circumstellar matter parameters determ. 0-109492
 Centaurus X-3, neutron star characts. from correlated spin-up and X-ray luminosity meas. 0-101648
 central star of Abell 46, eclipsing binary 0-73027
 U Cephei, accretion discs obs. 0-82412
 U Cephei, anal. of radial velocity curve of B9 component 0-94829
 NY Cephei, massive eclipsing binary star, progress report from UVB photometry 0-67789
 VV Cephei, supergiant, UV spectrum 0-82415
 U Cephei, three colour light curve perturbations and orbital element determ. (*French*) 0-67787
 EM Cephei, UVB, photometry rel. to constancy or variability of period 0-105286
 VV Cephei, UV spectrum obs. during chromospheric eclipse phase 0-109498
 VW Cephei, W Ursae Majoris star, orbital period decrease and B-V colours rel. to physical status 0-109495
 VW Cephei, W Ursae Majoris star, rot. line broadening rel. to shape and mass ratio 0-109494
 VW Cephei W Ursae Majoris system, period and colour change mass transfer model 0-77453
 XY Ceti, revised photometric elements 0-109458
 Z Chamaeleontis, eruptive binary, model from photoelectric data anal. 0-72961
 RS Chamaeleontis, four-colour photometry rel. to photometric elements, absolute dimensions and He abundance 0-67783
 Z Chamaeleontis, gravitational waves from eclipsing cataclysmic binary 0-90439
 RS and RZ Chamaeleontis, photometric elements of detached systems 0-90473
 close binaries, narrow-band photometry and differential effects 0-67780
 close binaries, period distrib. from secondary maxima 0-109467
 close binary stars props. before and after mass transfer, obs. and theory comparison 0-62187
 close eclipsing binary stars, near IR photometry rel. to mass transfer rates 0-67784
 contact binaries, envelope energy transfer model 0-90478
 contact binaries, orbital periods sudden changes due to third component 0-109497
 contact binaries, solar type, initial mass ratio distrib. function 0-109496
 contact binaries, theories of struct. 0-109493
 contact binaries with age-zero components, secular stability 0-67786
 AI Crucis, revised photometric elements 0-109459
 31 and 32 Cygni, ζ Aurigae stars, UV spectroscopic obs. 0-109499
 EM Cygni, cataclysmic variable, red and white dwarf binary, period change, B photometry 0-90434
 V444 Cygni, new light curve anal. techniques appl. 0-82417
 GO Cygni, orbital period changes 0-72999

eclipsing binary stars continued

- SW Cygni, period changes, mass transfer and third body effects 0-62183
 CC Cygni, photometric obs. of RS Canum Venaticorum type binary, interpretation 0-62182
 V380 Cygni, revised photometric elements 0-109458
 SW Cygni, semi-detached Algol type binary, period study, photometry and spectra obs. 0-82424
 V1329 Cygni (HBV 475), symbiotic variable, photometric and spectroscopic history 0-62148
 CI Cygni symbiotic star, UV and optical spectrum changes during eclipse 0-105258
 Cygnus X-3, X-ray polarisation obs. from OSO 8 0-90571
 detached, period variations, review 0-109474
 RZ Draconis, photoelectric light curve and orbital period study 0-109461
 CD Eridani, photometric soln. for eclipsing binary system 0-62185
 YY Geminorum, photometry and orbital period study 0-105287
 U Geminorum, visual magnitude estimates during outburst (1980 Oct.) 0-109439
 in globular clusters, preliminary report on eclipsing binaries and cataclysmic variables 0-109505
 HD 153919 (=4U 1700-37), supergiant-neutron star, optical variability 0-82419
 HD 197406, WN7 type binary orbital data, UV obs. 0-85952
 Hercules X-1, accretion disc viscosity determ. using slaved disc model 0-62110
 Hercules X-1 (HZ Herculis) binary system, pre-supernova parameters 0-62318
 HZ Herculis, 1978 UBv photometry of active state 0-62189
 AM Herculis, cyclotron lines in spectrum of nova-like star (*Russian*) 0-67753
 DQ Herculis, emission line eclipse phenomena, visible spectra obs. 0-94800
 HZ Herculis, light curve, radiation pressure effects 0-105280
 AM Herculis, polar, IR photometric obs. 0-98687
 DI Herculis, relativistic motion of periastron 0-94830
 AM Herculis, spectrophotometric obs. at min. light min. light 0-98692
 u Herculis, two new light curves 0-90472
 AM Herculis, visual magnitude estimates (1980 March-June) 0-82428
 AM Herculis, X-ray eclipsing binary, UV and visible spectra anal. 0-109563
 AM Herculis (3U 1809+50), polarimetry and spectrophotometry rel. to mag. field 0-94835
 AM Herculis (3U 1809+50), simultaneous three-channel photometry rel. to optical flickering mechanism 0-82411
 AM Herculis (3U 1809+50), UV spectrum obs. 0-67782
 AM Herculis (4U 1814+50), X-ray emitting mag. white dwarf binary, review of props. 0-105403
 HZ Herculis (Hercules X-1), 35 day clock mechanism 0-73070
 HZ Herculis (Hercules X-1), Ariel V X-ray spectra 0-90580
 HZ Herculis (Hercules X-1), implications of cyclotron features in X-ray spectrum 0-86015
 HZ Herculis (Hercules X-1), IUE obs. spectrum and light var. 0-73069
 HZ Herculis (Hercules X-1), optical and UV obs. 0-109487
 HZ Herculis (Hercules X-1), X-ray continuum and Fe line emission during X-ray low state 0-105393
 HR 5110, Algol type RS Canum Venaticorum star, H α , yu photometry obs. 0-105276
 TT Hydrae, absolute dimensions of β Persei type eclipsing binary 0-62184
 EX Hydrae, dwarf nova, IR and optical light curves 0-67747
 EX Hydrae, dwarf nova lightcurve, periodic and secular vars. 0-77413
 HS Hydrae, photometric elements of detached system 0-90473
 EX Hydrae, spectra of dwarf nova 0-98670
 VW Hydris, dwarf nova, IR light curves 0-67747
 instantaneous spectra determ. by inversion technique 0-82218
 SW Lacertae, W Ursae Majoris star, photoelectric obs. and epochs of min. light 0-62196
 LB 3479, subdwarf system, evolutionary model comment 0-90426
 light curve analysis by Fourier techniques 0-72993
 light curve analysis by Fourier techniques 0-72994
 light curves linear analysis, fractional light loss anal. 0-82416
 light curves soln. using LIGHT computer program 0-77454
 β Lyrae, CNO abundances in atmosphere, IR spectra (*Russian*) 0-67794
 β Lyrae, current knowledge 0-105289
 β Lyrae, orbital period variability 0-72997
 TY Mensae, contact eclipsing binary, evolutionary stage from UBv light curve anal. 0-105278
 AU Monocerotis, mathematical anal. of photometric peculiarities 0-77448
 AU Monocerotis, photoelec. obs. 0-73002
 MW Pavonis, W Ursae Majoris system, evolutionary stage from UBv light curve anal. 0-105278
 BB Pegasi, BV photoelectric lightcurve analysis 0-62194
 X Persei, gaseous ring struct., H I alpha obs. 0-109482
 β Persei, Mg II 280 nm line profile, calcs. and UV obs. 0-82421
 RY Persei, spectroscopy and physical parameters of atmospheres 0-101618
 β Persei, UV obs., from TD-1A satellite 0-77447
 RY Persei, visible spectra obs., model 0-67795
 β Persei (Algol), primary component rot. 0-72996
 β Persei (Algol) eclipsing binaries, mass loss and mass transfer theory 0-62191
 SZ Piscium, RS Canum Venaticorum star, photometric obs. rel. to starspot model 0-109490
 VV Puppis, AM Herculis type binary, optical absorpt. spectrum, cyclotron interpretation and models 0-73003
 VV Puppis, polar, IR photometric obs. 0-98687
 radial velocity curves of close binary systems, anal. 0-90470
 WZ Sagittae, 1978-9 outburst of dwarf nova, spectra 0-94801
 WZ Sagittae, eruptive binary, model from hot spot eclipses anal. 0-72962
 WZ Sagittae, image-tube spectroscopic obs. of 1978 Dec. outburst 0-72958
 WZ Sagittae, outburst of December 1978, UV obs. 0-72982
 WZ Sagittae, recurrent nova, IUE obs. in outburst 0-109448
 WZ Sagittae, recurrent nova, spectroscopic obs. and model for superhump phenomena 0-82368
 V1357 Sagittarii, visible obs. 0-77452
 V701 Scorpis, dimensions and evolution of early-type contact binary 0-62188

eclipsing binary stars continued

- V861 Scorpis, upper limit on X-ray emission, and non-coincidence with (OAO 1653-40) 0-73072
 μ Scorpis, UV obs. from TD-1A satellite 0-77447
 RY Scuti, ephemeris and UBv photometry 0-94832
 RZ Scuti, JKL IR obs., light curves 0-101615
 sd-d type, struct. and dimens. 0-82423
 semidetached systems, revised photometric elements 0-62193
 W Serpentis stars, new class, accretion onto nondegenerate stars 0-109483
 Y Sextantis, W Ursae Majoris system, UBv obs., light curve soln. by computer program 0-77454
 Stepanyan's star, obs. of G8 V absorpt. spectrum and emission spectrum 0-67788
 Stepanyan's star, possible cataclysmic variable, eclipses obs. and orbital period refinement 0-62195
 RW Tauri, gaseous ring struct., H I alpha obs. 0-109482
 λ Tauri, mass loss from UV spectra obs. 0-109485
 CD Tauri, orbital element determ., BV photometer obs. 0-73000
 BL Telescopii A, yellow variable supergiant near Cepheid instability strip, VBLUW photometry 0-98672
 RW Trianguli, nova-like binary, radial vels., dimens. from visible spectra 0-82418
 4U 1700-37 (=HD 153919), X-ray obs. 0-86016
 4U 1700-37 (HD 153919), X-ray binary, high-energy X-ray obs. 0-86014
 XY Ursae Majoris, observational evidence for large-scale spot activity on primary component 0-109491
 AN Ursae Majoris, polar, IR photometric obs. 0-98687
 W Ursae Majoris stars, rot. line broadening functions rel. to stellar shapes 0-109494
 UX Ursae Majoris time series photometry 0-77446
 W Ursae Majoris type stars, secular stability of contact binaries with age-zero components 0-67786
 V444 Cygni, light curve anal. by new method 0-109374
 V80 in dwarf spheroidal galaxy in Ursa Minor, eclipsing binary star with RRc primary 0-109505
 ER Vulpeculae, W Ursae Majoris star, rot. line broadening rel. to shape and mass ratio 0-109494

ecology

- conference, Osaka, Japan (Nov. 1979) 0-98756
 environmental background monitoring program 0-81518
 modelling, temperate ecosystem, literature review 0-81949
 nuclear waste ponds and streams, Hanford, ecological search for radiation effects 0-89804
 OTEC power system development and environmental impacts 0-66990
 radioactive effluent, Pu and Am inventory of ecosystem near a nuclear facility 0-97820
 review of ecology and systematics (book) 0-67945
 sonic boom of supersonic transport aircraft, effects on ecological environment 0-106661
 tropical rain forests, exploitation causing destruction (*German*) 0-101137
 vegetation thermal IR emissivity, ecological variations 0-104557

economic and sociological effects

- see also *demography; personnel*
 air pollution, material damage functions 0-76693
 air pollution damage, economic evaluation 0-76692
 energy storage, social implications 0-67001
 fusion reactor, Tandem Mirror Reactor power plant, maintenance and handling economics 0-102311
 Indian scientists' role in policy making process, critical assessment 0-90653
 information technology, conference, London, England (Nov. 1979) 0-90599
 MIT undergraduate physics students, goals, aspirations and attitudes 0-57022
 nuclear power, environmental issues 0-94121
 nuclear power station, operation, socio-economic effects on demography, finance and local activities of region (*French*) 0-74038
 physics and arms race, physicists participation explored for general education students 0-57023
 road traffic noise, a socioeconomic approach to subjective responses 0-67022
 Soddy, F., nuclear science, economics and social responsibility, holistic approach 0-90640
 wind power generation in North Sea, feasibility and economics 0-97759

economics

- air-conditioning, energy saving control system, using heat storage tank (*Japanese*) 0-72087
 alternative energy sources, energy accounting study 0-76589
 artificial satellites, future applications, reliability and cost considerations (*Italian*) 0-109334
 cellulosic waste disposal by conversion to ethanol 0-61502
 desalination plants, MSF, solar powered 0-61281
 diamond tool bit machining, comparison with conventional optical process 0-69569
 electrochemical processes, energy use analysis (*Dutch*) 0-72019
 electrochemical processes, energy use optimisation (*Dutch*) 0-72020
 energy conservation, hard and soft paths compared 0-89584
 energy conservation in Britain, main options 0-76620
 energy resources, economic choice for rural India, methodology 0-104499
 energy-political questions nationally and internationally for West Germany (*German*) 0-101072
 fibre optic market trends, worldwide 0-38699
 finance for space research, the role of private funding in European space ventures 0-77121
 fission reactors, fast breeder, using uranium-plutonium cycle, Na-cooled, technical and economic viewpoints of application (*German*) 0-99202
 flat-plate non-tracking ground mounted photovoltaic array structures, cost reduction anal. 0-94038
 flat-plate photovoltaic array design optimisation 0-94037
 flywheel energy storage and conversion system for photovoltaic appl., economic anal. 0-94116
 fusion reactor, LARTS, extended burn operation, physics, engineering and economics 0-95440
 fusion reactor, multiple mirror, coil design and economic optimisation 0-99284
 fusion reactors, committed site development, technical and economic aspects 0-95437

economics continued

- fusion reactors, symbiotic energy system, U fuelled, economic anal. using SYMECON code 0-106172
- fusion reactors, Tokamaks, maintenance design requirements and economics 0-99285
- fusion symbiotic system, managing fusion burn, economic analysis 0-106173
- geothermal energy resources for electricity generation, discounted cash flow anal. 0-85263
- horizontal-axis wind-turbine system for pumping duties in Third World agriculture, economic aspects 0-61259
- hybrid solar photovoltaic/solar thermal electric power system, simulation 0-94025
- hydraulic coal trunk pipeline transport systems, methods of improving economic effectiveness 0-106837
- international symbiotic nuclear energy parks using breeders and advanced converters, economic feasibility 0-57825
- Kitt Peak National Observatory telescopes, cost effectiveness in terms of publications and citations 0-90334
- KS-7F solar kitchen, economic effects on economy 0-89590
- metallurgy, automatic barrel line type ATS closed system, small parts electroplating, after-treatment and drying (*German*) 0-84861
- neutral beam source, cryopumping and mag. shielding, fabrication and operating cost 0-106229
- nuclear fusion reactor materials, social aspects (*Dutch*) 0-106153
- nuclear power stations, cost comparison of PWR and PHWR in Korea 0-57821
- optical fibre transmission systems, 1.2-1.5 μm , economic evaluations and forecasts 0-87533
- optical precision instrument manufacture, microcomputer appl. (*German*) 0-95116
- optical shop interferometric instrumentation as a cost-effective production tool 0-74535
- photovoltaic system sizing anal. 0-94039
- photovoltaic systems break-even cost anal. for rural Mexico 0-94027
- power generation, hydroelectric, economic assessment of fuel savings (*Russian*) 0-97760
- power stations, steam-gas combined, based on natural gas resources from North Sea, economics and possibilities (*Norwegian*) 0-101073
- solar cell fabrication, photovoltaic process based on thick film technique 0-94016
- solar cells, thin film, technical and economical eval. 0-94012
- solar energy, Middle Eastern research programmes 0-66939
- solar input and solar data computation for engineering of solar systems, transients simulation 0-94060
- solar photovoltaic arrays, optimisation of total annual energy output from constant/adjustable tilt systems 0-94059
- solar photovoltaic power systems for rural areas of developing countries, technology, reliability, economics and appls. 0-61286
- solar power, technical-economic validation of resources as energy sources 0-89593
- solar powered residential water heating 0-61311
- solar thermoelectric generators, metallic thermo-electric materials utilisation, economic characts. 0-101122
- solar voltaic power systems, comparison to fuel energy, for telecommunications 0-61381
- solar water heating systems, economic assessment based on measured performance 0-97807
- space heating, solar collectors combined with ground heat pumps, advantages (*German*) 0-76605
- space-manufactured satellite power systems, costs anal. using lunar materials 0-97767
- superconductive energy storage magnet, single layer, design and cost-related parameters 0-108815
- symbiotic system economic evaluation using SYMECON 0-106177
- transducers of electrical variables, modular, third-generation individual and group arrangements, NC series (*Czech*) 0-62645
- underground pressurised saturated hot water storage for peak lopping appls., economic aspects 0-76653
- university engineering education courses economics 0-67973
- wind energy conversion systems, value to electric utility, economic model 0-61257
- wind power, recent developments aid economic aspects 0-61238
- wind power plants, integration into existing power systems, implications 0-61258
- CdS-Cu₂S thin-film solar cells, low-cost manufacturing process outline, economic anal. 0-93930
- Si photovoltaic industry, environmental control, economic and ecological requirements 0-94026
- Si solar cells, low cost processes for fabrication 0-94013

eddy current losses

- domain wall dynamics, eddy current dominated, and magnetisation losses 0-88778
- estimation method, in large steel plate having one-phase excitation (*Polish*) 0-93145
- ferromagnetic plates eddy current phenomena numerical computation method (*German*) 0-65952
- fusion reactor, TFTR, eddy current theory for structural materials 0-95427
- plate, nonmagnetic, thin, with multiparallel system of conductors, losses calc. 0-78743
- Fe powder-plastic composite, soft mag. material, mag. and mech. props. 0-75812
- Fe-Si (3 wt.%), grain-oriented, domain struct. regulation and power loss reduction 0-88779
- Fe-Si (3 wt.%), grain-oriented, power loss and domain wall variation with lamination thickness 0-88814
- Fe-Si (3 wt.%), grain-oriented, energy loss reduction by lowering sheet thickness 0-88816
- Fe-Si (3 wt.%), oriented, losses and domains, mech. stress effects 0-88852
- Nb-Ti superconducting single layered multifilamentary coil, eddy current loss depend. on demagnetisation 0-97040

eddy currents

- see also induction heating
- coating ZZ 0-77775
- complex shape product inspection, local eddy current transducer 0-108671
- conducting cylinders in field of conductors perpendicular to side surfaces (*German*) 0-106415

eddy currents continued

- cylindrical products, diameter meas., interfering factors elimination 0-77755
- double-ended eddy current transducers, signal calc. for nonferromag. cylindrical products 0-89443
- electrical conductivity meas., standard models 0-86343
- feed through eddy current transducer, numerical anal. or operating mode during ferromagnetic rod inspection 0-108670
- ferromagnetic plates eddy current phenomena numerical computation method (*German*) 0-65952
- flaw detection, suppression of interf. parameters 0-89442
- flaw detection of long ferromag. products, magnetizing device parameters 0-89447
- imaging flaw detection system 0-89426
- irregularly shaped plates, slow ramped field, eddy current heating, anal. 0-91722
- metal, eddy current response to solidification in one dimension 0-104140
- metallic objects with complex shape, eddy-current inspection 0-89446
- MHD channel, anisotropically conducting plasma in inhomogeneous elec. and mag. fields, current calc. (*Russian*) 0-74995
- multifrequency eddy current inspection with continuous wave methods 0-71844
- non-magnetic tubular conductors, eddy current study (*French*) 0-83541
- nonmagnetic conducting tubes appl., special study (*French*) 0-83540
- nuclear power station heat exchangers, eddy current probe for nondestructive testing of transfer tubes (*Japanese*) 0-81246
- plate, metallic, eddy current distrib. after step function of external magnetic field 0-69293
- Poisson's ratio, eddy current determination 0-65116
- polymer mixture, metal fraction contents and properties meas. method (*Russian*) 0-76571
- steel, cold-rolled, isotropic, specific magnetic loss meas. at high frequency 0-101808
- steel, structural ties, NDT by eddy current transducer, optimum parameters and capabilities 0-108669
- testing of wire and bar 0-71819
- Tokamak fusion reactor vacuum vessel, eddy currents when plasma current is disrupted, calc. (*German*) 0-68937
- toroidal deflection yokes, eddy current compensation 0-95762
- transducer, feed-through, approx. calc. of mag. field, non ferromag. media 0-78746
- transducer, matrix eddy-current, with magnetic circuit, design and construction 0-68228
- transducer with electrical commutation of excitation field, NDT 0-105633
- ultrasonic and eddy current testing of welded titanium tubes (*Japanese*) 0-108651
- Young's modulus, eddy current determination 0-65116
- Fe-Ni-Mn, Invar, RF collapse and thermal effects, Mossbauer study 0-100624
- Pb-Sn (20wt.%), eddy current study of solidification 0-104141
- Si monocrystal peripheral fusion channelling under HF heating (*Russian*) 0-59627

edge dislocations

- cholesteric, liquid crystals, disclinations, rotation defects, topology (*French*) 0-79679
- climb process, of edge dislocation, effect of glide forces 0-70195
- crack propagation effect of 2- or 3-dimensional macrodefect (*Japanese*) 0-104261
- cracks, plane elasticity, curvilinear crack edges concentrated forces and edge dislocations, numerical soln. 0-58970
- dechannelling mechanism due to dislocations, anal. 0-59538
- diamond crystals, synthetic, etch-pit formation on cube faces, electron microscopy obs. 0-75232
- electron microscopy, high resolution, dislocation core studies, image calc. methods 0-96535
- electronic localised state at edge dislocations, parabolic dispersion law (*Russian*) 0-65479
- free surface in undeformed and deformed crystals, differential geometry, distortion, torsion, Burgers circuit 0-64996
- magnetically ordered cryst., dislocation drag, magnetoelastic waves 0-103332
- point defect-edge dislocation interaction near solid surface 0-79834
- screening in metals and superconductors, metal softening (*Russian*) 0-64997
- stability under shear stress, hydrostatic press. 0-59462
- superconductors, type II, vortex pinning at edge dislocations, electrostatic mechanism 0-103802
- superdislocations, resist. to motion, temp. depend. expressions (*Russian*) 0-79789
- surface dislocations, universal concept, rel. to disclinations and grain boundaries 0-100231
- triglycine fluoborillate, deuterated, dislocation line defect X-ray topographic analysis 0-59465
- two-face dislocation boundary, energy and induced stresses (*Russian*) 0-103331
- web dendrites, dislocations, stacking faults, X-ray topographic study (*Chinese*) 0-88148
- Al bicrystal, high resolution electron microscopy obs. of dislocations 0-103347
- Al-Mg (0.3 wt.%) single cryst., dislocations obs. by high voltage electron microsc. 0-79796
- Al₂O₃, sapphire, edge dislocation loop obs. by high resolution lattice imaging 0-103346
- Au/Cu, bilayers, interdiffusion phenomena, lattice dislocations, TEM obs. 0-59736
- Bi anisotropic crystal, dislocation wall stress field and strain energy 0-100233
- CdS, acoustic wave attenuation, phonon viscosity and dislocation drag 0-70319
- Cu alloys, FCC, climb of extended dislocations due to irradiation in HVEM 0-103343
- Cu, electrical resistance of edge dislocations (*German*) 0-96859
- Cu, single crystals, neutron irradiated, stresses and secondary slip between overlapping and dislocation arrays 0-88162
- Cu, single crystals, cyclically and unidirectionally deform. X-ray diff. study 0-89319
- Cu-Cd (1.0 wt.%), yield stress and flow stress 0-97524
- (Cu-Au)-Co, single crystals, solid soln. and particle strengthening, superposition 0-97495

edge dislocations continued

- Fe, epitaxial growth on Au platelets, dislocations 0-96760
 Fe-Al, single crystals, deform. at high temps. 0-81125
 $\text{Ga}_{1-x}\text{Al}_x\text{As}_{1-y}\text{P}_y$ epitaxial layer heterojunction, nonradiative recombination at misfit dislocations 0-96901
 GaSb, acoustic wave attenuation, phonon viscosity and dislocation drag 0-70319
 Ge bicrystal, high resolution electron microscopy obs. of dislocations 0-103347
 Ge, dissociated dislocations, constriction correlation with jogs 0-79801
 Ge, energy spectra of dislocations 0-70637
 LiF bicrystal, high-angle tilt boundary and edge dislocation intersection effects 0-79836
 LiF crystal, contact damage obs. by cathodoluminesc. 0-71728
 LiF, dislocation structure, influence of variable defect. temp. 0-70211
 MgO crystal, contact damage obs. by cathodoluminesc. 0-71728
 MgO crystal, yield strength and dislocation mobility 0-93601
 MgO, electron irradiation damage, cryst. defects 0-107320
 MgO, single cryst., tensile creep, stress induced dislocation structs. 0-96539
 MgO single crystals, dislocation processes, obs. by HVEM in-situ deform. 0-103340
 $\text{MgO}:\text{Fe}^{3+}$, point defect complex-edge dislocation interaction energies, atomistic calc. 0-107314
 NaCl, dislocation density in monocrystal deformed under high hydrostatic press. 0-70216
 NaCl, dislocation mobility under high press., temp. depend. 0-75235
 NaCl, dislocation ordering influence on integrated X-ray coeff. 0-103357
 NaCl, edge dislocation, core struct. and props., theory 0-70194
 NaCl, electric field gradients near dislocations, resulting NMR lineshapes 0-75225
 NaCl, high resolution TEM and radiation sensitivity, dislocation obs. on deformed crystals. 0-107260
 NaCl, polarisation caused by charged dislocation motion 0-59463
 NaClO_3 , dislocations rel. to growth mechanism from aq. soln., X-ray topography 0-59464
 Ni-H, thermally charged, serrated yielding 0-85007
 Si, Czochralski grown crystals, swirl-type defect obs. 0-100236
 Si, dislocation generation in local oxidation 0-107245
 Si, energy spectra of dislocations 0-70637
 Si:P, dislocation disloc. mode obs. by weak-beam TEM 0-107259
 Te, a-edge dislocated crystals, mobility anisotropy 0-107781
 YAG crystals, dislocations and inclusions, birefringence topography obs. 0-107248
 Zn, line energy of basal screw dislocation, exptl. determ. 0-88154
 Zr alloys, creep and growth, irradiation induced, microstruct. depend. 0-93602
 Zr, irradiation growth, reaction rate theory calcs. 0-88212

education

- see also educational aids; educational courses; teaching; training*
 air-dielectric interface, EM wave reflection and transmission in terms of polarisation 0-105458
 black hole energy emission, Heisenberg's uncertainty principle 0-105454
 damped oscillator motion, expansion in normal modes 0-67951
 de Broglie waves, dispersion relation 0-67949
 Earth's core discovery 0-105486
 electrical and electronic engineering design education and training conference, London, England 0-67971
 electrical and electronic engineering undergraduate courses, engineering design importance 0-67972
 electrostatic potential, laboratory and theoretical comparison 0-105461
 engineering education, importance of research and design for satisfying industrial needs 0-67974
 Euler's three-body problem, eqns. of motion 0-67953
 extremum sufficient condition in classical action integral, eigenvalue problem 0-105462
 formal reasoning patterns, study using Piagetian tasks, appls. to science education 0-77560
 International Commission on Physics Education, activities 0-101682
 Lorentz transform law for EM field, fluxoid motion example 0-67954
 magnetic field from charges in arbitrary motion 0-105460
 magnetic multipole expansion 0-105456
 mathematics module, description and evaluation 0-86056
 meteorology, survey of weather forecasting games at American Universities 0-98770
 microscopy, course at North Carolina State University 0-95135
 MIT undergraduate physics students, goals, aspirations and attitudes 0-57022
 national science curriculum, impact on content-free cognitive outcomes, in Tasmania 0-77559
 nonlinear oscillators, turning point approx. and appl. 0-67952
 obstetric practice, the place of real-time and static B-mode scanning, educational syllabus 0-86057
 particle in selfgravitating spherical dust shell, adiabatic invariance 0-105459
 physics and arms race, physicists participation explored for general education students 0-57023
 quantum tunneling through a rectangular barrier using $|\psi|^2$ and flux 0-105457
 quantum oscillators, matrix element diagrams 0-105455
 resistive hose instability in relativistic electron beam 0-67947
 school curricula, science and mathematics development 0-86055
 schools specialised in physics and mathematics (Hungarian) 0-67956
 Schrodinger equation, exactly soluble with bistable pot. 0-67950
 teaching at an independent day school in USA, a typical day 0-57045
 university engineering education courses economics 0-67973

educational aids

- see also student laboratory apparatus*
 audio-visual learning aids laboratory in teaching of analytical chemistry 0-94944
 ball-bearing electric motor construction 0-67997
 bi-lingual audio-visual aids for technical education in developing Arab countries 0-94943
 castor oil dielectric fluid, microwave propag., permittivity effect, demonstration 0-105468
 college astronomy and physics texts, readability 0-77583
 compact solar camera, student project 0-67975
 computer terminal to audiovisual device interface 0-67986
 digital timer with memory, appl. to dynamics experiments, principles of electronic circuitry 0-67994

educational aids continued

- Einstein and Brownian motion, student project 0-68000
 Foucault's rotating mirror method for meas. speed of light 0-67996
 hazemeter for window pollution assessment 0-67995
 holographic movie camera and projection system 0-78808
 information technology, conference, London, England (Nov. 1979) 0-90599
 least square fitting, pocket calculator program with variable precision 0-67976
 light velocity fibre optic wink-around expt. 0-90628
 mathematics teaching by computer, long-division practice program in BASIC 0-98775
 microcomputer systems, appls. for chemistry CAI 0-57042
 microcomputers in education, hardware, software and personnel problems 0-98771
 microcomputers in schools, software and equipment choice 0-98772
 music practice rooms, user requirements 0-74606
 nodal slide, experimental and theoretical thick lens parameters comparison 0-67998
 numerical analysis, interactive teaching package 0-86058
 optical-to-tactile converter 0-57041
 PET 2001, multidisciplinary summer course for schoolchildren 0-98774
 physics teaching aids, convention of secondary school physics teachers (Hungarian) 0-67957
 physics teaching using SWTP 6800 system in BASIC 0-98776
 shuttlecock, terminal vel. in vertical fall 0-90627
 slide/tape modules use in teaching SEM 0-68005
 strain gauge data logger, for educational purposes 0-73353
 teaching aids and materials 0-94942
 TRS-80, teaching at Keene High School 0-98773
 TV microscopy system for teaching and quality control 0-82817
 ultrasound propagation in liqs., undergraduate expt. 0-69608
 video tapes in SEM teaching, evaluation 0-68004
 weather forecasting games at American Universities, survey 0-98770

educational computing

- see also computer-aided instruction*
 astronomy, use of computers in schools 0-73126
 microcomputers in education, hardware, software and personnel problems 0-98771
 orbital motion on an interactive-graphics terminal 0-73152
 physics laboratory experiments, graphic computer simulations 0-105470
 student appraisal system, computer automated sign-on, item anal. 0-62430
 test generation program design for astronomy courses 0-90622

educational courses

- alkali metals, cohesive energy 0-90630
 approximation methods for 0-105474
 biomedical engineers and technicians in developing countries, training 0-62408
 computerised test generation program design for astronomy courses 0-90622
 electronics, undergraduate laboratory course 0-105478
 fibre optical communications, course status and effectiveness 0-62413
 geophysics, applied MSc programme in Nigeria 0-105463
 integrated optics graduate survey course at Georgia Inst. of Technology 0-62414
 localised interference fringes 0-101680
 master's level graduate training in medical physics at the University of Colorado Health Sciences Center 0-82603
 mathematics, remedial work for university students in engineering courses 0-86054
 Modern Optics Project Laboratory course at MIT, programme 0-62421
 musical acoustics, teaching of blind students 0-77584
 optical engineering education at Carnegie-Mellon University, programmes review 0-62419
 optical radiation detector laboratory, graduate-level, expts. 0-62432
 optics, graduate training at Optical Sciences Centre, programmes 0-62418
 optics and lasers, San Diego State University, programme 0-62423
 optics at Texas Tech. University, programme methods 0-62424
 optics education, graduate, at Air Force Inst. of Technology, programme 0-62417
 optics education at Georgia Tech, development and current status overview 0-62420
 optics graduate degree programme, on-site, case study 0-62416
 optics laboratory, undergraduate, in American universities, status 0-62411
 optics programmes and opportunities in US 0-62412
 optics programmes in US, attacks and recommendations 0-62409
 optics teaching by faculty of Inst. of Optics, profile 0-62422
 optics technology programmes in US, development 0-62410
 physics 13: teaching modern physics through science fiction 0-90626
 scientific revolutions, Einstein and Lorentz examples 0-82594
 SEM coordinated, multidiscipline courses 0-67965
 solar eclipse predictions using vector method for intermediate level astronomy courses 0-105452
 solid surfaces, surface processes, and solid/gas interactions 0-73125

e.g. see electroencephalography**effective mass (band structure)**

- exchange interactions in semiconductors and insulators, mean free path and energy gap effects 0-88522
 graphite intercalated with AsF_5 , quantum oscillatory phenomena 0-107823
 graphite surface, adsorbed He, band struct. and thermodynamic props. 0-80349
 metal, work function, pseudopot. calc. 0-96970
 MOS structure, 2D electron gas, for IR Faraday rotation 0-80389
 neutral bound excitons, accurate binding energies, variational method calc. 0-107715
 polar crystal, Frenkel exciton effective mass temp. depend., lattice displacement interactions (Chinese) 0-84429
 polar crystal, polaron effective mass temp. depend., electron interaction (Chinese) 0-84436
 polytypes, one-dimens. Kronig-Penney model and calcs. 0-75494
 pyrolytic graphite, magnetoresistance positive-negative transition (Russian) 0-96923
 semiconductor, elec. cond., hopping model, semi-classical, effective mass and carrier mobility calc. 0-96872
 semiconductor, shielding by electron gas in magnetic field 0-107727
 semiconductor superlattice, transverse electron effective mass 0-100429

effective mass (band structure) continued

- semiconductors, ferromagnetic multivalley anisotropic, electron autolocalisation (*Russian*) 0-92848
 superconductor, effect of varying electronic density of states 0-75672
 tunnelling MIS structures photovoltaic energy conversion, band struct. 0-92995
 two-valley semiconductor, hot electron instability, intervalley scatt. (*Russian*) 0-92921
 Au-SiO₂-Si system, oxide film 16-36 Å thick, tunnel currents 0-70842
 Cd,Hg_{1-x}Te epitaxial graded gap layers, plasma reflection and magnetoreflection 0-71391
 Cd,Hg_{1-x}Te layers, epitaxial graded-gap, nonlinear elec. effects 0-100468
 p-CdSnAs₂, Hall effect, thermo EMF, thermomagnetic effects 0-107822
 p-CdSnAs₂, heavily doped, elec. transport props. under elastic deformation 0-96915
 CdTe:Li(Cl), acceptor states study by donor acceptor pair excitation luminesc. 0-100683
 CdTe-HgTe superlattice on CdTe layers, evanescent states, tight binding calcs. 0-70611
 CoS₂, galvanomagnetic effect of single cryst. 0-96912
 Cu, Fermi surface, electron mass enhancement, orthornormal function enhancement 0-96777
 CuCl, exciton spatial dispersion determ., two-photon Raman scatt. via excitonic mol. state 0-60595
 Ga_xAl_{1-x}As, photodetector diode on GaAs substrate dark currents, tunnelling, energy gaps, effective masses 0-70805
 GaAs, conduction band effective mass, influence of high uniaxial stress 0-80162
 GaAs-Al_xGa_{1-x}As heterojunction interface, two-dimensional hole gas obs., Shubnikov-de Haas meas. 0-80357
 Ga_xIn_{1-x}As_yP_{1-y}, electron effective mass, cyclotron reson. and magnetophonon effect meas. 0-103618
 Gd-Ni, ferromag., elec. resist. temp. depend. 0-96843
 Ge, donor polarizability, multivalley effective mass calc. 0-96817
 Ge, effective masses of heavy and light holes, from ohmic mobility data 0-80160
 GeTe, effective masses for cond., density of states 0-88472
 GeTe-Sb₂Te₃, solid solutions, cond., density of states 0-88472
 Hg_{0.82}Cd_{0.18}Te, electronic anomalous mass near reson. acceptor level, Shubnikov-de Haas meas. 0-80163
 HgTe, mobility of electrons and holes, 4 to 100K 0-107821
 In_{1-x}Ga_xAs_yP_{1-y}, electron effective mass from Shubnikov-de Haas meas. 0-80298
 In_{1-x}Ga_xAs_yP_{1-y}, evidence for alloy scatt. from press. induced changes of electron mobility 0-88548
 In_xGa_{1-x}As_yP_{1-y} photodetector diode on InP substrate dark currents, tunnelling, energy gaps, effective masses 0-70805
 In_xGa_{1-x}P_yAs_{1-y}, electron effective mass and Dingle temp., Shubnikov-de Haas oscills. 0-59859
 Mo, effective mass meas. and electron velocities 0-96773
 Nb, Fermi surface, electron mass enhancement, orthornormal function enhancement 0-96777
 Ne, solid, hole band struct., Bratsev wave function calcs. (*Russian*) 0-65437
 p-Pb_{1-x}Ge_xTe film, cyclotron reson. above and below struct. phase transition 0-88879
 PbS, anomalous magnetoresist. 0-107813
 Pb_xSn_{1-x}Se solid solns., photoluminesc. spectra, energy band parameter determ. 0-71484
 Pb_{1-x}Sn_xTe, hole effective mass near zero bandgap, IR refl. study 0-108205
 Pb_{1-x}Sn_xTe, lattice and electronic props. and g-value 0-80161
 Si, deep-level point defects, effective-mass nature 0-59922
 Si, donor polarizability, multivalley effective mass calc. 0-96817
 Si, effective masses of heavy and light holes, from ohmic mobility data 0-80160
 Si, electron and hole effective mass, intrinsic conc., temp. depend. 0-107692
 n-Si, Faraday rot. temp. depend., effective mass determ. 0-71392
 p-Si, heavily doped, intra- and interband Raman scatt. by free carriers 0-108208
 Si, local pseudopotential, Gaussian band charge model 0-88477
 Si on sapphire thin film, Hall effect, magnetoresistance (*French*) 0-65601
 Si p-channel MOS structure, stress effects on elec. props., press. transducer props. 0-100526
 Si:Li, electron-phonon scatt., in intermediate conc. region 0-65180
 Sn, liq., optical props., 0.62-3.7 eV 0-75996
 Sn, white, band masses and deformation pots., OPW pseudopotential model 0-100430
 α-U, Fermi surface and effective masses, de Haas-van Alphen meas. 0-65426
 V, electronic structure, model potential calcs. (*Russian*) 0-100431

effusion

- vapour pressure computer-automated meas. by simultaneous Knudsen torsion-effusion method 0-73334
 Fe-Zn, homogeneous phases, Gibbs free energies of form., Knudsen effusion method 0-66481
 URu₃, sublimation thermodynamics 0-97722

EHD *see electrohydrodynamics***EHT calculations**

- alkanes, H⁺ chemical shifts, extended Huckel calcs. with gauge in variant atomic orbitals 0-102449
 benchtrotene, EHT method calcs., parametrisation, population anal. (*French*) 0-58157
 benzene, H⁺ chemical shifts, extended Huckel calcs. with gauge in variant atomic orbitals 0-102449
 trans-butadiene, polarisability, nonlinear elec. susceptibility, SCF calcs. 0-95547
 dibenzylchromium, EHT method calcs., parametrisation, population anal. (*French*) 0-58157
 ethylene, polarisability, nonlinear elec. susceptibility, SCF calcs. 0-95547
 ethylenic compounds, H⁺ chemical shifts, extended Huckel calcs. with gauge in variant atomic orbitals 0-102449
 ferrocene, EHT method calcs., parametrisation, population anal. (*French*) 0-58157
 hexatriene, polarisability, nonlinear elec. susceptibility, SCF calcs. 0-95547
 III-V compounds, (110) surface, energy distrib. of dangling-orbital surface states 0-80347

EHT calculations continued

- organometallic compounds, EHT method calcs., parametrisation, population anal. (*French*) 0-58157
 overlap and electron interaction effects, rel. to NDO LCAO theories 0-95536
 α-quartz, CNDO/2 calcs., electronic props. of perfect cluster, EPR parameters of O²⁻ vacancy 0-107701
 relative Raman line intensities, extended Huckel valence basis sets 0-106329
 self-consistent charge Xα method, appl. to small mols. 0-91449
 self-consistent charge Xα method, theory 0-91448
 Si (111), surface relax., EHT and cluster calcs. (*Chinese*) 0-59762
 (TCNQ)₂, dimeric interactions, MO calcs., applicability to crystal struct. 0-75215
 (TTF)₂, dimeric interactions, MO calcs., applicability to crystal struct. 0-75215
 TTF-TCNQ, dimeric interactions, MO calcs., applicability to crystal struct. 0-75215
 Ag latent image particles, electronic effects 0-82840
 GaAs (110), surface electronic struct. calcs. 0-80343
 GaAs, (110) surface structure, rotational relaxation, cluster model (*Chinese*) 0-107621
 GaAs, pure and N doped, extended Huckel theory appl. 0-59916
 GaP, pure and N doped, extended Huckel theory appl. 0-59916
 NbSe₃, electronic struct., chem. interpret. of geom. deform., oxidation state formalism 0-107690

eigenfunctions *see eigenvalues and eigenfunctions***eigenvalues and eigenfunctions**

- acoustic signal processing, eigenvector decomposition of correlation matrices 0-96118
 acoustics, eigenmode analysis of the interference patterns in reverberant sound fields 0-96112
 anharmonically coupled oscillators, semiclassical calcs. of eigenvalues 0-95514
 anti-commutative, self-inverse matrices and transformations in eigenvalue problems (*Chinese*) 0-101951
 asymptotic distribution of eigenvalues for the multidimensional Schrödinger equation 0-94985
 atomic eigenfunctions, nodal structure 0-57122
 beams flexural-torsional problem by series expansion in eigenfunctions 0-83732
 biological systems, symmetry 0-81519
 boson field, damping superoperator eigenvalue problem, direct soln. 0-57180
 buckling, bifurcation and limit point instability of dual eigenvalue third order systems 0-87727
 chemical reaction diffusion equation, nearly degenerate bifurcations, mode interactions 0-85149
 circle theorems for inviscid steady flows 0-59043
 climatology of global solar radiation in California and an interpolation technique based on orthogonal functions 0-67402
 coupled second-order differential eqns., numerical soln. method for eigenvalue problems 0-94976
 cubic crystals, perfect, nonBloch electron state density 0-75487
 cylindrical orthotropic shell stability problems, spectrum singularities 0-99950
 determination by continued fraction 0-105490
 diatomic mols., spurious avoided crossing detection 0-87057
 diffusion, two-way, separation of variables, decaying and growing eigenfunctions 0-62594
 diffusion and convection in parallelogram cross-section pipe with plug flow (*German*) 0-100000
 diffusion equation, from space-time transport eqn., for anisotropic random media 0-62595
 double well Schrödinger operators 0-90698
 doubly anharmonic oscillator, class of exact solns. 0-105531
 education, eigenvector of general rot., geometrical construction 0-57025
 elastic shell, cylindrical, isotropic, elastic stability, critical load analysis 0-83744
 empirical eigenfunction anal., appl. to prediction of beach changes in S. California 0-98305
 evolution equations, nonlinear, inverse spectral transform, generalisation of Klein-Gordon problem 0-68055
 evolution systems and convection-diffusion, stiffness and stability, Gershgorin theory 0-77626
 extreme eigensolution calculation method for high order real symmetric matrix 0-90703
 extremum sufficient condition in classical action integral, eigenvalue problem, education 0-105462
 fermion field with broken SU₂ symm., two-dimensional isotopic model (*Russian*) 0-73616
 finite chain, with random dil. impurities, localisation characts., amplitude anal. 0-96825
 fluid dynamics, Poiseuille flow in circular pipe, linear stability 0-79399
 fluid dynamics, stationary superpionic gas stream conical flow about plane wedge and circular cone 0-74912
 fluid structure vibr. eigenvalue problems, finite elements, modal methods 0-96269
 galaxies, global instability of polytropic gaseous discs with Toomre density distrib. 0-98725
 Gelfand-Levitan equation, non-self adjoint operators, eigenfunctions, spectral representations 0-86131
 general SCF coupling operators, arbitrariness 0-99439
 hadronic matter, string junction model and spectrum energy density of string 0-57556
 harmonic oscillator, ground and first excited state energies, g⁰ quantum field theory 0-62839
 harmonic oscillators, position and momentum eigenstates, superposed coherent states 0-57135
 Henon-Heiles Hamiltonian system, vibr. energy levels in quasiperiodic and stochastic regimes, props. 0-91529
 Huckel matrix, degenerate eigenvalues investigated under insertion of additional bond or centre 0-78542
 Hulthen potential energies for l≠0, screening parameter 0-101731
 hypervirial scaling iterative method 0-73196
 ideal string, extremal solutions of inverse eigenvalue problems with finite spectral data 0-101712
 image methods for constructing Green's functions and eigenfunctions for domains with plane boundaries 0-94979
 irregular finite element meshes, grading rules 0-68045

eigenvalues and eigenfunctions continued

- isospectral matrices, finite transforms 0-105529
- Josephson junction, current biased, eigenstates and eigenvalues 0-60148
- Klein-Gordon equation, inverse spectral transform 0-68055
- Kramers equation, eigenvalues calc., Fokker-Planck eqn. for Brownian motion in a potential 0-86215
- layered composites, heat conduction eigenvalue problems 0-74702
- linear microscopic equations in irreversible thermodynamics, eigenvalue problem 0-57227
- linear transport equation, continuously varying spatial media, elementary solns. 0-86229
- magnetic resonance results, eigenvectors and eigenvalues, error estimation by linear data-fitting technique 0-68018
- mechanical systems, follower load type, time invariant functionals 0-77609
- molecular energy levels 0-58123
- molecule, nonrigid, sum of states, isometric group, symmetry no., thermodynamic functions 0-58186
- momentum eigenfunctions in complex momentum plane, Hartree Fock functions 0-63517
- N-electron system, Schrodinger eqn. soln. using antisymmetrisation 0-106246
- narrow resonances, high energy mag. resonances, exactly soluble model 0-86134
- neutron transport theory, ω mode transport eqn., asymptotic soln. 0-102231
- nonlinear second order system, eigenfunction expansion solutions of Fokker-Planck eqn. 0-73172
- nuclear octupole vibration, collective, wave functions, spherical harmonics 0-68532
- nuclear structure, quasiclassical soliton solutions of Hartree eqn., Newtonian interaction with screening 0-68569
- numerical integration leading to Bohr-Sommerfeld formula, alternative to JWKB calcs. 0-86119
- ocean trench waves, dispersion curves and eigenfunctions 0-72547
- optical bare resonator eigenvalue analysis, matrix methods 0-78927
- optical fields, broadband coherence-separable, free-space propag. model 0-78763
- optical inhomogeneous circular waveguide, asymptotic eigenvalues of vector waves 0-96010
- optical leaky dielectric waveguide, planar hollow structure, eigenmode analysis 0-78973
- optical-fibres, graded-index, mode eigenfunction computation, propagating beam method 0-95988
- orbital angular momentum eigenvalues, integrality calcs. 0-67977
- oscillator, quartic, zeta function 0-62532
- oscillators, quartic, eigenfunction zeroes 0-73197
- partition functions, coherent states and upper bounds in Hilbert space 0-57173
- plasma drift waves, eigenmodes with arbitrary radial wavelengths, stability 0-64710
- plasma instabilities, resistive-g and ion temp. gradient in sheared magnetic field 0-64708
- polarons, energy eigenvalue, systematic calculation procedure 0-84439
- polychromatic speckle pattern, dominant eigenvalues to evaluate intensity probability density function 0-106451
- polymer diffusion equation with hydrodynamic interaction, equiv. normal coord. 0-79966
- post-buckling behaviour of structures using a finite element-nonlinear eigenvalue technique 0-92078
- potential problems, non-local, Perey effect, WKB method 0-68077
- pseudo Coulomb problem, group $O(2,1)$, irreducible representation 0-73209
- quadrupole-phonon states, fifth label generating operator, props. and eigenvalues 0-79887
- quantum energy levels, statistical mechanics method, perturbative variational approach 0-62513
- quantum field theory, inverse problem method 0-68377
- quantum mechanical systems, moment method of eigenvalue and expectation value determ. 0-62534
- quantum mechanics, decaying states in rigged Hilbert space formulation 0-62521
- quantum pendulums, classical, semiclassical and quantum aspects, teaching 0-101679
- quantum tunnelling, reaction coord. method 0-62500
- quark confinement, coupling constant inverse, energy perturbation expansion and eigenvalue 0-86658
- quasiclassical estimates on moments of the energy levels 0-98806
- radial Schrodinger equation, eigenvalues, matrix elements, phase shifts 0-86133
- radiative transfer integral equation spectrum, eigenfunctions asymptotic behaviour 0-67540
- random matrix ensembles, joint eigenvalue distrib. 0-101748
- relativity, spherically symmetric space-times with vanishing curvature scalar 0-68096
- resonance eigenvalues, accuracy criteria 0-91423
- resonance theory in indefinite metric spaces 0-101730
- ring laser, open cavity matrix eqns. in diffraction theory 0-69429
- rotated hamiltonians, complex-coordinate rotation and least-squares variational method 0-68075
- rotating harmonic oscillator, eigenvalues 0-82675
- rotating strings, elastic, heavy, nonlinear eigenvalue problems, bifurcating branches of solns. 0-73174
- scalar diffraction, inverse theory, eigenvalue formulation 0-102613
- scattering, relativistic, separable representation of square well potential 0-82922
- Schrodinger eqn., $r^{-(s+2)}$ type, $SL(2,R)$ acting on quaternions 0-57125
- Schrodinger equation, exactly soluble with bistable pot. 0-67950
- Schrodinger equation, existence of eigenvalues of infinite multiplicity 0-94989
- Schrodinger equation, linear potential wavefunctions, generalised hypergeometric functions 0-62512
- Schrodinger equation, nonlinear field equations, quantum inverse scattering transform method, 2-D ice and ferroelectric lattices 0-68348
- Schrodinger equation, three-body problem with hard cores, 1-D, reduction to 2-D Helmholtz eqn. 0-62523
- Schrodinger equation, three-body problem with hard cores, 1-D, eigenvalue lower bounds 0-68069
- Schrodinger equation eigenvalues, perturbation theory calc. without complete set of eigenfunctions 0-105519

eigenvalues and eigenfunctions continued

- Schrodinger equations, three-body problem, bound state eigenvalues lower bounds, upper bounds by Rayleigh-Ritz method 0-68068
- Schrodinger operator, point spectrum, non-existence of eigenvectors of compact support (French) 0-68063
- semi-simple Lie groups, Casimir operator eigenvalues, symmetric power sum expansions 0-86604
- semifinite strip with clamped sides, bending, Papkovitch-Fadle eigenfunction completeness 0-58929
- sine-Gordon equation, nonlinear field equations, quantum inverse scattering transform method, 2-D ice and ferroelectric lattices 0-68348
- single eigenvalue distrib. for non-zero mean matrix ensembles, correct form 0-73198
- soliton, extended particle, quantisation, degeneracy of eigenstates 0-73594
- sound propagation in parallel sheared flows in ducts, mode estimation 0-79026
- star counts, eigenvectors anal. for space densities derivation 0-85932
- Sturm Liouville eqns., numerical anal. and eigenvalue problems 0-90655
- SU(N) gauge theories, $1/N$ expansions, singular integral operator 0-57511
- SU(N) symmetric quantum dynamical systems, $N \rightarrow \infty$, energy spectrum for singlet and adjoint states 0-62880
- thermal convection in closed gas centrifuge, eigenvector soln. of linearised eqns. 0-83797
- tight lower bounds to eigenvalues of the Schrodinger equation 0-94984
- toroidal resonators for EM waves, Maxwell eqns. for toroidal geometry 0-102598
- unbounded Hermitian operators, low-lying eigenstates, method 0-98812
- unified theory of atoms and atomic aggregates, self consistent theory 0-102418
- unstable resonator, half-symmetric, with coated rear cone, polarisation effects 0-74402
- vibration, transverse, of rectangular plate with eccentric circular inner boundary 0-106737
- waves, shallow water, with quasi-periodic boundary conditions, eigensolutions of elliptic problem 0-83804
- Cu IV, wavelength region 700-1200 Å, extended analysis 0-99473
- H, degenerate 3s-3d levels, in mag. field, eigenvalues, Bender-Wu formulas 0-83275
- H hyperfine splitting inside paraboloidal surfaces 0-99445
- H₂O, excited stretching vibr., quantum mechanics. 0-91535
- He⁺, electron impact excitation cross-sections, reson. parameters calcs. 0-91686
- NiVI, sixth spectrum analysis 220-335 and 890-1325 Å regions 0-95565
- YIG thin film gyromag. waveguide, on GGG substrate, optical propag. props. Faraday effect 0-74513
- eigenvectors** see *eigenvalues and eigenfunctions*
- eightfold way** see *SU₃ theory*
- Einstein-de Haas effect**
 - see also *gyromagnetic ratio*
 - history, Einsteins' expt. work 0-98783
- einsteinium**
 - see also *nuclei with*
 - No entries
- einsteinium compounds**
 - No entries
- elastic aftereffect**
 - α -Fe, neutron irradiated, mobile C atom trapping, anelastic and magnetic relaxations 0-100306
 - Fe powders, cold-pressed, props., effect of air 0-100810
 - Ta-H(D), anelasticity due to long-range diffusion 0-60904
 - V-H(D), anelasticity due to long-range diffusion 0-60904
- elastic constants**
 - see also *elastic moduli*
 - alkali halides, elastic constants, temp. depend., pseudopot. calc. 0-65120
 - alkali halides, photoelastic consts., short range polarisability effect 0-80748
 - alkali metal halides, elastic consts., anomalous temp. depend., phonon-lattice interaction 0-107354
 - alkali metals, effective ion-ion potential, compressibility and force consts. 0-70158
 - alkali metals, phonon dispersion binding energy, compressibility, elastic consts. electron screening and Ashcroft pot. calcs. 0-65174
 - alkaline earth chalcides with NaCl-type structure, third-order elastic consts. 0-70292
 - aniline hydrobromide, ferroelastic, acoustic softening near transition temp. 0-96617
 - biphenyl-D₁₀, Brillouin scatt. at room temp. 0-71433
 - chevron notched short bar specimens, compliance and stress intensity coefficients 0-96232
 - clinical support surfaces, mech. compliance evaluation 0-92053
 - crack at the boundary between two materials with a branch into one of them in the case of antiplane strain 0-79231
 - critical behaviour near elastic phase transitions 0-100299
 - crystals, rel. to surface waves propagation over liquid and crystalline layers 0-76924
 - diamond, Cosserat continuum model, elastic props., lattice dynamics 0-59552
 - EBBA, IR absorpt. spectra, elec. field effects, orientational order parameter determ. by IR dichroism, bend elastic consts. 0-80778
 - FCC polycryst., under hydrostatic pressure 0-107356
 - ferroelectric, uniaxial, crit. behaviour, electrostrictive coupling role 0-71329
 - ferroelectric ceramic, polycryst., elasticity props., neutron bombardment effects 0-79856
 - ferromagnet, itinerant electron, magnetoelastic contribs. to US vel., elastic consts., and susceptibility 0-75829
 - fibre cross-reinforced layered composites, moment effects in plane problem 0-64393
 - fibre reinforced composites, three-dimensionally reinforced with short fibres, effective elastic consts. 0-58910
 - fibre reinforced polymer matrix composites, space environmental effects 0-71721
 - frontal method for structural mechanics, algorithm for excluding unknowns 0-79157
 - garnet solid soln. series, elastic props. inferred from expts. on pyrope 0-76968
 - glass-ceramic, machinable, elastic const. temp. depend. 0-79852
 - hard sphere crystal, thermoelasticity in relation to melting 0-107353

elastic constants continued

Invar, phase stability, spinodal decomposition 0-88327
invariance relations for elastic waves in crystals 0-84250
Ising spin system, coupled to acoustic and optic lattice modes, critical behaviour 0-71044
Jahn-Teller cooperative T-systems, dynamics, elastic props. 0-65511
liquid crystals, NMR spin-lattice relax. time near phase transitions 0-71222
liquid crystals, prep. and phys. props., book 0-105444
MBBA, IR absorpt. spectra, elec. field effects, orientational order parameter determ. by IR dichroism, bend elastic consts. 0-80778
metal, textured cubic, residual stress evaluation 0-89435
metals, elastic constants and moduli of axial textures 0-75286
metals, Morse potential appl. in molecular-metallic framework 0-79742
nematic liquid crystals, orientation fluctuations in high mag. field, quenching, birefringence effects 0-64892
neopentane, diamond force const., rel. to crystal elastic consts., Raman freq., bulk compressibility and freq. assignments 0-65183
non-elastic phase transitions, elastic const. crit. behaviour 0-100298
noncontact material testing using laser energy deposition and interferometry 0-71846
orthotropic composite model materials, photoelastic calibration 0-87715
pentyl-cyano-biphenyl, nematic, hydrodynamic parameters meas. with and without applied elec. field 0-100297
polydimethylsiloxane end-linked chains, nonGaussian effects 0-65127
polydomain ferroelec. crystals, phys. consts., self consistent calcs. 0-88942
polyethylene terephthalate, shear compliances meas. of oriented sheet 0-104363
quartz, elastic constants and piezoelec. props. 0-92590
tris-sarcosine calcium chloride, elastic props., US damping 0-84229
squaric acid, layered, antiferroelec., phase transition mechanism 0-97210
squaric acid, two dimensional antiferroelec., Brillouin scatt. at structural phase transition, hypersonic elastic consts. determ. 0-71430
steel, austenitic stainless, N-alloyed 0-108490
steel, Cr-Mn (13, 19 wt.%), elastic const. behaviour, anomalous, low temp. 0-97521
stiffness, exact straight line element calc. 0-79138
p-terphenyl-(d₄), Brillouin scatt. at room temp. 0-71433
trabecular bone from human vertebral body, elastomech. props. 0-67141
uniaxial crystals, third-order elastic consts., review 0-65119
vinylidene fluoride-trifluoroethylene film, cryst. phase transition 0-66120
wurtzite-type crystals, lattice dynamics including the effect of electronic extension 0-59586
AgCl-AgBr mixed crystals., elastic consts. and cryst. symm. 0-70290
Al, energy and elastic constants 0-59435
Al, metallic, phonon freq., binding energy, compressibility, elastic const. and energy band gap calcs., linear pot. 0-88284
BaTiO₃, paraelectric crystal, nonlinear props. 0-84699
BaTiO₃, polydomain ferroelec. crystals., phys. consts., self consistent calcs. 0-88942
BeO, wurtzite-type crystals, lattice dynamics including the effect of electronic extension 0-59586
Bi₂FeO₂₀, longitudinally vibrated bars, reson. freq., DC elec. field effects, elastic coupling polarising correction terms 0-60503
Bi₂SiO₂₀ crystal, piezoelec. and saw props. 0-75949
Cd₂Hg_{1-x}Se, phase transition and elastic consts., US vel. study 0-75354
CdIn₂S₄, Brillouin scatt., elastic and photoelastic consts. determ. 0-60619
CdS, elastic, piezoelec. and dielec. props. 0-108157
CdS, elastic, piezoelectric, and dielec. props., 4.2 to 300K 0-60508
CdS, resonant Brillouin scatt., photoelastic const., imag. part contrib. 0-108218
CdS_{1-x}Se_x, mixed crystals, deformation effects on free excitons 0-76073
CdTe, lattice dynamics and phonon parameters bond bending force model 0-59595
CePd₃ single crystal Czochralski growth and characterisation 0-60767
CeSn₃, mode softening and elastic consts., acoustic vel. meas. 0-88242
Cr, lattice dynamics, improved Fieλεκ model 0-59598
Cr, spin-flip transition temperature, press. depend. from elastic const. meas. 0-65944
CsMnCl₂·2H₂O, diagonal elastic const., thermal expansion coeffs., ultrasonic velocity meas. 0-79853
Cs₂NaM³⁺Cl₆ (M³⁺=Bi,Nd,Pr), ferroelastic phase transitions, thermal expansion, elasticity, and X-ray anal. 0-70393
Fe, powder-forged, elastic consts., density depend. 0-84987
Fe-C (graphite, 0.3 wt.%), powder-forged, elastic consts., density depend. 0-84987
Fe-Ni(Pt) Invars, elastic and mag. props., magnetoelastic interaction effects (*Russian*) 0-84631
Fe₂O₄, magnetocrystalline anisotropy, anomalies in magnetostriction and elastic constants 0-60244
GaAs crystal growth, thermal and elastic const. evaluation 0-92586
GaAs, lattice dynamics, phonon freq., bond bending force model calcs. 0-70335
GaP, lattice dynamics and phonon parameters bond bending force model 0-59595
GaP, thermal expansion below room temp., press. depend. of elastic stiffness consts. and phonon frequencies 0-79963
Ga₂(Se), layer compound, long-wavelength phonons and elastic consts. 0-65175
GaSb, lattice dynamics, phonon freq., bond bending force model calcs. 0-70335
GaSe, lattice dynamics and elastic props., Born-von Karman model study 0-70337
InP, lattice dynamics and phonon parameters bond bending force model 0-59595
InSe, layer compound, long-wavelength phonons and elastic consts. 0-65175
K, appl. of model pseudopot. to elastic consts. 0-59845
K₂Ba(NO₃)₂, elastic props. 0-96588
(K_{1/2}Bi_{1/4})(Zn_{1/6}Nb_{5/6}O₃), cation disordered perovskite, elastic consts. and thermal expansion 0-96587
KBr_{1-x}(CN)_x, mixed mol. cryst., coupled rot. and translational modes 0-84267
KCN, inelastic neutron scatt. by coupled rot. and translational modes 0-79895
KCl(F)(Br)(I), elastic constants, temp. derivatives at constant volume 0-59549
KD₂PO₄, acoustic phonon dispersion, elastic stiffness, light scatt. obs. 0-103966
KD₃(SeO₃)₂, phase transition, neutron scatt. study 0-75351

elastic constants continued

KH₂(SeO₃)₂ and KD₃(SeO₃)₂, ferroelastic phase transition, mech. stress effect 0-70394
K₂Hg(CN)₄, third order elastic consts. 0-84231
K₂ReCl₆, softening of acoustic modes, obs. by Brillouin scattering 0-71440
K₂SeO₄, elastic props. at commensurate-incommensurate transition, Brillouin scatt. and US study 0-93248
K₂SnCl₆, elastic consts., inelastic neutron scatt. and US meas. 0-59553
K₂SnCl₆, softening of acoustic modes, obs. by Brillouin scattering 0-71440
K₂Zn(CN)₄, third order elastic consts. 0-84231
LaAg_{1-x}In_x, phonon dispersion, elastic consts. and struct. instability, soft mode behaviour 0-103436
LaP₂O₁₄, continuous ferroelastic transition elastic and mechanical props. 0-92668
LaP₂O₁₄, coupling effects between soft optic and acoustic modes at ferroelastic transition 0-70358
Li, energy and elastic constants 0-59435
Li single cryst., US attenuation and vel. measurements in vicinity of martensitic phase transformation 0-75358
LiCl(F)(Br)(I), elastic constants, temp. derivatives at constant volume 0-59549
Mn-Cn (25, 62 wt.%), temp. depend., 170-300K (*Russian*) 0-81095
NiO, antiferromag., temp. depend. of elastic consts., US study 0-79854
Mo, lattice dynamics, improved Fieλεκ model 0-59598
MoSi₂ film, elastic stiffness and thermal expansion coeffs. 0-107451
(NH₄)₂BeF₄, elastic props., US damping 0-84229
(NH₄)₂SiF₆, softening of acoustic modes, obs. by Brillouin scattering 0-71440
(NH₄)₂SnCl₆, softening of acoustic modes, obs. by Brillouin scattering 0-71440
Na, appl. of model pseudopot. to elastic consts. 0-59845
NaCl(F)(Br)(I), elastic constants, temp. derivatives at constant volume 0-59549
Nb-H system, lattice dynamics, local frequency spectrum, mean thermal displacement of H 0-59604
Nb_{5/3}Ta_{4/3}, effects of hydrostatic pressure on changes in elastic consts. caused by addition of H 0-75287
NiTi equiatomic alloy, single cryst. elastic consts. near martensitic transform. 0-75283
Pb, filamentary crystals, third-order elastic consts. combinations 0-92585
PbF₂, US vel. near press. induced cubic-to-orthorhombic transform. 0-103476
Pb₃(GeO₄)(VO₄)₂, Pb₃(SiO₄)(VO₄)₂, and Pb₃GeO₁₁, elastic nonlinearity and acoustic losses 0-59554
Pb(Mg_{1/3}Nb_{2/3}O₃), cation disordered perovskite, elastic consts. and thermal expansion 0-96587
Pb₃(P,V_{1-x}O₄)₂, ferroelastic phase transition, DTA, dilatometric and Brillouin scatt. study 0-70398
Pb(Zn_{1/3}Nb_{2/3}O₃), cation disordered perovskite, elastic consts. and thermal expansion 0-96587
Pd-H system, lattice dynamics, local frequency spectrum, mean thermal displacement of H 0-59604
Pd₂Si and PdSi films, on Si, stress obs. 0-80145
PrSn₃, thermal expansion and transverse elastic const. near mag. phase transition 0-60394
Pr₂Tl, thermal expansion and transverse elastic const. near mag. phase transition 0-60394
PtSi films, on Si, stress obs. 0-80145
RbCaF₃, first order improper ferroelastic phase transition at 194K, phenomenological description 0-70397
RbCl(F)(Br)(I), elastic constants, temp. derivatives at constant volume 0-59549
SiN film, elastic stiffness and thermal expansion coeffs. 0-107451
Si₃N₄ film, elastic stiffness and thermal expansion coeffs. 0-107451
SrTiO₃, critical elastic compliance, acoustic resonance meas. 0-65118
Ta, shear elastic constant, anomalous temp. behaviour, US study 0-79855
Ta-H system, lattice dynamics, local frequency spectrum, mean thermal displacement of H 0-59604
TaSi₂ film, elastic stiffness and thermal expansion coeffs. 0-107451
TeO₂, paratellurite, single crystals., third-order elastic constants 0-88243
α-Ti alloys VT1 and VT5, struct. and phys. props., H₂ effect 0-108576
α-β Ti Widmanstätten alloy interfaces, elastic interact. stresses, effect on plastic flow onset 0-104218
TiSi₂, film, elastic stiffness and thermal expansion coeffs. 0-107451
TmSe, first obs. of negative elastic const. 0-103409
V, effects of hydrostatic pressure on changes in elastic consts. caused by addition of H 0-75287
V-H single crystals., elastic consts., temp. depend., H effects 0-66563
V-H system, lattice dynamics, local frequency spectrum, mean thermal displacement of H 0-59604
WO₃, acoustic instability near monoclinic orthorhombic phase transition, X-ray scatt. 0-65215
WSi₂ film, elastic stiffness and thermal expansion coeffs. 0-107451
ZnO, elastic, piezoelec. and dielec. props. 0-108157
ZnS, lattice dynamics, phonon freq., bond bending force model calcs. 0-70335
ZnS(Se)(Te), thermal expansion and lattice dynamics under press. 0-100316
ZnTe, lattice dynamics and phonon parameters, bond bending force model lattice dynamics and phonon parameters bond bending force model 0-59595

elastic deformation

see also bending; elasticity; electrostriction; stress/strain relations; torsion
absorbing media, acoustic pulse deform., numerical calc. algorithm (*Russian*) 0-96591
alloys, machining damage, depth of surface layers determ. 0-85094
bars, phase boundary propagation, dynamic elastic bar theory, sound wave interactions 0-69706
beam modelling, linear shape function for axial displacement approx., finite element anal. 0-69665
beams, spatially curvilinear elastic, geometrically nonlinear theory 0-96189
beams, straight, homogeneous and isotropic, linear flexural theory (*French*) 0-74743
collagen with planar crimp, tensile deformation 0-84235

elastic deformation continued

- colloidal systems, surface forces, direct meas., elastic deform. effect 0-93805
- complex idealised bar, deformation processes, bifurcational elastic eqn. soln., pseudobifurcation (*Russian*) 0-58945
- composite ribbed multilayer cylindrical shells, stability and optimal design 0-58949
- contact, frictionally heated, thermoelastic deform. 0-83764
- crack, oblique edge, in semi-infinite plate, stress anal. 0-64463
- crack closure in bending, elastic plates, sixth order anal. 0-96231
- cracktip under incipient creep deform., stress field and modified J-integral (*Japanese*) 0-103411
- crystals, monatomic, nonlinearly elastic, twinning 0-58903
- defect dynamics, field equations, four dimensional space-time setting 0-96521
- deformation wave processes, corrected nonlinear eqns., stresses and strains 0-102998
- edge dislocation screening in metals and superconductors, metal softening (*Russian*) 0-64997
- epoxides, dielectric relax. and deform props., cross-link density effect (*Russian*) 0-60942
- fatigue, hydrostatic stress-sensitive relationship for biaxial stress conditions 0-74805
- FCC polycryst., under hydrostatic pressure 0-107356
- fibre reinforced composites, stress redistribution dynamics during fibre rupture 0-64394
- filaments, slender, with planar crimp, tensile deformation 0-84235
- finite elasticity with general loading, uniqueness for deformed surface 0-79153
- glass, viscous deformation during heating and cooling 0-89314
- grinding, role of elastic and plastic behaviours (*Japanese*) 0-100868
- hybrid deformation elements for elastic media 0-92049
- hyperelastic materials, anisotropic, compressible, finite plane strain, universal deformations 0-69667
- incompressible elastic materials with different moduli in compression and tension, dynamic problems 0-79141
- indentation hardness and hot pressing, calc. methods 0-58981
- laminated plates, symmetric, specially orthotropic, thermoelastic anal. 0-92058
- layer pressed against substrate, separation and slip caused by tensile load 0-96536
- lung, deforms. at minimal vol. 0-97977
- mirror, nonaxisymmetric, fabrication by stressed mirror polishing 0-99885
- non-associated plasticity and elastoplasticity, rate boundary value problems, variational principles 0-87726
- nonlinear cantilever beam statics (*German*) 0-106726
- nonlinearly elastic body at eqn., relation between stability and continuous dependence 0-92063
- optical fibre preform rod, refractive index profile meas. by transverse diffractive interferogram 0-64141
- ordered regions near macroscopic defects and percolation phase transform. in crystals (*Russian*) 0-92665
- panels, stiffened, eight-stringer, with rectangular cut-out, stresses and deformations, eccentric tensile load (*Japanese*) 0-64467
- particle falling in viscous fluid, deform. 0-79149
- penny-shaped crack problem, deformed incompressible elastic solid 0-92085
- plexiglass composite, long term strength and durability 0-75294
- polydimethylsiloxane end-linked chains, nonGaussian effects 0-65127
- polyethyleneterephthalate-polycapromide melts, two-phase blend, rheological props. (*Russian*) 0-58997
- polymer-metal sliding, wear eqn. in terms of fatigue and topography of sliding surfaces 0-108597
- polyurethane, segmented, domain struct., deform. effect 0-93623
- red blood cells, minimum energy anal. of membrane deform. 0-72141
- regularly layered half-space, deformation, vibrational loading 0-99933
- ring, plane deformation, determ. of stresses and displacements, composite boundary conditions (*Russian*) 0-74738
- rock, fracture, role of crack inertia 0-109138
- rod, curved, deformed by end loads (*Russian*) 0-74745
- rotating viscoelastic tapered cantilever, circulatory force at free end, influence of angle of attack on stability 0-69686
- rubber, natural, crosslinked by dicumyl peroxide, modulus, swelling relations 0-59551
- rubber covered rolls, contact and deformation nonlinear elastic problem, stress anal. 0-79239
- rubber cylinder, circular, uniformly heated, combined extension and torsion 0-92057
- shells, isotropic thin elastic, nonlinear theory (*Russian*) 0-79147
- single crystals under large loads, theoretical elastic behaviour, review and appl. 0-71681
- size effect, thermodynamical model for constrained and unconstrained bodies 0-58900
- sphere, deformation and sticking to a rigid plane, mol. force effect 0-106720
- steel shell, mech. behaviour during solidification 0-81043
- steel SW7M, low-cycle fatigue at high hardness levels (*Polish*) 0-89323
- stress and configuration, elastic and plastic strain increments 0-87718
- stress measurement, temporary and residual stresses, high-temps. 0-64498
- tendon, viscoelastic deform. obs. 0-101211
- textiles with planar crimp, tensile deformation 0-84235
- thermodynamics, eqn. of state for solids 0-96589
- thermoelastic deformation, second order effects 0-92051
- thermoelastic solids, thermomechanical constraint, internal, constitutive equations, material anisotropy 0-58897
- thermoelasticity of anisotropic cylindrical shells 0-92059
- thick plates, 3-dimens. refined elasticity theory, bending and torsion 0-64375
- torsion free axisymmetric deformations, two function expression for displacements 0-64367
- trapezoid plate, freely rotating, mechanical effects, calc. method (*German*) 0-106728
- tubes, thick-walled, bifurcation under axial loading 0-79150
- urinary bladder interferometry, holography of bladder deforms. in vitro, rabbit expt. 0-67201
- urinary bladder interferometry, tumour and lesion detect. by holography 0-67202
- β -BaF₂, stress wave profiles 0-96593

elastic deformation continued

- CrO₂, semidry refractory, struct. and mech. props., surface-active agents effect 0-89304
- Cu, theoretical strength 0-104229
- Fe-Ni alloys props. of materials used in electromechanical filter resonators (*Czech*) 0-76318
- GaAs-Ga_{1-x}In_xP heterostructure, elastic stresses and substrate/epitaxial film mismatch, X-ray diff. method 0-92794
- Ge single crystals, photopiezoelectric effect under elastic deform. 0-107856
- KCl, pure and Ba doped, symm. of elastic fields due to defect displacements, diffuse X-ray scatt. 0-70256
- Nb₂O₅-SiO₂ glass, scoring, deform. and fracture mech. approach 0-89332
- Pd alloys, effect of alloying on activation energy of H₂ diffusion 0-107571
- Si, diffusion of P, elastic deform. relax. and dislocation generation 0-79997
- Si, stretched, lattice vibr. anharmonicity, influence of stress on elastic moduli, Raman spectra 0-80791
- ZrO₂, porous, sintered stabilised microspheres, strength and fracture studies 0-85019
- elastic hysteresis**
- nonlinear nonideally elastic materials, relationships between stresses and strains (*Russian*) 0-90675
- steel, age hardened, dynamics of cyclic plasticity (*Czech*) 0-108464
- steel, type AC/HT-2, grain diameters, US attenuation 0-89429
- K(D,H_{1-x})₂(SeO₃)₂, ferroelastic, anelastic and elastic infra-low freq. props. 0-70304
- V₂Si, mixed state, hysteresis in elastic characteristics (*Russian*) 0-103799
- elastic limit**
- shell stability during axial compression, hardening beyond elastic limit 0-99931
- steel, structural, elastic limit determ. by acoustic emission 0-66716
- Fe, cast, contact deformation, reverse slipping effect (*Russian*) 0-97591
- Pb(Zr,Ti_{1-x})O₃, meas. of Hugoniot curve with commercial manganin stress gauges 0-70362
- α -Ti, determination of microflow parameters from compression tests 0-66584
- elastic moduli**
- see also Poisson ratio; shear modulus; Young's modulus
- alkali halide elastic dielectrics, Gruneisen parameter, effective ionic charge volume derivative 0-84273
- alkali halides, mixed, bulk modulus, temp. variation 0-92588
- alkali halides, repulsive hardness parameters, crystal-independent 0-64947
- alkali halides, repulsive softness parameter anal. 0-107102
- alkali metals, bulk modulus and eqns. of state under press. 0-88293
- alkali silicate glasses, secondary relax. transitions 0-88261
- body loading with cracks, energy conditions for brittle failure (*Russian*) 0-96234
- Brillouin scatt. and refr. index measurements 0-76035
- ceramic multilayer capacitors, fracture mechanics approach to structural reliability assessment 0-89328
- coke, metallurgical, industrial strength meas. methods, critique 0-85117
- colloids, model, elastic moduli, Monte Carlo methods 0-108754
- composite elastic medium, effective bulk and shear moduli 0-99927
- composites, overall elastic moduli prediction 0-75285
- concrete, elasticity modulus and strength, aggregate conc. effect 0-66591
- concrete, flowing, expt. studies (*Japanese*) 0-89298
- concrete, high strength, made with a special cement admixture, mech. props. (*Japanese*) 0-89297
- concrete, strain rate effect on strength and deform. during hardening process (*Japanese*) 0-93616
- cranial bone, fetal, elastic modulus obs., appl. to fetal head moulding biomechanics 0-67128
- cylinder, thin-walled, laminated, non-uniform, elastic equilib. with surface loads and displacements 0-69671
- cylindrical three layer pipe, stress-strain state, filler compressibility effects (*Russian*) 0-58901
- diamond, compressibility, appl. of Murnaghan eqn. of state, Morse pot. 0-79861
- diaphragm muscle, canine, in vivo stiffness props., obs. and meas. system 0-97988
- ebonite, viscoelastic, linearity conservation 0-108492
- elastic deformation, thermodynamics of, eqn. of state for solids 0-96589
- elastomers, rel. between relax. behaviour and tensile strength (*German*) 0-66604
- elastomers, soot filled, mech. relax. behaviour (*German*) 0-84985
- epoxy resin, filled and unfilled, subjected to extensional creep, dynamic props. 0-71697
- epoxy/E-glass continuous fibre composite type 3M Scotchply, complex moduli, comparison of meas. with estimated bounds 0-93590
- filled polymer mechanical properties, particle shape effect, review 0-100864
- fluoride crystals, rutile-type, interionic pots., cohesive energy, bulk modulus, calc. 0-79741
- garnet solid soln. series, elastic props. inferred from expts. on pyrope 0-76968
- glass bead reinforced nylon, design parameters, fibre orientation effect 0-81141
- glass bead reinforced polycarbonate, design parameters, fibre orientation effect 0-81141
- glass fibre reinforced nylon, design parameters, fibre orientation effect 0-81141
- glass fibre reinforced plastics, ageing by boiling in water, effect on physico-mech. props. 0-60892
- glass fibre reinforced polycapromide, viscoelastic, linearity conservation 0-108492
- glass fibre reinforced polycarbonate, design parameters, fibre orientation effect 0-81141
- graphite, pyrolytic commercial, high-temp. thermal and mech. props. 0-75372
- graphite fibre filled polyimide composite laminates, space environment, phys. and mech. response 0-81140
- Hashin-Shtrikman bounds, effective elastic moduli, hexagonal, trigonal and tetragonal polycryst. 0-75282
- Hashin-Shtrikman bounds, effective elastic moduli, monoclinic polycryst. 0-70291
- hybrid glass fibre/C fibre reinforced epoxy-phenolic, elastic characts. prediction 0-108491

elastic moduli continued

- incompressible elastic materials with different moduli in compression and tension, dynamic problems 0-79141
 Jahn-Teller crystals, ferroelectric transitions, elastic and dielectric anomalies, microscopic model 0-71332
 latex, shear waves, elastic moduli determined, light scattering 0-58956
 liquid, Gruneisen parameter rel. to Rao's acoustical parameter 0-92581
 magnetically ordered crystal, dislocation drag, magnetoelastic waves 0-103332
 metals, elastic constants and moduli of axial textures 0-75286
 metals, simple, elastic moduli, chemical trends, pseudopotential method 0-107355
 methane, crystalline, structure and compression at high pressure, room temperature 0-107199
 nylon 6 (polycapromamide), salted, glass transition temperature and elastic modulus, moisture effect 0-103465
 oxide crystals, rutile-type, interionic potentials, cohesive energy, bulk modulus, calculation 0-79741
 plexiglass composite, long term strength and durability 0-75294
 polyamide, aromatic, fibre, high modulus, molecular and supramolecular structure 0-79710
 polyamide, viscoelastic, linearity conservation 0-108492
 polyamides, extended chain aromatic, fibres, tensile strength and moduli 0-81021
 polycapromamide, oriented filaments, mechanical properties 0-66550
 polycrystal, linear, E and G moduli, crystallisation effect (*German*) 0-59556
 polydimethylsiloxane, end-linked chains, model elastomeric networks, Gaussian, nonGaussian and ultimate properties 0-103260
 polydimethylsiloxane chains, end-linked, swollen model networks, stress/strain isotherms and elastic modulus 0-79668
 polydimethylsiloxanes, rubbery and liquid, hypersonic sound velocity, Brillouin spectra measurements 0-75308
 polyester resin, unsaturated, chalk filled, properties (*German*) 0-104228
 polyester resin concrete, effects of styrene-unsaturated polyester ratio on properties (*Japanese*) 0-89299
 polyester/E-glass chopped fibre composites types PPG SMC-R25 and PPG SMC-R65, complex moduli, comparison of measurements with estimated bounds 0-93590
 polyester/E-glass hybrid chopped/continuous fibre composite type PPG XMC-3, complex moduli, comparison of measurements with estimated bounds 0-93590
 polyethylene, high density, solid state coextrusion, geometric factors effect 0-71704
 polyethylene flow crystallisation, in extensional flow developed by convergent capillaries, properties 0-84111
 polymer networks, stochastic cross-linked, modulus of elasticity, functionality effects (*German*) 0-59555
 polymer-metal sliding, wear equation in terms of fatigue and topography of sliding surfaces 0-108597
 polymers filled with agglomerated particles, dynamic mechanical properties 0-66569
 polyolefins, ultra-high modulus, production by tensile drawing and hydrostatic extrusion 0-81022
 polystyrene, viscoelastic, linearity conservation 0-108492
 PTFE and filled PTFE, nonlinear creep, compression bulk modulus 0-66593
 pyrope, elasticity of single crystal, implications for garnets 0-76968
 rare gas solids, third order elastic constants, second order elastic constant pressure derivatives 0-70501
 sandwich composite beams, stress distribution measurements under four-point bending, multilayer built-up theory 0-96190
 second-order phase transitions in crystals, equilibrium configurations, thermoelectricity theory 0-70364
 silicate glasses, longitudinal and transverse elastic wave velocities, temperature and composition variations 0-88258
 single crystals under large loads, theoretical elastic behaviour, review and application 0-71681
 solids, evaluation of finite strain equations of state using lattice models 0-96620
 spring-loaded mass system vibration analysis (*German*) 0-96224
 steel, austenitic stainless, types 304 and 316, environment effect on crack growth, under creep and fatigue conditions 0-85035
 stochastically inhomogeneous structures, macroscopic third-order elastic moduli 0-69672
 transition metal alloys, cohesive properties and pressure-volume relation 0-92476
 unidirectional fibre composites, anisotropic constituents, effect elastic moduli and other properties 0-58911
 viscoelastic material, failure and instability in tension 0-87720
 Zircaloy-4, elastic properties, O additions effect 0-66565
 α -Al₂O₃ fibre FP reinforced Al and Mg composites, fabrication and properties 0-81004
 Al₂O₃-SiO₂ refractory concrete, elastic properties 0-89280
 Ar, solid, equilibrium properties, uncorrelated pairs approx. 0-84303
 Bi, deformation calculations, band structure variation, electron phase transitions due to deformation (*Russian*) 0-65137
 Bi_{1-x}GeO₂₀, third-order elastic moduli determined 0-65121
 Bi_{1-x}Sb_x, deformation calculations, band structure variation, electron phase transitions due to deformation (*Russian*) 0-65137
 Bi_{1-x}SiO₂₀, third-order elastic moduli determined 0-65121
 C fibre reinforced composites for spacecraft use, preparation, properties and structure 0-71625
 C fibre reinforced nylon, design parameters, fibre orientation effect 0-81141
 C fibre reinforced polycarbonate, design parameters, fibre orientation effect 0-81141
 Cu-Ag (0.1 wt.%), cold-worked, internal friction peaks in kHz range 0-89276
 DyVO₄ Jahn-Teller crystal, deformation induced transitions, elastic and dielectric characteristics (*Russian*) 0-80726
 Fe-Ni alloys, properties of materials used in electromechanical filter resonators (*Czech*) 0-76318
 Ge, pure and n-type, US velocity and attenuation, second and third order elastic moduli 0-70325
 HfO₂, stabilised compounds, elastic properties rel. to porosity and temperature 0-81096
 Ho,Tb_{1-x}Co_x rare phase compounds, elastic properties, temperature and magnetic field dependence 0-60393
 K, self-diffusion, high temperature, bulk modulus determined 0-79976
 KCl_{1-x}Br_x, bulk modulus, room temperature, to 400°C 0-92588
 Li, phonon limited resistivity structure depend., Umklapp scattering, elastic constants 0-88532

elastic moduli continued

- Li₂O-Al₂O₃-SiO₂ glass, study of elastic properties 0-104205
 Mn₂Si₂, elastic moduli, phase transitions, ultrasonic velocity 0-92589
 Na, phonon limited resistivity structure depend., Umklapp scattering, elastic constants 0-88532
 Nb₂Sn, softening of surface phonons in (100) plane 0-107627
 Ni-based TaC eutectic, directionally solidified, elastic moduli 0-84984
 Pb(Zr,Ri)O₃:Ni-silicon rubber flexible composite pyroelectric, dielectric properties 0-80704
 Pb(Zr,Ti)O₃ ceramics with ladder type structure, preparation and properties 0-75945
 Pd alloys, effect of alloying on activation energy of H₂ diffusion 0-107571
 Se, trigonal, normal mode calculations 0-84259
 Si, ground state properties in density-functional pseudopotential approach 0-92803
 Si, pure and n-type, US velocity and attenuation, evaluation using elastic moduli 0-70325
 Si, stretched, lattice vibration anharmonicity, influence of stress on elastic moduli, Raman spectra 0-80791
 Si, total energy calculations by r-space method, Wannier functions 0-88503
 SiC-coated C fibre, compatibility with Al (*Japanese*) 0-71700
 Si₃N₄, bending strength, deformability, elastic moduli and brittleness 0-81191
 SiO₂-Al₂O₃-Cu₂O glass alkaline durability, corrosion rate, heat capacity and elastic moduli 0-93673
 SiO₂-Al₂O₃-Y₂O₃-La₂O₃-TiO₂ glasses with high elastic moduli, alkaline durability 0-85071
 Sn, Fermi surface, dilational strain dependence, elastic moduli and torque observations 0-70586
 Ta, acoustic emission induced by hydride formation 0-76257
 TbFe₂, magnetic field dependence, acoustic transducer application 0-87698
 TiBr-TiI(Cl) crystals, photoelastic moduli 0-97230
 V, determination of effect of H based on US velocity measurements 0-75288
 V-H single crystals, elastic constants, temperature dependence, H effects 0-66563
 (V_{1-x}Cr_x)₂Si, elastic moduli, 4.2 to 290K, softening near superconduct transition (*Russian*) 0-92582
 V₂Si, magnetic susceptibility, density of states model for lattice transformation in A-15 compounds 0-65219
 V₂Si, mixed state, hysteresis in elastic characteristics (*Russian*) 0-103799
 W, self-diffusion, high temperature, bulk modulus determined 0-79976
 Y₂O₃ ceramics, strength under mechanical and thermal actions 0-97554
 ZnP₂, Brillouin scattering and optical properties measurements 0-76041
 ZrO₂, porous, sintered stabilised microspheres, strength and fracture studies 0-85019
- elastic moduli measurement**
 acoustic insulating material complex elastic modulus measurements and transfer function theory (*Hungarian*) 0-106765
 ceramic layers on metallic substrates, mechanical properties measurements (*French*) 0-104375
 complex elastic modulus, temperature frequency variation for soft elastic materials (*German*) 0-106764
 piezoelectric transducer automatic setup, for continuous measurements of internal friction and elastic moduli of solids 0-108652
 plasma coatings, elastic properties, acoustic measurements (*Russian*) 0-97519
 refractories, US method for up to 2000K (*French*) 0-104373
 Young's modulus measurements using audio generator amplifier and speaker 0-62427
 Al₂O₃, US method for up to 2000K (*French*) 0-104373
- elastic scattering of atoms and molecules**
 angular correlations, summary of review papers 0-63757
 atomic metastability exchange collisions, Pauli principle effects 0-99536
 atomic spin exchange collisions, Pauli principle effects 0-99535
 benzene+bromomethane, microwave line width and quadrupole moments, perturbation theory 0-69190
 benzene+OCS, microwave line width and quadrupole moments, perturbation theory 0-69190
 classical many-body collision model incorporating Heisenberg and Pauli principles 0-63511
 electronic and atomic collisions, conference, Kyoto, Japan (Aug.-Sept. 1979) 0-57011
 electronic and atomic collisions, conference, Kyoto, Japan (Aug.-Sept. 1979) 0-62394
 molecular collisions in laser field, basis set selection and rotating-wave approx. 0-58341
 potentials, anisotropic, from rotationally inelastic and elastic cross sections, direct inversion method 0-69090
 ring laser, collision model, averaged, in active medium polarizability theory 0-95924
 translational nonequilibrium in resonant EM field, rel. to atom-buffer gas collision cross-section differences 0-96340
 $\mu\text{p}+\text{p}$, elastic scattering cross section of muonic H atoms 0-69278
 Ar⁺+He, integral elastic scattering, repulsive potentials derivation 0-63744
 C₃ inert gas, three body interaction, fluorescence spectra principal series lines and secondary satellites 0-83313
 H, positron elastic scattering, S-wave phase shifts calculation, least squares method 0-106374
 HCl+Ar, differential cross section, quasiclassical close coupling approx. 0-63743
 H(1s)+Cs, differential electron attachment and elastic scattering, 30-528 eV 0-63745
 He+H⁺, differential scattering, 1-12 eV, high resolution beam measurements 0-58348
 He+NaK collisions studied using circularly polarised laser fluorescence, molecular reorientation observations 0-69215
 He(2¹S, 2³S), transition probabilities, potentials 0-58371
 Ne⁺+Ar integral elastic scattering, repulsive potentials derivation 0-63744
 Ne(P₂) elastically scattered, metastable, angular distribution, conventional rel. to Doppler shift methods 0-58418
- elastic scattering of electrons by atoms and molecules**
 see also gas phase electron diffraction
 atomic electron scattering, in IR radiation field, theory 0-83487
 atoms, electron scattering, in strong radiation fields, review 0-63801
 coaxial electron and atomic beams sequential multiple scatterings, random walk approach 0-99574
 diatomic molecule, electron scattering, low energy, multichannel variational calculations, static exchange approx. 0-83483
 distorted wave matrix elements for inverse power potentials, approximate analytic evaluation 0-83442
 dosimetry of electrons, scatter effects, plane ⁹⁰Sr-⁹⁰Y medical applicator 0-61699

elastic scattering of electrons by atoms and molecules continued

- eikonal exchange amplitudes 0-69235
 electron scatt. and photoionisation, shape-resonance enhanced nuclear motion effects 0-63603
 electron-matter interactions rel. to electron microscopy 0-89097
 electronic and at. collisions, conf., Kyoto, Japan (Aug.-Sept. 1979) 0-57011
 electronic and at. collisions, conference, Kyoto, Japan (Aug.-Sept. 1979) 0-62394
 exchange perturbation theory for electron scatt., appl. elastic scatt. from H 0-78709
 gases, multiple scatt. effect on electron mobility 0-58383
 light atom, intermediate energy, differential cross-sections calc. 0-106394
 molecular electron scatt. resons. near threshold, vibr. induced narrowing 0-91673
 multicentre molecules, intratarget diffr., extended Glauber theory 0-58380
 negative ions, Feshbach type reson. scatt., Glauber approx. calcs. 0-102570
 nonpolar molecules, slow scatt. 0-91666
 polar molecules, electron impact, elastic scatt. and vibr. excitation, effective range theory 0-83485
 pseudostates wave functions determ. in modified close-coupling calcs. 0-99572
 reduced phase space approach calcs. 0-83438
 resonant phenomena, complex stabilisation method 0-78515
 slow positrons and electrons, meas. of angular distrib. using TOF spectrometer 0-86496
 theory and calc. techniques 0-63841
 trifluorodimethylmercury, gas phase mol. struct., electron diffr. and micro-wave spectra obs. 0-78609
 Ar, electron scatt. and ejection, electron energy loss spectra 0-58394
 Ar, positron annihilation decay rates, high temp. behaviour 0-58389
 Ar total scattering cross sections for low-energy electrons 0-58417
 CO, electron elastic scatt., low energy, static exchange approx. calcs. 0-69236
 CO, electron scatt., low energy, multichannel variational calcs., static exchange approx. 0-83483
 CO₂, electron elastic scatt. and vibr. excitation by 4, 10, 20 and 50 eV electrons 0-83484
 H, E_g ≥ 100 eV, ang. distrib. calc. 0-74248
 H, elastic electron scatt., pseudostates wave functions determ. in modified close-coupling calcs. 0-99572
 H, elastic electron scatt., 20-50 eV, Born calcs. of differential cross section 0-102571
 H, electron elastic scatt., exchange perturbation theory 0-78709
 H, electron scattering, optical pot. methods 0-102569
 H + e⁽⁺⁾, elastic and inelastic scatt., relativistic spin-dependent amplitude, Glauber approx. 0-63818
 H₂, 100-2000 eV, scatt. amplitude and cross-section 0-87228
 H₂, electron scatt., absolute total cross-sections, 0.2-100 eV 0-91674
 H₂, electron scatt., elastic and inelastic, Glauber approx. 0-91695
 H₂, electron scatt., low energy, multichannel variational calcs., static exchange approx. 0-83483
 H₂, electron scatt., Schwinger variational principle, static-exchange approx. 0-63820
 H₂, Gaussian basis Glauber approx., elastic and vibrorotational excitation cross sections 0-58399
 H₂⁺, electron elastic scatt., phaseshifts, quantum defect and two electron excited states 0-91671
 HCN, electron elastic scatt., differential cross-sections, effective range theory 0-83485
 HCl, electron elastic scatt., exchange and polarisation 0-91668
 H(1s) electron scattering, variable-charge Coulomb-projected Born approximation 0-58392
 H(2s), optical model approach to elastic scattering of electrons, polarisation effects 0-58382
 He atoms, matrix effective potential for electronic response in 30-400 eV electron scatt. 0-58388
 He, elastic scatt. of electrons in second-order eikonal approximation 0-91667
 He, electron elastic scatt., 5 to 200 eV, cross-sections meas., calibration 0-63822
 He, electron elastic scatt., two-pot. eikonal approx. calcs. 0-99573
 He, electron scatt., Glauber-Bonham-Ochkur exchange amplitudes 0-69237
 He, electron scattering, optical pot. methods 0-102569
 He, total scatt. cross sections for low-energy electrons 0-58417
 Hg atoms, elastic electron scatt., relativistic effects 0-102568
 Hg, electron elastic scattering, 8 to 18 eV, electron spin polaris. 0-91669
 Hg electron resonant elastic and inelastic scatt. (Russian) 0-78710
 Hg, positron scatt. at low energy 0-91670
 Li, electron elastic scatt., two-pot. eikonal approx. calcs. 0-99573
 LiF, electron elastic scatt., differential cross-sections, effective range theory 0-83485
 LiF, electron scattering; differential cross sections, three part hybrid method 0-58381
 LiH, electron scatt., low energy, multichannel variational calcs., static exchange approx. 0-83483
 N₂, elastic and inelastic electron scatt., state to state cross section 0-78708
 N₂, electron scatt., absolute total cross-sections 0-83486
 N₂, electron scatt., elastic and inelastic, Glauber approx. 0-91695
 N₂, electron scatt., local exchange pot. comparison 0-78707
 N₂, electron scatt., low energy, multichannel variational calcs., static exchange approx. 0-83483
 N₂, multiple scatt. method, scatt. cross section calc. 0-63816
 Na, electron scatt., crossed beam study 0-91672
 Na, excited, electron scatt. at low energy, total cross section 0-63821
 O₂, A¹Π_g, state pot. energy curve, MCSCF calcs. 0-63565
 O₃, low energy elastic and inelastic electron scatt., rot. transitions, close coupling calc. 0-78706

elastic waves

- see also *acoustic waves*; *Love waves*; *magnetoelastic waves*; *Rayleigh waves*; *seismic waves*; *vibrations*
 absorbing media, acoustic pulse deform., numerical calc. algorithm (Russian) 0-96591
 acoustic beam interaction with elastic hollow sphere in acoustic fluid (Ukrainian) 0-69710

elastic waves continued

- anisotropic media, asymptotic equipartition of kinetic and strain energy 0-92081
 bars, phase boundary propagation, dynamic elastic bar theory, sound wave interactions 0-69706
 beam, thin, semi-infinite, transversal displacement 0-74802
 brittle materials, water drop impacted, damage thresholds 0-81149
 capacitative excitation of elastic oscillations 0-71862
 composite materials, fibre reinforced, rectangular rods, elastic wave propagation (French) 0-83749
 composites, fibrous, elastic shear waves propagation 0-58963
 coupled dynamic thermoelasticity problem for a half space with thermal 'memory', thermoelastic waves 0-83753
 crystals, special surfaces and directions, elastic surface wave existence 0-92604
 cylindrical rod, periodic structure, torsional vibrations, interfacial elastic parameters 0-96215
 deformation wave processes, corrected nonlinear eqns., stresses and strains 0-102998
 diffraction by a crack of a cylindrical longitudinal pulse 0-92082
 diffraction by wedge, three dimensional nonstationary problem 0-69723
 edge effect analysis of the linear theory of elastic continua mixture (Ukrainian) 0-69711
 edge notched brittle plates, virgin waves and boundary reflections at fracture 0-79233
 exceptional surface waves in triclinic crystals, existence problems, general props. 0-92603
 excitation and propagation of elastic waves, book 0-94937
 excitation by laser beam, through thermoelastic effect 0-103503
 finite plate, propag. mode III crack, dynamic stress intensity factor, reflected stress waves 0-103001
 fluid filled cavities in elastic solids, fluid identification using resonance method 0-64452
 frictional interface, elastic wave reflection, refraction and absorption, SH motion 0-64437
 front excitation and diffr., by point source with semi-infinite shield 0-79202
 Griffith crack-antiplane shear wave interaction at interface of two bonded elastic half-spaces, geophys., seismological appl. 0-92087
 half space, plane elastic wave scatt., reciprocity and power flow theorems 0-102997
 impact, internal meas. of shear and compression waves, gauge lead effects 0-74817
 inclusions, thin, elastic wave scatt. 0-65151
 incompressible elastic solids, finite amplitude circularly pol. elastic wave reflection and transmission 0-64448
 infinite elastic medium, diffraction of torsional waves by flat annular crack 0-64447
 infinite elastic space with cavity and shell, micropolar elastic wave propag. 0-58950
 infinite elastic space with cavity and shell, micropolar torsional elastic wave propag. 0-58951
 interface wave guided by thin film between two solids 0-100385
 isotropic half space with embedded anisotropic layer, elastodynamic Green's tensor 0-69732
 isotropic medium, elastic waves, mag. field effects 0-58955
 latex, shear waves, elastic modulus determ., light scatt. 0-58956
 layered systems, film-substrate characts. of phase-velocity dispersion and struct. of waves 0-59775
 lenticular martensite growth by transformation wave propag. 0-81055
 linear wave motions study using FFT, NDT appl. 0-92038
 longitudinal, transversally isotropic cylinder with initial stress 0-99934
 martensitic transformation, elastic wave generation comparable to Bain deform., role of multiphonon processes (Russian) 0-84246
 matrix method of optimal truncation, appl. to scatt. from voids and rigid obstacles 0-62480
 metals, ultrasonic inspection, echo-mirror method with transform. of elastic waves 0-108663
 micropolar space with cylindrical or spherical hollow, elastic wave propagation 0-87731
 neutron beam channelling and focusing in ferromagnets (Russian) 0-107351
 nonlinear hereditary elastic medium, longitudinal wave weak distortion process 0-62473
 nonlinear mechanics eqns. and entropy growth across a shock, symmetric form 0-69705
 perfectly conducting elastic sphere, in vacuum, radial vibr. freq., mag. field effects 0-58955
 periodically layered composites in plane strain, dispersion eqn. for waves 0-79212
 piezoelectric crystals, elastic surface waves 0-103558
 piezoelectric medium, semibounded, body waves and quasi-body surface waves 0-107367
 plate, deformed elastic, thickness oscillations 0-64439
 plate, surface wave generation by turbulent boundary layer flow 0-74843
 plate, thin elastic, suddenly punched hole, plane stress unloading waves 0-69729
 polyvinylidene fluoride piezoelectric film, Lamb and SH wave attenuation (French) 0-79196
 porous structure, water-saturated, elastic wave speeds, Biot's theory confirmation 0-103418
 progressing torsional loads along a bore in an elastic medium 0-79197
 pulse propag. in media with freq. dependent Q, theory 0-72438
 quasilayered elastic strip, modulated propagating normal wave transform. 0-74800
 reflected wave field changes in cylinder caused by surface curvature changes (German) 0-106767
 rod, elastic oscillations, wave operator fundamental solutions, asymptotic formulae 0-69722
 rods and plates, strain-rate-sensitive material, elastic-plastic wave propag. mech. 0-69724
 rods with variable cross section, elastic wave propag. 0-64450
 scalar-wave propag. in random elastic layer 0-83754
 scattering by elastic sphere embedded in isotropic elastic medium 0-96214
 scattering from weak inhomogeneities, deterministic inverse problem 0-75300
 scattering of elastic waves by an elastic sphere 0-83747
 SH-waves incident on cylindrical tunnel dynamic stress anal. of elastic liner 0-79201
 shear, and compression wave propag. in impacted solids 0-83755

elastic waves continued

- shear wave scattering by cracks in elastic medium, stress intensity factors 0-74787
- shear waves in an elastic-plastic material due to a supersonic surface step load 0-102999
- shells, two fluid-coupled cylindrical elastic, transient response to incident press. pulse 0-58966
- silicate glasses, longit. and transverse elastic wave vels., temp. and comp. variations 0-88258
- specific directions of plane elastic waves in thin quartz crystal plates 0-92601
- spherical cavity in infinite medium, radial vibr. freq., mag. field effects 0-58955
- steel layer types St3+OKh13, acoustic emission parameters, brittle fracture, crack propagation (*Russian*) 0-93633
- steel layers, types St3+Kh18N9T, acoustic emission parameters, brittle fracture, crack propagation (*Russian*) 0-93633
- stimulated acoustooptical effects due to nonlinear photoelasticity 0-103941
- Stoney wave on the fluid and preliminarily stressed body interface (*Ukrainian*) 0-69708
- Stoney waves at (001) interface between cubic symm. cryst. 0-100388
- strain wave propagation in viscoelastic bars due to longitudinal impacts anal. (*Japanese*) 0-96223
- strength of materials, empirical determ., cleavage fracture in plane waves 0-96225
- temperature compensation and travel times of waves 0-69731
- thermoelastic half-space, dynamic response to energy flux, stress wave evolution (*French*) 0-74795
- tube filled with streaming incompressible fluid, pressure wave propagation 0-96228
- two bonded elastic solids interface, penny shaped crack, torsional wave interaction 0-64484
- viscoelastic bar, transient wave propag. 0-106745
- viscoelastic layered composites, wave propag., dispersion and dissipation effects 0-102982
- viscoelastic media, two-dimensional wave problem, Volterra method solns. 0-69727
- viscoelastic plate, guided harmonic waves 0-79194
- viscoelastic solid, plane and spherical wave propagation 0-106738
- viscoelastic wave propagation, integration contour deform. for Laplace transform inversion 0-74801
- viscous materials, heat-conducting, with hidden variables, shock waves and acceleration waves 0-74788
- weakly anisotropic elastic bodies with cubic symmetry, surface waves (*Russian*) 0-79198
- Al rod, exponentially varying shape, impact by steel spheres, elastic wave propagation 0-74791
- BaTiO₃, elastic props., singularities near tetragonal-cubic phase transition 0-70303
- GaS, elastic prop. anisotropy, Debye temp. (*Russian*) 0-88244
- GaS(Se), elastic characteristics, Debye temp., ultrasonic study (*Russian*) 0-79872
- KD-PO₄, neutron scattering from coupled polar-elastic waves 0-92623
- NaCl-NaBr, elastic wave damping, 300 to 1500 MHz, impurity effects 0-92602
- PbMoO₄, elastic wave excitation and amplification by laser radiation 0-103419
- W, elastic wave scatt. from oblate spheroidal WC inclusion 0-65151
- YAG:Er, elastic wave damping, 300 to 1500 MHz, impurity effects 0-92602

elasticity

- for crack problems in elasticity see crack-edge stress field analysis
- see also elastic constants; elastic moduli; elasticity of liquids; elastoplasticity; photoelasticity; rheology; thermoelasticity
- A15 compound, superconducting transition depend. on non-hydrostatic stress 0-107948
- aeroelastic behaviour, large Darricus rotors derived from behaviour of 5.5 m rotor 0-61251
- aeroelastic stability, large wind turbines 0-61249
- analytical continuous solns., harmonic displacement field representation 0-62472
- annular plates, nonsymmetric postbuckling behaviour, numerical analysis 0-102968
- anti-median elastic problem, N-harmonic solutions 0-99928
- arteries, human, intracranial and extracranial, stiffness and elastic behaviour 0-85436
- arteries, small, pulmonary, elasticity in the cat 0-108942
- axisymmetric elastic problems, stress function solns. (*Japanese*) 0-64371
- bar under tension, torsion appl., 2nd order effects, energy method 0-79158
- beam, cracked, dynamic weight function from finite element soln. 0-79234
- beam, dynamically loaded circular, on elastic foundation, natural freqs. 0-79209
- beam bending on Pasternak foundation, reciprocal variational inequalities 0-92091
- beam on elastic foundation subjected to nonconservative load, stability 0-79191
- beams, skew-curved, static anal. for loading and response, closed form soln. 0-64368
- beams, spatially curvilinear elastic, geometrically nonlinear theory 0-96189
- beams, straight, homogeneous and isotropic, linear flexural theory (*French*) 0-74743
- beams, uniform elastic, lateral buckling, perturbation methods 0-64417
- beams, elastic, under tension, nonlinear transverse vibrs. 0-74803
- bending, axisymmetric elastic bodies with arbitrary boundary conditions, semianal. boundary integral 0-102969
- bending of plates and shells, small parameter method 0-99930
- bicrystal, elastic incompatibility stresses (*Japanese*) 0-107361
- body with plane cracks of normal fracture, 3D problems (*Russian*) 0-79219
- bonded wedge shaped stamp apex singularity, Green's functions for elastic half space 0-64489
- boundary problems in static elasticity, distortion trivector pot., variational principle (*Russian*) 0-79146
- cantilevers, flutter load, discontinuity, variational technique 0-58944
- Cauchy elastic materials, canonical representation using Darboux classification theorem 0-83735

elasticity continued

- circular plate of variable thickness, bending with symmetrical loading 0-69699
- elastic plate on elastic foundation, bending and contact problems 0-96235
- closed-end cylindrical shell under line load along a generator, elastic anal. based on discrete element method and Vlasov eqns. 0-69675
- coiled multilayer shell, stress anal. of elastic and elastoplastic work 0-79156
- colliding cylinders, resulting stress field for linearly elastic material (*Russian*) 0-79237
- column, elastic, axially loaded, optimum linear tapering design 0-64379
- composite material, mechanical behaviour, book 0-94935
- composite rib stiffened constructions, design criteria 0-102977
- composite shell structs., stress-strain state, elastic equilib. 0-74748
- cone cylinder jointed shell, ring stiffened, external hydrostatic pressure, elastic stability (*Chinese*) 0-64412
- conical shell, skew, truncated, external hydrostatic pressure, elastic stability (*Chinese*) 0-64413
- constant deformable dielectrics, coupled mechanoelastic fields, piezoelectricity and Lamb problem 0-58899
- contact on a transversely isotropic half-space, or between two transversely isotropic bodies 0-64488
- contact problem for a layer with two stamps 0-69653
- coupled bending-torsion flutter in cascades, aeroelastic stability boundaries 0-64424
- crack at the boundary between two materials with a branch into one of them in the case of antiplane strain 0-79231
- crack emanation, from circular hole in infinite sheet, Green's function methods 0-92084
- crack tip lattice trapping, relation between macroscopic and microscopic thermodynamic surface energies 0-59572
- cracks, edge, interface, energy release rate calc. based on M-integral 0-87742
- cracks, penny-shaped, in elastic sphere embedding in infinite elastic space, thermal stresses 0-64460
- cracks, penny-shaped, transverse tension, stresses, micropolar elasticity 0-64459
- cracks, plane, occupying two-connected domain, elasticity theory problems (*Ukrainian*) 0-74804
- cracks, plane elasticity, curvilinear crack edges concentrated forces and edge dislocations, numerical soln. 0-58970
- cracks dynamic propagation in anti-plane shear, anal. by finite differences 0-84240
- cracks with a corner point, stress intensity factors, modified Lobatto-Chebyshev method, 0-99972
- critical loads for elastic bodies, lower bounds, stability 0-79185
- crystal surface elastic props., surface tension tensor, volume stress (*Russian*) 0-100389
- curvilinear elastic rods, vibrations 0-57095
- cylinder, circular, transversely isotropic, concentrated loads, 3-D anisotropic elasticity theory 0-83734
- cylinder, thick-walled heteromodular, subjected to underwater waves, numerical calc. 0-74746
- cylinder, thin-walled, laminated, non-uniform, elastic equilib. with surface loads and displacements 0-69671
- cylinder, transversally isotropic with initial stress, longitudinal waves 0-99934
- cylinder dynamic behaviour in the vicinity of the fundamental radial-mode frequency (*Ukrainian*) 0-69709
- cylinder under torsion elastic, spherical cavity effect in stress-strain state 0-101717
- cylinder with inserts and holes, torsion problem, integral eqn. soln. method 0-106717
- cylinder with oblate spheroidal cavity or internal penny shaped crack under tension, stresses 0-69736
- cylinders, constrained, elastic stress analysis by special finite element method 0-106718
- cylinders in elastohydrodynamic contact, lubricant layer thickness and resistance to rolling 0-96236
- cylindrical cavity in elastic half-space, Rayleigh wave loading, stress spectral representation 0-64453
- cylindrical tube, isotropic elastic, holographically meas. surface displacement, stress/strain extrapolation 0-64374
- damaged zone steady state dynamic propagation (*French*) 0-74737
- dielectrics, hyperelastic, with saturated polarisation, variational and invariance principles 0-74730
- dielectrics with polarisation gradient, boundary value problem exact soln. 0-58898
- disc and coaxial ring, partial contact, loaded by external pressure (*Russian*) 0-74814
- disc inclusion, rigid, embedded in with transversely isotropic elastic medium 0-83763
- discontinuous deformation gradients near crack tip in finite anti-plane shear 0-58973
- dynamic elasticity, irregular finite element meshes, grading rules 0-68045
- dynamic elasticity, linear, discrete time approx. of initial boundary value problems, error estimates 0-73175
- dynamic elasticity, tensor spherical harmonics appl. to Navier eqn. 0-98296
- dynamic response of a slab of elastic-viscoplastic material that exhibits induced plastic anisotropy 0-83737
- dynamic shear loading at boundary between elastic space and cylindrical rigid enclosure (*German*) 0-58896
- edge cracked sheets with mixed boundary conditions, stress intensity factors, displacements, stresses 0-64477
- elastic mechanical systems, vibr. damping by dampers with filled voids (*Russian*) 0-58954
- electroelasticity for piezoelectric medium with cuts, 2-D boundary value problems 0-73139
- electronic structure and solid props., rel. to chemical bonding, book 0-86044
- elliptic stamp moving at constant speed on an elastic half-space 0-69654
- equilibrium determination given the stress on a contour (*German*) 0-105505
- ethylene-vinyl acetate copolymers, extrusion and heavy duty films, radiation crosslinking, struct. effect 0-66844
- extruded billets, residual stress determ. from acoustoelastic meas. 0-76467
- fatigue cracks, elastic transpositions, numerical calc. 0-74809
- fibre reinforced composite waveguides, axisymm. elastic vibrs. 0-102995

elasticity continued

fibre reinforced elastic slab subjected to axial loads, instability and buckling 0-64420
 finite elasticity with general loading, uniqueness for deformed surface 0-79153
 finite element analysis of elastic behaviour near an open circular hole (*Japanese*) 0-74750
 fluid filled cavities in elastic solids, fluid identification using resonance method 0-64452
 fracture, brittle, energy release rate, equivalent to Rice integral (*French*) 0-64457
 Fredholm conditions in Signorini's perturbation method 0-62471
 frictional interface, elastic wave reflection, refraction and absorption, SH motion 0-64437
 frictionless stamp impression in elastic half space, contact problem with semiunknown boundary of the contact region 0-69744
 fully stressed state of an elastic continuum 0-92050
 fundamental frequency of vibration of a rectangular plate on a nonlinear elastic foundation 0-69712
 gas diffusion in linear elastic solid, stress-assisted 0-65294
 gels of rodlike macromolecules, nonlinear elasticity in condensed state 0-104199
 general relativistic formulation, elastic rotating cylinder 0-82642
 geometrically nonlinear elasticity theory, dual variational principle 0-94958
 glass fibre reinforced plastic, cemented joint of cylindrical shell with cover, stressed state 0-69668
 Griffith crack-antiplane shear wave interaction at interface of two bonded elastic half-spaces, geophys., seismological appl. 0-92087
 gyroscope with tuned elastic suspension, dynamical characts. 0-79133
 gyroscopic eigenvalue problems in elasticity, nonconservative 0-101708
 half space, elastic, edge cracks, dynamic growth 0-58972
 half space, elastic field due to ellipsoidal inclusions with uniform dilatational eigenstrains 0-58913
 half space, rectangular cylinder penetration, contact problem, stress fields 0-64490
 harmonic holes for nonconstant stress fields, deloids and cardeloids 0-64373
 helical compression springs, finite elements for dynamical anal. 0-96191
 Hertzian impact of two elastic spheres in the presence of surface damping 0-69743
 honeycomb sandwich beams with laminated faces, flexural wrinkling 0-79183
 Hooke's law, potential energy curve 0-67961
 horizontal axis wind turbine blades, aeroelastic stability and response 0-61250
 hyperelastic materials, anisotropic, compressible, finite plane strain, universal deformations 0-69667
 impact load impulse form determination by the displacements and strains of a circular plate (*Russian*) 0-74751
 incompressible elastic materials with different moduli in compression and tension, dynamic problems 0-79141
 incompressible elastic solids, finite amplitude circularly pol. elastic wave reflection and transmission 0-64448
 infinite elastic medium, diffraction of torsional waves by flat annular crack 0-64447
 infinite elastic medium with cylindrical inclusion, external crack in torsion, stress distrib. 0-79216
 infinite elastic space with cavity and shell, micropolar elastic wave propag. 0-58950
 infinite elastic space with cavity and shell, micropolar torsional elastic wave propag. 0-58951
 infinite transversely isotropic solid, containing penny-shaped crack, stress intensity factor 0-69738
 laminated reinforced elastic shells, stability 0-58948
 laminates, multilayer, thick, hybrid-stress finite element formulation 0-92043
 linear elastic beams, shells and plates, elementary theories review 0-69677
 linear elastostatics, Liouville theorems, uniqueness, analytic continuation, continuous dependence 0-64372
 linear elastostatics, unified boundary-integral eqn. method 0-57092
 longitudinal-shear crack refraction, Wiener-Hopf method calcs. 0-87743
 lung, dynamic compliance, freq. dependence, anal. from 1 breathing cycle 0-97967
 lung elastic recoil rel. to ageing healthy males and females 0-67117
 membranes, stability of nonlinear oscillations from Liapunov method 0-96212
 metals, BCC, under elastic stress, Snoek peak height determ. 0-65153
 micropolar continua, static problems, nonhomogeneous eqn. of equilibrium, Green's functions and Fourier transforms 0-58905
 micropolar space with cylindrical or spherical hollow, elastic wave propagation 0-87731
 mixed periodic problems, quadrature solution 0-86088
 mode I loading three-dimensional elastostatic problems, soln. method 0-92086
 multiply connected domains with cyclic and mirror symmetry, plane elasticity problem 0-96188
 nonlinear, effect on capture efficiency of dislocation loops 0-59461
 nonlinear elastic bodies, of different tensile and compression-strengths, stress and strain (*Ukrainian*) 0-69661
 nonlinear elastic continuum, one-dimens. description (*German*) 0-106725
 nonlinear hereditary elastic medium, longitudinal wave weak distortion process 0-62473
 nonlinear nonideally elastic materials, hysteresis, relationships between stresses and strains (*Russian*) 0-90675
 nonlinear shell theory, boundary value problem solutions 0-57094
 nonlinear theory, dynamic problems, existence and uniqueness theorem 0-69658
 nonlinearly elastic body at eqn., relation between stability and continuous dependence 0-92063
 nonlocal theory, stationary boundary problems, reciprocity principle and Green's tensors 0-68046
 nonsymmetric structs., static and dynamic imperfection sensitivity, buckling model modification 0-79190
 notch stress anal. in elastic bodies, energy variations 0-64378
 one-dimensional wave propagation in materials with different moduli in tension and compression 0-83746
 penny-shaped crack problem, deformed incompressible elastic solid 0-92085
 periodic problem in elasticity theory, soln. uniqueness 0-69674

elasticity continued

piecewise homogeneous bodies, two-dimens. elasticity theory stress problems 0-74749
 piecewise homogeneous body, elasticity spatial problems, approx. solutions, R-functions 0-69670
 piecewise-homogeneous plate with slits on elliptic line separating materials 0-99932
 plane elastic crack, dynamics under variable loading (*Russian*) 0-79222
 plane elastic wave diffraction by wedge, three dimensional nonstationary problem 0-69723
 plane elastostatic boundary value problems, Rizzo's integral and Kupradze's functional eqns. 0-57093
 plane elastostatics, integral equations for mixed boundary value problem 0-79143
 plane with const. tangential stress at free boundary, expt. stress anal. of subdomains 0-99978
 plane-strain buckling of cracks in incompressible elastic solids 0-79186
 plate, annular, elastically supported, with central rigid mass, free vibrations (*Japanese*) 0-96226
 plate, circular, elastically supported, with conc. mass at centre, large amplitude vibrs. (*Japanese*) 0-96227
 plate, deformed elastic, thickness oscillations 0-64439
 plate, elastic, containing through crack, skew symmetric loading, transverse shear effects 0-64478
 plate, impact force meas. method 0-79242
 plate, rectangular with asymmetrically reinforcing beams, contact interaction 0-99975
 plate, thin elastic, suddenly punched hole, plane stress unloading waves 0-69729
 plate, variable thickness, on elastic foundation, bending, closed form soln. 0-79179
 plate stability conditions, variational formulations 0-69701
 plate with initial crack subject to extension, brittle fracture energy conditions (*Russian*) 0-103002
 plates, anisotropic skew, large amplitude vibrs., transverse shear, rot. inertia, theory 0-79207
 plates, anisotropic skew, large amplitude vibrs., transverse shear and rot. inertia, numerical results 0-79208
 plates, rectangular elastic, secondary buckling states 0-74782
 plates, rigidity matrix, triangular finite elements (*Russian*) 0-74739
 plates, semicircular, displacement due to concentrated force at a point, Green's function technique 0-58904
 plates, V-notched elastic, symm. loaded, stress intensity factors, caustic method 0-83770
 plates on elastic foundations, variational approach 0-79160
 point defect interaction with grain boundaries 0-59483
 polycrystals, elastic stress and strain microinhomogeneity, finite element method 0-79155
 polydimethylsiloxane end-linked chains, nonGaussian effects 0-65127
 polyester laminates, glass fibre reinforced, enhanced elasticity, chem. resist. tests (*Polish*) 0-60901
 polyester resins unsaturated, enhanced elasticity, chem. resist. tests (*Polish*) 0-60901
 polyethylenes, extrusion and heavy duty films struct. parameters influence on cross-linking by radiation 0-66844
 polyoxymethylene, transitions and relaxation spectrograph 0-65204
 poroelastic cylinder, twisted pore effect on fluid flow, solid deformation and stress 0-64377
 poroelastic cylinders, torsional vibrs., wavelength, phase and group vel. 0-79214
 postbuckling analysis of elastic structures by the finite element method 0-96209
 precipitate and dislocation loop strain and stress field calcs. using affine transformations 0-106722
 prestressed elastic body, 3-D contact problem 0-69655
 prismatic bar of linearly elastic material, maximum theorem appl. for complementary energy functional 0-83733
 progressing torsional loads along a bore in an elastic medium 0-79197
 propoxylated bisphenol A, mech. props., effect of polyester copolymers modified with polypropylene glycol addition (*Polish*) 0-60902
 pulmonary interstitial fluid space compliance, estimation in isolated perfused rabbit lung 0-104605
 quartz, electron irradiation effects on optical, dielec., elastic props. 0-59521
 quartz plates, rotated-Y-cuts, high frequency vibrations 0-96216
 quasistationary Rayleigh waves on inhomogeneous anisotropic elastic body surface 0-69721
 rectangular parallelepiped, natural vibrs. from 3D elasticity and plate theory (*Russian*) 0-79199
 rectangular plate bending, superpower degeneration of boundary layer of angular points (*Russian*) 0-74776
 rectilinear anisotropic solids, mixed-mode crack anal. using conservation laws of elasticity 0-84239
 reflex stiffness of man's anti-gravity muscles during knee bends while carrying extra weights 0-61601
 regularly layered half-space, deformation, vibrational loading 0-99933
 reinforcement material distrib. for specified stress field criteria, plane elasticity hybrid problem 0-64376
 rigid indenter and elastic halfspace, dynamic contact with perfect adhesion and frictional slip 0-58980
 rigid punch bonded to elastic half plane, stress singularities 0-64491
 rigid sphere embedded in elastic medium, response to incident stochastic waves 0-64451
 rigid stamp, elastic layer indentation under complete adhesion conditions 0-58979
 rod, curved, deformed by end loads (*Russian*) 0-74745
 rod, elastic oscillations, wave operator fundamental solutions, asymptotic formulae 0-69722
 rod, thin elastic, non-conservative torsion (*German*) 0-106723
 rod, thin elastic, with causally mixed inputs, iterative numerical soln. 0-79161
 rod with clamped ends, axial and transverse loading, stability, plane elasticity theory (*Russian*) 0-79184
 rods, elastic, high-freq. long wave vibrs. 0-96211
 rough elastic bodies, plane and axisymmetric contact problems 0-74812
 rough spheres, elastic contact, anal. approx. 0-79240
 rubber, natural, crosslinked by dicumyl peroxide, modulus, swelling relations 0-59551
 rubber covered rolls, contact and deformation nonlinear elastic problem, stress anal. 0-79239
 rubber seal technology, advances 0-93730

elasticity continued

- Saint Venant's solns. in rod and beam theories 0-69676
 saturated elastic half-space with partially embedded elastic bar, quasi-static bending 0-79145
 second order beam theory 0-58908
 second order effects in an elliptic hole stressed at infinity 0-96192
 shell, cylindrical, closed, laminated, longitudinal crack, elastic eqn., energy approach (*Russian*) 0-87740
 shell, cylindrical, isotropic, elastic stability, critical load analysis 0-83744
 shell, cylindrical elastic, dynamic response in potential fluid 0-64446
 shell, elastic, cylindrical, stability, Liapunov's second method 0-64410
 shell, elastic cylindrical, ribbed, with weight on springs, free vibr. freqs. 0-69725
 shell, high-shallow, with rib of equal resistance, contact interaction, tangential stress distrib. (*Russian*) 0-87745
 shell, viscous plastic layers, viscous elastic filler, variable loading (*Russian*) 0-69695
 shell design by finite element method, deformation and elasticity theory 0-74747
 shell of revolution, orthotropic, thick, stress-strained state, finite element method (*Russian*) 0-87713
 shell problems, finite element anal. (*Ukrainian*) 0-69662
 shell stability during axial compression, hardening beyond elastic limit 0-99931
 shells, circular cylindrical, in axial compression, axisymmetric creep buckling, isotropic elasticity 0-69704
 shells, curvilinear tubular, elastic equilb., finite element anal. (*Russian*) 0-79148
 shells, cylindrical, and of revolution, path independent integrals 0-87711
 shells, cylindrical, dynamic stability, in-plane inertia and disturbance effects 0-79181
 shells, cylindrical, finite element anal., solid of rev., thin shell and inter-phase elements 0-74744
 shells, isotropic thin elastic, nonlinear theory (*Russian*) 0-79147
 shells, Kirchhoff-Love, structural stability, mixed variational principles and non holonomic constraints (*French*) 0-74779
 shells, spatial stability problems in elastic systems, modified energetic procedure (*Russian*) 0-58943
 shells, thick hyperelastic, spherical, large amplitude free and forced oscillations 0-74794
 shells, thin, doubly curved, numerical integration of triangular finite element 0-92044
 shells, thin elastic spherical, large axisymmetrical deflection states 0-79154
 shells, two fluid-coupled cylindrical elastic, transient response to incident press. pulse 0-58966
 Signorini problem for a Cosserat plate 0-69666
 single crystals under large loads, theoretical elastic behaviour, review and appl. 0-71681
 single mass vibroimpact system, response to white noise random excitation 0-64454
 solid deformable body, residual stresses by creating holes, holographic interferometry appl. (*German*) 0-79243
 sphere, deformation and sticking to a rigid plane, mol. force effect 0-106720
 stability, response to finite strain 0-79187
 steel, stainless, global bending response analysis of elastic and viscoplastic nuclear shipping cask structures subjected to impact loading 0-76301
 steel, type K12M, rel. between structural inhomogeneity and wear resist. (*Russian*) 0-66672
 strain energy of elastic prismatic bar, theorems (*German*) 0-79142
 stress intensity and elastic equilibrium of a wedge with a crack 0-69733
 stress tensor, Kauderer's postulates (*German*) 0-64364
 stress-strain state at brittle crack vertex, geometric nonlinearity effects (*Russian*) 0-79221
 strip, elastic, Griffith crack interactions, mixed boundary value problem 0-58969
 strip or beam, state of stress, rectilinear thin walled inclusion effects 0-96187
 strips, seizure, elastic stresses, extra loading moments (*Russian*) 0-69664
 supports for straight fluid-carrying pipes, critical velocity calc., w.r.t. vibrations production (*German*) 0-58914
 surface concentrated loading, axisymmetric problem for homogeneous medium (*French*) 0-92041
 symmetrical branches at end of crack, effects on growth 0-103003
 tensionless contact without friction between elastic layer and elastic foundation 0-64487
 thermodynamic behaviour of non-hyperelastic elastic materials, mathematical model 0-73290
 thick plates, 3-dimens. refined elasticity theory, bending and torsion 0-64375
 thin electroelastic sheets, fluttering, thermodynamic effects (*German*) 0-106749
 thin tubes conveying fluid, hydroelastic stability, in plane boundary conditions, shearing loads 0-64419
 three-layer plates, circular, stability 0-79188
 Timoshenko beam, shear coeff. (*German*) 0-106729
 torsion investigation by approx. methods for inhomogeneous elastic layer 0-98799
 torsion of elastic sphere by elastic punches 0-99929
 track compliance, influence on running, model and expts. 0-61602
 traction problem, strain energy bound in finite elasticity with nonzero surface data 0-58909
 truss, pin-jointed, with cyclic symmetry, structural rigidity, static and kinematic indeterminacy 0-58906
 two bonded elastic solids interface, penny shaped crack, torsional wave interaction 0-64484
 two-phase anisotropic medium, interfacial dislocation, stresses, displacements and energy calc. 0-79786
 two-phase transversely isotropic elastic materials, Green's function solns. 0-58912
 unbounded elastically isotropic medium, fields generated by moving dislocations, multipole-moment expansion (*Russian*) 0-103330
 unilateral contact problem in linear elasticity 0-79238
 unloading wave propagation in cylindrical, semi-infinite, elastic-plastic rod, asymptotic behaviour 0-69659
 vibration of partially adhering stamp 0-69656
 vibroisolation parameter selection method and stability for two machines on elastic beam 0-87738
 viscoelasticity rods with nonlinear elasticity relation and nonlinear internal friction, parametrically excited oscils. 0-99947

elasticity continued

- Vlasov theory of cylindrical shells, boundary conditions 0-69660
 weakly anisotropic elastic bodies with cubic symmetry, surface waves (*Russian*) 0-79198
 wedge, symmetric cracking by transverse displacements, stress intensity factors 0-79226
 $Al_2O_3 \cdot B_2O_3 \cdot SiO_2$ sheet glass, solar energy appl., optical and mech. props. 0-87447
 Cu-Al, dislocation core cut-off parameter, estimation from stacking fault nodes 0-103370
 Fe-Ni, single cryst., solid soln. softening, effect of interstitial N 0-97496
 Fe-Ni alloys props. of materials used in electromechanical filter resonators (*Czech*) 0-76318
 Pu, elastic constants at elevated temps., noncontact meas. tech. 0-104405
 $SrTiO_3$, critical elastic compliance, acoustic resonance meas. 0-65118
 $V_{0.5}Si_{1-x}Ge_x$, elastic props., 77 to 290K, rel. to supercond. transition temp. (*Russian*) 0-66560
 $V_{0.5}Si_{1-x}Ge_x$ solid soln., longitudinal and transverse US wave propag. rate, 4.2 to 300K (*Russian*) 0-103423
 WO_3 , reduced, elastic strain energy in cryst. shear planes 0-75239
- elasticity of liquids**
 see also compressibility of liquids
 p-n-alkoxybenzoates of p-n-alkoxyphenyl, smectic A phases mol. struct. and elastic behaviour 0-59382
 elastohydrodynamic lubrication, non-Newtonian effects of volume relaxation 0-103009
 smectic C liq. cryst. film, mol. orientation fluctuations in two-dimens., light scatt. obs. 0-93355
- elasto-optical effects** see photoelasticity; piezo-optical effects
- elastomers**
 see also rubber
 butadiene styrene elastomers, cross-linked, mech. relax. behaviour (*German*) 0-84986
 cellular elastomer selection for use in biomechanical capacitive force transducers, measuring device (*German*) 0-85545
 diene oligomers with hydroxyl groups, prep. by rubber oxidation (*German*) 0-85175
 laminated elastomeric bearings, high-capacity, finite-element anal. 0-96197
 polydimethylsiloxane, end-linked chains, model elastomeric networks, Gaussian, nonGaussian and ultimate props. 0-103260
 polyether-polyester, differential scanning calorimetry, crit. points (*Japanese*) 0-75344
 polyether-polyester elastomers, differential scanning calorimetry by using poly(oxy-1,4-butylene glycol) as soft segment (*Japanese*) 0-79916
 polyurethanes, cross-linked, mol. mobility and struct., thermomechanical and NMR obs. (*Russian*) 0-69285
 relaxation behaviour, rel. to tensile strength (*German*) 0-66604
 silicones, dental impression materials, dimens. stability, holographic and interferometric study 0-67204
 soot filled, mech. relax. behaviour (*German*) 0-84985
 surface roughness, friction and adhesion 0-66674
 thermal spectroscopic study 0-89445
 urethane elastomer, thermoplastic, dilute soln., viscosity and sedimentation 0-103512
 urethane polyester elastomers, dielectric relax., spatial network density (*Russian*) 0-71310
 vacuum seal materials, practical selection 0-77797
- elastoplasticity**
 $\sigma \sim \epsilon$ relation variant for variable loading of elastic-plastic bodies 0-58933
 asymptotic behaviour of elastoplastic bodies under periodic loading 0-83740
 boundary element method, initial stress approach 0-74762
 cavity, cylindrical, stress distrib., photoelastic investigations, successive elastic solns. (*Polish*) 0-64391
 coiled multilayer shell, stress anal. of elastic and elastoplastic work 0-79156
 columns, elastoplastic, thin and vertical, postbuckled, deflections 0-87728
 constitutive theory, thermodynamic treatment 0-64390
 convexity condition in an elastic-plastic material (*German*) 0-106734
 crack tips, blunt, elastic-plastic stress field, plane stress and plane strain (*Chinese*) 0-64469
 cylinders, discretely stiffened, buckling under axial compression 0-64408
 damaged body, unknown boundary value problem explicit solution (*French*) 0-79166
 disc, annular, axially symmetric, with rigid inclusion, decohesive carrying capacity (*Russian*) 0-69688
 discs, doubly-connected, elastoplastic, full yielding at collapse, noncircular shapes 0-74755
 discs, doubly-connected, noncircular, full yielding at collapse, photoplastic verification 0-74756
 doubly connected region, numerical solution of two dimensional elastoplastic problems 0-99946
 elastic-viscoplastic frames, dynamic responses, strain hardening effects 0-79178
 elastic-viscoplastic materials, strain rate effects on necking 0-58918
 elastic-viscoplastic materials, uniaxial cyclic loading, stresses, relaxation, creep 0-64402
 existence-uniqueness result for some models of thermoplasticity 0-92077
 flow rule for lowering buckling stresses (*Japanese*) 0-99949
 formulation of laws for plastic anisotropic elastic materials in volume expansion (*German*) 0-106732
 fracture stress obtained from the elastic crack tip enclave model 0-71730
 high strain rate behaviour, incremental elastic-viscoplastic constitutive eqns. integration 0-85138
 integrated load increment method for finite elasto-plastic stress analysis 0-92072
 localisation of deformation, bifurcation modes 0-79167
 metallic materials, elastic-plastic transition behaviour model (*German*) 0-75295
 metals, inelastic cyclic strain under nonuniform stress state conditions, residual stresses effect 0-81132
 non-associated plasticity and elastoplasticity, rate boundary value problems, variational principles 0-87726
 perfectly plastic medium, elastic-plastic field at tip of steadily growing crack (*Chinese*) 0-58968
 plain strain contained plastic deformation, elastic-plastic laws, finite element anal. 0-92073
 plane elastoplasticity, subject to large strains, finite element anal. (*Japanese*) 0-96207

elastoplasticity continued

- plane V-notched specimen, elastic-plastic limit load anal. 0-69684
 plane-strain crack growth, comparison of theory and experiment 0-108560
 plate, elastic-plastic, flexed in its plane, stress concentrations, method of small parameter (*Russian*) 0-74759
 plate, thin, elastoplastic, buckling model (*French*) 0-74778
 plate weakened by equal-armed cross-shaped crack, plastic strain and fracture 0-69740
 plates, elastic viscoplastic, transient dynamic large deflection anal., finite element method 0-69683
 polycrystals elastic-plastic deformation, plane geometrical model and finite element calc. 0-79860
 porous metals, plasticity, stress-strain curves, yield stresses, strain vectors 0-83738
 Rakhmatulin elastic-plastic model, dynamic 3-dimens. eqns. 0-58927
 rate problems in finite strain classical elastoplasticity energy theorems, Lagrangians 0-74766
 relaxing media, shock waves struct., dislocation model 0-58961
 rod, elastoplastic, dynamic bending and residual deformation (*Russian*) 0-75293
 rod of rate-sensitive material, elastic-plastic tension-torsion analysis 0-83741
 rods and plates, strain-rate-sensitive material, elastic-plastic wave propag. mech. 0-69724
 shakedown, partial, under thermomechanical loading path (*French*) 0-74757
 shakedown problems for elastic plastic solids with piecewise linear yield surface 0-79173
 shear waves in an elastic-plastic material due to a supersonic surface step load 0-102999
 shell, rectangular flexible elastoplastic, yield theory and deformation theory appl. 0-74773
 shells, axisymmetric, unsymmetrical bending, elastoplastic anal. 0-92065
 shells, elastic-plastic circular cylindrical, under internal pressure, bifurcation 0-64421
 slab with elliptical opening, flexed in its own plane, small parameter method (*Russian*) 0-74760
 solid free boundary, slip line initial development, elastic-plastic problem 0-96196
 spherical body, instability under uniform loading 0-58946
 stability of thin-walled pressure vessels of elastic-plastic linear hardening material 0-92075
 steel, low C, crack initiation at root of circumferential notch of round bar specimens (*Japanese*) 0-60947
 steel, type 4052Kh, thermomechanical working influence on mech. props. (*Russian*) 0-93578
 steel casting, calc. method of thermal and thermo-visco-elasto-plastic processes (*German*) 0-79859
 steel continuous casting, thermal, thermo-visco-elasto-plastic processes (*German*) 0-81044
 steel plates, explosively clad, fatigue crack propagation behaviour (*Japanese*) 0-104262
 strength of materials, empirical determ., cleavage fracture in plane waves 0-96225
 stress measurement, temporary and residual stresses, high-temps. 0-64498
 stress wave propag. (*Czech*) 0-108507
 supplementary strain method, appl. 0-96205
 thermal elastoplastic stress analysis based on initial strain method (*Japanese*) 0-77620
 thin plate elastic-plastic buckling, Hencky effects, von Karman nonlinear strain (*French*) 0-58942
 tube, thick-walled, axisymmetric deformation in presence of upper yield point (*Russian*) 0-74758
 tubes, thick-walled, thermoelastoplastic creep stress anal. 0-58922
 viscoplastic materials, elastic, rate-independent limit of constitutive eqns. 0-74753
 viscoplastic model, cyclic load, stress evolution, asymptotic behaviour (*French*) 0-64382
 viscoplastic/elastic media, constitutive eqn. covering wide range of strain rates (*Japanese*) 0-79862
 Al-Cu-Si-Mg, deform. simulation using torsional test, elastoplastic constitutive eqn. 0-93594
 Al-Cu-Si-Mn, type 2017S-T4, crack initiation at root of circumferential notch of round bar specimens (*Japanese*) 0-60947
 Al-Zn-Mg-Cu (6, 2.5, 1.5 wt.%), deform. simulation using torsional test, elastoplastic constitutive eqn. 0-93594
 Fe₃₀Ni₄₀P₁₄B₆, metallic glass, bending tests, evidence of ideal elastic-plastic deform. 0-97543
 Ti-Al-Mo-Zr, type VT-9, creep eqns. rel. to extension and compression props. 0-100875

elastoresistance

- Si on sapphire, residual strain effect on elec. props. (*Japanese*) 0-84522

ELDOR

- actomyosin, X-irradiated ENDOR and ELDOR obs. 0-63689
 myosin, X-irradiated ENDOR and ELDOR obs. 0-63689
 polycrystalline dipeptides, X-irradiated ENDOR and ELDOR obs. 0-63689

electrets

- see also dielectric devices; electrostatics; photoelectrets; thermoelectrets
 applications to transducers, filters and pyroelectric devices, book contrib. 0-80709
 bioelectrets, electrets in biomaterials and biopolymers 0-80686
 diamagnetic anisotropy of thermoelectret and magnoelectret states 0-97053
 discharge model 0-88908
 discharge model 0-88909
 EL2 telephone transmitter, technology development 0-83723
 fibre, non-woven, high-efficiency filtering medium 0-76691
 fundamental aspects of research, book 0-77552
 hexamethyldisiloxane plasma polymerised thin film, charge trapping char-acts. 0-96895
 magnoelectrets, possible mech. of biological effects of mag. fields 0-93157
 metallised, mech. instabilities (*French*) 0-88906
 novolac and novolac allyl ether electrets, thermal depolarisation, chem. struct. effect 0-71297
 photoresist, KTRF, thermally stimulated discharge current studies 0-75924

electrets continued

- physical principles 0-80682
 piezoelectric and pyroelectric props. 0-80685
 plastic films, charge distribution determ. (*German*) 0-75920
 polystyrene film, thermally stimulated discharge currents 0-71300
 prepolarised, meas. microphones appl. 0-74649
 radiation-induced charge storage and polarisation effects 0-80684
 RNA, solid hydrated samples, hysteresis loops, nonlinear dielectric properties 0-71294
 thermal pulsing technique for spatial distrib. of charge and polarisation 0-93235
 thermally stimulated discharge 0-80683

electric actuators

- thread grinder, high precision, laser interferometric auto-correcting system 0-90830

electric admittance

- hemispherical monopole surrounded by plasma layer, Tonks-Dattner reson. and input admittance 0-87887
 macroion solutions, theory of effect of small ions on electrical admittance 0-71914
 p-n heterojunction differential admittance theory in the presence of surface electron states 0-96981
 CaF₂-H₂, ionic cond. determ. from admittance and dielec. loss meas. (*French*) 0-107479
 Si ion-controlled diodes, acid-base exposure effects, Si-SiO₂ interface state density 0-96984
 Ta₂O₅, amorphous and cryst., elec. cond. mechanism, admittance meas. 0-70705

electric admittance measurement

- MIS/SIS solar cells, automated surface states anal. 0-93966
 PbS-Si p-n heterojunctions, AC admittance meas. 0-96979

electric amplifiers see amplifiers**electric arc furnaces** see arc furnaces**electric arc welding** see arc welding**electric arcs** see arcs (electric)**electric breakdown**

- see also electric breakdown of gases; electric breakdown of liquids; electric breakdown of solids
 dielectric conduction and breakdown, conf., Gainesville, FL, USA (Oct.-Nov. 1979) 0-82564
 heavy ion counters based on MOS structure 0-69032
 ion beam extraction, computer simulation, finite element method 0-96387
 numerical description of treeing for dielectric breakdown in polymethylmethacrylate 0-100633
 plasma sheath breakdown to glow transition in plasma filled gap 0-100105
 testing, Voyager spacecraft, JPL, Pasadena, USA 0-92415
 vacuum gap breakdown initiation by microparticle impact 0-96413
 wire-plane electrodes, breakdown voltage, effect of vacuum conditions 0-64798
 As₂S₃ film, evaporated, switching effects 0-96952
 Cu electrodes, breakdown voltage, prebreakdown current in vacuum, crossed elec. mag. fields depend. 0-79604
 Kr-Ar, phase matched, generation of Lyman- α radiation 0-91845
 Kr-Xe, phase matched, generation of Lyman- α radiation 0-91845
 Si, thermally oxidised-electrolyte system, features of cathodic breakdown (*Russian*) 0-107907

electric breakdown of gases

- see also electron avalanches
 air, electrode surface roughness effects 0-84018
 air, heated, breakdown parameters 0-103202
 air at Ti surface, optical breakdown, interferometric investigation 0-100064
 air gaps, 1 to 9 cm, with heated electrodes, investigation (*German*) 0-107010
 breakdown wave propagation in ionised gas in nanosecond discharges 0-87890
 coaxial plasma guns, breakdown phase, optical and elec. meas. 0-70036
 compressed SF₆, repeated breakdown field strength in uniform field perturbed by protrusion 0-96406
 crossed magnetic field, equivalent reduced electric field concept 0-64805
 dielectric gases and gas mixtures, maximum electric strength and vapour pressure relationships 0-92249
 flowing gas spark gaps, electric breakdown study, improved method 0-64821
 HF breakdown, lower-hybrid waves, focusing and channelling (*Russian*) 0-106890
 insulating replacement gases for SF₆ 0-59313
 ionising wave propag. mechanisms 0-83941
 laser gas breakdown, shock and ionisation waves, photographic absorpt. obs. 0-87967
 laser-supported breakdown, finite absorpt. length model 0-107005
 metal carbonyl vapours, pulsed laser breakdown, ultra-fine metal particle form. 0-84881
 molecular ion reactions influence on optical breakdown 0-96341
 multiply-charged plasma, temp. kinetics and population levels (*Russian*) 0-106952
 overvoltage breakdown development at high gas press. 0-84021
 prebreakdown stage, review 0-106868
 rod-to-plate system, initial corona voltage calculated according to Townsend's Theory (*Czech*) 0-87961
 space charge ionising waves, high velocity propagation 0-87889
 sparking potential in longit. mag. fields 0-106996
 Townsend primary ionization coefficients and breakdown voltages of cycloparaffin vapours 0-79602
 vacuum breakdown, Trump-Van de Graaff condition anal. 0-79613
 vacuum breakdown in elec. field in range (5-7) $\times 10^6$ V/cm 0-87973
 Ar, heated, breakdown parameters 0-103202
 Ar plasma, RF breakdown pot. microwave scanning technique 0-64773
 CCl₄F₂-CO₂ gas mixture, field breakdown gradients calc. method 0-92248
 CCl₄F₂-N₂ gas mixture, field breakdown gradients calc. method 0-92248
 CO₂ TEA pulsed, UV preionized, high power laser, development and performance 0-106539
 He, heated, breakdown parameters 0-103202
 He, laser-induced breakdown 0-96339
 He, pulsed breakdown at low temp. 0-103216
 SF₆ corona-stabilised breakdown, computations and obs. 0-64804

electric breakdown of gases continued

SF₆ impulse breakdown characteristics for nonuniform field gaps for switchgear design 0-84024
SF₆ insulation breakdown characts. under operating conditions in HV apparatus 0-96414
XeCl discharge, KrF laser induced preionization 0-84020

electric breakdown of liquids

bubbles behaviour obs. 0-71313
dielectric liquid high field carrier transport, electron multiplication and breakdown, mol. struct. depend. 0-84694
dielectric liquids, ion mobility meas. and breakdown process, optical methods 0-84692
dielectric liquids, qualitative model of elec. breakdown process, effects of external field 0-84693
hydrocarbons, electric breakdown, light emission investigation 0-93241
pulsed breakdown, interferometric obs. 0-80696
silicon fluids, positive discharge propag., rel. to transformer oil 0-88926
transformer oil, positive discharge propag., rel. to silicone fluids 0-88926
water, electrical breakdown in μ s regime with Cu, brass, steel and Al electrodes 0-103917
water, for applied electric fields in range 200-500 kV/cm in the 2-10 microsecond time domain 0-71316
N₂, dielec. breakdown, press. depend. of polarity effect 0-75936

electric breakdown of solids

see also impact ionisation: partial discharges; Zener effect
cast-epoxy resins, AC breakdown-voltage characts. (Japanese) 0-88927
dielectric materials, spacecraft, charging and discharging 0-71315
dielectric solids, electric breakdown 0-66111
dielectric surface, photoinduced surface discharge 0-88929
dielectrics, thermal breakdown, theory 0-75938
electret discharge model 0-88908
electret discharge model 0-88909
ethylene propylene rubber, effect of electrode profile on dielec. breakdown voltage, epoxy resin insulation system 0-60502
gaseous model, macroscopic channel development in strong elec. field, tree growth and return streamer 0-84696
high field conduction and breakdown in solid dielectrics, review 0-84691
insulators, detection of US emission prior to breakdown 0-88924
intense electric fields, tree-shaped phenomena in solid insulating materials (Rumanian) 0-63885
laser pulse produced breakdown, SHG increase evidence for large carrier conc. 0-102769
mica, pulse electric breakdown under pressure, lamination effects 0-66110
physical basis dielec. localisation and memory track 0-88925
polyethylene:Br₂(l), films, electron-beam induced carrier mobility and elec. breakdown 0-80429
polyethylene, cable grade crosslinked, effect of electrode profile on dielec. breakdown voltage, epoxy resin insulation system 0-60502
polyethylene, dielectric props., investigation for morphology changes created by mechanical drawing and annealing 0-84697
polyethylene, electron beam crosslinking process for high voltage power cable 0-66846
polyethylene, halogen-doped, carrier transport and breakdown characteristics (Japanese) 0-96889
polyethylene terephthalate polymer insulator, conduction and breakdown mechanism (German) 0-100469
polymer, dielec. breakdown theories, mol. and morphological features rel. to elec. strength, review (Japanese) 0-60501
polymer, dielectric breakdown, DC trees caused by space charge accumulation, carrier injection and trapping effects 0-84695
polymeric insulating materials, water treeing initiation and growth, effects on cable service life 0-84698
polystyrene:Br₂(l), films, electron-beam induced carrier mobility and elec. breakdown 0-80429
polystyrene, halogen-doped, carrier transport and breakdown characteristics (Japanese) 0-96889
polyvinylidene fluoride, dielec. breakdown and elec. cond., room temp. to 150°C 0-60500
pulsed surface flashover mechanism involving electron-stimulated desorption 0-70055
semiconductors, effect of freq. on applied voltage 0-75592
stator windings, failure mechanisms under thermal cycling (Japanese) 0-104189
BaTiO₃ ceramic, degradation under high AC elec. field 0-60499
MoS₂ oxide film, dielec. props. and growth kinetics 0-81215
NaCl, optical strength, effect of irradi. in mechanically stressed state 0-80695
RbCl films, breakdown on appl. of electric voltage pulses 0-66109
Si p-n junction, subnanosec. current drops in delayed breakdown 0-75633
Si p-n junction, subnanosec. current drops in delayed breakdown 0-75634
Si planar semiconductor junctions, disruptive voltage calc., ionisation coeff. (Rumanian) 0-103746
Tm₂O₃ film, between Al electrodes, prep. and elec. props. 0-60103
ZnO ceramic varistors, thermal breakdown 0-88928
ZnSe:In, highly compensated single crystals, thermally initiated current breakdown, current-voltage characts. 0-65579

electric cables see cables (electric)

electric capacity see capacitance

electric cells see cells (electric)

electric charge

see also space charge
EHD flow, nonstationary, with charge diffusion, nonlinear and linear wave processes 0-59124
electrets in plastic films (German) 0-75920
ferroelectric, interaction energy between a charge and domain wall 0-88939
material charging in space environment 0-109327
paper sheets, charge decay and resistance parameters correlation determ. 0-70795
radiating particles of finite size, Dirac's subtraction formalism (German) 0-91740
rocket payload, charge neutralisation during electron beam emission, laboratory studies 0-77258
spacecraft, charge neutralisation via electron emitter (Japanese) 0-94673

electric coils see coils

electric condensers see capacitors

electric conductance see electric admittance

electric conductance measurement see electric admittance measurement

electric conduction processes see electrical conductivity

electric conductors see conductors (electric)

electric connectors

see also cable jointing
additive-free hard Au appls. 0-108718
lead-ins with composite seal for high pressure chambers 0-105665

electric control equipment

see also controllers; electric actuators; electric sensing devices; switches; telecontrol equipment; telemetering equipment
LMFBR ML-3 Na circuit, electrical and control installations (Spanish) 0-57819
slide projector, dissolve control unit provides cross-fading and operational sequence recording 0-77833

electric control gear see electric control equipment

electric current

see also arcs (electric); corona; critical currents; current density; current distribution; current fluctuations; eddy currents; electrojets; fault currents; leakage currents; short-circuit currents; sparks
Alaska oil pipeline, induced elec. currents meas. by gradient fluxgate and SQUID magnetometers 0-98231
bipolar trickle reactors, electric current versus potential plots 0-76521
heliosphere, elec. currents rel. to model of mag. field configuration 0-94670
Jupiter magnetosphere, currents generation by Io interaction with plasma torus 0-98604
solar atmosphere, elec. currents as solar wind energy source 0-94768
solar flares, expt. on merging of two current carrying plasma columns (Japanese) 0-94775

electric current measurement

see also ammeters; galvanometers
AC, using magneto-optical methods, principles and advantages (Polish) 0-105676
ampere, absolute meas. using NMR 0-98941
ampere realization and gyromag. ratio of proton meas. at NPL 0-98940
ampere realization by means of current balance at NPL 0-105678
ampere realization expts. at NBS 0-98938
bipolar cell stacks, leakage currents 0-76526
charged particle beam in range 100 μ A-300 mA, magnetomodulation device 0-68993
DC currents, low, new system of meas. 0-82791
insulating materials under high elec. field, determination of complex permittivity (French) 0-98933
laser light measuring techniques (Japanese) 0-86342
magnetic defectoscopes, nonsinusoidal periodic currents meas. 0-104386
moving-coil expt. for meas. of current and EMF, vel. control technique 0-98939
multijunction thermal convertors for AC-DC transfer standards 0-98874
nonsinusoidal periodic current meas. using standard DC shunt with magnetic powder monitoring, frequency errors 0-104398
optical fibre, current measurement appl. 0-96015
optical fibre, single-mode, for current meas. system, birefr. induced by bends and twists 0-99832
reproduction of ampere at German ASMW 0-98944
RMS measurement errors quantified 0-57274
transients, fast digital technique (Polish) 0-86340
ultrashort current pulse generation and meas. using Josephson devices 0-90827

electric discharge machining see spark machining

electric discharges see discharges (electric)

electric domain walls

double quadratic kink soln. to ferroelec. domain wall dynamic polarisability 0-66135
ferroelastic, roughening transition suppression by long range elastic forces 0-75991
ferroelectric, interaction energy between a charge and domain wall 0-88939
ferroelectric ceramic, mech. and elec. losses, correl., theory and expt. 0-66133
ferroelectric ceramics, materials and dielec. props., review 0-75957
piezoelectric ceramic, nonlinear charge release under uniaxial press. 0-80706
roughening transition, Peierls force against Peierls divergence 0-75991
TGS: α -alanine, single crystals, dielec. spectrum in RF range (Russian) 0-66097
BaTiO₃, electron microscopy investigs. of ferroelec. substances, review (Japanese) 0-71366
BaTiO₃, periodic domain struct. and opalescence at tetragonal to orthorhombic transition 0-66131
BaTi_{0.95}Sn_{0.05}O₃, ferroelec. film, switching process 0-60518
Gd₂(MoO₄)₃, ferroelec., amorphous Si:H coating, domain wall motion, image scanning 0-83663
Gd₂(MoO₄)₃, matrix-addressed analogue ferroelec. memory 0-103926
LiNbO₃, crystal defects, X-ray diffr. topographic study (Chinese) 0-84173
NaD₃H_{3(1-x)}(SeO₃)₂, ferroelec. dispersion 0-66129
PLZT, mech. and elec. losses, correl., theory and expt. 0-66133
Pb(Zr,Ti)O₃, porosity-permittivity relations, depolarising factors determ. and pore effects (Japanese) 0-97189

electric domains

see also electric domain walls; ferroelectric materials
dicalcium strontium propionate, ferroelec. domains, direct optical visibility 0-84704
exciton dielectric, inhomogeneous current state phase transition, free energy (Russian) 0-84703
ferroelectric plate, domain struct. near first-order phase transition resembling second-order-transition 0-93139
ferroelectric substances, electron microscopy investigations, review (Japanese) 0-71366
ferroelectric tetragonal ceramics, 90° domain-rot. fraction after polarisation, X-ray determ. 0-75992
ferroelectrics, domain structure as outcome state for poling procedure 0-80728
guanidine aluminium sulphate hexahydrate, SEM obs. of ferroelec. domain struct. in single crystals 0-97219
guanidinium aluminium sulphate hexahydrate, surface obs., SEM and AES expts. 0-71362
guanidinium aluminium sulphate hydrate, ferroelec., decoration patterns on cleavage surface, domain obs. 0-97218

electric domains continued

- guanidinium uranyl sulphate hydrate, ferroelec., decoration patterns on cleavage surface, domain obs. 0-97218
 semiconductor heating, thermal domain investigation, current voltage char-acts. 0-70711
 semiconductors, exciton and domain luminesc., book 0-82588
 SLC, chiral structure in electric field, dielectric permeability, spontaneous polarisation (*Russian*) 0-75159
 smectic liquid crystals, ferroelec., submicrosecond bistable electro-optic switching 0-84051
 tetragonal ferroelectric irradiated by laser pulses, spatial temp. and bound-charge distrib. 0-103927
 TGS, effect of Fe^{3+} admixture on phys. props. 0-76052
 TGS, ferroelec. activation field change 0-71358
 TGS, internal field prod. in layer periodical domain struct. by X-ray irradiation 0-71359
 TGS, kinetics of domain formation during phase transition 0-66130
 triglycine sulphate, ferroelec., decoration patterns on cleavage surface, domain obs. 0-97218
 BaTiO_3 ceramics, PTC-type, grain boundary study using TEM 0-107267
 BaTiO_3 , periodic domain struct. and opalescence at tetragonal to orthorhombic transition 0-66131
 BaTiO_3 , polydomain ferroelec. crystals, phys. consts., self consistent calcs. 0-88942
 BaTiO_3 , pure and doped crystals, surface and domain struct., AES and SEM expts. 0-71363
 Fe_2O_3 lattice parameters, NMR freqs., and magnetoelec. pots. near 12K 0-71146
 n-Ga, In, Sb Gunn diode, high field domain characts. 0-59992
 $\text{Gd}_2(\text{MoO}_4)_3$, electron microscopy investigs. of ferroelec. substances, review (*Japanese*) 0-71366
 $\text{Gd}_2(\text{MoO}_4)_3$, one-dimensional ferroelectric image sensor with polymer photoconductor 0-80729
 Ge:Cu, surface waves at static domain boundaries (*Russian*) 0-80288
 $(\text{Li}_2\text{B}_2\text{O}_7)_{1-x}(\text{WO}_3)_x$, dipolar glass, space charge injection, thermally stimulated depolarisation currents 0-66103
 LiNbO_3 , crystal defects, X-ray diffr. topographic study (*Chinese*) 0-84173
 LiTaO_3 crystals for commercial SAW TV IF filters, fabrication 0-80961
 NH_4HSO_4 , ferroelec. props. rel. to struct. 0-71345
 $\text{NaH}_2(\text{SeO}_3)_2$, domain struct. realignment and Barkhausen effect 0-71361
 NaZnGeO_4 :Mn, electrolum., ionisation domains 0-84787
 Ni-I single crystals, mag. and dielectric props. 0-93095
 PLZT ceramic, visible light scatt. depend. on photoferroelectric space charge fields 0-80806
 $\text{Pb}_3(\text{PO}_4)_2$, ferroelastic, dielectric anomalies, phase transitions, permittivity, relaxation (*Russian*) 0-71293
 PbTiO_3 , phase transform., different kinetic types 0-71347
 $\text{Pb}(\text{Zr,Ti})\text{O}_3$, tetragonal ferroelec. ceramic, 90° domain-rot. fraction after polarisation, X-ray determ. 0-75992
 RbHSeO_4 , ferroelec. props. rel. to struct. 0-71345
 $\text{Sr}_{1-x}\text{Ba}_x\text{Nb}_2\text{O}_6$, photorefractive in space charge field, phase transitions 0-97229
 $\text{Sr,Ba}_{1-x}\text{Nb}_2\text{O}_6$, domain struct. influence on electrooptical props. 0-93283
 ZnS, prebreakdown electrolum., domain form. and negative resist. effects 0-84788
 ZnS:Mn AC thin film devices, domain electrolum. 0-66303
- electric double refraction** *see electro-optical effects*
- electric drives**
see also electric propulsion
 dual capstan drive tape recorder (*German*) 0-95092
 laser grating mount, stepping motor controlled 0-87402
 linear asynchronous motor drive system, for rotating optical components inside vac. system 0-102874
 stepper motor drives for use in synchronous interlock systems for cinematographic special effects 0-98991
- electric field effects**
see also acoustoelectric effects; discharges (electric); electrical conductivity; electro-optical effects; electrochemistry; electrodynamics; electrokinetic effects; electroluminescence; electromechanical effects; electromigration; electron field emission; electrophoresis; field emission ion microscop; field evaporation; field ion emission; field ionisation; high field effects; magnetoelectric effects; particle optics
 60 Hz electric field, 240 kV/m, long-term effects on mice 0-89784
 60 Hz high intensity electric fields, behavioural and biological effects in living organisms 0-89740
 aniline, liq., far IR absorpt. spectra, electric field effects 0-95625
 atomic interactions, retarded energy shift and pair polarisability, field theoretical perturbation theory 0-102560
 bone stimulation devices, anal. of sinusoidal EM fields 0-108990
 cylinder in still air, DC corona cooling obs. 0-70071
 fogging effect of an electric field on a photographic film (*Russian*) 0-62783
 heat pipes, electric field effects on characts. 0-83728
 high electric field biological effects on human nervous systems 0-89739
 human beings, effects of elec. and mag. fields, HV lines to 800 kV (*French, English*) 0-72209
 hyperthermia, localised current field heating as an adjunct to radiation therapy 0-98056
 lipid bilayer, alkane solubility modified by elec. field 0-97874
 liquids, potential and flux conserving static equilibria in elec. or mag. fields, determ. 0-88399
 MHD channel, anisotropically conducting plasma in inhomogeneous elec. and mag. fields, current calc. (*Russian*) 0-74995
 R. sphaeroides, polarisation of photosynthetic membranes and reaction centres in elec. field 0-94277
 rats, lack of effect of elec. field exposure, data re-evaluation 0-72210
 rats influence of 45-Hz vertical elec. fields 0-76784
 relativistic charged particle in electric field, spin rot., curved crystal p.e. channelling (*Russian*) 0-63907
 retardation of electrolytic mass transport in collinear electric-magnetic fields 0-104443
 Ar, absorpt. spectra, field induced autoionisation near ionisation threshold 0-106301
 BaMoO_4 crystals, growth in SiO_2 gel under influence of elec. field 0-93469
 Bi and Bi-Sb (12 at.%), cryst. growth from melt, impurity distrib. control by electrotransfer method (*Russian*) 0-66418

electric field effects continued

- Kr, absorpt. spectra, field induced autoionisation near ionisation threshold 0-106301
 Mn thin films, vacuum deposited in elec. field, resist., struct. 0-103761
 Mo, film, formation by reduction of MoCl_5 0-93491
 Ni-Si melt refining by electric fields, ionic conduction of Ni, Si (*Russian*) 0-65273
 $\text{Se}_{0.95}\text{Te}_{0.05}$, glass crystallisation, effect of an alternating electric field 0-88054
 Sn film, vacuum deposited, substrate and substrate temp. effects on struct. 0-107677
 TiAsS_3 , glass, crystallisation, effect of an alternating electric field 0-88054
- electric field measurement**
see also field plotting
 electrostatic voltage sensor (*Japanese*) 0-105632
 gaseous insulating materials, potential meas. by corona probe 0-82790
 isotropic RF electric/magnetic field strength meter, design 0-82751
 optical sensor for measurement of high electric field intensity 0-69509
 VHF noise field strength at 95 MHz over India, meas. techniques and obs. 0-109294
 N-O mixtures, positive glow corona in quasi-uniform fields 0-100104
- electric field strength measurement** *see electric field measurement*
- electric fields**
see also electric field effects; electric field measurement; electromagnetic fields; electromagnetic waves; field plotting
 axisymmetric field problem soln. by Gaussian surface charge simulation 0-95758
 calculation by floating random walk method 0-95760
 charged microparticles productions under high electric field intensity in ultra high vacuum, measurement (*Japanese*) 0-96411
 computation by charge simulation and finite element methods 0-95759
 computation using SCOFF program (*German*) 0-78740
 difference frequency generation by stimulated Raman scatt. using inhomogeneous electrostatic field 0-95954
 discharge, volumetric, semi-self-maintaining, excited by electron beam, current maintenance in cathode layer 0-59322
 drift diffusion unipolar conduction between parallel plate electrodes, closed form steady state solutions 0-91720
 electron beam, relativistic, electrostatic field rel. to propag. in strong mag. field (*Japanese*) 0-91737
 fast insulator surface flashover, investigation using electro-optical elec. field meas. 0-64820
 field analysis computers, colloquium, London, England (March 1980) 0-94964
 finite elements in electrical and magnetic field problems, book 0-62399
 fluid nonpolar polarisable, local field at large distances from charge or dipole rel. to dielec. constant 0-83534
 gap between flat plate and cylindrical electrode with cone-shaped end, calc. method (*Croatian*) 0-99600
 inhomogeneous media, galvanomag., stratified, elec. fields 0-63888
 intense electric fields, tree-shaped phenomena in solid insulating materials (*Rumanian*) 0-63885
 intensity, numerical calculation methods (*French*) 0-106413
 moving sources in conducting medium, multipole expansion 0-106417
 multilayer, electric field distrib. and laser damage reduction 0-87420
 piezoelectric transducers, electric field, nonuniform, expt. study 0-102955
 powers determination using direct analogue method (*Czech*) 0-69290
 solar wind, elec. field fluctuations rel. to plasmadynamical processes (*German*) 0-109323
 static electric field determ., numerical methods, monodielec./multidielec. regions, iterative solns. (*Spanish*) 0-106419
 static field problems, numerical soln. algorithms 0-95757
 stationary potential fields, theory, complementarity principle 0-63894
 transponder dipole antennas in and near three-layered body 0-98181
 variable space charge density, design, between hyperboloidal conic electrode and grounded plate (*Czech*) 0-87258
 CO_2 laser, pulsed, elec. field distrib. in vol. discharge controlled by electron beam 0-58505
 SF_6 impulse breakdown characteristics for nonuniform field gaps for switchgear design 0-84024
- electric filters** *see filters*
- electric furnaces**
see also arc furnaces; resistance furnaces
 laboratory, considerations for the prospective buyer 0-77788
- electric fuses**
 constant current test method for fuseable links 0-73390
 Al foil fuse, electrically exploded, surrounding medium effect 0-103207
- electric generators**
see also magnetohydrodynamic converters; turbogenerators; Van de Graaff generators
 cooling, H_2 production, onsite, by H_2O electrolysis 0-72097
 explosive-magnetic generators, energy take-off to inductive load using circuit breaking 0-59323
- electric glow** *see corona*
- electric heaters** *see electric heating*
- electric heating**
see also domestic appliances; drying; electric furnaces; induction heating; ovens; radiofrequency heating; space heating
 compound conductors, impulse heating, Cu vapour conc. determ. 0-75346
 fixed-pitch propeller wind-power plants, appl. 0-61260
 fusion reactor, Doublet III, ohmic heating E-coil vacuum breaker system, function and operation 0-102323
 fusion reactor magnetic coil, Large Coil Program, test heater conceptual designs 0-91251
 LMFB ML-3 Na circuit, electrical and control installations (*Spanish*) 0-57819
 long rod, direct-heating meas., interpretation 0-102964
 metals, heat content correlation under fast heating (*Russian*) 0-70426
 optical communication fibre endface preparation by AC discharge heating and stretching 0-64232
 sintering, ohmic, diffusion processes, temp. distrib. influence 0-92704
 steel, high and low C, wires, electroheated, thermal cycling and corrosion behaviour 0-61006
- electric ignition**
 No entries
- electric impedance**
see also electric reactance; electric resistance
 alternating current electrode processes, review 0-61107

electric impedance continued

antennas, horizontal, above infinite plane Earth, input impedance and current distrib. 0-90259
conducting solutions, bridge method for meas. dielectric relaxation 0-82793
electrochemical cells, multicomponent impedance diagrams, resolution technique 0-66959
metal, surface impedance near anomalous skin-effect limit, electron-electron N processes 0-100497
plasma, complex nonlinear impedance of flat antenna 0-103130
polystyrene, particles in dil. soln., bridge method for meas. dielectric relaxation 0-82793
sonar transducer, Langevin type, made from Pb(Zr,Ti)O₃ type 1 ceramic, performance characts. 0-79095
 β -Al₂O₃-Na₂O, single cryst., non-Debye capacitance 0-107497
Cd film, surface RF impedance in strong mag. fields (*Russian*) 0-92920
Ni, electrocrystallisation, reaction mechanism, appl. of impedance meas. (*French*) 0-103597
PdO, free energy of form. using impedance dispersion analysis 0-108728
TiO₂ electrodes, chemically modified, nature of surface states 0-107905
n-TiO₂-electrolyte interface impedance, freq. depend., equiv. cct. 0-100516
W film, surface RF impedance in strong mag. fields (*Russian*) 0-92920
WO₃ thin film, Li diffusion, appl. of AC techniques 0-70468
Yb₂O₃, electronic cond. rel. to partial press. of O₂ of high temp. (*French*) 0-59979
Zn, electrocrystallisation, reaction mechanism, appl. of impedance meas. (*French*) 0-103597

electric impedance measurement

see also *electric reactance measurement*; *electric resistance measurement*
complex impedances in RF range, meas. using Maxwell bridges 0-98931
complex mutual inductance concept for bioelectric impedance transformer bridge 0-63886
cross-capacitor method (*Chinese*) 0-77815
electrochemical system, LF impedance meas. technique using on-line computer 0-57339
electrode, accuracy of parameter meas. 0-61108
impedance probe calibration, for vacuum meas. in single component two-phase mixture (*Italian*) 0-62677
oesophageal geometry changes in swallowing, transduction, for animal grazing studies 0-76888
superconducting thin film, RF complex impedance meas. 0-84573

electric machine testing see machine testing

electric machine theory see machine theory

electric machines

see also *electric generators*; *electric motors*; *machine bearings*; *machine insulation*; *machine testing*; *machine theory*; *rotors*; *small electric machines*; *stators*; *superconducting machines*
acoustic noise generation mechanisms and characteristics, selecting quiet equipment and correcting noisy devices 0-64286
acoustic noise meas. errors (*Hungarian*) 0-96102
active parts electrodynamic equations general solutions using orthotropic modelling (*Russian*) 0-99601
end zone magnetic field calc. using approx. analytic method 0-106416
power plant dynamics and control, conf. Hyderabad, India (Feb. 1979) 0-91215
volts-per-bar and flashover, causal mechanisms and preventive measures 0-92408

electric moments

see also *atomic electric moment*; *molecular moments*; *nuclear electric moment*
baryon electric dipole moments in CP noninvariant Kobayashi-Maskawa theory (*Russian*) 0-105897
t-cyanobutane, dielectric relaxation study, complex permittivity 0-80688
dipole pseudo-spin glasses, collective excitations 0-59617
dipole relaxation in electric field, teaching 0-90625
DNA solution, elec. birefringence, stabilised induced dipole behaviour 0-85349
poly(1,3-diolepane), dipole moments, dielectric const. meas 0-66099
polyelectrolytes, saturation of induced dipole moment, orientation mechanism and electro-optical effects 0-84785
polynucleotide solution, elec. birefringence, stabilised induced dipole behaviour 0-85349
polystyrene interfacial colloidal crystals., microscopic obs. 0-97737
quark electric dipole moment in Kobayashi-Maskawa theory with gluonic corrections (*Russian*) 0-86688
radially symmetric reradiating scatterers in EM fields, formulae for simple treatment (*German*) 0-87270
e dipole moment, experimental searches 0-77996
 μ dipole moment, experimental searches 0-77996
n electric dipole moment, CP violation in gauge theories 0-91041
Ar+N₂(O₂, CO), molecular fluid mixtures, equilibrium props. 0-64867
Au, surface dipole moment calc. 0-60060
n, electric dipole moment using ultracold neutrons 0-82974
N₂+O₂, molecular fluid mixtures, equilibrium props. 0-64867
Pt, surface dipole moment calc. 0-60060
SrO:Co, noncentral and interstitial ion complexes, ESR obs. 0-71169
W, surface dipole moment calc. 0-60060

electric motors

see also *d.c. motors*; *linear motors*; *permanent magnet motors*; *stepping motors*
ball-bearing electric motor construction 0-67997
gearless telescopic drive, transference from elec. motor to polar axis 0-67571
ribbed frames with external fans, heat transfer coefficient measurements (*Hungarian*) 0-87709
Fe-Si, non-oriented sheets, production and props. 0-88797

electric networks see networks (circuits)

electric noise measurement

600 MHz to 1 GHz coaxial thermal noise standard 0-98875
amplifiers, noise figure, measurement by connecting source resistance between input and output (*French*) 0-68214
solar cell device reliability estimation using noise spectral density meas. 0-93896
thermal noise, zero point energy noise term presence 0-68213
transistors, noise figure, measurement by connecting source resistance between input and output (*French*) 0-68214
Al thin films 1/f noise, depend. on internal mech. stresses 0-65711

electric potential

see also *contact potential*; *overvoltage*; *surface potential*; *voltage control*; *voltage measurement*
back diode amplifier, use at low temp. 0-57324
electromotive force: Volta's forgotten concept 0-73143
electrostatic potential, laboratory and theoretical comparison 0-105461
ferromagnets, cyclically remagnetised, discrete spectra of induction calcs., demagnetising factor 0-103859
gap between flat plate and cylindrical electrode with cone-shaped end, calc. method (*Croatian*) 0-99600
gas flow, nonequib. ionisation and Hall EMF 0-69981
glow discharge tube, EM MM-wave detection properties in mag. field 0-70059
graphite arc, in Ar flow, meas. of anode voltage drop 0-84022
ionosphere, high-latit., elec. pot. soln. for field-aligned current sources 0-72674
metal-dielectric interface, static point charge in dielec. pot. distrib. (*Russian*) 0-60088
stationary potential fields, theory, complementarity principle 0-63894
Sylvester's criterion applied to Poisson's eqn., quantitative proof of Earnshaw's theorem 0-87261
thermocouples stability obs., Nicrosil-Nisil, 538°C to 1177°C, production furnaces appl. 0-68198
Ag- β -Al₂O₃, test for solid electrolyte by EMF meas on Ag/Au couples (*German*) 0-104307
Ag-Zn, molten, EMF meas. of activities using ZrO₂ solid electrolytes (*Japanese*) 0-88339
Au-Zn, molten, EMF meas. of activities using ZrO₂ solid electrolytes (*Japanese*) 0-88339
Cu₂O, standard free energy of formation, by EMF method with solid oxide electrolyte at low temps. (*Japanese*) 0-88338
Fe-Mo system, thermomech. props. 0-89208
Fe-Ni (32 wt.%), EMF appearance during $\gamma \rightarrow \alpha$ transform. (*Russian*) 0-89215
Fe₂O₄, standard free energy of formation, by EMF method with solid oxide electrolyte at low temps. (*Japanese*) 0-88338
Fe₂O, standard free energy of formation, by EMF method with solid oxide electrolyte at low temps. (*Japanese*) 0-88338
Na₂O-B₂O₃-NiO melts, NiO activity and solubility meas. by EMF method (*Japanese*) 0-92677
PbO, standard free energy of formation, by EMF method with solid oxide electrolyte at low temps. (*Japanese*) 0-88338
Sb₂O₃, standard free energy of formation, by EMF method with solid oxide electrolyte at low temps. (*Japanese*) 0-88338

electric power generation

see also *direct energy conversion*; *power stations*; *wave power generation*
energy storage technology and solar energy use, worldwide trends (*German*) 0-72086
FBR, electric power generation, research, development and demonstration, risk and timing 0-57837
fuel cells, H₂PO₄ and molten carbonate fuel cell developments 0-66966
geothermal resource field development 0-66934
hydroelectric, economic assessment of fuel savings (*Russian*) 0-97760
photovoltaic power system elements, efficiency and terminology summary 0-97790
refuse fuel, conversion to elect. energy at St. Louis refuse fuel demonstration project 0-93846
reverse electrodialysis of brine solns., elec. cell design and cost 0-85271
rural electrification by solar power, photovoltaic arrays efficiency 0-66974
salinity gradient power utilising vapour pressure differences in water 0-76652
solar ponds, electric power generation at Salton Sea, CA, USA 0-94113
solar thermochemical electric power generation, reversible chemical reactions 0-61394
water power development, feasibility, economics 0-61274
wind energy for electricity production, windmill construction (*French*) 0-66925
wind power generation in North Sea, feasibility and economics 0-97759
wind power plants, experimental projects in progress, design problems and results achieved (*Italian*) 0-72007
H₂PO₄ fuel cell designs for residential and commercial cogeneration 0-66970

electric propulsion

see also *electric drives*; *electric vehicles*; *traction*
vehicle battery systems available and under development, review (*Dutch*) 0-72025
vehicle power sources, battery design requirements for commercial use (*Dutch*) 0-72024
vehicle power sources, fuel cell/secondary battery hybrid appls. (*Dutch*) 0-72037
LiAl(Si)/FeS(S₂) battery developments for electric vehicle propulsion and load levelling appls. 0-61325
Na/S traction batteries, development progress and problems, review 0-61326

electric reactance

see also *capacitance*; *inductance*
GaAs solar cells, photoreactance of p-n junction diodes 0-81464
Si solar cells, photoreactance of p-n junction diodes 0-81464

electric reactance measurement

see also *capacitance measurement*; *inductance measurement*
No entries

electric relays see relays

electric resistance

bevelled shallow junctions, spreading resistance data correction 0-80358
electrode, impedance meas., accuracy 0-61108
human body, electrostatic spark discharges obs., nature and incendiary behaviour 0-72406
microelectrodes, open tip glass, influence of diffusion, double layer, and glass conduction on elec. resistance 0-67300
toroidal field coils, EM parameters calcs. of current paths in homogeneous media (*Japanese*) 0-106155

electric resistance furnaces see resistance furnaces

electric resistance measurement

see also *ohmmeters*
contact resistance of metal-semiconductor interface 0-105672
earthing checking instrument, meas. of resist. of ground at various levels and of earthing connections (*German*) 0-98936

electric resistance measurement continued

- high, review of accuracy and sensitivity of various instruments and techniques 0-57331
 high loss materials at high freqs. 0-62686
 instrument for crack measurement 0-100984
 loudspeaker moving coil temp. meas. systems (Hungarian) 0-106698
 metals, low-cycle failure investigation, elec. resist. meas. appl. 0-85109
 ohmic contacts to semiconductor, meas. of contact resistance using transmission line model 0-70826
 reproduction of ohm at German ASMW 0-98944
 semiconductor spreading-resistance meas. for doping profile determ., prep-processing of data for resistivity calcs. 0-57265
 skin resistance biofeedback, using frequency controlled oscillator detector 0-101156
 solar concentrator cells, effects of temp. variations 0-93944
 steel, low C, low-cycle failure investigation, elec. resist. meas. appl. 0-85109
 temperature dependence of thermoelectromotive force and resistance 0-57330
 Ge resistance thermometers, stability data at 3 temperatures 0-86307

electric resistors *see resistors***electric sensing devices**

- see also instruments; measurement*
 acceleration sensors, lower limiting frequency and indication threshold (German) 0-95093
 analogue digital double integration joulemeter, AC loss meas. in superconducting magnets 0-57325
 atmosphere temperature sensors, humidity effects and sea salt contamination 0-82095
 bioelectrochemical sensor using immobilised enzyme electrodes (Japanese) 0-109071
 bipolar IC temperature transducer, intrinsic bandgap voltage as reference, Fahrenheit, Celsius or arbitrary scale operation 0-82761
 butterfly-valve inductive orientation detector as means of measuring angular displacements 0-68193
 capacitance sensors for phase percentage determ. in multiphase pipelines 0-62625
 capacitive sensor of soil pressure, using polyurethane foam dielectrics (Slovak) 0-86281
 conductivity probe design for use with bridge instrument, wide range of test solns. 0-95110
 contact cryogenic fluid level sensor 0-73371
 electrochemical sensors for partial press. meas. in blood 0-67303
 electronic gas detection, Pellistor, VQ and TGS sensors (Spanish) 0-93832
 electrostatic voltage sensor (Japanese) 0-105632
 ferroelectrics hysteresis loop sensing (Czech) 0-82792
 gas chromatographic air analyser fabricated on Si wafer 0-73343
 gas detector, all-electric, using laser beam and Stark cell 0-74417
 gas sensor, using $\alpha\text{-Fe}_2\text{O}_3$ semiconductor ceramics (Japanese) 0-61498
 gas-sensitive sensor with ultrafine particle film deposited on monolithic IC chip (Japanese) 0-105630
 Humicera-III, ceramic sensor, multifunctional sensor to detect humidity and gases (Japanese) 0-105659
 humidity sensor, Al_2O_3 , ageing improvement (Japanese) 0-100863
 humidity sensor, capacitive, Panahume (Japanese) 0-105658
 isotropic RF electric/magnetic field strength meter, design 0-82751
 laser-operated, photographic paper quality improvement, colour spots detection (German) 0-57412
 level and volume meas. in conductive liquids using array of point sensors 0-68177
 liquid level measurement transducer, cascade transistor cct., level to freq. converter 0-73310
 magnetic field sensor, Wiegand module (German) 0-62694
 magnetic induction gauge consisting of 3 Hall transducers 0-105682
 NTC thermistor sensors, cct. designs and design calculation tables 0-68201
 pressure and differential-pressure sensors, seven types (German) 0-77772
 PVDF pyroelectric IR detector (Japanese) 0-105714
 pyroelectric polymer IR detector (Japanese) 0-105713
 quantum sensors, use in instrument for digital recording of submarine irradiance and photoperiod 0-98474
 ring-core magnetometer sensor for articulatory meas. of jaw movements 0-101243
 'smart sensors', role in remote sensing of Earth from space, book 0-62402
 solid electrolyte gas sensor developments 0-61217
 spectrophone, low-noise, using continuous laser beam 0-74418
 SQUID, appl. to cardiac recording, phase and amplitude relationships of elec. and mag. events 0-104695
 water vapour sensor of P_2O_5 type 0-98907
 Ag^+ ion automatic sensor-analyser for photographic fixing bath regeneration systems (Russian) 0-95172
 Ge sensors, He level gauge appl. 0-57277
 Ge: Au film strain gauges, press. sensor (Japanese) 0-105631
 LiNbO₃ sensor for elec. hygrometer (Japanese) 0-95103
 $\text{MgCr}_2\text{O}_4\text{-TiO}_2$ porous ceramic humidity sensors 0-86325
 O₂ analysis, electrochemical sensors 0-93816
 O₂ sensors, solid electrolyte, noncatalytic electrodes 0-76573
 PLZT pyroelectric detectors, delayed onset of piezoelec. oscills. 0-75953
 Pt thin-film temp. sensor (Japanese) 0-105645
 Si diaphragm pressure sensor, integrated signal conditioning 0-76859
 Si ion-controlled diodes, acid-base exposure effects, Si-SiO₂ interface state density 0-96984
 Si, on sapphire, Schottky magnetodiode, integrated mag. sensor 0-68223
 SnO₂ gas sensor, fast-detecting, prep. 0-61497

electric shielding, nuclear *see nuclear screening***electric shocks**

- see also protection; safety*
 50/60-Hz AC, ventricular fibrillation tests on animals (German) 0-101154

electric spark machining *see spark machining***electric sparks** *see sparks***electric strain gauges** *see strain gauges***electric strength**

- see also electric breakdown*
 dielectric gases and gas mixtures, maximum electric strength and vapour pressure relationships 0-92249

electric strength continued

- mica, pulse electric breakdown under pressure, lamination effects 0-66110
 polymer, dielec. breakdown theories, mol. and morphological features rel. to elec. strength, review (Japanese) 0-60501
 polyvinylidene fluoride, dielec. breakdown and elec. cond., room temp. to 150°C 0-60500
 rare earth aluminate, scandate and zirconate film coatings, electrophys. props. w.r.t. prep. technology 0-60781
 spark gaps, SF₆, limiting sparkover voltage values determ. and dielectric strength testing in power equipment (Czech) 0-87962
 Al_2O_3 , anodic film, trapped O₂ and effect on dielec. stability 0-100634
 BaTiO₃ ceramic films, dielec. strength, statistical anal. 0-75935
 $\text{CCl}_3\text{F}_2\text{-CO}_2$ gas mixture, field breakdown gradients calc. method 0-92248
 $\text{CCl}_3\text{F}_2\text{-N}_2$ gas mixture, field breakdown gradients calc. method 0-92248
 NaCl, optical strength, effect of irradiation in mechanically stressed state 0-80695
 Ta₂O₅ film on Al, Cu, Au, Ag electrode, electric strength of MIS system 0-96999

electric susceptance *see electric admittance***electric susceptibility** *see optical susceptibility***electric switchgear** *see switchgear***electric transformers** *see transformers***electric utilities** *see electricity supply industry***electric variables measurement**

- see also attenuation measurement; capacitance measurement; charge measurement; dielectric measurement; electric admittance measurement; electric current measurement; electric field measurement; electric impedance measurement; electric noise measurement; electric reactance measurement; electric resistance measurement; electrical conductivity measurement; frequency measurement; gain measurement; inductance measurement; phase measurement; power factor measurement; power measurement; Q-factor measurement; voltage measurement*
 200 kW Gedser windmill in Denmark, performance meas. 0-61431
 A/D converter with special appl. to medium precision Pt resist. thermometry 0-86297
 carrier lifetime measurements from transient elect. photoresponses in solar cells 0-61346
 conference on precision EM meas., Braunschweig, Germany (Jun. 1980) 0-98903
 contact electrification of polymers, meas. using computer-controlled apparatus 0-86341
 Hall effect measurement, liq. semiconds. 0-65594
 high pressure chamber designed according to opposed anvil principles, thermoelectric force meas. (German) 0-90863
 insulating particles in insulating liquids, high field electrophoresis 0-90865
 Josephson AC effect applications in precision metrology and novel voltage source (German) 0-70902
 LV short-circuit testing station, equipment and measurement methods (Polish) 0-77773
 MIS structure, elec. parameter meas. of second order equivalent ccts. 0-57332
 model for 1/f noise 0-98945
 pyroelectric materials, automated simultaneous meas. of electrical properties 0-57335
 Seebeck coefficient measurement of disc-shaped samples by AC method (Japanese) 0-73392
 standardising laboratory for developing countries 0-101774
 transducers, third-generation, Czechoslovak (Metra Blansko) range (Czech) 0-73340

electric vehicles

- see also electric drives; electric propulsion*
 batteries, criteria for electric vehicle and energy storage applications 0-72031
 battery systems available and under development, review (Dutch) 0-72025
 dispersed electrodes appl., Zn electrode development (French) 0-72023
 high speed ground transportation vehicles gas-flow-controlled arcs for power collection 0-70054
 power sources, battery design requirements for commercial use (Dutch) 0-72024
 power sources, fuel cell/secondary battery hybrid appls. (Dutch) 0-72037
 social implications of energy storage 0-67001
 LiAl/FeS(S₂) battery developments for electric vehicle propulsion and load leveling appls. 0-61325

electric welding

- see also arc welding; electron beam welding; resistance welding; welding electrodes*
 electroslag, using plate electrodes for Al busbar component parts welding 0-81083
 fusion welding of Al alloys, weld susceptibility to hot cracking 0-81143

electrical conduction in condensed matter

- see also carrier density; carrier lifetime; carrier mean free path; carrier mobility; carrier relaxation time; dislocation scattering; electrical conductivity of liquids; electrical conductivity of solids; electrical conductivity transitions; electron density (metals); electron mean free path (metals); electron mobility (metals); electron-phonon interactions; electron relaxation time (metals); high field effects; hopping conduction; impurity scattering; Lorenz number; minimum metallic conductivity; minority carriers; mixed conductivity; negative resistance effects; one-dimensional conductivity; photoconductivity; point defect scattering; size effect; skin effect; small polaron conduction; space-charge-limited conduction; spin disorder resistivity; surface conductivity; surface scattering; thermally stimulated currents; tunnelling*
 Anderson localisation, self-consistent diagrammatic theory 0-107746
 inhomogeneous media, galvanomag., stratified, elec. fields 0-63888
 inhomogeneous medium, effective cond., iteration series and variational estimates, Herring method 0-70663
 Monte Carlo calc., book contrib. 0-100458
 randomly-inhomogeneous conducting media, generalised charac. computation using random function theory (Russian) 0-75535
 H₂⁺ system, quantum oscillations in tunnelling, oscill. freq., tunnelling currents (Russian) 0-60065

electrical conductivity

- see also electrical conduction in condensed matter; electrical conductivity of gases; electron mobility; ion mobility; space-charge-limited conduction*
 disperse systems, depend. on conducting component content 0-92954

electrical conductivity continued

fluid system, electric conduction in relativistic thermodynamics 0-105498
polystyrene particles, monodisperse, dil. and conc. aqueous dispersions, elec. cond., surface cond. and double-layer polarisation 0-89533

electrical conductivity measurement

antistatic polymer film surfaces, microammeter meas. method 0-98932
biological conductivity monitor for isolated nerve preparation expts. 0-67301
conductometer to record rapidly varying electrical conductivity 0-61184
contact transducers, threshold sensitivity meas. 0-62688
contactless measurement of sheet conductivity and mobility of semiconductor wafer by using eddy current 0-62693
electron microscope, HV, in-situ elec. resistivity meas. 0-101893
electrooptic crystal voltage-induced birefr. obs. for very high resist. meas. 0-73386
gas chromatographic bipolar pulse differential electrolytic cond. detector 0-93814
gas-electrolyte dispersions, void fraction meas. using conductivity method 0-76525
'Impul's' conductometer (USSR), elimination of dilute soln. instability 0-77813
ionic conductivity, four-probe AC bridge technique 0-57340
liquid metals, contactless resistivity meas., impedance change of a coil 0-73388
liquids, gases, conducting, high press., temp. elec. cond. meas., four electrode method 0-62685
metal-semiconductor interface, meas. of resistivity 0-105672
metallic thin film, thickness dependence, quantum size affect (*German*) 0-86344
metals and alloys, critical temperatures determination, elec. resist. method, IMASH-5S-69 installation 0-71827
organic liquid conductivity and bulk charge determ. cell (*Russian*) 0-57328
particulate layer, thin, under ionic bombardment 0-68218
patient electrical conductivity and permittivity imaging, computing tomography technique 0-98055
photoconduction decays, fast, measurement, DC-10 MHz low noise amplifier system 0-57326
potential single-sonde method for inhomogeneity meas. of InAs, InSb 0-65549
probe design for use with bridge instrument, wide range of test solns. 0-95110
resistance variation with temperature 0-77575
rotating sample magnetometer for contactless conductivity meas. 0-73391
SEM technique, appl. to TTF-TCNQ 0-86507
standard models for measuring elec. cond. 0-86343
water, monitoring using conductivity cell for wave height probe 0-57280
water, pure ($10^{-1} \mu\text{S/cm}$), at steady temperature and flow (*Czech*) 0-62684
Ag halide microcrystal, photoconductivity meas. by microwave technique 0-103719
PbO₂ powder, electronic conductivity, separation of particle core and surface resistance 0-104442
Si:P film, polycryst., heavily doped, mobility and carrier conc., optical determ. 0-66314

electrical conductivity of amorphous metals and alloys
see also dislocation scattering; electron density (metals); electron mean free path (metals); electron mobility (metals); electron relaxation time (metals); electronic conduction in metallic thin films; impurity scattering; point defect scattering; surface scattering
alloy, thermal stability, crystn., DSC and elec. resist. study 0-107060
alloys, amorphous, exhibiting Mossbauer spectra, elec. props. (*French*) 0-80244
finite disordered system, resistance probability distrib. (*Russian*) 0-103657
glassy metals, structure, transport props., magnetic behaviour, review 0-70138
metallic glass, electron transport theory, diff. model appl. 0-80245
metallic glass, prep. and phys. props. development 0-81003
metallic glasses, elec. resist., press. depend. 0-96841
metallic glasses, electronic lifetime, noncommutative two-level model 0-103663
metallic glasses, electronic structure rel. to elec. cond., supercond. and mag. props. 0-65429
metallic glasses, production and properties, technological appl. 0-71105
metallic glasses, stability 0-75184
rare earth-transition metal alloys, amorphous, electronic and mag. props. 0-93093
Al-Cu, superconducting amorphous films of high stability 0-70889
Au-Ge-Si, influence of struct. on elec. resist. of glass forming alloys 0-65518
Au, Si_{1-x} amorphous alloy, crystallisation, elec. cond. study 0-103246
Au, Si_{1-x} amorphous films, phys. studies 0-75476
Ce₈₀Au₂₀, metallic glass, mag. ordering and cryst. field effects, speromagnetism 0-80531
Co-B-Si amorphous alloy, liq. quenched, elec. resist. and cyclic deform. 0-59949
Co-Gd-Mo amorphous films, resist. and extraordinary Hall effect, thermal annealing effect 0-70852
CoP amorphous alloy, heat treatments influence on opt. props., struct. and DC resist. obs. 0-80892
Co_{1-x}P_x amorphous alloy film, elec. resistance, temp. depend. (*Russian*) 0-103660
Cu-Ag-P(6-14, 11-14 wt.%) amorphous, crystn. and elec. props., X-ray diff., elec. resist. and DTA meas. (*Japanese*) 0-84088
Fe and Fe-Ni Metglas alloys, ohmic and Hall resist. 100-700K, mag. behaviour 0-80254
Fe-B, amorphous ferromag., temp. depend. of resist., appl. of extended Ziman theory 0-59950
Fe-B-Cr(Mo), metallic glasses, mag., struct., and elec. props. 0-88751
Fe-B-Si amorphous alloy, liq. quenched, elec. resist. and cyclic deform. 0-59949
Fe-Ni-B-Mo, crystn. temp. and elec. cond. correl., Mo effect 0-75179
Fe₈₀B₂₀, metallic glass, Doppler broadening of positron annihilation γ -radiation and elec. resist. 0-66321
Fe₈₄B₁₆, metallic glass, electrical resistivity and crystallisation 0-88526
Fe₈₄B₁₆, metallic glass, electrical resistivity and crystallisation 0-88526
Fe₇₈Mo₂₂, metallic glass, Doppler broadening of positron annihilation γ -radiation and elec. resist. 0-66321
Fe₄₀Ni₄₀B₂₀, amorphous, phase transforms., resistometric anal. 0-75538

electrical conductivity of amorphous metals and alloys continued

Fe₂Ni_{80-x}B₂₀ and Fe₂Ni_{80-x}P₁₄B₆ metallic glasses, low temp. resist. and galvanomag. effects, mag. state influence 0-84461
Fe₂Ni_{80-x}B₂₀ glass, resist., magnetoresist., and thermoelec. power 0-70681
Fe₃₂Ni₃₆Cr₁₄P₁₂B₆, metallic glass, Doppler broadening of positron annihilation γ -radiation and elec. resist. 0-66321
Fe₃₂Ni₃₆Cr₁₄P₁₂B₆ metallic glass, crystn. kinetics by TEM 0-75186
Fe₄₀Ni₄₀P₁₄B₆, amorphous, resistometric study of short-range ordering rel. to heat treatment 0-70140
Fe₂Ni_{80-x}P₁₄B₆ glass, resist., magnetoresist., and thermoelec. power 0-70681
Fe₇₉P₁₃B₈ amorphous alloys, splat cooled, Mn, Cr and V substituted, mag. and transport props. 0-84593
Fe₂Ni_{1-x} amorphous alloy, elec. resist. 0-80246
Gd-Al(C)(Cu)(Ga)(Ni)(Pd)(Rh) alloys, amorphous, mag. and elec. props. 0-80499
Gd-Ti(V)(Cr)(Mg)(Nb)(Ge)(Si)(Au) amorphous films, spontaneous Hall effect and elec. resist. 0-80251
Hf_{1-x}Fe_x amorphous alloys, formation, crystallisation and electrical resistivity 0-96838
La-Ag alloys, amorphous, elec. resist. and supercond. 0-70885
La-Au, splat-quenched, Mossbauer effect and elec. resist., amorphous struct. 0-84676
Mn-Bi micromagnetic alloy, mag., elec. and elastic props. (*Russian*) 0-108028
Nb-Ge, amorphous supercond. alloy, resistivity, transition temp. 0-60126
Nb-ir(Rh) system glasses, form., crystn. and microhardness, resist. obs. 0-89178
Ni-Fe based metallic glasses, Curie pt. anomalies 0-60256
Ni-Y, elec. resist., press. depend. 0-96841
NiP amorphous alloy, heat treatments influence on opt. props., struct. and DC resist. obs. 0-80892
Ni₂Zr_{1-x} metallic glass, crystallisation kinetics, elec. resist. and mag. susceptibility meas. 0-103659
Pd-Au-Si, influence of struct. on elec. resist. of glass forming alloys 0-65518
Pd-Ni-Si amorphous alloys, crystn. process during isothermal ageing 0-89275
R_{1-x}Co_x, rare earth amorphous alloys, thermal stability, elec. cond. enthalpy 0-100172
Ta-ir(Rh) system glasses, form., crystn. and microhardness, resist. obs. 0-89178
W-Re amorphous alloys, phase-slip and localisation diffusion lengths 0-107747
W-Re films, amorphous, one-dimensional quantum localisation 0-80413
WSi₂, sputtered, props. for MOS IC appl. 0-70831

electrical conductivity of amorphous semiconductors and insulators

see also carrier density; carrier lifetime; carrier mean free path; carrier mobility; carrier relaxation time; dislocation scattering; electrical conductivity transitions; electronic conduction in insulating thin films; high field effects; hopping conduction; impurity scattering; minority carriers; negative resistance effects; photoconductivity; point defect scattering; small polaron conduction; surface scattering
chalcogenide glasses, electronic transport mechanisms and coeffs. 0-80282
chalcogenides, Poole-Frenkel effect, charged dangling bonds model 0-59994
cytochrome c₃, anhydrous film, elec. cond., temp. and ambient press. depend. 0-85327
dispersive transport, computer simulation, time of flight signals 0-70696
doped amorphous semiconductors, electronic props. 0-80283
finite disordered system, resistance probability distrib. (*Russian*) 0-103657
glass, electron migration and spectral relax., random-walk model 0-80280
glasses, elec., mag., and optical props., conference, Troy, NY, USA (Aug. 1979) 0-105417
glassy polymers, elec. resist., corresponding states relationship 0-59704
Hall conductivity in random-phase model 0-65599
Kapton, pyrolysed, cond. polymer, transport and mag. props. 0-96887
localised states and cond. mechanism in amorphous semicond. (*Japanese*) 0-84467
metallomacrocycles, mixed valent, cofacial assembly, cond. polymeric material 0-70143
oxide semiconducting glasses, electronic cond. mechanism 0-65562
perspex, electric conduction and isothermal dielectric relax. 0-80285
poly(ethyl vinyl ketone) film, reacted with phosphoryl chloride, elec. cond. 0-97599
poly(p-phenylene), AsF₆ doped, highly cond. charge transfer complexes, elec. and optical props. 0-70778
poly-N-vinylcarbazole thin amorphous film, hole drift mobility, mol. mass. depend. 0-75663
cis-polyacetylene:AsF₆, conductivity meas., non-Ohmic effects 0-96891
polyacetylene:Br(Pd), ion implantation effect on elec. props. 0-65026
polyacetylene:SbF₆, elec. cond. meas. 0-60055
polyacetylene, variable density, synthesis, elec. cond., thermopower 0-60016
polyacetylene films, doping effect on elec. cond., chem. and optical props. 0-65572
polyacetylene films, electrical properties (*Japanese*) 0-96888
polycarbonate: tri-p-tolylamine, chemical control of conductivity 0-59984
polycarbonate, and charge-transfer complex modifications, isothermal dark currents 0-88559
polyethylene, dielectric props., investigation for morphology changes created by mechanical drawing and annealing 0-84697
polyethylene, elec. cond. of high and low density samples, oxidation effects 0-107784
polyethylene terephthalate polymer insulator, conduction and breakdown mechanism (*German*) 0-100469
polymer film, bulk elec. cond. parallel to film surface 0-92889
polypyrrole films, electrochemical prep., chem. and phys. characterisation 0-70708
polyvinylquinazoline-I₂ complexes, absorpt. spectra and elect. cond. 0-92891
review of structural and electronic props. 0-64901
semiconductor, amorphous, field effect and capacitance-voltage meas. anal., localised density of states 0-103686
semiconductor characterisation, cond. type determ. by pot. profiling 0-73387

electrical conductivity of amorphous semiconductors and insulators continued
 semiconductors, amorphous, electronic transport mechanisms and coeffs. 0-80282
 semiconductors, temp. depend. electronic cond., review 0-59975
 p-terphenyl, hopping cond. among localised states 0-70861
 tetracene, hopping cond. among localised states 0-70861
 Ag₂Se thin film, switching and Ag movement, point contact technique 0-60107
 As-Ge-Te, chalcogenide glass, elec. cond. and dielec. const. 0-75567
 As-Se glasses, elec. transport studies 0-103695
 As-Te-Si-Ge amorphous chalcogenide semiconductor, thin film interface, meas. (Korean) 0-97014
 As₁₀Ge₁₅Te₇₅Ag_x glass, elec. and dielec. props., Ag additions effect 0-65558
 As₂S₃ glasses, DC elec. cond. and thermo-elec. power 0-96865
 (As_{0.9}S_{0.6})_{100-x}Cu_x glassy, struct. and elec. cond. study 0-59399
 As₂Sb₂Se₉ glassy semiconductors, electronic props. 0-103712
 As₂Se₃ glassy films, current-voltage characts., temp. depend., SCL current 0-92902
 As₂Se₃, transient electrical transport, general and unified treatment 0-59977
 As₂Se₃:Ag amorphous, freq. depend. cond. 0-88565
 As₂Se₃:Pt, glass, effect of impurities on elec. props. 0-103699
 As₂Te₃ and As₂Te₂Ge, amorphous, AC cond. at low temps. 0-80269
 Au-Si_{1-x} amorphous films, phys. studies 0-75476
 B₂O₃-V₂O₅-P₂O₅ glass, mech. and elec. props 0-84228
 BaO-V₂O₅-CuO semiconducting glasses, impurity effects, elec. resist. and EPR study 0-103692
 C-H films, amorphous, elec. props., chem. modifications 0-84523
 CdO-P₂O₅ glass, thin film, elec. cond., high and low fields 0-80427
 CdSn_{0.9}O_{1.1} films, transparent conducting, deposited by RF sputtering from CdO-SnO₂ target 0-76179
 Fe(OH), thin films, elec. cond. var. with temp., amorphous struct. 0-75566
 Ga-Ge-Se chalcogenide glasses, rare earth element doped, elec. props. 0-96885
 Ge amorphous films, structural relaxation and crystallisation 0-100170
 Ge film, prepared by evap. or sputtering, AC loss meas. 0-65560
 N-Ge-Bi-Se glass, elec. and optical props. 0-65550
 Ge-Ga amorphous alloy, co-evaporated elec. and optical props. 0-70860
 Ge-Si-Ga amorphous thin film, memory switching effects 0-88605
 Ge-Sb-Se glass, elec. props, comp. depend. 0-70697
 Ge₂₀Bi₁₀Se_{70-x} semicond. glass, resist., thermoelec. power, optical absorpt. 0-88555
 Ge₂₀Bi₁₀Se_{70-x}Te₁₀ semicond. glass, resist., thermoelec. power, optical absorpt. 0-88555
 Ge₄₂S₅₈ amorphous, bulk and film forms, elec. props. and ESR study 0-103691
 GeSe₂-As₂Se₃-Sb₂Se₃, elec. cond. over wide range of temp. 0-88564
 GeSe₂-Te amorphous layers, prep. and elec. props. 0-97436
 Ge_{1-x}Sn_xTe film, amorphous, elec. cond. 0-93016
 HgSe film, anomalous photocond., electron microscope study 0-65623
 InTe thin films, flash evaporation, electrical props. 0-65722
 LiCl-Li₂O-P₂O₅ glass system, vitreous domain, struct., elec. cond. (French) 0-70135
 Li₂O-B₂O₃-P₂O₅ glass, mech. and elec. props 0-84228
 Na₂O-3SiO₂-Fe²⁺, Fe³⁺ glasses, Mossbauer and ESR spectra and internal friction 0-100865
 Na₂O-B₂O₃-Bi₂O₃ glass with metallic Bi granules, elec. cond. 0-84493
 Na₂O-B₂O₃-P₂O₅ glass, mech. and elec. props 0-84228
 Na₂O-B₂O₃-SiO₂-As₂O₃(As₂O₅) glasses, DC and AC resist., bipolaronic hopping cond. 0-88558
 Na₂O-K₂O-B₂O₃-SiO₂ glass, character of elec. cond. 0-103516
 Na₂O-SiO₂ glass, OH⁻ content effect on mech. and other props. 0-89337
 Nb₂O₅-V₂O₅-P₂O₅ glasses and glass ceramics, elec. cond., struct. 0-84466
 PbO-B₂O₃-Bi₂O₃ glass with metallic Bi granules, elec. cond. 0-84493
 Ru_xTi_{1-x}O₂ films, percolation elec. cond. in strong electric fields (Russian) 0-84471
 S-based amorphous semicond. film, prep. by plasma decomp. of H₂S-N₂-NH₃, and characterisation 0-80422
 SbSe, amorphous thin film high field charge transport and quasi-Fermi level location 0-70863
 Se, amorphous, elec. cond., activation energy, density, cryst. Se effect 0-65548
 Se, amorphous film, photocond., dark cond., rel. to crystn. 0-88596
 Se, transient electrical transport, general and unified treatment 0-59977
 Se-Ge-Te, chalcogenide glass, elec. cond. and dielec. const. 0-75567
 Se-Te-Sb glasses, electronic transport 0-88579
 Se_{1-x}Te_x amorphous, optical and elec. props. 0-84506
 Se₁₂Te₄₉As₂₉Ge₁₀ semiconductor amorphous films, field effect, trapping 0-84472
 Si, amorphous, EPR and spin-dependent effects 0-80592
 Si, amorphous, ion implantation method, B and P ions 0-100274
 Si, amorphous co-sputtered doped, photovoltaic material appl. 0-93488
 Si, amorphous film, RF plasma deposition from SiCl₄-H₂, characterisation 0-66435
 Si, amorphous film, TSC, density of localised states distrib. 0-65587
 Si, amorphous films, halogenated and hydrogenated, elec. and optical props. 0-97016
 Si, amorphous films, hopping conduction, dangling bond generation by high temp. annealing 0-60115
 Si, amorphous films, RF sputtering prep. at high Ar press., props. obs. 0-80418
 Si, elec. props., ion implantation effects 0-79828
 Si film, hopping cond. control by ion bombard. induced struct. modification 0-92898
 Si, sputtered, resist. control by ion implantation 0-100262
 Si, transient electrical transport, general and unified treatment 0-59977
 Si, transport results, interpretation 0-80260
 Si:Au, O(H), film, amorphous, elec. cond. meas. 0-80423
 Si:BP, ion implanted crystalline and amorphous laser annealing 0-97509
 Si:F, amorphous, heat resistant, prep., elec. cond., IR absorpt., annealing 0-65719
 Si:H, amorphous, discharge prod., optically induced cond. changes 0-96937
 Si:H, amorphous, Schottky diodes, elec. props., light-induced effects 0-103741
 Si:H,B, amorphous, field effect and thermoelec. power 0-96924

electrical conductivity of amorphous semiconductors and insulators continued
 Si:H,P film, elec. cond., thickness and temp. depend. 0-65559
 Si:H amorphous films, conductivity and temp. dependence of optical gap 0-100462
 Si:H amorphous films, ESR, optical gap and elec. cond. meas. 0-75842
 Si-H:P amorphous film, dark cond., struct., Raman scatt. 0-88588
 Si_{1-x}H_x:Al, amorphous, co-sputtered Al modification, electronic and optical props. 0-100461
 SiO₂, transient electrical transport, general and unified treatment 0-59977
 SnO₂:P, CVD films, elec. props., cryst. to amorphous transition effects 0-107933
 SnO₂:Sb film on glass substrates, elec. props. 0-88652
 Ta₂O₅ anodic films, elec. cond. mechanism, admittance meas. 0-70705
 Te_{50-x}Se₅₀Sn_x, thin films, elec. cond. and thermoelectric power meas. (French) 0-80335
 V₂O₅ amorphous layers, gel deposited, semicond. props. 0-92887
 V₂O₅-As₂O₃-RO, R=Ba, Ca, Pb, semicond. glass, electronic props. 0-88557
 V₂O₅-V₂O₄-BaZnO₂ glass, V ion states, mag. and elec. props. 0-88556
 VTe, mag. and elec. transport props. 0-92897
 WO₃-B₂O₃-ZnO semiconducting glasses, DC cond. and optical absorpt. 0-107783
 Y₂O₃-AlN-SiO₂ oxynitride glasses, elec. props. 0-80267

electrical conductivity of crystalline metals and alloys

see also dislocation scattering; electron density (metals); electron mean free path (metals); electron mobility (metals); electron relaxation time (metals); electronic conduction in metallic thin films; impurity scattering; point defect scattering; surface scattering
 alkali metals, electron-electron scatt., thermal and elec. resistivity 0-59956
 alkali metals, thermopower and elec. cond., relationship at low temps. (Russian) 0-92882
 alloys, resistivity evolution during decomposition, theory (French) 0-75546
 alloys, substitutional, electrical resist., long and short range orders effect 0-107761
 binary alloys, elec. resist. near crit. point 0-96847
 coherently decomposing alloys, extra resistivity calc., X-ray small angle scatt. 0-92873
 copper quaternary thiospinels, mag. and elec. props. (French) 0-65771
 critical temperatures determination, elec. resist. method, IMASH-5S-69 installation 0-71827
 dilute alloy, perturbation expansion for the asymmetric Anderson Hamiltonian 0-80202
 dilute alloys, elec. transport and deviations from Matthiessen's rule 0-65524
 disordered alloy, residual resistivity due to clustering, ageing effects 0-65521
 electron theory, contrib. of Sir Rudolf Peierls, 1928-1935 0-57054
 electron-dislocation scattering and negative deviations from Matthiessen's rule 0-80248
 electron-impurity scattering, lattice distortion effects, phase shifts, calc. 0-96860
 eutectics, HgTe-PbTe and Au-PbTe, prep. and thermoelectric behaviour characts. 0-107774
 ferromagnetic Fermi-liquid model, electron-impurity system hydrodynamics, elec. cond. 0-103835
 ferromagnetic metal, uniaxial, anisotropic spin fluctuations and anisotropic band struct. effects on resist. near T_c 0-65543
 ferromagnetic metals, resist. anisotropy, crit. behaviour and temp. depend. 0-96858
 ferromagnetic metals, transport props., crit. behaviour 0-65522
 impure metals at low temperatures, conductivity 0-103669
 ion polarisation and point defect resistivity in metals 0-103672
 lattice defects and diffusion processes in solids, book 0-107207
 linearized Boltzmann eqn. soln., resist. and deviation from Matthiessen's rule 0-65523
 metal, electron Boltzmann eqn. solns., energy depend. 0-88537
 metal-H systems, temp. depend. of impurity resist. 0-65529
 metallic ferromagnet, antiresonance region, EM wave propag., Maxwell's eqns. soln. 0-66038
 metals, electrical and thermal resistance, influence of static atomic displacements 0-103674
 metals, electrical conductivity, high pressure effects 0-92879
 metals, phonon-phonon scatt. role in lattice thermal cond., phonon drag, elec. cond. 0-70483
 metals, quantum magneto-dimensional effects, open Fermi surfaces, conduction electrons (Russian) 0-80487
 metals, two and one interstitial model explanation of elec. cond. variations 0-88143
 minimal metallic cond., localisation scaling theory (Russian) 0-103671
 mixed valence cpds., elec. cond., periodic Anderson model, memory function approach 0-84458
 N-S boundary resistivity, tunnelling contact resistance (Russian) 0-93048
 noble metal alloys, dil., deviations from Matthiessen rule 0-65525
 polycrystalline metallic conductivity, grain-boundary scatt. model 0-88530
 polyvalent metal alloys, dil., deviations from Matthiessen rule 0-65525
 rare earth alloys, RBe₁₃, resist. and susceptibility study 0-71565
 rare earth ion intermetallics, RFe₂, (R=Sc, Lu, Y), mag. props., 80-1300K (Russian) 0-75750
 rare earth metal impurity in metallic host, exchange interaction, electrical resistivity 0-84453
 simple metals, model pseudopot. appl. to various props. 0-59845
 spin fluctuations, mag. field effect, electronic sp. ht. and elec. resist. 0-108026
 steel, austenitic stainless, Cr-Ni, resist. damage rate during neutron irradi. at 23K 0-96571
 steel, maraging, ageing kinetics and struct. of N12K7M5TYu, effect of high temp. deform. of austenite (Russian) 0-84960
 steel, maraging 18%Ni, calorimetric anal. of ageing (Japanese) 0-89264
 thermoelectric materials, B₂C₃ and (B,Si)₂C₃-p-type LaS_x-N-type alloys, fabrication and thermoelectric props. 0-107771
 thin metallic plate in strong mag. field, electron scatt. elec. cond. theory (Russian) 0-59974
 thin wires, exptl. study of Anderson localisation 0-96849
 transition metals, thermophysical data at high temps., submicrosecond-pulse-heating method 0-103459
 very thin wires, effect of inelastic electron scatt. on cond. 0-80259

electrical conductivity of crystalline metals and alloys continued

- wire, cylindrical, elec. resist., scatt. processes, Monte Carlo calc. 0-75560
 Ag, low temp. resist. and thermoelec. ratio, electron-electron scatt. contrib. 0-70670
 Ag, virtual bound states due to 4d- and 5d-transition metal impurities 0-70667
 AgZn, β' - γ transformation, effect of additional elements 0-66507
 Al dilute alloys, elec. resist., impurity and temp. depend. 0-65526
 Al foil, electrical conduction, electron mean free path, surface scatt. 0-88535
 Al, granular supercond., normal state cond. 0-88529
 Al, low temp. resist. and thermoelec. ratio, electron-electron scatt. contrib. 0-70670
 Al, small spheres, bulk plasmons damping 0-75561
 Al, with linear lattice defects, temp. depend. of magnetoresist. and Matthiessen's rule departure (*Russian*) 0-84456
 Al-Cu (2-5 wt.%), precipitation total surface influence on resistivity (*French*) 0-71650
 Al-Sc, elec. resist. determ. 0-92876
 Al-Si-Cu-Zr, ageing kinetics (*Russian*) 0-76274
 Al-Y, specific elec. resist., variation with Y conc. 0-84455
 Al-Zn (10 wt.%), ageing at low temp., effects of fluctuation of solute conc. 0-76287
 Al-Zn (10 wt.%), ageing at low temp., effects of fluctuation of solute conc. 0-76288
 Al-Zn (8-25 wt.%), solid solns., residual resist. during clustering 0-97483
 Al-Zn-Mg alloy, Ag addition and pre-precipitation treatment, influence on GP zone growth 0-71658
 Al₂O₃-NiCr composite, plasma sputtering of electroheating coatings, elec. props. (*Russian*) 0-108350
 AlZn, disordered, residual resistivity due to clustering, ageing effects 0-65521
 Au, deformed, annealing kinetics of vacancies (*Japanese*) 0-88139
 Au, low temp. resist. and thermoelec. ratio, electron-electron scatt. contrib. 0-70670
 Au, virtual bound states due to 4d- and 5d-transition metal impurities 0-70667
 Au-Cr, dil., elec. resist., generalised phase shift anal. of Kondo effect 0-75556
 Au-Cr, dil. alloys, elec. resist., deviations from Matthiessen's rule 0-75541
 Au-Pd (150 wt.%), quenched, vacancy annihilation and short-range order formation, elec. resist. 0-108487
 Au_{50-x}Pd_{50-x} (0 ≤ x ≤ 15.02) β' -phase, Hall effect and elec. cond. 0-107768
 Au_{100-x}Zn_x (47 ≤ x ≤ 52), β' -phase, Hall effect and elec. cond. 0-107768
 Be, sintered, physicochem. props. anisotropy, BeO inclusions effect 0-60804
 Bi whiskers, persistent metallic behaviour, elec. resist. meas. 0-75544
 Bi-Sb (6 at.%) whiskers, persistent metallic behaviour, elec. resist. meas. 0-75544
 (Ce, La)In₃, heat capacity and elec. resist. 0-71049
 α-Ce, exchange-enhanced, elec. resist. T² depend., press. effect 0-96845
 γ-Ce, Kondo-like anomaly 0-96857
 CeAl₃, resistivity and volumetric meas., phase diagrams, comparison with CeS 0-107789
 CeBe₃, intermediate valence state, XPS, resist. and susceptibility study 0-71565
 Ce(In, Sn), heat capacity and elec. resist. 0-71049
 Ce_{1-x}La_x, dil., γ-α transition temp. and press., elec. resist. meas. up to 10 kbar 0-59643
 CeTi₃, mag. susceptibility, magnetisation, neutron diff., elec. resist., and sp. ht. meas. 0-75733
 Co-Cr eutectic alloy, thermal conductivity and electric resist. at high temp. 0-103668
 β-Co₂Ga₈, negative TCR obs. 0-75543
 Co₂Ga_{2-x}Fe_x, elec. resist., temp. and mag. field depend., mag. contrib. 0-96846
 Co₂(Ni_{0.4}Cu_{0.6})_{1-x}Fe_xO₄ ferrite, relation between elec. cond. and mag. anisotropy 0-75548
 Co(S, Se_{1-x})₂, galvanomag. effects, obs. and interpretation 0-70726
 Cr, volt ampere characteristics during electron melting process (*Russian*) 0-75336
 Cr-Co, dil., antiferromag., elec. resist. min., press. and impurity effects 0-59970
 Cr-Fe, dil., antiferromag., elec. resist. min., press. and impurity effects 0-59970
 Cr-Mo, elec. resist. and thermo-EMF, conc. depend., 4.2 to 1500K (*Russian*) 0-80247
 Cr-Mo, electrical resistivity, spin density wave gap, Neel temp. 0-88534
 Cr-Si-V, (2, 0.1 at.%), paramag. to commensurate spin density wave transition 0-65875
 CrAs, high press. paramag. antiferromag. transitions, elec. props., band model development (*Russian*) 0-60277
 Cs, metal impurity effect on residual elec. resistance (*Russian*) 0-84457
 Cs, supercond., elec. resist. and phase transforms. under high press. (*German*) 0-107763
 Cu, electrical resistance of edge dislocations (*German*) 0-96859
 Cu, low temp. resist. and thermoelec. ratio, electron-electron scatt. contrib. 0-70670
 Cu, microalloyed with B, elec. cond. and strength props. (*Polish*) 0-89285
 Cu wire, negative longitudinal magnetoresist. size effect 0-80252
 Cu-Al, short range order and static distortion contribution to residual elec. resistivity (*Russian*) 0-70672
 Cu-Al films, elec. cond. of vacuum condensates depend. on composition, annealing (*Russian*) 0-65709
 Cu-Au alloys, vacancy and divacancy migration activation energies, elec. cond. meas. 0-88140
 Cu-Fe system, ageing and reversion phenomena study 0-89274
 Cu-Ga (17 wt.%), elec. resist. and TEM studies 0-108604
 Cu-Mn alloy, manganin, hysteresis-corrected calibration under shock loading 0-74818
 Cu-Nb multifilamentary composite, dislocation resistivity 0-70671
 Cu-Ni (30-90 wt.%), elect. resist. rel. to cold working and heat treatment 0-71655
 Cu₂Au, electrical resistivity and LRO, energy gap formation in Fermi surface 0-88533
 Cu_{1-x}Cr₂Se₆, influence of excess Cu on physical props. 0-103836
 Cu₂Mn_{1-x}Sn_x alloy, compositional SRO, hyperfine interactions 0-71065
 Cu₂NiSn, Heusler alloy, elec. resist., 4.2 to 300K 0-75547
- electrical conductivity of crystalline metals and alloys continued**
 Cu(Rh_{1-x}Cr_x)₂S₄, spinel system, susceptibility and metallic resistivity, anomalies due to s-d interaction 0-70958
 Cu(SCN)_{1/3}, synthesis and high elec. cond., activated and metallic cond. obs. 0-96957
 DyAg_{1-x}In_x, elec. and Hall resist. 0-96844
 ErFe₂-YFe₂, and ErFe₂-LuFe₂, mag. props., 80-1300K (*Russian*) 0-75750
 ErRh_{1-x}Sn_{3-x}, synthesis, supercond. and mag. props. 0-100547
 Eu, electrical resistivity of solid and liquid phases, thermopower, melting temp. 0-59955
 EuGd₂S₄, nonstoichiometric, elec. transport props., semicond. and metallic cond. 0-107786
 Eu_{1-x}Sm_xS, ESR, exchange interaction, susceptibility, elec. cond., thermoelectric power 0-93174
 Fe, purification, recryst. temp. and elec. resistivity (*Japanese*) 0-100780
 Fe-Al (40 at.%) and Fe-Al (50.5 at.%) ordered alloys, 20K neutron irradiation effects, stoichiometry depend., resist. obs. (*French*) 0-84215
 Fe-Co-Mo-Nb(Ta) semihard mag. alloy, mag. props., thermal expansion, elec. resistivity and hardness (*Japanese*) 0-88789
 α-Fe-N, supersaturated solid solns., N atom precip. kinetics, resist. meas. 0-60864
 Fe-Ni alloys, enthalpy change between α'-γ and α-γ transformations 0-93550
 Fe-Ni-Co-W(Mo) (18.65, 8.99, 4.87 wt.%), ageing characts., 380-530°C 0-60876
 Fe-Pd Invar alloys, elec. and mag. props. and thermal expansion 0-75732
 Fe-Si (3 to 5 wt.%) sinters, mag. props., Si and Fe-Si additions effect 0-71104
 Fe-Ti, solubility and diffusivity of H and D in mixed crystal phase, elec. cond. meas. (*German*) 0-107575
 Fe-Ti (V)(W), dil., thermophysical props. and elec. cond., temp. depend. 0-96842
 Fe₃Al, electrical resistivity and LRO, energy gap formation in Fermi surface 0-88533
 Fe₂NbSe₂, transport props. and mag. ordering 0-65527
 Fe₂Ni₂Mn₁, disordered, mag. struct. near ferro-antiferromagnetic transition 0-60211
 B-Ga, metastable, elec. props. in normal and supercond. states (*Russian*) 0-65520
 Gd, ferromag., transport props., crit. behaviour 0-65522
 Gd-Ni, ferromag., elec. resist. temp. depend. 0-96843
 GdAg_{1-x}In_x, elec. and Hall resist. 0-96844
 GdCu, electrical resistivity and length changes with temp., hysteretic behaviour 0-97600
 (Gd_{1-x}Y_x)₂Co₃, Curie temp. and resist.-temp. curves, comp. depend. 0-71020
 Hg, solid, resistivity ratio, 1.65 to 234K 0-59952
 Hg₂Mo₂S₈ Chevrel phase, synthesis, stability and characts. 0-71608
 Ho-Cu intermetallics, resist. and magnetoresist., mag. ordering obs. 0-70677
 HoCu₂, mag. struct. and elec. resist., neutron diff. obs. 0-60206
 Ho₂Y_{1-x}Sb_x system, magnetisation, elec. resist., and sp. ht. meas. 0-60213
 Ir, thermophysical props. at temps. up to 7000K 0-103497
 K, low temp. resist. and thermoelec. ratio, electron-electron scatt. contrib. 0-70670
 K, metal impurity effect on residual elec. resistance (*Russian*) 0-84457
 (La,Nd)Sn₃, reverse Kondo effect in presence of crystalline elec. field splitting 0-103684
 La-Gd (8 at.%), FCC, under hydrostatic pressure, resistivity meas., comparison with positive-J spin glasses 0-59958
 Li, phonon limited resistivity struct. depend., Umklapp scatt., elastic consts. 0-88532
 Li-Mg, Matthiessen's rule, elec. and thermal deviations, impurity scatt. 0-88536
 Li-Pt, phase diagram for comp. range 0-40 at.% Pt, mag. and elec. props. (*German*) 0-84912
 LiAl, anomalous elec. resistivity near critical composition 0-103673
 Mg, H₂ dissolution, resistometric study under press. 0-70417
 Mg-Nd-Zn dilute alloy, metallography and precip. kinetics 0-71655
 Mn_{2-x}Fe_xSi₂, elec. resist. and mag. susceptibility, ferromag. to antiferromag. transition 0-80504
 Mo, elec. resist., quadratic contrib., 2 to 40K (*Russian*) 0-92874
 Mo, volt ampere characteristics during electron melting process (*Russian*) 0-75336
 Mo-V, elec. resist. and thermo-EMF, conc. depend., 4.2 to 1500K (*Russian*) 0-80247
 Mo₂Ge, Al₅ cpd., normal state, low temp. resist. 0-107762
 Mo₂GeRh_{1-x}Te_x, synthesis, struct., and elec. props. 0-92877
 Mo₂Ku₂Te₈, synthesis, struct., and elec. props. 0-92877
 Na, metal impurity effect on residual elec. resistance (*Russian*) 0-84457
 Na, phonon limited resistivity struct. depend., Umklapp scatt., elastic consts. 0-88532
 Nb, elec. resist. due to interstitial H (D) 0-96848
 Nb, volt ampere characteristics during electron melting process (*Russian*) 0-75336
 Nb-Rh, α-phase alloy, superconductivity and resistance behaviour 0-70882
 Nb-Ta(V)(Ti)(Mo), resistivity due to H incorporation 0-70666
 Nb₃Al, Al₅ cpd., normal state, low temp. resist. 0-107762
 Nb₃Al, temp.-depend. of elec. resist. 0-103675
 Nb₃Ge, temp.-depend. of elec. resist. 0-103675
 Nb₃Ge, Al₅ cpd., normal state, low temp. resist. 0-107762
 Nb₃Sn, Al₅ cpd., normal state, low temp. resist., disorder effects 0-107762
 (Nb_{0.99}Ti_{0.01})_{1-x}Ge_x, high T_c, resist. meas. 0-88531
 NdSn₃, elec. cond., cryst. field effect, spin disorder contrib. 0-65540
 Ni, push-pull fatigued polycrystals, point defects, elec. excess resist. meas. 0-100910
 Ni-Cu-H systems, Curie temp. during phase transitions under high press. H₂ 0-71029
 Ni-S solid solns., residual elec. resist. (*Russian*) 0-70465
 Ni₃Fe single crystals, longitudinal magnetoresist. meas. 0-70675
 Ni₃(Fe_{1-x}Nb_x), temp. and conc. depend. of anomalous Hall effect (*Russian*) 0-70674
 NiO, dipole orientation from bound polaron hopping 0-84437
 NiPt, quenched, ordering kinetics and domain struct. form. during isothermal tempering (*Russian*) 0-66502
 NiTi, premartensitic transformation of B2 phase, shape memory 0-84931
 PbAs (~0.01 wt.%), enhanced precip. phenomena, invest. of mechanism by elec. resist. meas. 0-104162

electrical conductivity of crystalline metals and alloys continued

- Pb-Sb-As (1.1-1.8, ~0.01 wt.%), enhanced precip. phenomena, invest. of mechanism by elec. resist. meas. 0-104162
 Pb(Ag) alloys, effect of Ag content on yield strength 0-76322
 PbMo₃S₂Fe, elec. cond. anomalous temp. depend., mag. moments (*Russian*) 0-92878
 Pd alloy-H system, α - β phase transformations, hysteresis of press., elec. resistance, review 0-60859
 Pd, elec. resist. due to interstitial H (D) 0-96848
 Pd-Co (0.1-45.7 at.%), thermo EMF at 4.2-300K (*Russian*) 0-92881
 Pd-Cr, dil., temp. dependent scatt. 0-59973
 Pd-Fe (0.54-8.0 at.%), thermo EMF at 4.2-300K (*Russian*) 0-92881
 Pd-H system, α - β phase transformations, hysteresis of press., elec. resistance, review 0-60859
 Pd-Ni (15-90 at.%), thermo EMF at 4.2-300K (*Russian*) 0-92881
 β' -PdIn, electrical resistance, mag. susceptibility and IR freq. dispersion (*Russian*) 0-107759
 (Pd₅Rh₅)₂H₂, elec. resistivity studies 0-59957
 Pr, localised 4f shell breakdown under press. 0-70411
 PrIr₂(Pt₂)(Rh₂)(Ru₂), sp. ht., differential susceptibility and elec. resist. meas. 1.4-40K 0-71063
 Pt, recovery spectrum after thermal neutron irradi., resist. obs., Au addition effect and defect conc. depend. 0-65057
 Pt-Fe alloy, ordered, T-c phase diagram, antiferro- and ferromagnetism (*Russian*) 0-65871
 Pt-transition metal, dil., impurity resist. 0-92875
 Rb, elec. resist. and phase transforms. under high press. (*German*) 0-107763
 Rb, metal impurity effect on residual elec. resistance (*Russian*) 0-84457
 Re, elec. resist., quadratic contrib., 2 to 40K (*Russian*) 0-92874
 Ru, elec. resist., quadratic contrib., 2 to 40K (*Russian*) 0-92874
 Sc thin films, obtained in vac. of 10^{-5} - 10^{-6} Torr, struct. and elec. resist. 0-107931
 Sc-Gd, dil., reverse resist. anomaly and negative magnetoresist. 0-84459
 ScAl₂-Eu, intermediate valence on Eu ions, Mossbauer isomer shift 0-84587
 Si, metallic, superconducting transition temp., press. effects, elec. cond. 0-103777
 Sm, electron radiation damage, elec. resistivity change rates 0-59954
 Sm, magnetoresistivity and elec. resist., 4.2 to 300K (*Russian*) 0-88539
 Sn, galvanomagnetic props., temp. depend. meas. in single cryst. 0-96850
 SrCo₃O₇ ($0 < \delta < 0.5$), ferromag. metallic elec. props. 0-70668
 Ta, elec. resist. due to interstitial H (D) 0-96848
 Ta, resistivity due to H incorporation 0-70666
 Ta, thermophysical props. and neutron absorpt. 0-103488
 Ta-Rh, ϕ -phase alloy, superconductivity and resistance behaviour 0-70882
 TbAg_{1-x}Nx, elec. and Hall resist. 0-96844
 TbZn, elec. resist., behaviour at mag. crit. points 0-65901
 Th-Gd(Tb)(Dy)(Ho)(Er)(Tm)(Lu) (1 at.%), Heisenberg exchange, residual resist. meas. 0-75558
 α -Ti alloys VT1 and VT5, struct. and phys. props., H₂ effect 0-108576
 Ti, polycrystal, discontinuous electrical resistivity, low temp. active straining (*Russian*) 0-103666
 Ti-Mo-V-Al-Cr-Fe (4.8, 4.7, 5.2, 1.1, 1.0 wt.%), structural changes during heating up to 1000°C, DTA study (*Russian*) 0-93552
 Ti-Ni, multiplicity of structural transitions, phase diagrams, elec. cond. meas. 0-71649
 Ti-Ni-Fe, multiplicity of structural transitions, phase diagrams, elec. cond. meas. 0-71649
 Ti-Pb in solid and liquid state, specific electric resistance 0-103662
 Tm magnetic transitions, effect of H₂ in solid solns., elec. resist. meas. 0-100585
 UAl₂, spin fluctuations, mag. field effect, electronic sp. ht. and elec. resist. 0-108026
 U(Co_{1-x}Fe_x)₂, ferromag. onset, susceptibility and resist. meas. 0-70967
 UMo₂, transport props., influence of lattice distortion 0-100452
 UNi₂, mag. phase transition, elec. resist. meas. 0-97094
 V, elec. resist. due to interstitial H (D) 0-96848
 V, thermophysical props. at temps. up to 7000K 0-103497
 V, volt ampere characteristics during electron melting process (*Russian*) 0-75336
 V₂Sn, A-15 cpd., normal-state elec. resist. 0-75542
 W, elec. resist., quadratic contrib., 2 to 40K (*Russian*) 0-92874
 W, volt ampere characteristics during electron melting process (*Russian*) 0-75336
 Y, electrical resistivity of solid and liquid phases, thermopower, melting temp. 0-59955
 Y, electron radiation damage, elec. resistivity change rates 0-59954
 Y-Gd, dil., reverse resist. anomaly and negative magnetoresist. 0-84459
 YNi₃, magnetism resurgence, neutron diffr. and mag. props. study 0-65819
 Yb, electron radiation damage, elec. resistivity change rates 0-59954
 Zn, single cryst., contribution of basal dislocations to residual elec. resist. (*Russian*) 0-75539

electrical conductivity of crystalline semiconductors and insulators

- see also carrier density; carrier lifetime; carrier mean free path; carrier mobility; carrier relaxation time; dislocation scattering; electronic conduction in crystalline semiconductor thin films; electronic conduction in insulating thin films; high field effects; hopping conduction; impurity scattering; minority carriers; negative resistance effects; photoconductivity; point defect scattering; small polaron conduction; surface scattering
 β -Al₂O₃-Cu₂O, phys. and chem. props., use in determ. of thermodynamics of Cu-Sn alloys 0-107502
 algorithm for calc. of impurity concentration from sheet resistivity and sheet Hall coefficient data 0-70246
 anthracene single crystals, hole trapping by photo-oxidation products, injection currents (*Russian*) 0-92904
 compensated semiconductor, cluster scattering, DC resist., energy-loss method 0-96862
 copper quaternary thiospinels, mag. and elec. props. (*French*) 0-65771
 DBTTF halogen complexes, IR, UV spectra, EPR study 0-108215
 2,6-N,N-diacetylaminopyridine elec. cond., γ dose and temp. (303-363K) effects 0-103696
 diamond:Sb, implanted, radiation damage and annealing study 0-100263
 2,6-N,N-dibenzoyldiaminopyridine elec. cond., γ dose and temp. (303-363K) effects 0-103696
 dielectrics containing impurities, carrier distrib. and currents, numerical simulation (*French*) 0-70718
 electron-hole plasma and elec. field, stratification at low temp. 0-60020

electrical conductivity of crystalline semiconductors and insulators continued

- ferroelectric semiconductors, props., book 0-82590
 ferromagnetic semiconductor, energy and mobility of spin polarons 0-70982
 ferromagnetic semiconductor, spin polaron props., effect on carrier scatt. 0-60233
 ferromagnetic semiconductors, hot electron relax. time 0-59996
 GaAs, polycrystalline, grain boundary resistance meas. effect on solar cell performance 0-93891
 graphite, resistivity and magnetoresistance, 4.2 to 293K 0-100459
 graphite-K intercalation compounds, electronic props., resistivity, Hall effect and magnetoresistance 0-75585
 haematite, elec. resist. and phase transition under shock compression 0-72496
 hopping model, semi-classical, effective mass and carrier mobility calc. 0-96872
 ionic semiconductors, cyclotron resonance, elec. cond., electron-phonon interactions 0-93180
 IV-VI semiconductors, structural phase transitions, anomalous resist., electron-soft phonon interactions 0-108167
 lattice defects and diffusion processes in solids, book 0-107207
 lattice parameters, mag. and elec. props. 0-100578
 lead acetate trihydrate:Mn²⁺, ESR, elec. cond. 0-93165
 lead phthalocyanine:O₂(I), Schottky barrier effect on AC current response 0-75623
 metal colloids in ionic cryst., preparation, optical, mag. resonance, elec. props. 0-59459
 MgAl₂-Fe₂O₃ solid solution system, solid state properties study 0-93094
 naphthalene, charge carrier drift mobility, semi empirical anal. 0-65553
 naphthalene, electron and hole off-diagonal mobility component determ. 0-65552
 nematic liquid crystal, elec. conduct. based on injection-contact phenomena theory (*Russian*) 0-107807
 periclas refractories, props. after testing at over 2000°C 0-104317
 perovskite oxides, point defects, elec. cond., and electron energy spectra 0-70706
 phenothiazine derivatives, semicond. elec. props., optical spectra, and EPR 0-103693
 phthalocyanines, elec. cond., compensation effect 0-100455
 plasma effects, strongly elongated electron distrib., normal oscils. 0-60021
 polyacetylene:I, dc microwave cond., permittivity 0-107843
 polyethylene, elec. cond. of high and low density samples, oxidation effects 0-107784
 polystyrene, plasma polymerised, free radicals, transient elec. current, EPR, heat treatment 0-71178
 rare earth chalcobismuthites, RbTe₃, prep., elec. props., and crystallographic data 0-59981
 rare earth oxides, perovskite-like, synthesis, struct., elec. props. 0-65554
 rare earth sulphides, EuR₃, R=La, Ce, Pr, Nd, Sm, Gd, elec. cond. meas. 0-65555
 rare earth-CrO₃, elec. transport 0-70700
 review, electronic transport in insulators (*Spanish*) 0-84464
 ruthenates, ACu₂Ru₄O₁₂, A=Na,Ca,Sr,Cd,La,Pr,Nd, synthesis, cryst. struct., mag. and elec. props. (*French*) 0-107151
 semiconductor, electron quantum states, nonequilibrium current fluctuations in quantised mag. fields (*Russian*) 0-107704
 semiconductor characterisation, cond. type determ. by pot. profiling 0-73387
 semiconductors, temp. depend. electronic cond., review 0-59975
 semiconductors, thermoelectrically anisotropic, carrier kinetics at low temp. 0-92893
 semiconductors, thermoelectrically anisotropic 0-92894
 semiconductors with impurities, electron cond. temp. and freq. depend., two band model (*Russian*) 0-75564
 spreading-resistance meas. for doping profile determ., preprocessing of data for resistivity calcs. 0-57265
 TCNQ salts, elec. cond. spectrum fine struct. 0-96884
 tetraselenotetracene iodides, struct. and physical props., DC electrical cond. and EPR linewidth meas. 0-103312
 thallium hexanoate, soliton conduction, elec. cond. field and temp. depend. anomaly (*Russian*) 0-103703
 thinned semiconductor device, SEM, electron beam induced cond. of defects, rel. to TEM 0-107027
 (TMTSF)₂PF₆ (AsF₆), linear-chain conductor, semicond.-metal transition in small elec. field 0-103730
 transition metal chalcogenides, quasi-one-dimens., elec. mag., and supercond. props., review (*Russian*) 0-93022
 AgI group superionic conduction, phase transition detection by thermoelectric power method 0-92669
 AgN₃, high-resist. explosive cpd., elec. and galvanomag. props., temp. depend. 0-103728
 Ag₂N_{2-x}Te_{2-x}Te_{3-x}VO₁₄, (x=0,4), mixed tellurate, cryst. chem. and elec. cond. (*French*) 0-107150
 Al-anodised Ta₂O₃/native oxide-n-GaAs MOS structure evaluation 0-84514
 AlB₂, α - and β -forms, elec. props. at high temps. and in strong elec. fields, thermistor appls. 0-92903
 Al₂O₃:Cr, pure and doped, electron irradi. induced cond., TSC and EPR study 0-80277
 Al₂O₃:Zr ceramic, elec. props., additives effect, and interaction with steel melt 0-104305
 B, β -rhombohedral, elec. props. at high temps. and in strong elec. fields, thermistor appls. 0-92903
 BC, sintered, struct. and props. 0-104181
 Ba₂C, thermophysical props. and neutron absorpt. 0-103488
 BaFe₂O₁₉, ferrite, DC cond., dielec. props., lattice consts. 0-80272
 BaHfO₃, BaSnO₃ and BaZrO₃, high-density ceramics prep. and elec. props. 0-60812
 Ba₃Sc₂O₉, Ba₃Sc₂WO₉ and Ba₃ScTaO₉, elec. cond. nature, depend. on comp. and medium thermodynamic parameters 0-70773
 Ba₉Sr₆Nb₃O₂₆, electronic props. and photoresponses 0-92925
 BaTiO₃:C, solubility of C at low O₂ potentials, 800°C 0-100334
 BaTiO₃:La, Sb, second phase effect on elec. and mag. props. 0-60986
 BaTiO₃:Nb, elec. props., contact material influence 0-70848
 Bi₂O₃, polymorphic transformation and elec. resistivity (*Japanese*) 0-93555
 Bi_{0.88}Sb_{0.12}, semiconducting transport props., 2 to 100K 0-59989
 Bi_{2-x}Sb_xTe_{3-x}Se_x, elec. cond. and thermoelec. props., neutral defects influence 0-60017

electrical conductivity of crystalline semiconductors and insulators continued

Bi₂Te₃-Bi₂Se₃-Sb₂Te₃, solid solution, single crystal, elec. cond., thermoelectric props. 0-88550
(Bi₂Te₃)_{0.9}(Sb₂Te₃)_{0.5}(Sb₂Se₃)_{0.05} n-type alloy for thermogenerators, thermo-EMF, elec. cond. and thermoelec. efficiency factor, 300-600K 0-70735
Bi₂Te₃O₁₂, elec. characts., phase transition obs. 0-60517
Bi₂WO₆, ferroelectric, dielectric props., elec. cond. and relaxation phenomena obs. 0-80692
C₈BrCl_{1-x} intercalate, crystallographic, elec., mag. props. 0-107184
C₂₄Rb, intercalated graphite, resistivity and specific heat anomalies 0-107440
CaSnO₃ and CaZrO₃, high-density ceramics prep. and elec. props. 0-60812
CdCr₂S₄ crystal growth, structural defects, physical properties 0-60759
CdCr₂Se₄, ferromag. semicond., conc. anomalies rel. to red shift of absorpt. edge 0-70732
CdCr₂Se₄:In(Ga), elec. resist. and magnetoresist., 2 to 200K 0-96876
CdF₂-YF₃, thermal ionisation energy of monovalent centres 0-80207
n-Cd₂GeO₄, electronic and cond. props. rel. to prep. conditions and defect struct. 0-107787
Cd₂Hg_{1-x}Te crystals, donor compensation, low temp. cond. study 0-75571
CdS thin layers, recryst. from CdS-Cr₂O₃ mixtures, phys. and photoelec. props. 0-96935
CdS:In, impurity resist., Matsubara-Toyozawa theory extension 0-80264
CdS_{1-x}Te_x, recryst. from CdS_{1-x}Te_x-Cr₂O₃ mixtures, photocond. props. 0-96936
p-CdSiAs₂, electron irradi. elec. props. annealing, lattice defects 0-100465
p-CdSnAs₂, Hall effect, thermo EMF, thermomagnetic effects 0-107822
p-CdSnAs₂, heavily doped, elec. transport props. under elastic deformation 0-96915
CdTe, elec. and photoelec. props. due to double injection, quenching spectra 0-70765
CdTe-CdS heterojunctions, growth by closed-tube chem. transport, elec. props. 0-60070
CdTe_{1-x}Se_x(Te₄):Au, elec. cond., density, dielectric const., changes on fusion 0-88553
Cd₂Zn_{1-x}S films, chem. sprayed, carrier density and mobility 0-60121
CeB₆, crystal preparation, elec. resistance, phase transitions 0-97427
CePd₃-MPd₃ mixed valent systems, nonlinear conc. depend. of resist. 0-65528
CeS, resistivity and volumetric meas., phase diagrams, comparison with CeAl₃ 0-107789
Co complex, 2,6-N,N-diacetylaminopyridine-Co(II) elec. cond., γ dose and temp. (303-363K) effects 0-103696
Co complex, 2,6-N,N-dibenzoyldiaminopyridine-Co(II) elec. cond., γ dose and temp. (303-363K) effects 0-103696
Co²⁺Mo⁴⁺O₃, defect spinel struct., elec. and mag. props. 0-70176
Co₃Mo₃S₆O₂, O-containing Chevrel phases, synthesis and props. 0-108368
Co₂RhS₄, mag. semicond., mag. and elec. props. 0-93121
CoS₂, galvanomagnetic effect of single cryst. 0-96912
CoS₂, narrow-band ferromag., high press. effect on anomalous elec. resist. 0-70698
Co₂Z ferroxplana form. process peculiarities 0-89368
Co₂Zn_{1-x}Fe₂O₄, ferrite, DC cond., dielec. props., lattice consts. 0-80272
CrNbO₄, elec. cond. meas. 0-100463
CrVO₄, elec. cond. meas. 0-100463
CsClO₄, AC elec. cond. temp. and freq. depend., obs. and unified defect struct. model 0-88554
CuB₂, elec. props. at high temps. and in strong elec. fields, thermistor appls. 0-92903
CuCl, pressure depend. of structural, chemical, elec. and mag. props. 0-96596
CuCrSe₂, influence of excess Cu on physical props. 0-103836
CuInTe₂ single crystals, directional freezing growth and doping, resist. changes on annealing 0-60768
Cu₃Mo₃S₆O₂, O-containing Chevrel phases, synthesis and props. 0-108368
Cu(SCN)_{1/3}, synthesis and high elec. cond., activated and metallic cond. obs. 0-96957
CuSbS₂ crystals, growth and characterisation 0-60770
CuWO₄, elec. cond., thermoelectric power and dielectric constant temp. depend. 0-96886
EuB₆, electronic struct., transport and mag. props. 0-96782
EuB₆, Hall effect and resistivity data, ferromagnetic ordering temp., pressure depend. 0-60010
EuB₆, resistivity press. variation, lattice consts. 0-100456
EuGd₂S₄, nonstoichiometric, elec. transport props., semicond. and metallic cond. 0-107786
Eu₂IrH₈, prep., cryst. struct., mag. and elec. props. 0-88117
EuO, physical and physicochem. props., review 0-96875
EuO:Gd, elec. cond. under hydrostatic press., Curie temp. 0-96881
EuO:Gd, pure and doped, elec., mag., and optical props. rel. to electronic conc. 0-96880
Eu₂O₃, thermophysical props. and neutron absorpt. 0-103488
EuO(Se), complex elec. cond. anomalies 0-107812
EuTe, magnetic impurity states, mag. and transport props. 0-96913
Eu_{1-x}Yb_xTe, (0<x<1), mag. semicond., elec., mag. and optical props. 0-97070
FEPS₃, layered semiconductors, optical and electronic props. 0-70761
Fe_{0.2}Co_{0.8}S₂, narrow-band ferromag., high press. effect on anomalous elec. resist. 0-70698
Fe_{1-x}Co_xSi solid solution, semiconductor-metal transition 0-103627
Fe_{1-x}Cu_xCr₂S₄, ESR spectra, elec. and mag. props., Curie temp. 0-97137
FeF₂ thin film, polarisation mechanism, AC and TSC study 0-66104
FeGa₂Se₄, elec. cond., mag. susceptibility 0-88301
Fe₂O₃-Al₂O₃ mixed oxide, X-ray diffr. and elec. cond. 0-79954
Fe₂O₃, magnetite, and related Jente spinels, mag. crit. point behaviour 0-60342
FeRh₂S₄, mag. semicond., mag. and elec. props. 0-93121
FeS, pressure effect on elec. resist. and thermoelec. power 0-70308
Fe(Sb_{1-x}Te_x)₃ system cpds., prep., cryst. struct., elec. and mag. charact. 0-108349
Fe₂SiO₄, fayalite, elec. cond. obs. under shock compression 0-81873
 θ -Fe₂V₂O₅, spin glass and paramag. props., susceptibility, EPR and Mossbauer studies 0-75782
n-Ga_{1-x}Al_xAs:Si, room-temp. cond. and band struct. 0-96869

electrical conductivity of crystalline semiconductors and insulators continued

n-GaAs, current-voltage characts., dislocation etch pits and perfect cryst. 0-70695
GaAs device isolation with deuteron bombardment 0-75248
GaAs, electrical conductivity and thermoelectric power charge due to melting 0-100490
GaAs, epitaxial, residual donor identification by far IR photoconductivity meas. 0-103717
GaAs, H⁺ irradiation, effect on electrical props. 0-65567
GaAs, heavily doped, fluctuation-induced tunnelling cond. 0-65516
GaAs, ion implanted, laser annealing 0-107296
GaAs, point defects, laser annealing 0-107224
GaAs:Cr, carrier equilibrium effects, impurity states, elec. resistivity 0-65488
GaAs:CrO semi-insulating monocrystal development and four-level model 0-88191
GaAs:Cr semi-insulating wafer, heat treatment technique for no thermal conversion 0-100857
GaAs:O, electrolum., photolum., negative differential resist. rel. to recomb. processes 0-66304
GaAs:Se, Ga, dual species ion implantation, elec. characts. 0-103377
GaAs:Se ion implanted samples, Q-switched ruby laser annealing, improvement in elec. props. 0-100460
GaAs:Zn, implanted, laser annealing, elect., Rutherford backscattering and SEM meas. 0-100273
Ga_{1-x}Mn_xSb, elec. cond., mag. susceptibility, Hall const., and thermo-EMF, 80 to 1000K (Russian) 0-88549
GaSb LEC single crystal growth, novel encapsulant material 0-93475
Ga₂Se₃, solid solution, elec. cond. 0-88301
Ga₂Se₃-FeSe, phase diagram, elec. cond., mag. susceptibility 0-88301
GaTe, transport properties under hydrostatic pressure 0-75589
GdBi₆, crystal preparation, elec. resistance, phase transitions 0-97427
Gd_{1-x}S_x, ferromag., elec. props. near Curie temp. 0-107788
Gd_{1-x}□_xS₄, transport and mag. props., mag. Wigner localisation 0-97069
Ge, electron-hole droplets, percolation theory of cond., expt. 0-92896
n-Ge, laser irradi., accumulation of defects, effect on elec. props. 0-107317
Ge, magnetoresistance of electron-hole liq., percolation model 0-96920
Ge, oscillatory exciton breakdown, microwave cond. 0-103716
Ge:As, Sb, Hall mobility, temp. dependence 0-96919
Ge:O, slow thermal relax. of cond. rel. to donor complexes 0-70704
Ge:Sb, heavily doped semicond., scatt. mechanism, resist. and Hall coeff. maxima 0-75586
Ge-Si alloys, n-type, phosphorous doped, precipitation effects due to heat treatment 0-107833
H_{1.6}MoO₃, electronic props., mag. susceptibility and spectra 0-80266
Hg_{1-x}Cd_xTe epitaxial layers, elec. props. 0-96910
Hg_{1-x}Cd_xTe-type semimetals, kinetic props., local acceptor level effects 0-65557
HgSe, elec. resist., high press. phase transform., band gap 0-70707
HgTe, mobility of electrons and holes, 4 to 100K 0-107821
InAs, electrical conductivity and thermoelectric power charge due to melting 0-100490
InAs, resist. inhomogeneity meas. with single-sonde potential method 0-65549
InAs:Cd, Te, donor-acceptor interaction, elec. cond. and Hall coeff. meas. 0-59988
In_{1-x}Ga_xSb films, elec. props., preparation 0-100473
InP, electron transport props., mag. field and temp. depend. 0-92888
n-InP, γ -ray and electron irradi., annealing of radiation point defects, elec. cond. and Hall coeff. meas. 0-65051
InS₇, single crystal, switching effect and memory. (Russian) 0-70774
p-InSb, influence of plastic deform. on elec. props. 0-103711
InSb, neutron irradi., defect cluster form., effect on elec. props. 0-65062
InSb, resist. inhomogeneity meas. with single-sonde potential method 0-65549
InSb, thermal cond., elec. cond., and thermoelec. power, press. depend. 0-59744
InSb:Cd (Zn) (Ge), ion-irradiated, p-n conversion during heat treatment 0-96558
n-InSb:Cr, deep impurities, elec. cond. and Hall coeff. meas., 4.2 to 120K 0-107791
KCl: CdCl₂, elec. cond., role of electrode material, surface precipitation effects 0-59985
K₂Te^{VI}Te₃O₁₂, mixed tellurate, cryst. chem. and elec. cond. (French) 0-107150
LaCrO₃-Cr ceramic, prep., phase comp. and elec. cond. (Polish) 0-71621
La_{1-x}Sr_xFeCoO₃ (0.5≤x≤0.9), ferromag., elec. props., itinerant electron model 0-107785
LiAl, transport props., rel. to semimetallic band struct. 0-88581
LiNbO₃:Fe, elec. resist., temp. and conc. depend. 0-80275
LuRhO₃, elec., mag. and photoelectrochemical props. 0-96925
MgAl₂O₄, γ -irradiated crystal, TSC, thermoelec. power, thermolum. and afterglow 0-75583
MgCr₂O₄-TiO₂, porous ceramics, humidity-sensitive electrical conduction 0-107782
Mg₂Fe_{1-x}O, diffusion of ⁵⁹Fe and elec. cond. 0-59700
MgO, sintered, refractories, props. after testing at over 2000°C 0-104317
Mg_{0.2}Zn_{0.75}Fe₂O₄, ferrite, DC cond., dielec. props., lattice consts. 0-80272
(Mn,Zn)Fe₂O₄:Si, Ca, Ti, second phase effect on elec. and mag. props. 0-60986
MnAs_{0.95}P_{0.05}, anisotropy of elec. cond. and Hall effect 0-92908
Mn²⁺Mo⁴⁺O₃, defect spinel struct., elec. and mag. props. 0-70176
Mo₂Ru₂Se₈, synthesis, struct., and elec. props. 0-92877
MoS₂ solid lubricant, antifriction and elec. props. depend. on oxidation temp., dopant influence 0-108584
Mo₂S₃ Chevrel phases with group IIIa metals, Nb, Hg, Pb and Cu, synthesis, stability and characts. 0-71608
Mo_{0.5}W_{0.5}Se₂, single cryst. vapour growth, characterisation 0-93466
NH₄Cl(Br), effect of NH₄⁺ internal motion on elec. and optical props. 0-100454
NH₄ClO₄, AC elec. cond. temp. and freq. depend., obs. and unified defect struct. model 0-88554
NaNbO₃, elect. cond. mech., resist., Hall coeff. and thermoelec. power meas. 0-65603
NbO₂, on-state decay rel. to recomb. and nonlinear props. 0-84492
Nb₂O₅-V₂O₅-P₂O₅, glasses and glass ceramics, elec. cond., struct. 0-84466

electrical conductivity of crystalline semiconductors and insulators continued

- NbSe₂ solid lubricant, antifriction and elec. props. depend. on oxidation temp., dopant influence 0-108584
 Nb_{1-x}V_xSe₂, elec. and mag. anomalies at CDW transition 0-107722
 Nd_{1-x}Ca_xVO₃, solid solutions, elec. props. 0-96866
 Ni complex, 2,6-N,N-diacyldiaminopyridine-Ni(II) elec. cond., γ dose and temp. (303-363K) effects 0-103696
 Ni complex, 2,6-N,N-dibenzoyldiaminopyridine-Ni(II) elec. cond., γ dose and temp. (303-363K) effects 0-103696
 Ni_{1-x}Co_xS₂, elec. cond., thermoelec. power and optical meas. 0-59986
 Ni_{1-x}Cr_xS₂, elec. transport, mag. susceptibility and DTA meas. 0-96954
 NiFe₂O₄, electronic phase transition 0-65640
 Ni₃Fe₂O₄, DC and low freq. cond. and influence of microstruct. 0-70699
 Ni₃Mo₂S₂O₂, O-containing Chevrel phases, synthesis and props. 0-108368
 NiO, doped and undoped, elec. props. and surface characts. 0-65571
 NiPS₃, layered semiconductors, optical and electronic props. 0-70761
 NiS_{2-x}Se_x, elec. cond., thermoelec. power and Hall effect meas. 0-65561
 NiWO₃, AC elec. conductivity, thermoelec. power and dielec. const. 0-70736
 PLZT, thin, elec. cond. and pyroelectric behaviour 0-75954
 Pb_{0.94-x/2}Bi_{0.06}Nb_{1-x}O₃, Nb dopant morphology effect on microstructure 0-81005
 Pb_{1-x}Ge_xTe solid solns., phase transition influence on elec. props., 77 to 450K 0-103689
 Pbl₂, dielectric props., elec. cond., space charge polarisation 0-100631
 PbMo₂S₂O₂, O-containing Chevrel phases, synthesis and props. 0-108368
 PbS-Sb₂S₃ semicond., optical and photoelec. behaviour 0-96938
 Pb_{1-x}Sn_xSe, transport phenomena in solid solutions with band inversion 0-107792
 Pb_{0.87}Sn_{0.13}Te, film, effect of hydrostatic pressure on props. 0-70862
 Pb_{1-x}Sn_xTe, thermoelectric effects, characteristics at low temps. 0-107831
 Pb_{1-x}Sn_xTe:In, dielectric state, avalanche breakdown in strong elec. fields (Russian) 0-92901
 PbTe:In, electron mobility, temp.-independent part, Hall effect and elec. cond. meas. 0-92914
 PbTe-InTe system, phase interactions and solid soln. form., physicochem. and elec. characteris. 0-104129
 Pb(Zr,Ti)O₃:Fe(Nb) ceramic, elec. and electromechanical props., depend. on dopants 0-81212
 PtSb₂, high field elec. props., impact ionisation 0-96892
 RbAg₂S₃, superionic conductor, phase transition detection by thermoelectric power method 0-92669
 RbClO₄, AC elec. cond. temp. and freq. depend., obs. and unified defect struct. model 0-88554
 Rb₂WO₃ bronze, elec. resist. meas., anisotropy 0-75569
 Ru₂Ge_{3-x}Sn_x and Ru₂Ge_{3-x}Si_x, diffusionless phase transitions, elec. and mag. props. 0-96871
 RuO₃, thermal conductivity meas., rel. to elec. cond. 0-65317
 S, single crystal, photoelectron, electronic transport and Mott-Gurney transition (Spanish) 0-84464
 Sb₂S₃, defect drift in elec. fields and bistable switching 0-92947
 Sb₂Se₃ crystals, mag. and elec. props. 0-96873
 (Sb₂Se₃)_{0.7}(Bi₂Se₃)_{0.3}, solid soln., prep. and elec. properties of layered crystals 0-70762
 Sb₂Te₃, thermoelectric properties and phase transition, under hydrostatic pressure up to 9 GPa 0-65609
 Se₂O₃, liq. and solid phase elec. cond., high temp. meas. 0-84468
 Se₂O₃, solid and liq. phases, thermophysical and electrophysical props. 0-103495
 Se powder compacts, sintered, electrical cond. 0-70693
 P-Si, conductivity and carrier lifetime, high injection effects 0-70719
 Si crystal, impurities determ. and resistivity after reactor neutron irradi. 0-65563
 p-Si, Czochralski grown, microdistrib. of O, SEM and spreading resist. obs. 0-79830
 n-Si, deformed, thermal treatment effect on elec. cond. and dislocation mobility 0-107265
 n-Si, elec. cond. control by hot electron intervalley transfer 0-59993
 p-Si, elec. resist., shock wave compression effects 0-80265
 Si, electrical conductivity, inertia of electron heating, expt. and theory 0-65613
 n-Si, electron heating by static elec. field 0-96894
 Si, enhanced conductivity in plasma hydrogenated films, thermionic emission 0-70692
 Si, epitaxial layer thickness meas. using phase correction function of substrate resistivity (Rumanian) 0-90812
 Si, high-resistivity layer form. during electron irradi. 0-80352
 n-Si, ion-implanted, elec. characts. after laser annealing 0-88562
 p-Si, laser irradi., accumulation of defects, effect on elec. props. 0-107317
 Si, multigrained, grain boundary elec. and compositional props., surface anal. 0-76575
 n-Si, piezoresist. rel. to piezothermoelec. power, electron-phonon drag region 0-70737
 Si, point defects, laser annealing 0-107224
 Si, poly crystalline, electronic behaviour of grain boundaries, solar cell appl. 0-92859
 Si, radiation defects, influence of dislocations on accumulation, elec. props. 0-92558
 Si wafers, Czochralski grown, minority carrier transport props., laser beam scan for homogeneity anal., photovoltaic cell appls. 0-92905
 Si:Al(Ga), spreading resist. calibration using Si:B 0-103690
 Si:As, diffused, laser irradi., stability study 0-65547
 Si:As, heavily As-diffused, Hall mobility and resist. rel. to carrier conc. 0-107815
 Si:As, ion implanted, low temp. thermal annealing 0-96552
 Si:As⁺, implanted, CW laser annealing, electron-beam induced current 0-100709
 p-Si:B(Al), radiation defect form. and annealing study using Hall effect, cond. and carrier diffusion length 0-84214
 Si:B(P), ion implanted crystalline and amorphous laser annealing 0-97509
 Si:Fe(Al), compensated substrates for solar cells, effects of Fe and Al 0-94009
 a-Si:H alloys, sputter deposited thin film coatings, property-comp. relationships 0-80975
 Si:P, heavily doped semicond., scatt. mechanism, resist. and Hall coeff. maxima 0-75586

electrical conductivity of crystalline semiconductors and insulators continued

- Si:P, implanted low temp. annealed, elec. activation, damage depend. 0-88182
 Si:P, incoherent light flash annealing, elec. props., backscattering spectra 0-97504
 Si:P, neutron transmutation doping, elec. props. rel. to neutron fluence 0-96555
 Si:P, neutron transmutation doping, resist. homogeneity rel. to compensation ratio 0-96556
 n-Si:P(B), elec. cond. oscills., electron instability effects due to dislocations 0-103704
 SiAs, cryst. growth from melt, elec. props. 0-76170
 SiC, diffusion of B, elec. cond. meas. 0-96696
 SmB₆, crystal preparation, elec. resistance, phase transitions 0-97427
 SmB₆, mixed valent semicond., transport props. and electronic struct., review 0-96877
 SmB₆, resistivity press. variation, lattice consts. 0-100456
 SmS, physical and physicochem. props., review 0-96875
 SnF₂, phase transitions, X-ray diffr., elec. cond. and thermal anal. studies 0-100329
 SnO₂-based gas sensors, resist. temp. depend. on exposure to CO, H₂, and propane 0-103694
 SrFe₂O₁₉/Si, Sr, second phase effect on elec. and mag. props. 0-60986
 SrMnO_{3-x}, O-deficiency induced polymorphs and elec. cond. 0-71643
 Sr₂Nb₂O₇, electronic props. and photoresponses 0-92925
 SrSnO₃ and SrZrO₃, high-density ceramics prep. and elec. props. 0-60812
 TTT₂3+8 complex, influence of press. on metal-dielectric phase transition (Russian) 0-92818
 α -Ta₂O₅, elec. cond. mechanism, admittance meas. 0-70705
 Ta₂O₅, 1T and 1H polytypes, fast neutron irradi., defect prod., effects on resist. and charge density waves 0-65060
 Ta₂O₅ (1T) electron irradiated, lattice contraction 0-59520
 Tb(NO₃)₃·Fe(NO₃)₃·(NH₄)₂CO₃·H₂O system, cpd. form., comp. and props. 0-100832
 Te, a-edge dislocated crystals, mobility anisotropy 0-107781
 Te-(Bi,Sb,-)₂Te₃ eutectic, electrophys. props., directed crystn. conditions influence and comp. depend. 0-107827
 Te-based eutectics, crystn. rate effect on electrophys. props. mutual solubility effect 0-60774
 TiO₂:Cr(Ta), slightly doped, elec. cond. and defect struct., charge compensation and point defect model 0-75568
 TiSe, impurity effects on elec. props. 0-80263
 Ti_{0.33}WO₃ bronze, elec. resist. meas., anisotropy, supercond. 0-75569
 TmSe, Anderson lattice resist. for antiferromag. ordering 0-65556
 UC, quenched in defects, formation, migration and resistivity 0-64990
 UCN, quenched in defects, formation, migration and resistivity 0-64990
 (V_{1-x}Cr_x)₂O_{3+x}, elec. props. and struct. 0-84494
 V₂O₅, ferroelec. semicond., dielec. and elec. meas. 0-60516
 WS₂ solid lubricant, antifriction and elec. props. depend. on oxidation temp., dopant influence 0-108584
 Y oxides, perovskite-like, synthesis, struct., elec. props. 0-65554
 Y₂O₃, liq. and solid phase elec. cond., high temp. meas. 0-84468
 YbB₆, resistivity press. variation, lattice consts. 0-100456
 Yb₂O₃, electronic cond. rel. to partial press. of O₂ of high temp. (French) 0-59979
 ZnAs₂, homogeneity region and electrophys. props. 0-60833
 p-Zn_{0.1}Cd_{0.9}Sb, thermoelec. anisotropic semicond., carrier kinetics at low temps. 0-92893
 Zn_{0.1}Cd_{0.9}Sb, thermoelectrically isotropic semicond., carrier kinetics in intrinsic cond. range 0-92894
 ZnCr₂Se₄, electroconductivity, thermoelectromotive force, Hall effect (Russian) 0-70694
 ZnCr₂Se₄:In, magnetoresist. and elec. resist. above and below Neel temp. (Russian) 0-88576
 Zn²⁺Mo⁴⁺O₃, defect spinel struct., elec. and mag. props. 0-70176
 ZnO, elec. cond. at high fields 0-80287
 ZnO, non-ohmic ceramic, degradation props. under AC and DC bias 0-80262
 ZnO varistor ceramics, current-voltage characts., inhomogeneities and single barriers 0-80273
 ZnO:Ba, Co, rare earth metal varistors, microstructure-prop. relations 0-100249
 ZnO:Bi, Sb, Co, second phase effect on elec. and mag. props. 0-60986
 α -ZnP₂, doped, single crystal, electrical properties 0-92892
 Zn₃P₂, elec. cond., Hall effect, P interstitial effects 0-84465
 ZnSb, thermoelec. anisotropic semicond., carrier kinetics at low temps. 0-92893
 p-ZnSiAs₂, electron irradi. elec. props. annealing, lattice defects 0-100465
 4.26ZrO₂·Nb₂O₅, elec. cond. meas. 0-100463
 6.14ZrO₂·Ta₂O₅, elec. cond. meas. 0-100463
 ZrS₃, quasi one-dimens. semicond., elec. transport props. 0-107790
 ZrTe₅, giant resistivity anomaly 0-107794

electrical conductivity of electrolytic liquids

- see also electrochemical analysis; electrolytic ion mobility; Wien effect
 dielectric liquids, ion mobility meas. and breakdown process, optical methods 0-84692
 gas chromatographic bipolar pulse differential electrolytic cond. detector 0-93814
 Cu complexes of 2-amino-5-methyl-1,3,4-thiadiazole and 2,5-dimethyl-1,3,4-thiadiazole, conductometric and IR meas. 0-87121
 CuSO₄, aq. solns., densities, viscosities, elec. cond. meas., 20 to 70°C 0-95688
 CuSO₄/H₂SO₄ electrolytes, densities, elec. cond., viscosities 0-107455
 Ho(NO₃)₃ solns., f-f transitions, intensity anal., correl. with cond. and US absorpt. 0-97292
 KCl solution, elec. cond. obs. for seawater salinity scale 0-72646
 LiCl-KCl, molten mixture, struct., diffusion, cond., mol. dynamics calc. 0-64871
 NaCl, water-HMPT soln., ionic diffusion coeffs. meas. (French) 0-65265
 PbO-SiO₂, melt, elec. cond. and struct. 0-88020

electrical conductivity of gases

- see also space-charge-limited conduction
 conductance for the gas flow of an accelerating tube 0-102359
 ethane, gas, liq., and crit., electron mobility, density and temp. effects 0-92246
 ethane, supercritical, electron mobility as function of density and temp. 0-59163
 excited gas, resonant optical discharge 0-92343

electrical conductivity of gases continued

- fluid, two dims. motion, mag. field evolution, anti-dynamo theorem extension (*Russian*) 0-59127
 imperfect high temp. plasma, elec. cond. meas. (*Russian*) 0-100072
 Cs vapour, electrical cond. near saturation point 0-69967
 H₂-O₂ seeded system for MHD generator, elec. cond. 0-76642

electrical conductivity of liquids

see also *electrical conductivity of electrolytic liquids*

- acetone, macroscopic model for solvated ion dynamics, cation conductance calcs. 0-65261
 acetonitrile, macroscopic model for solvated ion dynamics, cation conductance calcs. 0-65261
 alkali metals, liq., Fermi energy, density of states, electronic props., exchange and correl. effects 0-96774
 benzene, gaseous, critical and liquid, electron transport 0-64673
 cholesteryl laurate-cholesteryl caprylate (75 wt.%), polymorphic behaviour, optical, elec. and dielec. meas. 0-65208
 trans-decalene-cyclohexane liq. mixtures, hole mobility, percolation model 0-65551
 diphenylanthracene in benzene soln., extrinsic photocond. kinetics 0-92691
 ethane, gas, liq., and crit., electron mobility, density and temp. effects 0-92246
 fluid, two dims. motion, mag. field evolution, anti-dynamo theorem extension (*Russian*) 0-59127
 glass melt, multiphase electric current field (*Czech*) 0-84310
 hexafluorobenzene liq., electron mobility, percolation model 0-65551
 hexafluorobenzene-benzene liq. mixture, electron mobility, percolation model 0-65551
 n-hexane-ethanol liq. mixtures, electron mobility, percolation model 0-65551
 'Impul's' conductometer (USSR), elimination of dilute soln. instability 0-77813
 low conductivity media, unipolar injection, forced diffusion model 0-92692
 metals of groups IIB, IIIB, and IV, thermoelectric power, pseudopotential calc. 0-59959
 methanol solution in benzene, dielec. relax. time by RF cond. meas. 0-71302
 microemulsion system, existence of bicontinuous zone 0-104466
 microemulsions, light scattering, rel. tp percolation phenomena 0-104467
 organic liquid conductivity and bulk charge determ. cell (*Russian*) 0-57328
 polar liquids in double layer capacitors, RF conduction, ion diffusion effect 0-107883
 polar molecules, viscosity activation energy and relax. time, RF cond. meas. 0-96677
 pyridine, macroscopic model for solvated ion dynamics, cation conductance calcs. 0-65261
 rubrene, in benzene soln., extrinsic photocond. kinetics 0-92691
 semiconductor, Hall conductivity in random-phase model 0-65599
 silicone oil, ionic behaviour, carrier mobility and viscosity 0-107453
 thermal props. at high temp. 0-75536
 thin film thickness measurement, conductometric method 0-77751
 toluene, gaseous, critical and liquid, electron transport 0-64673
 water-toluene-sodium dodecyl sulphate-butanol 1 mixture, interface light scatt., interface tension meas. 0-76039
 α -AgI, activation vol. for ionic cond., appl. to molten salts 0-59711
 Ar, condensed, electron drift, Davydov electron energy distribution function, diffusion (*Russian*) 0-80339
 Au-Ge-Si, influence of struct. on elec. resist. of glass forming alloys 0-65518
 CaF₂, melts, elec. cond., surface tension, viscosity, density (*Russian*) 0-92758
 CaF₂-MgO-SiO₂, melts, elec. cond., surface tension, viscosity, density (*Russian*) 0-92758
 CaF₂-MgO(SiO₂), melts, elec. cond., surface tension, viscosity, density (*Russian*) 0-92758
 Cd-Zn binary systems, melts, elec. resist., 0-700°C 0-65517
 CdTi₂(Te₂)₂:Au, elec. cond., density, dielectric const., changes on fusion 0-88553
 Cu alloys, and thermal cond. 0-103661
 Cu, and thermal cond. 0-103661
 Cu-Al(Ga)(In) alloys, temp. and conc. depend., model interpret. and alloy struct. (*Russian*) 0-88528
 D-T, liq., dielectric constant and elec. cond. 0-84680
 Eu, electrical resistivity of solid and liquid phases, thermopower, melting temp. 0-59955
 GaAs, electrical conductivity and thermoelectric power charge due to melting 0-100490
 GeSe₂-As₂Se₃-Sb₂Se₃, elec. cond. over wide range of temp. 0-88564
 Hg, melting line determ., pressures up to 1200 MPa 0-84281
 Hg, supercritical, elec. cond., four electrode method 0-62685
 In, liq., thermal props. at high temp. 0-75536
 In-Zn binary system, melts, elec. resist., 0-700°C 0-65517
 InAs, electrical conductivity and thermoelectric power charge due to melting 0-100490
 Ir, thermophysical props. at temps. up to 7000K 0-103497
 Li-Cd alloy, elec. resist. and Knight shift 0-75537
 Li-Mn liquid alloys, form factor effects, pseudopotentials, resist. calc. 0-103608
 Li-Pb liquid alloys, elec. resistivity, negative temp. coeff. 0-88527
 Mo, elec. resist., melting pt. to boiling pt., temp. depend. 0-96839
 Na, linear pot. and elec. resist., calcs. 0-65519
 Pb, liq., elec. resist. calcs., pseudopot. depend. 0-96840
 Pd-Au-Si, influence of struct. on elec. resist. of glass forming alloys 0-65518
 Pt, thermodynamic characterisation, by isobaric expansion meas. 0-103494
 Sc₂O₃, liq. and solid phase elec. cond., high temp. meas. 0-84468
 Sc₂O₃, solid and liq. phases, thermophysical and electrophysical props. 0-103495
 Se, electronic transport props., equation of state, to 1900K and 1800 bars 0-65574
 Se, liq., dielectric relax. and elec. cond. 0-108150
 Se-Tl-S alloys, liq., dielectric relax. and elec. cond. 0-108150
 Sn-Te, molten, elec. cond. and phase diagram 0-84454
 Te-transition metal, liq. semicond., elec. props. 0-96870
 Ti, elec. resist., melting pt. to boiling pt., temp. depend. 0-96839
 Ti, liq., thermal props. at high temp. 0-75536

electrical conductivity of liquids continued

- Tl-Pb, in solid and liquid state, specific electric resistance 0-103662
 TlTe, melt, elec. cond., surface tension, microhardness, influence of impurities 0-88551
 Tl₂Te, melt, resistivity, surface tension, microhardness, influence of impurities 0-88552
 Tl₂(Te,Se_{1-x}) mixtures, magnetic susceptibility and elec. cond. 0-88715
 V, elec. resist., melting pt. to boiling pt., temp. depend. 0-96839
 V, thermophysical props. at temps. up to 7000K 0-103497
 W, elec. resist., melting pt. to boiling pt., temp. depend. 0-96839
 Y, electrical resistivity of solid and liquid phases, thermopower, melting temp. 0-59955
 Y₂O₃, liq. and solid phase elec. cond., high temp. meas. 0-84468

electrical conductivity of one-dimensional systems see one-dimensional conductivity**electrical conductivity of plasmas see plasma transport processes****electrical conductivity of solids**

see also *electrical conductivity of amorphous metals and alloys; electrical conductivity of amorphous semiconductors and insulators; electrical conductivity of crystalline metals and alloys; electrical conductivity of crystalline semiconductors and insulators; electronic conduction in crystalline semiconductor thin films; electronic conduction in insulating thin films; electronic conduction in metallic thin films; ionic conduction in solids; recovery; superconductivity*

- Anderson model, non-orthogonal elec. resist. 0-59947
 anisotropic percolation, square random network conductivity (*French*) 0-68142
 binary crystals, electrical conductivity versus interatomic bond character 0-59948
 body with large number of cracks, effective cond. taking into account capacitance and action of mech. loads 0-84242
 cellulose acetate membrane, asymmetric, elec. and electroosmotic transport behaviour in dialysis-osmosis expts. 0-108745
 cermet film granular media, dielectric function theory, permittivity, percolation transport props. 0-88498
 disordered electronic systems, spin interaction effects, loop expansion and exact relations among local gauge invariant modes 0-80221
 disordered Fermi systems, in two dimensions, interaction effects 0-75655
 disordered materials, fluctuation-induced tunnelling cond. 0-65516
 disordered system, AC cond. tensor in mag. field 0-92870
 dithiocarbamate complexes of Cr, Mn, Sn and Pb IR, electronic and mass spectra, mag. susceptibility, cond. meas. 0-97270
 epoxy polyester, PE-933, metal-filled, elec. cond., theory and expt. 0-60057
 fibre reinforced composite, single ply, thickness effect on percolation and conductivity 0-92953
 graphite intercalation cpds., high elec. cond., engineering appl. 0-70780
 graphite intercalation cpds. with AsF₆ and SbF₆, synthesis and elec. props. 0-70781
 graphite nitrates, elec. props. perpendicular to layers, resistance, magnetoresistance, charge transport mechanisms 0-80268
 graphite salts, C₈M_F (M=Os, Ir, As), struct. and elec. props. 0-70183
 graphite/epoxy composite, single ply, elec. cond. meas. 0-92953
 hopping conduction, master eqn. approach in presence of mag. field 0-103697
 inflowing structure, Anderson localisation, elec. cond. temp. depend. (*Russian*) 0-103639
 inhomogeneous conductors, cond. anisotropy and Hall effect near percolation threshold 0-107755
 Israel Physical Society 1980 annual meeting, Rehovot, Israel (April 1980) 0-94909
 layered structures, intercalation, crack propag. theory 0-97559
 magnetic semiconductors, critical behaviour of electronic properties, theory 0-96861
 metallic fibre reinforced composite materials 0-100450
 Mott's formula for thermopower and for Wiedemann-Franz law 0-84462
 multicomponent percolation, conduction 0-92871
 nonuniform systems, effective conductivity from percolation and conduction theory 0-62597
 one dimensional disordered system, cond. and electron localisation 0-103658
 one-dimensional electron system, distorted, dynamical elec. cond. calc. 0-59962
 percolation in square lattice, temp. depend., effective medium theory 0-96837
 percolation network samples, cond. near crit. point 0-105578
 phosphate glass-Al alloy seals, and mech. props., glass transition 0-81018
 polymer, metal-filled, elec. cond., theory and expt. 0-60057
 polymer/metal powder compacts, cond. threshold, particle size ratio effect 0-80337
 polymeric conductors and graphite intercalation cpds., struct. and phys. props., symposium, San Jose, USA (March 1979) 0-62379
 projection operator formalism appl. to cyclotron reson. on semicond. surfaces 0-88524
 PVC-C composite, fluctuation-induced tunnelling cond. 0-65516
 PVC-Cu composites with chemically deposited ultrafine copper particles 0-93534
 quasi-two dimensional conductor, galvanomagnetic props., optical analogy (*Russian*) 0-60108
 random trees theory, appl. to conductance networks 0-65515
 serum albumin, bovine, hydrated, dielec. and elec. props. 0-97854
 site percolation, infinitesimal renormalisation group transform. 0-88525
 site percolation threshold in random networks 0-80241
 solid state physics, book 0-101676
 spin glasses, elec. resist., thermal resist. and thermopower 0-65542
 superconductors, granular, percolation model, specific heat, elec. resistance 0-93025
 thermally stimulated relaxation in solids, transport phenomena, book 0-77553
 titanomagnetite sand from New Zealand, density, elec. and mag. prop. 0-98311
 TTF-TCNQ, anisotropic cond., X-ray effects 0-96855
 TTF-TCNQ complex, trans-diethyl-dimethyl TTF-TCNQ, one-dimens. cond. 0-96853
 two-dimensional disordered systems, effects of interactions on non-metallic behaviour 0-92869
 wustite solid solns., props. connected with localised electron state 0-107734

electrical conductivity of solids continued

- Ag particles embedded in dielec. KCl medium, search for maximum metallic resist. 0-107756
 Ar, condensed, electron drift, Davydov electron energy distribution function, diffusion (*Russian*) 0-80339
 C films with high conductivity, prep. and props. 0-80983
 $C_{12}^{-2}PtF_6$, struct. and elec. props. 0-70183
 $Cr_{3.2}Se_4$, struct., elec. and mag. props. 0-107160
 $CsSnI_3$, surface props., Auger study, elec. cond. meas., photochem. study 0-66339
 Cu powder, sp. ht. cond. and sp. elec. cond. meas., Wiedemann Franz Lorenz law (*German*) 0-92872
 $ErFe(CN)_6 \cdot 5H_2O$, powder, elec. transport props. obs. 0-70701
 Fe, carbonyl powder, specific elec. conductivity, 5 to 200 MPa (*German*) 0-70664
 $Fe-Al_2O_3$ granular films, superparamagnetism and relax. effects 0-71118
 $HoFe(CN)_6 \cdot 5H_2O$, powder, elec. transport props. obs. 0-70701
 I, metallic, mol. and monatomic phase, elec. resist. at high press. and low temp. 0-65638
 IrO_2 film, A-C response 0-107926
 $KClO_4$, AC electrical conductivity meas. between temp. range 25-325°C, automated technique 0-59699
 $KClO_4:CrO_3^{2-}(SO_4^{2-})$, AC electrical conductivity meas. between temp. range 25-325°C, automated technique 0-59699
 $Mn-SiO_2$, annealed cermet films, elec. resist., composition depend. 0-97007
 $MoSi_2$ refractory formation by As^+ ion beam bombardment 0-107286
 Na-zeolite, matrix, Te cluster superlattices, N and S type volt-ampere characts., elec. cond. (*Russian*) 0-70665
 $Pt-SiO_2$ cermet films, struct. and props. 0-96956
 $ReSi_2$, atomic volume deviations and supercond. T_c and elec. cond. 0-75203
 $TaSe_2-Se_2$ (1T), transport props. 0-103710
 $TaSi_2$ refractory formation by As^+ ion beam bombardment 0-107286
 $TeO_2-MoO_3-V_2O_5$, phase comp. determ. using X-ray diff., electron microscopy and DTA (*German*) 0-88046
 UC, UC_2 , U_2C_3 , and $UC+UC_2$, elec. resist., 4 to 1900K 0-59953
 WSi_2 refractory formation by As^+ ion beam bombardment 0-107286
 $YbFe(CN)_6 \cdot 5H_2O$, powder, elec. transport props. obs. 0-70701
 ZrO_2 stabilised with lime at high temp. (*Rumanian*) 0-65575

electrical conductivity transitions

- see also metal-insulator transition
 chalcogenide glass films, threshold switching 0-96950
 chalcogenide glasses, memory effect, local doping, switching 0-107873
 inhomogeneous thin amorphous chalcogenide films, reversible switching, thermal stability criteria 0-70856
 MIM, thin film, use as non-heated source of electrons, review 0-84516
 MIS diode, thin-insulator, switching phenomena, current-control-type negative resist. characts. 0-107915
 MOS capacitor, direct current/voltage relns. as function of oxide doping 0-88635
 photodiode, switching process and plasma effects, theory 0-65667
 phthalocyanine layers, metal-free, between Ag and Al electrodes, switching effects 0-65706
 polyacetylene:AsF₆, thermopower and transport props. 0-65611
 polyacetylene:SbF₆, elec. cond. meas. 0-60055
 polyacetylene, doped, elec. cond. and thermopower 0-96951
 polyacetylene, doped, fluctuation-induced tunnelling cond. in metallic regime 0-65516
 polyacetylene films, doping effect on elec. cond., chem. and optical props. 0-65572
 PVC in metal sandwich struct., switching props., voltage- and current-controlled negative resist. 0-103767
 semiconductors with impurities, electron cond. temp. and freq. depend., two band model (*Russian*) 0-75564
 TCNQ salt, dibenzo-TTF-TCNQCl₂, one-dimens. mag. semicond., mag. and elec. props. 0-88601
 TCNQ salt, MEM(TCNQ)₂, dielec. const. obs., DC and microwave cond. obs. 0-59663
 (TMTSF)₂PF₆ (AsF₆), linear-chain conductor, semicond.-metal transition in small elec. field 0-103730
 $Fe_2O_3-Bi_2O_3$ sintered material, elec. switching effects due to thermal ionic breakdown (*Korean*) 0-70776
 $Ag_{2.1}W_{0.9}O_{16}$, solid electrolyte, anisotropic elec. cond., low temp. phase transitions 0-65289
 Ag₂Se thin film, switching and Ag movement, point contact technique 0-60107
 AlB₁₂, α - and β -forms, elec. props. at high temps. and in strong elec. fields, thermistor appls. 0-92903
 $As_{10}Ge_{15}Te_{75}Ag_x$ glass, elec. and dielec. props., Ag additions effect 0-65558
 As₂S₃ film, evaporated, switching effects 0-96952
 B, β -rhombohedral, elec. props. at high temps. and in strong elec. fields, thermistor appls. 0-92903
 BN films, humidity sensitive elec. props. and switching characts. 0-107938
 C films with high conductivity, prep. and props. 0-80983
 CuB_{24} , elec. props. at high temps. and in strong elec. fields, thermistor appls. 0-92903
 $CuCl$ powder compacts, DC voltage depend. resist. under press. 0-80334
 $\alpha-Fe_2O_3$, elec. resist. and phase transition under shock compression 0-72496
 $Fe_2O_3-Bi_2O_3$ sintered material, elec. switching effects for temp. range 700-850°C (*Korean*) 0-70775
 GaAs, electrical conductivity and thermoelectric power charge due to melting 0-100490
 GaAs:Fe, p-n-n struct., photoelec. props. 0-107862
 GaAs:Fe reverse biased p-n-n struct., switching effect 0-88628
 GaAs:O, electrolum., photolum., negative differential resist. rel. to recomb. processes 0-66304
 GaAs(P), semiconductor-metal transition, press. calibration above 100 kbars fixed points 0-77808
 GdBr₃ single crystals, mag. behaviour and structure change at low temp. 0-71018
 Ge-S-Ga amorphous thin film, memory switching effects 0-88605
 $Ge_{20}Bi_2Se_{80-x}$, semicond. glass, resist., thermoelec. power, optical absorpt. 0-88555
 $Ge_{20}Bi_2Se_{80-x}Te_{10}$, semicond. glass, resist., thermoelec. power, optical absorpt. 0-88555
 $Ge_{1-x}Sn_xTe$ film, amorphous, elec. cond. 0-93016

electrical conductivity transitions continued

- Hg-Xe vapour deposited films, cond. transitions, effect of disorder on supercond. 0-88659
 I, metallic, mol. and monatomic phase, elec. resist. at high press. and low temp. 0-65638
 InAs, electrical conductivity and thermoelectric power charge due to melting 0-100490
 InAs, two dimensional accumulation layer, Anderson localisation 0-107871
 InAs-GaSb superlattices, mag. field induced semimetal-semicond. transition 0-65656
 n-InP, impurity and minimum metallic cond. in mag. field 0-103731
 In_2S_3 , single crystal, switching effect and memory (*Russian*) 0-70774
 $InSb_{1-x}Bi_x$, multitarget RF sputtering, metastable phase, conductivity transition 0-76178
 $KTa_{0.7}Nb_{0.3}O_3$, pressure-induced resistance and colour change obs. 0-75608
 LiAl, anomalous elec. resistivity near critical composition 0-103673
 $LiNH_4SO_4$, DC elec. cond. 0-88603
 $Mg, Fe_{1-x}O_x$, polycryst., Verwey type transition, resist., magnetisation, Mossbauer effect and permeability obs. 0-75764
 $Na_2O-B_2O_3-Bi_2O_3$ glass with metallic Bi granules, elec. cond. 0-84493
 $Na_2Se_2P_2O_7$, fast-ion conductor, struct. phase transition 0-88362
 NbO_2 , on-state decay rel. to recomb. and nonlinear props. 0-84492
 $Nd_{1-x}Ca_xVO_3$, solid solutions, elec. props. 0-96866
 $PbO-B_2O_3-Bi_2O_3-Bi_2O_3$ glass with metallic Bi granules, elec. cond. 0-84493
 Pr, localised 4f shell breakdown under press. 0-70411
 S-Ni-Fe system containing monosulphide solid soln., elec. and struct. relations 0-90038
 Sb_2S_3 , defect drift in elec. fields and bistable switching 0-92947
 Se, metallic state, press. induced, elec. cond. meas. 0-96949
 Se powder compacts, sintered, electrical cond. 0-70693
 Si, amorphous films, RF sputtering prep. at high Ar press., props. obs. 0-80418
 Si amorphous films, switching, electrothermal model 0-80407
 p-Si, elec. resist., shock wave compression effects 0-80265
 Si film, amorphous, hopping cond. control by ion bombard. induced struct. modification 0-92898
 Si, metallic state, press. induced, elec. cond. meas. 0-96949
 Si, static compression in [100] and [111] directions, elec. resist. obs. 0-65637
 Si/ In_2O_3 -SnO₂ thin film junctions, polarity dependent memory switching effects 0-70814
 $(Sm_{1-x}Gd_x)_2S_4$ mixed valence compound, elec. cond. transition 0-70777
 SnO_2 , O chemisorption, elec. cond. and EPR meas. correlation 0-84369
 $SrCl_2$, fast ion cond., specific heat anomaly, mol. dynamics study 0-65283
 $SrCl_2$, ionic cond., self-diffusion, rel. to defect motion, mol. dynamics study 0-65282
 Ta_2 (1T) electron irradiated, lattice contraction 0-59520
 Te, metallic state, press. induced, elec. cond. meas. 0-96949
 $Te_{50-x}Se_{50}Sn_x$, thin films, elec. cond. and thermoelectric power meas. (*French*) 0-80335
 Ti-Se, liquid mixtures, press. effect on two-phase region 0-75347
 TlTe, melt, elec. cond., surface tension, microhardness, influence of impurities 0-88551
 U_3O_{8-x} phase transition to U_6O_{21+x} study by elec. cond. meas. 0-100489
 VO_2 single cryst., noise in presence of current filament 0-92952
 VO_2 single crystal, elec. switching 0-92946
 V_2O_5 , impurity doping effects, elec. props. obs. 0-75609
 $V_2O_5-P_2O_5-Nb_2O_5$ glasses, switching 0-88604
 WO_3 , semiconductor-metal transition, structural phase transition 0-107870
 $ZnIn-S_4$ crystals, switching effect, electric field distribution 0-107872
 $ZnIn-S_4$, S-type negative resist. and switching effects 0-65581
 $ZnTe(S)$, semiconductor-metal transition, press. calibration above 100 kbars fixed points 0-77808

electrical contacts

- see also contact potential; contact resistance; ohmic contacts; point contacts
 pulsed high currents in Tokamak device, design and testing 0-70029
 Ag in H₂S atmospheres, formation of contaminating layers (*German*) 0-71811
 Ag-Zn, internally oxidized, elec. contact characts., alloying additions effect (*Japanese*) 0-88619
 AgCdO, powder metallurgy production, for switchgear in power engineering 0-104094
 Al-Au couple, electroformed, nonohmic characts. and electron emission 0-60066
 Al-Cr, thin film metal contact, sheet resistance changes 0-80356
 Au surface, lubrication by plasma-deposited thin films of fluorocarbon polymer 0-89157
 Au-Cd, Hg_{1-x}Te(CdTe) contacts, photo-effect in the 77-300K range, barrier height estimation 0-107850
 Bi₂Te₃, surface prep. by etching for electroplating elec. contacts 0-108647
 Cu H₂S atmospheres, formation of contaminating layers (*German*) 0-71811
 Cu, slip ring, elemental surface composition as function of temp. 0-66901
 In-Cd, Hg_{1-x}Te(CdTe) contacts, photo-effect in the 77-300K range, barrier height estimation 0-107850
 Pd-Ag in H₂S atmospheres, formation of contaminating layers (*German*) 0-71811
 Si device metallisation, TiN and TaN as diffusion barriers 0-65304
 Si solar cells, low cost, Ni contacts 0-94017

electrical engineering

- see also high-voltage engineering
 electrical and electronic engineering undergraduate courses, engineering design importance 0-67972
 electronics, undergraduate laboratory course 0-105478

electrical engineering applications of computing see electrical engineering computing**electrical engineering computing**

- see also computerised control; computerised instrumentation; power system analysis computing; power system CAD
 dry etched line edge profiles 0-71780
 electric field computation using SCOFF program (*German*) 0-78740

electrical engineering computing continued

ion milling, string segment motion algorithm 0-71779
 solar energy DC-AC inverter design, effect of meteorological conditions, computer simulation 0-61373
 toroidal field coils, EM parameters calcs. of current paths in homogeneous media (*Japanese*) 0-106155
 transformer oil diagnosis (*Czech*) 0-97744

electrical fault location *see* **fault location****electrical forming** *see* **electroforming****electrical insulation** *see* **insulation****electrical noise** *see* **noise****electrical power systems** *see* **power systems****electrical properties of substances**

see also **dielectric properties of substances; discharges (electric); electric conductivity; flexoelectricity; thermoelectricity**
 No entries

electrical resistance measurement *see* **electric resistance measurement****electrical transport processes** *see* **electrical conductivity****electricity**

see also **atmospheric electricity; electric charge; electric current; electrical properties of substances; electromagnetism; terrestrial electricity**
 theory of, book 0-86051

electricity supply industry

advanced reactor and fuel cycle systems, potentials and limitations for United States utilities 0-106106
 biological risk involved in power production 0-98209
 effects of world energy resources on economy (*German*) 0-89583
 FBR, electric power generation, research, development and demonstration, risk and timing 0-57837
 thermal energy storage, US DOE research program for aquifer waste heat utilisation 0-97808
 tidal power stations, technical details and operating experience 0-72009
 underground pressurised saturated hot water storage for peak lopping appls. 0-76653
 wind energy conversion systems, value to electric utility, economic model 0-61257

electro-optical devices

see also **electrochromic devices; liquid crystal devices; optical modulation; Q-switching**

active optical devices, seminar, San Diego, CA, USA (August 1979) 0-101664

bistable devices, optical regenerative oscill. and monostable pulse generation 0-106612

bistable mirrorless device, monostable pulse generation and optical regenerative oscill. 0-96002

bistable optical device development from integrated two-arm interferometer, appls. (*French*) 0-69555

bistable optical devices, overshoot switching 0-58776

ceramics, transparent ferroelectric, composition selection for appl. in light modulators (*Russian*) 0-91869

channel waveguide interferometric modulator for EM field detection 0-74498

conference, Minneapolis, MN, USA (June 1979) 0-77535

deflector of blazed grating type, multistage system 0-106625

discharge gap characts., laser-radiation-triggered, influence of discharge medium, electrooptic switch control appls. 0-64818

electric field intensity meas., electro-optical sensor with fibre transmission line 0-69509

electrical resistivity meas. method, using electrooptic cryst. voltage-induced birefr. 0-73386

electrostatic field distribution calc. (*Russian*) 0-87514

fact directional coupler switch/modulators, novel ps optical pulse sampling method 0-58784

ferroelectrics, photoelectric states in real time spatial light modulators, photorefractive effect 0-80676

GaAs homojunction rib waveguide directional coupler switch 0-69554

heterostructure planar waveguides guided-to-radiation mode conversion and appl. to light modulation 0-87557

hologram electronic heterodyne recording and self-interference term rejection 0-91756

holographic one-tube goggle system engineering 0-78988

imagery, 2-D sampled, aliasing and blurring effects 0-99635

integrated optics, electrooptical channel waveguide matrix switch using total internal reflection 0-58810

integrated optics sub-ps gate 0-58809

interference polarisation filter, Q-switching ruby laser with high-frequency control of lasing conditions 0-74363

laser modulator for optical coherent transient generation 0-102776

laser pulse shaping on multiple rot. lines, using electro-optical cryst. modulator 0-78879

laser unequal path interferometer with electro-optical camera and mini-computer, fabrication/test appl. 0-77847

light modulator with small nonactive losses 0-78981

light shutter array, large area electronically controllable, using polyvinylidene fluoride bimorph vanes 0-58696

linear interferometric modulator for electromagnetic field detection 0-58782

liquid crystal electro-optic switch, four-port, for unpolarised fibre light 0-58715

Mach-Zehnder type modulator, RF modulation characts. meas. method 0-74480

Michelson interferometer, active stabilization by electrooptically tuned laser 0-86386

modulator, asymmetrical, electric field config. anal. (*Russian*) 0-91885

multicavity IR electro-optical tunable filter 0-102831

multivibrator operation, in optical bistable device 0-58674

nephelometer, integrating, characterisation of nonspherical atm. aerosol particles 0-77106

optical preprocessor, use in Earth-resources satellites 0-67430

phase contrast microscope attachment for weak phase object visibility 0-86396

photopolarimeter, electrooptic four-modulator, for Mueller matrix meas. 0-73417

picosecond optical sampling, cascade of waveguide interferometers driven by microwaves 0-99849

Pockels cell driver of fast rise time and high repetition rate using thyatron 0-69537

Pockels cell modulator, max. depth of light modulation 0-102819

electro-optical devices continued

Pockels cells, optically timed, electrooptic prepulse suppression for fusion laser systems 0-102743

polarisation-conversion wavelength-selective fibre switches 0-58736

reflector, controlled, temp. fields, thermal distortions 0-96021

remote sensing multichannel data sets, integrated optical comparator 0-64213

ruby laser with electrooptical shutter, emission spectrum narrowing and single freq. giant pulse lasing 0-78877

semiconductor ridged waveguides for electrooptic radiation modulators 0-91925

shutter for laser pulse shaping, Pockels cell with programmable transmission control 0-64162

space-time light modulator 0-69526

spatial light modulator resolution, stored point charge effects 0-106616

surface prism laser deflector, for field destructive interference 0-87492

system aspects of electro-optics, seminar, Huntsville, AL, USA (May 1979) 0-94921

system manufacture, test and process control changes 0-96044

systems analysis using two-dimensional FFT algorithm 0-78986

thin film electrooptic deflector using induced grating with variable blaze angle 0-99862

three-dimensional topographic mensuration, laser electro-optic system 0-99784

travelling wave optical modulator using a directional coupler LiNbO₃ waveguide 0-96035

tunable filters, programmable 0-102830

tunable filters and polarisation conversion devices 0-102829

turbidity meter, multichannel 0-67423

video signal conversion device for SEM 0-57423

Bi₁₂SiO₂₀ PROM device, image recording and erasure mechanism 0-74490

CdTe crystal Pockels modulator, PCM of CO₂ TEA laser pulse 0-102742

GaAlAs light intensity modulators using p-n junctions 0-99871

GaAs 400 MHz TW laser modulator 0-87541

GaAs, Franz-Keldysh effect modulator parameters for integrated optics systems 0-106624

GaAs-Al_xGa_{1-x}As electro-optic frequency- and polarisation-modulated injection laser 0-91810

KD₂PO₄ crystal, electro-optical extraction of Nd:YAG laser pulses (*German*) 0-87416

KD₂PO₄ crystal electron-beam spatial light modulator, resolution 0-74503

KD₂PO₄ photo-spatial light modulator, optical data processing 0-102839

KH₂PO₄ electro-optic modulator crystals, piezoelec. induced acoustic transients 0-70316

LiNbO₃ crystal two-stage electrooptic deflector 0-106625

LiNbO₃ waveguide, planar electro-optic prism array beam splitter 0-64209

LiNbO₃ waveguide modulators and switches, Ti-diffused, fabrication on directional coupler principle 0-83678

LiNbO₃:Ti, coupled waveguided TE/TM mode splitter 0-64142

LiNbO₃:Ti, planar optical waveguides, processing and props. 0-78965

LiNbO₃:Ti channel waveguide high-speed cutoff modulator 0-64195

LiNbO₃:Ti diffused optical waveguide, guided light scatt. sources 0-78966

LiNbO₃:Ti diffused optical waveguide, efficient tapered gap prism coupling 0-78967

LiNbO₃:Ti digitally driven integrated optics amplitude modulator 0-58808

LiNbO₃:Ti electro-optic TE-TM mode convertor structure 0-64215

LiNbO₃:Ti optical branching waveguide, characts. 0-83681

LiNbO₃:Ti optical waveguide electrooptic devices polarisation independ. directional coupler switch and wavelength filters 0-58783

LiNbO₃:Ti phase-matched waveguide electro-optic TE=TM mode convertor 0-58749

LiNbO₃:Ti single mode electrooptic waveguide modulator, high-speed operation 0-91915

LiNbO₃:Ti waveguide electro-optic TE=TM mode converter-wavelength filter 0-64210

Nd³⁺:YAG laser, high repetition rate electrooptic Q-switching, birefringence 0-69430

PLZT ceramic, modulator for optical communication 0-78964

PLZT electro-optic shutter stereoscopic display applications 0-90826

PLZT/TFPD thermal/flash protective lens assembly, polarised delamination investigation 0-78929

PLZT/TFPD thermal/flash protective lens assembly, polarised delamination investigation 0-78929

PLZT/TFPD thermal/flash protective lens assembly, polarised delamination investigation 0-78929

PLZT/TFPD thermal/flash protective lens assembly, polarised delamination investigation 0-78929

PLZT/TFPD thermal/flash protective lens assembly, polarised delamination investigation 0-78929

PLZT/TFPD thermal/flash protective lens assembly, polarised delamination investigation 0-78929

PLZT/TFPD thermal/flash protective lens assembly, polarised delamination investigation 0-78929

PLZT/TFPD thermal/flash protective lens assembly, polarised delamination investigation 0-78929

PLZT/TFPD thermal/flash protective lens assembly, polarised delamination investigation 0-78929

PLZT/TFPD thermal/flash protective lens assembly, polarised delamination investigation 0-78929

PLZT/TFPD thermal/flash protective lens assembly, polarised delamination investigation 0-78929

PLZT/TFPD thermal/flash protective lens assembly, polarised delamination investigation 0-78929

PLZT/TFPD thermal/flash protective lens assembly, polarised delamination investigation 0-78929

PLZT/TFPD thermal/flash protective lens assembly, polarised delamination investigation 0-78929

PLZT/TFPD thermal/flash protective lens assembly, polarised delamination investigation 0-78929

PLZT/TFPD thermal/flash protective lens assembly, polarised delamination investigation 0-78929

PLZT/TFPD thermal/flash protective lens assembly, polarised delamination investigation 0-78929

PLZT/TFPD thermal/flash protective lens assembly, polarised delamination investigation 0-78929

PLZT/TFPD thermal/flash protective lens assembly, polarised delamination investigation 0-78929

PLZT/TFPD thermal/flash protective lens assembly, polarised delamination investigation 0-78929

PLZT/TFPD thermal/flash protective lens assembly, polarised delamination investigation 0-78929

PLZT/TFPD thermal/flash protective lens assembly, polarised delamination investigation 0-78929

PLZT/TFPD thermal/flash protective lens assembly, polarised delamination investigation 0-78929

PLZT/TFPD thermal/flash protective lens assembly, polarised delamination investigation 0-78929

PLZT/TFPD thermal/flash protective lens assembly, polarised delamination investigation 0-78929

PLZT/TFPD thermal/flash protective lens assembly, polarised delamination investigation 0-78929

PLZT/TFPD thermal/flash protective lens assembly, polarised delamination investigation 0-78929

PLZT/TFPD thermal/flash protective lens assembly, polarised delamination investigation 0-78929

PLZT/TFPD thermal/flash protective lens assembly, polarised delamination investigation 0-78929

PLZT/TFPD thermal/flash protective lens assembly, polarised delamination investigation 0-78929

PLZT/TFPD thermal/flash protective lens assembly, polarised delamination investigation 0-78929

PLZT/TFPD thermal/flash protective lens assembly, polarised delamination investigation 0-78929

PLZT/TFPD thermal/flash protective lens assembly, polarised delamination investigation 0-78929

PLZT/TFPD thermal/flash protective lens assembly, polarised delamination investigation 0-78929

PLZT/TFPD thermal/flash protective lens assembly, polarised delamination investigation 0-78929

PLZT/TFPD thermal/flash protective lens assembly, polarised delamination investigation 0-78929

PLZT/TFPD thermal/flash protective lens assembly, polarised delamination investigation 0-78929

electro-optical effects continued

- DNA, calf-thymus and superhelical PM2 aq. solns., electro-optic obs. of γ -irrad. damage 0-85452
- DNA, dye labelled elec. dichroism and birefringence, comparison with mol. props. from polarised fluoresc. 0-84785
- DNA, Hg (II) and Ag (I) complexes in soln., theoret. interpret. of elec. dichroism obs. 0-85347
- DNA solution, elec. birefringence, stabilised induced dipole behaviour 0-85349
- EBBA, IR absorpt. spectra, elec. field effects, orientational order parameter determ. by IR dichroism, bend elastic consts. 0-80778
- electric current and voltage meas. using laser light (*Japanese*) 0-86342
- electric dichroism measurement instrument with digital processing 0-82800
- electro-optic crystals, hologram formation arbitrary transport length anal., photovoltaic effects 0-78802
- fast insulator surface flashover in vacuum, mechanism, electro-optical investig. 0-103206
- ferroelectric semiconductors, appl. to optical storage (*Russian*) 0-80749
- graded index planar lightguide, electrooptical diffraction 0-78995
- holographic recording in electrooptic crystals, photogalvanic effect mechanism of nonlinear wave interaction 0-102672
- hydroscopic particle humidification process, electrooptic scatt. meas. 0-77107
- laser beam propagating in liquid, polarization, DC elec. field influence 0-91828
- liquid crystal alignment films prod. by RF plasma beam technique 0-76198
- macromolecular solution, alternating elec. field light scatt., low angle approx. 0-84721
- macromolecular solution, dynamic light scatt. by flexible macromols. in fluctuating elec. field 0-84722
- macromolecular solution, rot. diffusion coeff. calc. method w.r.t. mol. struct., elec. birefringence relax. time data interpret. 0-85331
- macromolecular solution, transient elec. birefringence in reversing fields of arbitrary strength and duration 0-84719
- macromolecules and colloids, conf., Uxbridge, England (Apr. 1978) 0-82577
- materials for modulator, display, and storage appls., review 0-74450
- MBBA, IR absorpt. spectra, elec. field effects, orientational order parameter determ. by IR dichroism, bend elastic consts. 0-80778
- MBBA, positive space charge influence on texture, domain form. factor, polarised light study 0-88037
- MBBA-EBBA, controllable liq. cryst. transparency, electrooptical characts. 0-78996
- MIS photosensitive high resolution struct., spatial light modulation with liq. cryst. 0-96026
- nematic liquid cryst., ZhK-440, transparency, electrooptical characts. 0-78996
- nematic liquid cryst. mixture, ZLI-207, nonideally oriented layers, Fredericksz transition dynamics 0-100163
- nematic liquid crystal, elect. conduct. based on injection-contact phenomena theory (*Russian*) 0-107807
- nematic liquid crystal transducers, dynamic scatt., pre-excitation 0-88021
- p-n-nonyloxybenzoic acid, smectic C phase, electro-optical effect (*Russian*) 0-92458
- nucleosomes and nucleosomal DNA, electro-optical props., relax. times and chain struct. 0-85350
- 4-n-octyl-4'-cyanobiphenyl/4-n-decyl-4'-cyanobiphenyl mixture, dynamic characts. of electrooptical effect with memory 0-108183
- trans-p-n-octyloxy- α -methyl-p'-cyanophenyl cinnamate, mag. and elec. birefr. in isotropic phase 0-80744
- parametric effects anal., in optics 0-102619
- phase shifting at 94 GHz using bulk crystals, microwave electro-optic coeffs. determ. 0-71382
- PLZT coarse-grained solid solutions, electro-optical processes induced by longitudinal electric field (*Russian*) 0-80750
- poly-4-vinylpyridine, electro-optic study of conformational changes induced by heavy metal ions 0-84725
- polydisperse dilute suspensions, of rod-like particles, anisotropy of electric polarisability 0-85224
- polyelectrolytes, saturation of induced dipole moment, orientation mechanism and electro-optical effects 0-84785
- polynucleotide solution, elec. birefringence, stabilised induced dipole behaviour 0-85349
- polynucleotide solution, elec. field induced orientation and effects 0-85348
- polypeptides, ionic and non-ionic, electro-optical studies of conformation 0-71379
- polyribonucleotides, dye tagged, aqueous solns., elec. induced fluoresc. changes 0-85346
- polyvinylidene fluoride, electro-optic and elasto-optic effects 0-80754
- polyvinylidene fluoride, thermodynamic model and appl. 0-75955
- purple membrane fragment suspensions, elec. dichroism obs., trimer model interpret. 0-89728
- quartz, electro-optical props. near phase transition 0-80756
- relaxation distribution function, approx. methods and num. inversion of Laplace transform. 0-84720
- ruby ring laser with forced mode locking 0-95915
- semiconductor, elec. field induced optical SHG theory, Brillouin zone integral 0-69457
- semiconductors, EM wave absorption in quantising electric field 0-108182
- sepiolite, electric polarisability, anisotropy, length depend. of ionic contrib. 0-85224
- sepiolite, size distributions, transient electric birefringence 0-85223
- single-mode fibres, electro-optical polarisation control 0-91899
- smectic A phase, dynamic characts. of electrooptical effect with memory 0-108183
- smectic C liquid crystals, ferroelec., fundamentals and display appl. 0-79676
- smectic liquid crystal, chiral, optics and electro-optics, kinematical diff. theory 0-92461
- smectic liquid crystals, ferroelec., submicrosecond bistable electro-optic switching 0-84051
- sodium bentonite, Wyoming, suspension, comparison of optico-optical scattering and birefringence 0-85226
- solutions and suspensions, polarised fluoresc. in elec. field, mol. props. deriv. 0-84785
- suspension of absorbing particles, simultaneous meas. of dichroism and birefringence in elec. field., photocurrent signal obs. 0-82801
- electro-optical effects continued**
- tunable single-sideband generation in IR 0-78876
- uniaxial crystals, local field influence on electron contribution to linear electro-optical effect (*Russian*) 0-88968
- viologen films, on transparent oxide electrodes, morphology, electro-optical obs. 0-100703
- Al_{0.5}Ga_{0.5}As, modified-strip buried-heterostructure lasers, CW electro-optical properties 0-74359
- Bi₁₂SiO₂₀, electrooptic photorefractive crystals for optical information processing 0-74313
- Bi₁₂SiO₂₀, optical sensor for measurement of high electric field intensity 0-69509
- CaWO₄, centrosymmetric cryst., linear electrogyration study 0-60540
- CdTe linear electro-optic translation of IR laser wavelengths 0-78878
- CdTe single cryst., linear electro-optical props., temp. depend. 0-71376
- Co₂, electrooptical consts., 2 ν_3 band induced component 0-78626
- copper phthalocyanine, size distributions, transient electric birefringence 0-85223
- CsCuCl₃, phase transition, refr. index, electrooptic coeff., pyroelec. signal, and NQR meas. 0-70386
- CSH₂PO₄, ferroelec. transition, electrooptic 0-76005
- Cu single cryst., linear electro-optical props., temp. depend. 0-71376
- GaAs, photoluminescence, electron gas coding influence in ion-bombarded layers 0-108272
- GaAs single cryst., linear electro-optical props., temp. depend. 0-71376
- GaAs:Cr, photoluminescence in strong electric fields 0-108270
- GaAs-Al_{0.5}Ga_{0.5}As DH laser, MBE grown, CW electro-optical props. 0-102725
- Gd₂(MoO₄)₃, spontaneous rot. of plane of polarisation of light in external field 0-93282
- n-InSb submillimetric-wave free-carrier Faraday effect in strong longitudinal elec. field 0-66164
- K₂Li₂Nb₂O₇ films for optical waveguides epitaxial growth and characterisation 0-79016
- LiNbO₃, cleaved, crystallographic and electrooptic props. 0-59575
- LiNbO₃, electrooptic photorefractive crystals for optical information processing 0-74313
- LiNbO₃, optical waveguides by ion implantation 0-106622
- MnNbO₃, tetragonal, electronic struct., optical anisotropy 0-70599
- PLZT slim-loop and linear ceramics, longit. electrooptic effects, display appl. 0-80751
- xPb_{1-x}GeO₄(VO₄)₂, (1-x)Pb_{1-x}SiO₄(VO₄)₂, solid solution of centrosymmetric crystals, electrically induced optical activity 0-108180
- PbMoO₄, centrosymmetric cryst., linear electrogyration study 0-60540
- SbSI, absorption edge, elec. field effect rel. to ferroelec. props. 0-97240
- Sr₂Ba_{1-x}Nb₂O₆, domain struct. influence on electrooptical props. 0-93283
- SrMoO₄, centrosymmetric cryst., linear electrogyration study 0-60540
- STiO₃, monodomain, O-D and O-H stretching vibrs., IR spectra 0-71449
- WO₃, anodic oxide films, quadratic electro-optic and electrostrictive effects, ellipsometry 0-108184
- ZnS, linear electrooptic coeff. dispersion 0-71380
- Zn single cryst., linear electro-optical props., temp. depend. 0-71376
- ZnSe single cryst., linear electro-optical props., temp. depend. 0-71376
- electroabsorption**
- semiconductor with complex valence band, polarisation props. of interband electroabsorption 0-66152
- As₂Se₃, cryst., electroabsorption on indirect gap 0-80812
- GaAs electroabsorption signal, depend. on elec. field 0-103942
- GaSe thin films, electroabsorpt. spectra, exciton line splitting 0-107716
- GaTe, single cryst. prep. and electroabsorpt. spectra investig. 0-103968
- InSb n⁺-p junctions, photocurrent spectrum near long wavelength edge of fundamental absorption band 0-100483
- p-InSb, shift of fundamental absorpt. edge in crossed elec. and mag. fields 0-76034
- WO₃-B₂O₃-ZnO semiconducting glasses, DC cond. and optical absorpt. 0-107783
- electroacoustic effects** see *acoustoelectric effects*
- electroacoustic generators** see *acoustic generators*
- electrocaloric effects** see *pyroelectricity*
- electrocardiogram** see *electrocardiography*
- electrocardiography**
- see also *bioelectric potentials; biomagnetism; cardiology*
- ambulatory, computer processing system 0-89897
- analysis system, long term recordings, quantitative evaluation of rhythm disturbances (*German*) 0-76847
- arrhythmia ambulatory anal. in real-time with minicomputer 0-85523
- arrhythmia detection, edit and recall system, microprocessor-based 0-89891
- arrhythmia detection with a multi-microprocessor system for distributed and parallel processing 0-85524
- arrhythmia identification and verification by 3-channel eval. of long-term ECG records 0-85518
- arrhythmia monitoring, single scan algorithm for QRS-detect. and feature extraction 0-85520
- arrhythmia quantification, template matching algorithm evaluation 0-85519
- artifact in referential EEG recordings, minimisation by computer subtract 0-94390
- automated monitoring, new electrode system 0-89898
- automatic analysis on minicomputer-based system, 24 hr ECG 0-89889
- avian ECG, radiotelemetry system 0-98202
- beat counter, versatile digital SAMI 0-85510
- body surface potential mapping, microcomputer processing system (*Japanese*) 0-72347
- body surface potential mapping project 0-104794
- calibrator for ECG/respiration monitor 0-98159
- computer based instrument complex using SK-2 cylindrical coordinator (*Russian*) 0-76856
- computer processing, measurement error determ. 0-94401
- computerised tomography, ECG-gated, motion phantom 0-98115
- contour analysis system utilising decision tables, real-time, microprocessor-based 0-89830
- contour map production for electrophysiology 0-72340
- coronary artery disease, preclinical, detect. in male subjects using the omnigram 0-81767
- data reduction using a microcomputer (*German*) 0-81748
- diagnosis improvement by nonlinear feature extraction methods 0-85530

electrocardiography continued

- diagnostic functions of ECG signals, effect of random noise (*Croatian*) 0-98169
- digital ECG systems testing 0-81756
- echocardiography, high-resolution, computerised US signal processing 0-76814
- EKIT Malyshech equipment, operational errors 0-61717
- emission computerised tomography, ECG-gated, cardiac blood pool 0-98117
- epicardial excitation spread, method for registration (*German*) 0-76845
- epicardial mapping, computerised display system (*Japanese*) 0-101279
- equilibrium left ventricular ejection fraction determ., background noise estimation 0-94365
- extrastyle monitor using FIFO 0-72360
- Frank xyz signal interpretation by unmodified 12-lead computer system 0-94400
- frequency-domain analysis 0-85521
- gated blood pool scan, radioisotope evaluation of ventricular performance 0-85483
- heart block computer detect. by correl. of surface and endocardial ECG 0-94410
- HG ECG, computer methods for anal. 0-72352
- His-bundle activity detect., theoretical anal. of error during signal averaging 0-94392
- Holter recordings, low cost arrhythmia analyser, GRETA 0-94403
- Holter tape high speed digital anal. with full editing capability 0-89896
- lead CAD 0-85526
- left ventricular hypertrophy study in borderline hypertensive young men 0-109050
- left ventricular performance parameters rel. to max. dZ/dt 0-101159
- long-term recordings, comparison of techniques for exam. 0-72349
- magnetocardiography recording, props. of ideal system, appl. of ECG theory 0-104700
- microprocessor-based body surface isopotential and topological maps 0-72361
- microprocessor-based evaluation system for conventional leads 0-89894
- monitor, heart rate meter and alarm eval., proposed standard test tapes 0-89899
- monitoring, anal. of 24 hr recording, operator-controlled computer system 0-89888
- multichannel recording using TDM 0-101283
- myocardial ischaemia and necrosis monitoring in acute myocardial infarction 0-85525
- nuclear cardiology, beat-by-beat validation of ECG gating [nuclear medicine] 0-98071
- nuclear cardiology, performance characts. of a commercial ECG gate 0-98073
- optimisation, conf., Halifax, Nova Scotia, Canada (Jan. '79) 0-76850
- pressure-induced changes in cardiac conduction, action pot. correls. 0-81572
- prototype waveforms generation by piecewise correlational averaging 0-109053
- QRS detector/delineator devel. and eval. 0-89892
- R and T waves in ECG and magnetocardiography 0-104699
- R-wave enhancement for heart rate determ., abdominal-lead fetal ECG 0-67264
- recording on tape, correction of timing errors due to tape speed variation 0-72354
- rhythm analysis, syntactic approach 0-89900
- signal-averaging system, flexible, computerised 0-67270
- simulation using a microprocessor 0-61726
- sinus rhythm, diagnosis by IBM ECG anal. program (*Japanese*) 0-67278
- SQUID, appl. to cardiac recording, phase and amplitude relationships of elec. and mag. events 0-104695
- stress/duress automated detect. system 0-76852
- supraventricular arrhythmia rapid anal. from long-term oesophageal recordings, drug assessment 0-89904
- surface mapping, interpolation methods in FORTRAN 0-81750
- T-wave location by computer, R-T interval 0-76854
- telephone transmission, analogue and digital, errors and noise 0-94398
- time-selective filtering using computer 0-89895
- torso surface isopotential simulation using simple conduction-elec. field model with Neumann boundary 0-89706
- vectorcardiogram information enhancement, automatic pre-processing 0-94402
- vectorcardiographic microprocessor system (*Bulgarian*) 0-61722
- vectorcardiography, 3-dimens. 0-94405
- ventricular arrhythmia model 0-89893
- ventricular fibrillation signal anal. 0-85522
- waveform, statistical algorithm and struct. anal. 0-72341

electrocataphoresis *see electrophoresis***electrochemical analysis**

- see also electrochemistry; polarography; voltammetry (chemical analysis)*
- boiler feedwater redox potential meas. by Pt thin-layer electrodes 0-89578
- C U determination by constant current coulometric titration in 5 to 20 mg range 0-78381
- conductometer to record rapidly varying electrical conductivity 0-61184
- flow cell for use with O₂ membrane electrode, glucose, glucose oxidase determ. appl. 0-61736
- flow coulometry, with ring-disk electrode 0-71966
- flue gas, in 200 MW plant, trial operation with Westinghouse O₂ probe (*Czech*) 0-89562
- Kalousek electromechanical switch, for potentiostatic conditions 0-85236
- polarisation studies, electrode design 0-93761
- polymer mixture, metal fraction contents and properties meas. method (*Russian*) 0-76571
- potentiometric titration apparatus, microprocessor controlled, for equilib. studies 0-89579
- potentiostat, P-04, for electrochem. meas. 0-61185
- single crystal surface, electrochemistry, surface struct., superlattice struct. 0-76519
- solid electrolyte gas sensor developments 0-61217
- steel, ferritic stainless, Cr-Mo (12.1wt.%) microstructure influence on localised corrosion behaviour 0-61018
- steel, W-Co-Mo-Cr-V-C (8.5, 8.1, 4.5, 3.5, 2.2, 1.02 wt.%), phase composition, struct. and props. 0-104163
- surface water continuous analysis by NH₄⁺-sensitive plastic membrane electrode 0-89701
- titrimetric analyser with ammeter pick-up (*Russian*) 0-71984

electrochemical analysis continued

- variable-potential coulometer analyser integration error analysis 0-93831
 - Cl₂ residual, in saline cooling waters, determ. via modified amperometric membrane probes 0-82112
 - Cl⁻ ions in nuclear reactor water coolant, determination by flow-type porous metallic Ag electrode 0-89577
 - Cu binary alloy, polarisation studies, electrode design 0-93761
 - Cu₂S-CdS solar cells, Cu₂S growth kinetics and composition analysis by absorbance transient and galvanic electrochemical measurements 0-92797
 - Fe-Cr alloys, in acid and neutral solns., thickness and optical constants of passive and transpassive films 0-66698
 - Li/TiS₂(TiSe₂)(Ti_{1-x}S₂), electrochem. obs. of Li intercalation 0-61216
 - Li₁₋₃₃Si, cryst. struct. and electrochem. anal. (*German*) 0-88132
 - O₂ analysis, electrochemical sensors 0-93816
 - O₂ sensors, solid electrolyte, noncatalytic electrodes 0-76573
 - PdO-Pd miniature pH electrode description and use 0-89886
 - Pu safeguarding, computer-assisted controlled potential coulometric determ. 0-78384
 - ZrO₂ based solid electrolyte, use for study of O₂ solubility and diffusivity in liq. metals 0-59669
- electrochemical batteries** *see cells (electric)*
- electrochemical electrodes**
- see also electrochemistry*
 - alternating current electrode processes, review 0-61107
 - anode behaviour in cyanide-Ag baths (*German*) 0-61103
 - bioelectrochemical sensor using immobilised enzyme electrodes (*Japanese*) 0-109071
 - boiler feedwater redox potential meas. by Pt thin-layer electrodes 0-89578
 - catecholamines, HPLC and continuous flow anal. using flow cell based on rotating disk electrode 0-66894
 - catheter tip pH electrodes for continuous intravascular recording 0-81755
 - cathodic protection for small plant using Ti electrodes (*German*) 0-100943
 - corrosion rate measurement, with dual electrodes 0-85180
 - dispersed, three-dimensional, hydro-metallurgy appl. (*French*) 0-71919
 - dispersed, Zn, for primary and secondary cells, electric vehicles appl. (*French*) 0-72023
 - electrocatalysis, surfaces modified by metal adatoms, review 0-61110
 - electrochemical reactors with three-dimensional electrodes, characterisation using electrochemical tracer method 0-76520
 - electrochemically formed layers, ageing effects, kinetic and structural consequences 0-61109
 - fast ion transport in solids, conf., Lake Geneva, USA (May 1979) 0-57006
 - fast ion transport in solids, conf., Lake Geneva, USA (May 1979) 0-105427
 - fixed-bed, three-dimensional, porous, mass and charge transfer (*French*) 0-71920
 - glassy C electrodes for photogalvanovoltaic and photovoltaic cells 0-89630
 - graphite fluorides, (CF)_n and (C₂F)_n, prep., struct., discharge characts., electrode props. 0-89502
 - holder for electrochem. stress corrosion expts. at high temp. and press. 0-61102
 - impedance measurement, accuracy of electrode props. determ. 0-61108
 - intercalation compound, NMR investigs., review 0-60432
 - intercalation compound, thermodynamic and transport props. 0-66963
 - ion-selective electrodes for determination of urine-electrolytes (*German*) 0-94384
 - ion-selective membrane, Ag⁺ and F⁻ based ceramic materials appl. (*Japanese*) 0-61203
 - layer and tunnel compounds, fast ion transport and electrochem. storage 0-61324
 - molten carbonate fuel cell, electrolyte comp. effect on electrode kinetics 0-101092
 - oxide semiconductors in photoelectrochemical conversion of solar energy, use as cell anodes 0-101120
 - photoelectrochemical cells with semiconductor electrodes for solar energy conversion and storage (*French*) 0-61386
 - photosynthetic reaction centre from bacteria working on SnO₂ electrode 0-94092
 - polarisation studies, electrode design 0-93761
 - ring-disk electrode, in flow coulometry 0-71966
 - single crystal surface, electrochemistry, surface struct., superlattice struct. 0-76519
 - static mercury drop, voltametry appls. 0-97740
 - steel electrodes, pitting corrosion currents rel. to conc. of inhibitive and corrosive anions under corrosion conditions 0-85181
 - surface, anisotropy of optical props. 0-60534
 - surface water continuous analysis by NH₄⁺-sensitive plastic membrane electrode 0-89701
 - thionine-coated electrode for photogalvanic cells, electrochem. and XPS anal. 0-72071
 - three-dimensional, with loose support, principles and appl. (*French*) 0-71918
 - three-dimensional reactors, dimensioning, w.r.t. mass transfer phenomena (*French*) 0-71921
 - transition metal chalcogenides, reversible electrodes appls. 0-61112
 - Ag, adsorbed rhodamine B, anisotropy of optical props. 0-60534
 - Ag covered Ti electrodes for cathodic protection for small plant (*German*) 0-100943
 - Ag, monomolecular films of Pb, anisotropy of optical props. 0-60534
 - Ag porous metallic electrode, for determ. of Cl⁻ ions in nuclear reactor water coolant 0-89577
 - Ag, surface, adsorption of pyridine on graphitic C overlayer, Raman spectra obs. 0-103954
 - AgCl covered Ti electrodes for cathodic protection for small plant (*German*) 0-100943
 - Ag(s)/Ag₂SO₄+Na₂SO₄(l) high temp. ref. electrode, study 0-76622
 - Al alloy electrode, corroding, acoustic emission 0-60997
 - Al-(Mn), effects of Mn on electrode or free corrosion potentials 0-100942
 - Al-Mg (7 wt.%), bare surface reaction rates in aq. solns. 0-101022
 - Al₂O₃, anodic, passified, inhibition of reaction with water 0-89390
 - Au, adsorbed Br₂, anisotropy of optical props. 0-60534
 - C, glassy, electrolytic durability 0-66809
 - CdSe, chemically sprayed thin films as photoanode in photoelectrochem. cells, power charact. meas. 0-85293

electrochemical electrodes continued

- CdSe film photoanodes for electrochem. photovoltaic cells, fabrication and evaluation 0-76641
 CdSe photoanode improved efficiency by photoelectrochem. etching 0-104512
 Cd₂SnO₄ and Cd₂SnO₄:CdO, thin film electrodes in H₂SO₄ electrolytes, reduction, AES and SEM 0-65674
 n-CdTe, semiconductor electrode, electrochem. behaviour in nonaqueous media (*French*) 0-66808
 Cu anode, passivating behaviour and illum. effects in alkaline soln. 0-104449
 Cu binary alloy, polarisation studies, electrode design 0-93761
 Cu, flat electrode, ionic mass transfer coeffs. determ. in open channels 0-59110
 Cu phthalocyanine thin film electrodes, near IR photoelectrochemical responses 0-93766
 Fe, corrosion and passivation in LiCl soln., peripheral velocity effect 0-61000
 Fe-air batteries, bifunctional air electrode 0-72028
 p-GaAs electrode, flatband pot. determ. from differential stress meas. 0-75638
 n-GaP electrode, photoanodic dissolution rate, effect on surface electronic band energies 0-103748
 p-GaP semiconducting photoelectrode 0-101119
 HF electrode, surface oxide film, impedance and pot. behaviour 0-61001
 IrO₂ anodic film electrochromic cell, fabrication and display device use 0-61320
 IrO₂ anodic films, electrochromism and ionic cond., model 0-59706
 Li incorporated transition metal oxides, topochem. reactions, chem. prep. and characterisation 0-61115
 Li-Si, electrode pot., Li utilisation determ. 0-81427
 LiAl/FeS₂ battery system research developments at ANL 0-61323
 Li₂CoO₂, cathode material for batteries of high energy density 0-101089
 Li₂Fe₂ (0 < x ≤ 2) cathodic system, chem. and electrochem. studies 0-85188
 Li₂O-GeO₂-Ga₂O₃ glass, electrode props., dissolution kinetics 0-89387
 Li₂Ta₂O₇ and Li₂Ti₂O₇, chem. diffusivity of Li at 30°C 0-59737
 n-Si, Fe₂O₃-coated, heterostruct. photoanode for photoelectrolysis of water 0-61384
 Ni-Cd sealed battery electrode performance meas. 0-66962
 Pb electrode, in situ surface phase study by laser Raman spectroscopy 0-103542
 PdO-Pd miniature pH electrode description and use 0-89886
 Pt electrodes, polymeric surface film form. by electrooxidation of phenolic cpds., ellipsometric study 0-104450
 Pt, on C electrode, surface area loss in H₃PO₄ 0-101091
 Pt, oxide layers on electrode surface anisotropy of optical props. 0-60534
 Pt/ZrO₂ porous electrode/solid electrolyte system, interface polarisation effects 0-61114
 Si:H, amorphous, photoelectrochem. behaviour 0-81480
 Si-SiO₂ electrode, electronic cond., luminesc. obs. 0-61111
 SnO₂, effect of DC on corrosion in lead glass melt 0-85075
 n-SrTiO₃ electrode, flatband pot. determ. from differential stress meas. 0-75638
 SrTiO₃ semicond. electrodes, electroreduction process kinetics, cathodic dark current meas. 0-66807
 TiO₂, doping processes, influence on photoelectrochem. behaviour 0-79822
 n-TiO₂ electrode, flatband pot. determ. from differential stress meas. 0-75638
 n-TiO₂ electrode, photo-oxidation of acetate and iodide 0-81331
 n-TiO₂ electrode in AlCl₃-NaCl melt, electrochem. and photoelec. props. 0-81328
 TiO₂ electrodes, chemically modified, nature of surface states 0-107905
 TiO₂/Nb semicond. electrodes, electroreduction process kinetics, cathodic dark current meas. 0-66807
 WO₃ electrodes, electrochromic processes, digital simulation model 0-76518
 Zn, electrode in alkaline soln., exam. of surface state by potentiodynamic voltammetry 0-85187

electrochemical machining *see electrolytic machining*

electrochemical polishing *see electrolytic polishing*

electrochemistry

- see also Debye-Huckel theory; electrical conductivity of electrolytic liquids; electrochemical analysis; electrochemical electrodes; electrolysis; electrolytic devices; electrophoresis*
 adsorbed molecule, Raman scattering 0-60563
 bipolar cell stacks, leakage currents, simulation program 0-76526
 bipolar trickle reactors, electric current versus potential plots 0-76521
 bipolar trickle reactors, flow models for hydrodynamic characts. and reaction rate constants, 0-76522
 bipolar trickle reactors, study using electrochemical tracer method 0-76523
 cathodic protection for small plant, economic method (*German*) 0-100943
 charge transfer reactions in biological systems, mech. of coupling 0-76889
 cobalt phthalocyanine, electrochromism and oxidation 0-93768
 condensed adsorption layers, effect on electrode reaction rates 0-93769
 corrosion rate measurement, with dual electrodes 0-85180
 current distribution cell for qualitatively predicting differences in barrel plating performance of electroplating solutions 0-71917
 electric double layer, primitive models, pot. difference and charge density 0-76515
 electrical double layer, ion adsorpt. and discrete charge effects, self-consistent calcs. 0-76516
 electrical double layers, repulsive electrostatic interaction, statistical mech. theory 0-92432
 electrocapillary acceleration meters, electrolyte composition selection 0-73331
 electrocapillary acceleration meters with electrolyte in gel form 0-73330
 electrocatalysis, radiotracer method investig. appls. 0-70525
 electrochemical mass transfer, drag-reducing polymers, effects, comparative study 0-76528
 electrochemical reactor characterisation, marker pulse method improvements 0-76524
 electrochemical reactors with three-dimensional electrodes, characterisation using electrochemical tracer method 0-76520
 electrochromic cell using solid proton conductor electrolyte, HUO₂PO₄·4H₂O 0-89497
 energy conversion analysis (*Dutch*) 0-72019
 energy use optimisation (*Dutch*) 0-72020

electrochemistry continued

- fixed-bed electrodes, three-dimensional, mass and charge transfer (*French*) 0-71920
 gas-electrolyte dispersions, void fraction meas. using conductivity method 0-76525
 glass, molten, reactions with conducting materials 0-85186
 heterogeneous catalysis, conference, Varna, Bulgaria (Oct. 1979) 0-82578
 instrumentation 0-71916
 iodide, charge transfer to solvent spectra, spectral shift data, Madelung const. determ. 0-85204
 ion electrostatic interaction at electrode surface, ion field penetration 0-81333
 ion implantation, chemical and electrochem. aspects, review 0-100271
 Leclanche cell, impedance spectrum of an undischarged cell 0-89604
 multicomponent impedance diagrams, resolution technique 0-66959
 multicomponent systems, phase diagrams and thermodynamic data, electrochem. determ. 0-71922
 nuclear track emulsions, electrochemical etching of fast neutron induced recoil tracks in cellulose triacetate 0-91406
 polydicarboxylic acids, electrophoretic and viscometric props. 0-66811
 polypyrrole films, electrochemical prep., chem. and phys. characterisation 0-70708
 potentiostat, electronic instrument for electrochemical kinetic measurements 0-105675
 power sources and energy science 0-101023
 reactors, dimensioning, with three-dimensional electrodes, mass transfer phenomena (*French*) 0-71921
 reduced Ni oxide, H absorption 0-76529
 retardation of electrolytic mass transport in collinear electric-magnetic fields 0-104443
 reverse pulsed polarography, reversibility characterisation, electrode reaction product determ. 0-66889
 secondary cells, Ni-Cd, plastic-bonded electrodes positive active layer study 0-101088
 secondary cells, Zn-Br, performance anal. in electric vehicle and utility applications 0-101086
 secondary cells with C-air electrodes in alkaline electrolytes, ageing mechanism study 0-101087
 single crystal surface, electrochemistry, surface struct., superlattice struct. 0-76519
 solid state cells with RbAg₄I₅ electrolyte, contact between electrode and electrolyte, electrochemical investigation 0-76527
 steady-state conversion-rate rel. to surface reaction process, catastrophe theory 0-108717
 steel, alloy, hardened, electrochem. characts. and stress corrosion cracking, ageing and cold treatment effects 0-108639
 steel, austenitic stainless, stress corrosion crack growth, electrochem. aspects 0-97620
 steel, mild, cyclic strain enhanced dissolution in NH₄NO₃, corrosion fatigue props. 0-85083
 steel, notched specimens in sea water, endurance limit enhancement, specimen size, freq. effects 0-93678
 steel, stainless, pitting corrosion in chloride media, electrochem. aspects 0-61007
 steel 45-antifrictional alloys friction pairs, electrochem.-mech. investigation (*Russian*) 0-76367
 steel electrodes, pitting corrosion currents rel. to conc. of inhibitive and corrosive anions under corrosion conditions 0-85181
 thermal battery cells using molten nitrates as electrolyte and oxidiser 0-76624
 trifluoromethanesulphonic acid, and salts, electrochem. characts. in nonaqueous solvents 0-89499
 velocity sensor, freq. characts. calcs. 0-96675
 zinc phthalocyanine, electrochromism and oxidation 0-93768
 Ag-Sn alloys and amalgams, electrochem. considerations, corrosion in physiological soln. 0-93760
 Ag(s)/Ag₂SO₄+Na₂SO₄(l) high temp. ref. electrode, study 0-76622
 Al₃Ga₁-Sb solid soln., electrochem. deposition of Ni and Pd 0-93505
 δ-Bi₂O₃, thermoelectric power, heat of transport of O²⁻ ions 0-92713
 Cd₂SnO₄ and Cd₂SnO₄:CdO, thin film electrodes in H₂SO₄ electrolytes, reduction, AES and SEM 0-65674
 Cr, electrochemical behaviour, in molten V₂O₅ (*Japanese*) 0-89498
 Cu, coadsorption of H₂O and Br, on (100) face, Helmholtz layer model system 0-92777
 Cu, electrochem. nucleation and growth on Te and Al, TEM 0-104451
 Cu-Sn alloy, thermodynamics of Cu and Sn solns. using copper β-alumina solid electrolyte, 800-1100K 0-107502
 Fe corrosion in aq. H₂S, FeS polymorph form. 0-81231
 Fe, electrochemical behaviour, in molten V₂O₅ (*Japanese*) 0-89498
 Fe, film growth under organic coatings, qualitative ellipsometric-electrochem. approach 0-104344
 Fe₂O₃, semicond. anode in aq. electrolyte, electrom. and electrochem. 0-76080
 Fe₈₀P₁₃C₇, amorphous and crystalline, electrochemical and semicond. behaviour (*Russian*) 0-101021
 GaAs anodic oxide, states, electrochemical meas. 0-80176
 H-Cl electrochemically regenerative fuel cell, electrode kinetics and cell perform. 0-89610
 H₂ thermochemical production using H₂SO₄-SO₂ cycle, electrochem. aspects 0-97812
 Li/SOCl₂ primary cells, SOCl₂ reduction mech. in supporting electrolyte 0-108792
 Li-Al system, Li solubility and chem. diffusion in Al, electrochem. study 0-107432
 Li₂FeS₂ (0 < x ≤ 2) cathodic system, chem. and electrochem. studies 0-85188
 β-Li₂V₂O₇, bronze, thermodynamics of ordering 0-84302
 Li₂VSe₄, intercalation cpds., electron chem., ionicity 0-89501
 Li₂WO₄, electrochem. and chem. Li incorporation, cryst. struct. 0-88131
 Mg-AgCl seawater battery, performance and EMF at great ocean depths 0-76623
 MnO₂, doped, dry cell depolariser, hydrazine reduction kinetics 0-89603
 MnO₂, preparation and characterisation of doped samples for appl. as dry-battery depolarisers 0-89602
 n-MoSe₂ based liq. junction solar cell, nonaqueous electrolyte system employing Cl₂/Cl⁻ couple 0-81432
 NO, electrocatalytic decomp. on electrochem. reduced zirconia surface 0-61113
 Na₂O-SiO₂-(CaO) glass, molten, metal ion diffusion and redox behaviour, electrochemical studies 0-81332

electrochemistry continued

- Ni₂, electrochemical behaviour, in molten V₂O₅ (*Japanese*) 0-89498
 O²⁻ low partial press., thermogalvanic meas. using O²⁻ ion conductors 0-73389
 Pb-acid cells, PbO₂ formation on Pb and antimonial Pb alloy 0-76628
 PbO₂ powder, electronic conductivity, separation of particle core and surface resistance 0-104442
 PdO, free energy of form. using impedance dispersion analysis 0-108728
 Pt and Pt/Ru electrocatalysts for methanol oxidation in acid electrolyte with improved steady state activity for fuel cell appls. 0-76629
 SrTiO₃, semicond. anode in aq. electrolyte, electrolum. and electrochem. 0-76080
 SrTiO₃ semicond. electrodes, electroreduction process kinetics, cathodic dark current meas. 0-66807
 Ti electrochemical machining, electrolytes development, electrochem. in static solns. 0-85182
 Ti electrochemical machining, electrolytes development, electrochem. studies in flowing solns. 0-85183
 Ti:Pd, ion implanted, corrosion behaviour and Rutherford backscatt. anal. 0-71792
 TiO₂, semicond. anode in aq. electrolyte, electrolum. and electrochem. 0-76080
 TiO₂:Nb semicond. electrodes, electroreduction process kinetics, cathodic dark current meas. 0-66807
 V₂S₅, amorphous, electrochemistry in Li cells 0-76626
 W, oxidation, WO₃ amorphous anodic film growth in acidic soln. 0-81232
 WO₃, film, electrochem. injection kinetics of Li, LF AC meas. 0-57339
 WO₃, semicond. anode in aq. electrolyte, electrolum. and electrochem. 0-76080
 ZnSO₄ electrolytes containing Ge and Co, polarisation charact., exam. by cyclic voltammetry 0-104444

electrochromic devices

- cell using solid proton conductor electrolyte, H₂O₂.PO₄.4H₂O 0-89497
 short circuit memory in electrochromic displays 0-97238
 p-GaAs/heptyl viologen system, appl. in photoelectrochemical cells and photoelectrochromic displays 0-76640
 H₂O₂.PO₄.4H₂O, film fabrication and appl. as solid electrolyte in electrochromic displays 0-70462
 IrO₂, anodic film electrochromic cell, fabrication and display device use 0-61320
 IrO₂, anodic films, electrochromic props. and device uses 0-61319
 WO₃-electrolyte electrochromic cells, proton injection phenomena 0-71448
 WO₃:LiI, solid-state electrochromic cell, fabrication and characts. (*Japanese*) 0-84717

electrochromism

- cholesteryl chloride+cholesteryl laurate, binary compensated, rhodamine 6G guest, electro-optical colour effect 0-71378
 cobalt phthalocyanine, electrochromism and oxidation 0-93768
 cyclic ketones, electrochromism and electric dichroism for studying transitions to second excited singlet 0-63692
 dye in polymer matrices, electrochromic props. and use as probe of matrix softening around T_g 0-84724
 polymer-modified electrodes, electrochromic characts. 0-66149
 short circuit memory in electrochromic displays 0-97238
 viologens, solutions for display appl., oxidant impurities elimination 0-78922
 zinc phthalocyanine, electrochromism and oxidation 0-93768
 IrO₂ anodic films, electrochromism, anion mechanism 0-100647
 IrO₂ film, A-C response 0-107926
 IrO₂ anodic films, electrochromism and ionic cond., model 0-59706
 IrO₂ anodic films, electrochromic props. and device uses 0-61319
 IrO₂ anodically grown film as electrochromic material 0-71377
 IrO₂, electrochromic, oxidation state changes and struct. 0-100950
 Li₂B₂O₇, ferroelectric glass, phase transition, permittivity, electrochromism, photochromism 0-80719
 Rh oxide film, anodic, two-colour electrochromic system 0-66150
 TeO₂, ferroelectric glass, phase transition, permittivity, electrochromism, photochromism 0-80719
 WO₃ electrodes, electrochromic processes, digital simulation model 0-76518
 WO₃ film, Au surface layer effect on electrochromic behaviour 0-76004

electrodeposited coatings *see electrodeposits***electrodeposited films** *see electrodeposits***electrodeposited layers** *see electrodeposits***electrodeposition**

- see also electrodeposits; electroplating*
 crystal face, growth behaviour in presence of screw dislocations 0-103276
 metal, electrocatalysis, surfaces modified by metal adatoms, review 0-61110
 metal chalcogenides, using nonaqueous solvents 0-76200
 metal cluster growth and props., photography and catalysis appl., conf., Villeurbanne, France (Sep. '79) 0-105431
 multicomponent systems, electrodeposition, theoretical model 0-65396
 polyphenylene oxide thin films, electrochem. prep., impurity effects on cond., electroforming 0-88655
 resistive layer above pit, stabilisation 0-93506
 steel surface corrosion protection, propargyl alcohol film growth, ellipsometric obs. (*Rumanian*) 0-60996
 tetramethylammonium silver iodide superionic film, electrodeposition, electrochem. cells 0-107478
 Ag electrodeposition, on (100) face of single crystal Ag in presence of sulphadiazine 0-89161
 Ag, on (111) face, habit modification caused by Cl⁻ 0-71600
 Al₂O₃, anodic oxide film, behaviour of emulsion particles during electrodeposition 0-104357
 Au film electrodeposition, substrate effects on film props. 0-81329
 CdSe film, soln. growth 0-66437
 CdSe film deposition, and reaction sequence of H₂SeO₃ reduction 0-71603
 CdTe thin film polycrystalline solar cells prepared by electrodeposition 0-93948
 Co-W alloy electrodeposition, influence of MgSO₄ and gum arabic additives (*Russian*) 0-80991
 Cr film, trivalent, cathodic deposition, as bonding interface between Cu and polyethylene 0-76201
 Cu diffusion layer cathodic deposition and anodic dissolution rates 0-93503
 Cu electrocrystallisation on graphite electrodes, nucleation 0-93504

electrodeposition continued

- Cu electrodeposition, on a Cu single cryst. (110) face in presence of sulphaguanidine 0-76203
 Cu electrodeposition, on Cu single cryst. (111) plane in presence of sulphaguanidine 0-76204
 Cu, electroless bath, electrochem. control system 0-71601
 Cu, epitaxial nucleation and growth, on (111)Ag 0-104081
 Ge powder electrodeposition, from molten fluoride mixtures 0-60797
 MoS₂ Chevrel phases with group IIIa metals, Nb, Hg, Pb and Cu, synthesis, stability and characts. 0-71608
 Ni, electrocrystallisation, reaction mechanism, appl. of impedance meas. (*French*) 0-103597
 Ni, on to Al₂Ga_{1-x}Sb solid soln. 0-93505
 Ni-Co-W, electrodeposition, surface morphology and cryst. struct. 0-71602
 Ni-P amorphous alloys, electrodeposited and melt-quenched atomic and electronic structures 0-88062
 Ni-P coating, electroless, ultra-black surface production by chemical treatment 0-76647
 Pb, underpotential adsorption, cathodic deposition, on Ag(111) and (100) (*German*) 0-108363
 PbSe film, soln. growth 0-66437
 Pd, on to Al₂Ga_{1-x}Sb solid soln. 0-93505
 Re, electrodeposited from fused salts, (101) texture (*Russian*) 0-92791
 n-Si-Cu Schottky contacts, electrochem. deposition, barrier height and ideality factor 0-75641
 Tl, underpotential adsorption, cathodic deposition, on Ag(111) and (100) (*German*) 0-108363
 Zn, electrocrystallisation, reaction mechanism, appl. of impedance meas. (*French*) 0-103597
 Zn electrodeposition, on Zn and Al single crystals, from H₂SO₄ bath, SEM obs. (*Japanese*) 0-93502
 Zn, fine powder, electrodeposition 0-60802
 Zn hot galvanisation, production components, installation and power supply (*French*) 0-66686
 Zn, on Pt single crystal spheres, critical overvoltage 0-104080

electrodeposits*see also electroplated coatings*

- adhesion after strain hardening, test device 0-71837
 metals, electrolytic cell for making standard samples 0-85106
 multi-layer, thicknesses meas. circuit, using decade counter (*Czech*) 0-95071
 multilayer Ni deposits, simultaneous thickness and electrochemical potential determination for individual layers 0-71813
 spectrally selective surfaces for photothermal conversion of solar energy 0-101125
 tensile testing device 0-100988
 thickness determination by profilography 0-85095
 Al₂Ga_{1-x}Sb-Pd contacts, struct., preparation elec. props. 0-65684
 Au, Co-hardened, characterisation by Mossbauer spectroscopy, Co precip. formation 0-80108
 CdSe film, electrodeposited, for photoelectrochemical cell for solar energy conversion 0-94093
 Co, electrodeposited, influence of soln. pH on microstruct. 0-65399
 Co-P, electrodeposited alloys, heat-induced structural changes (*Japanese*) 0-89263
 Co-P, electrodeposited amorphous alloys with high permeability, thermal treatment with and without field 0-89372
 Co-P films with various preferred orientations, mag. props. 0-100604
 CoP, and CoNiP, cylindrical amorphous electrodeposited layers, mag. props., torsion influence 0-88848
 Co₂P₁₈, amorphous alloys, electronic struct., γ-ray Compton scatt. study (*Japanese*) 0-84422
 Cr-Cr₂O₃, black chrome electrolytic coatings for solar collectors 0-94100
 Cu, electrolytic coating, brightness and adsorption of surface-active additives 0-100963
 Fe coated medium C steel, distrib. of bounded fatigue limits 0-81198
 Fe-P electrodeposited foil, amorphous, mag. domains 0-75821
 Fe-Zn, galvanization study (*French*) 0-66447
 Ni, electrodeposited film, thermal anal., occlusion of gases rel. to mag. props. 0-59823
 Ni electrodeposition on Cu (001), three-dimens. epitaxial crystallites, TEM image contrast 0-88457
 Ni-P, electrodeposited film, thermal anal., occlusion of gases rel. to mag. props. 0-59823
 Ni-S, electrodeposited film, thermal anal., occlusion of gases rel. to mag. props. 0-59823
 Ni₈₁P₁₉, amorphous alloys, electronic struct., γ-ray Compton scatt. study (*Japanese*) 0-84422
 Si/In(Cd), Si/Cd Schottky contacts, electrochemically deposited 0-88633
 Sn-Ni electrodeposited equatonic alloy, cryst. struct., X-ray, electron diffraction 0-79748
 Zn electrodeposition, on Zn and Al single crystals, from H₂SO₄ bath, SEM obs. (*Japanese*) 0-93502

electrodes

- see also anodes; cathodes; electrochemical electrodes; electron tube components; microelectrodes; welding electrodes*
 algae, living electrode for biophotolysis of water, long-lived photoconverter 0-104510
 arbitrarily electrodeposited piezoelec. plate acoustic spatial response determ. 0-99910
 brass, in high repetition rate spark switches, surface ageing 0-106997
 catalyst for water photolysis, I-V model 0-108721
 diathermy indifferent electrodes, performance electrodes. 0-72367
 diffrillator electrodes, recovery curves for different materials 0-67283
 ECG automated monitoring, new electrode system 0-89898
 electrical breakdown of air gaps, 1 to 9 cm, with heated electrodes, investigation (*German*) 0-107010
 electrophoresis, laser Doppler, high current-density electrodes 0-89500
 electrosurgical dispensing electrodes metal-foil, dry thermal props., skin temp. rises 0-98171
 EM flowmeter theory and application 0-96328
 filters as selective electrodes for synthetic penetrating ions 0-104821
 fuel cell electrodes, galvanostatic switching curve shapes 0-66965
 fuel cell O₂ electrodes, galvanostatic transients, curve shape, 0 to 5 msec. 0-93868
 fusion reactor, long pulse high current ion source electrode cooling 0-91360

electrodes continued

- geophysical arrays for induced polarisation (IP) sounding, effects of EM coupling over uniform half-space 0-101324
 high-current arc electrode vapour influence and estimation 0-70070
 HV electrodes, epoxy resin insulation, effect on dielec. breakdown voltage of polymer sheets 0-60502
 hypodermic needle Po_2 electrode 0-98156
 intense electric fields in needle/cylinder electrodes, distribution (*Rumanian*) 0-63885
 ion electrostatic interaction at electrode surface, ion field penetration 0-81333
 IR point-contact diode tunnelling and rectification rel. to electrode geometry 0-57378
 magnetite, electrode, polycrystn., differential capacitance 0-66136
 mass transfer to continuous moving surface 0-69821
 membrane, chalcogenide ceramic, Cu-selective electrode (*Chinese*) 0-81357
 multipoint electrode for biological pot. recording 0-104784
 noncatalytic, for solid-electrolyte O_2 sensors 0-76573
 organic liquid conductivity and bulk charge determ. cell (*Russian*) 0-57328
 PDX neutral beam injector, multi-aperture ion accel. electrodes thermal anal. 0-102371
 pH measurements using polarizable electrodes 0-76514
 plasma electrode, electric field compression 0-64736
 plasma-electrode contact processes, microplasma diagnostics 0-59325
 polymer-modified electrodes, electrochromic characts. 0-66149
 porous electrodes, effect of porosity 0-66815
 rare earth chromite based electrode material development for MHD generators 0-84893
 screening, discharge phenomena with UHV positive and negative lightning and switching pulses for dimensioning (*German*) 0-87963
 secondary cells, Ni-Cd, plastic-bonded electrodes positive active layer study 0-101088
 solid solution electrodes, characterisation and performance, secondary battery appl. 0-72033
 spark gap electrodes, erosion characts. 0-103204
 spark gaps with parallel plane electrodes, erosion characts. 0-70076
 spark-gap, electrodes, acoustic phenomena in erosion 0-64796
 stimulating electrodes of different materials implanted in cat skeletal muscles, threshold meas. 0-101297
 supraventricular arrhythmia rapid anal. from long-term oesophageal recordings, drug assessment 0-89904
 surface potential meas., guarded electrode design which has small gap between electrode and guard ring 0-68215
 surface roughness, effect on electric breakdown in air 0-84018
 teflon, C-loaded, for chronic EEG recordings in microwave research 0-67305
 vacuum gap breakdown initiation by microparticle impact 0-96413
 on vibrating sphere, mass transfer 0-61106
 water, electrical breakdown in μs regime with Cu, brass, steel and Al electrodes 0-103917
 wire-plane electrodes, breakdown voltage, effect of vacuum conditions 0-64798
 Al, charge effects on insulating films obs., PET and SiO_2 0-75625
 Al, in high repetition rate spark switches, surface ageing 0-106997
 C, used in emission spectrography, isotopic labelling study, plasma appl. (*Hungarian*) 0-106976
 C-fibre, elec. props. and EEG apps. 0-72355
 CdTe electrode, redox reaction due to complex $\text{M}(\text{CN})_6^{3-/4-}$ (*French*) 0-89482
 Cu-BN composite electromachining tools, dynamic hot pressing 0-84889
 Cu-selective electrode, chalcogenide ceramic membrane (*Chinese*) 0-81357
 Mo electrode, corrosion rate in molten glass (*Chinese*) 0-66687
 Mo, low-temperature thermionic converter with an expanded-area collector 0-70045
 Pb-Bi counterelectrode Pb alloy Josephson junctions 0-65743
 $\text{Pb}(\text{Zr,Ti})\text{O}_3$, internally electroded with Pt, resonance behaviour 0-84701
 Ti electrodes, RuO_2 coated, corrosion during O evolution rel. to electrode prep. (*French*) 0-76420
 W electrodes, C segregation and arc damage 0-64795
 WCs, preparation method effects on catalytic activity for H_2 evolution 0-101024
 ZnTe electrode, redox reaction due to complex $\text{M}(\text{CN})_6^{3-/4-}$ (*French*) 0-89482

electrodynamics

- see also *electron beams; electron optics; electron tubes; ion beams; ion optics; ion sources; quantum electrodynamics*
 anisotropic artificial dielectrics, dispersion props, investigation, electrodynamic method 0-88903
 boundary conditions for media with spatial dispersion and transition layers (*German*) 0-78742
 boundary problem solution for complex shape regions 0-69300
 boundary problems, method for solving 0-95773
 charged particle, gyrating, adiabatic invariants 0-83544
 charged particle in homogeneous magnetic field, Cartesian and polar wave functions 0-68061
 charged particle motion at vac.-medium interface, transient radiation emission spectral distrib. 0-63901
 charged particle motion in alternating elec. fields, scaling conditions 0-63903
 charged particle orbits in helical magnetic fields 0-99613
 colloids, interfacial electric polarisability, and interactions 0-108751
 deformable bodies with electric and magnetic quadrupoles 0-62492
 dipole particles in axisymmetric electrostatic and magnetostatic fields, meridional trajectories 0-78750
 discharges in condensed media, electrodynamics problems, theoretical investigation (*Russian*) 0-75116
 education, Brewster angle in semi-infinite dielectric moving perpendicularly to interface 0-57034
 Einstein-de Sitter universe, classical predictive electrodynamics 0-86175
 elastic media, dissipative, relativistic electrodynamics 0-73219
 electrodynamics of superconductors as a consequence of local gauge invariance (*German*) 0-103778
 electron acceleration in EM field, new field theory appl. (*Chinese*) 0-62494
 electron band structure, optically induced in external plane wave field 0-106432

electrodynamics continued

- energy density convexity and hyperbolicity of partial differential eqns. in nonlinear electrodynamics (*French*) 0-62491
 equation of motion for radiating charged particle 0-57110
 Fourier transform, fractional order, appl. to quantum mechanics and electron motion in magnetic field 0-82665
 free electron in external field, wavefunctions, nonrelativistic treatment 0-99611
 free electron laser, saturation effects, classical theory 0-95864
 free relativistic electron in external field 0-99612
 heterogeneous gyrotropic media electrodynamics, antisymmetric reciprocity principle conditions fulfilment (*Russian*) 0-74287
 Lienard-Wiechert eqns., rel. to electron mass (*Spanish*) 0-82654
 magnetic field motion of charged particle 0-90690
 MHD accelerators, electrodynamic characts. 0-64788
 moving sources in conducting medium, multiple expansion 0-106417
 neutron stars, electrodynamics in curved space 0-90465
 neutron stars, electrodynamics of disk accretion, magnetic field structure 0-85973
 particle motion delocalisation in non-uniform HF field with finite correl. time 0-58450
 path-dependent Lagrangians in relativistic electrodynamics 0-90670
 projection methods, applicability limit 0-91734
 quantisation of matter without quantising related fields 0-105525
 relativistic, electromagnetic waves dispersion equations in moving media 0-57089
 resonant antenna system, anomalous radiation and electrodynamic characts. 0-69302
 rheometric structure theory, convective differentiation and continuum electrodynamics 0-86087
 spherical particles beam, focusing by axisymmetric mag. fields 0-78755
 transparent medium, energy-momentum and ang. momentum emission rates of moving charge, covariant electrodynamics 0-57108
 two charged particles problem, Lagrangian and Hamiltonian up to fourth-order terms 0-91736
 vector product formulation of special relativity and electromagnetism 0-105496
 Hg films, superconducting, far-IR and electrodynamic props. meas. 0-103957
- electrodynamometers** see *dynamometers*
- electroencephalograms** see *electroencephalography*
- electroencephalography**
 see also *bioelectric potentials; biomagnetism; brain*
 21-channel EEG monitor with real-time result colour display 0-72364
 alpha-contingent visual stimulation, detect. of cerebral lateralisation of function 0-94190
 alpha-rhythm, neural vet model 0-76719
 auditory brain stem responses, cat, effects of lesions 0-85407
 auditory brain stem responses, cat, intracranial and extracranial recordings 0-85406
 auditory brainstem frequency, response to waveform envelope periodicity 0-61590
 auditory evoked brain stem pot., sex differences in amplitudes and latencies 0-89767
 auditory evoked brain stem pots., effects of analogue and digital filtering 0-89878
 auditory evoked potentials, event-related obs. in schizophrenics 0-85405
 auditory evoked resonances, comparison of narcoleptics, primary insomniacs and normal controls 0-61579
 automated monitoring of long-term implanted electrodes in human brain (*Russian*) 0-76857
 automatic interpretation, background activity anal. 0-85503
 autoregressive analysis, a method for detect. of EEG changes in newborns to tones 0-108982
 biofeedback of slow cortical pots., time series anal. 0-89736
 brain stem auditory evoked potentials and blink reflex in quiescent multiple sclerosis 0-67091
 cerebral activity monitor, using biofeedback rhythms inducing cct. (*Spanish*) 0-72359
 classification, automatic, decision rules comparison 0-109054
 coherence estimates, significance in determ. of central α and μ activities 0-61720
 decision P350, waveform and neural mechanism, auditory click and elec. finger stimuli 0-61528
 deconvolution procedure for information extraction from average evoked response signals 0-61724
 discriminant analysis based scoring system 0-81766
 distortion by volume conduction, compensation by spatial deconvolution 0-94391
 dot-density topogram, simple, computer-generated 0-94407
 ECG artifact in referential EEG recordings, minimisation by computer subtract 0-94390
 elderly patient EEGs, technical and other considerations 0-98150
 electrode, C-fibre, elec. props. and EEG apps. 0-72355
 electrodes, C-loaded teflon, for chronic EEG recordings in microwave research 0-67305
 epilepsy diagnostics, EEG trace coding (*French*) 0-67277
 epileptic spike morphology, quantitative obs. 0-98153
 equipment for measuring potentials (*French*) 0-85516
 event-related potential changes in chronic alcoholics 0-67076
 evoked potential estimation, effectiveness of Wiener filtering 0-61723
 evoked potential records, comparative freq. anal. 0-67269
 evoked potentials, appl. in brain mechanism studies and diagnosis (*German*) 0-61535
 evoked potentials, event-related, in normal, mentally retarded and autistic children 0-85388
 evoked potentials, math. model for source localisation, somatosensory stimulation 0-89774
 evoked responses, peripheral versus foveal, multiple sclerosis early diagnosis appl. 0-67276
 EVOQ: a system configurable for automatic simulation and recording of mean evoked potentials on a minicomputer (*French*) 0-85507
 focal interictal epileptiform discharges rel. to spinal field pots., rat 0-94191
 focal slow waves localisation 0-94406
 hierarchical modelling of EEG signals 0-109052
 histological marking with multiple thin-film electrode probe for intracortical recording 0-67297
 human sleep EEG, spindle pattern recognition by real time anal. (*Japanese*) 0-89903

electroencephalography continued

- intellectual activity, classification of normal and anomalous forms, quantised-wave theory of coherent brain appl. (*Russian*) 0-76722
- intellectual activity, psychoheuristic relationship of psychotism structs. and giftedness structs. introduction, quantised wave theory of coherent brain appl. (*Russian*) 0-76723
- interictal spiking, spontaneous, awake kindled rat 0-67058
- intracortical recording of field pots., 16-fold semi-microelectrode 0-67298
- jet aeroplane noise, effects on facial expression, EEG and manual responses, human subjects 0-98006
- Kullback Leibler-nearest neighbour rule classification, population 0-85504
- LED true checkerboard pattern reversal stimulator for visually evoked pots. study 0-61658
- medical electronics, appl. to otology (*Japanese*) 0-67268
- microcomputer-based period and amplitude anal. system 0-72353
- neural basis of EEG waves 0-108868
- neurostimulation automatic triggering as function of several EEG parameters, apparatus 0-98203
- neurosurgical intensive care, non-invasive monitoring techniques 0-81757
- newborns, healthy, right mid-temporal sharp transients 0-94192
- NREM sleep, period and amplitude anal., young adults 0-85376
- pattern visual evoked pots., age-dependent latency change obs. 0-85390
- patterns during cognitive tasks, controlled tasks anal. 0-67059
- patterns during cognitive tasks, methodology and complex behaviours anal. 0-61531
- phase-locked loop spindle detect. system, human and automatic validation 0-98154
- piezoelectric earphones, usefulness in recording brain stem auditory evoked pots. 0-94389
- polygraphic sleep recordings, computerised scoring method 0-109049
- pulse-time-coded, freq. anal. (*Russian*) 0-72357
- real-time detection using two-component wave model 0-104788
- recording system, portable pulse-interval modulation telemetry/multiplexing system, home use 0-67261
- sensory evoked potentials, use in monitoring residual function of injured spinal cords 0-81747
- serial quantitative EEG 0-61728
- sleep, small spike obs. during rapid eye movements stage in man 0-101155
- sleep state analysis, automatic real-time practical method, computerised 0-67263
- slow potential shifts and decision P350 interactions, auditory and elec. stimuli 0-61529
- somatosensory evoked potentials, reduction during movement, cat extralemniscal pathways recordings 0-85421
- spectral band analysis, contrib. to attentional processes study (*French*) 0-61721
- syntactic anal. software system 0-104787
- technology, conf., Atlanta, USA (Sept. 1979) 0-90601
- theta rhythm, dipole-like neuronal sources, anesthetized rat obs. 0-61527
- topographical display of epileptiform transients based on a statistical approach 0-108833
- tracing processing system, software development (*Japanese*) 0-94409
- transient detection by matched inverse digital filtering 0-85506
- visual evoked cortical potential meas., signal optimisation using Kalman filter (*Japanese*) 0-72348
- visual evoked potential, N1-P2 corrs. of reaction time at the single trial level 0-85389
- visual evoked potentials, single-trial classification using stepwise discriminant anal. 0-85387
- visually evoked electrocortical response rel. to microwave-induced hyperthermia, guinea pig 0-61627
- visually evoked potential, microsecond sensitivity of human system to irregular flicker 0-81586
- visually evoked potentials, speed methods for vision assessment, normal and amblyopic eyes 0-61661
- visually evoked potentials and sensory dimensions 0-61548
- visually evoked potentials to electronic pattern reversal, latency variations 0-94202
- visually evoked response, simultaneous recording to flashes at different retinal locations. 0-72279
- visually evoked response to bar gratings, linear extrapolation to threshold, visual acuity assessment 0-67080
- voluntary movement evoked cortical pots., comparative study, man and monkey 0-94189
- Walsh spectral estimates with appls. to classification of EEG signals 0-104789

electroendosmosis *see* electrophoresis

electroerosive machining *see* spark machining

electrofluidynamics *see* electrohydrodynamics

electrofluorescence *see* electroluminescence

electroforming

- metal sheet, circular, impulsive press. by underwater wire explosions, dynamic plastic deform. 0-84866
- polyphenylene oxide thin films, electrochem. prep., impurity effects on cond., electroforming 0-88655
- BN films, humidity sensitive elec. props. and switching characts. 0-107938
- Pt-polymer-Au capacitor, electroforming, negative resist., electron emission 0-80406
- Te-Se-Cd rectifying sandwich structs., elec. forming action, Schottky junction form. 0-80371

electrogasdynamics *see* electrohydrodynamics

electrohydrodynamics

- compressible liquid, bubble deformation in electric field 0-64618
- convective instability in dielectric fluid between two coaxial cylinders 0-74994
- dielectric fluid, flow and heat transfer in annular channel, electric field effect 0-103077
- dielectric liquid, elec. stressed, motion due to Coulomb, electromech. forces, schlieren image obs. 0-100037
- dielectric liquids, boiling process in narrow horizontal channels due to action of elec. field (*Russian*) 0-74707
- dielectric organic liquid, concentric annuli, heat and momentum transfer, electric field effects 0-96315
- drops, direct contact heat transfer with intermittent electric field 0-74869
- drops, EHD flow, with small Reynolds number, resulting deformation 0-59126

electrohydrodynamics continued

- electrically conducting media with nonlinear heat release, turbulence props. 0-103024
- electrokinetic flow in a narrow cylindrical capillary 0-92233
- electroviscous effect, AC characteristics, pressure-drop fluctuations 0-107457
- Freon electrohydrodynamic flow, jet dynamic pressure obs. (*Russian*) 0-59117
- heat pipes, electric field effects on characts. 0-83728
- integration of electrodynamic equations by direct methods 0-92235
- laser Doppler anemometry on transparent turbulent electromagnetically driven flow 0-103090
- liquid insulants, elec. stressed, bulk electroconvection 0-87814
- metals, liq., infiltration in medium with interconnected pores, during passage of elec. current 0-100033
- nematic director in dielec. regime, dynamical behaviour, EHD instabilities (*Japanese*) 0-59387
- nematic liquid crystal in contact with photoconductor EHD instability, nematic liquid crystal in contact with photoconductor 0-79695
- nematics, EHD instabilities, white noise effect 0-70115
- nonstationary flows with charge diffusion, nonlinear and linear wave processes 0-59124
- pentyl-cyano-biphenyl, nematic, hydrodynamic parameters meas. with and without applied elec. field 0-100297
- rubrene, electrochemilum. by DC, highly organised EHD convection obs. 0-71499
- sphere in current carrying liq., convection mass transfer, num. anal. 0-83851
- thermoelectric MHD, pipe end problem, boundary layers and rotation 0-69942
- transformer oil electrohydrodynamic flow, jet dynamic pressure obs. (*Russian*) 0-59117
- H₂O vapour under point corona discharge, microprocessor control for vapour generator and EHD phenomena 0-106852

electrojets

see also ionosphere

- Alaska oil pipeline, elec. current induced by electrojet 0-61756
- auroral electrojet, empirical relations to interplanetary parameters 0-105118
- auroral electrojet activity, rel. to LF/MF transmissions non-linear demodulation and ELF signals generation 0-94639
- auroral electrojet during isolated substorm event 0-105132
- auroral electrojets, movements during high-latitude substorms 0-109315
- auroral radio backscatter at 42 MHz, amplitude rel. to Doppler shift 0-61955
- auroral zone currents, obs. in morning sector pass 0-98510
- counter electrojet caused by vertical wind, equator region 0-85795
- eastward electrojet over auroral arc, rocket obs. of N-edge 0-101481
- equatorial, fading records near edge of jet over Tiruchirappalli, full correl. anal. 0-101473
- equatorial, plasma instability and electron density irregularities, HF radar obs. 0-105112
- equatorial, three metre irregularities depend. on Zenith angle, radar obs. 0-105109
- equatorial, type II irregularities, nonlinear theory 0-61958
- equatorial anomaly, counter electrojet assoc. changes, upward drift reversal 0-109292
- equatorial anomaly, counter electrojet assoc. changes, upward drift reversal obs. 0-109297
- equatorial counter-electrojet, electron drift vel., radar obs. 0-82126
- equatorial electrojet, type I radar echoes with double-peaked Doppler spectra 0-67458
- equatorial electrojet strength, rel. to ionospheric 0-82129
- field-aligned current closure and Joule heating near Harang discontinuity 0-72682
- lunar tide influence on equatorial electrojet 0-61937
- pressure and rel. fluctuations caused by auroral electrojet 0-82118
- substorm intensified eastward electrojet, 3-D current flow 0-85796

electrokinetic effects

see also electrohydrodynamics; electrophoresis

- biological particle surface, elec. double layer phenomena (*Rumanian*) 0-94144
- dimethylketone, streaming current and cross-coeff. meas. in electrokinetic processes 0-76531
- electroosmotic permeability coefficient in charged membrane model 0-108749
- estuarine environment, natural suspended matter flocculation and electrokinetic pot. (*French*) 0-61817
- flat plate streaming potential investigations: hydrodynamics and electrokinetic equivalency 0-106777
- flow in narrow cylindrical capillary 0-92233
- KCl solution, streaming current and cross-coeff. meas. in electrokinetic processes 0-76531

electroluminescence

see also phosphors

- infrared electroluminescence as a diagnostic tool for polycrystalline GaAs solar cells 0-93885
- MIM cathode, local electron emission and electroluminescence patterns obs. 0-108327
- organic substances, electrochemiluminescence as possible source of coherent radiation, and role in biological processes (*Russian*) 0-76093
- polyethylene terephthalate, TSC and thermolum. due to electron detrapping by local mol. motions 0-96898
- refractories, luminescence characteristics of pure surfaces acted on by flux of field emission electrons 0-100695
- rubrene, electrochemilum. by DC, highly organised EHD convection obs. 0-71499
- semiconductors, exciton and domain luminesc., book 0-82588
- tandem solar cells, detailed balance limit of efficiency 0-72056
- p-terphenyl, cryst., double injection and electrolum. 0-97342
- AlGaAs heterojunction photocell with luminesc. wavelength converter 0-108800
- Al_{0.5}Ga_{0.5}P, LPE, crystallographic obs. and electrolum. 0-88445
- Au, discontinuous films, electroluminescence obs. 0-103998
- Au/ZnSe:Mn/n-GaAs low threshold thin film DC electrolum. cell, pulse-excited characts. 0-76081
- Au-ZnS electrolum. Schottky barrier diode, S⁺-implanted, blue emission 0-76082
- BaTiO₃, pure and Fe doped, ferroelec., switching and electrolum. 0-76079

electroluminescence continued

- CaS:Pd phosphors, trap and luminescent centre location, photo-, thermo- and electroluminescence studies 0-71482
 CdF₂:NaF thin films, electroluminescence obs. at 77K (*French*) 0-80866
 CdSnAs₂-InP, n-p heterojunction, elec. props., electroluminesc., band struct. 0-75632
 Cu cathodes, broad area type, electrolum. regions, current-voltage char- acts. 0-84019
 Fe₂O₃, semicond. anode in aq. electrolyte, electrolum. and electrochem. 0-76080
 GaAlAs DH lasers, self-sustained pulsation suppression, effect of SiO₂ facet coating films 0-95894
 GaAs, electroluminescent study of irradiated induced struct. damage, athermal annealing 0-108280
 GaAs:O, electrolum., photolum., negative differential resist. rel. to recomb. processes 0-66304
 GaAs:Si p-n junction LED, electroluminesc. efficiency 0-71491
 GaAs/(Ga,Al)As, DH laser diode, electroluminescence near 1 eV 0-60682
 GaAs:P₂N, photolum. and electrolum. study of N isoelectronic traps 0-89061
 GaN, luminesc. centres 0-93405
 GaN, polarised electroluminescence emission, microstructure investigations 0-97344
 GaN:Zn, n-i struct., anomalous luminesc. 0-80865
 GaP electroluminescent diode struct. prep. by SSD and Czochralski methods, dynamic props. (*Czech*) 0-97425
 GaP:Bi,N, photoluminesc., electroluminesc., 4.2 to 300K, excitons and hole traps 0-108275
 p(GaP:Zn)-electrolyte interface, electrochemical LED, luminescence obs. 0-84507
 GaSb:Sn, p-n junction, electroluminesc. and photoluminesc. 0-66306
 GaSe, exciton-phonon quasibound states, photocond. and luminesc. study 0-96800
 Ge-Sb, far IR emission stimulation by impact ionisation 0-66301
 n-Ge-ZnSe:Mn²⁺-In₂-Sn₂O₃-y thin film electrolum. cell with low-threshold voltage 0-84786
 InAs and solid solutions, recombination mechanisms of excess carriers, luminesc. obs. 0-97337
 InGa_{1-x}As_xSi p-n structs., electrolum. spectra, 77 to 300K 0-93408
 InGaAsP-InP DH LED, high temp. aged, dark-spot defects, TEM obs. 0-66300
 KBr:Ti, electroluminescence, spectra and quantum yield activator conc. depend., cond. changes 0-89070
 KCl:Ti, electroluminescence, spectra and quantum yield activator conc. depend., cond. changes 0-89070
 KCl:Ti (0.003 to 0.27 mol.%), electrolum. 0-71490
 Mo (111), electroluminescence in 200 to 630 nm range 0-103997
 NaZnGeO₄:Mn, electrolum., ionisation domains 0-84787
 PbS_{0.9}Se_{0.1} 4.6 μm LED, room temp., band gap and electrolum. 0-66302
 Si p-n junction, reverse bias high voltage, secondary surface breakdown 0-70813
 Si:Al, localised exciton bound to isoelectronic trap 0-66283
 Si-SiO₂ electrode, electronic cond., luminesc. obs. 0-61111
 SiC (6H), blue-emitting diodes by CVD 0-97439
 SiC LED, defect luminesc. 0-89069
 SiC LEDs prepared by overcompensation method, photon assisted tunnelling 0-97341
 SiC p-n junction, electroluminesc. 0-97343
 SiC p-n junction, epitaxial, grown by sublimation, elec. and struct. props. (*Chinese*) 0-60067
 SiC p-n junctions, electrolum. spectra and kinetics 0-66305
 SnO₂-copper phthalocyanine-Ag systems, elec. and electroluminescent behaviour 0-80864
 SnO₂-Cu₂S-ZnS:Mn,Cu-Al₂O₃-Al, light-emitting struct., cond. and electrolum., heat treatment 0-97345
 SrTiO₃, semicond. anode in aq. electrolyte, electrolum. and electrochem. 0-76080
 Ta (111), electroluminescence in 200 to 630 nm range 0-103997
 TiO₂, semicond. anode in aq. electrolyte, electrolum. and electrochem. 0-76080
 W, surface adsorption processes following electron excitation, cathode-luminescence studies 0-100390
 WO₃, semicond. anode in aq. electrolyte, electrolum. and electrochem. 0-76080
 ZnO:Ce(Tb) phosphors, electrolum. brightness, voltage and freq. depend. 0-60681
 ZnO:Dy(Yb)(Nd)(Sm)(Pr)(Gd)(La)(Er), electrolum. brightness, field strength and freq. depend. 0-100696
 ZnS crystals in electrolyte, electrolum. and elec. props. 0-93407
 ZnS films, electrolum., bistable excitation 0-93406
 ZnS, post field recomb. in pulsed electrolum. 0-71488
 ZnS powder phosphors electroluminescent cells, AC electrolum. characts. (*Japanese*) 0-71489
 ZnS, prebreakdown electrolum., domain form. and negative resist. effects 0-84788
 ZnS thin films, effect of fabrication parameters on electroluminescence and related props. (*Japanese*) 0-76083
 ZnS:Cu, Cl, Mn film, AC electrolum. 0-60680
 ZnS:Cu, Mn DC electroluminescent powder panels, bulk and junction effects 0-89068
 ZnS:Mn, Cu, Cl films, AC electrolum. 0-60679
 ZnS:Mn AC thin film devices, domain electrolum. 0-66303
 ZnS:Tb, Cu(Ag) phosphors, luminesc. props. 0-100690
 ZnSe, low resistance ohmic contacts using In-Ga liquid alloy, LED fabrication appl. 0-70823
 ZnTe, low voltage green LED, struct. double diffusion procedure 0-100697

electrolysis

- see also anodisation; electrical conductivity of electrolytic liquids; electrodeposition; electroforming; electrolytic dissociation; electrolytic ion mobility; electrolytic machining; electrolytic polishing
 ageing effects, kinetic and structural consequences 0-61109
 alternating current electrode processes, review 0-61107
 anodic electrolysis of radioactive isotopes (*Hungarian*) 0-93765
 bubble growth rate, during electrolysis in supersaturated liq. 0-61104
 cathodes, phosphate pickled mild steel, behaviour during deep electrolytic water enrichment, T meas. 0-93764
 cells, high current density, high press. advanced cells for H₂ production 0-61441

electrolysis continued

- ion discharge, periodic 0-66813
 organic substances, electrochemiluminescence as possible source of coherent radiation, and role in biological processes (*Russian*) 0-76093
 polymer solutions, diffusion of ionic species, meas. by diffusion controlled electrolysis 0-74920
 polystyrene lattices, electro-flotation, collection efficiency 0-74946
 pulse electrolysis, theoretical aspects 0-85191
 steam electrolysis at high temp. for H₂ production 0-61440
 steel, Ni-Cr, anodic dissoln. in NaCl solns. at high current densities (*Russian*) 0-76396
 steels, obs. and anal. of sulphides, using non-aqueous electrolyte-potentiostatic etching method (*Japanese*) 0-89433
 water, CW and flash photoelectrolysis using ferroelectric photoanodes 0-81339
 water, photoelectrolysis, using Fe₂O₃-coated n-Si heterostruct. photoanode 0-61384
 water, photoelectrolysis with TiO₂ catalyst 0-60755
 water photoelectrolysis, rel. to charge transfer via surface states of semicond. 0-75636
 Al-Al₃Ni, electrolytic prep. of Al₃Ni fibres, SEM and anodic polarisation studies 0-100817
 Cd₂GeO₄ anode for H₂O photoelectrolysis 0-108716
 CdIn₂O₄ anode for H₂O photoelectrolysis 0-108716
 Cd₂SnO₄ anode for H₂O photoelectrolysis 0-108716
 Cr-W, anodic dissoln. at high current densities (*Russian*) 0-76395
 CuSO₄ soln., electrochemical analogue of Benard instability, isothermal and potentiostatic conditions 0-76530
 Fe-Ni-C, quenched martensite, annealing during cathodic hydrogenation, 200°C (*French*) 0-93573
 HBr electrolysis for H₂ production 0-97816
 H₂O, alkaline electrolysis using inorganic-membrane-electrolyte for H₂ prod. 0-72092
 H₂O, design and operation of advanced H₂O electrolyzers for H₂ prod., review 0-61449
 H₂O electrolysis in fused NaOH for H₂ prod. 0-76660
 H₂O, H₂ production, module design, geometry, capacity, operating temps., pressures, electrode types 0-72098
 H₂O, high temperature electrolysis of steam H₂ production, fusion reactors, synfuel production 0-72099
 H₂O, nucleate boiling, vapour bubble behaviour, heat and mass diffusion 0-67013
 H₂O photoelectrolysis, H₂/hydrocarbon fuel prod. via biomass conversion wastes 0-89653
 H₂O, production of H₂, on-site, for electric generator cooling 0-72097
 H₂O, with solid polymer electrolyte, for H₂ production 0-61442
 Li₂O-SiO₂ glass, protonated, field-driven guest proton redistrib. 0-107474
 Mo foils, device for electrolytic thinning from wire, for electron microscopy 0-85105
 Na₂O-CaO-SiO₂ molten glass, electrolysis reactions 0-89496
 Ni-Cr, anodic dissoln. in NaCl solns. at high current densities (*Russian*) 0-76396
 NiH₂ formation, electrolytic charging of pure Ni 0-71626
 P reduction in sewage effluent by electrochemical process 0-104445
 ZnCl₂-KCl-NaCl, molten system, containing Ni²⁺ ions, appl. to electrowinning, polarographic study 0-66810

electrolytes

- for solid electrolytes see superionic conducting materials
 see also electrolysis; superionic conducting materials
 aerosol OT-n-heptane-water, reversed micellar solution; addition of electrolyte, neutron small angle scattering 0-104468
 alkaline, W monocryst. anode soln., surface orientation and anode current effects (*Russian*) 0-75360
 aqueous electrolyte solutions, vel. correls., improved representation 0-59360
 aqueous media, ion-pairing, hard sphere model 0-96428
 binary electrolytes, pair distrib., osmotic coeff. in conc. up to 1 mol/l 0-61148
 bright plating, from zincate electrolytes, progress 0-66442
 charged hard-sphere fluid, electrified interface pot., extended mean spherical approx. calcs. 0-84502
 Coulomb systems, equilib. distrib. functions expansion in power of density 0-64681
 crystalline stoichiometric hydrates, struct., Raman spectra, H-bond interactions (*German*) 0-80804
 dipolar hard sphere solvent with charged hard spheres, hypernetted chain approx. 0-61130
 electric double layer, primitive models, pot. difference and charge density 0-76515
 electrocapillary acceleration meters, electrolyte composition selection 0-73331
 electrocapillary acceleration meters with electrolyte in gel form 0-73330
 electroplating, rack parts or bulk goods, in GTL-barrel units, Zn coating using acid electrolyte (*German*) 0-84862
 fluoride mixtures, molten, for Ge powder electrodeposition 0-60797
 gas-electrolyte dispersions, void fraction meas. using conductivity method 0-76525
 generalised polymer problems, Flory exponents 0-107039
 inorganic-membrane electrolytes for H₂ prod. by H₂O alkaline electrolysis 0-72092
 ionic drift from 50 Hz supply, pulse echo technique 0-70314
 ionic mass transfer in narrow rectangular conduits 0-61105
 ionic systems, weakly screened, evaluation of convolution integrals appearing in integral eqn. describing pair correlations 0-84044
 lithium salt electrolyte submillimetric absorption obs. 0-60611
 macroion solutions, theory of effect of small ions on electrical admittance 0-71914
 macromolecule, charged, in external elec. field, spherical case 0-75145
 mass transfer, ionic, in open channels, electrolyte probe determ. 0-59110
 mixed salt solution approximating seawater composition, dielec. and radiation characts. 0-97184
 nonionic surfactants, stabilisation of bubble nuclei in agarose gels 0-76562
 outer-sphere electron transfer in polar solvents, Debye theory 0-93762
 polyelectrolyte soln., counterion condensate around line charge as δ-function, nonlinear Poisson-Boltzmann theory 0-85184
 polyelectrolytes, saturation of induced dipole moment, orientation mechanism and electro-optical effects 0-84785
 polymer electrolytes, solid, H₂O electrolysis, H₂ technology 0-67012

electrolytes continued

- polystyrene, sulphonated, polyelectrolyte solution, correlations and dynamics 0-104446
 primitive model electrolytes, grand canonical Monte Carlo calculations 0-92427
 primitive model electrolytes, symmetrical, canonical Monte Carlo calcs. 0-92428
 sodium polystyrene sulphonate in aq. soln., quasi-elastic light scatt. 0-100661
 solid polymer electrolyte H₂O electrolysis, appl. to H₂ prod. 0-61442
 solution containing spherical particles, appln. of hypernetted chain approximation to particle interaction 0-85185
 solutions, aqueous, apparent molal isochoric heater. capacities at 25°C 0-59671
 solutions, electron energy 0-66812
 solutions in alcohols, ultrasonic vel. and density meas. used to calc. compressibility, intermol. free length and salivation no. 0-96150
 symmetric electrolytes, charged surface electrostatic repulsion, numerical procedure 0-104441
 thermal battery cells using molten nitrates as electrolyte and oxidiser 0-76624
 trifluoromethanesulphonic acid, and salts, electrochem. characts. in nonaqueous solvents 0-89499
 Ag-Sb alloy coating deposition (*Bulgarian*) 0-93763
 Bi₂O₃/Bi³⁺/electrolyte system, field and temp. depend. of electronic current 0-66814
 CsCl, activation coefficients and solvation numbers in mixed methanol solvents 0-81334
 CuBr₂(Cl₂), aq. soln., structural transition, neutron diffr. study 0-64872
 CuCl₂(Br₂), aq. solns., EXAFS meas. 0-60714
 CuSO₄/H₂SO₄ electrolytes, densities, elec. cond., viscosities 0-107455
 KBr, activation coefficients and solvation numbers in mixed methanol solvents 0-81334
 KCl, activation coefficients and solvation numbers in mixed methanol solvents 0-81334
 KNO₃, activation coefficients and solvation numbers in mixed methanol solvents 0-81334
 Li closoboranes as electrolytes in Li solid cathode cells 0-108794
 Li salt based solid electrolyte, synthesis and characterisation, secondary cell appl. (*French*) 0-72034
 LiAlCl₄, solid and molten electrolyte, thermodynamic stability 0-107447
 LiCl aqueous solns., dynamical props., by ultrasonic propag. meas. 0-76517
 LiCl electrolyte influence of lasing props. of rhodamine G solutions 0-91788
 NH₄Cl, activation coefficients and solvation numbers in mixed methanol solvents 0-81334
 NaCl, activation coefficients and solvation numbers in mixed methanol solvents 0-81334
 NaCl, monoelectrolyte, highly mineralised salt soln., dielec. and radiation characts. 0-97184
 NaClO₂ electrolyte influence on lasing props. of rhodamine G solutions 0-91788
 NiCl₂, aq. soln., structural transition, neutron diffr. study 0-64872
 NiCl₂(Br₂), aq. solns., EXAFS meas. 0-60714
 SrBr₂, aq. solns., EXAFS meas. 0-60714
 Ti electrochemical machining, electrolytes development, electrochem. in static solns. 0-85182
 Ti electrochemical machining, electrolytes development, electrochem. studies in flowing solns. 0-85183
 Zn secondary batteries, props. of alternate electrolytes 0-104502
 ZnBr₂, aq. solns., EXAFS meas. 0-60714
 ZnCl₂, aq. soln., structural transition, neutron diffr. study 0-64872
 ZnCl₂-KCl-NaCl, molten system, containing Ni²⁺ ions, appl. to electrorefining, polarographic study 0-66810
 ZnSO₄ electrolytes containing Ge and Co, polarisation charact., exam. by cyclic voltammetry 0-104444

electrolytes, solid see superionic conducting materials**electrolytic capacitors**

- power, dielectric liquids flammability and degradation 0-88944
 Al solid, pit etching method for improving freq. and temp. characts. 0-100944

electrolytic conductivity of liquids see electrical conductivity of electrolytic liquids**electrolytic deposition see electrodeposition****electrolytic devices**

No entries

electrolytic dissociation

see also electrolytic ions

- electroviscous effect, AC characteristics, pressure-drop fluctuations 0-107457
 ion trajectories in weak electrolytes, dissociation and recomb. of ions 0-85189
 GeO₂-Na₂O, Na⁺ partial dissociation investigated by elec. meas. 0-92716

electrolytic ion mobility

see also electrophoresis

- polar liquids in double layer capacitors, RF conduction, ion diffusion effect 0-107883
 Al-Nb superimposed metallic layers, ionic movements during anodization, Rutherford backscatt. and nuclear microanal. 0-71913
 γ-Al₂O₃ interface with electrolyte solns., adsorption of ions, surface conductance, ion mobility and surface pot. 0-75622
 Nb-Al superimposed metallic layers, ionic movements during anodization, Rutherford backscatt. and nuclear microanal. 0-71913
 Nb-Ta superimposed metallic layers, ionic movements during anodization, Rutherford backscatt. and nuclear microanal. 0-71913
 Ta-Nb superimposed metallic layers, ionic movements during anodization, Rutherford backscatt. and nuclear microanal. 0-71913
 ZrF₄-based glasses, elec. transport props. 0-79983

electrolytic ions

see also electrical conductivity of electrolytic liquids; electrolytic dissociation; electrolytic ion mobility
 trajectories in weak electrolytes, dissociation and recomb. of ions 0-85189

electrolytic machining

see also electrolytic polishing

- steel, Ni-Cr, anodic dissoln. in NaCl solns. at high current densities (*Russian*) 0-76396

electrolytic machining continued

- tools, Cu-BN composite, dynamic hot pressing 0-84889
 Al foil electrolytic perforation, surface film phase composition obs. (*Russian*) 0-61004
 Cr-W, anodic dissoln. at high current densities (*Russian*) 0-76395
 Mo foil electrolytic perforation, surface film phase composition obs. (*Russian*) 0-61004
 Ni foil electrolytic perforation, surface film phase composition obs. (*Russian*) 0-61004
 Ni-Cr, anodic dissoln. in NaCl solns. at high current densities (*Russian*) 0-76396
 Ti alloys, electrochemical working, film form. and surface roughness (*Russian*) 0-76397
 Ti electrochemical machining, electrolytes development, electrochem. in static solns. 0-85182
 Ti electrochemical machining, electrolytes development, electrochem. studies in flowing solns. 0-85183
 Ti foil electrolytic perforation, surface film phase composition obs. (*Russian*) 0-61004

electrolytic polishing

see also electrolytic machining

- cathode polishing effect, nanosecond discharge in vac. 0-79599
 Incoloy 800, steam oxidised, oxide coating anal. 0-89399
 metal, high melting point, electrolytic polishing and etching to reveal struct. (*German, English*) 0-89417
 metal spheres, electromechanical polishing and etching 0-68188
 procedures for electrolytic polishing of a number of special materials (*German, English*) 0-89382
 Ag and alloy electron microscope specimens, noncyanide electropolishing method 0-100967
 Ti, optical props. from 1.8 to 3 eV 0-85088
 W, polishing technique as prep. for TEM 0-71851

electromagnetic absorption see electromagnetic wave absorption**electromagnetic compatibility**

see also frequency allocation

- controlled fusion expt. shielding and earth loop elimination using fibre optics 0-74007
 international calibration cycles of field intensity and power density, measurements 0-82752
 TEM lines used in EMC tests 0-83536

electromagnetic corrections

"electromagnetic corrections" is distinguished in use from "radiative corrections" by application to elementary particle and nuclear interactions

see also radiative corrections

- Higgs boson decay, QED and QCD radiative corrections 0-95275
 SU(2)_L × U(1) theory, radiative corrections, simple renormalisation framework 0-101973
 weak and EM radiative corrections to low-energy processes 0-95274
 e⁺e⁻ → μ⁺μ⁻, radiative corrections around Z⁰, Weinberg-Salam model 0-99103
 μp deep inelastic scatt., inclusive cross section, lepton pair EM prod. contrib. (*Russian*) 0-105904
 ν_ee⁻ → ν_μe⁻, weak and EM radiative corrections, sensitivity test 0-105880

electromagnetic decays

- baryon resonances, EM transitions, multipole moments in single quark transition model 0-62985
 charmonium electromagnetic decay, relativistic eval. 0-68459
 flavour changing weak radiative decays, short and long distance effects 0-73712
 light meson radiative decay, Zweig law (*Russian*) 0-102051
 meson photocoupling in quark model 0-82954
 meson-antimeson hadronic molecules, spectrum, leptonic and radiative decays (*Russian*) 0-57602
 tensor meson radiative decay in SU(6) × O(3) broken symmetry quark model 0-73710
 vector meson radiative decays, SU(3) symmetry viewpoint 0-95273
 vector meson radiative decays, vector dominance model in broken SU(3) 0-73711
 vector mesons, EM decay in broken SU(3) 0-82976
 vector mesons, radiative decay, single parameter scheme 0-86720
 B → B'πγ, contribs. of B → B'γ process 0-78066
 χ → ππγ, charmonium E1 radiative transitions and quark mag. moments 0-86721
 D⁺, charmed tensor meson, strong and EM decay modes 0-68451
 e⁺e⁻ → γγ, 9.4-31.6 GeV, differential cross section, T → γγ decay limits 0-91073
 e⁺e⁻ initiated γγ processes, charged pair prod., f⁰ → γγ width 0-91123
 η(η') → γγ, quark model tests 0-78067
 η → γγ(π⁺π⁻γ), chiral quark model anal. (*Russian*) 0-105900
 η → μ⁺μ⁻γ, branching ratio and η EM form factor 0-105899
 η → ππγ, quark loop model, SU(3) splitting of quark masses 0-62990
 η → ργ(γγ), C-even meson radiative decay, SU(3), and VDM anal. (*Russian*) 0-68460
 η' EM decay, η-η' mixing and gluons 0-62981
 η' → γγ(π⁺π⁻γ), chiral quark model anal. (*Russian*) 0-105900
 η' → π⁺π⁻γ(γγ), quark model descript. 0-62970
 F₁ → F₂γ, nondiagonal transition amplitude for arbitrary fermion charges (*Russian*) 0-86722
 F⁺⁺, charmed tensor meson, strong and EM decay modes 0-68451
 K_s⁰ → γγ, (π⁺π⁻γ), chiral quark model anal. (*Russian*) 0-105900
 K⁺ → K⁰γ, quark loop model, SU(3) splitting of quark masses 0-62990
 K⁰ → K_s⁰γ, SU(3) and isospin symmetry breaking effects 0-95272
 K_s⁰ → K_s⁰γ and Primakoff conversion of K_s⁰ to K_s⁺ 0-73695
 μ⁺ → e⁺γ, upper limit for branching ratio 0-78051
 P → γ⁺γ⁺, EM characts. for pseudoscalar meson decay in nonlocal quark model (*Russian*) 0-102050
 φ → ηγ, quark loop model, SU(3) splitting of quark masses 0-62990
 π⁺ → e⁺γ, isospin-breaking, chiral limit, conserved-vector-current violation, σ model 0-62988
 π⁺ → e⁺γ, modified quark loop model, form factors, struct. functions, radiative decay 0-91088
 π⁺ → e⁺γ and SU(3) × SU(3) σ-model 0-78054
 π⁰ → 2γ, decay width as signal for nuclear matter phase transition, Primakoff effect 0-86842
 π⁰ → 2γ, tensor-trace and triangle anomalies 0-73709
 π⁰ → γγ(π⁺π⁻γ), chiral quark model anal. (*Russian*) 0-105900
 π⁺ → p-η(η'), 8.45 GeV/c, differential cross section ratio, η' decay branching 0-78094
 ψ → 3γ, heavy narrow state search, η' and η_c branching ratios 0-57600

electromagnetic decays continued

- $\psi \rightarrow \eta \gamma$, QCD, width, exclusive OZI violating radiative decay 0-68458
- $\psi \rightarrow \eta(\eta') \gamma$, quark model tests 0-78067
- $\psi \rightarrow \eta \gamma$, conflict with single parameter scheme for radiative decays of vector mesons 0-86720
- ψ radiative decay width from glueball model 0-62941
- ψ , ψ decay branching ratios, isospin and flavour symmetry breaking 0-95264
- ψ and ψ decay ratios, composite particle matrix elements 0-95266
- $\psi \rightarrow \chi \gamma$, charmonium E1 radiative transitions and quark mag. moments 0-86721
- $\psi \rightarrow \psi \gamma \gamma$, $\psi \rightarrow \gamma \chi$, $\chi \rightarrow \gamma \psi$ branching ratios 0-57601
- (qq) $\rightarrow (\bar{q}q') \gamma$, width, exclusive OZI violating radiative decay 0-68458
- $\rho \rightarrow \pi \gamma$, radiative decay width from pion excitation anal. 0-57599
- $\sigma \rightarrow 2\gamma$, tensor-trace and triangle anomalies 0-73709
- $\Sigma^+ \rightarrow p \gamma$, $1/2^-$ resonance poles to parity-violating amplitude, two-quark weak transitions 0-78062
- $\tau \rightarrow \nu \pi \gamma$, π form factors, axial-vector and structure dependent, vector meson dominance model 0-62989

electromagnetic energy *see electromagnetic waves***electromagnetic field theory**

- see also electromagnetic waves; electromagnetism*
- 3D nonlinear EM field anal. using computer program TOSCA 0-95765
- antenna-potential approx. of EM field 0-68060
- canonical formulation of the classical electromagnetic field 0-86095
- charged particle config., stability 0-57109
- coupled-bar problems, conformal transformations combined with numerical techniques 0-83538
- dielectric, damped integrodifferential eqns., asymptotic bounds to system of solns. 0-62493
- dual representation with circuit theory, Poynting's theorem 0-94963
- education, classical mechanics gauge invariance, derivation of Maxwell's eqns. 0-73131
- energy flow vector of EM field 0-83537
- Galilei covariant theory, minimal EM coupling 0-77634
- gauge invariance, EM four pot., transformation properties 0-91002
- gauge transformation, distribution of fields and sources of singular vector potential 0-73190
- geometric unification of classical gravitational and EM interactions 0-57165
- interaction of electron beams with microwave-frequency field, of planar gap 0-106431
- irregular boundaries problems, direct noniterative numerical soln. using network analogues 0-95766
- magneto-dipole configurations in general relativity 0-67539
- Maxwell equation integration in laminar media 0-68059
- molecular interaction with EM fields, classical theory 0-95686
- nonstationary and inhomogeneous, time-space-dependent power spectrum 0-77635
- scatterer surface current density, calc. using numerical technique 0-78747
- spinor representation of Maxwell's eqns., algebraic props. 0-86097
- spinor representation of Maxwell's eqns. 0-86096
- torison, effect on gauge invariance, semi-minimal coupling principle 0-77675
- variational principles for Maxwell's equations 0-78744
- vector product formulation of special relativity and electromagnetism 0-105496

electromagnetic fields

- channel waveguide interferometric modulator for EM field detection 0-74498
- charged particles motion, Lagrangian and Hamiltonian up to fourth-order terms 0-91736
- circumferential stress in large high field magnet coils, thick-thin cylinder approach 0-95761
- crystalline slab, EM field in 0-96463
- detection of HF EM fields by nerve cell membranes, possibility discussion (Russian) 0-76785
- Earth, boundary conditions for EM field above two-dimensional inhomogeneous struct. 0-85595
- Earth, EM field subsurface propag. from horizontal elec. dipoles 0-98229
- electric machine active parts electrodynamic equations general solutions using orthotropic modelling (Russian) 0-99601
- electron band structure, optically induced in external plane wave field 0-106432
- entomological experiments on teratogenic effects of EM fields 0-85446
- excitation in cavity in conducting shell by penetrating radiation 0-87263
- ferromagnetic conductor, cylindrical, acoustic wave propag., EM field behaviour 0-88857
- flowmeter with moving field, fluid flow and moving field equations (Rumanian) 0-64663
- health effects regulation from AC transmission line electromagnetic fields 0-94286
- LF, problem of conducting ellipsoid 0-58444
- LF seabed sounding (Russian) 0-67431
- liquid crystals, thermooptical effects used to visualise EM fields 0-62723
- Lorentz transform law for EM field, fluxoid motion example 0-67954
- magnetic oblique rotator, EM field prod., exact vacuum soln. 0-58442
- magnetosphere boundary layer, EM fluctuations excitation by field-aligned currents 0-67473
- MHD laminar flow, longitudinal dynamic effects determination for Na, Al, Sn and Hg (Rumanian) 0-64792
- neutron stars, electrodynamics in curved space 0-90465
- plate-conductors system, multiparallel, losses calc. 0-78743
- radially symmetric reradiating scatterers in EM fields, formulae for simple treatment (German) 0-87270
- radiation from vertical electrical vibrator, located on axis of ideally conducting disc 0-106418
- resonant energy transfer from electrons to a slow electromagnetic wave 0-83545
- static and stationary, determ. using variation calculus (Hungarian) 0-87259
- Stormer problem, equilb. points in planar mag. binary problem 0-82178
- TEM lines, EMC tests 0-83536
- transducer, straight-through screened circular primary, between multilayer cylinder and tube, EM field 0-71856
- transient, steady-state solns. in cylindrical enclosure 0-83535
- vertical magnetic dipole on two-layer Earth 0-76906
- welding arc, EM forces effect on plasma flows, calc. 0-83912
- Zeeman effect, linear, relativistic correction, Coulomb field 0-102484

electromagnetic induction*see also inductance*

- Alaska oil pipeline, elec. current induced by electrojet 0-61756
 - conducting ellipsoid in LF EM field, induced elec. and mag. moments 0-58444
 - cross-borehole EM probing, location of high-contrast anomaly 0-72639
 - cryogenic rings, current induction and decay 0-106972
 - current-carrying coil, moving above conducting plate, forces and moments 0-87264
 - Earth, boundary conditions for EM field above two-dimensional inhomogeneous struct. 0-85595
 - Earth, VLF response of laterally inhomogeneous anisotropic ground 0-85754
 - Earth surface impedance, N-layered half space theory 0-76909
 - eddy current field in screened transducer field, dynamic anal. (German) 0-95763
 - eddy currents in cylindrical core of induction coil considering winding helix (German) 0-95764
 - electrode arrays for Earth induced polarisation (IP) sounding, effects of EM coupling over uniform half-space 0-101324
 - ferromagnetic plates eddy current phenomena numerical computation method (German) 0-65952
 - flowmeter with moving field, fluid flow and moving field equations (Rumanian) 0-64663
 - geoelectric, EM induction in thin sheet conductivity anomalies at Earth's surface 0-76907
 - geoelectric sounding of buried axial conductor, time-domain response 0-105059
 - geoelectric sounding of conductive circular cylinder, expt. and theoretical results 0-105058
 - geomagnetic induction in central Australia, meas. 0-72424
 - geomagnetic transfer functions at pulsation periods 0-72417
 - geophysical, model of E. coast region of N.America 0-98235
 - geophysical sounding of dipping half plane embedded in conducting rock 0-90236
 - geophysical surveying, transient time-domain EM method 0-98227
 - geothermal energy resources in Oregon, USA, elec. and EM sounding obs. 0-97761
 - history of Arago's, Babbage and Herschel's and Faraday's experiment 0-68013
 - homopolar disc dynamo system, magnetic instability 0-81808
 - layered Earth with surface-loop inductor, transient response, theory 0-72410
 - magnetic induction, large-scale demonstration 0-101699
 - magnetotelluric apparent resistivity, effect of localised source 0-72429
 - ocean coast effects 0-76908
 - ocean current induced EM fields, theory 0-61805
 - ocean electric current induced by Sq, around land masses 0-72413
 - ocean EM induction affecting Sq during IGY 0-72428
 - scatterer surface current density, calc. using numerical technique 0-78747
 - Sierra Nevada batholith, elec. conductivity of crust 0-72411
 - sounding of layered structure of Earth, time domain anal. 0-72641
 - steel, nitrified layer depth, electroinduction meas. method 0-104379
 - sulphide prospect in California copper belt, broadband EM study 0-72503
 - superconducting solenoids fields meas., automatic, using NMR 0-57344
 - Vancouver Island region, terrestrial EM induction 0-104879
 - Venus magnetic tail, unipolar induction effects 0-62060
- electromagnetic interference**
- see also radiofrequency interference; television interference*
 - angular scattering of water drops and ice particles [electromagnetic interference], frequencies above 10 GHz appl. 0-109183
 - electric equipment testing laboratory, movable, type ETL-35, design (Russian) 0-95088
 - nuclear power plant equipment electromagnetic interference and RFI effects 0-57880
 - X-ray image intensifier (German) 0-105761
- electromagnetic lenses** *see magnetic lenses*
- electromagnetic oscillations**
- see also cavity resonators; lasers; masers; ring lasers*
 - ferrite spheres, magnetisation, resonance oscillation freq. determ. 0-71106
 - semiconductor plasma, longitudinal oscillations 0-88583
- electromagnetic radiation** *see electromagnetic waves*
- electromagnetic theory of light**
- losslessness of optical systems in a vectorial treatment 0-83558
- electromagnetic wave absorption**
- see also electromagnetic wave propagation in plasma; gamma-ray absorption; light absorption; spectra; X-ray absorption*
 - aerosol, thin flat, EM wave scatt. and absorpt. 0-91723
 - atmosphere, propag. of microwaves, refr. and absorpt. coeffs., optimal orthogonal expansion props. 0-98414
 - black hole, Reissner-Nordstrom, coupled gravitational and EM perturb., scatt. matrix, energy conversion, quasi-normal modes 0-67775
 - cloudy atm., long distance meas. by radiometry 0-90196
 - crystalline slab of point molecules, dielec. theory 0-97222
 - dielectric fluid, Debye absorption at crit. liq.-vapour transition 0-100322
 - diffraction by strip under mixed boundary conditions 0-87268
 - dissipative structures, formation and stability 0-108950
 - EM absorbing wall with resistive sheets, circular freq. locus 0-106428
 - energy deposition in inhomogeneous block model of man for near-field irradiation conditions 0-89788
 - holographic unslanted transmission and reflection gratings, modal theory, EM wave propag. 0-83673
 - intergalactic radiation field, absorpt. due to pyrolytic graphite whiskers rel. to microwave background 0-94866
 - ionosphere, A1 absorption measurements at 2.4 and 5.6 MHz 0-82132
 - ionosphere, global absorpt. meas. on board ships 0-98500
 - ionosphere radio wave absorption, morphological features of winter absorpt. anomaly at middle latits. 0-67459
 - ionosphere winter absorption anomaly, implications of eddy diffusion models for mesosphere and lower thermosphere 0-109198
 - microwave absorption in atmosphere of giant planets induced by collisions of H molecules 0-90350
 - microwave power absorption differences between normal and malignant tissue 0-104640
 - neutron stars, magnetic, photons free-free absorpt. rel. to radiative heat transfer in plasma layers 0-94826
 - paramagnetic crystal, quantum amplification and absorpt. of EM wave in moderating structure 0-87361

electromagnetic wave absorption continued

- planetary nebulae, He II λ α photons absorpt. rel. to forbidden lines intensities 0-67833
 rain attenuation, radiometric determ. at millimetre wavelengths, multiple-scatt. effects metric determ. at millimetre wavelengths, multiple-scatt. effect 0-90260
 resonant energy transfer from electrons to a slow electromagnetic wave 0-83545
 semiconductor with superlattice in quantising electric field 0-108182
 semiconductors, electron-phonon interactions, combined phonon resonance (Russian) 0-75321
 small-radius scatterers, cyclotron resonance harmonics 0-71183
 superconductor, EM wave nonlinear absorpt. near one-photon threshold 0-60142
 thin absorbing films, plane-wave interaction 0-95767
 thin finite dielectric cylinder, scattering and absorption of EM waves 0-74281
 Bi, EM wave dispersion and damping, Voigt configuration, non-local calcs. 0-100475
 GdTb, ferromag., magnetisation and microwave absorpt. 0-65816
 He I 584 Å transfer in quasars and gaseous nebulae, photon destruction efficiency 0-67550
 n-InSb, degenerate plasma, Coulomb collision photon absorpt. dynamic screening (Russian) 0-92924

electromagnetic wave attenuation *see electromagnetic wave absorption; electromagnetic wave scattering*

electromagnetic wave diffraction

- see also electromagnetic wave propagation in plasma; gamma-ray diffraction; light diffraction; X-ray diffraction*
 anisotropic media, EM wave diffraction, threshold effects (Wood anomalies) 0-99608
 antenna potential method (Russian) 0-63899
 curvilinear surfaces with inhomogeneous admittance 0-69296
 cylindrical obstacle, high freq. two-dimens. diff. of incident anisotropic cylindrical wave 0-95770
 cylindrical pulse diff. by metallic half plane, boundary value problem, direct transform technique 0-69573
 cylindrical surfaces, ribbed, EM wave diff. 0-106424
 cylindrical wave diff. by cylindrical obstacle with arbitrary cross-section, asymptotic series solns. 0-99609
 diffraction by strip under mixed boundary conditions 0-87268
 diffraction grating props., theoretical model 0-91732
 electrodynamic boundary problem solution for complex shape regions 0-69300
 extended path with single obstacle, attenuation factor calc. 0-95775
 geometrical theory of diffraction for EM waves, book 0-73121
 grating EM theoretical developments 0-106633
 gravitational lens effect, EM wave diff. in Schwarzschild space-time 0-90750
 H-polarised EM wave, diff. by semiconductor strip 0-91730
 Helmholtz equation, direct quadrature soln., three-dimens. problems 0-74285
 Hertzian waves, reflection and diffraction by moving layers (German) 0-87266
 holographic gratings under grazing incidence in X-ray and XUV region, EM theory 0-90962
 by infinitely long perfectly conducting screens of finite width and thickness (German) 0-91724
 inhomogeneous medium, EM wave propagation, phase function method 0-69295
 inverse theory of scalar diff., eigenvalue formulation 0-102613
 magnetic field diff. meas. on axes of disks and apertures, Babinet principle, complex spirals 0-102599
 nonorthogonal series method in EM wave diff. problems 0-69299
 plane stationary diffraction of E-pol. EM waves by curvilinear screens (Ukrainian) 0-69294
 projection method, properties of parametric system of basic functions 0-87269
 projection methods, applicability limit 0-91734
 ray optical anal. of scattering from dielectric coated conducting cylinder 0-83542
 scalar wave scattering by periodic surfaces, general modal theory 0-87271
 spatially dispersive crystal, reflectivity and transmittivity 0-99604
 strips illuminated at grazing incidence, uniform geometrical theory of diff. soln. 0-58447
 two-dimensional wave beam diffraction by stripline grid 0-87273

electromagnetic wave diffusion *see electromagnetic wave scattering*

electromagnetic wave interference

- see also atmospheric; electromagnetic wave interferometers; electromagnetic wave interferometry; electromagnetic wave propagation in plasma; light interference; Moire fringes*
 No entries

electromagnetic wave interferometers

- see also electromagnetic wave interferometry; light interferometers*
 IR interferometer diamond anvil cell interface with beam condenser 0-86384
 Michelson interferometer with time resolved IR Fourier transform spectroscopy, practical aspects 0-86464
 optical fibre ring interferometer, Sagnac effect (Russian) 0-101835
 Wharton and Gardner microwave interferometer for plasma density meas. 0-87948
 X-ray interferometer, LLL type, interfering beam phase rels. 0-90973
 X-ray interferometer for meas. of K-edge dispersion anomalies in Se 0-90956

electromagnetic wave interferometry

- see also light interferometry; Moire fringes*
 3C 119, 286, 345, 454.3, quasars, 5 milliarsecond resolution maps at 1.67 GHz 0-82531
 3C 147, 3C 286, quasars, VLBI obs. at 329 MHz 0-67898
 3C 345, quasar, VLBI obs. at 1.67 GHz 0-94885
 compound conductors, impulse heating, Cu vapour conc. determ. 0-75346
 CTA 102, quasar, 5 milliarsecond resolution maps at 1.67 GHz 0-82531
 gravitational wave interferometer, quantum mechanical radiation press. fluctuations 0-90770
 heterodyne interferometers, quasilinear filtration theory appl. to signal processing (Russian) 0-82807
 impulse spark study using two-wavelength interferometry 0-86391

electromagnetic wave interferometry continued

- interstellar dark clouds, radio continuum interferometric search for newly formed H II regions 0-98699
 interstellar dark clouds, radio continuum interferometry rel. to newly formed H II regions physical props. 0-105301
 K-band microwave interferometry for measurements of high surface vels. 0-77761
 liquid dielectric, pulsed breakdown, interferometric obs. 0-80696
 NGC 1275, Seyfert galaxy, radio interferometer study of nucleus struct. (Russian) 0-62288
 Orion methanol masers, interferometric and multitransitional study 0-67891
 Pioneer Venus Differential Long Baseline Interferometry expt. 0-67578
 radio astrometry, influence of troposphere on radio-interferometric meas. of coordinates 0-67581
 radio interferometry obs. of Haystack-Westford base line vector, comparison with geodetic obs. 0-89929
 radiointerferometry, Mandel'shtam's research 0-105488
 radioimage mapping with uncalibrated visibility data 0-77295
 SS 433, change in radio struct., 1980 January to June, from VLBI obs. 0-109557
 superheterodyne tracking cct. for mm-wave measurements 0-59288
 three dimensional spatial autocorrelation function meas. rel. to sky brightness 0-67576
 Venus microrrelief irregularities mean height, determination from radio transillumination data 0-72807
 BaTiO₃, ferroelectric mechanisms, anharmonic couplings by scanning IR interferometry 0-75978

electromagnetic wave propagation

- see also atmospheric electromagnetic wave propagation; atmospheric light propagation; backscatter; electromagnetic wave absorption; electromagnetic wave diffraction; electromagnetic wave interference; electromagnetic wave propagation in plasma; electromagnetic wave reflection; electromagnetic wave refraction; electromagnetic wave scattering; guided electromagnetic wave propagation; light propagation; light transmission; radiowave propagation*
 3 GHz surface and lateral EM wave meas. 0-103742
 air-dielectric interface, EM wave reflection and transmission in terms of polarisation, education 0-105458
 anisotropic layered media, 4×4 matrix algebra 0-106445
 averaged Maxwell equations in severe random nonuniformities 0-69298
 azimuthally gyrotropic medium, EM wave spectrum, theory 0-91735
 circumsolar plasma, Venera 10 radio signal spectral meas. 0-109326
 coal, microwave propag. expts. rel. to anisotropic elec. props. 0-98312
 coherent propagation through sparse particle conc. 0-91729
 cubic crystals, paramagnetic nonlinear Faraday effect, EM wave propagation (Russian) 0-80761
 depth sounding interpretation, master tables, book 0-86043
 discontinuous or layer media, unidimensional propag. of transient signals 0-87265
 doped conducting media, low-freq. props., EM wave reflection 0-103715
 Earth, comprehensive study of subsurface propag. from horizontal elec. dipoles 0-98229
 Earth surface layer, EM wave refl. and transmission coeffs., linear ramp model 0-61759
 education, Brewster angle in semi-infinite dielectric moving perpendicularly to interface 0-57034
 EM radiation in media with spatial dispersion, spatial coherence formation and polarisation increase 0-106442
 ferromagnets with conduction electron spin, EM wave propagation with discrete spectrum 0-92923
 gyromagnetic media, energy-flow eqns. for bandlimited signals (German) 0-91725
 gyrotropic medium, Green's function and field of moving charges 0-58445
 heterogeneous media, long-wavelength EM propag. 0-63892
 holographic gratings, sharp boundaries, modal theory, EM wave propag. 0-83672
 holographic unsalted transmission and reflection gratings, modal theory, EM wave propag. 0-83673
 inhomogeneous medium, EM wave propagation, phase function method 0-69295
 inhomogeneous plasma, polarised radiation transfer 0-99607
 interface plane wave reflection and refraction, positron polarisation effects (Russian) 0-79431
 lake ice, microwave propag. rel. to radar and radiometry remote sensing meas. 0-85691
 laminated composites, bonding material influence 0-91726
 layer decomposition method for radiation propag. anal. (French) 0-95772
 linear wave growth in periodic structures, instabilities, amplification and stop bands 0-87276
 minimum autonomous blocks method for propagation of radiation in nonlinear medium 0-87274
 moving media, plane waves and refl. from moving interfaces 0-63890
 nematic liquid cryst., orientational fluctuations effect on evanescent modes of transmitted EM wave 0-64889
 nonlinear anisotropic dielectrics, nondispersive waves, EM disturbance propag. and reflection 0-106429
 nonlinear dissipative media, circularly polarised EM waves 0-63891
 nonlinear EM wave propagation, in strong mag. fields, second harmonic generation 0-77988
 planetary nebulae, EUV radiation transmission rel. to central stars temps. determ. 0-67724
 point source in one-dimensional, randomly inhomogeneous medium, with specularly reflecting walls 0-105514
 polarization effects in cosmological models with anisotropic curvature 0-94903
 problems connected with special source structs., review 0-87272
 projection methods, applicability limit 0-91734
 quasi-optical parabolic approx., in randomly inhomogeneous media, validity analysis 0-106422
 radiating system, EM wave transformation directionality diagrams 0-87275
 radio waves in ionospheres of Jupiter and Saturn, spectral broadening meas. by Pioneers 10 and (11) 0-109391
 ray surface equation and Fermat's principle, in moving anisotropic media 0-106425
 semiconductor with superlattice, EM wave propag., mag. field effect 0-70745

electromagnetic wave propagation continued

- semiconductors, EM wave interaction in weakly nonlinear medium with superlattice 0-93257
- slow EM wave theory in conducting jets 0-91731
- solar wind turbulent plasma, radio wave propag. meas. using three satellites 0-101518
- subsurface radar using video pulse for deep probing in Earth, pulse propag. in lossy media using LF window 0-74282
- uniaxial plasma or dielec. half-space, EM radiation from line source, theory 0-99605
- Al, electromagnetic wave propagation, demonstration 0-73149
- Bi, EM wave dispersion and damping, Voigt configuration, non-local calcs. 0-100475
- Bi₂-Sb₂, EM wave propag. for rot. of mag. field from Faraday to Voigt config. 0-84419
- Cu film, optical const. deduced from surface EM wave propag. 0-60697
- SiO₂ film on Cu substrate, surface EM wave absorpt., optical const. (Russian) 0-108216

electromagnetic wave propagation in plasma

- see also *ionospheric electromagnetic wave propagation; light propagation in plasma; magnetospheric electromagnetic wave propagation*
- absorption and dual propagation in warm, plasma half-space, density and temp. depend. 0-75048
- absorption at electron cyclotron freq. 0-79457
- air plasma, radiowave interaction, electron velocity, collision cross-section depend. 0-103155
- bragg effects in microwave transmission through stationary plasma structures 0-83944
- caviton, dissipative three-dimens. Langmuir soliton, formation (Russian) 0-83943
- circumsolar plasma, radio signal spectral lines formation 0-92330
- collisionless magnetoplasma, EM wave conversion to extraordinary wave 0-79451
- complex nonlinear impedance of flat antenna 0-103130
- complex ray analysis for plasmas 0-83902
- Cotton-Mouton effect in Jupiter ionosphere and magnetosphere, rel. to decametric radio emission modulation 0-67643
- cylindrically confined cold plasma, overdense and steep density, plane EM wave scattering 0-70005
- DC arc plasma, alterations in spectral line intensities due to external mag. fields 0-79621
- delay line simulation, wave propag. in dispersive and attenuating media 0-82606
- dense pinch, electron-positron pair production in EM field (Russian) 0-100092
- depolarisation in plasma with MHD turbulence (Russian) 0-103154
- diffraction radiation characts. of an open conducting periodic struct., temp. and elect. conc. determ. (Ukrainian) 0-70004
- dipole antenna in magnetoactive plasma EM field distrib. 0-100079
- dispersion, of plasma waves propagating along mag. field in strongly anisotropic relativistic plasma 0-67542
- electric field fluctuations spectrum, laser fluoresc. spectroscopy meas. 0-87946
- electron beam, relativistic mirror feature, perp. temp. effects 0-78749
- electron beam produced inert gas plasmas, UV to near IR laser lines 0-92334
- electron magnetised plasma, stability in circularly polarised EM wave field 0-87897
- electrostatic pulse generation by two electromagnetic pulses 0-92295
- EM soliton propagation in nonequilibrium dispersive media (Russian) 0-106933
- EM wave penetration into plasma, permittivity sign changes (Russian) 0-100477
- emission, absorption and transfer of waves in astrophysical diffuse magnetised plasmas, book 0-105446
- energy transport from 1.06 μ m and 0.53 μ m laser plasmas interactions at 10^{15} W cm⁻² 0-92261
- flame plasma with presence of current, EM radiation obs. (Russian) 0-103126
- H-polarised EM wave by isotropic moving plasma, transient response 0-64731
- heating by EM wave transmission in mag. field (Russian) 0-103167
- heavy-particle acceleration by charge-density waves in vacuum and in plasma 0-70044
- HF discharge, ionisation overheat instability in EM wave field (Russian) 0-106990
- high-frequency heating of inhomogeneous plasma in $\omega \geq \omega_{Hi}$ freq. range (Russian) 0-106946
- high-frequency wave propag. in strongly magnetised plasma 0-103158
- hot collisional plasma filled waveguide, wave propag. 0-92331
- hydrogenic ion lines, red shift in plasma 0-103128
- impulse response of Lorentz medium 0-59242
- inhomogeneous magnetoactive plasma, EM waves linear interaction 0-96364
- interaction of photons with electrons in dielectric media (German) 0-103117
- interaction of plasma with strong EM wave, efficient transformation of radiation frequency 0-106931
- ion-acoustic fluctuations, CO₂ laser study 0-83946
- ion-acoustic pulse generation by 2 EM pulses at difference freqs. in collisionless plasma 0-79475
- ionosphere, decametric freq. shift of magnetoionic component 0-105104
- kilometric radiation in Jupiter magnetosphere, ray tracing 0-72866
- Langmuir system, kinetic theory of mag. field generation 0-69974
- laser light parametric absorpt., convective parametric instability 0-100073
- laser radiation propagation, scatt., third harmonic freq. radiation flux density 0-87901
- laser-plasma interaction and ablative acceleration of thin foils at 10^{12} - 10^{15} W/cm² 0-83963
- layered plasma, use of Fuchsian differential eqns. 0-75060
- low Z plasma, 1.06 μ m low pulse reson. absorption 0-87903
- magneto-active plasma, parametric instabilities set up by EM radiation (Russian) 0-106889
- magnetoactive plasma, total absorpt. of EM wave (Russian) 0-106944
- magnetoplasma, interpretation of 6-component measurements of wave field 0-83921
- magnetoplasma, refr. index profiles in layered media, extraordinary mode 0-77223

electromagnetic wave propagation in plasma continued

- maser emission, by plasma produced electrons orbiting a positively charged wire 0-92272
- mass renormalization in stochastic acceleration of particles (Russian) 0-100066
- modulational instability of nonlinear wave propagation in relativistic plasmas 0-106911
- neutral atoms in plasma background, strong EM radiation effects 0-103157
- nonlinear estimates of Brillouin scatter in plasma 0-87895
- nonlinear interaction, electron collision freq., self-consistent eqn. (Russian) 0-75055
- nonlinear scattering of upper hybrid laser radiation by electron Bernstein modes in a plasma 0-64720
- nonlinear subharmonic wave generation in nonuniform plasmas 0-106912
- nonstationary plasma, anomalous radiation intensity 0-87898
- nonuniform Vlasov plasma, wave propagation theory 0-79508
- p-polarised EM wave struct. near point of reflection (Russian) 0-103118
- plasma column, overdense, reson. microwave absorpt. 0-64732
- polarisation of picosecond excited continuous X-ray radiation (Russian) 0-59190
- ponderomotive craters, in phased waveguide array plasma, form. by microwave irradi. 0-83885
- power reflection, transmission and absorption coefficients for a moving plasma slab in a rectangular waveguide 0-106925
- pulsed RF-trapped particle interaction stochastic effects in tokamak 0-59245
- quasi-static potential oscillations of thin conductor, instability 0-87900
- radar signal reflection from Sun, efficiency of four-plasmon interactions 0-101582
- radiowave dispersion by plasma ejected from BL Lacertae objects 0-82516
- radiowave propag. in turbulent shearing plasma, pulsar microstructure 0-94822
- ray and wave optics of integrable and stochastic systems, WKB method 0-59244
- reflection from moving ionis. front in const. mag. field (Russian) 0-106927
- relativistic effects near cyclotron resonances 0-59243
- relativistic nonlinear EM waves, in cold plasma, propag. modes and effects 0-79507
- relativistic plasma, EM wave dispersion relations from hydrodynamical eqns. 0-79559
- relativistic plasma, nonlinear dispersion relation for transverse wave 0-87939
- resonance absorption, self-consistent density profiles for obliquely incident light 0-64758
- resonant Balmer line irradi. of H plasma, theory and laser spectrosc. meas. 0-75099
- RF anomalous penetration in collisionless plasma 0-64730
- second harmonic generation suppression effect (Russian) 0-87899
- second-harmonic generation of upper-hybrid radiation in a plasma 0-79506
- self precession and freq. shift of EM wave in dissipative medium 0-79504
- self-trapping of intense optical beams in plasmas 0-92329
- stimulated Brillouin rescattering 0-87896
- stimulated Brillouin scattering initiated by ponderomotive force density fluctuations 0-103129
- stimulated Raman and Brillouin backscattering along mag. field 0-69983
- stimulated scattering processes, saturation by electrostatic daughter waves nonlinear decay 0-79509
- stochastic heating, relativistic electron generation (Russian) 0-83952
- temperate multi-species plasma around ion cyclotron freq. range, plane wave propagation 0-75050
- Tokamak, JFT-2, parametric heating by RF near lower hybrid freq. 0-70023
- two Langmuir wave parametric decay instability, self-trapped EM pump wave effects 0-96357
- uniaxial plasma or dielec. half-space, EM radiation from line source, theory 0-99605
- Vlasov theory for magnetised plasma, coherent state approach 0-64675
- wave penetration into half-space collisional plasma 0-106928
- wave radiation by oscillating electric dipole in moving warm plasma 0-87868
- waveguide, rectangular, filled with uniaxial anisotropic relativistic warm plasma, EM wave propag. and attenuation 0-59246
- whistler propagation in magnetospheric plasma 0-90294
- Ar plasma parameters, microwave scanning technique 0-64773
- Cs(Ar-Cs) plasmas, electron momentum transfer cross section, cyclotron reson., temp., cond., and vel. meas. 0-106930
- Xe rarefied plasma, emission characts. 0-103122

electromagnetic wave reflection

- see also *electromagnetic wave propagation in plasma; light reflection; X-ray reflection*
- air-dielectric interface, EM wave reflection and transmission in terms of polarisation, education 0-105458
- biological substances, dielectric props. meas. at RF and microwave freq. by coaxial line reflection methods 0-109065
- black hole, Reissner-Nordstrom, coupled gravitational and EM perturb., scatt. matrix, energy conversion, quasi-normal modes 0-67775
- doped conducting media, low-freq. props., EM wave reflection 0-103715
- E-region, appl. of group and phase height meas. to electron density profile distortion meas. 0-109299
- Earth surface layer, EM wave refl. and transmission coeffs., linear ramp model 0-61759
- electrodynamical boundary problems, method for solving 0-95773
- electron beam, relativistic mirror feature, perp. temp. effects 0-78749
- Gaussian beam wave refl. by inhomogeneous slab with permitt. perturbation 0-63897
- H-polarised EM wave by isotropic moving plasma, transient response 0-64731
- Hertzian waves, reflection and diffraction by moving layers (German) 0-87266
- incremental reflection coeff. at permittivity profile inflection, generalised WKB and Katsenelenbaum's methods comparison 0-91728
- interface plane wave reflection and refraction, positron polarisation effects (Russian) 0-79431
- ionosphere, effect of gravity waves on 100 kHz Loran-C signals 0-109304

electromagnetic wave reflection continued

- ionosphere, evidence for reflecting layer below classical D-region 0-98508
- low latitude whistlers, lower and upper freq. cut-off explanation 0-82131
- moving media, plane waves and refl. from moving interfaces 0-63890
- nonlinear anisotropic dielectrics, nondispersive waves, EM disturbance propagation, and reflection 0-106429
- nonlinear medium with one-dimensional random nonuniformities, statistical analysis 0-106421
- radar reflectivity profile classified by rain types 0-101420
- radar signal reflection from sea surface, spatial intensity fluctuations 0-109170
- radar signal reflection from Sun, efficiency of four-plasmon interactions 0-101582
- spatially dispersive crystal, reflectivity and transmittivity 0-99604
- statistical analysis, wave reflected from randomly inhomogeneous layer description, by series satisfying causality condition 0-106420

electromagnetic wave refraction

- see also electromagnetic wave propagation in plasma; light refraction*
- atmosphere, propagation of microwaves, refr. and absorpt. coeffs., optimal orthogonal expansion props. 0-98414
- Earth interior, refr. index distrib. image reconstruction via iterative ray tracing between boreholes 0-98466
- electrodynamical boundary problems, method for solving 0-95773
- interface plane wave reflection and refraction, positron polarisation effects (Russian) 0-79431
- Jupiter magnetosphere, kilometric radiation refr. by Io plasma torus 0-72866
- radiowave refraction corrections for exponential atmosphere, real-time computational method 0-98432
- VHF refraction in atmospheres of giant planets 0-98608

electromagnetic wave scattering

- see also backscatter; electromagnetic wave propagation in plasma; gamma-ray scattering; light scattering; X-ray scattering*
- aerosol, thin flat, EM wave scatt. and absorpt. 0-91723
- angular scattering of water drops and ice particles [electromagnetic interference], freq. above 10 GHz appl. 0-109183
- axially incident plane wave scattering by body of revolution 0-74284
- background slab affecting scatt., profile reconstruction algorithm 0-94644
- black hole, Reissner-Nordstrom, coupled gravitational and EM perturb., scatt. matrix, energy conversion, quasi-normal modes 0-67775
- buried inhomogeneities, general three-dimens. formalism 0-95769
- charged particles internal forces, moving faster than light in a medium 0-78751
- circumstellar dust shells, polarisation by Mie scatt., Monte Carlo anal. 0-98650
- circumstellar envelopes scatt., radiation linear polarisation spectrum rel. to mag. field determ. (Russian) 0-90344
- cylinder, direct and inverse scatt. problems, Dirichlet boundary conditions 0-95774
- cylinder, infinite tilted, linearly polarised incidence at arbitrary angle 0-58457
- cylinder, inverse scattering problem, determ. of shape from far field data 0-83543
- dielectric body, long EM wave scatt. 0-74283
- dielectric circular cylinders, elimination of resonant solns. of integral eqns. 0-63896
- diffusion equation derived from space-time transport equation 0-78772
- exterior scattering from spheroidal composite objects, soln. 0-87267
- extinction cross section for single particles at 100 GHz 0-82116
- frequency selective surfaces, EM wave scatt. from periodic screens, waveguide and optics appls. 0-87278
- Gaussian beam wave by two semicylindrical bosses on infinite perfectly cond. plane 0-63898
- gyrotropic media, artificial, EM scattering 0-106423
- holographic gratings, sharp boundaries, modal theory, EM wave propagation 0-83672
- holographic unslanted transmission and reflection gratings, modal theory, EM wave propagation 0-83673
- inverse electrodynamic scattering problem, general prop. of field with passive scatterers 0-63893
- ionosphere, incoherent scattering, total cross section 0-72690
- ionosphere, metallic ions of meteor origin effect in VHF forward scattering, contribution to sporadic-E formation 0-67461
- ionosphere, nonlinear scatt. of microwaves from solar power satellite, theoretical anal. (Japanese) 0-94634
- ionosphere, plasma parameters, incoherent scatt. of EM waves, EISCAT project (French) 0-82142
- ionosphere, scintillation, power law phase screen model, strong scatt. 0-61962
- ionosphere, scintillation, power law phase screen model, weak scatt. 0-61961
- ionosphere, whispering-gallery type mode scattering 0-98514
- microwave cosmic background, scattering in clusters of galaxies, 9 mm obs. 0-105366
- microwave cosmic background radiation, scattering in clusters of galaxies 0-105367
- Mie scattering improved algorithms 0-78771
- multiple, point source in one-dimensional, randomly inhomogeneous medium, with specularly reflecting walls 0-105514
- multiple scattering by random distribts. of discrete scatterers with coherent pot. and quantum mech. formalism 0-95768
- nonhomogeneous layer above reflecting surface, scattering of waves 0-58449
- nonlinear medium with one-dimensional random nonuniformities, statistical analysis 0-106421
- nonlinear theory of stimulated coherent scatt. of EM wave by relativistic electron beams (Russian) 0-102601
- one-dimensional direct and inverse scattering in causal space 0-102600
- plane EM scattering by conducting rectangular cylinder 0-106427
- plane EM wave two-dimens. multiple scatt. by N slits array, asymptotic formula 0-99610
- plane wave, by metal cone, near its symmetry axis 0-106426
- polarisation of scattered radiation, in medium with internal energy sources 0-67541
- projection method, properties of parametric system of basic functions 0-87269
- prolate spheroid and half prolate spheroid on plane, EM wave scatt. with axial incidence (French) 0-91727
- radially symmetric reradiating scatterers in EM fields, formulae for simple treatment (German) 0-87270

electromagnetic wave scattering continued

- radio waves, transionospheric, scintillation time struct. under weak and strong scatt. conditions 0-90281
- rain, multiple-scatt. effect on radiometric determ. of radiowave attenuation at millimetre wavelengths 0-90260
- ray optical anal. of scattering from dielectric coated conducting cylinder 0-83542
- resonance ponderomotive effects in EM wave scatt. and emission 0-69301
- scalar wave scattering by periodic surfaces, general modal theory 0-87271
- semi-infinite dielectric slabs, plane EM wave scatt. anal. using Helmholtz eqn. 0-63895
- sinusoidal surfaces, scatt. patterns 0-58448
- solar corona, efficiency of four-plasmon interactions in radar signal refl. from Sun 0-101582
- statistical analysis, wave reflected from randomly inhomogeneous layer description, by series satisfying causality condition 0-106420
- statistically rough surface, wave scatt., book 0-73116
- successive approximation method appl. for scattering from round dielectric cylinder (Russian) 0-63889
- surface wave electromagnetic scattering from notches in ground plane covered by dielectric slab 0-87277
- thin finite dielectric cylinder, scattering and absorption of EM waves 0-74281
- Thomson scattering in strong mag. field, vacuum polarisation effects 0-86632
- tropospheric long-distance propagation, multiple scatt. effect 0-109229
- VHF waveguide dielectric scatt. model for pulse-probe data interpretation (Russian) 0-62682

electromagnetic waves

- see also bremsstrahlung; Cherenkov radiation; electromagnetic field theory; electromagnetism; gamma-rays; heat radiation; light; microwaves; radiofrequency cosmic radiation; solar radiofrequency radiation; sunlight; synchrotron radiation; transition radiation; undulator radiation; whistlers; X-rays*
- amplification and generation based on Doppler-effect, nonlinear theory 0-63902
- bio-electromagnetic research, reviews 0-85444
- black body radiation, sound scattering analogue, outdoor sound propagation and reflection from ground and buildings 0-69579
- defective dielectrics, EM heating with time depend. param., WKB calcs. 0-71367
- Einstein-Maxwell equations, EM and gravitational wave spacetimes, similarity solutions 0-57154
- electron channelling, photon prod. 0-79846
- intrinsic waves in azimuthally magnetised bigyrotropic medium 0-91733
- Jupiter magnetosphere, kilometric radiation spatial and temporal studies 0-77328
- line sources, elec. and mag., interaction with moving magnetoplasma slab, EM radiation 0-67537
- living tissues, simulated, temp. distrib. in EM irradi. 0-85354
- low-temperature blackbody source 0-73355
- magnetically ordered crystals, absorbent, EM waves polarisation 0-108189
- monocrystals, EM radiation of relativistic positrons and electrons during axial and planar channelling 0-79845
- multifrequency N-th order coherence functions, path integral approach 0-95771
- Poynting vector theory, light beam shifts, total internal refl. 0-78764
- related fast processes measurement, present methods in USSR, future prospects 0-57271
- resonant antenna system, anomalous radiation and electrodynamic characteristics 0-69302
- volume holography, coupled-wave theory generalisations 0-106495

electromagnetism

- see also electric fields; electrodynamics; electromagnetic field theory; electromagnetic induction; electromagnetic oscillations; electromagnetic waves; magnetic fields; magnetism*
- acceleration through random classical radiation, thermal effects 0-73191
- averaged Maxwell equations in severe random nonuniformities 0-69298
- complementary variational principles for Maxwell's equations 0-99603
- diffraction gratings, theoretical method, numerical appl., Maxwell eqns. in curvilinear coords. 0-95786
- Dirac-gauge in Maxwell's theory 0-90687
- education, exterior algebra and exterior differential forms for electromagnetic problems 0-57037
- electrodynamic boundary conditions for media with spatial dispersion and transition layers (German) 0-78742
- ferrofluid, nonlinear surface waves, bifurcation theory approach 0-58439
- interfacial EM props. using singular fields, charge density and currents 0-90691
- Maxwell eqn. invariance algebra 0-82923
- Maxwell equations, boundary value approx. using finite element anal. (German) 0-91718
- Maxwell equations reformulation of weakly guiding optical fibre propagation 0-78974
- Maxwells eqn. integration, implicit scheme, space and time discretisation 0-90688
- metal surface, mol. vibr. energy transfer, classical EM theory 0-96806
- method of virtual power, electromag. continua appl., coupled fields 0-58438
- microtron electromagnet, mag. field distrib. using mag. scalar pot. 0-102597
- motion of charged particle in uniform magnetic field motion of charged particle 0-90690
- resistance variation with temperature 0-77575
- static EM angular momentum, in vacuo obs. 0-73631
- symmetries and vacuum Maxwell's equations 0-86178
- theory and applications, book 0-86051
- theory of electricity, book 0-86051
- toroidal resonators for EM waves, Maxwell eqns. for toroidal geometry 0-102598
- variational principles for Maxwell's equations 0-78744
- welding arcs, gas velocity fields modelling 0-75039

electromagnets

- see also coils; superconducting magnets*
- bubble chamber, SKAT, main parameters and magnetic field meas. 0-69022
- circumferential stress in large high field magnet coils, thick-thin cylinder approach 0-95761

electromagnets continued

- fusion reactor, compact ignition test reactor, engineering design using Bitter type magnet 0-102310
- fusion reactor, Heliotron E, helical coil design, mag. field perturbations 0-99300
- microtron electromagnet, mag. field distrib. using mag. scalar pot. 0-102597
- permanent magnet and coil combination for large dia. ion source 0-74066
- Fe pole pieces, in electromagnets, mag. anisotropy effect on mag. field homogeneity (*Japanese*) 0-93111

electromechanical effects

- dielectric liquid, elec. stressed, motion due to Coulomb, electromech. forces, schlieren image obs. 0-100037
- electroelasticity problems, numerical soln. 0-80707
- SAW vel. and electromech. coupling factor 0-75422
- steel, austenitic, tensile strength, elec. current impulse effect down to 4.2K 0-81131
- TGS, ferroelec. single crystal, low freq. nonlinear effects 0-84490
- NH₂H₂PO₄, Z-cut, SAW props. 0-84358
- Pb(Zr,Ti)O₃:Fe(Nb) ceramic, elec. and electromechanical props., depend. on dopants 0-81212
- RbHSO₄, ferroelec., dielec. dispersion 0-97179
- V₃Si, supercond. structure and properties (*German*) 0-93631

electromechanical filters

- resonators, props. of materials used (*Czech*) 0-76318

electrometers

- see also charge measurement
- electrophotographic films, surface charge meter using electrostatic induction (*Japanese*) 0-77886
- fixed-capacitor and resistive methods compared 0-90866
- fluid insulator used in gas phase ions investigation 0-57336
- Keithley model 642 portable electrometer, critical input design 0-68209

electrometry see *electrometers***electromigration**

- ballistic electron wind theory, quantum mech. generalisation 0-75379
- Feynman-Hellmann theorem and oscillator strengths, force on atom in electrostatic field 0-65275
- III-V semiconductors, point defects and deep traps, thermodynamic history, model 0-59908
- jellium, driving force, strong-coupling theory 0-65300
- multicomponent systems, rel. to electroepitaxy, theoretical model 0-65396
- proton transport in solids 0-79974
- quartz, synthetic, deuteration, EPR and IR absorpt. characterisation 0-92721
- semiconductor, enhanced electrodiffusion purification in mag. field, GaAs epitaxial film appl. 0-66409
- thin film conductor, mass transport and assoc. failures 0-59694
- velocity sensor, freq. charact. calcs. 0-96675
- Al, deposited metallic thin films, H incorporation effects on stress and electromigration 0-80139
- Al thin film stripes, electromigration lifetimes width depend. 0-92799
- Al-Cu (0.5 wt.%), evaporated layers, electromigration, linewidth depend. 0-65277
- Au thin film, electromigration, adhesion layer effects 0-96685
- CdS:Cu(Ag), charge and transport mechanism of impurities, electrodiffusion doping 0-59725
- CdS:Li(Cu), pure and doped, electrodiffusion of shallow donors, photocurrent, TSC, and exciton luminesc. meas. 0-79992
- Cu thin film, electromigration, adhesion layer effects 0-96685
- Mo₂Si₃ of Si 0-92708
- Se, photosensitive particle migration, electrophotographic film structure and process 0-101863
- Si, heavily doped films, electromigration obs. 0-65295
- SnO₂:Sb film, amorphous, electrotransport phenomena obs., under DC electric field 0-59840

electromotive force see *electric potential***electron absorption**

- see also beta-ray absorption
- barium stearate film, low energy electron range meas. using radioisotope Auger electrons 0-70257
- SiO₂ massive dielectric target, 5-25 keV electrons penetration charact. 0-70260

electron accelerators

- see also betatrons; electron ring accelerators; microtrons
- current density meas. method for electron acceleration 0-102366
- energy spectrum monitoring of electron beam 0-68994
- future technologies in high-energy physics, collective accelerators, laser accelerators, single-pass collectors 0-78466
- inertial confinement fusion, Angara 5 features and design principles 0-63384
- Kharkov linear electron accelerator for obtaining beam of quasischromatic linearly polarized photons, 2-crystal goniometric setup 0-68976
- linear accelerator with S-band subharmonic prebuncher for picosecond single electron pulse (*Japanese*) 0-78460
- linear electron accelerator for 1-mA average current, 10 μsec duration 0-68978
- long duration pulsed electron beams, development 0-68980
- nanosecond beam dynamics in linear electron accelerator 0-86996
- optical reflector for energy extraction for electron synchrotron 0-78467
- pulse generator, repetitively pulsed electron beam system using cold-cathode electron gun 0-68981
- self-acceleration expts., regulation of magnetization of ferrite 0-63425

electron affinity

- atomic, optimum pot. model used to generate numerical pot., energies and electron affinities determ. 0-99534
- benzyl radicals, monomethyl- and dimethyl-substituted, electronic spectra and electron affinity 0-63618
- exciplexes and excited aromatic molecules, donor-acceptor props., comparison of fluorescence quenching 0-69174
- first row elements, electron affinity, semiempirical predictions 0-63555
- glyoxal, electron affinity at centrosym. trans geometry 0-87225
- halogen mols., electron dissociative attachment 0-91694
- hydronaphthyl radicals embedded in naphthalene cryst., optical transition energies and ionisation energies 0-78595
- methyl glyoxal, electron affinity at centrosym. trans geometry 0-87225
- methylamine, affinities for H⁺(Li⁺)(K⁺)(CH₃⁺), ab initio SCF calculations 0-102443

electron affinity continued

- molecules containing C, N, O and H atoms, electron affinities and ionisation pot., semiempirical calcs. 0-78535
- positronium nitrate, [NO₃⁻e⁺], existence, Hartree-Fock-Roothaan calcs. 0-83254
- positronium nitrite, [NO₂⁻e⁺], existence, Hartree-Fock-Roothaan calcs. 0-83254
- second row elements, electron affinity, semiempirical predictions 0-63555
- SCF(C₂)⁺ pot. energy curves calc. using SCF, MCSCF and CI methods, dissociation energies, bond lengths, electron affinity 0-95523
- CN⁻, electron propagator theory, mol. electron affinities calcs. 0-83521
- Cl₂⁻, electron propagator theory, mol. electron affinities calcs. 0-83521
- GaAs epitaxial thin films with neg. electron affinity, photoelectron energy distrib. 0-100755
- GaP:Cs-O simultaneous adsorption, oxidation interface chemical struct. 0-103584
- GeH₃⁻, electronic struct., electron affinity, inversion barrier, ab initio SCF Gaussian basis calc. 0-63552
- H, electron affinity, semiempirical predictions 0-63555
- H₂, electron dissociative attachment 0-91694
- He, electron affinity, semiempirical predictions 0-63555
- I₂(I₂⁺)(I₂⁻), HF and SCF calcs., pot. curves, electron affinity and quadrupole moment determ. 0-95527
- In, meas. by dissociation of InBr, InI (*French*) 0-63849
- LiNbO₃, thermionic emission charact. 0-104034
- NH₃, affinities for H⁺(Li⁺)(K⁺)(CH₃⁺), ab initio SCF calculations 0-102443
- Ne isoelectronic series, second order correl. energy, Z depend. of irreducible-pair energies 0-91417
- O⁻(O₂⁻), optimum pot. model used to generate numerical pot., energies and electron affinities determ. 0-99534
- Tl, meas. by dissociation of TlBr, TlI (*French*) 0-63849
- UF₆:MF (M=Na or K), ion-molecule equilibria, heat of form. and dissociation and electron affinities determ. 0-104480

electron annihilation see *electron-positron interactions***electron attachment**

- N-bromosuccinimide, X-irrad., ESR study of Br and σ⁺ radical 0-66037
- chlorofluoromethanes, electron attachment, electron swarm method 0-69245
- halogen mols., electron dissociative attachment 0-91694
- molecule and mol. clusters, electron attachment electron-mol. collision, Rydberg electron exchange 0-63843
- perfluorobenzene, electron attachment, radiative and dissociation, negative ion lifetimes, ion cyclotron reson. spectra 0-74251
- perfluorocyclobutane, electron attachment, radiative and dissociation, negative ion lifetimes, ion cyclotron reson. spectra 0-74251
- perfluoromethylcyclohexane, electron attachment, radiative and dissociation, negative ion lifetimes, ion cyclotron reson. spectra 0-74251
- perfluorotoluene, electron attachment, radiative and dissociation, negative ion lifetimes, ion cyclotron reson. spectra 0-74251
- CO, X²⁺, vibr. levels, UPS electron attachment obs. 0-95683
- H₂, electron dissociative attachment 0-91694
- HBr, electron impact ionisation, vibr. excitation spectra threshold peaks, negative ion effects 0-106322
- HCl, dissociative electron attachment, differential cross section, Feshbach reson. 0-83508
- HF, Feshbach reson., predissoc. investig. 0-83433
- H(1s)+Cs, differential electron attachment and elastic scatt., 30-528 eV 0-63745
- O₂, attachment cooling, press. depend. 0-91663
- O₂, electron attachment threshold photoelectron spectra, vibr. excitation 0-83422
- O₂-N₂ mixture, attachment cooling, press. depend. 0-91663
- SF₆-N₂ mixture, electron swarm development, Boltzman eqn. anal. 0-87841
- SF₆-N₂ mixtures, attachment coeffs. and ionic mobilities, 1.2-4 eV 0-96338
- SF₆+Rydberg atom, reaction channels, expt. vs. theory 0-63755

electron avalanches

- gas, high press. breakdown in strong static elec. field, plasma mechanism 0-79614
- laser spark, electron conc. limitation, electrodynamic mechanism (*Russian*) 0-59333
- optical discharges by laser radiation, continuous equilb. plasma maintenance 0-59259
- SF₆ discharge inception voltage affected by avalanche growth space charge (*German*) 0-75109
- Ar, cathode dark space ionisation avalanche with cold cathode (*Russian*) 0-84013
- Ar, electron avalanche development, exact Boltzmann eqn. anal. 0-59318
- CO₂ self-sustained laser system, electron avalanche and electron-ion recomb. coeffs. meas. 0-102694

electron beam absorption see *electron absorption***electron beam applications**

- see also electron beam deposition; electron beam lithography; electron beam machining; electron beam welding; radiation therapy
- adhesion determination, thin films 0-71833
- calorimeter, high-temperature, containerless 0-73366
- double-sided electron beam generator for KrF laser excitation, fusion appl. 0-68956
- electron beam high resolution thermal wave microscopy 0-95158
- integrated grating circuit for guided-beam multiple division fabricated by electron-beam direct writing 0-91934
- magnetosphere sounding, beam-plasma interaction expt. by JIKIKEN satellite (*Japanese*) 0-94655
- medicine, therapy of mycosis fungoides 0-72286
- metals heat treatment principle and appl. (*French*) 0-66558
- Nb, pure, production by carbothermic reduction-electron beam melting combination method 0-89177
- polymeric, cable insulation, radiation modification using electron beams 0-66848
- projector having a thermoplastic target and operator's eye, charact. 0-96023
- scanned electron beams, activation of low dose Si implants in GaAs 0-75246
- semiconductor depth profiling by electron beam induced junction current meas. 0-96977
- semiconductor laser, electron beam pumped, use of periodic structs. with special profiles 0-95923

electron beam applications continued

- semiconductor laser, electron beam pumping efficiency, coating effect 0-91795
 spark gap, electron beam triggered, characts., investig. 0-107001
 Al:Si(Zn), ion implanted electron beam annealing, ion backscatt. and TEM meas. 0-59500
 Ar-N₂ mixture, electron beam pumped, lasing obs. at 337, 358, 380 and 406 nm 0-102700
 As-Se-S-G chalcogenide amorphous film, computer-generated holograms using electron beam irradi. 0-95846
 CO₂-N₂-He laser media excitation by electron beams admitted through gasdynamic windows 0-99694
 Ga_{1-x}In_x-As_{1-y}Sb_{1-y} tunable electron-beam-pumped laser parameters 0-106524
 HF chemical laser initiation by relativistic electron beam 0-64005
 SF₆+H₂ chemical laser, electron beam pumping 0-91784
 Xe₂ excimer laser, electron beam excitation, VUV fluoresc., lasing 0-87379
 XeCl(B) formation in electron beam assisted Xe/HCl laser discharge 0-63988

electron beam deposition

- dielectric coatings, optical characts., effect of electric field during film condensation 0-69539
 ion plating, evaporation sources, gaseous media, and transport modes 0-80984
 thin film deposition process, line-edge profile simulation appl. 0-104068
 thin films fabrication techniques 0-76176
 vacuum, using electron beam techniques, technical problems (*German*) 0-84850
 Al-Zn thin film, prep. using Sn-Zn evaporant source 0-100789
 In₂O₃ films, electron beam evaporation, elec. and optical props. (*Japanese*) 0-60784
 Mo-Ru(-Si), amorphous superconductors, prep. by electron beam evaporation and liq. quenching, crit. temp. 0-103776
 Nb₃Al film, electron-beam coevaporated, prep. and characts. 0-76187
 Nb₃Ge coevaporated film, high supercond. transition temp., nucleation and growth 0-76185
 Nb₃Pb superconducting film, prep., vac. deposition 0-89149
 Si films, electron beam evaporated, for MIS solar cells 0-93490
 Ta-Ta₂O₅-InP thin refractory MIS struct. deposition 0-75647
 Tm₂O₃ film, between Al electrodes, prep. and elec. props. 0-60103
 ZnSe-Si heterojunctions, IR quenching of photocapacitance 0-92968
 ZrO₂ thin film, optical props. rel. to cryst. struct. 0-97357

electron beam effects

- see also beta-ray effects; cathodochromism; cathodoluminescence; electron impact; plasma-beam interactions*
 absorbed dose distrib. in thin layers rel. to electron beam incidence 0-83226
 adsorbate distribution, electron-stimulated desorption ion imaging 0-103572
 alkali halide, irradi. stability obs. using X-ray emission meas. (*Russian*) 0-66326
 alkali halides, irradiated at room temperature, stored energy 0-79839
 alkali metal halides, F-colouring role of impurities 0-64995
 alkaline earth oxide irradi. stability obs. using X-ray emission meas. (*Russian*) 0-66326
 alloy, solute redistrib. during in situ irradi. in HVEM 0-107324
 anthracene, pulsed electron excitation, triplet excitons, spectral and electrical investigations 0-78288
 atom displacement radiation damage, in electron microscopes 0-103394
 Auger scanning microprobe, approach to damage-free anal. 0-89581
 auroral electron bunching near artificial electron beam 0-98511
 brain, caudate nucleus, neurotransmitter activity transient alterations after irradi., rat expts. 0-72267
 catalase, glucose embedded, measurement and reduction of radiation damage in frozen hydrated crystalline specimens 0-89810
 cellular repair rates determined by split-dose and dose-rate methods, comparison 0-104680
 cellulose, degradation by high voltage electrons 0-100283
 ceramics, glassy, struct. and electron beam sensitivity 0-79841
 copper phthalocyanine, chlorinated, radiation damage mechanism 0-88000
 α' copper phthalocyanine and chlorinated derivative mol. crystals, radiation damage in electron microscope 0-107328
 covalent crystals, nanosec. electron beam effects, size depend., Ioffe effect 0-88211
 creep and growth, radiation induced, fundamental mechanisms 0-92596
 crystalline and organic materials, knock-on process, review 0-79840
 crystalline materials, in situ deform. by high voltage electron microscopy 0-103352
 cytochrome c oxidase, macromolecular struct., electron microscopy and image anal. 0-89716
 degassing metals for extreme low pressures 0-98924
 diamond, electron irradiated, photochromism 0-71454
 diamond, thermal conductivity, high temp., electron irradi. effects 0-65318
 diamond, vacancy enhanced N aggregation, electron irradiation effects IR spectra 0-70245
 dielectric surface, charge accumulation, losses, electron-beam treatment (*Russian*) 0-75931
 discharge, volumetric, semi-self-maintaining, excited by electron beam, current maintenance in cathode layer 0-59322
 displacement damage simulation in HVEM irradi. 0-107325
 DNA, radiation induced mol. size change, electron irradiated, effect of p-nitroacetophenone 0-89807
 DNA double strand breaks rel. to radiation dose, yeast cell obs. 0-72232
 dynamic and dosimetric characterisation of irradi. solids, laser and holographic interferometry obs. (*Rumanian*) 0-90886
 electron microscope, high resolution, obs. at liq. He temps., radiation damage effects 0-86517
 electron microscopy, correlation analysis of radiation damage 0-100282
 electron-matter interactions rel. to electron microscopy 0-89097
 5-fluorocytosine, electron beam damage assessed by EELS 0-89809
 Frenkel defects, form. and collapse, defect migration, electron irradi. effects, computer simulation 0-92523
 glass, adsorption of Au, AES study, electron bombardment effects 0-65380
 glutamine synthetase macromolecular struct., electron microscopy and image anal. 0-89716
 graphite, synergistic effect of electrons on atomic H activity 0-106112

electron beam effects continued

- Hastelloy B-2, corroded surface, electron bombardment effect during Auger electron anal. 0-61014
 homogeneous electron irradiation (*German*) 0-102603
 ionic crystals, nanosec. electron beam effects, size depend., Ioffe effect 0-88211
 irradiation effects on surface prop. of solids 0-70261
 lipid peroxide formation in irradi. synthetic diets, storage effects 0-101025
 magnetosphere, wave emissions prod. by JIKIKEN electron beam-plasma interaction expt. (*Japanese*) 0-94655
 mammalian cells, lethally damaged, proliferation obs. after irradi. by various particles 0-108971
 metal, irradi., elastic point defect-dislocation interactions, defect dragging model extension 0-65050
 metal, irradi., selfinterstitial atomic defect interaction radii, recovery expts. and error sources 0-65049
 metals, interstitial loop growth, pulsed irradi. effects 0-88210
 metals, submicroscopic defects, influence on HVEM in-situ expts. 0-103392
 metals, two and one interstitial model explanation of elec. cond. variations 0-88143
 methylmethacrylate soln., aqueous, polymerisation under pulse electronic accelerator irradiation 0-66802
 mica, natural, high γ - and electron-irrad. doses effect on annealing behaviour, thermal decomp. resist. 0-60897
 microscopy of frozen hydrated crystalline specimens, meas. and reduction of damage 0-85552
 MNOS structures, electron-beam-irrad., interface defects, high temp. H₂ anneal 0-96745
 monocrystals, EM radiation of relativistic positrons and electrons during axial and planar channelling 0-79845
 Ni, adsorption residual C removal by electron beam irradi. and heat treatment (*Chinese*) 0-88421
 Nimonic PE-16, irradi. in HVEM, void growth, vacuum environment influence 0-107323
 oxidation induced by ion or electron bombardment, AES-SIMS study 0-108606
 paraffin, single crystal, STEM versus CTEM beam damage 0-103393
 PMMA, space radiation effects evaluation 0-70263
 polybutadienes, radiation chemically cross-linked, charact. by pyrolysis gas chromatography (*German*) 0-81348
 polyethylene:Br₂(I₂), films, electron-beam induced carrier mobility and elec. breakdown 0-80429
 polyethylene, single crystal, electron microscopy study 0-103273
 polyethylene, space radiation effects evaluation 0-70263
 polymer composite matrix materials, spacecraft, space radiation effects evaluation 0-70263
 polymer spacecraft materials, electron and proton irradi. effects 0-70262
 polystyrene:Br₂(I₂), films, electron-beam induced carrier mobility and elec. breakdown 0-80429
 protein, electron radiation damage on primary and secondary struct. level 0-89808
 quartz, dislocations, electron irradi. induced vitrification 0-107252
 α -quartz, electron irradi., defect struct. and radiolysis 0-107321
 quartz, electron irradiation effects on optical, dielec., elastic props. 0-59521
 radiation damage problems in electron microscopy 0-59517
 semiconductor, ion implanted, pulsed laser and electron beam annealing comparison 0-92547
 semiconductor-electron beam interactions, review 0-101911
 p-Si, electron irradi. effect on Hall mobility temp. depend. 0-60011
 solar corona, heating by fast electron streams 0-105228
 solid, high energy electron scatt., Monte Carlo calcs. 0-96422
 solid target, electron probe penetration and energy loss characts., diffusion model 0-96585
 solid-electron and X-ray interaction (*Chinese*) 0-70253
 solids, interaction with electrons and X-rays (*Chinese*) 0-80896
 spacecraft thermal control coatings, electron and proton irradi. effects 0-70262
 steel, austenitic stainless, creep dependence on electron irradi., in type SS316 steel, dislocation motion (*Russian*) 0-108495
 steel, austenitic stainless, irradi. creep of type 316 in HVEM 0-97523
 steel, austenitic type KO 34, microstruct. changes on electron beam welding (*Hungarian*) 0-104252
 steel, low C, HF oscillations during electron beam welding (*Russian*) 0-76273
 steel, stainless, radiation damage by 1 MeV electrons, dislocation struct., brittleness (*Russian*) 0-75226
 steel, stainless, vacuum components, pre-vacuum surface finish influence on electron stimulated desorption in ultrahigh vacuum 0-57320
 steel, stainless, voids, TEM, diff. contrast 0-75218
 steels, stainless, electron irradiated, dislocation damage, HVEM study 0-103389
 stilbene, pulsed electron excitation, triplet excitons, spectral and electrical investigations 0-92828
 superconductors, low temp. SEM appl. 0-80443
 surface processes, interatomic forces, theories 0-107632
 thulium phthalocyanine, mol. image in high resolution electron microscopy, radiation damage effect 0-107203
 5-trifluoromethyluracil, electron beam damage assessed by EELS 0-89809
 uridine-5'-phosphate.2Na⁺ single crystals, radiation damage, ESR obs. 0-108964
 Zircaloy, foil, dislocation loop nucleation and growth during 1 MeV electron irradi. 0-88152
 Zircaloy-2, electron irradiation damage, direct obs. 0-84212
 Al, dislocation loops, interstitial, size distrib. for metal irradiated in high voltage electron microscope (*Russian*) 0-103335
 Al fracture speed during phase explosion due to electron beam irradi. (*Russian*) 0-76336
 Al, interstitial loop form., effects of repeated electron irradi. 0-75220
 Al:Ga, pulsed electron-beam annealing, lattice site location improvement 0-107303
 Al-Cu (1 wt.%), electron irradiated, dislocation damage, HVEM study 0-103389
 Al-Mg, dilute, dislocation loops, interstitial, size distrib. for metal irradiated in high voltage electron microscope (*Russian*) 0-103335
 Al₂O₃, β - and β'' -phases, defect struct. obs. by high resolution TEM, battery ageing relevance 0-107501
 Al₂O₃, irradi. stability obs. using X-ray emission meas. (*Russian*) 0-66326

electron beam effects continued

- Al₂O₃:Cr, pure and doped, electron irradi. induced cond., TSC and EPR study 0-80277
- AlPO₄, synthetic berlinite, electron irradi. effects, ESR, ENDOR, optical spectral study 0-80608
- Au, thin foil, enhanced electron energy deposition heated, soft X-ray vacuum UV spectra 0-80901
- Au₃Si₆₅, amorphous vacuum-deposited and liquid-quenched films, diffusion and crystn. 0-84094
- CO₂ laser, pulsed, elec. field distrib. in vol. discharge controlled by electron beam 0-58505
- CaF₂, electron irradi. defect aggregates, ordering, U and Th impurity effects 0-75216
- CdS, dislocation motion due to heating by electron beam in TEM 0-79799
- p-CdSiAs₂, electron irradi. elec. props. annealing, lattice defects 0-100465
- Cr-SiO₂-Si MIS solar cells, photovoltaic performance and interface states, nucl. radiation effects 0-94004
- Cu alloys, FCC, climb of extended dislocations due to irradiation in HVEM 0-103343
- Cu, dislocation pinning rate, neutron and electron irradi., meas. by internal friction method 0-96570
- Cu, electron-irradiated, monovacancy migration during stage III annealing, NQR study 0-107576
- Cu foils, electron-irradiated, point defect agglomerates, HVEM invest. during in-situ annealing 0-84213
- Cu fracture speed during phase explosion due to electron beam irradi. (Russian) 0-76336
- Cu, irradi., elastic point defect-dislocation interactions, defect dragging model extension 0-65050
- Cu, irradi., migration and thermal conversion of defects, 100 to 330K 0-59519
- Cu, neutron and electron irradi., interstitial formation, dislocation pinning, internal friction meas. 0-100284
- Cu single crystals Au ion implanted, pulsed electron beam irradi. 0-65019
- Cu-Al, dislocations, dissociated, climb mechanism, nucleated loops, Burgers vectors 0-65002
- Cu-Al alloy, irradi. in HVEM, climb of dissociated dislocations and point defect absorpt. 0-107257
- Cu-Fe (1.5 wt.%), precipitation-effect on void formation during electron irradiation 0-84211
- Cu-Fe (1.5 wt.%) alloy, void form. during irradi. in HVEM, reactor irradi. simulation and ageing effects 0-107327
- Fe, electron-irradiated, positron lifetime meas. 0-93431
- Fe, irradiated with electrons then annealed, magnetoresistance at 20K (French) 0-103677
- Fe, pure and doped, electron irradi., mag. aftereffect 0-88838
- α -Fe-C, electron irradi., vacancy-C interaction, positron lifetime meas. 0-75264
- Fe-C, electron-irradiated, positron lifetime meas. 0-93431
- Fe-Cr-Ti-Mo-TiO₂ (13, 3.5, 1.5, 2 wt.%) dispersion hardened, void swelling 0-65046
- Fe-Ni alloy, martensitic transform, influence of thermal and electron irradi. treatment of austenite (Russian) 0-66509
- Fe-Si (3 at%), deformation and electron bombardment, influence on dislocation struct., 20-500°C (Russian) 0-92536
- Fe-Si (3 wt.%), electron irradiated, yield strength and elongation 0-76325
- Fe_{0.5}Co_{0.5-x}Cr_x films, vacuum-deposited cryst. and mag. struct. (Russian) 0-93081
- GaAs, dislocation-free, point defects and rad. damage 0-88141
- GaAs, electroluminescent study of irradi. induced struct. damage, athermal annealing 0-108280
- GaAs, electron beam induced current, minority carrier generation distrib. 0-96900
- n-GaAs, electron irradi. defects, carrier removal rate, annealing effects 0-75269
- GaAs, electron irradi. induced defect levels, hydrostatic press. effect 0-92858
- GaAs, electron-beam excited, efficient generation of electron-hole plasma 0-76051
- GaAs, epitaxial layers, electron irradi. deep level trap energy depend. 0-80205
- GaAs, laser annealing of point defects 0-107224
- GaAs on Ga_{0.9}Al_{0.1-x}As, electron scatt., cathodoluminesc., loss spectra 0-104023
- GaAs, primary radiation defect separation by elec. field 0-92522
- GaAs shallow-homojunction solar cells, electron radiation effects 0-97798
- GaAs solar cells, electron and proton radiation damage 0-94034
- GaAs solar cells, simultaneous radiation damage and annealing 0-94033
- GaAs:Se ohmic contacts, pulsed electron beam annealing donor density, mobility 0-65678
- GaAs:Si, Li, IR absorpt., microstruct., charge compensation 0-107565
- GaAs-GaAlAs wafers, defects and degradation, transmission cathodolum. evaluation 0-65395
- GaP crystals, radiation defects, TSC obs. 0-65588
- GaP, IR absorpt. spectra depend. on compensating defects and thermal treatment (Russian) 0-71465
- Ge crystals, electron beam induced changes of real struct., HVEM 0-81390
- Ge, electron beam irradi., {111} faults, nature and origin 0-70258
- Ge epitaxial film, ion implantation and electron beam anneal effects on carrier conc. 0-75255
- Ge, lattice images of defects and radiation damage applies. 0-107210
- p-Ge:Au,Sb,Hg(Zn), radiation-defect form., Au influence 0-92911
- Ge:Sb,Cu, photoelec. props., fast electron irradi. effects 0-60036
- Hg, X-ray microanal., quantification of losses 0-85261
- n-In_{1-x}Ga_xP, direct-gap semiconductor, cathodoluminesc., electron irradi. effects 0-108283
- InP film, electron-beam annealed, surface conduction 0-84500
- n-InP, γ -ray and electron irradi., annealing of radiation point defects, elec. cond. and Hall coeff. meas. 0-65051
- KBr, defect accumulation under electron irradi. at 4K 0-107233
- KCl, F-centre relaxation kinetics, temp. depend. following electron irradi. 0-92527
- KCl(I), electron range-energy relation, thermally created lattice vacancies effect 0-92574
- K₂Pt(CN)₄Br_{0.3}3H₂O, anisotropic radiation damage in electron microscopy, diff. spot fading rate obs. 0-107329
- LiCl, radiation effects on decay time of F-centre emission 0-93381

electron beam effects continued

- LiNbO₃ surfaces, ion and electron bombard., photoelectron spectroscopy and electronic props. 0-71559
- LiNbO₃, XPS and UPS from surface defects 0-76136
- LiYF₄, electron-irradi. induced defects, optical and EPR study, impurity effects 0-66238
- Mg-Ag, ion implanted, recovery stage characterisation by electron irradi. 0-107295
- MgAl₂O₄, irradi. stability obs. using X-ray emission meas. (Russian) 0-66326
- MgAl₂O₄, radiation damage, optical absorpt., F-centres 0-64994
- MgO crystals, radiation damage influence on deform. in HVEM 0-103391
- MgO, electron irradiation damage, cryst. defects 0-107320
- Mo alloys, dil., HVEM bombarded, neutron damage simulation, defect cluster and dislocation obs. 0-107330
- Mo, irradi. in HVEM, anisotropy of damage prod. 0-107322
- MoS₂, lattice images of defects and radiation damage applies. 0-107210
- NaCl, high resolution TEM and radiation sensitivity, dislocation obs. on deformed crystals. 0-107260
- Na₂O-MgO-Al₂O₃, β'' -alumina, high-resolution electron microscopy 0-75208
- NaReO₄, EPR spectra of paramag. centres and free radicals 0-108072
- Nb, adsorbed H distrib., electron-stimulated desorption ion imaging 0-103572
- Nb₂Ge, low temperature electron, neutron irradi. effects on critical temp. (French) 0-75669
- Nb₂Sn, Al₁₅ cpd., normal state, low temp. resist., disorder effects 0-107762
- Nb₂Sn, monofilaments, radiation-enhanced diffusion growth, crit. current density 0-65758
- Ni, irradi. in HVEM, interstitial loop growth 0-107326
- Ni-Cr-Fe alloys, radiation enhanced precip. and dissolution of precipitates, point defect kinetics and dislocation obs. 0-108467
- Ni-Cu, electron-irradi., neutron-scatt. studies 0-75268
- Ni₃Fe, disaccommodation meas. after low temp. electron and neutron irradi. 0-88832
- PbS, photosensitive film, electron bombard. effect on elec. cond. 0-93019
- Pd, silicide formation due to laser and electron beam annealing 0-84849
- Pt, silicide formation due to laser and electron beam annealing 0-84849
- RbCl, electron bombard., colour centre photoemission, surface contamination and escape depth 0-66392
- RbMnF₃:Fr, pure and doped, unirradiated and electron irradi., energy transfer 0-108254
- Sb, electron microscope irradiation effects, agglomeration of point defects, dislocation climb and loops (French) 0-59518
- Si, advanced material for space solar cell 0-94007
- Si diode radiation detector, stabilisation of radiation damage 0-91377
- Si, electron beam annealing, beam voltage effect modeling 0-75275
- Si, electron beam irradi., {111} faults, nature and origin 0-70258
- Si, electron beam scan annealed, deep levels 0-65481
- Si, high-resistivity layer form. during electron irradi. 0-80352
- Si, ion implanted, electron beam annealing, surface struct. study using SEM 0-70235
- Si, laser annealing of point defects 0-107224
- Si, lattice images of defects and radiation damage applies. 0-107210
- Si materials, advanced, preliminary evaluation for space solar cells 0-94006
- Si, migration of Au, electron bombardment effects 0-100362
- Si n⁺-p junction solar cells, electron irradi., DLTS spectra and defect effects 0-93999
- Si n⁺-p solar cells, effect of elec. bus during 1 MeV electron irradi. and isochronal annealing, elec. characts. and deep level pop. 0-94086
- Si, neutron and electron bombard., radiation defect recomb., photoelec. props. meas. 0-60039
- Si p-n junction depletion layer, electron beam damage inhibition 0-70817
- Si p-n junctions, spin depend. surface recomb., electron irradiation effect 0-88627
- Si processing technology, appls. of scanning CW lasers and electron beams 0-100932
- n-Si, quenched, fast electron irradiated, annealing of defects 0-89259
- Si, radiation induced defects in high-voltage electron microscope 0-65048
- Si, radiative recomb. centre accumulation due to high temp. electron irradi. 0-93394
- Si solar cells, n⁺-p, Li-counterdoped, radiation damage 0-94000
- Si solar cells, radiation damage annealing mechanisms and low temp. annealing 0-94003
- Si solar cells, ultrathin, electron and proton effects 0-94002
- Si substrate for PMMA electron sensitive layer, 400 Å linewidth electron beam lithography 0-65392
- Si, surface, pulsed electron beam processing, doping, annealing 0-75254
- Si surface electron beam deposited silicide formation using scanning CW laser beam 0-66862
- Si wafer, ion implanted, electron beam annealing, computer simulation 0-96569
- Si:Al, electron irradi. induced defects, transient capacitance study 0-59516
- Si:As, scanning electron beam annealing, spreading resistance, junction depth 0-75267
- Si:As high-dose implanted single crystals, pulsed electron-beam annealing 0-103373
- Si:As⁺, implanted, CW laser annealing, electron-beam induced current 0-100709
- p-Si:B(Al), radiation defect form. and annealing study using Hall effect, cond. and carrier diffusion length 0-84214
- Si:P implanted, multicannan electron beam annealing 0-75242
- Si:P(O) p⁺-n⁺ solar cells, comparison rel. to resistance to 1.5 MeV electron irradi., majority carrier trapping 0-94087
- Si:Sb vacuum deposited coating, p-n junction, pulsed electron beam annealing doping, diffusion 0-75480
- Si-SiO₂ interface in MOS structs. low-energy electron beam irradi., charge accumulation process anal. 0-65701
- SiO₂ coatings on SiO₂ substrate, cathodoluminescence spectra, electron irradi. 0-76085
- Sm, electron radiation damage, elec. resistivity change rates 0-59954
- Ta₂S₃ (1T) electron irradiated, lattice contraction 0-59520
- TiC, electron irradi. damage, electron microsc. study 0-84210
- Tl-Hg, excimer band emission from electron beam initiated discharge in Tl-Hg 0-78841
- Tl-Xe, excimer band emission from electron beam initiated discharge in Tl-Xe 0-78840
- U₂Si, reversible twinning, in-situ obs. 0-104241

electron beam effects continued

- V₂O₅, electron beam induced decomposition, appearance pot. spectroscopy 0-85203
 W (110) stepped surface, electron stimulated desorption of O, atomic steps and defects influence 0-80091
 W surface, adsorbed CO, electron-stimulated desorption, photoemission, relax. energy 0-100401
 Y, electron radiation damage, elec. resistivity change rates 0-59954
 YIG, electron and γ -irrad., photomagnetic effect 0-103877
 Yb, electron radiation damage, elec. resistivity change rates 0-59954
 ZnO, irradiation in high voltage electron microscope dislocation loops study 0-88157
 ZnO UV laser, electron-beam pumped 0-99753
 ZnS UV laser, electron-beam pumped 0-99753
 p-ZnSiAs₂, electron irradi. elec. props. annealing, lattice defects 0-100465
 ZnTe, irradiation induced radiative centers obs. 0-66290
 Zr, electron irradiation damage, direct obs. 0-84212
 Zr, foil, dislocation loop nucleation and growth during 1 MeV electron irradi. 0-88152
 Zr, void swelling during electron irradi., HVEM study 0-92559
 Zr-Nb(0.1, 2.5 wt.%), foil, dislocation loop nucleation and growth during 1 MeV electron irradi. 0-88152
 Zr-Sn(Fe)(Ni) (0.15 wt.%), electron irradiation damage, direct obs. 0-84212

electron beam impact *see electron impact***electron beam lithography**

- see also electron resists*
 conference on electron, ion and proton beam technology, conf., Boston, MA, USA (29 May-1 June, 1979) 0-67927
 flying spot scanner for conversion of SEM to lithography system 0-86512
 Josephson junction fabrication by ion implantation, electron beam lithography and dry etching 0-88693
 low profile electron collector system 0-68292
 microfabrication for guided-wave optical devices 0-58812
 microgratings for guided-beam deflection, electron-beam direct-writing fabrication 0-102856
 NMOS VLSI circuits manufacture process and problems (Norwegian) 0-60090
 toroidal deflection yokes, eddy current compensation 0-95762
 triple slit scheme for high current variable-shaped beam forming 0-68290
 x-ray zone plates fabricated using electron-beam and X-ray lithography 0-88335
 Si₃N₄ sample substrates, high resoln. electron beam fabrication using STEM 0-104104

electron beam machining

- integrated optical grating circuit fabrication by electron beam direct writing 0-64214
 spatial charge and beam radius determination (Russian) 0-74290

electron beam welding

- fusion reactor, Heliotron E, vacuum chamber construction using electron beam welding 0-106180
 spatial charge and beam radius determination (Russian) 0-74290
 steel, austenitic, KO 34 samples, electron beam welded, Charpy test expts. (Hungarian) 0-104252
 technology, principles and applications 0-82756

electron beams

- see also electron impact; electron optics; Schwarz-Hora effect*
 aberration elimination, electron beam scanning systems 0-78756
 accelerators for long duration pulsed electron beams, development 0-68980
 annular, prod. by foillless diodes 0-95779
 broadening effects caused by discreteness of space charge 0-69309
 bunching at mag. field discontinuity 0-63905
 classical stimulated bremsstrahlung, electron beam bunching 0-69306
 coaxial electron and atomic beams sequential multiple scatterings, random walk approach 0-99574
 compact cold cathode electron beam gun, appl. CO₂ laser (German) 0-86501
 compensated Pierce instability 0-102606
 conference on electron, ion and proton beam technology, conf., Boston, MA, USA (29 May-1 June, 1979) 0-67927
 cylindrical-mirror electrostatic analyser for beta spectroscopy of beams 0-63446
 deflected electron probe, correction of distorted spot shape using dynamic focusing and stigmator 0-57427
 deflection error assessment, expt. technique 0-78757
 electron bunching, scattering and bremsstrahlung in cryst. lattice in strong EM field 0-65113
 energy broadening, Boersch effect 0-69308
 energy coupling to expanding thick-shelled target 0-96365
 energy spectrum monitoring in low-energy electron accelerators 0-68994
 flare stars, fast electrons hypothesis rel. to flare emission spectrum 0-67731
 guiding system including automatic capture circuitry 0-99005
 hollow beam pot. in magnetically insulated diode 0-70046
 intense electron beam propagation between two plane conductors 0-91744
 intense relativistic electron beam generation by foillless diodes, simulation 0-63438
 interaction with microwave-frequency field, of planar gap 0-106431
 ion acceleration by space charge plasma waves in straight-line beam 0-103166
 JIKIKEN satellite, electron beam emission for magnetosphere beam-plasma interaction expt. (Japanese) 0-94655
 laser pulse amplification through energy exchange with electron beam via nonlinear radiation press. effects 0-95776
 magnetic electron deflection system, high accuracy, shielding ferrite tube 0-102602
 magnetized, flowing through cavity, self-consistent potential calculation 0-91743
 magnetosphere, counterstreaming electron beams at altitudes of 1 R_E over auroral zone 0-67474
 merged electron-ion beam experiment, determ. overlap integral from differential-scanning meas. 0-87282
 mirror electron microscopy, contrast form. 0-68299
 modulated electron beam, non-linear oscillation theory (Russian) 0-106898
 monoenergetic, energy recuperation collector 0-87281
 neutral molecule motion control by electron beams 0-99582
 overlapping, use for interal confinement fusion 0-91242
 pulse generator, repetitively pulsed electron beam system 0-68981

electron beams continued

- pulsed, measurement of current density distrib. and energy spectrum 0-63426
 relativistic, coherent X-ray emission 0-91739
 relativistic, EM instability and stopping power of plasma 0-92289
 relativistic, gradB transport, bunching and focusing 0-96345
 relativistic, intense, guiding with axial mag. field 0-87006
 relativistic, passage at high current through matter 0-91745
 relativistic, propag. along a wire in vacuum guide 0-74291
 relativistic, theoretical scheme for axial compression 0-96367
 relativistic, with variable charge neutralisation degree, equil. state 0-59249
 relativistic electron beam, propag. in strong mag. field (Japanese) 0-91737
 relativistic electron beam in magnetised plasma, relax. processes, non-linear theory, instability (Russian) 0-103162
 relativistic electron beam in plasma, relaxation (Russian) 0-103161
 relativistic electron beam in stimulated coherent scatt. of EM wave (Russian) 0-102601
 relativistic electron beam relaxation in dense gas, radiative energy transfer 0-69968
 relativistic electron beams with finite energy spread and improved emittance, development and investigation 0-91741
 relativistic free-electron wave generators, electrically pumped 0-91742
 relativistic inhomogeneous electron beam, space charge oscills. 0-78759
 relativistic mirror feature, perp. temp. effects 0-78749
 rockets, payload charge neutralisation during electron beam emission, laboratory studies 0-77258
 self magnetically insulated electron flows, line voltage determination 0-69318
 self-acceleration expts., regulation of magnetization of ferrite 0-63425
 self-bunching in resonantly absorbing medium, radiation amplification feasibility 0-102605
 self-focused, relativistic, filamentation instability 0-74289
 solar corona, electron beam injections rel. to type IV radio burst quasisperiodic struct. 0-62097
 spatial charge and beam radius determination (Russian) 0-74290
 spatial electron beam-matter interaction, model calcs. for Cu (German) 0-84815
 spatially modulated electron beam, parametric instability, periodic mag. field effect 0-87285
 thermal particle motion effect on autoresonance acceleration process (Russian) 0-69007
 vacuum beam diodes, repetitively pulsed, lifetime and stability 0-63386
 KD₂PO₄ crystal electron-beam spatial light modulator, resolution 0-74503

electron capture

- see also charge exchange; electron attachment*
 atom+ion multielectron collisions, charge transfer at intermediate energy, atomic model 0-91652
 cytochrome c₃-hydrogenase, reduction kinetics, Mossbauer spectra 0-67031
 electronic and at. collisions, conference, Kyoto, Japan (Aug.-Sept. 1979) 0-62394
⁵⁷Fe, isomer-shift calibration by lifetime variations in electron capture decays of ⁵²Fe 0-75902
 hydrogenic ions, electron capture by charge particles at relativistic energies 0-102565
 ion collisions, electron capture, atomic excited state polarisation, optical detection 0-58377
 multicharged ion and nucleus electron capture during collisions (Russian) 0-87850
 multicharged ions, classical trajectory eikonal approx. 0-69233
 multielectron target+multiply charged ion, electron capture, review 0-63812
 multiply charged atom+H, electron capture, unitarised distorted wave approx. 0-63814
 multiply charged ion, electron capture into different excited states in plasma 0-64679
 multiply charged ion+atom, autoionisation, electron and photon emission 0-63813
 multiply charged ion+one-electron target, electron capture, review 0-63811
 plasma chromatography and electron capture detector, comparison between two techniques 0-61176
 quinones-Zn porphyrin, quinones sensitised reduction in vesicle systems 0-71897
 spectroscopy, technique for surface science and ferromagnetism 0-92766
 Ag latent image particles, electronic effects 0-82840
 Ar+multicharged ion collisions, one electron capture from inner shells 0-58376
 Ar²⁺+Ar (Kr)(Xe), single electron capture excitation, photon emission, VUV spectroscopy 0-58379
 Ar⁶⁺+H₂ collisions, excitation and ionisation 0-78683
 C+H⁺ collision, electron capture cross section 0-63804
 CO₂-N₂-He-O₂ discharge mixture, three body electron attachment to O₂ 0-64779
 Cl^{q+}+Cu, K X-ray production and radiative electron capture, fluoresc. yield determ. 0-99553
 Cs+H⁺(H), single-electron capture total cross sections 0-91656
 H like atom alignment due to electron capture in particle-atom collisions (Russian) 0-106379
 H, one-electron capture by fast multiply charged ions, q³ scaling 0-91658
 H+B^{q+}(C^{q+})(N^{q+})(O^{q+}), (2≤q≤4, 5), cross sections at keV energies 0-78705
 H+He²⁺, electron transfer, plane-wave factor, mol. state treatment 0-63807
 H+Xeⁿ⁺(Ar^{q+})(Fe^{q+}), electron capture by heavy multicharged ions at low velocities total cross sections meas. 0-99548
 H⁰+N³⁺, electron loss cross section 0-63805
 H⁺+H, ionisation and electron capture to continuum 0-58366
 H⁺+He(1s²), K-shell electron capture collision, static pot. effect 0-91660
 H₂+Xeⁿ⁺(Ar^{q+})(Fe^{q+}), electron capture by heavy multicharged ions at low velocities total cross sections meas. 0-99548
 He-like target+fast projectile, electron capture cross-sections 0-69231
 He+He⁺, double collision spectroscopy 0-58378
 He⁺+H₂(He)(N₂)(O₂)(CO₂)(methane)(ethane)(propane), 0.7-2 MeV, charge-changing collisions, electron capture 0-58372
 K+H⁺(H), single-electron capture total cross sections 0-91656

electron capture continued

- Li+doubly charged ions, electron capture excitation, theoretical predictions in fusion plasma 0-63810
- Li+positron, positronium formation in highly excited states, first Born approx. 0-58420
- Mg-H⁺ 2p_{1/2} vacancy alignment electron capture role 0-83465
- Na+H⁺(H), single-electron capture total cross sections 0-91656
- Ne²⁺+Ar (Kr)(Xe), single electron capture excitation, photon emission, VUV spectroscopy 0-58379
- Ne²⁺+Xe, electron capture collisions, 15 to 50 keV, excitation 0-102566
- O⁴⁺+inert gas, electron transfer meas., 60-200 keV 0-83480
- O⁴⁺+He, charge exchange measurements using double-tandem accelerator-decelerator source of low-energy highly-stripped O ions 0-81317
- O₂ electron capture rate from geminate ion recombination fluoresc. data 0-74245
- O₂ in liquid Xe, electron capture 0-102402
- Pb₁₋₃, Sn, Te, In, tunnelling impurity self-localisation, anomalous props. nature (Russian) 0-59915
- Rb+H⁺(H), single-electron capture total cross sections 0-91656

electron capture, nuclear *see nuclear electron capture***electron density**

see also carrier density; current density; electron density (metals); plasma density

- air, electron drift velocity at 293K 0-103102
- Z Andromedae, atmosphere electron densities from IUE obs. 0-109450
- atoms, electron densities and electrostatic pot. calc. 0-102430
- atoms, electrostatic pot.-electronic density relationships 0-69206
- aurora, N(²D) emission and ion chemistry, satellite obs. 0-72673
- aurora, pulsations of electron and ion intensity 0-61934
- aurora modelling, time-depend. study 0-72672
- auroral oval, electron density distrib. rel. to auroral arcs global form. 0-67446
- azaaromatics, neutral and protonated, excited singlet and triplet states, charge densities, INDO calcs. 0-58152
- breakdown, ionising wave propag. mechanisms 0-83941
- D-region, electron density profiles, statistical model 0-61964
- DC arc plasma, alterations in spectral line intensities due to external mag. fields 0-79621
- discharges in gases, pulsed, theoretical and expt. study 0-92416
- E-region electron density profile, distortion meas. using group and phase height meas. 0-109299
- F₂-layer, mid-latitudes, mag. storm effects 0-61970
- F₂-layer, parameters at high latitude during quiet conditions 0-105106
- F₂-layer, peak electron density using servo model 0-101486
- F-layer electron density inhomogeneity, thermodiffusion mechanism (Russian) 0-85791
- F-region, cleft region perturbation during substorm 0-101483
- F-region, electron density and ion temp. profiles rel. to airglow ground-based obs. anal. 0-98496
- F-region, equatorial irregularities and electron density, radar obs. 0-77222
- F-region, winter anomaly causes 0-85793
- F-region during mag. storm, electron content by satellite VHF signal obs. 0-101471
- F-region peak electron density, diurnal and solar cycle variation 0-61949
- gas discharge columns with electron prod. and loss rates linear and quadratic in electron density, electron density distrib. 0-96400
- interplanetary medium, electron density vars. physical form from scintillation spectra 0-72741
- interstellar irregularities from pulsar scintillations freq. time struct. 0-101608
- interstellar medium, electron density determ. from low-latit. pulsars dispersion meas. and distances 0-101606
- ionosphere, bottomsides, mid-latitude trough discovery 0-109300
- ionosphere, calc. technique for ground and satellite obs. 0-90275
- ionosphere, combined ground and satellite measurements, IRI model extension 0-61911
- ionosphere, cond. and electron density of reflecting layer below classical D-region 0-98508
- ionosphere, electron concentration profile, vert. struct. 0-61936
- ionosphere, electron density and temp. rel. to primary ion-electron prod. rates changes 0-72675
- ionosphere, electron distrib. rel. to production rate and heating 0-105103
- ionosphere, HF heating expt. for fluctuations of electron density 0-82140
- ionosphere, O⁺/electron density ratio in 140-200 km height range 0-105102
- ionosphere, plasma bubbles spatial relationship with 1 m equatorial spread-F irregularities 0-67457
- ionosphere, polarisation electric field vert. distrib. in topside 0-61935
- ionosphere, radar obs. of electron density revealing gravity waves 0-77182
- ionosphere, sporadic-E and F₂ layers, electron fluctuation origins 0-101475
- ionosphere, topside, electron density rel. to electron temp. models 0-67460
- ionosphere, total electron content comparative study 0-98516
- ionosphere, total electron content fluctuations rel. to scintillation of VHF and GHz waves 0-109302
- ionosphere, use of regularisation method 0-72679
- ionosphere, vertical density gradients rel. to equatorial electrojet type 1 radar echoes with double-peaked Doppler spectra 0-67458
- ionosphere electron density of Delhi and latitudinal depend., INTASAT Faraday fading obs. 0-109293
- ionosphere equatorial anomaly, dissimilar forms in E.Asia and India 0-109301
- ionosphere equatorial bubbles, model computations of assoc. radio wave scintillation 0-94641
- ionosphere total electron content, nighttime enhancements at low latits. 0-72677
- lower ionosphere, electron density profile from radiowave data 0-67462
- magnetosphere, evidence for trapped flux limit from pulsating aurorae 0-72666
- magnetosphere, local electron density and mag. field meas. via JIKIKEN (EXOS-B) satellite stimulated plasma wave expts. (Japanese) 0-94649
- magnetosphere, whistler duct struct. and formation 0-94659
- magnetosphere radiation belts, electron intensity fluctuations meas. from Cosmos 484 satellite 0-72698
- molecular similarity, electron density function meas. 0-91413
- molecules, electron densities and electrostatic pot. calc. 0-102430

electron density continued

- Mossbauer atoms, electron densities at nuclear centre and surface, calcs. using Dirac-Fock eqn. 0-74100
- outer radiation belt electron intensity rise, link with magnetosphere disturbance 0-77225
- PHL 1092, narrow line quasar, Fe II emission region electron density and temp. 0-77508
- plasma, laser-created, asymmetric electron density profile, interferometric meas. 0-75085
- plasma diagnostics using X-ray spectrometer, high-speed, multichannel 0-57445
- plasmopause, electron density profile meas. stimulated plasma wave results (Japanese) 0-94650
- plasmosphere, mid-latitude, nighttime electron content, geophysical disturbance effects, 1974 August to November 0-94642
- protonosphere depletion assoc. with mag. storm, and recovery 0-85784
- pulsed laser discharges, interferometric meas. 0-96393
- Saturn, ionosphere electron density from Pioneer II radio occultations 0-94751
- semiconductors, electron-electron collision effect on current voltage characts. in quantising mag. field 0-103705
- solar corona, density model for N.polar hole at 1973 June 30 eclipse 0-98627
- solar corona, rel. to photosphere mag. field strength 0-85913
- solar flares, determ. from X-ray spectra 0-82326
- solar flares, electron density enhancement rel. to O I 1355.6 Å and C I 1355.8 Å lines obs. 0-90381
- universal variational functionals of electron densities, first-order density matrices, and natural spin-orbitals and solution of the *r*-representability problem 0-95516
- UV galaxies, double nuclei, visible spectra obs. (Russian) 0-77495
- UV photoplasma, electron density, microwave meas. 0-75097
- Ar plasma, radial distrib. of excited atoms prod. by surface wave (French) 0-96349
- CO₂ self-sustained laser system, electron avalanche and electron-ion recomb. coeffs. meas. 0-102694
- F₂-layer, low latitude, electron density eqn. of continuity soln. 0-101472
- H spark, laser-triggered, electron densities meas. 0-106975
- H spark gap arc discharges, laser-triggered, electron density meas. 0-64822
- H₂⁺, mol. electron density distrib., binding/antibinding anal. 0-95534
- He-I⁺ laser discharge, positive-column, particle densities 0-103215
- He-metal vapour lasers, positive column electron densities, experimental study (Japanese) 0-69376
- Hg vapour, electron drift velocity at 573K 0-103103
- Mg vapour, electron momentum transfer cross section, from 0.1-5 eV 0-103104
- N₂-methane, rapidly developing discharge, streak camera records interpretation 0-59280
- N₂-SF₆ pulsed discharge laser with CW X-ray preionisation 0-95910
- Na-Xe, excimer lasers, high-power discharges, models 0-69373
- O₂, low energy electron drift velocity at 293K 0-103101
- electron density (crystallography)** *see crystallography*
- electron density (metals)**
- alkali metals, partial pressure contributions to equation of state 0-107401
- metal, electron density behaviour near impurity charge 0-75518
- metals, ground state of solids, spin density functional method, binding energy, compressibility 0-65477
- nontransition metals, electron density, bulk and surface props. relation 0-103609
- surface, self-consistent electron theory, review 0-88616
- unidimensional metals, plasmon freq., effect of nonuniform electron density profile (Russian) 0-59896
- Au-transition metal alloys, ¹⁹⁷Au Mossbauer isomer shift cellular atomic model 0-84673
- BiSb (>20 wt.%), electronic band struct. 0-107698
- Co(GaTiV) alloys, ferromag. onset, electron conc. depend. 0-60203
- Cr-Fe, elastic moduli, electron conc., pulse echo overlap meas. 0-59550
- B-Ga, metastable, elec. props. in normal and supercond. states (Russian) 0-65520
- Ni films, electronic struct. calc., effects of chemisorption; contact pot. and surface magnetisation 0-103734
- Ni-Fe, electronic struct. calc., effects of chemisorption; contact pot. and surface magnetisation 0-103734
- Ti-V, elastic moduli, electron conc., pulse echo overlap meas. 0-59550
- electron density of states** *see electronic density of states*
- electron density of states (condensed matter)** *see electronic density of states*
- electron detachment**
- excited atom ionisation due to collisions in their own gas (Russian) 0-91654
- ion electron impact detachment, ionisation, excitation, dissociation and recombination 0-63832
- negative ion+atom, electron detachment, zero range Fermi approach 0-63798
- negative ions, at. and mol. collisions electron detachment for energies near threshold 0-63797
- negative ions, electron impact detachment cross sections, classical scaling theory appls. 0-83492
- negative ions, photoabsorption spectra, long-range field effect 0-91521
- resonance partial widths and partial photodetachment rate using the rotated-coordinate method 0-91428
- Ar+Ar⁺(Ar²⁺)(Ar³⁺), electron stripping cross-sections meas. 0-83477
- Br+H₂(D₂)(O₂)(N₂)(CO)(CO₂)(methane), total electron detachment cross sections for energies around threshold 0-99550
- Cl⁺+H₂(D₂)(O₂)(N₂)(CO)(CO₂)(methane), total electron detachment cross sections for energies around threshold 0-99550
- H⁺, ion beam diagnostics using laser beam 0-95497
- H⁺, photoabsorption spectra, long-range field effect 0-91521
- H⁺, two-electron photodetachment threshold, blackbody radiation effects 0-91524
- H⁺+H(He), electron detachment in adiabatic regime, mechanisms 0-63800
- H⁺+He, electron detachment, theoretical obs. 0-63799
- H⁺+inert gas, negative ion detachment cross section determ. 0-63796
- K⁺, photodetachment and at. polarisability 0-91522
- Ne+H⁺(D⁺), electron detachment, dynamical phenomenon 0-106305
- electron detection and measurement**
- backscattered electron detector, multi-purpose 0-102404
- backscattered electrons in SEM by conversion to secondary electrons 0-62804

electron detection and measurement continued

- dose-rate conversion factors for external exposure to photons and electrons, modifications to DOSFACTOR code 0-104775
- electron-matter interactions rel. to electron microscopy 0-89097
- film photon and electron absorbed-dose detector 0-91379
- Johnston electron multiplier, low energy ion counting efficiency 0-63479
- mica dosimeters, for visualisation of electron isodose curves in a medium 0-99349
- microchannel plate based detector for a heavy ion beam spectrometer 0-58018
- photoelectrons, phase-sensitive vidicon detector for angle-resolved electron spectroscopy 0-90933
- relativistic electron energy loss distrib. in thin gas layers of proportional counters 0-99429
- relativistic electrons, 0.1 to 6.0 GeV superheated superconducting colloid shower detector 0-91398
- scintillator detector, detection efficiency and performance estimation, of HV STEM 0-101899
- STEM, quadrant detector, appls. 0-77914
- STEM multichannel detector system 0-68331
- subnanosecond plastic scintillators, 100 keV electron detection 0-69037
- CaF₂:Eu, scintillation detector, in STEM 0-101897
- FeSO₄ dosimetry for electrons, a re-evaluation 0-68963
- MgO coated detector for SEM backscatter to secondary electron conversion 0-68332
- Pb-scintillator sandwich EM shower detector, perform. characts. 0-102385
- Si(Li)-emulsion shower counter for cosmic ray electron obs. 0-58033

electron device noise

- charge injection device as stellar tracking sensor 0-85861
- cyclic queue models of semiconductor noise and vehicle fleet operations 0-80336
- electronics for the physicist with applications, book 0-62403
- HgCdTe/CdTe, limited diffusion volume photodiode, characterisation 0-75627
- model for 1/f noise 0-98945
- quantum noise at low temperature 0-103733
- semiconductor laser intrinsic noise in optical communication systems 0-69394
- semiconductor lasers 0-58538
- superconducting tunnel junctions, quantum noise effects in 0-1 mV bias range 0-80449
- Fe³⁺:TiO₂, 86-88 GHz low-noise TW maser 0-69354
- (GaAl)As-GaAs narrow stripe laser, improved optical communication system performance 0-102733
- GaAs injection lasers, direct modulation enhancement effect of HF noise 0-83608
- HgCdTe reverse-biased photodiodes for wideband appls., excess noise 0-107876
- InGaAsP avalanche photodiode, 1.3 μ m, noise performance, -190°C 0-57370
- Si diffused junction photodiode performance characteristics 0-80367
- TlInSe₂, monocrystal, photoelec. props. (Russian) 0-70752

electron device testing

- see also *integrated circuit testing; semiconductor device testing*
- capacitors, ceramic, using scanning laser acoustic microscopes, comparison with SEM and optical microscopy results 0-58875
- deflection system performance using resolution test specimen 0-69311
- quartz resonator surface patterns obs., using SEM 0-71323
- SAW voltage contrast obs., using SEM 0-69618
- space radiation environment for electronic components, laboratory simulation 0-94689

electron diffraction

- see also *electron diffraction crystallography; electron diffraction examination of materials; gas phase electron diffraction; high energy electron diffraction; low energy electron diffraction*
- microscope resolving power limitations 0-86528

electron diffraction crystallography

- see also *crystal atomic structure; Debye-Waller factors*
- 3-beam elastic intensities, inversion for scalar scattering by centrosymmetric cryst. 0-107023
- backscattering patterns, in field emission gun SEM 0-100142
- bent molecular organic crystals, electron diff. intensities 0-100132
- bicrystals, theory 0-75122
- bonding charge densities, determ. 0-75125
- centrosymmetric cryst., inversion of 3-beam intensities for scalar scattering 0-107023
- computer indexing of point diffraction patterns 0-100136
- convergent beam, development and appls. 0-75124
- convergent beam electron diffraction 0-103220
- convergent-beam diffraction patterns obtained by beam-rocking method, signal processing 0-70085
- cubic crystal, image contrast of dislocation loops, elastic anisotropy depend. 0-103349
- defect imaging, analytical contrast calcs. in two-beam case 0-100134
- defect symmetry, electron diff. contrast, theory 0-96418
- defect symmetry and diff. contrast 0-79778
- digenite-type disordered crystals, diff. pattern, cluster theory 0-75123
- double crystal interferometer, dynamical theory 0-100135
- dynamical theory of scattering, crystal with equidistantly bent reflecting planes (Russian) 0-70078
- dynamical theory, approximations 0-87997
- electron diffraction symmetries 0-100138
- frozen hydrated crystalline specimens, meas. and reduction of damage 0-85552
- graphite, zone-axis pattern maps 0-100137
- inelastic electron scattering in crystals, extension of Yoshioka theory 0-103219
- inelastic scattering, dynamical diffraction and generalised dielec. response function 0-75120
- lattice defects, characterisation 0-103320
- lattice fringe imaging theory 0-103225
- lattice image calculations for imperfect crystals, superlattice approach 0-107030
- lattice images of defects, computer simulation of high resolution images 0-107208
- many-beam lattice images from thicker crystals 0-88004
- microdiffraction patterns, point group symmetry from dislocation cores 0-100140
- phase determination, superposed diffraction patterns 0-100141

electron diffraction crystallography continued

- slow electron diffraction, from thin crystal struct., theory (Russian) 0-64843
- spherically symmetrical coherency strain contrasts, S-matrix theory calcs. 0-100133
- spot broadening, resolution, X-ray and electron beam diff. patterns (German) 0-84033
- STEM application, two-dimens. diff. patterns obs. and recording system 0-79650
- superlattice fringe images of ordered alloys, computer simulation 0-103296
- textures, reflection sphere curvature influence on reflection location geometry 0-87996
- two-phase cryst. structures, orientational electron microdiff. anal. with aid of OMEGA program 0-103218
- Bi, intervalley scattering processes, surface struct., transverse electron focusing study (Russian) 0-84352
- Mo extinction length χ_{220} meas., electron energy influence 0-90935
- Si crystal, contrast depend. of Kikuchi patterns on primary electron beam energy (Russian) 0-64844

electron diffraction examination of materials

- see also *gas phase electron diffraction; high energy electron diffraction; low energy electron diffraction; reflection high energy electron diffraction*
- adsorbate vibrations, large-angle inelastic electron scatt., theory 0-75427
- adsorbed layers, photoelectron diff. azimuthal patterns, struct. sensitivity 0-107644
- Al-Zn-Mg (5.1 wt.%), decomp. process, TEM study 0-71660
- alloys, high resoln. diff. and imaging characterisation 0-104050
- alloys, phase transition premonitory phenomena, exam. by electron diff. and microscopy (French) 0-59651
- amorphous metals, geometric struct. models and diffraction exam. techniques 0-79700
- anthanthrene, mol. cryst. images in electron diff. patterns 0-103315
- Bloch wave model for ECP contrast in Si, Cu, Ag, Au 0-96419
- γ - brass type alloys, superstructures and defect obs. 0-107284
- catalase, glucose embedded, measurement and reduction of radiation damage in frozen hydrated crystalline specimens 0-89810
- cellulose, degradation by high voltage electrons 0-100283
- ceramics, high resoln. diff. and imaging characterisation 0-104050
- chaotite, a new allotropic form of carbon, produced by shock compression 0-80997
- convergent beam electron microscopy, appl. in materials science 0-107028
- crystalline materials, struct. of grain boundaries using diff. techniques 0-59478
- 1,2,6-cyclononatriene, mol. struct. and conformation, gas phase electron diff. 0-106400
- diacetylene monocarboxylic acids, multilayers, struct. phase transitions and polymerisability 0-80129
- 1,1-difluoroethane, mol. struct., gas phase electron diff. obs. 0-58385
- dislocation core, symmetry of dynamical electron microdiffraction patterns 0-100140
- DNA helix destabilising protein cryst. 0-85338
- F 0-76244
- film adsorbed on graphite, two-dimensional phase transitions 0-107653
- film defect growth and nucleation, electron microscopy and diffraction exam. (French) 0-59824
- glasses and ceramics, characterisation with analytical electron microscope 0-84068
- graphite, zone-axis pattern maps 0-100137
- graphite-Rb, intercalation cpd., superlattice struct., electron diff. study 0-75214
- n-hexatriacontane film, vacuum deposited on alkali halide crystals, structure and heat treatment 0-103600
- II-VI semiconductors, thin epitaxial layer, direct synthesis (German) 0-104070
- 2-iodoacetamide, mol. struct., electron diff. obs. 0-63819
- liquids, single beam microdensitometer 0-86370
- martensitic transformations, electron microscope study of cryst. geometry (Russian) 0-108441
- metal oxide smoke particles prepared by gas evap., morphology and coalescence growth 0-97738
- octadecylacrylamide films, oriented ultrathin, radiation-induced solid state polymerisation 0-80128
- PbO-Nb₂O₅ system, X-ray and electron microscopic phase and struct. determ. (French) 0-92508
- phthalocyanines, metal free, mol. cryst. images in electron diff. patterns 0-103315
- polyethylene spherulites, thin melt-cast films, high density, deform. process in non-equatorial regions 0-81124
- protein, cryst. struct. analysis by electron diff., single scatt. approx., domains of validity 0-101150
- protein crystal, wet, low dose electron diff. 0-85550
- steel, austenitic stainless, unlubricated, friction, wear and microstruct. of types 304, 316 and Nitronic 60 0-108589
- steel, austenitic stainless, welded explosively, induced martensites morphology 0-104153
- surface films on solids, TEM study method 0-65409
- tetrafluoro-p-benzoquinone, mol. struct., gas phase electron diff. obs. 0-58386
- tetramethyl-p-benzoquinone, mol. struct., gas phase electron diff. obs. 0-58386
- trifluoroethene-d₆-d₁₁, mol. struct., microwave and electron diff. obs. 0-58384
- tris(trimethylstannyl)amine, gas phase electron diffraction 0-106401
- vacuum deposited film, orientation axis tilt rel. to vapour angle of incidence 0-88456
- Zircaloy-2, hydride precipitation and growth at crack tips, electron optical obs. 0-108449
- Ag-Al (26 at.%), massive transform, $\beta \rightarrow \zeta$, crystallography and morphology 0-97475
- AgI aerosol particle size, struct. rel. to ice forming activity 0-61164
- Al-(Mg)(Fe), pure (dilute), large wire drawing plastic deform. 0-108508
- Al-Cu, superconducting amorphous films of high stability 0-70889
- Al-Mg, oxidation control study, electron opt. techniques eval. 0-85089
- Al-Mg₂Si, ageing sequence study by electron microdiff. 0-81068
- Al₂O₃ films, DC reactively sputtered, struct. 0-96764
- Al₂O₃, grain boundary thickness obs. using electron diff. techniques 0-79811

electron diffraction examination of materials continued

- Au films, vac. condensed at oblique vapour incidence, oriented cryst. growth, electron diff. study 0-97432
- Au, grain boundary thickness obs. using electron diff. techniques 0-79811
- Au, pentagonal symmetry, icosahedral struct. (*French*) 0-79729
- Au, thin film bicrystal, diffraction effects from inclined grain boundaries 0-103362
- Au thin films, electron diff. investigation of Debye temp. 0-88420
- Au-Si thin film double layer, silicide form., electron diff. study 0-80005
- Au₁₁Mn₄ ordered phase formation, electron diff. and microscopy study 0-107418
- Au₂Mn thin film study 0-92793
- Au₂Si₁₋₂ amorphous films, phys. studies 0-75476
- BaFe₂O₄ amorphous film, prep. by RF sputtering, crystallisation 0-76183
- Ba_{1-x}Fe_xS₄ electron diff. study, orientation anomaly 0-107152
- BaTiO₃ ceramics, PTC-type, grain boundary study using TEM 0-107267
- Ba₂YbF₆ single crystals, electron diff. cryst. struct. anal. (*French*) 0-92507
- Be₂N₂-BeSiN₂ system, crystallography and phase relationships, TEM and electron diff. study 0-92502
- Bi film, structure and electronic props. 0-70562
- BiVO₄, ferroelastic domains, electron microscopy and electron diff. obs. 0-100254
- C fibre structure, recent advances 0-81069
- C, filamentous catalytic, rel. crystallographic orientations of C and metal 0-89240
- C, thin foil, irradiation with 1.2 MeV Ar⁺, electron diffraction study 0-103397
- Ca₂(Al,Fe,Cr)O₅ solid soln., planar interfaces, TEM obs. 0-65008
- Ca₂Si₂O₇(OH)₂, xenotile, polytype identification 0-72519
- Cd₃As₂ films, nucleation processes, on NaCl substrates 0-59813
- Cd₁ polytypes, vapour growth mechanism 0-84124
- CdIn₂Se₄, high resolution electron microscopic study of polytypism 0-88119
- CdS, epitaxial growth and nucleation, on monocryst. ZnS, substrate real struct. influence 0-88455
- CdS epitaxial layers on sapphire, exciton struct. of absorpt., photoluminesc. and photocond. spectra 0-89027
- Co-P, electrodeposited alloys, heat-induced structural changes (*Japanese*) 0-89263
- Co-P alloys, geometric struct. models and diffraction exam. techniques 0-79700
- Co-Ti-Fe (3, 1 to 2 wt.%), spinodal decomposition 0-100839
- Co_{3-x}Mo_xO₄ films, prep., struct. and elec. characteris. 0-108353
- Cr film, obtained by thermo ionic precipitation, phase composition, lattice parameters (*Russian*) 0-96756
- CrO₂ and CrO(OH), fine particle obs. of cryst. morphology and topotaxy 0-65969
- Cr_{2.8}V_{0.7}Fe_{3.4}C₃, stacking fault study, morphology, comp. and struct. 0-84190
- CsTi₂NbO₆, layer struct., X-ray and electron diff. study 0-79753
- Cu films, vac. condensed at oblique vapour incidence, oriented cryst. growth, electron diff. study 0-97432
- Cu, grain boundaries, intrinsic struct., electron diff. anal. 0-84186
- Cu, thin film, oxidation, RMEED/SEM studies 0-100968
- Cu-Al-Ge, Hume-Rothery glass form. 0-96449
- Cu-Al-Sn system, coexistence of different and brass like phases 0-89206
- Cu-Bi, grain boundary thickness obs. using electron diff. techniques 0-79811
- Cu-Ni-Al (5, 2.5 at.%), precip. hardening (*Japanese*) 0-71663
- Cu-Ni-Sn (10, 6 wt.%), spinodal decomposition, X-ray and electron diff. study 0-81063
- Cu-Sn alloy system, long period superlattice obs. and impurity effects 0-103297
- CuInS₃ films, RF sputtered, growth and props. 0-80124
- CuIn₂S₈, sulphospinel, electron microscopy study 0-88080
- Cu₄₀Nb₃₀X₃₀ (X=Ti, Zr, Hf), superconductors with metastable ordered structs. 0-108484
- Cu_{3-x}Te₂, non-stoichiometric phases, electron microscopic and electron diffraction studies 0-64977
- Fe sputtered film, amorphous, Mossbauer study and electron diff. obs. 0-75897
- Fe vacuum deposits on Ni(Cu)(Ag) (111) FCC substrates, orientation relationships 0-59836
- α-Fe whiskers, pure, ductile fracture, microscopic obs. of initiation mechanism 0-85044
- Fe-Cr-Al-Y, oxidation resistance, heat treatment and Al⁺ ion implantation 0-71785
- Fe-Ni-Mn (20, 5 wt.%), rel. orientation between adjacent martensite laths 0-76254
- Fe-Si (3wt.%), grain-oriented, secondary recryst., grain growth inhibition 0-89245
- Fe-X-C (X=Cr, Mo, W), quenched rapidly from melts, nonequilib. phases (*Japanese*) 0-71630
- Fe₂O₃-Fe₂O₃ thin film on passivated Fe, electron diff. study (*German, English*) 0-89418
- Fe₂Sn₁₋₂ amorphous film, struct. and mag. props. 0-65972
- FeTi-D(H), γ-phase, neutron and electron diff. 0-84156
- GaAs, dislocation-free, point defects and rad. damage 0-88141
- Gd-Co amorphous films, mag. struct., mag. bubbles, electron diff. study (*Chinese*) 0-71126
- Ge amorphous films, structural relaxation and crystallisation 0-100170
- GeO, Cu, amorphous thin film, impurity effects on struct. 0-107054
- α-HgS films, sputter-deposited in Hg vapour, growth and props. 0-75467
- InP single crystals, uniaxial compression deform. characts. 0-84991
- InTe thin films, flash evaporation, electrical props. 0-65722
- KNiCl₃, disorder as observed by electron diff. 0-75213
- K₂Pt(CN)₄Br_{0.3}H₂O, anisotropic radiation damage in electron microscopy, diff. spot fading rate obs. 0-107329
- La-Al amorphous alloys, internal friction, relaxation process 0-92607
- LaNbO₄, room temp. form., symmetry determ. by convergent beam electron diff. 0-79723
- La₂O₃, cryst. struct., X-ray powder diff. and electron diff. study 0-107161
- MgCa(CO₃)₂, dolomite, partial thermal decomp. into MgO and CaCO₃, product cryst. growth 0-108706
- Mn thin films, vacuum deposited in elec. field, resist., struct. 0-103761
- NaCl-gas reactions, atmospheric, in situ TEM studies 0-104544
- Nb₄₀Fe₄₀P₁₄B₆, metallic glass, explosive compaction, mech. props. 0-89176

electron diffraction examination of materials continued

- Nb₂Ge, sputtered on Cu, film-substrate interface obs. by electron microscopy 0-65398
- 4NbO_{0.76} thin film, FCC cell struct. investigation 0-92796
- 3Nb₂O₃·8WO₃, circular diffuse scattering studied by 1 MV high resolution electron microscopy 0-59350
- NdNbO₄, room temp. form., symmetry determ. by convergent beam electron diff. 0-79723
- Nd₂O₃, cryst. struct., X-ray powder diff. and electron diff. study 0-107161
- Ni-Al-Mo (12.7, 21.6 wt.%), directionally solidified eutectic composite, precipitation 0-108454
- Ni-Cu-X (X=Sn, Nb, Ti), spinodal decomp. alloys, linear expansion coeff. influence on morphological anisotropy (*Japanese*) 0-70431
- OPBr₃, mol. struct., electron diff. and spectroscopic vibr. amplitude 0-58387
- PLZT ferroelectric thin films, epitaxial growth and optical props. 0-70543
- Pb_{1-x}Sn_x-Te-PbTe heterostructures, MBE produced on mica and LiNbO₃, elec. props. study 0-88629
- Pb₃(VO₄)₂, ferroelastic, phase transitions, boundary walls 0-107419
- Pd₈₀Si₂₀, amorphous alloy, partial struct. functions, X-ray, electron and neutron diff. studies (*Japanese*) 0-88050
- (SN)_x, halogenated, struct. behaviour, TEM obs. 0-70126
- SPBr₃, mol. struct., electron diff. and spectroscopic vibr. amplitude 0-58387
- Sb_{0.2(0.4)}Mo_{0.3(1)}, synthesis, struct. and oxidation state (*French*) 0-64971
- Sch₂, electron diff. investigation 0-107112
- Si, ion bombardment induced defect distrib., IR and electron diff. study 0-65074
- Si, oxide scale microstruct. of oxidised single cryst. 0-108613
- Si:N wafers, Si₃N₄ layer growth by high dose implantation and annealing, elec. props. 0-70227
- Si-CoSi₃Si, double heteroepitaxy, solid phase and MBE 0-104063
- SiC, HVEM obs. of various polytypes 0-76248
- SiC, oxide scale microstruct. of oxidised single cryst. 0-108613
- SiC polytypes, lattice imaging studies on intergrowth structs. 0-107025
- Sn film, vacuum deposited, substrate and substrate temp. effects on struct. 0-107677
- Sn polycrystalline films, elec. props. and crystallite size, 4.2K to room temp. (*Russian*) 0-93011
- 2Ta₂O₃ thin film, FCC cell struct. investigation 0-92796
- Ta₂O₅, with hexagonal lattice in thin layers, atomic struct., electron diff. 0-84160
- Te, Kikuchi patterns, of non-centrosymmetrical crystal 0-100202
- α-Ti-Al-Sn, alloy Ti-679, electron diff. anal. of Ti₃Si phase (*Chinese*) 0-64845
- Ti-Mo alloys, structural stability under high-pressure soaking 0-104151
- Ti-Mo-Zr-Sn (11.5, 6.0, 4.5 wt.%) alloy, struct. as affected by processing history 0-84972
- Ti-Si amorphous alloy, melt-quenched, transform. studies and mech. props. 0-100838
- Ti-V (10 at.%), α-ω transformation, electron diff. evidence of intermediate BCC phase 0-81051
- V-H(D), phase diagrams, struct. studies 0-66491
- V-O alloys, quenched, local ordering of O, electron microscopy and diff. 0-59453
- V-Ti-C, high temp. carbide form., electron microscopy study 0-89228
- VO₂, metal-insulator transition and electronic struct., ion bombard. effects 0-92948
- VO₂, V₂O₃ and V₂O₅, film prep. under equil. conditions, struct. and elec. props. 0-108352
- V₂O₅, amorphous semicond., solubility and fibrous texture 0-75162
- V₂Si, supercond. structure and properties (*German*) 0-93631
- W {100}, anisotropy of inelastic electron refl., energy loss effects 0-79642
- W, SEM expts., anomalous patterns (*Chinese*) 0-59349
- YFe₂O₄, extra electron reflections 0-100139
- YIG, thermomag. anal. by electron diff. 0-108035
- YbFe₂O₄, extra electron reflections 0-100139
- Yb₂Fe₂O₇, extra electron reflections 0-100139
- Yb₂Fe₂O₁₀, extra electron reflections 0-100139
- Zn film deposition on Al, TEM and electron diff. obs. 0-75460
- ZnSn ion beam etching, topographic changes, amorphisation, luminescence study 0-76078
- Zr, hydride precipitation and growth at crack tips, electron optical obs. 0-108449
- Zr-Nb (2.5 wt.%), hydride precipitation and growth at crack tips, electron optical obs. 0-108449
- ZrO₂-CaO (15 mol.%), precipitation and ordering 0-100837
- ZrO₂-Y₂O₃ (9 mol.%), precipitation and ordering 0-100837

electron-electron double resonance see ELDOR

electron-electron interactions

see also electron-electron scattering

No entries

electron-electron scattering

see also electron-electron interactions

No entries

electron emission

see also cathodes; electron field emission; exoelectron emission; photoemission; secondary electron emission; spin polarised electron emission; thermionic electron emission; work function

conference, Leningrad, USSR, (Jan. 1979) 0-98754

ferroelectric electron emitter with negative electron affinity 0-100762

heavy ion induced collective electron emission 0-80926

semiconductor, electron emission from surface subband, reduced work function 0-60757

steel, type 40 Kh, electron emission depend. on surface mechanical treatment (*Russian*) 0-100945Cu, electron emission depend. on surface mechanical treatment (*Russian*) 0-100945

LiF, ion and electron emission following ion impact 0-100729

NaCl, ion and electron emission following ion impact 0-100729

Si, ion and electron emission following ion impact 0-100729

Zn, electron emission depend. on surface mechanical treatment (*Russian*) 0-100945

electron energy bands see band structure

electron energy loss spectra

acetylene, higher excited states, electron energy loss spectra 0-91664

electron energy loss spectra continued

- actinides and their fluorides, interband, collective and atomic (p,d) excitations, Z-160 eV, fast EELS 0-93443
adsorbed molecule, angle-resolved and variable impact energy electron vibr. excitation spectroscopy 0-76119
adsorbed molecules, electron-impact vibr. excitation, specular selection rule 0-80051
analytical tool, data handling and processing 0-81407
atoms, near threshold struct. in K-shell spectra, photoionisation or fast charged particle ionisation 0-87064
chemical analysis, filtered images 0-101062
direct elemental analysis 0-71998
dislocations and microplasma sites, STEBIC/STEM/EELS correlation 0-96528
electron microscope, analytical 0-86521
energy losses due to diffraction radiation (*Ukrainian*) 0-75278
5-fluorocytosine, electron beam damage assessed by EELS 0-89809
inelastic electron scattering: surface vibrational spectroscopy 0-107347
inelastic electron-matter interactions 0-104024
inert gas solids, collective excitations and EELS, calc. 0-92842
inner-shell electron impact excitation, developments in electron energy loss spectroscopy 0-63842
magnetic spectrometer, corrected second-order aberrations 0-87013
metallic thin films, electron backscattering, empirical study 0-108310
metallic thin films, Everhart theory extension of backscattered electron energy spectra 0-108309
microanalysis, quantitative approach to inner shell losses 0-101059
microspectrometry, using energy loss electrons in electron microscopes, review 0-104025
molecules, energy loss spectra, state-to-state rot. transition cross sections 0-91665
nitromethane, variable angle electron-impact excitation, transitions in 7-12 eV energy-loss range 0-69244
plasmons and interband transitions, electron excitation, book 0-77555
poly(vinyl cinnamate), excited state, low-energy EELS and INDO/S calcs. 0-106407
polyacetylene:AsF₆(I), pure and doped, electronic excitations, momentum depend., EELS study 0-76121
quantitation methods, recent progress 0-73542
radiation damage, meas. of loss of gaseous elements from thin samples 0-96568
rare earth oxides, segregation study by electron energy-loss spectroscopy 0-79953
rare earths and their oxides and fluorides, interband, collective and atomic (p,d) excitations, Z-160 eV, fast EELS 0-93443
resolution optimisation, wing electron lenses between TEM specimen and electron spectrometer 0-101886
SEM technique exam., ultra-high vacuum, secondary electron emission dependence on electron beam density dose 0-61209
STEM, appl. to materials science 0-103228
STEM, multi-channel averaging 0-101061
STEM, spectrograph, recording of energy loss spectra 0-86525
STEM, structural and chemical analysis, appls. 0-88003
TCNQ salt, decamethylferrocenium, monomeric and dimeric, optical and EELS study 0-100660
TEM, image contrast from single-electron excitation 0-59353
TEM, standard, implanted Si 0-99017
TEM, theory and instrum. 0-81405
TEM image and electron energy loss spectrum display by self-scanned linear Si photodiode arrays 0-68330
thin films, chem. anal. by energy loss spectroscopy 0-104493
3d transition metal films, EELS, anomalous L₃/L₂ white-line ratios 0-93444
transmission, microanalysis of precipitates in Ni-base superalloy 0-104492
5-trifluoromethyluracil, electron beam damage assessed by EELS 0-89809
water, chemisorbed on Pt (111), EELS spectra, vibr. freqs. 0-80920
Ag, photoionisation cross sections, electron-impact inverse mean free paths, and stopping powers for each subshell 0-69113
Ag, thin targets, electron transmission below 3 keV (*French*) 0-60725
Al, L-shell ionisation by 80 keV electrons, transmission electron energy loss spectroscopy 0-60721
Al, small spheres, bulk plasmons damping 0-75561
Ar, electron energy loss spectra, Compton defect characterised by shift and asymmetry parameters 0-95723
Ar, electron scatt. and ejection, electron energy loss spectra 0-58394
Ar, energetic electron degradation spectra and initial yields 0-95724
Ar-high energy electron spectroscopy techniques 0-62740
Au, core-electron excitation edges 0-66345
Au-Si interface, critical Au-film thickness obs. for room temp. interfacial reaction 0-75390
Au-Si interface, electron energy loss and AES meas. 0-89096
Ba monoatomic film on W (110), characteristic electron energy loss 0-100720
Be film, on W (110), growth mode, work function, thermal desorption, and struct. 0-75477
CO, adsorbed on Cu (100), vibr. excitation cross-sections 0-75441
Cd, oxidation, chemisorption and oxide regimes, UPS and EELS study 0-81236
Cu (100), adsorbed formate and acetate species, EELS study 0-76120
Cu, core-electron excitation edges 0-66345
Cu, thin targets, electron transmission below 3 keV (*French*) 0-60725
CuO, on Cu, identification by electron spectroscopic methods 0-60747
Cu₂O, on Cu, identification by electron spectroscopic methods 0-60747
EuO (100), EELS, Eu valence in surface region and high energy giant reson. 0-84816
Fe, O, films, electron microscopy and energy-loss spectroscopy 0-80137
GaAs film, electron scatt., cathodoluminesc. meas., energy depend. of electron deposition depth determ. 0-104023
Ge, volume plasmon, cryst. orientation influence 0-80921
HBr, electron impact ionisation, vibr. excitation spectra threshold peaks, negative ion effects 0-106322
Hf, electronic excitations, charact. energy loss meas. up to 50 eV 0-60723
HfO₂, electronic excitations, charact. energy loss meas. up to 50 eV 0-60723
LiF film, surface phonons and thickness variation, EELS meas. 0-92774
Mg (0001) face, incipient oxidation, EELS and LEED studies 0-81237
N₂, electron impact dissoc., EELS, N⁻ autoionisation 0-106397
N₂ gas, electron energy degradation, Monte Carlo study 0-69969

electron energy loss spectra continued

- Nb, electron energy losses due to H, obs. by scanning TEM 0-79850
Nd₂O₃, EELS, low loss peak due to plasmon 0-79953
Nd₂O₃-Y₂O₃ film, segregation obs. by EELS 0-79953
Ne, electron energy loss spectra, Compton defect characterised by shift and asymmetry parameters 0-95723
Ne, electron impact excitation of 2s2p³s and 2s2p³p configs., energy loss obs. 0-91685
Ne, electron impact K-shell excitation, EELS 0-106396
Ni (100), dissociative chemisorption and mol. adsorption of NO 0-65373
Ni (111), adsorbed H, angle-resolved and variable impact energy electron vibr. excitation spectroscopy 0-76119
Ni, core-electron excitation edges 0-66345
Ni, dielectric matrix, analytic model 0-75512
Ni film, interaction with O₂, AES, EELS, work function, and gravimetric meas. 0-75433
Ni superalloy, STEM microanal. of precipitates and their nuclei 0-81067
Pd surface, segregated S state, AES, EELS, UPS and XPS study 0-93452
Pt (111), adsorption of NO, EELS, thermal desorption, LEED, and AES study 0-80086
Pt (111), chemisorption of mol. O₂, XPS, UPS, EELS, and work function meas. 0-76139
Pt, core-electron excitation edges 0-66345
Pt, surface, (111), O₂ interactions, UPS, EELS and thermal desorption study 0-100409
Rh (111), chemisorption of acetylene and ethylene, EELS, LEED and thermal desorption mass spectrometry 0-80057
Sc, electronic excitations, charact. energy loss meas. up to 50 eV 0-60723
Sc, interband, collective and atomic (p,d) excitations, Z-160 eV, fast EELS 0-93443
Sc₂O₃, electronic excitations, charact. energy loss meas. up to 50 eV 0-60723
Sc₂O₃, interband, collective and atomic (p,d) excitations, Z-160 eV, fast EELS 0-93443
Si, amorphous, scanning TEM studies of cryst. inclusions 0-79699
Si, amorphous film, EELS microanalysis 0-100722
Si, bulk plasmon dispersion, electron energy loss spectra meas. 0-59899
Si, identification of oxide precipitates 0-100723
Si, L-shell ionisation by 80 keV electrons, transmission electron energy loss spectroscopy 0-60721
Si-Au, interface study using EELS 0-97391
Si-Ge heterojunction form., microscopic aspects, EELS meas. 0-80368
Si-SiO₂-Si₃N₄, MNOS structure, chem. comp. and electronic states, Auger and energy loss spectra obs. 0-92999
Si₃N₄, Si(LVV) Auger spectra, ion bombardment, electron energy loss spectra 0-80911
SiO₂ amorphous film, Si(LVV) Auger spectra, ion bombardment, electron energy loss spectra 0-80911
SrTiO₃, adsorption of O₂, electron energy-loss spectra obs. 0-89521
TiH₂ and TiD_{0.9}, surface characts., AES, EELS, SIMS, and XPS study 0-65343
V, electron energy losses due to H, obs. by scanning TEM 0-79850
V-Ti-C, elemental anal. by EELS 0-101069
V-Ti-C, high temp. carbide form., electron microscopy study 0-89228
W (100), adsorbed H, angle-resolved and variable impact energy electron vibr. excitation spectroscopy 0-76119
W (100), H adsorbate low energy electron vibrational excitation 0-84375
W {100}, anisotropy of inelastic electron refl., energy loss effects 0-79642
W, chemisorbed H₂, vibr. spectra characts., adsorption sites 0-70535
XeF₄ molecules with Jahn-Teller pseudo-effect, ang. depend. of inelastic scatt. of electrons 0-69246
Y, electronic excitations, charact. energy loss meas. up to 50 eV 0-60723
Y, interband, collective and atomic (p,d) excitations, Z-160 eV, fast EELS 0-93443
Y₂O₃, electronic excitations, charact. energy loss meas. up to 50 eV 0-60723
Y₂O₃, interband, collective and atomic (p,d) excitations, Z-160 eV, fast EELS 0-93443
ZnO polar surfaces, H and O₂ exposed, ion irradi., and heat treated, cond., EELS study 0-71525
Zr, electronic excitations, charact. energy loss meas. up to 50 eV 0-60723
ZrO₂, electronic excitations, charact. energy loss meas. up to 50 eV 0-60723
- electron energy states (condensed matter)**
see also band structure; band theory models and calculation methods; deep levels; defect electron energy states; dopplers; electron energy states of amorphous solids; electron energy states of liquid metals; electron energy states of liquid semiconductors; electron gas; electron traps; electronic density of states; exchange interactions (electron); excitons; Fermi level; Fermi surface; field interactions (condensed matter); heli-cons; hole traps; impurity electron states; Landau levels; localised electron states; magnetic breakdown; magnons; metal-insulator transition; metal theory; plasmons; polar semiconductors; polarons; positron states; ripplons; spin-orbit interactions; spin-phonon interactions; surface electron states; triplet state
alkali dithioferates (III), electronic struct. and hyperfine interactions, Xa calcs. 0-100448
Bloch electrons, dynamics in constant elec. fields 0-88463
Bloch electrons in magnetic field, quantum numbers 0-96768
coherent states in solids using Bravais lattice operator 0-75490
conduction electrons, thermodynamic method for quantitative anal. 0-59946
disordered systems, systematic approach, averaged Green functions calc. 0-80150
energy band structure for one-dimensional case (*Russian*) 0-59851
KKR method, structure constants, electronic struct. 0-80152
local density kinetic energy expressions for electronic struct. calc. 0-65473
phase integral approximations, advantages over JWKB approx. 0-87027
properties of solids and electronic struct., chemical bond physics, book 0-86044
semiconductor, electron excitation spectra in field of two travelling waves 0-65514
small metal particles, thermodynamic props. of electrons 0-59844
TCNQ salt, n-methyl-n-ethylmorpholinium, unpaired electron states, IR refl. study 0-75491

electron energy states (condensed matter) continued

- TEM, image contrast from single-electron excitation 0-59353
two dimensional system of electrons in uniform neutralizing positive background, absence of cryst. order 0-103610
universal variational functionals of electron densities, first-order density matrices, and natural spin-orbitals and solution of the ν -representability problem 0-95516
Cu₂ Zn clusters, electronic structures, SCF-X α -SW method 0-88468
Cu₄ clusters, electronic structures, SCF-X α -SW method 0-88468
LaLiO₃IrO₃, perovskite, prep. and mag. study 0-80486
Zn₄ clusters, electronic structures, SCF-X α -SW method 0-88468

electron energy states of amorphous solids

- see also Anderson model*
band theory, rel. to appls. of amorphous materials 0-107693
disordered system with correls., density of states at band tail 0-80154
II-VI amorphous semiconductors, electronic states, sublattice one-band Hamiltonian transform. 0-59861
III-V amorphous semiconductors, electronic states, sublattice one-band Hamiltonian transform. 0-59861
laser irradiated amorphous materials, electronic struct., one-electron approx. 0-70576
metal, muffin-tin model, s-phase-shift model 0-88473
metallic glass, prep. and phys. props. development 0-81003
metallic glasses, electronic structure rel. to elec. cond., supercond. and mag. props. 0-65429
polyacetylene:I, electronic structure, XPS and UPS meas. 0-66385
polyacetylene, electronic energy states and charge density contours studied muffin tin orbitals technique 0-80164
polyacetylenes, fluorinated, electronic struct., tight-binding LCAO-SCF-MO calcs., prep. 0-70591
polyenes, long chain, electronic struct. in Peierls-PPP model 0-84423
polyethylene, electronic energy states and charge density contours studied muffin tin orbitals technique 0-80164
polyethylene, solid liq., secondary electron emission spectroscopy 0-80916
polymer, conjugated and saturated chain, electronic struct., review 0-59860
PTFE, electronic energy states and charge density contours studied muffin tin orbitals technique 0-80164
review of structural and electronic props. 0-64901
semiconductor, density of states determ. from field effect data 0-107688
semiconductors, amorphous, electronic transport mechanisms and coeffs. 0-80282
semiconductors, amorphous, optical absorption, theory 0-80818
semiconductors, defects, band gap states 0-80215
semiconductors, doped, electronic props. 0-80283
semiconductors, electronic states, theoretical methods 0-80167
As-S amorphous chalcogenide thin film, transient photoinduced phenomena 0-80884
As₂S₃ and As₂S₄ vapour-deposited films, valence states, thermal and photo-induced changes UPS study 0-93459
B, evaporated, electronic struct., XPS, SXS and isochromat investig. 0-76143
Co₈P₁₈, amorphous alloys, electronic struct., γ -ray Compton scatt. study (*Japanese*) 0-84422
Fe_{1-x}(P,B)_x, amorphous and crystalline, photoemission and band structure 0-60754
Fe₇₂P₂₈, amorphous alloy, electronic struct., KKR calc. 0-96775
Fe₇₉P₂₁B₈ amorphous alloys, sput cooled, Mn, Cr and V substituted, mag. and transport props. 0-84593
Na₂O-SiO₂ glasses, elementary electronic excitations, refl., luminesc., and photoemission meas. 0-84778
Ni-P amorphous alloys, electrodeposited and melt-quenched atomic and electronic structures 0-88062
Ni₈₁P₁₉, amorphous alloys, electronic struct., γ -ray Compton scatt. study (*Japanese*) 0-84422
Pd-Si-(Cu), amorphous, Hall effect meas. and electronic struct. 0-75551
Pd-Si-(Cu) amorphous ribbons, low temp. sp. ht., density of states trends 0-79957
Se, amorphous, electronic struct. and optical props., pseudopot. calc. 0-65428
Se, layer, localised states in band gap 0-59928
Se, photoelectronic behaviour, in glass transition region 0-60045
Se, trigonal and amorphous, electronic struct. and nonempirical calc. of struct. props. 0-59866
Se-As, photoelectronic behaviour, in glass transition region 0-60045
Se-Te-Sb glasses, electronic transport 0-88579
Si, elec. props., ion implantation effects 0-79828
Si, glow discharge deposited, mobility edge calc. 0-80220
Si, random-network model, charge-density variation 0-80165
Si, transport results, interpretation 0-80260
Si:H, amorphous, Auger electron spectrosc. obs. 0-76112
Si:H, amorphous thin film, ion plating, IR absorpt. meas. 0-84857
a-Si:H, electronic states and bonding config. 0-64900
Si₃Ge_{1-x}O₂, amorphous, electronic struct. 0-80166
Si₃N₄, electronic struct., LCAO calc. 0-96776
Si₃N₄, Si(LVV) Auger spectra, ion bombardment, electron energy loss spectra 0-80911
SiO₂ amorphous film, Si(LVV) Auger spectra, ion bombardment, electron energy loss spectra 0-80911
Te, amorphous, electronic struct. and optical props., pseudopot. calc. 0-65428
Te, trigonal and amorphous, electronic struct. and nonempirical calc. of struct. props. 0-59866
Zr-Co, amorphous and crystalline, d-band struct., alloying effects 0-59862
Zr-Ni, amorphous and crystalline, d-band struct., alloying effects 0-59862

electron energy states of glassy solids *see electron energy states of amorphous solids***electron energy states of liquid metals**

- alkali metals, liq., Fermi energy, density of states, electronic props., exchange and correl. effects 0-96774
muffin-tin model, s-phase-shift model 0-88473
perturbation theory, extension to dense partially ionised plasmas 0-75500
structured medium approximation 0-84421
Co, liquid, Hall effect, band struct. and exchange scatt. 0-80250
Cu, liq., electronic structure, structured medium approx. 0-84421
Fe, liquid, Hall effect, band struct. and exchange scatt. 0-80250
Fe, liquid, N solubility depend. on added elements, mechanism (*Russian*) 0-65223

electron energy states of liquid metals continued

- Hg, reflection spectra, electronic density of states, calc. 0-66229
Ni, liquid, Hall effect, band struct. and exchange scatt. 0-80250

electron energy states of liquid semiconductors

- density of states at band tail 0-80154
Ag-S(Se)(Te), liq., mag. susceptibility meas., electron localisation and chem. bonding 0-60178
In-Se(Te), liq., mag. susceptibility meas., electron localisation and chem. bonding 0-60178
Sn-Se(Te), liq., mag. susceptibility meas., electron localisation and chem. bonding 0-60178
Te-transition metal, liq. semicond., elec. props. 0-96870

electron field emission

- borosilicate glass, field-induced electron emission into ultra-high vacuum 0-104048
elliptic emission functions used in calc. of electron emission from surfaces 0-89124
field at the surface of a field-emission cathode 0-100757
field emission medium energy diode, electron flow, HF oscills. 0-79582
gun lenses props. calc. and obs., electrostatic 0-62809
metal cathodes subjected to pulsed electric fields, electron field emission charact. 0-71580
metallic multi-point field emission source, prep. by cathodic growth 0-100758
micro Auger analysis, using field emission source 0-104020
MIM, thin film, use as non-heated source of electrons, review 0-84516
MIM cathode, local electron emission and electroluminescence patterns obs. 0-108327
MIM cathodes, LF noise sources and reduction 0-108328
nanosecond pulse duration investigations, construction of expt. arrangement 0-105750
Nottingham effect, region of localisation increase at low temp. 0-100756
photostimulated field emission, triangular barrier pot. model 0-100759
STEM with field emission gun, X-ray analysis of metals and ceramics inhomogeneities 0-59354
superconductors, critical parameters during field emission of electrons 0-88682
thermal field, use of W(100), TiC whisker, Re, ThW and Zr 0-66403
thermal field emission source for high resolution, high current e-beam microprobes 0-68297
Ag/p-In_{0.77}Ga_{0.23}As photocathode, field assisted photoemission to 2.1 microns 0-76130
Al-Au couple, electroformed, nonohmic characts. and electron emission 0-60066
Au film, nonohmic characts. and electron emission 0-60066
Au film, quantum size effect, field emission study 0-70849
Cr₃C, cathodic needle growth, at lower electric fields from Cr(CO)₆ vapour 0-76161
Eu chalcogenides, cond. band spin struct. 0-71577
Ge, field-emission current-voltage characts., effect of earlier measurements 0-71579
InGaP/InGaAs struct. for transferred electron photocathodes, VPE growth and characterisation 0-76193
InP-InGa_{1-x}As alloy photocathodes, semiconductor photoemitters, field-assisted, 1-2 μ m range 0-97396
Ir, field emission spectrosc. from (111) flat and stepped planes 0-76157
Mo, field emission anomalies in mag. field (*Russian*) 0-93462
Mo fine tip cathode, field emission stability, rel. to passivation 0-100760
Mo islet films, effect of external elec. field on electron emission 0-80952
Mo₃C, cathodic needle growth, at lower electric fields from Mo(CO)₆ vapour 0-76161
Nb, field emission anomalies in mag. field (*Russian*) 0-93462
Pb, electron field emission, temp. effect 0-60756
Pd film, quantum size effect, field emission study 0-70849
Si field emission photocathodes, emission current noise characts. 0-100746
Si multiple tip field emission photocathode, photokinetics 0-100480
W (110) mobility and two-dimens. compressibility of adsorbed Xe, field emission current fluctuation method 0-80089
W (110) plane, tunnelling of H in surface diffusion, field emission fluctuation method meas. 0-75416
W [310] tip, prep. from rolled sheet 0-97447
W, adsorption of Dy, Ho, Er, field emission electron study 0-100393
W, field emission, mag. field effects 0-93463
W, field emission anomalies in mag. field (*Russian*) 0-93462
W fine tip cathode, field emission stability, rel. to passivation 0-100760
W-EuS, amorphous, memory effect in field emission 0-89126
W-Zr field emitter, time-of-flight atom-probe study 0-80949
Zr-O-W (100) thermal field emitters, operational experience 0-71576

electron gas

- see also cathode ray tubes; electron optics*
adiabatic de Haas-van Alphen effect at low temp., Fermi fluid interaction and chem. pot. effects (*Russian*) 0-84442
alkali metals, electron-electron scatt., thermal and elec. resistivity 0-59956
Boltzmann electron gas in Gaussian random potential, mean field approach 0-107721
channelled heavy ions, electron pick-up from free electron gas in thin solid film 0-107349
chemisorption, image charge effects, surface plasmons 0-84381
chemisorption, image charge effects on adsorbate valence spectra, perturbational study 0-84380
condensed matter physics, dynamic correlations, book 0-86046
crystallisation, zero-order, Bethe-Fermi homework potential 0-63117
degenerate, in metal or semicond. slabs, surface plasmon damping 0-88501
degenerate, with elastic scatt., form of memory function 0-101753
degenerate electron liquid, skipping orbit cyclotron resonance, surface state transitions 0-103889
degenerate relativistic electron gas, electron collisions, thermal conductivity 0-109355
diamagnetism and surface currents 0-88496
dielectric constant, local-field correction, review 0-107731
dielectric function, degenerate electron gas at metallic densities, nonlocal interactions, compressibility and dispersion 0-107730
dielectric function, dynamical exchange decoupling, plasmon dispersion, SDW and CDW 0-59900
disordered conduction, dielectric function, phenomenological derivation 0-77692
disordered Fermi systems, in two dimensions, interaction effects 0-75655

electron gas continued

- dynamical local field corrections in dielectric function 0-88500
electron interaction with optical phonon directional flux 0-59893
fast ion in solid, oscillatory wake, trapped electron binding energy, RPA calc. 0-96575
ferromagnet, excitonic, zero-sound excitations, Fermi liq. model 0-93101
ferromagnetic semiconductors with hot electrons, instability of coupled spin-helical waves 0-107841
free electron gas, n-dimens., eqn. of state (*Spanish*) 0-82718
ground state, stochastic method calcs. 0-95031
Hohenberg Kohn theorem, extension to excited states 0-80197
inelastic positron scatt. in electron gas, plasmon excitation 0-92843
inhomogeneous, virial and Hellmann-Feynman theorems 0-88494
inhomogeneous electron gas, exchange effects and nonzero temps. 0-84444
intermediate valency compounds, conduction processes, metal-insulator transition 0-96787
ion motion in crystal, effect of polarisation field 0-103406
jellium, two- and three-dimens., CDW, appl. to liq. He surface and semiconductors 0-65476
many-electron systems, self-interaction corrected approach, beyond local spin density approx. 0-92844
metal, electron density behaviour near impurity charge 0-75518
metal lattice heating by radiation, plasma effects, degenerate electron gas calcs. 0-70742
metal surface, SHG, hydrodynamic theory of electron gas 0-87437
metal surfaces, SHG, non-linear response to optical fields 0-83645
metallic surface, self-consistent electron theory, review 0-88616
metals, ground state of solids, spin density functional method, binding energy, compressibility 0-65477
metals, polar states and free electron gas (*Russian*) 0-84415
metals, simple, quasiparticle props., density functional approx., electron gas calc. 0-96808
MIS, magnetooptic absorption by electron gas, optical phonon effects 0-97248
MOS structure, 2D electron gas, far IR Faraday rotation 0-80389
MOSFET, two-dimens. electron gas, determ. of fine struct. const. based on quantised Hall resist. 0-96997
multiple-band systems, dielec. function in generalised relax-time approx. 0-103637
nonrelativistic electron in const. parallel elec. and mag. fields, thermodynamic characteristics 0-90777
one-dimensional, interacting, ground-state energy in mean field approx. and instabilities 0-88493
p-wave electronic recoil spectra in perturbed electron gas 0-107724
plasma, ionic, dynamics, electronic screening of ionic motions 0-64678
quasi-two dimensional conductor, galvanomagnetic props., optical analogy (*Russian*) 0-60108
Ruderman-Kittel interaction at finite temp. (*Russian*) 0-96835
screening of proton, Anderson model calc. 0-59895
semiconductor, heavily doped, scatt. mech., resist. and Hall effect maxima 0-75586
semiconductor shielding in magnetic field 0-107727
semiconductors, degenerate, energy band structure effect on transverse magnetoresistance 0-88580
semiconductors, narrow-gap, plasmon-phonon interaction effect on optical phonon dispersion 0-103435
spin polarised, correlation energies for local spin density calcs. 0-107725
stopping power for slow neutrons, damping effects 0-65098
surface, He atom scattering pot., surface electron density depend. 0-104027
thermal desorption and dissociation catalyzed by a solid surface 0-108734
two-dimensional, in mag. field, polarisability 0-107888
two-dimensional, internal energy, specific heat effective mass, temp. depend. 0-75513
two-dimensional electron fluid, second order exchange energy, correlation energy 0-107729
uniform, electronic props. of H and He impurities 0-96807
Wigner distribution for cylindrically symmetric system 0-65475
Bi, film, size effect of carrier heating, surface scatt. (*Russian*) 0-100474
GaAs, photoluminescence, electron gas coding influence in ion-bombarded layers 0-108272
GaAs-AlGaAs heterojunction superlattices, inelastic light scatt. by two-dimens. electron gas 0-93360
He, liquid surface quasi-one dimensional electron chain instability, string-zig zag transition (*Russian*) 0-65335
K, liquid, interionic interaction theory, pseudopotential calcs. (*Russian*) 0-79675
Na liquid, interionic interaction theory, pseudopotential calcs. (*Russian*) 0-79675
Si, (100) inversion layer, electromigration in two dimensional electron gas, driving force 0-84441
Si surface, MOS struct. band structure, minigaps, magnetoresistance, cond., space charge layers 0-92980

electron guns

- beam current control for improved stability 0-84814
Boersch effect, energy broadening 0-69313
coaxial diode electron beam system for excimer laser excitation 0-86509
compact cold cathode electron beam gun, appl. CO₂ laser (*German*) 0-86501
crossed-field, pot. min. determ. 0-95188
cylindrical relativistic diode, space charge limited, voltage distrib. and current calc. 0-63437
electron gun, for computer driven STEM, image registration 0-104838
electrostatic and electromagnet lenses 0-99007
field emission, comparison of cold and thermal types used in the same electron microscope 0-101890
field emission, noise and energy broadening 0-101889
field emission, off-axis electron holography 0-101905
field emission, Philips EM 400 TEM/STEM performance 0-57441
field emission, STEM appl., X-ray analysis of metals and ceramics inhomogeneities 0-59354
field emission gun for sub-angstrom resolution TEM 0-82851
field emission gun SEM column electron-optical performance obs. and model 0-68328
field-emission source, theoretical investigation of rotationally symmetric gun 0-99006
large-area cold-cathode grid-controlled for Antares CO₂ laser amplifier 0-68955

electron guns continued

- lenses props. calc. and obs., electrostatic, for high-brightness field emitters 0-62809
microscope Cambridge University 600 kV high resolution, engineering performance 0-82849
plasma cathode and built-in gas generator 0-106947
pulse generator, repetitively pulsed electron beam system using cold-cathode electron gun 0-68981
pulsed desorption slot, cathode, operating stability 0-87002
SEM, photographic recording system 0-101903
single-pole magnetic lens as condenser for field emission electron gun 0-68325
STEM, computer driven, image registration 0-104838
STEM, thermal cathode illumination system, for round beam electron probe systems 0-57436
surface change method, computer anal. of characteristics 0-101891
triode and diode guns, electron optics numerical determ. of beam profile 0-106435
LaB₆ gun, 100 kV, combined CTEM and STEM 0-86516
Zr-O-W (100) thermal field emitters, operational experience 0-71576

electron-hole avalanches *see impact ionisation***electron-hole drops**

- bulk compressibility and surface energy of electron-hole liquids 0-65465
direct gap semiconductors, electron-hole droplet condensation 0-103630
electron-hole binding and exciton formation (*Russian*) 0-65468
energy condensation, comparison with ball lightning (*Russian*) 0-107712
mobility (*Chinese*) 0-65466
phonon wind, electron-hole droplet theory 0-107707
polar semiconductor, strongly anisotropic, electron-hole liq. in mag. field 0-59890
semiconductor, electron-hole liquid, 'neutrality' question of impurities 0-92822
semiconductors, electron-hole drop formation, phonon wind influence (*Russian*) 0-92825
semiconductors, particle complexes, N=1 to ∞ , book contrib. 0-80194
CdS, electron-hole pairs behaviour in energetic ion tracks 0-65457
n-CdSe, laser excited stimulated emission, optical gain spectrum 0-76050
CuCl, electron-hole pairs behaviour in energetic ion tracks 0-65457
GaP, electron-hole drops, self-consistent surface calculation 0-65464
Ge, carrier relaxation rate temp. depend. and pair density in large electron-hole drop 0-75509
Ge, electron-hole drop drag by ultrasound (*Russian*) 0-100437
Ge, electron-hole drop drag, interaction with thermal pulses 0-103631
Ge, electron-hole drop freq. depend. damping 0-88482
Ge, electron-hole droplet cloud kinetics, thermalisation phonons 0-88483
Ge, electron-hole droplets, percolation theory of cond., expt. 0-92896
Ge, electron-hole droplets distrib., and phonon wind 0-103629
Ge, electron-hole liquid, MHD effects 0-80190
Ge, exciton condensation, electron-hole drop investigation in UHF field, nucleation (*Russian*) 0-80193
Ge, exciton condensation, light scatt. by electron-hole drops 0-84435
Ge, inhomogeneous stressed, electron-hole drop light scatt. and absorption 0-108212
Ge, mag. field luminesc. lifetime, quantum oscills., phonon wind effects 0-93385
Ge, magnetoresistance of electron-hole liq., percolation model 0-96920
Ge, nonequilibrium charge carrier-mag. field interaction electron-hole drops, recombination (*Russian*) 0-75511
Ge, oscillatory exciton breakdown, microwave cond. 0-103716
Ge, pure, electron hole size distribution at pulse optical excitation 0-59883
Ge strain-confined large electron-hole drop characteristics 0-65469
Ge, uniformly deformed, free carrier cyclotron resonance, electron-hole drops (*Russian*) 0-71182
Ge:In (Sb) and pure cryst., kinetics of strain-confined large electron-hole drop and its clinging exciton system 0-75508
Ge:Sb, electron-hole drop lifetime, quenching temp. influence 0-59889
NH₄Br:Ti, and pure crystals, luminesc., VUV irradiated at 80K (*Russian*) 0-84763
PbI₂ direct gap polar semicond., electron hole liquid phase diagram (*Russian*) 0-93314
Si, stressed, one- and two-component electron-hole liq. at T=0 0-80189
n-Si:P(B), elec. cond. oscills., electron instability effects due to dislocations 0-103704

electron-hole recombination*see also carrier mobility*

- Auger recombination of carriers bound to centres involving phonons 0-107805
CdS, green edge luminescence spectrum, temp. depend. 0-108274
deep centres, ODMR (*French*) 0-60461
dielectrics containing impurities, carrier distrib. and currents, numerical simulation (*French*) 0-70718
diffusion length and lifetime meas. and assessment by SEM 0-96902
electron-beam-induced current, minority carrier generation vol. influence 0-84475
ferromagnet-semiconductor contact, spin-depend. recomb. and scatt. on electron injection 0-65654
HgCdTe/CdTe, limited diffusion volume photodiode, characterisation 0-75627
homojunction direct gap solar cells, theoretical limit efficiency 0-97795
III-V semiconductors, radiative recomb., optical evaluation review 0-60647
kinetics, subject to allowance for correl. between particles 0-80858
minority carrier recombination 0-65591
MOS pulsed capacitor, minority carrier lifetime meas. influence of Si-wafer surface state density 0-60098
MOSFET, recomb. lifetime determ. 0-62683
narrow gap semiconductors, recombination mechanisms, review 0-96905
p-n junction, diffused, space-charge recombination current 0-88623
p-n junction solar cells, determ. of lifetime and recombination currents 0-89637
photogalvanic effect under electron-hole interaction conditions 0-88591
polar semiconductor crystalline thin films, surface vibr. states, IR absorpt. spectra obs. (*Russian*) 0-60606
polydiacetylene-toluene-sulphonate, photocond. meas., 0.62-3.1 eV 0-70757
Schottky barrier solar cells, back-illuminated, theoretical performance 0-61345
semiconductor, ambipolar hot-carrier size effect kinetics 0-107799

electron-hole recombination continued

- semiconductor, Auger recombination rate, nonequilibrium carrier distrib. 0-65578
 semiconductor, biexcitons, one-photon radiative recomb. 0-70621
 semiconductor, graded-gap, internal photo-effects, excess carrier distrib. 0-107847
 semiconductor, magnetodiode and magnetoconcentration effects, influence of field effect 0-107903
 semiconductor, photomagnetolectric effect, injection-level dependent lifetime 0-80319
 semiconductor, spin dependent recomb., theory 0-103708
 semiconductor depth profiling by electron beam induced junction current meas. 0-96977
 semiconductors, narrow-gap, recomb. instability under crossed elec. and mag. fields 0-70712
 semiconductors, optical saturation for high carrier recomb. freq. (*Russian*) 0-88585
 semiconductors, photocond., photoelec. effects, book contrib. 0-84488
 semiconductors, radiative recomb., book contrib. 0-84784
 n-Si, recombination centres and carrier lifetimes after γ -irrad. 0-60004
 solar cell, Auger recombination limit on efficiency at high level of illumination 0-108797
 solar cell, p-n junction, polycryst., grain boundary influence on recomb. 0-93913
 solar cells, $\text{Cu}_{1-x}\text{S}-\text{CdS}$, collection coefficient theoretical anal. at conjunction 0-101094
 solar cells, polycryst., recomb. at grain boundaries, effect on photoresponse 0-108796
 solar cells, surface recombination velocity and diffusion length meas. 0-93965
 p-terphenyl, cryst., double injection and electrolum. 0-97342
 AgBr, photoexcited electrons and holes in latest image form., review 0-73496
 AgCl, luminescence fatigue, adsorbed Ag atoms 0-66281
 AlGaAs heterojunctions, nonradiative recomb. vel. estimate from edge luminesc. props. 0-65668
 AlGaAs-GaAs proton irradiated solar cells, deep level defects and recombination parameters 0-94032
 $\text{Al}_{1-x}\text{Ga}_x\text{As}$:Cu, variable-gap semicond., impurity props., carrier recomb. 0-96907
 $\text{Al}_{1-x}\text{Ga}_x\text{As}$ -GaAs quantum-well heterostructures, phonon-assisted recomb. and stimulated emission 0-74358
 $\text{Al}_{1-x}\text{Ga}_x\text{As}$ -GaAs quantum-well heterostruct., exciton in recomb. 0-103990
 $\alpha\text{-Al}_2\text{O}_3$, recombination luminescence mechanism 0-71477
 Al_2O_3 :Cr, pure and doped, electron irradi. induced cond., TSC and EPR study 0-80277
 Au-n-Si Schottky barrier solar cells, recombination in space charge region 0-61351
 n-Cd, Hg_{1-x}Te crystals, carrier recomb. in extrinsic conduction range 0-70722
 CdS, charged impurity centres, drift during passage of photocurrent 0-70767
 CdS, highly excited, stimulated emission processes, electron-hole plasma recomb. 0-97307
 CdS, quasimonopolar semicond., recombination in near surface space charge region (*Russian*) 0-88574
 CdS:Ni, nonradiative recomb., photocond. spectra 0-70764
 n-CdSe, laser excited stimulated emission, optical gain spectrum 0-76050
 CdSe, recombination mechanism at dislocations, photoluminescence 0-103993
 Cu, hot cathodoluminescence study, electron-hole recombination 0-93410
 $\text{Cu}_2\text{S}-\text{CdS}$ solar cells, interface recombination phenomena and tunnel effect 0-66978
 (Ga,Al)As:Si(Ge), epitaxial layers, radiative recomb., compensation, cathodolum. study 0-66307
 $\text{Ga}_{1-x}\text{Al}_x\text{As}_{1-y}\text{P}_y$ epitaxial layer heterojunction, nonradiative recombination at misfit dislocations 0-96901
 GaAs, electron-beam excited, efficient generation of electron-hole plasma 0-76051
 GaAs, electron-spin relaxation and recomb. kinetics, time-resolved luminesc. study 0-108074
 GaAs, γ - and electron irradiation, influence on recomb. characts. near surface 0-71478
 GaAs, H ion bombard., carrier removal effects 0-92542
 GaAs, proton irradiated, low energy, deep level defects and hole diffusion length meas. 0-60000
 GaAs, spin-depend. recomb., photoluminesc. obs. 0-60666
 GaAs, surface recomb. vel., psec. optical techniques 0-70784
 GaAs:O, electrolum., photolum., negative differential resist. rel. to recomb. processes 0-66304
 GaAs:Si, influence of stoichiometry on recomb. processes 0-93396
 GaP:Si(Se), donor bound exciton excited states 0-66284
 GaSe, exciton luminesc. kinetics, intermediate electron-hole states 0-93389
 Ge, ambipolar hot-carrier size effect kinetics 0-107799
 Ge, nonequilibrium charge carrier-mag. field interaction electron-hole drops, recombination (*Russian*) 0-75511
 Ge, photomagnetic effect, space inhomogeneous nonequilibrium carrier lifetimes (*Russian*) 0-71152
 Ge surface states, recomb. centres, regularities, electrolyte contact effects (*Russian*) 0-65652
 Ge:Mn, Sb, recombination waves, convective instability development 0-70721
 Ge:P(Sb)(Bi), γ -irrad., carrier trapping and recomb. at point radiation defects 0-107810
 Ge:Sb, electron-hole drop lifetime, quenching temp. influence 0-59889
 Ge:Sb, Ni(Mn), recombination wave spectrum, two-level traps 0-96906
 Ge-GaAs heterojunction, elec. and recomb. props., interface defect effects 0-80365
 GeSe₂, glassy, powdered and bulk, fatigue of photolum. 0-80855
 HgCdTe-CdTe photodiode, 1.33 μm , grown by LPE, phys. props. 0-107892
 $\text{Hg}_{1-x}\text{Cd}_x\text{Te}$, recombination processes using impact ionization capture cross sections 0-75577
 $\text{In}_{0.53}\text{Ga}_{0.47}\text{As}$ photodiodes with dark current limited by generation-recombination and tunneling 0-107893
 InGaAsP DH, luminesc., quantum efficiency determ. 0-108273
 InGaAsP/InP DH lasers, temp. depend. characts. 0-58541
 InGaAsP-InP DH lasers, interfacial recomb., influence on oscill. characts. 0-87393

electron-hole recombination continued

- InGaAsP-InP DH laser, threshold current, temp. depend. 0-106521
 $\text{In}_{1-x}\text{Ga}_x\text{P}$, direct-gap semiconductor, cathodoluminesc., electron irradi. effects 0-108283
 $\text{In}_{1-x}\text{Ga}_x\text{P}_{1-y}\text{As}_y\text{In}_{1-x}\text{Ga}_x\text{P}_{1-y}\text{As}_y$, visible spectrum multiple-quantum-well heterostruct. lasers 0-106537
 InP, surface recomb. vel., psec. optical techniques 0-70784
 InSb, Auger-governed decay of laser-induced plasma, optical probing 0-76105
 InSb, high-resistivity p-type or crystals of n-type, recombination processes, photocond. and photomag. effect meas. (*Russian*) 0-88567
 InSb, reabsorbed radiative recomb. and photon recycling 0-76076
 InSb, recombination processes using impact ionization capture cross sections 0-75577
 KBr(I), photostimulated recomb., electron spin polarisation 0-60673
 KCl:SnCl₂, photostimulated hole recombination luminesc. (*Russian*) 0-80833
 MgO doped powder phosphors, photo- and thermostimulated luminesc. obs. (*Russian*) 0-66263
 NbO₂, on-state decay rel. to recomb. and nonlinear props. 0-84492
 Pb chalcogenides, Auger recomb., theory 0-65586
 $\text{Pb}_{1-x}\text{Sn}_x$ epitaxial layers, radiative and nonradiative recomb. processes 0-60670
 PbTe photovoltaic detector, detectivity limits 0-105709
 RbI, photostimulated recomb., electron spin polarisation 0-60673
 Si, amorphous, EPR and spin-dependent effects 0-80592
 Si, amorphous and crystalline, heating by Q-switched laser radiation 0-84963
 Si, amorphous hydrogenated solar cells, field depend. quantum efficiency, electron-hole recombination 0-66971
 Si based MOS device irradiation with γ -rays, minority carrier generation, CV characts. 0-88637
 n-Si, bipolar ohmic contact with macroscopic recomb. centres. 0-80379
 Si, carrier capture at amphoteric deep level defects 0-88569
 P-Si, conductivity and carrier lifetime, high injection effects 0-70719
 Si, dense plasma dynamics during pulsed laser annealing, carrier density, recombination 0-84479
 Si, hole-hole-electron Auger recombination 0-70720
 Si, laser induced dense plasma, dynamics 0-65612
 Si polycrystalline solar cells, recombination, electron-beam-induced current characterisation 0-81470
 Si solar cells, polycrystalline p-n junctions, recombination currents, physical models 0-93892
 Si:F,H, amorphous efficient carrier generation for solar photovoltaic energy conversion 0-92906
 Si:H, amorphous, defect photoluminesc. meas. 0-97334
 Si:H, amorphous, geminate recombination model for photoluminescence decay 0-71481
 Si:H, amorphous, optical studies of excess carrier recomb., evidence for dispersive diffusion 0-76059
 Si:Li, photolum. of bound exciton and bound multiexciton complex, Zeeman effect 0-108265
 Si:O, carrier recomb. processes, role of vacancy-O complexes 0-65592
 Si:O, heat treated, excess carrier recomb. rate, defect levels 0-75579
 n-Si:P(B), elec. cond. oscills., electron instability effects due to dislocations 0-103704
 Si-H, amorphous, sputtered, photolum. obs. 0-80856
 Si,Ge_{1-x}As_x heterojunction, elec. and recomb. props., interface defect effects 0-80365
 TiGaSe₂, monocrystal, processes of recombination and trapping levels, photocond. meas. (*Russian*) 0-70751
 Zn_2P_2 -metal contacts, photoelectric props. 0-92930
 ZnSe, near band edge photoluminescence, electron-hole recombination 0-80835
 ZnSe, residual cond., recomb. of photoexcited carriers, Hall coeff. 0-75605
- electron impact**
 see also atomic electron impact excitation; atomic electron impact ionisation; molecular electron impact dissociation; molecular electron impact excitation; molecular electron impact ionisation; secondary electron emission
 atomic and surface physics, conf., Salzburg, Austria (Feb. 1980) 0-57010
 dielectric materials, spacecraft, charging and discharging 0-71315
 electron reflection from metal surfaces, surface roughness, IR absorpt. 0-71526
 electron-matter interactions rel. to electron microscopy 0-89097
 inelastic electron scattering: surface vibrational spectroscopy 0-107347
 inelastic electron-matter interactions 0-104024
 ionisation in Nier-type electron impact ion source, repeller curve interpretation 0-57421
 molecular solids, interaction with 0-15 eV electrons, formation of charged excitonic complexes 0-107708
 photographic sensitive material, short time exposure, expt. technique 0-86477
 PVC, Cu evaporated film, electron-induced metalochromic reaction for metal image formation 0-86476
 reflection and transmission through surface pot. barrier, Schrodinger eqn. 0-87998
 secondary electron kinetic emission from electron and ion bombardment 0-66342
 solid, compression wave interaction, pulsed electron beam initiation 0-79877
 spatial electron beam-matter interaction, model calcs. for Cu (*German*) 0-84815
 spectroscopy of molecular excitation functions, trapped electron restrictions 0-69184
 X-ray microanalysis, spatial resolution in thin foils 0-101065
 Ag (100) and (111) surfaces, positronium form. due to slow positron trapping 0-107748
 Ag, electron backscatt. by bulk target, theoretical model (*French*) 0-60722
 Al, electron backscatt. by bulk target, theoretical model (*French*) 0-60722
 Al film, electron transmission, calc. 0-60724
 Au film, electron transmission, calc. 0-60724
 Cu (111) surface, positronium form. due to slow positron trapping 0-107748
 Cu, electron backscatt. by bulk target, theoretical model (*French*) 0-60722
 Cu film, electron transmission, calc. 0-60724

electron impact continued

- Si, oxidation induced by ion or electron bombardment, AES-SIMS study 0-108606
- Ti, Tokamak plasma, atomic struct., highly ionized states 0-75086
- W (100 and (111), O₂ electron stimulated desorption patterns, computer simulations 0-75443
- W (110) and (111) surfaces, KCl adsorption-desorption behaviour 0-75442
- W surface, (100), photon and electron stimulated desorp. of O 0-100397

electron interactions see *elastic scattering of electrons by atoms and molecules; electron attachment; electron beam effects; electron beams; electron-electron interactions; electron-electron scattering; electron impact; electron-nucleon interactions; electron-nucleon scattering; electron-nucleus reactions; electron-nucleus scattering; electron-positron interactions; electron-positron scattering; electron spectra; hadron electroproduction; neutrino-electron interactions; neutrino-electron scattering; secondary emission*

electron ionisation see *electron impact*

electron lenses

- see also *aberrations; electron microscopes; electron optics; electrostatic lenses; magnetic lenses*
- aberration correction, round lenses 0-78758
- aberrations, reduction by optimisation techniques 0-87290
- cathode lens having a quasiparabolic field 0-95782
- charged particle trajectory calc. in electrostatic field, teaching 0-90635
- condenser objective, single field, advantages and limitation for min.-exposure 0-87292
- condenser-objective, combined CTEM and STEM 0-86516
- crossed lenses, theoretical and expt. study 0-95780
- electron gun, with electrostatic and electromagnetic lenses 0-99007
- electrostatic crossed lens, for electron microscopic devices 0-87289
- energy-loss spectral resolution optimisation using electron lenses between TEM specimen and electron spectrometer 0-101886
- foil lens, spherically corrected, for electron phase microscopy (German) 0-83546
- gun, electrostatic, for field emission 0-62809
- image reconstruction, computerized, fragment size choice 0-78785
- magnetic spectrometer, corrected second-order aberrations 0-87013
- multi-element electrostatic cylinder lenses, computer program for calc. of electron trajectories 0-87283
- objective, with compensated axial chromatic aberration, for electron microscope 0-87293
- one and two-lens electron-optical system parameter comparison 0-87284
- probe forming systems, optimisation with respect to aberrations and vertical beam landing 0-68291
- SEM, photographic recording system 0-101903
- SEM lens system design, snorkel or condenser-objective 0-57438
- single-pole electron lens finite element analysis 0-69315
- STEM, single atom microscopy, instrumental aspects 0-86522
- superconducting, for imaging organic materials in electron microscope 0-73553
- triple slit scheme for high current variable-shaped beam forming 0-68290
- twin, Philips EM 400 TEM/STEM performance 0-57441

electron lifetime (metals) see *electron relaxation time (metals)*

electron mean free path (metals)

- granular materials, size effects in cond. and supercond. 0-77581
- metals, sound pulse spike like transport near acoustic cyclotron resonance (Russian) 0-100617
- polycrystalline-thin metal films, thermoelectric power, mean free path model 0-107770
- thin metallic plate in strong mag. field, electron scatt. elec. cond. theory (Russian) 0-59974
- wire, cylindrical, elec. resist., scatt. processes, Monte Carlo calc. 0-75560
- Ag film, defect density, thickness depend., elec. resist. obs. 0-70568
- Ag film, in situ resistivity meas. 0-97008
- Al foil, electrical conduction, electron mean free path, surface scatt. 0-88535
- Au, thin film, self-sustaining, electron mean free path meas. 0-92883
- Au-Cu-Fe spin glass alloys, impurity mag. resist. meas. 0-59972
- Cd film, surface RF impedance in strong mag. fields (Russian) 0-92920
- B-Ga, metastable, elec. props. in normal and supercond. states (Russian) 0-65520
- Gd-Al(C)(Cu)(Ga)(Ni)(Pd)(Rh) alloys, amorphous, mag. and elec. props. 0-80499
- (Nb_{0.99}Ti_{0.01})₂-xGe₂, high T_c, resist. meas. 0-88531
- Pd film, elec. resist. 0-93013
- Pd thin film, temp. coeff. of resist. meas. 0-107930
- Rh, thin films, polycryst., resistivity and temp. coeff. of resistivity 0-88648
- W film, surface RF impedance in strong mag. fields (Russian) 0-92920

electron micrographs see *electron microscope examination of materials; electron microscopy*

electron microprobe analysers see *electron probe analysis*

electron microprobes see *electron probes*

electron microscope applications

- see also *electron microscope examination of materials; scanning electron microscope applications*
- backscattered electron images of biological specimens 0-104827
- biological application, quarter-micron serial sectioning and stereoscopy 0-72384
- Earth sciences, use of electron microscopy 0-105091
- HV, in-situ elec. resistivity meas. 0-101893
- medical diagnosis using clinical pathology liver and kidney samples, computer assisted 0-85485
- n-p junctions, determ. of transport parameters of minority carriers using electron microscope 0-65665
- plant root transport studies using ion localisation, freeze substitution method 0-85569
- size determination of sonicated vesicles, spray freezing method 0-98188
- stylus examination, roughness meas. of engineering surfaces (German) 0-68182
- Si₃N₄ sample substrates, high resoln. electron beam fabrication using STEM 0-104104

electron microscope examination of materials

- see also *electron microscope applications; electron microscopy; scanning electron microscope examination of materials; scanning-transmission electron microscope examination of materials; transmission electron microscope examination of materials*
- alkali halide, crystal, irradiation-induced defects 0-107316
- alloy, solute redistrib. during in situ irradiation in HVEM 0-107324

electron microscope examination of materials continued

- alloys, high resoln. diffraction and imaging characterisation 0-104050
- alloys, phase transition premonitory phenomena, exam. by electron diffraction and microscopy (French) 0-59651
- amphiboles, high-resolution electron microscopy 0-75241
- animal plasma membranes, study using freeze-fracture technique 0-104842
- anodic film, behaviour of emulsion particles during electrodeposition 0-104357
- Antarctic aerosols particle anal., comp. 0-77091
- asbestos fibres concentration meas., in air and liquid, analytical methods review 0-72120
- bacterial cell wall, surface charge and morphogenesis of regular arrays of macromols. 0-85366
- Bloch wave model for ECP contrast in Si, Cu, Ag, Au 0-96419
- cellulose, degradation by high voltage electrons 0-100283
- ceramics, glassy, struct. and electron beam sensitivity 0-79841
- ceramics, high resoln. diffraction and imaging characterisation 0-104050
- chloritoid intergrown polypoly identification by electron multiple scatt. 0-70184
- chromites high-resolution observations 0-75241
- colloidal photochromic dyes, quasi-crystals produced in applied electric field 0-85225
- compound eye of worker honey bee, cell junctions 0-85383
- conference of Electron Microscopy Society of Southern Africa, Port Elizabeth, S.Africa (Feb. 1980) 0-73099
- convergent beam electron microscopy for materials science 0-107028
- copper phthalocyanine, chlorinated, radiation damage mechanism 0-88000
- copper phthalocyanine, simulated mol. images, point models and kinematical contrast, amplitudes 0-103223
- coronene, minimal exposure high resolution electron microscopy 0-79653
- cowpea chlorotic mottle virus packing in crystalline monolayers 0-89922
- crack tip strain meas. by electron micrograph stereoscopy 0-69752
- crystalline materials, semiconductors, developments in high resolution imaging 0-99001
- cytochrome c oxidase, macromolecular struct., electron microscopy and image anal. 0-89716
- diamond crystals, synthetic, etch-pit formation on cube faces 0-75232
- dislocation loops in cubic metal, black-white contrast 0-75234
- dislocation velocity, thermal activation exam. of applied stress and temp. depend., expt. methods (French) 0-59474
- dislocations, collective behaviour, velocity of slip band and mobile dislocation densities, HVEM study (French) 0-65006
- DNA, spreading of large associations, dark field electron microscopy 0-85563
- DNA kinetoplast, ultrastruct., interpretation of dark field electron microscopy images of isolated purified networks 0-85369
- enzymes, molecular struct. reconstruction from electron microscopy images 0-89715
- epoxy resin, plastic deform. effect on crack propag. 0-97563
- ferroelectric substances, electron microscopy investigations, review (Japanese) 0-71366
- film, evaporated at oblique incidence, columnar grains inclination angle 0-75468
- film defect growth and nucleation, electron microscopy and diffraction exam. (French) 0-59824
- foil, dislocation loop nucleation and growth during 1 MeV electron irradiation 0-88152
- geometrical and chemical knowledge at high resolution, electron microscopy and inner shell excitations 0-79646
- glial smooth endoplasmic reticulum acid phosphatase transport into damaged axons, role of microtubules 0-85381
- glomerular permeability in foetal rabbit 0-85372
- glutamine synthetase macromolecular struct., electron microscopy and image anal. 0-89716
- grain boundaries, high angle, plane matching secondary relaxations 0-103363
- graphite FeCl₃ intercalate, interpenetration of 'stages' direct imaging 0-84037
- haemocyanin of Limulus polyphemus, quaternary struct. 0-85337
- hexadecachlorophthalocyanato-copper discrimination of individual atoms in mol. images 0-100226
- II-VI semiconductors, thin epitaxial layer, direct synthesis (German) 0-104070
- jimthompsonite and anthophyllite from Swiss Alps, disordered intermediate minerals imaging 0-72518
- lipid bodies, saturated, in organ pipe cactus visualisation by cytochem. technique 0-76873
- magnetic domain wall observation device for use with 1 MeV electron microscope 0-101882
- martensitic transformations, electron microscope study of cryst. geometry (Russian) 0-108441
- material wear, electron metallography using SEM, TEM 0-76455
- metallography, feasibility and methodology of in situ experimentation (French) 0-68301
- metals, FCC, deformed single crystals, struct. evolution at heating 0-103337
- metals, submicroscopic defects, influence on HVEM in-situ expts. 0-103392
- microtubules in optic nerves of temperature acclimated goldfish, electron microscopy 0-85395
- milk fat globule membrane, cryst. struct. 0-85364
- mitochondrial complex III membranes preps., cryst. struct. 0-85365
- multilite-corundum ceramics, electron microscopy of damaged surface 0-88413
- naphthalene crystal nucleation on anthracene microcrystals suspended in vapour-gas stream 0-76165
- neutron-bombarded, diffuse X-ray scattering (Russian) 0-92560
- Nimonic 80A superalloy, contrast from cavities in HVEM 0-79780
- Nimonic PE-16, irradiation in HVEM, void growth, vacuum environment influence 0-107323
- nucleic acids, electron microscopy using basic protein film method 0-104844
- Nylon 6 g yarn, fine struct. change in twisting, annealing and untwisting, X-ray and electron microscopy obs. 0-84904
- oocyte paracrystalline structures, mouse, Mus cervicolor poppaeus 0-89731
- optic tectum, goldfish, fine struct. 0-85396
- ovale, minimal exposure high resolution electron microscopy 0-79653
- ovarian cortex effect of daily prenatal gamma irradiation in beagle pups 0-85453

electron microscope examination of materials continued

- Permalloy film, mag. microstruct. obs. in nonlinear ripple magnetis. case (*Russian*) 0-65971
- photographic emulsion grains, latent image distrib., etching and recrystn. effects of solns. 0-77890
- pigeonite, inverted, from SW Norway, precipitation temp. estimation 0-72500
- PMMA, electron beam scattering, Monte Carlo simulation 0-100148
- poly-m-toluenylsilsesquioxane mesomorphic struct., form. during polymerisation (*Russian*) 0-61095
- polyacetylene films, stretch-aligned, prep. and morphology 0-66471
- polyacrylic acid film, structuration and mech. props., EM obs. (*Russian*) 0-59406
- polyalkane imides, crystallisability, supermol. and crystalline structures 0-84100
- polyamide, aromatic, fibre, high modulus, mol. and supramol. struct. 0-79710
- polybutadiene-poly- α -methylstyrene copolymers, struct. obs., prep. (*French*) 0-59401
- polycarbonate styrene-acrylonitrile copolymer mixture, determ. of phase structure 0-103272
- polyethylene, linear, melt-crystallised sharp fraction, lamellar morphology 0-84099
- polyethylene, single crystal, electron microscopy study 0-103273
- polyethylene/ethylene vinyl acetate copolymer mixture, rel. between hypermol. struct. and stability (*German*) 0-64929
- polymer film, microprobe localisation 0-103271
- polymers, HVEM in-situ deform. 0-104215
- polyoxymethylene, nascent, morphology, optical and electron microscopic obs. 0-59403
- polystyrene-polyethylene/propylene block copolymer, micelle form. in lubricating oil 0-61171
- Porphyra osmoregulation, struct. aspects 0-85370
- protein supramolecular structure, ordered, electron micrographs, image processing 0-89923
- quartz dislocation fine structure under electron irradi. 0-70213
- quaterylene, minimal exposure high resolution electron microscopy 0-79653
- Rene 80, dislocation behaviour during plastic deform. (*Japanese*) 0-108504
- retina, rat, rod and cone-type photoreceptors in post-equatorial region 0-85384
- Rhacopholus embryo yolk platelets, freeze fracture study of crystalline struct. 0-104552
- rock magnetism, domain structure obs. by Lorentz electron microscopy 0-72502
- semiconductor, dislocation struct. and elec. props. 0-70201
- semiconductor materials, microcharacterisation 0-101911
- semiconductor thin sample etching for electron microscope exam. 0-86272
- semiconductors, appl. of analytical techniques to crystal growth and defects 0-73546
- semiconductors, conf., Oxford, England (April 1979) 0-67928
- shape memory alloy, martensite boundaries, lattice imaging study 0-107359
- silicate HV high-resolution electron microscopy 0-70096
- steel, 0.7% C, welded zone, fatigue strength and microstruct. (*Japanese*) 0-89339
- steel, 35NiCr18, bainite transformation, study with aid of hot stage microscope 0-76253
- steel, alloy type, photoemission electron microscope obs. of high temp. precip. behaviour 0-108456
- steel, austenitic, type 70, cold brittleness structural depend., fracture mechanisms (*Russian*) 0-97571
- steel, austenitic stainless, irradi. creep of type 316 in HVEM 0-97523
- steel, austenitic stainless, precipitation of $M_{23}C_6$ type carbide on twin boundaries 0-89226
- steel, En 24, Cr, V, deform. effect on decomp. of austenite, carbide precipitation 0-84938
- steel, eutectoid, Si partitioning during pearlite transform., analytical electron microscopy applic. 0-108458
- steel, low Si, martensite struct. and mech. props. (*Korean*) 0-93614
- steel, maraging, ageing kinetics and struct. of N12K7M5TYu, effect of high temp. deform. of austenite (*Russian*) 0-84960
- steel, pearlitic, struct. variations under plastic strain and subsequent heating, cementite decomp. (*Russian*) 0-84954
- steel, stainless, fracture micromechanism when kept isothermally in sulphur pulp 0-76355
- steel, stainless, radiation damage by 1 MeV electrons, dislocation struct., brittleness (*Russian*) 0-75226
- steel, stainless 304, crack propagation under fatigue-creep conditions and fractography (*Japanese*) 0-104267
- steel, structural, supercooled austenite, structural characts. of decomposition 0-60870
- steel, W-Co-Mo-Cr-V-C (8.5, 8.1, 4.5, 3.5, 2.2, 1.02 wt.%), phase composition, struct. and props. 0-104163
- steel ball bearing, fatigued, phase changes, nomenclature 0-89198
- steel turbine casings, residual life determ. 0-93585
- steels, stainless, electron irradiated, dislocation damage, HVEM study 0-103389
- styli of electrical surface roughness meas. instrums., examination of wear (*German*) 0-101782
- TCNQ salt, Ag.TCNQ, cryst. struct. 0-70186
- 2,3,4,5-tetraacetoxymercurithiophene, dark-field imaging, computer simulation 0-100151
- thin foil, X-ray microanalysis in electron microscope (*French*) 0-61191
- transition metal oxide catalysts, reduction, cryst. defects influence, in-situ electron microscopy 0-81322
- viral infections diagnosis, contrib. of electron microscopy (*Italian*) 0-109024
- viroid RNA, covalently closed circular mols., conform. states 0-85340
- zinc oxalate, isothermal crystallisation from soln. 0-108336
- Ag, (111) surface electron microscopy 0-103556
- Ag and alloy electron microscope specimens, noncyanide electropolishing method 0-100967
- Ag, electrodeposit, on (111) face, habit modification caused by Cl^- 0-71600
- Ag, multiply twinned particles, internal and surface struct. by electron microscopy 0-84189
- Ag powder, ultrafine, sintering, coalescence growth stage 0-89174

electron microscope examination of materials continued

- AgBr, Herschel effect, latent image centre struct. changes under laser irradi. 0-77900
- AgBr layer, sensitised, topography of developed centres 0-73491
- AgI hydrosols, kinetics and mechanics of colloid systems formation 0-101045
- Ag₃Mg, periodic antiphase boundaries, electron microscopy study (*French*) 0-59481
- Al, Al ion irradiated, void swelling and annealing of voids, electron microscopy study 0-88216
- Al, dislocation loops, interstitial, size distrib. for metal irradiated in high voltage electron microscope (*Russian*) 0-103335
- Al film, dislocation observation by electron microscope using convergent beam (*French*) 0-96532
- Al, interstitial loop form., effects of repeated electron irradi. 0-75220
- Al, laser strengthening, struct., hardness and dislocation density (*Russian*) 0-76399
- Al, low-order Fourier coeff. of pot., modified thickness fringe method 0-75130
- Al, polycrystalline, movement of 3-fold nodes of boundaries in high temp. creep 0-89317
- Al, polycryst., HVEM in-situ investigation of creep mechanism 0-104214
- Al-Ag, type-II superconductor, torque oscillations in mag. field (*Russian*) 0-103800
- Al-Cu (1 wt.%), electron irradiated, dislocation damage, HVEM study 0-103389
- Al-Cu (2-5 wt.%), precipitation total surface influence on resistivity (*French*) 0-71650
- Al-Fe-X-Si (X=transition metal), struct. and comp. by electron microscopy 0-88093
- Al-Mg, dilute, dislocation loops, interstitial, size distrib. for metal irradiated in high voltage electron microscope (*Russian*) 0-103335
- Al-Mg, oxidation control study, electron opt. techniques eval. 0-85089
- Al-Mg (0.3 wt.%) single cryst., dislocations obs. by high voltage electron microsc. 0-79796
- Al-Mg-Zn alloys, evaporation effect of alloying elements Mg and Zn in in-situ EM studies 0-103388
- Al-Ti alloy spark alloying, cathode weight change and hardened layer obs. (*Russian*) 0-61005
- Al-Zn, grain boundary reaction sites, determ. of struct. aspects 0-103359
- Al-Zn (70, 30 wt.%), decomp. study, 25-160°C (*Czech*) 0-89225
- Al-Zn-Mg (3.6, 1.95 wt.%), ageing and plastic deform., effect on structure, electron microsc. and X-ray diff. study (*Russian*) 0-81108
- Al-Zn-Mg (91, 6, 3, wt.%), H embrittlement and trapping, HVEM obs. 0-76364
- Al-Zn-Mg alloy, Ag addition and pre-precipitation treatment, influence on GP zone growth 0-71658
- Al₃Mg₂, diffusionless phase transformation 0-104150
- Al₂O₃, derived from boehmite, phase transformations and microstruct. 0-60857
- α -Al₂O₃, grain boundary segregation 0-103361
- Al₂O₃, grain boundary thickness obs. using electron diff. techniques 0-79811
- β -Al₂O₃, long-period structs., electron microscope obs. 0-92501
- β' -Al₂O₃, Mg- and Li-stabilised, high-resoln. electron microscopy images 0-107277
- Au, (111) surface electron microscopy 0-103556
- Au, atomic cluster, on W support film, computer simulation of phase contrast 0-100150
- Au film, integrated condensation coeff. on NaCl cleavage faces, Rutherford ion backscatt. obs. and electron microscopy 0-59827
- Au, grain boundary structure, high resolution HVEM 0-103360
- Au, grain boundary thickness obs. using electron diff. techniques 0-79811
- Au, interstitial, calc. images and diffraction patterns 0-100152
- Au, multiply twinned particles, internal and surface struct. by electron microscopy 0-84189
- Au, pentagonal symmetry, icosahedral struct. (*French*) 0-79729
- Au powder, ultrafine, sintering, coalescence growth stage 0-89174
- Au, tilt boundary, $\Sigma=11$, simulated and observed struct., vibr. of individual atoms at grain boundary 0-88167
- AuMn alloy, ordered, vacuum deposited epitaxial films, orientation control by external stress 0-100426
- Au₁Mn₄ ordered phase formation, electron diff. and microscopy study 0-107418
- Au₃Si₆, amorphous vacuum-deposited and liquid-quenched films, diffusion and crystn. 0-84094
- Au₃Si_{1-x} amorphous films, phys. studies 0-75476
- Ba_{1+x}Fe₂S₄, electron diff. study, orientation anomaly 0-107152
- BaTiO₃, electron microscopy investigations of ferroelec. substances, review (*Japanese*) 0-71366
- BaTiO₃, ferroelectric, polarisation reversal, electric field induced phase transform. 0-103925
- Bi₂CaNa_{1-x}Nb₂O_{10+x}, intergrowth, IMV high-resolution electron microscopy 0-107436
- BiVO₄, ferroelastic domains, electron microscopy and electron diff. obs. 0-100254
- C fibre structure, recent advances 0-81069
- C, film, image contrast rel. to inelastic scattering 0-100154
- C, hard, heat-treated under pressure, characterisation of carbon phase by electron microscope 0-60855
- C, nongraphitizable, catalytic graphitization by Cr₂O₃, MnO₂ 0-97440
- Ca₂YFeO₁₃, cryst. struct., electron microscopy and X-ray diff. study 0-88116
- Cd₃As₂, film on NaCl substrate, vacuum deposition, growth morphology, microstructure 0-75479
- CdIn₂Se₄, high resolution electron microscopic study of polytypism 0-88119
- Co intercalation compound, electron microscopy 0-84164
- Co-Fe-Si-B, decomp. of amorphous state during annealing below recryst. temp. (*Russian*) 0-75164
- Co-Ti-C, secondary precipitation and allotropic transform., TEM obs. 0-108453
- CrBr₂, ferromag. domains, using liq. He mag. specimen stage 0-103855
- CsI:Tl, precipitation of Tl solid solns. 0-70419
- Cu, (111) surface electron microscopy 0-103556
- Cu complex, hexadecachlorophthalocyanatocopper (II), atomic resolution by computer image processing from electron micrographs 0-100149
- Cu foils, electron-irradiated, point defect agglomerates, HVEM invest. during in-situ annealing 0-84213

electron microscope examination of materials continued

- Cu, foils, faulted defect formation by moving boundaries 0-107281
 Cu phthalocyanine, grain boundary struct., crystallographic planes 0-103366
 Cu, polycrystn., strain localisation during hot deform. 0-104195
 Cu, single crysts., (110) oriented, tensile deformation, HVEM of recrystn., recrystallised state 0-89256
 Cu, tensile deformed (110) oriented single cryst., recrystn., high voltage electron microscopy study 0-84958
 Cu thin foils, intrinsic struct. in grain boundaries and boundary mobility 0-103368
 Cu-Al, dislocation core cut-off parameter, estimation from stacking fault nodes 0-103370
 Cu-Al, dislocations, dissociated, climb mechanism, nucleated loops, Burgers vectors 0-65002
 Cu-Al (11 at.%) single cryst., dislocation reactions during deform. twinning 0-79795
 Cu-Al alloy, ordered, superlattice fringe images, computer simulation 0-103296
 Cu-Al(Au) alloys, HV electron microscopy, crit. voltages depend. on comp., temp. and short-range order 0-100146
 Cu-Bi, grain boundary thickness obs. using electron diffr. techniques 0-79811
 Cu-Fe (1.5 wt.%), precipitation-effect on void formation during electron irradiation 0-84211
 Cu-Fe (1.5 wt.%) alloy, void form. during irradiation in HVEM, reactor irradiation simulation and ageing effects 0-107327
 Cu-Si (6.5 at.%), plastic deformation, HVEM study (French) 0-66605
 Cu-Si (8 wt.%), intrinsic struct. in grain boundaries and boundary mobility 0-103368
 Cu-Zn, interface sliding of FCC and BCC boundaries 0-104240
 Cu-Zn-Al, β' martensite crystal crossing rel. to reversible shape memory effect (Japanese) 0-108499
 CuAu alloy, ordered, vacuum deposited epitaxial films, orientation control by external stress 0-100426
 Cu₃Au, alloys, superlattice-fringe imaging theory, images formed from two beams 0-79649
 CuIn₂S₄ sulphospinel electron diffr. study 0-88080
 Cu₂O polycrystals., dislocation obs. by electron microscope (Spanish) 0-75230
 Cu₃Pd, periodic antiphase boundaries, electron microscopy study (French) 0-59481
 Cu₃-Te₂, non-stoichiometric phases, electron microscopic and electron diffraction studies 0-64977
 Fe based alloy, amorphous, liq. quenched, struct., thermal stability and mech. props. 0-88059
 Fe intercalation compound, electron microscopy 0-84164
 Fe polycrystals, grain misalignment, electron microscope determ. (Russian) 0-103358
 Fe, stray mag. fields above stripe domains, electron microscope and μ^* -tensor determ. 0-71089
 α -Fe whiskers, pure, ductile fracture, microscopic obs. of initiation mechanism 0-85044
 Fe-Al, single crystals, deform. at high temps. 0-81125
 Fe-Al alloy, ordered, superlattice fringe images, computer simulation 0-103296
 Fe-Au bimetal epitaxial films, examination of interaction at temps. $\geq 600^\circ\text{C}$ 0-75482
 Fe-B, rapidly quenched, metastable phases 0-76234
 Fe-C-Mn-V, austenite microstruct. memory (German) 0-84977
 Fe-Co-(Ni), annealing effect on microstruct. rel. to mag. and mech. props. 0-89267
 Fe-Cr, high-temp. oxidation, borate inhibitors 0-66705
 Fe-Cr (9 wt.%), extrinsic grain boundary dislocations, low C content influence 0-107273
 Fe-Cr-Co permanent magnet system, miscibility gap, microstruct. and mag. props. obs. 0-76228
 Fe-Cr-Ni, foil, in situ oxidation in HVEM 0-104354
 Fe-Cr-Ni (18.14 wt.%), γ to ϵ to α martensitic transform., external stress effect, double tensile deform. exam. 0-108438
 Fe-Cr-Ti-Mo-TiO₂ (13, 3.5, 1.5, 2 wt.%) dispersion hardened, void swelling 0-65046
 Fe-Cu (4.54 wt.%) alloy, scaling behaviour, 700-1000°C, 1 atm. O₂ 0-93679
 Fe-Mn, mechanical twinning of close-packed hexagonal ϵ -phase during plastic deform. (Russian) 0-60909
 Fe-Ni (4 wt.%), extrinsic grain boundary dislocations, low C content influence 0-107273
 Fe-Ni-C (30, 0.5 wt.%) single cryst., stress induced martensitic transform. 0-60860
 Fe-Ni-Co-W(Mo) (18.65, 8.99, 4.87 wt.%), ageing characts., 380-530°C 0-60876
 Fe-Ni-Mo, martensitic transformation, annealing, influence on struct. of austenite (Russian) 0-81057
 Fe-Si (3 wt.%) high-permeability grain-oriented steel, quenching effect on primary recrystn. texture development 0-84956
 Fe-Zn, quenched, martensite struct. and hardness, electron microscope exam. (Russian) 0-66619
 Fe₃Al, alloys, superlattice-fringe imaging theory, images formed from two beams 0-79649
 (Fe_{1-x}M_x)₂O₃, yH₂O, M=Cr,Cu,Ni, crystal growth, characterisation by Mossbauer spectroscopy, mag. meas. and electron microscopy (French) 0-80655
 Fe₂O₃ ultrafine particles in PTFE matrix, EPR and Mossbauer study 0-100625
 Fe₂O₃ films, electron microscopy and energy-loss spectroscopy 0-80137
 β -FeOOH, dehydration 0-79767
 Fe₂Pt, atomic thermal vibr. anisotropy, martensitic transform. model (French) 0-70355
 GaAs, semi-insulating, optical and electron microscopy exam., line dislocation precipitates 0-70205
 Gd₂(MoO₄)₃, ferroelectric, polarisation reversal, electric field induced phase transform. 0-103925
 Gd₂SiO₅, atomic positions, high resolution electron microscopy 0-100220
 Ge amorphous film, bright-field hollow cone images 0-75136
 Ge amorphous films, structural relaxation and crystallisation 0-100170
 Ge, dislocation electron image filtering in electron microscopy 0-75129
 Ge, electron beam irradiation, {113} faults, nature and origin 0-70258
 Ge, epitaxial growth of very thin electron microscopy specimens 0-100793
 Ge-O, Cu, amorphous thin film, impurity effects on struct. 0-107054

electron microscope examination of materials continued

- Ge-GaAs, heteroepitaxial systems, misfit dislocations obs. using HV electron microscopy 0-100242
 Hf, polymorphic transition, emission images obs. in temp. range 1800-2100°K 0-100836
 Hg, atom, on C support film, signal-to-noise enhancement by incoherent superposition 0-101906
 Hg, condensation, two-dimensional, on W 0-107666
 Hg_{1-x}Fe_xTe, struct. invest. using X-ray diffr. and electron microscopy 0-75365
 HgSe film, anomalous photocond., electron microscope study 0-65623
 In-Sn alloy crystals, phase changes and shape memory effect (Japanese) 0-108502
 InSb, single crystal, chem. and ion etching, surface changes (French) 0-108614
 IrO₂, electrochromic, oxidation state changes and struct. 0-100950
 K₂Pt(CN₄)Br_{0.3}·3H₂O, anisotropic radiation damage in electron microscopy, diff. spot fading rate obs. 0-107329
 Li₂+2P₂O₃+11P₂O₅, polyphosphate, melting and crystallisation 0-70376
 Mg-Nd-Zn dilute alloy, metallography and precip. kinetics 0-71655
 MgO crystals., geometrical-statistical parameters of dislocation interactions with point obstacles 0-103341
 MgO crystals., radiation damage influence on deform. in HVEM 0-103391
 MgO, high temperature prestrain effect on plastic props., dislocation struct. 0-79866
 MgO single crystals, surface atomic steps obs. by electron microscopy, dark- and bright-field techniques 0-84040
 MgO single crystals., dislocation processes, obs. by HVEM in-situ deform. 0-103340
 MgO-CdO, interface, coincidence-site-lattice relations 0-103588
 Mn thin films, vacuum deposited in elec. field, resist., struct. 0-103761
 MnAlGe film, mag. domains and amorphous to cryst. phase transition, electron microscopy obs. 0-71129
 MnGaGe film, mag. domains and amorphous to cryst. phase transition, electron microscopy obs. 0-71129
 Mo alloys, dil., HVEM bombarded, neutron damage simulation, defect cluster and dislocation obs. 0-107330
 Mo, dislocation structure of diffusional welding zone (Russian) 0-96531
 Mo extinction length l_{200} meas., electron energy influence 0-90935
 Mo, irradiation in HVEM, anisotropy of damage prod. 0-107322
 Mo polycrystals, grain misalignment, electron microscope determ. (Russian) 0-103358
 Mo, single and polycrystals., struct. change during work softening, HVEM 0-103336
 MoS₂, molybdenite crystal, direct imaging of atom configuration projected onto the basal plane 0-64847
 Na-A zeolite, struct. obs. by high-resolution electron microscopy 0-84175
 NaCl, cleavage faces, evaporation pattern determ. by decoration method in electron microscopy (German) 0-107626
 NaCl, impurity precipitation and grain boundary diffusion 0-107567
 NaCl, monatomic step struct., decoration technique 0-103554
 Na₂O-B₂O₃-Bi₂O₃, glass with metallic Bi granules, elec. cond. 0-84493
 Na₂O-CaO-Al₂O₃-SiO₂ glass, crystn. for the purpose of obtaining vitrocramics (French) 0-75163
 Na₂O-CaO-SiO₂ glass foils, HVEM in-situ straining expts. 0-104216
 Na₂O-MgO-Al₂O₃, β'' -alumina, high-resolution electron microscopy 0-75208
 Na₂Ti₂O₉, orthorhombic, unit-cell twinning of monoclinic Na₂Ti₂O₉, cryst. struct. 0-107155
 (Na₂Ti₂O₉)_n(BaTi₂O₉)_m, tunnel struct. intergrowth, electron, microscopy investigations 0-100218
 Nb-H(D), H ordering, review 0-60850
 Nb₂O₅·8H₂O, circular diffuse scattering studied by 1 MV high resolution electron microscopy 0-59350
 Ni alloys, plasticity, heat treatment effect 0-76277
 Ni base superalloy Nimonic 80A, microstruct. anal. by high-resolution electron microscopy 0-76459
 Ni based alloy, amorphous, liq. quenched, struct., thermal stability and mech. props. 0-88059
 Ni, dislocation structure evolution after hydroextrusion (Russian) 0-96530
 Ni, electron irradiation in HVEM, interstitial loop growth 0-107326
 Ni intercalation compound, electron microscopy 0-84164
 Ni, single cryst., cyclically deformed, HVEM in-situ deform. study 0-103339
 Ni, stray mag. fields above stripe domains, electron microscope and μ^* -tensor determ. 0-71089
 Ni-ceramic coating structure, influence of micropowder inclusion (Russian) 0-59820
 Ni-Cr, (30 wt.%), collective dislocation movements, in situ study 0-100243
 Ni-Cr, high temp. thermomech. treatment effect on tensile diagrams of KhN77TYuR (Russian) 0-60884
 Ni-Cr (33 at.%), plastic deformation, HVEM study (French) 0-66605
 Ni-Fe-Co-Ti, electron microscopy and mag. meas. 0-71097
 γ -Ni₃(Al,Ti), single crystal, dislocation movement, HVEM obs. (Japanese) 0-108503
 NiFe, single and multilayer thin films, strip domains, inplane magnetisation 0-103866
 NiFe, mag. film, pulse switching at low temp. 0-103868
 NiPt, quenched, ordering kinetics and domain struct. form. during isothermal tempering (Russian) 0-66502
 P, amorphous, struct. by electron microscopy 0-84065
 Pb foil, type I supercond., crit. current density, pinning force density, shadow electron microscopy obs. 0-88696
 Pb, melting, changes in electron image contrast 0-100147
 PbO-B₂O₃-Bi₂O₃, glass with metallic Bi granules, elec. cond. 0-84493
 PbS islands, vacuum deposited, electron microscope obs. 0-103601
 Pb₃(VO₄)₂, ferroelastic, phase transitions, boundary walls 0-107419
 Pd, (111) surface electron microscopy 0-103556
 Pd-Si metallic glass, high-resolution electron microscopy 0-84097
 Pt complex, [2, 2', 2"-terpyridine PtCl]⁺, motion of Pt atoms, electron microscopy obs. 0-103314
 Pt intercalation compound, electron microscopy 0-84164
 Sb, cleavage faces, evaporation pattern determ. by decoration method in electron microscopy (German) 0-107626
 Sb₂Te₃, cleavage faces, evaporation pattern determ. by decoration method in electron microscopy (German) 0-107626
 Si, (110) oriented, electron optical conditions for struct. image form. 0-75131

electron microscope examination of materials continued

- Si crystals, dynamic processes associated with stacking faults and deformation, HVEM in-situ obs. 0-103369
 Si crystals, in-situ HVEM obs. of dislocation processes during high temp. deform. 0-103342
 Si, electron beam irradiation, {113} faults, nature and origin 0-70258
 Si, HVEM struct. images of extended 60° and screw dislocations 0-59466
 Si, ion-implanted amorphous, laser epitaxial recrystallisation threshold energy 0-70571
 Si, laser annealing of SiO₂ layers 0-97505
 Si, radiation induced defects in high-voltage electron microscope 0-65048
 Si wafer, thin surface layers, amorphous to cryst. transform, obs. technique 0-107288
 Si-SiO₂-Mg-Cu powder compact, nitridation to form Si₃N₄ whiskers (Japanese) 0-93674
 SiC polytypes, lattice imaging studies on intergrowth structures. 0-107025
 SiO₂, ultrathin oxide on Si, struct. obs. by high-resolution electron microscopy 0-103592
 SmCo₅, mag. domain structure rel. to crystal defects 0-103856
 SmCo₅, sintered magnets, eutectoid decomp. 0-89219
 SrTiO₃, ferroelectric, polarisation reversal, electric field induced phase transform. 0-103925
 Ta-H(D), H ordering, review 0-60850
 TeO₂-MoO₃-V₂O₅, phase comp. determ. using X-ray diffr., electron microscopy and DTA (German) 0-88046
 Ti-Al, elec. spark Al doping of VT-18, surface struct. and props. (Russian) 0-76398
 Ti-Al-Mo, type BT22, phase transformations under step-by-step heat treatment (Russian) 0-108436
 Ti-Mo, structure associated with BCC to omega transform. (Russian) 0-108432
 β-Ti-Mo-Zr-Sn(11.5, 6, 4.5 wt.%), metastable phase III, microstruct. and age hardening response 0-84945
 Ti-Si amorphous alloy, melt-quenched, transform. studies and mech. props. 0-100838
 TiC, electron irradiation damage, electron microsc. study 0-84210
 V-H(D), hydrogen ordering, review 0-60850
 V-O alloys, quenched, local ordering of O, electron microscopy and diffr. 0-59453
 V-Ti-C, high temp. carbide form., electron microscopy study 0-89228
 V₂O₅ and lower oxides, defect structures and related props. 0-59454
 WO₃, reduction, defect role, in situ HVEM obs. 0-81323
 YAG, simulated mol. images, point models and kinematical struct. amplitudes 0-103223
 Y₂O₃, dislocation and plasticity dissociation 0-107247
 Zn-Al (0.4 wt.%), intergranular slip during in situ superplastic deform. 0-96538
 Zn-Al (1.1 wt.%) superplastic alloy, grain size determ. (Czech) 0-81118
 Zr, foil, dislocation loop nucleation and growth during 1 MeV electron irradiation 0-88152
 Zr, void swelling during electron irradiation, HVEM study 0-92559
 Zr-H alloy, precip. of γ-ZrH, shear mechanism 0-104170
 Zr-Nb (0.1, 2.5 wt.%), foil, dislocation loop nucleation and growth during 1 MeV electron irradiation 0-88152
 ZrO₂-CaO, stabilised microspheres, structure, mechanical props. (Russian) 0-100379
 ZrO₂-Y₂O₃, stabilised microspheres, structure, mechanical props. (Russian) 0-100379

electron microscopes

- see also electron microscopy; field emission electron microscopes; scanning electron microscopes; scanning-transmission electron microscopes; transmission electron microscopes
 200 kV electron microscope with resolution limit less than 0.25 nm 0-101881
 analytical, for electron energy loss anal. 0-86521
 ANL HVEM-TANDEM accelerator facilities 0-101896
 Cambridge University 600 kV high resolution, engineering performance 0-82849
 conference, Toronto, Canada (Aug. 1978) 0-82579
 construction, operation and special types, review 0-86529
 contamination by surface diffusion of adsorbed hydrocarbon molecules, theory 0-99013
 contamination due to surface diffusion of hydrocarbons and elimination method 0-73545
 cooling stage, high-resolution double-tilt, for 1.2 MV HVEM 0-68322
 high resolution, 600 kV electronic mechanical and electron-optical engineering design features 0-86518
 high resolution, developments in imaging crystalline materials 0-99001
 high resolution, obs. at liq. He temps. 0-86517
 high resolution JEOL 200CX, performance eval. and apps. 0-82850
 historical development 0-68320
 HV 3 MV type, mech. vibr. sources and effects (French) 0-82848
 image converters, for HVEM 0-104839
 magnetic specimen stage, liq. He, investigation of ferromag. domains in CrBr₃ 0-103855
 magnetic spectrometer, corrected second-order aberrations 0-87013
 mirror electron microscope, microprocessor system 0-62798
 optical diffractometer analogue 0-69494
 optical model, design and use 0-86534
 photographic system, external 0-101902
 resolving power limitations 0-86528
 sample holder, Be, EDS spectral contamination 0-101907
 shadow type, stereo images form. 0-95195
 single-polepiece objective and projector lenses 0-68326
 specimen devices, for in-situ experiments 0-101910
 spiral distortion correction double-lens system 0-68327
 superconducting lens system for 500 kV electron microscope 0-68321
 vacuum pump, high-performance oil-free design 0-99011
 LaB₆ cathodes, mounting methods and operating charact. 0-57437
 LaB₆ cathodes, single crystal, of <100> and <110> orientations, brightness meas. from 1500 to 1950K 0-62808

electron microscopy

- see also electron microscope applications; electron microscope examination of materials; electron microscopes; field emission electron microscopy; metallography; scanning electron microscopy; scanning-transmission electron microscopy; specimen preparation; transmission electron microscopy
 aberration correction 0-86531

electron microscopy continued

- analytical electron microscope optimization of X-ray microanalysis, instrum. problems 0-73540
 analytical microscopy at 200 keV 0-73547
 atom displacement radiation damage, in electron microscopes 0-103394
 atom resolution, in mol. images 0-100226
 automatic investigation of electron microscope images 0-92425
 autoradiograms of serial sections, preparation for electron microscopy 0-67312
 autoradiography of isolated mols. 0-85564
 autotutorial methods utilizing sound-on-slide presentations 0-73534
 bacteriophages, freeze drying method for electron microscopy 0-104826
 beam scattering, in organic specimen, Monte Carlo simulation 0-100148
 biological autoradiography, soln. of reverse problem 0-94419
 biological macromolecule, high resolution struct. determ. by electron microscopy 0-89717
 biological specimen replication at -150°C with improved freeze-fracture apparatus 0-85560
 biological specimens, electron exposure-dependent contrast transfer 0-104837
 biological X-ray microanalysis, principles 0-73566
 bright field images, signal-to-noise enhancement by incoherent superposition 0-101906
 bright-field hollow cone illumination 0-75136
 cartilage proteoglycan simultaneous localisation by light and electron microscopy 0-85571
 cell membrane particle diameters meas. by computer from electron micrographs 0-101307
 cell ultrastructure, computer anal. 0-85555
 combined scanning microdensitometer and diffractometer 0-73529
 computer image processing, atomic resolution from 500 kV electron micrographs 0-100149
 conference, electron microscopy and analysis, Brighton, England (Sept. 1979) 0-67936
 conference, Melbourne, Australia (Feb. 1980) 0-82572
 conference, Toronto, Canada (Aug. 1978) 0-82579
 conference of Electron Microscopy Society of Southern Africa, Port Elizabeth, S.Africa (Feb. 1980) 0-73099
 conically tilted projections, 3-D reconstruction 0-99618
 convergent beam electron diffraction 0-103220
 convergent beam electron microscopy, appl. in materials science 0-107028
 crystal orientation determ. from selected area channelling patterns 0-70092
 crystal structures and cryst. defects, electron microscope imaging 0-88006
 crystal surface, in-situ cleaning by ion sputtering 0-101895
 crystalline materials, high resolution imaging techniques 0-99001
 crystalline materials, in situ deform. by high voltage electron microscopy 0-103352
 dark field image calculation 0-75137
 dark-field imaging, computer simulation 0-100151
 decoration method, rel. to crystal growth (German) 0-103222
 decoration technique, surface step struct. determ. 0-103554
 defect imaging, analytical contrast calcs. in two-beam case 0-100134
 defect symmetry, electron diffr. contrast, theory 0-96418
 differential sensitivity of neurosecretory and non-neurosecretory neurones of an aphid 0-98195
 dislocation, Burgers vector determ. by weak-beam image in HVEM (Japanese) 0-70199
 dislocation core studies in high resolution microscopy, image calc. methods 0-96535
 displacement damage simulation in HVEM irradiation 0-107325
 Doppler shift of electron waves, illustration using electron mirror interference microscope 0-95783
 dynamic phenomena, in situ appl. of DC electric field 0-103925
 electrocyte stacks of torpedine ray, assembly for quick-freezing tissues 0-67316
 electron gun, with electrostatic and electromagnetic lenses 0-99007
 electron-matter interactions rel. to electron microscopy 0-89097
 electrostatic crossed lens, for electron microscopic devices 0-87289
 EM, electron exposure-dependent contrast transfer 0-104837
 energy loss microanalysis system with high collection efficiency 0-86508
 failure analysis tools comparison and selection 0-71865
 foil lens, spherically corrected, for electron phase microscopy (German) 0-83546
 freeze fracture, size determination of sonicated vesicles, spray freezing method 0-98188
 freeze fracture autoradiography, red blood cell plasma membrane 0-98192
 freeze-etching improvement using evaporated film 0-85558
 freeze-fracture technique, appl. to study of animal plasma membranes 0-104842
 frozen hydrated crystalline specimens, meas. and reduction of damage 0-85552
 grain boundary reaction sites, determ. of struct. aspects 0-103359
 HEED, critical voltage effect, zone axis, interpret. using atomic string approx. 0-96421
 high resolution, appl. of Fraunhofer holography 0-99016
 high voltage, materials testing in situ experiments, feasibility and methodology (French) 0-68301
 high voltage, quantitative anal. of in situ straining experiments, strong frictional force 0-100244
 holey film preparation by ion-etching method 0-105751
 holographic filter, for electron micrography image improvement 0-99680
 homogeneous electron irradiation (German) 0-102603
 HV, in situ obs. techniques and apps., review (Japanese) 0-59351
 HV, in situ oxidation of Fe-Cr-Ni foils 0-104354
 image accumulation, digital storage and processing system 0-101901
 image contrast, of cluster atoms, rel. to inelastic scattering 0-100154
 image formation, propag. problems connected with special source structures. 0-87272
 image processing system for micrographs based on minicomputer 0-73549
 image reconstruction from projections, blurring due to object movement 0-78784
 image reconstruction of low and high dose micrographs of neg. stained glutamine synthetase 0-85551
 image recording system, detection quantum efficiency 0-99009
 image wavefunction asymptotic approx., extension to biprism edges 0-95193

electron microscopy continued

- imaging and diffraction, from localised defects and disorder 0-100152
 imaging of thin phase objects, tilted and extended 0-99617
 immunoelectronmicroscopy in detect. of antibodies to rabies virus 0-85567
 inelastic electron-matter interactions 0-104024
 lattice fringe imaging applications 0-88005
 lattice fringe imaging theory 0-103225
 lattice image calculations for imperfect crystals, superlattice approach 0-107030
 light optical diffractometer, for electron microscope images operating on line 0-101900
 magnetic domain wall observation device for use with 1 MeV electron microscope 0-101882
 many-beam lattice images from thicker crystals 0-88004
 many-beam structure images, optimal comput. techniques 0-95203
 membrane preparatory procedures, for electron microscopic anal., at mol. level resoln. 0-104843
 metallographic sample preparation, procedures 0-57272
 microdensitometer-computer correlation analysis of ultrastructural periodicity 0-85553
 microfractography (*Japanese*) 0-71841
 minimal exposure high resolution, organic materials 0-79653
 mirror electron microscopy, contrast form. 0-68299
 molecule images, simulation by point models and kinematical struct. amplitudes 0-103223
 neurons, section embedding technique for sequential light and electron microscopic exam. 0-67317
 nonperiodic objects, reconstruction from electron micrographs using correlation methods 0-86527
 numerical aperture and f-stop utilisation 0-105753
 organic materials, imaging with superconducting lenses 0-73553
 phase contrast simulation, of Au cluster atoms on W support film 0-100150
 phase problem, partial coherent illumination influence 0-62800
 phase problem, rel. to holography 0-99681
 phosphorylase A crystals, automated struct. determ., from micrographs 0-92425
 photoemission, principles and appls. 0-89424
 planar defect 'on edge', electron wave function in vicinity 0-88002
 pore-channel marking, electron microscopy of polymer films 0-103271
 preparation of structural fragile cell-biological specimens, exchange method 0-98190
 prevention of losses and damage during X-ray microanalysis 0-73567
 protein film method, basic, in electron microscopy of nucleic acids 0-104844
 protein supramolecular structure, ordered, electron micrographs, image processing 0-89923
 radiation damage, correl. anal. 0-100282
 radiation damage problems in electron microscopy 0-59517
 replica technique, glue films for detaching single-stage C replicas 0-61038
 resolution estimation in electron microscopy 0-77911
 resolution improvement for crystal structure imaging and atomic movement dynamic obs. 0-70090
 ribosome subparticle fine struct. investigation by optical filtration of electron microscope images 0-81779
 screening effect by dielectric support film 0-86504
 secretory granule membrane, particle clustering induced by centrifugation, freeze-fracture anal. 0-85559
 semiconductor applications of electron microscopy, advances 0-101911
 specimen deposition and fabrication by ion beam sputtering 0-82855
 stereo imaging in shadow microscope 0-95195
 superconducting lens, electron microscope appl. 0-86530
 support film phase contrast, Fourier spectrum analysis 0-95199
 symposium, Toledo, Ohio, USA (Aug. 1979) 0-82571
 thin film, thickness determ., by electron backscattering 0-101904
 three dimensional, minimal dose technique 0-86526
 tilted illumination imaging, contrast transfer functions 0-95198
 ultramicroscopy in scanning microscopes 0-95137
 weak-beam images of dislocation dipoles and multipoles, calc. 0-75231
 work function variations, mirror electron microscopy meas. 0-86505
 Al₂O₃ supermicrogrid preparation and props. for use as support film in high resolution electron microscopy 0-99010
 Ge, dislocation electron image filtering in electron microscopy 0-75129

electron mobility

- see also carrier mobility; electron mobility (metals)*
 air, electron drift velocity at 293K 0-103102
 benzene, gaseous, critical and liquid, electron transport 0-64673
 dense gases, electrons and positrons, review 0-103106
 ethane, gas, liq., and crit., electron mobility, density and temp. effects 0-92246
 ethane, supercritical, electron mobility as function of density and temp. 0-59163
 gases, multiple scatt. effect 0-58383
 nonpolar fluid, excessive electrons near crit. points 0-92836
 swarm transport coefficients, iterative method calcs. 0-96336
 toluene, gaseous, critical and liquid, electron transport 0-64673
 transport properties of electrons with narrowly defined bands at low temp. (*Russian*) 0-103656
 Ar, electron avalanche development, exact Boltzmann eqn. anal. 0-59318
 Ar, liq., compressed, excess electron mobility theory 0-80338
 CO₂, ratio of lateral diffusion to mobility for electrons at moderate E/N 0-59160
 He, gaseous, positron mobility edge 0-83880
 Hg vapour, electron drift velocity at 573K 0-103103
 Mg vapour, electron momentum transfer cross section, from 0.1-5 eV 0-103104
 N₂, dense vapour, electron localisation 0-87840
 NH₃ vapour, supercrit. and subcrit. 0-59162
 O₂, low energy electron drift velocity at 293K 0-103101

electron mobility (metals)

- Au film, ultrathin evaporated, acoustoelectric meas. of electron mobility and diffusion 0-65707
 Bi, film, size effect of carrier heating, surface scatt. (*Russian*) 0-100474
 B-Ga, metastable, elec. props. in normal and supercond. states (*Russian*) 0-65520

electron multipliers

- channel, high count rate, exponential decay and recovery of model gains 0-87022

electron multipliers continued

- counting characts. dependence of secondary-electron multipliers on residual gas pressure 0-106239
 Johnston, low energy ion counting efficiency 0-63479
 mass spectroscopy, electron multiplier gains determ. for various ions by pulse counting method 0-57418
 microdensitometer system for use in TEM 0-95197
 narrow energy distribution of output electrons from modified single channel electron multiplier 0-57337
 secondary electron open-type, for X-ray spectroscopy and electron microprobe anal. 0-99027

electron nuclear double resonance *see* ENDOR**electron-nucleon interactions**

- see also electron-nucleon scattering; electron-proton interactions*
 deep inelastic scatt., heavy lepton mixings, Weinberg-Salam model 0-62992
 deep inelastic scatt., quark model, field-theoretic, quark indistinguishability, nucleon structure function 0-62993
 QCD and short range nuclear phenomena 0-91060
 relativistic theory of P violation in many-electron atoms 0-91042
 target mass effects in polarized electroproduction 0-78072
 eN, 50, 100, 300 GeV, in emulsion, cascade showers 3-dimens. development 0-86724
 eN deep inelastic scatt., QCD anal. 0-95276
 eN \rightarrow eX, SU(2)_L \times U(1) gauge theory distinguished from SU(2)_L \times SU(2)_R \times U(1), neutral currents, z-bosons 0-62908
 en \rightarrow en π , pol. e, P-odd asymmetry and cross sections, SU(2) \times U(1), SU(3) \times U(1) calcs. (*Russian*) 0-62998
 e⁻N, inclusive pion production due to $\gamma q \rightarrow \pi q'$ process, quark-parton model (*Russian*) 0-78073
 e⁻N \rightarrow e⁻ Δ (3/2, 3/2), P-odd asymmetry, P nonconserving neutral current interaction 0-57611

electron-nucleon scattering

- see also electron-nucleon interactions; electron-proton scattering*
 polarised e scattering, elastic and deep inelastic covariant formulation 0-78069
 eN elastic scatt., pol. e, nucleon form factors, P violating symmetry, Weinberg-Salam calcs. 0-68461
 eN elastic scatt. in nuclei, P violating asymmetry due to weak neutral currents 0-73713

electron-nucleus reactions

- for inelastic electron-nucleus scattering, see "electron-nucleus scattering"*
see also electron-nucleon interactions; nuclear electron capture
 deep inelastic scatt., Δ (1232) production 0-57772
 excitation, giant monopole, energy-weighted isoscalar sum rules 0-63174
 heavy nucleus, coherent and inclusive prod. of hadrons with low P_T, Coulomb excitation and decay of projectile 0-83100
 pion electroproduction from the nucleon near threshold 0-68651
 QCD and short range nuclear phenomena 0-91060
 relativistic theory of P violation in many-electron atoms 0-91042
 (e,X) 4.5 GeV heavy particle production semicond. telescopic detection setup (*Russian*) 0-63461
 (γ ,d), odd-Z light nuclei, from (e,e'd), cross section, E2 transistors giant resonance and clusters 0-63169
²¹Al(e,x), electrodisintegration charged particle yield, α to t cross section ratio (*Russian*) 0-86902
⁹Be(e, π^+), 1848 MeV, virtual photon spectrum, virtual photon theory test 0-102183
¹²C(e,e'), role of two-particle scatt. (*Russian*) 0-91178
¹²C(e, π^+), ¹²B analogue states at 4.5 MeV giant resonance region, strong spin-isospin mode 0-78250
¹¹¹Cd, 1330 keV level excitation cross section from positron annihilation 0-68583
⁵⁶Fe(e, α), E2 isoscalar resonance sum rule, DWBA anal. 0-68621
²H(e,e,p) 1180 MeV electrons, proton distribution, neutron momentum distribution (*Russian*) 0-68652
³H(e,n,p), disintegration and Coulomb excitation cross sections in channelled nuclei 0-59539
³He(e,e,p), cross-section, Fadeev technique, nucleon-nucleon interaction (*Russian*) 0-73842
⁴He(e,e'p) reaction cross-section and ground state shell model calcs. (*Russian*) 0-78283
⁴He(e, π^+), ⁴He 2⁺ resonance evidence at 40 MeV 0-86880
¹³⁹La(e,p), 15-25 MeV, T₀+1 giant dipole resonance and characteristic decay mode 0-78247
⁶Ni(e,p), (e, α), A=58, 60, 62, electrodisintegration cross sections, E1, E2 absorption, DWBA anal. 0-106052
 Ni(e, α), E2 strength in resonance regions statistical decay 0-91146
²³⁷Np(e,f), 10-34 MeV, electrofission cross section, E2 transition mode and giant resonances 0-106084
¹⁶O(e, π^+), 180.4 MeV, virtual photon spectrum, virtual photon theory test 0-102183
¹⁴¹Pr(e,p), 15-25 MeV, T₀+1 giant dipole resonance and characteristic decay mode 0-78247
²⁶⁴Pu, muonic atom direct electroprod., finite nuclear size effects (*Russian*) 0-69272
^AW(e,f), A=182,184,186, 35-55 MeV, fission barriers, pairing strength deformation depend., stat. anal. 0-57810
⁹⁰Zr(e, α), 135-66.5 MeV, (γ , α) statistical and pre-equilibrium cross sections and multipolarities 0-68646

electron-nucleus scattering

- see also electron-nucleon scattering*
 semileptonic weak and EM interactions, multipole operators, HO single particle matrix elements 0-73840
 (e,e), c.m. motion effects in oscillator shell model 0-106050
 (e,e'), 70 MeV, 1p shell nuclei, shell model cross sections, giant M2, transversal E1 resonances 0-63143
 (e,e'), A=12, 24, 28, isovector M1 excitations, current and spin contribs. 0-68582
 (e,e'), cross section near quasielastic maximum, shell and optical models (*Russian*) 0-91179
 (e,e'), light and medium nuclei, high energy approx. anal., transition densities and probabilities (*Russian*) 0-63129
²⁰⁷(e,e'), transverse scatt. amplitude suppression, form factors, neutron hole states 0-91129
²⁷Al(e,e'), 70-340 MeV, odd parity state electroexcitation, form factors, transition probs. 0-78208
²⁷Al(e,e'), cross sections, shadowing effect at small four momentum transfer 0-63176

electron-nucleus scattering continued

- ²⁷Al(e,e) multiple operators in semileptonic weak and electromagnetic interactions 0-73840
¹³C(e,e), $1^+(T=1, 15.1 \text{ MeV})$ state excitational pionic modes, M1 form factor 0-78195
¹³C(e,e), cross sections, shadowing effect at small four momentum transfer 0-63176
¹²Cl(e,e), 25-115 MeV, ground state charge distrib. and RMS charge radius 0-57672
^ACa(e,e), backward scatt., $A=40, 42, 44, 48$, mag. dipole ground state transition search 0-106009
⁴⁸Ca(e,e), 757.5 MeV, elastic cross section 0-63175
⁴¹Cl(e,e), 116, 194 MeV, $A=35, 37$, charge distrib. and RMS charge radius 0-102109
⁵⁹Co(e,e), magnetic e scatt., exchange current effects, plane wave Born approx. 0-78282
^AFe(e,e), 100-275 MeV, $A=54, 56, 57$, cross sections and muonic X-ray meas., charge distrib. systematics 0-86801
⁵⁶Fe(e,e), Coulomb form factor for $O^+ \rightarrow 4^+$ transition, collective 4^+ states, shell model 0-57664
⁵⁶Fe(e,e), longitudinal and transverse inelastic response functions and cross sections 0-57771
²H(e,e'), 56.4 MeV, cross sections, form factors, meson exchange current contrib. 0-68649
²H(e,e), EM form factors, relativistic formulae, moment corrections 0-63075
²H(e,e), form factors, tensor pol., and two-nucleon force calcs. 0-106045
²He(e,e) energy weighted sum rules (*Russian*) 0-86900
³He(e,e'), nuclear high momentum components and y scaling 0-106051
³He(e,e), charge formfactors, second Born approx. and pole model 0-78133
³He(e,e), relationship to $^3\text{He}(\pi^-, \pi^-)$ 0-78323
⁶Li(e,e'), 102, 123 MeV, excitation form factor, $^3\text{H}-^3\text{He}$ cluster model 0-78190
⁶Li(e,e'), 76-141 MeV, form factors, appl. to (π^-, γ) , phenomenological model 0-83068
⁶Li(e,e), charge formfactors, second Born approx. and pole model 0-78133
⁶Li(e,e), elastic and inelastic charge form factors from shell model wave functions 0-68523
⁷Li(e,e') at first πN resonance, cross section longitudinal and transverse components (*Russian*) 0-86901
⁹³Nb(e,e), magnetic e scatt., exchange current effects, plane wave Born approx. 0-78282
^ANi(e,e), 100-275 MeV, $A=58, 60, 62, 64$, cross sections and muonic X-ray meas., charge distrib. systematics 0-86801
¹⁶O(e,e'), 799, 996, 1178 MeV, cross sections (*Russian*) 0-68653
¹⁶O(e,e'), 80-165.7 MeV, giant dipole and quadrupole resonances, form factors 0-102168
¹⁶O(e,e'), isovector mag. dipole and quadrupole transitions, analogues, $(\pi^- \gamma)$ relation 0-106010
²⁰⁸Pb (e,e'), 2- giant resonance twist mode excitation, $B(M2)$ values, form factors 0-78246
²⁰⁸Pb(e,e'), 70-335 MeV, natural parity high spin state excitation 0-63060
^ASi(e,e'), 126-293 MeV, $A=28, 29$, levels and form factors, particle-phonon coupling anal. 0-105977
²⁵Si(e,e'), 6- T=1 resonance form factor, mag. strength quenching, meson exchange currents 0-86882
⁸⁷Sr(e,e), magnetic e scatt., exchange current effects, plane wave Born approx. 0-78282
⁴⁹Ti(e,e), magnetic e scatt., exchange current effects, plane wave Born approx. 0-78282
⁵¹V(e,e), magnetic e scatt., exchange current effects, plane wave Born approx. 0-78282
^AZn(e,e), 100-275 MeV, $A=64, 66, 68, 70$, cross sections and muonic X-ray meas., charge distrib. systematics 0-86801
⁹⁰Zr(e,e'), 2- giant resonance twist mode excitation, $B(M2)$ values, form factors 0-78246

electron optics

- see also beta-ray spectrometers; electron beams; electrostatic lenses; ion optics; magnetic lenses; particle optics*
aberration elimination, electron beam scanning systems 0-78756
aberrations, reduction by optimisation techniques 0-87290
beam deflection error assessment, expt. technique 0-78757
bipolar electron-optical image converter as a circuit element 0-78994
Boersch's electron optical bench, modifications 0-87286
Boersch effect, energy broadening 0-69313
Boersch effect in electron-optical instruments 0-69308
bright field TEM, partially coherent attenuation envelope shape 0-101885
bright-field image contrast and resolution in STEM and conventional TEM 0-95200
cathode lens having a quasispherical field 0-95782
charged particle trajectory calc. in electrostatic field, teaching 0-90635
computer image processing, atomic resolution of 500 kV electron micrograph 0-100149
condenser objective, single field, advantages and limitation for min-exposure 0-87292
conference on electron, ion and proton beam technology, conf., Boston, MA, USA (29 May-1 June, 1979) 0-67927
conically tilted projections, 3-D reconstruction 0-99618
crossed lenses, electron optical charact., trajectory anal., aberrations from axial pot. profile 0-63909
crossed lenses, theoretical and expt. study 0-95780
crystal structures and cryst. defects, electron microscope imaging 0-88006
CTEM, on-line electron-optical correlation computing 0-99008
cylindrical-mirror electrostatic analyser for beta spectroscopy of beams 0-63446
deflection system performance using resolution test specimen 0-69311
diffraction radiation generators, echelette use, electron flow (*Russian*) 0-69314
distortion correction and deflection calibration by laser interferometry in exposure system 0-69310
Doppler shift of electron waves, illustration using electron mirror interference microscope 0-95783
electron gun, with electrostatic and electromagnetic lenses 0-99007
electron probe, compensation of aberrations, dynamical focusing with stigmator 0-87291

electron optics continued

- electrostatic crossed lens, for electron microscopic devices 0-87289
electrostatic energy filter, telescopic, with cylindrical mirror analysers 0-87296
field emission gun SEM column electron-optical performance obs. and model 0-68328
foil lens, correction of spherical aberration, appl. to STEM 0-87294
foil lens, spherically corrected, for electron phase microscopy (*German*) 0-83546
gun lenses, electrostatic for high-brightness field emitters 0-62809
image formation, partially coherent, two dimens., computer simulation 0-106434
image reconstruction, computerized, fragment size choice 0-78785
imaging of thin phase objects, tilted and extended 0-99617
incoherent illumination method with conventional electron microscope, granular noise elimination 0-95201
interference microscopy, image wavefunction asymptotic approx., extension to biprism edges 0-95193
low profile electron collector system 0-68292
magnetic energy filter, without second-order aberrations 0-86524
magnetic imaging filter, electron optical experiments 0-87295
magnetic prism, design, for TEM energy filter 0-86523
magnetic spectrometer, corrected second-order aberrations 0-87013
microscope, high resolution, 600 kV, electronic mechanical and electron-optical engineering design features 0-86518
microscope resolving power limitations 0-86528
microscopy, high resolution, appl. of Fraunhofer holography 0-99016
microscopy, phase problem, partial coherent illumination influence 0-62800
minimal exposure high resolution, electron microscopy, organic materials 0-79653
monochromator, telescopic, in CTEM, with cylindrical mirror analysers 0-87296
nonperiodic objects, reconstruction from electron micrographs using correlation methods 0-86527
objective lens, with compensated axial chromatic aberration, for electron microscope 0-87293
one and two-lens electron-optical system parameter comparison 0-87284
optimisation of electron optical systems using orthogonal functions 0-63908
probe forming systems, optimisation with respect to aberrations and vertical beam landing 0-68291
protein supramolecular structure, ordered, electron micrographs, image processing 0-89923
scanning electron probe voltage contrast, device ground level floatation 0-73527
SEM, photographic recording system 0-101903
SEM lens system design, snorkel or condenser-objective 0-57438
sextupole corrector limitations 0-102604
STEM, differential phase contrast role 0-95202
STEM, image formation, 2-D computer simulation of heavy atom model compounds 0-75135
STEM, images, matching illum. to specimen struct. 0-73551
STEM, multi-signal detection and processing 0-73552
support film phase contrast in electron microscopy, Fourier spectrum analysis 0-95199
tilted illumination imaging in electron microscopy, contrast transfer functions 0-95198
transverse focusing at large emitter currents (*Russian*) 0-87280
triode and diode guns, electron optics numerical determ. of beam profile 0-106435
triple slit scheme for high current variable-shaped beam forming 0-68290
undulator radiation, irregularity effects 0-99614
use of light optical diffractometer 0-101900
variable-shaped beam systems, adjustment accuracy requirements for sub-micron pattern prod. 0-69312
LaB₆ cathodes for Kohler illum. and brightness meas. 0-68296
Si, (110) oriented, electron optical conditions for struct. image form. 0-75131
Si, electron beam annealing, beam voltage effect modeling 0-75275
Si:As, scanning electron beam annealing, spreading resistance, junction depth 0-75267
- electron pair annihilation** *see electron-positron interactions*
- electron pair production**
black holes, primordial, electron-positron radiation, spectrum rel. to galactic radio spectrum 0-62179
dense pinch, electron-positron pair production in EM field (*Russian*) 0-100092
near threshold screening effects, partial wave calc., energy shift screening theory 0-57768
neutron stars, pair formation and electric field boundary conditions at magnetic poles 0-101613
photoproduction on nuclei, 1-10 GeV, total cross section meas. 0-78280
pulsars, pair creation model rel. to source of coherent radio emission 0-82403
pp, 53, 63 GeV, massive electron pair prod., T ang. decay, scaling function 0-68495
pp, 53, 63 GeV, T and ψ prod., dielectron decay angles 0-68496
 $p\bar{p} \rightarrow e^+e^-$ annihilation, weak neutral current effects (*Russian*) 0-105837
 $\text{Ge}(\gamma, e^+e^-)$, cross section near threshold, atomic electron screening effects 0-87279
- electron pairs**
see also electron pair production; positronium
No entries
- electron paramagnetic resonance** *see paramagnetic resonance*
- electron-phonon interactions**
see also phonon drag; strong-coupling superconductors; tunnelling spectra; tunnelling spectroscopy; Umklapp process
A 15 type superconductors, acoustic phonon spectra, electronic density of state function (*French*) 0-80444
acoustic waves, parametric excitation in presence of electron currents (*Russian*) 0-80328
acoustoelectric effect, electron drag by coherent Lamb phonons in quantising magnetic field 0-80330
adsorbate vibrations, large-angle inelastic electron scatt., theory 0-75427
adsorbed layer, electronic transforms, near boundary separating mag. and nonmag. states 0-92961
alkali metals, thermopower and elec. cond., relationship at low temps. (*Russian*) 0-92882

electron-phonon interactions continued

alloys, binary, supercond. transition temp. lowering by nonmagnetic impurities 0-100546
 alloys, dil., of polyvalent and noble metals, deviations from Matthiessen rule 0-65525
 amorphous metals, superconducting properties rel. to ordering 0-65735
 Auger recombination of carriers bound to centres involving phonons 0-107805
 binary alloys, random, specific heat enhancement and electron-phonon interaction 0-65242
 binary compound, Kohn anomaly in optical phonon branch 0-92626
 bound polaron, non-perturbative variational method 0-88485
 brass, lattice thermal cond. component, 4.2 to 30K, microscopic mechanisms 0-107757
 CDW transition temperature, scatt. effects 0-107720
 close packed compounds, superconducting T_c , heterogeneous hybridisation (Chinese) 0-107940
 conductors, quantum acoustic bleaching, acoustic zones 0-70324
 cyclotron resonance lineshape arising from electron-phonon interactions 0-97142
 dilute alloy, Seebeck coefficient, electron-phonon enhancement 0-70685
 dilute magnetic alloys, electron sound absorpt., disordered mag. impurities, spin glasses (Russian) 0-80503
 disordered system, AC cond. tensor in mag. field 0-92870
 electron gas, electron interaction with optical phonon directional flux 0-59893
 electron gas, one-dimens., interacting, ground-state energy in mean field approx. and instabilities 0-88493
 electron-hole binding accompanied by Wannier-Mott exciton form. 0-59887
 ferroelectrics, vibronic, band struct. temp. depend. 0-70598
 ferromagnet, itinerant electron, magnetoresist. and anomalous Hall effect due to electron-phonon interactions 0-70680
 ferromagnetic semiconductors, free carrier absorpt. of radiation 0-97227
 granulated superconductors, phase transitions, Josephson energy (Russian) 0-84540
 hopping promoted by electron-electron coupling 0-59987
 impure metals at low temperatures, conductivity 0-103669
 impurity atom in solid, reson. fluoresc., transient spectrum, intensity, and intensity correl. 0-84777
 impurity centres, electron-phonon coupling from structured optical spectra, review 0-89038
 ionic semiconductors, cyclotron resonance, elec. cond., electron-phonon interactions 0-93180
 itinerant electron ferromagnets, elastic props. and electronic struct. 0-66001
 IV-VI semiconductors, structural phase transitions, anomalous resist., electron-soft phonon interactions 0-108167
 Jahn-Teller cooperative T-(e+t) system, thermal cond. 0-70479
 kinetic equation, chronological and antichronological T-products 0-70627
 localised system, strongly coupled, photon echo phenomenon 0-64118
 metal, electron-phonon interaction effects on spin susceptibility 0-93108
 metal, ferromag., antiferromag., magnetoelastic coupling effect on magneto-elec. reson. 0-75837
 metal, monovalent, contrib. of John Bardeen 0-57057
 metal-semiconductor interface, photoelectron injection, quantum mech. transmission and optical phonon scatt. 0-84511
 metals, electrical and thermal resistance, influence of static atomic displacements 0-103674
 metals, positron trapping by defects influence of positron-phonon and electron-phonon interactions (Russian) 0-93425
 metals, superconductivity studied by electron-phonon and Coulombian e-e coupling strength and quasi particle mass 0-88666
 mixed valence cpds., elec. cond., periodic Anderson model, memory function approach 0-84458
 mixed valence systems, theory 0-70343
 molecular chain, 1-D electron motion, electron-phonon interaction, acoustic solitons 0-70628
 molecular crystals, electronic transport theory, local linear electron phonon coupling 0-65545
 Mott's formula for thermopower and for Wiedemann-Franz law 0-84462
 multiple band electron-phonon transport eqn. derivation 0-100318
 multiple band transport theory, generating functional approach 0-92633
 naphthalene, doped, role of nonequilibrium phonons in stimulated radiation emission 0-103971
 n-octane-3,4,6,7-dibenzpyrene impurity, fluorescence impurity spectra, phonon free line broadening (Russian) 0-108279
 one-dimensional conductor, lattice stability, phonon dispersion, Kohn anomaly 0-96603
 p-n tunnel junctions, photoinduced transitions, theory 0-65669
 parametric excitation in solids, quantum calcs. 0-103714
 Peierls transition, Frohlich model, one-dimens., CDW stability, electron-phonon coupling 0-65452
 point contacts between identical metals, HF rectification at low temp. 0-105706
 polar crystal, polaron effective mass temp. depend., electron interaction (Chinese) 0-84436
 polar semiconductor crystalline thin films, surface vibr. states, IR absorpt. spectra obs. (Russian) 0-60606
 polar semiconductors, secondary cyclotron emission giant oscillations of intensity and line shape 0-66192
 polaron bound to Coulomb pot., energy 0-88487
 polarons, generalised path integral formalism, ground state energy corrections 0-84438
 quasi-one-dimensional electron-phonon system, electron jump effect on phase transition (Russian) 0-92673
 quasi-two dimensional conductor, galvanomagnetic props., optical analogy (Russian) 0-60108
 quench-condensed films, superconducting transition temp., elastic stress and strain effects 0-70883
 quinzarin in alcohol glasses, electron-phonon coupling, photochemical hole burning 0-97265
 rare earth systems with valence transitions, phonons 0-96611
 relaxation times in solid-state theory and one-dimensional molecular systems (Russian) 0-100640
 semiconductor, degenerate, surface optical phonons 0-70520
 semiconductor, magnetophonon resonance oscils., peak shape, theory 0-107824
 semiconductor, n-type, nonequilibrium photoelectron distrib. and absolute negative cond. in quantising mag. fields 0-65622
 semiconductor, noncoherent interaction of a light pulse 0-106561

electron-phonon interactions continued

semiconductor, optical phonon amplification by EM wave field in presence of mag. field 0-65181
 semiconductor, phonon induced hopping between Stark levels 0-92900
 semiconductor, Seebeck and Hall coeffs. Lorenz number, anisotropy, theory (German) 0-65608
 semiconductor surface, cyclotron reson., projection operator formalism 0-88524
 semiconductor thin film, polaron near-threshold spectrum 0-65471
 semiconductor thin films, ferroelectric properties, quantum size effect 0-97201
 semiconductors, degenerate, energy band structure effect on transverse magnetoresistance 0-88580
 semiconductors, electron-electron collision effect on current voltage char-acts. in quantising mag. field 0-103705
 semiconductors, electron-phonon interactions, combined phonon resonance (Russian) 0-75321
 semiconductors, heat pulse absorpt. in nonquantising mag. fields 0-60054
 semiconductors, hot electron transverse escape galvanomagnetic effects (Russian) 0-80289
 semiconductors, magnetic, spin wave electron amplification theory 0-97083
 semiconductors, piezoelec., degenerate, transverse magnetoresist. in strong field, quantum effect 0-80299
 semiconductors, polar, resonance electron-phonon Raman scatt., cross-section oscils. 0-60598
 semiconductors, van Hove critical point region, electron-phonon interactions, dispersion law 0-70344
 solid, impurity atom fluoresc. radiation, intensity correlation, low temp. limit 0-80847
 superconductivity and lattice instability 0-88663
 superconductivity and phonons, review 0-84543
 superconductor, amorphous, Eliashberg function, tunnelling and crit. temp. anal. 0-80455
 superconductor order parameter singularities, tunnelling currents, Fermi surface calcs. (Russian) 0-80458
 superconductors, phonon Raman scatt. 0-100657
 surface exciton energies and radii 0-92829
 tetrabutylammonium europium yttrium isothiocyanate, conc.-depend. electron-phonon coupling, and self-quenching 0-60657
 tight-binding metals, electronic struct. and kinetic props. at high temp. 0-59848
 trans-polyacetylene, intrinsic, electron-phonon coupling 0-79901
 transition metal compounds, reduced ionisation potentials as parameters in superconducting transition temp. calcs. 0-75671
 transition metals, generalisation of modified tight-binding approximation 0-88288
 transition metals, paramagnetic susceptibility, phonon instability, mixed localised-collective electron states 0-103811
 transport properties of electrons with narrowly defined bands at low temp. (Russian) 0-103656
 TTF-TCNQ, elec. resist., electron-phonon scatt. 0-92884
 Ag₂Se, electronic and electrogalvanic props. in α -phase region (French) 0-107820
 Al and dilute alloys with Ge and Zn, magnetoresist. depend. on temp., 4.2-70K 0-70682
 Al dilute alloys, elec. resist., impurity and temp. depend. 0-65526
 Al, magnetoresistance, path integral method calc. 0-65537
 Al, pure and dil. alloys, diffusion thermopower, inelastic electron-phonon interaction 0-96851
 Al_{0.8}Ga_{0.2}As-GaAs DH laser operation, phonon contrib. 0-102724
 Al_{0.8}Ga_{0.2}As-GaAs quantum-well heterostructures, phonon-assisted recomb. and stimulated emission 0-74358
 AlH₃, electronic struct. and electron-phonon interaction, hydrogenation effect, rel. to supercond. 0-107694
 As-Se-Ge(-S), photostructural change in Urbach tail 0-76021
 Bi bounded semimetals, phonon two-stage drag of electrons, thermoelectric power, scatt. mechanism 0-92919
 CdS, polaron cyclotron resonance freq. shifts, halfwidths, cumulant expansion method calcs. (Russian) 0-88880
 Cr, diffuse electron scatt. (Russian) 0-103438
 Cr, spin density wave, Nambu-Eliashberg eqns. for k-state electron-hole pairing 0-97050
 Cu and dilute Cu-Au alloy, magnetoresist. depend. on temp., 4.2-70K 0-70682
 CuCl crystal resonant Raman scatt. and luminescence competition (Japanese) 0-80770
 Cu_{1.8}Mo_{0.2}S₈, supercond. Chevrel phase, electron tunnelling spectroscopy expts. (German) 0-107966
 Cu₂NiSn, Heusler alloy, elec. resist., 4.2 to 300K 0-75547
 EuTe, mag. 'Bragg' scatt. obs. through Raman scatt. 0-66179
 Fe, electron-phonon coupling, point contact spectroscopy obs. (Russian) 0-70342
 Fe, purification, recrystn. temp. and elec. resistivity (Japanese) 0-100780
 Fe_{1-x}Mn_xCl₂, low-lying electronic excitations in antiferromag. and paramag. phases Raman scatt. study 0-71414
 Fe₂O₄, Verwey transition, charge density-phonon condensation 0-65217
 GaAs, surface exciton energy 0-92829
 p-GaSb, heavily doped, LO phonon-carrier interaction, Raman interf. line-shapes 0-93319
 Gd(OH)₃, dynamical effects of interaction between 4f electrons and optical phonons 0-108196
 Ge, amorphous film, persistent photoconductivity, dangling bonds 0-84487
 Ge:P, phonon drag thermoelectric power at low temp. 0-107828
 GeS, absorpt. spectra, electron-phonon interactions 0-80810
 InP, compensation ratio, electron mobility and free-carrier absorpt. 0-80261
 InSb, CESR at high mag. fields, scatt. mechanisms 0-93177
 p-InSb, heavily doped, LO phonon-carrier interaction, Raman interf. line-shapes 0-93319
 n-InSb, phonon-assisted cyclotron reson. strongly depend. on surface condition 0-70755
 InSe, exciton and polaron anisotropies, reson. Raman scatt. study 0-76033
 K, ultrasonic attenuation at low temp., spherical Fermi surface model 0-84255
 KI, perturbed by Jahn-Teller centres, lattice dynamics 0-107394
 MgO:Co²⁺, electronic and impurity-induced Raman scatt. 0-100659
 Mo, diffuse electron scatt. (Russian) 0-103438
 Mo, effective mass meas. and electron velocities 0-96773

electron-phonon interactions continued

- Mo, elec. resist., quadratic contrib., 2 to 40K (*Russian*) 0-92874
 NO_2^- ion in nitrite salt cryst., $^{13}\text{B}_{1-11}\text{A}_1$ transition spectra, reasons for diffuseness 0-97276
 NaF, quasimolecular struct. characts. of NaL_{1111} absorpt. edge 0-93436
 NaI:F, electron-lattice coupling of F-centres, optical props. 0-60641
 Nb, diffuse electron scatt. (*Russian*) 0-103438
 Nb, effect of changes in $\alpha^2(\Omega)\text{F}(\Omega)$ on the zero-temp. energy gap 0-97025
 Nb, electron-phonon interaction, relativistic, APW calc. 0-92837
 Nb, superconducting, thermodynamic props. 0-107955
 Nb-Al, diffuse electron scatt. (*Russian*) 0-103438
 Nb₃Sn, effect of changes in $\alpha^2(\Omega)\text{F}(\Omega)$ on the zero-temp. energy gap 0-97025
 Nb_{1-x}V_xSe₂, elec. and mag. anomalies at CDW transition 0-107722
 Nd(OH)₃, dynamical effects of interaction between 4f electrons and optical phonons 0-108196
 Ni, electron-phonon coupling, point contact spectroscopy obs. (*Russian*) 0-70342
 Pb, effect of changes in $\alpha^2(\Omega)\text{F}(\Omega)$ on the zero-temp. energy gap 0-97025
 Pb, pure and dil. alloys, diffusion thermopower, inelastic electron-phonon interaction 0-96851
 PbMo₃S₈, supercond. Chevrel phase, electron tunnelling spectroscopy expts. (*German*) 0-107966
 Re, elec. resist., quadratic contrib., 2 to 40K (*Russian*) 0-92874
 Re, Fermi surface, RF size effect, temp. depend. 0-65424
 Ru, elec. resist., quadratic contrib., 2 to 40K (*Russian*) 0-92874
 RuO₂, thermal conductivity meas., rel. to elec. cond. 0-65317
 Si, laser induced dense plasma, dynamics 0-65612
 Si, non thermal laser induced ordering, plasma life time, phonon interactions 0-84481
 Si:Li, electron-phonon scatt., in intermediate conc. region 0-65180
 Si:Li, thermal cond., low temp. phonon scatt., internal strain effects 0-96706
 Si:P, thermal cond., electron-phonon interaction at low temps. 0-92730
 Si-SiO₂ interface, remote polar phonon scatt. in Si inversion layers 0-80095
 SmS, lattice dynamical model 0-96610
 Sm_{1-x}Y_xS, mixed valence system, theory 0-70343
 SnTe, dispersive transform., interband electron-phonon interactions, phase diagram 0-93252
 SnTe, structural phase transition threshold instability in strong EM field 0-103477
 Ta, effect of changes in $\alpha^2(\Omega)\text{F}(\Omega)$ on the zero-temp. energy gap 0-97025
 Ta, electron-phonon interaction, relativistic, APW calc. 0-92837
 Tb(OH)₃, dynamical effects of interaction between 4f electrons and optical phonons 0-108196
 TbZn, ferromag., thermoelec. power, temp. depend. and crit. behaviour 0-96852
 Tc, rel. to superconductivity and Fermi surface calcs. 0-70873
 Ti-Cr, diffuse electron scatt. (*Russian*) 0-103438
 Ti-Mo, diffuse electron scatt. (*Russian*) 0-103438
 Ti-Nb, diffuse electron scatt. (*Russian*) 0-103438
 TI films, supercond. amorphous, effective phonon spectrum and lattice sp. ht. 0-70895
 V, electron-phonon coupling constant calc. (*Russian*) 0-70624
 V, electronic structure, model potential calcs. (*Russian*) 0-100431
 V oxides, change in phonon damping due to metal-insulator transition 0-103625
 V_{1-x}, mag. 'Bragg' scatt. obs. through Raman scatt. 0-66179
 VO₂, magnetic susceptibility in insulating and metallic phases, electron-electron and electron-lattice interactions 0-96788
 VO₂, metal-insulator transition and electronic struct., ion bombard. effects 0-92948
 W, elec. resist., quadratic contrib., 2 to 40K (*Russian*) 0-92874
 Y(OH)₃, dynamical effects of interaction between 4f electrons and optical phonons 0-108196
 Zn_{1-x}Hg_xSe, current carrier scattering mechanism 0-65546
 ZnSe crystals, doped and undoped, optical absorption edge 0-60626
 ZnSe, multiphonon ionisation of deep point centres in a charged dislocation field (*Russian*) 0-100281
 ZnTe:Li, electron-phonon interactions in Raman scatt. 0-60594
 Zr, H(D) implanted, superconductivity enhancement obs. 0-70884
 ZrS₃, quasi one-dimens. semicond., elec. transport props. 0-107790

electron-positron inclusive interactions

- annihilation, 12-31.6 GeV, τ production and decay branching ratios, lifetime 0-78052
 annihilation, 30 GeV, inclusive K^0 prod. $\text{K}^0\text{K}^+/\mu^+\mu^-$ prod. ratio 0-91103
 annihilation, charge current asymmetry as QCD test, neutral gluons 0-57616
 annihilation, charged Higgs boson prod. signatures, Weinberg-Salam parametrisation 0-57620
 annihilation, CM energies 29.90-31.46 GeV, narrow resonance search upper limit 0-63003
 annihilation, hadron and lepton prod., τ -lepton decay, K^{\pm} , p, \bar{p} yields, quark flavours 0-73725
 annihilation, hadron prod. total cross section, CM energies 1.4-2.0 GeV 0-57619
 annihilation, narrow resonance search upper limit at PETRA, 29.90-31.46 GeV 0-57618
 annihilation, QCD and jet acollinearity, quark-gluon coupling 0-105914
 annihilation, QCD and semilocal duality (hadrons/ $\mu^+\mu^-$) cross section ratio 0-78085
 annihilation, quark fragmentation in field-theoretic model of composite hadrons 0-82986
 annihilation, quark jet fragmentation into mesons and baryons, chain decay model 0-63001
 annihilation, superheavy flavour prod., weak current effects, Z^0 effects 0-57614
 annihilation, three-jet analysis, minimisation of sum of squares of transverse momenta 0-63008
 annihilation and deep inelastic leptonproduction, structure functions, QCD and parton model 0-63010
 annihilation and deep inelastic reactions, jet anal., thrust distrib., summing leading logs 0-63004
 annihilation and hadron-induced events, multiplicity ratio 0-105877
 annihilation cross section, fourth-order QCD contribs. 0-82987
 charmed meson produced in e^+e^- annihilation 0-91106

electron-positron inclusive interactions continued

- e^+e^- —hadrons, 9.4-10.4 GeV, three T states, mass spacings, lepton pair widths 0-68465
 hadron multiplicity at 10 to 40 GeV 0-63007
 hadron production, inclusive study, momentum distrib., energy and multiplicity 0-57613
 hadron production, multiplicity distribution, Regge like parton model (*Russian*) 0-78100
 hard processes, large rapidity separation of baryonic number, partons, and dual topology 0-95255
 heavy particle pair production, secondary particle distribs., τ properties 0-62960
 Higgs particle search at PETRA using Wilczek mechanism 0-105838
 high energy data from PETRA, QCD anal., QCD coupling constants 0-82985
 high energy interactions (*Chinese*) 0-78074
 inclusive hadron prod., polarisation and p nonconservation asymmetries, π , K^{\pm} , D^{\pm} prod. 0-78084
 jet structures of leptons, quarks and gluons, perturbative QCD, process dependence 0-68470
 jets, colour-singlet subsystems, large rapidity gaps 0-68469
 jets, two-particle distribs. from single-particle fragmentation functions, effects of heavy quark flavours 0-68468
 meson production, b-quark quantum number mesons, cross-section from equivalent photon approx. 0-68467
 new particles observed in e^+e^- annihilation 0-95283
 PETRA results for fluons, nuclear forces, t-quarks and quark-lepton symmetry 0-86731
 prospects at high energies 0-91074
 QCD jet simulation, cutoff choice effects 0-102015
 quark jets, transverse momentum profile 0-57621
 spacelike features and asymptotic behaviour of e^+e^- annihilation 0-86630
 spin dependent photon structure functions from Drell-Yan and e^+e^- reactions 0-82973
 U(1)×SU_c(2)×SU(3) theory, integer charge quarks, lepton hadronic processes (*Russian*) 0-86653
 weak interactions, summer school, Varenna, Italy (Jul. 1977) 0-90597
 $\text{D}-\text{K}^*\mu^-$, in e^+e^- annihilation, T-odd asymmetry in CP violation model (*Russian*) 0-105885
 e^+e^- —jets, on-shell QCD quark form factor from two particle correlations 0-86740
 e^+e^- —jets, transversely polarised annihilation, charged gluon jets, Pati-Salam model 0-86739
 e^+e^- —3 jets, integer charge quark model, gluon jets 0-91101
 e^+e^- —3 jets, three gluon coupling in perturbative QCD 0-105913
 e^+e^- —4 jets, differential 4-jet acoplanarity distribs., QCD predictions, heavy quark prod. 0-78083
 e^+e^- annihilation, gluon jets, multiplicity and ang. distribs. asymmetries 0-91105
 e^+e^- annihilation, opposite side quantum number correlations 0-105863
 e^+e^- annihilation, Q^2 duality test with nonrelativistic potentials 0-102011
 e^+e^- annihilation, recent DORIS results 0-91107
 e^+e^- annihilation at high energies and search for the t-quark continuum contribution 0-102012
 e^+e^- —bb, heavy quark masses and C- and P-odd asymmetries, Weinberg-Salam model (*Russian*) 0-102060
 e^+e^- —charmed hadrons, quark mass effect on fragmentation functions 0-91098
 e^+e^- collisions, jet prod. and two-photon annihilation, hadron spectra 0-91121
 e^+e^- —DD, above charm threshold at energy corresponding to $\psi(3770)$ 0-73723
 e^+e^- — $\Delta\chi$, polarisation effects in nonperturbative parton model, scaling 0-105912
 e^+e^- — e^+e^- BB, cross-section from equivalent photon approx. 0-68467
 e^+e^- — e^+e^- X, virtual 2 photon processes, luminosity functions, rapidity distrib., QED factors 0-86734
 e^+e^- — e^+e^- +2 jets, $\gamma\gamma$ — $q\bar{q}$ contrib. to cross section, QCD corrections 0-78106
 e^+e^- — e^+e^- χ_{bb} , cross-section from equivalent photon approx. 0-68467
 e^+e^- — e^+e^- η_{bb} , cross-section from equivalent photon approx. 0-68467
 e^+e^- — e^+e^- $q\bar{q}(q\bar{q})$ + jet, $\gamma\gamma$ initiated 3 jet events in QCD 0-102057
 e^+e^- —gluon and quark jets 0-91100
 e^+e^- — $\gamma\chi$, angular asymmetries, weak contribs. 0-101976
 e^+e^- — $\gamma\chi$, obs. at DORIS 0-102058
 e^+e^- — $\gamma^*\text{e}^+\text{e}^-$ + hadrons, QCD predictions 0-63009
 e^+e^- — γ^* —hadrons, hadron calorimetric meas., QCD predictions, gluon emission 0-91102
 e^+e^- —hadrons, 12, 30 GeV, jets, quark fragmentation and coupling constant, QCD comparison 0-105915
 e^+e^- —hadrons, 12, 30 GeV, $\pi, \text{K}, \text{p}, \bar{\text{p}}$ production 0-105916
 e^+e^- —hadrons, 33-35.8 GeV, new quark flavour search, cross sections and thrust 0-86736
 e^+e^- —hadrons, fourth T state observation in annihilation events 0-86737
 e^+e^- —hadrons, higher order QCD corrections 0-95280
 e^+e^- —hadrons, jets from heavy quarks, QCD perturbation theory 0-63012
 e^+e^- —hadrons, non-perturbative QCD vacuum, total cross section corrections 0-86735
 e^+e^- —hadrons, parton model and QCD 0-105860
 e^+e^- —hadrons, QCD test 0-102006
 e^+e^- —hadrons, R problem, QED and QCD corrections, quarks and leptons 0-95281
 e^+e^- —hadrons, semiinclusive hadron prod., quark fragmentation function corrections, QCD 0-63013
 e^+e^- —hadrons, two and three point energy correlations, QCD struct. 0-102019
 e^+e^- —hadrons, T, T', T'' states, mass differences, leptonic width ratio 0-68466
 e^+e^- —hadrons, T'' observation at CESR, mass and leptonic width 0-86738
 e^+e^- —hadrons ($\mu^+\mu^-$), T(9.46) muonic branching ratio, total and leptonic width 0-86703
 e^+e^- —jets, energy cone distrib. around jet axis, QCD anal. 0-86732
 e^+e^- —jets, exclusive calcs. for QCD jets, Monte Carlo approach 0-105911
 e^+e^- —jets, jet ang. momentum, ang. distrib., oblateness and invariant mass, QCD calcs. 0-73722
 e^+e^- —jets, particle ratios from quark statistical model 0-73724

electron-positron inclusive interactions continued

- $e^+e^- \rightarrow$ jets, t-quark pair prod. effects in annihilation, Kobayashi-Maskawa model 0-86733
 $e^+e^- \rightarrow$ multihadrons, planar three jet events, gluon bremsstrahlung, strong coupling constant 0-57617
 $e^+e^- \rightarrow \pi^+\pi^-\pi^0$, 1.45-1.875 GeV, ω behaviour at 1.55 GeV 0-82984
 $e^+e^- \rightarrow \pi^+\pi^-\pi^+\pi^-$, 1.45-1.875 GeV, ρ behaviour at 1.55 GeV 0-82984
 $e^+e^- \rightarrow \psi(3770)$, cross section, ψ mass, total width and e^+e^- partial width 0-73696
 $e^+e^- \rightarrow$ QQ, heavy quark study approach 0-105859
 $e^+e^- \rightarrow$ q \bar{q} g, (3g), jet-mass spectra, perturbative QCD 0-63006
 $e^+e^- \rightarrow$ q \bar{q} g, cross sections and ang. distrib. 0-102061
 $e^+e^- \rightarrow$ q \bar{q} g, gluon bremsstrahlung, neutral current and beam polarisation effects 0-99106
 $e^+e^- \rightarrow$ q \bar{q} g, gluon fragmentation, polarised 0-82988
 $e^+e^- \rightarrow$ q \bar{q} g, long, polarised beams, beam-event asymmetry, massless QCD null result 0-91104
 $e^+e^- \rightarrow$ quark jet, dimensionally regularised box graphs, zero mass case 0-102005
 $e^+e^- \rightarrow$ quark jet, two particle correlations in QCD 0-105858
 $e^+e^- \rightarrow$ three jets, acoplanar angle relative to beam polarisation, vector/scalar gluons 0-63005
 $e^+e^- \rightarrow \tau^+\tau^-H^0$, Higgs scalar boson production, Weinberg model calcs. (Russian) 0-68442
 $e^+e^- \rightarrow$ VX, parton model, polarisation effects (Russian) 0-63002
 $e^+e^- \rightarrow$ VX, polarisation states and differential cross sections for πA_1 and $\rho^+\rho^-$ (Russian) 0-102059
pp, 62 GeV/c, multiparticle prod. mech., e^+e^- comparison in parton model 0-78103
q \bar{q} decay, semiclassical model, vacuum polarisation by colour field 0-63011
qq \bar{q} diquonium states, production in e^+e^- processes 0-57615
 $\tau \rightarrow K^*\pi\nu$, in e^+e^- annihilation, T-odd asymmetry in CP violation model (Russian) 0-105885

electron-positron interactions

- see also *electron-positron inclusive interactions; electron-positron scattering; positron annihilation in liquids and solids*
errors on ratios of small numbers of events 0-105879
hadron polarization operator nonsuperrenormalizable model, rainbow approx. of $(\lambda/2)\Phi^4$ model 0-105821
pair annihilation in superstrong magnetic fields, appl. to neutron stars 0-85847
 $SU_1(2) \times U(1)$ and $SU_1(2) \times SU_3(2) \times U(1)$ predictions at high Q^2 , neutral currents, Z-bosons 0-63029
 $e^+e^- \rightarrow e^+e^-(\gamma\gamma)$, 27.7-31.6 GeV, QED test, Weinberg angle 0-77995
 $e^+e^- \rightarrow e^+e^-(\mu^+\mu^-)(\gamma\gamma)$, 12-31.6 GeV, QED test and Weinberg angle 0-91027
 $e^+e^- \rightarrow e^+e^-(\mu^+\mu^-)(\tau^+\tau^-)$, high energy colliding beams, Mark J detector study 0-95282
 $e^+e^- \rightarrow FF(B\bar{B})$, $\tau\nu$ decay signature for F^\pm and B^\pm detection 0-91099
 $e^+e^- \rightarrow \gamma\gamma$, 9.4-31.6 GeV, differential cross section, T- $\gamma\gamma$ decay limits 0-91073
 $e^+e^- \rightarrow \gamma\mu\bar{\mu}$, neutrino counting, $e^+e^- \rightarrow 3\gamma$ background 0-68441
 e^+e^- initiated $\gamma\gamma$ processes, charged pair prod., $R_{\gamma\gamma}$ width 0-91123
 $e^+e^- \rightarrow l^+l^-$, neutral current effects around vector resonances, polarisation 0-105878
 $e^+e^- \rightarrow \mu^+\mu^-$, 9.4 GeV, QED test 0-101965
 $e^+e^- \rightarrow \mu^+\mu^-$, radiative corrections around Z^0 , Weinberg-Salam model 0-99103
 $e^+e^- \rightarrow$ O particle, decay, mass, prod. from Zweig rule intermediate vector particle model (Chinese) 0-73697
 $e^+e^- \rightarrow \pi^+\pi^-(K^+K^-)$, $\sqrt{s}=1.5$ GeV, EM timelike form factors for π and K 0-91089
 $e^+e^- \rightarrow \pi^+\pi^-\pi^0$, 750-1100 MeV, ω and ϕ meson interference 0-105910
 $e^+e^- \rightarrow W^+W^-(\gamma e^+e^- W^+W^-)$, Yang-Mills coupling 0-68443
 $e^+e^- \rightarrow W^+$ hadrons, from Z^0 pole to threshold 0-105917
 $\gamma^*\gamma^* \rightarrow 2$ jets in e^+e^- , parton model QCD corrections for doubly deep processes 0-73758
He, positron decay rate nonlinear density depend. 0-71509

electron-positron scattering

- see also *electron-positron interactions*
QED test at 9.4 to 31.6 GeV 0-101965
 $e^+e^- \rightarrow e^+e^-$, T(9.46) electronic branching ratio and total width 0-86702
 $e^+e^- \rightarrow e^+e^-(\gamma\gamma)$, 27.7-31.6 GeV, QED test, Weinberg angle 0-77995
 $e^+e^- \rightarrow e^+e^-(\mu^+\mu^-)(\gamma\gamma)$, 12-31.6 GeV, QED test and Weinberg angle 0-91027
 $e^+e^- \rightarrow e^+e^-(\mu^+\mu^-)(\tau^+\tau^-)$, high energy colliding beams, Mark J detector study 0-95282

electron probe analysers see *electron probe analysis***electron probe analysis**

- Auger scanning microprobe, approach to damage-free anal. 0-89581
backscattering theory, using Boltzmann transport equation 0-57439
bone and cartilage, calcification studies using X-ray microanalysis 0-76885
 α - β brass, interface segregation 0-89231
brass, nondestructive determ. of in-depth profile 0-93836
coal particles and composition determ., computer evaluation of SEM images 0-71994
conference, electron microscopy and analysis, Brighton, England (Sept. 1979) 0-67936
correction procedure for quantitative microanalysis, crit. appraisal 0-85242
daguerreotypes, plates and process obs. 0-68286
diamond, industrial, anal. cathodoluminesc. studies in SEM 0-81410
dispersion influence on lateral resolution of X-ray microanalysis in STEM 0-85257
energy dispersive X-ray spectrometry, qualitative and quantitative analysis problems 0-85249
energy-loss analysis, single crystals, in TEM, diff. conditions influence 0-81406
energy-loss analysis, theory and instrum. 0-81405
energy-loss spectroscopy, as analytical tool, data handling and processing 0-81407
field emission micro SEM, for UHV surface anal. 0-86519
films, orientation effects in quantitative X-ray microanal. 0-85259
films on substrates, charact. fluoresc. effects calc. 0-81408
fracture surfaces, quantitative analysis problems in energy dispersive X-ray spectrometry with Si(Li) diodes (French) 0-89571
glaze/glass-ceramic, interface reactions, electron microprobe anal. 0-84398

electron probe analysis continued

- Hastelloy-X, Ni-Cr-Fe-Mo, cyclic oxidation resist. improvement by high temp. etching treatment 0-97627
in-situ gas reaction cell, for field emission SEM 0-81415
Inconel 617, creep, morphological changes of carbides, affect on creep props. 0-108509
kaolin bodies, effect of mineralizers on firing shrinkage, microstruct. and strength 0-97488
light elements, ultrasoft X-ray spectroscopy, local anal., electron-microprobe excited radiation 0-99027
LSI surface analytical techniques applied to electronic components [Si LSI chip inspection] 0-81392
microbeam analysis, lateral resolution 0-101064
mineral fibre characterisation using energy dispersive X-ray spectrometry in TEM (French) 0-82857
mineralogical use of energy dispersive X-ray spectrometry with Si(Li) diodes (French) 0-85251
minerals, Na and K determ., low temp. sample holder design (French) 0-85248
Murchison carbonaceous chondrite meteorites, Si in metal grain, electron probe anal. 0-77363
peak-to-background method for quantitative anal. of single particles, development progress 0-73541
portland cement, doped with ZnO, struct. and props. 0-60914
scanning cathodoluminescence microprobe analyser 0-81409
scanning microprobe microscopy, conf., Paris, France (Oct. 1979) 0-82569
SEM electron probe microanal. by means of X-ray spectrometers, review 0-95194
steel, Al semikilled, (Fe,Mn_{1-x})O.Al₂O₃ inclusions, deoxidation, thermodynamic conditions 0-60830
steel, Al-Cr, FeO.(Al,Cr)_{1-x}O₃ inclusions, thermodynamics 0-60831
steel, austenitic stainless steels, unalubricated, friction, wear and microstruct. of types 304, 316 and Nitronic 60 0-108589
steel, austenitic type 304, sensitised, intergranular stress corrosion cracking inhibition study 0-100939
steel, ball bearing, fatigue damage, influence of dispersed phases in martensitic matrix 0-108549
steel, Cr (10 wt.%), precip. free ferrite form., STEM 0-84941
steel, Cr-Mo, ferritic, grain boundary segregation, X-ray microanal. by STEM 0-66740
steel, Cr-Mo, oxidised, mechanism of crack decoration of oxides by electrodeposition 0-97560
steel, eutectoid, Si partitioning during pearlite transform., analytical electron microscopy applic. 0-108458
steel, ferritic Cr-Mo type, microanalysis of precipitates using TEM 0-108688
steel, stainless, corrosion and grain boundary penetration on exposure to coal gasification environment 0-61003
steel, structural, supercooled austenite, structural characts. of decomposition 0-60870
steel, tool and high-speed, high freq. induction melting and centrifugal casting in instrumental anal. 0-84886
steel foil, microanalysis by energy dispersive X-ray spectrometry (French) 0-85250
steels, stainless, surface characterisation rel. to adhesive bonding chem. etching, SEM, AES, XPS and electron probe microanal. 0-88416
STEM, precipitates in Ni-base superalloy 0-104492
STEM, structural and chemical analysis, appls. 0-88003
surface microstructure determ. and microanalysis by ultrahigh vacuum field emission gun SEM 0-96423
TEM, appl. to Nb₃Sn thin films 0-104491
TEM, contamination reduction using liq. N₂ cold trap assembly 0-101056
TEM/STEM performance, Philips EM 400, with field emission gun and twin lens 0-57441
thin foil, X-ray microanalysis in electron microscope (French) 0-61191
ultrathin tissue sections, P standards for electron probe X-ray microanalysis 0-98193
window glass, knots and cords, EPMA characterisation 0-84085
X-ray microanalysis, in TEM up to 1000 kV 0-101063
X-ray microanalysis, quantitative investigation of thin specimens 0-101068
X-ray microanalysis, spatial resolution in thin foils 0-101065
X-ray microchemical analysis, optimising conditions 0-101067
X-ray quantum counters, dead time determ., accuracy estimation 0-99022
X-ray spatial resolution, for SEM and STEM specimens 0-101066
Ag-In-Sn, internal oxidation, precipitation behaviour of oxide (Japanese) 0-66515
AgMg two phase bicrystal, growth by solid state diffusion couple method 0-60773
Al, small spheres, bulk plasmons damping 0-75561
Al-Mg-Li alloy, metastable S'-phase, struct. (Russian) 0-103291
Al-Si (0.57 at.%), Si precipitate dissolution kinetics 0-84935
Al₂O₃, sintering temperature effect of titanate additions 0-60808
Al₂O₃-glass seals, diffusion of Al, electron microprobe study 0-107577
3.Al₂O₃.2SiO₂, mullite, decomposition by SiO₂ volatilisation 0-61082
Au, thin foil, spatial resolution of X-ray microanalysis 0-101065
B-Si, (0 to 14.3 at.%), phase charact., regions of existence (French) 0-104117
B-Si alloys, B-rich, prep., anal. and cryst. growth (French) 0-104091
CdS_{1-x}Se_x, chem. comp. and luminescence obs. 0-80869
Cd_{1-x}Zn_xS solar cell thin films, microprobe characterisation (French) 0-61349
CePd₂, single crystal Czochralski growth and characterisation 0-60767
Co-Ge binary system, phase diagram rel. to that of Ni-Ge (French) 0-97463
Co-mischmetall system, phase relations, microstruct., mag. props. 0-104118
Co-WC hard alloys, rapidly quenched struct. 0-76233
CoF₂, antiferromag. crit. props., neutron scatt. obs. 0-88749
Co₂Sm crystals, microstruct., homogeneous precip. and nucleation 0-104160
Co_{1-x}Zn_xF₂, antiferromag. crit. props., neutron scatt. obs. 0-88749
Cr, corrosion in SO₂, 700-1000°C 0-97642
Cr-Ge system, phase diagram, thermal anal., X-ray diff., microhardness, and electron probe anal. (French) 0-97462
Cr₂₃V_{0.7}Fe_{3.4}C₃, stacking fault study, morphology, comp. and struct. 0-84190
Cu/Sn-Ni/Au tricouples, electrodeposited, interdiffusion obs. 0-84331

electron probe analysis continued

- Cu-Ga, binary alloy constituent EDS anal., secondary fluorescence, SEM study (*Chinese*) 0-85231
 Cu-Ni-Ti system, phase equilibria in Cu rich region and Cu-Ti quasi-binary constitution (*Japanese*) 0-89203
 Fe, cast, tensile strength, Al addition effects (*Korean*) 0-71736
 Fe-Cr-O system, phase relations at 1200°C using diffusion couple technique 0-89205
 Fe-Mn cast alloys, homogenisation annealing and chemical diffusion (*Czech*) 0-66551
 Fe-Ni, grain boundary segregation, X-ray microanal. by STEM 0-66740
 Fe-Ni-Cr (30.6, 21.3 wt.%), Alloy 800, high temp. oxidation at low O₂ press., SEM, AES and electron probe microanal. study 0-93688
 Fe-Ni-Cr-Al-Y, oxidation mechanism, Y addition effect on kinetics and oxide adherence 0-97623
 Fe-Ni-(P), phase diagram determ., 700 to 300°C 0-108399
 Fe-Si (3wt.%), grain-oriented, secondary recryst., grain growth inhibition 0-89245
 Fe₃Ni₃Cr₁₄B₆ metallic glass, crystn. kinetics by TEM 0-75186
 GaAs, binary alloy constituent EDS anal., secondary fluorescence, SEM study (*Chinese*) 0-85231
 GaP-N LED structures, local dopant conc. determ. using SEM cathodolum. spectra 0-101057
 Gd₂O₃-Ga₂O₃ system, phase diagram relationships of garnet-perovskite transform. 0-97460
 HF with interstitial O, quantitative TEM obs. of small agglomerates 0-107227
 Hg, quantification of losses in X-ray microanal. 0-85261
 KMn_{1-x}Ni_xF₃, antiferromag. crit. props., neutron scatt. obs. 0-88749
 LaNi₄B₆, H₂ absorpt. props. 0-88432
 La₂Si₂O₇N₂ single cryst. growth by floating zone method with SiO₂-Si₃N₄ additions 0-93481
 LiNbO₃/Ti, planar and channel optical waveguides, anisotropic diffusion expts. 0-64200
 Lu_{2-x}Si₂O₇Eu_x, synthesis and spectroscopic study 0-84846
 MnSi-Si system, striations and cryst. struct. of matrix 0-103292
 Mo powder, influence of powder reduction processes on props. 0-89175
 NaCl-KCl system, interdiffusion, miscibility, Kirkendall effect 0-107568
 Na₂O-CaO-SiO₂ molten glass, electrolysis reactions 0-89496
 Na₂O-TiO₂-SiO₂ glass, co-ordination of Ti, X-ray emission spectra study 0-84072
 NbGa₂O₃, O stabilised cpd., struct. determ. 0-103301
 Nb₃Sn-Cu multifilamentary composite wire, Nb₃Sn filament morphology and grain size 0-100855
 Ni-(Co)-Cr, aluminide coating, microstruct. and chem. 0-76189
 Ni-Al (2 and 6 wt.%), oxidation, α -Al₂O₃ growth, microstruct., precip. 0-108626
 Ni-Al-Nb ternary system, electron microprobe analysis of nickel-rich region at 1473K 0-71631
 Ni-Co-Al alloys, continuous precip., SEM, TEM, X-ray diffr. study 0-89220
 Ni-Cr-Ta system, phase equilib. of Ni rich region at 1523 and 1273K 0-93541
 Ni-Ge binary system, phase diagram rel. to that of Co-Ge (*French*) 0-97463
 NpO₂ single crystal growth, gas phase chemical transport method (*French*) 0-60760
 Pb₂GeO₁₁, sputtered ferroelec. films, prep. struct. and dielec. props. 0-75452
 Si diode, impurity profiles, scanning electron microprobe anal. 0-79832
 SiO₂-Al₂O₃ porous catalysts, EPMA quantitative anal., new correction calc. method, modified ZAF method (*Japanese*) 0-93822
 SiO₂-MgO porous catalysts, EPMA quantitative anal., new correction calc. method, modified ZAF method (*Japanese*) 0-93822
 Sm₂O₃-Ga₂O₃ system, garnet-perovskite transform., phase diagram relationships 0-97460
 Ti-TiB (4.32 wt%), high temp. oxidation kinetics under 1 bar pressure, 1255-1471K 0-89410
 Ti-Ta (4.37 wt%), oxidation kinetics, 1258-1473K, and at pressure of 0.013, 0.133 and 1.0 bar 0-89411
 (U,Ce), U self-diffusion 0-92711
 (U,La)C, U self-diffusion 0-92711
 (U,Pu)C, sintering, role of Ni as sintering additive 0-84892
 (U,Y)C, U self-diffusion 0-92711
 (U,Zr)C, U self-diffusion 0-92711
 U-Y-C FBR nuclear fuels, phase anal., 1400°C 0-66485
 UC, sintering, role of Ni as sintering additive 0-84892
 UO₂-PuO₂ fuel pin, hyperstoichiometric, post irradiation examination 0-63258
 VSe_{2-x}S_x (0<x<2) solid solutions, characterisation 0-88730
 WC-Co DC and RF sputtered coatings, bias effect, struct., X-ray-Auger study 0-70565

electron probe microanalysis *see electron probe analysis*

electron probe microscopy *see electron probe analysis*

electron probes

- see also electron probe analysis*
 aberration compensation, dynamical focusing with stigmator 0-87291
 Auger scanning microprobe, approach to damage-free anal. 0-89581
 beam deflection error assessment, expt. technique 0-78757
 correction of distorted spot shape using dynamic focusing and stigmator 0-57427
 field emission source advantages for restricted divergence probe 0-68324
 scanning electron probe voltage contrast, device ground level floatation 0-73527
 solid target, electron probe penetration and energy loss characts., diffusion model 0-96585
 STEM, thermal cathode illumination system, for round beam electron probe systems 0-57436
 thermal field emission source for high resolution, high current e-beam microprobes 0-68297
 variable-shaped beam systems, adjustment accuracy requirements for sub-micron pattern prod. 0-69312

electron-proton interactions

- see also electron-proton scattering*
 deep inelastic scatt., σ_L/σ_T ratio from quark model 0-82979
 deep inelastic scatt., quark-parton model with logarithmic scaling violation 0-78071
 ep \rightarrow epK⁺ π^+ K⁻ π^- , 1.8, 2.1, 2.5 GeV/c², meson resonance observ. 0-82982

electron-proton interactions continued

- ep \rightarrow ep $\pi^+\pi^-\pi^+\pi^-$, 1.8 GeV/c², meson resonance observ. 0-82982
 e \rightarrow p \rightarrow Wp ν , from Z⁰ pole to threshold 0-105917

electron-proton scattering

- see also electron-proton interactions*
 polarised scattering, asymmetries, gauge models 0-62991
 ep, deep inelastic scatt., higher order asymptotic freedom corrections 0-105903

electron radiation

- channelled electrons in crystals quasi-synchrotron radiation characts. 0-92572
 stimulated electron radiation due to wiggled magnetic field 0-58451

electron relaxation time (metals)

- alkali metals, elec. and thermal cond. in weak mag. fields 0-65535
 alloys, binary, elec. resist. near crit. point 0-96847
 dilute alloys, elec. transport and deviations from Matthiessen's rule 0-65524
 metallic glasses, electronic lifetime, noncommutative two-level model 0-103663
 W-Re amorphous alloys, phase-slip and localisation diffusion lengths 0-107747

electron resists

- conference on electron, ion and proton beam technology, conf., Boston, MA, USA (29 May-1 June, 1979) 0-67927
 PMMA, cross-linked positive electron resist, synthesis and props. 0-76221
 positive resist, plasma etching durability, additive effects 0-66683

electron ring accelerators

- compression system, IPP-Japan 0-95490
 EM induction conductor accelerator efficiency increase method 0-99355

electron scattering *see elastic scattering of electrons by atoms and molecules; electron beam effects; electron beams; electron-electron interactions; electron-electron scattering; electron impact; electron-nucleon interactions; electron-nucleon scattering; electron-nucleus reactions; electron-nucleus scattering; electron-positron interactions; electron-positron scattering; electron spectra; hadron electroproduction; neutrino-electron interactions; neutrino-electron scattering; secondary emission*

electron solvation *see solvation*

electron spectra

- see also Auger effect; conversion electron spectra; electron energy loss spectra; electron impact; electron spectroscopy; photoelectron spectra*
 acetophenones, di- and trisubstituted, $\pi^*\pi$ systems, UV electronic absorpt. spectra 0-74132
 acetophenones, mono substituted, semi empirical π -electron calcs. 0-74131
 anthracene surface, Ar impact, Penning ionisation electron spectra and photoelectron spectra 0-66352
 astronomical synchrotron radiation component, effect of interstellar mag. field inhomogeneities 0-85849
 electronic and at. collisions, conference, Kyoto, Japan (Aug.-Sept. 1979) 0-62394
 F-region, energetic electrons spectra meas. by Hadamard energy spectrometer (*Japanese*) 0-94637
 graphite fluorides, (CF)_n and (C₂F)_n, prep., struct., discharge characts., electrode props. 0-89502
 heterocyclic aromatic molecules, Penning electron spectra and photoelectron spectra, rel. intensities 0-95725
 ionosphere, winter, thermal electrons energy distrib. obs. by S-310-5 rocket (*Japanese*) 0-94636
 magnetopause, energetic electron spectrum meas. from Prognost 3 0-72697
 molecules, electronic excitation functions by low electron impact spectroscopy, trapped electron restrictions 0-69184
 multiply charged ion+atom, autoionisation, electron and photon emission 0-63813
 Penning ionisation processes investig. by electron spectroscopy 0-58364
 semiconductor detector active volume, determ. from gamma ray interactions, Monte Carlo method 0-63448
 Ar⁺+H, assoc. ionis., rovibronic struct. in electron energy spectrum 0-106380
 As₂Se₃-Pt, glass, effect of impurities on elec. props. 0-103699
 Cd, 5th P₁ autoionising state, 150 eV electron impact excitation, (e, 2e) ang. distrib. study 0-83495
 GaAs thin films, reactively sputtered, ESCA/XPS study 0-97430
 H₂, statistical fluctuations in ionisation yield, rel. to electron degradation spectrum 0-99581
 HF, Feshbach resons., predissoc. investig. 0-83433
 Ne⁺ scatt. electron spectra, distinction from neutral autoionising states 0-83482
 Ne⁺+H, assoc. ionis., rovibronic struct. in electron energy spectrum 0-106380
 O₂ electron coincidence spectrosc., valence electron momentum distrib. and binding energies 0-102583

electron spectrometers

- see also beta-ray spectrometers*
 cylindrical mirror, eqns. of motion of electrons theory 0-86503
 electron energy analyser used in Vacuum Generators HB5 STEM 0-73543
 electrostatic cylindrical electron vel. analyser, 127°, relativistic effects 0-86506
 electrostatic spectrometer, in plasma analyser expt. on Pioneer Venus Orbiter 0-67498
 Hadamard energy spectrometer, appl. to F-region energetic electrons spectra meas. (*Japanese*) 0-94637
 magnetic, corrected second-order aberrations 0-87013
 position sensitive multidetector based on charge coupled imaging device 0-86502
 retarding energy analyser, potential distribution of high resolution energy (*Japanese*) 0-68302
 trochoidal electron monochromator, optimization of parameters 0-86511
 two-channel coincidence, 0.7 ns resolution 0-91363

electron spectroscopy

- see also electron spectra; photoelectron spectroscopy*
 adhesion, surface chemistry studies, anal. appls. 0-88440
 alkali tetrachloroaluminate, vapor characterisation by photoelectron spectrosc. 0-81388
 alkali tetrafluoroaluminate, vapor characterisation by photoelectron spectrosc. 0-81388

electron spectroscopy continued

- ammonium tetrachloroaluminate, vapor characterisation by photoelectron spectrosc. 0-81388
 atomically clean surfaces, instruments for anal. and imaging 0-105749
 Auger microprobe, microcomputer controlled 0-81414
 binding energy and charge density meas., electron coincidence spectroscopy 0-63817
 cylindrical-mirror electrostatic analyser for beta spectroscopy of beams 0-63446
 electron capture spectroscopy, technique for surface science and ferromagnetism 0-92766
 energy loss, measurement of radiation damage 0-96568
 energy loss microanalysis system with high collection efficiency 0-86508
 energy-loss, as analytical tool, data handling and processing 0-81407
 energy-loss analysis, theory and instrum. 0-81405
 energy-loss spectral resolution optimisation using electron lenses between TEM specimen and electron spectrometer 0-101886
 failure analysis tools comparison and selection 0-71865
 gas atmosphere quantitative analysis adsorption chamber 0-85234
 graphite, electron-spectroscopic analysis of neutron-irradiated pyrographite 0-63261
 high resolution techniques 0-62740
 impact electron spectroscopy of molecular excitation functions, trapped electron restrictions 0-69184
 inelastic electron scattering: surface vibrational spectroscopy 0-107347
 inner-shell electron spectroscopy, for microanal. 0-68303
 ionising excited atom thermal energy collisions, electron spectrometric studies 0-63788
 kaolin bodies, effect of mineralizers on firing shrinkage, microstruct. and strength 0-97488
 magnetic prism beta spectrometer for low energies 0-99403
 metal oxides, ESCA, Madelung pot. effects 0-104036
 scanning Auger electron microscope, calc. of effects of backscattered electrons on spatial resolution 0-81412
 scanning Auger microscopy, developments 0-101909
 scanning Auger microscopy, resolution, quantification and sensitivity 0-81411
 steel, ferritic stainless, effect of Cl ions on passive layers 0-59766
 steels, stainless, passive state, electron spectroscopy anal. 0-59765
 surface anal. tools review 0-103540
 surfaces and interfaces, analysis by combined Auger, X-ray and SEM studies 0-81413
 surfaces and thin film studies by combined system of SIMS, AES and XPS 0-86536
 thin films, chem. anal. by energy loss spectroscopy 0-104493
 Al-Mg (2.5wt.%) sheet, surface oxide state and weldability 0-59769
 Fe-Cr-Al-Y, oxidation resistance, heat treatment and Al³⁺ ion implantation 0-71785
 n-InP, epitaxial layer, (100) surface chemistry, ESCA study 0-103552
 Li⁺+Ne collisions, vel. dependence of Ne 2s and 2p, vacancy production, electron spectroscopy 0-58344
 Ni passivation, S influence study by Auger and electron spectroscopy 0-65347
 Si, amorphous film, RF plasma deposition from SiCl₄-H₂, characterisation 0-66435
 Te compounds, electron spectroscopic studies (*French*) 0-108770

electron spin

- Dirac equation, mechanical sphere, magnetic momentum and lines of force (*Hungarian*) 0-68344

electron spin-lattice relaxation

- acoustic, liquids 0-97128
 benzil, cryst., excited triplet state spin-lattice relax. probabilities, temp. depend. (*Russian*) 0-88860
 benzophenone, migration of triplet excitons, EPR profiles and phosphoresc. decay data 0-84641
 ferromagnetic metals and semiconductors, electron spin-lattice relaxation (*Russian*) 0-103823
 Ga₂Al_{1-x}As, optically oriented electron, nuclei spin instability (*Russian*) 0-70660
 inhomogeneous systems, line broadening, spin-spin and spin-lattice relax. rate meas. 0-58292
 nitroxide free radicals in liquids, electron spin-echo obs. 0-63685
 ruby:Cr, relaxation behaviour, EPR study, environmental effects 0-66021
 ruby:Ti³⁺(V³⁺), cross-relax. 0-71163
 tris-sarcosine calcium chloride:Mn²⁺ ferroelec. dynamics, EPR and ENDOR study 0-75972
 uranyl phenanthraquinone radical ion complex, longitudinal spin-lattice relax. time determ. 0-108076
 β -Al₂O₃-Na₂O, colour centre ESR by localised tunnelling states 0-108073
 CdTe:Mn, spin-lattice coeffs. of Mn²⁺ 0-84646
 Ce₂Mg₃(NO₃)₁₂, spin-lattice relax., dynamic susceptibility meas., liq. He contact effects 0-66011
 Fe³⁺(⁶S) paramagnetisations, spin lattice relaxation Mossbauer study, dynamic spin Hamiltonian formalism 0-97173
 GaAs, electron-spin relaxation and recomb. kinetics, time-resolved luminesc. study 0-108074
 Gd³⁺ impurity ions, EPR spectra, linewidth narrowing due to spin-lattice relax. of lanthanide Kramers host ions 0-108061
 n-InSb, spin polarisation, anisotropic size effect, effect on CESR signal 0-70743
 K halides, spin-lattice relax. of O₂⁻ centre 0-88863
 KCr alum, relaxation behaviour, EPR study, environmental effects 0-66021
 LaF₃:Er³⁺, optically excited, direct-process spin-lattice relaxation 0-93378
 MgO:Cr²⁺, APR under applied stress 0-88865
 MgO:Cr³⁺, ODMR study, Cr³⁺ ions in tetragonal symm. sites 0-88892
 MgO:Fe³⁺, spin-lattice relax. time, meas. 0-66020
 MgO:Mn²⁺, spin-lattice relax. time, meas. 0-66020
 Mn II-lecithin lipid-water system, NMR and EPR obs. 0-61168
 NiSiF₆, dilute, single-spin cross-relax. calcs. 0-97129
 NiSiF₆·6H₂O, non-Kramers system, spin-lattice relaxation at strong fields 0-100612
 Rb halides, spin lattice relaxation meas. of O₂⁻ centre 0-88863
 Si:Cr(Mn), spin-lattice relax. of Jahn-Teller centres, coexistence of minima with different symmetries 0-80602
 TiO₂, Mn³⁺ ion electron spin-lattice relaxation 0-108054
 Y₂SiO₅:Ce³⁺(Nd³⁺)(Er³⁺)(Yb³⁺), EPR and spin-lattice relax. 0-108063
 YbCl₃·6H₂O:Gd³⁺, EPR, temp. depend., spin-lattice relax. time 0-93173

electron spin-lattice relaxation continued

- zinc formate dihydrate: Co, spin lattice relax. of Co²⁺ ions 0-75847
 Zn(BF₄)₂·6H₂O:Ni, phase transition study, EPR of diluted Ni²⁺, 98-298K 0-75846
 ZnTe:Mn, spin-lattice coeffs. of Mn²⁺ 0-84646

electron spin polarisation

- see also CIDEPI: spin polarised electron emission*
 atomic and electronic collisions, polarisation phenomena, review 0-83501
 bacterial photosynthetic reaction centres, light induced electron spin polarisation 0-63681
 bremsstrahlung by transversely polarised electrons, azimuthal asymmetry due to spin-orbit coupling 0-60705
 chemical reactions, spin polarisation analysis using intermolecular interactions theory, chemical polarisation, exchange repulsion 0-76510
 chemically induced dynamic spin polarisation, orientation depend. 0-63656
 ferromagnetic semiconductor, doped, electron spin polarisation and conduction band struct. 0-65449
 ferromagnetic semiconductors, electronic quasiparticle spectrum 0-97051
 Heusler alloys, ferromag. alignment rel. to conduction electron polarisation 0-60235
 LEED, spin-polarised, symm. props. 0-96420
 LEED, spin-polarized, time reversal and spatial symmetries 0-87999
 magnetic surface props., polarised electron scatt. study 0-93160
 metals, spin and charge polarisation around mag. impurities 0-75714
 photoelectrons, ang. depend. of spin polarisations 0-78652
 rare earth intermetallic compounds, NMR anal. of indirect mag. interactions 0-71193
 rare earth intermetallics, RAl₂, orbital and spin polarisations of cond. electrons 0-65791
 semiconductor, spin-dependent recomb. and scatt. in presence of optical orientation of electrons 0-96908
 semiconductors, doped, local spin-density-functional method, appl. to metal-insulator transition 0-96789
 spin dependent phenomena in electron-atom collisions 0-63830
 transition metal 3d monoxides, specific vol. and mag. moment calcs. 0-65822
 Am, 5f-electron delocalisation 0-70595
 EuB₆, ferromag., spin-polarised energy band struct., APW calc. 0-96779
 EuO:Gd, surface mag. props. 0-71566
 Fe, ferromag. film, surface states, surface magnetisation and electron spin polarisation 0-65648
 GaAs, electron-spin relaxation and recomb. kinetics, time-resolved luminesc. study 0-108074
 p-GaP:Zn,S, spin polarisation of donors and acceptors in mag. field, optical and microwave study 0-93393
 H, spin-polarised, Bose condensation, phenomenological description 0-77699
 H, spin-polarised, Bose-Einstein condensation 0-77698
 Hg, electron elastic scattering, 8 to 18 eV, electron spin polaris. 0-91669
 n-InSb, spin polarisation, anisotropic size effect, effect on CESR signal 0-70743
 KBr(I), photostimulated recomb., electron spin polarisation 0-60673
 Ni, ferromag. film, surface states, surface magnetisation and electron spin polarisation 0-65648
 Ni(001) surface states, surface magnetisation, electron spin polarisation 0-88612
 Pd, metallic, positive muon Knight shift 0-71280
 RbI, photostimulated recomb., electron spin polarisation 0-60673
 W (001), adsorption of N₂, effect on LEED electron spin polarisation and intensity profiles 0-65377
 W crystal-atom and W(001) surface, low-energy positron diffraction, theoretical study 0-83004
 W-EuS, amorphous, memory effect in field emission 0-89126
- electron spin relaxation** *see electron spin-lattice relaxation*
electron spin resonance *see paramagnetic resonance*
electron states, impurity *see impurity electron states*
electron states, surface *see surface electron states*
electron streams *see electron beams*
electron structure of solids (crystallography) *see crystallography*
electron structure of solids and liquids (energy structure) *see electron energy states (condensed matter)*
electron theory
see also Dirac equation; quantum electrodynamics
 Casimir model, self-stress in dielectric and conducting balls 0-86625
 gyromagnetic ratio in Coulomb field 0-82870
 spin, Dirac equation, mechanical sphere, magnetic momentum and lines of force (*Hungarian*) 0-68344
- electron theory of metals** *see metal theory*
electron traps
see also colour centres; hole traps; impurity electron states
 activation energy determ. by different trap spectroscopy techniques 0-75582
 bulk trap energetic distribution props., space charge limited current meas. use 0-80293
 carbohydrate compounds, X-irrad., trapped electrons, ESR and ENDOR obs. 0-93161
 chalcogenide glass films, threshold switching 0-96950
 covalent semiconductors, low temp. galvanomag. effects, shallow attractive traps 0-88575
 dibenzofuran:anthracene, cryst., prompt fluoresc., temp. depend., trap effects (*German*) 0-93400
 dielectric, solid thermally stimulated characts., dipolar relaxation time, trap levels and ionic space charge polarisation 0-84685
 DLTS, photo-excited, minority carrier trap meas. 0-96816
 electro-optical spatial light modulator resolution, stored point charge effects 0-106616
 energetical trap distrib., first principles model, linear finite defect chain 0-59912
 ESR and ENDOR obs. 0-93161
 ferrocene films, plasma-polymerised, carrier trapping, elec. cond. meas., 300 to 525K 0-100543
 III-V semiconductors, point defects and deep traps, thermodynamic history, model 0-59908
 lattice migration, diffusive and percolative excitons 0-59879
 lead acetate trihydrate:Mn²⁺, ESR, elec. cond. 0-93165
 MIS structures, dielectric layer, transient processes during charge trapping for injecting contact 0-70844

electron traps continued

- MOS interface states density, photoemission obs. using photocurrent and photocapacitance meas. 0-92990
 MOS structures, inversion layer near electrode edge, pot. and charge density distribution 0-88642
 MOS structures, quasistatic and nonequilibrium phenomena with constant gate-current bias 0-80385
 naphthalene, electron trapping, one-carrier TSC and SCL currents 0-70715
 phthalocyanine layers, metal-free, between Ag and Al electrodes, switching effects 0-65706
 poly- α -naphthol, semicond., isothermal depolarisation currents, electron trap parameters 0-60492
 poly-p-xylylene films, carrier traps, X-ray induced TSC, thermolum. and dielec. loss study 0-88570
 polycarbonate, and charge-transfer complex modifications, TSC 0-88572
 polyethylene, dielectric props., investigation for morphology changes created by mechanical drawing and annealing 0-84697
 polyethylene, space-charge storage under high DC voltage condition, TSC meas. (German) 0-75576
 polyethylene films, corona charged, charge trapping 0-88571
 polyhydroxy compounds, X-irrad., trapped electrons, ESR and ENDOR obs. 0-93161
 polymer, dielectric breakdown, DC trees caused by space charge accumulation, carrier injection and trapping effects 0-84695
 polystyrene atactic carrier transport and photogeneration 0-80318
 polystyrene thin films, TSC and surface charge meas. 0-103769
 polyvinylidene fluoride, X-ray induced TSC 0-75578
 quasifree excitons and electrons, impurity trapping 0-59880
 semiconductor, impact ionization, review 0-65577
 semiconductor, nonlinear conductivity, vortex waves, carrier mobility and lifetime 0-96893
 semiconductor lasers, triggerable, light-coupled logic appl. 0-74360
 semiconductor with arbitrary energy spectrum of trapped states, surface region of space charge 0-107811
 semiconductors, photocond., photoelec. effects, book contrib. 0-84488
 semiconductors, thermally stimulated conductivity luminescence, defect levels, traps, book contribution 0-80296
 space charge limited current-voltage charact., steady state, validity of anal. eqns. 0-107800
 sucrose, single cryst., absorption spectrum of electron traps, pulse radiolysis obs. 0-93369
 1,2,4,5-tetrachlorobenzene, mol. solid, heat pulses, phonon-induced delocalisation of trapped excited triplet states 0-89053
 thermally stimulated electron emission, dependence on heating rates, conduction electron retrapping probability (Russian) 0-84826
 thermoluminescence method for trap depth determ. 0-80211
 TSC, trap depth determ. theory 0-70716
 TSC with slow retrapping, trap depth determ. 0-59998
 TSC with two trapping levels, calc. 0-60489
 Ag specie nucleation and phase formation in latent image 0-97716
 Al/Al₂O₃/Al structures with organic monomolecular layer, cond. at high elec. fields 0-80402
 Al-Al₂O₃-Si structure, study of charge trapping 0-60097
 AlGaAs semiconductor lasers, single-mode stabilisation by traps 0-95893
 Al_{0.5}Ga_{0.5}As triggerable semiconductor lasers made by deep proton bombardment 0-69408
 Al₂O₃ anodic films, trapping levels study using TSC 0-103768
 Al₂O₃:Cr, pure and doped, electron irradi. induced cond., TSC and EPR study 0-80277
 As₂Se₃, modulated photocurrent, analysed for trap-limited case (Japanese) 0-60030
 BaTiO₃, reduction inhibition by impurity ions 0-101018
 CaF₂:Eu, Mn, cathodoluminescence SEM appl., stroboscopic 0-70088
 CaS:Pd phosphors, trap and luminescent centre location, photo-, thermo- and electroluminescence studies 0-71482
 Cd, positron trapping at low temp. lifetime spectra 0-84799
 CdS, electron and hole trapped centres, EPR, photoluminescence, photoconductivity study 0-108071
 CdS:Cu, C-V curves of MIS diode used to examine trapping levels 0-65697
 CdS:Cu, Cl films, photocond. growth and decay time 0-60041
 CdS-Cu₂S junctions, carrier trap density, deep level defects 0-107801
 n-CuInS₂, mag. props., obs. 0-70939
 (GaAl)As injection lasers operating with optical fibre resonators 0-91812
 Ga_{0.5}Al_{0.5}As, epitaxial, radiative deep states 0-76061
 GaAs, deep centre free energy level determ. by transient capacitance technique 0-103641
 GaAs, epitaxy by metallorganic and chloride depositions, defect characterisation at growth interface 0-59817
 n-GaAs, MBE, correl. between electron traps and growth processes 0-65387
 GaAs MOS structures, leakage current for anodic oxide layers, space charge trapping effects 0-60091
 GaAs, organometallic VPE, with varying As/Ga ratios, deep states 0-65480
 GaAs, proton irradiated, low energy, deep level defects and hole diffusion length meas. 0-60000
 GaAs Schottky barrier structure, defects from proton irradiation, thermal transients and optical capacity (French) 0-59534
 n-GaAs surface barrier diodes for nuclear radiation detection, deep trapping centres 0-92849
 GaAs type FET with buffer, bias effects due to deep centres in struct. (French) 0-107917
 GaAs:Cr, deep acceptor level, DLTS and optical DLTS study 0-92852
 GaAs:Cr, thermally grown, DLTS study of Cr trap density 0-96815
 GaAs_{1-x}P_xN, photolum. and electrolum. study of N isoelectronic traps 0-89061
 GaP crystals, radiation defects, TSC obs. 0-65588
 GaP:Ni(Fe), multivalence impurities, EPR and optical absorpt. meas. 0-75844
 Ge p⁺-n⁺ structures, large-scale trap charact. 0-92966
 Ge:P(Sb)(Bi), γ -irrad., carrier trapping and recomb. at point radiation defects 0-107810
 Ge:Sb, Ni(Mn), recombination wave spectrum, two-level traps 0-96906
 Ge-Si₃N₄ system, potential barriers determ. from photoinjection carriers trapping 0-103756
 H₂O, crystalline ice, localised excess electrons yield studied as function of dose rate 0-97712
 Hg_{1-x}Cd_xTe photodiodes, long cutoff wavelength, effect of trap tunnelling on IR detector performance 0-73451

electron traps continued

- α -HgS, trapping parameters determ. by TSC meas. 0-59997
 In_{0.5}Ga_{0.5}As_{1-x}P_x, epitaxial layers, characterisation and relation to lattice matching 0-100540
 InP:Fe shallow trap thermally stimulated cond. spectroscopy, photocond. spectrum under DC conditions 0-65585
 InSb MOS struts., energy spectrum of traps in oxide layer 0-107922
 La₂O₃:S:Eu, slow phosphoresc., high press. study 0-80839
 LiF TLD phosphor, residual thermoluminescence effect on sensitisation 0-108287
 LuYScO₄:Er³⁺(Tm³⁺)(Ho³⁺), thermolum. meas. 0-97354
 MgO doped powder phosphors, photo- and thermostimulated luminesc. obs. (Russian) 0-66263
 NaOH:CrO₄²⁻(NO₂⁻), electron tunnelling, pulse radiolysis 0-108722
 NaOH:Fe(Cn)₆³⁻, electron tunnelling, pulse radiolysis 0-108722
 Sb₂S₃ film, coevaporated, elec. cond. meas. 0-65726
 Se, modulated photocurrent, analysed for trap-limited case (Japanese) 0-60030
 Se₁₂Te₄₉As₂₉Ge₁₀ semiconductor amorphous films, field effect, trapping 0-84472
 Si junction diode, diffused, with deep level traps, negative capacitance 0-96976
 Si, n⁺-p diode, γ -radiation defects, annealing and recomb. props. 0-65045
 Si n⁺-p solar cells, degradation mechanisms associated with Ti impurities 0-81465
 Si p-n junctions, spin depend. surface recomb., electron irradiation effect 0-88627
 Si, polycryst., energy distrib. of trapping states, from impedance of MOSS struct. 0-65691
 Si, polycrystalline, phenomenological model for mobility 0-65564
 Si thin film, polycryst., CVD, elec. props. 0-107934
 n-Si wafer, trap centres of self-interstitials 0-75516
 Si:Al, localised exciton bound to isoelectronic trap 0-66283
 Si:Au, C-V curves of MIS diode used to examine trapping levels 0-65697
 Si:H, amorphous, defect photoluminesc. meas. 0-97334
 Si:H, amorphous, solar cells, trap spectroscopy using transient current techniques 0-104508
 Si:P(O) p⁺-n⁺ solar cells, comparison rel. to resistance to 1.5 MeV electron irradi., majority carrier trapping 0-94087
 Si:Se, photocapacitance and photoconductivity 0-107859
 Si:V p-n junctions, thermal emission rates and capture cross sections of majority carriers at V centres 0-96980
 Si-insulator interface, non-avalanche charge injection, expt. study, charge trapping effects 0-60099
 Si-SiO₂, MOS interface states density, meas. techniques and model development 0-92988
 Si-SiO₂, MOS interface states density, transient capacitance meas. eval. 0-92989
 Si-SiO₂-Mo-Si₃N₄-Al MNOS structures with metal grains, charge transport at SiO₂-Si₃N₄ interface 0-65693
 SiC, spin-flip scatt. of laser light from photoexcited excitons 0-93330
 SiO₂, As-implanted, electron trapping and detrapping charact. 0-65692
 SiO₂ layer used for MOSFETs, electron trapping behaviour 0-92981
 SiO₂ layers on Si, ionis. thresholds of electron traps 0-92983
 SiO₂ MOS capacitor, defect current obs. 0-92987
 SiO₂ thin films, radiation-induced trapping centres, rel. to MOS transistor technology 0-107804
 SiO₂, vitreous, charged defect centres 0-107745
 SiO₂, vitreous, paramag. centres associated with bonding defects 0-80609
 SiO₂:As⁺ implanted layers in MOS struct., electron trapping and detrapping charact. 0-92982
 SrFCl, thermolum. and optical absorption spectra 0-66309
 Sr:Nd, phosphorescence decay, trapping levels 0-104003
 TiGaSe₂, monocrystal, processes of recombination and trapping levels, photocond. meas. (Russian) 0-70751
 Zn₃P₂, thermoluminescence glow curve method for radiation induced traps 0-60689
 Zn₃(PO)₂, thermoluminescence glow curve method for radiation induced traps 0-60689
 ZnS, low-temp. trap anal. thermally stimulated luminesc. model extension 0-80877
 ZnS:Se₂₋, electron trap associated with anion vacancy, DLTS study 0-80210
 ZnSe, electron trap associated with anion vacancy, DLTS study 0-80210
 ZnSe, heat-treated in controlled partial press. of Zn or Se, TSC 0-59910
 ZnTe:Li, O, Hagemark theory, O modification isoelectronic trap 0-75517
 ZrS₂O₄, X-irradiated, trapping and emission centres, thermolum. meas. 0-89076
- electron tube components**
 see also electron guns
 Sm-Co ring magnets for BWO, 110 to 170 GHz, design and appl. (German) 0-105684
- electron tube diodes** see diodes
- electron tube manufacture**
 vacuum-deposited layers, stable structure formation 0-80979
- electron tube rectifiers** see rectifier tubes
- electron tubes**
 see also cold-cathode tubes; diodes; electron emission; microwave tubes; relativistic electron beam tubes; tetrodes; thermionic tubes; triodes; ultra-high frequency tubes; X-ray tubes
 No entries
- electron tunnelling** see tunnelling
- electron valves** see electron tubes
- electron-wave tubes**
 see also klystrons; magnetrons; travelling-wave-tubes
 No entries
- electronegativity**
 atomic electronegativity, density functional theory 0-99440
 atoms in molecules, diatom. shieldings rel. to electronegativity 0-102524
 binary compounds, energy gap trends, correl. with electron transfer parameters from optical spectroscopy 0-80174
 bases, liquid, thermodynamic props. (German) 0-66482
 carbenes, heterosubstituted, singlet-triplet splitting depend. on heteroatom electronegativity and conform. 0-63553
 diatomic mol., electronegativity, bond charge and chemical pot. approach 0-91703
 quartz, low, CC Si-O bond characteristics 0-84132

electronegativity continued

- AgBF₄, ionic radii and chem. shifts, correl. with electronegativity 0-66054
 Al chalcogenate and chalcogenite double salts, form. laws and acid-base props. 0-101070
 CsBF₄, ionic radii and chem. shifts, correl. with electronegativity 0-66054
 CsI crystals, relation of struct. and bond type to slip geometry 0-88165
 Cu-M-O ternary liquid alloys, thermochem. calcs. 0-85209
 Ga chalcogenate and chalcogenite double salts, form. laws and acid-base props. 0-101070
 H₂, electronic chemical pot., natural orbitals occupation numbers and electronegativity 0-63509
 In chalcogenate and chalcogenite double salts, form. laws and acid-base props. 0-101070
 LiF crystals, relation of struct. and bond type to slip geometry 0-88165
 NH₄BF₄, ionic radii and chem. shifts, correl. with electronegativity 0-66054
 PbS, crystals, relation of struct. and bond type to slip geometry 0-88165
⁶⁷Zn Mossbauer spectroscopy with 93 keV reson. 0-66095

electronic calculators

- for calculator applications see under relevant applications e.g. engineering computing; natural sciences computing
 desktop calculator library module, for advanced composite materials anal. 0-77764
 least square fitting, pocket calculator program with variable precision 0-67976
 programmable pocket calculator, short circuit current calc. (German) 0-68186

electronic conduction in crystalline semiconductor thin films

for electronic conduction in amorphous thin films, see "electrical conductivity of amorphous semiconductors and insulators"
 see also electrical conductivity of amorphous semiconductors and insulators; electrical conductivity of crystalline semiconductors and insulators; electrical conductivity transitions

- adenine film, polycryst., energy conversion processes, quantum yields, 4 to 10 eV 0-88589
 CdTe thin film on ferroelectric TGS, influence of polarisation reversal on elec. cond. 0-65720
 double injection in transverse mag. field, theory 0-80421
 films, elec. and galvanomag. props., microstruct. 0-70859
 germanium phthalocyanine, elec. cond. temp. depend. 0-80271
 ion beam milling, amomalous sputter yield behaviour 0-108624
 Kane semiconductor films, thermomag. and thermoelec. effects, theory 0-70864
 organic semiconductor films, Schrieffer effect 0-60118
 silicon phthalocyanine, elec. cond. temp. depend. 0-80271
 solar cells, thin film polycrystalline materials, resistivity and Hall effect meas. 0-93899
 p-terphenyl, polycryst., charge carrier transport and DC cond. 0-70858
 thymine film, polycryst., energy conversion processes, quantum yields, 4 to 10 eV 0-88589
 AgInS₃, and AgInS₃, spray pyrolysis, film struct., elec. and optical props. 0-71592
 Ag₂Re films, galvanomag. props. and quantum size effects, obs. 0-70866
 Al_{0.5}Ga_{0.5}As, compensated, electron mobility temp. depend. 0-96868
 Ba_{0.8}Sr_{0.2}TiO₃ films, DC conductivity, strong microwave field effect 0-65727
 Bi thin film, structure and electronic props. 0-70562
 Cd_{0.9}Hg_{0.1}Te layers, epitaxial graded-gap, nonlinear elec. effects 0-100468
 CdO-SnO₂ DC reactively sputtered films, elec. and optical props. 0-103763
 CdS films, prep. by reactive pulverisation, chemical, crystallographic and electronic props. (French) 0-60112
 CdS polycrystalline films, high strain sensitivity 0-93017
 CdS thin films, growth and evaluation for fabrication of high performance photovoltaic solar cells 0-93501
 CdS thin films on brass substrates, nondestructive resistivity meas. tech. 0-93898
 CdS:Cu, Cl films, photocond. growth and decay time 0-60041
 CdS:Cu(Cl) thin films, surface and bulk photocond. 0-88653
 CdTe film, photogenerated carrier transport props. 0-88590
 CdZnS thin films, growth and evaluation for fabrication of high performance photovoltaic solar cells 0-93501
 Cd_{1-x}Zn_xS films, thermal evaporation prep., phys. props. 0-84410
 Co_{0.5}Mn_{0.5}O₄, prep., struct. and elec. characteris. 0-108353
 CuIn_{0.7}Ga_{0.3}Se₂ epitaxial layers, on GaAs substrates, struct. and elec. props. 0-107670
 CuInS₂ films, RF sputtered, growth and props. 0-80124
 CuInS₂ thin films for solar cells, radiofrequency sputtering technique, elec. props. 0-93487
 CuInTe₂ epitaxial layers, on GaAs, growth and props. 0-108359
 Cu₂S, 1 ≤ x ≤ 2, quantum temp. size effect and magnetism (Russian) 0-103764
 EuS films, mag. and elec. props. rel. to stoichiometry and defects 0-97122
 Ga_{1-x}Al_xS₂:Zn, acceptor energy level and elec. props. 0-65482
 GaAs, compensated, electron mobility temp. depend. 0-96868
 GaAs compensated VPE thin film, electron Hall mobilities 0-107932
 n-GaAs, epitaxial, high temp. carrier transport 0-65725
 GaAs epitaxial layers on polycryst. GaAs substrates, LPE growth characts. 0-75471
 GaAs, ion-implanted layers, close contact capless annealing, elec. props. 0-84192
 GaAs:Ge film, MBE grown, heavily doped, elec. props. rel. to growth parameters 0-100537
 GaAs:Se(Zn) polycrystalline film, Hall effect, resistivity meas. 0-96911
 GaAs:Si, accelerated growth rate effect on MBE, Hall mobility and photolum. meas. 0-104067
 GaInAs-InP, growth by low-pressure metalorganic CVD 0-71595
 Ga_{1-x}In_xAs, on (111)B InP, LPE growth, characterisation of high purity lattice 0-104082
 Ga_{1-x}In_xAs-InP, MBE film growth, composition control obs. 0-84399
 GaN, VPE growth rate influence on elec. and luminesc. props. 0-100702
 Ge epitaxial film, ion implantation and electron beam anneal effects on carrier conc. 0-75255
 Ge epitaxial film, vac. deposited on GaAs, doping effect of annealed GaAs surface 0-65718

electronic conduction in crystalline semiconductor thin films continued

- Ge heteroepitaxial film, ethanol pulsed adsorption effect on elec. cond. 0-93014
 Hg_{1-x}Cd_xTe, epitaxial layers, elec. properties in the range 4.2 to 300K (French) 0-65721
 In₂O₃:Sn, RF magnetron sputtered film, elec. and optical props. 0-104065
 InAs films, MBE grown on GaAs, electron mobilities, lattice mismatch effect 0-80419
 p-In_{0.53}Ga_{0.47}As:Zn on InP, elec. and optical props. 0-75662
 In_{1-x}Ga_xAs:P_{1-y}, hole mobility over temp. range 77 to 300K 0-60111
 In₂O₃ films, activated reactive evaporation technique of prep. 0-80989
 In₂O₃ films, electron beam evaporation, elec. and optical props. (Japanese) 0-60784
 In₂O₃ films, reactively evaporated, elec. props. 0-84521
 In₂O₃, thermally evaporated film, struct. and elec. props. 0-104066
 In₂O₃, thin film, sputter deposition form., optical and elec. props. 0-60123
 In₂O₃:Sn, films, activated reactive evaporation technique of prep. 0-80989
 In₂O₃:Sn films; vac. deposited, elec. props. 0-100542
 In₂O₃:SnO₂ thin film, Hall mobility, temp. depend., grain boundary effects 0-75658
 InP epitaxial films, grown on heavily doped substrates, carrier mobility study, magnetoresist. meas. 0-60116
 InP, ion-implanted layers, close contact capless annealing, elec. props. 0-84192
 InSb recrystallised thin films on mica substrate, elec. props. 0-70867
 InSb, thin films, electrophysical props. obs. 0-103765
 InSb_{1-x}Bi_x, multitarget RF sputtering, metastable phase, conductivity transition 0-76178
 InSe films, residual photocond., field quenching 0-60037
 In₂Si₂O₇, thin film, sputter deposition form., optical and elec. props. 0-60123
 InTe thin films, flash evaporation, electrical props. 0-65722
 PBS, photosensitive film, electron bombard. effect on elec. cond. 0-93019
 PbS-PbO vacuum evaporated films, elec. cond. and photocond. 0-75656
 PbSe films, current carrier conc. and type control, elec. cond., synthesis process (Russian) 0-100412
 Pb_{1-x}Sn_xTe epitaxial films, adsorption-induced accumulation layer form. on surface 0-60117
 PbTe film, electronic thermal cond. and thermoelec. power 0-93018
 n-PbTe:In(Cu) epitaxial films, elec. transport props. 0-75659
 Sb, semimetalline film, elec. cond., grain boundary scatt. effects 0-103766
 Sb₂S₃ film, coevaporated, elec. cond. meas. 0-65726
 n-Si channel (100) inversion layer MOSFET, valley splitting, conductivity 0-70840
 Si, epitaxial layer deposition by ion beam methods 0-100417
 Si film, low press. CVD prep., struct., elec. and optical props. 0-70548
 Si, graphoepitaxy on fused SiO₂ using surface micropatterns and laser crystn. and characterisation 0-70554
 Si on sapphire, residual strain effect on elec. props. (Japanese) 0-84522
 Si, P implanted low pressure CVD polycryst. films, elect. characts. 0-60114
 Si polycrystalline film resistivity reduction by Nd:YAG laser annealing 0-100539
 Si thin film, polycryst., CVD, elec. props. 0-107934
 Si:Ar, ion-implanted, epitaxial regrowth by laser annealing, microstruct. 0-84404
 Si:As, polycrystalline, As segregation at grain boundaries, elec. props. meas. 0-75259
 Si:N wafers, Si₃N₄ layer growth by high dose implantation and annealing, elec. props. 0-70227
 Si:P, polycryst. films, elec. props., EPR, defect states, doping effects 0-75660
 Si:P film, polycryst., heavily doped, mobility and carrier conc., optical determ. 0-66314
 p-Si:P implanted films, piezoresist. stress tensors, ion dose depend., -80 to 120°C 0-100538
 Si-F-H-P, film, dark cond., struct., Raman scatt. 0-88588
 SnO₂ CVD coating on glass, elec. resist. rel. to cryst. microstruct. 0-84520
 SnO₂:P, CVD films, elec. props., cryst. to amorphous transition effects 0-107933
 SnO₂:Cu,S-ZnS:Mn,Cu,Al₂O₃:Al, light-emitting struct., cond. and electrolum., heat treatment 0-97345
 Te, oriented films, semiconducting props., Hall coeff., band structure 0-70854
 Te:Cu films, elec. transport props. 0-60120
 VO₂, V₂O₃ and V₂O₅, film prep. under equil. conditions, struct. and elec. props. 0-108352
 Zn,Cd_{1-x}S films, spray pyrolysis, elec. props. 0-75657
 Zn,Cd_{1-x}S, thin solid soln. films, vapour deposited, elec. and optical characts. 0-60110
 ZnO, CVD of epitaxial films on sapphire, SAW interdigital transducer fabrication 0-66430
 ZnO epitaxial film, nonuniform cond. due to H chemisorption (Russian) 0-65723
 ZnO films, RF sputtered single-cryst., on sapphire, struct. and SAW props. 0-80105
 ZnO sputtered films, undoped and Ga doped, props. rel. to deposition conditions 0-107935
 ZnSe layers, cond. type determ. by pot. profiling 0-73387
 ZnSe, MBE growth, elec. and optical props. 0-75462
 ZnTe, MBE growth, elec. and optical props. 0-75462
 ZnTe films, simple and modified Poole-Frenkel cond. 0-97017
 ZnTe:Cu films, high cond., elec. and optical props. 0-88651

electronic conduction in insulating thin films

- see also electrical conductivity of amorphous semiconductors and insulators; electrical conductivity of crystalline semiconductors and insulators
 alkali halide thin films, high-field electron injection, ionic cond., photocond. 0-75665
 ferrocene films, plasma-polymerised, carrier trapping, elec. cond. meas., 300 to 525K 0-100543
 fluorocarbon polymer, plasma-deposited thin films for lubrication of Au contact surfaces 0-89157
 Langmuir-Blodgett films, elec. and photoelec. transport props., device appl. 0-80431
 PMMA film in small area lateral MIMS device, cond., switching 0-97003

electronic conduction in insulating thin films continued

- polyacetylene films, undoped, nonlinear current-voltage charact. 0-75574
 polycarbonate, and charge-transfer complex modifications, isothermal dark currents 0-88559
 polyethylene films electrical conductivity under various conditions (*French*) 0-70869
 polyethylene terephthalate films, current peaks obs. with linearly increasing voltage 0-88654
 polyimide films, transient current in time range 10^{-4} to 10 s at temps. 180 to 280°C 0-65729
 polymer thin films formed in RF discharge using monomer organic semi-cond., elec. props. obs. 0-80432
 polyphenylene oxide thin films, electrochem. prep., impurity effects on cond., electroforming 0-88655
 polystyrene:1 films, thermally stimulated discharge, I conc. and polarisation temp. depend. 0-107937
 polystyrene films, soln. grown, elec. cond. meas. 0-97020
 polystyrene thin films, TSC and surface charge meas. 0-103769
 PTFE grafted membranes, struct.-properties relationships (*French*) 0-61136
 PVC films, soln. grown, DC cond. mechanisms, field and temp. depend. 0-97021
 PVC in metal sandwich struct., switching props., voltage- and current-controlled negative resist. 0-103767
 resistive layer above pit, stabilisation 0-93506
 AlF₃ in Al-AlF₃-Al MIM thin film structures, dielec. and elec. props. (*Slovak*) 0-100536
 AlN films, RF glow discharge deposited, current-voltage charact. 0-84515
 BN films, humidity sensitive elec. props. and switching charact. 0-107938
 In₂O₃:Sn transparent conducting films, homeotropic orientation of liquid crystals (*Russian*) 0-108181
 In₂SnO₃ film, effect of ambient atmosphere during annealing, elec. props. 0-97510
 NiF₂ film preparation and characterisation 0-59815
 PTO₂ films, electronic struct., reduction processes, photoemission, optical absorpt. and resist. meas. 0-80931
 Si₃N₄ polycrystalline, electrode shape effects on oxide conduction 0-96890
 Si₃N₄ films, CVD in MNOS and MNS structs., elec. resist. 0-97019
 Si₃N₄ thin film, reactively sputtered, struct. and elec. props. 0-88656
 SiO₂ amorphous film, dye-sensitised steady-state photocond. in Au-dye-SiO₂-Au struct. 0-107924
 SiO₂ films, grown in presence of O₂-trichloroethylene, room temp. negative bias instability 0-60102
 SiO₂ films in poly-oxide poly Si structures, elec. cond. and charge distrib. 0-92984
 SiO₂ MOS capacitor, defect current obs. 0-92987
 SiO₂ thin film dielec., in MIM struct., interfacial props. rel. to non-stoichiometry 0-80399
 Ta-Al-N thin film resistors with improved elec. props. 0-100544
 Ta₂N₃ and TaN_x films, thermal oxidation and resist. 0-60125
 Ta₂O₅ anodic films, elec. cond. mechanism, admittance meas. 0-70705
 TbF₃ thin films, AC conduction obs. 0-70868
 TiN films, reactively RF sputtered, struct. and elec. props., substrate bias effects 0-96763
 TiO₂ film, ion plated, DC cond. study 0-100457
 Tm₂O₃ film, between Al electrodes, prep. and elec. props. 0-60103

electronic conduction in metallic thin films

- see also discontinuous metallic thin films; electrical conductivity of amorphous metals and alloys; electrical conductivity of crystalline metals and alloys*
 conduction electron focusing by inhomogeneous mag. field (*Russian*) 0-70850
 disordered electronic systems, low-dimensionality, Anderson localisation, resist. 0-84491
 grain boundary and surface scatt., statistical model 0-103762
 grain boundary scatt., Hall coeff., theory 0-88649
 granular materials, size effects in cond. and supercond. 0-77581
 linear variations with thickness 0-103760
 metal film, temperature coefficient of total resistance 0-70853
 metallic films, metal-dielectric boundary thermal resistance, nonlinear elec. resistance (*Russian*) 0-65530
 metallic thin films, hot electron distribution function, nonlinear elec. resistance (*Russian*) 0-65717
 metallic thin films, resistivity strain coeff. calcs. 0-100449
 nonmetallic conduction at low temps. 0-97012
 Permalloy RF sputtered films, O effects in mag. and elec. props. 0-100603
 polycrystalline film, superimposed effects of three arrays of scattering planes on electrical conductivity 0-80412
 polycrystalline-thin metal films, thermoelectric power, mean free path model 0-107770
 size effect, Umklapp processes of charge carriers and anomalous transmittance in RF range (*Russian*) 0-70851
 size effects and resist., approximate expressions 0-88645
 superconducting inhomogeneous film, cond. near superconducting transition temp. 0-93031
 temperature-fluctuation noise of substrate supported films 0-92949
 thermal strains, effect of support, theory 0-88647
 thermoelectric power, thermal stress effects, theory 0-65714
 thickness dependence, quantum size affect (*German*) 0-86344
 thin wires, exptl. study of Anderson localisation 0-96849
 wire, thin-film, possible explanation of nonlinear cond. 0-97011
 Ag, appl. of percolation theory 0-65712
 Ag, defect density, thickness depend., elec. resist. obs. 0-70568
 Ag film, Ge coated, electrical resistance and ageing (*Russian*) 0-103759
 Ag film, in situ resistivity meas. 0-97008
 Ag, thin film, elec. resist., effect of annealing In electrodes 0-80416
 Al, deposited metallic thin films, H incorporation effects on stress and electromigration 0-80139
 Al film, lattice and bulk heat capacity meas. for normal and supercond. states 0-92684
 Al film on Si(111) substrate, struct., props. depend. on vapour flow, ionisation (*Russian*) 0-75453
 Al films, resistance changes due to bombardment by N, C, or Ar ions 0-103670
 Al, granular, transition to localisation, elec. resist. 0-70877
 Al thin conducting film, electromigration under superimposed DC and noise powers 0-107879

electronic conduction in metallic thin films continued

- Al, thin film, elec. resist., effect of annealing In electrodes 0-80416
 Al, thin film, thermal cond. meas., size effect 0-65715
 Al-Cr, thin film metal contact, sheet resistance changes 0-80356
 Al-Cu, superconducting amorphous films of high stability 0-70889
 Al-Si, DC magnetron-sputtered, residual gas influence on props. 0-80968
 Au film, adatom surface diffusion at low temps., elec. resist. study (*French*) 0-65376
 Au film, quantum size effect, field emission study 0-70849
 Au film, ultrathin evaporated, acoustoelectric meas. of electron mobility and diffusion 0-65707
 Au, nonohmic charact., and electron emission 0-60066
 Au, thin film, discontinuous, high resist., Hall effect meas. 0-65716
 Au, thin film, elec. resist., effect of annealing In electrodes 0-80416
 Au-TiO₂W_{0.1}, thermal annealing study of metallisation on Si 0-80134
 Au₂Si_{1-x} amorphous films, phys. studies 0-75476
 Bi, amorphous metal films, crystallisation with and without mag. field 0-70570
 Bi film, adatom surface diffusion at low temps., elec. resist. study (*French*) 0-65376
 Bi films, resistance changes due to bombardment by N, C, or Ar ions 0-103670
 Bi, thin film, resistivity, rel. to thickness 0-107928
 Cd film, surface RF impedance in strong mag. fields (*Russian*) 0-92920
 Cr containing Cr₂O₃ film struct., oxide percentage determ. and temp. coeff. of resist. 0-103607
 Cr, preparation by decomp. of bis-arene cpds., struct. and phys. props. 0-60785
 Cu films, resistance changes due to bombardment by N, C, or Ar ions 0-103670
 Cu, thin film, elec. resist., effect of annealing In electrodes 0-80416
 Cu-Al films, elec. cond. of vacuum condensates depend. on composition, annealing (*Russian*) 0-65709
 Cu-Ni thin films, ferromag., Hall effect meas. 0-80428
 Cu-Ni/Au-Ni multilayer films, ohmic behaviour, use as strain gauge 0-65713
 Fe-Cr-Al, Kanthal films, vac. deposited, evaporation charact., comp., struct. and elec. props. 0-88646
 Fe-Ni films, on glass substrate, thermoelec. effect 0-107769
 Ga, amorphous metal films, crystallisation with and without mag. field 0-70570
 B-Ga, metastable, elec. props. in normal and supercond. states (*Russian*) 0-65520
 Gd films, electrical props. correlation with microstructure 0-97009
 (Gd_{1-x}Co_x)_{1-x}Ar, amorphous mag. film, elec. and mag. prop. depend. on Ar 0-80410
 Hg-Xe vapour deposited films, cond. transitions, effect of disorder on supercond. 0-88659
 LaNi₅, H₂ absorption in thin film hydriding alloys 0-65238
 Mn film, elec. resist., deposition rate effect 0-97010
 Mn thin film, DC resist., activation energy, thickness depend. 0-84518
 Mn, vacuum deposited, in elec. field, resist., struct. 0-103761
 Mn-SiO cermet thin film, DC resist., activation energy, thickness depend. 0-84518
 MnBi film, electrical props., in situ annealing effect 0-65708
 Mo, evaporated, annealing behaviour, SEM obs. 0-65397
 Mo film, evaporated, grain size and resist. 0-88650
 Mo, sputtered, elec. resist., annealing and struct. effects 0-60109
 Mo, thin film deposition by high current ion beam sputtering, struct. and elec. props. 0-59837
 Ni, evaporated, elec. resist. and galvanomagnetic props. 0-80411
 Ni films, adsorption and decomp. of ethylene, coverage depend. meas. 0-96743
 Ni-Cr films implanted with N ions, electric properties (*Russian*) 0-107927
 Pb film, monocryst., heteroepitaxial growth, struct. defects, and elec. props. (*Russian*) 0-84403
 Pd film, elec. resist. 0-93013
 Pd film, quantum size effect, field emission study 0-70849
 Pd thin film, temp. coeff. of resist. meas. 0-107930
 Rh, thin films, polycryst., resistivity and temp. coeff. of resistivity 0-88648
 Sc thin films, obtained in vac. of 10^{-5} - 10^{-6} Torr, struct. and elec. resist. 0-107931
 Sm thin film, elec. props. 0-107929
 SmCo₅, H₂ absorption in thin film hydriding alloys 0-65238
 Sn polycrystalline films, elec. props. and crystallite size, 4.2K to room temp. (*Russian*) 0-93011
 SnO₂ films, non-stoichiometric, DC reactively sputtered, elec. props. 0-80415
 Ta thin film, elec. cond., strain gauge factor, ion bombardment effects 0-80417
 Ta, thin film deposition by high current ion beam sputtering, struct. and elec. props. 0-59837
 Ti-W films, bias-sputtered, quantitative anal. 0-80114
 V film, vac. evaporated, elec. props. 0-80414
 W film, surface RF impedance in strong mag. fields (*Russian*) 0-92920
 W-Re films, amorphous, one-dimensional quantum localisation 0-80413
 WSi₂, sputtered, props. for MOS IC appl. 0-70831
 Yb, amorphous metal films, crystallisation with and without mag. field 0-70570

electronic data processing see data processing**electronic density of states**

- A15 compounds, supercond. crit. temp. for model density of state using Eliashberg gap eqns. 0-93034
 A-15 compounds, density of states model for lattice transforms. 0-65219
 A-15 compounds, disordered, resist. and supercond. transition temp. 0-107944
 adatom density of states, impurity atom effects 0-92958
 adatom valence-level position variation on metal surface 0-88611
 adsorption of atoms on metals, Green's function formalism for studying electronic struct., local density of states calc. 0-107884
 alkali metals, liq., Fermi energy, density of states, electronic props., exchange and correl. effects 0-96774
 alloy thin film, thickness depend. of CPA electronic densities of states 0-65644
 alloys, magnetisation calc. method based on moments of density of states 0-65770
 alloys, substitutional, self consistent cluster theory for off diagonal disordered systems 0-84272

electronic density of states continued

- amorphous alloys, density of states of n-components 0-80153
 amorphous materials, laser irradi., electronic struct., one-electron approx. 0-70576
 amorphous semiconductors, density of states determ. from field effect data 0-107688
 amorphous semiconductors, doped, electronic props. 0-80283
 atoms, exchange energy as function of electron density 0-91426
 Auger lineshape anal. of molecules and solids 0-76113
 binary linear chain, electronic props., short-range order effects 0-96769
 central peak in the density of states of a disordered linear chain 0-100428
 cubic crystals, perfect, nonBloch electron state density 0-75487
 dilute alloy, perturbation expansion for the asymmetric Anderson Hamiltonian 0-80202
 disordered alloys, electronic density of states in muffin tin model 0-88467
 disordered one-dimensional lattice systems, diffusion and hopping conductivity 0-59991
 disordered system, one-dimens., density of states and wavefunction shape, periodic boundary condition influence 0-80223
 disordered system with correls., density of states at band tail 0-80154
 electron gas, screening of proton, Anderson model calc. 0-59895
 exponential tail in random potential 0-65423
 Fermi systems, disordered in two dimensions, interaction effects 0-75655
 ferromagnetic metals, spin fluctuation theory, Curie temp., mag. susceptibility 0-65937
 ferromagnetic semiconductor, two-band s-d model hybridization 0-65446
 graphite, electronic struct. exact exchange HF calcs. 0-65438
 graphite intercalation cpds., Fermi surface and transport props., LCAO model 0-80159
 heavily doped semiconductor, density of states at band tail 0-80154
 II-VI amorphous semiconductors, electronic states, sublattice one-band Hamiltonian transform. 0-59861
 III-V amorphous semiconductors, electronic states, sublattice one-band Hamiltonian transform. 0-59861
 insulator-to-metal transition for half-filled Hubbard band in paramagnetic state 0-92817
 linear Brillouin zone integration method, generalised susceptibility calcs. 0-88462
 liquid, electronic structure, structured medium approx. 0-84421
 liquid metal, electronic density of states, pseudopotential calcs. 0-70578
 liquid metals, strong binding model, electronic density of states, Green's function calcs. (Russian) 0-70111
 liquid semiconductor, density of states at band tail 0-80154
 Lloyd formula and muffin-tin CPA local density of states 0-70577
 magnetic alloys, conc., density of states, Kondo effect, theory 0-65780
 metal particles, small, characterisation and props., book contrib. 0-84417
 metal-tunnel oxide-Si junctions, processing condition depend. 0-80380
 metals, amorphous and liq., s-phase-shift model 0-88473
 MNOS p-channel transistor, memory characts., H₂ anneal effects 0-80388
 molecular crystals, electronic transport theory, local linear electron phonon coupling 0-65545
 muffin-tin potentials, arbitrary array, local density of states 0-92805
 one-dimensional metal crystals., surface density of states, rel. to adsorbed molecule 0-107889
 one-dimensional oscillator systems, density of states-frequency theorem 0-82602
 one-dimensional superlattice, exact solns. 0-75488
 α -quartz, electronic struct., local disorder influence 0-59870
 rare earth metals, density of 4f states below and above Fermi level, XPS and bremsstrahlung isochromat spectroscopy 0-76140
 recursion method for the extended impurity problem 0-96814
 semiconductor, amorphous, field effect and capacitance-voltage meas. anal., localised density of states 0-103686
 semiconductor, complex energy band under optical excitation, high-frequency negative cond. and population inversion 0-107858
 semiconductor, doped, impurity band density in atomic limit 0-107735
 semiconductor, doped, metal-insulator transition, anal. 0-88478
 semiconductor, with defects or impurities, local density of electron states 0-92857
 semiconductor surface, chemisorption of mol. complexes, bond orbital model (German) 0-59807
 semiconductor/adsorbate system, local density of states calcs. (German) 0-60062
 semiconductors, amorphous, electronic states, theoretical methods 0-80167
 semiconductors, amorphous, electronic transport mechanisms and coeffs. 0-80282
 semiconductors, optical props. under press., book contrib. 0-84715
 semiconductors, van Hove critical point region, electron-phonon interactions, dispersion law 0-70344
 solids, chemical bonding studied using scattering theory concepts 0-103289
 superconductor, effect of varying electronic density of states 0-75672
 superconductors with energy depend. electronic density of states, gap and crit. temp. 0-84538
 thin film, 11-layered, CPA calc. of local density of electronic states 0-65643
 tight-binding metals, electronic struct. and kinetic props. at high temp. 0-59848
 Tomonaga-Luttinger model, one particle temp. Green's function 0-57182
 transition metal alloys, binary, state density curves, relation between short-range order and Fermi level position, CPA calculations 0-107687
 transition metal-H systems, energy and electron density of states, improvements to theory 0-70636
 transition metals, core levels between surface and bulk atoms, variation of binding energy shifts 0-88615
 transition metals, ferromag., dil. H electronic struct. 0-70638
 valence electron distribution, in crystals, diff. data processing 0-92418
 Al, 3d impurities, self-consistent spin density functional calcs. 0-70635
 Al, Auger spectra, KLL and KLV, screening effects and plasmon gains 0-80913
 Al, K X-ray absorption, K-emission spectrum, band struct. using APW method 0-97380
 Al₂O₃/La-rare earth metal tunnel junctions, cond. meas., cryst. field effects 0-88694
 AlH₃, electronic struct. and electron-phonon interaction, hydrogenation effect, rel. to supercond. 0-107694

electronic density of states continued

- As₂S₃ 100-x(Se_{100-x}), localised states density near valence band edge (Russian) 0-103638
 Au, energy band structure, X-ray emission spectra, APW calc. 0-92811
 Au(Ag)(Cu)-Sn liquid, optical reflectivity spectra of virtual bound states 0-89021
 BN, electronic struct., exact exchange HF calcs. 0-65438
 BaTiO₃ (001), LEED and UPS studies 0-100747
 BaTiO₃, K-edge X-ray absorpt., cond. band states 0-97382
 BaTiO₃, valence band UPS and partial p and d density of states 0-71560
 Be, electronic struct., NMR study 0-108085
 BeNi, dil., electronic struct., NMR study 0-108085
 CO molecular adsorbed on Mo (110) surface, electronic states, photoemission spectra 0-65363
 CdF₂, UPS and XPS spectra, rel. to optical props. 0-66386
 CdS, surface energy struct. changes during ion cleaning and thermal annealing 0-92962
 p-CdSnAs₂, Hall effect, thermo EMF, thermomagnetic effects 0-107822
 CoMn(Cr)(V)(Ti), dil., low temp. specific heat and magnetisation 0-65925
 Cr₂Si, mag. susceptibility, 2 to 300K, rel. to electron energy spectrum 0-60185
 Cu (100), electronic struct., self-consistent local-orbital calc. 0-80348
 Cu, bulk and (001) films, extended tight-binding calcs. 0-70592
 Cu, liq., electronic structure, structured medium approx. 0-84421
 Cu-Ni, density of states of d-electrons, tight binding approx. calcs. 0-59863
 EuMo₂S₆, Chevrel phase, mag. interactions, LMTO energy band studies 0-70606
 GaAs (110), surface electronic struct. calcs. 0-80343
 GaTe, transport properties under hydrostatic pressure 0-75589
 Gd, magnetic crystalline anisotropy, Fermi level, electronic density of states 0-84596
 GdMg, noncollinear mag. struct., nonlinear band behaviour 0-75706
 GdRh₂B₄, magnetic and electrostatic props., NMR study 0-93195
 Ge (100), density of states, simple modelistic treatment of virtual surface states 0-103739
 Ge, mag. field luminesc. lifetime, quantum oscills., phonon wind effects 0-93385
 Ge_{0.5}Si_{0.5}, elec. cond., density of states, impurity and temp. depend 0-65568
 GeTe, effective masses for cond., density of states 0-88472
 GeTe-Sb₂Te₃, solid solutions, cond., density of states 0-88472
 Hg, reflection spectra, electronic density of states, calc. 0-66229
 In_{0.65}Tl_{0.35}, supercond. transition temp., specific heat, pseudopotential form factor 0-97026
 Ir, energy band structure, X-ray emission spectra, APW calc. 0-92811
 LiC₆ and LiC₁₂, intercalation cpds., electronic struct. calcs. 0-70613
 LiNbO₃, valence band UPS and partial p and d density of states 0-71560
 LuRh₂B₄, magnetic and electrostatic props., NMR study 0-93195
 MOS capacitor, photoionisation cross section and interface state density 0-92974
 Mg, Auger spectra, KLL and KLV, screening effects and plasmon gains 0-80913
 MnAu₂, helical antiferromag., optical absorpt., density of states 0-66224
 MnCl₂, lattice dynamics, density of states and sp. ht. calc. 0-92624
 MnP, spin polarised energy band struct., electronic specific heat, APW calcs. 0-65431
 MnSi, electronic energy band struct., self-consistent APW calc. 0-65433
 Na, adsorbed on Al, adatom valence-level position variation 0-88611
 Na, Auger spectra, KLL and KLV, screening effects and plasmon gains 0-80913
 Nb chalcogenides and chalcogenide halides, geometrical struct. and metal-metal bonding 0-80172
 Nb_{0.75}Ga_{0.25}, A 15 phase high transition temp., sp. ht. determ. 0-60140
 Nb₂Nb_{1-x}Si_x(Ge)_x, impurity stabilised A15 supercond., transition temp., lattice consts., specific heat 0-93026
 NbS₂ and Nb₂S₄, electronic struct. and predicted cond. props. 0-92815
 NbSe₂, pure and intercalated with ethylenediamine, positron annihilation study 0-84801
 Ni clusters local densities of states 0-88466
 Ni, ferromagnetic, electronic struct. by real space approach 0-65432
 Ni-Co(Fe)(V)(Ti), dil., optical absorpt., electronic struct. 0-108277
 Ni(Fe,Cr) and Ni₂(Fe,Cr), electron states density model and mag. characts. calcs. (Russian) 0-92804
 Ni₂Fe alloys, low-temperature specific heat, long and short range order effects 0-100339
 NiSb, bandstructure and density of states calc. 0-70580
 Pb, ab initio band struct. calcs. 0-75502
 PbMo₂S₆, Fe, elec. cond. anomalous temp. depend., mag. moments (Russian) 0-92878
 PbO-SiO₂ glass, reduced channel-plate, variable range hopping conductivity 0-107466
 Pb_{1-x}Sn_xTe:In, Hall effect and photoconductivity (Russian) 0-103720
 Pd-Si(Cu) amorphous ribbons, low temp. sp. ht., density of states trends 0-79957
 Pt band-structure determ., angle-resolved photoemission 0-66398
 Pt, energy band structure, X-ray emission spectra, APW calc. 0-92811
 PtO₂ films, electronic struct., reduction processes, photoemission, optical absorpt. and resist. meas. 0-80931
 Rb halides, role of quantum effects in lattice dynamics, Debye temp., shell model calcs. 0-70336
 Sc, band structure, density of states, absorpt. spectra, KKRZ calc. 0-70593
 Sc-Zr(Mg), low-temp. heat capacity 0-75370
 Se, amorphous, electronic struct. and optical props., pseudopot. calc. 0-65428
 Se, amorphous layer, localised states in band gap 0-59928
 Se, electronic struct. of cryst. phases and hydrostatic press. effects 0-59865
 Se, photoelectronic behaviour, in glass transition region 0-60045
 Se, trigonal and amorphous, electronic struct. and nonempirical calc. of struct. props. 0-59866
 Se-As, photoelectronic behaviour, in glass transition region 0-60045
 Si, (001) (2X1) reconstructed surface, dimer model self consistent calcs. 0-88613
 Si (111) 7X7 clean surface and O chemisorbed stage valence band density of states from L_{2,3}VV Auger spectra 0-100717
 Si, amorphous film, TSC, density of localised states distrib. 0-65587

electronic density of states continued

- Si, amorphous films, halogenated and hydrogenated, elec. and optical props. 0-97016
 Si, amorphous films, hopping conduction, dangling bond generation by high temp. annealing 0-60115
 Si, Auger spectra, KLL and KLV, screening effects and plasmon gains 0-80913
 Si, hydrogenated amorphous, gap states, comparison of photoemission and photocond. results 0-103724
 Si:F,H, amorphous, elec. and optical props. 0-60031
 n-Si:H, amorphous, bulk density of deep states, DLTS meas. 0-88518
 Si:H,B, amorphous, field effect and thermoelec. power 0-96924
 Si:Li, electron-phonon scatt., in intermediate conc. region 0-65180
 Si-SiO₂ interface, density of states, theory 0-80395
 Si-SiO₂ interface, improved characterisation, refined quasistatic and cond. methods 0-96990
 Si-SiO₂ MOS interface, surface-state density and minority carrier generation rate, meas. by DLTS, hot hole effect 0-100527
 Si₃Ge_{1-x}O₂, amorphous, electronic struct. 0-80166
 SiO₂, Auger line shapes, final state correlation effects 0-89095
 SiO₂, vitreous, low temperature heat capacity enhancement model 0-75369
 SnMo₂S₈, Chevrel phase, mag. interactions, LMTO energy band studies 0-70606
 SrF₂, UPS and XPS spectra, rel. to optical props. 0-66386
 SrTiO₃, (100), LEED and UPS studies 0-100747
 SrTiO₃, calc. of matrix element effects in freq. dependent dielectric function 0-70632
 SrTiO₃, K-edge X-ray absorpt., cond. band states 0-97382
 SrTiO₃, valence band UPS and partial p and d density of states 0-71560
 Te, amorphous, electronic struct. and optical props., pseudopot. calc. 0-65428
 Te, electronic struct. of cryst. phases and hydrostatic press. effects 0-59865
 Te, trigonal and amorphous, electronic struct. and nonempirical calc. of struct. props. 0-59866
 Te-transition metal, liq. semicond., elec. props. 0-96870
 Th, photoelectron spectra study, core and valence levels 0-66394
 Th, valence and 5f states, XPS and bremsstrahlung isochromat spectroscopy 0-66393
 ThC₂N₄, NMR, Knight shift and spin-lattice relax. 0-100621
 ThN, photoelectron spectra study, core and valence levels 0-66394
 Ti alloys, Fermi sphere limiting electronic capacitance, Brillouin zones (*Russian*) 0-92808
 TiBe₂, de Haas-van Alphen effect, Fermi surface, theory 0-103614
 TiC₂N_{1-x}(O_{1-x}), electronic struct., KKR-ATA method 0-65447
 TiFe_{1-x}Co_x, electronic struct. and mag. moment calcs. 0-65821
 TiN_{1-x}, substoichiometric, electronic density of states, CPA method calcs. 0-88464
 TiN₂O_{1-x}, electronic struct., KKR-ATA method 0-65447
 TiO₂, rutile, K-edge X-ray absorpt., cond. band states 0-97382
 TiS₂(Se₂), valence density of states, Gilat-Raubenheimer method 0-88465
 TiCl₄, ground-state props., Wannier functions, and electronic struct., ab initio self-consistent calc. 0-80178
 Ti₂(Te,Se_{1-x}) mixtures, liq., electrical conductivity, magnetic susceptibility 0-88715
 U compounds, NaCl struct. type, relativistic energy bands, LMTO calcs. 0-65442
 U, photoelectron spectra study, core and valence levels 0-66394
 U, valence and 5f states, XPS and bremsstrahlung isochromat spectroscopy 0-66393
 UN, photoelectron spectra study, core and valence levels 0-66394
 UO₂, photoelectron spectra study, core and valence levels 0-66394
 US(Se)(Te), electronic struct. and exchange band splitting, optical refl. meas. 0-66226
 U,Th_{1-x}As (Sb), electronic struct., relativistic KKR-averaged T-matrix approx. method 0-107702
 V, electronic structure, model potential calcs. (*Russian*) 0-100431
 V₂(Hf,Zr), NMR and mag. susceptibility, density of states determ. (*Russian*) 0-66053
 V,Hf_{1-x}Zr_x, normal and supercond. state, transition temps., mag. susceptibility and specific heat determ. (*Russian*) 0-60132
 V_{2-x}Nb_xHf, NMR of ⁵¹V and mag. susceptibility, 20-300K (*Russian*) 0-93192
 V₂O₅, energy band structure, bonding props., projected density of states anal. 0-70603
 V₂Si, magnetic susceptibility, density of states model for lattice transformation in A-15 compounds 0-65219
 W surface, (110), chemisorpt. effects on dielec. function, refl. spectra 0-75616
 ZrB₂, self-consistent band struct., XPS, reflectance, NQR, Hall effect and density of states meas. 0-107689
 ZrS₂(Se₂), valence density of states, Gilat-Raubenheimer method 0-88465
 ZrZn₂, de Haas-van Alphen effect, Fermi surface, theory 0-103614

electronic density of states of amorphous solids *see electron energy states of amorphous solids*

electronic density of states of liquid semiconductors *see electron energy states of liquid semiconductors*

electronic desk calculators *see electronic calculators*

electronic engineering computing

- see also circuit analysis computing; computerised instrumentation*
 bevelled shallow junctions, spreading resistance data correction 0-80358
 capacitor charging, polymer filled, injection times obs. 0-70796
 coupled-bar problems, conformal transformations combined with numerical techniques 0-83538
 MOST structure modelling, using hybrid computer, Poisson partial differential equation solution (*Slovak*) 0-75643
 thin film deposition process, line-edge profile simulation appl. 0-104068

electronic equipment manufacture

- ellipsometer measurement of thin films on wafers, real time, computer assisted 0-73418
 IR pyrometer performance parameters and applications (*German*) 0-86315
 PC fabrication, detrimental effect of aged Sn-Pb surfaces 0-108625
 surface measurements in manufacturing processes, precise mechanical test method (*German*) 0-62624

electronic equipment manufacture continued

- thin films fabrication techniques, evaporation and sputtering 0-76176
 wires electroplating, uniform, rotating cell design with helicoidally shaped internal surface 0-80990
electronic equipment testing
 cardiac monitor, heart rate meter and alarm eval., proposed standard test tapes 0-89899
 digital recording system for tipping bucket raingauges, description and field testing 0-77161
 solar cell arrays, flat plate PV modules, elec. and environmental testing requirements for terrestrial apps. 0-61368
electronic music
see also musical acoustics; musical instruments
 four-channel percussion synthesiser using 5700 type modules, construction details 0-106681
 percussion synthesizer, construction and operating controls 0-106682
 PMOS programmable sound generator, microprocessor-compatible, electronic music apps. (*German*) 0-79092
 portable electronic organ 0-96148
 RE electronic piano, organ pedal cct. construction, tone cct. elements (*Dutch*) 0-99904
 tone filters for electronic organs, tone spectra and source waveforms 0-106683
electronic structure, atomic *see atomic structure*
electronic structure, molecular *see molecular electronic states*
electronic switching systems
 microelectronic apps., conf., Calcutta, India (Jul. 79) 0-96755
electronics applications of computing *see electronic engineering computing electronics*
see also beta-rays; cosmic ray electrons; positrons
 anapole moment, static parity violating coupling to EM field, unified gauge theory 0-68390
 arbitrary plane wave EM field, electron motion, radiational corrections, mass operator (*Russian*) 0-57534
 band structure, optically induced in external plane wave field 0-106432
 Earth bow shock, energetic electrons meas. in upstream solar wind 0-90308
 electron-muon symmetry of Callan-Symanzik function: two-lepton case 0-73627
 inertial mass, Mach's Principle 0-62538
 magnetic moment, muon effects in QED 0-62899
 magnetic moments, anomalous, QED test 0-77996
 magnetosheath, Prognost 4 obs. of ≤ 2 MeV electrons and cold plasma 0-90296
 magnetosphere, high energy electron flux obs. and comparison with VLF emissions by EXOS-B satellite (*Japanese*) 0-94652
 magnetosphere energetic electrons, obs. in magnetosheath and solar wind 0-90310
 muon-electron mass ratio in a semi-classical model 0-91072
 inner radiation belt, electron flux vars. near trapping zone boundary during substorms 0-67470
 outer radiation belt, maximum fluxes of electrons with E>1 MeV (1958-1971) 0-61968
electrooptics *see electro-optical effects*
electroosmosis *see osmosis*
electrophoresis
see also electrophoretic coating techniques
 agarose gel immunoelectrophoretic determination of molecular weights of tubulin antigens 0-67313
 biological cell electrophoretic mobility meas. using new automatic method 0-67322
 biological particle surface, elec. double layer phenomena (*Rumanian*) 0-94144
 dielectrophoretic force, theory expt. 0-72403
 display device, for large area X-ray image receptor 0-98091
 enamelling of domestic electric and gas cooking equipment using electrophoresis, installation and process details (*French*) 0-108719
 gas discharge, DC, time-depend. cataphoretic gas separation with end volumes 0-79603
 insulating particles in insulating liquids, high field electrophoresis 0-90865
 insulating particles in insulating liquids, high-field electrophoresis, basic transport mechs. 0-93767
 Ioncote coating process, using field emission systems for corrosion and abrasion protection (*German*) 0-76205
 laser Doppler, high current-density electrodes 0-89500
 macromolecule, charged, in external elec. field, spherical case 0-75145
 mast cells, rat, electrophoretic mobility distrib. alteration after immunological activation 0-67047
 motor-car corrosion protection improvement, primer paint appl. by electrocoating effect (*Dutch*) 0-71915
 phthalocyanine-alkane interface, charge transfer, rel. to photoelectrophoretic image form. 0-65616
 polydicarboxylic acids, electrophoretic and viscometric props. 0-66811
 proteins in intercellular bridges 0-89734
 serum-electrophoresis, quantitative, by digital picture processing (*German*) 0-94306
 synaptic vesicles and synaptosomal membranes, electrokinetic props. 0-67055
 He-Ne mixture, cataphoretic gas separation in DC glow discharge with end volumes 0-79428
 Ne, isotope separation by cataphoresis in DC gas discharge 0-103213
electrophoretic coating techniques
 enamelling of domestic electric and gas cooking equipment using electrophoresis, installation and process details (*French*) 0-108719
 Ioncote coating process, using field emission systems for corrosion and abrasion protection (*German*) 0-76205
 pigment separation and deposition, electron sensitive (*German*) 0-108365
electrophoretic coatings
 Cr₃C₂, electrophoretic alloy coatings on C steel, sintered, struct. form., Ni-P undercoat effect 0-61027
 Cr₃C₂, electrophoretic coatings on steel, sintering 0-66707
electrophotography
 amorphous materials apps. 0-107693
 bit capacity limitation, toner size and deposition 0-62762
 developer, size distrib., particle charge and toner-carrier force (*German*) 0-73493
 document copy machine, physics (*Japanese*) 0-82842
 electret applications, book contrib. 0-80709

electrophotography continued

- electrostatic calculation of electrographic development 0-77888
 films, surface charge meter using electrostatic induction (*Japanese*) 0-77886
 image information content and noise analysis 0-101861
 imaging system requirements interacting with copier architecture 0-77895
 insulating particles in insulating liquids, high field electrophoresis 0-90865
 insulating particles in insulating liquids, high-field electrophoresis, basic transport mechs. 0-93767
 laser recording and information handling, seminar, San Diego, CA, USA (Aug. 1979) 0-101663
 latent electrostatic image transfer (*Japanese*) 0-73487
 materials sensitivity, deterioration of coloured images due to illum. in diaprojector (*Russian*) 0-62782
 noise perception and level of graininess 0-62753
 photoactive pigment electrophotographic imaging system, dark charge exchange process 0-62758
 photoconductor image charge transfer to electrographic film 0-101864
 photosensitivity of electrophotographic molecular recording media during nanosecond exposures (*Russian*) 0-73516
 pictorial electrographic printing, tone reproduction and screen design 0-62752
 PVK/PVK-TNF/TNF.PMG system, electrophotographic characts. 0-62759
 scientific basis of process 0-68287
 toner, recycled in xerographic development system, cycle distrib. 0-62760
 transparent electrophotographic film for high-resolution holographic recorders 0-102671
 X-ray images, electronic recording 0-62815
 CdInGaS₂, pure and Cu-doped, electrophotography layers (*Russian*) 0-68282
 HgI₂/CdS binder layer photoreceptor, surface charge characts. thickness depend. 0-57409
 Se, appl. to xerography 0-57415
 Se, electrophotographic characts. of films rel. to viscosity of bulk specimens (*Russian*) 0-73505
 Se, photosensitive particle migration, electrophotographic film structure and process 0-101863
 Se:As X-ray plates, electronic transport (*German*) 0-80290
 Se-As alloys, appl. to xerography 0-57415
 SeTe/Se multilayer photoreceptor, transient photoconductivity (*Japanese*) 0-75596

electrophotoluminescence *see* electroluminescence; photoluminescence

electrophysiology *see* bioelectric phenomena

electroplated coatings

- additive-free hard Au for electric connections and PCB contacts 0-108718
 barrier layers, against diffusion 0-66444
 electrolytes for Ag-Sb alloy coating deposition (*Bulgarian*) 0-93763
 Ag-Cu surface alloyed films, laser melt quenched, microstruct. 0-76423
 Au, electrodeposited and sputtered, hard, reactive softening, X-ray diff. studies 0-100414
 Co-W alloy electrolytic coatings, heat treatment effects on coercivity, hysteresis and structure (*Russian*) 0-60381
 Cr plated steel, factors influencing durability 0-108643
 Cr-Cr₂O₃ black, electroplated solar collector coatings, high temp. optical and struct. degradation 0-66995
 Cr-Cr₂O₃ black solar absorber surfaces, microstruct. rel. to electroplating parameters 0-61418
 Cu, Ni alloy protection against hydrogen embrittlement, aerospace engine appl. 0-76416
 Sn/Cu electroplated bimetallic films, interfacial reaction 0-96765
 Zn deposition by pulse plating (*German*) 0-60792

electroplating

- anode behaviour in cyanide-Ag baths (*German*) 0-61103
 automatic barrel line type ATS closed system, small parts electroplating, after-treatment and drying (*German*) 0-84861
 bright plating, from zincate electrolytes, progress 0-66442
 brush plating, for wear resist. appls. 0-66443
 current distribution cell for qualitatively predicting differences in barrel plating performance of electroplating solutions 0-71917
 embrittlement protection of Ni alloy, by Cu electrodeposits, aerospace engine appl. 0-76416
 injection laser diode mode structure enhancement by backface plating 0-64056
 levelling, geometric and true, in electroplating, study using stylus methods 0-66445
 metal barrier-layer protective deposits, inorganic finish selection and appl. 0-71812
 pulse electrolysis, theoretical aspects 0-85191
 steel, Cr-Mo, oxidised, mechanism of crack decoration of oxides by electrodeposition 0-97560
 steel, mild wire nails, with Ni, Zn and Cu, barrel plating efficiency 0-100964
 thin film prep. for solar energy utilisation 0-84847
 wires, uniform, rotating cell design with helicoidally shaped internal surface 0-80990
 Au and Sn-Pb alloys, comparison (*French*) 0-89158
 Co concentration monitoring, by automatic colorimeter 0-105691
 Cr trivalent plating solns., prod. experience 0-71606
 Cu barrel plating C steel nails, efficiency 0-100964
 Cu electrodeposition in cylindrical pores by pulse plating 0-81330
 Cu electroplating method for sensitizing stress meas. (*Japanese*) 0-68197
 Ni barrel plating C steel nails, efficiency 0-100964
 Ni electroless plating of Fe powder 0-61026
 Ni films, self-supporting, electroplating method of prep. 0-66436
 Ni, structure-internal stress relationship 0-70561
 Sn, autocatalytic deposition on steel, Ni, Cu, polypropylene and ABS 0-100965
 Zn barrel plating C steel nails, efficiency 0-100964
 Zn bright coating, rack parts or bulk goods, in GTL-barrel units (*German*) 0-84862
 Zn deposition by pulse plating (*German*) 0-60792

electropolishing *see* electrolytic polishing

electroreflectance

- zincblende-type crystals, electromodulation, piezomodulation, theory 0-93281
 Ag (110), surface state contrib. 0-80755
 n-Al_{0.5}Ga_{0.5}As, ion implanted films, optical and luminesc. props. 0-60699

electroreflectance continued

- As₂Se₃, single crysts., fine struct. of direct gap from electrorefl. spectra 0-93280
 Au (110), surface state contrib. 0-80755
 Cu (110), surface state contrib. 0-80755
 GaAs, exciton quenching, obs. at room temp. using electrolyte electroreflectance 0-60546
 n-GaAs, ion implanted films, optical and luminesc. props. 0-60699
 GaAs, Schottky barrier electrorefl. meas. by sample rotating technique 0-60544
 GaAs Schottky-barrier, linear and quadratic electroreflectance, minicomputer-controlled meas. 0-97241
 n-GaAs, spectra, light induced, electrolyte and Schottky barrier techniques of meas. 0-76046
 n-GaP, ion implanted films, optical and luminesc. props. 0-60699
 N-Ge, electrorefl. spectra, light induced, electrolyte and Schottky barrier techniques of meas. 0-76046
 InGaAsP, bandgap energy by electroreflectance and photoluminesc. spectra 0-107700
 In_{1-x}Ga_xP_{1-y}As_y, lattice matched to InP, electroreflectance obs. 0-93416
 In₂O₃, thermally evaporated film, struct. and elec. props. 0-104066
 Mg₂Cd_{1-x}Te, electroreflection spectra, comp. depend. 0-66230
 Pb(Zr,Ti)O₂ ceramic, surface barrier electroreflectance, hysteresis, ageing 0-80752
 Si, amorphous, hydrogenated film, electroreflectance study 0-88967
 Si, ion implanted films, optical and luminesc. props. 0-60699

electrospark machining *see* spark machining

electrostatic accelerators

see also Van de Graaff accelerators

- charge-exchange accelerator for fast-neutron spectrometer 0-63440
 conductance for the gas flow of an accelerating tube 0-102359
 direct-action accelerators with inductive energy storage and exploding conductors 0-68974
 fusion reactor, PDX neutral beam injector, ion accel. structural anal. 0-102375
 low energy, high current accelerator for 14 MeV neutron production 0-99353
 neutral beam, continuously operating, convectively cooled ion accelerator, mech. design and fabrication 0-102374
 ultrasensitive mass spectrometry with tandem electrostatic accelerators 0-101876
 C⁻ ion source for radiocarbon dating using tandem accelerators 0-94620

electrostatic coating techniques

- efficiency obs., discharges in electrostatic coatings meas. 0-71593
 enamelling by electrostatic frit powder spraying 0-97428
 integral glass covering of spacecraft solar cells by electrostatic bonding 0-93676
 metallic coatings, electric field atomisation from melt 0-76174
 terrestrial photovoltaic arrays, electrostatic bonding as encapsulation technique 0-94020

electrostatic coatings

- discharges obs., using image intensifier and laser Doppler anemometer 0-71593

electrostatic devices

- see also* capacitors; dielectric devices; electrostatic accelerators; electrostatic lenses; electrostatic precipitators
 aerosol particle size classifier, parallel plate electrostatic device 0-95070
 copying processes of latent electrostatic image transfer (*Japanese*) 0-73487
 electro-gas dynamic technologies, corona discharge industrial applications, qualitative analysis (*Rumanian*) 0-70061
 electrophotographic films, surface charge meter using electrostatic induction (*Japanese*) 0-77886
 filter, electret fibre, non-woven, high efficiency 0-76691
 ion analysers for laser prod. plasma detection, space charge effects 0-96392
 microcantilever electrostatic deflection system for transmission optical modulator array 0-87512
 mirror, plane electrostatic, resolution improvement method 0-78753
 optical component protection in dusty environments, electrostatic techniques 0-58657
 piezoelectric receivers, amplitude-freq. response determ. for acoustic emission 0-87699
²H-³H fuel pellet electrostatic injection (*Japanese*) 0-78434

electrostatic fields *see* electric fields

electrostatic lenses

- see also* aberrations; focusing; particle beams
 coaxial lens, soln. techniques 0-69307
 coaxial lenses 0-74061
 crossed lenses, electron optical characts., trajectory anal., aberrations from axial pot. profile 0-63909
 doublet of crossed electrostatic lenses, characts. 0-99615
 gun, for high-brightness field emitters 0-62809
 immersion crossed lens, trajectory, anal. 0-99616

electrostatic microphones *see* microphones

electrostatic precipitation *see* electrostatic precipitators; precipitation (physical chemistry)

electrostatic precipitators

- charge measurement, positive and negative corona 0-96403
 corona discharge theory analytic developments (*Rumanian*) 0-70062
 dust particles, charged, vel. meas. using laser Doppler velocimeter 0-95083
 dusts, electrostatic precipitation (*German*) 0-89532
 mists, electrostatic precipitation (*German*) 0-89532
 particle velocity, laser Doppler anemometry study 0-59144
 particulate layer deposition, resistivity meas. under ionic bombardment 0-68218

electrostatics

- see also* electrets; electric charge; electric fields; electrostatic devices; static electrification; triboelectricity
 capacity of two-unequal adhering spheres 0-91719
 circular membrane reflector made by surface bending due to electrostatic tension 0-91876
 conference, Oxford, England (Apr. 1979) 0-67932
 cooling effects exam., steel plate at 500°C 0-69628
 cylinders, circular 2-D electrostatic problems, integral eqn. soln. 0-83533
 dielectric ellipsoid or elliptic cylinder, Laplace eqn. soln. to electrostatic boundary value problem 0-63884

electrostatics continued

- discharge energy determ., using mathematical and physical models 0-70065
 electro-aerosols, precipitation in the airways, effect of electrostatic scatter 0-108929
 electrographic development, electrostatic calc. 0-77888
 electron beam, magnetized, flowing through cavity, self-consistent potential calculation 0-91743
 electrophotographic developer, size distrib., particle charge and toner-carrier force (*German*) 0-73493
 field near charged surface, integral evaluation method 0-99599
 fuel cell electrodes, galvanostatic switching curve shapes 0-66965
 imaging problems with plane boundaries, demonstration 0-90629
 Jupiter magnetosphere, electrostatic waves obs. 0-72865
 magnetosphere, electrostatic waves rel. to inverse loss cone electrons temp. anisotropy relaxation (*Russian*) 0-109314
 magnetosphere, mode of propag. electrostatic plasma waves and radio waves determ. using stimulated plasma wave results (*Japanese*) 0-94650
 planar electrostatics, teaching 0-90623
 plasma, electrostatic shear flow instability theory and appl. to magneto-pause and solar wind 0-96359
 potential, laboratory and theoretical comparison 0-105461
 spark discharges from body, nature and incendiary behaviour obs. 0-72406
 sparks detection and characts., by radio methods 0-68217
 surface dipole layers, forces between plates 0-70793
 toroidal charge and current configurations, static fields described in terms of ring multipoles 0-78741
 unequal adhering spheres, electrostatic field generation 0-99598

electrostriction

- see also *piezoelectric materials; piezoelectricity*
 acoustic waves, parametric excitation in presence of electron currents (*Russian*) 0-80328
 Born model, electrostriction rel. to dielec. and thermoelastic props. 0-71322
 capacitance type AC dilatometer for piezoelectric and electrostriction const. meas. 0-77747
 ferroelectric, uniaxial, crit. behaviour, electrostrictive coupling role 0-71329
 liquids, photoacoustic and photorefractive detect. of small absorpts., electrostrictive limits 0-108171
 paraelectric-ferroelectric-antiferroelectric phase transitions, electrostrictive effects 0-97209
 plane-parallel absorbing layer, nonlinear optical props. 0-58631
 relaxor ferroelectrics, electrostrictive effects 0-66112
 stimulated Brillouin scatt., three dimensional, for focused Gaussian beam 0-69456
 TGS, electrostrictive and dielec. coeffs., neutron diff. study 0-75943
 BaTiO₃ ceramic, degradation under high AC elec. field 0-60499
 BaTiO₃, paraelectric crystal, nonlinear props. 0-84699
 N₂ liq., photoacoustic and photorefractive detect. of small absorpts., electrostrictive limits 0-108171
 Pb(Mg_{1/3}Nb_{2/3})O₃, electrostrictive effect 0-66113
 Pb(Mg_{1/3}Nb_{2/3})O₃:PbTiO₃, ceramic dielectric, electrostriction, relaxation, polarisation 0-80700
 Pb(Zr,Ti)O₃:Ba, paraelectric ceramic, electrostrictive effect 0-80701
 RbH₂PO₄, electrostrictive effects, US rel. 0-75941
 WO₃, anodic oxide films, quadratic electro-optic and electrostrictive effects, ellipsometry 0-108184

electrosynchronisation see *synchronisation***electroviscous effect**

- see also *colloids; viscosity*
 AC characteristics, pressure-drop fluctuations 0-107457

element origin

- see also *cosmic ray origin; cosmology*
 cosmological and stellar nucleosynthesis, review 0-62359
 galactic cosmic ray Fe nuclei source, neutron excess from isotopic comp. 0-72729
 galactic disc chemical evolution, inflow problem 0-62279
 r-nuclei prod. sites in Galaxy 0-72932
 solar system s-process elements, difficulties, with ²²Ne as neutron source 0-72926
²⁶Al, synthesis in explosive H burning 0-85929
 Ar, galactic nucleosynthesis rel. to low Ar abundances in three halo planetary nebulae 0-82443
¹¹B, neutrino-induced prod. in stellar C layer 0-82337
¹⁴C in groundwater, possible subsurface prod. rel. to dating 0-85690
 Fe group elements, prod. in supernova outburst (*Russian*) 0-62167
⁴He production, nonzero neutrino rest mass effects 0-105413
⁸⁶Kr in meteorite, s-process nucleosynthesis and s-process neutron capture time scale 0-73080
 O, enrichment rate in Galaxy determ. from planetary nebulae O/H ratios age depend. 0-105328
¹⁰⁷Pd, solar system prod. rel. to isotopically anomalous Ag in Santa Clara and Pion Fe meteorites 0-85902

element relative abundance

- see also *isotope relative abundance*
 Abec meteorite, C rich material with high volatile element content, implications 0-85908
 Allende meteorite, tracer elements loss mechanism after heating to 1400°C rel. to primitive meteorites thermal metamorphism 0-109401
 Allende meteorite (C3V), tracer element loss after heating to 1400°C, rel. to primitive meteorites thermal metamorphism 0-109402
 Antarctic aerosols particle anal., comp. 0-77091
 atmospheric trace elements in UK, 1978 survey 0-90208
 C2 chondrite meteorites, evidence for chemical fractionations 0-109400
 3C 120, Seyfert galaxy, assoc. nebulosity O/H and N/O ratios 0-67890
 carbonaceous chondrites, ion beam analysis 0-62089
 α Centauri binary system, spectroscopic chemical anal. 0-62128
 cosmological light elements, constraint for G var., comment on errors 0-72767
 Cretaceous mid-ocean ridge basalt (MORB), Nd and Sr isotopic comps. and rare earth element abundances 0-94520
 Cretaceous-Tertiary boundary event, Os and Ir enrichment of sediments 0-76976
 Cygnus Loop, SNR, abundances and filament shock vel., UV obs. 0-94848
 30 Doradus nebular complex, chemical comp. and struct. obs. 0-62226
 Earth inert gas composition, origin from solar nebula 0-61785
 elliptical galaxies, chemical evolution 0-67843

element relative abundance continued

- galactic disc chemical evolution, inflow problem 0-62279
 galaxies, chemical evolution, review 0-77486
 γ Geminorum, differential abundance anal. rel. to α Lyrae standard 0-82362
 halogen content of ultramafic nodules, determ. by gamma-ray spectroscopy and radioactivity meas. 0-76945
 igneous lithic clasts from mesosiderites and howardites, petrography and chemistry compared with eucrites and diogenites 0-72890
 interplanetary dust grains collected from stratosphere, neutron activation study 0-82319
 interstellar gas near 30 Doradus, element abundances from UV absorpt. lines obs. 0-85978
 interstellar Sc II in ζ Ophiuchi spectrum, abundance upper limit 0-82445
 Jupiter atmosphere, cloud struct. and C/H ratio from methane line profiles near 1.1 μ 0-62067
 herzolites, comp. rel. to comp. of Earth mantle 0-76940
 lunar regolith samples from Luna-24, element abundance determ., neutron activation obs. 0-67597
 lunar soil samples from Luna 24, inert gas element and isotope composition 0-67593
 lunar soil samples from Luna-24, N₂ abundance, neutron activation obs. 0-67594
 M32, metallicity and galaxy age from spectral synthesis 0-67842
 Markarian 59, supergiant H II region in SBm galaxy NGC 4861, metal abundance from spectroscopic obs. 0-98705
 Mars, chem. composition of interior, cosmochemical model 0-72813
 metal content of Hyades star cluster rel. to solar colour 0-101569
 metallicity of NGC 6635 globular star cluster 0-90483
 metals in H II regions and stellar populations in bright galaxy nuclei 0-98708
 Morasko meteorite, composition and origin 0-77359
 NGC 1851, 6624, globular cluster, abundance gradients spectroscopic investigation 0-82437
 NGC 7027, planetary nebula, CNO elements abundances from UV spectrum 0-82459
 nuclear waste from extraterrestrial civilisations, stellar spectra 0-82230
 Orion Nebula, Cl and Fe abundances from forbidden Cl II and Fe II near IR mapping 0-62217
 planet interior differentiation processes, trace elements as probes 0-98584
 planetary nebulae, abundances from weak diagnostic spectral lines 0-109531
 planetary nebulae, abundances of He, Ne, Ar, N, and Cl 0-109532
 planetary nebulae, classification according to abundance, chem. kinetic and spatial props. 0-109509
 planetary nebulae, hot stellar wind model for refractory elements gas-phase abundances 0-109516
 planetary nebulae, implications for galaxy abundance 0-109530
 planetary nebulae central star abundances corrections from UV flux determ. 0-72945
 planetary nebulae in M31 (Andromeda galaxy) and companions, comps. rel. to nucleosynthesis and cosmic He abundance 0-109520
 planetary nebulae in Magellanic Clouds, He, N and O abundances, effects of excitation class 0-109519
 planetary nebulae of galactic halo, photoionisation models and chemical abundances of K 648, 49+88.1° and (108-76.1°) 0-109507
 rainfall in Trinidad comp. determ. 0-82045
 rare earth elements, geochemistry in Archaean metasedimentary rocks from Kambalda, Western Australia 0-109143
 rare earths in HD 187473, Si star 0-98671
 rare earths in Melrose-b howardite 0-101566
 rare gases in volcanic rocks, mass fractionation as indicator of gas transport to or from magma 0-98292
 s-process elements, effects of unthermalised isomeric states and time-varying neutron flux on branching ratios 0-90410
 siderophile elements, fractionation in enstatite chondrites 0-98617
 solar flare cosmic rays, element abundance in 2≤Z≤28 range 0-90382
 solar nebula, rare earth element condensation and fractionation 0-72796
 solar system, comparison with galactic halo stars (*French*) 0-72933
 in spiral galaxies, chemical enrichment correl. with density wave energy 0-98715
 subdwarf stars, odd-Z and r-process elements abundances from spectroscopic anal. 0-62122
 supernova remnants, evidence for element depletion from far UV spectrophotometry 0-90498
 trace elements in basalts from Nauru Basin 0-94499
 U, conc. and isotopic comp. in Edwards carbonate aquifer, Texas, rel. to aquifer oxidation/reduction state 0-98362
 γ Ursae Majoris, Am star, microturbulence and metal content determ. 0-82377
 W50, supernova remnant, N overabundance from optical spectrum 0-90557
 Al in cool halo stars, implications for galaxy abundance 0-105232
 Ar/H, low abundances meas. in three halo planetary nebulae 0-82443
¹¹B, abundance from neutrino-induced prod. in stellar C layer 0-82337
⁹Be/H in Population I giant stars, theoretical surface abundances 0-94796
 C abundance in planetary nebula IC 418, determ. from UV spectra 0-67832
 C in Orion Nebula and IC 418 from visible and IUE obs. 0-82451
 C, O abundances in planetary nebula NGC 7662, determ. from photoionisation model 0-62233
 C/H in high excitation planetary nebulae, IUE satellite obs. 0-94860
 C/H in Uranus atmosphere, evidence for enhancement over solar ratio from methane-spectrum 0-98609
 C/H ratio for Jupiter from 8.9 μm IR spectrum 0-67638
 C/N abundances on first giant branch of NGC 6752 globular cluster 0-67719
 C/O ratio in Orion Nebula, determ. from long-slit spectroscopy in rocket UV 0-105297
 CNO abundances in atmosphere of β Lyrae, IR spectra (*Russian*) 0-67794
 CNO abundances in B-type stars in associations and general field 0-67702
 CNO in Population I giant stars, theoretical surface abundances 0-94796
 CNO var. in massive binary stars, Wolf-Rayet appls. 0-94802
 Ca, abundances in F-type supergiants in Magellanic Clouds 0-98655
 Ca in giant stars in globular clusters 0-72940
 Cd, concs. in fractions of H3 chondrites Tieschitz and Brownfield correl. with isotope fractionation 0-94764
 Ce depletion in Melrose-b howardite 0-101566

elemental relative abundance continued

- Fe Abell 1060 galaxy cluster, abundance from X-ray spectrum obs. by (HEAO A-2) 0-82518
 Fe conc. determ. in Vellar estuary 0-77015
 Fe group elements, relative abundances from prod. in supernova outburst (*Russian*) 0-62167
 Fe in Centaurus galaxy cluster, abundance from X-ray spectrum obs. by (HEAO A-2) 0-82518
 Fe meteorites of groups IAB and IIICD, element abundances rel. to origin 0-109404
 Fe/H abundance in 628 stars, catalogue 0-98579
 Fe/H calibration of subdwarf star 37-45 colour excess 0-82363
 Fe/H of F- and G-dwarf stars, determ. using CORAVEL radial vel. scanner 0-94791
 H 1/He I, ratio in local interstellar medium rel. to ionisation state 0-90502
 H II regions, metal rich, abundance determ. errors 0-82461
 H II regions near nucleus of spiral galaxy NGC 3310, metal abundance and N/O ratio 0-62235
 H in anisotropic universe, mass fraction rel. to primaeval radiation polarisation 0-82552
 H/He ratio in ν Eridani, atm. parameter determ. 0-67739
 H₂/H₂+He abundance on Saturn from Pioneer 11 IR radiometry obs. 0-82290
 He abundance in galactic H II regions, recombination line obs. 0-98703
 He abundance in white dwarf HZ 43, stellar struct. from soft X-ray obs. 0-72944
 He and heavy element abundance in H II region in NHC 2366, visible and radio obs. 0-77475
 He in chaotic Friedmannian Universe 0-67920
 He in Earth interior, incorporated from immature Sun (*Russian*) 0-81856
 He, ionisation struct. and abundance in Orion Nebula, SHF obs. 0-105315
 He universal abundance 0-62356
 He/C, C/O ratios in C₂ white dwarf LP 145-141, rel. to strong UV absorpt. 0-67715
 He/H in Sagittarius B2, He recombination line obs. interpretation 0-62300
 I/Xe, IIE iron meteorites, Weekeroo Station and Netschaev 0-77360
 Li, abundance in atmospheres of M-type supergiants (*Russian*) 0-72950
 Li abundance in Luna 24 soil samples 0-67590
 Li in tektites and impact glasses 0-61799
⁷Li/H in Population I giant stars, theoretical surface abundances 0-94796
 Mg/Ca in He-rich white dwarf star Ross 640, UV spectra 0-94790
 Mn in NE-Pacific water 0-101384
 N/C in Q0353-383, QSO abundance anomalies, UV and visible spectral obs. 0-82532
 N/O ratio in Venus upper atmosphere, Pioneer Venus Orbiter meas. 0-77310
 N/S in spiral galaxy NGC 5236, radial var. of abundance ratio from emission line obs. 0-82497
 Na in M13 red giants, evidence for protocloud gas inhomogeneities 0-82439
 Na in nightglow from Na I D doublet excitation obs. 0-98497
 Nd/Sm ratio of lower continental crust, constraints from mantle Nd-Sr isotope correl. 0-94498
 Ni I solar photosphere from oscillator strength obs. 0-98625
 Ni in Cu alloy of Mayfield chondritic meteorite 0-67671
 O, abundance in emission clumps of irregular galaxy (Markarian 325) 0-67869
 O, Fe in globular cluster stars, influence on horizontal-branch morphology 0-67695
 O/H ratios in planetary nebulae, meas. rel. to Galaxy O enrichment 0-105328
 P/H ratio for Jupiter from 8-9 μ m IR spectrum 0-67638
 Pb in subalpine pond sediments, anthropogenic source var. 0-85315
¹⁰⁸Pd/¹⁰⁹Ag in Santa Clara and Pinon Fe meteorites, meteorites, rel. to isotopically anomalous Ag origin 0-85902
²⁴⁴Pu/²³⁸U, ratio in St. Severin chondrite 0-72889
²²⁶Ra, behaviour in Pee Dee River-Winyah Bay estuary, S.Carolina 0-98360
 Rb/Sr ratio of lower continental crust, constraints from mantle Nd-Sr isotope correl. 0-94498
¹⁸⁷Re/¹⁸⁶Os in Earth mantle, rel. to use of Os isotopes as petrogenetic and geological tracers 0-89989
 S in Martian lithosphere, possible overabundance 0-72832
 S in planetary nebulae, abundance from IR line meas. 0-82444
 Th/U in sedimentary rocks, rel. to crustal evolution and sedimentary recycling 0-85654
 Zn, solar photosphere abundance, discrepancy with meteorite abundance 0-72897

elemental semiconductors

- amorphous, high field transport, impact ionisation, carrier mobility 0-80286
 c Si-SiO₂ layers, physics, electron and ion motion, Cl, Na and K ion effects (*Dutch*) 0-60093
 crystal growth aspects of electronic materials, review 0-66405
 diamond-Sb, implanted, radiation damage and annealing study 0-100263
 diamond, accelerator irradiation, heavy ion irradiation damage 0-100291
 diamond, defect electronic struct. and lattice config., MO approaches 0-65495
 diamond, homogeneous formation in gas phase, laser beam effects (*Russian*) 0-104052
 diamond, ion-doped with Li electron transport 0-92917
 diamond, Jahn-Teller coupling at neutral vacancy 0-71453
 diamond, sound excitation orientational effect due to channelled electrons 0-84254
 diamond, two-phonon bound state, Raman freq. 0-65179
 diamond, uniaxial stress splitting of E to E transitions at trigonal centres in cubic crystals 0-97312
 films, elec. and galvanomag. props., microstruct. 0-70859
 force variation due to charged defects 0-92634
 Ge-Si sandwich struct., sputter profiling, combined Auger-X-ray anal. 0-66909
 graphite, resistivity and magnetoresistance, 4.2 to 293K 0-100459
 graphite, thermoelectric power, low temperature, anomaly rel. to phonon drag 0-65610

elemental semiconductors continued

- group IV, Mossbauer spectroscopy of defects, radiation damage and deep levels 0-59533
 ion beam milling, amomalous sputter yield behaviour 0-108624
 ion implanted layers, complex refr. index profile, ellipsometric meas. 0-93262
 irradiation induced crystalline to amorphous transition, Gibbs energy 0-70371
 p-type, infrared absorption and plasma reflection 0-97284
 photon drag detector design and choice of semiconductor 0-57374
 photovoltaic technology, conf., San Diego, CA, USA (Jan. 1980) 0-86041
 ribbon growth using scanned focused CO₂ laser beams 0-66417
 semiconductor depth profiling by electron beam induced junction current meas. 0-96977
 Si:In growth by Czochralski crystal pulling, characterisation for extrinsic IR detectors, focal-plane arrays 0-76168
 p-Si, anodic etching for discriminating between elec. active and inactive defects 0-108605
 p-Si, electron irradiation effect on Hall mobility temp. depend. 0-60011
 Si, ion implanted by high energy C ions structural and optical props. 0-107292
 n-Si, recombination centres and carrier lifetimes after γ -irrad. 0-60004
 Si (111), surface relax., EHT and cluster calcs. (*Chinese*) 0-59762
 Si epitaxy, vapour phase deposition technology 0-75472
 n⁺-Si-Al ohmic contacts, metallisation structs. for very shallow n⁺/p junctions 0-60084
 solar cells, minority carrier MIS diodes appl. (*Slovak*) 0-97792
 SOS structures, high-field electron transport, drift vel. meas. 0-80387
 surface structure, chem. and spectroscopy, review 0-59764
 surface/adsorbate systems, local density of states calcs. (*German*) 0-60062
 uniaxially compressed crystal, exciton molecule radiation (*Russian*) 0-108264
 web dendrites, dislocations, stacking faults, X-ray topographic study (*Chinese*) 0-88148
 Ag-In₂S₃-Si layered struct., Hall effect, I-V characts., surface states (*Russian*) 0-97001
 Al-amorphous Ge-nSi, photoelectric props. 0-70822
 Al-In₂S₃-Si layered struct., Hall effect, I-V characts., surface states (*Russian*) 0-97001
 Al-Si₃N₄-SiO₂-Si, MNOS structures degradation under UV irradiation effect 0-107923
 As, amorphous, absence of photodarkening 0-103970
 As, amorphous, defects, band gap states 0-80215
 As, amorphous, short-range order, theory and probes 0-79698
 Au-Si thin film double layer, silicide form., electron diffraction study 0-80005
 Au-SiO₂-nSi, tunnelling MIS struct. 0-92995
 B, β -rhombohedral, elec. props. at high temps. and in strong elec. fields, thermistor appls. 0-92903
 C:H, film, amorphous elec. props., chem. modifications by doping 0-84523
 Ge (100), dimer reconstruction, photoemission obs. 0-80939
 Ge (111), electron struct., photoelec. props. 0-100493
 Ge (111), spectroscopy of electron subbands 0-71422
 Ge (111) clean surface, O₂ adsorption rate and electron work function 0-59779
 Ge, acceptor complex spectra, tunnelling H systems 0-89036
 Ge acousto-optical deflector performance at 10.6 μ m 0-102835
 Ge, ambipolar hot-carrier size effect kinetics 0-107799
 Ge, amorphous, defects, band gap states 0-80215
 Ge, amorphous, ideal surface, definition and characts. 0-107623
 Ge, amorphous, laser crystallisation, for production of large grained sheets for solar cells 0-93570
 Ge amorphous film, crystn. front velocity during scanned laser crystn. 0-107662
 Ge, amorphous film, DC sputter deposited, effect of trapped Ar on minimum temp. for impulse stimulated explosive crystallisation 0-100422
 Ge amorphous film, disorder induced phonon absorpt. meas. using double beam Fourier spectrometer 0-105725
 Ge, amorphous film, persistent photoconductivity, dangling bonds 0-84487
 Ge amorphous films, structural relaxation and crystallisation 0-100170
 Ge and Ge-diamond bolometers operated at 4.2, 2.0, 1.2, 0.3, 0.1K, design and construction 0-77868
 Ge, anomalous avalanche breakdown 0-80284
 n-Ge, anomalously enhanced plasma diffusion transverse to mag. field 0-96931
 Ge bicrystals, high angle tilt boundaries, TEM (*French*) 0-70224
 Ge, black, solar selective absorber characterisation 0-80112
 Ge, Bragg reflection in case of multiple X-ray scatt. 0-100127
 Ge, carrier relaxation rate temp. depend. and pair density in large electron-hole drop 0-75509
 Ge, compensated, impurity photocond. relax times 0-88592
 Ge, compensated, sub mm radiation absorpt., temp. depend. 0-66331
 Ge, compensated by thermal defects, recomb. and optical props. 0-64989
 Ge complanar X-ray resonator circulating beam, high symm. multiple wave configurations (*Russian*) 0-78875
 Ge crystals, orientational depend. of photoacoustic effect (*Russian*) 0-65167
 Ge crystals., electron beam induced changes of real struct., HVEM 0-103390
 n-Ge, D⁻ state struct. rel. to photocond. expts. 0-59924
 Ge, deep impurity levels, activation energy 0-107742
 Ge detector, high purity, fast neutron damage 0-59526
 Ge, dislocation electron image filtering in electron microscopy 0-75129
 Ge, dislocation electron states, from press. depend. of photocond. 0-96819
 Ge, dislocations under high stress, stacking fault energies, TEM study 0-70202
 Ge, dissociated dislocations, constriction correlation with jogs 0-79801
 Ge, donor polarizability, multivalley effective mass calc. 0-96817
 Ge, EXAFS amplitudes, many-body effects 0-97379
 Ge, EXAFS at high press. 0-97376
 Ge, effective masses of heavy and light holes, from ohmic mobility data 0-80160
 Ge, electron beam irradiation, {111} faults, nature and origin 0-70258
 Ge, electron-hole drop drag by ultrasound (*Russian*) 0-100437
 Ge, electron-hole drop drag, interaction with thermal pulses 0-103631
 Ge, electron-hole drop freq. depend. damping 0-88482
 Ge, electron-hole droplet cloud kinetics, thermalisation phonons 0-88483

elemental semiconductors continued

Ge, electron-hole droplets, percolation theory of cond., expt. 0-92896
 Ge, electron-hole droplets distrib., and phonon wind 0-103629
 Ge, electron-hole liquid, MHD effects 0-80190
 N-Ge, electrorefl. spectra, light induced, electrolyte and Schottky barrier techniques of meas. 0-76046
 Ge, energy gap, impurity conc. depend., calc. 0-80170
 Ge, energy loss spectra of C^{2+} ions 0-65114
 Ge, energy spectra of dislocations 0-70637
 Ge epitaxial film, ion implantation and electron beam anneal effects on carrier conc. 0-75255
 Ge epitaxial film, vac. deposited on GaAs, doping effect of annealed GaAs surface 0-65718
 Ge, epitaxial growth of very thin electron microscopy specimens 0-100793
 Ge, exciton condensation, electron-hole drop investigation in UHF field, nucleation (Russian) 0-80193
 Ge, exciton condensation, light scatt. by electron-hole drops 0-84435
 Ge, exciton droplets, energy condensation (Russian) 0-107712
 Ge, far IR photon drag and radiation pressure in refractive media 0-60048
 Ge, faulted dipoles, high-resolution TEM study 0-103345
 Ge, field-emission current-voltage characts., effect of earlier measurements 0-71579
 Ge film, amorphous, prepared by evap. or sputtering, AC loss meas. 0-65560
 Ge film bolometer, radiation loss from JFT-2 Tokamak, meas. 0-95141
 n-Ge, Hall effect, uniaxial deform. effects 0-65605
 Ge, heavily doped, microcreep breakdown 0-97549
 Ge, heterodiffusion due to H atom surface recombination stimulation, Cu, Zn, In coated (Russian) 0-59726
 Ge heteroepitaxial film, ethanol pulsed adsorption effect on elec. cond. 0-93014
 Ge, high refl. phase conjugation at 10 μ m, intracavity CO_2 laser techniques 0-78894
 p-Ge, IR light free hole absorpt., nonvertical optical transitions (Russian) 0-80802
 Ge, illumination influence on surface cond. irreversible elec. cond. increase (Russian) 0-92963
 Ge, impurity spectral linewidth meas., free electron effects 0-71463
 p-Ge, infrared absorption and plasma reflection 0-97284
 Ge, inhomogeneous stressed, electron-hole drop light scatt. and absorption 0-108212
 Ge, internal Stark effect on impurity states, low-temp. magnet. absorption meas. 0-60636
 p-Ge, intervalence-band transitions, saturation, theory 0-75997
 Ge, intervalley electron-electron scattering effect on optical transitions 0-108267
 Ge, ion beam irradi., defects prod. by individual displacement cascades, TEM study 0-70265
 Ge, ion bombardment-induced photon emission as function of target temp. 0-100698
 Ge, ion-implanted, laser pulse annealing, TEM and channelling study 0-100264
 Ge, ionisation rates, cryst. orientation depend. 0-103700
 n-Ge, laser irradi., accumulation of defects, effect on elec. props. 0-107317
 Ge, laser pulse annealing, induced nucleation, crystal growth 0-84966
 p-Ge, laser radiation excited, gradient EMF anisotropy 0-75604
 Ge, lattice dynamics under press 0-92627
 n-Ge, low temp. galvanomag. effects, shallow attractive traps 0-88575
 Ge, low-field study of p^+nn^+ or p^+pn^+ structs. on forward direction 0-60072
 Ge, mag. field luminesc. lifetime, quantum oscills., phonon wind effects 0-93385
 Ge, magnetoresistance of electron-hole liq., percolation model 0-96920
 p-Ge modulation of 3.39 μ m abs. by CO_2 laser irradi. (Japanese) 0-74410
 Ge, muonium relaxation rates 0-75912
 p-Ge, negative magnetoresist. and Hall effect, press. and field depend. 0-70733
 Ge, neutron irradi., absorpt. edge 0-93320
 Ge, neutron-irradiated, positron lifetime 0-97374
 Ge, nonequilibrium charge carrier-mag. field interaction electron-hole drops, recombination (Russian) 0-75511
 Ge, nonlinear susceptibility, 10 μ m, determ. by time resolved ellipse rotation 0-83633
 p-Ge, odd magnetoresist. under weak carrier heating conditions 0-96917
 Ge optical props. in 2.5-15 micron region 0-80775
 Ge, oscillatory exciton breakdown, microwave cond. 0-103716
 Ge $p^+n^+n^+$ structures, charge transport under impurity freezeout conditions 0-92965
 Ge p-n junction, photo-EMF generation in saturation region 0-75635
 Ge, Pendellosung fringe shape depend. on specimen-film distance (Russian) 0-87994
 Ge, photomagnetic effect, space inhomogeneous nonequilibrium carrier lifetimes (Russian) 0-71152
 Ge, photothermal cond., low temp. depend. 0-70756
 p-Ge, piezo Hall effect meas. 0-96883
 Ge, piezoresistive vibrating circular membrane, reflectance light modulation 0-97232
 Ge, plastically deformed under high temp. creep conditions, elec. props. 0-92915
 n-Ge, proton and γ irradi., minority carrier recombination 0-65591
 Ge, pure, electron hole size distribution at pulse optical excitation 0-59883
 Ge, pure and n-type, US velocity and attenuation, second and third order elastic moduli 0-70325
 Ge ribbon single crystals, grown from melt, dislocation struct. form. under thermal stress 0-107082
 p-Ge, saturable absorption of picosecond CO_2 laser pulses 0-95956
 Ge, saturation of transmitted intensity of CO_2 laser pulses 0-64111
 Ge, self-diffusion, activation energy and entropy factors 0-88353
 Ge single crystals, constitutional supercooling growth conditions, structural and chem. inhomogeneities 0-93473
 Ge single crystals, photopiezoelectric effect under elastic deform. 0-107856
 Ge, spectral diffusion in acceptor-hole system at low temp., ultrasonic hole-burning expt. 0-92610
 Ge, spin Hamiltonian and anomalous muonium states 0-71286
 Ge, stationary creep depend. on deform. stabilisation of material struct. (Russian) 0-100300

elemental semiconductors continued

Ge strain-confined large electron-hole drop characteristics 0-65469
 Ge, supercond. at high press., crit. temp. 0-60130
 Ge surface, (111), ion-bombarded and annealed, spectroscopic ellipsometry study 0-103543
 Ge, surface, Hall effect study, channel cond. (Russian) 0-92909
 Ge surface states, recomb. centres, regularities, electrolyte contact effects (Russian) 0-65652
 Ge, thermal conductivity of semiconductors, quantum acoustical method, thermal phonon lifetimes 0-65312
 n-Ge, thermal phonon scatt., piezo-thermal cond. 0-70482
 n-Ge, thermoelec. power in quantising mag. field, phonon-phonon interactions 0-107832
 Ge thin films on glass substrates, annealing by Ar ion bombardment 0-80136
 Ge, uniformly deformed, free carrier cyclotron resonance, electron-hole drops (Russian) 0-71182
 Ge, vacancy formation and stability due to noncentral force 0-70192
 Ge, volume plasmon, cryst. orientation influence 0-80921
 Ge X-ray detector, Au contact layer thickness meas. 0-62627
 Ge, ^{119m}Sn , impurity lattice dynamics, Mossbauer spectra, Debye temp. 0-84262
 Ge:Ag(Ni), gamma ray effects on impurity states 0-96822
 Ge:As, Sb, Hall mobility, temp. dependence 0-96919
 p-Ge:As,Sb,Hg(Zn), radiation-defect form., Au influence 0-92911
 Ge:As film strain gauges, press. sensor (Japanese) 0-105631
 Ge:B(Al)(Ga), shallow acceptor spectral line intensities 0-88517
 Ge:Be, p, absorption of radiation, 0.6-2.8 mm, 4.2 to 20K 0-66332
 Ge:Cu, solubility and behaviour of Cu, internal friction investigations 0-92678
 Ge:Cu, surface waves at static domain boundaries (Russian) 0-80288
 Ge:Ga, resonant scattering of phonons by bound holes in temp. range 1 to 5K 0-75393
 Ge:In (Sb) and pure cryst., kinetics of strain-confined large electron-hole drop and its clinging exciton system 0-75508
 Ge:In(Hg), impurity characterisation from thermal carrier meas. 0-65595
 Ge:Li, Cu p-n junctions, current stimulated LiCu complex formation, photocurrents 0-107897
 Ge:Mn, Sb, recombination waves, convective instability development 0-70721
 n-Ge:Ni p^+n-n^+ structs., double-injection current-voltage characts. 0-60074
 Ge:O, Cu, amorphous thin film, impurity effects on struct. 0-107054
 Ge:O, IR absorpt. at low temp. (Chinese) 0-108228
 Ge:O, slow thermal relax. of cond. rel. to donor complexes 0-70704
 Ge:P, charact. temp. and lattice thermal cond. 0-59743
 Ge:P, phonon drag thermoelectric power at low temp. 0-107828
 Ge:P(Sb)(Bi), γ -irrad., carrier trapping and recomb. at point radiation defects 0-107810
 Ge:Pb, ion implanted damaged layer, laser induced reorder 0-84201
 Ge:Pd and pure, photoelectric props., surface states (Russian) 0-60043
 Ge:Sb, electron-hole drop lifetime, quenching temp. influence 0-59889
 Ge:Sb, excited donor states, double optical transitions, reson. absorpt. meas. 0-93371
 Ge:Sb, heavily doped, mass anisotropy, and multiple scattering effects 0-107802
 Ge:Sb, heavily doped semicond., scatt. mechanism, resist, and Hall coeff. maxima 0-75586
 n-Ge:Sb, high-field Hall effect spectroscopy 0-65600
 Ge:Sb, Ni(Mn), recombination wave spectrum, two-level traps 0-96906
 Ge:Sb, Zn(Hg), photoelec. props., 70 to 300K 0-65621
 Ge:Sb,Cu, high resist. compensated, impurity of photocond., pulsed unipolar injection carriers 0-92935
 Ge:Sb,Cu, photoelec. props., fast electron irradi. effects 0-60036
 Ge:Sn, ion implantation of radioactive ^{119}Sn 0-59495
 Ge:Zn photoresistor, current responsivity rel. to nonequilib. hole lifetime 0-60035
 Ge:Zn 11 , G and D lines, stress induced components 0-71447
 Ge:Zn 11 carrier lifetime, nonequilibrium, phase method for determ. 0-65629
 Ge/GaAs (110) heterojunction, valence band discontinuity in XPS spectra, precise determ. 0-84834
 Ge-GaAs, heteroepitaxial systems, misfit dislocations obs. using HV electron microscopy 0-100242
 Ge-GaAs heterojunction, elec. and recomb. props., interface defect effects 0-80365
 Ge-InAs based MIS struct., avalanche carrier multiplication 0-88566
 n-Ge-metal Schottky barrier contacts, IR optoelectronic props., quantum detector appls. 0-75640
 n-Ge-n-GaAs isotype heterojunctions, modelling, characts. 0-103747
 Ge-Sb, far IR emission stimulation by impact ionisation 0-66301
 Ge-Si $_3$ N $_4$ system, potential barriers determ. from photoinjection carriers trapping 0-103756
 n-Ge-ZnSe:Mn $^{2+}$ -In $_2$ -Sn $_2$ O $_3$ - γ thin film electrolum. cell with low-threshold voltage 0-84786
 Ge(Li) detector, fast neutron damage 0-59525
 Ge(111) surface, diffuse scatt. at high temp., RHEED study 0-80043
 (In $_2$ -Sn $_2$) $_2$ O $_3$ - γ Si solar cells, degradation 0-94047
 In $_2$ -Sn $_2$ O $_3$ -insulator-poly-Si solar cells, photovoltaic conversion parameters 0-101093
 LiNbO $_3$ -Si, acoustoelectronic memory, effect of band-bending 0-70771
 MIS solar cells, comparison of majority- and minority carrier 0-85280
 n $^+$ -n-pGe avalanche photodiode, noise factors, internal quantum efficiency 0-70803
 n-Si, (111) inversion layers, valley splitting, Shubnikov de Haas oscills. 0-65698
 n-Si, Fe, O_2 -coated, heterostruct. photoanode for photoelectrolysis of water 0-61384
 NaX-Se semiconductor superlattice absorpt. edge, light scatt. (Russian) 0-71438
 PbS-Si heterojunction, space charge capacitance, PbSn film thickness depend. 0-88630
 PbS-Si heterojunction, PbS film growth and struct. 0-96762
 Pd-Si structure, epitaxial silicide growth, LEED and AES study 0-103590
 Pt-Si:As, silicide form. during laser irradi., p-n junctions and ohmic contacts 0-84397
 Se, amorphous and liquid state, Raman spectra, crystn. processes 0-60608
 Se, amorphous, bulk, Raman scatt. near Tg 0-60596
 Se, amorphous, bulk, reson. Raman scatt. 0-60597

elemental semiconductors continued

- Se, amorphous, elec. cond., activation energy, density, cryst. Se effect 0-65548
 Se, amorphous, electronic struct. and optical props., pseudopot. calc. 0-65428
 Se, amorphous, luminescence 0-80862
 Se, amorphous, transient electrical transport, general and unified treatment 0-59977
 Se, amorphous, US attenuation at low temp., internal friction peak 0-65152
 Se, amorphous, US relaxation and retardation of deform. near T_g point 0-84256
 Se, amorphous and liq. state, mol. structure, local atomic arrangement at intrinsic bonding defects 0-59374
 Se, amorphous film, dielec. activity obs. near glass transition temp. 0-75933
 Se, amorphous film, highly disordered, UPS study 0-76148
 Se, amorphous film, influence of wavelength on optical quenching of photoconductivity 0-60046
 Se, amorphous film, photocond., dark cond., rel. to crystn. 0-88596
 Se, amorphous films, evaporated, ageing and crystn., DTA 0-65413
 Se, amorphous layer, localised states in band gap 0-59928
 Se, appl. to xerography 0-57415
 Se, bonding coordination defects 0-59927
 Se, charge density, self-consistent OPW and pseudopot. calcs. 0-92813
 Se, electronic struct. of cryst. phases and hydrostatic press. effects 0-59865
 Se films, Ag diffusion, effect on interferometric thickness meas. 0-96695
 Se, glassy, localised electronic states, photoluminesc. and ESR studies 0-65501
 Se, liq., electronic transport props., equation of state, to 1900K and 1800 bars 0-65574
 Se, metallic state, press. induced, elec. cond. meas. 0-96949
 Se, modulated photocurrent, analysed for trap-limited case (*Japanese*) 0-60030
 Se, photoelectronic behaviour, in glass transition region 0-60045
 Se, polycryst., low-frequency coupled photocurrent and temp. oscillation 0-60044
 Se powder compacts, sintered, electrical cond. 0-70693
 Se, rhombohedral, IR absorpt. spectrum 0-103949
 Se, SAW vel. and electromech. coupling factor 0-75422
 Se, thin film selective absorber coatings, prod. using an oblique vacuum deposition technique 0-81488
 Se, trigonal, acoustoelectric current saturation 0-60053
 Se, trigonal, behaviour of optical gap under press. 0-80171
 Se, trigonal, normal mode calcs. 0-84259
 Se, trigonal, Raman scatt. at very high press. 0-60566
 Se, trigonal, transverse magnetoresistance meas., influence of illumination 0-65607
 Se, trigonal and amorphous, electronic struct. and nonempirical calc. of struct. props. 0-59866
 Se, trigonal and amorphous, positron lifetimes, positronium form. 0-60711
 Se, trigonal and vitreous, sp. ht. and thermal cond., 3 to 300K 0-59676
 Se:As, amorphous film, dielec. activity obs. near glass transition temp. 0-75933
 Se:As X-ray plates, electronic transport (*German*) 0-80290
 Se:I, vitreous, crystn, kinetics determ. (*German*) 0-79936
 Si, (001) (2×1) reconstructed surface, dimer model self consistent calcs. 0-88613
 Si, (001) and (111), geometrical and electronic struct., review 0-80039
 Si (001) substrate for Pd:Si epitaxial islands 0-96748
 Si (001) surface struct., high energy ion scatt. study 0-59772
 Si (001) wafer, pyramidal hillocks, TEM obs. during chemical etching 0-70508
 Si (1,1,0) direction, channelled particle radiation spectra, emitted quanta angular distrib. 0-96578
 Si (100), (111) substrates for rare earth metal silicide thin film formation, backscattering study 0-70542
 Si (100), dimer reconstruction, photoemission obs. 0-80939
 Si (100), H adsorption, MeV ion scatt. study 0-80071
 Si (100), vicinal, LEED obs. of stepped surface 0-59773
 Si, (100) inversion layer, electromigration in two dimensional electron gas, driving force 0-84441
 Si (100) reconstructed surface struct. study using thermal energy He diff. 0-60731
 p-Si, (100)-oriented, n-channel inversion layers, MOS field-effect devices, mag. quantisation effect on surface capacitance 0-70834
 Si, (110) oriented, electron optical conditions for struct. image form. 0-75131
 Si, (110) plane, quantum state observation during fast electron channelling (*Russian*) 0-59541
 Si (111), intermediate oxidation state, core photoelectron absorpt. vs. chemical shifts 0-81220
 Si (111), ion bombard., struct. changes, AES obs. 0-79842
 Si (111), nitridation, AES and LEED results 0-80041
 Si (111), surface structure, high temp. RHEED obs. using metal-backed fluoresc. screen 0-75126
 Si (111) 7×7 clean surface and O chemisorbed stage valence band density of states from $L_{23}VV$ Auger spectra 0-100717
 Si (111) 7×7 surface structure investigation, RHEED 0-96723
 Si, (111) surface, proton dechannelling under channelling, blocking and double alignment conditions 0-88235
 Si, (111) surface structure phase transform, screw dislocations RHEED study 0-88153
 Si, (111) surface substrate for NiSi₂ epitaxial film, interfacial order, backscatter, channelling study 0-65390
 Si (111) surface substrate for Al film, struct., props. depend. on vapour flow (*Russian*) 0-75453
 Si (111) surfaces, cleaved, electronic structure following Al adsorption 0-75610
 Si (111)- 1×1 , electronic struct. of surface, model pseudopot. calc. 0-65651
 Si, advanced material for space solar cell 0-94007
 Si, ambient effect of O precipitation, self interstitial mechanisms, IR spectra, TEM study 0-66510
 Si, amorphous, defects, band gap states 0-80215
 Si, amorphous, doped, electronic props. 0-80283
 Si, amorphous, EPR and spin-dependent effects 0-80592
 Si, amorphous, elec. props., ion implantation effects 0-79828

elemental semiconductors continued

- Si, amorphous, epitaxial regrowth, structure and impurities effect 0-84401
 Si, amorphous, glow discharge deposited, mobility edge calc. 0-80220
 Si, amorphous, glow discharge produced, defect creation, high optical excitation 0-97327
 Si, amorphous, hydrogenated, electron drift mobility meas. 0-75565
 Si, amorphous, hydrogenated film, electroreflectance study 0-88967
 Si, amorphous, hydrogenated and deuterated, struct. 0-103245
 Si, amorphous, hydrogenation using DC and HF plasma treatment 0-59497
 Si, amorphous, ideal surface, definition and characts. 0-107623
 Si, amorphous, implanted, recrystn. induced by scanning CW laser, reaction rates, analytical model 0-66334
 Si, amorphous, ion implantation, negative magnetoresist., localised mag. states 0-70731
 Si, amorphous, ion implantation method, B and P ions 0-100274
 Si, amorphous, laser crystallisation, for production of large grained sheets for solar cells 0-93570
 Si, amorphous, Lifshitz constant for calc. of van der Waals force between two solids (*French*) 0-107658
 Si, amorphous, luminescence 0-80862
 Si, amorphous, opaque, surface phonon attenuation, Brillouin scatt. 0-80808
 Si, amorphous, prep. by reactive RF sputtering in Ar-silane mixtures, undoped, n-type and p-type targets 0-76182
 Si, amorphous, pure and H doped, picosecond relax. of optically induced absorption 0-97302
 Si, amorphous, pure and hydrogenated, far IR absorption coeff. meas. 0-108213
 Si, amorphous, random-network model, charge-density variation 0-80165
 Si, amorphous, solar cells, design considerations 0-85277
 Si, amorphous, solar cells, barrier props. determ. by differential I-V characts. meas. 0-94053
 Si, amorphous, sputtered, resist. control by ion implantation 0-100262
 Si, amorphous, substrate orientation effect on regrowth by laser pulses, channeling, backscatter 0-84409
 Si, amorphous, transient electrical transport, general and unified treatment 0-59977
 Si, amorphous, transport results, interpretation 0-80260
 Si, amorphous, UHV evaporated, annealing behaviour of spin density 0-93163
 Si, amorphous, undoped, photocond., continuous illum. effect 0-84486
 Si, amorphous and crystalline, heating by Q-switched laser radiation 0-84963
 Si, amorphous and crystalline, ion implanted, UPS meas. 0-97411
 Si, amorphous and polycryst. thin film solar cells, perform. parameters, review 0-93882
 Si, amorphous co-sputtered doped, photovoltaic material appl. 0-93488
 Si, amorphous evaporated, picosecond optoelectronic detect., sampling and correlation meas. 0-100478
 Si amorphous film, acoustic study using Rayleigh waves 0-75312
 Si, amorphous film, analytical techniques, review 0-80120
 Si amorphous film, anisotropic etching phenomenon, appl. as solar selective absorber surfaces 0-72054
 Si, amorphous film, EELS microanalysis 0-100722
 Si, amorphous film, glow discharge deposition, rate enhancement by mag. field 0-65412
 Si, amorphous film, RF plasma deposition from SiCl₄-H₂, characterisation 0-66435
 Si, amorphous film, selective laser recrystn. over heavily doped lines 0-84947
 Si, amorphous film, TSC, density of localised states distrib. 0-65587
 Si, amorphous films, halogenated and hydrogenated, elec. and optical props. 0-97016
 Si, amorphous films, hopping conduction, dangling bond generation by high temp. annealing 0-60115
 Si, amorphous films, RF sputtering prep. at high Ar press., props. obs. 0-80418
 Si, amorphous hydrogenated, fabrication method 0-80956
 Si, amorphous hydrogenated solar cells, field depend. quantum efficiency, electron-hole recombination 0-66971
 Si, amorphous layer prod. by ion implantation, diffusion broadening, ESR study 0-92552
 Si amorphous layer recrystallisation by laser beam 0-93566
 Si amorphous layers, glow-discharge, laser-annealed, elec. props. 0-75661
 Si, amorphous layers, RF-sputtered on sapphire, crystallisation by CW ion laser annealing 0-80109
 Si, amorphous layers, recrystallisation, pulsed laser annealing 0-65404
 Si amorphous p-n junctions, high current, characts. 0-70807
 Si, annealed, neutron-irradiated, EPR centre (S=1), characts. 0-71177
 Si, annealed, photoluminesc. anal. of defects 0-80836
 Si, annealing, using laser pulses, impurity incorporation at melt-cryst. interface 0-59504
 Si, annealing during Czochralski growth, influence on defect density 0-60769
 Si anodic oxidation in RF induced O plasma 0-100931
 Si, anodisation at low substrate temp. by low pressure O₂ plasma 0-104314
 Si, anomalous avalanche breakdown 0-80284
 Si, anomalous etch structures using ethylenediamine-pyrocatechol-water based etchants and their elimination 0-81217
 Si, anomalous sputter yields of interfacial species, cascade mixing process for interpretation 0-76122
 Si, Ar ion etching, carbide form. 0-81222
 Si, as-grown Czochralski crystal, multiple p-n junction structure obtained by heat treatment, appl. to solar cells 0-101099
 Si, Auger spectra, KLL and KLV, screening effects and plasmon gains 0-80913
 Si, Auger spectra induced by 100 keV Ar⁺ impact 0-84820
 Si back surface field solar cell degradation at high intensity due to base cond. modulation loss 0-94085
 Si based alloys, amorphous, photovoltaic behaviour, solar cell appl. 0-94051
 Si based MIS negative barrier contact for induced back surface field solar cell 0-101101
 Si based MIS structure, photoelectric characts. carrier injection levels (*Russian*) 0-96946
 Si based MOS capacitors, scanning photovoltage investigation 0-80396
 Si based MOS device irradiation with γ -rays, minority carrier generation, CV characts. 0-88637

elemental semiconductors continued

- Si, bent crystal, γ -radiation beam deflection due to 900 MeV channelled electrons 0-84223
 n-Si, bipolar ohmic contact with macroscopic recomb. centres. 0-80379
 Si, blistering due to 400 to 1800 keV $^4\text{He}^+$ ions, modal range determ. 0-100289
 n-Si, bound excitons and bound multiexciton complexes, excitation spectra 0-96792
 Si, bound-exciton spectral lines, conc. broadening at high impurity concs. 0-80826
 Si, bulk deep centres, continuous energy spectrum, isothermal capacitance relaxation method 0-107741
 Si, bulk plasmon dispersion, electron energy loss spectra meas. 0-59899
 Si, CVD, surface anal. during growth using RHEED and Auger spectroscopy 0-66433
 Si, CVD amorphous films, effect of surface characts. on visible and UV optical props. 0-60698
 Si, CVD from $\text{SiH}_4\text{-HCl-H}_2$ system, rate-determining reactions and surface species 0-84405
 Si, carrier capture at amphoteric deep level defects 0-88569
 Si, carrier lifetime depth distrib. due to Ar ion implantation 0-70232
 Si, cast, growth structure and photovolt. props. of solar cells 0-94008
 Si, cast polycryst., laser annealed for solar cells 0-93918
 Si, cast polycryst. p-n junction solar cell, hydrogenation effects 0-93916
 n-Si channel (100) inversion layer MOSFET, valley splitting, conductivity 0-70840
 Si, channelling of relativistic protons in bent crystals, theory 0-96581
 Si, chemisorption of XeF_2 and SiF_4 , XPS and Auger spectra, surface chemistry 0-81358
 Si chip manufacture for fibre alignment in lightguide cable connectors 0-64188
 Si coated with Pd, interference effects on irradiation with laser beam 0-66333
 Si, commercial, nitridation, effect of BaF_2 0-81359
 Si, compensated by thermal defects, recomb. and optical props. 0-64989
 Si, compensated monocrystal, IR absorption spectra, Fourier transform obs. 0-60644
 Si concentrator cells, high efficiency, design, fabrication and meas. 0-93938
 Si concentrator solar cells, new technology for fabrication 0-81457
 Si concentrator solar cells, effects of nonuniform illumination 0-93942
 Si concentrator solar cells, high efficiency, state-of-the-art design and processing 0-93958
 P-Si, conductivity and carrier lifetime, high injection effects 0-70719
 Si conductor-insulator-semiconductor solar cells, automated-production, outlook 0-94021
 Si, controlled dislocation formation, struct. density (Russian) 0-107244
 Si, core exciton binding energies 0-80188
 Si, core structure of glide-set 90° and 30° partial dislocations 0-96523
 Si, crack-tip dislocation pattern, X-ray topography (French) 0-107253
 Si, crucible grown, virgin and implanted, laser irradiation effects on surface structure 0-92768
 Si crystal, contrast depend. of Kikuchi patterns on primary electron beam energy (Russian) 0-64844
 Si crystal, Czochralski grown, enhanced Borrmann effect 0-70191
 Si crystal, impurities determ. and resistivity after reactor neutron irradiation 0-65563
 Si, crystal defects and impurities interaction obs. by electron microscopic methods 0-65003
 Si crystal growth, for electronic devices 0-66419
 Si crystal microcrack detection by ultrasonoreflection 0-66733
 Si, Czochralski grown, dislocation free, swirl defect form., doping effect 0-92519
 p-Si, Czochralski grown, microdistrib. of O, SEM and spreading resist. obs. 0-79830
 Si, Czochralski grown, oxide precip. homogeneous nucleation 0-65221
 Si, Czochralski grown, oxide precipitates, diffusion-limited growth 0-97484
 Si, Czochralski grown crystal, O precip., nucleation behaviour and dislocation loop form. (Japanese) 0-59664
 Si, Czochralski grown crystals, swirl-type defect obs. 0-100236
 Si, DC MOSFET dopant profile method 0-70244
 Si, deep impurity levels, activation energy 0-107742
 Si, deep level defects, struct. bonding, amphoteric centres 0-88506
 Si, deep-level point defects, effective-mass nature 0-59922
 n-Si, defect charge states, complex form., gamma-ray effects 0-96564
 Si, defects, divacancy and split 100 interstitial, electronic structure calc. 0-65494
 Si, deformed, annealed and recrystallized, struct., implications for solar cells 0-60922
 n-Si, deformed, thermal treatment effect on elec. cond. and dislocation mobility 0-107265
 Si dendritic web for solar cells 0-89634
 Si, dense plasma dynamics during pulsed laser annealing, carrier density, recombination 0-84479
 Si, deposition on rotating disc, one-dimens. model 0-75461
 Si, deposition using solar furnace 0-89148
 Si devices, metallisation, TiN and TaN as diffusion barriers 0-65304
 Si, dielectric function spectra, ellipsometric determ., many-particle effects at E_g -transition 0-93363
 Si, diffracted X-ray channelling by special deform. fields 0-100295
 Si, diffusion and power spectral density and correl. function of vel. fluctuation for electrons 0-65576
 Si, diffusion coefficient determ. from carrier conc. depth profile 0-107566
 Si diffusion in Au-refractory thin film systems obs., by combination of scattering techniques 0-65308
 Si, diffusion mechanism of P, migration channels along vacancies and interstices 0-79996
 Si, diffusion of B from CVD BN covered with Si_3N_4 , appl. to master slice p-MOS IC 0-107564
 Si, diffusion of P, elastic deform. relax. and dislocation generation 0-79997
 Si diode, impurity profiles, scanning electron microprobe anal. 0-79832
 Si diode radiation detector, stabilisation of radiation damage 0-91377
 Si dislocation free, quantitative determ. of microdefect density by preferential chem. etching 0-65001
 Si, dislocation generation in local oxidation 0-107245
 Si, dislocation motion from indentation rosette 0-79798
 Si, dislocation-free, deep centres formed after high temp. treatment 0-96824
 Si, donor polarizability, multivalley effective mass calc. 0-96817

elemental semiconductors continued

- Si, doping impurity distrib., during cryst. growth by Czochralski method (Russian) 0-100276
 Si, EFG ribbon, characterisation by ion beam tech. 0-79833
 Si, effect of disorder on H content 0-75258
 Si, effective masses of heavy and light holes, from ohmic mobility data 0-80160
 Si, elasto-optic constants, real and imaginary, direct absorpt. and Raman scatt. meas. 0-97234
 n-Si, elec. cond. control by hot electron intervalley transfer 0-59993
 p-Si, elec. resist., shock wave compression effects 0-80265
 Si, electrical conductivity, inertia of electron heating, expt. and theory 0-65613
 Si, electron and hole effective mass, intrinsic conc., temp. depend. 0-107692
 Si, electron beam annealing, beam voltage effect modeling 0-75275
 Si, electron beam irradiation, {113} faults, nature and origin 0-70258
 Si, electron beam scan annealed, deep levels 0-65481
 Si, electron drift in high elec. fields, long-time tail of autocorrelation function 0-103702
 n-Si, electron heating by static elec. field 0-96894
 Si, electron-irradiated crystals, positron trapping, temp. depend. 0-104009
 Si, electronic interface states in intrinsic stacking-faults 0-75522
 Si, electrotransfer in Mo_2Si_3 0-92708
 Si, energy gap, impurity conc. depend., calc. 0-80170
 Si, energy spectra of dislocations 0-70637
 Si, enhanced conductivity in plasma hydrogenated films, thermionic emission 0-70692
 Si, epitaxial, on sapphire, characterisation, X-ray rocking curves 0-75458
 Si, epitaxial (111) surface, etching observation of stacking faults, dislocations, S-pits, etch pits (Chinese) 0-70197
 Si epitaxial film, containing struct. defects formed during growth, positron annihilation 0-93433
 Si epitaxial film on sapphire, microtwins, TEM exam. 0-70555
 Si epitaxial films on Czochralski sapphire, optimisation of deposition conditions in $\text{SiH}_4\text{-H}_2$ system 0-75464
 Si, epitaxial growth on sapphire by partially ionised vapour deposition, RHEED-AES obs. 0-80985
 Si, epitaxial layer deposition by ion beam methods 0-100417
 Si epitaxial layer regrowth due to laser annealing mechanism, liquid and solid phase regimes 0-100712
 Si, epitaxial layer thickness meas. using phase correction function of substrate resistivity (Hungarian) 0-90812
 Si epitaxial layers, grown in vac. at low temps. P and Sb doping 0-88189
 Si epitaxial layers, meas. of doping profiles (Hungarian) 0-70545
 Si, epitaxial layers, stacking defect distrib. anal. using ion channelling tech. 0-100294
 Si epitaxial layers, vacuum deposited, conditions for impurity migration from B, P, Sb doped sources (Russian) 0-107570
 n-Si epitaxial layers on oppositely conducting substrates, two layer Hall coeff. meas. technique 0-80297
 Si epitaxial thin film growth on sapphire and spinel by MBE 0-76186
 Si, epitaxial wafer, saucer pit microdefects reduction by intrinsic gettering 0-75450
 Si epitaxy, autodeposition effects 0-100259
 Si, etching by CF_4 , plasma deposition reactor gas phase characts., mass spectra 0-70566
 Si, etching characts. using reactive ion etching with tetrafluoromethane- Cl_2 gas mixture 0-104313
 Si, etching in He-F_2 plasma, etch rates, mass spectra, direct ion sampling study 0-79510
 Si, etching in reactive plasmas 0-71778
 Si, F-enhanced plasma growth of native layers, Auger profiles 0-93662
 Si, far IR photon drag and radiation pressure in refractive media 0-60048
 n-Si, Faraday rot. temp. depend., effective mass determ. 0-71392
 Si film, amorphous, glow discharge deposited, for low cost solar cells 0-61355
 Si film, amorphous, hopping cond. control by ion bombard. induced struct. modification 0-92898
 Si film, ion bombarded, crystalline-to-amorphous transition, defect-rich film prep. 0-65071
 Si film, low press. CVD prep., struct., elec. and optical props. 0-70548
 Si film, MBE, cryst. defect props., substrate treatment effects 0-70551
 Si film, polycryst., grain struct. and surface roughness, TEM study 0-70556
 Si film, polycryst., laser-induced CVD growth from SiCl_4 0-84852
 Si film, semi-insulating, with 40 at. % O, AES and PES study 0-107939
 Si films, electron beam evaporated, for MIS solar cells 0-93490
 Si films, RF sputtered, Ar conc. as function of operation frequency and discharge pressure 0-65393
 Si films, ribbon-against-drop process, physical and chemical characterisation 0-92798
 Si, fine structure of lowest exciton state (Russian) 0-96801
 Si, float zone, meas. of deep levels by photovoltage spectroscopy 0-103723
 Si, float zone, process-induced effects on carrier lifetime and defects 0-81216
 Si, float zone crystal, dislocation creation and elimination 0-107072
 Si for integrated optics high quantum efficiency waveguide coupled photodetectors 0-58805
 Si, free excitons, drift and diffusion, luminesc. obs. 0-84434
 Si, furnace preannealed (111) ion implanted, laser irradiation 0-65015
 Si, gettering by ion damage, minority carrier lifetime and backscatt. study 0-100286
 Si, grain boundary defects in thin semicrystalline material 0-93889
 Si, grain boundary elec. props./impurity correl. using surface anal. of multigrained samples by SIMS and AES 0-79816
 Si, graphoepitaxy on fused SiO_2 using surface micropatterns and laser crystn. 0-70554
 Si, ground state props. in density-functional pseudopot. approach 0-92803
 Si, HYEM struct. images of extended 60° and screw dislocations 0-59466
 Si, heavily doped, excess intrinsic carrier density, deionisation of impurities as explanation 0-96864
 p-Si, heavily doped, intra- and interband Raman scatt. by free carriers 0-108208
 Si, heavily doped, microcreep breakdown 0-97549
 Si, heavily doped, minority-carrier transport parameters meas. 0-80291

elemental semiconductors continued

p-Si, heavily doped contact layers on IR detectors, IR transmissivity 0-108190
Si, heavily doped films, electromigration obs. 0-65295
Si, heavy ion induced disorder in surface and at shallow depths 0-59535
Si, high dislocation density crystals, photoelectret state investigation 0-97191
Si, high dose self-irrad., spatial correl. between primary and secondary defect profiles 0-59536
Si high efficiency solar cells, laser annealing, reviews 0-93976
Si, high electronic current density in anodic oxidation 0-89386
Si, high rate reactive ion etching 0-85070
Si, high-dose Ar implantation, X-ray topographic obs. of strains and damage 0-59496
Si, high-resistivity layer form. during electron irrad. 0-80352
Si, hole-hole-electron Auger recombination 0-70720
Si, hydrogenated amorphous, laser annealing 0-100713
Si, hydrogenated amorphous, gap states, comparison of photoemission and photocond. results 0-103724
Si, implantation, microstruct., fabrication, ion channelling effects 0-70230
Si, implanted crystal, laser induced annealing and diffusion behaviour 0-88202
Si, implanted with low solubility dopants, laser annealing, TEM study 0-70233
Si, impurity content characterisation, exciton luminesc. 0-60653
Si, impurity solubility limit after laser induced melting 0-107426
Si, impurity states, localised orbital approach 0-92851
Si in MOS structure Pt diffused, hysteresis and memory props. 0-96992
a-Si $In_xSn_{1-x}O_2$ /YZ 0-101113
n-Si inversion layers, electronic g-factor, spin-split Landau levels 0-80346
Si inversion layers, harmonic generation due to hot electrons 0-65694
Si inversion layers, mobility temp. depend., Coulomb and surface roughness scatt. 0-80390
Si, inversion layers, nonmetallic cond. at low temp. 0-70833
Si inversion layers, phase diagram in strong mag. fields 0-88492
n-Si inversion layers, resist. temp. depend. at liq. He temps. 0-80391
Si, ion beam irrad., defects prod. by individual displacement cascades, TEM study 0-70265
Si, ion bombardment, anomalous surface damage from channelling-backscatt. meas. 0-84222
Si, ion bombardment induced defect distrib., IR and electron-diffr. study 0-65074
Si, ion damage TEM study of laser annealing 0-88215
Si, ion implantation, channelled, through metal silicide film 0-70231
Si, ion implantation, channelling, alignment effects 0-88183
Si, ion implantation, high dose, solid phase epitaxial regrowth 0-103380
Si, ion implantation by laser annealing, characterisation, solar cell applications 0-70247
Si, ion implanted, annealing of heavy ion cascade damage, channelling meas. 0-89255
Si, ion implanted, annealing by ion beam heating 0-103382
Si, ion implanted, CW laser annealing 0-92550
Si, ion implanted, complex annealing behaviour of amorphous layers, TEM obs. of defect struct. 0-107299
Si, ion implanted, damage profiles, Rutherford backscattering 0-100733
Si, ion implanted, damage struct. obs. using TEM and cross section specimens 0-107298
Si, ion implanted, defect struct., dislocation loops and elongated defects 0-107300
Si, ion implanted, dopant depend. of oxidation rate 0-89384
Si, ion implanted, electron beam annealing, surface struct. study using SEM 0-70235
Si, ion implanted, radiation defect production at different temps. 0-103398
Si, ion implanted, scanning CW and pulsed laser annealing 0-92549
Si, ion implanted, self implanted, self annealing using high ion current density treatment 0-89254
Si, ion implanted, standard for TEM, EELS 0-99017
Si, ion implanted films, optical and luminesc. props. 0-60699
Si, ion penetration, computer program 0-88185
Si ion-controlled diodes, acid-base exposure effects, SiO_2 -Si interface state density 0-96984
Si, ion-implanted, annealing using scanning CW laser system 0-100265
n-Si, ion-implanted, elec. characts. after laser annealing 0-88562
Si, ion-implanted, impurity activation monitoring by SAW techniques 0-65020
Si, ion-implanted, laser pulse annealing, TEM and channelling study 0-100264
Si, ion-implanted amorphous, laser epitaxial recrystallisation threshold energy 0-70571
Si ion-implanted dopant redistribution under laser annealing 0-70242
Si, ion-implanted layers, crystn. by ns laser pulses, TEM and RHEED 0-100421
Si, ion-implanted layers, epitaxial regrowth by laser beam and flash annealing 0-100420
Si ion-implanted solar cells, factors controlling efficiency 0-81451
Si ion-implanted solar cells 0-81452
Si, isolated dislocation motion, velocity determ. (*Chinese*) 0-107243
Si, isolated vacancy, electronic struct., SCF method 0-80208
Si, joining and recrystallisation using thermomigration process 0-65298
Si junction diode, diffused, with deep level traps, negative capacitance 0-96976
Si junction diodes, fabrication by LPE on Si:B substrates, and characts. 0-80363
Si, L-shell ionisation by 80 keV electrons, transmission electron energy loss spectrometry 0-60721
Si large grain films on metallurgical Si substrates, chem., struct., elect. and photovoltaic props. 0-61357
Si laser annealed, nonequilibrium solubility and segregation 0-84296
Si, laser annealing, nonlinear dynamic transport processes 0-93437
Si, laser annealing mechanisms, disordered overlayers, crystalln. 0-84967
Si, laser annealing of semiconductors, review 0-107301
Si laser annealing of SiO_2 layers 0-97505
Si, laser damage statistics rel. to structural defect statistics 0-91829
Si, laser heating of lightly damaged material, carrier diffusion effect 0-84809
a-Si, laser induced crystallisation mechanism, epitaxial regrowth 0-84962
Si, laser induced dense plasma, dynamics 0-65612
p-Si, laser irrad., accumulation of defects, effect on elec. props. 0-107317
Si, laser pulsed heating, lattice temp., Raman meas. 0-80780

elemental semiconductors continued

Si, lattice dynamics under press 0-92627
Si, lattice strains induced by localized oxidation, high temp. real-time X-ray topographic studies 0-108489
n-Si, lattice vibr. excitation conditions, vol. charge redistrib. effect (*Russian*) 0-103427
Si layer, on buried SiO_2 layer formed by high-dose, O ion implantation, TEM, AES, and XPS obs. 0-88172
Si layers amorphized by molecular ions, laser annealing 0-103379
Si, lifetime in Ar^+ ion implant damage getterred, MOS voltage ramping 0-75247
Si lightguide connector component characts. 0-69544
Si, liq., dissolution of quartz, effect of C, rel. to melt growth 0-70414
Si, liquid, interaction with die material during edge defined film fed growth 0-104060
Si, local pseudopotential, Gaussian band charge model 0-88477
Si MIS capacitors, C-V curves, outer oxide surface conditions effects 0-97000
Si MIS grating solar cells on minority carrier blocking back surface field substrates 0-94078
Si MIS phototransistors, photoelec. props. at high illum. intensities 0-60101
Si MIS solar cells with Cr, Hf, Be, Sc and Y as barrier forming metals, expt. investigation 0-94077
Si MIS/inversion layer solar cells 0-94075
Si, MOS capacitor, interface state parameter determ. by DLTS 0-65642
Si, MOS diode, dependence of minority carrier bulk generation on HCl concentration 0-88639
Si MOS tunnel junctions, processing condition depend. of props. 0-80380
Si materials, advanced, preliminary evaluation for space solar cells 0-94006
Si, melt grown crystals, impurity incorporation, calcs. 0-79718
Si, metallic state, press. induced, elec. cond. meas. 0-96949
Si, metallurgical grade, impurity gettering of polycrystalline solar cells 0-81441
Si, microcracks detection using US sonoprobe 0-76462
Si, migration of Au, electron bombardment effects 0-100362
Si, minority carrier lifetime improvement through laser damage gettering 0-65589
Si minority carrier MIS solar cells, design and expt. results 0-81445
Si minority carrier MIS solar cells, AM1 efficiencies 0-93975
Si monocrystal peripheral fusion channelling under HF heating (*Russian*) 0-59627
Si monocrystalline sheet fabrication for solar cells, CLF Czochralski furnace and enhanced slicing technology 0-93476
Si multicrystalline solar cell material prep., fast-pulled float zone, CZ and cast ingot and foil methods 0-93483
Si, multigrained, grain boundary elec. and compositional props., surface anal. 0-76575
Si, multigrained, impurity segregation to grain boundaries, AES and SIMS obs. 0-65027
n-Si, multivalued Sasaki effect 0-107795
Si, μSR , spin Hamiltonian and anomalous muonium states 0-71286
Si n/n^+ epitaxial layers, anomalies of Sb distrib. 0-65035
Si, n^+ -p diode, γ -radiation defects, annealing and recomb. props. 0-65045
Si n^+ -p junction solar cells, electron irrad., DLTS spectra and defect effects 0-93999
Si n^+ -p solar cell, forward and reverse bias tunnelling 0-85274
Si n^+ -p solar cells, degradation mechanisms associated with Ti impurities 0-81465
Si n^+ -p solar cells, effect of elec. bus during 1 MeV electron irrad. and isochronal annealing, elec. characts. and deep level pop. 0-94086
p-Si, n-channel inversion layers, mag. susceptibility of electrons in presence of quantising mag. field. 0-76560
Si, neutron and electron bombard., radiation defect recomb., photoelec. props. meas. 0-60039
Si, non thermal laser induced ordering, plasma life time, phonon interactions 0-84481
Si noncrystalline film, struct., interatomic distances, SRO 0-107053
p-Si, odd magnetoresist. under weak carrier heating conditions 0-96917
Si on ceramic, coating with inverted meniscus (SCIM) technique, solar cell appl. 0-89163
Si, on sapphire, epitaxial, crystalline quality improvement by ion implantation and furnace regrowth 0-88452
Si on sapphire, residual strain effect on elec. props. (*Japanese*) 0-84522
Si, on sapphire, Schottky magnetodiode, integrated mag. sensor 0-68223
Si on sapphire, stress-relieved regrowth by laser annealing 0-65389
Si on sapphire film, laser annealing /non-thermal theory expt. test 0-89273
Si on sapphire thin film, Hall effect, magnetoresistance (*French*) 0-65601
Si, optical consts. by unpolarised incident radiation 0-76044
Si, optical spectrum, many particle effects, band struct. 0-89024
Si, oxidation, solubility and transport behaviour of water, dissolution 0-93801
Si, oxidation, thermal growth mechanisms of vitreous oxide layers 0-93675
Si, oxidation induced by ion or electron bombardment, AES-SIMS study 0-108606
Si, oxidation stacking faults, shrinkage and growth, bulk O_2 effects 0-96546
Si, oxidation-induced Frank sessile dislocation loops, struct. change 0-75228
Si, oxidation-induced stacking faults, distinction between clean and decorated faults by etching 0-79818
Si, oxide scale microstruct. of oxidised single cryst. 0-108613
Si, P implanted low pressure CVD polycryst. films, elect. characts. 0-60114
Si p^+ -i- n^+ field induced junction solar cells, conversion efficiency limit in concentrated sunlight 0-85282
Si p^+ - n - n^+ back surface field concentrator solar cells 0-93939
Si p^+ - n^+ back-surface-field solar cells, physics underlying performance 0-85283
Si p-channel MOS structure, stress effects on elec. props., press. transducer props. 0-100526
Si p-i-n structure, ESR of conduction electrons 0-93179
Si, p-n junction, current-voltage characts., misfit dislocations, high press. effects 0-65671
Si p-n junction, reverse bias high voltage, secondary surface breakdown 0-70813

elemental semiconductors continued

- Si p-n junction, small signal equivalent circuit, finite carrier multiplication 0-65664
 Si p-n junction, subnanosec. current drops in delayed breakdown 0-75633
 Si p-n junction, subnanosec. current drops in delayed breakdown 0-75634
 Si p-n junction depletion layer, electron beam damage inhibition 0-70817
 Si p-n junction diodes and solar cells, minority carrier diffusion length 0-107894
 Si p-n junctions, avalanche breakdown anisotropy 0-70811
 Si p-n junctions, electron emission from depletion layers 0-100509
 Si p-n junctions, spin depend. surface recomb., electron irradiation effect 0-88627
 Si, p-n junctions, voltage-current characts., fast neutron irradiation effects (Russian) 0-65659
 Si, phonon-assisted Auger recomb., direct calc. of overlap integrals 0-107808
 n-Si, phonon-phonon relaxation 0-96609
 Si, phonon-phonon relaxation investigation for conventional and neutron doped crystals 0-96927
 Si, photocapacitive MIS IR detector, spectral response, noise characts. 0-75644
 Si photoconducting films, amorphous, undoped, I-V characts. of vacuum deposited films 0-60049
 Si photodiode for optical channel waveguides 0-102805
 Si, photon emission due to Ar^{+} ion bombard., adsorbed and recoil-implanted O effect 0-80872
 Si, photovoltaic and photomagnetic effects, rel. to intervalley electron transfer 0-60034
 Si, photovoltaic cell, absolute spectral sensitivity calibration, radiometry, photometry (Chinese) 0-86367
 Si photovoltaic low series resistance concentrator for high intensity appl. 0-93940
 Si, piezobirefringence in opaque region 0-60541
 n-Si, piezoresist. rel. to piezothermoelec. power, electron-phonon drag region 0-70737
 n⁺nn⁺ Si planar device, hot electron flicker noise at 78K 0-103732
 Si planar semiconductor junctions, disruptive voltage calc., ionisation coeff. (Rumanian) 0-103746
 Si, plasma effects during pulsed laser annealing 0-84480
 Si, plastically deformed, dislocation structure with different sample orientation 0-70207
 Si, point defects, H passivation 0-75515
 Si, point defects, laser annealing 0-107224
 Si, poly crystalline, electronic behaviour of grain boundaries, solar cell appl. 0-92859
 Si, poly-oxide-poly struct., elec. cond., charge distrib. in SiO_2 films 0-92984
 Si, polycryst., anisotropic plasma etching 0-85069
 Si, polycryst., CVD, recrystn. on heating 0-80107
 Si, polycryst., deposition as example of pyrolytic CVD process 0-84407
 Si, polycryst., energy distrib. of trapping states, from impedance of MOSS struct. 0-65691
 Si, polycryst., layer structure dependence on carrier gas moisture and O_2 content (Bulgarian) 0-59811
 Si, polycryst., oxidation, morphological aspects 0-76388
 Si, polycryst. p-n junction solar cells, grain-boundary and intragrain recombination currents 0-81442
 Si, polycrystalline, As segregation at grain boundaries, elec. props. meas. 0-75259
 Si, polycrystalline, electrode shape effects on oxide conduction 0-96890
 Si, polycrystalline, grain boundary obs. by TEM, solar cell appl. 0-72057
 Si, polycrystalline, Hall mobility 0-60006
 Si polycrystalline, low cost conversion into sheet by heat exchange method and fixed abrasive slicing technique 0-93479
 Si, polycrystalline, phenomenological model for mobility 0-65564
 Si, polycrystalline, solar cells, grain-boundary hydrogenation technique for improvement 0-85273
 Si, polycrystalline, thermal oxide anomalous stress 0-93661
 Si, polycrystalline barrier heights and passivation of grain boundaries 0-93890
 Si, polycrystalline Czochralski-grown, MIS solar cell characterisation using scanned laser response exam. 0-93884
 Si polycrystalline film, effect of defects/grain boundaries on photovoltaic mech. 0-93883
 Si polycrystalline film resistivity reduction by Nd:YAG laser annealing 0-100539
 Si, polycrystalline films, meas. of effective diffusion length, by surface photovoltage meas. 0-80424
 Si, polycrystalline layers on C substrates, RAD process, solar cells appl. 0-89635
 Si, polycrystalline multilayer support struct., control of deform. in dielec. isolated substrates 0-107681
 Si polycrystalline solar cells fabricated from refined metallurgical-grade Si, impurity gettering 0-94011
 Si, polycrystalline structure stability, stacking defects, twins grain struct. (Russian) 0-100248
 Si, polycrystalline-metal contacts, minority carrier injection 0-103750
 Si polycrystalline-metal Schottky barrier solar cells, elec. and photovoltaic contact props. 0-93936
 Si, porous layer form. mechanism by anodisation in HF soln. 0-71769
 Si, precipitation of O, 650°C, IR absorpt. and X-ray diff. 0-76258
 Si, prod. of polySi vapour deposited coatings for solar cells, cost anal. 0-93495
 Si, pure, lattice parameters, and topographic meas., using double-beam triple-cryst. X-ray spectrometer 0-77915
 Si, pure and n-type, US vel. and attenuation, evaluation using elastic moduli 0-70325
 Si purification, plasma melting zone technique (French) 0-89141
 Si purification, plasma melting zone technique, optimisation (French) 0-89142
 Si, quantitative anal. with SIMS 0-101052
 n-Si, quenched, fast electron irradiated, annealing of defects 0-89259
 Si RF sputter-etched surface, cryst. damage, spectroscopic ellipsometry obs. 0-103538
 Si, radiation defects, influence of dislocations on accumulation, elec. props. 0-92558
 Si, radiation induced defects in high-voltage electron microscope 0-65048
 Si, radiative recomb. centre accumulation due to high temp. electron irradi. 0-93394
 Si, reactive ion beam etching expts., selectivity, anisotropy 0-104308
 Si, reflectivity time dependence during pulsed laser annealing 0-66214

elemental semiconductors continued

- n-Si, relaxation of electron energy, carrier-density dependence 0-107809
 Si, residual stress and defects induced by scribing 0-60990
 Si ribbon, dendritic web growth from melt, solar cell module fabrication 0-93478
 Si ribbon, EFG, C contaminant conc. determ. by nuclear techniques and SIMS 0-59506
 Si ribbon, low angle sheet growth technique, direct shaping characts. 0-93480
 Si ribbon crystal growth, 10 cm wide, temp. distrib. meas. in die 0-104059
 Si ribbon crystals, edge-defined film-fed growth technique for solar cells 0-89633
 Si ribbon growth by EFG, thermal sensitivity and stability 0-107080
 Si ribbon solar cells, defect anal. using laser scanner 0-94089
 Si ribbon solar cells, var. of minority-carrier diffusion length with light intensity, heavy metal doping effects 0-93937
 Si ribbons, edge-defined film-fed growth technique for solar cells 0-89138
 Si ribbons for solar cells, ultra high speed growth, elec. props. 0-89162
 Si ribbons grown by capillary action shaping technique, surface quality and impurity distrib. 0-108343
 Si rich SiO_2 - SiO_2 -Si rich SiO_2 layers for dual electron injector struct. 0-96991
 Si, SOC (Si on ceramic) continuous coating for solar cells 0-93904
 Si, screw dislocation networks, TEM study 0-70204
 Si selective anodic oxidation in O_2 plasma 0-108610
 Si, selective etching rel. to SiO_2 by $CBrF_3$ plasma without undercutting 0-76380
 Si, self-diffusion, activation energy and entropy factors 0-88353
 Si, self-scanned photodiode array, evaluation for integrated optics spectrum analyser 0-58806
 Si, semi-empirical APW calc. of band structure 0-84424
 Si semiconductor plates, control of quality of surface treatment, using Al spraying technique 0-60989
 Si, semicrystalline vs. single crystal for photovoltaics 0-93917
 Si, shallow contact formation substrate temp. depend., Pd-W alloys 0-96963
 Si shallow junction device, silicide contact 0-70819
 Si sheet, high speed growth, heat transport analysis 0-107669
 Si sheet casting for solar cells 0-89139
 Si sheet-form solar cells, efficiency improvement, minority carrier diffusion length limitations 0-93925
 Si, single crystal, fracture under several liq. environments 0-81157
 Si single crystal, improved horizontal ribbon growth technique 0-108345
 Si single crystal ingot growth from metallurgical grade Si, inhomogeneities 0-59416
 Si, single crystals, thermal conductivity calculation (Hungarian) 0-65311
 Si single crystals, mech. polishing with reagent, activation energy effects (Japanese) 0-89379
 n-Si, size-induced magnetoresist. in strong elec. fields 0-65582
 Si, slip, room temp., TEM obs. 0-79804
 Si, slip dislocation nucleation during laser annealing 0-84179
 Si solar cell arrays, fixed-base, flat panels, possible developments for more competitive power production 0-72050
 Si solar cell arrays, for earth orbital and orbit transfer missions 0-94044
 Si solar cell fabrication from multiple ingots using melt replenishment Czochralski method, cell anal. 0-93477
 Si solar cell parameters, grain size dependence 0-94049
 Si solar cell processing, pulsed laser techniques for annealing ion-implantation damage 0-81453
 Si solar cells, all-plate low cost contact system 0-93992
 Si solar cells, analysis of short-circuit current 0-85285
 Si solar cells, base resist. influence on temp. characts. 0-89618
 Si solar cells, capacitance transient spectra of processing- and radiation-induced defects 0-61340
 Si solar cells, design for limit conversion efficiency 0-93960
 Si solar cells, effects of metallic impurities 0-85278
 Si solar cells, fabrication using continuous or pulsed lasers (French) 0-61350
 Si solar cells, fundamental efficiency limitations 0-93963
 Si solar cells, high open circuit voltage, P implantation 0-89642
 Si solar cells, inhomogeneities and their influence on cell performance 0-93967
 Si solar cells, ion implantation and annealing technology 0-93996
 Si solar cells, ion implanted grating type 0-101102
 Si solar cells, ion-implanted, expt. study of efficiency controlling factor 0-93997
 Si solar cells, junction formation techniques using spray-on polymer dopants, cost effective, high throughput 0-94014
 Si solar cells, limit efficiency evaluation 0-93973
 Si solar cells, low cost, Ni contacts 0-94017
 Si solar cells, low cost processes for fabrication 0-94013
 Si solar cells, manufacturing cost anal. of flat plate vs. concentrator solar cells 0-93949
 Si solar cells, metallurgical-grade, fabrication by epitaxial growth or direct diffusion 0-101104
 Si solar cells, n⁺-p, Li-counterdoped, radiation damage 0-94000
 Si solar cells, Ni-Cu conductor system 0-93991
 Si solar cells, $POCl_3$ gettering of Ti, Mo and Fe-contaminated cells 0-94010
 Si solar cells, photoreaction of p-n junction diodes 0-81464
 Si solar cells, polycrystalline p-n junctions, recombination currents, physical models 0-93892
 Si solar cells, polycrystalline, from recrystallized plasma deposited thin films 0-104509
 Si solar cells, preparation using laser processing 0-81454
 Si solar cells, production process effect on fracture strength 0-93656
 Si solar cells, proton irradiated, processing influence on elec. performance 0-94001
 Si solar cells, radiation damaged, origin of reverse annealing 0-76630
 Si solar cells, radiation damage annealing mechanisms and low temp. annealing 0-94003
 Si solar cells, realisation by laser induced diffusion of deposited Sb 0-93998
 Si solar cells, review and current developments 0-108801
 Si solar cells, review of physics underlying recent improvements 0-93974
 Si solar cells, single-crystal, HV, multijunction, parameters and characteristics 0-89615
 Si solar cells, solid source diffusion process for fabrication 0-93994
 Si solar cells, spray-on TiO_2 antireflection coatings 0-80963

elemental semiconductors continued

- Si solar cells, surface passivation by SnO_2 films, effect on cell transport props. and short circuit current 0-61360
- Si solar cells, TiO_2 AR coating by spray deposition 0-104511
- Si solar cells, ultrathin, electron and proton effects 0-94002
- Si solar cells, unified model of fundamental limitations 0-81448
- Si solar cells, updating limit efficiency 0-81447
- Si solar cells using minority carrier MISS 0-101103
- Si solar cells with fire through contacts printed on anti-reflection coating 0-93993
- Si solar cells with screen printed diffusion and metallisation 0-94015
- Si solar concentrator cell, effects of nonuniform illumination and temp. profiles under concentrated sunlight 0-93941
- Si, solute loss on laser annealing solute out diffusion 0-100840
- Si source for vacuum deposition, with two independent filaments 0-76190
- Si spectroscopic applications of structures produced by orientation-dependent etching 0-93668
- Si, sputtered atom ang. distrib. for keV Ar^+ bombard. 0-84819
- Si, square single crystals, Czochralski growth 0-97422
- Si, stacking faults, weak-beam contrast in TEM 0-75132
- Si, static compression in [100] and [111] directions, elec. resist. obs. 0-65637
- Si, stationary creep depend. on deform. stabilisation of material struct. (Russian) 0-100300
- Si, stressed, one- and two-component electron-hole liq. at $T=0$ 0-80189
- Si, stretched, lattice vibr. anharmonicity, influence of stress on elastic moduli, Raman spectra 0-80791
- Si substrate, for wet thermal oxide film, trap emptying kinetics 0-92983
- Si substrate for Al film, annealing effect on eutectic point (Russian) 0-100850
- Si substrate for epitaxial crystn. of GaP films by ns laser pulses 0-107674
- Si substrate for PMMA electron sensitive layer, 400 Å linewidth electron beam lithography 0-65392
- Si substrate for Pd and Pt, silicide formation by laser, electron beam annealing 0-84849
- Si substrate for RF sputtered ferroelectric BaTiO_3 films, ferroelectric props. 0-80697
- Si substrate for SiO_2 film, ellipsometric spectra, thickness determ. (Chinese) 0-86379
- Si, substrate for ZnS , Na_3AlF_6 films, H_2O absorpt., IR anal. 0-75446
- Si substrate prep. for epitaxial solar cells, low-cost, unidirectional solidification process 0-93924
- Si substrate solar cells, upgraded metallurgical grade, epitaxial growth 0-93905
- Si, substrate temp. influence on shallow contact formation on Si, shallow contact formation substrate temp. depend., Pt-W alloys 0-96963
- Si substrate thinness, device design, solar cell processing, empirical study of interaction 0-93995
- Si surface, (111), energy states, computer renormalisation-group calc. 0-75617
- Si surface, depth profiling, optoacoustic technique 0-65337
- Si surface, ion bombardment enhanced mixing of Ag layers, Rutherford backscatt. meas. 0-65034
- Si surface, laser-annealed, characterisation by ellipsometry 0-103544
- Si surface, MOS struct. band structure, minigaps, magnetoresistance, cond., space charge layers 0-92980
- Si, surface, pulsed electron beam processing, doping, annealing 0-75254
- Si surface, reduction growth, autopotaxy (Russian) 0-107672
- Si surface, thermal oxidation induced defects, origin and growth (Chinese) 0-66681
- Si, surface and films on sapphire, quality determ. using IR and UV specular reflectance meas. 0-108684
- Si surface electron beam deposited silicide formation using scanning CW laser beam 0-66862
- Si surface formation during etching of thin thermally grown oxide layers, ellipsometric control (Russian) 0-104315
- Si, surface topography changes due to pulsed laser annealing 0-84348
- Si, surface treatment by the low-energy ions of plasma accelerators 0-97608
- Si surfaces etched in CF_4 or $\text{CF}_4\text{-O}_2$ plasma, morphology 0-93671
- Si, temperature during CW laser heating, Raman scatt. meas. 0-76109
- Si terrestrial solar cells, stress tested, contact integrity testing 0-94018
- Si, thermal annealing study of Au- $\text{Ti}_{0.3}\text{W}_{0.7}$ metallisation 0-80134
- Si, thermal oxidation, role and effects of Cl 0-108622
- Si, thermal oxidation kinetics, steady-state transport anal. 0-71773
- Si, thermal oxidation kinetics, theoretical perspective 0-76387
- Si, thermally oxidised surfaces, electron mobility in inversion and accumulation layers, MOS devices 0-103753
- Si thick-film growth using contiguous capillary coating on porous C substrates 0-93507
- Si thin film, polycryst., CVD, elec. props. 0-107934
- Si thin film for solar cells, thermal expansion shear separation technique 0-81439
- Si thin p-n junction solar cells, minority carrier mirrors and optical confinement for high efficiency (27%) 0-93933
- Si thin ribbon grown at high speed, thermal stresses, reduced thermal buckling 0-107078
- Si, thin slabs, vibr. freq. calcs., dimens. effect 0-60585
- Si thin-film polycrystalline vacuum-deposited solar cells, TiB_2 bottom electrode, 10% efficiency 0-93489
- Si, total energy calcs. by r-space method, Wannier functions 0-88503
- Si tube growth by EFG process 0-108344
- Si, uniaxially stressed, excitonic molecule emission spectra, electron valley degeneracy effects 0-60669
- Si, V-grooves formed by etching, phosphosilicate glass bridge struct. 0-104312
- p-Si, vacancy, charge states, Jahn-Teller stabilisation energy 0-80209
- Si vacancy, electron states, Anderson negative-U system 0-96820
- Si, vacancy formation and stability due to noncentral force 0-70192
- Si wafer, ion implanted, electron beam annealing, computer simulation 0-96569
- Si wafer, slotted mask, direct deposition of metal contact pattern on MIS solar cells 0-97786
- Si wafer, thin surface layers, amorphous to cryst. transform., obs. technique 0-107288
- n-Si wafer, trap centres of self-interstitials 0-75516
- Si wafer processing, CO_2 laser heating dynamics 0-76106
- Si wafer stacking faults, preoxidation gettering by reverse side P diffusion-induced misfit dislocations 0-60988

elemental semiconductors continued

- Si wafers, Czochralski grown, minority carrier transport props., laser beam scan for homogeneity anal., photovoltaic cell appls. 0-92905
- Si wafers, floating-zone, etch struct. on microdefects as affected by dopants and surface treatment 0-79773
- Si wafers, saw damage reduction in lubricant environment 0-108585
- Si wide ribbon, high speed edge-defined film-fed growth 0-104058
- Si, with dislocations, noise spectrum 0-107881
- Si, X-ray section topography in the Bragg case 0-79637
- Si: As(Pb), high-dose ion implanted and annealed, implant redistribution 0-107309
- Si: ^{119}mSn , impurity lattice dynamics, Mossbauer spectra, Debye temp. 0-84262
- Si: ^{57}Co (^{57}Fe), implanted, Mossbauer spectra, study of dose dependence 0-75900
- Si:Al, electron irradi. induced defects, transient capacitance study 0-59516
- Si:Al, localised exciton bound to isoelectronic trap 0-66283
- Si:Al, polycryst. film, grain boundary diffusion, Auger sputter profiling 0-75388
- Si:Al(Ga), O_2 diffusion, conc. profile meas. 0-79990
- Si:Al(Ga), spreading resist. calibration using Si:B 0-103690
- Si:Ar, As, ion implanted, laser annealing, doping profiles, channelling 0-97506
- Si:Ar, ion-implanted, epitaxial regrowth by laser annealing, microstruct. 0-84404
- Si:Ar(Ne)(O)(N), ion-implanted, defect reverse annealing, 550-650°C 0-88875
- Si:As, CVD, doping using $\text{SiH}_4\text{-H}_2\text{-AsH}_3$ system 0-79823
- Si:As, diffused, laser irradi., stability study 0-65547
- Si:As, diffusion model, degeneracy and partial ionisation effects 0-96693
- Si:As, heavily As-diffused, Hall mobility and resist. rel. to carrier conc. 0-107815
- Si:As, ion implanted, formation of As complexes 0-59511
- Si:As, ion implanted, low temp. thermal annealing 0-96552
- Si:As, ion implanted, pulsed ion beam annealing 0-103395
- Si:As, ion implanted, pulsed laser annealing, partial solid-state regrowth 0-103591
- Si:As, MBE with simultaneous ion implant doping 0-66432
- Si:As, scanning electron beam annealing, spreading resistance, junction depth 0-75267
- Si:As, shallow junctions by high-dose implants 0-96694
- Si:As, solid solubility and thermal behaviour of metastable 0-75359
- Si:As high-dose implanted single crystals, pulsed electron-beam annealing 0-103373
- Si:As ion implanted layers, annealing by CO_2 laser, doping profile shift 0-84965
- Si:As ion implanted shallow junction 0-70228
- Si:As laser annealing, heat and mass transport model 0-92546
- Si:As $^+$, implanted, CW laser annealing, electron-beam induced current 0-100709
- Si:As $^+$ (P $^+$) ion implanted, laser annealed, correlation of struct. and elec. props 0-70855
- Si:As(B), heavy-doping effects and impurity segregation during high-pressure oxidation 0-65014
- Si:As(P), ion implanted, TEM study after laser and furnace annealing 0-70234
- Si:As(P)(Sb), donor-polarizability enhancement as the insulator-metal transition is approached from the insulating side 0-80184
- Si:As(Pb), ion-implanted, impurity redistrib. during laser irradi. 0-100280
- Si:As(Sb), ion implanted, lattice location of impurities after pulsed laser annealing 0-88196
- Si:Au, C-V curves of MIS diode used to examine trapping levels 0-65697
- Si:Au, EPR spectrum, strong nucl. quadrupole effect 0-93172
- Si:Au, O(H), film, amorphous, elec. cond. meas. 0-80423
- Si:Au, P-induced point defects influence on Au gettering mechanism 0-65030
- Si:Au, precipitation of solid soln., effect of gamma irradiation 0-59515
- Si:Au deep level parameter determ. by isothermal capacitance transient spectroscopy 0-88507
- Si:Au p $^+$ -n junction, small area, acceptor level conc., determ. from TSC curves 0-75631
- Si:B, anomalous B profiles prod. by BF_3 implantation 0-75252
- Si:B, bound many-exciton complexes, luminescence spectra, mag. props. 0-103994
- Si:B, He $^+$ irradiation-induced diffusion, effect on impurity distrib. 0-70470
- Si:B, high conc. effects in ion implantation 0-75245
- Si:B, ion implanted, structure defects /formation and behaviour under annealing in various ambients 0-65033
- Si:B, layer resist. depend. on implanting and annealing conditions (German) 0-96551
- Si:B, P, long range enhancement of B diffusivity by P diffusion 0-103386
- Si:B, resonant scattering of phonons by bound holes in temp. range 1 to 5K 0-75393
- Si:B, use of BN source to achieve high surface concentration of B (Russian) 0-107639
- Si:B (0.2 wt.%) ion implanted, B atom displacement due to low temp. irradi. 0-88234
- Si:B diffusion at Si-SiO $_2$ interface, Auger spectra, Rutherford backscattering 0-70471
- Si:B implanted wafers, ionis. assisted annealing and effects 0-100257
- Si:B ion implanted, strain profiles from X-ray rocking curves 0-107290
- Si:B ion implanted grating-type solar cells, var. of junction depth, collection efficiencies 0-93934
- Si:B ion implanted layers, light refl. and transmission coeffs., computer program 0-66316
- Si:B photodiode front region collection efficiency models 0-96899
- Si:B radiation damage and minority carrier lifetime, SEM-EBIC obs. 0-96573
- Si:BF $_3^+$, ion implantation appl. in semicond. device production 0-103383
- p-Si:(Be)(Al), radiation defect form. and annealing study using Hall effect, cond. and carrier diffusion length 0-84214
- Si:(Be)(Li) ion implanted, channelling and random equivalent depth distrib. 0-100293
- Si:(P), dislocations under high stress, stacking fault energies, TEM study 0-70202
- Si:(P), ion implanted crystalline and amorphous laser annealing 0-97509

elemental semiconductors continued

- Si:B(P), proton-irrad., impurity uphill diffusion, vacancy mechanism 0-92719
- Si:B(P)(As)(Sb)(Cu)(Fe), ion implanted, doping profile, pulsed laser annealing effects 0-88197
- Si:Be, ion implanted, correl. of atomic distrib. and implantation induced damage profiler 0-88199
- Si:Bi, ion implanted, channelling obs. of pulsed Q-switched ruby laser annealing 0-59542
- Si:Bi, ion-implanted, solid phase epitaxial growth during annealing, super-saturated solid soln. form. 0-103384
- Si:C, impurity determ. by IR absorpt. spectroscopy, room temp. and low temp. meas. comparison 0-108237
- Si:Co, minority carrier lifetime investigation 0-80292
- Si:C⁰(Mn⁺), spin-lattice relax. of Jahn-Teller centres, coexistence of minima with different symmetries 0-80602
- Si:Cu, precipitate morphology, IR microscopy study (*Chinese*) 0-103539
- Si:F, amorphous, heat resistant, prep., elec. cond., IR absorpt., annealing 0-65719
- Si:F, amorphous alloys, RF sputtering prep. in SiF₄-Ar gas mixture, spectra 0-80772
- Si:F,H, amorphous, elec. and optical props. 0-60031
- Si:F,H, amorphous efficient carrier generation for solar photovoltaic energy conversion 0-92906
- Si:Fe, ion implanted, laser annealing studies using Mossbauer spectroscopy 0-79827
- Si:Fe(Al), compensated substrates for solar cells, effects of Fe and Al 0-94009
- Si:Ga, IR absorption of dopant centres, spectral depend. on doping, impurity conc. and temp. 0-76053
- n-Si:Ga laser doped, segregation, Rutherford backscattering 0-103483
- Si:Ga(As), laser-doped, impurity distrib., Rutherford backscatt. and channelling anal. 0-59507
- Si:Gd(Pr), photoconductivity anomalies due to mag. impurities (*Russian*) 0-103722
- Si:Ge, recryst. after implantation using different temp. and energy sequences 0-84196
- Si:H, amorphous, 2p level shift, XPS obs. 0-97401
- Si:H, amorphous, Auger electron spectrosc., obs. 0-76112
- Si:H, amorphous, band tail absorpt., photocurrent meas. for Schottky barrier solar cell 0-60032
- n-Si:H, amorphous, bulk density of deep states, DLTS meas. 0-88518
- Si:H, amorphous, defect photoluminesc. meas. 0-97334
- Si:H, amorphous, defect states, luminesc. and ESR obs. 0-76075
- Si:H, amorphous, discharge prod., optically induced cond. changes 0-96937
- Si:H, amorphous, HV photovoltaic cells, design parameters 0-101105
- Si:H, amorphous, image pickup devices 0-100481
- Si:H, amorphous, optical studies of excess carrier recomb., evidence for dispersive diffusion 0-76059
- Si:H, amorphous, photoelectrochem. behaviour 0-81480
- n-Si:H, amorphous, photoelectromagnetic effect 0-107845
- Si:H, amorphous, Pt film growth, AES and LEED study 0-88447
- Si:H, amorphous, Schottky diodes, elec. props., light-induced effects 0-103741
- Si:H, amorphous, short-range order, theory and probes 0-79698
- Si:H, amorphous, solar cells, trap spectroscopy using transient current techniques 0-104508
- Si:H, amorphous, solar-cells, charge collection and spectral response 0-85275
- Si:H, amorphous, sputtered on Gd₂(MoO₄)₃, ferroelec. domain wall motion, image scanning 0-83663
- Si:H, amorphous, sputtered Schottky barrier solar cells, conduction mechanism 0-104506
- Si:H, amorphous, stacked solar cells, development 0-94050
- Si:H, amorphous, surface states distribution using MOS tunnel junctions 0-103735
- Si:H, amorphous, temp. depend. of photolum. 0-89063
- Si:H, amorphous Schottky solar cells, prep. and characts. of diode RF reactive cathodic sputtered films (*French*) 0-61347
- Si:H, amorphous thin film, ion plating, IR absorpt. meas. 0-84857
- Si:H, amorphous thin film solar cells 0-81478
- a-Si:H, electronic states and bonding config. 0-64900
- a-Si:H, influence of H on optical props., H conc. and H bonds 0-76098
- Si:H,B, amorphous, field effect and thermoelec. power 0-96924
- Si:H,Li, amorphous, photoluminescence obs. 0-66280
- Si:H,P amorphous film, elec. cond., thickness and temp. depend. 0-65559
- Si:H alloy, amorphous, dihydride model of vibrational spectra 0-80827
- a-Si:H alloys, sputter deposited thin film coatings, property-comp. relationships 0-80975
- Si:H amorphous, solar cell structure, optical absorption by gap states 0-94052
- Si:H amorphous films, conductivity and temp. dependence of optical gap 0-100462
- Si:H amorphous films, ESR, optical gap and elec. cond. meas. 0-75842
- Si:H amorphous films, IR spectrum and struct. 0-97277
- Si:H amorphous films, reactively sputtered, prep. and characterisation 0-100785
- Si:H amorphous MIS solar cell, loss mechanisms and photovoltaic parameters, overview 0-93923
- Si:H film, amorphous, H-associated disorder modes, PMR spin-lattice relax. time meas. 0-93202
- Si:H film, amorphous, plasma-deposited, small angle X-ray and neutron scatt. studies 0-59826
- a-Si:H film, glow discharge deposited, H profiles, doping level 0-84202
- a-Si:H highly homogeneous, for low-cost solar cell fabrication 0-72053
- Si:In, absorpt. spectra, impurity excited state lines 0-108243
- Si:In, clustering and precipitation, time-dependent perturbed ang. correlation meas. 0-65234
- Si:In, dopant energy levels, Hall meas. interpretation 0-107736
- p-Si:In, ion implanted, doping profiles from capacitance-voltage characts. 0-88203
- Si:In extrinsic IR detector material with high responsivity compensated by neutron transmutation, float-zone growth 0-75597
- Si:K, bound exciton luminescence in mag. field (*Russian*) 0-108278
- Si:Li, bound-exciton excited states, uniaxial anal. 0-71475
- Si:Li, defect electronic struct. and config., semi-empirical calc. 0-107739
- Si:Li, electron-phonon scatt., in intermediate conc. region 0-65180
- Si:Li, photolum. of bound exciton and bound multiexciton complex, Zeeman effect 0-108265

elemental semiconductors continued

- Si:Li, thermal cond., low temp. phonon scatt., internal strain effects 0-96706
- Si:Mn,Bi, standard, doubly implanted, Rutherford backscattering meas. at MeV energies, screening corrections 0-88204
- Si:N, high energy ion implantation of buried insulating layers 0-88188
- Si:N, implantation at high doses, annealing conditions for homogeneous buried insulating layer (*French*) 0-59498
- Si:N, ion implanted, oxidation characts. 0-89385
- Si:N, laser-annealed, Jahn-Teller distorted donor, EPR meas. 0-84642
- Si:N wafers, Si₃N₄ layer growth by high dose implantation and annealing, elec. props. 0-70227
- Si:N(P), ion implanted, IR transmission and rel. spectra study 0-108244
- Si:O, A centre, theoretical study 0-75521
- Si:O, carrier recomb. processes, role of vacancy-O complexes 0-65592
- Si:O, Czochralski crystal, oxygen striation and thermally induced microdefects 0-100275
- Si:O, heat treated, excess carrier recomb. rate, defect levels 0-75579
- Si:O, IR absorpt. at low temp. (*Chinese*) 0-108228
- Si:O, incorporation of O during pulsed-laser irradi. 0-96557
- Si:O, kinetics of donor formation, under heat treatment in 450-900°C range 0-75523
- Si:O,H amorphous, time resolved luminesc. 0-66288
- Si:O(C), implant redistribution, annealing effects, SIMS meas. 0-96561
- Si:O(C) wafers, impurity meas. by Fourier transform IR spectra 0-89030
- Si:O(C) wafers, impurity meas. by Fourier transform IR spectra at low temp. 0-89031
- Si:P, annealing after ion implantation, ellipsometric study 0-65018
- Si:P, dielec. susceptibility meas., polarisation catastrophe at metal-insulator transition 0-59873
- Si:P, doping during growth from gas phase, thermodynamic analysis 0-59489
- Si:P, heavily doped semicond., scatt. mechanism, resist, and Hall coeff. maxima 0-75586
- Si:P, homogeneous nuclear transmutation technique, thyristors appl. 0-70236
- Si:P, implanted low temp. annealed, elec. activation, damage depend. 0-88182
- Si:P, incoherent light flash annealing, elec. props., backscattering spectra 0-97504
- Si:P, ion implanted, regrowth of damage structs. by laser annealing 0-107289
- Si:P, ion implanted, subsurface damage, TEM and channelled Rutherford backscatt. study 0-107337
- Si:P, ion implanted with small doses, defect annealing by nanosecond laser pulses 0-107297
- Si:P, luminescence circular polarisation, emission by many exciton complexes 0-93398
- Si:P, measurement techniques for determining P densities 0-75262
- Si:P, neutron transmutation doping, elec. props. rel. to neutron fluence 0-96555
- Si:P, neutron transmutation doping, resist. homogeneity rel. to compensation ratio 0-96556
- n-Si:P, piezothermoelec. power in electron-phonon SRS region, anisotropy 0-70738
- Si:P, polycryst., channelling of implanted P during MOS device processing 0-65017
- Si:P, polycryst. films, elec. props., EPR, defect states, doping effects 0-75660
- Si:P, polycrystalline laser recrystallised film on Si substrate, cryst. struct., thermal oxidation 0-65391
- Si:P, thermal cond., electron-phonon interaction at low temps. 0-92730
- Si:P bipolar transistors, interstitial supersaturation and misfit dislocation climb, TEM study 0-70203
- Si:P film, polycryst., heavily doped, mobility and carrier conc., optical determ. 0-66314
- Si:P implanted, multiscanning electron beam annealing 0-75242
- p-Si:P implanted films, piezoresist. stress tensors, ion dose depend., -80 to 120°C 0-100538
- Si:P polycrystalline layer, role in lattice defect reduction assoc. with P predeposition 0-70229
- p-Si:P semiconductor detector in radiometric inspection problems 0-62819
- Si:P(As)(B), nonequilibrium solid solutions obtained by heavy ion implantation and laser annealing 0-92544
- n-Si:P(B), elec. cond. oscills., electron instability effects due to dislocations 0-103704
- Si:P(O) p⁺-n-n⁺ solar cells, comparison rel. to resistance to 1.5 MeV electron irradi., majority carrier trapping 0-94087
- p-Si:P(P⁺) photocytic props. in HF 0-89504
- Si:Pt, hole capture cross-section at E_g+0.34 eV, capacitance meas. (*French*) 0-65493
- Si:Pt, implanted and laser annealed, segregation and increased dopant solubility 0-65016
- Si:S, deep level characterisation, implantation predeposition technique 0-100444
- Si:Sb, high dose Sb ion implantation, buried layer appls. 0-88186
- Si:Sb, ion implanted, Sb diffusion during oxidation, snow-plough effect 0-88366
- Si:Sb, ion implanted and annealed, influence of implantation temp. on dislocation generation 0-88158
- Si:Sb, laser doping, evaporation loss and diffusion of Sb, under pulsed laser irradi. 0-59508
- Si:Sb, low energy ion implantation, profile determ. 0-88176
- Si:Sb, low energy ion implantation Schottky barrier diodes and resistors 0-88177
- Si:Sb, MBE film, doping technique 0-79821
- Si:Sb, Mossbauer spectroscopy of ¹¹⁹Sn defect struct. 0-97174
- Si:Sb, produced by ion implantation and laser annealing, Sb behaviour above solid solubility 0-88200
- Si:Sb,P, double implants, residual defect reduction after damage anneal 0-88170
- Si:Sb vacuum deposited coating, p-n junction, pulsed electron beam annealing doping, diffusion 0-75480
- Si:Sb(Ga)(Bi)(In), dopant solubility limit, laser irradi. effects 0-84295
- Si:Sc, photocapacitance and photoconductivity 0-107859
- Si:Se, impurity states, A- and B-centres, electron, hole thermionic emission rates 0-96813
- Si:Sn, Mossbauer study of defects due to ¹¹⁹In implantation 0-80641
- Si:Te, laser melting, surface Te atom accumulation, profiles 0-100258
- Si:Te, Mossbauer spectra of ¹¹⁹Sn defect struct. 0-97175

elemental semiconductors continued

- Si:Ti substrate for epitaxial solar cells 0-61341
 Si:V p-n junctions, thermal emission rates and capture cross sections of majority carriers at V centres 0-96980
 Si:Y, photoelectric props. 0-107860
 Si:Zn, minority carrier lifetime investigation 0-80292
 Si/Al and Si/Al-Si(Cu), Si regrowth minimisation through overlying Al or Al alloy film 0-70569
 n-Si/As-Te-Ge film, heterojunction, elec. and photovolt. props. 0-100514
 Si/In₂O₃-SnO₂ thin film junctions, polarity dependent memory switching effects 0-70814
 Si/In(-Cd), Si/Cd Schottky contacts, electrochemically deposited 0-88633
 Si/Pd system, solid phase epitaxial growth control by C ion implantation 0-75466
 p-Si/rare earth metal contacts, surface pot. barrier 0-60086
 Si/refractory metal-Ni(Pd)(Pt) interactions, phase separation 0-65303
 Si-Ag interfaces, solar cell contacts 0-92973
 p-Si-Al, ohmic contacts, Si dissoln. and recrystn. effects, computer calc. 0-103749
 Si-Al Schottky barrier solar cell, using polycryst. Si, grain boundary effects on elec. behaviour 0-85279
 Si-Al₂O₃-Al structure, study of charge trapping 0-60097
 Si-Al₂O₃ system, solid phase Si regrowth on sapphire 0-100413
 Si-Au, interface study using EELS 0-97391
 Si-Au interface, critical Au-film thickness obs. for room temp. interfacial reaction 0-75390
 n-Si-Au Schottky barrier solar cells, recombination in space charge region 0-61351
 Si-CoSi₂Si, double heteroepitaxy, solid phase and MBE 0-104063
 Si-Cr interfaces, metallurgical and electrical props. 0-60081
 Si-Cr₂O₃-Al, current-voltage characts., oxide film effects 0-70841
 n-Si-Cu Schottky contacts, electrochem. deposition, barrier height and ideality factor 0-75641
 Si-F-H amorphous solar cells, DC glow discharge fabrication 0-72041
 Si-F-H-P, film, dark cond., struct., Raman scatt. 0-88588
 Si-GaSe n-p heterojunction, elec. characts., interface states 0-70812
 Si-Ge heterojunction form., microscopic aspects, EELS meas. 0-80368
 Si-H-P amorphous film, dark cond., struct., Raman scatt. 0-88588
 Si-In₂O₃-SnO₂-y SIS heterostructure solar cells, spray-deposited 0-101106
 Si-insulator interface, non-avalanche charge injection, expt. study, charge trapping effects 0-60099
 Si-metal contact, transport theory of Schottky barriers 0-80372
 Si-metal contacts, analytical techniques, review 0-80120
 Si-metal interface, silicide formation, interface marker technique obs. 0-59734
 Si-Mo sputtered contacts, contact resistance 0-92970
 Si-Mo substrate-film interface, reaction on heat treatment, silicide formation 0-79999
 Si-on-ceramic solar cells, short-circuit current density meas. using light-beam-induced-current tech. 0-93887
 Si-Pb heterojunction, RHEED, Mossbauer spectroscopy and I-V characts. 0-70828
 Si-PbS heterojunction, effect of Si substrate orientation on struct. and interface props. 0-80097
 Si-PbS n-p heterojunctions, AC admittance meas. 0-96979
 n-Si-Pd diodes, chemical reduction process for fabrication 0-60082
 n-Si-Pd₂Si contact, interface struct. and Schottky barrier height, correl. obs. using TEM 0-100504
 Si-Pd-Si structure, epitaxial growth, backscattering and transmission electron microscopy studies of layered structures 0-80123
 Si-Pd-Ti, silicide form. in evaporated films 0-80006
 Si-Pt Schottky barrier, laser formation and characts. 0-60079
 Si-PtSi interface, impurity effects 0-80037
 n-Si-Re(Os) Schottky contact barrier height meas. 0-65675
 Si-refractory metal contacts, thermally cleaned surfaces 0-100521
 Si-refractory metal structs., interface modification by ion implantation 0-70475
 Si-Si interface, elec. cond. rel. to interface state population 0-65672
 Si-Si₃N₄ interface in MNS capacitors, surface state density investigation 0-60100
 Si-SiO₂, influence on frequency-temp. coeff. of SAW devices 0-79066
 Si-SiO₂, interface, doping depend. of interface states and charges 0-92992
 Si-SiO₂, interface, stress meas. technique 0-84395
 Si-SiO₂, ion implantation through SiO₂ film, recoil implantation of O, EPR study 0-88180
 Si-SiO₂, MOS interface states density, meas. techniques and model development 0-92988
 n-Si-SiO₂, MOS structures, radiation states 0-103758
 Si-SiO₂, recoil implanted O profile after ion implantation through SiO₂ 0-88198
 Si-SiO₂, two layer system, P⁺-ion penetration tails, expt. and computer anal. 0-75249
 Si-SiO₂, abrupt interface form. by very high dose O⁺ ion implantation 0-75253
 Si-SiO₂, boundary, surface charge transport in valence band of Si 0-70789
 Si-SiO₂, electrode, electronic cond., luminesc obs. 0-61111
 Si-SiO₂, in MOSFETs, inversion layer carrier mobility, theory 0-60094
 Si-SiO₂, interface, (001) vicinal planes, minigaps in inversion layers, far IR absorpt. meas. 0-107919
 Si-SiO₂, interface, barrier height in MOS tunnelling structures 0-88644
 Si-SiO₂, interface, density of states, theory 0-80395
 Si-SiO₂, interface, improved characterisation, refined quasistatic and cond. methods 0-96990
 Si-SiO₂, interface, remote polar phonon scatt. in Si inversion layers 0-80095
 Si-SiO₂, interface, thermal SiO₂ sputter induced roughness, Auger sputter profiling study 0-75244
 Si-SiO₂, interface, thermally grown, surface pot. inhomogeneities after stress ageing 0-92993
 Si-SiO₂, interface in MOS capacitors, lateral diffusion of Na⁺, neutralisation 0-92986
 Si-SiO₂, interface in MOS solar cells, operational characts. and struct. 0-93901
 Si-SiO₂, interface states, deposition of H containing layers and annealing 0-92991
 Si-SiO₂, inversion layer, n-channel, anomalous magnetoresist., model 0-96996

elemental semiconductors continued

- Si-SiO₂, laminar ion-implanted systems, struct. change investig. by MSSI method (*Russian*) 0-107918
 Si-SiO₂, MIS systems, dynamic props. of switching, appl. to charge transfer devices 0-92997
 Si-SiO₂, MOS capacitors, relationship between trapped holes and interface states 0-70830
 Si-SiO₂, MOS interface states density, transient capacitance meas. eval. 0-92989
 Si-SiO₂, structure, alkali metal ion migration and accumulation, interface struct. 0-107574
 Si-SiO₂, structures, B ions implanted, energy spectra of shallow traps at various implantation energies 0-80392
 Si-SiO₂-Al, interface barrier energies for tunnel oxides, internal photoemission meas. 0-84512
 Si-SiO₂-Al, internal photoemission, pot. barrier height determ. 0-65699
 Si-SiO₂-Al MOS surface channel influence on channel-to-contact diode charact. 0-92994
 Si-SiO₂-Al structures, SiO₂ thin dielec. film elec. props. with DC voltage (*Slovak*) 0-88634
 Si-SiO₂-Al with thick dielec. layer, photoelec. props. 0-92979
 Si-SiO₂-Au Schottky barrier solar cells, back-illuminated, theoretical performance 0-61345
 Si-SiO₂-Au system, oxide film 16-36 Å thick, tunnel currents 0-70842
 Si-SiO₂-CdS solar cell, I-V characteristics 0-89621
 Si-SiO₂-Si capacitor, polycryst., capacitance voltage characterisation 0-70794
 Si-SiO₂-Si thin film MOS structures, elec. props. with applied DC voltage (*Slovak*) 0-92977
 Si-SiO₂-Si₃N₄ MNOS structure, chem. comp. and electronic states, Auger and energy loss spectra obs. 0-92999
 Si-SiO₂-Si MOS structures, charge motion, TSC meas. 0-100534
 Si-SiO₂-polySi thin film structures, dielectric props. (*Slovak*) 0-75934
 Si-SiO₂, interfaces, carrier transport processes, electron states, conference, Durham, England (July 1979) 0-90612
 Si-Sn heterojunction, RHEED, Mossbauer spectroscopy and I-V characts. 0-70828
 Si-TiO₂-Al, current-voltage characts., oxide film effects 0-70841
 Si-V₂O₅-Al, current-voltage characts., oxide film effects 0-70841
 p⁺-Si₃-Ge, n-Si junction diodes, lattice misfit effects on I-V characts. 0-70804
 Si(Li) X-ray detector, Au contact layer thickness meas. 0-62627
 Si(111), ion-bombard., O₂ adsorption, SIMS study 0-70522
 Si(111) reconstructed 7×7 surface superlattices, microdomain model 0-107625
 Si(111)-Pb ion implanted amorphous layers, recrystallisation, impurity out-diffusion model (*Chinese*) 0-88363
 Si(111)/Pt/Ni Schottky diodes, current-voltage characts. and comp. profiles 0-84508
 Si(111)-(7×7), and impurity stabilised Si(111)-(1×1) surface, photoemission studies 0-104041
 Si(111)-√3×√3-Ag structure, atomic arrangement, low energy ion scatt. spectroscopy 0-96724
 Si(111)(7×7) surface models, LEED anal. 0-75418
 substrate, thin film of Ag or Al, work function Si (*French*) 0-80353
 T-metal, thin film contact, time evolution of photovoltaic effect 0-65687
 Te, a-edge dislocated crystals, mobility anisotropy 0-107781
 Te, acousto-optical props. at wavelength of 10.6 μm 0-76001
 Te, amorphous, electronic struct. and optical props., pseudopot. calc. 0-65428
 Te amorphous and liquid state, Raman spectra, crystn. processes 0-60608
 Te, cyclotron reson. in pulsed high mag. fields, cond. band struct. 0-59867
 Te, electronic struct. of cryst. phases and hydrostatic press. effects 0-59865
 Te film, stability in moist air, rel. to information storage capability, atmospheric corrosion model 0-71774
 Te film, surface morphology depend. on vacuum deposition angle 0-103553
 Te film, vacuum deposited, growth and morphology of crystals 0-96766
 Te, growth of single crystals by Czochralski method 0-66423
 Te, impurity spectroscopy 0-65499
 Te, metallic state, press. induced, elec. cond. meas. 0-96949
 Te, negative photoconductivity, intraband absorpt. (*Russian*) 0-107854
 Te, oriented films, semiconducting props., Hall coeff., band structure 0-70854
 Te, photoconductivity in strong mag. fields, doping effects, impurity levels 0-75602
 Te, SHG under two-photon reson. conditions 0-99803
 Te, strained and unstrained, SHG and propag. of CO₂ laser radiation 0-58641
 Te, thin film selective absorber coatings, prod. using an oblique vacuum deposition technique 0-81488
 Te, trigonal, Raman scatt. at very high press. 0-60566
 Te, trigonal and amorphous, electronic struct. and nonempirical calc. of struct. props. 0-59866
 Te, two types of carriers 0-60013
 Te:Cu films, elec. transport props. 0-60120
 Te-Ag thin film system, stress-relief appearance conditions 0-65416
 Te-Bi multilayer thin film struct. thermoelec. props. 0-92964
 Te-Bi thin film system, stress-relief appearance conditions 0-65416
 Te-Se-Cd, sandwich structure, fabrication and characteristics 0-60089
 Te-transition metal, liq. semicond., elec. props. 0-96870

elementary particle coupling constants

- Adler-Weisberger sum rule and the σ -commutator for the kaon-proton system 0-101956
 Adler-Weisberger sum rule and the σ -commutator for the kaon-neutron system 0-101957
 Glauber approach and the triple-pomeron coupling 0-68435
 quark mass, electroweak contrib. 0-101990
 SU(4), symmetry breaking effects on strong coupling const., charmed and uncharmed B BP couplings calc. 0-105802
 e⁺e⁻→hadrons, 12, 30 GeV, jets, quark fragmentation and coupling constant, QCD comparison 0-105915
 e⁺e⁻ high energy data from PETRA, QCD anal., QCD coupling constants 0-82985
 e⁺e⁻→multihadrons, planar three jet events, gluon bremsstrahlung, strong coupling constant 0-57617
 e⁺e⁻→ $\pi^+\pi^-\pi^0$, 750-1100 MeV, ω and ϕ meson interference 0-105910

elementary particle coupling constants continued

- $\eta \rightarrow \pi\pi\eta$, $\delta\eta/\pi$ and $\delta\eta/\pi$ coupling constant ratio, $\delta(980)$ quark content 0-82955
- $K^-p \rightarrow \Lambda\eta$, 6 GeV/c, baryon exchange reactions, ηNN coupling constant, A polarisation, nucleon-Regge exchange 0-78098
- $K^-p \rightarrow \Lambda\pi^0$, 6 GeV/c, baryon exchange reactions, ηNN coupling constant, A polarisation, nucleon-Regge exchange 0-78098
- NN forward scatt., two and three pion cut contribs., nucleon exchange model 0-63103
- $\nu(\bar{\nu})p$, 2 GeV elastic scatt., charged current/neutral current event ratio 0-57582

elementary particle decay

- see also *electromagnetic decays; elementary particle coupling constants; hadron decay; leptonic decays; muon decay; nonleptonic decays; semileptonic decays*
- explosive cascade-decays of leptons, quarks, virtual photons, weak vector bosons and Higgs scalars 0-86641
- geometrical approach to elementary particles 0-105865
- hadron production, quark fragmentation and triple Regge models, quark decay functions 0-62921
- heavy quark infrared safe weak decay, dimensional regularisation techniques, gluonic corrections 0-102087
- intermediate vector boson decay, QED and QCD radiative corrections, hadronic jets 0-73759
- lepton \rightarrow hadrons, coherent and inclusive, due to lepton-nucleus collisions 0-83100
- moment and Fokker-Planck eqns. 0-82709
- $\nu(\bar{\nu})N$, heavy lepton prod. and decay, differential cross sections (*Russian*) 0-105940
- $\tau \rightarrow K^*\pi$, in e^+e^- annihilation, T-odd asymmetry in CP violation model (*Russian*) 0-105885
- $\tau \rightarrow \mu e$, flavour changing neutral current search 0-105836
- $\tau \rightarrow \nu\eta\pi$, T-violation effects, neutrino mass (*Russian*) 0-95294
- $\tau \rightarrow \nu\rho\pi$, spin parity anal. 0-105941
- τ^- decays, SPEAR, Mark II detectors, recent results 0-74045
- τ decay as QCD test 0-102006

elementary particle electromagnetic interactions

- see also *Weinberg model*
- bagged complex scalar field, EM interaction, fine struct. const., possible dynamic origin 0-86635
- electron-photon beams from proton accelerators, EM interaction investigation (*Russian*) 0-106214
- Higgs boson couplings, charged, K_L - K_S mass differences 0-62917
- QED, fine-structure constant, coupled Maxwell and Dirac eqns., lepton and quark-like solutions 0-62894
- pp, heavy lepton prod. and decay, supersymmetrical model of weak and EM interactions (*Russian*) 0-86748

elementary particle gravitational interactions

- see also *supergravity*
- cosmological ν sea, EM wave propagation, torsionic background 0-77283
- gravitationally induced CP effects, quantum gravodynamics, QCD quark sector 0-86616
- Kerr-like neutrino-gravitational solutions 0-95240
- quark energy nonconserving fluctuations and strong forces 0-57551
- QED, fine-structure constant, coupled Maxwell and Dirac eqns., lepton and quark-like solutions 0-62894
- SU(3) group strong interactions in gravitational field 0-91047
- unified gauge theory of gravitational and strong interactions 0-95016

elementary particle inclusive interactions

- see also *electron-positron inclusive interactions; elementary particle large momentum transfer interactions; pion-nucleon inclusive interactions; proton-proton inclusive interactions*
- additive quark model and multiparticle production off emulsion nuclei at 50 GeV 0-68491
- axiomatic field theory, analytic structure of the 3 \rightarrow 3 forward amplitude 0-68376
- bag model, isobaric ensemble and multiplicity distrib. (*Russian*) 0-82952
- cluster model, multi-Regge, comparison with multiparticle transverse and longitudinal data 0-62952
- cross section decrease at fixed angles, planarity at high energies, analyticity 0-78105
- deep inelastic and semi-inclusive annihilation structure function factorisation in Bjorken limit, mass singularities 0-86713
- deep inelastic lepton-hadron scatt., semiinclusive hadron prod., quark fragmentation function corrections, QCD 0-63013
- deep inelastic scatt., inclusive observables and hard gluon emission 0-99094
- diffractive hadronic reactions, statistical description of multipion prod. 0-95260
- forward jet production meas. in high transverse momentum hadron-proton collisions 0-101989
- forward scattering, single particle inclusive spectra, Cos θ plane singularities effects 0-102083
- gluon and quark jets in a recursive model motivated by quantum chromodynamics, T decay 0-62936
- gluon and quark population evolution in QCD jets, numerical estimates 0-101987
- gluon fragmentation, polarised, in e^+e^- , e^+q and hadron scattering 0-82988
- hadron+hadron, cluster model, field theoretic, multiperipheral production, Feynman scaling violation 0-57576
- hadron+hadron $\rightarrow \gamma\gamma X$, scaling and quark mass dependence, quark parton model 0-73749
- hadron+hadron inclusive cross section of symmetric hadron pairs produced, hard scatt., parton model and QCD 0-63052
- hadron+nucleus, spatial temporal development, nuclear hadronic cascades 0-63040
- hadron beam jets structure at small P_T 0-102014
- hadron inclusive prod. cross sections at large P_T A-depend., quark-parton model (*Russian*) 0-86771
- hadron induced multiparticle reactions, S-1500 GeV, resonance prod. correlations, jet model (*German*) 0-91118
- hadron interactions, inclusive, large momentum transfer, quark counting, EM form factors 0-68498
- hadron interactions, inclusive processes, multiplicity and scaling, resonance production, additive quark model, SU(6) theory, review 0-63043
- hadron jets, rapid parton and hadron distribution 0-86693
- hadron leptonproduction, nuclear targets, quark-nucleon inclusive cross section, heavy lepton pairs 0-57607
- hadron physics at high p_T 0-73743

elementary particle inclusive interactions continued

- hadron production, quark fragmentation and triple Regge models, quark decay functions 0-62921
- hadron-hadron, in H, AL, inclusive particle distribs., QCD predictions 0-99112
- hadron-hadron 3-jet collisions, charge conjugation asymmetries and tri-linear gluon coupling 0-105934
- hadron-hadron inclusive interactions, charmed particle production, η_c , ψ and other cc bound states 0-63036
- hadron-nucleus, 50-200 GeV/c, multiparticle production, multiplicities, cross sections and ang. distribs. 0-86768
- hadron-nucleus, rapidity distrib., 22.8, 50, 400 and ≥ 1000 GeV in emulsion, multiperipheral models 0-91117
- hadron-nucleus (nucleon), relativistic secondary multiplicities, constituent quark rescatt. 0-63034
- hadronic collisions, jet structure, two-jet events, glueball-Pomeron identity, dual field theory 0-63051
- hadronic events, inelastic, non-diffractive, charge correlations in jets, quantum number effects 0-86764
- hadronic lepton pair production, QCD jets 0-62994
- hard processes, large rapidity separation of baryonic number, partons, and dual topology 0-95255
- heavy quark mesons, inclusive hadronic prod. (*Russian*) 0-86770
- high energy hadron-nucleus interactions, mean slow particle multiplicity mass depend. 0-102081
- higher order QCD jets in photoproduction 0-99087
- higher-twist effects in QCD, deep inelastic scattering and the Drell-Yan process 0-102020
- inclusive vector meson production in fragmentation regions of meson at small P_T 0-105931
- jet decay models, group-theoretical and four-momentum variables 0-73684
- jet phenomenon and Lorentz deformation 0-105806
- jet production on nuclei, strong A depend. (*Russian*) 0-102084
- large p_T photoproduction, gluon fragmentation function extraction, scaling 0-105853
- large p_T hadronic collisions, QCD sensitive test, quark and gluon jets 0-57647
- lepton+nucleon, quark and gluon jets, Breit frame, QCD 0-62995
- local number fluctuation in multiparticle production 0-57574
- mean multiplicity depend. on transferred momentum, expt. and geometric approach (*Russian*) 0-95293
- mean multiplicity of secondary particles in hadron-nuclear interactions, multiple scatt. theory (*Russian*) 0-68502
- multiparticle hadronic reactions, phenomenological parametrisation 0-99110
- multiple hadron production and struct. from 10 GeV to 10 TeV interactions 0-57653
- particle multiple prod. cross section in model with pomeron intercept $\alpha_p > 1$ (*Russian*) 0-82959
- QCD, high P_T hadron prod. in pionisation region and vacuum singularity (*Russian*) 0-86772
- QCD and short range nuclear phenomena 0-91060
- QCD hadron jets, branching processes, multiplicity distrib., KNO scaling (*Russian*) 0-101998
- quark and hadron jets, charge and energy flow in cascade models 0-102017
- quark fragmentation functions for inclusive hadron production, Regge formalism 0-68462
- quark fragmentation jets in QCD, cascade model 0-78045
- scaling hypothesis for the rapidity distributions and information theory 0-73747
- singular gauge fields, effect on inclusive differential cross sections 0-105782
- soft gluon resummation formulae for hard parton processes in QCD 0-105842
- space-time structure of jet hadronization 0-91024
- totally inclusive leptonprod., scaling anal., target mass corrections in QCD parton model 0-102052
- transverse momentum correlations for secondaries, rapidity cluster, stat. model 0-73754
- BB annihilation process, simple geometrical picture 0-95291
- eN, 50, 100, 300 GeV, in emulsion, cascade showers 3-dimens. development 0-86724
- e $^-$ N, inclusive pion production due to $\gamma q \rightarrow \pi q'$ process, quark-parton model (*Russian*) 0-78073
- γ +hadron-lepton pair, perturbative QCD, twist-2 photon operator, parton subprocesses 0-73716
- γ N, inclusive pion production due to $\gamma q \rightarrow \pi q'$ process, quark-parton model (*Russian*) 0-78073
- γ N-jet+X, QCD cross sections 0-73715
- γ N- $\mu\bar{\mu}X$, QCD cross sections 0-73715
- γ N- π^+X , QCD cross sections 0-73715
- γp , 40-70 GeV, inclusive D^0 photoprod. cross sections, pair and associated prod. 0-91097
- $\gamma p \rightarrow (pp)p$, inclusive and exclusive pp photoprod. S(1936) prod. 0-86729
- $\gamma p \rightarrow \pi^+ \pi^- \pi^+ \pi^- \pi^+$ p, diffractive production, jet-like structure 0-57606
- $\gamma p \rightarrow X$, large p_T , perturbative QCD 0-86723
- $\gamma p \rightarrow q\bar{q}$, quark-antiquark jet diffractive photoprod. in perturbative QCD 0-73714
- $h_1 h_2 \rightarrow l\bar{l}X$, massive lepton pair prod., polarisation and spin effects 0-105929
- in deep inelastic scattering, quark jet as trigger for gluon jet 0-62996
- K structure functions from inclusive prod. data, nonstrange quark distribs. 0-86715
- $K^-N \rightarrow \mu^+ \mu^- X$, K^-/π^- structure function ratio using Drell-Yan process 0-86718
- $K p$, 70 GeV/c, total and differential cross-sections for π and K production 0-63050
- kp, large P_T pion 0 prod., meson structure functions, quark distrib. functions 0-86714
- $K^- p$, 10, 16 GeV/c, S^+ , S^- inclusive prod. A prod. comparison 0-86766
- $K^- p$, 110 GeV/c, charged multiplicity distrib. 0-78101
- $K^- p \rightarrow \Delta^+ X$, 32 GeV, inclusive and total cross sections 0-105936
- $K^- p \rightarrow \Delta^+ X$, 32 GeV/c, total and differential cross sections, energy dependence 0-63048
- $K^- p \rightarrow \pi^+ (1385) X$, 32 GeV, inclusive and total cross sections 0-105936
- $K^+ p$, 147 GeV/c, inclusive Δ^{++} prod., cross section energy depend. 0-57651
- $K^+ p$, 70 GeV/c, cross sections and charged multiplicity distribs. 0-63053

elementary particle inclusive interactions continued

- k^+p , multiple production processes regularities, Monte Carlo model 0-102082
 $K^+p \rightarrow \pi^- \pi^+ X$, 32 GeV/c, two-pion correlations, Monte Carlo model 0-83008
 K^+p , 130, 200 GeV, jet prod. cross sections, QCD anal. and scale breaking 0-99111
 K^+p , fireball model, universal scaling function 0-57646
 K^+p , π^+/π^- inclusive ratio in quark recombination model 0-102022
 $K^+p \rightarrow K^+ X$, triple Pomeron coupling, Reggeon treatment 0-68488
 $L_d \rightarrow \Delta X$, deep inelastic scatt., isobar admixture possibility (Russian) 0-91095
 μN , 10^{12} eV, T muoprod. limits from tritium final states 0-105909
 μN -hadron shower, charm-pair production effects 0-73748
 μN in Fe, 280 GeV, dimuon prod. cross sections 0-91094
 μN in Fe, 280 GeV, tritium event cross sections 0-99104
 μp deep inelastic scatt., inclusive cross section, lepton pair EM prod. contrib. (Russian) 0-105904
 $\mu p \rightarrow K^+ X$, 225 GeV, deep inelastic scatt., strange neutral particle prod. 0-105902
 $\mu p \rightarrow \Lambda(\Lambda^0) X$, 225 GeV, deep inelastic scatt., strange neutral particle prod. 0-105902
 NN , 10^{12} eV, rapidity gap distrib., Snider multiperipheral cluster model 0-73757
 $np \rightarrow \pi X$, baryonium exchange, triple-Regge couplings 0-86763
 $pd \rightarrow A^+ X$, high energy charmed baryon prod. obs. 0-105881
 pN , K^0 and π^- prod. rates, SU(3) symmetry violation in quark jet 0-82966
 pN -hadron shower, charm-pair production effects 0-73748
 $pN \rightarrow \psi X$, neutral current ψ prod., Z^0 -gluon fusion model 0-78015
 $p p$, multiple production processes regularities, Monte Carlo model 0-102082
 $p p$ charged current interaction, inclusive ρ^0 prod. 0-62963
 pd , 70 GeV, π^+ , K^+ , p , \bar{p} prod. with 0.5-2.2 GeV/c transverse momenta, yield ratio, QCD (Russian) 0-83012
 pN , 400 GeV, in emulsion, two-particle rapidity correlation 0-63054
 pN , 67 GeV, multiperipheral cluster production 0-73689
 pN , 67 GeV, rapidity dispersion and cluster production 0-78104
 pN , 67 GeV/c, in Be, Al, Cu, inclusive π^+ , K^+ , p , \bar{p} prod. cross sections (Russian) 0-86769
 pN , 67 GeV/c, nuclear targets, π^+ , K^+ , p , \bar{p} yields (Russian) 0-68501
 pN , 70 GeV in emulsion, pion cluster obs. 0-86762
 pN -charm particles, obs. in high resolution streamer chamber 0-73742
 pN -hadron shower, charm-pair production effects 0-73748
 pN in emulsion, 200, 400 GeV/c, multiparticle prod., azimuthal and rapidity effects 0-63035
 pN in Fe, 400 GeV/c, $\psi(3100)$ prod. 0-57650
 $pN \rightarrow l^+ l^- X$, scaling predictions, Drell-Yan model 0-73756
 $pN \rightarrow \Lambda^0 X$, inclusive cross section, constituent-constituent multiple scatt. model for dependence on atomic number 0-83101
 π , structure functions from inclusive prod. data, nonstrange quark distrib. 0-86715
 π^0 high p_T prod. ang. depend., inclusive cross sections, scaling 0-91119
 πN , 6-200 GeV, amplitude anal. in impact parameter representation, non-zero polarisation, shell struct. (Russian) 0-86752
 πN , 16, 22 GeV, dimuon prod. parton intrinsic transverse momentum, QCD perturbation 0-63037
 πn , 40 GeV/c, many pion systems in inclusive reactions, transverse momentum effects (Russian) 0-57654
 πN , 40 GeV/c in ^{12}C , multinuclear inclusive process correlation functions (Russian) 0-68500
 πN , in ^{12}C , 40 GeV/c, one- and multi-nucleon interactions, secondary charged particle multiplicity (Russian) 0-83013
 πN , in C, S 5 GeV/c, π^0 and n inclusive spectra, cascade model (Russian) 0-68490
 $\pi N \rightarrow \gamma X$, 50 GeV, gamma prod. characteristics in emulsion reactions 0-68492
 πN in Ne, 25, 50 GeV/c, secondary particle multiplicity and multiple scatt. model anal. (Russian) 0-83014
 $\pi N \rightarrow \mu^+ \mu^- X$, K^-/π^- structure function ratio using Drell-Yan process 0-86718
 $\pi n \rightarrow p X$, 21, 205 and 360 GeV/c, reggeised one-pion-exchange 0-57649
 $\pi N \rightarrow \psi X$, 225 GeV, bottom meson pair production limit 0-73750
 πp , 150 GeV/c, leading particles and diffraction dissociation, 2-, 4- and 6-prong events 0-68486
 $\pi^+ \pi^- \rightarrow$ mesons, multimeson inclusive spectra and recombination model, multi-quark structure functions, predictions 0-73751
 $K^+p \rightarrow \pi^+ X$, 32 GeV, topological cross sections 0-102085
 pN , 350 GeV in Ne, D^+ prod. cross section and lifetime 0-68494

elementary particle interaction models

- see also bootstrapping; composite models of hadrons; diffraction model; duality and dual models; peripheral models; statistical models; vector meson dominance model; Weinberg model
conference, particles and fields, Montreal, Canada (Oct. 1979) 0-73090
inclusive processes, cross section decrease at fixed angles, planarity at high energies, analyticity 0-78105
leptons, topological bootstrap approach, rishon model 0-78046
P+I model, flavour and baryon number renormalisation 0-78050
quarks and leptons, topological bootstrap approach, rishon model 0-78047
twist selection rule, mass zero representation partons 0-78027
Z(N) strings and hadron structure 0-86572
 ψ^+ (3.772), ground state admixture in potential model 0-102033

elementary particle interactions

- see also cosmic ray effects and interactions; elementary particle coupling constants; elementary particle electromagnetic interactions; elementary particle gravitational interactions; elementary particle inclusive interactions; elementary particle large momentum transfer interactions; elementary particle scattering; elementary particle strong interactions; elementary particle weak interactions; hadron-deuteron interactions; hadron-hadron interactions; high-energy cosmic ray interactions; lepton-deuteron interactions; lepton-hadron interactions; lepton-lepton interactions; photon-deuteron interactions; photon-hadron interactions; photon-lepton interactions; photon-photon interactions; polarisation in elementary particle interactions; quantum field theory of interactions; unified field theories; vertex functions
cluster decomposition of many dimens. phase space, appl. to high energy collisions 0-102027

elementary particle interactions continued

- conference, particles and fields, Montreal, Canada (Oct. 1979) 0-73090
event recording and analysis by computer (French) 0-63496
forces between leptons and quarks, a gauge field phenomena 0-91008
fundamental constituents of matter and unification of weak and electromagnetic interactions 0-62940
high-energy physics, particles and interactions, accelerators 0-77944
polarisation in atomic and nuclear physics 0-63162
Rutherford Laboratory, particle physics experiments 1979 0-105942
tachyon exchange in two-body interactions 0-82960
unified theory of elementary-particle forces 0-105827
elementary particle large momentum transfer interactions
see also elementary particle inclusive interactions
elastic scattering, small and large momentum transfer relations (Russian) 0-86698
hadron+hadron, large-angle scattering, quasi-potential approach, pre-asymptotic effects 0-68484
hadron+hadron inclusive cross section of symmetric hadron pairs produced, hard scatt., parton model and QCD 0-63052
hadron inclusive prod. cross sections at large p_T A-depend., quark-parton model (Russian) 0-86771
hadron interactions, inclusive, large momentum transfer, quark counting, EM form factors 0-68498
hadron physics at high p_T 0-73743
hadronic events, inelastic, non-diffractive, charge correlations in jets, quantum number effects 0-86764
high-transverse-momentum symmetric-particle-pair spectra and correlations 0-95250
large p_T photoproduction, gluon fragmentation function extraction, scaling 0-105853
large p_T hadronic collisions, QCD sensitive test, quark and gluon jets 0-57647
lepton pair production, QCD and hard-scatt. model, spin-spin asymmetries 0-63014
mean multiplicity depend. on transferred momentum, expt. and geometric approach (Russian) 0-95293
QCD, high p_T hadron prod. in pionisation region and vacuum singularity (Russian) 0-86772
 $\gamma p \rightarrow \pi X$, large p_T , perturbative QCD 0-86723
 kp , large p_T pion 0 prod., meson structure functions, quark distrib. functions 0-86714
 NN large angle elastic scatt., spin-spin asymmetries and flavour depend., quark interchange 0-86743
 p production, compared to π , large transverse momentum, rearrangement of hard scattered partons 0-62934
 pp , 100, 200 GeV, elastic scatt., polarisation effects at large momentum transfer, quark model (Russian) 0-83005
 pp , 31-63 GeV, direct photon prod. at large p_T , π^0/γ prod. ratio 0-63038
 pp , 62.4 GeV/c, direct single photon prod. at large p_T 0-91113
 pp , ISR energies, high p_T π^0 and single photon events, associated charged particle multiplicity 0-63039
 pp , large p_T pion 0 prod., meson structure functions, quark distrib. functions 0-86714
 pp elastic scatt. at high energies and large momentum transfer, review (Russian) 0-105926
 $pp \rightarrow pp$, large momentum transfer, multiple-scattering model, three-quark proton 0-63031
 $pp \rightarrow pp$, Van der Waals type model 0-73740
 $pp \rightarrow \pi X$, large- p_T reactions in broken color gauge theory 0-95292
 pp scatt. cross section at high momentum transfer, geometrical scaling, energy depend. (Russian) 0-102064
 π^0 high p_T prod. ang. depend., inclusive cross sections, scaling 0-91119
 πp , direct photon prod., Compton and annihilation process contrib. 0-105925
 πp , large p_T pion 0 prod., meson structure functions, quark distrib. functions 0-86714
 $\pi p \rightarrow \pi p$, large momentum transfer, multiple-scattering model, three-quark proton 0-63031
 πp , 40 GeV/c, correlation between π and accompanying large transverse momentum particle (Russian) 0-86758
ed elastic scatt. at high momentum transfer 0-82977

elementary particle mass

- see also baryon mass; lepton mass; mass differences; mass formulae; meson mass
fermions, light, mass hierarchy, grand unification, SU(N) theory 0-62911
heavy quarks, mass power law 0-62955
quark mass, electroweak contrib. 0-101990
quarks, EM form factors in instanton fields 0-99102
SU(5) grand unification, heavy coloured Higgs scalars, b-quark mass 0-57543
transverse lattice QCD, hadron mass spectrum 0-57568
Weinberg-Salam model with two massless Higgs doublets, particle masses, perturbation constraint 0-57541
t-quark mass predictions from Glashow determinant condition 0-86677
W, mass in SU(5) grand unified theory 0-68411
Z, mass in SU(5) grand unified theory 0-68411

elementary particle scattering

- see also bootstrapping; elementary particle interactions; hadron-deuteron scattering; hadron-hadron scattering; lepton-deuteron scattering; lepton-hadron scattering; lepton-lepton scattering; Mandelstam representation; photon-deuteron scattering; photon-hadron scattering; photon-lepton scattering; photon-photon scattering; polarisation in elementary particle scattering; Pomeronchuk poles and trajectories; quantum field theory of elastic scattering; Regge poles and trajectories; relativistic scattering theory; S-matrix theory
elastic scattering, small and large momentum transfer relations (Russian) 0-86698
non-relativistic scattering by stationary external metrics and Yang-Mills potentials 0-101938
off-shell particle scattering, total cross sections, QCD 0-68418
total cross sections, asymptotic upper bound 0-105938

elementary particle strong interactions

- see also composite models of hadrons; duality and dual models; hadron classification schemes; peripheral models; quantum field theory of strong interactions
effective hamiltonian for $\Delta C=1$ nonleptonic interactions in the Kobayashi-Maskawa model 0-86667
Planck energy nonconserving fluctuations and strong forces 0-57551

elementary particle strong interactions continued

- QED, fine-structure constant, coupled Maxwell and Dirac eqns., lepton and quark-like solutions 0-62894
 stellar environment, nucl. struct. and reactions 0-72765
 strong gravity, field equations, strong interactions, de Sitter microsphere idea of hadrons 0-68111
 SU(2)×U(1) gauge model, chiral SU(2)×SU(2) symmetry and electron mass 0-57542
 SU(3) group strong interactions in gravitational field 0-91047
 unified gauge theory of gravitational and strong interactions 0-95016
 K⁰-K⁰ mixing, strong interaction corrections in six quark model, QCD calcs. 0-82957
 K⁺→π⁺e⁺e⁻, neutral-current process, strong interaction corrections 0-62968
 K⁺p→π⁺Σ⁺, box diagram calcs. unitarity corrections in strong interactions 0-91110
 NN→πππ, kinematic singularity free helicity amplitudes, crossing matrix anal. props. 0-95285
 pp, 23.4-62 GeV, scatt. amp., differential cross section from eikonal model (Russian) 0-57642
 πN→πN, kinematic singularity free helicity amplitudes, crossing matrix anal. props. 0-95285

elementary particle symmetry

- see also *chiral symmetries; conservation laws; discrete symmetries; dynamical symmetry; helicity (elementary particles); isotopic spin (elementary particles); nonlinear symmetries; spontaneous symmetry breaking; SU_n theory; supersymmetry*
 charmed baryons, weak decays, quark model framework 0-62976
 dynamical groups, symmetries and constants of motion for electric and mag. charges 0-101945
 Lie-admissible deformation of self-adjoint systems 0-101941
 SU(3)×U(1) electroweak model, strong extension, flavour and colour gauge exchange symmetries (Chinese) 0-101975
 symmetries and differential equations 0-105807
 tensor meson dominance, internal symmetries, and meson mixing for the new particles 0-102036
 unitary symmetry in baryon-antibaryon systems (Chinese) 0-102000

elementary particle theory

- see also *Bethe-Salpeter equation; complex angular momentum plane; current algebra; dispersion relations; electron theory; elementary particle interaction models; elementary particle symmetry; Feynman diagrams; form factors (elementary particles); group theoretical schemes; helicity (elementary particles); isotopic spin (elementary particles); Lee model; mass formulae; quantum field theory; S-matrix theory; scaling phenomena; structure functions; sum rules; vertex functions*
 advances towards a unified theory 0-91039
 anomalous magnetic moment, perturbative expansion divergence 0-78063
 anti-commutative, self-inverse matrices and transformations in eigenvalue problems (Chinese) 0-101951
 basic course in modern weak-interaction theory 0-91044
 Bernard Gregory 1979 lectures 0-77992
 boson, Green function, rainbow approach of scalar model (Russian) 0-68436
 charm, elementary particle theories, properties (Spanish) 0-73681
 cluster decomposition of many dimens. phase space, appl. to high energy collisions 0-102027
 cosmological approach, review, book contrib. 0-68440
 electron-muon symmetry of Callan-Symanzik function: two-lepton case 0-73627
 hadron building blocks, pionic mass intervals in narrow and S-state resonances 0-105875
 hadronic matter, anisotropic superfluidity, analytic formulation 0-105869
 heavy lepton prediction in weak interaction theories 0-73657
 identical particle indistinguishability, field quantisation Lie algebraic approach 0-77984
 lepton charge, geometric interpretation (Hungarian) 0-73691
 space-time approach to the description of cumulative-type processes (German) 0-68439
 stable particles as building blocks of matter 0-57577
 superconductivity theory development, (1950s to 1980s) (Czech) 0-80440
 trilocal structures, expansions 0-57460

elementary particle weak interactions

- see also *neutral currents; quantum field theory of weak interactions; Weinberg model*
 basic course in modern weak-interaction theory 0-91044
 effective hamiltonian for ΔC=1 nonleptonic interactions in the Kobayashi-Maskawa model 0-86667
 electroweak gauge models with heavy W bosons, SU₂×U₁×U₁' scheme (Russian) 0-86652
 heavy lepton prediction in weak interaction theories 0-73657
 Higgs boson couplings, charged, K_L-K_S mass differences 0-62917
 mass scale of weak interactions 0-91045
 milliweak gauge models of CP violation 0-73633
 neutral weak current interactions, review 0-73654
 neutral-current weak interaction without electroweak unification 0-105835
 neutrino interactions in neutron stars, pulsation damping 0-77439
 neutron decay, weak interaction meas., coincidence type ion electron converter detector obs. 0-58100
 QED, fine-structure constant, coupled Maxwell and Dirac eqns., lepton and quark-like solutions 0-62894
 relativistic theory of P violation in many-electron atoms 0-91042
 six- and eight-quark models, weak interactions 0-99086
 stellar interiors, sd-shell nuclei, appl. to supernovae 0-82336
 SU₂×U₁ and the origin of the Cabibbo angle, charged gauge boson mixing 0-73639
 SU(2)_c⊗SU(2)_l⊗U(1) weak model, ν mass and spontaneous P nonconservation 0-62884
 SU(3)×U(1) gauge theory, electro-weak interaction, helicity mixed representation 0-78013
 unconfined colour quark models, weak interactions and neutral currents (Russian) 0-105841
 weak interactions, summer school, Varenna, Italy (Jul. 1977) 0-90597
 n electric dipole moment, CP violation in gauge theories 0-91041
 N form factors, weak, asymptotic behaviour within QCD dipole and tri-pole formulae 0-62987
 ν oscillations in weak interaction model 0-78014
 pp, heavy lepton prod. and decay, supersymmetrical model of weak and EM interactions (Russian) 0-86748
 pp scatt., <300 MeV P-odd asymmetry for pol. p (Russian) 0-102063

elementary particles

- see also *bosons; charm particles; composite particles; cosmic rays; fermions; gamma-rays; hadrons; hypothetical particles; leptons; quantum field theory; strange particles*
 antimatter, origin, whereabouts 0-62340

elements (chemical)

- for specific metals and non-metals see appropriate chemical names
 see also *element origin; element relative abundance; periodic system of elements*
 mantle related thermodynamic props. and reactions at high press. and temp. 0-81874

Eliashberg strong-coupling model see *strong-coupling superconductors***Elinvar**

- No entries

ellipsometers

- see also *ellipsometry*
 conference, Berkeley, CA, USA (Aug. 1979) 0-101665
 instrumentation, review 0-101819
 measurement of thin films on wafers, real time, computer assisted 0-73418
 perpendicular-incidence microellipsometer 0-101824
 single-element rotating-polarizer ellipsometer 0-101823
 spinning analyser ellipsometer, meas./magneto-optic rotation and ellipticity (Japanese) 0-73419
 vacuum automatic ellipsometer for condensing film homogeneity determ. 0-101825

ellipsometry

- see also *ellipsometers; polarimetry*
 angle-of-incidence derivative ellipsometry and reflectometry, implementation and appl. 0-73420
 anisotropic layered media, 4×4 matrix algebra 0-106445
 anisotropic object, single zone method for ellipsometric parameter determ. 0-68240
 anodised films on metals, ellipsometer obs. interpretation using film form. models 0-101828
 carbon tetrachloride, surface study, ellipticity coeff., ellipsometric method 0-84343
 conference, Berkeley, CA, USA (Aug. 1979) 0-101665
 corrosion inhibitor action obs., of propargyl alcohol, film growth on steel surfaces (Rumanian) 0-60996
 data analysis aided by derivative plots in n,κ-space 0-86378
 1,2-dimyristoyl-sn-glycero-3-phosphoserine multilayers, phase transitions, temp. depend., ellipsometric study 0-108846
 1,2-dipalmitoyl-sn-glycero-3-phosphocholine multilayers, phase transitions, temp. depend., ellipsometric study 0-108846
 factor VIII, native and modified, surface adsorption and mol. interactions, ellipsometric obs. 0-104555
 fibrinogen, native and modified, surface adsorption and mol. interactions, ellipsometric obs. 0-104555
 four-photon spectroscopy of condensed media, nonlinear spectroscopy developments 0-91860
 glasses, high vol. low cost, as solar reflectors, compositions and weathering effects 0-106589
 goniometric attachment for ellipsometers 0-90883
 ice, surface transition layer, ellipsometric study 0-103545
 instrumentation, review 0-101819
 ion implanted layers, complex refr. index profile, ellipsometric meas. 0-93262
 Kramers-Kronig relations and sum rules, Lorentz oscillator model 0-102617
 linearly polarised light depolarisation effective ellipse phase and amplitude 0-86381
 liquid crystal thin layer, polarised light ellipticity after passage 0-88036
 metallic films and surfaces, nonlocal effects, theory 0-104006
 metals, solid and liq., optical props. by spectroscopic ellipsometry, review 0-103929
 microscopical equipment, methods, appls. and related topics, bibliography 0-73124
 Mueller-Stokes calculus, conventions and formulas 0-102618
 optical surfaces, ellipsometric charact. determ. using nanosecond laser pulses 0-101822
 pyrocarbon coatings, refl. anisotropy and struct. determ. by perpendicular incidence microellipsometer 0-101824
 reflectance-aided null ellipsometry for film-substrate systems 0-101827
 rotating-analyser ellipsometers, cell window imperfection effects 0-101826
 semiconductor film growth, multilayer systems, spectroscopic ellipsometry, review 0-103603
 spectroscopic, appl. to in situ meas. and anal. of plasma-grown GaAs oxides 0-76386
 stabilised two-frequency laser, use in ellipsometry 0-101820
 stress measurement in birefringent medium by fast three-dimens. ellipsometry 0-101821
 surface structure, submonolayer and monolayer films, ellipsometric study, review 0-103546
 surfaces, laser-annealed, characterisation by ellipsometry 0-103544
 transparent films on transparent substrates, theory 0-104007
 uniaxial crystals, refl. ellipsometry nonlinear eqn. inversion 0-95120
 Van der Waals film adsorbed on graphite, two-dimensional phase transitions 0-107653
 Ag film, ellipsometric response to CO adsorption 0-103571
 Al₂O₃ films, DC reactively sputtered, struct. 0-96764
 Ar, liquid, surface study, ellipticity coeff., ellipsometric method 0-84343
 Au film, evap., temp. change and gas adsorpt. effect on opt. const., ellipsometric obs. (German) 0-89081
 Au, optical props., dielec. function, void model, sample effects 0-76048
 Bi₂Te₃, anodic film form., in situ ellipsometric study 0-104318
 Co-Gd(Tb)(Sm) film, magneto-optic coeff. and refr. index, ellipsometric determ. 0-71501
 Co-Si interface, glassy layer, ellipsometric charact. 0-103589
 Cu adsorption of O₂, N₂O on (100) surface, reaction with CO 0-103583
 Cu anode, passivating behaviour and illum. effects in alkaline soln. 0-104449
 Fe, film growth under organic coatings, qualitative ellipsometric-electrochem. approach 0-104344
 Fe, passive film form. in phosphate soln., intensity-following ellipsometry study 0-104345
 Fe-Cr alloys, in acid and neutral solns., thickness and optical constants of passive and transpassive films 0-66698

ellipsometry continued

- Fe-Gd(Tb) film, magneto-optic coeff. and refr. index, ellipsometric determ. 0-71501
GaAs anodisation, ellipsometric study (*Japanese*) 0-97610
GaAs, ion-implantation induced damage profile, ellipsometric study, annealing 0-103400
GaAs oxides, plasma-grown, in situ meas. and anal. with spectroscopic ellipsometry 0-76386
GaAs-GaAlAs superlattices, metalorganic VPE growth, in sites ellipsometry monitoring 0-70547
GaSe, anodic film form., in situ ellipsometric study 0-104318
Ge surface, (111), ion-bombarded and annealed, spectroscopic ellipsometry study 0-103543
Hg optical props. by spectroscopic ellipsometry, review 0-103929
InSb, ion implanted, ellipsometric study 0-60537
InSb, refractive index and absorpt. coeff., cryst. orientation depend. 0-60536
KCl surface, VUV irradi., colour centre layer, angle-of-incidence derivative ellipsometry and reflectometry 0-73420
Li, optical props. by spectroscopic ellipsometry, review 0-103929
MgF₂-Na₃AlF₆ thin film deposits, quenched ageing by chopping 0-97364
Na, optical props. by spectroscopic ellipsometry, review 0-103929
Nd(NO₃)₃, aqueous soln., single photon absorpt. band struct., electronic resons. coherent ellipsometry 0-90881
Ni (100), adsorption of O₂ and reduction of surface oxide by H₂ 0-108741
Ni, anodic passive film form. in NaOH soln., refl. and ellipsometric study 0-104447
Ni, corrosion and passivation in phosphate soln., pH depend., ellipsometric study 0-104448
Ni film, evaporated, chemisorpt. of CO, ellipsometric investig. (*German*) 0-61156
Pt electrodes, polymeric surface film form. by electrooxidation of phenolic cpds., ellipsometric study 0-104450
Ru (1120), adsorption of O₂, H₂, and CO, ellipsometry-LEED study 0-103570
Si, dielectric function spectra, ellipsometric determ., many-particle effects at E_g-transition 0-93363
Si oxides, steam grown, index of refr. ellipsometric meas. 0-75995
Si RF sputter-etched surface, cryst. damage, spectroscopic ellipsometry obs. 0-103538
Si surface formation during etching of thin thermally grown oxide layers, ellipsometric control (*Russian*) 0-104315
Si wafers layers, multilayer ellipsometry, layer thickness and refr. index determination of layers 0-95121
Si:As, CW CO₂-laser annealing, comparison with thermal annealing 0-84193
Si:P, annealing after ion implantation, ellipsometric study 0-65018
Si-SiO₂ interface, thermally grown oxide, spectroscopic ellipsometric anal. 0-107659
SiO₂ film on 6H-SiC substrate, ellipsometric meas., accuracy and sensitivity 0-77840
SiO₂ films, desorption from Si single cryst., ellipsometric obs. 0-100410
SiO₂ films on Si, ellipsometric spectra, thickness determ. (*Chinese*) 0-86379
SiO₂, thin films on rough polycryst. Si surfaces, oxide thickness and refractive index meas. 0-93422
SiO₂ ultrathin layers, refr. index meas. 0-103936
SiO₂-Na₂O-CaO-MgO float glass, surface SnO₂ distrib., ellipsometry and XPS study 0-84346
SiO₂ thin films, deposition and characterisation study 0-80133
Sn, liq., optical props., 0.62-3.7 eV 0-75996
Sn, liq., optical props. by spectroscopic ellipsometry, review 0-103929
Ti, electropolished, optical props. from 1.8 to 3 eV 0-85088
WO₃, anodic oxide films, quadratic electro-optic and electrostrictive effects, ellipsometry 0-108184
Yb₂O₃ thin film on Cr substrate, refr. index depend. on thin film thickness 0-108290

elliptical polarisation see polarisation

elongation

- see also deformation; thermal expansion
acrylourethane coatings, radiation curable, tensile, elongation and modulus props. appl. techniques 0-66847
 α -brass, plane stress ductile fracture, prestrain effects 0-108532
 α -brass, single cryst., yielding behaviour rel. to low temp. annealing treatment (*Japanese*) 0-93582
brittle fibre reinforced composite, static strength depend. on component separation boundaries (*Russian*) 0-76304
effect of simulated fission products on mech. props. 0-73922
epoxy-rubber particulate composite, toughness and fracture mech. 0-71727
ethylene-Co copolymers and -SO₂ copolymers prep. by catalysis and ⁶⁰Co γ -radiation, mech. props. 0-66841
ethylene-vinyl acetate copolymers, extrusion and heavy duty films, radiation crosslinking, struct. effect 0-66844
fibre reinforced laminated hybrid, tensile first cracking strain and strength 0-81175
filled polymer mechanical properties, particle shape effect, review 0-100864
metal, thin-walled cylinder, elongation upon torsion 0-64386
Mylar film/adhesive/Al foil laminate, mech. interactions 0-81112
polyethylene-polypropylene blend, extruded, thermal swelling and mech. characterisation 0-81110
polyacetylene films, tensile props. and partial alignment 0-104210
1,2-polybutadiene crosslinked in strain states; entanglement networks, stress-birefr. relations 0-66590
polydimethylsiloxane, crosslinked, stress/strain relations from large compression to high elongation 0-66589
polydimethylsiloxane, end-linked chains, model elastomeric networks, Gaussian, nonGaussian and ultimate props. 0-103260
polydimethylsiloxane end-linked chains, nonGaussian effects 0-65127
polyethylene, photodegradation mechanism, from yield strength, elongation and mol. wt. studies (*Japanese*) 0-76311
polyethylenes, extrusion and heavy duty films struct. parameters influence on cross-linking by radiation 0-66844
polyphenylene sulphide, high mol. wt. soluble resin, prep., mech. props. 0-60828
rubber, natural, crosslinked by dicumyl peroxide, modulus, swelling relations 0-59551

elongation continued

- SEM, combined deformation/heating stage, acoustic emission rate meas. 0-101892
siloxane, temp. transitions, linear dilatometry and X-ray diffr. obs. (*Russian*) 0-59404
stator windings, failure mechanisms under thermal cycling (*Japanese*) 0-104189
steel, alloy, deformation, rapid dynamic, at -196°C 0-104220
steel, austenitic stainless, type 304, cyclic creep during unbalanced tension-compression loading at elevated temp. 0-97545
steel, C, plates, residual elements effect on through-thickness props. 0-66660
steel, C, tensile props. in high press. H₂ at room temp. (*Japanese*) 0-108501
steel, Cr-Mo, effect of Mo on high-temp. props. 0-85005
steel, Cr-Mo (10-14, 2-6 wt.%), heat-resist., creep-rupture strengths 0-104271
steel, ferritic stainless, embrittlement 0-85041
steel, high alloy Cr-Mo-W, splat quenched, formation of metastable austenite 0-84974
steel, microalloyed, types V1599, V1600, V1286, NbCN precipitation in undeformed austenite 0-89230
steel, Ni, welded joints on LNG carriers mech. props. and fracture toughness 0-85017
steel, stainless, deformation, rapid dynamic, at -196°C 0-104220
steel, stainless, fracture micromechanism when kept isothermally in sulphur pulp 0-76355
steel, stainless 301, stress corrosion cracking in MgCl₂ soln., environment effect on initiation and propag. (*Japanese*) 0-104338
steel, V-Nb and Cr-Mo-V-Nb, supercooled austenite isothermal decomp., struct., strength and fracture characts. 0-60966
steel (*German*) 0-100869
steel sheet, hot and cold rolled, cold formability, notched tensile test and stretch bend test (*German*) 0-61031
steels, austenitic stainless, stress corrosion cracking, correl. between electrochem. and mech. parameters 0-97613
steels, types SS41, SB42, SM50A, STK55, liq. Zn embrittlement (*Japanese*) 0-81164
telohelic, chain extension, qualitative aspects 0-95752
torsional deformation testing for plastic deformation, fracture (*Hungarian*) 0-97659
TZM-Mo alloy, mech. props., effect of exposure to high temp. He containing O₂, room temp. study 0-93639
viscoelastic material, failure and instability in tension 0-87720
Ag-Ni (10 wt.%) wire, plastically deformed, fracture struct. (*German*) 0-71744
Al alloy-mica particle composite, cast prep. and mech. props., bearing appl. 0-71613
Al notched bars, deform. behaviour and strength having biaxial state of stress at notch root (*Japanese*) 0-81116
Al-Cu-Mg/mica particulate composite mech. props. 0-100919
Al-Cu(Si)(Mg) binary and ternary alloys, dimensional changes in heat treatment 0-89271
Al-Cu(0-10 wt.%) sintered compacts, mech. props. rel. to sintering 0-76210
Al-Mg-Si alloys, cast, precip-rich zones on grain boundaries, soln. heat treatment conditions effect on mech. props. 0-104176
Al-Zn-Ti(Mn), mech. props., Ti or Mn addition effect (*Korean*) 0-93613
Al₂O₃, vacuum condensate, struct. and mech. props., second phase effect (*Russian*) 0-71705
B₂O₃-SiO₂-Na₂O phase-separated glass, creep fracture morphology 0-81151
Co-Fe-V-Ni, mag. and mech. props., heat treatment and stress effects 0-60363
Cu single crystals, deformed, HVEM study of recrystn. texture 0-104179
Cu-Cd (1.0 wt.%), yield stress and flow stress 0-97524
Cu-Cr (0.75 wt.%), deformation characts., fully reversed cyclic strain with fatigue cracks and dislocation struct. 0-81148
 α -Fe whiskers, pure, ductile fracture initiation, macroscopic obs. of deform. history and failure 0-85043
 α -Fe whiskers, pure, ductile fracture, microscopic obs. of initiation mechanism 0-85044
Fe-Cr-Al (7, 5 wt.%), expt. stainless alloys, phys. and mech. props. 0-97637
Fe-Ni-C alloy with single-component martensite texture, α - γ transform., changes in shape (*Russian*) 0-104152
Fe-Si (3 wt.%), electron irradiated, yield strength and elongation 0-76325
GdCu, electrical resistivity and length changes with temp., hysteretic behaviour 0-97600
MgCd wire, elongation during disorder-order transform. (*Russian*) 0-104148
Mo, mech. props., effect of exposure to high temp. He containing O₂, room temp. study 0-93639
Mo powder, influence of powder reduction processes on props. 0-89175
NbC, vacuum condensate, struct. and mech. props., second phase effect (*Russian*) 0-71705
Ni, ductility and fracture, nonmetallic inclusions effect 0-104221
Ni thin-walled cylinder, elongation upon torsion 0-64386
Ni-Cr Nimonic alloys, mech. props., high-temp. irradi. effects 0-100885
Pd₄₀Si₂₀ amorphous alloy, skip deform. and crit. shear stress, using tensile testing machine 0-89321
Ti-Al-Mo-Zr, type VT-9, creep eqns. rel. to extension and compression props. 0-100875
Ti-Al-V (6.4 wt.%), microstruct. effect of base metals on diffusion welding (*Japanese*) 0-89296
Ti-Al-V (6.4 wt.%) superplastic alloy, maximum attainable ductility 0-60919
Ti-Al-V (6.4 wt.%) cast alloy, with improved microstruct., mech. props. (*Japanese*) 0-71701
 β -Ti-Mo, thermal instability, hardness and tensile deform. (*Japanese*) 0-71703
Ti-Mo-V-Al-Cr-Fe (4.8, 4.7, 5.2, 1.1, 1.0 wt.%), structural changes during heating up to 1000°C, DTA study (*Russian*) 0-93552
TiB₂, TiC, vacuum condensate, struct. and mech. props., second phase effect (*Russian*) 0-71705
U-Mo (2 wt.%), depleted, effect of microstruct. on mech. props. 0-108497
Zn-Al(Cu), mech. and technological props. (*Polish*) 0-89286

elongation continued

- Zr-Al (8.6 wt.%), fast neutron irradiated, tensile props. and fracture toughness 0-84994
 ZrO₂, ZrB₂, vacuum condensate, struct. and mech. props., second phase effect (*Russian*) 0-71705

e.m. waves *see electromagnetic waves***embrittlement**

- see also ductile-brittle transition; hydrogen embrittlement; liquid metal embrittlement*
 Admiralty Metal, transgranular stress corrosion crack propag. 0-89402
 alloys, embrittling residuals categorisation by Auger electron spectroscopy 0-66739
 alloys, temper embrittlement, impurities and alloying elements role, review 0-66649
 chemically assisted fracture, atomic models of crack growth 0-64466
 chemically assisted fracture, general reaction rate theory and thermodynamics 0-64465
 engineering materials, intergranular fragility index 0-66637
 metallic glasses, annealing behaviour, thermal stability and crystn. 0-75167
 steel, alloy, temper embrittlement, comp. influence 0-66658
 steel, alloy 10G2S1 welds, fracture, subjected to low-temp. fatigue 0-89350
 steel, austenitic stainless, embrittlement by He in ³H handling facilities 0-102285
 steel, cast automatic couplings, yield strength, crack propag. resistance and ductile-brittle transition temp. 0-104281
 steel, continuously cast, segregation at halfway cracks 0-60869
 steel, Cr-Mo (2.25, 1.0 wt.%), temper embrittlement, effect of P, Sn, comp. and carbide precip. 0-85036
 steel, Cr-Mo (2.25, 1.0 wt.%), temper embrittlement, effect of Mn, Si, comp. and carbide precip. 0-85037
 steel, Cr-Mo weld metal, trace element embrittlement suppression by creep strength effects 0-66656
 steel, Cr-Mo-V low-alloy, high-temp. ductility and crack growth, impurities effect 0-66652
 steel, Cr-Mo-V low-alloy, prior austenite grain boundary embrittlement by B 0-66657
 steel, Cr-Ni-C (3, 1, 0.6 wt.%), grain boundary sulphide precip. and hot ductility (*Japanese*) 0-71654
 steel, ferritic stainless, embrittlement 0-85041
 steel, heating effect on phase composition, microstruct. and mech. props. 0-100859
 steel, high strength weld metal, fractography, microstructure and reheated zone toughness effects (*Japanese*) 0-108543
 steel, hot shortness, high-temp. embrittlement, residual and trace elements influence 0-66644
 steel, low alloy, 15Kh2MFA and 15Kh2NMFa, neutron irradiation embrittlement, effect of P, Sb and Sn impurities 0-85055
 steel, low alloy, temper embrittlement and ternary equilib. segregation 0-60958
 steel, low C, stress ageing embrittlement under short term thermally stressed cycle (*Russian*) 0-60885
 steel, low-alloy, impurities, segregation and creep embrittlement 0-66653
 steel, machining, 12L14, effect of Pb and Te on hot-shortness mechanism 0-104190
 steel, martensitic 12% Cr, temper embrittlement 0-66650
 steel, Mn-Mo-Ni, embrittling effects of residual elements 0-66655
 steel, Ni-Cr, temper embrittlement, intermediate tempering treatments 0-60944
 steel, Ni-Mo-Cr, embrittling effects of residual elements 0-66655
 steel, rail, toughness, effect of Sn, SEM exam. 0-97569
 steel, stainless, ferrite to austenite decomp. 0-93554
 steel, tempered martensitic, type AISI 410, role of C in embrittlement phenomena 0-93652
 steels, solute segregation and intergranular fracture 0-60957
 TZM-Mo alloy, mech. props., effect of exposure to high temp. He containing O₂, room temp. study 0-93639
 Al-Cu-Mg-Li alloy extrusions, microstruct., embrittlement and fracture props. 0-60965
 Al-Zn-Mg, crack-arrest markings on intergranular stress corrosion fracture surfaces 0-89405
 Co-Ni-Mo-C, amorphous alloys, med. props. and thermal stability (*Japanese*) 0-85049
 Cu-Bi (0.02 wt.%) alloy, intergranular fracture, Kossel X-ray diff. in SEM obs. 0-108579
 Fe, hot shortness, high-temp. embrittlement, residual and trace elements influence 0-66644
 Fe-Co-Mo-C, amorphous alloys, med. props. and thermal stability (*Japanese*) 0-85049
 Fe-Cr-Co, ductile magnet alloys, mech. props. 0-85001
 Fe-Mn-B, B effect on intergranular embrittlement 0-108555
 Fe-Ni-C, intercrystalline embrittlement in tempered martensite, elimination by reautenitization (*Slovak*) 0-108548
 Fe-Ni-Mo-C, amorphous alloys, med. props. and thermal stability (*Japanese*) 0-85049
 Fe₂₀Ni₄₀P₁₄B₆ amorphous alloy, temper embrittlement 0-76295
 Mo, mech. props., effect of exposure to high temp. He containing O₂, room temp. study 0-93639
 Ni-Cr, heat-resist., high-temp. ductility and embrittlement 0-76314
 Ni-Si-B, amorphous, thermal stability of ductility 0-76327
 Pt crucibles, surface changes rel. to Fe anal. 0-61192
 steels, Cr-C-Mn(Ni), struct. prop. rel., design of struct. steels for high strength and toughness 0-97491
 W-Cu (92.8, 7.2 wt.%), liq.-phase sintered, embrittlement and interfacial impurity segregation 0-66647
 Zr-Nb (2.5 wt.%), nuclear fuel channels, neutron effects on ultimate fracture strength, 293 to 573K 0-85054

e.m.c. *see electromagnetic compatibility***emergency power supply**

- Li long life battery systems, standby power for data retention in volatile memory systems, selection criteria 0-61337
 Ni-Cd batteries for standby power systems 0-104500
 Pb acid battery plants, current and future trends, telecommunications emergency power supply 0-61333
 Pb-acid 'G-cell', construction and design and performance charact. for UPS systems 0-61335
 Pb-acid storage batteries for uninterrupted power supply appls. 0-61334

e.m.f. *see electric potential***emission nebulae** *see nebulae***emission spectra** *see spectra***emissivity***see also brightness*

- atmospheric IR properties relevant to building envelope heat losses 0-58895
 baffled blackbody diffused cavities, integrated emissivity, precise calc. 0-96180
 blackbody cavities, directional emissivity calc., Monte Carlo method 0-83729
 building envelope heat radiation losses and countermeasures 0-58894
 cirrostratus clouds, IR emissivity meas. by remote sounding 0-82061
 cirrus clouds, IR emissivity calc. from lidar and radiometer meas. 0-82060
 crystalline material optical absorption meas. 0-105718
 Earth surface, microwave emissivity remote sensing by NIMBUS-6 0-98485
 fog, thermal emissivity 0-95795
 Fresnel's relations in IR, verification and determ. of emissivity and compound index (*French*) 0-84309
 glass, IR emissivity calc., strongly absorbing media surface refl. 0-107452
 IR imaging systems, sensibility equation modification (*Chinese*) 0-102806
 liquids, opaque and diathermanous, total normal emissivity meas. at high temp. 0-102965
 measurement using IR thermography (*French*) 0-103507
 metal surface, rough, hemispherical emittance 0-70434
 metals and alloys, emissivity determ. using low-inertia opt. dilatometry 0-59684
 pyrographite, IR spectral emissivity at high temperatures 0-103505
 radiation temperature, reflectivity, emissivity meas. of room temp. materials (*Chinese*) 0-101814
 refractories, integral radiant capacity, calorimetric meas. method 0-65259
 schist containing clay and sand, integrated normal emissivity with low heat conductivity coeffs. 0-103504
 schist dust; integrated normal emissivity with low heat conductivity coeffs. 0-103504
 solar absorber, high temp., spectral selectivity, thermal emissivity calc. 0-61403
 steel, stainless, emittance, oxidation and surface roughness effects 0-96673
 steel, stainless, emittance meas. rel. to surface roughness parameters 0-100342
 steel, type Kh23N18, integrated normal emissivity with low heat conductivity coeffs. 0-103504
 surface emittance, determ. total hemispherical calorimetric emissometer 0-86309
 terrestrial surface, emissivity correction for thermal radiation interpretation 0-82092
 thermal radiation property meas. of materials 0-96181
 Tokamak, enhanced plasma-frequency radiation (*Chinese*) 0-59185
 water pollution, dielectric props. and determ. of microwave emissivity 0-101142
 Ce-Cu, liquid, normal spectral emissivity 0-103506
 Fe, monocryst. and polycryst., thermal emission, magneto-optic circular polarisation obs. 0-70435
 Ni, polycryst., thermal emission, magneto-optic circular polarisation obs. 0-70435
 Pt, emissivity, integral, meas., modulation technique 0-62672
 Re, carburised, spectral emissivity at 0.65 μ m 0-75374
 SiO₂ glasses, spectral emittance at high temps. 0-96674
 SnO₂ films, selective, optical characterisation by thermodynamical method 0-84796
 Ta surface, nonstationary heating and oxidation in low temp. plasma flow, heat and charge transfer obs. (*Russian*) 0-104341
 Ta, thermal cond. and emissivity meas. using imaging furnace 0-103667
 Ti, during nonstationary high temp. heating by Ar flow (*Russian*) 0-84308
 V, radiance temperature at melting point, surface roughness depend. 0-59683
 W (100), total hemispherical emissivity meas., sensitivity to O₂ adsorption 0-79964

emitters *see television camera tubes***employees** *see personnel***employment***see also personnel*

No entries

emulsions*see also nuclear track emulsions; photographic emulsions*

- cluster size distribution for the Ornstein-Zernike correlation 0-97734
 concentrated, rheological props. 0-99981
 creamed, vol. fraction, effect of film thickness and contact angle 0-81370
 deposition, in pores of Al₂O₃ anodic oxide film 0-104357
 drop of water-fuel emulsion, microexplosive boiling of metastable overheated water, microblast (*Russian*) 0-74930
 ethylene-vinyl acetate copolymer, powdered, prep. by emulsion polymerisation (*Japanese*) 0-104110
 latex solids, agglomerating and dewatering 0-104470
 light scattering, rel. tp percolation phenomena 0-104467
 microemulsion system, existence of bicontinuous zone 0-104466
 microemulsions, heat transfer meas. by laser-induced thermal blooming 0-91833
 microemulsions, quasi-elastic light scatt. 0-108755
 SEM preparation technique for emulsion particles, freeze drying 0-62799
 surfactant solutions, aggregation, micelle and microemulsion form. 0-89547
 thin liquid films in emulsions, contact angles 0-92761
 viscosity, dynamic, effect of inertia for dilute emulsion in pure straining motion 0-87797
 water-in-oil emulsion, boiling, bubble formation, cinemicrophotography 0-74961
 water-in-oil microemulsions, electro-optical phenomena in lyotropic liquid crystals 0-107050
 water-in-oil microemulsions, structural relaxation by thermal current anal. 0-107049

emulsions continued

water-oil microemulsions, optical matching 0-61157
water-petroleum emulsions, mean particle diameter and conc. determ. by light scatt. 0-89538

emulsions (nuclear track) see nuclear track emulsions**emulsoids see emulsions****encapsulation**

see also packaging

composite drop formation, hydrodynamics 0-64603
photovoltaic cells using silicone materials, encapsulation 0-94019
solar cells automated production, with wraparound contacts 0-76635
solar cells encapsulation using ethylene-vinyl acetate double vac. technique 0-93510
terrestrial photovoltaic arrays, development of glass encapsulation technique 0-94020
GaAs:Cr, semi-insulating, Cr redistrib. during thermal annealing as function of encapsulant and implant fluence 0-84199
GaAs:Cr,Se, ion-implanted, semi-insulating effects of Cr redistrib. on elec. characts. when encapsulated with Si_3N_4 0-59982

encoding

see also codes; decoding

auditory-nerve fibre encoding of 2-tone approximations to steady-state vowels 0-61582
coherent codes, iterative improvement algorithm 0-87330
colour film archival storage, white light processing technique 0-99637
hearing, temporal perceptions, effects of early auditory deprivation 0-76761
information encoding by complex zeros, analytic Fourier optics, comment 0-87326
linear predictive coded speech quality problems and expts. 0-91982
multiplex image coding, astronomical IR speckle interferometry appl. (French) 0-67580
myocardial ^{201}Tl scintigram anal., nonredundant coded aperture tomographic method 0-94364
nerve fibre membrane analogue-code conversion, ionic mechanisms 0-81575
nerve impulse encoding, elec. processes 0-76718
nuclear medicine, coded aperture imaging, qualitative and quantitative 0-89843
optical processing, incoherent imagery system, introduction of partial coherence by holographic components 0-95853
parametric coding of speech spectra, computer studies 0-96137
PCM encoding and decoding for optical memories 0-102658
perceptual coding in the cosing transform domain 0-102635
picture direct transmission via single optical fibre 0-106628
polychromatic processing technique for colour image transparencies 0-86473
pseudocolour density encoding, white-light, using contrast reversal 0-83560
quasistationary processes and universal codes 0-91994
speech, parametric coding of speech spectra 0-96136
speech, signal models for low bit-rate coding 0-106674
speech encoding in auditory nerve, effects of nonlinearities 0-108913
speech quality and intelligibility measures and their correlations 0-91978

ENDOR

N-acetylglycine, X-irrad., stable radical electronic and mol. struct., ENDOR and ESR 0-80637
actomyosin, X-irradiated ENDOR and ELDOR obs. 0-63689
adamantane, γ -irrad., free radicals EPR and ENDOR 0-69170
bacteriorhodopsin radicals, role in primary charge separation of Rhodospseudomonas viridis 0-63688
bacteriopheophytin b radicals, role in primary charge separation of Rhodospseudomonas viridis 0-63688
carbohydrate compounds, X-irrad., trapped electrons, ESR and ENDOR obs. 0-93161
cytochrome c oxidase, Cu ENDOR 0-94170
dibenzenechromium-dibenzenevanadium, proton HFS data, ENDOR obs. 0-66073
dipotassium glucose-1-phosphate, X-irrad., ESR-ENDOR obs 0-60419
electron spin echo envelope modulation, 2-dimens. Fourier transform 0-63680
haemoglobin, human, maleimide spin labeled, proton ENDOR spectra obs. 0-89719
hippuric acid, X-irrad. single cryst., ^{14}N and ^1H ENDOR study; 0-71240
ionic crystal defects, mag. reson. studies 0-108066
isobacteriochlorins, π cation radicals, implications for NO_2^- , SO_2^- reductases 0-63684
KBr(I):D, inelastic light scattering of localised vibration of interstitial H atom in alkali halides 0-88998
lanthanum nicotinate dihydrate, cryst., nucl. quadrupole interactions, D atom coords., ENDOR obs. 0-97161
myosin, X-irradiated ENDOR and ELDOR obs. 0-63689
organic doublet radicals in nematic and smectic liq. crystals, ENDOR obs. 0-91585
polycrystalline dipeptides, X-irradiated ENDOR and ELDOR obs. 0-63689
polyhydroxy compounds, X-irrad., trapped electrons, ESR and ENDOR obs. 0-93161
potassium hydrogen malonate, room-temperature ENDOR spectra obs. 0-106339
quick access sample system for low temp. K-band ESR and ENDOR 0-57352
ruby, distant nuclei ESR and ENDOR experiments, dipole-dipole reservoir importance 0-71241
trapped electrons, ESR and ENDOR obs. 0-93161
tris-sarcosine calcium chloride: Mn^{2+} ferroelec. dynamics, EPR and ENDOR study 0-75972
urea-malonic acid, room-temperature ENDOR spectra obs. 0-106339
 $\beta\text{-Al}_2\text{O}_3\text{-Na}_2\text{O}$, ENDOR meas. of defects 0-66074
 $\beta\text{-Al}_2\text{O}_3\text{-Na}_2\text{O}$, X-ray induced defects, EPR and ENDOR study 0-60456
 AlPO_4 , synthetic berlinite, electron irradi. effects, ESR, ENDOR, optical spectral study 0-80608
 $\text{BaMgF}_2\text{:Mn}^{2+}$ ferroelec., EPR and ENDOR study, cryst. field tensor 0-71162
 CdS:Ti^{2+} , superhyperfine interact., ENDOR study at 4.2K 0-80639
 $\text{Cs}_2\text{SO}_4\text{-Al}_2(\text{SO}_4)_3\text{-24H}_2\text{O}$, $^{33}\text{Cr}^{3+}$ ENDOR Lines, RF ENDOR power and modulation freq. effects 0-75884
Cu complex, $\text{Cu}(\text{H}_2\text{O})_6^{2+}$, ligand hyperfine interactions, orbital angular momentum contrib. 0-96833

ENDOR continued

Cu complex, $\text{Cu}(\text{II})$ bis(dithiocarbamate), ^1H ENDOR 0-87154
Fe dicyclopentadienyl-dibenzenevanadium, coalescence temps., full proton HFS tensor, ENDOR obs. 0-66073
GaAs: $^{56}\text{Fe}^{3+}$, paramag. centres, identification from ESR and ENDOR spectra 0-80600
GaP: $^{67}\text{Fe}^{3+}$ (^{53}Cr), paramag. centres, identification from ESR and ENDOR spectra 0-80600
GaP:Ge, ENDOR study, superhyperfine interactions 0-93210
KCl:H, ENDOR and ESR study of anion sites 0-108118
 KH_2AsO_4 , γ -irradiated, free radicals, EPR and ENDOR study of consequences of ferroelec. transition (French) 0-93209
 KMgF_3 , F-centre ENDOR study 0-108117
 $\text{KMgF}_3\text{:Yb}^{3+}$, perovskite type cryst., ENDOR meas. 0-80638
 $\text{KZnF}_3\text{:Yb}^{3+}$, perovskite type cryst., ENDOR meas. 0-80638
 $\text{LiBaF}_3\text{:Mn}^{2+}$, having inverse periodic struct., ENDOR study 0-97162
 $\text{Mg}(\text{NH}_4)_2(\text{SO}_4)\cdot 6\text{H}_2\text{O:VO}(\text{H}_2\text{O})_5^{2+}$, proton ENDOR meas. used to determine hyperfine coupling tensors 0-66075
 $\text{RbAl}(\text{SO}_4)_2\cdot 12\text{H}_2\text{O}$, spin-Hamiltonian with trigonal S^3I terms for describing $^{87}\text{Fe}^{42}$ ENDOR spectra 0-75885
 $\text{RbGa}(\text{SO}_4)_2\cdot 12\text{H}_2\text{O}$, spin-Hamiltonian with trigonal S^3I terms for describing $^{87}\text{Fe}^{42}$ ENDOR spectra 0-75885
 $\text{SrCl}_2\text{:Gd}^{3+}$ hyperfine interaction, X-band ENDOR 0-60457
 ZnTe:Mn^{2+} , forbidden transitions of Mn^{2+} induced by hyperfine interactions 0-60458

energies, molecular dissociation see molecular dissociation energies**energy, binding see binding energy****energy, lattice see lattice energy****energy, surface see surface energy****energy bands see band structure****energy bands, electron see band structure****energy control see power control****energy conversion, direct see direct energy conversion****energy gap**

see also superconducting energy gap

amorphous, photogeneration, thermalisation model calcs., band gap (French) 0-75595
amorphous semiconductors, defects, band gap states 0-80215
binary compounds, energy gap trends, corrl. with electron transfer parameters from optical spectroscopy 0-80174
education, deep one-dimens. periodic pot., zero energy gaps, Kronig-Penney model 0-62426
education, forbidden energy gap meas. in Si and Ge p-n junctions 0-57027
exchange interactions in semiconductors and insulators, mean free path and energy gap effects 0-88522
graphite, diamagnetism with quasilinear dispersion law, orbital susceptibility, valence bands (Russian) 0-80475
Hubbard model, narrow-band region, quasiparticles, electron relax. and transport props. 0-80151
Hubbard model, split-band solution and energy gap, narrow-band region 0-75484
II-VI quaternary semiconductor alloys, energy bandgap and lattice constant contours 0-103622
III-V semiconductors, optical transitions, effect of perturbed k-selection and gap shrinkage 0-66257
insulator, many-electron systems, self-interaction corrected approach, beyond local spin density approx. 0-92844
intrinsic semiconductors, indirect exchange interaction, finite temp., valence bands and energy gaps effect 0-59943
metal, antiferromag., thermoelec. power in mag. field 0-70686
metal-dielectric transition, two-band model, Coulomb interactions, self consistent calcs. (Russian) 0-80185
MIS negative barrier contact for induced back surface field solar cell 0-101101
narrow-gap semiconductor, carrier quasienergy spectrum in strong EM wave field 0-92922
oxide semiconductors in photoelectrochemical conversion of solar energy, use as cell anodes 0-101120
polyacetylene films, AsF_5 doped, photocond. and junction props. 0-70770
polyacetylene films, doping investigation, insulator-metal transition, optical transmission meas. 0-103729
polyethylene, intrinsic photocond. under vacuum UV irradi. 0-70759
porphyrin films, methine bridge substituted, surface photovolt. depend. on fabrication method 0-60119
semiconducting powders, band-gap energies, photoacoustic meas. 0-70579
semiconductor, graded-gap, internal photo-effects, excess carrier distrib. 0-107847
semiconductor, Moss formula, refr. index rel. to energy gap 0-108173
semiconductor epitaxial layers, varizional, parameter determ. by photoluminescence method (Russian) 0-108291
semiconductors, exciton effect in interband electronic Raman scattering 0-103946
semiconductors, forbidden gap width, relation to refractive index, single oscillator calcs. (Russian) 0-71372
semiconductors, population inverted, resonant Brillouin scatt., photoelastic consts. 0-89015
semiconductors polarised light nonlinear rotation 0-93268
superconductor, metal-insulator transition, electron pairing, effect on optical props. 0-60139
transition metals, alloys, and cpds., XPS asymmetry of core electrons and electronic struct. parameters 0-93460
tunnelling MIS structures photovoltaic energy conversion, band struct. 0-92995
UV high-power laser material, refractive props. and optical constants 0-106555
Al, metallic, phonon freq., binding energy, compressibility, elastic const. and energy band gap calcs., linear pot. 0-88284
 AlGaAs buried heterostructure lasers, gain and absorpt. spectra meas. 0-91792
 AlGaAs p-n diodes, I-V characts., tunnelling 0-100510
 $\text{AlGa}_{1-x}\text{As}_x\text{:Cu}$, variable-gap semicond., impurity props., carrier recomb. 0-96907
 $\text{AlGa}_{1-x}\text{Sb-Pd}$ contacts, band gap depend. of barrier height 0-65685
As-Se amorphous system, photocond. props. 0-88587
a- As_2S_3 , energy gap meas., by Faraday rotation 0-66161
 $\text{As}_2\text{S}_{100-x}$ amorphous films, optical props. and photoinduced changes 0-60700
 As_2Se_3 , cryst., electroabsorption on indirect gap 0-80812

energy gap continued

- As₂Se₃, single crystals, fine struct. of direct gap from electrorefl. spectra 0-93280
- Au-n-Ga_{1-x}Al_xAs-n-GaP narrow-band variable-gap surface-barrier photo-detector 0-96944
- Au-SiO₂-Si system, oxide film 16-36 Å thick, tunnel currents 0-70842
- B:H amorphous films, optical band gap, thermal treatment effect 0-93415
- BaAl₂O₉, refr. index and optical absorpt. 0-66139
- Ba_{0.5}Sr_{0.5}Nb₂O₆, electronic props. and photoresponses 0-92925
- BaTiO₃ (001), LEED and UPS studies 0-100747
- BiI₃ film, exciton-phonon interaction, optical const., Faraday effect, permitt. 0-59884
- CdCr₂Se₄, Mott ferromagnetic semiconductor, optical absorption edge, critical behaviour 0-97226
- CdGa₂(S_{1-x}Se_x)₄ solid solns., band struct. behaviour w.r.t. comp. (French) 0-107699
- Cd₂GeO₄ anode for H₂O photoelectrolysis 0-108716
- n-Cd₂GeO₄, electronic and cond. props. rel. to prep. conditions and defect struct. 0-107787
- Cd_{1-x}Hg_xGa₂S₄ solid solns., band struct. behaviour w.r.t. comp. (French) 0-107699
- CdIn₂O₄ anode for H₂O photoelectrolysis 0-108716
- Cd_{1-x}Mn_xSe, fundamental optical props. 0-84751
- CdO-SnO₂ DC reactively sputtered films, elec. and optical props. 0-103763
- Cd₂SnO₄ anode for H₂O photoelectrolysis 0-108716
- CdTe:Cl, semi-insulating, impurity photocond. spectra, local state distrib. in band gap 0-107865
- CdTe-HgTe superlattice on CdTe layers, evanescent states, tight binding calcs. 0-70611
- Cr, antiferromag., transverse magnetoresist., electron interference oscils. 0-65534
- CsBr, (110) surface, electronic struct. of valence bands calc. (Russian) 0-75621
- CsCl, (110) surface, electronic struct. of valence bands calc. (Russian) 0-75621
- CsI, (110) surface, electronic struct. of valence bands calc. (Russian) 0-75621
- Cu (111), final state band gap effects in UPS 0-89120
- Cu₃Au, electrical resistivity and LRO, energy gap formation in Fermi surface 0-88533
- CuGa_{0.5}In_{0.5}Se₂/Zn_{0.25}Cd_{0.75}S heterojunction solar cell, preparation and props. 0-101110
- CuInSe₂, influence of impurities and free carriers on optical props. 0-108225
- CuSbS₂ crystals, growth and characterisation 0-60770
- de Haas-van Alphen freq. and Fermi surface anisotropy press. depend. 0-59856
- Dy_{1-x}Sm_x, magnetoresist. of polycryst. specimens in fields up to 44 kOe (Russian) 0-92880
- Fe₂Al, electrical resistivity and LRO, energy gap formation in Fermi surface 0-88533
- FeP₃, layered semiconductors, optical and electronic props. 0-70761
- Ga_{1-x}Al_xAs, intervalley energy gaps, temp. junction, expl. determ. 0-80179
- Ga_{1-x}Al_xAs, photodetector diode on GaAs substrate dark currents, tunnelling, energy gaps, effective masses 0-70805
- GaAs:Fe(Co)(Cu)(Ni), substitutional impurity elec. struct. 0-88513
- GaAs_{1-x}Sb_x (x≤0.05), band gap, temp. depend., from edge photolum. meas. 0-71486
- n-Ga_{1-x}In_xP photoelectrochemical cells, bandgap energy, electronic transition mode, and diffusion length 0-72070
- GaN epitaxial films, cathodoluminesc. spectra 0-71496
- Gd₂O₃, B-type monoclinic, DC(AC) elec. cond., thermoelectric power, dielectric const., temp. depends. 0-59980
- Ge, energy gap, impurity conc. depend., calc. 0-80170
- Ge:Pd and pure, photoelectric props., surface states (Russian) 0-60043
- N-Ge-Bi-Se glass, elec. and optical props. 0-65550
- Ge-Si₃N₄ system, potential barriers determ. from photoinjection carriers trapping 0-103756
- Ge₂₀Bi_{80-x}Se_x, semicond. glass, resist., thermoelec. power, optical absorpt. 0-88555
- Ge₂₀Bi_{80-x}Te_x, semicond. glass, resist., thermoelec. power, optical absorpt. 0-88555
- ³He, superfluid B-phase, collective excitations in presence of superflow 0-92744
- Hg, reflection spectra, electronic density of states, calc. 0-66229
- Hg_{1-x}Cd_xTe epitaxial layers, elec. props. 0-96910
- HgCr₂Sd_{4-x}Te_x, ferromag. semicond., zero bandgap transition 0-96783
- HgSe, elec. resist., high press. phase transform., band gap 0-70707
- HgSe, interband $\Gamma_6-\Gamma_8$ magnetoabsorption, temp. study 0-76032
- In_{1-x}Al_xAs, band gap, IR absorpt. spectra meas. 0-66205
- InGaAsP, bandgap energy by electroluminescence and photoluminesc. spectra 0-107700
- InGaAsP-InP layers, grown by LPE techniques, lattice const., bandgap, thickness and surface morphology meas. 0-59818
- In_{1-x}Ga_xAs_{1-y}P_y, electron effective mass from Shubnikov-de Haas meas. 0-80298
- In_{0.9}Ga_{0.1}As_{1-y}P_y photodetector diode on InP substrate dark currents, tunnelling, energy gaps, effective masses 0-70805
- In_{1-x}Ga_xSb, energy gap, temp. depend. and photovoltaic effect 0-70746
- In₂O₃, thermally evaporated film, struct. and elec. props. 0-104066
- InSb (110), cleaved, gap states, field effect meas. 0-84501
- InSe, photo-absorption of green exciton 0-80816
- InTeBr, intermediate phase, cryst. struct. 0-100834
- KCl, photoelectric emission in photon energy region 1.0 to 6.0 eV 0-108321
- LiNbO₃ surfaces, ion and electron bombard., photoelectron spectroscopy and electronic props. 0-71559
- LuRhO₃, elec., mag. and photoelectrochemical props. 0-96925
- MoS₂, molybdenite band structural props. rel. to supercond. and semicond. 0-96781
- Nb chalcogenides and chalcogenide halides, geometrical struct. and metal-metal bonding 0-80172
- Ni_{1-x}Co_xS₂, elec. cond., thermoelec. power and optical meas. 0-59986
- NiPS₃, layered semiconductors, optical and electronic props. 0-70761
- PbI₂:KI alloys, fundamental abs. edge, potential as solar convertor 0-101128
- Pb_{1-x}Mn_xTe, photovoltaic effect, p-n junction, energy gap determ. 0-92931

energy gap continued

- PbS_{0.9}Se_{0.1} 4.6 μm LED, room temp., band gap and electrolum. 0-66302
- PbS(Se)(Te), energy gap and dielec. props., 77 to 373K 0-66100
- PbSnF₄, anionic conductor, thin films and ceramics 0-107556
- Pb_{1-x}Sn_xSe, transport phenomena in solid solutions with band inversion 0-107792
- Pb_{1-x}Sn_xSe, X=0.03-0.07, monocrystal film, edge of intrinsic absorpt. (Russian) 0-71368
- Pb_{1-x}Sn_xTe, hole effective mass near zero bandgap, IR refl. study 0-108205
- Pb_{1-x}Sn_xTe, X=0.2, monocrystal, edge of intrinsic absorpt. (Russian) 0-71368
- Pb_{1-x}Sn_xTe:In, Hall effect and photoconductivity (Russian) 0-103720
- Pb_{1-x}Sn_xTe_{1-y}Se_y solid solutions with constant lattice parameter, phase comp. 0-108417
- Ru₂Ge_{3-3x}Sn_{3x} and Ru₂Ge_{3-3y}Si_{3y}, diffusionless phase transitions, elec. and mag. props. 0-96871
- S-based amorphous semicond. film, prep. by plasma decomp. of H₂S-N₂-NH₃, and characterisation 0-80422
- SMS, band struct. and semicond. metal phase transition 0-80180
- Se, amorphous layer, localised states in band gap 0-59928
- Se, photoelectronic behaviour, in glass transition region 0-60045
- Se, trigonal, behaviour of optical gap under press. 0-80171
- Se-As, photoelectronic behaviour, in glass transition region 0-60045
- Si, amorphous films, hydrogenated and hydrogenated, elec. and optical props. 0-97016
- Si, energy gap, impurity conc. depend., calc. 0-80170
- Si, hydrogenated amorphous, gap states, comparison of photoemission and photocond. results 0-103724
- Si p-n junction diodes and solar cells, minority carrier diffusion length 0-107894
- Si, semi-empirical APW calc. of band structure 0-84424
- Si:H, amorphous thin film, ion plating, IR absorpt. meas. 0-84857
- Si:H amorphous, solar cell structure, optical absorption by gap states 0-94052
- Si:H amorphous films, conductivity and temp. dependence of optical gap 0-100462
- Si:H amorphous films, ESR, optical gap and elec. cond. meas. 0-75842
- Si-SiO₂ interface, (001) vicinal planes, minigaps in inversion layers, far IR absorpt. meas. 0-107919
- Si-SiO₂ MOS capacitors, relationship between trapped holes and interface states 0-70830
- Si_{1-x}H_{2x}Al_x amorphous, co-sputtered Al modification, electronic and optical props. 0-100461
- SiO₂, HCl-grown oxides, characterisation of surface states using MOS transient currents 0-65696
- Sm₂O₃, B-type monoclinic, DC(AC) elec. cond., thermoelectric power, dielectric const., temp. depends. 0-59980
- Sn₂P₃S₆, investigation of p-T diagram near a singular point (Russian) 0-88937
- Sn₂P₂(Se₂S_{1-x})₆, ferroelec. tricrit. phase transform., light transmission study 0-71355
- Sr, monochalcogenides, electronic energy band struct., APW calcs. 0-65439
- Sr₂Nb₂O₇, electronic props. and photoresponses 0-92925
- SrTiO₃ (100), LEED and UPS studies 0-100747
- SnTiO₃ (111), O₂, H₂ and H₂O chemisorption, UPS and XPS studies, illum. effects 0-71572
- Tb₂O₃, B-type monoclinic, DC(AC) elec. cond., thermoelectric power, dielectric const., temp. depends. 0-59980
- TiO₂, rutile, optoelectronic props., band struct., theory 0-80175
- Tm₂O₃ film, between Al electrodes, prep. and elec. props. 0-60103
- UO₂, electronic distributions by X-ray spectroscopy 0-97407
- Zn-In-S thin layers, ternary phases, optical props. near long-wavelength intrinsic absorpt. edge 0-80887
- ZnGeP₂, bandgap absorption edge, spectra, electron transitions (Russian) 0-97305
- ZnP₂, Brillouin scattering and optical props. meas. 0-76041
- α-ZnP₂, resonant Brillouin scatt. near indirect band gap 0-93350
- Zn₃P₂, optical props., transition energies from transmission and refl. meas. 0-60532
- ZnSe, band-edge photoluminesc., far-below band-gap excitation 0-76063
- ZnTe, pure and P(As) doped, shallow-acceptor, donor, free-exciton, and bound-exciton states 0-60667
- ZnTe:Bi, laser annealing, channelling, reflectivity spectra 0-66215

energy gap, superconducting see superconducting energy gap

energy level crossing

see also Hanle effect

- atoms, oscil. strength in presence of level crossings 0-99480
- diatomic mol., spurious avoided crossing detection 0-87057
- 1,8-dichlorooctane, quadrupolar relax. centres, limited spin diffusion 0-100649
- laser-induced collisional energy transfer, level crossing expansion 0-83461
- molecular collisions in laser field, multiphoton vibrational excitation enhancement, semiclassical theory 0-58350
- photon counting distribution second factorial moment meas. for level crossing detection 0-99485
- Ba I, light shift induced zero-field level crossing 0-58220
- Cd, broadening of ⁵P₁ level 0-83479
- ³He atom forbidden singlet-triplet anticrossings, D levels 0-99491
- Hg, two photon excitation, time resolved spectroscopy 0-87075
- Li(2p)+H₂(N₂), Li(2p) excitation, alignment and orientation obs. 0-63794
- Sml, Zeeman coherence, transient and stationary, polarisation spectroscopy 0-58212
- Yb, 4f¹⁴6s6p ³P₁ and ¹P₁ levels, Stark effect, tensor polarisabilities 0-87080

energy level transitions, atomic see atomic spectra

energy level transitions, molecular see molecular spectra

energy level transitions, nuclear see nuclear energy level transitions

energy levels see energy states

energy levels, atomic see atomic structure

energy levels, molecular see molecular energy levels

energy levels, nuclear *see nuclear energy levels*

energy levels in solids and liquids *see electron energy states (condensed matter)*

energy loss of particles
see also channelling; electron energy loss spectra; radiation effects
amorphous targets, energetic in transport, Monte Carlo program 0-102411
anisotropic point source in infinite medium, energy deposition 0-88228
atom-atom collision cascades localisation, impurity and thermal vibr. influence, computer simulation method 0-88227
beryl, natural and synthetic, ion channelling transmission ratios 0-75277
cascade processes of particle passage through substance, fluctuations 0-92579
cellulose nitrate, energy loss critical rate for charged particles 0-74082
charged particle energy loss in cryst., theory 0-79847
composite interatomic potential, validity over large atomic separation 0-84225
conference, atomic collisions in solids, Hamilton, Canada (Aug. 1979) 0-62375
conversion electron penetration through metallic and oxidized thin layers 0-102414
diamond, half wavelength and stopping power of planar channelled protons 0-65087
Doppler shift attenuation in layered targets 0-102409
electron beam scattering, in organic specimen, Monte Carlo simulation 0-100148
electron channelling pattern, large angle, generation and appl. 0-100296
electron energy deposition in Ar, Monte Carlo calcs. 0-69242
electron energy losses due to diffraction radiation (*Ukrainian*) 0-75278
electron gas, stopping power for slow neutrons, damping effects 0-65098
electron probe penetration and energy loss characts. in solid target, diffusion model 0-96585
energetic ions near solid surface, energy loss 0-96580
energy spectra of δ -rays produced due to high energy particles with biological systems 0-108951
fission fragments in gases, stopping powers and energy distribts. 0-78499
frictional quantum mechanical system, one-dimens. scatt. model for coherence in stopping power problem 0-101736
heavy charged particle specific energy losses meas. using densitometric method (*Russian*) 0-63482
heavy ion ranges, Z_1 oscillations 0-65096
heavy ions, channelled, stopping power Z_1 oscillation vel. depend. 0-65101
heavy ions, energy loss in 0.5 to 1.4 MeV/amu range 0-65103
heavy ions, low vel., channelling stopping power oscills. 0-103404
heavy ions in solids, electronic stopping cross-section, Z_2 -oscills., target struct. effects 0-70285
heavy nonrelativistic ions in matter, semiclassical theory 0-84224
heavy particles, expt. results for W-values 0-78500
heavy-ion stopping-power calculations 0-78505
heterogeneous media, energy deposition of slowing down particles 0-88230
ion backscattering and implantation, H and He ions, computer simulation, comparison of MARLOWE and TRIM codes 0-66350
ion implantation, range parameters, nucl. stopping power, ion backscatt. determ. 0-88232
ions, low energy surface scatt., inelastic energy loss 0-70278
ions in solids, Lindhard's dielec. theory 0-65077
KERMA values, consistent set for H, C, N, and O for neutrons from 10 to 80 MeV 0-68967
levinson's theorems in classical scattering 0-90729
metal and metal oxide spacecraft thermal control materials, low-energy proton effects 0-70288
metal target preparation for stopping power meas. of channelled ions in low energy region 0-63431
mica, 210 keV electrons, Vavilov-Cherenkov radiation, ang. distrib. half width, spectral depend. (*Russian*) 0-71505
modified Firsov model, sensitivity to atomic electron speed 0-65100
monoenergetic electron continuous slowing down approx., range and projected range 0-78497
multiple scattering corrections to energy loss measurements for slow ions 0-95511
muons, Z_1 correction meas. 0-78502
muons in shielded scintillator, energy loss calcs. 0-63490
near surface yield enhancement for He ions in noncryst. solids 0-65105
neutron cross-sections and kerma values for C, N and O from 20 to 50 MeV 0-101217
polystyrene, energy losses and straggling for H^+ and He^+ beams (*Russian*) 0-84226
projectile size dependence of stopping power 0-65099
proton attenuation lengths in paraffin, concrete and iron around targets 0-102412
protons, 600 MeV, luminescent detector efficiency, mass stopping power calc. 0-99346
recoil atoms of heavy ion reactions, local lattice damage, TDPAD meas. 0-84220
recoil mixing in high-fluence ion implantation 0-65095
recoil mixing in solids by energetic ion beams 0-59531
relativistic charged particle in electric field, spin rot., curved crystal p.e. channelling (*Russian*) 0-63907
relativistic electron energy loss distribts. in thin gas layers of proportional counters 0-99429
resonant energy transfer from electrons to a slow electromagnetic wave 0-83543
Rossi counter equivalent dose meas. in high-energy radiation fields 0-94376
solids, stopping values of energetic ions, predicted with energy loss model 0-88229
soliton solution in the wake interaction due to virtual plasmon exchange 0-65108
stopping power of liquids for alpha particles, meas. apparatus 0-88224
swift ions, electron state energy shift in passing through solids 0-65107
transient magnetic field effects on particles slowing in solids 0-65106
 α track registration, solid state track detectors in solutions of actinides 0-63486
Ag, energy losses and straggling for H^+ and He^+ beams (*Russian*) 0-84226
Ag film, energy losses of electrons, microcalorimetric meas. 0-59543
Al, energy losses and straggling for H^+ and He^+ beams (*Russian*) 0-84226

energy loss of particles continued
Al film, energy losses of electrons, microcalorimetric meas. 0-59543
Al, ion-induced electron emission, ion charge depend. 0-108315
Al, low mass particles, A<16, charge-exchange effects in energy-loss straggling 0-65104
Al, positron penetration depth and energy loss 0-92578
Al projected range distrib. of 5-25 keV $^{16}N^+$ ions 0-65094
Al single crystal, $^{18}O^+$ ions implantation in channelling directions, stopping power meas. from max. range 0-65078
Ar $^{+}$ energy and ang. distrib. in passing through C, Cu, Ag films 0-100292
Au, energy losses and straggling for H^+ and He^+ beams (*Russian*) 0-84226
Au film, energy losses of electrons, microcalorimetric meas. 0-59543
Au, range distributions for 25-200 keV $^{14}N^+$ ions 0-103405
Au, stopping power for ^{107}Ag , ^{109}Ag and ^{150}Sm 0-70284
Au, thin film, anomalous stopping power effects 0-65102
Be, fusion reactor material, range profiles of Li^+ , appl. of (n,p) and (n, α) reactions 0-61200
Be, projected range distrib. of 5-25 keV $^4He^+$ 0-65094
Be, stopping power for protons, 20 to 120 keV 0-91411
Br $^{6+}$, 42 MeV, stopping power and radial dose distrib. obs. in tissue-equivalent gas 0-101218
C, electronic stopping power of heavy ions, empirical relation 0-92571
Cu, differential ranges of fission products by a coulometric method 0-65097
Cu, energy losses and straggling for H^+ and He^+ beams (*Russian*) 0-84226
Cu, projected range distrib. of 5-25 keV $^4He^+$ 0-65094
Cu:O single crystal, $^{18}O^+$ ions implantation in channelling directions, stopping power meas. from max. range 0-65078
Fe, range distributions for 25-200 keV $^{14}N^+$ ions 0-103405
Gd, stopping power and energy straggling of $^4He^+$ ions in vacuum-evaporated films 0-88231
Ge, energy loss spectra of C^{2+} ions 0-65114
 H^+ + $H_2(CO_2)$, vibr. excitation, 10-30 MeV 0-58358
 He^+ , energy and ang. distrib. in passing through C; Cu, Ag films 0-100292
 4He stopping power, 0.15 to 1 MeV, backscatt. determ. 0-88233
KCl(l), electron range-energy relation, thermally created lattice vacancies effect 0-92574
 ^{86}Kr , stopping power meas. at 3-5 MeV/nucleon 0-102410
Li projectiles, electronic stopping cross section meas., intermolecular interactions 0-75279
 N^+ , electronic stopping power in solids, range distrib. energy depend. 0-92575
 N_2+H^+ collision, total ionis. cross section and stopping power for protons 0-69228
Nb, projected range distrib. of 5-25 keV $^4He^+$ 0-65094
 Ne^+ , energy and ang. distrib. in passing through C, Cu, Ag films 0-100292
Ni, energy loss spectra of C^{2+} ions 0-65114
Ni film, amorphous layer covered, target prep. for channelled ion stopping power meas. 0-63431
Ni, range distributions for 25-200 keV $^{14}N^+$ ions 0-103405
Ni, stopping power for ^{107}Ag , ^{109}Ag and ^{150}Sm 0-70284
Ni:O single crystal, $^{18}O^+$ ions implantation in channelling directions, stopping power meas. from max. range 0-65078
O ions, non-equilibrium charge state distrib. charge exchange cross-sections in solid targets 0-65109
 ^{208}Pb , stopping power meas. at 3-5 MeV/nucleon 0-102410
 S^{4+} , travelling in solids, K α X-ray spectra 0-100706
Si, blistering due to 400 to 1800 keV $^4He^+$ ions, modal range determ. 0-100289
Si, energy loss and multiple scattering of non-channelled α -particles (*German*) 0-59544
Si, half wavelength and stopping power of planar channelled protons 0-65087
Si, ion penetration, computer program 0-88185
Si-SiO $_2$, two layer system, P^+ -ion penetration tails, expt. and computer anal. 0-75249
SiO $_2$ massive dielectric target, 5-25 keV electrons penetration characts. 0-70260
Ti, energy loss spectra of C^{2+} ions 0-65114
 ^{238}U , stopping power meas. at 3-5 MeV/nucleon 0-102410
W, atomic density, effect on proton energy loss and dechannelling 0-65088
W, enhanced penetration of low energy He along (100) channel 0-65093
 ^{132}Xe , stopping power meas. at 3-5 MeV/nucleon 0-102410
ZnO, spacecraft thermal control material, low-energy proton effects 0-70288
Zr, range distributions for 25-200 keV $^{14}N^+$ ions 0-103405

energy measurement *see power measurement*

energy-range relations *see energy loss of particles*

energy resources
see also fuel; solar energy concentrators; solar power; wind power
advanced energy conversion for electrical power generation (*Japanese*) 0-93865
alternative energy resources, review (*Italian*) 0-66917
alternative energy sources, energy accounting study 0-76589
alternative versus conventional energy sources, economic comparison (*German*) 0-72002
ambient energy systems for energy conservation 0-61316
biomass, review of possible energy conversion processes (*French*) 0-93843
biomass conversion technology 0-89601
biomass energy, development, availability, and storage possibilities (*French*) 0-89587
biomass energy production and the photosynthetic pathway 0-61393
biomass for energy production, economic eval. (*Swedish*) 0-93844
biomass production utilising geothermal low temp. heat 0-66932
brown coal basins of Hungary, Eocene, geophys. exploration (*Hungarian*) 0-104938
Bullaren lineament, SW Sweden, heat extraction potential 0-76602
conf. San Diego, CA, USA (Feb. 1980) 0-62395
conservation, hard and soft paths compared 0-89584
economic choice for rural India, methodology 0-104499
electricity supply industry, effects of world energy resources on economy (*German*) 0-89583
energy conservation in Britain, main options 0-76620

energy resources continued

- energy-political questions nationally and internationally for West Germany (German) 0-101072
 ethanol, as petrol substitute, increased use in USA (Dutch) 0-72004
 forecasting models and their validity 0-89582
 future reserves projections to 2050 (Dutch) 0-61221
 geopressed geothermal energy production plant, environmental effects 0-97764
 geothermal, 5 MW pilot plant, anal. of binary thermodynamic cycle with dual boiling 0-97763
 geothermal, coaxial well for space heating and cooling 0-66933
 geothermal, feasibility and demonstration of low-grade heat energy from deep aquifers, Canada 0-61278
 geothermal, future prospects in world energy strategy 0-72012
 geothermal district heating system, planning assessment, financing and design optimisation 0-61279
 geothermal electric power generation, types of plants 0-61276
 geothermal electric power generation 0-66937
 geothermal energy, development, availability, and storage possibilities (French) 0-89587
 geothermal energy, utilisation for thermal and electric energy, geochem. engineering and materials 0-61275
 geothermal energy and biofuel production in agriculture 0-66932
 geothermal energy extraction from penny-shaped reservoir made in hot dry rock 0-108784
 geothermal energy in Hungary, non-electric usage 0-76601
 geothermal energy in Sweden, investigations in Bohus granite area 0-85631
 geothermal energy recovery from hot dry rock, use of weighted brine 0-101076
 geothermal energy resource exploitation, conf. Sept., Landerello, Italy 0-81418
 geothermal energy resources for electricity generation, discounted cash flow anal. 0-85263
 geothermal energy resources in Oregon, USA, elec. and EM sounding obs. 0-97761
 geothermal energy resources utilisation possibilities (German) 0-108785
 geothermal hot water for controlled horticulture 0-108783
 geothermal power, demonstration projects for technical and economic feasibility 0-66936
 geothermal power, near-term supply curve for elec. appls. based on prod. costs 0-61277
 geothermal power developments and environmental pollution 0-61470
 geothermal reservoir, transient steam flow, Kawah Kamojang, Java 0-77018
 geothermal resource development, power station planning and siting 0-66935
 geothermal resource field development for electric power generation 0-66934
 geothermal resources, low-temp., in E. United States 0-85264
 geothermal resources in USA, National Exploration Program 0-72011
 geothermal technology, development into an exact science 0-61781
 Hawaii Geothermal Project, groundwater geochem. study 0-72567
 heat and energy savings and coordination and planning of resources expansion (Russian) 0-89585
 hot dry rock geothermal reservoir fracture mapping techniques 0-81419
 hydrocarbons production by photosynthesis 0-89661
 hydropower potential in Burundi 0-81417
 industrial utilisation of energy, book 0-61222
 instrumentation 0-72001
 logistic substitution model, appl. to energy systems 0-89600
 municipal refuse, utilisation of heat energy 0-66919
 national energy policy anal. and planning models 0-101071
 nuclear power, US energy policy 0-81426
 nuclear power and US energy policymaking, suggested revision of production/consumption patterns 0-66954
 ocean energy potential 0-66956
 ocean energy sources and their exploitation 0-89588
 ocean thermal energy, development, availability, and storage possibilities (French) 0-89587
 oil shales of Green River, USA, thermal decomposition rel. to elec. cond. obs. 0-104495
 photovoltaic cells, Galileo works activities (Italian) 0-60029
 photovoltaic conversion comparative evaluation (Italian) 0-60023
 power generation, hydroelectric, economic assessment of fuel savings (Russian) 0-97760
 power station waste heat utilisation for fish farming and agriculture (German) 0-101080
 power stations, steam-gas combined, based on natural gas resources from North Sea, economics and possibilities (Norwegian) 0-101073
 research and development in Britain, general survey (German) 0-72000
 review of long-term energy systems and the role of nuclear and solar energy 0-66918
 review of new sources including solar and wave energy (Spanish) 0-81420
 salinity gradient power utilising vapour pressure differences in water 0-76652
 solar power, alternative fuel source, predictions for future and technical-economic possibilities 0-89591
 solar-radiation meter, automatic 0-89592
 St. Lucia, Sulphur Springs geothermal field model 0-94494
 supply, transition from fossil fuel to nuclear and regenerative sources, technical, economic and ecological aspects 0-66955
 synthesis of energy system, soft solar energy option 0-76614
 system modelling, New Zealand appl. 0-76590
 technological forecasting, uK energy modelling system 0-72003
 N. Thailand, hot springs and geothermal gradients 0-94495
 tidal energy, flexible water barriers and compressed air energy 0-61273
 tidal power, Korea, prefeasibility study 0-61271
 Travale-Radicondoli geothermal area (Tuscany), dipole elec. sounding method appl. 0-97762
 utilisation in USA, city lights obs. by satellite 0-104494
 water power, review of possible developments in Sweden (Swedish) 0-93847
 water power development, feasibility, economics 0-61274
 wave power, development, availability, and storage possibilities (French) 0-89587
 wind power plants, experimental projects in progress, design problems and results achieved (Italian) 0-72007
 wood energy in W. Virginia 0-72006
 H₂, biophotolytic production from H₂O 0-61457

energy resources continued

- H₂, photolytic prod. using biological and artificial catalysts 0-61444
 H₂ production by H₂O decomposition using solar energy conversion 0-97813
 H₂ production by steam reforming of natural gas, chemical kinetics 0-97815
 H₂ production using high temp. reactors 0-97814
 H₂ production using hybrid cycles with HBr electrolysis 0-97816
 H₂, thermochem. prod., H₂O pyrolysis using Fe-Cl cycle, chem. engineering anal. 0-97811
 H₂, thermochemical production using H₂SO₄-SO₂ cycle, electrochem. aspects 0-97812
 U exploration and prospecting methods 0-85768
 U, international resources assessment 0-99215
 U resources and accessibility, reliability of nuclear fuel supply 0-99216
 U₂O₈ demand projections using a disaggregated market penetration model 0-99214
 U₂O₈ recovery from seawater, R and D program 0-99217
²³⁵U, recovery from enrichment plant tailings by laser isotope separation 0-83212
- energy states**
 see also atomic structure; electron energy states (condensed matter); energy level crossing; molecular energy levels; nuclear energy levels; population inversion
 orbital angular momentum eigenvalues, integrality calcs. 0-67977
- energy states in solids and liquids** see electron energy states (condensed matter)
- energy storage**
 see also capacitor storage; direct energy conversion; energy storage devices
 batteries, electric vehicle and power storage appl. 0-72031
 battery appls. and developments, conf., Brussels, Belgium (Jan. 1979) 0-72032
 chemical conversion and storage of solar energy, book 0-86045
 chemical fuel production by solar energy conversion 0-61318
 environmental impact of energy storage technology development 0-61471
 fast ion transport in solids, conf., Lake Geneva, USA (May 1979) 0-57006
 fast ion transport in solids, conf., Lake Geneva, USA (May 1979) 0-105427
 flywheel energy storage and conversion system for photovoltaic appl., economic anal. 0-94116
 fusion reactor, FTFR, energy conversion and storage systems, fault detection and protection 0-95431
 H₂ absorption in thin film hydriding alloys, LaNi₅ and SmCo₅ 0-65238
 heat storage in a solar heating system using Na salt hydrates 0-67005
 heat storage in solar heating system using Na salt hydrates, based on extra water principle 0-67006
 heat storage tank, energy saving control system for air conditioning (Japanese) 0-72087
 homopolar generator design for fusion reactor energy storage 0-68953
 inductive storage systems for cylindrical imploding plasma drives 0-70019
 large-scale elec. energy storage, review 0-89676
 latent heat storage, physical and chemical processes at low temps. 0-72091
 materials needs, in energy conservation and storage 0-66958
 phase change materials, thermal energy storage, cycle life tester 0-72090
 social implications of solar and H₂ energy storage and electric vehicles 0-67001
 solar, desalination process appl. multistage flash evaporation, demonstration project 0-61283
 solar chemical storage, chemical bond energy of SiO₂ and ammoniates undergoing thermal decomposition 0-76656
 solar collector, water-trickle type, with massive concrete slab for heat storage 0-108814
 solar collector design and suntracking control for PORSHE concept 0-61425
 solar energy, chemical storage, effect of micellar phase on photo-induced reactions 0-89678
 solar energy, storage and power supply for building heating, optimal conditions (French) 0-61297
 solar energy chemical conversion and storage using norbornadiene-quadracyclic photoisomeric interconversion 0-89664
 solar energy chemical storage, photo-induced electron transfer reactions in solution, organised assemblies and at interfaces 0-89677
 solar energy chemical storage, photosensitization mechanisms for energy storing isomerizations 0-89679
 solar energy chemical storage using novel photocyclization reactions of 1-alkenyl-2-pyridones 0-89680
 solar energy collection and storage, latent heat diode walls, space heating (French) 0-61298
 solar energy collection and storage, space heating (French) 0-61299
 solar energy conversion and storage using artificial photosynthetic systems 0-89662
 solar energy electricity storage, battery appls. potential 0-72067
 solar energy storage, molten salts, heat transfer salt (French) 0-61434
 solar energy storage by metal hydride, review 0-61455
 solar energy storage methods for large-scale appls., eval. 0-89675
 solar energy storage system, ammoniated salt heat pump using MgCl₂·CaCl₂, NH₄Cl 0-81484
 solar heat pump and thermal storage system based on CaCl₂ and methanol vapour reaction for space heating 0-85307
 solar heating system, annual cycle thermal energy storage, sensitivity anal. 0-67007
 solar HVAC system, thermal storage, materials, labour and insulation costs 0-72088
 solar ponds, non-convecting, review 0-61407
 solar space heating, two-tank storage system using seasonal and diurnal tanks 0-72016
 solar thermal energy accumulator using stones, operating principles (German) 0-72085
 solar-H₂ energy systems, review 0-61447
 solar-H₂ systems using metal hydrides 0-61464
 superconducting magnetic energy storage system with superconducting rotary machines as I/O system (Japanese) 0-85306
 technology and solar energy use, worldwide trends (German) 0-72086
 thermal, optimally distrib. insulation for in-ground heat storage tanks 0-94119

energy storage continued

thermal, rock bed storage for solar energy systems, comparison of meas. and predicted performance 0-67004
 thermal, using phase change material, time variation of storage and release 0-67008
 thermal, waste heat utilization with annual aquifer storage for space heating appls. 0-97809
 thermal energy storage, US DOE research program for aquifer waste heat utilisation 0-97808
 thermal energy storage for solar appls. 0-72089
 thermal energy storage in industry and power stations 0-67002
 thermal energy storage in salt hydrates for solar heating systems, storage material props. 0-101134
 thermal energy transport using benzene/cyclohexane reversible chemical reaction systems 0-67009
 thermal storage, convolution model of packed bed units 0-94118
 thermal storage in density stratified fluids and phase change materials 0-67003
 thermal storage in solar heating appls. in northern latitudes, insolation modelling 0-66941
 thermal storage of solar energy using chabazitic tuff, a zeolitic rock 0-94117
 underground pressurised saturated hot water storage for peak lopping appls. 0-76653
 Ag-H₂ electrochemical cell design using rolled stack configuration 0-101084
 CaCl₂·2CH₃OH, solar heat pump and thermal storage system for space heating 0-85307
 CaCl₂·6H₂O, heat transfer props. for heat of fusion energy storage 0-76654
 CaO-Ca(OH)₂, reversible hydration-dehydration for solar energy storage 0-97810
 H absorption-desorption characts. on TiCo_{1-x}Mn_x 0-96735
 H, biophotolytic production from H₂O 0-61457
 H sorption at press. up to 1500 atm. on rare earth alloys, RM_x (M=Co, Ni) 0-97819
 H storage in metal hydrides 0-61445
 H₂ and O₂ production from H₂O using solar energy, eval. of a hybrid process 0-104519
 H₂ as an energy source 0-108816
 H₂, atomic at 1K, energy storage appls. (*German*) 0-89681
 H₂, biologically-assisted production, use of polymeric viologen mediators in a bioreactor based on hydrogenase-catalysed Na₂S₂O₄ decomposition 0-61460
 H₂ bulk storage using TiFe-based hydrides 0-61463
 H₂, comparison of technologies and economics for fixed site storage 0-67011
 H₂ distribution in natural gas equipment, operating, safety and material problems 0-61468
 H₂ electrolytic production by high temp. steam electrolysis 0-61440
 H₂ electrolytic production, development and operation of advanced electrolysis cell 0-61441
 H₂ electrolytic production, design and operation of advanced H₂O electrolyzers, review 0-61449
 H₂ energy research programs in Japan 0-61435
 H₂, HYCSOS chemical heat pump, low grade heat enhancement using LaNi_{5-x}Al_x 0-61467
 H₂, photobiological prod., key enzymes and biochem. systems, tech. problems of H₂ prod., review 0-61446
 H₂ photochemical production by H₂O dissociation utilising solar energy, review 0-61452
 H₂, photochemical production using visible light on aqueous solns. of a Ru complex 0-85192
 H₂ photolytic production using chlorophyll-catalysed H₂O photolysis and solar energy storage 0-61458
 H₂ production, H₂O electrolysis module design, geometry, capacity, operating temps., pressures, electrode types 0-72098
 H₂ production and storage utilising solar energy conversion, book 0-57017
 H₂ production by alkaline electrolysis using inorganic-membrane-electrolyte 0-72092
 H₂ production by biological and biochemical solar energy conversion, review 0-61454
 H₂ production by direct solar energy conversion at sea, review 0-61456
 H₂ production by direct thermal decomposition of H₂O utilising solar energy, thermodynamics, review 0-61450
 H₂ production by H₂O electrolysis, nucleate boiling, vapour bubble behaviour, heat and mass diffusion 0-67013
 H₂ production by H₂O electrolysis, compression and storage 0-72097
 H₂ production by H₂O electrolysis in fused NaOH 0-76660
 H₂ production by H₂O photolysis using solar radiation, feasibility of large scale generation 0-72095
 H₂ production by H₂O radiolysis, thermoradiation dehydrogenation using nuclear power, kinetic anal. 0-67010
 H₂ production by H₂O solar photolysis using Pt/(chlorophyll a.2H₂O) reaction 0-89663
 H₂ production by solid polymer electrolyte H₂O electrolysis 0-61442
 H₂ production by solid polymer electrolyte H₂O electrolysis 0-67012
 H₂, production from natural gas, naphtha and coal on industrial scale 0-61438
 H₂ production from water using biomass feedstock and bromination process 0-61459
 H₂ production in fusion-synfuel blanket, thermal hydraulics 0-106176
 H₂, review 0-61453
 H₂ solution in TiCr_{1.8}, enthalpy, solubility and mol. vibr. determ., comparison with soln. in metals and binary alloys 0-79951
 H₂ storage, high pressure gas storage using microcavity structures 0-61462
 H₂ storage, transmission and distrib., review 0-61439
 H₂, storage as metal hydrides, props. and appls. 0-76661
 H₂ storage at fixed sites for distribution 0-61461
 H₂ storage in amorphous plasma-sprayed Sm-Co, effect of H₂ atm. on crystn. and mag. props. 0-64898
 H₂ storage in Fe-Ti hydrides, specific heat meas. at room temp. 0-65248
 H₂ storage in form of metal hydrides 0-72096
 H₂ storage properties of Zr(V_{1-x}Co_x)₂, rel. to electronic struct. 0-76662
 H₂ storage using hydride beds, thermal transport enhancement using high conductivity materials 0-61466
 H₂ storage using Mg-La(Ce)(mischmetal) alloys 0-72093
 H₂, thermal efficiency of H₂ compression using hydrides 0-61465

energy storage continued

H₂, thermo-electro-chemical production by Westinghouse H₂SO₄ process, heat penalty and economic anal. 0-61437
 H₂, thermochemical compression for hydride thermosorption, theory (*Ukrainian*) 0-76657
 H₂, thermochemical prod. by H₂O decomposition utilising solar heat 0-61451
 H₂, thermochemical production, plasmochemical H₂O decomposition using nuclear energy source 0-61436
 H₂, thermochemical production using fusion energy using metal oxide thermochem. cycles 0-76658
 H₂, thermochemical production by Mark-13 cycle, development of laboratory-scale plant 0-76659
 H₂, using Ti-Mn alloy systems (*Japanese*) 0-61443
 H₂/hydrocarbon fuel prod. via biomass conversion wastes by solar H₂O photoelectrolysis 0-89653
 H₂-Br₂ cell for energy storage appls. 0-72029
 KCl-CuCl eutectic fused salt, potential as intermediate temp. solar heat transfer and storage medium 0-101135
 TiFe_{0.8}Be_{0.2} alloys for H₂ storage 0-97817

energy storage devices

heat storage device, off-peak, ambient temp. observer/predictor control system 0-66950
 inductive storage element, pulsed discharge into fluid gap, electrohydraulic effect (*Russian*) 0-100117
 large-scale elec. energy storage, review 0-89676
 secondary batteries, 1979 status and prospects (*Japanese*) 0-76655
 secondary cells, Ni-Cd, plastic-bonded electrodes positive active layer study 0-101088
 secondary cells with C-air electrodes in alkaline electrolytes, ageing mechanism study 0-101087
 solar seasonal storage devices, economic optimisation of storage capacity and collector area 0-101133
 superconductive energy storage magnet, single layer, design and cost-related parameters 0-108815
 thermal storage in fluid/solid packed beds, design and rating (*French*) 0-61433
 H-Cl electrochemically regenerative fuel cell, electrode kinetics and cell perform. 0-89610

energy transfer collisions, molecular *see molecular inelastic collisions*

engineering

see also biomedical engineering; civil engineering; design engineering; electrical engineering; environmental engineering; maintenance engineering; mechanical engineering; naval engineering; systems engineering; value engineering
 earthquake engineering, implications of seismic body waves propag. in S. Kanto Region (*Japanese*) 0-94481
 C fibres, engineering applications, production requirements and mech. props. 0-89168

engineering applications of computing *see engineering computing*

engineering computing

see also aerospace computing; chemical engineering computing; communications computing; electrical engineering computing; electronic engineering computing; mechanical engineering computing; nuclear engineering computing
 solar input and solar data computation for engineering of solar systems, transients simulation 0-94060

engineering societies *see societies*

engines

see also aerospace engines; heat engines; internal combustion engines; ion engines
 engine intake noise, high freq., ray-theory approach 0-69595

enthalpy

see also heat of
 acrolein, s-trans and s-cis, trapping from thermal mol. beams and UV-induced isomerisation in Ar matrices, enthalpy determ. 0-97688
 air enthalpy meas. by LiCl humidity sensors 0-90858
 alkali metal fluoroaluminate, dissoc. enthalpies, mass spectrometric determ., heat of form. 0-97720
 biomolecules+chloranil, charge transfer interaction, equilib. const., enthalpy and enthalpy determ., mol. polarisability 0-89708
 butane, liq., enthalpy difference between rot. isomers, IR spectrosc. obs. 0-106404
 t-butyl acetate, rot. isomerism, dielect. and Raman spectra 0-106328
 t-butyl formate, rot. isomerism, dielect. and Raman spectra 0-106328
 ethylene, diatomics-in-mols., semiempirical valence bond π -electron theory 0-99461
 excess enthalpy and excess entropy functions derivation by direct method from TX phase diagram, heats of mixing calc. 0-75366
 glass making system, continuous, energy balance 0-89189
 glass structure, isobaric variation, phenomenological theory (*French*) 0-59393
 glasses, order parameter model, vol. and enthalpy relax. 0-88008
 graphite, pyrolytic commercial, high-temp. thermal and mech. props. 0-75372
 intercalation compound electrodes, thermodynamic and transport props. 0-66963
 intermetallic phases, B2 struct., substitutional and triple defects, enthalpies of formation 0-96520
 ion solvation, correlation of total and partial enthalpies, vel. to nucleation energy barrier 0-89514
 ionic crystals, migration volumes calc. 0-103324
 liquids, order parameter model, vol. and enthalpy relax. 0-88008
 metals, heat content correlation under fast heating (*Russian*) 0-70426
 micellar systems, aqueous, thermochemistry 0-61133
 multicomponent systems, phase diagrams and thermodynamic data, electrochem. determ. 0-71922
 natural gas mixtures, simulated, enthalpy and phase equil., correl. with modified Starling eqn. 0-61127
 pentane, liq., enthalpy difference between rot. isomers, IR spectrosc. obs. 0-106404
 polycarbonate, glassy state, enthalpy relax., thermal density fluctuations 0-59678
 polyethylene, low-density, environmental stress cracking, surfactant soln. effect 0-89376
 polymer glasses, enthalpy relax., scanning calorimetry technique 0-90851
 pure gas, enthalpy, Carlson-Thodos van der Waals eqn. calcs. 0-83878
 solid electrolytes, fabrication and props. 0-70463

enthalpy continued

- superplastic flow, activation enthalpy determ. from strain rate changes in tensile tests 0-81127
 water, random network model, liq. and ice polymorphs enthalpy and heat content 0-64869
 Ag thin evaporated films, rel. between microstruct. and excess free energy, TEM 0-70427
 Ag-Ge eutectic alloy, heat capacity meas. over temp. range 800-1200K (*French*) 0-88331
 Ar + Xe⁺, XeAr⁺ form., dissociation energy, reaction equilib. and rate consts. 0-61071
 Au-Sn, zeta and AuSn phases, heats of form. and heat contents 0-60837
 BF₂ radical, thermomechanical studies by mass spectrometry, enthalpy of form. and ionisation pot. determ., chem. bonds 0-81382
 BaO-B₂O₃-V₂O₅ glass, oxidation-reduction of V, thermodynamics 0-85169
 CaCu₂, γ -phase in Ca-Cu system, calorimetric determ. of enthalpy of form. (*French*) 0-84915
 CaWO₄, cryst. growth from solns. in melts, kinetics parameters and thermodynamic props. 0-59424
 CdTe_{1-x}Te_x, single and polycryst. samples, linear expansion, heat capacity and thermodynamic props. 0-103489
 Cl⁻ hydration complexes, gas phase, electrostatic calcs. 0-100055
 Cr, enthalpy and specific heat, empirical eqn. (*Russian*) 0-92683
 Cu dilute binary solid solutions, enthalpies of mixing and excess free enthalpies (*French*) 0-107427
 Eu₂Sn₂S₁₂, mag. and thermodynamic props., metamagnetism 0-60273
 Fe-Ni alloys, enthalpy change between α' - γ and α - γ transformations 0-93550
 Fe₂₃Ni₁₃Cr₁₄P₁₇B₈ metallic glass, effect of pre-ageing on glass transition temp. 0-100326
 GeP, thermodynamic characts. 10-300K, interatomic bond elasticity 0-59677
 H₂O₂(As)₄O₄H₂O, water deficiency, enthalpy of dehydration, thermogravimetric anal. 0-65251
 I⁻ hydration complexes, gas phase, electrostatic calcs. 0-100055
 Ir, thermophysical props. at temps. up to 7000K 0-103497
 KHSO₄·Fe³⁺, DC cond. meas., mechanism 0-65285
 LaNi₅/H system, thermodynamics of H trapping 0-107444
 La₁₀W₂O₂₁, enthalpy and heat capacity at high temp. 0-70424
 α -La₂WO₆, enthalpy and heat capacity at high temp. 0-70424
 La₂W₂O₁₅, enthalpy and heat capacity at high temp. 0-70424
 MgAl₂O₄ spinel refractory, enthalpy and specific heat determs. 0-88334
 MgCr₂O₄ spinel refractory, enthalpy and specific heat determs. 0-88334
 N-Fe solid soln. in equilibrium with N₂ gas, partial molar enthalpy and excess entropy 0-60838
 Nb, liq. and solid, enthalpy meas. by levitation calorimetry 0-103499
 Nb, solute trapping of H, symmetry of O-H pair 0-108488
 R₁-Co₂, rare earth amorphous alloys, thermal stability, elec. cond. enthalpy 0-100172
 Se₂O₃, solid, enthalpy investig. at high temp. 0-103498
 β -SiC, thermodynamic props., temp. depend., 5 to 300K 0-96666
 SiP, thermodynamic characts. 10-300K, interatomic bond elasticity 0-59677
 Sn, thermally induced vacancies, positron trapping 0-89083
 SrWO₄ cryst. growth, from Na₂WO₄ melts, thermodynamic props. 0-107084
 ThC_n(n=1 to 6), Knudsen effusion mass spectrometric investigations, enthalpies and heat of formation calcs. 0-66858
 TiCr_{1.8}, H and D soln., enthalpy, solubility and mol. vibr. determ., comparison with soln. in metals and binary alloys 0-79951
 U(C,N), N vapour pressures and thermodynamic props. 0-84918
 UC_x, partial molar thermodynamic quantities, semi-invariant cumulants method 0-65250
 UN, N vapour pressures and thermodynamic props. 0-84918
 V, thermophysical props. at temps. up to 7000K 0-103497
 W, relative enthalpy, 273 to 1173K, electronic heat capacity coeff. 0-103496
 ZrI₄, high-temp. enthalpy, X-ray powder diffr. data 0-107446
 ZrO₂, enthalpy and heat capacity at 1100-2500K 0-103472

entropy

- see also *entropy of substances*
 adsorption thermodynamics, symmetrical, case of noninert adsorbent 0-80059
 binary system, isobaric and isothermal phase transform., exchange processes, entropy meas. (*German*) 0-90798
 biomolecules + chloranil, charge transfer interaction, equilib. const., enthalpy and entropy determ., mol. polarisability 0-89708
 classical entropy, relationship with quantum-mechanical entropy 0-73298
 complexity and time in physics (*Chinese*) 0-81285
 conductors, rigid, thermodynamic anal., hyperbolic heat conduction eqn. 0-64334
 continuous distribution based on non-standard anal., new definition 0-82736
 cosmological fluctuations, spontaneous prod. 0-94902
 defects, or inhomogeneities, entropy of formation equation validity 0-79960
 deterministic dynamics to probabilistic descriptions 0-68029
 dipole relaxation in electric field, teaching 0-90625
 dislocations and melting in two and three dimensions 0-103454
 early Universe, inhomogeneity and origin of entropy 0-62350
 education, Brownian motion, melting, surface tension and rubber networks, thermodynamic anal. 0-73132
 elastic materials, non-hyperelastic, thermodynamic behaviour, mathematical model 0-73290
 elastic media, dissipative, relativistic electrodynamics 0-73219
 excess enthalpy and excess entropy functions derivation by direct method from TX phase diagram, heats of mixing calc. 0-75366
 gas, monatomic, time average problem, statistical entropy change over constant energy path 0-68123
 gas flows, entropy prod. determ. using Boltzmann's H-theorem, Knudsen effusion 0-106867
 gases, ideal, entropy of mixing, Gibbs paradox, indistinguishability 0-57226
 generation, heat transfer augmentation techniques 0-79118
 granular materials, shear deformation, entropy model 0-84233
 ground-state entropy and algebraic order at low temperatures 0-86234
 heat engines, minimum entropy prod. and optimisation 0-85297
 hot Universe perturbations, primordial struct. evol. 0-105411

entropy continued

- information entropy, and law of large numbers, opacity of statistics (*French*) 0-73288
 information theoretic approach, exptl. and inherent uncertainties 0-82733
 inhomogeneous medium, effective cond., iteration series and variational estimates, Herring method 0-70663
 invariant transforms. of entropy prod., extended irreversible thermodynamics 0-73293
 Ising model, bond random, ferromagnetic-antiferromag. mixture, triangular cactus tree, statistical theory 0-75702
 Lyapunov variable, entropy and meas. in quantum mechs. 0-77739
 maximum entropy spectral estimation of frequency and arrival angle 0-96129
 Maxwell demon and correspondence between information and entropy 0-86241
 measure of degree of material organisation using information quantity based on entropy (*Polish*) 0-57232
 micropolar fluids, thermodynamical aspects, non-linear approach 0-105598
 mixtures, simple, non-equilib. thermodynamics 0-76543
 multicomponent systems, phase diagrams and thermodynamic data, electrochem. determ. 0-71922
 neutron gas system in stationary power reactor with decoupling thermodynamics and distrib. function 0-86950
 nonequilibrium thermodynamics, stochastic measures 0-86240
 nonlinear mechanics eqns. and entropy growth across a shock, symmetric form 0-69705
 nonlinear response of a system in connection with entropy maximum 0-95047
 one particle distributions, entropy bounds 0-62607
 optical systems, entropy and negentropy (*French*) 0-102608
 Ott relativistic temperature variation, comment on derivation 0-86084
 phase transitions, first-order, finite-size rounding rel. to entropy, system size 0-59623
 polytype relative stabilities, entropy contribs. 0-100197
 radiation entropy and its role during photosynthesis 0-108858
 radiographic granularity, of screen-film systems, assessment by entropy method 0-98070
 soft discs, two-dimens. melting, phase transition boundary 0-96629
 spin wave parametric excitation, stochastic auto-oscill., Kolmogorov entropy (*Russian*) 0-75749
 statistical entropy, and law of large numbers, opacity of statistics (*French*) 0-73288
 superadditivity and concavity, black hole systems 0-98867
 supersaturated vapour, critical clusters, theory and Monte Carlo simulation, review 0-82734
 terrestrial planet, cratered surface entropy 0-101541
 TLD elements, transmitted information 0-89860
 valence transition, entropy and phase diagram 0-59877
 Van der Waals gases, adiabatic and isothermal spinodal curves 0-92034
 wear, entropy production model 0-74815
 CaWO₄ cryst. growth from solns. in melts, kinetics parameters and thermodynamic props. 0-59424
 Cl⁻ hydration complexes, gas phase, electrostatic calcs. 0-100055
 Cu, NMR study on nuclear ordering below 1 μ K 0-93187
 CuSO₄ soln., electrochemical analogue of Benard instability, isothermal and potentiostatic conditions 0-76530
 H + H₂, reaction probability, max. entropy derivation, statistical theories 0-66781
 I⁻ hydration complexes, gas phase, electrostatic calcs. 0-100055
 SrWO₄ cryst. growth, from Na₂WO₄ melts, thermodynamic props. 0-107084
- entropy of substances**
 alkaline earth fluoride, doped with trivalent rare earths, migration entropy for bound fluorine motion 0-71303
 atomic and plastic crystals, melting transitions, thermodynamic props. 0-96452
 benzene-hexa-n-hexanoate, phase transitions and mesophase form., sp. ht. and IR spectra, 13 to 393K 0-79955
 block copolymers, microphase separation, thermodynamic treatment (*Chinese*) 0-79947
 brass, liquid, thermodynamic props. (*German*) 0-66482
 communal entropy and glass transition, theory 0-70131
 copolymer globule model, orientationally-ordered liq. cryst. state (*Russian*) 0-59389
 crystal orientational disordering, thermodynamic props., stat. mech. model 0-96453
 cyclo-hexyl-ammonium-copper-trichloride, specific heat, ferromagnetic chain system 0-103491
 di(alkylammonium)CdCl₂Br₂, solid-solid phase transitions 0-84290
 dielectric fluid, Debye absorption at crit. liq.-vapour transition 0-100322
 entropy change on melting of simple substances, thermal expansion, configurational entropy 0-59630
 ionic crystals, migration volumes calc. 0-103324
 liquid crystal, binary mixtures, phase transition, entropy, relation to smectic plane tilt angle 0-65203
 liquid crystal surface, statistical thermodynamics, local order parameter 0-88023
 liquid crystals, thermodynamic props. calc. 0-103464
 metals, dislocations and shock compression, thermodynamics 0-100235
 metals, entropies and heats of fusion 0-103458
 methane, melting transitions, thermodynamic props., positional disordering energies 0-96452
 micellar systems, aqueous, thermochemistry 0-61133
 minerals, dislocations and shock compression, thermodynamics 0-100235
 polydiphenylsiloxane, thermodynamics of fusion 0-84280
 polymer, polydisperse, glass transition temp., mol. mass depend. 0-92656
 polymer protonated and deuterated mixtures, partial miscibility 0-107037
 polymers, solidification, as dissipative process 0-65205
 pyridine, deuterium substituted, Raman and IR vibr. spectra 0-84739
 rare earth (III) complexes, cysteinates, thermodynamics of form. 0-89515
 solid-liquid interface free energy anisotropy clustering influence 0-80054
 steel, aluminising, thermodynamic anal. of phase transforms. 0-76413
 steel, medium and high C, deformation ageing, entropy, free energy, dislocations (*Russian*) 0-66581
 vacancy formation parameters from specific heat data 0-75221
 viscous liquids, glass transition, nonconfig. contribs. to excess entropy 0-92654
 water, random network model, entropy calc. 0-64870

entropy of substances continued

Wolff model, thermodynamic props., local moments in dil. alloys, var. method 0-65781
 α -AgI, superionic cond., statistical thermodynamic description (French) 0-65281
Al₃Mg₁₇-c liquid alloys, vols. and entropies of mixing, calc. 0-75363
alkali metals, liquid, internal energy, heat of mixing, entropy, dielectric function 0-88340
Ar, melting transitions, thermodynamic props., positional disordering energies 0-96452
BaCl₂(F₂), sp. ht. meas., Schottky-type diffuse phase transitions, defect form. energies and entropies 0-107441
 δ -Bi₂O₃, thermoelectric power rel. to fast ionic conduction 0-107549
 δ -(Bi₂O₃)_{1-x}(Y₂O₃)_x, thermoelectric power rel. to fast ionic conduction 0-107549
CaGa₂O₄ and CaGa₂O₇, cryst., thermodynamic parameters of reactions of form., thermodynamic stability 0-108726
CdS, polytype relative stabilities, entropy contrbs. 0-100197
CdTe, single and polycryst. samples, linear expansion, heat capacity and thermodynamic props. 0-103489
CeB₆, anomalous sp. ht. intrinsic mag. phase transitions obs. 0-108027
Cr-Ge, thermophysical props., at elevated temp. 0-103493
CuMn spin glass, specific heat and entropy 0-60354
Cu₂S, Cu₁₁S₈, α - β transition, thermographic investigation of heats, entropies and activation energies 0-88314
DyFe₂H₁₂, thermodynamic props., H₂ desorption isotherm meas. 0-89516
ErFe₂H₁₂, thermodynamic props., H₂ desorption isotherm meas. 0-89516
EuB₆, ferromag. and antiferromag. sp. ht. meas., 1.8-77K 0-65948
Eu₂Sn₃S₁₂, mag. and thermodynamic props., metamagnetism 0-60273
Fe-Cu liquid alloy, heats of mixing, mixing entropies (Russian) 0-65224
GeP, thermodynamic characts. 10-300K, interatomic bond elasticity 0-59677
³He, liq. B-phase at equilb., formalism 0-88384
³He, solid, ordering obs. at melting press. in high mag. fields 0-84341
³He, solid, spin ordered, melting press. and entropy 0-84340
³He, solid magnet, spin-lattice models 0-88394
³He-Z near A. phase transition, collective oscill. hybridisation (Russian) 0-80020
⁴He, solid-fluid, eqn. of state, melting props. under press. 0-96721
K-Rb, internal energy, heat of mixing, entropy, dielectric function 0-88340
LaMnO₃, stoichiometric manganite form. reaction, thermodynamic characts. 0-108727
LaNi₅/H system, thermodynamics of H trapping 0-107444
Li-Pb liquid compound forming alloy, entropy of mixing 0-88328
LiAlCl₄, solid and molten electrolyte, thermodynamic stability 0-107447
Li₂N, vapourisation, studied by Knudsen effusion method 0-92662
Li_{2-x}P₂O_{3-x}, polyphosphate, melting and crystallisation 0-70376
Mn-Ge, thermophysical props., at elevated temp. 0-103493
Mn₂Ga₂N, sp. ht., 6 to 350K, mag. and crystallographic phase transitions 0-71060
Mn₂ZnN, sp. ht., 6 to 350K, mag. and crystallographic phase transitions 0-71060
N-Fe solid soln. in equilibrium with N₂ gas, partial molar enthalpy and excess entropy 0-60838
Na-Cs, internal energy, heat of mixing, entropy, dielectric function 0-88340
Na-Cs, liq., struct. factor, free energy of mixing, and electrochem. pot., thermodynamic calc. 0-96436
Na-K, internal energy, heat of mixing, entropy, dielectric function 0-88340
NaAlH₄ and Na₃AlH₆, molar heat capacity and thermodynamic functions, 10 to 300K 0-65243
NaI:Ca²⁺, pure and doped, lattice defects, entropy and enthalpy of formation and migration 0-96687
Ni alloys, aluminising, thermodynamic anal. of phase transforms. 0-76413
Pb, thermodynamic characterisation, by isobaric expansion meas. 0-103494
PbF₂, sp. ht. meas., Schottky-type diffuse phase transitions, defect form. energies and entropies 0-107441
Pd-D, crystallite size effects, simultaneous sorption and X-ray study 0-65237
Pr(OH)₃, electronic heat capacity, 0.45 to 4.2K, phase transition at 1.21K 0-59673
PuRu₂, intermetallic cpd., sublimation thermodynamics 0-96639
ScP, thermodynamics and high temp. vapourisation 0-88310
Sc₂S₃, order-disorder transition, ionic model appl. 0-107096
Si-C, polytype relative stabilities, entropy contrbs. 0-100197
 β -SiC, thermodynamic props., temp. depend., 5 to 300K 0-96666
SiP, thermodynamic characts. 10-300K, interatomic bond elasticity 0-59677
SnSe₂, sublimation, temp. depend. of equilb. constants 0-88312
SrCl₂, sp. ht. meas., Schottky-type diffuse phase transitions, defect form. energies and entropies 0-107441
Th₃As₄, heat capacity meas., 3-500K 0-88769
U₃As₄, heat capacity, 5-300K, ferromag. transition obs. 0-88769
UC, partial molar thermodynamic quantities, semi-invariant cumulants method 0-65250
UF₄, vapourisation behaviour 0-84283
V-Ge, thermophysical props., at elevated temp. 0-103493
V,Hf_{1-x}Zr_x, normal and supercond. state, transition temps., mag. susceptibility and specific heat determ. (Russian) 0-60132
YbGa₂, mag. props. between 44-600 mK 0-80517
ZnS, polytype relative stabilities, entropy contrbs. 0-100197
Zr₁₄, high-temp. enthalpy, X-ray powder diff. data 0-107446

environmental engineering

see also air conditioning; cooling; ergonomics; lighting; safety; space heating; temperature control; ventilation
advances in environmental science and engineering, book 0-105448
coal conversion technologies, health and environmental effects 0-81493
fusion reactors, JT-60, seismic anal., design changes 0-95425
high electric field biological effects on human nervous systems 0-89739
nuclear power plants, environment protection problems during construction (French) 0-76663
nuclear power plants, environmental research data implementation (French) 0-74037
nuclear power plants, environmental studies organisation (French) 0-76664

environmental engineering continued

nuclear power plants, hydrobiological studies, conception and data obtained (French) 0-76665
RWE environment protection organisation outline and functions (German) 0-101552
safety and environmental pollution (German) 0-63370
Si photovoltaic industry, environmental control, economic and ecological requirements 0-94026
environmental requirements see environmental engineering
environmental testing
see also corrosion testing
birefringent filter mechanical tuning techniques 0-102834
chamber, Oblako universal gas-water vapour generator, humidity test facility 0-62653
composite insulating materials, fatigue behaviour, influence of superposition of elec., mech. and environmental stresses 0-97590
Darrieus rotar windmill arrays, wake interaction, wind tunnel simulation 0-61245
electronic components, space radiation environment effects, laboratory simulation 0-94689
graphite fibre filled polyimide composite laminates, space environment, phys. and mech. response 0-81140
multiple shaker testers, production and military applications 0-64276
photovoltaic modules testing, reliability and performance 0-94063
solar photovoltaic flat panel procurement, qualification test results 0-94064
steel, stainless, 18Cr-2Mo-Ti, atmospheric corrosion 0-85078
thin solar cells, advanced module technique 0-94041
Al-brass tubes, passivation treatment for atmospheric corrosion protection during storage and transport 0-85079
Cu-Ni-Zn alloy, surface comp., outdoor exposure influence 0-59770
Cu-Sn alloy, surface comp., outdoor exposure influence 0-59770
Cu-Zn alloys, surface comp., outdoor exposure influence 0-59770
Cu₂-S-CdS ceramic solar cells, solar batteries operating characts. 0-93874
Li/SOCl₂ cells, abuse tests 0-97776
Ni-H₂ battery for satellite energy storage 0-81430
Si solar cells, base resist. influence on temp. characts., temp. cycling 0-89618
epitaxial growth
see also liquid phase epitaxial growth; vapour phase epitaxial growth
diamond-like semiconductor film epitaxial growth, computer simulation 0-70560
incommensurate epitaxies at finite temps., substrate pot. effect 0-88451
metastable compound synthesis with high supercond. transition temp. 0-93024
Au-Ge contacts on GaAs, SEM and TEM obs. of struct. 0-100522
GaP films on Si, epitaxial crystallisation by nanosecond laser pulses 0-107674
Ni, ion-implanted and virgin, laser irr. effect, epitaxial lattice regrowth 0-108306
Pd-Si structure, epitaxial silicide growth, LEED and AES study 0-103590
Si, amorphous, epitaxial regrowth, structure and impurities effect 0-84401
Si, amorphous layers, recrystallisation, pulsed laser annealing 0-65404
Si epitaxial layer regrowth due to laser annealing mechanism, liquid and solid phase regimes 0-100712
Si, graphoepitaxy on fused SiO₂ using surface micropatterns and laser crystn. 0-70554
Si, ion implantation, high dose, solid phase epitaxial regrowth 0-103380
Si, ion implanted, annealing by ion beam heating 0-103382
Si, ion-implanted layers, crystn. by ns laser pulses, TEM and RHEED 0-100421
Si, ion-implanted layers, epitaxial regrowth by laser beam and flash annealing 0-100420
Si substrate solar cells, upgraded metallurgical grade, epitaxial growth 0-93905
Si surface, reduction growth, autoepitaxy (Russian) 0-107672
Si:Ar, ion-implanted, epitaxial regrowth by laser annealing, microstruct. 0-84404
Si:As, ion implanted, laser annealed, lattice defects, epitaxial regrowth 0-103334
Si:As, ion implanted, pulsed laser annealing, partial solid-state regrowth 0-103591
Si:Bi, ion-implanted, solid phase epitaxial growth during annealing, super-saturated solid soln. form. 0-103384
Si:Sb,P, double implants, residual defect reduction after damage anneal 0-88170
Si/Pd system, solid phase epitaxial growth control by C ion implantation 0-75466
Si-CoSi₃Si, double heteroepitaxy, solid phase and MBE 0-104063
Si-Pd-Si structure, epitaxial growth, backscattering and transmission electron microscopy studies of layered structures 0-80123
Si(111) reconstructed 7x7 surface superlattices, microdomain model 0-107625
epitaxial layers
see also magnetic epitaxial layers; metallic epitaxial layers; semiconductor epitaxial layers
anthraquinone, UV light effect on nucleation during crystallisation on anthracene surface 0-75478
anthrone, UV light effect on nucleation during crystallisation on anthracene surface 0-75478
film/substrate interface, misfit dislocation obs. using electron microscopy 0-103605
n-nitroaniline, UV light effect on nucleation during crystallisation on anthracene surface 0-75478
thulium phthalocyanine, mol. image in high resolution electron microscopy, radiation damage effect 0-107203
AgBr(Cl) vapour-deposited epitaxial film, surface structure 0-59814
(Bi,Tm)₂(FeGa)₂O₁₂ ion implanted epitaxial garnet film, bubble domains, cryst. struct. disorder 0-93150
CoO, XPS obs. of formation on Co (0001) 0-66396
NiSi₂ epitaxial film on (111) Si substrate, interfacial order, backscatter, channelling study 0-65390
Pd:Si epitaxial islands on Si (001) substrate 0-96748
Si:Al epitaxial layers, nuclear microanalysis of Al impurities ²⁷Al(d, α)²⁵Mg 0-61193
Si:Bi, ion-implanted, solid phase epitaxial growth during annealing, super-saturated solid soln. form. 0-103384

epitaxial layers continued

- SiC, reaction-bonded, 'REFEL', microstruct. characterization 0-97490
 TiBr, polymorphism, XPS obs. 0-97398
 TiCl, polymorphism, XPS obs. 0-97398
 W epitaxy on W(110) substrate, work function meas., LEED investigation 0-80103

epitaxy see epitaxial growth**EPR line breadth**

- aluminium copper tetrahalides, exchange, mag. anisotropy, and spin diffusion contribs. to EPR linewidth 0-80597
 benzophenone, migration of triplet excitons, EPR profiles and phosphoresc. decay data 0-84641
 charge transfer crystals, mixed, exciton transport, low-dimensional, statistical model and experiments 0-65461
 conducting media, EPR line shape, magnetoresist. effect 0-84638
 DEM(TCNQ)₂, ESR study 0-97127
 diamond, ultradisperse, ESR, particle size and lattice microdistortions 0-97140
 diethylammonium manganese chloride, Heisenberg magnet, spin diffusion, EPR study 0-66019
 dynamic Jahn-Teller effect in ESR spectra, Green's functions calcs. 0-84643
 inhomogeneous systems, line broadening, spin-spin and spin-lattice relax. rate meas. 0-58292
 manganese stearate: cadmium stearate, dil. quasi two-dimensional, ESR line width 0-71155
 mesophase pitch, magnetically-oriented, phys. props., mol. struct. 0-64885
 metals, cond. electron and spin scatt. due to dislocations 0-75856
 nitroxide spin probes, unresolved hyperfine broadening convection in EPR, linewidth and Heisenberg spin exchange freq. determ. 0-71180
 peroxylamine disulphonate, EPR lineshape, dispersion vs. absorpt. plots, modulation broadening and instrumental distortion 0-58290
 piperidinyloxy 2,2,6,6-tetramethyl radical, recrystallised samples, EPR study 0-100615
 poly-4-vinylpyridine, intramol. mobility and local density in soln. spin mark method obs. (Russian) 0-70107
 poly-4-vinylpyridine, mol. dynamics and local density in conc. soln., spin mark method obs. (Russian) 0-70108
 polyacetylene, mag. soliton defect ESR study 0-80590
 praseodymium ethylsulphate:Sm, one-dimens. X-Y system, spin dynamics, electron spin echo meas. 0-66031
 quinolinium (TCNQ)₂, random exchange Neisenberg antiferromag. chain, intermediate field magnetisation meas. 0-103857
 rare earth impurity, ESR, exchange induced broadening in low lying crystalline field system 0-108062
 rare earth pseudobinary intermetallic compounds, ESR studies 0-108064
 RE-1306 radiospectrometer improvement for crystals obs., use of LF modulation of magnetic field 0-57350
 ruby, distant nuclei ESR and ENDOR experiments, dipole-dipole reservoir importance 0-71241
 semiconductor with transition metal impurity states, EPR linewidth calc. 0-80599
 TCNQ salt, K-TCNQ, EPR linewidth, ang. and freq. depend. 0-80591
 1,2,4,5-tetrachlorobenzene, triplet exciton, ESR and optical absorption lines 0-96791
 tetramethylammonium(0), Li(CH₃NH₂)₄, existence, conduction- and localised-electron spin reson. 0-66035
 (TMTSF)₂PF₆, ESR g-factor, linewidth, spin susceptibility, metal-insulator transition 0-103887
 (TMTSF)₂PF₆ (AsF₆), linear-chain conductor, semicond.-metal transition in small elec. field 0-103730
 Ag foil, or film, conduction electron spin disorientation at surface 0-75855
 Al₂O₃:Cr³⁺, inhomogeneous spin system, time evolution towards saturated state 0-88869
 Au-Er, dil., EPR at 100 mK to 1K 0-66028
 Au-Yb, dil., EPR at 100 mK to 1K 0-66028
 C films with high conductivity, prep. and props. 0-80983
 CaF₂:Tm²⁺, ultra-low nuclear spin temp., low field behaviour, EPR study 0-100614
 CdCr₂Se₄, Crit. relax. processes, mag. reson. expts. 0-60425
 CdCr₂Se₄:Cu(Ag), ferromag. reson. and ESR line widths 0-60413
 CrN, antiferromagnetic EPR spectra, binding energy, isotropic exchange and ordering (German) 0-80604
 CsMnBr₃, EPR linewidth anisotropies 0-103878
 Cu complex, N,N'-ethylenbis(salicylaliminato) copper (II)-thiourea, in solns., bond strength and hyperfine linewidth, EPR 0-74186
 Cu complex, N,N'-o-phenylenebis(salicylaliminato) copper (II)-thiourea, in solns., bond strength and hyperfine linewidth, EPR 0-74186
 Cu foil, conduction electron spin disorientation at surface 0-75855
 Cu-Mn, exchange-coupled localised moments, Korringa relaxation rate 0-75851
 CuCr₂Se₄, Crit. relax. processes, mag. reson. expts. 0-60425
 EuLa_{1-x}Al₂, cryst. fields and exchange parameters, ESR meas. 0-71175
 Fe₃Ni₆Cr₄P₁₂B₆, Metglas 2826A, EPR at 20 GHz 0-75848
 Fe₂O₃ ultrafine particles in PTFE matrix, EPR and Mossbauer study 0-100625
 Gd³⁺ impurity ions, EPR spectra, linewidth narrowing due to spin-lattice relax. of lanthanide Kramers host ions 0-108061
 Gd(Fe,Al)_{1-x}, magnetic behavior 0-108079
 GdLa_{1-x}Al₂, cryst. fields and exchange parameters, ESR meas. 0-71175
 Gd₂Ni_{7-x}Al₃, EPR of Gd³⁺ ions 0-97139
 HgCr_{2-x}Al_xSe₄ and HgCr_{2-x}Ga_xSe₄, temp. depend. of ESR linewidth, 105-300K 0-71161
 K₂MnF₇, crit. EPR line broadening near Neel temp. 0-71165
 K₂Mn₂G_{8-x}F₁₆, impure two-dimensional system, ESR line reson. shift due to low symmetric spin distrib. 0-93162
 La-Gd, exchange-coupled localised moments, Korringa relaxation rate 0-75851
 LaBe₁₃Er, ESR, appl. of exchange induced broadening in low lying crystalline field system 0-108062
 (La_{0.3}O_{0.95}Co_{0.05})_{0.05}:Mn²⁺, X-band EPR study 0-60409
 MgO:Co²⁺, ESR linewidths of Co²⁺ 0-80596
 Mn II-lecithin lipid-water system, NMR and EPR obs. 0-61168
 Mn₂Al₂Si₂O₁₂, amorphous, spin-glass, insulating, Mn²⁺ mag. reson. 0-65918
 xMnO₂(100-x)[19TeO₂.PbO] glasses, EPR studies of Mn²⁺ ion distribution 0-71167
 O₂, liquid, exchange interaction, EPR absorpt. line shape anal. 0-71158

EPR line breadth continued

- PrIn₃:Gd, indirect nuclear exchange interactions, ESR-linewidth meas., sp. ht. determ. 0-103825
 PrNi₂-Gd, dil., single crystal, ESR study 0-75850
 RbMnBr₃, EPR linewidth anisotropies 0-103878
 SrTiO₃:Fe³⁺, order-disorder and central peak behaviour, EPR study 0-75970
 V₂O₅-CuO-BaO glass, unpaired electron localisation, ESR study 0-66026
 YbCl₃.6H₂O:Gd³⁺, EPR, temp. depend., spin-lattice relax. time 0-93173
 zinc formatedihydrate:Co, spin lattice relax. of Co²⁺ ions 0-75847
 Zn(BF₄).6H₂O:Ni, phase transition study, EPR of diluted Ni²⁺, 98-298K 0-75846
 (ZrO₂)_{0.9}(Y₂O₃)_{0.1}:Cr, Mn, stabilised single crystal, EPR of Mn²⁺ and Cr³⁺ 0-66024
 ZrSiO₄, natural, radiation defect centre, EPR obs. 0-75853

epsilon meson resonances see eta meson resonances**equalisers**

- outdoor classical music sound reinforcement systems compared 0-92011
 room acoustics correction, using Shure analyser (German) 0-58873

equations

- see also *Bethe-Salpeter equation; differential equations; equations of state; functional equations; integral equations; nonlinear equations*
 black holes, spherically symmetric, perturbations, linearised Einstein-Maxwell eqns. 0-72992
 convolution equation solution, problems arising, auditory appl. 0-94147
 Hill's equation in celestial mechanics, new exact method (Chinese) 0-105152
 Navier equation of dynamic elasticity, appl. of tensor spherical harmonics 0-98296

equations of state

- see also *equations of state of gases; equations of state of liquids; equations of state of solids; phase transformations; thermodynamics*
 ferrofluids, phase diagrams and eqn. of state 0-60280
 free boson gas in weak external pot. 0-86203
 free electron gas, n-dimens., eqn. of state (Spanish) 0-82718
 interstellar medium, eqns. of state rel. to role of OB stars in interstellar clouds form. 0-109506
 Ising model, one-dimensional transverse-field, in complex longitudinal field, real-space renormalization group method, T=0 0-103806
 liquid-vapour transition, non-Ising-like effects, eqn. of state, renormalisation group calc. 0-84286
 minimum energy reaction paths, virial theory implications 0-97686
 modified cell theory, eqn. of state for hard spheres 0-103445
 neutron stars, eqn. of state with pion condensate rel. to cooling 0-77443
 neutron stars, rotating, eqns. of state rel. to props. in bi-metric theory of gravitation 0-90466
 nucleon matter, eqn. of state at subnuclear densities 0-77278
 Peng-Robinson and Benedict-Webb-Rubin equations, calculations using TI-59 0-77738
 percolation, universal critical amplitude ratios 0-101765
 plasma, classical one-component, improved equation of state 0-83887
 second virial coeff. inversion for complete pot. energy functions 0-91628
 second virial coefficient, functional equations 0-103442
 second virial coefficient data, complete iterative inversion method calcs. 0-83448
 single phase liquids, thermodynamic stability limit and eqns. of state 0-92037
 spherically symmetric fluid, general relativity, equation of state, no slow uniform contraction 0-62544
 square well fluid, eqn. of state well width depend., Monte Carlo calc. 0-64853
 superdense celestial bodies, theory 0-67773
 supernovae, effects of core eqn. of state on outcome of stellar collapse 0-85928
 virial inequalities, quantum and relativistic 0-62609
 CO, second virial coeffs. 0-83440
 H, spin-polarised, mag. eqn. of state 0-100374
 He II, excitation spectrum and second virial coefficient calc. 0-102549
 Li plasma, elec. cond. at 12.5-50 MPa, (7-50)×10⁴K 0-64685
 Li-D equation of state under extreme conditions, solid state to plasma region 0-69976
 N₂, second virial coeffs. 0-83440
 SF₆, pair polarisability anisotropy, point atom polarisability approx. calcs. 0-87244
 Y₂O₃ plasma, eqn. of state investig. 0-75027

equations of state of gases

- binary solutions of dense liquids and gases, isothermal eqn. of state calcs. (Russian) 0-88292
 binary vapours, enthalpies of mixing 0-93791
 compressed gas, radial distrib. function hard sphere model 0-69961
 heterogeneous nonideal chemically reacting system, comp., thermodynamic props. calcs. 0-76492
 high-pressure gas equation-of-state meas. interferometry 0-77810
 multipole gases, second virial coeff. meas. 0-69959
 saturated steam parameters in reactor containments with escape of coolant, simplified calc. 0-68764
 supersaturated vapour, equilib. press. depend. on nucleating drop radius 0-69960
 thermophysical props. inversion, anisotropic pot. energy function generation 0-99531
 vapour pressure, prediction using equation of state 0-103443
 water vapour, perturbed-hard-sphere eqn. of state 0-96331
 weakly ionised gas non-ideal behaviour, virial eqn. of state and fugacity coeffs. 0-79424
 Ar, Clausius-Mossotti second virial coefficient 0-79426
 CO, heat capacity, calc. by modified Redlich-Kwong eqn. of state 0-69963
 H₂O, metastable state, fundamental equation 0-103447
 He, Clausius-Mossotti second virial coefficient 0-79426
 He-Xe, eqn. of state, Monte Carlo calcs. 0-59158
 He, gas, second virial coeff., acoustic determ., 1.28-2.13K 0-69965
 N₂, structural second virial coeff., intermol. pot. and mag. scatt. 0-78678
 Ne, Clausius-Mossotti second virial coefficient 0-79426
 O₂, structural second virial coeff., intermol. pot. and mag. scatt. 0-78678

equations of state of liquids

- alkali metals, crystalline and alkaline, eqns. of state, zero compression isotherms (Russian) 0-103446
 benzene, equation of state studied using statistical theory results 0-84276
 binary solutions of dense liquids and gases, isothermal eqn. of state calcs. (Russian) 0-88292

equations of state of liquids continued

- carbon tetrachloride, equation of state studied using statistical theory results 0-84276
 charged hard sphere dense classical fluid, equation of state and crit. point 0-64849
 dumbbells, nearly-Hookean, dilute soln., rheological equation of state 0-100321
 glass forming liquids, vol. relax. 0-96429
 hard core fluid with two-Yukawa tail, appl. to Ar 0-59618
 hard core fluids, asymptotic behaviour of virial expansions 0-88010
 hard disc fluid, infinite dilution solute chemical pot. by Monte Carlo simulation 0-88009
 hard sphere, surface tension, compressibility, bulk modulus press. coeffs. and Rao's acoustical parameter 0-80027
 hard spheres, quantum mechanical virial coeff., two point Pade approx. 0-79657
 hard spheres mixtures, equations of state for calc. thermodynamic props. 0-84301
 liquids, simple, thermodynamically self-consistent theories, radial distrib. function, functional derivative 0-92435
 metals, isothermal compressibility and eqn. of state at m.p. 0-79673
 mixtures, asymmetric, Henry's constants and second virial coefficients from perturbed-hard-chain theory 0-96621
 PET, P-V-T relationships 0-107400
 poly-4-methylpentene-1, P-V-T relationships 0-107400
 polyacrylamide, aq. soln., thermodynamic props., light scatt. obs. (Russian) 0-71439
 polybutadiene and butadiene-styrene in tetrahydrofuran, second virial coeffs. 0-65188
 polybutene-1, P-V-T relationships 0-107400
 polyethylene, branched, P-V-T relationships 0-107400
 polymer melt, eqn. of state analysis w.r.t. Ising fluid model 0-79907
 polypropylene, P-V-T relationships 0-107400
 polysulphone, P-V-T relationships 0-107400
 PTFE, P-V-T relationships 0-107400
 seawater, eqn. of state at high press. 0-101369
 simple fluids, hard and soft-core eqns. of state, termination temps., Kihara pot. 0-70360
 simple liqs. with repulsive forces, thermodynamically self-consistent theory 0-75139
 vapour pressure, prediction using equation of state 0-103443
 vinyl polymers, precip. from solns., temp. determ. (German) 0-85208
 Ar, liq., equation of state studied using statistical theory results 0-84276
 Ar modified droplet model, mean droplet interaction below T_c 0-70363
 D₂O, liquid, volumetric and derived thermal characteristics at low temp. and high pressure 0-107352
 F, hard sphere model with attractive interactions 0-96434
 H₂O, metastable state, fundamental equation 0-103447
 H₂O, modified droplet model, mean droplet interaction below T_c 0-70363
 Na equation of state, melting curve 0-103448
 O₂, modified droplet model, mean droplet interaction below T_c 0-70363
 Se, electronic transport props., equation of state, to 1900K and 1800 bars 0-65574

equations of state of solids

- alkali metals, bulk modulus and eqns. of state under press. 0-88293
 alkali metals, crystalline and alkaline, eqns. of state, zero compression isotherms (Russian) 0-103446
 alkali metals, partial pressure contributions to equation of state 0-107401
 anorthite, thermal eqn. of state up to 120 GPa, appl. to Earth mantle 0-109136
 crystals, anharmonic, with complex lattice, equations of state 0-107399
 densely packed crystals with strong sixth-order anharmonicity, eqns. of state 0-92637
 diamond, compressibility, appl. of Murnaghan eqn. of state, Morse pot. 0-79861
 Earth interior, Gruneisen function evaluated in harmonic approx. 0-72474
 elastic deformation, thermodynamics of, eqn. of state for solids 0-96589
 finite strain equations of state, evaluation using lattice model 0-96620
 Gruneisen coefficient at Earth interior conditions 0-72474
 guanidine aluminium sulphate hexahydrate:Cr³⁺, ESR spectra fine struct. 0-93169
 ionic crystals, binding forces and eqns. of state, inner electron contrib., calc. 0-64950
 metal, simple, non muffin-tin corrections to eqn. of state (French) 0-59906
 methane, crystalline, struct. and compression at high press., room temp. 0-107199
 molecular solids, melting curves, Lennard-Jones Devonshire theory 0-65201
 polyethylene, equation of state for semicrystalline, crystalline polymers 0-65187
 polypropylene, isotactic, equation of state for semicrystalline, crystalline polymers 0-65187
 porous solid, generalised p - α model, eqn. of state, sound vel. 0-65154
 reinforced plastics, equations of state, taking account of mech. damage 0-97553
 steel, high-strength, dynamic yield strengths, phase transition press. and Hugoniot parameters 0-75331
 Al, constitutive equation for porous materials with strength, press. effects 0-79875
 Al, shock wave data, 'solid Hugoniot' rel. to 'fluid Hugoniot' 0-65155
 Be, solid-state models, comparison 0-75332
 CaO, eqn. of state at high press., appl. to Earth core and mantle 0-109122
 Ce, high pressure phase transition, anomalous Gruneisen parameter behaviour 0-79934
 Cu, shock wave data, 'solid Hugoniot' rel. to 'fluid Hugoniot' 0-65155
 FeO, eqn. of state at high press., appl. to Earth core and mantle 0-109122
 *He, solid-fluid, eqn. of state, melting props. under press. 0-96721
 KBr crystals, binding forces and eqns. of state, inner electron contrib., calc. 0-64950
 (Mg,Fe)SiO₃, shock deform. expts., Hugoniot data implications 0-94497
 Na equation of state, melting curve 0-103448
 NaCl, eqn. of state to 32 kbar and 500°C, length change meas. 0-70361
 Pb(Zr,Ti)_{1-x}O₃, meas. of Hugoniot curve with commercial manganin stress gauges 0-70362
 p-H, solid, constant volume heat capacity and eqn. of state, temp. depend. 0-65334

equations of state of solids continued

- TiO₂, rutile phase, shock induced phase transition anisotropic behaviour 0-103475
 U, Hugoniot data, ultrahigh press. (TPa) shockwave from underground nuclear explosion 0-59580
equilibrium, chemical *see chemical equilibrium*
equilibrium, phase *see phase equilibrium*
equilibrium constants *see chemical equilibrium*
equilibrium diagrams *see phase diagrams*
equivalent circuits
see also network parameters; network synthesis
 Josephson junctions, coupled, I-V charact., model calc. 0-84559
 MHD generator, channel electrical characts., equivalent ccts. 0-75106
 MIS structure, elec. parameter meas. of second order equivalent ccts. 0-57332
 MOS capacitor formed over p-on-n semiconductor structure, G-V characts. 0-100532
 nonlinear magnetic field simulator for electromagnetic fields anal. (Japanese) 0-95756
 p-n heterojunction differential admittance theory in the presence of surface electron states 0-96981
 p-n junction, small signal equivalent circuit, finite carrier multiplication 0-65664
 photoconductor image charge transfer to electrographic film 0-101864
 piezo-transducer, broadband matching for acousto-optical devices (Russian) 0-64329
 solar cells, faulty, scanning light spot anal. 0-89625
 sonar transducer, Langevin type, made from Pb(Zr,Ti)O₃ type 1 ceramic, performance characts. 0-79095
erbium
see also nuclei with
 adsorption on W, field emission electron study 0-100393
 atom, L-shell internal excitation accompanying L-capture 0-95726
 Debye-Waller factor and Lindemann parameter, temp. depend., lattice dynamical model calcs. 0-59610
 L-line emission spectrum diagram line 0-84808
 magnetisation, quantum jump 0-60369
 silicide thin film formation on (100) and (111)Si substrate, backscattering study 0-70542
 vaporisation, heat of sublimation, meas. 0-103471
 Bi₂GeO₁₀:Er, luminesc., emission and excitation spectra 0-103975
 CaF₂:Er, defect structure, quenching effect, dielec. relax. and optical absorption 0-65031
 CaF₂:Er, near-Debye dielectric responses 0-71291
 Ca_{1-x}Sr_xF₂:Er³⁺ mixed crystal, luminesc. transition, inhomogeneous line broadening calc. 0-97332
 CdF₂:Er³⁺, Tm³⁺, evidence for Er³⁺→Tm³⁺ energy transfers, fluoresc. expts. 0-60655
 Er³⁺:KLu(WO₄)₂, room temp. stimulated emission obs. 0-106527
 LaBe₃:Er, ESR, appl. of exchange induced broadening in low lying crystalline field system 0-108062
 LaF₃:Er³⁺, optically excited, direct-process spin-lattice relaxation 0-93378
 LiYF₄:Er³⁺, electron-irrad. induced defects, optical and EPR study 0-66238
 LuCrO₃:Er³⁺, doping effect on ⁵¹Cr NMR in domain walls 0-71219
 LuYScO₄:Er³⁺, thermolum. meas. 0-97354
 RbMnF₂:Er, unirradiated and electron irrad., energy transfer 0-108254
 RbMnF₂:Er³⁺, absorption, emission, excitation and lifetime meas. 0-71460
 ScH₃:Er, proton distrib. and site energies, ESR meas. 0-59509
 SeOCl₂:Er³⁺, SbCl₅ acidified, Racah and Judd-Ofelt parameters in laser liqs. 0-106516
 YAG:Er, elastic wave damping, 300 to 1500 MHz, impurity effects 0-92602
 YH₃:Er, proton distrib. and site energies, ESR meas. 0-59509
 Y₂SiO₅:Er³⁺, EPR and spin-lattice relax. 0-108063
 ZnO:Er, electrolum. brightness, field strength and freq. depend. 0-100696
erbium alloys
 Au-Er, dil., EPR at 100 mK to 1K 0-66028
 Au-Er, ESR studies 0-108064
 CePd-Er, dil., low field mag. susceptibility, electro-nuclear effects 0-60189
 Co₆₇Er₃₃, amorphous alloy, sputtered, local order and amorphous struct. 0-88061
 Er-La, HCP, mag. phase diagram, neutron diff. meas. 0-70950
 ErCo₂, mag. excitations, RPA theory 0-65830
 ErCo₂, sorption at press. up to 1500 atm. 0-97819
 Er_{1-x}Co_x, amorphous alloys, thermal stability, elec. cond. enthalpy 0-100172
 ErFe₂, mag. excitations, RPA theory 0-65830
 ErFe₂-LuFe₂ (10, 90 wt.%), mag. props., 80-1300K (Russian) 0-75750
 ErFe₂-YFe₂ (30, 70 wt.%), mag. props., 80-1300K (Russian) 0-75750
 ErFe₂ and Er₂Fe₃, magnetostriction, room temp. to 80K 0-65993
 Er₂Fe₃, magnetostriction, temp. depend., 20 to 350K 0-65994
 ErFe₂H₃, multiplet absorption isotherms, theory 0-103564
 ErFe₂H₃, thermodynamic props., H₂ desorption isotherm meas. 0-89516
 Er_{1-x}Gd_xAl₃, effective mol. field at ¹⁶⁷Er, NMR meas. 0-71197
 Er_{1-x}Ho_xRh_{1-x}B₄, mag. and supercond. transitions, cryst. field effects 0-107950
 Er₂In, mag. props. 0-108009
 Er₂Ir₂, cryst. struct. 0-96473
 Er₂La_{1-x}Be₃, ESR studies 0-108064
 Er₂La_{1-x}Be₃, mag. sp. ht. and ESR, cryst. field interactions 0-60290
 ErNi₂, sorption at press. up to 1500 atm. 0-97819
 Er₂Os, cryst. struct. 0-96474
 ErPt₂, low temp. mag. susceptibility 0-93075
 ErPt, mag. susceptibility meas., mag. transitions obs. 0-60222
 ErRh_{1-x}Sn_{3-x}, new supercond./mag. cpds., X-ray powder diff. data 0-100215
 ErRh_{1-x}Sn_{3-x}, synthesis, supercond. and mag. props. 0-100547
 Er_{1-x}Tm_xRh_{1-x}B₄, mag. and supercond. transitions, cryst. field effects 0-107950
 Th-Er (1 at.%), Heisenberg exchange, residual resist. meas. 0-75558
 Ti-Er(Y), effects of Er and Y additives on deformation behaviour 0-81121

erbium compounds

- see also *erbium alloys*
 $\text{ErCO}_3\text{Y}^{3-}$, ($\text{Y} = \text{ethylenediaminetetracetate ion}$), formation constants (French) 0-104458
 triethyl sulphate, single cryst., H^+ coords., NMR 0-97152
 $\text{CsEr}(\text{MoO}_4)_3$, permittivity temp. depend., polymorphic transition 0-92670
 $(\text{Er,Nd})_3\text{PO}_7$, IR and Raman spectra, vibr. assignments, cryst. struct. characts. 0-97258
 Er_3Al_5 , Ga_2O_3 , LPE, spectroscopic props. 0-93419
 ErAsO_4 , ferroelectricity, dielec. meas. 0-60515
 $\text{ErCl}_3 \cdot 6\text{H}_2\text{O}$, single cryst., H^+ coords., NMR 0-97152
 ErCo_2Si_2 , mag. props. 0-107988
 ErD_2 , thin film, degradation during film processing, investigation 0-101047
 $\text{ErFe}(\text{CN})_6 \cdot 5\text{H}_2\text{O}$, powder, elec. transport props. obs. 0-70701
 ErFeO_3 , field induced spin reorientation, Mossbauer spectroscopy 0-65878
 ErFeO_3 , Raman scatt. from magnons, anisotropy const. determ. 0-66178
 ErFeO_3 , SAW meas. of magnetoelastic effects 0-75839
 ErFeO_3 , weak ferromagnet, μSR study 0-93226
 ErIG , high-field magnetisation, low temp. mag. anisotropy 0-75802
 ErIG , spontaneous Faraday rot. rel. to sublattice magnetisation 0-66159
 ErIG , superexchange operator and cryst. field interactions 0-59931
 ErMo_2Se_6 , mag. supercond., neutron scatt. obs. 0-70952
 ErN , miscibility with UC (German) 0-96654
 ErNi_2Si_2 , mag. props., 4.2-200K 0-84602
 $\text{Er}_2\text{O}_3\text{-GeO}_2$ system cpds., physicochem. characteris. 0-97469
 $\text{ErP}_2\text{O}_{14}$, X-ray cryst. struct. determ. 0-96486
 ErRh_2B_4 , ferromag. superconductor, vortex phase 0-80441
 ErRh_2B_4 , long ferromag. supercond., metastable supercond. state 0-103771
 ErRh_2B_4 , mag. supercond., NMR study of ^{11}B 0-107957
 ErRh_2B_4 , superconducting, magnetic dilemma 0-75680
 ErRh_2B_4 , superconducting thin films, crystal mag. field 0-75693
 ErTiO_3 , bulk mag. and struct. props., ferrimag. order 0-107993
 ErTiO_3 , magnetic structure determination, neutron scatt. study 0-65809
 $\text{Er}_2\text{Y}_{1-x}\text{Rh}_2\text{B}_4$, mag. and supercond. transitions 0-70874
 $\text{EuEr}_2\text{Ga}_{10}\text{Fe}_2\text{O}_{12}$, garnet thin films, magnetisation orientation, temp. depend. 0-71125
 Kf-ErF_3 , phase diagram 0-92645
 $\text{Na}_3\text{-Li}_x\text{ErSi}_4\text{O}_{12}$, solid electrolytes for Na/TiS_2 cells, synthesis, characts. and utilisation 0-107518
 $(\text{YErCa})_3(\text{Fe Ge})_2\text{O}_{12}$, mag. loss and domain wall mobility 0-65980
 $\text{Y}_{1-x}\text{Yb}_x\text{Er}_2\text{OCl}_2$, Er ion excited state decay and population (Russian) 0-100694

erection

- shrouded wind turbine, pilot plant construction 0-66931
 vertical axis wind turbines 0-66929
 wind turbine, variable pitch vertical axis, 2.4 m dia. prototype 0-61265

ergodic theorem see *statistical mechanics***ergonomics**

- see also *human factors; man machine systems*
 acoustic noise effect on performance of a psychomotor task, sorting during 90 dB(A) of pink noise 0-64283
 car drivers, work spectacles and functional visual fields (Italian) 0-108875
 design of materials satisfying acoustical and mechanical criteria 0-64234
 effect of vibration on reading numeric displays 0-104582
 ergometer for small-animal research 0-101295
 open-plan offices, role of acoustic screening 0-87650
 recording studios, leisure facilities for performers 0-69601

erosion

- Atlantic coastline, behaviour in Landes and Basque regions (French) 0-76987
 Baltic coastal beach scouring and accumulation by moderate sea disturbances (Russian) 0-81867
 SE. Baltic mainland shore moderately accumulative section morphodynamics (Russian) 0-67359
 channel bottom, kinematic characts. of nonuniform flow, limiting stability, erosion 0-94547
 chemical weathering of rock, meas. technique using U isotope ratio 0-77142
 cirques in Bear River Range, north-central Utah, numerical anal. 0-72510
 cohesionless bottom sediments, limiting stability in turbulent channel flow, erosion 0-94546
 cohesionless soils on channel bottom and sloping sides, onset of motion 0-94548
 Deimos, loose material downslope movement obs. 0-94737
 granular bed material, erosional capacity of smoothly varying streams, particle size 0-94545
 landform erosion simulation program 0-85650
 lunar rocks, erosion mechanisms rel. to microcrater and accretionary grain populations development 0-94732
 Mars outflow channels erosion, implications of sediment transport modes in channelled water flows 0-98363
 regolith reprocessing by cratering, erosion of material layer which loses charact. props. 0-62053
 river bank erosion rate, obs. in Devon, England 0-105002
 riverbeds, channel deformations, hydraulic modelling 0-77024
 rockfall from cliff face, seasonal variation obs. in N.Ireland 0-105001
 submarine canyons south of Iceland, obs. 0-90068
 CaCO_3 accumulations, erosion effects in Ontong-Java Plateau box cores 0-61793

error analysis

- see also *error correction; error detection*
 atmospheric precipitation acidity measurement, error anal. applied to indirect methods 0-72108
 ballistic galvanometer, error due to non-transient impulses, integral expression 0-86349
 Brorfelde transit circle, diameter corrections 0-105164
 concentricity, round parts, profile determ. (German) 0-57249
 correlation methods, signal parameter meas. 0-57241
 corrosion rates, error anal. in using 2 and 3 electrode polarisation resist. meas. 0-100930
 DC currents, low, new system of meas. 0-82791
 digital tachometers 0-90832
 electron diffraction patterns, of textures, reflection sphere curvature influence on reflection location geometry 0-87996

error analysis continued

- geodetic networks connection problems, stiffening problem, error anal. 0-81799
 graded index fibre, error estimates fo first order WKB calc. method 0-87488
 gravity base points, repeated meas. accuracy estimation (Chinese) 0-76892
 least squares method, generalisation 0-62028
 measurement error determination techniques, meas. of mass 0-57237
 measurement systematic multiplicative algorithm (Russian) 0-86245
 potential field data, constrained inversion, use of pseudohyperellipsoids 0-85752
 Seasat scanning multichannel microwave radiometer, antenna pattern corrections error analysis algorithm 0-94683
 seismic refraction method, vel. determ. and error anal. 0-90229
 stellar absolute luminosity calibrations, error discussion rel. to consistency 0-62111
 variable-potential coulometer analyser integration error analysis 0-93831
 X-ray small-angle scattering, information content and error anal., Shannon sampling 0-59340
 Pt resistance thermometers, temp. range influence on error to non-linearity (Russian) 0-90841
 W ribbon-filament temperature lamps, radiation error estimation 0-64128

error compensation

- see also *error correction*
 Fourier transform spectrometer, SNR enhancement by elec. filter compensation of slide velocity errors 0-95151
 interferometric measurement of sphericity standards (German) 0-87569
 multijunction thermal convertor AC/DC transfer, Thomson effect error reduction 0-103679
 optical multilayer filters, non normal incidence, optical monitoring, allowable tolerances (French) 0-87526
 thermoresistive convertor error compensation methods (Russian) 0-73363

error correction

- atmosphere measurements by double theodolite technique, control of inherent uncertainties 0-77160
 chopping pyrometer for remote meas. below 200°C (German) 0-86313
 cone absorption calorimeter for pulsed laser meas. 0-98980
 Earth EM sounding, VLF-EM profiles topographic correction based on model studies 0-101452
 electron diffraction patterns, of textures, reflection sphere curvature influence on reflection location geometry 0-87996
 monochromator scanning control system using microprocessor, spectral line shift correction (Japanese) 0-57384
 seismometer, long-period, drift corrections using borehole seismometer with stable period (Japanese) 0-67417
 systematic uncertainties, randomisation and quantitative assessment 0-98869
 thermocouple psychrometry, effect of and correction for different wet and dry bulb response 0-98472
 tomographic image, with aid of computer simulation 0-85470

error correction codes

- speech transmission, forward and backward prediction in adaptive differential PCM over nonideal channels 0-99902

error detection

- see also *error analysis*
 ECG, computer processing, measurement error determ. 0-94401
 optical storage focus error detection, skew beam and Foucault knife-edge techniques 0-102649

error recovery (computers) see *system failure and recovery***error statistics**

- 800 Mbit/s optical transmission experiments with dispersion-free fibres at 1.5 μm 0-58680
 hierarchical systems, calibration errors influence on end item performance 0-98788
 image registration using material information 0-99664
 probabilities of error in research statistical interpretation 0-90658

errors

- see also *measurement errors*
 atmosphere transmittance, algorithm accuracies 0-101429
 Earth surface temperature in mountainous terrain, diurnal var. prediction and errors 0-82011
 ECG, His-bundle activity detect., theoretical anal. of error during signal averaging 0-94392
 ECG telephone transmission, analogue and digital, errors and noise 0-94398
 elastodynamics, linear, discrete time approx. of initial boundary value problems, error estimates 0-73175
 image alignment errors due to aliasing 0-106480
 myoelectrically controlled systems, five-state, error rate obs. 0-72376
 neutrino physics, errors on ratios of small numbers of events 0-105879
 nuclear power stations, HTGR risk assessment, operator actions, event and fault tree anal. 0-63330
 refractive error stability of contact lens wearers 0-108879
 solar energy concentrators, generalised optical design technique, consideration of various errors 0-95979
 stellar spectral classification prediction from uvby β photometry, errors 0-67700
 stereo-pair images, correlation error prediction 0-102636
 system reliability in face of human (operator) errors, bibliography 0-94940
 tensile test, regulated, strength and deform. characteristic values, consistency (German) 0-93712
 VMOS dynamic memory, 65536-bit, investigation of alpha-particle induced soft errors 0-88223
 e^+e^- physics, errors on ratios of small numbers of events 0-105879

Esaki diodes see *tunnel diodes***Esaki effect** see *tunnelling***ESCA** see *electron spectroscopy; spectrochemical analysis; X-ray photoelectron spectra***estimation theory**

- see also *information theory*
 blind deconvolution, zero phase blurring function estimation 0-106482
 identifiable sound source location from time differences of arrival 0-91951
 linear state estimator design, updating budget, meas. theory 0-95058
 partitioned sub-optimal linear estimator, separate channel implementation 0-94949

estimation theory continued

passive sonar, errors in range and bearing estimation 0-79030
 signal-dependent film-grain noise, optimal image estimation 0-102659
 time series, conference, Nottingham, England (Mar. 1977) 0-82580
 variance-covariance-component estimation of Helmert type, introduction 0-101318

eta meson resonances

nonperturbative QCD, large N_c , QCD bag model, instantons and η' mass 0-57559
 η_c mass and other props, review from theoretical models 0-102025
 η (957) meson, quark model description for prod. and decay 0-62970
 $\eta \rightarrow \pi\pi\pi$, amplitude satisfying Adler conditions, relativistic quark pair creation model 0-95262
 $\eta \rightarrow \gamma\gamma(\pi^+\pi^-)$, chiral quark model anal. (Russian) 0-105900
 $\eta \rightarrow \pi\pi\pi$, $\delta\eta\pi$ and $\delta\eta\pi$ coupling constant ratio, $\delta(980)$ quark content 0-82955
 $\eta_c \rightarrow \psi\gamma$, charmonium, hyperfine interaction, nonperturbative treatment 0-62944
 $\gamma p \rightarrow \pi^+p$, 0.6 to 1.8 GeV, backward angles, η -cusp 0-57609
 $P \rightarrow \gamma l^+ l^-$, EM characts. for pseudoscalar meson decay in nonlocal quark model (Russian) 0-102050
 $\bar{p}p$ resonant annihilation, η_c charmonium state prod. cross section 0-82991
 $\pi^- p \rightarrow \eta(\eta')n$, 8.45 GeV/c, differential cross section ratio, η' decay branching 0-78094
 $\psi \rightarrow 3\gamma$, heavy narrow state search, η' and η_c branching ratios 0-57600

eta mesons

EM decay, η - η' mixing and gluons 0-62981
 hadron-hadron inclusive interactions, charmed particle production, η_c , ψ and other $c\bar{c}$ bound states 0-63036
 $M_{\psi-\eta_c}$ and $M_{\eta-\eta_c}$ lower bounds, concave and convex pots. 0-91057
 $\eta(\eta') \rightarrow \gamma\gamma$, quark model tests 0-78067
 $\eta \rightarrow \gamma\gamma(\pi^+\pi^-)$, chiral quark model anal. (Russian) 0-105900
 $\eta \rightarrow \mu^+\mu^-$, γ , branching ratio and η EM form factor 0-105899
 $\eta \rightarrow \pi\pi\gamma$, quark loop model, SU(3) splitting of quark masses 0-62990
 $\eta \rightarrow \gamma\gamma(\gamma\gamma)$, C-even meson radiative decay, SU(3), and VDM anal. (Russian) 0-68460
 η_c candidate evidence from SPEAR, crystal ball detector, recent results 0-74046
 η_c associated with gluon, hadronic prod. 0-105846
 $\eta \rightarrow \pi\pi\pi$, current algebra techniques, pole plus remainder model, chiral symmetry breaking and QCD 0-62972
 $K^- p \rightarrow \Lambda\eta$, 6 GeV/c, baryon exchange reactions, η NN coupling constant, Λ polarisation, nucleon-Regge exchange 0-78098
 $P \rightarrow \gamma l^+ l^-$, EM characts. for pseudoscalar meson decay in nonlocal quark model (Russian) 0-102050
 $\pi^- p \rightarrow \eta n$, Regge pole model with phenomenological residue functions 0-102077
 $\pi^- p \rightarrow \eta(\eta')n$, 8.45 GeV/c, differential cross section ratio, η' decay branching 0-78094
 $\pi^- p \rightarrow n\eta'$, 1.3 to 3.8 GeV/c, differential and total cross-sections 0-83000
 $\pi^- p$, 32 GeV/c, π and ρ^0 inclusive prod., f and η cross section estimates (Russian) 0-68499
 $\psi \rightarrow 3\gamma$, heavy narrow state search, η' and η_c branching ratios 0-57600
 $\psi \rightarrow \eta\gamma$, conflict with single parameter scheme for radiative decays of vector mesons 0-86720

etalons see interferometers**etchants see etching****etching**

see also crystal defects; dislocation etching; sputter etching
 active abrasive conc. determ. by static method based on etch figure stars count 0-74544
 CR-39 plastic, electrochem. etching, optimum conditions 0-95505
 diamond:Sb, implanted, radiation damage and annealing study 0-100263
 diamond, synthetic, oxidized in fused salts, etch features 0-97604
 diamond crystals, synthetic, etch-pit formation on cube faces, electron microscopy obs. 0-75232
 dry etched line edge profiles, computer simulation 0-71780
 electrochemical etching of fast neutron induced recoil tracks in cellulose triacetate 0-91406
 electrochemical etching studies of the CR-39 plastic solid state nuclear track detectors 0-91391
 electron microscopy on etched thin foils, comparative SEM, STEM and TEM analysis 0-100144
 freeze-etching improvement using evaporated film 0-85558
 glass shell, built-up, local strengthening influence on supporting capacity 0-71714
 Hastelloy-X, Ni-Cr-Fe-Mo, cyclic oxidation resist. improvement by high temp. etching treatment 0-97627
 hexafluoroethane, RF discharge chem., added acetylene effect, mechanistic model for fluorocarbon plasmas 0-84017
 Inconel 625, organic contamination removal by plasma cleaning and etching 0-97645
 ion milling, string segment motion algorithm 0-71779
 Josephson junction fabrication by ion implantation, electron beam lithography and dry etching 0-88693
 leucosapphire, Cr influence as impurity on thermochem. etching 0-88190
 lithography, heavy ion, tool for object investigation and replication 0-90931
 LR-115 plastic track detector, etching behaviour 0-99423
 metal, high melting point, electrolytic polishing and etching to reveal struct. (German, English) 0-89417
 metal, laser-photoinduced etching, photodissociation of dissolved complexed halogens in soln. 0-100929
 metal spheres, electromechanical polishing and etching 0-68188
 metal surface, plasma cleaning and etching, removal of C 0-97645
 MIS solar cells, etched slotted mask for direct deposition of metal contact pattern 0-97786
 narrow double-current-confinement channelled-substrate-planar laser fabrication by double etching 0-64073
 natural quartz SSNTD, etching characts. 0-91401
 particle track detectors, electron microscopy of etch pits 0-99424
 photographic emulsion grains, latent image distrib., etching and recrystn. effects of solns. 0-77890
 planar optical waveguide interconnection method 0-58671
 plasma etching, problems with creating vacuum (French) 0-101803
 plasma etching during NMOS VLSI circuits manufacture process and problems (Norwegian) 0-60090

etching continued

plasma industrial utilisation, synthesis, powder, metallurgical and surface treatments, review (French) 0-96398
 polystyrene, high impact, etching in $\text{CrO}_3\text{-H}_2\text{SO}_4$ soln. (Russian) 0-81223
 positive resist, plasma etching durability, additive effects 0-66683
 ruby, Cr influence as impurity on thermochem. etching 0-88190
 semiconductor, laser-photoinduced etching, photodissociation of dissolved complexed halogens in soln. 0-100929
 semiconductor, photosensitive etching in nonoxidising etchants 0-78813
 semiconductor films, production of oblique cuts 0-104309
 semiconductor photosensitive etching for hologram recording, attainable spatial freqs. 0-69343
 semiconductor thin sample etching for electron microscope exam. 0-86272
 p-Si, anodic etching for discriminating between elec. active and inactive defects 0-108605
 solid state nuclear track detectors, development of etched nuclear tracks 0-91384
 solid state nuclear track detectors, effect of etching conditions on energy resolution of phosphate glass and polycarbonate detectors 0-91390
 solid state nuclear track detectors, track registration and development efficiency 0-91385
 solid state nuclear track detectors, track registration and development efficiency 0-91386
 solid state nuclear track detectors, visualization of latent damage trails etching, decoration and observation techniques, review 0-91382
 steel, austenitic stainless, phosphide analysis using nonaqueous electrolyte potentiostatic etching method (Japanese) 0-89221
 steel, C, hot plastic deform., vac. colour etching investigation 0-61036
 steel, C, phosphide analysis using nonaqueous electrolyte potentiostatic etching method (Japanese) 0-89221
 steel, Cr, cold roll, frictional heating surface damage 0-76289
 steel, etchant for revealing austenite grain boundaries 0-85098
 steel, ferritic stainless, phosphide analysis using nonaqueous electrolyte potentiostatic etching method (Japanese) 0-89221
 steel, high strength dual phase, martensite/bainite differentiation using improved etching technique 0-100951
 steel, martensitic-ageing, etching technique, for revealing struct. inhomogeneities 0-61035
 steel, Nb microalloyed dual phase, etching technique 0-71809
 steel, stainless, Cr-Ni-Ti, metallographic detection of (Ti,Ni)₆C 0-66721
 steel, stainless, O₂ desorpt. during laser irradi., etching, AES study 0-66338
 steel, surface state influence on etching effect 0-81235
 steel sheet, surface anal. by ion etching and atomic absorb. spectroscopy (German) 0-81377
 steels, obs. and anal. of sulphides, using non-aqueous electrolyte-potentiostatic etching method (Japanese) 0-89433
 steels, stainless, surface characterisation rel. to adhesive bonding chem. etching, SEM, AES, XPS and electron probe microanal. 0-88416
 thin film deposition process, line-edge profile simulation appl. 0-104068
 track etch detectors, neutron energy depend. and threshold energy 0-61703
 transition metal silicides, refractory for ICs, review 0-100820
 triglycine sulphate, deuterated, reticulated target for pyroelectric vidicon, IR imaging 0-77858
 vacuum technique problems, with modern semiconductor processes (German) 0-86330
 Zircaloy-2, hot-pressed, influence of diffused C on structure and oxidation 0-61016
 AgCl, ionic space charge and dissolution 0-107431
 Al and Al alloy anodised oxide films, for adhesive bonding appls., AES and SEM study 0-66689
 Al film, and native oxide film, etching in carbon tetrachloride plasmas 0-76407
 Al foils, etching wastes appl. to corundum ceramics prod. 0-108376
 Al plasma etching, undercutting phenomena 0-97635
 Al solid electrolytic capacitors, pit etching method for improving freq. and temp. characts. 0-100944
 Al surface, plasma cleaning and etching, removal of C 0-97645
 Al-poly-Si Schottky-barrier solar cells, grain boundary effects on electrical behaviour 0-85279
 (AlGa)As DH lasers, comparison of 'normal' lasers and lasers exhibiting light jumps 0-106519
 As₂S₃ chalcogenide glass films, photographic Ag photodoping to produce negative relief image 0-59490
 Au, ¹⁹F recoil ranges by irradiation of O₂ with ³He and ⁴He particles 0-71931
 Au-GaAs Schottky barrier solar cells, effect of interfacial oxide layer on cell characts. 0-61365
 BaF₂ crystal, selective etching and dissolution kinetics 0-71775
 Bi₂Te₃, surface prep. by etching for electroplating elec. contacts 0-108647
 Cd-Sn alloy, superconductivity and microstructure 0-107949
 CdS thin film solar cell fabrication, HCl etching 0-81474
 CdSe photoanode improved efficiency by photoelectrochem. etching 0-104512
 Cu single crystals, neutron irradiated, secondary slip 0-88161
 Cu surface, plasma cleaning and etching, removal of C 0-97645
 Fe, cast, austenitic grain size determ. 0-81255
 Fe, sintered, influence of metallographic treatment on pore analysis 0-76417
 Fe-Si (2-8 wt.%), single crystals, growth striations, X-ray studies 0-79774
 (Ga,Al)As narrow double-current-confinement channelled-substrate planar laser fabrication, double etching technique 0-74371
 GaAs based MOS capacitors, scanning photovoltage investigation 0-80396
 GaAs etch solns. containing H₂O₂, correl. between etch and surface film characts. 0-71770
 GaAs, laser-induced microscopic etching 0-76379
 GaAs, vapor-phase etching, mechanisms and kinetics 0-100934
 GaAs wafer, double-etching technique for submicron channel fabrication, laser fabrication appl. 0-74387
 GaAs(Sb), electrochemical sectioning and surface finishing 0-108611
 GaInAsP-InP stripe laser, etched mirrors fabricated by wet chem. etch 0-99744
 GaP, vapor-phase etching, mechanisms and kinetics 0-100934
 Ge, black, solar selective absorber characterisation 0-80112
 H₂SO₄ etchant, for revealing struct. inhomogeneities in martensite-ageing steel 0-61035

etching continued

- HfC, etchant for revealing microstructure 0-85097
 n-InP, epitaxial layer, (100) surface chemistry, ESCA study 0-103552
 InP, laser-induced microscopic etching 0-76379
 InP p-n junction, grain boundary etching 0-96541
 InSb, optical constants and oxidation with various surface treatment (*Russian*) 0-88955
 n-InSb, phonon-assisted cyclotron reson. strongly depend. on surface condition 0-70755
 InSb, refractive index and absorpt. coeff., cryst. orientation depend. 0-60536
 InSb, single crystal, chem. and ion etching, surface changes (*French*) 0-108614
 Nb, mono- and polycrystn., crystallographic orientation, etching technique determ. 0-71814
 Nb-N(O)(C) system, specimen prep. for metallography (*German, English*) 0-89439
 NbC, etchant for revealing microstructure 0-85097
 Se-Ge amorphous films, obliquely deposited, photoinduced chem. changes 0-76385
 Se, Te, x_{Se} , growth of single crystals by Czochralski method 0-66423
 Si (001) wafer, pyramidal hillocks, TEM obs. during chemical etching 0-70508
 Si amorphous film, anisotropic etching phenomenon, appl. as solar selective absorber surfaces 0-72054
 Si, anomalous etch structures using ethylenediamine-pyrocatechol-water based etchants and their elimination 0-81217
 Si based MOS capacitors, scanning photovoltage investigation 0-80396
 Si blazed holographic grating fabrication by selective etching 0-74320
 Si chip manufacture for fibre alignment in lightguide cable connectors 0-64188
 Si compounds, plasma etching, gas flow-rate depend. 0-97603
 Si, Czochralski grown crystal, O precip., nucleation behaviour and dislocation loop form. (*Japanese*) 0-59664
 Si dislocation free, quantitative determ. of microdefect density by preferential chem. etching 0-65001
 Si, epitaxial (111) surface, etching observation of stacking faults, dislocations, S-pits, etch pits (*Chinese*) 0-70197
 Si, epitaxial wafer, saucer pit microdefects reduction by intrinsic gettering 0-75450
 Si, etching by CF_4 , plasma deposition reactor gas phase characts., mass spectra 0-70566
 Si, etching in $He-F_2$ plasma, etch rates, mass spectra, direct ion sampling study 0-79510
 Si film, MBE, cryst. defect props., substrate treatment effects 0-70551
 Si, optical waveguides along both sides of groove 0-96006
 Si, oxidation-induced Frank sessile dislocation loops, struct. change 0-75228
 Si, oxidation-induced stacking faults, distinction between clean and decorated faults by etching 0-79818
 Si photovoltaic low series resistance concentrator for high intensity appl. 0-93940
 Si, reactive ion beam etching expts., selectivity, anisotropy 0-104308
 Si semiconductor plates, control of quality of surface treatment, using Al spraying technique 0-60989
 Si solar cells, junction formation techniques using spray-on polymer dopants, cost effective, high throughput 0-94014
 Si spectroscopic applications of structures produced by orientation-dependent etching 0-93668
 Si surfaces etched in CF_4 or CF_4-O_2 plasma, morphology 0-93671
 Si, V-grooves formed by etching, phosphosilicate glass bridge struct. 0-104312
 Si wafers, floating-zone, etch struct. on microdefects as affected by dopants and surface treatment 0-79773
 Si/SiO₂ interface, precise wet-chemical etching, using rapidly rotating sample 0-93669
 Si₃N₄ antireflection coating for solar cells, reactive plasma process for forming metal grid patterns 0-93990
 Si₃N₄ layers produced by ion implantation, oxidation inhibition and etching 0-103374
 Si₃N₄, surface etching by laser-generated free radicals 0-71772
 Si₃N₄(SiO₂) plasma etching, plasma processes involved in dry processing using CF_4 active etchant species 0-79581
 SiO₂, etching characts. in trifluoromethane gas plasma 0-76392
 SiO₂, etching in $He-F_2$ plasma, etch rates, mass spectra, direct ion sampling study 0-79510
 SiO₂ film, prep. using high press. O_2 , residual stress, chemical etch rate, refr. index and density meas. 0-71768
 SiO₂ films sputtered in H-Ar mixed gas, enhanced step coverage 0-75470
 SiO₂, HF vapour phase etching, prod. viability for semicond. manufacturing and reaction model 0-81219
 SiO₂, masking film in alkaline etching 0-71771
 SiO₂, plasma etching with hexafluoroethane in radial flow reactor 0-76391
 SiO₂, plasma-chemical etching, spectroscopy 0-85243
 SiO₂, reactive ion beam etching expts., selectivity, anisotropy 0-104308
 SiO₂ relief, plasma etching, tapered wall prod. 0-97606
 SiO₂, surface etching by laser-generated free radicals 0-71772
 SiO₂, surfaces etched in CF_4 or CF_4-O_2 plasma 0-93671
 SiO₂ thermal film, freon ion beam etching, IR study (*Russian*) 0-76095
 SiO₂ thin thermally grown oxide layers etching in HCl, ellipsometric control of Si surface form. (*Russian*) 0-104315
 SiO₂-Al₂O₃-B₂O₃ glass mech. strength increased by etching 0-97609
 SiO₂-P₂O₅ glass film, CVD, P conc. profile by etch rate technique 0-96450
 SnO₂:P, CVD growth and etching characts., doping effects 0-107667
 Ta-N(O)(C) system, specimen prep. for metallography (*German, English*) 0-89439
 TaC, etchant for revealing microstructure 0-85097
 Te, growth of single crystals by Czochralski method 0-66423
 U prospecting using microdistrib. anal. of Siwalik vertebrate fossils by nuclear Track Etch tech. 0-98489
 V-N(O)(C) system, specimen prep. for metallography (*German, English*) 0-89439
 W [310] tip, prep. from rolled sheet 0-97447
 W, stacking fault stability determ. 0-96548
 ZnS ion beam etching, topographic changes, amorphisation, luminescence study 0-76078
- ether drift *see special relativity*
 Ettingshausen effect *see thermomagnetic effects*
 europium
see also nuclei with
 adsorption by Al₂O₃, radioactive waste storage 0-99240
 alkali halide:Eu²⁺, spin-Hamiltonian parameters, superposition model calcs. 0-96830
 alkaline earth halides:Eu²⁺, fluorescence lifetime and quantum efficiency for 5d-4f transitions 0-100681
 atom, electron impact excitation cross section, Born and Ochkur approx. 0-87230
 electrical resistivity of solid and liquid phases, thermopower, melting temp. 0-59955
 electronic struct. investigation by electron spectroscopy method 0-92812
 Al₂(WO₄)₃:Eu, and undoped crystals, luminesc. obs. 0-89047
 Ba₂SiO₄Br₂:Eu, blue emitting X-ray luminescent material for intensifying screens (*French*) 0-66260
 BeF₂:Eu³⁺ glass, luminesc. of Eu³⁺, transition probabilities 0-80845
 BeF₂:Eu³⁺ glass, struct. and optical props. 0-84067
 BeF₂:Eu³⁺ glass, struct., Monte Carlo simulations 0-96448
 Bi₂Al₂O₉:Eu³⁺, luminesc. expts. 0-60656
 CaF₂:Eu, dimer reorientation activation volume 0-107285
 CaF₂:Eu, CaF₂:Eu,Mn(Gd), single crystal predisintegration phenomena, SEM cathodolum. obs. 0-59502
 CaF₂:Eu²⁺, photoluminesc. mag. circ. polaris. 0-89056
 CaF₂:Eu²⁺, Sm³⁺, relaxed resonance acoustic phonons in vibronic anti-Stokes luminescence (*Russian*) 0-93404
 CaF₂:Eu³⁺, ¹⁹F NMR studies 0-60429
 CaF₂:Eu³⁺, VUV absorpt. spectra, dopant clustering 0-108230
 CdF₂:Eu²⁺, EPR spectra, hydrostatic press. and temp. effects 0-84648
¹⁵¹Eu (¹⁵³Eu) excitation transfer, effect on selective photoionisation 0-99538
 Eu²⁺ impurities in cubic crystals, 5d-4f radiative transition probability calc. 0-71474
 Eu³⁺ fluorescence spectra in rare earth oxyhalides (*French*) 0-89042
 Eu³⁺, rare-earth ions, charge transfer and crystal field theory 0-70654
 Eu+Sr, absorptive collisional energy transfer, laser induced excitation spectra 0-63584
 Eu+Sr, laser induced collisional energy transfer profile, high resolution study 0-83471
 Eu³⁺+UO₂²⁺ solution, nuclear pumped liq. lasers, LASL program 0-64011
 KCl:Eu, Eu²⁺ concentration effect on lattice parameter and density of crystals 0-88169
 KCl:Eu²⁺ crystals, photostimulated afterglow investigation at room temp. 0-108259
 KY₂F₁₀:Eu³⁺, cryst. field parameters and intensity parameters, J-mixing effects 0-59932
 La:Eu²⁺, liquid, γ -ray spectra observation of exchange interaction 0-84672
 La₂O₃:Eu, high press. effect on luminesc. efficiency and lifetime, charge transfer absorpt. 0-66266
 La₂O₃:Eu, slow phosphoresc., high press. study 0-80839
 LiNbO₃:Eu³⁺, luminesc. props., Li/Nb ratio effect 0-97323
 Lu₂(WO₄)₃:Eu, and undoped crystals, luminesc. obs. 0-89047
 NaCl:Eu, secondary Eu phase dissolution, EPR and optical absorpt. study 0-96655
 NaPO₃:Eu³⁺, luminesc. of Eu³⁺, transition probabilities 0-80845
 Sc₂(WO₄)₃:Eu, and undoped crystals, luminesc. obs. 0-89047
 SrB₂O₄:Eu²⁺, luminesc. of high-press. phases 0-100680
 Y₂O₃:Eu, cathodoluminesc. investig., appl. to cathode ray tube screening 0-108282
 Y₂O₃:Eu, high press. effect on luminesc. efficiency and lifetime, charge transfer absorpt. 0-66266
 YVO₄:Eu, cathodoluminesc. investig., appl. to cathode ray tube screening 0-108282
 ZrF₄:Eu³⁺ glass, luminesc. of Eu³⁺, transition probabilities 0-80845
- europium alloys
 indirect magnetic interactions, NMR anal. 0-71193
 EuAl₂Ga₂, synthesis, NMR and X-ray absorpt. studies 0-108083
 EuCu₂Si₂, interconfiguration fluctuation, NMR expts. 0-66069
 Eu₂La_{1-x}Al₂, cryst. fields and exchange parameters, ESR meas. 0-71175
 Eu₂La_{1-x}Al₂, dil. EPR, cryst. fields and effective exchange interaction 0-66029
 Eu_{1-x}La_xS, electron struct., lattice constns., X-ray spectral study (*Russian*) 0-100432
 EuPt₂ compounds, partial valence change, ¹⁵¹Eu Mossbauer and magnetisation obs. 0-70167
 Gd-Eu, magnetocrystalline anisotropy, magnetisation and torque curve meas. 0-65859
 La_{0.9}Eu_{0.1}Ni_{4.6}Mn_{0.4}, absorption-desorption props. of H₂, degradation mechanism, Mossbauer study 0-88431
 ScAl₂:Eu, intermediate valence on Eu ions, Mossbauer isomer shift 0-84587
 Sm-Eu, dil., mag. and elec. hyperfine interac., TDPAD obs., paramag. behaviour, exchange integral 0-103908
- europium compounds
see also europium alloys
 chalcogenides, cond. band spin struct. 0-71577
 chalcogenides, mag. polaron stability 0-96803
 chalcogenides, resonant Raman scattering model via magnetic exciton in ferromagnetic phase 0-93326
 chalcogenides, spin-dependent Raman scatt. from phonons 0-97274
 double metaphosphates with alkali metals or H, luminesc. props. 0-100675
 EuSe, photocond. and photodiffusive voltage spectra 0-96940
 niobates, mixed metal, Eu oxidation state, mag. props., Mossbauer study 0-66080
 sulphides, EuR₄, R=La, Ce, Pr, Nd, Sm, Gd, elec. cond. meas. 0-65555
 tantalates, mixed metal, Eu oxidation state, mag. props., Mossbauer study 0-66080
 tetrabutylammonium europium yttrium isothiocyanate, conc.-depend. electron-phonon coupling, and self-quenching 0-60657
 BeF₂-KF-CaF₂-AlF₃-EuF₃ fluoroberyllate glass, Eu³⁺ fluoresc. linewidth 0-66285
 C₂Eu intercalation compounds, three dimensional continuous melting 0-59631
 Eu complex, europium benzoyltrifluoroacetate chelate layers, fluorescence lifetime changes induced by variable optical environments 0-9³386

europium compounds continued

- Eu solid solutions with lanthanides, monosulfides, and oxides, vacant d states, X-ray absorpt. 0-103623
 Eu-B-C ternary and binary boundary systems, preparation techniques, X-ray analysis 0-60840
 Eu-Sr-S, spin glass materials, mag. field dependence of susceptibility peak 0-103840
 Eu₄As₄, mag. susceptibility and EPR meas. 0-71173
 EuAsO₄, ferroelectricity, dielec. meas. 0-60515
 EuB₆, electronic struct., transport and mag. props. 0-96782
 EuB₆, ferromag., spin-polarised energy band struct., APW calc. 0-96779
 EuB₆, ferromag. and antiferromag. sp. ht meas., 1.8-77K 0-65948
 EuB₆, Hall effect and resistivity data, ferromagnetic ordering temp., pressure depend. 0-60010
 EuB₆, resist., Hall effect, and magnetoresist. under hydrostatic press., 4.2 to 300K 0-96879
 EuB₆, resistivity press. variation, lattice const. 0-100456
 EuB₆, thermal expansion, X-ray method, room temp. to 1300 C 0-96670
 EuB₆, valence state of Eu, X-ray line displacement meas. 0-70633
 EuB₂O₇, X-ray cryst. struct. determ. 0-107135
 EuCu₂Si₂, mixed valence system, X-ray absorption spectroscopic study 0-80906
 EuEr₂Ga₂O₇Fe₃O₁₂, garnet thin films, magnetisation orientation, temp. depend. 0-71125
 EuF₂, thermal props. (*German*) 0-81355
 EuF₂, thermodynamic data compared with SrF₂ (*German*) 0-81355
 EuGa₂S₄(Se₄), mag. susceptibility and EPR meas. 0-71173
 Eu_{1-x}Gd_xO₃, mag. props., transport meas. 0-97117
 EuGd₂S₄, nonstoichiometric, elec. transport props., semicond. and metallic cond. 0-107786
 Eu_{1-x}Gd_xS, spin glass, transition temp., freq. depend. 0-97113
 EuLg:Ga(Al), pure and doped, mag. anisotropy, magnetisation meas. 0-60240
 Eu₂IrH₆, prep., cryst. struct., mag. and elec. props. 0-88117
 Eu₂Ir₂O₇, pyrochlore, sp. ht. below 20K, Debye temp. 0-65241
 Eu₂La_{1-x}Ta_xO₁₀, polycryst., luminesc. and excitation spectra 0-60659
 EuLiH₃, transferred hyperfine fields at Eu nuclei, NMR meas. 0-71195
 (EuLu)₂(FeAl)₂O₁₂, film epitaxial growth on Gd₃GaO₁₂ substrate, mag. props. 0-65402
 EuMo₂S₃, Chevrel phase, mag. interactions, LMTO energy band studies 0-70606
 EuNa₂Mg₂(VO₄)₃, disordered, thermal quenching of luminesc. 0-71472
 EuO (100), EELS, Eu valence in surface region and high energy giant reson. 0-84816
 EuO, Brillouin-Mandelstam scattering from thermal and excited magnons 0-70980
 EuO, cryst. field parameters due to 4f^{N-1}5D configs. 0-80230
 EuO, electronic struct. investigation by electron spectroscopy method 0-92812
 EuO, ferromagnetic electronic structure, absorption, thermoreflection and thermotransmission spectra (*French*) 0-97300
 EuO, ferromagnetic piezotransmission behaviour in magnetic field 0-97272
 EuO film threshold characteristics in holographic and bit recording (*Russian*) 0-63944
 EuO, light scatt. from spin waves and magneto-optic hysteresis meas. 0-97244
 EuO magnetic semiconductor, quasiparticle lifetimes, CPA study 0-65443
 EuO, magnetic susceptibility critical exponent, corrections to scaling 0-103846
 EuO nonstoichiometric film, ESR spectra and exchange interaction 0-93176
 EuO, spin order and fluctuations, Raman scatt. study 0-97273
 EuO, spin wave lifetime, theory compared with expt. 0-60228
 EuO, transmission and resistivity, stress modulation effect near Curie temperature 0-96874
 EuO:Gd, elec. cond. under hydrostatic press., Curie temp. 0-96881
 EuO:Gd, ferromag. semicond., electron spin polarisation and conduction band struct. 0-65449
 EuO:Gd, pure and doped, elec., mag., and optical props. rel. to electronic conc. 0-96880
 EuO:Gd, surface mag. props. 0-71566
 EuO:La(Gd), photothreshold changes below mag. ordering temp. 0-97406
 EuO:Sm³⁺, hyperfine field at Sm, TDPAC meas. 0-93215
 EuO_{1-x} single crystals, Faraday effect, near IR, effect of carriers 0-71395
 Eu₂O₃, thermophysical props. and neutron absorpt. 0-103488
 Eu₂O₃-Y₂O₃ solid soln. phases, synthesis 0-104132
 EuO(S)(Se)(Te), spin order and fluctuations, Raman scatt. study 0-97273
 EuO(Se), complex elec. cond. anomalies 0-107812
 EuO₂Sb₁₂, prep. and cryst. struct. 0-100211
 EuP₂O₁₄, luminesc. of Eu³⁺, transition probabilities 0-80845
 Eu₂PO₇ and (Eu,Nd)PO₇, IR and Raman spectra, vibr. assignments, cryst. struct. charact. 0-97258
 Eu_{1-x}R_xO_{1-x} (R=Nd, Eu, Gd), lattice parameters, mag. and elec. props. 0-100378
 EuRu₂Sb₁₂, prep. and cryst. struct. 0-100211
 EuS, amorphous, on W, memory effect in field emission 0-89126
 EuS, ferromag. semicond., high field susceptibility, spin waves 0-75735
 EuS, ferromagnetic electronic structure, absorption, thermoreflection and thermotransmission spectra (*French*) 0-97300
 EuS films, mag. and elec. props. rel. to stoichiometry and defects 0-97122
 EuS, light scatt. from spin waves and magneto-optic hysteresis meas. 0-97244
 EuS, single cryst., high-field susceptibility meas., temp. range 2.5 to 16.5K 0-84589
 EuS, spin order and fluctuations, Raman scatt. study 0-97273
 EuS, spin-assisted phonon Raman scatt., mag. phase depend. 0-71413
 EuS, thin film, Brillouin scattering from spin waves 0-65843
 EuS-Ga₂S₃-GeS₂, chalcogenide glasses, conditions of form. of glassy prod. (*French*) 0-100325
 Eu₂S₄, metal-insulator transition, cond. processes 0-96787
 EuSe, magnetic phase transitions, thermal modulation spectroscopy study (*French*) 0-97301
 EuSe, spin order and fluctuations, Raman scatt. study 0-97273
 EuSe, spin-assisted phonon Raman scatt., mag. phase depend. 0-71413
 EuSe, VPE by hot-wall technique 0-80958

europium compounds continued

- EuSe_{1-x}Te_x, transferred hyperfine fields at Eu nuclei, NMR meas. 0-71195
 Eu_{1-x}Sm_xS, ESR, exchange interaction, susceptibility, elec. cond., thermoelectric power 0-93174
 Eu_{1-x}Sm_xS, electron config. of Sm ions, X-ray L-absorpt. spectroscopy 0-60715
 Eu₂Sn₂Mo₆S₈, supercond. props. 0-97023
 Eu₂Sn₂S₁₂, mag. and thermodynamic props., metamagnetism 0-60273
 Eu_{0.4}Sr_{0.6}S, spin glass, spin dynamics, neutron scatt. study 0-65907
 Eu₂Sr_{1-x}S, Heisenberg spin glass system, excitations 0-84610
 Eu₂Sr_{1-x}S, insulating spin glass, sp. ht. near ferromag. onset 0-97106
 Eu₂Sr_{1-x}S, mag. clusters, spinodal decomp. trend 0-65923
 Eu₂Sr_{1-x}S, mag. ordering in dil. Ising and Heisenberg systems with competing interactions 0-65914
 Eu₂Sr_{1-x}S, magneto-optical redshift in absorpt. and photoluminesc., mag. short-range order 0-71388
 Eu₂Sr_{1-x}S, paramag. susceptibility, expt. and comparison with high temp. series expansion 0-60176
 Eu₂Sr_{1-x}S, spin glass, spin wave modes and low temp. sp. ht. 0-80538
 Eu₂Sr_{1-x}S, spin glass, transition temp., freq. depend. 0-97113
 Eu₂Sr_{1-x}S, spin glass to ferromag. transition, neutron scatt. and susceptibility meas. 0-60254
 Eu₂Sr_{1-x}S, spin-glass props. and mag. transition 0-97105
 (Eu₂Sr_{1-x})₂S, transferred hyperfine fields, NMR 0-71196
 (Eu₂Sr_{1-x})₂S, very dil., magnetisation dynamics 0-65915
 EuTe, antiferromag. semicond., Raman scatt., spin-phonon interactions 0-66185
 EuTe, high-temperature evaporation and reactivity 0-103469
 EuTe, mag. 'Bragg' scatt. obs. through Raman scatt. 0-66179
 EuTe, magnetic impurity states, mag. and transport props. 0-96913
 EuTe, magnetic phase transitions, thermal modulation spectroscopy study (*French*) 0-97301
 EuTe, spin order and fluctuations, Raman scatt. study 0-97273
 EuTe, spin-assisted phonon Raman scatt., mag. phase depend. 0-71413
 Eu_{1-x}Yb_xTe, (0<x<1), mag. semicond., elec., mag. and optical props. 0-97070
 Gd₂Eu_{1-x}B_x, solid solns., mag. susceptibility, 80 to 1000K (*Russian*) 0-88713
 La₂Eu_{1-x}B_x solid solns., thermal cond., 300 to 2000K 0-59741
 Tm_{1-x}Eu_xSe, semicond. with valence instabilities, cryst. chem. considerations 0-100213
 Tm_{1-x}Eu_xSe, valence instabilities, phase diagram 0-70651
 TmSe-EuSe, semiconductor-metal transitions 0-96953
 (YEuCa)₂(FeGeSi)₂O₁₂, mag. loss and domain wall mobility 0-65980
 (YEuTm)₂(GaFe₂)₂O₁₂ ferrite garnet films, mag. bubbles, translational motion, mechanism for inertial effects 0-100606
- eutectic alloys**
 binary, distribution coeffs., estimation from Van Laar and Hayes-Chipman relations 0-84293
 dendrite growth—the coupled zone 0-97489
 eutectics, HgTe-PbTe and Au-PbTe, prep. and thermoelectric behaviour charact. 0-107774
 glassy alloy prod. using low temp. melt spinning device 0-100825
 lamellar eutectoids(ic), stability principles 0-89195
 quasi binary eutectic systems, with inclusive phases, hardness, transform., decomposition (*Russian*) 0-97572
 single grained, directionally solidified, anisotropic yielding behaviour 0-103412
 steel, eutectoid, mech. behaviour, thermomech. treatment effects 0-84970
 Ag-Ge eutectic alloy, heat capacity meas. over temp. range 800-1200K (*French*) 0-88331
 Ag-Sm system, phase diagram, eutectic temps., microstruct. (*German*) 0-104119
 Al-Al₃Ni, electrolytic prep. of Al₃Ni fibres, SEM and anodic polarisation studies 0-100817
 Al-Al₃Ni eutectic, temp. gradients, microstructural changes 0-84971
 Al-Ca-Zn (5.5 wt.%) superplastic sheet alloy, mechanical properties, superplastic forming behaviour 0-60920
 Al-Cu (33 wt.%) eutectic, solidification under reduced gravity, behaviour of suspended Al₂O₃ particles (*German*) 0-60853
 Al-CuAl₃ eutectics, microstruct. after solidification, heat pipe influence 0-76243
 Al-Si, quasiisotropic, rheological deformation theory 0-79165
 Al-Si eutectic alloy, banded struct., SEM and optical microscopy 0-104144
 Al-Si(Ge) eutectic alloys in screened ohmic contacts for solar cells 0-94090
 Au-Co, liquidus line determ. by mag. meas. 0-60250
 Au-Ge/GaInAsP, ohmic contact, elec. charact. 0-80376
 Au-Si thin film double layer, silicide form., electron diff. study 0-80005
 Bi-Cd(Sn), eutectic, contact melting kinetics (*Russian*) 0-70377
 Bi-MnBi eutectic region, of Bi-Mn phase diagram 0-81034
 Cd-Ge broken lamellar eutectic composite, tensile and compressive props. 0-71694
 Cd-Sn binary system, high press. study 0-93539
 Cd-Tl binary alloy system at high press. 0-97461
 Cd-Zn binary systems, melts, elec. resist., 0-700°C 0-65517
 Cd-Zn eutectics, microstruct. after solidification, heat pipe influence 0-76243
 Co base alloy, creep-fatigue interaction in aligned eutectic and solid soln. 0-108554
 Co-(Cr,Co)₂C₃ eutectic, oxidation effect on toughness and strength 0-89404
 Co-Cr-C eutectic alloy, thermal conductivity and electric resist. at high temp. 0-103668
 Cr-(Cr,Co)₂C₃ eutectic, oxidation effect on toughness and strength 0-89404
 Cu-Cu₂e eutectic alloy, cast and directionally solidified, struct. and props. (*Russian*) 0-104138
 Fe-B(-Si), glassy, field-induced mag. anisotropy near eutectic comp. 0-93110
 Fe-C-Si, high purity, vacuum melted, nodular graphite form. 0-108452
 Fe-MuS eutectics, unidirectional solidification (*German*) 0-100827
 GaSb based eutectics, thermal cond. and diffusivity, 300-700K, phonon mechanism 0-103526
 Ge-Au eutectic alloys, field ion sources 0-97414
 Hg-Tl, phase limits, determ. by enthalpy functions along liquidus (*French*) 0-84911
 Hg-Tl amalgam, viscosity meas. 0-88349

eutectic alloys continued

- In-Zn binary system, melts, elec. resist., 0-700°C 0-65517
 InSb based eutectics, thermal cond. and diffusivity, 300-700K, phonon mechanism 0-103526
 Ir-Y eutectic alloy, supercond. transition enhancement due to lattice softening 0-103775
 Li-Pb eutectic alloys for fusion reactor solid breeder blankets, reactions with water 0-102297
 Li-Pb-cooled blanket for tandem mirror fusion reactor, neutronic anal. 0-99273
 Mo-Mo₂C(HfC)(TiC)(ZrC), eutectic formation of regular struct., crystn. (Russian) 0-66496
 Nb-Th, eutectic composition 0-100828
 Ni-Al-Cr₃C₂, directionally solidified, oxidation resistance, influence of Y 0-89409
 Ni-based TaC eutectic, directionally solidified, elastic moduli 0-84984
 Ni-Cr-Al-TaC, eutectic composite, microstructure, fatigue props. 0-85038
 Ni-Cr-NbC (18, 10 wt.%) eutectic composite, unidirectional solidification, thermal cycling, temp. range effect on microstructural degradation 0-89272
 Ni-NbC (10 wt.%), directional solidification and struct. (Russian) 0-84922
 Ni-Ni₃B eutectic, high temp. X-ray anal. 0-71639
 Ni-TaC, eutectic alloys, chem. incompatibility of ceramic nitrides for directionally solidifying 0-81046
 Ni-TaC eutectic superalloy, casting, furnace atm. effects 0-84880
 Pb-Sb, thermal analysis in non-faceted/faceted eutectic systems 0-71637
 Pb₂Li, ISSEC selection for fusion reactor 0-57950
 Si-Au eutectic alloys, field ion sources 0-97414
 Sn-Bi, thermal analysis in non-faceted/faceted eutectic systems 0-71637
 Sn-Pb (26%), liq. eutectic alloy Seebeck coeff. 0-84463
 Te-(Bi,Sb_{1-x})₂Te₃, electrophys. props., directed crystn. conditions influence and comp. depend. 0-107827
 Ti-Ag (10 to 17.5 wt.%), eutectoid system, $\beta \rightarrow \alpha_m$ transform., nucleation kinetics 0-97474
 Ti-Au, (9.9 wt.%), eutectoid system, $\beta \rightarrow \alpha_m$ transform., nucleation kinetics 0-97474
 Ti-Th, eutectic composition 0-100828
 Zn-Al (22 wt.%), eutectoid, low stress and superplastic creep behaviour 0-81120
 Zr-ZrC, eutectic formation of regular struct., crystn. (Russian) 0-66496

eutectic structure

- eutectics, HgTe-PbTe and Au-PbTe, prep. and thermoelectric behaviour chars. 0-107774
 irregular eutectic, branching limited growth 0-81042
 lamellar eutectoids(ic), stability principles 0-89195
 multi-component crystal growth, kinetic equation theory, binary system crystallisation 0-88071
 pattern selection in non-equilib. processes, marginal stability theory, eutectic solidification model 0-60852
 Al-Al₃Pt₂, eutectic alloys, unidirectionally solidified, struct. study 0-108394
 Al-Si alloy, quasisotropic, rheological deformation theory 0-79165
 Au-Ge contacts on GaAs, SEM and TEM obs. of struct. 0-100522
 CaF₂-AlF₃-Na₂AlF₆-(Al₂O₃), phase equilibria, X-ray diffr. and DTA meas. 0-108409
 Fe-Cr(W)-M, (M=Si,Mo,Ni,Mn,P,Cr), cellular growth of S-pearlite formed by carburisation 0-108486
 Fe-M, (M=Cr,W,Mo,V,Ti), morphology and growth kinetics of δ -pearlite formed by carburisation 0-108485
 Fe-Ni-Cr (35, 15 wt.%) superalloy, stress rupture and tensile props., C and B additions effect (Chinese) 0-104244
 KCl-CuCl eutectic fused salt, potential as intermediate temp. solar heat transfer and storage medium 0-101135
 La-CrO₃-W(Mo)(Cr) eutectics, prep. and microstruct. 0-108380
 Mo-TiC lamellar eutectic composite, deformation and strength, room temp. to 2073K (Japanese) 0-71702
 Te-based eutectics, crystn. rate effect on electrophys. props. mutual solubility effect 0-60774
 YCrO₃-W(Mo)(Cr) eutectics, prep. and microstruct. 0-108380

eutectoid steel see carbon steel**evaluation**

- see also computer selection and evaluation*
 building heat loss diagnostics, IR image evaluation requirements 0-86424
 dereverberation process evaluation by normal and impaired listeners 0-91974
 eye movement in target tracking using EOG 0-109057
 holographic interferogram quantitative evaluation procedures (German) 0-87344
 international collaboration among calibration services 0-101773
 lubricant evaluation, of oils used in cold rolling of steel 0-85068
 magnetically hard material demagnetisation curve evaluation 0-90869
 optical sensor system simulation and evaluation 0-96030
 physical optics farfield inverse scatt., mathematical inversion technique for nondestructive eval. 0-69580
 solid propellant stress transducer evaluation 0-81245
 standard sample homogeneity evaluation, optimal obs. planning 0-93721
 superfluous, meas. elimination, precision evaluation 0-90805

evaporated layer production see vapour deposition**evaporation**

- see also drying; field evaporation*
 aerosol, single droplet, size and mass meas. using electrodynamic balance 0-89535
 Amazon Basin, water recycling, ¹⁸O conc. study 0-81955
 atmosphere, continental maps of evapotranspiration (German) 0-98368
 atmosphere, surface evaporation rate rel. to steam fog form. in Fenland 0-98431
 atmosphere boundary layer, evaporation studies using portable differential psychrometer system 0-105072
 benzene adsorbent mesopores, capillary evaporation and struct. 0-107614
 BO₂-BO₂ 0-65252
 boiling point drying by volumetric abs. of RF and MW EM energy, heat and mass transfer chars. 0-79130
 bubbles, evaporating, surface condensation of vapours of high boiling substance 0-59021
 climate, evaporation rel. to water balance of Britain, 50000 yr BP to present day 0-72566
 crystal rough surface smoothing, during evaporation or condensation 0-103470

evaporation continued

- cutting fluid, hydrolysed polyacrylonitrile based, operational characteristics 0-89359
 desalination evaporator, falling-film, with vertically finned surfaces, hydrodynamics and heat transfer 0-58891
 evaporator design, for gas phase electron diffraction 0-57424
 hydrology, force-restore method for ground surface temp. prediction 0-98469
 infinite plate, thin liquid film evaporation, surface temp. and heat transfer 0-64346
 intensive evaporation processes, lifetime of drop rapidly evaporating in a heated gas medium (Russian) 0-74725
 lakes and rivers, evaporation from surface, scaling theory 0-109179
 laser radiation action on condensed medium, hydrodynamic effects 0-93439
 liquid, absorbing intense IR radiation, behaviour of pressure 0-102749
 plane evaporation boundary instability in laser radiation-matter interactions (Russian) 0-76111
 polymers, high-temp. pyrolysis, heat transfer processes at gas/solid surface (Russian) 0-61152
 porous cermet, heat transfer and stability for moving evaporating coolant 0-64563
 river watershed evaporative losses, Tigris and Euphrates 0-81957
 seawater boundary layer during evaporation, optical interferometry (Russian) 0-61919
 soil moisture, role in flood forecasting model 0-81951
 solar desalination unit with evaporation chamber, test results 0-96178
 solar evaporation and refrigeration units, assurance of specified energy parameter values, statistical analysis 0-93848
 spherical droplet, evaporation and condensational growth, mass transport calcs. 0-97736
 statistical mechanical theory of the kinetics of phase transitions, review, book contrib. 0-73270
 surfaces subject to cooling effects, nonlinear eqns. numerical soln. (German) 0-58893
 thin absorbing films, laser-induced removal, two-phase mechanism 0-97384
 thin films fabrication techniques 0-76176
 thin liquid films with extensive evaporation, heat transfer (German) 0-99920
 two-dimensional Lennard-Jones system, phase transitions, calc. 0-59621
 water, evaporation through monolayer free and monolayer covered surfaces, temp. gradients meas. 0-88402
 water evaporative cooling, convection and mass transfer, fog formation in boundary layers 0-79293
 water evaporative cooling, heat and mass transfer coeffs., fog formation effects 0-79294
 Al-Mg-Zn alloys, evaporation effect of alloying elements Mg and Zn in in-situ EM studies 0-103388
 BeO, heated on W, thermal anal. using mass spectrometric, technique, vapourisation behaviour 0-79932
 CaO, heated on W, thermal anal. using mass spectrometric, technique, vapourisation behaviour 0-79932
 Cd, inert gas effect on rate of evaporation 0-84285
 Co, particle formation by evap., electron microscopy obs. of interaction processes 0-104053
 Cr-Zr source improvement, diffusion barrier layer deposition for IC metallurgy 0-76163
 Cs₂CrO₄, mol. beam obs. of evap., saturated vapour press., 656.8 to 1151K 0-107411
 Cu-Ni, evaporation limited segregation 0-70513
 Cu₂S, Cu₃S, $\alpha \rightarrow \beta$ transition, thermographic investigation of heats, entropies and activation energies 0-88314
 EuTe, high-temperature evaporation and reactivity 0-103469
 Fe, particle formation by evap., electron microscopy obs. of interaction processes 0-104053
 He superfluid films, geometry induced third sound splitting 0-96712
 Hg, deposition, on W, evaporation energies 0-107666
 MgO, heated on W, thermal anal. using mass spectrometric, technique, vapourisation behaviour 0-79932
 N₂ adsorbent mesopores, capillary evaporation and struct. 0-107614
 Na evaporation from slot type capillary structs., crit. heat fluxes 0-74854
 Na, liquid, evaporation from capillary-porous struct., capillary restriction in initial stages 0-107609
 NaCl, cleavage faces, evaporation pattern determ. by decoration method in electron microscopy (German) 0-107626
 NaCl crystal rough surface smoothing, during evaporation or condensation 0-103470
 Na₂O-B₂O₃-GeO₂ system glass-forming melts, mass spectrometry obs. of thermodynamic props. 0-97468
 Na₂O-B₂O₃-GeO₂ vitreous melts, thermodynamic props. from mass spectra 0-65253
 Ni, particle formation by evap., electron microscopy obs. of interaction processes 0-104053
 Sb, cleavage faces, evaporation pattern determ. by decoration method in electron microscopy (German) 0-107626
 Sb₂Te₃, cleavage faces, evaporation pattern determ. by decoration method in electron microscopy (German) 0-107626
 Si:Sb, laser doping, evaporation loss and diffusion of Sb, under pulsed laser irradi. 0-59508
 SiO₂-water system, inorg. polymer struct. form., globular crystn. 0-101042
 YbTe, high-temperature evaporation and reactivity 0-103469
 Zn, inert gas effect on rate of evaporation 0-84285
 (Zn_{0.2}Co_{0.8}(Ni_{0.8})O)Al₂O₃, ZnO evaporation in vac. 0-59640

Evershed effect see sunspots**evolution (biological)**

- biosatellite Cosmos-782, biological expts. 0-61710
 ferredoxins, evolution of chloroplast-type from S. platensis [2Fe-2S] type and struct. of latter 0-94165
 interstellar molecules in prebiological evolution 0-94726
 land life emergence, implications of atmospheric O₂ content evolution 0-98400
 magnetic field of Earth, role in evolution 0-104883
 origin of life, chem. evolution (bibliography) 0-90620
 origin of life, mol. biophys. basis 0-94158
 palynofloral change at Cretaceous-Tertiary, boundary, Rb/Sr age from Hell Creek, Montana (Z coal) 0-94487
 review of ecology and systematics (book) 0-67945

exchange forces in nucleus *see nuclear forces*

exchange interactions (electron)

see also antiferromagnetism; ferromagnetism; RKKY interaction; superexchange interactions
actinide mononitrides, anomalous mag. props., planar coupling theory 0-60245
adsorbed layers, autoionisation bands due to one-centre resonances, theory 0-59790
aluminium copper tetrahalides, exchange, mag. anisotropy, and spin diffusion contribs. to EPR linewidth 0-80597
alkali dithioferates (III), electronic struct. and hyperfine interactions, $X\alpha$ calcs. 0-100448
alkali metals, magnetic property volume depend., Knight shifts, electron spin response 0-88729
alloys, magnetic anisotropy, influence of local symmetry (*Russian*) 0-93109
aluminoborate glass, Fe and Cr ion interaction, mag. and spectral props. 0-103883
amorphous alloys, indirect exchange interaction and paramag. Curie temp. 0-75752
amorphous Heisenberg and Ising chains, thermodynamics 0-108022
Anderson model, orbitally degenerate, exchange coupling in atomic limit, rel. to two-site Hubbard model 0-108000
anisotropic exchange interactions, effect on singlet ground state system 0-65852
Anisotropic magnetic ordering via combined spin and orbital exchange scattering of conduction electrons 0-65863
anisotropic spin-phonon coupling model, exact solutions (*Russian*) 0-100590
antiferromagnet, amorphous, spin waves, exchange fluctuations, calc. 0-65847
antiferromagnet, FCC, Ising model, mag. phase diagram, ordering, Monte Carlo calc. 0-103833
antiferromagnet chain, renormalisation group nearest neighbour interactions 0-60357
asperomagnetism, short-range order, in Heisenberg magnet 0-65941
Bloembergen-Rowland approximation, indirect exchange interaction, mean free path effects 0-60238
borosilicate glass, Fe and Cr ion interaction, mag. and spectral props. 0-103883
chemically induced dynamic spin polarisation, orientation depend. 0-63656
copper, benzoate, one-dimens. antiferromag., heat capacity, field-induced crossover of spin-dimensionality 0-97099
copper acetate, deuterated, dimeric, single crystals., inelastic neutron scatt. 0-92867
crystals, mag. struct., exchange multiplets 0-60202
cyclohexyl ammonium copper chloride, one dimensional spin $1/2$ ferromag., mag. props. 0-71000
degenerate narrow bands, intraatomic Coulomb and exchange energies 0-84452
diethylammonium copper tetrabromide, mag. struct., NMR meas. 0-71192
diisopropylammonium copper chloride, mag. interactions, susceptibility, 2-230K 0-60237
diluted Ising and Heisenberg systems with competing interactions, mag. ordering, appl. to Eu_2S_2 0-65914
dimethylammonium copper tetrachloride, ferromag., quasi two-dimensional, ordering temp., press. depend. 0-84601
disordered condensed media, with impurities, energy transfer 0-80217
dynamical local field corrections in dielectric function 0-88500
electron gas, dielectric function, dynamical exchange decoupling, plasmon dispersion, SDW and CDW 0-59900
electron gas, inhomogeneous, exchange effects and nonzero temps. 0-84444
electron gas, two-dimensional, internal energy, specific heat effective mass, temp. depend. 0-75513
electron scattering, exchange perturbation theory 0-78709
Falicov-Kimball model at atomic limit 0-65505
ferredoxin, Fe atoms at active centre, exchange integral of antiferromag. interaction 0-76697
ferromagnetic Neel mode with helical mode, coupling energy study (*French*) 0-70999
ferrites, ferroelec., coupled ferroelec. and spin waves, exchange interactions 0-70995
ferrites, inhomogeneous exchange interaction influence on ferromagnetic resonance line moments 0-75864
ferromagnet, effects of biquadratic exchange and uniaxial anisotropy on T_c 0-60329
ferromagnet, Heisenberg model, two-magnon reson. in absence of bound states, calc. 0-60423
ferromagnet, linear mag. birefr. (*Russian*) 0-93284
ferromagnet, magnon-phonon interactions, Heisenberg exchange red. 0-80494
ferromagnet, one dimensional, effect of biquadratic exchange on solitary waves 0-65836
ferromagnet, one-dimensional localised nuclear magnon modes 0-93098
ferromagnet, photoelectric effect rel. to saturation magnetisation 0-65618
ferromagnetic Ising model, band-mixed square-lattice: approx. crit. surface 0-70921
ferromagnetic systems, singlet-triplet, excitation spectrum, double-time Green's functions 0-84603
ferrous formate dihydrate, paramagnetic specific heat, decoration iteration transformation anal. 0-70938
films, ferromagnetic, perpendicularly magnetised, surface and vol. magnetoelastic waves (*Russian*) 0-93151
graphite, electronic struct. exact exchange HF calcs. 0-65438
guanidine aluminium sulphate hexahydrate: Cr^{3+} , ESR spectra fine struct. 0-93169
harmonic rotor model, interactions, spirals and phase transitions with and without long range order 0-60350
heavily doped semiconductor, n-type, disordered mag. system, hierarchy of exchange interactions 0-80235
Heisenberg antiferromagnet, one-dimens., impure, mag. susceptibility 0-60168
Heisenberg ferromagnetic system with biquadratic exchange interactions, spin wave theory (*Chinese*) 0-88755
Heisenberg model, disordered ferromag. states, random exchange integrals 0-80550

exchange interactions (electron) continued

Heisenberg multi-quadratic isotropic model, LRO, phase transf., exchange interactions (*Chinese*) 0-88756
Heusler alloys, ferromag. alignment rel. to conduction electron polarisation 0-60235
indirect exchange in Bloembergen-Rowland approx., ellipsoidal Fermi surface and relax. process effects 0-107754
intrinsic semiconductors, indirect exchange interaction, finite temp., valence bands and energy gaps effect 0-59943
(iron, chromium) carboxylates, heteronuclear trimer exchange clusters, ESR spectra 0-80603
Ising and Heisenberg inhomogeneous mixture, quenched system, critical temp. 0-88770
Ising chain, with next-nearest neighbour interactions, mag. responses to spin-Peierls transition 0-71054
Ising ferromagnet and antiferromagnet, two-dimens. square, ground state, apparent 3-spin interactions 0-88709
Ising model, random-bond, upper bond to sp. ht. on Nishimori's line 0-71068
itinerant electron ferromagnets, elastic props. and electronic struct. 0-66001
itinerant electron model, susceptibility, local exchange approx. calc. 0-60169
magnetic alloys, conc., density of states, Kondo effect, theory 0-65780
magnetic insulators with Jahn-Teller ions, temp. depend. of exchange integrals 0-103827
magnetic materials, symmetry and macroscopic dynamics 0-107973
magnetic semiconductor, indirect exchange interaction, mean free path effects 0-97088
magnetic systems with random interactions, upper bounds to be quenched free energy 0-103845
magnetically ordered crystals, exchange symm., mag. struct. (*Russian*) 0-65785
manganese stearate: cadmium stearate, dil. quasi two-dimensional, ESR line width 0-71155
many-electron systems, self-interaction corrected approach, beyond local spin density approx. 0-92844
Mattis model, modified, mag. relax. 0-65947
metal, electron-phonon interaction effects on spin susceptibility 0-93108
metal, indirect coupling between localised mag. moments by narrow band electrons 0-70942
metallic surface energy, exchange and correl. contrib., wave-vector decomp. 0-75615
metamagnet, compressible, renormalisation group theory of pseudocritical point 0-60337
multiple scattering method, eliminating α exchange parameter 0-103652
Neel mode, ferrimagnetic-helical [hh0] mode coupling vector model (*French*) 0-75770
NMR hybrid relaxation and multiple pulse methods for studying chemical, physical and spin exchange 0-80629
noncollinear magnetic order and spin wave spectrum in presence of competing exchange interactions 0-65834
nonequilibrium superconductors, ferromag. ordering of quasi-particles and rise of domains 0-107958
nonmagnetic metal, s-d exchange model exact solution, mag. susceptibility, mag. impurity interactions (*Russian*) 0-70943
one-dimensional random Glauber model, magnetisation relax. 0-80523
ordered magnetic cpds., selective sublattice dilution, percolation problem 0-103850
paramagnet, anisotropic, spin dynamics, exchange-bond dilution effects 0-88763
periodic systems electronic struct., LCAO SCF ab initio HF calcs. method 0-65419
polyvinyl alcohol film containing Cu^{2+} complexes, photoconductivity 0-107849
porous anisotropic magnets, approach to mag. saturation 0-93146
quinolinium (TCNQ)₂, random exchange Neisenberg antiferromag. chain, intermediate field magnetisation meas. 0-103857
rare earth binary insulating compounds, exchange interactions, paramag. susceptibility expts. 0-60177
rare earth impurity, ESR, exchange induced broadening in low lying crystalline field system 0-108062
rare earth intermetallic compounds, quadrupolar interactions, parastriction 0-60400
rare earth iron intermetallics, RFe_2 , (R=Sc, Lu, Y), mag. props., 80-1300K (*Russian*) 0-75750
rare earth metal impurity in metallic host, exchange interaction, electrical resistivity 0-84453
rare earth metals, magnon dispersions in ferromag. and screw structs., nonlinear s-f exchange interaction effect 0-75746
rare earth pseudobinary intermetallic compounds, ESR studies 0-108064
rare earth sesquioxides, exchange interactions, paramag. susceptibility expts. 0-60177
semiconducting surface inversion layers, exchange and correl. 0-75618
semiconductor, intrinsic, indirect exchange interaction, finite temp. effects 0-71003
semiconductor-based spin glass, indirect exchange interaction of localised spins 0-88768
semiconductors, indirect exchange interaction between localised moments 0-93079
semiconductors and insulators, mean free path and energy gap effects 0-88522
simple metals, ground state energy, structural expansion 0-88497
spin system, exchange energy near singular points or lines 0-93106
spin-1/2 cubic lattice, with anisotropic exchange, configs. 0-65926
strip films, bulk and surface spin oscils., mag. reson. 0-97149
superconductor with magnetic impurities, coexistence of superconductivity and ferromag., BCS and Zener models 0-88676
superradiance, dynamical behaviour in model mag. insulator 0-87358
TCNQ complexes, disordered, thermodynamics of random exchange models 0-103826
1,2,4,5-tetrachlorobenzene, triplet excitons, zero field ODMR 0-88891
transition metal, chemisorption of H, effect of surface spin fluctuations 0-75613
3d-transition metal ions, s-doublet struct., appl. of exchange correlation mass operator approx. 0-106266
trimethylammonium cobalt trichloride, metamagnet, AC susceptibility and exchange const. 0-70961
TTF-CuBDT, inter- and intra-chain exchange couplings, proton spin-lattice relax. time meas. 0-71220

exchange interactions (electron) continued

- two-dimensional electron fluid, second order exchange energy, correlation energy 0-107729
 X-Y model, biquadratic, spin one, variation of Curie temp. 0-97102
 Ag, valence-core electron exchange interactions, local approx. 0-91416
 Ar, solid, energy bands, depend. on choice of exchange-correlation pot. 0-70607
 Au-Gd(Y), dil., conduction electron-local moment exchange interaction meas. 0-60191
 BN, electronic struct., exact exchange HF calcs. 0-65438
 Ba₂NbRu₂O₁₂ and Ba₂TaRu₂O₁₂, (Ru₂O₁₂)¹³⁻ cluster obs. in presence of orbital degeneracy and spin-orbit coupling (*French*) 0-70655
 BaO-V₂O₅-CuO semiconducting glasses, impurity effects, elec. resist. and EPR study 0-103692
 CaLaFeO₃, two-dimens. mag. ordered, structural and mag. props. (*French*) 0-70173
 CdBr₂Co²⁺, exchange-coupled Co²⁺ pairs, optical absorpt. and Zeeman studies 0-66242
 CdCr₂S₄(Se₄), spontaneous magnetisation temp. depend., nuclear resonance freq. depend. (*French*) 0-80483
 CdCr₂Se₄, ferromag. semicond., conc. anomalies rel. to red shift of absorpt. edge 0-70732
 Cd_{1-x}Mn_xTe, indirect exchange interaction 0-97087
 Cd_{1-x}Mn_xTe, semimagnetic, exchange interactions between localised and delocalised electrons 0-97245
 CdS, doped, amorphous antiferromagnet model, susceptibility and spin-flip Raman scatt. meas. 0-97057
 α-Ce, exchange-enhanced, elec. resist. T² depend., press. effect 0-96845
 Ce mononitrides, anomalous mag. props., planar coupling theory 0-60245
 Ce₂Al₁₁, competition between ferro- and antiferromag. interactions 0-60258
 CeB₆, anomalous sp. ht. intrinsic mag. phase transitions obs. 0-108027
 CeB₆, mag. and electronic props. 0-71048
 CeC₂, mag. props. 0-108008
 CeDy_{1-x}C_x, mag. props. 0-108008
 Ce₂Mg₃(NO₃)₁₂·24H₂O, ground state with dipole-dipole and exchange interactions in external mag. field 0-84582
 Ce_{0.08}Y_{0.92}Sb, dilute f-electron system in cluster regime, crystal field and exchange splittings 0-97062
 Co complex, Co(II)(1,2,4-triazole)₂(NCS)₂ quasi two-dimens. canted S=1/2 antiferromag. 0-70976
 Co, energy band dispersion and mag. exchange splitting, angle-resolved photoemission meas. 0-71567
 Co, energy band dispersions and mag. exchange splitting 0-76146
 Co, liquid, Hall effect, band struct. and exchange scatt. 0-80250
 Co-CoO films, evaporated, exchange anisotropy 0-88841
 Co_{1-x}Te, fluctuating localised mag. moments, d band motion, Mossbauer study 0-65768
 CrN, antiferromagnetic EPR spectra, binding energy, isotropic exchange and ordering (*German*) 0-80604
 Cr₄(OH)₆(NH₃)₂Cl₆·4H₂O, exchange coupled mol. Cr³⁺ tetramers, inelastic neutron scatt. 0-65792
 Cs₂FeF₆, mag. struct. and one-dimens. antiferromagnetism 0-60209
 CsMnCl₂·2H₂O, subthreshold two-magnon absorpt., depend. on freq., temp. and mag. field, exchange coupling const. (*Russian*) 0-71184
 CsNiF₃, quasi-one-dimensional ferromagnet, subthreshold parallel pumping of magnons 0-75745
 Cu complex, Cu₂Cl₂(H₂O)₂·2 tetramethylsulphone, mag. interactions, susceptibility, 2-230K 0-60237
 Cu, NMR study on nuclear ordering below 1 μK 0-93187
 Cu-Mn, exchange-coupled localised moments, Korringa relaxation rate 0-75851
 n-CuInS₂, mag. props., obs. 0-70939
 CuSeO₅, strongly antiferromag. coupled Cu linear chain, orbital props. 0-100580
 DyAG, antiferromag., induced staggered mag. fields 0-65810
 Dy_{1-x}Sm_x, magnetoresist. of polycryst. specimens in fields up to 44 kOe (*Russian*) 0-92880
 ErFe₂YFe₂ and ErFe₂-LuFe₂, mag. props., 80-1300K (*Russian*) 0-75750
 Eu solid solutions with lanthanides, monosulfides, and oxides, vacant d states, X-ray absorpt. 0-103623
 Eu₂La_{1-x}Al₃, cryst. fields and exchange parameters, ESR meas. 0-71175
 Eu₂La_{1-x}Al₃, dil. EPR, cryst. fields and effective exchange interaction 0-66029
 EuO nonstoichiometric film, ESR spectra and exchange interaction 0-93176
 EuO:Gd, surface mag. props. 0-71566
 EuO:Sm³⁺, hyperfine field at Sm, TDPAC meas. 0-93215
 EuS, single cryst., high-field susceptibility meas., temp. range 2.5 to 16.5K 0-84589
 Eu_{1-x}Sm_xS, ESR, exchange interaction, susceptibility, elec. cond., thermoelectric power 0-93174
 Fe complex, Fe(1,2,4-triazole)₂(NCS)₂, quasi-2-dimens. S=1/2 antiferromag., mag. props., hidden canting 0-107986
 Fe, energy band dispersion and mag. exchange splitting, angle-resolved photoemission meas. 0-71567
 Fe garnets, sublattice magnetisation curves, Mossbauer study 0-75808
 Fe group, mol. Jahn-Teller reson. states as possible antecedents to magnetism 0-75701
 Fe, intercell exchange energy, Hartree-Fock approx. 0-60239
 Fe, liquid, Hall effect, band struct. and exchange scatt. 0-80250
 Fe, spin susceptibility, high-field, spin-density functional formalism 0-70959
 γ-Fe-Ni, local magnetisation of Fe atoms, Mossbauer effect meas. 0-75891
 FeF₂:Mn, antiferromag. reson. and local magnon mode, FIR laser study 0-66042
 FeF₃, amorphous, struct. and mag. props., computer model 0-96446
 (Fe_{1-x}Ni_x)₂P, Curie temp., press. depend. meas. 0-97091
 Fe₈₀P_{20-x}C_x(Si_{1-x}Ge_x), amorphous, size effect of metalloids on mag. props. 0-84594
 Fe₂Pt Invar alloy, anomalous Curie const., susceptibility meas. 0-75731
 Fe₂Pt Invar alloy, thermal expansion and spontaneous magnetisation, Invar anomalies, low spin model 0-71001
 FeSO₄, α- and β-forms, magnetic interactions, neutron inelastic scatt. study 0-107980
 Fe_{1-x}Te, fluctuating localised mag. moments, d band motion, Mossbauer study 0-65768
 Fe_{1-x}Zn_xF₂, dil. antiferromag., electronic and mag. props., Raman scatt. and optical absorpt. study 0-108207

exchange interactions (electron) continued

- Fe₈₀P_{20-x}C_x(Si_{1-x}Ge_x), amorphous, size effect of metalloids on mag. props. 0-84594
 Gd-Ni, ferromag., elec. resist. temp. depend. 0-96843
 GdAlO₃, canted antiferromagnetic, Mossbauer meas. 0-97171
 GdCo₅Ni_{1-x}Se_x, intrinsic coercivity, anisotropy, exchange and cryst. field interactions 0-75806
 Gd(Fe,Al_{1-x})₂, magnetic behavior 0-108079
 Gd₂La_{1-x}Al₃, cryst. fields and exchange parameters, ESR meas. 0-71175
 GdNi_{1-x}(x=3, 3.5, 8.5), ferrimag., mag. reson. above and below Curie temp. 0-97148
 Gd₂Ni_{17-x}Al_x, EPR of Gd³⁺ ions 0-97139
 Ge, spectral diffusion in acceptor-hole system at low temp., ultrasonic hole-burning expt. 0-92610
 H₂, relative magnitudes of direct and indirect exchange, Heitler-London calcs. 0-69069
³He, HCP, and adsorbed ³He with triangular lattice, exchange and mag. order 0-107606
³He, liq., exchange model 0-88387
³He liquid, exchange model, antiferromagnetic exchange field, susceptibility-specific heat ratio (*French*) 0-80019
³He, solid, four spin exchange model and magnetism 0-92752
 HgCr₂Se₄, spontaneous magnetisation temp. depend., nuclear resonance freq. depend. (*French*) 0-80483
 Hg_{1-x}Mn_xTe, indirect exchange interaction 0-97087
 Hg_{1-x}Mn_xTe, non-parabolic zero-gap semicond., indirect exchange interaction 0-80498
 Hg_{1-x}Mn_xTe, semimagnetic, exchange interactions between localised and delocalised electrons 0-97245
 Hg_{1-x}Mn_xTe, transverse magnetoresistance in quantised mag. fields 0-96922
 KCuF₃, one-dimens. antiferromag., spin waves, neutron scatt. study 0-65848
 K₂FeF₆, mag. struct. and one-dimens. antiferromagnetism 0-60209
 KMn₂Mg_{1-x}F₃, randomly diluted Heisenberg paramag. nucl. relax. 0-60444
 KZnF₃, exchange interactions of transition metal ions in orbitally degenerated excited states 0-65512
 La:Eu²⁺, liquid, γ-ray spectra observation of exchange interaction 0-84672
 La-Fe alloy, amorphous, sputtered at high rate, mag. props. 0-75753
 La-Gd, exchange-coupled localised moments, Korringa relaxation rate 0-75851
 LaAlO₃, exchange interactions of transition metal ions in orbitally degenerated excited states 0-65512
 LaBe₁₃:Er, ESR, appl. of exchange induced broadening in low lying crystalline field system 0-108062
 La_{1-x}Tb_xAl₃, competing paramag. anisotropy from cryst. field and indirect quadrupolar coupling 0-60180
 MgO:Fe²⁺ single cryst., exchange energy 0-96834
 MgO:Ni²⁺, near IR luminesc. from isolated and exchange-coupled Ni²⁺ ion pairs, temp. depend. 0-93382
 Mn-Bi micromagnetic alloy, mag., elec. and elastic props. (*Russian*) 0-108028
 Mn(CN)₃(H₂O)₃, mag. interactions, theory 0-97085
 Mn₂N, mag. struct. non-collinearity, neutron diff. obs. 0-65796
 MnP, ferro-spiral transition, neutron scatt. studies 0-65876
 Mn₂Sb, spin-wave dispersion relations, exchange interactions, neutron inelastic scatt. 0-65832
 α-MnSeO₄, magnetic interactions, neutron inelastic scatt. study 0-107980
 Na₂O-B₂O₃:Cu²⁺, Mn²⁺ glasses, Cu²⁺-Mn²⁺ interaction studied by ESR 0-93166
 Ne, solid, energy bands, depend. on choice of exchange-correlation pot. 0-70607
 Ni, band struct. and multielectron excitations, angle-resolved photoemission determ. 0-76147
 Ni, energy band dispersion and mag. exchange splitting, angle-resolved photoemission meas. 0-71567
 Ni, exchange splitting of 3d bands, angle-resolved photoemission meas. 0-71568
 Ni, ferromag., exchange integral maximisation, neutron scatt. obs. and ten-fold degenerate Hubbard model comparison 0-71004
 Ni, ferromag. props., teaching expt. 0-82608
 Ni, liquid, Hall effect, band struct. and exchange scatt. 0-80250
 Ni-Fe Invar, thermal expansion and spontaneous magnetisation, Invar anomalies, low spin model 0-71001
 Ni-Pd, high mag. field effects, mag. isotherms near Curie point, exchange splitting energies 0-60272
 Ni-Pd, mag. moment distrib., one-mag.-species model calc. 0-65788
 Ni-Rh, mag. moment distrib., one-mag.-species model calc. 0-65788
 Ni₃Co_{3-x}O₃, composition depend antiferromagnetic-ferrimagnetic ordering, mag. susceptibility meas. 0-70973
 NiPtCl₆·6H₂O, singlet-ground-state magnets, ESR at low temps. 0-97132
 NiSnCl₆·6H₂O, singlet-ground-state magnets, ESR at low temps. 0-97132
 Ni_{1-x}Te, fluctuating localised mag. moments, d band motion, Mossbauer study 0-65768
 Ni(001) surface states, surface magnetisation, electron spin polarisation 0-88612
 Ni(110), mag. exchange splitting of electronic surface states 0-88610
 O₂, liquid, exchange interaction, EPR absorpt. line shape anal. 0-71158
 Pb₉Sn₁₀F₂, NMR study of F atom motion (*French*) 0-100622
 PbTe:Fe, single crystals, state and behaviour of Fe, mag. props. 0-93080
 Pd₉₉Fe₀₁Gd₀₀₁, Pd-Gd exchange const., neutron diffuse scatt. meas. 0-71002
 Pd₂MnIn_{1-x}Sn_x and Pd₂MnIn_{1-x}Sb_x, Heusler alloys, mag. order, disorder effects 0-88723
 Pr₂Ca₂MnO₇, struct. and magnetisation study 0-65804
 PrCo₂, strongly exchange-enhanced paramagnetism, susceptibility 0-60179
 PrFe₂, Laves phase, mag. props., Mossbauer spectra, crystalline field mag. anisotropy 0-65851
 PrIn₃, nucl. orientation of ¹⁴⁴Pm in singlet ground state, exchange interaction and cryst. field splitting obs. 0-71275
 PrIn₃:Gd, indirect nuclear exchange interactions, ESR-linewidth meas., sp. ht. determ. 0-103825
 PrNi₂-Gd, dil., single crystal, ESR study 0-75850
 Rb, valence-core electron exchange interactions, local approx. 0-91416
 Rb₂FeF₆, mag. struct. and one-dimens. antiferromagnetism 0-60209
 Sc-Gd, dil., reverse resist. anomaly and negative magnetoresist. 0-84459
 SiC, laser Raman spin-flip scatt. from excitons, luminesc. 0-80786

exchange interactions (electron) continued

- Sm-Eu alloy, dil., mag. and elec. hyperfine interac., TDPAD obs., paramag. behaviour, exchange integral 0-103908
 Sm₂Se₄, valence fluctuation, mag. susceptibility meas. 0-97056
 SnTe:Mn, NMR shift meas. 0-97154
 TbCo₂, magnetocrystalline anisotropy and spontaneous magnetostriiction 0-75831
 TbCo₅, sublattice magnetisation, temp. depend., neutron diffr. anal. (Russian) 0-103815
 TbP (As)(Sb)(Bi), mag. transitions, quadrupolar interaction effects 0-80512
 TbZn, mag. excitations meas. 0-70979
 TeCr₂O₆, exchange interactions within binuclear entity (Cr₂O₁₀)¹⁴⁻ 0-60236
 Th-Gd(Tb)(Dy)(Ho)(Er)(Tm)(Lu) (1 at.%), Heisenberg exchange, residual resist. meas. 0-75558
 Tm-Zn, paramagnetism, mag. excitations, exchanges interactions 0-88718
 TmSe, intermediate valence cpd., susceptibility, single-ion approach 0-70935
 TmSe, mag. props. 0-97086
 TmSe, valence mixing, mag. props. obs. 0-70648
 U(SiSe)(Te), electronic struct. and exchange band splitting, optical refl. meas. 0-66226
 V₂O₅-CuO-BaO glass, unpaired electron localisation, ESR study 0-66026
 WCr₂O₆, exchange interactions within binuclear entity (Cr₂O₁₀)¹⁴⁻ 0-60236
 WV₂O₆, exchange interactions within binuclear entity (V₂O₁₀)¹⁴⁻ 0-60236
 WV₂O₆, magnetic susceptibility, behaviour in terms of quasi-isolated binuclear units 0-97073
 Y-Gd, dil., reverse resist. anomaly and negative magnetoresist. 0-84459
 Y_{1-x}R_xCo₂, R=Gd,Tb,Nd, ferrimag., magnetisation, exchange interactions, mag. anisotropy 0-80565
 YbFe₂, cryst. elec. field and exchange interac., ¹⁷⁰Yb Mossbauer obs., magnetostriiction contrib. 0-108124
 ZnGa₂O₄Cr³⁺, weak exchange interaction determ., ESR study 0-93107
 Zn_{1-x}Ge_xFe_{2-x}O₄, double exchange magnetism, Mossbauer study 0-66087

exchange models see peripheral models**exchanges (chemical) see chemical exchanges****exchanges (telephone) see telephone exchanges****excimer lasers**

- atomic and molecular lasers appl. to collision physics 0-63596
 backward Raman amplifier for excimer laser pulse compression, parasitic superfluoresc. suppression 0-69453
 book, gaseous electronics and gas lasers 0-73120
 discharge pumped multiwavelength lasers (Chinese) 0-102703
 electric discharge pumped excimer laser model 0-58516
 electron beam system for laser excitation, coaxial diode 0-86509
 inert gas, electroionisation discharge, negative cathode pot. drop 0-79615
 inert gas halide lasers, 60-ns electron beam excitation 0-74340
 inert gas halides, exciplex mol. form., rel. to laser operation 0-81318
 inert gas halides, laser mechanism, excitation methods and appls. 0-95871
 inert gas mixture, electrophotoionization discharge, laser pumping 0-91781
 inert gas nuclear pumped lasers, prod. efficiency of excited states 0-63998
 inert gases, self-sustained discharge possibility with bulk photoionisation impurities 0-75113
 nuclear generated plasmas, ³He and ²³⁵UF₆ excitation, spectra obs. 0-83997
 optically pumped mol. lasers, review 0-58519
 photoionisation excimer laser chars. 0-102712
 pumping, quasi-reson. energy and charge exchange processes, new transitions 0-58526
 XeF laser wavelengths, transient absorpt. in electron-beam excited inert gases 0-83592
 Ar-Hg-Cl₂, elec. discharge, electron inelastic collision props. 0-79617
 Ar-Kr-F₂, nucl. pumped laser, high energy beam deposition 0-63999
 Ar-N₂ mixture, electron beam pumped, lasing obs. at 337, 358, 380 and 406 nm 0-102700
 Ar-N₂ mixture, lasing at four lines 0-99713
 ArF excimer laser, electron-beam pumped, efficiency and gain 0-78844
 ArF excimer laser multiphoton ionisation mass spectra 0-81381
 CO* prod. from Ar*+CO₂, use in laser systems 0-63824
 C^{III}, effective lifetime in N and air 0-102704
 ClF UV laser system 0-83597
 Cs-Xe solar-pumped MHD excimer laser, modelling 0-95873
 F₂ UV laser system 0-83597
 H₂ laser, VUV, with sealed gas-discharge tube 0-74399
 HgBr₂+ inert gas metastable atom (N₂(A³Σ_u⁺)), dissociation 0-63774
 HgCl₂(Br₂), low lying excited state electronic struct. and photodissoc., appl. to lasers 0-63560
 HgH, two-level laser system, discharge simulations 0-74351
 HgTl excimer laser, kinetics, optical excitation obs. 0-58527
 I₂, efficient laser action on 342 nm band, ArF laser pumping 0-99703
 I₂ laser, three-level, pumped by CW dye laser 0-63993
 I₂ molecule B-X electron transition during Cu vapour laser optical pumping (Russian) 0-78845
 IF emission spectrum and form. kinetics in electron-beam-produced plasma 0-102533
 KrCl, B and C states, energy ordering from temp. depend. of emission spectra 0-78837
 KrCl laser, lifetime extension by H addition 0-91773
 KrF 1J avalanche discharge laser unstable resonator expts., beam divergence 0-74404
 KrF electroionisation laser, energetic, threshold and spectral chars. 0-99705
 KrF, electron beam pumped laser medium, time depend. fluoresc. spectrum in high current density range 0-78842
 KrF, excimer lasers, state of art 0-95879
 KrF laser, kinetic model, limiting behaviour and scaling 0-78838
 KrF laser driven methane backward Raman amplifier, high-efficiency energy extraction 0-106533
 KrF laser induced preionization of XeCl discharge 0-84020
 KrF mini-laser operation at high repetition rate 0-74396
 KrF, photoionisation excimer laser chars. 0-102712

excimer lasers continued

- KrF* laser, generation of high-spectral-brightness tunable XUV radiation at 83 nm 0-91846
 KrF* nuclear pumped lasers, excited state prod. rate and fission power pulse shape matching 0-63998
 KrF* tunable ultrahigh spectral brightness excimer laser source 0-64046
 Li₂, ³Σ_g⁺+³Σ_g⁺ excimer emission, ab initio calcs. 0-91608
 MgXe excimer bands, emission intensities and excited-state densities meas. 0-92413
 N₂ helical TE laser, tube geometry simplification 0-69406
 N₂ high power discharge laser excited through high dielectric constant ceramic materials 0-58572
 N₂, IR laser transition, excitation process 0-87383
 N₂ laser, 406 nm emission on C-B band 0-64047
 N₂ laser, appl. of pulsed transversally excited discharge (French) 0-107009
 N₂ laser, construction and properties, axial or cross-field discharge 0-69418
 N₂ laser 337.1 nm transition, rotational struct. variation 0-78836
 N₂ multi-stage TEA laser 0-95912
 N₂ pulsed laser, construction and theoretical explanation (Slovak) 0-95874
 N₂ superfluorescent UV laser, demonstration 0-105475
 N₂ UV pulsed laser with Blumlein pulse generator, fabrication (Japanese) 0-69417
 N₂-He plasma, laser produced, high press. amplified stimulated emission 0-78843
 N₂-SF₆ pulsed discharge laser with CW X-ray preionisation 0-95910
 Na-Xe, high-power discharges, models 0-69373
 Na₂, ³Σ_g⁺+³Σ_g⁺ excimer emission, ab initio calcs. 0-91608
 S₂, optically pumped superfluorescence molecular laser 0-63990
 Ti-Hg, excimer band emission from electron beam initiated discharge in TlI-Hg 0-78841
 Ti-Xe, excimer band emission from electron beam initiated discharge in TlI-Xe 0-78840
 Xe, atm. press. and low e-beam excitation rates, expt. studies 0-78863
 XeF two module discharge laser, gain and temporal chars. 0-87385
 Xe₂ excimer laser, electron beam excitation, VUV fluoresc., lasing 0-87379
 XeBr, B and C states, energy ordering from temp. depend. of emission spectra 0-78837
 XeBr electric discharge pumped laser (Chinese) 0-102701
 XeCl, B and C states, energy ordering from temp. depend. of emission spectra 0-78837
 XeCl, electric discharge excimer laser with intense preionisation 0-63991
 XeCl electroionisation laser, energetic, threshold and spectral chars. 0-99705
 XeCl, excited by discharge stabilised by electron beam 0-63992
 XeCl frequency-tuned laser, coherent tunable vacuum UV near H Ly-β transition 0-99798
 XeCl, high-energy subnanosecond pulse amplification 0-99770
 XeCl laser, B-X, form. and quenching kinetics 0-74341
 XeCl laser, lifetime extension by H addition 0-91773
 XeCl mini-laser operation at high repetition rate 0-74396
 XeCl, UV picosecond pulse amplification 0-74372
 XeCl+HCl(inert gas atom), ground state destruction, quenching rate consts. meas. 0-63758
 XeCl, triatomic excimer, transient gain meas. at 488.0, 497.6, 514.5 nm 0-58511
 XeCl triatomic excimer laser in visible 0-64048
 XeCl(B) formation in electron beam assisted Xe/HCl laser discharge 0-63988
 XeF, direct pumping by electron beam pulses, gain and laser oscill. obs. in blue-green 0-102699
 XeF, electric discharge excimer laser with intense preionisation 0-63991
 XeF electroionisation laser, energetic, threshold and spectral chars. 0-99705
 XeF electron-beam-pumped laser, chars., 300-600K 0-78839
 XeF, excited by discharge stabilised by electron beam 0-63992
 XeF, ground state kinetics, multilevel model of energy transfer 0-99707
 XeF laser, output control by injection locking 0-74405
 XeF laser performance, ground state population effect 0-63987
 XeF* nuclear pumped laser obs. 0-63996

excimers**see also excimer lasers**

- anthracenes, exciplex form. with amines, form. kinetics and luminesc. props. 0-66792
 bis(9-anthryloxy)polyoxalkanes, intramolecular excimer form. and photodimerisation, kinetic anal., rate constants determ. 0-66800
 benzene, nanosecond laser photolysis 0-66825
 conformational mobility, fluorescence obs. 0-63877
 flexible chain molecules, mutual interpenetration, fluorescence obs. 0-63877
 gas mixture, self sustained volume photoionisation discharge existence conditions 0-79610
 heteroexcimers, intramolecular, picosecond time-resolved fluorescence studies 0-83401
 impurity centres, electron-phonon coupling from structured optical spectra, review 0-89038
 inert gas halides, exciplex mol. form., rel. to laser operation 0-81318
 inert gas-SF₆ mixture, formation of inert gas fluorides in AC discharge 0-64817
 methine dyes, spectral props., solvent effects 0-69181
 molecule formation in plasma by halide ion recomb. or alkali metal charge exchange 0-75026
 naphthalene, singlet and triplet excimer interactions, exciton resons. 0-95535
 1-β-naphthyl-2-N-piperidinoethane, intramol. exciplex form., ground state conform. control 0-102547
 phosphatidylcholine bilayers, fluidity changes and phase transitions, intramol. excimer fluoresc. obs. 0-85342
 PMMA film, doped, time resolved absorpt. spectra, decay kinetics of exciplex state 0-84098
 poly-N-vinyl carbazole, pulsed laser excitation, time resolved fluoresc., 0-89041
 polyacenaphthalene, glassy soln., fluoresc. yield, polarisation and decay, temp. depend. 0-89043
 polyacenaphthalene-methylmethacrylate copolymer 0-89043
 porphyrins in liquid crystal, oriented photoexcited triplets, EPR study 0-84636

excimers continued

- pyrene crystals, anomalous emission excited near absorption edge 0-100682
 pyrene dodecanoic acid, lateral diffusion at air-water interface, monomer excimer dynamics 0-92693
 pyrene excimer fluorescence, erythrocyte membrane fluidity changes after X-irrad. obs. 0-72262
 triplet exciplexes, rapid rot., spin-selective depopulation of sublevels, heavy atom-induced mag. field effect 0-95552
 zinc pyrochlorophyllide in nematic liquid crystals, oriented photoexcited triplets, EPR study 0-84636
 Ar-Kr-F₂ mixture, nucl. induced excimer fluoresc. for I laser excitation 0-78846
 Li₂, $^3\Sigma_g^- + ^3\Sigma_g^-$ excimer emission, ab initio calcs. 0-91608
 Na₂, $^3\Sigma_g^- + ^3\Sigma_g^-$ excimer emission, ab initio calcs. 0-91608
 Na₂, triplet satellite band obs. in self-broadened D-line very far blue wing 0-95688
 SF₆-R-H(Ar) ternary mixtures, formation of inert gas fluorides in AC discharge 0-64817
 Xe+Ne, quenching of excited Xe*(³P₂, ³P₁, ¹P₁) states 0-63578
 XeI*, production via laser absorpt. processes at 193 nm, quenching kinetics 0-91466
 Xe₂*, synchrotron radiation excited, time resolved spectroscopy 0-69092

exciplexes see excimers

excitonic molecules

- anthracene, cryst., exciton aggregate possible form. under intense optical pumping, fluoresc. spectra 0-84772
 biexcitons, nonlinear laser spectrosc., multiphoton transitions 0-84433
 Frenkel biexcitons, eigenstates and transition spectra 0-88480
 many-valley semiconductor, bound multi-exciton complexes, density-matrix functional approach 0-96794
 perylene crystal, molecular exciton system, resonance Raman and fluorescence studies, dynamical effects 0-66169
 semiconductor, biexcitons, one-photon radiative recomb. 0-70621
 semiconductor, single-quantum radiative recomb. of biexcitons due to biexciton-exciton interactions 0-96793
 semiconductors, coherent biexcitons, two-photon nutation effect (Russian) 0-59892
 semiconductors, particle complexes, N=1 to ∞, book contrib. 0-80194
 semiconductors, two-photon nutation of coherent biexcitons 0-80191
 surface biexciton in polar semicond., binding energy calc. 0-96796
 uniaxially compressed crystal, exciton molecule radiation (Russian) 0-108264
 CdS electronic two- and one-photon Raman scatt. via biexcitons, stimulated config. obs. mag. field shift 0-103963
 CdS, photocond., spectral depend. at high excitation intensity, exciton effects 0-65619
 Cd_{1-x}Zn_xS heteroepitaxial single-cryst. layers, photoluminesc. props. 0-100692
 CuBr, biexciton dispersion, two-photon absorpt. 0-76045
 CuCl, dielectric function for semiconductors with high exciton conc. 0-84443
 CuCl, exciton spatial dispersion determ., two-photon Raman scatt. via excitonic mol. state 0-60595
 GaSe, deep free and constrained excitons and biexcitons, collective interactions (Russian) 0-66282
 α-O₂, cryst., exciton, exciton-magnon, and biexciton absorpt. at 1.5K 0-84750
 α-O₂ crystals, absorpt. line polarisation biexciton existence (Russian) 0-108242
 α-O₂ crystals, absorption line biexciton polarisation (Russian) 0-89028
 n-Si, bound excitons and bound multiexciton complexes, excitation spectra 0-96792
 Si, uniaxially stressed, excitonic molecule emission spectra, electron valley degeneracy effects 0-60669

excitons

see also excitonic molecules; phonon-exciton interactions

- absorption spectra, exciton peak, temp. depend., calc. 0-59885
 acceptor-donor-acceptor complex, Frenkel excitons and ionic excited states 0-92824
 adenine film, polycryst., energy conversion processes, quantum yields, 4 to 10 eV 0-88589
 alkali cyanides, mol. excitons, X-ray excited emission spectra obs. 0-66287
 alkali metal halides, defect production in cation sublattice, mechanisms 0-96510
 annihilation phenomena in low dimensionality finite lattice, master eqn. 0-92821
 anthracene, cryst., exciton aggregate possible form. under intense optical pumping, fluoresc. spectra 0-84772
 anthracene, cryst., heat pulse propag., exciton condensation, time-resolved fluoresc. spectra 0-84771
 anthracene, orientationally disordered cryst., lattice relax. effect 0-107278
 anthracene, pulsed electron excitation, triplet excitons, spectral and electrical investigations 0-92828
 anthracene, singlet exciton transitions, energies and oscillator strengths, boson theory with PPP wavefunctions 0-92820
 anthracene, thick crystals, excitation spectrum of fluorescence 0-76068
 anthracene crystals, orientationally disordered, exciton trap depths 0-88481
 anthracene films, optical props., comparison between free and optical contact mounting 0-89079
 anthracene-phenanthrene-TCNB, exciton transport obs. 0-65461
 anthracene-phenanthrene-tetracyanobenzene, CT-cryst., mini-excitons and lattice dynamics, ESR, optical and Raman spectra 0-60406
 antiferromagnets, exciton motion 0-70617
 benzophenone, cryst., charge carrier generation by exciton-exciton collisions 0-88568
 benzophenone, migration of triplet excitons, EPR profiles and phosphoresc. decay data 0-84641
 Bose condensation and superdiamag. current prod. possibility 0-65456
 canted magnetic structured materials, exciton spectra, optical props. 0-70622
 charge transfer crystals, mixed, exciton transport, low-dimensional, statistical model and experiments 0-65461
 chromophore aggregates in Frenkel exciton model, dynamic perturbation effects on circular dichroism intensity 0-93273
 coherent and incoherent motion in continuous time random walk framework 0-59882

excitons continued

- coherent phonons and excitons in biological systems, Bose condensation 0-67042
 covalent crystal, dynamical correlation effects on quasiparticle Bloch states 0-88499
 crystal optical characteristics, relax. processes exciton dispersion 0-107709
 cubic symmetry cryst., quadrupole exciton theory 0-103632
 γ-cyclopropyl-bis (1,3,3-trimethylindolenine-2-yl)pentamethinium fluoroborate, exciton surface polaritons, reflecting faces obs. 0-65645
 dibromonaphthalene, quasilinear chain excitons, Stark effects 0-97239
 p-dichlorobenzene-p-dibromobenzene mixed crystals, triplet exciton migration, time resolved emission spectroscopy 0-89052
 4,4'-dichlorobenzophenone single crystals, mutual annihilation of triplet excitons, 1.5 and 4.2K, phosphoresc. obs. 0-80850
 dielectric, inhomogeneous current state phase transition, free energy (Russian) 0-84703
 disordered systems, electronic energy transfer, generalized master eqn. 0-57221
 droplets, energy condensation, comparison with ball lightning (Russian) 0-107712
 dye monomolecular layers, energy transfer between sensitizers and acceptors 0-80861
 electron-hole binding accompanied by Wannier-Mott exciton form. 0-59887
 electron-hole binding and exciton formation (Russian) 0-65468
 electron-hole liquids, relation between bulk compressibility and surface energy 0-65465
 electron-hole paired systems, ferromagnetic ordering phase diagram 0-97097
 energy levels, influence of exciton gas and electron-hole plasma 0-96795
 ethylammoniumtetrachlorochromate, optical absorption intensity, short-range spin correlation 0-108185
 excitonic polaritons, classical and quantum mechanical aspects (French) 0-103634
 ferromagnet, excitonic, zero-sound excitations, Fermi liq. model 0-93101
 ferromagnetic metal, exciton condensation effects on props., Hubbard model 0-60171
 fluorene:pyrene-d₁₀, single cryst., host-guest triplet pairs, mag. field effect 0-60649
 Frenkel, weakly excited, energy bands calculation in number representation (Japanese) 0-107714
 heavily doped semicond., photoemission lineshapes of impurity levels, p-wave resonance 0-76154
 inert gas solids, collective excitations and EELS, calc. 0-92842
 insulator in mag. field, two-band model 0-80192
 insulators with spontaneous currents, impurity scatt. effect on phase transitions 0-80242
 ionic crystal, exciton mechanism model for defect form. 0-80187
 ionic crystal, fundamental luminescence at high ionisation levels (Russian) 0-103985
 Ising model, nonlinear excitations and coherent states in transverse field 0-68143
 laser pulse propagation in solid under conditions of excitonic state resonance 0-87430
 lattice migration, diffusive and percolative excitons 0-59879
 layered crystal, wave functions, exciton spectrum, light absorpt. (Russian) 0-100436
 many-valley semiconductors, donor impurity levels and excitons, shallow-deep instabilities 0-75520
 metals, exciton effects on X-ray absorption edges 0-108298
 methylammoniumtetrachlorochromate, optical absorption intensity, short-range spin correlation 0-108185
 molecular crystals, disordered, incoherent, electronic energy transfer in impurity band 0-75525
 molecular crystals, electronic excitation energy transfer, external elec. field effect 0-84431
 molecular crystals, exciton-phonon coupling and exciton transport 0-84430
 molecular crystals, phononless exciton band lineshape, excitation transfer, stochastic models 0-107711
 molecular crystals, weakly disordered theory of time evolution of exciton coherence 0-65455
 molecular solids, interaction with 0-15 eV electrons, formation of charged excitonic complexes 0-107708
 Mott insulators, excitonic spin polarons, appl. of Nagaoka's theorem for electron-hole pair 0-107978
 multi-component, LT mixed mode, dispersion relation 0-65470
 Nakajima-Zwanzig generalised master eqn. for exciton motion in mol. crystals 0-65462
 naphthalene:anthracene, pure and doped, delayed fluoresc. (French) 0-80846
 naphthalene, singlet and triplet excimer interactions, exciton resons. 0-95535
 naphthalene, singlet and triplet exciton percolation, tunnelling and thermalisation 0-84432
 naphthalene, singlet exciton transitions, energies and oscillator strengths, boson theory with PPP wavefunctions 0-92820
 naphthalene, vibr. relax. studied by four wave mixing (CARS), spectral lineshapes obs. 0-80762
 naphthalene-β-naphthol, concentration effects in exciton absorption region 0-108241
 naphthalene-β-naphthol mixture, exciton absorpt. depolarisation 0-103972
 naphthalene-h₈ and d₈, isotopic mixed crystals, exciton spectra in IR region 0-71400
 narrow gap semiconductor, diamagnetic excitons in two-band Dirac model 0-59888
 neutral bound excitons, accurate binding energies, variational method calc. 0-107715
 neutron scattering from equilibrium and non-equilibrium phonons, excitons and polaritons 0-84032
 p-nitrofluorene crystal film, exciton spectrum, IR absorpt. and Raman scatt. 0-80771
 nonequilibrium excitonic insulator, possible diffusion instability 0-59891
 nonlinear luminescence quenching at high pumping levels, microscopic theory 0-89040
 nonstationary processes 0-107710
 organic molecular crystal, doped, two-particle electronic excitation, optical cooperative excitation 0-93368
 organic molecular crystals, charge carrier generation by exciton-exciton collisions 0-88568

excitons continued

- pentacene, singlet exciton transitions, energies and oscillator strengths, boson theory with PPP wavefunctions 0-92820
 phase transition to incommensurate excitonic phase 0-75510
 polar crystal, Frenkel exciton effective mass temp. depend., lattice displacement interactions (*Chinese*) 0-84429
 poly-2,4-hexadiyne-1,6-diol bis (p-toluene sulfonate), exciton surface polaritons, reflecting faces obs. 0-65645
 poly-N-vinylcarbazole-biacetyl, triplet exciton quenching, exciton trapping model 0-66267
 polycarbonate, intrinsic conformational defect states 0-65500
 polydiacetylene, intrinsic conformational defect states 0-65500
 polymer, conjugated and saturated chain, electronic struct., review 0-59860
 pyrene, luminescence of free and self-trapped excitons 0-108250
 pyrene, triplet state, excitonic energy transfer, phosphoresc. and delayed fluoresc., 2 to 300K 0-84776
 quasifree, impurity trapping, finite coherence effects 0-59880
 relaxation times in solid-state theory and one-dimensional molecular systems (*Russian*) 0-100640
 resonance light scattering and hot luminesc. of self-trapping excitons 0-93336
 resonant Raman scattering via virtual exciton 0-71412
 semiconductor, dielectric liq. of Wannier-Mott excitons 0-65458
 semiconductor, direct band gap type, polariton theory of reson. electronic Raman scatt. on neutral donor levels 0-108194
 semiconductor, nonlinear coherence phenomena in exciton region 0-99806
 semiconductor, resonant Brillouin scattering of exciton polaritons 0-93357
 semiconductor, single-quantum radiative recomb. of biexcitons due to biexciton-exciton interactions 0-96793
 semiconductor films, exciton light absorption coefficient (*Russian*) 0-71504
 semiconductor thin films, ion implanted, optical and luminesc. props. 0-60699
 semiconductors, core exciton binding energies 0-80188
 semiconductors, doped, shallow impurity states, Hubbard bands and donor excitonic states, HF calc. 0-100443
 semiconductors, exciton and domain luminesc., book 0-82588
 semiconductors, exciton effect in interband electronic Raman scattering 0-103946
 semiconductors, exciton-impurity state with low binding energy 0-103646
 semiconductors, particle complexes, N=1 to ∞ , book contrib. 0-80194
 semiconductors, two-dimensional, Mott exciton formation in high mag. fields (*Russian*) 0-65467
 semiconductors with direct band gaps, exciton-polariton interactions, Green's function approach 0-92831
 spatial dispersion exponential model, boundary conditions (*Russian*) 0-75994
 stilbene, adsorbed rhodamine 6Zn, mol. cryst., role of excitonic and radiative mechs. of energy transport 0-108276
 stilbene, pulsed electron excitation, triplet excitons, spectral and electrical investigations 0-92828
 surface exciton energies and radii 0-92829
 TCNQ salt, decamethylferrocenone, monomeric and dimeric, optical and EELS study 0-100660
 p-terphenyl, cryst., exciton phosphoresc. at 300K 0-108277
 tetracene, singlet exciton transitions, energies and oscillator strengths, boson theory with PPP wavefunctions 0-92820
 1,2,4,5-tetrachlorobenzene, exciton states in crystals and dimers 0-70620
 1,2,4,5-tetrachlorobenzene, mol. solid, heat pulses, phonon-induced delocalisation of trapped excited triplet states 0-89053
 1,2,4,5-tetrachlorobenzene, triplet exciton, ESR and optical absorption lines 0-96791
 1,2,4,5-tetrachlorobenzene, triplet excitons, zero field ODMR 0-88891
 thymine film, polycryst., energy conversion processes, quantum yields, 4 to 10 eV 0-88589
 trialkylammonium, iodides, absorpt. and luminesc. spectra of self-localized excitons 0-97340
 triplet exciton annihilation rate, magnetic field depend. effect of spin-lattice relaxation 0-65459
 Wannier excitons, electronic spectrum, in quasi-two-dimensional structures 0-65460
 Wannier excitons, radiative decay in thin crystal fields 0-92823
 AgBr, cyclotron reson. of polarons at high density excitation 0-75859
 AgBr, photoluminesc. study of excitons in high mag. fields 0-80843
 Ag₂O, exciton luminesc. spectra, mag. field influence 0-80860
 Al-Formvar-Sn coupled films, Ginzburg's excitonic supercond. model 0-97039
 AlAs(Sb), fine structure of lowest exciton state (*Russian*) 0-96801
 AlGa_{1-x}As-GaAs quantum-well heterostruct., exciton in recomb. 0-103990
 AlN, absorpt. edge shape interpretation, Wannier excitons absorpt. in charge impurity elec. field 0-66233
 AlN, luminesc. excitation spectrum and band struct. 0-84783
 Ar atoms in Ne matrix, radiative and nonradiative lifetimes in excited states 0-69106
 Ar:OCS, O(¹S) and S(¹S) photodissociative prod., photoluminesc. excitation spectra, exciton energy transfer 0-89508
 As₂S_{3-x}Se_x, amorphous, picosecond relax. of optically induced absorption 0-97302
 BiI₃, structure, exciton states and physicochem. characteristics (*Russian*) 0-100435
 Cd_{1-x}Mn_xTe, exchange induced ionization of bound excitons, luminesc. meas. 0-97328
 Cd_{1-x}Mn_xTe, semimagnetic, exchange interactions between localised and delocalised electrons 0-97245
 CdS, additional waves and polariton dispersion, reflectivity, transmittivity spectra 0-71443
 CdS crystals, one-photon pumping, active layer structure, light amplification 0-78858
 CdS crystals, radiative recombination, high excitation rates 0-108269
 CdS, electron-hole pairs behaviour in energetic ion tracks 0-65457
 CdS, electron-hole plasma, gain and refl. spectra study 0-66227
 CdS epitaxial layers on sapphire, exciton struct. of absorpt., photoluminesc. and photocond. spectra 0-89027
 CdS, highly excited, stimulated emission processes, exciton-exciton (electron) scatt. 0-97307
 CdS, photocond., spectral depend. at high excitation intensity, exciton effects 0-65619
 CdS plane parallel slab, optical const. determ. methods 0-60531

excitons continued

- CdS, subMM radiation excitation by N₂ laser pulse 0-60678
 CdS, three-branch exciton-polariton dispersion, direct meas. by reson. Brillouin scatt. 0-60620
 CdS:Li(Cu), pure and doped, electrodiffusion of shallow donors, photocurrent, TSC, and exciton luminesc. meas. 0-79992
 CdS_{1-x}Se_x, mixed crystals, deformation effects on free excitons 0-76073
 n-CdSe, laser excited stimulated emission, optical gain spectrum 0-76050
 CdSe, single crystals, luminesc. of electron-hole plasma 0-60675
 CdSe:Li, pure and doped, reson. Raman and Brillouin scatt., elastic exciton-defect scatt. 0-80788
 CdTe crystals, exciton luminescence spectra rel. to shallow impurity conc. 0-97335
 CdTe, exciton magnetoreflectance spectra, multicomponent polaritons, Zeeman splitting 0-88974
 CdTe film, exciton spectra, press. and temp. depend. 0-80886
 p-CdTe, photocond., photoluminesc., spectral studies 0-88593
 CdTe, recombination radiation due to high-density excitons 0-93392
 CdTe:Mn²⁺, exciton refl. spectra and mag. susceptibility 0-66253
 CdTe:Mn²⁺, luminesc. and magnetooptic reson., mag. field effect 0-93390
 CoCO₃, LF exciton and Raman spectra, one-magnon and two-magnon scatt. 0-93333
 CoCO₃, two-sublattice noncollinear antiferromag., exciton-magnon light absorpt. mechanisms (*Russian*) 0-89017
 CsCoBr₃, quasi 1D Ising antiferromag., polarised Raman scatt. from mag. excitations 0-66182
 CsI:Na⁺(K⁺), luminesc. processes 0-103989
 CsMnCl₃·2H₂O, antiferromag. insulator, self-trapping of excitons 0-70619
 CsMnF₃, exciton migration, excitation and luminesc. study (*Russian*) 0-66264
 CsMnF₃, exciton-magnon interactions in optical transition, absorpt. and emission spectra meas. 0-70981
 CsPbCl₃, electronic struct. and optical props. in fundamental absorpt. region 0-93367
 CuCl, electron-hole pairs behaviour in energetic ion tracks 0-65457
 CuCl, interface supercond., piezoelec. hypothesis 0-60128
 Cu₂O, exciton luminesc. spectra, mag. field influence 0-80860
 Cu₂O, reson. Raman scatt. from stress-split forbidden excitons 0-93332
 Cu₂O, uniaxial stress effects on excitons 0-60589
 Cu₂O:Ag⁺, exciton-neutral and exciton-charged impurity scatt. cross sections 0-70618
 Eu chalcogenides, resonant Raman scattering model via magnetic exciton in ferromagnetic phase 0-93326
 FeBO₃, mag. linear dichroism and absorpt. spectra, exciton-magnon absorpt. mechanism 0-66160
 Fe_{1-x}Mn_xCl₂, disordered, Raman scatt. from Fe²⁺ and Neel temp. 0-60579
 Fe_{1-x}Mn_xCl₂, low-lying electronic excitations in antiferromag. and paramag. phases Raman scatt. study 0-71414
 Ga, reson. photoemission shake-up and Auger processes at 3p photothreshold 0-100748
 GaAs core exciton binding energies 0-80188
 GaAs, donor-acceptor-type complex 0-80837
 GaAs, excited luminescence, influence of IR illumination 0-76072
 GaAs, exciton effects in photocond., photoluminesc. 0-96797
 GaAs, exciton quenching, obs. at room temp. using electrolyte electroreflectance 0-60546
 GaAs, excitons in arbitrary mag. fields 0-96798
 GaAs, fine structure of lowest exciton state (*Russian*) 0-96801
 p-GaAs, MBE grown, photolum. lines due to defect-induced bound exciton radiative recomb. 0-103974
 GaAs, surface exciton energy 0-92829
 GaAs_{1-x}P_x, indirect-gap, evidence for exciton localization by alloy fluctuations, photolum. 0-66276
 GaAs_{1-x}P_x(Te), bound exciton stress depend., piezoluminescence, photoluminescence 0-82006
 GaP, anomalous photoeffect on connected excitons (*Russian*) 0-92929
 GaP, core exciton binding energies 0-80188
 GaP, donor states theory, camel's back struct. influence 0-59921
 GaP, reson. photoemission shake-up and Auger processes at 3p photothreshold 0-100748
 p-GaP, spin-flip Raman scattering, review 0-108209
 GaP:Bi, photoluminesc., electroluminesc., 4.2 to 300K, excitons and hole traps 0-108275
 GaP:N, bound exciton absorpt. line asymmetry, electroabsorption spectra 0-71459
 GaP:S, ground and excited states of bound exciton complex, stress effects 0-65463
 GaP:S(Se), donor bound exciton excited states 0-66284
 Ga_{0.99}As_{0.01}N, luminesc. of N bound state excitons, local-environment effects 0-100691
 GaS(Se), reson. Brillouin scatt. 0-89010
 GaSb, core exciton binding energies 0-80188
 GaSe, deep free and constrained excitons and biexcitons, collective interactions (*Russian*) 0-66282
 GaSe, exciton luminesc. kinetics, intermediate electron-hole states 0-93389
 GaSe thin films, electroabsorpt. spectra, exciton line splitting 0-107716
 GaTe, single cryst. prep. and electroabsorpt. spectra investig. 0-103968
 Ge, carrier relaxation rate temp. depend. and pair density in large electron-hole drop 0-75509
 Ge, exciton condensation, electron-hole drop investigation in UHF field, nucleation (*Russian*) 0-80193
 Ge, exciton condensation, light scatt. by electron-hole drops 0-84435
 Ge, nonequilibrium charge carrier-mag. field interaction electron-hole drops, recombination (*Russian*) 0-75511
 Ge, oscillatory exciton breakdown, microwave cond. 0-103716
 Ge strain-confined large electron-hole drop characteristics 0-65469
 Ge:In (Sb) and pure cryst., kinetics of strain-confined large electron-hole drop and its clinging exciton system 0-75508
 GeS, physical basis for Urbach's rule 0-93366
 GeSe₂, amorphous film, laser induced oscillatory phenomena 0-84711
 H₂, cryst. ortho-para mixtures, vibr. coherence decay 0-78903
 Hg_{1-x}Cd_xTe, near band-gap photoluminesc., bound exciton luminesc. obs. 0-103973
 In_{0.95}Ga_{0.05}P, N free and implanted, photoluminescence study 0-97322
 InP, luminescence, hot electron effects 0-66277
 InSb, absorpt. edge, exciton struct. 0-93321
 p-InSb, photoexcited exciton spin-flip scatt. 0-74434

excitons continued

- p-InSb, spin-flip Raman scattering, review 0-108209
 InSe, photo-absorption of green exciton 0-80816
 KBr, cation defects creation mechanism 0-75224
 KBr, colour centre form. under polarised UV irr., dichroism in absorption spectra 0-107232
 KBr, decay and time resolved emission spectra from σ -excitons produced by heavy-ion irradiation 0-89071
 KBr, self-trapped exciton form. via thermally induced defect reactions 0-60687
 KCN, Cl_{1-x}, finite field local field catastrophe phenomena in spectra 0-92830
 K⁺CN₂-Cl_{1-x}, influence of structural disorder on exciton spectra 0-108224
 KCl, F-centre formation at highly excited triplet states of self-trapped excitons 0-76066
 KCl:Cu⁺, exciton bands, optical absorpt. and MCD spectra 0-80821
 KCl(Br), cation defects creation mechanism 0-75224
 K₂CoF₆, 2-dimens. Ising antiferromag., mag. excitons, Raman scatt. obs. 0-66181
 KI, self trapped exciton form. time at Σ_u^+ state under pulsed electron beam in ps range 0-97347
 KI, self-trapped exciton form. via thermally induced defect reactions 0-60687
 KI:Cu⁺, exciton bands, optical absorpt. and MCD spectra 0-80821
 Kr atoms in Ne matrix, radiative and nonradiative lifetimes in excited states 0-69106
 Kr:OCS, O(¹S) and S(¹S) photodissociative prod., photoluminesc. excitation spectra, exciton energy transfer 0-89508
 LiH(D), isotope effect on Wannier-Mott exciton levels 0-103633
 Mn,Cd_{1-x}Se single crystals, photoluminesc., composition depend. 0-80854
 MoSe₂, exciton spectra 0-97296
 α -N₂, mol. cryst., theory of time evolution of exciton coherence 0-65455
 N₂, solid, exciton-phonon coupling in strong coupling limit, temp. depend. 0-92616
 NH₄Br:Ti, and pure crystals, luminesc., VUV irradiated at 80K (Russian) 0-84763
 NaCl, pure and doped, 20K X-ray irradiation, thermolum. and recovery processes 0-93412
 NaCl, self-trapped exciton form. via thermally induced defect reactions 0-60687
 NaCl(Br), X-ray or UV irradiated, cation defects creation mechanism 0-75224
 NaMnCl₂, antiferromag. insulator, self-trapping of excitons 0-70619
 NbS₂Cl₂(Br₂)(I₂), absorpt. edge spectrum, fine struct. 0-66219
 Ne, solid, bulk excitons, expt. 0-92827
 Ne, solid, bulk excitons, theory 0-92826
 Ne:H, exciton states and L₁,L₂ emission 0-93372
 α -O₂, antiferromagnetic polycrystal, splitting of exciton absorpt. lines in mag. field (Russian) 0-103943
 α -O₂, cryst., exciton, exciton-magnon, and biexciton absorpt. at 1.5K 0-84750
 α -O₂ crystals, spin ordering effect on light absorpt. (Russian) 0-89029
 PbCl_{2-2x}Br_{2x}, luminesc. and reflection spectra (Russian) 0-84762
 PbI₂ direct gap polar semicond., electron hole liquid phase diagram (Russian) 0-93314
 PbI₂, first-order 2H-4H polytype transition, exciton spectroscopic study 0-59647
 PbI₂, photoexciton interaction, luminescence spectra, polariton dispersion diagram 0-93397
 PbO, single crystals, exciton and impurity luminesc. 0-60674
 PbO, visible absorpt. spectra rel. to indirect exciton transitions 0-60628
 RbBr, self trapped exciton form. time at Σ_u^+ state under pulsed electron beam in ps range 0-97347
 RbCl(Br), cation defects creation mechanism 0-75224
 RbCoF₆, 2-dimens. Ising antiferromag., mag. excitons, Raman scatt. obs. 0-66181
 Rb₂CrCl₄, optical absorption intensity, short-range spin correlation 0-108185
 S, orthorhombic, photogeneration of charge carriers 0-107844
 n-Si, bound excitons and bound multiexciton complexes, excitation spectra 0-96792
 Si, bound-exciton spectral lines, conc. broadening at high impurity concs. 0-80826
 Si, core exciton binding energies 0-80188
 Si, fine structure of lowest exciton state (Russian) 0-96801
 Si, free excitons, drift and diffusion, luminesc. obs. 0-84434
 Si, impurity content characterisation, exciton luminesc. 0-60653
 Si, optical spectrum, many particle effects, band struct. 0-89024
 Si:Al, localised exciton bound to isoelectronic trap 0-66283
 Si:B, bound many-exciton complexes, luminescence spectra, mag. props. 0-103994
 Si:K, bound exciton luminescence in mag. field (Russian) 0-108278
 Si:Li, photolum. of bound exciton and bound multiexciton complex, Zeeman effect 0-108265
 Si:P, luminescence circular polarisation, emission by many exciton complexes 0-93398
 SiC, laser Raman spin-flip scatt. from excitons, luminesc. 0-80786
 SiC polytypes, free exciton luminesc. meas., phonon energies 0-80852
 p-SiC, spin-flip Raman scattering, review 0-108209
 SiC, spin-flip scatt. of laser light from photoexcited excitons 0-93330
 SiO₂, exciton study, luminescent centres as exciton detectors 0-66278
 SiO₂, fused, broken bond defect generation mechanisms 0-88044
 SnO₂, exciton luminescence spectra, absorpt. spectra 0-89064
 SrCl₂:Cu⁺, exciton bands, optical absorpt. and MCD spectra 0-80821
 TiBr₃, exciton luminescence spectra, absorpt. spectra 0-89064
 TiBr₃, resonant polaron coupling and excitons under mag. field 0-71383
 Xe atoms in Ne matrix, radiative and nonradiative lifetimes in excited states 0-69106
 YVO₄:Nd³⁺, energy transfer processes, laser-excited time-resolved spectroscopy 0-84765
 ZnAs, Schottky diodes, elec. and photoelec. props., excitons 0-65653
 Zn,Cd_{1-x}Se, exciton reflection spectra anomalies (Russian) 0-97304
 ZnCr₂O₄, antiferromag. spinel, absorpt. and luminesc. spectra 0-66225
 ZnO, electron-hole plasma, gain and refl. spectra study 0-66227
 ZnO, exciton luminesc., 16 to 77K 0-97329
 ZnP, Schottky diodes, elec. and photoelec. props., excitons 0-65653
 ZnS, cathodolum. emission spectra, exciton lines 0-76084
 ZnSe, blue photoluminesc. excited with strong laser radiation 0-93391
 ZnSe, exciton emission, halfwidths, thermal and optical activation energies obs. (French) 0-66268

excitons continued

- ZnSe, exciton refl. spectra, temp. depend. 0-59886
 ZnSe, near band edge photoluminescence, electron-hole recombination 0-80835
 ZnSe, resonance Raman scatt., exciton-polariton luminescence (Russian) 0-97287
 ZnSe, thermally treated crystals, photoluminesc. 0-60661
 ZnSe(Te), fine structure of lowest exciton state (Russian) 0-96801
 ZnTe crystals, polariton effects in luminesc. 0-103988
 ZnTe, edge luminesc. excited by electron bombard. 0-66308
 ZnTe film, exciton spectra, press. and temp. depend. 0-80886
 ZnTe, pure and P(As) doped, shallow-acceptor, donor, free-exciton, and bound-exciton states 0-60667
 ZnTe, secondary emission, transient behaviour under band-to-band excitation 0-108266
 p-ZnTe, spin-flip Raman scattering, review 0-108209
 ZrS₃, excitonic transition, reson. Raman spectra, Franck-Condon factors 0-97252
 ZrS₃, photolum. from excitons 0-66274

exhibitions

No entries

exobiology see extraterrestrial life

exoelectron emission

- exoemission phenomena, TSC, thermionic emission, book contribution 0-80954
 oxidised surface, oxidising conditions effect on thermally stimulated exoelectron emission (Japanese) 0-89127
 Al anodic films, acoustic and electron-emission during deform. 0-80143
 Al₂O₃:Li, TSEE, Li doping effects 0-80953
 BaTiO₃, electron exoelectron unipolarity associated with phase transitions 0-97415
 BeO, field-assisted thermally stimulated exoelectron emission 0-100761
 BeO, photostimulated exoelectron emission under discontinuous stimulation 0-108329
 BeO, TSEE, effect of surface SiO₂ 0-76159
 LiNbO₃:Fe, exoelectron emission in pyroelectric regime 0-76158
 MgO, exoelectron emission, mean energy, temp. depend. 0-76160
 MgO, thermally stimulated exoelectron emission (German) 0-66404
 NiO, powder compact surface, oxidising conditions effect on thermally stimulated exoelectron emission (Japanese) 0-89127
 NiO, single cryst. cleavage plane, oxidising conditions effect on thermally stimulated exoelectron emission (Japanese) 0-89127
 Pt, tension-strained, thermally stimulated exoelectron emission, excitation mechanism (Russian) 0-71581
 TiO₂, thermally stimulated exoelectron emission (German) 0-66404
 V₂O₅, thermally stimulated exoelectron emission (German) 0-66404
 ZnO, thermally stimulated exoelectron emission (German) 0-66404

exosphere

- escape of ions to space, ion chem. and low altitude accel. effects 0-85798
 protonosphere depletion assoc. with mag. storm, and recovery 0-85784
 temperatures of high latit. exosphere, geomag. activity effects 0-109286
 Li⁺ diffusion and ion-neutral interactions, laser sounding obs. (French) 0-82115
 O atom corona, of fast atoms during solar max., airglow obs. 0-101469
 O atoms, polar corona atom distrib. 0-82120

exotic atoms

see also hadronic atoms; muonic atoms

- ^AH, A=1,2,3, \bar{p} radiative atomic recombination, antiprotonic atoms 0-83527
⁴He, muonic, formation and hyperfine struct. 0-91707

expanding universe see cosmology

expansion, thermal see thermal expansion

expansion chambers see cloud chambers

exploding foils see exploding wires and foils

exploding wires and foils

see also discharges (electric); plasma production

- accelerators, direct-action, using inductive storage device with commutation by exploding conductors 0-68974
 burst phase, simulation by one-dimens. MHD code 0-75080
 electrically exploded foil opening switches, basic performance 0-70019
 electrohydraulic forming of circular metal sheet 0-84866
 explosive-magnetic generators, energy take-off to inductive load using circuit breaking 0-59323
 fused metal foil operating switch for inductively driven plasma implosions generation 0-70018
 liquid cavity collapse, accompanied by RF emission 0-87790
 MHD instability effects in imploding plasma liners 0-75081
 microsecond stratified pulsed discharge 0-87975
 solving transient process in electrical explosion of conductor in restricted volume of liquid (Russian) 0-100088
 stratified pulsed discharge with limited surface area 0-87974
 Al foil fuse, electrically exploded, surrounding medium effect 0-103207

explosion bubbles see bubbles

explosions

see also accidents; detonation; nuclear explosions; safety; shock waves

- air suspension homobaric flow in presence of physicochemical transform. 0-87820
 Asama Volcano, spectral studies of explosion earthquakes assoc. with 1973 eruptions (Japanese) 0-67340
 axially symmetric explosion in magnetogasdynamics 0-62007
 black holes, primordial, explosion rate upper limit from gamma-ray bursts search 0-67911
 centrifuge cratering 0-72522
 cloud development, effect of explosions (Chinese) 0-82042
 concrete slab, explosive shock resist., tensile fracture 0-85065
 containment vessel, cylindrical, submerged, dynamic plastic response, design formulae 0-83759
 crater formation modelling, meteorite impact effects 0-90088
 detonation, similarity and differences between conditions for initiation and failure 0-103038
 detonation wave magnification by pulsation energy 0-59075
 disc galaxies nuclei, superdense gaseous cores form. rel. to periodic explosions 0-90526
 dust explosion, flame propag. vel., uniform dispersion of single sized particles 0-66803
 electrical conductivity of high temp. imperfect gas (Russian) 0-100072
 graphite, shock wave, prod. by explosion, vel. meas. 0-59074
 hydrodynamic cumulation regimes during lining collapse, cumulative jet 0-69891

explosions continued

- magnetized spheroids, anisotropic explosions 0-67532
- metallic shell, explosive expansion, deform. and rupture modes and mechanisms 0-85064
- metallic shell, explosive expansion, rupture behaviour 0-85063
- nuclear power stations, industrial activities nearby causing hazards 0-78408
- ocean blast wave propagation, theory for stratified ocean (*Russian*) 0-81904
- PMMA, radical form. in explosive loading, electron spin reson. obs. 0-63678
- quarrying, use of electronic transient recorders for meas. explosion noise and vibration 0-67023
- seismic explosions at Tateyama, Japan, appl. to seismic waves vel. change in S.Kanto area (*Japanese*) 0-67338
- shock wave propagation investigations on suitability of piezoelectric and magnetoelastic detectors (*Polish*) 0-79351
- shock waves instability in a relaxing medium 0-100013
- solar chromosphere flares, initial phase parameters determ. from gas-dynamic explosion model 0-62104
- spiral galaxies, normal, post-explosion gas depletion in central regions 0-62272
- supernova core, Rayleigh-Taylor convective overturn rel. to explosion 0-77429
- underground explosion, seismic radiation pattern 0-61780
- vacuum technique problems, with modern semiconductor processes (*German*) 0-86330
- viscous fluid under cyclic deform., self-heating, hydrodynamic thermal explosion 0-58993
- water, explosive shock wave propagation, energy hypothesis 0-92179

exposure meters *see photometers***extended Huckel theory calculations** *see EHT calculations***extensive air showers** *see cosmic ray showers and bursts***extensometers**

- capacitance type AC dilatometer for piezoelectric and electrostriction const. meas. 0-77747
- dilatometer for PVT meas. of liquids and plastic crystals at low temperature 0-68208
- dilatometric measurements, high temp. method accuracy 0-73308
- emissivity determination, metals and alloys, using low-inertia opt. dilatometry 0-59684
- photoresistor dilatometer, for polymer materials testing 0-81251
- porcelain-metal cermet, stress determ., meas. method (*German*) 0-76425
- quartz dilatometer based on mechanon for meas. linear expansion coeff. 0-105639

external flows

- circular cylinders, surface-roughness effects on mean flow, turbulent boundary layers 0-92128
- cylinder, transverse curvature and turbulence effects on axisymmetric liquid flow (*Russian*) 0-59015
- ideal gas supersonic flow around blunt wedge, sonic line shape 0-64577
- longitudinal blunt circular cylinder, axisymmetric separated and reattached flow, turbulence 0-79285
- nozzle in different jet regimes, internal and external flows, separation and wakes 0-100023
- rectangular body, laminar flow, separation bubble and stagnation line 0-64514
- sphere immersed in a fluidised bed, mass transfer (*French*) 0-92214
- stagnation flow turbulence about circular cylinder, visual study 0-96248
- steady flow about blunt bodies, finite difference methods 0-96280
- steady viscous flow past circular cylinder, numerical study, vortices and separation 0-92108
- Stokes flow, slender body theory for viscous incompressible fluid 0-92160
- streaming in vicinity of plate possessing propagating longitudinal strain wave 0-87758
- streamline flow round an array of profiles in a magnetic field perpendicular to the plane of the flow 0-83856
- turbomachines, boundary layer charact., influence of external flow turbulence 0-87811

extraordinary ray *see birefringence***extrapolation**

- creep rupture data analysis, development of correlation and extrapolation methods 0-58975
- Josephson junctions, voltage response, functional relation, extrapolation technique for accelerating computation 0-107963
- rate equations for elevated temperature creep 0-65141

extraterrestrial atmospheres

- see also comets; planetary atmospheres; stellar atmospheres*
- comet comae, effect of solar photodissociative ionisation 0-90370
- Comet Kohoutek (1973 XII), ion tail dynamical response to solar wind interaction 0-85897
- Comet West (1976 VI), coma mols. and dust distrib., visible emission profiles 0-101562
- comets neutral atmospheres, average random walk model for mol. phot. dissociation 0-77351
- Ganymede, atmosphere erosion by radiation belt energetic atomic particles 0-72736
- Io, global SO₂ abundance upper limit 0-77332
- Io plasma torus, effects on Jupiter kilometric radiation ray tracing 0-72866
- Io plasma torus, effects on Jupiter kilometric radiation spatial and temporal distrib. 0-77328
- Moon exosphere simulation, Monte Carlo methods 0-67588
- Moon exosphere simulation, Monte Carlo methods 0-67589
- Periodic Comet Stephan-Oterma (1980g), total visual magnitudes and coma diameters, (1980 September 7 to 11) 0-109397

extraterrestrial life

- artificial objects located at Earth-Moon libration points, unsuccessful search 0-98647
- bibliography, chem. evolution and the origin of life 0-90620
- comets, primordial, elementary life forms origin in radiogenically melted interiors 0-67659
- detection from nuclear waste spectrum in stellar spectra 0-82230
- habitable zones around main-sequence stars rel. to climatic models 0-82049
- interstellar bacterial grains, prod. of 3 μ spectral feature in galactic IR sources 0-62227
- interstellar molecules in prebiological evolution 0-94726
- interstellar travel and communication, bibliography 0-101677

extraterrestrial life continued

- Mars, organic compound search by Viking, final conclusions 0-67627
- Mars, Viking mission results 0-82255
- radiocommunication using Sun as gravitational lens 0-62040
- search for signals from extraterrestrial civilisations, simulation approach 0-62039
- SETI at 18 cm, high sensitivity search 0-82229

extraterrestrial radiofrequency radiation *see radiofrequency cosmic radiation***extremum control** *see optimal control***extrusion**

- ethylene-methyl acrylate, random copolymer, review 0-108330
- ethylene-vinyl acetate copolymers, extrusion and heavy duty films, radiation crosslinking, struct. effect 0-66844
- glass fibre, forming process, characts., anal. techniques 0-58827
- high strain rate processes, review 0-84864
- invariant system with switched element, design and evaluation for heat processes control during extrusion of plastic materials (*Russian*) 0-100854
- nonferrous metal, semi-brittle, high-speed backward extrusion using superimposed hydrostatic press. 0-84865
- plastic resins, secondary coating of optical fibres, effect on transmission props. 0-58704
- plastics sheet blowing and extruding, process identification for automatic process control (*German*) 0-81023
- PMMA, hydrostatic extrusion 0-108479
- polyethylene-polypropylene blend, extruded, thermal swelling and mech. characterisation 0-81110
- polyethylene, high density, solid state coextrusion, geometric factors effect 0-71704
- polyethylene, high density, solid state coextrusion, technique for ultradrawing thermoplastics 0-84979
- polyethylene, high-density, solid-state coextrusion, mol. wt. distrib. effect 0-104212
- polyethylene fibre, high-strength high-modulus, morphology and tensile prop. relations 0-103264
- polyethylene film, minimum running thickness, biaxial extensional flow study 0-100993
- polyethylene melt, high density, oscillating flow during extrusion, model anal. 0-100016
- polyethylene melt, oscillatory flow through capillary 0-103046
- polyethylenes, extrusion and heavy duty films struct. parameters influence on cross-linking by radiation 0-66844
- polyolefins, ultra-high modulus, production by tensile drawing and hydrostatic extrusion 0-81022
- reverse cold impact extrusion, appl. of ultrasonic radial oscillations (*Russian*) 0-97441
- thermally induced extrudate swell, Galerkin method 0-79312
- Ag halide optical fibres, extrusion, visible and IR transmission 0-58829
- Al billet, hot extrusion, nonsteady state temp. distrib., numerical method 0-60886
- Nb₃Sn A15 composite superconductors, hydrostatic extrusion (*French*) 0-104090
- Ni, dislocation structure evolution after hydroextrusion (*Russian*) 0-96530
- ZrO₂, partially stabilized, props. and appl. to extrusion dies 0-97507

eye

- see also contact lenses; vision*
- accommodation, reaction and response times obs. 0-67073
- accommodation and vergence static behaviour, computer simulation of interactive dual-feedback system 0-94205
- accommodation microfluctuation dynamics studied with highly sensitive IR optometer 0-81580
- accommodative responsiveness rel. to contrast sensitivity for sinusoidal gratings 0-61552
- adaptation, technique for estimating the contrib. of photomech. responses 0-85547
- aerial image modulation lowering, contrbs. of retina and eye optical system 0-81584
- amblyopia, human, differences in neural basis, effect of mean luminance 0-72156
- amblyopia, lack of normalcy of dominant eye 0-97898
- amblyopia, monocular, prevalence among anisometropes 0-67071
- aquatic eyes, retinoscopy, refractive error considerations 0-61750
- bifoveate retina of lizard, light microscopic study 0-101165
- binocular retinal image motion during active head rotation 0-72158
- binocular vision, artificial aniseikonia, geometrical explanation of induced size effect 0-72173
- binocular vision deprived humans, binocular interactions tuned to size and orientation 0-81606
- blink reflex, effects of elec. stimulus freq. during rest and a task 0-61547
- blinking and suppression of visual stimulation 0-97909
- brain stem auditory evoked potentials and blink reflex in quiescent multiple sclerosis 0-67091
- chromatic aberration meas. with chromoretinoscopy 0-81581
- chromatic aberration rel. to accommodation, meas. using dynamic laser speckle pattern 0-81582
- chromoretinoscopy and its instrumentation 0-94201
- cinema photography 0-67186
- compound eye of Cicindela tranquebarica herbst, fine struct. 0-85382
- compound eye of worker honey bee, cell junctions, electron microscopy 0-85383
- concomitancy testing, new method 0-94305
- conditioning auditory stimuli and the cutaneous eyeblink reflex, human obs. 0-67090
- cone, computer-driven hardware model, response obs. 0-72402
- cone outer segments, light-induced changes in membrane current, tiger salamander and turtle 0-108899
- cone spectral mechanisms, ERG and psychophysical obs. 0-61565
- contrast sensitivity as a function of position on the retina 0-61561
- contrast thresholds versus border enhancement, scatt. light effect 0-94213
- corneal damage induced by near-UV laser, cumulative effects 0-85448
- corneal pressures due to soft contact lenses and corneal asymmetry 0-104621
- corneal sensitivity and thickness after wearing PMMA and gas-permeable contact lenses 0-61544
- corneal temperature range, implications in prediction of laser thermal damage 0-108848
- cortical plasticity in monocularly deprived immobilized kittens, eye movement dependence 0-81588

eye continued

dark-adaptation, comments on the testing of 2 prominent hypotheses 0-108896
 detection, effect of photon noise 0-61559
 disc vasculature in Down's Syndrome 0-67069
 displacement thresholds, foveal and peripheral, rel. to stimulus luminance, line length, movement duration 0-101183
 divergence excess strabismus, optometric therapy 0-97902
 ERG, human, nonlinear kernels 0-61545
 ERG, oscillatory pots., analogue circuit model and frog obs. 0-89750
 ERG recording, computer assisted standardised quantitative method 0-109048
 evoked potentials, speed methods for vision assessment, normal and amblyopic eyes 0-61661
 far peripheral retina, spectral sensitivity 0-104586
 figure perception, role of eye movements 0-101186
 fixation distance changes, ocular translation and cyclotorsion obs. 0-89752
 fluorescein angiography of the ocular fundus 0-67185
 focus on retina, best value for various fixation distances, phakic and aphakic eyes 0-108882
 foveal fixation, functional test based on differential cone directional sensitivity 0-85399
 foveal increment threshold, lateral effect of oscill. of peripheral luminance gratings 0-108904
 fundus photography in optometric practice 0-67183
 glasses, prescription meas. 0-67981
 gonioscopy in optometry 0-67182
 gonioscopic method for grading of the anterior chamber angle 0-108993
 heterophoria, prism-induced, oculomotor adaption 0-108880
 historical paper by Jean Mery written in 1704 0-57050
 holocamera for 3-D micrography of the alert human eye 0-98057
 holography applications in ophthalmology 0-67200
 hummingbird colour vision to near UV light 0-97914
 illumination and reflection edges, recognition by human visual system 0-94209
 insect colour vision, effected by one visual pigment and filters 0-94212
 instrument focusing to take account of eye accommodation 0-101811
 intensity discrimination capacity of tree shrew retinal ganglion cells 0-61556
 jerk nystagmus, some new findings 0-67074
 keratoconus, position of corneal apex 0-94200
 lateral inhibition in composite eye of limulus, expt. (French) 0-89705
 Limulus ommatidia, resonant response of neural model to double freq. stimulation 0-76734
 luminance flicker enhancement by colour-opponent mechanisms, monkey obs. 0-61549
 lumirhodopsin, photoconversion at 77K, quantum efficiency estimation 0-67081
 Macular pigment, role in polarised light detect., meas. technique 0-61560
 magnetophosphores, quantitative anal. of thresholds 0-72184
 mental activity evoking pupil dilation, link with intelligence 0-61532
 metarhodopsin transition, triggering of light-induced change in Ca binding, rod disk membranes 0-94211
 microsaccades, role in high acuity observational tasks 0-108893
 microscope, scanning mirror, with optical sectioning characts., ophthalmology appls. 0-85461
 monocular deprivation, unequal, alternating, cause of asymmetric visual fields in cats 0-104584
 monocular light exclusion, reduction of retinal directional sensitivity obs. 0-81592
 monocular vergence movements produced by external visual feedback 0-108883
 motion kinetics in moving target pursuit, oculomotor abnormalities in neurological disorders detect. 0-108888
 motor systems of eye and hand, optimal response in pointing at a visual target 0-61567
 movement in luminance edge threshold effect, stabilised viewing conditions 0-81589
 movements, role in detection of stationary structs., theoretical model 0-81594
 movements control, effects of frontal eye field and superior colliculus ablations 0-72154
 MTF of defocused optical system for incoherent monochromatic light, human eye 0-67072
 myopia in developing chicks following monocular and binocular lid closure 0-61543
 Nephrops norvegicus (L.), circadian rhythmicity, neurohumoral basis 0-108889
 neurons, cat eye, stereotaxic method for recording from single cells 0-89913
 night convergence and presbyopia (Spanish) 0-89746
 nonlinear visual processing in cat's retina, model 0-85385
 nonlinearity, analytical derivation 0-67082
 nystagmus, automatic on-line anal. (German) 0-76846
 ophthalmic photography, external 0-67180
 ophthalmic photography instrumentation, survey of clinical impressions 0-67188
 orientation sensitivity of visual movement detection system activating landing response of blowflies 0-101176
 oscillatory responses of the Limulus retina 0-101166
 outer isopter perimetric response variability obs. in old subjects 0-108894
 perceptive field sizes fovea and periphery, light- and dark-adapted obs. 0-61574
 peripheral contrast sensitivity for sine-wave gratings and single periods 0-61562
 photodocumentation, conf., Birmingham, USA (Dec. 1977) 0-62362
 photography, new instrumentation and techniques 0-67187
 photoreceptor membrane interfacial pots., light-induced 0-72161
 photoreceptor membranes, incorporation into a multilamellar film 0-89907
 photoreceptor optics, formalism and excitation 0-61540
 position determination for communications system, IR system 0-76821
 position measurement, method for implantation of mag. search coils 0-85548
 projector having a thermoplastic target and operator's eye, characts. 0-96023
 proprioception, input to horizontal oculomotor system of crayfish, expt. obs. 0-72181
 pupillary light reflex system, modelling and identification 0-61554
 rapid eye movement analysis during sleep 0-76870

eye continued

reading without a fovea 0-76748
 receptor optics and orientation, vertebrate 0-81585
 reduced eye, expts. in life science labs. 0-82617
 refractive error meas. using dynamic laser speckle pattern 0-81583
 refractive state of ground squirrel 0-67070
 retina, albino rabbit, X-ray effects, SEM obs. 0-104674
 retina, bovine, R2 component of early receptor pot. rel. to metarhodopsin II form. 0-97904
 retina, frog, morphometric anal. of internal horizontal cells 0-108892
 retina, rat, rod and cone-type photoreceptors in post-equatorial region, electron microscopy 0-85384
 retina, serial reconstruct. of adjacent ganglion cells 0-89749
 retina injuries, magnetoretiographic meas. using SQUID magnetometer 0-104702
 retinal chromophore, reson. Raman spectra obs. of struct. 0-94168
 retinal damage from a white-light laser, thresholds and mechanisms, rhesus monkey obs. 0-108955
 retinal ganglion cell layer, cat, newly identified presumptive microneurons population 0-67077
 retinal ganglion cells, class I, in the toad, Bufo spinulosus 0-85393
 retinal ganglion cells, orientation bias, cat expts. 0-94206
 retinal ganglion cells in the galago, size and topographic arrangement 0-67078
 retinal image cinematographic recording, accommodation microfluctuation appl. 0-81579
 retinal images, defocused and spatially filtered, stereoscopic acuity 0-101177
 retinal neuron firing rates, lack of predictability from interspike interval statistics 0-67075
 retinal photoreceptors, response increase and noise decrease by circadian clock in Limulus brain 0-94210
 retinal research and study, selected review 0-108874
 retinotectal projection in goldfish to an inappropriate region with a reversal in polarity 0-72153
 retrolental fibroplasia, A-mode ultrasonography and oculometry 0-89816
 rods, toad, spontaneous quantal events induced by pigment bleaching 0-108895
 saccades, differential responses of 'simple' and 'complex' cells of cat's striate cortex 0-85394
 saccades, small, lack of useful purpose considerations 0-61553
 saccadic eye movements, small, perceptual function 0-61577
 saccadic latency predictability in a novel voluntary oculomotor task 0-72157
 screening-pigment migration in retinula cells of crayfish, spectral sensitivity 0-72165
 senile macular degeneration, colour discrimination rel. to visual acuity 0-108897
 shields, individualised, for electron beam therapy and low-energy photon irradi. 0-109040
 simulator of human visual system (Russian) 0-76877
 slit lamp, hand-held, with lid opener for ocular exam. 0-67179
 slit lamp photodocumentation of ocular structure 0-67181
 smallest channel in early human vision 0-101178
 smooth pursuit movements, target position and vel. as stimuli 0-85392
 spectral eye fatigue, school lighting effects 0-76732
 spectral reflectance photography of the ocular fundus 0-67184
 spectral sensitivity of human eye, colour coordinates number triple (Russian) 0-76741
 spectral sensitivity of human eye, deductive derivation of mathematical model (Russian) 0-76740
 specular reflections by polaroid films, pot. eye hazard 0-85447
 strabismic cats, eye movement obs. 0-89748
 strabismus, fusional convergence ranges using random dot stereograms, operant conditioning 0-108900
 striate cortex functional architecture quantitative model 0-89747
 tapetum lucidum, cat, morphology obs. 0-108878
 target tracking, eye movement evaluation using EOG 0-109057
 transient sensitisation by a contrast flash 0-72162
 two eyes constituting separate visual channels, expts. 0-97923
 US in ophthalmic diagnosis 0-81673
 vergence and accommodation static behaviour, computer simulation of interactive dual-feedback system 0-94205
 vergence control, role of spatial freq. tuned channels 0-101170
 vertebrate retina modelling and simulation, extended networks 0-108884
 vertebrate retina neuronal activities modelling and simulation 0-85386
 vertebrate retinas, outer segment layer, light-induced Ca fluxes 0-94207
 vertical fixation disparity, correction by horizontal prism 0-67281
 vestibular control of oculomotor and postural mechanisms 0-72151

F-centres

see also A-centres; M-centres; R-centres; Z-centres

alkali chlorides, positron-trapping colour centre dynamics, positron annihilation study 0-108294
 alkali halide: H⁻ (D⁻), local modes and colour centre absorpt. bands, analogy 0-60632
 alkali halide hologram, high-efficiency recording by selective colloidal centre destruction 0-63955
 alkali halides, divalent cation doped, irradiated, first-stage F-centre prod. 0-107231
 alkali halides, emission band of F-centre 0-76071
 alkali halides, F-centre accumulation, radiation induced, temp. depend. 0-59460
 alkali halides, F-centres, ESR in different states of relaxed configuration 0-108067
 alkali halides, gamma and additively coloured, dissolving in pure water, lyoluminesc. mechanism 0-100693
 alkali halides, saddle-point configuration, molecular model parameter 0-107234
 alkali halides, Z₁-centres, peculiarities of thermolum. 0-103999
 alkali metal chloride crystal, F centre energy level shift and splitting in O⁻ field 0-70640
 alkali metal halides, F-colouring role of impurities 0-64995
 dilute metal solutions in molten salts, optical absorption, F-centre model for bound state 0-89023
 dislocation influence on optical props. 0-108234
 laser used for IR optogalvanic spectrosc. of He positive column discharge 0-78563
 lasers, colour centre, thermal strains in active elements, theory 0-91804
 NaCl, dislocation charge photostimulated variation kinetics (Russian) 0-79806

F-centres continued

- sapphire, F-centre, fluorescence decay below 75K 0-60664
 sapphire, neutron bombard., F-centre fluorescence, photoluminescence 0-100676
 β -Al₂O₃-Na₂O, X-ray induced defects, EPR and ENDOR study 0-60456
 Ca fluorapatites, carbonated, B-type, EPR of F⁺-centre after X-irrad. (French) 0-108065
 CaF₂:M, M=Mn, Fe, Co, Ni, X-irrad., impurity effects on defect prod. 0-92525
 CaO, EPR of colour centres, 295K (Russian) 0-84649
 CaO, obs. of dipolar induced spin dephasing, coherent optical-microwave spectroscopy 0-103900
 CaO, photoionisation of F-centre, luminesc. and photocond. meas. 0-66270
 CaS, EPR of colour centres, 295K (Russian) 0-84649
 CdS, electron and hole trapped centres, EPR, photoluminescence, photoconductivity study 0-108071
 Cs halides, F-centre energy levels, ion-size effects, calc. 0-96519
 CsBr, F-centre absorpt., uniaxial stress effects 0-60634
 KBr, colour centre form. under polarised UV irrad., dichroism in absorption spectra 0-107232
 KBr, defect accumulation under electron irrad. at 4K 0-107233
 KBr, F-centre lifetime, perturbation effects, luminesc. meas. 0-108252
 KBr, gamma-irrad., hologram recording by F-centre bleaching 0-78814
 KBr, recomb. in ionic crystals., defect interaction 0-84206
 KBr, recomb. in ionic crystals., defect interactions 0-84207
 KBr, self-trapped exciton form. via thermally induced defect reactions 0-60687
 KBr(I), photostimulated recomb., electron spin polarisation 0-60673
 KCl, F-centre formation at highly excited triplet states of self-trapped excitons 0-76066
 KCl, F-centre relaxation kinetics, temp. depend. following electron irrad. 0-92527
 KCl, γ -irrad., F-centre absorpt., flash-stimulated changes 0-92524
 KCl surface, VUV irrad., colour centre layer, angle-of-incidence derivative ellipsometry and reflectometry 0-73420
 KCl, thermoluminesc., halogen and alkali impurity effects 0-97352
 KCl, X-ray irradiated, first-stage F-centre prod. 0-107231
 KCl:Ag, X-irrad., thermoluminesc. study of Ag centres 0-80874
 KCl:Na, F_B centre energy levels 0-107738
 KCl:Pb²⁺, pure and doped, electrolytically coloured, elec. cond. and optical absorpt. meas. 0-100668
 KCl:Pb²⁺, X-ray irrad., electron-trapped centres, Pb⁺ and Pb⁰, optical absorpt. spectra 0-71461
 KCl(Br), F-centre emission, mag. circular polarisation 0-108251
 KCl:Br₂, mixed crystals, thermolum. and optical absorption studies 0-104000
 KCl(I), electron range-energy relation, thermally created lattice vacancies effect 0-92574
 KI, self trapped exciton form. time at ¹S₀⁺ state under pulsed electron beam in ps range 0-97347
 KI, self-trapped exciton form. via thermally induced defect reactions 0-60687
 KMgF₃, F-centre ENDOR study 0-108117
 LiCl, radiation effects on decay time of F-centre emission 0-93381
 LiF, F-centres, defect electron struct., extended-ion model calcs. 0-59907
 LiF:Mg,Ti, defect states, ESR and ionic cond. study 0-108058
 LiH, defect form. at low temp., EPR, thermolum. and TSC study 0-107222
 LiH, formation and annihilation of Li colloids and H bubbles 0-107228
 LiF pellets, sintered, neutron irradiated, ESR study 0-92566
 LiYF₄, electron-irrad. induced defects, optical and EPR study, impurity effects 0-66238
 MgAl₂O₄, radiation damage, optical absorpt., F-centres 0-64994
 Na₂Al₂(Si_{0.95}Ge_{0.05})₂O₂₄.2NaBr, Ge-doped sodalite powders, UV absorpt. band 0-71452
 Na₂Al₂Si₂O₂₄(NaX)₂, X=Cl, Br or I, sodalites, thermal destruction of colour centres (Russian) 0-84169
 Na₂Al₂Si₂O₂₄.Cl(Br)(I), cathodochromic sodalites, coloured crystals, tunnel and recomb. luminesc., temp. depend. (Russian) 0-66261
 Na₂Al₂Si₂O₂₄.NaX₂(₂₋₉), (X=Cl, Br, I), X-ray irrad., thermal-erase cathodochromism and dihalide mol. centres (Russian) 0-66236
 NaBr(I), optically activated F⁻F⁺ centre conversion in mag. field 0-108253
 NaCl, amplitude phase hologram recording on colloid type centres (Russian) 0-69347
 NaCl crystals, electronic and hole centres and surface, quantum-chemical calcs. 0-65489
 NaCl, F-centers, laser irrad. optical bleaching kinetics 0-66244
 NaCl, γ -irrad., F-stimulated inversion of sign of dislocation charge 0-59475
 NaCl, pure and doped, 20K X-ray irradiation, thermolum. and recovery processes 0-93412
 NaCl, self-trapped exciton form. via thermally induced defect reactions 0-60687
 NaCl:Cu⁺, electrolytically coloured, electron trapping, optical absorpt. 0-100672
 NaCl:Mn²⁺, thermolum. spectra, mechanisms 0-80873
 NaF:Mn, role of Mn²⁺ in thermolum. 0-97353
 NaF:U, luminesc. spectra, Vib. struct. 0-80840
 NaI:F, electron-lattice coupling of F-centres, optical props. 0-60641
 NaMgF₃, defects induced by X- and vacuum UV irrad., optical and elec. study 0-107319
 RbBr, self trapped exciton form. time at ¹S₀⁺ state under pulsed electron beam in ps range 0-97347
 RbCl, electron bombard., colour centre photoemission, surface contamination and escape depth 0-66392
 RbCl:Ca²⁺, thermolum. and optical absorption studies 0-104002
 RbCl(Br), F-centre emission, mag. circular polarisation 0-108251
 RbI, photostimulated recomb., electron spin polarisation 0-60673
 RbMnF₃:Fr, pure and doped, unirradiated and electron irrad., energy transfer 0-108254
^{85,87}RbCl isotope enriched cryst., optical registration of EPR F-centres (Russian) 0-103886
 Y₂O₃:Zr³⁺, F-centre charge state, ESR and thermally stimulated luminesc. obs. 0-60418
 ZnO, defect struct. calc., doping effects 0-107218
 ZrSiO₄, X-irradiated, trapping and emission centres, thermolum. meas. 0-89076
- F₂-centres** see *M-centres*
F₃-centres see *R-centres*
F₄-centres see *A-centres*
F-layer see *F-region*
F-region
 airglow, anal. of consistency of ground-based obs. with satellite results 0-98496
 airglow of at. O rel. to short wave radio absorpt. 0-77184
 aurora associated with magnetospheric cusp 0-90273
 auroral convection over 60°≤Δ≤75°: Millstone Hill incoherent scatter obs. 0-67454
 bubbles in equatorial spread F, nonlinear evolution 0-85801
 bubbles seen in topside soundings of spread F, characts. 0-85800
 collisional Rayleigh-Taylor instability in equatorial spread F 0-82138
 critical frequency, rel. to ionosphere global scale electrodynamic coupling of high and low latit. regions 0-77194
 current convective instability in auroral F-region 0-72680
 diffusion equations, coupled time-dependent, numerical method using self-diffusion coeff. 0-109285
 disturbances, large scale periodic, Faraday fading of satellite 40 MHz signals 0-101475
 drift variability above Tiruchirappalli, rel. to electrojet strength 0-82129
 electron density inhomogeneity, thermomdiffusion mechanism (Russian) 0-85791
 electron energy distrib. above aurora, secondary peaks driving instability 0-82135
 electron temp. model, Aeros-A data compared to radar obs. 0-67465
 energetic electrons spectra, meas. by Hadamard energy spectrometer (Japanese) 0-94637
 equatorial, drift measurement of Ba cloud, spaced receiver technique 0-72678
 equatorial anomaly, counter electrojet assoc. changes, upward drifts reversal 0-109292
 equatorial anomaly, counter electrojet assoc. changes, upward drift reversal obs. 0-109297
 equatorial spread-F, coincident radar and rocket obs. 0-105111
 equatorial spread-F, seasonal and solar cycle vars. in American zone 0-109298
 equatorial spread-F in American and Indian zones, seasonal var. 0-72689
 equatorial spread-F irregularities, spatial relationship with plasma bubbles 0-67457
 equatorial spread-F meas. by Altair incoherent scatter radar 0-61927
 F₁-layer, ion comp. and temp. profiles from incoherent scatter radar studies 0-72654
 F₁-layer at nighttime, ion composition near mag. equator 0-72683
 F₂-layer, bottomsides, electron depletion obs. assoc. with mid-latit. ionosphere trough 0-109300
 F₂-layer, parameters at high latitude during quiet conditions 0-105106
 F₂-layer, seasonal difference in ionisation and height due to neutrals 0-61951
 F₂-layer during daytime, servo model 0-101486
 F₂-layer electron density, mag. storm effects 0-61970
 fading records over Tiruchirappalli (1973-5), cross spectral anal. 0-101478
 global electron temp. distrib. model, 300-700 km altitude 0-67464
 heating by powerful radio emission with random modulation of carrier freq. 0-109310
 ion convection at high-latitude, nighttime 0-85797
 ionisation enhancements, rel. to localised nighttime auroral zone scintillation enhancements 0-98506
 irregularities and background density of equator region, VHF and UHF radar obs. 0-77222
 large-scale artificial inhomogeneity spectrum 0-98515
 magnetic storms affecting electron composition, 140 MHz obs. 0-101471
 neutral zonal winds, contrib. to interhemispheric ion transport 0-98509
 peak electron density, diurnal and solar cycle variation 0-61949
 perturbation by electron precipitation in cleft region during substorm 0-101483
 plasma cloud, intermediate wavelength EXB gradient drift instability 0-105114
 plasma cloud striations, study of outer scale size 0-90279
 radiowave heating using HF signal, plasma line enhancement 0-82140
 radiowave propag., generalized magnetoionic formulae 0-61963
 spread-F, range and frequency spread occurrence at Kodaikanal 0-72676
 spread-F formation 0-72712
 spread-F in equatorial ionosphere, assoc. with radio scintillations 0-77191
 spread-F plasma bubbles in equatorial topside region 0-72694
 strong mag. storms affecting equatorial f_o 0-77197
 temperature and ion chemistry at nighttime, 400-450 km altitude, Ogo 6 data 0-90267
 temperature and wind measurement Fabry-Perot-interferometer imaging system appl. 0-101441
 thermal parametric instability, effect of recomb. processes and plasma nonisothermability 0-61967
 TID phenomena at nighttime, distrib. and occurrence 0-77206
 TID phenomena in F-region, influences of thermosphere winds 0-109305
 VHF radar aurora and strong HF backscat. comparison 0-61960
 winds affecting O⁺ and H⁺ equal ionisation level 0-90280
 winter anomaly causes 0-85793
 Ba cloud release, computer simulation of gradient drift instability 0-85802
 F₂-layer, plasma ambipolar diffusion and vertical drift at low latitude 0-101472
 F₂-layer electron density var. with latitude during geomag. storm. 0-101474
 N atom and O ions in dynamic model, daytime high-latitude 0-72693
 N⁺ photochem. rel. to solar cycle phase 0-85783
 O⁺+N₂(O₂), excited ion reactions, charge transfer coeffs. at thermal energy 0-95721
 O⁺+N₂(O₂), metastable ion reactions, rate consts. and ion mobility at 300K 0-95722
- f-values** see *oscillator strengths*
faces (crystal) see *crystal faces*
facsimile
 see also *video signals*
 METEOSAT 1 weather satellite pictures, amateur reception (German) 0-81982
 picture direct transmission via single optical fibre 0-106628
 weather chart transmission for military apps. 0-90206
 weather satellite picture processor for TIROS-N series, visible and IR pictures 0-67439

facsimile communication *see facsimile*

facsimile document reproduction *see photocopying*

facsimile signals *see video signals*

facsimile transmission *see facsimile*

faculae *see Sun*

fading

see also radiowave propagation

E-region, fading records over Tiruchirapalli (1973-5), full correl. anal. 0-101473

ionosphere, E- and F-regions over Tiruchirapalli (1973-5), cross spectral anal. 0-101478

ionosphere, spaced fading obs. of ionisation irregularity drift motion 0-82133

ionosphere electron density of Delhi and latitudinal depend., INTASAT Faraday fading obs. 0-109293

Mitra-type fading near travelling ionospheric disturbances, cross spectral anal. 0-82128

spaced receiver fading obs. at Thumba 0-109296

sporadic-E affecting ELF wave propag. at nighttime 0-77202

sporadic-E layer, VHF fading evidence for F-region disturbances 0-101475

VLF atmospherics anomalies rel. to rainy days over Calcutta 0-82127

failure (mechanical)

see also fracture; mechanical strength; plastic deformation

alloys, statistical model, in conditions of monotonous cyclic loading (*Bulgarian*) 0-70296

composite materials, tension stability, deformation up to failure (*Russian*) 0-75289

composites under complex loading, failure criteria 0-81206

geological materials failure, role of acoustic fluidisation 0-85653

metals, statistical model in conditions of monotonous cyclic loading (*Bulgarian*) 0-70296

solar cell life prediction using physical chemical failure progression modelling 0-61370

stator windings, failure mechanisms under thermal cycling (*Japanese*) 0-104189

surface profilometry, role in diagnosis 0-66676

viscoelastic material, failure and instability in tension 0-87720

failure analysis

see also wear

aircraft metal fatigue crack detection using nondestructive evaluation (NDE) methods 0-71826

fatigue failure, rupture, continuous damage mechs., uniaxial homogeneous state of stress 0-74806

fission reactors, failure probability distrib. from observed failure data, beta distrib. 0-63335

fission reactors, shutdown heat removal system failure, fault tree, common-cause anal. 0-63334

fission reactors, shutdown heat removal systems, reliability fault tree anal. and β -factor method 0-63331

fractography, fractures preservation and cleaning 0-71866

implanted prosthesis failure analysis techniques and results 0-89906

metallisation corrosion, IR microscopy technique 0-98976

metals structural failures, for industrial appl. 0-76429

micromechanical models in risk anal. 0-108572

plates, symmetrically laminated cross-ply rectangular, initial flexural failure anal. 0-64461

safety determ. from defect evaluation rel. to fracture mech. (*German*) 0-100908

solar cell fault analysis using scanning light spot and distrib. network model 0-81473

spacecraft materials failure, metallurgical exam. 0-71868

stress corrosion cracking failure, predictive approaches 0-97611

tools comparison and selection 0-71865

fallout

see also air pollution

W.Cumbria, Pu and ^{137}Cs concs. in environmental samples and possible maritime effect 0-108817

N.Europe air radionuclide conc., due to Chinese nucl. explosion 0-108826

sediment mixing and accumulation, fallout tracer obs. 0-81864

Ural disaster questioned, possible fallout from atmospheric test 0-76666

^{24}Am concs. in sediments from coastal basins off California and Mexico 0-98303

^{14}C pollution of Atlantic from nucl. weapons tests 0-89683

^{113}Cd in marine organisms and sediment around Marshall Island nucl. test site 0-109174

Pu fallout detection using fission tracks prod. with neutron irradi. spectra 0-95479

Pu in alkaline, saline lakes 0-97826

^{24}Pu concs. in sediments from coastal basins off California and Mexico 0-98303

Faraday effect

atomic system, nonlinear variations in strong mag. field 0-79429

cubic crystals, paramagnetic nonlinear Faraday effect, EM wave propagation (*Russian*) 0-80761

dye ring laser, CW, optical diode to enforce one-direction travelling wave operation 0-69427

electric current measurement, AC, using magneto-optical methods, principles and advantages (*Polish*) 0-105676

ferromagnet, microwave modulation of light using magnetodynamic resonance 0-71393

fibre Faraday rotators in fibre Raman lasers 0-58775

garnet films, meas. using magneto-optical apparatus 0-105680

garnets, IR refl., ATR, Voigt and Faraday expts. 0-66180

Hubbard model, Green function method, conc. depend. of Hall and Verdet coeffs. 0-80240

inhomogeneously magnetised media, Faraday effect, polarisation plane rotation (*Russian*) 0-66154

ionosphere, Faraday effect meas. at 140 MHz using two-channel polarimeter first results 0-61912

ionosphere, Faraday rot. meas. rel. to dissimilar forms of equatorial anomaly in E.Asia and India 0-109301

lightguide, magneto-optical props., weak microwave field meas. 0-73463

low Verdet constant material in Faraday rotator 0-69520

M87 radio emission, Faraday rot. in radio/X-ray halo 0-67844

measurement in pulsed mag. field 0-80758

measurement of magneto-optic rotation and ellipticity, spinning analyser ellipsometer (*Japanese*) 0-73419

Faraday effect continued

MHD devices, plasma ionization instability, dynamic suppression, switching modelling 0-59308

MOS structure, 2D electron gas, far IR Faraday rotation 0-80389

Neel ferrimagnets, phase transitions, field-induced spin-orientational 0-75767

optical fibre, highly birefringent, Faraday rotation 0-58672

optical quanta counting procedure, magneto-optical transition radiation, Cherenkov radiation (*Russian*) 0-80760

paramagnetic centre crystals, nonlinear optical Faraday effect 0-99811

paramagnetic system with quadrupole splitting, magneto-optical effects, magnetic resonance saturation 0-60404

plasma, hot, mag. field determ. using Faraday rot. (*Rumanian*) 0-87950

plastic:Eu $^{3+}$, Faraday rotation sign oscill. in very strong mag. fields (*Russian*) 0-88973

rare earth garnets, RIG, (R=Tb, Dy, Ho, Er), spontaneous Faraday rot. rel. to sublattice magnetisation 0-66159

semiconductor, p-type, Faraday effect due to free holes 0-97247

superconductor Faraday effect obs. in polarising microscope 0-70892

toroidal controlled fusion poloidal mag. field meas. by far IR Faraday rotation 0-59303

transparent synchrotron astronomical sources, internal Faraday rot. effect 0-72760

a-As $_2$ S $_3$, energy gap meas., by Faraday rotation 0-66161

Bi, Faraday effect and magnetic circular dichroism 0-83399

Bi $_3$ film, exciton-phonon interaction, optical consts., Faraday effect., permitt. 0-59884

CaF $_2$:U $^{3+}$, anomalous magneto-optic props., optical detection of ESR and cross-relax. resonances 0-93287

CdTe AC Faraday rotation devices for far IR laser intracavity polarisation modulation 0-58613

(Co,Cr,Fe) $_2$ O $_4$, (Co,Rh,Fe) $_2$ O $_4$ film magneto-optical switches, for laser beam synchronisation 0-58615

EuO film threshold characteristics in holographic and bit recording (*Russian*) 0-63944

EuO $_2$ single crystals, Faraday effect, near IR, effect of carriers 0-71395

Fe $_2$ BO $_6$, Faraday rotation and birefringence 0-100650

Fe $_2$ O $_4$, IR refl., ATR, Voigt and Faraday expts. 0-66180

GaP:Fe, optical absorption spectrum and Faraday effect 0-108245

GaSe, Faraday rot. near absorpt. edge, optical dispersion meas. 0-80757

(Gd, Bi) $_2$ (Fe, Ga) $_2$ O $_7$ magneto-optic LPE garnet films, high-energy heavy ion irradi., props. 0-71390

GdFeBi, amorphous ferrimag. films, magneto-optical props., optical spectra 0-76008

Gd $_2$ Ga $_2$ O $_7$, IR refl., ATR, Voigt and Faraday expts. 0-66180

GdIG, IR refl., ATR, Voigt and Faraday expts. 0-66180

Ge, standard measures of magneto-optical rotation of plane of polarisation in IR region 0-60551

InP, Faraday interband effect subjected to quantising mag. fields 0-97246

n-InSb, Faraday effect in strong EM fields 0-93286

InSb, intensity depend. interband Faraday rot. obs., saturation and reson. enhancement effects 0-108186

InSb, standards for magneto-optical rotation, charge carrier density determ. in semiconductors 0-60551

n-InSb submillimetric-wave free-carrier Faraday effect in strong longitudinal elec. field 0-66164

KMgF $_2$:Ni $^{2+}$, acoustic Faraday and Cotton-Mouton effects, theory 0-65987

KMnF $_3$, Faraday effect mechanism in paramag. phase 0-60552

MnSb $_{1-x}$ Sn $_x$ films, Faraday rotation, optical absorpt. coeffs. 0-97242

NO vibr. overtone band, mag. rot. spectrosc. obs. 0-86446

Na $_2$ O.SiO $_2$.Tb $_2$ O $_3$ glass magneto-optical study 0-88976

Nb $_2$ S $_3$, flux density gradient determ. by Faraday effect 0-107969

Ni, paramag. region, Fe and Co impurity effects on susceptibility, Faraday obs. (*Russian*) 0-88731

OH, fundamental vibr. band, mag. rot. spectrosc. obs. 0-86446

Pb $_1-x$ Ge $_x$ Te magnetoplasma reflectivity and transmission spectra 0-71428

RbMnF $_3$, Faraday effect mechanism in paramag. phase 0-60552

n-Si, Faraday rot. temp. depend., effective mass determ. 0-71392

SiO $_2$.Na $_2$ O.Nd $_2$ O $_3$ glass, magneto-optical props., absorpt. spectrum 0-88969

Tl $_2$ (Te,Se) $_{1-x}$ mixtures, liq., electrical conductivity, magnetic susceptibility 0-88715

UO $_2$, electronic transitions, crystal field effects and phonons, phase transition 0-97303

YFe $_4$ Ga $_6$ O $_7$ domains, neutron depolarisation and Faraday rotation study 0-93137

Y $_2$ Fe $_4$ Ga $_6$ O $_7$, domain struct., neutron depolarisation and Faraday rot. 0-71084

YIG, Faraday effect, influence of mag. field on sublattice contributions 0-88975

YIG, one-magnon Raman scatt., Faraday rot. 0-66156

YIG thin film gyromag. waveguide, on GGG substrate, optical propag. props. Faraday effect 0-74513

YIG:Tb garnet, Faraday effect in strong mag. field (*Russian*) 0-100651

(YRb)(FeAl) $_2$ O $_7$ films, R=Gd, Yb, Faraday effect in transverse mag. field, orientation depend. 0-88971

farming

field burning practice, downwind particulate pollution 0-97836

photovoltaic powered 20-hp DC/AC irrigation system and 3-kW N generator 0-89645

fast amplifiers *see pulse amplifiers*

fast Fourier transforms

air coils, FFT calc. of mag. fields 0-74280

double beam interferometer for background suppression and spectral detection 0-95129

gamma ray spectra anal., fast Fourier transform (*Chinese*) 0-77762

heart fourth sound studied by FFT 0-94397

image recognition by generalised harmonic analysis (*Russian*) 0-63930

image restoration for invariant pointspread functions 0-69332

linear wave motions study using FFT, NDT appl. 0-92038

nuclear reactor component vibration investigation using fast Fourier transform analysers 0-63315

optical fibre diameter measurement using fast Fourier transform 0-91894

optical systems analysis using two-dimensional FFT algorithm 0-78986

plano-plano interferometer modes, FFT computation, Fresnel numbers 0-86392

fast Fourier transforms continued

- SEM diffractogram online computation 0-70095
- spectrum analyser appl. (*Spanish*) 0-90825
- speech adaptive noise cancellation by short-time Fourier transform 0-91976

fastening see joining processes**fatigue**

- for corrosion fatigue see stress corrosion cracking; for thermal fatigue see thermal stress cracking
- see also fatigue cracks; fatigue testing
- acoustic emission 0-97673
- after-effects in thermo-elasticity 0-106724
- alloys, high temperature, creep failure criteria 0-65150
- aortic valve tissue, porcine, glutaraldehyde-treated, mech. fatigue study 0-67112
- bluntly notched members, fatigue life estimates 0-100999
- brass, spring alloys, microplastic deform. and endurance limit 0-81197
- α - β brass, two phase bicrystal, fatigue 0-108520
- cables design and testing, optical fibre, w.r.t. stress-strain behaviour 0-69551
- ceramics, subcrit. crack extension charact. (*German*) 0-100888
- complex stress state, equivalent stress in theory of fatigue fracture 0-79230
- composite insulating materials, fatigue behaviour, influence of superposition of elec., mech. and environmental stresses 0-97590
- composite laminates, proof test and fatigue study 0-93643
- damage analysis under nonproportional cycling 0-97556
- dislocation structures, and fracture surfaces in fatigue (*Japanese*) 0-65144
- failure, rupture, continuous damage mechs., uniaxial homogeneous state of stress 0-74806
- fatigue limit, in bi-freq. loading 0-104289
- ferromagnetic solids, magnetomechanical effects, magnetostriction, hysteresis, stress, yielding, fatigue damage, crack growth (*Polish*) 0-71150
- fibre, single-mode, numerical aperture effects 0-69548
- fibre reinforced composite aircraft materials, design allowables 0-81204
- fibre reinforced plastics, under random loadings, mathematical model and digital simulation (*Japanese*) 0-85032
- fibres, optical, high-strength, use of surface compression cladding 0-69549
- fusion reactor first-wall structures, fatigue life criteria 0-86980
- glass, fracture and fatigue, crack tip radii influence 0-89335
- glass fibre reinforced plastic, fatigue fracture kinetics studied by diffusion scatt. of luminous fluxes 0-76446
- glass fibre reinforced plastic, fatigue processes, review 0-81176
- glass fibre reinforced plastic laminates, strength and deformability, artificial ageing effect 0-60893
- glass reinforced polyamide 6, fatigue strength after heat treatment, ageing and coating of Al-containing lacquer (*Polish*) 0-89347
- graphite fibre reinforced epoxy, US attenuation as an indicator of fatigue life 0-85118
- graphite/epoxy laminate, T300/5208, proof testing under cyclic tension-tension fatigue 0-81249
- graphite/epoxy laminates, statistical fatigue, high load effect 0-93642
- hydrostatic stress-sensitive relationship for biaxial stress conditions 0-74805
- hydroxylapatite, dense, fatigue and fracture strength from diametral tests, after various treatments 0-60953
- laminate, anal. 0-104253
- life determination for structural elements, based on fatigue crack propag. theory 0-81182
- life distribution estimation, from S-N curve (*Japanese*) 0-71737
- lightguide fibre, ensuring mechanical reliability 0-79001
- linear fracture mechanics parameters, in fatigue life estimation, sensitivity study (*Japanese*) 0-64468
- metal, notched, cyclic stress/strain behaviour, random fatigue life (*German*) 0-100907
- metal fatigue crack detection using nondestructive evaluation (NDE) methods 0-71826
- metal fatigue tests for plastic deformation (*Hungarian*) 0-97665
- metallic materials, fatigue life distrib. theoretical obs. near fatigue limit 0-59569
- metals, fatigue resistance, processes leading to failure 0-94907
- metals, inelastic cyclic strain under nonuniform stress state conditions, residual stresses effect 0-81132
- micromechanisms of crack extension, conf., Cambridge, England (March 1980) 0-105421
- mortar specimens, repeated impact bending load study (*Japanese*) 0-93622
- numerical expressions of fatigue results (*Japanese*) 0-62455
- optical fibre, UV cured epoxy acrylate coated, zero stress ageing effect on strength 0-58753
- optical fibres, $\text{GeO}_2\text{-B}_2\text{O}_3\text{-SiO}_2$, ageing effects of moisture on fatigue and tensile strength 0-66539
- optical fibres, mech. reliability 0-91909
- optical fibres, tensile strength and static fatigue, analysis using Weibull distribution for optimum design 0-85011
- PMMA, fatigue life enhancement, prior crazing 0-89331
- polymer, crack tip failure mechanism modelling 0-108565
- polypropylene, microstruct. changes during large strain cyclic deform. 0-66627
- powder metallurgy, fatigue strength significance (*German*) 0-60946
- PVC, fatigue life, influence of cyclic loading conditions 0-76350
- radial impeller blades, unsteady aerodynamic forces and moments, singularity method obs. 0-58952
- rectangular parallelepiped, fatigue fracture in complex stress state 0-79229
- rolls in hot strip mills, contact fatigue failure 0-60950
- scale effect in the resistance to fatigue in the complex stressed state 0-74807
- solar collectors with multilayer cylinder heat exchangers, heat balance eqn. and thermal stress anal. 0-58977
- statistical methods for creep, fatigue and fracture data analysis 0-58936
- steel, 0.7% C, welded zone, fatigue strength and microstruct. (*Japanese*) 0-89339
- steel, 12Cr1MoV, thermal fatigue and creep effect in fracture 0-104297
- steel, (0.36 wt.% C) Ni-Cr-Mo, electrosag refined, fracture toughness and fatigue behaviour 0-81171
- steel, Al-killed, fatigue life for program loading of multiple repeated two step stresses (*Japanese*) 0-66632

fatigue continued

- steel, alloy, 15KhM1 and 20KhM1, plastic deform. with thermal cycling 0-89310
- steel, alloy, quenched carbonitrided, multicycle fatigue failure 0-104283
- steel, alloy 10G2S1 welds, fracture, subjected to low-temp. fatigue 0-89350
- steel, austenitic stainless, fretting corrosion of orthopaedic implant materials by bone cement 0-104813
- steel, austenitic stainless, nonsensitized, fatigue strength, intergranular corrosion effect (*Japanese*) 0-85027
- steel, austenitic stainless, supercond. magnets, mech. and phys. props. at 4K 0-86976
- steel, austenitic stainless, thermal fatigue, fractographic features of failure 0-76349
- steel, austenitic stainless, type SUS 304, low cycle fatigue strength reduction factor (*Japanese*) 0-104259
- steel, austenitic stainless, types 304 and 316, environment effect on crack growth, under creep and fatigue conditions 0-85035
- steel, austenitic stainless type 304, time-depend. fatigue, mechanistic model 0-100925
- steel, austenitic stainless type SUS 316, low cycle fatigue tests, freq. effect on notch sensitivity at elevated temps. (*Japanese*) 0-104260
- steel, ball bearing, fatigue damage, influence of dispersed phases in martensitic matrix 0-108549
- steel, C, rolling contact fatigue, tufftriding effect on 0.2% C cylindrical specimen 0-100954
- steel, C, type SFVV1, low cycle fatigue strength reduction factor (*Japanese*) 0-104259
- steel, C, unnotched, fatigue life estimation, under combined torsion and bending (*Japanese*) 0-93647
- steel, Cr-Mn, low-cycle fatigue at 20 and -196°C 0-81196
- steel, Cr-Mo, notched specimens, fatigue strength distrib. (*Japanese*) 0-66633
- steel, Cr-Mo (2.25, 1 wt.%), creep and high temp. low-cycle fatigue tests 0-85061
- steel, Cr-Mo (2.25, 1 wt.%) pipe, high temp. fatigue and creep strength 0-85060
- steel, eutectoid, mech. behaviour, thermomech. treatment effects 0-84970
- steel, fatigue and cyclic plasticity rel. to struct. inhomogeneity 0-81184
- steel, fatigue damaged, fracture toughness 0-89353
- steel, fatigue life, influence of cyclic loading conditions 0-76350
- steel, fatigue limit assessment, progressive load methods (*German*) 0-61058
- steel, fatigue strength, low cycle overload effect 0-60967
- steel, fracture in low-cycle fatigue tests in H_2 (*Russian*) 0-76332
- steel, high-strength, fatigue, interaction effects between trace impurities and environment 0-66651
- steel, high-strength, low cycle fatigue, hysteresis loops, cyclic strain curves, fatigue diagrams (*Polish*) 0-66638
- steel, high-strength, type 4340, new inhibitors for crack arrestment in corrosion fatigue 0-100941
- steel, hot forging die type, fractography (*Japanese*) 0-108547
- steel, low alloy, high strength, fatigue crack growth, in presence of welding residual stresses (*Russian*) 0-71739
- steel, low and medium C, fatigue strength, small defect effect 0-104255
- steel, low C, cyclic loading, change in mech. props. rel. to heat treatment 0-104282
- steel, low C, fatigue life, variable strain ranges (*Czech*) 0-60956
- steel, low C, type 38NCD4, fatigue life improvement by N ion implantation, dose depend. 0-76328
- steel, low-C, fatigue strength and crack propag. behaviour under impact program loading conditions (*Japanese*) 0-66635
- steel, martensitic, fatigue life, low-cycle, temp. and strain rate effects 0-85056
- steel, medium C, electrolytic Fe coated, distrib. of bounded fatigue limits 0-81198
- steel, mild, cyclic strain enhanced dissolution in NH_4NO_3 , corrosion fatigue props. 0-85083
- steel, Mn-Si, fatigue, level of prior cyclic stresses effect 0-89348
- steel, Ni, high-strength, impact fatigue strength, heat treatment conditions effect 0-76285
- steel, Ni-P plated, electroless, fatigue strength and plated layer microstruct. (*Japanese*) 0-93645
- steel, notched specimens in sea water, endurance limit enhancement, specimen size, freq. effects 0-93678
- steel, plain C, having ferrite-martensite mixed structs., microstructural parameters effect on fatigue strength (*Japanese*) 0-71735
- steel, powder forged, fatigue, surface treatment effect 0-85048
- steel, rolled, anisotropic, fatigue fracture surface obs. (*Japanese*) 0-108546
- steel, shafts, type 45, fatigue strength improvement after glow discharge treatment 0-108573
- steel, sheets bonded with low density polyethylene, static fatigue (*French*) 0-108522
- steel, spring alloys, microplastic deform. and endurance limit 0-81197
- steel, stainless, austenitic, deform. substruct. and annealing, stacking fault tetrahedra form 0-107282
- steel, stainless, orthopaedic, type En58J, Mo ion-plating, corrosion fatigue 0-66694
- steel, stainless, type 316, low cycle fatigue props. in vac., fracture mode 0-85021
- steel, stainless 304, crack propagation under fatigue-creep conditions and fractography (*Japanese*) 0-104267
- steel, stainless 304 sol. of annealed and thermally-aged, high-cycle fatigue behaviour 0-100923
- steel, strain-hardened subsurface layer, residual stress change in fatigue 0-81185
- steel, tempering effect on fatigue strength 0-60891
- steel, TRIP, fatigue strength 0-108552
- steel, tufftrided, type S15CK, fatigue strength, estimation of size effect (*Japanese*) 0-81166
- steel, type IN-787, for use in Arctic, low temp. effects on mech. props. 0-76310
- steel, type Man-Ten, and KQC-100, fatigue life estimates of bluntly notched members 0-100999
- steel, type SAE 1008, finite fatigue life distrib., various load-time histories 0-97589
- steel, US strengthening treatment effect on fatigue resistance 0-81193
- steel (*French*) 0-66670
- steel 1Kh17N25h, fatigue failure, surface finishing influence 0-60972
- steel ball bearing, fatigued, phase changes, nomenclature 0-89198

fatigue continued

- steel bearing, surface-ground, residual stress fatigue property comparison 0-60975
- steel SW7M, low-cycle fatigue at high hardness levels (*Polish*) 0-89323
- steels, low-C, aged after quenching, rel. between micro-cracks and coarsening effect (*Japanese*) 0-81159
- steels and alloys, fatigue limit, static and cyclic loading 0-71755
- strength prediction, U_0^* procedure using Woehler tests (*German*) 0-71850
- test data, statistical anal. (*Japanese*) 0-62452
- UHV fatigue drive, design and performance 0-86328
- Weibull distribution, adding static and dynamic fatigue effects 0-70298
- Weibull distribution, three parameter estimation rel. to parameter estimation of fatigue life distrib. (*Japanese*) 0-65130
- Zircaloy-2 fuel tubes, cumulative damage fatigue tests at room temp. and 300°C 0-93638
- Zircaloy-2 fuel tubes, low cycle fatigue studies at room temp., 300 and 350°C 0-93637
- Al aircraft alloy, fatigue resistance improvement by laser shock 0-93654
- Al alloy RR58, low cycle fatigue at 423K, prior treatment effect 0-104254
- Al alloys, (5083, 6061, 2219), supercond. magnets, mech. and phys. props. at 4K 0-86976
- Al, cyclic loading, change in mech. props. rel. to heat treatment 0-104282
- Al, fatigue life, influence of cyclic loading conditions 0-76350
- Al, high temp., cyclic grain boundary migration phenomena 0-85053
- Al-Ag (7.27 wt.%), peculiarities exhibited during fatigue loading (*Chinese*) 0-71723
- Al-Cu, high strength, type 2024-T3, crack growth, fatigue induced surface deform., holographic detect. 0-85120
- Al-Mg-Si, type 6061-T6, 6063-T6, effective stress range factor in fatigue 0-100924
- Al-Mg-Zn-Cu, type 7050, calorimetric study of fatigue induced microstructural changes 0-85034
- Al-Zn, type 7075-T6, coldworked hole specimens, residual stresses, fracture mech. anal. 0-97587
- Al₂O₃, polycrystn., high-temp. fatigue and strength 0-60954
- C fibre reinforced composites for spacecraft use, prep., props. and struct. 0-71625
- Co base alloy, creep-fatigue interaction in aligned eutectic and solid soln. 0-108554
- Co-B-Si amorphous alloy, liq. quenched, elec. resist. and cyclic deform. 0-59949
- Cr-Mo steel types JIS SCMP 2, SCMV 3 and SCMV 4, high-temp. high-cycle fatigue props., press. vessel appls. (*Japanese*) 0-93650
- Cu alloys, low-cycle fatigue and cyclic creep, -196-20°C 0-100913
- Cu, cyclic loading, change in mech. props. rel. to heat treatment 0-104282
- Cu-Al (5 wt.%), subjected to tension-compression fatigue, deform. and fracture strength (*Japanese*) 0-93644
- Fe, cast, low-cycle fatigue, theory 0-89349
- Fe electrolytic coated medium C steel, distrib. of bounded fatigue limits 0-81198
- Fe polycrystalline, two ferromag. methods for eval. of fatigue limit 0-89438
- Fe-B-Si amorphous alloy, liq. quenched, elec. resist. and cyclic deform. 0-59949
- MgO single cryst., impact wear characts. 0-76374
- Mo, fatigue of single crystals, dislocation struct. and strain localisation (*Russian*) 0-71741
- Mo polycrystn., cyclically deformed, dislocation arrangements 0-108506
- Ni alloy, fatigue and cyclic plasticity rel. to struct. inhomogeneity 0-81184
- Ni alloy, heat resistant, fatigue limit comparison in torsion and tension-compression 0-81181
- Ni, push-pull fatigued polycrystals, point defects, elec. excess resist. meas. 0-100910
- Ni spring alloys, microplastic deform. and endurance limit 0-81197
- Ni-Cr superalloy, interactions between creep and low cycle fatigue (*Chinese*) 0-66572
- Ni-Cr-Al-TaC, eutectic composite, microstructure, fatigue props. 0-85038
- Ni-Cr-Co-Ti-Mo-W-Al (14, 9.8, 5, 4, 3.9, 3 wt.%), low cycle fatigue, prior heat treatment effect 0-60962
- Ni-Cr-Ta-Ti-Si, EP557 precipitation hardening alloy, mech. props., heat treatment effect 0-60877
- Si₃N₄, high-speed rolling bearings, fatigue strength 0-93655
- SiO₂ fibre lightguides, fused, zero stress strength reduction and transitions in static fatigue 0-87523
- SiO₂, fused silica fibre lightguide, static fatigue transitions 0-58744
- Ti alloy VT3-1, fatigue failure, surface finishing influence 0-60972
- α -Ti, fatigue crack growth, influence of grain orientation, SEM study 0-108550
- Ti, fatigue damage, SEM, X-ray diffr. and surface trace anal. 0-85040
- Ti-Al-Cr-Mo-V(Fe), low cycle fatigue in repeated tension 0-76348
- Ti-Al-V (6, 4 wt.%), fretting corrosion of orthopaedic implant materials by bone cement 0-104813
- Ti-Al-V (6.4 wt.%), H related fatigue fracture 0-76344
- Ti-V-Fe-Al (10, 2, 3 wt.%), fracture toughness and stress corrosion resistance 0-100904

fatigue cracks

- asymptotic stress intensity factors for fatigue crack-growth calculations 0-108529
- α -brass, fatigue crack growth micromechanisms at low stress intensities 0-108570
- α -brass, fatigue crack propag., role of dislocation substruct. 0-60963
- ceramics, lifetimes and slow crack growth prediction (*German*) 0-104250
- ceramics, subcritical crack extension meas. with double-torsion specimens (*German*) 0-104359
- coke, breakage behaviour rel. to struct. 0-85026
- crack propagation, quantifying the parameters 0-100891
- crack propagation, under variable stresses (*Japanese*) 0-86028
- crack tip, plastic deform., metallographic anal. by recrystn. 0-85029
- cumulative damage model, fatigue crack growth appl. 0-79232
- cylinder, hollow with internal circular crack, axially symmetric torsion determ. 0-64456
- detection and rating by acoustic emission, review 0-104380
- device for producing fatigue cracks in specimens 0-61051
- effective stress range factors in fatigue crack propag. 0-100924

fatigue cracks continued

- elastic transpositions, numerical calc. 0-74809
- fission reactor materials, failure analysis by remote fatigue crack growth meas. system 0-68790
- growth retardation model, based on critical damage approach 0-99960
- growth testing, using computer-controlled stress intensity gradient technique 0-76432
- Hastelloy-X, low cycle fatigue crack propagation at 25°C and 760°C 0-104270
- metal, fatigue crack growth micromechanisms at high stress 0-108569
- metal fatigue crack detection using nondestructive evaluation (NDE) methods 0-71826
- metallic materials, fatigue life distrib. theoretical obs. near fatigue limit 0-59569
- metallic materials, tenacity parameters 0-60973
- metallic structures initial fatigue quality characterisation using equivalent-initial-flaw-size distribution 0-58978
- metals, fatigue lives, eval. using crack initiation model (*Japanese*) 0-104258
- metals, fatigue resistance, processes leading to failure 0-94907
- microcrystalline alloys, metastable, rapidly quenched particulates, props. appl. and production 0-84887
- nuclear reactor materials, PWR, H₂-assisted fatigue-crack growth model 0-71745
- nucleation from particles, statistical aspects, expt. test 0-89345
- polycarbonate, glassy, fatigue crack initiation in high strain fatigue tests 0-97564
- polymer-metal sliding, wear eqn. in terms of fatigue and topography of sliding surfaces 0-108597
- polypropylene, microstruct. changes during large strain cyclic deform. 0-66627
- potential methods, for crack length determ. of fatigued specimens (*German*) 0-81167
- pressure vessels, AE during fatigue crack expansion 0-108675
- propagation, effect of 2- or 3-dimensional macrodefect (*Japanese*) 0-104261
- propagation investigations, US testing equipment 0-81247
- PVC, glassy, fatigue crack initiation in high strain fatigue tests 0-97564
- SEM of bulk specimens using imaging of subgrains 0-66609
- sero-hydraulic test system, for fatigue crack propagation studies under biaxial loading 0-76431
- steel, (0.36 wt.% C) Ni-Cr-Mo, electroslag refined, fracture toughness and fatigue behaviour 0-81171
- steel, A533B alloy, fatigue crack growth of irradiated pressure vessel steels in simulated, reactor-grade water environment 0-97582
- steel, Al-killed, fatigue life for program loading of multiple repeated two step stresses (*Japanese*) 0-66632
- steel, austenitic stainless, fatigue crack propagation, effect of neutron irradiation 0-97583
- steel, austenitic stainless, fatigue crack propagation, influence of neutron irradiation 0-97584
- steel, austenitic stainless, types 304 and 316, environment effect on crack growth, under creep and fatigue conditions 0-85035
- steel, austenitic stainless type 304, time-depend. fatigue, mechanistic model 0-100925
- steel, austenitic stainless type SUS 316, low cycle fatigue tests, freq. effect on notch sensitivity at elevated temps. (*Japanese*) 0-104260
- steel, ball bearing, fatigue damage, influence of dispersed phases in martensitic matrix 0-108549
- steel, C, crack initiation and propagation life under repeated impact tensile loads (*Japanese*) 0-104264
- steel, C, fatigue crack propagation in sheet, influence of struct. of ferrite-pearlite bands (*French*) 0-76338
- steel, Co-Cr-Mo, type HY 180 correl. between advanced NDT evaluation methods and fracture mech. parameters 0-97675
- steel, Cr-Mo, impact fatigue crack growth at low temps. (*Japanese*) 0-104266
- steel, Cr-Mo, notched specimens, fatigue strength distrib. (*Japanese*) 0-66633
- steel, Cr-Ni-Mn, AISI 4340, correl. between advanced NDT evaluation methods and fracture mech. parameters 0-97675
- steel, ductile structural, fatigue crack propag. rate and striation spacing 0-93635
- steel, fatigue crack propag., quantifying the parameters 0-100891
- steel, fatigue crack propag. near to threshold stress intensity 0-100898
- steel, fatigue crack tip plastic deform., X-ray diffr. investigation (*Russian*) 0-104251
- steel, ferritic, clad with austenitic steel 309, US detection of undercladding microcracks (*Italian*) 0-108683
- steel, ferritic-martensitic, fatigue crack tip plastic zone (*Japanese*) 0-71738
- steel, high strength 4340, fatigue crack growth resistance, fracture mechanism effect (*Japanese*) 0-104265
- steel, high-strength, fatigue crack growth rate and crack tip shapes, cyclic bending (*Russian*) 0-71740
- steel, low alloy, high strength, fatigue crack growth, in presence of welding residual stresses (*Russian*) 0-71739
- steel, low C, high cycle fatigue, crack initiation model (*Japanese*) 0-104258
- steel, low C ferritic, fatigue crack growth micromechanisms at low stress intensities 0-108570
- steel, low-C, fatigue strength and crack propag. behaviour under impact program loading conditions (*Japanese*) 0-66635
- steel, low-C, types 535C, SB 42-B, fatigue crack propag. and crack closure behaviour under plain strain conditions (*Japanese*) 0-81160
- steel, mild, fatigue crack arrest and retardation, load stepdown effect 0-108527
- steel, mild, fatigue crack propagation, stress ratio effect 0-71733
- steel, mild, fractography study of shear mode fatigue crack growth by etch pits (*Japanese*) 0-108545
- steel, Ni-Mo-V, fatigue crack growth, H₂ gas environment effect (*Japanese*) 0-104340
- steel, notched specimens in sea water, endurance limit enhancement, specimen size, freq. effects 0-93678
- steel, plain C having ferrite-martensite mixed structs., microstructural parameters effect on fatigue strength (*Japanese*) 0-71735
- steel, sintered, fracture of residual pores 0-76352
- steel, stainless, fatigue props. of low-fluence neutron irradi. samples 0-97585
- steel, stainless, low-cycle fatigue characteristics of neutron irradi. samples 0-97586

fatigue cracks continued

steel, stainless 316, fatigue behaviour of materials containing significant amounts of irradiation-induced He 0-100917
 steel, stainless type 316, thermally aged, accelerated creep-fatigue crack propag. 0-89326
 steel, type Man-Ten, and KQC-100, fatigue life estimates of bluntly notched members 0-100999
 steel plates, explosively clad, fatigue crack propagation behaviour (Japanese) 0-104262
 steels, mild and type 304, fatigue crack growth and threshold measured at very high frequencies 0-71742
 stresses due to acoustically induced vibration aircraft skin panels, prediction of edge crack growth 0-69737
 stretch zone width and striation spacing. The comparison of theories and experiments 0-85051
 surface reaction, and transport controlled crack growth, model 0-75299
 US test procedure for early detect. and remaining life prediction 0-71848
 US visualization, advantages over pulse-echo methods 0-66738
 Al alloy, types L73 and L88, fatigue crack propagation, stress ratio effect 0-71733
 Al alloy 2219-T851, noncontinuum crack tip deform. of surface cracks 0-104273
 Al alloy sheets, type 7075-T6 used in aircraft, early detection of fatigue cracks 0-66730
 Al alloy type 7010-T7651, high toughness, cyclic and monotonic crack propag. 0-108528
 Al alloys, fatigue crack initiation, computer simulation 0-100893
 Al alloys, fracture relief formed in fatigue crack growth, rel. to failure mechanism 0-76347
 Al bicrystals, isoxial, fatigue crack initiation in grain boundary affected regions (Japanese) 0-89338
 Al, fatigue crack initiation, pre-existing subgrain effect 0-97565
 Al, fatigue crack propag., quantifying the parameters 0-100891
 Al-Cu, high strength, type 2024-T3, crack growth, fatigue induced surface deform., holographic detect. 0-85120
 Al-Cu, type 1100, synchrotron radiation microradiography 0-85121
 Al-Cu, type 2219-T851, fracture mechanics and surface chemistry of fatigue crack growth 0-81168
 Al-Cu-Mg-Li alloy extrusions, microstruct., embrittlement and fracture props. 0-60965
 Al-Cu-Mn, type 2219, synchrotron radiation microradiography 0-85121
 Al-Mg, alloy A5083-O, fatigue crack propag. and crack closure behaviour under plain strain conditions (Japanese) 0-81160
 Al-Zn, type 7075-T6, coldworked hole specimens, residual stresses, fracture mech. anal. 0-97587
 Al-Zn-Mg, atmosphere effect on fatigue crack propag. (Japanese) 0-81161
 Al-Zn-Mg-Cu (6.2, xwt.%) type alloy, fatigue crack propag., Cu content and recryst. effect 0-60960
 Cu, fatigue crack growth and threshold measured at very high frequencies 0-71742
 Cu, fatigue crack propag., role of dislocation substruct. 0-60963
 Cu, fatigue crack propag., influence of specimen thickness (German) 0-66669
 Cu-Cr (0.75 wt.%), deformation charact., fully reversed cyclic strain with fatigue cracks and dislocation struct. 0-81148
 Fe, Armco, fatigue crack propag., influence of specimen thickness (German) 0-66669
 Fe, Armco, plastic zone around fatigue crack, vac. effect 0-100914
 Fe, ductile, influence of crack tip sharpness and morphology of graphite on K_{IC} (Chinese) 0-81144
 Fe-C (0.64 wt.%), fatigue crack bifurcation 0-71748
 Fe-Si, fatigue fracture fractography in broad strain-amplitude range, in air and vacuum 0-81186
 α -Ti, fatigue crack growth, influence of grain orientation, SEM study 0-108550
 α -Ti, fatigue crack growth micromechanisms at low stress intensities 0-108570
 Ti, fatigue damage, SEM, X-ray diffr. and surface trace anal. 0-85040
 Ti-Al-Sn-Zr (6.19, 1.92, 1.43 wt.%), fatigue fracture facet investigation by selected area electron channelling 0-89344
 Ti-Al-V (6.4 wt.%), β -annealed, subsurface fatigue crack initiation 0-108553
 Ti-Al-Zr-Mo-Si (5.97, 4.73, 0.49, 0.34 wt.%), fatigue fracture facet investigation by selected area electron channelling 0-89344
 Ti-Al-Zr-Mo-Si (6, 5, 0.5, 0.25 wt.%), β -processed, fatigue props., hold time effect 0-60961
 β -Ti-V metastable alloys, fatigue crack propag. 0-60964

fatigue failure see *fatigue*

fatigue fracture see *fatigue*

fatigue life see *fatigue*

fatigue testing

for corrosion fatigue testing, see *corrosion testing*
 ceramics, lifetimes and slow crack growth prediction (German) 0-104250
 ceramics, subcrit. crack extension meas. with double-torsion specimens (German) 0-104359
 crack growth rates, meas. method based on crack opening 0-61032
 creep and fatigue testing installation for wide range of strain rates 0-76447
 cyclic stress-strain curve determination (Czech) 0-89434
 denture base materials, multi-station machine for fatigue testing 0-108648
 denture base polymers, test machine 0-66712
 fastening materials, specimen for testing 0-61050
 fibres, biaxial rotation fatigue testing, torque development 0-71840
 fusion reactor, PDX toroidal field coil joint fatigue testing 0-91252
 fusion reactor, TFTR, vacuum vessel bellows, strength and fatigue anal. 0-95455
 laboratory tests automation, using 500 kN and 2.5 MN ATE (Czech) 0-66710
 life prediction method for conditions of multistep cyclic loading 0-76346
 loads and load histories, test methods devel. 0-100970
 metallic materials, tenacity parameters 0-60973
 metals, low-cycle failure investigation, elec. resist. meas. appl. 0-85109
 metals, method using EM pulsator 0-89440
 metastable austenitic steels, test machine and fatigue strength temp. dependence (Japanese) 0-71842
 mill stand in-situ fatigue testing, devices for automatic emergency protecting (Russian) 0-93717

fatigue testing continued

nuclear power engineering materials certification testing for safety and reliability 0-78360
 nuclear steam generator tubes testing and evaluation, using CIS/DASIO system (Czech) 0-63301
 optical fibre, dynamic fatigue and strength degradation 0-58719
 optical high-strength fibre production and proof-testing 0-64204
 servo-hydraulic testing machines 0-108649
 steel, austenitic stainless type SUS 316, low cycle fatigue tests, freq. effect on notch sensitivity at elevated temps. (Japanese) 0-104260
 steel, C, crack initiation and propagation life under repeated impact tensile loads (Japanese) 0-104264
 steel, C-Cr (1.0, 1.5 wt.%), 52100 bearing steel, control of surface residual stress by heat treatment 0-97501
 steel, low C, low-cycle failure investigation, elec. resist. meas. appl. 0-85109
 steel, mild, fatigue softening and hardening detected from Barkhausen noise 0-76428
 steel, type SAE 1008, finite fatigue life distrib., various load-time histories 0-97589
 steel, weldable, fatigue data, low and high cycle compatibility (Czech) 0-89343
 steel discs, austenitic and ferritic biaxial fatigue testing under changing temps. (German) 0-71759
 strain and damage electrical measurement method (French) 0-71854
 strain range partitioning method for anal. of material creep fatigue behaviour 0-104361
 textile fibres, multistation apparatus using biaxial rotation over a pin 0-66726
 US fatigue systems, deform. amplitude determ. 0-97676
 wire fatigue properties, fast testing method using 23 kHz US frequency 0-89460
 Woehler tests, U_0 * procedure for reliable prediction of random fatigue strength (German) 0-71850
 Zircaloy-2 fuel tubes, cumulative damage fatigue tests at room temp. and 300°C 0-93638
 Zircaloy-2 fuel tubes, low cycle fatigue studies at room temp., 300 and 350°C 0-93637
 Al alloys, struct., accelerated fatigue test method 0-100981
 Cu-Cr (0.75 wt.%), deformation charact., fully reversed cyclic strain with fatigue cracks and dislocation struct. 0-81148
 Mo, fusion reactor appl., quick heating thermal fatigue test, ultra-high vac. environment (Japanese) 0-93716

fault currents

see also *flashover; leakage currents; short-circuit currents*
 fusion reactor, JT-60, fault current anal. in grounding system 0-99307

fault location

digital multimeter, Avo DA117, overview of field servicing appls. 0-68210
 industrial NDT computed transverse axial tomography system 0-89430
 long-haul communications optical fibre fault location method 0-64193
 optical fibres, backscatter meas. 0-64183
 optical time domain reflectometry by photon counting 0-95122

f.d.m. see *frequency division multiplexing*

feature extraction see *pattern recognition*

feedback

see also *control systems; control theory*
 analogue and digital optical image processing, feedback systems 0-102650
 auditory perception nonlinear model with autocorrel. feedback 0-81615
 auroral arcs global formation, numerical simulation in feedback theory 0-67446
 Fourier transform spectrometer, high resolution ruggedized 0-95152
 high-speed optical systems at 0.85 μ m, modal noise and optical feedback 0-87323
 integrated astable optical multivibrator using Mach-Zehnder interferometric optical switches 0-87560
 machine tool position feedback by laser interferometer 0-73438
 Michelson interferometer, active stabilization by electrooptically tuned laser 0-86386
 monochromatic light source with electronically variable wavelength 0-102791
 optical coherent feedback, flexible filter operations 0-87337
 optical feedback in incoherently illuminated systems 0-87336
 optical feedback processing by TV-optical method 0-87335
 optical image processing, analogue and digital, feedback, review 0-102639
 optical incoherent feedback using TV 0-87334
 optical processor, confocal feedback system for partial differential eqn. analogue soln. 0-102630
 photomultiplier gain stabilisation with high counting rate, feedback resistor series effect appl. 0-106232
 preamplifier circuit in Fourier spectrometer, using InSb photodiode, improved noise compensation 0-73474
 prosthesis, sensory feedback system for above knee prosthesis (Japanese) 0-72372
 satellites attitude control, inertially fixed pitch stabilisation by solar radiation press. 0-101523
 semiconductor injection laser, external optical feedback effect on props. 0-58535
 semiconductor laser nonlinear distortions on modulation linearity improvement by negative feedback (German) 0-69395
 two-resonator CRM oscillator with external feedback 0-87362
 voice amplification, adaptive method for feedback suppression (German) 0-106676
 walking, connections between different legs, quantitative model 0-101161
 walking, individual leg control, model 0-101160
 He-Ne ^{127}I , stabilised laser source for Michelson interferometer, optical feedback obs. 0-106545

Fermi-Dirac statistics see *quantum statistical mechanics*

Fermi gas see *fermion systems*

Fermi level

alkaline earth fluorides, orbital binding energy and ionicity relations, XPS meas. 0-97399
 electron gas, perturbed, p-wave electronic recoil spectra 0-107724
 excitonic insulator in mag. field, two-band model 0-80192
 glasses, defect reactions, ionicity dependence, negative-U states 0-88510
 graphite, diamagnetism with quasilinear dispersion law, orbital susceptibility, valence bands (Russian) 0-80475

Fermi level continued

- graphite intercalation compound, interaction between one or two s orbitals (French) 0-65440
- III-V semiconductor-oxide interface states, photoemission obs. of energy levels induced by adsorpt. 0-93000
- inflowing structure, Anderson localisation, elec. cond. temp. depend. (Russian) 0-103639
- insulator-semicond. interface, impurity-band hopping conduction in surface layers 0-75649
- intermediate valence system, local polaron model 0-107717
- liquid metals of groups IIB, IIIB, and IV, thermoelectric power, pseudo-potential calc. 0-59959
- metal lattice heating by radiation, plasma effects, degenerate electron gas calcs. 0-70742
- metals and alloys, electrons at Fermi surface, book 0-105445
- periodic systems electronic struct., LCAO SCF ab initio HF calcs. method 0-65419
- rare earth aluminate, scandate and zirconate film coatings, electrophys. props. w.r.t. prep. technology 0-60781
- rare earth metals, density of 4f states below and above Fermi level, XPS and bremsstrahlung isochromat spectroscopy 0-76140
- semiconductor, Fermi level, monotonous shift with increasing temp. 0-92809
- semiconductors, isothermal and non-isothermal C-V deep level meas. using Schottky contacts 0-88515
- semiconductors, temp. depend. electronic cond. 0-59975
- semiconductors, thermally stimulated relaxation processes, book contribution 0-80295
- substitutional alloys of intermediate valence systems, static mag. susceptibility con. and temp. depend. 0-84586
- transition metal alloys, binary, state density curves, relation between short-range order and Fermi level position, CPA calculations 0-107687
- transition metals, ferromag., dil. H electronic struct. 0-70638
- zincblende-symmetry narrow-gap semicond., Fermi energy and Fermi-Dirac integrals 0-70604
- Ag, thin film deposited on Si, work function (French) 0-80353
- Al (001), enhanced photoexcitation 0-80937
- Al, thin film deposited on Si, work function (French) 0-80353
- Al-anodised Ta₂O₃/native oxide-n-GaAs MOS structure evaluation 0-84514
- Au-3d transition metal alloys, UPS study, localised states 0-93449
- Au-n-Si Schottky barrier solar cells, recombination in space charge region 0-61351
- Be, electronic struct., NMR study 0-108085
- BeNi, dil., electronic struct., NMR study 0-108085
- Bi, giant quantum attenuation anomalies of sound waves at high mag. field, temp. and freq. depend. 0-70587
- C:H films, amorphous, elec. props., chem. modifications 0-84523
- p-CdSiAs₂, electron irradi. elec. props. annealing, lattice defects 0-100465
- Cr₂Si, mag. susceptibility, 2 to 300K, rel. to electron energy spectrum 0-60185
- Cu, hot cathodoluminescence study, electron-hole recombination 0-93410
- Eu, electronic struct. investigation by electron spectroscopy method 0-92812
- EuO, electronic struct. investigation by electron spectroscopy method 0-92812
- Fe₂S₃, pyrrhotite, thermocond. and thermoelec. power 0-96926
- GaAlAs, surface vacancies, bound state energy levels calc. 0-80340
- Gd, magnetic crystalline anisotropy, Fermi level, electronic density of states 0-84596
- Ge_{0.8}Si_{0.2}, elec. cond., density of states, impurity and temp. depend. 0-65568
- p-GeTe, reflectance, and thermoref. spectra 0-80814
- HfC_{1-x}N_{1-x}, X-ray valence photoelectron spectrum, 4f signal calc. 0-66391
- Hg_{1-x}Cd_xTe, optical absorpt., quasilocal acceptor level effects, theory 0-92853
- InP, Γ_4 symm. acceptor centre hole mag. props. (Russian) 0-88733
- In, Ga, and In_{0.5}As_{0.5}P_{1-x} binary and quaternary cpds., surface and dielec. semicond. interface props. 0-93001
- InP, surface vacancies, bound state energy levels calc. 0-80340
- KCl, photoelectric emission in photon energy region 1.0 to 6.0 eV 0-108321
- LiC₆ and LiC₁₂, intercalation cpds., electronic struct. calcs. 0-70613
- LuRhO₃, elec., mag. and photoelectrochemical props. 0-96925
- MnP, spin polarised energy band struct., electronic specific heat, APW calcs. 0-65431
- MnSi, electronic energy band struct., self-consistent APW calc. 0-65433
- Na, equilibrium struct. and phys. props., pseudopot. method 0-96778
- NbSe₂ pure and intercalated with ethylenediamine, positron annihilation study 0-84801
- Ni₂Fe alloys, low-temperature specific heat, long and short range order effects 0-100339
- NiSb, bandstructure and density of states calc. 0-70580
- PbO-SiO₂ glass, reduced channel-plate, variable range hopping conductivity 0-107466
- Pb_{1-x}Sn_xTe:Ge, anomalous behaviour of impurity centres under press. (Russian) 0-65491
- Pd-Si-(Cu), amorphous, Hall effect meas. and electronic struct. 0-75551
- Pt-transition metal, dil., impurity resist. 0-92875
- SbSe, amorphous thin film high field charge transport and quasi-Fermi level location 0-70863
- Si:H, amorphous, Schottky diodes, elec. props., light-induced effects 0-103741
- Si_{1-x}H_xAl, amorphous, co-sputtered Al modification, electronic and optical props. 0-100461
- SmB₆, mixed valent semicond., transport props. and electronic struct., review 0-96877
- TbZn, ferromag., thermoelec. power, temp. depend. and crit. behaviour 0-96852
- Te-transition metal, liq. semicond., elec. props. 0-96870
- TdC₂N₂, NMR, Knight shift and spin-lattice relax. 0-100621
- TiN_{1-x}, stoichiometric, electronic density of states, CPA method calcs. 0-88464
- V_{2-x}Nb_xHf, NMR of ⁵¹V and mag. susceptibility, 20-300K (Russian) 0-93192
- V₂Si, magnetic susceptibility, density of states model for lattice transformation in A-15 compounds 0-65219
- p-ZnSiAs₂, electron irradi. elec. props. annealing, lattice defects 0-100465

Fermi liquid *see fermion systems***Fermi resonance**

- acetic acid-d₆(-d₁), Fermi reson., IR spectra band profiles 0-60569
- methanol, aqueous, damped coupled oscillator model used to study Fermi resonance 0-69152
- methyl alcohol-d₃, Fermi resonance due to large amplitude vibr. 0-83519
- N-methylacetamide, solid, Fermi resons. 0-97266
- trans-polyacetylene obtained by polymerisation on TiO₂, Raman spectrum (Spanish) 0-88988
- polyatomic molecules, radiationless transitions, Fermi resons. and quasiscrete spectrum 0-95665
- CO₂, dipole moment functions 0-87094
- CO₂, near critical point Rayleigh and Raman scatt., Fermi diad 0-80765
- CO₂, solid, Fermi reson. press. tuning, Raman spectra 0-93293
- H-bonded systems, frequency shift rel. to IR bandwidth 0-99502
- α -LiIO₃, Fermi resonance in surface polariton spectra (Russian) 0-71423
- N₂O, dipole moment functions 0-87094

Fermi surface

- alkali metals, Fermi surface topological changes due to uniaxial stresses 0-92810
- alloys, dil., of polyvalent and noble metals, deviations from Matthiessen rule 0-65525
- anisotropic superconductors, upper critical field theory 0-75692
- edge dislocation screening in metals and superconductors, metal softening (Russian) 0-64997
- exciton dielectric, inhomogeneous current state phase transition, free energy (Russian) 0-84703
- graphite intercalation cpds., Fermi surface and transport props., LCAO model 0-80159
- graphite-K intercalation compounds, electronic props., de Haas-van Alphen effects and Fermi surfaces 0-75498
- graphite-K intercalation compounds, electronic props., resistivity, Hall effect and magnetoresistance 0-75585
- indirect exchange in Bloembergen-Rowland approx., ellipsoidal Fermi surface and relax. process effects 0-107754
- metal, antiferromag., thermoelec. power in mag. field 0-70686
- metal, Pippard sound-attenuation oscillating angular depend. (Russian) 0-103613
- metal, soft X-ray emission spectra and Fermi surface, contrib. of John Bardeen 0-57057
- metal, strained, interpolation functions for Fermi surface 0-65425
- metal surface region, electrostatic energy and screened charge interaction for different Fermi surface shape 0-70631
- metal-dielectric transition, two-band model, Coulomb interactions, self consistent calcs. (Russian) 0-80185
- metallic films, ultrasound attenuation, size magnetoacoustic effect (Russian) 0-107869
- metallic ultrathin filaments, dielectric and superconducting fluctuations, Peierls transition (Russian) 0-65742
- metals, electron theory, internal press. 0-92802
- metals, ground state energy, structural expansion, HF approx. 0-65420
- metals, inelastic scatt. of fast electron, plasma oscillations effect 0-100439
- metals, quantum magneto-dimensional effects, open Fermi surfaces, conduction electrons (Russian) 0-80487
- metals, sound absorption and dispersion temp. depend. associated with Fermi surface plateaus (Russian) 0-65166
- metals and alloys, electrons at Fermi surface, book 0-105445
- pyrolytic graphite, magnetoresistance positive-negative transition (Russian) 0-96923
- quasi-one-dimensional electron-phonon system, electron jump effect on phase transition (Russian) 0-92673
- rare earth metals, electronic sound attenuation anomalies at transition to helical phase, Fermi surface topology (Russian) 0-92807
- simple metals, model pseudopot. appl. to various props. 0-59845
- sound attenuation in magnetic field at the 2^{1/2}-order phase transition (Russian) 0-100487
- superconducting band gap anisotropy, Eliashberg eqns., review (Spanish) 0-84544
- superconductor order parameter singularities, tunnelling currents, Fermi surface calcs. (Russian) 0-80458
- superconductors, strongly anisotropic, nonmag. impurities effect on supercond. transition temp. 0-93035
- transition metal compounds, reduced ionisation potentials as parameters in superconducting transition temp. calcs. 0-75671
- Al, magnetoresistance, path integral method calc. 0-65537
- Al, superconducting band gap anisotropy and Fermi surface anisotropy (Spanish) 0-84544
- Au, self-consistent relativistic band struct. 0-75501
- Be, Fermi surface, stress-induced changes 0-96770
- Bi, deformation calculations, band struct. variation, electron phase transitions due to deform. (Russian) 0-65137
- Bi, giant quantum attenuation anomalies of sound waves at high mag. field, extra attenuation peaks 0-70588
- Bi, magnetoresistance, high temp. oscils., props. (Russian) 0-65606
- Bi, quantum-EM excitations 0-88471
- BiSb, alloys, semimetallic, camera, dispersion relations 0-59854
- Bi_{1-x}Sb_x, deformation calculations, band struct. variation, electron phase transitions due to deform. (Russian) 0-65137
- Bi_{1-x}Sb_x, EM wave propag. for rot. of mag. field from Faraday to Voigt config. 0-84419
- Bi_{1-x}Sb_x, semiconducting alloy, band struct. study, Shubnikov-de Haas effect (Russian) 0-80181
- Bi₈₆Sb₁₄Te, single crystal, dispersion of magnetoplasma waves (Russian) 0-70739
- Cd, Fermi surface, stress-induced changes 0-96770
- Co, Fermi surface under press., de Haas-van Alphen effect meas. 0-75499
- Cr, diffuse electron scatt. (Russian) 0-103438
- Cr, Fermi surface under press., de Haas-van Alphen effect meas. 0-75499
- Cr, Neel temperature and Fermi energy, nonmag. impurity effects 0-65888
- Cr-Si, dilute alloy, mag. susceptibility and Neel temp. meas. 0-71017
- Cs, Fermi surface and quasiparticle props., density functional approx. 0-96771
- Cs, Fermi-surface-press. dependence 0-96772
- Cs, metal impurity effect on residual elec. resistance (Russian) 0-84457

Fermi surface continued

- Cu, Fermi surface, electron mass enhancement, orthonormal function enhancement 0-96777
 Cu, quenched, Hall coefficient, relaxation times, Fermi surface 0-84460
 Cu, strained, interpolation functions for Fermi surface 0-65425
 Cu₂Au, electrical resistivity and LRO, energy gap formation in Fermi surface 0-88533
 CuH dilute alloy, Hall coefficient, relaxation times, Fermi surface 0-84460
 de Haas-van Alphen freq. and Fermi surface anisotropy press. depend. 0-59856
 Fe, Fermi surface under press., de Haas-van Alphen effect meas. 0-75499
 Fe, mag. breakdown and Hall resist., theory and model calcs. 0-75552
 Fe₃Al, electrical resistivity and LRO, energy gap formation in Fermi surface 0-88533
 FeGe₂, antiferromag., Fermi surface, stress effects, oscillatory magnetotri-
 ction and torque meas. 0-103616
 K, metal impurity effect on residual elec. resistance (*Russian*) 0-84457
 K, ultrasonic attenuation at low temp., spherical Fermi surface model 0-84255
 LaAl₃, calc. of energy band-structure and Fermi surface by APW method 0-70590
 LaAl₃, electronic struct., APW method and local-spin-density approx. 0-65434
 LaB₆, de Haas-van Alphen effect, low-field 0-75497
 LaB₆, electronic struct., APW method and local-spin-density approx. 0-65434
 Li, Fermi surface and quasiparticle props., density functional approx. 0-96771
 Mo, diffuse electron scatt. (*Russian*) 0-103438
 Mo, effective mass meas. and electron velocities 0-96773
 Mo, longwave dopplers, nonlocal Hall effect, surface impedance, size effect (*Russian*) 0-80253
 Mo, vol. depend. of extremal cross sectional areas of Fermi surface from de Haas-van Alphen meas. 0-70589
 MoO₂:Re(V), current carrier sign, Fermi surface cross section variations (*Russian*) 0-84420
 Na, Fermi surface distortions, model pot. 0-80157
 Na, metal impurity effect on residual elec. resistance (*Russian*) 0-84457
 Nb, diffuse electron scatt. (*Russian*) 0-103438
 Nb, Fermi surface, electron mass enhancement, orthonormal function enhancement 0-96777
 Nb-Al, diffuse electron scatt. (*Russian*) 0-103438
 Nb-Zr alloy, BCC- ω phase transition, electronically driven nature, rel. to Fermi surface features 0-103433
 NbSe₂, CDW form., supercond. and Fermi surface determ., press. study 0-70891
 NbSe₂, mag. susceptibility, CDW effect 0-88716
 Ni, Fermi surface under press., de Haas-van Alphen effect meas. 0-75499
 β -NiAl, electronic struct. and optical props. 0-97228
 Os, thermal EMF quantum oscils. (*Russian*) 0-88543
 Pb, ab initio band struct. calcs. 0-75502
 Pd-Cu compound, KKR electronic struct. 0-59864
 Rb, Fermi surface and quasiparticle props., density functional approx. 0-96771
 Rb, Fermi-surface press. dependence 0-96772
 Rb, metal impurity effect on residual elec. resistance (*Russian*) 0-84457
 Re, Fermi surface, Landau quantum oscill. meas. in magnetotri-
 ction, stress and strain derivatives 0-107691
 Re, Fermi surface, RF size effect, temp. depend. 0-65424
 ReO₃, mag. breakdown above compressibility collapse transition 0-103617
 Sb, electronic struct., depend. on hydrostatic pressure 0-80158
 SiP₂, with pyrite struct., Fermi surface calc. 0-65427
 Sn, Fermi surface, dilatational strain depend., elastic moduli and torque obs. 0-70586
 Sn, magnetic breakdown orbits 0-103615
 Sn, white, band masses and deformation pots., OPW pseudopotential model 0-100430
 Sn, white, Fermi surface, dilatational strain depend., OPW calcs. 0-84418
 TaN, energy band struct. calc., symmetrised APW method 0-96784
 Tc, superconductivity and Fermi surface calcs. 0-70873
 Ti alloys, Fermi sphere limiting electronic capacitance, Brillouin zones (*Russian*) 0-92808
 Ti-Cr, diffuse electron scatt. (*Russian*) 0-103438
 Ti-Mo, diffuse electron scatt. (*Russian*) 0-103438
 Ti-Nb, diffuse electron scatt. (*Russian*) 0-103438
 TiBe₂, de Haas-van Alphen effect, Fermi surface, theory 0-103614
 α -U, Fermi surface and effective masses, de Haas-van Alphen meas. 0-65426
 V, electron-phonon coupling constant calc. (*Russian*) 0-70624
 V, electronic structure, model potential calcs. (*Russian*) 0-100431
 VO, investigation of Fermi surface from electron energy spectrum (*Russian*) 0-75496
 W, (110) surface, conduction electron interaction with diffracting electrons (*Russian*) 0-79643
 W, longwave dopplers, nonlocal Hall effect, surface impedance, size effect (*Russian*) 0-80253
 ZnTe clean and adsorbed O₂ (110) surfaces, UV photoemission spectra (*Japanese*) 0-93456
 ZnZn₂, de Haas-van Alphen effect, Fermi surface, theory 0-103614

Fermi-Thomas model see *Thomas-Fermi model***fermion systems**

- see also *electron gas; liquid helium-3*
 alkali halide crystals, defect fermion properties, ionic cond. calcs. 0-59457
 antiferromagnetic Fermi liquid, critical phenomena, neutron scatt., Neel point (*Russian*) 0-71077
 broken SU₂ symmetry field, two-dimensional isotopic model (*Russian*) 0-73616
 degenerate system, heavy impurity mobility 0-70493
 disorder variables and para-fermions in two-dimensional statistical mechanics 0-98853
 disordered Fermi systems, in two dimensions, interaction effects 0-75655
 dressed fermion bubble, real-space equivalent calcs. 0-101751
 electron liquid, spin-dependent, correlation energies for local spin density calcs. 0-107725

fermion systems continued

- electron liquid on liq. He surface, high freq. cond. electron correlation effects 0-107589
 electron system, two-dimensional, melting curve, phase diagram 0-57179
 ferromagnetic Fermi-liquid model, electron-impurity system hydrodynamics, elec. cond. 0-103835
 functional integral formalism for quantum spin systems 0-82714
 generalized Grassmann algebras with applications to Fermi systems 0-57174
 giant MIT bag, hot quark matter, from relativistic ideal Fermi gas 0-99083
 hard-sphere Fermi system, energy and momentum distrib., Jastrow variational wave functions 0-73261
 Hartree Fock solns. 0-98852
 many-fermion quantum mechanics, coherent-state representation 0-94988
 metallic ultrathin filaments, dielectric and superconducting fluctuations, Peierls transition (*Russian*) 0-65742
 metals, localised dynamic perturbations 0-73262
 momentum distrib., Fermi-hypernetted-chain theory 0-82716
 non-relativistic fermions, Ward identity 0-86633
 nuclear matter model, momentum distrib., Fermi-hypernetted-chain theory 0-82716
 one particle distributions, entropy bounds 0-62607
 operator ordering, functional integrals 0-62574
 para-Fermi quantization in the representation of SO(n) 0-86554
 para-Grassmann algebras with applications to para-Fermi systems 0-57175
 partial level density for widely varying values of the range of interaction 0-58120
 quadratic Hamiltonian diagonalisation 0-82719
 quantum mechanics of ground state 0-82713
 relativistic fermion fields, bosonisation, Luttinger model, thermodynamic correlation functions 0-68356
 SO(2N+1) algebra, time-dependent Hartree-Bogoliubov theory, quantisation 0-62575
 superconducting Fermi-liquid, electromagnetic response, formal solutions 0-100548
 superfluid neutron fluid, stationary flow in ³P₂ paired state (*Russian*) 0-103527
 temperatures, inverse, equilibrium states, C*-algebra and continuous one-parameter automorphism group 0-82712
 trilocal structures, secular eqn. 0-90776
 zincblende-symmetry narrow-gap semicond., Fermi energy and Fermi-Dirac integrals 0-70604
 F₁-F₂, nondiagonal transition amplitude for arbitrary fermion charges (*Russian*) 0-86722
 D, atomic, Fermi fluid, stabilisation 0-100374
³He, ground state of polarised and unpolarised fluid, Monte Carlo calcs. 0-92748

fermions

- see also *baryons; fermion systems; leptons*
 generations in grand unified theories, SU(8) model 0-78012
 mass hierarchy, light fermions, grand unification, SU(N) theory 0-62911
 phase locked cavity, inertial mass and anomalous ang. momentum, fermion model 0-86159
 quantum field theory, large order perturb. theory, more than one coupling constant 0-77940
 Reggeization of elementary fermions in arbitrary renormalizable gauge theories 0-68367
 relativistic quantum theory with correct conservation laws 0-82677
 Schwinger model, Ward identity, fermion axial vector current divergence, chiral invariant regulator field 0-57524
 SU(2)×U(1) model, fermion and Higgs multiplet structure, universality 0-62909
 SU(5) grand unification, superheavy fermions and proton lifetime (*Russian*) 0-91036
 unified gauge theories, electroweak mixing angle, sequential triplets scheme of fermions 0-86650
 unified scalar-free theory, order-R vacuum functional, with spontaneous scale breaking 0-78003

fermium

- see also *nuclei with*
 No entries

fermium compounds

- No entries

ferrimagnetic properties of substances

- see also *ferrimagnetism; ferrites; garnets; magnetic semiconductors*
 anisotropy energy density 0-88742
 (Ca_{0.6}Fe_{0.3}O₃)₇(La₂O₃)₃ compounds, effects of Nd₂O₃ substitution on magnetic props. (*Japanese*) 0-108010
 MgAl₂-Fe₂O₄ solid solution system, solid state properties study 0-93094
 oxides, R₂Cu₃Mn₂O₁₂, R=La to Lu, Y, synthesis and mag. props. 0-75717
 rare earth alloys, R₂Pt (R=Gd, Tb, Dy, Ho, Er), magnetic susceptibility meas., mag. transition obs. 0-60222
 rare earth titanium oxides, RTiO₃ type, bulk mag. and struct. props., ferrimag. order 0-107993
 rare earth-Ag alloy, amorphous, model calcs., of mag. props. 0-84616
 rare earth-transition metal alloys, amorphous, ferrimag., spin arrangements in large fields 0-75718
 rare earth-transition metal alloys, disordered, magnetisation behaviour 0-71099
 BaO-Fe₂O₃-(Na₂O) glass, rapidly quenched, mag. and ferrimag. props. 0-75744
 Ba₃WFe₂O₈ and Ba₃WFe₂O_{8.42}, crystallographic and mag. props., comparative study 0-103303
 (Co,Cr,Fe)₃O₄, (Co,Rh,Fe)₃O₄ film magneto-optical switches, for laser beam synchronisation 0-58615
 CoCr₂S₄, ferrimag. semicond., magnetocrystalline anisotropy 0-71012
 CsCoBr₃, ID Ising antiferromagnet, spin dependent Raman scattering from phonons and electronic excitations 0-103948
 Dy₂O₃SO₄, mag. ordering, magnetisation, AC susceptibility and Zeeman effect meas. 0-60205
 DyPt, low temp. mag. susceptibility 0-93075
 ErCo₂(Fe₂), mag. excitations, RPA theory 0-65830
 Eu_{1-x}²⁺Nd_x³⁺O_{1-x}N_x, lattice parameters, mag. and elec. props. 0-100578
 Fe_{0.5}Cu_{0.5}Cr₂S₄, ESR spectra, elec. and mag. props., Curie temp. 0-97137

ferrimagnetic properties of substances continued

- $\text{Fe}_2\text{Mg}_{1.3}\text{Zn}_{0.7}\text{Ti}_{0.3}\text{O}_4$ spinel system, X-ray diffraction, Fe Mossbauer effect 0-88900
 Fe_2O_4 , magnetite, magnetoresist., applied mag. field effects 0-80301
 Fe_2S_8 , pyrrhotite, thermocand. and thermoelec. power 0-96926
 Gd-Co based amorphous sputtered films, microstruct. variability and mag. anisotropy, implanted ion effects 0-88459
 (Gd,Co) $_{1-x}$ ($x=1$), Ar, amorphous films, effective anisotropy field, ferromag. reson. obs. 0-71123
 Gd(Fe,Al) $_{1-x}$, magnetic behavior 0-108079
 GdFeBi, amorphous ferrimag. films, magneto-optical props., optical spectra 0-76008
 GdNi $_x$ ($x=3, 3.5, 8.5$), ferrimag., mag. reson. above and below Curie temp. 0-97148
 HoCo $_2$, mag.excitations, neutron inelastic scatt. meas. 0-60231
 HoCo $_2$, spin wave excitations, 4.8 and 78K 0-60230
 HoCo $_{0.5-1}$ Mn $_{0.5}$ (Fe) $_{0.5}$ (Ni) $_{0.5}$ (Cu) $_x$, cryst. struct. and mag. props. 0-75800
 Ho $_2$ O $_3$ SO $_4$, mag. ordering, magnetisation, AC susceptibility and Zeeman effect meas. 0-60205
 HoSb, mag. phase diagram, quadrupolar interactions 0-65820
 Li $_2$ B $_2$ O $_7$ -LiFeO $_8$ glass, rapidly quenched, mag. and ferrimag. props. 0-75744
 Mn(CN) $_3$ (H $_2$ O) $_{0.57}$, mag. interactions, theory 0-97085
 Mn $_{1.85}$ Cr $_{0.15}$ Sb, antiferromag.-ferrimag. transition, neutron crit. scatt. and crossover effect 0-71023
 MnSb, spin-wave dispersion relations, exchange interactions, neutron inelastic scatt. 0-65832
 NaMnCrF $_6$, mag. struct., neutron Laue diff. method 0-70951
 Nd $_{50}$ Ag $_{50}$, amorphous, mag. props. 0-60182
 NdPt $_5$, low temp. mag. susceptibility 0-93075
 Ni $_3$ Co $_{1-x}$ O, composition depend antiferromagnetic-ferrimagnetic ordering, mag. susceptibility meas. 0-70973
 Pt-Cr, ferrimag., magnetisation density, polarised neutron diff. meas. 0-60204
 RbNiF $_2$ spin lattice, susceptibility, Heisenberg model (Russian) 0-65893
 Sm $_2$ Mn $_{23-x}$ Fe $_x$, magnetic behaviour, temp. and comp. depend. 0-93090
 SrFe $_2$ Al $_2$ O $_{19}$, thin film LPE growth and mag. props. 0-80992
 Tb-Fe amorphous thin films, magnetic after-effect, Kerr magneto-optic effect obs. 0-97123
 TbCo $_2$, magnetocrystalline anisotropy and spontaneous magnetostriction 0-75831
 TmPt $_5$, low temp. mag. susceptibility 0-93075
 U $_2$ S $_3$, sp. ht. at low temps., mag. behaviour 0-60353
 Y $_{1-x}$ R $_x$ Co $_2$, R=Gd,Tb,Nd, ferrimag., magnetisation, exchange interactions, mag. anisotropy 0-80565

ferrimagnetic resonance

- (Gd,Tm,Y) $_2$ (Fe,Ga) $_2$ O $_{12}$ LPE garnet thin films, magnetocrystalline anisotropy 0-93147
 Gd(Fe,Al) $_{1-x}$, magnetic behavior 0-108079
 GdNi $_x$ ($x=3, 3.5, 8.5$), ferrimag., mag. reson. above and below Curie temp. 0-97148
 (Ho $_{0.58}$ Tb $_{0.22}$)Fe $_2$, microwave mag. props. 0-65860
 Li $_{0.5}$ Fe $_{2.5-x}$ Cr $_x$ O $_4$ press. depend. of anisotropy consts. 0-65865
 Sm $_{0.4}$ Y $_{2.6}$ Fe $_{3.8}$ Ga $_{1.2}$ O $_{12}$ epitaxial films, uniaxial mag. anisotropy, ferrimag. reson. study 0-80577

ferrimagnetism

- see also ferrimagnetic properties of substances*
 amorphous thin films, struct. and mag. props., review 0-93148
 Bloch wall oscil., viscosity coeffs. freq. depend., permeability and mag. losses 0-71094
 ferrimagnetic Neel mode with helical mode, coupling energy study (French) 0-70999
 magnetic polaritons in two sub-lattice ferrimagnets 0-65845
 magnetisation theoretical models, for uniparametric materials 0-65960
 Neel ferrimagnets, phase transitions, field-induced spin-orientational 0-75767
 Neel mode, ferrimagnetic-helical [hh0] mode coupling vector model (French) 0-75770

ferrite applications

- see also ferrite devices*
 proton synchrotrons, magnetisation of ferrites in tunable accelerating resonators 0-68983

ferrite devices

- see also ferrite applications; magnetostatic wave devices*
 ELF antenna for Magion satellite for 0.1 to 16 kHz freq. range (Czech) 0-85775
 (YBiEr) $_3$ (Fe,Ga) $_2$ O $_{12}$ ferrite-garnet film, micron cylindrical mag. domains, high recording density 0-65978

ferrites

- see also ferrimagnetic properties of substances; ferrimagnetism; ferrite applications; ferrite devices*
 350 NNI ferrite for use in superhigh vacuum systems, prep. 0-108478
 adsorption of CO, catalytic oxidation, IR spectrosc. investig. 0-89524
 antiferroelectric, coupled magnetoelc. oscil. and high freq. susceptibility tensor (Russian) 0-93152
 (CaO.6Fe $_2$ O $_3$) $_{97}$ (La $_2$ O $_3$) $_3$ compounds, effects of Nd $_2$ O $_3$ substitution on magnetic props. (Japanese) 0-108010
 CO $_2$ ferrite, crystal structure, X-ray absorpt. spectra, chemical shifts 0-88118
 composite semiconductor-ferrite struct., surface magnetostatic spin wave interactions (Russian) 0-88739
 dielectric constants and permeability of microwave ferrites (Chinese) 0-66096
 electron-stimulated absorption of bulk spin waves 0-70992
 epitaxial ferrite-garnet films with inversion layers, behaviour of cylindrical mag. domains, visual tracking method 0-71139
 ferrite materials and components, laboratory meas. automation (Polish) 0-101789
 ferroelectric ferrites, coupled ferroelec. and spin waves, exchange interactions 0-70995
 frequency tripling of spin waves due to longitudinal pumping excitation (Russian) 0-88740
 hexagonal, with M, W and Y structures containing Fe $^{2+}$ and Fe $^{3+}$ mag. ions, saturation moment and anisotropy 0-71009
 industrial ferrites type 1500 NMZ and 2000 NMI, mag. susceptibility depend. on heating (Russian) 0-108603
 inhomogeneous exchange interaction influence on ferromagnetic resonance line moments 0-75864
 lightguide, ferrite film, for nonreciprocal optical systems 0-99880

ferrites continued

- magnetic bubble materials, props. and preparation models, review (Rumanian) 0-93149
 magnetic permeability, initial, determination for toroidal samples as function of temp. 0-57346
 magnetization, regulation in expts. on self-acceleration of electron beam 0-63425
 magnetostriction due to Co $^{2+}$ ions, effect of excited states 0-65990
 orthoferrite cryst. films, local coercivity of domains boundaries (Russian) 0-80578
 p 0-75807
 parametric spin wave excitation (Russian) 0-93099
 polycrystalline ferrites, anisotropy const. meas. 0-97090
 rare earth ferrite garnets, phase transitions, field-induced spin-orientational 0-75767
 rare earth orthoferrites, domain wall dynamics 0-65957
 rare earth orthoferrites, mag. anisotropy in cryst. field approx. 0-60241
 rare earth orthoferrites, muon states, local mag. fields 0-75911
 rare earth orthoferrites, Raman scatt. from magnons, anisotropy consts. determ. 0-66178
 soft, production and props. 0-88801
 soft, spray firing for presintered powder prep. 0-89181
 spheres, magnetisation, resonance oscillation freq. determ. 0-71106
 spinels, mag. crit. point behaviour 0-60342
 thin films, Brillouin scattering from spin waves 0-65843
 window cores, magnetoelastic props., compressive stresses influence measurements using photo stress method (Polish) 0-93134
 B $_2$ O $_3$ Fe $_2$ O $_3$ nMO $_2$ ($n=2$ or 4, M=Mg, Co, Ni, Cu), mag. props., transitions 0-75763
 Ba ferrite, FMR in uniaxial crystal plate with bubble domain lattice 0-93182
 Ba hexaferrite, irradiated by fast neutrons, mag. props. 0-97116
 Ba, plastic magnet appl. anisotropic, based on moulding ferromagnetic powder material with plastics (Japanese) 0-60829
 Ba $_2$ Co $_{1.65}$ Fe $_{0.35}$ Fe $_{28}^{2+}$ O $_{46}$, temp.-mag. field phase diagram, torque method 0-60276
 BaFe $_{12-2x}$ M $_x$ Ti $_x$ O $_{19}$ (M=Co, Ni, Zn), mag. props. determ. 0-75759
 BaFe $_{12}$ O $_{19}$, bubble and stripe lattice domain wall oscil. 0-97115
 BaFe $_2$ O $_9$, Ca $^{2+}$ substitution effect on hexaferrite lattice and mag. props. 0-60243
 BaFe $_2$ O $_9$, ferrite, DC cond., dielec. props., lattice consts. 0-80272
 BaFe $_2$ O $_9$, microparticles, magnetisation reversal, hysteresis loop obs. 0-75813
 BaFe $_2$ O $_9$ particles, magnetic domain study by colloid-SEM method 0-97120
 BaFe $_2$ O $_9$ powder, hysteresis of microwave absorpt. and magnetisation reversal 0-75814
 BaFe $_2$ O $_9$, powder, milled and annealed, phase composition, lattice consts. and crystallite size 0-71677
 BaFe $_2$ O $_9$ powders, fast reaction presintering 0-97445
 Ba $_6$ Fe $_2$ O $_3$, ferrite polycryst., depend. of domain width on sample thickness 0-108031
 BaSr $_2$ Ca $_{1-x}$ Fe $_x$ O $_8$, substituted hexagonal ferrites, mag. split Mossbauer spectra obs. and X-ray struct. data 0-71250
 BaZn $_2$ Fe $_{16-x}$ M $_x$ O $_{27}$ (M=Al, Ga, In, Sc), mag. props. and Mossbauer effect 0-75766
 Ba $_3$ Zn $_2$ Fe $_{24}$ O $_{41}$, ferromag. reson., low power nonlinear effects 0-75861
 Ca ferrite, composition and mag. props., anisotropy field, magnetisation 0-71109
 Ca $_2$ (Al,Fe,Cr)O $_5$ solid soln., planar interfaces, TEM obs. 0-65008
 CaLaFeO $_4$, two-dimens. mag. ordered, structural and mag. props. (French) 0-70173
 Ca $_3$ Ni $_{1-x}$ Fe $_x$ O $_4$, X-ray struct. anal., determ. of lattice constant and interplanar distances (French) 0-96487
 CaO-SrO-Fe $_2$ O $_3$ system, phase relations, Sr hexaferrite field occurrence 0-93545
 (Co,Cr,Fe) $_3$ O $_4$, (Co,Rh,Fe) $_3$ O $_4$ film magnetooptical switches, for laser beam synchronisation 0-58615
 CoFe $_2$ O $_4$ mag. fluid particles, comp., struct., and mag. props. 0-60374
 CoFe $_2$ O $_4$, mag. hyperfine fields, Mossbauer spectra 0-108139
 CoFe $_2$ O $_4$ ultrafine particles, prep. and mag. props. 0-71116
 Co $_2$ (Ni $_{0.5}$ Cu $_{0.5}$) $_{1-x}$ Fe $_x$ O $_4$ ferrite, relation between elec. cond. and mag. anisotropy 0-75548
 Co $_3$ Ni $_{1-x}$ Fe $_x$ O $_4$, induced mag. anisotropy consts., conc. and temp. depend. 0-108001
 Co $_3$ Ni $_{1-x}$ Fe $_x$ O $_4$, ferrite, DC cond., dielec. props., lattice consts. 0-80272
 Cu ferrite films, Mn-, Ni- and Al-substituted, LPE growth 0-96752
 CuFe $_2$ O $_4$, Jahn-Teller type crystal distortions 0-103904
 Cu $_{0.5}$ Fe $_{2.5}$ O $_4$ -ZnFe $_2$ O $_4$, cation distrib., mag. moment, Mossbauer spectra, chem. anal. 0-75210
 DyFeO $_3$, field induced spin reorientation, Mossbauer spectroscopy 0-65878
 DyFeO $_3$, spin reorientation transitions induced by magnetic fields, Mossbauer study 0-71246
 DyFeO $_3$, weak ferromagnet, μ SR study 0-93226
 Dy $_2$ O $_3$ Ho $_2$ O $_3$ FeO $_3$ orthoferrite, domain struct., temp. depend. 0-71086
 ErFeO $_3$, field induced spin reorientation, Mossbauer spectroscopy 0-65878
 ErFeO $_3$, SAW meas. of magnetoelastic effects 0-75839
 ErFeO $_3$, weak ferromagnet, μ SR study 0-93226
 Fe $_{10.92}$ K $_{1.55}$ O $_17$, ferrite, cryst. struct., nonstoichiometry, ion-ion correlations 0-88130
 (Fe $_{0.19}$ $^{2+}$ Mg $_{0.56}$ $^{2+}$ Mn $_{0.25}$) [Fe $_{1.87}$ $^{3+}$ Al $_{0.13}$ $^{3+}$ O $_2$] $^{2-}$, influence of Fe $^{2+}$ ion substitution on electron hopping, Mossbauer study 0-71247
 (Fe $_{0.545}$ $^{2+}$ Mg $_{0.32}$ $^{2+}$ Mn $_{0.03}$ $^{2+}$ Cu $_{0.10}$ $^{2+}$) [Fe $_{7.4}$ $^{3+}$ Al $_{0.6}$ $^{3+}$ O $_2$] $^{2-}$, influence of Fe $^{2+}$ ion substitution on electron hopping, Mossbauer study 0-71247
 Fe $_2$ O $_4$, dielec. function and polar Kerr rotation, 0.5-3.6 eV 0-66221
 Fe $_2$ O $_4$, IR refl., ATR, Voigt and Faraday expts. 0-66180
 Fe $_2$ O $_4$, magnetocrystalline anisotropy, anomalies in magnetostriction and elastic constants 0-60244
 HoFeO $_3$, field induced spin reorientation, Mossbauer spectroscopy 0-65878
 La ferrite, composition and mag. props., anisotropy field, magnetisation 0-71109
 Li ferrite, linear electric field effects in mag. anisotropy and ferromag. reson. 0-65854
 Li ferrites, MW dielectric losses, causes and reduction (Chinese) 0-75930
 Li ferrites, porous, porosity effect on saturation of magnetisation 0-108036
 Li matrix ferrites, coercivity, synthesis, thermostability control 0-80569

ferrites continued

Li-Co ferrite, mag. anisotropy induced by thermomag. treatment, ionic order effect, magnetostriction meas. 0-103830
Li-Zn, (Li, Zn, Ti, Cr substituted), Mossbauer spectrometry, effect of supertransferred hyperfine fields and relaxation (*French*) 0-80654
 $\text{Li}_{0.5}\text{Fe}_{2.5-x}\text{Cr}_x\text{O}_4$, press. depend. of anisotropy consts. 0-65865
 $\text{Li}_{0.5}\text{Fe}_2\text{O}_4$, magneto-optical Kerr effect, reflectivity spectra 0-66157
 $\text{Li}_{0.5}\text{Fe}_2\text{O}_4$ milled ferrite powder, substruct. and sinterability 0-84894
 $\text{Li}_{0.5}\text{Fe}_2\text{O}_4$ Ru substitution effect on struct. and mag. props., and max. solubility determ. 0-75364
 $\text{Li}_{0.5}\text{Mn}_{0.15}\text{Fe}_{2.35}\text{O}_4$ ferrite cores with rectangular hysteresis loops, pulse parameters, effect of Fe_2O_3 heat treatment 0-60370
LiZn ferrosilicates, mol. field. coeff. conc. depend. 0-97114
 $\text{Mg}_x\text{Fe}_{3-x}\text{O}_4$ crystals, first mag. anisotropy const., 7-295K 0-65855
 $\text{Mg}_x\text{Fe}_{3-x}\text{O}_4$, polycryst., Verwey type transition, resist., magnetisation, Mossbauer effect and permeability obs. 0-75764
 $\text{Mg}_{0.25}\text{Zn}_{0.75}\text{Fe}_2\text{O}_4$, ferrite, DC cond., dielec. props., lattice consts. 0-80272
(Mn,Zn) Fe_2O_4 :Si, Ca, Ti, second phase effect on elec. and mag. props. 0-60986
Mn ferrite, magnetic permeability, photoinduced reduction (*Rumanian*) 0-75794
Mn-Zn ferrites, grain boundary exam. using TEM and AES 0-107268
 MnFe_2O_4 , additional spin echo of ^{55}Mn nuclei 0-60455
 $\text{Mn}_x\text{Fe}_{3-x}\text{O}_4$, dielec. function and polar Kerr rotation, 0.5-3.6 eV 0-66221
MnZn ferrite, initial mag. permeability rel. to mag. anisotropy 0-80557
MnZn ferrite, microstructure and initial permeability, presintering process effect 0-89367
MnZn ferrite powder prep., wet method 0-89180
MnZn ferrite powders, reactive, mag. materials obtained by compaction 0-89182
MnZn ferrites, internal friction and ΔE effect depend. on demagnetisation method 0-80584
MnZn ferrites, post sinter-cooling rates effects 0-89369
MnZn ferrous ferrite, initial mag. permeability second-order magnetocrystalline anisotropy influence 0-88820
MnZn ferrous ferrites, mag. permeability stress depend. 0-88822
MnZn, form. of comp. heterogeneity during high-temp. sintering 0-60818
 $\text{Mn}_{1-x}\text{Zn}_x\text{Fe}_2\text{O}_4$, prepared by wet method, neutron diff. and high field Mossbauer expts. 0-75719
 $\text{Na}_{0.9}\text{Ti}_1\text{Fe}_{0.9}\text{O}_4$, short period β -alumina type cpds., cryst. struct. and superionic cond. 0-107499
Ni ferrite, quenched, Neel temp. and initial susceptibility 0-75762
Ni-ferrite powders, form. in presence of Li_2SO_4 - Na_2SO_4 molten salts, prep. and characts. 0-84869
Ni-Zn-Co, synthesis from solid solns. of schoenite-type salts 0-93511
 $\text{Ni}_{1-x}\text{Cd}_x\text{Fe}_2\text{O}_4$, mag. props. rel. to ionic struct. 0-75756
NiFe, prep. of single crystal by chem. transport with TeCl_4 0-104051
 NiFe_2O_4 ferrite, mag. props., neutron irradi. 0-103858
 NiFe_2O_4 mag. fluid particles, comp., struct., and mag. props. 0-60374
 NiFe_2O_4 milled ferrite powder, substruct. and sinterability 0-84894
 $\text{Ni}_x\text{Fe}_{3-x}\text{O}_4$, DC and low freq. cond. and influence of microstruct. 0-70699
 $\text{Ni}_x\text{Fe}_{3-x}\text{O}_4$, magnetostriction, 80 to 300K, depend. on comp. and electron ordering on octahedral sites 0-65995
 $\text{Ni}_x\text{Fe}_{3-x}\text{O}_4$, spinels, fine particles, magnetic properties obs. 0-71031
NiZn ferrite, dielec. props., Jahn-Teller ion effects 0-97181
NiZn ferrites, density and mag. props., isostatic pressure effect 0-60816
NiZn ferrites, internal friction and ΔE effect depend. on demagnetisation method 0-80584
NiZn ferrites, nonstoichiometric, initial susceptibility and microstruct. 0-84591
NiZn ferrites, V_2O_5 induced mag. aftereffects 0-60379
NiZn, magnetoelastic Villari effect 0-88847
NiZn, prep. of single crystal by chem. transport with TeCl_4 0-104051
NiZn, ZrO_2 additions influence on sintering and physicochem. props. 0-108369
NiZnCo ferrites, switching time and coeff., hydrostatic press. effect 0-88802
NiZnCo ferrites, voltage response under sinusoidal and pulse magnetisation effected by hydrostatic press. 0-88846
 $\text{Ni}_{0.25}\text{Zn}_{0.75}\text{Fe}_2\text{O}_4$, Mossbauer study, spin fluctuations 0-60471
 $\text{Ni}_{0.25}\text{Zn}_{0.75}\text{Fe}_2\text{O}_4$, Mossbauer study, noncollinear spin struct. 0-60472
 $\text{Ni}_{0.25}\text{Zn}_{0.75}\text{Fe}_2\text{O}_4$, structural phase transition, X-ray and neutron diff. study 0-79735
 $\text{Ni}_{0.5}\text{Zn}_{0.5}\text{Fe}_2\text{O}_4$ coarse grain polycryst. ferrite, diffusional creep (*Japanese*) 0-104238
 $\text{Ni}_{0.85}\text{Zn}_{0.15}\text{Fe}_2\text{O}_4$ ferrite, mag. anisotropy compensation under neutron irradi. 0-75807
 $\text{Ni}_{1-x}\text{Zn}_x\text{Fe}_2\text{O}_4$, polycryst., domain wall energy rel. to anisotropy 0-71090
 $\text{PbFe}_{1-x}\text{O}_{10}$, bubble and stripe lattice domain wall oscils. 0-97115
 $\text{PbFe}_{1-x}\text{O}_{10}$, single crystal, Mossbauer spectra 0-84670
Sr, plastic magnet appl., anisotropic, based on moulding ferromagnetic powder material with plastics (*Japanese*) 0-80829
 $\text{SrFe}_{12-x}\text{Cr}_x\text{O}_{19}$, hexagonal ferrite series, Mossbauer study 0-71258
 $\text{SrFe}_2\text{Ga}_2\text{O}_{13}$ ferrite, mag. struct., Mossbauer study 0-93087
 $\text{SrFe}_2\text{O}_{19}$, Ca^{2+} additives effect on hexaferrite lattice and mag. props. 0-60243
 $\text{SrFe}_2\text{O}_{19}$:Si, Sr, second phase effect on elec. and mag. props. 0-60986
 TbFeO_3 , mag. susceptibility, temp. depend., effective field at Tb ion sites 0-75742
 TmFeO_3 , acoustic vel. and attenuation shifts at spin reorientation phase transition 0-65986
(YEuTm) $_3(\text{GaFe})_2\text{O}_{12}$ ferrite garnet films, mag. bubbles, translational motion, mechanism for inertial effects 0-100606
YFeO₃, domain boundary inertia during mag. reversals (*Russian*) 0-88776
YFeO₃, mag. anisotropy in cryst. field approx. 0-60241
YFeO₃, orthoferrite, crit. domain wall vel. 0-71135
(YGdTm) $_3(\text{FeGa})_2\text{O}_{12}$ epitaxial film, formation of lattice of cylindrical mag. domains from stripe domains (*Russian*) 0-80579
(YGDYbBi) $_3(\text{FeAl})_2\text{O}_{12}$ ferrite-garnet films, effect of in-plane field on dynamics of domain walls 0-65979
 $\text{ZnCr}_2\text{Fe}_{1-x}\text{O}_4$, Mossbauer spectra, quadrupole splitting, Debye temp. 0-93218
 $\text{Zn}_x\text{Cu}_{0.1}\text{Fe}_{2.9-x}\text{O}_4$, ferromag. relax. 0-60422
 $\text{Zn}_x\text{Cu}_{0.1}\text{Fe}_{2.9-x}\text{O}_4$, ferromag. reson., g-factors, Jahn-Teller ion effects 0-66043

ferrites continued

$\text{Zn}_x\text{Fe}_{3-x}\text{O}_4$ ferrite, mag. struct., Mossbauer spectra and magnetisation study, 4.2K 0-103818
 $\text{Zn}_x\text{Fe}_{3-x}\text{O}_4$, ferromag. reson., g-factors, Jahn-Teller ion effects 0-66043
ferroacoustic resonance
No entries
ferroelasticity
see also shape memory effects
aniline hydrobromide, ferroelastic, acoustic softening near transition temp. 0-96617
aniline hydrobromide, ferroelastic phase transition, Raman scatt. study 0-108195
dislocation-phonon interactions, phase transition effects in proper ferroelastic 0-59600
domain wall, roughening transition suppression by long range elastic forces 0-75991
F 0-100329
ferrodistortive spin-phonon systems, crit. props. 0-88315
ferroelectric-elastic phase transition, modelling, appl. to KH_2PO_4 and $\text{LiNH}_4\text{C}_4\text{H}_9\text{O}_2\cdot 2\text{H}_2\text{O}$ (*Russian*) 0-75961
ferroc crystals, prototypic point group, physical props., model 0-80715
ferroc phase transitions, non-mag., unified classification 0-70387
macroscopic quadrupole effects as method of obs. of struct. transforms in crystals 0-71321
memory alloy, pseudoelastic, model for first-order phase transition 0-92642
polymorphic transition region, mech. hysteresis 0-79942
tetramethylammonium tetrachlorocuprate crystal, incommensurate-ferroelastic (commensurate) phase transition obs. 0-75352
tris-sarcosine calcium chloride: Mn^{2+} ferroelec. dynamics, EPR and ENDOR study 0-75972
 $\text{Ba}_2\text{NaNb}_2\text{O}_{15}$, incommensurate refls. near ferroelastic transition, neutron and X-ray precession obs. 0-70395
 BaTiO_3 , ferroic materials, fracture processes 0-79869
 BiVO_4 , ferroelastic domains, electron microscopy and electron diff. obs. 0-100254
 BiVO_4 , ferroelastic phase transition, birefringence meas. using rotating-analyser method 0-80742
 BiVO_4 , ferroelastic phase transition, birefringence meas. at simultaneous high pressure and temp. 0-80743
 $\text{Cs}_3\text{NaM}^{3+}\text{Cl}_6$ ($\text{M}^{3+}=\text{Bi}, \text{Nd}, \text{Pr}$), ferroelastic phase transitions, thermal expansion, elasticity, and X-ray anal. 0-70393
 DyVO_4 , Jahn-Teller crystal, deform. induced transitions, elastic and dielectric characts. (*Russian*) 0-80726
 $\text{Gd}_2(\text{MoO}_4)_3$, ferroelec.-ferroelastic, photolum. and photocond. meas. 0-84768
 Hg_2Br_2 , nonintrinsic ferroelastic, thermal expansion and thermodynamic potential 0-88344
 Hg_2Cl_2 , neutron and Raman scatt. studies, ferroelastic transitions 0-76015
 $\text{K}_2\text{Ba}(\text{NO}_3)_2$, elastic props. 0-96588
 $\text{K}(\text{D}, \text{H}_{1-x})(\text{SeO}_3)_2$, anelastic and elastic infra-low freq. props. 0-70304
 $\text{KD}_3(\text{SeO}_3)_2$, phase transition, neutron scatt. study 0-75351
 $\text{KFe}(\text{MoO}_4)_2$, phase transitions at 312 and 139K 0-70396
 $\text{KH}_2(\text{SeO}_3)_2$ and $\text{KD}_3(\text{SeO}_3)_2$, ferroelastic phase transition, mech. stress effect 0-70394
 $\text{KH}_2(\text{SeO}_3)_2$, ferroelastic transition under uniaxial press., EPR study 0-59562
 LaP_2O_4 , continuous ferroelastic transition elastic and mechanical props. 0-92668
 LaP_2O_4 , coupling effects between soft optic and acoustic modes at ferroelastic transition 0-70358
 Na_2CO_3 , phys. props. related to phase transitions 0-96643
 $\text{NaH}_2(\text{SeO}_3)_2$, domain struct. realignment and Barkhausen effect 0-71361
 NdP_2O_4 , ferroelastic, hydrostatic press. effect on phase transition temp. 0-70293
 $\text{Pb}_3(\text{PO}_4)_2$, ferroelastic, dielectric anomalies, phase transitions, permittivity, relaxation (*Russian*) 0-71293
 $\text{Pb}_3(\text{P}_{0.95}\text{V}_{0.05}\text{O}_4)_2$, ferroelastic transition, soft mode, inelastic neutron scatt. study 0-70357
 $\text{Pb}_3(\text{P}_{1-x}\text{V}_x\text{O}_4)_2$, ferroelastic phase transition, DTA, dilatometric and Brillouin scatt. study 0-70398
 $\text{Pb}_3(\text{VO}_4)_2$, ferroelastic, phase transitions, boundary walls 0-107419
 $\text{Pb}(\text{Zr,Ti})\text{O}_3$, ferroic materials, fracture processes 0-79869
 RbCaF_3 , first order improper ferroelastic phase transition at 194K, phenomenological description 0-70397
 SnF_2 , second order $\beta\rightleftharpoons\gamma$ transition, neutron diff. and NMR obs. 0-107095
 $\text{Tb}(\text{MoO}_4)_3$ cryst. struct. in ferroelec., ferroelastic, antiferroelec. and paraelastic phases 0-75205
 VO_2 , ferroelastic metal-insulator transition, electronically triggered crystallographic phase transition 0-70614
 WO_3 , acoustic instability near monoclinic orthorhombic phase transition, X-ray scatt. 0-65215
ferroelectric Curie temperature
domain struct. near first-order phase transition resembling second-order transition 0-93139
extended defect system, phase transform., critical props. 0-103455
extrinsic ferroelectrics, transition, polarisation, dielectric divergence 0-80718
ferroelectric materials for dielectric power conversion, dielectric prop. anal. 0-80712
ferroelectrics with hydrogen bonds, phase transition into coherent state, two-level proton calcs. (*Russian*) 0-71356
methyl ammonium aluminium sulphate, ferroelec., proton spin-lattice relax. time anomaly 0-60440
methylammonium alums, dielec. relax. near transition point 0-71301
narrow-gap ferroelectric, phase transition due to strong mag. field 0-103924
oxyfluoride ferroelectrics, chemical bonding, Curie temp., spontaneous polarisation 0-75981
rare earth arsenates, RAsO_4 , ferroelectricity, dielec. meas. 0-60515
Rochelle salt, dehydration kinetics in ferroelec. and paraelec. phases, surface acoustic waves influence 0-97204
(Rochelle salt) $_x$ (ammonium Rochelle salt) $_{1-x}$, phase transitions, hydrostatic press. effects 0-93246
TGS, autostabilised state, elec. second harmonic generation 0-103921
TGS, ferroelec. single crystal, low freq. nonlinear effects 0-84490
TGS, static crit. phenomena, lattice defect influence 0-71336

ferroelectric Curie temperature continued

- TGS, US relax. time constant 0-84257
 TGSSe, autostabilised state, elec. second harmonic generation 0-103921
 vinylidene fluoride-trifluoroethylene film, cryst. phase transition 0-66120
 As₂Sb_{1-x}SI mixed crystals, phonon coupling, ferroelectric phase transition, Raman study 0-108165
 BaTiO₃, electron exoemission unipolarity associated with phase transitions 0-97415
 Cs(H_{1-x}D_x)₂PO₄, dielec. props., temp. meas. 0-71335
 KH₂AsO₄, NQR of ⁷⁵As, press. and temp. depend., 77K to Curie temp. 0-71227
 K(H_{1-x}D_x)₂PO₄, polarisation relaxation time and Landau kinetic coeff. rel. to degree of deuteration 0-84251
 KH₂PO₄, crit. behaviour, dilatometer study 0-92689
 KH₂PO₄, ferroelectric transition, order-disorder character of hydrogen bond 0-93251
 KH₂PO₄ type ferroelectrics, Green's function theory of phase transitions with pseudo-spin-lattice coupled mode model 0-71354
 K_{1-x}Na_xTaO₃ quantum ferroelectric, dielec. susceptibility 0-103922
 K_{1-x}Ta_xNbO₃ quantum ferroelectric, dielec. susceptibility 0-103922
 Li_{1+y}Ta_{1-y}Ti_yO₃ (0 ≤ y ≤ 0.028), non-stoichiometric phase, crystallographic and dielec. props. 0-75212
 NH₄HSeO₄, ferroelec. props. rel. to struct. 0-71345
 NH₄HSeO₄, ferroelec., phase transitions, permittivity and pyroelectricity meas. 0-71350
 (NH₄)₂SO₄, static and dynamic dielec. behaviour 0-71337
 Na_{1-x}Li_xNbO₃ mixture, ferroelec.-paraelec. transitions, dielec. props. meas. 0-66125
 Na₂R(WNb₂)O₆F₆ (R=Y, Nd, Eu, Gd, Dy, Lu), synthesis, cryst.-chem. and dielec. study (*French*) 0-108164
 PLZT ceramics, modified by Ca²⁺(Sr²⁺)(Nd³⁺)(Y³⁺), dielec. behaviour 0-60519
 PLZT modified high voltage dielectric, permittivity, Curie temp., loss meas. 0-80720
 Pb₃(Ge_{1-x}Si_x)O₁₁, electrogyration, phase transition and dielectric props. 0-93269
 PbSc_{2/3}Te_{1/3}O₃-PbSc_{1/3}W_{1/3}O₃(PbFe_{2/3}Te_{1/3}O₃) ferroelec. props. and lattice consts. 0-60520
 PbZrO₃, ferroelec. solid solns., atom shifts, polarisation and Curie temps. 0-100636
 RbHSeO₄, ferroelec., dielec. dispersion 0-97179
 RbHSeO₄, ferroelec. props. rel. to struct. 0-71345
 RbH₃(SeO₃)₂, dielec. relax. near ferroelec. Curie temp. 0-97207
 RbH₃(SeO₃)₂, US vel. and absorpt. near ferroelec. Curie temp. 0-97206
 TGS, ferroelectric phase transition, high resolution NMR study 0-97214
 V₂O₅, ferroelec. semicond., dielec. and elec. meas. 0-60516

ferroelectric devices

- conference, Minneapolis, MN, USA (June 1979) 0-77535
 converters of shockwave mech. energy into elec. power 0-61429
 phase shifting at 94 GHz using bulk crystals, microwave electro-optic coeffs. determ. 0-71382
 photoferroelectric image storage in antiferroelectric-phase PLZT ceramics 0-71353
 piezoceramic aperiodic transducer, mech. load study 0-87700
 Gd₂(MoO₄)₃, ferroelec., amorphous Si:H coating, domain wall motion, image scanning 0-83663
 Gd₂(MoO₄)₃, matrix-addressed analogue ferroelec. memory 0-103926
 PLZT pyroelectric detectors, delayed onset of piezoelec. oscils. 0-75953
 PLZT thermal, flash, ferroelectric protective goggles 0-81746

ferroelectric domains see electric domains**ferroelectric materials**

- see also antiferroelectric materials; electric domain walls; ferroelectric semiconductors; ferroelectric thin films; ferroelectric transitions; lattice dynamics of ferroelectric crystals
 ammonia Rochelle salt, temp. depend. of optical axis angle, phase transitions (*Russian*) 0-97216
 ammonium Rochelle salt, thermodynamics of ferroelec. transition 0-84702
 1,6-bis(2,4-dinitrophenoxy)-2,4-hexadiyne, obs. of apparent ferroelec. transition 0-66121
 bulk photovoltaic effect response coeff. 0-65631
 ceramic, polycryst., elasticity props., neutron bombardment effects 0-79856
 ceramics, materials and dielec. props., review 0-75957
 ceramics, transparent ferroelectric, composition selection for appl. in light modulators (*Russian*) 0-91869
 conference, Minneapolis, MN, USA (June 1979) 0-77535
 copper formate tetrahydrate, ice rule ferroelectric, polarisation correlations 0-97190
 deformable, coupled acousto-optic modes 0-96093
 deformable, coupled electroacoustic eqns. 0-96092
 dicalcium lead propionate, improper ferroelectric, dielectric props., IR radiation pyroelectric detection 0-80711
 dicalcium strontium propionate, ferroelec. domains, direct optical visibility 0-84704
 dielectric constant meas. using automatic system (*German*) 0-90864
 dielectric power conversion, dielectric prop. anal. 0-80712
 DOBAMBC, chiral smectic, ferroelec., press. and solute effects 0-103920
 DOBAMBC, ferroelec. liq. crystals, elec. and optical props., appls. (*Japanese*) 0-88943
 DOBAMBC, smectic A and ferroelec. smectic phases, ¹³C NMR study 0-75153
 electro-optical and nonlinear-optical materials, review 0-74450
 electron microscopy investigations, review (*Japanese*) 0-71366
 EPR, elec. field modulated 0-75841
 esters, SLIC, ferroelectric behaviour, specific heat, spontaneous polarisation 0-75958
 extrinsic ferroelectrics, transition, polarisation, dielectric divergence 0-80718
 glycine sulphate-L-alanine, unirradiated, optical spectroscopy of scintillations 0-80863
 guanidine aluminium sulphate hexahydrate, SEM obs. of ferroelec. domain struct. in single crystals 0-97219
 guanidinium aluminium sulphate hexahydrate, surface obs., SEM and AES expts. 0-71362
 guanidinium aluminium sulphate hydrate, ferroelec., decoration patterns on cleavage surface, domain obs. 0-97218
 guanidinium uranyl sulphate hydrate, ferroelec., decoration patterns on cleavage surface, domain obs. 0-97218
 halide ferroelectrics, transitions, formulae, structural data 0-75980

ferroelectric materials continued

- heterogeneous states, statistics (*Russian*) 0-80721
 hysteresis loop sensing (*Czech*) 0-82792
 large-gap type, vibronic theory and opt. props., anomalous bulk photovoltaic effect 0-103939
 liquid crystals, chiral smectic C phase, phys. props., review 0-75150
 lithium thallium tartrate, sp. ht., 0.3 to 25K, second-order ferroelec. transition 0-59674
 methyl ammonium aluminium sulphate, ferroelec., proton spin-lattice relax. time anomaly 0-60440
 methylammonium aluminium sulphate dodecahydrate, single crystals, high-order EPR transitions of Cr³⁺ 0-108052
 methylammonium alums, dielec. relax. near transition point 0-71301
 oxyfluoride ferroelectrics, chemical bonding, Curie temp., spontaneous polarisation 0-75981
 photoelectric states in real time spatial light modulators, photorefractive effect 0-80676
 PLZT ceramic, ageing, dielec. props. 0-88940
 PLZT coarse-grained solid solutions, electro-optical processes induced by longitudinal electric field (*Russian*) 0-80750
 polar materials, appl. to SAW and other devices 0-66114
 polydomain ferroelec. crystals, phys. consts., self consistent calcs. 0-88942
 polyvinylidene fluoride, electro-optic and elasto-optic effects 0-80754
 polyvinylidene fluoride, hysteresis phenomena under high elec. field 0-66134
 polyvinylidene fluoride film, hysteresis and dipolar orientation 0-97217
 pyroelectricity, primary and secondary, review 0-93243
 PZT ceramics, ferroelec. energy conversion under shock loading 0-108163
 rare earth arsenates, RAsO₄, ferroelectricity, dielec. meas. 0-60515
 (rare-earth), Ti₂O₇, (RE=La-Nd, Sm, Gd, Y), ferroelec., layer type struct., cryst. growth 0-108348
 relaxor ferroelectrics, electrostrictive effects 0-66112
 Rochelle salt, dehydration kinetics in ferroelec. and paraelec. phases, surface acoustic waves influence 0-97204
 Rochelle salt, ferroelectric, Raman and IR study 0-71406
 salicidenanilins, SLIC, ferroelectric behaviour, specific heat, spontaneous polarisation 0-75958
 tris-sarcosine calcium chloride, elastic props., US damping 0-84229
 smectic C liquid crystals, ferroelec., fundamentals and display appl. 0-79676
 Tanane, ferroelec. mol. cryst.; strong piezoelec. coupling 0-75942
 TBACA, chiral, smectic C* and H* phases, mol. orientational ordering, ¹⁴N NQR study 0-75152
 tetragonal ceramics, 90° domain-rot. fraction after polarisation, X-ray determ. 0-75992
 tetragonal ferroelectric irradiated by laser pulses, spatial temp. and bound-charge distrib. 0-103927
 tetramethylammonium cobalt tetrachloride, ferroelectricity, triple 60 Hz D-E hysteresis loops 0-71365
 tetramethylammonium cobalt tetrachloride, Raman spectra near incommensurate phase transitions 0-76013
 tetramethylammonium tetrachlorocobaltate, ferroelec., pressure-temp. phase diagrams 0-97205
 tetramethylammonium tetrachloroferrate, press. induced ferroelectricity, dielec. and DTA meas. 0-80722
 tetramethylammonium tetrachlorozincate, ferroelec., pressure-temp. phase diagrams 0-97205
 tetramethylammonium tetrachlorozincate, incommensurate phase study, ferroelectric-paraelectric phases (*French*) 0-88318
 tetramethylammonium tetrachlorozincate, X-ray study of incommensurate phase 0-71351
 tetramethylammonium zinc tetrachloride, ferroelectricity, triple 60 Hz D-E hysteresis loops 0-71365
 tetramethylammonium zinc tetrachloride, incommensurate phase transitions, ¹³C NMR study 0-75968
 tetramethylammonium zinc tetrachloride, Raman spectra near incommensurate phase transitions 0-76013
 TGS:α-alanine, single crystals., dielec. spectrum in RF range (*Russian*) 0-66097
 TGS: nitroaniline, dielec. and pyroelec. props. 0-75916
 TGS:L-alanine, unirradiated, optical spectroscopy of scintillations 0-80863
 TGS, autostabilised state, elec. second harmonic generation 0-103921
 TGS, crit. behaviour of thermal expansion, neutron diff. study 0-75371
 TGS, deuterated, ferroelec., dielec. nonlinearity 0-75959
 TGS, effect of Fe³⁺ admixture on phys. props. 0-76052
 TGS, electrostrictive and dielec. coeffs., neutron diff. study 0-75943
 TGS, ferroelec., vacuum cleaved, charge compensation 0-60510
 TGS, ferroelec. activation field change 0-71358
 TGS, ferroelec. single crystal, low freq. nonlinear effects 0-84490
 TGS, ferroelectric hysteresis, dielectric and pyroelectric props. (*Chinese*) 0-88938
 TGS, internal bias field, hysteresis loops (*Chinese*) 0-84705
 TGS, internal field prod. in layer periodical domain struct. by X-ray irradi. 0-71359
 TGS, kinetics of domain formation during phase transition 0-66130
 TGS, L-α-alanine disordered regions, dielec. prop. changes in transition region 0-108159
 TGS, perfect and imperfect, sp. ht. and sound vel., crit. anomalies 0-71331
 TGS, spontaneous polarisation, low temp. meas. 0-75921
 TGS, static crit. phenomena, lattice defect influence 0-71336
 TGS (-d₃₁), sp. ht. near ferroelec. phase transition 0-70420
 TGS and deuterated cpd., ferroelec. US relax. time constant 0-84257
 TGS crystals., effects of radiation induced defects on internal bias field 0-88941
 TGS powders, dielec. dispersion 0-97180
 TGS substrate, influence of polarisation reversal on elec. cond. of CdTe thin film 0-65720
 TGSe, ferroelec., dielec. nonlinearity 0-75959
 TGSe, autostabilised state, elec. second harmonic generation 0-103921
 thiourea, ferroelectric, Raman and IR study 0-71406
 thiourea, incommensurate phase, soft modes, condensation of even-order harmonics 0-103313
 thiourea, incommensurate phase transition, X-ray and neutron scatt. study 0-75963
 thiourea, X-ray diffuse scattering studies using high-pressure and low-temp. cell 0-86336
 triglycine fluoborilate, deuterated, dislocation line defect X-ray topographic analysis 0-59465

ferroelectric materials continued

- triglycine sulphate, ferroelec., decoration patterns on cleavage surface, domain obs. 0-97218
 tris-sarcosine calcium chloride: Mn^{2+} ferroelec. dynamics, EPR and ENDOR study 0-75972
 tris-sarcosine calcium chloride, ferroelec. transitions, soft modes, Raman scatt. spectra obs. 0-80763
 tris-sarcosine calcium chloride, phase transition, hydrostatic press. effect, dielec. const. meas. 0-71327
 trissarcosine calcium chloride, ferroelec. phase transition, Raman and Brillouin scatt. studies 0-71340
 twisted smectic C phase, mol. conformation and orientational order, NMR studies, review 0-75151
 vinylidene-fluoride-trifluoroethylene copolymer, piezoelectricity 0-88930
 $Zn_2B_4O_{13}Br$, ferroelec. 43m-mm2 phase transition, molar heat capacity meas. 0-93249
 $AgNa(NO_2)_2$, ^{23}Na elec. field gradient tensor from NMR satellite lines near phase transition 0-71191
 $AgNa(NO_2)_2$, crit. dynamics, hydrostatic press. effect, dielec. props. meas. 0-71328
 $AgNa(NO_2)_2$, ferroelec. cryst., Raman spectrum, phase transition, comparative anal. with $NaNO_2$ 0-88935
 $AgNa(NO_2)_2$, order-disorder ferroelec., influence of hydrostatic press. on polarisation dynamics 0-103913
 $As_0.7Sb_{0.3}Si$ cryst., ferroelec., soft mode Raman and IR spectroscopy 0-76016
 $As_2Sb_{1-x}Si_x$ mixed crystals, phonon coupling, ferroelectric phase transition, Raman study 0-108165
 $(Ba,Sr)TiO_3$, ferroelec. props., press. depend., anharmonic oscillator model 0-80716
 $BaHfO_3$, $BaSnO_3$ and $BaZrO_3$, high-density ceramics prep. and elec. props. 0-60812
 $BaMgF_4:Mn^{2+}$ ferroelec., EPR and ENDOR study, cryst. field tensor 0-71162
 $BaMn_{0.99}Co_{0.01}F_4$, magnetoec. phenomena, dielec. behaviour near Neel temp. 0-71151
 $BaMnF_4$, pure and Co doped, ferroelec. antiferromag., dielec. anomalies 0-71288
 $BaMnF_4$, spectroscopy near ferroelec. transition, dielec. anomalies near mag. ordering temp. 0-75965
 $Ba_2NaNb_2O_{15}$, cryst. comp. effect on low temp. phase transition 0-71346
 $Ba_2NaNb_2O_{15}$, growth layer form., crystallization conditions effect, light diff., Curie temp. 0-100778
 $Ba_2NaNb_2O_{15}$, high press. phase transitions, Raman scatt. studies 0-71402
 $Ba_2NaNb_2O_{15}$, incommensurate refls. near ferroelastic transition, neutron and X-ray precession obs. 0-70395
 $Ba_2NaNb_2O_{15}$, local states, thermoluminesc. study 0-60690
 $BaO-Nd_2O_3-TiO_2-Bi_2O_3$ system ceramics, high stability low loss dielectric preparation 0-81008
 $(Ba,Sr_{1-x})TiO_3$ 0-60514
 $Ba,Sr_{1-x}Nb_2O_6:Ce$, pure and doped, photoelec. props. and photorefractive 0-60538
 $Ba,Sr_{1-x}TiO_3$, ferroelec. film, heteroepitaxial growth in cathode sputtering 0-93486
 $BaTiO_3$, band struct. calc., interpretation of XPS and UPS spectra 0-70597
 $BaTiO_3$ ceramic, degradation under high AC elec. field 0-60499
 $BaTiO_3$ ceramic dielectric capacitor, processing prop. relations, hysteresis, permittivity 0-80730
 $BaTiO_3$ ceramics, PTC-type, grain boundary study using TEM 0-107267
 $BaTiO_3$, crystn. from melts, comparison of different prospective oxy-anion solvents 0-71583
 $BaTiO_3$, elastooptic effect near ferroelec. transition, temp. depend. 0-97233
 $BaTiO_3$, electron exoemission unipolarity associated with phase transitions 0-97415
 $BaTiO_3$, electron microscopy investigs. of ferroelec. substances, review (Japanese) 0-71366
 $BaTiO_3$, ferroelec. cryst., IR and Raman spectra, mode coupling 0-66194
 $BaTiO_3$, ferroelectric mechanisms, anharmonic couplings by scanning IR interferometry 0-75978
 $BaTiO_3$, ferroic materials, fracture processes 0-79869
 $BaTiO_3$ film, struct. and dielec. props. 0-60514
 $BaTiO_3$, internal stress and strength, failure mechanism 0-66128
 $BaTiO_3$, intrinsic luminesc. 0-71467
 $BaTiO_3$, K-edge X-ray absorpt., cond. band states 0-97382
 $BaTiO_3$, mean square atomic displacement temp. depend., sublattice vibration anharmonicity 0-79890
 $BaTiO_3$, Mossbauer spectroscopy, sample prep. and results 0-66078
 $BaTiO_3$, paraelec. phase, stabilisation of soft mode 0-75985
 $BaTiO_3$, paraelectric crystal, nonlinear props. 0-84699
 $BaTiO_3$, periodic domain struct. and opalescence at tetragonal to orthorhombic transition 0-66131
 $BaTiO_3$, polycryst., phase transition obs. in -170 to 220°C range (Russian) 0-103474
 $BaTiO_3$, polycrystalline ferroelectric, grain-size dependent props. 0-71352
 $BaTiO_3$, polydomain ferroelec. crystals, phys. const., self consistent calcs. 0-88942
 $BaTiO_3$, polymorph, hexagonal, low temp. and surface CO_2 adsorption and desorption 0-80713
 $BaTiO_3$, powders, Bragg reflection integral intensities due to structural anomalies 0-107098
 $BaTiO_3$, pure and doped crystals, surface and domain struct., AES and SEM expts. 0-71363
 $BaTiO_3$, pure and Fe doped, ferroelec., switching and electrolum. 0-76079
 $BaTiO_3$, reduction inhibition by impurity ions 0-101018
 $BaTiO_3$, soft mode spectroscopy IR refl. meas. 0-88982
 $BaTiO_3$, spontaneous polarisation, low temp. meas. 0-75921
 $BaTiO_3$, surface microrelief after ion irradi. 0-59774
 $BaTiO_3$, surface study using AES and ion scatt. spectroscopy 0-65339
 $BaTiO_3$ type crystal, thermodynamic analysis of struct. phase transitions (Russian) 0-103473
 $BaTiO_3$, valence band UPS and partial p and d density of states 0-71560
 $BaTiO_3$, vibronic theory and opt. props. 0-103939
 $BaTiO_3:BaTi_2O_7$, dielec. props. and microstruct. 0-60481
 $BaTiO_3:C$, solubility of C at low O_2 potentials, 800°C 0-100334
 $BaTiO_3:Co$, tricritical point, X-ray diff. meas. 0-71341
 $BaTiO_3:Fe^{3+}$, local position determ. by EPR 0-108057

ferroelectric materials continued

- $BaTiO_3-BiFeO_3$ solid solns., ferroelec.-antiferromag., magnetoelectric effect at ferroelec. transition 0-100637
 $Ba_2Ti_9O_{20}$ single crystals, prep. and unit-cell parameters 0-103302
 $BaTi_0.98Sn_{0.02}O_3$, ferroelec. film, switching process 0-60518
 $Ba(Ti_{1-x}Sn_x)O_3$ film, struct. and dielec. props. 0-60514
 $BiFeO_3$, ferroelec., antiferromag., cryst. and mag. struct., neutron diff. study 0-65786
 $Bi_4Ti_3O_{12}$, elec. characts., phase transition obs. 0-60517
 Bi_2WO_6 , ferroelectric, dielectric props., elec. cond. and relaxation phenomena obs. 0-80692
 Bi_2WO_6 layered ferroelectric, anomalous photovoltaic effect, photovoltaic current 0-75603
 $CaSnO_3$ and $CaZrO_3$, high-density ceramics prep. and elec. props. 0-60812
 $Ca_{1-x}Sr_{x/2}Ba_{x/2}Zr_{1-x}Ti_xO_3$, ceramic system, dielectric props., microwave resonator application 0-80674
 $Cr_3B_2O_3Cl$, ferroelec. 43m-mm2 phase transition, molar heat capacity meas. 0-93249
 $Cs,CdBr_4$, struct. phase transitions, NQR study 0-71343
 CsD_2PO_4 , pseudo-one-dimensional ferroelectric transition, ^{31}P chemical shift and relaxation study 0-66123
 CsD_2PO_4 , pseudo-one-dimens. ferroelec. transition, DMR and relax. study 0-71223
 CsD_2PO_4 , pseudo-one-dimensional ferroelec. and antiferroelec. transitions, phase diagram obs., soft modes 0-93245
 $Cs(H_{1-x}D_x)_2PO_4$, dielec. props., temp. meas. 0-71335
 CsH_2PO_4 and CsD_2PO_4 , pseudo one-dimens. ferroelec. ordering dynamics, ^{31}P NMR study 0-75971
 CsH_2PO_4 , ferroelec. transition, electrooptic 0-76005
 CsH_2PO_4 , ferroelec., X-ray struct. study at room temp. 0-88113
 CsH_2PO_4 , ferroelec. transition, neutron diff. study 0-93247
 $Cs_3MoO_3F_3$, ferroelec., transition obs. 0-75989
 $CsK(MoO_4)$ R=Dy, Ho, Er, permittivity temp. depend., polymorphic transition 0-92670
 $Cs_3RbMoO_3F_3$ and $Cs_3RbWO_3F_3$, ferroelec., transition obs. 0-75989
 $Cs_3WO_3F_3$, ferroelec., transition obs. 0-75989
 $Cu-Cl$ boracite, pyroelec. coeff. meas. 0-75951
 $Cu_3B_2O_3Cl$, ferroelec. 43m-mm2 phase transition, molar heat capacity meas. 0-93249
 $Fe-I$ boracite, pyroelec. coeff. meas. 0-75951
 $Fe_3B_7O_{13}I$, ferroelec. 43m-mm2 phase transition, molar heat capacity meas. 0-93249
 $Fe_3B_7O_{13}I$, improper ferroelectric, dielectric props., IR radiation pyroelectric detection 0-80711
 $(Fe,Cr_{1-x})_2O_3$ corundum-type solid solution single crystal growth, chem. vapour transport 0-93465
 Fe_2O_3 , lattice parameters, NMR freqs., and magnetoec. pots. near 12K 0-71146
 $Gd_2(MoO_4)_3$, domain wall motion dynamics 0-108030
 $Gd_2(MoO_4)_3$, electron microscopy investigs. of ferroelec. substances, review (Japanese) 0-71366
 $Gd_2(MoO_4)_3$, ferroelec., amorphous Si:H coating, domain wall motion, image scanning 0-83663
 $Gd_2(MoO_4)_3$, ferroelec.-ferroelastic, photolum. and photocond. meas. 0-84768
 $Gd_2(MoO_4)_3$, one-dimensional ferroelectric image sensor with polymer photoconductor 0-80729
 $Gd_2(MoO_4)_3$, surface study using AES and ion scatt. spectroscopy 0-65339
 HCl and $HCl-DCI$, ferroelec. transition, ^{35}Cl NQR study 0-71233
 KD_2AsO_4 , ferroelec., high temp. phase transition, Raman spectra 0-71338
 KD_2AsO_4 , high temp. phase transitions, proton dynamics 0-76023
 $KD_2H_2(1-x)PO_4$ crystals, $0 < x < 0.98$, light scatt. by polaritons 0-96802
 $K(D_2H_{1-x})_2(SeO_3)_2$, ferroelastic, anelastic and elastic infra-low freq. props. 0-70304
 KD_2PO_4 , acoustic phonon dispersion, elastic stiffness, light scatt. obs. 0-103966
 KD_2PO_4 , coexistence states during first order transition, optical obs. 0-75350
 KD_2PO_4 , neutron scattering from coupled polar-elastic waves 0-92623
 KD_2PO_4 , phase transitions study, role of cryst. struct. determ. 0-75197
 KD_2PO_4 , polarisation fluctuations, wavevector depend. 0-71295
 KD_2PO_4 , X-irradiated, hysteresis effects obs. by ESR 0-103928
 $KD_2PO_4:Ti^{2+}$, EPR of ferroelec. and paraelec. phases 0-66012
 KD_2PO_4 -type ferroelectrics, parametric tunnelling-like reson. 0-66119
 $K_2Fe(CN)_6 \cdot 3H_2O$, ferroelec. and paraelec. phases, dielec. props. meas. 0-60494
 KH_2AsO_4 , ferroelec., high temp. phase transition, Raman spectra 0-71338
 KH_2AsO_4 , ferroelectric phase transition under high hydrostatic press., mol. dynamics, NQR study 0-75880
 KH_2AsO_4 , γ -irradiated, free radicals, EPR and ENDOR study of consequences of ferroelec. transition (French) 0-93209
 KH_2AsO_4 , high temp. phase transitions, proton dynamics 0-76023
 KH_2AsO_4 , NQR of ^{75}As , press. and temp. depend., 77K to Curie temp. 0-71227
 KH_2AsO_4 , proton modes, dielec. spectroscopy 0-75915
 $K(H_{1-x}D_x)_2PO_4$, polarisation relaxation time and Landau kinetic coeff. rel. to degree of deuteration 0-84251
 $KH_2(1-x)D_2PO_4$, proton modes, dielec. spectroscopy 0-75915
 KH_2PO_4 , Brillouin-Rayleigh scatt. studies near ferroelec. transition temp. 0-76036
 KH_2PO_4 , crit. behaviour near tricritical point, phenomenological interpretation 0-70389
 KH_2PO_4 , crit. behaviour, dilatometric study 0-92689
 KH_2PO_4 , critical and tricritical phenomena, susceptibility, exponents 0-75976
 KH_2PO_4 , family of crystals, proton modes, dielec. spectroscopy 0-75915
 KH_2PO_4 , ferroelectric transition, order-disorder character of hydrogen bond 0-93251
 KH_2PO_4 , phase transitions study, role of cryst. struct. determ. 0-75197
 KH_2PO_4 , single crystal neutron diffraction study at high pressure 0-92497
 KH_2PO_4 , spontaneous polarisation, low temp. meas. 0-75921
 KH_2PO_4 , X-irradiated, hysteresis effects obs. by ESR 0-103928
 $KH_2PO_4:Ti^{2+}$, EPR of ferroelec. and paraelec. phases 0-66012
 $KH_2PO_4-KD_2PO_4$ mixed crystals, dielec. spectra, sub-mm wavelengths 0-80724
 KH_2PO_4 -type ferroelectrics, tunnelling integral 0-70156

ferroelectric materials continued

- KH_2PO_4 -type ferroelectrics, dielec. props., four-cluster approx. 0-97202
 $\text{KH}_2(\text{SeO}_3)_2$ and $\text{KD}_3(\text{SeO}_3)_2$, ferroelastic phase transition, mech. stress effect 0-70394
 $\text{KH}_2(\text{SeO}_3)_2$, ferroelastic transition under uniaxial press., EPR study 0-59562
 $\text{K}_2\text{MoO}_4\text{F}_3$, ferroelec., transition obs. 0-75989
 $\text{K}_{1-x}\text{Na}_x\text{TaO}_3$ quantum ferroelectric, dielec. susceptibility 0-103922
 KNbO_3 , cubic, temp. depend. of intensity of X-ray interference 0-59613
 KNbO_3 , domain struct. at transitions from twinned phase, appl. to tetragonal-orthorhombic transition 0-71360
 KNbO_3 , ferroelec. cryst., IR and Raman spectra, mode coupling 0-66194
 KNbO_3 reduced, phase hologram recording sensitivity, energy transfer, photovoltaic effects 0-78799
 K_2SeO_4 , dielec. dispersion, 5-900 MHz, near incommensurate-commensurate transition 0-60522
 K_2SeO_4 , ferroelectricity, triple 60 Hz D-E hysteresis loops 0-71364
 K_2SeO_4 , Raman spectra, effects of temp., substitutional cations, and stress 0-71405
 $\text{KTA}_{1-x}\text{Nb}_x\text{O}_3$, holographic storage using photorefractive effect, dielectric const. 0-78800
 $\text{KTA}_{1-x}\text{Nb}_x\text{O}_3$, quantum ferroelectric, dielec. susceptibility 0-103922
 $\text{KTAO}_3\text{-Li}$, ferroelec. transition and atomic motions, ^7Li NMR study 0-75872
 $\text{K}_2\text{WO}_4\text{F}_3$, ferroelec., transition obs. 0-75989
 K_2ZnCl_4 , ferroelectricity, triple 60 Hz D-E hysteresis loops 0-71365
 K_2ZnCl_4 , incommensurate phase transitions, ^{35}Cl NQR study 0-75968
 K_2ZnCl_4 , modulated struct. in ferroelec. phase, X-ray obs. 0-64970
 $\text{La}_2\text{Ti}_2\text{O}_7$, layered ferroelectric anomalous photovoltaic effect, photovoltaic current 0-75603
 $\text{Li}_2\text{B}_2\text{O}_7$, ferroelectric glass, phase transition, permittivity, electrochromism, photochromism 0-80719
 $(\text{Li}_2\text{B}_4\text{O}_7)_{1-x}(\text{WO}_3)_x$, dipolar glass, space charge injection, thermally stimulated depolarisation currents 0-66103
 $\text{LiGa}_2(\text{MoO}_4)_3$, single crystals, cryst. growth, optical props. 0-60763
 $\text{LiH}_2(\text{SeO}_3)_2$, ferroelec., absolute atomic arrangement and spontaneous polarisation, neutron diff. study 0-59442
 $\alpha\text{-LiIO}_3$, depolarisation current, dielectric const. relaxation behaviour (Chinese) 0-88905
 $\alpha\text{-LiIO}_3$, surface defect layer struct. due to mechanical working (Russian) 0-100238
 LiNH_4SO_4 and LiND_4SO_4 , dielec. pyroelec., and thermal props. 0-60509
 LiNH_4SO_4 , DC elec. cond. 0-88603
 LiNbO_3 , appl. in sub-100 ps pyroelec. detectors, 10.6 μm damage threshold meas. 0-77859
 LiNbO_3 , crystal defects, X-ray diff. topographic study (Chinese) 0-84173
 LiNbO_3 , ferroelec., displacive type phase transition, far IR reflection spectra 0-71339
 LiNbO_3 , Fourier transform IR spectroscopy of vibr. states at high temp. 0-97256
 LiNbO_3 , hologram storage depend. on envelope field, space charge field 0-78801
 LiNbO_3 , light induced ultrasonic wave velocity change, refractive index 0-97236
 LiNbO_3 pure and Fe doped, IR induced acousto-photorefractive memory effect 0-80746
 LiNbO_3 , pure and Fe doped, two-photon photorefractivity 0-80753
 LiNbO_3 single crystals, growth from melt, Czochralski method (Chinese) 0-76171
 LiNbO_3 single crystals grown by automatic diameter control, power striations (Chinese) 0-81080
 LiNbO_3 , spontaneous polarisation, low temp. meas. 0-75921
 LiNbO_3 , thermionic emission characts. 0-104034
 LiNbO_3 , valence band UPS and partial p and d density of states 0-71560
 LiNbO_3 , XPS and UPS from surface defects 0-76136
 $\text{LiNbO}_3\text{-Cu(Fe)}$, light induced charge transport, photovoltaic effects, impurity states 0-80317
 $\text{LiNbO}_3\text{-Fe}$, impurity charge states after UV irradiation 0-60462
 $\text{LiNbO}_3\text{-Fe}$, white-light image processing 0-87321
 $\text{LiNbO}_3\text{-Fe}$ (0.05%), hologram recording γ radiation effect 0-78812
 $\text{LiNbO}_3\text{-Ni}$ optical absorpt. spectra 0-71450
 $\text{LiNbO}_3\text{-Ti}$, planar optical waveguides, processing and props. 0-78965
 $\text{LiNbO}_3\text{-Ti}$ diffused optical waveguide, guided light scatt. sources 0-78966
 $\text{LiNbO}_3\text{-Ti}$ diffused optical waveguide, efficient tapered gap prism coupling 0-78967
 $\text{LiNbO}_3\text{-CdSe}$ layer structure, SAW absorpt., elec. field effects 0-65355
 LiTaO_3 , appl. in sub-100 ps pyroelec. detectors, 10.6 μm damage threshold meas. 0-77859
 LiTaO_3 , crystals for commercial SAW TV IF filters, fabrication 0-80961
 LiTaO_3 , ferroelec., displacive type phase transition, far IR reflection spectra 0-71339
 LiTaO_3 , Fourier transform IR spectroscopy of vibr. states at high temp. 0-97256
 $\text{LiTaO}_3\text{-Cu(Fe)}$, light induced charge transport, photovoltaic effects, impurity states 0-80317
 $\text{Li}_{1+x}\text{Ta}_{1-y}\text{Ti}_y\text{O}_3$ ($0 \leq y \leq 0.028$), non-stoichiometric phase, crystallographic and dielec. props. 0-75212
 MnBO_3 , orthorhombic, electronic struct., SCF-MS-X α calc. 0-70600
 MnBO_3 , tetragonal, electronic struct., optical anisotropy 0-70599
 $(\text{ND}_4)_2\text{BeF}_4$ and $(\text{NH}_4)_2\text{BeF}_4$, incommensurate phase, ^9Be NMR study 0-75973
 $(\text{NH}_4)_2\text{SO}_4$, ferroelectricity, triple 60 Hz D-E hysteresis loops 0-71364
 $(\text{NH}_4)_2\text{BeF}_4$, elastic props., US damping 0-84229
 $(\text{NH}_4)_2\text{BeF}_4$, far-infrared and submillimetre dielectric response 0-80782
 $(\text{NH}_4)_2\text{BeF}_4$, ferroelectricity, triple 60 Hz D-E hysteresis loops 0-71364
 $(\text{NH}_4)_2\text{BeF}_4$, linear and nonlinear optical props. in incommensurate phase 0-69452
 $(\text{NH}_4)_2\text{BeF}_4$, paraelec. phase, X-ray and neutron diff. cryst. struct. anal. 0-84159
 $(\text{NH}_4)_2\text{Cd}_2(\text{SO}_4)_3$, dielec. and spontaneous polarisation, -195 to -180°C, particle size depend. 0-97200
 NH_4HSeO_4 , cryst. struct., dielec. and ferroelec. props. 0-60528
 NH_4HSeO_4 , ferroelec. phase transition, pyroelec. props. 0-60513
 NH_4HSeO_4 , ferroelec. props. rel. to struct. 0-71345
 NH_4LiSO_4 , point group symm. at high press. phase 0-70150
 $(\text{NH}_4)_{1-x}(\text{Rb})_x\text{SO}_4$, isomorphous impurity effect on dielec. and nonlinear optical props. 0-88911

ferroelectric materials continued

- $(\text{NH}_4)_2\text{SO}_4$, paraelectric, N-quadrupole coupling meas. by proton-N double resonance 0-60459
 $(\text{NH}_4)_2\text{SO}_4$, static and dynamic dielec. behaviour 0-71337
 $(\text{NH}_4)_2\text{ZnCl}_4$, commensurate-incommensurate phase transition, ^{35}Cl NQR study 0-75966
 $(\text{NH}_4)_2\text{ZnCl}_4$, ferroelectricity and incommensurate-commensurate phase transitions 0-60523
 $\text{Na}_0.5\text{Bi}_{0.5}\text{TiO}_3$, phase transition, hysteretic behaviour 0-71330
 $\text{NaD}_3\text{H}_{3(1-x)}(\text{SeO}_3)_2$, ferroelec. dispersion 0-66129
 $\text{NaH}_2(\text{SeO}_3)_2$, β to δ ferroelec. transition under press. Raman spectra study 0-80725
 $\text{NaH}_2(\text{SeO}_3)_2$, domain struct. realignment and Barkhausen effect 0-71361
 $\text{NaH}_2(\text{SeO}_3)_2$, ferroelec., proton motion within H bonds, neutron scatt. study 0-75986
 $\text{Na}_{1-x}\text{Li}_x\text{NbO}_3$ mixture, ferroelec.-paraelec. transitions, dielec. props. meas. 0-66125
 NaNO_2 , ^{23}Na elec. field gradient tensor from NMR satellite lines near phase transition 0-71191
 NaNO_2 , ferroelec., dielec. and thermal behaviour 0-80680
 NaNO_3 , nuclear quadrupole coupling const. and spontaneous polarisation 0-71229
 NaNbO_3 , hydrostatic press. effect on permittivity, phase transition, hysteresis 0-80670
 $\text{Nd}_2\text{Ti}_2\text{O}_7$, layered ferroelectric, anomalous photovoltaic effect, photovoltaic current 0-75603
 $\text{Ni}_3\text{B}_2\text{O}_{13}\text{Br}$, ferroelec. 43m-mm2 phase transition, molar heat capacity meas. 0-93249
PLTZ ceramic, bonded lens assembly manufacture 0-79018
PLTZ ceramic, proton implanted, photoferroelectric effect for image storage and display devices 0-80315
PLTZ ceramic, thin wafer electrode slotting process 0-79017
PLTZ ceramic, thin wafer production polishing process 0-81214
PLTZ ceramic, visible light scatt. depend. on photoferroelectric space charge fields 0-80806
PLTZ ceramics, elastooptic effect, stress induced birefr. 0-60543
PLTZ ceramics, modified by $\text{Ca}^{2+}(\text{Sr}^{2+})(\text{Nd}^{3+})(\text{Y}^{3+})$, dielec. behaviour 0-60519
PLTZ ceramics photosensitivity enhancement by H- and He-ion implantation 0-96934
PLTZ, diffuse phase transitions; Curie temp., dielectric props. 0-75979
PLTZ, mech. and elec. losses, correl., theory and expt. 0-66133
PLTZ modified high voltage dielectric, permittivity, Curie temp., loss meas. 0-80720
PLTZ powder preparation, hydrolysis ball mixing 0-81006
PLTZ slim-loop and linear ceramics, longit. electrooptic effects, display appl. 0-80751
PLTZ slugs, powder hot pressing technique 0-81007
PLTZ thermal, flash, ferroelectric protective goggles 0-81746
PLTZ, thin, elec. cond. and pyroelectric behaviour 0-75954
PLTZ/TFPD thermal/flash protective lens assembly, polarised delamination investigation 0-78929
 $(\text{Pb,Ba})(\text{Zr,Ti})\text{O}_3$, diffuse phase transitions, Curie temp., dielectric props. 0-75979
 $(\text{Pb,Sr})_2\text{Ge}_2\text{O}_{11}$, single crystals, growth and X-ray and dielec. investigations 0-88127
 $(\text{Pb}_{1-x}\text{Ba}_x)_2\text{Ge}_2\text{O}_{11}$, ferroelec. phase transition, dielec. const. and quasi-elastic light scatt. 0-71289
 $\text{Pb}_{0.94-x/2}\text{Ba}_{0.4}\text{Nb}_x\text{Zr}_{1-x}\text{O}_3$, Nb dopant morphology effect on microstructure 0-81005
 $\text{Pb}_{1-x}(\text{Cs,Bi})_x\text{Ge}_2\text{O}_{11}$ 0-75960
 $\text{Pb}_2\text{GeO}_{11}$, elastic nonlinearity and acoustic losses 0-59554
 $\text{Pb}_2\text{GeO}_{11}$, lattice dynamics parameters anisotropy, X-ray diff. study 0-59612
 $\text{Pb}_2\text{GeO}_{11}$, pulsed polarisation switching process depend. on illumination 0-93253
 $\text{Pb}_2\text{GeO}_{11}\text{-Gd}^{3+}$, displacive phase transition, S ion spin Hamiltonian parameter dependence on order parameter 0-70356
 $\text{Pb}_2\text{GeO}_{11}\text{-Gd}^{3+}$, ferroelec. transition, temp. depend., EPR study 0-66127
 $\text{Pb}_2(\text{Ge}_{1-x}\text{Si}_x)\text{O}_{11}$, electrogyration, phase transition and dielectric props. 0-93269
 PbHPO_4 , crystals, ferroelec. phase transition, hydrostatic press. influence, dielec. meas. 0-88936
 PbHPO_4 , phase transitions study, role of cryst. struct. determ. 0-75197
 $\text{PbIn}_{0.5}\text{Nb}_{0.5}\text{O}_3$, ferroelectric, dielectric props. 0-103923
 $\text{Pb}(\text{Mg}_{1/3}\text{Nb}_{2/3})\text{O}_3$, cation disordered perovskite, elastic const. and thermal expansion 0-96587
 $\text{Pb}(\text{Mg}_{1/3}\text{Nb}_{2/3})\text{O}_3$, electrostrictive effect 0-66113
 $\text{Pb}_2\text{MgNb}_2\text{O}_9\text{-PbTiO}_3$, relaxor ferroelectrics, electrostrictive effects 0-66112
 $\text{Pb}_{1-x}\text{Nd}_x\text{Ge}_2\text{O}_{11}$, ferroelec. props. 0-75960
 $\text{PbO-MoO}_3\text{-MO}$ and $\text{PbO-WO}_3\text{-MO}$ systems, M=Ca, Ba, Mg, Sr, perovskite type cpds. detection 0-108404
 $\text{PbSc}_{0.5}\text{Nb}_{0.5}\text{O}_3$, single cryst., dielec. props. 0-66126
 $\text{PbSc}_{2/3}\text{Te}_{1/3}\text{O}_3$, ferroelec., high-frequency permittivity, temp. depend. 0-71325
 $\text{PbSc}_{2/3}\text{Te}_{1/3}\text{O}_3\text{-PbSc}_{2/3}\text{W}_{1/3}\text{O}_3(\text{PbFe}_{2/3}\text{Te}_{1/3}\text{O}_3)$ ferroelec. props. and lattice const. 0-60520
 $\text{Pb}_{0.95}\text{Sr}_{0.05}(\text{Zr}_{1-x}\text{Ti}_x)\text{O}_3\text{-Nb}_2\text{O}_5$, phase coexistence range, lattice const. 0-92680
 PbTiO_3 , optical birefringence in low temp. region 0-93276
 PbTiO_3 , phase transform., different kinetic types 0-71347
 PbTiO_3 , vibronic theory and opt. props. 0-103939
 $\text{Pb}(\text{Zn}_{1/3}\text{Nb}_{2/3})\text{O}_3$ single crystal, pyroelec. props., meas. under laser beam illum. 0-66117
 $\text{Pb}(\text{Zr,Ti})\text{O}_3$ ceramics, low temp. sintering, elec. and mech. props. 0-71616
 $\text{Pb}(\text{Zr,Ti})\text{O}_3$, ferroic materials, fracture processes 0-79869
 $\text{Pb}(\text{Zr,Ti})\text{O}_3$, fracture and deform. 0-79870
 $\text{Pb}(\text{Zr,Ti})\text{O}_3$, porosity-permittivity relations, depolarising factors determ. and pore effects (Japanese) 0-97189
 $\text{Pb}(\text{Zr,Ti})\text{O}_3$, shock depoled ferroelec. ceramic, anal. of ideal response 0-60511
 $\text{Pb}(\text{Zr,Ti})\text{O}_3$, tetragonal ferroelec. ceramic, 90° domain-rot. fraction after polarisation, X-ray determ. 0-75992
 $\text{Pb}(\text{Zr,Ti})\text{O}_3\text{-Cr}_2\text{O}_3$ ceramics, reson. freq. comp. and temp. depend. 0-70413
 $\text{Pb}(\text{Zr,Ti})\text{O}_3\text{-Fe(Nb)}$ ceramic, elec. and electromechanical props., depend. on dopants 0-81212

ferroelectric materials continued

- PbZrO₃, ferroelec., crystallographic shear planes as nonstoichiometric defects 0-59484
 PbZrO₃, ferroelec. solid solns., atom shifts, polarisation and Curie temps. 0-100636
 PbZrO₃:La, appl. in sub-100 ps pyroelec. detectors, 10.6 μ m damage threshold meas. 0-77859
 Pb(Zr_{0.52}Ti_{0.48})O₃, polycrystalline ferroelectric, grain-size dependent props. 0-71352
 PbZr_{1-x}Ti_xO₃ ceramics, morphotropic phase boundary 0-81035
 Pb(Zr_{1-x}Ti_x)O₃, meas. of Hugoniot curve with commercial manganin stress gauges 0-70362
 Pr₂Ti₂O₇, layered ferroelectric, anomalous photovoltaic effect, photovoltaic current 0-75603
 RbH₂PO₄, critical and tricritical phenomena, susceptibility, exponents 0-75976
 RbH₂PO₄, electrostrictive effects, US rel. 0-75941
 RbH₂PO₄, ferroelec. phase transition, birefringence studies 0-108162
 RbH₂PO₄, proton modes, dielec. spectroscopy 0-75915
 RbH₂PO₄, X-irradiated, hysteresis effects obs. by ESR 0-103928
 RbHSO₄, ferroelec., dielec. dispersion 0-97179
 RbHSeO₄, ferroelec. props. rel. to struct. 0-71345
 RbHSeO₄, ferroelec., far IR spectra 0-71404
 RbH₂(SeO₃)₂ crystal, incommensurate phase, quadrupole moment study 0-97213
 RbH₂(SeO₃)₂:VO²⁺, EPR spectra, spin Hamiltonian parameters 0-100609
 Rb₂KMoO₄F₃ and Rb₂KWO₄F₃, ferroelec., transition obs. 0-75989
 Rb₂MoO₄F₃, ferroelec., transition obs. 0-75989
 Rb₂WO₄F₃, ferroelec., transition obs. 0-75989
 Rb₂ZnBr₄, ferroelectricity, triple 60 Hz D-E hysteresis loops 0-71365
 Rb₂ZnBr₄, ferroelec., photovoltaic and photorefractive phenomena 0-75598
 Rb₂ZnBr₄, modulated struct., far IR transmission, temp. depend. 0-71408
 Rb₂ZnBr₄, soft modes obs. by Raman scatt. 0-97283
 Rb₂ZnBr₄(Cl₄), Raman spectra near incommensurate phase transitions 0-76013
 Rb₂ZnCl₄, commensurate-incommensurate phase transition, crit. behaviour, sp. ht. meas. 0-71342
 Rb₂ZnCl₄, commensurate-incommensurate phase transition, ³⁵Cl NQR study 0-75966
 Rb₂ZnCl₄, dielec. dispersion, 5-900 MHz, near incommensurate-commensurate transition 0-60522
 Rb₂ZnCl₄, ferroelectricity, triple 60 Hz D-E hysteresis loops 0-71365
 Rb₂ZnCl₄, incommensurate phase transition, ⁸⁷Rb NMR study 0-75967
 Rb₂ZnCl₄, incommensurate phase transitions, ³⁵Cl NQR study 0-75968
 Rb₂ZnCl₄, phase transitions, thermal expansion coeff. 0-100638
 SbSBr, single crystals, birefringence meas., ferroelec. transition obs. 0-88933
 SbSI, absorption edge, elec. field effect rel. to ferroelec. props. 0-97240
 SbSI, ferroelectric, dark current and spontaneous polarisation, ferroelectric transitions obs. 0-60521
 SbSI-SbSBr system, ferroelec., anharmonic effects in far IR reflectivity spectra 0-76014
 Sr Nb₂O₆, crystallography, polymorphism and isomerism, X-ray diff. and DTA study 0-100216
 Sr_{0.75}Ba_{0.25}Nb₂O₆, ceramic ageing, dielec. props. 0-88940
 Sr_{1-x}Ba_xNb₂O₆, photorefractive in space charge field, phase transitions 0-97229
 Sr_{1-x}Ba_xNb₂O₆, appl. in sub-100 ps pyroelec. detectors, 10.6 μ m damage threshold meas. 0-77859
 Sr_{1-x}Ba_xNb₂O₆, domain struct. influence on electrooptical props. 0-93283
 Sr_{1-x}Ba_xNb₂O₆, high press. phase transitions, Raman scatt. studies 0-71402
 Sr_{1-x}(Na_{0.5}Bi_{0.5})_{1-x} solid solutions, piezoelec. and ferroelec. props. (French) 0-108158
 Sr_{1-x}(Na_{0.5}Bi_{0.5})_{1-x}TiO₃ ferroelec. ceramic, hot pressing, numerical simulation (French) 0-76220
 Sr₂Nb₂O₇, high press. phase transitions, Raman scatt. studies 0-71402
 Sr₂Nb₂O₇, layered ferroelectric, anomalous photovoltaic effect, photovoltaic current 0-75603
 SrSnO₃ and SrZrO₃, high-density ceramics prep. and elec. props. 0-60812
 SrTiO₃, calc. of matrix element effects in freq. dependent dielectric function 0-70632
 SrTiO₃, ceramic, electrocaloric effects for refrigeration at cryogenic temp. 0-77789
 SrTiO₃, cubic, temp. depend. of X-ray reflection intensities 0-107021
 SrTiO₃, disorder manifestation, light scatt. spectra, high temp. 0-76017
 SrTiO₃, ferroelectric, first order structural phase transition, anharmonic oscillator model 0-86239
 SrTiO₃, heavily reduced, soft mode behaviour 0-71409
 SrTiO₃, mean square atomic displacement temp. depend., sublattice vibration anharmonicity 0-79890
 SrTiO₃, monodomain, O-D and O-H stretching vibrs., IR spectra 0-71449
 SrTiO₃, Mossbauer spectroscopy, sample prep. and results 0-66078
 SrTiO₃, optical SHG near phase transition 0-71348
 SrTiO₃, surface microrief after ion irradi. 0-59774
 SrTiO₃, undispersive nonlinear dielectric, third harmonic generation (Russian) 0-95955
 SrTiO₃, valence band UPS and partial p and d density of states 0-71560
 SrTiO₃:Fe³⁺, order-disorder and central peak behaviour, EPR study 0-75970
 TBSe, crit. behaviour, electrostrictive coupling role 0-71329
 TGS, crit. behaviour, electrostrictive coupling role 0-71329
 TGS, ferroelectric phase transition, high resolution NMR study 0-97214
 Tb(MoO₄)₃ cryst. struct. in ferroelec., ferroelastic, antiferroelec. and paraelectric phases 0-75205
 Tb₂(MoO₄)₃, improper ferroelectric, dielectric props., IR radiation pyroelectric detection 0-80711
 TeO₂, ferroelectric glass, phase transition, permittivity, electrochromism, photochromism 0-80719

ferroelectric phenomena *see ferroelectricity***ferroelectric semiconductor materials** *see ferroelectric semiconductors***ferroelectric semiconductors**

- band bending in surface layer 0-60061
 book 0-82590

ferroelectric semiconductors continued

- ferroactive fluids, advanced appls. 0-80714
 IV-VI semiconductor, vibronic model of lattice instability 0-80723
 perovskite oxides, point defects, elec. cond., and electron energy spectra 0-70706
 thin films, ferroelectric properties, quantum size effect 0-97201
 Ag₃AsS₃, proustite, phonons and soft modes at ferroelec. transition 0-60524
 Ba_{0.5}Sr_{0.5}TiO₃ films, DC conductivity, strong microwave field effect 0-6527
 BaTiO₃ ceramic surface, neutralisation of bombarding ion beam 0-71528
 BaTiO₃, XPS and UPS from surface defects 0-76136
 BaTiO₃:Co, voltaic current appearance on proton irradi. 0-104032
 BaTiO₃:Nb, elec. props., contact material influence 0-70848
 Cd₂Nb₂O₇, photolum. and carrier drift mobility at ferroelec. transition 0-71469
 KNbO₃, reduced, phase hologram recording, energy transfer and sensitivity 0-69338
 KTa_{0.7}Nb_{0.3}O₃, pressure-induced resistance and colour change obs. 0-75608
 LiNbO₃ surfaces, ion and electron bombard., photoelectron spectroscopy and electronic props. 0-71559
 LiNbO₃:Fe, elec. resist., temp. and conc. depend. 0-80275
 LiNbO₃:Fe, electro-optic cryst., light induced charge transport, holographic obs. 0-70747
 LiNbO₃:Fe, exoelectron emission in pyroelectric regime 0-76158
 LiTaO₃:Fe, electro-optic cryst., light induced charge transport, holographic obs. 0-70747
 NaNbO₃, elect. cond. mech., resist., Hall coeff. and thermoelec. power meas. 0-65603
 PbMg_{1/3}Nb_{2/3}O₃, electro-optical and elasto-optical props., appl. to optical storage (Russian) 0-80749
 PbMg_{1/3}Nb_{2/3}O₃, photolum. and carrier drift mobility at ferroelec. transition 0-71469
 PbMg_{1/3}Ta_{2/3}O₃ electro-optical and elasto-optical props., appl. to optical storage (Russian) 0-80749
 PbTiO₃, photolum. and carrier drift mobility at ferroelec. transition 0-71469
 PbZn_{1/3}Nb_{2/3}O₃ electro-optical and elasto-optical props., appl. to optical storage (Russian) 0-80749
 SbSBr glass, IR reflectivity spectra 0-71403
 SbSI, anomalous photovoltaic effect 0-70749
 SbSI, ferroelec. phase transition and nonlinear props. 0-75988
 SbSI, photolum. spectra in ferroelec. phase, 600-800 nm., 14-100K 0-71468
 SbSI_{0.8}Br_{0.2}, anomalous photovoltaic effect 0-70749
 Sn₂P₂S₆, ferroelec. semicond., phase transition and lattice dynamics 0-60526
 Sn₂P₂S₆, investigation of p-T diagram near a singular point (Russian) 0-88937
 Sn₂P₂S₆, soft mode props., Raman scatt. study 0-60525
 Sn₂P₂(Se₂S_{1-x})₆, ferroelec. tricitr. phase transform., light transmission study 0-71355
 SnTe, dispersive transform., interband electron-phonon interactions, phase diagram 0-93252
 n-SrTiO₃ electrode, flatband pot. determ. from differential stress meas. 0-75638
 SrTiO₃ ferroelectric modes, Raman spectra, neutron scatt. meas. 0-80727
 SrTiO₃, photolum. and carrier drift mobility at ferroelec. transition 0-71469
 SrTiO₃ semicond. electrodes, electroreduction process kinetics, cathodic dark current meas. 0-66807
 SrTiO₃, soft modes, zone boundary mode 0-71357
 TiSe type crystals, possible second-order phase transitions, group-theoretical anal. 0-92672
 V₂O₅, ferroelec. semicond., dielec. and elec. meas. 0-60516

ferroelectric switching

- characteristics investigation using cct. containing bipolar square pulse generator 0-62687
 hysteresis loops and butterfly plots, macroscopic theory 0-66132
 smectic liquid crystals, ferroelec., submicrosecond bistable electro-optic switching 0-84051
 TGS, ferroelec. activation field change 0-71358
 TGS substrate, influence of polarisation reversal on elec. cond. of CdTe thin film 0-65720
 (Ba,Sb_{1-x})₂TiO₃ 0-60514
 BaTiO₃ film, struct. and dielec. props. 0-60514
 BaTiO₃, pure and Fe doped, ferroelec., switching and electrolum. 0-76079
 BaTi_{0.98}Sn_{0.02}O₃, ferroelec. film, switching process 0-60518
 Ba(Ti_{1-x}Sn_x)₂O₃ film, struct. and dielec. props. 0-60514
 Pb₂GeO₁₁, pulsed polarisation switching process depend. on illumination 0-93253

ferroelectric thin films

- ferroactive thin films, physical prop. optimisation 0-80698
 phthalocyanine metal free films, TSC, ferroelectric-semiconductor transition 0-66105
 semiconducting, ferroelectric properties, quantum size effect 0-97201
 (Ba,Sb_{1-x})₂TiO₃ 0-60514
 Ba,Sr_{1-x}TiO₃, ferroelec. film, heteroepitaxial growth in cathode sputtering 0-93486
 BaTiO₃ film, struct. and dielec. props. 0-60514
 BaTiO₃ RF sputtered ferroelectric film on Si substrate, ferroelectric props. 0-80697
 BaTi_{0.98}Sn_{0.02}O₃, ferroelec. film, switching process 0-60518
 Ba(Ti_{1-x}Sn_x)₂O₃ film, struct. and dielec. props. 0-60514
 K₂Li₂Nb₂O₅ films for optical waveguides epitaxial growth and characterisation 0-79016
 LiNbO₃:Na structure field stability limits, LPE film growth, SAW velocity 0-80102
 LiNbO₃:Na⁺ (Co²⁺, Zr⁴⁺) film, improvement in temp. stability and SAW device appl. 0-75939
 PLZT ferroelectric thin films, epitaxial growth and optical props. 0-70543
 Pb₂GeO₁₁, sputtered ferroelec. films, prep. struct. and dielec. props. 0-75452
 Pb(Zr,Ti)O₃ films, ferroelec., ion beam deposition sputtered from multi-component targets 0-80974
 Pb(Zr,Ti_{1-x})O₃ films, deposition by focused ion beam sputtering 0-76177

ferroelectric transitions

- see also critical fluctuations; displacive transformations; ferroelectric Curie temperature; order-disorder transformations
- ammonia Rochelle salt, temp. depend. of optical axis angle, phase transitions (*Russian*) 0-97216
- ammonium Rochelle salt, thermodynamics of ferroelec. transition 0-84702
- antiferroelectric ferrites, coupled magnetoelc. oscills. and high freq. susceptibility tensor (*Russian*) 0-93152
- antiferroelectrics, multicritical points in structural phase transitions, renormalisation 0-75982
- antiferromagnet, ferroelec., phase transformations (*Russian*) 0-93114
- benzil, phase transition, far IR spectroscopy meas. 0-71407
- 1,6-bis(2,4-dinitrophenoxy)-2,4-hexadiene, obs. of apparent ferroelec. transition 0-66121
- converters of shockwave mech. energy into elec. power 0-61429
- D_{3d} crystals, structural phase transitions, soft modes, group theory 0-92638
- defect-containing crystals, US absorpt. near displacive phase transitions, anomalous temp. depend. 0-92612
- Devil's staircase and harmless staircase, oscillating interactions through elastic stairs or other harmonic fields 0-88296
- diatomic linear chain, ferroelec. soft modes 0-70353
- dielectric spectroscopy, transitions, permittivity 0-75914
- displacive and order-disorder type, thermal cond. at low temps. 0-75391
- displacive phase transition, S ion spin Hamiltonian parameter dependence on order parameter 0-70356
- domain structure as outcome state for poling procedure 0-80728
- dynamic critical phenomena 0-75962
- electron microscopy investigations, review (*Japanese*) 0-71366
- exciton dielectric, inhomogeneous current state phase transition, free energy (*Russian*) 0-84703
- exciton insulators with spontaneous currents, impurity scatt. effect on phase transitions 0-80242
- extended defect system, phase transform., critical props. 0-103455
- extrinsic ferroelectrics, transition, polarisation, dielectric divergence 0-80718
- ferroelastic, dislocation-phonon interactions, phase transition effects 0-59600
- ferroelectric materials for dielectric power conversion, dielectric prop. anal. 0-80712
- ferroelectrics with hydrogen bonds, phase transition into coherent state, two-level proton calcs. (*Russian*) 0-71356
- ferroic phase transitions, non-mag., unified classification 0-70387
- halide ferroelectrics, transitions, formulae, structural data 0-75980
- heterogeneous states, statistics (*Russian*) 0-80721
- hydrogen-bonded ferroelectric, central peak, thermal cond. 0-93250
- improper and incommensurate phase transitions, neutron scatt. studies 0-75974
- incommensurate crystal phases, symm. props., superspace groups 0-75195
- incommensurate phase transitions 0-75964
- incommensurate polar phase form. 0-71344
- IV-VI semiconductor, vibronic model of lattice instability 0-80723
- IV-VI semiconductors, structural phase transitions, anomalous resist., electron-soft phonon interactions 0-108167
- Jahn-Teller crystals, elastic and dielec. anomalies, microscopic model 0-71332
- light generation at impurity atoms in ferroelectrics and LC, fluctuation effects (*Russian*) 0-91767
- lithium thallium tartrate, sp. ht., 0.3 to 25K, second-order ferroelec. transition 0-59674
- macroscopic quadrupole effects as method of obs. of struct. transforms in crystals 0-71321
- magnetoelc. effect at ferroelec. and antiferroelec. transitions 0-100637
- modelling of ferroelectric-elastic transition, appl. to KH_2PO_4 and $LiNH_4C_4H_9O_2 \cdot 2H_2O$ (*Russian*) 0-75961
- narrow-gap ferroelectric, phase transition due to strong mag. field 0-103924
- order-disorder, pseudo-one-dimens. kinetic Ising model 0-71333
- p-alkoxybenzylidene-p'-amino-2-chloropropyl-cinnamate, chiral smectic, dielec. props. 0-96441
- paraelectric-ferroelectric-antiferroelectric phase transitions, electrostrictive effects 0-97209
- phthalocyanine metal free films, TSC, ferroelectric-semiconductor transition 0-66105
- PZT ceramics, ferroelec. energy conversion under shock loading 0-108163
- quantum transition suppression, pyroelectric, electrocaloric effects, specific heat 0-75984
- Rochelle salt, ferroelec. phase transition, Raman scatt. study 0-97211
- Rochelle salt, ferroelec. phase transitions in pseudo-spin lattice coupled mode model 0-108161
- Rochelle salt, ferroelectric, Raman and IR study 0-71406
- tris-sarcosine calcium chloride, elastic props., US damping 0-84229
- semiconductor thin films, ferroelectric properties, quantum size effect 0-75201
- semiconductors, ferroelec., book 0-82590
- squaric acid, antiferroelec., struct. phase transition mechanism 0-75969
- squaric acid, layered, antiferroelec., phase transition mechanism 0-97210
- squaric acid, two-dimens. phase transition, Raman scatt. study 0-71401
- static critical behaviour, structural phase transitions 0-92640
- structural phase transition at low temps. 0-75990
- structural phase transitions, ultrasonic velocity and attenuation meas. 0-75977
- Tanane, ferroelec. mol. cryst., strong piezoelec. coupling 0-75942
- tetramethylammonium cobalt tetrachloride, Raman spectra near incommensurate phase transitions 0-76013
- tetramethylammonium tetrachlorocobaltate, ferroelec., pressure-temp. phase diagrams 0-97205
- tetramethylammonium tetrachlorozincate, ferroelec., pressure-temp. phase diagrams 0-97205
- tetramethylammonium tetrachlorozincate, incommensurate phase study, ferroelectric-paraelectric phases (*French*) 0-88318
- tetramethylammonium tetrachlorozincate, X-ray study of incommensurate phase 0-71351
- tetramethylammonium zinc tetrachloride, incommensurate phase transitions, ^{13}C NMR study 0-75968
- tetramethylammonium zinc tetrachloride, Raman spectra near incommensurate phase transitions 0-76013
- TGS, crit. behaviour of thermal expansion, neutron diff. study 0-75371

ferroelectric transitions continued

- TGS, kinetics of domain formation during phase transition 0-66130
- TGS, $L\alpha$ -alanine disordered regions, dielec. prop. changes in transition region 0-108159
- TGS, perfect and imperfect, sp. ht. and sound vel., crit. anomalies 0-71331
- TGS ($-d_1$), sp. ht. near ferroelec. phase transition 0-70420
- thermal conductivity, anomalies near structural phase transitions (*Russian*) 0-75394
- thermal expansion of crystals, book 0-73115
- thiourea, ferroelectric, Raman and IR study 0-71406
- thiourea, incommensurate phase, soft modes, condensation of even-order harmonics 0-103313
- thiourea, incommensurate phase transition, X-ray and neutron scatt. study 0-75963
- tris-sarcosine calcium chloride: Mn^{2+} ferroelec. dynamics, EPR and ENDOR study 0-75972
- tris-sarcosine calcium chloride, ferroelec. transitions, soft modes, Raman scatt. spectra obs. 0-80763
- tris-sarcosine calcium chloride, phase transition, hydrostatic press. effect, dielec. const. meas. 0-71327
- trissarcosine calcium chloride, ferroelec. phase transition, Raman and Brillouin scatt. studies 0-71340
- trissarcosine calcium chloride, press. effect 0-84681
- uniaxial ferroelectrics, crit. behaviour, electrostrictive coupling role 0-71329
- uniaxial ferroelectrics, Urbach rule and polarisation fluctuations, optical absorpt. edge 0-88910
- unit cell multiplication during phase transform., spontaneous polarisation 0-75983
- vibronic ferroelectrics, band struct. temp. depend. 0-70598
- vinylidene-fluoride-trifluoroethylene copolymer, piezoelectricity 0-88930
- $Zn_3B_2O_3Br$, ferroelec. 43m-mm2 phase transition, molar heat capacity meas. 0-93249
- $[(NH_4)_2H(SO_4)]_{1-x}[(ND_4)_2D(SO_4)]_x$ system, ferroelectric transitions 0-108160
- Ag_3AsS_3 , proustite, phonons and soft modes at ferroelec. transition 0-60524
- $Ag_2x_{18}W_{16}$, superionic conductor, order-disorder type transitions, ionic conductivity meas. 0-66122
- $AgNa(NO_2)_2$, ^{23}Na elec. field gradient tensor from NMR satellite lines near phase transition 0-71191
- $AgNa(NO_2)_2$, crit. dynamics, hydrostatic press. effect, dielec. props. meas. 0-71328
- $AgNa(NO_2)_2$, ferroelec., Raman scatt. and phase transitions 0-71349
- $AgNa(NO_2)_2$, ferroelec. cryst., Raman spectrum, phase transition, comparative anal. with $NaNO_2$ 0-88935
- $As_2S_3Sb_2SI$ cryst., ferroelec., soft mode Raman and IR spectroscopy 0-76016
- $BaMnF_4$, spectroscopy near ferroelec. transition, dielec. anomalies near mag. ordering temp. 0-75965
- $Ba_2NaNb_5O_{15}$, cryst. comp. effect on low temp. phase transition 0-71346
- $Ba_2NaNb_5O_{15}$, high press. phase transitions, Raman scatt. studies 0-71402
- $BaTiO_3$, displacive ferroelectric, effective charge determ. 0-97212
- $BaTiO_3$, elastic props., singularities near tetragonal-cubic phase transition 0-70303
- $BaTiO_3$, elastooptic effect near ferroelec. transition, temp. depend. 0-97233
- $BaTiO_3$, electron exoemission unipolarity associated with phase transitions 0-97415
- $BaTiO_3$, ferroelectric mechanisms, anharmonic couplings by scanning IR interferometry 0-75978
- $BaTiO_3$, ferroic materials, fracture processes 0-79869
- $BaTiO_3$, internal stress and strength, failure mechanism 0-66128
- $BaTiO_3$, paraelec. phase, stabilisation of soft mode 0-75985
- $BaTiO_3$, periodic domain struct. and opalescence at tetragonal to orthorhombic transition 0-66131
- $BaTiO_3$, polycrystalline ferroelectric, grain-size dependent props. 0-71352
- $BaTiO_3$, pure and Fe doped, ferroelec., switching and electrolum. 0-76079
- $BaTiO_3$, soft mode spectroscopy IR refl. meas. 0-88982
- $BaTiO_3$, thin film, polarisation reversal, electric field induced phase transform. 0-103925
- $BaTiO_3/Co$, tricritical point, X-ray diff. meas. 0-71341
- $BaTiO_3-BiFeO_3$ solid solns., ferroelec.-antiferromag., magnetoelectric effect at ferroelec. transition 0-100637
- $Ba(Ti_{1-x}Sn_x)_3O_3$ thick film, ferroelec., phase transitions and dielec. props. 0-97215
- $BiFeO_3$, ferroelec., antiferromag., cryst. and mag. struct., neutron diff. study 0-65786
- $Bi_4Ti_3O_{12}$, elec. characs., phase transition obs. 0-60517
- Bi_2WO_6 , ferroelectric, dielectric props., elec. cond. and relaxation phenomena obs. 0-80692
- $Ca_2Nb_2O_7$, ferroelectric phase transitions, dielec. constant and thermal expansion rel. to temp. 0-88934
- $Cd(NO_3)_2$, phase transition, SHG, optical and dielec. meas. 0-71334
- $Cd_2Nb_2O_7$, photolum. and carrier drift mobility at ferroelec. transition 0-71469
- $Cr_2B_2O_7Cl$, cubic, approx. nonlinear optical susceptibility 0-78904
- $Cr_2B_2O_7Cl$, ferroelec. 43m-mm2 phase transition, molar heat capacity meas. 0-93249
- $CsCaCl_3:Co(Mn)$, EPR, 4.2 to 450K, ferroelec. transition 0-60414
- Cs_2CdBr_4 , struct. phase transitions, NQR study 0-71343
- CsD_2PO_4 , pseudo-one-dimensional ferroelectric transition, ^{31}P chemical shift and relaxation study 0-66123
- CsD_2PO_4 , pseudo-one-dimens. ferroelec. transition, DMR and relax. study 0-71223
- CsD_2PO_4 , pseudo-one-dimensional ferroelec. and antiferroelec. transitions, phase diagram obs., soft modes 0-93245
- CsH_2PO_4 and CsD_2PO_4 , pseudo one-dimens. ferroelec. ordering dynamics, ^{31}P NMR study 0-75971
- CsH_2PO_4 , ferroelec. transition, electrooptic 0-76005
- CsH_2PO_4 , ferroelec. transition, neutron diff. study 0-93247
- $Cu_2B_2O_7Cl$, cubic, approx. nonlinear optical susceptibility 0-78904
- $Cu_2B_2O_7Cl$, ferroelec. 43m-mm2 phase transition, molar heat capacity, meas. 0-93249
- $DyVO_4$ Jahn-Teller crystal, deform. induced transitions, elastic and dielectric characs. (*Russian*) 0-80726
- $Fe_3B_2O_7Cl$, cubic, approx. nonlinear optical susceptibility 0-78904

ferroelectric transitions continued

Fe₃B₂O₇, ferroelec. 43m-mm2 phase transition, molar heat capacity meas. 0-93249
Gd₂(MoO₄)₃, electron microscopy investigs. of ferroelec. substances, review (*Japanese*) 0-71366
Gd₂(MoO₄)₃, thin film, polarisation reversal, electric field induced phase transform. 0-103925
H-bonded ferroelectrics, phonon relax. mechanism 0-79906
HCl and HCl·DCl, ferroelec. transition, ³⁵Cl NQR study 0-71233
KCN, dynamics of CN⁻ ions near phase transitions at 83K 0-80717
KCN, mean field theory 0-92830
KD₂AsO₄, ferroelec., high temp. phase transition, Raman spectra 0-71338
KD₂AsO₄, high temp. phase transitions, proton dynamics 0-76023
KD₂PO₄, phase transitions study, role of cryst. struct. determ. 0-75197
KD₂PO₄, polarisation fluctuations, wavevector depend. 0-71295
KD₂PO₄·Ti³⁺, EPR of ferroelec. and paraelec. phases 0-66012
KH₂AsO₄, ferroelec., high temp. phase transition, Raman spectra 0-71338
KH₂AsO₄, ferroelectric phase transition under high hydrostatic press., mol. dynamics, NQR study 0-75880
KH₂AsO₄, γ-irradiated, free radicals, EPR and ENDOR study of consequences of ferroelec. transition (*French*) 0-93209
KH₂AsO₄, high temp. phase transitions, proton dynamics 0-76023
K(H_{1-x}D_x)₂PO₄, polarisation relaxation time and Landau kinetic coeff. rel. to degree of deuteration 0-84251
KH₂PO₄, Brillouin-Rayleigh scatt. studies near ferroelec. transition temp. 0-76036
KH₂PO₄, crit. behaviour near tricritical point, phenomenological interpretation 0-70389
KH₂PO₄, critical and tricritical phenomena, susceptibility, exponents 0-75976
KH₂PO₄, ferroelectric transition, order-disorder character of hydrogen bond 0-93251
KH₂PO₄, phase transitions study, role of cryst. struct. determ. 0-75197
KH₂PO₄·Ti³⁺, EPR of ferroelec. and paraelec. phases 0-66012
KH₂PO₄-KD₂PO₄ mixed crystals, dielec. spectra, sub-mm wavelengths 0-80724
K₃H(SO₄)₂, and K₃D(SO₄)₂, dielec. props. and phase transitions 0-60482
KNbO₃, displacive ferroelectric, effective charge determ. 0-97212
KNbO₃, domain struct. at transitions from twinned phase, appl. to tetragonal-orthorhombic transition 0-71360
K₂SeO₄, dielec. dispersion, 5-900 MHz, near incommensurate-commensurate transition 0-60522
K₂SeO₄, elastic props. at commensurate-incommensurate transition, Brillouin scatt. and US study 0-93248
K₂SeO₄, hexagonal-orthorhombic transition, Brillouin scatt. study 0-97208
K₂SeO₄, incommensurate to ferroelec. transition, hydrostatic press. effects, neutron scatt. study 0-108166
KTaO₃·Li, ferroelec. transition and atomic motions, ⁷Li NMR study 0-75872
K₂ZnCl₄, incommensurate phase transitions, ³⁵Cl NQR study 0-75968
Li₂B₂O₇, ferroelectric glass, phase transition, permittivity, electrochromism, photochromism 0-80719
LiNH₂SO₄ and LiND₂SO₄, dielec. pyroelec., and thermal props. 0-60509
LiNH₂SO₄, DC elec. cond. 0-88603
LiNbO₃, ferroelec., displacive type phase transition, far IR reflection spectra 0-71339
LiNbO₃, Fourier transform Ir spectroscopy of vibr. states at high temp. 0-75256
LiTaO₃, displacive ferroelectric, effective charge determ. 0-97212
LiTaO₃, ferroelec., displacive type phase transition, far IR reflection spectra 0-71339
LiTaO₃, Fourier transform Ir spectroscopy of vibr. states at high temp. 0-97256
(ND₂)₂BeF₄ and (NH₄)₂BeF₄, incommensurate phase, ⁹Be NMR study 0-75973
ND₂D₂AsO₄, protonic cond. near antiferroelec. Neel temp. 0-59703
(NH₄)₂BeF₄, elastic props., US damping 0-84229
(NH₄)₂BeF₄, far-infrared and submillimetre dielectric response 0-80782
(NH₄)₂H(SO₄)₂, phase transitions, dielec. study at low temps. 0-88902
NH₄HSeO₄, cryst. struct., dielec. and ferroelec. props. 0-60528
NH₄HSeO₄, ferroelec. phase transition, pyroelec. props. 0-60513
NH₄HSeO₄, ferroelec., phase transitions, permittivity and pyroelectricity meas. 0-71350
(NH₄)₂SO₄, paraelectric, N-quadrupole coupling meas. by proton-N double resonance 0-60459
(NH₄)₂ZnCl₄, commensurate-incommensurate phase transition, ³⁵Cl NQR study 0-75966
(NH₄)₂ZnCl₄, ferroelectricity and incommensurate-commensurate phase transitions 0-60523
Na_{0.5}Bi_{0.5}TiO₃, phase transition, hysteretic behaviour 0-71330
NaH₂(SeO₃)₂, β to δ ferroelec. transition-under press. Raman spectra study 0-80725
NaH₂(SeO₃)₂, ferroelec., proton motion within H bonds, neutron scatt. study 0-75986
Na_{1-x}Li_xNbO₃ mixture, ferroelec.-paraelec. transitions, dielec. props. meas. 0-66125
NaNO₂, ²³Na elec. field gradient tensor from NMR satellite lines near phase transition 0-71191
NaNO₂, ferroelec., dielec. and thermal behaviour 0-80680
NaNO₂, optical harmonic generation near ferroelec. transition 0-91858
NaNbO₃, hydrostatic press. effect on permittivity, phase transition, hysteresis 0-80670
Na₂R(WNb₂)O₃F₃ (R=Y, Nd, Eu, Gd, Dy, Lu), synthesis, cryst.-chem. and dielec. study (*French*) 0-108164
Ni-I single crystals, mag. and dielectric props. 0-93095
Ni₂B₂O₇Br, cubic, approx. nonlinear optical susceptibility 0-78904
Ni₂B₂O₇Br, ferroelec. 43m-mm2 phase transition, molar heat capacity meas. 0-93249
O²⁻ polarisability rel. to ferroelec. phase transitions 0-71326
PLZT ceramic, ageing, dielec. props. 0-88940
PLZT, diffuse phase transitions, Curie temp., dielectric props. 0-75979
(Pb,Ba)(Zr,Ti)O₃, diffuse phase transitions, Curie temp., dielectric props. 0-75979
(Pb_{1-x}Ba_x)₂Ge₂O₁₁, ferroelec. phase transition, dielec. const. and quasi-elastic light scatt. 0-71289
Pb_{0.94-x}La_{0.06}Nb₂Zr_{1-x}O₃, Nb dopant morphology effect on microstructure 0-81005

ferroelectric transitions continued

Pb₂Ge₂O₁₁, ferroelec. transition, US and elasto-optic props. 0-60527
Pb₂Ge₂O₁₁, lattice dynamics parameters anisotropy, X-ray diff. study 0-59612
Pb₂Ge₂O₁₁·Gd³⁺, ferroelec. transition, temp. depend., EPR study 0-66127
Pb₃(Ge_{1-x}Si_x)₃O₁₁, electrogyration, phase transition and dielectric props. 0-93269
PbHPO₄, crystals, ferroelec. phase transition, hydrostatic press. influence, dielec. meas. 0-88936
PbHPO₄, phase transitions study, role of cryst. struct. determ. 0-75197
PbIn_{0.5}Nb_{0.5}O₃, ferroelectric, dielectric props. 0-103923
PbMg_{1/3}Nb_{2/3}O₃, photolum. and carrier drift mobility at ferroelec. transition 0-71469
PbSc_{0.5}Nb_{0.5}O₃, single cryst., dielec. props. 0-66126
PbTiO₃, photolum. and carrier drift mobility at ferroelec. transition 0-71469
Pb(Zr,Ti)O₃, ferroic materials, fracture processes 0-79869
Pb(Zr_{0.52}Ti_{0.48})O₃, polycrystalline ferroelectric, grain-size dependent props. 0-71352
PbZr_{1-x}Ti_xO₃·Nb₂O₅ ceramic, ferroelec. transitions, polarisation meas. (*French*) 0-66124
PbZr_{1-x}Ti_xO₃ ceramics, morphotropic phase boundary 0-81035
RbH₂PO₄, critical and tricritical phenomena, susceptibility, exponents 0-75976
RbH₂PO₄, ferroelec. phase transition, birefringence studies 0-108162
RbH₂PO₄, phase transitions study, role of cryst. struct. determ. 0-75197
Rb₂H(SO₄)₂, and Rb₃D(SO₄)₂, dielec. props. and phase transitions 0-60482
RbHSeO₄, ferroelec., far IR spectra 0-71404
RbH₂(SeO₃)₂ crystal, incommensurate phase, quadrupole moment study 0-97213
RbH₂(SeO₃)₂, dielec. relax. near ferroelec. Curie temp. 0-97207
RbH₂(SeO₃)₂, US vel. and absorpt. near ferroelec. Curie temp. 0-97206
RbNbW₂O₉ crystals, growth and props. 0-104054
Rb₂ZnBr₄, modulated struct., far IR transmission, temp. depend. 0-71408
Rb₂ZnBr₄, soft modes at phase transforms., far IR spectrum study 0-107398
Rb₂ZnBr₄, soft modes obs. by Raman scatt. 0-97283
Rb₂ZnBr₄(Cl₄), Raman spectra near incommensurate phase transitions 0-76013
Rb₂ZnCl₄, commensurate-incommensurate phase transition, crit. behaviour, sp. ht. meas. 0-71342
Rb₂ZnCl₄, commensurate-incommensurate phase transition, ³⁵Cl NQR study 0-75966
Rb₂ZnCl₄, dielec. dispersion, 5-900 MHz, near incommensurate-commensurate transition 0-60522
Rb₂ZnCl₄, incommensurate phase transition, ⁸⁷Rb NMR study 0-75967
Rb₂ZnCl₄, incommensurate phase transitions, ³⁵Cl NQR study 0-75968
SbSBr, single crystals, birefringence meas., ferroelec. transition obs. 0-88933
SbSi, ferroelec. phase transition and nonlinear props. 0-75988
SbSi, ferroelectric, dark current and spontaneous polarisation, ferro-paraelectric transitions obs. 0-60521
SbSi-SbSBr system, ferroelec., anharmonic effects in far IR reflectivity spectra 0-76014
Sn₂P₂Se₆, ferroelec. semicond., phase transition and lattice dynamics 0-60526
Sn₂P₂Se₆, investigation of p-T diagram near a singular point (*Russian*) 0-88937
Sn₂P₂Se₆, soft mode props., Raman scatt. study 0-60525
Sn₂P₂(Se₂S_{1-x})₆, ferroelec. tricrit. phase transform., light transmission study 0-71355
Sr_{0.7}Ba_{0.3}Nb₂O₆, ceramic ageing dielec. props. 0-88940
Sr_{1-x}Ba_xNb₂O₆, photorefractive in space charge field, phase transitions 0-97229
Sr_{1-x}Ba_xNb₂O₆, domain struct. influence on electrooptical props. 0-93283
Sr_{1-x}Ba_xNb₂O₆, high press. phase transitions, Raman scatt. studies 0-71402
Sr_{1.8}Na_{0.2}Nd_{0.1}Ta_{0.7}O₇, solid soln., ferroelectric phase transitions, dielec. constant and thermal expansion rel. to temp. 0-88934
Sr₂Nb₂O₇, ferroelectric phase transitions, dielec. constant and thermal expansion rel. to temp. 0-88934
Sr₂Nb₂O₇, high press. phase transitions, Raman scatt. studies 0-71402
Sr₂Ta₂O₇, ferroelectric phase transitions, dielec. constant and thermal expansion rel. to temp. 0-88934
SrTiO₃, optical SHG near phase transition 0-71348
SrTiO₃, photolum. and carrier drift mobility at ferroelec. transition 0-71469
SrTiO₃, semiconductor, soft modes, zone boundary mode 0-71357
SrTiO₃, thin film, polarisation reversal, electric field induced phase transform. 0-103925
SrTiO₃·Fe³⁺, order-disorder and central peak behaviour, EPR study 0-75970
TGS, ferroelectric phase transition, high resolution NMR study 0-97214
Tb(MoO₄)₃, cryst. struct. in ferroelec., ferroelastic, antiferroelec. and paraelectric phases 0-75205
TeO₂, ferroelectric glass, phase transition, permittivity, electrochromism, photochromism 0-80719
TiSe type crystals, possible second-order phase transitions, group-theoretical anal. 0-92672

ferroelectricity

see also antiferroelectricity; ferroelectric devices; ferroelectric materials; ferroelectric switching; ferroelectric transitions
anomalous photovoltaic effect of ferroelectrics, review 0-65628
antiferroelectrics, multicritical points in structural phase transitions, renormalisation 0-75982
bibliography (Aug.-Dec. 1978) 0-62405
ceramic, mech. and elec. losses, correl., theory and expt. 0-66133
conference, Portoroz, Yugoslavia (Sep. 1979) 0-73092
continual model, boundary conditions 0-93244
dielectric behaviour of materials undergoing dipole alignment transitions 0-88922
dielectric spectroscopy, transitions, permittivity 0-75914
domain wall, interaction energy with elec. charge 0-88939
double quadratic kink soln. to ferroelec. domain wall dynamic polarisability 0-66135
electron emitter with negative electron affinity 0-100762

ferroelectricity continued

- ferrites, ferroelec., coupled ferroelec. and spin waves, exchange interactions 0-70995
 ferroactive fluids, advanced appls. 0-80714
 ferroelectric crystals, polariton light scatt. freq.-angle spectra, nonlinear susceptibility interference (*Russian*) 0-92834
 ferroic crystals, prototypic point group, physical props., model 0-80715
 hysteresis loops and butterfly loops, macroscopic theory 0-66132
 incommensurate crystals, first order Raman scatt. from unbounded phonons 0-88990
 multistable self-wave media 0-86094
 negative capacitances, comparison with negative viscosities 0-66118
 optically induced internal fields in ferroelectrics 0-107855
 order-disorder, displacive transformations, tunnelling, phonons 0-75975
 photogalvanic current in ferroelectrics 0-70748
 powders, phonon electroacoustic echoes, storage mechanisms 0-75606
 quantum transition suppression, pyroelectric, electrocaloric effects, specific heat 0-75984
 structural phase transitions, ultrasonic velocity and attenuation meas. 0-75977
 unit cell multiplication during phase transform., spontaneous polarisation 0-75983
 vibronic ferroelectrics, band struct. temp. depend. 0-70598
 $\text{Ca}_2\text{Mg}(\text{Co})(\text{Zn})(\text{Mn})(\text{Cd})(\text{Ca})\text{TeO}_6$, optical SHG study of acentricity, ferroelec. of low temp. phases 0-71324
 $\text{Cd}_2\text{Mg}(\text{Co})(\text{Zn})(\text{Mn})(\text{Cd})(\text{Ca})\text{TeO}_6$, optical SHG study of acentricity, ferroelec. of low temp. phases 0-71324
 $\text{Sr}_2\text{Mg}(\text{Co})(\text{Zn})(\text{Mn})(\text{Cd})(\text{Ca})(\text{Sr})\text{TeO}_6$, optical SHG study of acentricity, ferroelec. of low temp. phases 0-71324

ferrofluids *see magnetic fluids***ferromagnetic-antiferromagnetic transitions**

- see also metamagnetism; Morin temperature*
 dimethylammonium copper tetrachloride, layer compound $(\text{CH}_3\text{NH}_3)_2\text{Cu}(\text{Cl},\text{Br})_{1-x}$, antiferro- to ferromag. transition 0-108005
 metamagnetic transition in absence of mag. field, model 0-97092
 temperature induced antiferromagnetic-ferromagnetic phase transition, s-f two-band Hubbard model 0-60253
 $\text{CoMnSi}_{1-x}\text{Ge}_x$, amg. props. 0-60270
 $\text{Cu}_2\text{MnAl-Pd}$, MnAl mixed Heusler alloys, mag. props. 0-60269
 $\text{Cu}_{1-x}\text{Pd}_x\text{MnSb}$, mag. phase transition 0-60268
 Dy, domain effects near order-disorder and order-order ferromagnetic transitions 0-65886
 Dy, magnetic domain structure, hysteresis, thermal modulation study 0-71082
 Dy, magnetocaloric effect and mag. phase transitions, 80 to 300K 0-60279
 FeCl_2 , magnetic transition and sublattice mag. moment rotation nonequivalence (*Russian*) 0-100586
 $\text{Fe}_{55}\text{Ni}_{28}\text{Mn}_{17}$, disordered, mag. struct. near ferro-antiferromagnetic transition 0-60211
 FePt, metamagnetic transitions in external fields 0-60272
 $\text{Hg}_{1-x}\text{Zn}_x\text{Cr}_2\text{Se}_4$, magnetic struct., neutronographic and mag. investigation (*Russian*) 0-88726
 $(\text{La}_{0.9}\text{Ca}_{0.1})\text{MnO}_{3+y}$, mag. props., Faraday method meas. 0-103832
 MnB_2 , polycryst., magnetoresist. and mag. props. (*Russian*) 0-92907
 $\text{Mn}_{1-x}\text{Fe}_x\text{Si}_3$, elec. resist. and mag. susceptibility, ferromag. to antiferromag. transition 0-80504
 Pt-Fe ordered alloy, multiply mag. phase transitions 0-60264
 Tb, magnetisation intensity in antiferromag. state and mag. field induced phase transforms. (*Russian*) 0-65811

ferromagnetic Curie temperature *see Curie temperature***ferromagnetic-paramagnetic transitions**

- see also Curie temperature*
 amorphous magnet, random anisotropy axis model in the infinite-range limit 0-88761
 ferromagnet, disordered, phase transitions, mol. field and Landau-Ginzburg theories 0-93118
 ferromagnetic Fermi-liquid model, electron-impurity system hydrodynamics, elec. cond. 0-103835
 inhomogeneous ferromagnets, phase transitions, micromagnetic theory 0-65942
 metals, ferromagnetic metals, resist. anisotropy, crit. behaviour and temp. depend. 0-96858
 rare earth compounds, Curie constant rel. to valence bond strength 0-60251
 rare earth cpds., $\text{RMO}_6\text{S}_8(\text{Se}_8)$ and RRh_4B_4 , coexistence of supercond. and mag. ordering (*Russian*) 0-84542
 $\text{CdCr}_2\text{Se}_4(\text{Se}_4)$, thermoreflexance, photoconductance, Raman scatt. near mag. phase transition 0-97298
 CdCr_2Se_4 , Crit. relax. processes, mag. reson. expts. 0-60425
 $\text{Co}_2\text{Ga}_{1-x}\text{Fe}_x$, elec. resist., temp. and mag. field depend., mag. contrib. 0-96846
 $\text{Co}(\text{S},\text{Se})_2$, metamagnetic transitions in external fields 0-60272
 CuCr_2Se_4 , Crit. relax. processes, mag. reson. expts. 0-60425
 $\text{EuO}(\text{S})$, spin order and fluctuations, Raman scatt. study 0-97273
 Fe, magnetic moments, local short range order, high temp. effects 0-65902
 Fe-Cr, hyperfine magnetic fields, Mossbauer spectra 0-97165
 Gd, coil noise due to permeability fluctuations at phase transition temp. 0-84598
 Gd, domain effects near order-disorder and order-order ferromagnetic transitions 0-65886
 Gd, thermal conductivity critical behaviour near Curie point 0-75540
 HgCr_2Se_4 , thermoreflexance, photoconductance, Raman scatt. near mag. phase transition 0-97298
 K_2CuF_4 , layered spin system, planar rotator symmetry, phase transition 0-65951
 K_2CuF_4 , spin relax., crit. behaviour, high freq. susceptibility meas. 0-65936
 $(\text{La}_{0.9}\text{Ca}_{0.1})\text{MnO}_{3+y}$, mag. props., Faraday method meas. 0-103832
 MnP, Lifshitz point, transverse differential susceptibility meas. 0-84599
 $\text{Ni}_{1-x}\text{Cu}_x$, phase transform. influence on surface chem. reaction 0-108737
 Pd-Ni, thermal expansion and magnetostriction meas. near crit. conc. for ferromagnetism 0-65881
 Rb_2ZnCl_4 , phase transitions, thermal expansion coeff. 0-100638
 TbZn, elec. resist., behaviour at mag. crit. points 0-65901
 TmSe, Curie constant rel. to valence bond strength 0-60251
 $\text{U}_{1-x}\text{Nd}_x\text{S}$, mag. phase diagram 0-71027
 $\text{U}_{1-x}\text{Pr}_x\text{S}$, mag. phase diagram 0-71027

ferromagnetic properties of substances

- see also ferromagnetic relaxation; ferromagnetic resonance; ferromagnetism; magnetic semiconductors*
 actinide elements and compounds, book contrib. 0-75727
 aluminium copper tetrahalides, exchange, mag. anisotropy, and spin diffusion contribs. to EPR linewidth 0-80597
 alloys, d-metal, magnetic susceptibility and Knight shift meas. 0-66055
 alloys, surface spin waves, cluster Bethe lattice approach 0-70983
 Alnico 8, permanent magnetic alloy, topography of precipitate phase (*Chinese*) 0-66512
 aluminoborate glass, Fe and Cr ion interaction, mag. and spectral props. 0-103883
 amorphous ferromagnets, book contrib. 0-75743
 anisotropy energy density 0-88742
 borosilicate glass, Fe and Cr ion interaction, mag. and spectral props. 0-103883
 coal, mag. susceptibility and Mossbauer meas. 0-60464
 copper formate anhydrate, cryst. struct. and mag. props. 0-79768
 cyclo-hexyl-ammonium-copper-trichloride, specific heat, ferromagnetic chain system 0-103491
 cyclohexyl ammonium copper chloride, one dimensional spin $1/2$ ferromag., mag. props. 0-71000
 cylindrical ferromag. conductor, acoustic wave propag., EM field behaviour 0-88857
 diethylammonium copper tetrabromide, mag. struct., NMR meas. 0-71192
 dimethylammonium copper manganese chloride, two-dimens. mixed magnet, EPR 0-66030
 dimethylammonium copper tetrachloride, crit. slowing down and anomalous relax. near Curie temp. 0-71053
 dimethylammonium copper tetrachloride, ferromag., quasi two-dimensional, ordering temp., press. depend. 0-84601
 dimethylammonium copper tetrachloride-tetrabromide mixed cryst., mag. transition 0-65874
 eddy-current flow detection of long ferromag. products, magnetizing device parameters 0-89447
 electron spin-lattice relaxation (*Russian*) 0-103823
 ethylammoniumtetrachlorochromate, optical absorption intensity, short-range spin correlation 0-108185
 ferric solution ferromagnetic liquid insulation in redox flow battery, quantum parameters separation 0-61338
 flow detected by high freq. magnetization, harmonic content in mag. field 0-71857
 Heusler alloys, ferromag. alignment rel. to conduction electron polarisation 0-60235
 Invar, Fe-Ni and Fe-Pt, magnetoelastic contribs. to US vel., elastic const., and susceptibility 0-75829
 Invar, magnetic structure, depend. on absorbed H, Stoner's band model calcs., Mossbauer spectra 0-65787
 Invar film, superline mag. struct. (*Russian*) 0-80572
 irreversible magnetising processes, random propag. 0-88818
 isopermalloy, permeability stability calc. rel. to texture (*Chinese*) 0-65959
 magnetizing device for inspection of products of ferromagnetic materials according to parameters of Barkhausen discontinuity 0-89457
 metal, electron-phonon interaction effects on spin susceptibility 0-93108
 metallic, glasses, soft-magnetic properties (*German*) 0-71108
 metallic glass, micromag. calcs. and props. 0-80501
 metallic glass, sput cooled, mag. props. 0-80491
 metallic glasses, Brillouin-Mandelstam scattering from thermal and excited magnons 0-70980
 metallic magnets investigation, present state (*Polish*) 0-107987
 metals, electron spin-lattice relaxation (*Russian*) 0-103823
 metals, max. in acoustic attenuation at low mag. fields 0-93158
 metals, thermal oxidation rate determ. using nanowebmeters 0-61045
 metals, transport props., crit. behaviour 0-65522
 metals, ultrasound attenuation and EM generation 0-108046
 Metglas 2605 ribbon, saturation magnetostriction meas. by small-angle magnetisation rot. 0-60391
 Metglas 2826 ribbon, saturation magnetostriction meas. by small-angle magnetisation rot. 0-60391
 methylammoniumtetrachlorochromate, optical absorption intensity, short-range spin correlation 0-108185
 mischmetal-Co system, thermomagnetic analysis of intermediate phases 0-93115
 nuclear fuel shell inspection, mag. method for detecting ferromag. particles 0-66746
 oxides, $\text{RCu}_2\text{Mn}_4\text{O}_{12}$, R=La to Lu, Y, synthesis and mag. props. 0-75717
 Permalloy, 50NP, and 79NM, magnetic properties and structure, environment effect during annealing 0-60366
 Permalloy, reference materials characts. obs., temperature effect 0-80563
 Permalloy film, mag. microstruct. obs. in nonlinear ripple magnetis. case (*Russian*) 0-65971
 Permalloy films, RF sputtered on Au, coercivity 0-80575
 Permalloy films with band domain struct., thermomag. recording, resolving power (*Russian*) 0-75769
 Permalloy RF sputtered films, O effects in mag. and elec. props. 0-100603
 Permalloy-Cu(Al) two-layer films, mag. anisotropy, grain boundary diffusion (*Russian*) 0-71122
 rare earth alloy, amorphous, ferromag. state, non-axial elec. field gradient effect 0-75728
 rare earth alloys, $\text{R}_{60}\text{Ni}_{31}$, amorphous, Curie temp., mag. susceptibility and coercive force, 4.2 to 300K 0-93092
 rare earth amorphous alloys, random anisotropy magnetism 0-65853
 rare earth compounds, RCO_2 metamagnetic transitions in internal fields 0-60272
 rare earth cpds., $\text{RMO}_6\text{S}_8(\text{Se}_8)$ and RRh_4B_4 , coexistence of supercond. and mag. ordering (*Russian*) 0-84542
 rare earth intermetallic compounds, book contrib. 0-75726
 rare earth intermetallics, RAI_2 , orbital and spin polarisations of cond. electrons 0-65791
 rare earth iron intermetallics, RFe_2 , (R=Sc, Lu, Y), mag. props., 80-1300K (*Russian*) 0-75750
 rare earth iron intermetallics, RFe_2 , magnetostrictive, book contrib. 0-75838
 rare earth metals, heavy, liq., mag. susceptibility meas. 0-75740
 rare earth metals, magnon dispersions in ferromag. and screw structs., nonlinear s-f exchange interaction effect 0-75746
 rare earth metals and alloys, book contrib. 0-75725

ferromagnetic properties of substances continued

rare earth-transition metal alloys, disordered, magnetisation behaviour 0-71099
rare earth-Zn alloys, parastriction and magnetoelastic coeffs. 0-65996
round bar, high energy alternating field stray flux testing technique 0-100972
semiconductor, red shift effect, optical absorpt. edge calc. 0-66140
semiconductors, ferromagnetic multivalley anisotropic, electron autolocalisation (*Russian*) 0-92848
semiconductors, magnetic, spin wave electron amplification theory 0-97083
steel, B-Si, grain-oriented, high induction, Cu impurity effects 0-89366
steel, C, magnetomechanical acoustic emission for residual stress NDT 0-71149
steel, cold-rolled, isotropic, specific magnetic loss meas. at high frequency 0-101808
steel, elect., mag. props. determ. with Epstein hysteresis tester 0-60364
steel, electrical, mag. hysteresis representation in numerical modelling of mag. fields 0-88813
steel, ferritic, magnetomechanical acoustic emission for residual stress NDT 0-71149
steel, high-speed, low temp. mag. cycling effects on ferromag. struct. 0-100928
steel, martensitic, sp. ht. and magnetisation meas. 1.2 to 10K 0-71059
steel, mild, fatigue softening and hardening detected from Barkhausen noise 0-76428
steel, Si, grain-oriented, high permeability, dissoln. and precip. of AlN and MnS 0-89223
steel, Si, nonoriented sheet prod. with texture of {100} (ovw) 0-89246
steel, Si, permeability change due to stress variation after demagnetization in Rayleigh region 0-88854
steel, stainless, Ferralloy, creep-rupture props., 650-800°C 0-97535
steel, structural, 34KhN3M, heat treatment effect on magnetostriction 0-104306
steels Kh18N(10-25), mag. susceptibility, 4.2 to 300K, and magnetoelasticity (*Russian*) 0-65812
superconductor, magnetic, shape effects 0-103773
thin film, direct determ. of mag. domain wall profiles, using split detector STEM 0-103867
TMNC, quasi one dimensional planar ferromag., low temp. NMR study im mag. field 0-97157
transition metal, chemisorption of H, effect of surface spin fluctuations 0-75613
transition metal alloys, amorphous, mag. props., chem. short-range order 0-75739
transition metal alloys, amorphous, mag. props., structure and preparation 0-75737
transition metal alloys, dilute, spin glasses, mag. ordering, book contrib. 0-75787
transition metal alloys, dilute ferromagnetic, itinerant d-electron(hole) degenerate, spin stiffness constant 0-70930
transition metal intermetallic cpds., H absorption and mag. props. 0-60224
transition metals, ferromag., dil. H electronic struct. 0-70638
two-layer mag. structures, thermomag. recording 0-100588
 γ -Al-Mn-C, permanent magnetism and microstruct. 0-75811
Au-Co, liquidus line determ. by mag. meas. 0-60250
Au-Fe alloys, spin correlations, neutron diff. meas. 0-80482
Ba₂Co_{1.65}Fe_{0.35}²⁺Fe₂₈³⁺O₄₆, temp.-mag. field phase diagram, torque method 0-60276
CdCr₂S₄, photothreshold changes below mag. ordering temp. 0-97406
CdCr₂S₄(Se₄), spontaneous magnetisation temp. depend., nuclear resonance freq. depend. (*French*) 0-80483
CdCr₂Se₄, Crit. relax. processes, mag. reson. expts. 0-60425
CdCr₂Se₄, ferromag. semicond., conc. anomalies rel. to red shift of absorpt. edge 0-70732
CdCr₂Se₄ magnetic semiconductor, photoinduced centre kinetics 0-71110
CdCr₂Se₄, magnetisation, study of photoinduced charges 0-80567
CdCr₂Se₄, Mott ferromagnetic semiconductor, optical absorption edge, critical behaviour 0-97226
CdCr₂Se₄, reactor radiation influence on ferromagnetic phase transform. (*Russian*) 0-75760
CdCr₂Se₄-Ga(In), photoconductivity, photomagnetoconductance near Curie point (*Russian*) 0-100485
CdCr₂Se₄(S₄), thermoreflectance, photoconductance, Raman scatt. near mag. phase transition 0-97298
CeAl₃, sp. ht., Kondo effect and ferromag. order coexistence 0-65927
CeAl₁₁, competition between ferro- and antiferromag. interactions 0-60258
CeAl₁₁, sp. ht., Kondo effect and ferromag. order coexistence 0-65927
Ce₂Co₇, and ternary hydride, mag. props. 0-108007
CeCo₂H₄, mag. props. 0-108007
Ce₂Mg₃(NO₃)₁₂·24H₂O, ground state with dipole-dipole and exchange interactions in external mag. field 0-84582
CeNi₄Al, mag. susceptibility, H adsorption-desorption cycle effects 0-107990
(Ce_{1-y}Y_y)Fe₂, mag. susceptibility and Mossbauer meas., lattice parameters 0-97068
(Co_{0.9}Fe_{0.1})₈₀B₂₀ glass, induced anisotropy and time changes of permeability 0-75815
Co alloys, amorphous, effects of metalloids on mag. props. 0-75738
Co, energy band dispersion and mag. exchange splitting, angle-resolved photoemission meas. 0-71567
Co epitaxial films, even magneto-optical effects 0-76007
Co, Fermi surface under press., de Haas-van Alphen effect meas. 0-75499
Co, ferromagnetic micropowder, cryst. struct., coercivity, remanence, saturation 0-65967
Co film, mag. anisotropy study using NMR spin echo method 0-60384
Co film, mag. domain wall obs. by electron holography 0-80582
Co fine particles in Cu, interface magnetisation 0-88858
Co, fundamental and secondary mag. props., book contrib. 0-75724
Co, interstitial site determ., μ SR technique 0-71287
Co-B-(Cr) thin film glasses, mag. props. and corrosion resist. 0-80576
Co-CoO films, evaporated, exchange anisotropy 0-88841
Co-Cr mag. film, crystallographic texture formation effects on props. (*Russian*) 0-108471
Co-Fe, dil., hyperfine mag. fields, press. effect, Mossbauer meas. 0-71277
Co-Fe, soft mag. props. rel. to metallurgical aspects 0-88810

ferromagnetic properties of substances continued

Co-Fe amorphous alloys, worked, perminvar type mag. hysteresis loop, longit. Kerr effect obs. 0-65958
Co-Fe-Si-B, ferromag., magneto-optical spectra in amorphous and cryst. states (*Russian*) 0-84749
Co-Fe-V-Ni, mag. and mech. props., heat treatment and stress effects 0-60363
Co-Gd(Tb)(Sm) film, magneto-optic coeff. and refr. index, ellipsometric determ. 0-71501
Co-mischmetall system, phase relations, microstruct., mag. props. 0-104118
Co-Mn alloys, ferromagnetic, high field mag. susceptibility meas. 0-75729
Co-Mn-Ni-Fe-Si-B amorphous alloys, mag. props., low magnetostriction 0-75832
Co-P, amorphous, domain struct., mag. anisotropy origin 0-80554
Co-P films with various preferred orientations, mag. props. 0-100604
Co-Pt ferromagnetic alloy, 6 T ultrasonic study of magnetoelastic coupling 0-93154
Co-Si-B, amorphous ribbon, saturation magnetostriction meas. by small-angle magnetisation rot. 0-60391
Co-V, Co rich, mag. moments, Curie temp., and NMR spectrum 0-70964
Co-V, ferromag. struct. in nucl. spin echoes 0-60453
Co-W alloy electrolytic coatings, heat treatment effects on coercivity, hysteresis and structure (*Russian*) 0-60381
Co_{100-x}B_x, amorphous, mag. struct., mag. susceptibility meas. 0-80485
Co₂B, glassy and cryst., hyperfine field distrib., ⁵⁹Co spin echo spectra 0-80635
Co₂Fe_{1-x}, ferromagnetism and spatial long-range order 0-60159
(Co_{0.93}Fe_{0.07})_{75-x}Cr_{0.07}Si₁₅B₁₀ amorphous alloy, thermal stability, Cr conc. effects, DTA expts. 0-59395
(Co_{0.89}Fe_{0.11})₇₂Mo_{0.18}Si₁₅B₁₀, metallic glass, strain- and field-induced mag. anisotropy 0-108004
Co₅₇Fe₄₃Ni₁₀(Si₂B)₂₈, amorphous, soft mag. props., switched-mode power supply apps. 0-88850
Co_{70.4}Fe_{4.4}Si₁₅B₁₀, amorphous, mag. aftereffect spectra and annealing props. 0-88831
 β -Co₅₂Ga₄₈, negative TCR obs. 0-75543
Co₂Ga_{2-x}Fe_x, elec. resist., temp. and mag. field depend., mag. contrib. 0-96846
Co₂Ga_{2-x}Fe_x, mag. field depend. of resist., 5.80K 0-70676
Co(GaTiV) alloys, ferromag. onset, electron conc. depend. 0-60203
(Co_{1-x}Mn_x)₂B, magnetocrystalline anisotropy meas., 4.2-300K 0-71006
CoMn(Cr)(V)(Ti), dil., low temp. specific heat and magnetisation 0-65925
Co₅₀Mn_{50-x}, ordering and disordering phenomena, mag. study 0-70154
CoMnP, cryst. mag. struct., neutron diff. study (*French*) 0-59439
CoMnSi_{1-x}Ge_x, amg. props. 0-60270
Co₇₃Mo₂Si₁₅B₁₀, metallic glass, strain- and field-induced mag. anisotropy 0-108004
CoP, and CoNiP, cylindrical amorphous electrodeposited layers, mag. props., torsion influence 0-88848
CoPd, single crystals, domain struct., temp. and field depend. 0-71085
CoRhS₄, mag. semicond., mag. and elec. props. 0-93121
Co(S, Se)₂, metamagnetic transitions in external fields 0-60272
CoS₂, galvanomagnetic effect of single cryst. 0-96912
CoS₂, itinerant ferromagnet, ferromag. reson. and EPR meas. 0-66044
CoS₂, narrow-band ferromag., high press. effect on anomalous elec. resist. 0-70698
Co(S, Se_{1-x})₂, galvanomag. effects, obs. and interpretation 0-70726
CoSm crystals, microstruct., homogeneous precip. and nucleation 0-104160
CoTi_{1-x}Al_x, mag. and electronic props., ferromag. and paramag. state 0-65814
Co₉₀Zr₁₀, ferromag. amorphous alloy, crystn. and domain struct. study 0-107056
Cr-Co-Fe, low Co, phase separation, TEM and Mossbauer spectra obs. 0-71269
Cr-Fe, dil., magnetisation, Fe local moments 0-60215
Cr-Fe, dil., spin correlations and neutron scatt. near crit. conc., theory 0-60327
Cr-Ge system, XPS, X-ray and neutron diff. and mag. meas. to study chem. bonding and electronic struct. 0-60749
CrBr₂, ferromag. domains, using liq. He mag. specimen stage 0-103855
CrBr₃, HF spectra, susceptibility, spin waves in domain walls (*Russian*) 0-80909
CsFeCl₃, pseudo-one-dimens. singlet ground state ferromag., mag. excitations, neutron scatt. study 0-97064
CsMnF₄, planar ferromag., cryst. and /mag. struct., Jahn-Teller effect 0-75715
CsNiF₃, 1D ferromag., optical absorption and spin dynamics 0-71417
CsNiF₃, anisotropic Heisenberg chain, nonlinear excitations 0-70927
CsNiF₃, low frequency dynamics in external mag. field 0-108020
CsNiF₃, nonlinear excitations, 1D-ferromag., neutron scatt. 0-70949
CsNiF₃, one dimensional planar model with symm. breaking fields, thermodynamics, static props. 0-97111
CsNiF₃, one-dimens. magnet, local magnon modes 0-65829
CsNiF₃, one-dimensional ferromagnet, optical absorpt. and static spin correlation functions 0-71415
CsNiF₃, quasi one dimensional planar ferromag., low temp. NMR study im mag. field 0-97157
CsNiF₃, quasi-one-dimensional ferromagnet, subthreshold parallel pumping of magnons 0-75745
CsNiF₃, stochastic motion of Sine-Gordon-solitons, spin-correlation function 0-93105
CsNiF₃, subthreshold parallel pumping of magnons and antiferromag. reson. 0-71185
Cu HCP film, uniaxial, mag. domain struct. 0-60385
Cu:Co precipitates, mag. anisotropy, precipitate shape, coercive force 0-80500
Cu-Au-Fe, ferromag. ordering in FCC γ -Fe precipitates, Mossbauer study 0-71267
Cu-Mn-Al, Heusler alloys, ferromag. inclusions, mag. props. and struct. study (*Russian*) 0-80570
Cu-Mn-Al alloys, displaced hysteresis loop and microstructure obs. 0-84613
Cu-Ni, random ferromag. alloy, local mag. moment calc. 0-70974
Cu-Ni films, compositionally modulated, magnetic anisotropy, magnetisation curves 0-88840

ferromagnetic properties of substances continued

- Cu-Ni-Co, mag. props. of system of disperse ferromag. particles, 73 to 673K (*Russian*) 0-65968
 Cu-Ni-Fe, magnetic properties, heat treatment and compressive stress effects 0-60367
 CuCr₂S₄-xSe₂ spinels, NMR spin echo study 0-71238
 CuCr₂Se₄, Crit. relax. processes, mag. reson. expts. 0-60425
 Cu₂Cr₂Se₄-xBr₂, Hall effect 0-60012
 Cu₂MnAl_{1-x}Sn_x, Mossbauer effect study 0-60473
 Cu(Rh_{1-x}Cr_x)S₄, spinel system, susceptibility and metallic resistivity, anomalies due to s-d interaction 0-70958
 Dy, interstitial site determ., μ SR technique 0-71287
 Dy, magnetic domain structure, hysteresis, thermal modulation study 0-71082
 DyBi, mag. behaviour 0-71025
 Dy(Co,Ni)₂, intrinsic mag. aftereffect meas., domain wall motion 0-71121
 DyFe₃ and Dy₂Fe₂₃, magnetostriction, room temp. to 80K 0-65993
 Dy₂Fe₁₇, domain structures and anisotropy constant. 0-93136
 Dy_{1-x}Sm_x, magnetoelast. of polycryst. specimens in fields up to 44 kOe (*Russian*) 0-92880
 ErFe₂-YFe₂, and ErFe₂-LuFe₂, mag. props., 80-1300K (*Russian*) 0-75750
 ErFe₃ and Er₂Fe₂₃, magnetostriction, room temp. to 80K 0-65993
 Er₂Fe₂₃, magnetostriction, temp. depend., 20 to 350K 0-65994
 Er_{1-x}Ho_xRh₄B₄, mag. and supercond. transitions, cryst. field effects 0-107950
 ErRh₄B₄, ferromag. superconductor, vortex phase 0-80441
 ErRh₄B₄, long ferromag. supercond., metastable supercond. state 0-103771
 ErTiO₃, magnetic structure determination, neutron scatt. study 0-65809
 Er_{1-x}Tm_xRh₄B₄, mag. and supercond. transitions, cryst. field effects 0-107950
 Eu chalcogenides, cond. band spin struct. 0-71577
 Eu chalcogenides, resonant Raman scattering model via magnetic exciton in ferromagnetic phase 0-93326
 Eu chalcogenides, spin-dependent Raman scatt. from phonons 0-97274
 EuB₆, electronic struct., transport and mag. props. 0-96782
 EuB₆, ferromag., spin-polarised energy band struct., APW calc. 0-96779
 EuB₆, ferromag. and antiferromag. sp. ht meas., 1.8-77K 0-65948
 EuB₆, Hall effect and resistivity data, ferromagnetic ordering temp., pressure depend. 0-60010
 Eu₂IrH₃, prep., cryst. struct., mag. and elec. props. 0-88117
 EuLiH₃, transferred hyperfine fields at Eu nuclei, NMR meas. 0-71195
 EuO, ferromagnetic piezotransmission behaviour in magnetic field 0-97272
 EuO film threshold characteristics in holographic and bit recording (*Russian*) 0-63944
 EuO, magnetic susceptibility critical exponent, corrections to scaling 0-103846
 EuO, physical and physicochem. props., review 0-96875
 EuO, spin wave lifetime, theory compared with expt. 0-60228
 EuO, transmission and resistivity, stress modulation effect near Curie temperature 0-96874
 EuO:Gd, elec. cond. under hydrostatic press., Curie temp. 0-96881
 EuO:Gd, ferromag. semicond., electron spin polarisation and conduction band struct. 0-65449
 EuO:Gd, pure and doped, elec., mag., and optical props. rel. to electronic conc. 0-96880
 EuO:Gd, surface mag. props. 0-71566
 EuO:La(Gd), phototreshold changes below mag. ordering temp. 0-97406
 EuO:Sm³⁺, hyperfine field at Sm, TDPAC meas. 0-93215
 EuO(S), ferromagnetic electronic structure, absorption, thermoreflexion and thermotransmission spectra (*French*) 0-97300
 EuO(S), spin order and fluctuations, Raman scatt. study 0-97273
 EuPt₃ compounds, partial valence change, ¹⁵¹Eu Mossbauer and magnetisation obs. 0-70167
 Eu_{1-x}R_x²⁺O_{1-x}N_x (R=Eu,Gd), lattice parameters, mag. and elec. props. 0-100578
 EuS, ferromag. semicond., high field susceptibility, spin waves 0-75735
 EuS films, mag. and elec. props. rel. to stoichiometry and defects 0-97122
 EuS, single cryst., high-field susceptibility meas., temp. range 2.5 to 16.5K 0-84589
 EuS thin film, Brillouin scattering from spin waves 0-65843
 Eu,Sr_{1-x}S, Heisenberg spin glass system, excitations 0-84610
 Eu,Sr_{1-x}S, insulating spin glass, sp. ht. near ferromag. onset 0-97106
 Eu,Sr_{1-x}S, magneto-optical redshift in absorpt. and photoluminesc., mag. short-range order 0-71388
 Eu,Sr_{1-x}S, spin glass to ferromag. transition, neutron scatt. and susceptibility meas. 0-60254
 (Fe,Co,Ni)-Si(B), amorphous mag. alloy, magnetostriction rel. to soft mag. props. 0-84633
 Fe, 90° walls, stable orientations, theory and X-ray observations (*Japanese*) 0-60359
 Fe alloys, amorphous, effects of metalloids on mag. props. 0-75738
 Fe alloys, amorphous, mag. saturation, spin wave stiffness, temp. depend. 0-75741
 Fe alloys, amorphous, saturation magnetisation, Curie temp. and size effect 0-65815
 Fe and Fe-Ni Metglas alloys, ohmic and Hall resist. 100-700K, mag. behaviour 0-80254
 Fe, BCC, high field Knight shift and hyperfine anisotropy of ⁵⁷Fe 0-71205
 α -Fe, cold work aftereffects 0-88830
 Fe, dynamic exponent, crossover obs., TDPAC Meas. 0-108021
 Fe, electron tunnelling 0-60104
 Fe, electron-phonon coupling, point contact spectroscopy obs. (*Russian*) 0-70342
 Fe, energy band dispersion and mag. exchange splitting, angle-resolved photoemission meas. 0-71567
 Fe epitaxial films, even magneto-optical effects 0-76007
 γ -Fe, FCC film, epitaxial growth on CuAu (111) surfaces, strong ferromagnetism 0-70557
 Fe, Fermi surface under press., de Haas-van Alphen effect meas. 0-75499
 Fe, ferromag. film, surface states, surface magnetisation and electron spin polarisation 0-65648
 Fe, ferromagnetic, partial circular polarisation of thermal emission in mag. field 0-71387

ferromagnetic properties of substances continued

- Fe, ferromagnetic micropowder, cryst. struct., coercivity, remanence, saturation 0-65967
 Fe film, coated, interface magnetism by Mossbauer spectroscopy 0-75890
 Fe film, nuclear spin system dynamics Mossbauer study in FMR conditions (*Russian*) 0-80651
 Fe films, ferromagnetic reson., photoacoustic detection 0-80613
 Fe films, thickness variations in extraordinary and spontaneous Hall coeffs. 0-97013
 Fe, fundamental and secondary mag. props., book contrib. 0-75724
 Fe garnets, sublattice magnetisation curves, Mossbauer study 0-75808
 Fe group, mol. Jahn-Teller reson. states as possible antecedents to magnetism 0-75701
 Fe, H₂ embrittlement and H₂ adsorption 0-89401
 Fe, high purity, magnetomechanical damping, magnetic field variations 0-93156
 Fe, intercell exchange energy, Hartree-Fock approx. 0-60239
 Fe, interstitial site determ., μ SR technique 0-71287
 Fe, mag. aftereffect meas., phenomenological description 0-88835
 Fe, mag. breakdown and Hall resist., theory and model calcs. 0-75552
 Fe, mag. hyperfine field at ¹²⁹I, press. depend., nucl. gamma reson. 0-71256
 Fe, magnetic moments, local short range order, high temp. effects 0-65902
 Fe, magnetism at high temps. 0-75721
 Fe, magnetomechanical acoustic emission for residual stress NDT 0-71149
 α -Fe, neutron irradiated, mobile C atom trapping, anelastic and magnetic relaxations 0-100306
 Fe particles, dispersed in Hg, mag. props., aggregate form. 0-60375
 Fe particles, spin collinearity, Mossbauer spectra study 0-71114
 Fe, polarised, ferromag., evidence for K-shell polarisation of ¹²C ions via mol. orbital promotion 0-71273
 Fe polycrystalline, two ferromag. methods for eval. of fatigue limit 0-89438
 Fe, positive muon diffusion, press. depend. 0-75907
 Fe powder-plastic composite, soft mag. material, mag. and mech. props. 0-75812
 Fe, pure and doped, electron irradiat., mag. aftereffect 0-88838
 Fe, spin susceptibility, high-field, spin-density functional formalism 0-70959
 Fe, spontaneous volume magnetostriction 0-65989
 Fe sputtered film, amorphous, Mossbauer study and electron diffr. obs. 0-75897
 Fe, stray mag. fields above stripe domains, electron microscope and μ^* -tensor determ. 0-71089
 Fe thin film, Brillouin scattering from spin waves 0-65843
 Fe thin layers, vacuum coated on PMMA, mag. behaviour during mech. stress cycles (*German*) 0-80581
 Fe whisker, domain theory, quasi-dislocation theory appl. (*Japanese*) 0-60358
 Fe whisker, magnetisation curve meas. using SQUID system 0-86347
 Fe, whisker, magnetoresistance, deviations from Kohler's rule 0-70673
 Fe, whisker single crystals, ferromag. reson. and surface anisotropy 0-71187
 Fe-Al, domain struct. and magnetostriction, heat treatment effect 0-60398
 Fe-Al (4 wt.%) alloy, mag. anisotropy induced by cold rolling (*Russian*) 0-84595
 Fe-Al(Ti), O containing, mag. aftereffect and disaccommodation meas., time depend., activation energy, and ageing props. 0-88836
 Fe-Al(24.3 at.%)C alloy, magnetic permeability disaccommodation, 260-400K 0-93144
 Fe-B, amorphous, induced anisotropy, development by mag. annealing and under applied mech. stress 0-65868
 Fe-B, amorphous, induced anisotropy by heat treatment in mag. field and under applied mech. stress 0-75758
 Fe-B, amorphous, mag. aftereffect, initial susceptibility time depend. 0-88829
 Fe-B, amorphous alloy, mag. props. 0-84618
 Fe-B, amorphous ferromag., temp. depend. of resist., appl. of extended Ziman theory 0-59950
 Fe-B, liq., mag. susceptibility meas. 0-75740
 Fe-B amorphous alloy, annealed, microstruct. and mag. domain changes 0-75790
 Fe-B amorphous alloys, mag. aftereffect 0-65970
 Fe-B metallic glasses, struct., stability and crystn. 0-75173
 Fe-B metallic ribbons, correl. between quenching temp. and mech. and mag. props. 0-89373
 Fe-B phase ferromag. amorphous alloys, stiffening below Curie temp., pole effect (*Japanese*) 0-84632
 Fe-B ribbon, microhardness, and static coercive force, melt overheating effect 0-84978
 Fe-B-C, amorphous, effects of replacement of B by C on mag. props. 0-84621
 Fe-B-C amorphous alloy, formation, mag. props., thermal stability and density 0-75796
 Fe-B-C amorphous alloys for use in power transformers 0-88808
 Fe-B-C amorphous alloys with high saturation induction 0-84617
 Fe-B-Cr(Mo), metallic glasses, mag., struct., and elec. props. 0-88751
 Fe-B-Cr(Si) thin film glasses, mag. props. and corrosion resist. 0-80576
 Fe-B-Si-C amorphous alloys, prep. and props. 0-88748
 Fe-B(Si), glassy, field-induced mag. anisotropy near eutectic comp. 0-93110
 Fe-B(P) amorphous alloys, anomalous thermal expansion, ΔE effect, Invar and Elinvar characts., delay time 0-80589
 Fe-Ci (3 wt.%), local magnetisation losses, grain orientation effect 0-88817
 Fe-Co, 3d ferromagnet nuclear spin-lattice relaxation 0-80627
 Fe-Co, ferromagnetic micropowder, cryst. struct., coercivity, remanence, saturation 0-65967
 Fe-Co-Mo-Nb(Ta) semihard mag. alloy, mag. props., thermal expansion, elec. resistivity and hardness (*Japanese*) 0-88789
 Fe-Co-Ni Perminvar, mag. props. singularities in region of mag. anisotropy (*Russian*) 0-84614
 Fe-Co-Si-B, amorphous soft ferromagnet with high mag. induction 0-84619
 Fe-Co-Si-B, zero magnetostrictive amorphous alloy with high saturation induction, mag. annealing 0-60362
 Fe-Co-Si(B), amorphous ferromagnet, mag. after effect on soft mag. props. 0-84626

ferromagnetic properties of substances continued

- Fe-Co-Ti(V)(Cr)(Mn), sp. ht. in ordered and disordered phases 0-71061
 Fe-Co-V(Ni), annealing effect on microstruct. rel. to mag. and mech. props. 0-89267
 Fe-Cr, hyperfine magnetic fields, Mossbauer spectra 0-97165
 Fe-Cr, random ferromag. alloys, local mag. moment calc. 0-70974
 Fe-Cr-Al (12, 3 wt.%), internal friction and rigidity modulus, strain amplitude depend. (*Japanese*) 0-92606
 Fe-Cr-Co (28, 10.5 wt.%) ductile magnet alloy, humidity-induced H_2 embrittlement 0-89406
 Fe-Cr-Co alloy, coercive force mechanism 0-71103
 Fe-Cr-Co alloys, (5-9 wt.% Co), obtained by slow cooling under mag. field, permanent magnet props. 0-75797
 Fe-Cr-Co permanent magnet system, miscibility gap, microstruct. and mag. props. obs. 0-76228
 Fe-Cr-Co-Mo high energy permanent magnets, mag. props. 0-97119
 Fe-Gd(Tb) film, magneto-optic coeff. and refr. index, ellipsometric determ. 0-71501
 Fe-Ni, Invar, Curie point, annealing effects and time depend. 0-80508
 γ -Fe-Ni, local magnetisation of Fe atoms, Mossbauer effect meas. 0-75891
 Fe-Ni, magnetisation calc. method based on moments of density of states 0-65770
 Fe-Ni, secondary recryst. and mag. props. 0-89247
 Fe-Ni (308-44.1 at.%) Invar alloys, anomalous mag. anisotropy and thermal expansion 0-75755
 Fe-Ni (32.3 at.%), mag. struct. in commensurate approx., neutron diffraction study 0-60212
 Fe-Ni (33-38 at.%), low-angle neutron diffraction, anomalous crit. scatt. (*Russian*) 0-60193
 Fe-Ni alloy type YundK25B, anomalous magnetocaloric effect 0-60278
 Fe-Ni based metallic glass, Metglas 2826 MB, Mossbauer study 0-75897
 Fe-Ni Invar, magnetovolume coupling enhancement factor, temp. depend. 0-88851
 Fe-Ni Invar alloys, sputter quenched, mag. props. 0-75799
 Fe-Ni Invar alloys of crit. conc., mag. props., flow theory methods (*Russian*) 0-65894
 Fe-Ni Invar anomalies, explanation in terms of itinerant electron magnetism 0-75705
 Fe-Ni-B-Si, amorphous, mag. props., heat treatment effects 0-89370
 Fe-Ni-B(P), ferromag., magneto-optical spectra in amorphous and cryst. states (*Russian*) 0-84749
 Fe-Ni-C, Invar, coated, Mossbauer spectra, effect of applied RF mag. field 0-80645
 Fe-Ni-Co-Cu-Ti YundKT alloys, impaired mag. props. with C and S additions 0-60368
 Fe-Ni-Cr, mag. props. in weak mag. fields (*Russian*) 0-75771
 Fe-Ni-Mn, Invar, RF collapse and thermal effects, Mossbauer study 0-100624
 Fe-Ni-Mo, martensitic transformation, annealing, influence on struct. of austenite (*Russian*) 0-81057
 Fe-Ni-P-B, metallic glasses, struct. relax., annealing effects on mag. props. 0-89261
 Fe-Ni(Al), mag. aftereffect meas., phenomenological description 0-88835
 Fe-Ni(Pt) Invars, elastic and mag. props., magnetoelastic interaction effects (*Russian*) 0-84631
 Fe-Ni(35.4 at.%) Invar alloys, T^2 term contribution to magnetisation 0-71096
 Fe-P electrodeposited foil, amorphous, mag. domains 0-75821
 Fe-P(Ga)(As)(Sb), dil., short range order, NMR study 0-71237
 Fe-Pd, magnetic after-effect of H isotopes 0-75817
 Fe-Pd Invar alloys, elec. and mag. props. and thermal expansion 0-75732
 Fe-Pt Invar alloys, magnetocrystalline anisotropy const. determ. 0-65861
 Fe-rare earth alloys, amorphous, magnetoelasticity and moment rot., US vel. calc. and neutron scatt. meas. 0-65992
 Fe-Sb-Ni(Cr), dil., short range order, NMR study 0-71237
 Fe-Si, grain oriented, misorientation effects on mag. props. 0-88792
 Fe-Si, grain oriented sheet, grain struct. by computer mapping 0-88168
 Fe-Si, grain oriented sheet, AC hysteresis, surface struct. and elastic stress effects 0-88791
 Fe-Si, grain oriented transformer sheets, permeability and magnetostriction, tensile stress effects 0-88843
 Fe-Si, grain-oriented sheets, high permeability, low losses, review 0-88790
 Fe-Si, loss meas. at high flux densities 0-88799
 Fe-Si, mag. props., stress and reannealing effects 0-88844
 Fe-Si, non-oriented sheets, production and props. 0-88797
 Fe-Si, power loss and permeability meas. by means of Hall probes and stochastic ergodic correl. 0-86350
 Fe-Si, single cryst., mag. domain wall motion, X-ray topography study 0-65953
 Fe-Si, stator core, grain-oriented and non-oriented, magnetic flux and loss distrib. 0-88798
 Fe-Si (3 to 5 wt.%) sinters, mag. props., Si and Fe-Si additions effect 0-71104
 Fe-Si (3 wt.%), domain wall spacing and core loss, forsterite and stress coatings effect 0-88780
 Fe-Si (3 wt.%), ferromag. domains, imaging by neutron interferometry 0-71087
 Fe-Si (3 wt.%), grain oriented, mag. props., effect of decarburization (*Chinese*) 0-103821
 Fe-Si (3 wt.%), grain-oriented, domain struct. regulation and power loss reduction 0-88779
 Fe-Si (3 wt.%), grain-oriented, domain wall profiles throughout magnetisation cycle 0-88781
 Fe-Si (3 wt.%), grain-oriented, stacking effect on power loss, mag. props. 0-88795
 Fe-Si (3 wt.%), grain-oriented, power loss and domain wall variation with lamination thickness 0-88814
 Fe-Si (3 wt.%), grain-oriented, energy loss reduction by lowering sheet thickness 0-88816
 Fe-Si (3 wt.%), high permeability, use in transformer cores 0-88793
 Fe-Si (3 wt.%), internal friction, instantaneous, depend. on phase of torsional oscills. (*Russian*) 0-71142
 Fe-Si (3 wt.%), losses, demagnetisation freq. and grain orientation depend. 0-88796
 Fe-Si (3 wt.%), mag. domain wall contrast in synchrotron X-ray topographs 0-75792
 Fe-Si (3 wt.%), mag. loss and magnetostriction, DC flux alternation effects 0-88794

ferromagnetic properties of substances continued

- Fe-Si (3 wt.%), magnetisation variation during bending oscills., rel. to ΔE effect (*Russian*) 0-65983
 Fe-Si (3 wt.%), nonoriented sheets, magnetisation, tensile stress effects 0-88845
 Fe-Si (3 wt.%), oriented, losses and domains, mech. stress effects 0-88852
 Fe-Si (3 wt.%), power losses at extremely low freqs. 0-88815
 Fe-Si (3 wt.%), stripe domain structure, dynamic behaviour at high mag. induction values (*Russian*) 0-80553
 Fe-Si (3 wt.%), texture, Mossbauer expts. 0-71262
 Fe-Si (3 wt.%) alloy, mag. anisotropy induced by cold rolling (*Russian*) 0-84595
 Fe-Si (3 wt.%) laminations, magnetostriction behaviour associated with closure domain spikes 0-75834
 Fe-Si (3 wt.%) laminations, grain oriented, plastically deformed, anomalous losses 0-88853
 Fe-Si (3.25 wt.%) alloy, single cryst. with (007) planes, domain struct. influence on mag. torque 0-108034
 Fe-Si (3wt.%), grain-oriented, secondary recryst., grain growth inhibition 0-89245
 Fe-Si (6.5 wt.%) filament, formation by modified Taylor technique, and mag. props. 0-75795
 Fe-Si (6.5 wt.%) ribbon, sputter-cooled, mag. props. 0-88805
 Fe-Si-Al, Sendust, ribbon-form, prep. by rapid quenching, mech. and mag. props. 0-71611
 Fe-Si-Al (9.6, 5.4 wt.%), ribbon-form Sendust alloy, mag. props., annealing effects 0-88800
 Fe-Si-Al ribbon-form Sendust alloy made by rapid roll quenching, mag. props., recording head appls. 0-81001
 Fe-Si-B, high induction, hot rolling treatment 0-89266
 Fe-Si-B, magnetic metallic glasses, mag. props. 0-84620
 Fe-Si-B glassy alloys, mag. props., comp. effects 0-88752
 Fe-SiO multilayer films, interface magnetisation 0-88858
 Fe-Tb, magnetoelastic hysteresis, elastic stress and mag. field depend. (*Russian*) 0-65982
 Fe-V, ferromag. struct. in nucl. spin echoes 0-60453
 Fe-W-Cr-Mo system, mag. and mech. props. rel. to production methods (*Japanese*) 0-71107
 Fe-Zn alloys, coercive force anisotropy after cold plastic deform. (*Bulgarian*) 0-75809
 Fe₃Pt, ordered ferromagnetic alloy, magnetic excitation obs. 0-70978
 (Fe-Ni-Mo)₈₀(P-B)₂₀, amorphous, mag. aftereffects and struct. instabilities 0-88833
 Fe₃Al(Si), electronic structure, magnetic moments 0-107695
 Fe_{1-x}B_x, amorphous, hyperfine fields and local mag. moments, Mossbauer study 0-75895
 Fe_{100-x}B_x, amorphous, mag. struct., mag. susceptibility meas. 0-80485
 Fe₈₀B₂₀, amorphous, Brillouin scatt. from magnons, ferromag. reson. 0-65844
 Fe₈₀B₂₀, amorphous, mag. permeability aftereffect during annealing 0-88834
 Fe₈₀B₂₀, amorphous ferromagnet, Mossbauer hyperfine fields, mag. struct. 0-75894
 Fe₈₀B₂₀ amorphous ribbon, initial susceptibility time lag 0-100579
 Fe₈₀B₂₀ glass, magnetisation reorientation, Mossbauer effect 0-66092
 Fe₈₀B₂₀ metallic glass, crystn. and struct. relax., Mossbauer effect study 0-75182
 Fe₈₀B₂₀ metallic glasses, stability and transforms. 0-75174
 Fe_{81.4}B_{6.6}, amorphous, mag. props. and microstruct., cooling rate and melt overheating effects 0-65965
 Fe_{81.4}B_{6.6} amorphous, mag. props., melt overheating and cooling rate effects 0-89371
 Fe_{1-x}Co_xAl, site preference and local environment effects, Mossbauer and NMR meas. 0-71264
 (Fe_{0.5}Co_{0.5})_{1-x}B_x, amorphous, hyperfine fields and local mag. moments, Mossbauer study 0-75895
 Fe₂Co₇₅B₂₀, amorphous, magnetisation reversal and domain boundary configs. 0-88809
 Fe₃₅Co₃₇B₂₀Si₁₀Al₃, stress-induced variation in magnetisation and dynamic magnetostrictive charact. 0-88855
 Fe₂Co_{1-x}Cl₂, metamagnet, mag. phase diagram by mag. induced light scatt. 0-65883
 Fe_{0.5}Co_{0.5-x}Cr_x films, vacuum-deposited cryst. and mag. struct. (*Russian*) 0-93081
 Fe_{0.3}Co_{0.8}S_{0.2}, narrow-band ferromag., high press. effect on anomalous elec. resist. 0-70698
 (Fe_{1-x}Co_x)₇₅Si₁₀B₁₂, amorphous, roll mag. anisotropy 0-75757
 (Fe₂Co_{1-x})₇₅Si₁₀B₁₄, amorphous, saturation magnetostriction, strain modulated FMR obs. 0-75863
 Fe₂Cr_{1-x} spin-wave evolution crossing from ferromag. to spin-glass regime 0-97080
 Fe₂Mg_{1-x}Cl₂, metamagnet, mag. phase diagram by mag. induced light scatt. 0-65883
 (Fe_{1-x}Mn_x)₂Y(B), Mn effect on Fe mag. moments, Mossbauer and mag. meas. 0-71016
 (Fe_{1-x}Ni_x)₈₃B₁₇, amorphous alloys ferromagnetic resonance 0-108080
 Fe₄₀Ni₄₀B₂₀, amorphous, RF annealing effects 0-108037
 Fe₄₀Ni₄₀B₂₀ and Fe₄₀Ni₄₀P₁₄B₆, amorphous, mag. aftereffect spectra and annealing props. 0-88831
 Fe_{80-x}Ni₂₀ and Fe_{80-x}Ni₁₄P₄B₆ amorphous alloys, microhardness correl. with mag. props. 0-88826
 Fe_{80-x}B₂₀ and Fe_{80-x}P₁₄B₆ metallic glasses, low temp. resist. and galvanomag. effects, mag. state influence 0-84461
 Fe₈Ni_{80-x}B₂₀ glass, resist., magnetoresist., and thermoelec. power 0-70681
 (Fe_{1-x}Ni_x)_{0.8}B_{0.2-x}P_x, amorphous, hyperfine fields and local mag. moments, Mossbauer study 0-75895
 Fe_{80-x}Ni_{20-y}P_y, amorphous, Rayleigh region and coercive force 0-88806
 (FeNi)₄₀Bi_{17.5}Al₅Si_{0.5}, stress-induced variation in magnetisation and dynamic magnetostrictive charact. 0-88855
 Fe₄₀Ni₄₀C₁₂P₄, amorphous film, dislocation and mag. struct., neutron diffraction study 0-70956
 Fe₄₀Ni₄₀(Mo₅Si₅)₂₀, amorphous, soft mag. props., switched-mode power supply appls. 0-88850
 Fe₄₀Ni₃₈Mo₄B₁₈, amorphous, mag. anisotropy, Mossbauer study 0-65864
 Fe₄₀Ni₃₈Mo₄B₁₈ and Fe₇₂Mo₂B₂₀ amorphous ribbons, magnetoelastic effects in as-quenched and stress-relieved states 0-80588
 (Fe_{1-x}Ni_x)₂P, Curie temp., press. depend. meas. 0-97091

ferromagnetic properties of substances continued

- (Fe_{1-x}Ni_x)₈₀P₂₀, amorphous, ferromagnetic alloys, mag. anomalies of Invar type (*Russian*) 0-93089
 Fe₂₀Ni₈₀P₁₄B₆, amorphous ferromagnet, Mossbauer hyperfine fields, mag. struct. 0-75894
 Fe₄₀Ni₄₀P₁₄B₆, amorphous, mag. polarisation in approach to ferromag. saturation 0-80560
 Fe₄₀Ni₄₀P₁₄B₆, amorphous, mag. permeability aftereffect during annealing 0-88834
 Fe₄₀Ni₄₀P₁₄B₆, amorphous ferromag., spin wave excitations 0-97079
 Fe₄₀Ni₄₀P₁₄B₆, amorphous ribbon, mag. domains and anisotropy distrib. 0-108029
 (Fe,Ni)_{1-x}Si₈₀P₁₀B₁₀, amorphous, magnetisation reversal and domain boundary configs. 0-88809
 Fe₈₀Ni₂₀-P₁₄B₆ glass, resist., magnetoresist., and thermoelec. power 0-70681
 (Fe_{1-x}Ni_x)₇₇Si₁₀B₁₃, amorphous, Landau-Ginzburg theory, magnetisation and Curie temp. 0-75700
 (Fe_{0.2}Ni_{0.8})_{1-x}(SiO)_x, Permalloy material, magnetisation, temp. and impurity atom conc. depend., band model calcs. (*Russian*) 0-93088
 Fe₂P, spin wave excitations meas. 0-65831
 Fe₂P₁₃B₆, amorphous alloys, sput cooled, Mn, Cr and V substituted, mag. and transport props. 0-84593
 Fe₉₀P₁₀-C₂(Si)₂(Ge)₂, amorphous, size effect of metalloids on mag. props. 0-84594
 Fe₉₀Pd₁₀, order-disorder transition, Mossbauer study 0-71268
 Fe₃P Invar alloy, anomalous Curie const., susceptibility meas. 0-75731
 Fe₃P Invar alloy, thermal expansion and spontaneous magnetisation, Invar anomalies, low spin model 0-71001
 FeRh₂S₄, mag. semicond., mag. and elec. props. 0-93121
 FeSi, single crystals, domain struct., temp. and field depend. 0-71085
 FeSi_{1-x}, amorphous film, magneto-optic Kerr effect 0-66158
 Fe₈₀Si₁₅, amorphous, soft mag. props. and potential uses 0-88807
 Fe₈₀Sn₁₅, amorphous film, struct. and mag. props. 0-65972
 Fe₂Ta₂S₂, metallic, mag. susceptibility at low temp. 0-70972
 FeV (2 at.%), NMR spin echoes, domain wall effects 0-75883
 Fe₈₀P₂₀-C₂(Si)₂(Ge)₂, amorphous, size effect of metalloids on mag. props. 0-84594
 Ga_{1-x}Mn_xSb, elec. cond., mag. susceptibility, Hall const., and thermo-EMF, 80 to 1000K (*Russian*) 0-88549
 Gd, ferromag., transport props., crit. behaviour 0-65522
 Gd, ferromagnetic, crit. sp. ht. and thermal expansion 0-60343
 Gd, interstitial site determ., μ SR technique 0-71287
 Gd, meas. of easy direction of magnetisation with aid of phase theory 0-65963
 Gd-Al(Cu)(Ga)(Ni)(Pd)(Rh) alloys, amorphous, mag. and elec. props. 0-80499
 Gd-Co(Ni)(Cu)(Rh)(Ru)(Pd)(Ga), amorphous, mag. props. and ferromag. reson. 0-75862
 Gd-Ni, ferromag., elec. resist. temp. depend. 0-96843
 Gd-Ti(V)(Cr)(Mg)(Nb)(Ge)(Si)(Au) amorphous films, spontaneous Hall effect and elec. resist. 0-80251
 Gd-Y alloys, mag. crit. temp. gap 0-60260
 Gd_{1-x}Ca_xAl₂, mag. props. and phase relations 0-107991
 GdCo₂, dilute ferromagnets, press. effect on Curie temp. 0-65873
 GdCo₂Ni₅₋₅₀, intrinsic coercivity, anisotropy, exchange and cryst. field interactions 0-75806
 (Gd_{0.5}Fe_{0.5})₉₀B₁₀, amorphous, mag. props., Mossbauer study 0-93093
 GdMg, noncollinear mag. struct., nonlinear band behaviour 0-75706
 Gd₂(MoO₄)₃, domain wall motion dynamics 0-108030
 GdN, and GdN_{1-x}O_x, mag. interactions 0-60218
 GdN_{1-x}O_x, magnetic interaction and carrier conc. 0-71005
 Gd₂Nd_{1-x}Zn, ferromag., mag. susceptibility and magnetisation, temp. depend. 0-70975
 Gd(OH)₃, dynamical effects of interaction between 4f electrons and optical phonons 0-108196
 Gd_{1-x}S_x, ferromag., elec. props. near Curie temp. 0-107788
 GdTb, ferromag., magnetisation and microwave absorpt. 0-65816
 Gd₉₀Tb₁₀, magnetisation, AC susceptibility and microwave absorption meas. 0-60221
 (Gd_{1-x}Y_x)Al₂, ferromag. and spin glass like behaviour, magnetisation meas. 0-75734
 (Gd_{1-x}Y_x)₄Co₃, Curie temp. and resist.-temp. curves, comp. depend. 0-71020
 Gd_{1-x}Y_xZn, ferromag., mag. susceptibility and magnetisation, temp. depend. 0-70975
 GdZrFe₂, hyperfine field at Gd, TDPAC meas. 0-93214
 Gd_{3-x}□_xS₄, transport and mag. props., mag. Wigner localisation 0-97069
³He, HCP, and adsorbed ³He with triangular lattice, exchange and mag. order 0-107606
 HgCr₂Sd_{4-x}Te_x, ferromag. semicond., zero bandgap transition 0-96783
 HgCr₂Se₄, n-type ferromag. semicond., galvanomagnetic props. 0-70727
 HgCr₂Se₄, spontaneous magnetisation temp. depend., nuclear resonance freq. depend. (*French*) 0-80483
 HgCr₂Se₄, thermoreflectance, photoconductance, Raman scatt. near mag. phase transition 0-97298
 HoCo₂Si₂, mag. props. 0-107988
 HoCu₅, resist. and magnetoresist., mag. ordering obs. 0-70677
 HoFe₂ and Ho₂Fe₂₃, magnetostriction, room temp. to 80K 0-65993
 HoFe₂₃, magnetostriction, temp. depend., 20 to 350K 0-65994
 HoRh₂B₄, low temperature magnetic properties 0-88728
 HoTb_{1-x}Co₂, laval phase compounds, elastic props., temp. and magnetic field dependence 0-60393
 K₂CuF₄, layered spin system, planar rotator symmetry, phase transition 0-65951
 K₂CuF₄, magnon condensation obs. in quasi-2D planar ferromag. phase 0-60232
 K₂CuF₄, spin relax., crit. behaviour, high freq. susceptibility meas. 0-65936
 K₂CuZn_{1-x}F₄, Curie temp., Cu conc. depend. 0-60255
 La-Fe alloy, amorphous, sputtered at high rate, mag. props. 0-75753
 LaMnO₃, phase diagram, mag. moments, neutron diff. study 0-108414
 La_{1-x}Sr_xCoO₃, (0.5 ≤ x ≤ 0.9), ferromag., elec. props., itinerant electron model 0-107785
 LiHoF₄, uniaxial dipolar ferromag., critical behaviour, mag. susceptibility meas. 0-80528
 LiRf₂ (R = Tb, Ho, Er), cryst. field parameters, mag. susceptibility meas., 0.3 to 100K 0-60214
 LiTbF₄, uniaxial dipolar ferromag., critical behaviour, mag. susceptibility meas. 0-80528

ferromagnetic properties of substances continued

- LiTb_{0.5}Y_{0.5}F₄, uniaxial dipolar ferromag., critical behaviour, mag. susceptibility meas., effect of Y³⁺ dilution 0-80528
 LuFe₂, ferromag., magnetisation density, neutron diff. study 0-60217
 δ -Mn₂ paramag., antiferromag. and ferromag., magnetic moment calcs. 0-60223
 Mn-Al-C, ferromag. alloy, transform. kinetics 0-76229
 Mn-Al-C, fine-grained cast struct., remanence and coercive force 0-60365
 Mn-Al-C (70, 29.5 wt.%) alloy magnet, Almax, anisotropic, mag. props. (*Japanese*) 0-60371
 τ -MnAl, estimated theoretical limit of mag. moment 0-97072
 MnAlGe film, mag. domains and amorphous to cryst. phase transition, electron microscopy obs. 0-71129
 MnAs_{1-x}P_x, double exchange ferromag. coupling, magnetisation meas. 0-75751
 MnBi, domain boundary inertia during mag. reversals (*Russian*) 0-88776
 MnBi films, prep. by ionised-cluster beam deposition technique, magnetooptical props. 0-100790
 Mn_{1-x}Cr_xAs, double exchange ferromag. coupling, magnetisation meas. 0-75751
 Mn_{5-x}Fe_xSi₃, elec. resist. and mag. susceptibility, ferromag. to antiferromag. transition 0-80504
 MnGaGe film, mag. domains and amorphous to cryst. phase transition, electron microscopy obs. 0-71129
 MnP, Lifshitz point, transverse differential susceptibility meas. 0-84599
 Mo oxides, magnetic susceptibility meas., temp. effect 0-103822
 NdFe₂, high field Mossbauer study 0-75893
 Nd(OH)₃, dynamical effects of interaction between 4f electrons and optical phonons 0-108196
 Ni, 109° and 71° walls, stable orientations, theory and X-ray observations (*Japanese*) 0-60359
 Ni (100) films, spin density by self-consistent linear APW method 0-65710
 Ni (110), polarised LEED study of magnetism 0-71102
 Ni, anisotropic magnetisation meas., 4-250K 0-65862
 Ni, diffusion and orientation aftereffects 0-88830
 Ni, dynamic exponent, crossover obs., TDPAC meas. 0-108021
 Ni, electron tunnelling 0-60104
 Ni, electron-phonon coupling, point contact spectroscopy obs. (*Russian*) 0-70342
 Ni, energy band dispersion and mag. exchange splitting, angle-resolved photoemission meas. 0-71567
 Ni epitaxial films, even magneto-optical effects 0-76007
 Ni, exchange integral maximisation, neutron scatt. obs. and ten-fold degenerate Hubbard model comparison 0-71004
 Ni, exchange splitting of 3d bands, angle-resolved photoemission meas. 0-71568
 Ni, Fermi surface under press., de Haas-van Alphen effect meas. 0-75499
 Ni, ferromag. film, surface states, surface magnetisation and electron spin polarisation 0-65648
 Ni, ferromag. props., teaching expt. 0-82608
 Ni, ferromag. struct. in nucl. spin echoes 0-60453
 Ni, ferromagnetic, electronic struct. by real space approach 0-65432
 Ni, ferromagnetic, electronic struct. and hyperfine field of nonmag. impurities, calc. 0-70658
 Ni, ferromagnetic metals, ultrasound attenuation, EM generation 0-108046
 Ni film, evaporated, for use as variable delay SAW device, magnetostrictive effects 0-71144
 Ni films, electronic struct. calc., effects of chemisorption; contact pot. and surface magnetisation 0-103734
 Ni films, ferromagnetic reson., photoacoustic detection 0-80613
 Ni fundamental and secondary mag. props., book contrib. 0-75724
 Ni, internal friction, instantaneous, depend. on phase of torsional oscils. (*Russian*) 0-71142
 Ni, internal friction and rigidity modulus, strain amplitude depend. (*Japanese*) 0-92606
 Ni, interstitial site determ., μ SR technique 0-71287
 Ni, magnetic neutron scattering by dislocations, temp. depend. 0-103820
 Ni, magnetoelastic contribs. to US vel., elastic consts., and susceptibility 0-75829
 Ni, magnetostrictive vibr. obs. by laser interferometric technique 0-66000
 Ni, polarised, ferromag., evidence for K-shell polarisation of ¹³C ions via mol. orbital promotion 0-71273
 Ni, positive muon diffusion, press. depend. 0-75907
 Ni, stray mag. fields above stripe domains, electron microscope and μ^* -tensor determ. 0-71089
 Ni-B thin film glasses, mag. props. and corrosion resist. 0-80576
 Ni-Co, high-field susceptibility, spin-wave spectrum, CPA calc. 0-65818
 Ni-Co (25 wt.%), single crystals, mag. annealing effect on magnetostriction and magnetisation at high temps. 0-108047
 Ni-Cu, ferromag., mag. moment, local environment effects, HF CPA cluster calc. 0-65817
 Ni-Cu, high-field susceptibility, spin-wave spectrum, CPA calc. 0-65818
 Ni-Cu-H systems, Curie temp. during phase transitions under high press. H₂ 0-71029
 Ni-Cu(Zn)(Ga)(Ge)(As)(Se)(Br)(Kr), dil., ferromagnetic, hyperfine field and relax. time obs. of impurity heavy nuclei 0-75533
 Ni-Fe, dil., hyperfine mag. fields, press. effect, Mossbauer meas. 0-71277
 Ni-Fe, electronic struct. calc., effects of chemisorption; contact pot. and surface magnetisation 0-103734
 Ni-Fe, high-field susceptibility, spin-wave spectrum, CPA calc. 0-65818
 Ni-Fe, orientation aftereffect 0-88830
 Ni-Fe, power losses at extremely low freqs. 0-88815
 Ni-Fe, soft mag. props. rel. to metallurgical aspects 0-88810
 Ni-Fe, thermal fluctuation aftereffect meas. by pulse field method 0-88837
 Ni-Fe (19 wt.%) alloy, mag. anisotropy induced by cold rolling (*Russian*) 0-84595
 Ni-Fe (36 to 50 wt.%), initial permeability, domain struct. model 0-88811
 Ni-Fe based metallic glasses, Curie pt. anomalies 0-60256
 Ni-Fe film, thermally activated domain wall motion 0-88777
 Ni-Fe films, energy change of Bloch wall with angle to easy axis, calc. (*Slovak*) 0-103863
 Ni-Fe Invar, thermal expansion and spontaneous magnetisation, Invar anomalies, low spin model 0-71001
 Ni-Fe-Co-Ti, electron microscopy and mag. meas. 0-71097

ferromagnetic properties of substances continued

- Ni-Fe-Cr-Mo-Ti-Al, PE 16, thermally activated domain wall motion 0-88777
- Ni-Fe-Nb-Mo-Al, head material for mag. recording, DC and AC mag. props. 0-88812
- Ni-H, ferromag., H impurities and μ SR, self-consistent calc. 0-84447
- Ni-Mn, dil., mag. moment distrib. and environmental effects, neutron scatt. obs. 0-60247
- Ni-Mn, ordered and disordered, press. effect on Curie temp. 0-71148
- Ni-Mn (17-27 at. %), low-angle neutron diff., anomalous crit. scatt. (*Russian*) 0-60193
- Ni-Mn alloys, ferromagnetism-to-spin glass phase transition and strong mag. field effect 0-75773
- Ni-Mn-H solid solutions, mag. props. 0-88753
- Ni-Pd, high mag. field effects, mag. isotherms near Curie point, exchange splitting energies 0-60272
- Ni-Pd, mag. moment distrib., one-mag.-species model calc. 0-65788
- Ni-Pd-Mn ternary alloys, mag. characts., use for thermoseed 0-107995
- Ni-Pt alloys, magnetic-moment distrib. neutron study 0-97066
- Ni-Rh, mag. moment distrib., one-mag.-species model calc. 0-65788
- Ni-Ru (≤ 4 at. %), influence of alloying on mag. anisotropy 0-71010
- Ni-SiO multilayer films, interface magnetisation 0-88858
- Ni₃Al(Ga), off-stoichiometric alloy, inverse mag. susceptibility rel. to defect conc. 0-60216
- Ni_{100-x}B_x, amorphous, mag. struct., mag. susceptibility meas. 0-80485
- Ni(Fe,Cr) and Ni₂(Fe,Cr), electron states density model and mag. characts. calcs. (*Russian*) 0-92804
- NiFe thin films, magnetoresistance, quasi-static characts. 0-107766
- Ni₃Fe alloys, low-temperature specific heat, long and short range order effects 0-100339
- Ni₃Fe, compression induced magnetic anisotropy, annealing effect 0-93112
- Ni₃Fe, disaccommodation meas. after low temp. electron and neutron irradi. 0-88832
- Ni₃Fe, domain struct. after tensile deform., dislocation effects 0-71083
- Ni₃Fe single crystals, longitudinal magnetoresist. meas. 0-70675
- Ni₃₆Fe₂₃Cr₁₄P₁₂B₆ metallic glass, mech. props. and thermal stability 0-76362
- (Ni_{1-x}Fe_x)₈₀P₁₀B₁₀, amorphous, Curie temp., press. effect 0-75833
- Ni₉₂M₈, M=impurity metal, formation of MH(D)-complexes 0-65236
- NiMnGe_{1-x}Si_x, mag. props., neutron diff. and magnetometric meas., 80-600K 0-65793
- NiTi alloy single cryts., ferromag. reson., g-value and linewidth 0-71186
- Ni(001) surface states, surface magnetisation, electron spin polarisation 0-88612
- Ni(110), ferromag., surface magnetisation, polarised LEED expt. 0-97118
- Ni(110), mag. exchange splitting of electronic surface states 0-88610
- NpCu₂Si₂, mag. struct., neutron diff. determ. 0-93084
- Pd-Co, dil., breakdown of ferromag. order, magnetoresist. obs. 0-71046
- Pd-Co, normal Hall effect (*Russian*) 0-103676
- Pd-Fe, magnetic anisotropy near Curie point, quasi domain struct. (*Russian*) 0-65867
- Pd-Fe, normal Hall effect (*Russian*) 0-103676
- Pd-Fe-Mn, ferromagnet-spin glass, thermal expansion forced, magnetostriiction and magnetisation under high press. 0-65255
- Pd-Fe(Co)(Ni), dilute ferromagnets, press. effect on Curie temp. 0-65873
- Pd-Mn, ferromagnetism to spin glass behaviour transition 0-71062
- Pd-Ni, normal Hall effect (*Russian*) 0-103676
- Pd-Ni, thermal expansion and magnetostriiction meas. near crit. conc. for ferromagnetism 0-65881
- Pd_{0.98}Fe_{0.01}Gd_{0.01}, Pd-Gd exchange const., neutron diffuse scatt. meas. 0-71002
- (Pd_{0.9985}Fe_{0.0015})_{1-x}Mn_x, mag. behaviour at Fe sites, Mossbauer effect meas. 0-66085
- Pd_{1-x}MnSb Heusler alloys, magnetic hyperfine fields on ¹¹¹Cd, TDPAC and magnetisation meas. 0-93219
- Pd_{2-x}MnSb, struct., appl. as improved neutron polariser 0-60199
- Pd₂Mn₂V_{1-x}Sn, Heusler alloy, structural disorder, Mossbauer study 0-80650
- Pd₃₅Zr₆₅, mag. susceptibility meas. 0-75740
- PrAg₃, low temp. mag. meas. 0-107989
- Pr_{1-x}Ca_xAl₂, mag. props. and phase relations 0-107991
- PrFe₂, high field Mossbauer study 0-75893
- PrFe₂, Laves phase, mag. props., Mossbauer spectra, crystalline field mag. anisotropy 0-65851
- PrIr₂(Pt₂)(Rh₂)(Ru₂), hyperfine sp. ht. and magnetisation meas. at 4.2K 0-75775
- Pr₅Se₄(S₄), induced ferromagnet, mag. props. under hydrostatic press. 0-60395
- Pr₃Tl, thermal expansion and transverse elastic const. near mag. phase transition 0-60394
- Pt-Co system, low temp. susceptibility 0-65920
- Pt-Fe, dil., breakdown of ferromag. order, magnetoresist. obs. 0-71046
- Pt-Fe alloy, ordered, T-c phase diagram, antiferro- and ferromagnetism (*Russian*) 0-65871
- Pt-Fe ordered alloy, multiply mag. phase transitions 0-60264
- Pt-Fe(Co), dilute ferromagnets, press. effect on Curie temp. 0-65873
- PtCr, AC susceptibility near percolation limit, ordered and disordered alloy 0-65900
- Pt_{0.75}(Cr_{1-x}Mn_x)_{0.25}, pseudobinary, magnon energy derivation 0-107996
- Rb₃CrCl₄, 2D-ferromag., renormalisation of long wavelength spin waves, neutron scatt. 0-60229
- Rb₃CrCl₄, optical absorption intensity, short-range spin correlation 0-108185
- Rb₃CrCl₄, planar ferromag., spin waves 0-65835
- RbFeCl₃, one-dimens. ferromagnet, lowest excitation, far IR study 0-66186
- RbFeCl₃, pseudo-one-dimens. singlet ground state ferromag., mag. excitations, neutron scatt. study 0-97064
- Rh₂MnPb, hyperfine fields, ferromag., NMR and Mossbauer effect studies 0-71259
- Rh₂MnSb, hyperfine fields, ferromag., NMR and Mossbauer effect studies 0-71259
- Ru₂FeSn, ferromag. Heusler alloys, hyperfine fields at nonmagnetic atoms in various sites, Mossbauer effect and NMR meas. 0-66089
- Sc-Gd, dil., reverse resist. anomaly and negative magnetoresist. 0-84459
- Si_{1-x}Fe_{0.00-x} polycryst. ribbon, prep. by rapid quenching, and props. 0-75803

ferromagnetic properties of substances continued

- Sm-Co, amorphous, plasma-sprayed, role of Ar or H₂ atm. in mag. props. and crystn., rel. to H₂ storage 0-64898
- SmCo₅, amorphous, supermag.-ferromag. transition and directional crystallisation 0-65891
- SmCo₅, high coercivity isotropic plasma-sprayed magnet, eutectoid decomp. 0-80568
- SmCo₅, isotropic plasma-sprayed high coercivity magnet, eutectoid decomp. 0-75810
- SmCo₅, nucleation of reversed domains at Co₂Sm₂ precip. 0-75791
- SmCo₅, sintered, hard mag. material, magnetisation behaviour 0-75805
- SmCo₅, sintered, mag. after-effect, expt. and model 0-75816
- Sm₂Co₇, coercive force depend. on annealing temp. 0-65964
- Sm₂Co₇, sintered magnets, coercive force and constitution, annealing temp. depend. (*Russian*) 0-88786
- SmFe₃ and Sm₂Fe₂₃, magnetostriiction, room temp. to 80K 0-65993
- SmS, physical and physicochem. props., review 0-96875
- SmZn, ferromag., cond. band antiparallel polarisation exceeding 4f moment 0-60207
- Sn_{1-x}Mn_xTe, electronic struct., transport props., mag. ordering effects 0-65441
- SrCoO_{3-x} ($0 < \delta < 0.5$), ferromag., metallic elec. props. 0-70668
- SrCoO_{3-x}, mag. and neutron diff. study 0-65805
- Tb, ferromagnetic domain structures down to 95K 0-71080
- Tb, magnetisation, AC susceptibility and microwave absorption meas. 0-60221
- Tb, magnetisation in basal plane, calc. 0-70969
- Tb, neutron elastic scattering, high-angle, anal. 0-80480
- TbCo₅, sublattice magnetisation, temp. depend., neutron diff. anal. (*Russian*) 0-103815
- TbCo₅Si₂, mag. props. 0-107988
- Tb_{0.27}Dy_{0.73}Fe₂, vertically zoned, magnetomechanical coupling and magnetostriiction 0-65999
- Tb_{0.3}Dy_{0.7}Fe₂, prep. by powder metallurgy, magnetostriictive props. 0-75826
- TbFe₃ and TbFe₂₃, magnetostriiction, room temp. to 80K 0-65993
- TbFeO₃, mag. susceptibility, temp. depend., effective field at Tb ion sites 0-75742
- (Tb_{1-x}La_x)Be₁₃, mag. struct., cryst. field effects, neutron diff. study 0-65789
- Tb(OH)₃, dynamical effects of interaction between 4f electrons and optical phonons 0-108196
- TbPt₃, low temp. mag. susceptibility 0-93075
- TbZn, ferromag., thermoelec. power, temp. depend. and crit. behaviour 0-96852
- TbZn, mag. excitations meas. 0-70979
- TiBe_{2-x}Cu_x, high press. study of Curie temp. and mag. susceptibility 0-84600
- Ti(Fe, Co), off-stoichiometric alloy, inverse mag. susceptibility rel. to defect conc. 0-60216
- TiFe_{1-x}Co_x, electronic struct. and mag. moment calcs. 0-65821
- Tm ferrogarnet film, cylindrical mag. domain motions, domain boundary oscils. (*Russian*) 0-71140
- TmFe₃ and Tm₂Fe₂₃, magnetostriiction, room temp. to 80K 0-65993
- U₃As₄, ferromag., mag. field induced phase transitions 0-65887
- U₃As₄, heat capacity, 5-300K, ferromag. transition obs. 0-88769
- U(Co_{1-x}Fe_x)₂, ferromag. onset, susceptibility and resist. meas. 0-70967
- UF₆, giant magnetoelastic deform. of cryst. struct. mag. props. (*Russian*) 0-93159
- UF₆B₃(B₄), Mossbauer effect of ⁵⁷Fe nuclei, mag. props. 0-103907
- U₂P₄, press. effects on elec. resist. and Curie temp. 0-75559
- UTE, crit. exponents, neutron and magnetisation meas. 0-88823
- U₂Th_{1-x}Sb_x, valence change of U accompanied by singlet-ground-state ferromag. 0-70965
- V-Pt, sp. ht. and mag. meas. in ordered and disordered phases 0-70422
- Y-Gd, dil., reverse resist. anomaly and negative magnetoresist. 0-84459
- Y-Sm ferrogarnet (*Russian*) 0-71140
- YCo₃ amorphous films, ⁵⁹Co spin echo study 0-80636
- Y₆Fe₂₃, magnetostriiction, temp. depend., 20 to 350K 0-65994
- Y(Fe_{1-x}Co_x)₂, NMR study 0-75882
- Y(Fe_{1-x}Co_x)₂, x ≤ 0.2 , mag. props. and Mossbauer meas. 0-75798
- (Y₂GdYbBi₃)(FeAl)₂O₁₂ epitaxial garnet film, uniaxial ferromagnet domain struct., phase transition (*Russian*) 0-108044
- Y₆Mn₂₃, low temp. specific heat determ. 0-65896
- YNi₃, magnetism resurgence, neutron diff. and mag. props. study 0-65819
- Y(OH)₃, dynamical effects of interaction between 4f electrons and optical phonons 0-108196
- YbFe₂, cryst. elec. field and exchange interac., ¹⁷⁰Yb Mossbauer obs., magnetostriiction contrib. 0-108124
- YbFe₂, high field Mossbauer study 0-75893
- ZnCr₂Se₄, electroconductivity, thermoelectromotive force, Hall effect (*Russian*) 0-70694
- Zn_{1-x}Ge_xFe_{2-x-3x}Fe_{2x+2+4x}O₄, double exchange magnetism, Mossbauer study 0-66087
- Zr(Fe_{1-x}Al_x)₂, Curie temp., magnetisation, and cryst. struct., conc. depend. 0-75730
- Zr(Fe_{1-x}Co_x)₂, NMR study 0-75882
- Zr(Fe_{1-x}Co_x)₂, thermal expansion and forced volume magnetostriiction 0-75830
- ZrZn₂, high press. study of Curie temp. and mag. susceptibility 0-84600

ferromagnetic relaxation*see also ferromagnetic resonance*

- ferrofluid, relax. in external mag. field, cubic cryst. case 0-71113
- CdCr₂Se₄, Crit. relax. processes, mag. reson. expts. 0-60425
- CoCr₂Se₄, Crit. relax. processes, mag. reson. expts. 0-60425
- Fe₃₀B₇₀ amorphous ribbon, initial susceptibility time lag 0-100579
- Ni, cold-worked, rel. between dislocation and ferromag. damping 0-107369
- Zn₃Cu_{0.1}Fe_{2.9-x}O₄, ferromag. relax. 0-60422
- ferromagnetic resonance**
- see also ferromagnetic relaxation*
- alloy, HTR material, oxidation and carburization in He 0-108645
- alloys, ferromagnetic disordered, spin wave and ferromag. reson. linewidth 0-66045
- Brillouin-Mandelstam scattering from thermal and excited magnons 0-70980
- dimethylammonium copper tetrachloride, two-dimens. ferromag., saturation of parallel-pumped magnons 0-97147

ferromagnetic resonance continued

- ferrites, inhomogeneous exchange interaction influence on ferromagnetic resonance line moments 0-75864
 ferromagnetic conductor, plasma effects, selective transparency near antiresonance region 0-100476
 Heisenberg ferromagnet, two-magnon reson. in absence of bound states, calc. 0-60423
 linear electric field effects 0-65854
 magnetic surface states, theory, review 0-84654
 magnetodynamic resonance, microwave modulation of light appl. 0-71393
 magnon-photon interaction in ferromagnets, construct. and radiation effects 0-71188
 metallic ferromagnet, antiresonance region, EM wave propag., Maxwell's eqns. soln. 0-66038
 strip films, bulk and surface spin oscills., mag. reson. 0-97149
 thick ferromagnetic film, reson. transmission of EM energy via phonons 0-60382
 Ba ferrite, FMR in uniaxial crystal plate with bubble domain lattice 0-93182
 BaFe_{12-2x}M_xTi_xO₁₉ (M=Co, Ni, Zn), mag. props. determ. 0-75759
 Ba₃Zn₂Fe₂O₄₁, ferromag. reson., low power nonlinear effects 0-75861
 CdCr₂Se₄, Crit. relax. processes, mag. reson. expts. 0-60425
 CdCr₂Se₄Cu(Ag), ferromag. reson. and ESR line widths 0-60413
 Co₂(Ni_{0.5}Cu_{0.5})_{1-x}Fe_xO₄ ferrite, relation between elec. cond. and mag. anisotropy 0-75548
 Co₉₀P₁₀, noncrystalline ferromagnet, electroless deposited, struct. and microscopic mag. props. 0-88063
 Co₂Pd_{80-x}Si₂₀, amorphous, structural and mag. heterogeneities 0-80484
 CoS₂, itinerant ferromagnet, ferromag. reson. and EPR meas. 0-66044
 CsMnF₃, parametric excitation of magnons, effect of RF modulation of mag. field 0-65842
 CuCr₂Se₄, Crit. relax. processes, mag. reson. expts. 0-60425
 CuCr₂Se₄, mag. reson. and valence state of Cu and Cr ions 0-60413
 Fe film, nuclear spin system dynamics Mossbauer study in FMR conditions (Russian) 0-80651
 Fe films, ferromagnetic reson., photoacoustic detection 0-80613
 Fe thin films, surface demagnetisation due to chemisorption, ferromagnetic reson. study 0-80616
 Fe, whisker single crystals, ferromag. reson. and surface anisotropy 0-71187
 Fe-Al₂O₃ granular films, superparamagnetism and relax. effects 0-71118
 Fe₈₀B₂₀, amorphous, Brillouin scatt. from magnons, ferromag. reson. 0-65844
 (Fe_{1-x}Co_x)₇₈Si₈B₁₄, amorphous, saturation magnetostriction, strain modulated FMR obs. 0-75863
 (Fe_{1-x}Ni_x)₈₃B₁₇, amorphous alloys ferromagnetic resonance 0-108080
 Fe₂Pd_{80-x}Si₂₀, amorphous, structural and mag. heterogeneities 0-80484
 Gd-Co, amorphous films, mag. props. ferromag. reson. meas., 20-520°C (Russian) 0-97144
 Gd-Co(Ni)(Cu)(Rh)(Ru)(Pd)(Ga), amorphous, mag. props. and ferromag. reson. 0-75862
 (Gd_{1-x}Co_x)_{1-x}Ar_x, amorphous films, effective anisotropy field, ferromag. reson. obs. 0-71123
 Gd₇₁Tb₂₉, magnetisation, AC susceptibility and microwave absorption meas. 0-60221
 K₂CuF₄, two-dimens. ferromag., saturation of parallel-pumped magnons 0-97147
 MnCO₃, parametric excitation of magnons, effect of RF modulation of mag. field 0-65842
 MnSb, magnetic losses, ferromagnetic resonance and antiresonance 0-100618
 Ni films, ferromagnetic reson., photoacoustic detection 0-80613
 Ni, thin films, surface demagnetisation due to chemisorption, ferromagnetic reson. study 0-80616
 NiTi alloy single cryts., ferromag. reson., g-value and linewidth 0-71186
 RbFeCl₂2H₂O, spin cluster excitation expts. 0-66039
 Tb, magnetisation, AC susceptibility and microwave absorption meas. 0-60221
 Y₃Fe_{5-x}Co_{x/2}Si_{x/2}O₁₂, spin reorientation, NMR and ferromag. reson. meas. 0-65890
 YIG film, periodically corrugated, insertion loss, reson. linewidth effect 0-80614
 YIG, magnetic domain wall motion in high drive fields 0-65955
 YIG, open die hot pressing, spin wave and FMR line width 0-89170
 YIG:La,Ga, film, LPE-grown, Ga incorporation, depend. of magnetisation on growth rate 0-84627
 YIG:La(Ga) films, ferromagnetic resonance, ion implantation effect 0-97145
 YIG:Sm³⁺, mag. anisotropy, effect of Sm³⁺ ferromag. reson. study 0-80615
 Y_{2.85}La_{0.15}Fe_{3.75}Ga_{1.25}O₁₂ LPE films, ion implantation effect on spin waves 0-71124
 Zn₂Cu_{0.9}Fe_{2.9-x}O₄, ferromag. reson., g-factors, Jahn-Teller ion effects 0-66043
 Zn₂Fe_{3-x}O₄, ferromag. reson., g-factors, Jahn-Teller ion effects 0-66043

ferromagnetism

- see also ferromagnetic properties of substances; ferromagnetic relaxation; ferromagnetic resonance; Ising model; spin waves
 alloy, pseudobinary, magnon energy derivation 0-107996
 alloys, binary, ferromagnetism and spatial long-range order 0-60159
 alloys, disordered cryst. and amorphous, mag. dipolar field distrib., computer simulation 0-65790
 amorphous, Landau-Ginzburg theory, magnetisation and Curie temp. 0-75700
 amorphous, structural instabilities and mag. permeability relax., 77 to 400K 0-80559
 amorphous alloys, indirect exchange interaction and paramag. Curie temp. 0-75752
 amorphous ferromagnets, asperomagnets and spin-glasses, spin waves, theory 0-75747
 amorphous ferromagnets, hidden excitations, theory 0-75748
 amorphous Heisenberg and Ising chains, thermodynamics 0-108022
 amorphous magnet, random anisotropy axis model in the infinite-range limit 0-88761
 amorphous thin films, struct. and mag. props., review 0-93148
 anisotropic, uniaxial two-sublattice ferromagnet, thermodynamic and mag. props. 0-65866
 anisotropic ferromagnet, one-dimensional Landau-Lifshits eqn. multi-soliton solutions (Russian) 0-71014
 anisotropic ferromagnet with external field, crit. pts. derivation 0-103837

ferromagnetism continued

- anisotropic ferromagnets, influence of spatially varying field on phase transitions 0-60339
 anisotropic Heisenberg chain, nonlinear excitations 0-70927
 anisotropic magnet in external mag. field, continuous phase transition existence 0-108011
 asperomagnetism, short-range order, in Heisenberg magnet 0-65941
 biaxial Lifshitz point problem in 3-dimens., spin wave theory 0-88759
 conducting cryst., dynamics of s-d model in alternating mag. field (Russian) 0-65825
 conduction electron spin, EM wave propagation with discrete spectrum 0-92923
 conductor, plasma effects, selective transparency near antiresonance region 0-100476
 cubic crystal, texture analysis, generalisation of dispersion theory 0-80556
 cubic lattices, fully frustrated, phase transitions, Gaussian and spherical model, free energy calcs. 0-60281
 Curie temperature, effects of biquadratic exchange and uniaxial anisotropy 0-60329
 cyclically remagnetised ferromagnets, discrete spectra of induction calcs., demagnetising factor 0-103859
 disaccommodation in ferromagnets, electronic device for automatic measurement (Japanese) 0-68227
 disordered, phase transitions, mol. field and Landau-Ginzburg theories 0-93118
 disordered binary alloys of ferromag. crystals, mag. dipole fields at interstitial sites 0-97176
 domain boundary parade motion, low freq. (Russian) 0-103852
 domain struct. near first-order phase transition resembling second-order transition 0-93139
 domain structure obs. using dry colloid observation apparatus, 90K to 290K 0-73394
 domain theory, quasi-dislocation theory appl. (Japanese) 0-60358
 domain wall mobility, damping, dipole-dipole interaction 0-93140
 easy plane amorphous wire, magnetisation, variational calc. 0-71098
 easy-plane anisotropy, HF magnon energies, kinematic consistency 0-93097
 easy-plane ferromagnet, magnetic anisotropy, temp. and field depend., classical model 0-71008
 eddy current phenomena in ferromagnetic plates, numerical computation (German) 0-65952
 elastic hard ferromagnets, relaxation effects, vectorial internal variables, rational thermodynamics 0-75828
 elastic solid, ferromagnetic, two coplanar Griffith cracks, singular stresses 0-65985
 electron capture spectroscopy, technique for surface science and ferromagnetism 0-92766
 exciton condensation effects on props., Hubbard model of ferromag. metal 0-60171
 excitonic, zero-sound excitations, Fermi liq. model 0-93101
 extended Hubbard model, ferromag. solns. 0-80473
 ferroic crystals, prototype point group, physical props., model 0-80715
 ferromagnet, nuclear magnetisation motion, hyperfine field microscopic inhomogeneity, NMR freq. shift (Russian) 0-80623
 ferromagnet magnetisation, influence of high intensity longitudinal sound waves 0-103875
 ferromagnetic semiconductor, spectral density approach for s-f model quasiparticle concept 0-80173
 ferromagnetic superconductor, paramagnetic fluctuations, influence on superconductivity 0-70900
 ferromagnetic superconductors, self-induced vortices, magnetisation, Gibbs free energy 0-70916
 ferromagnets and spin glasses, supercond. and mag. order 0-93029
 field theory, critical exponents, Borel transform. 0-80541
 film, dynamics near transition pt. from homogeneous to inhomogeneous magnetis. state 0-108038
 film, heterogeneity influence on static and dynamic props. of domain walls (Russian) 0-65974
 films, perpendicularly magnetised, surface and vol. magnetoelastic waves (Russian) 0-93151
 FK G inequalities and fluctuations, probabilistic approach 0-77712
 geomagnetic field sensitivity in animals, ferromag. coupling to muscle receptors as basis 0-72185
 harmonic rotor model, interactions, spirals and phase transitions with and without long range order 0-60350
 Heisenberg, ferromagnet, classical, with dipole-dipole interaction, renormalisation group and crit. exponents 0-60351
 Heisenberg amorphous ferromagnet, magnetisation and Curie temp., CPA calc. 0-75703
 Heisenberg chain, classical, nearest-neighbour, low temp. dynamics 0-80524
 Heisenberg chain, weakly bound magnon states (Russian) 0-100591
 Heisenberg ferromagnet, anisotropic, collective Green's function, dynamical RPA 0-70925
 Heisenberg ferromagnet, classical one-dimensional, transfer integral and collective coordinate results for free energy 0-93067
 Heisenberg ferromagnet, correlation functions in ferromagnetic and paramagnetic regions, RPA 0-71075
 Heisenberg ferromagnet, critical dynamics of impurity spin below T_c 0-71076
 Heisenberg ferromagnet, cubic, with next nearest neighbour interactions, two-magnon bound states 0-70977
 Heisenberg ferromagnet, disordered two-dimens., CPA theory of bond model 0-60163
 Heisenberg ferromagnet, linear, with applied mag. field, second-magnon like excitations 0-65837
 Heisenberg ferromagnet, magnon renormalisation 0-65849
 Heisenberg ferromagnet, spin-wave renormalisation, S_z≥1 0-71070
 Heisenberg ferromagnet, transition temp., mean field upper bound 0-97048
 Heisenberg ferromagnet, two-dimensional, soln. 0-60166
 Heisenberg ferromagnet, two-magnon reson. in absence of bound states, calc. 0-60423
 Heisenberg ferromagnetic system with biquadratic exchange interactions, spin wave theory (Chinese) 0-88755
 Heisenberg model, critical dynamics spin wave theory, dynamic scaling hypothesis failure 0-97082
 Heisenberg model, disordered ferromag. states, random exchange integrals 0-80550

ferromagnetism continued

Heisenberg model, nearest-neighbour spin-spin correl. functions calc. 0-80537
 Heisenberg model, point singularities in micromagnetic systems with radial symmetry 0-107976
 Heisenberg ferromagnet, surface magnetisation profile and localised magnons 0-70985
 higher harmonic method, ferromag. object inspection, difference schemes 0-89444
 ideal Heisenberg ferromagnet, phonon renormalisation and spin waves 0-88754
 impurity relaxation in nonresonance field, phonon amplification (*Russian*) 0-100310
 inhomogeneous ferromagnets, phase transitions, micromagnetic theory 0-65942
 intrinsic semiconductors, indirect exchange interaction, finite temp., valence bands and energy gaps effect 0-59943
 irreversible and reversible magnetising processes, impressed propag. 0-88819
 Ising, kinetic chain relaxation, randomly signed exchange 0-70919
 Ising ferromagnet, comparison with plane rotor 0-60348
 Ising ferromagnet, diamond lattice, phase transition, crit. props. 0-93127
 Ising ferromagnet, gaussian fluctuations of mol. field, magnetisation and free energy 0-70918
 Ising ferromagnet, linearisation assumption, crit. correlation function 0-60158
 Ising ferromagnet, phase coexistence, translation invariance and stability 0-80513
 Ising ferromagnet and antiferromagnet, two-dimens. square, ground state, apparent 3-spin interactions 0-88709
 Ising ferromagnetic half-plane, surface, pinned domain wall, free energy and magnetisation profile 0-60361
 Ising model, bond random, ferromagnetic-antiferromag. mixture, triangular cactus tree, statistical theory 0-75702
 Ising model, bond-dil. two-dimens., phase transition 0-60320
 Ising model, constant-coupling approx., successive phase transitions 0-97108
 Ising model, ferromagnetic, band-mixed square lattice, approx. crit. surface 0-70921
 Ising model, one-dimens., with phase transition, thermodynamic props. calc. 0-80536
 Ising model, randomly dilute, conc. expansion study 0-60315
 Ising model, spin-one three dimensional, single-ion anisotropy, crit. behaviour 0-80540
 Ising model, two-dimens., ferromagnet-spin glass transition, Monte Carlo calc. 0-60287
 Ising model, two-dimens., order parameter and induced susceptibility 0-71036
 Ising model, with transverse field, ferromagnetic and antiferromagnetic susceptibilities 0-60160
 Ising model with competing interactions, critical properties and exact results 0-93129
 Ising spin glass, d-dimensional, frustration effect 0-108019
 Ising spin glass, d-dimensional, frustration effect and dilution problems 0-108018
 Ising spin glasses, in effective interaction approx. 0-60288
 itinerant electron ferromagnet, magnetoelastic contribs. to US vel., elastic consts., and susceptibility 0-75829
 itinerant electron ferromagnet, magnetoresist. and anomalous Hall effect due to electron-phonon interactions 0-70680
 itinerant electron ferromagnet, magnon spectrum just below T_c , theory 0-65833
 itinerant electron ferromagnet, temp. depend. of angle-resolved photoemission 0-76142
 itinerant electron ferromagnets, elastic props. and electronic struct. 0-66001
 itinerant electron ferromagnets, magneto-volume effects 0-60397
 itinerant electron model, contrib. of Conyers Herring in 1930s 0-57056
 itinerant electron model, susceptibility, local exchange approx. calc. 0-60169
 itinerant ferromagnet, mag. props., temp. depend., functional integral approach 0-60170
 itinerant ferromagnet, spin waves, surface effects, RPA calc. 0-60226
 itinerant ferromagnets, magnetoelastic props., thermodynamic aspects 0-66002
 Landau-Lifschitz equation, nonlinear, exact integration 0-80495
 light scattering from bulk and surface spin waves in ferromag. slab, theory 0-71389
 linear mag. birefr. (*Russian*) 0-93284
 magnetic aftereffects, review 0-88830
 magnetic order coexistence with charge density waves 0-97096
 magnetic susceptibility, spin and charge density waves, Curie temp. (*Russian*) 0-100581
 magnetically ordered cryst., indirect nuclear spin interactions 0-103847
 magnetically ordered substances, book 0-73112
 magnetisation stimulation by nonresonance AC mag. field (*Russian*) 0-65962
 magneto-volume effect and Invar phenomena ferromagnetic metals, magneto-volume effect, Invar phenomena 0-66007
 magnetomechanical effects, magnetostriction, hysteresis, stress, yielding, fatigue damage, crack growth (*Polish*) 0-71150
 magnon-phonon interactions, Heisenberg exchange red. 0-80494
 metal, magnetoelastic coupling effect on magnetoelc. reson. 0-75837
 metal, uniaxial ferromag. anisotropic spin fluctuations and anisotropic band struct. effects on resist. near T_c 0-65543
 metallic ferromagnet, antiresonance region, EM wave propag., Maxwells' eqns. soln. 0-66038
 metals, electronic struct. and magnetism, review 0-70573
 metals, polar states and free electron gas, mag. moments (*Russian*) 0-84415
 metals, resist. anisotropy, crit. behaviour and temp. depend. 0-96858
 metals, spin fluctuation theory, Curie temp., mag. susceptibility 0-65937
 microwave modulation of light using magnetodynamic reson. 0-71393
 mixed valence compounds, dynamic susceptibility, RPA study of Anderson lattice 0-97075
 Mossbauer lineshape in ferromagnet 0-71251
 Mott insulators, excitonic spin polarons, appl. of Nagaoka's theorem for electron-Hole pair 0-107978
 neutron beam channelling and focusing in ferromagnets (*Russian*) 0-107351

ferromagnetism continued

nonequilibrium superconductors, ferromag. ordering of quasi-particles and rise of domains 0-107958
 nuclear spin waves, surface and bulk, Green function formalism 0-70984
 one dimensional ferromagnets, effect of biquadratic exchange on solitary waves 0-65836
 one dimensional randomly dilute Ising ferromagnet, dynamics 0-70922
 one-dimensional, localised nuclear magnon modes 0-93098
 one-dimensional ferromagnet, algebraic soliton in mag. field directed along anisotropy axis 0-75785
 one-dimensional Heisenberg magnet, in mag. field, dynamic correlations 0-70926
 ordered regions near macroscopic defects and percolation phase transform. in crystals (*Russian*) 0-92665
 particle suspensions in non-conducting and metallic liqs., review 0-60372
 photoelectric effect rel. to saturation magnetisation 0-65618
 pinned domain wall motion, magnetic damping studies 0-65956
 planar cyclic remagnetisation, of isotropic ferromagnet with two mutually orthogonal sinusoidal mag. intensities (*Russian*) 0-80561
 planar Ising ferromagnet solvable model with roughening transitions 0-71069
 polaritons, asymmetrical guided mag., in ferromag. slab 0-88738
 polycrystalline ferromagnetic material, magnetic texture anal. 0-108002
 Potts lattice gas, crit. and tricrit. exponents using Kadanoff transform. 0-101768
 quantum critical dynamics with mode coupling 0-108023
 quantum Heisenberg ferromagnets and stochastic exclusion processes 0-88712
 random anisotropy model in Ising model, Monte Carlo simulation 0-80546
 random ferromagnets, Ginzburg criterion, critical fluctuations 0-71032
 random quenched ferromagnet, crit. behaviour, effective exponents, renormalisation 0-60326
 randomly disordered alloys, ferromagnetism onset, mag. inhomogeneity 0-75774
 reverse magnetostrictive effect in stressed ferromagnetic bar (*Rumanian*) 0-84630
 s-d model, electronic spectrum struct., moments method 0-97052
 semiconductor, energy and mobility of spin polarons 0-70982
 semiconductor, ferromag., doped, electron spin polarisation and conduction band struct. 0-65449
 semiconductor, ferromag., localised magnon mode relax. theory 0-70986
 semiconductor, ferromag., polaron solitary waves 0-70625
 semiconductor, ferromag., short wavelength magnon generation 0-70987
 semiconductor, ferromag., spin polaron props., effect on carrier scatt. 0-60233
 semiconductor, ferromag., surface localised low energy electron-magnon states (*Russian*) 0-88734
 semiconductor, ferromag. two-band s-d model hybridization 0-65446
 semiconductor, mag. polaron stability 0-96803
 semiconductor-ferromagnet contact, spin-depend. recomb. and scatt. on electron injection 0-65654
 semiconductors, electronic quasiparticle spectrum 0-97051
 semiconductors, ferromagnetic with hot electrons, instability of coupled spin-helical waves 0-107841
 semiconductors, free carrier absorpt. of radiation 0-97227
 semiconductors, s-f interaction on conduction band, red shift effect theory 0-59872
 simple ferromagnets, crit. behaviour 0-60331
 singlet-triplet ferromagnet, Dyson eqn. derivation 0-107974
 singlet-triplet ferromagnetic systems, excitation spectrum, double-time Green's functions 0-84603
 slab, finite thickness, spin correl. functions 0-80522
 solid state physics, 1933-40, contrib. of Sir Nevill Mott 0-57055
 spin glass-ferromagnetic phase, mean field theory 0-103841
 spin glasses, dilute, at zero temperature, low concentration series expansion 0-93131
 spin glasses, dilute ferromagnets, ferromagnetic modes 0-93133
 spin subsystem thermodynamics, spin-phonon interactions, mag. order parameter 0-103848
 spin wave excitation due to parallel pumping, mag. impurity interactions (*Russian*) 0-80497
 spin-1/2 cubic lattice, with anisotropic exchange, configs. 0-65926
 spinel structure ferromagnets, prediction of existence using cybernetic computer learning methods 0-108048
 subdominant critical indices for the ferromagnetic susceptibility of the spin-1/2 Ising model 0-100574
 superconductivity-ferromagnetism coexistence in two-band model (*Russian*) 0-84539
 superconductor with magnetic impurities, coexistence of superconductivity and ferromag., BCS and Zener models 0-88676
 surface spin fluctuations and light scatt. 0-84727
 surface spin waves, Brillouin light scatt. 0-93359
 susceptibilities of $S=1/2$ XY model on the square lattice at $T=0$ 0-88732
 systems far from thermodynamic equilb., dissipative structures, broken symm. equilb. phase transition theory 0-65827
 thick film, reson. transmission of EM energy via phonons 0-60382
 thin film alloys, surface magnetism props., Curie temp., Ising model 0-108039
 thin films, parametric oscill. with biaxial anisotropy 0-103861
 tight-binding model ferromagnet, surface magnetisation 0-103807
 transition metal, band theory of linear magnetostriction 0-71141
 uniaxial anisotropy, first order magnetisation processes theory 0-60242
 uniaxial ferromagnetic with intrinsic mag. field, domain struct. 0-93141
 uniaxial ferromagnet, domain struct. in mag. field 0-103853
 vacancy distribution along mag. sublatitics in β -brass type ferro and antiferromagnetic alloys (*Russian*) 0-79783
 X-Y model, biquadratic, spin one, variation of Curie temp. 0-97102
 X-Y model, $S=1/2$, on triangular lattice, ground state props. 0-60165
 Y garnet, inhomogeneous collective magnon oscill. excited by RF field (*Russian*) 0-100582

ferromagnets see *ferromagnetic properties of substances; ferromagnetism*

ferrous alloys see *iron alloys*

Feshbach resonances see *atomic resonant states; molecular resonant states*

f.e.t. see *field effect transistors*

few-nucleon reactions see *nuclear reactions involving few nucleon systems*

few-nucleon scattering see *nuclear scattering involving few nucleon systems*

few-nucleon systems see *nuclei with mass number 1 to 5*

Feynman diagrams

$(\phi^3)_6$ field theory, deep inelastic lepton-headron scatt., cut vertex theory and reciprocity relation 0-57466
 ϕ^4 theory, Euclidean, local existence of Borel transform of Schwinger functions 0-77932
 amplitude circuit breakers 0-86558
 atomic interactions, retarded energy shift and pair polarisability, field theoretical perturbation theory 0-102560
 chiral field, supersymmetric, $1/N$ perturbation theory and quantum conservation laws 0-68373
 Coulomb gas 2-D, interaction potential, screening length, critical temp. 0-62571
 Euclidean quantisation of gauge theories, Weinger integral and nonstandard analysis 0-68358
 Euclidean quantum field theory, n-point functions, renormalised G-convolution 0-68341
 Feynman path integral and gauge invariance 0-82601
 group weight and vanishing graphs 0-57482
 Klein-Gordon particles, charged, quantum kinetic theory, Feynman rules and thermal eqn. 0-57177
 light-cone gauge, QCD calcs., non-singlet quark struct. function 0-57464
 multi-loop dimensionally regularised Feynman diagram evaluation 0-86586
 multiperipheral parton model, deep inelastic processes 0-82961
 n-point functions, renormalised G-convolution, convergence in Euclidean case 0-77930
 one-loop diagrams, reduction, scalar field theory (*Russian*) 0-62864
 operator ordering, interaction Hamiltonian noncommuting operators, S-matrix expansion, Feynman rules 0-57472
 planar diagrams, $SU(N)$ asymmetric model, semiclassical approach 0-77957
 regularization method 0-62844
 renormalised Feynman amplitude, high energy behaviour 0-86555
 scattering amplitudes, sixth-order, Yang-Mills fields, finite-diagram theory 0-73585
 $SU(N)$ symmetric quantum dynamical systems, $N \rightarrow \infty$, energy spectrum for singlet and adjoint states 0-62880
 subtracted Feynman amplitudes, low energy asymptotic anal. 0-99040
 zero-mass behaviour of Feynman amplitudes 0-68353
 π EM form factor factorisation and asymptotic behaviour in QCD 0-91090

fibre optics

acoustic noise level meas. using optical fibre interferometric hydrophone 0-87673
 acoustic sensing with single coiled monomode fibre 0-102826
 acoustic sensor, fibre-optic, modulation processes 0-58771
 acoustical detector probe 0-91916
 asymmetric fiber power splitter 0-83661
 birefringent fibre interferometric secondary light source 0-105702
 bistable optical devices: an overview 0-58625
 brain reflectance, mapping technique using optical fibres 0-72381
 Brillouin ring laser, fibre-optic, use for inertial sensing 0-87411
 bundles and single fibres, appls. (*Japanese*) 0-78998
 coherent fibre optics testing techniques 0-78992
 concentrated solar energy transmission, high-power lightpipe development 0-87481
 diode laser wavelength monitoring using fibre interferometer 0-74413
 electric field intensity meas., electro-optical sensor with fibre transmission line 0-69509
 endoscopic miniature camera with fibre-optic faceplate 0-77896
 Faraday effect in lightguide, weak microwave field meas. 0-73463
 Faraday rotators in fibre Raman lasers 0-58775
 fibrescopes using leached fibre image bundles, manufacture 0-83670
 Fourier hologram recording using Selfoc-type optical fibres 0-95850
 glass tubing dia. and wall thickness meas., P-329M instrum. 0-86262
 graded-index, multimode, differential mode delay and attenuation meas., optimal excitation calc. 0-99842
 holographic interferometry with optical fibres, hearing mechanism obs. 0-76879
 hydrophone, fibre-optic, description and advantages 0-58770
 hydrophone, optical interferometric, with homodyne detection, signal stabilization by light source tuning 0-87477
 hydrophones, comments on mechanism of transduction 0-58882
 illuminating fibre bundles, improved characts. due to glasses type VS 1637 and VO 720 0-102844
 industrial IR thermometer using fibre-optic lightguides 0-86302
 interferometer, single mode optical fibre, small phase shift meas. 0-57366
 interferometer gyro, thermally induced nonreciprocity 0-58665
 interferometers for length, temp., pressure and force meas. 0-98971
 interferometric sensor for acoustic detect., thermally induced optical phase effects 0-74479
 interferometry through single-mode fibres 0-73442
 introduction to theory and applications, book 0-90617
 laser Doppler velocimeter, follow-up-type, using single-mode optical fibres 0-74476
 laser fusion reactor, NOVA, pulsed power control system, fibre-optic multi-tapped computer bus 0-95443
 laser plate for digital image processing, all-optical parallel logic operation 0-106463
 laser radiation damage of fibre optic elements 0-102747
 lens, gradient-index rod, aberrations in multimode optical fibre devices 0-69487
 low-loss optical fibre evolution 0-69532
 magnetic field sensors 0-69510
 market trends, worldwide 0-58699
 modulated fibre ring interferometer, laser appl. 0-74506
 monomode fibre selective excitation for differential group delay meas. 0-99876
 multimode fibre coupler-type acoustic sensor, optical intensity modulation 0-102945
 multimode fibre optic interferometry, applications 0-86387
 nonlinear effects, appl. to active and passive device fabrication 0-58638
 optical path meas. using fibre optics, theoretical investigations of path transducers (*German*) 0-106608
 optomechanical pressure transducers, designing and testing 0-105662
 parametric oscillator, sequence freq. generation 0-83636
 passive optical rotation sensors using guided waves, developments 0-58781

fibre optics continued

pH sensor, miniature, for physiological use 0-109074
 photoelectric detection improvements 0-91919
 polariser, in-line, formation and props. 0-106603
 probe, angular position transducer, IR source 0-86257
 Raman lasers, fibre 0-102767
 remote inelastic light scatt. probe, use of optical fibres 0-58769
 research and development, advances, conf., Kingston, RI, USA (June 1978) 0-57005
 rotation sensor, all-waveguide configuration, key element tests 0-58796
 rotation sensor with low drift 0-69530
 Schlieren multimode fibre-optic hydrophone 0-102938
 sensors appl. (*Japanese*) 0-78997
 sensors for measurement and control appls. 0-58780
 signal processing devices 0-58768
 single mode CVD fibre, bend-induced birefringence obs. 0-58723
 single mode fibre analysis and fabrication for low polarisation birefringence 0-58722
 single mode fibre for current meas. system, birefr. induced by bends and twists 0-99832
 single mode fibre polarisation stabilisation 0-58724
 single-mode fibres, fractional wave devices and polarisation controllers 0-106606
 state-of-the-art and available equipment (*German*) 0-87484
 switch, crossbar 0-74497
 systems and field trials, review 0-58700
 temperature meas. appl. using phosphors as sensors 0-73360
 tension-coiled single-mode fibres, high birefr. 0-99858
 training, educational course status and effectiveness 0-62413
 US pressure sensor 0-58878
 viewing instrument appls., flexible fibre light-guides 0-87545
 wavelength division multiplexer using optical fibre pieces 0-91917
 welded optical fibre signal splitter 0-102814
 white light, information processing and transmission 0-95833
 GaAs lasers, current research 0-83613
 GaAs lasers, optical fibre coupled arrays 0-69393

fibre reinforced composites

see also *carbon fibre reinforced composites; glass fibre reinforced plastics*
 ? 0-100817
 aircraft materials, design allowables 0-81204
 angle ply, delamination mechanics and failure mode 0-79236
 asbestos fibre reinforced cement, strength and fracture props. 0-108533
 bagasse fibre reinforced phenol formaldehyde, tensile strength and Young's modulus, SEM study 0-60952
 bent thin-wall constructions, rupture 0-64472
 brittle fibre reinforced composite, static strength depend. on component separation boundaries (*Russian*) 0-76304
 brittle fracture, crack interactions 0-65149
 characterisation by differential scanning calorimetry 0-71869
 composite beams, effects of fibre orientations on free vibrations 0-87734
 cord-rubber laminates, two-ply balanced, interlaminar-shear strain study 0-97526
 cracks, emanating from circular hole in unidirectional specimen, anal. 0-100301
 cross-reinforced layered, moment effects in plane problem 0-64393
 deformability characteristics, reinforcement scheme effect 0-58930
 elastic shear waves propagation 0-58963
 elastic slab subjected to axial loads, instability and buckling 0-64420
 epoxy laminates, interlaminar failure 0-81207
 epoxy resin composites, cooldown residual thermal stresses, viscoelastic response 0-60941
 fatigue behaviour under random loadings, mathematical model and digital simulation (*Japanese*) 0-85032
 fibre composite structure, thermal field techniques for NDT 0-66737
 fibre glass laminate in tension, creep 0-71718
 fracture, mixed mode, in unidirectional samples 0-100302
 fracture, theory 0-89351
 fracture processes modelling, digital computer appl. 0-65147
 glass fibre reinforced cement, durability in wet and dry conditions, fibre length and content effect 0-71726
 glass-fibre reinforced cement, strength study by reliability concept, fibre concept and temp. depend. (*Japanese*) 0-66586
 graphite fibre epoxy composites, eutectic coating moisture barriers 0-81228
 graphite fibre epoxy laminates, low thermal expansivity, design considerations 0-81031
 graphite fibre filled phthalocyanine composites, cure cycle investigation 0-81030
 graphite fibre filled polyimide composite laminates, space environment, phys. and mech. response 0-81140
 graphite fibre filled polyimide composite prepreg laminates, room-temp. ageing effect 0-81093
 graphite fibre reinforced composites, damage by moisture, diffusion anal. 0-81227
 graphite fibre reinforced glass, impact damage tolerance and reliability 0-81177
 interfacial interactions and bonding, fibre surface props. 0-80046
 Kapron fibre reinforced phenolic resin, fracture kinetics, interface props. 0-66640
 kevlar-epoxy composites pressure vessels, holographic nondestructive eval. 0-81275
 laminated hybrid, tensile first cracking strain and strength 0-81175
 linen-cloth-reinforced phenolic resin, epoxy resin laminate, sliding behavior against Cu or Al spheres at cryogenic 0-66671
 metallic, electrical conductivity, fibre effects 0-100450
 micro- and macrocracks 0-65148
 organic textolite, long-term strength in plane stressed state 0-60930
 organoplastics, fracture characts., effect on strength 0-66642
 plastic matrix, props., implications for structural design 0-81174
 plastic matrix, stress distributions along short fibre 0-60913
 plates, anisotropic skew, large amplitude vibrs., transverse shear and rot. inertia, numerical results 0-79208
 plates, symmetrically laminated cross-ply rectangular, initial flexural failure anal. 0-64461
 polymer matrix, soaking, wetting and compounding of materials during production (*German*) 0-93535
 polymer matrix, space environmental effects 0-71721
 polymer multilayer composites, wire-reinforced, dynamically loaded, crack propagation and arrest 0-97567

fibre reinforced composites continued

- polypropylene fibre reinforced polyoxyethylene, fracture kinetics, interface props. 0-66640
 polypropylene fibrillated film reinforced cement matrix for low cost sheeting 0-80996
 propagation of plane harmonic waves, infinite isotropic medium having embedded doubly periodic array of cylindrical fibres 0-87607
 quasi-one-dimensional heat conduction, nonlinear mixture theory 0-64335
 quasi-static crack propagation in single cells of fibre reinforced materials under tension (*German*) 0-106759
 reinforcement scheme optimisation with respect to deformability at assigned stresses 0-69689
 rods, rectangular, elastic wave propagation (*French*) 0-83749
 sapphire fibre reinforced Mo, strength at rupture 0-104286
 short fibre distribution 0-71882
 single fibre-brittle zone model, fracture behaviour 0-97570
 single ply, thickness effect of percolation and conductivity 0-92953
 slender fibre-reinforced materials, non-dilute, thermal and mechanical props. 0-103524
 slender nearly-perfect conductors, dilute, bulk thermal properties 0-103525
 steel fibre reinforced Al, thermophys. props. 0-59745
 steel fibre reinforced concrete, vibr. compaction, pressure compaction and curing (*Japanese*) 0-89179
 stress redistribution dynamics during fibre rupture 0-64394
 structure optimisation in stability problems 0-58947
 tensile strength, struct. parameters depend. 0-65134
 tension stability, deformation up to failure (*Russian*) 0-75289
 thermal conductivity bound calculations, for short-fibre unidirectional composites 0-92727
 thermal NDT using liquid crystals, fibreglass laminates 0-93709
 three-dimensionally reinforced with short fibres, effective elastic consts. 0-58910
 unidirectional fibre composites, anisotropic constituents, effect elastic moduli and other props. 0-58911
 waveguides, axisymm. elastic vibrs. 0-102995
 wire reinforced Al, stress-deformed state, elastic, strength props. (*Russian*) 0-76303
 wood fibre reinforced Portland cement composite, strength 0-100822
 Al-B fibre-D16 alloy welded composites, structure, strength and fracture props. (*Russian*) 0-108524
 AlN filamentary crystal reinforced mullite-corundum ceramics, filaments strength, eval. 0-104230
 α -Al₂O₃ fibre FP reinforced Al and Mg composites, fabrication and props. 0-81004
 α -Al₂O₃ filamentary crystal reinforced mullite-corundum ceramics, filaments strength, eval. 0-104230
 B fibre reinforced Al, impact damage tolerance and reliability 0-81177
 B fibre reinforced Al, thermophys. props. 0-59745
 B fibre reinforced epoxy composites, notched, tensile strength and failure modes 0-81205
 B₄C-phenolic fibre reinforced composite for nuclear shielding appls. 0-102353
 Cr₂C₂ fibre reinforced Ni-based composite, oxidation and creep, Y additions effect 0-66685
 Mo fibre reinforced Cu, rule of mixtures of deform. parameters in stage III 0-97532
 Mo fibre reinforced Cu with weak interfaces, stability of tensile deform. 0-97533
 Nb fibre glass composites, new technique for producing fine metal fibres 0-108384
 NbC fibre reinforced Ni-Cr, eutectic, unidirectional solidification, thermal cycling, temp. range effect on microstruct. 0-89272
 Nb₃Sn microfilamentary superconducting composite, critical currents, fracture props. 0-107970
 Ni-Al-Mo (12.7, 21.6 wt.%), directionally solidified eutectic composite, precipitation 0-108454
 Ni-Cr-NbC eutectic composite, unidirectional solidification, thermal cycling, temp. range effect on microstructural degradation 0-89272
 Pb(Zr,Ti)_{0.5} fibre arrays in epoxy cement, ferroelectric ceramic-plastic composites 0-81015
 SiC fibre reinforced Al, thermophys. props. 0-59745
 SiC fibre reinforced Al, plasma-formed semifinished products, props. 0-84890
 SiC fibre reinforced Al, synthesis by liquid pressing method 0-100816
 W fibre reinforced Cu composites, correl. between thermal cycling-induced microstructural changes at interphase boundaries and tensile behaviour (*Japanese*) 0-71674

fibres

- see also carbon fibres; composite materials; fibre reinforced composites; glass fibres; optical fibres
 Agave cantala natural fibre, small-angle X-ray scatt. of densely packed colloidal system, scatt. inhomogeneities 0-76565
 asbestos fibres concentration meas., in air and liquid, analytical methods review 0-72120
 basalt, cement reinforcing fibre, alkali resist. 0-89377
 cellulose fibre, gamma-irrad., and storage effects on props. (*Russian*) 0-61121
 cellulose fibre formation in stirred dimethyl sulphoxide-paraformaldehyde soln. 0-104440
 cellulose fibres, elec. anisotropy 0-97220
 cellulose fibres, with planar crimp, tensile deformation 0-84235
 collagen fibres, mech. props., role of struct. organisation 0-72207
 elastic filaments, tensile test method, and treatment of expt. data 0-85111
 environmental, convergent beam electron microscopy obs. 0-108689
 fatigue testing, biaxial rotation, torque development 0-71840
 filter, fibrous, distrib. of fluid vels., flow resist., random flow model 0-79393
 fir-tree textures, possible existence 0-76269
 graphite Raman microprobe-microscope appl. 0-62737
 jute, cement reinforcing fibre, alkali resist. 0-89377
 Kevlar aramid fibre, regular fine bands obs. by polarization microscopy 0-107064
 low-density structure, centrifugal method for mech. prop. obs. 0-71823
 metallic fibre knitted gauze permeable materials, mech. props. 0-66607
 mineral fibre characterisation using energy dispersive X-ray spectrometry in TEM (*French*) 0-82857
 monofilament, substitute particles for optical single-particle-size spectrometer testing 0-58819

fibres continued

- nitrocellulose fibres, polarised light study 0-80736
 Nylon 6 gut yarn, fine struct. change in twisting, annealing and untwisting, microbeam X-ray obs. 0-81026
 Nylon 6 gut yarn, fine struct. change in twisting, annealing and untwisting, X-ray and electron microscopy obs. 0-84904
 para-polyamide based, struct. deform. props. 0-60928
 polyamide, aromatic, fibre, high modulus, mol. and supramol. struct. 0-79710
 polyamide, differently matted, meas. of diffuse reflectance spectra, using SPEKOL spectrophotometer 0-78336
 polyamides, extended chain aromatic, fibres, tensile strength and moduli 0-81021
 polyester-hydrazide, aromatic, fibres and films, synthesis and props. (*Japanese*) 0-108387
 polyethylene, flow-induced fibril form. from soln. 0-59402
 polyethylene fibre, high-strength high-modulus, morphology and tensile prop. relations 0-103264
 polyethylene fibre, production by hot drawing 0-60894
 polyethylene fibre prod. by surface growth method, mech. props. 0-104108
 polyethylene-paraffin wax, blends, rapid cooling processing techniques 0-84905
 polyethylene/polypropylene blends, surface growth of fibres and films 0-66470
 refractory thermal insulation effective thermal cond., fibre diameter effects 0-104105
 sapphire, strength at rupture 0-104286
 small particle spectral diffuse IR reflectivity meas. 0-68276
 textile filaments, with planar crimp, tensile deformation 0-84235
 textiles, fatigue testing, multistation apparatus using biaxial rotation over a pin 0-66726
 α -Al₂O₃ fibre FP, manufacture, strength and modulus 0-81013
 B, CVD, morphologies, influencing factors, temp. range 1390-1640K 0-89154
 BaTiO₃ fibres synthesised from Ba(OH)₂+2K₂O.11TiO₂.3H₂O fibre hydrothermal reaction (*Japanese*) 0-93527
 CaSiO₃, fibrous, controlled crystallisation and anisotropy 0-59425
 Si-SiO₂-Mg-Cu powder compact, nitridation to form Si₃N₄ whiskers (*Japanese*) 0-93674
 SiO₂ fibres, freeze formed from polysilicic acid aq. soln. 0-71609
 SiO₂ fibres, LF optical phonons, Raman spectra 0-80789
 Ti base alloys, melt-extracted polycryst., mech. props. 0-76360
 V₂O₅, amorphous semicond., solubility and fibrous texture 0-75162
field, crystal internal see crystal field interactions
field effect devices
 see also field effect integrated circuits; field effect transistors; metal-insulator-semiconductor devices
 hybrid field-effect liquid-crystal light valve, optical data processing performance 0-99860
 magnetodiode and magnetoconcentration effects, influence of field effect 0-107903
field effect integrated circuits
 see also charge-coupled device circuits
 CMOS ICM 7555 capacitance meter cct., using radio receiver indicator 0-62692
 p-MOS, master slice, appl. of B diffusion into Si from CVD Bn covered with Si₃N₄ 0-107564
 MOS, properties of sputtered WSi₂ as gate electrode and interconnecting material 0-70831
 MOSFET amplifier, fabrication on Si wafer, integrated acoustic transducer arrays 0-74683
 PMOS programmable sound generator, microprocessor-compatible, electronic music appls. (*German*) 0-79092
 SOS MOST, electronic props. at Si-sapphire interface 0-96993
 VMOS dynamic memory, 65536-bit, investigation of alpha-particle induced soft errors 0-88223
field effect transistor circuits
 Used for general papers and papers where the use of field effect transistors is significant
 photodetector with automatically adjustable threshold level, design considerations 0-62724
field effect transistors
 see also field effect integrated circuits; insulated gate field effect transistors; junction gate field effect transistors; Schottky gate field effect transistors
 GaAs photo-FET high speed photoconductive integrated optical receiver 0-58816
 noise figure, measurement by connecting source resistance between input and output (*French*) 0-68214
 GaAs Schottky-gate FET and GaAlAs injection DH laser, monolithic integration 0-58593
 GaAs:Cr, FET, influence of Cr on mobility of electrons 0-92910
 GaAs:Ge MBE power FETs with Sn surface impurities 0-80374
 GaAs-n-Al_xGa_{1-x}As heterojunctions, selectively doped, FET 0-80364
 In_{0.53}Ga_{0.47}As p-i-n photodiode-FET photoreceiver for 1.0 to 1.7 μ m wavelength optical fibre communications systems 0-58794
field emission, electron see electron field emission
field emission electron microscopes
 see also field emission electron microscopy
 electron gun, comparison of cold and thermal types used in the same electron microscope 0-101890
 electron gun, noise and energy broadening 0-101889
 electron holography, off-axis 0-101905
 glass, for investigation of emission probs. of single cryst. faces 0-101879
 gun lenses, electrostatic for high-brightness field emitters 0-62809
 in-situ gas reaction cell, for field emission SEM 0-81415
 micro SEM, for UHV surface anal. 0-86519
 monochromator, telescopic, in CTEM, with cylindrical mirror analysers 0-87296
 probe size to current relationship, advantages for restricted divergence probe 0-68324
 rotationally symmetric gun, theoretical investigation 0-99006
 scanning, high resolution image 0-86520
 scanning-transmission, for X-ray microanal. 0-85260
 SEM field emission gun column electron-optical performance obs. and model 0-68328
 single-pole magnetic lens as condenser for field emission electron gun 0-68325
 STEM, improved spatial resolution of X-ray microanalysis 0-104490

field emission electron microscopes continued

STEM, phase contrast characteristics 0-100153
ultrahigh vacuum field-emission SEM 0-62812

field emission electron microscopy

see also field emission electron microscopes
electron backscattering patterns, in field emission gun SEM 0-100142
electron work function of individual cryst. faces 0-101879
surface microstructure determ. and microanalysis by ultrahigh vacuum field emission gun SEM 0-96423
transmission, sub-angstrom resolution 0-82851
virtual surface states, simple modelistic treatment 0-103739
Co film, mag. domain wall obs. by electron holography 0-80582
Hg, condensation, two-dimensional, on W 0-107666
Mo (111) planes, adsorption of NH_3 , preferential nitriding, FEM study 0-66877
W (110) surface, adsorbed Pd, growth, struct., stability, desorption 0-59794
W, adsorption of NO and NO_2 0-84390
W, coadsorption of La and B, field emission and field ion microscopy 0-104049

field emission ion microscopes

see also field emission ion microscopy
atomic probe, field ion microscope with time-of-flight mass spectrometer, recording unit 0-73520
Ga ion source, emission characts. obs. 0-62810

field emission ion microscopy

see also atom probe field ion microscopy; field emission ion microscopes
field emitter surface, elec. field empirical formula 0-97413
gas supply function, expt. determ. from adsorption rate 0-100402
metals and alloys, defects and chemical inhomogeneities (German) 0-57431
protein adsorbed layers on field-emitter tips, removal by UV radiation 0-104836
Al alloy, FIM and microanalysis, developments 0-100155
Au-W interface struct., FIM obs. 0-65384
Cs, VPE on W emitter, FEM obs. 0-70552
Fe, oxidation, FIM obs. 0-89388
 $\text{Fe}_{80}\text{B}_{20}$ amorphous wire, crystn. by annealing at 780°C 0-100177
 LaB_6 and $\text{La}_{0.38}\text{Sm}_{0.62}\text{B}_6$, FIM study 0-71578
Mo surface, adsorbed Ga and Sn, struct., FIM obs. 0-103576
Ni surface, single-atom self-diffusion FIM study 0-103548
Ni-Ta (70, 30 wt.%) metallic glass, struct. and crystn. (Russian) 0-70136
 SmB_6 , FIM study 0-71578
Th, atomic struct. by field ion microscopy 0-59437
W (110) surface, adsorbed Pd, growth, struct., stability, desorption 0-59794
W (123) plane, clean and H saturated, surface diffusion of single W atoms 0-80081
W, coadsorption of La and B, field emission and field ion microscopy 0-104049
W, low-energy ion bombardment, depth of sputtering damage obs. by FIM 0-60734
W, stacking fault stability determ. 0-96548
W surface, adsorbed W, Ga, Sn, struct., FIM obs. 0-103576
W surface self-diffusion, ion impact induced, FIM study 0-103549

field evaporation

ions, post-ionisation by tunnelling into substrate 0-80951
Ga liquid metal ion source, energy distrib. meas. 0-95493
 W^{3+} field ion evaporated from ionic bonding states, appearance energies 0-81225

field intensity patterns (antenna) *see antenna radiation patterns***field interactions (condensed matter)**

see also crystal field interactions; hyperfine field interactions (condensed matter)
 $\text{BeF}_2\text{:Eu}^{3+}$ glass, struct. and optical props. 0-84067
 $\text{Ce}_{80}\text{Au}_{20}$, metallic glass, mag. ordering and cryst. field effects, speromagnetism 0-80531
 PbO-SiO_2 glasses, high temp. ESR of Fe(III) 0-60410
 $\text{Fe}_{21}\text{Ag}_{79}$, amorphous, sp. ht. at low temp. 0-75780
 $\text{Sm}_{21}\text{Ag}_{79}$, amorphous, sp. ht. at low temp. 0-75780

field ion emission

field emitter surface, elec. field empirical formula 0-97413
metallic multi-point field emission source, prep. by cathodic growth 0-100758
Bi, liquid, field ion source emission characts. 0-74059
Cu, electrodes, breakdown voltage, prebreakdown current in vacuum, crossed elec. mag. fields depend. 0-79604
Ga ionisation mechanism on W field emitter 0-76156
Ga, liquid, field ion source emission characts. 0-74059
Ga liquid metal field emission ion source, characts. 0-108326
Ga liquid metal ion source, energy distrib. meas. 0-95493
Ge-Au eutectic alloys, field ion sources 0-97414
Ir, adsorbed gases, field desorption from field ion tips 0-59793
Si-Au eutectic alloys, field ion sources 0-97414
W (111), field adsorption of He, array model 0-59800
W, adsorbed gases, field desorption from field ion tips 0-59793
W surface, adsorbed K, field emission flicker noise power 0-59795
 W^{3+} field ion evaporated from ionic bonding states, appearance energies 0-89125

field ion microscopy, atom-probe *see atom probe field ion microscopy***field ionisation**

diethyl ether, field ionisation, thermal energy distribution and energy deposition 0-95732
evaporated ions, post-ionisation by tunnelling into substrate 0-80951
hexanes, isomeric, 0-95732
hexanes, isomeric, unimol. decomp. processes following field ionisation, temp. depend. 0-95733
metal surface, field desorption and field ionisation of Cs, H, and He 0-104047
negative ion formation by field ionisation 0-89123
surface-atom polarisability derivation from field-ion energy deficits 0-76155
Au, liq., ion source fabrication and emission characts. 0-68995
Ga ion source, liquid, emission characts. obs. 0-62810
Ga ionisation mechanism on W field emitter 0-76156
Ga, ionisation ionisation at field emitter, optical emission 0-93461
GaAs, field ionisation speed of shallow impurity levels, quantum-mechanical estimates 0-97412

field ionisation continued

H, Stark spectrum and field ionisation, density of continuum states, normalised wavefunctions 0-83317
 H_2 and rare gas field ion source with high angular current 0-68996

field measurement, electric *see electric field measurement***field measurement, magnetic *see magnetic field measurement*****field plotting**

see also field strength measurement
biomedical surface mapping, interpolation methods, in FORTRAN 0-81750
ECG, microprocessor-based body surface isopotential and topological maps 0-72361
ECG body surface potential mapping project 0-104794
EEG, simple computer-generated dot-density topogram 0-94407
electrophysiology, automated production of contour maps 0-72340
epicardial mapping, computerised display system (Japanese) 0-101279

field strength measurement

see also electric field measurement; magnetic field measurement
EM fields using linear interferometric electro-optical modulator 0-58782
HF field distrib. in cavity resonators 0-98930
international calibration cycles of field intensity and power density, measurements 0-82752

field theories, unified *see unified field theories***field theory, classical *see classical field theory*****field theory, crystal *see crystal field interactions*****field theory, electromagnetic *see electromagnetic field theory*****field theory, meson *see meson field theory*****field theory, quantum *see quantum field theory*****fields, electric *see electric fields*****fields, magnetic *see magnetic fields*****filament lamps**

calibration of incandescent lamps for spectral irradiance by absolute radiometers 0-102788
halogen, standard apparatus, to produce and meas. thermal radiation flux densities 0-62674
Kr-Ag-N gas mixture, thermal conduction coefficient calculational methods (Russian) 0-96335
slit lamp, hand-held, with lid opener for ocular exam. 0-67179
standard temperature, with W-ribbon filaments 0-95102
W halogen lamp and mirror furnace at Czochralski growth 0-60766
W ribbon-filament temperature lamps, radiation error estimation 0-64128
W-halogen quartz envelope lamp, polarization characteristics 0-95970
Zr ribbon filament lamp, calibrated source for IR radiometer 0-83653

file management *see file organisation***file organisation**

see also data handling; data structures; database management systems
EVOQ: a system configurable for automatic simulation and recording of mean evoked potentials on a minicomputer (French) 0-85507

filled polymers

acoustic impedance and ultrasonic velocity calculation, simple approx. method 0-64314
agglomerated filler particles, dynamic mech. props. 0-66569
characterisation, by TEM 0-103270
cumulative internal damage, US assessment 0-97653
dynamic shear modulus and acoustic velocity, filler content depend. 0-60900
elastomers, soot filled, mech. relax. behaviour (German) 0-84985
epoxy, mica filled, polishing by abrasive papers and lapping cpds. 0-108620
epoxy based, creep and recovery under hydrostatic compression in programmed loading 0-100881
epoxy composites, with different degrees of hardening, bulk-creep prediction 0-104223
epoxy polyester, PE-933, metal-filled, elec. cond., theory and expt. 0-60057
epoxy resin, glass bead filled, subjected to extensional creep, dynamic props. 0-71697
epoxy resin/particle composites, particle size effect in thermal expansion, filler effects on T_g 0-84305
equations of state, taking account of mech. damage 0-97553
fibre reinforced, space environmental effects 0-71721
fibre reinforced epoxy laminates, interlaminar failure 0-81207
glass bead reinforced nylon, design parameters, fibre orientation effect 0-81141
glass bead reinforced polycarbonate, design parameters, fibre orientation effect 0-81141
glass fibre reinforced nylon, design parameters, fibre orientation effect 0-81141
glass fibre reinforced polycapromide, viscoelastic, linearity conservation 0-108492
glass fibre reinforced polycarbonate, design parameters, fibre orientation effect 0-81141
graphite fibre epoxy composites, eutectic coating moisture barriers 0-81228
graphite fibre epoxy laminates, low thermal expansivity, design considerations 0-81031
graphite fibre filled phthalocyanine composites, cure cycle investigation 0-81030
graphite fibre filled polyimide composite laminates, space environment, phys. and mech. response 0-81140
graphite fibre filled polyimide composite prepreg laminates, room-temp. ageing effect 0-81093
kevlar-epoxy composites pressure vessels, holographic nondestructive eval. 0-81275
lignocellulose polymer composites as γ -dosimeters in the kilorad range 0-95465
mechanical properties, particle shape effect, review 0-100864
mechanical test unit, with intense high-temp. heating 0-100987
metal-composite rods, compressed, delamination 0-64396
metal-filled, elec. cond., theory and expt. 0-60057
natural rubber vulcanisate, network changes during physical testing 0-60936
organic textolite, long-term strength in plane stressed state 0-60930
organoplastics, fracture characts., effect on strength 0-66642
phenolic resin, Kapron fibre reinforced, fracture kinetics, interface props. 0-66640

filled polymers continued

- PMMA, effect of fillers on molecular motions, dielectric relax. meas. 0-80691
 PMMA, quartz- and glass-particle reinforced, abrasive wear 0-97594
 polyester based, creep and recovery under hydrostatic compression in programmed loading 0-100881
 polyester polymer concrete, longitudinal deform. modulus study is creep conditions (*Bulgarian*) 0-71685
 polyester resin, unsaturated, chalk filled, props. (*German*) 0-104228
 polyester-E glass composites, types SMC-25, SMC-65 and SMC-30EA, moisture absorpt. 0-93799
 polymer concretes, hydrothermally stable, hydraulic cement-type fillers 0-85144
 polyoxyethylene, polypropylene fibre reinforced, fracture kinetics, interface props. 0-66640
 polystyrene, γ -Fe₂O₃ powder filled, mag. films, packing and particle orientation (*Japanese*) 0-104115
 polyvinyl acetate, γ -Fe₂O₃ powder filled, mag. films, packing and particle orientation (*Japanese*) 0-104115
 polyvinyl butyral, γ -Fe₂O₃ powder filled, mag. films, packing and particle orientation (*Japanese*) 0-104115
 PTFE based, nonlinear creep, compression bulk modulus 0-66593
 PVC, waste soft, oil absorptive filler effect on heat distortion temp. (*Japanese*) 0-108389
 PVC-C composite, fluctuation-induced tunnelling cond. 0-65516
 sheet moulding compound, material, process and performance 0-81032
 spheroplastic, spherical shells, supporting capacity 0-87723
 spheroplastics, mech. characts, calc. 0-60931
 urea-formaldehyde resin/wood materials, book 0-73114
 viscoelasticity theory, appl. 0-64397
 B fibre reinforced epoxy composites, notched, tensile strength and failure modes 0-81205
 C fibre reinforced nylon, design parameters, fibre orientation effect 0-81141
 C fibre reinforced polycarbonate, design parameters, fibre orientation effect 0-81141

films

- see also adsorbed layers; coatings; foils; helium films; Langmuir films; liquid films; monolayers; optical films; polymer films; replicas; thick films; thin films*
 glue, appl. in detaching single-stage C replicas 0-61038
 protein film, at liq. interfaces, dilatational props. 0-94255
 protein film, at liq. interfaces, shear rheologica props. 0-94256
 surface film phase transitions, conf., Eric, Sicily, Italy (Jun. 1979) 0-105429
 zinc dialkyldithiophosphate surface film, prep. and nature 0-104300

filtering and prediction theory

- see also information theory; Kalman filters; random processes*
 adaptive filter structures, for seismic signals deconvolution 0-98451
 air pollution, Venice region, real-time forecast, Kalman predictor 0-72103
 airborne target tracking filter configurations compared 0-96130
 automatic speaker recognition, cepstral/spectral and linear prediction techniques compared 0-91993
 chalcogenides of ABX₂ type comp., cybernetic prediction of form. possibility 0-101004
 clock error with a Wiener predictor and by numerical calculation 0-82748
 digital filtering of US data by deconvolution 0-106669
 digital speech processing, linear prediction parameter estimation using Kalman filtering (*German*) 0-96134
 EMG, rectified surface, time constant in low pass filtering 0-67266
 event location by recursive least squares prediction 0-96131
 flood event real-time predictors, stochastic model 0-67383
 heterodyne interferometers, quasilinear filtration theory appl. to signal processing (*Russian*) 0-82807
 neuronal spike train data, adaptive filtering 0-67265
 oil-bearing layer with input parameter correction, discrete dynamic model 0-83778
 optimal restoration filter for Poisson noise impaired and linearly blurred images 0-106481
 orthogonal transforms program for medical scintigrams 0-72365
 partial spatial coherence blur correction by postdetection image processing 0-78792
 passive tracking acoustic array evaluation, nonlinear filtering lower bound algorithms 0-96088
 road traffic noise abatement, noise propag. characts. identification under different conditions, Kalman filter theory appl. (*German*) 0-99896
 segmentation of band-limited speech signals using linear prediction 0-91970
 seismic signals deconvolution, adaptive filter structs. 0-98451
 shape variation detection, two-component chromatographic peaks resolution 0-71971
 spectra differentiation, filtering props. of polynomial methods 0-66900
 speech analysis, homomorphic filter in ARMA model (*Japanese*) 0-87666
 stellar spectroscopy, appl. of linear filtering theory to line profiles (*Italian*) 0-90340
 target discrimination methodology in remote sensing 0-58470
 wind, stochastic predictors, AR and ARMA models 0-67400

filters

- see also active filters; band-pass filters; crystal filters; digital filters; electromechanical filters; Kalman filters; low-pass filters; matched filters; microwave filters; optical filters; passive filters; spatial filters*
 comb filter, use for describing time-varying biological rhythmicities 0-97852
 electrostatic energy filter, telescopic, with cylindrical mirror analysers 0-87296
 energy, background current elimination in RF mass spectrometer, expt. results (*Japanese*) 0-82844
 Fourier transform spectrometer, SNR enhancement by elec. filter compensation of slide velocity errors 0-95151
 mica nuclear track microfilters, prod. and props. 0-96574
 multistage parallel-serial time averaging filters to reduce time jitter in scintillation counter time meas. 0-102405
 narrowband, SAW resonators at 1.43 GHz appl. 0-87687
 Nuclepore, characterization measurements 0-86324
 tone filters for electronic organs, tone spectra and source waveforms 0-106683
 Wiener filters, effectiveness in evoked pot. estimation 0-61723

filters, optical *see* optical filters**filtration**

- cellulose acetate membrane, asymmetric, elec. and electroosmotic transport behaviour in hyperfiltration expts. 0-108746
 constant pressure filtration, filter medium fast plugging, mathematical models 0-100030
 fibrous filter, distrib. of fluid vels., flow resist., random flow model 0-79393
 flow through heterogeneous earthen dam, problem solvability 0-90110
 flow through porous media, filtration theory problem soln. (*Russian*) 0-74970
 glomerular filtration rate meas., comparison of 4 commercial preps. of ^{99m}Tc(Sn)DTPA 0-81704
 metal gauzes, porous, hydraulic resist. in laminar filtration 0-100034
 microvascular filtration, comparison of characts. in isolated and intact lungs, dog expts. 0-97974
 optimal impulse control, separation theorem for classical filtering model (*French*) 0-90659
 plane filtration, of underground waters, convective mass transfer, boundary problems (*Russian*) 0-83793
 pulse-jet fabric filter, high vel., dust retention effect on pressure drop 0-103072
 steel, stainless, porous sheet, pore dimensions, filtration and permeability (*Russian*) 0-76480
 Na-fire aerosol filtration in nuclear reactors 0-68853
 NaF filter material interaction mechanism with Al melt (*Russian*) 0-108743

FIM, atom-probe *see* atom probe field ion microscopy**fine structure, atomic *see* atomic fine structure****fine structure, molecular *see* molecular fine structure****finite automata**

- stochastic cellular systems theory (*German*) 0-90661

finite element analysis

- 3D nonlinear EM field anal. using computer program TOSCA 0-95765
 acoustic transmission/radiation systems, appl. to horn and silencer design 0-87589
 atmosphere turbulent boundary layer, finite-element numerical modelling 0-77061
 atmospheric transport problems, contaminant movement, Galerkin finite element method 0-74902
 beam, cracked, dynamic weight function from finite element soln. 0-79234
 beam modelling, linear shape function for axial displacement approx., finite element anal. 0-69665
 bending of plates, finite difference variational method 0-92045
 biaxial strength tests, finite element anal. 0-89431
 boundary layer, numerical soln. of linearised Navier-Stokes eqns., effect of cell Reynolds number 0-106780
 boundary layer problems, finite difference methods, nonuniform grid generation 0-83780
 brittle solids, unstable growth of tension cracks 0-106756
 circular segment shaped plates vibration anal. 0-58957
 coiled multilayer shell, stress anal. of elastic and elastoplastic work 0-79156
 compressible flow, conservation equations, characteristic method of lines soln. 0-59064
 constrained viscoelastic damping composites, noise and vibration insulation 0-83743
 container subjected to forced pitching oscillation, liquid motion, nonlinear anal. 0-96270
 convex analysis and variational inequalities (*Japanese*) 0-77606
 cord-rubber laminates, two-ply balanced, interlaminar-shear strain study 0-97526
 coupled structural-acoustic radiation system, appl. to loudspeaker charact. calc. 0-83691
 curved beams, nonlinear dynamic anal., finite element method 0-96213
 cylindrical punch, three-dimensional stress field, photoelastic studies 0-93272
 cylindrical three layer pipe, stress-strain state, filler compressibility effects (*Russian*) 0-58901
 diffusion-convection equation, stability of finite difference approximations 0-82730
 direct radiator loudspeaker model, vibrating shell and closed cavity radiating into semi-infinite acoustic space 0-69622
 drops, rotating, captive between co-rotating parallel faces, shapes and stability, capillarity eqns. 0-64592
 duct entrance region, laminar heat transfer, finite element method 0-69836
 dynamic finite element analysis of cracked bodies subjected to impact loading 0-69742
 dynamic fracture toughness, influence on dynamic crack propag. 0-99966
 dynamics analysis, rotationally periodic large space structures, transfer matrix combined method 0-74731
 Einstein's gravitational field eqns., finite element method soln. 0-86177
 elastic behaviour near an open circular hole (*Japanese*) 0-74750
 elastic plate, crack closure in bending, sixth order anal. 0-96231
 elastic shell problems, finite element anal. (*Ukrainian*) 0-69662
 elastic shells, cylindrical, finite element anal., solid of rev., thin shell and interphase elements 0-74744
 elastic shells, thin, doubly curved, numerical integration of triangular finite element 0-92044
 elastic stress analysis of constrained cylinders by special finite element method 0-106718
 elastic-plastic problems, supplementary strain method, appl. 0-96205
 elasticity, beam bending on Pasternak foundation, reciprocal variational inequalities 0-92091
 elasticity, hybrid-stress finite element formulation for thick multilayer laminates 0-92043
 elasticity, thick orthotropic shell of revolution, stress-strained state, finite element method (*Russian*) 0-87713
 elastodynamics, irregular finite element meshes, grading rules 0-68045
 elastodynamics, linear, discrete time approx. of initial boundary value problems, error estimates 0-73175
 elastomeric bearings, high-capacity, laminated, finite-element anal. 0-96197
 elastoplasticity, finite strain, rate problems, energy theorems, Lagrangians 0-74766
 electric field computation by charge simulation and finite element methods 0-95759

finite element analysis continued

- electric fields, intensity, numerical calculation methods (*French*) 0-106413
- electrical and magnetic field problems, book 0-62399
- electroelasticity problems, numerical soln. 0-80707
- embedded semicircular surface crack, stress intensity factors, superposition methods 0-79217
- EURDYN, nonlinear transient dynamics programs for fast reactor safety 0-91234
- EURDYN-IM, safety studies on LMFBR, computer program 0-99267
- evolution systems and convection-diffusion, stiffness and stability, Gershgorin theory 0-77626
- extrudate swell, thermally induced, Galerkin method 0-79312
- fetal head moulding, finite element model investigation 0-67129
- fibre reinforced composites, angle ply, delamination mechanics and failure mode 0-79236
- field analysis computers, colloquium, London, England (March 1980) 0-94964
- field problems, multi-terminal representations appl., graph theoretical field model 0-90689
- fission reactor fluid dynamic transient analysis using ASWR method with staggered meshes (*German*) 0-83176
- flow in porous media, diphasic incompressible, diffusion-convection eqn., mixed finite element method, water flooding 0-74969
- fluid discontinuities, subgrid resolution in tracking methods 0-105506
- fluid dynamics, 2-D incompressible Navier-Stokes flow, finite element MAC scheme 0-74824
- fluid dynamics, axisymmetric Newtonian jets, die-swell, Galerkin finite element method 0-83830
- fluid dynamics, boundary deform., Galerkin finite element technique for multidimensional flow 0-86089
- fluid dynamics, groundwater flow, finite element eqns., Newton iteration and modified conjugate gradient method 0-77622
- fluid dynamics, laminar flow, viscous fluid in toroidal tube, oscillations 0-79253
- fluid dynamics, laminar flow in entrance region of ducts, marching technique 0-69761
- fluid dynamics, lined ducts, eigenvalue problem, Hermitian elements 0-74983
- fluid dynamics, Navier-Stokes equations, finite difference approx. with second-order accuracy 0-87756
- fluid dynamics, Navier-Stokes equations, finite element soln., applied to blood flow 0-94269
- fluid dynamics, Newtonian fluid, recirculating flow in rectangular cavity, free convective flow in enclosed container 0-74852
- fluid dynamics, non-Newtonian, finite element routine using mixed method 0-103045
- fluid dynamics, partly elliptic flows, EMIT numerical procedure 0-79255
- fluid dynamics, Poisson equation, non-uniform grid, finite-difference, matrix decomp. technique 0-69756
- fluid dynamics, porous flow, new mathematical models 0-83837
- fluid dynamics, pseudo-upstream finite difference scheme for advection 0-106773
- fluid dynamics, small-disturbance transonic flow, nonlinear mixed elliptic hyperbolic eqn., finite element anal. 0-83814
- fluid dynamics, stationary Navier-Stokes eqn., discretisation, splitting of linear operators, iterative methods 0-69755
- fluid dynamics, transonic flow problems, modified FLIC method, finite element anal. 0-74911
- fluid dynamics, two-phase flow with condensation, U enrichment by photochemical laser, mathematical model (*French*) 0-74029
- fluid dynamics, unsteady compressible 3-D boundary layer flow 0-103011
- fluid dynamics, viscous flow, unsteady, around elliptic cylinder, heat transfer, finite difference method (*Japanese*) 0-69831
- fluid dynamics, viscous flow, laminar flow, Navier-Stokes eqns., central difference scheme 0-69762
- fluid dynamics, viscous-convective type flow, mixed finite element soln., discrete least squares approach 0-74851
- fluid dynamics, water boundary layer along heated cylinder, buoyancy and variable viscosity effects 0-79256
- fluid flow simulator, free boundaries, surface tension effects 0-82647
- fluid structure vibr. eigenvalue problems, finite elements, modal methods 0-96269
- fracture analysis, 2D linear, elastic, finite element anal. vs. the edge function method 0-99963
- free vibrations of conical solid horn with flange (*Japanese*) 0-79045
- frequencies of orthotropic circular plates elastically restrained against rotation, large amplitude axisymmetric vibrations 0-83750
- frontal method for structural mechanics, algorithm for excluding unknowns 0-79157
- fusion reactor, magnetic confinement, structural anal., combined interactive/batch computer environment 0-91255
- fusion reactor, PDX, toroidal field coil and frame struct., anal., finite element anal. 0-106165
- fusion reactor, PDX power test results, struct. finite element anal. 0-91265
- fusion reactor, PDX Tokamak, finite element anal. using computer graphics 0-95424
- fusion reactor, PDX Tokamak, struct. anal. by finite element method 0-106166
- fusion reactor, SLPX TF coil, stress anal. using COE IC-NASTRAN 0-106168
- fusion reactor toroidal field coil finite element stress anal. 0-91256
- gas-liquid interaction in turbulent reacting flows, mathematical model 0-83862
- gas-particle flow in shock tube, finite difference calc. (*Japanese*) 0-79390
- glass fibre reinforced plastic, cemented joint of cylindrical shell with cover, stressed state 0-69668
- gravity wave problem, upstream difference method 0-106806
- Hastelloy-X, low cycle fatigue crack propagation at 25°C and 760°C 0-104270
- heat and mass transfer, finite element soln., for chemically reacting system 0-68153
- heat conduction, fluid in contact with surface, transient temp. field, mesh refinement method 0-69825
- heat conductivity, temperature distrib. (*Russian*) 0-74701
- helical compression springs, finite elements for dynamical anal. 0-96191
- Homalite-100 plates, modified compact-tension specimens, dynamic anal. 0-97561
- horizontal fluid layer in porous medium, convective instability, critical Rayleigh number 0-64564

finite element analysis continued

- horn loudspeaker, anal. of acoustic radiation by finite element method 0-96171
- human torso surface isopotential simulation using simple conduction-elec. field model with Neumann boundary 0-89706
- hydrodynamic model using smooth elements, estuarine appl. 0-98356
- hydrodynamics simulations, frontal solution method, finite element anal. 0-74825
- IGFET, simulation of semiconductor transport using coupled and decoupled solution techniques 0-65695
- Inconel, steam generator tubing, mag. probe inspection 0-85119
- infinite cracked isotropic sheet, under symmetric loads, Green's functions for stresses, stress intensity factors and displacements 0-99967
- integrated load increment method for finite elasto-plastic stress analysis 0-92072
- ion beam extraction, computer simulation, finite element method 0-96387
- isotropic plane sandwich plates, constant shear theory 0-99943
- laminates, angle ply, 3D finite difference soln. of free edge effect 0-79152
- laminates, cross-ply, edge effects, traction-free-edge condition satisfaction 0-79151
- laminates, damage zone failure analysis 0-85059
- light beam propagation through moving aqueous aerosol cloud containing medium 0-91750
- linear viscoelasticity, finite element method variant 0-69692
- loudspeaker cones, effect of voice-coil and surround on vibration and sound pressure level 0-96172
- lung, finite element model for macroscopic deform. 0-108945
- lung, macroscopic deformation, finite element model 0-89781
- magnetic fields, numerical analysis, fundamental equations and historical evolution (*Portuguese*) 0-78739
- magnetic fields, two-dimensional graph-theoretical model 0-87260
- magnetic lens design, finite element program improvement 0-69316
- mantle convection model, finite element method 0-67354
- Maxwell equations, boundary value approx. using finite element anal. (*German*) 0-91718
- Maxwell fluid, die swell, finite element anal. 0-83822
- metals, high temp. stress anal. by finite element method 0-96203
- neutron diffusion equations, finite element soln. tech. using imaginary nodal points and element subdivision 0-68721
- neutron transport theory, nonuniform lattice problems, 2-D constrained finite element anal. 0-86952
- nonlinear materials, Mode I fracture behaviour, finite element anal. 0-84237
- nonuniform grids in finite difference approximations, application to fluid flow problems 0-105507
- nuclear cross-section adjustment and evaluation, finite element basis in data adjustment 0-68612
- optical fibre, single-mode, single-polarisation, with refractive-index pits on both sides of core 0-99846
- optical waveguides, finite element anal. 0-87558
- oscillation rods in viscous fluids, added mass and damping, finite element anal. 0-58967
- partial differential equations, conference, Bethlehem, PA, USA (June 1979) 0-86039
- pipe elbow element, linear anal., bending axial and torsional displacements, ovalisation 0-79177
- plain strain contained plastic deformation, elastic-plastic laws, finite element anal. 0-92073
- plane elastoplasticity, subject to large strains, finite element anal. (*Japanese*) 0-96207
- plane V-notched specimen, elastic-plastic limit load anal. 0-69684
- plasma MHD, nonlinear time-dependent hydromagnetic model, spatial and temporal finite-difference techniques 0-59192
- plasma MHD, stability code, ERATO, convergence of solns. 0-83906
- plastic anal. of thin-walled beams of open cross section, finite-element model 0-74767
- plastic deformation, necked bar, void growth, finite element anal. 0-64383
- plastic flow, isotropic body, finite element method for volume integration 0-74770
- plasticity theory for porous metals 0-83738
- plate structure, crack simulation computer program (*Japanese*) 0-79218
- plates, elastic viscoplastic, transient dynamic large deflection anal., finite element method 0-69683
- plates, laminated anisotropic composite, penalty plate bending element 0-96200
- plates, rigidity matrix, triangular finite elements (*Russian*) 0-74739
- plates, thin and moderately thick, serendipity cubic displacement hybrid stress element 0-96202
- PMMA plates with flawed fastener holes, static fracture testing 0-97651
- pollutant transport eqn., 3-D, numerical algorithm 0-106811
- polycarbonate plates, modified compact-tension specimens, dynamic anal. 0-97561
- polycrystalline materials, effect of grain boundary sliding on anelasticity 0-96592
- polycrystalline metals, effect of grain boundary sliding on steady creep 0-96590
- polycrystals, elastic stress and strain microinhomogeneity, finite element method 0-79155
- polymers, glassy, craze surface displacements, model 0-93651
- post-buckling behaviour of structures using a finite element-nonlinear eigenvalue technique 0-92078
- postbuckling analysis of elastic structures by the finite element method 0-96209
- potential flow, 3-D, about arbitrarily shaped bodies, direct matrix embedding technique 0-64511
- Prandtl punch problem, finite element model for plane-strain plasticity 0-58940
- propagation of plane harmonic waves, infinite isotropic medium having embedded doubly periodic array of cylindrical fibres 0-87607
- punch stretching, localised necking, finite element anal. 0-102971
- reinforced plastic cylindrical shells, optimal design under dynamic constraints 0-102996
- resonance frequencies of non-rectangular reverberation chambers, calculation by numerical methods 0-64324
- ribbed plates with large openings, design optimisation, finite element anal. appl. 0-87724
- rotating beam with tip mass, vibration 0-58960
- rotating liquid drops, asymmetric shapes and stability 0-87796

finite element analysis continued

- rotationally periodic large space structures, finite element transfer matrix dynamic analysis, 100 m parabolic dish 0-74731
 sea model, hydrodynamic, 3-D, variable vertical eddy viscosity, finite element anal. 0-85661
 seismic depth migration after stack, finite-difference method 0-98254
 seismic depth migration before stack, finite-difference method 0-98255
 seismic surface waves in three-dimens. struct. 0-61765
 shell design by finite element method, deformation and elasticity theory 0-74747
 shells, curvilinear tubular, elastic equilib., finite element anal. (Russian) 0-79148
 shells, large inelastic deformations for arbitrary shape, TRUMP element appl. 0-92068
 shells of revolution, computer program for linear and geometrically non-linear static analysis (Japanese) 0-64500
 shells of revolution under axisymmetric and asymmetric loadings, linear elastic dynamic analysis program using finite element analysis (Japanese) 0-106719
 single-pole electron lens 0-69315
 smoke-motion, numerical anal. by finite-element method (Japanese) 0-69910
 smooth spline-like finite-element differentiation, of full field experimental data over arbitrary geometry 0-62454
 spinal cord electrical stimulation, 2D anal. 0-98054
 spine, human, finite element model for in vivo freq. response anal. 0-104623
 steady state convection-diffusion eqn., quadratic finite element solns. 0-92019
 stiff bending plates, stress-strain states, finite element effectiveness, polynomial approx. (Russian) 0-58921
 stiffness, exact straight line element calc. 0-79138
 Stokes flow, stress-hybrid finite element method 0-99985
 strength of materials and mechanical systems dynamics computing, based on three-dimensional models (German) 0-58976
 stress-strain states, 3-D elasticity, finite element method (Russian) 0-74728
 subsonic plane pot. flows, least squares finite element anal. (Chinese) 0-59063
 tectonic visco-elastic system modelling 0-104930
 thermal characteristics of finite element and finite difference calcs. for transient problems, comments 0-69633
 thermal elastoplastic stress analysis based on initial strain method (Japanese) 0-77620
 thermoelectric cooler, single stage, finite element thermal stress anal. 0-108807
 thin plates, bending anal. hybrid stress finite element model 0-96201
 three-dimensional stress anal., transition finite elements 0-92042
 tidal motion on sphere, geodesic finite-difference method for curved domains 0-109153
 Timoshenko rod, straight axis, free bending oscillations investigation (Hungarian) 0-89327
 transition finite elements for axisymmetric stress analysis 0-92048
 tsunami, island of Hawaii, 1979 November 25, numerical anal. by finite-element method 0-72449
 tuning fork for HF operation, second-mode, finite element anal. and expts. 0-102980
 two-phase flow, nonlinear test case 0-96293
 UNCLE finite element scheme, input specification 0-95512
 vibrating plate, variable thickness, spline technique method 0-79195
 viscous incompressible non-Newtonian flow, finite element method, Bingham fluid 0-92184
 vortex flows, between rotating cylinders, axisymmetric Navier-Stokes equations 0-59044
 Al-Cu-Si-Mn, type 2017S-T4, crack initiation at root of circumferential notch of round bar specimens (Japanese) 0-60947
 B fibre reinforced epoxy composites, notched, tensile strength and failure modes 0-81205
 Fe, cast flake and nodular, rupture strength, circumferential notch (Japanese) 0-93649
 H bound states in strong mag. field 0-99438
 H₂⁺ bound states in strong mag. field 0-99438
 He⁺, electron scatt., reson. state assoc., incomplete spectrum of Hamiltonian matrix 0-99568
 Si-Ge thermoelectric generators, approximation errors when using averaged properties solutions for required heat rates estimation 0-108808

finite state automata *see finite automata***Finlay-Freundlich red-shift hypothesis** *see gravitational red shift***fires**

- see also accidents; combustion; flames; safety*
 human use of fire, history and effects on Earth albedo and climate 0-81893
 IR forest fire alarm system 0-86429
 nuclear power stations, industrial activities nearby causing hazards 0-78408
 pyroclumulus cloud over North Canterbury, New Zealand, 1878 April 10, obs. 0-109240
 spark discharges from body, electrostatic, nature and incendiary behaviour obs. 0-72406

fission

- see also fission of plutonium; fission of uranium; photofission; spontaneous fission*
²³⁸U, high spin pot. energy surfaces, fission barrier, α -, γ -decay half lives, yrast spectrum 0-73764
 A=200 region, macroscopic fission barriers, isospin depend., liquid drop model 0-57811
 barrier props., expt. studies and statistical anal. review 0-102216
 beta strength function, half life and delays, nuclear- and astro-physics consequences 0-102149
 beta strength function structures, nuclear- and astro-physics consequences 0-99152
 binary fission saddle points, shape parametrization for liquid-drop studies 0-106086
 conference on nuclear physics, Mikolajki, Poland (2-14 Sept. 1979) 0-101662
 deformation process mass parameter, liquid drop model 0-102221
 discovery, research of 1930's, '40's, Otto Hahn 0-57063
 electron-collision cross-section data for atom or molecule, rel. to radiation physics 0-63829

fission continued

- fissionability, target mass depend. for π , γ , α , p, cascade-evaporation and liquid drop calcs. (Russian) 0-106089
 fragment excitation, prompt neutron distrib., renormalised gas model calcs. 0-99169
 hadron induced fission, low energy evaporative particle emission from emulsion nuclei (Russian) 0-86943
 isomers, spectrosc. props. 0-105966
 low energy fission, charge distrib., quantum mechanical phenomenon of GDR 0-86945
 mechanisms, recent progress (French) 0-78274
 mesoatoms, prompt fission internal γ -ray conversion, fragment radiative transitions (Russian) 0-86944
 multi-chance high-spin fission, fragment anisotropy, stat. model anal. 0-57812
 muon induced, response tail to high threshold reaction 0-83075
 pre-actinide nuclei, fission barriers, level density collective effects (Russian) 0-106092
 saddle point, statistical fluctuations, Suzuki's scaling limit 0-86946
 trans-uranium nuclei, fission barrier and (neutron width-fission width), nucleon contents depend. (Russian) 0-106093
 (n,n'), thermal, parity violation from opposite parity rot. states 0-95303
 (n, γ), (n, γ), low energy γ -transitions between compound states, statistical theory 0-57737
²³²UZZ 0-95329
¹⁰⁷AgZZ 0-95329
 Ag(p,f), 1 GeV, binary fission, possible mass instability of correlated fragments 0-83133
²⁴¹Am(n,f), 14.8 MeV, cross-section meas. using mica track detectors 0-95330
²⁴³Am(n,f), low energy, far-out asymmetric mass distrib. 0-83132
⁴⁰Ar(X), 222-340 MeV, A=116-197, charged particle emission, early collision evolution, fission and evaporation cross sections 0-106072
¹⁴⁷Au⁴⁰Ar, f, 340 MeV, H and He emission, rapid energy equilib., to ang. distrib. 0-86936
¹⁹⁷AuZZ 0-95329
¹⁹⁷Au(²²Ne, f), 178 MeV, α -particles and fission fragments, spectra and cross sections (Russian) 0-91203
¹⁹⁷Au(d,f), 80 MeV, post neutron emission fission products 0-83136
⁸Be fission mode, large amplitude collective motion, adiabatic TDHF calcs. 0-86786
²⁰¹Bi (α ,f), 23-140 MeV, Γ_{crit} from fragment ang. distrib. anal. 0-106087
²⁰⁹Bi (n, xnf), fission high energy neutrons (Russian) 0-106091
²⁰⁹BiZZ 0-95329
²⁰⁹Bi(¹³⁶Xe,X), 940 MeV bombarding energy depend., fragment deformation, sequential fission 0-86938
²³²Cf scission point configuration, α -ang. distrib., trajectory calcs. for LRA fission 0-83134
²⁴³Cm(n,f), thermal neutron fission cross section and fission-resonance integral 0-86942
²⁴⁵Cm (n,f), thermal, charge distrib., ¹³⁵I and ¹⁹⁰Ba fractional cumulative yields 0-63074
¹⁶²Er compound nucleus fission at high ang. momentum, fragments from ³⁰Si(¹³²Xe,f) 0-99196
⁵⁵Fe(⁵²Cr, X), entrance channel mass asymmetry effects on reaction mechanism, fission and fusion 0-106077
⁹²Mo(¹⁶O,X), entrance channel mass asymmetry effects on reaction mechanism, fission and fusion 0-106077
⁴Np(n,f), A=234, 235, low energy, far-out asymmetric mass distrib. 0-83132
²³⁷Np muonic, prompt fission, fragment atomic muon capture 0-95312
²³⁷Np, muonic atom lifetimes from muon induced fission 0-69269
²³⁷Np(e,f), 10-34 MeV, electrofission cross section, E2 transition mode and giant resonances 0-106084
²³⁷Np(n,f), intermediate struct. line fitting, subthreshold fission resonances 0-102214
²³⁷Np(n,f), thermal neutron sub-barrier fission ¹³⁴I and ¹³⁵Xe yields 0-86935
²³⁷Np(p,f), 11-26 MeV, product yield 0-91197
²⁰⁷PbZZ 0-95329
²⁰⁸Pb(²⁰⁸Pb, H), 7-7.5 MeV/N, product energy and element distrib., fission probab., energy losses 0-86916
¹⁵³Tb, fission barrier at 28.5 MeV 0-91202
²³⁰Th(n,f), 0.68-1.10 MeV, fission fragment ang. distrib., resonance and moment of inertia 0-102219
²³²Th(n,f), 2-8 MeV, fission product yields and mass distrib. 0-86939
²³²Th(p,f), 29-97 MeV, Rb, In and Cs relative indep. yields, charge division 0-102218
²³²Th(p,p,f), 52.5 MeV, fission probability 0-99195
⁴W(¹²C,f), A=182, 183, 184, 186, 80 to 115 MeV, lifetime meas. by crystal-blocking tech. 0-91198
⁴W(¹⁶O,f), A=182, 183, 184, 186, 80 to 115 MeV, lifetime meas. by crystal-blocking tech. 0-91198
⁴W(e,f), A=182,184,186, 35-55 MeV, fission barriers, pairing strength deformation depend., stat. anal. 0-57810

fission counters

- fission track spark counting method for neutron monitoring 0-58080
 high sensitivity neutron spectroscopy and dosimetry appl. (French) 0-58078
 neutron dosimetry system, based on fission counter for fuel processing plant 0-57981
 position sensitive parallel plate avalanche fission detector, particle induced fission coincidence measurements 0-63485
 BF₃ detector assembly for photofission and photoneutron studies 0-63484
 Xe proportional scintillation detector, energies and angles of emission of ²³²Cf fission fragments 0-63488

fission of plutonium

- Pu²³⁹, product separation asymmetry in fission by slow polarised neutrons (Russian) 0-106088
⁴Pu(n,f) A=239,242,244, 14.8 MeV, cross-section meas. using mica track detectors 0-95330
⁴Pu, A=239,242, muonic, prompt fission, fragment atomic muon capture 0-95312
⁴Pu, A=239,242, muonic atom lifetimes from muon induced fission 0-69269
⁴Pu(n,f) A=240,241, 14.8 MeV, meas. of reaction parameters using solid state nuclear track detectors 0-91201
²³⁹Pu(n,f), fission-fragment yields of neutron fission in FBR 0-83102
²³⁸Pu(n,f), intermediate struct. line fitting, subthreshold fission resonances 0-102214

fission of plutonium continued

- ²³⁹Pu, fission product beta decay, $\bar{\nu}$ spectra 0-102150
²³⁹Pu(γ ,f), 15-55 MeV, photofission symmetric and asymmetric yields 0-83135
²³⁹Pu(n,f), far-out asymmetric mass distrib. 0-83132
²³⁹Pu(n, γ), thermal, fission product $\bar{\nu}_e$ spectrum, β -decay characs. 0-78340
²⁴⁰Pu, effect of spontaneous fission on energy release in a nuclear explosive 0-95464
²⁴⁰Pu fission barrier, deformation energy curve, constrained HF calc. 0-83053
²⁴²Pu(μ ,f), radiationless muonic transition induced fission, fission dynamics probe, friction coeff. 0-78336

fission of uranium

- fission track dating using U glasses, error analysis 0-95503
 fission track determ. of U abundance in Himalayan plants 0-101305
 solid-state nuclear track detectors, review of appls. in fission physics 0-91396
 U²³³, product separation asymmetry in fission by slow polarised neutrons (Russian) 0-106088
 U²³⁵ in pegmatites, homogenised fission track anal. using solid state track detector 0-97719
^AU, A=235,238, fission product beta decay, $\bar{\nu}$ spectra 0-102150
^AU, A=235,238, muonic atom lifetimes from muon induced fission 0-69269
^AU^m, A=236,238, isomeric to prompt fission ratios; fission fragments from (d,pf), (d,pnf) 0-86940
^AU(γ ,X), A=235, 236, 238, 5-18.3 MeV, photoneutron and photofission cross sections, giant resonance and deformations 0-68712
^AU(γ ,f), A=235,238, 15-55 MeV, photofission symmetric and asymmetric yields 0-83135
^AU(μ ,f), A=235,238, prompt and delayed fission, absolute yields and lifetimes 0-78337
^AU(n,f), A=233,235, ejection fission products angular depend. on thermally polarised neutron capture (Russian) 0-86941
^AU(n,f), A=235, 238, fission-fragment yields of neutron fission in FBR 0-83102
^AU(n,f), A=235, 238, low energy, far-out asymmetric mass distrib. 0-83132
²³²U production and decay, nonproliferation aspect of ²³³U-Th fuel cycle 0-57839
²³³U(n,f), thermal polarised neutrons, neutron emission P-odd asymmetry (Russian) 0-78338
²³³U(ρ ,f), alpha-particle angular and energy spectra, cross-section anisotropy 0-57809
²³⁴U(n,f), intermediate struct. line fitting, subthreshold fission resonances 0-102214
²³⁵U fission fragment thermonuclear superheavy nuclei synthesis, prod. cross sections 0-95331
²³⁵U, thermal neutron fission, fission product decay energy release rates, effect on LWR LOCA 0-57894
²³⁵U, thermal neutron induced fission, nuclear charge distribution in fission products 0-57808
²³⁵U(n,f) thermal 3 MeV, ¹³⁶I isomeric ratio (French) 0-68709
²³⁵U(n,f), symmetric fission, proton scatt. by fission fragments in neck area 0-83130
²³⁵U(n,f), thermal, fragment ionisation, charge distrib., stat. and instant perturbation theory (Russian) 0-63219
²³⁵U(n, γ), thermal, d, t, He emission probabilities from stable core model (Russian) 0-68713
²³⁵U(n, γ), thermal, fission product $\bar{\nu}_e$ spectrum, β -decay characs. 0-78340
²³⁵U(n, γ f), X-ray yield fluctuations, γ -transitions in ²³⁶U 0-106085
²³⁶U fission as multi-dimensional Brownian motion, Fokker-Planck soln. (Chinese) 0-99197
²³⁶U isomeric and prompt fission, nuclear superfluidity evidence from ²³⁵U(d,pf) 0-68711
²³⁸U subbarrier photofission, cross section and half-life, double hump model 0-102217
²³⁸UZZ 0-95329
²³⁸U(²³⁸U,f), 1785 MeV, exam. of multiprong events due to multiple sequential fission using solid state track detectors 0-91199
²³⁸U(⁸⁴Kr,f), 806 MeV, exam. of multiprong events due to multiple sequential fission using solid state track detectors 0-91199
²³⁸U(γ ,f), ¹³⁵Xe, direct meas. of absolute and fractional independ. yields 0-78341
²³⁸U(γ ,f), BF₃ detector assembly for photofission and photoneutron studies 0-63484
²³⁸U(γ ,f) 20 MeV, computer program for yield determ. of short-lived products 0-102215
²³⁸U(n,f), 5 eV-2.5 MeV, fission cross section, fission barrier second well parameters, resonances 0-63217
²³⁸U(p,f), 11-29 GeV, three dims. charge dispersion curves, isobaric yields 0-102111

fission products

- A=134-144, fission yields from spectroscopic meas., γ -branching and half-lives 0-78213
 A=135-143, odd A fission products, delayed n, decay studies and Q _{β} meas. 0-78227
 air over N.Atlantic, obs. of radioactivity and source region identification 0-77074
 BWR spent fuel safeguarding, nondestructive assay using gamma spectrometry 0-68802
 carbide fuels, effect of burn-up and temp. on appearance of optically visible fission gas bubbles 0-63251
 ceramic nuclear fuels, irradi. induced rare gas diffusion 0-59524
 conference on nuclear spectroscopy of fission products, Grenoble, France (May 1979) 0-77546
 decay energy release rates following ²³⁵U fission, effect on LWR LOCA 0-57894
 decoupling model for fission fragment transitional nuclei, odd-odd and even mass 0-78174
 delayed neutrons and P_n values 0-78339
 even-even neutron-rich fission products, de-excitation spectra, β -decay, deformation 0-78203
 FBR, role of fission gas swelling and release in reactor accidents 0-57854
 FBR oxide fuels, dynamic response of grain boundary cavities to stress and temperature changes under conditions of continuous gas generation 0-66544

fission products/continued

- FEBIAD ion source for fission fragment isotope separation 0-78483
 fissioning plasma from gas phase nucl. reactor, appl. 0-64794
 gamma-ray spectra analysis of fission products, automatic general-purpose program GSAP (Chinese) 0-69013
 gas, release from Na-bonded carbide fuel pins in OSIRIS (French) 0-73916
 gas release from high burn-up oxide fuel, predictions in ELESIM code 0-57864
 gases in HTGR fuel particles, content meas. apparatus 0-68793
 HTGR, fission product playout in primary cooling system, in situ meas. using Ge(Li) spectrometer 0-73881
 ion source fission product separators 0-78479
 ISOLDE as a source of neutron-rich nuclei 0-78480
 LMFBR advanced MX-type fuels, fission gas swelling, temp. depend. 0-57842
 LMFBR advanced MX-type fuels, low-temp. microscopic swelling, phenomenological model 0-57851
 LMFBR advanced MX-type fuels, swelling mechanism anal. 0-57850
 LMFBR fuel, fission gas behaviour during overpower transient, calcs. using COREF-1 code 0-57853
 LMFBR fuel behaviour during HCDA, intragranular fission gas behavior under isothermal conditions 0-102236
 LWR spent fuel, non-destructive anal. using inherent and induced neutron radiation (Russian) 0-68805
 magic and doubly magic nuclei, A=129, 131, 133 chains, 0⁺ states, spectroscopy 0-78165
 mesoatoms, prompt fission internal γ -ray conversion, fragment radiative transitions (Russian) 0-86944
 mixed oxide fuels, SEM obs. of gas bubble morphology 0-57843
 multi-chance high-spin fission, fragment anisotropy, stat. model anal. 0-57812
 neutron rich fission fragments, excited state spin assignment, various methods 0-78506
 neutron rich nuclei, beta decay half lives, expt. techniques 0-78224
 neutron rich transitional fission fragments, spectroscopy, 0⁺ states and octupole vibrs. 0-78204
 nuclear far from β -stability, delayed neutron energy spectra, structure effects 0-78226
 nuclear fuel swelling, fission gas precipitation into intra- and intergranular porosity, theory 0-57849
 nuclear fuels fission gas behaviour, conf. Karlsruhe, Germany (Oct. 1978) 0-56992
 nuclear materials safeguards, collection and analysis of measured fission product data 0-95354
 nuclei far from stability, β -decay energies, γ -rays, Q _{β} values and masses 0-78225
 odd nuclei, soft and deformed, rotor plus quasiparticle approach, moments, transition probabilities 0-78214
 odd-odd fission products, level schemes, rot. bands, shell model states 0-78167
 PWR fuel clad failure characterisation based on fission product activity, PROFIP 3 code 0-95365
 PWR irradiated fuel, monitoring by gamma spectrometry nondestructive meas. (French) 0-63288
 rapid automated nuclear chemistry, short lived fission products, reactor safety 0-81353
 reactor fuel burn-up and cooling time determ. using gamma spectrometry 0-63289
 reactor fuel burn-up determination using gamma spectrometric nondestructive assay for IAEA safeguards 0-68806
 reactor fuel burn-up determination using gamma spectrometry, IAEA safeguards experience in Czechoslovakia 0-63292
 reactor fuel burn-up measurement using spatial power distrib. eval. and gamma spectrometry 0-68803
 reactor spent fuel safeguards verification using gamma spectrometry 0-63290
 saddle point, statistical fluctuations, Suzuki's scaling limit 0-86946
 SIRIUS facility for neutron rich fission fragment studies 0-78484
 SISAK 2, chemical separation method for short lived fission products in spectroscopic studies 0-74068
 Sphere-Pac mixed carbide fuel, effect of early gas release in temp. calcs. 0-102235
 TRISTAN II mass separator, ion source, beam optics, computer system 0-78481
 TRISTAN II mass separator at Brookhaven HFBR, research programme for fission products 0-78482
 unsolved fission product separators, gas filled JOSEF, parabola LOHENGRIN 0-78478
 Z=37-43, neutron rich fission products, mass energy surface, decay props. 0-78228
 Ag(p,f), 1 GeV, binary fission, possible mass instability of correlated fragment 0-83133
¹⁴Au(⁴⁰Ar, f), 340 MeV, H and He emission, rapid energy equilib., to ang. distrib. 0-86936
¹⁹Au(²²Ne, f), 178 MeV, α -particles and fission fragments, spectra and cross sections (Russian) 0-91203
¹⁹Au(d,f), 80 MeV, post neutron emission fission products 0-83136
¹⁴⁰Ba, fractional cumulative yield from ²⁴³Cm(n,f) 0-63074
²⁰¹Bi (α ,f), 23-140 MeV, $t_{1/2}$ from fragment ang. distrib. anal. 0-106087
²³²Cf fission, neutron deficient fragments, search for positron activity (Russian) 0-63218
²⁵²Cf spontaneous fission, fission product β spectra (Russian) 0-91204
²⁵²Cf spontaneous fission, prompt γ -ray differential angular distrib. 0-102220
²⁵⁴Cf spontaneous fission, neutron-rich fragments, even-even products 0-78342
 Cs, fission fragment, delayed neutron branches from γ -spectroscopy 0-78230
 Cs, ground state spins, moments, charge radii by laser spectroscopy 0-78147
 Cs migration effects on fuel-cladding mech. interaction in (U,Pu)₂O₇ fuel pins 0-102250
¹³⁷Cs/¹³⁷Cs activity ratio for LWR fuel burn-up determ. (Russian) 0-68804
¹⁶²Er compound nucleus fission at high ang. momentum, fragments from ³⁰Si(¹³²Xe,f) 0-99196
 He release from UO₂-Zr high burnup nuclear fuel rods 0-57846
 I, radioactive, air sampling system, separation into gaseous and particulate fractions 0-57962

fission products continued

- ¹³¹I, behaviour during rinsing in in-pile loop after fission product release expt. 0-73879
- ¹³⁴I, fractional independ. yield from ²³⁸U(γ ,f) 0-57814
- ¹³⁴I, yield from ²³⁷Np(n,f) 0-86935
- ¹³⁵I, fractional cumulative yield from ²⁴⁵Cm(n,f) 0-63074
- ¹³⁶I, isomeric ratio, γ -spectra thermal neutron and 3 MeV fission of ²³⁵U (French) 0-68709
- Kr, from ²⁴⁸Cm and ²⁵⁰Cf in meteorites 0-63215
- Kr release from UO₂-Zr high burnup nuclear fuel rods 0-57846
- ¹⁰²Mo fission product decay, ¹⁰²Tc decay scheme and γ -intensities 0-78229
- ²³Np muonic, prompt fission, fragment atomic muon capture 0-95312
- Pd, corrosion of SiC coating of HTGR coated particle fuels 0-102237
- ²³⁹Pu, product separation asymmetry in fission by slow polarised neutrons (Russian) 0-106088
- ^APu, A=239,242, muonic, prompt fission, fragment atomic muon capture 0-95312
- ²³⁹Pu, fission product beta decay, $\bar{\nu}$ spectra 0-102150
- ²³⁹Pu(n,γ), thermal, fission product $\bar{\nu}_e$ spectrum, β -decay characts. 0-78340
- Rb, fission fragment, delayed neutron branches from γ -spectroscopy 0-78230
- Rb, ground state spins, moments, charge radii by laser spectroscopy 0-78147
- ¹³²Sn levels, isomers, lifetimes and transition probabilities from fission 0-78163
- Tc decay, ^{104,106,108}Ru level scheme and transitions, collective model anal. 0-78166
- ²³⁰Th(n,f), 0.68-1.10 MeV, fission fragment ang. distrib., resonance and moment of inertia 0-102219
- ²³²Th(n,f), 2-8 MeV, fission product yields and mass distrib. 0-86939
- ²³²Th(p,f), 29-97 MeV, Rb, In and Cs relative independ. yields, charge division 0-102218
- (U, Pu) C, nuclear fuel, irradiation induced creep meas. 0-93605
- (U,Pu)C FBR fuel pins, fission gas release 0-57847
- (U,Pu)O₂ 0-63252
- (U,Pu)O₂, fission gas release and retention in irradiated nuclear fuels 0-57841
- U, assay of natural samples, meas. of gamma- or neutron activity of short-lived fission products 0-61179
- ^U²³³, product separation asymmetry in fission by slow polarised neutrons (Russian) 0-106088
- UC, nuclear fuels, irradi. induced kinetics, diffusion and fission gas resoln. 0-59523
- UO₂ 0-63252
- UO₂, fission gas release and retention in irradiated nuclear fuels 0-57841
- UO₂, high burnup nuclear fuels, relation between fission product release and fuel microstruct. 0-57845
- UO₂, nuclear fuels, distribution and size of intragranular fission gas bubbles 0-57840
- UO₂, nuclear fuels, fission gas release at high burn-ups 0-57852
- UO₂, nuclear fuels, irradi. induced kinetics, diffusion and fission gas resoln. 0-59523
- UO₂, volatilization pot. of metallic inclusions in irradiated nuclear fuel during LOF overheating transients 0-57895
- ^AU, A=235,238, fission product beta decay, $\bar{\nu}$ spectra 0-102150
- ^AU^m, A=236,238, isomeric to prompt fission angular; fission fragments from (d,pf), (d,pnf) 0-86940
- ^AU(n,f), A=233,235, ejection fission products angular depend. on thermally polarised neutron capture (Russian) 0-86941
- ²³⁴U under barrier photofission, 4-5.7 MeV, fragment ang. distrib. (Russian) 0-106090
- ²³⁵U fission fragment thermonuclear superheavy nuclei synthesis, prod. cross sections 0-95331
- ²³⁵U fission product γ radiation for short irradiated times, energy distrib. 0-73929
- ²³⁵U(n,f), symmetric fission, proton scatt. by fission fragments in neck area 0-83130
- ²³⁵U(n,f), thermal, fragment ionisation, charge distrib., stat. and instant perturbation theory (Russian) 0-63219
- ²³⁵U(n,f), thermal neutron induced fission, nuclear charge distribution in fission products 0-57808
- ²³⁵U(n, γ), thermal, d, t, He emission probabilities from stable core model (Russian) 0-68713
- ²³⁵U(n, γ), thermal, fission product $\bar{\nu}_e$ spectrum, β -decay characts. 0-78340
- ²³⁸U(γ ,f) 20 MeV, computer program for yield determ. of short-lived products 0-102215
- ²³⁸U(p,f), 11-29 GeV, three dimensions charge dispersion curves, isobaric yields 0-102111
- Xe fission gas release and microscopic swelling in LMFBR highly-rated MX-type fuels 0-57848
- Xe, from ²⁴⁸Cm and ²⁵⁰Cf in meteorites 0-63215
- Xe, radial distribution of bonded fission gas in mixed carbide fuel pins 0-57844
- Xe release from (U,Pu)C_{1-x}N_x LMFBR MX-type fuels 0-73921
- Xe release from UO₂-Zr high burnup nuclear fuel rods 0-57846
- ¹³⁵Xe, direct meas. of absolute and fractional independ. yields from ²³⁸U(γ ,f) 0-78341
- ¹³⁵Xe yield from ²³⁷Np(n,f) 0-86935

fission reactor cooling and heat recovery

- see also cooling: fission reactor core control and monitoring
- 7-pin bundle simulation during flow rundown transient 0-68879
- AGR once-through nuclear boiler at 14.5 MPa, hydrothermal and chemical conditions 0-63232
- AGR once-through high press. boiler feedwater solutes behaviour 0-63233
- boiling crisis, nuclear reactor safety and performance, state of the art review 0-63312
- Browns Ferry BWR, load following test 0-68892
- BWR, calc. of shutdown dose rate around recirculation pipes, radioactive corrosion products in primary cooling water 0-68734
- BWR, feedwater and recirculation control system coordination 0-73880
- BWR, heating, ventilation and air conditioning systems (Japanese) 0-91212
- BWR, iron oxide deposition on heated surfaces, model 0-73902
- BWR, primary containment vessel, spray heat removal characteristics 0-73972

fission reactor cooling and heat recovery continued

- BWR, safety relief valve discharge loads, dynamic effects on structures and eqpt. 0-99236
- BWR, steam chugging during LOCA, general transient anal. 0-73903
- BWR, TRAB transient analysis program for pressure vessel and subsystems 0-73978
- BWR cluster geometry, enthalpy and mass flow distribution 0-78359
- BWR condensate feedwater system, dynamic model 0-73883
- BWR containment system, effect of torus wall flexibility on hydro-structure interaction 0-83195
- BWR coolant pipes, intergranular stress cracking, in-service inspection influences 0-68887
- BWR decay heat removal systems, probabilistic risk assessment, fault and event tree anal. 0-63333
- BWR LOCA, hydrodynamic lead characteristics of primary containment vessel 0-73972
- BWR LOCA, phased mission analysis of ECCS failures 0-68851
- BWR LOCA, press. oscill. phenomena induced by steam condensation, in containment with press. suppression system 0-68848
- BWR LOCA, steam fraction determ. in flowing air/stream mixtures by meas. of IR rad. attenuation 0-75010
- BWR LOCA analysis, jet pump modelling using RELAP4 0-68850
- BWR long-term cooling, closed form analytical model 0-78355
- BWR NSSS structural integrity programs at GEC 0-99230
- BWR pressure-suppression system, steam chugging anal., heat transfer and fluid mechanics characts. 0-95339
- BWR turbine trip transient analysis using ALMOS plant model (German) 0-83177
- condensation heat transfer, nonequilibrium temp. profiles, mass transfer engineering calc. 0-63227
- condensation-driven fluid motions, nuclear reactor safety 0-63228
- conference, Berlin, Germany (Aug. 1979) 0-77539
- coolant flow rate determ. using ¹⁶N decay activity meas. 0-73955
- coolant interchannel interaction for prolonged flow around bunches of rods 0-73888
- countercurrent flow limitation, heater rod dynamics effects 0-73906
- critical two-phase flow, bubble nuclei 0-64615
- critical two-phase flow models, nuclear reactor safety 0-63229
- departure from nucleate boiling ratio safety limit to modelling parameters in COBRA IIIC/MIT 0-73901
- depressurisation studies, transient density, press., temp. variations, during discharge 0-57833
- Dounreay test reactor, fast breeder test experience 0-86961
- drag disk dynamic anal. in transient two phase flow 0-73907
- ducts, one-dimensional models for transient gas-liquid flows 0-64614
- dynamics of nuclear power facilities upon deterioration of heat exchange 0-63234
- electrical system design for future AGR power stations 0-57935
- EURDYN-1M, safety studies on LMFBR, computer program 0-99267
- fast breeder test reactor operator training simulator model development 0-91219
- fast reactor fuel, thermohydraulic performance for low duct dilation 0-73893
- fast reactor fuel assembly, turbulent laminar flow characteristics (Czech) 0-68738
- FBR safety and economics, leak detection, cooling, waste disposal 0-63303
- FBR thermal hydraulics, sensitivity theory for general systems of non-linear equations 0-86954
- feedwater systems, auxiliary, fault tree anal. 0-63332
- flow anomaly diagnosis, autoregressive model appl. (Japanese) 0-83146
- flow boiling dynamics in film region 0-83142
- flow structure for critical discharge conditions of boiling water through cyl. channels 0-83145
- fluid dynamic transient analysis using ASWR method with staggered meshes (German) 0-83176
- fuel rod bundle, cross flow heat transfer via the fuel elements 0-63226
- fuel thermocouples and liquid-level probes for core monitoring 0-99239
- GCFR, core thermal hydraulics and pumping power anal. code JUPITER 0-73889
- heat transfer downstream of blockage with discrete permeability in rectangular channel 0-69915
- HTGR, dynamic characts., primary loop characts. (Japanese) 0-57832
- HTGR, fission product plateau in primary cooling system, in situ meas. using Ge(Li) spectrometer 0-73881
- HTGR, hydrogen secondary cooling system, construction and performance tests (Japanese) 0-91210
- HTGR radiative gas heat exchangers, radiation effects at high temps. 0-95338
- HWR, shutdown heat removal systems, reliability fault tree anal. and β -factor method 0-63331
- inverted annular film boiling heat transfer formulation 0-73899
- Isar BWR power station, transient expts. during startup and initial operation (German) 0-83187
- lightly damped tubular arrays, damping props, flow induced vibr. tests 0-68760
- liquid level detector based on level sensitive transducer for PWR environment 0-57874
- LMFBR, chemical leak detection, effects of NaOH in Na 0-63326
- LMFBR, diffusion type H₂ meter in Na loop 0-68728
- LMFBR, hydrodynamics of large-scale fuel-coolant interactions 0-78409
- LMFBR, molten UO₂ fuel-Na coolant thermal interaction, characterisation of fragmented fuel 0-68774
- LMFBR, Na boiling detection, power spectral density surveillance systems 0-68740
- LMFBR, Na purification system, cold traps and plugging indicator 0-99209
- LMFBR, Na-H₂O steam generators, safety problems and their solution in the USSR 0-63318
- LMFBR, pool type, natural circulation cooling 0-102289
- LMFBR, pressure transient analysis in piping systems including the effects of plastic deformation and cavitation 0-74775
- LMFBR, rod bundle, static press. meas. 0-73969
- LMFBR, shutdown heat removal systems, reliability fault tree anal. and β -factor method 0-63331
- LMFBR, surface temp. distrib. of peripheral fuel elements, approx. thermal modelling 0-63237
- LMFBR, two-phase flow calculations in low-pressure systems 0-103068
- LMFBR, wire wrapped rod bundles, coolant mixing, peripheral flow prediction 0-73891

fission reactor cooling and heat recovery continued

- LMFBR coolant flow rate meas. using electromagnetic converter 0-73887
- LMFBR cooling systems, reliability 0-57838
- LMFBR fuel and blanket transient thermal performance characteristics 0-68880
- LMFBR fuel intra-assembly flow mixing uncertainty, statistical determination methodology 0-73890
- LMFBR fuel rod subassembly, thermal-hydraulic anal. as distrib. parameter system (*Japanese*) 0-68736
- LMFBR HCDA, energetics of bubble expansions, potential attenuation mech. 0-83197
- LMFBR HCDA, I-D compressible coolant dynamics, numerical anal. using EULFCL code 0-68733
- LMFBR intersubassembly transient heat transfer code, TCLUS1 0-63231
- LMFBR LOCA, dynamics of natural circulation 0-57836
- LMFBR mesh-packed cold traps, O₂ impurity deposition, computational program 0-57824
- LMFBR ML-3 Na circuit, electrical and control installations (*Spanish*) 0-57819
- LMFBR outlet plena, stratification criteria 0-73892
- LMFBR rotating shield plug annulus, Na vapour deposition rates and gas flow patterns 0-68732
- LMFBR steam generator stability, STMFREQ code 0-73908
- LMFBR subassembly pressure loss, expt. study and evaluation 0-73894
- LMFBR triangular rod array, flow resistance wall shear stress in interior subchannel 0-63244
- LMFBR vented fuel assembly, thermodynamic modelling and testing 0-83144
- LMRBR, interchangeable core assessment, coolant orifice zoning 0-102229
- LOCA, data analysis using computer-aided models (*Czech*) 0-73949
- LOCA analysis in small compact reactors using RELAP4/MOD5 thermal hydraulic code 0-68852
- LOCA consequences, hydrodynamics mass method anal. 0-73909
- LOFT, contribution to nuclear reactor safety 0-106139
- LOFT, requalification following LOCE 0-57904
- LOFT drag disc turbine meter rakes for two-phase flow measurement 0-102260
- LOFT reactor secondary cooling system, waterhammer phenomena 0-57905
- loss-of-coolant accidents, German Risk Study (*German*) 0-57866
- LWR critical heat flux calc., anal. of empiric relations using CRISIS code (*Bulgarian*) 0-68766
- LWR LOCA, fission product decay energy release rates following ²³⁵U fission 0-57894
- LWR LOCA, modelling of press. and temp. changes in two-phase, two-component flow (*Bulgarian*) 0-68904
- LWR LOCA, rewetting models, review and comparison 0-83194
- LWR LOCA, two-phase flow instrumentation for safety anal. 0-102259
- LWR materials of primary-circuit components, safety concepts, quality (*German*) 0-73914
- LWR piping, intergranular stress-corrosion cracking 0-81234
- LWR safety, condensation heat transfer in stably stratified systems 0-63311
- mass exchange rates in ¹⁶N tagged slug flow 0-73911
- monitoring of boiling water and of steam content using Cherenkov radiation 0-73957
- natural-circulation steam generator model for optimal steam generator water level control 0-68876
- nuclear heating in thick iron slabs at the ORR pool side facility 0-63241
- nuclear power station PWR, ice condenser system (*Japanese*) 0-91214
- nuclear power stations, accumulation ponds cooling possibility analysis (*Slovenian*) 0-91208
- once through steam generator, Na-heated, stability anal. nuclear reactor systems model 0-91218
- PBHTGR, core behaviour following massive air ingress, graphite corrosion eval. (*German*) 0-83181
- PBHTR, afterheat removal system failure, radiant heat transfer anal. 0-95364
- pebble bed HTR, delayed after heat removal (*German*) 0-106102
- piping system design, rationalisation of power plant pipe break criteria 0-99205
- PNP-3000, prototype nuclear process heat reactor, core temp. transients, heat transfer calc. (*German*) 0-83180
- power reactor, water cooled and moderated, tube film boiling heat transfer coeffs. 0-73877
- power system equipment and components, multiphase flow prediction 0-64616
- pressure boundary leakage detection system 0-63306
- primary coolant circuit service life, working condition effects (*Czech*) 0-73885
- primary coolant flowmeter 0-73912
- PWR, core reflooding, progress of hardening front (*French*) 0-91211
- PWR, critical heat flux in fuel bundles at low mass vel. 0-73900
- PWR, dynamic pressure, scale flow modelling of random press. power spectral density 0-83143
- PWR, fluid, structure interactions, numerical anal. method 0-73884
- PWR, scaling air-water flooding 0-73904
- PWR, shutdown heat removal systems, reliability fault tree anal. and β -factor method 0-63331
- PWR, two circuit system, licensing and design, European view 0-57930
- PWR, two phase flow modelling for LOCA (*French*) 0-78349
- PWR boiler steam generators, two-phase flow problems in low press. transients (*French*) 0-78350
- PWR boiler tubes, denting type corrosion, control by use of neutralisers 0-106109
- PWR constructional elements vibrations, due to cooling medium flow, meas. and evaluation (*Hungarian*) 0-63304
- PWR core barrels with and without holes, various edge conditions, hydrodynamic vibrations 0-78406
- PWR critical heat flux in rod bundles using round tube correlation 0-73898
- PWR dynamical behaviour modelling in FORTRAN 0-91217
- PWR fuel clad failure characterisation based on fission product activity, PROFIP 3 code 0-95365
- PWR LOCA, average void fraction estimate in vertical two phase flow channel 0-73878
- PWR LOCA, opening and extension of circumferential cracks in pipe 0-78364

fission reactor cooling and heat recovery continued

- PWR LOCA, pump behaviour conveying two-phase flow (*French*) 0-78351
- PWR LOCA reflood, effect of low containment press. on peak cladding temp. 0-57897
- PWR nuclear power station, heating, ventilating and air conditioning systems (*Japanese*) 0-91213
- PWR power station secondary water chemistry study, progress report 0-106108
- PWR pressuriser behaviour during operational transient, math. model 0-63230
- PWR primary and secondary water chemistry, European experience 0-106110
- PWR vessel and primary circuits estimation of reliability, probabilities and adaptive models 0-106125
- safety, fault tree anal. using Monte Carlo and anal. methods (*Spanish*) 0-57870
- saturated steam parameters in reactor containments with escape of coolant, simplified calc. 0-68764
- shutdown heat removal system failure, fault tree, common-cause anal. 0-63334
- small bore piping, field support to ASME Section III rules 0-63346
- SNR-300 LMFBR, accidents in tertiary system, dynamic behaviour of steam generators (*German*) 0-83141
- SNR-300 LMFBR, ECCS, decay heat removal during heat sink failure, accident anal. using NOTUNG code (*German*) 0-83185
- stability analysis and characts. for two-phase flow eqn. systems with viscous terms 0-59103
- steam content, calculation of the true volume proportion of steam in the driving section of a natural-circulation loop 0-86957
- steam generator thermal hydraulics 0-95342
- steam generator tube performance in water cooled reactors in 1978 0-78399
- steam generator tubes testing and evaluation, using CIS/DASIO system (*Czech*) 0-63301
- subchannel void drift model, analytic derivation 0-68759
- subchannel void drift model, analytic derivation 0-73905
- temperature noise in one-phase heat transfer: stochastic models 0-68726
- tensor formulation of the fluid-solid interaction force for multidimensional, two-phase flow within tube arrays 0-92211
- thermal mixer, advanced design, performance 0-63243
- thermal reactor, rapid decomposition effects on bubble transition 0-73897
- thermal reactor convective heat transfer coefficient enhancement in two-phase nonboiling flow 0-73895
- thermal reactors, film boiling destabilisation due to pressure shock arrival 0-73896
- thermal-hydraulics, quality influence on the departure from nucleate boiling in cross flows through bundles 0-95340
- thermomechanical instability of a heat releasing granular layer, GCR model 0-92134
- two phase flow modelling, theoretical foundation, appl. to fission reactor fluid flow and heat transfer 0-103065
- two-phase flow in pin bundle, two fluid model 0-91209
- two-phase flow operating conditions (*French*) 0-78348
- two-phase stratified horizontal flow, averaged and local instantaneous formulations, stability 0-64613
- two-phase-flow instrumentation development at Brookhaven National Laboratory 0-102261
- void-distribution effects in void measurements using scattered/uncollected neutrons 0-73910
- vortex diodes in post accident heat removal systems 0-106100
- walls, permeable, cooling characts., heat exchange, rad. emitter design 0-64535
- water chemistry of reactor coolant (*Japanese*) 0-68737
- CO₂ fundamental condensation cycles in steam and nucl. power plants, performance characts. 0-63368
- EBR-II Na system cold traps for control of O₂, H₂, T impurities 0-78411
- N₂O₄ fission reactor coolant, heat transfer on condensation (*Russian*) 0-57860
- N₂O₄ turbulent dissoc. flow, along heated tubes, heat transfer 0-63225
- SiC ceramic heat exchanger, cost-effective design 0-95341
- UF₆-CF₄ mixture, gas core fission reactor, fission based plasma engine 0-63366
- UO₂ fuel-coolant interaction, film boiling and vapor explosion phenomena 0-95363

fission reactor core control and monitoring

- see also fission reactor safety; fission research reactors; nuclear engineering; nuclear reactor instrumentation
- accelerator-driven breeding blankets, neutron-return effects, implications for fuel enrichment without reprocessing 0-57914
- Browns Ferry BWR, load following test 0-68892
- BWR, ASEA-ATOM, core supervision system 0-68883
- BWR, in-core neutron detector noise, local component modelling 0-68866
- BWR computer based control systems 0-83211
- BWR condensate feedwater system, dynamic model 0-73883
- BWR control cell core design concept 0-68763
- BWR core calculations using improved coarse mesh methods 0-68849
- BWR core concept, WNS-type fuel, equilibrium cycle performance 0-68762
- BWR decay heat removal systems, probabilistic risk assessment, fault and event tree anal. 0-63333
- BWR fuel preconditioning, initial pressurisation, fuel temps., fission product release 0-63357
- BWR fuel preconditioning 0-63360
- BWR fuel rod relocation, gap conductance anal. 0-83192
- BWR in-core neutron detector sensitivity to control rod vibr. using neutron noise anal. 0-57910
- BWR LOCA, phased mission analysis of ECCS failures 0-68851
- BWR LOCA, pool swell modelling and small-scale expts., comparative eval. 0-95362
- BWR LOCA, pool swell reduced scale simulations, scaling law limitations 0-99238
- BWR reflectors, effective albedo parameter determination 0-68756
- CANDU-PHW 600 MWe reactors, channel power mapping and calibration routing 0-57892
- control and instrumentation designs beyond the 1980s 0-57872
- control guidelines 0-106119
- control theory, steady-state accuracy of neutron field regulation 0-63319

fission reactor core control and monitoring continued

coolant flow rate determ. using ^{16}N decay activity meas. 0-73955
 coolant interchannel interaction for prolonged flow around bunches of rods 0-73888
 coupled-core nuclear reactor, distributed parameters identification, pseudorandom perturbation and correlation anal. 0-86966
 critical assembly fuel elements, apparatus for determ. of relative fission density release (*Russian*) 0-73973
 critical facility, fast neutron spectrum meas. using (n, α) and (n, p) reactions 0-78403
 digital computer applications in reactor instrumentation and control 0-106134
 directional fully encapsulated gamma detector for in-core reactor meas. 0-63307
 Doppler feedback use in control rod drop transients, Maine Yankee expt. 0-68895
 Dounreay test reactor, fast breeder test experience 0-86961
 EBR-II, in-reactor measurement of neutron absorber performance, He release of B_2C 0-73951
 EBR-II reflector assembly irradiated induced bowing, implications for core restraint design 0-104234
 energy distribution, algorithm for extremal control 0-83209
 failed fuel element detection, delayed neutrons meas. (*Polish*) 0-73952
 failure location algorithm for complex networks 0-99228
 Fast Breeder Blanket Facility reaction rate and neutron energy spectrum meas. 0-68865
 fast breeder core with internal blanket 0-68870
 fast reactor analysis, composition self shielding factors 0-73965
 fast reactor pulsed neutron die-away dispersion laws, modelling method 0-68867
 FBR, neutron spectra in the MeV range in fast critical assemblies 0-83210
 FBR, space dependent simulation of transient behaviour using KINTIC-2 code (*German*) 0-83182
 FBR, zero-power neutron noise expt. anal., power spectral density and subcritical reactivity 0-57911
 FBR blanket facility, gamma-ray heating rate meas. in stainless steel and Pb 0-57912
 FBR containment code, structural deform., SEURBNUK-2 0-78404
 FBR containment code validation program, SEURBNUK 0-78405
 FBR fuel pin safety expts. at SLSF, centerline fuel thermocouple performance 0-102283
 FBR HCDA, convective heat transfer correlations for molten core debris pools growing in concrete 0-83196
 FBR transient fuel behaviour maps, fuel response to thermal transients 0-57926
 FBR transient fuel behaviour maps, fuel response to thermal transients 0-68874
 FDR type reactors, transient anal., neutron power and temp. form factors, depend. on time and power level 0-83178
 fission reactor fuel performance modelling, pellet-cladding interaction 0-63264
 Ford reactor, equilibrium core calcs. with reduced enrichment fuel 0-68885
 Ford reactor, neutronic anal. using low enrichment fuel 0-68886
 Ford reactor, reduced enrichment fuel effects on performance and utilisation 0-63344
 FTR, criticality expts. with concrete reflected fuel pins in water 0-78410
 fuel bundle thermal-hydraulic anal., comparison of computational techniques in COBRA-IIIC and COBRA-IIIP (*Japanese*) 0-95374
 fuel preconditioning, power shock anal. and sipping 0-63358
 fuel preconditioning, TVA Browns Ferry Nuclear Plant, in-core management and core manoeuvring 0-63359
 fuel thermocouples and liquid-level probes for core monitoring 0-99239
 FUGEN LWR, reactor physics tests 0-68893
 FUGEN plant dynamic tests 0-68894
 gas tagging of fuel failure, simultaneous identification of multiple failures using barycentric-coords. tech. 0-83191
 guard line circuits dual microprocessor system, decision-making and self-testing 0-57901
 HCDA, bubble worth variation in molten cores 0-68854
 HCDA, neutronics and hydrodynamics equations, energy release, DISCAL code 0-68842
 hot pellet nuclear reliability factors 0-68754
 HTGR, nonlinear dynamic anal. of prismatic graphite fuel elements, response to seismic excitation 0-99237
 HTR, Xe dynamics, 2D reactor models, axially collapsing methods (*German*) 0-68731
 HWR TV-O, active core neutron spectrometry using Bonner spheres (*Czech*) 0-73948
 in-reactor fuel temperature, transient response of centreline thermocouples, appl. to fuel modelling 0-95372
 instrumentation and control test loop diagrams 0-68890
 integral parameter correlations, reactor performance using data covariances 0-68869
 intermediate energy standard neutron field, ENDF/B-V cross sections 0-63325
 linear extrapolation distance for a black cylindrical control rod with the pulsed neutron method 0-68839
 LMCBR, heterogeneous, core power distrib., sensitivity to localised reactivity insertion 0-68881
 LMFBR, gas tag identification of failed assemblies, anal. methods 0-95369
 LMFBR, heterogeneous, breeding performance improvements 0-68882
 LMFBR, hydrodynamics of large-scale fuel-coolant interactions 0-78409
 LMFBR, rod bundle, static press. meas. 0-73969
 LMFBR, safeguards system for monitoring of fissile material inventory 0-63293
 IMFBR fuel and blanket transient thermal performance characteristics 0-68880
 LMFBR HCDA, energetics of bubble expansions, potential attenuation mech. 0-83197
 LMFBR HCDA, US meas. of penetration of liquid Na into limestone concrete 0-78412
 LMFBR HCDA aerosol behaviour, kinetic corrections to aerosol gravitational collisional efficiency 0-95386
 LMFBR TOP accident, implications of in-channel fuel plugging 0-78414
 LOCA, reflooding phase, flow film boiling, void fraction meas. 0-92207
 LWR, thermal neutron disadvantage factors for $\text{PuO}_2\text{-UO}_2$ and UO_2 lattices 0-73945

fission reactor core control and monitoring continued

LWR core analysis, qualification of SIMULATE against the Hatch-1 end-of-cycle 1 gamma scan 0-57921
 LWR core, few group 2-D diffusion eqns. in hexagonal geometry, HEXAB-II-30E code (*Bulgarian*) 0-68765
 LWR core, minimisation of energy distrib. inhomogeneities 0-63321
 LWR critical heat flux calc., anal. of empiric relations using CRISIS code (*Bulgarian*) 0-68766
 LWR irradiated fuel assemblies, nondestructive exam. using γ -ray and neutron techniques 0-66760
 LWR LOCA, two-phase flow, horizontal stratified, 1-D two-fluid eqns. 0-91226
 LWR refuelling shutdown, multiple controlled-cell removal 0-99252
 Magnox reactors, Trawsfynydd, computerised monitoring and control system 0-86965
 material safeguards, unirradiated fuel control in BOR-60 fuel assemblies (*Russian*) 0-68809
 materials safeguarding, fuel assembly identification using US signatures, statistical aspects 0-69620
 materials safeguarding, remote-controlled and long-distance unique identification of reactor fuel elements or assemblies 0-63296
 materials safeguards, in situ verification techniques for fast critical assembly cores 0-78390
 metallic fuel cladding eutectic formation during postirradiation heating in EBR-II 0-102241
 microprocessor controlled multipoint recorder with graphical video output for reactor core temperatures 0-57873
 microprocessor-based flux wire evaluation and anal. system 0-63353
 MIT research reactor, flux synthesis techniques for routine core physics calcs. 0-68868
 monitoring of boiling water and of steam content using Cherenkov radiation 0-73957
 monitoring system improvement due to improved computer technology 0-57882
 multicore reactor, optimal control determ. from energy release profile (*Russian*) 0-73974
 NBS standard neutron fields, average fission cross-section meas., error anal. 0-68857
 neutron absorption, control poison optimisation, depletion calcs. 0-57906
 neutron fluence meas. using solid state nuclear track detectors with Au and In foils 0-69035
 neutron noise analysis in PWR and BWR power reactors 0-86964
 neutron-physical characteristics of Soviet BABETs reactors, startup experience 0-73953
 non-destructing testing of reactor components using acoustic emission (*Spanish*) 0-57871
 nondestructive neutron assay for nuclear materials accountability and criticality control 0-66759
 nonlinear reactor noise anal., appl. of Langevin eqn. with system-size expansion 0-68727
 optical instrumentation methods for two-phase reactor flows 0-63313
 Palisade PWR, physics model verification 0-63322
 pattern recognition systems, ORNL expts. 0-63351
 PB-HTGR, control-rod induced flux perturbations, numerical anal. using out-of-force instrumentation (*German*) 0-83179
 PBHTGR, core behaviour following massive air ingress, graphite corrosion eval. (*German*) 0-83181
 PBHTR, afterheat removal system failure, radiant heat transfer anal. 0-95364
 plant diagnostics—the integrated approach 0-68899
 PNP-3000, prototype nuclear process heat reactor, core temp. transients, heat transfer calc. (*German*) 0-83180
 power coefficient measurement based on reactor coolant system average temp. 0-57909
 power density limitation system development 0-68884
 power spectral density measurements with ^{252}Cf for a light-water-moderated research reactor, determ. of reactivity of far-subcritical systems 0-57913
 pressure tube-type reactors, moderator temp. coeffs. of reactivity meas. 0-57893
 prompt neutron yield calcs. from neutron induced fission 0-68858
 protection system software validation, quality assurance experience 0-57886
 PWR, clad free pellet recriticality possibilities 0-68863
 PWR, dynamic pressure, scale flow modelling of random press. power spectral density 0-83143
 PWR, eval. of annular fuel economic benefits 0-57919
 PWR, evaluation of fuel performance (*Japanese*) 0-99226
 PWR, neutron noise diagnostics of 2-D control rod vibrs. 0-68840
 PWR, three loop, simulation in advanced recycle methodology program 0-68856
 PWR control rod digital position indicating system (*Japanese*) 0-63314
 PWR core analysis, effects of improved UO_2 once-through fuel cycle 0-57917
 PWR core analysis, methods and data validation 0-57924
 PWR core analysis, steady-state core physics and thermal-hydraulic reload design calcs. 0-57923
 PWR core analysis, transport-to-diffusion theory for gadolinia-loaded fuel pins 0-57908
 PWR core analysis using EPRI ARMP program, calc. and meas. reactor physics parameters 0-57925
 PWR core analysis verification, reactivity rundown and power distrib. accuracy 0-57922
 PWR core barrels with and without holes, various edge conditions, hydrodynamic vibrations 0-78406
 PWR core control, multistage mathematical programming 0-91227
 PWR core power manoeuvres, fuel duties and fuel preconditioning, FLAIR-CENSOR 0-63337
 PWR engineered safety features actuation system follow-up system logic 0-57879
 PWR fuel cycle alternatives, reactor physics anal. 0-57918
 PWR fuel induced cladding deformation, Zircaloy creep correl., in-pile meas. 0-97547
 PWR tight-pitch cores, reactor physics of fuel cycles 0-57920
 PWR with wide vessel to concrete air gaps, ex-core detector sensitivity studies 0-73970
 reactivity coefficient charges in Soviet RBMK reactors 0-73954
 reactivity coefficients, perturbation effects from point-kinetics model (*Hungarian*) 0-78346
 reactor core gamma dosimetry, solid state nucl. track detector appl. 0-95466

fission reactor core control and monitoring continued

- reactor noise, AR-MA anal. hidden state variables 0-73944
- reactor physics considerations in design for improved BWR fuel cycles 0-57916
- remote multiplexing for nuclear reactor instrumentation and control circuits 0-57885
- resonance absorption calculations in thermal reactors 0-86955
- self absorption factor of gamma radiation in reactor fuel assemblies 0-63320
- SNR-300 LMFBR control and load following performance (*German*) 0-83184
- space dependent stochastic neutron kinetics with Gaussian parametric excitation 0-63223
- space independent low power model, multigroup energy formalism for reactor stochastic eqns. 0-63224
- steam generator tubes testing and evaluation, using CIS/DASIO system (*Czech*) 0-63301
- STF 3/4 critical assembly, worth and reaction rate calcs. 0-68864
- subcritical cyclostationary nuclear reactor, neutron counting statistics, sinusoidally modulated neutron source 0-99203
- thermal power determ. using neutron flux density meas. 0-73955
- thermal reactor assemblies, effective neutron diffusion parameters 0-73874
- thermocouples, 2200°C fuel centerline for LOFT program 0-57877
- Three Mile Island incident, operator/instrumentation interactions 0-57890
- TMI-2 accident, analysis of high readings by startup channel neutron detectors 0-102265
- TMI-2 accident, nuclear reactor safety, role of instrumentation and control (*Japanese*) 0-73947
- track-etch monitor for reactor power anal., evaluation 0-78418
- transport lag, stability effect on reactor control 0-57891
- TRIGA III reactor, anal. of standard and FLIP fuel mixed loading patterns 0-57855
- US thermometry appls. 0-73365
- US viewing system for reactor fuel assemblies under liquid Na 0-57875
- Westinghouse reactors, secondary neutron source, benefit of early removal 0-63343
- wire-wrapped core assemblies, turbulent flow split modelling and expts. 0-95370
- Yankee reactor physics method verification 0-63323
- ZPPR, critical experiments for 600-700 MW LMFBRs 0-68859
- ZPPR pin geometry, SDX cell homogenisation code validation 0-86962
- ZPPR-9, control rod interaction meas. 0-63324
- ZPPR-9, stimulated hodoscope slot effect in STF critical assembly 0-68860
- BWR, primary containment vessel, spray I₂ removal characteristics 0-73972
- CF₄-UF₆ mixture, gas core fission reactor, fission based plasma engine 0-63366
- platinum self-powered in-core detectors for PWR core power distrib. monitoring 0-73971
- (U,Pu)₂O₇ fuel pin behaviour during FFTF 3c/s reactivity insertion event, TREAT expt. anal. 0-102240
- UF₆, high temp. fissioning plasma core reactors, fluid mechanical confinement 0-63248
- ²³⁸U, neutron capture self-indication meas., shape anal. 0-68753

fission reactor fuel

- see also claddings; fission of plutonium; fission of uranium; fission reactor fuel preparation and reprocessing; isotope separation; radioactive waste
- accountability, U and P NDA of crated waste by gamma-ray and neutron coincidence counting 0-83166
- accounting and safeguarding, spent fuel bundle counter for 600 MW CANDU reactor 0-63269
- alpha waste production and proliferation hazard of different fuel cycles 0-83214
- Alpha-Gamma Hot Cell Facility at Argonne-East 0-68779
- autoradiographic inventory methods for nondestructive assay of reactor fuels and fuel assemblies 0-71875
- burn-up determination using gamma spectrometric nondestructive assay for IAEA safeguards 0-68806
- burn-up determination using gamma spectrometry, IAEA safeguards experience in Czechoslovakia 0-63292
- burn-up measurement using spatial power distrib. eval. and gamma spectrometry 0-68803
- burnup determination using Aragonit γ detector 0-63262
- BWR core operation flexibility for improved fuel cycles 0-57915
- BWR fuel cycle improvements, reactor physics considerations 0-57916
- BWR fuel preconditioning, initial pressurisation, fuel temps., fission product release 0-63357
- BWR fuel preconditioning 0-63360
- BWR fuel rod relocation, gap conductance anal. 0-83192
- BWR spent fuel element storage, neutron physical aspects 0-68841
- BWR spent fuel safeguarding, nondestructive assay using gamma spectrometry 0-68802
- Caramel fuel cladding rupture, development and detection at OSIRIS experimental reactor (*French*) 0-95371
- carbide fuel pins, Na-bonded, fission gas release studies (*French*) 0-73916
- carbide fuels, effect of burn-up and temp. on appearance of optically visible fission gas bubbles 0-63251
- ceramic nuclear fuels, irradiated rare gas diffusion 0-59524
- clad failure prediction during FBR overpower transiency, JANE code 0-78363
- computer system for automatic inspection of fuel pellets 0-68795
- computerised tomography appl. for fuel-element inspection 0-73927
- conference, Berlin, Germany (Aug. 1979) 0-77539
- CRBRP fuel rod design analysis, life limiting criteria on ductility limited strain and cumulative damage function 0-102252
- creep, irradiation induced, transient state, kinetic eqn. treatment 0-88251
- criticality safety analysis in nuclear fuel cycle (*Japanese*) 0-99225
- distribution of speculative uranium resources 0-78369
- EBR II, metallic driver fuel, irradiated, perform. at high burn-up, fuel-cladding interactions 0-95348
- element cladding, corrosion product deposition, heat transfer model (*Bulgarian*) 0-71818
- enriched U, lower costs 0-106111
- failed fuel element detection, delayed neutrons meas. (*Polish*) 0-73952
- failure, performance modelling, pellet-cladding interaction 0-63264

fission reactor fuel continued

- fast reactor fuel, thermohydraulic performance for low duct dilation 0-73893
- FBR, role of fission gas swelling and release in reactor accidents 0-57854
- FBR fuel development, international development programs 0-102248
- FBR fuel handling, radiation safety 0-73985
- FBR fuel pin safety expts. at SLSF, centerline fuel thermocouple performance 0-102283
- FBR oxide fuels, dynamic response of grain boundary cavities to stress and temperature changes under conditions of continuous gas generation 0-66544
- FBR transient fuel behaviour maps, fuel response to thermal transients 0-57926
- FBR transient fuel behaviour maps, fuel response to thermal transients 0-68874
- FBR UO₂-fuelled blanket assembly design considerations 0-102254
- FFTF, instrumented fuel test at the fuels open test assembly 0-102247
- FFTF fuel systems design criteria 0-102251
- fissile materials safeguards, quantity and isotopic comp. meas. (*Russian*) 0-63287
- fission gas behaviour, conf. Karlsruhe, Germany (Oct. 1978) 0-56992
- French contribution to reduced enrichment research and test reactor program 0-68931
- fuel pin rupture detection system using meas. of time differential of acoustic emissions 0-102282
- fuel pins, fast breeder, fuel-cladding mech. interaction, obs. and anal. 0-86959
- fusion-fission symbiosis, nuclear fuel trajectories, fissile and fusile fuel characterisations 0-68947
- future nuclear power technology, impact of nuclear research in India 0-95345
- gas release and swelling, operational model, grain boundary gas 0-95346
- gas tagging of fuel failure, simultaneous identification of multiple failures using barycentric-coords. tech. 0-83191
- gas-discharge reactor, fuel element component conc., plasma temp. profile instabilities 0-63253
- grain boundary loss terms, use in fission gas release and swelling models 0-63257
- high U density fuel for test and research reactors 0-68801
- hot cell extension optical profilometer 0-68789
- HTGR, nonlinear dynamic anal. of prismatic graphite fuel elements, response to seismic excitation 0-99237
- HTGR coated particle fuels, SiC coating corrosion by fission product Pd 0-102237
- HTGR fuel particles, fission gas content meas. apparatus 0-68793
- HTGR fuel rod fabrication, estimation and control 0-83215
- in-core irradiation facilities, development and expt. using JRR-2 and JMTR research reactors, Japan (*Japanese*) 0-63256
- in-reactor fuel temperature, transient response of centreline thermocouples, appl. to fuel modelling 0-95372
- international resources assessment 0-99215
- irradiated fuel assemblies, burn-up and cooling time determ. using gamma spectrometry 0-63289
- irradiated LWR fuel, European transport experience 0-63309
- irradiated nuclear reactor fuel rod components, EM separation, feasibility 0-99224
- irradiation test facility for high U-loaded fuel plates as part of reduced enrichment program 0-68932
- isotopic correlations in irradiated fuel from VVER power reactors (*Russian*) 0-68838
- LMFBR, gas tag identification of failed assemblies, anal. methods 0-95369
- LMFBR, heterogeneous, fuel element performance, impact of design and operating parameters 0-102249
- LMFBR, hydrodynamics of large-scale fuel-coolant interactions 0-78409
- LMFBR, molten UO₂-fuel-Na coolant thermal interaction, characterisation of fragmented fuel 0-68774
- LMFBR advanced MX-type fuels, fission gas swelling, temp. depend. 0-57842
- LMFBR advanced MX-type fuels, low-temp. microscopic swelling, phenomenological model 0-57851
- LMFBR advanced MX-type fuels, swelling mechanism anal. 0-57850
- LMFBR fuel, fission gas behaviour during overpower transient, calcs. using COREF-1 code 0-57853
- LMFBR fuel behaviour during HCDA, intragranular fission gas behavior under isothermal conditions 0-102236
- LMFBR fuel disruption following LOF accident, in-pile expt. using high-speed cinematography 0-78366
- LMFBR fuel rod subassembly, thermal-hydraulic anal. as distrib. parameter system (*Japanese*) 0-68736
- LMFBR heterogeneous core design with interchangeable oxide/carbide fuel, CDS development program 0-102253
- LMFBR highly-rated MX-type fuels, fission gas release and microscopic swelling 0-57848
- LMFBR metal fuel elements, development and performance 0-57856
- LMFBR TOP accident, implications of in-channel fuel plugging 0-78414
- LMFBR universal core layout, interchangeability of hetero(homo)geneous cores and oxide/carbide fuels 0-102228
- LMRBR, interchangeable core assessment, coolant orifice zoning 0-102229
- LMRBR interchangeable core assembly design 0-102230
- LOFT, contribution to PWR fuel behaviour 0-106139
- LWR, irradiated fuel assemblies, burn-up meas. for nuclear material safeguards, IAEA experience 0-68807
- LWR fuel burn-up determ. from ¹³⁴Cs/¹³⁷Cs activity ratio (*Russian*) 0-68804
- LWR fuel rod, transient pellet-cladding interaction, ISUNE-4 computer anal. 0-91228
- LWR irradiated fuel assemblies, nondestructive exam. using γ -ray and neutron techniques 0-66760
- LWR power stations, incremental fuel cost calcs. using FAPMAN-IC program module 0-95356
- LWR reference fuel rods, acquisition and safeguards verification 0-68813
- LWR spent fuel, alpha spectrometric meas. for SNM verification 0-78424
- LWR spent fuel, non-destructive anal. using inherent and induced neutron radiation (*Russian*) 0-68805
- LWR spent fuel, nondestructive meas. and verification for materials safeguards 0-78420

fission reactor fuel continued

- LWR spent fuel elements, gamma spectrometric meas. of burnup U:Pu ratio and cooling time for materials safeguards 0-78423
 LWR Sphere-Pac oxide fuel, eval. of thermal conductivity 0-102234
 metallic fuel cladding eutectic formation during postirradiation heating in EBR-II 0-102241
 mixed carbide fuels, radial distrib. of bonded fission gas 0-57844
 mixed oxide fuels, SEM obs. of gas bubble morphology 0-57843
 neutron detector for determ. of transuranic element comp. of nuclear fuel cladding hulls 0-63471
 nondestructive element and isotope assay of Pu and U in nuclear materials 0-71870
 nondestructive measurement of U and Th conc. and quantities using XFA and gamma spectrometry 0-71877
 nuclear energy materials, anal. techniques 0-93834
 nuclear fuel, coated HTR particles, failure statistics calc., effect of SiC fracture stress and kernel porosity 0-73920
 optimised nuclear fuel rod array design for PWRs 0-106118
 oxide nuclear fuel, fission gas release and swelling, simple operational model 0-92565
 PCI-resistant fuel rod designs 0-102239
 post-irradiation examination, hot cell complex test facilities in Japan (Japanese) 0-63255
 preconditioning, power shock anal. and sipping 0-63358
 preconditioning, TVA Browns Ferry Nuclear Plant, in-core management and core manoeuvrability 0-63359
 pressure drop along longitudinally-finned seven-rod cluster nuclear fuel elements 0-83149
 PWR, eval. of annular fuel economic benefits 0-57919
 PWR, evaluation of fuel performance (Japanese) 0-99226
 PWR core analysis, effects of improved UO₂ once-through fuel cycle 0-57917
 PWR core power manoeuvres, fuel duties and fuel preconditioning, FLAIR-CENSOR 0-63337
 PWR dynamical behaviour modelling in FORTRAN 0-91217
 PWR fuel clad failure characterisation based on fission product activity, PROFIP 3 code 0-95365
 PWR fuel cycle alternatives, reactor physics anal. 0-57918
 PWR irradiated fuel, monitoring by gamma spectrometry nondestructive meas. French 0-63288
 PWR tight-pitch cores, reactor physics of fuel cycles 0-57920
 Quad City 1, fuel performance meas. following third irradiation cycle 0-68778
 radiation enhanced kinetics in the fuel lattice 0-59522
 radiological implications of Pu recycling in HTGR fuels 0-68777
 reactor fuel anal. using radioactive thermal neutron capture gamma rays 0-61214
 research reactor fuel element loadings with reduced U enrichment 0-68933
 safeguarding: 0-68835
 safeguarding, determ. of U and Pu content of fuels using isotope correlation tech. 0-68834
 safeguarding, fuel assembly identification using US signatures, statistical aspects 0-69620
 safeguarding, remote-controlled and long-distance unique identification of reactor fuel elements or assemblies 0-63296
 safeguards, materials accounting in a LWR fuel reprocessing plant 0-83173
 safeguards, nondestructive, energy-dispersive, X-ray fluorescence analysis of product-stream concentrations from reprocessed nuclear fuels 0-83163
 safeguards, sensitivity anal. of the MUF variance for large HEU fabrication plant 0-83169
 safeguards scheme for 600-MW CANDU generating stations 0-63291
 safeguards surveillance at reprocessing plants, fuel history anal. French 0-68837
 safeguards verification of spent fuel using gamma spectrometry, burn-up, cooling time and fission product conc. determ. 0-63290
 shell inspection, mag. method for detecting ferromag. particles 0-66746
 spent fuel bundle counters for CANDU reactors, appl. of safeguards design principles 0-63347
 spent fuel cooling time determ. utilising gamma-ray meas. 0-63268
 spent fuel safeguards, containment and surveillance at fuel reprocessing facilities 0-95351
 spent fuel storage, supercriticality through optimum moderation 0-57896
 spent fuel subassemblies, nondestructive assay, comparison of calcs. and meas. 0-78421
 spent fuel transportation, commercial experience in US 0-63310
 spent fuel verification by gamma-ray spectroscopy for materials safeguards 0-78422
 spent fuel waste products, delayed neutron nondestructive assay instrumentation, Monte Carlo calculational design 0-81271
 spent nuclear fuel elements, intermediary storage, stationary temp. level determ. calc. method 0-91223
 Sphere-Pac mixed carbide fuel, effect of early gas release in temp. calcs. 0-102235
 structural analysis of fuel element codes 0-78362
 swelling, fission gas precipitation into intra- and intergranular porosity, theory 0-57849
 synthetic and fissile fuel prod. by Cat-D fueled SAFFIRE reactors 0-99280
 thermal-hydraulic anal., comparison of computational techniques in COBRA-IIIC and COBRA-IIIP (Japanese) 0-95374
 transient heat conduction problem in composite region, simulation capability of elec. heater (Japanese) 0-68772
 TRIGA III reactor, anal. of standard and FLIP fuel mixed loading patterns 0-57855
 underwater solution to nuclear fuel storage problem 0-86963
 USA Reduced Enrichment Research and Test Reactor Program, current status 0-68930
 wire-wrapped core assemblies, turbulent flow split modelling and expts. 0-95370
²³³U-Th, optimisation and growth potential in LMFBR 0-73930
 Pu accountability, nondestructive assay using neutron counting, calorimetry and gamma spectrometry 0-63266
 Pu accountability and control, field nondestructive assay measurements as applied to process inventories 0-63265
 Pu, assay of large samples using portable neutron coincidence counter 0-69041
 Pu, calorimetric nondestructive assay for in-field meas. 0-71874
 Pu content in nuclear fuels, appl. of isotopic safeguards tech. 0-99210

fission reactor fuel continued

- Pu, elastic constants at elevated temps., noncontact meas. tech. 0-104405
 Pu, input accountability in reprocessing plants, tracer tech. using Mg and Pb 0-73919
 Pu, isotope composition, determ. using gamma spectrometry 0-66915
 Pu, isotopic analysis by resin-bead mass spectrometry for materials safeguards 0-78392
 Pu, isotopic composition, determ. using thermal ionisation spectrometry with automatic data eval. 0-66913
 Pu, isotopic composition, determ. using precise absolute gamma spectroscopic meas. 0-66916
 Pu nondestructive analysis, calibration by calorimetric assay 0-71878
 Pu, nondestructive assay of large samples 0-71871
 Pu passive assay using Euratom variable dead-time neutron counter 0-69042
 Pu, production and availability, uses, reprocessing, fast reactor fuel cycles 0-68767
 Pu safeguarding, automated ion-exchange system for rapid Pu separation from impurities 0-78383
 Pu safeguarding, computer-assisted controlled potential coulometric determ. 0-78384
 Pu safeguarding using resin bead mass spectroscopy 0-73984
 Pu safeguards, fissile material accountability using controlled potential coulometry 0-63298
 Pu safeguards, fuel reprocessing product soln. accounting, using K-edge densitometer 0-95352
 Pu safeguards, nondestructive assay using automated in-line instrumentation 0-95353
 Pu safeguards, product soln. gamma-ray NDA using K-absorption edge densitometer 0-83162
 Pu safeguards accountability, gamma-ray meas. of Pu and Am in molten salt residues 0-83165
 Pu safeguards assay, isotopic meas. by gamma ray spectrometry using two-detector method 0-83161
 Pu safeguards verification methods for input-accountability meas. at reprocessing plant 0-95349
 Pu-Th, optimisation and growth potential in LMFBR 0-73930
 Pu(C₂O₃)₂ precipitator, dynamic process model for nuclear materials safeguards 0-83150
 PuO₂, particle size meas. in UO₂-PuO₂ tablets, image analysis by LEITZ-TAS with process computer 0-68773
²³⁹PuO₂, stoichiometric, high-temp. deformation 0-81111
²³⁹Pu, evaluation of portal monitors for the detection of nuclear materials 0-63406
 (Th,U)C advanced FBR fuels, radiological assessment of reprocessing 0-73983
 (Th,U)O₂, burnup simulated, high O₂ pot., chem. state 0-91220
 Th-based, fuel cycles, nonproliferation aspect of ²³²U presence in ²³³U-Th fuel cycle 0-57839
 Th-based metal alloy fuels for FBRs, determ. of solidus temperature 0-104124
 Th-Pu (20 wt.%) metal fuels, compatibility with cladding alloys for FBR appls. 0-102242
 Th-Pu-U-Zr (20, 4, 8 wt.%) metal fuels, compatibility with cladding alloys for FBR appls. 0-102242
 Th-U (20 wt.%) metal fuels, compatibility with cladding alloys for FBR appls. 0-102242
 ThN-rare earth nitride mixed system, quasibinary existence (German) 0-91221
 ThO₂ microspheres, coated, coating permeability meas. 0-95343
²³²Th(n,γ), ratio to (n,2n) in fast reactor, direct meas. 0-102233
 (U, Pu) C, nuclear fuel, irradiation induced creep meas. 0-93605
 (U,Pu)(C,N) and (U,Pu)N, high burn-up simulated, Pu self diffusion 0-92712
 (U,Pu)C FBR fuel pins, irradiation behaviour 0-57847
 (U,Pu)C LMFBR fuel, Na-bonded, consequences of rapid Na loss on fuel behaviour 0-102238
 (U,Pu)C, pellet and sphere-pac nuclear fuels, comparative irradiation tests 0-78367
 (U,Pu)C_{1-x}N_x LMFBR MX-type fuels, fission gas release and microscopic swelling 0-73921
 (U,Pu)O₂ 0-63252
 (U,Pu)O₂, fission gas release and retention in irradiated nuclear fuels 0-57841
 (U,Pu)O₂ fuel pin behaviour during FFTF 3c/s reactivity insertion event, TREAT expt. anal. 0-102240
 (U,Pu)O₂ fuel pins, Cs migration effects on fuel-cladding mech. interaction 0-102250
 (U,Pu)O₂, nondestructive active assay of ²³⁵U and ²³⁹Pu 0-71873
 U enrichment by laser isotope separation (Japanese) 0-68960
 U, gaseous fueled reactor use as power supply for nuclear pumped laser system 0-63247
 U, impact of fusion-fission hybrid reactors on world demand 0-95404
 U, irradiation growth during fission fragment and proton bombard. 0-92568
 U, isotopic analysis by resin-bead mass spectrometry for materials safeguards 0-78392
 U, isotopic composition, determ. using thermal ionisation spectrometry with automatic data eval. 0-66913
 U, isotopic composition, determ. using thermal ionisation mass spectrometry 0-66914
 α-U, mech. props. at very high strain rates, double-notch shear test use 0-85131
 U ore costs, optimisation of LWR and FBR power prod. strategy 0-99253
 U plasma fueled reactor, use as power supply for nuclear pumped laser system 0-63247
 U resources and accessibility, reliability of nuclear fuel supply 0-99216
 U safeguarding, 5 to 20 mg determ. by constant current coulometric titration 0-78381
 U safeguarding, determ. of trace amounts by pulsed laser fluorimetry 0-78382
 U, safeguarding using resin bead mass spectroscopy 0-73984
 U safeguards, fissile material accountability using controlled potential coulometry 0-63298
 U/Pu fuel reprocessing solutions, NDA using X-ray L-edge densitometer for materials safeguards 0-83167
 U-²³⁸Pu-²³⁹Np GCRF fuel cycle to produce isotopically denatured Pu for LWR 0-78427
 U-Ba-C FBR nuclear fuels, phase anal., 1400°C 0-66487
 U-Pr-C FBR nuclear fuels, phase anal., 1400°C 0-66486

fission reactor fuel continued

- U-Sr-C FBR nuclear fuels, phase anal., 1400°C 0-66487
- U-Y-C FBR nuclear fuels, phase anal., 1400°C 0-66485
- UAl₃ dispersion nuclear fuels, development and irradiation performance 0-78368
- UAl₃ fuel, development, irradiation performance in test reactors 0-68799
- UC, chemical compatibility with Cr-Fe-Ni cladding alloys, thermodynamic model 0-63263
- UC, irradiation induced kinetics, diffusion and fission gas resolution 0-59523
- UC, miscibility with rare earth nitrides (*German*) 0-96654
- UC, quenched-in defects, formation, migration and resistivity 0-64990
- UCN, quenched-in defects, formation, migration and resistivity 0-64990
- UF₄-LiF(KF) molten binary mixtures, viscosity meas. 0-65270
- UF₆ conversion and its role in the 1980s 0-99266
- UF₆, gaseous fuel reactor applications 0-63367
- UF₆, safeguarding of enriched UF₆ bulk transfers 0-68814
- UN, synthesis from UO₂ through carbide 0-73980
- UO₂ 0-57852
- UO₂ 0-63252
- UO₂ burnup determ. in PWR and BWR using NDA of neutron emission rates 0-83148
- UO₂ crystn., specific heat anomaly 0-84299
- UO₂ fission gas release and retention in irradiated nuclear fuels 0-57841
- UO₂ fuel-coolant interaction, film boiling and vapor explosion phenomena 0-95363
- UO₂ gas bubble mobility 0-91222
- UO₂ high burnup nuclear fuels, relation between fission product release and fuel microstruct. 0-57845
- UO₂ intragranular fission gas bubbles, size and distrib. 0-57840
- UO₂ irradiation induced kinetics, diffusion and fission gas resolution 0-59523
- UO₂ low enriched coated fuel particles for HTGR, anal. of O₂ partition equilibrium 0-68769
- UO₂ low enriched fuel rods, storage and transportation, critical separation in water with fixed neutron poisons 0-73918
- UO₂ nuclear fuel, exam. of neutron yield on O(α ,n) reaction 0-86912
- UO₂ pellets, sinterability, particle size effect 0-104098
- UO₂ single-cryst. neutron diffraction data, reanal. using third cumulants 0-100130
- UO₂ sputtering by thermal neutrons, depend. of ejection coeff. on neutron flux 0-83157
- UO₂ surface energy, determ. by Hertzian indentation 0-93641
- UO₂ volatilization pot. of metallic inclusions in irradiated fuel during LOF overheating transients 0-57895
- UO₂-PuO₂ fuel pellets, porosity meas. methods (*German*) 0-73915
- UO₂-PuO₂ fuel pin, hyperstoichiometric, post irradiation examination 0-63258
- UO₂-UC microspheres, coated, coating permeability meas. 0-95343
- UO₂-Zr high burnup nuclear fuel rods, Xe, Kr, He release 0-57846
- U₃O₈ demand projections using a disaggregated market penetration model 0-99214
- U₃O₈ enrichment standards, gamma-ray spectra 0-78378
- U₃O₈ maximal fabricable conc. in Al base fuel elements 0-68800
- U₃O₈ recovery from seawater, R and D program 0-99217
- U₃O₈ two near-term alternatives for improved nuclear fuel utilization in PWR 0-95347
- U_{0.77}Pu_{0.23}O_{2±x} oxygen potential in temp. range 1523 to 1822K 0-106113
- UZrH fuels, development for TRIGA reactors 0-68798
- ^AU, A=234, 236, minor isotope concentration meas. for safeguarding U enrichment cascade 0-63283
- ²³⁵U safeguards, expt. nondestructive assay using a random driver 0-83164
- ²³⁵U fission product γ radiation for short irradiation times, energy distrib. 0-73929
- ²³⁸UO₂ grains distrib. in graphite matrix, effect on resonance integral 0-68768

fission reactor fuel preparation and reprocessing

- see also *isotope separation; radioactive waste*
- accelerator-driven breeding blankets, neutron-return effects, implications for fuel enrichment without reprocessing 0-57914
- accountability enhancement in first solvent extraction cycle, state estimation technique 0-83216
- actinide radioactive waste, biological hazards, consequences for LMFBR fuel recycling 0-86960
- actinides, decay heat estimation, summation calcs. and Standard eqns., review 0-63317
- alpha waste production and proliferation hazard of different fuel cycles 0-83214
- availability calculations for nuclear material processing facilities 0-73988
- Babcock & Wilcox hot cell facility 0-68910
- Barnwell Nuclear Fuel Plant, remote handling systems, overview 0-68920
- Battelle Hot Cell Laboratory 0-68913
- BWR fuel preconditioning, initial pressurization, fuel temps., fission product release 0-63357
- BWR fuel preconditioning 0-63360
- criticality safety analysis in nuclear fuel cycle (*Japanese*) 0-99225
- decommissioning of fuel reprocessing facility, nondestructive assay of ²³⁵U content of materials 0-81269
- density measuring meter, digital, remotely operated 0-68927
- direct enrichment and self-protected fissile fuel prod. using hybrid reactors 0-95390
- exhaust air, environmental radiation exposure (*German*) 0-57940
- extraction processing of nuclear fuel fluxes, effect of flux oscill. on Pu accumulation, math. simulation 0-63355
- extractor design data and flowsheets, comparison of selected reprocessing plants (*German*) 0-57938
- FBR driver fuel pins, integrated quality status and inventory tracking system 0-78431
- FBR fuel, development of secure automated fabrication systems 0-102287
- FBR fuel development, international development programs 0-102248
- FBR fuel fabrication using advanced secure automated system 0-102286
- FBR fuel handling, radiation safety 0-73985
- fission products, decay heat estimation, summation calcs. and Standard eqns., review 0-63317
- French contribution to reduced enrichment research and test reactor program 0-68931
- fuel cycle, extraction, concentration, UF₆ conversion, isotope separation (*French*) 0-63354
- fuel element fabrication (*French*) 0-73979

fission reactor fuel preparation and reprocessing continued

- fuel elements recycling and thermal re-irradiation, technical, economic and safety problems (*German*) 0-99269
- fuel pellets, computerized fabrication and inspection for SNM accountability 0-78432
- Fuels and Materials Examination facility, design and construction 0-73986
- gaseous fuel reactor applications 0-63367
- Hanford hot cell facility 0-68911
- homogeneous fluid-fueled reactors capable of in-situ fuel reprocessing nitride-liquid Sn concept 0-57834
- Hot Fuel Examination Facility Complex, history and status 0-68909
- HTGR fuel rod fabrication, estimation and control 0-83215
- HTR spent fuel reprocessing facility, real-time data acquisition and processing system (*German*) 0-106148
- inertial confinement fusion reactor, appl. PWR fuel rod re-enriching 0-106174
- International Fuel Service Centres for U resource conservation and proliferation resistance 0-57941
- irradiated fuel elements recycling plant design modifications and safety of used nuclear fuel during storage and disposal (*German*) 0-99219
- irradiated fuel inspection station 0-68917
- irradiation test facility for high U-loaded fuel plates as part of reduced enrichment program 0-68932
- linear accelerator fuel enricher regenerator and fission product transmuter 0-63365
- LWR fuel cycle, diversion anal. for material safeguarding 0-63274
- LWR multigoal fuel cycle optimization including nonproliferation objectives 0-73982
- LWR spent fuel, head-end part of fuel reprocessing facility, unloading installations, handling and transfer techniques (*German*) 0-57939
- LWR spent fuel, receiving and shearing system 0-68928
- materials, safeguarding; 0-68835
- materials, safeguarding, material accountability control automation at fuel reprocessing plant 0-68832
- materials, safeguarding, meas. of fissile materials entering a reprocessing plant (*French*) 0-68828
- materials, safeguarding, verification of reprocessing plant input and output analyses 0-68830
- materials safeguard techniques capability in nuclear fuel facilities 0-63279
- materials safeguarding, advanced accountability techniques for breeder fuel fabrication facilities 0-73939
- materials safeguarding, advanced detection systems to prevent LWR spent fuel diversion 0-68822
- materials safeguarding, advanced instrumental systems and techniques for fuel reprocessing plant 0-68821
- materials safeguarding, determ. of U and Pu content of fuels using isotope correl. tech. 0-68834
- materials safeguarding, dynamic materials accounting in chemical separations, conversion, and fuel fabrication facilities 0-73938
- materials safeguarding, nondestructive measurements of irradiated fuel assemblies at a reprocessing facility 0-95392
- materials safeguarding, possible ways of verifying the input of a reprocessing facility 0-68826
- materials safeguarding, tracer techniques for Pu input accountability in reprocessing plants 0-68827
- materials safeguarding at fuel reprocessing plant to prevent materials diversion 0-68824
- materials safeguarding at reprocessing plants, inspection of hulls at La Hague (*French*) 0-68831
- materials safeguarding at U fuel fabrication facility US/IAEA system 0-63284
- materials safeguards, appl. of semidynamic material control in spent-fuel reprocessing plant 0-83174
- materials safeguards, deviations from mass transfer equilibrium and mathematical modeling of mixer-settler contactors 0-83171
- materials safeguards, dynamic materials accounting for solvent-extraction systems 0-83172
- materials safeguards, microscopic process monitoring [for nuclear materials safeguards] of fuel reprocessing facilities to prevent material diversion 0-83153
- materials safeguards, model for the application of IAEA safeguards at mixed-oxide fuel fabrication facilities 0-63286
- materials safeguards, nondestructive, energy-dispersive, X-ray fluorescence analysis of product-stream concentrations from reprocessed nuclear fuels 0-83163
- materials safeguards, sensitivity anal. of the MUF variance for large HEU fabrication plant 0-83169
- materials safeguards and materials control, meas. tech. conf. Charleston, SC, USA (November 1979) 0-77544
- materials safeguards procedures in fuel reprocessing plant 0-68823
- materials safeguards surveillance at reprocessing plants, fuel history anal. (*French*) 0-68837
- materials safeguards system for highly enriched U fuel fabrication plant 0-63285
- materials safeguards system of back-end facilities with emphasis on waste management 0-83175
- materials safeguards techniques appl. to Eurodif gas diffusion plant (*French*) 0-63281
- materials safeguards techniques at Tokai fuel reprocessing plant 0-68833
- microsphere handling techniques and equipment 0-68924
- multiservice utility plug for remote fuel processing 0-68926
- neutron dosimetry system, based on fission counter for fuel processing plant 0-57981
- nonproliferation, nuclear fuel cycles and radiation damage 0-68934
- nuclear materials safeguards technology based on separation nozzle process for U enrichment facility 0-63280
- on-line radiation monitoring at a nuclear fuel reprocessing plant 0-95469
- ORNL Transuranium Processing Plant, current status 0-68915
- pin bowing in AGR fuel elements, meas. by camera device 0-106146
- political, ecological, social and economic aspects of nuclear fuel reprocessing, closed fuel cycle (*Dutch*) 0-106147
- powder batching system development 0-68922
- powder transfer in fuels refabrication by negative pressure pneumatic transport 0-68923
- preconditioning, power shock anal. and sipping 0-63358
- preconditioning, TVA Browns Ferry Nuclear Plant, in-core management and core manoeuvrability 0-63359
- production process improvements 0-83213

fission reactor fuel preparation and reprocessing continued

- Pu holdup in glove-gox exhaust filter, in-line monitoring by gamma ray detection 0-78458
- Purex kinetics, U extraction with tributylphosphate (*German*) 0-57937
- Purex process, first extraction, Pu accumulation, computer simulation, SEPHIS code 0-68907
- Purex-type reprocessing plants, schematic flowsheet comparison (*German*) 0-57936
- PWR core power manoeuvres, fuel duties and fuel preconditioning 0-63337
- PWR irradiated fuel assemblies, remote operations 0-68918
- remote fuel refabrication laboratory concepts 0-68925
- remote system mock-up testing for Idaho Chemical Reprocessing plant 0-73987
- research reactor fuel element loadings with reduced U enrichment 0-68933
- safeguarding a gas centrifuge pilot plant in Japan 0-63282
- safeguards, fuel reprocessing product soln. accounting, using K-edge densitometer 0-95352
- safeguards, materials accounting in a LWR fuel reprocessing plant 0-83173
- safeguards containment and surveillance concepts at fuel reprocessing plant 0-95350
- safeguards instrumentation for Pu processing facility 0-63362
- Savannah River Plant, Purex process, 25 years of remote handling 0-68921
- shielded cubicle and equipment for examination of coated fuel particles 0-68929
- SNM safeguards, assay of dissolver solns. by totally sampled wavelength dispersive X-ray fluorescence 0-83160
- spent fuel disassembly and Canning at Barnwell Fuel Plant 0-68919
- spent fuel safeguards, containment and surveillance at fuel reprocessing facilities 0-95351
- thermal reactor fuel cycles, actinide wastes toxicity limitations (*German*) 0-99220
- toxicity reduction in Auger fusion reactor 0-106175
- TRIGA Penn State Beazale reactor, fuel management 0-63361
- US decontamination system for reactor fuel transfer pool, remotely operated 0-68916
- USA Reduced Enrichment Research and Test Reactor Program, current status 0-68930
- Vallecitos Nuclear Center Hot Cells 0-68912
- waste storage and reprocessing of fuels, nuclear burning and types of reactor (*French*) 0-91235
- Whiteshell Nuclear Research Establishment Hot Cell facility 0-68914
- Al capsule dissolution and solidification from neutron irradiation. UO_2 fuel rod 0-73981
- Pu accountability, computerised gamma spectrometer system for meas. isotopic and total Pu conc. in solns. 0-63363
- Pu accountability and control, field nondestructive assay measurements as applied to process inventories 0-63265
- Pu accountability by ceric oxidation, ferrous reduction and dichromate titration for nuclear materials safeguards 0-63364
- Pu analysis in irradiated fuel reprocessing solns., spectrophotometric determ. in near IR 0-78433
- Pu concentration in irradiation, fuel dissolver solns., determ. by isotope dilution alpha spectrometry 0-78428
- Pu content in nuclear fuels, appl. of isotopic safeguards tech. 0-99210
- Pu extraction, solvent choice effect 0-106149
- Pu fuel facility damage from high winds, risk anal. 0-63356
- Pu, input accountability in reprocessing plants, tracer tech. using Mg and Pb 0-73919
- Pu, production and availability, uses, reprocessing, fast reactor fuel cycles 0-68767
- Pu safeguarding using resin bead mass spectroscopy 0-73984
- Pu safeguards, fuel reprocessing product soln. accounting, using K-edge densitometer 0-95352
- Pu safeguards, product soln. gamma-ray NDA using K-absorption edge densitometer 0-83162
- Pu safeguards verification methods for input-accountability meas. at reprocessing plant 0-95349
- $\text{Pu}(\text{C}_2\text{O}_4)_2$ precipitator, dynamic process model for nuclear materials safeguards 0-83150
- (Th,U)C advanced FBR fuels, radiological assessment of reprocessing 0-73983
- Th-U fuel reprocessing facility, computerised analytical process control system for material safeguards 0-78429
- U concentration in fuel reprocessing streams, acid-compensation dual-wavelength spectrochem. anal. 0-78430
- U enrichment, centrifuge process, LWR fuel (*German*) 0-68905
- U enrichment by photochemical laser, two-phase flow with condensation, mathematical model (*French*) 0-74029
- U, nuclear fuel conversion plant, nondestructive assay 0-66761
- U, safeguarding using resin bead mass spectroscopy 0-73984
- U/Pu fuel reprocessing solutions, NDA using X-ray L-edge densitometer for materials safeguards 0-83167
- $\text{U}^{238}\text{Pu}^{237}\text{Np}$ GCRF fuel cycle to produce isotopically denatured Pu for LWR 0-78427
- UAl₃ dispersion nuclear fuels, development and irradiation performance 0-78368
- UAl₃ fuel, development, irradiation performance in test reactors 0-68799
- $\text{UF}_4\text{-CF}_4$ mixture, gas core fission reactor, fission based plasma engine 0-63366
- UF_6 continuous gas flow control simulation (*German*) 0-78416
- UN, synthesis from UO_2 through carbide 0-73980
- UO_2 dense microsphere production by sol-gel technique (*Czech*) 0-68906
- UO_2 , green pellet with zinc stearate as additive, effect on sintering 0-68908
- UO_2 preparation, emanation thermal anal. for characterisation of uranyl gel microspheres 0-95391
- U_2O_8 maximal fabricable conc. in Al base fuel elements 0-68800
- U_2O_8 , A=234, 236, minor isotope concentration meas. for safeguarding U enrichment cascade 0-63283
- $\text{U}^{238}\text{U}^{235}\text{Th}$ fuel recycle plant, materials safeguarding, control and accountability system 0-73942
- U^{235}U , recovery from enrichment plant tailings by laser isotope separation 0-83212

fission reactor instrumentation see nuclear reactor instrumentation**fission reactor materials**

- see also claddings; fission reactor fuel; fusion reactor materials; materials handling; moderators; radioactive waste
- accountability, fuel burn-up measurement using spatial power distrib. eval. and gamma spectrometry 0-68803
- accountability, in-tank measurement of solution density 0-78391
- accountability, tank volume calibration algorithm 0-83159
- accountability tanks, automated calibrator 0-83158
- aerodynamic and thermodynamic effects on environment of nuclear power plants (*German*) 0-61469
- ageing at high temp., effect on creep props. SEM 0-97516
- alkali metal, liq., reactions with refractory metals and oxides, relevance to reactor technology 0-85173
- alkali metals, liquid, O_2 pot. and O_2 distrib. coeffs. between alkali and struct. metals 0-65231
- assay and accountability of special nuclear materials using neutron correlation meas. tech. 0-69015
- automated ultrasonic testing system for piping in nuclear power plant (*Japanese*) 0-71839
- BWR containment vessels of prestressed concrete, pressure tests 0-81254
- carbonaceous matrix materials for HTGK fuel rods, irradiation-induced dimensional changes 0-65052
- clad failure prediction during FBR overpower transients, JANE code 0-78363
- clad strain, power history effect, in-reactor meas. 0-78357
- cladding, corrosion product deposition, water chemistry effect 0-106116
- cladding, eddy-current integrity testing at HFER 0-68788
- cladding strain, effect of fuel density and fuel relocation, in-reactor meas. 0-104408
- containment of special nuclear materials for storage, transfer and nondestructive assay meas. 0-63267
- crack-front tunnelling, investigated by single specimen compliance technique 0-70300
- creep, irradiation induced, correlation of theory with expt. evidence 0-88255
- creep testing, extensometric method, for inside nuclear reactor channels 0-100998
- Croley steel for LMFBR steam generator, meas. of T permeation 0-68775
- decommissioning of fuel reprocessing facility, nondestructive assay of ^{235}U content of materials 0-81269
- defectoscopy of gamma-active objects in their natural radiation (*Bulgarian*) 0-71867
- elastic-plastic linear hardening material for thin-walled pressure vessels, stability and yield stress anal. 0-92075
- engineering materials certification for safety and reliability testing 0-78360
- failure analysis by remote fatigue crack growth meas. system 0-68790
- FBR cladding dilatation, effect of radial temp. gradient 0-68776
- FBR containment code, structural deform., SEURBNUK-2 0-78404
- FBR containment code validation program, SEURBNUK 0-78405
- FBR core materials studies for improving reactor performance, trends 0-102232
- FBR fuel pin failure, fuel porosity and crack effects on transient overpower analysis 0-71760
- flow induced vibrations and fretting wear damage 0-95357
- fuel pins, fast breeder, fuel-cladding mech. interaction, obs. and anal. 0-86959
- fuel sheaths, neck growth during high temp. transients in steam 0-78396
- gamma-heating effects, calorimetric validation of TLD measurements 0-63254
- GCFR advanced alloy cladding, oxidation behaviour in the environment 0-104350
- General Atomic Hot Cell modification and refurbishment 0-68786
- graphite: Ba impregnated, sorption of Cs, thermodynamic modelling of multicomponent sorption behaviour 0-102243
- graphite, coarse grained, fracture toughness (*German*) 0-76358
- graphite, corrosion by CO_2 , CO production radiologically induced gas pressure effects 0-106115
- graphite, Cs sorption kinetics modelling 0-102244
- graphite, electron-spectroscopic analysis of neutron-irradiated pyrographite 0-63261
- graphite, neutron irradiation effects on thermal shock resist. and fracture toughness (*Japanese*) 0-66622
- graphite, quantitative microanalysis by laser emission spectroscopy 0-81384
- graphite, synergistic effect of electrons on atomic H activity 0-106112
- graphite, thermal conductivity, effect of porosity 0-65314
- graphite corrosion in PBHTGR process heat reactor following massive air ingress (*German*) 0-83181
- heavy ion bombardment damage, comparison of analytical and Monte Carlo computer codes 0-102245
- heavy water dielectric constant meas. over temp. range 473K to 643K 0-103912
- hot cell measurement and test equipment, calibration control 0-68787
- in-core irradiation facilities, development and expt. using JRR-2 and JMTR research reactors, Japan (*Japanese*) 0-63256
- Incoloy 800, nuclear grade boiling tubing superalloy, Co and C content anal. 0-78397
- Inconel, steam generator tubing, mag. probe inspection 0-85119
- Inconel 600, nuclear grade boiling tubing superalloy, Co and C content anal. 0-78397
- Inconel 600, nuclear reactor boiler corrosion, XPS 0-66709
- Inconel 600, nuclear reactor boiler corrosion, XPS 0-71816
- Inconel 600 safe-end cracking failure at Duane Arnold reactor 0-104295
- LMFBR, liquid Na-limestone concrete interaction following HCDA, US meas. 0-78412
- LMFBR, Na purification system, cold traps and plugging indicator 0-99209
- LMFBR fuel channels, measurement of irradiation creep in bending 0-104406
- LMFBR fuel pin bundles in flowing Na, design and operation of SLSF test trains for safety tests 0-102281
- LMFBR materials, interstitial loop nucleation and growth during irradiation, Fokker-Planck equation, numerical soln. 0-57857
- LMFBR materials, interstitial loop nucleation and growth during irradiation, Fokker-Planck equation, numerical soln. 0-68796
- LMFBR structural materials, development of an instrumented materials irradiation test for FFTF 0-57858

fission reactor materials continued

LMFBR structural materials, development of an instrumented materials irradiation test for FFTF 0-68797
 LMFBR structure materials in liquid Na, capsule type creep tester (*Japanese*) 0-108653
 LWR materials of primary-circuit components, safety concepts, quality (*German*) 0-73914
 LWR piping, intergranular stress-corrosion cracking 0-81234
 LWR wastes, treatment and disposal methods (*German*) 0-57868
 management, safeguarding and accounting, conf. Albuquerque, NM, USA (July 1979) 0-62382
 metal surfaces, radioactive contamination 0-68771
 metallic fuel cladding eutectic formation during postirradiation heating in EBRII 0-102241
 metals and alloys, stress relaxation, in-reactor study at low temps. 0-93588
 Nimonic PE16, irradiation creep data obtained in fast and thermal neutron spectra correlation with displacement cross-sections 0-84993
 Nimonic PE-16, electron irradi. in HVEM, void growth, vacuum environment influence 0-107323
 Nippon Nuclear Fuel Development Co. hot laboratory, present status 0-68781
 non-destructive assay techniques for irradiated fissile material in extended configurations 0-71872
 nondestructive analysis, results of international collaboration in the ESARDA working group 0-71879
 nondestructive assay equipment, calibration using reference materials for fissile material assay 0-71880
 nondestructive neutron assay for nuclear materials accountability and criticality control 0-66759
 nuclear energy materials, anal. techniques 0-93834
 nuclear reactor components, NDT using acoustic emission (*Spanish*) 0-57871
 O-arai Engineering Centre post irradiation examination facilities 0-68780
 Oak Ridge, hot cell facilities, history 0-68784
 Oak Ridge National Laboratory Ceramic Fuels Alpha Facility 0-68783
 on-line radiation monitoring at a nuclear fuel reprocessing plant 0-95469
 ORNL Radioactive Materials Analytical Laboratory 0-68785
 pneumatic system for transferring radioactive samples at Savannah River Laboratory 0-68794
 pressure vessels, strain measurements 0-79865
 PWR, H₂-assisted fatigue-crack growth model 0-71745
 PWR, metals and alloys (*Spanish*) 0-95344
 PWR core barrels with and without holes, various edge conditions, hydrodynamic vibrations 0-78406
 PWR piping, circumferential cracks, opening and extension, MARC finite element program 0-78364
 PWR power station secondary water chemistry study, progress report 0-106108
 PWR primary and secondary water chemistry, European experience 0-106110
 pyrocarbon coating, isotropic, gas permeability, neutron irradiation effect (*French*) 0-63260
 pyrocarbon coating, isotropic, gas permeability meas. (*French*) 0-63259
 radiation damage, ion penetration distance calculations with multigroup transport computer codes 0-102246
 refractory metals and oxides, reactions of liq. alkali metals, relevance to reactor technology 0-85173
 remote maintenance at Fuels and Materials Examination Facility 0-68792
 safeguard role of standard reference materials in achieving measurement traceability 0-78371
 safeguard techniques capability in nuclear fuel facilities 0-63279
 safeguarding; 0-68835
 safeguarding, advanced accountability techniques for breeder fuel fabrication facilities 0-73939
 safeguarding, advanced detection systems to prevent LWR spent fuel diversion 0-68822
 safeguarding, advanced instrumental systems and techniques for fuel reprocessing plant 0-68821
 safeguarding, appl. of mobile nondestructive assay system 0-71876
 safeguarding, application of an improved volume calibration system to the calibration of accountability tanks 0-68829
 safeguarding, containment and surveillance devices 0-63349
 safeguarding, determ. of U and Pu content of fuels using isotope correl. tech. 0-68834
 safeguarding, development of containment and surveillance measures for IAEA safeguards 0-63350
 safeguarding, diverse forms of fissile material, large stocks verification 0-73932
 safeguarding, dynamic material accountability in an integrated safeguards system 0-73940
 safeguarding, dynamic materials accounting in chemical separations, conversion, and fuel fabrication facilities 0-73938
 safeguarding, dynamic materials control, development, test and eval. program 0-73936
 safeguarding, dynamic materials control 0-68819
 safeguarding, gamma spectrometric techniques and standards (*French*) 0-68811
 safeguarding, isotopic correl. tech., R and D by ESRADA 0-68836
 safeguarding, isotopic inventory prediction employing a Monte Carlo Dan-coff factor 0-73924
 safeguarding, judging the results of analytical verification meas. 0-68817
 safeguarding, material accountability control automation at fuel reprocessing plant 0-68832
 safeguarding, material control and accountability for ²³³U/Th fuel recycle plant 0-73942
 safeguarding, meas. of fissile materials entering a reprocessing plant (*French*) 0-68828
 safeguarding, measurement errors 0-73935
 safeguarding, measurement standardisation 0-68812
 safeguarding, nondestructive measurements of irradiated fuel assemblies at a reprocessing facility 0-95392
 safeguarding, nuclear materials control system in the THTR-300 high-temperature pebble-bed reactor 0-73941
 safeguarding, optimal estimates of inventory and losses using nuclear material accountability data 0-68818
 safeguarding, possible ways of verifying the input of a reprocessing facility 0-68826
 safeguarding, SNM control and accounting, role of certified reference materials 0-68815

fission reactor materials continued

safeguarding, SNM dynamic materials control and accountability system 0-73937
 safeguarding, statistical anal. of materials accountability, computer simulation 0-73933
 safeguarding, stratification of nuclear materials for control and accountability 0-68816
 safeguarding, survey assay meter developments at BNL for nuclear materials safeguarding appls. 0-69038
 safeguarding, tracer techniques for Pu input accountability in reprocessing plants 0-68827
 safeguarding, two-stage sampling for detection of SNM diversions 0-73934
 safeguarding, unirradiated fuel control in BOR-60 fuel assemblies (*Russian*) 0-68809
 safeguarding, use of automated electromanometer at fuel processing facility 0-99211
 safeguarding, VACOSS electronic sealing system 0-63348
 safeguarding, verification of reprocessing plant input and output analyses 0-68830
 safeguarding a gas centrifuge pilot plant in Japan 0-63282
 safeguarding at fuel reprocessing plant to prevent materials diversion 0-68824
 safeguarding at reprocessing plants, inspection of hulls at La Hague (*French*) 0-68831
 safeguarding at U fuel fabrication facility US/IAEA system 0-63284
 safeguarding isotopic correlations in irradiated fuel from VVER power reactors (*Russian*) 0-68838
 safeguarding of critical facilities to detect diversion of nuclear materials 0-68808
 safeguarding of materials from U/Th fuel cycle, nondestructive meas. 0-76457
 safeguarding SNM control and accountability, reliability of nondestructive assay techniques 0-76456
 safeguards, accountability system for nuclear materials control in research centres 0-63499
 safeguards, accounting and control in BOR-60 FBR (*Russian*) 0-63295
 safeguards, appl. of semidynamic material control in spent-fuel reprocessing plant 0-83174
 safeguards, burn-up meas. of irradiated LWR fuel assemblies 0-68807
 safeguards, collection and analysis of measured fission product data 0-95354
 safeguards, computerised nondestructive assay for materials management 0-78388
 safeguards, definition and objectives of IAEA safeguards 0-83155
 safeguards, deviations from mass transfer equilibrium and mathematical modeling of mixer-settler contactors 0-83171
 safeguards, diversion anal. of LWR fuel cycle 0-63274
 safeguards, diversion protection using personnel portal detectors 0-78389
 safeguards, dynamic materials accounting for solvent-extraction systems 0-83172
 safeguards, experience at the International Atomic Energy Agency in processing safeguards information 0-63497
 safeguards, experience gained with Euratom's nuclear materials accounting and reporting system 0-63271
 safeguards, experience in the application of IAEA inspection practices 0-63270
 safeguards, facility design features relevant to improved IAEA safeguards 0-63277
 safeguards, IAEA, technical criteria for design, operation and evaluation 0-63272
 safeguards, IAEA containment and surveillance measures 0-68810
 safeguards, IAEA quantitative goals for measurement systems 0-83168
 safeguards, improvement of material accountability verification procedure 0-63273
 safeguards, in situ verification techniques for fast critical assembly cores 0-78390
 safeguards, integrated quality status and inventory tracking system for FBR driver fuel pins during manufacture 0-78431
 safeguards, inventory verification methods in DOE safeguards inspections 0-78386
 safeguards, inventory verification using high resolution gamma spectroscopy 0-69016
 safeguards, isotopic measurements on Kr and Xe, behaviour of the quadrupole mass-spectrometer towards various noble gases 0-63300
 safeguards, LASL analytical chemistry program 0-78380
 safeguards, mathematical simulation of calorimeters used for rapid nuclear fuel assay 0-95355
 safeguards, meas. of fissile material in accounting tanks 0-68825
 safeguards, microscopic process monitoring [for nuclear materials safeguards] of fuel reprocessing facilities to prevent material diversion 0-83153
 safeguards, model for the application of IAEA safeguards at mixed-oxide fuel fabrication facilities 0-63286
 safeguards, Monte Carlo simulation of MUF distrib. 0-83170
 safeguards, nuclear materials analysis using plasma desorption mass spectrometry isotope ratio determ. using TOF mass spectrometry 0-78375
 safeguards, performance and eval. of international analytical intercomparison expt. 0-78374
 safeguards, performance goals and criteria 0-83154
 safeguards, prototype, reference materials for nondestructive assay 0-78372
 safeguards, quantitative determ. of unauthorised removal of nuclear materials, using changes in spectral indices (*Russian*) 0-63294
 safeguards, reference materials and meas. traceability 0-78370
 safeguards, simulated neutron tomography for nondestructive assays 0-99218
 safeguards, systems design for materials accountability 0-78393
 safeguards, ultrasonically identified security seals for CANDU safeguard systems 0-63297
 safeguards, uniform data description for a generalized real-time nuclear materials control system 0-63498
 safeguards, verification and control, instrument requirements in static locations 0-63299
 safeguards and materials control, meas. tech., conf. Charleston, SC, USA (November 1979) 0-77544
 safeguards applications of far infrared radiometric techniques for the detection of contraband 0-73925
 safeguards applications of far infrared radiometric techniques for the detection of contraband 0-83156
 safeguards approaches and evaluation methods 0-73923

fission reactor materials continued

safeguards containment and surveillance concepts at fuel reprocessing plant 0-95350
 safeguards for avoiding diversion of fissile materials using quasi-total containment (*French*) 0-63276
 safeguards in LWR power stations, design features and instrumentation (*Russian*) 0-63278
 safeguards in Th-U, fuel reprocessing facility, computerised analytical process control system 0-78429
 safeguards measurement system anal., appl. of controllable unit approach to materials control 0-68820
 safeguards procedures in fuel reprocessing plant 0-68823
 safeguards reference measurement system utilizing resonance neutron radiography for nondestructive assay meas. 0-78377
 safeguards spectrochemical anal. of U, Pu, Th by alpha spectrometry using liquid scintillation methods 0-78379
 safeguards surveillance at reprocessing plants, fuel history anal. (*French*) 0-68837
 safeguards system for highly enriched U fuel fabrication plant 0-63285
 safeguards system for LMFBR, monitoring of fissile material inventory 0-63293
 safeguards system in Japan 0-83152
 safeguards system of back-end facilities with emphasis on waste management 0-83175
 safeguards systems parameters for IAEA 0-63275
 safeguards techniques appl. to Eurodif gas diffusion plant (*French*) 0-63281
 safeguards techniques at Tokai fuel reprocessing plant 0-68833
 safeguards technology, conf. Vienna, Austria (Oct. 1978) 0-62391
 safeguards technology based on separation nozzle process for U enrichment facility 0-63280
 safeguards within Euratom framework, NUMSAS data processing system for statistical accountability 0-73926
 seismically qualified piping, failure probability, ASME code limits 0-78365
 SNM, nondestructive assay techniques for control and accountability 0-81270
 SNM accountability, computerised fabrication and inspection of fuel pellets 0-78432
 SNM safeguards, assay of dissolver solns. by totally sampled wavelength dispersive X-ray fluorescence 0-83160
 SNM safeguards, IAEA Meas. requirements and experience 0-78385
 SNM safeguards, LASL DYMAC accountability system, software development 0-99212
 SNM safeguards, US NRC material control and accountability inspection program 0-78387
 stainless steel, neutron dose determ., from isotope abundance ratio, mass spectra obs. 0-61220
 steam generator thermal hydraulics 0-95342
 steam generator tube performance in water cooled reactors in 1978 0-78399
 steam generator tubes testing, and evaluation using CIS/DASIO system (*Czech*) 0-63301
 steel, A533B alloy, fatigue crack growth of irradiated pressure vessel steels in simulated, reactor-grade water environment 0-97582
 steel, alloy A533B1, neutron irradi., flow growth characts. by acoustic monitoring 0-100918
 steel, austenitic, types M316, FV548, 304, irradiation creep data obtained in fast and thermal neutron spectra correlation with displacement cross-sections 0-84993
 steel, austenitic (03KH18N10T), heat treatment for fission reactor appls. 0-66454
 steel, austenitic stainless, creep, effect of temp. and dose rate variations, Dounreay fast reactor 0-93603
 steel, austenitic stainless, fatigue crack propagation, effect of neutron irradiation 0-97583
 steel, austenitic stainless, fatigue crack propagation, influence of neutron irradiation 0-97584
 steel, austenitic stainless, neutron dose rate depend. of swelling in fission reactors 0-104233
 steel, austenitic stainless, stress corrosion cracking, factors influencing susceptibility 0-97617
 steel, austenitic stainless, type 316, irradi. induced creep 0-93606
 steel, ferritic, Cr-Mo (2.25, 1 wt.%), C and Nb influence on structural transformations (*French*) 0-84925
 steel, fracture toughness of nuclear pressure vessels 0-81172
 steel, low alloy, 15Kh2MFA and 15Kh2NMFA, neutron irradi. embrittlement, effect of P, Sb and Sn impurities 0-85055
 steel, low-C, kinetics of void development in fracturing A533B tensile bars 0-76357
 steel, Mn-Mo-Ni, embrittling effects of residual elements 0-66655
 steel, Mn-Mo-Ni (A533 B), ductile-brittle transition, material fracture temp. depend., Gauss distrib. function 0-97574
 steel, Ni-Mo-Cr, embrittling effects of residual elements 0-66655
 steel, stainless, 304, bend test ductility of irradi. specimens for LMFBR appls. 0-104235
 steel, stainless, 316, oxidation behaviour in the environment, appl. to GCFR fuel claddings 0-104350
 steel, stainless, austenitic, dynamic uniaxial and biaxial stress-strain relationships 0-81122
 steel, stainless, cladding dimensional changes in FBR (U,Pu)₂O₂ fuel pins due to swelling and inelastic strain 0-104296
 steel, stainless, EBR-II reflector assembly irradi. induced bowing, implications for core restraint design 0-104234
 steel, stainless, fast neutron irradiated, solution annealed tubing, residual stress behaviour 0-65054
 steel, stainless, fatigue props. of low-fluence neutron irradi. samples 0-97585
 steel, stainless, FBR blanket facility, gamma-ray heating rate meas. 0-57912
 steel, stainless, FeCrAlloy, creep-rupture props., 650-800°C 0-97535
 steel, stainless, low-cycle fatigue characteristics of neutron irradi. samples 0-97586
 steel, stainless, LWR fuel cladding material evaluation 0-99213
 steel, stainless, stress corrosion susceptibility in high purity water, O₂ and temp. effects 0-61002
 steel, stainless, type 316, low cycle fatigue props. in vac., fracture mode 0-85021
 steel, stainless, type 316, modelling effects of fast neutron irradiation in mech. behaviour 0-84234

fission reactor materials continued

steel, stainless, type 316 20% cold worked fission reactor fuel cladding, axial stress effects on transient mech. response 0-71743
 steel, stainless 316, Fokker-Planck eqn. describing evolution of interstitial loop microstruct. during irradiation 0-107215
 steel, stainless 316, soln. annealed, cavity alignment and precipitation during dual ion bombardment 0-70273
 steel, stainless type 316, irradi. induced nuclear cladding swelling, empirical development of design equation 0-59527
 steel, stainless type 316, irradiation induced creep under 60 MeV alpha irradiation 0-92597
 steel, type 12X18H10T, defect development in contact area with coolant (*Russian*) 0-57859
 steel pressure vessel plates, US examination, PISC project 0-57861
 steel pressure vessel US examination, PISC trials result anal. scheme 0-57863
 steels, irradiated pressure vessel, reference fracture toughness curves 0-100921
 steels, nuclear reactor pressure vessel steels, optimum chem. comp. rel. to props. 0-93517
 steels, radiational swelling of two-phase austenitic-ferritic stainless steels 0-65063
 Stellite-6, XPS obs. of aqueous oxidation, surface comp. and gaseous oxidation effect 0-81238
 strain measurement, extensometric method, for inside nuclear reactor channels 0-100998
 stress corrosion cracking, prediction in 10% NaOH soln. at 315°C 0-97616
 structural reliability, conference, Berlin, Germany (Aug. 1979) 0-105422
 thermomechanical transient anal., strain-rate dependent plasticity 0-79864
 TRIGA reactor at HFER, neutron radiography studies 0-68758
 undersaturated alloys, irradiated, solute segregation kinetics, via drift and defect-solute complexes 0-60872
 void swelling, nucleation theory 0-65038
 weld metal, submerged arc irradiated, reference fracture toughness curves 0-100921
 Winfrith Hot Cells-1964-1979 0-68782
 Zircaloy, LWR fuel rod cladding, damage accumulation during I₂-induced stress corrosion cracking 0-71810
 Zircaloy, PWR fuel induced cladding deformation, creep correl., in-pile meas. 0-97547
 Zircaloy, textured, interactive creep and growth, upper-bound evaluation 0-89293
 Zircaloy, unirrad., stress corrosion cracking, I₂-induced, effect of test temp., alloy comp. and heat treatment 0-97632
 Zircaloy cladding, crud deposition 0-106117
 Zircaloy cladding, enhanced steam oxidation by deformation under LWR LOCA 0-73917
 Zircaloy cladding, stress corrosion cracking, inner surface texture effect 0-66695
 Zircaloy cladding stress corrosion cracking due to I (*Japanese*) 0-78361
 Zircaloy fuel cladding, irradiation-induced in-reactor corrosion in CANDU reactors 0-104352
 Zircaloy PWR cladding, deformation in LOCA 0-106114
 Zircaloy PWR fuel cladding deformation tests under mainly convective cooling conditions 0-57862
 Zircaloy sheath, fission gas absorpt. following irradi., power history effects 0-78395
 Zircaloy sheaths, oxidation rate calc. method 0-78394
 Zircaloy-2, anodic oxidation kinetics, in 0.05M oxalic acid (aq. and alcoholic) 0-104331
 Zircaloy-2, hot-pressed, influence of diffused C on structure and oxidation 0-61016
 Zircaloy-2, irradiation growth, reaction rate theory calcs. 0-88212
 Zircaloy-2, irradiation growth, shape and volume changes 0-92562
 Zircaloy-2, mech. props. after exposure to I₂-methanol solutions, SEM study 0-93689
 Zircaloy-2, neutron irradi. damage, TEM characts. 0-107332
 Zircaloy-2, oxide coating thermal cond. meas. 0-80009
 Zircaloy-2, pressure tubes, irradi. creep and growth, anisotropy factors 0-97536
 Zircaloy-2 fuel tubes, cumulative damage fatigue tests at room temp. and 300°C 0-93638
 Zircaloy-2 fuel tubes, low cycle fatigue studies at room temp., 300 and 350°C 0-93637
 Zircaloy-2 pressure tube, elongation in Douglas Point CANDU reactor 0-78398
 Zircaloy-2 pressure tube elongation, neutron induced creep and growth, meas. and anal. 0-93628
 Zircaloy-4, creep rupture at superimposed non-stationary stress and temp. loading 0-66630
 Zircaloy-4, elastic props., O additions effect 0-66565
 Zircaloy-4, failure strain prediction under non-stationary loading conditions 0-93640
 Zircaloy-4, fuel cladding, burst criteria under LOCA conditions 0-73931
 Zircaloy-4, resistance-welded, microstruct. of weld region 0-66549
 Zircaloy-4, stress-relieved and cold-worked, stress relaxation in bending at 673K 0-93609
 Zircaloy-4 BWR channels, corrosion resistance 0-104351
 Zircaloy-4 cladding deformation under LOCA transient heating conditions, analytical modelling 0-104236
 Al, neutron damage, positron annihilation 0-65056
 Al-Cu (4 wt.%) alloy, neutron irradi., weak-beam dark-field obs. of dislocations near θ' precipitates 0-107333
 Al-Mg (0.1 at.%), neutron damage, positron annihilation 0-65056
 B₂C neutron absorber for EBR-II, He release, in-reactor meas. 0-73951
 B₂C, thermophysical props. and neutron absorpt. 0-103488
 B₂C-304 stainless steel cermet for nuclear shielding appls. 0-102352
 B₂C-Cu cermet fabrication for neutron shielding appls. 0-102354
 B₂C-phenolic fibre reinforced composite for nuclear shielding appls. 0-102353
 Be, irradiated with He⁺ at 20 keV, surface damage and gas trapping profile meas. (*French*) 0-84218
 C-graphite materials for HTR and fusion reactors 0-73928
 CC Fe-Ni-Cr (35, 15 wt.%) Nb(Ti)(Mo), corrosion in HTGR He environment 0-61021
 Cd thermal neutron filter, in-cell US inspection 0-68791
 Ce, gettering of H, mass spectrometry and microgravimetry study, rel. to HTGR gas purification 0-73374

fission reactor materials continued

- Cr-Fe-Ni alloys, claddings, chemical compatibility with UC nuclear fuels, thermodynamic model 0-63263
 Cu, irradiated with 20 keV He⁺, surface damage and gas trapping profile meas. (*French*) 0-84219
 Cu, proton-irradiated, H₂ gas-bubble struct., study at 300K 0-92569
 Cu-Fe (1.5 wt.%), precipitation-effect on void formation during electron irradiation 0-84211
 Cu-Fe (1.5 wt.%) alloy, void form. during irradi. in HVEM, reactor irradi. simulation and ageing effects 0-107327
 Eu₂O₃, thermophysical props. and neutron absorpt. 0-103488
 Fe base superalloy, type A-286, elevated temp. fracture toughness testing of thin section irradi. materials 0-61063
 Fe-Al (40 at.%) and Fe-Al (50.5 at.%) ordered alloys, 20K neutron irradi. effects, stoichiometry depend., resist. obs. (*French*) 0-84215
 Fe-Cr-Ni (12, 15 wt.%) austenitic alloy, Ni⁶⁺ irradiated, void swelling and phase stability, Si and Ti effects 0-65055
 Fe-Cr-Ti-Mo-TiO₂ (13, 3.5, 1.5, 2 wt.%) dispersion hardened, void swelling 0-65046
 H₂ permeation reduction using Pd foil in liquid metal (*Japanese*) 0-68770
 H₂ permeation through HTGR heat exchanger tubes, reduction using calorising method (*Japanese*) 0-100360
 Hf and Zr, trace elements, simultaneous determ. in soln. using X-ray fluorescence anal. 0-97752
 MgAl₂O₃, faulted defect aggregates prod. by neutron-irradi. 0-107331
 N₂O₄, fission reactor coolant, heat transfer on condensation (*Russian*) 0-57860
 N₂O₄, viscosity and thermal cond., approx. polynomials (*Russian*) 0-59739
 Ni, creep, irradi. induced with 17 MeV deuterons 0-93607
 Ni-Cr-Al-Ti, stress corrosion cracking, factors influencing susceptibility 0-97617
 Ni-Cr-Fe, stress corrosion cracking, factors influencing susceptibility 0-97617
 Ni-Cr-Fe alloys, radiation enhanced precip. and dissolution of precipitates, point defect kinetics and dislocation obs. 0-108467
 Pb, FBR blanket facility, gamma-ray heating rate meas. 0-57912
 Pt, neutron damage, positron annihilation 0-65056
 Pu safeguards, preparation of ²⁴⁴Pu standard reference material 0-78373
 Pu-bearing materials, environmental impact of transportation, linear regression anal. 0-85308
 Ta, thermophysical props. and neutron absorpt. 0-103488
 Ti alloys, corrosion in saline radioactive waste isolation environments 0-104349
 Ti, gettering of H, mass spectrometry and microgravimetry study, rel. to HTGR gas purification 0-73374
 (U,Pu)C FBR fuel pins, fuel/clad compatibility 0-57847
 (U,Pu)C, sintering, role of Ni as sintering additive 0-84892
 α-U, strain rate effect on tensile flow and fracture 0-84992
 U(C,N), N vapour pressures and thermodynamic props. 0-84918
 UC, sintering, role of Ni as sintering additive 0-84892
 UC:Y(Zr)(La)(Ce), U self-diffusion 0-92711
 UN, N vapour pressures and thermodynamic props. 0-84918
 (U_{0.9}Pu_{0.1})O_{1.98} fuel pin, post-irrad. examinations 0-78400
 U₂Si, reversible twinning, in-situ obs. 0-104241
²³⁵U/²³⁸U isotope ratio determ. in UF₆ samples using gas quadrupole mass spectroscopy 0-78376
 UF₆, mass spectrometric determ. of ²³⁵U content 0-68961
 Zircaloy, foil, dislocation loop nucleation and growth during 1 MeV electron irradi. 0-88152
 Zircaloy-2, effect of simulated fission products on mech. props. 0-73922
 Zircaloy-2, electron irradiation damage, direct obs. 0-84212
 Zircaloy-4, deformation behaviour between 77 and 900K 0-71686
 Zr alloys, creep and growth, irradiation induced, rate theory approach 0-89294
 Zr alloys, irradiation growth, influence of microstructure and test conditions 0-92561
 Zr and alloys, neutron irradi. at 573 to 923K, damage struct. 0-107334
 Zr and Hf, trace elements, simultaneous determ. in soln. using X-ray fluorescence anal. 0-97752
 Zr, breakaway oxidation kinetics at 623K, SEM study 0-97633
 Zr, electron irradiation damage, direct obs. 0-84212
 Zr, foil, dislocation loop nucleation and growth during 1 MeV electron irradi. 0-88152
 Zr, foil bending by in situ ion irradi., neutron damage simulation, room temp. oxide growth 0-107342
 Zr, gettering of H, mass spectrometry and microgravimetry study, rel. to HTGR gas purification 0-73374
 Zr, irradiation growth, influence of microstructure and test conditions 0-92561
 Zr, irradiation growth, reaction rate theory calcs. 0-88212
 Zr, void swelling during electron irradi., HVEM study 0-92559
 Zr-Al (8.6 wt.%), dimensional stability struct. and mech. props, effects of neutron irradi. 0-92563
 Zr-Hf (2.2 wt.%), high temp. oxidation in flowing O₂, 873-1173K 0-93687
 Zr-Nb (0.1, 2.5 wt.%), foil, dislocation loop nucleation and growth during 1 MeV electron irradi. 0-88152
 Zr-Nb (2.5 wt.%), channel tubes, in-reactor creep and irradi. growth 0-93604
 Zr-Nb (2.5 wt.%), cold-worked, pressure tubing, metallography and mech. props. 0-89269
 Zr-Nb (2.5 wt.%), high temp. oxidation in flowing O₂, 873-1173K 0-93687
 Zr-Nb (2.5 wt.%), nuclear fuel channels, neutron effects on ultimate fracture strength, 293 to 573K 0-85054
 Zr-Nb (2.5 wt.%), pressure tubes, irradi. creep and growth, anisotropy factors 0-97536
 Zr-Nb (2.5 wt.%) pressure tube rel. between stress intensity factor, crack opening displacement and J-integral 0-100920
 Zr-Nb (97.5, 2.5 wt.%) nuclear reactor pressure tube material, H embrittlement study by TEM 0-76363
 Zr-Nb-Sn (3.0, 1.0 wt.%), high temp. oxidation in flowing O₂, 873-1173K 0-93687
 Zr-Sn (1.5 wt.%), electron irradiation damage, direct obs. 0-84212
 Zr-Sn-Fe-Ni (1.5, 0.1, 0.15 wt.%), electron irradiation damage, direct obs. 0-84212
 Zr-Sn(Fe)(Ni) (0.15 wt.%), electron irradiation damage, direct obs. 0-84212

fission reactor materials continued

- Zr₃Al, deformed and irradi., lattice defects obs., superlattice dislocations and defect clusters 0-107261
⁹⁴Zr(n,α)⁹¹Sr, fast n, fission spectrum averaged cross section 0-63177
- fission reactor operation**
 see also *fission reactor cooling and heat recovery; fission reactor core control and monitoring; fission reactor safety*
 BWR, Enrico Fermi-2, system turnover, test and startup program 0-63338
 BWR, Finland's TVO 1, commissioning and startup 0-68888
 BWR, power upgrading, feasibility, benefit, cost anal. 0-68877
 BWR core operation flexibility for improved fuel cycles 0-57915
 BWR designed for improved operation at Grand Gulf 0-106121
 control rooms, human factors design approaches, improvement of man-machine interface, error reduction 0-63327
 CRNL NOS/BE 1.3 system, dynamic core allocation 0-78425
 decontamination by liquid waste elimination without reactor defuelling, CAN-DECON process 0-73943
 digital simulator software development, kinetic equations integration, numerical solution method 0-68901
 EDF graphite-gas reactors, role of nuclear calculations in operation (*French*) 0-95373
 failure probability distrib. from observed failure data, beta distrib. 0-63335
 FBR core materials studies for improving reactor performance, trends 0-102232
 FBR power prod., optimised strategy rel. to U ore costs 0-99253
 gaseous fuel reactor applications 0-63367
 HTGR, surveillance robot for fuel and reflector element inspection 0-68873
 LMFBR power stations, electric power generation and fuel fabrication 0-57928
 LWR maintenance problems for remote technology appl. 0-68871
 LWR power prod., optimised strategy rel. to U ore costs 0-99253
 Maine Yankee power station update history 0-73967
 molten salt fusion-fission symbiotic systems, nuclear performance calcs. of catalysed D-D and D-T reactors 0-57948
 nuclear power station with VVER-400 reactor, primary circuit coolant pressure and quantity control (*Polish*) 0-91231
 nuclear power stations, load factors and availability achieved with light water and heavy water reactors (*Slovenian*) 0-68843
 operator reliability, Weibull distrib. model 0-63336
 power upgrading, combustion engineering Inc. experience 0-73968
 power upgrading, regulatory perspective 0-73966
 power uprating, hardware and safety aspects 0-63342
 Project Manager organisation in nuclear plant turnover and startup 0-63339
 start-up experience of IBR-2 pulsed research reactor 0-73956
 startup, conduct of operations, organisation and personnel 0-63340
 startup, staffing program, scope, tasks, resources, constraints, anal., implementation 0-63341
 teleoperator systems for reactor maintenance, technology assessment 0-68872
 training simulator, design characteristics (*Spanish*) 0-58007
 university type reactors, economic success, project update 0-68900
 Westinghouse power plants, uprating capacity 0-68878
 CO₂ fundamental condensation cycles in steam and nucl. power plants, performance characts. 0-63368
 He cooled reactor turbine control experiences Fort St. Vrain HTGR (*German*) 0-57927
 UF₄-CF₄ mixture, gas core fission reactor, fission based plasma engine 0-63366
- fission reactor safety**
 see also *fission reactor cooling and heat recovery; fission reactor core control and monitoring*
 7-pin bundle simulation during flow rundown transient 0-68879
 accident at Three Mile Island, lessons learned in maintenance and reliability 0-57929
 accident management, automated notification of reactor data to off-site personnel 0-95388
 accidents, Three Mile Island nuclear power station, viewpoint of member of Commission of Enquiry 0-83190
 aircraft impact, structural response, reaction-time and impact area-time curves 0-78407
 ALARA, it is being achieved, utility and navy records 0-68898
 ARMP model appl. to Beaver Valley Unit 1 0-68862
 aRMP reload safety evaluation methods for application to Kewaunee 0-68861
 aseismic bearing foundation system for power station earthquake protection 0-83206
 availability of redundant safety systems with common-mode and undetected failures 0-91230
 BABEL, multigroup neutron library for fast reactor, shielding design studies 0-68745
 Biblis B nuclear power station risk study, results and conclusions (*German*) 0-68902
 boiling crisis, nuclear reactor safety and performance, state of the art review 0-63312
 Boltzmann equation, P₁ approx. in presence of delayed neutron emission 0-78347
 Browns Ferry BWR, load following test 0-68892
 BWR, calc. of shutdown dose rate around recirculation pipes, radioactive corrosion products in primary cooling water 0-68734
 BWR, iron oxide deposition on heated surfaces, model 0-73902
 BWR, primary containment vessel, spray heat removal characteristics 0-73972
 BWR, safety relief valve discharge loads, dynamic effects on structures and eqpt. 0-99236
 BWR, steam chugging during LOCA, general transient anal. 0-73903
 BWR, TRAB transient analysis program for pressure vessel and subsystems 0-73978
 BWR containment system, effect of torus wall flexibility on hydro-structure interaction 0-83195
 BWR coolant pipes, intergranular stress cracking, in-service inspection influences 0-68887
 BWR decay heat removal systems, probabilistic risk assessment, fault and event tree anal. 0-63333
 BWR LOCA, hydrodynamic lead characteristics of primary containment vessel 0-73972
 BWR LOCA, phased mission analysis of ECCS failures 0-68851

fission reactor safety continued

BWR LOCA, pool swell modelling and small-scale expts., comparative eval. 0-95362
 BWR LOCA, pool swell reduced scale simulations, scaling law limitations 0-99238
 BWR LOCA, press. oscill. phenomena induced by steam condensation, in containment with press. suppression system 0-68848
 BWR LOCA anal. using homogeneous critical flow model, expt. determ. of blowdown flow rate 0-106120
 BWR LOCA analysis, jet pump modelling using RELAP4 0-68850
 BWR NSSS structural integrity programs at GEC 0-99230
 BWR radioactivity releases reported to Licensee Event Report file 0-68889
 BWR turbine trip transient analysis using ALMOS plant model (*German*) 0-83177
 cable tests to IEEE standards 0-57884
 CANDU reactors, seismic design criteria and requirement 0-78358
 Caramel fuel cladding rupture, development and detection at OSIRIS experimental reactor (*French*) 0-95371
 component vibration investigation using fast Fourier transform analysers 0-63315
 computerised reactor protection systems, reliability anal. using Markov methods 0-91229
 condensation-driven fluid motions, nuclear reactor safety 0-63228
 conference, Berlin, Germany (Aug. 1979) 0-77539
 conference, design, safety requirements, London, UK (Apr. 1980) 0-57013
 containment building, Mark III, advantages, Grand Gulf Nuclear Station project 0-106122
 containment structure design and service loads 0-106138
 containment testing by TVA 0-68897
 coolant depressurisation studies, transient density, press., temp. variations, during discharge 0-57833
 coolant pressure boundary leakage detection system 0-63306
 core meltdown accident, radioactive pollution consequences from liquid pathways 0-104778
 critical two-phase flow models, nuclear reactor safety 0-63229
 criticality safety analysis in nuclear fuel cycle (*Japanese*) 0-99225
 current nuclear power plant safety issues, 1980 conf. preview 0-95360
 Czechoslovak Research Institute activities, safety, waste disposal and personnel training (*Slovak*) 0-83188
 decontamination by liquid waste elimination without reactor defuelling, CAN-DECON process 0-73943
 departure from nucleate boiling ratio safety limit to modelling parameters in COBRA IIIC/MIT 0-73901
 digital computer applications in reactor instrumentation and control 0-106134
 Doppler feedback use in control rod drop transients, Maine Yankee expt. 0-68895
 DOT 3.5, use in fast power reactor shield configuration calcs. 0-68749
 Dounreay PFR, plant improvements 0-57933
 Dounreay test reactor, fast breeder test experience 0-86961
 electrical auxiliary systems, safety design for AGR's 0-57934
 electrical equipment, qualification concept 0-57883
 electrical system design for future AGR power stations 0-57935
 emergency planning and preparedness 0-57887
 environmental protection, reactor safety and waste handling (*Hungarian*) 0-91224
 environmental protection in Hungary (*Hungarian*) 0-91225
 equipment qualification for dynamic loads 0-99233
 EURDYN, nonlinear transient dynamics programs for fast reactor safety 0-91234
 EURDYN-1M, safety studies on LMFBF, computer program 0-99267
 failure location algorithm for complex networks 0-99228
 failure probability distrib. from observed failure data, beta distrib. 0-63335
 fast neutron criticality monitor, response to prompt critical bursts 0-63398
 fault tree anal. using Monte Carlo and anal. methods (*Spanish*) 0-57870
 FBR, role of fission gas swelling and release in reactor accidents 0-57854
 FBR, space dependent simulation of transient behaviour using KINTIC-2 code (*German*) 0-83182
 FBR fuel pin failure, fuel porosity and crack effects on transient over-power analysis 0-71760
 FBR fuel pin safety expts. at SLSF, centerline fuel thermocouple performance 0-102283
 FBR HCDA, convective heat transfer correlations for molten core debris pools growing in concrete 0-83196
 FBR safety and economics, leak detection, cooling, waste disposal 0-63303
 FBR transient fuel behaviour maps, fuel response to thermal transients 0-57926
 FBR transient fuel behaviour maps, fuel response to thermal transients 0-68874
 FDR type reactors, transient anal., neutron power and temp. form factors, depend. on time and power level 0-83178
 feedwater systems, auxiliary, fault tree anal. 0-63332
 FFTF TOP analysis, uncertainty in accident consequences calculated by large codes due to uncertainties in input 0-78413
 fluid dynamic transient analysis using ASWR method with staggered meshes (*German*) 0-83176
 Fort St. Vrain HTGR, afterheat predictions and meas. 0-68891
 FTR, criticality expts. with concrete reflected fuel pins in water 0-78410
 fuel accounting and safeguarding, spent fuel bundle counter for 600 MW CANDU reactor 0-63269
 fuel pin rupture detection system using meas. of time differential of acoustic emissions 0-102282
 fuel rod gas pressure meas. during LOFT, sensor description 0-57876
 fuel thermocouples and liquid-level probes for core monitoring 0-99239
 FUGEN plant dynamic tests 0-68894
 gamma rays, 6 MeV, penetrating shielding materials, energy and ang. flux density spectra 0-63393
 German Risk Study, social risk assessment (*German*) 0-57866
 guard line circuits dual microprocessor system, decision-making and self-testing 0-57901
 Harrisburg reactor accident in 1979, lessons to be learned (*German*) 0-91233
 HCDA, bubble worth variation in molten cores 0-68854
 HCDA, neutronics and hydrodynamics equations, energy release, DISCAL code 0-68842

fission reactor safety continued

HTGR, nonlinear dynamic anal. of prismatic graphite fuel elements, response to seismic excitation 0-99237
 HTGR risk assessment, operator actions, event and fault tree anal. 0-63330
 human factors, normal operation and emergency procedures, errors, safety, maintenance, working conditions 0-63328
 HWR, shutdown heat removal systems, reliability fault tree anal. and β -factor method 0-63331
 industrial activities nearby causing hazards, deterministic and probabilistic studies 0-78408
 Isar BWR power station, transient expts. during startup and initial operation (*German*) 0-83187
 JOYO experimental fast reactor, radiation protection monitoring programme 0-57992
 liquid level detector based on level sensitive transducer for PWR environment 0-57874
 LMFBF, chemical leak detection, effects of NaOH in Na 0-63326
 LMFBF, filtration of Na-fire aerosols 0-68853
 LMFBF, gas tag identification of failed assemblies, anal. methods 0-95369
 LMFBF, hydrodynamics of large-scale fuel-coolant interactions 0-78409
 LMFBF, inherent safety features 0-106145
 LMFBF, LOF-driven TOP, FCI related material movements 0-73946
 LMFBF, molten UO₂ fuel-Na coolant thermal interaction, characterisation of fragmented fuel 0-68774
 LMFBF, Na boiling detection, power spectral density surveillance systems 0-68740
 LMFBF, Na boiling hazard (*French*) 0-78402
 LMFBF, Na-H₂O steam generators, safety problems and their solution in the USSR 0-63318
 LMFBF, pool type, natural circulation cooling 0-102289
 LMFBF, pressure transient analysis in piping systems including the effects of plastic deformation and cavitation 0-74775
 LMFBF, shutdown heat removal systems, reliability fault tree anal. and β -factor method 0-63331
 LMFBF accident, contained radioactive suspension behavior anal. 0-99227
 LMFBF cooling systems, reliability 0-57838
 LMFBF fuel, fission gas behaviour during overpower transient, calcs. using COREF-1 code 0-57853
 IMFBF fuel and blanket transient thermal performance characteristics 0-68880
 LMFBF fuel disruption following LOF accident, in-pile expt. using high-speed cinematography 0-78366
 LMFBF fuel pin bundles in flowing Na, design and operation of SLSF test trains for safety tests 0-102281
 LMFBF HCDA, energetics of bubble expansions, potential attenuation mech. 0-83197
 LMFBF HCDA, I-D compressible coolant dynamics, numerical anal. using EULFC1 code 0-68733
 LMFBF HCDA, US meas. of penetration of liquid Na into limestone concrete 0-78412
 LMFBF HCDA aerosol behaviour, kinetic corrections to aerosol gravitational collisional efficiency 0-95386
 LMFBF HCDA analysis, uncertainty in accident consequences calculated by large codes due to uncertainties in input 0-78413
 LMFBF subassembly, fuel coolant interaction anal.model and computer code SAMI 0-106136
 LMFBF TOP accident, implications of in-channel fuel plugging 0-78414
 LOCA, data analysis using computer-aided models (*Czech*) 0-73949
 LOCA, reflooding phase, flow film boiling, void fraction meas. 0-92207
 LOCA analysis in small compact reactors using RELAP4/MOD5 thermal hydraulic code 0-68852
 LOCA consequences, hydrodynamics mass method anal. 0-73909
 LOF overheating transients, volatilization pot. of metallic inclusions in irradi. UO₂ fuel 0-57895
 LOFT, contribution to nuclear reactor safety 0-106139
 LOFT, requalification following LOCE 0-57904
 LOFT drag disc turbine meter rakes for two-phase flow measurement 0-102260
 LOFT reactor secondary cooling system, waterhammer phenomena 0-57905
 loss of coolant studies, gamma densitometer detector comparison 0-57881
 Lovisa-1 Nuclear Power Station, in Finland, safety during design, building, and operating stages (*Russian*) 0-106128
 LWPR, radiological emergency monitoring and instrumentation, Federal guidance 0-57961
 LWR, human operator errors, analytical model 0-63329
 LWR fuel rod, transient pellet-cladding interaction, ISUNE-4 computer anal. 0-91228
 LWR LOCA, enhanced steam oxidation of Zircaloy cladding by deformation 0-73917
 LWR LOCA, fission product decay energy release rates following ²³⁵U fission 0-57894
 LWR LOCA, modelling of press. and temp. changes in two-phase, two-component flow (*Bulgarian*) 0-68904
 LWR LOCA, rewetting models, review and comparison 0-83194
 LWR LOCA, two-phase flow, horizontal stratified, I-D two-fluid eqns. 0-91226
 LWR LOCA, two-phase flow instrumentation for safety anal. 0-102259
 LWR maintenance problems for remote technology appl. 0-68871
 LWR piping, intergranular stress-corrosion cracking 0-81234
 LWR power stations, R and D for improving seismic safety 0-99231
 LWR refuelling shutdown, multiple controlled-cell removal 0-99252
 LWR safety, condensation heat transfer in stably stratified systems 0-63311
 microprocessor controlled multipoint recorder with graphical video output for reactor core temperatures 0-57873
 natural-circulation steam generator model for optimal steam generator water level control 0-68876
 neutron radiography appl. (*Slovak*) 0-76430
 neutron-physical characteristics of Soviet BABETs reactors, startup experience 0-73953
 non-destructing testing of reactor components using acoustic emission (*Spanish*) 0-57871
 nuclear heating in thick iron slabs at the ORR pool side facility 0-63241
 nuclear power plant equipment electromagnetic interference and RFI effects 0-57880
 Nuclear Safety Chain concept development to increase operator awareness 0-57931

fission reactor safety continued

nuclear simulation programme based on a quality system (*German*) 0-57902
 operator reliability, Weibull distrib. model 0-63336
 optical instrumentation methods for two-phase reactor flows 0-63313
 PBHTGR, core behaviour following massive air ingress, graphite corrosion eval. (*German*) 0-83181
 PBHTR, afterheat removal system failure, radiant heat transfer anal. 0-95364
 pebble bed HTR, delayed after heat removal (*German*) 0-106102
 piping system, crack initiation and propagation, fracture mechanics 0-83193
 plant diagnostics—the integrated approach 0-68899
 PNP-3000, prototype nuclear process heat reactor, core temp. transients, heat transfer calc. (*German*) 0-83180
 power density limitation system development 0-68884
 power reactor, water cooled and moderated, tube film boiling heat transfer coeffs. 0-73877
 pressure vessel steels, fracture toughness 0-81172
 pressure vessels, thick steel sections, inspection by US nondestructive examination 0-102258
 primary coolant circuit service life, working condition effects (*Czech*) 0-73885
 principles underlying IAEA nuclear safety programme 0-95361
 probabilistic methods, reliability and risk analysis, Fed. Rep. Germany 0-106124
 probabilistic methods in safety analysis and regulations in France 0-106123
 probabilistic risk assessment, methodology and appls. 0-63352
 probabilistic siting analysis, atmospheric releases, health effects 0-106130
 protection system and engineered safeguard system separation review program 0-57820
 protection system design criteria 0-68935
 protection system software validation, quality assurance experience 0-57886
 PWR, clad free pellet recriticality possibilities 0-68863
 PWR, core reflooding, progress of hardening front (*French*) 0-91211
 PWR, shutdown heat removal systems, reliability fault tree anal. and β -factor method 0-63331
 PWR, two circuit system, licensing and design, European view 0-57930
 PWR, two phase flow modelling for LOCA (*French*) 0-78349
 PWR accident prevention, extra instrumentation for Ringhals 2 station, Sweden 0-63369
 PWR and PHWR-Candu types, qualitative comparison of nuclear safety features (*Slovenian*) 0-95358
 PWR boiler steam generators, two-phase flow problems in low press. transients (*French*) 0-78350
 PWR boiler tubes, denting type corrosion, control by use of neutralisers 0-106109
 PWR containment air monitoring system 0-57965
 PWR containment vessel optimisation 0-106137
 PWR containments following LOCA, heat transfer coefficient 0-86958
 PWR design and plant layout, safety criteria 0-102288
 PWR engineered safety features actuation system follow-up system logic 0-57879
 PWR fuel clad failure characterisation based on fission product activity, PROFIP 3 code 0-95365
 PWR LOCA, average void fraction estimate in vertical two phase flow channel 0-73878
 PWR LOCA, opening and extension of circumferential cracks in pipe 0-78364
 PWR LOCA, pump behaviour conveying two-phase flow (*French*) 0-78351
 PWR LOCA reflood, effect of low containment press. on peak cladding temp. 0-57897
 PWR pressuriser behaviour during operational transient, math. model 0-63230
 PWR vessel and primary circuits estimation of reliability, probabilities and adaptive models 0-106125
 quality assurance, need for sensible interpretation 0-57932
 quantitative methods of assessing risks 0-57903
 radioisotope relays, operation, construction and appl. (*Polish*) 0-106129
 rapid automated nuclear chemistry, short lived fission products, reactor safety 0-81353
 reliability analysis, unavailability of systems under periodic test and maintenance 0-95368
 remote US inspection unit for piping and vessel inspection 0-104394
 risk assessment in European Community 0-106135
 seismic qualification of Class 1E eqpt. 0-99234
 seismic qualification tests of elect. eqpt., damage severity factor concept 0-99235
 seismic safety margins research program of the US Nuclear Regulatory Commission 0-99229
 seismic safety of mechanical eqpt., R and D program 0-99232
 seismically qualified piping, failure probability, ASME code limits 0-78365
 shielding benchmark calcs. by Discrete Ordinates and Monte Carlo methods 0-73886
 shutdown heat removal system failure, fault tree, common-cause anal. 0-63334
 small bore piping, field support to ASME Section III rules 0-63346
 SNR-300 LMFBR, accidents in tertiary system, dynamic behaviour of steam generators (*German*) 0-83141
 SNR-300 LMFBR, ECCS, decay heat removal during heat sink failure, accident anal. using NOTUNG code (*German*) 0-83185
 SNR-300 LMFBR, response to reactivity insertions (*German*) 0-83183
 snubber evaluation program 0-63345
 stability analysis and characters. for two-phase flow eqn. systems with viscous terms 0-59103
 steam generator tube performance in water cooled reactors in 1978 0-78399
 structural reliability, conference, Berlin, Germany (Aug. 1979) 0-105422
 TAPIRO fast research reactor, computerised protection system 0-63308
 Thailand's first nuclear power plant, radiation monitoring programme 0-57996
 thermocouples, 2200°C fuel centerline for LOFT program 0-57877
 Three Mile Island, accident, malfunction development, prevention (*Hungarian*) 0-68846
 Three Mile Island incident, Atmospheric Release Advisory Capability, response and support 0-57889

fission reactor safety continued

Three Mile Island incident, operator/instrumentation interactions 0-57890
 Three Mile Island incident, Pennsylvania's emergency preparedness and response 0-57888
 Three Mile Island malfunction, monitoring, radiation exposure 0-57960
 TMI, Kemeny Commission report, conclusions and recommendations, summary 0-63302
 TMI, role of analytical chemistry in accident control, assessment and recovery 0-95389
 TMI-2 accident, analysis of high readings by startup channel neutron detectors 0-102265
 TMI-2 accident, cause, radiological consequences, NRC action 0-102262
 TMI-2 accident, nuclear reactor safety, role of instrumentation and control (*Japanese*) 0-73947
 TMI-2 accident analysis, ¹³¹I release, steam explosions and molten fuel concrete interactions 0-102264
 TMI-2 accident analysis using two-loop RETRAN model 0-102263
 two-phase-flow instrumentation development at Brookhaven National Laboratory 0-102261
 US decontamination system for reactor fuel transfer pool, remotely operated 0-68916
 US viewing system for reactor fuel assemblies under liquid Na 0-57875
 vent filtered containment, feasibility and effectiveness issues 0-68875
 vortex diodes in post accident heat removal systems 0-106100
 VVER type nuclear reactors, in Soviet Union, biological shielding problems 0-106127
 West German policy (*German*) 0-57865
 worldwide ISO standards for nuclear technology safety 0-102266
 Zircaloy PWR cladding, deformation in LOCA 0-106114
 ZPPR-9, stimulated hodoscope slot effect in STF critical assembly 0-68860
 BWR, primary containment vessel, spray I₂ removal characteristics 0-73972
 EBR-II Na system cold traps for control of O₂, H₂, T impurities 0-78411
 I, radioactive, air sampling system, separation into gaseous and particulate fractions 0-57962
¹³¹I, behaviour during rinsing in in-pile loop after fission product release expt. 0-73879
 (U,Pu)O₂ fuel pin behaviour during FFTF 3c/s reactivity insertion event, TREAT expt. anal. 0-102240
 UF₆-CF₄ mixture, gas core fission reactor, fission based plasma engine 0-63366
 UO₂ fuel-coolant interaction, film boiling and vapor explosion phenomena 0-95363

fission reactor theory and design
see also fission reactors; fission research reactors; neutron transport theory
 advanced reactor and fuel cycle systems, potentials and limitations for United States utilities 0-106106
 AMPX code, operating experience 0-68743
 AMPX code for coupled multigroup n- γ cross section sets 0-68741
 AMPX code implementation problems at KFA Jülich 0-68742
 BABEL, multigroup neutron library for fast reactor, shielding design studies 0-68745
 Boltzmann equation, P₁ approx. in presence of delayed neutron emission 0-78347
 BWR, improved core design 0-68761
 BWR condensate feedwater system, dynamic model 0-73883
 BWR control cell core design concept 0-68763
 BWR core calculations using improved coarse mesh methods 0-68849
 BWR core concept, WNS-type fuel, equilibrium cycle performance 0-68762
 BWR in-core neutron detector sensitivity to control rod vibr. using neutron noise anal. 0-57910
 BWR LOCA anal. using homogeneous critical flow model, expt. determ. of blowdown flow rate 0-106120
 BWR reflectors, effective albedo parameter determination 0-68756
 CANDU reactors, seismic design criteria and requirement 0-78358
 conference, design, safety requirements, London, UK (Apr. 1980) 0-57013
 control and instrumentation designs beyond the 1980s 0-57872
 control theory, steady-state accuracy of neutron field regulation 0-63319
 critical assemblies, bare homogeneous, anal., interrelating differential and integral nuclear data 0-68739
 departure from nucleate boiling ratio safety limit to modelling parameters in COBRA IIIC/MIT 0-73901
 design basis R and D of power stations to cut costs and schedules 0-99204
 design management, plant replication for low-cost nuclear power, Philippines National Power Corp. 0-63242
 DOT 3.5, use in fast power reactor shield configuration calcs. 0-68749
 double criticality of uniform-power-reflected reactors 0-57828
 EBR-II reflector assembly irradi. induced bowing, implications for core restraint design 0-104234
 electrical auxiliary systems, safety design for AGR's 0-57934
 electrical system design for future AGR power stations 0-57935
 ENDF/B-V uncertainty data processing into multigroup covariance matrices 0-68752
 energy distribution, algorithm for extremal control 0-83209
 engineering test facility as a test device for inertially confined fission 0-57831
 fast breeder core with internal blanket 0-68870
 fast reactors, ²³⁹Pu decay heat evaluation 0-63239
 FBR, electric power generation, research, development and demonstration, risk and timing 0-57837
 FBR, nonstationary prompt-neutron diffusion, multigroup treatment 0-86956
 FBR, zero-power neutron noise expt. anal., power spectral density and subcritical reactivity 0-57911
 FBR analysis, general multigroup nodal procedure based on response matrix principles [for FBR analysis] 0-57827
 FBR thermal hydraulics, sensitivity theory for general systems of non-linear equations 0-86954
 FBR UO₂-fuelled blanket assembly design considerations 0-102254
 FDR type reactors, transient anal., neutron power and temp. form factors, depend. on time and power level 0-83178
 fluidised bed concept, diffusion theory 0-68729

fission reactor theory and design continued

FMSR, physics performance of a centrally moderated fast reactor concept 0-99208
 GAM library data formation in energy groups, PWR appl. 0-68746
 gamma-power of hot circuit, calc., effect of flow hydrodynamics of process materials 0-63235
 GCFR, core thermal hydraulics and pumping power anal. code JUPITER 0-73889
 homogeneous fluid-fueled reactors capable of in-situ fuel reprocessing nitride-liquid Sn concept 0-57834
 hot pellet nuclear reliability factors 0-68754
 HTGR, dynamic characts., primary loop characts. (*Japanese*) 0-57832
 HTGR development and its process heat, steam-cycle and gas turbine appls. 0-63250
 HTGR prestressed concrete pressure vessels, design of removable closures for large cavities 0-78356
 HTR, Xe dynamics, 2D reactor models, axially collapsing methods (*German*) 0-68731
 hybrid reactor analysis, separation technique for transport eqn. and sensitivity theory 0-57823
 inertial confinement hybrid reactor design with flowing Li/molten salt 0-95405
 integral parameter correlations, reactor performance using data covariances 0-68869
 international symbiotic nuclear energy parks using breeders and advanced converters, economic feasibility 0-57825
 irradiation loop containing nonfissile material, optimality criterion based on γ -ray flux losses 0-63236
 large LMFBRs, balance-of-plant design considerations 0-106107
 LMFBR, breeding ratio and multiplication factor uncertainties 0-86953
 LMFBR, current developments in nuclear breeder technology 0-57835
 LMFBR, heterogeneous, fuel element performance, impact of design and operating parameters 0-102249
 LMFBR, neutron elastic removal cross sections, interference effect of strong scattering resonances 0-68658
 LMFBR, review of worldwide R and D 0-63249
 LMFBR, wire wrapped rod bundles, coolant mixing, peripheral flow prediction 0-73891
 LMFBR fuel cycles that reduce nuclear weapon material proliferation 0-106105
 LMFBR fuel intra-assembly flow mixing uncertainty, statistical determination methodology 0-73890
 LMFBR heterogeneous core design with interchangeable oxide/carbide fuel, CDS development program 0-102253
 LMFBR universal core layout, interchangeability of hetero(homo)geneous cores and oxide/carbide fuels 0-102228
 LMFBR vented fuel assembly, thermodynamic modelling and testing 0-83144
 LMFBRs, national development programmes, status assessment 0-106104
 LMRBR, interchangeable core assessment, coolant orifice zoning 0-102229
 LMRBR interchangeable core assembly design 0-102230
 LOFT, contribution to nuclear reactor safety 0-106139
 LWBR, symbiotic system using ^{238}U -Pu and ^{233}Th - ^{233}U fuel cycles 0-57822
 LWR core, few group 2-D diffusion eqns. in hexagonal geometry, HEXAB-II-30E code (*Bulgarian*) 0-68765
 LWR core, minimisation of energy distrib. inhomogeneities 0-63321
 LWR core analysis, qualification of SIMULATE against the Hatch-1 end-of-cycle 1 gamma scan 0-57921
 LWR design codes EPRI-CELL and CPM, implementation 0-68751
 LWR parameter sensitivity to neutron scatt. kernel models and data 0-63240
 LWR power stations, design features and instrumentation for materials safeguards (*Russian*) 0-63278
 materials safeguards, facility design features relevant to improved IAEA safeguards 0-63277
 MORSE continuous weights code 0-68748
 multicore reactor, optimal control determ. from energy release profile (*Russian*) 0-73974
 multigroup charged-particle transport calcs., temp. effects on cross sections 0-57818
 NBS standard neutron fields, average fission cross-section meas., error anal. 0-68857
 neutron absorption, control poison optimisation, depletion calcs. 0-57906
 neutron diffusion, relationship among the various anisotropic diffusion coefficients for periodic lattices 0-57826
 neutron flux distribution, transmission probability method 0-106101
 neutron thermalisation, THERMOS spectrum code, accurate reduced mesh model 0-57829
 neutron transport, 3-D integral transport code SHETAN 0-63238
 neutron transport theory, ω mode transport eqn., asymptotic soln. 0-102231
 neutron transport theory, P_N -value of asymptotic decay constant 0-57830
 nonlinear reactor noise anal., appl. of Langevin eqn. with system-size expansion 0-68727
 nuclear power reactor systems, dynamical behaviour modelling 0-91216
 Nuclear Safety Chain concept development to increase operator awareness 0-57931
 parameter identification using the irreversible circulation of fluctuation 0-73882
 PBR, neutron flux distrib. in multisphere configs., diffusion-theoretical model (*German*) 0-73875
 pebble bed HTR, heterogeneity effects in temp. coeff. calcs. 0-68757
 piping system design, rationalisation of power plant pipe break criteria 0-99205
 point reactor kinetic eqn. with Gaussian reactivity fluctuation, exact soln. 0-68735
 power coefficient measurement based on reactor coolant system average temp. 0-57909
 probability-based design criteria for nuclear structures 0-99207
 prompt neutron yield calcs. from neutron induced fission 0-68858
 protection system and engineered safeguard system separation review program 0-57820
 PWR, two circuit system, licensing and design, European view 0-57930
 PWR containments following LOCA, heat transfer coefficient 0-86958
 PWR core analysis, effects of improved UO_2 once-through fuel cycle 0-57917
 PWR core analysis, methods and data validation 0-57924
 PWR core analysis, steady-state core physics and thermal-hydraulic reload design calcs. 0-57923

fission reactor theory and design continued

PWR core analysis, transport-to-diffusion theory for gadolinia-loaded fuel pins 0-57908
 PWR core analysis using EPRI ARMP program, calc. and meas. reactor physics parameters 0-57925
 PWR core analysis verification, reactivity rundown and power distrib. accuracy 0-57922
 PWR design and plant layout, safety criteria 0-102288
 PWR dynamical behaviour modelling in FORTRAN 0-91217
 PWR tight-pitch cores, reactor physics of fuel cycles 0-57920
 reactivity coefficient changes in Soviet RBMK reactors 0-73954
 reactivity reserve and K_{eff} estimation (*Russian*) 0-73913
 reactor dynamics, numerical integration using real integrating factors 0-68730
 reactor physics, review 0-63245
 reactor physics considerations in design for improved BWR fuel cycles 0-57916
 reactor physics considerations of PWR fuel cycle alternatives 0-57918
 resonance absorption calculations in thermal reactors 0-86955
 seed-blanket calcs., 2-D, one-channel synthesis method, transport and diffusion 0-73876
 self-shielding factors, discrepancies between ETOX and TIMS codes 0-68744
 shielding benchmark calcs. by Discrete Ordinates and Monte Carlo methods 0-73886
 small bore piping, field support to ASME Section III rules 0-63346
 space dependent stochastic neutron kinetics with Gaussian parametric excitation 0-63223
 space independent low power model, multigroup energy formalism for reactor stochastic eqns. 0-63224
 structural response to dynamic loads, simulation of dynamic environments for design verification 0-99206
 subcritical cyclostationary nuclear reactor, neutron counting statistics, sinusoidally modulated neutron source 0-99203
 thermal reactor benchmark calculations with the MCNP Monte Carlo code 0-68755
 transport codes DOT and TWOTRAN as standards for diffusion in pebble bed reactors 0-68750
 unified neutron transport theory for reactor analysis 0-63246
 WIMS-D performance in cell parameters calculation for $\text{UO}_2\text{-D}_2\text{O}$ systems 0-68747
 ZPPR pin geometry, SDX cell homogenisation code validation 0-86962
 $^{230}\text{Pu}(n,f)$, fission-fragment yields of neutron fission in FBR 0-83102
 UF_6 , high temp. fissioning plasma core reactors, fluid mechanical confinement 0-63248
 $^A\text{U}(n,f)$, $A=235$, 238, fission-fragment yields of neutron fission in FBR 0-83102
 ^{238}U , neutron capture self-indication meas., shape anal. 0-68753

fission reactors
 see also fission reactor materials; fission reactor operation; fission reactor theory and design; fission research reactors; hybrid reactors; nuclear engineering; nuclear physics; nuclear power stations
 American Nuclear Society proceedings (conf. Las Vegas, NV, June 1980) 0-94920
 BWR computer based control systems 0-83211
 BWR designed for improved operation at Grand Gulf 0-106121
 CANDU, decommissioning 0-95394
 CANDU and HTGR thermal reactors, principles and charac. review (*Dutch*) 0-68847
 CANDU system, general review 0-95393
 CANDU-OCR power station options and costs 0-73989
 cost comparison of PWR and PHWR nuclear power plants in Korea 0-57821
 Dounreay PFR, plant improvements 0-57933
 Dounreay test reactor, fast breeder test experience 0-86961
 fast breeder, using uranium-plutonium cycle, Na-cooled, technical and economic viewpoints of application (*German*) 0-99202
 fast breeder reactors, French national program 0-99271
 fast reactor developments in various countries (*French*) 0-86967
 fast reactors, ^{239}Pu decay heat evaluation 0-63239
 FBR, review 0-57943
 fissioning plasma from gas phase nucl. reactor, appl. 0-64794
 FUGEN LWR, reactor physics tests 0-68893
 future nuclear power technology, impact of nuclear research in India 0-95345
 HTGR and alternative nuclear strategies (*Chinese*) 0-78353
 long-term nuclear energy strategies, role of fission and fusion 0-78354
 molten salt breeder reactor technology, recent progress (*Japanese*) 0-91236
 nuclear power reactor systems, dynamical behaviour modelling 0-91216
 nuclear power station with VVER, for semi-peak load generation, mathematical model 0-68936
 pattern recognition systems, ORNL expts. 0-63351
 power plant dynamics and control, conf. Hyderabad, India (Feb. 1979) 0-91215
 PWR, core reflooding, progress of hardening front (*French*) 0-91211
 PWR, three loop, simulation in advanced recycle methodology program 0-68856
 PWR radioactive gaseous effluents, release trends in US 1977 0-95481
 Quad City 1, fuel performance meas. following third irradiat. cycle 0-68778
 steels, nuclear reactor pressure vessel steels, optimum chem. comp. rel. to props. 0-93517
 Super-Phenix fast reactor power station, in France (*French*) 0-86967
 Triga Mark III nuclear reactor, as intense gamma radiation source (*Spanish*) 0-83232
 VVER 440, design and engineering props., production and assembly 0-91207
 YAYOI FBR, prod. of epithermal neutron field for ^{10}B neutron capture therapy 0-61692
 H_2 production using high temp. reactors 0-97814
 U, gaseous fueled reactor use as power supply for nuclear pumped laser system 0-63247
 U plasma fueled reactor, use as power supply for nuclear pumped laser system 0-63247

fission research reactors
 see also fission reactor core control and monitoring; fission reactor theory and design; nuclear reactor instrumentation
 CRBRP, gas tag identification of failed assemblies, anal. methods 0-95369

fission research reactors continued

- Demokritos, fast neutron irradi. facility 0-99270
 EBR II, metallic driver fuel, irradi. perform. at high burn-up, fuel-cladding interactions 0-95348
 EBR II, reactor subassembly removal using gripper device 0-57942
 EBR-II, in-reactor measurement of neutron absorber performance, He release of B_4C 0-73951
 EBR-II reflector assembly irradi. induced bowing, implications for core restraint design 0-104234
 engineering test facility as a test device for inertially confined fission 0-57831
 Fast Breeder Blanket Facility reaction rate and neutron energy spectrum meas. 0-68865
 fast breeder test reactor operator training simulator model development 0-91219
 FFTF, development of an instrumented materials irradi. test for LMFBR structural materials 0-57858
 FFTF, development of an instrumented materials irradi. test for LMFBR structural materials 0-68797
 FFTF, gas tag identification of failed assemblies, anal. methods 0-95369
 Ford reactor, equilibrium core calcs. with reduced enrichment fuel 0-68885
 Ford reactor, neutronic anal. using low enrichment fuel 0-68886
 Ford reactor, reduced enrichment fuel effects on performance and utilisation 0-63344
 French contribution to reduced enrichment research and test reactor program 0-68931
 fuel element loadings with reduced U enrichment 0-68933
 HIFAR materials testing reactor, spent fuel safeguards verification using gamma spectrometry 0-63290
 high U density fuel for test and research reactors 0-68801
 IBR-2 pulsed research reactor, start-up experience 0-73956
 irradiation test facility for high U-loaded fuel plates as part of reduced enrichment program 0-68932
 Japan, reactor fuel and material development and expt. using JRR-2 and JMTR research reactors (Japanese) 0-63256
 LOFT, requalification following LOCE 0-57904
 LOFT reactor secondary cooling system, waterhammer phenomena 0-57905
 metallic fuel cladding eutectic formation during postirradiation heating in EBR-II 0-102241
 MIT research reactor, flux synthesis techniques for routine core physics calcs. 0-68868
 NBS reactor, activity summary July 1978 to June 1979 0-106103
 OSIRIS, Caramel fuel cladding rupture, development and detection (French) 0-95371
 PBHTGR process heat reactor, core behaviour following massive air ingress (German) 0-83181
 PNP-3000, prototype nuclear process heat reactor, core temp. transients, heat transfer calc. (German) 0-83180
 power spectral density measurements with ^{252}Cf for a light-water-moderated research reactor, determ. of reactivity of far-subcritical systems 0-57913
 protection system design criteria 0-68935
 RA reactor, fuel burn-up measurement using spatial power distrib. eval. and gamma spectrometry 0-68803
 Rossendorf ECH-I irradiated fuel assemblies, burn-up and cooling time determ. using gamma spectrometry 0-63289
 STF 3/4 critical assembly, worth and reaction rate calcs. 0-68864
 thermal-neutron-driven 14-MeV neutron generator 0-95496
 TRIGA III reactor, anal. of standard and FLIP fuel mixed loading patterns 0-57855
 TRIGA Penn State Beazale reactor, fuel management 0-63361
 TRIGA reactor at HFER, neutron radiography studies 0-68758
 university type reactors, economic success, project update 0-68900
 USA Reduced Enrichment Research and Test Reactor Program, current status 0-68930
 water trap, polarised-neutron beam shut-off 0-87004
 ZPPR, critical experiments for 600-700 MW LMFBRs 0-68859
 ZPPR-9, control rod interaction meas. 0-63324
 ZPPR-9, stimulated hodoscope slot effect in STF critical assembly 0-68860
 EBR-II Na system cold traps for control of O_2 , H_2 , T impurities 0-78411
 UAl_x fuel, development, irradi. performance in test reactors 0-68799
 UF₆, high temp. fissioning plasma core reactors, fluid mechanical confinement 0-63248
 U_3O_8 maximal fabricable conc. in Al base fuel elements 0-68800
 UZrH fuels, development for TRIGA reactors 0-68798

fluxes see cracks**flame sprayed coatings**

- Fe-Si gas-flame spray deposited protective coating, for C steel heat exchanger 0-61025

flame spraying

No entries

flames

see also chemically reactive flow; combustion; fires

- acetylene-air flame, $Li(Na)(K)(Mg)(Ca)$ damping consts., Lorentz collisions, mag. field effect 0-66805
 advection and propagation in fluid 0-59097
 air-acetylene flame, multichannel apparatus detect. limits using atomic absorpt. spectra 0-76586
 CARS spectrometer for gases and flames 0-95154
 deflagration waves, heterogeneous, flame model for gas phase, nonlinear differential eqn. 0-81326
 deflagration waves, heterogeneous, flame model for gas phase, partial differential eqn. 0-85177
 dust explosion, flame propag. vel., uniform dispersion of single sized particles 0-66803
 gasoline-air flame, laser induced fluorescence spectra obs. 0-91587
 kerosene-air flame laser induced fluorescence spectra obs. 0-91587
 laminar flames, premixed, non-adiabatic, nonlinear theory 0-93757
 laser Doppler velocity measurements in turbulent flames using spark discharge particle generator 0-59139
 local turbulence props., Raman spectroscopy meas. 0-64648
 luminous flares, heat of radiation calcs. (German) 0-68154
 plane flame, flameholder influence on static stability 0-101020
 propane flame, wake stabilized, response to sudden accel. or deceleration of free stream 0-61096
 pyrolysing slab, laminar wake flame heights 0-76513

flames continued

- Raman spectroscopy, remote spontaneous, new trends in recording of signals 0-73485
 swirling, temp. distrib. 0-61098
 temperature, meas. using unresolved rot. struct. of mol. spectra 0-86300
 temperature measurement, 5 laser-excited fluoresc. methods, theoretical basis 0-101793
 temperature measurement using laser induced fluoresc. spectrosc. of OH 0-90839
 thermal diffusion flame, two dimens. cellular struct. formation 0-69947
 Ar-H flame, Se trace amount determ. by hydride generation-nondispersive flame at fluoresc. spectroscopy 0-89553
 $BaO+Ar(CO_2)_n$ in Ar flame, rot. and translational relax. by sub-Doppler optical-optical double reson. 0-95583
 CO flame rise vel. meas. by particle track method 0-89489
 CO, output spectra from $CS_2-O_2-CO_2(N_2O)$ flame lasers 0-83601
 Ca, laser saturation broadening in flames, fluoresc. excitation profile obs. 0-95568
 H supersonic flames, chemical kinetics and unmixedness effects on burning 0-64649
 In, laser saturation broadening in flames, fluoresc. excitation profile obs. 0-95568
 $Li(2^2P_{1/2,3/2})$, laser induced flame chemistry, saturated mode fluoresc. meas. 0-89491
 Na, laser saturation broadening in flames, fluoresc. excitation profile obs. 0-95568
 $Na(3^2P_{1/2,3/2})$, laser induced flame chemistry, saturated mode fluoresc. meas. 0-89491
 OH $A^2\Sigma^+$ state, laser excited, vibr. energy transfer, flame thermometry appls. 0-58349
 OH in flames, laser excitation dynamics 0-74201
 SeH_2 , atomisation in cool H_2-O_2 flame burning in quartz tube atomiser 0-76581
 Sr, laser saturation broadening in flames, fluoresc. excitation profile obs. 0-95568

flare stars see stars**flares, solar see solar flares****flash lamps**

- flashlamps, coaxial and preionised linear, comparison as pumping sources for high power dye lasers 0-102730
 photoflash units, chemical and electronic, temporal spectral characts., meas. method 0-95171
 photographic flash light meas. instruments development (Hungarian) 0-57411
 photographic flash sequencer, using thyristor control 0-62749
 photographic flashlamp trigger circuit 0-62750
 slave triggers for photographic flash 0-95168
 sound triggered electronic photo flash unit, using variable time delay 0-57407
 sound triggered flash cct., using variable time delay 0-57414
 triggered light pulse generator for recording fast processes 0-105727
 Xe and Ar flashlamps for vacuum UV radiation 0-106590
 Xe flashlamp efficiency for photoinitiation of HF pulsed laser 0-69403
 Xe Kh-122-PM pump/lamp module operating conditions, for Nd laser system 0-91815

flash photolysis see photolysis**flashover**

- air, rod-to-plane gap, space charges, impulse voltage meas. (Japanese) 0-87970
 dielectric materials spacecraft, surface discharge arc propag. and damage 0-71314
 electric machines, volts-per-bar and flashover, causal mechanisms and preventive measures 0-92408
 fast insulator surface flashover, investigation using electro-optical elec. field meas. 0-64820
 fast insulator surface flashover in vacuum, mechanism, electro-optical investig. 0-103206
 insulators, HV, influence of air pollution on dielectric rigidity (Slovenian) 0-64801
 insulators, HV for transmission lines, power arcs occurring in networks and laboratories, comparisons 0-87983
 pulsed surface flashover mechanism involving electron-stimulated desorption 0-70055
 spark gaps, long air, disruptive voltage calc. with positive switch voltages (German) 0-87964

flaw detection see crack detection**flexoelectricity**

- p,p'-dihexyloxytolan, flexoelec. coeff. in nematic phase, thermal depend. 0-79685
 MBBA, flexoelec. coeff. in nematic phase, thermal depend. 0-79685
 nematic liquid crystal, total internal reflection, review 0-96445
 nematic liquid crystals, paramagnetic, flexomagnetoec. effects 0-75158
 p,p'-octyloxycyanobiphenyl, flexoelec. coeff. in nematic phase, thermal depend. 0-79685
 4,n-pentylphenyl (pentylbenzoyloxy)-3-chlorobenzoate, flexoelec. coeff. in nematic phase, thermal depend. 0-79685

flexural strength see bending strength**flicker noise see random noise****flip-chip devices**

see also thin film circuits

No entries

flip-flops

- bistable optical devices: an overview 0-58625
 electro-optical multivibrator operation, in optical bistable device 0-58674
 optical image processing, analogue and digital, feedback, review 0-102639

floating zone method (crystal growth) see zone melting**floating zone refining see zone refining****floculation**

see also colloids; sedimentation

- depletion stabilisation and depletion flocculation, theory 0-89534
 estuarine environment, natural suspended matter flocculation and electrokinetic pot. (French) 0-61817
 turbulent, mathematical model (Japanese) 0-79389
 SiO_2 -water system, inorg. polymer struct. form., globular crystn. 0-101042

flow

see also chemically reactive flow; compressible flow; Couette flow; external flows; flow instability; flow measurement; flow through porous media; Knudsen flow; laminar flow; magnetohydrodynamics; multiphase flow; non-Newtonian flow; plasma flow; Poiseuille flow; pulsatile flow; rotational flow; shear flow; stratified flow; supersonic flow; transonic flow
benthic ocean, flow struct. 0-72532
static electrification effects, progress up to 1979 0-69292
Stokes flow, stress-hybrid finite element method 0-99985

flow birefringence

colloidal solution, flow alignment, transition from isotropic to nematic phase 0-84060
critical fluids under flow, large flow birefringence 0-103938
equilibrium birefringence for weakly ionised molecular gas in strong mag. field 0-83881
localized, induced behind obstacles in polymer soln. (French) 0-93275
molecular liqs., Maxwell effect relax. time and light scatt. line broadening 0-76040
poly-m-phenylene-isophthalamide in dimethylacetamide, flow birefringence (Russian) 0-66148
polycaprolactam, and copolymers, optical anisotropy and rigidity 0-88959
polycarbonate, secondary flow and stress birefringence patterns in pressure hole 0-64590
polycyclohexanamide, and copolymers, optical anisotropy and rigidity 0-88959
polymer melt, flow birefringence meas., influence of parasitic birefringences 0-88963
polymer solutions, liquid cryst., rheo-optics of shear and elongational flow, quiescent and flow birefringent characts. 0-83773
polystyrene solution, constitutive models, expl. tests based on birefringence data 0-100015
As-S, melt struct., orientation birefr., viscosity, refr. index, and density 0-84713

flow control

cooling water flow control in continuous casting process, vortex flowmeters 0-64655
fusion reactor, TFTR, T gas injection system transient response 0-102337
nuclear fuel production, continuous gas flow control simulation (German) 0-78416
orifice, cavitating, under reattached flow conditions, noise and vibration characteristics 0-83829
H₂O vapour under point corona discharge, microprocessor control for vapour generator and EHD phenomena 0-106852
O₂ regulator, solid-state, high-temperature 0-57301

flow instability

absolute and convective instabilities, distinction and appl. to interstellar medium 0-98539
annulus, tall, vertical, conduction regime of natural convection stability 0-99987
asymptotic stability of unsteady inviscid stratified flows 0-83832
atmosphere, dissipative effects, convective instability (French) 0-77058
atmosphere, preferred mode of Ekman conditional instability of second kind (CISK) 0-72617
Benard convection, stability of horizontal layer of fluid heated from below 0-87767
Bernard convection, and linear fluctuation theory, Markovian processes and irreversibility 0-87766
binary alloy indirectional solidification, convective and interfacial instabilities 0-60851
binary liq. layer, microgravity, thermoconvective stability 0-74866
boundary layer flow, laminar, over porous flexible surface, oscillatory flow 0-92107
buoyancy-thermocapillary convection layers with free surface, energy stability theory 0-87768
centrifugal instabilities in finite containers, periodic model 0-106783
centrifugal instabilities of circumferential flow in finite cylinders, non-linear theory 0-99989
channel bottom, kinematic characts. of nonuniform flow, limiting stability, erosion 0-94547
channel flow, plane, shear rate dependent viscosity, effect on stability (German) 0-87809
channel flow stability, influence of nonparallelism 0-83845
chemically driven convection of dissociating Navier Stokes fluid, instabilities 0-59128
cholesteric liquid crystals, oscillatory convective instabilities, caused by heating from below 0-103239
cohesionless bottom sediments, limiting stability in turbulent channel flow, erosion 0-94546
combined convection flow along vertical surface, fluctuating boundary layers 0-96254
composite mixture, flow through porous medium, Rayleigh-Taylor instability 0-69912
compressible axisymmetric jet sound radiation by instability waves 0-69792
compressible fluid layer through porous medium, thermal instability 0-92114
concentric rotating cylinders, temp. gradient effect on stability 0-79263
continuity equation, 1-dimens., for unsteady flow 0-82598
Couette-Taylor flow, laser Doppler velocimetry obs. of transition to turbulence 0-92163
critical mixtures, shear and critical fluctuations, instantaneous mapping of velocity gradients 0-79420
deep water waves, instabilities, review, book contrib. 0-96274
dust-gas flows, steady and oscill., mean heat transfer 0-89536
early nonperiodic transitions in Couette flow 0-59056
EHD, convective instability in dielectric fluid between two coaxial cylinders 0-74994
energy stability of the Eulerian-mean motion in the upper ocean to three-dimensional perturbations 0-92149
ethane, flow continuity in arterial capillary systems in cryogenic heat pipes 0-64536
external noise effect on transition to turbulent convection 0-96263
ferromagnetic fluid, stability in vertical magnetic field, variational approach (German) 0-96316
fingers in fluid surfaces, stability to instability transition 0-79260
finite-amplitude thermal convection and geostrophic flow in a rotating magnetic system 0-87813

flow instability continued

fission reactor safety, stability analysis and characts. for two-phase flow eqn. systems with viscous terms 0-59103
flowmeters, stabilizing liquid flows 0-103084
fluid dynamic transient analysis using ASWR method with staggered meshes (German) 0-83176
fluid layer between co-axial cylinders, instability of natural convection 0-64558
fluidised beds, instability waves and bubble origin, two-fluid eqns. 0-92205
foam stability relation to structure, criteria derivation w.r.t. drainage stage 0-69904
forced oscillations of separated shear layer, appl. to cavity flow-tone effects 0-64256
galaxies, global instability of polytropic gaseous discs with Toomre density distrib. 0-98725
gas stream, supersonic, stationary, conical flow about plane wedge and circular cone 0-74912
Gortler stability at rigid and elastic plane plates (Russian) 0-79261
Gortler vortex type perturbation profiles in boundary layers problem on curved surface (Russian) 0-74834
graphite-air mixture steady and oscill., mean heat transfer 0-89536
Hartmann flow, nonlinear stability, monoharmonic analysis 0-83850
heat flux-flow coupling effects in the stability of vapour generators (German) 0-74967
horizontal fluid layer in porous medium, convective instability, critical Rayleigh number 0-64564
hydraulic jumps with waves, kinematic approach, extension of Rayleigh's method 0-69854
hydrodynamic instabilities and turbulence, flow states, examples and meas. methods 0-92116
hydromagnetic capillary instability of a liquid jet with an axial flow 0-74990
hydromagnetic flow, stability in temp. field 0-92231
immiscible incompressible fluids, interfacial convective instability, diffusional exchanges, adsorption-desorption processes 0-70504
immiscible liquid two-phase flow in porous media, unstable displacement 0-92213
inclined fluid layer, double diffusive instability, linear stability anal. 0-92113
inclined fluid layer, double diffusive instability, secondary convecting layers 0-92112
inclined open channel, stability of permanent roll waves 0-64629
inclined surfaces, wave instability of laminar mixed convection flow 0-69837
incompressible viscoelastic fluid, Rayleigh-Taylor instability 0-79363
interstellar radiative shocks, thermal instability rel. to maser condensations form. 0-67821
inviscid, rotating, compressible fluid, linear stability 0-92161
inviscid linearly-sheared parallel flow, characterisation of acoustic disturbances 0-69848
jet, magnetisable liquid, stability 0-83831
jet noise and large scale instability waves, effect of upstream tones 0-69790
jets undergoing mass transfer, break-up effect of nonlinear concentration profiles 0-79371
Kelvin-Helmholtz instability in stellar winds, influence on turbulent mixing with interstellar gas 0-67701
Kelvin-Helmholtz instability in supersonic and super-Alvenic fluids 0-87816
laminar flowing liquids, concurrent, in horizontal cylindrical channel 0-79397
liquid film, instability on surface of rot. sphere 0-59006
liquid layer flowing down inclined plane, heating and cooling effects on stability 0-79254
liquids in longwave limit, static and dynamic stability, heat diffusion 0-92138
Lorentz equation derivation for unstable dispersive physical systems 0-83786
Lorenz model dynamics for convective instability 0-59007
magnetic fluids, instabilities, leading to rupture of continuity 0-59003
magnetogasdynamic parallel flows, inviscid stability 0-69933
metastable flows of water, spontaneous boiling 0-106709
MHD fluid layer, thermal instability in transverse field 0-87812
micropolar fluid layer subject to magnetic field, thermal instability 0-64585
Navy vessel fracture mechanics and flow separation 0-99971
nematic liquid crystals, nonlinear stability of motion 0-83784
non-linear hydrodynamic stability, unipolar injection of insulating liquid, Galerkin method 0-74835
nonisothermal magnetisable fluid, thermal convective stability, modulated mag. field effects 0-64646
nonlinear effects in laminar stability theory (French) 0-103012
nonlinear focusing and Kelvin-Helmholtz instability 0-83785
nonsteady one-dimensional liquid flow, analytic method calcs. 0-59009
ocean, expl. study of nonlinear baroclinic instability and mode selection in large basin 0-85669
ocean solitary Rossby waves over variable relief, analytical theory rel. to stability 0-101371
ocean solitary Rossby waves over variable relief, numerical expts. rel. to stability 0-101372
ocean upper layer, hydrodynamic instability rel. to equilib. Langmuir circulation model 0-101381
oscillating two-stream instability, exact soln. 0-92115
overstability in horizontal layer of binary liq. mixture with Soret effect 0-106782
PAA, nonlinear soft mode at Rayleigh-Benard instability, neutron cond. spectrosc. obs. 0-79266
particulate sedimentation, stability, two-dimens. anal. 0-69768
periodic MHD oscillations, stability, perturbation theory 0-83858
plane channel flow, subcrit. turbulence transition 0-106787
plane jet, stability and autooscillations from channel anal. 0-100018
plane Poiseuille flow, nonlinear stability by high order amplitude expansions 0-74975
plasma focus, pinch column form. and stability 0-96380
Poiseuille flow in circular pipe, linear stability 0-79399
polyethylene melt, oscillatory flow through capillary 0-103046
polymer solution, highly elastic, vel. meas. in die entry region of capillary rheometer 0-99988
porous cermet, heat transfer and stability for moving evaporating coolant 0-64563

flow instability continued

radiative thermal instabilities in relativistic flows, rel. to compact synchrotron sources-variability 0-105369
 Rayleigh-Benard convection, randomly forced, initial value problem 0-79314
 Rayleigh-Benard convection, turbulence and intermittency, expt. 0-99998
 Rayleigh-Benard instability, n-component reactive fluids 0-69945
 Rayleigh-Benard instability, reactive binary fluids 0-69944
 Rayleigh-Benard instability in p-oxoanisole, fluctuations, real time obs. by neutron scatt. 0-59390
 Rayleigh-Bernard convection, forced phase diffusion 0-103019
 Rayleigh-Taylor instability, thermal cond. and compressibility effects 0-79262
 Rayleigh-Taylor instability in oscillating mag. field 0-59008
 relativistic fluids flow through channels, self similar solns. and stability rel. to radio galaxies 0-62006
 ripple and dune formation on erodible bed by low Froude number flow 0-106784
 rivulets, static, moving contact lines and rivulet instabilities 0-79264
 rotating Boussinesq viscous fluid, inertial instability, appl. to atm. 0-90131
 rotating cylindrical annulus, transition to Taylor vortices, Ekman layers 0-87776
 rotating disc boundary layer transition regime, spiral vortices 0-59040
 rotating stratified fluid, parallel shear flow, baroclinic and barotropic instability 0-98328
 saturated porous layer, sudden temp. rise, stability, linear and energy methods, convection 0-74972
 self-gravitating fluid column, modulational instability 0-85848
 semi-infinite porous medium bounded by horizontal surface, mixed convective flow, vortex instability 0-79304
 shear flows, inviscid and parallel, instability 0-79265
 shear layer instability noise produced by various jet nozzle configurations 0-69791
 shell, uniformly imploded ablatively driven, fluid instabilities 0-92111
 shock waves instability in a relaxing medium 0-100013
 shock waves of arbitrary strength, with viscosity and heat conduction, stability 0-59076
 silicone oil, Newtonian, vel. meas. in die entry region of capillary rheometer 0-99988
 slowly spreading jets, MHD instability 0-87818
 slowly varying wavetrains, dissipation and dispersion effects 0-64573
 smectic-A liquid crystals, oscillatory convective instabilities, caused by heating from below 0-103239
 solar atmosphere, penetrative instabilities theory in presence of thermal dissipation 0-109406
 spiral vortex flow stability, experimental investigation 0-79327
 stable surface chemical reactions, interfacial hydrodynamic instability 0-66874
 steady flows, stability criteria of perfect incompressible fluid with a free boundary 0-69767
 stratified fluid, duct, equilibrium breakdown, thermosiphon work (French) 0-59114
 stratified fluids in open channel, critical flow conditions 0-74956
 subsonic flow, diverging, stability aspects, time-dependent method 0-74906
 superimposed miscible liquids, dynamic stabilization, turbulent transport through diffuse boundary layer 0-74844
 surge and rot. stall, flow instabilities 0-106803
 tangential discontinuity on fluid interface, two-dimens. perturbation development 0-96245
 Taylor 0-59044
 Taylor cells hydrodynamics instability and vortex currents in Couette flow 0-64571
 Taylor vortices near oscillating cylinder, subharmonic destabilisation 0-92162
 thermal diffusion flame, two dimens. cellular struct. formation 0-69947
 three dimensional growing boundary layers, linear stability 0-74833
 three dimensional parallel shear flows, stability and transition for rot. disc 0-74887
 three-wave decay interaction, steady-state turbulence spectrum 0-96249
 Timoshenko bar, aerodynamic stability, time- and space-harmonic balance (German) 0-83812
 triple correlation of the pressure in subsonic circular jets and nonlinear interaction of instability waves 0-69893
 tubes, viscous liquid turbulent unsteady flow, pressure drop in transition region 0-74978
 turbulent shear layer, instability waves, radiation of sound 0-79341
 two viscous incompressible fluids in parallel uniform shearing motion, hydrodynamic stability 0-59010
 two-phase flow, horizontal stratified, 1-D two-fluid eqns. for LWR LOCA 0-91226
 two-phase stratified horizontal flow, averaged and local instantaneous formulations, stability 0-64613
 unstable flow past cavity, three-dimens. nature, obs. 0-59053
 unstable laminar boundary layers, nonlinear evolution and breakdown 0-92109
 unsteady 3-dimens. compressible flow, implicit finite difference simulations, transonic appl. 0-64576
 unsteady axisymmetric 1-dimens. motions of ideal incompressible liquid, small perturbations 0-59004
 unsteady boundary layer separation, mathematical criterion 0-69884
 unsteady hydromagnetic thermal boundary layer problem, numerical treatment 0-92227
 unsteady inviscid 2-D flow analogy using stretched membrane and moire fringes 0-64658
 unsteady laminar separation and stall from aerodynamic surfaces 0-59090
 unsteady motion of finite mass of fluid 0-59005
 viscoelastic fluid, stability of steady shearing flows, energy method and parabolic maximum principle 0-74926
 viscous fluid, stability of steady vertical flow 0-64520
 viscous liquid film instability under the influence of an adjacent gas flow 0-92110
 viscous stratified shear flow, stability eqns., completeness obs. 0-64519
 vortex shedding flowmeter, stabilisation in low Reynolds number range 0-83865
 vortex-induced wake buffeting and its suppression 0-103030
 water, apparent Weissenberg effect 0-83787
 water jets sensitive to sound, two-dimensional, velocity fluctuations behaviour (Japanese) 0-100020

flow instability continued

water near 4°C, plane-parallel convective flow instability 0-92137
 water-air two phase flow, oscillatory flow instabilities 0-83833
 wavefronts in reaction-diffusion systems, instability and turbulence 0-106855

flow measurement

see also *anemometers; flow visualisation; flowmeters; laser velocimeters*
 air flow consumption meas., respiratory process parameters determ. using electric model (Bulgarian) 0-76867
 air/water mixture mass flow meas. by drag devices and γ densitometer 0-79385
 airflow rate, with electrical indication and automatic data logging system 0-75014
 airflow through cascade of turbine blades, laser anemometry 0-59146
 axisymmetric jets, coherent structs. using optical technique, convection vel. 0-69888
 blood flow, regional, assessment by intravenous injection of ^{99m}Tc pertechnetate 0-104732
 blood flow measurements by NMR of the intact body 0-81680
 bubbles, acoustical meas. of gas bubble volumes and gas flow rates 0-62633
 capillary blood flow, dual beam laser velocimeter anal. 0-75015
 cerebral blood flow, meas. in pig by ^{133}Xe clearance technique 0-94421
 coal dust mass flow meas. methods (German) 0-92242
 desorption-permeation time lags of permanent gases through microporous plugs 0-59137
 direction, pressure probes, yaw meter sensitivity for null reading technique 0-69954
 direction probes for turbomachine technology 0-87824
 dispersed phase of two-phase flow, holographic anal. 0-103061
 Doppler anemometry, velocity and photomultiplier bias effects 0-59140
 echocardiography, pulsed Doppler, variable sample vol. dimension 0-76816
 electrodiffusion velocity sensor, freq. characts. calcs. 0-96675
 electrostatic precipitator, particle velocity, laser Doppler anemometry study 0-59144
 EM velocity transducer with a multipole mag. 0-83868
 end effects in a flow-rate transducer with a cylindrical magnet 0-83869
 fast flowing wet steam, electrical meas. of droplet size 0-64659
 fission reactor coolant flow rate determ. using ^{16}N decay activity meas. 0-73955
 flame ionization detector, meas. fluctuating conc., in turbulent flows 0-92240
 flames, local turbulence props., Raman spectroscopy meas. 0-64648
 fluid section flow pattern speckle photography 0-103096
 fluidised bed bubble observation using probes and X-rays 0-79379
 gas-liquid two-phase flow, response of small pitot tubes 0-92209
 heated circular jet, outer part, temp. and vel. simultaneous meas. errors 0-87830
 heated flows, fine scale turbulence, hot and cold wire sensitivity corrections 0-69956
 high pressure piston flowmeter with digital readout (Polish) 0-64661
 highly viscous fluid emerging from slit onto plate, flow development and meas. 0-59142
 horizontal gas-liquid stream, flow vel. meas. 0-96301
 hydrodynamic factors, calibration of flowmeters, meas. errors 0-96322
 hydrodynamic instabilities and turbulence, flow states, examples and meas. methods 0-92116
 jet displacement transducers, relation between dynamic and precision characts. 0-64660
 laser anemometry, fundamental limitation and accuracy 0-87829
 laser interferometry appl. 0-75018
 laser-Doppler anemometry and photon correlation for turbulence length scales 0-87828
 liquid, energy approach reproduction method 0-96321
 liquid flow rates through pipes, applicability of experimental meas. methods 0-100044
 LMFBR coolant flow rate meas. using electromagnetic convertor 0-73887
 Ludwig tube, steady flow duration extension, reservoir orifice method, variable opening area effect 0-64579
 magneto-inductive flowmeters, installation (German) 0-64662
 mass flow instrumentation performance, during LOFT nonuclear test series 0-69952
 mass flow meter using Coriolis principle, electro-optical force sensing techniques 0-103094
 mass flow rate measurements, estimates of probability characts. 0-73302
 mean velocity very close to a wall, hot-wire anemometer meas. errors 0-79413
 neonatal peripheral circulation, human, characterisation by US pulsed Doppler technique 0-76815
 NMR flowmeters, vortex meters, and mass flowmeters, calibration 0-92239
 nozzle flowmeter instantaneous flow rate meas. in pulsating water flow (Japanese) 0-59133
 omnidirectional wall shear stress meter 0-106860
 optical instrumentation methods for two-phase reactor flows 0-63313
 organ blood flow measurements, effect of instantaneous partition coeff. of Xe 0-101256
 periodic fluid flows by laser anemometry, periodic sampling 0-64657
 photon correlation techniques in fluid mech., conf., Cambridge, England (March 1979) 0-56998
 pipe flow, spatial cavitation-nuclei-measurements by means of laser velocimeter 0-64593
 pipeline film flow speed, electromagnetic system 0-79417
 polydispersed flows, Doppler signal spectrum 0-103081
 polymer melts, rheological properties at low shear stresses, meas. using sandwich type creep rheometer 0-59153
 polymer soln. highly elastic, vel. meas. in die entry region of capillary rheometer 0-99988
 probe, 4-hole cylindrical cantilever, for 3D flow meas. 0-87833
 probe, spherical Pitot, construction and calibration (Italian) 0-69957
 pulmonary blood flow, method for noninvasive bedside determ. 0-81762
 pulsating turbulent pipe flow, velocity field and press. gradients 0-64641
 pulse-compensation method of meas. liquid flow-rate based on NMR 0-103088
 radiolabelled microspheres, use in meas. of regional blood flows during +G, stress 0-81786
 random, statistics analysed by photon correlation anemometry 0-64522

flow measurement continued

Rayleigh-Bernard flow, equal velocity fringes by speckle photography 0-75005
resonant hydraulic circuit pulsatile water flow meas. using laser Doppler velocimeter 0-103091
rotating flow around circular cylinder, azimuthal velocity in gas centrifuge 0-74890
rotating turbulent flow, method for meas. vel. vector and stress tensor components (*Russian*) 0-83867
spermatozoa, human, motility evaluation, photon correlation meas. 0-61745
state-of-the-art review, special features and appls. 0-64654
stirred vessel, velocity measurement and flow trajectory, using image sensor 0-69950
thermal measurement systems for flow rate and flow composition (*Russian*) 0-69953
thermosiphon solar water heaters, transient flow meas. using laser doppler anemometer 0-61413
three-dimensional characs., using five-hole probes, calibration and appl. 0-69951
tissue perfusion measurements made with thermal diffusion probe, effect of probe geometry 0-104802
triple-sensor probes for turbulent flow-field investigations 0-100043
truncated autocorrelation functions, numerical inversion 0-57097
tumour blood flow, meas. by photon activation, ¹⁵O decay technique 0-104755
turbulent mixing flow, velocity biasing resulting from non-uniform seeding 0-59143
turbulent supersonic flows, freq. response of constant temp. hot-wire anemometers 0-59149
two phase flow, computerised tomography meas. technique 0-59135
two phase flow pattern characterisation by electrical conductance probe 0-106857
two phase one component, single substance flows, probe method for phase concentration determ. 0-74954
two-phase flow, isotopic computerised tomography meas. 0-59136
two-phase flow, measurement techniques, recent progress (*French*) 0-79411
two-phase flow instrumentation for safety anal. of LWR LOCA 0-102259
two-phase flow meas. in nuclear reactors, LOFT drag disc turbine meter rakes 0-102260
unsteady inviscid 2-D flow analogy using stretched membrane and moire fringes 0-64658
vaneless diffuser of centrifugal compressor, flow velocity meas. using laser Doppler anemometer 0-59147
velocity and direction of water flow, meas. method 0-96318
velocity gradients and laminar and turbulent diffusion, direct optical meas. 0-59132
velocity measurements inside a rotating cylindrical cavity with a radial outflow of fluid 0-96275
visualisation by foreign particle or energy optical tracing 0-96329
vortex shedding principle appl. (*German*) 0-79419
water, cavitation expts. using shock tube 0-87789
X-hot wire probe method for two-dimensional nonsteady air flow (*Japanese*) 0-59134
Fe₄₀Ni₄₀P₁₄B₆, metallic glass, glass transition, viscous flow and differential scanning calorimetry meas. 0-96635

flow resistance see viscosity

flow separation

aeronautics, infinite swept attachment line boundary layer, turbulence 0-74840
air flow over rearward facing step, flow separation meas. 0-69885
axisymmetric afterbodies, separated turbulent flows, wakes, exhaust plume effects 0-74885
blunt flat plates, air flow, 2-D, thermal boundary layer characteristics, nose shape effects 0-92121
body of revolution with heating and cooling, boundary layer transition and separation 0-64518
boundary layer, laminar, subsonic, strong slot injection, triple deck theory 0-74831
boundary layer flow past circular cylinder, rapidly convergent series soln. 0-96244
boundary layers, laminar, compressible, Prandtl=0.72, sharp pressure rise effect 0-83782
channel flow stability, influence of nonparallelism 0-83845
channel flows, severe nonsymmetric constriction, curving or cornering, separation 0-92222
circular cylinder in liquid Na crossflow, local heat transfer, numerical study 0-64539
circular cylinders, surface-roughness effects on mean flow, turbulent boundary layers 0-92128
corner interaction of boundary layer and shock wave, flow separation 0-96287
cylinder, axisymmetric, with slanted base, near-wake flow 0-74886
cylinder on β -plane, prograde and retrograde rot. flows, boundary layer separation 0-92189
detached flow around bodies with local vortex sheets 0-87778
detached flows past a cylinder with a flat end, subsonic and transonic vels. 0-92187
disc normal to wall, turbulence intensities and local mean vels., separated flow 0-64531
gas, perfect, vortex sheet, separation from smooth body at large Reynolds number (*French*) 0-74908
gas jet blowing into supersonic flow without 3-dimens. boundary layer separation, nozzle shape 0-100009
gas-liquid pipe flow, influence of return bends on velocity ratio 0-74962
gaseous microbubble growth in laminar separation bubbles 0-106821
incompressible separated boundary layers including viscous-inviscid interaction, transition bubble 0-64515
leading edge bubble formation, peaky airfoil (*French*) 0-64524
longitudinal blunt circular cylinder, axisymmetric separated and reattached flow, turbulence 0-79285
nose separation for laminar boundary layers on body of revolution 0-59091
open pipe exits, flow during acoustic resonance, vortices and boundary layers 0-92224
periodic wavy surface, laminar boundary layer, nonlinear anal. for long waves, separation 0-87759

flow separation continued

permeable contour in flow with jet separation, impulses and impact effects 0-92196
plate, Kirchhoff-Rayleigh flow, separation, wakes and vortices 0-69839
porous medium, saturated, mixed convection boundary layer flow on vertical surface 0-106798
rearward facing step, turbulent incompressible reattaching flow, adverse press. gradient effects 0-69773
rectangular body, laminar flow, separation bubble and stagnation line 0-64514
rectangular body in forced convection, heat transfer study, flow separation 0-74874
semi-infinite body, two-dimensional linear and nonlinear stern waves, separation point 0-69852
shock wave interaction with turbulent boundary layer disturbed by injection 0-74916
steady viscous flow past circular cylinder, numerical study, vortices and separation 0-92108
Stokes flow, effect of separation on drag and torque 0-106818
stratified flow, averaged formulation, high order dispersion effects in separated flow models 0-74960
supersonic flow over compression ramp, laminar separation, second order asymptotic soln. 0-83828
supersonic separation flow, 2- and 3-dimens., turbulent boundary layer and shock wave 0-100017
three-dimensional boundary-layer separation 0-92188
three-dimensional flow over wings with leading-edge vortex separation 0-74927
tube, round, vortex streams, radius of separation (*Russian*) 0-69841
two-phase stratified horizontal flow, averaged and local instantaneous formulations, stability 0-64613
unsteady, behind normal plate, discrete-vortex model, modified velocity-point scheme (*Japanese*) 0-79331
unsteady, behind normal plate, discrete-vortex model, velocity-point scheme (*Japanese*) 0-79330
unsteady boundary layer separation, mathematical criterion 0-69884
unsteady laminar separation and stall from aerodynamic surfaces 0-59090
vortex tube input parameters, effect on rate of rotation of flows (*Russian*) 0-96264
wedge impulsively set into motion, boundary layer development 0-79259
wedge like sharp edge starting vortex, flow visualisation expts. 0-59046
wedges, high Reynolds number flow, base pressure in near wake 0-59038

flow through porous media
aerosol particles, dendritic deposition in fibrous, inertial impaction and interception 0-74945
air injected through porous surface, shock wave interaction with turbulent boundary layer 0-74916
Barenblatt's problem, flow through media with double porosity, anal. using continuum theory of mixtures 0-83841
binary mixtures flowing through activated C, adsorpt. interference 0-107635
boundary layer flow on vertical surface, mixed convection 0-106798
channel with porous walls, convective diffusion and mass transfer (*French*) 0-79305
composite mixture, flow through porous medium, Rayleigh-Taylor instability 0-69912
compressible fluid layer through porous medium, thermal instability 0-92114
constant pressure filtration, filter medium fast plugging, mathematical models 0-100030
Couette flow, plane, past permeable bed, buoyancy effect 0-92215
cylinder immersed in porous medium, unsteady heat transfer, Darcy flow 0-83794
cylindrical porous medium, free convection boundary conditions, mean heat transfer 0-79302
dam seepage, variational inequality appl. to flow through porous media 0-100028
diffusion, 2-D, transient, along high-diffusivity lamina bisecting half-space 0-106841
dispersion resulting from flow through spatially periodic porous media 0-92216
dynamic behaviour of a porous medium saturated by a Newtonian fluid 0-83840
Earth crust, implications of dilatancy-fluid diffusion theory for aftershock sequences 0-85604
elastoviscous liquid, combined free and forced convection flow through porous channel 0-103073
erythrocyte, flow resistance into pores 0-61609
fibrous filter, distrib. of fluid vels., flow resist., random flow model 0-79393
filtration in heterogeneous earthen dam, problem solvability 0-90110
filtration theory problem soln. (*Russian*) 0-74970
fluidised beds, combustion facility, radiation heat transfer, particle size and flow parameter effects 0-69641
free convection flow past vertical porous plate set in impulsive motion 0-69818
gas, circulating, forced convection through porous cavity, solar heating (*French*) 0-69626
gas, nonsteady flow through semipermeable screen to vacuum 0-100029
gas absorption, plastic packed column, mass transfer characteristics, proposal of packed column blood oxygenator 0-74968
gas flow, recirculating, in packed columns, mass transfer and mixing, cell model 0-69913
gas flow through multilayered regions 0-59108
gas flow through porous materials, pressure loss 0-64623
gas in porous sorbent, initial impurity content 0-64624
gas injection into liquid through porous plate, squeezing out of liq. 0-64622
gas screen, subsonic turbulent boundary layer, friction behind permeable section 0-92127
granular materials, particle density measurement by pycnometry 0-69903
heat pipe, filled with porous material, glycol water circulation 0-69896
heat transfer downstream of blockage with discrete permeability in rectangular channel 0-69915
heated porous body, impregnation with viscous liquid 0-79392
heterogeneous porous medium, two-phase flow, multidimensional problem (*Chinese*) 0-64608
horizontal fluid layer in porous medium, convective instability, critical Rayleigh number 0-64564

flow through porous media continued

- horizontal tubes in fluidised beds, local heat transfer coeffs. 0-74875
- hydromagnetic free convection flow in Stokes problem, for porous vertical limiting surface with const. suction 0-90328
- hydromagnetic squeeze film between porous circular disks with velocity slip 0-74997
- hydrothermal flows, two-phase, in permeable media, struct. 0-85693
- immiscible liquid two-phase flow in porous media, unstable displacement 0-92213
- laminar flow over porous flexible boundary, oscillatory flow 0-92107
- laminar isothermal flow of two immiscible compressible fluid phases 0-69919
- laminar viscous flow down an open inclined channel with naturally permeable bed 0-69764
- leaching from model porous bodies by reflection spectroscopy 0-100031
- magnetic fluid, penetration through porous medium with uniform mag. field oblique to interface 0-59107
- magnetic fluids, response to mech., mag. and thermal forces 0-59122
- mathematical model 0-83837
- metal gauzes, hydraulic resist. in laminar filtration 0-100034
- metals, liq., infiltration in medium with interconnected pores, during passage of elec. current 0-100033
- MHD flow through porous straight channel 0-69932
- MHD forced convection in channel bounded by plate and permeable bed, Hall effects 0-69934
- microporous plugs, measurement of desorption-permeation time lags of permanent gases 0-59137
- Monte Carlo models for water circulation study (*Rumanian*) 0-69917
- moving-bed solid flow in inclined pipe leading to fluidised bed., gas leakage 0-64619
- moving bed solids flow in inclined pipe leading to fluidised bed 0-64620
- natural convection in a vertical cylindrical well filled with porous medium 0-79297
- numerical methods for flows through porous media. II 0-69914
- one-dimensional moisture migration caused by temp. gradients 0-96305
- permeable contour in flow with jet separation, impulses and impact effects 0-92196
- pipes, porous, complementary variational principles for steady and unsteady Poiseuille flow 0-92225
- plasmatron, discharge stabilised, by gas blown through porous wall 0-75105
- platelet interaction with vessel surface, blood rheological factor influences 0-61612
- polymer solutions, flow through sand filters, flow resistance 0-79395
- porous cermet, heat transfer and stability for moving evaporating coolant 0-64563
- porous flow through rectangular dam, proof of free boundary convexity using maximum principle 0-69916
- porous medium being dried, moisture flow, generalised model (*Hungarian*) 0-83839
- porous pipe in a pipe heat exchanger, laminar flow, vel. changes 0-64512
- porous structures for cooling laser reflectors, theoretical study 0-91809
- rectangular cavity with porous filling, steady convection and boundary layers 0-79309
- Reynolds eqn., generalised form for porous boundaries 0-87803
- rocks, microporous, movement of solutes through aqueous fissures 0-94553
- rocks, of water, shear thinning and shear thickening polymer additives 0-72100
- rotating disc and porous disc. fluid flow 0-64569
- saturated porous layer, sudden temp. rise, stability, linear and energy methods, convection 0-74972
- second order fluid, natural convection flow from porous plate, suction and injection effects 0-59029
- semi-infinite porous medium bounded by horizontal surface, mixed convective flow, vortex instability 0-79304
- semibounded compressible stream, optimal suction at heat-cond. porous surface (*Russian*) 0-79346
- semifluidised bed, mass transfer rate 0-59105
- spouted beds of spherical particles, spout termination, parameters 0-64621
- stationary flow between porous rotating cylinders in a radial magnetic field 0-83857
- steel, stainless, porous sheet, pore dimensions, filtration and permeability (*Russian*) 0-76480
- Stokes problem, effects of free convection on oscillatory flow past infinite porous vertical limiting surface 0-109348
- supersonic flow around a cone, power-law injection, bease influence 0-100010
- tensor formulation of the fluid-solid interaction force for multi-dimensional, two-phase flow within tube arrays 0-92211
- thermal convection in porous media, dispersion effects 0-103027
- two immiscible liquids, flow inhibition due to differential wettability 0-87802
- two moderately rotating porous discs, heat transfer 0-103028
- two-dimensional infiltration in unsaturated soils, nonlinear diffusion eqn. numerical soln. 0-69918
- two-phase incompressible flow, diffusion-convection eqn., mixed finite element method, water flooding 0-74969
- velocity and longitudinal dispersion, deterministic model 0-83842
- viscous fluid, incompressible, hydromagnetic free convective flow past vertical porous wall, mass transfer 0-64645
- viscous incompressible fluid, laminar divergent flow through porous cone (*French*) 0-83838
- walls, permeable, cooling characts., heat exchange, rad. emitter design 0-64535
- water impurity concentration in steam-generating channels with capillary-porous structure 0-103071
- water transport in soils, review, book contrib. 0-96308
- wire gauzes resistance coefficient measurement at low air velocity (*Japanese*) 0-106843
- CO₂ laser amplifiers, porous tube generated flow field, heat and mass diffusion 0-63969

flow visualisation

- body of revolution with heating and cooling, boundary layer transition and separation 0-64518
- cavitation in water jets, flow visualisation using holography 0-106862
- Couette-Taylor flow, laser Doppler velocimetry obs. of transition to turbulence 0-92163

flow visualisation continued

- critical mixtures, shear and critical fluctuations, instantaneous mapping of velocity gradients 0-79420
- curved wall power fluidics characts. 0-103053
- electrochemical reactors with three-dimensional electrodes, characterisation using electrochemical tracer method 0-76520
- glycerin-water solns., visualization of standing vortices behind cylinder 0-59151
- haemofol mitral valve, results of flow visualisation expts. 0-104632
- laser Doppler anemometry on transparent turbulent electromagnetically driven flow 0-103090
- pipe-exit flow visualisation using high-speed photography 0-106863
- plane mixing layer vortex digital image processing 0-103095
- rheometer, analytical, optical sliding contact, for flow visualisation at articular surface 0-104847
- stagnation flow turbulence about circular cylinder, visual study 0-96248
- surface patterns using O quenching of dye fluorescence 0-79422
- turbulent horseshoe vortex 0-103016
- two-dimensional random field model for image structural analysis (*Russian*) 0-63932
- unsteady airfoil, Kutta condition (*Japanese*) 0-92155
- unsteady inviscid 2-D flow analogy using stretched membrane and moire fringes 0-64658
- velocity measurements inside a rotating cylindrical cavity with a radial outflow of fluid 0-96275
- water-in-oil emulsion, boiling, bubble formation, cinemicrophotography 0-74961
- wedge like sharp edge starting vortex, flow visualisation expts. 0-59046

flowmeters

- see also *anemometers*; *flow measurement*; *laser velocimeters*
- animal research, totally implantable directional Doppler flowmeters 0-67293
- blood flow detection in human heart, US pulsed Doppler flowmeter system, microcomputer based 0-104690
- blood flowmeter US implantable bidirectional pulsed Doppler device, timing and signal processing ICs 0-76812
- Coanda fluidic digital gas flowmeter 0-59138
- contact-type flowmeter working in thermal boundary layer, temp. error determination 0-103093
- contactless, construction principles (*Russian*) 0-87823
- contactless thermal, calibration characts. 0-103085
- cooling water flow control in continuous casting process, vortex flowmeters 0-64655
- dynamic errors, mobile weighing system 0-96326
- electromagnetic flowmeter with moving field, fluid flow and moving field equations (*Rumanian*) 0-64663
- electrostatic, effect of arrangement of electrodes on accuracy 0-103087
- EM flowmeter theory and application 0-96328
- EM velocity transducer with a multipole mag. 0-83868
- end effects in a flow-rate transducer with a cylindrical magnet 0-83869
- fission reactor primary coolant flowmeter 0-73912
- flange tap orifice flowmeters, Stolz and ASME-AGA orifice eqns., lab. data comparison 0-64604
- gas flow meas. with vortex meter and microcomputer (*German*) 0-92241
- high pressure piston flowmeter with digital readout (*Polish*) 0-64661
- hydrodynamic factors, calibration and meas. errors 0-96322
- liquid, design nomogram 0-96323
- liquid flow rates through pipes, applicability of experimental meas. methods 0-100044
- magneto-inductive flowmeters, installation (*German*) 0-64662
- mass, meas. Coriolis effect on mols., electro-optical sensing 0-96327
- mass flow meter using Coriolis principle, electro-optical force sensing techniques 0-103094
- mechanical, engineering meas., conf., Johannesburg, South Africa, (Feb. 1979) 0-75016
- mechanical, readout conversion to electrical output 0-75012
- movable orifice type, meas. principle, design and trial meter results (*Japanese*) 0-59148
- nasal flowmeter for preterm infants, self-retaining 0-98158
- NMR flowmeters, vortex meters, and mass flowmeters, calibration 0-92239
- nozzle, instantaneous flow rate meas. in pulsating water flow (*Japanese*) 0-59133
- nuclear reactor 0-99268
- oil, differential, mechanical to electrical readout conversion 0-75013
- pipe bends as flowmeters (*Italian*) 0-69958
- precision, commercial instruments survey (*French*) 0-83871
- pulse-compensation method of meas. liquid flow-rate based on NMR 0-103088
- reference, development for irrigation water mains 0-96325
- reference installations, development prospects for meas. computer complexes 0-96320
- respiratory, hot-wire, evaluation for clinical appls. 0-72346
- selection, performance-application compromise 0-87822
- stabilizing liquid flows for flowmeter appls. 0-103084
- tachometric, testing with volumetric dynamic flowmeter installation 0-96324
- test system based on anal. of synthetic model 0-103082
- testing, design principles for comparative testers 0-96319
- thermal measurement systems for flow rate and flow composition (*Russian*) 0-69953
- transducer calibration, using computerised system 0-79416
- transfer function, determination using hydropulsator 0-103083
- two phase flow in pipe lines, on-line holdup or quality meter 0-106858
- ultrasonic, wide beam 0-106856
- US, PLL cct. (*Japanese*) 0-79414
- US, recal. of characts. and calibration 0-103086
- US compensation-type flowmeters (*Russian*) 0-83866
- US flowmeter, multichannel 0-103089
- US pulse Doppler, arterial flow in man 0-104805
- vortex, development and appl. trends 0-75017
- vortex flowmeter design, theoretical and practical aspects (*Polish*) 0-103092
- vortex shedding flowmeter, stabilisation in low Reynolds number range 0-83865

fluctuations

- see also *Brownian motion*; *critical fluctuations*; *current fluctuations*; *noise*; *random processes*
- W. Antarctic ice sheet, fluctuations in Antarctic Peninsula area 0-94549

fluctuations continued

antiferromagnet, crit. fluctuation of staggered magnetisation, AC susceptibility meas. 0-60219
atmosphere humidity fluctuations meas., correction for different wet and dry bulb response in thermocouple psychrometry 0-98472
atmosphere scintillation, theory for millimetre and submillimetre wavebands 0-61884
atmosphere surface layer temperature, fluctuations investigation via acoustic method 0-67434
atmosphere temperature fluctuations, heat flux and struct. functions meas. with acoustic Doppler sodar 0-105023
atmospheric precip., daily precip. fluctuations modelling with Markov-I chain 0-101401
atmospheric turbulence effects on IR and near-millimetric-wave propagation 0-61902
Bernard convection, and linear fluctuation theory, Markovian processes and irreversibility 0-87766
Boltzmann equation, stochastic, hydrodynamic fluctuations 0-68158
book 0-73104
Boussinesq fluids in turbulent convection, power spectra of temp. and vel. fluctuations 0-98543
chaos, onset and characteristics 0-82723
chemical instabilities, stochastic approach, anomalous fluctuation and transient behaviour 0-89465
chemical system, equilibrium fluctuations, deviations from Poisson behaviour, molecular dynamics 0-86211
classical plasma dynamics 0-83888
classical system with long-range forces, eqn. props., BBGKY eqn., neutrality, screening, sum rules 0-62569
colloids, interfacial electric polarisability, and interactions 0-108751
contracted description of fluctuating systems 0-90781
cosmic microwave background small-scale fluctuations (Russian) 0-109576
cosmological fluctuations, spontaneous prod. 0-94902
critical mixtures, shear and critical fluctuations, instantaneous mapping of velocity gradients 0-79420
dielectrics with periodic boundary conditions, fluctuation theorems 0-80735
disordered materials, fluctuation-induced tunnelling cond. 0-65516
early universe density-temp. fluctuations, present observability 0-82554
Earth annual polar motion, many-year var. rel. to atmospheric circulation many-year fluctuation (Chinese) 0-104848
FKG inequalities and fluctuations, probabilistic approach 0-77712
Florida Current, fluctuations in transport at periods between tidal and two weeks 0-72551
fluid dynamics, Rayleigh-Benard convection, randomly forced 0-79314
fluids, simple, thermally induced surface fluctuations 0-88403
Fokker-Planck model, transport equation renormalisation 0-82732
four-point field coherence function, strong fluctuations of wave intensity 0-63927
gamma-Lorentzian intensity fluctuations, integrated, statistics 0-102685
gas-lasers, single-mode, fluctuations of laser beam diameter, lens effect 0-64090
gaussian fluctuations of mol. field 0-70918
gravitational wave interferometer, quantum mechanical radiation press. fluctuations 0-90770
heat flux fluctuations, Fokker Planck eqn. in extended irreversible thermodynamics 0-86205
Heisenberg chain, classical, energy fluctuations 0-80472
Heisenberg chain, one dimensional classical energy fluctuations 0-70924
hydrodynamical fluctuation theory far from equilibrium 0-98856
incommensurate epitaxies at finite temps., substrate pot. effect 0-88451
incommensurate systems, discrete lattice effects 0-107402
intensity fluctuations and fourth-order coherence function in random media 0-78774
intensity fluctuations at two wavelengths in turbulent medium 0-87318
ionosphere, total electron content fluctuations rel. to scintillation of VHF and GHz waves 0-109302
ionosphere, turbulent fluctuations, rel. to strong turbulence in partially ionised plasmas 0-79499
ionosphere electric field, ULF fluctuations obs. in dayside auroral oval 0-98505
ionosphere F-layer, large-scale artificial inhomogeneity spectrum 0-98515
Ising ferromagnet, gaussian fluctuations of mol. field, magnetisation and free energy 0-70918
laser beam, intensity fluctuations in snowfall (Russian) 0-94602
laser beam amplitude fluctuation statistics in turbulent atmosphere 0-106458
L.F. dissipation and relaxation props., universality 0-84687
light intensity fluctuations behind lens, receiving aperture shape effect 0-95980
Ligurian Sea continental shelf, currents low-freq. fluctuations rel. to wind fluctuations 0-85675
liquid, ionic, binary mode coupling theory of charge fluctuation spectrum 0-92451
Lorenz model, turbulence in dissipative dynamical systems 0-90784
macromolecules, internal coordinates fluctuations, effect on dimensions 0-74266
Markov process generated by Langevin equations, WKB-type expansion 0-86212
mathematical formulation, review, book contrib. 0-73267
metastability, rigorous molecular theory, review, book contrib. 0-73271
molecular low dimensional system, spontaneous symm. distortion 0-96456
nematic liquid cryst., orientational fluctuations effect on evanescent modes of transmitted EM wave 0-64889
non-gaussian field, clipped time autocorrelation function of intensity fluctuations 0-106472
nonequilibrium steady states, irreversible processes, Lyapunov functions 0-95049
nonequilibrium fluctuations in driven systems 0-86210
nonlinear irreversible processes and fluctuations 0-82724
nonlinear oscillator with fluctuating parameters, dynamics, thermal noise 0-101729
nonpolar fluid, excessive electrons near crit. points 0-92836
ocean upper layer, small-scale temp. fluctuations statistical regularities (Russian) 0-94528
one-dimensional conductors, disordered, resistance fluctuations 0-80256
open dynamic subsystem, nonlinear eqn. with fluctuating parameters derivation 0-94991
open dynamical system, equations with fluctuating parameters 0-62584

fluctuations continued

optical beams in randomly inhomogeneous media, strong fluctuations of fields 0-99634
optical phase fluctuations, interferometric anal. of deep random-phase screens 0-101834
partially coherent beam intensity fluctuation calc. in turbulent atmosphere 0-78775
percolation theory, fluctuations of infinite network 0-73278
perturbed flow, moisture form. kinetics 0-79387
phase transitions, nonequilibrium transient behaviour 0-93732
photon counting with dead time, inversion problem 0-99682
polyacetylene, doped, fluctuation-induced tunnelling cond. in metallic regime 0-65516
polycarbonate, glassy state, enthalpy relax., thermal density fluctuations 0-59678
polymer blends, fluctuation dynamics, spinodal decomp. 0-79943
precipitation, seasonal, in Jerusalem, temporal fluctuations 0-72618
pulsed laser radiation intensity fluctuations, thermal selfinteraction in turbulent medium 0-102781
PVC-C composite, fluctuation-induced tunnelling cond. 0-65516
pyroelectric thin film detector, temp. fluctuation noise 0-77861
radar signal reflection from sea surface, spatial intensity fluctuations 0-109170
radiation counting rate meter output at threshold, fluctuation and arrival shift by computer simulation 0-106240
radiation fluctuations from light source 0-95857
radio emission of cloudy atmosphere, expt. characts. of fluctuation 0-67399
random, moment behaviour of soln. processes for nonlinear stochastic differential eqns. (Japanese) 0-95039
randomly inhomogeneous layer, statistical moments of wave field, strong fluctuations of wave intensity 0-57107
randomly inhomogeneous medium, fluctuations in phase arrival angle and freq. correl. of spherical waves 0-106456
Schrödinger equation, randomly fluctuating interaction term, uncertainty in nature 0-62499
semiconductors, mobility-fluctuation description of 1/f noise 0-84496
shock tube driver gas flow with fluctuations 0-96282
simple fluids, fluctuation expressions for nonequilib. distrib. functions in adiabatic flows 0-92441
simplified hydrodynamic theory of nonlocal stationary state fluctuations 0-98857
solar constant fluctuations, prod. by convection zone struct. adjustments 0-82321
solar continuum brightness, fluctuations rel. to trapped gravity waves in solar atmosphere 0-72898
solar radio noise storm, drifting pulsations obs. 0-62105
solar wind plasma, density fluctuations from three-satellite radio wave propag. meas. 0-101518
solid laser, fluctuations in laser theories 0-83587
starlight interstellar polarisation, fluctuation theory 0-82442
statistical mechanical theory of the kinetics of phase transitions, review, book contrib. 0-73270
statistical theories, nonlinear, fluctuation effects, truncation schemes of cumulant hierarchies 0-68133
stellar mass loss from O and Of stars, fluctuation theory involving stochastic accel. 0-90413
stochastic gravitational fluctuations in a self-consistent mean field theory, review 0-90734
stochastic one-variable system, growth of fluctuations from marginal eqn. 0-86213
structural phase transitions, Landau theory 0-92639
superfluorescence delay times, intrinsic quantum fluctuations 0-58492
superfluorescent pulse fluctuation 0-58490
symmetry breaking in the decay of unstable states 0-57188
thermodynamics, irreversible, extended, hydrodynamical fluctuations 0-86235
thin films, substrate supported, temp. fluctuation noise 0-92949
turbulence in systems with small parameters 0-105571
turbulence in the motion of a free particle and de Broglie waves 0-57189
two-level system, Rabi oscillations in partially coherent field 0-102688
underwater sunlight fluctuations in sea spatial and temporal correlation 0-94533
universe, Friedmann model, with decoupled radiation field, density perturbations growth 0-109567
Universe, tenacious myths about cosmological perturbations larger than horizon size 0-105408
Universe density perturbations, consequences for evolution nonlinear stage of neutrino rest mass (Russian) 0-105414
Universe density perturbations spectrum, consequences of neutrino rest mass (Russian) 0-109576
Yang-Mills multi-instantons, quantum fluctuations, Seeley coeffs. 0-77934
Al film, lattice and bulk heat capacity meas. for normal and supercond. states 0-92684
GaAs, heavily doped, fluctuation-induced tunnelling cond. 0-65516
H II regions density fluctuations, statistical approach 0-77468
³He, liquid, surface fluctuation influence on free energy, surface tension (Russian) 0-92746
⁴He, superfluid, fluctuations in turbulent counterflow, vortex line density fluctuation power spectra 0-84335
Ni-Fe, thermal fluctuation aftereffect meas. by pulse field method 0-88837
Pb_{1-x}Li_x(As)(Ag)(In)(Sn)(Sb)(Te)(Au)(Ti)(Bi), liquid alloys, local fluctuations and quadrupolar relaxation 0-66060
Tl₂Te-Tl liquid system, conc. fluctuation, time-of-flight quasielastic neutron scatt. obs. 0-88324

fluctuations in superconductors
used only for thermal (thermodynamic) fluctuations around the order parameter near the critical point
ferromagnetic superconductor, paramagnetic fluctuations, influence on superconductivity 0-70900
granular microbridges, fluctuations and crit. current determ. 0-84562
granular microcylinder, flux quantisation phenomena above T_c (Russian) 0-70899
hard superconductor, critical state stability and oscillations 0-107959
metal, granular superconductivity, instability 0-103796
metal inhomogeneous granular, superconductivity 0-103795
metallic ultrathin filaments, dielectric and superconducting fluctuations, Peierls transition (Russian) 0-65742

fluctuations in superconductors continued

- nonequilibrium state stability with respect to finite fluctuations 0-103782
 nonequilibrium superconductors, ferromag. ordering of quasi-particles and rise of domains 0-107958
 rare earth cpds., $\text{RMO}_2\text{S}_2(\text{Se}_2)$ and RRh_2B_4 , coexistence of supercond. and mag. ordering (*Russian*) 0-84542
 selfconsistent treatment of fluctuations in superconductors 0-100549
 ultra-thin films, transition temp., interface and fluctuation phenomena 0-84527
 Al particles, small supercond. nuclear spin-lattice relax. meas. 0-88681
 Al-Ag, type-II superconductor, torque oscillations in mag. field (*Russian*) 0-103800
 Ga ultrathin metallic filaments, appearance of dielec. instability, coexistence with supercond. 0-103784
 Hg ultrathin metallic filaments, appearance of dielec. instability, coexistence with supercond. 0-103784
 In ultrathin metallic filaments, appearance of dielec. instability, coexistence with supercond. 0-103784
 NBN granular films, supercond., crit. props. 0-88661
 Sn, film, superconducting fluctuations, transition temp. (*Russian*) 0-65740
 Sn superconducting films, Ge-covered, effect on excess elec. cond. 0-65741
 Sn ultrathin metallic filaments, appearance of dielec. instability, coexistence with supercond. 0-103784

fluctuations of cross sections *see statistical theory of nuclear reactions and scattering***fluid composition control** *see chemical variables control***fluid composition measurement** *see chemical variables measurement***fluid dynamics**

- see also aerodynamics; biological fluid dynamics; drag reduction; electrohydrodynamics; flow; hydrodynamics; Navier-Stokes equations; rarefied fluid dynamics; relativistic fluid dynamics; surface waves (fluid); turbulence; wakes*
 advection, pseudo-upstream finite difference scheme 0-106773
 astrophysics, higher order fluid eqns. for multicomponent nonequilib. stellar atmospheres and star clusters 0-105156
 boundary deform., Galkerkin finite element technique for multidimensional flow 0-86089
 calculation of force of resistance of a medium to motion of particles of various shapes at Reynolds numbers exceeding unity 0-106775
 chaotic flows of autonomous dissipative systems 0-73176
 computer simulation of fluid structure and dynamical props. using Monte Carlo and mol. dynamic methods (*German*) 0-69757
 Cosserat continuum, kinetic energy, linear and angular momentum densities, invariance 0-74829
 counterflow processes, nonlinear modelling using weighted residual methods 0-69754
 discontinuities, subgrid resolution in tracking methods 0-105506
 drops, liquid, charged, dynamics, symmetric and asymmetric stabilities 0-79366
 duct flow eigenvalue problem, FEM soln. with Hermitian elements 0-74983
 Earth fluid core with inward growing boundaries, dynamics 0-76934
 fission reactor fluid dynamic transient analysis using ASWR method with staggered meshes (*German*) 0-83176
 flow in curved tube, finite difference anal. method 0-106846
 free boundary flow, surface tension effects, finite element fluid flow simulators 0-82647
 geophysical fluid dynamics theory, book 0-105443
 gravity current, front motion down incline 0-106819
 gravity current slumping 0-103052
 groundwater flow, finite element eqns., Newton iteration and modified conjugate gradient method 0-77622
 hyperbolic systems, high-order methods, dynamic problems 0-68033
 image processing applications at IBM Madrid Scientific Center 0-102657
 incompressible flow including heat and mass transfer, vel.-press. coupling treatment 0-69832
 incompressible fluid flow, one dimensional, calc. 0-79402
 liquid, ideal incompressible flow, topological measuring of canonical Clebsch variables 0-69758
 liquids, momentum transfer, cooperative effects 0-68160
 momentum theory, generalised formulation for transient phenomena 0-62474
 multiparameter splitting schemes for solution of spatially three-dimensional nonstationary problems 0-68047
 Newtonian fluid, incompressible, between parallel plates, effect of wall slip on drag flow and pressure flow (*German*) 0-87810
 nonhomogeneous fluid, compact manifold boundary, Euler equations 0-62476
 oil-bearing layer with input parameter correction, discrete dynamic model 0-83778
 piston problem, one-dimensional, in non-ideal gas, time-dependent soln. 0-82185
 Poisson equation, non-uniform grid, finite-difference, matrix decomp. technique 0-69756
 potential flow, 3-D, about arbitrarily shaped bodies, direct matrix embedding technique 0-64511
 pulsating incompressible fluid in elastic tube, pressure wave propagation through tube 0-96228
 reverse pseudo-unsteady aerodynamic calculation methods (*French*) 0-69759
 shallow water theory, exact solns. to eqns., appls. 0-58998
 solar wind, plasma fluid aspects 0-90313
 Stokes problem, for infinite vertical plate with const. heat flux 0-79108
 Stokes problem, second-order difference scheme 0-90678
 stratosphere, Lagrangian motion of air parcels 0-109215
 thin body with ventilated cavity, inclined entry into ideal imponderable liquid 0-99984
 transformation group techniques appl. to nonlinear fluid and plasma eqns. (*French*) 0-77623
 universality class of asymmetric fluid critical points 0-57098
 viscous fluid, incompressible, motion in curved pipe of elliptical cross-section 0-74989
 viscous fluid, shear processes, local order theory 0-59687

fluid flow *see flow***fluid instability** *see flow instability***fluid mechanics**

- see also capillarity; cavitation; compressibility of gases; compressibility of liquids; fluid dynamics; hydrostatics; Mach number*
 annual review of fluid dynamic, book 0-94927
 computer simulation of fluid structure and dynamical props. using Monte Carlo and mol. dynamic methods (*German*) 0-69757
 falling horizontal cylinder, low Reynolds number, horizontal plane boundary effect 0-87757
 incompressible viscous fluid, slow motion of small sphere outside cylinder 0-96239
 photon correlation techniques in fluid mech., conf., Cambridge, England (March 1979) 0-56998
 relation to statistical physics, book contrib. 0-94959

fluid theory, dense *see liquid theory***fluid valves** *see valves***fluidic devices**

- attached jet characteristics, aspect ratio effect (*Japanese*) 0-87791
 curved wall power fluidics characts. 0-103053

fluidised beds

- 100 MW fluidised bed combustion district heating plant burning high S content residual oils 0-108777
 200 MW atmospheric fluidised-bed combustion steam generator, comparison of three designs 0-108776
 atmospheric fluidised-bed combustion boiler development facility, first year of operation 0-108775
 bubble observation using probes and X-rays 0-79379
 bubbles of gas, rise velocities 0-64610
 bubbling fluidised beds, theoretical bounding relations, for bubble void fraction 0-96296
 combustion facility, radiation heat transfer, particle size and flow parameter effects 0-69641
 critical height reduction anal. of particle ejection 0-106842
 dehydration of solutions and suspensions, rel. to granulation 0-81373
 drag force generated at high Reynolds numbers, effect of particle proximity 0-96306
 fission reactors, fluidised bed concept, diffusion theory 0-68729
 geological materials, acoustic fluidisation prod. by strong transient wave field, theory and appls. 0-85653
 heat transfer between a freely-rising slug and a fluidised bed 0-96307
 heat transfer between air fluidised beds and horizontal Cu tubes 0-79317
 heat transfer coeff. between bed and vertically inserted tube wall 0-74971
 heat transfer in fluidised bed with immersed horizontal tubes (*Russian*) 0-74880
 heterogeneous fluidised system, aerodynamic aspects of transfer processes, crit. state 0-79394
 horizontal tubes in fluidised beds, local heat transfer coeffs. 0-74875
 instability waves and bubble origin, two-fluid eqns. 0-92205
 kinetic energy of particles in fluidised bed rel. to bubbling phenomena, theoretical anal. (*Russian*) 0-74965
 liquid, axial dispersion obs. 0-59106
 liquid fluidised bed, mass transfer time fluctuations 0-79380
 mass transfer, Karman-Pohlhausen method and concentric spheres free surface model 0-79378
 mass transfer to power law fluids in fluidised beds 0-100032
 moving bed solid flow in inclined pipe leading to fluidised bed., gas leakage 0-64619
 moving bed solids flow in inclined pipe leading to fluidised bed 0-64620
 multifuel fluidised bed combustion packaged boiler to supply 10000 lb/h saturated steam at 100 psig 0-108779
 semifluidised bed, mass transfer rate 0-59105
 sphere immersed in a fluidised bed, mass transfer (*French*) 0-92214
 spouted beds of spherical particles, spout termination, parameters 0-64621
 steam generating system to supply 100000 lb/h of saturated steam burning high S coal 0-108778
 surface temperature measurement using infrared photoresistors (*Russian*) 0-82763

fluidised powders *see powders***fluidity** *see viscosity***fluids**

- see also bubbles; classical theories of fluid structure; disperse systems; fluid mechanics; fluidised beds; gases; gravity waves; liquids; non-Newtonian fluids; quantum fluids; quantum theories of fluid structure*
 No entries

fluorescence

- see also atomic fluorescence; fluorescent lamps; fluorescent screens; molecular fluorescence; nonradiative transitions; X-ray fluorescence analysis*
 5-acetyl-5H-benzo[b]carbazole-5H-benzp[b]carbazole, singlet-singlet energy transfer (*German*) 0-93402
 adenine film, polycryst., energy conversion processes, quantum yields, 4 to 10 eV 0-88589
 alkali-alumino-phosphate:U, rontgenoluminesc. and fluoresc., radiative transitions obs. 0-103977
 alkaline earth halides:Eu²⁺, fluorescence lifetime and quantum efficiency for 5d-4f transitions 0-100681
 anthracene, cryst., exciton aggregate possible form. under intense optical pumping, fluoresc. spectra 0-84772
 anthracene, cryst., heat pulse propag., exciton condensation, time-resolved fluoresc. spectra 0-84771
 anthracene, thick crystals, excitation spectrum of fluorescence 0-76068
 anthracene-phenanthrene-tetracyanobenzene, CT-cryst., mini-excitons and lattice dynamics, ESR, optical and Raman spectra 0-60406
 automatic fluorescence microscop photometry data processing and display (*German*) 0-86369
 backward Raman amplifier for excimer laser pulse compression, parasitic superfluoresc. suppression 0-69453
 benzene, soln., fluoresc., quenching in pulsed proton and alpha particle irradi., radiation quality effects 0-66259
 benzene cryst., electron irradi., phenylcyclohexadienyl radical form., absorpt. and fluoresc. spectra study 0-89035
 calcite, luminescence spectral anal. of polycyclic aromatic hydrocarbon impurities 0-71483
 cellular fluorescence polarisation measurements in flow systems, epillumination optical design 0-89908
 condensed phase fluoresc., double reson. excitation spectroscopy 0-86438

fluorescence continued

- cooperative resonance fluorescence, multiple sidebands, semiclassical calcs. 0-99685
- cytofluorometric measurements by fluorescence extinction through a diaphragmed objective 0-67319
- decay time, phase-shift and modulation techniques, pulsed light sources high harmonic content 0-69179
- dibenzofuran:anthracene, cryst., prompt fluoresc., temp. depend., trap effects (*German*) 0-93400
- dilute systems, donor fluorescence at high trap concentration 0-71479
- diquinolinyl cyanomethane, fluoresc. quantum yields, viscosity effects 0-60646
- donor fluorescence, t-matrix analysis 0-100679
- dye molecules adsorbed on Ag, Au and Cu films, absorpt. and luminesc. study 0-103981
- films on substrates, electron probe anal., charact. fluoresc. effects calc. 0-81408
- fluorene:pyrene- d_{10} , single cryst., host-guest triplet pairs, mag. field effect 0-60649
- fluorescein angiography of the ocular fundus 0-67185
- fluorescent materials, reflective radiance factor meas. by two-monochromator method (*Japanese*) 0-68237
- frozen gas matrix, refr. index determ. by emission spectrosc. 0-90884
- glass:Nd³⁺, spectral props. (*Chinese*) 0-60645
- Hercules X-1, fluorescent origin of Fe K-line emission during X-ray low state 0-105393
- impurity atom in solid, reson. fluoresc., transient spectrum, intensity, and intensity correl. 0-84777
- impurity centres, electron-phonon coupling from structured optical spectra, review 0-89038
- indigo derivatives, fluorescence decay times, meas. by synchroscan streak camera 0-84759
- internal combustion engine, conc. fluctuation meas. 0-71973
- 4-isocyanate-trans-stilbenes, donor substituted, anisotropic fluoresc. in low viscosity solvents (*German*) 0-93401
- level crossing detection through photon counting distrib. second factorial moment meas. 0-99485
- line narrowing, line-shape deconvolution 0-89039
- membrane surfaces, antibody association kinetics with spin-label haptens 0-66787
- membranes, structural order of lipids and proteins, fluoresc. anisotropy data eval. 0-97873
- microscopy, incident light, specimen prep. method 0-82755
- microscopy of living cells, low level, appls. of image intensification 0-94432
- molecular solid, intermolecular interactions, laser induced phonon probe 0-79891
- muscle, cross bridge rotation during contraction, fluctuations in polarised fluoresc. 0-97856
- muscle, tryptophan fluorescence polarisation 0-97877
- naphthalene:anthracene, pure and doped, delayed fluoresc. (*French*) 0-80846
- n-octane-3,4,6,7-dibenzpyrene impurity, fluorescence impurity spectra, phonon free line broadening (*Russian*) 0-108279
- organic molecular crystals, intermolecular interactions, spectroscopic studies, review 0-103958
- pentacene in naphthalene (p-terphenyl), mol. mixed crystals., optical dephasing and vibronic relax. 0-95957
- pentacene in p-terphenyl, intermolecular interactions, laser induced phonon probe 0-79891
- perylene, intermolecular interactions, laser induced phonon probe 0-79891
- phenanthrene, two-photon excitation spectra, exciton-phonon and intramol. vibronic coupling 0-84774
- photobleaching recovery method, bleaching light effect on membrane diffusion meas. 0-94434
- photosynthesis, chloroplast fluorescence, investigated using laser spectrofluorimetry 0-81558
- photosynthetic apparatus repression b 2-deoxy-D-glucose, low-temp. fluoresc. spectra of intact *Chlorella* cells 0-81559
- phthalocyanine, doped photovoltaic cell, photoconductivity, elec. field induced fluoresc. quenching, charge carrier photogeneration 0-84485
- planet surface, environmental remote sensing, molecular absorpt. methods 0-72651
- polyacenaphthalene, glassy soln., fluoresc. yield, polarisation and decay., temp. depend. 0-89043
- polyacenaphthalene-methylmethacrylate copolymer 0-89043
- polyaspartamides, soluble, fluorescent labelling 0-58426
- polyribonucleotides, dye tagged, aqueous solns., elec. induced fluoresc. changes 0-85346
- pressure calibration system improvement using ruby R₁ fluorescence 0-98928
- pseudo-Kossel lines in high press. X-ray diffr. pattern using diamond anvil cell 0-79623
- pyrene, triplet state, excitonic energy transfer, phosphoresc. and delayed fluoresc., 2 to 300K 0-84776
- pyrene crystals, anomalous emission excited near absorption edge 0-100682
- rare earth oxyhalides: Eu³⁺, fluorescence spectra obs. (*French*) 0-89042
- resonance fluorescence in Markovian stochastic fields 0-83573
- ruby, quantum efficiency, photoacoustic meas. 0-73472
- ruby fluorescence line shift, condensed gas phase transitions obs. in diamond-anvil cell 0-73381
- ruby R₁ zero phonon line, resonance fluoresc. meas. 0-89055
- sapphire, F-centre, fluorescence decay below 75K 0-60664
- sapphire, neutron bombard., F-centre fluorescence, photoluminescence 0-100676
- sapphire, optical detection of acoustic phonons at THz freqs. 0-75320
- semiconductor-liquid junction solar cells, use of fluorescent windows in cell design 0-10114
- sodium fluorescein-rhodamine B, energy transfer in luminescent mixed solutions 0-103976
- solid, impurity atom fluoresc. radiation, intensity correlation, low temp. limit 0-80847
- solid laser dynamics, Auger recombination effects 0-63998
- solutions and suspensions, polarised fluoresc. in elec. field, mol. props. deriv. 0-84785
- spectroscopy using pulsed lasers, time-resolved 0-57393
- p-terphenyl cryst., low lying single state 0-97320
- tetrabenzo[a, od, j, lm]perylene evaporated film, crystn., time depend. as function of purity 0-88449

fluorescence continued

- tetrabutylammonium europium yttrium isothiocyanate, conc.-depend. electron-phonon coupling, and self-quenching 0-60657
- tetracene, disordered, vapour deposited on glass substrate, fluoresc. and energy transfer 0-84761
- tetracene, unrelaxed fluoresc., direct picosecond obs. 0-89046
- thymine film, polycryst., energy conversion processes, quantum yields, 4 to 10 eV 0-88589
- uniaxial liq. crystal polarised fluoresc. emission 0-80838
- Venus upper atmosphere, solar Lyman α fluoresc. scatt. rel to dayglow spectrum 1250 to 1430 Å. 0-77311
- very weak, photon correlator for meas. transient waveforms 0-87250
- Al₂O₃:Cr³⁺, ruby, reson. scatt. and trapping of 29 cm⁻¹ acoustic phonons 0-93403
- Al₂O₃-SiO₂ glass ceramic, surface streaks and blisters, UV fluoresc. study 0-84347
- BeF₂:Eu³⁺ glass, struct., Monte Carlo simulations 0-96448
- BeF₂-KF-CaF₂-AlF₃-EuF₃ fluoroberyllate glass, Eu³⁺ fluoresc. linewidth 0-66285
- CaF₂, optical detection of acoustic phonons at THz freqs. 0-75320
- CaO, photoionisation of F-centre, luminesc. and photocond. meas. 0-66270
- CdF₂:Er³⁺, Tm³⁺, evidence for Er³⁺==Tm³⁺ energy transfers, fluoresc. expts. 0-60655
- CH³⁺+Cu, K X-ray production and radiative electron capture, fluoresc. yield determ. 0-99553
- CsMnF₃, exciton-magnon interactions in optical transition, absorpt. and emission spectra meas. 0-70981
- Eu complex, europium benzoyltrifluoroacetate chelate layers, fluorescence lifetime changes induced by variable optical environments 0-93386
- F+H₂(D)₂ZZ 0-81303
- KBr:L⁺, OH⁻, luminesc. of interstitial atomic H 0-89062
- KCl:Eu²⁺ crystals, photostimulated afterglow investigation at room temp. 0-108259
- LaBr₃:Nd³⁺, energy level anal., polarised absorpt. and fluoresc. spectra 0-76056
- LaCl₃:Nd³⁺, energy level anal., polarised absorpt. and fluoresc. spectra 0-76056
- LaCl₃:Nd³⁺, phonon-induced relax. in excited optical states, linewidth temp. depend. meas. 0-100688
- LaCl₃:U³⁺, cryst., spectrum anal., cryst. field parameters 0-76057
- LaF₃:Er³⁺, optically excited, direct-process spin-lattice relaxation 0-93378
- LiCl:Ag, fluoresc. and UV absorpt. spectra 0-80844
- LiNbO₃, luminesc. props., Li/Nb ratio effect 0-97323
- Lu₂-Si₂O₇:Eu₃, synthesis and spectroscopic study 0-84846
- NaBr(I), optically activated F⁻F' centre conversion in mag. field 0-108253
- Na₃La_{1-x/3}Ce_{x/3}(PO₃)₂, optical props. (*French*) 0-103991
- Nd³⁺:LaCl₃, laser-induced fluoresc., hyperfine structs. 0-100677
- Nd³⁺:LaCl₃, laser-induced fluoresc. energy transfer effects 0-100678
- NdP₂O₄, fluoresc. lifetime meas., IR and photoacoustic spectroscopy 0-60632
- P₂O₅-R₂O₃-M₂O(M'O), (M=alkali metal, M'=alkaline earth, R=Y or rare earth), metaphosphate glass phosphors, fluoresc. props., activation conc. effect 0-89058
- POCl₃:Pr³⁺, fluoresc. and lifetimes of excited states 0-71466
- RbBr:L⁺, OH⁻, luminesc. of interstitial atomic H 0-89062
- SrF₂, optical detection of acoustic phonons at THz freqs. 0-75320
- U, sputtered atoms, laser fluorescence spectroscopy 0-66359
- YVO₄:Nd³⁺, energy transfer processes, laser-excited time-resolved spectroscopy 0-84765
- ZnO phosphor fired with Zn, luminesc. in green and red region 0-66265
- ZnS:Tm²⁺, charge compensation and polytypism influences on fluorescence 0-89051
- fluorescence of atoms** see atomic fluorescence
- fluorescence of molecules** see molecular fluorescence
- fluorescent lamps**
colour-reference-standard fluorescent lamp with colour rendering index of 99 0-78925
phosphors, charact. of emission and absorption (*Japanese*) 0-89067
- fluorescent screens**
see also electroluminescence
metal-backed, appl. to high temp. RHEED obs. 0-75126
phosphors, cathodoluminesc. investig., appl. to cathode ray tube screening 0-108282
X-ray intensifying screen, role of reflective layer 0-62816
- fluorimetry** see spectrochemical analysis
- fluorine**
see also nuclei with
atom, ab initio effective valence shell Hamiltonian for neutral and ionic valence states 0-74117
atom, spin-orbit splitting and ²P_{1/2} radiative lifetime, absorpt. spectrosc. meas. 0-87063
combustion studies, 2-compartment bomb calorimeter 0-57300
discharge, stationary vol., reduced-power meas. 0-75115
F+dichloromethane, reaction products, modulated mol. beam mass spectrosc. obs. 0-97742
fluorination of Fe-Ni alloys, chem. nature of fluoride film 0-101035
formaldehyde+F reactions, rate consts. by EPR 0-93736
isoelectronic sequence, X-ray spectra 0-87071
K α X-ray satellite struct. and KLL Auger electron spectra, solid-state effects 0-89089
laser, discharge pumped multiwavelength (*Chinese*) 0-102703
liquid, hard sphere model with attractive interactions 0-96434
molecule, electron impact excitation, dissociation of lowest electronic state 0-63839
molecule, He(II) photoelectron spectra 0-91601
molecule, pseudopot. calcs. 0-91446
molecule, relativistic Dirac-Fock multiconfig. SCF calcs. 0-99456
molecule, UV laser system 0-83597
X-ray spectra from light ion bombard. studies 0-71518
Ar-Kr-F₂, nucl. pumped laser, high energy beam deposition 0-63999
Ar-Kr-F₂ discharge, inelastic electron collisions, energy distrib. and rate consts. 0-87980
Ar-Kr-F₂ mixture, nucl. induced excimer fluoresc. for I laser excitation 0-78846
Cu+F₂, chemiluminesc. reactions, mol. beam study 0-97702
F⁻ ions in Kr and Xe; mobilities and diffusion coeffs. determ. 0-100048

fluorine continued

- F^- , second order correl. energy, Z depend. of irreducible-pair energies 0-91417
 $F+CO$ in Ar matrix, vibr. and electronic spectra, valence force potential determ., mol. photodissoc. obs. 0-85170
 F +ethylene (benzene) derivatives, deuterated, IR chemiluminesc. 0-102506
 $F+H_2$, reactivity-selectivity, bounds derivation 0-66763
 $F+H_2(D_2)$, rate consts., temp. depend. 0-81302
 $F+H_2(D_2)ZZ$ 0-81303
 $F+H_2$ -HF+H, DWBA transition amplitude kernel 0-81310
 $F+HCl(HBr)(DBr)(HI)$, H abstraction reactions, temp. depend., laser photolysis IR fluorecs. obs. 0-93744
 $F+HCl$ -HF+Cl, time resolved vibr. chemiluminesc. and rate consts. 0-61069
 F +methyl radical, IR chemiluminescence obs. 0-61080
 $F+O_3$ reaction, $FO(X^2\Pi)$ radical VUV photoelectron spectra 0-104455
 F^++Kr^++Ar , three body ion-ion recombination probability, Monte Carlo simulation 0-85160
 $F^++Si(S)(Ar)(Kr)$, inner-shell ionisation, X-ray cross sections 0-58369
 $F_2+K_2(Cs_2)$, ionisation reactions, absolute cross sections 0-99565
 $F_2+Kr(Xe)$, XeF, KrF form., relax. and quenching 0-81314
 F_2+XeF^++Xe , temp. dependent quenching rate constants 0-63701
 $FO(X^2\Pi)$ radical from $F+O_3$ reaction, VUV photoelectron spectra 0-104455
 ^{18}F penetration in Ge single crystals, charged particle activation anal. 0-93828
 ^{18}F , prep. with an electron linear accelerator, medical and biological appls. 0-98136
 ^{18}F recoil ranges in Au by irradiation of O, with 3He and 4He particles 0-71931
 ^{18}F -5-fluorouracil studies in humans and animals 0-109000
 ^{18}F -labelled acetic acid, carrier-free, production via a recoil labelling method 0-104756
 $^{18}F+H_2$, hot atom reaction, nonequilibrium time-depend. theory 0-61126
 ^{18}F +hexafluoropropylene nonequilibrium effects in moderated nuclear recoil experiments 0-89509
 ^{18}F +methane, nonequilibrium effects in moderated nuclear recoil experiments 0-89509
 F^++H_2 , quenching of excited state, semiclassical studies, comparison between reactive and nonreactive processes 0-106375
 H_2/F_2 laser, initiation using surface spark discharge UV light source 0-78923
 H_2+F_2 , branched chain reaction, role of thermally nonequilibrium atoms and molecules 0-76507
 $He-F$ mixture, RF discharge, mass spectroscopy, floating double probe meas. 0-84016
 $InSb:F$, acceptor props. and diffusion coeff. of F 0-70643
 $Na:F$, electron-lattice coupling of F-centres, optical props. 0-60641
 $Si:F$, amorphous, heat resistant, prep., elec. cond., IR absorpt., annealing 0-65719
 $Si:F$, amorphous alloys, RF sputtering prep. in SiF_4 -Ar gas mixture, spectra 0-80772
 $Si:F,H$, amorphous, elec. and optical props. 0-60031
 $Si:F,H$, amorphous efficient carrier generation for solar photovoltaic energy conversion 0-92906
 $Si-F-H:P$, film, dark cond., struct., Raman scatt. 0-88588
 $SiO+F_2$, matrix reaction, $OSiF_2$ prod., IR spectra and force consts. calcs. (German) 0-97718
 $SiO_2:F$, ion implanted, F influence on oxidation-induced stacking faults 0-65011
 $Xe-F$ two module discharge laser, gain and temporal characts. 0-87385

fluorine compounds

- alkaline earth fluorides, cryst. growth in reactive atmosphere 0-80962
 ESCA shifts and effective charges 0-78648
 fluoride crystals, rutile-type, interionic pots., cohesive energy, bulk modulus, calc. 0-79741
 fluoride mixtures, molten, for Ge powder electrodeposition 0-60797
 fluoride solid electrolytes 0-70464
 fluorides, electric field gradient, time-differential-angular-distrib. method 0-60463
 $F+H_2$, gas phase H-atom transfer reactions, struct.-reactivity correl., pot. energy surfaces 0-104433
 FBr^- centre in alkali halides, analysis of spin-Hamiltonian parameters of heteronuclear XY^- defects 0-88509
 FCN , ^{14}N quadrupole coupling consts., ab initio calcs. 0-58283
 FCN , CW for IR mol. laser, optical pumping with $^{16}CO_2$ and $^{18}CO_2$ lasers 0-74343
 FCO , radical, struct. and props. calcs. 0-74112
 FCP , microwave spectrum, struct., dipole moment and vibr.-rot. props. obs. 0-91549
 FCI^- centre in alkali halides, analysis of spin-Hamiltonian parameters of heteronuclear XY^- defects 0-88509
 $FD+H(D)$, low barrier quantum model, vibr. deactivation 0-69216
 $FH+H(D)$, low barrier quantum model, vibr. deactivation 0-69216
 $FH+H(D)$, low barrier quantum model, vibr. deactivation 0-69216
 $F^-(H_2O)_n(n=1,2)$, FSGO-pair-pot. calcs. (German) 0-74278
 $FNNF$, mol. struct., cis effect 0-91434
 F_2O , geometry, electron spectrum, vert. ionis. pot. ab initio calc. 0-58187
 FOO radical, struct. and props. calcs. 0-74112
 FSO (FOS), struct. and props., SCF calcs. 0-106260
 FSS , struct. and props., SCF calcs. 0-106260
 N_2F_4 , collisionless dissociation kinetics in highpower IR radiation field 0-66853
 SO_2F_2 , dye laser excitation of vibr. levels of upper electronic state, mol. fluorecs. meas. 0-83402

flux (magnetic) see magnetic flux**flux (neutron) see neutron flux****flux creep**

see also flux pinning

No entries

flux crystal growth see crystal growth from solution**flux flow**

see also flux pinning

- composite superconductor, flux jumps and training 0-70911
 ferromagnetic superconductors, self-induced vortices, magnetisation, Gibbs free energy 0-70916
 granular films as weak link in Josephson devices, vortex flow model 0-88685
 Lorentz transform law for EM field, fluxoid motion example 0-67954

flux flow continued

- superconducting loop broken by damped Josephson junction, anomalous flux penetration 0-97033
 thin film superconductors, flux lattice melting, phase diagram 0-84571
 type II superconducting wire, nonideal, flux penetration in transverse mag. field (Japanese) 0-60154
 type II superconductors, longitudinal currents in a system of Abrikosov vortices, Ginzburg-Landau eqn. anal. 0-70914
 Al superconducting film, transition to zero vorticity, long-range topological order 0-93039
 Cu-Nb₃Sn multifilamentary tapes, in situ formed, crit. current density anisotropy 0-84576
 In-Bi, mixed state, pinning centre distrib. statistics, I-V characts. (Russian) 0-100571
 Nb-Zr, crit. current, flow-flow resist. depend., allowance for superheating (Russian) 0-93061
 Nb₃Ge, amorphous film, supercond., flux flow resist., vortex pair dissociation 0-88701
 NbN weak links, granular, Josephson behaviour 0-75681
 (Nb_{0.99}Zr_{0.01})₃Sn, AC power losses in parallel AC and DC mag. fields 0-97041
 Sn-Sn₃O₄-Sn long Josephson tunnel junction, flux flow, crit. conditions 0-80452

flux-line lattice

- antiferromagnetic superconductor, isolated vortex line 0-70912
 films with periodic thickness modulation, pinning effects 0-88702
 Josephson tunnel junction, nonresonant vortex motion 0-97037
 superconducting order parameter perturbation flux pinning 0-103801
 superconductor, type II, longit. current, continuous vortex cutting 0-88704
 superconductor Faraday effect obs. in polarising microscope 0-70892
 thin film superconductors, flux lattice melting, phase diagram 0-84571
 type II superconductor, bounded, intermediate state struct. form. near crit. field, role of surface 0-80465
 type II superconductor, nonideal, with dense pinning centres, threshold criterion 0-88703
 type II superconductors, flux-line-cutting threshold 0-88705
 type II superconductors, longitudinal currents in a system of Abrikosov vortices, Ginzburg-Landau eqn. anal. 0-70914
 type II superconductors, order parameter change near H_{c2} , influence of transport current 0-75690
 vortices, local mag. flux density and elec. current density 0-84572
 Al granular films, vortex noise at supercond. transition 0-84530
 Al, supercond. cylinder, order parameter enhancement by microwave irradiation 0-70896
 ErRh₂B₄, ferromag. superconductor, vortex phase 0-80441
 V (-Ti), supercond., rotating discs, hysteresis losses and mag. phenomena 0-75695

flux line motion see flux flow**flux pinning**

see also flux creep; flux flow

- films with periodic thickness modulation, pinning effects 0-88702
 hard superconductor, flux trapping, penetration depth determ. 0-100572
 loss-free current, max. possible, of type-II supercond. with flux pinning 0-84579
 superconducting order parameter perturbation flux pinning 0-103801
 superconductors, type II, vortex pinning at edge dislocations, electrostatic mechanism 0-103802
 trapped flux removal by thermal gradient technique 0-75694
 type II superconductor, nonideal, with dense pinning centres, threshold criterion 0-88703
 Al₂O supercond. film, RF complex impedance meas., dynamic pinning 0-84573
 Al-Ag, torque oscillations in mag. field (Russian) 0-103800
 In-Bi, mixed state, pinning centre distrib. statistics, I-V characts. (Russian) 0-100571
 (Mo_{0.6}Ru_{0.4})₈₀Si₁₀B₁₀, amorphous supercond. matrix, flux pinning by MoRu precipitates 0-65756
 Nb, critical current density, deviation from critical state model 0-84578
 Nb film, struct. and electrophys. props. at 4.2K 0-80436
 Nb, peak effect due to vortex pinning in subsurface layer (Russian) 0-93060
 Nb, single crystals, fluxoid pinning by small nitride precipitates 0-70913
 Nb-Ti, pinning curves, high field J_c and scaling behaviour 0-93064
 Nb-Ti-Ta, pinning curves, high field J_c and scaling behaviour 0-93064
 Nb-Ti(Mo), AC loss minimum, pinning, flux distribution 0-84574
 Nb₃Sn bronze process, flux pinning scaling law depend. on strain 0-75696
 Nb₃Sn, flux density gradient determ. by Faraday effect 0-107969
 Pb foil, crit. current density, pinning force density, shadow electron microscopy obs. 0-88696
 Pb-Na (8.4 at.%), supercond., surface flux pinning, crit. state model 0-97044
 V₃Si, supercond. mixed state, low temp. tetragonal-domain-reorientation phenomena, US expts. and thermal props. 0-60141

flux vortex flow see flux flow**flux vortex lattice see flux-line lattice****fluxmeters**

see also magnetic field measurement; magnetic flux

- development review, 1980 status (French) 0-95114
 MIS-3M magnetic measuring system (USSR), testing small permanent magnets 0-62699
 superconducting, quantum, with 15 to 20 kHz passband 0-57345

fluxoid array see flux-line lattice**foams**

see also bubbles

- black foam films stability, review 0-104463
 nozzle, convergent-divergent, choked foam flow 0-74940
 polyethylene, electron beam crosslinking process for high voltage power cable 0-66846
 polyurethane, foaming parameters determ. from US wave vel. 0-71885
 polyurethane foam, processing machines and systems, motor car components appl. (German) 0-71955
 polyurethane solid foams, creep laws (German) 0-65139
 soap foam, arrangement of cells in a net rel. to grain sections of polycryst. 0-70225
 stability relation to structure, criteria derivation w.r.t. drainage stage 0-69904

foams continued

- syneresis in Plateau-Gibbs channels of foams with high press. gradients, capillary press. 0-74948
- urea-formaldehyde resins, book 0-73114
- US characts. of open-cell polyurethane foam layers for airborne appls. 0-96597

focused collision sequences *see sputtering***focusing***see also self-focusing*

- adaptive focusing of light in inhomogeneous nonlinear medium, interf. criteria 0-99633
- atomic beam focusing by reson. radiation press., quantum fluctuations influence 0-58217
- charged particle motion in alternating elec. fields, scaling conditions 0-63903
- contact microscope for medical laboratory use 0-85540
- cyclotron, AVF, central region, changes of puller shape, axial focusing 0-74050
- cylindrical capacitor with oblique ends, ion optical coefficients determ., first-order focusing 0-63912
- deformation measurement, out-of-plane, using holographic interferometry and speckle photography, comparative accuracy 0-78804
- diffused channel waveguides, direct index meas. 0-87562
- dynamically focused electronic sector scanner based on CCDs 0-98042
- electron micrograph, 500 kV, atomic resolution, computer image processing 0-100149
- electron microscope resolution improvement for crystal structure imaging and atomic movement dynamic obs. 0-70090
- electron microscopy, imaging of thin phase objects, tilted and extended 0-99617
- electron probe, compensation of aberrations, dynamical focusing with stigmator 0-87291
- electrons, transverse focusing at large emitter currents (*Russian*) 0-87280
- electrostatic crossed lens, for electron microscopic devices 0-87289
- electrostatic energy filter, telescopic, with cylindrical mirror analysers 0-87296
- electrostatic lenses, focusing of GeV particle beams 0-74061
- fibre, gradient-index light-focusing, image enhancement 0-69501
- flat-field spectrograph design, holographic grating appl. 0-68264
- focometer, F-1, for lens focal length meas. 0-64138
- gas, resonance four-photon shift, optimal focusing of high-power pumping 0-95574
- gradient-index imaging, theory 0-69331
- grainless focusing screen for cameras and microscopes, light scatter reduction appl. 0-101836
- grating coupler, chirped and curved, for focusing beam 0-78979
- gravitational lens effect, focusing by slowly rotating relativistic spherical mass 0-105155
- image formation with ultracold-neutron waves 0-78752
- instrument focusing to take account of eye accommodation 0-101811
- laser beam focused in plane target, jet form., investigation using wavefront method 0-75103
- laser focus movement, nonlinear optical technique 0-74446
- lens, gradient-index rod, evaluation by imaging 0-69485
- lens-array photographic system, depth of sharp focusing, resolution 0-62763
- light beam, in moving nonlinear media, using gradient method 0-106578
- magnetic prism, design, for TEM energy filter 0-86523
- magnetic spectrometer, corrected second-order aberrations 0-87013
- microscope, focusing technique for digital image anal. system 0-68250
- microscope objective, piezoelec. and electrodynamic automatic focusing servo mechanisms 0-73445
- neutrons, imaging and focusing by zone plate 0-106433
- optical fibre preform, refractive index profile and cross-sectional geometry meas. method 0-91893
- optical microscope, accommodation focusing control 0-82814
- optical storage focus error detection, skew beam and Foucault knife-edge techniques 0-102649
- optimum focusing conditions for twelfth optical harmonic generation (*German*) 0-64098
- pancratic objectives, aberration stabilisation, during focusing 0-102799
- particle accelerator, laser focusing, phase-adjusted 0-63434
- particle beams, superconducting magnets appl. 0-68990
- phase anomaly in focused light beams, intuitive explanation 0-99622
- plasma lower-hybrid waves, focusing and channelling during HF-breakdown of gas (*Russian*) 0-106890
- radiography, RMS focal spot, validity considerations 0-81691
- reflex cameras, lens-array focusing system tests 0-86479
- refractive index, profile determ. of light focusing rod, Interphako interf. microscopy method 0-101832
- rod, tapered gradient-index, geometrical optics 0-69322
- self-imaging multiplexer and branching couplers 0-106629
- Selfoc lens, aberration improvement by glass composition and ion exchange process parameter choice 0-69486
- single-polepiece magnetic lens axial field distrib. 0-69317
- single-polepiece objective and projector lenses for electron microscope 0-68326
- spherical particles beam, focusing by axisymmetric mag. fields 0-78755
- STEM, defocus and astigmatism, automatic correction method 0-68298
- STEM, non-optimal apertures 0-62801
- step-stare spaceborne optical system smear compensation by focal plane manipulation 0-82172
- stimulated Brillouin scatt., three dimensional, for focused Gaussian beam 0-69456
- stress wave focusing in paraboloids of revolution, internal fractures 0-83762
- symmetry properties of focused fields 0-83550
- TEM, contrast of fold domain boundaries and microsectors in polyethylene single crystals 0-107065
- US flaw detection, focusing probes 0-104383
- X-ray diffraction focusing, with (n,m)-positioning of crystals 0-87989
- CO₂ laser fusion system alignment by IR Smartt interferometer 0-74425
- CO₂ laser Gemini fusion system optical performance 0-74392
- CO₂ laser Helios fusion target positioning with orthogonal telescopes 0-74421
- N₂-He plasma, laser produced, high press. amplified stimulated emission 0-78843

focusing, particle *see focusing; particle optics***fog**

- aerosol size distribution by inverting spectral turbidity data 0-95796

fog continued

- California coast, marine fog: form and fog-stratus systems development 0-77060
- DMSP visible imagery, fog as cause of anomalous grey shades 0-77111
- glory formation, diff. model 0-82053
- heterogeneous photocondensation process initiation by laser radiation 0-67410
- IR broadband transmission rel. to meteorological events 0-85744
- Irkutsk airport, fog prediction model 0-85736
- laser beacon visibility in fog, range extension technique 0-101434
- laser beam off-axis propag. in low visibility weather conditions, non-small-angle scatt. 0-102621
- real-time holographic viewing in moving fog 0-102676
- spectral transmission data, IR propag. and performance modelling 0-90218
- steam fog in Fenlands, obs. after heavy rain, (1979 May 1) 0-98431
- temperature profiles in fog, meas. via shipboard use of low-level atmospheric thermograph 0-105073
- thermal emissivity 0-95795
- visual range and radiation-fog microphysics 0-109195
- water evaporative cooling, convection and mass transfer, fog formation in boundary layers 0-79293
- water evaporative cooling, heat and mass transfer coeffs., fog formation effects 0-79294

foils

- alloy, solute redistrib. during in situ irradiation in HVEM 0-107324
- alloy, X-ray fluorescence correction in thin foil analysis 0-85256
- alloy, X-ray microanal., thin foils, data correction for absorpt. effects 0-85255
- β -brass, spinodally decomposed, morphology and characts. 0-60863
- cellulose nitrate thin foil manufacture for α particle track detector (*Spanish*) 0-74091
- electron microscopy on etched thin foils, comparative SEM, STEM and TEM analysis 0-100144
- electron probe analysis, orientation effects in quantitative X-ray microanal. 0-85259
- Incoloy 901, foil prep. for TEM exam. 0-88001
- metal foils, low energy heavy ion multiple scatt. in finite range potential 0-70283
- metal powder, method for TEM study 0-84038
- mounting technique, wrinkle-free 0-77767
- steel, microanalysis by energy dispersive X-ray spectrometry (*French*) 0-85250
- steel, stainless, TEM foils, white band contrast 0-75134
- thermally induced structural changes, specimen surface influence 0-103559
- thickness measurement method, X-ray microanal. technique 0-85256
- X-ray microanalysis in electron microscope (*French*) 0-61191
- Ag, conduction electron spin disorientation at surface 0-75855
- Ag foil, interface with liq., oxide props., refl. and scatt. light spectroscopy 0-60702
- Ag, surface plasma-wave reflectance and roughness-induced scatt. 0-66228
- Ag, surface-plasmon resonance, roughness-induced wavelength corrections 0-108288
- Al, anodising, behaviour of emulsion particles during electrodeposition 0-104357
- Al, α -particle irradiation under fusion reactor conditions, He bubble alignment during deform. 0-107345
- Al foil, electrical conduction, electron mean free path, surface scatt. 0-88535
- Al foil, internal friction changes during low temp. plastic deform. (*Russian*) 0-100304
- Al foil, laser irradiation, fracture props. (*Russian*) 0-108523
- Al foil, secondary electron emission due to α -particle irradiation. (*Russian*) 0-66344
- Al foil electrolytic perforation, surface film phase composition obs. (*Russian*) 0-61004
- Al, high strength, vapour deposited on curved surfaces, quantitative characterisation 0-80144
- Al, influence of O₂-pressure on oxidation rate, TEM study 0-104355
- Al-Mg, oxidation in O₂ atm., TEM study 0-104356
- Au, grain boundary structure, high resolution HVEM 0-103360
- Au, spatial resolution of X-ray microanalysis 0-101065
- Au, thin film bicrystal, diffraction effects from inclined grain boundaries 0-103362
- Au, thin foil, enhanced electron energy deposition heated, soft X-ray vacuum UV spectra 0-80901
- C foil, extreme UV induced forward photoemission 0-76137
- C foil, H₂⁺ transmission yield 0-100732
- C foil, He⁺ and HeH⁺ impact, quantum beat pattern depend. on foil thickness 0-58343
- Cr, irradiation with 1.2 MeV Ar⁺, electron diffraction study 0-103397
- Cr, K α incident, equilib. charge state distrib. and multiple scatt. angles 0-59532
- Cfoil, HeH⁺ impact, dissociation, emitted light polarisation meas. 0-58361
- Cr foil, laser irradiation, low-angle X-ray scatt., angular block misalignment and hardness (*Russian*) 0-103413
- Cu, conduction electron spin disorientation at surface 0-75855
- Cu foil, laser irradiation, low-angle X-ray scatt., angular block misalignment and hardness (*Russian*) 0-103413
- Fe-Cr-Ni, in situ oxidation in HVEM 0-104354
- Ge, [110] oriented, seven-beam lattice images of defects 0-107209
- Ge, epitaxial growth of very thin electron microscopy specimens 0-100793
- Mo, device for electrolytic thinning from wire, for electron microscopy 0-85105
- Mo foil electrolytic perforation, surface film phase composition obs. (*Russian*) 0-61004
- Na₂O-CaO-SiO₂ glass foils, HVEM in-situ straining expts. 0-104216
- Nb, electron energy losses due to H, obs. by scanning TEM 0-79850
- Ni foil electrolytic perforation, surface film phase composition obs. (*Russian*) 0-61004
- Ni superalloy, STEM microanal. of precipitates and their nuclei 0-81067
- Ni thin foil, single crystal, cyclically deformed, HVEM in-situ deform. study 0-103339
- Ni-Al(Si), ion irradiation, surface effects on precip. morphology 0-104168
- Ni-Co-Cr TEM foils, white band contrast 0-75134
- Pb, type I supercond., crit. current density, pinning force density, shadow electron microscopy obs. 0-88696

foils continued

- Si, computer simulation of high resolution images of defects 0-107208
 Sn foils, 1-3.5 GeV electron impact, transition X-ray emission, comparison with theory (*Russian*) 0-60704
 Ti foil electrolytic perforation, surface film phase composition obs. (*Russian*) 0-61004
 V, electron energy losses due to H, obs. by scanning TEM 0-79850
 Zr, foil bending by in situ ion irradi., neutron damage simulation, room temp. oxide growth 0-107342

Fokker-Planck equation

- absorptive optical bistability, transmitted light spectrum and dynamic response function 0-99789
 absorptive optical bistability transient, local relax., quantum statistical treatment 0-91838
 atomic system, two-level, collective behaviour in external field, thermodynamics 0-86236
 atoms, reson. radiation force, quantum mech. fluctuations, influence on at. motion 0-58233
 bistable potentials, diffusion, Schrodinger and Fokker-Planck equations 0-62528
 butane, flexible chain molecules, momentum space diffusion eqns. 0-75142
 channelling of relativistic protons in bent crystals, theory 0-96581
 chemical systems, single variable, master eqn. approximation by Fokker-Planck type eqns. 0-77702
 colloidal solution, flow alignment, transition from isotropic to nematic phase 0-84060
 constrained systems, Hamiltonian construction and diffusion eqns. derivation 0-73258
 coupled random walk process theory, Fokker-Planck eqn. calcs. 0-77710
 DITE Tokamak, beam driven current meas. 0-106940
 eigenvalues of Fokker-Planck operators 0-98863
 electron distribution function, steady state response to applied electric field, e^-e^- collisions 0-83883
 fast charged particle, dechannelling from planar channel, stochastic theory 0-96579
 ferrofluids, dissipative process in non-homogeneous mag. field 0-59119
 fluctuations and nonlinear irreversible processes. II 0-82724
 gases, weakly ionised, electron motion, stochastic theory of homogeneous systems, review 0-77735
 gross variables, microdynamics and nonlinear stochastic processes 0-101754
 heat flux fluctuations, Fokker Planck eqn. in extended irreversible thermodynamics 0-86205
 Kramers equation, eigenvalues calc., Fokker-Planck eqn. for Brownian motion in a potential 0-86215
 Langevin equations, Fokker Planck Dynamics approach 0-57194
 laser Fokker-Planck equation solutions, polynomial expansion method 0-91771
 laser plasmas, hot electron energy relaxation and transport (*Japanese*) 0-96347
 limit cycle fluctuations near bifurcation point, Fokker Planck, Langevin eqn. calcs. 0-77709
 Liouville problem, quasi-particle dynamics from a given kinetic eqn., inverse 0-101749
 LMFB materials, interstitial loop nucleation and growth during irradiation, Fokker-Planck equation, numerical soln. 0-57857
 LMFB materials, interstitial loop nucleation and growth during irradiation, Fokker-Planck equation, numerical soln. 0-68796
 molecular rotation and translation interaction 0-69262
 moment and Fokker-Planck eqns. for growth and decay of small objects 0-82709
 multidimensional bistable potential, diffusion, WKB calc. 0-101770
 multigroup formalism to solve the Fokker-Planck equation characterizing charged particle transport 0-68159
 multistationary behaviour systems, stochastic approaches 0-98854
 nonlinear second order system, eigenfunction expansion solutions of Fokker Planck eqn. 0-73172
 nonMarkovian Langevin n-dimensional eqn. approx. 0-57191
 optical bistability in bad cavity limit, Fokker Planck eqn. approach 0-64116
 optical stability, absorptive, two-level atom system, photon antibunching 0-58486
 path integral soln. for eqn. with spatial coordinate-dependent moments 0-77688
 plasma, electron beam injection, collisional relax., Fokker Planck computational treatment 0-64738
 quasiadiabatic solutions, time-dependent drift, fluctuation coefficients 0-90785
 stochastic one-variable system, growth of fluctuations from marginal eqn. 0-86213
 stochastic quantisation processes, review, Markov processes, Martingales, quantum dynamics 0-94969
 superionic conductors, theoretical models, review 0-107465
 symmetry breaking in the decay of unstable states 0-57188
 Tokamak plasma, beam driven currents, trapped electrons effect 0-70011
 toroidal plasmas, beam driven currents, trapped electrons effect 0-70011
 transport equation renormalisation 0-82732
 transport properties of electrons with narrowly defined bands at low temp. (*Russian*) 0-103656
 trapped ion, laser cooling, theory 0-58414
 triatomic molecules, C_2 , symm., vector statistical distrib., mol. dynamics computer simulation 0-63734
 unstable state decay, trajectory time spread, laser photon statistics 0-83585
 weak diffusion master eqn. expansion, critical points 0-57228
 ^{238}U fission as multi-dimensional Brownian motion, Fokker-Planck soln. (*Chinese*) 0-99197

food processing industry

- ultrasonic inspection, welded joints in sugar extraction diffusion apparatus 0-93703

forbidden gap *see energy gap*Forbush decreases *see cosmic ray variations*

force

- see also atomic forces; coercive force; Coriolis force; force measurement; molecular force constants; nuclear forces*
 education, momentum flow as force, alternative conceptualisation for teaching mechanics 0-67993

force continued

- Faraday and the concept of force 0-57048
 Galaxy disc, local K_z -force field rel. to interstellar matter z-distrib. 0-62271
 force constants *see lattice dynamics; molecular force constants*
 force measurement
see also dynamometers
 bone mechanical properties characterisation by dynamic response 0-76782
 cellular elastomer selection for use in biomechanical capacitive force transducers, measuring device (*German*) 0-85545
 fibre optical interferometers for length, temp., pressure and force meas. 0-98971
 friction apparatus for meas. normal displacement of sliding body 0-99977
 load cell design and development for materials testing 0-105628
 load cells and force transducers 0-86276
 semiconductor force transducer suitable for use with small muscles 0-72395
 shearing forces on the sole of the foot, meas. system 0-72342
 state of the art and development prospects in the USSR 0-62621
 strain gauge dynamometer system, body of rotation form, non axially symm. load 0-73350
 tensile force measurement instruments developed as first order reference standards (*German*) 0-105635
 tensometer, semicond., with parallel channel, operation principle (*Russian*) 0-73352

force meters *see force measurement*forecasting, technological *see technological forecasting*

forecasting theory

- pollution episodes in Venetian region, real-time forecasting via Kalman predictor 0-82046
 streamflow, model, identification of seasonal water supply forecasting models using Akai's information criterion 0-67386
 time series, conference, Nottingham, England (Mar. 1977) 0-82580

forging

- steel, friction and wear during hot forging 0-89358
 steel, powder forged, fatigue, surface treatment effect 0-85048
 Fe, powder-forged, elastic const., density depend. 0-84987
 Fe-C (graphite, 0.3 wt.%), powder-forged, elastic const., density depend. 0-84987
 NaCl Czochralski crystal growth for large CO_2 laser windows 0-74525
 Ti-Al-Sn, alloy 6242, dynamic effects of flow and fracture during isothermal forging 0-76343

form factors, atomic *see atomic structure*

form factors (elementary particles)

- see also form factors (nuclear)*
 $(\phi)_6$ theory, composite particle form factor, asymptotic behaviour 0-86595
 baryon resonances, EM transitions, multipole moments in single quark transition model 0-62985
 composite particle EM form factors, asymptotic behaviour 0-62927
 double-logarithmic quark and form factors and the evolution of parton jets 0-68421
 hadron interactions, inclusive, large momentum transfer, quark counting, EM form factors 0-68498
 hadronic form factor asymptotics in QCD (*Russian*) 0-62983
 hadronic wave functions at short distances and the operator product expansion, QCD tests 0-57564
 mesons, bound state wave function, probability interpretation, form factors, Bethe-Salpeter eqn. (*Chinese*) 0-101930
 quarks, EM form factors in instanton fields 0-99102
 scaling, deep inelastic scattering, form factors, Tauberian theorems in quantum field theory 0-68375
 singlet quark form factor exponentiation in leading logarithm approx. 0-91091
 weak nucleon formfactors in modified vector dominance model (*Russian*) 0-68437
 D inelastic screening, form factor at $t \neq 0$ 0-91070
 $D \rightarrow K\pi\nu$, charm-changing weak hadronic current, models 0-57585
 dnp vertex form factor, ed elastic scatt. at high momentum transfer 0-82977
 ed \rightarrow ed, nucleon forces, meson exchange current effects, impulse approx., review 0-57603
 ed elastic scatt. at high momentum transfer, form factors at γNN and dnp vertices 0-82977
 $e^+e^- \rightarrow$ jets, on-shell QCD quark form factor from two particle correlations 0-86740
 $e^+e^- \rightarrow \pi^+\pi^-(K^+K^-)$, $\sqrt{s}=1.5$ GeV, EM timelike form factors for π and K 0-91089
 eN elastic scatt., pol. e, nucleon form factors, P violating symmetry, Weinberg-Salam calcs. 0-68461
 $\eta \rightarrow \mu^+\mu^- \gamma$, branching ratio and η EM form factor 0-105899
 γNN vertex form factor, ed elastic scatt. at high momentum transfer 0-82977
 K, bound state relativistic effective range approx., EM form factors and charge radii 0-95270
 K $^-$ EM form factor direct meas. from elastic scatt. cross section 0-86716
 $K_1^{*-} \rightarrow \pi^+\pi^-\nu$, K^{*+} decay spectrum and form factors 0-57587
 $K_1^0 \rightarrow \pi^+\pi^-\nu$, transverse polarisation of μ , violation of time-reversal invariance 0-68448
 $K_1^0 \rightarrow \pi^+\pi^-\nu$, form factors 4-momentum depend., μ e universality (*Russian*) 0-68449
 K_{14} decay vector form factor (*Russian*) 0-105900
 $N \rightarrow \Delta(1232)$ electromagnetic transition form factor and pion-nucleon dynamics at moderate energies 0-57598
 n electric polarisability, from photoabsorption cross-section 0-57597
 N form factor, isovector, meson field theory, pseudoscalar πN interaction 0-62986
 N form factors, weak, asymptotic behaviour within QCD dipole and triple pole formulae 0-62987
 N* EM transition form factors 0-102049
 $np \rightarrow np$, polarisation phenomena in close-to-forward scatt., intermediate energy region 0-78086
 ν , EM form factors and mag. moments, Weinberg-Salam model and extensions (*German*) 0-62904
 p electric polarisability, from photoabsorption cross-section 0-57597
 $pd \rightarrow e^+e^-n$, proton EM form factors, pp annihilation (*Russian*) 0-68457

form factors (elementary particles) continued

- $pp \rightarrow e^+e^-$, magnetic nucleon form factor, p-meson type contribs. 0-57596
 $pp \rightarrow pp$, polarisation phenomena in close-to-forward scatt., intermediate energy region 0-78086
 π , modified quark loop model, form factors, struct. functions, radiative decay 0-91088
 π EM form factor asymptotics in QCD perturbation theory, partonic interpretation (*Russian*) 0-62984
 π EM form factor factorisation and asymptotic behaviour in QCD 0-91090
 $\pi \rightarrow e \gamma$ and $SU(3) \times SU(3)$ σ -model 0-78054
 π form factors, axial-vector and structure dependent, vector meson dominance model 0-62989
 $V \rightarrow \rho \mu^+ \mu^-$, vector meson decay EM form factors in bag model (*Russian*) 0-62982

form factors (nuclear)

- [CC] $^{12}\text{C}(\gamma, \pi^+)^{12}\text{B}$, nuclear critical opalescence study 0-105988
 deuteron form factors and spectroscopic factors in heavy spherical nuclei, shell model (*Russian*) 0-63078
 EM isovector form factors of bound nucleons 0-78134
 few nucleon correlations from high energy scatt., review (*Russian*) 0-68549
 momentum and mass distrib., form factors, short range correlation effects 0-105959
 off shell form factor model, NN scatt. appl. 0-86800
 particle-vibration coupling form factor from simple model 0-57663
 radial wave functions of valence nucleons 0-73788
 rotational nuclei, A=159-181, transverse form factors from projected HF approach 0-105965
 (e, e'), cross section near quasielastic maximum, shell and optical models (*Russian*) 0-91179
 NNN bound state problems, hyperspherical harmonic expansion, review 0-91136
 $^{207}\text{Pb}(e, e')$, transverse scatt. amplitude suppression, form factors, neutron hole states 0-91129
 $^{27}\text{Al}(e, e')$, 70-340 MeV, odd parity state electroexcitation, form factors, transition probabs. 0-78208
 ^4C , A=12, 13, nuclear critical opalescence, M1 form factor, pion field and condensation 0-73809
 $^{12}\text{C}^1(T=1, 15.1 \text{ MeV})$ state excitational pionic modes, M1 form factor for (p, p'), (e, e') 0-78195
 $^{12}\text{C}^2$, level, transverse EM form factor, convection current contrib. 0-63076
 ^{12}C M1 form factor, pion field critical opalescence, ρ role, polarisation phenomena 0-68552
 ^{12}C M1 form factor, pion field, rho meson role 0-105970
 $^{12}\text{C}(K^+, K^+)$, form factors, cross sections, interior probing capability 0-78366
 $^{12}\text{C}(\rho, \alpha)$, 45.2 MeV, cross sections, finite range DWBA anal., cluster form factors 0-68666
 $^{42}\text{Ca}(p, t)$ form factor, hole and continuum contribs. for pick-up reactions 0-78256
 ^{57}Co , ($3/2^+$ state), anomalous analyzing power, DWBA calc. from $^{60}\text{Ni}(p, \alpha)$ 0-86894
 $^{56}\text{Fe}(e, e')$, Coulomb form factor for $O^+ \rightarrow 4^+$ transition, collective 4^+ states, shell model 0-57664
 $^1\text{H}(\gamma, \pi^+)$, 3.4-18 GeV, π NN form factor and differential cross sections, one pion exchange 0-68526
 ^1H charge operator, retardation, quasipot. eqns. and rel. corrections 0-99122
 $^1\text{H}(e, e')$, 56.4 MeV, cross sections, form factors, meson exchange current contrib. 0-68649
 $^1\text{H}(e, e)$, EM form factors, relativistic formulae, moment corrections 0-63075
 $^1\text{H}(e, e)$, form factors, tensor pol., and two-nucleon force calcs. 0-106045
 $^1\text{H}(p, p)$ large angle elastic scatt., d form factor at large q^2 0-102189
 $^1\text{H}(\pi, \pi)$, 142, 256 MeV, form factor-backward scatt. correlation, tensor polarisation 0-99189
 ^1H , EM form factors, 3-nucleon wave function calc. 0-95302
 ^1H , meson exchange currents, effect on charge form factors 0-105990
 ^1H , EM form factors, 3-nucleon wave function calc. 0-95302
 ^1H , meson exchange currents, effect on charge form factors 0-105990
 ^1H , nuclear charge form factor, two-boson exchange charge density π, ρ, ω exchanges 0-63073
 ^1H , one-body charge form factor computer code listing 0-57673
 $^1\text{H}(e, e)$, charge formfactors, second Born approx. and pole model 0-78133
 $^1\text{H}(e, e)$, relationship to $^1\text{H}(\pi^-, \pi^-)$ 0-78323
 $^1\text{H}(\pi^-, \pi^-)$, 145, 180 and 195 MeV, relationship to $^1\text{H}(e, e)$ 0-78323
 $^1\text{H}(\pi^-, \pi^0)$, form factor sensitivity in Glauber multiple scatt. formalism 0-105964
 $^4\text{He}(\pi^-, \pi^- p)$, 5 GeV/c, quasielastic scatt., cross section, form factor, final state interactions 0-99190
 ^4He nuclear charge density determ. using form factor analyticity 0-63077
 $^6\text{Li}(e, e')$, 102, 123 MeV, excitation form factor, $^3\text{H}-^3\text{He}$ cluster model 0-78190
 $^6\text{Li}(e, e')$, 76-141 MeV, form factors, appl. to (π^-, γ), phenomenological model 0-83068
 $^6\text{Li}(e, e)$, charge formfactors, second Born approx. and pole model 0-78133
 $^6\text{Li}(e, e)$, elastic and inelastic charge form factors from shell model wave functions 0-68523
 ^7Li charge form factor with resonating group wave function, quad. moment, charge radius 0-102110
 ^7Li , 3α forces, ground state energy and form factor 0-86817
 $^{16}\text{O}(e, e')$, 80-165.7 MeV, giant dipole and quadrupole resonances, form factors 0-102168
 $^{208}\text{Pb}(e, e')$, 2⁺ giant resonance twist mode excitation, B(M2) values, form factors 0-78246
 ^{208}Pb region, mag. transition strength, core polarisation effects, form factor shape 0-86850
 $^4\text{Si}(e, e')$, 126-293 MeV, A=28, 29, levels and form factors, particle-phonon coupling anal. 0-105977
 $^{28}\text{Si}(e, e')$, 6⁺ T=1 resonance form factor, mag. strength quenching, meson exchange currents 0-86882

form factors (nuclear) continued

- $^{90}\text{Zr}(\alpha, \alpha)$, form factor, coupling between real and imaginary optical potential 0-68680
 $^{90}\text{Zr}(e, e')$, 2⁺ giant resonance twist mode excitation, B(M2) values, form factors 0-78246

formal logic

foundational studies, A. Mostowski, book 0-57015

formation, heat of *see* heat of formation**forming processes**

- see also* casting; electroforming
 explosive forming, computer numerical simulation 0-59560
 fusion reactor, TFTR outer poloidal field coil insulation and mould design 0-91261
 high strain rate processes, review 0-84864
 hot metal, dynamic yield characts. during multistage deform., plastometer design 0-85135
 optical element polishing simulation calc. and results (*German*) 0-87566
 PVC, oriented mouldings, struct. order 0-60896
 shells, plastic, explosive forming, computer numerical simulation 0-59560
 steel, high-speed tool, properties, powder metallurgy prep. method (*Czech*) 0-60800
 Al-Ca-Zn (5.5 wt.%) superplastic sheet alloy, mechanical properties, superplastic forming behaviour 0-60920
 Al-Mg-Si, type 6100, microstruct. characts. influence on formability, heat treatment 0-81090
 Na₂O-CaO-SiO₂ glass, vol. relaxation and thermal history during forming process 0-70130

FORTRAN

- complete computer program in FORTRAN, for analysis of variance and means 0-98792
 PWR dynamical behaviour modelling in FORTRAN 0-91217

Foucault currents *see* eddy currents**fountain effect** *see* superfluid helium-4**Fourier analysis**

- see also* Fourier transforms; harmonic analysis; waveform analysis
 2A 0311-227 optical counterpart, binary star, light curve Fourier anal. 0-82549
 β Canis Majoris, β Cephei star, Fourier anal. of radial vel. changes 0-105246
 β Carinae, Cepheid variable, Fourier anal. of light var. 0-90442
 Cherenkov effect in spatially dispersive media 0-105516
 diffusion-convection equation, stability of finite difference approximations 0-82730
 Earth surface temperature, determ. of diurnal var. in mountainous terrain 0-82011
 eclipsing binary stars, light curve analysis by Fourier techniques 0-72993
 eclipsing binary stars, light curve analysis by Fourier techniques 0-72994
 electron micrograph, 500 kV, atomic resolution, computer image processing 0-100149
 electron microscopy, conically tilted projections, 3-D reconstruction 0-99618
 ν Eridani, β Cephei star, Fourier anal. of radial vel. changes 0-105246
 forces exerted in walking and running 0-94266
 gamma ray spectra anal., fast Fourier transform (*Chinese*) 0-77762
 geophysical data acquisition (*Italian*) 0-102954
 heat conduction, nonlinear Fourier eqn. soln., minorant-majorant aprox. 0-79105
 inhomogeneous medium, effective cond., iteration series and variational estimates, Herring method 0-70663
 parallel optical Fourier transform techniques for Fourier spectroscopy 0-95161
 physical optics farfield inverse scatt., mathematical inversion technique for nondestructive eval. 0-69580
 pinhole and continuous projections, limited angle 3-D reconstruction 0-61667
 resonant antenna system, anomalous radiation and electrodynamic characts. 0-69302
 scattering, inverse problem, determ. of shape of cylindrical obstacle 0-83543
 σ Scorpii, β Cephei star, Fourier anal. of radial vel. changes 0-105246
 segmental cylindrical shells vibrations 0-58958
 solitary wave, diffraction by circular island in ocean, shallow-water theory (*French*) 0-83803
 stellar spectral line profiles, Fourier deconvolution for mag. fields detect. 0-72949
 tomography, computed, 3-D image reconstruction, Fourier deconvolution method 0-61669
 truncated autocorrelation functions, numerical inversion 0-57097
 Cu, bulk and (001) film, extended tight-binding calcs. 0-70592

Fourier series *see* series (mathematics)**Fourier transform optics**

- see also* Fourier transform spectroscopy
 2-D acoustic Fourier transform of optical images 0-74308
 aberrated diffraction pattern obs. with computer-generated holograms 0-102681
 ambiguity processing by joint Fourier transform holography 0-58468
 analogue data processing systems, polarised modulation of light (*Russian*) 0-91884
 apodisation, optimal, Fourier spectrometry 0-99641
 biological cell size meas. by static light scatt. Fourier transform 0-81793
 chirped grating lenses anal. 0-87563
 chromosome metaphase spread, automatic finding, prep. and eval. of object spectra 0-98168
 circularly symmetric positive filter function realisation by transparent rings 0-87343
 coherence properties modification of light beam, optical processing appls. 0-78769
 coherent information processing by a pair of lenses in spherical wave illumination 0-95816
 coherent optical implementation of generalized two-dimensional transforms 0-95835
 coherent optical iterative extrapolation of 2-D band-limited signals 0-78780
 colour image archival storage using Fourier multicolour holograms 0-102674
 colour image evaluation from tristimulus values transfer functions measurements 0-87333
 computer-generated hologram spectrum shaping and image reconstruction, iterative method 0-106475

Fourier transform optics continued

- confocal scanning microscope, image form. 0-68249
- correlation function of single-mode radiation in a quasi-classical approximation 0-95815
- cylindrical surface two-wavelength speckle pattern intensity distrib. at optical transform plane 0-106487
- deflection contour generation, Fourier filtering of white light speckle patterns 0-98881
- disordered crysts., optical transforms 0-78783
- driven equilibrium Fourier transform sensor operating at 100 MHz 0-74612
- education, geometrical optics, lens Fourier transform properties 0-57024
- electro-optical spatial light modulator resolution, stored point charge effects 0-106616
- electron optical systems, optimisation using orthogonal functions 0-63908
- fast image recognition by generalised harmonic analysis (*Russian*) 0-63930
- fibre waveguide mode properties, computation by propagating beam method 0-69502
- fibres, graded-index, multimode, differential mode delay and attenuation meas., optimal excitation calc. 0-99842
- fibres with arbitrary index profile, pulse propag. and dispersion 0-78984
- fluid section flow pattern speckle photography 0-103096
- geophysical mapping and remote sensing by optical filtering 0-101458
- graded-index optical fibres, mode eigenfunction computation propagating beam method 0-95988
- high-contrast point-image holography in turbulent atmosphere (*Russian*) 0-63943
- hologram recording in optical system with synthetic aperture 0-95852
- holograms, stacked Fourier, reconstruction 0-87348
- holographic disc with high data transfer rate, audio response memory appl. 0-58477
- holographic lensless Fourier transform, spherical wave illum. 0-74312
- holographic lensless Fourier transform, wavelength difference between recording and reconstructing wavefronts 0-58471
- image irradiance moments optical calc., wave optical accuracy limitations 0-74302
- image reconstruction, iterative computer method 0-102634
- implicit sampling for noncoherent optical data processing 0-99652
- incoherent optical discrete Fourier transform processing system 0-74303
- information encoding by complex zeros, analytic Fourier optics, comment 0-87326
- integrated optical multimode waveguides, Fourier domain propagation calc. 0-64219
- interferometric determination of complex Fourier spectra 0-87327
- laser pulse autocorrelation by optical processing of Fabry-Perot spectrograms 0-58465
- lens, spatial invariance test 0-69492
- lens design, least squares fitting of Zernike's polynomials to wave aberration function 0-83660
- light pencil and interferometer for amplitude and phase profiles 0-102680
- long-wave imaging with super-resolution by wavelength diversity 0-102675
- matched filter visibility effects on the correlation function 0-96031
- matched filtering improvements for coherent optical pattern recognition 0-78786
- microscope, scanning and conventional, Fourier imaging of phase information 0-73444
- multichannel long integration time techniques 0-91751
- object restoration beyond Rayleigh limit in presence of noise 0-102661
- optical fibre diameter measurement using fast Fourier transform 0-91894
- parallel optical Fourier transform techniques for Fourier spectroscopy 0-95161
- paraxial approx. of scalar diffraction theory without using Kirchhoff integral 0-95838
- particle motion detection in transparent liquids, Fourier transform acousto-optical system performance 0-87680
- pattern recognition by thermoplastic complex filter 0-99656
- perceptual coding in the cosing transform domain 0-102635
- photodichroic spatial light modulator for joint Fourier transform correlation 0-106617
- plano-plano interferometer modes, FFT computation, Fresnel numbers 0-86392
- projector having a thermoplastic target and operator's eye, charact. 0-96023
- radiographs, signal and graininess relationship 0-95808
- real-time incoherent subtraction of irradiance 0-74301
- reconstruction, three-dimensional, from planar projections 0-99639
- regularized object restoration, resolution beyond the diff. limit 0-87324
- scatterplate interferometer, scalar diffraction theory 0-73432
- scatterplate interferometer principles, limitations and tolerances 0-73436
- self-imaging, light-optical experiments (*German*) 0-63938
- speckle interference fringes, lens aberration effects 0-105700
- spherical-cylindrical lens combination, combined 1-D image-orthogonal Fourier transform processing 0-58658
- surface-wave acousto-optic signal processors 0-102640
- systems analysis using two-dimensional FFT algorithm 0-78986
- tomography, transaxial scanners for reconstructing objects from their X-ray projections, review 0-102632
- two-dimensional structure in-plane vibr., stress analysis by laser speckle method 0-103006
- uneven interface of media with different refractive indices, statistical charact. of images 0-87331
- variable-scale single-lens optical transform systems 0-58656
- CO₂ laser Antares fusion system optical diffraction computation 0-74424
- CO₂ laser fusion system optical design and analysis 0-74391

Fourier transform spectroscopy

- absorption cell for heated gas IR spectroscopy 0-98987
- air pollutant measurement by absorption spectrum Fourier transform 0-81514
- apodisation, optimal, Fourier spectrometry 0-99641
- capillary column gas chromatography at nanogram resolution using dual beam Fourier transform IR spectroscopy 0-89554
- coal, cleaved surface, photoacoustic IR spectra 0-87104
- coal and mineral content characterisation by Fourier transform IR spectroscopy 0-104474
- complex systems, pyrolysis and combustion charact., Fourier transform IR spectroscopy 0-86462

Fourier transform spectroscopy continued

- differential absorption at high modulation frequencies using a Fourier transform infrared spectrometer 0-95160
- diffuse reflectance Fourier transform IR spectroscopy using diamond anvil cell 0-101855
- double-beam spectrometer, for weak IR absorpt. meas. 0-105725
- double-pass rapid-scanning spectrometer, for plasma diagnostics 0-103190
- electron spin echo envelope modulation, 2-dimens. Fourier transform 0-63680
- far IR, spectrum distortion by multiple reflections using Michelson interferometer 0-82837
- far IR and near MM wave power energy meter calibration 0-57373
- far IR modular Fourier interferometer construction, very high resolution 0-57401
- field meas. Fourier transform spectrometer 0-86470
- fixed groove depth lamellar grating Fourier transform spectrometer 0-77885
- Fourier transform NMR spectroscopy, review 0-104486
- FT NMR, digitisation and data processing 0-95115
- gases, high resolution vibr. spectra by Fourier transform far IR spectroscopy 0-86461
- ghostline intensity in far IR 0-73480
- interferometric data from GC Fourier transform IR spectroscopy, functional group anal. 0-89548
- interferometry, multimode fibre optic, applications 0-86387
- ion cyclotron reson. mass spectroscopy, freq. sweep excitation 0-101810
- IR, dual beam Fourier transform spectrometer, sensitivity improvement by using Digilab 496 interferometer 0-90910
- IR Fourier spectrometers, grid polarisers 0-105724
- IR spectrometer software package for phase correction 0-95162
- Ku-band microwave Fourier transform spectrometer, construction, appls. 0-68265
- laser wavelength calibration using optogalvanic effect, atlas 0-62727
- light pipe gas cell, Au coated internally, for gas chromatography/Fourier transform IR spectroscopy 0-89555
- liquid chromatography effluents on line anal., micro liq. chromatography-interfaced Fourier transform IR spectrophotometer 0-73483
- Michelson Fourier transform stellar spectrometer 0-98552
- Michelson type Fourier interferometer and gaseous molecular spectra 0-68275
- microreactor assembly to study heterogeneous catalyst system, IR emission spectral anal. 0-98988
- multichannel long integration time techniques 0-91751
- multiplex and high throughput spectroscopy 0-95145
- narrowband optical signal, spectral width estimation 0-102627
- neopentane adsorbed on graphite, quasi two-dimens. fluid, NMR 0-102525
- new developments—passive heterodyne spectrosc. and diode laser absorpt. spectrosc. 0-95148
- NMR, computer programmable digital pulse generator 0-98959
- NMR, pulsed field gradient system 0-57353
- NMR spectrometer, magic-angle rot. 0-105688
- NMR thermometer, for multinuclear Fourier transform NMR 0-57292
- noise compensation, using improved InSb photodiode preamplifier circuit 0-73474
- NQR, electronics appls. 0-63668
- oxide crysts., Fourier transform IR spectroscopy of vibr. states at high temp. 0-97256
- parallel optical Fourier transform techniques for Fourier spectroscopy 0-95161
- pentachlorotoluenes, positional isomers, ¹³C Fourier transform NMR spectroscopy, struct. and compositional anal. 0-91576
- photoacoustic FT IR spectroscopy of liquid and solid samples 0-90911
- polystyrene, isotactic gel film, Fourier transform IR spectrum 0-104465
- power transmission spectroscopy, use of approx. expressions 0-98982
- pseudocolour density encoding, white-light, using contrast reversal 0-83560
- PTFE, γ-ray effects on 19 and 30°C phase transitions, Fourier transform IR spectroscopy 0-103387
- pulsed NQR, automation for Zeeman studies of single crystals 0-66066
- rapid scanning, very high resolution, data processing aspects 0-95150
- rapid scanning Fourier transform time resolved spectroscopy, practical aspects 0-86464
- reflection dispersive Fourier interferometer window eliminating backlash error 0-57402
- SNR enhancement by elec. filter compensation of slide velocity errors 0-95151
- solar spectra, Fourier transform spectroscopy at South Pole 0-98448
- solids, IR photoacoustic Fourier transformed spectroscopy 0-86465
- specimen holder for transmission dispersive far IR Fourier transform spectroscopy 0-86468
- spectrometer, balloon-borne, using focal plane detector array 0-95147
- spectrometer, high resolution ruggedized 0-95152
- spectrometer performance, instrumentation for assessment 0-95165
- stratosphere trace molecule Fourier transform spectrometer optical design 0-82099
- tetrachloromethane, fluid, collision induced light scatt. intensity 0-103955
- tetrahedral mol. fluids, collision induced light scatt. intensity 0-103955
- Tokamak, PLT, electron cyclotron radiation Fourier transform diagnostics 0-59292
- Tokamak diagnostic Fourier transform spectrometer calibration by liquid N₂ cooled microwave absorber 0-59304
- Tokamak far IR Fourier transform spectroscopic Michelson interferometer 0-59294
- Tokamak far IR Fourier transform spectroscopy resolution limits 0-59298
- variable-thickness cell for liquid MM-wave Fourier transform and laser spectroscopy 0-57403
- ArHBr, ArHCl, and isotopic forms, rot. spectra, mol. struct., mol. consts. 0-58246
- CO-myoglobin, mol. tunnelling, isotope effect, time resolved IR Fourier transform obs. 0-72126
- Cs₂ZnCl₄·Cu²⁺ electron spin echo envelope, Fourier transform ¹³³Cs modulation 0-58291
- DF⁺ prod. from D+PTFE, Fourier transform IR spectroscopy 0-87105
- FePO₄ coating on Armco Fe, Fourier transform IR absorpt.-reflection spectra 0-71500
- GaAs:Ge,Se transmutation shallow donor transition obs. 0-59925
- In_{1-x}Ga_xAs:P_{1-y} far IR reflection spectrum 0-60612
- K₂O₈Cl₆, Cl NQR spectra by Fourier transform methods 0-75879

Fourier transform spectroscopy continued

- KrHBr, KrCHI, and isotopic forms, rot. spectra, mol. struct., mol. consts. 0-58246
^{138,139}La, Fourier transform NMR 0-57354
^{14,15}N₂, Fourier spectrometry and IR emission spectra 0-83368
 NH₃, atmospheric, IR emission studied using Fourier spectroscopy 0-95628
 NO, Fourier transform spectra, intensity and self-broadening coeff. meas. 0-102503
 NO, IR emission Fourier transform spectroscopy, mol. rot.-vibr., RKR potential curve calc. 0-95618
 P I, IR spectra and HFS 0-91478
 P I, spectra and term anal. 0-91481
 Pb_{1-x}Ge_xTe magnetoplasma reflectivity and transmission spectra 0-71428
 SeF₆, in Kr matrix, temp. reversible IR spectral changes, site struct. dynamics 0-102505
 Si compensated monocrystal, IR absorption spectra 0-60644
 Si:O(C) wafers, impurity meas. by Fourier transform IR spectra 0-89030
 Si:O(C) wafers, impurity meas. by Fourier transform IR spectra at low temp. 0-89031

Fourier transforms

- see also *fast Fourier transforms; Fourier analysis; Fourier transform optics*
 acoustooptic effect calc., integrated 0-91944
 atomic scatt. factors and momentum densities, asymptotic form 0-74105
 diffusion equation, from space-time transport eqn., for anisotropic random media 0-62595
 diffusion equation, with non-linear terms, Fourier transform 0-103514
 discrete, passive sonar appl., using directional transducer arrays (*Spanish*) 0-69586
 elasticity, micropolar continua, static problems, nonhomogeneous eqn. of equilibrium, Green's functions and Fourier transforms 0-58905
 elastostatic problems, three-dimens., mode I loading, soln. method 0-92086
 electrodynamic suspension system, current coil interaction with semiinfinite superconducting sheet (*Russian*) 0-83539
 electron microscopy support film, phase contrast, Fourier spectrum analysis 0-95199
 gamma emitting organs, 2 and 3-dimens. digital Fourier reconstruction 0-101705
 granular solids, cracks, stress concentrations and shapes, Fourier transform methods 0-83761
 Hubbard and similar models, functional Fourier transform 0-84416
 Lie groups, nilpotent, smooth functions Fourier transforms 0-99067
 α Lyrae (Vega) rot. rate determ. from line profile photoelec. obs., Fourier transforms 0-77408
 musical scale, 12-tone, tempered Fourier transform 0-87671
 particle dimension determination, by direct Fourier cosine transformation, of expt. SAXS data 0-79624
 partitioned signal detection by discrete cross-spectrum analysis 0-91966
 quantum mechanical appl. of fractional order Fourier transform 0-82665
 radiographic imaging, 3-dimens. 0-85486
 radionuclide angiography technique for assessment of regional wall motion abnormalities 0-85488
 retinal photoreceptors, small angle X-ray data processing 0-81536
 sarcoplasmic reticulum membranes, small angle X-ray data processing 0-81536
 SL(2,R), universal covering group, Plancherel formula 0-68393
 Slater is orbital four centre mol. integrals, Fourier transforms 0-74104
 STEM and conventional TEM, bright-field image contrast and resolution 0-95200
 two-centre charge distrib., Fourier transform, STO general expression derivation 0-58119
 vision, receptive fields in area 17 of cat visual cortex, linear and nonlinear properties 0-104583

fractionation see *distillation***fracture**

- see also *brittle fracture; crack-edge stress field analysis; cracks; creep fracture; ductile-brittle transition; ductile fracture; embrittlement; fatigue; fracture toughness; stress corrosion cracking*
 adhesion bonds, stressed state and strength during breaking (*Russian*) 0-76478
 angled elliptic notch problem under biaxial loading, strain failure criterion 0-79235
 annular crack at spherical voids, stress intensity factor estimates 0-106757
 atomic chain, loaded, phonon model of breaking 0-70301
 beams in pure bending, distributed damage theory, cracks, fracture 0-64474
 bearings, plain, fracture 0-81170
 bone, crack velocity depend. of longitudinal fracture, bovine tibia 0-97965
 brass, two phase α/β bicrystal, transgranular slip and fracture across an interface 0-81150
 brass (37%Zn), workhardened thin specimens, fracture, anisotropy coeff. role (*French*) 0-104276
 brittle solid, atomically sharp cracks, TEM study 0-71729
 brittle solids, microfracture resulting from anisotropic shape changes 0-88254
 BWR fuel rod relocation, gap conductance anal. 0-83192
 cellulose fibre hydrolysability increase on gamma-irrad. (*Russian*) 0-61121
 ceramic building materials, breakdown kinetics by X-ray diffr. 0-108526
 ceramics, cracking characterisation by double torsion test (*French*) 0-104369
 ceramics, fracture mech., probability, micromech. models of crack growth 0-108571
 chemically-assisted fracture, atomic modelling at crack tips 0-106754
 composite materials, crack growth, conc. criterion 0-65146
 composite materials, stochastic fracture models, and strength test results statistical anal. 0-64470
 composite materials, unidirectional, three-dimens. fracture 0-64471
 crack growth law derivation, linear viscoelastic solids, fracture process zone concept 0-92088
 crack trajectory, unstable crack extension, stress field anal. 0-64462
 cropping and blanking, plastic flow, fracture, crack propagation 0-74761
 crystalline bodies, plastic strain and microcrack propag. 0-81199
 crystalline materials, fracture, stress relaxation effect 0-88256
 cutting tools, diffusive wear, mag. field effect 0-60985

fracture continued

- cylinder, rupture under wave conditions, stress-strain state for explosive loading (*Russian*) 0-79220
 defect dimension determination by acoustic emission 0-104381
 dislocation distrib., fracture relation, plastic flow at crack tip, slip line theory 0-64482
 dislocation structures, and fracture surfaces in fatigue (*Japanese*) 0-65144
 effect of simulated fission products on mech. props. 0-73922
 elastic body with plane cracks of normal fracture, 3D problems (*Russian*) 0-79219
 elastic crack tip enclave model, fracture stress 0-71730
 elastic fracture analysis, 2D linear, finite element anal. vs. the edge function method 0-99963
 epoxide resin, low temp. crack propag. 0-85020
 epoxy materials, crack blunting mechanisms 0-66624
 epoxy resin, plastic deform. effect on crack propag. 0-97563
 epoxy resins, expt. exam. of fracture by peeling method (*Russian*) 0-71761
 failure micromechanisms, classification according to failure type (*Russian*) 0-108557
 fibre cross-reinforced layered composites, moment effects in plane problem 0-64393
 fibre reinforced composites, fracture processes modelling, digital computer appl. 0-65147
 fibre reinforced composites, micro- and macrocracks 0-65148
 fibre reinforced composites, stress redistribution dynamics during fibre rupture 0-64394
 fibre reinforced composites, theory 0-89351
 fibre reinforced composites, unidirectional, mixed mode fracture 0-100302
 fibre reinforced composites with high work of fracture 0-81029
 fibre reinforced epoxy laminates, interlaminar failure 0-81207
 fibre reinforced laminated hybrid, tensile first cracking strain and strength 0-81175
 fibre reinforced plastic, props., implications for structural design 0-81174
 fibre reinforced plastics, bent thin-wall constructions, rupture 0-64472
 fission reactor materials, clad failure prediction during FBR overpower transiency, JANE code 0-78363
 flaws, 2D, irregularly shaped, fracture mechanics transfer function 0-99970
 fracture mechanism maps, usefulness 0-84245
 fragile materials, mech. props. and fracture mech. (*French*) 0-104274
 fusion reactor blanket structures, linear elastic fracture mech. anal. 0-86979
 glass fibre reinforced cement, durability in wet and dry conditions, fibre length and content effect 0-71726
 glass fibre reinforced plastic, fracture dynamics 0-100906
 glass fibre reinforced plastic laminates, failure models, reinforcement struct. effect 0-66641
 glass fibre reinforced plastics, cylindrical shells, compressive and flexural strength (*Japanese*) 0-81115
 glass fibre reinforced plastics, damage summation in nonstationary cyclic loading 0-60969
 glass fibres, flaw generation by indentation fracture technique 0-81156
 glass rods, compressively clad, residual stresses, comparison of optical and fractographic meas. 0-108539
 glasses and fragile materials, fracture energy, direct meas. (*French*) 0-104376
 grain boundaries decohesion energy, solute adsorption influence 0-65009
 granite, failure expts., pore press. stabilisation 0-90079
 graphite fibre filled polyimide composite laminates, space environment, phys. and mech. response 0-81140
 graphite ring, eccentric, under radial thermal load, stress state 0-76351
 high strain rate processes, review 0-84864
 Homalite-100 plates, modified compact-tension specimens, dynamic anal. 0-97561
 hot dry rock geothermal reservoir fracture mapping techniques 0-81419
 Inconel 600 safe-end cracking failure at Duane Arnold reactor 0-104295
 interfacial cohesion, adsorption-induced losses 0-65010
 Kapron fibre reinforced phenolic resin, fracture kinetics, interface props. 0-66640
 lattice instability theory 0-84244
 layered structures, intercalation, crack propag. theory 0-97559
 lecture on fracture toughness (*Japanese*) 0-90595
 linear fracture mechanics parameters, in fatigue life estimation, sensitivity study (*Japanese*) 0-64468
 linear theory of elasticity, in fracture mechanics 0-64458
 longitudinal-shear crack refraction, Wiener-Hopf method calcs. 0-87743
 macrofracture of solids, mechanism and kinetics 0-92600
 magnesite-dolomite refractories, tar bound, fracture and wear 0-104287
 mechanics of cracking, computing, based on three-dimensional models and finite element analysis (*German*) 0-58976
 metal rods, stress state and fracture in pulsed mag. field 0-81201
 metallised coating on polyethylene terephthalate film, fracture under laser irrad. (*Russian*) 0-76333
 metallurgical coke, mech. behaviour charact. (*French*) 0-104371
 meteoroids atmospheric breakup, effects on crater field form. 0-94760
 meteors thermal fracture, detached particles mean dia. 0-62081
 microanalysis of fracture surfaces by energy dispersive X-ray spectrometry with Si(Li) diodes (*French*) 0-89571
 microfractography (*Japanese*) 0-71841
 micromechanical models in risk anal. 0-108572
 Mylar film/adhesive/Al foil laminate, mech. interactions 0-81112
 Ni-base wrought superalloy, creep and stress rupture behaviour in air and vacuum 0-60918
 Nimonic 105, creep and stress rupture props., trace elements influence 0-66602
 nonlinear materials, Mode I fracture behaviour, finite element anal. 0-84237
 nuclear reactor materials, crack-front tunnelling, investigated by single specimen compliance technique 0-70300
 nuclear reactor piping system, crack initiation and propagation, fracture mechanics 0-83193
 nuclear reactors, seismically qualified piping, failure probability, ASME code limits 0-78365
 optical waveguide long-term stress failure probability estimation 0-58745
 organopolitics, fracture characts., effect on strength 0-66642
 parabolics of revolution, internal fractures due to stress wave focusing 0-83762

fracture continued

- Phobos, impact fracturing rel. to grooves distrib., morphology and possible origin 0-72837
 along planar slip bands 0-107262
 plastic fracturing materials, work inequalities and stress-strain relations 0-103000
 plates under uniaxial load, optimum hole shapes, cracks and fracture appl. 0-64479
 plexiglass composite, long term strength and durability 0-75294
 polycarbonate plates, modified compact-tension specimens, dynamic anal. 0-97561
 polyethylene, high-density unorientated, damage buildup kinetics under creep conditions, during prolonged loading 0-60932
 polyethylene, nonoriented partially cryst., kinetic damage accumulation cure 0-71753
 polymeric materials, thin-wall tubes, rupture time determ. 0-64473
 polymers, specific fracture surface energy, meas., review (French) 0-104275
 polypropylene, (Moplen) influence of temp. and mol. wt. on high speed fracture mechanics 0-76341
 polypropylene, oriented, microcracks diagnostics by paramag. probe method 0-66736
 polypropylene fibre reinforced polyoxyethylene, fracture kinetics, interface props. 0-66640
 polypropylene fibrillated film reinforced cement matrix for low cost sheeting 0-80996
 prediction on basis of acoustic emission 0-104382
 preservation and cleaning, for fractography 0-71866
 pyrex glass, statistical analysis of Hertzian fracture using Weibull distribution function 0-66623
 reactor fuel pin rupture detection system, using meas. of time differential of acoustic emissions 0-102282
 reactor technology, conference, Berlin, Germany (Aug. 1979) 0-77539
 resin matrices and their contribution to composite properties 0-81028
 rock half-space, impact of steel cylinder and effects 0-85649
 rubber, fracture in viscoelastic systems under cyclic loading 0-81195
 ruby, structural defects due to laser irradi. (Russian) 0-100303
 solid popellant, delayed fracture and crack propagation (French) 0-108521
 statistical methods for creep, fatigue and fracture data analysis 0-58936
 steel, austenitic, types 304 and 316, fracture-mechanisms, tensile specimens 0-85039
 steel, austenitic stainless, ageing at high temp., effect on creep props. SEM 0-97516
 steel, austenitic stainless, liquation cracking during welding, comp. influence 0-66645
 steel, cast, heat-resist., subcrit. crack growth 0-97581
 steel, cast automatic couplings, yield strength, crack propag. resistance and ductile-brittle transition temp. 0-104281
 steel, Charpy type bars of AISI 4340, varying notch root radii, fracture initiation and propag. at notch root 0-85050
 steel, Cr-Mo-P (2.25, 1 wt.%), stress relief cracking, effect of P segregation 0-89324
 steel, Cr-Mo (2.25, 1.0 wt.%), fracture-mechanisms, tensile specimens 0-85039
 steel, Cr-Mo weld metal, reheat cracking, residual elements and microstruct. influence 0-66553
 steel, Cr-Mo-V low-alloy, mech. props. and stress relief cracking, effects of impurities and deoxidation practice 0-66599
 steel, Cr-Mo-V low-alloy, stress relief cracking, impurity and alloy content effects 0-66654
 steel, Cr-Mo-V low-alloy with high residual element content, cavitation control 0-66663
 steel, Cr-Mo-V pressure vessel, microstruct. parameters and yielding rel. to plastic deform. 0-89318
 steel, Cr-Ni-Mn, adiabatic shear band determ. by surface obs. 0-97579
 steel, Cr-Ni-Mo, 'spots' (Chinese) 0-104248
 steel, crack resistance, -196 to 500°C 0-71750
 steel, high C, tensile strength, working and heat treatment effects (Japanese) 0-104209
 steel, high strength, dislocation sweeping model for hydrogen assisted subcritical crack growth 0-97577
 steel, high strength, subcritical crack growth, role of time delayed H₂ assisted plastic zone growth 0-97576
 steel, low-alloy, hardened deoxidised, delayed failure, influence of internal adsorpt. of impurities 0-60974
 steel, martensitic-aged, plastic deformation influence in type N17K12M5T steel on mech. props. (Russian) 0-76305
 steel, medium C, Ni-Cr-Mo, overheated, fractographic study (Chinese) 0-66616
 steel, Mn-C-Si-Cu (0.95, 0.85, 0.25, 0.16 wt.%), fibrous-banded fracture mechanism 0-104280
 steel, Mn-Nb-Al-C, crack propag. and hot ductility during straightening concast strand 0-66646
 steel, sintered, fracture of residual pores 0-76352
 steel, stainless, creep limit, cyclic load component effect at high temps. 0-104231
 steel, stainless, fracture micromechanism when kept isothermally in sulphur pulp 0-76355
 steel, structural, impurity effect on crack initiation, dynamical loading (Czech) 0-60955
 steel, structural, macroscopic and microscopic features of fracture 0-81179
 steel, type 4052Kh, thermomechanical working influence on mech. props. (Russian) 0-93578
 steel fracture mode, determ. from shear lip width 0-60968
 steel sheet, hot and cold rolled, cold formability, notched tensile test and stretch bend test (German) 0-61031
 steels, solute segregation and intergranular fracture 0-60957
 stress intensity factor determ. along crack path., numerical method 0-74808
 superplasticity, region I characteristics 0-107357
 surface anal. by SEM microtopography 0-79824
 tensile fracture device for Auger electron spectroscopy 0-73530
 torsional deformation testing for plastic deformation, fracture (Hungarian) 0-97659
 Weibull parameter estimation, for fracture characterisation 0-79224
 Zircaloy-4, failure strain prediction under non-stationary loading conditions 0-93640
 Zircaloy-4, fuel cladding, burst criteria under LOCA conditions 0-73931

fracture continued

- Ag-Ni (10 wt.%) wire, plastically deformed, fracture struct. (German) 0-71744
 Al alloy, creep crack growth 0-60976
 Al alloy AK4-1, crack growth rate prediction under creep conditions 0-85107
 Al alloys, fracture relief formed in fatigue crack growth, rel. to failure mechanism 0-76347
 Al anodic films, acoustic and electron-emission during deform. 0-80143
 Al foil, laser irradi., fracture props. (Russian) 0-108523
 Al, fracture mechanism 0-100903
 Al fracture speed during phase explosion due to electron beam irradi. (Russian) 0-76336
 Al, workhardened thin specimens, fracture, anisotropy coeff. role (French) 0-104276
 Al-B fibre-D16 alloy welded composites, structure, strength and fracture props. (Russian) 0-108524
 Al-Cu, type 2219-T851, fracture mechanics and surface chemistry of fatigue crack growth 0-81168
 Al-Cu (4 wt.%), supersaturated and aged conditions, high strain deform. 0-60907
 Al-Cu (4.6 wt.%), cold work and ageing influence on ductility and fracture behaviour (Japanese) 0-89295
 Al-Cu-Mg-Li alloy extrusions, microstruct., embrittlement and fracture props. 0-60965
 Al-Cu(Mg), liquid impact erosion 0-108598
 Al-Li-Mn (2.8, 0.3 wt.%), recrystallised sheet, fracture behaviour, SEM and TEM study 0-97566
 Al-Mg (2 wt.%), hardening and fracture characts., β -phase dissolution role 0-81178
 Al-Mg-Si, type 6010, microstruct. characts. influence on formability, heat treatment 0-81090
 Al₂O₃ (96 wt.%), fractographic criteria for subcritical crack growth boundaries 0-81155
 Al₂O₃, atomically sharp cracks, TEM study 0-71729
 Al₂O₃, hot pressed, fracture stress-reflecting spot relations 0-71731
 Al₂O₃-TiC, composite, fracture behaviour in three-point bending 0-60951
 Au, metallised coating on polyethylene terephthalate film, fracture under laser irradi. (Russian) 0-76333
 B₂C, TEM investigation using C replicas 0-61034
 BN, TEM investigation using C replicas 0-61034
 BaTiO₃, ferroic materials, fracture processes 0-79869
 Be, fracture and strength properties, dynamic ageing effects 0-81202
 CaF₂, strength-controlling fracture energy depend. on flaw-size to grain-size ratio 0-81152
 Ca₂SiO₅, fracture surfaces, quantitative anal. using energy dispersive X-ray spectrometry (French) 0-89571
 Co-CoAl, two phase, interaction between deform., fracture initiation and propag. 0-85006
 Cu fracture speed during phase explosion due to electron beam irradi. (Russian) 0-76336
 Cu, metallised coating on polyethylene terephthalate film, fracture under laser irradi. (Russian) 0-76333
 Cu wire, tough-pitch, cupping fracture, Cu₂O particle size effect 0-66668
 Cu-Bi, grain boundary struct. intergranular fracture, segregation role 0-66648
 Fe, cast, grey, fracture surface after dynamic fracture, Mg conc. effect 0-100909
 Fe, pure, fracture-mechanisms, tensile specimens 0-85039
 Fe-Cr-Co, ductile magnet alloys, mech. props. 0-85001
 Fe-Ni-Al-Co-Cu-Ti YUNDK type, S effect on mech. props. 0-60927
 Fe-Ni-Cr (35, 15 wt.%) superalloy, stress rupture and tensile props., C and B additions effect (Chinese) 0-104244
 Fe-Ni-Cr based alloy, KhN35VTYu, temp. depend. of energy of fracture, influence of γ' phase (Russian) 0-81147
 Fe-Si, rapid cracks self-arrest potential, -196-0°C 0-100911
 Fe-Si (2.6 wt.%) single cryst., crack propag., controlled plastic crack tip opening rate 0-60943
 GaP/Si heterostruct., differential thermal contraction, plastic deform., fracture 0-108494
 Ge, atomically sharp cracks, TEM study 0-71729
 H₂, embrittlement cracking and impurity atom migration (Chinese) 0-104247
 Ir-W (0.3%), grain boundary comp., trace element additions effect 0-66661
 Li₂O-Al₂O₃-SiO₂ glass-ceramic, near-zero thermal-expansion heat treatment effect in fracture behaviour 0-66537
 MgAl₂O₄, strength-controlling fracture energy depend. on flaw-size to grain-size ratio 0-81152
 Mo, fracture and crack tip plastic zones, in situ obs. 0-108686
 Mo-W (30 wt.%), wrought, fracture, characteristic features 0-104278
 Mo-Zr (0.15 wt.%), wrought, fracture, characteristic features 0-104278
 Na₂O-CaO glass, (K₁,V) diagram determ. (French) 0-108558
 Na₂O-CaO glass, abrasion-resistant, high strength 0-76369
 Na₂O-SiO₂ glass, microcracking about NiS inclusions, fracture mech. description 0-89333
 Na₂O-SiO₂ glass, OH⁻ content effect on mech. and other props. 0-89337
 Na₂O-SiO₂ glass, scoring, deform. and fracture mech. approach 0-89332
 Nb₃Sn microfilamentary superconducting composite, critical currents, fracture props. 0-107970
 Ni alloys, liquation cracking during welding, comp. influence 0-66645
 Ni, ductility and fracture, nonmetallic inclusions effect 0-104221
 Ni films, adhesion on graphite 0-80141
 Ni, metallised coating on polyethylene terephthalate film, fracture under laser irradi. (Russian) 0-76333
 Ni-Cr-Al sintered alloy, hot vac. pressure, fracture and mech. characts. 0-66667
 Ni₃Fe₂Cr₁₄P₂B₆ metallic glass, mech. props. and thermal stability 0-76362
 Pb(Zr,Ti)O₃, ferroic materials, fracture processes 0-79869
 Pb(Zr,Ti)O₃, fracture and deform. 0-79870
 Pd₉₀Si₁₀ glass, deform. localisation, plastic instabilities and fracture 0-89320
 239PuO₂, stoichiometric, high-temp. deformation 0-81111
 Si, atomically sharp cracks, TEM study 0-71729
 Si, elastically bent, strain conc. determ. by microfluorescent densitometry of X-ray topography 0-79245
 Si, near (111), fracture by painted indenter, SEM study 0-71734
 Si, single crystal, fracture under several liq. environments 0-81157

fracture continued

- Si-Al C fibre composite technological coatings, liquid phase method preparation (*Russian*) 0-108375
 SiC, atomically sharp cracks, TEM study 0-71729
 SiC, pressureless-sintered, high temp. strength (*Japanese*) 0-104299
 SiC, TEM investigation using C replicas 0-61034
 Si₃N₄, cracking characterisation by double torsion test (*French*) 0-104369
 Ti-Al-Sn, alloy 6242, dynamic effects of flow and fracture during isothermal forging 0-76343
 Ti-Al-V (6.4 wt.%), effect of air exposure on fracture characts. 0-100890
 α -U, strain rate effect on flow and fracture 0-100887
 α -U, strain rate effect on tensile flow and fracture 0-84992
 W bicrystals, crack propag. across grain boundaries, crack speed meas. technique appl. 0-108575
 Y₂O₃ ceramics, strength under mech. and thermal actions 0-97554
 Y₂O₃, strength-controlling fracture energy depend. on flaw-size to grain-size ratio 0-81152
 Zn-Al(Cu), mech. and technological props. (*Polish*) 0-89286
 Zr-Nb (2.5 wt.%) pipe, fracture resistance, hydrogenation effect 0-104279
 ZrO₂, partially stabilized, processing defects 0-97558
 ZrO₂, porous, sintered stabilised microspheres, strength and fracture studies 0-85019

fracture strength *see* fracture toughness

fracture strength testing *see* fracture toughness testing

fracture toughness

see also notch brittleness; notch ductility; notch strength

- ABS-rubber modified, two-phase struct. influence on fracture toughness (*German*) 0-66666
 acoustic emission, amplitude distrib. anal. 0-66713
 Araldite B specimens, dynamic fracture toughness, influence on dynamic crack propag. 0-99966
 asbestos fibre reinforced cement, strength and fracture props. 0-108533
 brittle fracture, statistical theory, dislocation mechanism, crack propagation (*Chinese*) 0-106755
 brittle materials, water drop impacted, damage thresholds 0-81149
 ceramic multilayer capacitors, fracture mechanics approach to structural reliability assessment 0-89328
 ceramics, coarse-grained, dimensional anal. of grain size depend. of fracture strength 0-70299
 ceramics, crack extension micromechanisms, review 0-108567
 ceramics, transformation toughening, martensitic transforms. in crack-tip stress fields 0-104154
 ceramics and brittle solids, abrasive wear, role of plastic deform. and fracture 0-108594
 ceramics containing metastable tetragonal ZrO₂, grinding induced tempering 0-89260
 chevron notched short bar specimens, compliance and stress intensity coefficients 0-96232
 coke, breakage behaviour rel. to struct. 0-85026
 coke, metallurgical, industrial strength meas. methods, critique 0-85117
 composite, crack extension micromechanism 0-108566
 composites, single fibre-brittle zone model, fracture behaviour 0-97570
 concrete slab, explosive shock resist., tensile fracture 0-85065
 crack tip, plastic deform., metallographic anal. by recrystn. 0-85029
 dynamic fracture toughness, influence on dynamic crack propag. 0-99966
 epoxy, elastomer-modified, loading rate depend. fracture prop. 0-76342
 epoxy-rubber particulate composite, toughness and fracture mech. 0-71727
 ethylene-vinyl acetate-vinyl chloride graft copolymers, rel. between morphology and toughness (*German*) 0-66665
 fibre reinforced composites, unidirectional, mixed mode fracture 0-100302
 fracture mechanism maps, usefulness 0-84245
 glass, annealed and tempered, impact damage, strength 0-85025
 glass systems, binary and ternary, structure toughness-composition relationship 0-104257
 graphite, coarse grained, fracture toughness (*German*) 0-76358
 graphite, neutron irradiation effects on thermal shock resist. and fracture toughness (*Japanese*) 0-66622
 graphite, thermal shock resistance and fracture toughness during graphitising heat treatment (*Japanese*) 0-71843
 Homalite-100 plates, modified compact-tension specimens, dynamic anal. 0-97561
 hydroxylapatite, dense, fatigue and fracture strength from diametral tests, after various treatments 0-60953
 lecture on fracture toughness (*Japanese*) 0-90595
 microcrystalline alloys, metastable, rapidly quenched particulates, props. appl. and production 0-84887
 NASICON solid electrolyte, processing and phys. props. 0-60820
 Navy vessel fracture mechanics and flow separation, instability phenomena 0-99971
 nitrided layer, fracture toughness determ. from hardness impressions (*German, English*) 0-97575
 nuclear reactor materials, crack-front tunnelling, investigated by single specimen compliance technique 0-70300
 optical fibre, fracture surface anal. 0-58754
 phosphate glass-Al alloy seals, elec. and mech. props., glass transition 0-81018
 phthalocyanine polymer, dynamic mech. props. and fracture energy 0-100866
 PMMA, instantaneous crack resist. during stable crack propag. 0-85058
 polycarbonate plates, modified compact-tension specimens, dynamic anal. 0-97561
 polyester resin, cross-linked unsaturated, synthesis and fracture toughness 0-93634
 polyphenylene sulphide, high mol. wt. soluble resin, prep., mech. props. 0-60828
 polystyrene, rubber modified, two-phase struct. influence on fracture toughness (*German*) 0-66666
 porcelain, crack propag. data applicability to failure prediction 0-81154
 PVC, rigid plate, notching method effect on Charpy impact values, fractographic considerations (*Japanese*) 0-108541
 PVC-Cu composites with chemically deposited ultrafine copper particles 0-93534
 quasi-cleavage fracture, characteristic length parameter, correlation with fracture toughness (*Chinese*) 0-104246
 reference curve development 0-97588
 sapphire fibre reinforced, Mo, strength at rupture 0-104286

fracture toughness continued

- steel, (0.36 wt.% C) Ni-Cr-Mo, electroslag refined, fracture toughness and fatigue behaviour 0-81171
 steel, Al-Ti-(Mo), Al-Ti-V-(Mo), Al-Ti-Nb-(Mo) and Al-V-(Mo) low-alloy, toughness improvement through Ti additions 0-66525
 steel, alloy, sheet, crack-propag. resist. in heat-affected zone in presence of H₂ rolling direction and preliminary plastic tensile strain effects 0-60971
 steel, austenitic, strength, ductility and fracture toughness, N and Cr effects 0-100878
 steel, austenitic stainless, supercond. magnets, mech. and phys. props. at 4K 0-86976
 steel, C, plates, residual elements effect on through-thickness props. 0-66660
 steel, C, residual elements, effect on props. 0-66643
 steel, Co-Cr-Mo type HY-180M, mech. props. and SCC, overaging effect 0-108634
 steel, Cr-Mo, effect of Mo on high-temp. props. 0-85005
 steel, Cr-Mo (10-14, 2-6 wt.%), heat-resist., creep-rupture strengths 0-104271
 steel, Cr-Ni-Sr (18.15, 17.64, 2.4 wt.%), rare-earth additions effect on impact fracture (*Chinese*) 0-66617
 steel, Cr-Si-Mn-Ni-Mo-C, resist. to deform. and fracture, C effect 0-71757
 steel, fatigue damaged, fracture toughness 0-89353
 steel, ferritic, cleavage fracture toughness, temp. and strain rate depend. 0-85028
 steel, ferritic-martensitic, fatigue crack tip plastic zone (*Japanese*) 0-71738
 steel, fibrous crack extension, micromechanisms 0-108563
 steel, fracture toughness of nuclear pressure vessels 0-81172
 steel, high Mn-Cr, austenitic struct. stability and low-temp. toughness (*Japanese*) 0-76356
 steel, high speed, props. after electroslag remelting 0-104139
 steel, high strength, heat resistant, fracture resistance at low temps. 0-104284
 steel, high strength, produced by extrusion of Ni-coated steel powder, enhanced fracture resist. 0-81169
 steel, high strength weld metal, fractography, microstructure and reheated zone toughness effects (*Japanese*) 0-108543
 steel, high-speed, fracture toughness, carbides influence (*French*) 0-108559
 steel, high-strength structural type StE47, specimen geometry and plastic deform. effect on fracture mechanics (*German*) 0-66613
 steel, high-strength tool steel D7KhFN, remelting effect on mech. props. 0-76284
 steel, hot forging die type, fractography (*Japanese*) 0-108547
 steel, low alloy, strength, Cr and N effects 0-104277
 steel, low C structural, fracture toughness and X-ray diffr. obs. of surface (*Japanese*) 0-66634
 steel, low Si, martensite struct. and mech. props. (*Korean*) 0-93614
 steel, low-alloy, residual elements, effect on props. 0-66643
 steel, low-C, kinetics of void development in fracturing A533B tensile bars 0-76357
 steel, maraging stainless, phase transformation and mech. props. rel. to heat treatment (*Chinese*) 0-66501
 steel, medium C, Cr-Mn-Mo, austenising temp. effect on microstruct. and fracture toughness (*Chinese*) 0-66542
 steel, Mn-C-Si-Cu (0.95, 0.85, 0.25, 0.16 wt.%), fibrous-banded fracture mechanism 0-104280
 steel, Mn-Mo, castings, mech. props., Cu and Sn trace elements effect 0-66596
 steel, Ni, welded joints on LNG carriers mech. props. and fracture toughness 0-85017
 steel, Ni-Co-Cr, high-strength medium C, Cr effect on props. 0-76339
 steel, Ni-Cr-Mo SNCM8, delayed fracture, specimen thickness and threshold stress intensity effect (*Japanese*) 0-104268
 steel, pearlitic, heat treatment effect on fracture resistance, microstruct. and mech. props. 0-104191
 steel, rail, toughness, effect of Sn, SEM exam. 0-97569
 steel, stainless, strength down to 4.2K; influence of stress raisers 0-71754
 steel, steam pipes, 12Cr1MoV, selection of allowable stresses based on minimum possible strength data 0-104237
 steel, structural, second phase particle effects on impact strength 0-108581
 steel, structural, type St 37, microstruct. rel. to fracture toughness and fracture load of bending specimens (*German*) 0-89352
 steel, toughness, review of joint tests (*German*) 0-65142
 steel, V-Nb and Cr-Mo-V-Nb, supercooled austenite isothermal decomp., struct., strength and fracture characts. 0-60966
 steels, irradiated pressure vessel, reference fracture toughness curves 0-100921
 steels, wide plate and V-notch bending tests evaluation on basis of materials mechanics (*German*) 0-66571
 steels, with yield pt. of about 260 to 800 N/mm², specimen thickness influence of fracture mechanics parameters (*German*) 0-66614
 steels, with yield pt. of about 420 to 720 N/mm², correlation between yield pt./tensile strength ratio and toughness (*German*) 0-66615
 stretch zone width and striation spacing. The comparison of theories and experiments 0-85051
 stretched zone anal. by means of stereo matching method (*Japanese*) 0-108544
 thin sheet impact strength study (*Czech*) 0-59571
 weld metal, submerged arc irradiated, reference fracture toughness curves 0-100921
 wood, fracture toughness variations with specimen size, statistical approach 0-100889
 wood fibre reinforced Portland cement composite, strength 0-100822
 Al alloys, (5083, 6061, 2219), supercond. magnets, mech. and phys. props. at 4K 0-86976
 Al-Mg, fracture resistance at low temps. 0-104284
 Al-Si-Cu, fracture resistance at low temps. 0-104284
 Al-Zn-Mg, atmosphere effect on fatigue crack propag. (*Japanese*) 0-81161
 Al-Zn-Mg, type 7075-T651 plate, thickness direction inhomogeneity of mech. props. and fracture toughness 0-100892
 Al₂O₃, fracture toughness determ. using four-point-bend specimens 0-108536
 Al₂O₃, polycrystn., high-temp. fatigue and strength 0-60954
 Al₂O₃ refractories, fracture, J-integral meas. 0-108537
 Al₂O₃ substrates, tape-casted, fracture strength analysis 0-60948

fracture toughness continued

- Al₂O₃-B₂O₃-SiO₂ sheet glass, solar energy appl., optical and mech. props. 0-87447
 β'' -Al₂O₃-Na₂O solid electrolyte, processing and phys. props. 0-60820
 β'' -Al₂O₃-Na₂O solid electrolyte, strength degradation under electrolytic conditions 0-61329
 3Al₂O₃-2SiO₂-ZrO₂ composites, sintered, in situ-reacted, fracture props. 0-81158
 B fibre reinforced epoxy composites, notched, tensile strength and failure modes 0-81205
 Co-(Cr,Co)₇C₃ eutectic, oxidation effect on toughness and strength 0-89404
 Co-Zr, amorphous phase form. in Zr-poor region, hardness and fracture strength (Japanese) 0-84914
 Cr-(Cr,Co)₇C₃ eutectic, oxidation effect on toughness and strength 0-89404
 Cu-Al (5 wt.%), subjected to tension-compression fatigue, deform. and fracture strength (Japanese) 0-93644
 Fe, cast flake and nodular, rupture strength, circumferential notch (Japanese) 0-93649
 Fe, ductile, influence of crack tip sharpness and morphology of graphite on K_{IC} (Chinese) 0-81144
 Fe-Cr-Mo, white cast, optimising fracture toughness and abrasion resist. 0-85042
 Fe-Cr-Mo alloy castings, thick-section, factors affecting 0-108374
 Fe-Mn-B, B effect on intergranular embrittlement 0-108555
 Fe-Mo-Ta, ternary Laves phase strengthening 0-108466
 Fe-Ni-Al-(Cu) (12, 0.5, 0.5 to 3 wt.%), Cu addition strengthening at 77K, mech. props. 0-60875
 Fe-Ni-Ti-(Cu) (12, 0.25, 2 wt.%), Cu addition strengthening at 77K, mech. props. 0-60875
 Fe-Ni-V-(Cu) (12, 2, 2 wt.%), Cu addition strengthening at 77K, mech. props. 0-60875
 Fe-Ni-(Cu) (12, 0.5 to 3 wt.%), Cu addition strengthening at 77K, mech. props. 0-60875
 Fe-Zr, amorphous phase form. in Zr-poor region, hardness and fracture strength (Japanese) 0-84914
 Mo-TiC lamellar eutectic composite, deformation and strength, room temp. to 2073K (Japanese) 0-71702
 Na₂O-B₂O₃-SiO₂ glass fibre, plastic coating influence on strength 0-58697
 Na₂O-B₂O₃-SiO₂ glass-Ni compact, indented, strength and fracture toughness 0-93636
 Na₂O-B₂O₃-SiO₂ glass, fracture toughness, effect of microheterogeneous struct. 0-104256
 Na₂O-B₂O₃-SiO₂, mechanical strength and swelling in liq. 0-85024
 Nb fibre glass composites, new technique for producing fine metal fibres 0-108384
 Nb₄₀Fe₄₀P₁₄B₆, metallic glass, explosive compaction, mech. props. 0-89176
 Ni alloys, heat resistant EI437B and EI929, surface condition, air stream effect 0-76409
 Ni alloys, plasticity, heat treatment effect 0-76277
 Ni-Fe-Cr superalloy 718, heat treatment effect on room temp. and elevated temp. fracture toughness response 0-100922
 Ni-Zr, amorphous phase form. in Zr-poor region, hardness and fracture strength (Japanese) 0-84914
 PbO-B₂O₃ phase-separated glass, fracture toughness, Vickers indentation method 0-85023
 SiC, fracture toughness and high-temp. slow crack growth 0-81153
 Si₃N₄, hot-pressed, fracture toughness determ. using specimens with chevron and straight through notches 0-108538
 Si₃N₄, hot-pressed, strength anisotropy origins 0-89330
 SiO₂-B₂O₃-Na₂O-K₂O glass, strengthening by partial leaching 0-60993
 Ti-Al-Mo-V (8, 1, 1 wt.%), Widmanstätten colonies, fracture toughness 0-85031
 Ti-V-Cr-Mo, fracture resistance at low temps. 0-104284
 Ti-V-Fe-Al (10, 2, 3 wt.%), fracture toughness and stress corrosion resistance 0-100904
 TiC coated WC-Co cemented carbides, fracture toughness 0-85046
 WC-Co alloys, fracture toughness model 0-84243
 Zr-Al (8.6 wt.%), fast neutron irradiated, tensile props. and fracture toughness 0-84994
 Zr-Nb (2.5 wt.%), nuclear fuel channels, neutron effects on ultimate fracture strength, 293 to 573K 0-85054
 Zr-Nb (2.5 wt.%) pipe, fracture resistance, hydrogenation effect 0-104279
 ZrO₂, partially stabilised ceramics, strengthening, post-sintering heat treatment 0-97518

fracture toughness testing

- see also notch testing
 bar-to-block based testing method for materials characteris. in high-vel. tension 0-85133
 biaxial strength tests, finite element anal. 0-89431
 brass, crack initiation at high strain rates, uniaxial and biaxial tests 0-85141
 chevron notched short bar specimens, compliance and stress intensity coefficients 0-96232
 compact specimen, for plane strain crack arrest toughness testing 0-76433
 dynamic stress/strain measurements under superimposed high press., torsion bomb machine 0-85130
 fastening materials, specimen for testing 0-61050
 glass components, life testing under flexing load (French) 0-89432
 glass fibre reinforced plastic, woven-roving type, high-speed punching, failure mechanisms 0-85143
 Griffith fracture tests, for plastic deform. (Hungarian) 0-97666
 impact machines, pendulum, energy meas. using optical system 0-69746
 J integral, work for failure and work for plastic deform. 0-61061
 laboratory tests automation, using 500 kN and 2.5 MN ATE (Czech) 0-66710
 limestone tubes, dynamic torsional failure obs. 0-85648
 metals, crack resistance determination, cyclic loading, methodological instructions 0-108660
 PMMA plates with flawed fastener holes, static fracture testing 0-97651
 polyethylene, high-density, impact fracture behaviour, adiabatic heating at crack tip 0-85142
 radial expansion technique for fracture strain meas. at high strain rates 0-85134

fracture toughness testing continued

- refractories, strength and thermal properties, automated test system 0-100986
 refractory concrete fracture strength, test apparatus simulating usage conditions 0-71824
 refractory products, toughness measurement, expt. problems (French) 0-104368
 split Hopkinson pressure bar application 0-85140
 statistical processing of results, cold brittleness crit. temps. determ. 0-100980
 steam turbines, structural stresses, experimental anal. 0-93727
 steel, alloy, single specimen determ. for J_{IC} 0-100989
 steel, alloy A533B1, neutron irradi., flow growth characts. by acoustic monitoring 0-100918
 steel, cast, cold resistance determination, quick method 0-100997
 steel, fracture initiation moment, I-integrals critical value determ., ultrasonic method 0-61049
 steel, low-alloy, fracture toughness characts., loading rate effect 0-100897
 steel, low-alloy, testing cracked specimens for impact bending, expt. planning method appl. 0-71831
 steel, stainless, thin sheet, fracture resist., critical opening of crack criterion 0-61048
 steel, structural, wide plate tensile testing eval. (German) 0-100969
 steel, types A533B and KAS, fracture toughness meas. using elect. potential method (Japanese) 0-93722
 steel 45G2, fracture resistance, from impact bending tests and oscillograms 0-61047
 structural materials, crack resist. determ. 0-81258
 Stycast-1266, mechanical props. at low temps. 0-57286
 Al alloy, crack initiation at high strain rates, uniaxial and biaxial tests 0-85141
 Fe base superalloy, type A-286, elevated temp. fracture toughness testing of thin section irradi. materials 0-61063
 Fe, pig, white, mech. props. meas. (French) 0-104370
 Si solar cells, production process effect on fracture strength 0-93656
 Si₃N₄, hot-pressed, fracture mech. parameters, indentation-precracking and double-torsion methods 0-104364
 WC/Co cemented carbides, fracture toughness testing 0-104410
- francium**
 see also nuclei with
 atom, radioisotopes, hyperfine spectroscopy, nucl. props. 0-57677
- francium compounds**
 No entries
- Franck-Condon factors**
 bent triatomic mol., photodissoc. rot. distrib. 0-95694
 benzaldehyde in methylcyclohexane, $n^*\pi^*$ spectra 0-63627
 bound continuum vibr. transitions, Franck Condon matrix elements calcs. 0-69191
 diatomic molecule, Franck Condon factors, vibr. rot. interaction effect 0-74198
 diatomic molecule, vibr.-rot. states, high accuracy wave functions and energies 0-74159
 electronic transitions, band shape in multimode weak coupling limit, multidimens. subspace theory 0-87178
 local mode mols., normal mode spectra 0-95687
 molecule core 1s and 1b, photoelectron bands, vibr. excitations, ab initio calc. 0-63543
 photochemistry two-photon, photo-fragment distrib., isotope separation appl. 0-81344
 polyenes, photoisomerisation, triplet pot. energy surfaces and normal mode anal. 0-108700
 thiophosgene, second excited singlet state emission spectroscopy 0-69157
 vibration frequency change influence 0-106312
 Wigner distrib. function 0-99520
 Br₂, B²Π(O_g⁺) predissoc. rates, analytical interpretation 0-91617
 C₂, A¹Π_u state, orbital angular momentum 0-78514
 CN⁻, spectrosc. consts. for ground and excited states, ab initio, CI calcs. 0-78551
 CO, X²Σ⁺, vibr. levels, UPS electron attachment obs. 0-95683
 CO₂, A¹Σ_g⁺-X²Σ_g⁺ system, laser induced fluoresc., pot. energy curve and mol. consts. 0-58307
 Ca₂, vibr.-rot. states, high accuracy wave functions and energies 0-74159
⁶³Cu, A¹Π_u-X¹Σ_g⁺ transition, Franck-Condon factors and r-centroids 0-95690
 GaAs/O₂, deep level, Franck-Condon shift, photocond. and Hall effect study 0-70642
 H+Cl₂, stochastic-collision complex model theory 0-108696
 H+LiF, laser-induced nonadiabatic collision process, classical model 0-77701
 H₂, predissoc., interference effects, lineshape obs. 0-83432
 HCN predissoc. Franck-Condon amplitudes 0-95694
 HD, predissoc., interference effects, lineshape obs. 0-83432
 H₂O threshold PES, OH⁺ fragment obs. 0-78647
 HOCl, photodissoc. rot. distrib. 0-95694
 H₂S⁺, ²B₁, ²A₁ and ²B₂ electronic states, pot. energy curves, CI calcs. 0-87048
 He+OCS, emission spectra in He afterglow 0-87139
 He⁺+CS₂, dissoci. charge-transfer, CS⁺(B²Σ⁺-A²Π_g) emission prod., Morse pot. Franck-Condon factors calc., vibr. anal. 0-99539
 He⁺+OCS, dissoci. charge-transfer, CS⁺(B²Σ⁺-A²Π_g) emission prod., Morse pot. Franck-Condon factors calc., vibr. anal. 0-99539
 I₂, B-X fluoresc. band system, intensity and relative band strengths meas. 0-102540
 I₂ lines, Franck-Condon factors, Ar⁺, Kr⁺ and He-Ne laser excitation 0-58320
 LaO, Franck-Condon factors rot. depend. 0-58319
 MgO, Franck-Condon factors rot. depend. 0-58319
¹⁴N₂, Fourier spectrometry and IR emission spectra 0-83368
 NH₃, vibr. excitation in soft X-ray emission and core ESCA spectra 0-69163
 NaOH:CrO₄²⁻(NO₂⁻), electron tunnelling, pulse radiolysis 0-108722
 NaOH:Fe(Cn)₆³⁺, electron tunnelling, pulse radiolysis 0-108722
 SiO, Franck-Condon factors rot. depend. 0-58319
 SO₂, single vibronic level fluoresc. spectra 0-91597
 SiS₂, chemiluminescent flame spectra, electronic states and rot. struct. obs., vibr. assignments, Franck-Condon factors determ. 0-85179
 TiO, Franck-Condon factors rot. depend. 0-58319
 TiO, γ-system, Franck-Condon factors, r-centroids and Einstein coefficients calcs. 0-74163

Franck-Condon factors continued

ZrO₂, Franck-Condon factors rot. depend. 0-58319
 ZrS₂, excitonic transition, reson. Raman spectra, Franck-Condon factors 0-97252

Frank-Read sources

metals, time dependent plastic deformation, thermodynamic model 0-76309
 personal recollections of F.C. Frank 0-62442
 plasticity, rate-independent, axiomatic model 0-87717
 Si:B, ion implanted, structure defects formation and behaviour under annealing in various ambients 0-65033
 Zn, line energy of basal screw dislocation, exptl. determ. 0-88154

Fraunhofer lines *see solar spectra***free-electron approximation**

alkali metals, cohesive energy, teaching 0-90630
 education, deep one-dimens. periodic pot., zero energy gaps, Kronig-Penney model 0-62426
 HF wave dispersion for complex wave numbers, ordinary waves 0-70740
 metal, electron density behaviour near impurity charge 0-75518
 metals, electron theory, internal press. 0-92802
 one-dimensional conductivity, with arbitrary bandfilling, Peierls instability 0-59968
 Sn, liq., optical props., 0.62-3.7 eV 0-75996

free electron lasers

classical theory, saturation, perturbation calcs. 0-83580
 coherent dynamics, conservation law, small signal theory and gain-spread relation 0-83582
 coherent dynamics with arbitrary magnet geometry 0-83581
 coherent states in single mode and multimode cases 0-102689
 energy transfer, computer simulation 0-83578
 free charged particle interacting with intense laser pulse, energy momentum gain 0-101963
 intense-beam free electron laser, beam quality expts. 0-58619
 IR and millimetric waves and applications, conf., Miami Beach, USA (Dec. 1979) 0-57009
 low gain, analytic soln. of quasi-Bloch eqns. 0-87363
 multiphoton analysis 0-78826
 nonlinear free electron laser dynamics with space charge and wiggler effects 0-58500
 nonlinear saturation, thermal effects using EM pump 0-87364
 nonlinear wave equation for free electron lasers driven by single-particle currents 0-69355
 oscillation characts. of free electron laser based on stimulated Raman scatt. by relativistic electron beam 0-99688
 physical processes and construction problems 0-102691
 pulse amplification through energy exchange with electron beam via nonlinear radiation press. effects 0-95776
 pulsed laser dynamics, coherent picosecond pulse propag. calcs. 0-95860
 quantum mechanical and classical theories 0-83579
 quantum theory for strong fields 0-83583
 reaction kinetics measurement and control using laser technology, free electron laser appl. 0-81349
 saturation effects, classical theory 0-95864
 small signal gain of free electron lasers with nonuniform wigglers 0-58499
 small signal theory for gain in strong axial mag. field 0-78825

free energy

adsorption thermodynamics, symmetrical, case of noninert adsorbent 0-80059
 alkali metals, condensed phase, free energy, Debye-Huckel theory calcs. 0-79958
 alloy, binary, with arbitrary mole fraction, order disorder transition in case of FCC lattice 0-88295
 amorphous magnet, random anisotropy axis model in the infinite-range limit 0-88761
 antiferromagnet, linear-chain, sine-Gordon solitons 0-80543
 bounds, upper and lower, renormalisation group methods 0-68162
 brass, liquid, thermodynamic props. (German) 0-66482
 t-butyl alcohol, self-assoc., linear and nonlinear dielec. effects obs. 0-60484
 n-butylamine-n-propanol, isothermal vapour-liquid equilib. 0-59639
 colloids, rel. to thermodynamic stabilisation 0-81369
 commensurate phases, spatially modulated, in simple Ising model 0-79909
 crystallisation of phase A from A+B melt, Helmholtz free energy 0-79911
 cubic lattices, fully frustrated, phase transitions, Gaussian and spherical model, free energy calcs. 0-60281
 degenerate semiconductors, heterogeneous state, first-order phase transition, Ginzberg-Landau method analogue 0-70372
 dicalcium lead propionate, improper ferroelectric, dielectric props., IR radiation pyroelectric detection 0-80711
 dilute metal solutions in molten salts, optical absorption, F-centre model for bound state 0-89023
 dipole relaxation in electric field, teaching 0-90625
 Earth mantle elements compounds and modifications, high press. and temp. thermodynamics 0-81874
 elastic media, dissipative, relativistic electrodynamics 0-73219
 ferroelectric, uniaxial, crit. behaviour, electrostrictive coupling role 0-71329
 ferroelectric substances, electron microscopy investigations, review (Japanese) 0-71366
 ferromagnetic Ising model, spin-one three dimensional, single-ion anisotropy, crit. behaviour 0-80540
 ferromagnetic superconductors, self-induced vortices, magnetisation, Gibbs free energy 0-70916
 first order phase transitions, droplet models, renormalisation, singularities 0-90500
 granulated superconductors, phase transitions, Josephson energy (Russian) 0-84540
 group IIIa dihydrides, structs. and stabilities 0-107146
 harmonic crystals, Helmholtz free energy, vacancy defects interactions calc. by cell cluster method 0-107443
 harmonic crystals, thermodynamic props., effects of vacancy defects determ. by cell cluster method 0-79959
 Heisenberg ferromagnet, classical one-dimensional, transfer integral and collective coordinate results for free energy 0-93067
 Heisenberg metamagnet, collinear, mag. phase diagram 0-71035
 Heisenberg model, classical spin, with three or four spin interactions, linear chain 0-70923

free energy continued

inhomogeneous charged fluids, density functional theory, rel. to molten salts surfaces 0-79660
 intercalation compound electrodes, thermodynamic and transport props. 0-66963
 interfacial tension var. with supersaturation, one-layer adsorpt. model 0-103563
 ionic clusters, struct., thermodynamic functions, energy surfaces and SIMS 0-63881
 ionic crystals, thermodynamic ion-vacancy complexes (Spanish) 0-75222
 irradiation induced crystalline to amorphous transition, Gibbs energy 0-70371
 Ising chain, random bond, low temp. behaviour 0-57211
 Ising chain of alternating spins of 1/2, and general S, appl. of transfer matrix method 0-80529
 Ising ferromagnet, gaussian fluctuations of mol. field, magnetisation and free energy 0-70918
 Ising ferromagnetic half-plane, surface, pinned domain wall, free energy and magnetisation profile 0-60361
 Ising magnet coupled to isotropic elastic medium, first order transition, renormalisation method 0-68151
 Ising model, modulated phase with solitons, phasons and devil's staircase 0-95044
 Ising model strip, spin 1/2, critical wall perturbations and a local free energy functional 0-80533
 Ising spin glass, three-dimensional mag. correlations 0-103849
 Josephson effect higher harmonics, flux tunnelling, thermodynamic free energy 0-60147
 kaolinite rare-earth complexes, relax., molar free energy of activation for dipole relax. 0-88919
 liquid crystals (Chinese) 0-79696
 liquids, diatomic, hard and soft core, free energy difference, Monte Carlo calcs. 0-92436
 magnetic objects, current loops, thermodynamics, teaching 0-90633
 magnetic systems with random interactions, upper bounds to be quenched free energy 0-103845
 metals, melting theory for small particles, Helmholtz free energy 0-59629
 micellar systems, aqueous, thermochemistry 0-61133
 microcluster formation, free energy, curvature-depend. surface tension effect 0-100056
 micropolar fluids, thermodynamical aspects, non-linear approach 0-105598
 mixtures, binary and ternary, activity coeffs. rel. to excess Gibbs free energies 0-96665
 mobile pinning points on dislocations, equilibrium distrib. 0-79792
 molecule desorption and surface diffusion from critical deposition rate 0-92786
 2(4)-monooxypyrimidines, gaseous, matrix, soln., tautomeric equilib., IR and UV absorpt. spectra 0-58256
 Mott transition in Hubbard long range model, isostructural instability, thermodynamic props. (Russian) 0-65454
 multicomponent systems, phase diagrams and thermodynamic data, electrochem. determ. 0-71922
 narrow band electron systems, unified theory of magnetism 0-70928
 NLC, effective ion mass and mobility calcs. (Russian) 0-79694
 nonuniform one dimensional classical fluids, Lennard-Jones pot. interactions, Percus Yevick approx. and density functional calcs. 0-64864
 paraelectric-ferroelectric-antiferroelectric phase transitions, electrostrictive effects 0-97209
 PET, crystallization, lamellar growth kinetics and thickness 0-103266
 phase boundaries in first-order phase transitions, dynamics stability 0-107403
 Planck function, replacement for free energy function 0-62603
 polar mol.+ion, statistical and thermodynamic theory 0-99562
 poly(vinylidene fluoride) phase II, field induced phase transitions 0-96640
 poly-arylate-dimethyl siloxane, polyblock copolymers, struct., thermodynamic stability (Russian) 0-64931
 polymer melting, theoretical aspects 0-59633
 polymer protonated and deuterated mixtures, partial miscibility 0-107037
 polystyrene-methylcyclohexane, coexistence curve, comparison obs. and free energy calc. 0-88323
 polyvinylidene fluoride, cryst., struct. phase transition theory, free energy, uniaxial stress 0-64924
 Potts s-state model on Cayley tree Bethe-Peierls critical coupling 0-103844
 quantum compressible Ising model, critical behaviour 0-108016
 rare earth (III) complexes, cysteinates, thermodynamics of form. 0-89515
 simple liqs. with repulsive forces, thermodynamically selfconsistent theory 0-75139
 small polaron theory, translational symm. breaking transform. 0-92838
 solid-liquid interface free energy anisotropy clustering influence 0-80054
 solvent-rod mixture, two phase, interfacial free energies, quartic van der Waals theory 0-59377
 spin glass, infinite range model, stability and susceptibility in Parisi's soln. 0-88762
 spin glass, principle of minimum free energy 0-88773
 spin glass transition, cumulant expansion of free energy of disordered systems 0-71067
 spin glasses, free energy, order parameter expansion, random bond model 0-84609
 spin glasses, metastable states, crit. free energy 0-88764
 spin-glasses, order parameter expansion of free energy, random site model 0-88772
 steel, aluminising, thermodynamic anal. of phase transforms. 0-76413
 steel, medium and high C, deformation ageing, entropy, free energy, dislocations (Russian) 0-66581
 structural and mag. phase transforms., integral rational basis of invariants (Russian) 0-62602
 substitutional solid solutions, new phase nucleation mechanism 0-61135
 superconducting order parameter perturbation flux pinning 0-103801
 superconductors, magnetic impurity low temp. behaviour, transition temp., specific heat, free energy 0-88691
 supersaturated vapour, critical clusters, theory and Monte Carlo simulation, review 0-82734
 symmetry principles and 1/f noise 0-68136
 temperature induced antiferromagnetic-ferromagnetic phase transition, s-f two-band Hubbard model 0-60253

free energy continued

- transition metal dichalcogenides, trigonal-prismatically coordinated layers, phenomenological theory of CDW state 0-80200
 triangular lattice, thermodynamic props., effect of vacancy defects determ. by cell cluster method 0-79959
 TTF-TCNQ, Landau theory of phase transitions 0-92666
 two dimensional real matter, low density free energy in canonical thermodynamics plasmas 0-87852
 two-centre Lennard-Jones liquids, free energy, perturbation theory 0-79656
 type II superconductor, bounded, intermediate state struct. form. near crit. field, role of surface 0-80465
 type-II superconductors, anisotropic, lower crit. field 0-60153
 Ag-Zn, molten, EMF meas. of activities using ZrO_2 solid electrolytes (Japanese) 0-88339
 AgCl: Cd²⁺, heavily doped, free energy and point defect distrib., integral eqn. method 0-107219
 Al₂₀Cu₂₅Zr₅₅ metallic glass, inelastic deform., free energy spectra 0-71699
 Ar, solid, equil. props., uncorrel. pairs approx. 0-84303
 Au-Zn, molten, EMF meas. of activities using ZrO_2 solid electrolytes (Japanese) 0-88339
 AuCu-Al thin film bilayer system, phase formation, backscattering spectra 0-96728
 Ba, silicates, solid state reactions, thermodynamics and kinetics (German) 0-76236
 BaMnF₄, pure and Co doped, ferroelec. antiferromag., dielec. anomalies 0-71288
 Ba₂TiO₄, Ba₂Ti₇O₄₀, standard Gibbs free energy of formation, EMF meas. at 673K 0-85207
 Bi-S liquid soln., S activities meas. by EMF method (Japanese) 0-70425
 C-C interaction energy, thermodynamics of steels 0-93793
 CaGa₂O₄ and CaGa₄O₇, cryst., thermodynamic parameters of reactions of form., thermodynamic stability 0-108726
 CaWO₄, cryst. growth from solns. in melts, kinetics parameters and thermodynamic props. 0-59424
 Ce-S-O equilibrium in molten Fe (Chinese) 0-104423
 Cl⁻ hydration complexes, gas phase, electrostatic calcs. 0-100055
 Cr, spin density wave state, phenomenological free energy density description 0-75720
 Cr-Ge, thermophysical props., at elevated temp. 0-103493
 Cs-SiO₂-Al₂O₃ system interactions, getter development for radiocaesium 0-83208
 CsNiF₃, one dimensional planar model with symm. breaking fields, thermodynamics, static props. 0-97111
 Cu₂O, standard free energy of formation, by EMF method with solid oxide electrolyte at low temps. (Japanese) 0-88338
 Cu₄₀Zr₆₀, Cu₅₆Zr₄₄, and Cu₆₀Zr₄₀ metallic glass, inelastic deform., free energy spectra 0-71699
 ErRh₂B₄, ferromag. superconductor, vortex phase 0-80441
 Fe, Gibbs energy in BCC and liquid states rel. to FCC, Fe-C and Fe-N phase diagrams 0-60846
 Fe-C phase diagram, thermodynamic anal. 0-60846
 Fe-N phase diagram, thermodynamic anal. 0-60846
 Fe-Zn, homogeneous phases, Gibbs free energies of form., Knudsen effusion method 0-66481
 Fe₂B₂O₇, improper ferroelectric, dielectric props., IR radiation pyroelectric detection 0-80711
 Fe₂O₄, standard free energy of formation, by EMF method with solid oxide electrolyte at low temps. (Japanese) 0-88338
 Fe₂O₃, standard free energy of formation, by EMF method with solid oxide electrolyte at low temps. (Japanese) 0-88338
 Ga-Ge-Zn ternary alloys, thermodynamic props., EMF meas. 0-81033
 Ge-Si, phase diagrams near melting point, Helmholtz free energy, heat of solution 0-70379
 GeP, thermodynamic characts. 10-300K, interatomic bond elasticity 0-59677
 H₂, embrittlement adsorption or decohesion, mechanism 0-97643
 H₂O, liquid, free energy calcs. by random network model 0-92688
³He, liquid, surface fluctuation influence on free energy, surface tension (Russian) 0-92746
 HF, liquid, viscosity at melting point, free energy (Russian) 0-92699
 Hg₂Br₂, nonintrinsic ferroelastic, thermal expansion and thermodynamic potential 0-88344
 I⁻ hydration complexes, gas phase, electrostatic calcs. 0-100055
 K, self-diffusion, high temp. bulk modulus determ. 0-79976
 KCl-NaCl mixed crystals, contact angles and free energies at solid/melt interface 0-64937
 LaMnO₃, stoichiometric manganite form. reaction, thermodynamic characts. 0-108727
 Li/TiS₂(TiSe₂)(Ti₁₁S₂), electrochem. obs. of Li intercalation 0-61216
 LiAlCl₄, fast ionic conductor, thermodynamic and phase props. 0-89211
 LiAlCl₄, solid and molten electrolyte, thermodynamic stability 0-107447
 Li₂MO₂ (M=transition metal), thermodynamic investigations 0-89210
 Li₂N, vaporisation, studied by Knudsen effusion method 0-92662
 LiRbSO₄, order-disorder phase transitions with many-minimum potential, thermodynamic props. 0-96623
 Mn-Ge, thermophysical props., at elevated temp. 0-103493
 NH₄HSeO₄, ferroelec. phase transition, pyroelec. props. 0-60513
 (NH₄)₂SO₄(BeF₄), order-disorder phase transitions with many-minimum potential, thermodynamic props. 0-96623
 Na-Cs, liq., struct. factor, free energy of mixing, and electrochem. pot., thermodynamic calc. 0-96436
 Na₂O-B₂O₃-GeO₂ system glass-forming melts, mass spectrometry obs. of thermodynamic props. 0-97468
 Nb₂Al, prep. by reduction of Nb₂O₅ and Al₂O₃ by CaH₂, thermodynamic calc. 0-100809
 Ni alloys, aluminising, thermodynamic anal. of phase transforms. 0-76413
 Ni-Cr(Fe)(Cu) alloy, matrix effect in SIMS anal. using O₂⁺ primary beam 0-76576
 PbO, standard free energy of formation, by EMF method with solid oxide electrolyte at low temps. (Japanese) 0-88338
 PdO, free energy of form. using impedance dispersion analysis 0-108728
 Pd₉₀Si₁₀ metallic glass, inelastic deform., free energy spectra 0-71699
 Sb, liquid, diffusion of O₂, activity coeff. 0-65267
 Sb₂O₃, standard free energy of formation, by EMF method with solid oxide electrolyte at low temps. (Japanese) 0-88338
 Si-Ge, impurity states, A- and B-centres, electron, hole thermionic emission rates 0-96813
 β-SiC, thermodynamic props., temp. depend., 5 to 300K 0-96666

free energy continued

- SiP, thermodynamic characts. 10-300K, interatomic bond elasticity 0-59677
 Sr Nb₂O₆, crystallography, polymorphism and isomerism, X-ray diffr. and DTA study 0-100216
 SrWO₄, cryst. growth, from Na₂WO₄ melts, thermodynamic props. 0-107084
 Ta BCC lattice, strain ordering in interstitial solutions 0-107420
 Tb₂(MoO₄)₃, improper ferroelectric, dielectric props., IR radiation pyroelectric detection 0-80711
 (Th,U)O₂, burnup simulated, high O₂ pot., chem. state 0-91220
 Ti, liquid, viscosity at melting point, free energy (Russian) 0-92699
 V, liquid, viscosity at melting point, free energy (Russian) 0-92699
 V-Ge, thermophysical props., at elevated temp. 0-103493
 VO₂, metal-insulator transition, electron correls. and spin dimerization, thermodynamical study 0-70615
 W, self-diffusion, high temp. bulk modulus determ. 0-79976
 Zr, liquid, viscosity at melting point, free energy (Russian) 0-92699
 Zr₁₄, high-temp. enthalpy, X-ray powder diffr. data 0-107446
 ZrO₂, doped, ionic cond., theoretical model 0-107552

free field rooms see anechoic chambers

free induction decay (optical) see optical coherent transients

free radical reactions

- acetylperoxy radicals, absorpt. spectrum and reaction kinetics 0-91571
 benzophenone ketyl radical, in micelle, decay rate in mag. field, photolysis meas. 0-85154
 bromotrifluoromethane, IR multiphoton selective dissoc., effect of acceptor radicals 0-66854
 chemically induced dynamic polarisation in strong mag. field, radical rotation influence 0-76509
 iodotrifluoromethane, IR multiphoton selective dissoc., effect of acceptor radicals 0-66854
 methyl radical + O(F), infrared chemiluminescence obs. 0-61080
 pentafluoroacetone, IR laser induced decomp., free radical mechanism 0-71924
 photolytically initiated, high temp. kinetics meas. technique 0-61085
 recombination probability in liqs., HF mag. field, reson. effect 0-93737
 thiamine (vitamin B₁₂), aq. soln., radiation induced reactions 0-93779
 AgBr crystal produced by action of free radicals, developability 0-66838
 C₃+NO(O₂), reaction kinetics, laser induced fluoresc. obs. of allene photolysis 0-66820
 ClO+formaldehyde, expt. showing no reactivity, stratospheric implications 0-90119
 ClO+HO₂, reaction rate constns. and products at 298K, discharge flow mass spectra 0-67391
 HO₂+HO₂, gas phase reaction mechanism, FT IR spectrosc. obs. 0-85163
 NF+H(NF), electronically-excited free radical reactions 0-97707
 NF₂+H(O₂N), electronically-excited free radical reactions 0-97707
 NH₂+O₃, reaction mechanism, flash photolysis obs. 0-104425
 O+methane →OH+methyl reaction, photolytically initiated, high temp. kinetics meas. technique 0-61085
 OH+gaseous S compounds, lower atmos. chem. 0-61870
 OH+H₂O₂ →HO₂+H₂O, reaction rate constns., laser induced fluoresc. 0-101017
 OH+H₂SO₄, collisional reaction probabilities atmospheric chem. 0-90168
 OH+OCS(CS₂), lower atmosphere chem. 0-61870
 OH+RH →H₂O+R, radical substitution reaction 0-81321
 OH+trans-2-butene, reaction products, O₂ and NO₂ effects obs. 0-85156

free radicals

- see also free radical reactions; paramagnetic resonance of free radicals
 σ*, ESR of radical in N-bromosuccinimide, X-irrad. 0-66037
 N-acetylglycine, X-irrad., stable radical electronic and mol. struct., ENDOR and ESR 0-80637
 acetylperoxy radicals, absorpt. spectrum and reaction kinetics 0-91571
 adamantane, γ-irrad., free radicals EPR and ENDOR 0-69170
 alkyl halide and σ* anion radicals, stability 0-89468
 allyl radical, restricted SCF and MC SCF calc. of C_{2v} and C_s structs. 0-83289
 bacteriorhodophyll radicals, role in primary charge separation of Rhodospseudomonas viridis 0-63688
 bacteriopheophytin b radicals, role in primary charge separation of Rhodospseudomonas viridis 0-63688
 benzene radical cation in solid Ar, fluorescence spectra obs. 0-83382
 benzophenone ketyl radical, in micelle, decay rate in mag. field, photolysis meas. 0-85154
 N-benzoylaminoethyl radical, from X-irrad. hippuric acid, ¹⁴N and ¹H ENDOR study 0-71240
 benzyl bromide, photolysis, free radical form., investig. 0-102523
 benzyl chloride, photolysis, free radical form., investig. 0-102523
 benzyl radical, ¹²B₂-³B₂ transition in absorpt. spectrum, extinction coeffs. 0-102523
 benzyl radicals, monomethyl- and dimethyl-substituted, electronic spectra and electron affinity 0-63618
 bromobenzene -d₀(-d₅) radical cation, electron impact dissoc., secondary isotope effect 0-63836
 α-bromofluoro alkyl pi-radical, signs of hyperfine and quadrupole couplings, ESR determ. 0-97141
 bromofluoromethylene radical, laser-induced fluoresc., ¹A*⁻¹A' transition 0-91589
 chlorophyll a, cation radical formation by pulse radiolysis, oxidation and demetallation rate constns. 0-61505
 chlorophyll-a radical cation lifetime in water-acetonitrile soln. 0-72136
 comets neutral atmospheres, average random walk model for mol. phot. dissociation 0-77351
 difluoroethene, cis- and trans-, photoelectron-photoion coincidence study, fluoresc. obs. 0-95678
 doublet states, positive ion potential anal. in CNDO/BW calc. 0-91452
 ethyl radical, C-C bond barrier rot., IR spectra 0-76536
 fluorobenzene radical cations in solid Ne, laser-induced fluoresc. spectra, vibr. struct. of excited and ground states 0-95671
 formaldehyde anion radical, hyperfine coupling constns., vibr. depend., ab initio calcs. 0-87150
 halogermane radical anions, ESR spectra and struct. 0-87153
 5-halouracils, solid, radiation damage, free radicals in 5-fluorouracil single crystals. 0-71926
 hexafluorobenzene anion-radicals in squalane, ESR spectrum optical detection 0-95655

free radicals continued

- hexafluorobenzene radical anion, ^{13}C hyperfine interaction, EPR obs. 0-83392
- 1,3,5-hexatriene radical cation, in Ne matrix, laser induced fluoresc. and emission spectra 0-87163
- 1-hydronaphthyl radical, 4.2K absorpt. spectrum (*French*) 0-80809
- hydronaphthyl radicals embedded in naphthalene cryst., optical transition energies and ionisation energies 0-78595
- hyperfine struct., EPR cepstra method determ. 0-102531
- iodomethyl radical, vibr. excited, photofragmentation IR emission obs. 0-87162
- isopropyl radical, Ar matrix isolated, IR spectra and UV photolysis 0-66827
- lipids of membranes, free radical formation on UV irradiat. 0-81647
- metalloporphyrin, cation radical formation by pulse radiolysis, oxidation and demetalation rate consts. 0-61505
- methoxy, Jahn-Teller induced rovibronic effect, nuclear spin-electron spin hyperfine Hamiltonian 0-83298
- methoxy radical, LMR spectra anal. 0-63677
- methoxy radical and deuterate, vibronic level fluoresc. spectrum 0-58305
- methoxy radical prod. from 266 nm photolysis of methyl nitrite 0-76534
- methoxy radical UV emission spectra from methanol+Ar(Kr) reactions 0-91572
- methyl radical, hyperfine coupling consts., vibr. depend., ab initio calcs. 0-87150
- methyl radical, vibr. excited, photofragmentation IR emission obs. 0-87162
- methylene, $^1\text{B}_1\text{-}^1\text{A}_1$ separation, ab initio 0-106251
- methylene+HD(D_2)(H_2), isotopic exchange, interstellar implications 0-61087
- methylene peroxide, struct., energy levels, ab initio UHF and MRUHF NO CI calcs. 0-83287
- muonic radicals, μSR spectra obs. 0-69279
- naphthalenes, methyl substituted radical cations, UHF spin densities, additivity model calcs. 0-58139
- nitroxide free radicals in liquids, electron spin-echo obs. 0-63685
- nitroxyl radicals, cyclic, conform. flexibility, EPR obs. 0-91581
- organic, solid, selective pulse NMR expts. 0-60452
- organic doublet radicals in nematic and smectic liq. crystals, ENDOR obs. 0-91585
- peroxy chain radicals, reactivity and struct., EPR spectra, trapped in PTFE 0-66783
- phenol biradical prod. from O+benzene(-d), crossed mol. beam investig. 0-71902
- phenylcyclohexadienyl radical form in electron irradiat. benzene cryst., absorpt. and fluoresc. spectra study 0-89035
- piperidinyloxy 2,2,6,6-tetramethyl radical, recrystallised samples, EPR study 0-100615
- planar cyclic radicals, C-H proton isotropic hyperfine consts., C hybridisation 0-95646
- pyrene solutions, radical ion pairs, pulse radiolysis, time resolved EPR spectra meas. by ODMR of fluoresc. 0-83395
- radical radiation formation in solid organic compounds 0-85201
- RX^\cdot , radical anion stability conditions, pot. energy diagrams 0-85161
- spin exchange, anisotropic spin-density distrib. 0-102526
- stilbene anion radicals, photoinduced isomerisation, 77K 0-66818
- BF_2 radical, thermomechanical studies by mass spectrometry, enthalpy of form. and ionisation pot. determ., chem. bonds 0-81382
- BO_2^\cdot , II vibronic states, laser induced fluoresc. obs. 0-58301
- BeOH , struct. and electronic props., ab initio calcs. 0-74113
- BrO , free radical, Ar matrix absorpt. spectra, mol. vibronic states obs., spectroscopic const. determ. 0-83387
- C_2 , ($a^1\Pi_u$), prod. from IR multiphoton dissoc. of acrylonitrile 0-63723
- C_2 +NO, laser-induced chemilum. reaction 0-61101
- C_2 + O_2 , $\text{C}_2(\text{X}^1\Sigma_g^+)$ and $\text{C}_2(a^1\Pi_u)$ intersystem crossing and free radical kinetics 0-95668
- C_2 + $\text{O}_2(\text{NO})$, IR laser photolysis of polyat. mols. photochem. appls. 0-66835
- C_3 production by IR multiphoton allene photolysis, vibr. relax., chem. kinetics 0-66820
- CCO radical, heat of form. calc., geometries excitation energies and vibr. freq. calc. using POL-CI wave functions 0-89512
- CCl, reaction rate const. determ. using laser-induced fluoresc. technique 0-97682
- CCl_2 , reaction rate const. determ. using laser-induced fluoresc. technique 0-97682
- CClF, reaction rate const. determ. using laser-induced fluoresc. technique 0-97682
- $\text{CCl}(\text{X}^1\Pi)+\text{methylhalosilanes}$, reaction rate const. determ. by kinetic absorpt. spectroscopy 0-97683
- CF_2+H , IR matrix isolation spectra 0-97706
- CH_2 , formed by laser photolysis of methylamine fluoresc. obs. 0-97710
- CH radical, SCF theory, multiconfig., direct orbital optimisation 0-87049
- CH radical, sputtered, rotational and vibrational excitation 0-69224
- $\text{CH}(\text{A}^2\Delta)$ radicals, electronically excited, lifetimes and quenching rate constants meas. 0-69188
- CHF radical, $\text{A}^1\text{A}^1\text{-X}^1\text{A}^1$ transition, laser induced fluoresc. 0-95660
- CN, ($\text{A}^2\Pi_i\text{-X}^2\Sigma^+$) and ($\text{B}^2\Sigma^+\text{-X}^2\Sigma^+$) yields from HCN photodissoc. 0-87141
- CN, ($\text{X}^2\Sigma^+$), prod. from IR multiphoton dissoc. of acrylonitrile 0-63723
- CN, $\text{B}^2\Sigma^+\text{-A}^2\Pi$ 0-0 and 1-0 bands, laser excitation spectra 0-91588
- CN formed by laser photolysis of methylamine, fluoresc. obs. 0-97710
- CN free radical, $\text{A}^2\Pi\text{-X}^2\Sigma$ Red system, perturbation analysis 0-87247
- CN, internal energy distrib. following vinyl cyanide photodissoc., temp. depend. 0-78638
- CN^* , $\text{B}^2\Sigma^+$ state, fluoresc. decay dynamics, collisional quenching and radiative lifetimes 0-58306
- ^{13}C , CIDNP, obs. in reactions of organic and inorganic radicals during pulse radiolysis 0-63660
- CiCO radical, struct. and props. calcs. 0-74112
- ClO, free radical, Ar matrix absorpt. spectra, mol. vibronic states obs., spectroscopic const. determ. 0-83387
- ClOO radical, struct. and props. calcs. 0-74112
- FCO, radical, struct. and props. calcs. 0-74112
- FOO radical, struct. and props. calcs. 0-74112
- $\text{FO}(\text{X}^1\Pi)$ radical from F+ O_2 reaction, VUV photoelectron spectra 0-104455
- HO radical form. from $\text{H}_2+\text{N}_2\text{O}$ reaction on Pt surface, laser-induced fluoresc. obs. 0-108738

free radicals continued

- HO_2 free radical, dipole moments and Stark effects from microwave spectra 0-63623
- HO_2 prod. from $\text{H}+\text{O}_2+\text{Ar}$, rate const. calc. 0-101026
- HO_2+HO_2 , gas phase reaction mechanism, FT IR spectrosc. obs. 0-85163
- HO_2+O_3 , reaction kinetics, laser mag. reson. obs. 0-102528
- HSO radical, Doppler-limited dye laser excitation spectroscopy, rot., distortion and spin-rot. interaction const. determ. 0-83383
- IO, free radical, Ar matrix absorpt. and emission spectra, mol. vibronic states obs., spectroscopic const. determ. 0-83387
- KPF $_6$, γ -irrad., trapped free radicals EPR obs. 0-63683
- MgOH, struct. and electronic props., ab initio calcs. 0-74113
- ND, singlet-triplet transitions, high resolution spectrosc. with new emission source (*French*) 0-57383
- $\text{NF}+\text{H}(\text{NF})$, electronically-excited free radical reactions 0-97707
- $\text{NF}_2+\text{H}(\text{O})(\text{N})$, electronically-excited free radical reactions 0-97707
- NH, singlet-triplet transitions, high resolution spectrosc. with new emission source (*French*) 0-57383
- NH_2 radical, mag. hyperfine interactions, zero-point vibr. effects 0-58167
- NH_2+O_3 , reaction mechanism, flash photolysis obs. 0-104425
- NH_3^+ radical, mag. hyperfine interactions, zero-point vibr. effects 0-58167
- N_2H_4^+ radical, mag. hyperfine interactions, zero-point vibr. effects 0-58167
- $\text{NH}(\text{NH}_2)$ obs. in laser photolysis of methylamine, fluoresc. obs. 0-97710
- NO_3 , detect. in polluted troposphere by differential optical absorpt. 0-77036
- OH, fundamental vibr. band, mag. rot. spectrosc. obs. 0-86446
- OH in flames, laser excitation dynamics 0-74201
- OH, optimum mol. consts. and term values, $\text{X}^2\Pi$ and $\text{A}^2\Sigma^+$ states, vibr.-rot. and microwave freqs. 0-95577
- OH, Pt catalytic oxidation of H_2 and D_2 , matrix isolation and laser fluoresc. obs. of prods. 0-66865
- OH+gaseous S compounds, lower atmos. chem. 0-61870
- $\text{OH}+\text{H}_2\text{O}_2\rightarrow\text{HO}_2+\text{H}_2\text{O}$, reaction rate consts., laser induced fluoresc. 0-101017
- OH+OCS(CS_2), lower atmosphere chem. 0-61870
- OH+organic compounds photooxidation reactions in atmosphere, rates, reactivity and mechanism 0-72104
- $\text{OH}+\text{RH}\rightarrow\text{H}_2\text{O}+\text{R}$, radical substitution reaction 0-81321
- OH+trans-2-butene, reaction products, O_2 and NO_2 effects obs. 0-85156
- SO_2F , dye laser excitation of vibr. levels of upper electronic state, mol. fluoresc. meas. 0-83402
- Si biradical, six-coordinate, mol. mobility two-spin probe investig. 0-102529
- SiH , emission spectroscopy, in $\text{H}_2\text{-SiH}_4$ glow discharge 0-69984
- SiH_3 radical, hyperfine coupling consts., vibr. depend., ab initio calcs. 0-87150
- XeF^* , $\text{B}^2\Sigma^+$ and $\text{C}^2\Pi_{3/2}$ states, fluoresc. decay dynamics, collisional quenching and radiative lifetimes 0-58306

freezing

see also refrigeration

- bacteriophages, freeze drying method for electron microscopy 0-104826
- biological specimen freeze drying technique for SEM 0-104828
- biological specimen replication at -150°C with improved freeze-fracture apparatus 0-85560
- cells, mouse embryo, innocuous freezing during warming 0-94175
- cells, volumetric changes during freezing and thawing, thermodynamic model 0-108863
- ceramic compounds, lyophilisation parameters, freeze-drying synthesis 0-97453
- concrete, flowing, expt. studies (*Japanese*) 0-89298
- freeze-etching improvement using evaporated film 0-85558
- ice nucleation on AgI, exptl. verification of ice-forming activity theory 0-101406
- metal fixed points, limitations caused by trace impurities 0-105644
- monolayers, Lennard-Jones system, melting in external field, freezing, temp. determ. 0-65362
- plant root transport studies using ion localisation, freeze substitution method 0-85569
- polymorphous material, Stefan problem, melting or freezing, interfacial boundaries 0-64350
- red blood cell freezing, cryopreservation and refrigeration 0-67262
- Ross Ice Shelf (Antarctica), basal freezing, confirmed by core drilling 0-101393
- secretory granule membrane, particle clustering induced by centrifugation, freeze-fracture anal. 0-85559
- spherical particles, force exerted by freezing interface 0-107083
- supercooled aqueous solution, freezing, generalised analytical soln. 0-92142
- TEM specimen freeze drier, all-glass design 0-82854
- water droplet freezing process under supercooled conditions 0-65192
- C-O white dwarf freezing, C-O eutectic model 0-77405

Frenkel defects

- acceptor-donor-acceptor complex, Frenkel excitons and ionic excited states 0-92824
- alkali halides, irradiated at room temperature, stored energy 0-79839
- diffusion-controlled defect annealing, theory 0-92520
- ionic crystal, influence of defect interaction upon their recomb. 0-84207
- semiconductors, glassy, diamag., photostructural changes, mechanism 0-92557
- steel, austenitic stainless, Cr-Ni, resist. damage rate during neutron irradiat. at 23K 0-96571
- superionic conductor, with fluorite struct., activation vol. 0-107557
- unstable, form. and collapse, defect migration, electron irradiat. effects, computer simulation 0-92523
- AgBr(Cl), ionic transport, defect form. and migration energies, quasiharmonic model 0-107538
- AgCl, ionic mobility, diffusion coeffs., defect mobility energies 0-65284
- AgCl(Br), enhanced defect form., mean field theory 0-107220
- Ag $_2$ Se, electronic and electrogalvanic props. in α -phase region (*French*) 0-107820
- $\text{BaCl}_2(\text{F}_2)$, sp. ht. meas., Schottky-type diffuse phase transitions, defect form. energies and entropies 0-107441
- BaF_2 , ionic cond., activation vols., freq. depend. cond., press. effects 0-100354
- BeF_2 , vitreous, ionic transport and defect struct. 0-107472

Frenkel defects continued

- CaF₂, ionic cond., activation vols., freq. depend. cond., press. effects 0-100354
 CaF₂, mol. dynamics studies of superionic conductors 0-107547
 CdF₂, ionic cond., activation vols., freq. depend. cond., press. effects 0-100354
 Cu₂O:Mn, photomemory mobility components, charged centre conc. 0-103725
 Fe, irradiated with electrons then annealed, magnetoresistance at 20K (*French*) 0-103677
 GaAs, primary radiation defect separation by elec. field 0-92522
 Ge:Se, electron-hole drop lifetime, quenching temp. influence 0-59889
 Hg_{1-x}Cd_xTe, grown from melt, Kirkendall and Frenkel effects 0-100365
 KBr, cation defects creation mechanism 0-75224
 KBr, defect accumulation under electron irradi. at 4K 0-107233
 KBr, recomb. in ionic crystals, defect interactions 0-84207
 KCl, ionic cond., defect parameters, diffusion coeffs. 0-79978
 KCl:S²⁺(SO₄²⁻), ionic cond., defect parameters, diffusion coeffs. 0-79978
 KCl:S²⁺(SO₄²⁻), defect parameters, self-consistent set, ionic cond. meas. 0-107487
 LiH, defect form. at low temp., EPR, thermolum. and TSC study 0-107222
 MgO, electron irradiation damage, cryst. defects 0-107320
 Na₂Al₂Si₂O₇(NaX)_{2n}, X=Cl, Br or I, sodalites, thermal destruction of colour centres (*Russian*) 0-84169
 NaBr Frenkel pairs, interactions forming enrichment centres 0-96518
 NaCl(Br), X-ray or UV irradiated, cation defects creation mechanism 0-75224
 PbBr₂(Cl₂)(I₂), ionic cond. and activation volumes, high press. effects 0-100353
 PbF₂, sp. ht. meas., Schottky-type diffuse phase transitions, defect form. energies and entropies 0-107441
 RbCl(Br), cation defects creation mechanism 0-75224
 n-Si, defect charge states, complex form., gamma-ray effects 0-96564
 SrCl₂, pure and doped, disorder and defect props. 0-107217
 SrCl₂, sp. ht. meas., Schottky-type diffuse phase transitions, defect form. energies and entropies 0-107441
 SrF₂, ionic cond., activation vols., freq. depend. cond., press. effects 0-100354
 ZnO, defect struct. calc., doping effects 0-107218
 ZnTe, irradiation induced radiative centers obs. 0-66290

frequency allocation

- EM spectrum, overcrowding and use by radio astronomy 0-85874
 space appl. and research, WARC 1979 impact 0-105147

frequency changers *see frequency converters***frequency control**

- see also automatic frequency control*
 quartz clock, accuracy, radio signal control (*French*) 0-95079

frequency converters

- see also mixers (circuits); optical frequency conversion*
 tunable IR solid-state laser characteristics and principles 0-87406
 CdTe linear electro-optic translation of IR laser wavelengths 0-78878

frequency division multiplexing

- contradirectional frequency-selective couplers for guided-wave optics 0-102803
 incoherent optical correlation operations 0-99650
 multimode digital system wavelength multiplexing constraints in 850 nm region 0-63942

frequency-domain analysis

- ECG frequency-domain analysis 0-85521
 glass fibre drawing process, characterization and control 0-58826
 graded-index optical fibre intermodal dispersion, frequency-domain meas. 0-58729
 speech adaptive noise cancellation by short-time Fourier transform 0-91976

frequency measurement

- see also atomic clocks*
 atomic time and frequency standards development at Shanghai observatory, China 0-105617
 automatic frequency meters, construction and performance (*French*) 0-62658
 clock error with a Wiener predictor and by numerical calculation 0-82748
 CMOS ICM 7216B multifunction counter used for time, frequency or period measurement (*German*) 0-74092
 digital filter appl. (*Russian*) 0-57264
 electromagnet. meas., precision, conf., Braunschweig, Germany (Jun. 1980) 0-98903
 error probability anal. (*Russian*) 0-90823
 instantaneous frequency measurement of micro-wave range by two different point detected signals (*Japanese*) 0-73327
 laser, far IR optically pumped, monitoring by piezoelec. transducers 0-102729
 laser frequency measurement using supercond. point contacts 0-90824
 lasers, precise meas. in submm. and IR regions 0-99698
 methyl alcohol laser, freq. meas. at 4.25 THz using Josephson harmonic mixer and phase lock techniques 0-95078
 quantum oscillator, phase automatic freq. control parameters, optimal values (*Russian*) 0-77814
 spectrum analyser using FFT (*Spanish*) 0-90825
 standards comparison, improved accuracy 0-95062
 users' manual on time and freq. meas. 0-94934
 CO₂ laser, stabilized, meas. of freq. 0-99699
 CO₂ laser transitions, absolute freq. meas. by multiplication of CO₂ difference freq. 0-105618
 Cs clocks made by Oscilloquartz Company, investigation of metrological characts. 0-101787
 D₂O laser phase locking to freq. standard, CO₂-OsO₄ laser freq. meas. 0-95080
 H maser frequency, nonuniform magnetic field effect 0-99687
 H masers, with automatically tuned resonators 0-95859
 He-Ne laser, methane-stabilized at 88 THz 0-73304
 He-Ne laser, methane-stabilized, meas. of freq. at 88 THz accurate to ± 3 parts in 10⁹ 0-99700
 He-Ne laser, stabilized, meas. of freq. 0-99699
 NH₃ 81.5 μ m subMM laser, freq. meas. by CO₂ laser difference freq. comparison 0-74415
 W-Ni(Co) point-contact diodes as harmonic generators and mixers, DC bias dependence 0-75653

frequency meters

- automatic, construction and performance (*French*) 0-62658
 Heathkit IM-4100 multi-function, circuit diagrams and performance data (*French*) 0-73348
 Watford Electronics 0-050 MHz digital frequency meter measures frequency and time intervals 0-68191

frequency modulation

- coupled laser oscillators, injection modulation 0-99773
 electrooptic polarization modulated injection laser 0-58591
 flow-detection apparatus, noise immunity, sounding signal freq. modulation 0-89441
 hearing, theory of detection for low modulation freqs. 0-61586
 ionosphere, heating by powerful radio emission with random modulation of carrier freq. 0-109310
 laser gas analysers, freq. modulation appls. 0-85246
 laser interferometers, AM and FM operation and applications (*German*) 0-86389
 optical fibre analogue signal transmission system (*German*) 0-58679
 shot noise limited stimulated Raman gain laser system for monolayer vibr. spectroscopy 0-62744
 CO₂ laser, detuning effects of FM mode-locking 0-69434
 Ga_{1-x}Al_xAs DH injection laser, FM at microwave freq. rates 0-58610
 He-Ne 3.39 μ m laser, FM eliminated CH₄ locked freq. stabilisation in dual feedback control 0-99772
 He-Ne laser, beat freq., high displacement sensitivity meas. 0-95926

frequency regulation *see frequency control***frequency response**

- back diode amplifier, use at low temp. 0-57324
 concatenated fibre-optic cable, cumulative baseband frequency response models 0-78983
 far IR laser hybrid output couplers, metal mesh dielectric mirror design and fabrication 0-58554
 loudspeaker system amplitude and phase response rel. to driver alignment on baffle 0-92010
 MOS inversion layers, freq. response of charge transfer 0-88638
 multielement acoustic array characterisation by acousto-optic diffraction 0-99911
 piezoelectric receivers, amplitude-freq. response determ. for acoustic emission 0-87699
 pulse preamplifier for fast photocond. decays meas. 0-57326
 SAW devices, automatic response measurements for large time-bandwidth SAW devices 0-74677
 He cooled reactor turbine control experiences Fort St. Vrain HTGR (*German*) 0-57927
 Se photocell optical vibration transducer 0-77768
 Si accelerometer, batch fabricated 0-73328

frequency stability

- see also frequency control; laser frequency stability*
 electron cyclotron maser, fundamental mode, linear theory 0-58496
 IMPATT source, frequency-stabilised, 115 GHz 0-67573
³He gas thermometer secondary standard for 0.5 to 40K 0-82762
 Rb maser oscillator, freq. domain meas. 0-83574

frequency synthesizers

- see also frequency converters*
 digital synthesis of low-freq. signals, performance data for LEA GSN 20 and GSN 80 series (*French*) 0-73393

frequency synthesizers *see frequency synthesizers***friction**

- see also internal friction; lubrication*
 abraded surfaces, topography rel. to contact area and abrasion mechanism 0-58986
 air turbulent flow in heated channel, effect of gravitational field 0-64533
 asymmetrical friction in piston-cylinder device and effect on melting curves of In, Bi 0-86292
 N. Atlantic Ocean, bottom friction rel. to wind-induced sea level changes on Scotian shelf 0-72531
 brass, α - β phase transformation caused by friction 0-76378
 brass, cold rolling, inhomogeneous texture 0-89251
 Brownian motion, bistability effects in periodic potentials 0-68139
 camera lens shutters, friction coefficient nonreproducibility evaluation 0-62765
 circular cylinder, local heat transfer by turbulence of free-stream flow of viscous liquid, theoretical determ. of influence (*Russian*) 0-96252
 Colmonoy hardfacing materials, friction characts. in high temp. Na (*Japanese*) 0-89356
 composite friction and bearing materials, development, friction and wear theory, review 0-60979
 composite materials, water lubrication, wear studies 0-60984
 contact, frictionally heated, thermoelastic deform. 0-83764
 contact platform effect, roughness, friction and wear 0-64497
 Coulomb friction, elast. solid with one-sided contact (*French*) 0-64485
 dry sliding wear, role of dynamic recrystallisation 0-108599
 education, circular motion with friction, numerical and analytical solns. 0-57029
 education, speed and displacement relations for tire skids, program for PET 0-57038
 elastomers, surface roughness, friction and adhesion 0-66674
 elastometric materials, friction testing using reciprocating friction and wear tester 0-76451
 external friction reduction by forced piezoelec. oscillation 0-92096
 film rupture in laminar and turbulent lubrication, inertia forces effect 0-74813
 floors, small mobile apparatus for meas. coeff. of friction 0-69747
 fluorocarbon polymer thin films for lubrication of Au contact surfaces 0-89157
 gas flow through cracks, surface roughness influence 0-69929
 high speed rubbing, thermomechanical interactions 0-83769
 Inconel hardfacing materials, friction characts. in high temp. Na (*Japanese*) 0-89356
 liquid-friction bearing tester, description and improvements over existing designs 0-64503
 materials under melting, intensity calc. 0-103416
 metal cutting, direct SEM obs. of adhesion and frictional sliding 0-104412
 metal-insulator pairs, frictional heating at cryogenic temps., rel. to supercond. magnet technology 0-66671
 metallic glasses, friction coeff. determ. using sliding friction rig 0-89355
 metallic powder materials, deform., boundary conditions on sliding surfaces 0-60978

friction continued

- metals, rheological interpretation of planar deformed state in extremal friction regime (*Russian*) 0-64385
- metalworking, role of friction, and energy saving in deep drawing 0-76271
- polymers, entanglement, topological theory, chain centre-friction coeffs. 0-91709
- PTFE, wear, sliding speed, contact press. and rubbing surface temp. 0-76372
- quadratic friction quantisation, point object in viscous field 0-68076
- rectangular vibrating plates separated by liquid filled gaps, viscosity friction calc. (*German*) 0-105504
- rigid indenter and elastic halfspace, dynamic contact with perfect adhesion and frictional slip 0-58980
- rubber, friction against paper and polymer film surfaces, microroughness effect 0-71763
- self-excited vibrations in lubricated friction 0-58984
- shear loaded interface crack, friction effects, contact zones, stress fields 0-79225
- shuttlecock, terminal vel. in vertical fall 0-90627
- slab, surface displacements for high speed rubs 0-83767
- sliding bodies, friction apparatus for meas. normal displacement 0-99977
- sliding contact, friction, wear, temp. anal. 0-93659
- steel, austenitic, friction in vacuum of type U8 steel under microshock loading (*Russian*) 0-108583
- steel, austenitic stainless, unlubricated, friction, wear and microstruct. of types 304, 316 and Nitronic 60 0-108589
- steel, friction and wear during hot forging 0-89358
- steel, friction measuring test for use under conditions of high normal interfacial force 0-76454
- steel, stainless, Cr-Ni-Mo-Mn (16.55, 10.23, 2.28, 1.34 wt.%), hardfacing materials, friction characts. in high temp. Na (*Japanese*) 0-89356
- steel 45-antifrictional alloys friction pairs, electrochem.-mech. investigation (*Russian*) 0-76367
- stellite hardfacing materials, friction characts. in high temp. Na (*Japanese*) 0-89356
- stochastic quantisation, nonlinear wave eqn. 0-98825
- straining experiments, in situ, strong frictional force, quantitative anal. 0-100244
- tester, variable speed 0-100990
- thermal pipes, sonic restriction on power at high temp. 0-103023
- turbulent boundary layer, surface friction meas. using plane Pitot tube 0-79284
- variable resistance boundary layers, frictional resist. effects on motion of bodies 0-96243
- viscous liquid flow through annular clearance over rotating inner cylinder 0-64626
- wear and friction, material aspects in manufacturing processes 0-81210
- wheel temperature in railroad service, effect of brake shoes 0-93660
- zinc dialkyldithiophosphate surface film, prep. and nature 0-104300
- Ag, cold rolling, inhomogeneous texture 0-89251
- Al, cold rolling, inhomogeneous texture 0-89251
- C diamondlike layers, RF plasma deposited, frictional props. 0-71762
- Cd film, dry lubrication on C steel, tribological behaviour 0-89364
- Co base alloys, unlubricated, adhesive wear study 0-108593
- friction surface structural investigation, O₂ surface diffusion (*Russian*) 0-96726
- Cu pin against steel ring, dry sliding wear, role of dynamic recrystallisation 0-108599
- Cu pin-on-disc friction and wear under boundary lubrication, dissolved O₂ effect 0-76365
- Cu-Sn industrial bronzes, Sn diffusion in deform. zone influence on wear resistance, friction (*Russian*) 0-108582
- MoS₂ solid lubricant, antifriction and elec. props. depend. on oxidation temp., dopant influence 0-108584
- NbSe₂ solid lubricant, antifriction and elec. props. depend. on oxidation temp., dopant influence 0-108584
- Ni base alloys, unlubricated, adhesive wear study 0-108593
- Ti alloys, lubrication by chloroparaffins, friction and wear (*Russian*) 0-93657
- Ti base composite sintered bearing materials, metallic solid lubricant infiltrated, antifriction props. 0-60981
- Ti, friction surface structural investigation, O₂ surface diffusion (*Russian*) 0-96726
- Ti-Al-V alloy, friction coeff. reduction on injection with TiC particles 0-85086
- TiC, frictional characts. and contact-zone deform. in homogeneity range 0-66673
- UO₂ powder compaction, friction between particles and die walls 0-71620
- WC-Co hard alloys, hot-pressed, wear resist. under abrasive friction, heat treatment effect 0-66555
- WS₂ solid lubricant, antifriction and elec. props. depend. on oxidation temp., dopant influence 0-108584

friction, internal *see internal friction***frictional electricity** *see triboelectricity***fuel**

- see also coal; fission reactor fuel; pulverised fuels*
- 100 MW fluidised bed combustion district heating plant burning high S content residual oils 0-108777
- alcohol, diesel engines auxiliary fuels 0-61230
- alcohol, ethanol and methanol, fuel for vehicles, gas turbines, and boilers, Brazil 0-61229
- biochemistry and biotechnology, conf., Helsinki, Finland, 27-31 Aug. 1979 0-57001
- biomass, H₂ production from water using biomass feedstock and bromination process 0-61459
- biomass energy R and D 0-66922
- biomass options for the Big Island of Hawaii 0-66921
- coal gasification, potential fuel source 0-93842
- coke, metallurgical, microstruct., using refl. light microscopy and image anal. 0-66732
- energy-political questions nationally and internationally for West Germany (*German*) 0-101072
- ethanol, as petrol substitute, increased use in USA (*Dutch*) 0-72004
- fossil, appl. of cross-polarisation ¹³C NMR with magic angle spinning 0-77819
- fossil fuel utilisation, reliability, maintainability and availability engineering 0-61234
- fossil fuels for use in MHD power stations 0-72074

fuel continued

- future reserves, projections to 2050 (*Dutch*) 0-61221
- liquid fuel supplies and synthetic fuel prod. 0-97753
- liquid fuels from biomass, biotechnology appls. 0-61225
- methane production from cellulose by sewage bacteria 0-72005
- methanol derivation from lignite, fuel appl. 0-61223
- petroleum spills on water, control using gellants 0-61496
- polymer interrelations, raw material 0-63876
- refuse derived, conversion to elect. energy at St. Louis refuse fuel demonstration project 0-93846
- solid propellant stress transducer evaluation 0-81245
- synthetic and fissile fuel prod. by Cat-D fueled SAFFIRE reactors 0-99280
- synthetic fuel manufacture using peat 0-97754
- synthetic fuel prod. by direct radiolysis using fusion radiation sources 0-61227
- synthetic fuels from wood, gasification of biomass in developing countries 0-61231
- UK policy suggestions for future, coal to oil and gas conversion, nuclear power 0-61224
- waste materials as fuels, refuse derived fuels, pyrolysis, hydrolysis, fluidised beds 0-66920
- wood energy in W. Virginia 0-72006
- wood energy program; industrial, New England 0-61233
- wood fuel resource, coordinated energy sources for production of heat, steam, electricity 0-61232
- wood sawdust, flash pyrolysis, cyclone, solar gas-solid chemical reactor (*French*) 0-61296
- wood waste gasification using flash pyrolysis and concentrated solar energy (*French*) 0-61226
- wood-waste fired power plants, economic feasibility anal. 0-66923
- C-based fuel production by CO₂ thermochem. reduction using solar energy 0-76610
- H storage in metal hydrides 0-61445
- H₂ as an energy source 0-108816
- H₂ for single cylinder diesel engines 0-61228
- H₂ internal combustion engines, electronic fuel injection techniques 0-72094
- H₂ photocatalytic production by carbohydrate conversion using RuO₂/TiO₂/Pt photocatalyst powder 0-94120
- H₂ production, electrolysis of steam, high temperature, in fusion reactors, synfuel production 0-72099
- H₂ production, high temperature fusion blanket design for synthetic fuel plant 0-99275
- H₂ production from coal by centrifugal separation from gasification products 0-76643
- H₂ storage as metal hydrides, props. and appls. 0-76661
- H₂ storage in form of metal hydrides 0-72096
- H₂/hydrocarbon fuel prod. via biomass conversion wastes by solar H₂O photoelectrolysis 0-89653
- fuel batteries** *see fuel cells*
- fuel cells**
- anode, electrochemical oxidation of H₂ and CO in fused alkali metal carbonates 0-72040
- cathodes, voltage losses 0-104503
- developments in electrochemical energy sources (*German*) 0-97770
- electric power generation, H₃PO₄ and molten carbonate fuel cell developments 0-66966
- electric vehicle power sources, fuel cell/secondary battery hybrid appls. (*Dutch*) 0-72037
- electrochemistry, power sources and energy science 0-101023
- honeycomb-type structures for high power batteries and fuel cells, possible use 0-72027
- materials needs, in energy conservation and storage 0-66958
- methanol-air, 50 W, with hydrophobic air electrodes 0-89609
- molten carbonate, development of S-tolerant compounds 0-72039
- molten carbonate fuel cell, electrolyte comp. effect on electrode kinetics 0-101092
- molten carbonate fuel cell performance, H₂S effect, mixed pot. anal. 0-81431
- molten carbonate fuel cell power plant, eng. development 0-66969
- oxygen electrodes, galvanostatic switching curve shapes 0-66965
- power plants for utility appls. 0-66967
- power station, 4.8 MW DC 0-89608
- types and construction principles (*Dutch*) 0-72038
- H-Cl electrochemically regenerative fuel cell, electrode kinetics and cell perform. 0-89610
- H₂-air-H₃PO₄ fuel cell performance, effect of NH₃ 0-108795
- H₃PO₄, assessment of alternative fuel cell designs for residential and commercial cogeneration 0-66970
- H₃PO₄ fuel cells, commercial prototype plant for dispersed electric power generation 0-66968
- NH₃ high temperature solid electrolyte, overpot. and product selectivity characts. 0-104504
- O₂ electrodes, galvanostatic transients, curve shape, 0 to 5 msec. 0-93868
- Pt and Pt/Ru electrocatalysts for methanol oxidation in acid electrolyte with improved steady state activity for fuel cell appls. 0-76629
- Pt, on C electrode, surface area loss in H₃PO₄ 0-101091
- S-tolerant components development for molten carbonate cell 0-89611
- fugacity**
- see also kinetic theory of gases*
- weakly ionised gas non-ideal behaviour, virial eqn. of state and fugacity coeffs. 0-79424
- full wave rectification** *see rectification*
- full wave rectifiers** *see rectifiers*
- function approximation**
- see also Chebyshev approximation; interpolation*
- furnaces, walking-beam, numerical soln. of two-dimens. temp. field, boundary condition modification (*Polish*) 0-87706
- function generators**
- see also pulse generators; square-wave generators; time bases*
- Echosimulator, function generator for meas. of US diagnostic equipment characts. (*German*) 0-104685
- Mossbauer effect work, function generator using IC 0-68334
- sinewave, simultaneous supply of fifty strain transducers, ship vibration testing 0-62652
- sweep, x-y recorder, sweep speed dependent on four terminal network transfer charact. 0-62649

functional analysis*see also harmonic analysis*

- bar, rectangular, torsion crack problem, harmonic function continuation technique soln. 0-99969
- composite multidimensional function decomposition into its components 0-79625
- dynamical systems, homoclinic and heteroclinic points in Hemon mapping, analyticity 0-82634
- fracture analysis, 2D linear, elastic, finite element anal. vs. the edge function method 0-99963
- gauge field theory, double counting, collective coordinate resolution of identity of unity 0-68359
- gauge theories, quantisation, without fixing gauge, functional technique 0-57471
- Helmholtz equation, 1-D three-body problem, Sommerfeld Maluzhinetz transformation 0-62524
- Ising model, critical temperature, modulated Pade approximant 0-84605
- Markov process generated by Langevin equations, WKB-type expansion 0-86212
- mechanical systems, follower load type, time invariant functionals 0-77609
- neural transformations of random signals, Wiener and of functionals of Markov chain 0-76727
- noise distorted function resolution into sum of exponentials, characteristic eqn. coeffs. 0-77707
- one dimensional function, resolution into sum of exponentials, roots of polynomial 0-77603
- Pade approximant, modulated, applied to Ising model critical temperature 0-84605
- quantum field theory, nonperturbative generating functionals for Green's functions 0-73588
- quantum mechanics, Feynman path integrals with Gaussian measure, Laplace transform method 0-62522
- relaxation distribution function, approx. methods and num. inversion of Laplace transform. 0-84720
- thermal conductivity, nonlinear, variational formulation, counter functional, exactness of soln. (Russian) 0-90800
- wave equation, reduced, fixed incident field, inverse problem 0-62484

functional equations

- closed time path Green's functions, transform. props. (Chinese) 0-105491
- composite multidimensional function decomposition into its components 0-79625
- metals, ground state of solids, spin density functional method, binding energy, compressibility 0-65477
- multiplicative functionals on diffusion processes 0-73286
- nonlinear differential equation, compactness of bounded trajectories of dynamical systems 0-82636
- optimal control, differential eqn., canonical, functional relation expressed by Volterra series (French) 0-73159
- random functional equations, stochastic approx. in Banach space (Japanese) 0-95038

functionals *see functional equations***functions***see also Bessel functions; Boolean functions; Green's function methods; random functions; recursive functions; transfer functions; vertex functions*

- f-function regularisation, symmetric spaces of rank 1, physical instabilities 0-57519
- exponential, single-step numerical method anal., approx. of exponential function 0-94950
- H-function of radiative transfer integral eqn. spectrum, calc. for semi-infinite medium 0-67540
- Laguerre functions, appl. to nuclear medicine washout curves 0-81521
- Meijer's G-function, differential props. 0-86072
- mixtures, multicomponent, anal., by method of additions 0-61187
- zeta function of quartic oscillator 0-62532

fundamental constants *see constants***fundamental law tests**

Aspect experiment, objective reality, causality in QED 0-99076

fundamental particles *see elementary particles***fundamental physics concepts** *see physics fundamentals***fundamentals of physics** *see physics fundamentals***furnaces***see also electric furnaces; refractories*

- gradient and mirror furnaces for Swedish materials science expt. in Texas 1 and 2 sounding rockets 0-104362
- graphite furnace atomic absorpt. spectrometry heated by capacitive discharge, determ. of elements 0-66892
- imaging furnace, appl. to thermal cond. and emissivity meas. of Ta 0-103667
- LPE, multi-layer, furnace design and fabrication (Japanese) 0-108366
- melting furnace of high efficiency using hot plate and spherical mirror 0-68202
- metallic thin films, vacuum deposition, ultra-high vac. technique 0-100791
- mirror furnace at Czochralski growth 0-60766
- Mossbauer furnace for amorphous alloy investigations 0-98916
- production, Nicrosil-Nisil thermocouples appl., 538°C to 1177°C 0-68198
- pyrometer, temp. meas. of bodies heated in solar furnaces 0-86312
- RF, floating-zone melting with viscous torque control 0-89140
- solar, Pd membrane diffusion-cell for separation H₂ containing mixtures 0-92245
- solar, thin films production appl. 0-89148
- space solar furnaces, for materials-science expts. 0-108786
- technology, IR applications 0-86431
- walking-beam, numerical soln. of two-dimens. temp. field, boundary condition modification (Polish) 0-87706
- C fibres, thermal expansion coeff. meas. using TEM fitted with furnace 0-102966

Furry theorem *see quantum electrodynamics***fuses, electric** *see electric fuses***fusion** *see melting***fusion, nuclear** *see nuclear fusion***fusion-fission reactors** *see hybrid reactors***fusion reactor ignition***see also fusion reactor materials; plasma heating; plasma production*
100 kJ CO₂ laser, Antares, status report 0-64075**fusion reactor ignition continued**

- ablative laser fusion implosion, scaling laws and spatial struct. 0-87915
- Antares CO₂ laser power amplifier, design 0-69423
- Antares laser fusion project, 300 kJ, 200 kA Marx energy storage module 0-68954
- automatic target alignment of Helios CO₂ laser system 0-74416
- black body radiation imploding in small cavity as inertial confinement fusion driver 0-86984
- catalysed D fusion reactor start-up chars. (Japanese) 0-86983
- chain reactions, kinetics, high electron temps., interactions with D-T plasma 0-68945
- characterization techniques for high quality ICF targets 0-86986
- Chinese research 0-78447
- compact ignition test reactor, engineering design using Bitter type magnet 0-102310
- conference, controlled fusion and plasma physics, Oxford, England (Sept. 1979) 0-77545
- conference, inertial confinement fusion technical digest, San Diego, CA, USA (Feb. 1980) 0-57012
- dense matter, laser driven fusion, laboratory expts. 0-75077
- double-sided electron beam generator for KrF laser excitation, fusion appl. 0-68956
- electron accelerator for inertial confinement fusion, Angara 5 features and design principles 0-63384
- electron beam, energy coupling to expanding thick-shelled target 0-96365
- electron beam fusion, pellet and pellet-blanket neutronics and photonics 0-74006
- electron gun, large-area cold-cathode grid-controlled, for Antares CO₂ laser amplifier 0-68955
- Engineering Test Facility/International Tokamak Reactor, plasma physics chars. 0-95420
- exploding liner gas confinement, liner velocity effects 0-79541
- exploding-pusher-tamper areal density, neutron activation meas. 0-91237
- focused beam ray tracing for laser fusion 0-83218
- gas-filled microballoons, radiation effects MEDUSA code calcs. 0-83220
- heavy ion acceleration, time-depend. study, fusion ignition appl. 0-86997
- heavy-ion fusion preaccelerator, 1.5 MeV, fibre-optic remote control system 0-73993
- hot-ion-mode ignition in a Tokamak reactor 0-73999
- ICF, production and energy flux concentration of REB accelerator 0-74026
- inertial confinement fusion, pulsed power aspects, overview 0-63382
- inertial confinement fusion reactors, appl. of intense charged particle beams overlap 0-91242
- inertial confinement fusion reactors, use of black-body radiation as fusion driver 0-91241
- inertial confinement pellet fusion, perturbation theory for sensitivity and uncertainty anal. 0-68946
- inertial fusion reactors, feedback-controlled laser-guided pellets 0-73997
- inertial fusion results from Shiva 0-92358
- inertially confined fusion, high density effects 0-86981
- intense ion beam propag. in z-discharge plasma channels, straight and tapered 0-83948
- inertial confinement fusion, implosion of black body radiation 0-73990
- ISX-B neutral beam injector expt. on prototype beam line 0-74039
- JIPP T-II, simultaneous neutral beam injection and lower hybrid heating 0-79516
- laser driven inertial confinement fusion, pulse power technology 0-63385
- laser focus movement, nonlinear optical technique 0-74446
- laser fusion, progress at Lawrence Livermore Lab., USA 0-57945
- laser fusion cryogenic target characterisation by wavefront shearing interferometer 0-74008
- laser fusion experiments at KMSF 0-92355
- laser fusion physical processes, investigation 0-74024
- laser fusion research, progress in Europe 0-74025
- laser fusion system, CO₂ eight beam, SF₆ saturate absorber effects on optical performance 0-106577
- laser fusion system beam quality, Laser Optical Train Simulation code 0-78886
- laser fusion systems, electrooptic prepulse suppression using Pockels cells 0-102743
- laser fusion targets, cryogenic technology 0-68939
- laser inertial containment, principles and problems (French) 0-78437
- magnetic-gun igniter for controlled thermonuclear fusion, travelling wave linac. 0-91238
- magnetogasdynamical energy storage in controlled thermonuclear fusion 0-57951
- neutral beam injection, energy and power requirements for Tokamak reactors 0-91243
- Nova, mechanical design, overview 0-91279
- particle beam interactions with plasma, inertial fusion appls. 0-59250
- plasma, subignited, α -particle heating 0-92340
- polymer-coated laser fusion targets, compression to 10¹¹ liq. DT density 0-83964
- pulsed power acceleration for fusion reactor ignition 0-63383
- radiation absorption in magnetoplasma, rel. to laser fusion 0-92273
- second-harmonic generation of upper-hybrid radiation in a plasma 0-79506
- shell target monitoring by X-ray Schlieren method 0-86263
- spherical laser target hydrodynamic compression stability (Russian) 0-106159
- Tokamak ignition equilibria and thermal stability 0-74005
- Tokamak plasma overheated underdense, two-zone model and 1-D transport code 0-63376
- Tokamak plasmas, advanced-fuel, ignition and thermal stability 0-86970
- Tokamak reactor, fuel injection, dynamic burn control 1-D transport code 0-68948
- Tokamak reactor, toroidal magnetic field ripple, burn control 0-63375
- tritium filling and monitoring apparatus for particle beam inertial confinement fusion targets 0-57949
- vacuum beam diodes, repetitively pulsed for inertial confinement fusion 0-63386
- X-ray emission in laser imploded targets, three-dimens. reconstruction 0-79563
- X-ray microradiographs of laser fusion targets, improved image analysis techniques 0-79562
- Ar^{16,17+} filled glass shell, symmetric laser compression 0-64759
- CO₂ laser Antares fusion system power amplifier optics 0-74394
- CO₂ laser Antares fusion system beam alignment 0-74422
- CO₂ laser Antares fusion system, mirror quality specifications 0-74423
- CO₂ laser Antares fusion system optical diffraction computation 0-74424

fusion reactor ignition continued

- CO₂ laser beam-diagnostics techniques, laser beam parameter monitoring 0-64089
 CO₂ laser fusion system optical design and analysis 0-74391
 CO₂ laser fusion system alignment by IR Smartt interferometer 0-74425
 CO₂ laser fusion system wavefront correction, deformable mirror design 0-74427
 CO₂ laser fusion system phase conjugation 0-74429
 CO₂ laser fusion system, optical design considerations 0-78868
 CO₂ laser Gemini fusion system optical performance 0-74392
 CO₂ laser Gemini fusion system, wavefront error correction by deformable mirror 0-74426
 CO₂ laser Helios fusion system, multicomponent gaseous saturable absorber optimisation 0-74393
 CO₂ laser Helios fusion system, beam simultaneity system 0-74419
 CO₂ laser Helios fusion system alignment 0-74420
 CO₂ laser Helios fusion target positioning with orthogonal telescopes 0-74421
 CO₂ laser Helios fusion system beam diagnostics 0-78882
 CO₂ laser system, pulsed, for fusion research 0-58556
 CO₂ long-pulse 2 GW single longit. mode source for laser-matter expts. 0-78860
 D-T compression, explosion-induced, cylindrical system with heavy inertial layer, neutron yield 0-68944
 Li⁺doubly charged ions, electron capture excitation, theoretical predictions in fusion plasma 0-63810
 Nd:glass laser system, multichannel, for fusion experiments, model 0-58557

fusion reactor materials

see also *fission reactor materials*; *radioactive waste*

- alkali metal, liq., reactions with refractory metals and oxides, relevance to reactor technology 0-85173
 alternative advanced fuels, cat-D, D-T and D-³He comparison 0-99310
 blanket material impurity hazardous activity and dose rates, biological hazard pot. 0-102315
 Chinese research 0-78447
 cryogenic inertial confinement fusion target fabrication system operable inside room-temp. chamber 0-106152
 CTR first wall, high power ion-irrad. test 0-78443
 CTR first walls, high power ion-irrad. test 0-68941
 Doublet III, toroidal field coils, Cu alloy plate defect size restrictions 0-91257
 electron beam fusion, pellet and pellet-blanket neutronics and photonics 0-74006
 first wall, fusion product. bombard., prompt and non-prompt contrib. 0-106156
 first wall, radiation damage simulation using fission reactor test facilities 0-57950
 fusion reactor first-wall performance under ion bombardment and cyclic stresses, in-reactor materials testing 0-104407
 fusion-fission symbiosis, nuclear fuel. trajectories, fissile and fusile fuel characterisations 0-68947
 graphite, conditioning of surface by atomic H 0-93665
 graphite, degassing rate measurement 0-102306
 graphite, ion bombarded, light gases, structural study using TEM 0-92570
 hybrid blanket data and development, review, simulation test facilities 0-106170
 ICFR, first walls, void growth, analytical model 0-63377
 ICFR, interstitial loop formation, point defect clustering 0-63378
 Inconel 625, electron yields under ion bombardment for clean and oxidised surfaces 0-66368
 inertial confinement fusion target, formation of uniform solid fuel layers 0-95432
 irradiation creep by the climb-controlled glide mechanism in Tokamaks 0-102304
 irradiation effects, Fusion Materials Irradiation Test facility initial target design 0-95410
 low energy ion erosion expts., Kaufman source appl. 0-68942
 low Z coating development program 0-106182
 magnetic confinement system, surface problems caused by dissolved H₂ 0-57946
 MFTF, intense neutron environment, test cell side wall design, shielding materials 0-102318
 neutron 14 MeV irradiation, Fusion Materials Irradiation Test Facility 0-91361
 neutron irradiation effects on organic insulators at 5K for superconducting magnets 0-107336
 neutron multipliers for D-T solid breeder fusion reactors to improve T breeding ratio 0-102296
 nuclear, social aspects (*Dutch*) 0-106153
 pellet fusion reactor, thermomech. dynamic behaviour of solid wall 0-95396
 post-irradiation examination, hot cell complex test facilities in Japan (*Japanese*) 0-63255
 refractory metals and oxides, reactions of liq. alkali metals, relevance to reactor technology 0-85173
 refractory oxide development for fusion reactor first walls, chem. environment effects 0-83221
 refuelling pellet penetration depth and fuel deposition 0-78446
 review of props. (*Dutch*) 0-68938
 solid breeding blanket for commercial Tokamak reactors, materials and design 0-95441
 solid H pellet interaction with magnetised plasma 0-78451
 stainless steel, neutron dose determ., from isotope abundance ratio, mass spectra obs. 0-61220
 steel, austenitic stainless, microarcing studies in low temp. RF-plasma 0-96407
 steel, stainless, design of materials irradiation experiments utilizing spectral tailoring 0-102305
 steel, stainless, oxidised, sputtering yield meas. by atomic fluoresc. spectroscopy 0-80922
 steel, stainless, Type 316, neutron irrad. effects on tensile props. and microstruct. 0-65059
 steel, stainless 316, fatigue behaviour of materials containing significant amounts of irrad.-induced He 0-100917
 structural materials, accident-related dose rate calc. 0-95411
 symbiotic energy system, U fuelled, economic anal. using SYMECON code 0-106172
 symbiotic system, managing fusion burn, economic analysis 0-106173

fusion reactor materials continued

- Thor Tokamak, wall conditioning by cleaning H discharges 0-78440
 Tokamak plasma fusion products, deposition and thermalisation 0-83895
 Tokamak plasmas, advanced-fuel, ignition and thermal stability 0-86970
 void, and interstitial loop evolution in pulsed fusion reactors 0-84217
 Al, Al ion irradiated, void swelling and annealing of voids, electron microscopy study 0-88216
 Al, expt. and statistical model determ. of α -prod. by 14.8 MeV neutrons 0-95397
 Al foil, α -particle irrad. under fusion reactor conditions, He bubble alignment during deform. 0-107345
 Al, laser fusion target simulation, press. ionisation 0-63374
 Ar, response to spherical blast waves, effect on first wall protection 0-91245
 B₄C, low energy ion erosion expts., Kaufman source appl. 0-68942
 B₄C reflector-shield concept for fusion reactor designs 0-10293
 Be, low energy ion erosion expts., Kaufman source appl. 0-68942
 Be range profiles of Li⁺, appl. of (n,p) and (n, α) reactions 0-61200
 BeO film, 5 keV D implantation 0-100268
 Bi, breeding zone in molten-salt blanket, effect on ²³²Th and ²³⁵U fission rates 0-99272
 C, low energy ion erosion expts., Kaufman source appl. 0-68942
 C-graphite materials for HTR and fusion reactors 0-73928
 Co, (n,2n) 14 MeV cross sections 0-91181
 Cr, (n,2n) 14 MeV cross sections 0-91181
 Cu, expt. and statistical model determ. of α -prod. by 14.8 MeV neutrons 0-95397
 Cu, low energy ion erosion expts., Kaufman source appl. 0-68942
 D-T fusion reaction, D+T \rightarrow n+⁴He, chain carriers 0-86969
 Fe, (n,2n) 14 MeV cross sections 0-91181
 Li liq., deuteron activated, shielding 0-99286
 Li liq. blanket, T removal by Y 0-95434
 Li, liquid, coolant and T fuel source, safety anal. and support facilities 0-63380
 Li Tokamak breeding blankets, T breeding perform. comparative eval. 0-95398
 Li-D equation of state under extreme conditions, solid state to plasma region 0-69976
 Li-Pb eutectic alloys for fusion reactor solid breeder blankets, reactions with water 0-102297
 Li-Pb-cooled blanket for tandem mirror fusion reactor, neutronic anal. 0-99273
 Li₃N, vaporisation, studied by Knudsen effusion method 0-92662
 Li₂O, 2.7 MeV triton recoil range from ⁶Li(n, α)³H 0-63372
 Li₂O blanket breeding material, single crystal synthesis using vacuum fusion technique 0-71585
 Li₂O, neutron irrad. effects, optical absorpt. spectra 0-75271
 Li₂O pellets, neutron irradiated, temp. distrib. 0-86968
 Li₂O pellets, sintered, neutron irradiated, ESR study 0-92566
 Li₂O, porosity, dependence on thermal diffusivity and thermal conductivity, 200-900°C 0-92726
 Li₂O Tokamak breeding blankets, T breeding perform. comparative eval. 0-95398
 Li₃Pb₂, T breeding fusion blanket with boiling water coolant 0-99274
 Li₃Pb, Tokamak breeding blankets, T breeding perform. comparative eval. 0-95398
 Mn, (n,2n) 14 MeV cross sections 0-91181
 Mo, (n,2n) 14 MeV cross sections 0-91181
 Mo, activation anal., charged particle prod. cross sections by 14 MeV neutrons 0-93829
 Mo alloys (MCHVP and TsM10VD), erosion, effect of ion bombardment dose and previous surface treatment 0-89419
 Mo, fusion reactor appl., quick heating thermal fatigue test, ultra-high vac. environment (*Japanese*) 0-93716
 Mo impurity flux, time resolved, in DITE Tokamak 0-63373
 Mo, low energy ion erosion expts., Kaufman source appl. 0-68942
 Mo surface, rolled, H₂⁺ ion bombard, large blister form. 0-75274
 NaK, liquid metal, blanket coolant, natural convection under transverse magnetic field 0-69827
 Nb, (n,2n) 14 MeV cross sections 0-91181
 Nb, activation anal., charged particle prod. cross sections by 14 MeV neutrons 0-93829
 Nb:He, mech. props. and microstruct. 0-85003
 Ni, (n,2n) 14 MeV cross sections 0-91181
 Pb, breeding zone in molten-salt blanket, effect on ²³²Th and ²³⁵U fission rates 0-99272
 T breeding in TFTR, tritium breeding test blanket module design 0-99304
 T gas, container prep. effect on growth of protium and methane impurities 0-78436
 T separation from Li at low conc. using Y 0-83219
 Ti, (n,2n) 14 MeV cross sections 0-91181
 Ti impurity flux, time resolved, in DITE Tokamak 0-63373
 Ti spongy metallic protective gettered coating for thermonuclear reactor walls (*Russian*) 0-106154
 Ti:D, ion implanted, depth profiles, temp. depend. 0-100270
 Ti-70A superalloy, fusion reactor blanket structures, radiation resistance 0-63379
 Ti-Al-V, fusion reactor blanket structures, radiation resistance 0-63379
 Ti-Al-V (6.4 wt.%), ion irradiated, microstruct. study using TEM 0-96572
 Ti-Fe-C-N, ion irradiated, microstruct. study using TEM 0-96572
 TiB₂, plasma sprayed, low energy ion erosion expts., Kaufman source appl. 0-68942
 TiD₂, nucleation and growth in D₂⁺ implanted Ti, TEM study 0-97717
 VBe₂, low energy ion erosion expts., Kaufman source appl. 0-68942
 Zr alloys, creep and growth, irradiation induced, microstruct. depend. 0-93602
 Zr-Al getter modules, transient getter scheme for Tokamak fusion test reactor 0-79584

fusion reactors

- see also *fusion reactor ignition*; *fusion reactor materials*; *hybrid reactors*; *plasma heating*
 advanced fuel fusion reactor wall loading limitations and stability index beta 0-99311
 Alcator Tokamak, radiative and particle power losses, bolometric meas. 0-73996
 Alcator-A Tokamak, D₂ thermal desorption meas. 0-79588
 American Nuclear Society proceedings (conf. Las Vegas, NV, June 1980) 0-94920

fusion reactors continued

ASDEX, assembly and commissioning, review 0-102334
 ASDEX, extraction grid for high power ion source 0-102372
 ASDEX, neutral beam injection, beam line design 0-99395
 ASDEX, neutral beam injectors, HV power supply system, thyristor control 0-99332
 Auegan, fission prod. toxicity reduction 0-106175
 axial shock heating applied to compact toroid plasma formation 0-95402
 bakeable seals development for large noncircular ports on Tokamak fusion test reactor 0-82777
 Beta II, field reversed expt., device description 0-91274
 beta limits for Tokamak experiments 0-83937
 Beta-II, magnetised coaxial plasma gun mechanical design and construction 0-91271
 blanket, high-temp. design for synthetic fuel plant 0-99275
 blanket, NOEL (No External Leak), thermal anal. and tests 0-95459
 blanket design, impact of module size on the tritium breeding and energy conversion experiments in an ETF/INTOR reactor 0-102295
 blanket structures, linear elastic fracture mech. anal. 0-86979
 blankets, structure mechanics at elevated temps. and high fluences 0-86978
 breakeven condition on hot-ion mode 0-78439
 bremsstrahlung cross-sections, 1- and 2-photon, Debye shielding corrections 0-106157
 burn period plasma current maintenance, rectifying first wall, oct. anal. 0-102307
 Chinese research 0-78447
 cluster test facility, design 0-90835
 committed site development, technical and economic aspects 0-95437
 compact ignition test reactor, engineering design using Bitter type magnet 0-102310
 compact reverse-field pinch for small demonstration fusion reactor 0-95413
 compact toroidal ignition experiment, support struct. anal. by numerical code 0-106167
 component development, mag. systems and plasma engineering, programs status review 0-99299
 conference, controlled fusion and plasma physics, Oxford, England (Sept. 1979) 0-77545
 conference, inertial confinement fusion technical digest, San Diego, CA, USA (Feb. 1980) 0-57012
 conference, San Francisco, USA (Nov. 1979) 0-91248
 cryosorption pumping of He by charcoal, cryopump design for fusion reactor 0-105654
 Culham conceptual Tokamak, remotely operated shield door 0-74009
 Demonstration Power Tokamak Reactor, vacuum outer containment and metal seals feasibility study 0-95458
 development, review of expt. accomplishments, program strategies and system test facilities 0-57958
 development of fusion power, pure and hybrid reactor options, review 0-63389
 development research at Debrecen, Hungary (*Hungarian*) 0-91240
 DITE, behaviour review including injection and bundle divertor 0-74021
 DITE Phase II ion source, characteristics 0-83223
 DITE Tokamak bundle divertor, Mk.II design 0-91268
 DITE-II, neutral beam ion source particle beam identification 0-99397
 DIVA Tokamak, confinement and MHD characs. of very low q discharges 0-64765
 divertorless Tokamaks, limiter pumping system 0-95463
 Doublet III, computer control system 0-99321
 Doublet III, limiter performance, design and material selection 0-106162
 Doublet III, neutral beam injection system, two-gap magnet design and performance 0-92379
 Doublet III, neutral beam injector system, instrumentation and control 0-99322
 Doublet III, neutral beam interlock system using IR detector 0-106228
 Doublet III, neutral beam test tank design 0-99301
 Doublet III, ohmic heating E-coil vacuum breaker system, function and operation 0-102323
 Doublet III, plasma density, shaping and characteristics 0-74018
 Doublet III, plasma shape control, 1.5 Megawatt DC chopper power supply 0-102333
 Doublet III, possible Dee configs. 0-91269
 Doublet III, toroidal field coils, Cu alloy plate defect size restrictions 0-91257
 Doublet III, vacuum vessel neutral beam armour 0-95462
 Doublet III beamline, review, component relation and config., design constraints 0-99382
 Doublet III beamline calorimeter, three dims. heat transfer anal. 0-99381
 Doublet III neutral beam injector system, outgassing rate meas. and residual gas anal., coating props. 0-95457
 Doublet-III, frequency generator-rectifier system performance 0-102326
 DTHR, advanced bundle divertor design 0-92821
 EBT heating, electron-cyclotron absorption and microwave propagation 0-64749
 eddy currents in vacuum vessel when plasma current is disrupted, calc. (*German*) 0-68937
 electron beam driven Tokamaks, review 0-99317
 ELMO Bumpy Torus, microwave coupling 0-99328
 ELMO Bumpy Torus, ring power balance optimisation 0-99316
 ELMO Bumpy Torus, scaling studies 0-78444
 ELMO Bumpy Torus Proof-of-Principle, proposed mag. system 0-99296
 Engineering Test Facility: progress and plans 0-95418
 Engineering Test facility, R and D program 0-95419
 ETA-BETA II, reverse field pinch, expt. tests and performance 0-102312
 ETA-BETA II RFP, diffuse pinch, temp. and confinement results 0-74028
 ETA-BETA II RFP, vacuum system design and operation 0-95450
 ETF, design considerations 0-95438
 ETF, design considerations for remote maintenance 0-68950
 ETF, engineering challenges, review 0-95422
 European thermonuclear fusion programme, role of technology 0-86982
 fibre optics, use in controlled fusion expt. shielding and earth loop elimination 0-74007
 field reversed mirror neutral beam startup, hybrid plasma code simulation 0-99313
 FINTOR-D, T breeding blanket, Monte Carlo calcs. 0-99283
 first wall, life extension by periodic annealing 0-102344
 first wall blanket, cylindrical module, reference design 0-106181
 first-wall structures, fatigue life criteria 0-86980

fusion reactors continued

FT Tokamak, non-thermal electron distrib. function 0-83891
 FT Tokamaks, expt. results 0-74014
 FT-I Tokamak, electron cyclotron heating expt. 0-75071
 FT-I Tokamak, lower hybrid heating, energy balance 0-79523
 FTR, equilib. field coils, electrical supply system, optimisation and computer aided performance anal. 0-91288
 fueling and thermonuclear instability, cold plasma layer surface fueling source 0-59196
 future nuclear power technology, impact of nuclear research in India 0-95345
 heavy-ion-beam fusion reactor conceptual design 0-95414
 Heliotron E, helical coil design, mag. field perturbations 0-99300
 Heliotron E, neutral beam injector ion source power supply 0-99333
 Heliotron E, vacuum chamber construction using electron beam welding 0-106180
 HFCTR, demonstration reactor conceptual design, high force density magnets and modularisation 0-95439
 high temperature efficient energy conversion 0-86985
 homopolar generator design for fusion reactor energy storage 0-68953
 HYPERFUSE: a novel inertial confinement system utilizing hypervelocity projectiles for fusion energy production and fusion waste transmutation 0-102300
 inertial confinement, advanced engineering requirements, review 0-95421
 inertial confinement, advanced fuel D pellets, opaque tamper requirements 0-102303
 inertial confinement, ion-beam wet-wood-burners using limited mass targets 0-102301
 inertial confinement, preliminary assessment of heavy ion fusion 0-102299
 inertial confinement, T self-sufficient A-FLINT pellet, optimised design 0-102302
 inertial confinement, USA research 0-78448
 inertial confinement fusion reactor, appl. PWR fuel rod reenriching 0-106174
 inertial confinement fusion reactor system integration 0-102298
 inertial confinement fusion technology in USA, status (*German*) 0-68952
 international cooperation on fusion research (*Japanese*) 0-63371
 international fusion technology program, review 0-95423
 International Tokamak Reactor (INTOR) Workshop, R and D status report 0-95417
 ISX-B, electron cyclotron microwave heating 0-99329
 ISX-B, high power neutral beam injection studies 0-79545
 ISX-B, neutral beam power system 0-91283
 ISX-B, neutral beam system 0-99388
 ISX-B, with bundle divertor, structural anal. 0-91254
 ISX-B tokamak, design of bundle divertor expt. 0-102341
 ISX-B Tokamak, expt. program, review 0-78435
 ISX-B toroidal field coil finger joints, fatigue life, structural evaluation 0-91253
 Japanese Tokamak research, impurity control, low-q discharge, scaling law, RF heating 0-74015
 JET, control system, communications, diagnostics, data storage and anal., NORD computers 0-68943
 JET, design, construction, physics 0-74023
 JET, extraction element design for long pulse multi-megawatt neutral beam 0-102373
 JET, neutral injector overvoltage injection system 0-99398
 JET, periplasmion ion source for intense neutral beam 0-99380
 JET, transport calcs. for approach to ignition 0-92263
 JFT-2 Tokamak, impurity ion sputtering 0-79554
 JIPP T-II, neutral beam injection system, design and expt. test 0-106226
 JT-60, fault current anal. in grounding system 0-99307
 JT-60, grounding system design 0-102313
 JT-60, grounding system pot. rise during lightning strike, anal. 0-102314
 JT-60, poloidal field DC power supply developments 0-102325
 JT-60, poloidal field power supply system, AC voltage behaviour, simulation 0-91287
 JT-60, prototype neutral beam injector unit 0-106225
 JT-60, seismic anal., design changes 0-95425
 JXFR, neutral beam injection system, gas-beam interaction secondary particles 0-106227
 JXFR, superconducting mag. system conceptual design 0-99295
 Large Coil Program, coil winding development support 0-106190
 Large Coil Program, General Dynamics Convair/IGC manufacturing engineering 0-106169
 Large Coil Program, insulation system cryogenic elec. test 0-91263
 Large Coil Program, low temp. stability, joints, design method 0-106195
 Large Coil Program, Nb₃Sn forced flow superconducting test coil, Westinghouse design 0-99337
 Large Coil Program, NbTi, superconducting test coil, General Dynamics Convair Division, Intermagnetics General Corp. design 0-99338
 Large Coil Program, NbTi superconducting test coil, General Electric design and manufacture program 0-102319
 Large Coil Program, pool boiling mag. quench press. calc. 0-106199
 Large Coil Program, research and development activity 0-99336
 Large Coil Program, superconducting mag. coil struct. design status 0-106189
 Large Coil Program, test heater conceptual designs 0-91251
 large coil Program, Westinghouse coil cooldown and warmup 0-106193
 Large Coil Program, Westinghouse coil stability testing, pulsed induction heating 0-106194
 Large Coil Program, Westinghouse superconducting mag. elec. design 0-91250
 Large Coil Task, CC NbTi, pool cooling superconducting test coil, Japanese design 0-99340
 Large Coil Task, CC NbTi forced flow superconducting test coil, Swiss design 0-99341
 Large Coil Task, NbTi, forced flow superconducting test coil, EURATOM design 0-99339
 Large Coil Test Facility, instrumentation system design 0-95446
 Large Coil Test Facility, liq. He cooling system 0-102321
 Large Coil Test Facility test stand design description 0-102320
 LARTS, extended burn operation, physics, engineering and economics 0-95440
 laser fusion, wavelength scaling, benefits of lasers with wavelength less than one micron 0-75073
 laser fusion process heat systems, criteria for industrial applications 0-57953
 laser produced nuclear fusion, review 0-63381
 laser target, cylindrical shell, thermal vibrs., general soln. 0-95433

fusion reactors continued

linear magnetic solenoid reactor plasmas, dynamic behaviour 0-64751
 linear spheromak, conceptual design 0-95412
 liner implosion, anomalous transport processes in radially compressed reversed-field configurations, numerical simulation 0-64689
 LINUS, imploding liq. liner system, engineering anal. 0-99315
 liquid metal linear implosion systems with blade lattice for rotational stabilisation 0-73994
 LMFBF, inherent safety features 0-106145
 LMFBFs, national development programmes, status assessment 0-106104
 long pulse extraction from modified duoPIGatron for neutral beam fusion reactor system 0-91355
 long pulse high current ion source electrode cooling 0-91360
 long-term nuclear energy strategies, role of fission and fusion 0-78354
 low power Tokamak experimental fusion power plant, scoping studies with empirical scaling, SISYFUS code 0-102309
 LPTT, engineering design 0-102308
 magnet, high current density superconducting coils, cryostability 0-106201
 magnet stability, press. induced flow cooling, highly stable superconducting mag. systems 0-106192
 magnet systems for commercial power reactors, structural design 0-86975
 magnetic, Tokamak and tandem mirror reactors, neutral beam injection and superconducting magnets 0-63391
 magnetic confinement, structural anal., combined interactive/batch computer environment 0-91255
 magnetic confinements, international collaboration 0-63390
 magnets, constitutive model for struct. anal. of elastic-plastic and slip deformation 0-86977
 MFTF, BBC CQK 200-4 modulator tube for sustaining neutral beam power supply 0-99290
 MFTF, cryogenic system 0-106163
 MFTF, electrical systems, overview 0-91278
 MFTF, end loss region high energy plasma gettering 0-102343
 MFTF, exception handling control system 0-99325
 MFTF, ion and neutral beams dumps, design 0-102317
 MFTF, mag. cryostability 0-106198
 MFTF, neutral beam accel power supply protection 0-102380
 MFTF, neutral beam module component design and development 0-91270
 MFTF, neutral beam source development 0-102368
 MFTF, plasma buildup, contaminant control 0-95461
 MFTF, plasma diagnostics system 0-95444
 MFTF, plasma streaming system, description 0-91280
 MFTF, power supply system, digital simulation using EMTP code 0-91286
 MFTF, start up neutral beam power supply system 0-91281
 MFTF, superconducting mag. quench vent rate 0-106197
 MFTF, supervisory control and diagnostics system, database management system 0-99326
 MFTF, supervisory control and diagnostics system, database management system, data structs. 0-99327
 MFTF, supervisory control and diagnostics system software 0-99324
 MFTF, sustaining neutral beam power supply, cct. anal. using ASTAP and EMTP codes 0-91284
 MFTF, sustaining neutral beam power supply, shunt preconditioner, IBM-ASTAP anal. 0-102332
 MFTF, sustaining neutral beam power supply system, modelling with ASTAP code 0-91285
 MFTF plasma diagnostics Data Acquisition System 0-99319
 MFTF superconducting mag. design and construction 0-101008
 MFTF-B, full tandem extension, description 0-99294
 Mirror Fusion Test Facility, superconductor core manufacturing and quality 0-93521
 mirror machines, 2XIIB neutral-beam-heated, extreme UV spectroscopy 0-74002
 molten-salt blanket, effect of Pb and Bi neutron multiplication zones on the fission rates of ^{232}Th and ^{235}U 0-99272
 moving plasmoid reactors using advanced fuel, modularisation 0-99312
 multimewatt gyron design for controlled thermonuclear reactor heating 0-59256
 multiple mirror, coil design and economic optimisation 0-99284
 multipole fusion confinement with 2 MA levitated superconducting coil 0-106191
 muon catalysis of d-t fusion 0-78438
 Nagoya Bumpy Torus, confinement studies 0-78445
 neutral beam injection, 120 keV, ion source 0-91357
 neutral beam injection, 24 MW 400 keV H beam 0-91356
 neutral beam injection, trace identification of Cs and Na 0-95401
 neutral beam injection reionisation power losses in duct, model 0-99385
 neutral beam injecto cryogenic pumping panel chevron baffles, black coating materials, selection 0-95456
 neutral beam injector, continuous operation, water cooled U-tube extraction grid 0-99392
 neutral beam injector mag. cusp plasma source, design and fabrication 0-99377
 neutral beam injector vacuum system transient simulation anal. 0-95453
 neutral beam source, 40 kV for TMX, engineering design 0-91358
 neutron source, 3 ns pulsed beam-target, thermonuclear neutron burst simulation 0-87008
 neutron yield depend. on interelectrode insulating system shape 0-74027
 neutronics, fundamental problems (Japanese) 0-57944
 neutronics analysis using generalised variational principles 0-57947
 non-circular Tokamak field shaping coils, current optimisation 0-95426
 non-superconducting magnet structures for near-term, large fusion experimental devices, magnet and structural design 0-86973
 nonelectrical applications, review 0-57952
 NOVA, high speed rot. mech. shutter design for pre-pulse protection 0-96032
 NOVA, pulsed power control system, fibre-optic multi-tapped computer bus 0-95443
 nuclear, social aspects (Dutch) 0-106153
 oil shale extraction in situ retort utilising fusion reactor 0-108780
 ORNL/TNS and ETF, tokamak reactor poloidal field system study 0-95436
 particle-beam fusion reactors, first wall protection by inert cavity gases 0-91245
 PDX, 6 MW Neutral Beam Project, overview 0-106223
 PDX, assembly, description 0-99308

fusion reactors continued

PDX, data acquisition systems, networking and distrib. processing improvements 0-99318
 PDX, flexible work platform and balcony design 0-106161
 PDX, initial operation 0-79555
 PDX, large Tokamak, design and future use 0-79534
 PDX, neutral beam elec. power system, ion source supply upgrade 0-102330
 PDX, ORNL prototype neutral beam injection system, ion source development 0-99391
 PDX, shaping field-equilib. field power supply rectifier upgrade study 0-91290
 PDX, toroidal field coil and frame struct., anal., finite element anal. 0-106165
 PDX neutral beam injector, ion accel. structural anal. 0-102375
 PDX neutral beam injector, multi-aperture ion accel. electrodes thermal anal. 0-102371
 PDX neutral beam injector development 0-99375
 PDX power test results, struct. finite element anal. 0-91265
 PDX Tokamak, finite element anal. using computer graphics 0-95424
 PDX Tokamak, struct. anal. by finite element method 0-106166
 PDX Tokamak, surface analysis station 0-79586
 PDX toroidal field coil joint fatigue testing 0-91252
 pellet re-fuelling feasibility, review 0-91246
 pellet refuelling of a divertor Tokamak 0-91247
 PETULA Tokamak, lower hybrid heating expts. 0-83958
 PGFR seismic risk anal. 0-99298
 PHIBEX, poloidal field power supply for ignition, computer based cct. anal. 0-102329
 plasma contamination, sputtered particles, energy and mass distrib. 0-84822
 plasma fuelling, collisional drift modes, anomalous skin effect, enhanced particle penetration nonlinear theory 0-64703
 plasma heating and confinement, review 0-63388
 plasma heating by collisional slowing of fast ions in noncircular Tokamaks 0-95403
 PLT, D₂ flux and energy incident on probe, power balance, impurity generation 0-79553
 PLT, data acquisition systems, networking and distrib. processing improvements 0-99318
 PLT, fusion neutron yield during D neutral beam injection 0-79522
 PLT, ICRF heating for two-ion regime 0-83959
 PLT, neutral beam duct reionisation losses, obs. and power loss model 0-99383
 PLT, neutral beam injection, power input and plasma temp. reconciliation 0-106224
 PLT, neutral beam injection and ICRF heating, charge exchange meas. 0-83892
 projected inertial confinement fusion reactor target evaluation by buoyancy analysis 0-78442
 R-OM stellarator, MHD resonant HF heating 0-79518
 rectangular plasma generator, advanced ion source for ion injectors 0-99376
 reversed field mirror reactors, startup using coaxial plasma guns, scaling laws 0-99279
 reversed field pinch, RFX constructional details 0-91277
 RF driven current generation by lower hybrid waves in Tokamak 0-103116
 RINGBOOG II, toroidal discharges with cold blankets 0-83901
 rotating plasma reactors, longitudinal confinement, stability equilibrium and heating problems 0-74001
 RST, RF driven steady state toroidal expt., design 0-91276
 RST, support struct. 0-102342
 safety and environmental pollution (German) 0-63370
 safety of superconducting fusion magnets: twelve problem areas 0-102348
 SAFFIRE, Cat-D fueled, synthetic and fissile fuel prod. 0-99280
 shielding and maintainability in an experimental Tokamak 0-99287
 SLPX, Superconducting Long-Pulse Experiment, scoping study 0-91275
 SLPX TF coil, stress anal. using COSMIC-NASTRAN 0-106168
 solid breeder blankets for D-T reactors, operating temp. limits for T release and recovery 0-102294
 solid breeding blanket for commercial Tokamak reactors, materials and design 0-95441
 Spheromak fusion reactors, MHD equilib. and stability, numerical anal. 0-74000
 Starfire, commercial Tokamak power plant, conceptual design 0-57957
 STARFIRE project, an overview 0-106183
 STARFIRE project, design parameters 0-106184
 STARFIRE project, first wall and blanket design 0-106188
 STARFIRE project, impurity control system 0-102345
 STARFIRE project, maintenance considerations 0-102346
 STARFIRE project, superconducting poloidal coils design study 0-106185
 STARFIRE project, T handling and vacuum requirements 0-106187
 STARFIRE project, toroidal field coil system preliminary assessment 0-106186
 stationary ion source construction 0-91359
 stellarator, plasma losses, quasi-neoclassical law 0-79544
 stellarators, equilibrium and stability calcs. 0-83982
 stellarators, magnetic hill effects on equilibrium 0-79558
 stellarators, research status 0-74013
 superconducting fusion magnetic systems, struct. anal. methods and standards 0-86972
 superconducting magnet for magnetic flux compression, compression generator, PULSAR, design optimisation 0-68957
 superconducting magnet joints, resistance welding 0-91259
 superconducting magnets, pulsed, stability studies, fusion reactor appls. (Japanese) 0-106158
 superconducting magnets, structural alloys, props. at 4K 0-86976
 superconducting magnets, structural design 0-86974
 superconductor coils appl., based on Nb-Ti (French) 0-95399
 superconductor optimisation for 12 Tesla toroidal field coils from Nb-Ti and Nb-Ti-Ta alloys 0-91272
 synfuel blanket design for mirror or Tokamak reactors 0-95407
 synfuel blanket module in neutron beam, 2-D heating anal. by computer simulation 0-95406
 tandem mirror fusion reactors, axisymmetric sloshing-ion plugs 0-73998
 tandem mirror plasmas, alpha particle dynamics 0-83986
 Tandem Mirror Reactor, end plug mag. system design 0-102347
 Tandem Mirror Reactor power plant, maintenance and handling economics 0-102311

hydrogen continued

- Si-H, amorphous, Schottky diodes, elec. props., light-induced effects 0-103741
 Si-H, amorphous, solar cells, trap spectroscopy using transient current techniques 0-104508
 Si-H, amorphous, solar-cells, charge collection and spectral response 0-85275
 Si-H, amorphous, sputtered on $Gd_2(MoO_4)_3$, ferroelec. domain wall motion, image scanning 0-83663
 Si-H, amorphous, sputtered Schottky barrier solar cells, conduction mechanism 0-104506
 Si-H, amorphous, stacked solar cells, development 0-94050
 Si-H, amorphous, surface states distribution using MOS tunnel junctions 0-103735
 Si-H, amorphous, temp. depend. of photolum. 0-89063
 Si-H, amorphous Schottky solar cells, prep. and characts. of diode RF reactive cathodic sputtered films (*French*) 0-61347
 Si-H, amorphous thin film, ion plating, IR absorpt. meas. 0-84857
 Si-H, amorphous thin film solar cells 0-81478
 a-Si-H, electronic states and bonding config. 0-64900
 a-Si-H, influence of H on optical props., H conc. and H bonds 0-76098
 Si:H,B, amorphous, field effect and thermoelec. power 0-96924
 Si:H, Li, amorphous, photoluminescence obs. 0-66280
 Si:H,P, amorphous film, elec. cond., thickness and temp. depend. 0-65559
 Si-H alloy, amorphous, dihydride model of vibrational spectra 0-80827
 a-Si:H alloys, sputter deposited thin film coatings, property-comp. relationships 0-80975
 Si-H amorphous, solar cell structure, optical absorption by gap states 0-94052
 Si-H amorphous films, conductivity and temp. dependence of optical gap 0-100462
 Si-H amorphous films, ESR, optical gap and elec. cond. meas. 0-75842
 Si-H amorphous films, IR spectrum and struct. 0-97277
 Si-H amorphous films, reactively sputtered, prep. and characterisation 0-100785
 Si-H film, amorphous, H-associated disorder modes, PMR spin-lattice relax. time meas. 0-93202
 Si-H film, amorphous, plasma-deposited, small angle X-ray and neutron scatt. studies 0-59826
 a-Si:H film, glow discharge deposited, H profiles, doping level 0-84202
 a-Si:H highly homogeneous, for low-cost solar cell fabrication 0-72053
 Si-F-H:P, film, dark cond., struct., Raman scatt. 0-88588
 Si-H:P, amorphous film, dark cond., struct., Raman scatt. 0-88588
 SiC:H amorphous reactively sputtered film, H content effect on film props. 0-75459
 Si_{1-x}C_xH glow discharge films, local atomic struct., XPS and AES study 0-93448
 Si_{1-x}C_xH₂ amorphous films, IR absorpt. bands 0-100705
 Ti alloy, crack initiation on planar shear bands, H₂ assisted 0-71749
 UF₆-H₂/HF nuclear pumped laser, characts. 0-78847
 W (100), H adsorbate low energy electron vibrational excitation 0-84375
 WCs, preparation method effects on catalytic activity for H₂ evolution 0-101024
 Zr-H, implanted, superconductivity enhancement obs. 0-70884

hydrogen bonds

- acetate-ferrihemoglobin, X-ray struct. anal., 3D refinement at resol. of 2.0 Å 0-104554
 acetonitrile-HCl complex in liq. Xe, IR spectral study 0-95626
 alcohol H-complexes interactions, H-bond vibr. freq., anharmonic calcs. 0-99453
 alkali metal acid oscilates, neutron inelastic scatt. spectra in 2200-200 cm⁻¹ range 0-70327
 amidinium salts, ¹⁴N NQR spectra, H⁺ relax. times 0-60448
 azo dyes, UV-visible spectrophotometric 0-61207
 binary complexes, small H-bonded mols. electronic structs., ab initio calcs. 0-74108
 bioenergetics, H bonded chain theory 0-76699
 chemical reactivity, reliability of quantum mechanical predictions, config. of reaction prod., H-bonded species 0-108691
 D-chloroform, soln., Raman scattering tensor components 0-99508
 D-chloroform-dimethylsulphoxide, soln., Raman scattering tensor components 0-99508
 clusters, small, formation, struct. and props. 0-58437
 α-cyanoacrylate adhesive in first monolayer on bulk Al surface, IR spectra, H-bond form., stretching vibr. 0-87119
 decanoic acid, associated vapours, homogeneous nucleation 0-96638
 diatomic molecules, shortening of energy relax. time of excited mol. vibr. in dense medium by form. of H-bonds 0-91553
 difluoroacetic acid, soln., polarisable H bonds, IR spectrosc. obs. 0-58408
 dihydroxy benzenes in ethyl alcohol, dielec. dispersion charact. 0-75932
 dihydroxy toluene in ethyl alcohol, dielec. dispersion charact. 0-75932
 dimer, partially deuterated, microwave spectra and struct. 0-74212
 dimethylamine-HCl systems, H-bonded complexes studied by ab initio MO method, dipole moments determ. 0-83253
 DNA, proton radiationless transitions for hydrogen bonds (*Russian*) 0-97857
 electrolyte, soln. and cryst. (*German*) 0-80804
 enolate anion from acetone, gas phase, negative ion chemistry 0-87060
 ethanol, H-bonding investigated with supersonic mol. beam using photoionisation quadrupole mass spectrometer 0-102543
 ethylene-vinyl alcohol copolymers, H bonding study by near-IR spectra (*Japanese*) 0-78734
 F 0-92515
 ferroelectric, H-bonded, central peak, thermal cond. 0-93250
 ferroelectrics, H-bonded, phonon relax. mechanism 0-79906
 ferroelectrics with hydrogen bonds, phase transition into coherent state, two-level proton calcs. (*Russian*) 0-71356
 formic acid, cryst., H bonded, IR spectrum computer simulation 0-97253
 formic acid, soln., polarisable H bonds, IR spectrosc. obs. 0-58408
 glasses, oxide type, internal friction 0-92605
 graphical enumeration of hydrogen-bonded structures 0-106403
 heptanoic acid, associated vapours, homogeneous nucleation 0-96638
 β-hydroxy acrolein, lower excited states, electronic struct. and H-bonding, ab initio SCF and CI calcs., photochemical mechanism 0-83278
 p-hydroxy-trans-cinnamic acid, cryst. struct. basis for absence of thermal mesomorphism 0-96509
 liquid mixtures, binary, US vel. determ., hydrogen bond interactions 0-79881
 manganese adipate dihydrate, cryst. struct., H-bonding and O atom coordination 0-96506

hydrogen bonds continued

- methanol, aqueous, damped coupled oscillator model used to study Fermi resonance 0-69152
 methanol (-d), H-bonding investigated with supersonic mol. beam using photoionisation quadrupole mass spectrometer 0-102543
 methotrexate-dihydrofolate reductase complex form., conform., laser Raman obs. 0-104553
 2-methoxyethylamine, microwave spectra, H-bond, torsional motion and mol. vibr. obs., rot. isomerism, mol. moments determ. 0-95603
 methylamine-HCl systems, H-bonded complexes studied by ab initio MO method, dipole moments determ. 0-83253
 molecules, bridge angle, vibr. behaviour, simplified and accurate calcs. 0-95735
 monodipate-tetraquo-cobalt (II), cryst. struct., H-bonding scheme 0-96504
 2(4)-monoxopyrimidines, gaseous, matrix, soln., tautomeric equilib., IR and UV absorpt. spectra 0-58256
 myristic acid, associated vapours, homogeneous nucleation 0-96638
 naphthol complexes, H-bonded, form. of ion pairs in presence of crown ethers, proton-transfer photochemical reactions 0-85199
 nitroxide groups in crystals, H bonds and short intermolecular contacts 0-63855
 oriented DNA, hydration, neutron scatt. obs. 0-89714
 oxytocin, H bond linking ring and tail β-turns, biofunctional evaluation 0-61511
 penninite, one-layer triclinic chlorite, neutron diffraction study 0-84144
 phenol-phenyl complex, electrostatic mol. pot. contour maps, MODPOT and VRDDO calcs. 0-102463
 potassium hydrogen malonate, carboxylic proton chem. shift tensor 0-58280
 1,2-propane diol-dipropylene glycol, dielec. dispersion charact. 0-75932
 propionitriles (-O, NH, S), conformational investig., NMR, IR and semiempirical MO methods 0-95650
 propyl acetate-propyl alcohol, dielec. dispersion charact. 0-75932
 protein, structure and bonding, quantum theory, ab initio calcs. 0-61509
 proton semiconductors, with H-bonds, quantum theory of proton cond. 0-65641
 pyridine-H-bond donors, D spin-lattice relax. meas., mol. interactions anal. (*French*) 0-87151
 pyridines, monosubst., H₂O complexes, n-π* transitions, H bonding, MO theory 0-95550
 pyrrole-acetonitrile, H-bonded complex, ab initio MO calcs. 0-102440
 strontium maleate tetrahydrate, cryst. struct., H-bonding scheme 0-96505
 tetra-isomyl phosphonium bromide hydrate, clathrate, cryst. struct., X-ray study 0-64987
 tetramethylammonium hydrogen bis-trichloroacetate (-d₉), ³⁵Cl NQR study 0-66064
 thiones, N-H-S weak and medium strong H bonds, IR spectra 0-69132
 2-(2-tosylaminophenyl)-4H-3,1-benzoxazine-4-one, cryst. and mol. struct. 0-84167
 2,4,6-tribromophenol, Raman and IR spectra, hydrogen bonds 0-84735
 2,4,6-trichlorophenol, Raman and IR spectra, hydrogen bonds 0-84735
 trichlorosilane liquid, Si-H stretching mode vibr. dephasing, Raman study 0-84736
 trifluoroacetic acid, soln., polarisable H bonds, IR spectrosc. obs. 0-58408
 trifluoroethanol, H-bonding investigated with supersonic mol. beam using photoionisation quadrupole mass spectrometer 0-102543
 trimethylcarbinol complexes in soln., weakly H-bonded, IR bandshapes 0-106354
 triphenylcarbinol complexes in soln., weakly H-bonded, IR bandshapes 0-106354
 tris(ethylenediamine)metal(III), H bonding (*French*) 0-87241
 vibrational predissociation in hydrogen bonded complexes 0-61078
 water, chemisorbed on Pt (111), EELS spectra, vibr. freqs. 0-80920
 water-imidazole, H bond interrupted chain, cooperative effects, STO-3G ab initio calcs. 0-63535
 XH-Y complexes, IR absorpt. spectra, intramol. coupling influence, pot. energy surfaces derivation 0-91624
 BeBH₃, H bridged system, floating spherical Gaussian model 0-78518
 CO-HBr, weakly bound, rot. spectra 0-91544
 CO-HCl, weakly bound, rot. spectra 0-91544
 CO-HF, weakly bound, rot. spectra 0-91544
 Ca₂(NH₄)₂(H₂PO₄)₂·2H₂O, X-ray cryst. struct., PO₄ ion with 3 symmetric H bonds 0-64956
 Ca₂[B₃O₆](C₂H₅O)₂·hilgardite, PMR of water mol. 0-84655
 Ca[Fe(CN)₆](NO₃)₄·4H₂O, X-ray cryst. struct. determ., heavy-atom method 0-92494
 Ce₂(SO₄)₃·9H₂O(D₂O), polarised Raman spectra, vibr. props. and role of lattice H₂O 0-66201
 ClH-dimethyl ether, vibr. rot. IR spectra, quantum and classical mechanics 0-91561
 Co complexes, Co(en)₂Cl₂·Cl₂·HCl·2H₂O, temp. dependence of NQR frequencies 0-66068
 Co(H₂O)₆[SnF₆], crystal structure (*French*) 0-59441
 Cr₂H₂(SO₄)₂·24H₂O, X-ray cryst. struct. determ., H bond study 0-92491
 CROOH(D), barrier to proton or deuteron tunnelling 0-70156
 CsH₂PO₄, ferroelec., X-ray struct. study at room temp. 0-88113
 Cs₂[FeCl₄(H₂O)]₂, X-ray cryst. struct. determ. 0-107129
 H₂+Pt(111) surfaces, interactions, bond breaking activity, model pot. 0-108744
 HAl_{1/2}O₁₇, H β-alumina, IR absorpt. study 0-100655
 HBO₂, cubic, monoclinic and orthorhombic forms, H bonding, IR and Raman spectra 0-76029
 HCl, liquid, struct. and mol. dynamics studied using intermolecular force models 0-83445
 HF molecules, infinite linear chain, equilibrium structure and stabilisation energy 0-63856
 HF-HCl, SCF energy hypersurface, stationary points, thermodynamics of form. 0-102436
 H₂F₂ and H₂F₃ clusters, molecular structures, ab initio calcs. 0-83532
 H⁺(H₂O)_n, ion-induced water clusters, mass spectra, IR continuum absorpt. 0-87257
 H₂O, charged clathrates, model for formation and stabilisation 0-91714
 H₂O-HF heterodimer, H bonding, microwave rot. spectrum, mol. geometry and moment 0-99501
 H₂O+H₂O, pair pot. near H bonded equil. config., amorphous and crystalline solid and liq. 0-64946
 (H₂O)₂, difference electrostatic mol. pot. contour maps, basis set superposition effect 0-102462

hydrogen bonds continued

- HUO₂AsO₄·4H₂O and HUO₂PO₄·4H₂O layered cpds., struct. investigs. below antiferroelec. transition temps., H bond ordered structs. 0-107416
 K salt of β -ketoaldehyde, configurations of anions in solutions studied by IR spectroscopy, H-bond form. 0-87117
 K₂Ca[B₄O₅(OH)₂]₂·8H₂O, synthetic, X-ray cryst. struct. study, H bond geometries 0-92509
 KD₂AsO₄, ferroelectric, high temp. phase transitions, proton dynamics 0-76023
 KD₂PO₄, polarisation fluctuations, wavevector depend. 0-71295
 KH₂AsO₄, ferroelectric, high temp. phase transitions, proton dynamics 0-76023
 KH₂PO₄, ferroelectric transition, order-disorder character of hydrogen bond 0-93251
 KH₂PO₄, single crystal neutron diffraction study at high pressure 0-92497
 K₂InCl₃·H₂O, crystal structure and H-bonding 0-64978
 KPhI₂·2H₂O, X-ray cryst. struct. determ. 0-64958
 Li salt of β -ketoaldehyde, configurations of anions in solutions studied by IR spectroscopy, H-bond form. 0-87117
 LiBH₄, H bridged system, floating spherical Gaussian model 0-78518
 LiBeH₃, H bridged system, floating spherical Gaussian model 0-78518
 LiCH₃, H bridged system, floating spherical Gaussian model 0-78518
 LiNO₃·3H₂O, neutron diffr. studies at 120 and 295K, H bond studies 0-88099
 Mg₉IO₄·4Mn₁·89(SO₄)₂(OH)₂₆·8H₂O, mooreite, X-ray cryst. struct. determ. and refinement 0-92488
 (ND₄)₂D₂IO₆, neutron diffr. study 0-88098
 (NH₄)₂GeF₆, cryst., highly bent H bonds, IR spectrosc. investig. 0-93292
 (NH₄)₂H₂IO₆, neutron diffr. study 0-88098
 NH₄HSO₄, ferroelec. props. rel. to struct. 0-71345
 NH₄NO₃, crystals, NH₄⁺ ion symmetry in phases II-V, Raman spectra obs. 0-66200
 (NH₄)₂SO₄, paraelectric, N-quadrupole coupling meas. by proton-N double resonance 0-60459
 (NH₄)₂SiF₆, cryst., highly bent H bonds, IR spectrosc. investig. 0-93292
 (NH₄)₂SnF₆, cryst., highly bent H bonds, IR spectrosc. investig. 0-93292
 (NH₄)₂TiF₆, cryst., highly bent H bonds, IR spectrosc. investig. 0-93292
 Na salt of β -ketoaldehydes, configurations of anions in solutions studied by IR spectroscopy, H-bond form. 0-87117
 NaH₂(SeO₃)₂, ferroelec., proton motion within H bonds, neutron scatt. study 0-75986
 NaIn(SO₄)₂·6H₂O, X-ray cryst. struct. determ., H bond system 0-92511
 Na₂SbS₄·9H₂O(D₂O), vibrational spectra, internal SbS₄ and H₂O(D₂O) vibr. assignments 0-66199
 RbHSO₄, ferroelec. props. rel. to struct. 0-71345
 RbIn(SO₄)₂·4H₂O, refinement of cryst. struct., interatomic distances, bonds 0-59448
 Rb₂[C₂O₄]₂·D₂O₂, neutron profile refinement at 5K 0-88103
 Si₂H₆, amorphous, discharge prod., optically induced cond. changes 0-96937
 a-Si-H, influence of H on optical props., H conc. and H bonds 0-76098

hydrogen compounds

- see also deuterium compounds; hydroxonium ion; ice; steam; tritium compounds; water
 acetonitrile-HCl complex in liq. Xe, IR spectral study 0-95626
 complexes, H-bonded, frequency shift rel. to IR bandwidth 0-99502
 halides, rot. relax. with inert buffer gas, comment 0-69221
 halides, rot. relax. with inert buffer gas, reply 0-69222
 HCl-inert gas mixtures, van der Waals molecules, far IR spectra 0-95610
 HF chemical laser, CW, with unstable telescopic resonator, radiation field structure 0-91786
 hydrides, aq. dissoc., solvation, MINDO/S calcs. solvation theory 0-97708
 hydrides, first row, bending pot. calc. using MINDO approx., force const., equilb. geometry 0-95544
 meson capture, chemical, hydrogen and H isotope effects 0-69277
 metal hydrides, chemical heat pump, hydride conversion and storage system 0-72077
 metal hydrides as hydrogen storage media 0-61445
 PVC thermal degradation, reinitiation - mechanism of HCl catalysis 0-71944
 steel, mild, descaling by HCl (*French*) 0-108642
 steel, mild, electrodes, in H₂SO₄, H evolution reaction kinetics 0-97630
 struct. and props., SCF calcs. 0-106260
 Al anodic oxidation, in H₂SO₄, pH-values effect (*German*) 0-76419
 Al₂O₃·H₂O⁺, β and β' phases, protonic, conductance and spectroscopy 0-70450
 β -Al₂O₃·H₂O⁺, struct. basis for superionic cond. 0-107498
 β -Al₂O₃·NH₄⁺·H₂O⁺, single cryst. PMR and proton motion 0-108101
 Ar-HBr, intermol. pot. energy surfaces calcs. 0-91625
 Ba+HF—BaF+H, dual mol. beam excitation difference spectroscopy, state-to-state vibr. resolved dynamics 0-89474
 ClH-dimethyl ether, vibr.-rot. IR spectra, quantum and classical mechanics 0-91561
 DF-HBr CW optical resonance transfer laser 0-64003
 Fe-Cr (12 wt.%), corrosion in o-phosphoric acid 0-97622
 H+HCO—H₂+CO, classical trajectory study 0-93750
 H₂-air-H₂PO₄, fuel cell performance, effect of NH₃ 0-108795
 (H-He)⁺, ab initio calcs. 0-63799
 HAl₁O₁₇, H β -alumina, IR absorpt. study 0-100655
 HBr rot. relaxation, diffusion theory 0-106313
 HBF₂ and DBF₂, harmonic force field and ground-state average struct. determ. 0-83342
 HBO₂, band strengths, shock tube IR spectrosc. meas. 0-106358
 HBO₂, cubic, monoclinic and orthorhombic forms, H bonding, IR and Raman spectra 0-76029
 HBr, absorpt. coeffs. meas. in Nd laser emission band 0-78620
 HBr electrolysis for H₂ production 0-97816
 HBr, electron impact ionisation, vibr. excitation spectra threshold peaks, negative ion effects 0-106322
 HBr, fine struct. in dissociative attachment cross sections 0-87248
 HBr, photoelectron angular distrib. 0-58318
 HBr, vac. UV absorpt. cross section 0-91574
 HBr-CO, weakly bound, rot. spectra 0-91544
 HBr+Ba, laser induced fluoresc. study at different collision energies 0-91632
 HBr+CO(CO₂)(N₂O)(NO)(N₂O)(O₂), rate consts. for vibr. energy transfer meas. using laser induced fluorescence technique 0-87206

hydrogen compounds continued

- HBr+Cl⁺—HCl+Br⁺, vibr. product state distrib., IR chemiluminesc. obs. 0-81309
 HBr+ethylene, low temp. chain hydrobromination, kinetics and mechanism 0-93735
 HBr+F, H abstraction reactions, temp. depend., laser photolysis IR fluoresc. obs. 0-93744
 HBr+HCl, single quantum vibr. energy transfer 0-69223
 HCCF, CW for IR mol. laser, optical pumping with ¹⁶CO₂ and ¹⁸CO₂ lasers 0-74343
 HCL, fluid states, mol. dynamics simulation 0-79671
 HCL+HF, HF(v=3) relax. and rate consts. 0-61069
 HCN and HNC, mm wave emission obs. of interstellar clouds 0-90503
 HCN, electron elastic scatt., differential cross-sections, effective range theory 0-83485
 HCN emission in W3 H II region, LF obs. 0-82446
 HCN, Fermi and Coulomb correl. holes, SCF and CI wave functions 0-69085
 HCN formed by laser photolysis of methylamine, mol. fluoresc. obs. 0-97710
 HCN, ground state pot. surfaces, analytical functions 0-83304
 HCN, harmonic force consts., vibr. freqs., integrated intensities, MINDO/3 method 0-58411
 HCN in neutral cometary atmospheres, photodissoc. rel. to CN prod. 0-82303
 HCN in smoke, tunable diode laser meas. 0-89559
 HCN, interstellar, absorpt. lines obs. towards Cassiopeia A 0-101624
 HCN, interstellar, distrib. in vicinity of young B-type stars (*Russian*) 0-105321
 HCN, interstellar, in ¹ Σ state, collisional excitation by H₂ 0-109508
 HCN, intravalence triplet-triplet electronic transition, geometrical struct. and rel. energies determ. 0-99586
 HCN, J=4—3, 354 GHz transition in Orion Molecular Cloud 0-101636
 HCN, modified virtual orbitals, systematic CI procedure 0-83294
 HCN, photodissoc., photoabsorpt., photoemission and CN form. obs. 0-87141
 HCN predissoc. Frank-Condon amplitudes 0-95694
 HCN, relationships between higher-transition frequencies 0-69119
 HCN synthesis in HF plasma torch 0-61099
 HCN temp. depend. adsorption by activated and impregnated C 0-89522
 HCN⁺, ² Σ^+ and ² Π states, SCF and CI calcs. for determ. optimum linear geometries, bond angles calc. 0-74114
 HCN-CO complex, charge transfer theory, Mulliken population, ab initio calc., multiconfiguration scheme 0-106392
 HCN+LiH, rot. inelastic collision, energy transfer 0-87211
 HCN+He, translational-vibrational energy transfer, quantum dynamical study 0-63746
 HCN+He(H₂)(CH₃F), HCN 0-102498
 HCO⁺+CO, isotopic exchange, interstellar implications 0-61087
 HCP, force fields and force consts. of electronically excited states 0-69116
 HCSI-HSiC, isomerisation energies, ab initio MRD-CI calcs. 0-106271
 HCl, absorpt. coeffs. meas. in Nd laser emission band 0-78620
 HCl additive effects on ²⁷Al spin-lattice relax. in AlCl₃ aq. soln. 0-66058
 HCl and HCl-DCl, ferroelec. transition, ³⁵Cl NQR study 0-71233
 HCl, atmospheric measurements using ground based IR spectroscopy (*French*) 0-81975
 HCl, C¹H-X¹ Σ^+ system, (0, 0) and (0, 1) bands, oscillator strength determ. and UV spectra 0-91570
 HCl concentration, effect on H absorpt. of steel, and aniline surfactants effectiveness 0-108638
 HCl dissociation for XeCl(B) formation in electron beam assisted Xe/HCl laser discharge 0-63988
 HCl, dissociative electron attachment, differential cross section, Feshbach resons. 0-83508
 HCl, electron elastic scatt., exchange and polarisation 0-91668
 HCl, electrostatically interacting molcs., CI multipole function calcs. convergence 0-91458
 HCl, from H+Cl⁺, vibr. state distrib. 0-66794
 HCl in diffuse interstellar clouds, abundance and chem. models 0-91570
 HCl, in stratosphere, volume mixing ratios meas. 0-72587
 HCl liq., time correlation function, computer simulation 0-79670
 HCl, liq., vibr. relax., IR double reson. 0-95712
 HCl, liquid, struct. and mol. dynamics studied using intermolecular force models 0-83445
 HCl, nucl. spin-spin coupling consts., ab initio calcs. 0-95647
 HCl, one electron props. and polarizability, SCF and CI calcs. 0-58159
 HCl, one-electron props., corrections, Moller-Plesset perturbation theory calc. 0-95519
 HCl, overtone vibr.-rot. bands, intracavity dye laser techniques meas. 0-91532
 HCl, polar liqs. models, mol. polarisability effect 0-92444
 HCl, pseudopot. calcs. 0-91446
 HCl release in coastal atm. 0-90113
 HCl rot. relaxation, diffusion theory 0-106313
 HCl, second order mag. props., coupled Hartree-Fock perturbation theory 0-87042
 HCl, vac. UV absorpt. cross section 0-91574
 HCl, vibr. emission from ClF-H₂ chem. laser 0-97709
 HCl, vibr. excitation in electric discharge 0-87978
 HCl-CO, weakly bound, rot. spectra 0-91544
 HCl-inert gas rot.-vibr. line pressure broadening and shift calc. 0-69124
 HCl-Xe, liq., enthalpy of mixing, calorimetric meas. 0-59661
 HCl+Ar, differential cross section, quasiclassical close coupling approx. 0-63743
 HCl+Ar, inelastic scatt. exponential perturbation theories 0-74217
 HCl+Ba, laser induced fluoresc. study at different collision energies 0-91632
 HCl+Ca⁺, (Sr), reaction performed under high resolution, luminescence obs. 0-95662
 HCl+Cl(Br)(H), vibr. relaxation and reaction rates determ. 0-108698
 HCl+D, HCl dissociative ionisation, H⁺ signal origin, mol. beam obs. 0-66778
 HCl+D(O)(Cl)(Br), relax. and chem. reaction, time resolved IR fluoresc. and mass spectrometry obs. 0-69177
 HCl+F, H abstraction reactions, temp. depend., laser photolysis IR fluoresc. obs. 0-93744
 HCl+F—HF+Cl, time resolved vibr. chemiluminesc. and rate consts. 0-61069
 HCl+H, semi-empirical pot. energy surfaces calc. by diatomics-in-molecules method 0-95556

hydrogen compounds continued

- HCl+HBr, single quantum vibr. energy transfer 0-69223
 HCl+I₂ gas, weak collisions, HCl spectral line broadening of IR spectra 0-74161
 HCl+N₂(O₂)(D₂)(H₂), HCl ν_1 band perturbations, linewidth and shifts calcs., IR spectra obs. (French) 0-58251
 HCl+XeCl, ground state destruction, quenching rate consts. meas. 0-63758
 H₂CrO₄, chemical treatment of glass fibre reinforced epoxy laminate (German) 0-93670
 HD+CH₃⁺(CD₃⁺), isotopic exchange, interstellar implications 0-61087
 HDSe, high resolution IR spectra, anal. of 2 ν_1 band, rot. ground state const. determ. 0-95616
 H₂-_nD_nSe(n=0, 1 and 2) ⁷⁷Se NMR on XL-100 spectrometer, isotope effects and spin-lattice relax. 0-71211
 HD($\nu=5$)+HD($\nu=0$)-H₂+D₂, mol. H₂ exchange, reaction mechanism 0-85167
 HEu(PO₃)₄, luminesc. props. 0-100675
 HF, atmospheric measurements using ground based IR spectroscopy (French) 0-81975
 HF CW chemical laser, longit. and transverse mode competition in stable, unstable resonators 0-95917
 HF CW chemical laser, spatial homogeneity of radiation improvement using telescopic resonator 0-106549
 HF chemical laser initiation by relativistic electron beam 0-64005
 HF chemical TE laser, 16 μ m emission 0-83600
 HF, correl. energy, fourth order diagrammatic, many body Rayleigh Schrodinger perturbation theory 0-63556
 HF, electrostatically interacting mol., CI multipole function calcs. convergence 0-91458
 HF, Feshbach resons., predissoc. investig. 0-83433
 HF, fine struct. in dissociative attachment cross sections 0-87248
 HF in absorption, anomalous dispersion meas. 0-95881
 HF, in stratosphere, volume mixing ratios meas. 0-72587
 HF, intermolecular interaction energies calcs. using minimal basis sets 0-78681
 HF, laser field interaction, Floquet theory, dynamic Stark shift, broadening 0-63716
 HF laser with flow-through chem. active medium, pulsed-periodic regime realisation 0-106513
 HF laser with resistive Ge electrodes, for optical studies of semiconductors 0-64061
 HF, molecular energy quantities from localised charge densities, dependence on geometry and basis set 0-63525
 HF molecules, infinite linear chain, equilibrium structure and stabilisation energy 0-63856
 HF, orbital relax. energy for single and double ionis. from valence shells 0-106253
 HF, polar liqs. models, mol. polarisability effect 0-92444
 HF premixed chain reaction CW laser, spectral output 0-95882
 HF, pseudopot. calcs. 0-91446
 HF pulsed chemical laser of HI-SF₆ system 0-106514
 HF pulsed chemical laser of HI-SF₆ system 0-106515
 HF pulsed laser, appl. of CW X-ray preioniser 0-64037
 HF pulsed laser, Xe flashlamp efficiency for photoinitiation 0-69403
 HF, pulsed laser numerical modelling, rot. relax. 0-87388
 HF, relativistic Dirac-Fock multiconfig. SCF calcs. 0-99456
 HF, SCF theory, multiconfig., direct orbital optimisation 0-87049
 HF TEA laser, He-free, with MW output 0-64060
 HF, vibr.-rot. band, absorpt. line self-broadening, rot. relax. 0-87213
 HF/UF₆, H₂ nuclear pumped laser, characts. 0-78847
 HF-CO, weakly bound, rot. spectra 0-91544
 HF-DF simultaneous laser excited by ferroelec. ceramic capacitatively coupled discharge 0-69413
 HF-HCl, SCF energy hypersurface, stationary points, thermodynamics of form. 0-102436
 HF+Ar, state-to-state cross sections for rot. to translational energy transfer determ. 0-91644
 HF+Ba, product rot. and vibr. distributions and reaction cross sections depend. on reagent translational energy 0-93745
 HF+C₂H₃⁺, interaction, struct. and stability, ab initio calcs. 0-58347
 HF+H, low barrier quantum model, vibr. deactivation 0-69216
 HF+H₂(D₂)(N₂), 200K and 295K vibr. relax. rates 0-63766
 HF+HCl(CO₂)(N₂O)(CO)(N₂)(O₂), HF($\nu=3$) relax. and rate consts. 0-61069
 HF+HF, rot. relax. collision, scaling theory anal. 0-74232
 HF+HF (methane)(methane-d₄), collision relaxation rate constants and rot. equilibration time meas. 0-69213
 HF+Li-LiF+H, pot. energy surface, SCF and CI calcs. 0-71904
 HF+Sr, endothermic reaction, comparison of effectiveness of vibr. and translational excitation 0-93746
 H₂F₂ and H₂F₃ clusters, molecular structures, ab initio calcs. 0-83532
 HF-HF, vibrational predissociation in hydrogen bonded complexes 0-61078
 HHe⁺, N-electron system, Schrodinger eqn. soln. using antisymmetrisation 0-106246
 HHe⁺+Ar, ab initio pot. energy data, SCF-LCAO calcs. 0-63530
 HI nuclear quadrupole HFS in IR spectrum, obs. using tunable diode laser 0-58412
 HI, photoelectron angular distrib. 0-58318
 HI, vac. UV absorpt. cross section 0-91574
 HI-SF₆ system, HF pulsed chemical laser 0-106514
 HI-SF₆ system, HF pulsed chemical laser 0-106515
 HI+Cl₂-HCl+I⁺, vibr. product state distrib., IR chemiluminesc. obs. 0-81309
 HI+D, HI dissociative ionisation, H⁺ signal, mol. beam obs. 0-66778
 HI+F, H abstraction reactions, temp. depend., laser photolysis IR fluoresc. obs. 0-93744
 HIO₃, PMR spectra, homonuclear and heteronuclear broadening separation 0-77828
 H_{0.9}MoO₃ and H_{1.7}MoO₃ bronzes, NMR relax. obs. at 77<T<450K, H diffusion 0-108089
 H_{1.6}MoO₃ bronze, proton shift tensors PMR meas. 0-71202
 H_{1.6}MoO₃, electronic props., mag. susceptibility and spectra 0-80266
 HN₃, UV photolysis 0-101027
 H¹⁴N₃, rotational-vibrational Raman spectrum of ν_2 band 0-91564
 HN₃+NH(NH₂), rate consts. from HN₃ UV photolysis data 0-101027
 HNC, and HCN, ¹⁴N quadrupole coupling consts., ab initio calcs. 0-58283
 HNC⁺, ² Σ^+ and ² Π states, SCF and CI calcs. for determ. optimum linear geometries, bond angles calc. 0-74114

hydrogen compounds continued

- HNCO, rot. spectrum, ground and vibr. state reson., centrifugal distortion coupling 0-83364
 HNF₂, photoelectron spectra, vibr. struct. obs. ionisation pot. determ., ab initio calcs. of ionic geometry 0-83418
 HNF₂, vertical ionisation pot. calc. by perturbation corrections to Koopmans' theorem 0-83520
 HNNN, substitution struct., rot. consts. calcs. 0-91534
 HNO A¹A' excited state dipole moment, optical-optical double reson. Stark spectrosc. obs. 0-106337
 HNO isomerism, low lying electronic states, ab initio MRD-CI calcs. 0-83291
 HNO, low-lying states, pot. energy surfaces calcs. 0-102460
 HNO₂, air pollution obs. in W.Europe 0-72106
 HNO₂, concentration in stratosphere, simultaneous inference using inversion algorithm 0-82000
 HNO₂, corrosion of Ag-Au and Cu-Au 0-85091
 HNO₂, IR spectra, 865.5-871.0 and 884.5-887.0 cm⁻¹ regions, equiv. width meas., atm. spectrum appl. (French) 0-87114
 HNO₂ in marine air of equatorial Pacific 0-85702
 HNO₂, in stratospheric in situ obs. 0-105077
 HNO₂, particulate nitrate and acidity measurement in ambient air, filter media 0-104541
 HNO₂, VUV photodissoc., vibr. and rot. distrib. 0-87191
 HNP-HPN, isomerisation energies, ab initio MRD-CI calcs. 0-106271
 HO, detection by laser excited fluoresc., press. depend. of fluoresc. and photolytic interferences 0-95666
 HO radical form. from H₂+N₂O reaction on Pt surface, laser-induced fluoresc. obs. 0-108738
 HO₂, free radical, dipole moments and Stark effects from microwave spectra 0-63623
 HO₂, struct. and props., SCF calcs. 0-106260
 HO₂+ClO, free radical reaction rate consts. and products at 298K, discharge flow mass spectra 0-67391
 HO₂+ClO, reaction product distrib. 0-72586
 HO₂+HO₂, gas phase reaction mechanism, FT IR spectrosc. obs. 0-85163
 HO₂+O₃, reaction kinetics, laser mag. reson. obs. 0-102528
 H₂ mass sources in galactic plane, southern hemisphere survey 0-73054
 H₂O masers, 22 GHz galactic plane survey, 14 new sources 0-77464
 H₂O⁺, spin and rot. fine struct., orbital angular momentum 0-83247
 H₂O⁺, vibr. and rot. struct., intensity factors and orbital angular momentum 0-83246
 H₂O-HF heterodimer, H bonding, microwave rot. spectrum, mol. geometry and moment 0-99501
 H₂O₂, sum of states, isometric group, symmetry no., thermodynamic functions 0-58186
 H₂O₂, twisted mol., optical rot. strength calcs. 0-95793
 H₂O₂-H₂O, isolation of singular component for heat capacities of supercooled H₂O 0-107437
 H₃O⁺ (D₃O⁺), plasma dissociative ion electron recomb., rate coeffs. 0-63747
 HOCl, photodissoc. rot. distrib. 0-95694
 H₃O⁺(H₂O)_{0.1,2}+D₂O reactions, SIFT studies, review 0-58435
 H₃O⁺(H₂O)_n+D₂O(NH₃), binary reactions, rate coeffs. and product ion distributions determ. 0-81305
 HONO (nitrous acid), obs. in urban atmosphere by differential optical absorpt. 0-76677
 HO₂NO, UV absorpt., spectra, photodissoc. lifetime meas. 0-83386
 HOS-HSO, isomerisation energies, ab initio MRD-CI calcs. 0-106271
 HPN-HNP, isomerisation energies, ab initio MRD-CI calcs. 0-106271
 H₂PNH₂, inversion-rot. mechanism, basis set and geometry optimisation effects 0-83273
 HS_n⁺, n=1-4, electronic struct., ab initio Hartree-Fock-Slater calcs. 0-74107
 HS₂²⁺, n=1-4, electronic struct., ab initio Hartree-Fock-Slater calcs. 0-74107
 H₂S, aq., Fe corrosion, FeS polymorph form. 0-81231
 H₂S atmospheres, formation of contaminating layers on elec. contact materials (German) 0-71811
 H₂S, bond bending, bond orbitals rel. to nucl. motion 0-95513
 H₂S effect on molten carbonate fuel cell performance, mixed pot. anal. 0-81431
 H₂S, nucl. spin-spin coupling consts., ab initio calcs. 0-95647
 H₂S, photoionisation cross sections and asymmetry parameters, SCF X α scatt. wave calcs. 0-63542
 H₂S pollutant in troposphere, photochemical sources 0-90112
 H₂S, SS 0-78620
 H₂S, second order mag. props., coupled Hartree-Fock perturbation theory 0-87042
 H₂S+Cl⁺, reactions at room temp. 0-93749
 H₂S+K, collisional ionisation, positive and negative ion energy spectra obs. 0-63775
 H₂S+N₂⁺, deactivation, from laser-induced CO₂ fluoresc. obs. 0-63776
 H₂S₂, rot. barriers, internal rot. and electronic struct., valence electron study 0-83344
 H₂S₂, n=1-4, electronic struct., ab initio Hartree-Fock-Slater calcs. 0-74107
 H₂S(D₂S) photodissoc., SH internal energy distribution 0-95697
 HSO radical, Doppler-limited dye laser excitation spectroscopy, rot., distortion and spin-rot. interaction const. determ. 0-83383
 HSO-HOS, isomerisation energies, ab initio MRD-CI calcs. 0-106271
 H₂SO₄ aerosol, filter sampling of air, possible artifacts 0-82079
 H₂SO₄ aerosol in coastal atm., form. of particulates 0-90113
 H₂SO₄ aerosols, heterogeneous atmospheric reactions and role as tropospheric sinks 0-72612
 H₂SO₄, air pollutant measurement techniques 0-104542
 H₂SO₄ and (NH₄)₂S₂O₈ etchant, for NbC, TaC and HfC 0-85097
 H₂SO₄, atm. aerosol, extinction, absorpt., backscattering and mass content relations 0-101403
 H₂SO₄ atmosphere-aerosol study of Venus cloud microstructure and optical props. 0-72808
 H₂SO₄ etchant, for revealing struct. inhomogeneities in martensite-ageing steel 0-61035
 H₂SO₄ mist monitor, semicontinuous 0-61495
 H₂SO₄ polydisperse aerosol number and mass conc. meas. by elect. aerosol anal. 0-108753
 H₂SO₄ vapour pressure rel. to gas-particle conversion 0-94560
 H₂SO₄-H₂O aerosols nucleation rate in presence of ionisation source 0-104464

hydrogen compounds continued

- H₂SO₄-H₂O-ion aerosol particles, ultrafine, stratospheric form., ion-induced nucleation 0-72608
 H₂SO₄-Mn²⁺-KBrO₃-oxalacetic acid, chaos type reactions anal. 0-85165
 HSO₃F-graphite, intercalation compound, Raman spectral study (*French*) 0-60581
 HSS, struct. and props., SCF calcs. 0-106260
 HSBCl₆·3H₂O, cryst. struct., cation H₃O₂²⁺ (*German*) 0-107133
 H₂Se₂, rot. barriers, internal rot. and electronic struct., valence electron study 0-83344
 H₂SeO₃, reduction, reaction sequence and CdSe film deposition 0-71603
 HSIC-HCSi, isomerisation energies, ab initio MRD-CI calcs. 0-106271
 H₂SiO, electronic struct., dipole moments, mol. polarisability, force fields, ab initio calcs. 0-78531
 H₂Te₂, rot. barriers, internal rot. and electronic struct., valence electron study 0-83344
 HUO₂AsO₄·4H₂O and HUO₂PO₄·4H₂O layered cpds., struct. investigs. below antiferroelec. transition temps., H bond ordered structs. 0-107416
 HUO₂AsO₄·4H₂O and HUO₂PO₄·4H₂O layered cpds., single and polycryst., proton cond. behaviour w.r.t. antiferroelec. transition temps. 0-107481
 H_{n-2}UO₂(IO₆)_n·4H₂O, n=0.5 to 2.0, high proton cond. 0-107562
 HUO₂PO₄·4H₂O, film fabrication and appl. as solid electrolyte in electrochromic displays 0-70462
 HUO₂PO₄·4H₂O solid proton conductor, appl. as electrochromic cell 0-89497
 H₂WO₃ bronzes, Anderson transition, XPS 0-107705
 HuO₂P(As)O₄·4H₂O, water deficiency, enthalpy of dehydration, thermogravimetric anal. 0-65251
 KBr·I⁻, OH⁻, luminesc. of interstitial atomic H 0-89062
 Kr-HCl, intermol. pot. energy surface calcs. 0-91625
 NH₂Br, dislocation influence on phase transition and light scatt. (*Russian*) 0-59648
 N₂H₆FeF₆, one-dimensional antiferromagnetism, Mossbauer study 0-65872
 (NH₄)₂S₂O₈-HCl-H₂O dislocation etchant for β-brass crystals. 0-65004
 O+H₂O→OH+OH, energy partitioning 0-101009
 OH+H₂O→HO₂+H₂O, reaction rate consts., laser induced fluoresc. 0-101017
 RbBr·I⁻, OH⁻, luminesc. of interstitial atomic H 0-89062
 T+HD, variational transition field theory and unified statistical model 0-97700

hydrogen embrittlement

- adsorption model, and equilibrium crack growth meas. 0-108574
 adsorption or decohesion, mechanism 0-97643
 cracking and impurity atom migration (*Chinese*) 0-104247
 fracture analysis of failure in service (*Japanese*) 0-104337
 Hastelloy, C-276, H-induced crack growth 0-71747
 Hastelloy, H₂ embrittlement in H₂S environments, impurity segregation effects 0-71724
 low C steel, explosive-thermal treatment, sulphide cracking decrease, hydrogen embrittlement (*Russian*) 0-108477
 metals, effect on props. 0-104290
 metals, hydrogen brittleness measurement 0-104291
 metals, reversible H embrittlement 0-104292
 Ni-Co, H₂ embrittlement, heat treatment and impurities effect 0-76331
 nuclear reactor materials, PWR, H₂-assisted fatigue-crack growth model 0-71745
 plasma magnetic confinement system, surface problems 0-57946
 steel, 4340, H₂ embrittlement, stress state, thickness and delayed failure in bending 0-71746
 steel, austenitic, explosive-thermal treatment, sulphide cracking decrease, hydrogen embrittlement (*Russian*) 0-108477
 steel, austenitic stainless, cathodically charged, H₂ embrittlement, α' martensite effect 0-71725
 steel, bimetal, alloy with austenitic stainless, H permeability 0-107572
 steel, carbon type, hydrogen press. effect on morphology of hydrogen attack 0-85052
 steel, Co-Cr-Mo HY 180M, SCC in NaCl, temp. effect 0-108633
 steel, Cr-Mo, H embrittlement in H₂S environment, Mo effect 0-76415
 steel, effect of H₂ on phys. and mech. props. 0-101657
 steel, effect on band strength 0-104293
 steel, fracture in low-cycle fatigue tests in H₂ (*Russian*) 0-76332
 steel, H embrittlement mechanism, microcrack formation, dislocation model (*Russian*) 0-65143
 steel, high strength, dislocation sweeping model for hydrogen assisted subcritical crack growth 0-97577
 steel, high strength, subcritical crack growth, role of time delayed H₂ assisted plastic zone growth 0-97576
 steel, high-strength, H distrib. and delayed brittle fracture 0-108577
 steel, mild, electrodes, in H₂SO₄, H evolution reaction kinetics 0-97630
 steel, mild, US detect. of H embrittlement 0-71822
 steel, Ni-Cr-Mo-V, corrosion fatigue crack growth in NaOH soln., cathodic pot. effect 0-89403
 steel, Ni-Mo-V, fatigue crack growth, H₂ gas environment effect (*Japanese*) 0-104340
 steel, SAE 1045, permeation meas. of H trapping, rel. to cryst. microstruct. 0-84328
 steel, welded-joints, H₂ induced cracking, S content effect 0-97562
 steel welds, bead-on-plate, H₂ diffusion and trapping 0-96697
 stress corrosion cracking, role of H₂, state of art review 0-61017
 trap theory, of H embrittlement 0-89325
 Al-Zn-Mg (91, 6, 3, wt.%), H embrittlement and trapping, HVEM obs. 0-76364
 Fe, effect of H₂ on phys. and mech. props. 0-101657
 Fe, H₂ embrittlement and H₂ adsorption 0-89401
 Fe, H₂ permeation, rel. to embrittlement, organic inhibitors, surface treatment 0-108635
 Fe, polycrystalline, H₂ adsorpt. and embrittlement, work function changes 0-96741
 Fe, pure, cathodic charging effect on creep and tensile deformation 0-76320
 Fe, pure, hydrogen-charged, initial cracking obs. 0-108580
 Fe, whiskers, H₂ effect on mech. props. 0-108556
 Fe-Cr-Co (28, 10.5 wt.%) ductile magnet alloy, humidity-induced H₂ embrittlement 0-89406
 Fe-Ni-C, quenched martensite, annealing during cathodic hydrogenation, 200°C (*French*) 0-93573
 Fe-Ti, Ti as H trap for embrittlement control 0-66662

hydrogen embrittlement continued

- LaNi₅Fe, H₂ absorpt. cracking, acoustic emission characts. (*Japanese*) 0-66631
 Ni alloy protection, by Cu electroplating, aerospace engine appl. 0-76416
 Ta single crystal, H₂ embrittlement (*Japanese*) 0-66636
 Ta-H system, acoustic emission study 0-76257
 Ti alloys, delayed brittle fracture, H₂ effect 0-100912
 Ti alloys, hydrogenation at 200-600°C and up to 10000 kPa 0-107435
 α-Ti alloys VT1 and VT5, struct. and phys. props., H₂ effect 0-108576
 Ti-Al-V (6.4 wt.%), H related fatigue fracture 0-76344
 Ti-Al-V-Sn (5.5, 5.5, 2 wt.%), crack growth, slow, H-induced 0-104272
 U-Mo (2 wt.%), depleted, effect of microstruct. on mech. props. 0-108497
 Zr-Nb (2.5 wt.%) pipe, fracture resistance, hydrogenation effect 0-104279
 Zr-Nb (97.5, 2.5 wt.%) nuclear reactor pressure tube material, H embrittlement study by TEM 0-76363

hydrogen ion activity see pH**hydrogen ion concentration see pH****hydrogen ions**

- backscattering from Au(Cs), fraction reflected 0-60741
 Earth's upper atmosphere, coupled time-dependent diffusion eqns. 0-109285
 field ion source with high angular current 0-68996
 hydrogenic ions, electron capture by charge particles at relativistic energies 0-102565
 ionisation rates, shock tunnel meas. 0-75022
 isoelectronic sequence, electron impact ionisation cross section 0-91688
 line broadening and shift due to plasma ions (*Russian*) 0-96350
 proton beam characts. control by laser-induced selective multiplet processes 0-61122
 pulsed proton source, Penning type, beam parameters 0-87001
 quantum oscillations in tunnelling, oscill. freq., tunnelling currents (*Russian*) 0-60065
 two photon ionisation in presence of one photon ionisation, cross section calc. 0-83327
 H II, Zeeman splitting of high-n recomb. lines 0-58210
 H⁺, ^p(1) and ^p(1) resonances associated with n=3 hydrogenic threshold 0-78557
 H⁺ backscatt. from solid surface due to proton bombardment 0-99554
 H⁺, classical many-body collision model incorporating Heisenberg and Pauli principles 0-63511
 H⁺, DC Stark broadening of ¹p⁰ shape reson. 0-63585
 H⁺, double excited states below N=3 threshold, arrangement of resonances in series converging exponentially 0-99462
 H⁺ form. by surface and vol. processes, neg. ion source appl., review 0-58375
 H⁺, formation by HCl dissociative electron attachment, differential cross section, Feshbach resons. 0-83508
 H⁺, ion beam diagnostics using laser beam 0-95497
 H⁺, many-body perturbation theory with radially restricted basis functions 0-78526
 H⁺, photoabsorption spectra, long-range field effect 0-91521
 H⁺ photofragments angular distribution, parity favoured electric dipole transitions 0-58330
 H⁺ production cross sections in H⁰+Cs collisions 0-78698
 H⁺ production in foil breakup of H₂⁺, inhibition effect 0-99549
 H⁺ resonances in electric field 0-63607
 H⁺, two-electron photodetachment threshold, blackbody radiation effects 0-91524
 H⁺ ion mobility in He, expt. 0-96337
 H⁺, prod. by electron impact dissociation of H₂, kinetic energy, ang. distrib. 0-63838
 H⁺-H₂ system, pot. energy surfaces 0-74215
 H⁺-affinities of methylamine, ab initio SCF calculations 0-102443
 H⁺-affinities of NH₃, ab initio SCF calculations 0-102443
 H⁺-He²⁺ mixture, fully ionised, two-component plasma, mean spherical model 0-87854
 H⁺+H(He), electron detachment in adiabatic regime, mechanisms 0-63800
 H⁺+He, electron detachment, theoretical obs. 0-63799
 H⁺+¹⁰⁶Cd, simultaneous nucl. and K-shell excitation, ¹⁰⁷In lifetime meas. 0-63130
 H⁺+Ag, excited X-ray polarisation, Born approx. calcs. (*Russian*) 0-78566
 H⁺+Ag(Zr)(Fe)(Cu)(Ti) 0-106390
 H⁺+Al(Cu), K-shell ionisation 0.5 to 40 MeV, meas. and PWBA-BEA calcs. 0-78699
 H⁺+alkali metal, charge exchange, eikonal approx. calcs. 0-78703
 H⁺+Ar, charge exchange excitation, alignment tensor components, coincidence method 0-63795
 H⁺+Ar, Hα and Hβ emission cross section 0-63783
 H⁺+atom, emission electron angular and energy distribution 0-87222
 H⁺+atoms (Z=27 to 34), K shell ionisation, nuclear Coulomb effect 0-91650
 H⁺+CO, computed cross section vibr. threshold effects 0-63759
 H⁺+CO (^Σ), ground state pot. energy surface, ab initio SCF calc., protonated equilib. geometry 0-83301
 H⁺+CO₂, vibr. excitation, isotope and time effects 0-63773
 H⁺+CO(^Σ), vibr. excitation calc., close coupling and sudden approx. 0-78561
 H⁺+Cs(Rb)(K)(Na), single-electron capture total cross sections 0-91656
 H⁺+D₂, collisional complex form. 0-58339
 H⁺+H, H excitation, angular differential cross sections 0-63784
 H⁺+H, ionisation and electron capture to continuum 0-58366
 H⁺+H high energy collision, excitation multipole moments, classical trajectory approx. 0-106389
 H⁺+H₂, rot. and vibr. excitation, energy loss obs. 0-63773
 H⁺+H₂, sudden approx. of Cross, computational tests, cross section factorisation, scatt. phenomena 0-58352
 H⁺+H₂, vibr. excitation, ab initio CI pot. energy surface calcs. 0-74228
 H⁺+H₂, vibr.-rot excitation, ab initio CI pot. energy surface calcs. 0-74229
 H⁺+H₂(CO₂), vibr. excitation, 10-30 meV 0-58358
 H⁺+He, differential scatt., 1-12 eV, high resolution beam meas. 0-58348
 H⁺+Li, charge exchange, eikonal approx. calcs. 0-78703
 H⁺+Li⁺, charge transfer and ionisation, total cross sections for production of Li²⁺ determ. 0-91657

hydrogen ions continued

- H^+ + methane- H_2^+ + methyl radical, quantum 0-71911
 H^+ + N_2 collision, total ionis. cross section and stopping power for protons 0-69228
 H^+ + SF_6 , mode selective vibr. excitation 0-58351
 H_2^+ , free free absorpt. coeffs. dipole length formulation and two centre close coupling calc. 0-83345
 H_2^+ , bound states in strong mag. field 0-99438
 H_2^+ , differential cross section rel. to charge exchange cross sections of fragments 0-78704
 H_2^+ , dissoci. recombination, doubly excited Rydberg states 0-83506
 H_2^+ , electron elastic scatt., phaseshifts, quantum defect and two electron excited states 0-91671
 H_2^+ , exchange perturbation theory 0-63518
 H_2^+ , ground state, pot. energy curves, $1/R$ expansion coeff. calcs. 0-91472
 H_2^+ , mol. electron density distrib., binding/antibinding anal. 0-95534
 H_2^+ , photodissoc., mass spectra 0-86489
 H_2^+ , polarised Balmer radiation due to scatt. from Nb surface, adsorbed O_2 effects 0-99569
 H_2^+ , transmission yield through thin C-foil meas. 0-100732
 H_2^+ + Ar, endothermic charge transfer reaction, low energy crossed beam study 0-95720
 H_2^+ + Ar, low energy proton transfer reactions, crossed beam studies 0-108697
 H_2^+ + D_2 , H^+ + H , product angular and vel. vector distributions meas. by crossed beam expt. 0-101012
 H_2^+ + H_2 , state selected reaction cross sections, coincidence technique obs. 0-66797
 H_2^+ + methanol, dissoci. charge transfer reaction studied at rel. translational energies from 600 eV to 5000 eV 0-104432
 H_2^+ , IR spectrum, ν_2 band obs. 0-99506
 H_2^+ , ion beam prod. by coaxial electron impact ion source 0-62795
 H_2^+ , rot.-vibr. spectrum, ab initio calcs. 0-95595
 H_2^+ , vibr. excitation, ab initio CI pot. energy surface calcs. 0-74228
 HD^+ , Hellmann-Feynman theorem anomaly 0-63510
 H_2^+ (D^+) + H_2 (D_2) collisions, slow ion production, charge transfer cross sections 0-106378
 $H125\alpha$ recomb. line in M82, SHF obs. 0-82486
 $Li + H^+$, Li core excitation cross section, correlation and reorganisation effect 0-87215
 $Na + H^+$, $2p^3s^2p_{3/2}$ state alignment, collisionally induced, impact parameter calc. 0-83474
 $Ne + H^+$ (D^+), electron detachment, dynamical phenomenon 0-106305

hydrogen neutral atoms

- 1S Lamb shift and 1S-2S isotope shift 0-91464
 1s resonance, stabilisation method calcs., convergence 0-91492
 adsorbed on He surface, Bose condensation, adsorption isotherms and stability 0-107638
 adsorption, on graphite (0001) surface, vibr. spectrum, at. beam scatt. obs. 0-92779
 atoms produced by IR multiphoton dissociation of alkenes, IR detection 0-83356
 Balmer γ line profiles and masses of DA white dwarf stars 0-77399
 Balmer lines, formation in bright prominences spectra (Russian) 0-77377
 bombardment of graphite surface 0-93665
 bound states in strong mag. field 0-99438
 chemisorbed, surface charge fluctuations effect on spectral density 0-65368
 chemisorbed on cluster, indirect interactions, Grimley-Pisani model and tight-binding calc. 0-65370
 Cherenkov line radiation, QSO emission-like spectra (Chinese) 0-105378
 collapsing pre-galactic gas cloud, local stability, linear perturbation anal. 0-82513
 conversion by electron impact, eikonal exchange amplitude in Coulomb break-up processes 0-87232
 detection by resonance fluoresc., coherent tunable VUV generation near Ly- β transition 0-99798
 diffusion coeff., in H_2 , luminesc. intensity meas. 0-103098
 dilute hard-sphere Bose-gas model, low-density atomic H gas property-calc. 0-87194
 Dirac atom, relativistic, energy level splitting 0-77938
 Dirac field, self-interacting, charged nonlinear spinor field in Coulomb-like potential, localised solns. 0-68351
 double-quantum saturation spectroscopy, laser and RF 0-77880
 elastic electron scatt., 20-50 eV, Born calcs. of differential cross section 0-102571
 elastic electron scattering, pseudostates wave functions determ. in modified close-coupling calcs. 0-99572
 elastic scattering of electrons, optical model approach, polarisation effects 0-58382
 electron capture by fast multiply charged ions, q^3 scaling 0-91658
 electron elastic scatt., exchange perturbation theory 0-78709
 electron elastic scatt. at low intermediate energies 0-106393
 electron excitation, matrix elements by Faddeev approach 0-78714
 electron impact, 1s-2s and 1s-2p excitation, electron-photon coincidence meas. 0-87233
 electron impact excitation, 1s-2s transition, exact second Born amplitude 0-102572
 electron impact excitation, cross-sections, multipole moments, quasiclassical calcs. 0-63828
 electron impact excitation, electron-photon coincidence, large angle expt. 0-83500
 electron impact excitation of $n=2$ to $n=3$ transition, algebraic variational method close coupling calcs. 0-91678
 electron impact ionisation, polarised Coulomb-projected Born approx. 0-106395
 electron scatt., atomic optical potential model 0-99578
 electron scatt. information obtained using symmetrically coupled partial differential eqn. 0-102574
 electron scattering, elastic, $E_e \geq 100$ eV, ang. distrib. calc. 0-74248
 electron scattering, optical pot. methods 0-102569
 electron-photon angular correlation meas. for excitation of 2P state 0-91636
 EM vacuum fluctuations, ground state energy in multiply connected universes 0-87050
 emission-line spectrum from a slab of hydrogen at moderate to high densities 0-72759
 energy levels and bound-bound transitions in strong mag. field 0-58134

hydrogen neutral atoms continued

- energy spectra, angular distrib. from HeH^+ collisions with thin foils 0-66355
 Fermi contact interaction, spin density calcs., Hiller Sucher Feinberg identity 0-69061
 fine structure $3S_{1/2}$ - $3^2D_{5/2}$ interval, separated oscillatory field meas. 0-99482
 finite chains, HF solns. stability and symmetry breaking, independent particle model calcs. 0-87035
 form factor for arbitrary states, dipole moment component matrix element calcs. (Russian) 0-58143
 fusion reactor neutral beam injection, 24 MW 400 keV H beam 0-91356
 galaxies, IR magnitude/H I vel. width relation rel. to distance scale and Universe expansion rate outside Local Supercluster 0-105325
 gaseous, high-resolution mag. reson. study, 1 to 1.3K 0-95560
 $H + FH(FD)$, low barrier quantum model, vibr. deactivation 0-69216
 hydrogenlike atoms, spin-orbit terms derivation 0-73148
 hyperfine splitting inside paraboloidal surfaces 0-99445
 interplanetary H I, $L\alpha$ emission profiles reanal. rel. to local interstellar gas temp. and vel. 0-105141
 interstellar absorption in galactic centre direction 0-77465
 ionisation in AC and DC elec. fields, time depend. 0-63585
 ionisation potential and energies in mag. field 0-99585
 Jupiter atmosphere, hydrocarbon and H I photochemistry rel. to Lyman α albedo 0-105194
 Kepler problem for n-dimensional atoms, dynamical symmetries 0-58121
 line profiles in RY Persei spectra, visible obs. 0-67795
 longit. excited states in intense mag. fields, rel. to pulsars 0-91469
 Lyman α albedo of Jupiter, Copernicus UV obs. 0-94747
 Lyman α albedo of Jupiter rel. to solar activity 0-98601
 Lyman α effect on non-LTE model atmospheres of A-type stars 0-90422
 Lyman α emission from Jupiter, Voyager 2 EUV obs. 0-77338
 inner M101 galaxy group, H I obs. 0-67885
 mesic, atomic X-ray yields 1s and 2p level shifts and widths, cascades, calc. 0-78730
 mesonic atoms, formation in mixtures of lightest elements 0-87252
 mesosphere and thermosphere composition UV dayglow Lyman α and β obs. 0-109290
 multiphoton ionisation of H like atoms, Pade-Sturmian approach 0-87089
 muonic, formation at extremely low press. 0-74263
 muonic atom + Y, muon transfer mechanism from free muonic hydrogen 0-69218
 negative mesons in H, atomic capture 0-69276
 NGC 1023 galaxy group, H I obs. and possible intergalactic H I cloud discovery 0-67886
 NGC 1052, elliptical galaxy, field, H I emission mapping and line profiles 0-98719
 NGC 7538 and Shapley 159, H II region/mol. cloud complex, H I aperture synthesis obs. 0-90510
 in NGC 925, barred spiral galaxy, high-resolution H I obs. 0-105329
 one-dimens., $\Psi(x) = \Psi(-x)$ even states, teaching 0-90638
 optical harmonic coefficients, third order, at low freqs. 0-78905
 Orion Nebula, radio obs. of nearby H I distrib. and vels. 0-105322
 oscillator, four-dimensional, rot. invariance of coordinate transform., appln. to Stark problem 0-99436
 perturbation theory and Pade approx. in electric field 0-91493
 photoionisation, absolute cross-sections, expt. meas. techniques 0-63598
 photoionisation in homogeneous elec. field (Russian) 0-106309
 photon emission, Bohr theory covariant eqns., teaching 0-105482
 pulsar crust, crust, infinitely magnetised H atom theory 0-77282
 quasars, large-red shift, spectra, implications of neutrino rest mass for H I obs. problem (Russian) 0-105414
 quasi-stationary states in field of strong monochromatic wave, perturbation theory calcs. (Russian) 0-58145
 redshifted H I 21 cm line assoc. with Stephan's Quintet of galaxies 0-67882
 relativistic energy levels in strong mag. fields 0-102454
 Rydberg consts., saturated absorpt., spectroscopy meas. 0-105604
 in Sa spiral galaxies, H I study 0-98714
 Sharpless 159 and NGC 7538, H II region/mol. cloud complex, H I aperture synthesis obs. 0-90510
 spin-polarised, Bose condensation, phenomenological description 0-77699
 spin-polarised, Bose-Einstein condensation 0-77698
 Stark and photoabsorption spectrum, density of oscillator strengths, atom c.f. semiconductor spectra 0-83318
 Stark effect, high orders of perturbation theory for excited states 0-87079
 Stark effect, iteration procedure for any field strength 0-69104
 Stark effect, second order correction for energy (Rumanian) 0-74147
 Stark effect studied by scattering theory methods 0-63586
 Stark spectrum and field ionisation, density of continuum states, normalised wavefunctions 0-83317
 in static multipole field, logarithmic perturbation expansion 0-91431
 superpermeability, in interaction with Pd membrane 0-81365
 trapping and thermal detection using superconducting magnet at low temp. 0-73396
 Virgo cluster spiral galaxies, H I deficiency from 21 cm obs. 0-62277
 VUV radiation, narrowband tunable, at Lyman- α wavelength 0-78907
 K^+p atom and $\Lambda(1405)$, KN interaction model 0-68479
 μ^+p , elastic scattering cross section of muonic H atoms 0-69278
 p radiative atomic recombination, antiprotonic atoms 0-83527
 $Ar^+ + H$, collisional quenching rates 0-95548
 Ge, heterodiffusion due to H atom surface recombination stimulation, Cu, Zn, In coated (Russian) 0-59726
 H, degenerate 3s-3d levels, in mag. field, eigenvalues, Bender-Wu formulas 0-83275
 H I α observations of Algol type stars 0-109484
 H I halo round Seyfert galaxy Markarian 348, 21 cm obs. 0-82504
 H I halo round Seyfert galaxy Markarian 348, rel. to nucl. activity 0-82505
 H-like atoms, dipole polarisability of arbitrary hybrid bound states 0-87237
 H + alkali metal atom, interaction potentials 0-63736
 H + Ar, H α and H β emission cross sections 0-63782
 H + $Ar^+(Ne^+)$, assoc. ionis., rovibronic struct. in electron energy spectrum 0-106380
 H + Ar(Kr)(Xe), ion pair formation, curve crossing model 0-87216
 H + $B^{3+}(C^{4+})(N^{5+})(O^{6+})$, ($2 \leq q \leq 4, 5$), cross sections at keV energies 0-78705
 H + Br $_2$ reaction, Br prod., matrix isolated ESR 0-106336

hydrogen neutral atoms continued

- H+CF₂, IR matrix isolation spectra 0-97706
H+CN(NC)(NSI), bimolecular exchange reactions, dynamical-statistical method calcs. 0-104435
H+Cl₂, pot. energy surfaces, inversion calcs. 0-93734
H+Cl₂, stochastic-collision complex model theory 0-108696
H+Cl → HCl+e, associative reaction, product vibr. state distrib. 0-66794
H+Cs(Rb)(K)(Na), single-electron capture total cross sections 0-91656
H+D, close coupling calc., resonant spin-flip process, Ramsauer-Townsend effects 0-99547
H+D₂, collinear motion, energy transfer and dissociation, collision dynamics 0-99563
H+D₂ reaction, transition state theory calculations, kinetic isotope effect explanation 0-66784
H+e (e⁻), elastic and inelastic scatt., relativistic spin-dependent amplitude, Glauber approx. 0-63818
H+H, electron loss cross section, four-body trajectory calcs. 0-99566
H+H, spin-exchange and freq. shift cross sections at low temps. 0-83452
H+H interaction, second order dispersion energy, Borel integral investigation 0-74218
H+H₂, collinear quantum mech. reactive scatt., hyperspherical coords. 0-108694
H+H₂, collinear reaction, Delves radial coord. S-matrix propag. calcs. 0-108695
H+H₂, exponential gap relation, rot. inelasticity 0-78693
H+H₂, reaction probability, max. entropy derivation, statistical theories 0-66781
H+H₂, reactions and collisions in IR laser field, collision-induced absorpt. spectra 0-76499
H+H₂, scatt. wave function modal struct. and global behaviour 0-81307
H+H₂, sudden rot. reactive scatt., 3-dimens., approx. quantum mech. calcs. 0-76498
H+H₂(Cl₂), reactivity-selectivity, bounds derivation 0-66763
H+H₂(D₂)(T₂) reactions, accurate pot. energy surface, isotope effects, quasiclassical trajectory study 0-97698
H+H₂(v=1), exchange reaction, integral and differential cross sections determ. 0-85153
H+H₂ → H₂+H three dimens. chem. reaction, distorted-wave calcs. 0-81294
H+H⁺, electron detachment in adiabatic regime, mechanisms 0-63800
H+H⁺, H excitation, angular differential cross sections 0-63784
H+H⁺, ionisation and electron capture to continuum 0-58366
H+HCO → H₂+CO, classical trajectory study 0-93750
H+HCl, semi-empirical pot. energy surfaces calc. by diatomics-in-molecules method 0-95556
H+HCl, vibr. relaxation and reaction rates determ. 0-108698
H+HF, low barrier quantum model, vibr. deactivation 0-69216
H+H⁺, electron loss cross section, four-body trajectory calcs. 0-99566
H+He²⁺, electron transfer, plane-wave factor, mol. state treatment 0-63807
H+He(Ar), collisional coherent excitation, meas. of Lyman α-photons 0-99552
H+LiF, laser-induced nonadiabatic collision process, classical model 0-97701
H+methane, abstraction and exchange reaction, barrier height calc. using POL-Cl wave functions 0-81304
H+multiply charged ion, electron capture, unitarised distorted wave approx. 0-63814
H+N³⁺, multicharged ion thermal charge exchange reaction, rel. to astrophysics 0-63815
H+NF, electronically-excited free radical reactions 0-97707
H+NF₂, electronically-excited free radical reactions 0-97707
H+Ne(Ar), electron energy loss 0-87217
H+O₂+Ar, HO₂ free radical prod., rate const. calc. 0-101026
H+O₂(N₂), collisional coherent excitation, meas. of Lyman α-photons 0-99552
H+O₂ → HO₂+O(³P), yields 0-71900
H+O²⁺(Nⁿ⁺)(Cⁿ⁺)(Bⁿ⁺), charge transfer cross sections, oscillatory behaviour in low-energy collisions 0-63806
H+OH → H₂+hw, radiative association reaction for mol. synthesis in interstellar clouds 0-90509
H+T₂, H-exchange studied by crossed molecular beam experiments 0-93747
H+Xeⁿ⁺(Arⁿ⁺)(Feⁿ⁺), electron capture by heavy multicharged ions at low velocities total cross sections meas. 0-99548
H³+Cs collisions, H⁺ production cross sections 0-78698
H³+N³⁺, electron loss cross section 0-63805
H⁺+H₂ high energy collision, excitation multipole moments, classical trajectory approx. 0-106389
H₂+Cl(Br)(I)(F), gas phase H-atom transfer reactions, struct.-reactivity correl., pot. energy surfaces 0-104433
H₂ and H₂ spectral profiles from neutral beams and plasmas in high mag. fields 0-83999
H₂, dynamic Stark effect for elec. field-strength meas. in waveguide 0-69103
H(²S)+Ar(³P_{0,2}), energy transfer collisions, Lyman-α emission profile obs., in microwave discharge and reaction cell 0-58359
¹H, pionic, pion mass high accuracy meas. from transitions 0-106406
H⁺+H(Li), resonant ionisation, cross section and ionisation probability 0-63785
H110α radio recomb. line in galactic radio sources, SHF obs. 0-77472
H(1s) electron scattering, variable-charge Coulomb-projected Born approximation 0-58392
H(1s)+Cs, differential electron attachment and elastic scatt., 30-528 eV 0-63745
H(2S)+He(N)(Ar), excitation and ionisation contributions to sum-rule Born cross sections 0-99551
Hα and Hβ, Stark profiles, ion-motion effect 0-63592
NH₃+H₂, NH₃ inversion transition, linewidths and T₁/T₂ ratio 0-99499
Ne:H, exciton states and L_αL_β emission 0-93372

hydrogen neutral molecules

- ²S and ³S state pots., diatomic transition operators, L² basis expansions 0-63519
ab initio SCF intermolecular interaction energy calcs. 0-78537
adsorption on Rh-TiO₂ catalyst., surface states, NMR spectrosc. investig. 0-103891
chloropentafluoroethane-H₂, multiphoton dissoc., ¹³C enrichment factor, CO₂ laser wavelength and fluence depend. 0-58331

hydrogen neutral molecules continued

- classical many-body collision model incorporating Heisenberg and Pauli principles 0-63511
contamination in He plasma, satellites of He 492.2 nm line, fine struct. interpretation 0-59235
dynamic dipole polarisabilities calcs. 0-74110
E,F¹Σ⁺ state, collisional and radiative props. 0-58357
electron degradation spectrum, statistical anal. of. ionisation yield 0-99581
electron dissociative attachment 0-91694
electron impact dissoc. ionisation 0-83510
electron impact excitation, H_α and H_β lines emission, intensity decay curves meas. 0-83505
electron impact excitation, low energy, distorted wave approx. cross-sections 0-83511
electron impact excitation, to high Rydberg states, by threshold energy collision 0-83509
electron impact H⁺ prod., kinetic energy, ang. distrib. 0-63838
electron impact ionisation cross section 0-78718
electron repulsion matrix elements, asymptotic form, adiabatic representation 0-87038
electron repulsion potentials calcs. 0-91427
electron scatt., absolute total cross-sections, 0.2-100 eV 0-91674
electron scatt., elastic and inelastic, Glauber approx. 0-91695
electron scatt., low energy, multichannel variational calcs., static exchange approx. 0-83483
electron scatt., Schwinger variational principle, static-exchange approx. 0-63820
electron scattering, Gaussian basis Glauber approx., elastic and vibrorotational excitation cross sections 0-58399
electron scattering, iterative approach to Schwinger variational principle 0-99580
electron scattering, total cross section meas. at very low energies 0-58398
electron scattering elastic, 100-2000 eV, scatt. amplitude and cross-section 0-87228
electronic chemical pot., natural orbitals occupation numbers and electronegativity 0-63509
electronic struct., valence bond model, pairwise correlation 0-78543
four-body system, adiabatic representation 0-91530
infrared spectrum of matrix isolated H₂, mol. rot. and vibr. const. determ. 0-78617
interstellar gas clouds, spherically symm., gravitational collapse, effect of H₂ form. 0-101628
interstellar H₂, collisional excitation of linear mol. CO, OCS, SiO, HCN and HC₃N in ¹²S state 0-109508
interstellar H₂, OH rot. excitation rel. to maser emission 0-62232
interstellar H₂ form. in diffuse clouds, influence of Lyman band absorpt. of UV radiation (*Russian*) 0-73026
liquid, moon capture rate meas. 0-69275
lowest singlet and triplet states, interactions, electronic force calcs. 0-63742
magnetic susceptibility calcs. vector pot. variation method, effective selection of gradient transform. functions 0-69258
microwave absorption in atmosphere of giant planets induced by collisions of H molecules 0-90350
NGC 7027, planetary nebula, H₂ emission spatial distrib. obs. 0-98698
nonadiabatic coupling matrix elements by Hellmann-Feynman theory and HF 0-83263
ortho-para conversion, magneto-catalytic reaction, quantum formulation 0-108750
photoelectron asymmetry parameters 0-95684
photoelectron spectra, rot. intensity distrib. 0-91605
polarisabilities, variation-perturbation calcs. 0-87243
polarisability, dipole, coupled perturbed Hartree-Fock method improvement 0-58148
predissoc., interference effects, lineshape obs. 0-83432
preions, and predissoc., rel. to spectral line shape 0-63724
relativistic Dirac-Fock multiconfig. SCF calcs. 0-99455
relativistic Dirac-Fock multiconfig. SCF calcs. 0-99456
singlet superexcited levels, radiative emission 0-83415
solid, fundamentals, static props., review 0-75403
states velocity auto-correl. function, relax. time, neutron scatt. obs. 0-58401
static polarisability, ab initio SCF wave functions 0-74106
sticking and accommodation on low-temp. substrate, mol. beam expts. 0-84368
valence bond orbital method for understanding electronic struct. 0-106268
vertical ionis. pot., many-body Green's function calcs. 0-102439
vibrational and rotational transitions, CARS, optical Stark effect 0-99512
Zeeman effect, Bender-Wu formula and SO(4,2) dynamical group, perturbation coeffs. determ. 0-95674
Ar⁺(²P)+H₂, Ar⁺ two spin orbit state, reaction cross section, direct determ. 0-93748
Br+H₂, proximity induced electric dipole moment effect in laser field 0-83456
Cs-H₂ vapour, resonant character of laser induced formation of particles 0-89481
¹⁸F+H₂, hot atom reaction, nonequilib. time-depend. theory 0-61126
H⁺+He(1s²), K-shell electron capture collision, static pot. effect 0-91660
H₂, field ionisation under nonequilibrium conditions 0-74244
H₂, high resolution electron spectroscopy 0-62740
H₂ in Ar, vibr. energy relax. 0-106384
H₂, optical polarisation following electron impact 0-63831
H₂, rotational Raman intensities and polarisability anisotropy change meas. with internuclear distance 0-63641
H₂, triplet state, molecular polarisability, ab initio calcs. 0-63860
H₂ vibrationally excited 2 μm lines toward molecular clouds 0-94853
H₂-Ar, states velocity auto-correl. function, relax. time, neutron scatt. obs. 0-58401
H₂-H₂ dimers, hyperfine struct. in zero mag. field 0-95700
H₂-H₂ intermol. pair pot., ab initio SCF-Cl surface 0-91457
H₂+⁴He, inelastic collision, R-matrix study 0-87204
p-H₂+⁴He, vibr. relax., analytical approx. 0-63761
H₂+Ar⁺, collisions, ionisation and excitation resulting from electron capture 0-78683
H₂+C⁺(N⁺)(O⁺), reactant ion electronic states, effect on charge transfer cross sections 0-63809
H₂+CH_n⁺, isotopic exchange, interstellar implications 0-61087

hydrogen neutral molecules continued

- $H_2 + CO$, coadsorption on Cu-Ni (110) single cryst. surface, TDS and UPS obs. 0-80052
 $H_2 + CO$, rot. excitation, rel. between tensorial cross sections 0-83454
 $H_2 + CO_2$, exponential gap relation, rot. inelasticity 0-78693
 $H_2 + CO_2$, rot. transfer, ab initio intermol. pot. energy surface 0-58354
 $H_2 + C(S_0)$ 0-74241
 $H_2 + Cd(P_1) \rightarrow CdH + H$, product initial rot. state distrib., pump and probe laser obs. 0-85158
 $H_2 + Cl^+$, reactions at room temp. 0-93749
 $H_2 + D$ reaction, transition state theory calculations, kinetic isotope effect explanation 0-66784
 $H_2 + D$ rearrangement collision, vibr. excitation effects 0-71910
 $H_2 + D_2$, reactive and inelastic scatt., semiempirical pot. energy surfaces calcs. 0-74140
 $H_2 + D(O)(Cl)(Br)$, relax. and chem. reaction, time resolved IR fluoresc. and mass spectrometry obs. 0-69177
 $H_2 + F$, absolute rate coeffs. at 295 to 765K 0-81303
 $H_2 + F$, rate consts., temp. depend. 0-81302
 $H_2 + F_2$, branched chain reaction, role of thermally nonequilibrium atoms and molecules 0-76507
 $H_2 + F^+$, quenching of excited state, semiclassical studies, comparison between reactive and nonreactive processes 0-106375
 $H_2 + F \rightarrow HF + H$, DWBA transition amplitude kernel 0-81310
 $H_2 + H$, collinear quantum mech. reactive scatt., hyperspherical coords. 0-108694
 $H_2 + H$, collinear reaction, Delves radial coord. S-matrix propag. calcs. 0-108695
 $H_2 + H$, exponential gap relation, rot. inelasticity 0-78693
 $H_2 + H$, reaction probability, max. entropy derivation, statistical theories 0-66781
 $H_2 + H$, reactions and collisions in IR laser field, collision-induced absorpt. spectra 0-76499
 $H_2 + H$, reactivity-selectivity, bounds derivation 0-66763
 $H_2 + H$, scatt. wave function modal struct. and global behaviour 0-81307
 $H_2 + H$, sudden rot. reactive scatt., 3-dimens., approx. quantum mech. calcs. 0-76498
 $H_2 + H_2$, exponential gap relation, rot. inelasticity 0-78693
 $H_2 + H_2$, rot. relax. collision, scaling theory anal. 0-74232
 $H_2 + H_2$, state selected reaction cross section, coincidence technique obs. 0-66797
 $H_2 + H_2^+ \rightarrow H_3^+ + H$, state-selected ion-molecule reactions threshold electron-secondary ion coincidence technique obs. 0-85166
 $H_2 + H_2O^+$, rate constants determ. as function of relative kinetic energy 0-81292
 $H_2 + H^+$, rot. and vibr. excitation, energy loss obs. 0-63773
 $H_2 + H^+$, vibr. excitation, 10-30 meV 0-58358
 $H_2 + H^+$, vibr. excitation, ab initio CI pot. energy surface calcs. 0-74228
 $H_2 + H^+$, vibr.-rot. excitation, ab initio CI pot. energy surface calcs. 0-74229
 $H_2 + H^+(Li^+)$, sudden approx. of Cross, computational tests, cross section factorisation, scatt. phenomena 0-58352
 $H_2 + HCN$, HCN excited vibr. state, T_2 meas. 0-102498
 $H_2 + HCl$, HCl v_0-v_1 band perturbations, linewidth and shifts calcs., IR spectra obs. (French) 0-58251
 $H_2 + H(D)(T)$ reactions, accurate pot. energy surface, isotope effects, quasiclassical trajectory study 0-97698
 $H_2 + H \rightarrow H + H_2$, three dimens. chem. reaction, distorted-wave calcs. 0-81294
 $H_2 + He$, exponential gap relation, rot. inelasticity 0-78693
 $H_2 + He$, inelastic scatt., vibr. adiabatic basis functions calcs. 0-102551
 $H_2 + He$, inelastic scatt. exponential perturbation theories 0-74217
 $H_2 + He$, mol. energy transfer by quasiclassical trajectory methods, vibr. relax. and dissoci., rot. effect 0-99557
 $H_2 + He$, pot. energy surface, ab initio calcs., van der Waals const. determ. 0-106372
 $H_2 + He$, vibr. relax. cross section 0-99494
 $H_2 + He^+$, 0.7-2 MeV, charge-changing collisions, electron capture 0-58372
 $H_2 + HgBr$, vibr. relax., rate coeffs., fluoresc. obs. 0-63697
 $H_2 + Hg(P_1)$, quenching rate constants determ. with nanosecond light pulser with Hg vapour 0-100111
 $H_2 + Kr^{2+}$, charge transfer reactions, rate coeffs. and product-ion distributions meas. 0-104431
 $H_2 + Li$, exponential gap relation, rot. inelasticity 0-78693
 $H_2 + Li^+$, exponential gap relation, rot. inelasticity 0-78693
 $H_2 + Li^+(2P_1)$, collision induced quenching and fine struct. transition rate coefficients meas. 0-74221
 $H_2 + Li(2p)$, Li(2p) excitation, alignment and orientation obs. 0-63794
 $H_2 + N_2^+$, collisional disoc. cross-section, 2.4-24.3 keV 0-58373
 $H_2 + N_2O$, HO radical form. on Pt surface, laser-induced fluoresc. obs. 0-108738
 $H_2 + N_2 + N_2H_4$, mixtures with nonthermal vibr. excitation of mol. N_2 , formula for calc. equilb. const. 0-76545
 $H_2 + N^+$, electron capture and ion loss cross-section, 2.4-24.3 keV 0-58373
 $H_2 + Ne^{2+}$, energy-loss scaling in 0.5-3.5 keV 0-63768
 $H_2 + Ne^{2+}$, charge transfer reactions, rate coeffs. and product-ion distributions meas. 0-104431
 $H_2 + Ni^+$, endothermic reactions, investig. 0-97692
 $H_2 + O$, classical trajectory calcs., ab initio surface, singlet state, rate consts. 0-66786
 $H_2 + O$, pot. energy surfaces and reaction rates, ab initio calcs. 0-63531
 $H_2 + O_2$, combustion, kinetic modeling and sensitivity anal. 0-89490
 $H_2 + OH \rightarrow H_2O + H$, reaction product vibr. distrib., quasiclassical trajectory, calcs. 0-85162
 $H_2 + Pt(111)$ surfaces, interactions, bond breaking activity, model pot. 0-108744
 $H_2 + vinylidene$, addition reaction, MINDO/3 study 0-108705
 $H_2 + Xe^{n+}(Ar^{n+})(Fe^{n+})$, electron capture by heavy multicharged ions at low velocities total cross sections meas. 0-99548
 $H_2 + Y$, high temp. equilb. meas. 0-66780
 H_3 , diatomic state mixing parameter 0-74139
 H_3 , emission spectra, rot. struct. obs. mol. const. determ., predissociation 0-106331
 H_3 , relative magnitudes of direct and indirect exchange, Heitler-London calcs. 0-69069
 H_3 , Rydberg states, spectroscopic B_0 consts. 0-74109
 H_4 , pot. energy surfaces, valence bond calcs. 0-74129
 $H_4 + H_2$, hexadecapolar U-branch transitions in IR fundamental band 0-91631

hydrogen neutral molecules continued

- HD, 5-0 transition, intracavity photoacoustic detector spectrosc. obs. 0-77877
 HD detection in Uranus atm. from visible spectra obs. 0-82296
 HD, electron impact disoc. ionisation 0-83510
 HD electron scattering, total cross section meas. at very low energies 0-58398
 HD, perturbation var. calc. with contact interaction, effect of approx. zero order wavefunctions 0-58107
 HD, predissoc., interference effects, lineshape obs. 0-83432
 HD, spin-dipolar term, spin-spin coupling const. corrections, Fermi contact terms calcs. 0-99448
 HD, spin-spin coupling constant convergence, comparative study 0-63536
 HD + D_2 , state-resolved $\Delta j = 2$ rot. transitions 0-63772
 HD + Ni^+ , endothermic reactions, investig. 0-97692
 $H_3^+ + (D_3^+ + H_2(D_2))$ collisions, slow ion production, charge transfer cross sections 0-106378
 HF + $H_2(D_2)(N_2)$, 200K and 295K vibr. relax. rates 0-63766
 He + H_2 , adiabatic distorted-wave infinite order sudden approx. 0-99558
 He + $H_2(D_2)$, dissociative charge transfer, 78-330K 0-61079
 $H_2(v_1=1) + H$, exchange reaction, integral and differential cross sections determ. 0-85153
 $N_2 + He$, rot. inelastic scatt., appl. of sudden approx. 0-95705
 $O_3 + He(D_2)(H_2)$, vibr. relax. rate consts. 0-74231
 SF₆ + H_2 , chemical laser, electron beam pumping 0-91784
 UF₆- H_2 gas dissociation in pulsed IR and UV laser fields 0-91620

hydrological techniques

- annual streamflow record extension by correl. methods 0-81950
 climatology, hydrology, atmospheric research and meteorology from space, conference, Ajaccio, Corsica (1979 November 12 to 16) 0-62397
 daily river flow, non parametric Markov model, appl. to Cheyenne river 0-81948
 dialysis of stream water, meas. of dissolved forms of trace elements 0-97851
 flood forecasting, loss of runoff due to water absorpt. by soil 0-109178
 flood forecasting model from rainfall catchment and evaporation data, retention hysteresis 0-81951
 flood inundation of agricultural land, LANDSAT digital image anal. 0-61913
 flow through heterogeneous earthen dam, problem solvability 0-90110
 glacier thickness and water content, radar measurement technique 0-98369
 ground surface temperature prediction, force-restore method investigation 0-98469
 groundwater recharge in Ganges Basin, alternative methods for water supply 0-81952
 groundwater salinity and ionic strength determination method 0-109176
 groundwater searches in Ukrainian Shield fracture zones, appl. of geothermal survey peculiarities (Russian) 0-104935
 groundwater vel. determ. using organic solute-mineral surface interactions 0-98492
 groundwater velocity determ. using natural He 0-82111
 hydrothermal system, temp. measurement scale based on chem. comp. of gas fraction 0-98277
 ice, dielectric relax. meas. by blocking layer method 0-103914
 lake ice, microwave radar and radiometric remote sensing meas. 0-85691
 lakes, latent and sensible heat fluxes prediction from surface water temps. 0-72562
 microwave remote sensor development and appl. to hydrology 0-105082
 optical methods of water quality determ., turbid waters spectral scatt. props. 0-72560
 particulate concs., remote sensing of lakes 0-105056
 precipitation measurement, dual-gauge and Wyoming shield systems 0-61928
 prospecting in Africa, geophysical techniques 0-61818
 radar subsurface sounding of groundwater in deserts and glaciers 0-67437
 rainfall measurement by weather radar, appl. to hydrology 0-90263
 rainfall of short duration, runoff calc. method (French) 0-77143
 rainfall prediction for short response time basins 0-98491
 river longitudinal slope determ. 0-82108
 River Tiber, physical processes related to discharge into sea, aerospatial obs. 0-108831
 rivers downstream pollution, one-dimensional transient model for short-term prediction 0-81496
 runoff from steppe zone river, estimation method for spring norm 0-85694
 snow parameters, investigation by radiometry in 3 to 60 mm wavelength region 0-72561
 soil moisture, basic hydrophys. charact., determ. method 0-85696
 soil moisture, determ. in Africa by soil thermal inertia cartography (CITHARE project) 0-76980
 soil moisture content meas., quick drying procedure 0-82109
 space-borne remote sensing (Italian) 0-109333
 subsurface water detection methods, in Armenia, elec. profiling and sounding 0-85753
 sulphate determ. in brines, indirect anal. by atomic absorpt. 0-89556
 surface water continuous analysis by NH_4^+ -sensitive plastic membrane electrode 0-89701
 turbid water, instrument of meas. light absorpt. coeff. 0-82076
 water-resource development project design, optimal apportionment scheme appl. (French) 0-77019
 P determination, automated procedure 0-81517
 ^{22}Ra in public water supplies, conc. determ. (German) 0-94138
 Rn groundwater monitoring systems for earthquake prediction 0-94467
 Se (-II,0), (-IV) and (-VI) composition of water, by gas chromatography method 0-81928

hydrology

- see also groundwater; lakes; rivers
 aquifer inverse problem, statistical method case study 0-98371
 Brazil, precipitable water, distrib. maps 0-77075
 Britain, water balance, 50000 yr BP to present day 0-72566
 conference, on climatology, hydrology, atmospheric research and meteorology from space, Ajaccio, Corsica (1979 November 12 to 16) 0-62397
 Dakota drainage pattern mapping IR thermal imagery remote sensing 0-81892
 Darling River system floods, chronological evolution, Nimbus-5 radiometry. obs. 0-94543
 drainage basin characteristics, network power model 0-61823
 drainage density estimation from topological variables 0-61831

hydrology continued

- drainage network change in Britain 0-81934
- drainage network mapping of Pantanal Brazil, Landsat-2 imagery 0-81944
- drought definitions 0-105010
- drought in streamflow series, statistical characts. 0-105009
- evaporation from water surface, scaling theory 0-109179
- floods and their causes, in India 0-101389
- floods in Plynlmon expt. catchments, Wales, geomorphological effectiveness 0-81932
- ground surface temperature prediction, force-restore method investigation 0-98469
- independent mixed models, range, drought effects 0-81954
- Kirishima volcanoes, Japan, heat discharge and H₂O emission rates, hydrothermal survey (*Japanese*) 0-67357
- mid-ocean ridges, obs. and implications of ridge crest hot springs 0-98304
- potential evapotranspiration, continental maps based on Penman concept calcs. (*German*) 0-98368
- reservoir flooding, for oil recovery, shear thinning and shear thickening polymer additives 0-72100
- runoff from land receiving animal wastes, pollutant transport, review 0-97831
- runoff kernel for basin, mathematical derivation 0-61832
- soil moisture, basic hydrophys. charact., determ. method 0-85696
- soil moisture, cartography in Africa by geostationary satellite (CITHARE project) 0-76980
- spring-flood forecasting and runoff loss due to water absorpt. by soil 0-109178
- streamflow record synthesis, feature prediction model appl. 0-98372
- wadi flood water sampler 0-98493
- S.Wales floods of late December 1979, meteorological anal. 0-98429

hydromagnetic waves see magnetohydrodynamic waves

hydromagnetics see magnetohydrodynamics

hydrometers

- see also density measurement
- No entries

hydrophones

- see also sonar
- acoustical tracking, ocean current profiling 0-67427
- arrays, underwater, appl. in passive sonar (*Spanish*) 0-69586
- CW coherence meas. at low freq. for long underwater paths 0-106654
- fibre-optic, comments on mechanism of transduction 0-58882
- fibre-optic, description and advantages 0-58770
- fibre-optic, modulation processes 0-58771
- fibre-optic pressure sensor 0-58878
- gain limitations of passive vertical line array in shallow water 0-96117
- membrane hydrophone for 0.5 to 15 MHz range, press. meas. in US fields 0-108987
- multipath separation and passive localisation using horizontal wavenumber spectrum 0-91952
- noise level meas. using optical fibre intermetric hydrophone 0-87673
- optical interferometric, with homodyne detection, signal stabilization by light source tuning 0-87477
- SAW sensor using resonator-controlled oscillators 0-74631
- Schlieren multimode fibre-optic hydrophone 0-102938
- spatial noise spectrum meas. in ocean for small observation baseline 0-102902
- tracking of slowly sinking floats, meas. vertical profiles of oceanic current and Richardson number 0-67378
- underwater signal phase stability, meas. using moving source 0-87623
- Pb,Sr_{1-x}(Zr,Ti,Nb)₃O₁₂, hydrophone ceramic, effect of one-dimensional uniaxial stress 0-80705
- Pb(Zr,Ti)O₃, research grade, hydrophone ceramic, effect of one-dimensional uniaxial stress 0-80705

hydrophotometers see photometers

hydrostatics

- cellulose nitrate, nonlinear viscoelastic deform., hydrostatic press. and third invariant of deviatoric stress tensor 0-93587
- fatigue, hydrostatic stress-sensitive relationship for biaxial stress conditions 0-74805
- ferrofluids, Landau and Lifshitz hydrostatic press., thought expts. 0-59111
- weighing in immiscible liquids, for porosity determ. of coatings 0-66714

hydrothermal crystal growth see crystal growth from solution

hydroxonium ion

- complexes, produced by collisional dissoc. method, mass spectrometric study, dissoc. energies determ. 0-95707
- inversion barrier, high-order replacements inclusion in CI calc. 0-63504

hydroxyl group see oxygen compounds

hygiene

- see also medicine
- No entries

hydrometers

- see also humidity measurement
- heated electrolytic sensor 0-109262
- humidity sensor, capacitive, Panahume (*Japanese*) 0-105658
- hygrometry testing scheme for the Soviet countries 0-57312
- psychrometer, portable differential system construction and operation 0-105072
- yaRV-2 compact automatic nuclear resonance hygrometer 0-105657
- LiCl heated electrical, modified instrum. 0-95104
- LiNbO₃ sensor for elec. hygrometer (*Japanese*) 0-95103
- SiC thin-film thermistors with high thermal response (*Japanese*) 0-105629

hyperfine field interactions (condensed matter)

- see also crystal hyperfine field interactions; nuclear screening
- 4-amino-2,2,6,6-tetramethylpiperidine-N-oxyl and deuterated derivatives, mag. resonance study 0-63686
- Lorentzian lineshapes and isotropic distrib. of molecules, analytical expressions derived for powder samples 0-60401
- Ni-Pd-P, metallic glass, electronic structure, pulsed NMR study 0-75869
- nitroxide radical, long range Y-P hyperfine coupling, ESR spectra obs. 0-75858
- nitroxide spin probes, unresolved hyperfine broadening convection in EPR, linewidth and Heisenberg spin exchange freq. determ. 0-71180
- Co₂B, glassy and cryst., hyperfine field distrib., ⁵⁹Co spin echo spectra 0-80635

hyperfine field interactions (condensed matter) continued

- Cs-Au liq. alloy, formation of localised electronic states, NMR obs. 0-93201
- Cu(II)-DL-proline complex, ESR, magnetic susceptibility and optical absorption 0-93167
- Fe_{1-x}B_x, amorphous, hyperfine fields and local mag. moments, Mossbauer study 0-75895
- Fe₈₀B₂₀, amorphous struct., Mossbauer spectroscopy investigation 0-84677
- (Fe_{0.5}Co_{0.5})_{1-x}B_x, amorphous, hyperfine fields and local mag. moments, Mossbauer study 0-75895
- FeF₃, amorphous, struct. and mag. props., computer model 0-96446
- Fe(H₂O)₆²⁺ ion, amorphous frozen soln., Mossbauer study, hyperfine struct. 0-80644
- Fe₄₀Ni₄₀B₂₀, amorphous, RF annealing effects 0-108037
- (Fe_{1-y}Ni_y)_{0.8}B_{0.2-x}P_x, amorphous, hyperfine fields and local mag. moments, Mossbauer study 0-75895
- La₇₅Ga₂₅, amorphous, local symmetry around glass-former sites, elec. quadrupole effects, NMR 0-80618
- La_{80-x}Pr_xAu₂₀, amorphous, mag. and supercond. props. 0-75713
- Mo₇₀B₃₀, amorphous, local symmetry around glass-former sites, elec. quadrupole effects, NMR 0-80618
- Mo₄₀Ru₃₂B₂₀, amorphous, local symmetry around glass-former sites, elec. quadrupole effects, NMR 0-80618
- Ni-Pt-P, metallic glass, electronic structure, pulsed NMR study 0-75869
- Ni₇₈P₂₂B₀, amorphous, local symmetry around glass-former sites, elec. quadrupole effects, NMR 0-80618
- ¹⁷O, naturally abundant, nuclear quadrupole resonance spectrum for fine struct. detection 0-75881

hyperfine field interactions in crystals see crystal hyperfine field interactions

hyperfine structure, atomic see atomic hyperfine structure

hyperfine structure, molecular see molecular hyperfine structure

hyperfragments see hypernuclei

hypernuclei

- orbital excitation of the hyperon in hypernuclei 0-106001
- (K,K), isobar doorway model, optical pot., Λ -nuclear matter binding energy 0-106079
- ANN correlations and Λ binding in nuclear matter 0-106000
- NN tensor force effect on Λ separation energy 0-86845
- Σ to Λ conversion widths (*Russian*) 0-106003
- Σ -hypernuclear state width, model estimation 0-57719
- Σ N effective complex pot. from Σ -atoms and scatt. lengths 0-57717
- ⁹Be(K⁻, Π^-), 720 MeV/c, Sigma hypernuclei prod., missing mass spectrum 0-57721
- ⁹Be, excited states and spectra, continuum effects calcs. 0-57720
- ⁴H _{Λ} , binding energy, Fadeev equation in coord. space, Lambda-nucleon potential 0-63120
- ³H _{Λ} , short range repulsion, separation energy, K-harmonics calcs. 0-86846
- ³He _{Λ} , Λ -N pot. Majorana component on B _{Λ} value, overbinding 0-99144
- ⁶He _{Λ} , short range repulsion, separation energy, K-harmonics calcs. 0-86846
- ⁶Li _{Λ} , supermultiplet struct. and decay props. of hypernuclear 1⁺ resonances from (K⁻, π^-) 0-78186
- ⁸Li _{Λ} , possible γ -transition from ⁹Be(K⁻, π^-) 0-106002
- ⁴Li _{Λ} , A=6,7, excited states and spectra, continuum effects calcs. 0-57720
- ^{AA}Li, A=10, 11, double hypernuclei, prod. and decay from (K⁻, X), emulsion 0-57718
- ¹⁶O _{Λ} , Λ -N residual interactions, Λ spin-orbit splitting and effective mass 0-57722

hyperon absorption

- No entries

hyperon capture

- see also hypernuclei
- No entries

hyperon decay

- flavour changing weak radiative decays, short and long distance effects 0-73712
- nonleptonic decays, Weinberg-Salam and harmonic oscillator quark model 0-102048
- nonleptonic hyperon decays, final state interactions with inelastic effects, comments 0-99099
- nonleptonic hyperon decays, QCD corrections 0-91087
- Λ hyperon polarisation, meas. by hybrid Monte Carlo tech. 0-99431
- $\Lambda^0 \rightarrow p e^- \bar{\nu}$, absolute rate, $\Lambda(\Gamma^0 \rightarrow p e^- \bar{\nu})/\Gamma(\Lambda^0 \rightarrow p \pi^-)$ precise meas. 0-57593
- $\nu p \rightarrow \mu^- p k^+ \pi^+ \pi^0 \Sigma^+$ prod. and decay 0-86710
- $\Omega \rightarrow \Lambda K$, QCD and valence quark approx. 0-105893
- $\Omega \rightarrow \Theta e(\mu) \bar{\nu}$ or $\Theta^* e(\mu) \bar{\nu}$, branching ratios and lepton energy spectra 0-73701
- $\Omega \rightarrow \Sigma^* \pi(\Sigma^0 \pi^-)$, nonleptonic hyperon decays, QCD description, PCAC anal. 0-95269
- pp, ISR energies, p fragmentation, D⁺ prod. from Λ_c^* and Λ_b decay 0-102080
- $\Sigma^- \rightarrow \Lambda K$, QCD and valence quark approx. 0-105893
- $\Sigma^+ \rightarrow p \gamma$, 1/2⁻ resonance poles to parity-violating amplitude, two-quark weak transitions 0-78062
- $\Sigma^+ \rightarrow p \nu e$, flavour changing neutral current search 0-105836
- Σ^\pm , lifetimes and longitudinal accel. 0-86709
- Σ^\pm , lifetimes, decay asymmetry and nonleptonic decay branching ratio, $|\Delta I|=1/2$ rule 0-78061
- Σ^+ , mass and mean life from high energy cosmic ray data (*Chinese*) 0-102045
- Σ^+ , production and decay obs. 0-105894
- Y⁻3g, angular patterns and front-back moments, QCD 0-73702

hyperon detection and measurement

- No entries

hyperon-deuteron interactions

- see also hyperon-deuteron scattering
- No entries

hyperon-deuteron scattering

- see also hyperon-deuteron interactions
- No entries

hyperon effects

- No entries

hyperon interactions *see* hyperon-nucleon interactions; hyperon-nucleus reactions; kaon-hyperon interactions; lepton-hadron interactions; photon-hadron interactions; pion-hyperon interactions

hyperon magnetic moment

No entries

hyperon mass

$K^- d \rightarrow \Xi^- K^0 p$, 1.45, 1.65 GeV/c, $\Xi^- p$ invariant mass enhancement 0-57639
 Λ , charmed baryon mass in SU(1,4) dynamical group theory 0-62882
 Σ , charmed baryon mass in SU(1,4) dynamical group theory 0-62882
 Σ_c^+ , mass and mean life from high energy cosmic ray data (Chinese) 0-102045

hyperon-nucleon interactions

see also hyperon-nucleon scattering

hadron interactions, effective radius quantum number depend., quark sum rules (Russian) 0-102062
 ΛN distrib. function, Λ -binding to nuclear matter, Fermi hypernetted chain approx. 0-78131
 ΣN effective complex pot. from Σ -atoms and scatt. lengths 0-57717
 3H_A , binding energy, Faddeev equation in coord. space, Lambda-nucleon potential 0-63120

hyperon-nucleon scattering

see also hyperon-nucleon interactions

No entries

hyperon-nucleus reactions

for inelastic hyperon-nucleus scattering, *see* "hyperon-nucleus scattering"

see also hyperon capture; hyperon-nucleon interactions

No entries

hyperon-nucleus scattering

see also hyperon-nucleon scattering

No entries

hyperon production

$K^- d \rightarrow \Xi^- \Lambda p$, pole in 3S_1 hyperon-nucleon scattering amplitudes 0-102068
 $K^- d \rightarrow \Xi^- K^0 p$, 1.45, 1.65 GeV/c, $\Xi^- p$ invariant mass enhancement 0-57639
 $K^- p$, 10, 16 GeV/c, Σ^+ , Σ^- inclusive prod. A prod. comparison 0-86766
 $K^- p \rightarrow \Lambda + X$, 32 GeV/c, total and differential cross sections, energy dependence 0-63048
 $K^- p \rightarrow \Lambda \eta$, 6 GeV/c, baryon exchange reactions, ηNN coupling constant, Λ polarisation, nucleon-Regge exchange 0-78098
 $K^- p \rightarrow \Lambda \pi^0$, 6 GeV/c, baryon exchange reactions, ηNN coupling constant, Λ polarisation, nucleon-Regge exchange 0-78098
 $K^- p \rightarrow \pi^- \Sigma^+$ and $\pi^- p \rightarrow K^- \Sigma^+$, exchange degeneracy 0-57634
 $K^- p \rightarrow \pi^- Y^+$, $Y^+ = \Sigma^+$ or $Y^* (1385)$, 7 GeV/c, hypercharge exchange in line-reversed $\pi^- p$ and $K^- p$ 0-82998
 $K^- p \rightarrow \pi^- \Sigma^+$, box diagram calcs. unitarity corrections in strong interactions 0-91110
 $K^- p \rightarrow \rho^- Y^+$, $Y^+ = \Sigma^+$ or $Y^* (1385)$, 7 and 11.5 GeV/c, hyperon polarisation, vector meson decay angular distrib. 0-82997
 $K^- p \rightarrow \Sigma^- \pi^+$, backward differential cross section 0-63024
 $K^- p \rightarrow \Sigma^- \pi^+ \pi^0$, 4.15 GeV/c, nondiffractive A_1 production, double-Regge model 0-78097
 $K^- p \rightarrow \sigma^+$ (1385)X, 32 GeV, inclusive and total cross sections 0-105936
 Λ hyperon polarisation, meas. by hybrid Monte Carlo tech. 0-99431
 $\mu p \rightarrow \Lambda^0 (\Lambda^0) X$, 225 GeV, deep inelastic scatt., strange neutral particle prod. 0-105902
 $\nu d \rightarrow \Lambda_c^+ X$, high energy charmed baryon prod. obs. 0-105881
 $\nu p \rightarrow \mu^- p k^- \pi^+ \pi^0$, Z_c^+ prod. and decay 0-86710
 (p, Λ^+) , inclusive cross section, constituent-constituent multiple scatt. model for dependence on atomic number 0-83101
 $pN \rightarrow \Lambda^+ X$, inclusive cross section, constituent-constituent multiple scatt. model for dependence on atomic number 0-83101
 pp , 300 GeV/c, inclusive prod. of K^0 , Λ^0 $K^+ \Xi^-$ (890) and $\Sigma^+ \Xi^-$ (1385) 0-95290
 pp , high energies, $\Sigma^+ (1385)$ inclusive prod., minimised wave function model calcs. (Russian) 0-63047
 pp , probabilistic quark-model approach to p fragmentation 0-63049
 $pp \rightarrow \Delta^{++} (1232) X$, 32 GeV, cross sections 0-105937
 $pp \rightarrow \Xi (1385) X$, 3.6 GeV, factorisation hypothesis test 0-102055
 $\pi^- p$, 100, 200, 360 GeV/c, inclusive prod. of π^0 , K_S^0 , Λ^0 , $\bar{\Lambda}^0$, cross sections 0-73745
 $\pi^- p \rightarrow K^0 \Lambda$, 3.5 GeV/c, Λ polarisation, high statistics meas. 0-57637
 $\pi^- p \rightarrow K^0 \Sigma^0$, 1395 to 2375 MeV/c, differential cross-section and polarisation 0-57635
 $\pi^- p \rightarrow K^0 (890) \Lambda^0 \Sigma^0$, 10 GeV/c, K^0 polarisation meas. in hypercharge exchange reaction 0-63017
 $\pi^- p \rightarrow \Lambda K$, low energy, amplitude anal., Lagrangian model 0-82995
 $\pi^+ p \rightarrow K^+ \Sigma^+$ and $K^- p \rightarrow \pi^- \Sigma^+$ exchange degeneracy 0-57634
 $\pi^+ p \rightarrow K^+ Y^+$, $Y^+ = \Sigma^+$ or $Y^* (1385)$, 7 GeV/c, hypercharge exchange in line-reversed $\pi^+ p$ and $K^- p$ 0-82998
 $\pi^+ p \rightarrow K^+ (890) Y^+$, $Y^+ = \Sigma^+$ or $Y^* (1385)$, 7 and 11.5 GeV/c, hyperon polarisation, vector meson decay angular distrib. 0-82997
 Σ_c^+ , production and decay obs. 0-105894
 $\gamma p \rightarrow K^+ \lambda (\Sigma^0)$, $\pi^+ n$, $\pi^- p$, $K^+ \Lambda$, $K^+ \Sigma^0$ final state comparisons above resonance region 0-105906

hyperon resonances

$\Sigma^+ \rightarrow \pi \gamma$, $1/2^-$ resonance poles to parity-violating amplitude, two-quark weak transitions 0-78062
 Σ_c^+ , production and decay obs. 0-105894

hyperon scattering *see* hyperon-nucleon scattering; hyperon-nucleus scattering; kaon-hyperon scattering; lepton-hadron scattering; photon-hadron scattering; pion-hyperon scattering

hyperon spin and parity

No entries

hyperons

see also hyperon resonances

beam physics, review, book contrib. 0-68503
 Λ (1405) and kaonic H atom, KN interaction model 0-68479
 A_c , structure of hadrons containing heavy quark, MIT bag model 0-86672
 Σ_c^+ , lifetimes and longitudinal accel. 0-86709
 Σ_c^+ , structure of hadrons containing heavy quark, MIT bag model 0-86672

hypersonic flow

aerodynamical anal. of body in hypersonic source flow field (Chinese) 0-59066
boundary layer, laminar, nonequil. ionis. problem 0-59129

hypersonic flow continued

chemical laser, low pressure, line-shape flattening resulting from hypersonic nozzle wedge flow 0-91783
chemically reactive flow, aerodynamic heating of blunt bodies 0-74998
compressible fluid flow past degenerate star-red giant interacting binary stars 0-67779
disintegrating blunt bodies, radiative heating in H_2 -He atms. 0-69865
dissociated high enthalpy hypersonic laminar air flow, heat transfer to flat plate 0-69828
gas, shock wave under continuous energy supply 0-103042
gas compression in heavy piston, hypersonic speed, shock waves 0-69869
nonequilibrium free jet expansion, rotational temp. meas. for N_2 0-69890
nonequilibrium free jet expansion, translational temp. meas. in N_2 0-64600
nozzles, high enthalpy supersonic flow conversion to hypersonic flow 0-74937
teflon gas injected into shock layer flow, hypersonic flow past blunt body 0-74998
three-dimensional shapes, optimal surfaces and total drag coeffs. 0-59068
vehicle hypersonic wake, radiation from injected small particles, free molecular regime 0-64650

hypersorption *see* sorption

hypertritons *see* hypernuclei; tritons

hypervirial theorem *see* quantum theory

hypochromism *see* light absorption

hypothesis formation *see* heuristic programming

hypothetical particles

see also charm particles; heavy leptons; intermediate bosons; magnetic monopoles; quarks; tachyons
dyons, spatial volume integral of Tr F(tilde) F, Yang-Mills theory 0-77943
magnetoelectric charge states of matter-energy, magnetoelec. ionisation and magnetoelectrophoresis 0-99114
magnetoelectric dipole structure hypothesis, biological and cosmic appls. 0-91124
magnetoelectric dipoles, appl. to biological effects of mag. fields 0-93157
magnetoelectric monopoles, delocalisation prediction, possibility for detect. 0-99115
relic θ particle concentration in the Universe (Russian) 0-86026
Universe, very massive unstable particles, prop. bounds 0-82558
L-particles, existence: possibility from anomalous cosmic ray events 0-86701

hysteresis

see also coercive force; dielectric hysteresis; elastic hysteresis; magnetic hysteresis; remanence
ceramic materials, fine-grained, cyclic plastic deform. as cause for thermal expansion hysteresis 0-89290
degenerate four-wave mixing, hysteresis and optical bistability 0-69446
Fabry-Perot nonlinear interferometer, beam profile hysteresis variations 0-86393
gas laser, linearly polarized waves, interaction with longitudinal mag. field 0-95936
laser, multimode, containing saturable absorbers, bistable operation 0-91862
microscopic theory 0-80731
MIS structure, elec. parameter meas. of second order equivalent ccts. 0-57332
MOS structure Pt diffused, hysteresis and memory props. 0-96992
optical SHG, temperature phase-matching curve hysteresis 0-91852
periodic capillary tube, two phase fluid flow and hysteresis 0-107615
periodic capillary tube, two phase fluid flow and hysteresis 0-107616
steel, high-strength, low cycle fatigue, hysteresis loops, cyclic strain curves, fatigue diagrams (Polish) 0-66638
superconductor, long thin-film, paradox in crossover of mech. causing hysteresis 0-107971
TCNQ salts, crystallisation versus electrical conductivity 0-92885
Cu-Mn alloy, manganin, hysteresis-corrected calibration under shock loading 0-74818
Fe, carbonyl powder, specific elec. conductivity, 5 to 200 MPa (German) 0-70664
GdCu, electrical resistivity and length changes with temp., hysteretic behaviour 0-97600
Nb, mixed state, hysteresis of US attenuation 0-84549
 PbF_2 , ionic cond., activation volumes and high press. phase transitions 0-70461
Pd alloy-H system, α - β phase transformations, hysteresis of press., elec. resistance, review 0-60859
Pd-H system, α - β phase transformations, hysteresis of press., elec. resistance, review 0-60859
Pd-H system, solvus hysteresis 0-71659
 $SrCl_2$, ionic cond., activation volumes and high press. phase transitions 0-70461

I-II-VI₂ semiconductors *see* ternary semiconductors

I-III-VI₂ semiconductors *see* ternary semiconductors

IC *see* integrated circuits

IC engines *see* internal combustion engines

ice

see also glaciology; snow

aerosol, thin flat, EM wave scatt. and absorpt. 0-91723
age category differentiation through location and temp. observations using microwaves 0-67380
Antarctic ice, cryst. size and climatic record down to last ice age 0-94544
W. Antarctic ice sheet, fluctuations in Antarctic Peninsula area 0-94549
Arctic ice cover, attenuation of 8 and 20-cm EM waves 0-67379
Arctic sea ice, decay following CO_2 -induced atmospheric temp. rise 0-61802
atmosphere, hexagonal ice crystals as cause of 46° halo and its arcs 0-82065
atmospheric, AgI surface adsorption, effective pair pot. model 0-100394
Baltic beach sedimentary material stratification (autumn/winter 1976-7) (Russian) 0-76962
cirrus cloud, sunpillar form. theory 0-85747
climate effects of ice cap-albedo feedback, in 2-D energy balance model 0-67407
climate model with ice-sheet dynamics, stable periodic solns. 0-90210
cloud, ice nucleation by aerosol particles 0-61864
cloud, ice splinter production during riming, NH_3 addition expts. 0-72585

- ice continued
clouds, ice particle concs. rel. to Climax and Wolf Creek Pass cloud seeding expts. 0-82094
continental ice sheet, stochastically driven with planetary wave feedback, model 0-77025
crystal habit change mechanism, ice disc growth from vapour 0-84117
crystallisation, and melting rate in laminar stream of liquid 0-100770
crystallisation phenomenon of icicles, growth mechanism, structure and shape 0-59423
crystals, light scatt. expts. (*Russian*) 0-94601
cubic, D₂O isolated, H⁺ exchange and Bjerrum defect migration, direct spectroscopic obs. 0-88356
dielectric relaxation in presence of ionic impurities, block layer meas. tech. 0-103914
dislocation vel. theory, glide plane influence 0-79805
fast ice, crystal c-axis alignment, Arctic Alaska coast 0-67375
on Galilean satellites, IR spectral reflectance obs. 0-82263
GL 2591, protostellar source, 3 μ m ice absorpt. band, linear polarisation obs. 0-105303
glacial ice, upwelling in stratified ocean due to melting 0-81897
lapetus, water ice identification from relative reflectance meas. at 1.6 and 2.2 μ m 0-98607
Icelandic, thermal and physical characts. of subglacial volcanism 0-101350
Ih, elastic diffuse neutron scattering due to D-D correlation functions 0-96493
impact craters in ice and ice-saturated sand, Martian implications 0-67614
initiation in cumulus congestus clouds unmixed updraught cores 0-81997
ion beam erosion effects, energy depend. 0-65067
lake ice, microwave radar and radiometric remote sensing meas. 0-85691
long-period gravity waves in ice-covered sea 0-67372
Mars surface evidence for H₂O ice from reflectance spectroscopy 0-72834
mechanical properties of sea ice, in-situ meas. using flatjack methods 0-69751
morphology of ice crystals grown from vapour, influence of vapour diffusion and heat diffusion 0-64933
nucleation on AgI, exptl. verification of ice-forming activity theory 0-101406
nucleation on AgI, influence of aerosol particle size, struct. 0-61164
nuclei, tropospheric, in summer, background levels in Greenland 0-72609
orientational correlation parameter, water mol. dipole moment for ice VI 0-59407
passive microwave obs. from Nimbus satellites 0-101422
permafrost, active layer heat transfer medium (*Russian*) 0-81943
permafrost beneath the Beaufort Sea: near Prudhoe Bay, Alaska 0-94552
permafrost on Mars, thermodynamics 0-67621
permittivity at mm wavelengths 0-66098
phase transition, ice VII-ice VIII, second-order, Haus-Tanaka model 0-70385
plastic deformation, ultrasonic wave attenuation by dislocations (*French*) 0-59564
platelets, radiation attenuation effectiveness factor determ., IR absorpt. 0-66141
Raman spectra of O-H and O-A stretching vibrations of ices II and IX 0-66166
random network model, liq. and ice polymorphs enthalpy and heat content 0-64869
rime deposits as indicators of wind direction 0-98428
riming process, laboratory expts. 0-105037
Ross Ice Shelf (Antarctica), basal freezing, confirmed by core drilling 0-101393
sea ice, Danish studies using Landsat and airborne sensor data 0-94527
sea ice, remote sensing, appls. 0-77176
sea ice and glacial development in Late Cenoic N.Hemisphere 0-90098
sea ice in Beaufort Sea, August ice cover vars. rel. to mesoscale weather conditions 0-101366
sea ice meltwater in E.Canadian Arctic, isotope study 0-77002
sea ice underside, geometrical roughness props. 0-98334
sea-ice, climate feedback systems involving ocean temp. and CO₂ 0-98443
secondary crystal prod., rel. to charge separation in atmosphere 0-81998
surface transition layer, ellipsometric study 0-103545
surface viscosity, activation energy, vacancy migration 0-107458
transverse flexure, refined Reissner anal. 0-88247
VI phase, shock compression expts. for Hugoniot function 0-84248
water-water, pair pot. near H bonded equilb. config., amorphous and crystalline solid and liq. 0-64946
wind interaction with dry snow and bare ice surface 0-109181
AgI aerosol, ice forming activity, UV irr. effect 0-71950
- iconoscopes** see television camera tubes
- identification**
see also control theory; correlation methods; frequency response; modelling; parameter estimation; simulation; state estimation
cardiovascular system, mathematical models and identification problems 0-89780
neural transformations of random signals, Wiener and of functionals of Markov chain 0-76727
pupillary light reflex system, modelling and identification 0-61554
sampling stroboscopic convertor identification by Hammerstein model (*Russian*) 0-74495
speech waveform coders, objective quality meas. equipment and method 0-91981
streamflow, model, identification of seasonal water supply forecasting models using Akai's information criterion 0-67386
- iets** see tunnelling spectra; tunnelling spectroscopy
- IEXE** see ion microprobe analysis
- i.f. amplifiers** see intermediate-frequency amplifiers
- i.g.f.e.t.** see insulated gate field effect transistors
- ignition**
see also electric ignition
gas mixture, by electric sparks, Kesaev cathode cell formation 0-70066
internal combustion engine, conc. fluctuation meas. 0-71973
stagnation flow at a heated curved wall, ignition condition 0-96242
Na arc lamp, light-induced ignition method 0-77599
- II-III₂-VI₄ semiconductors** see ternary semiconductors
- II-IV-V₂ semiconductors** see ternary semiconductors
- II-VI semiconductors**
amorphous semiconductors, electronic states, sublattice one-band Hamiltonian transform. 0-59861
CdS, green edge luminescence spectrum, temp. depend. 0-108274
CdS, single crystals, laser emission from surface diffraction grating 0-95900
CdTe thin film on ferroelectric TGS, influence of polarisation reversal on elec. cond. 0-65720
crystal growth, optimal synthesis methods 0-100764
deep centres, ODMR (*French*) 0-60461
HgCdTe/CdTe, limited diffusion volume photodiode, characterisation 0-75627
II-VI compounds, charged dislocations and plastic deform. 0-107264
lattice dynamics, eight-parameter bond-bending forces model 0-70334
quaternary alloys, energy bandgap and lattice constant contours 0-103622
resonant secondary emission spectra, relax. of energy and polarisation 0-93331
SHG efficiency at 77K under high field condition 0-84470
solar cells, polycrystalline and tandem, for high efficiencies, using compound semiconductors 0-72052
sphalerite, hydrothermal single crystals, feasibility of optical methods for quality control 0-89065
surface structure, chem. and spectroscopy, review 0-59764
thin epitaxial layer, direct synthesis (*German*) 0-104070
ZnS-V₂⁺, impurity states by Green's function method 0-92855
Au-CdTe-Au structure, current transport props. 0-80408
(Cd,Hg)Te epitaxial structures, comp. profile depend. on deposition parameters 0-100795
Cd chalcogenides, thin films, VPE, needle-like cryst. growth 0-80148
Cd,Hg_{1-x}Te, elec. characts., impurity effects 0-92890
Cd,Hg_{1-x}Se, phase transition and elastic const., US vel. study 0-75354
CdHgTe, anomalous avalanche breakdown 0-80284
CdHgTe photoelectromagnetic detector for 10.6 μ m radiation, non-cooled, performance 0-82818
Cd_{0.15}Hg_{0.85}Te, photothermagnetic effect in mm range 0-92932
Cd_{0.17}Hg_{0.83}Te-Au(In) contacts, photo-effect in the 77-300K range, barrier height estimation 0-107850
Cd_{0.2}Hg_{0.8}Te, ion implantation doping for realisation of IR detectors, responsivity meas., ion range straggling 0-73452
Cd_{0.2}Hg_{0.8}Te recrystallisation for supercooled IR detector production (*German*) 0-86403
n-Cd_{0.2}Hg_{0.8}Te, excess generation-recombination noise 0-107880
n-Cd_{0.3}Hg_{0.7}Te, photoelec. props. at 78K, relax. time, minority carrier extraction 0-107864
Cd,Hg_{1-x}Te, carrier lifetime, effect of comp. fluctuations and second-phase inclusions 0-80294
n-Cd,Hg_{1-x}Te crystals, carrier recomb. in extrinsic conduction range 0-70722
Cd,Hg_{1-x}Te crystals, donor compensation, low temp. cond. study 0-75571
Cd,Hg_{1-x}Te, dislocation motion, effect of lattice defects on microhardness (*Russian*) 0-70220
Cd,Hg_{1-x}Te epitaxial graded gap layers, plasma reflection and magnetoreflection 0-71391
Cd,Hg_{1-x}Te, epitaxial growth from stoichiometric melt, crystn. and diffusion 0-75475
Cd,Hg_{1-x}Te, epitaxial layer p-n junction, current-voltage characteristics of photovoltaic detectors, 1 to 15 μ m 0-86407
Cd,Hg_{1-x}Te films, growth by cathodic sputtering in Hg vapour plasma 0-97431
Cd,Hg_{1-x}Te, graded gap epitaxial layers, spectral characts. of photoelectromagnetic effect 0-60022
Cd,Hg_{1-x}Te, graded-gap layers, galvanomag. props. at low temp. and in weak mag. field 0-75664
Cd,Hg_{1-x}Te layers, epitaxial graded-gap, nonlinear elec. effects 0-100468
Cd,Hg_{1-x}Te, long term stability at 300K, rel. to device appl. 0-59978
n-Cd,Hg_{1-x}Te, recombination due to surface excitation, photoconductivity, impurity states (*Russian*) 0-60042
Cd,Hg_{1-x}Te, tunnelling effect in p-n junctions 0-75630
Cd,Hg_{1-x}Te, vacancy electron states, acceptor behaviour, electron mobility 0-70193
CdO, aqueous-deposited films, struct. and electronic props. for solar cell appls. 0-100797
Cd(S, Se) film grown on InP substrate, mismatch dislocations and lattice distortion, dangling bond density 0-84406
CdS, acoustic wave attenuation, phonon viscosity and dislocation drag 0-70319
CdS, acousto-voltaic effect, asymmetric electron ejection from trap levels (*Russian*) 0-65634
CdS, additional waves and polariton dispersion, reflectivity, transmittivity spectra 0-71443
CdS, aqueous-deposited films, struct. and electronic props. for solar cell appls. 0-100797
CdS, charged impurity centres, drift during passage of photocurrent 0-70767
CdS crystal growth from vapour, preferential deposition, elec. field effects 0-84122
CdS crystals, electron-hole plasma, carrier optical orientation 0-100689
CdS crystals, one-photon pumping, active layer structure, light amplification 0-78858
CdS crystals, orientational depend. of photoacoustic effect (*Russian*) 0-65167
CdS crystals, radiative recombination, high excitation rates 0-108269
CdS, defect struct. and config. produced by irr., elastic scatt. expts. 0-84178
CdS, dislocation motion, TEM obs. 0-79799
CdS, doped, amorphous antiferromagnet model, susceptibility and spin-flip Raman scatt. meas. 0-97057
CdS, EPR of adsorbed oxygen radicals, temp. depend. 0-80612
CdS, elastic, piezoelec. and dielec. props. 0-108157
CdS, elastic, piezoelectric, and dielec. props., 4.2 to 300K 0-60508
CdS, electro-acoustically active, AC impedance meas. 0-103726
CdS, electron and hole trapped centres, EPR, photoluminescence, photoconductivity study 0-108071
CdS, electron-hole pairs behaviour in energetic ion tracks 0-65457
CdS, electron-hole plasma, gain and refl. spectra study 0-66227

II-VI semiconductors continued

- CdS electronic two- and one-photon Raman scatt. via biexcitons, stimulated config. obs. mag. field shift 0-103963
- CdS, epitaxial growth and nucleation, on monocrystrn. ZnS, substrate real struct. influence 0-88455
- CdS epitaxial layers on sapphire, exciton struct. of absorpt., photoluminesc. and photocond. spectra 0-89027
- CdS, exciton droplets, energy condensation (*Russian*) 0-107712
- CdS film, chemical bath deposited, solar energy conversion by photoelectrochem. cells 0-108804
- CdS film spray fabrication, physical props., Cu_2S -CdS solar cell applications (*French*) 0-60113
- CdS films, chem. deposited, growth kinetics and polymorphism 0-75463
- CdS films, prep. by reactive pulverisation, chemical, crystallographic and electronic props. (*French*) 0-60112
- CdS, flux exclusion, superconductivity at high temp. 0-97058
- CdS, generation of optical radiation in direction of propag. of streamer 0-69401
- CdS γ -ray dosimeters with elevated stability under irradiation 0-86995
- CdS, highly excited, stimulated emission process at 80K 0-97307
- CdS, hydrogenlike donor negative ion, ground and excited states, obs. 0-70645
- CdS monocrystral petal lasers, single-photon excitation (*Russian*) 0-99736
- CdS, nonlinear self-action effect and absolute two-photon absorption coeff. 0-83649
- CdS phosphor, powdered, in host material, solar cells wavelength shifting 0-85286
- CdS, photocond., spectral depend. at high excitation intensity, exciton effects 0-65619
- CdS photoconductivity, spatial homogeneities exam. using DC and microwave techniques 0-93895
- CdS platelet laser, emission spectra, optical coupling between partial resonators 0-69400
- CdS platelet lasers, optically pumped, spatial and spectral distribution of laser emission 0-64032
- CdS, polaron cyclotron resonance freq. shifts, halfwidths, cumulant expansion method calcs. (*Russian*) 0-88880
- CdS polycrystalline films, high strain sensitivity 0-93017
- CdS, polytype relative stabilities, entropy contribs. 0-100197
- CdS, population-inverted, resonant Brillouin scattering and photoelastic consts. 0-76042
- CdS, pure spin diffusion without charge transport, spin flip Raman scatt. obs. 0-93329
- CdS, quasimonopolar semicond., recombination in near surface space charge region (*Russian*) 0-88574
- CdS, rock-salt type high-press. phase synthesis using metal sulphide additives 0-104084
- CdS single cryst., lasing action excited by ruby laser picosecond pulses 0-64035
- CdS single cryst., vaporization and form. of negative whiskers 0-92659
- CdS, single crystals, US luminesc. obs. 0-76092
- CdS, single-quantum radiative recomb. of biexcitons due to biexciton-exciton interactions 0-96793
- CdS, spectra of refl. and transmission coeffs. near exciton absorpt. line 0-88951
- CdS, spectroscopic study of local centre interaction, change with external illumination 0-80323
- CdS, stimulated Mandelstam-Brillouin scatt. on acoustic phonon amplification (*Russian*) 0-71437
- CdS, subMM radiation excitation by N_2 laser pulse 0-60678
- CdS, surface energy struct. changes during ion cleaning and thermal annealing 0-92962
- CdS, surface photovoltage, characterisation 0-60033
- CdS thin film solar cell fabrication, HCl etching 0-81474
- CdS thin films, growth and evaluation for fabrication of high performance photovoltaic solar cells 0-93501
- CdS thin films on brass substrates, nondestructive resistivity meas. tech. 0-93898
- CdS thin layers, recryst. from $\text{CdS-Cr}_2\text{O}_3$ mixtures, phys. and photoelec. props. 0-96935
- CdS, thin plates, piezosemiconductors, second harmonic acoustoelectric current obs. 0-80329
- CdS, three-branch exciton-polariton dispersion, direct meas. by reson. Brillouin scatt. 0-60620
- CdS, two-photon absorpt. effect on hyper-Raman scatt. 0-74441
- CdS, XPS, secondary illumination effects, band bending, level shifts 0-108324
- CdS:Cu, C-V curves of MIS diode used to examine trapping levels 0-65697
- CdS:Cu, Cl films, photocond. growth and decay time 0-60041
- CdS:Cu, photocurrent, elec. field effect on recombination processes (*Russian*) 0-100484
- CdS:Cu, photosensitivity degradation mechanism 0-107851
- CdS:Cu sintered layers, relaxation photocurrent kinetics (*Russian*) 0-108852
- CdS:Cu(Ag), charge and transport mechanism of impurities, electrodiffusion doping 0-59725
- CdS:Cu(Cl) thin films, surface and bulk photoconc. 0-88653
- CdS:D⁺, binding energy of D⁺ ion 0-92541
- CdS:Ga crystal cathodoluminescence, SEM analysis 0-97349
- CdS:In, impurity resist., Matsubara-Toyozawa theory extension 0-80264
- CdS:In(Cl) concentration quenching mechanism of luminescence 0-97336
- CdS:Li, complex luminescence centres, recombination-stimulated conversion 0-108268
- CdS:Li, luminescence bands, photocurrent spectra (*Russian*) 0-60677
- CdS:Li, pure and doped, green edge luminesc., complex nature of centres 0-60671
- CdS:Li, single crystals, anisotropic luminesc. centres 0-80857
- CdS:Li(Cu), pure and doped, electrodiffusion of shallow donors, photocurrent, TSC, and exciton luminesc. meas. 0-79992
- CdS:Mn, vacuum deposited film, Mn migration, EPR and X-ray study 0-65411
- CdS:Na, Hagemark theory, green edge emission line intensity 0-75517
- CdS:Ni, nonradiative recomb., photocond. spectra 0-70764
- CdS:Ni²⁺, Zeeman effect at Ni impurities 0-60633
- CdS:Te-based photoelectrochem. cell, luminesc., thermal manipulation of deactivation processes 0-81479
- CdS:Ti²⁺, superhyperfine interact., ENDOR study at 4.2K 0-80639
- CdS/Cu₂S heterojunction solar cells diffusion length determ. using minority carrier SEM 0-61359

II-VI semiconductors continued

- CdS/Cu₂S solar cells, polycryst. thin film photovoltaic materials, photon loss anal., expt. determ. 0-93888
- CdS/Cu₂S thin film heterojunctions, photocapacitance meas. of solar cell parameters 0-93897
- CdS/Cu₂S, sequential evap. for solar cell applic. 0-93902
- CdS/InP epitaxial thin films on NaCl, HEED and TEM study 0-88446
- n-CdS/p-InP/p-InP heterostructure solar cell with ultrathin window layer, computer anal. 0-97788
- n-CdS/p-ZnIn₂Se₄ thin film solar cell, photovoltaic props. 0-89628
- CdS-Al(Au) interfaces, bonding and interdiffusion, XPS obs. 0-80000
- CdS-Au contacts, electronic states, vacuum UV photoelectron spectra 0-80827
- CdS-CdTe p-n junction screen printed thin film solar cells 0-72055
- CdS-Cu₂S ceramic solar cells, solar batteries operating characts. 0-93874
- CdS-Cu₂S heterojunction solar cells, carrier transport, nonmonotonic band profiles 0-61361
- CdS-Cu₂S heterojunction, energy-band struct., capacitance-voltage characts., illumination effects 0-96982
- CdS-Cu₂S heterophotocells based on CdS films of stoichiometric composition, elec. and photoelec. props. 0-93873
- CdS-Cu₂S junctions, carrier trap density, deep level defects 0-107801
- CdS-Cu₂S solar cell fabrication by magnetron reactive sputtering deposition 0-61363
- CdS-Cu₂S solar cells, microstructural study of heterojunction materials 0-93978
- CdS-Cu₂S thin film planar junction devices, quantitative photon loss anal. 0-61362
- CdS-Cu₂S thin-film solar cells, low-cost manufacturing process outline, economic anal. 0-93930
- CdS-Cu₂S thin-film solar cells, high open-cct. voltage and low refl. losses 0-94088
- CdS-Cu₂S solar cell, prep. and characts. (*Croatian*) 0-93876
- CdS-CuInSe, solar cell, polycrystalline thin film, high photocurrent, characts. 0-61339
- CdS-InP(CdTe)(GaAs)(Ge), solar cell heterojunctions, CVD fabrication, photovoltaic response 0-93878
- CdS-SiO₂ (glass) layered system, characts. of phase-velocity dispersion and struct. of surface waves 0-59775
- CdS-SiO₂-Si solar cell, I-V characteristics 0-89621
- CdS(Se), electrodeposition, using nonaqueous solvents 0-76200
- CdS(Se), piezoelec. semicond., sound absorption 0-60051
- CdS_{1-x}Se_x, chem. comp. and luminescence obs. 0-80869
- CdS_{1-x}Se_x, mixed crystals, deformation effects on free excitons 0-76073
- CdS_{1-x}Se_x monocrystral petal lasers, single-photon excitation (*Russian*) 0-99736
- CdS(Se)(Te) charged dislocations, flow of charge with plastic deform. 0-85010
- CdS(Se)(Te), determ. of wurtzite, zincblende and rocksalt phases 0-100219
- CdS(Se)(Te), positron annihilation study 0-60713
- CdS(Se)(Te), vacuum deposited film, orientation axis tilt rel. to vapour angle of incidence 0-88456
- CdS₂Te_{1-x}, recryst. from $\text{CdS}_2\text{Te}_{1-x}\text{-Cr}_2\text{O}_3$ mixtures, photocond. props 0-96936
- CdSe 16 μm parametric amplification with HF laser pumping 0-78910
- CdSe, chemically sprayed thin films as photoanode in photoelectrochem. cells, power charact. meas. 0-85293
- CdSe film, soln. growth 0-66437
- CdSe film deposition, and reaction sequence of H_2SeO_3 reduction 0-71603
- CdSe film photoanodes for electrochem. photovoltaic cells, fabrication and evaluation 0-76641
- CdSe film polycryst., thermal diffusion of Cr, 240-400°C 0-80001
- CdSe films, oriented, epitaxial growth by epitaxial nucleation in submicroscopic holes method 0-59834
- CdSe films, solar energy conversion using electrodeposited films for photoelectrochemical cell 0-94093
- CdSe, fundamental absorpt. edge, influence of laser radiation intensity (*Russian*) 0-71445
- n-CdSe, laser excited stimulated emission, optical gain spectrum 0-76050
- CdSe photoanode improved efficiency by photoelectrochem. etching 0-104512
- CdSe photoanodes, S substitution during operation and mech. of surface protection 0-107906
- CdSe, recombination mechanism at dislocations, photoluminescence 0-103993
- CdSe, single crystals, luminesc. of electron-hole plasma 0-60675
- CdSe, temp. depend. phase-matched nonlinear optical devices 0-99794
- CdSe thin film transistor on Cr substrate, cryst. struct., substrate defect effects 0-70563
- CdSe thin-film solar cells 0-93970
- CdSe, undoped and Cr doped, far IR transmission and reflectance spectra 0-71429
- CdSe:Cu, impurity photocurrent, kinetics and oscills. 0-65624
- CdSe:Li, pure and doped, reson. Raman and Brillouin scatt., elastic exciton-defect scatt. 0-80788
- CdSe-Au contacts, electronic states, vacuum UV photoelectron spectra 0-70827
- CdSe-Sb₂Se₃ heterojunction, photoelec. props. 0-70816
- CdSe-SiO₂ (glass) layered system, characts. of phase-velocity dispersion and struct. of surface waves 0-59775
- CdSe(Te) and solid solns., optimal synthesis conditions for single cryst. growth 0-100776
- CdSe_{0.65}Te_{0.35}, polysulphide photoelectrochem. solar cell 0-72073
- p-CdTe, barrier heights of metals on etched surface 0-80378
- CdTe, crystal size depend. of photoplastic effect 0-92592
- CdTe crystals, exciton luminescence spectra rel. to shallow impurity conc. 0-97335
- CdTe, diffusion and solubility of Ge, 630-800°C, prep. conditions depend. 0-103519
- CdTe, elec. and photoelec. props. due to double injection, quenching spectra 0-70765
- CdTe electrode, redox reaction due to complex $\text{M}(\text{CN})_6^{3-/4-}$ (*French*) 0-89482
- CdTe, electron mean free path, 350-1450 eV 0-103707
- CdTe, energy bands and optical props. calc., tight-binding model with spin-orbit interaction 0-65448
- CdTe, exciton magnetoreflectance spectra, multicomponent polaritons, Zeeman splitting 0-88974

II-VI semiconductors continued

- CdTe film, exciton spectra, press. and temp. depend. 0-80886
 CdTe film, photogenerated carrier transport props. 0-88590
 CdTe films, oriented, epitaxial growth by epitaxial nucleation in submicroscopic holes method 0-59834
 CdTe, growth of epitaxial layers, activation by UV and IR radiation 0-71598
 CdTe, lattice dynamics and phonon parameters bond bending force model 0-59595
 n-CdTe layers, growth and characterisation, heterojunctions and Schottky barriers fabrication (*German*) 0-89151
 CdTe linear electro-optic translation of IR laser wavelengths 0-78878
 CdTe, low temp. thermal cond., growth parameter influence 0-92725
 CdTe metal-semiconductor-metal γ -ray detector characts. 0-57451
 CdTe, minority carrier diffusion length from photocurrent meas. in semiconductor-electrolyte boundary 0-65584
 p-CdTe, nondoped, heat treatment in vacuum, dissociation obs. effects on struct. and props. (*Japanese*) 0-60662
 p-CdTe, photocond., photoluminesc., spectral studies 0-88593
 CdTe, recombination radiation due to high-density excitons 0-93392
 n-CdTe, semiconductor electrode, electrochem. behaviour in nonaqueous media (*French*) 0-66808
 CdTe single cryst., linear electro-optical props., temp. depend. 0-71376
 CdTe surface, sputter cleaning and dry oxidation, XPS and LEED study 0-108618
 CdTe thin film polycrystalline solar cells prepared by electrodeposition 0-93948
 CdTe thin films, oriented, VPE growth, infrared transmission, photovoltaic cells 0-59825
 CdTe, vapour-phase-grown, cathodoluminesc. study 0-76086
 CdTe:As(P), ion implanted, elec. props. 0-65021
 CdTe:Cl, semi-insulating, impurity photocond. spectra, local state distrib. in band gap 0-107865
 CdTe:Cu films, impurity behaviour, Hall mobility and hole density meas. 0-80420
 CdTe:Fe, Mn, Cr, introduction of elec. active defects 0-103647
 CdTe:Fe²⁺, reson. relax. time for impurity electrons and localised phonons interaction, appl. to thermal cond. 0-59590
 CdTe:In precipitation and out-diffusion of solute during cooling 0-100840
 CdTe:Li(Cl), acceptor states study by donor acceptor pair excitation luminesc. 0-100683
 CdTe:Mn, spin-lattice coeffs. of Mn²⁺ 0-84646
 CdTe:Mn²⁺, exciton refl. spectra and mag. susceptibility 0-66253
 CdTe:Mn²⁺, luminesc. and magneto-optic reson., mag. field effect 0-93390
 CdTe:Si(Cl), force variation due to charged defects 0-92634
 CdTe/Hg_{1-x}Cd_xTe multilayers, LPE growth 0-80104
 CdTe-Au contacts, electronic states, vacuum UV photoelectron spectra 0-70827
 CdTe-Au(In) contacts, photo-effect in the 77-300K range, barrier height estimation 0-107850
 CdTe-CdS heterojunctions, growth by closed-tube chem. transport, elec. props. 0-60070
 CdTe-CdS heterojunction, photocapacitance and photocond. 0-96978
 CdTe-CdS thin film p-n solar cells, spectral response temp. depend. 0-93871
 CdTe-HgTe superlattice on CdTe layers, evanescent states, tight binding calcs. 0-70611
 CdTe-In system, equilib. phase diagram and liq. phase epitaxial growth of CdTe from In soln. (*Japanese*) 0-71634
 p-CdTe-Langmuir film interface, prep., characters. and MIS struct. 0-92998
 CdTe-ZnS(Se) solid solns., optimal synthesis conditions for single cryst. growth 0-100776
 CdTe(Se):Co, impurity luminescence no phonon line depend. on temp., Debye temp. 0-66273
 CdTe_{1-x}Se_x, multiband model of impurity complexes 0-65497
 CdZnS thin films, growth and evaluation for fabrication of high performance photovoltaic solar cells 0-93501
 Cd_{1-x}Zn_xS films, thermal evaporation prep., phys. props. 0-84410
 Cd_{1-x}Zn_xS heteroepitaxial single-cryst. layers, photoluminesc. props. 0-100692
 Cd_{1-x}Zn_xS solar cell thin films, microprobe characterisation (*French*) 0-61349
 Cd,Zn_{1-x}S films, chem. sprayed, carrier density and mobility 0-60121
 CuGa_{0.5}In_{0.5}Se₂/Zn_{0.25}Cd_{0.75}S heterojunction solar cell, preparation and props. 0-101110
 Cu₂S-CdS heterojunction interface, depth distribution profiles, Auger spectra 0-88622
 Cu₂S-CdS heterojunctions, role of deep levels in controlling photovoltaic props. 0-92941
 Cu₂S-CdS solar cells, Cu₂S film growth methods 0-80980
 Cu₂S-CdS solar cells, optimised grid patterns 0-108798
 Cu₂S-CdS solar cells with interdigitated grid, current-voltage analysis 0-93981
 Cu₂S-CdS sprayed solar cells, chemical spray deposition 0-93979
 Cu₂S-Zn_{1-x}Cd_xS and Cu₂S-CdS thin film solar cells by solid state reaction, comparison 0-101109
 Cu₂-_xS-CdS p-n heterojunction, optical energy convertor, struct. and recomb. props. 0-72065
 Cu₂S-CdS thin film solar cells, using all film vacuum deposited process 0-93977
 HgCdTe epitaxial material, ion implantation, junction form. 0-100260
 HgCdTe photodiodes formed by double-layer LPE 0-104078
 HgCdTe reverse-biased photodiodes for wideband appls., excess noise 0-107876
 HgCdTe solid solution photodiode for CO₂ laser active medium study 0-95868
 HgCdTe-CdTe photodiode, 1.33 μ m, grown by LPE, phys. props. 0-107892
 Hg_{0.6}Cd_{0.4}Te LPE layer growth from Te-, Hg-, and HgTe-rich solns., comparison 0-76199
 (Hg_{0.6}Cd_{0.4})_{1-x}Te_x, defect anal., intrinsic material parameters 0-75519
 Hg_{0.74}Cd_{0.25}Te thin film deposition on Si substrates by RF triode-sputtering, large-area photodetector arrays 0-80965
 Hg_{0.77}Cd_{0.23}Te nonlinear optical IR generation 0-58642
 Hg_{0.8}Cd_{0.2}Te surface, sputter cleaning and dry oxidation, XPS and LEED study 0-108618
 Hg_{0.82}Cd_{0.18}Te, electronic anomalous mass near reson. acceptor level, Shubnikov-de Haas meas. 0-80163

II-VI semiconductors continued

- Hg_{1-x}Cd_xTe breakdown-limited MIS device, increased charge capacity using ramped gate voltage 0-103751
 Hg_{1-x}Cd_xTe, degenerate four-wave mixing of 10.6 μ m radiation 0-95943
 Hg_{1-x}Cd_xTe, Einstein relation for inversion layers 0-103706
 Hg_{1-x}Cd_xTe, epitaxial layers, elec. properties in the range 4.2 to 300K (*French*) 0-65721
 Hg_{1-x}Cd_xTe epitaxial layers, elec. props. 0-96910
 Hg_{1-x}Cd_xTe, grown from melt, Kirkendall and Frenkel effects 0-100365
 Hg_{1-x}Cd_xTe, Hall coeff., anomalous temp. depend., 4.2 to 70K 0-65604
 Hg_{1-x}Cd_xTe hot-electron photoconductive detection of near mm wave radiation 0-57377
 Hg_{1-x}Cd_xTe, implanted with Hg, Al, damage and lattice location study 0-103381
 Hg_{1-x}Cd_xTe, near band-gap photoluminesc., bound exciton luminesc. obs. 0-103973
 Hg_{1-x}Cd_xTe, optical absorpt., quasilocal acceptor level effects, theory 0-92853
 n-Hg_{1-x}Cd_xTe, optical phase conjugation 0-83644
 Hg_{1-x}Cd_xTe photodiodes, long cutoff wavelength, effect of trap tunnelling on IR detector performance 0-73451
 Hg_{1-x}Cd_xTe, recombination processes using impact ionization capture cross sections 0-75577
 Hg_{1-x}Cd_xTe, segregation, compositional characterisation 0-107434
 Hg_{1-x}Cd_xTe, theory of optical absorpt., contribution by quasilocal acceptor levels (*Russian*) 0-71451
 Hg_{1-x}Cd_xTe-In contact, diffusion of In 0-103520
 Hg_{1-x}Cd_xTe-type semimetals, kinetic props., local acceptor level effects 0-65557
 HgS, electrodeposition, using nonaqueous solvents 0-76200
 α -HgS, gas-phase and solid-state Hg 5d photoionisation processes, direct comparison 0-76149
 α -HgS, trapping parameters determ. by TSC meas. 0-59997
 HgSe, band struct. and spin splitting Shubnikov de Haas study 0-65445
 HgSe, elec. resist., high press. phase transform., band gap 0-70707
 HgSe film, anomalous photocond., electron microscope study 0-65623
 HgSe, interband Γ_6-1 magnetoabsorption, temp. study 0-76032
 HgSe, two-phonon resonant effect, far-infrared reflectivity 0-108203
 HgTe, 1.5 to 30K, thermal expansion and heat capacity meas. 0-59681
 HgTe, energy bands and optical props. calcs., tight-binding model with spin-orbit interaction 0-65448
 HgTe, growth of epitaxial layers, activation by UV and IR radiation 0-71598
 HgTe, Γ_8 symm. acceptor centre hole mag. props. (*Russian*) 0-88733
 HgTe, mobility of electrons and holes, 4 to 100K 0-107821
 HgTe, phonon dispersion relations, neutron study 0-70340
 HgTe surface, sputter cleaning and dry oxidation, XPS and LEED study 0-108618
 HgTe, vacancy electron states, acceptor behaviour, electron mobility 0-70193
 InSe, photo-absorption of green exciton 0-80816
 LiNbO₃-CdSe layer structure, SAW absorpt., elec. field effects 0-65355
 PbSe film, soln. growth 0-66437
 n-Pb_{0.88}Sn_{0.12}Te spin flip Raman laser pumped by TE CO₂ laser, characts. 0-87397
 Pb_{1-x}Sn_xTe LPE film IR detector performance 0-86422
 PbTe, effect of pressing and sintering, study of induced defects by SEM 0-59983
 n-PbTe(InCu) epitaxial films, elec. transport props. 0-75659
 SnO₂-Cu₂S-ZnS:Mn,Cu,Al₂O₃-Al, light-emitting struct., cond. and electrolum., heat treatment 0-97345
 Zn chalcogenides, thin films, VPE, needle-like cryst. growth 0-80148
 Zn S-CdS:Ag(Cu), cathodoluminesc. investig., appl. to cathode ray tube screening 0-108282
 Zn,Cd_{1-x}S film, optimal synthesis conditions for single cryst. growth 0-100776
 Zn,Cd_{1-x}S films, spray pyrolysis, elec. props. 0-75657
 Zn,Cd_{1-x}S monocrysal photol. lasers, single-photon excitation (*Russian*) 0-99736
 Zn,Cd_{1-x}S, thin solid soln. films, vapour deposited, elec. and optical characts. 0-60110
 Zn,Cd_{1-x}S-Cu₂S heterojunction solar cells, props., comp. meas. of interfacial region 0-81472
 Zn_{1-x}Cd_xSe, mixed crystals, antireson. in phonon spectrum, Raman spectroscopy 0-88992
 Zn,Cd_{1-x}Se, exciton reflection spectra anomalies (*Russian*) 0-97304
 Zn,Hg_{1-x}Se, current carrier scattering mechanism 0-65546
 Zn,Hg_{1-x}Se, vacancy electron states, acceptor behaviour, electron mobility 0-70193
 ZnO, adsorbing p- and n-type dyes, surfaces pot., UV light illum. effect 0-75624
 ZnO, aqueous-deposited films, struct. and electronic props. for solar cell appls. 0-100797
 ZnO, CVD of epitaxial films on sapphire, SAW interdigital transducer fabrication 0-66430
 ZnO, defect struct. calc., doping effects 0-107218
 ZnO, elastic, piezoelec. and dielec. props. 0-108157
 ZnO, elec. cond. at high fields 0-80287
 ZnO, electron-hole plasma, gain and refl. spectra study 0-66227
 ZnO epitaxial film, nonuniform cond. due to H chemisorption (*Russian*) 0-65723
 ZnO, exciton luminesc., 16 to 77K 0-97329
 ZnO film on glass substrate, high-rate deposition using DC reactive magnetron sputtering 0-80978
 ZnO film on oxidised Si, optical measure of acoustic quality 0-80893
 ZnO films, RF sputtered single-cryst., on sapphire, struct. and SAW props. 0-80105
 ZnO, influence on frequency-temp. coeff. of SAW devices 0-79066
 ZnO non-ohmic ceramic, degradation props. under AC and DC bias 0-80262
 ZnO nonohmic ceramic, formation mechanism 0-60813
 ZnO phosphor fired with Zn, luminesc. in green and red region 0-66265
 ZnO polar surfaces, H and O₂ exposed, ion irradi., and heat treated, cond., EELS study 0-71525
 ZnO RF sputtered films for SAW transducers, X-ray characterisation 0-80138
 ZnO RF sputtered films, post deposition annealing behaviour 0-100416
 ZnO, single cryst., photo- and thermoluminescence 0-66311
 ZnO, single crystals, photocond. lifetimes, Zn⁺ hole traps 0-75581
 ZnO sputtered films, undoped and Ga doped, props. rel. to deposition conditions 0-107935

gallium compounds continued

- p-Ga_{1-x}In_xPyAs_{1-y}/Au-Zn, specific contact resist. 0-84509
 Ga_{1-x}In_xSb, electron transport in RF field, Monte Carlo simulation 0-96932
 Ga_{1-x}In_xSb, Ga-rich, prep. by Czochralski technique 0-60771
 n-Ga_{1-x}In_xSb Gunn diode, high field domain characts. 0-59992
 Ga_{1-x}Mn_xSb, elec. cond., mag. susceptibility, Hall const., and thermo-EMF, 80 to 1000K (*Russian*) 0-88549
 Ga₂Mo₃S₄ Chevrel phase, synthesis, stability and characts. 0-71608
 GaN, electron struct., ESCA study 0-89116
 GaN epitaxial films, cathodoluminesc. spectra 0-71496
 GaN, initial growth, on Al₂O₃ and spinel (*German*) 0-107664
 GaN, luminesc. centres 0-93405
 GaN, photoluminesc. spectra, energy distrib. 0-97339
 GaN, polarised electroluminescence emission, microstructure investigations 0-97344
 GaN preparation in sealed fused silica ampoules 0-80982
 GaN, VPE growth rate influence on elec. and luminesc. props. 0-100702
 GaN:Zn, n-i struct., anomalous luminesc. 0-80865
 GaN/Ga layered films, Ga whisker growth 0-92800
 GaNbO₄, polymorphic transition under high press. 0-100835
 GaO₂N, based multiple insulating layers for surface passivation of GaAs 0-93006
 n-GaP, acoustoelectric effect due to piezoelectrically active wave 0-80331
 GaP, adsorption and desorption of Cs, LEED, AES, and photoemission meas. 0-70532
 GaP, anomalous avalanche breakdown 0-80284
 GaP, anomalous photoeffect on connected excitons (*Russian*) 0-92929
 GaP, comparison of contact resistances of Au-Zn, Au-Zn-Sb, Au-Ge-Ni and Au-Ge-Ni-Sb alloyed contacts 0-70825
 GaP, complex ¹¹⁹Sn impurity-defect, Mossbauer study 0-75898
 GaP, core exciton binding energies 0-80188
 GaP, crystal, growth conditions rel. to dislocation struct. 0-88151
 GaP crystals, radiation defects, TSC obs. 0-65588
 GaP, donor states theory, camel's back struct. influence 0-59921
 n-GaP electrode, photoanodic dissolution rate, effect on surface electronic band energies 0-103748
 GaP electroluminescent diode struct. prep. by SSD and Czochralski methods, dynamic props. (*Czech*) 0-97425
 GaP, electron-hole drops, self-consistent surface calculation 0-65464
 GaP films on Si, epitaxial crystallisation by nanosecond laser pulses 0-107674
 GaP, green cathodolum. from cryst. defects, SEM, TEM study 0-80870
 GaP, IR absorpt. spectra depend. on compensating defects and thermal treatment (*Russian*) 0-71465
 GaP, impurity-containing single crystals, refl. spectra 0-80823
 n-GaP, ion implanted films, optical and luminesc. props. 0-60699
 GaP LED, SEM study of charge collection and cathodoluminesc. 0-65661
 GaP, lattice dynamics and phonon parameters bond bending force model 0-59595
 GaP, light scatt. by LO phonons, high-resolution study 0-80798
 GaP, liquid interaction parameters determ., 580-670°C 0-65197
 GaP, optical transitions, effect of perturbed k-selection and gap shrinkage, theory comparison with expt. 0-66257
 p-GaP photocathode, charge transfer via surface states, water photoelectrolysis anal. 0-75636
 GaP, pure and N doped, extended Huckel theory appl. 0-59916
 GaP, radiative recombination, optical evaluation review 0-60647
 GaP, Raman scatt. from plasmon-phonon coupled modes 0-93337
 GaP, reson. photoemission shake-up and Auger processes at 3p photothreshold 0-100748
 n-GaP, Schottky barrier height data for several contact systems 0-60080
 p-GaP, Schottky barriers on polar (111) and (111) surfaces 0-88631
 p-GaP semiconducting photoelectrode 0-101119
 GaP semiconductor Raman laser 0-78864
 GaP, semiconductor-metal transition, press. calibration above 100 kbars fixed points 0-77808
 GaP single cryst., defect distrib. near abraded surface 0-92533
 p-GaP, spin-flip Raman scattering, review 0-108209
 GaP, temp. coeff. of induced birefringence 0-93277
 GaP, thermal expansion below room temp. 0-79963
 GaP, VPE layer structures for LED's, SEM, and TEM obs. of dislocation density reduction expt. 0-100425
 GaP, vapor-phase etching, mechanisms and kinetics 0-100934
 GaP:⁵⁶Fe(⁵⁷Fe)(⁵³Cr), paramag. centres, identification from ESR and ENDOR spectra 0-80600
 GaP:Bi,N, photoluminesc., electroluminesc., 4.2 to 300K, excitons and hole traps 0-108275
 GaP:Ce(Dy)(Pr) epitaxial films, photoluminesc. spectra 0-66294
 GaP:Co, optical spectra and Zeeman anal. of Co 3d⁷ state 0-66247
 GaP:Co(Ni), photolum. excitation spectroscopy 0-80841
 p-GaP:Cr, hole traps, ESR studies 0-75843
 GaP:Cr epitaxial layers, Cr conc. profile determ. 0-65029
 GaP:Cs-O simultaneous adsorption, oxidation interface chemical struct. 0-103584
 GaP:Fe, double Fe-thermal acceptor centre, energy states 0-96823
 GaP:Fe, optical absorption spectrum and Faraday effect 0-108245
 GaP:Fe³⁺, ESR spectrum, elec. field, uniaxial compression influence 0-103882
 GaP:Ge, ENDOR study, superhyperfine interactions 0-93210
 GaP:N, bound exciton absorpt. line asymmetry, electroabsorption spectra 0-71459
 GaP:N LED structures, local dopant conc. determ. using SEM cathodolum. spectra 0-101057
 GaP:Ni(Fe), multivalence impurities, EPR and optical absorpt. meas. 0-75844
 GaP:S, defect struct. and tetrahedral precipitates, TEM study 0-107246
 GaP:S, ground and excited states of bound exciton complex, stress effects 0-65463
 GaP:S(Se), donor bound exciton excited states 0-66284
 GaP:Ti(Co)(Ni), positron annihilation meas. rel. to deep levels study 0-60712
 GaP:Zn, O, influence of impurity-absorbed illumination on luminesc. 0-93395
 p-GaP:Zn,S, spin polarisation of donors and acceptors in mag. field, optical and microwave study 0-93393
 p/GaP:Zn-electrolyte interface, electrochemical LED, luminescence obs. 0-84507
 GaP/Si heterostruct., differential thermal contraction, plastic deform., fracture 0-108494

gallium compounds continued

- GaP-GaAsP planar heterostructure strip ridged waveguide under mech. load, polarisation modulation 0-96038
 GaP-Pd contact system, low temp. alloyed contact formation 0-100519
 GaP-Si, heteroepitaxial growth, electronic and optical props. 0-104075
 GaP-Si, heterostructure, zincblende-on-diamond type systems, MBE growth, (110) orientation as preferred orientation 0-80099
 GaP,As_{1-x}N_x, luminesc. of N bound state excitons, local-environment effects 0-100691
 GaP(Sb), surface (110), energy distrib. of dangling-orbital surface states 0-80347
 n-GaP, Bridgman crystals, hole traps, photocond. and thermal quenching study 0-75580
 GaS, elastic prop. anisotropy, Debye temp. (*Russian*) 0-88244
 GaS, infrared optical props., polarisation depend., vibr. modes 0-100658
 GaS, layer compound, long-wavelength phonons and elastic consts. 0-65175
 GaS, reson. Brillouin scatt. 0-89010
 GaS, shallow core level spectra 0-104037
 GaS₂ glass (*French*) 0-71369
 GaS,Ge_{1-x}N_x, valence band states, composition depend., photoemission spectra study 0-100434
 GaS(Te)(Se), elastic characteristics, Debye temp., ultrasonic study (*Russian*) 0-79872
 GaSb (110), surface core-level binding-energy shifts 0-103737
 GaSb (110)/Au interface, heat-treated, struct. and chem. state, angle-resolved XPS 0-97400
 GaSb, accumulation layer localised carriers interaction with LO phonons, Raman interference lineshapes 0-93338
 GaSb, acoustic wave attenuation, phonon viscosity and dislocation drag 0-70319
 GaSb, adsorption and desorption of Cs, LEED, AES, and photoemission meas. 0-70532
 GaSb based eutectics, thermal cond. and diffusivity, 300-700K, phonon mechanism 0-103526
 GaSb, bulk and epitaxial, IR reflect. meas., carrier conc. and mobility determ. 0-80769
 GaSb, core exciton binding energies 0-80188
 GaSb, defect concentration determ. Hall effect 0-103385
 GaSb, diffusion of In, 520 to 712°C 0-79995
 GaSb, electrochemical sectioning and surface finishing 0-108611
 GaSb, electroliquid epitaxial growth 0-89160
 GaSb film, polycrystalline, Hall mobility 0-97015
 GaSb films, elemental incorporation probability modification by ion bombard. during growth 0-80118
 p-GaSb, heavily doped, LO phonon-carrier interaction, Raman interf. lineshapes 0-93319
 GaSb interface with oxide, photoemission obs. of energy levels induced by adsorpt. 0-93000
 GaSb, LEC growth, Hall coeff. 0-89133
 GaSb LEC single crystal growth, novel encapsulant material 0-93475
 GaSb, lattice dynamics, phonon freq., bond bending force model calcs. 0-70335
 GaSb, piezoresistive vibrating circular membrane, reflectance light modulation 0-97232
 p-GaSb, saturation characts. over CO₂ laser spectrum 0-83646
 GaSb, solid solns., impact ionisation, cond. and valence band effects 0-65583
 GaSb substrate for Al₂O₃ film, ion beam etching defect detection 0-89155
 GaSb:Sn, p-n junction, electroluminesc. and photoluminesc. 0-66306
 GaSb-InAs system, (110) surface and interface electronic struct. 0-100494
 (GaSb)_{1-x}Ge_x films, single-cryst. metastable semicond., growth and phase stability 0-80115
 GaSe, ¹¹⁰Ag diffusion, temp. depend. and solution (*Russian*) 0-70467
 GaSe, anodic film form., in situ ellipsometric study 0-104318
 p-GaSe, back wall Schottky barrier cells, diffusion length, RT spectral response meas. 0-107806
 GaSe, deep free and constrained excitons and biexcitons, collective interactions (*Russian*) 0-66282
 GaSe, exciton luminesc. kinetics, intermediate electron-hole states 0-93389
 GaSe, exciton-phonon quasibound states, photocond. and luminesc. study 0-96800
 GaSe, Faraday rot. near absorpt. edge, optical dispersion meas. 0-80757
 GaSe films, optical props. at lattice vibr. freqs., IR and Raman spectra 0-60696
 e-GaSe films, optical props. in IR region, metal substrate effect 0-71502
 GaSe, impurity photocond., induced illumination corresponding to fundamental absorption region 0-92933
 GaSe, lattice dynamics and elastic props., Born-von Karman model study 0-70337
 GaSe, layer compound, long-wavelength phonons and elastic consts. 0-65175
 e-GaSe, long-wavelength lattice vibr. 0-92631
 GaSe, press. induced metallic and supercond. state 0-75666
 e-GaSe, Raman scatt., hydrostatic press. effect 0-84745
 GaSe, reson. Brillouin scatt. 0-89010
 GaSe, shallow core level spectra 0-104037
 GaSe thin films, electroabsorpt. spectra, exciton line splitting 0-107716
 GaSe, thin layers, far IR refractive index 0-80799
 GaSe:Sn, ¹¹³Sn diffusion, temp. depend. and Sn solubility (*Russian*) 0-70466
 p-GaSe:Sn, majority carrier drift mobility meas. 0-92895
 GaSe-SnO₂, heterojunctions, photoelec. props. 0-96945
 α(β)-Ga₂Se₃, cryst. growth, optical, X-ray diffr. and SEM study 0-71587
 Ga₂Se₃, solid solution, elec. cond. 0-88301
 Ga₂Se₃-FeSe, phase diagram, elec. cond., mag. susceptibility 0-88301
 GaSe_{1-x}Te_x, Raman scatt., optical phonons and phase transition 0-66202
 GaSe_{1-x}Te_x, Raman spectra, phonon freq. 0-97286
 GaTe, ¹¹⁰Ag diffusion, temp. depend. and solution (*Russian*) 0-70467
 GaTe, cryst. struct., TEM and X-ray diffr. study 0-79757
 GaTe, layer cryst., polarised IR refl. spectra 0-97279
 GaTe monocrystal, far IR polarised complex reflectivity obs. 0-60609
 α-GaTe, single cryst., Raman scatt. 0-60599
 GaTe, single cryst. prep. and electroabsorpt. spectra investig. 0-103968
 GaTe, transport properties under hydrostatic pressure 0-75589
 GaTe-SnO₂ heterojunctions, photoelec. props. 0-96945
 (Ga_{1-x}V_x)₂O₃, impurity doping effects, elec. props. obs. 0-75609

gallium compounds continued

- Ga, Brillouin spectra, light scatt. cross section for surface ripples 0-71434
 Gd₂O₃-Ga₂O₃ system, phase diagram relationships of garnet-perovskite transform. 0-97460
 Ge-S-Ga amorphous thin film, memory switching effects 0-88605
 GeS₂, single crystal, far IR transmission 0-80800
 HgCr₂-Ga₂Se₃, temp. depend. of ESR linewidth, 105-300K 0-71161
 In-Ga-P ternary system, low temp. phase diagram rel. to epitaxial growth 0-84916
 InAs-GaSb superlattices, mag. field induced semimetal-semicond. transition 0-65656
 InAsSb/GaSb broad-spectral-band IR detector, backside-illum. heterostructure approach 0-73450
 InGaAsP avalanche photodiode, 1.3 μ m, noise performance, -190°C 0-57370
 InGaAsP avalanche photodiodes, breakdown mechanism, donor conc. effect 0-70710
 InGaAsP, bandgap energy by electroreflectance and photoluminesc. spectra 0-107700
 InGaAsP DH, luminesc., quantum efficiency determ. 0-108273
 InGaAsP, LPE, diffusion-limited step-cooling technique, layer thickness and composition 0-84402
 InGaAsP LPE heterostructs., interface grading, Auger depth profile 0-103585
 InGaAsP strip-buried heterostructure laser, high output power, operation 0-58559
 InGaAsP-InP buried heterostructure lasers emitting at 1.3 μ m, accelerated ageing characts. 0-95898
 InGaAsP-InP DH laser, 1.55 μ m, low temp. LPE growth for room-temp. CW operation 0-64045
 InGaAsP-InP DH LED, high temp. aged, dark-spot defects, TEM obs. 0-66300
 InGaAsP-InP DH lasers, perturbed InP growth, photoluminesc. study 0-106518
 InGaAsP-InP DH laser, threshold current, temp. depend. 0-106521
 InGaAsP-InP high-gain heterojunction phototransistor 0-103745
 InGaAsP-InP layers, grown by LPE techniques, lattice const., bandgap, thickness and surface morphology meas. 0-59818
 In_{1-x}Ga_xAs_{1-y}P_{1-y}, electron effective mass from Shubnikov-de Haas meas. 0-80298
 In_{1-x}Ga_xAs_{1-y}P_{1-y} epitaxial layer, far IR refl. spectra, lattice vibrs. 0-97282
 In_{1-x}Ga_xAs_{1-y}P_{1-y}, evidence for alloy scatt. from press. induced changes of electron mobility 0-88548
 In_{1-x}Ga_xAs_{1-y}P_{1-y}, Hall mobility, comp. depend. 0-75587
 In_{1-x}Ga_xAs_{1-y}P_{1-y}, hole mobility over temp. range 77 to 300K 0-60111
 In_{1-x}Ga_xAs_{1-y}P_{1-y}, surface and dielec.-semicond. interface props. 0-93001
 InGaP/InGaAs struct. for transferred electron photocathodes, VPE growth and characterisation 0-76193
 In_{0.9}Ga_{0.1}P, N free and implanted, photoluminescence study 0-97322
 n-In_{1-x}Ga_xP, direct-gap semiconductor, cathodoluminesc., electron irradi. effects 0-108283
 In_{1-x}Ga_xP, epitaxial layers, compositional inhomogeneity 0-88444
 In_{1-x}Ga_xP, proportional ingredient content determ. by X-ray fluorescence 0-97747
 InGaPAs LPE layers, compositional inhomogeneity, photoluminesc. obs. 0-75451
 In_{1-x}Ga_xP_{1-y}As_{1-y}, lattice-matched epitaxial layers, LPE growth on GaAs(100), characterisation 0-75465
 In_{1-x}Ga_xP_{1-y}As_{1-y}, lattice matched to InP, electroreflectance obs. 0-93416
 In_{1-x}Ga_xP_{1-y}As_{1-y}, In_{1-x}Ga_xP_{1-y}As_{1-y}, visible spectrum multiple-quantum-well heterostruct. lasers 0-106537
 In_{1-x}Ga_xP_{1-y}As_{1-y}, InP coupled multiple quantum-well heterostructure laser diodes, threshold current temp. depend. 0-78855
 In_{1-x}Ga_xP_{1-y}As_{1-y}, electron effective mass and Dingle temp., Shubnikov-de Haas oscils. 0-59859
 In_{1-x}Ga_xSb, energy gap, temp. depend. and photovoltaic effect 0-70746
 In_{1-x}Ga_xSb films, elec. props., preparation 0-100473
 InP homojunction solar cell, antirefl. coated, high-efficiency 0-104505
 InP/In_{1-x}Ga_xAs_{1-y}P_{1-y} interfaces, sputter-profiled, depth resolution degradation by cone form. 0-80094
 InP-GaInAsP buried heterostructure lasers of 1.5 μ m region, fabrication and characts. 0-74388
 InP-InGaPAs heterojunction lasers and LEDs, 1.0 to 1.2 μ m 0-74362
 In₂-Sn_{0.3}O₃-Ga_{0.7}In_{0.3}(P-InP_{0.5}As_{0.5}) heterojunction solar cells, chemistry and prep. 0-94073
 La₂S₃-Ag₂S-Ga₂S₃ glass system, prep., thermal and elec. props. (French) 0-89192
 Li₂O-Ga₂O₃, rapidly quenched glasses, Li ion cond., elec. cond. 0-100346
 Li₂O-GeO₂-Ga₂O₃ glass, electrode props., dissolution kinetics 0-89387
 Na₂O-Ga₂O₃ system β and β' phases, fast ion cond., prep. and phase comp. 0-59716
 NbGa₂O₄, O stabilised cpd., struct. determ. 0-103301
 PbTe-Ga₂Te₃, phase interaction, DTA, XPA and microstructural anal. 0-96625
 RbGa(SO₄)₂·12H₂O, spin-Hamiltonian with trigonal S³I terms for describing ⁵⁷Fe³⁺ ENDOR spectra 0-75885
 Si-GaSe n-p heterojunction, elec. characts., interface states 0-70812
 Sm₂O₃-Ga₂O₃ system, garnet-perovskite transform., phase diagram relationships 0-97460
 V₂O₅-GaNbO₄ system, interfacial reactions, efficient boundary conditions and solid state reactivity 0-76542
 YGaIG, magnetoelastic wave propagation time dispersion reduction 0-75836
 YIG:Ga, films, ferromagnetic resonance, ion implantation effect 0-97145
 Y_{2.8}La_{0.15}Fe_{2.85}Ga_{1.15}O₁₂ garnet, mag. props., ion implantation effect, Mossbauer study 0-97166
 ZnGa₂S₄, band struct., pseudopot. method 0-92816

gallium phosphide light emitting diodes *see light emitting diodes***galvanomagnetic effects**

- see also Hall effect; magnetoresistance; Suhl effect; thermomagnetic effects*
 alloys, dil. mag., transport props. in mag. field, impurity-electron scatt. 0-65541
 covalent semiconductors, low temp. galvanomag. effects, shallow attractive traps 0-88575
 disordered system, AC cond. tensor in mag. field 0-92870
 disordered system in mag. field, frequency dependence of conductivity tensor, theoretical investigation 0-70725

galvanomagnetic effects continued

- gapless semiconductor, transport coeffs. in quantum limit 0-80302
 hopping conduction, master eqn. approach in presence of mag. field 0-103697
 longitudinal magnetoconductivity, effect of multiple scatt. 0-96836
 metal, ferromag., antiferromag., magnetoelastic coupling effect on magnetoec. reson. 0-75837
 semiconductor, magnetodiode and magnetoconcentration effects, influence of field effect 0-107903
 semiconductor layers, double injection in transverse mag. field, theory 0-80421
 semiconductors, hot electron transverse escape galvanomagnetic effects (Russian) 0-80289
 space-time symmetry restrictions on transport coefficients 0-70662
 spatially inhomogeneous magnetic field effect on semiconductor carriers 0-92916
 Ag₂Re films, galvanomag. props. and quantum size effects, obs. 0-70866
 Ag₂Se, electronic and electrogalvanic props. in α -phase region (French) 0-107820
 Bi, thermoelectric power, electronic thermal cond., in mag. field 0-60015
 B-Ga, metastable, elec. props. in normal and supercond. states (Russian) 0-65520
 n-Ge, anomalously enhanced plasma diffusion transverse to mag. field 0-96931
 Hg_{1-x}Cd_xTe-type semimetals, kinetic props., local acceptor level effects 0-65557
 n-InSb, ionized impurity scatt. limited mobility, expt. 0-80274
 p-InSb, magnetoconcentration effect, negative differential conductance 0-70729
 n-Si, multivalued Sasaki effect 0-107795
 Te, photoconductivity in strong mag. fields, doping effects, impurity levels 0-75602

galvanomagnetism *see electromagnetism***galvanometers**

- ballistic galvanometer, error due to non-transient impulses, integral expression 0-86349
 laser beam resonant chopper performance characteristics and limitations 0-64084
 oscillograph, construction for fast process recording 0-73346

galvanothermomagnetic effects *see thermomagnetic effects***game theory**

- see also information theory*
 assignment problem, mixed, strategy game, utility function maximisation, equilibrium points 0-68028
 differential encounter-evasion game, nonstationary, theorem on the alternative 0-68026
 differential games, control systems with aftereffect 0-68025
 differential games, stable position control 0-68024
 quandle, rel. to quantum non-locality detections 0-86143

gamma fission reaction *see photofission***gamma radiation** *see gamma-rays***gamma-ray absorption**

- Fe, photon penetration, photon backscatt. incidence angle depend. 0-104008
 organ doses from isotropic γ -ray fields, review 0-109026
 polystyrene, photon penetration, photon backscatt. incidence angle depend. 0-104008
 pulmonary oedema of intact dogs, meas. by transthoracic γ -ray attenuation 0-81787
 water irradiated by photons up to 2 MeV, initial energies of Compton electrons and photoelectrons 0-108320
 Al, photon penetration, photon backscatt. incidence angle depend. 0-104008
 Pd concentration determ. by gamma-ray absorption from ¹¹⁹Sn^m 0-108123
¹¹⁹Sn, total mass absorpt. coeff. of gamma quanta, chem. binding influence, determ. using Mossbauer effect 0-99467

gamma-ray angular distribution*see also gamma-ray spectra*

- gamma reactions initiated by polarised particles, Legendre polynomial coeffs. 0-73107
 linear polarisation mixing coeffs. for mixed dipole and quadrupole γ -radiations, Compton polarimeter 0-73110
¹²C(p,p'), 22-27 MeV, ¹⁺ state de-excitation γ -ray ang. distrib., tensor force effects, DWBA anal. 0-68580
⁴⁰Ca, A=44.46, excited states and transition ang. distrib. from Ti(¹⁴C,¹⁶O) 0-95308
¹⁴¹Ce collective M1 excitation effects on γ -ang. distrib., direct semidirect model of ¹⁴⁰Ce(n, γ) 0-57733
²⁵²Cf spontaneous fission, prompt γ -ray differential angular distrib. 0-102220
⁶³Cu(p,p') negative parity level excitation, gamma ray obs., test for core excitation model 0-68534
⁴Fe(p, γ)Co, A=54.56, giant dipole resonance splitting, direct-semidirect capture model anal. 0-106055
¹⁰⁹In high spin states, γ -transitions, ang. distrib. from ¹⁰⁸Cd(α ,2np) 0-73783
⁷⁹Kr, low lying levels from ⁷⁹Br(p,n γ) 0-105972
⁵³Mn fragmented $g_{9/2}$ isobaric analogue resonance, γ -spectra and excitation functions from ⁵²Cr(p, γ) 0-68627
⁶⁰Ni high spin states, J⁺, T_{1/2}, ang. distrib. and polarisations from ⁵⁶Fe(⁷Li, p2n γ) 0-99116
²⁰⁴Pb(n,n' γ), 1.5-3.1 MeV, levels, J⁺, excitation functions and mixing ratios 0-102123
¹⁴⁷Pm, level scheme and transitions following ¹⁴⁷Nd 0-83073
¹⁴¹Pr, positive parity levels, gamma-ray yields and ang. distrib. 0-105962
¹⁶⁰Tb-¹⁶⁰Dy, γ -transitions and angular distributions 0-83060
⁴Ti, A=48.50, excited states and transition ang. distrib. from Cr(¹⁴C,¹⁶O) 0-95308
¹⁶⁷Tm, energy level scheme from ¹⁶⁵Ho(α ,2n γ) (German) 0-88576
¹⁶⁷Tm(HI,n γ), ang. distrib., multipolarities (French) 0-68575

gamma-ray applications*see also radiation therapy*

- air/water mixture mass flow meas. by drag devices and γ densitometer 0-79385
 density of fluid meas., theory, practices and appl. 0-73325
 ethylene-Co copolymers and -SO₂ copolymers prep. by catalysis and ⁶⁰Co γ -radiation, mech. props. 0-66841

gamma-ray applications continued

fluid meas. in mechanical engineering, conf., Johannesburg, South Africa, (Feb. 1979) 0-75016
 geophysical prospecting, allowance for scattered gamma radiation (*Russian*) 0-105067
 multibeam sonde, stand for adjusting 0-85103
 polyethylene, irradiation, crystallinity and crosslinking efficiency 0-66843
 polyethylene-glass fibre composites, gamma-irradiated filler 0-66840
 quartz dental composites, acrylic acid grafted on particles by gamma-radiation 0-66840
 rubber-metal facings, vulcanisation degree determ., γ -ray method 0-61043

gamma-ray astronomical observations

burst obs. in 1978 November, ISEE 3 high-resolution spectroscopy 0-67907
 burst source in Sculptor measured by Venera 11, 12 and Prognos 7, identification attempt (*Russian*) 0-77520
 burst sources, ISEE 3 obs. and expt. 0-98546
 3C 273, search for 1-20 MeV gamma rays, balloon-borne obs. of QSO 0-67912
 CG 135+1, search for 1-20 MeV gamma rays, balloon-borne obs. of QSO 0-67912
 CG 135+1, spectrum obs. 20 keV-25 MeV 0-105398
 cosmic γ quanta, short-term fluctuations obs. 0-67483
 Cygnus X-1 and X-3, search for 1-20 MeV gamma rays, balloon-borne obs. 0-67912
 fast intense gamma-ray transient (1979 March 5), detect. 0-73073
 galactic background, structure from gamma ray obs. 0-98743
 galactic disc, obs. between $-45^\circ < l < 45^\circ$ in 80 keV to 8 MeV energy range 0-82540
 gamma-ray burst, distance and spectrum of 1972 April 27 event 0-67903
 N49, SNR in LMC, Pioneer Venus Orbiter obs. of 1979 March 5 gamma-ray transient 0-77518
 NGC 4151, search for 1-20 MeV gamma rays, balloon-borne obs. of Seyfert galaxy 0-67912
 observational test of cosmological particle production theories 0-109574
 PSR 1822-09, balloon-borne gamma-ray obs. 0-105269
 Sun, gamma-ray lines from flare, HEAO 1 obs. 0-67682
 transient gamma-ray event of 1979 March 5, location 0-73074
 ultra high energy gamma-ray bursts from celestial sources, unsuccessful search 0-67911

gamma-ray astronomy

see also *gamma-ray sources (astronomical)*
 active aperture imaging for direction meas. of high energy γ -rays 0-62022
 conference, non-solar gamma-rays (Bangalore, India, May-June 1979) 0-77548
 COS-B, instrument description (*Danish*) 0-82544
 cosmic gamma ray spectroscopy, review 0-67582
 cosmic rays in the galactic centre, predicted from high energy γ ray observations 0-72731
 electron-positron pair track analysis in multilayer gamma-ray telescope 0-63469
 galactic background, structure from gamma ray obs. 0-98743
 ISEE 3 experiment and obs. of burst sources 0-98546
 Lixoscope, X-ray and gamma-ray telescope system 0-62020
 Pioneer Venus Orbiter Gamma Burst Detector 0-67505
 solar gamma ray emissions study, Solar maximum mission, detector assembly and electronic assembly 0-63476
 Space Shuttles, Gamma Ray Observatory launch instrums. and operations 0-109365
 spectrometers, cooled Ge, on P78-1 satellite 0-58019
 stellar nucleosynthesis constraints from detect. of ^{26}Al gamma ray line 0-94780
 telescope for high energy X-rays, large sensitivity, energy and angular resolution 0-62016
 telescope for medium energy gamma-rays scintillation counter time-of-flight system 0-62017
 ultra-high energy γ -ray astronomy (10^{11} - 10^{13} eV) 0-101649

gamma-ray detection and measurement

see also *gamma-ray spectrometers; radioactivity measurement*
 activated thick foil close to NaI detector crystal, gamma counting and self-shielding efficiency 0-69043
 air ionisation probe for α , β , γ and shoe monitor 0-58084
 astronomy, high energy, γ -ray telescope, large sensitivity, energy and angular resolution 0-62016
 astronomy medium energy gamma-ray telescope, scintillation counter time-of-flight system 0-62017
 autoradiographic inventory methods for nondestructive assay of reactor fuels and fuel assemblies 0-71875
 BWR spent fuel safeguarding, nondestructive assay using gamma spectrometry 0-68802
 Cherenkov ring imaging counter, single photon detectors 0-58036
 directional fully encapsulated gamma detector for in-core reactor meas. 0-63307
 dose-rate conversion factors for external exposure to photons and electrons, modifications to DOSFACTER code 0-104775
 film photon and electron absorbed-dose detector 0-91379
 fission reactor loss of coolant studies, gamma densitometer detector comparison 0-57881
 gamma camera, appls. for three-dimensional emission tomography using scattered photon information 0-98134
 gamma-ray spectrometers; calc. of radioactivity induced during spaceflight 0-102382
 lignocellulose polymer composites as γ -dosimeters in the kilorad range 0-95465
 luminescent detector efficiency for 600 MeV protons, mass stopping power calc. 0-99346
 LWR irradiated fuel assemblies, nondestructive exam. using γ -ray and neutron techniques 0-66760
 LWR spent fuel, nondestructive meas. and verification for materials safeguards 0-78420
 Marinelli type vessel, geometry in γ -ray activity determ. (*Japanese*) 0-91409
 megachannel pulse height analyser for gamma-ray coincidence analysis 0-99430
 mixed β - γ dosimetry, ionisation and scintillation counters 0-57975
 Mossbauer effect, inelastic scattering intensity meas. 0-71245
 multialayer γ -telescope spark chambers, 5-200 MeV e^+e^- pair track anal 0-63469

gamma-ray detection and measurement continued

nuclear accident dosimetry system, Czechoslovakia 0-57978
 nuclear energy level lifetime measurement using on-line computer and registration time shift compensation 0-68577
 nuclear fuel burnup determination using Aragonic γ detector 0-63262
 nuclear materials accountability, U and P NDA of crated waste by gamma-ray and neutron coincidence counting 0-83166
 nuclear materials safeguarding, gamma spectrometric techniques and standards (*French*) 0-68811
 on-line radiation monitoring at a nuclear fuel reprocessing plant 0-95469
 particle detectors, microprocessor-controlled data acquisition system for temporal/angular correl. between β - and γ -ray emission (*Spanish*) 0-106238
 passive personnel portal detectors for nuclear materials diversion protection using gamma-ray and neutron detectors 0-78389
 personal monitoring, effect of environmental radiation, thermoluminescent dosimeter (*Japanese*) 0-61707
 photon position monitors for CHES synchrotron source, using split photoelectron detectors and ionisation chamber 0-91336
 photon radiation meas. in nuclear power stations 0-63403
 plastic track detectors, structural charges due to high dose γ -rays 0-95500
 position sensitive gamma ray detection system, 3-D, fabrication and efficiency 0-63483
 proton accelerator beam scraper, photon dose rate calc. 0-99367
 pulse shape analyser, effect of pulse pile-up on discrimination between neutrons and gamma rays 0-91402
 PWR irradiated fuel, monitoring by gamma spectrometry nondestructive meas. (*French*) 0-63288
 Q-values of β^- decay, rapid meas. from electron and gamma energy decays 0-78220
 reactor core gamma dosimetry, solid state nucl. track detector appl. 0-95466
 reactor fuel burn-up and cooling time determ. using gamma spectrometry 0-63289
 reactor fuel burn-up determination using gamma spectrometric nondestructive assay for IAEA safeguards 0-68806
 reactor fuel burn-up determination using gamma spectrometry, IAEA safeguards experience in Czechoslovakia 0-63292
 reactor fuel burn-up measurement using spatial power distrib. eval. and gamma spectrometry 0-68803
 reactor spent fuel safeguards verification using gamma spectrometry 0-63290
 reference material, based on silicate glass 0-78454
 rocks and soils, Ge(Li) detectors for γ -radioactivity meas. 0-67418
 seawater γ -ray field, meas. system (*Russian*) 0-109268
 segmented scanning device for gamma-ray meas. of Pu and Am in molten salt residues 0-83165
 self absorption factor of gamma radiation in reactor fuel assemblies 0-63320
 semiconductor detector active volume, determ. from gamma ray interactions, Monte Carlo method 0-63448
 SF5 lead glass Cherenkov counter, high energy photon position determ. 0-58032
 spherical detectors, calc. of γ -ray recording efficiency 0-83236
 thermal neutron capture γ -ray meas. using neutron guide tube 0-58099
 TLD phosphors, sensitised, photon energy dependence 0-78498
 TLD system, automated, for gamma radiation monitoring 0-57964
 γ -emitting radioelements, meas. of weak doses (*French*) 0-91410
 ^{10m}Ag , gamma-ray intensities, precision meas. 0-102139
 ^{70}Be , 477.6 keV, Analytic fitting of full-energy peaks in Ge(Li) spectra at high count rates 0-99147
 $\text{Bi}_2\text{Ge}_2\text{O}_7$, 38 mm scintillator, γ -ray response 0-58048
 ^{207}Bi , gamma-ray intensities, precision meas. 0-102139
 $\text{CaF}_2(\text{Eu})$ Phoswich detector, evaluation for ^{90}Sr in situ anal. 0-58067
 $\text{CaSO}_4:\text{Dy}$ TLD, low exposure rate depend. meas. 0-102408
 CdS γ -ray dosimeters with elevated stability under irradiation 0-86995
 CdTe gamma backscatt. assay meter 0-58070
 CdTe matrix γ -camera, biomedical appl. 0-76827
 CdTe metal-semiconductor-metal γ -ray detector characts. 0-57451
 ^{56}Co , gamma-ray intensities, precision meas. 0-102139
 ^{134}Cs , gamma-ray intensities, precision meas. 0-102139
 $^{\text{A}}\text{Eu}$, A=152,154, gamma-ray intensities, precision meas. 0-102140
 Ge detectors, high purity, event timing, compared to Ge(Li) detectors 0-69018
 Ge p^+-n^+ structures, large-scale trap characts. 0-92966
 Ge semiconductor detector efficiency determ. using a standard Marinelli beaker geometry 0-63450
 Ge(Li) and HPGe detectors, coincident sum peaks 0-63447
 Ge(Li) detector, gamma pulse pileup, random summing losses 0-58023
 Ge(Li) detectors, gamma-ray intensity standards for calibration 0-74083
 Ge(Li) gamma-ray spectra analysis of fission products, automatic general-purpose program GSAP (*Chinese*) 0-69013
 Ge(Li), peaks in gamma spectra analysis, analytic approx. 0-102395
 Ge(Li) semiconductor, used simultaneously with NaI(Tl) scintillation spectrometer, in neutron activation cross-section meas. 0-78485
 ^3He ionisation chamber, improved time resolution in n - γ coincidence meas. 0-99416
 HgI_2 , soln. grown crystals, low-energy gamma-ray cond. type detectors 0-97418
 ^{121}I , variation of γ -counting efficiency with sample composition 0-83238
 ^{192}Ir , gamma-ray intensities, precision meas. 0-102140
 NaI scintillation counter, calc. of self-shielding and detector efficiency 0-99419
 NaI(Tl) crystals for volume cylindrical sources, efficiency of detection 0-63457
 NaI(Tl) detectors, response functions to terrestrial γ -radiation, computer program C-83233
 NaI(Tl) scintillation spectrometer, used simultaneously with Ge(Li) semiconductor, in neutron activation cross-section meas. 0-78485
 NaI(Tl) well-type detectors, photopeak efficiency values, expts. and calcs. 0-63454
 NaI(Tl) scintillator detectors for neutron-gamma discrimination 0-102386
 Pu holdup in glove-box exhaust filter, in-line monitoring by gamma ray detection 0-78458
 Pu, isotope composition, determ. using gamma spectrometry 0-66915
 Pu, isotopic composition, determ. using precise absolute gamma spectroscopic meas. 0-66916
 Pu safeguards, product soln. gamma-ray NDA using K-absorption edge densitometer 0-83162

gamma-ray detection and measurement continued

- Pu safeguards assay, isotopic meas. by gamma ray spectrometry using two-detector method 0-83161
⁷¹Li(Li), peaks in gamma spectra analysis, analytic approx. 0-102395
¹¹⁹Sn, total mass absorpt. coeff. of gamma quanta, chem. binding influence, determ. using Mossbauer effect 0-99467
⁸⁵Sr, 514.0 keV, Analytic fitting of full-energy peaks in Ge(Li) spectra at high count rates 0-99147
 U, assay of natural samples, meas. of gamma- or neutron activity of short-lived fission products 0-61179
 Xe high pressure proportional, scintillation camera for X- and γ -ray imaging 0-99412
⁸⁸Y, gamma-ray intensities, precision meas. 0-102139

gamma-ray diffraction

- FeO₃, suppression effect under hyperfine quadrupole splitting, Mossbauer study (*Russian*) 0-75906

gamma-ray effects

- see also *biological effects of gamma-rays; radiolysis*
 adamantane, γ -irrad., free radicals EPR and ENDOR 0-69170
 alkali halides, irradiated at room temperature, stored energy 0-79839
 borosilicate glasses, gamma irradiation effect on density, refractive index, thermal expansion 0-79838
 cellulose fibre, gamma-irrad., and storage effects on props. (*Russian*) 0-61121
 cephalosporins, radiation-sterilisation 0-66822
 2,6-N,N-diacetylaminopyridine elec. cond., γ dose and temp. (303-363K) effects 0-103696
 2,6-N,N-dibenzoyldiaminopyridine elec. cond., γ dose and temp. (303-363K) effects 0-103696
 FBR blanket facility, gamma-ray heating rate meas. in stainless steel and Pb 0-57912
 fission reactor irradiation loop containing nonfissile material, optimality criterion based on γ -ray flux losses 0-63236
 fission reactors, gamma-power of hot circuit, calc., effect of flow hydrodynamics of process materials 0-63235
 glutaric acid, γ -irrad. single crystals, free radical EPR obs. at 77K 0-81340
 1-hydronaphthyl radical, 4.2K absorpt. spectrum (*French*) 0-80809
 lipid peroxide formation in irrad. synthetic diets, storage effects 0-101025
 metals, thickness meas. by backscatt. γ radiation 0-101781
 mica, natural, high γ and electron-irrad. doses effect on annealing behaviour, thermal decomp. resist. 0-60897
 mixed fluoride crystals, nucl. radiation effects 0-80831
 nuclear power reactor materials calorimetric validation of TLD-measured heating effects 0-63254
 octadecylacrylamide films, oriented ultrathin, radiation-induced solid state polymerisation 0-80128
 optical fibre, γ -irrad., differential interferometric meas. of refr. index changes 0-78952
 optical fibre, neutron and gamma induced transient absorpt. and luminesc. 0-58763
 oxide glasses, γ -irrad., CuO effects on EPR 0-84645
 photochromic glass, darkening effect due to γ -irrad. 0-96566
 PMMA, neutron and gamma irradiation effects 0-66839
 polycarbonate, γ -irradiated, dielec. behaviour and glass transition 0-97182
 polyethylene, γ -irrad., asymmetric 002 X-ray line profiles, analysis 0-96567
 polyethylene, vinyl group reactions during γ -irrad., crystallinity effect, absorbance obs. 0-81346
 polystyrene, neutron and gamma-irradiation effects 0-66839
 potassium antimonyl tartrate, neutral aq. soln., gamma radiolysis 0-101030
 PTFE, γ -ray effects on 19 and 30°C phase transitions, Fourier transform IR spectroscopy 0-103387
 quartz, surface damage by X-rays, γ -rays, neutrons, SEM study 0-79837
 ruby, radiation-induced optical processes, impurity effects 0-66310
 semiconductor, space charge region thickness, deep level props., determ. by γ -ray absorpt. 0-59995
 n-Si, recombination centres and carrier lifetimes after γ -irrad. 0-60004
 steel, stainless, type 4301, radiation enhanced permeation of H₂ 0-59732
 superheated water, flashing kinetics, γ -radiation effects 0-92025
 Teflon, gamma irradiated, free four-term analysis of positron lifetime spectra 0-76101
 TGS crystals, effects of radiation induced defects on internal bias field 0-88941
 thymidine monophosphate aqueous solution, gamma irrad. effect on base damage, phosphate release 0-89806
 B₂C-phenolic fibre reinforced composite for nuclear shielding appls. 0-102353
 CaSO₄:Dy, thermoluminescent glow peaks, post γ -irrad. annealing study 0-89077
 CaSO₄:Dy TLD phosphor, γ radiation changes in glow curve 0-60688
 Co complex, 2,6-N,N-diacetylaminopyridine-Co(II) elec. cond., γ dose and temp. (303-363K) effects 0-103696
 Co complex, 2,6-N,N-dibenzoyldiaminopyridine-Co(II) elec. cond., γ dose and temp. (303-363K) effects 0-103696
⁶⁰Co, polyethylenes loss tangent variation (*German*) 0-75266
 CsBr(Cl):Cu⁺, γ -irradiated, thermolum. emission 0-104001
 CsH₂AsO₄ crystals, dielectric radiation effects, γ -radiation 0-93234
 GaAs, electroluminescent study of irrad. induced struct. damage, athermal annealing 0-108280
 n-GaAs, nature of low temp. field generation of carriers, liberation from surface states 0-92960
 n-Ge, proton and γ irrad., minority carrier recombination 0-65591
 Ge:Ag(Ni), gamma ray effects on impurity states 0-96822
 Ge:P(Sb)(Bi), γ -irrad., carrier trapping and recomb. at point radiation defects 0-107810
 n-InP, γ -ray and electron irrad., annealing of radiation point defects, elec. cond. and Hall coeff. meas. 0-65051
 KBr, gamma-irrad., hologram recording, by F-centre bleaching 0-78814
 KCl, γ -irrad., F-centre absorpt., flash-stimulated changes 0-92524
 KCl, pure and Ba doped, symm. of elastic fields due to defect displacements, diffuse X-ray scatt. 0-70256
 KH₂AsO₄, γ -irradiated, free radicals, EPR and ENDOR study of consequences of ferroelec. transition (*French*) 0-93209
 KMg₂[AlSi₃O₁₀]F₂, with excess Al, synthetic fluorophlogopite, radiation-induced paramag. O⁻ centres 0-60417
 K₂O-B₂O₃-Fe₂O₃, γ -irrad., Mossbauer spectroscopic study 0-108132

gamma-ray effects continued

- KPF₆, γ -irrad., trapped free radicals EPR obs. 0-63683
 LiCl, radiation effects on decay time of F-centre emission 0-93381
 LiCl single crystals, γ -irrad., thermolum. meas. 0-80880
 LiF, γ -irrad. induced defects, positron capture and annealing obs. 0-60707
 LiF, γ -irrad. pure and Mg-doped, phonon scatt. and interstitial clusters 0-70254
 LiF TLD phosphor, γ -irrad. induced sensitisation, UV effects 0-108286
 LiF TLD phosphor, residual thermoluminescence effect on sensitisation 0-108287
 LiF:OH:Mg, γ -irrad. induced oxyhydril complexes 0-92555
 LiNbO₃, hologram recording, γ radiation effect 0-78812
 LiNbO₃:Fe (0.05%), hologram recording γ radiation effect 0-78812
 Li₂O-Al₂O₃-SiO₂:Cd⁺, glass, ESR study 0-103879
 Li₂O-TiO₂-Al₂O₃-SiO₂ glass, γ -irrad., struct. position of Ti, EPR study 0-84644
 MgAl₂O₄, γ -irradiated crystal, TSC, thermoelec. power, thermolum. and afterglow 0-75583
 MgO-TiO₂-Al₂O₃-SiO₂ glass, γ -irrad., struct. position of Ti, EPR study 0-84644
 Mo, gamma irradiated defects, interaction with positrons (*Russian*) 0-97372
 NaCl, γ -irrad., F-stimulated inversion of sign of dislocation charge 0-59475
 NaCl, optical strength, effect of irrad. in mechanically stressed state 0-80695
 NaCl:Cd²⁺, dielectric loss following plastic deform. 0-84690
 Na₂O-SiO₂:CuO glass, gamma-irradiated, EPR and optical spectra 0-103885
 Na₂O-TiO₂-Al₂O₃-SiO₂ glass, γ -irrad., struct. position of Ti, EPR study 0-84644
 NaReO₄, EPR spectra of paramag. centres and free radicals 0-108072
 Nd:glass laser, influence of neutron and γ irrad. on generating characts. (*Russian*) 0-69402
 Ni complex, 2,6-N,N-diacetylaminopyridine-Ni(II) elec. cond., γ dose and temp. (303-363K) effects 0-103696
 Ni complex, 2,6-N,N-dibenzoyldiaminopyridine-Ni(II) elec. cond., γ dose and temp. (303-363K) effects 0-103696
 PbTe, diffusion of Ag, effect of gamma irradiation 0-59515
 S, allotropic modifications and activity distrib. 0-70255
 Si based MOS device irradiation with γ -rays, minority carrier generation, CV characts. 0-88637
 n-Si, defect charge states, complex form., gamma-ray effects 0-96564
 Si, n⁺-p diode, γ -radiation defects, annealing and recomb. props. 0-65045
 Si, radiation defects, influence of dislocations on accumulation, elec. props. 0-92558
 Si:Au, precipitation of solid soln., effect of gamma irradiation 0-59515
 n-SiO₂, MOS structures, radiation states 0-103758
 YIG, electron and γ -irrad., photomagnetic effect 0-103877

gamma-ray interactions

see also *gamma-ray scattering*

No entries

gamma-ray lasers

- computerised analysis, collaboration collection report 0-73106
 kinetics, quasi-classical approach (*Russian*) 0-74332
 negative light absorption by medium with selective freq. modulation of quantum oscillators 0-106501
 three-level Mossbauer gamma-ray lasers, two-stage pumping 0-78857

gamma-ray polarisation

- Mossbauer 14.4 keV gamma-ray source, design, calibration and polarimeter 0-86535

gamma-ray production

- electron-photon beams from proton accelerators, EM interaction investigation (*Russian*) 0-106214
 Mossbauer 14.4 keV gamma-ray source, design, calibration and polarimeter 0-86535
 Triga Mark III nuclear reactor, as intense gamma radiation source (*Spanish*) 0-83232
 tunable narrow band radiation production using laser saturation 0-57680
¹⁸²Ta Mossbauer sources (*French*) 0-74064

gamma-ray scattering

see also *Compton effect; gamma-ray interactions*

- bone, mineral content, coherent scatt. of photons 0-67238
 geophysical prospecting, allowance for scattered gamma radiation (*Russian*) 0-105067
 inelastic scattering intensity meas. using Mossbauer effect 0-71245
 lung density, Compton scatt. meas., multiple photon interactions 0-67146
 photon, spectra of gamma rays backscattered by infinite air (skyshine) 0-101436
 Li₃N, electron density study using Compton scattering 0-79750

gamma-ray sources see *gamma-ray production***gamma-ray sources (astronomical)**

- Apollo 16 gamma-ray burst, distance and spectrum of 1972 April 27 event 0-67903
 background isotropic radiation excess at 1 MeV, possible Seyfert galaxy origin 0-77522
 burst obs. in 1978 November, ISEE 3 high-resolution spectroscopy 0-67907
 burst source in Sculptor measured by Venera 11, 12 and Prognoz 7, identification attempt (*Russian*) 0-77520
 Cassiopeiae A supernova remnant and surrounding H II region, γ -ray generation 0-85989
 CG195.5+4.5, upper limit to 59.35 s periodic radio emission at 18 cm 0-86018
 CG 135+01 (=LS 1+61°303), X-ray emission detect. 0-105400
 CG 135+1, spectrum obs. 20 keV-25 MeV 0-105398
 CG 353+16 not assoc. with ϕ Ophiuchi region 0-94896
 Compton emission models, constraints from gamma-ray data 0-67902
 conference, non-solar gamma-rays (Bangalore, India, May-June 1979) 0-77548
 Crab nebula, model for pulsed γ -ray and X-ray emission 0-62230
 dwarf stars, degenerate accreting, thermonuclear burst assoc. with chromosphere γ -ray emission 0-96864
 fast intense gamma-ray transient (1979 March 5), detect. 0-73073
 galactic burst sources, review of models 0-82494
 galactic disc, obs. between $-45^\circ < l < 45^\circ$ in 80 keV to 8 MeV energy range 0-82540

gamma-ray sources (astronomical) continued

- galactic gamma rays sources, shock region between stellar wind and interstellar matter 0-77512
galactic small-scale structure from obs. of discrete sources 0-98743
galactic sources, obs. with COS-B (*Danish*) 0-82544
Galaxy gamma-ray emission, fluxes determ. from cosmic ray electron spectrum 0-62257
Kerr black hole, low-freq. radiation from infalling particle 0-62176
N49, SNR in LMC, Pioneer Venus Orbiter obs. of 1979 March 5 gamma-ray transient 0-77518
N49 supernovae remnant as source of March 1979 γ -ray burst 0-105270
neutron stars, accreting, thermonuclear burst assoc. with chromosphere γ -ray emission 0-98684
NGC 4151, Seyfert galaxy, gamma-ray emission, Compton scatt. model 0-98711
protogalaxy formation age and γ -ray background 0-62325
PSR 0531+21, Crab pulsar, γ -ray obs. with COS-B (*Danish*) 0-82544
PSR 0833-45, Vela pulsar, γ -ray obs. with COS-B (*Danish*) 0-82544
PSR 1822-09, balloon-borne gamma-ray obs. 0-105269
pulsars, gamma-ray production mechanism 0-77433
pulsars, rotational energy loss, slowing down index and time derivs., gamma radiation 0-67762
quasars, Comptonised spectrum, Monte Carlo simulation 0-90566
relativistic electron spectra, inference from meas. of inverse Compton radiation 0-90339
supernova, nearby, UV and gamma radiation effects on terrestrial atmosphere 0-94584
supernovae, gamma-ray emission, continuum intensity and spectrum 0-101602
transient gamma-ray event of 1979 March 5, location 0-73074
ultra high energy gamma-ray bursts from celestial sources, unsuccessful search 0-67911
ultra-high energy sources (10^{11} to 10^{13} eV) 0-101649
Vela pulsar (PSR 0833-45), radiation model 0-94824

gamma-ray spectra

- see also *gamma-ray angular distribution; gamma-ray spectra of liquids and solids; nuclear decay theory*
biological systems interacting with high energy particles 0-108951
bremsstrahlung contribution from low energy electrons to scattered gamma ray spectra 0-78192
calibration materials for X and γ -ray spectrometers, decay data 0-106221
cosmic gamma ray spectroscopy, review 0-67582
electron beam fusion, pellet and pellet-blanket neutronics and photonics 0-74006
fast Fourier transform anal. (*Chinese*) 0-77762
LWR spent fuel elements, gamma spectrometric meas. of burnup U/Pu ratio and cooling time for materials safeguards 0-78423
measurement standards, National Bureau of Standards (USA) 0-90807
nuclear fuels, nondestructive measurement of U and Th conc. and quantities using XFA and gamma spectrometry 0-71877
nuclear materials, nondestructive element and isotope assay of Pu and U 0-71870
nuclear materials safeguards, inventory verification using high resolution gamma spectroscopy 0-69016
radioactive nuclides, quantum radiation, data handbook 0-94933
spent nuclear fuel cooling time determ. utilising gamma-ray meas. 0-63268
thermal neutron capture γ -ray meas. using neutron guide tube 0-58099
^{110m}Ag, gamma-ray intensities, precision meas. 0-102139
⁷Be, 477.6 keV, Analytic fitting of full-energy peaks in Ge(Li) spectra at high count rates 0-99147
⁹Be(γ, γ'), 32 MeV, energy spectra, d prod. process (*Russian*) 0-91177
²⁰⁷Bi, gamma-ray intensities, precision meas. 0-102139
¹²C gamma line Doppler broadening in ¹²C(n,n γ)¹²C and ⁹Be($\alpha, n\gamma$)¹²C, 4438 keV 0-91147
¹⁰⁴Cd quasiro. ground state band and γ -transition from ¹⁰²Pd($\alpha, 2n\gamma$) 0-105955
⁵⁶Co, gamma-ray intensities, precision meas. 0-102139
¹²³Cs (^{123m}Cs), gamma and conversion electron radiation 0-106017
¹³⁴Cs, gamma-ray intensities, precision meas. 0-102139
¹⁴Eu, A=152, 154, gamma-ray intensities, precision meas. 0-102140
⁵⁵Fe resonances, levels, J^o, valence capture γ -ray spectrum from ⁵⁴Fe(n, γ) 0-86852
¹⁴Gd, A=152, 154, γ -transition energy and intensity meas. from Eu decay 0-73818
Ge(Li) and HPGe detectors, coincident sum peaks 0-63447
Ge(Li) detector, gamma pulse pileup, random summing losses 0-58023
¹⁹²Ir, gamma-ray intensities, precision meas. 0-102140
⁷Li(γ, γ'), 32 MeV, energy spectra, d prod. process (*Russian*) 0-91177
¹¹Li beta decay, γ activity 0-106018
¹⁷²Lu decay, identification of γ -spectra unplaced energies by delayed coincidence meas. 0-78221
¹⁴N(γ, γ'), 32 MeV, energy spectra, d prod. process (*Russian*) 0-91177
²³Na(n, X γ), 0.2 to 20 MeV, reaction cross sections 0-99172
¹⁶O ions, mag. hyperfine interactions, PAC meas. 0-95734
Pu safeguards, product soln. gamma-ray NDA using K-absorption edge densitometer 0-83162
Pu safeguards accountability, gamma-ray meas. of Pu and Am in molten salt residues 0-83165
Pu safeguards assay, isotopic meas. by gamma ray spectrometry using two-detector method 0-83161
¹⁵²Sm, γ -transition energy and intensity meas. from ¹⁵²Eu decay 0-73818
⁸⁵Sr, 514.0 keV, Analytic fitting of full-energy peaks in Ge(Li) spectra at high count rates 0-99147
⁴⁸Ti, weak EI transitions examined using γ -ray, γ - γ coincidence and n- γ coincidence techniques 0-57724
²³⁵U fission product γ radiation for short irradi. times, energy distrib. 0-73929
²³⁵U, radioactive series decay, computer simulation 0-102160
²³⁸U, radioactive series decay, computer simulation 0-102160
⁸⁸Y, gamma-ray intensities, precision meas. 0-102139

gamma-ray spectra of liquids and solids

- see also *Mossbauer effect*
Allende, S content, neutron capture gamma-ray spectroscopy 0-94728
crystal sources, geometrical coeffs. for interpretation of γ -ray perturbed angular correl. with quadrupole interactions 0-73109
electric quadrupole interactions measured by nuclear orientation and NMR on oriented nuclei, review 0-92868

gamma-ray spectra of liquids and solids continued

- fluorides, electric field gradient, time-differential-angular-distrib. method 0-60463
intermediate state perturbation in low temperature nuclear orientation 0-97168
lunar rock, S content, neutron capture gamma-ray spectroscopy 0-94728
method and alloys, liquidus and solidus temperatures, determ. by γ -ray method 0-65193
recoil atoms of heavy ion reactions, local lattice damage, TDPAD meas. 0-84220
relaxation phenomena and magnetic hyperfine fields of isolated Ce ions in liquid and solid metals 0-108137
stratified crystal structs., strongly bound γ -rays 0-80895
ultrarelativistic particle radiation in cryst., γ - γ correlations obs. 0-71274
Au lattice location in Zn, gamma-spectral study 0-80227
BN, ¹⁵N zero point vibr. energy from nuclear photon scattering 0-59593
BeF₂ aqueous solns., mag. and quadrupole relax. 0-71226
Cd conc. in kidney and liver, neutron activation anal., organ depth determ. 0-72321
¹¹¹Cd, nucl. orientation coeffs. with axially symm. elec. field gradient 0-97168
Co-⁴⁸V, nucl. orientation of ⁴⁸V, γ -ray anisotropy obs. 0-97169
Cr, hyperfine interactions on ¹¹¹Cd-probe nuclei, TDPAC meas. 0-75904
EuO:Sm³⁺, hyperfine field at Sm, TDPAC meas. 0-93215
Fe, dynamic exponent, crossover obs., TDPAC Meas. 0-108021
Fe, polarised, ferromag., evidence for K-shell polarisation of ¹²C ions via mol. orbital promotion 0-71273
Fe, transient magnetic low velocity field 0-80642
Fe-⁴⁸V, nucl. orientation of ⁴⁸V, γ -ray anisotropy obs. and NMR meas. 0-97169
GdZrFe₂, hyperfine field at Gd, TDPAC meas. 0-93214
Hf(SO₄)₂, elec. quadrupole interaction, TDPAC technique, coincidence system 0-93216
Hg electric field gradients at different Be lattice sites, gamma-spectral study 0-80224
Hg, quadrupole interactions in Zn, lattice location, gamma spectral study 0-80227
HoVO₄, below 1K, nuclear orientation study of Van Vleck enhanced nuclear antiferromagnet 0-88899
¹¹¹In, nucl. orientation coeffs., nucl. mag. moment 0-97168
La:Eu²⁺, liquid, γ -ray spectra observation of exchange interaction 0-84672
Mg, quadrupole interaction of ¹⁸¹Ta, gamma-spectral study 0-80228
NH₄Cl, ¹³N zero point vibr. energy from nuclear photon scattering 0-59593
Ni alloys, dil., hyperfine field distribs., DPAC meas. 0-93222
Ni dynamic exponent, crossover obs., TDPAC meas. 0-108021
Ni, polarised, ferromag., evidence for K-shell polarisation of ¹²C ions via mol. orbital promotion 0-71273
Ni, self implantation damaged, crit. behaviour, perturbed ang. distrib. meas. anal. 0-60476
Ni-Cu(Zn)(In), implantation damaged, crit. behaviour, perturbed ang. distrib. meas. anal. 0-60476
Pd_{1-x}MnSb Heusler alloys, magnetic hyperfine fields on ¹¹¹Cd, TDPAC and magnetisation meas. 0-93219
PrIn₃, nucl. orientation of ¹⁴⁴Pm in singlet ground state, exchange interaction and cryst. field splitting obs. 0-71275
Sc-Ru, elec. field gradient and temp. depend. TDPAC meas. 0-60477
Si:In, clustering and precipitation, time-dependent perturbed ang. correlation meas. 0-65234
Sm-Eu alloy, dil., mag. and elec. hyperfine interac., TDPAD obs., paramag. behaviour, exchange integral 0-103908
Tb-Ta(Cd), elec. quadrupole interaction, temp. and press. depend., TDPAC meas. 0-60469
U₃O₈ enrichment standards, gamma-ray spectra 0-78378
Y-Ru, elec. field gradient and temp. depend. TDPAC meas. 0-60477

gamma-ray spectrometers

- see also *gamma-ray spectra*
Compton-suppression spectrometer, Ge control detector, dead layer minimisation 0-99400
computerised gamma spectrometer system for meas. isotopic and total Pu conc. in solns. 0-63363
large capacity sample changer for fully automated gamma ray spectroscopy 0-58021
Mossbauer furnace for amorphous alloy investigations 0-98916
Mossbauer spectrometer NP 255, measuring capacity enlargement (*Czech*) 0-73558
multi-channel analyser, portable microprocessor controlled, accessories, data acquisition 0-63474
ninety-channel Cherenkov mass spectrometer for high-energy electrons and gamma quanta (the 'photon' installation) 0-91362
Pioneer Venus Orbiter Gamma Burst Detector 0-67505
protection and operation simplification, by relay device attachment 0-57447
pulse shape analyser, effect of pulse pile-up on discrimination between neutrons and gamma rays 0-91402
scintillation detector, gain stabilising scheme, gated radioactive source and broad digital window 0-63453
spent fuel verification by gamma-ray spectroscopy for materials safeguards 0-78422
stabilized spectrometer for scattered γ -radiation, analysis of operating quality 0-69009
CdTe detector, performance compared to HgI₂ detector 0-58062
Ge spectrometers, cooled, on P78-1 satellite 0-58019
Ge(Li) detector efficiency determ. for gas bomb geometries 0-78486
Ge(Li) detectors for γ -radioactivity in rocks and soils 0-67418
Ge(Li), in situ meas. of fission product plateau in HTGR 0-73881
Ge(Li) semiconductor, used simultaneously with NaI(Tl) scintillation spectrometer, in neutron activation cross-section meas. 0-78485
Ge(Li) summing-up effects, optimisation of detector-target geometry for in-beam γ -spectroscopy 0-74070
HgI₂ detector, performance compared to CdTe detector 0-58062
HgI₂ detectors, γ - and X-ray detection, solution grown crystals 0-63452
NaI 4 γ multidetector system for exam. of nuclear struct. and reactions at high ang. momentum, theory 0-74071
NaI(Tl) scintillation spectrometer, used simultaneously with Ge(Li) semiconductor, in neutron activation cross-section meas. 0-78485
Pu, isotopic composition, nondestructive anal. using gamma spectrometry 0-63392

gamma-ray transport see photon transport theory

gamma-rays

No entries

gamma transition see glass transition

Gamow-Teller transitions see beta-decay

garnets

includes ferrimagnetic insulators, $M_3Fe_2O_{12}$; for rock-type garnets, $MM'(SiO_3)_2$, see minerals

see also ferrimagnetic properties of substances

bubble film, magnetoelastic interactions 0-65976

bubble garnet film, non-implanted, surface mag. struct. 0-84628

bubble garnet film, saturation velocity, in-plane field effects 0-108041

domain wall oscillations, bubble domain wall motion 0-108042

epitaxial ferrite-garnet films with inversion layers, behaviour of cylindrical

mag. domains, visual tracking method 0-71139

epitaxial film, stress induced magnetocrystalline anisotropy 0-71013

epitaxial films, easy magnetisation axis orientation 0-60383

films, meas. of Faraday effect and susceptibility using magneto-optical

apparatus 0-105680

films with orthorhombic anisotropy, domain wall motion 0-80580

growth induced anisotropies, large, arising from preferential occupation of

Ir^{4+} and Mg^{2+} on Fe sites 0-75754

IR reflectivity, ATR, Voigt and Faraday expts. 0-66180

large growth-induced anisotropy to preferential occupation of Fe sites

0-75754

magnetic bubble materials, props. and preparation models, review

(Rumanian) 0-93149

magnetic properties and applications, structural props. 0-65760

rare earth ferrite garnets, phase transitions, field-induced spin-orientational

0-75767

rare earth garnets, RIG, ($R = Tb, Dy, Ho, Er$), spontaneous Faraday rot.

rel. to sublattice magnetisation 0-66159

rare earth iron, two-sublattice ferrimags., mag. polaritons 0-65845

rare earth iron garnets, anisotropic, mag. props., high field and low temp.

0-75801

superexchange operator and cryst. field interactions 0-59931

two-layer mag. structures, thermomag. recording 0-100588

YIG films, spin wave dispersion eqn. for delay lines (Russian) 0-88736

Bi-garnet thick layers, regular domain structure, magneto-optical diffr. of

light 0-108188

(BiTm) $_3$ (FeGa) $_2$ O $_2$ ion implanted epitaxial garnet film, bubble domains,

cryst. struct. disorder 0-93150

Ca $_2$ Fe $_2$ Ge $_2$ O $_2$ garnet, light absorpt. spectral study 0-93322

Ca $_2$ Mn $_2$ Ge $_2$ O $_2$ garnet, metamagnetic transition, high anisotropy peculiarities

(Russian) 0-60274

DyAG, antiferromag., induced staggered mag. fields 0-65810

DyAG, antiferromag., induced staggered magnetic fields, microscopic

mech. 0-80527

DyAG, electrostatic model of cryst. field 0-59945

Dy $_2$ Ga $_2$ O $_2$, dipolar magnet, sp. ht. and magnetisation meas. 0-60344

Dy $_2$ Ga $_2$ O $_2$, induced staggered mag. fields, neutron diffr. study 0-60196

ErIG, high-field magnetisation, low temp. mag. anisotropy 0-75802

ErIG, superexchange operator and cryst. field interactions 0-59931

EuEr $_2$ Ga $_2$ O $_2$, garnet thin films, magnetisation orientation, temp.

depend. 0-71125

EuIG:Ga(Al), pure and doped, mag. anisotropy, magnetisation meas.

0-60240

(EuLu) $_2$ (FeAl) $_2$ O $_2$, film epitaxial growth on Gd $_3$ Ga $_2$ O $_2$ substrate, mag.

props. 0-65402

Fe garnet, optical radiation interaction with magnetostatic waves

0-76009

Fe garnets, sublattice magnetisation curves, Mossbauer study 0-75808

(Gd, Bi) $_3$ (Fe, Ga) $_2$ O $_2$ magneto-optic LPE garnet films, high-energy

heavy ion irradiat. props. 0-71390

(Gd,Tm,Y) $_3$ (Fe,Ga) $_2$ O $_2$ LPE garnet thin films, magnetocrystalline anisotropy

0-93147

GdAG, electrostatic model of cryst. field 0-59945

Gd $_3$ Ga $_2$ O $_2$, flux growth and nucleation temp. determ. (Chinese) 0-60761

Gd $_3$ Ga $_2$ O $_2$, IR refl., ATR, Voigt and Faraday expts. 0-66180

Gd $_3$ Ga $_2$ O $_2$, mag. phase diagram, AC susceptibility meas. 0-60265

Gd $_3$ Ga $_2$ O $_2$, X-ray topography and double-crystal diffraction 0-92534

Gd $_3$ Ga $_2$ O $_2$:Ho $^{3+}$, stimulated emission at low temps. 0-106526

GdIG, IR refl., ATR, Voigt and Faraday expts. 0-66180

GdIG, local mag. anisotropy in stress field of single dislocation 0-88744

(LaTmCa) $_3$ (FeGe) $_2$ O $_2$, mag. loss and domain wall mobility 0-65980

LuAG, electrostatic model of cryst. field 0-59945

Lu $_3$ Al $_2$ O $_2$:Ho $^{3+}$, stimulated emission at low temps. 0-106526

Nd $_3$ Ga $_2$ O $_2$, floating zone method growth, interface shapes 0-60775

Nd $_3$ Ga $_2$ O $_2$:Nd $^{3+}$, radiationless decay processes, laser photoacoustic spectroscopy

meas. 0-84766

SmIG, mag. phase transitions, Mossbauer spectroscopy obs. 0-80509

(SmLu) $_3$ (FeAl) $_2$ O $_2$, film epitaxial growth on Gd $_3$ Ga $_2$ O $_2$ substrate, mag.

props. lattice mismatch 0-65402

Sm $_2$ Y $_2$ Fe $_3$ Ga $_2$ O $_2$, epitaxial films, uniaxial mag. anisotropy, ferrimag.

reson. study 0-80577

TbAG, reson. electronic Raman effect, interferences, lifetime meas.

0-93294

TbIG, [111] magnetoelastic props., rel. to Cotton-Mouton birefringence,

90-500K 0-103876

Tb $_{0.75}$ Y $_{0.25}$ Fe $_2$ O $_2$ garnet, mag. transition, mag. props. anomaly 0-93120

Tm ferrogarnet film, cylindrical mag. domain motions, domain boundary

oscills. (Russian) 0-71140

TmAG, Mossbauer study of crystal field props. 0-66082

Tm $_2$ Ga $_2$ O $_2$, Mossbauer study of crystal field props. 0-66082

(Y,Sm,Ca) $_3$ (FeGe) $_2$ O $_2$ epitaxial films, mag. props., growth condition

effects 0-97124

Y garnet, inhomogeneous collective magnon oscill. excited by RF field

(Russian) 0-100582

Y-Sm ferrogarnet (Russian) 0-71140

YAG, as substrate for Er $_3$ Al $_3$ -Ga $_2$ O $_2$ LPE film for solid laser 0-93419

YAG crystals, dislocations and inclusions, birefringence topography obs.

garnets continued

YAG:Er, elastic wave damping, 300 to 1500 MHz, impurity effects

0-92602

YAG:Ho $^{3+}$, spectroscopy, stimulated emission 0-93374

YAG:Ho $^{3+}$, stimulated emission at low temps. 0-106526

YAG:Nd crystal, orientation influence on thermally induced birefringence

(Chinese) 0-88958

YAG:Nd $^{3+}$, radiationless decay processes, laser photoacoustic spectroscopy

meas. 0-84766

Y $_3$ (Al $_{0.5}$ Ga $_{0.5}$) $_2$ O $_2$:Nd $^{3+}$, radiationless decay processes, laser photoacoustic

spectroscopy meas. 0-84766

Y $_3$ Al $_2$ O $_2$ crystal growth from melt, gas bubble capture theory 0-64941

(YBiEr) $_3$ (FeGa) $_2$ O $_2$ ferrite-garnet film, micron cylindrical mag. domains,

high recording density 0-65978

(YErCa) $_3$ (FeGe) $_2$ O $_2$, mag. loss and domain wall mobility 0-65980

(YEuCa) $_3$ (FeGeSi) $_2$ O $_2$, mag. loss and domain wall mobility 0-65980

(YEuTm) $_3$ (GaFe) $_2$ O $_2$ ferrite garnet films, mag. bubbles, translational

motion, mechanism for inertial effects 0-100606

YFe $_{5-x}$ Al $_x$ O $_2$, impurity redistrib. kinetics, temp. depend., vacancy effects

0-75263

Y $_3$ Fe $_{5-x}$ Al $_x$ O $_2$, permeability spectra rel. to microstruct. 0-71100

Y $_3$ Fe $_{5-x}$ Al $_x$ O $_2$, mixed garnet, cation distrib., temp. depend., magnetisation

study 0-79831

Y $_3$ Fe $_{5-x}$ Co $_x$ Si $_2$ O $_2$, spin reorientation, NMR and ferromag. reson.

meas. 0-65890

YFe $_4$ Ga $_2$ O $_2$ domains, neutron depolarisation and Faraday rotation study

0-93137

YFe $_{5-x}$ Ga $_x$ O $_2$, impurity redistrib. kinetics, temp. depend., vacancy effects

0-75263

Y $_3$ Fe $_4$ Ga $_2$ O $_2$, domain struct., neutron depolarisation and Faraday rot.

0-71084

Y $_3$ Fe $_{5-x}$ Ga $_x$ O $_2$, mag. domains and cryst. defects 0-75789

Y $_3$ Fe $_{5-x}$ Ga $_x$ O $_2$, mixed garnet, cation distrib., temp. depend., magnetisation

study 0-79831

Y $_3$ Fe $_{5-x}$ Gd $_x$ O $_2$, permeability spectra rel. to microstruct. 0-71100

Y $_3$ Fe $_2$ O $_2$ LPE growth on Gd $_3$ Ga $_2$ O $_2$ substrates, substrate orientation

effect 0-66438

YGaIG, magnetoelastic wave propagation time dispersion reduction

0-75836

Y $_3$ Ga $_2$ O $_2$:Nd $^{3+}$, radiationless decay processes, laser photoacoustic spectroscopy

meas. 0-84766

Y $_{2.5}$ Gd $_{0.5}$ GaFe $_2$ O $_2$, garnet thin films, magnetisation orientation, temp.

depend. 0-71125

YGGdIG, with various domain wall orientations, natural spin reson.

0-66040

YGGdIG film, amorphous, mag. bubbles obs. and structural transformation

0-75824

YGdTmFe $_4$ Ga $_2$ O $_2$ epitaxial films, bubble-domain lattices with specified

parameters 0-60386

(YGGdM) $_3$ (FeGa) $_2$ O $_2$ epitaxial film, formation of lattice of cylindrical

mag. domains from stripe domains (Russian) 0-80579

(YGGdYbBi) $_3$ (FeAl) $_2$ O $_2$ ferrite-garnet films, effect of in-plane field on

dynamics of domain walls 0-65979

(YGGdYbBi) $_3$ (FeAl) $_2$ O $_2$ epitaxial garnet film, uniaxial ferromagnet

domain struct., phase transition (Russian) 0-108044

YIG, Bi-substituted, LPE, domain wall reson. 0-60387

YIG, Bloch line mass and mobility in a domain boundary (Russian)

0-93138

YIG, Brillouin-Mandelstam scattering from thermal and excited magnons

0-70980

YIG crystals, bulk growth from high temp. solns., props. 0-66413

YIG, cylindrical mag. domains, translational motion 0-108043

YIG, domain wall mobility and mass meas. method (Russian) 0-108033

YIG, electron and γ -irrad., photomagnetic effect 0-103877

YIG, electrostatic model of cryst. field 0-59945

YIG, Faraday effect, influence of mag. field on sublattice contributions

0-88975

YIG film, magnetostatic surface wave propag. in nonuniform mag. field

0-80574

YIG film, periodically corrugated, insertion loss, reson. linewidth effect

0-80614

YIG, floating zone method growth, interface shapes 0-60775

YIG, MW dielectric losses, causes and reduction (Chinese) 0-75930

YIG, magnetic domain wall motion in high drive fields 0-65955

YIG, magneto-optical Kerr effect, reflectivity spectra 0-66157

YIG, magnetoelastic wave propagation time dispersion reduction 0-75836

YIG, multiple mag. layer structures, magnetostatic surfacewave propag.

0-88839

YIG, Neel point behaviour in stoichiometry vicinity 0-88750

YIG, nonreciprocal attenuation of magnetoelastic Rayleigh waves

0-60399

YIG, one-magnon Raman scatt., Faraday rot. 0-66156

YIG, open die hot pressing, spin wave and FMR line width 0-89170

YIG, permeability, domain rot. and wall displacement contrib. 0-80564

YIG, permeability spectra rel. to microstruct. 0-71100

YIG, polycryst., initial and reversible parallel susceptibilities, hydrostatic

press. effects 0-75835

YIG sandwiched between grounded dielectric layers, magnetostatic bulk

wave propagation 0-60380

YIG single crystals, liq. flux growth, obs. 0-66416

YIG, sound vel., temp. depend., phonon scatt. processes 0-96598

YIG, spin wave parametric excitation threshold at low temp. 0-97084

YIG, substituted, magnetite nucleation in transitional zone, ionic process,

lattice imaging 0-70424

YIG, thermomag. anal. by electron diffr. 0-108035

YIG, thin film, Brillouin scattering from spin waves 0-65843

YIG thin film gyromag. waveguide, on GGG substrate, optical propag.

props. Faraday effect 0-74513

YIG, thin films, magnetostatic modes at Q-band freq. 0-65828

YIG, vitreous electric-field-gradient distrib., Mossbauer quadrupole splitting

meas. 0-75901

YIG: Si single crystals, mag. props. 0-107981

YIG:Ga, oxidising effects of high temp. annealing in reducing atmosphere

0-66696

YIG:Co film, influence of stress induced anisotropy on domain struct.

0-100605

YIG:Ga(Sc), magneto-optical Kerr effect, reflectivity spectra 0-66157

YIG:La,Ga, film, LPE-grown, Ga incorporation, depend. of magnetisation

on growth rate 0-84627

YIG:La(Ga) films, ferromagnetic resonance, ion implantation effect

0-97145

III-V semiconductors continued

- GaP single cryst., defect distrib. near abraded surface 0-92533
 p-GaP, spin-flip Raman scattering, review 0-108209
 GaP, temp. coeff. of induced birefringence 0-93277
 GaP, thermal expansion below room temp. 0-79963
 GaP, VPE layer structures for LED's, SEM, and TEM obs. of dislocation density reduction expt. 0-100425
 GaP, vapor-phase etching, mechanisms and kinetics 0-100934
 GaP:⁵⁶Fe(⁵⁷Fe)(⁵³Cr), paramag. centres, identification from ESR and ENDOR spectra 0-80600
 GaP:Bi,N, photoluminesc., electroluminesc., 4.2 to 300K, excitons and hole traps 0-108275
 GaP:Ce(Dy)(Pr) epitaxial films, photoluminesc. spectra 0-66294
 GaP:Co, optical spectra and Zeeman anal. of Co 3d⁷ state 0-66247
 GaP:Co(Ni), photolum. excitation spectroscopy 0-80841
 p-GaP:Cr, hole traps, ESR studies 0-75843
 GaP:Cr epitaxial layers, Cr conc. profile determ. 0-65029
 GaP:Cs-O simultaneous adsorption, oxidation interface chemical struct. 0-103584
 GaP:Fe, double Fe-thermal acceptor centre, energy states 0-96823
 GaP:Fe, optical absorption spectrum and Faraday effect 0-108245
 GaP:Fe³⁺ ESR spectrum, elec. field, uniaxial compression influence 0-103882
 GaP:Ge, ENDOR study, superhyperfine interactions 0-93210
 GaP:N, bound exciton absorpt. line asymmetry, electroabsorption spectra 0-71459
 GaP:N LED structures, local dopant conc. determ. using SEM cathodolum. spectra 0-101057
 GaP:Ni(Fe), multivalence impurities, EPR and optical absorpt. meas. 0-75844
 GaP:S, ground and excited states of bound exciton complex, stress effects 0-65463
 GaP:S(Se), donor bound exciton excited states 0-66284
 GaP:Ti(Co)(Ni), positron annihilation meas. rel. to deep levels study 0-60712
 GaP:Zn, O, influence of impurity-absorbed illumination on luminesc. 0-93395
 p-GaP:Zn,S, spin polarisation of donors and acceptors in mag. field, optical and microwave study 0-93393
 p-GaP:Zn-electrolyte interface, electrochemical LED, luminescence obs. 0-84507
 GaP/Si heterostruct., differential thermal contraction, plastic deform., fracture 0-108494
 GaP-GaAsP planar heterostructure strip ridged waveguide under mech. load, polarisation modulation 0-96038
 GaP-Pd contact system, low temp. alloyed contact formation 0-100519
 GaP-Si, heteroepitaxial growth, electronic and optical props. 0-104075
 GaP-Si, heterostructure, zincblende-on-diamond type systems, MBE growth, (110) orientation as preferred orientation 0-80099
 GaP(As), liquid interaction parameters determ., 580-670°C 0-65197
 GaP,As_{1-x}N, luminesc. of N bound state excitons, local-environment effects 0-100691
 GaSb (110), surface core-level binding-energy shifts 0-103737
 GaSb (110)/Au interface, heat-treated, struct. and chem. state, angle-resolved XPS 0-97400
 GaSb, accumulation layer localised carriers interaction with LO phonons, Raman interference lineshapes 0-93338
 GaSb, acoustic wave attenuation, phonon viscosity and dislocation drag 0-70319
 GaSb, adsorption and desorption of Cs, LEED, AES, and photoemission meas. 0-70532
 GaSb based eutectics, thermal cond. and diffusivity, 300-700K, phonon mechanism 0-103526
 GaSb, bulk and epitaxial, IR reflect. meas., carrier conc. and mobility determ. 0-80769
 GaSb, core exciton binding energies 0-80188
 GaSb, defect concentration determ. model, Hall effect 0-103385
 GaSb, diffusion of In, 520 to 712°C 0-79995
 GaSb, electrochemical sectioning and surface finishing 0-108611
 GaSb, electroliquid epitaxial growth 0-89160
 GaSb films, elemental incorporation probability modification by ion bombard. during growth 0-80118
 p-GaSb, heavily doped, LO phonon-carrier interaction, Raman interf. lineshapes 0-93319
 GaSb interface with oxide, photoemission obs. of energy levels induced by adsorpt. 0-93000
 GaSb, LEC growth, Hall coeff. 0-89133
 GaSb LEC single crystal growth, novel encapsulant material 0-93475
 GaSb, lattice dynamics, phonon freq., bond bending force model calcs. 0-70335
 GaSb, piezoresistive vibrating circular membrane, reflectance light modulation 0-97232
 p-GaSb, saturation characts. over CO₂ laser spectrum 0-83646
 GaSb, solid solns., impact ionisation, cond. and valence band effects 0-65583
 GaSb:Sn, p-n junction, electroluminesc. and photoluminesc. 0-66306
 GaSb-InAs system, (110) surface and interface electronic struct. 0-100494
 GaSb(As) substrates for Al₂O₃ film, ion beam etching defect detection 0-89155
 GaSe films, optical props. at lattice vibr. freqs., IR and Raman spectra 0-60696
 Ga, Brillouin spectra, light scatt. cross section for surface ripples 0-71434
 Ge-GaAs, heteroepitaxial systems, misfit dislocations obs. using HV electron microscopy 0-100242
 Ge-GaAs heterojunction, elec. and recomb. props., interface defect effects 0-80365
 Ge-InAs based MIS struct., avalanche carrier multiplication 0-88566
 n-Ge-n-GaAs isotype heterojunctions, modelling, characts. 0-103747
 Hg-InP Schottky-barrier diode, contact times, I-V characts. 0-96971
 (In,Ga)(As,P) binary, ternary and quaternary, hydride vapour phase epitaxy, cryst. growth and props. 0-66434
 In-Ga-P ternary system, low temp. phase diagram rel. to epitaxial growth 0-84916
 p-In_{0.77}Ga_{0.23}As/Ag photocathode, field assisted photoemission to 2.1 microns 0-76130
 In_{1-x}Al_xAs, band gap, IR absorpt. spectra meas. 0-66205
 In,Al_{1-x}P, proportional ingredient content determ. by X-ray fluoroscopy 0-97747

III-V semiconductors continued

- InAs and solid solutions, recombination mechanisms of excess carriers, luminesc. obs. 0-97337
 InAs, anomalous avalanche breakdown 0-80284
 InAs, electrical conductivity and thermoelectric power charge due to melting 0-100490
 InAs films, MBE grown on GaAs, electron mobilities, lattice mismatch effect 0-80419
 InAs, intensity of 3-phonon diffuse scattering of X-rays 0-84027
 InAs, melt, mutual diffusion of components 0-88345
 n-InAs, photoelectric props., inhomogeneous impurity distrib. 0-107867
 InAs, resist. inhomogeneity meas. with single-sonde potential method 0-65549
 p-InAs, saturation characts. over CO₂ laser spectrum 0-83646
 InAs, thermal oxidation, growth rate and chem. comp., temp. depend. 0-108619
 InAs, transient dynamic response calculation by Monte Carlo techniques 0-107796
 InAs, two dimensional accumulation layer, Anderson localisation 0-107871
 InAs:Cd, Te, donor-acceptor interaction, elec. cond. and Hall coeff. meas. 0-59988
 InAs:Mn²⁺, Jahn-Teller effect for ion impurities 0-107753
 InAs:S(Mg), ion implanted, photocond., photo-EMF, and optical absorpt. spectra 0-70763
 InAs:Sn, single crystals, defect formation 0-88606
 InAs-GaSb superlattices, mag. field induced semimetal-semicond. transition 0-65656
 InAs,P_{1-y} alloy, composition effects in growth by MBE 0-59816
 InAsSb/GaSb broad-spectral-band IR detector, backside-illum. heterostructure approach 0-73450
 InBi single crystal, deform. mode under dynamic indentation 0-88163
 InGaAs, LPE, diffusion-limited step-cooling technique, layer thickness and composition 0-84402
 InGaAs-InP punch-through type photodetector fabricated by VPE 0-68253
 In_{0.1}Ga_{0.9}As, quantitative anal. with SIMS 0-101052
 In_{0.53}Ga_{0.47}As p-i-n photodiode-FET photoreceiver for 1.0 to 1.7 μm wavelength optical fibre communications systems 0-58794
 In_{0.53}Ga_{0.47}As photodiodes with dark current limited by generation-recombination and tunneling 0-107893
 p-In_{0.53}Ga_{0.47}As-InP on InP, elec. and optical props. 0-75662
 In_{0.53}Ga_{0.47}As-InP avalanche photodiode with guard-ring struct., characts. 0-96939
 In_{0.53}Ga_{0.47}As-InP avalanche photodiode structure for 1 to 1.6 μm region 0-98978
 In_{1-x}Ga_xAs layer on InP, misfit dislocation free, LPE growth 0-108364
 In_xGa_{1-x}As:Si p-n structs., electrolum. spectra, 77 to 300K 0-93408
 In_xGa_{1-x}As:Zn, lattice matching to InP, LPE growth conditions 0-70541
 InGaAsP, anodic oxidation, refractive indices 0-97601
 InGaAsP avalanche photodiode, 1.3 μm, noise performance, -190°C 0-57370
 InGaAsP avalanche photodiodes, breakdown mechanism, donor conc. effect 0-70710
 InGaAsP, bandgap energy by electroreflectance and photoluminesc. spectra 0-107700
 InGaAsP DH, luminesc., quantum efficiency determ. 0-108273
 InGaAsP DH lasers with etched reflectors, fabrication, current density 0-64050
 InGaAsP LED sources, for near-IR absorpt. meas. 0-77135
 InGaAsP, LPE, diffusion-limited step-cooling technique, layer thickness and composition 0-84402
 InGaAsP LPE heterostructs., interface grading, Auger depth profile 0-103585
 (InGa)(AsP) laser system, VPE growth using metal organic sources or halide transports 0-99748
 InGaAsP photodetector, improved two wavelength demultiplexing 0-58795
 InGaAsP single-mode CW ridge-waveguide laser emitting at 1.55 micron 0-58584
 InGaAsP strip-buried-heterostructure high-output power laser 0-58540
 InGaAsP strip-buried heterostructure laser, high output power, operation 0-58559
 InGaAsP/InP DH lasers, temp. depend. characts. 0-58541
 InGaAsP/InP DH stabilised 1.3 μm laser diode-isolator module for hybrid optical integrated cct. 0-58583
 InGaAsP/InP injection lasers for long wavelength (1.1 to 1.6 μm) optical communication 0-58582
 InGaAsP/InP phototransistors, fabrication by LPE, photodetectors 0-95139
 InGaAsP-InP buried crescent injection laser emitting at 1.3 μm with low threshold current 0-87404
 InGaAsP-InP buried heterostructure lasers emitting at 1.3 μm, accelerated ageing characts. 0-95898
 InGaAsP-InP CW lasers, 1.5-1.7 μm, VPE 0-78861
 InGaAsP-InP DH laser, 1.55 μm, low temp. LPE growth for room-temp. CW operation 0-64045
 InGaAsP-InP DH LED, high temp. aged, dark-spot defects, TEM obs. 0-66300
 InGaAsP-InP DH lasers, interfacial recomb., influence on oscill. characts. 0-87393
 InGaAsP-InP DH lasers, spatial hole burning, spontaneous emission saturation, direct obs. 0-95892
 InGaAsP-InP DH lasers, temp. dependence of threshold and elect. characts. 0-99725
 InGaAsP-InP DH lasers, perturbed InP growth, photoluminesc. study 0-106518
 InGaAsP-InP DH laser, threshold current, temp. depend. 0-106521
 InGaAsP-InP high-gain heterojunction phototransistor 0-103745
 (InGa)(AsP) laser system, 1 μm wavelength, lattice matching techniques 0-99748
 InGaAsP-InP layers, grown by LPE techniques, lattice const., bandgap, thickness and surface morphology meas. 0-59818
 In_{0.83}Ga_{0.17}As_{0.37}P_{0.63}, reactive ion etching of III-V compounds 0-58813
 In_{1-x}Ga_xAs_yP_{1-y} DH lasers for 1.3 and 1.5 μm optical fibre communications 0-91817
 In_{1-x}Ga_xAs_yP_{1-y}, electron effective mass from Shubnikov-de Haas meas. 0-80298
 In_{1-x}Ga_xAs_yP_{1-y} epitaxial layer, far IR refl. spectra, lattice vibrs. 0-97282

III-V semiconductors continued

- In_{1-x}Ga_xAs_{1-y}P_y, evidence for alloy scatt. from press. induced changes of electron mobility 0-88548
 In_{1-x}Ga_xAs_{1-y}P_y, far IR reflection spectrum 0-60612
 In_{1-x}Ga_xAs_{1-y}P_y, Hall mobility, comp. depend. 0-75587
 In_{1-x}Ga_xAs_{1-y}P_y, hole mobility over temp. range 77 to 300K 0-60111
 In_{1-x}Ga_xAs_{1-y}P_y/InP 1.5 μm room-temp. CW laser fabrication and operation 0-64070
 In_{1-x}Ga_{1-x}As_{1-y}P_y, epitaxial layers, characterisation and relation to lattice matching 0-100540
 In_{1-x}Ga_{1-x}As_{1-y}P_y, photodetector diode on InP substrate dark currents, tunnelling, energy gaps, effective masses 0-70805
 In_{1-x}Ga_{1-x}As_{1-y}P_y, surface and dielec.-semicond. interface props. 0-93001
 InGaP/InGaAs struct. for transferred electron photocathodes, VPE growth and characterisation 0-76193
 In_{0.3}Ga_{0.7}P, N free and implanted, photoluminescence study 0-97322
 n-In_{1-x}Ga_xP, direct-gap semiconductor, cathodoluminesc., electron irradiation effects 0-108283
 In_{1-x}Ga_xP, epitaxial layers, compositional inhomogeneity 0-88444
 In_{1-x}Ga_{1-x}P, proportional ingredient content determ. by X-ray fluorescence 0-97747
 InGaPAs LPE layers, compositional inhomogeneity, photoluminesc. obs. 0-75451
 In_{1-x}Ga_{1-x}P_{1-y}As_y, lattice-matched epitaxial layers, LPE growth on GaAs(100), characterisation 0-75465
 In_{1-x}Ga_{1-x}P_{1-y}As_y, lattice matched to InP, electroluminescence obs. 0-93416
 In_{1-x}Ga_{1-x}P_{1-y}As_y, In_{1-x}Ga_{1-x}P_{1-y}As_y, visible spectrum multiple-quantum-well heterostruct. lasers 0-106537
 In_{1-x}Ga_{1-x}P_{1-y}As_y, InP coupled multiple quantum-well heterostructure laser diodes, threshold current temp. depend. 0-78855
 In_{1-x}Ga_{1-x}P_{1-y}As_y, electron effective mass and Dingle temp., Shubnikov-de Haas oscills. 0-59859
 In_{1-x}Ga_{1-x}Sb, energy gap, temp. depend. and photovoltaic effect 0-70746
 In_{1-x}Ga_{1-x}Sb films, elec. props., preparation 0-100473
 InN film growth by reactive sputtering in Ar-N₂ discharge, mechanism 0-89107
 In₂O₃-InN film growth by reactive sputtering in N₂-O₂ discharge, mechanism 0-89108
 In₂O₃-SnO₂-InP solar cell junctions, efficiency, InP surface props. 0-85288
 InP (110) surfaces, cleaved and polished-sputtered-annealed, LEED and AES study 0-103550
 InP avalanche photodiodes, microplasmas, investigation 0-60018
 n-InP, compensated, elec. props., space-charge effects 0-65569
 InP, compensation ratio, electron mobility and free-carrier absorpt. 0-80261
 InP, depend. of phonon spectrum on hydrostatic press., Raman spectra 0-93315
 InP detector, unbiased, using Schottky-barrier diode, operation in submm. wave region 0-105707
 InP, electron transport props., mag. field and temp. depend. 0-92888
 InP, epitaxial, kinetics of VPE 0-60790
 InP epitaxial films, grown on heavily doped substrates, carrier mobility study, magnetoresist. meas. 0-60116
 n-InP, epitaxial layer, (100) surface chemistry, ESCA study 0-103552
 InP, Faraday interband effect subjected to quantising mag. fields 0-97246
 p-InP field-assisted photocathodes, quantum efficiency 0-84831
 InP film, electron-beam annealed, surface conduction 0-84500
 InP films, organometallic VPE grown, props. 0-96753
 InP grown by LPE, method for free In removal from surface 0-84860
 n-InP, γ-ray and electron irradiation, annealing of radiation point defects, elec. cond. and Hall coeff. meas. 0-65051
 n-InP, heat treatment in controlled P vapour 0-88137
 InP homojunction solar cell, antiref. coated, high-efficiency 0-104505
 InP, impact ionisation by electrons and holes 0-100467
 n-InP, impurity and minimum metallic cond. in mag. field 0-103731
 InP integrated optical communication components, overview 0-79012
 InP interface with oxide, photoemission obs. of energy levels induced by adsorpt. 0-93000
 InP inversion-type MISFET with SiO₂ gate insulation interface props., elec. drift 0-93002
 InP, ion-implanted layers, close contact capless annealing, elec. props. 0-84192
 InP, LEC growth of dislocation free crystals 0-89134
 InP, laser-induced microscopic etching 0-76379
 InP, lattice dynamics and phonon parameters bond bending force model 0-59595
 InP, lattice matching to In_{1-x}Ga_{1-x}As_{1-y}Zn, LPE growth conditions 0-70541
 InP, luminescence, hot electron effects 0-66277
 InP, MBE, substrate temp. related degradation mechanisms 0-65385
 InP MIS devices, diffusion, chemical reactions, contamination, AES and SIMS 0-72066
 n-InP, MOS solar cells, electrical and photovoltaic characteristics 0-85276
 InP, model for ~1.10 eV emission band 0-66289
 InP n⁺-p⁺ homojunction solar cells, high efficiency, LPE layer growth, photolithographic fabrication 0-93929
 InP, noise calc. using Monte-Carlo method 0-75575
 p-InP, ohmic contact using Be-Au metalisation, low contact resist. 0-65677
 InP p⁺-n abrupt junctions, ionisation coeffs., photomultiplication meas. 0-65655
 InP p-n junction, grain boundary etching 0-96541
 InP photodiodes, dark current and breakdown characs. 0-70806
 InP, photoluminescence meas. using diamond-anvil press. cell 0-108256
 InP, press. depend. of direct absorption edge 0-93365
 InP, reactive ion etching of III-V compounds 0-58813
 InP single crystals, uniaxial compression deform. characs. 0-84991
 InP solar cells, thin film growth tech. and characterisation 0-89631
 InP, surface, pulsed electron beam processing, doping, annealing 0-75254
 InP, surface and dielec.-semicond. interface props. 0-93001
 InP, surface passivation using composite Al₂O₃ and native oxide, MIS characs. 0-93004
 InP, surface phonon polariton dispersion and damping, frustrated total internal refl. meas. 0-80792
 InP, surface recomb. vel., spec. optical techniques 0-70784
 InP, surface vacancies, bound state energy levels calc. 0-80340
 InP, VPE growth for MESFET's 0-103602
 InP, Zn diffused single-crystal, substitutional dopant and hole conc. meas. 0-75260

III-V semiconductors continued

- InP:Cd, doping by UV laser photodeposition 0-84191
 InP:Cd, p⁺-n⁻ junction form. by diffusion doping 0-84504
 InP:Cd(Zn), avalanche photodiode characs., impurity diffusion effects 0-70709
 n-InP:Cr, press. depend. of elec. resist. and Cr ionisation energy 0-80281
 InP:Cr²⁺, Jahn-Teller effect for ion impurities 0-107753
 InP:Fe shallow trap thermally stimulated cond. spectroscopy, photocond. spectrum under DC conditions 0-65585
 InP:SSD growth of low dislocation density crystals 0-89135
 InP/CdS epitaxial thin films on NaCl, HEED and TEM study 0-88446
 InP/In_{1-x}Ga_xAs_{1-y}P_y interfaces, sputter-profiled, depth resolution degradation by cone form. 0-80094
 InP/InGaAs heterojunction phototransistor, high-sensitivity 0-100505
 InP/InGaAsP avalanche photodiodes, with guard ring structure 0-100506
 p-type InP/Langmuir film MIS diodes, characs. 0-80384
 InP/SiO₂ interface formation, thermodynamic considerations 0-100529
 InP-Al interface struct., low temp. interaction, AES study 0-107661
 p-InP-Cd(Zn), ohmic contact formation on InP by laser photochemical doping 0-80369
 InP-Cu contact system, low temp. alloyed contact formation 0-100519
 InP-GaInAsP buried heterostructure lasers of 1.5 μm region, fabrication and characs. 0-74388
 InP-In_{1-x}Ga_xAs_{1-y}P_y-InP 1.55 μm DH room-temp. CW laser fabrication and operation 0-64071
 InP-In_{1-x}Ga_xAs_{1-y}P_y-InP 1.53 μm single-mode CW ridge-waveguide laser 0-64072
 InP-In_{1-x}Ga_{1-x}As_{1-y} alloy photocathodes, semiconductor photoemitters, field-assisted, 1-2 μm range 0-97396
 InP-InGaAsP p-n junction avalanche photodiodes, surface passivation techniques 0-100508
 InP-InGaAs heterojunction lasers and LEDs, 1.0 to 1.2 μm 0-74362
 InP-Si₃N₄ (SiO₂), interface props., plasma deposited dielectrics, n-channel MOSFET action 0-93003
 InP-SiO₂ interface, CVD problems, ESCA profiles 0-93497
 InP-SnO₂ heterojunctions, elec. and photovoltaic characs. 0-75628
 InP(As), liquid interaction parameters determ., 580-670°C 0-65197
 InP(Sb)(As) substrates for Al₂O₃ film, ion beam etching defect detection 0-89155
 InSb (110), cleaved, gap states, field effect meas. 0-84501
 InSb (110), surface struct. by elastic LEED, comparison with GaAs(110) and ZnTe(110) 0-80040
 InSb (110) surface, LEED intensity dynamical anal. 0-88412
 InSb, absorpt. edge, excitation study 0-93321
 InSb, accumulation layer localised carriers interaction with LO phonons, Raman interference lineshapes 0-93338
 InSb, anomalous avalanche breakdown 0-80284
 n-InSb, anomalous three LO phonon assisted cyclotron resonance 0-108078
 InSb, Auger-governed decay of laser-induced plasma, optical probing 0-76105
 InSb based eutectics, thermal cond. and diffusivity, 300-700K, phonon mechanism 0-103526
 n-InSb based MIS struct., carrier generation under nonequilibrium conditions 0-88640
 n-InSb, Brillouin instability in magnetostatic field 0-78909
 InSb, CESR at high mag. fields, scatt. mechanisms 0-93177
 InSb, carrier heating by microwave field, inertia effects 0-65580
 n-InSb, cond. electron cooling induced by CO laser and non-ohmic DC field 0-96941
 n-InSb, cond. electron spectra in quantised mag. field, impurity resonance scatt. (Russian) 0-93178
 InSb, convection in melts, and cryst. growth under large inertial accelerations 0-66421
 InSb, crystal growth from melt, facets and twin formation obs. (Chinese) 0-59409
 InSb, current-voltage characteristics at room temperature and high hydrostatic pressure 0-88560
 InSb, depletion layer, plasma and vibr. plasma type guided polaritons (Russian) 0-96933
 InSb, Einstein relation for inversion layers 0-103706
 InSb, electron-hole plasma instabilities, impact ionisation conditions, microwave emission 0-107840
 InSb, extrinsic and intrinsic, interaction of transverse magnetoresist. effects 0-65596
 n-InSb, Faraday effect in strong EM fields 0-93286
 InSb film, grown by MBE, RHEED study 0-100415
 InSb films, elemental incorporation probability modification by ion bombard. during growth 0-80118
 InSb, films, X-ray fluoresc. anal. method, long-term stability 0-61212
 InSb, galvanomagnetic props. of annealed single crystals 0-96909
 InSb, growth angle determ. from cryst. lateral face shape and solidified separation drops 0-103282
 p-InSb, heavily doped, LO phonon-carrier interaction, Raman interf. lineshapes 0-93319
 InSb, helicon beam form. during microwave transmission in mag. field 0-80308
 InSb, high-resistivity p-type or crystals of n-type, recombination processes, photocond. and photomag. effect meas. (Russian) 0-88567
 n-InSb, hot electron noise temp., Monte Carlo Calc. 0-107877
 InSb, impact ionisation and magneto-transport, high crossed elec. and mag. fields 0-107797
 InSb, impurity distribution, during epitaxial growth from liq. phase 0-88443
 p-InSb, influence of plastic deform. on elec. props. 0-103711
 InSb, intensity depend. interband Faraday rot. obs., saturation and reson. enhancement effects 0-108186
 InSb, ion implantation, anomalous radiation disordering 0-92553
 InSb, ion implanted, ellipsometric study 0-60537
 n-InSb, ionized impurity scatt. limited mobility, expt. 0-80274
 InSb lattice, static dielec. const. and carrier conc. meas. via gyrotropic sphere reson. 0-97143
 InSb MIS diode, anodised, C-V characs., effect of high elec. field pulse 0-60092
 n-InSb, MIS diode, time-dependent photovoltaic effect 0-75601
 p-InSb MIS struct., field effect studies 0-80386
 InSb MIS structure, effect of room background on noise props. 0-103755
 InSb MOS struct., capacitance of n-channel inversion layers, elec. field effects 0-80393
 InSb MOS structs., energy spectrum of traps in oxide layer 0-107922

III-V semiconductors continued

- InSb, magnetoacoustic wave excitation by acoustic wave propagation 0-88597
 p-InSb, magnetoconcentration effect in extrinsic cond. range 0-65593
 p-InSb, magnetoconcentration effect, negative differential conductance 0-70729
 n-InSb, microwave helicon resonances, carrier density, mobility, dielectric const. 0-96930
 InSb, morphological and structural changes due to ion bombardment 0-79843
 InSb n^+p junctions, photocurrent spectrum near long wavelength edge of fundamental absorption band 0-100483
 n-InSb, negative longit. magnetoresist., carrier conc. and mobility depend., 77K 0-60007
 InSb, neutron irradi., defect cluster form., effect on elec. props. 0-65062
 InSb, noise calc. using Monte-Carlo method 0-75575
 n-InSb, non-degenerate, linear longitudinal elec. cond., US wave effects in DC mag. field 0-88599
 InSb, nonlinear transmission of picosecond 10.6 μm pulses 0-106559
 InSb, optical constants and oxidation with various surface treatment (*Russian*) 0-88955
 InSb, phonon dispersion relations, eight-parameter bond-bending forces model 0-70334
 n-InSb, phonon-assisted cyclotron reson. strongly depend. on surface condition 0-70755
 n-InSb, photoconductivity mechanism, 4.2 to 77K 0-70766
 p-InSb, photoexcited exciton spin-flip scatt. 0-74434
 n-InSb, piezoelectric nondegenerate semicond., magnetoacoustic effects of nonparabolic band struct. 0-96948
 InSb, pinch effect at room temp. 0-65615
 n-InSb, proton irradi. defects energy level scheme, transport props. meas. 0-96576
 n-InSb, quasi-helicon waves instability 0-70741
 InSb, Raman scattering study of unoxidised Sb in anodic oxide films 0-88985
 InSb, reabsorbed radiative recomb. and photon recycling 0-76076
 InSb, recombination processes using impact ionization capture cross sections 0-75577
 InSb recrystallised thin films on mica substrate, elec. props. 0-70867
 InSb, refractive index and absorpt. coeff., cryst. orientation depend. 0-60536
 InSb, resist. inhomogeneity meas. with single-sonde potential method 0-65549
 n-InSb, semiconductors, plasma oscills. within submillimetre freq. range 0-84473
 p-InSb, shift of fundamental absorpt. edge in crossed elec. and mag. fields 0-76034
 InSb, single crystal, chem. and ion etching, surface changes (*French*) 0-108614
 n-InSb, spin polarisation, anisotropic size effect, effect on CESR signal 0-70743
 p-InSb, spin-flip Raman scattering, review 0-108209
 n-InSb, spin-magnetophonon resonance 0-96918
 n-InSb submillimetric-wave free-carrier Faraday effect in strong longitudinal elec. field 0-66164
 InSb substrate, room temp. CVD of Si_3N_4 0-71597
 n-InSb substrates, MIS struct. form. by reactive deposition of Si_3N_4 , C/V meas. 0-103752
 InSb, surface helicons in semiconductor plasma, theory 0-60019
 InSb, thermal cond., elec. cond., and thermoelec. power, press. depend. 0-59744
 InSb, thin films, electrophysical props. obs. 0-103765
 InSb, undoped and Te-doped, anomalous impurity segregation, Hall and mass spectrum meas. (*Chinese*) 0-59501
 InSb, X-ray topographic evidence of asymmetrical pre-yield behaviour 0-75229
 InSb: Cd, thermal conductivity down to 0.38K 0-107582
 InSb: Cd (Zn) (Ge), ion-irradiated, p-n conversion during heat treatment 0-96558
 n-InSb: Cr, deep impurities, elec. cond. and Hall coeff. meas., 4.2 to 120K 0-107791
 InSb: Cr, Zn and InSb: Zn, impurity centre behaviour, impurity conc. and Hall coeff. meas. 0-65490
 InSb: F, acceptor props. and diffusion coeff. of F 0-70643
 p-InSb: Ge, proton irradi. defects energy level scheme, transport props. meas. 0-96576
 InSb: Te, cryst. growth from melt, pulling method, US effects on facet growth 0-76169
 InSb-Au contact system, low temp. alloyed contact formation 0-100519
 InSb-NiSb, photovolt. effects rel. to theory of semicond. with internal elec. short circuits 0-65620
 InSb $_{1-x}$ Bi $_x$, metastable epitaxial film, phase diagram 0-76238
 InSb $_{1-x}$ Bi $_x$, multitarget RF sputtering, metastable phase, conductivity transition 0-76178
 In $_{1-x}$ Sn $_x$ O $_3$ -y-Ga $_x$ In $_{1-x}$ P(-InPAs $_{1-y}$) heterojunction solar cells, chemistry and prep. 0-94073
 n-Inb, anomalous Hall effect, stress depend. 0-65598
 Si $_x$ Ge $_{1-x}$ -GaAs, heterojunction, elec. and recomb. props., interface defect effects 0-80365
 SiO $_2$ -GaAs, vacuum evaporated system, acoustoelec. signal, interface props. 0-75646

III-VI semiconductors

- Al $_x$ Ga $_{1-x}$ As, modified-strip buried-heterostructure lasers, CW electro-optical properties 0-74359
 GaAs, polycrystalline films, meas. of effective diffusion length by SEM 0-80424
 GaAs-GaSe n-p heterojunction, elec. props., interface states 0-65670
 n-GaS, Bridgman crystals, hole traps, photocond. and thermal quenching study 0-75580
 GaS, elastic prop. anisotropy, Debye temp. (*Russian*) 0-88244
 GaS, infrared optical props., polarisation depend., vibr. modes 0-100658
 GaS, layer compound, long-wavelength phonons and elastic consts. 0-65175
 GaS, shallow core level spectra 0-104037
 GaS, Ge $_{1-x}$ valence band states, composition depend., photoemission spectra study 0-100434
 GaS $_{1-x}$ Se $_x$, mixed crystals, IR reflectivity spectra 0-66204
 GaS(Te)(Se), elastic characteristics, Debye temp., ultrasonic study (*Russian*) 0-79872
 GaSb film, polycrystalline, Hall mobility 0-97015

III-VI semiconductors continued

- GaSe, ^{110}Ag diffusion, temp. depend. and solution (*Russian*) 0-70467
 GaSe, anodic film form., in situ ellipsometric study 0-104318
 p-GaSe, back wall Schottky barrier cells, diffusion length, RT spectral response meas. 0-107806
 GaSe, deep free and constrained excitons and biexcitons, collective interactions (*Russian*) 0-66282
 GaSe, exciton luminesc. kinetics, intermediate electron-hole states 0-93389
 GaSe, exciton-phonon quasibound states, photocond. and luminesc. study 0-96800
 GaSe, Faraday rot. near absorpt. edge, optical dispersion meas. 0-80757
 e-GaSe films, optical props. in IR region, metal substrate effect 0-71502
 GaSe, impurity photocond., induced illumination corresponding to fundamental absorption region 0-92933
 GaSe, lattice dynamics and elastic props., Born-von Karman model study 0-70337
 GaSe, layer compound, long-wavelength phonons and elastic consts. 0-65175
 e-GaSe, long-wavelength lattice vibr. 0-92631
 GaSe, press. induced metallic and supercond. state 0-75666
 e-GaSe, Raman scatt., hydrostatic press. effect 0-84745
 GaSe, shallow core level spectra 0-104037
 GaSe thin films, electroabsorpt. spectra, exciton line splitting 0-107716
 GaSe, thin layers, far IR refractive index 0-80799
 GaSe: Sn, ^{113}Sn diffusion, temp. depend. and Sn solubility (*Russian*) 0-70466
 p-GaSe: Sn, majority carrier drift mobility meas. 0-92895
 GaSe-SnO $_2$ heterojunctions, photoelec. props. 0-96945
 $\alpha(\beta)$ -Ga $_2$ Se $_3$, cryst. growth, optical, X-ray diffr. and SEM study 0-71587
 Ga $_2$ Se $_3$, solid solution, elec. cond. 0-88301
 Ga $_2$ Se $_3$ -FeSe, phase diagram, elec. cond., mag. susceptibility 0-88301
 GaSe $_{1-x}$ Te $_x$, Raman scatt., optical phonons and phase transition 0-66202
 GaSe $_{1-x}$ Te $_x$, Raman spectra, phonon freq. 0-97286
 GaTe, ^{110}Ag diffusion, temp. depend. and solution (*Russian*) 0-70467
 GaTe, cryst. struct., TEM and X-ray diffr. study 0-79757
 GaTe, layer cryst., polarised IR refl. spectra 0-97279
 GaTe monocrystal, far IR polarised complex reflectivity obs. 0-60609
 α -GaTe, single cryst., Raman scatt. 0-60599
 GaTe, single cryst. prep. and electroabsorpt. spectra investig. 0-103968
 GaTe, transport properties under hydrostatic pressure 0-75589
 GaTe-SnO $_2$ heterojunctions, photoelec. props. 0-96945
 GeS $_2$, single crystal, far IR transmission 0-80800
 In-Se(Te), liq., mag. susceptibility meas., electron localisation and chem. bonding 0-60178
 InGaAsP, epitaxial growth by chloride CVD process, thermodynamic anal. 0-64936
 InS $_7$, single crystal, switching effect and memory (*Russian*) 0-70774
 n-InSb, degenerate plasma, Coulomb collision photon absorpt. dynamic screening (*Russian*) 0-92924
 InSe, ^{110}Ag diffusion, temp. depend. and solution (*Russian*) 0-70467
 γ -InSe, 3R struct. type refinement 0-64962
 InSe, exciton and polaron anisotropies, reson. Raman scatt. study 0-76033
 InSe films, residual photocond., field quenching 0-60037
 InSe, layer compound, long-wavelength phonons and elastic consts. 0-65175
 InSe, photoconductivity anisotropy at high optical excitation levels (*Russian*) 0-103721
 InSe solar cells, photovoltaic conversion efficiency 0-61356
 InSe thin film, sputter growth and chem. anal. by XPS/ESCA 0-80976
 InSe-SnO $_2$ n-n heterojunctions, photoelec. props. 0-96945
 In $_x$ Se $_{1-x}$ -SnO $_2$ amorphous film-SnO $_2$ system, photovoltaic spectra, annealing effect (*Japanese*) 0-92926
 InTe thin films, flash evaporation, electrical props. 0-65722
 PbTe-Ga $_2$ Te $_3$, phase interaction, DTA, XPA and microstructural anal. 0-96625
 Si-GaSe n-p heterojunction, elec. characts., interface states 0-70812
 TiInS $_2$, layered structure crystals, refractive index meas. method 0-98966
 TiSe type crystals, possible second-order phase transitions, group-theoretical anal. 0-92672
 TiTe, melt, elec. cond., surface tension, microhardness, influence of impurities 0-88551
 Ti $_2$ Te, melt, resistivity, surface tension, microhardness, influence of impurities 0-88552

illumination see lighting

image amplifiers see image intensifiers

image converters

see also fluorescent screens; image intensifiers

- alkali metal vapour, IR image upconversion using two-photon resonant optical four-wave mixing 0-58632
 biplanar electron-optical image converter as a circuit element 0-78994
 HVEM, for biological specimens 0-104839
 hybrid field-effect liquid-crystal light valve, optical data processing performance 0-99860
 IR-to-visible image conversion with a thick-layer hologram 0-87355
 liquid crystal image transducer, optical props. at normal incidence, off-state behaviour 0-64160
 liquid crystal transducer, performance effects of liquid crystal thickness 0-102838
 liquid-crystal image transducer, normal incidence, on-state optical performance 0-99852
 oil layer, deformable, spatial light modulator as incoherent to coherent image transformer 0-96008
 photocathode sensitivity uniformity over surface, distortion of zone charact. by interference in substrate 0-58709
 pulsed electron optical converter, dynamic spatial MTF estimate 0-74502
 sampling stroboscopic converter identification by Hammerstein model (*Russian*) 0-74495
 subnanosecond optical detector developments 0-77870
 thermo-optical converter with liq. modulating medium 0-91927

image iconoscopes see television camera tubes

image intensifiers

- channel plate image intensifier, for high-speed image information processor 0-78982
 electron microdensitometer system for use in TEM 0-95197
 electronic detectors to enhance optical information from telescopes, image intensifiers and CCDs (*French*) 0-67569
 Fabry-Perot-interferometer imaging system for thermospheric temp. and wind meas. 0-101441

image intensifiers continued

- fibre, gradient-index light-focusing, image enhancement 0-69501
- fluorescence microscopy of living cells, low level, appls. of image intensification 0-94432
- holographic one-tube goggle system engineering 0-78988
- laser projection microscope, transmitted light, Cu vapour laser as image amplifier 0-73446
- laser projection microscope with image-brightness amplifier using Pb and Mn vapour 0-106541
- multifunction image intensifier tube for optical image processing 0-99825
- night vision goggles, military low-cost, design and development 0-78990
- optoelectronics, appl. in measuring gas discharge phenomena 0-107007
- photochron picrosec. streak cameras for linear photoelec. recording 0-86365
- time-gated optical imaging system meas. of laser target emitted light angular distrib. 0-79572
- TV, EM image accumulation, digital storage and processing system 0-101901
- X-ray, magnetic interferences (*German*) 0-105761
- X-ray, noise evaluation, digital method 0-98097
- X-ray intensifying screen, role of reflective layer 0-62816

image orthicons *see television camera tubes***image processing** *see picture processing***image sensors***see also television camera tubes*

- C-CD camera, appl. to Einstein X-ray Observatory fields RI photometry 0-62315
- C-CD camera on Galileo Jupiter Orbiter Mission 0-85859
- C-CD imager, edge enhancement using 3×3 pixel neighbourhood operator functions 0-102644
- CCD 800×800 detector arrays on Space Telescope 0-109370
- charge injection device as stellar tracking sensor 0-85861
- CTEM image recording using CCD 0-68329
- electron spectrometer using new multidetector based on charge-coupled imaging device 0-86502
- fast solid-state camera for high-speed event diagnostics 0-78985
- flexible high-resolution film recorder system 0-102827
- flexible high-resolution film recording system design 0-102828
- forward-looking IR sensor image segmentation by maximum likelihood parameter estimation 0-99662
- Image Understanding Program philosophy and results 0-95818
- IR sensor figures of merit 0-86419
- IR sensor noise reduction algorithms, Monte Carlo evaluation 0-95824
- IR staring mosaic sensor background suppression and tracking 0-86415
- liquid velocity measurement and flow trajectory, using image sensor, appl. to stirred vessel 0-69950
- mosaic sensor test and calibration facility for focal plane arrays 0-86425
- scanstor, luminous line coord. meas. 0-96019
- step-stare IR sensor design for aerospace vehicle detection 0-86418
- thermal imaging tube, pyroelectric, sensitivity and geometrical resolution improvement (*German*) 0-105715
- vidicon, Si-intensified-target, low intensities meas., astronomy appl. (*German*) 0-98545
- Gd₂(MoO₄)₃, ferroelec., amorphous Si:H coating, domain wall motion, image scanning 0-83663
- Gd₂(MoO₄)₃, one-dimensional ferroelectric image sensor with polymer photoconductor 0-80729

image storage tubes

No entries

images, optical *see optical images***imaging, acoustic** *see acoustic imaging***imaging, infrared** *see infrared imaging***IMMA** *see ion microprobe analysis***impact (mechanical)***see also ballistics; impact strength*

- acoustic radiated noise level calc. of mechanical impact using tapping machine (*French*) 0-87639
- asteroids, high vel. impact, catastrophic destruction mechanism 0-82257
- brittle materials, water drop impacted, damage thresholds 0-81149
- buoyant cylinder released underwater, impact motion on a surface body 0-68041
- centrifuge cratering 0-72522
- colliding cylinders, resulting stress field for linearly elastic material (*Russian*) 0-79237
- concrete, impact bending capacity (*Japanese*) 0-89341
- crater formation 0-94765
- crater slumping, role of acoustic fluidisation 0-85653
- craters, modification by fallback ejecta 0-82317
- craters in ice and ice-saturated sand, Martian implications 0-67614
- cylindrical beam, impact effect on rigid wall (*German*) 0-106763
- cylindrical punch, three-dimensional stress field, photoelastic studies 0-93272
- dynamic finite element analysis of cracked bodies subjected to impact loading 0-69742
- Earth, ring system form. assoc. with Eocene terminal event 0-76890
- elastic plate, impact load impulse form determination by the displacements and strains of a circular plate (*Russian*) 0-74751
- elastic sphere torsion by elastic punches 0-99929
- epoxy resin, stresses arising during high-speed droplet impact 0-71764
- floor sound insulation, analysis using L_c and L_w (*Japanese*) 0-79054
- floors, elastic coverings, effect of thickness and hardness on impact sound insulation props. (*Japanese*) 0-79053
- frame, plane, impulsively loaded, large deflections, mode approx. technique extension 0-83757
- gas gun, short-barrelled, for impact studies 0-64501
- glass, annealed and tempered, impact damage, strength 0-85025
- graphite/epoxy laminates, stress wave damage 0-93611
- Hertzian impact of two elastic spheres in the presence of surface damping 0-69743
- indentation hardness and hot pressing, calc. methods 0-58981
- indentation hardness and microhardness test methods for plastic deform. (*Hungarian*) 0-97664
- internal meas. of shear and compression waves, gauge lead effects 0-74817
- Joule's constant determination, large scale 19th century expt. method 0-77572
- lunar highlands, effects of meteorite bombardment on primordial crust 0-109381

impact (mechanical) continued

- lunar rocks, microcrater and accretionary grain populations under meteoroid and solar wind bombardment 0-94731
- lunar rocks, microcrater and accretionary grain populations from lunar surface and Apollo samples obs. 0-94732
- metal, ductile, jet-impingement solid-particle erosion testing, halo effect 0-76376
- metal, strong, compressive stress/strain props. meas. at very high strain rates, modified Hopkinson bar system 0-85128
- metal tube, dynamic lateral compression, strain rate effects 0-83758
- meteorite crater field formation, effects of meteoroid atmospheric breakup 0-94760
- meteorite parent body, impact melting rel. to origin of Fe meteorites of groups IAB and IIICD 0-109404
- micrometeoroid impact on thin film of detector, lab. expts. 0-77292
- mirror/flaw-size relations, residual contact stresses effect 0-107363
- mortar specimens, repeated impact bending load study (*Japanese*) 0-93622
- nonlinear oscillator and reflectors, periodic vibr. and impact characteristics 0-92089
- pendulum impact machines, energy meas. using optical system 0-69746
- Phobos, Stickney crater impact rel. to grooves distrib., morphology and possible origin 0-72837
- planetary satellites, effect of proximity to Roche limit on dynamical behaviour of ejecta 0-98592
- plastic wave theory, comparison of predictions with impact expts. 0-83742
- plate, impact force meas. method 0-79242
- polystyrene, atactic, indentation recovery 0-84988
- PZT ceramics, ferroelec. energy conversion under shock loading 0-108163
- regolith reprocessing by cratering, erosion of material layer which loses charact. props. 0-62053
- rock half-space, impact of steel cylinder and effects 0-85649
- shear, and compression wave propag. in impacted solids 0-83755
- shell, cylindrical, impact on surface of compressible fluid, numerical method (*Russian*) 0-87746
- shell, spherical, impact on surface of compressible fluid, numerical method (*Russian*) 0-87747
- single mass vibroimpact system, response to white noise random excitation 0-64454
- sphere impacting on thin square plate, acoustic generation mechanism 0-74591
- split Hopkinson pressure bar application to fracture dynamics 0-85140
- steel, C, crack initiation and propagation life under repeated impact tensile loads (*Japanese*) 0-104264
- steel, Cr-Mo, effect of Mo on high-temp. props. 0-85005
- steel, Cr-Mo-Ni-V, dynamic stress intensity factor meas., possibilities and limits (*German*) 0-93719
- steel, Cr-Ni-Sr (18.15, 17.64, 2.4 wt.%), rare-earth additions effect on impact fracture (*Chinese*) 0-66617
- steel, ferritic stainless, embrittlement 0-85041
- steel, high Mn-Cr, austenitic struct. stability and low-temp. toughness (*Japanese*) 0-76356
- steel, low C, dynamic stress intensity factor meas., possibilities and limits (*German*) 0-93719
- steel, low-alloy, testing cracked specimens for impact bending, expt. planning method appl. 0-71831
- steel, low-C, fatigue strength and crack propag. behaviour under impact program loading conditions (*Japanese*) 0-66635
- steel, low-C, kinetics of void development in fracturing A533B tensile bars 0-76357
- steel, Mn-V reinforcing type, strain ageing characts. rel. to mech. props. 0-84969
- steel, Ni-Co-Mo, dynamic stress intensity factor meas., possibilities and limits (*German*) 0-93719
- steel, stainless, global bending response analysis of elastic and viscoplastic nuclear shipping cask structures subjected to impact loading 0-76301
- steel, types S25C and S45C surface damage produced by pulsating impact contact load (*Japanese*) 0-104263
- steel 45G2, fracture resistance, from impact bending tests and oscillograms 0-61047
- structural member, dynamic loading and plastic response, review 0-83756
- testing, deform. meas. accuracy improvement 0-81259
- two degrees of freedom system, effect of damping on impact response 0-74587
- Al, 6061-T6, pressure shear impact in transverse displacement interferometer, plastic flow 0-81137
- Al rod, exponentially varying shape, impact by steel spheres, elastic wave propagation 0-74791
- Al, ultimate tensile strength for brief impact 0-70309
- Al-Bi(Cd)(Pb)-Ti, containing low-melting pt. inclusions, mech. props. 0-93632
- Al-Zn-Mg, type V-95, ultimate tensile strength for brief impact 0-70309
- C fibre reinforced composite, split Hopkinson press. bar test, opt. and strain gauge methods comparison 0-85132
- Cu, polycryst., surface layer hardening by multiple impact 0-108469
- InBi single crystal, deform. mode under dynamic indentation 0-88163
- MgF, polycryst., quartz particle impacts no. effect on erosion in elastic-plastic response regime 0-81209
- MgO single cryst., impact wear characts. 0-76374
- MgO single cryst., impact wear damage 0-76375
- Na₂O-CaO glass, shear deform. under pyramidal indentations 0-84989
- Na₂O-CaO-SiO₂ glass, high-vel. liq. impact, oblique impact anomaly 0-89329
- PbO-B₂O₃ phase-separated glass, fracture toughness, Vickers indentation method 0-85023
- Ti-Al-V (6.4 wt.%), effect of air exposure on fracture characts. 0-100890
- Ti-Al-V (6.4 wt.%) cast alloy, with improved microstruct., mech. props. (*Japanese*) 0-71701

impact avalanche transit-time diodes *see IMPATT diodes***impact ionisation**

- amorphous, high field transport, impact ionisation, carrier mobility 0-80286
- anomalous avalanche breakdown 0-80284
- electron-hole avalanches with constant ionisation coefficient, comment and reply 0-75572
- heterojunction multilayered structs., effective impact ionisation rates 0-88621
- narrow gap semiconductors, recombination mechanisms, review 0-96905

gauge field theory continued

fermionic solitons in gauge theories and their quantum corrections 0-101927
 Feynman path integral and gauge invariance 0-82601
 fiber bundle structure of gauge field and reduction by the Higgs mechanism 0-82885
 fibre bundles and topology 0-105793
 Fock quantisation for indefinite metric gauge fields 0-77942
 forces between leptons and quarks, a gauge field phenomena 0-91008
 free automorphic quantum field theory, gauge transformations and field algebras 0-86546
 free EM field quantisation, gauge invariant fields 0-105817
 free tensor potential equivalence in QED 0-73579
 fundamental monopoles and multimonomole solutions for arbitrary simple gauge groups 0-77952
 gauge equivalent fields, existence near instantons (*Russian*) 0-62865
 gauged $N > 4$ supergravity, vanishing one loop β -function, infinite renormalisation 0-86186
 geometrical unification of gauge and Higgs fields 0-99077
 ghost-free axial gauge in supergravity 0-57162
 Gibow vacuum copies in terms of harmonic maps for SU_2 gauge theories 0-57488
 glueball spectra, prod. and decay for QCD and $SU(n)$ gauge theories 0-62941
 gluon mass, lower bound in integer-quark-charge model 0-78042
 grand unification from neutral currents in gauge models 0-78009
 grand unified gauge theories, running coupling constants and unifying mass scale 0-91029
 Grassman number systems, Hamiltonian formalism, canonical quantisation by Feynman path-integral 0-77697
 gravitation, spinor formalism 0-90762
 gravitation as gauge theory of Poincaré group 0-86189
 gravitation theory with alternative to black holes 0-57168
 gravitational bubbles, radiative corrections to covariant massless quartically self-interacting meson theory 0-62826
 gravitational field gauge theories, review 0-98848
 gravitational gauge theory with no black holes 0-82702
 gravitino, axial current anomaly, Faddeev-Popov ghosts 0-68120
 graviton scatt. amplitude, gauge invariance 0-82700
 gravity and supergravity, conformal, Yang-Mills-like Lagrangians 0-62560
 Green's functions, nonperturbative generating functionals 0-73588
 group weight and vanishing graphs 0-57482
 hadronic gauge couplings in meson decays 0-102037
 hadrons, QCD model, asymptotically free field theory, anomalous dimensions of composite particles 0-73665
 Hamilton-Jacobi formalism for strings, string-gauge theory link 0-78048
 Hamiltonian classical mechanics, gauge theory for long range fields 0-86077
 hidden ghosts in antisymmetric tensor gauge fields coupled to gravity 0-82889
 Higgs and gauge fields, group actions on principle bundles and dimensional reduction 0-105770
 Higgs boson couplings, charged, K_L - K_S mass-differences 0-62917
 Higgs field zeros for axially symmetric multi-monopole configurations 0-82887
 high spin fields with antisymmetric tensor-spinors and Maxwell-like field equations 0-105772
 high-energy physics, particles and interactions, accelerators 0-77944
 horizontal symmetries dynamical symmetry breaking and neutrino masses 0-105830
 infrared attractive fixed points, gauge symmetries, QED and anti-grandunification 0-95213
 instanton system weakly interacting with anti-instanton system, external electric fields, structure and stability 0-77956
 instantons, generation of meson mass spectrum, current algebra, mixing angles 0-86567
 instantons, gravitational, flavour currents of QCD, Green's functions, foam-like structure of space-time 0-62825
 instantons in $N \rightarrow \infty$ limit, weak and strong coupling β -functions 0-95217
 instantons in nonAbelian gauge theories and QCD mesons 0-105777
 intense field electrodynamics, Goppert-Mayer gauges 0-99075
 interacting instanton-antiinstanton system under external colour mag. fields in $SU(2)$ gauge 0-101920
 interaction potentials for multi-quark states from instantons and other background gauge field configurations 0-101995
 isotropic cosmological models, vacuum stress energy tensor and particle creation (*German*) 0-94901
 K-M matrix calc. using horizontal gauge (*Chinese*) 0-101931
 lattice gauge theories, boxiton scatt. cross section 0-82890
 lattice gauge theories, chiral symmetry dynamical breaking 0-99061
 lattice gauge theories, vortex free energy, strong and intermediate coupling string tension 0-105786
 lattice gauge theories, $Z(N)$ system phase struct., dual variables 0-62848
 lattice QCD₂, Wilson's loop eqn. soln. for large N limit 0-78030
 lattice regularised field theory, renormalised and bare coupling constants 0-77960
 lattice $SU(N)$ gauge theory, vacuum structure, large-scale 0-57470
 left-right symmetric gauge models, parameter constraints from neutral current data 0-86588
 lepton structure model 0-91063
 leptons, $SU(3)$ electroweak theory 0-86638
 lh theory of leptons and hadrons, unification in $GA_{4,R}$ gauge 0-86639
 Lie-admissible deformation of self-adjoint systems 0-101941
 local gauge symmetry, dynamical stability and large distance behaviour 0-90991
 loop-space representation and the large- N behavior of the one-plaquette Kogut-Susskind Hamiltonian 0-99060
 magnetic flux metamorphosis in spontaneously broken gauge theories 0-99047
 manifestly conformally covariant field equations and a geometrical understanding of mass 0-105788
 massless 't Hooft model, tachyonic modes, vanishing of scalar density 0-77949
 massless $[g\phi^4]_4$ theory, functional integrals, complex instantons and asymptotic perturbation series 0-86571
 membrane models and generalized Z_2 gauge theories, renormalisation props. 0-86587
 meronic solution class for charged particle conformal invariant interaction 0-90983
 milliweak gauge models of CP violation 0-73633

gauge field theory continued

model $U(N)$ lattice gauge theories, exactly soluble, $N = \infty$ phase transition 0-86583
 models of dynamically broken gauge theories 0-77974
 molecules under static mag. field, gauge invariance 0-102587
 momentum subtraction scheme, quark mass depend. cancellation in anomalous dims. 0-77965
 $n \neq 4$ axial vector anomaly, noncontribution 0-62858
 neutral currents, Higgs flavour-changing, suppression in $SU(2)_L \times SU(2)_R \times U(1)$ left-right symmetric gauge theory 0-78016
 neutrino mass problem, gauge hierarchy 0-90989
 neutron matter-quark matter phase transition, QCD and extended Higgs model, instantons 0-91062
 neutron oscillation phenomenology in gauge model with spontaneously broken B-L symmetry 0-90996
 new gauge transformation for a generalized quantum representation 0-86136
 non Abelian gauge theories in external electromagnetic fields (*Russian*) 0-57533
 non-Abelian gauge fields, physical degrees of freedom 0-105778
 non-Abelian gauge theories, high energy behaviour, reggeon field theory, QCD 0-62822
 non-Abelian gauge theory with many flavours, high energy processes, asymptotical behaviour (*Russian*) 0-101935
 non-Abelian theories, dual formulation 0-82902
 nonAbelian gauge theory, transformation into Abelian gauge theory 0-99041
 nonAbelian lattice gauge theories, phase structure critical temp. 0-86592
 noncovariant effects in the perturbation theory of two-dimensional gauge theories 0-57495
 nonleading logarithm struct. in terms of β -function and anomalous dims. 0-77964
 nonperturbative QCD, large N_c , QCD bag model, instantons and η' mass 0-57559
 nonrelativistic gauge theories, massive fields with nontrivial field eqns. 0-105773
 $O(10)$, $SU(4)$ colour subgroup, fractional charged gauge boson, proton half-life 0-73644
 $O(3)$ nonlinear σ -model, mass generation in dense instanton gas approx. 0-82880
 one loop equivalent gauges, one loop infinities and renormalisation constants 0-62842
 operator formalism of statistical mechanics of gauge theory in covariant gauges 0-86591
 operator ordering, gauge fixing in non-Abelian theories 0-77975
 operator ordering and Feynman rules in gauge theories 0-101926
 path dependent formulation and origin of field, copies in non-Abelian case 0-86594
 Pati-Salam model, higher order parton transition effects in deep inelastic scatt. 0-78008
 perturbation theory, gauge symmetry hierarchies upper bounds 0-77958
 phase diagrams, dynamic mass generation and renormalisations 0-68365
 Poincaré group gauge theory, geometric meaning, equivalence to Einstein-Cartan gravitation 0-62845
 pre-quarks and fractional charges 0-91048
 primordial magnetic monopoles in unified gauge theories 0-91035
 QCD, anomalous dimensions of gauge-invariant three-fermion local operators of twist three 0-86662
 QCD, gauge field propagator and the number of fermion fields 0-62928
 QCD, Gell-Mann-Low function in 3 loop approx., nonAbelian gauge theory with fermions 0-86675
 QCD, lattice and continuum, Λ parameters connections 0-82945
 QCD, stagnant gauge for gluon propagator 0-57554
 QCD axial gauge, $O(\alpha_s)$ infra-red divergences, deep inelastic quark struct. function 0-86676
 QCD renormalisation in two loop approx. in arbitrary gauge 0-102002
 QCD vacuum of background $SU(2)$ gauge field, colour mag. permeability 0-78023
 QDD, quantum dath dynamics, $SU(3)$ model for composite quarks and leptons 0-91055
 QED, conformal-invariant, Ward identity of dilation current 0-68401
 QED, covariant, renormalised transition amplitudes, gauge independence, Green functions 0-57530
 QED, relativistic two particle bound state energy levels, gauge invariance 0-77989
 quadratic lagrangians in a space with torsion and the theory of the spinor gauge field 0-91006
 quantisation in finite volume without constraints or A_0 ambiguity 0-73605
 quantised $SU(2)$ gauge theory, Monte Carlo study 0-77973
 quantum contour field equations, renormalisation and string like eqn. 0-86581
 quantum gauge anomalies axial vector current derivation method calcs. (*Russian*) 0-62863
 Quantum inequivalence of different field representations, supergravity appl. 0-95214
 quark structure model 0-91063
 quasiconfinement in colour gauge symmetry, unconfined quarks and gluons 0-86686
 radiation theory, multipolar Hamiltonian QED and quantum optics 0-86634
 random spin systems, gauge symm., phase transitions (*Russian*) 0-77929
 Reggeization of elementary fermions in arbitrary renormalizable gauge theories 0-68367
 regularity constraints and quantised actions 0-73601
 renormalisation theory, perturbative, general features, quantum action principles, pure Yang-Mills theory 0-105794
 restricted theory as subset of nonAbelian gauge theory 0-62851
 right translation invariant metrics and variational principles on principal bundle, gauge theories (*Chinese*) 0-101743
 S-matrix, gauge singlet operators instead of bound states 0-99063
 scale invariant gauge theories, instanton role, short distance limit 0-101924
 self-dual $SU(2)$ fields in Eguchi-Hanson space 0-57483
 sine-Gordon equation, discrete, on $SU(2)$ lattice, group theory aspects 0-57486
 singular gauge fields, effect on inclusive differential cross sections 0-105782
 $SO(3,2)$ de Sitter symmetry, spontaneously broken, gravitational holonomy group 0-57149

gauge field theory continued

SO(3) Georgi-Glashow model, field-strength description of non-Abelian gauge theories 0-62856
 SO(4n+2) gauge theory, dynamical symmetry breaking 0-86580
 space-dispersion approach to the explanation of the Higgs-mechanism 0-90975
 spin 5/2 fields, gauge theory 0-73583
 spinning particle in metric-torsion field, eqn. of motion 0-62543
 standard electroweak gauge model with light W and Z bosons 0-95236
 stochastic quantisation processes, review, Markov processes, Martingales, quantum dynamics 0-94969
 strings as collective field theory of U(N) gauge fields 0-62849
 strong gravity, field equations, strong interactions, de Sitter microsphere idea of hadrons 0-68111
 strongly interacting Higgs bosons, gauged nonlinear σ -model, $SU(2)_L \times U(1)$ extension 0-86656
 $SU_L(2) \times U(1)$ and $SU_L(2) \times SU_R(2) \times U(1)$ predictions at high Q^2 , neutral currents, Z-bosons 0-63029
 SU_N/Z_N gauge invariant theory, phase factor operators and soliton fields 0-77947
 $SU(2)_C \times (T_3)_R \times U_V(1)$ gauge group, grand unification, symmetry breaking and Z bosons 0-73641
 $SU(2)_C \times U(1)$, strong CP-violating phase, one-loop corrections, Higgs particles 0-62910
 $SU(2)_C \times U(1)$ gauge model, mixing angles and CP violation 0-73648
 $SU(2)_C \times U(1)$ gauge theory, four flavours, Cabibbo angle natural relations and bounds 0-57550
 $SU(2) \times U(1)$ gauge model, chiral $SU(2) \times SU(2)$ symmetry and electron mass 0-57542
 $SU(2) \times U(1)$ gauge model, muon anomalous mag. moment, charged Higgs boson contrib. 0-78011
 $SU(2) \times U(1)$ model, fermion and Higgs multiplet structure, universality 0-62909
 $SU(2) \times U(1)$ theories, weak isospin breaking, higher order corrections 0-95235
 $SU(2) \times U(1)$ unified gauge field, Euclidean space and O_4 invariance 0-91031
 $SU(2)$ gauge field, Hamiltonian formulation in interaction with external source 0-62850
 $SU(2)$ gauge field theory, nonlinear scalar field eqn., spherical symmetric exact solns. (Chinese) 0-62886
 $SU(2)$ gauge fields coupled to strong gravity, Coulomb like solutions 0-82701
 $SU(2)$ gauge theory, external charges, topological classification for Yang-Mills eqns. 0-90977
 $SU(2)$ theory, asymptotic freedom scales calc. using Monte Carlo methods 0-90988
 $SU(2)$ Yang's monopole, quaternionic gauge fields on S^7 0-57473
 $SU(3)_{\text{colour}} \times SU(2) \times U(1)$ gauge, full operator structure of the non-leptonic $|\Delta S|=1$ weak Hamiltonian 0-99089
 $SU(3) \times U(1)$ electroweak model, strong extension, flavour and colour gauge exchange symmetries (Chinese) 0-101975
 $SU(3) \times U(1)$ gauge theory, electro-weak interaction, helicity mixed representation 0-78013
 $SU(3)$ colour gauge group, coloured monopoles 0-68360
 $SU(3)$ theory, asymptotic freedom scales calc. using Monte Carlo methods 0-90988
 $SU(5)$, gauge invariance and fermion mass dimensions 0-62907
 $SU(5)$, symmetry breaking patterns, Higgs fields 0-101953
 $SU(5)$ gauge model, masses, mixing angles, CP violation and b-quark decay 0-78006
 $SU(5)$ unified gauge theory, non-Abelian electric and mag. flux 0-57545
 $SU(8)$ grand unification, natural embedding of $SU(3)$ horizontal symmetry 0-86646
 $SU(N)$ Coulomb and Landau gauge theories vacuum struct., Gribov ambiguities, harmonic anal. 0-68363
 $SU(N)$ gauge theories, $1/N$ expansions, singular integral operator 0-57511
 $SU(n)$ gauge theories, spontaneous symmetry breaking pattern 0-95228
 $SU(N)$ gauge theory with scalar fields, effective Lagrangian 0-82897
 $SU(N)$ lattice gauge theories, weak to strong coupling crossover 0-95212
 $SU(N)$ symmetric quantum dynamical systems, $N \rightarrow \infty$, energy spectrum for singlet and adjoint states 0-62880
 $SU(N)$ theories, order and disorder parameter inequalities 0-99051
 superconducting early Universe, cosmological baryon prod., CP invariance grand unification 0-90592
 supergrand exceptional unification and quark-lepton constituents 0-91030
 supergrand unification in E_8 , quark-lepton assignments, symmetry breaking scheme 0-68408
 supergravity, trivial solution identification, gauge transformation to Einstein vacuum soln. 0-68115
 superspace gauge theories, superspace Maxwell and Yang-Mills actions 0-86582
 supersymmetric and nonsupersymmetric, regularisation by dimensional reduction 0-77951
 supersymmetric QED, supercurrent gauge invariance, α -independ. 0-95233
 supersymmetry and developments in gauge theory (Chinese) 0-77978
 systematics of higher-spin gauge fields 0-57478
 T-baryonium system, four-body potential in multiquark states 0-101996
 temporal gauge $A_0=0$ 0-90984
 three-loop charge renormalization effects due to quartic scalar self-interactions 0-57489
 topless model for grand unification 0-73653
 tumbling gauge theories with chiral fermion fields, symmetry breaking 0-99042
 twisted lattice gauge fields, local order parameter, phase transitions 0-77966
 two dimensional space time, gauge theory path ordered operator formalism 0-77967
 U(1) chiral symmetry breaking from $SU(1)$ gauge theory 0-86617
 U(1) lattice gauge model, phase transition in four-dimensional compact QED 0-105820
 U(1) lattice gauge theory, four dims., nonconfining phase, existence proof 0-73602
 U(N) gauge theory, Nambu-Gato string like equation 0-105785
 U(N) lattice gauge theory as $N \rightarrow \infty$, planar diagram sums in terms of statistical ensembles 0-99052
 unification of fundamental forces, review 0-95238
 unified gauge theories, grand, asymptotic freedom constraints 0-62914

gauge field theory continued

unified scalar-free theory, order-R vacuum functional, with spontaneous scale breaking 0-78003
 unified theories 0-73652
 unified theory of EM and weak interactions, local gauge invariance 0-82928
 vacuum spacetimes, stationary and axially symmetric, homogeneous Hilbert problem, Kinnersley-Chitre transformations 0-68349
 vacuum states for pure gauge fields on coset, topological props. 0-68372
 vacuum structure in gauge theories, strong CP violation and cosmology 0-86578
 Ward-Takahashi identities for gauge-ghost field proper vertices (Chinese) 0-99062
 wave function renormalisation constants, gauge independ. in gauge field theories 0-82883
 wave mechanics, gauge invariant and Power-Zienau-Woolley transformation 0-99073
 weak gauge boson doubling in standard $SU(2) \otimes U(1)$ model, W, Z bosons 0-62916
 Wilson's lattice, local chiral symmetry for gauge theories 0-105774
 Wilson loop critical point behaviour in gauge and lattice gauge theories 0-90993
 Z_2 lattice gauge Higgs theories, Monte-Carlo calcs. 0-86593
 Z_2 four dimensional lattice gauge theories, series anal. 0-99050
 Z_2 lattice gauge theory coupled to Higgs field, phase diagrams 0-57485
 Z_N symmetric models phase transitions 0-101922
 $Z(2)$ gauge theories, hidden fermions 0-82899
 $Z(2)$ gauge theory, phase transition, variational calcs. 0-99049
 $Z(2)$ lattice gauge theory, variational approach, two phase struct., phase transition 0-68361
 $Z(2)$ lattice gauge theory in 2+1 dims., fermion representation 0-82900
 $Z(N)$ and $U(1)$ lattice theories in three-dims., phase diagram 0-82901
 $Z(N)$ gauge theories, phase transitions 0-73609
 $Z(N)$ strings and hadron structure 0-86572
 $eN \rightarrow eX$, $SU(2)_L \times U(1)$ gauge theory distinguished from $SU(2)_C \times SU(2)_R \times U(1)$, neutral currents, z-bosons 0-62908
 $en \rightarrow en\pi$, pol. e, P-odd asymmetry and cross sections, $SU(2) \times U(1)$, $S(3) \times U(1)$ calcs. (Russian) 0-62998
 $e N \rightarrow e \Delta(3/2, 3/2)$, P-odd asymmetry, P nonconserving neutral current interaction 0-57611
 ep , polarised scattering, asymmetries, gauge models 0-62991
 $F_i \rightarrow F_j$, nondiagonal transition amplitude for arbitrary fermion charges (Russian) 0-86722
 n electric dipole moment, CP violation in gauge theories 0-91041
 νN , heavy-quark production, t and b-quarks, $SU(2) \times SU(2) \times U(1)$ gauge group mixing angles 0-68445
 $\nu N \rightarrow \nu X$, $SU(2)_L \times U(1)$ gauge theory distinguished from $SU(2)_C \times SU(2)_R \times U(1)$, neutral currents, z-bosons 0-62908
 $pp \rightarrow \pi X$, large- P_T reactions in broken color gauge theory 0-95292
 $Z \rightarrow l^+ l^-$, deviations from lepton universality in renormalisable gauge models 0-91122

Gaussian noise see random noise
Gaussian orbital calculations see GO calculations
Gaussian-type orbital calculations see GTO calculations
Ge-Si alloys
 amorphous, solar cells, tandem multiple gap 0-94029
 diffused p-n junction, elec. and photoelectric props. 0-101095
 electronic structure, short-range order effects, calc. 0-92861
 hot-pressed, fine-grained, boundary scatt. of phonons, lattice thermal cond. 0-107583
 hot-pressed, fine-grained, boundary scatt. of phonons, theory 0-107584
 IR spectra, calc. for imperfect homopolar crysts., lattice dynamics 0-59601
 n-type, phosphorous doped, precipitation effects due to heat treatment 0-107833
 phase diagram, lattice const. var. effects 0-97470
 phase diagrams near melting point, Helmholtz free energy, heat of solution 0-70379
 thermoelectric alloys, phase diagrams, and imperfection chemistry 0-108422
 thermoelectric materials, high temperature 0-89659
 Ge-Si-Te, solid solns., donor states energy spectrum 0-88516
 Ge_0Si_{10} , elec. cond., density of states, impurity and temp. depend 0-65568
 $NiMnGe_{1-x}Si_x$, mag. props., neutron diffr. and magnetometric meas., 80-600K 0-85793
 $Si_3Ge_{1-x}Ga_xAs$, heterojunction, elec. and recomb. props., interface defect effects 0-80365

gegenstein see zodiacal light
Geiger counters
 background determ. by hard cosmic radiation 0-69027
 compensated count rate cct. for portable survey meter 0-99426
 coordinate counters for UV and X-ray photons 0-69026
 gas-chromatography, beta radi effluents, window flow counter 0-93824
 needle counter, small size low-level 0-58075
 radiation overload warning system for Geiger-Muller detectors 0-78492
 self-quenching, anode surface changes with ageing 0-58025
 Ag-activated Geiger counter calibration for neutron yield determ. in Frascati plasma focus expt. 0-99409

Geiger Muller counters see Geiger counters
gelatin
 see also gels
 chromatized gelatin layers, processing for holographic recording (Russian) 0-91762
 diazo salt sensitised gelatin for holographic recording, grating form. 0-78798
 fine-grained bleached emulsion scatt. model and expt. 0-102670
 gels, in water and glycerol/water mixtures, dynamic viscoelastic props. 0-64508
 IR absorption spectra of pure layers and layers with AgBr emulsion layer (Russian) 0-62776
 layer, dry, aqueous soln. penetration 0-85221
 phosphorescence kinetics curves of gelatin layers with and without $AgNO_3$ (Russian) 0-62776
 photographic layers, permeation of photographic developer, potentiometric exam. (Russian) 0-73500
 thiosulphate determ. in photographic gelatine, spectrophotometric method (Hungarian) 0-66905

gelatin continued

- Ag halide film physical props., effect of gelatin structure 0-97715
 Ag halide sensitised gelatin processing, phase volume hologram form. 0-78797

gels

- agarose gels, bubble prod., stabilisation by nonionic surfactants 0-76562
 amylopectin, glycerin impregnated, dynamic viscoelasticity (*Japanese*) 0-104203
 amylose, glycerin impregnated, dynamic viscoelasticity (*Japanese*) 0-104203
 correlated percolation, ϵ expansion, appl. to gels 0-77714
 N,N-diethylacrylamide, cross-linked copolymer, improved mech. props. 0-61091
 dipalmitoyl lecithin bilayer, mol. tilt, X-ray diffraction obs. in gel phase 0-84059
 electrocapillary acceleration meters with electrolyte in gel form 0-73330
 ethidium bromide E-DNA, intercalated birefringent fibres, microspectrophotometric investig. (*German*) 0-57392
 ethylene-vinyl acetate copolymer, powdered, prep. by emulsion polymerisation (*Japanese*) 0-104110
 gelatin gels, in water and glycerol/water mixtures, dynamic viscoelastic props. 0-64508
 gelatin sol-gel transition, viscosity meas. method 0-85219
 heterogeneous two-phase, permeability 0-76563
 ionomer solutions, in water, gel form. and demixing transition 0-61172
 medical US phantoms, water-based gels 0-81671
 mesomorphic monolayers, quasi-two dimens., theoretical models 0-76713
 poly(dihydroxypropyl methacrylate), surface charact., by contact angle methods 0-61140
 poly(hydroxyethyl methacrylate), surface charact., by contact angle methods 0-61140
 poly(m-xylene adipamide), molten, gel form. kinetics (*Japanese*) 0-108757
 poly(methoxyethyl methacrylate), surface charact., by contact angle methods 0-61140
 polyacrylamide gel and single chain in soln., laser light scatt. obs. near phase transitions 0-93808
 1,2-polybutadiene, crosslinked in states of strain, entanglement networks, swelling anisotropy obs. 0-79666
 polydimethylsiloxane chains, end-linked, swollen model networks, stress/strain isotherms and elastic modulus 0-79668
 polymethacrylic acid, swollen networks, viscoelastic photoelastic behaviour 0-59366
 polystyrene, conform. and near all-trans extended-chain model relevant in gels, X-ray diff. patterns interpret. 0-79707
 polystyrene, isotactic gel film, Fourier transform IR spectrum 0-104465
 polystyrene networks swollen in cyclohexane, swelling equil. and light scatt. at theta conditions 0-107036
 polyvinyl alcohol networks, swelling equil. with dil. salt solns., thermoelastic behaviour, hydroxyl group interact. 0-79667
 rodlike macromolecules, nonlinear elasticity in condensed state 0-104199
 rods, elastic dilatational mode, light beam positional modulation 0-64167
 silicate gardens, growth morphology, mechanisms 0-100765
 sol-gel transition, UV attenuation meas. 0-101043
 sol-gel transition kinetics 0-85218
 starch, glycerin impregnated, dynamic viscoelasticity (*Japanese*) 0-104203
 unsaturated polyester resins, gelation, viscosity meas. (*Polish*) 0-59690
 uranyl gel microsphere characterisation by emanation thermal anal. for ^{235}U fuel prep. 0-95391
 Al_2O_3 ultrafine gel particle form. from $\text{NH}_3\text{-AlCl}_3$ solution 0-93807
 $\text{Na}_2\text{O-CaO-SiO}_2\text{-H}_2\text{O}$ system gels, metastable nature 0-71952
 SiO_2 gel, BaMoO_4 crystals grown under influence of elec. field 0-93469
 SiO_2 gel, internal and surface struct. by X-ray scatt. 0-84074
 SiO_2 -water system, inorg. polymer struct. form., globular crystn. 0-101042
 Zr gels, thermal and related studies 0-71937
 $\text{ZrO}_2\text{-SiO}_2\text{-(Na}_2\text{O)}$ glass fibres, prep. from metal alkoxides, resistance to NaOH soln. 0-97454

general relativity

- see also cosmology; gravitation; gravitational red shift; Schwarzschild metric; space-time configurations; unified field theories
 Ψ collapse and relativistic covariance (*French*) 0-82682
 acceptance in Canada 0-68012
 algebraic computations by CAMAL 0-94998
 anholonomic Cauchy problem in general relativity 0-86166
 anisotropic fluids with two-perfect-fluid components, Einstein eqn. soln. 0-105554
 approximation methods 0-73235
 asymptotic structure of isolated systems 0-73230
 asymptotic symmetries, energy-momentum and angular momentum at future null infinity 0-73231
 axial symmetric space-times, canonical forms 0-105545
 axially symmetric Brans-Dicke solutions for Einstein's field eqns. 0-90753
 axially symmetric stationary perfect fluid solns. of Einstein's field eqn. 0-86157
 bell's inequalities from the field concept in general relativity 0-105771
 Bells inequality, quantum generalisations for different space-time regions 0-101728
 Bianchi type II exact cosmological model with matter and EM field 0-105560
 Bianchi type-I cosmologies and spinor fields 0-62347
 black holes, primordial, radiation accretion in early Universe 0-67918
 black holes, spherically symmetric, perturbations, linearised Einstein-Maxwell eqns. 0-72992
 black holes, thermally evaporating, Raychaudhuri eqn. 0-109457
 Brans-Dicke-Jordan theory connection, general relativity extension 0-62547
 Casimir cancellations in half an Einstein universe 0-86161
 Cauchy problem formulation for Einstein eqns., coordinate conditions, reference frame theory 0-37150
 caustics and singularities, gravitational converging effects 0-77654
 cavity, vanishingly small, gravitational field inside matter 0-95012
 charged fluid sphere, general relativity soln., Einstein-Maxwell eqns. 0-68088
 charged particles, motion in relativistic fields 0-57146
 charged singularities, repulsive effects 0-90731
 collapse of axially symmetric star, initial data 0-85960
 colour geometrodynamics, eightfold way, review 0-95243

general relativity continued

- conformal invariance 0-90736
 cosmic censorship and test particles, black hole destruction 0-105552
 cosmic microwave background spectrum, G-varying cosmology 0-86020
 cosmological rotating metrics, scalar perturbations 0-62348
 cosmology, Lagrangian or Hamiltonian formulations, shift vector field restrictions, symmetry group 0-67923
 Coulomb interaction in Riemann space 0-90737
 creation and gnosiological lessons 0-98780
 cylindrical systems, numerical codes 0-67549
 de Sitter metric, elliptical space temporal closed Universe 0-109570
 dielectric tensor and magnetic permeability in the weak field approximation of general relativity 0-90751
 differential forms, complex vectorial formalism 0-57144
 Doppler effect, gravitational, explored using geostationary satellite 0-109351
 dualism of field and matter in the general theory of relativity (*German*) 0-90748
 dust, charged, rotating, cylindrically symmetric interior soln. of Einstein-Maxwell eqns. 0-82688
 dynamics, Hamiltonian approach 0-73236
 education, Einstein's General Theory of Relativity and press reaction 0-57075
 education, speed, Galilean and Einsteinian concepts, vel., rapidity and celerity 0-73130
 Einstein's contribution to cosmology 0-77530
 Einstein's equations, exact solns. for spinning mass 0-105548
 Einstein's equations, spherically symmetric case, orthonormal tetrads 0-68095
 Einstein's equations, stationary axially symmetric case, Painleve's transcendental functions (*French*) 0-73218
 Einstein's equations, stationary axisymmetric soln. 0-95005
 Einstein's gravitational field eqns., finite element method soln. 0-86177
 Einstein's impact on theoretical physics 0-77677
 Einstein's non-symmetric unified field theory, universal symmetry and Klotz metric 0-62555
 Einstein's theory of gravitation, review 0-90745
 Einstein dynamics without special-relativistic kinematics 0-77657
 Einstein equation in lifted Finsler spaces 0-77665
 Einstein equations, general cosmological solution, singularity problems 0-82686
 Einstein equations, $[(2+1)+1]$ -formalism, apparent horizons in space-time with rotational Killing vector 0-73222
 Einstein field eqns. of gravitation from general principle of relativity (*German*) 0-68086
 Einstein field equations, characteristic initial value problem in general relativity 0-73238
 Einstein field equations, plane symmetric static and homogeneous vacuum solns. 0-86164
 Einstein Maxwell equations, source-free EM field plus pure radiation 0-77678
 Einstein Maxwell field with null fluid present 0-77668
 Einstein pseudotensor, gravitational energy-momentum 0-98833
 Einstein symposium, Berlin, Germany (Mar. 1979) 0-90596
 Einstein-de Sitter universe, classical predictive electrodynamics 0-86175
 Einstein-Dirac equation, new soln. 0-90742
 Einstein-Maxwell eqn., N soliton solutions (*Russian*) 0-105556
 Einstein-Maxwell equations, inhomogeneous stationary cosmological solns. 0-62556
 Einstein-Maxwell equations, static electrovac solns., complexification technique 0-68114
 Einstein's equations, harmonic solns. 0-90744
 elastic media, dissipative, relativistic electrodynamics 0-73219
 EM fields in space-times with local rotational symmetry 0-82694
 EM propagation between physical source and constant vel. receiver in vacuo 0-105502
 EM tensor fields in space-time V_4 of general relativity 0-77674
 EM wave transmission from isolated system 0-73247
 empty space-times, four-parametric set of solutions to $G_{\mu\nu}=0$ 0-95007
 energy-momentum quantised field tensor vacuum means 0-73227
 equations of motion and radiation reaction 0-73232
 equations of motion from generalised Einstein eqn. 0-90738
 Ernst equation, vacuum soln. family 0-62551
 evolution from equivalence principle 0-98779
 experimental testing, results (*German*) 0-73255
 experimental verification of the general theory of relativity 0-98850
 extended bodies, description and motion 0-73233
 Finsler relativity theory, basic principles 0-73226
 Finsler space, scalar curvature, Einstein tensor 0-77655
 Finsler spaces, physical aspects underlying the field theory 0-101745
 Finsler theory of relativity, basic principles 0-73228
 fluid ball problem, global anal. 0-98834
 fluid cylinders, static, and plane layers, general relativity solns. 0-68090
 free particle propagator covariant WKB expansion in Riemannian space 0-68100
 Friedmann model, expanding Universe, nonlinear acoustic effects (*French*) 0-67921
 Galilean invariant Schrodinger eqn., relativistic wave eqn. derivation, Lie algebra 0-105555
 gauge theory with no black holes 0-82702
 generalized Einstein-Maxwell field theory, asymptotic behaviour 0-86184
 genesis of general relativity 0-90747
 ghost free gravity Lagrangians with propag. torsion 0-86173
 global relativity, recent advances 0-90746
 gravitation and dynamical space, geometrical framework, Mach's principle 0-95001
 gravitation and space-time, general relativity 0-68104
 gravitation as gauge theory of Poincare group 0-86189
 gravitation with torsion field, propagation eqns. for bodies with spin and rotation 0-77670
 gravitational bremsstrahlung in post-linear fast-motion approximation 0-62549
 gravitational collapse, bimetric general relativity theory 0-85853
 gravitational energy loss in scattering problems 0-73244
 gravitational field and arbitrary gauge field, equations of motion, Heisenberg and classical, force term, spin-curvature coupling 0-57158
 gravitational fields, axially symmetric, Weyl's class of static vacuum solutions 0-68089
 gravitational fields, spinor fields, and groups of motions 0-98832
 gravitational monopoles, path depend. approach for Einstein's eqn. 0-77682

general relativity continued

gravitational radiation, collapsed objects and exact solns., Einstein Century Summer School, Perth, Australia, 1979 January 0-105434
gravitational radiation, relativistic corrections and spectrum fine structure for binary stars 0-90479
gravitational radiative corrections as the origin of spontaneous symmetry breaking 0-86192
gravitational theory with nonmetric connection, integrability conditions 0-105546
gravitational wave detection, astrophysical sources, resonant mass, laser interferometer and Doppler ranging methods 0-68122
gravitational wave field, conformal coupling to curvature 0-68105
gravity theories with propagating torsion 0-57161
Hagedorn temperature and Dirac's large numbers hypothesis 0-105410
Hawking effect, temp. relativity, axiomatic field theory 0-109456
DI Herculis, eclipsing binary, relativistic motion of periastron 0-94830
hierarchical cosmology, mathematical formalism and Einstein eqns. 0-82555
homogeneous space-times of the Godel type 0-105553
inhomogeneous Universe, gravitational wave effects, on orbital motions 0-61998
interaction theory formalism 0-90735
inverted black holes, anisotropic collapse, static vacuum, electrovacuum field struct. 0-67776
isolated gravitating systems, summer school, Varenna on Lake Como, Italy (Jun-Jul 1976) 0-73089
jet bundles and path structures 0-82684
Kerr metric effect on EM wave plane of polarization 0-94827
Kerr-Schild-Vaidya fields with axial symmetry 0-95000
Kerr-type particle, uniformly accelerating and rotating, Schwarzschild, Rindler and Kerr surfaces of red shift 0-85855
killing vectors and maximal slicing 0-77667
kinks and cobordism in field theories, general relativity fermions 0-98835
Kinnersley-Chitre spinning mass field 0-105550
Lagrangians in flat space-time 0-86169
length prescription for generalised radial observer, Schwarzschild and Reissner-Nordstrom line elements 0-73223
Lichnerowicz equation, global solns. on asymptotically Euclidean complete manifold 0-101738
Lie group broken symmetry of transformation generating general relativistic theories 0-98836
light deviation in invariant mechanics (*French*) 0-90740
linear stellar structure model in general relativity 0-94709
linearised gravity, eqns. of motion, charged rotating sources 0-77663
linearised gravity, equations of motion, four momentum radiation 0-77662
local simultaneity in general relativity 0-86167
Lorentzian manifold, Kahler-metrics 0-73251
 M_4 factorisation, spinor algebra, Dirac equation geometrical, interpretation 0-62838
magnetisable media, relativistic models, and energy-momentum tensor of EM field (*Russian*) 0-86180
magneto-dipole configurations 0-67539
massive spheres, non-rigid with slowly varying density, eqn. solns. 0-101612
massive spheres with an isothermal core 0-82405
mathematical origins of general relativity and of unified field theories 0-95009
matter and light wave interferometry in gravitational fields 0-94997
maximal hypersurfaces, boundary value problem 0-82687
maximal hypersurfaces and positivity of mass 0-73237
mechanical oscillator, relativistic spin quadrupole gravitational effect (*Russian*) 0-68103
Minskowski space time, real analytic local extension 0-77656
motion of continuous medium in given space-time, four-velocity 0-68091
Nariai's boundary condition in general relativity 0-57148
negative mass and positive mass matter, hypothetical coexistence, causal paradoxes 0-82685
neutrino systems, relativistic kinetic theory of transport processes 0-73283
neutron interference, gravity and inertial effects, principle of equivalence at quantum level 0-77669
neutron interferometer expt., role of gravity in quantum theory 0-86176
neutron stars, electrodynamics in curved space 0-90465
nonstatic gravitational fields of an ideal fluid without shear and rotation 0-90741
Novikov coordinates, equivalent to Kruskal, transformaton from Schwarzschild coordinates 0-68098
null hyperspace initial data 0-101740
oscillations, Einstein's field eqns. 0-73217
perfect fluid cosmology with geodesic world lines 0-67924
perfect fluids, Hamiltonian formalism 0-82689
phase locked cavity, inertial mass and anomalous ang. momentum, fermion 0-86159
physicists' reactions and popular attitudes, historical account 0-77602
Plebanski classification of the tensor of matter 0-101737
polarisable media, relativistic models, and energy-momentum tensor of EM field (*Russian*) 0-86180
polytropic fluid spheres with negative index, struct. and stability (*Chinese*) 0-57143
propagation of the general relativistic blast wave 0-105549
PSR 1913+16, binary pulsar, relativistic observable effects 0-77438
PSR 1913+16, binary system, test of relativistic effects (*Dutch*) 0-62172
pure massless scalar geon from Einstein scalar field eqns. 0-86174
pure radiation fields and gravitational waves 0-77673
quantum field theory, indefinite-metric, boson field, equal-time commutator 0-68119
quantum field theory, Lagrangian formulation, conservation laws, relativistic gravitation (*Russian*) 0-68337
quantum gravity, choral of symmetries in general relativity 0-105565
quantum many-particle systems in curved spacetime 0-98751
quantum mechanical one-particle state, interfering neutron beam expt. 0-95025
radiating fluid spheres, interior solns., boundary conditions 0-77672
radiation damping, solvable model 0-73243
recursive calculation of axially symmetric stationary Einstein fields 0-77661
Reissner-Nordstrom perturbations, coupled Einstein-Maxwell eqns. 0-68108
relativistic gas stationary macroscopic motions, relations to gravitational field symm. 0-62552

general relativity continued

Ricci tensor, classification in space-times with four parameter group of motions 0-77660
Ricci tensor classification in space-times admitting four parameter group of motions 0-77659
Riemannian manifolds, symmetric vectors and algebraic classification 0-68094
rigidly rotating relativistic dust cylinder, Riemann tensor, ultrarelativistic case 0-86158
rotating black holes, superradiance, spin thermodynamic explanation 0-86179
rotating dust sphere, slow rotation limit, maximal slicing condition 0-73246
rotating systems, Einstein equations 0-68101
scalar field, exterior case, identification of variational principles (*French*) 0-73220
scale covariant gravity theories, astrophysical tests 0-73216
selfgravitating systems, strongly interacting, perturbation methods 0-73234
semiclassical relativity, weak field limit 0-57169
seven-dimensional relativity, 4-D gravity coupled to Yang-Mills fields 0-82699
shear hell holes and anisotropic universes 0-95011
shock wave propagation, stationary approx. 0-86172
singularities at real points of H space 0-98831
slow-motion approximation in radiation problems 0-73242
SO(3,2) de Sitter symmetry, spontaneously broken, gravitational holonomy group 0-57149
some electrovac models of homogeneous gravitational force fields in general relativity 0-95014
space-time events, nonlocalisability 0-94972
space-times, co-ordinate dependent investigation of limits 0-95003
spherically symmetric fluid, general relativity, equation of state, no slow uniform contraction 0-62544
spherically symmetric space-times with vanishing curvature scalar 0-68096
spinning particle in grav. field with torsion, eqns. of motion (*Chinese*) 0-62546
spinning particle in metric-torsion field, eqn. of motion 0-62543
star clusters, relativistic, with high central redshift 0-105293
static charged gas spheres, field eqns. solns. 0-101739
static general relativistic stellar models, props. 0-86165
static gravitational solitons, singularities, horizons, field behaviour at infinity (*Russian*) 0-73229
stationary Einstein-Maxwell equations, gravitational and EM potentials 0-86185
stationary Einstein-Maxwell fields, electrovacuum solution 0-73225
statistical formulation of gravitational radiation reaction 0-90749
stellar aberration, classical rel. to relativistic theory 0-67517
stellar dynamics, stability of spherical systems, binding energy criterion 0-94837
string thickening, null-string dust, bivector field 0-77671
string thickening, perfect dust, timelike bivector field 0-90732
strings and Maxwell fields of rank 2, local correspondence 0-73245
strong gravitational field and general relativity 0-67548
superpotential forms and total energy/momentum vanishing in closed forms 0-98828
symmetries and vacuum Maxwell's equations 0-86178
tangent bundle, geodesics, correspondence with spinning particles 0-68099
tests at quantum level 0-98849
theory of motion, electromagnetism, gravitation 0-105500
thermodynamics, relativistic, nonstationary, hidden variable approach 0-68097
thin sandwich problem, geometry 0-73239
Tomimatsu-Sato $\delta=3$ metric, Weyl conform tensor, invariants 0-68087
torsion effect on macroscopic gyroscope 0-98830
Trautman's radiation condition 0-73241
twisting type-N solutions 0-73221
twistor field equations 0-57145
two-body problem in linearised gravity 0-86160
two-body relativistic interactions, Hamiltonian formalism 0-77666
unified field theory, five-dimensional theory of interacting scalar, electromagnetic, and gravitational fields 0-105833
unified field theory, nonsymmetric, metric hypothesis, spinor analysis 0-68404
unified gauge theory of gravitational and strong interactions 0-95016
uniform field metric derivation without field eqns. 0-90739
uniform rotating sphere, five parameter internal gravit. field family (*Russian*) 0-95008
vacuum field equations, fifth dimension, ratio of EM to gravitational force 0-77679
vacuum superfluidity near anisotropic singularity, phase transitions (*Russian*) 0-94905
Vaidya's metric, complexification, radiative and nonradiative, parts of energy-momentum tensor 0-68093
variable rest mass field theory and the cosmological singularity models 0-77525
variational principle for perfect and imperfect fluids in general relativity 0-90733
vector field with zero covariant deriv., general metric 0-68092
velocity matrix in six-dimensional space-time 0-86171
velocity of light, Mossbauer meas., isotropy 0-95026
Vlasov-Einstein eqns. in spherical symmetry, self-similar analysis 0-67535
weak conservation law covariant formulation 0-73224
Weyl's theory and principle of least action, Riemannian manifold laws of motion (*French*) 0-62542
Weyl metrics, pseudo 0-95002
Yano vector fields and conformally related spaces 0-98829
zitterbewegung, atoms with point particles 0-57147

generator coordinate method

see also nuclear structure theory
cluster systems, normalisation kernels, SU(3) prop., generator coordinate theory 0-73814
Griffin-Hill-Wheeler equation soln. for scatt. problems 0-73813
matrix elements between arbitrary single particle wavefunctions, generator coordinate method 0-57751
*Be collective excitation spectra from generalised hyperspherical functions method (*Russian*) 0-91133

generator coordinate method continued

- ¹²C(α,α), generator coordinate multichannel calc., levels and resonances 0-78149
⁴He(α,α), s-wave, Coulomb amplitudes from generator coordinate theory 0-83107
⁴He(α,α), size change of α effect on phase shift, generator coordinate and variational methods (*Chinese*) 0-68683

generators, acoustic *see acoustic generators***generators, electric** *see electric generators***geochemistry**

- see also Earth structure; geology*
 anorthositic massif of Labrador's Nain complex, Proterozoic magma origin 0-94500
 apatite solubility in magma, laboratory expts. 0-72504
 Archaean metasedimentary rocks from Kambalda, Western Australia, rare earth element geochemistry 0-109143
 N.Atlantic mantle, chemistry and Pb, Nd, Sr isotopic correl. 0-90023
 basalt of back-arc basin, compositional evolution of mantle source 0-72471
 calc-alkaline volcanic rocks of Cerro Galan, NW Argentina, Sr isotope evidence for crustal contamination 0-98318
 Caledonian granites petrogenesis, isotopic evidence for continental crust provenance 0-109146
 continent to ocean fluxes of water-soluble K, Ca and Mg, contri. of atmospheric aerosols 0-72598
 Cretaceous-Tertiary boundary event, Os and Ir enrichment of sediments 0-76976
 crustal evolution and sedimentary recycling, evidence from Th and U abundances in sedimentary rocks 0-85654
 deep seismic zone, Tohoku, Japan, freq.-magnitude obs. rel. to geochem. changes 0-72447
 Earth's mantle, chemical evolution, nature and timing of mantle's differentiation 0-90043
 Galapagos spreading centre, volcanic rock differentiation trends 0-104937
 granitic magma of Bushveld Complex, trace element abundances rel. to crystallisation history 0-109145
 granitoid rocks, Nd-Sr isotopic relationship and continental crust development, chemical approach to orogenesis 0-94522
 groundwater, movement of solutes through aqueous fissures in porous rocks 0-94553
 Hawaii Geothermal Project, groundwater geochem. study 0-72567
 hydrothermal alteration of hot spring deposits 0-76974
 hydrothermal system, temp. measurement scale based on chem. comp. of gas fraction 0-98277
 Indian Ocean, physicochemical studies of coastal pollution off Bombay 0-104522
 SE Indian Ridge, seafloor mag. anomalies rel. to chem. of mid-ocean ridge basalt 0-109102
 Kerguelen Islands igneous rocks origin, role of enriched oceanic mantle sources 0-98319
 Laccadive Sea, chemical oceanography 0-104995
 Laccadive Sea, trace metals concs. 0-104997
 Laccadive Sea waters, total Hg concs. 0-104996
 Lake Michigan, surface microlayer and subsurface element concs. 0-77022
 lithosphere, present struct. and struct. evolution (*Russian*) 0-81857
 magma chamber, fluid dynamics model of differentiation and layering 0-76939
 mantle, lithophile elements depletion rel. to continental crust comp. and nature of lower crust 0-94498
 mantle chemical heterogeneity, evidence, conf., Nov. 1978, London 0-85623
 mantle Nd and Sr isotopes, differentiation occurring in episodes 0-67352
 mantle xenoliths, equilibrated Nd and unequilibrated Sr isotopic comp. meas. 0-98321
 Mid-Atlantic Ridge basalts, geochem. variation along length of ridge 0-90027
 Mid-Cayman Rise spreading centre, basalt glasses geochemical var. and petrogenesis 0-101364
 mid-ocean ridge basalts, composition restrictions 0-90025
 mid-ocean ridge basalts, source evolution from Bay of Islands ophiolite complex Nd and Sr isotopic study 0-85651
 ocean chemistry, role of ridge crest hot springs 0-98304
 ocean N cycle, implications of N₂O meas. in tropical E.Pacific Ocean 0-94542
 oceanic upper mantle, depletion by partial melting rel. to Owen fracture zone ultramafics petrology 0-94519
 oil shales of Green River, USA, thermal decomposition rel. to elec. cond. obs. 0-104495
 ophiolite petrogenesis in oceanic crust, Nd and Sr isotope study 0-61782
 orogenic herzolite petrogenesis in oceanic crust, Nd and Sr isotope study 0-61782
 E.Pacific Rise geothermal system, limits on geothermal fluid temp. rel. to metal transport and sulphides deposition 0-101362
 rare gases in volcanic rocks, isotopes mass fractionation as indicator of gas transport to or from magma 0-98292
 rhyolitic ignimbrites origin, Batopilas area, Mexico, Sr isotope study 0-94501
 rock melts, prediction of major element mineral/melt equilibria 0-109125
 Roosevelt Hot Springs thermal area, Utah hydrothermal alteration prod. minerals, mass abundance 0-90008
 salt deposits, Upper Triassic, of N.Atlantic region, lateral fractionation model for comp. var. 0-94516
 E.Scotia Sea, back-arc basin, volatiles in submarine volcanic rock 0-67353
 Severn estuary, seasonal and spring neap tidal depend. of axial dispersion coeffs. 0-94534
 silicic volcanics, Jurassic, from Nevada, USA, thermochemical remanent magnetisation 0-98310
 sulphide deposits from E.Pacific Rise near 21°N, mineralogy and geochemistry 0-101361
 thermobarogeochemistry of inclusions (*Russian*) 0-104954
 Troodos ophiolite complex, major oxide geochemistry and origin 0-98317
 ultramafic xenolith petrology and upper mantle processes, Kapfenstein, Austria 0-76973
 ultramafic xenoliths/basanite magma reaction in Tahiti lava, implications for magma crystallisation 0-90086
 Vellar estuary, Fe precipitation, conc. determ. 0-77015
 water from geothermal wells at geothermal well water, chemical analyses 0-90104

geochemistry continued

- ²⁴¹Am from nuclear weapons testing, evidence for delayed fallout from concs. in ocean sediments 0-98303
⁴⁰Ar, excess, in Alpine biotites, evolution from ⁴⁰Ar-³⁹Ar anal. 0-94521
¹⁰Be geochemistry in North Pacific during Pliocene 0-101356
 CaO, solid, phase transition at high-pres., lower mantle implications 0-79876
 H₂O, concs. in hypersthenic magmas rel. to juvenile outgassing and transport 0-72507
 He in Earth interior, incorporated from immature Sun (*Russian*) 0-81856
 K deficiency of ocean ridge silicic rocks, by vap. phase transport 0-81877
¹⁷O+¹⁶O, fractionation by chemical equil. 0-89513
¹⁸O+¹⁶O, fractionation by chemical equil. 0-89513
 P determination in surface fresh waters, automated procedure 0-81517
²⁴¹Pu from nuclear weapons testing, evidence for delayed fallout from concs. in ocean sediments 0-98303
²²⁶Ra, behaviour in Pee Dee River-Winyah Bay estuary, S.Carolina 0-98360
 Re-Os geochemistry, rel. to use of Os isotopes as petrogenetic and geological tracers 0-89989
 Th, analytical geochemical prospecting methods 0-72635
 U, analytical geochemical prospecting methods 0-72635
 U, isotope fractionation in Edwards carbonate aquifer, Texas, rel. to aquifer oxidation/reduction state 0-98362
 U prospecting, geochemistry of inclosure radioactivity 0-85766

geochronology

- see also radioactive dating*
 Adelaide Geosyncline, Australia, Late Precambrian palaeomagnetism 0-101325
 SW Alaska, episodic accretion and plutonism 0-101346
 W.Antarctic ice sheet, fluctuations in Antarctic Peninsula area 0-94549
 Antarctica, deep ice age and Holocene/Pleistocene climatic record from ice crust. size 0-94544
 Antarctica, subglacially erupted rocks of Early Miocene 0-98287
 Anti-Atlas, Morocco, Pan-African province geodynamic interpretation from geology and geochronology (*French*) 0-76952
 Archaean rocks of E.Lac Seul region, English River subprovince, NW Ontario, Rb-Sr isotopic study 0-94486
 Archaean sedimentary basins, time history rel. to lithosphere thickness 0-89986
 Archaean greenstone belt, NW. Ontario, Zr-U-Pb geochronology 0-98272
 Bay of Islands ophiolite complex, Sm-Nd age and Nd and Sr isotopic study 0-85651
 beach ridges in S.Australia, palaeomag. chronology rel. to Milankovitch theory of ice ages 0-98307
 Butte mining district, Montana, palaeomagnetism, rock magnetism and aspects of structural deform. 0-101326
 calcite dating, appl. of luminesc. under N₂ laser excitation 0-60685
 Canary Islands, age and crustal struct. 0-67355
 Chibougamau pluton, Quebec, Precambrian Rb/Sr geochronology 0-98273
 Chile, Camaraca Formation of Middle Jurassic, palaeomag. and plate rotation 0-85586
 Coso Range, California 0-90049
 Cretaceous section of Chilean Andes, palaeomag. and K-Ar age 0-85585
 Cretaceous-Tertiary boundary (Z coal), Hell Creek, Montana, Rb/Sr age 0-94487
 Dellwood knolls, volcanic activity age rel. to role in triple junction tectonics off northern Vancouver Island 0-90067
 Devensian glaciation in Britain, effects on water balance, 50000 yr BP to present day 0-72566
 Donegal granite, Ireland, emplacement age by isotope chronology 0-67356
 Duxbury massif (2.5 Ga), Quebec, remobilised piece of pre 3.0 Ga sialic basement 0-76970
 Eocene terminal event, formation of ring system around Earth 0-76890
 fission track dating using U glasses, error analysis 0-95503
 Goat Paddock cryptoexplosion crater, W.Australia, Eocene age determ. 0-98322
 E Greenland, southern Caledonian fold belt polyorogenic nature from isotopic age study 0-76938
 Grenville series of Ontario, palaeomag. rel. to Ar isotope dating 0-98232
 Himalaya, uplift and cooling rates from geochronological data 0-85627
 Iapetus Ocean, evidence for Cambrian opening 0-98299
 SW Iceland, K-Ar ages, stratigraphy and palaeomagnetism of Esja, Eyrafljall and Akrafljall mountains 0-89950
 N.Iceland, lava succession, K-Ar dating, geological and palaeomagnetic obs. 0-109096
 Iceland Plateau, history from sea floor morphology and mag. anomalies N of Iceland 0-89953
 Indo-Australian plate, internal deform. chronology rel. to Himalayan orogenic stage 0-109134
 Japan, uplifted terraces ¹⁴C dating rel. to large earthquakes time-predictable recurrence model 0-85598
 Lepontine Alps, chrontours rel. to heat-flow distrib. temporal changes assoc. with metamorphism 0-101347
 Lower Ordovician rocks of NW Argentina, palaeomag. and K-Ar age 0-89938
 marine, sediment, ²³⁰Th age, α -scintillation counting method 0-72636
 Messina Layered Intrusion, Limpopo Mobile Belt, S.Africa, tectonic setting, geology and age 0-76969
 Munster Basin, NW Germany, Upper Cretaceous limestones magnetisation age and Cretaceous pole position 0-89949
 Newfoundland, Early Palaeozoic plate tectonic model 0-94509
 Norwegian eclogites, Caledonian Sm-Nd ages and crustal origin 0-76978
 Oxford Lake-Knee Lake greenstone belt, N.Manitoba, Rb-Sr ages 0-94485
 Quaternary palaeoclimate temp. and precip. chronology for N.America NW. coast region 0-98438
 rinneite, Rb-Sr dating of potash salt deposits 0-67429
 salt deposits, Upper Triassic, of western N.Atlantic, stratigraphic age 0-94516
 Santorini (Thera) eruption, 1450 BC, archaeological dating for tephra discovered at Rhodes 0-109129
 SW. Scottish Highlands, chrontours, rel. to heat-flow distrib. temporal changes assoc. with metamorphism 0-101347
 Searles Valley, California, lacustrine sediment core chronology from palaeomagnetic data 0-89955

geochronology continued

sediment core from Gulf of California, varve chronology rel. to ³²Si half life determ. 0-91153
sedimentary basins, heat flow and subsidence histories with finite crustal extension rates 0-89987
Sibley Group, Thunder Bay district, Ontario, Canada, stratigraphy and depositional setting 0-94517
Siebengebirge, Germany, K-Ar age of Tertiary volcanics 0-98280
Silurian-Devonian rocks of NW.Argentina, paleomag. and K-Ar age 0-89938
Sulawesi (E Indonesia) western arc, palaeomag. studies and fission-track dating rel. to tectonic history 0-89957
thermoluminescence and age determination (*German*) 0-105076
trondhjemitic basement enclave, near Favourable Lake volcanic complex, NW.Ontario, Canada, age 0-94518
vermiculite, fission track annealing and dating 0-81885
volcanic plagioclases, thermoluminescence dating 0-98475
Pb isotopes struct. of basic-ultrabasic layered complex 0-81847
U-Pb ages of pegmatites in Enderby Land, Antarctic 0-76946

geodesy

see also gravity
Afar triangle, geodetic evidence for rifting, model for vertical displacements 0-98295
Ancona geodetic network, design problem 0-85578
artificial satellite laser ranging, high precision, earthquake anal. 0-98215
British Isles 0-109086
crustal deformation analysis, models for estimation of parameters (*German*) 0-101319
data analysis by collocation method 0-77130
deep asymmetry of Earth, inertia rel. to convection currents 0-98269
densification of ground control networks, computer program package (*German*) 0-94452
Diablo Plateau region, W.Texas, new evidence for tectonic uplift 0-72481
displacement meas., small, using three-mode laser 0-77748
Earth deformation, mag. field effects 0-109085
Earth pear-shaped section, improved longitude-averaged meridional profile 0-94450
earthquake prediction based on tilt anomaly 0-104917
free nets, modification of Helmert-Wolf's soln. (*German*) 0-94453
geocentric position variation due to terrestrial fluid mass motion 0-76894
geodynamical changes, evaluation of Doppler satellite obs. 0-76893
geoid and global heights in Europe, collocation method analysis 0-76896
geoid height, spherical harmonic potential coeffs., use of area means 0-94449
geopotential from gravity measurements, levelling data and satellite results 0-101313
geopotential resonance, Skylab 1 rocket, 1973-27B, orbit determ. and anal. 0-67515
global gravity field compared to geomagnetic potential 0-104854
gravity perturbation due to ocean tide, series computation 0-104857
ground tilt, measurement via borehole long-period seismometer (BELS type 79) with stable period (*Japanese*) 0-67417
Haystack-Westford base line vector, geodetic meas. comparison with radio interferometry obs. 0-89929
horizontal networks, height-controlled three-dimens. adjustment 0-101444
hydrostatic ellipticity calculation algorithm 0-62055
N Iceland, gravity and height vars. during present rifting episode 0-90060
NE Iceland rift zone, geodetic meas. and horizontal crustal movements 0-89930
interference distance meas. using semicond. lasers 0-77175
Japanese Islands region, topography and gravity anomalies data compilation (*Japanese*) 0-67332
Krafla Caldera, NE Iceland, gravity and elevation changes caused by magma movement 0-90052
Krafla volcano area, N. Iceland subsidence events, (1975 to 1979) 0-90053
LAGEOS orbit, long-term evolution 0-94676
level surveying, atoms. refr. correction (*Russian*) 0-77127
levelling survey data, math. anal. for assumed const. vertical vel. (*German*) 0-82081
mantle (lower), density anomalies derived from geophys. data 0-89927
network connection problems, stiffening problem, error anal. 0-81799
networks design for crustal movements study (*German*) 0-76897
observatory at Graz-Lustbuehl, Austria, work and projects 0-77117
ocean, sea level transients obs. by Geos 3 coincident orbits 0-72535
optical systems, high-precision compensated levels, geodetic appl. 0-101813
Pacific sea-floor topography and isostatic compensation mechanism (Hawaii region) 0-104945
physical geodesy and surveying, objectives, meas. techniques and data processing methods (*German*) 0-101317
positive geoid height anomalies, correl. with subducted lithosphere and hotspots 0-90056
radio methods, quasi-single freq. Doppler-Faraday technique 0-77128
satellite altimetry data anal., combination solns. 0-76895
satellites gravity measurements, basic mechanical principles of gravimeters and gravity gradiometers (*German*) 0-101461
scale and orientation in combined Doppler and triangulation nets 0-101311
sea-mount loads affecting crust, isostatic compensation and geoid anomalies 0-109132
SEASAT radar altimeter, resolution capability preliminary estimates 0-72645
SeaSat-1 North Sea expt. (*German*) 0-81805
second-order derivatives in spheroidal and spherical coords. 0-101315
smoothing function recurrence relation 0-98213
spherical harmonic coefficients of Earth's field, orthogonality 0-104881
spherical harmonic potential coeffs., use of area means 0-94449
surface deformation detect., 500-m base laser interferometer 0-105087
tangent bundle, geodesics, correspondence with spinning particles 0-68099
tides in solid Earth, review (*Chinese*) 0-89925
trilateration network, adjustments to account for meteorological conditions 0-77131
W.USA, vertical crustal movement, anal. of levelling survey 0-72409
variance-covariance-component estimation of Helmert type, introduction 0-101318
Very Long Baseline Interferometry appl. to geodesy 0-109274

geodesy continued

Walvis Ridge, compensation mechanism 0-94448
zenith telescope geodetic meas. 0-98550

geodetics *see geodesy*

geoelectricity *see terrestrial electricity*

geology
see also rocks
acoustic fluidisation, new geological process, theory and appls. 0-85653
Adelaide Geosyncline, Australia, Late Precambrian geology and palaeomagnetism 0-101325
Afghan Pamir, geology and tectonics of Himalayas 0-72513
E.Afghanistan, Logar ultrabasic massif, geology and geomag. 0-72512
Antarctica, subglacially erupted rocks of Early Miocene 0-98287
Anti-Atlas, Morocco, Pan-African province geodynamic interpretation from geology and geochronology (*French*) 0-76952
apatite solubility in magma, laboratory expts. 0-72504
Appalachians, structural trends NE of Newfoundland and Trans-Atlantic correlation 0-85656
Archaean rocks of E.Lac Seul region, English River subprovince, NW.Ontario, Rb-Sr isotopic study 0-94486
Archaean rocks of Limpopo Mobile belt, showing early high-grade metamorphism 0-94502
Archaean sedimentary basins, geology rel. to lithospheric thickness 0-89986
Archean greenstone belt, NW. Ontario, Zr-U-Pb geochronology 0-98272
N.Atlantic, Mesozoic and Cainozoic, calcareous sediments depth distrib. 0-81866
Australia, tectonic, igneous and metallogenic provinces rel. to mantle convection and subcrustal stresses 0-72484
Baikal region hot springs (*Russian*) 0-94551
basalt of back-arc basin, compositional evolution of mantle source 0-72471
basic-ultrabasic layered complex, Pb isotope composition 0-81847
Bay of Islands ophiolite complex Nd and Sr isotopic study rel. to midocean ridge basalts source evolution 0-85651
Black Sea NW shallow, lithology and stratigraphy from seismic multi-dimensional vel. generalisation (*Russian*) 0-105068
Bohus granite area, SW Sweden, geothermal investigations 0-85631
Bonnet Plume Basin, Yukon Territory, Canada, gravity profile anal. as aid to coal basin evaluation 0-76898
British Isles, evidence for Cambrian opening of Iapetus ocean 0-98299
Bushveld Complex, geology, eastern compartment emplacement model 0-94505
Butte mining district, Montana, palaeomagnetism, rock magnetism and aspects of structural deform. 0-101326
Cainozoic intra-plate convection, rel. to mantle convection 0-98293
Canary Islands, palaeomagnetism and early magmatic history 0-72431
CaO-SiO₂-CO₂, subsolidus and liquidus phase relationships to 30 kbar 0-85643
carbonate mineral identification by CO₂ evolution on heating 0-90248
Carpathian Mountains, disjunctive dislocations revealed by interpretation of space television photographs (*Russian*) 0-104958
Cesano geothermal field, Italy, geological study 0-76975
chelonian cycles in continental crust evolution (*Chinese*) 0-89984
Chibougamau pluton, Quebec, Precambrian Rb/Sr geochronology 0-98273
Chilkat Peninsula, Alaska Upper Triassic rocks, regional implications 0-98271
cirques in Bear River Range, north-central Utah, numerical anal. 0-72510
coal seams, approx. seismic wave diffrac. theory for transparent half-planes 0-89974
Columbia Plateau, basalt flow, contact zone remanent magnetisation 0-81881
Coso Range, California 0-90049
Cretaceous species extinction explained by cometary impact 0-76977
Cretaceous-Tertiary boundary, plankton extinction and geochem. indicating extraterrestrial event 0-76976
Cretaceous-Tertiary boundary (Z coal), Hell Creek, Montana, Rb/Sr age 0-94487
E.Crimea, geological data rel. to deep crustal struct. (*Russian*) 0-104933
Dahomeyide orogenic belt, geology and struct. correl. with Volta Basin 0-109121
desert features created by wind, Western Desert of Egypt compared with Mars 0-72815
Donegal granite, Ireland, emplacement age by isotope chronology 0-67356
Dunnage Melange, Newfoundland, regional geology 0-81875
Duxbury massif (2.5 Ga), Quebec, remobilised piece of pre 3.0 Ga sialic basement 0-76970
earthflow slope formation in Hong Kong 0-109144
Elberton pluton, Georgia, USA, palaeomag. of granite 0-72423
electron microscopy, use in Earth sciences 0-105091
evaporite deposition from groundwater mobilised salt, coastal sabkhas, Libya 0-81883
extension veins of deformed rock, crack-seal mechanism 0-61798
faults and other linear features, detect. from LANDSAT images 0-77177
faults and shear zones, assoc. deep focus earthquakes 0-61786
Favourable Lake volcanic complex (Archaean), NW.Ontario, Canada, trondhjemitic basement enclave 0-94518
fluorite mineralisation of carbonate bearing rocks, dynamic model 0-81876
Franciscan formation, California, pedestrians guide to rock exposures 0-81849
Galapagos spreading centre, volcanic rock differentiation trends 0-104937
Garon Lake Archaean geothermal system, Matagami rock-water interaction 0-98283
Geotraverse Rhenoherynikum, fault zones investigation by seismic refl. and refr. studies 0-90046
glacial sediments of English Lake District, pre-Devensian till 0-94523
Goat Paddock cryptoexplosion crater, W.Australia struct. and shocked rocks petrology 0-98322
greenstone belts, numerical models of vertical Archaean tectonism 0-81861
Grenville Front Zone, Precambrian geological struct. of Labrador 0-8274
W.Himalaya, Central Crystallines, geology and tectonics 0-72516
Himalaya, Tethyan and Higher, geological description 0-72515

geology continued

- Himalaya and Indo-Gangetic Plains, geology and pre-Mesozoic orogeny 0-72514
 Himalayas region, conf., Mar. 1978, Katmandu, Nepal 0-72523
 human interference with geological medium, investigating methods 0-85323
 hydrogeological database characts. (Italian) 0-109255
 hydrothermal alteration of hot spring deposits 0-76974
 Iberian margin ocean-continent boundary struct., discovery of serpentinite diapir W. of Galicia Bank 0-94489
 NE Iceland, dyke swarms rel. to geomag. anomalies (ΔZ) 0-89951
 N Iceland, results of height meas., (1965 to 1977) 0-89931
 SW Iceland, stratigraphy and palaeomagnetism of Esja, Eyrafjall and Akrafjall mountains 0-89950
 igneous dikes, depth estimation via mag. anomaly sounding (Russian) 0-105069
 igneous layered rocks, magma double-diffusive crystallization 0-90081
 India, peninsular, fan faults rel. to origin of Himalayas 0-85630
 S.Indian craton, tectonic-framework deduced by LANDSAT imagery 0-98290
 Indo-Australian plate, deformed oceanic crust rel. to plate internal deform. 0-109134
 Indo-Gangetic Plains and Himalaya, geology and pre-Mesozoic orogeny 0-72514
 IR multispectral aircraft scanner data, image processing 0-98454
 Isua supracrustal belt (Early Precambrian), W. Greenland, cosmic grains discovery in Fe formation 0-72508
 Itapicuru greenstone belt, survey for ore bodies in Brazil 0-81879
 Jharia coalfield of India, survey of struct. and geol. 0-76972
 Jharia Gondwana sedimentary basin, India, geology rel. to geothermal meas. 0-98276
 josephinite, Widmanstaetten patterns as evidence of mantle origin 0-81887
 Lepontine Alps, metamorphism rel. to heat-flow distrib. temporal changes 0-101347
 limestone cave deposits, O isotopes for palaeotemp. of mid-Wisconsin 0-82069
 Longonot volcano, Central Kenya, geology, question of volumes of volcanic products 0-85633
 LWR spent fuel elements, disposal in geologic isolation, feasibility study report 0-106140
 magma chamber, fluid dynamics model of differentiation and layering 0-76939
 magnetic profiling of geological contact, harmonci inversion method 0-77137
 mantled gneiss domes of E.Finland, cluster pattern implying gravit. instability of Proterozoic crust 0-81848
 Messina Layered Intrusion, Limpopo Mobile Belt, S.Africa, tectonic setting, geology and age 0-76969
 metallic mineral deposits of Australia mag. induced polarisation survey results 0-98223
 meteorite crater field formation, effects of meteoroid atmospheric breakup 0-94760
 Mid-Atlantic Ridge, geology of submarine hydrothermal field at 26°N latit. 0-85641
 mineral identification in rocks, mag. rot. hysteresis loss meas. 0-67428
 Moenkopi formation, SE.Utah, USA, magnetostratigraphy 0-72422
 Moine thrust zone, differential stress determ. from deformation-induced microstructs. 0-85652
 Nain anorthositic complex, Labrador, examples of contrasted magmas commingling in plutonic environment 0-104959
 Nepal, basic intrusions of volcanic origin 0-72477
 Nepal Himalaya, struct. geology of Kusma-Sirkang section 0-72478
 Newfoundland, geology rel. to Early Palaeozoic plate tectonic model 0-94509
 Nias Island, Indonesia, sedimentology and palaeobathymetry of Neogene trench-slope deposits 0-104950
 Nias Island, Indonesia, structural geology implications for subduction zone tectonics 0-109120
 N.Nigeria, pipe in schist belt, geophys. anomaly study 0-76971
 North Sea basin, subsidence in post-mid-Cretaceous 0-109133
 ocean spreading ridge, silicic rocks, late-magma vap. transport of K 0-81877
 ophiolite petrogenesis in oceanic crust, Nd and Sr isotope study 0-61782
 ophiolitic melange of Late Precambrian, Egyptian desert, formation process 0-81884
 Ordovician basalt assoc. with Fe-rich deposits, in Scotland, ancient mid-ocean ridge? 0-81878
 orogenic lherzolite petrogenesis in oceanic crust, Nd and Sr isotope study 0-61782
 Oxford Lake-Knee Lake greenstone belt, N.Manitoba, Rb-Sr ages 0-94485
 E.Pacific Rise, geology of hot springs areas 0-101360
 plutophysical props. of ultramafic rocks, using factor analysis 0-90087
 plutonic intrusions, influence of temp. on deep magmatic diapir folds (Russian) 0-104957
 Proterozoic anorthositic massif of Labrador's Nain complex, magma origin 0-94500
 pyroxenes from planetary basalt, silicate mineralogy study 0-72802
 quartz cryst. axes orientation, in metamorphosed volcanic sediment 0-85655
 radioactive waste disposal in geologic formations, site selection criteria 0-106142
 remote sensing application 0-109279
 rhyolitic ignimbrites origin, Batopilas area, Mexico, Sr isotope study 0-94501
 rinneite, Rb-Sr dating of potash salt deposits 0-67429
 rock chem. weathering rate 0-77142
 rockfall from cliff face, seasonal variation obs. in N.Ireland 0-105001
 salt deposits, Upper Triassic, of western N.Atlantic, obs. from Newfoundland Grand Banks 0-94516
 San Andreas Fault, geodetic tilt obs. 0-81800
 SW. Scottish Highlands, metamorphism rel. to heat-flow distrib. temporal changes 0-101347
 sediment of continental shelf, anomalous declination due to slumping 0-76964
 SE Siberia, crust struct. and role of Archean folded ovals 0-101349
 Sibley Group, Thunder Bay district, Ontario, Canada, stratigraphy and depositional setting 0-94517
 Siebengebirge, Germany, K-Ar age of Tertiary volcanics 0-98280

geology continued

- silicate glasses of geologic interest; Mossbauer absorpt. of Fe III, effect of glass chem. comp. (French) 0-80658
 spent nuclear fuel stored in basalt, chances of reintroduction into biosphere, analysis 0-106144
 stratigraphic data, support for astronomical theory of climatic fluctuations 0-72509
 structural geology, conf. (1978), Toronto, Canada 0-101666
 structural geology, LANDSAT data anal. (Italian) 0-109281
 subduction zones, material transport within accretionary prisms and 'knocker' problem 0-101353
 sulphide prospect in California copper belt, broadband EM study 0-72503
 surface geology of glaciated area of USA, ground mode radiowave propag. 0-76979
 Texas, geological interpretation of National Uranium Resource Evaluation (NURE) aerial radiometric survey data 0-101438
 Theftford Mines ophiolites, Quebec, palaeomagnetism 0-61757
 SW.Tunguska syncline, platform structure from gravity surveys 0-98289
 ultramafic xenolith petrology and upper mantle processes, Kapfenstein, Austria 0-76973
 E.United States, geology rel. to low-temp. geothermal resources 0-85264
 United States Atlantic continental shelf, US Geological Survey core drilling 0-72511
 Volta Basin, geology and struct. correl. with Dahomeyide orogenic belt 0-109121
 Western Desert of Egypt, wind pitted and fluted rocks compared with Mars obs. 0-72816
 Yellowknife supergroup, Northwest Territories, volcanic rock density determ. from gravity obs. 0-98320
 Rn mapping in U exploration, exclusion of ^{220}Rn signal 0-61916
 U abundance in Himalayan plants, fission track method 0-101305

geomagnetic storms see magnetic storms

geomagnetic variations

- see also micropulsations
 ΣKp parameter, rel. to nighttime electron content of mid-latit. plasmasphere, 1974 August to November 0-94642
 A₁-index, 1964-1976, rel. to geomag. field and interplanetary field states 0-104866
 activity, effect on radar meteor rate 0-67662
 Adirondacks, geomag. fluctuations gradient anal. 0-89947
 archaeological ceramics, Peru, geomag. variations over last 2000 yrs. 0-94455
 archaeomagnetic field strength, Egyptian adobe bricks (3000-0BC) 0-104862
 auroral luminosity rel. to geomag. field changes 0-77187
 auroral oval, mag. fluctuations prod. by ionospheric Hall current 0-98501
 auroral zone, ground-based obs. of elec. currents using two-dimensional magnetometer array 0-90245
 Basque Provinces, Pyrenean folding, deep geomagnetic sounding (French) 0-67351
 coast effect, review 0-94458
 D_{st} index, negative change assoc. with whistler ducts formation 0-94659
 daily mag. variations meas. in Alaska, atmos. current system 0-85590
 daily magnetic variations influenced by interplanetary field 0-85591
 daily variation at equator affected by N. and S. hemisphere Sq currents 0-76904
 daily variations (lunar and solar) 0-109104
 diurnal variation of horizontal field component, correl. with ionospheric equatorial anomaly 0-109301
 earthquake precursory field changes, Nov. 1974 Hollister 'quake, California 0-104912
 EM induction, transfer functions at pulsation periods 0-72417
 equatorial geomagnetic field, daily variations, effect of sector boundary passage 0-67335
 excursions and Pyramid Lake, Nevada palaeomagnetic record 0-101321
 exosphere, mag. activity effects on temps. at high latits. 0-109286
 interplanetary mag. field caused by cyclical nature 0-81813
 K₁-index influence on equatorial P₂ pulsations fine struct. 0-72721
 K₁-index 3-hr range, geophys. meaning 0-82143
 local daytime energy spectra, depend. on solar wind vel. and interplanetary mag. field direction 0-67476
 Lunping, Taiwan, solar and lunar daily variations, 1966 to 1976 period 0-72416
 magnetic noise of low-freq. generated on auroral field lines 0-101494
 magnetometer for sea-floor mag. fluctuations, ULF-ELF 0-77152
 magnetosphere, geomag. fluctuations obs. by new space-borne ring-core type magnetometer (Japanese) 0-94671
 magnetosphere, large scale elec. fields and currents, related geomag. vars., review 0-105121
 Lower Matuyama epoch, geomagnetic events from palaeomag. obs. in SW Iceland 0-89950
 ocean currents due to geomag. field, theory 0-104962
 ocean electric current induced by Sq, around land masses 0-72413
 palaeointensity secular variation, meas. on postglacial lavas from Iceland 0-89952
 palaeomagnetic data analysis, elimination of secular variation 0-61755
 polarity reversals, role of fluid core dynamics with inward growing boundaries 0-76934
 Proterozoic Belt Supergroup in Montana and Idaho, palaeopoles and polarity zonation 0-72420
 Ps 6 magnetic disturbances, seasonal and diurnal var. 0-67477
 SW.Queensland, telluric currents assoc. with anomalous geomag. vars. 0-109089
 remote sensing at mesospheric heights 0-77124
 reversal chronology from Arizona volcanic sequence rel. to ocean floor polarity record 0-72419
 S₁ obs. from Alaskan meridian chain, ionosphere and magnetosphere currents 0-85813
 S₂ variation, magnetosphere or ionosphere dynamo? 0-109090
 San Andreas fault, local mag. field meas. rel. to fault creep obs. 0-85629
 secular impulse rel. to deep mantle conductivity 0-98236
 secular trends in daily mag. variations 0-109103
 secular variation, 1947-1977, implications for mantle elec. cond. 0-61754
 secular variation, dynamo theory frictional damping of Hide's mag. waves 0-98218
 secular variation, modelled on mantle elec. cond. inhomogeneity (German) 0-81806

geomagnetic variations continued

secular variation in Europe, analytical representation on basis of observational data 0-101323
secular variation in Finland, 1650-1970 period 0-67336
secular variation since 8500 BP 0-104865
secular variations, geomag. field models comparison with obs., rel. to broad scale anomaly studies 0-72425
secular variations, short period, meas. from palaeomag. records of N.Poland Holocene lake sediments 0-98221
secular variations from Iceland lava flow data, model 0-104871
short-period anomaly over Imandra-Varzuga structure (Kola Peninsula) (Russian) 0-85589
short-period variations, changes in direction of mag. vector before 1972
Sitka, Alaska, earthquake 0-76923
solar cycle variation, of geomag. external spherical harmonic coeffs. 0-85592
solar cycle variations, of first-degree spherical harmonic components of geomag. field 0-85593
Sq and EM induction of oceans, during IGY 0-72428
St. Vincent's Gulf, South Australia, island and coast effect in geomag. vars. 0-72426
strong disturbances, correl. with lower atmosphere instability at different seasons 0-61881
substorm variation field modeling, current system anal. 0-105130
substorms, high-latit., mag. vars. characts. 0-109315
substorms, negative bays rel. to electron flux vars. in inner radiation belt near trapping zone boundary 0-67470
thermosphere, magnetic activity effects on winds in N.Polar Cap 0-67445
total intensity secular trend at Bombay (1848-1967) rel. to sunspot nos. 0-81811
twelve month wave in an and as activity indices 0-72427
Vancouver Island region, terrestrial EM induction 0-104879
volcanomagnetic effect, piezomag. field assoc. with Mogi model for surface displacements 0-67334
vorticity area index at 500 mb, geomagnetic disturbance effects 0-61873
Yoldia Clay sequence from Denmark, 14-40000 yr B.P., geomag. variations 0-94454

geomagnetism

see also geomagnetic variations; magnetic storms
Adirondak mountains, mag. field components, fluctuation anal. 0-89946
E.Afghanistan, Logar ultrabasic massif, geology and geomag. 0-72512
N.America, E. coastal region, EM induction model 0-98235
animal sensitivity to geomag. field, ferromag. coupling to muscle receptors as basis 0-72185
anomalies, derivative harmonic function restoration (Russian) 0-85577
anomalies due to subsurface features, rel. to sloping contacts interpretation 0-98222
anomalies in Altai Sayan folded region USSR, due to deuteroorogenic stage complexes 0-101327
anomalies interpretation, separation from gravity anomalies of comparable horizontal dimensions 0-94606
anomalies of mag. and gravity field, anal. by unitary method 0-89932
anomalies over three-dimens. objects, inverse problem soln. 0-89939
anomaly due to 2-D assym. triangular prism, expression for total field 0-94457
anomaly due to magnetic body, parameters of body from pot. data 0-85581
anomaly inversion, generalised multibody model 0-98226
anomaly of thin dike, curve fit by calculator program 0-98228
anomaly sounding, estimation of cover thickness above magnetised mass (Russian) 0-105069
anomaly survey data analysis, curve-matching optimisation method (Chinese) 0-89935
central Australia, geomag. induction 0-72424
Australia, geophysical profile along 29°S 0-72460
Australian magnetic observatories 0-72632
bays rel. to geomagnetic activity and 1972 interplanetary magnetic field 0-105124
bow shock, DC mag. field obs. 0-90306
Canada, geomag. field models comparison with obs., rel. to broad scale anomaly studies 0-72425
Canada, long-wavelength mag. anomalies determ. using polynomial and upward continuation techniques 0-85594
Canada, magnetic observatories annual report (1977) (French, English) 0-72418
E. Canada, sedimentary cover thickness meas. by aeromag. survey 0-77138
Columbia Plateau, basalt flow, contact zone remanent magnetisation 0-81881
conductive cylinder, anomalous mag. field, induced by elec. current (Chinese) 0-104858
contact surface parameters, determ. using space domain filter method (Chinese) 0-89933
core-mantle boundary, magnetic contour map 0-104880
Coso Range, California, aeromagnetic and gravity surveys 0-89943
data reduction and analysis, data from satellite magnetometer 0-77141
Dead Sea Rift and N.Israel, mag. and gravity obs. and interpretation 0-98233
deep crustal struct. inferred from mag. anomalies of long-wavelength 0-72430
Dellwood knolls, mag. anomalies rel. to role in triple junction tectonics off northern Vancouver Island 0-90067
dipole axis precession rel. to auroral activity equatorial latitude 0-98499
dipole field, comparisons with cosmological expectations 0-67337
Djibouti Republic, magnetic anomaly map and tectonic interpretation 0-61753
dynamo action in rotating shell 0-81807
dynamo model of magnetic field, self-consistent treatment 0-81808
dynamo problem, dynamics of fluid core with inward growing boundaries 0-76934
dynamo theorems 0-81810
dynamo theory, core paradox reconsidered 0-90033
dynamo theory, spherical dynamo with anisotropic α -effect 0-81809
Earth deformation, mag. field effects 0-109085
EM depth sounding interpretation, master tables, book 0-86043
EM field above two-dimensional inhomogeneous struct., boundary conditions 0-85595
EM induction effects of ocean coast 0-76908

geomagnetism continued

EM sounding, iterative ray tracing between boreholes for underground image reconstruction 0-98466
EM sounding, VLF-EM profiles, topographic correction based on model studies 0-101452
EM soundings, multifrequency, topographic and misorientation effects study 0-101451
evolution of life, role of Earth's magnetic field and steady ozone layer 0-104883
external spherical harmonic coeffs., solar cycle var. 0-85592
first-degree spherical harmonic components, solar cycle vars. 0-85593
Galapagos Islands, t, spreading centre jumps 0-104877
geoelectric inhomogeneities, position determination by variable geomag. field method 0-89956
geological contact magnetic profiling, inverting by harmonic method 0-77137
gradiometer data integration in geomagnetic surveying 0-105064
NE.Iceland, elec. resist. model from magnetotelluric obs., correl. with temp. 0-89954
NE Iceland, mag. anomalies (ΔZ) and interpretation based on rock magnetic investigations 0-89951
Iceland, sea floor morphology and mag. anomalies N of Iceland 0-89953
SE Indian Ridge, seafloor mag. anomalies rel. to chem. of mid-ocean ridge basalt 0-109102
ionosphere, elec. currents and mag. field vector obs. by S-310-5 rocket (Japanese) 0-94635
ionosphere, mag. field obs. by Atmosphere Explorer C rel. to field-aligned currents and plasma drift vel. 0-72681
ionospheric records over Shanghai, March 1953 to June 1955, Earth mag. field intensity (Chinese) 0-77192
Itapicuru greenstone belt, Bahia, Brazil, mag. survey for ore bodies 0-81879
lightning direction finding, by mag. method 0-77078
magnetic induced polarisation techniques, effect of large cond. contrasts 0-98461
magnetic potential compared to global gravity anomaly field 0-104854
magneto-telluric response dispersion relations, inversion problem theory 0-104861
magnetosheath, high latit., mag. field lines rel. to ≤ 2 MeV electrons transport 0-90296
magnetosphere, field line MHD torsional oscill. rel. to mini-substorm and long-period Pi 2 event (Japanese) 0-94653
magnetosphere, force tube width rel. to turbulence development in longit. currents 0-67469
magnetosphere, local electron density and mag. field meas. via JIKIKEN (EXOS-B) satellite stimulated plasma wave expts. (Japanese) 0-94649
magnetosphere, mag. curl in front of magnetosphere boundary 0-85804
magnetosphere, quadrupole shape 0-101492
magnetosphere plasma sheet, variability of mag. field and dynamics during substorms 0-98518
magnetostatic field problem, soln. in high susceptibility case via method of subsections 0-105065
magnetotail, neutral sheet, particle accelerations 0-72696
magnetotelluric field of electrical currents in bottom and shore of Barents Sea 0-104864
magnetotelluric sounding, fundamental model 0-77167
marine magnetic anomalies, implications from Troodos ophiolite metamorphism 0-81812
marine magnetic anomalies origin, implications of palaeomagnetism of Thetford Mines ophiolites, Quebec 0-61757
metallic mineral deposits of Australia mag. induced polarisation survey results 0-98223
Moon recording Earth mag. field on fission origin from mantle 0-101537
ocean current induced EM fields, theory 0-61805
ocean ridge anomalies, mantle thermoconvective wave explanation 0-90064
oceanic crust magnetic reversal boundary, three dimens. modeling inversion of deep sea tour obs. 0-109098
E.Pacific Rise, mag. gradiometer meas. rel. to marine mag. anomalies origin 0-101360
piezomagnetic field, assoc. with Mogi model of surface displacements around volcanoes 0-67334
polarity in magnetotail neutral sheet, statistical determ. 0-72717
potential field modelling, end corrections 0-85580
quartz H magnetometer, calc. formula for horiz. component 0-105062
regional and local mag. fields, local function representations 0-98225
Reykjanes Ridge, mag. anomalous south of 60°N rel. to evolution between 40 and 12 Myr BP 0-90069
ring current magnetic field at magnetically quiet geomagnetic equator 0-105123
ring current magnetic field characts., spherical harmonic analysis 0-101493
Souss Basin, S.W. Morocco, mag. survey and crustal struct. 0-89958
spherical harmonic coefficients of Earth's field, orthogonality 0-104881
spherical harmonic spatial power spectra, for crust and core fields 0-104882
subsurface EM field propagation from horizontal elec. dipoles, comprehensive study 0-98229
surface vertical component from aeromagnetic survey, computational method 0-105061
Tohoku District mag. anomalies, high-altitude meas. by balloon-borne ring-core magnetometer (Japanese) 0-94608
twelve month wave in an and as activity indices 0-72427
Weddel Sea, geomagnetic, bathymetric and seismic obs. of crust 0-104929

geometrical optics

aerosol medium bleached zone, probe radiation propag., intensity and phase fluctuations 0-67411
analogue model, light reflection and refraction, teaching 0-67948
beam splitting device for use with smoke chamber ray optics demonstrations 0-67990
binocular vision, artificial aniseikonia, geometrical explanation of induced size effect 0-72173
bipolar spatial filtering, incoherent, review 0-102822
caustic point displacement due to generalised bending, third-order approx. 0-83656
circular cylinders, single scatt. phase matrix, ray optics and wave theory comparison 0-102610
complex ray analysis for plasmas 0-83902

geometrical optics continued

- concentrator, compound parabolic, phase space conservation for incoherent propag. 0-69491
 corner diffraction, Albertsen's coeff. testing via spectral domain approach 0-87304
 differential mode delay rel. to refr. index profile, geometrical optics treatment 0-69529
 diffraction and aberration effects, wave optical calc. 0-83549
 education, lens Fourier transform properties 0-57024
 education, matrix optics, principal plane concept generalisation 0-73140
 electron optics, charged particle trajectory calc. in electrostatic field, teaching 0-90635
 ELMO Bumpy Torus, ray tracing near electron cyclotron freq. 0-83975
 EM scattering from dielectric coated conducting cylinder, ray optical anal. 0-83542
 fibre, graded index, mode coupling due to perturbation of index profile 0-106598
 fibre scattering, ray theory 0-69528
 focused beam ray tracing for laser fusion 0-83218
 focused field, symmetry props. 0-83550
 focused light beams, phase anomaly, intuitive explanation 0-99622
 Gaussian beam propagation in 3-layered dielec. medium (*Japanese*) 0-87306
 Gaussian optics parameters, HP-67 calculator program 0-106439
 general optical concentrator, max. radiant power density at receiver 0-102794
 generalised ray tracing, caustic surfaces, bending and merit function for optical design 0-102612
 gradient-index imaging, theory 0-69331
 gravitational lens effect, focusing by slowly rotating relativistic spherical mass 0-105155
 holographic grating arbitrarily oriented in space, ray path calc. 0-99677
 homogeneous medium, Gaussian light beam propag., diffr. effects described using complex-ray method 0-78770
 ice crystals, atmospheric, ray tracing rel. to origin of 46° halo and its arcs 0-82065
 illumination, relative, easy calc. 0-63920
 interferometric length measurement with curved wavefronts (*German*) 0-77752
 laser beam divergence influence on axicon axial intensity distrib. 0-95934
 laser radiation absorption by spherical plasma, geometrical optics 0-59189
 launching and propagation of light in optical fibres 0-69504
 lens, gradient-index rod, aberrations in multimode optical fibre devices 0-69487
 lens paraxial eqn. dimensional analysis 0-74462
 linear Fresnel lens with grooves of finite size, solar radiation concentration 0-106592
 localised wave fields, nonlinear geometric optics (*German*) 0-69448
 lower hybrid waves in nonuniform plasmas, geometric optics 0-83924
 Mie scattering efficiencies, asymptotic behaviour 0-106452
 mirror lens systematisation according to extent of central obstruction (*German*) 0-102795
 mountain shadow phenomena, spike seen by off-summit observer 0-78761
 multimode fibres of arbitrary refr. index profile, pulse dispersion 0-74475
 multiple lens experiment 0-82596
 nonsymmetrical optical system, matrix representation 0-64130
 plasma, formalism 0-83925
 polymer lightguide, light propag., nonlinearity, quasi-optical approx. 0-99837
 quasiotics in anisotropic and dispersive media 0-91943
 radiation flaw detection, correction of shadow images 0-89456
 random phase screens, probability density for intensity of plane waves 0-87317
 randomly inhomogeneous medium, fluctuations in phase arrival angle and freq. correl. of spherical waves 0-106456
 ray and wave optics of integrable and stochastic systems, WKB method 0-59244
 ray surface equation and Fermat's principle, in moving anisotropic media 0-106425
 resonator, sensitivity to misalignment, anal. by ray contour method 0-58602
 ring laser, perturbed cavity calcs. 0-102739
 rod, tapered gradient-index, geometrical optics 0-69322
 Rowland circle, corrected, least-squares method derivation 0-64161
 scattering by ice crystals, geometric ray optics anal. (*Russian*) 0-94601
 solid bodies, optic-geometric method calc. of diffraction patterns (*Russian*) 0-91746
 speckle photography and holographic interferometry, scatt. geometry, topology, vector fields, theory 0-87347
 teaching to engineers, matrix algebra methods 0-62415
 telescope, image vergence variation with object distance change, general case 0-63934
 telescope-spectrometer combination, optical props. 0-87455
 telescopic systems, practical approach to parallax problems 0-99818
 wavefront aberration polynomial, calc. 0-102614
 wavefront estimation from wavefront slope meas., least-squares curve fitting model 0-106467
 waveguide, parabolic index with random dielectric constant gradient, Gaussian beam propag. 0-58698
 X-ray interferometer, LLL type, interfering beam phase rels. 0-90973
 HF CW chemical laser, spatial homogeneity of radiation improvement using telescopic resonator 0-106549

geometry

- see also *space time configurations*
 σ -models, conservation laws, infinite series, differential geometric content 0-62841
 Backlund transformations in several variables, differential geometric anal. 0-86073
 Bianchi model universes, hypersurfaces of transitivity, Riemann curvature 0-67922
 differential geometry methods in gauge and gravitational theories 0-90768
 dynamical systems, symmetries, first integrals and differential forms 0-77983
 geodesic balls, volume, and geometry of Riemannian manifold (*French*) 0-68085
 geometric quantization and quantum mechanics, book 0-94908
 gravitational axial superfield and the formalism of differential geometry (*Russian*) 0-57164

geometry continued

- left-flat space-times, null tetrad and restrictive conditions 0-62545
 Lorentzian manifold, Kahler-metrics 0-73251
 non-Euclidean geometry and structures prior to Einstein, speculations (*German*) 0-90651
 point-surface distance meas. adjustment, geometrical aspects (*German*) 0-86255
 quantum theory, physical geometry, group manifold 0-105522
 relativistic particles, with isotopic spin, kinematics, geometric quantisation 0-62871
 relativity, general, differential forms, complex vectorial formalism 0-57144
 supergravity, curvature in terms of torsion and covariant derivatives, Bianchi identities 0-62561
 thermodynamics, irreversible, near equilib., metric geometry 0-62604
 wave fronts defined by eikonal equations, structural stability, elementary catastrophes 0-73187
- geons** see *gravitons*
- geophones** see *seismometers*
- geophysical aspects of cosmic rays**
 diurnal anisotropy, anal. of 0-94660
 gamma-rays, quasi-periodic intensity variations in stratosphere (*Russian*) 0-90177
 heavy nuclei penetration into atmos., calc. 0-85826
 magnetosphere cosmic noise absorption during substorms 0-72727
 middle atmosphere chemical comp., importance of energetic particle precip. 0-109213
 muon charge ratio, sea level, phenomenological model 0-67487
 muons, parent nucleons, energy distrib., at sea level and underground, phenomenological model 0-61974
 neutron component vars. during September 1977, Mirny and Moscow obs. 0-105137
 nucleons, altitude variation, Feynman scaling hypothesis calcs. 0-77245
 radiofrequency noise 'absorbed' by E-region plasma waves 0-82139
 radiowave absorption ionosphere, impulsive quasi-periodic variations 0-105116
 short-term cosmic ray fluctuations, time anal. 0-67483
 solar flares near-Earth radiation hazard, dosage estimation technique 0-67482
 stratosphere obs., evidence for interplanetary modulation processes 0-101508
 supernova, nearby, cosmic radiation, effects on terrestrial atmosphere 0-94584
 two year variations in Earth atm., sonde obs. 0-101511
 underground muons, response functions for different depths 0-82160
⁷Be production in atm. and transport from Sun, tracer for terrestrial-solar relationship 0-98525
¹⁴C form. in atm., diffusion distrib. 0-105110
¹⁴C in tree rings, climatic vars. record rel. to solar variability 0-101424
- geophysical equipment**
 see also *atmospheric measuring apparatus; geophysical prospecting; geophysical techniques; meteorological instruments; oceanographic equipment; seismometers*
 airborne lidar system for geophysical and atmospheric expts. (*Italian*) 0-109277
 automatic spinner magnetometer for rock specimens 0-101455
 Cactus accelerometer on Castor satellite, flight results synthesis for accels. below 10⁻³ g 0-77251
 Canadian Magnetic Observatory Network, annual report (1977) (*French, English*) 0-72418
 carbonate mineral identification by CO₂ evolution on heating 0-90248
 colour plotter system for computer graphics output, appls. in geoscience 0-98467
 core drilling equipment for permafrost regions (*French*) 0-77140
 Earth tide recorder photoelec. compensation method to acquire data 0-77129
 electrode arrays for Earth induced polarisation (IP) sounding, effects of EM coupling over uniform half-space 0-101324
 EM sounding system, multifrequency, topographic and misorientation effects study 0-101451
 geothermal logging instrumentation, borehole measurements, developments 0-61909
 gradient magnetometers, appl. to induced elec. currents meas. in Alaska oil pipeline 0-98231
 gravimeters in artificial Earth satellites, basic mechanical principles (*German*) 0-101461
 gravity gradiometers in artificial Earth satellites, basic mechanical principles (*German*) 0-101461
 imaging photon detectors 0-86405
 laser interferometer, 500-m base, Earth surface deform. detect. 0-105087
 Laterolog borehole resist. logging device, function and applications 0-85755
 lensless scanning telescope, MTF 0-58655
 magnetometer, ring-core type, high sensitivity, for balloons, high-altitude mag meas. (*Japanese*) 0-94608
 magnetometer (quartz H type), calc. formula for horiz. component 0-105062
 magnetometer array, two-dimensional, for ground-based obs. of auroral zone elec. currents. 0-90245
 microscope photometer/semiautomatic image anal. instrument system for morphometric and photometric value meas. 0-82815
 Multi-detector Electro-optical Imaging Scanner for aircraft remote sensing 0-82085
 multichannel radiometer, programmable, for Earth remote sensing 0-77253
 multispectral scanner, for remote sensing, parametric model 0-77261
 multispectral scanner, high resolution, for Earth obs., optical design 0-82174
 multispectral sensor for satellite, analytical design 0-77262
 optical systems, high-precision compensated levels, geodetic appl. 0-101813
 opto-electronic device for aerial colour photograph interpretation (*Russian*) 0-61920
 radiometer for Earth radiation meas., fused silica filter performance 0-87473
 sampler for ephemeral wadi floods 0-98493
 satellite IR radiometer, calibration 0-101440
 seismic vibrator (electromagnetic), characts. for self-excited regime 0-90262
 seismic vibrator signals, non-sinusoidal, theory 0-82086

geophysical equipment continued

'smart sensors', role in remote sensing of Earth from space, book 0-62402
solar-radiation meter, automatic 0-89592
Space Borne Event Timer, NASA laser ranging system, meas. of Earth movement along San Andreas Fault 0-61984
SQUID magnetometers, dewar systems design 0-101462
step-stare spaceborne optical system image motion compensation 0-90322
superconductive gradiometers, for measuring magnetic effects of geophysical origin 0-101463
Thematic Mapper of Landsat-D, optical component design 0-77260
wire-line core barrels for exploratory drilling 0-98482
SiO₂-GeO₂/SiO₂ load bearing optical cable, geophys. appls. 0-91923

geophysical prospecting

see also minerals
acoustic logging data, on-line computer interpretation techniques 0-90239
acoustic sounding of ocean-bottom subsurface layered media, spatial parameter estimation 0-77134
aeromagnetic survey of sedimentary cover thickness, using 1-D spectral anal. 0-77138
anomalies of mag. and gravity field, anal. by unitary method 0-89932
borehole acoustic logging, calc. of transient acoustic waveform 0-72640
borehole EM wave exploration, digital holography technique appl. (Chinese) 0-82080
coal seismic prospecting, approx. diff. theory for transparent half-planes 0-89974
conference, Nov. 1979, New Orleans, USA 0-81891
core drilling equipment for permafrost regions (French) 0-77140
cross-borehole EM probing, location of high-contrast anomaly 0-72639
data analysis, interpretive patterns, influence of meas. noise and meas. device accuracy 0-90235
dipole electric sounding method and application to Tuscany geothermal area 0-97762
dipole-dipole deep geoelectric soundings over geological structures 0-101449
direct current resistivity method, elec. fields in random cond. layered Earth 0-77171
electric near zone field development method testing in NW.Kola Peninsula (Russian) 0-85761
electric potential probing of underground struct. (German) 0-82089
electric sounding data analysis, use of reciprocal geoelec. section 0-90237
electromagnetic sounding transient pulse induction method, one-loop version 0-101448
EM depth sounding interpretation, master tables, book 0-86043
EM induction in thin sheet conductivity anomalies at Earth's surface 0-76907
EM remote sensing, computerized geophysical tomography 0-77169
EM remote sensing, reconstruction algorithms for geophysical applications in noisy environments 0-77168
EM remote sensing of inhomogeneities in ground, numerical modelling 0-77165
EM response of dipping half plane embedded in conducting rock 0-90236
EM sounding, detectability of intermediate layers, time domain anal. 0-72641
EM wave refl. and transmission coeffs., linear ramp model of crust 0-61759
epithermal neutron fissions in nuclear geophysics (Russian) 0-85658
gamma-ray logging of boreholes, exact inverse filters 0-94609
gamma-ray surveys, allowance for scattered gamma radiation (Russian) 0-105067
geoelectric inhomogeneities, position determination by variable geomag. field method 0-89956
geoelectric sounding, controlled-source DC pot. problem by self-pot. Green's function 0-77136
geomagnetic depth sounding by means of oceanographic and aeromagnetic surveys 0-77166
geothermal energy resources in Oregon, USA, elec. and EM sounding obs. 0-97761
geothermal resources in USA, National Exploration Program 0-72011
gravity and magnetic sounding, separation of anomalies of comparable horizontal dimensions 0-94606
gravity anomaly data processing system, involving interactive computer graphics (French) 0-94610
gravity sounding, calc. of gravity field of three-dimensional masses 0-94451
horizontally multilayered Earth models, recurrence formulae for layer eigenfunctions 0-90246
Hungary Eocene brown coal basins, geophysical exploration by well logging methods (Hungarian) 0-104938
hydrothermal alteration minerals, near IR spectra for remote sensing use 0-81871
in situ capture gamma analysis of large mineral samples 0-61215
induced polarisation (IP) sounding, effects of EM coupling in electrode arrays over uniform half-space 0-101324
induced polarisation methods for ore body tracing (German) 0-82084
laterolog borehole resist. logging device, function and applications 0-85755
LF seabed sounding (Russian) 0-67431
magnetic anomaly of thin dyke, curve fit by calculator program 0-98228
magnetic anomaly sounding, estimation of cover thickness above magnetised mass (Russian) 0-105069
magnetic profiling of geological contact, harmonci inversion method 0-77137
magnetic sounding, magnetostatic field problem, soln. in high susceptibility case via method of subsections 0-105065
magnetotelluric sounding, fundamental model 0-77167
metallic mineral deposits of Australia mag. induced polarisation survey results 0-98223
natural gas in permafrost and speed of longitudinal sound in clathrate hydrates 0-88275
oil-gas province basement, gravity field studies (Russian) 0-85759
ore body, mag. survey of Itapicuru greenstone belt, Bahia, Brazil 0-81879
resistivity curves, finite difference evaluation method 0-89937
resistivity sounding by bipole-dipole method, theory 0-101450
seismic profiling of Black and Azov Sea floor, methods 0-89970
seismic prospecting, multiple reflected signal attenuation, least squares estimation procedure 0-85596
seismic refraction method, vel. determ. and error anal. 0-90229

geophysical prospecting continued

seismic sounding, common-depth-point method, prestack migration method for deformed refl. layer 0-98251
seismology, correlation refraction method, appl. to granite terrain weathered zone 0-90230
subsurface radar using video pulse for deep probing in Earth, pulse propagation in lossy media using LF window 0-74282
sulphide prospect in California copper belt, broadband EM study 0-72503
transient EM wave prospecting 0-76905
travel-time curves, theory 0-94473
vertical magnetic dipole on two-layer Earth, transient EM fields 0-76906
VLF surface mode propag., wave tilt meas. 0-77139
water detection in volcanic region of Armenia, elec. profiling and sounding methods 0-85753
water resources in Africa, techniques 0-61818
wave tilt sounding of multilayered structures 0-61926
well logging, electric, geometrical factors determ. from electrostatic field successive approx. (Chinese) 0-105057
wire-line core barrels for exploratory drilling 0-98482
Rn mapping in U exploration, exclusion of ²²⁰Rn signal 0-61916
²²²Rn mapping in U exploration, use of mat to avoid hole drilling 0-82087
Th, analytical geochemical prospecting methods 0-72635
U abundance in Himalayan plants, fission track method 0-101305
U, analytical geochemical prospecting methods 0-72635
U, exploration and prospecting methods 0-85768
U, geochemistry of inclosure radioactivity 0-85766
U ore detection, Rn gas concentration meas. using alpha sensitive plastic detectors 0-94617
U ore detection using integrated meas. of long-distance transport of ²²⁰Rn 0-98476
U ore exploration, Rn gas conc. meas. using alpha sensitive plastic films 0-94618
U, prospecting by active neutron logging, evaluation models 0-98480
U prospecting by γ -ray logging of borehole, factors affecting resolution 0-98463
U prospecting using microdistrib. anal. of Siwalik vertebrate fossils by nuclear Track Etch tech. 0-98489
U, sandstone-type ores, charged particle track analysis 0-91405
²³⁵U-fission track micromapping, exam. of U mobilisation processes in Precambrian sediments 0-98477

geophysical techniques

see also atmospheric techniques; hydrological techniques; ionospheric techniques; oceanographic techniques
acoustic logging data, on-line computer interpretation techniques 0-90239
aeromagnetic survey of sedimentary cover thickness, using 1-D spectral anal. 0-77138
aftershocks prediction, implications of dilatancy-fluid diffusion theory 0-85604
anomalies of mag. and gravity field, anal. by unitary method 0-89932
asymmetric bilateral rupture process anal. method (Chinese) 0-76911
atmosphere visibility trends, appl. of ridit anal. 0-82051
Australian magnetic observatories 0-72632
autoregressive technique, appl. to astronomy and geodynamics (Chinese) 0-85869
Bingham distrib. function in palaeomagnetic studies 0-72649
borehole acoustic logging, calc. of transient acoustic waveform 0-72640
borehole EM wave exploration, digital holography technique appl. (Chinese) 0-82080
carbonate mineral identification by CO₂ evolution on heating 0-90248
charged particle track analysis of sandstone-type U ore 0-91405
coal basin evaluation, appl. of gravity profile across Bonnet Plume Basin, Yukon Territory, Canada 0-76898
cross-borehole EM probing, location of high-contrast anomaly 0-72639
crustal deformation analysis, models for estimation of parameters (German) 0-101319
crustal radiogenic heat production, depth depend. modelling by variational approach 0-72464
data analysis, freq. estimator of truncated real sinusoids 0-73161
data analysis, interpretive patterns, influence of meas. noise and meas. device accuracy 0-90235
data analysis by collocation method 0-77130
data analysis of multivariate data set, canonical anal. 0-73333
data reduction, detrending and smoothing of random data 0-67425
dating methods using thermoluminescence (German) 0-105076
deep magnetotelluric sounding, surface geoelectric section effects (Russian) 0-85588
dielectric relaxation measurement of ice and rocks, blocking layer method 0-103914
digital data composition for satellite and radar imagery 0-67413
digital generation of accurate synthetic seismograms 0-85779
dike burial depth estimation by mag. palaeogeobarometric method 0-98220
dipole electric sounding method and application to Tuscany geothermal area 0-97762
Earth electrical parameters, determination from horizontal antennas input impedance meas. 0-90259
Earth interior Q-structure, determ. from seismic pulse rise time 0-72438
Earth strain measurement, He-Ne I₂ stabilised laser reliability as interferometer source 0-106545
Earth tide recorder photoelec. compensation method to acquire data 0-77129
earthquake epicentre determ. using P-wave arrival-time differences 0-101328
earthquake foreshocks, differentiation from earthquake swarms via seismic waveform variability (Japanese) 0-67342
earthquake frequencies, stochastic modelling (Japanese) 0-94480
earthquake magnitude determ. using undamped seismographs, appl. to Japanese earthquakes (1901 to 1925) (Japanese) 0-94484
earthquake maximum ground acceleration determ. using overturned gravestones (Japanese) 0-101453
earthquake pair technique for surface waves to study Reykjanes Ridge crest study 0-90021
earthquake parameter determ. computer technique (Chinese) 0-77126
earthquake precursory changes of He in soil, daily variation limitations 0-94469
earthquake prediction, changes in short-period geomag. vars. before 1972 Sitka, Alaska, earthquake 0-76923

indium compounds

- see also indium alloys; indium antimonide
 [CC] Ag-(100)InP, metal-semicond.cathode contact, metallurgical, physical, chemical processes 0-107911
 chalcogenate and chalcogenite double salts, form. laws and acid-base props. 0-101070
 α -In₂Te₃, I phase, order-disorder transform. for DO₂₂ struct., thermodynamic study 0-70155
 3-phonon diffuse scattering of X-rays, intensity calcs. 0-84027
 plectides, mixed, impurity induced Raman scatt. spectra 0-88983
 Ag-In-S₂-Si layered struct., Hall effect, I-V characts., surface states (*Russian*) 0-97001
 Ag-InP interface, Ag₂P formation during sintering 0-65309
 AgInS₂, and AgIn₂S₃, spray pyrolysis, film struct., elec. and optical props. 0-71592
 Al-In-S₂-Si layered struct., Hall effect, I-V characts., surface states (*Russian*) 0-97001
 As-Te-In, glass-forming, density and microhardness 0-103257
 CdInGaS₄, layered structure crystals, refractive index meas. method 0-98966
 n-CdS/n-InP heteroface solar cell with ultrathin window layer, computer anal. 0-97788
 CdS-InP solar cell heterojunctions, CVD fabrication, photovoltaic response 0-93878
 CdSnAs₂-InP, n-p heterojunction, elec. props., electroluminesc., band struct. 0-75632
 CuGa_{0.5}In_{0.5}Se₂/Zn_{0.29}Cd_{0.71}S heterojunction solar cell, preparation and props. 0-101110
 CuIn_{1-x}Ga_xSe₂(1-x)Te₂, pentenary alloy compounds for photovoltaic solar energy conversion 0-93971
 CuInS₃, single phase thin film prep. by flash evaporation 0-100796
 CuInS₃, influence of impurities and free carriers on optical props. 0-108225
 CuInSe₂, thin film fabrication by RF-sputtering for solar cell appls. 0-100786
 CuInSe₂, thin films, prep. by spray pyrolysis, struct., elect. and optical props. for solar cell appls. 0-100781
 CuInSe₂-CdS solar cell, polycrystalline thin film, high photocurrent, characts. 0-61339
 Cu₂In₂Zr_{1-x}S₂ system, struct. and cond. meas. (*French*) 0-88354
 Ga-In-Sb system, phase diagram calcs. in Ga+In rich region 0-60842
 GaAs/GaInP DH, MBE grown, optically pumped laser action at 77K 0-95890
 GaAs-Ga_{1-x}In_xP heterostructure, elastic stresses and substrate/epitaxial film mismatch, X-ray diff. method 0-92794
 GaAs-GaInAs structure, dislocation struct., TEM anal., appl. as IR LED 0-70206
 GaAs-In_{2-x}Sn_xO_{3-y} SIS heterostructure solar cells, spray-deposited 0-101106
 GaAs-InP heterojunction laser output wavelength control 0-74384
 GaInAs-InP, growth by low-pressure metalorganic CVD 0-71595
 Ga_{0.47}In_{0.53}As, HF carrier mobility, temp. depend., theory 0-75593
 Ga_{0.47}In_{0.53}As p-n junctions, band-to-band tunnelling current 0-107895
 Ga_{0.47}In_{0.53}As, photodetector applications 0-95140
 Ga_{1-x}In_xAs epitaxial layer growth by organometallic pyrolysis, homojunction LED prep. 0-76194
 Ga_{1-x}In_xAs, IR reflectivity, cluster effect on optical phonons 0-97259
 Ga_{1-x}In_xAs, organometallic VPE growth using trimethylarsenic 0-60788
 Ga_{1-x}In_xAs:Mn grown by LPE, elect. props. 0-100541
 GaIn_{1-x}As, on (111)B InP, LPE growth, characterisation of high purity lattice 0-104082
 Ga_{1-x}In_xAs-InP, MBE film growth, composition control obs. 0-84399
 GaInAsP alloys, materials and devices for long wavelength optical communication 0-99854
 GaInAsP DH laser emitting at 1.55 μ m, threshold currents 0-83609
 GaInAsP diode lasers, self-sustained pulsations in light output 0-64012
 GaInAsP LEDs, 1.3-1.6 μ m, appl. in long haul high data rate fibre optic communication systems 0-102854
 GaInAsP, rectifying and ohmic contacts 0-80376
 GaInAsP/InP 1.5-1.6 micron integrated twin-guide lasers with distributed Bragg reflectors 0-74380
 GaInAsP/InP buried heterostruct. laser, 1.6 μ m, fabrication and room temp. CW operation 0-58568
 GaInAsP/InP DH lasers emitting at 1.3 μ m, growth and characts. 0-64057
 GaInAsP/InP DH stripe geometry lasers emitting at 1.3 μ m, growth characterisation 0-69410
 GaInAsP/InP DH lasers, 1.3 μ m wavelength, LPE growth and characterisation 0-69411
 (100)GaInAsP/InP DH lasers, 1.5-1.6 μ m wavelength, two phase soln. LPE technique using anti-meltback layer 0-99750
 GaInAsP/InP integrated twin-guide lasers with distributed Bragg reflector, spectral behaviour 0-74381
 GaInAsP/InP lasers, 1.5 μ m emitting, high temp. CW operation 0-95889
 GaInAsP/InP lasers, LPE grown, effect of p-doping on carrier lifetime and threshold current density 0-99726
 GaInAsP/InP narrow planar stripe lasers, lasing characts. 0-95897
 GaInAsP-InP buried heterostructure lasers, 1.6 μ m wavelength 0-64055
 GaInAsP-InP integrated twin-guide lasers with first-order distributed Bragg reflectors, 1.3 μ m 0-58567
 GaInAsP-InP stripe-geometry monolithic laser with etched mirror and monitoring detector 0-64054
 GaInAsP-InP stripe laser, etched mirrors fabricated by wet chem. etch 0-99744
 Ga_{1-x}In_xAs_{1-y}P_y, electron effective mass, cyclotron reson. and magnetophonon effect meas. 0-103618
 Ga_{1-x}In_xAs_{1-y}P_y, IR refl. spectra 0-60602
 Ga_{1-x}In_xAs_{1-y}P_y/GaAs structure, LPE growth and lattice consfs. matching conditions 0-59822
 Ga_{1-x}In_xAs_{1-y}Sb_{1-y}, tunable electron-beam-pumped laser parameters 0-106524
 Ga_{1-x}In_xP MBE layers, comp., Rutherford scatt. and X-ray diff. meas. 0-75457
 n-Ga_{1-x}In_xP photoelectrochemical cells, bandgap energy, electronic transition mode, and diffusion length 0-72070
 Ga_{1-x}In_xP solid solns., isothermal liq. epitaxy 0-60793
 GaInAsP/InP heterostructure DFB laser under optical pumping, lasing characts. 0-87396
 Ga_{1-x}In_xP_{1-y}As_{1-y}/InP DFB injection laser, one-step LPE 0-58575
 p-Ga_{1-x}In_xPyAs_{1-y}/Au-Zn, specific contact resist. 0-84509
 Ga_{1-x}In_{1-x}Sb, Ga-rich, prep. by Czochralski technique 0-60771

indium compounds continued

- GaSb-InAs system, (110) surface and interface electronic struct. 0-100494
 Ge-InAs based MIS struct., avalanche carrier multiplication 0-88566
 Hg-InP Schottky-barrier diode, contact times, I-V characts. 0-96971
 In₂O₃/Sn, RF magnetron sputtered film, elec. and optical props. 0-104065
 I_{1-x}Te_x mixtures, high-temp. solids and melts, struct., thermodynamic props., Raman spectra obs. 0-66174
 (In,Ga)_{1-x}(As,P) binary, ternary and quaternary, hydride vapour phase epitaxy, cryst. growth and props. 0-66434
 In-Ga-P ternary system, low temp. phase diagram rel. to epitaxial growth 0-84916
 In-In₂O₃-Pb, Josephson tunnel junction fabrication for MM-wave detector 0-100427
 In-Se, liq., mag. susceptibility meas., electron localisation and chem. bonding 0-60178
 In-Te, liq., mag. susceptibility meas., electron localisation and chem. bonding 0-60178
 p-In_{0.77}Ga_{0.23}As/Ag photocathode, field assisted photoemission to 2.1 microns 0-76130
 In_{1-x}Al_xAs, band gap, IR absorpt. spectra meas. 0-66205
 In_{1-x}Al_xP, proportional ingredient content determ. by X-ray fluoroscopy 0-97747
 InAs and solid solutions, recombination mechanisms of excess carriers, luminesc. obs. 0-97337
 InAs, anomalous avalanche breakdown 0-80284
 InAs, electrical conductivity and thermoelectric power charge due to melting 0-100490
 InAs films, MBE grown on GaAs, electron mobilities, lattice mismatch effect 0-80419
 InAs, liquid interaction parameters determ., 580-670°C 0-65197
 InAs, melt, mutual diffusion of components 0-88345
 n-InAs, photoelectric props., inhomogeneous impurity distrib. 0-107867
 InAs, resist. inhomogeneity meas. with single-sonde potential method 0-65549
 p-InAs, saturation characts. over CO₂ laser spectrum 0-83646
 InAs, thermal oxidation, growth rate and chem. comp., temp. depend. 0-108619
 InAs, transient dynamic response calculation by Monte Carlo techniques 0-107796
 InAs, two dimensional accumulation layer, Anderson localisation 0-107871
 InAs₂Cd₂Te, donor-acceptor interaction, elec. cond. and Hall coeff. meas. 0-59988
 InAs:Mn²⁺, Jahn-Teller effect for ion impurities 0-107753
 InAs₂(Mg), ion implanted, photocond., photo-EMF, and optical absorpt. spectra 0-70763
 InAs:Sn, single crystals, defect formation 0-88606
 InAs-CdTe quasi-binary system, temp.-comp. diagram, physicochem. and thermodynamic analysis 0-104127
 InAs-GaSb superlattices, mag. field induced semimetal-semicond. transition 0-65656
 InAs₂P_{1-x} alloy, composition effects in growth by MBE 0-59816
 InAs₂B/GaSb broad-spectral-band IR detector, backside-illum. heterostructure approach 0-73450
 InBO₃Fe³⁺, ESR spectra, lattice parameters 0-93170
 InBi single crystal, deform. mode under dynamic indentation 0-88163
 InBi single crystals, Knight shifts and quadrupole interaction 0-84662
 InBr, electron impact dissoci. ions, In electron affinity meas. (*French*) 0-63849
 InBr₃, vibr. anal., pot. const. determ., mol., compliance and Coriolis coupling const. calc. 0-95579
 InBr₃-In₂Te₃ quasibinary system, phase relations 0-100834
 In₂CdI₆, solid electrolytes, ion transport mechanism and polarisability role, comparison with Cu⁺ and Ag⁺ cond. 0-107531
 InCl₃, intramolecular force fields, compliance const. and vibr. amplitudes 0-58234
 InCl₃, vibr. anal., pot. const. determ., mol., compliance and Coriolis coupling const. calc. 0-95579
 InCuAlO₄, rhombohedral oxides, symmetry group (*French*) 0-84157
 InFe₂Si_{0.5}O₄, rhombohedral oxides, symmetry group (*French*) 0-84157
 InGaAs, LPE diffusion-limited step-cooling technique, layer thickness and composition 0-84402
 InGaAs-InP punch-through type photodetector fabricated by VPE 0-68253
 In_{0.1}Ga_{0.9}As, quantitative anal. with SIMS 0-101052
 In_{0.53}Ga_{0.47}As p-n photodiode-FET photoreceiver for 1.0 to 1.7 μ m wavelength optical fibre communications systems 0-58794
 In_{0.53}Ga_{0.47}As photodiodes with dark current limited by generation-recombination and tunneling 0-107893
 p-In_{0.53}Ga_{0.47}As:Zn on InP, elec. and optical props. 0-75662
 In_{0.53}Ga_{0.47}As-InP avalanche photodiode with guard-ring struct., characts. 0-96939
 In_{0.53}Ga_{0.47}As-InP avalanche photodiode structure for 1 to 1.6 μ m region 0-98978
 In_{1-x}Ga_xAs layer on InP, misfit dislocation free, LPE growth 0-108364
 In_{1-x}Ga_xAs:Si p-n structs., electrolum. spectra, 77 to 300K 0-93408
 In_{1-x}Ga_xAs:Zn, lattice matching to InP, LPE growth conditions 0-70541
 InGaAsP, anodic oxidation, refractive indices 0-97601
 InGaAsP avalanche photodiode, 1.3 μ m, noise performance, -190°C 0-57370
 InGaAsP avalanche photodiodes, breakdown mechanism, donor conc. effect 0-70710
 InGaAsP, bandgap energy by electroluminescence and photoluminesc. spectra 0-107700
 InGaAsP DH, luminesc., quantum efficiency determ. 0-108273
 InGaAsP DH lasers with etched reflectors, fabrication, current density 0-64050
 InGaAsP, epitaxial growth by chloride CVD process, thermodynamic anal. 0-64936
 InGaAsP LED sources, for near-IR absorpt. meas. 0-77135
 InGaAsP, LPE, diffusion-limited step-cooling technique, layer thickness and composition 0-84402
 InGaAsP LPE heterostructs., interface grading, Auger depth profile 0-103585
 (InGa)(AsP) laser system, VPE growth using metal organic sources or halide transports 0-99748
 InGaAsP photodetector, improved two wavelength demultiplexing 0-58795

indium compounds continued

- InGaAsP single-mode CW ridge-waveguide laser emitting at 1.55 micron 0-58584
 InGaAsP strip-buried-heterostructure high-output power laser 0-58540
 InGaAsP strip-buried heterostructure laser, high output power, operation 0-58559
 InGaAsP/InP DH lasers, temp. depend. characts. 0-58541
 InGaAsP/InP DH stabilised 1.3 μ m laser diode-isolator module for hybrid optical integrated opt. 0-58583
 InGaAsP/InP injection lasers for long wavelength (1.1 to 1.6 μ m) optical communication 0-58582
 InGaAsP/InP phototransistors, fabrication by LPE, photodetectors 0-95139
 InGaAsP-InP buried crescent injection laser emitting at 1.3 μ m with low threshold current 0-87404
 InGaAsP-InP buried heterostructure lasers emitting at 1.3 μ m, accelerated ageing characts. 0-95898
 InGaAsP-InP CW lasers, 1.5-1.7 μ m, VPE 0-78861
 InGaAsP-InP DH laser, 1.55 μ m, low temp. LPE growth for room-temp. CW operation 0-64045
 InGaAsP-InP DH LED, high temp. aged, dark-spot defects, TEM obs. 0-66300
 InGaAsP-InP DH lasers, interfacial recomb., influence on oscill. characts. 0-87393
 InGaAsP-InP DH lasers, spatial hole burning, spontaneous emission saturation, direct obs. 0-95892
 InGaAsP-InP DH lasers, temp. dependence of threshold and elect. characts. 0-99725
 InGaAsP-InP DH lasers, perturbed InP growth, photoluminesc. study 0-106518
 InGaAsP-InP DH laser, threshold current, temp. depend. 0-106521
 InGaAsP-InP high-gain heterojunction phototransistor 0-103745
 (InGa)(AsP)-InP laser system, 1 μ m wavelength, lattice matching techniques 0-99748
 InGaAsP-InP layers, grown by LPE techniques, lattice const., bandgap, thickness and surface morphology meas. 0-59818
 In_{0.8}Ga_{0.17}As_{0.17}P_{0.63}, reactive ion etching of III-V compounds 0-58813
 In_{1-x}Ga_xAs_{1-y}P_{1-y} DH lasers for 1.3 and 1.5 μ m optical fibre communications 0-91817
 In_{1-x}Ga_xAs_{1-y}P_{1-y}, electron effective mass from Shubnikov-de Haas meas. 0-80298
 In_{1-x}Ga_xAs_{1-y}P_{1-y} epitaxial layer, far IR refl. spectra, lattice vibrs. 0-97282
 In_{1-x}Ga_xAs_{1-y}P_{1-y}, evidence for alloy scatt. from press. induced changes of electron mobility 0-88548
 In_{1-x}Ga_xAs_{1-y}P_{1-y} far IR reflection spectrum 0-60612
 In_{1-x}Ga_xAs_{1-y}P_{1-y}, Hall mobility, comp. depend. 0-75587
 In_{1-x}Ga_xAs_{1-y}P_{1-y}, hole mobility over temp. range 77 to 300K 0-60111
 In_{1-x}Ga_xAs_{1-y}P_{1-y}/InP 1.5 μ m room-temp. CW laser fabrication and operation 0-64070
 In_{0.9}Ga_{0.1}As_{1-y}P_y epitaxial layers, characterisation and relation to lattice matching 0-100540
 In_{0.9}Ga_{0.1}As_{1-y}P_y photodetector diode on InP substrate dark currents, tunnelling, energy gaps, effective masses 0-70805
 In_{0.9}Ga_{0.1}As_{1-y}P_y, surface and dielec.-semicond. interface props. 0-93001
 InGaP/InGaAs struct. for transferred electron photocathodes, VPE growth and characterisation 0-76193
 In_{0.3}Ga_{0.7}P, N free and implanted, photoluminescence study 0-97322
 n-In_{1-x}Ga_xP, direct-gap semiconductor, cathodoluminesc., electron irradi. effects 0-108283
 In_{1-x}Ga_xP, epitaxial layers, compositional inhomogeneity 0-88444
 In_{1-x}Ga_xP, proportional ingredient content determ. by X-ray fluorescence 0-97747
 InGaPAs LPE layers, compositional inhomogeneity, photoluminesc. obs. 0-75451
 In_{1-x}Ga_xP_{1-y}As_y, lattice-matched epitaxial layers, LPE growth on GaAs(100), characterisation 0-75465
 In_{1-x}Ga_xP_{1-y}As_y, lattice matched to InP, electroluminescence obs. 0-93416
 In_{1-x}Ga_xP_{1-y}As_y-In_{1-x}Ga_xP_{1-y}As_y visible spectrum multiple-quantum-well heterostruct. lasers 0-106537
 In_{1-x}Ga_xP_{1-y}As_y-InP coupled multiple quantum-well heterostructure laser diodes, threshold current temp. depend. 0-78855
 InGa_{1-x}P_xAs_{1-y}, electron effective mass and Dingle temp., Shubnikov-de Haas oscils. 0-59859
 InI, electron impact dissociation, ionis., In electron affinity meas. (French) 0-63849
 InI, high temp. solid and melt., struct., thermodynamic props., Raman spectra obs. 0-66174
 InI₃, high temp. solid and melt., struct., thermodynamic props., Raman spectra obs. 0-66174
 InI₃, high temp. solid and melt., struct., thermodynamic props., Raman spectra obs. 0-66174
 InI₃, vibr. anal., pot. const. determ., mol., compliance and Coriolis coupling const. calc. 0-95579
 In₂Mo₃S₈ Chevrel phase, synthesis, stability and characts. 0-71608
 InMo₆Se₆, X-ray cryst. struct. determ. 0-103299
 In₂Mo₃Se₁₉, superconducting chalcogenides containing Mo₆ and Mo₃ clusters 0-103804
 In₂Mo₃Se₁₉, X-ray cryst. struct. determ. 0-103299
 InMo₃Se₃(Te₃), synthesis and struct. 0-92498
 InN film growth by reactive sputtering in Ar-N₂ discharge, mechanism 0-89107
 InO₃/Sn transparent conducting films, homeotropic orientation of liquid crystals (Russian) 0-108181
 In₂O₃, films, activated reactive evaporation technique of prep. 0-80989
 In₂O₃ films, electron beam evaporation, elec. and optical props. (Japanese) 0-60784
 In₂O₃ films, reactively evaporated, elec. props. 0-84521
 In₂O₃ smoke particles prepared by gas evap., morphology and coalescence growth 0-97738
 In₂O₃, thermally evaporated film, struct. and elec. props. 0-104066
 In₂O₃, thin film, sputter deposition form., optical and elec. props. 0-60123
 In₂O₃-Sn, films, activated reactive evaporation technique of prep. 0-80989
 In₂O₃-Sn films; vac. deposited, elec. props. 0-100542
 In₂O₃-InN film growth by reactive sputtering in N₂-O₂ discharge, mechanism 0-89108
 In₂O₃-SnO₂ thin film, Hall mobility, temp. depend., grain boundary effects 0-75658

indium compounds continued

- In₂O₃-SnO₂/polySi, solar cell response exam. using electron-beam-induced current and scanning light spot tech. 0-81477
 In₂O₃-SnO₂-CdTe:P, p-n homojunction solar cell, elec., photovoltaic props., photoluminescence 0-81463
 In₂O₃-SnO₂-InP solar cell junctions, efficiency, InP surface props. 0-85288
 In₂O₃-SnO₂-Si SIS heterojunction solar cells 0-85281
 In₂O₃-SnO₂-Si SIS solar cells, reverse current-voltage characts. under illumination 0-89622
 In₂O₃-SnO₂-SiO₂-pSi solar cells, comparison between MIS and SIS 0-81443
 InP (110) surfaces, cleaved and polished-sputtered-annealed, LEED and AES study 0-103550
 InP (111), (110) and (001) substrates, Cd(S, Se) film growth, mismatch dislocations and lattice distortion 0-84406
 InP avalanche photodiodes, microplasmas, investigation 0-60018
 n-InP, compensated, elec. props., space-charge effects 0-65569
 InP, compensation ratio, electron mobility and free-carrier absorpt. 0-80261
 InP, depend. of phonon spectrum on hydrostatic press., Raman spectra 0-93315
 InP detector, unbiased, using Schottky-barrier diode, operation in submm. wave region 0-105707
 InP, electron transport props., mag. field and temp. depend. 0-92888
 InP, epitaxial, kinetics of VPE 0-60790
 InP epitaxial films, grown on heavily doped substrates, carrier mobility study, magnetoresist. meas. 0-60116
 n-InP, epitaxial layer, (100) surface chemistry, ESCA study 0-103552
 InP, Faraday interband effect subjected to quantising mag. fields 0-97246
 p-InP field-assisted photocathodes, quantum efficiency 0-84831
 InP film, electron-beam annealed, surface conduction 0-84500
 InP films, organometallic VPE growth, props. 0-96753
 InP grown by LPE, method for free In removal from surface 0-84860
 n-InP, γ -ray and electron irradi., annealing of radiation point defects, elec. cond. and Hall coeff. meas. 0-65051
 n-InP, heat treatment in controlled P vapour 0-88137
 InP, impact ionisation by electrons and holes 0-100467
 n-InP, impurity and minimum metallic cond. in mag. field 0-103731
 InP interface with oxide, photoemission obs. of energy levels induced by adsorpt. 0-93000
 InP inversion-type MISFET with SiO₂ gate insulation interface props., elec. drift 0-93002
 InP, ion-implanted layers, close contact capless annealing, elec. props. 0-84192
 InP, LEC growth of dislocation free crystals 0-89134
 InP, laser-induced microscopic etching 0-76379
 InP, lattice dynamics and phonon parameters bond bending force model 0-59595
 InP, lattice matching to InGa_{1-x}As_xZn, LPE growth conditions 0-70541
 InP, liquid interaction parameters determ., 580-670°C 0-65197
 InP, luminescence, hot electron effects 0-66277
 InP, MBE, substrate temp. related degradation mechanisms 0-65385
 InP MIS devices, diffusion, chemical reactions, contamination, AES and SIMS 0-72066
 n-InP, MOS solar cells, electrical and photovoltaic characteristics 0-85276
 InP, model for ~ 1.10 eV emission band 0-66289
 InP n⁺-p-p⁺ homojunction solar cells, high efficiency, LPE layer growth, photolithographic fabrication 0-93929
 InP, noise calc. using Monte-Carlo method 0-75575
 p-InP, ohmic contact using Be-Au metallisation, low contact resist. 0-65677
 InP n⁺-n abrupt junctions, ionisation coeffs., photomultiplication meas. 0-65655
 InP p-n junction, grain boundary etching 0-96541
 InP photodiodes, dark current and breakdown characts. 0-70806
 InP, photoluminescence meas. using diamond-anvil press. cell 0-108256
 InP, press. depend. of direct absorption edge 0-93365
 InP, reactive ion etching of III-V compounds 0-58813
 InP single crystals, uniaxial compression deform. characts. 0-84991
 InP solar cells, thin film growth tech. and characterisation 0-89631
 InP, surface, pulsed electron beam processing, doping, annealing 0-75254
 InP, surface and dielec.-semicond. interface props. 0-93001
 InP surface decomposition prevention in LPE growth 0-96749
 InP, surface passivation using composite Al₂O₃ and native oxide, MIS characts. 0-93004
 InP, surface phonon polariton dispersion and damping, frustrated total internal refl. meas. 0-80792
 InP, surface recomb. vel., psec. optical techniques 0-70784
 InP, surface vacancies, bound state energy levels calc. 0-80340
 InP thin films for photovoltaic devices 0-93972
 InP, VPE growth for MESFET's 0-103602
 InP, Zn diffused single-crystal, substitutional dopant and hole conc. meas. 0-75260
 InP:Cd, doping by UV laser photodeposition 0-84191
 InP:Cd, p⁺-p⁺-n junction form. by diffusion doping 0-84504
 InP:Cd(Zn), avalanche photodiode characts., impurity diffusion effects 0-70709
 n-InP:Cr, press. depend. of elec. resist. and Cr ionisation energy 0-80281
 InP:Cr²⁺, Jahn-Teller effect for ion impurities 0-107753
 InP:Fe shallow trap thermally stimulated cond. spectroscopy, photocond. spectrum under DC conditions 0-65585
 InP:SSD growth of low dislocation density crystals 0-89135
 InP/CdS epitaxial thin films on NaCl, HEED and TEM study 0-88446
 InP/InGa_{1-x}As_xP_{1-y} interfaces, sputter-profiled, depth resolution degradation by cone form. 0-80094
 InP/InGaAs heterojunction phototransistor, high-sensitivity 0-100505
 InP/InGaAsP avalanche photodiodes, with guard ring structure 0-100506
 p-type InP/Langmuir film MIS diodes, characts. 0-80384
 InP-Al interface struct., low temp. interaction, AES study 0-107661
 p-InP-Cd(Zn), ohmic contact formation on InP by laser photochemical doping 0-80369
 InP-Cu contact system, low temp. alloyed contact formation 0-100519
 InP-GaInAsP buried heterostructure lasers of 1.5 μ m region, fabrication and characts. 0-74388
 InP-In_{1-x}Ga_xAs_{1-y}-InP 1.55 μ m DH room-temp. CW laser fabrication and operation 0-64071
 InP-In_{1-x}Ga_xAs_{1-y}-InP 1.53 μ m single-mode CW ridge-waveguide laser 0-64072

indium compounds continued

- InP-InGa_{1-x}As alloy photocathodes, semiconductor photoemitters, field-assisted, 1-2 μ m range 0-97396
 InP-InGaAsP p-n junction avalanche photodiodes, surface passivation techniques 0-100508
 InP-InGaPAs heterojunction lasers and LEDs, 1.0 to 1.2 μ m 0-74362
 InP-Si₃N₄(SiO₂)_x interface props., plasma deposited dielectrics, n-channel MOSFET action 0-93003
 InP-SiO₂ interface, CVD problems, ESCA profiles 0-93497
 InP-SnO₂ heterojunctions, elec. and photovoltaic characts. 0-75628
 InP(As), surface (110), energy distrib. of dangling-orbital surface states 0-80347
 InP(Sb)(As) substrates for Al₂O₃ film, ion beam etching defect detection 0-89155
 InS₇, single crystal, switching effect and memory (*Russian*) 0-70774
 InSb, convection in melts, and cryst. growth under large inertial accelerations 0-66421
 InSb, noise calc. using Monte-Carlo method 0-75575
 n-InSb substrates, MIS struct. form. by reactive deposition of Si₃N₄, C/V meas. 0-103752
 InSb-Au contact system, low temp. alloyed contact formation 0-100519
 InSb_{1-x}Bi_x films, single-cryst. metastable semicond., growth and phase stability 0-80115
 InSb_{1-x}Bi_x, metastable epitaxial film, phase diagram 0-76238
 InSb_{1-x}Bi_x metastable films, elemental incorporation probability modification by ion bombard. during growth 0-80118
 InSb_{1-x}Bi_x, multitarget RF sputtering, metastable phase, conductivity transition 0-76178
 InSe, ¹¹⁰Ag diffusion, temp. depend. and solution (*Russian*) 0-70467
 γ -InSe, 3R struct. type refinement 0-64962
 InSe, exciton and polaron anisotropies, reson. Raman scatt. study 0-76033
 InSe films, residual photocond., field quenching 0-60037
 InSe, layer compound, long-wavelength phonons and elastic consts. 0-65175
 InSe, photo-absorption of green exciton 0-80816
 InSe, photoconductivity anisotropy at high optical excitation levels (*Russian*) 0-103721
 InSe solar cells, photovoltaic conversion efficiency 0-61356
 InSe thin film, sputter growth and chem. anal. by XPS/ESCA 0-80976
 InSe-SnO₂ n-n heterojunctions, photoelec. props. 0-96945
 In₂Se₃, transitions of high temp. α form (*French*) 0-92473
 In₂Se₃, vapour press. temp. depend., heat of evap. and form. 0-59642
 In₂Se₃-SnO₂ amorphous film-SnO₂ system, photovoltaic spectra, anneal-effect (*Japanese*) 0-92926
 InSeI, X-ray cryst. struct. determ. (*German*) 0-100214
 In₂Si₂O₇, thin film, sputter deposition form., optical and elec. props. 0-60123
 (In_{1-x}Sn_x)₂O_{3-y}-Si solar cells, degradation 0-94047
 In₂Sn₂Mo₆S₈, supercond. props. 0-97023
 In₂SnO₃ film, effect of ambient atmosphere during annealing, elec. props. 0-97510
 In_{2-x}Sn_xO_{3-y} solar cells, majority carrier conduction effects 0-97796
 In_{2-x}Sn_xO_{3-y}-Ga_{1-x}In_{1-x}P-(InP,As_{1-y}) heterojunction solar cells, chemistry and prep. 0-94073
 In_{2-x}Sn_xO_{3-y}-insulator-poly-Si solar cells, photovoltaic conversion parameters 0-101093
 In_{2-x}Sn_xO_{3-y}-poly Si SIS solar cells 0-97787
 In_{2-x}Sn_xO_{3-y}-SiO₂-Si SIS solar cells, loss mechanisms study for improvement of efficiency to above 12% 0-94080
 In_{2-x}Sn_xO_{3-y}-ZnSe:Mn²⁺-n-Ge thin film electrolum. cell with low-threshold voltage 0-84786
 InTa_{1-x}Nb_xO₄ system, structural and luminescent props. 0-84769
 InTe thin films, flash evaporation, electrical props. 0-65722
 InTe-PbTe system, phase interactions and solid soln. form., physicochem. and elec. characteris. 0-104129
 InTeBr, intermediate phase, cryst. struct. 0-100834
 InTeI, X-ray cryst. struct. determ. (*German*) 0-100214
 InVO₄, synthesis and thermal props. (*French*) 0-97443
 In₂Zn₄, solid electrolytes, ion transport mechanism and polarisability role, comparison with Cu⁺ and Ag⁺ cond. 0-107531
 K₂InCl₆·H₂O, crystal structure and H-bonding 0-64978
 PbIn_{0.5}Nb_{0.5}O₃, ferroelectric, dielectric props. 0-103923
 PbS-In₂S₃, phase investigation 0-66488
 RbIn(SO₄)₂·4H₂O, refinement of cryst. struct., interatomic distances, bonds 0-59448
 a-Si In_{2-x}Sn_xO_{3-y}/ZZ 0-101113
 Si/In₂O₃-SnO₂ thin film junctions, polarity dependent memory switching effects 0-70814
 Si-In_{2-x}Sn_xO_{3-y} SIS heterostructure solar cells, spray-deposited 0-101106
 SiO₂/InP interface formation, thermodynamic considerations 0-100529
 Ta-Ta₂O₅-InP thin refractory MIS struct. deposition 0-75647
 TiW-TiO₂-InP thin refractory MIS struct. deposition 0-75647
 TiInS₂, layered structure crystals, refractive index meas. method 0-98966
 TiInSe₂, monocrystal, photoelec. props. (*Russian*) 0-70752
 Zn-In-S thin layers, ternary phases, optical props. near long-wavelength intrinsic absorpt. edge 0-80887
 ZnIn₂S₄ crystals, switching effect, electric field distribution 0-107872
 ZnIn₂S₄, S-type negative resist, and switching effects 0-65581
 Zr_{1-x}In_{2x}O_{2-x}, ionic conductivity, lattice const. 0-96688

INDO calculations

- absorption bands, vibronic intensification obs., floating-orbital method 0-63619
 acetone, absorption bands, vibronic intensification obs., floating-orbital method 0-63619
 acetylcholine neurotransmitter, PCIL-INDO calcs. 0-58153
 N-acetylglycine, X-irrad., stable radical electronic and mol. struct., ENDOR and ESR 0-80637
 aniline-chlorophenol complexes, ³⁵Cl NQR, inter- and intramol. interactions 0-63666
 azaaromatics, neutral and protonated, excited singlet and triplet states, charge densities, INDO calcs. 0-58152
 benzyl radicals, monomethyl- and dimethyl-substituted, electronic spectra and electron affinity 0-63618
 butyl cation, H-elimination, energy partitioning, transition state geometry calc. using MINDO/3 0-104430
 chloroanisoles, ³⁵Cl NQR, inter- and intramol. interactions 0-63666
 chlorophenols, ³⁵Cl NQR, inter- and intramol. interactions 0-63666

INDO calculations continued

- 5,5'-diethylbarbituric acid, EPR and INDO-MO study of radical formation after irradiation 0-93774
 hippuric acid, X-irrad. single cryst., ¹⁴N and ¹H ENDOR study; 0-71240
 hydrocarbons, ¹³C chem. shifts, simplex optimised INDO calcs. 0-83284
 N-methyl-N-nitrosourea, electronic interactions with DNA, ESR obs. and INDO calcs. 0-94154
 nuclear spin-spin coupling constants, directly bonded C-C and C-H, CDOE/INDO LMO calcs. 0-95546
 organic molcs., relative Raman intensities, CNDO/2 INDO param. effect 0-95633
 PCIL-INDO method, theory and appls. 0-58153
 poly(vinyl cinnamate), excited state, low-energy EELS and INDO/S calcs. 0-106407
 SINDO/F theory of electronic struct., validity for transition metal cpds. 0-69075
 stilbene aza-analogues, lowest excited states, INDO/S calcs. 0-95545
 transition metal compounds, SINDO/F theory of electronic struct. 0-69075
 Co complex, Co(NO₂)₄⁴⁻, bond. props. and Jahn-Teller distortion, INDO-LCAO-MO calcs. 0-75532
 Cu complex, Cu(NO₂)₄⁴⁻, bond. props. and Jahn-Teller distortion, INDO-LCAO-MO calcs. 0-75532
 CuCl₂(Cl₄²⁻)(Cl₄⁴⁻), electronic struct. studies by SCF, MSX α and INDO method 0-74119
 CuF₂(F₄⁴⁻), electronic struct. studies by SCF, MSX α and INDO method 0-74119
 N₂, electron scatt., local exchange pot. comparison 0-78707
 NaNCO, val. band electronic struct., XPS meas., MOC and INDO calc. 0-95520
 O₂, spin-forbidden transition intensities, selective heavy atom effects 0-58240
 Pt complexes, INDO calcs. for predicting ground-state props., charge distributions and force const. determ. 0-83283

INDOR

see also nuclear Overhauser effect

No entries

induced anisotropy (magnetic)

- CdCr₂Se₄, magnetisation, study of photoinduced charges 0-80567
 (Co,Fe)₈₀B₂₀ glass, induced anisotropy and time changes of permeability 0-75815
 (Co_{0.89}Fe_{0.11})₇₂Mo₂Si_{1.8}B₁₀, metallic glass, strain- and field-induced mag. anisotropy 0-108004
 Co₇₃Mo₂Si_{1.8}B₁₀, metallic glass, strain- and field-induced mag. anisotropy 0-108004
 Co₂Ni_{1-x}Fe_xO₄, conc. and temp. depend. 0-108001
 Fe-Al (4 wt.%) alloy, mag. anisotropy induced by cold rolling (*Russian*) 0-84595
 Fe-B, amorphous, induced anisotropy by heat treatment in mag. field and under applied mech. stress 0-75758
 Fe-B(Si), glassy, field-induced mag. anisotropy near eutectic comp. 0-93110
 Fe-Si (3 wt.%) alloy, mag. anisotropy induced by cold rolling (*Russian*) 0-84595
 (Fe_{0.07}Co_{0.93})_{75-x}Cr_xSi₁₅B₁₀, amorphous, disaccommodation of mag. permeability and induced anisotropy 0-88741
 (FeNi)PB amorphous wires, surface oxidation and annealing influence on induced anisotropy 0-100957
 Li-Co ferrite, mag. anisotropy induced by thermomag. treatment, ionic order effect, magnetostriction meas. 0-103830
 Ni-Fe (19 wt.%) alloy, mag. anisotropy induced by cold rolling (*Russian*) 0-84595
 Ni₃Fe, compression induced magnetic anisotropy, annealing effect 0-93112
 (Y,Sm,Ca)₂(Fe,Gd)₂O₁₂ epitaxial films, mag. props., growth condition effects 0-97124
 YIG, large growth-induced anisotropy to preferential occupation of Fe sites 0-75754
 YIG:Co film, influence of stress induced anisotropy on domain struct. 0-100605
 (YRb)₃(FeAl)₂O₁₂ films, R=Gd, Yb, Faraday effect in transverse mag. field, orientation depend. 0-88971

inductance

- coils on infinite cylinder, mutual inductance 0-58443
 complex mutual inductance concept for bioelectric impedance transformer bridge 0-63886
 spheres and current carrying coils, integral representation of inductance 0-80469
 toroidal field coils, EM parameters calcs. of current paths in homogeneous media (*Japanese*) 0-106155

inductance measurement

No entries

induction, electromagnetic see *electromagnetic induction***induction heating**

see also electric furnaces; ovens

- eddy currents in cylindrical core of induction coil considering winding helix (*German*) 0-95764
 EM induction, irregularly shaped plates, slow ramped field, eddy current heating, anal. 0-91722
 fusion reactors, Large Coil Program, Westinghouse coil stability testing, pulsed induction heating 0-106194
 induction heating coils, 50 kA prototype superconducting cable, critical current 0-106196
 slab heating at steel plant 0-71672

induction machines see *asynchronous machines***induction motors**

- 3-phase, laminated cores, sound level theory, meas., and results (*Polish*) 0-92004
 linear asynchronous motor drive system, for rotating optical components inside vac. system 0-102874
 noise abatement for induction motors in air/air heat-exchangers for ventilation (*Hungarian*) 0-102923

inductor microphones see *microphones***industrial atmospheres** see *air pollution***industrial computer control**

see also manufacturing computer control

- optical precision instrument manufacture, microcomputer appl. (*German*) 0-95116

industrial economics *see economics*

industrial plants

hazards to nuclear power stations 0-78408
IR detector markets and device limitations 0-86432
IR instrumentation sources and optical components 0-87453
IR thermometry using fibre-optic lightguides 0-86302
methanol derivation from lignite, fuel appl. 0-61223
NDT computed transverse axial tomography system 0-89430
noise onset effects on physiological and psychological functions 0-91959
pollution, airborne metal conc. rels., nuclear anal. technique 0-72107

industrial research management *see research and development management*

industrial standards *see standards*

industries

this heading is restricted to those industries which are not covered by other specific headings
see also automobile industry; cement industry; ceramic industry; chemical industry; electricity supply industry; food processing industry; glass industry; metallurgical industries; mineral processing industry; paper industry; petroleum industry; plastics industry; textile industry
solar energy for process heat, energy requirement 0-76606
thermal energy storage in industry and power stations 0-67002

inelastic electron tunnelling spectra *see tunnelling spectra*

inelastic electron tunnelling spectroscopy *see tunnelling spectroscopy*

inert anodes *see anodes*

inert gas compounds

see also argon compounds; helium compounds; krypton compounds; neon compounds; radon compounds; xenon compounds
fluorides, formation in AC discharge 0-64817
halides, exciplex mol. form., rel. to laser operation 0-81318
halides, laser mechanism, excitation methods and appls. 0-95871

inert gases

see also argon; helium; krypton; neon; radon; xenon
adsorbates on simple metals, optical excitation, configurational switching, charge transfer 0-107643
adsorbed on graphite as microcluster, temp. depend., mol. dynamics study 0-80056
air monitoring systems for radioiodine and inert gases, evaluation 0-95480
atom, first excited config., intermediate coupling coeff. 0-83450
atom+alkali atom (ion), collision studies of quasi-one-electron systems 0-63750
atom+Ca, Ca metastable ³P-state, quenching reactions, fluoresc. meas. 0-102477
atom+Ca(Sr), ¹P₁-³P₁ excitation transfer 0-102559
atom+Cd, broadening of 5¹P₁ level 0-83479
atom+H⁺, negative ion detachment cross section determ. 0-63796
atom+halogen mol., halide form., relax. and quenching 0-81314
atom+Ne²⁺(Ar²⁺)(Kr²⁺)(Xe²⁺), low energy reactions, SIFT and drift tube obs. 0-97705
atom+ZnCl, ground state destruction, quenching rate consts. meas. 0-63758
atomic photoionisation, Dirac-Fock calcs., branching ratios and angular distrib. in p shells 0-63601
atoms+HgBr vapor, relax., rate coeffs., fluoresc. obs. 0-63697
binary mixtures, thermal diffusion factor meas. 0-79425
crystal, lattice vibrs. and radiative transitions of implanted ions (*Russian*) 0-69098
crystal, quasi-atomic and quasi-molecular exciton states (*Russian*) 0-103628
dense, rotational relax. of solute molecules reln. with local anisotropy fluc. 0-58183
dimers, Van-der-Waals type, electron impact ionis. 0-58400
discharge, isotope separation in travelling magnetic field 0-78719
discharge possibility, self-sustained, with bulk photoionisation impurities 0-75113
Earth inert gas composition, origin from solar nebula 0-61785
electroionisation discharge, negative cathode pot. drop 0-79615
electrophotoionization discharge, laser pumping 0-91781
field ion source with high angular current 0-68996
HCl-inert gas mixtures, van der Waals molecules, far IR spectra 0-95610
hydrogen halides rot. relax. with inert buffer gas, comment 0-69221
hydrogen halides rot. relax. with inert buffer gas, reply 0-69222
inert gas metastable atom+HgBr, dissociation excitation 0-63774
inert gases, atomic alignment in positive column (*Russian*) 0-87981
intermolecular spectroscopy and dynamical properties of dense systems, conf., Varenna, Italy (1978) 0-82581
ion laser, high voltage-low press. discharges, stationary props. 0-92400
ion laser mixtures, hollow cathode, CW operation and excitation mechanism 0-69363
lunar soil samples from Luna 24, inert gas element and isotope composition 0-67593
lung mathematical models, effect of common dead space on inert gas exchange 0-67126
mass spectrometer for noble gas anal., high-sensitivity pulse-counting spectrometer 0-95187
mixture, binary, μ -capture, near 5 atm., X-ray yield 0-58419
mixture, dipole autocorrelation function, Lennard-Jones and exponential dipole pots., classical calc. 0-64665
mixtures, high-press., collisional radiative recomb. 0-63595
noble gas-rich separates from H-type chondritic meteorites 0-85907
nuclear pumped lasers, electron impact cross section meas. 0-63985
nuclear pumped lasers, prod. efficiency of excited states 0-63998
Penning ionisation processes investig. by electron spectroscopy 0-58364
photoabsorption, local field effects, density-functional formalism 0-78766
planetary atmospheres, accretion from protoplanetary nebula, noble gas contents 0-109385
planetary nebulae, abundances of He, Ne, Ar, N, and Cl 0-109532
plasma, electron-beam produced, laser action of ionized and neutral atomic lines 0-106929
presolar gas components, isotopic anomalies in Murchison C2 chondrite 0-85904
resonance ionisation spectroscopy for transuranic trace analysis 0-93833
small clusters, structure, thermodynamic properties 0-88341
solid, collective excitations and EELS, calc. 0-92842
solid, Compton profiles, APW-X α calc. 0-80894
solid, contact electrification of 'ideal' insulators 0-70797
solid, melting curves, Lennard-Jones Devonshire theory 0-65201
solid, V₀-values, photoelectric determ. 0-92938

inert gases continued

stochastic description of exchange in living organs 0-81520
transient absorption, electron-beam excited inert gases at XeF laser wavelengths 0-83592
in volcanic rocks, isotopes mass fractionation as indicator of gas transport to or from magma 0-98292
Cd(P₁) radiation imprisonment lifetime, inert gas effect, phase-shift method 0-58213
Cs+inert gas, three body interaction, fluoresc. spectra principal series lines and secondary satellites 0-83313
HCl-inert gas rot-vibr. line pressure broadening and shift calc. 0-69124
HCl+inert gas, weak collisions, HCl spectral line broadening of IR spectra 0-74161
He²⁺+inert gas atom, electron capture into different excited states in plasma 0-64679
O²⁺+inert gas, electron transfer meas., 60-200 keV 0-83480
SF₆-inert gas mixture, high power cylindrical spark discharge, dynamic and visible charact. 0-64816

inertial navigation

gravity detection, covariance analysis of periodic traversing 0-95087

infinite series *see series (mathematics)*

inflammability *see combustion*

information analysis

see also classification; indexing
multiphase medium plasma dynamics, Soviet literature growth and duplication parameters (*Russian*) 0-59191

information dissemination

stellar photometric data 0-105179

information retrieval systems

astronomical database, BADAS, design and realisation (*Italian*) 0-98580
Chemical Registry System, tautomerism and alternating bonds, handling 0-63851
climate data archiving and quality control by computer 0-61907
MOLARS system of British National Meteorological Library 0-82068
SINC laboratory instrumentation information system, proposed structure 0-98908

information science

see also publishing
Indian scientific and technical Journals critical evaluation 0-94906

information services

British National Meteorological Library, MOLARS automation 0-82068
Chemical Registry System, tautomerism and alternating bonds, handling 0-63851
computer information, conference, London, England (Nov. 1979) 0-90599

information storage

climate data archiving and quality control by computer 0-61907

information storage systems *see information retrieval systems*

information systems, management *see management information systems*

information theory

see also codes; correlation theory; decision theory and analysis; estimation theory; filtering and prediction theory; modulation; signal detection; signal processing; speech intelligibility
concert hall problem, coherence length and diffuse reflection formulation 0-91962
entropy, information and statistical, and law of large numbers, opacity of statistics (*French*) 0-73288
experiments, indirect, maximising information, optimal initial state 0-77744
Gaussian signals in Gaussian noise transmitted over digital channel, degradation of S/N ratio 0-64298
image restoration using maximum information norm 0-106476
Maxwell demon and correspondence between information and entropy 0-86241
measurement techniques, error anal. using information, signal and system theory (*German*) 0-68164
medical imaging systems, information capacity considerations 0-98090
nonlinear experimental design, information measures 0-62616
quantum-mechanical kinetic energy as measure of information in distribution 0-101725
radiography, medical diagnosis, information storage requirements 0-98086
solar energy collection anal. using information theory 0-97799
streamflow, model, identification of seasonal water supply forecasting models using Akaike's information criterion 0-67386
turbulence, description and quantification (*German*) 0-106789

infrared astronomical observations

0957+561A, B, double quasar, IR obs. of quasar and intervening galaxy 0-73065
2A 0311-227, AM Herculis type binary star, IR photometry and polarimetry 0-77517
Am stars, τ Ursae Majoris and 15 Vulpeculae, energy distrib. from spectral obs. 0-85949
asteroids, IR reflectance spectra obs. and search for water of hydration 0-77318
Callisto, IR emission spectra 0-82264
Comet Bradfield (1979I), spectroscopic and photographic obs. in near IR 0-105205
compact IR sources in molecular clouds, near IR slit scans 0-105300
R Coronae Austrinae dark cloud stars, interstellar absorpt. spectra rel. to dust grain growth 0-67834
R Coronae Austrinae interstellar molecular cloud, for IR study and dust temp. profiles 0-62237
CPD -62° 1837 (HDE 308122), long-period variable member of triple 0-105260
 θ Cygni, F-type dwarf star, spectral type of faint distant companion 0-90481
P Cygni, H Paschen α obs. 0-62156
59 ν V832 Cygni, IR emission increase, spectrum scanner obs. 0-94809
V1016 Cygni, near-IR spectrographic obs. 0-94810
V1016 Cygni, symbiotic star, IR variability obs. from VJHKL photometry (*Russian*) 0-105263
V645 Cygni (GL 2789), IR and EHF spectroscopy 0-72956
Cygnus X region, far IR survey 0-82538
349 Dembowska, IR spectral obs., candidate for meteorite parent bodies 0-98595
DR 21/W75 complex, detection of H₂ vibrationally excited 2 μ m lines 0-94853
early-type stars in southern hemisphere, IR photometry 0-94786

infrared astronomical observations continued

- early-type stars with gas-dust envelopes, IR spectral energy distrib. 0-67732
 eclipsing binary stars, near IR photometry rel. to mass transfer rates 0-67784
 emission line stars in southern hemisphere, IR obs. 0-90496
 faint stellar images, colour-magnitude diagrams and clustering correl. functions rel. to star populations 0-82360
 G333.6-0.2, Ne II 12.81 μm forbidden line obs. at high resolution 0-85983
 galactic plane far IR emission, obs. at galactic longit. ($l^{\text{II}}=27.5^\circ$) 0-62231
 galaxies, distance scale from IR magnitude/H I vel.-width relation 0-82480
 galaxies, H I vel. widths and IR magnitudes rel. to distance scale and expansion rate outside Local Supercluster 0-105325
 galaxies, luminosity evolution from 2.2 μm of giant ellipticals 0-105358
 galaxies, V-K colours and IR Hubble diagram for giant ellipticals 0-105359
 Galilean satellites, water ice existence, IR spectral reflectance obs. 0-82263
 giant planets, atmospheric refraction indexes 0-98608
 GL 2591, protostellar source, 3 μm ice absorpt. band, linear polarisation obs. 0-105303
 GL 2636, star form. region in Cygnus-X, IR obs. 0-105302
 globular clusters, colours and interstellar reddening from integrated IR photometry 0-67575
 globular clusters near galactic centre, IR studies 0-82434
 HD 200775, possible protostar in reflection nebula NGC 7023, optical polarization and IR spectrum 0-85944
 HD 44179, binary star, 3.3 micron unidentified feature, high resolution spectra 0-82466
 HD 97048 (=HM 18), pre-main sequence star, unidentified IR features obs. 0-85943
 He2-442, UVK photometry and spectroscopic obs. (*Russian*) 0-94817
 Henize 715 (4U 1145-61), Be star, IR vars. rel. to circumstellar envelope disappearance 0-72979
 Herbig-Haro 2, detection of H₂ vibrationally excited 2 μm lines 0-94853
 Herbig-Haro objects exciting stars, 2 micron search 0-67720
 AM Herculis, polar, IR photometric obs. 0-98687
 HR 1099 (V711 Tauri), JHK photometry of noneclipsing RS Canum Venaticorum type star 0-72995
 EX Hydrae, dwarf nova, IR and optical light curves 0-67747
 VW Hydri, dwarf nova, IR light curves 0-67747
 Iapetus, relative reflectance meas. at 1.6 and 2.2 μm 0-98607
 IC 1396 interstellar molecular cloud, for IR study and dust temp. profiles 0-62237
 IC 342, Scd galaxy, central regions IR emission and star form. 0-62256
 III-106, CH star in globular cluster M22, CO in IR spectra 0-62131
 interstellar C₂, rot. fine-struct. lines obs. towards ϵ Persei 0-67811
 interstellar C in mol. clouds, 492 GHz line detection 0-90508
 interstellar grains, organic composition, IR obs. 0-77460
 interstellar grains comprised of organic cpds., 3.4 microns absorpt. obs. 0-109514
 interstellar medium, far IR fine structure line obs. 0-62253
 interstellar reddening in near IR, new results from JHK photometry of reddened stars 0-94857
 IR bright stars in region of galactic centre, catalogue and photometry 0-77299
 IRC+10216, variable C star 0-90568
 IRC+10216, C star, far IR size 0-82539
 Jupiter, C/H and D/H ratios from 8-9 μm IR spectrum 0-67638
 Jupiter, cloud distrib. between Voyager 1 and 2 missions, 5 micron obs. 0-77345
 Jupiter, IR spatial scans 0-82268
 Jupiter, methane line profiles near 1.1 μm as probe of cloud struct. and C/H ratio 0-62067
 Jupiter and Galilean satellites, Voyager 2 IR obs. 0-77335
 K-type giant stars, evidence for circumstellar shells from 0.4 to 20 μm photometry 0-90420
 Kuwano's novae-like object in Vulpecula, IR photometric obs. 0-62147
 BL Lacertae objects, polarisation, visual and IR photometry and polarimetry 0-77480
 late-type stars, anal. of balloon-borne near IR multicolour photometry 0-98654
 late-type stars, Ca II 8542 Å line as chromospheric activity indicator 0-62108
 CW Leonis (IRC+10216), IR C star, intrinsic polarisation obs. and origin 0-67730
 Liller 1 (MXB 1730-333), unusual burst in K-band (2.2 μm) 0-62319
 β Lyrae, CNO abundances in atmosphere, IR spectra (*Russian*) 0-67794
 M82, nuclear source nature from IR obs. 0-82485
 maser stars, late supergiants and long period variables 0-77410
 millimetre region cosmic background radiation, large scale anisotropy meas. 0-82553
 Mira variables, IR Photometry and OH maser pumping efficiency 0-82379
 molecular clouds, IR circular polarisation obs., interpretation 0-82469
 Monoceros R2, far IR obs. of young assoc. 0-73010
 MWC 349A, near-IR spectrographic obs. 0-94810
 MXB 1730-335, X-ray rapid burster, unsuccessful search for IR bursts 0-98740
 Neptune, albedo and brightness temp., 5 μm IR obs. 0-82300
 NGC 1068, type 2 Seyfert, recombination spectrum and reddening 0-90519
 NGC 2264, H II region, classification of optical, IR and radio obs. data 0-67818
 NGC 253, nuclear source nature from IR obs. 0-82485
 NGC 2903, spiral galaxy, nucleus identification and visual energy distrib. 0-62273
 NGC 7027, planetary nebula, 3.3 microns unidentified feature, high resolution spectra 0-82466
 NGC 7027, planetary nebula, H₂ emission spatial distrib. obs. 0-98698
 Nova Serpentis 1978, visible and IR photometry rel. to dust shell evolution 0-90430
 novae-like object in Vulpecula, light curve, photometric and spectroscopic obs. 0-67758
 O-type stars, C III 7901 to 9715 Å emission lines obs. 0-77401
 OB-type stars, search for H Paschen α 0-62156
 OH 205.1-14.1 in Lynds 1630 dark cloud, coincident IR source obs. 0-101630

infrared astronomical observations continued

- OMC-2, detection of H₂ vibrationally excited 2 μm lines 0-94853
 Omega Nebula (M17, W38, NGC 6618), S III, O III, N III, IR obs. 0-90495
 ρ Ophiuchi dark cloud stars, interstellar absorpt. spectra rel. to dust grain growth 0-67834
 Orion Molecular Cloud, HCN J=4-3 354 GHz transition detection 0-101636
 Orion Nebula, forbidden Cl II and forbidden Fe II near IR high resolution mapping 0-62217
 Orion Nebula, near IR photography with vacuum-cold camera 0-90341
 Pal 12, metal-rich globular cluster in outer galactic halo, optical and IR obs. 0-105290
 PKS 2126-15, QSO ($z=3.27$), JHK photometric obs. 0-94888
 planetary nebulae, advances in IR obs. 0-109525
 planetary nebulae, dust temp. and mass, IR photometry obs. 0-94850
 planetary nebulae, S abundance from IR and visible line meas. 0-82444
 planetary nebulae in southern hemisphere, IR and SHF obs. 0-90496
 VV Puppis, polar, IR photometric obs. 0-98687
 Q 0420-388, QSO ($z=3.13$), JHK photometric obs. 0-94888
 QSO 0957+561 AB, double quasar, IR spectrum confirms gravitational lens 0-77510
 quasars, IR spectra, H I line ratios 0-105391
 quasars, optical identification problems 0-105392
 S140 interstellar molecular cloud, for IR study and dust temp. profiles 0-62237
 S-type stars, Keenan and Wing bands, IR obs. 0-67722
 S-type stars, Keenan band identification problem, IR obs. 0-72946
 HM Sagittae, near-IR spectrographic obs. of young planetary nebulae 0-94810
 HM Sagittae, symbiotic star, IR variability obs. from VJHKL photometry (*Russian*) 0-105263
 Saturn, IR scans (1977 to 1978) 0-90363
 Saturn, PH₃ abundance, IR obs. 0-82278
 Saturn atmosphere, Pioneer 11, IR radiometry data 0-82290
 Saturn rings, unilluminated side, 20 μm brightness temp. 0-109392
 RZ Scuti, JKL IR obs., light curves for eclipsing binary 0-101615
 Serpens X-1, no IR bursts assoc. with Type I X-ray burst 0-98742
 Seyfert 1 galaxies, O I 8446 Å emission excitation mechanism, visible and IR obs. 0-85991
 Sh2-149, near IR photography with vacuum-cold camera 0-90341
 Sharpless 106 IR sources, 8-13 micron spectrophotometry 0-105305
 slow novae and symbiotic stars, late-type components spectral classifications 0-94813
 solar far-IR brightness temp. minima rel. to sunspot activity 0-62035
 solar quiescent prominence spectra, meas. of Ca⁺ 8542 and 8498 Å 0-90373
 solar spectrum, absorpt. lines asymmetry (*Russian*) 0-72901
 SS 433, IR variability obs. 0-98676
 stellar airborne spectrophotometry, 1.2-5.5 μm , spectra and absolute calibration 0-62117
 Sun, absolute brightness temp. meas. in far IR with balloon-borne interferometer 0-62095
 Sun, temperature minimum in far IR, var. with solar cycle 0-94769
 sunspot umbrae, IR Ca II lines 0-85918
 supergiant, B-type, assoc. IR source GL 2636, IR and visible obs. 0-105302
 symbiotic stars and slow novae, late-type components spectral classifications 0-94813
 Uranus, albedo and brightness temp., 5 μm IR obs. 0-82300
 Uranus, albedo and spectral features from IR obs. 0-82299
 Uranus and rings, obs. of stellar occultation, (1980 August 15 to 16) 0-98610
 AN Ursae Majoris, polar, IR photometric obs. 0-98687
 AI Velorum, BVRI photometry and photoelectric radial vels. rel. to nature of variable star 0-94815
 Venus, surface dust detected by Venera 9 and 10 radiant flux obs. 0-72803
 Vesta, IR spectral obs., candidate for meteorite parent bodies 0-98595
 W3 IRS 1, fine structure line radiation, dust UV opacity 0-90505
 W51-IRS 2 and W49 NW, compact H II regions, IR spectra obs. 0-90497
 WC stars, near IR spectrometry 0-94816
 Wolf Rayet stars, late type, 8-13 micron spectral obs. 0-101599
 X-ray source fields from Einstein Observatory, RI photometry with CCD camera 0-62315
 young variable stars, absorpt. and emission features, IR spectrophotometry obs. 0-72954
 zodiacal dust cloud, thermal emission at 11 and 20 microns 0-90367
 C stars, variable, IJHKL photometry obs. 0-98657
 He variable stars, IR excesses obs. 0-67733

infrared astronomy

- see also *infrared sources (astronomical)*
 airborne far IR Fabry-Perot astronomical spectrometer 0-109371
 airborne far IR Fabry-Perot spectrometer for astronomical fine structure lines 0-62026
 bandpass interference filters for 1-3 mm window 0-109368
 Cassegrain scanning system for IR images 0-82204
 conference, IR and MM waves and appls., Miami Beach, USA (Dec. 1979) 0-57009
 Cosmic Background Explorer, satellite instrumentation 0-61988
 3K cosmic background radiation, star form., nuclei of active galaxies 0-67958
 cosmic ray Cherenkov photons, effect on IR interferometric search for non-solar planets 0-98523
 detectors, trends in low-temp. thermal and photon detectors (*Russian*) 0-72778
 far IR astronomy, calibration source for balloon-borne telescopes 0-62027
 flux method for stellar temps. and diameter determ. 0-62030
 focal plane IR detector arrays for planetary missions 0-85862
 giant stars, IR radiation emission in final stages 0-72931
 high resolution image prod., use of totally computer controlled telescope 0-72785
 high resolution spectrometer, used for satellite astronomical measurements, cryogenically cooled 0-90914
 image contrast of diffraction-limited telescopes for circular incoherent sources of uniform radiance 0-82194
 Infrared Astronomical Satellite, features and performance 0-61989

infrared astronomy continued

- integrated IR photometry and wide field techniques for globular clusters 0-67574
- integrated IR photometry using wide field photometer for globular clusters 0-62029
- low-background astronomical integrated IR detector array development 0-85860
- Michelson interferometer on Voyager 0-77290
- multiplex image coding, astronomical IR speckle interferometry appl. (French) 0-67580
- photography, near IR, with vacuum-cold camera 0-90341
- Pioneer Venus Sounder Probe IR radiometer 0-67509
- planetary nebulae, advances in IR obs. 0-109525
- review of IR and submillimetric astronomy (Russian) 0-72773
- Salyut 6 Ge:B receiver for 60-130 μ m studies 0-67566
- sky survey telescope for wide field photography 0-105167
- space-borne interferometers, astrometry and planetary detection 0-109357
- star formation rate in inner Galaxy, IR obs. 0-67704
- Venus, clouds, IR absorption and scattering, particle size dispersion effect 0-109384
- InSb IR detectors, integrating preamplifier 0-90337

infrared communication see optical communication**infrared detectors**

see also bolometers; photodetectors

- 3-channel far IR detector based on coded Si;B, Ge:B, n-GaAs photoresistors 0-101839
- angular displacement transducer 0-86257
- atomic vapour quantum counter for upconversion of narrowband IR radiation in 1.5-20 μ m region, expt. results 0-73455
- balanced common module coolers 0-95142
- calibration standards requirements survey 0-57248
- chopping pyrometer for remote meas. below 200°C (German) 0-86313
- combustion technology, IR applications 0-86431
- conference, IR and MM waves and appls., Miami Beach, USA (Dec. 1979) 0-57009
- contactless temperature meas., IR techniques and detectors (German) 0-86314
- DH photodiodes, diffusion limited transient response 0-70809
- dicalcium lead propionate, improper ferroelectric, dielectric props., IR radiation pyroelectric detection 0-80711
- electronic gas detection, Pellistor, VQ and TGS sensors (Spanish) 0-93832
- far IR and near MM wave power energy meter calibration 0-57373
- focal plane IR detector arrays for planetary missions 0-85862
- forest fire alarm system 0-86429
- fusion reactor, Doublet III, neutral beam interlock system using IR detector 0-106228
- HgCdTe/CdTe, limited diffusion volume photodiode, characterisation 0-75627
- industrial IR detector markets and device limitations 0-86432
- industrial IR thermometry using fibre-optic lightguides 0-86302
- Josephson junctions, applications in plasma physics 0-103194
- laser low-level pulse meas. system at 1.064, transfer standards 0-86253
- laser pulse detector, fast nondamageable, using gaseous plasma 0-95138
- linearity, device for checking 0-101841
- low-background astronomical integrated IR detector array development 0-85860
- low-temperature thermal and photon detectors, astronomical appls. (Russian) 0-72778
- near IR (1 to 2 μ m) optical communications, colloquium, London, England (May 1980) 0-86040
- near IR mapping spectrometer design and testing for Galileo Jupiter Orbiter 0-90336
- nondispersive IR photometer selectivity improvement (German) 0-90880
- nonlinear responsivity characterisation 0-77853
- nuclear materials safeguards applications of far infrared radiometric techniques for the detection of contraband 0-73925
- optocoupler system, precision measurements non involving contact (German) 0-82823
- orbiting IR detector cooling by multitemission solid cryogen cooler 0-86423
- performance criterion of radiation detectors for thermal viewing systems 0-73459
- photometry, NDIR, partially layered detector, function and properties 0-105696
- photon drag detector design and choice of semiconductor 0-57374
- photoresistor, PbSe base, thermal stability over range 0°C to 60°C 0-73458
- Pioneer Venus Sounder Probe IR radiometer 0-67509
- point contact IR detector tunnelling and rectification characteristics, geometrical and multiple image interactions 0-57376
- point contacts between identical metals, HF rectification at low temp. 0-105706
- point-contact diode tunnelling and rectification rel. to electrode geometry 0-57378
- polyvinylidene fluoride film, pyroelec. camera tube for IR imaging, thermal diffusivity of Bi-Bi₂O₃ black layer 0-57369
- PVDF pyroelectric detector (Japanese) 0-105714
- pyroelectric, direct meas. of IR laser radiation multiphoton mol. absorpt. 0-102545
- pyroelectric, sub-100 ps, 10.6 μ m damage threshold meas. 0-77859
- pyroelectric 0-82820
- pyroelectric detector, performance evaluation method 0-82819
- pyroelectric detector for subnanosecond CO₂ laser pulse meas. 0-78884
- pyroelectric detectors, effect of substrate on current responsivity 0-73454
- pyroelectric ionisation upconverter for IR detection 0-77860
- pyroelectric polymers detector (Japanese) 0-105713
- pyroelectric thin film detector, temp. fluctuation noise 0-77861
- pyrometer performance parameters and applications (German) 0-86315
- radiometer with pyroelectric radiation receptor 0-101842
- rapid-scan polarising Michelson interferometer and InSb detector calibration 0-59305
- refracting objectives for 8 to 13 μ m 0-86421
- Schottky-barrier diode IR capacitive mixing and detect. at high, intermediate or modulation freqs. 0-77864
- self-scanned photodiode array as multichannel spectrometric detector 0-73466
- semiconductor IR photodetectors, comparison of extrinsic and intrinsic devices, temp. limitations 0-73456

infrared detectors continued

- seminar, optical radiation meas., San Diego, CA, USA (Aug. 1979) 0-86036
- sensor figures of merit 0-86419
- Si:In growth by Czochralski crystal pulling, characterisation for extrinsic IR detectors, focal-plane arrays 0-76168
- signal processors, continuous-time, for IR surveillance 0-78781
- signature classification system 0-86430
- slow-acting IR radiation receivers, meas. value correction (German) 0-105708
- solid thermal cond. and interface resistance meas. by radiation thermometry 0-86289
- spectrometer, cryogenic, detector-preamplifier, optimization 0-95164
- staring, military space and reconnaissance appln. 0-86406
- steam fraction determ. in flowing air/stream mixtures by meas. of IR rad. attenuation 0-75010
- step-stare IR sensor design for aerospace vehicle detection 0-86418
- submillimetre and IR review (Russian) 0-72773
- superconducting, space appl. 0-85836
- superconducting double multivibrator used as near- and medium-infrared radiation detector (German) 0-90892
- superconductive FIR detectors, Josephson-junction direct devices and transition edge bolometers, review 0-77865
- technology utilisation, symposium, San Diego, CA, USA (Aug. 79) 0-86037
- thermometer, non-contact (Polish) 0-90845
- three-dimensional thin pyroelectric IR detector simulation 0-57375
- two-scatter-plate low-speckle-noise integrator for atmospheric laser beam transmission meas. 0-90252
- CO concentration meas. in coal pulverising plant, IR gas analysers 0-89572
- CdHgTe photoelectromagnetic detector for 10.6 μ m radiation, non-cooled, performance 0-82818
- Cd_{0.7}Hg_{0.3}Te, ion implantation doping for realisation of IR detectors, responsivity meas., ion range straggling 0-73452
- Cd_{0.7}Hg_{0.3}Te recrystallisation for supercooled IR detector production (German) 0-86403
- Cd_{0.8}Hg_{0.2}Te, epitaxial layer p-n junction, current-voltage characteristics of photovoltaic detectors, 1 to 15 μ m 0-86407
- CdSb:Al, p-n junction formation by laser emission, photoelectric effects (Russian) 0-70815
- Fe₂B₂O₇, improper ferroelectric, dielectric props., IR radiation pyroelectric detection 0-80711
- GaAs, photocapacitive MIS IR detector, spectral response, noise characts. 0-75644
- Ga_{0.47}In_{0.53}As, photodetector applications 0-95140
- Ge and Ge-diamond bolometers operated at 4.2, 2.0, 1.2, 0.3, 0.1 K, design and construction 0-77868
- Ge-metal Schottky barrier photodetectors, near IR interband transitions and optical parameters 0-73449
- n-Ge-metal Schottky barrier contacts, IR optoelectronic props., quantum detector appls. 0-75640
- HgCdTe, nonlinear responsivity characterisation 0-77853
- HgCdTe reverse-biased photodiodes for wideband appls., excess noise 0-107876
- HgCdTe solid solution photodiode for CO₂ laser active medium study 0-95868
- Hg_{1-x}Cd_xTe photodiodes, long cutoff wavelength, effect of trap tunnelling on IR detector performance 0-73451
- InAsSb/GaSb broad-spectral-band IR detector, backside-illum. heterostructure approach 0-73450
- In_{0.43}Ga_{0.47}As-InP avalanche photodiode structure for 1 to 1.6 μ m region 0-98978
- InGaAsP avalanche photodiode, 1.3 μ m, noise performance, -190°C 0-57370
- InGaAsP-InP high-gain heterojunction phototransistor 0-103745
- InSb IR detectors, integrating preamplifier 0-90337
- LiNbO₃ intracavity upconverter for IR detect., limits to low noise equivalent power operation 0-74430
- LiTaO₃ monolithic pyroelectric array, IR detectors 0-77857
- LiTaO₃/CCD hybrid focal plane, IR imaging and detection, crosstalk 0-77856
- Nb thin film microbridge, video detection of far IR radiation (Japanese) 0-97038
- Pb_{0.97}Hg_{0.03}Te photovoltaic detector produced by Sb⁺ ion implantation 0-82821
- PbS, chem. deposited thin film, effect of morphological struct. on photosensitivity 0-70760
- PbS IR staring mosaic detector array module development 0-86413
- PbS mosaic array pulse-bias modulation 0-86414
- PbS-Si heterojunction, related optical and IR detector props. 0-77866
- Pb_{0.97}Sn_{0.03}Se, multispectral photovoltaic IR detectors 0-105710
- Pb_{1-x}Sn_xTe LPE film IR detector performance 0-86422
- PbTe photovoltaic detector, detectivity limits 0-105709
- PtSi Schottky-barrier monolithic IRCCD focal plane 0-86427
- Si extrinsic IR monolithic focal plane array detectors, I-V characts. of p⁺-p-p⁺ and n⁺-p-p⁺ structs. 0-77863
- p-Si, heavily doped contact layers on IR detectors, IR transmissivity 0-108190
- Si, photocapacitive MIS IR detector, spectral response, noise characts. 0-75644
- Si position-sensitive detector for CW and pulsed laser beams 0-78883
- Si:Au planar extrinsic IR detector, use of multiple internal refl. for increased sensitivity 0-77862
- Si:In extrinsic IR detectors with closely compensated residual impurities, model of responsivity temp. depend. 0-73453
- Si:In extrinsic IR detector material with high responsivity compensated by neutron transmutation, float-zone growth 0-75597
- Tb₂(MoO₄)₃, improper ferroelectric, dielectric props., IR radiation pyroelectric detection 0-80711

infrared imaging

- aircraft IR segmented composite window design 0-106621
- ATP-12M infrared imaging system (USSR), body temperature meas. 0-67280
- blackbody radiant flux calc. simplification 0-106710
- building heat loss diagnostics, IR image evaluation requirements 0-86424
- coherent fast IR wavefront aberration sensor interference problems 0-74499
- digital processing technique appl., thermal imager pictures delining 0-106466

infrared imaging continued

- Earth scene dynamics, satellite-borne mosaic sensor performance 0-90321
electron beam high resolution thermal wave microscopy 0-95158
emissivity meas. of good heat conducting materials (*French*) 0-103507
fibre composite structure, thermal field techniques for NDT 0-66737
fibreglass laminates, thermal NDT using liq. crystals. 0-93709
focal plane IR detector arrays for planetary missions 0-85862
forward-looking IR sensor image segmentation by maximum likelihood parameter estimation 0-99662
high resolution image prod., use of totally computer controlled telescope 0-72785
holographic scanner imaging systems, active and passive, 8 to 13 μm , characts. 0-91755
image registration and differencing by coherent optical pattern recognition 0-99648
image segmentation based on second-order grey level statistics 0-99663
industrial IR detector markets and device limitations 0-86432
IR non-destructive testing of bonded materials, theory and practice 0-93708
laser tracking system testing by 1 m unobscured IR collimator 0-78991
low-background astronomical integrated IR detector array development 0-85860
membraneous image translators, theory of basic characts. (*Russian*) 0-90838
microwave thermography, appl. in cancer diagnosis (*Spanish*) 0-67195
military, staring IR sensors, space and reconnaissance appln. 0-86406
mosaic IR image differencing for track assembly 0-86420
near-millimetric wavelength military systems 0-86428
noise reduction algorithms, Monte Carlo evaluation 0-95824
performance criterion of radiation detectors for thermal viewing systems 0-73459
photon detector for geophysical and astrophysical research 0-86405
pick-up tube, pyroelectric, sensitivity and geometrical resolution improvement (*German*) 0-105715
plasma sources, cooling pattern of acceleration grids meas. by IR scanning 0-86303
pyroelectric vidicons, figures of merit, material parameters 0-77855
quasi-staring IR sensor clutter rejection processor design 0-86417
refracting objectives for 8 to 13 μm 0-86421
scanning system modular design, assembly and alignment 0-78989
sensitivity equation modification (*Chinese*) 0-102806
Shroud of Turin, IR reflectance spectrosc. and thermographic investigations 0-87578
Shroud of Turin, scientific investigation 0-87576
Shuttle Orbiter re-entry, remote IR imagery and tracking 0-82171
Skylab conical multispectral scanner IR data statistics 0-90223
smoke/dust cloud temporal analysis algorithm 0-98484
staring mosaic sensor background suppression and tracking 0-86415
staring mosaic sensor performance, effect of spacecraft-induced line-of-sight jitter 0-86416
step-stare spaceborne optical system image motion compensation 0-90322
structural stress distrib. determ. by remote IR thermometry 0-87749
target discrimination methodology in remote sensing 0-58470
technology utilisation, symposium, San Diego, CA, USA (Aug. 79) 0-86037
thermal imaging scanners, mirror rotation axis optimisation 0-86426
thermal imaging with pyroelectric vidicon camera 0-86288
thermal inertia mapping by IR imagery, mathematical model 0-109280
thermo-optical convertor with liq. modulating medium 0-91927
thermography, reflectance errors 0-62661
thermoplastic layers, isothermal smoothing of surface deformation (*Russian*) 0-76394
thermovision law detector 'Stator-1', meas. channel 0-76449
triglycine sulphate, deuterated, reticulated target for pyroelectric vidicon, IR imaging 0-77858
US intensity pattern characterisation, thermographic-photographic technique 0-106689
 Cu_2S , Cu_1S , α - β transition, thermographic investigation of heats, entropies and activation energies 0-88314
Ge, polycrystalline thermal-imaging lens, optical requirements 0-69495
 $\text{LiTaO}_3/\text{CCD}$ hybrid focal plane, IR imaging and detection, crosstalk 0-77856
 SiC heat-exchanger tubing, IR techniques for evaluation 0-76435
 ZnS CVD IR window, optical and physical characteristics 0-106620
 $\text{Zn}_2\text{SiO}_4/\text{Mn}$, energy storage effect and retrieval 0-100684

infrared-infrared double resonance see optical double resonance

infrared radiometers see radiometers

infrared sources

- blackbody for energy calibration of infrared equipment 0-86377
blackbody radiant flux calc. simplification 0-106710
brightness determination of thermal source, use of optical parametric converter 0-98979
ChT-2R electric oven (USSR), calibration of radiometers using blackbody models 0-62722
classification system for isolated IR signatures 0-86430
conference, IR and MM waves and appls., Miami Beach, USA (Dec. 1979) 0-57009
far IR calibration source for balloon-borne telescopes 0-62027
fibre-optic communication system performance at 1.55 μm with single-longitudinal-mode laser 0-87556
fibreglass laminates, thermal NDT using liq. crystals. 0-93709
fluoromethane, $^{12}\text{CH}_3\text{F}$, far IR Raman laser line obs., CO_2 laser pumping 0-69381
fluoromethane high-power laser, tuning behaviour 0-63994
industrial IR instrumentation sources and optical components 0-87453
laser, mass spectroscopic analysis of gaseous impurity microconcentrations in nonconducting materials 0-73518
methanol far IR laser, twin optically pumped, for plasma diagnostics 0-59306
methanol twin optically pumped far IR laser for plasma diagnostics 0-103189
near IR (1 to 2 μm) optical communications, colloquium, London, England (May 1980) 0-86040
photoionisation, multiple, infrared laser 0-69194
quartz lamps, emitter for permeable walls cooling characts. investig. 0-64535
semiconductor light source for fibre optical communication 0-58653
storage ring design considerations for parasitic use of synchrotron radiation in the infrared 0-91340
- infrared sources continued**
tunable coherent IR and FIR sources utilising modulational instability 0-95967
tunable IR solid-state laser characteristics and principles 0-87406
tunable laser for semiconductor multiphoton spectroscopy (*French*) 0-82836
 CdS , subMM radiation excitation by N_2 laser pulse 0-60678
 Co:MgF_2 , tunable transition-metal-doped solid state lasers 0-58549
 $\text{Hg}_{0.77}\text{Cd}_{0.23}\text{Te}$ nonlinear optical IR generation 0-58642
 LiNbO_3 grating-tuned picosecond IR source with CdSe down-conversion 0-74435
 Ni:MgF_2 , tunable transition-metal-doped solid state lasers 0-58549
OCS laser, for 16 μm range, review (*Rumanian*) 0-87408
Pb salt tunable diode laser-integrating sphere system, output intensity characts. 0-78881
 $\text{PbS}_{0.1}\text{Se}_{0.9}$ 4.6 μm LED, room temp., band gap and electrolum. 0-66302
- infrared sources (astronomical)**
0957+561A, B, double quasar, IR obs. of quasar and intervening galaxy 0-73065
2A 0311-227, AM Herculis type binary star, IR photometry and polarimetry 0-77517
AFGL 2789 (V645 Cygni), Ae star, perplexing spectrum 0-73066
R Aquarii, symbiotic star, radio mol. maser line obs. 0-72960
Circinus X-1, changes in optical, IR and radio emission 0-67910
cocoon stars, numerical soln. of radiation transfer eqn. in spherical geometry 0-90329
compact IR sources in molecular clouds, near IR slit scans 0-105300
R Coronae Austrinae interstellar molecular cloud, for IR study and dust temp. profiles 0-62237
cosmic dust grains surrounding variable source of heating radiation, IR flux development 0-105324
V1016 Cygni, symbiotic star, IR variability obs. from VJHKL photometry (*Russian*) 0-105263
Cygnus X region, far IR survey 0-82538
early-type stars in southern hemisphere, search for IR excesses from JHKL photometry 0-94786
early-type stars with gas-dust envelopes, IR spectral energy distrib. 0-67732
emission line stars in southern hemisphere, IR obs. 0-90496
Equatorial Infrared Catalogue No.2 astronomical source distrib. 0-90346
galactic centre region, sources and obscuration 0-77487
galactic IR sources, 3 μ spectral feature identification 0-62227
galactic plane far IR emission, obs. at galactic longit. ($l^{\text{II}}=27.5^\circ$) 0-62231
galaxies, distance scale from IR magnitude/H I vel.-width relation 0-82480
galaxies, IR magnitude/H I vel. width relation rel. to distance scale and Universe expansion rate outside Local Supercluster 0-105325
galaxies, nearby, interstellar CO survey 0-62276
GL 2591, protostellar source, 3 μm ice absorpt. band, linear polarisation obs. 0-105303
GL 2636, star form. region in Cygnus-X, IR obs. 0-105302
GL 2789 (V645 Cygni), IR and EHF spectroscopy 0-72956
GL 333, vels. as affected by W4 ionisation front and assoc. shock 0-94843
globular clusters near galactic centre, IR studies 0-82434
HD 97048 (=HM 18), pre-main sequence star, unidentified IR features obs. 0-85943
He2-442, UVRR photometry and spectroscopic obs. (*Russian*) 0-94817
Herbig-Haro objects vicinity, exciting stars search and IR sources discovery 0-67720
IC 1396 interstellar molecular cloud, for IR study and dust temp. profiles 0-62237
IC 342, Scd galaxy, central regions IR emission and star form. 0-62256
interstellar medium, far IR fine structure line obs. 0-62253
IRC+10216, variable C star, IR spectra obs. 0-90568
IRC+10216 (CW Leonis), IR C star, intrinsic polarisation 0-67730
IRC+10274, IRC+10523, IR stars, H_2O maser emission detect. 0-62298
IRC+30219, variable C star, optical emission-line phase obs. 0-90569
IRC+10216, C star, far IR size 0-82539
K-type giant stars, IR excesses rel. to presence of circumstellar shells 0-90420
late-type stars, anal. of balloon-borne near IR multicolour photometry 0-98654
MXB 1730-335, X-ray rapid burster, unsuccessful search for IR bursts 0-98740
NGC 2903, spiral galaxy, nucleus identification and visual energy distrib. 0-62273
NGC 6334, far IR sources positions rel. to H_2O masers 0-73025
NGC 7027, planetary nebula, H_2 emission spatial distrib. obs. 0-98698
NGC 7538, IRS 1, formaldehyde maser, SHF band obs. 0-67822
O-type stars, C III 7901 to 9715 A emission lines obs. 0-77401
OMC-1, IR emission rel. to methanol masers excitation 0-67891
Orion Nebula, near IR photography with vacuum-cold camera 0-90341
planetary nebulae, advances in IR obs. 0-109525
planetary nebulae, southern, IR obs. 0-90496
protostellar envelope evolution, radiative transfer and spectrum 0-77384
quasars, optical identification problems 0-105392
review of IR and submillimetre astronomy (*Russian*) 0-72773
Roberts 22, bipolar nebula with OH emission, visual, radio and IR obs. 0-94859
RSO 1 catalogue cross correl. with IRC, AFGL and EIC catalogues 0-77511
S140 interstellar molecular cloud, for IR study and dust temp. profiles 0-62237
HM Sagittae, symbiotic star, IR variability obs. from VJHKL photometry (*Russian*) 0-105263
V818 Scorpii (Scorpius X-1), UV, visible, IR and X-ray obs. 0-82541
Seyfert galaxies, thermal IR emission vars. 0-67865
Sh2-149, near IR photography with vacuum-cold camera 0-90341
Sharpless 106 IR sources, 8-13 micron spectrophotometry 0-105305
slow novae and symbiotic stars, late-type components spectral classifications 0-94813
SS 433, IR variability obs. 0-98676
stars, IR bright, in region of galactic centre, catalogue and photometry 0-77299
supernova remnants in molecular clouds, struct. and emission 0-82450
symbiotic star candidates in LMC, optical spectroscopy and IR photometry 0-62139

infrared sources (astronomical) continued

symbiotic stars and slow novae, late-type components spectral classifications 0-94813
 SU Tauri, R Coronae Borealis star, IR excess discovery from optical and IR photometry 0-101601
 unidentified emission features, possible mechanism 0-82452
 W3 IRS 1, fine structure line radiation, dust UV opacity 0-90505
 W3/W4/W5 direction, IR sources correl. with heavy optical obscuration 0-62301
 W49 NW, compact H II regions, far IR spectrum 0-90497
 W51-IRS 2, compact H II regions, IR spectrum obs. 0-90497
 H II blisters, dusty, appearance at radio and IR wavelengths 0-85979
 H II regions, newly formed, in interstellar dark clouds, physical props. from radio continuum interferometry 0-105301
 He variable stars, IR excesses obs. 0-67733
 OH type I maser sources, model 0-90556

infrared spectra of diatomic inorganic molecules

diatomic molecule, vibr.-rot. states, high accuracy wave functions and energies 0-74159
 diatomic molecules, shortening of energy relax. time of excited mol. vibr. in dense medium by form. of H-bonds 0-91553
 gases, high resolution vibr. spectra by Fourier transform far IR spectroscopy 0-86461
 C₂, interstellar, rot. fine-struct. lines obs. towards ζ Persei 0-67811
 CO, adsorbed on Pd/Al₂O₃, IR study 0-108193
 CO₂, adsorbed on Ru (001), temp. depend. ordering processes 0-80773
 CO in IR spectra of III-106, CH star in M22 globular cluster 0-62131
 CO, oxidation on Ir films, IR absorpt. spectroscopy 0-71398
 CO, P(6) line absorpt. coeff. and halfwidth; temp. depend. 0-78618
 CO, rot. distrib. in supersonic beam, IR bolometry using tunable diode laser 0-63869
 CO-³He nuclear pumped laser, optimisation with 2 MeV protons 0-64000
 CO-myoglobin, mol. tunnelling, isotope effect, time resolved IR Fourier transform obs. 0-72126
 CS, rotation analysis of d³ Δ -a³ Π transition, IR spectra 0-78591
 Ca₂, vibr.-rot. states, high accuracy wave functions and energies 0-74159
 CdO, formed by matrix reactions, IR, Raman and visible spectra 0-87110
 Cs₂, dimer and higher polymer IR absorpt. bands, triplet state 0-63629
 D₂, matrix isolated, IR spectra, mol. rot. and vibr. const. determ. 0-87617
 DF* prod. from D+PTFE, Fourier transform IR spectroscopy 0-87105
 DT, vibr. rot. Raman anal. 0-87126
 H₂, matrix isolated, IR spectra, mol. rot. and vibr. const. determ. 0-87617
 H₂+D(O)(Cl)(Br), relax. and chem. reaction, time resolved IR fluoresc. and mass spectrometry obs. 0-69177
 H₂+H₂, hexadecapolar U-branch transitions in IR fundamental band 0-91631
 HBr(Cl), absorpt. coeffs. meas. in Nd laser emission band 0-78620
 HCl+D(O)(Cl)(Br), relax. and chem. reaction, time resolved IR fluoresc. and mass spectrometry obs. 0-69177
 HCl+tert gas, weak collisions, HCl spectral line broadening of IR spectra 0-74161
 HCl+N₂(O₂)(D₂)(H₂), HCl ν_0 - ν_1 band perturbations, linewidth and shifts calcs., IR spectra obs. (French) 0-58251
 HF in absorption, anomalous dispersion meas. 0-95881
 HI nuclear quadrupole HFS in IR spectrum, obs. using tunable diode laser 0-58412
^{14,15}N₂, Fourier spectrometry and IR emission spectra 0-83368
 N₂+Ar(Xe), $\Lambda^2\Sigma^+$ state energy pooling in flowing afterglow, Herman IR system 0-83503
 NH, IR emission studied using Fourier spectroscopy 0-95628
 NO, Fourier transform spectra, intensity and self-broadening coeff. meas. 0-102503
 NO, selectively excited rovibrational states, multiphoton ionisation spectra 0-69202
 NO, Zeeman modulation spectroscopy, line shape analysis 0-74197
 Na₂, vapour, IR absorpt. bands 0-102507
 OH, isotope effects, Zeeman effect, far IR laser mag-reson. spectra obs. 0-63674
 OH, Pt catalytic oxidation of H₂ and D₂, matrix isolation and laser fluoresc. obs. of prods. 0-66865
 PD⁺, IR emission spectra, rot. anal. and mol. parameters 0-69134
 PH⁺, IR emission spectra, rot. anal. and mol. parameters 0-69134
 Se₂, b'² Σ^+ -X'² Σ^+ near IR emission obs. 0-91556
 SeO, b'² Σ^+ -X'² Σ^+ near IR emission obs. 0-91556
 SeS, b'² Σ^+ -X'² Σ^+ near IR emission obs. 0-91556
 Te₂, B₀⁺-b'² Σ_g^+ system, transition assignment, IR and visible spectra obs. 0-58298
 TiO Φ system, near IR emission spectrum 0-69131
 YI, IR Π - Σ system, Fourier spectrometry, rovibrational anal. 0-83360
 ZnO, formed by matrix reactions, IR, Raman and visible spectra 0-87110
 ZrO, predicted IR spectrum and possible presence in S-type stars 0-62124
^{90,92,94}ZrO⁺, rot. anal. in near IR 0-74162

infrared spectra of inorganic solids

adsorbed layers, reflection-absorption IR spectroscopy, review, book contrib. 0-84747
 alkali germanate crystals and glasses, struct. and stability, IR spectra meas. 0-64911
 alkali halide:H (D⁻), local modes and colour centre absorpt. bands, analogy 0-60632
 alkali silicate glasses, struct. and thermal props. 0-84075
 aluminoborate glass, Fe and Cr ion interaction, mag. and spectral props. 0-103883
 antiferromagnet, IR absorption on impurity excitations near upper edge of spin-wave band 0-80829
 B₂O₃-Li₂O-LiCl, ionic conductor, IR refl. Raman study 0-66173
 benzil, phase transition, far IR spectroscopy meas. 0-71407
 biotite, Mossbauer and optical spectra, Fe²⁺-Fe³⁺ interactions 0-60470
 boracite, single cryst. prep. and phys. props. 0-100763
 borosilicate glass, Fe and Cr ion interaction, mag. and spectral props. 0-103883
 ceramics, piezoelectric, photoacoustic effect 0-84252
 o-chlorobenzoic acid: Nd³⁺(Pr³⁺) solid, vibrational spectra 0-84758
 trans-1,4-chloroiodocyclohexane, liquid, crystalline and amorphous state, conformation and vibr. spectra, IR obs. 0-60568

infrared spectra of inorganic solids continued

diamond, GR1 band, anal. of satellite lines by quadratic Jahn-Teller computing 0-97295
 diamond, vacancy enhanced N aggregation, electron irradiation effects IR spectra 0-70245
 diamond electron irradiated, photochromism 0-71454
 dickite, unusual crystal habit, structural disorder 0-59445
 diffuse reflectance Fourier transform IR spectroscopy using diamond anvil cell 0-101855
 dimethylammonium cadmium tetrachloride, far IR refractive index, extinction coeff. and dichroism obs. 0-66144
 electron reflection from metal surfaces, surface roughness, IR absorpt. 0-71526
 ferroelectric semiconductors, props., book 0-82590
 fibreglass insulating materials, radiative heat transfer rel. to optical props. 0-100367
 fluoride structures, superionic props., IR spectra 0-107483
 garnets, IR refl., ATR, Voigt and Faraday expts. 0-66180
 glass structure, vibr. spectroscopy studies 0-84732
 glasses, elec., mag., and optical props., conference, Troy, NY, USA (Aug. 1979) 0-105417
 ice, cubic, D₂O isolated, H⁺ exchange and Bjerrum defect migration, direct spectroscopic obs. 0-88356
 ice, O-H and O-D bond stretching vibrs., Raman spectra at atmospheric press. 0-66166
 ice platelets radiation attenuation effectiveness factor determ., IR absorpt. 0-66141
 intermolecular spectroscopy and dynamical properties of dense systems, conf., Varenna, Italy (1978) 0-82581
 metal particles, small, dielectric function and IR absorption 0-60607
 metallised coating on polyethylene terephthalate film, fracture under laser irradi. (Russian) 0-76333
 metals, coated, IR surface wave interferometry 0-63913
 minerals, near IR spectra of hydrothermally altered rocks 0-81871
 mixed valence compounds, anomalous IR absorption 0-66210
 molecular crystal IR spectral line shape and polarisation temp. depend. 0-88991
 near IR diffuse reflectance analysis anomalies 0-86383
 nosean identification, in sodalite and conversion of nosean sodalite 0-84907
 optical fibres, glass and plastic, neutron irradiated, optical absorpt. spectra 0.7 to 1.1 μ m 0-58762
 oxide crystals, Fourier transform IR spectroscopy of vibr. states at high temp. 0-97256
 perovskites, ordered cubic, cationic effect on intramolecular forces, stretching force const. 0-88979
 pnictide amorphous semiconductors, absence of photodarkening 0-103970
 polar semiconductor crystalline thin films, surface vibr. states, IR absorpt. spectra obs. (Russian) 0-60606
 polydiacetylene-toluenesulphonate, photocond. meas., 0.62-3.1 eV 0-70757
 polymer concretes, hydrothermally stable, hydraulic cement-type fillers 0-85144
 Pyrex, ion bombardment, form. of cpds., IR spectrosc. exam. (German) 0-88173
 quartz, electron irradiation effects on optical, dielec., elastic props. 0-59521
 quartz, Fourier transform IR spectroscopy of vibr. states at high temp. 0-97256
 quartz, IR radiation extinction coeff. rel. to mechanical Q 0-100653
 quartz, synthetic, deuteration, EPR and IR absorpt. characterisation 0-92721
 rare earth double orthophosphates with alkali metals, spectroscopic obs., struct. and chem. nature 0-100674
 rare earth oxyphosphates, IR and Raman spectra, vibr. assignments, cryst. struct. characts. 0-97258
 rare earth substituted lead apatites, Pb_{10-2x}R_xM_x(PO₄)₆Z₂, M=Na or K and Z=F or Cl, cryst. struct. and IR spectra 0-107167
 Rochelle salt, ferroelectric, Raman and IR study 0-71406
 rocks of volcanic origin, refl. characts., 400-800 nm 0-90073
 scheelite crystals., Davydov splitting of vibr. levels, short range interaction 0-71418
 semiconductor, p-type, infrared absorption and plasma reflection 0-97284
 semiconductors, amorphous, optical absorption, theory 0-80818
 semiconductors, optical props. due to phonons, book contrib. 0-80805
 semiconductors, weakly doped compensated IR light absorption by small scale fluctuations (Russian) 0-66255
 Si, ion implanted by high energy C ions structural and optical props. 0-107292
 silicate glass, hydration in steam atmosphere 0-85211
 silicate smokes, vapour condensed, IR absorpt. peaks compared to interstellar extinction curve 0-82180
 small-particle metal-insulator composites, anomalous far IR absorption 0-71427
 solid surface, microgravimetric-IR study 0-76577
 steel, BN extraction, and identification, IR anal. 0-85254
 thiourea, ferroelectric, Raman and IR study 0-71406
 (TMTSF)_xX, (X=PF₆⁻, AsF₆⁻, SbF₆⁻, BF₄⁻, NO₃⁻) highly conducting salts, props. 0-59969
 transition metal chalcogenophosphates, intercalation with n butyl-lithium, possible appl. in Li batteries 0-71446
 zero-gap semiconductors, anisotropy of IR absorpt. coeff., k.p. calc. 0-97285
 γ -Al₂O₃, physisorption and reaction of Mo(CO)₆, IR spectra obs. 0-80064
 [α]-SiC:H, prepared by reactive sputtering, layer props. (Japanese) 0-60695
 Ag electrodeposition, on (100) face of single crystal Ag in presence of sulphadiazine 0-89161
 Ag halide photochromic glasses, optical properties, effect of Cu ions 0-93364
 AgGaS₂-AgGaSe₂ system, phase diagram, lattice consts., and IR spectra 0-60841
 AgI-Ag₂O-MoO₃ glass glass superionic cond., struct. and transport props. 0-88602
 Al ultrafine particles, optical props., 0.3-2.5 μ m 0-76020
 β -AlO₂(Na,Li)₂O, NMR, Raman and IR spectra, and X-ray diffr., heat treatment induced changes 0-107508
 Al₂O₃, corundum, Fourier transform IR spectroscopy of vibr. states at high temp. 0-97256

glass continued

- Li₂O-SiO₂ glass, thermotransport props. 0-79985
 Li₂O-SiO₂ glasses, Li self-diffusion, mass spectrometric method 0-79982
 Li₂O-2SiO₂, short range struct. by pulsed neutron scatt. 0-59396
 Li₂SiO₄, piezoelectric glass ceramic, recrystallisation, pyroelectric response, permittivity 0-80703
 NaBaZn glass, Eu³⁺ centre symm. 0-100447
 NaF-SrF₂-CrF₃ glass transition, crystn. and melting temps., optical transmission (French) 0-64910
 Na₂O-2CaO-3SiO₂ glass, cryst. nucleation and growth, viscosity, thermodynamic props. 0-84079
 Na₂O-3SiO₂-Fe³⁺ glasses, Mossbauer and ESR spectra and internal friction 0-100865
 Na₂O-(CaO)-SiO₂, diffusion controlled attack by aq. solns. 0-81218
 Na₂O-Ca glass powders, mixed with CO₂ compounds, cellular-struct. glass fabrication 0-108382
 Na₂O-CaO, wettability, effect of cleaning procedures 0-65336
 Na₂O-CaO glass, (K₁,V) diagram determ. (French) 0-108558
 Na₂O-CaO glass, abrasion-resistant, high strength 0-76369
 Na₂O-CaO glass, shear deform. under pyramidal indentations 0-84989
 Na₂O-CaO glass phlogopite mica powders, composite fabrication, cellular struct. 0-84902
 Na₂O-CaO-SiO₂, formation of colour centres, linear absorption of UV radiation 0-103328
 Na₂O-CaO-SiO₂, grain-cleaning procedures effect on crushed glass chem. durability tests 0-66678
 Na₂O-CaO-SiO₂, proof testing 0-108654
 Na₂O-CaO-SiO₂ glass, vol. relaxation and thermal history during forming process 0-70130
 Na₂O-CaO-SiO₂ glass, leaching studies by sputter-induced photon spectrometry 0-80004
 Na₂O-CaO-SiO₂ glass, molten, metal ion diffusion and redox behaviour, electrochemical studies 0-81332
 Na₂O-CaO-SiO₂ glass, redox phenomena evaluation in melting-finishing process, SO₂ evolution 0-84900
 Na₂O-CaO-SiO₂ glass, high-vel. liq. impact, oblique impact anomaly 0-89329
 Na₂O-CaO-SiO₂ glass, hot erosion plastic flow and fracture 0-89354
 Na₂O-CaO-SiO₂ glass foils, HVEM in-situ straining expts. 0-104216
 Na₂O-CaO-SiO₂ glasses, Auger analysis, alkali signal decrease 0-61189
 Na₂O-CaO-SiO₂ molten glass, electrolysis reactions 0-89496
 Na₂O-CaO-SiO₂-Cr³⁺, absorpt. spectra, Fano antireson. and vibronic Lamb shift 0-71458
 Na₂O-CaO-SiO₂-Cr₂O₃ glass, redox equilibria of Cr ions, impurity effects 0-89477
 Na₂O-CaO-SiO₂-Fe₂O₃ molten glass, optical props., temp. depend. (French) 0-100667
 2Na₂O-CaO-3SiO₂ glass, cryst. nucleation rate, viscosity, heat treatment 0-84081
 Na₂O-Cs₂O-SiO₂ glasses, thermal diffusivity, heat capacity and thermal cond., laser flash method study 0-65310
 Na₂O-PbO-SiO₂, molten glass, reactions with conducting materials 0-85186
 Na₂O-PbO-SiO₂ glass-ceramic composite, directionally crystallised 0-107058
 Na₂O-SiO₂, fusion process study, EMF meas. (French) 0-89190
 Na₂O-SiO₂, ion bombardment, form. of cpds., IR spectrosc. exam. (German) 0-88173
 Na₂O-SiO₂, structure toughness-composition relationship 0-104257
 Na₂O-SiO₂ glass, acoustic and thermal Gruneisen parameters 0-59608
 Na₂O-SiO₂ glass, bridging to non-bridging ratio and correl. to glass density and refr. index, ESCA study 0-84832
 Na₂O-SiO₂ glass, bubble gas comp. change 0-79946
 Na₂O-SiO₂ glass, conduction and dielec. loss mechanisms, paired interstitial model 0-107468
 Na₂O-SiO₂ glass, evaporation by high temp. mass spectrometry 0-79927
 Na₂O-SiO₂ glass, internal and surface struct. by X-ray scatt. 0-84074
 Na₂O-SiO₂ glass, microcracking about NiS inclusions, fracture mech. description 0-89333
 Na₂O-SiO₂ glass, molten, metal ion diffusion and redox behaviour, electrochemical studies 0-81332
 Na₂O-SiO₂ glass, OH⁻ content effect on mech. and other props. 0-89337
 Na₂O-SiO₂ glass, scoring, deform. and fracture mech. approach 0-89332
 Na₂O-SiO₂ glass containing halogens glass formation 0-103254
 Na₂O-SiO₂ glass drops, quenched from liq. state, thermally treated, density profile 0-81083
 Na₂O-SiO₂ glass melt, dissoln. of O₂ and CO₂ gas bubbles 0-79945
 Na₂O-SiO₂ glasses, Auger analysis, alkali signal decrease 0-61189
 Na₂O-SiO₂ glasses, elementary electronic excitations, refl., luminesc. and photoemission meas. 0-84778
 Na₂O-SiO₂ glasses, water reactions at elevated temps. and press. 0-81312
 Na₂O-SiO₂:Au+CeO₂, Au particle nucleation 0-81066
 Na₂O-SiO₂:CuO glass, gamma-irradiated, EPR and optical spectra 0-103885
 Na₂O-SiO₂:CuO, γ -irrad., CuO effects on EPR 0-84645
 Na₂O-SiO₂:Fe₂O₃ glass, X-ray absorpt. spectra, effective co-ordination charges 0-84805
 Na₂O-SiO₂:MgO(CaO)(BaO) glasses, elec. cond., room temp. to 450°C 0-107473
 Na₂O-SiO₂:Tb₂O₃ magneto-optical study 0-88976
 Na₂O-TiO₂-SiO₂ glass, co-ordination of Ti, X-ray emission spectra study 0-84072
 NaOH:CrO₄²⁻(NO₃⁻), electron tunnelling, pulse radiolysis 0-108722
 NaOH:Fe(Cn)₃⁺, electron tunnelling, pulse radiolysis 0-108722
 5Na₂O:Fe₂O₃:8SiO₂ glass crystallisation study by Fe³⁺ EPR and Mossbauer spectra 0-64904
 Na₂O-2SiO₂, short range struct. by pulsed neutron scatt. 0-59396
 25Na₂O-75SiO₂ glass, thermal cond., temp. depend. at low temps. 0-65322
 Nd:glass laser with numerical programmed control (Russian) 0-91811
 Pb glass counter, automated calibration system 0-106233
 PbO-SiO₂, melt, elec. cond. and struct. 0-88020
 PbO-SiO₂, melt, polymer equilibria 0-88019
 PbO-SiO₂, structure toughness-composition relationship 0-104257
 PbO-SiO₂ glass, acoustic and thermal Gruneisen parameters 0-59608
 PbO-SiO₂ glass, reduced channel-plate, variable range hopping conductivity 0-107466
 PbO-SiO₂ glass, trimethylsilylation method for silicate ion anal. (Japanese) 0-71975

glass continued

- PbO-SiO₂ glasses, density-of-states and structural forms, Raman spectra study 0-97255
 PbO-SiO₂ glasses, high temp. ESR of Fe(III) 0-60410
 2PbO-SiO₂ melt, coding rate influence on constitution of silicate anions, crystn. kinetics 0-103248
 Sb-O-Cl(Br)(I), glass-forming regions 0-88057
 SiO₂, fused, surface crystn. by Li⁺ ion implantation and annealing 0-89383
 SiO₂, glass, acoustic and thermal Gruneisen parameters 0-59608
 SiO₂ glass, formation by hydrolysis of Si(OC₂H₅)₄ with NH₄OH and HCl soln., and characterisation 0-71622
 SiO₂ glass, low loss optical fibre, radiation-induced IR absorpt. 0-87521
 SiO₂ glasses, spectral emittance at high temps. 0-96674
 SiO₂, ion bombardment, form. of cpds., IR spectrosc. exam. (German) 0-88173
 SiO₂, three-component glass, liq. phase separation, with two oxide modifiers 0-103250
 SiO₂, vitreous, low temperature heat capacity enhancement model 0-75369
 SiO₂, vitreous, O and Si diffusion-controlled processes 0-79981
 SiO₂, vitreous Brillouin scatt., 35 GHz phonon vel. and absorpt. below 1K 0-100664
 SiO₂-CaO-Na₂O, layers near surface, anal. using SIMS 0-88041
 SiO₂-Li₂O, layers near surface, anal. using SIMS 0-88041
 SiO₂-Li₂O-Li₂SO₄ glass-forming region, struct. and ionic cond. 0-84320
 SiO₂-Na₂O alkali glass, grain-cleaning procedures effect on crushed glass chem. durability tests 0-66678
 SiO₂-Na₂O surface, Ca₃(PO₄)₂ film form., bonding to bond 0-85212
 SiO₂-Na₂O-CaO-MgO float glass, surface SnO₂ distrib., ellipsometry and XPS study 0-84346
 SiO₂-Na₂O-Nd₂O₃ glass, magneto-optical props., absorpt. spectrum 0-88969
 SiO₂-TiO₂, US vel. and absorption 0-107380
 TeO₂, ferroelectric glass, phase transition, permittivity, electrochromism, photochromism 0-80719
 TeO₂-MoO₃-V₂C₅, phase comp. determ. using X-ray diffr., electron microscopy and DTA (German) 0-88046
 TiO₂-SiO₂ glass form. by low temp. chem. polymerisation 0-84899
 TiO₂-SiO₂ glass system, Raman and hyper-Raman light scatt. spectra 0-66187
 U glass, fission track dating, error analysis 0-95503
 V₂O₅-As₂O₃-RO, R=Ba, Ca, Pb, semicond. glass, electronic props. 0-88557
 V₂O₅-CuO-BaO, unpaired electron localisation, ESR study 0-66026
 V₂O₅-V₂O₄-BaZnO₂ glass, V ion states, mag. and elec. props. 0-88556
 Y₂O₃-Al₂N₃-SiO₂ oxynitride glasses, elec. props. 0-80267
 ZrF₄:Eu³⁺ glass, luminesc. of Eu³⁺, transition probabilities 0-80845
 ZrF₄-BaF₂-MF₃ (M=Na, Ca, Ln, Th, n=1, 2, 3, 4), vitreous phases, network formers, modifiers and stabilisers (French) 0-64909
 ZrF₄-BaF₂-ThF₄-NaF(RF₃) (R=rare-earth) glass system, anion cond. 0-70460
 ZrF₄-BaF₂-ThF₄(LaF₃)(NdF₃)(PrF₃), F⁻ ion cond. glasses, cond. process 0-107477
 ZrF₄-based glasses, elec. transport props. 0-79983
 ZrF₄-ThF₄-BaF₂, IR-transparent, synthesis using reactive atm. processing technique 0-100826
 ZrO₂ glass, melting depend. on minute components, surface crystallisation 0-84278
 ZrO₂, glaze, liq. phase separation rel. to cryst. in glassy phase 0-103252

glass fibre reinforced plastics

- acoustic emission 0-104294
 ageing by boiling in water, effect on physico-mech. props. 0-60892
 cemented joint of cylindrical shell with cover, stressed state 0-69668
 chopped glass fibre reinforced polyester E, types SMC-65(-25 and -30EA), moisture absorpt. 0-93799
 cylindrical shells, compressive and flexural strength (Japanese) 0-81115
 E-glass type fibre, silane coupling agent deposited on surface, hydrolysis and drying effect on siloxane bonds 0-85072
 epoxy, braided filament reinforced, damage summation in nonstationary cyclic loading 0-60969
 epoxy laminates, exp. determ. of nonlinear shear behaviour 0-66575
 epoxy matrix, laminate, metallization by Cu and chem. treatment by H₂CrO₄ (German) 0-93670
 epoxy resin laminate, sliding behaviour against Cu or Al spheres at cryogenic temps. 0-66671
 epoxy resins, expt. exam. of fracture by peeling method (Russian) 0-71761
 epoxy-phenolic matrix, cyclically deformed under shear, energy dissipation, static tensile-compressive stress effect 0-104225
 epoxy/E-glass continuous fibre composite type 3M Scotchply, complex moduli, comparison of meas. with estimated bounds 0-93590
 fatigue damage monitoring of processes damaging elec. insulating materials 0-97673
 fatigue fracture kinetics studied by diffusion scatt. of luminous fluxes 0-76446
 fatigue processes, review 0-81176
 glass fibres-resin interface studies 0-93531
 glass reinforced polyamide 6, fatigue strength after heat treatment, ageing and coating of Al-containing lacquer (Polish) 0-89347
 high work of fracture composites, prep. and mech. tests 0-81029
 hybrid glass fibre/C fibre reinforced epoxy-phenolic, elastic characts. prediction 0-108491
 insulating materials, fatigue behaviour, influence of superposition of elec., mech. and environmental stresses 0-97590
 laminates, failure models, reinforcement struct. effect 0-66641
 laminates, strength and deformability, artificial ageing effect 0-60893
 nylon matrix, design parameters, fibre orientation effect 0-81141
 orthotropic laminates, torsion strength and shear modulus determ. 0-92587
 pipe, thin walled, finned, stress anal. and load bearing capacity 0-81100
 polycapromide, viscoelastic, linearity conservation 0-108492
 polycarbonate matrix, design parameters, fibre orientation effect 0-81141
 polyester, unidirectionally reinforced, damage summation in nonstationary cyclic loading 0-60969
 polyester laminates, glass fibre reinforced, enhanced elasticity, chem. resist. tests (Polish) 0-60901
 polyester matrix, crack growth micromechanism in corrosive environment 0-108615

glass fibre reinforced plastics continued

- polyester matrix, greenhouse sheets, ageing behaviour, natural and artificial weathering (*German*) 0-81226
- polyester/E-glass chopped fibre composites types PPG SMC-R25 and PPG SMC-R65, complex moduli, comparison of meas. with estimated bounds 0-93590
- polyester/E-glass hybrid chopped/continuous fibre composite type PPG XMC-3, complex moduli, comparison of meas. with estimated bounds 0-93590
- polyethylene-glass fibre composites, gamma-irradiated filler 0-66840
- resin matrices and their contribution to composite properties 0-81028
- shear characteristics of tubular specimens, strain gauge and clamp 0-85114
- sheet moulding compound, material, process and performance 0-81032
- stringed musical instrument resonant plates, use of synthetic materials 0-102937
- thermoplastic-based sheet materials, flexural anisotropy and stiffness assessment 0-76442
- unidirectional glass-plastic, fracture dynamics 0-100906
- wound martensitic steel welded composite vessels, glass fibre reinforced plastic wound, struct. strength 0-97552
- woven-roving type, high-speed punching, failure mechanisms 0-85143
- Young's modulus determination, dynamic high-speed method (*German*) 0-85123

glass fibres

- see also fibre optics; optical fibres*
- alkali borosilicate system, self-focusing fibres with aperture of 0.18 0-87548
- alkali lime germanosilicate GRIN fibre prep., losses and geometrical props. 0-69560
- clad-glass fibres, thermal stresses 0-107360
- crack growth during dynamic fatigue and effect on strength loss for tensile loading 0-89334
- drawing process, characterization and control 0-58826
- drawing process, extensional instabilities 0-89258
- E-glass type, silane coupling agent deposited on surface, hydrolysis and drying effect on siloxane bonds 0-85072
- fibre-optic communication in industry, appls., glass fibre props., connectors 0-87550
- fibre-glass insulating materials, radiative heat transfer rel. to optical props. 0-100367
- flaw generation, by indentation fracture technique 0-81156
- forming process, characs., anal. techniques 0-58827
- lightguide fibre, prototype drawing facility 0-64229
- lightguide fibre preform manufacture using modified CVD process 0-64228
- optical, preparation methods and performance factors 0-69557
- optical, step-index, nearly elliptical, with high eccentricity, fabrication for studying modes 0-95989
- for optical communications, colloquium, London, England (Jan. 1979) 0-67930
- optical fibre, fracture surface anal. 0-58754
- optical fibre, strengthening by molecular stuffing 0-58830
- optical fibre, UV cured epoxy acrylate coated, zero stress ageing effect on strength 0-58753
- optical fibre, vapour phase materials and processes, review 0-58825
- optical fibre communication advances, materials and techniques 0-102853
- optical fibres, mech. reliability 0-91909
- optical fibres, tensile strength and static fatigue, analysis using Weibull distribution for optimum design 0-85011
- optical graded-index fibre vapour-phase axial deposition method, fibre characteristics 0-58824
- optical transmission systems appls. (*German*) 0-69516
- preparation, appl. in Portland cement reinforcement, alkali resistance 0-81019
- resin interface studies 0-93531
- silicone and glass clad compound glass optical fibre comparison 0-69533
- BaO-GeO₂-Na₂O borosilicate core glasses for high numerical aperture fibres 0-69534
- GeO₂-Na₂O borosilicate glass fibre prod. by phase separation and leaching 0-69558
- Li₂O-SiO₂-P₂O₅ glass ceramic fibres, heat treatment, crystn., tensile strength 0-84995
- Na₂O-B₂O₃-SiO₂ glass fibre, plastic coating influence on strength 0-58697
- Na₂O-B₂O₃-SiO₂ glass fibre, plastic-coated, liq. N₂ strength 0-58707
- Na₂O-B₂O₃-SiO₂ glass, low-loss GRIN fibres, double-crucible prod., loss and bandwidth meas. 0-69559
- SiO₂/GeO₂, single-mode, numerical aperture effects on optical and mechanical props. 0-69548
- SiO₂ fibre lightguides, fused, zero stress strength reduction and transitions in static fatigue 0-87523
- SiO₂ fibres, fused, drawn from rods, oxy-H₂ flame, prep., strength, dia. var. 0-102868
- SiO₂ glass fibre, plastic-coated, liq. N₂ strength 0-58707
- SiO₂/P₂O₅, single-mode, numerical aperture effects on optical and mechanical props. 0-69548
- SiO₂-GeO₂/SiO₂ load bearing optical cable, geophys. appls. 0-91923
- ZrO₂-SiO₂-(Na₂O) glass fibres, prep. from metal alkoxides, resistance to NaOH soln. 0-97454

glass industry

- glass making system, continuous, energy balance 0-89189
- IR thermometry, readings interpretation 0-82765
- magneto-hydrodynamic phenomena, of mixing in the glass industry (*Polish*) 0-64647

glass-metal seals

- see also electron tube manufacture*
- interface study by Auger spectroscopy 0-76587
- phosphate glass-Al alloys seals, elec. and mech. props., glass transition 0-81018
- set point, of glass in glass-metal seals 0-108423

glass transition

- abietic acid, transverse US wave propag., glass and liquid transition region 0-79883
- AgPS₂-AgX (X=I, Br), glass-forming regions, struct. model (*French*) 0-100464
- alkali metaphosphate, M₂O-R₂O₃-P₂O₅ (R=Y or rare earth), glass transition temps. and coeffs. of linear thermal expansion 0-88343
- alkaline earth metaphosphate, MO-R₂O₃-P₂O₅ (R=Y or rare earth), glass transition temps. and coeffs. of linear thermal expansion 0-88343

glass transition continued

- chitin (poly-N-acetyl-D-glucosamine), dynamic mech. behaviour, effect of water 0-97522
- chitosan (poly-D-glucosamine), dynamic mech. behaviour, effect of water 0-97522
- chlorobenzene-cis-decalin, mixtures, dielec. const. and loss tangent in liq. and solid phases 0-100628
- copolymer globule model, orientationally-ordered liq. cryst. state (*Russian*) 0-59389
- epoxy resin, plastic deform. mechanism 0-97534
- epoxy resin/particle composites, particle size effect in thermal expansion, filler effects on T_g 0-84305
- ethylene-vinyl alcohol copolymer, drawn samples, annealing effect around T_g temps. on shrinkage and mol. orientation 0-79712
- liquid-glass transition, glass transition depend. on heating and cooling rates 0-79920
- macromolecules, linear, heat capacities, scanning calorimetry meas. 0-61134
- Nafion, densities and expansion coeffs. as function of various parameters 0-79711
- NR, glass-rubber transition, time-temp. superposition, shear creep compliance meas. 0-88309
- nylon 6 (polycapromide), salted, glass transition temp. and elastic modulus, moisture effect 0-103465
- phosphate glass-Al alloys seals, elec. and mech. props., glass transition 0-81018
- phthalocyanine polymer, dynamic mech. props. and fracture energy 0-100866
- PMMA, glass-rubber transition, time-temp. superposition, shear creep compliance meas. 0-88309
- poly(di-n-heptyl itaconate), alkyl side chain independent relax., double glass transition 0-59636
- polyaryloxyphosphazene copolymers, thermal, morphological and rheological props. 0-103265
- 1,2-polybutadiene, dynamic viscoelastic props. in curing process 0-76298
- polycarbonate, γ -irradiated, dielec. behaviour and glass transition 0-97182
- polycarbonate, bisphenol A, WAXS pattern, temp. effect and thermal history 0-93583
- polyether-polyester elastomers, differential scanning calorimetry, crit. points (*Japanese*) 0-75344
- polyether-polyester elastomers, differential scanning calorimetry by using poly(oxy-1,4-butylene glycol) as soft segment (*Japanese*) 0-79916
- trans-1,4-polyisoprene crystals, press. effect on growth rate 0-88064
- polymer, electrochromic dye probe for softening around T_g 0-84724
- polymer, polydisperse, glass transition temp., mol. mass depend. 0-92656
- polymer film, glassy and rubbery, isotope effect in H₂ and D₂ diffusion, T_g region behaviour 0-84327
- polymer latex film composite, glass transition temp. determ. using thermomech. curves 0-75342
- polymer mixing, heats 0-61132
- polymers, elec. resist., corresponding states relationship 0-59704
- polymers, solidification, as dissipative process 0-65205
- polyoxymethylene, transitions and relaxation spectrograph 0-65204
- polystyrene, glass-rubber transition, time-temp. superposition, shear creep compliance meas. 0-88309
- polystyrenes, anionic, TSC obs. of T_g and T_{II} transitions 0-84686
- polyurethanes, cross-linked, mol. mobility and struct., thermomechanical and NMR obs. (*Russian*) 0-69285
- polyvinylbutyral, elec. and dielec. props., mol. wt. effect on charge storage 0-97192
- PV, glass-rubber transition, time-temp. superposition, shear creep compliance meas. 0-88309
- PVC, glass-rubber transition, time-temp. superposition, shear creep compliance meas. 0-88309
- PVC-vinylchloride system, glass transition, vinylchloride influence (*German*) 0-79917
- spin-glass alloys, magnetoresistance, Boltzmann formalism calcs. 0-88540
- tetrabenzo[a, cd, j, lm]perylene evaporated film, crystn., time depend. as function of purity 0-88449
- viscous liquids, glass transition, nonconfig. contribs. to excess entropy 0-92654
- AgPO₃-AgX (X=I, Br), glass-forming regions, struct. model (*French*) 0-100464
- B₂O₃ and alkali borate glasses, Raman study at high temps. 0-93306
- BcF₃ glass transition, Monte Carlo study 0-75343
- EuS₂-Ga₂-GeS₂, chalcogenide glasses, conditions of form. of glassy prod. (*French*) 0-100325
- Fe₃₁Ni₃₄Cr₁₄P₁₃B₆ metallic glass, effect of pre-ageing on glass transition temp. 0-100326
- Fe₄₀Ni₄₀P₁₄B₆, metallic glass, glass transition, viscous flow and differential scanning calorimetry meas. 0-96635
- Fe₄₀Ni₄₀P₁₄B₆, Metglas 2826, hot forming 0-84980
- Li_{1+x}P₂O_{3+x+1}, polyphosphate, melting and crystallisation 0-70376
- Se, amorphous film, dielec. activity obs. near glass transition temp. 0-75933
- Se:As, amorphous film, dielec. activity obs. near glass transition temp. 0-75933
- SiO₂ fabric, structural stability rel. to brittleness, X-ray diffr. and IR spectrosc. studies 0-96634
- Te₆₀Ge₁₀Pb₃₀, DSC sensitivity to controlled ageing in glass transition region 0-71673
- Te₆₀Si_{20-x}Pb_x glasses, phase separation, double T_g presence 0-88306

glasses *see glass*

glassy state *see vitreous state*

glide, dislocation *see slip*

globular star clusters

- age and distance determ. using subdwarf photometry results 0-82435
- ages, effects of He settling in low mass stars 0-73013
- ages and composition, rel. to fundamental knowledge about galaxies evolution 0-90488
- brightness and density distrib., two parameter generalised isochronous models 0-67807
- ω Centauri, SEC Vidicon photometry of main sequence 0-90491
- core evolution, effect of gravitational catastrophe 0-67804
- E3 (ESO-037-SC 01) dying globular cluster, photometry and stellar content rel. to tidal truncation 0-105291
- galactic centre region, globular clusters IR studies 0-82434
- giant stars, Ca II H and K-lines and abundance 0-72940
- integrated IR photometry, colours and interstellar reddening 0-67575

infrared spectra of inorganic solids continued

- SiO(C) wafers, impurity meas. by Fourier transform IR spectra at low temp. 0-89031
 SiC (6H), IR absorpt., UV illumination effects, defect levels 0-66251
 SiC smokes, vapour condensed, IR absorpt. peaks compared to interstellar extinction curve 0-82180
 Si₃C_{1-x}H_x amorphous films, IR absorpt. bands 0-100705
 SiO evaporated film, dielec. function 8 to 33 μ m, spectrophotometric and refl. meas. 0-80883
 SiO₂ coatings on SiO₂ substrate, cathodoluminescence spectra, electron irradi. 0-76085
 SiO₂ deposited on Ge, optical constants, reflection spectra by Kramers Kronig method 0-76099
 SiO₂ fabric, structural stability rel. to brittleness, X-ray diffr. and IR spectrosc. studies 0-96634
 SiO₂ fibres, LF optical phonons, Raman spectra 0-80789
 SiO₂ film, on GaP substrate, N ion implantation, optical refl. and EPR meas. 0-84197
 SiO₂ film on Cu substrate, surface EM wave absorpt., optical consts. (Russian) 0-108216
 SiO₂, fused, for sealed ampoule cryst. growth, thermal transmission function 0-84731
 SiO₂, fused, surface crystn. by Li⁺ ion implantation and annealing 0-89383
 SiO₂ glass, formation by hydrolysis of Si(OiC₂H₅)₄ with NH₄OH and HCl soln., and characterisation 0-71622
 SiO₂ glass, ion bombardment, form. of cpds., IR spectrosc. exam. (German) 0-88173
 SiO₂ glass, low loss optical fibre, radiation-induced IR absorpt. 0-87521
 SiO₂, P-doped amorphous, porous and hydrophilic, water adsorpt. and IR spectra obs. 0-80061
 SiO₂ thermal film, freon ion beam etching, IR study (Russian) 0-76095
 SiO₂-B₂O₃ glass system, gel hot pressing synthesis and characterisation (French) 0-66468
 SiO₂-BPO₃ glasses and devitrificates prep., IR spectra (Polish) 0-71624
 SiO₂-NaAlSi₃O₈ glasses and devitrificates, prep. and vibr. spectroscopy study (Polish) 0-93530
 SiO₂ thin films, deposition and characterisation study 0-80133
 SiO₂-Ge, B, P, optical fibre, radiation induced optical absorpt. spectra, 0.4 to 1.7 μ m region 0-58761
 Sm₂S₃ films, refl. and transmission spectra at 300K 0-80889
 Sn-KCl granular superconductors, far IR absorpt. 0-84548
 SnS₂ mixed valence semiconductor, far IR refl. spectra 0-108191
 SrF₂, strain induced splitting and oscillator strength anisotropy of IR transverse optic phonon 0-92625
 SrF₂:Ce³⁺, cryst. field energies 0-59941
 SrF₂:Dy³⁺, cluster form., IR absorption study (French) 0-108240
 SrTa₂O₆, structural study X-ray diffr., IR absorpt. and Raman spectra (French) 0-107173
 SrTiO₃, monodomain, O-D and O-H stretching vibrs., IR spectra 0-71449
 Ta, and α -TaH₃, electronic struct., thermoreflectance studies 0-76047
 Tb(NO₃)₃·Fe(NO₃)₃·(NH₄)₂CO₃·H₂O system, cpd. form., comp. and props. 0-100832
 Tb₂O₃·H₂PO₄·H₂O system, cpd. form., comp. and props. 0-100832
 Te, oriented films, semiconducting props., Hall coeff., band structure 0-70854
 Ti, electropolished, optical props. from 1.8 to 3 eV 0-85088
 TiCl₃, phonon difference band absorpt., far IR laser spectroscopy 0-93325
 TiGaTe₂, TiInTe₂, and TiInSe₂, IR refl. spectra 0-60605
 Ti₆(M₂)₆¹²⁺(L₄)₂²⁻, (M=Pb, Ag, Au, (Bi₁₀Te₁₀)), struct., rel. to phonon spectra 0-71425
 α -U, polycryst., optical absorption meas. 0.15 to 2.0 eV 0-108223
 U(BH₄)₄, in Hf(BH₄)₄, excited state assignments and E-symmetry ground state, near IR MCD obs. 0-66153
 UO₂, 5f-magnetic semiconductor, spectroscopic data, review 0-97299
 UO₂, electronic transitions, crystal field effects and phonons, phase transition 0-97303
 US(Se)(Te), electronic struct. and exchange band splitting, optical refl. meas. 0-66226
 V, electronic struct., thermoreflectance studies 0-76047
 V₂O₃ and lower oxides, defect structures and related props. 0-59454
 V₂O₅ and lower oxides, electronic, optical, structural and surface props., review 0-88120
 V₄O₁₃, semicond., vibration spectra 0-88997
 α -VOPO₄, VPO₄, V₄(P₂O₇)₃ and (VO)₂P₂O₇, IR absorpt. spectra, bond freqs. 0-108192
 V₂Si thin film far IR laser thermal spectroscopy 0-60144
 W (100), chemisorbed H, ν , vibrational mode IR study 0-60582
 W, chemisorbed H₂, vibr. spectra characs., adsorption sites 0-70535
 W surface, (110), chemisorpt. effects on dielec. function, refl. spectra 0-75616
 WO₃-electrolyte electrochromic cells, proton injection phenomena 0-71448
 Y₂(CO₃)₃·nH₂O, tengerite, single cryst. hydrothermal growth 0-97417
 YIG:Zr, near IR absorpt. and magnetic circular dichroism 0-60580
 Y(OH)CO₃, ancylite like phase, hydrothermal cryst. growth (French) 0-108340
 ZnB₂O₄-RF, R=Mg, Ca, Sr, Ba, glass form., struct. and props. 0-84077
 ZnP₂, cryst., tetragonal, 2-phonon IR absorpt. 0-66176
 ZnP₂:In(Ga)(Ge)(S)(Se), doped and undoped, optical absorpt. spectra in range 0.5 to 2.2 eV 0-66250
 Zn₃P₂, optical props., transition energies from transmission and refl. meas. 0-60532
 ZnS, film on Si, fused quartz substrates, H₂O absorpt., IR anal. 0-75446
 ZnS cryst., IR absorpt., annealing effect 0-80774
 ZnSe, exciton refl. spectra, temp. depend. 0-59886
 ZnSe films, long wavelength IR polariton emission band thermal shift and broadening 0-92833
 ZnSe laser windows, AR coated, photoacoustic chopping freq. studies using CO₂ laser 0-83629
 ZnTe:As, impurity identification and characterisation, capacitance, luminescence and IR absorption 0-60639
 ZrF₄-THF₄-BaF₂ glass, IR-transparent, synthesis using reactive atm. processing technique 0-100826

infrared spectra of organic molecules and substances

see also molecular rotation; molecular vibration

- 1,1-dimethyl-1-silacyclopentane, IR and Raman spectra 0-60577
 acetaldehyde, UV photolysis, transient species IR spectra 0-86464
 acetic acid, and derivatives, vibr. spectra in soln. 0-63633

infrared spectra of organic molecules and substances continued

- acetic acid-d₀(-d₁), Fermi reson., IR spectra band profiles 0-60569
 acetone, adsorbed on ZnO, decomp., IR and kinetic obs. 0-59780
 acetonitrile, adsorption on MgO, IR and TPD study 0-70528
 acetonitrile, IR spectra, vibr. and reorientational and energy transfer wild separation, rot. const. determ. 0-87131
 acetonitrile-HCl complex in liq. Xe, IR spectral study 0-95626
 acetophenones, spectrosc. characs., using PPP SCF CI calcs. 0-102448
 acetylene, absorpt. coeffs. meas. in Nd laser emission band 0-78620
 acetylene, He-Ne laser line, high temp. absorpt., anal. by high resolution IR spectra 0-91554
 acid oxalate ion in aq. soln., vibr. studies, IR and Raman spectra 0-95589
 adsorbed layers, reflection-absorption IR spectroscopy, review, book contrib. 0-84747
 aliphatic ketones, freq.-topology-milieu relation, IR study, struct. and solvent effect (French) 0-95623
 alkanes, liq., mol. struct., selective deuteration and IR vibr. spectra 0-96432
 alkenes, IR multiphoton dissoci., IR detection of H atoms 0-83356
 p-alkoxybenzylidene-p-n-butylanilines, IR absorpt. spectra, elec. field effects, orientational order parameter determ. by IR dichroism 0-80778
 p-alkoxybenzylidene-p-aminocyananilines, IR absorpt. spectra, elec. field effect, orientational order parameter determ. by IR dichroism 0-80777
 alkyl metal carbonyls, phosphine monosubstituted, LF vibrs., IR and Raman spectra 0-95585
 allene-d₄, high resolution IR spectra 0-83365
 allylamine, laser-microwave double and triple reson. 0-83397
 2-amino-4-chlorophenol in solutions, IR absorpt. spectra 0-69135
 2-amino-p-cresol in solutions, IR absorpt. spectra 0-69135
 aminopyrazine, far IR spectra, barrier to planarity, pot. function and energy levels 0-69137
 4-aminopyridine hemiperchlorate, struct. determ. by neutron diffr. and IR spectra 0-92515
 aniline, liq., far IR absorpt. spectra, electric field effects 0-95625
 9,10-anthraquinone, lower triplet states, interactions and position, matrix isolation spectra 0-63634
 azulene vapour, IR and CO₂-laser absorpt. spectra 0-87120
 benzene, IR spectra, fine struct. of rot.-vibr. bands 0-102504
 benzene cryst., electron irradi., phenylcyclohexadienyl radical form., absorpt. and fluoresc. spectra study 0-89035
 benzene-hexa-n-hexanoate, phase transitions and mesophase form., sp. ht. and IR spectra, 13 to 393K 0-79955
 benzonitrile, IR absorpt. and Raman bands, half-band width conc.-depend. 0-74171
 bis(methylthio)alkanes, model compounds of polythioethers, vibr. spectra 0-58430
 bis [4-(n-butyl)-styryl dithiolato] Pt nematic complex with strong IR absorption 0-88305
 bisphenol A-phthalic anhydride epoxy resin, diglycidyl ether, Rayleigh scatt., Brillouin and IR spectra 0-66211
 butane, liq., enthalpy difference between rot. isomers, IR spectrosc. obs. 0-106404
 1-butene, adsorbed on δ -Al₂O₃, isomerisation, IR study 0-76554
 1-butene adsorption on delta alumina, microgravimetric-IR study 0-75432
 tri-n-butyl phosphate, quantitative IR absorpt. meas. 0-87106
 p-n-butyl-p'-heptanoyloxyazoxybenzene oriented on NaCl MgF₂ coated NaCl, surface phenomena and IR spectra 0-79678
 3-butyn-1-ol, vibr. spectra, assignments, rot. isomerism 0-58257
 calcium dipicolinate trihydrate, IR and Raman spectra, isotopic frequency shift, mol. vibr. obs., point groups determ. 0-89001
 calcium oxalate, anhydrous, IR and Raman spectra, vibrational studies 0-69139
 calcium oxalate monohydrate, IR and Raman spectra, vibrational studies 0-69139
 carbon tetrafluoride, liquid, comparison on interaction induced light scatt. and IR absorption 0-60561
 carbon tetrafluoride ¹²CF₄ laser, Doppler-limited absorption spectroscopy 0-74347
 carbon tetrafluoride laser, CF₄ molecule $\nu_3 + \nu_4$ band, optical pumping 0-74349
 carboxylic acid systems, H(D) complexes and dimers, ν_{CO} IR band intensities 0-63715
 1-chloro-2,2-dimethylpropane, IR and Raman spectra, vibr. assignment 0-74169
 1-chloro-2-methylpropane, IR and Raman spectra, vibr. assignment 0-74169
 trans-1,4-chlorobromocyclohexane, liquid, crystalline and amorphous state, conformation and vibr. spectra, IR obs. 0-60568
 chlorodifluoromethane, IR multiphoton dissoci., mag. field effect 0-93772
 trans-1,4-chloriodocyclohexane, liquid, crystalline and amorphous state, conformation and vibr. spectra, IR obs. 0-60568
 chloromethyl formate, conformation potential energy surfaces, ab initio calcs. 0-69065
 coal, cleaved surface, photoacoustic IR spectra 0-87104
 cyanoacetylene, ν_2 vibr.-rot. band, diode laser spectrum 0-91563
 α -cyanoacrylate adhesive in first monolayer on bulk Al surface, IR spectra, H-bond form., stretching vibr. 0-87119
 cyanomethane-d₀-d₃, soln., for IR spectra, band shape and moment anal. 0-58252
 cyclobutane, absorpt. of pulsed IR radiation and decomp., joulemeter and opto-acoustic obs. 0-58328
 cyclohexane, in benzene soln., mol. motion, correl. functions 0-96431
 cyclohexene vapour, IR spectra anal. 0-63628
 cyclopentadienylnhafniumdichloride, gaseous, far IR and Raman spectra 0-95624
 cyclopentadienylnitranium dichloride, gaseous, far IR and Raman spectra 0-95624
 cyclopentadienylnitraniumtrichloride, gaseous, far IR and Raman spectra 0-95624
 cyclopentadienylnitraniumdichloride, gaseous, far IR and Raman spectra 0-95624
 cyclopentylamine, vibr. spectra and struct. 0-102516
 cyclopropane, IR spectra studied by tunable laser, $\nu_{10} + \nu_{11}$ band anal. 0-95615
 cyclopropane-d₆, high resolution IR spectra, vibr. rot. band anal. 0-95621
 DBTTF halogen complexes, IR, UV spectra, EPR study 0-108215
 2,4-diamino-6-hydroxy-pyrimidine, IR absorption spectrum, vibr. anal., tautomerism 0-58253

infrared spectra of organic molecules and substances continued

- diatomic molecules, shortening of energy relax. time of excited mol. vibr. in dense medium by form. of H-bonds 0-91553
diazonium salts in aqueous solns. and polymer matrices, IR absorpt. spectra 0-76030
dicarboxylic acids, IR spectra Davydov splitting, methylene chain pendular vibrs. (*Russian*) 0-89008
2,6-dichlorobenzamide, IR spectrum, vibr. assignment 0-95608
2,2-dichlorobutane, liquid and solid, vibr. spectra, IR and Raman obs. 0-60567
dichloromethane-d₀-d₂, soln., far IR spectra, band shapes and moment anal. 0-58252
difluoroacetic acid, soln., polarisable H bonds, IR spectrosc. obs. 0-58408
1,1-difluoroethylene near-MM-wave emission assignments 0-58260
1,1-difluoroethylene submillimetric wave emission assignments 0-102708
2,3-dihydropyran vapour, IR spectra anal. 0-63628
dimethoxymethane, vibr. spectra and rot. isomerism 0-106325
dimethylphosphines, -d₀ (-d₁) force field interpretation of coupling between methyl rocking, PH bending and PC stretching 0-69141
dimethylsulphide, liq., solvated electrons, optical absorpt. spectrum obs. 0-97250
m-dinitrobenzene, oriented film, intermol. vibr. coupling, polarised IR spectra 0-97264
diphenyl anion salts, sublimed layer, electronic and IR absorpt. spectra 0-66189
dipicolinic acid, IR and Raman spectra, isotopic frequency shift, mol. vibr. obs., point groups determ. 0-89001
1,4-disilabutane, rot. isomerism, Raman and IR spectra 0-74168
dithiocarbamate complexes of Cr, Mn, Sn and Pb IR, electronic and mass spectra, mag. susceptibility, cond. meas. 0-97270
DNA hydrate, struct. conversions of sugar phosphate chain and nitrogenous bases 0-81530
DNA-lipid interaction, IR spectroscopic obs., DNA compactisation on disperse particles 0-104550
EBBA, IR absorpt. spectra, elec. field effects, orientational order parameter determ. by IR dichroism, bend elastic consts. 0-80778
EBBA, orientational order in glassy and nematic phases, IR dichroism meas. 0-64891
epifluorohydrin, IR and Raman spectra and conformations 0-60576
esters, long-chain, X- and Y-type multilayers, form. conditions and struct. characterisation 0-80127
ethane-1,1,1-d₃, gas-phase IR spectra, rot. fine struct. obs. 0-83359
ethyl radical, C-C bond barrier rot., IR spectra 0-76536
ethyl-furan-2-carboxylate, skeletal vibr. of IR spectra, conformational props., solvent polarity effect 0-87118
ethyl-p-azoxybenzoate, far IR and Raman spectra, smectic polymorphism 0-76022
ethylcyclopropane, solid, liquid, vapour phase, IR and Raman vibr. spectra 0-84740
ethylene, absorpt. cross sections at CO₂ laser wavelengths, temp. and press. depend. 0-78613
ethylene, He-Ne laser line, high temp. absorpt., anal. by high resolution IR spectra 0-91554
ethylene, IR absorpt. spectra of ν_1 , ν_{10} and ν_4 interacting band 0-83369
ethylene, narrow resonances of multiple-photon IR absorpt. 0-99529
ethylene, quadrupole moment tensor determ. by collision-induced absorpt. spectrum 0-91555
ethylene(-d₂) clusters, IR photodissoc. 0-89506
ethylene and propylene adsorbed on Ag, enhanced Raman spectra obs. 0-95607
ethylene-vinyl alcohol copolymers, H bonding study by near-IR spectra (*Japanese*) 0-78734
ethyloxirane, solid, liquid, vapour phase, IR and Raman vibr. spectra 0-84740
2-fluoro ethanol, Ar matrix, induced conformational isomerisation by IR irradi. 0-101010
fluoromethane+fluoromethane, collision induced mode selective energy transfer, fluoresc. obs. 0-69177
fluoromethyl formate, conformation potential energy surfaces, ab initio calcs. 0-69065
formaldehyde, isolated Voigt line, off-peak spectral absorpt. coeff. 0-106355
formaldehyde+Ar(N₂O), mol. isolated Voigt line, off-peak spectral absorpt. coeff. 0-106355
formaldehyde dimers, matrix isolated, struct., IR spectra 0-99504
formaldehyde-d₀(-d₁)(-d₂), matrix isolated, IR spectra, monomer absorpt. 0-95053
formic acid, cryst., H bonded, IR spectrum computer simulation 0-97253
formic acid, soln., polarisable H bonds, IR spectrosc. obs. 0-58408
formic acid dimer, vibr. spectra, CNDO/2 interpretation (*French*) 0-58155
formic acid-d₀(-d₁)(-d₂), vibr. spectra, CNDO/2 interpretation (*French*) 0-58155
furan, cryst., low freq. vibr. spectrum, temp. depend., 12 to 253K 0-84743
gases, IR fluoresc. by CO₂ laser 0-78619
2-haloethanols, torsional interaction, IR spectra, ab initio calcs., 2-dimens. model 0-74160
halomethanes, absorpt. coeffs. meas. in Nd laser emission band 0-78620
intermolecular spectroscopy and dynamical properties of dense systems, conf., Varenna, Italy (1978) 0-82581
iodomethane, P-line and ν_6 band spectra using CO₂ laser absorpt. 0-69142
iodotrifluoromethane, high vibr. state excitation in high-power laser field, spectral characts. 0-91562
isopropyl alcohol, adsorbed on ZnO, decomp., IR and kinetic obs. 0-59780
isopropyl radical, Ar matrix isolated, IR spectra and UV photolysis 0-66827
isopropylcyclopropane, solid, liquid, vapour phase, IR and Raman vibr. spectra 0-84740
liquid chromatography effluents on line anal., micro liq. chromatograph-interfaced Fourier transform IR spectrophotometer 0-73483
liquids and solids, gas chromatography-IR spectroscopy using Sadtler CIRA 101 analyser 0-93809
lithium oligopentadienyl and complexes, IR spectra (*Russian*) 0-71424
lithium salt electrolyte submillimetric absorption obs. 0-60611
malononitrile, cryst., phase transitions, Raman and IR obs. 0-88980
MBBA, IR absorpt. spectra, elec. field effects, orientational order parameter determ. by IR dichroism, bend elastic consts. 0-80778

infrared spectra of organic molecules and substances continued

- MBBA, orientational order in glassy and nematic phases, IR dichroism meas. 0-64891
methane, 2 ν_3 band, R₁ line, spectrum reconstruction using test response 0-77884
methane, ¹²C and ¹⁴C, line parameters for ν_2 and ν_4 bands, isotope shifts, appln. to planetary atmospheres 0-95622
methane, ¹³C and ¹²C, line strength ratios of 2 ν_3 singlet 0-78616
methane, absolute line strengths meas. using dual-beam diode laser spectrometer 0-101853
methane, IR anal. of ν_2 and ν_4 bands (*French*) 0-87113
methane, Jovian line profiles near 1.1 μ as probe of cloud struct. and C/H ratio 0-62067
methane, liquid, comparison on interaction induced light scatt. and IR absorption 0-60561
methane, saturated absorpt. meas. at 3.39 μ m using multipath cell 0-74442
methane, V-V energy transfer 0-83469
methane-d, 4.5 μ m absorpt., 2 ν_6 overtone band anal. 0-91557
methanes, ¹²CH₄ and ¹³CH₄, IR spectra obs., anal. of $\nu_2+\nu_3$ band 0-95614
methanol far IR laser line Stark splitting obs. 0-58313
methanol far IR Stark spectroscopy and 9-P(34) CO₂ laser line 0-69145
methanol-CO-H₂O-NH₃ solid mixture vibr. modes, IR spectra 0-90504
p-methoxy benzonitrile, IR absorpt. spectra, vibr. assignments 0-95609
methoxydifluorophosphine-d₀ and -d₃, IR and Raman spectra, mol. vibr. and struct. obs. 0-87103
methyl chloride, rot. anal. of IR absorpt. spectra, mol. vibr., rot. const. determ. 0-99505
methyl chloroform, vap., multiphoton dissoc. by CO₂ laser beam 0-61123
methyl furan-2-carboxylate, skeletal vibr. of IR spectra, conformational props., solvent polarity effect 0-87118
methyl furan-2-thiolcarboxylate, skeletal vibr. of IR spectra, conformational props., solvent polarity effect 0-87118
N-methylacetamide, solid, Fermi resons. 0-97266
methylacetylene, ν_5 band, microwave and IR laser Stark spectrosc. 0-91558
methylamine liquid, 293K, solvated electron decay kinetics obs. 0-71928
Michelson type Fourier interferometer and gaseous molecular spectra 0-68275
molecular crystal IR spectral line shape and polarisation temp. depend. 0-88991
molecular crystals, intermolecular interactions, spectroscopic studies, review 0-103958
molecular crystals, mol. orientation defects, effect on polarised IR and Raman spectra 0-88989
molecular monolayers, IR absorpt. enhancement by thin metal overlayers, ATR technique 0-88995
monochloroacetic acid, isolated molecules, internal rotation, CNDO/2 calcs., IR spectra 0-69254
2(4)-monoxypyrimidines, gaseous, matrix, soln., tautomeric equilib., IR and UV absorpt. spectra 0-58256
naphthalene-h₈ and d₈, isotopic mixed crystals, exciton spectra in IR region 0-71400
nitrobenzene, IR absorpt. and Raman bands, half-band width conc. depend. 0-74171
nitrocyclopropane, vibr. spectra struct. and bonding 0-102520
p-nitrotoluene crystal film, exciton spectrum, IR absorpt. and Raman scatt. 0-80771
nonafluorooisobutane, IR spectra, spectral bandshape and intensity of C-H chromophore 0-83355
Nylon-12 film, casting conditions effect on polymorphism 0-84903
octadecylacrylamide films, oriented ultrathin, radiation-induced solid state polymerisation 0-80128
optical fibres, glass and plastic, neutron irradiated, optical absorpt. spectra 0.7 to 1.1 μ m 0-58762
organometallic amines, IR spectra (*German*) 0-87133
oxalic acid in aq. soln., vibr. studies, IR and Raman spectra 0-95589
2,2-paracyclopentane, dimer vibration influence on emission spectrum 0-69133
pentacene, first excited singlet state, butterfly motion studied by fluoresc. spectra 0-78615
pentane, liq., enthalpy difference between rot. isomers, IR spectrosc. obs. 0-106404
PET, biaxial orientation, refr. index meas. by Raman and IR spectrosc. 0-60583
PET films, dyed, local mech. stresses, IR spectrosc. determ. 0-65418
PET films, one-way drawn, constant strain effects, IR meas. 0-60584
phosphine, IR spectrum, ν_1 and ν_2 band analysis 0-83366
photoionisation, multiple, infrared laser 0-69194
polar molecules in nonpolar solvent, far IR spectra and dielec. relax. 0-71312
poly(octadecyl ethylene), temp. depend. of 720 cm⁻¹ IR band 0-97281
poly(octadecyl ethylene oxide), temp. depend. of 720 cm⁻¹ IR band 0-97281
poly(p-phenylene), AsF₃ doped, highly cond. charge transfer complexes, elec. and optical props. 0-70778
polyacetylene, vibr. excitations of charged solitons 0-108201
polyacetylene films, doping effect on elec. cond., chem. and optical props. 0-65572
polyethylene, vinyl group reactions during γ -irrad., crystallinity effect, absorbance obs. 0-81346
polymer thin films formed in RF discharge using monomer organic semi-cond., elec. props. obs. 0-80432
polymers, aliphatic and aromatic, mean mol. orientation factors, from IR spectra and acoustic method 0-70142
polypropylenes, iso- and syndio-tactic, Raman tacticity bands, vibr. spectrum 0-66193
polysiloxene, irradi., linear, IR and solubility obs. 0-93775
polystyrene, isotactic gel film, Fourier transform IR spectrum 0-104465
polyvinylidene fluoride, corona-charged, surface effects 0-66102
porphyrin free base, vibr. and normal mode anal. 0-69122
principal component analysis, using computer (*Japanese*) 0-69143
propanal, methyl torsional pot. functions, LF Raman and IR vibr. spectra 0-95612
propionyl chloride(-d), 357-333 nm absorpt. system 0-69161
propionitriles (-O, NH, S), conformational investig., NMR, IR and semiempirical MO methods 0-95650
N-p-propoxybenzylidene-p-pentylaniline, orientational order in glassy and nematic phases, IR dichroism meas. 0-64891

gold continued

- Au-Ga_{1-x}Al_xAs Schottky diodes, band struct. from I-V, C-V meas. 0-96989
 Au-Ga_{1-x}Al_xSb Schottky barriers, barrier height 0-96986
 Au-GaAs MIS solar cells, effects of thin oxide layers on characts. 0-89624
 Au-GaAs polycrystalline Schottky barriers, transition with grain size from electrode-limit to bulk-limited cond. 0-65676
 Au-GaAs Schottky barrier solar cells, effect of interfacial oxide layer on cell characts. 0-61365
 Au-GaInAsP, rectifying contact, elec. characts. 0-80376
 Au-Ge Schottky barrier photodetectors, near IR interband transitions and optical parameters 0-73449
 Au-n-AlGaAs-n-GaAs Schottky-barrier solar cells, band readjustment effect 0-81458
 Au-n-Ga_{1-x}Al_xAs-n-GaP narrow-band variable-gap surface-barrier photodetector 0-96944
 Au-n-Si Schottky barrier solar cells, recombination in space charge region 0-61351
 Au-O bond energy glow discharge, mass spectrometry obs. 0-64808
 Au-oxide-n-GaAs MIS structures, reverse bias influence on photocurrent 0-107921
 Au-Pd-Au sandwich, obs. of strongly enhanced mag. susceptibility 0-93076
 Au-Si interface, critical Au-film thickness obs. for room temp. interfacial reaction 0-75390
 Au-Si interface, electron energy loss and AES meas. 0-89096
 Au-Si thin film double layer, silicide form., electron diff. study 0-80005
 Au-SiO₂-Si system, oxide film 16-36 Å thick, tunnel currents 0-70842
 Au-SiO₂-n-Si solar cells, comparison of majority- and minority-carrier silicon MIS solar cells 0-85280
 Au-SiO₂-n-Si, tunnelling MIS struct. 0-92995
 Au-Ti_{0.3}W_{0.7}, thermal annealing study of metallisation on Si 0-80134
 Au-W-GaAs Schottky barrier, elec. and chem. props., AES 0-96973
 Au-ZnS electrolum. Schottky barrier diode, S⁺-implanted, blue emission 0-76082
 Au+light and heavy ions, L-shell X-ray production and subshell ionisation cross sections meas. 0-91637
 Au₂, Harris-Pohl selected valence electron split-shell MO calcs. 0-91439
 Au⁺, ab initio SCF calcs. using relativistic effective core pot. 0-95524
 CdSnAs₂-Au, surface barrier junction, elec. props., temp. depend. 0-65686
 CdTe_{1-x}Se_x(Te₄):Au, elec. cond., density, dielectric const., changes on fusion 0-88553
 Cu/Sn-Ni/Au tricuiples, electrodeposited, interdiffusion obs. 0-84331
 Fe-Au bimetal epitaxial films, examination of interaction at temps. ≥600°C 0-75482
 films, vac. condensed at oblique vapour incidence, oriented cryst. growth, electron diff. study 0-97432
 Ge:Au, Sb, Hall mobility, temp. dependence 0-96919
 p-Ge:Au,Sb,Hg(Zn), radiation-defect form., Au influence 0-92911
 Ge:Au film strain gauges, press. sensor (*Japanese*) 0-105631
 InSb-Au contact system, low temp. alloyed contact formation 0-100519
 KBr:Au⁺, optical absorpt. bands and MCD, electron-lattice interaction 0-108236
 Ni:Au, ion-implanted, laser irradi. effect 0-108306
 Ni-Cr/Au films, interdiffusion processes and oxidation phenomena 0-59735
 PbI₂-Au, light sensitive, internal photoelectric emission 0-107910
 Pt-polymer-Au capacitor, electroforming, negative resist., electron emission 0-80406
 RbCl:Au⁺, optical absorpt. bands and MCD, electron-lattice interaction 0-108236
 Si:Au, amphoteric centre, struct. bonding of deep level defects 0-88506
 Si:Au, C-V curves of MIS diode used to examine trapping levels 0-65697
 Si:Au, EPR spectrum, strong nucl. quadrupole effect 0-93172
 Si:Au, O(H), film, amorphous, elec. cond. meas. 0-80423
 Si:Au, P-induced point defects influence on Au gettering mechanism 0-65030
 Si:Au, precipitation of solid soln., effect of gamma irradiation 0-59515
 Si:Au deep level parameter determ. by isothermal capacitance transient spectroscopy 0-88507
 Si:Au p⁺-n junction, small area, acceptor level conc., determ. from TSC curves 0-75631
 Si:Au planar extrinsic IR detector, use of multiple internal refl. for increased sensitivity 0-77862
 Si:Au, interface study using EELS 0-97391
 Si-SiO₂-Au Schottky barrier solar cells, back-illuminated, theoretical performance 0-61345
 SiO₂:Au, XPS line broadening and extra-atomic relax. energies 0-71561
 Sn/Au thin film diffusion couples, Kirkendall void form. 0-96698
 ZnTe:Au, elec. field and impurity conc. effect on ionisation energy 0-88514
 ZnTe:Au, impurity identification and characterisation, capacitance, luminescence and IR absorption 0-60639

gold alloys

see also gold compounds

- dilute, virtual bound states due to 4d- and 5d-transition metal impurities 0-70667
 electroplating, comparison with Sn-Pb alloy (*French*) 0-89158
 Ag-Au, corrosion in HNO₃ 0-85091
 Ag-Au alloys, EMF meas. employing Ag-β-Al₂O₃ (*German*) 0-104307
 Ag-Au-Cu, surface composition change on sputtering with 2 keV Ar ions 0-66365
 Ag₃Au_{1-x}Cu_x, phase relations, X-ray diff. and differential thermal anal. 0-108395
 Au-3d transition metal alloys, UPS study, localised states 0-93449
 Au-Ag, biccyst. thin film couples, interphase interfaces, TEM 0-70540
 Au-Ag (35 at.%), dechannelling of energetic He ions at dislocations 0-70275
 Au-Co, dil., valence and core level spectra, XPS study 0-84838
 Au-Co, electron scatt., spin-orbit effects 0-65533
 Au-Co, liquidus line determ. by mag. meas. 0-60250
 Au-Co electrodeposit, Co-hardened, characterisation by Mossbauer spectroscopy, Co precip. formation 0-80108
 Au-Cr, conc. spin glasses, thermopower 0-65538
 Au-Cr, dil., elec. resist., generalised phase shift anal. of Kondo effect 0-75556
 Au-Cr, dil. alloys., elec. resist., deviations from Matthiessen's rule 0-75541

gold alloys continued

- Au-Cu, Ising FCC and antiferromag., mag. phase diagram, ordering, Monte Carlo calc. 0-103833
 Au-Cu, surface conc. profile and surface energy 0-84350
 Au-Cu-Fe spin glass alloys, impurity mag. resist. meas. 0-59972
 Au-Dy, dil., hyperfine interaction, Mossbauer study, Kramers quartets 0-66083
 Au-Er, dil., EPR at 100 mK to 1K 0-66028
 Au-Er, ESR studies 0-108064
 Au-Fe, conc. spin glasses, thermopower 0-65538
 Au-Fe, dil., crit. dynamics 0-60325
 Au-Fe, dil., valence and core level spectra, XPS study 0-84838
 Au-Fe, spin glass, transition temp., freq. depend. 0-97113
 Au-Fe, spin glasses, alternating susceptibility 0-65912
 Au-Fe (1 at.%), spin glass, specific heat 0-60355
 Au-Fe (4 at.%), spin glass, magnetisation and energy relax. below T_g 0-65921
 Au-Fe (4.2 at.%), spin glass, DC magnetisation, field depend. 0-97103
 Au-Fe alloys, magnetism and atomic clustering 0-103810
 Au-Fe alloys, spin correlations, neutron diff. meas. 0-80482
 Au-Fe ion implanted alloy, Mossbauer conversion electron scatt. 0-88898
 Au-Gd, dil., conduction electron-local moment exchange interaction meas. 0-60191
 Au-Ge contacts on GaAs, SEM and TEM obs. of struct. 0-100522
 Au-Ge system, struct. of metastable phases (*German*) 0-108430
 Au-Ge/GaInAsP, ohmic contact, elec. characts. 0-80376
 Au-Ge-Ni/GaAs metal-semiconductor thermoelectric coolers, effects of contact resist. and dopant conc. 0-81481
 Au-Ge-Si, influence of struct. on elec. resist. of glass forming alloys 0-65518
 Au-Mn, conc. spin glasses, thermopower 0-65538
 Au-Mn alloys, reversible and irreversible DC magnetisation in spin glass regime 0-65908
 Au-Ni, dil., valence and core level spectra, XPS study 0-84838
 Au-Ni, surface segregation, strain effects 0-80042
 Au-Pd, biccyst. thin film couples, interphase interfaces, TEM 0-70540
 Au-Pd (1(50) wt.%), quenched, vacancy annihilation and short-range order formation, elec. resist. 0-108487
 Au-Pt-Pd-Ag-Cu, commercial dental alloy, age-hardening characts. 0-89235
 Au-Si formation at thin film interface, electron diff. study 0-80005
 Au-Sn, zeta and AuSn phases, heats of form. and heat contents 0-60837
 Au-Sn liquid, optical reflectivity spectra of virtual bound states 0-89021
 Au-Ti/SiO₂/p-Si MOS struct., interface state distrib., DC tunnelling spectra determ. 0-75611
 Au-transition metal alloys, ¹⁹⁷Au Mossbauer isomer shift cellular atomic model 0-84673
 Au-Y, dil., conduction electron-local moment exchange interaction meas. 0-60191
 Au-Yb, dil., EPR at 100 mK to 1K 0-66028
 Au-Yb thin films, ESR spectra, strain effects 0-71172
 Au-Zn, molten, EMF meas. of activities using ZrO₂ solid electrolytes (*Japanese*) 0-88339
 Au-Zn/p-Ga_{1-x}In_x/PyAs_{1-x}, specific contact resist. 0-84509
 AuCu-Al thin film bilayer system, phase formation, backscattering spectra 0-96728
 Au₃Cu_{1-x}Ag_x, phase relations, X-ray diff. and differential thermal anal. 0-108395
 AuFe spin glass, μ⁺ zero-field spin relax. probe for spin dynamics 0-97177
 Au₈₅Fe₁₅, and Au₈₂Fe₁₈, mag. props. 0-84592
 Au₇₇Ge₁₃Si₁₀, heat of crystn. and viscous behaviour 0-75166
 AuMg, B2 intermediate phase, slip system, ordering energy and atomic size ratio depend. 0-59471
 AuMn, mag. struct., phase transition, and magnon spectrum, random anisotropy effects 0-88722
 AuMn, ordered, vacuum deposited epitaxial films, orientation control by external stress 0-100426
 Au₁₁Mn₄ ordered phase formation, electron diff. and microscopy study 0-107418
 Au₃Mn thin films, electron diff. study 0-92793
 Au₂Mn, heat treated, short-range order, diffuse X-ray diff. study (*German*) 0-88092
 Au₃₅Ni₆₅, vapour quenched amorphous alloy, atomic arrangements 0-100173
 Au_{50-x}Pd₅₀ (0≤x≤15.02) β'-phase, Hall effect and elec. cond. 0-107768
 Au₃₅Si₆₅, amorphous vacuum-deposited and liquid-quenched films, diffusion and crystn. 0-84094
 Au₃Si_{1-x} amorphous alloy, crystallisation, elec. cond. study 0-103246
 Au₃Si_{1-x} amorphous films, phys. studies 0-75476
 Au₃Si_{1-x} metastable phase, substruct. unit cell (*German*) 0-88091
 Au_{100-x}Zn_x (47≤x≤52), β'-phase, Hall effect and elec. cond. 0-107768
 Be-Au, ohmic contact to p-InP, low contact resist. 0-65677
 Ce₈₀Au₂₀, metallic glass, mag. ordering and cryst. field effects, speromagnitism 0-80531
 Cs-Au, liq., molar vol. meas. 0-59546
 Cs-Au liq. alloy, formation of localised electronic states, NMR obs. 0-93201
 CsAu, molten, equimolar, structural evidence of ionic nature 0-64882
 Cu-Ag-Au, coherent phase diagram, theoretical calc. 0-70373
 Cu-Al spherical crystals, grown from drop of melt, topography 0-84353
 Cu-Au, corrosion in HNO₃ 0-85091
 Cu-Au, dil., magnetoresist., temp. depend. 0-70682
 Cu-Au, HV electron microscopy, crit. voltages depend. on comp., temp. and short-range order 0-100146
 Cu-Au (4 at.%), anneal hardening mechanism 0-60879
 Cu-Au alloys, vacancy and divacancy migration activation energies, elec. cond. meas. 0-88140
 Cu-Au system, two-phase mixtures, long-period superlattices 0-84140
 Cu-Au-Fe, ferromag. ordering in FCC γ-Fe precipitates, Mossbauer study 0-71267
 Cu-Au-O alloys, dil., O-metal interactions, activity coeff. meas. at 1423K 0-93792
 Cu-Mn-Au spin glasses, anisotropic exchange interactions, effect of non-mag. impurities 0-80534
 Cu-Ni/Au-Ni multilayer films, ohmic behaviour, use as strain gauge 0-65713
 Cu-Ti-Cu, wetting of Al₂O₃, alloying effects 0-107617
 (Cu-Au)-Co, single crystals, solid soln. and particle strengthening, superposition 0-97495

gold alloys continued

- Cu₃Ag_{1-x}Au_x, phase relations, X-ray diffr. and differential thermal anal. 0-108395
 CuAu, ordered, vacuum deposited epitaxial films, orientation control by external stress 0-100426
 Cu₃Au, alloys, superlattice-fringe imaging theory, images formed from two beams 0-79649
 Cu₃Au, disordered [001]-orientated single crystals, plastic deform., TEM and slip line studies 0-97541
 Cu₃Au, electrical resistivity and LRO, energy gap formation in Fermi surface 0-88533
 Cu₃Au, neutron irradi., displacement cascades, direct obs. method 0-107335
 Cu₃Au thin films, fine-grained and disordered, low temp. ordering 0-97433
 Cu₃Au-Co single cryst., precip. hardening (*German*) 0-84946
 Cu₃Au-Ni, antiphase domains morphology 0-108460
 CuMnAu, hysteresis, spin orbit scatt., effect on anisotropy in spin glass state, rel. to Au impurity conc. 0-71095
 Gd-Au amorphous films, spontaneous Hall effect and elec. resist. 0-80251
 Ge-Au eutectic alloys, field ion sources 0-97414
 HoAu, mag. phase diagram 0-75761
 La-Au, splat-quenched, Mossbauer effect and elec. resist., amorphous struct. 0-84676
 La-Sm-Au, amorphous, surface effects on Sm valence, XPS and X-ray absorption meas. 0-108325
 La₇₆Au₂₄, disordered ribbons, production of quenched samples using arc furnace 0-71612
 La_{80-x}Pr_xAu₂₀, amorphous, mag. and supercond. props. 0-75713
 γ-MnAu, antiferromag., phase diagram, X-ray diffr. and Young's modulus meas. 0-71024
 MnAu₂, helical antiferromag., optical absorpt., density of states 0-66224
 Ni-Ge-Au evaporated contacts on GaAs, TEM obs. 0-75449
 Pb-Au, interstitial and substitutional distrib. 0-84204
 Pb-In-Au base electrode film Josephson junctions, tunnel barrier oxide struct. 0-65750
 Pb_{1-x}Ag_x, liquid alloys, local fluctuations and quadrupolar relaxation 0-66060
 Pd-Au, alloys-H solid solutions, superconducting transition temp. behaviour (*Russian*) 0-70879
 Pd-Au-Si, influence of struct. on elec. resist. of glass forming alloys 0-65518
 PdAu (4.7 at.%), effect of alloying on activation energy of H₂ diffusion 0-107571
 (Pd₈₀Au₂₀Si₁₃)/Fe₃₀, compositionally modulated amorphous film, diffusion, struct. relax. 0-103518
 Pr₁La_{89-x}Au₂₀, amorphous, low temp. excitations, specific heat 0-100337
 Pt-Au, dil., recovery spectrum after thermal neutron irradi., Au effect and defect conc. depend. 0-65057
 Pt-Au, surface segregation, comp. depth profiles meas. using atom-probe field ion microscope 0-100380
 Sc-Au, dil., elec. field gradient, Mossbauer meas. 0-80665
 Si-Au eutectic alloys, field ion sources 0-97414
 Si-Au system, ion implanted induced giant gettering, annealing effects 0-88221
 Sm-Au, amorphous, surface effects on Sm valence, XPS and X-ray absorption meas. 0-108325
 TbAu₃, mag. phase diagram 0-75761
 Te-Au film, metastable supercond. alloys, produced by low temp. ion implantation 0-88670
 Ti-Au, (9.9 wt.%), eutectoid system, β→α_m transform., nucleation kinetics 0-97474
 YbAu₂, valence transition at surface of Yb 0-70652

gold compounds

- see also gold alloys*
 eutectics, HgTe-PbTe and Au-PbTe, prep. and thermoelectric behaviour characts. 0-107774
 AuF₆, produced from fast Cs+(AuF₅)_n collisions, ionisation cross section energy depend. 0-81300
 Au₂O₃, X-ray absorption, discontinuities and limits, chem. combination effects 0-93435
 Au₂P₃, melting temp., Au₂P₃-Au eutectic temp. 0-59628
 Cs₂PtCl₆, electronic state of Au at high press., Mossbauer spectra 0-60467

goniometers

- crystal cutting apparatus 0-86275
 crystal goniometric setup with electronic control system consisting of Kharkov linear electron accelerator 0-68976
 ellipsometer attachment 0-90883
 pulsed FT NQR spectrometer, automation for single crystal Zeeman studies 0-66066
 retroreflector photometric and goniometric accuracy 0-86375
 texture goniometer alignment of Schulz reflection technique, method for testing 0-81272
 Weissenberg rheogoniometer, R-17, axial compliance reduction for viscoelastic fluids 0-106859
 X-ray goniometer, for stress measurement in single crystals and coarse-grained specimens 0-64837
 X-ray powder diffractometry goniometer, with temp. control (*French*) 0-79631

GP zones *see* Guinier-Preston zones**grain boundaries**

- for grain boundary diffusion, see diffusion in solids; for grain boundary segregation, see segregation*
see also bicrystals; subboundary structure; twin boundaries
 adsorption-induced interface decohesion, pair bonding theory 0-88166
 bicrystal, elastic incompatibility stresses (*Japanese*) 0-107361
 β-brass bicrystals, shear-incompatible, grain boundary contrib. to Bauschinger effect 0-97550
 cavity growth anal. during superplasticity 0-60923
 ceramic materials, fine-grained, cyclic plastic deform. as cause for thermal expansion hysteresis 0-82920
 chloranil pellets, thermally stimulated discharge current and dielectric studies 0-93236
 creep and growth, irradiation induced, solute effects on defect precip. rate 0-88252
 creep and growth, radiation induced, fundamental mechanisms 0-92596
 creep damage and the remaining life concept 0-59574

grain boundaries continued

- creep fracture, failure mechanism involving grain boundary sliding and brittle crack extension 0-97557
 crystal orientation, determ. by zone axis method, appl. to grain boundaries, TEM 0-103226
 crystalline materials, struct. of grain boundaries using diffr. techniques 0-59478
 cubic materials, intergranular structures, geometrical approach, review (*French*) 0-59482
 cubic structures, symmetry of coincidence site lattices (*Russian*) 0-79807
 decohesion energy, solute adsorption influence 0-65009
 dislocation and diffusion creep transition 0-88253
 dislocations, effects on grain boundary processes of the steps in boundary plane 0-79785
 dislocations and lattice transformations, book contrib. 0-107242
 elastic interaction with point defects 0-59483
 electronic structure, development of analytical electron microscope 0-86521
 energy-misorientation relationship use in modelling grain boundary defects and props. 0-84188
 engineering materials, intergranular fragility index 0-66637
 epitaxial film, interfacial boundaries and transition regions (*Russian*) 0-103596
 FBR oxide fuels, dynamic response of grain boundary cavities to stress and temperature changes under conditions of continuous gas generation 0-66544
 FCC polycrystals, under hydrostatic pressure 0-107356
 ferrite-austenite (α-γ) interface, Fe self-diffusion compared with grain boundaries diffusion 0-65306
 fission fuel grain boundary loss terms, use in fission gas release and swelling models 0-63257
 fluorite, use of proton irradi. to reveal growth and deform. features 0-84216
 free surface segregation, rel. to grain boundary segregation 0-71657
 GaAs, polycrystalline, grain boundary resistance meas. effect on solar cell performance 0-93891
 Hastelloy, H₂ embrittlement in H₂S environments, impurity segregation effects 0-71724
 Incoloy 901, foil prep. for TEM exam. 0-88001
 Inconel, caustic stress corrosion cracking resistance, processing variables effect 0-71796
 Inconel 600, thermal treatment, grain boundary microstruct. and SCC resistance 0-71675
 Inconel 617, creep, morphological changes of carbides, affect on creep props. 0-108509
 Inconel X-750, deform. and fracture characts., 24-816°C 0-108551
 interfacial cohesion, adsorption-induced losses 0-65010
 interfacial structure effects on high temp. mechanical behaviour 0-59480
 intrinsic structure, in grain boundaries and boundary mobility 0-103368
 irradiation growth, contrib. of grain shape to anisotropy 0-92556
 liquid phase sintered systems, particle coalescence probability estimation 0-104086
 melting transition, grain-boundary, in two-dimensional lattice-gas model 0-59634
 metal, diffusion welding, migration of oriented intergranular boundary with pores (*Russian*) 0-84943
 metal, induced elastic interaction of dilatation centres with grain boundaries (*Russian*) 0-84205
 metal film, polycryst., superimposed effects of three arrays of scattering planes on electrical conductivity 0-80412
 metal film, temperature coefficient of total resistance 0-70853
 metallic conductivity, polycrystalline, grain-boundary scatt. model 0-88530
 metallic films, grain boundary scatt., Hall coeff., theory 0-88649
 metallic materials, fatigue life distrib. theoretical obs. near fatigue limit 0-59569
 metallic thin films, grain boundary and surface scatt., statistical model 0-103762
 metals, BCC, tilt boundaries, struct. 0-84184
 metals, FCC, twist boundaries, struct. invest. using computer simulation technique 0-84185
 metals, polycrystn., creep damage and cavity growth, assessment using density meas. 0-104217
 migration, TEM obs. on mechanism 0-79812
 migration kinetics, atom diffusion across boundary, theory 0-79809
 nuclear fuel, gas release and swelling, operational model, grain boundary gas 0-95346
 nuclear fuels, fission gas precipitation into intra- and intergranular porosity, theory 0-57849
 p⁺-n, n⁺-p solar cell structures on polycrystalline material, performance 0-89640
 Permalloy-Cu(Al) two-layer films, mag./anisotropy, grain boundary diffusion (*Russian*) 0-71122
 phase boundaries in first-order phase transitions, dynamics stability 0-107403
 photovoltaics and absorber/reflectors, diffusion, chemical reactions, contamination, AES and SIMS 0-72066
 plane coalescence, at grain boundaries 0-70221
 plane matching secondary relaxations, electron microscopy high angle, plane matching secondary relaxations, electron microscopy 0-103363
 plasticity 0-65135
 polycrystalline materials, effect of grain boundary sliding on anelasticity 0-96592
 polycrystalline metals, effect of grain boundary sliding on steady creep 0-96590
 precipitation reactions, determ. of struct. aspects, electron microscopy 0-103359
 properties, with reference to impurity effects (*Dutch*) 0-96544
 recrystallisation, phase boundary motion, heat release effect, self-consistent treatment 0-103449
 sapphire ribbon crystals, EFG growth and charact., voids, grain boundaries and dislocations 0-103283
 segregation, grain boundary, equilb. impurity conc. (*Russian*) 0-103478
 segregation at grain boundaries, critical assessment 0-75362
 semiconductor defects, spectroscopic techniques to study of electronic props. 0-84446
 semiconductor film, polycrystalline on optical props. grain boundary effects 0-80890
 sink strengths for thin film surfaces and grain boundaries 0-88207
 sintering, surface redistribution by grain boundary diffusion 0-84871
 skeletonization in quantitative metallography 0-101002

inorganic molecule configurations continued

- β -VOSO₄·5H₂O, X-ray cryst. struct. determ. and refinement (*French*) 0-107121
 XeF₂, pseudopotential SCF-MO studies, equilib. struct., stretch-stretch interaction force const. 0-95525
 XeF₄, pseudopotential SCF-MO studies, equilib. struct., stretch-stretch interaction force const. 0-95525
 XeF₄, pseudopot. SCF MO studies, steric aspects of struct. and force fields, Jahn-Teller effect 0-99444
 XeF₆, pseudopot. SCF MO studies, steric aspects of struct. and force fields, Jahn-Teller effect 0-99444

inorganic molecule electronic structure *see molecular electronic states***insolubility** *see solubility***inspection**

- see also quality control; reliability; testing*
 AMUR-6 instrument to detect defects and indicate their location 0-104402
 automatic inspection of materials using lasers 0-66734
 chromatographic method of calibrating leaks 0-77800
 coarse-structure materials, inspection of part quality using LF US methods, review 0-81264
 coating ZZ 0-77775
 complex shape product inspection, local eddy current transducer 0-108671
 component profile inspection equipment 0-105608
 composite piezotransducer for LF acoustic inspection using electrical models 0-104393
 contact lenses, back surface aspheric 0-66711
 contact media for US thickness meas. and defect inspection over wide temp. range 0-104395
 contactless laser interferometer sweep gauge for diamond-turned surfaces 0-73441
 cylindrical products, diameter meas., interfering factors elimination 0-77755
 dark-field surface inspection using total internal reflection 0-74519
 deposited metal, US echo inspection procedure 0-89425
 device for checking airtightness by parameter changes in object and medium 0-104404
 eddy current testing of wire and bar 0-71819
 eddy current transducer with electrical commutation of excitation field, NDT 0-105633
 eddy-current feed-through transducer, approx. calc. of mag. field, nonferromag. media 0-78746
 fatigue detection and rating by acoustic emission, review 0-104380
 feed through eddy current transducer, numerical anal. or operating mode during ferromagnetic rod inspection 0-108670
 ferromagnetic object inspection, method of higher harmonics, difference schemes 0-89444
 flexible scanning industrial X-ray fluoroscopic inspection 0-100971
 flexible scanning industrial X-ray/fluoroscopic inspection 0-89459
 heat treatment, electromagnetic quality inspection with specified intensity of internal field 0-108677
 international collaboration among calibration services 0-101773
 large monocrystal X-ray reflection/scanning and transmission topographic methods 0-96415
 magnetic particle inspection, nature of magnetic inks and powders 0-100974
 magnetized samples, defects, magnetostrictive conversion of US waves into EM fields 0-66008
 magnetizing device for inspection of products of ferromagnetic materials according to parameters of Barkhausen discontinuity 0-89457
 metallic objects with complex shape, eddy-current inspection 0-89446
 microtrons, appl. in nondestructive inspection of industrial products 0-81267
 nuclear fuel shell inspection, mag. method for detecting ferromag. particles 0-66746
 oil seal lubrication static contact shape and kinetic behaviour 0-97598
 optical fibre end face cut prep. and inspection techniques, review 0-74483
 optical microscope, large field, for use in semiconductor manufacture 0-82812
 piezoceramic transducers 0-104392
 plastic encapsulated and hermetic modules corrosion model 0-100937
 precision image isoon X-ray TV camera 0-101263
 pressure vessel crack detection by magnetic crack detection and dye-penetrant inspection 0-100994
 pressure vessels, AE during fatigue crack expansion 0-108675
 profile multiaxis meas. with vector drive 0-105609
 radio wave inspection with one sided access to object, conditions of coating and compensation 0-108679
 radiographic inspection algorithm speedup by array processor 0-108659
 radiographic inspection method, productivity 0-71861
 raw material acceptance testing for dielectric applications 0-97646
 receiver-transmitter for ultrasonic inspection units 0-89458
 rotatable microscope stage, used for hybrid microcircuits inspection 0-90889
 scanning acoustic microscopy for study of interfaces in solid-state devices 0-99907
 scanning optical microscope for semicond. materials and devices 0-95136
 soldering inspection using optical projection microscopes (*German*) 0-77849
 steel, ball bearing rods, inspection installation 0-81268
 steel, neutron quasialbedo thickness meas. of single layer product, optimization 0-105611
 steel, nitrided layer depth, electroinduction meas. method 0-104379
 steel, stainless austenitic welds, US inspection 0-71821
 steel, structural ties, NDT by eddy current transducer, optimum parameters and capabilities 0-108669
 steel case depth after quench hardening, inspection using coercimeters 0-104377
 thermovision flaw detector 'Stator-1', meas. channel 0-76449
 transducers, alternating-voltage, analogue, Soviet methods development 0-98872
 ultrasonic, welded joints in sugar extraction diffusion apparatus 0-93703
 US, inspection of metallic atomic power station equip., portable unit 0-104394
 US nondestructive inspection system, microprocessor utilization 0-71845
 US shadow flaw detectors, metrological peculiarities when inspecting thick rolled steel sheet 0-81263

inspection continued

- welded joint, radiographic inspection, standardization of sensitivity and flaw size 0-89455
 welded joint inspection by X-ray TV intrascope, photographic recording of images 0-86485
 welded joints, radiographic inspection, real flaws detectability evaluation 0-81266

instability *see stability***installation**

- EM flowmeter theory and application 0-96328
 optical fibres, transmission, applications and cable techniques (*Japanese*) 0-87493
 solar systems installation for domestic heating (*German*) 0-94103

instrumentation

- see also aerospace instrumentation; computerised instrumentation; digital instrumentation; digital readout; display instrumentation; nuclear instrumentation; physical instrumentation control*
 200 kW Gedser windmill in Denmark, performance and structural response meas. 0-61431
 fibre optics appl. survey 0-83665
 field instruments, winterisation without accessory heat 0-82758
 general purpose measuring instruments, microprocessor techniques appl. (*Spanish*) 0-62655
 measuring systems, systematic design 0-95094
 synchrotron radiation instrumentation, conf. Gaithersburg, MD, USA, June 1979 0-90607
 USSR State Bureau of Standards, metrological resource programmes 0-90809

instruments

- see also individual types of instruments, e.g. astronomical instruments, bridge instruments, optical instruments*
 innovation and business opportunity in instrument development 0-98909
 plastometer, cone type, for strength props. determ. of plastoviscous disperse systems 0-76426
 pneumatic feedback-monitoring, pressure variation effects 0-77743
 testing of measuring instruments, determ. of valid interval between tests values 0-57284
 thermocouple thermal inertia meas. (*Russian*) 0-62665

insulated gate field effect transistors

- Josephson FET, hybrid, feasibility 0-80451
 MNOS p-channel transistor, memory characts., H₂ anneal effects 0-80388
 MOS, unwanted effects of ions in SiO₂ layers on Si, review 0-92985
 MOS dopant profile, DC method 0-70244
 MOS field-effect devices, mag. quantisation effect on surface capacitance 0-70834
 MOSFET, n-Si inversion layers, electronic g-factor, spin-split Landau levels 0-80346
 MOSFET, n-Si inversion layers, resist. temp. depend. at liq. He temps. 0-80391
 MOSFET, near-ideal Si-SiO₂ interfaces using CVD, props. 0-80382
 MOSFET, negative magnetoresistance, 2-D random system 0-70728
 MOSFET, recom. lifetime determ. 0-62683
 MOSFET, Si-SiO₂ inversion layer carrier mobility, theory 0-60094
 MOSFET, surface quantum states, two-dimensionality of many-body effects 0-103740
 MOSFET, two-dimens. electron gas, determ. of fine struct. const. based on quantised Hall resist. 0-96997
 MOST, short channel, carrier saturation velocity, temperature effect (*French*) 0-70837
 MOST, short channel, output conductance, effect of ionising radiation 0-70836
 MOST structure modelling, using hybrid computer, Poisson partial differential equation solution (*Slovak*) 0-75643
 NMOS VLSI circuits manufacturing process and problems (*Norwegian*) 0-60090
 quasi-saturation mechanism associated with low doping level in drain region (*French*) 0-107920
 radiation-induced positive charge, thermal annealing 0-75648
 resistive gate, velocity-field curves for surface-free carrier in Si 0-60095
 semiconductor transport simulation using coupled and decoupled soln. techniques 0-65695
 surface depletion and inversion, arbitrary doping profile, theory 0-107912
 two-dimensional impurity bands, carrier-density dependence of activation energies associated with hopping 0-88561
 InP inversion-type MISFET with SiO₂ gate insulation interface props., elec. drift 0-93002
 InP-Si₃N₄(SiO₂)_x interface props., plasma deposited dielectrics, n-channel MOSFET action 0-93003
 n-Si, (111) inversion layers, valley splitting, Shubnikov de Haas oscills. 0-65698
 n-Si channel (100) inversion layer MOSFET, valley splitting, conductivity 0-70840
 Si, inversion layers, nonmetallic cond. at low temp. 0-70833
 Si-SiO₂ interface in IGFTs, anal. of CVD SiO₂ on (100) and (111) surfaces, near-ideal struts. 0-100528
 SiO₂ layer used for MOSFETs, electron trapping behaviour 0-92981
 SiO₂ thin films, radiation-induced trapping centres, rel. to MOS transistor technology 0-107804

insulated wires

- insulating and sheath materials for wire and cable, crosslinking by irradiation 0-66845
 polyolefin, cross-linked, insulation system for wire and cable for locomotives 0-66851
 polyolefin, cross-linked, irradiation appl. to provide improved insulation props. to wires and cables 0-66850
 PVC, cross-linked, irradiation appl. to provide improved insulation props. to wires and cables 0-66850
 PVC materials, cross-linkable, for wires and cable insulation 0-66849

insulating coatings

- see also varnish; waxes*
 oxide films, passivating, transient growth kinetics 0-93672
 rare earth aluminate, scandate and zirconate film coatings, electrophys. props. w.r.t. prep. technology 0-60781
 Fe-Si, grain oriented, phosphate coating anal. by IR spectroscopy 0-89570

insulating materials

- see also *asbestos; ceramics; composite insulating materials; dielectric materials; glass; insulating thin films; mica; organic insulating materials; thermal insulating materials*
- capacitors, power, dielectric liquids flammability and degradation 0-88944
- ferric solution ferromagnetic liquid insulation in redox flow battery, quantum parameters separation 0-61338
- fibreglass insulating materials, radiative heat transfer rel. to optical props. 0-100367
- gaseous, electric potential meas. by corona probe 0-82790
- intense electric fields, tree-shaped phenomena in solid insulating materials (Rumanian) 0-63885
- SF₆ impulse breakdown characteristics for nonuniform field gaps for switchgear design 0-84024
- SF₆ insulation breakdown characts. under operating conditions in HV apparatus 0-96414
- SF₆ with gaseous contaminants, arc decomposition kinetics investigation by combined gas chromatograph-mass spectrometry methods 0-92250
- SiO₂ fabric, prep. from E-glass, structural stability rel. to brittleness, X-ray diffr. and IR spectrosc. studies 0-96634

insulating materials, acoustic see *noise abatement***insulating materials, thermal** see *thermal insulating materials***insulating oils**

- composition, physical and chemical props. and determ. of free radicals (Rumanian) 0-97745
- liquid dielectrics, thermal performance estimation 0-88582
- oil immersed transformers, dissolved gas causes and phenomena, anal. (German) 0-76570
- silicon fluids, positive discharge propag., rel. to transformer oil 0-88926
- transformer, diagnosis by chromatographic analysis, computerised evaluation of results (Czech) 0-97744
- transformer oil, positive discharge propag., rel. to silicone fluids 0-88926
- transformer oil electrohydrodynamic flow, jet dynamic pressure obs. (Russian) 0-59117

insulating thin films

- see also *dielectric thin films; electronic conduction in insulating thin films*
- cadmium stearate based Langmuir films, deposition on p-CdTe, characts. and MIS struct. 0-92998
- hexamethyldisiloxane plasma polymerised thin film, charge trapping characts. 0-96895
- homogeneity during growth, determ. using vacuum automatic ellipsometer 0-101825
- PET, charge effects at Al electrodes obs. 0-75625
- polyacetonitrile in MIM capacitor, electroforming, negative resist., electron emission 0-80406
- polyethylene:Br₂(I₂), films, electron-beam induced carrier mobility and elec. breakdown 0-80429
- polystyrene:Br₂(I₂), films, electron-beam induced carrier mobility and elec. breakdown 0-80429
- polytetrahydrofuran in MIM capacitor, electroforming, negative resist., electron emission 0-80406
- rare earth aluminate, scandate and zirconate film coatings, electrophys. props. w.r.t. prep. technology 0-60781
- Al₂O₃, anodic film, trapped O₂ and effect on dielec. stability 0-100634
- Al₂O₃, anodic films, H conc. profiles meas. 0-75261
- Al₂O₃, anodic films, trapping levels study using TSC 0-103768
- Al₂O₃, CVD film on III-V semicond. substrate, ion beam etching, defect detection 0-89155
- Al₂O₃, thin film used in inelastic electron tunnelling spectroscopy, X-ray photoelectron spectrum 0-108319
- BaO, film, emission props. in relation to struct. 0-100501
- Bi₂O₃, thin film capacitor elec. props. under reduced press. 0-80397
- CaF₂, thin films, initial ionic thermocurrent meas. 0-97018
- Fe₂O₃, thin films, reactively sputtered, mechanical stresses rel. to deposition conditions 0-80146
- NiF₂ film preparation and characterisation 0-59815
- P₂O₅:SiO₂ glass film, thickness and IR spectrum changes on heat treatment in H₂ 0-70549
- RbCl films, breakdown on appl. of electric voltage pulses 0-66109
- Si-SiO₂ interfaces, carrier transport processes, electron states, conference, Durham, England (July 1979) 0-90612
- SiC, dielectric coating effect on surface polaritons, optical const. (Russian) 0-88489
- Si₃N₄, dielectric films made by NH₃-silane reaction, TEM study 0-84413
- Si₃N₄ films, prep., props. and appls., bibliography 0-94939
- Si₃N₄ layers deposition, high-temperature, in resistance furnace, temperature gradient and nitrogen flow influence obs. (Bulgarian) 0-80981
- Si₃N₄ layers produced by ion implantation, oxidation inhibition and etching 0-103374
- Si₃N₄, plasma-activated, passivation (Japanese) 0-85073
- Si₃N₄, room temp. CVD on InSb 0-71597
- Si₃N₄ sample substrates, high resol. electron beam fabrication using STEM 0-104104
- Si₃N₄, thermally stimulated depolarisation current meas. 0-88643
- SiO amorphous film, optical transmittance and reflectance, bulk optical props. determ. 0-88954
- SiO₂ CVD layer, high current injection from Si rich SiO₂ film 0-80430
- SiO₂ charge effects at Al electrodes obs. 0-75625
- SiO₂ deposited on Ge, optical constants, reflection spectra by Kramers Kronig method 0-76099
- SiO₂ film, on GaP substrate, N ion implantation, optical refl. and EPR meas. 0-84197
- SiO₂ film, prep. using high press. O₂, residual stress, chemical etch rate, refr. index and density meas. 0-71768
- SiO₂ films, DC plasma Si anodisation, dielectric const., O₂ pressure influence 0-70564
- SiO₂ films, growth on Si, role of defect structure 0-65403
- SiO₂ films, Si-rich, amorphous Si region obs. 0-84400
- SiO₂ films on Si, ellipsometric spectra, thickness determ. (Chinese) 0-86379
- SiO₂ in MOS structures, elec. props. with DC voltage (Slovak) 0-88634
- SiO₂ layer formation on polycryst. Si, morphological aspects 0-76388
- SiO₂ layer used for MOSFETs, electron trapping behaviour 0-92981
- SiO₂ layers on Si, ionic thresholds of electron traps 0-92983
- SiO₂, mobility and trapping of ions, Si-SiO₂ interface states 0-92985
- SiO₂, thermally grown films, thicknesses 30-600 Å, defect density meas. 0-84412

insulating thin films continued

- SiO₂ thin films, radiation-induced trapping centres, rel. to MOS transistor technology 0-107804
- SiO₂, thin films on rough polycryst. Si surfaces, oxide thickness and refractive index meas. 0-93422
- SiO₂ thin thermally grown oxide layers etching in HCl, ellipsometric control of Si surface form. (Russian) 0-104315
- SiO₂, ultrathin layers, refr. index meas. 0-103936
- SiO₂, vitreous layers, thermal growth on Si 0-93675
- SiO₂:As⁺ implanted layers in MOS struct., electron trapping and detrapping characts. 0-92982
- SiO₂, amorphous, acoustic study using Rayleigh waves 0-75312
- SiO₂, semi-insulating polycryst. films, AES and PES studies 0-107939
- SiO₂, thin films, deposition and characterisation study 0-80133
- WO₃, amorphous, struct. and crystn., TEM obs. 0-103606
- Y₂O₃, in MIM struct., electroforming props. 0-65705

insulation

- see also *cable insulation; electric breakdown; insulating coatings; insulating materials; insulators; machine insulation; transformer insulation*
- dielectric conduction and breakdown, conf., Gainesville, FL, USA (Oct.-Nov. 1979) 0-82564
- moistening diffusion kinetics, forecasting (Hungarian) 0-96692
- turbulent thermal insulation in magnetoplasma device, ion wave effects 0-106914
- X-ray tubes, rotary anode, HV insulation, discharges due to back scattered electrons elimination (German) 0-105758

insulation, thermal see *thermal insulation***insulation testing**

- cap-and-pin-type insulators, resistance to high current arcing for 110 and 400 kV power transmission lines (Polish) 0-70049
- composite insulating materials, fatigue behaviour, influence of superposition of elec., mech. and environmental stresses 0-97590
- crack inspection in foam insulation, using dye solution or X-ray opaque solution 0-76440
- electric insulating oils, composition, physical and chemical props. and determ. of free radicals (Rumanian) 0-97745
- epoxy resin insulation, adapted models selection problems for electric ageing (German) 0-89365
- fusion reactors, TFTR mag. field coil electrical insulation system and test results 0-93429
- insulators, HV for transmission lines, power arcs occurring in networks and laboratories, comparisons 0-87983
- power transformers, electromagnetic testing of partial discharges for failure and breakdown prevention (Russian) 0-97743
- SF₆ under impulse voltage stress, effects of pressure and vol. on firing delay (German) 0-87959

insulator-metal boundaries see *metal-insulator boundaries***insulator-semiconductor boundaries** see *semiconductor-insulator boundaries***insulators**

- i.e. *insulating devices*. For materials see *insulating materials*
- see also *insulation*
- contact electrification, expts. with solid rare gases 0-70797
- HV, influence of air pollution on dielectric rigidity (Slovenian) 0-64801
- HV for transmission lines, power arcs occurring in networks and laboratories, comparisons 0-87983
- thermal conductivity meas. of cast insulation materials 0-86293
- Al₂O₃ rod, damaged, mech. strength, surface defects effect, appl. as insulators (German) 0-76330

integer programming

- national energy policy anal. and planning models 0-101071
- nuclear power stations, optimal size and location in energy parks 0-95489

integral equations

- see also *integro-differential equations*
- acoustic radiation problem, Schenck numerical method (French) 0-69589
- alloys, binary, surface segregation kinetics 0-80044
- bending, axisymmetric elastic bodies with arbitrary boundary conditions, semianal. boundary integral 0-102969
- calculation of scattered sound fields near three dimensional objects 0-74558
- circular crack under general asymmetric loads, related integral eqns. 0-64483
- classical molecular fluids at equilibrium, integral equation derivation 0-64861
- complex resonator with internal diaphragm, diffr. losses and field distrib., integral eqns. 0-95921
- elasticity, nonlocal theory, stationary boundary problems, reciprocity principle and Green's tensors 0-68046
- electric arc, steady-state, energy eqn. soln., boundary value problem 0-79601
- electrodynamic suspension system, current coil interaction with semi-infinite superconducting sheet (Russian) 0-83539
- ELF propag. in nonstratified Earth-ionosphere waveguide, integral eqn. method 0-61959
- EM wave scattering by dielectric circular cylinders, elimination of resonant solns. of integral eqns. 0-63896
- equilibrium liq.-solid coexistence line, phase instability and direct correl. function integral eqn. 0-65196
- explicit integrals in celestial mechanics, new exact method for Hill's eqn. (Chinese) 0-105152
- extremum sufficient condition in classical action integral, eigenvalue problem, education 0-105462
- Fredholm 1st kind for acoustic calc. (Russian) 0-58834
- Galaxy stellar orbits, applicability of approximate third integral of motion 0-67798
- Griffith crack-antiplane shear wave interaction at interface of two bonded elastic half-spaces, geophys., seismological appl. 0-92087
- heat conduction, inverse problem, integral eqns. calcs. 0-74695
- hydrodynamics, half-immersed cylinder, virtual mass, integral equation method 0-87783
- Laplace eqn., axisymmetrical Koshi problem (Russian) 0-101713
- liquids, simple, thermodynamically self-consistent theories, radial distrib. function, functional derivative 0-92435
- nonmonotone stochastic integrals and stochastic differential calculus (French) 0-90779
- plane elastostatic boundary value problems, Rizzo's integral and Kupradze's functional eqns. 0-57093
- plane elastostatics, integral equations for mixed boundary value problem 0-79143

grain growth continued

- Mn-Al-C, fine-grained cast struct., remanence and coercive force 0-60365
 Mo film, evaporated, annealing behaviour, SEM obs. 0-65397
 Mo wire, struct. and high-temp. creep, dopant elements influence 0-66603
 Nb-Zr-Ni biphasic alloy, recrystallization annealing 0-104180
 Ni, alloying, influence on recrystn. and grain growth (*Russian*) 0-81071
 Pb, film, thermal strain, strain relax. above room temp. 0-59841
 Si, polycryst., CVD, recrystn. on heating 0-81017
 SiC-Al₂O₃ (0.61 to 1.2 wt.%), hot pressed, microstruct. 0-93563
 SrFe₁₂O₁₉-Si, Sr, second phase effect on elec. and mag. props. 0-60986
 α -Ti, cold rolled, primary recrystn., in situ investig. in HVEM 0-104185
 W wire, struct. and high-temp. creep, dopant elements influence 0-66603
 Zn-Al (22 wt.%), eutectoid, low stress and superplastic creep behaviour 0-81120
 Zn-Al (22 wt.%) superplastic alloy, grain growth texture 0-81075
 ZnO, fully dense, grain growth 0-93526
 ZnO:Bi, Sb, Co, second phase effect on elec. and mag. props. 0-60986

grain refinement

- steel, low alloy, ferritic-pearlitic, carbonitride hardening 0-104174
 Al-Ti alloy for use in aircraft, work hardening (*French*) 0-97502
 Al-Zn-Ti(Mn), mech. props., Ti or Mn addition effect (*Korean*) 0-93613
 Al-Zr (1-13 wt.%), rapidly quenched, extended solid solubility, grain refinement and age-hardening 0-76266
 steels, Cr-C-Mn(Ni), struct. prop. rel., design of struct. steels for high strength and toughness 0-97491
 Ti-Al-V (6.4 wt.%), β -annealed, subsurface fatigue crack initiation 0-108553

grain size

- see also grain growth; grain refinement
 Al thick probes, neutron transmission curves near Bragg-edge for grain size and texture eval. (*German*) 0-71667
 alloys, rapidly quenched crystalline, struct., and heat treatment effects 0-76292
 Baltic underwater coastal slope sand grain size and mineral composition (*Russian*) 0-76963
 body loading with cracks, energy conditions for brittle failure (*Russian*) 0-96234
 α -brass, fatigue crack propag., role of dislocation substruct. 0-60963
 brass, recrystallization during induction heating 0-97511
 brittle solids, microfracture resulting from anisotropic shape changes 0-88254
 [CC] Ag-(100)InP, metal-semicond.cathode contact, metallurgical, physical, chemical processes 0-107911
 ceramic materials, fine-grained, cyclic plastic deform. as cause for thermal expansion hysteresis 0-89290
 ceramics, coarse-grained, dimensional anal. of grain size depend. of fracture strength 0-70299
 ceramics containing metastable tetragonal ZrO₂, grinding induced tempering 0-89260
 Cr-Ni-Mo-V, austenite form. during heating, influence of recrystn. during tempering (*Russian*) 0-104188
 diamond, synthetic powder, thermal cond. 0-96702
 EPIQUANT, automatic structure analyser 0-85116
 F 0-100329
 ferrite, transform. kinetics, grain size, alloying element effect, carbide precip. 0-93560
 haematite, degree of reduction, potential relaxation due to cracks (*Russian*) 0-66770
 haematite reduction to magnetite, stress development mechanism (*Russian*) 0-93553
 ice, Antarctic, cryst. size and climatic record due to last ice age 0-94544
 Inconel 617, creep, morphological changes of carbides, affect on creep props. 0-108509
 Inconel 718, grain growth during sintering 0-97449
 kinetics of normal grain growth 0-71661
 metals, polycrystn., creep damage and cavity growth, assessment using density meas. 0-104217
 metals and alloys, BCC lattice, crit. embrittlement temp., struct. parameters effect (*Russian*) 0-66618
 monocrystal surface layer damage depend. on abrasive working parameters (*Russian*) 0-76368
 Ni-base wrought superalloy, creep and stress rupture behaviour in air and vacuum 0-60918
 nuclear fuel, gas release and swelling, operational model, grain boundary gas 0-95346
 olivine in Japanese peridotites, subgrain sizes rel. to uppermost mantle differential stress lateral var. 0-98275
 skeletonization in quantitative metallography 0-101002
 soap foam, arrangement of cells in a net. rel. to grain sections of polycryst. 0-70225
 stainless steel, machine faceted, low-energy ion erosion studies 0-80923
 steel, (0.36 wt.% C) Ni-Cr-Mo, electroslog refined, fracture toughness and fatigue behaviour 0-81171
 steel, austenitic, type 70, cold brittleness structural depend., fracture mechanisms (*Russian*) 0-97571
 steel, C, recrystallization annealing, grain growth, effect of type of deform. 0-100847
 steel, comp. and ferrite grain size influence on Ludwik eqn. constants (*German*) 0-81107
 steel, Cr-Mo (10-14, 2-6 wt.%), heat-resist., creep-rupture strengths 0-104271
 steel, creep rate mismatch interaction in stress relief cracking 0-97578
 steel, eutectoid, mech. behaviour, thermomech. treatment effects 0-84970
 steel, ferritic stainless, type 445 welds, ductility loss mechanism 0-85002
 steel, high alloy Cr-Mo-W, splat quenched, formation of metastable austenite 0-84974
 steel, high-speed tool, properties, powder metallurgy prep. method (*Czech*) 0-60800
 steel, low C, high cycle fatigue, crack initiation model (*Japanese*) 0-104258
 steel, low C type 08KP, plastic deform. depend. on grain size (*Russian*) 0-66580
 steel, low Si, martensite struct. and mech. props. (*Korean*) 0-93614
 steel, low-alloy, oxidation resist., N effect 0-66706
 steel, microalloyed, types V1599, V1600, V1286, NbCN precipitation in undeformed austenite 0-89230

grain size continued

- steel, Nb(V), (Al), hot-rolling, laboratory simulation, recrystn. of austenite 0-97512
 steel, pearlitic structural, austenite grains, growth rate during heating 0-100860
 steel, powder forged, fatigue, surface treatment effect 0-85048
 steel, stainless, shock loaded, residual martensite obs. 0-104414
 steel, stainless type 304, fabrication-related sensitisation 0-60887
 steel, structural, second phase particle effects on impact strength 0-108581
 steel, type 20Kh deformed, austenite grain size, inheritance effect with quenching and tempering 0-60881
 steel, type AC/HT-2, grain diameters, US attenuation 0-89429
 steel, W-Mo-Co, high-speed tool, struct. and props., cooling rate effect at primary crystn. temp. 0-76241
 steels, solute segregation and intergranular fracture 0-60957
 steels 4Kh4VMFSSh and 45Kh3V3MFSSh, grain size, hot deform. and austenitising effects 0-76286
 straight bar bending strength, brittle fracture energy conditions (*Russian*) 0-58974
 subgrain imaging, in bulk specimens to study localised plasticity using SEM 0-66609
 Zircaloy-2, pressure tubes, irradi. creep and growth, anisotropy factors 0-97536
 Al alloys, fatigue crack initiation, computer simulation 0-100893
 Al, cold rolling of 1100 plates, substruct. development 0-108476
 Al, creep behaviour, at high temp., influence of oxidation 0-97538
 Al film, lattice and bulk heat capacity meas. for normal and supercond. states 0-92684
 Al-Bi(Cd)(Pb)-Ti, containing low-melting pt. inclusions, mech. props. 0-93632
 Al-Mg (2 wt.%), hardening and fracture charact., β -phase dissolution role 0-81178
 Al-Ni (6 wt.%), fine-grained, deform. in tension and torsion 0-85008
 Al-Si, DC magnetron-sputtered, residual gas influence on props. 0-80968
 Al₂O₃ polycrystalline, effects of space charge, grain-boundary segregation and mobility differences on conductivity 0-79979
 Al₂O₃, vacuum condensate, struct. and mech. props., second phase effect (*Russian*) 0-71705
 Al₂O₃:Fe, pore form. during oxidative annealing, grain growth slowing 0-100856
 β -Al₂O₃:Na₂O, AC impedance, microstruct. and strength 0-100349
 β'' -Al₂O₃:Na₂O solid electrolyte, heat treatment effects on ionic cond. and microstruct. 0-65293
 Au, optical props., dielec. function, void model, sample effects 0-76048
 B fibre, US inspection, immersion method 0-66757
 BC, sintered, struct. and props. 0-104181
 BaTiO₃, polycrystalline ferroelectric, grain-size dependent props. 0-71352
 Bi₂MoO₆, superplasticity during phase transitions 0-108498
 Bi₂WO₆, superplasticity during phase transitions 0-108498
 CaF₂, strength-controlling fracture energy depend. on flaw-size to grain-size ratio 0-81152
 Cd, warm rolled, texture and grain size depend. of tensile props. 0-71720
 CdS-Cu₂S solar cells, microstructural study of heterojunction materials 0-93978
 CdSe thin film transistor on Cr substrate, cryst. struct., substrate defect effects 0-70563
 Cu, commercial, pure, vacuum environment end grain size effects on creep rupture props. at elevated temps. (*Japanese*) 0-81162
 Cu, creep damage and cavity growth, assessment using density meas. 0-104217
 Cu crystals, two-phase, recrystn. retardation, particle size, spacing effects 0-89242
 Cu, fatigue crack propag., role of dislocation substruct. 0-60963
 Cu, high-purity, grain size and strain rate influence on mech. behaviour, precursors existence 0-85016
 Cu, recrystallization annealing, grain growth, effect of type of deform. 0-100847
 Cu thick probes, subthermal neutron transmission curves, for Bragg grain size and texture eval. (*German*) 0-71667
 Cu-Cd (1.0 wt.%), yield stress and flow stress 0-97524
 CuInS₂ films, RF sputtered, growth and props. 0-80124
 Fe, Armco, Bauschinger effect, computerised evaluation method 0-93625
 Fe, Armco, grain size and strength depend. on nonmetallic inclusions (*Russian*) 0-100894
 Fe, cast, austenitic grain size determ. 0-81255
 Fe, creep at 77, 295K, formation of five struct. 0-60926
 Fe, grain growth, normal and abnormal, statistical distrib. of linear grain sizes 0-93581
 Fe thick probes, subthermal neutron transmission curves, for Bragg grain size and texture eval. (*German*) 0-71667
 Fe-Co-V(Ni), annealing effect on microstruct. rel. to mag. and mech. props. 0-89267
 Fe-Mn (1 at.%), strain age hardening 0-108472
 Fe-Ni, secondary recrystallisation singularities (*Russian*) 0-66528
 Fe-Ni-Al-Co-Cu-Ti YundK type, S effect on mech. props. 0-60927
 Fe-Ni-C (31.9, 0.02 wt.%) alloy, hardness of martensite-austenite mixtures 0-60959
 Fe-Ni-C (31.9, 0.02 wt.%), determ. of number and size distrib. of martensitic plates 0-76255
 Fe-Si, grain oriented sheet, AC hysteresis, surface struct. and elastic stress effects 0-88791
 Fe₃Pt austenitising conditions on M, temp. 0-81088
 GaAs, polycryst. solar cells, thin film growth and grain size, effect on cell efficiency 0-81471
 GaAs-Au polycrystalline Schottky barriers, transition with grain size from electrode-limit to bulk-limited cond. 0-65676
 Ge-Si alloys, hot-pressed, fine-grained, boundary scatt. of phonons, lattice thermal cond. 0-107583
 Ge-Si alloys, hot-pressed, fine-grained, boundary scatt. of phonons, theory 0-107584
 In_{0.9}Sn_{0.1}O_{3-x}, poly Si SIS solar cells 0-97787
 IrO₂, electrochromic, oxidation state changes and struct. 0-100950
 Li₂O-Al₂O₃-SiO₂ glass, crystallised, grain size and internal strain 0-103259
 MgAl₂O₄, strength-controlling fracture energy depend. on flaw-size to grain-size ratio 0-81152
 MgCa(CO₃)₂, dolomite, partial thermal decomp. into MgO and CaCO₃, product cryst. growth 0-108706
 Mn-Al-C, fine-grained cast struct., remanence and coercive force 0-60365

grain size continued

- MnZn ferrite powder prep., wet method 0-89180
 Mo alloy TSM-6, creep rate in vacuum, grain size effect 0-108514
 Mo film, evaporated, grain size and resist. 0-88650
 Mo film, sputtered, elec. resist., annealing and struct. effects 0-60109
 $\text{NH}_4\text{Cl}\cdot\text{H}_2\text{O}$, solidification microstructs., effect of reduced gravity 0-96632
 NaCl polycryst. containing Al_2O_3 dispersion, diffusive creep 0-97531
 Nb, creep rate in vacuum, grain size effect 0-108514
 Nb, granulated film, critical current temp. depend. (Russian) 0-103803
 NbC, vacuum condensate, struct. and mech. props., second phase effect (Russian) 0-71705
 Nb₃Ge, sputtered on Cu, film-substrate interface obs. by electron microscopy 0-65398
 NbN, granulated film, critical current temp. depend. (Russian) 0-103803
 Nb₃Sn, monofilaments, radiation-enhanced diffusion growth, crit. current density 0-65758
 Nb₃Sn multifilamentary composite supercond. wires, transverse sections prep., ion milling, TEM obs. of grain size 0-101000
 Nb₃Sn, powder metallurgically produced, microstruct. characts. 0-89233
 Nb₃Sn-Cu multifilamentary composite wire, Nb₃Sn filament morphology and grain size 0-100855
 Ni, creep at 77, 295K, formation of five struct. 0-60926
 Ni, creep rate at low stresses, effect of grain size 0-71707
 Ni-Co-Al alloys, continuous precip., SEM, TEM, X-ray diffr. study 0-89220
 NiO, stress relief and plastic flow in temp. range 1323-1473K 0-89302
 $\text{Ni}_{0.5}\text{Zn}_{0.5}\text{Fe}_2\text{O}_4$ coarse grain polycryst. ferrite, diffusional creep (Japanese) 0-104238
 Pb, film, hillock formation by grain boundary sliding 0-107673
 Pb, strength loss in supercond. state, size factor effect (Russian) 0-88677
 $\text{Pb}_{0.8}\text{Sn}_{0.2}\text{Te}$ crystals, Bridgman grown, X-ray perfection study 0-107018
 $\text{Pb}(\text{Zr,Ti})\text{O}_3$ films, ferroelec., ion beam deposition sputtered from multi-component targets 0-80974
 $\text{Pb}(\text{Zr}_{0.52}\text{Ti}_{0.48})\text{O}_3$, polycrystalline ferroelectric, grain-size dependent props. 0-71352
 239PuO_2 , stoichiometric, high-temp. deformation 0-81111
 Si, cast, growth structure and photovolt. props. of solar cells 0-94008
 Si solar cell parameters, grain size dependence 0-94049
 Si-SiO₂-Mo-Si₃N₄-Al MNOS structures with metal grains, charge transport at SiO₂-Si₃N₄ interface 0-65693
 Sn/Au thin film diffusion couples, Kirkendall void form. 0-96698
 Sn-Ni electrodeposited equatonic alloy, cryst. struct., X-ray, electron diffr. anal. 0-79748
 SnO₂-polySi solar cells, fabrication, grain size effects on device parameters 0-94045
 Steel, type 34Cr4, post-holding recrystallisation condition, use of NEOPHOT 2 and EPIQUANT 0-84949
 α -Ti, fatigue crack growth, influence of grain orientation, SEM study 0-108550
 Ti-Al-V (6.4 wt.%) superplastic alloy, maximum attainable ductility 0-60919
 TiB₂ thick film on low C steel substrate, CVD in US field, crystallite size 0-84854
 TiB₂, TiC, vacuum condensate, struct. and mech. props., second phase effect (Russian) 0-71705
 Va, creep rate in vacuum, grain size effect 0-108514
 WS₂, sputtered, props. for MOS IC appl. 0-70831
 $\text{Y}_2\text{Fe}_{10}\text{Al}_2\text{O}_{12}$, permeability spectra rel. to microstruct. 0-71100
 $\text{Y}_2\text{Fe}_{10}\text{Gd}_2\text{O}_{12}$, permeability spectra rel. to microstruct. 0-71100
 Y₂GdIG film, amorphous, mag. bubbles obs. and structural transformation 0-75824
 YIG, open die hot pressing, spin wave and FMR line width 0-89170
 YIG, permeability spectra rel. to microstruct. 0-71100
 Y₂O₃, strength-controlling fracture energy depend. on flaw-size to grain-size ratio 0-81152
 Zn-Al (1.1 wt.%) superplastic alloy, grain size determ. (Czech) 0-81118
 Zn-Al (22 wt.%), eutectoid, low stress and superplastic creep behaviour 0-81120
 ZnO sputtered films, undoped and Ga doped, props. rel. to deposition conditions 0-107935
 ZnO varistor ceramics, current-voltage characts., inhomogeneities and single barriers 0-80273
 ZnO:Ba, Co, rare earth metal varistors, microstructure-prop. relations 0-100249
 Zr-Nb (2.5 wt.%), pressure tubes, irradi. creep and growth, anisotropy factors 0-97536
 ZrO₂, partially stabilized, processing defects 0-97558
 ZrO₂, ZrB₂, vacuum condensate, struct. and mech. props., second phase effect (Russian) 0-71705

grain structure see crystal microstructure**grain subboundaries** see subboundary structure**grammars**

- parser for segmenting continuous speech into pseudo-syllabic nuclei 0-91985

gramophones

- signal rate of change, distribution meas. 0-79083

Granato-Lucke theory see dislocation damping**granular materials**

- see also granular structure
 abrasive, failure and strength characts. in US field, test unit 0-85112
 cracks, stress concentrations and shapes, Fourier transform methods 0-83761
 density measurement, plane strain conditions, acoustic method (Polish) 0-62635
 density measurement by pycnometry 0-69903
 elastohydrodynamic traction, granular behaviour 0-103008
 erevanit based glass, granulation and briquetting 0-60823
 flow from parallel sided bins, thickness of shear zone 0-81279
 flow round obstacles 0-103064
 fluidised beds, dehydration of solutions and suspensions, rel. to granulation 0-81373
 hot isostatic pressing in sheaths, process parameters calc. 0-84874
 inspection of part quality, coarse struct. materials, LF US methods 0-81264
 metal, granular superconductivity, instability 0-103796
 metal, inhomogeneous granular, superconductivity 0-103795
 metal granules, form. mechanism study during centrifugal atomisation of rotating blank 0-100798

granular materials continued

- metals, supercond. transition, increased resistance rel. to quasi-particle tunnelling 0-88689
 plastic flows, microscopic frictional effects, J₂-flow potential and yield function 0-64384
 random packing, statistical mech. considerations 0-104088
 rolling, granule kinematics 0-84875
 shear deformation, entropy model 0-84233
 Al alloy granules, lubricants for rolling 0-60980
 $\text{Al}_2\text{O}_3\cdot\text{ZrSiO}_4$, granular corundum-zircon refractory, development 0-66462
 CaHPO_4 , powder and granules with starch mucilage binder, surface topography variation under compression 0-80998
 $\text{Cr}_2\text{O}_3\cdot\text{ZrO}_2$ granules, from spray drying of suspensions 0-104100
 $\text{Fe-Al}_2\text{O}_3$ granular films, superparamagnetism and relax. effects 0-71118
 Nb granular films, ratio of supercond. transition temps. 0-84529

granular metallic thin films see discontinuous metallic thin films**granular structure**

see also granular materials

No entries

graph theory

see also trees (mathematics)

- aromaticity, reson. energy in graph theory 0-91412
 biological multistate systems, freq. of cyclic processes 0-108834
 field problems, multi-terminal representations appl., graph theoretical field model 0-90689
 infinite conjugated polymers, π -electron energy and energy gap, topological calcs. 0-91713
 mesh analysis using graph theory, generalised procedure, teaching 0-101681
 molecular energy levels 0-58123
 perturbation theory, diagrammatic, appl. to N₂, CO₂, BF 0-58131
 water-resource development project design, optimal apportionment scheme appl. (French) 0-77019

graphic equipment, computer see computer graphic equipment**graphics, computer** see computer graphics**graphite**

- (0001) surface adsorption of Xe, monolayer liquid and solid struct. 0-65400
 acceptor compounds, band struct. model and electrostatic effects 0-92814
 adsorbed Ar, Kr, overlayer-substrate spacing, LEED determ. 0-103579
 adsorbed Kr, submonolayer films, mol. dynamics simulation 0-88425
 adsorbed Kr monolayer, solid, commensurate to incommensurate transition 0-80079
 adsorbed Kr monolayers, commensurate-incommensurate transitions, low temp. theory 0-103582
 adsorbed layer of tetramethyltin, nature of 2 D diffusion 0-84372
 adsorbed neopentane, quasi two-dimens. fluid, NMR 0-102525
 adsorbed two-dimensional O₂, props. calc. 0-103568
 adsorption from Ar-N₂ liquid soln., mol. dynamics calc. 0-59806
 adsorption of ³He, selective, on (0001), level crossings 0-71556
 adsorption of Ar, multilayer adsorbed films, mol. theory 0-80058
 adsorption of H(D), on (0001) surface, vibr. spectrum, at. beam scatt. obs. 0-92779
 adsorption of He, surface band splitting, theory 0-60058
 adsorption of inert gas microcluster, temp. depend., mol. dynamics study 0-80056
 adsorption of O₂, partially localised, partially mobile monolayer films, adsorption isotherms 0-107646
 alkali intercalated graphite, C XXV Auger lineshape anal. 0-104019
 arc, in Ar flow, meas. of anode voltage drop 0-84022
 calorimeter in water phantom for absorbed dose meas. 0-74032
 carbyne form. in atm. of C stars and W Hydrae 0-67708
 chemisorption of O₂, influence of Fe as impurity 0-96732
 coarse grained, fracture toughness (German) 0-76358
 corrosion by CO₂, CO production radiolytically induced gas pressure effect 0-106115
 corrosion in PBHTGR process heat reactor following massive air ingress (German) 0-83181
 crucible material, Cu-Nb alloy prep. 0-84879
 cups for solid sample introduction into electrothermal atomiser 0-62734
 degassing rate measurement for fusion reactor appls. 0-102306
 diamagnetism with quasilinear dispersion law, orbital susceptibility, valence bands (Russian) 0-80475
 dispersed Al-Si, wear characts. (Korean) 0-93658
 dispersed particles in cast Al alloys, seizure resist. of composite alloys 0-89360
 Earth upper mantle, graphite abundance rel. to plate tectonics 0-81845
 electrode reactions with molten glass 0-85186
 electron-spectroscopic analysis of neutron-irradiated pyrographite 0-63261
 electronic struct., exact exchange HF calcs. 0-65438
 epoxy/graphite composite and cured epoxy resin, thermal expansion and swelling 0-92450
 epoxy/graphite laminate, T300/5208, proof testing under cyclic tension-tension fatigue 0-81249
 epoxy/graphite laminates, statistical fatigue, high load effect 0-93642
 fibre, surface anal. by XPS and polar/dispersive free energy anal. 0-65340
 fibre epoxy composites, eutectic coating moisture barriers 0-81228
 fibre epoxy laminates, low thermal expansivity, design considerations 0-81031
 fibre filled phthalocyanine composites, cure cycle investigation 0-81030
 fibre filled polyimide composite laminates, space environment, phys. and mech. response 0-81140
 fibre filled polyimide composite prepreg laminates, room-temp. ageing effect 0-81093
 fibre reinforced composites, damage by moisture, diffusion anal. 0-81227
 fibre reinforced epoxy, single ply, thickness effect of percolation and cond. 0-92953
 fibre reinforced epoxy composites, exposed to high temp., degradation of tensile and shear props. 0-81113
 fibre reinforced glass, impact damage tolerance and reliability 0-81177
 fibres, structure obs., Raman microprobe-microscope appl. 0-62737
 fluorides, (CF₃)₂ and (C₂F₆)_n, prep., struct., discharge characts., electrode props. 0-89502
 frequency distribution based on unfolding technique 0-92619
 gasification, Fe-catalysed, electron, microscopy 0-104358
 graphite, zone-axis pattern maps 0-100137
 graphite-air mixture steady and oscill., mean heat transfer 0-89536

integration continued

- objective and regular differentiation and integration, constitutive law and transport (*French*) 0-57090
- steady-state laminar flow in turbulence amplifier, numerical method (*Bulgarian*) 0-106779
- Fe, cast, US flow detection by boxcar integration 0-89437

integro-differential equations

- see also Boltzmann equation; Fokker-Planck equation; Liouville equation; master equation; Vlasov equation
- Brownian motion, generalised scalar case, computer simulation 0-77704
- dielectric, damped integrodifferential eqns., asymptotic bounds to system of solns. 0-62493
- nerve fields, topographic organisation 0-89742
- open systems, eqns. of motion in nonequilibrium. statistical mechanics 0-82710
- radiative transfer, time-dependent, exact soln. of integro-differential eqn. via Laplace transform 0-94703
- radiative transfer in finite atmosphere, exact soln. of basic eqn. via Laplace transform 0-94702
- three-dimensional neutron transport, discrete ordinate solution 0-63222
- Volterra equation, nonlinear, compactness of bounded trajectories of dynamical systems 0-82636
- wave reflected from randomly inhomogeneous layer description, by series satisfying causality condition 0-106420
- waves, gravity, on deep water, finite-amplitude steady irrotational inviscid waves 0-64575
- N, high intensity arcs, anode contraction region modeling 0-103210

intelligence, artificial see artificial intelligence**intelligibility, speech** see speech intelligibility**intensification** see amplification**intensity measurement**

- see also acoustic intensity measurement
- No entries

interacting control systems see multivariable control systems**interactive systems**

- see also interactive terminals; online operation
- electric field computation using SCOFF program (*German*) 0-78740
- interactive graphics system developed for NDT 0-66729
- molecular analysis system, MOLY, design of biologically active compounds 0-63852
- solar buildings, climatological design assessment interactive CAD techniques 0-61289
- Spectronic 2000 spectrophotometer, interactive microprocessor-controlled instrument 0-105716

interactive terminals

- see also interactive systems
- computer-aided optical design, optimisation and interactive graphics improvements 0-78933

interatomic potentials see potential energy functions**intercalation compounds**

- alkali intercalated graphite, C XV Auger lineshape anal. 0-104019
- alkali ionic conductors with sheet structures, ion mobility and influences 0-107522
- $C_8^+MF_6^-$ ($M=Os, Ir, As$), struct. and elec. props. 0-70183
- dichalcogenide hosts, intercalation and substitution-intercalation cpds., factors affecting ion mobility 0-59707
- electrode materials, thermodynamic and transport props. 0-66963
- ethidium bromide E-DNA, intercalated birefringent fibres, microspectrophotometric investig. (*German*) 0-57392
- graphite, electrostatic interactions and staging, nonlinear Thomas-Fermi eqns. 0-107732
- graphite, Fermi surface and transport props., LCAO model 0-80159
- graphite, struct. and phys. props., symposium, San Jose, USA (March 1979) 0-62379
- graphite acceptor compounds, band struct. model and electrostatic effects 0-92814
- graphite $FeCl_3$ intercalate, interpenetration of 'stages' direct imaging 0-84037
- graphite intercalated with AsF_5 , quantum oscillatory phenomena 0-107823
- graphite intercalation compound, interaction between one or two s orbitals (*French*) 0-65440
- graphite intercalation compounds with Br, K, ^{13}C NMR spectra 0-66048
- graphite intercalation cpds., high elec. cond., engineering appl. 0-70780
- graphite intercalation cpds. with AsF_5 and SbF_5 , synthesis and elec. props. 0-70781
- graphite intercalation with Li, Raman scatt. study 0-88999
- graphite nitrates, elec. props. perpendicular to layers, resistance, magnetoresistance, charge transport mechanisms 0-80268
- graphite- AsF_5 intercalated species, fractional ionisation and identification 0-97397
- graphite- Br_2 intercalation cpds., EXAFS study 0-71515
- graphite- Br_2 stage 2 cpds., Raman spectra 0-80787
- graphite- HSO_3F intercalation compound, Raman spectral study (*French*) 0-60581
- graphite-K, effect of H addition on superconducting transition temp. 0-70872
- graphite-K, electronic props., resistivity, Hall effect and magnetoresistance 0-75585
- graphite-K intercalation compounds, electronic props., de Haas-van Alphen effects and Fermi surfaces 0-75498
- graphite-Rb, superlattice struct., electron diff. study 0-75214
- layer and tunnel compounds, fast ion transport and electrochem. storage 0-61324
- layer structures, intercalation with N_2H_4 , charge density waves or artefacts 0-100221
- layered structures, intercalation, crack propag. theory 0-97559
- neutron scattering from adsorbed mol., surfaces and intercalates, review, book contrib. 0-84394
- NMR investigation in solid soln. electrodes, review 0-60432
- photo-intercalation: possible application in solar energy devices 0-108803
- staged, phase diagrams 0-60849
- transition model chalcogenophosphates, intercalation with n butyl-lithium, possible appl. in Li batteries 0-71446
- $Al(OH)_3$, intercalation with Li ions, X-ray diff. patterns and comp. determ. 0-76502
- AsF_5 -graphite intercalation compound nature 0-103308
- $C_8Br_xCl_{1-x}$ intercalate, crystallographic, elec., mag. props. 0-107184

intercalation compounds continued

- $C_6Eu(Yb)(Ba)$ intercalation compounds, three dimensional continuous melting 0-59631
- $C_{64}FeCl_3$, stage 1, dielec. response and intraband plasmon dispersion 0-59902
- $C_{12}^{2+}PtF_6^-$, struct. and elec. props. 0-70183
- $C_{24}Rb$, intercalated graphite, resistivity and specific heat anomalies 0-107440
- $C_{24}Rb$, intercalated graphite, order struct. determ. by neutron scatt. 0-107143
- Co, electron microscopy 0-84164
- Fe, electron microscopy 0-84164
- $Fe_{0.33}NbS_2$, lattice dynamics and hyperfine interactions, Mossbauer spectra study 0-108135
- $FeTiS_2$, lattice dynamics and hyperfine interactions, Mossbauer spectra study 0-108135
- KC₂₄, press. induced staging transition 0-79938
- Li incorporated transition metal oxides, topochem. reactions, chem. prep. and characterisation 0-61115
- Li intercalated atoms, host lattice strain effects 0-88082
- $LiTiS_2(TiSe_2)(Ti_1S_2)$, electrochem. obs. of Li intercalation 0-61216
- LiC_6 and LiC_{12} , electronic struct. calcs. 0-70613
- LiC_6 , intercalation compound, electronic struct., XPS meas. 0-59850
- $LiFePS_3(Se_3)$, $LiMnPS_3$ and $LiNiPS_3(Se_3)$, NMR and neutron diff. obs., mag. props. 0-60433
- $LiTaS_2$ and $LiTiS_2$, chem. diffusivity of Li at 30°C 0-59737
- $LiTiS_2$, alkali ion ordering, X-ray study 0-107165
- $LiVS_2$, intercalation cpds., electron chem., ionicity 0-89501
- $LiWO_3/LiTiS_2$, cyclable organic electrolyte cell, using 2 intercalation electrodes 0-76625
- Na-graphite intercalates, preparation, struct. 0-103307
- $NaTiS_2$, alkali ion ordering, X-ray study 0-107165
- $Na_2Y_2Zr_{1-x}S_{12}$, ionic cond. and NMR mobility obs., comp. depend. (*French*) 0-70459
- NbS_2 intercalate with tetraalkylammonium hydroxide, prep. and struct. 0-79752
- NbS_2 -(pyridine)_{1/2} intercalation complex, superlattice struct., NMR meas. 0-70180
- $NbSe_2$ pure and intercalated with ethylenediamine, positron annihilation study 0-84801
- Ni, electron microscopy 0-84164
- PbI_2 -pyridine(aniline)(pyridine), heat capacity of low temp., intercalation effect (*Russian*) 0-92682
- Pt, electron microscopy 0-84164
- TaS_2 and $Ta_2S_5Se_{0.4}$ intercalated with organic cpds., supercond., upper crit. fields and reduced dimensionality 0-70910
- TaS_2 intercalate with tetraalkylammonium hydroxide, prep. and struct. 0-79752
- TaS_2 intercalated with methylamine, supercond. layer cpd., crit. field enhancement and reduced dimensionality 0-60152
- TaS_2 -2H electrodes, topotactic reduction mechanism, neutron diff. obs. and intercalation cpd. form. 0-108748
- $Ta_2S_5(NH_3)$ and $Ta_2S_5(NH_3)_{1/3}(H_2O)_{2/3}$, incoherent inelastic neutron spectra 0-84163
- $(TiNbO_5)^-$ oxide layers, intercalation of alkylammonium ions 0-64985
- ZrB_2 , self-consistent band struct., XPS, reflectance, NQR, Hall effect and density of states meas. 0-70689

interdiffusion see diffusion**interface electron states**

- amorphous semiconductor-insulator boundary, density of states determ. from field effect data 0-107688
- anisotropic transition layer, surface polariton spectra in presence of resonance 0-88484
- covalent semiconductors, electronic interface states in intrinsic stacking-faults 0-75522
- defects, scatt. theory 0-84498
- epitaxial thin films with neg. electron affinity, photoelectron energy distrib. 0-100755
- III-V semiconductor based layered multielectronic systems, electronic process investig. survey (*Russian*) 0-107891
- III-V semiconductor-oxide interface states, photoemission obs. of energy levels induced by adsorp. 0-93000
- metal-semiconductor disordered interface, supercond. transition temp. enhancement by bipolaron interface centres 0-84528
- metal-tunnel oxide-Si junctions, processing condition depend. 0-80380
- MIS solar cells, computer simulation studies rel. to interface state meas. 0-72048
- MIS structure, surface state density, determ. from surface saturation photo-EMF meas. 0-75652
- MIS tunnel structure, injection and extraction effects, self-consistent model 0-92996
- MIS/SIS solar cells, automated surface states anal. 0-93966
- MOS capacitor, interface state parameter determ. by DLTS 0-65642
- MOS capacitors, n-type, optically active interface states study 0-60096
- MOS interface states density, photoemission obs. using photocurrent and photocapacitance meas. 0-92990
- MOS inversion layers, freq. response of charge transfer 0-88638
- MOS structure, semiconductor conductance and capacitance, extended AC conductance-bias method 0-96995
- MOS structure, space charge layer physics 0-92980
- MOS structures, quasistatic and nonequilibrium phenomena with constant gate-current bias 0-80385
- MOSFET, near-ideal Si-SiO₂ interfaces using CVD, props. 0-80382
- p-n heterojunction differential admittance theory in the presence of surface electron states 0-96981
- Schottky barrier solar cell, rel. to efficiency 0-76637
- Schottky-barrier diodes, resonant tunnelling spectroscopy, deep centre detection 0-96968
- semiconductor surface eval. using SAW convolver 0-97677
- semiconductor-insulator interface, microcomputer-aided interface-state analysis 0-80383
- superconductor-oxide interface, surface states, enhanced tunnel conductivity 0-80456
- $Al-Al_2O_3$ -p-GaAs MOS diode, capacitance-voltage characts. 0-107914
- Al-anodised Ta_2O_3 /native oxide-n-GaAs MOS structure evaluation 0-84514
- $Al_{0.33}Ga_{0.65}As$ -GaAs N-p heterojunction diodes, current suppression by cond. band discontinuity 0-80362
- Au-Si interface, electron energy loss and AES meas. 0-89096

interface electron states continued

- Au-Ti/SiO₂/p-Si MOS struct., interface state distrib., DC tunnelling spectra determ. 0-75611
- CdS-Au contacts, electronic states, vacuum UV photoelectron spectra 0-70827
- CdS-Cu₂S heterojunction, energy-band struct., capacitance-voltage characts., illumination effects 0-96982
- CdSe-Au contacts, electronic states, vacuum UV photoelectron spectra 0-70827
- CdSnAs₂-InP, n-p heterojunction, elec. props., electroluminesc., band struct. 0-75632
- CdTe-Au contacts, electronic states, vacuum UV photoelectron spectra 0-70827
- CdTe-CdS heterojunctions, growth by closed-tube chem. transport, elec. props. 0-60070
- CdTe-CdS heterojunction, photocapacitance and photocond. 0-96978
- p-CdTe-Langmuir film interface, prep., characters. and MIS struct. 0-92998
- Cr-SiO₂-Si MIS solar cells, photovoltaic performance and interface states, nucl. radiation effects 0-94004
- Cu (111)/Na interface, UPS study of surface electronic struct. 0-80350
- Cu₂S-CdS heterojunction solar cells, carrier transport, nonmonotonic band profiles 0-61361
- Cu₂S-CdS solar cells, interface recombination phenomena and tunnel effect 0-66978
- (Ga, Al, As) heterostructures and compounds, electronic props., empirical pseudopot. calc. 0-80366
- GaAs (110), with Al or Ga overlayers, interfacial electron states, UPS and LEED obs. 0-80377
- GaAs, surface passivation using Si₃N₄, interface characts. 0-93005
- GaAs type FET with buffer, bias effects due to deep centres in struct. (French) 0-107917
- GaAs/anodic oxide interface, characterisation of proposed model 0-103754
- GaAs-Al_{0.1}Ga_{0.9}As heterojunction interface, two-dimensional hole gas obs., Shubnikov-de Haas meas. 0-80357
- GaAs-AlGaAs heterojunction superlattices, inelastic light scatt. by two-dimens. electron gas 0-93360
- GaAs-GaSe n-p heterojunction, elec. props., interface states 0-65670
- n-GaAs-SiO₂ interface, MOS capacitors, surface states from conductance and capacitance meas. 0-100533
- GaSb-InAs system, (110) surface and interface electronic struct. 0-100494
- Ge/GaAs (110) heterojunction, valence band discontinuity in XPS spectra, precise determ. 0-84834
- InP, and In_{0.5}Ga_{0.5}As_{1-x}P_{1-y} binary and quaternary cpds., surface and dielec.-semicond. interface props. 0-93001
- InP inversion-type MISFET with SiO₂ gate insulation interface props., elec. drift 0-93002
- InP-Si₃N₄ (SiO₂), interface props., plasma deposited dielectrics, n-channel MOSFET action 0-93003
- n-InSb based MIS struct., carrier generation under nonequilibrium conditions 0-88640
- MOS capacitor, photoionisation cross section and interface state density 0-92974
- Pb_{1-x}Hg_xS-Si heterojunctions, elec. props. 0-100513
- PbS-Si heterojunction, space charge capacitance, PbSn film thickness depend. 0-88630
- Pd-SiO₂, work function changes due to adsorbed H₂, surface and interface dipoles 0-96972
- Si, cast polycryst. p-n junction solar cell, hydrogenation effects 0-93916
- Si-Au, interface study using EELS 0-97391
- Si-GaSe n-p heterojunction, elec. characts., interface states 0-70812
- Si-Ge heterojunction form., microscopic aspects, EELS meas. 0-80368
- Si-PbS heterojunction, effect of Si substrate orientation on struct. and interface props. 0-80097
- Si-Si interface, elec. cond. rel. to interface state population 0-65672
- Si-Si₃N₄ interface in MNS capacitors, surface state density investigation 0-60100
- Si-SiO₂, interface, doping depend. of interface states and charges 0-92992
- Si-SiO₂, MOS interface states density, meas. techniques and model development 0-92988
- Si-SiO₂, boundary, surface charge transport in valence band of Si 0-70789
- Si-SiO₂ interface, density of states, theory 0-80395
- Si-SiO₂ interface, electronic struct. calc. 0-100531
- Si-SiO₂ interface, improved characterisation, refined quasistatic and cond. methods 0-96990
- Si-SiO₂ interface, O₂ plasma effects on elec. props. 0-100523
- Si-SiO₂ interface, thermally grown, surface pot. inhomogeneities after stress ageing 0-92993
- Si-SiO₂ interface, unwanted effects of ions in SiO₂ layers, review 0-92985
- Si-SiO₂ interface in MOS device, indirect tunnelling involving intermediate states 0-92994
- Si-SiO₂ interface in MOS solar cells, operational characts. and struct. 0-93901
- Si-SiO₂ interface state density in ion-controlled diodes, acid-base exposure effects 0-96984
- Si-SiO₂ interface states, deposition of H containing layers and annealing 0-92991
- Si-SiO₂ interfaces, carrier transport processes, electron states, conference, Durham, England (July 1979) 0-90612
- Si-SiO₂ MOS capacitors, relationship between trapped holes and interface states 0-70830
- Si-SiO₂ MOS interface states density, transient capacitance meas. eval. 0-92989
- Si-SiO₂-Si₃N₄ MNOS structure, chem. comp. and electronic states, Auger and energy loss spectra obs. 0-92999
- SiO₂-GaAs, vacuum evaporated system, acoustoelec. signal, interface props. 0-75646
- TiO₂-Ni (100) interface, electronic props., struct., comp., chemical bonding 0-84499
- ZnO/Si SAW structs., anal. of charge injection 0-80049
- ZnO-grainboundary-ZnO junction in ceramic varistor, capacitance-voltage characts. 0-65689

interface phenomena

- see also adsorption; crystal surface and interface vibrations; interface structure; Kapitza resistance; semiconductor-electrolyte boundaries; surface phenomena
- 3 GHz surface and lateral EM wave meas. 0-103742
- adhesion, surface and interfacial aspects, review 0-108690
- adhesion, surface chemistry studies, anal. appls. 0-88440
- adhesion between solid surfaces 0-88438
- air-dielectric interface, EM wave reflection and transmission in terms of polarisation, education 0-105458
- alloys, binary dilute, solidification, planar interface stability (Czech) 0-89212
- amino acid residues, form. of mixed micelles and relative compatibility at interface 0-71951
- binary alloy interdirectional solidification, convective and interfacial instabilities 0-60851
- capillary wave propagation, experimental test of theories 0-69847
- charged hard-sphere fluid, electrified interface pot., extended mean spherical approx. calcs. 0-84502
- colloid system, forces of mol. attraction between solids, effect of EM lag 0-71949
- composites, single fibre-brittle zone model, fracture behaviour 0-97570
- contact behaviour of surfaces, of small nominal area 0-64493
- covalent or ionic-covalent crystals, dislocation-free contact 0-80096
- crack between dissimilar media, biaxial load effects 0-99968
- cylindrical rod, periodic structure, torsional vibrations, interfacial elastic parameters 0-96215
- drop deformation and orientation in shear and extensional flow fields, dynamic interfacial props. 0-107611
- drop dynamics in shear fields, role of dynamic interfacial effects 0-107612
- electrode surface, anisotropy of optical props. 0-60534
- ferrite-austenite (α - γ) interface, Fe self-diffusion compared with grain boundaries diffusion 0-65306
- ferromagnet-semiconductor contact, spin-depend. recomb. and scatt. on electron injection 0-65654
- fibre-resin composite, interfacial interactions and bonding, fibre surface props. 0-80046
- fluid/fluid interfaces, capillary phenomena, review 0-70506
- glass fibres-resin interface studies 0-93531
- hard spheres permeation through hard disc monolayers, interfacial mass transfer 0-107460
- immiscible incompressible fluids, interfacial convective instability, diffusional exchanges, adsorption-desorption processes 0-70504
- interfaces, co-segregation of metallic and non-metallic impurities 0-60868
- interfacial tension var. with supersaturation, one-layer adsorpt. model 0-103563
- ionic crystals, coupling of interfacial charge transfer and bulk transport 0-79986
- Kapton fibre reinforced phenolic resin, fracture kinetics, interface props. 0-66640
- liquid boundary layers, struct. and thermodynamic peculiarities 0-88408
- liquid-solid interface transmission IR spectroscopy 0-98985
- liquid-solid interfaces, scanning laser probe for acoustic wave phenomena observation 0-100386
- liquids, laminar flowing, concurrent, in horizontal cylindrical channel, mass transfer across interface of liquids 0-79397
- liquids, potential and flux conserving static equilibria in elec. or mag. fields, determ. 0-88399
- magnetic alloys, binary, spinodal decomp., computer simulation study of interface behaviour 0-84913
- metal-electrolyte interfaces, optical reflectance spectra, interpretation 0-93263
- MIS solar cells, interface problems, AES, SIMS and XPS study 0-89627
- monolayers, surface pressure at air-water interface, meas. technique 0-89526
- optical surface wave at a nonlinear interface 0-91867
- phthalocyanine-alkane interface, charge transfer, rel. to photoelectrochromic image form. 0-65616
- planar double layers, Derjaguin force formula 0-107890
- poly(dihydroxypropyl methacrylate), surface charact., by contact angle methods 0-61140
- poly(hydroxyethyl methacrylate), surface charact., by contact angle methods 0-61140
- poly(methoxyethyl methacrylate), surface charact., by contact angle methods 0-61140
- polypropylene fibre reinforced polyoxyethylene, fracture kinetics, interface props. 0-66640
- polystyrene interfacial colloidal crystals, microscopic obs. 0-97737
- protein film, at liq. interfaces, dilatational props. 0-94255
- pyrene dodecanoic acid, lateral diffusion at air-water interface, monomer excimer dynamics 0-92693
- radiation propagation analysis, layer decomp. method (French) 0-95772
- screw like dislocations behaviour with lattice frictional forces 0-64999
- semiconductor-electrolyte boundary, hot carrier injection, tunnelling from semiconductor states in depletion region 0-75637
- solid-liquid interface, wetting and adhesion, thermodynamic aspects 0-89525
- solid-liquid interface free energy anisotropy clustering influence 0-80054
- solid-solid interface chemistry, characterisation, theory 0-75448
- solvent structure, at polarisable interfaces, mol. models, review 0-59359
- spherical particles, force exerted by freezing interface 0-107083
- stability of interfaces which separate compressible bulk phases 0-107610
- stable surface chemical reactions, interfacial hydrodynamic instability 0-66874
- steel, austenitic stainless, MC precipitate comp., APFIM study 0-104161
- steel 45-antifrictional alloys friction pairs, electrochem.-mech. investigation (Russian) 0-76367
- superconducting ultra-thin films, transition temp., interface and fluctuation phenomena 0-84527
- supersaturated soln., shape stability of growing cylindrical particle due to diffusion and interface kinetics 0-79720
- surface thermodynamics, fundamental eqns. 0-107630
- thermoelectric cooling equipment, welded joints, heat emission effects on temp. distrib. (Russian) 0-69635
- total reflection and surface wave obs. 0-108292
- two-phase anisotropic medium, interfacial dislocation, stresses, displacements and energy calc. 0-79786
- Al₂O₃, fine grained, interface-controlled diffusional creep 0-60915
- GaAs MIS solar cells, effects of thin oxide layers on characts. 0-89624

interface phenomena continued

- GaAs-Au(Ag) Schottky barrier solar cells, interface problems, AES, SIMS and XPS study 0-89627
³He-⁴He mixture film, 2-D interface excitation spectrum 0-96718
³He/solid interface, refl. of transverse zero sound (*Russian*) 0-70492
⁴He, liquid-solid boundary, capillary sound motion, Kapitza resistance (*Russian*) 0-92737
 Ni films, electronic struct. calc., effects of chemisorption; contact pot. and surface magnetisation 0-103734
 Ni-Fe, electronic struct. calc., effects of chemisorption; contact pot. and surface magnetisation 0-103734
 Ni-Sn intermetallic phase growth kinetics at liq. Sn-solid Ni interface 0-71638
 PbSnF₆, anionic conductor, thin films and ceramics 0-107556
 Si-SiO₂ interface, stress meas. technique 0-84395
 Ti metal-metal interface, adhesion energy, surface treatment and ion implantation effects 0-107660
 U extraction by transfer between liq. phases, laser radiation effect 0-66795
 V₂O₅-AlNbO₄(GaNbO₄)(TiNb₂O₇) systems, interfacial reactions, efficient boundary conditions and solid state reactivity 0-76542

interface structure

- adhesion, surface anal. techniques appl. 0-65381
 analysis by combined Auger, X-ray and SEM studies 0-81413
 atomic structure, interface roughness, calc. (*Russian*) 0-103587
 bonded interface defect testing by differential interferometric Stoneley wave meas. 0-76444
 brass, two phase α/β bicrystal, transgranular slip and fracture across an interface 0-81150
 conductor-insulator-semicond. (CIS) solar cells, noncrystalline (poly and amorphous), interface importance 0-81466
 FCC crystal-melt interfaces, mol. dynamics simulation 0-79913
 glaze/glass-ceramic, interface reactions, electron microprobe anal. 0-84398
 grain boundaries, interfacial structure effects on high temp. mechanical behaviour 0-59480
 III-V semiconductors, surface and interface anal., secondary ion mass spectrometry technique 0-59763
 interface study by Auger spectroscopy 0-76587
 metal-dielectric interface, static point charge in dielec., pot. distrib. (*Russian*) 0-60088
 metal-semiconductor interfacial reaction, AES study (*Japanese*) 0-96701
 MNOS structures, electron-beam-irrad., interface defects, high temp. H₂ anneal 0-96745
 multilayer superlattice stacks, very thin nonideal, wavelength variation of transmissivity, refl. 0-100701
 polarisable interface, solvent struct., mol. models 0-59359
 rubber-metal interface, adhesion mechanism, XPS study 0-65382
 semiconductor film growth, multilayer systems, spectroscopic ellipsometry, review 0-103603
 SIMS, interfacial impurities, quantitative anal. 0-84396
 solid-solid interface chemistry, characterisation, theory 0-75448
 steel, dual phase HSLA, compositional anal., TEM 0-85253
 steel, spheroidization of pearlite, global microstruct. evolution 0-108482
 steel plates, explosively clad, fatigue crack propagation behaviour (*Japanese*) 0-104262
 thin films and interfaces, analytical techniques, review 0-80120
 Ag film growth on Pd substrate, interface cpd. form., AES study (*French*) 0-80131
 Ag-Al (26 at %), massive transform, β - β' , crystallography and morphology 0-97475
 Ag-InP interface, Ag₂P formation during sintering 0-65309
 Ag-Mg two phase bicrystal growth, orientation, interface struct. 0-60773
 Al/Cu thin film couples, TEM study of intermetallic nucleation at interface 0-65305
 Al-Ge(001) interface, struct., total-reflected X-ray diffr. 0-88441
 Al-Zn alloys, interfacial stability of planar solid-liq. interface during solidification 0-104145
 Al-Zn alloys, interfacial holes distrib. at beginning of interfacial instability in solidification 0-104146
 Al_{0.8}Ga_{0.2}As epitaxial layers on GaAs, struct. study by scanning Auger electron microscopy 0-80110
 Al₂O₃-glass seals, diffusion of Al, electron microprobe study 0-107577
 Au-Ag, bicryst. thin film couples, interphase interfaces, TEM 0-70540
 Au-Pd, bicryst. thin film couples, interphase interfaces, TEM 0-70540
 Au-Si thin film double layer, silicide form., electron diffr. study 0-80005
 Au-W, FIM obs. 0-65384
 BN, contact reactions with Ti and WC-Co at high pressures 0-61029
 CdGeAs, vertical Bridgman growth with control of interface shape and orientation 0-66420
 Cd(S, Se) film grown on InP substrate, mismatch dislocations and lattice distortion, dangling bond density 0-84406
 CdS-Al(Au) interfaces, bonding and interdiffusion, XPS obs. 0-80000
 CdS-Cu-S solar cells, microstructural study of heterojunction materials 0-93978
 Co-Si interface, glassy layer, ellipsometric charact. 0-103589
 Cu on Fe (001) substrate, orientation relationship 0-65415
 Cu-mild steel explosively welded interface, SEM examination (*German, English*) 0-96746
 GaAs based MOS capacitors, scanning photovoltage investigation 0-80396
 GaAs, polycryst., wet and dry oxides, comparative study by AES, SIMS and XPS 0-80116
 GaAs-Ga₂Al_{0.8}As_{0.2}Be, LPE, diffusion of Be into GaAs substrate 0-103517
 GaAs-Ge, heterostructure, zincblende-on-diamond type systems, MBE growth, (110) orientation as preferred orientation 0-80099
 n-GaAs-metal Schottky barrier, ultrathin native oxide, thickness determ. from C-V and photoresponse meas. 0-70821
 GaP, VPE layer structures for LEDs, SEM, and TEM obs. of dislocation density reduction expt. 0-100425
 GaP-Si, heterostructure, zincblende-on-diamond type systems, MBE growth, (110) orientation as preferred orientation 0-80099
 Ge-GaAs, heteroepitaxial systems, misfit dislocations obs. using HV electron microscopy 0-100424
 Ge-GaAs heterojunction, elec. and recomb. props., interface defect effects 0-80365
⁴He, solid-superfluid interface, struct., surface tension 0-88380
⁴He, solid-superfluid interface, roughening transition 0-103536

interface structure continued

- InGaAsP LPE heterostructs., interface grading, Auger depth profile 0-103585
 InP/In_{0.5}Ga_{0.5}As_{0.5}P_{0.5} interfaces, sputter-profiled, depth resolution degradation by cone form. 0-80094
 InP-Al interface struct., low temp. interaction, AES study 0-107661
 Li₃N thin film, vacuum evaporation on WO₃, retarded deposition 0-108351
 MgO-CdO, interface, coincidence-site-lattice relations 0-103588
 Mo-Si film-substrate interface, reaction on heat treatment, silicide formation 0-79999
 NaCl-KCl system, interdiffusion, miscibility, Kirkendall effect 0-107568
 Nb₂Ge, sputtered on Cu, film-substrate interface obs. by electron microscopy 0-65398
 Ni on Fe (001) substrate, orientation relationship 0-65415
 Ni-Al-Ta dendritic monocrysts., directionally solidified, coarsening kinetics 0-108425
 Ni-Cr(Fe)(Cu) alloy, matrix effect in SIMS anal. using O₂⁺ primary beam 0-76576
 Ni-Ge-Au evaporated contacts on GaAs, TEM obs. 0-75449
 Ni-Si(111), interface, reactivity and struct., ion channelling meas. 0-92788
 NiO-Al₂O₃ reaction at film-substrate interface, Rutherford backscatt. obs. 0-59733
 PbS-Si heterojunction, chem. struct., AES anal. 0-76115
 PbTe-In contacts, fabrication and props. 0-60078
 Pb_{1-x}Te-Pb_{1-x}Sn_xTe (x,y \leq 0.3), double heterostruct., LPE growth, heterostructure morphology 0-70550
 Pd-Si structure, epitaxial silicide growth, LEED and AES study 0-103590
 PtSi-Si, impurity effects 0-80037
 Si based MOS capacitors, scanning photovoltage investigation 0-80396
 Si, polycrystalline, thermal oxide anomalous stress 0-93661
 p-Si-Al, ohmic contacts, Si dissoln. and recrystn. effects, computer calc. 0-103749
 Si-metal interface, silicide formation, interface marker technique obs. 0-59734
 Si-PbS heterojunction, effect of Si substrate orientation on struct. and interface props. 0-80097
 n-Si-Pd₂Si contact, interface struct. and Schottky barrier height, correl. obs. using TEM 0-100504
 Si-Pd_{0.5}Si_{0.5}, amorphous, Pd₂Si layer form., shallow contact 0-103586
 Si-refractory metal struct., interface modification by ion implantation 0-70475
 Si-SiO₂ abrupt interface form. by very high dose O⁺ ion implantation 0-75253
 Si-SiO₂ interface, thermal SiO₂ sputter induced roughness, Auger sputter profiling study 0-75424
 Si-SiO₂ interface, thermally grown oxide, spectroscopic ellipsometric anal. 0-107659
 Si-SiO₂ structure, alkali metal ion migration and accumulation, interface struct. 0-107574
 Si₃Ge_{1-x}-GaAs, heterojunction, elec. and recomb. props., interface defect effects 0-80365
 SiO₂/GaAs, interface reaction during high-temp. heat-treatments 0-88439
 SiO₂/InP interface formation, thermodynamic considerations 0-100529
 SiO₂ ultrathin oxide on Si, struct. obs. by high-resolution electron microscopy 0-103592
 Sn/Cu electroplated bimetallic films, interfacial reaction 0-96765
 Te-Ag thin film system, stress-relief appearance conditions 0-65416
 Te-Bi thin film system, stress-relief appearance conditions 0-65416
 α - β Ti Widmanstätten alloy interfaces, elastic interact. stresses, effect on plastic flow onset 0-104218
 TiO₂-Ni (100) interface, electronic props., struct., comp., chemical bonding 0-84499
 ZnSe/water, laser-induced damage in ZnSe 0-102746
- interface tension** *see surface tension*
interface vibrations *see crystal surface and interface vibrations*
interfaces, computer *see computer interfaces*
interfaces, mechanical *see mechanical contact*
interfacial energy *see surface energy*
interfacial tension *see surface tension*
interfacial waves *see surface waves (fluid)*
- interference**
see also interference (signal); interference (wave)
 acoustic, eigenmode analysis of the interference patterns in reverberant sound fields 0-96112
 general relativity, quantum mechanical one-particle state, interfering neutron beam expt. 0-95025
- interference (signal)**
see also crosstalk; electromagnetic interference
 lunar noise effect obs., on satellite links (*Japanese*) 0-82239
 nuclear multichannel radiometer automatic channel separating system (*Russian*) 0-58094
- interference (wave)**
see also acoustic wave interference; electromagnetic wave interference
 neutron interference fringes due to gravitational potential, role of gravity in quantum mechanics 0-62495
- interference spectrometers**
 airborne far IR Fabry-Perot astronomical spectrometer 0-109371
 astronomical CCD spectrometer for 500 to 900 nm range 0-82207
 atmospheric pollutant interferential detector 0-108830
 Brilouin spectrometer with high contrast² and resolution, fully stabilized 0-57386
 etalon-spectrograph system, improved resolution over wide spectral range 0-101843
 Fabry-Perot, separation between maxima of interference fringes, difference record calcs. 0-62731
 Fabry-Perot spectrometer, reference channel for path difference determ. of interfering beams 0-77882
 Fabry-Perot spectrometer for airglow studies, with large aperture and high resolution 0-67424
 Fabry-Perot spectrometer for solar vel. field meas. 0-90333
 Fabry-Perot spectrometer instrumental function, HFS pressure effect determ. from absorption coeff. profiles 0-106299
 Fabry-Perot spectrometer parameter evaluation, deconvolution methods 0-105705

interference spectrometers continued

- far IR modular Fourier interferometer construction, very high resolution 0-57401
- field-widened interferometer spectrometers 0-95146
- Fourier spectrometer, balloon-borne, using focal plane detector array 0-95147
- Fourier transform spectrometer, high resolution ruggedized 0-95152
- Fourier transform spectrometer, rapid scanning, very high resolution, data processing aspects 0-95150
- Fourier transform spectrometer performance, instrumentation for assessment 0-95165
- grating spectrometers and spectrographs, design method 0-62742
- high resolution, appl. to study of laser modal configuration (*Spanish*) 0-86458
- IR Fourier spectrometers, grid polarisers 0-105724
- IR Michelson interferometer on Voyager 0-77290
- MATEC (matched tandem etalon camera), appl. to auroral obs. 0-101442
- Michelson type Fourier interferometer and gaseous molecular spectra 0-68275
- photoacoustic cell for mirror scan Michelson interferometer 0-68277
- reflection dispersive Fourier interferometer window eliminating backlash error 0-57402
- rocket-borne cryogenically cooled field-widened interferometer for the 2 to 8 μm spectral region 0-95163
- selective modulation interference spectrometer, far IR 0-57397
- solar interference spectrograph 0-109362
- stratosphere trace molecule Fourier transform spectrometer optical design 0-82099
- Tokamak far IR Fourier transform spectroscopic Michelson interferometer 0-59294
- variable-thickness cell for liquid MM-wave Fourier transform and laser spectroscopy 0-57403
- wavelength-modulating spectrometer implemented with photovoltaic photodiodes, comments 0-98981

interference spectroscopy

- see also *Fourier transform spectroscopy*
- coal and mineral content characterisation by Fourier transform IR spectroscopy 0-104474
- Fabry-Perot spectrograph, self-scanned photodiode array for image detect. (*French*) 0-73465
- Fourier spectrometry, optimal apodisation 0-99641
- interferometric data from GC Fourier transform IR spectroscopy, functional group anal. 0-89548
- laser pulse autocorrelation by optical processing of Fabry-Perot spectrograms 0-58465
- phase fluctuation optical heterodyne spectroscopy for molecular trace detect. 0-68266
- power transmission spectrometry, use of approx. expressions 0-98982
- solar rotation induced Doppler spectral shift meas. by scanning Fabry-Perot interferometer 0-77298

interference suppression

- astronomical plates deconvolution by maximum entropy, appl. to M87 jet 0-62032
- computed, low-dose X-ray imaging system 0-98092
- dynamic spatial filtering of coded optical image signals from noise 0-95826
- ECG, computerised, time-selective filtering 0-89895
- electron microscopy, microdensitometer-computer correlation analysis of ultrastructural periodicity 0-85553
- IR staring mosaic sensor background suppression and tracking 0-86415
- NMR, use of noise-reduction filter for resolution enhancement 0-73403
- noise compensation in Fourier spectrometer, using improved InSb photodiode preamplifier circuit 0-73474
- optics, spatial frequency plane filtering by dynamic coherent illumination 0-95825
- radiocardiography, equilibrium left ventricular ejection fraction determ., background noise estimation 0-94365
- Reticon spectrophotometer at Asiago Observatory, data anal. procedure (*Italian*) 0-98565
- RF mass spectrometer, background current elimination, using energy filter, expt. results (*Japanese*) 0-82844
- superconductive gradiometers, for measuring magnetic effects of geophysical origin 0-101463
- TEM images of dislocation core, optical filtering for noise removal 0-107254
- visual evoked cortical potential meas., signal optimisation using Kalman filter (*Japanese*) 0-72348

interferometers

- see also *acoustic wave interferometers; electromagnetic wave interferometers; interferometry*
- Josephson symmetric two-junction interferometers, self-induced reson., theory 0-107962
- neutron interferometer expt., role of gravity in quantum theory 0-86176

interferometry

- see also *acoustic wave interferometry; electromagnetic wave interferometry; holographic interferometry; interferometers*
- neutron interference, gravity and inertial effects, principle of equivalence at quantum level 0-77669
- neutron interference fringes due to gravitational potential, role of gravity in quantum mechanics 0-62495
- X-ray interferometry, appl. of synchrotron radiation 0-90954

intergalactic matter

- see also *clusters of galaxies; galaxies*
- Abell 401, X-ray galaxy cluster, hot intracluster gas rel. to radio emission distrib. 0-98731
- accretion by the galaxy in solar neighbourhood 0-67863
- black holes, primordial, number density limits from galactic radio spectrum 0-62179
- 4C 32.69, quasar, radio jet confinement by circum-quasar hot gas press. 0-105375
- 3C 351, quasar, interaction with intergalactic gas 0-105376
- clouds and QSO absorption lines 0-62311
- clouds rel. to origin of universe (*French*) 0-67874
- collapsing pre-galactic H gas cloud, local stability, linear perturbation anal. 0-82513
- evolution in clusters of galaxies, model 0-85992
- galactic evolution, effects of intergalactic matter, review 0-109543
- galaxy cluster X-ray sources, intracluster medium gas supply rate rel. to luminosity function evolution 0-62314

intergalactic matter continued

- gas accretion onto collapsed objects, source of cosmic X-ray background 0-90581
- gas envelopes round disk galaxies, infall and ejection 0-82483
- graphite, pyrolytic, whiskers, absorpt. effects rel. to cosmic microwave background 0-94866
- hot clumpy intergalactic medium emission contrib. to X-ray background 0-62335
- intracluster gas in Abell 2029, X-ray emission rel. to SAS 3 obs. 0-82519
- intracluster hot gas in compact groups, X-ray emission 0-90574
- intracluster medium, mass and metal abundance from elliptical galaxies chemical evolution 0-67843
- ionised gas in clusters of galaxies, microwave search 0-82477
- Magellanic Stream, possibly assoc. C star, visible obs. 0-77411
- Magellanic Stream H I regions, fine struct., 21 cm obs. 0-90523
- magnetic field interaction with hot intergalactic gas, magnetosphere existence 0-67876
- neutral clouds, collisions with galactic discs rel. to interstellar super-rings form. 0-98717
- NGC 4945, late-type spiral galaxy, evidence for infalling gas 0-109547
- Perseus X-ray cluster, form. of optical filaments in cooling gas round NGC 1275 galaxy 0-67862
- pressure gradient, determ. from double radio sources asymmetry and components flux ratio 0-67892
- quasar absorpt. line problem, visible obs. 0-67899
- relativistic and non-relativistic dust grains, rel. to high energy particles in EAS 0-61975
- shock waves, rel. to giant ellipsoidal shells around normal elliptical galaxies 0-86000
- Virgo cluster, evidence for confining environment for Virgo A (M87) from 610 MHz map 0-62302
- Virgo cluster, intracluster gas interaction with hot interstellar gas in elliptical galaxy (M86) 0-90535
- Virgo cluster, intracluster gas/galaxies interaction rel. to spiral galaxies H I deficiencies 0-62277
- X-ray background source possibility after heating by quasars 0-94898
- X-ray clusters of galaxies, large-scale struct. 0-82524
- C model abundance, X-ray absorpt. effects 0-62270
- H I, obs. in inner M101 group of galaxies 0-67885
- H I cloud in NGC 1023 galaxy group, discovery and redshift 0-67886
- H I in field of elliptical galaxy NGC 1052, evidence from 21 cm emission mapping and line profiles 0-98719
- H I in spectra of large-red shift quasars, consequences of neutrino rest mass (*Russian*) 0-105414
- H₂O, gravitational wave absorpt. by mols. 0-82189

intermediate bosons

- corrections, to spin $\frac{1}{2}$ heavy lepton decay 0-73761
- decay, neutrino number and isotropy of Universe in grand unified theories 0-85852
- decay, QED and QCD radiative corrections, hadronic jets 0-73759
- dim 5 and 6 operator mixing induced by Higgs scalars 0-86654
- electroweak gauge models with heavy W bosons, $SU_2 \times U_1 \times U_1$ scheme (*Russian*) 0-86652
- electroweak gauge models with sequential W and Z bosons 0-101971
- fermion asymmetry of the Universe and the W condensate, Weinberg-Salam model (*Russian*) 0-73087
- Glashow-Weinberg-Salam model, one-loop corrections to vector boson masses 0-57548
- heavy Higgs boson decay in Weinberg-Salam model 0-95241
- Higgs boson couplings, charged, K_L - K_S mass-differences 0-62917
- Higgs boson critical mass, baryon asymmetry from boson pair decay 0-90590
- Higgs boson decay, gluon final states, differential sphericity and thrust distrib. 0-86655
- Higgs boson decay, QED and QCD radiative corrections 0-95275
- Higgs boson photoproduction 0-78068
- Higgs particle search at PETRA using Wilczek mechanism 0-105838
- QCD corrections at Z_0 for hadron initiated lepton pair prod., renormalisation appl. 0-86678
- QCD corrections for Higgs-boson production 0-68419
- relativistic cosmology 0-90590
- rishon model, topological bootstrap approach 0-78046
- rishon model for quarks and leptons, topological bootstrap approach 0-78047
- Schwinger model, equivalent boson theory, anomaly-free Ward-Takahashi identities 0-82873
- standard electroweak gauge model with light W and Z bosons 0-95236
- strongly interacting Higgs bosons, gauged nonlinear σ -model, $SU(2)_L \times U(1)$ extension 0-86656
- $SU_2 \times U_1 \times U_1$ electroweak model, Weinberg-Salam intermediate bosons 0-105831
- $SU_4 \times U_1$ and the origin of the Cabibbo angle, charged gauge boson mixing 0-73639
- $SU(2)_L \times (T_3)_R \times U_V(1)$ gauge group, grand unification, symmetry breaking and Z bosons 0-73641
- $SU(2) \times U(1)$ gauge model, chiral $SU(2) \times SU(2)$ symmetry and electron mass 0-57542
- $SU(2) \times U(1)$ gauge model, muon anomalous mag. moment, charged Higgs boson contrib. 0-78011
- $SU(2) \times U(1)$ model, fermion and Higgs multiplet structure, universality 0-62909
- $SU(5)$, unification of weak, EM and strong interactions, review 0-105814
- $SU(5)$ grand unification, heavy coloured Higgs scalars, b-quark mass 0-57543
- subquark model of leptons and quarks, unification, currents and exotic states 0-86683
- unification of EM, weak and strong interactions, massless fermions coupling to vector mesons 0-73637
- weak gauge boson doubling in standard $SU(2) \otimes U(1)$ model, W, Z bosons 0-62916
- Weinberg-Salam model, extended, Higgs-induced neutral processes, natural-flavour conservation, K-symmetries 0-57539
- Weinberg-Salam model, Higgs mechanism (*French*) 0-77999
- Weinberg-Salam model with two massless Higgs doublets, particle masses, perturbation constraint 0-57541
- Weinberg-Salam model Yang-Mills theory of electro-weak interactions 0-73638
- Zweig forbidden processes, intermediate vector particle model, neutral vector mesons (*Chinese*) 0-62918

intermediate bosons continued

- $B^0 \rightarrow D^+ X(F^+ X)$, W-exchange dominance, decay rates 0-86706
 D^0 hadronic decay modes, W boson exchange model clean test 0-57592
 D^0 - D^0 mixing, flavour-changing Higgs bosons 0-62915
 e^+e^- , $SU_L(2) \times U(1)$ and $SU_L(2) \times SU_R(2) \times U(1)$ predictions at high Q^2 , neutral currents, Z-bosons 0-63029
 e^+e^- annihilation, charged Higgs boson prod. signatures, Weinberg-Salam parametrisation 0-57620
 e^+e^- annihilation, superheavy flavour prod., weak current effects, Z^0 effects 0-57614
 $e^+e^- \rightarrow \mu^+ \mu^-$, radiative corrections around Z^0 , Weinberg-Salam model 0-99103
 $e^+e^- \rightarrow \tau^+ \tau^- H^0$, Higgs scalar boson production, Weinberg model calcs. (Russian) 0-68442
 $e^+e^- \rightarrow W^+ W^- \gamma(e^+e^- W^+ W^-)$, Yang-Mills coupling 0-68443
 $e^+e^- \rightarrow W$ + hadrons, from Z^0 pole to threshold 0-105917
 $eN \rightarrow eX$, $SU(2)_L \times U(1)$ gauge theory distinguished from $SU(2)_L \times SU(2)_R \times U(1)$, neutral currents, Z-bosons 0-62908
 $e p \rightarrow W p \nu$, from Z^0 pole to threshold 0-105917
 $\gamma p \rightarrow W^+ n$, current algebra and sum rules high energy W^+ prod. 0-102039
 $\mu p \rightarrow \mu n W^+$, current algebra and sum rules high energy W^+ prod. 0-102039
 ν production, prompt sources, and axion decays and interactions, pN beam-dump experiment 0-63028
 $\nu n \rightarrow \mu p$, Higgs boson exchange effects on second-class currents 0-91075
 $\nu N \rightarrow eX$, $SU(2)_L \times U(1)$ gauge theory distinguished from $SU(2)_L \times SU(2)_R \times U(1)$, neutral currents, Z-bosons 0-62908
 $\nu N \rightarrow \mu X$, neutral current ν prod., Z^0 -gluon fusion model 0-78015
 $\bar{\nu} p \rightarrow \mu^+ n$, Higgs boson exchange effects on second-class currents 0-91075
 $\bar{p}p$, pp , pol. and unpolar. beams, hadronic jets, vector bosons, QCD and weak interference 0-57648
 $\bar{p}p$, pp , $SU_L(2) \times U(1)$ and $SU_L(2) \times SU_R(2) \times U(1)$ predictions at high Q^2 , neutral currents, Z-bosons 0-63029
W, mass in $SU(5)$ grand unified theory 0-68411
W searches with hadron beams, parton model anal. 0-91046
W-bosons, charged, mass spectrum, E_6 model of unified interactions, asymptotically free 0-73642
W-production via Z-decay in Weinberg-Salam model 0-101979
Z, mass in $SU(5)$ grand unified theory 0-68411
 $Z \rightarrow l^+ l^-$, deviations from lepton universality in renormalisable gauge models 0-91122

intermediate-frequency amplifiers

- 30 MHz amplifier for EPR spectrometer 0-98955

intermediate state

- electric field penetration and collective oscillations, review 0-88678
superconducting wire, intermediate state dynamics 0-88697
superconductors, type I, mixed state, Josephson condition, phase jumps (Russian) 0-107967
type II superconductor, bounded, intermediate state struct. form. near crit. field, role of surface 0-80465
In, superconductivity destruction singularities, intermediate state, hysteresis (Russian) 0-80460
Pb intermediate state, Meissner effect investigation by muon technique (Russian) 0-107954

intermediate valence compounds *see mixed valence compounds*intermetallic compounds *see alloys*

intermodulation

- nonlinear holography, multiple-reference-beam, intermodulation background noise suppression appl. 0-99674
volume phase holograms, non-sinusoidal high order modes 0-102665

intermodulation measurement

- No entries

intermolecular forces

see also Van der Waals forces

- acetone-toluene-tetrachloromethane, mol. interaction and thermodynamic props. 0-71935
acetonitrile-toluene-benzene, mol. interaction and thermodynamic props. 0-71935
atoms, identical, dispersion intermolecular pot. anomaly prod. by intense radiation field 0-58336
cholinesterase-acetylcholine soln., anion-cation site interactions, solvent effects on aggregate stability 0-61070
colloid system, forces of mol. attraction between solids, effect of EM lag 0-71949
Coulomb force for molecular dynamic calculations 0-91627
DNA interactions with cations, UV difference spectrosc. and Marcus theory 0-94153
ethane gas, local mode overtone bands 0-83444
factor VIII, native and modified, surface adsorption and mol. interactions, ellipsometric obs. 0-104555
fibrinogen, native and modified, surface adsorption and mol. interactions, ellipsometric obs. 0-104555
gas, diatomic, spherical source expansion 0-58356
hard sphere fluid near hard wall, diffusion coefficient, mol. dynamics simulation 0-64858
hard spheres permeation through hard disc monolayers, interfacial mass transfer 0-107460
hexamethylbenzene in tetrachloromethane soln., local mode overtone bands 0-83444
identical molecules, dispersion intermolecular pot. anomaly prod. by intense radiation field 0-58336
ion-dipole capture in noncentral field, variational and trajectory investigation 0-63739
liquid crystal ordering and theory of mol. dispersion forces and pair pots. 0-64886
N-methyl-N-nitrosourea, electronic interactions with DNA, ESR obs. and INDO calcs. 0-94154
molecular crystals, NQR freq., intermol. force effect 0-66065
neopentane, diamond force const., rel. to crystal elastic consts., Raman freq., bulk compressibility and freq. assignments 0-65183
neopentane liq., local mode overtone bands 0-83444
nitroxide groups in crystals, H bonds and short intermolecular contacts 0-63855
organic ternary liquid systems, intermolecular interaction, US vel. meas. 0-79879
oscillatory forces between two solid surfaces arising from struct. in intervening liq. meas. 0-70521
paradichlorobenzene, NQR freq., intermol. force effect 0-66065
poly- γ -benzyl-L-glutamate, soln., liquid crystal transitions anal. 0-65207

intermolecular forces continued

- polyatomic molecule, atomic force correlation functions for determ. vibr. relax. rates, role of mol. symmetry 0-83337
polyatomic mols. in liqs., vibr. energy relax. 0-63611
porphyrin in n-octane Shpol'skii matrix, defect props., Monte Carlo obs. 0-63533
primitive wave function in theory of intermolecular interactions 0-95703
real fluids, short range repulsions and long range attractions, simple pair pot. model 0-64850
rotational energy transfer, sensitivity anal. 0-63762
strongly coupled systems, one dimens. barriers, transfer rate 0-63735
tetramethylbutane in hexachlorobutadiene soln., local mode overtone bands 0-83444
 $Al^{3+}(H_2O)_n$ ($n=1,2,4,6$), FSGO-pair-pot. calcs. (German) 0-74278
Ar-HBr, intermol. pot. energy surfaces calcs. 0-91625
Ar-Ne(H_2), liquid solution, dielectric props., intermolecular interactions (Russian) 0-88904
Ar+CO₂(N₂), short-range intermol. pots., combined interatomic pots. calcs. 0-87198
Ar₂ van der Waals dimer, intermol. pot., SCF CI ab initio calcs. 0-106274
BaO+Ar(CO₂), in Ar flame, rot. and translational relax. by sub-Doppler optical-optical double reson. 0-95583
Be²⁺(H₂O)_n ($n=1,2,3,4,6$), FSGO-pair-pot. calcs. (German) 0-74277
CO₂, induced absorpt. spectral moment, mol. calcs. 0-63737
CO₂+Ar, short-range intermol. pots., combined interatomic pots. calcs. 0-87198
CO₂+Ne, intermol. pot. in repulsive short-range region, ab initio 0-69204
F⁺(H₂O)_n ($n=1,2$), FSGO-pair-pot. calcs. (German) 0-74278
H₂, expressions for calc. Coulomb repulsion between electrons using adiabatic basis 0-91427
H₂ molecule dimer, ab initio SCF intermolecular interaction energy calcs. 0-78537
H₂+He, vibr. relax. cross section 0-99494
HCl+N₂(O₂)(D₂)(H₂), HCl ν_{H-Cl} band perturbations, linewidth and shifts calcs., IR spectra obs. (French) 0-58251
H₂O, liquid, diamagnetism, temp. dependence, NMR chemical shift calcs., molecular interactions data 0-75707
H₂O+H₂O, pair pot. near H bonded equil. config., amorphous and crystalline solid and liq. 0-64946
(H₂O)₃, geometric config. energies, SCF LCAO MO calcs. 0-63551
H₂+H₂, inelastic collision, R-matrix study 0-87204
HgCl₂, NQR freq., intermol. force effect 0-66065
Kr-HCl, intermol. pot. energy surfaces calcs. 0-91625
Li⁺(H₂O)_n ($n=1,2,3,4,6$), FSGO-pair-pot. calcs. (German) 0-74277
Mg²⁺(H₂O)_n ($n=1,2,4,6$), FSGO-pair-pot. calcs. (German) 0-74278
N₂, liq. and gas, induced absorpt. spectral moment, mol. calcs. 0-63737
N₂ structural second virial coeff., intermol. pot. and mag. scatt. 0-78678
N₂+Ar, short-range intermol. pots., combined interatomic pots. calcs. 0-87198
Na⁺(H₂O)_n ($n=1,2,4,6$), FSGO-pair-pot. calcs. (German) 0-74278
O₂, liq. and gas, induced absorpt. spectral moment, mol. calcs. 0-63737
O₂ structural second virial coeff., intermol. pot. and mag. scatt. 0-78678
SO₂-¹⁸O mixtures, IR laser pumped, intermol. vibr. energy transfer dynamics obs. 0-87207

intermolecular mechanics

- see also association; intermolecular forces; kinetic theory of gases; liquid structure; liquid theory; Morse potential; potential energy functions*
acetone, ¹⁷O chemical shift and NMR linewidth meas., self-association equil. const. determ., mol. reorientations obs. 0-87148
adamantane-adamantane interactions, expansion of intermol. energy in set of symmetry-adapted functions 0-106371
n-alkanes, anisotropic London dispersion forces, surface effects 0-74214
aminoborilpolynes, intermolecular interaction through triple bonds, internal rot. 0-106370
aminopolynes, intermolecular interaction through triple bonds, internal rot. 0-106370
aniline-chlorophenol complexes, ³⁵Cl NQR, inter- and intramol. interactions 0-63666
chloroanisoles, ³⁵Cl NQR, inter- and intramol. interactions 0-63666
chlorophenols, ³⁵Cl NQR, inter- and intramol. interactions 0-63666
Coulomb centres with different charges, asymptotic expansions 0-69211
dense systems, intermolecular spectroscopy and dynamical props., conf., Varenna, Italy (1978) 0-82581
double well damped motion, proton tunnelling, transfer rate temp. depend. (German) 0-87058
dynamics, synchrotron radiation obs. appls. 0-66830
ethane, inclusion of nonbonded interactions in vibr. freq. calcs. 0-95590
ground state alkali molecules, mag. shielding and spin-rot. interaction 0-87186
homonuclear diatomic mols., force-torque correls. 0-87196
long-range anisotropic interactions between molecules of arbitrary symmetry, derivation by irreducible tensor method 0-69207
methane, intermolecular interaction energies calcs. using minimal basis sets 0-78681
methane, solid, plastic phase, mol. dynamics simulation 0-79715
methane-methane interactions, expansion of intermol. energy in set of symmetry-adapted functions 0-106371
molecular crystals, intermolecular interactions, spectroscopic studies, review 0-103958
molecular structure theory, quantum topology 0-106247
nonlinear oscillators, 1-D, intramolecular vibr. energy transfer, quantal, classical and statistical behaviour 0-91641
nonpolar molecules, intermol. interactions in intense radiation field 0-78679
optically active and inactive molecules, electric and mag. dispersion forces interaction 0-99533
organic molecular crystals, intermolecular interactions, spectroscopic studies, review 0-103958
phase and population relax., semigroup formalism 0-78519
polymer solution, Rayleigh scattering, intermolecular correlations effect 0-75146
polynes, intermolecular interaction through triple bonds, internal rot. 0-106370
pyridine-H-bond donors, D spin-lattice relax. meas., mol. interactions anal. (French) 0-87151
Schwinger and Kohn variational phase shift calculations, comparison 0-78672

intermolecular mechanics continued

- spin polarisation, analysis using intermolecular interactions theory, chemical polarisation, exchange repulsion 0-76510
 tetracene molecules in Ar clusters, excited state intramol. dynamics, laser-induced fluoresc. spectra obs. 0-78674
 triatomic molecules, C_2 , symm., vector statistical distrib., mol. dynamics computer simulation 0-63734
 bis-triazolopyridazines, conformation calcs. by mol. mechanics and CNDO/2 method 0-69079
 bis-triazolyls, conformation calcs. by mol. mechanics and CNDO/2 method 0-69079
 Ar+N₂(O₂, CO), molecular fluid mixtures, equilibrium props. 0-64867
 CO, second virial coeffs. 0-83440
 CS, liquid, Rayleigh and Raman bands, intensities of interaction induced components 0-63645
 DCl, plastic cryst. phase, struct. and dynamics 0-92469
 H₂-H₂ dimers, hyperfine struct. in zero mag. field 0-95700
 HCL, fluid states, mol. dynamics simulation 0-79671
 HCL, liquid, struct. and mol. dynamics studied using intermolecular force models 0-83445
 H₂O, intermolecular interaction energies calcs. using minimal basis sets 0-78681
 I₂, photolytic cage effect in gas phase 0-81345
 Li projectile, electronic stopping cross section meas., intermolecular interactions 0-75279
 N₂, ab initio MO-LCAO-SCF and Gordon-Kim intermolecular pot. for seven different orientations 0-95522
 N₂, second virial coeffs. 0-83440
 N₂+O₂, molecular fluid mixtures, equilibrium props. 0-64867
¹⁴N₂+CO, vibr.-vibr. energy transfer, long and short range pot. effect 0-99556
¹⁵N₂+CO, vibr.-vibr. energy transfer, long and short range pot. effect 0-99556
 (N₂)₂, Van der Waals molecule, struct. and internal rot. barriers determ., interaction pot. from ab initio calcs. 0-91626
¹⁴N¹⁵N+CO, vibr.-vibr. energy transfer, long and short range pot. effect 0-99556
 NO₂, hydrate clusters, ground-state HF pot., Monte Carlo simulation, energy surfaces and rot. barriers 0-106412
 Ne-Xe, equilibrium of coexisting phases 0-87197

intermolecular vibrations *see molecular rotational-vibrational energy transfer***intermolecular vibrations (molecular crystals)** *see lattice dynamics of molecular crystals***internal combustion engines**

- concentration fluctuations, meas. 0-71973
 diesel, exhaust noise, single monopole very low freq. noise source in air duct 0-64282
 diesel, piston slap, assessment of contribution to overall noise and vibration 0-79055
 diesel engine noise analysis, diagnosis and control 0-58857
 exhaust air pollution in Netherlands (*Dutch*) 0-101138
 fuel, alcohols as auxiliary fuels 0-61230
 H₂ powered, electronic fuel injection techniques 0-72094

internal conversion

- see also conversion electron spectra*
 E0-conversion, reduced probability, quadrupole moment effect 0-78138
 mesoatoms, prompt fission internal γ -ray conversion, fragment radiative transitions (*Russian*) 0-86944
 radionuclide decay, computer simulation, levels, transitions, internal conversion 0-63136
²⁴²Am, reduced E0 conversion due to mag. moment effects 0-83034
¹⁹⁵Au decay, K-shell capture fractions, internal conversion electrons, coincidence techniques 0-57743
 Dy K-shell internal conversion yields, gamma transition multiplicities from (α ,xn), (¹²C,xn) 0-78215
¹⁵⁷Eu, EM transitions, multipole, internal conversion coeffs. (*Russian*) 0-63121
⁵⁶Fe low lying levels, J^{*}, γ - γ coincidences, internal conversion from ⁵⁶Co β^+ -decay 0-86815
²²⁸Fr-²²⁸Ra, γ -rays, internal conversion, $\epsilon\gamma$ coincidence spectra meas. 0-78216
¹⁵⁷Ho-¹⁵⁷Dy decay, internal conversion electron spectra and $\epsilon\gamma$ coincidences (*Russian*) 0-68604
¹⁰⁸In high spin struct., in-beam spectroscopy, conversion electrons from ⁹⁸Mo(¹⁴N,4n γ) 0-73782
²⁰⁴Po, γ -rays, conversion electron spectra, $\gamma\gamma$ coincidences 0-83061
²²⁸Rn-²²⁸Fr-²²⁸Ra, γ -rays, internal conversion, $\epsilon\gamma$ coincidence spectra meas. 0-78216
⁷⁹Se, 96 keV transition, conversion coeff., γ -spectrum 0-63131
 Sn, internal conversion coeffs. for inner shells of atomic ions and relativistic ionic potentials 0-68600
¹⁸⁷Ta^m, β^- and EC branching ratios, K-internal conversion coeff., γ -intensities, T 1/2 0-68601
¹²⁰Te quasi-rot. band based on proton 4p-2h state, level scheme, transitions from ¹¹⁸Sn(α ,2n γ) 0-78119
²³⁷U internal conversion from 1/2⁺ isomeric state, U⁴⁺ electron configuration 0-58146
⁴⁵V level scheme, γ -rays, level lifetimes, internal conversion from ⁴⁰Ca(Li,xn) 0-63085

internal conversion in atoms *see Auger effect***internal conversion in molecules** *see nonradiative transitions***internal fields, crystal** *see crystal field interactions***internal friction**

- see also Bordoni effect; damping; Snoek effect; Zener relaxation*
 alkali silicate glasses, secondary relax. transitions 0-88261
 direct meas. of friction in solids with continuous variation of freq. 0-99979
 electric circuitry modifications for meas. on thin wire U-shape specimens 0-59579
 ferroelectric ceramic, mech. and elec. losses, correl., theory and expt. 0-66133
 glasses, oxide type, H bond interpretation 0-92605
 metals, BCC, under elastic stress, Snoek peak height determ. 0-65153
 metals, porous, plastic flows, microscopic frictional effects, J₂-flow potential and yield function 0-64384
 metals executing US torsional vibrations 0-58856
 minerals, ultrasonic damping due to internal friction, freq. depend. (*German*) 0-90078

internal friction continued

- piezoelectric transducer automatic setup, for continuous meas. of internal friction and elastic moduli of solids 0-108652
 plastic strain rate, and internal friction, phenomenological rel. 0-75301
 silicate glass, mechanical stress field influence on structural mobility 0-103421
 soil, plastic flows, microscopic frictional effects, J₂-flow potential and yield function 0-64384
 steel, austenitic, Cr-Mn-N, plastic deformation influence on internal friction, relaxation processes (*Russian*) 0-100870
 steel, austenitic stainless, internal friction due to H₂ gas molecules 0-71682
 steel, cold strained, defects interaction with carbide strengthening phases, carbide decom. degree (*Russian*) 0-84955
 steel, type Kh12M, rel. between structural inhomogeneity and wear resist. (*Russian*) 0-66672
 steel, type KVK, deform. strengthening of bayanite phase (*Russian*) 0-100851
 superconductors near critical temperature at acoustic frequencies, internal friction 0-100305
 test device for thin-walled tubular specimens 0-71836
 test method, for plastic deform. (*Hungarian*) 0-97662
 torsion pendulum, with anelastic solids of discrete relaxation spectra, resonant system 0-69687
 viscoelasticity rods with nonlinear elasticity relation and nonlinear internal friction, parametrically excited oscils. 0-99947
 Al dilute alloys, cold worked, internal friction peaks 0-97520
 Al foil, internal friction changes during low temp. plastic deform. (*Russian*) 0-100304
 Al, pure, cold worked, internal friction peaks 0-97520
 Al wire, grain boundary internal friction after recrystn. annealing (*Russian*) 0-66561
 Al-Cu(Mg), low freq. internal friction during plastic deform. (*Chinese*) 0-103420
 β -Al₂O₃, internal friction and Na transport 0-59578
 β -Al₂O₃-(Na,Li)₂O, ionic motion obs. using NMR and internal friction 0-108099
 Bi, Young's modulus and internal friction, 20°C to melting point (*Russian*) 0-89278
 Cd, Young's modulus and internal friction, 20°C to melting point (*Russian*) 0-89278
 Cu, acoustic losses due to strong ultrasonic and static stress fields 0-79886
 Cu, dislocation pinning rate, neutron and electron irradi., meas. by internal friction method 0-96570
 Cu, electron irradi., migration and thermal conversion of defects, 100 to 330K 0-59519
 Cu film, Gorsky effect, internal friction maxima, atom diffusional mobility (*Russian*) 0-70446
 Cu, neutron and electron irradi., interstitial formation, dislocation pinning, internal friction meas. 0-100284
 Cu-Ag (0.1 wt.%), cold-worked, internal friction peaks in kHz range 0-89276
 Fe, effect of H₂ on phys. and mech. props. 0-101657
 Fe, internal friction in plastic deformation process (*Chinese*) 0-88259
 Fe-Cr alloys, cold worked, internal friction due to H (*Japanese*) 0-70305
 Fe-Cr-Al (12, 3 wt.%), strain amplitude-depend. damping and modulus (*Japanese*) 0-92606
 Fe-Ni-Mo, martensitic transformation, annealing, influence on struct. of austenite (*Russian*) 0-81057
 Fe-Si (3 at%), deformation and electron bombardment, influence on dislocation struct., 20-500°C (*Russian*) 0-92536
 Fe-Si (3 wt.%), internal friction, instantaneous, depend. on phase of torsional oscils. (*Russian*) 0-71142
 Ge:Cu, solubility and behaviour of Cu, internal friction investigations 0-92678
 K(D,H_{1-x})₂(SeO₃)₂, ferroelastic, anelastic and elastic infra-low freq. props. 0-70304
 La-Al amorphous alloys, internal friction, relaxation process 0-92607
 MgO:(Li), polycrystn., internal friction (*German*) 0-59577
 MnZn ferrites, internal friction and ΔE effect depend. on demagnetisation method 0-80584
 NH₄Cl, acoustic absorption by soft modes of defects 0-59584
 NaCl, γ -irrad., F-stimulated inversion of sign of dislocation charge 0-59475
 Na₂O-3SiO₂:Fe²⁺, Fe³⁺ glasses, Mossbauer and ESR spectra and internal friction 0-100865
 Na₂O-K₂O-Al₂O₃-SiO₂, structure of modified surface layer, internal friction method 0-103258
 Nb, deformed polycryst., γ -peak obs. and interpret. in internal friction, 300-500K 0-81098
 Nb, dislocation damping, amplitude depend. 0-59469
 Nb, neutron irradiated, radiation anneal hardening (*Japanese*) 0-89243
 Nb, solute trapping of H, symmetry of O-H pair 0-108488
 Nb₂Ge(Si), amorphous films, thermally-activated internal friction peaks, structural obs. 0-80147
 Ni, cold-worked, rel. between dislocation and ferromag. damping 0-107369
 Ni, grain boundary internal friction, B solid solubility as function of grain size 0-60903
 Ni, H-charged cold-worked, internal friction peak 0-107368
 Ni, internal friction, instantaneous, depend. on phase of torsional oscils. (*Russian*) 0-71142
 Ni, strain amplitude-depend. damping and modulus (*Japanese*) 0-92606
 Ni-B, grain boundary internal friction, B solid solubility as function of grain size 0-60903
 Ni-Ti/Cu composite, plastic deform. influence on internal friction (*Russian*) 0-100871
 NiZn ferrites, internal friction and ΔE effect depend. on demagnetisation method 0-80584
 PLZT, mech. and elec. losses, correl., theory and expt. 0-66133
 Pb, Young's modulus and internal friction, 20°C to melting point (*Russian*) 0-89278
 xPbTiO₃+(1-x)PbCd_{1/3}Nb_{2/3}O₃, phase transition spread, polarisation relaxation, dielectric susceptibility (*Russian*) 0-75922
 Pb(Z,Ti,Mg,W)O₃, low-Q ceramics, props. and transducer appl. 0-75944
 Se, amorphous, US attenuation at low temp., internal friction peak 0-65152
 Sn, Young's modulus and internal friction, 20°C to melting point (*Russian*) 0-89278
 Ta, acoustic emission induced by hydride formation 0-76257

internal friction continued

- Ti-Ni, internal friction and US props. (*Russian*) 0-84247
 V, dehydrogenation by annealing with Zr foils, internal friction meas. 0-96736
 V wire, deformed in torsion, internal friction, H effect 0-76300
 Zn, internal friction anomalies in temp. initiated brittle-plastic transition (*Russian*) 0-96648

internal friction of liquids *see viscosity of liquids***internal mechanics, molecular** *see molecular vibration***internal mechanics of atoms** *see atomic structure***internal modes** *see molecular vibration in solids***internal stresses**

- alkali halides, thermally stimulated depolarisation of NCO⁻ centres 0-80678
 amorphous solid, structural defects, computer simulation study 0-88040
 anelasticity influence, on internal stress meas. in creep 0-70306
 bearings, plain, fracture 0-81170
 bicrystal, elastic incompatibility stresses (*Japanese*) 0-107361
 bounded domain undergoing sequential crystallisation, stress and strain investigation 0-100183
 cemented carbides, physical and chem. nature 0-76265
 coated optical fibre cable unit, internal stress due to compressive loads, optimum design 0-58717
 component hydropressing, residual stress distrib. (*Russian*) 0-93567
 composite three-layer cylindrical shells, initial stressed and deformed state 0-102974
 corundum, defect cryst. struct. study 0-103316
 crystal defects, elastic interaction under high hydrostatic press. 0-96512
 crystal growth, creation of stress and dislocations (*Russian*) 0-103277
 cubic crystals, response to (111) loading, internal energy, elastic moduli 0-84230
 cylinder with oblate spheroidal cavity or internal penny shaped crack under tension, stresses 0-69736
 diffusion motions of macroscopic inclusions in nonuniform compressive stress fields (*Russian*) 0-88351
 discs, circularly symmetric, rupture, ductile-brittle creep 0-69735
 FCC alloy, hardening by spinodal modulated structure 0-60874
 glass rods, compressively clad, residual stresses, comparison of optical and fractographic meas. 0-108539
 Jahn-Teller system, thermodynamic properties, internal stress effects 0-59679
 laminates, residual thermoelastic stresses 0-106721
 measurement, high-temp. 0-64498
 measurement, X-ray diffr. equipment, comparison 0-82858
 metal, textured cubic, residual stress evaluation 0-89435
 metals, dislocation-core movement and frictional stress 0-92529
 metals, inelastic cyclic strain under nonuniform stress state conditions, residual stresses effect 0-81132
 metals, residual stress on drawing calcs. by stress state changes variational principle (*Russian*) 0-65125
 mirror/flaw-size relations, residual contact stresses effect 0-107363
 multilayer cylindrical parts, residual stresses determ. 0-96206
 optical fibre, refractive index profile distortion, stress-induced 0-91889
 optical fibre, single mode, bending induced birefringence 0-87537
 PET films, dyed, local mech. stresses, IR spectrosc. determ. 0-65418
 PMMA, shock loaded, lateral compressive stresses meas. using Yb piezoresist. gauges 0-103007
 polyamide-polyurethane copolymer dispersions, structuration and relax. props., coating from props. 0-76559
 polycarbonate, ductile, large strain cyclic deform. 0-85000
 polyethylene, high density, ductile, large strain cyclic deform. 0-85000
 polyethylene film minimum running thickness, critical rupture stress 0-100993
 polypropylene, ductile, large strain cyclic deform. 0-85000
 pyrographite, initial stress state, neutron irradi. effect 0-97555
 rings, multilayer, circumferential residual stresses (*Russian*) 0-74729
 single crystals, internal stresses determ. with multicryst. X-ray spectrometer 0-64832
 solid solutions, dislocation-core movement and frictional stress 0-92529
 solidification front propagation, residual stress levels, polymerisation 0-59635
 steel, austenitic stainless, type SUS 304, welded joint, polarisation behaviour, boiling MgCl₂ soln. (*Japanese*) 0-93695
 steel, C, magnetomechanical acoustic emission for residual stress NDT 0-71149
 steel, C-Cr (1.0, 1.5 wt.%), 52100 bearing steel, control of surface residual stress by heat treatment 0-97501
 steel, carburized and quenched, residual stresses (*Japanese*) 0-89262
 steel, Cr plated, factors influencing durability 0-108643
 steel, Cr-Mo-P (2.25, 1 wt.%), stress relief cracking, effect of P segregation 0-89324
 steel, ferritic, magnetomechanical acoustic emission for residual stress NDT 0-71149
 steel, low alloy, high strength, fatigue crack growth, in presence of welding residual stresses (*Russian*) 0-71739
 steel, martensitic, ageing, effect of H₂ on stresses in process of $\gamma \rightarrow \alpha$ transformation (*Russian*) 0-76252
 steel, martensitic transform., stress calcs. using statistical model (*Russian*) 0-93557
 steel, medium, C, US attenuation, mag. field effect 0-89428
 steel, medium C, ground, residual stresses, X-ray evaluation 0-79863
 steel, Ni, 11.6%, quenched cylinder residual stresses, boring/turning and X-ray diffr. obs. (*German*) 0-93586
 steel, Si-Mn-P-S-Ni-Cr, residual stress meas. by X-ray diffr. 0-71688
 steel, stainless, fast neutron irradiated, solution annealed tubing, residual stress behaviour 0-65054
 steel, steam pipes, 12Cr1MoV, selection of allowable stresses based on minimum possible strength data 0-104237
 steel, strain-hardened subsurface layer, residual stress change in fatigue 0-81185
 steel, US strengthening treatment effect on fatigue resistance 0-81193
 steel bearing, surface-ground, residual stress fatigue property comparison 0-60975
 steel bearing rings, optimisation of thermomechanical working parameters (*Russian*) 0-93579
 steel plates, explosively clad, fatigue crack propagation behaviour (*Japanese*) 0-104262
 steels, alloy, stress relax. data anal. using total strain-time parametric method (*Japanese*) 0-104198

internal stresses continued

- Stepanov method shaped cryst. growth, physical problems, thermoelastic stresses 0-103279
 stochastic model for dip test in steady-state creep 0-58915
 styrene-butadiene-styrene block copolymer, stress relax. following steady-state flow, residual shear stress development 0-83772
 surface dislocations, universal concept, rel. to disclinations and grain boundaries 0-100231
 welds, residual stresses, evaluation by Barkhausen noise meas. 0-76436
 X-ray stress meas., computer-aided system (*Japanese*) 0-104366
 zincblende-type crystals, sublattice displacement from elect. or mech. deform. 0-81123
 Ag film, intrinsic stress meas. 0-71696
 Ag film deposition, thermal effects, influence on internal stress meas. 0-96767
 Ag powder, ultrafine, sintering, coalescence growth stage 0-89174
 Ag-Sn, splat-quenched, X-ray diffr. study 0-81094
 Al bicrystal, plastically deformed, slip heterogeneities 0-79858
 Al film, deform. under He ion bombardment 0-65073
 Al film, H incorporation effect on stress and electromigration 0-80139
 Al film, intrinsic stress meas. 0-71696
 Al, plastic deformation thermal activation parameters from creep kinetics and stress relaxation 0-71717
 Al thin films 1/f noise, depend. on internal mech. stresses 0-65711
 Al-Si alloy, eutectic, quasioisotropic 0-79165
 Al-Zn, type 7075-T6, coldworked hole specimens, residual stresses, fracture mech. anal. 0-97587
 Al-Zn-Mg-Cu alloys, heat treatment optimisation 0-60888
 Al_{0.9}Ga_{0.1}As:Cu, variable-gap semicond., impurity props., carrier recomb. 0-96907
 Au, electrodeposited and sputtered, hard, reactive softening, X-ray diffr. studies 0-100414
 Au film deposition, thermal effects, influence on internal stress meas. 0-96767
 Au film electrodeposition, substrate effects on film props. 0-81329
 Au powder, ultrafine, sintering, coalescence growth stage 0-89174
 Au-Ni, surface segregation, strain effects 0-80042
 BaTiO₃, ferroelectric ceramic, internal stress and strength, failure mechanism 0-66128
 BaTiO₃, ferroic materials, fracture processes 0-79869
 Cd films, struct. and props., X-ray diffr. spectra anal. 0-80119
 Cr condensates, lattice const., internal stresses (*Russian*) 0-107141
 Cr film, evaporated, concurrent ion bombard. effects 0-80142
 Cu film deposition, thermal effects, influence on internal stress meas. 0-96767
 Cu, plastic deformation thermal activation parameters from creep kinetics and stress relaxation 0-71717
 Cu-Ni (10 at.%), creep, substruct. and internal stresses (*Russian*) 0-97527
 Fe, Armco, ground, residual stresses, X-ray evaluation 0-79863
 Fe, magnetomechanical acoustic emission for residual stress NDT 0-71149
 α -Fe, nitrided, aging at room temp. 0-71679
 Fe-Mo(4.1 wt.%), steady state creep at high temps. 0-89316
 (FeNi)PB amorphous wires, surface oxidation and annealing influence on induced anisotropy 0-100957
 Fe₂O₃ thin films, reactively sputtered, mechanical stresses rel. to deposition conditions 0-80146
 n-GaAs epitaxial film, radiative recomb. under influence of mech. stresses 0-66291
 Ga_{1-x}Al_xAs laser diode, hetero-isolation stripe geometry for IR and visible radiation (*Japanese*) 0-83607
 GaAs-GaAlAs DH lasers, strain-enhanced luminesc. degradation, photoluminesc. obs. 0-69392
 GaAs-GaP heterostructure, radiative recomb. under influence of mech. stresses 0-66291
 Gd-Fe amorphous films, stress contrib. to perpendicular anisotropy 0-75819
 LiF film, intrinsic stress meas. 0-71696
 Li₂O-Al₂O₃-SiO₂ glass, study of elastic props. 0-104205
 Li₂O-Al₂O₃-SiO₂ glass, crystallised, grain size and internal strain 0-103259
 Mg films, struct. and props., X-ray diffr. spectra anal. 0-80119
 MgCd wire, elongation during disorder-order transform. (*Russian*) 0-104148
 Mn-Cr-Ti layers on low C steel, composite, residual stresses rel. to arc-spraying parameters (*German*) 0-104077
 Mo alloys, intercryst. fracture in ductile-brittle transition region, local internal stresses effect 0-81200
 Mo fibre reinforced Cu, rule of mixtures of deform. parameters in stage III 0-97532
 Mo films, sputtered from cylindrical-post magnetron with Ne, Ar, Kr and Xe, compressive stress and presence of inert-gas obs. 0-80140
 Na₂O-B₂O₃-SiO₂ glass, fracture toughness, effect of microheterogeneous struct. 0-104256
 Nb₃Sn, supercond. composite, residual stress state, crit. currents 0-80468
 Ni, creep, substruct. and internal stresses (*Russian*) 0-97527
 Ni, dislocation structure evolution after hydroextrusion (*Russian*) 0-96530
 Ni, electrodeposited film, thermal anal., occlusion of gases rel. to mag. props. 0-59823
 Ni electrodeposition, structure-internal stress relationship 0-70561
 Ni-Fe (36 to 50 wt.%), initial permeability, domain struct. model 0-88811
 Ni-P, electrodeposited film, thermal anal., occlusion of gases rel. to mag. props. 0-59823
 Ni-Si, electrodeposited film, thermal anal., occlusion of gases rel. to mag. props. 0-59823
 NiPt, quenched, ordering kinetics and domain struct. form. during isothermal tempering (*Russian*) 0-66502
 Pb(Ti,Zr)O₃ solid solutions, phase coexistence discrepancies 0-96662
 Pb(Zr,Ti)O₃ ceramics, DC field sintering preparation, piezoelectric props., ageing behaviour 0-81211
 Pb(Zr,Ti)O₃, ferroic materials, fracture processes 0-79869
 Pd-Si and PdSi films, on Si, stress obs. 0-80145
 PtSi films, on Si, stress obs. 0-80145
 Si, high-dose Ar implantation, X-ray topographic obs. of strains and damage 0-59496
 Si, polycrystalline, thermal oxide anomalous stress 0-93661
 Si, residual stress and defects induced by scribing 0-60990
 Si:B, implanted laser annealed, lattice strain, X-ray study 0-96554

internal stresses continued

- Si-Li, thermal cond., low temp. phonon scatt., internal strain effects 0-96706
 $\text{Si}_3\text{N}_4/\text{ZrO}_2$, hot-pressed, compressive surface stresses developed by oxidation induced phase change 0-60992
 SiO_2 film, prep. using high press. O_2 , residual stress, chemical etch rate, refr. index and density meas. 0-71768
 W fibre reinforced Cu composites, correl. between thermal cycling-induced microstructural changes at interphase boundaries and tensile behaviour (Japanese) 0-71674
 ZnS, film, intrinsic stress meas. 0-71696

internuclear double resonance *see* **INDOR****interplanetary magnetic fields***see also* **interplanetary matter**

- A_1 -index, 1964-1976, rel. to geomag. field and interplanetary field states 0-104866
 auroral electrojet, empirical relations to interplanetary parameters 0-105118
 B_1 and B_2 components, origin (Russian) 0-98611
 B_2 -component sign rel. to longit. position of magnetosphere polar cap plasma flow entry region 0-67472
 B_2 component, direction rel. to Earth bow shock three-dimensional shape 0-85832
 correlation with interplanetary cosmic ray protons 0-77243
 direction, influence on magnetosphere hydromag. energy spectra 0-67476
 Earth atmosphere elec. current systems and interplanetary field 0-105126
 Earth bow shock, DC mag. field obs. 0-90306
 Earth bow shock, initial ISEE mag. field obs. 0-90307
 Earth bow shock, theory of magnetic shocks in collisionless plasma 0-85854
 Earth bow shock interaction, backstreaming ions and interplanetary mag. field 0-101500
 Earth bow shock region, mag. field topology rel. to upstream particle events 0-77247
 Earth bow shock tangential mag. field line rel. to upstream energetic electrons 0-90308
 Earth bow shock vicinity, low-freq. waves obs. 0-90311
 Earth magnetosphere interaction, mag. curl in front of magnetosphere boundary 0-85804
 Earth satellite observations by Isee-1 and -3, reliability of method 0-85895
 geomagnetic activity, cyclical nature due to interplanetary field 0-81813
 geomagnetic daily variations influenced by interplanetary field 0-85591
 geomagnetic pulsations affected by interplanetary medium 0-77228
 Halley-Venus mission, Planet-A project for mag. meas. in interplanetary space (Japanese) 0-94672
 heliosphere magnetic field configuration, three-dimensional model 0-94670
 intensity, vars. during geomag. storms with gradual commencements (Russian) 0-105127
 magnetosheath, high latit., mag. field lines rel. to ≤ 2 MeV electrons transport 0-90296
 magnetosheath, mag. field direction rel. to obs. of energetic electrons of magnetospheric origin 0-90310
 magnetosphere interaction, correl. with auroral convection over ($60^\circ \leq \Delta \leq 75^\circ$) 0-67454
 magnetosphere merging with interplanetary field, half-wave rectifier response 0-72710
 magnetosphere-solar wind dynamo affected by IMF vector 0-85824
 north-south component in 1972 rel. to geomagnetic bays and geomagnetic activity 0-105124
 north-south field component, solar cycle dependent configurations in solar wind interaction regions 0-98529
 northward magnetic field, assoc. convection in magnetosphere polar cap 0-94658
 sector boundaries, rel. to Swan Cloud in Comet Kohoutek (1973 XII) and cometary plasma tails general morphology 0-98612
 sector boundaries at 1 AU, (1971-1973) 0-94668
 sector boundary passage effect on equatorial geomagnetic field, daily variations 0-67335
 sector structure, form. by large scale spiral waves in solar wind 0-85831
 sector structure, rel. to ionosphere global scale electrodynamic coupling of high and low latit. regions 0-77194
 sector structure (1926-1970), deduced from geomagnetic data 0-90368
 sector structure and anisotropy of 50-1000 GV cosmic rays 0-62072
 shock wave, 1978 January 3 to 4, Prognoz-6 energetic particle and solar wind meas. 0-90315
 shock waves, collisionless, mag. structs. thickness 0-90314
 solar wind, dynamic mag. struct. of large amplitude Alfvénic vars. 0-72734
 solar wind, mag. field direction rel. to obs. of energetic electrons of magnetospheric origin 0-90310
 solar wind, mag. field fluctuations rel. to plasmadynamical processes (German) 0-109323
 solar wind, mag. field rel. to Alfvén wave accel. 0-85923
 solar wind, mag. field rel. to plasma irregularities anisotropic struct. 0-67489
 solar wind, magnetic data anal. rel. to MHD turbulence 0-61977
 solar wind, obs. of fully developed anisotropic MHD turbulence 0-94669
 solar wind corotating interaction regions, energetic particles shock accel. 0-82159
 southward component, correl. with plasma sheet thinning during magnetospheric substorms 0-72705
 turbulence, character rel. to mean free path of low-rigidity cosmic rays 0-98524
 variation effects on solar flare cosmic ray particle intensity 0-77372
 Venus magnetic tail interaction, unipolar induction effects 0-62060
 vertical component origin and recurrency 0-90369

interplanetary matter*see also* **comets**; **cosmic dust**; **interplanetary magnetic fields**

- acceleration effect on solar cosmic rays, soln. to Fokker Planck eqn. 0-77242
 circumsolar dust cloud, inner F-corona, model and composition 0-82162
 circumsolar plasma, Venera 10 radio signal spectral meas. 0-109326
 cold-cloud aggregates, chemical energy and meteorite chondrule origin 0-105210
 collisional growth to planetesimals, relative vel. 0-82247
 corotating energetic particle events, origin 0-82161
 cosmic ray protons, 1-4.5 MeV, spectral anal. and correl. study 0-77243
 cosmic rays, flow lines and energy changes 0-82158

interplanetary matter continued

- cosmic rays, low-rigidity, weak turbulence diffusion theory rel. to mean free paths 0-98524
 cosmic rays propagation, rel. to large amplitude wave-trains of neutron intensity 0-94660
 dust, light scatt. intensity, theory 0-109324
 dust complex, azimuthal asymmetry mechanism from restricted three-body problem 0-85843
 dust components in inner Solar System 0-85914
 dust grain trace element anal., stratosphere collected particle 0-82319
 dust in stratosphere, visible absorpt. spectra 0-101554
 dust origin and evolution 0-101555
 dust particles, Mg isotopic composition 0-72879
 Earth bow shock, conference, Strasbourg, France (1978 August 31 to September 1) 0-82573
 Earth bow shock, first evidence and early studies, historical introduction 0-85816
 Earth bow shock, initial ISEE mag. field obs. 0-90307
 Earth bow shock, kinetic models of shocks in collisionless plasmas 0-90330
 Earth bow shock, obs. of backstreaming protons in upstream solar wind 0-90309
 Earth bow shock, review of upstream energetic-particle meas. 0-90308
 Earth bow shock, theory of magnetic shocks in collisionless plasma 0-85854
 Earth bow shock, three-dimensional shape 0-85832
 Earth bow shock plasma, possible generation mechanisms of low-freq. waves (≤ 50 Hz) 0-90312
 Earth bow shock vicinity, low-freq. waves obs. 0-90311
 electric currents, generation by solar activity rel. to solar wind energy source 0-94768
 electrons, energetic, of magnetospheric origin in magnetosheath and solar wind, obs. 0-90310
 heliosphere, model of mag. field configuration 0-94670
 ion fluxes from Jupiter, Voyager 1 and 2 obs. 0-94667
 Jupiter as source of electrons observed at Earth orbit 0-90357
 magnetic measurement in interplanetary space during Halley-Venus mission, Planet-A project (Japanese) 0-94672
 magnetosheath, Prognoz 4 obs. of ≤ 2 MeV electrons and cold plasma 0-90296
 magnetospheric storm, interplanetary shock wave with increased solar wind energy deposition 0-77237
 piston problem, one-dimensional, in non-ideal gas, time-dependent soln. 0-82185
 plasma, collisionless, stability of contact discontinuity, solar wind and magnetosphere boundary appls. 0-62002
 protoplanetary nebula formation of inhomogeneous Earth 0-90348
 scintillation, appl. to solar wind recurrence determ. at high heliographic latits. 0-62106
 scintillation spectra, radio spectrograph obs. rel. to electron density vars. physical form 0-72741
 scintillations, obs. rel. to solar wind plasma irregularities anisotropic struct. 0-67489
 shock wave, 1978 January 3 to 4, Prognoz-6 energetic particle and solar wind meas. 0-90315
 shock waves, collisionless, mag. structs. thickness 0-90314
 shock waves, collisionless shocks simulation and laboratory expts. 0-87893
 solar wind, He^+ flux after interplanetary shock, Imp 7 obs. 0-101520
 solar wind, low freq. continuum from ISEE 3, thermal electrostatic noise, LF obs. 0-10159
 solar wind, plasmadynamical processes review (German) 0-109323
 solar wind corotating structures, MHD model 0-90304
 solar wind interaction regions, N-S mag. field component solar cycle dependent configurations 0-98529
 solar wind sputtering rate 0-85835
 solar wind turbulent plasma, radio wave propag. meas. using three satellites 0-101518
 solar wind velocity determ. from interplanetary scintillation effects on 3C 279, SHF obs. (Russian) 0-77248
 Sun and heliosphere, conference, London, England (1979 April 3 to 4) 0-82574
 travelling interplanetary phenomena, space expts. related to Solar Maximum Year project 0-90404
 velocity distrib. from scintillation obs. 0-105143
 Venus environment, plasma wave investigation by Pioneer Venus Orbiter 0-67497
 zodiacal dust cloud, thermal emission at 11 and 20 microns 0-90367
 zodiacal light, new model for scatt. by irregular absorbing particles 0-67543
 H atoms from heliosphere, ionis. in near Sun region 0-105145
 H I, interstellar, interaction with solar wind 0-101506
 H I, $\text{L}\alpha$ emission profiles reanal. rel. to local interstellar gas temp. and vel. 0-105141
 He I, interstellar, obs. with gas absorpt. cell, implications for local interstellar medium struct. 0-62234
 He, interaction of solar wind with Sun's gravity focused He 0-105144
 He^+ , obs. in driver gas of interplanetary shock wave 0-72735

interplanetary medium *see* **interplanetary matter****interpolation***see also* **function approximation**

- biomedical surface mapping 0-81750
 computerised tomography, fan-beam to parallel-beam conversion by rubber sheet transformation 0-109009
 formant frequency and bandwidth conversion to reflection coefficients 0-91975
 two-beam interference fringe interpolation method 0-105703

interstellar dust *see* **cosmic dust****interstellar magnetic fields***see also* **interstellar matter**

- 3C 219, double radio galaxy, mag. field configurations from obs. at 1.48 and 4.89 GHz 0-77500
 3C 31, radio galaxy, mag. field struct. in radio jets 0-82526
 3C 58, supernova remnant, radioemission from mag. field interaction with relativistic electrons 0-73023
 Cassiopeia A, mag. field decrease rel. to radio spectrum secular flattening 0-101637
 direction correlation with planetary nebula major axes, hydromagnetic model 0-82473

H II regions continued

- Markarian 59, supergiant H II region in SBm galaxy NGC 4861 spectrum and struct. 0-98705
 in molecular clouds, evolution, effect of O-type star winds 0-94846
 N51D, bubble-like nebula in LMC, internal motions obs. 0-105295
 newly formed H II regions in interstellar dark clouds, physical props. from radio continuum interferometry 0-105301
 in NGC 1068, interpretation for emission line data 0-90519
 NGC 2264, classification of optical, IR and radio obs. data 0-67818
 in NGC 2366, dwarf galaxy, visible and radio obs. 0-77475
 in NGC 2997, morphology and hot spots around nucleus of galaxy 0-62282
 in NGC 3310, peculiar spiral galaxy, near nuclear H II regions exploratory investigation 0-62235
 in NGC 4314, barred spiral galaxy, distrib. from UBV surface photometry of central region 0-77482
 NGC 604, 5471, giant extragalactic H II regions, IUE UV spectra 0-77467
 NGC 604, in M 33, core-halo struct. 0-85984
 NGC 6334, H₂O masers mapping and star form. 0-73025
 NGC 6888, ring nebulae around Wolf-Rayet star HD 192163, spectra of filaments and smooth gas (*Russian*) 0-90515
 NGC 7000 (North America Nebula), rocket UV imagery 0-82440
 NGC 7000/IC 5070 complex, 28 W catalogue and sources at 610 MHz 0-105308
 NGC 7538, IRS 1, formaldehyde maser, SHF band obs. 0-67822
 NGC 7538 and Sharpless 159, H II region/mol. cloud complex, H I aperture synthesis obs. 0-90510
 observational properties rel. to planetary nebulae 0-109539
 origin from supernovae explosions 0-67877
 Orion A, H₂O maser source outburst obs. (*Russian*) 0-105320
 Orion Nebula, C abundance from visible and IUE obs. 0-82451
 Orion Nebula, forbidden Cl II and forbidden Fe II near IR high resolution mapping 0-62217
 Orion Nebula, He ionisation struct. and abundance, SHF obs. 0-105315
 Orion Nebula, IUE obs. of UV continuous spectrum 0-90499
 Orion Nebula, near IR photography with vacuum-cold camera 0-90341
 Orion Nebula, radio obs. of nearby H I distrib. and vels. 0-105322
 Orion Nebula (NGC 1976), long-slit spectroscopy in rocket UV 0-105297
 radio recombination lines, high-n, Zeeman splitting 0-58210
 S 213, assoc. with Berkeley 11 open cluster 0-94840
 Sh2-149, near IR photography with vacuum-cold camera 0-90341
 Sh2-156 (IC 1470), morphology, excitation and structure 0-67826
 Sharpless 106 IR sources, 8-13 micron spectrophotometry 0-105305
 Sharpless 115, evolved region, struct., UHF obs. 0-105313
 Sharpless 140, near IR slit scans of compact IR source (S140/IRS 1) 0-105300
 Sharpless 159 and NGC 7538, H II region/mol. cloud complex, H I aperture synthesis obs. 0-90510
 Sharpless 232, new background planetary nebula PN 173+3.1, visible obs. 0-105309
 Sharpless H II regions, assoc. H₂O maser emission detect. 0-62298
 shock fronts from OB-type stars H II regions, role in interstellar clouds form. 0-109506
 small H II regions with exciting stars, radio maps 0-62224
 in spiral galaxies, counts rel. to galaxy distance and luminosity 0-82484
 T Tauri nebula, ionisation and emission line spectrum calc. 0-67820
 in VV 126, multicomponent interacting galaxies, visible spectroscopy obs. (*Russian*) 0-77494
 in VV 794, photographic and spectral obs. (*Russian*) 0-77493
 W33, near IR slit scans of compact IR source in mol. cloud 0-105300
 W3, VLBI synthesis obs. and struct. of OH maser W3(OH) 0-105368
 W3 complex, CO, CS and HCN obs. LF obs. 0-82446
 W3 IRS 1, fine structure line radiation, dust UV opacity 0-90505
 W3 molecular cloud complex, model from mol. obs. 0-94843
 W3/W4/W5 region, heavy optical obscuration obs. 0-62301
 W49A, W51A, H109 α recomb. line, aperture synthesis obs. 0-105314
 W4, excitation by open cluster Ocl 352 0-94843
 W51-IRS 2 and W49 NW, IR spectra obs. 0-90497
 W58, galactic star-forming region, obs. of CO assoc. with H II region complex 0-67810
 W80 (Pelican Nebula), CO obs. of expanding mol. shell surrounding H II region 0-105296
¹²C¹⁸O and ¹²C¹⁶O J=2-1 transitions obs. 0-73022
 He abundance from 15 and 22 GHz recombination line obs. 0-98703
 OH type I maser sources, model 0-90556

hadron classification schemes

- hadron building blocks, pionic mass intervals in narrow and S-state resonances 0-105875
 trilocal structures, expansions 0-57460

hadron current

- see also current algebra
 No entries

hadron decay

- see also baryon decay; meson decay
 hadron production, coherent and inclusive, due to hadron-nucleus collision 0-83100
 pp collisions, high energy, fireball mass, rapidity, spin distrib. 0-57645

hadron-deuteron interactions

- see also hadron-deuteron scattering; hyperon-deuteron interactions; meson-deuteron interactions; proton-deuteron interactions
 inelastic screening, form factor at $t \neq 0$ 0-91070

hadron-deuteron scattering

- see also hadron-deuteron interactions; hyperon-deuteron scattering; meson-deuteron scattering; proton-deuteron scattering
 dd, gluon distribution 0-82939

hadron electroproduction

- baryon resonances, EM transitions, multipole moments in single quark transition model 0-62985
 charmed meson produced in e^+e^- annihilation 0-91106
 e^+e^- —hadrons, 9.4-10.4 GeV, three T states, mass spacings, lepton pair widths 0-68465
 meson electroproduction in correlating quark rearrangement model 0-86666
 new particles observed in e^+e^- annihilation 0-95283
 $c\bar{c}$ qq states, decay, hadronic and photo-prod., e^+e^- annihilation prod. 0-99092
 e^+e^- , hadron production, inclusive study, momentum distrib., energy and multiplicity 0-57613

hadron electroproduction continued

- e^+e^- 0-63010
 e^+e^- —jets, on-shell QCD quark form factor from two particle correlations 0-86740
 e^+e^- —3 jets, integer charge quark model, gluon jets 0-91101
 e^+e^- —3 jets, three gluon coupling in perturbative QCD 0-105913
 e^+e^- —4 jets, differential 4-jet acoplanarity distrib., QCD predictions, heavy quark prod. 0-78083
 e^+e^- annihilation, 10 to 40 GeV, hadron multiplicity 0-63007
 e^+e^- annihilation, charge current asymmetry as QCD test, neutral gluons 0-57616
 e^+e^- annihilation, gluon jets, multiplicity and ang. distrib. asymmetries 0-91105
 e^+e^- annihilation, hadron and lepton prod., τ -lepton decay, K^\pm , p, \bar{p} yields, quark flavours 0-73725
 e^+e^- annihilation, hadron multiplicity distribution, Regge like parton model (*Russian*) 0-78100
 e^+e^- annihilation, hadron prod. total cross section, CM energies 1.4-2.0 GeV 0-57619
 e^+e^- annihilation, QCD and semilocal duality (hadrons/ $\mu^+\mu^-$) cross section ratio 0-78085
 e^+e^- annihilation, QCD and jet acollinearity, quark-gluon coupling 0-105914
 e^+e^- annihilation, quark jet fragmentation into mesons and baryons, chain decay model 0-63001
 e^+e^- annihilation, three-jet analysis, minimisation of sum of squares of transverse momenta 0-63008
 e^+e^- annihilation and deep inelastic reactions, jet anal., thrust distrib., summing leading logs 0-63004
 e^+e^- collisions, jet prod. and two-photon annihilation, hadron spectra 0-91121
 e^+e^- — ΔX , polarisation effects in nonperturbative parton model, scaling 0-105912
 e^+e^- — e^+e^- qq(qq) + jet, $\gamma\gamma$ initiated 3 jet events in QCD 0-102057
 e^+e^- final states, qq decay, semiclassical model, vacuum polarisation by colour field 0-63011
 e^+e^- — γ^* — γ +hadrons, QCD predictions 0-63009
 e^+e^- — γ^* —hadrons, hadron calorimetric meas., QCD predictions, gluon emission 0-91102
 e^+e^- —hadrons, 12, 30 GeV, jets, quark fragmentation and coupling constant, QCD comparison 0-105915
 e^+e^- —hadrons, 12, 30 GeV, π, K, p, \bar{p} production 0-105916
 e^+e^- —hadrons, 33-35.8 GeV, new quark flavour search, cross sections and thrust 0-86736
 e^+e^- —hadrons, higher order QCD corrections 0-95280
 e^+e^- —hadrons, jets from heavy quarks, QCD perturbation theory 0-63012
 e^+e^- —hadrons, non-perturbative QCD vacuum, total cross section corrections 0-86735
 e^+e^- —hadrons, R problem, QED and QCD corrections, quarks and leptons 0-95281
 e^+e^- —hadrons, semiinclusive hadron prod., quark fragmentation function corrections, QCD 0-63013
 e^+e^- —hadrons, T, T', T'' states, mass differences, leptonic width ratio 0-68466
 e^+e^- —hadrons ($\mu^+\mu^-$), T(9.46) muonic branching ratio, total and leptonic width 0-86703
 e^+e^- inclusive hadron prod., polarisation and p nonconservation asymmetries, π, K^\pm, D^\pm prod. 0-78084
 e^+e^- —jets, energy cone distrib. around jet axis, QCD anal. 0-86737
 e^+e^- —jets, exclusive calcs. for QCD jets, Monte Carlo approach 0-105911
 e^+e^- —jets, jet ang. momentum, ang. distrib., oblateness and invariant mass, QCD calcs. 0-73722
 e^+e^- —jets, particle ratios from quark statistical model 0-73724
 e^+e^- —jets, t-quark pair prod. effects in annihilation, Kobayashi-Maskawa model 0-86733
 e^+e^- jets, two-particle distrib. from single-particle fragmentation functions, effects of heavy quark flavours 0-68468
 e^+e^- —multihadrons, planar three jet events, gluon bremsstrahlung, strong coupling constant 0-57617
 e^+e^- — $\pi^+\pi^-(K^+K^-)$, $\sqrt{s}=1.5$ GeV, EM timelike form factors for π and K 0-91089
 e^+e^- — $\pi^+\pi^-\pi^0$, 1.45-1.875 GeV, ω behaviour at 1.55 GeV 0-82984
 e^+e^- — $\pi^+\pi^-\pi^0$, 750-1100 MeV, ω and ϕ meson interference 0-105910
 e^+e^- — $\pi^+\pi^-\pi^+\pi^-$, 1.45-1.875 GeV, ρ behaviour at 1.55 GeV 0-82984
 e^+e^- —qqg, (3g), jet-mass spectra, perturbative QCD 0-63006
 e^+e^- —qqg, long. polarised beams, beam-event asymmetry, massless QCD null result 0-91104
 e^+e^- —three jets, acoplanar angle relative to beam polarisation, vector/scalar gluons 0-63005
 e^+e^- —VX, polarisation states and differential cross sections for πA_1 and $\rho^+\rho^-$ (*Russian*) 0-102059
 e^+e^- N, inclusive pion production due to $\gamma q \rightarrow \pi q'$ process, quark-parton model (*Russian*) 0-78073
 e^+e^- annihilation, 30 GeV, inclusive K^0 prod. $K^0 K^+/\mu^+\mu^-$ prod. ratio 0-91103
 e^+e^- annihilation, quark jets, transverse momentum profile 0-57621
 e^+e^- , high energy interactions (*Chinese*) 0-78074

hadron-hadron interactions

- see also baryon-baryon interactions; hadron-hadron scattering; meson-baryon interactions; meson-meson interactions
 charmed particle production, η_c, ψ and other $c\bar{c}$ bound states 0-63036
 cluster model, field theoretic, multiperipheral production, Feynman scaling violation 0-57576
 Drell-Yan muon prod., QCD correction uniqueness 0-78032
 forward hard scattering in hadron-hadron collisions in the energy region $\sim 10^{14}$ eV 0-86773
 forward jet production meas. in high transverse momentum hadron-proton collisions 0-101989
 hadron calorimeter expts., asymptotic power laws, QCD and parton model predictions 0-57560
 hadron induced multiparticle reactions, S-1500 GeV, resonance prod. correlations, jet model (*German*) 0-91118
 hadron production, multiplicity distribution, Regge like parton model (*Russian*) 0-78100
 hadron-hadron, in H, AL, inclusive particle distrib., QCD predictions 0-99112
 hadron-hadron 3-jet collisions, charge conjugation asymmetries and tri-linear gluon coupling 0-105934

hadron-hadron interactions continued

hadron-nucleus, pseudorapidity distrib., 24 GeV/c-4 TeV, energy and target depend. 0-91115
 hadron-nucleus, rapidity distrib., 22.8, 50, 400 and ≥ 1000 GeV in emulsion, multiperipheral models 0-91117
 hadron-nucleus (nucleon), relativistic secondary multiplicities, constituent quark rescatt. 0-63034
 hard processes, large rapidity separation of baryonic number, partons, and dual topology 0-95255
 heavy quark mesons, inclusive hadronic prod. (*Russian*) 0-86770
 high energy hadron-nucleus interactions, mean slow particle multiplicity mass depend. 0-102081
 high energy lepton pair prod. with pol. hadrons, P and C violations 0-99068
 inclusive cross section of symmetric hadron pairs produced, hard scatt., parton model and QCD 0-63052
 inclusive processes, large momentum transfer, quark counting, EM form factors 0-68498
 inclusive processes, multiplicity and scaling, resonance production, additive quark model, SU(6) theory, review 0-63043
 jet structure, two-jet events, glueball-Pomeron identity, dual field theory 0-63051
 jet structures of leptons, quarks and gluons, perturbative QCD, process dependence 0-68470
 Kopylov-Podgoretsky-Coconi formulation modification for hadron-hadron collisions 0-78044
 large p_T hadronic collisions, QCD sensitive test, quark and gluon jets 0-57647
 lepton pair production, QCD and hard-scatt. model, spin-spin asymmetries 0-63014
 lepton pair production, $q\bar{q}$ annihilation within same hadron, structure function anal. validity 0-57622
 mean multiplicity of secondary particles in hadron-nuclear interactions, multiple scatt. theory (*Russian*) 0-68502
 multiple hadron production and struct. from 10 GeV to 10 TeV interactions 0-57653
 neutron stars, determ. from pulsars and compact X-ray sources 0-77442
 partial inelasticity coefficients in hadron interactions with various targets (*Russian*) 0-68483
 photon production, AB- $\gamma\gamma X$, scaling and quark mass dependence, quark parton model 0-73749
 prompt lepton sources from hadronic collisions 0-73726
 QCD and short range nuclear phenomena 0-91060
 quark fragmentation functions for inclusive hadron production, Regge formalism 0-68462
 quark-parton cascades in nuclei and secondary hadron spectra from hadron-nucleus collisions (*Russian*) 0-57623
 s-channel resonance model based on peripheral resonances, exotic peaks 0-91069
 soft hadron-nucleus collisions, two chain parton model description 0-82944
 temperature parameter for thermal-like emission spectra, fluctuations 0-68482
 three hadron systems, resonance peaks, Brayshaw mechanism validity 0-73732
 $h_2 \rightarrow i\bar{l}X$, massive lepton pair prod., polarisation and spin effects 0-105929

hadron-hadron scattering

see also baryon-baryon scattering; hadron-hadron interactions; meson-baryon scattering; meson-meson scattering
 elastic hadron-hadron diffraction scatt. processes, scaling, conformal mapping without spurious cut 0-82992
 gluon fragmentation, polarised 0-82988
 hadronic diffraction, elastic scatt. as tunnelling phenomenon, dual model relation 0-57575
 hadronic interiors, meas. and charge distrib., hadronic diffraction scatt. 0-73817
 large-angle scattering, quasi-potential approach, pre-asymptotic effects 0-68484
 SU(1,3), dynamical group for non-charmed hadron scattering states 0-62883

hadron interactions *see hadron-deuteron interactions; hadron-hadron interactions; lepton-hadron interactions; photon-hadron interactions*

hadron leptonproduction

see also baryon production; hadron electroproduction; meson production
 deep inelastic lepton-hadron scatt., semiinclusive hadron prod., quark fragmentation function corrections, QCD 0-63013
 deep inelastic leptonproduction, normalising the renormalisation group anal., QCD twist effects 0-86690
 deep inelastic leptonproduction, meson bound state contrib. to σ_L/σ_T 0-78029
 lepton+nucleon, quark and gluon jets, Breit frame, QCD 0-62995
 nuclear targets, quark-nucleon inclusive cross section, heavy lepton pairs 0-57607
 nucleus+lepton, coherent and inclusive prod. of hadrons with low P_T , Coulomb excitation and decay of projectile 0-83100
 totally inclusive leptonprod., scaling anal., target mass corrections in QCD parton model 0-102052
 in deep inelastic scattering, quark jet as trigger for gluon jet 0-62996
 $\mu^- N \rightarrow$ hadron shower, charm-pair production effects 0-73748
 $\mu p \rightarrow K^0 X$, 225 GeV, deep inelastic scatt., strange neutral particle prod. 0-105902
 $\mu p \rightarrow \Delta^0(A^0)X$, 225 GeV, deep inelastic scatt., strange neutral particle prod. 0-105902
 $\nu N \rightarrow$ hadron shower, charm-pair production effects 0-73748
 $\tau \rightarrow \nu_\tau +$ hadron(s), decay modes and ν_τ mass 0-63057

hadron-nucleus reactions

see also hyperon-nucleus reactions; meson-nucleus reactions; nucleon-nucleus reactions
 baryonic inclusive spectra in hadron-, photon- and HI-nucleus collisions, fireball model 0-86892
 cascade model, space-time model, extension to photon- and lepton-nucleus collisions 0-68633
 deep inelastic electro-creation by polarised vector mesons (*Russian*) 0-102209
 hadron-hadron, in H, AL, inclusive particle distrib., QCD predictions 0-99112
 hadron-nucleus (nucleon), relativistic secondary multiplicities, constituent quark rescatt. 0-63034

hadron-nucleus reactions continued

heavy nucleus, coherent and inclusive prod. of hadrons with low P_T , Coulomb excitation and decay of projectile 0-83100
 high energy hadron-nucleus interactions, mean slow particle multiplicity mass depend. 0-102081
 independent particle model, extension to spectator-participant model for central heavy ion reactions 0-73861
 leading particle spectra on nuclear targets and multi-chain model 0-73829
 massive lepton pair production as a test of models for particle production on nuclei 0-102213
 mean multiplicity of secondary particles in hadron-nuclear interactions, multiple scatt. theory (*Russian*) 0-68502
 multi-chain model, recoil nucleon effect 0-83124
 multihadron production in nuclear matter and hadron struct., space-time description, review (*Russian*) 0-68571
 multiparticle production, multiplicities, cross sections and ang-distrib. 0-86768
 optical pot. eqns. for low and moderate energies (*Russian*) 0-63214
 pseudorapidity distrib., 24 GeV/c-4 TeV, energy and target depend. 0-91115
 QCD and short range nuclear phenomena 0-91060
 quark-parton cascades in nuclei and secondary hadron spectra from hadron-nucleus collisions (*Russian*) 0-57623
 rapidity distrib., 22.8, 50, 400 and ≥ 1000 GeV in nuclear emulsion 0-91117
 soft hadron-nucleus collisions, two chain parton model description 0-82944
 spatial temporal development, nuclear hadronic cascades 0-63040

hadron-nucleus scattering

see also hyperon-nucleus scattering; meson-nucleus scattering; nucleon-nucleus scattering
 No entries

hadron photoproduction

see also baryon photoproduction; meson photoproduction
 baryon resonances, EM transitions, multiple moments in single quark transition model 0-62985
 baryon spectroscopy and photoproduction couplings using new baryon wavefunctions 0-102016
 charm photoprod. with linearly pol. photons, QCD calcs., gluons 0-68464
 higher order QCD jets in photoproduction 0-99087
 large p_T photoproduction, gluon fragmentation function extraction, scaling 0-105853
 vector boson pair photoprod., theoretical cross sections 0-57610
 e^+e^- $q\bar{q}$ states, decay, hadronic and photo-prod., e^+e^- annihilation prod. 0-99092
 e^+e^- collisions, jet prod. and two-photon annihilation, hadron spectra 0-91121
 $e^+e^- \rightarrow e^+e^- + 2$ jets, $\gamma\gamma \rightarrow q\bar{q}$ contrib. to cross section, QCD corrections 0-78106
 $e^+e^- \rightarrow e^+e^- g(q\bar{q}) +$ jet, $\gamma\gamma$ initiated 3 jet events in QCD 0-102057
 e^+e^- initiated $\gamma\gamma$ processes, charged pair prod., $f_0 \rightarrow \gamma\gamma$ width 0-91123
 $\gamma^* \gamma^* \rightarrow 2$ jets in e^+e^- , parton model QCD corrections for doubly deep processes 0-73758
 γN , exclusive photoprod. reactions, Okubo-Zweig-Iizuka rule 0-95277
 γN , inclusive pion production due to $\gamma q \rightarrow \pi q$ process, quark-parton model (*Russian*) 0-78073
 $\gamma p \rightarrow \pi^+ n$, 600-1875 MeV, pol. p and γ , G and H polarisation parameters 0-99105
 $\rho'(1600)$ meson resonance from 2- and 4-pion distrib. in photoproduction data 0-95279

hadron production

see also baryon production; hadron leptonproduction; hadron photoproduction; meson production
 gluon-gluon interactions, hadron prod. and $\sigma(\text{total})$ growth at high energies 0-91049
 hadron+hadron, cluster model, field theoretic, multiperipheral production, Feynman scaling violation 0-57576
 hadron+hadron inclusive cross section of symmetric hadron pairs produced, hard scatt., parton model and QCD 0-63052
 hadron inelastic scatt., secondary hadron multiplicity distribution, Regge like parton model (*Russian*) 0-78100
 hadron interactions, inclusive, large momentum transfer, quark counting, EM form factors 0-68498
 inclusive hadron production, quark fragmentation and triple Regge models, quark decay functions 0-62921
 inclusive processes, multiplicity and scaling, resonance production, additive quark model, SU(6) theory, review 0-63043
 jet phenomenon and Lorentz deformation 0-105806
 multihadron production in nuclear matter and hadron struct., space-time description, review (*Russian*) 0-68571
 multiple hadron production and struct. from 10 GeV to 10 TeV interactions 0-57653
 nucleus+hadron, coherent and inclusive prod. of hadrons with low P_T , Coulomb excitation and decay of projectile 0-83100
 pp collisions, high energy, fireball mass, rapidity, spin distrib. 0-57645
 QCD, high P_T hadron prod. in pionisation region and vacuum singularity (*Russian*) 0-86772
 QCD hadron jets, branching processes, multiplicity distrib., KNO scaling (*Russian*) 0-101998
 quark fragmentation functions for inclusive hadron production, Regge formalism 0-68462
 quark-parton cascades in nuclei and secondary hadron spectra from hadron-nucleus collisions (*Russian*) 0-57623
 relativistic nuclei collisions, multi-hadron prod. mechanism 0-57763
 e^+e^- annihilation, jets, colour-singlet subsystems, large rapidity gaps 0-68469
 $e^+e^- \rightarrow e^+e^- (\mu^+ \mu^-) (\tau^+ \tau^-)$, high energy colliding beams, Mark J detector study 0-95282
 $pN \rightarrow$ hadron shower, charm-pair production effects 0-73748
 $pp \rightarrow$ hadrons, phase transition in Feynman-Wilson analogue fluid, multiplicities, plateaus, cross-sections 0-73744
 $pp \rightarrow X$, 205 GeV/c, leading p spectrum, random walk hypothesis, geometric bremsstrahlung model 0-68493
 $Y \rightarrow 3g$, angular patterns and front-back moments, QCD 0-73702

interstellar matter continued

- OH⁺ in interstellar clouds 0-67828
- S chemistry 0-101632
- S II in ζ Ophiuchi interstellar spectrum, abundance upper limit 0-82445
- Si IV column density towards early-type stars 0-73018

interstitials

see also Cottrell atmospheres; crowdions; Snoek effect

- alkali halide, crystal, irradiation-induced defects 0-107316
- alkali halide crystals, defect fermion properties, ionic cond. calcs. 0-59457
- alkaline earth fluoride, doped with trivalent rare earths, migration entropy for bound fluorine molecule 0-71303
- alkaline earth fluoride based solid solns., ion transport 0-107545
- alloys, interstitial atomic arrangement and mobility at high degrees of interstice filling (*Russian*) 0-107223
- BCC crystal lattice containing interstitial atom in split config., reson. and localised vibr. (*Russian*) 0-84268
- chemical potentials of structural elements of compounds and face or dislocation specificity, thermodynamic parameters 0-96514
- creep, irradi. induced in transient irradi. environments 0-92598
- creep, swelling and growth, radiation induced, bias factors estimated from self-consistent model 0-88249
- creep and growth, irradiation induced, solute effects on defect precip. rate 0-88252
- creep and growth, radiation induced, fundamental mechanisms 0-92596
- defect diffusion coeffs., site blocking, correlated defect motion 0-84315
- dislocation motion, lattice resist., effect of impurity interstitials 0-84170
- disordered binary alloys of ferromag. crystals, mag. dipole fields at interstitial sites 0-97176
- exotic atoms, conf., Erice, Sicily, (1979) 0-67939
- Fick's equations solutions for impurity diffusion, dislocations, interstitials, vacancies 0-70469
- Fokker-Planck eqn. describing evolution of interstitial loop microstruct. during irradiation 0-107215
- Frenkel defects, form. and collapse, defect migration, electron irradi. effects, computer simulation 0-92523
- fusion reactors, inertial confinement, interstitial loop formation, point defect clustering 0-63378
- glass, ionic conductivity, weak electrolyte theory 0-84322
- graphite, irradi., lattice expansion, vacancies and interstitials contrib., bond order role 0-65042
- HCP lattice, Huang diffuse scatt. from interstitials 0-88142
- intermetallic hydrides, interstitial site occupation by H atoms, quantitative model 0-96517
- interstitial site determ., μ SR technique 0-71287
- ion implantation, net recoil density 0-88175
- irradiation-induced, recombination rate with vacancies 0-96516
- LMFBR materials, interstitial loop nucleation and growth during irradiation, Fokker-Planck equation, numerical soln. 0-57857
- LMFBR materials, interstitial loop nucleation and growth during irradiation, Fokker-Planck equation, numerical soln. 0-68796
- mass flux, irradiation enhanced, dislocation interactions 0-88206
- metal, electron irradi., self-interstitial atomic defect interaction radii, recovery expts. and error sources 0-65049
- metal, H(D) diffusion, role of tunnelling, reson./nonreson. approaches 0-59718
- metal, ion implanted H(D), interstitial positions and vibr. amplitudes, fast ion channelling study, review 0-79848
- metal, irradi., containing pre-existing dislocations, interstitial loop form. kinetics 0-65040
- metal halides, fluoride structure, retarded ionic motion 0-88361
- metals, BCC, diffusion of H₂ and its isotopes, phonon-assisted quantum-mechanical tunnelling of interstitials 0-59730
- metals, dissolution of interstitial H₂ and D₂, diffusion coeffs., reverse isotope effect (*Russian*) 0-88368
- metals, dynamical props. of point defects, book contrib. 0-103317
- metals, FCC, H₂ diffusion, isotope depend. 0-59727
- metals, interstitial loop growth, pulsed irradi. effects 0-88210
- metals, light interstitials diffusion, multiphonon transition modes classification 0-70448
- metals, point defect diffusion controlled reaction theory, book contrib. 0-103318
- metals, point defect dynamic props. and diffusion controlled reactions, book 0-101674
- metals, two and one interstitial model explanation of elec. cond. variations 0-88143
- metals and alloys, FCC, interstitial diffusion, theory (*Russian*) 0-65296
- migration kinetics and thermodynamics 0-107461
- NMR spin relaxation, motion-induced, in low. temp. HF limit 0-60443
- non-metallic crystals, electric field influence on defect creation mechanism 0-70251
- nonstoichiometric compounds, physicochem. props. depend. on short-range order struct. 0-100227
- nuclear fuels, creep, irradiation induced, transient state, kinetic eqn. treatment 0-88251
- point-defect clustering during irradiation 0-92521
- radiation defect production, exact solns. of models for continuous and pulsed irradi., implications for stability and fluctuations 0-65041
- semiconductor, large-band-gap, self-compensation, role of impurities 0-92850
- solid solution, binary, radiation-induced instability, contrib. of dissipative processes 0-65039
- steel, stainless 316, Fokker-Planck eqn. describing evolution of interstitial loop microstruct. during irradiation 0-107215
- superionic fluorites, structure and transport 0-84318
- ternary BCC alloys, ordering process, effect of short-range order (*Russian*) 0-84908
- transition metal, BCC, neutron spectroscopy of fast H diffusion 0-59731
- transition metal-H systems, energy and electron density of states, improvements to theory 0-70636
- transition metals, BCC, interaction energy between self-interstitial and screw dislocation, calc. 0-70248
- triglycine calcium bromide:Cu²⁺, ESR studies 0-97136
- void, and interstitial loop evolution in pulsed fusion reactors 0-84217
- voids, coated, capture efficiency 0-96515
- Zircaloy-2, irradiation growth, reaction rate theory calcs. 0-88212
- Zircaloy-2, irradiation growth, shape and volume changes 0-92562
- Ag film, defect density, thickness depend., elec. resist. obs. 0-70568
- AgCl(Br), point defect form. energies, atomistic calc. and surface pot. meas. 0-107221

interstitials continued

- α -AgI, structural and dynamical behaviour 0-107544
- AgI: Cd, polycrystalline, thermoelectric power meas. 0-59698
- Al, film, superconducting transition temp. and lattice dynamics 0-93028
- Al, foil, influence of O₂-pressure on oxidation rate, TEM study 0-104355
- Al, interstitial loop form., effects of repeated electron irradi. 0-75220
- Al, proton irradiation, Al atomic displacement position study 0-103401
- Al-C interstitial solid solns., atomic static displacements and deform. interaction (*Russian*) 0-64953
- Al-Ge (0.1 wt.%), channelling meas. of Al interstitial atom trapping by Ge atoms 0-59537
- AlH₃, electronic struct. and electron-phonon interaction, hydrogenation effect, rel. to supercond. 0-107694
- β -Al₂O₃, conduction and dielec. loss mechanisms, paired interstitiality model 0-107468
- Al₂O₃, sapphire, edge dislocation loop obs. by high resolution lattice imaging 0-103346
- β -Al₂O₃-Na₂O, cond. plane struct. and energetics 0-92715
- Au, calc. images and diffraction patterns 0-100152
- Au, heavy ion irradi., cascade energy density effect on defect cluster type 0-107340
- B-Cr, paramagnetic centre struct. and defect form. 0-66034
- BaF₂, F⁻ interstitial and substitutional trivalent cations, phonon reson. and IR absorpt. 0-84752
- BaTiO₃:C, solubility of C at low O₂ potentials, 800°C 0-100334
- Be, ion-implanted, impurity lattice location, channelling meas., Monte Carlo calc. 0-107291
- CaF₂:Eu(Gd)(Dy)(Tb), dimer reorientation activation volume 0-107285
- CaF₂:alkali metal cation, thermal depolarisation study 0-108147
- CaF₂:O²⁻, CaF₂:Na⁺, O²⁻ and CaF₂:Y³⁺, O²⁻, thermal depolarisation obs. of defect clusters 0-71299
- CaF₂:Y³⁺, ionic cond. and thermal depolarisation obs. of defect clustering 0-71298
- CdF₂:Na(Nd), ionic cond. investigation by complex admittance method 0-100352
- CdF₂:Sm³⁺, photoconverted, thermally stimulated relax. 0-84476
- Cd, Hg_{1-x}Te, long term stability at 300K, rel. to device appl. 0-59978
- CdS, defect struct. and config. produced by irradi., elastic scatt. expts. 0-84178
- γ -Ce, FCC, localised vibration of interstitial H impurities 0-75322
- Ce, interstitial site determ., μ SR technique 0-71287
- Cs halides: H₂, luminesc. of interstitial atomic H 0-103986
- Cu, dislocation pinning rate, neutron and electron irradi., meas. by internal friction method 0-96570
- Cu, electron irradi., migration and thermal conversion of defects, 100 to 330K 0-59519
- Cu, H₂ diffusion, isotope depend. 0-59727
- Cu, ion bombard. by 5 keV Ar⁺, sub-surface damage 0-103399
- Cu, μ^+ diffusion data anal., theory of incoherent direct and indirect multiphonon transitions 0-70448
- Cu, neutron and electron irradi., interstitial formation, dislocation pinning, internal friction meas. 0-100284
- Cu, point and planar defects, computer simulation 0-59455
- Cu-M-O ternary liquid alloys, thermochem. calcs. 0-85209
- Cu_{2-x}S, and related disordered crystals, diffr. pattern, cluster theory 0-75123
- p-Cu₃VS₄, mixed conduction due to cationic interstitials 0-70772
- Dy, interstitial site determ., μ SR technique 0-71287
- Fe, pure and doped, electron irradi., mag. aftereffect 0-88838
- Fe, trapping of H, average trapping depth and trapping sites density 0-84297
- α -Fe:B(C)(N)(O), valency effect of interstitials 0-65502
- Fe-Al(Ti), O containing, mag. aftereffect and disaccommodation meas., time depend., activation energy, and ageing props. 0-88836
- Fe-Pd, magnetic after-effect of H isotopes 0-75817
- Fe_{0.49}Mn_{0.01}Ti_{0.5}H, localised vibrs., sp. ht. obs., room temp. 0-65248
- Fe_{0.545}Sb, temperature effect on lattice consts., Mossbauer spectra and density 0-88124
- Fe_{1-x}Sb, nonstoichiometry influence on mag. props. (*Russian*) 0-65813
- Gd, interstitial site determ., μ SR technique 0-71287
- Ge, electron beam irradi., [113] faults, nature and origin 0-70258
- Ge, ion beam irradi., defects prod. by individual displacement cascades, TEM study 0-70265
- Ge:Cu, solubility and behaviour of Cu, internal friction investigations 0-92678
- HF with interstitial O, quantitative TEM obs. of small agglomerates 0-107227
- HfV₂D₄, disordered solid solution, order-disorder transition 0-88321
- K- β -Al₂O₃, far IR absorpt., Bevers-Ross sites, interstitials 0-66240
- KBr, defect accumulation under electron irradi. at 4K 0-107233
- KBr:I⁻, OH⁻, luminesc. of interstitial atomic H 0-89062
- KCl, Born-Mayer parameters of He and Ar, interstitial interaction with neighbouring ions 0-100228
- KCl:Br⁻(I⁻), interstitial atomic H centres, formation kinetics and struct. M calc. and EPR studies 0-75854
- K₂OsCl₆, Cl NQR spectra by Fourier transform methods 0-75879
- K₂OsCl₆, impurity H⁺ ion motion, ³⁵Cl NQR obs., 77 and 298K 0-60451
- K₂OsCl₆, single cryst. with H⁺ interstitials, protonic cond. from dielec. meas. 0-107515
- LaNi₅/H system, thermodynamics of H trapping 0-107444
- LiF, γ -irrad. pure and Mg-doped, phonon scatt. and interstitial clusters 0-70254
- LiH, defect form. at low temp., EPR, thermolum. and TSC study 0-107222
- Li₃N, interstitial sites and anharmonic thermal vibrs. in cryst. struct., ionic cond. mechanism 0-107190
- Mg, HCP, vacancy clusters and interstitials, computer simulation study 0-64992
- Mg, HCP lattice, Huang diffuse scatt. from interstitials 0-88142
- MgAl₂O₄, faulted defect aggregates prod. by neutron-irrad. 0-107331
- MgO, electron irradiation damage, cryst. defects 0-107320
- Mo alloys, dil., HVEM bombarded, neutron damage simulation, defect cluster and dislocation obs. 0-107330
- Mo, H₂ diffusion enhanced by self-interstitial atoms, surface reaction const. determ. 0-75386
- Na, adsorbed on Al, adatom valence-level position variation 0-88611
- Na- β -Al₂O₃, far IR absorpt., Bevers-Ross sites, interstitials 0-66241
- NaCl, Born-Mayer parameters of He and Ar, interstitial interaction with neighbouring ions 0-100228

interstitials continued

- NaMgF₃, defects induced by X- and vacuum UV irradi., optical and elec. study 0-107319
 Na₂O-SiO₂ glass, conduction and dielec. loss mechanisms, paired interstitial model 0-107468
 Nb, elec. resist. due to interstitial H (D) 0-96848
 Nb, ion bombard. by 5 keV Ar⁺, sub-surface damage 0-103399
 Nb, solute trapping of H, symmetry of O-H pair 0-108488
 Nb-D-H, equilb. H/D separation factors 0-59668
 Nb-Ta(V)(Ti)(Mo), resistivity due to H incorporation 0-70666
 NbH₃, structural transform. rel. to order-disorder transform. 0-60858
 Ni, electron irradi. in HVEM, interstitial loop growth 0-107326
 Ni, interstitial site determ., μ SR technique 0-71287
 NiAl, nonstoichiometric, interstitial defect cluster obs. 0-107226
 Ni₂F₆, disaccommodation meas. after low temp. electron and neutron irradi. 0-88832
 Ni₁₀₀Sb, temperature effect on lattice const., Mossbauer spectra and density 0-88124
 Pb and Pb alloys, interstitial substitutional model for anomalous diffusion 0-84330
 Pb-Au, interstitial and substitutional distrib. 0-84204
 Pb_{1-x}Bi_xF_{2+x}, solid soln., struct. and ionic cond. correl., neutron diffr. study (*French*) 0-84324
 PbF₂ based solid solns., ion transport 0-107545
 Pd, elec. resist. due to interstitial H (D) 0-96848
 Pd-Ag-H(D), elastic energy dissipation peak 0-60905
 Pd-D-H, equilb. H/D separation factors 0-59668
 Pd-H system containing d impurities, chem. binding energies of point defects 0-107214
 Pd-H(D), elastic energy dissipation peak 0-60905
 Pd-Pt-H(D), elastic energy dissipation peak 0-60905
 Pd_{1-x}Pb_x, cryst. struct., X-ray study 0-103293
 Pt, ion irradi. damage, temp. depend., electron microscopy obs. of defect kinetics 0-107339
 Pt, recovery spectrum after thermal neutron irradi., resist. obs., Au addition effect and defect conc. depend. 0-65057
 RbBr:1⁻, OH⁻, luminesc. of interstitial atomic H 0-89062
 RbCl:Br⁻(I⁻), interstitial atomic H centres, formation kinetics and struct. MO calc. and EPR studies 0-75854
 RbMnF₃, pure and doped, unirradiated and electron irradi., energy transfer 0-108254
 Si, ambient effect of O precipitation, self interstitial mechanisms, IR spectra, TEM study 0-66510
 Si, amorphous layer prod. by ion implantation, diffusion broadening, ESR study 0-92552
 Si, Czochralski grown, dislocation free, swirl defect form., doping effect 0-92519
 Si, Czochralski grown crystal, O precip., nucleation behaviour and dislocation loop form. (*Japanese*) 0-59664
 Si, defects, divacancy and split 100 interstitial, electronic structure calc. 0-65494
 Si, diffusion mechanism of P, migration channels along vacancies and interstices 0-79996
 Si, electron beam irradi., [113] faults, nature and origin 0-70258
 Si, high dose self-irrad., spatial correlate. between primary and secondary defect profiles 0-59536
 Si, ion beam irradi., defects prod. by individual displacement cascades, TEM study 0-70265
 Si, ion implanted, interstitial generation and loop form. during annealing in oxidising medium 0-107225
 Si, oxidation stacking faults, shrinkage and growth, bulk O₂ effects 0-96546
 Si, thermal oxidation kinetics, steady-state transport anal. 0-71773
 Si, thermal oxidation kinetics, theoretical perspective 0-76387
 Si wafer, trap centres of self-interstitials 0-75516
 Si:Al, electron irradi. induced defects, transient capacitance study 0-59516
 Si:B (0.2 wt.%) ion implanted, B atom displacement due to low temp. irradi. 0-88234
 p-Si:B(Al), radiation defect form. and annealing study using Hall effect, cond. and carrier diffusion length 0-84214
 Si:Fe, solubility study by EPR and neutron activation anal. 0-75361
 Si:P bipolar transistors, interstitial supersaturation and misfit dislocation climb, TEM study 0-70203
 Si:Sb, Mossbauer spectra of ¹¹⁹Sn defect struct. 0-97174
 Si:Sn, Mossbauer study of defects due to ¹¹⁹Sn implantation 0-80641
 Si:Te, Mossbauer spectra of ¹¹⁹Sn defect struct. 0-97175
 Sm, electron radiation damage, elec. resistivity change rates 0-59954
 SmS type semiconductors, electronic struct., influence of point defects 0-70650
 α -Sn, ion implanted, defect struct., Mossbauer spectra 0-80214
 Sn:Cu, CVD coating on glass, elec. resist. rel. to cryst. microstruct. 0-84520
 SrCl₂, ionic cond., self-diffusion, rel. to defect motion, mol. dynamics study 0-65282
 SrCl₂, point defect parameters, ionic cond. study 0-107490
 SrCl₂, pure and doped, disorder and defect props. 0-107217
 SrF₂:La, type-I dipole reorientation, activation vol. determ. from dielec. const. 0-88916
 SrO:Co, noncentral and interstitial ion complexes, ESR obs. 0-71169
 Ta BCC lattice, strain ordering in interstitial solutions 0-107420
 Ta, elec. resist. due to interstitial H (D) 0-96848
 Ta, resistivity due to H incorporation 0-70666
 TaS₂ (1T) electron irradiated, lattice contraction 0-59520
 Ti, neutron irradiated, characterization of dislocation loops 0-88155
 Ti-Ta (4.37 wt%), oxidation kinetics, 1258-1473K, and at pressure of 0.013, 0.133 and 1.0 bar 0-89411
 γ -TiH₃, interstitial H diffusion mechanism, NMR spin-lattice relax. study 0-103515
 TiO₂, nonstoichiometry study, thermal emission of electrons 0-108317
 TiO₂:Cr(Ta), slightly doped, elec. cond. and defect struct., charge compensation and point defect model 0-75568
 TiO₂:Mo³⁺, interstitial EPR, g-tensor and hyperfine tensor 0-84647
 U, irradiation growth during fission fragment and proton bombard. 0-92568
 V, elec. resist. due to interstitial H (D) 0-96848
 V, electron-irradiated, positron annihilation study 0-70259
 V-H single crystals, elastic const., temp. depend., H effects 0-66563
 V-O alloys, quenched, local ordering of O, electron microscopy and diffr. 0-59453
 α -VD_{0.7}, vibrations of interstitial D, coherent neutron scatt. 0-96612

interstitials continued

- Y, electron radiation damage, elec. resistivity change rates 0-59954
 YH₃, location of H, PMR rigid-lattice second moment meas. 0-71198
 Y₂O₃, nonstoichiometry study, thermal emission of electrons 0-108317
 Yb, electron radiation damage, elec. resistivity change rates 0-59954
 Zn, HCP lattice, Huang diffuse scatt. from interstitials 0-88142
 Zn single cryst., dislocation velocity and plastic deform. 0-64998
 ZnO, irradiation in high voltage electron microscope dislocation loops study 0-88157
 Zn₃P₂, elec. cond., Hall effect, P interstitial effects 0-84465
 ZnSe, heat-treated in controlled partial press. of Zn or Se, TSC 0-59910
 ZnSe, self-compensation, role of impurities 0-92850
 Zr alloys, creep and growth, irradiation induced, rate theory approach 0-89294
 Zr alloys, creep and growth, irradiation induced, microstruct. depend. 0-93602
 Zr and alloys, neutron irradi. at 573 to 923K, damage struct. 0-107334
 Zr, irradiation growth, reaction rate theory calcs. 0-88212
 Zr, void swelling during electron irradi., HVEM study 0-92559

intersystem crossing see nonradiative transitions

intramolecular potentials see potential energy functions

intramolecular vibrations see molecular vibration; molecular vibration in solids

intrinsic magnetisation see spontaneous magnetisation

Invar

- magnetic structure, depend. on absorbed H, Stoner's band model calcs., Mossbauer spectra 0-65787
 magnetoelastic contribs. to US vel., elastic const., and susceptibility 0-75829
 phase stability, spinodal decomposition 0-88327
 RF collapse and thermal effects, Mossbauer study 0-100624
 superfine mag. struct. (*Russian*) 0-80572
 Fe-Ni, Curie point, annealing effects and time depend. 0-80508
 Fe-Ni (308-44.1 at.%) Invar alloys, anomalous mag. anisotropy and thermal expansion 0-75755
 Fe-Ni (36 wt.%) alloy 36N, effect of melting conditions on thermal expansion coeff. 0-65256
 Fe-Ni film, electrodeposited, struct. and mag. props. 0-107668
 Fe-Ni Invar, magnetovolume coupling enhancement factor, temp. depend. 0-88851
 Fe-Ni Invar alloys, splat quenched, mag. props. 0-75799
 Fe-Ni Invar alloys of crit. conc., mag. props., flow theory methods (*Russian*) 0-65894
 Fe-Ni Invar anomalies, explanation in terms of itinerant electron magnetism 0-75705
 Fe-Ni-C, coated, Mossbauer spectra, effect of applied RF mag. field 0-80645
 Fe-Ni(Pt) Invars, elastic and mag. props., magnetoelastic interaction effects (*Russian*) 0-84631
 Fe-Ni(35.4 at.%) Invar alloys, T² term contribution to magnetisation 0-71096
 Fe-Pd Invar, low temp. FCT phase obs. 0-93538
 Fe-Pd Invar alloy, Young's modulus, magnetostriction, Curie temp. 0-65988
 Fe-Pd Invar alloys, elec. and mag. props. and thermal expansion 0-75732
 Fe-Pt, Invar alloy, paramag. susceptibility 0-70940
 Fe-Pt, magnetoelastic contribs. to US vel., elastic const., and susceptibility 0-75829
 Fe-Pt Invar alloys, magnetocrystalline anisotropy const. determ. 0-65861
 Fe₂P, ordered ferromagnetic alloy, magnetic excitation obs. 0-70978
 Fe₂P Invar alloy, anomalous Curie const., susceptibility meas. 0-75731
 Fe₂P Invar alloy, thermal expansion and spontaneous magnetisation, Invar anomalies, low spin model 0-71001
 Fe₂P:Sn Invar alloy, Mossbauer shift temp. depend. 0-100626
 Ni-Fe Invar, thermal expansion and spontaneous magnetisation, Invar anomalies, low spin model 0-71001

invariance

see also conservation laws

- adiabatic invariance of particle in selfgravitating spherical dust shell 0-105459
 education, classical mechanics gauge invariance, derivation of Maxwell's eqns. 0-73131
 molecular geometry optimisations, invariance criteria, symmetry conservation rules 0-58406
 QCD, renormalisation group, confining and asymptotically free soln. 0-62881

inversion layers

- MIS inversion layer solar cells, two-dimensional model 0-89641
 MIS tunnel diode, minority-carrier, pot. barrier height 0-96998
 MISIM struct. inversion layer, symmetrical, carrier conc. calc. 0-75651
 MOS interface states density, photoemission obs. using photocurrent and photocapacitance meas. 0-92990
 MOS inversion layers, freq. response of charge transfer 0-88638
 MOS structure, 2D electron gas, for IR Faraday rotation 0-80389
 MOS structure with nonuniformly doped semiconductors, heavy inversion, definition for onset 0-96994
 MOS structures, inversion layer near electrode edge, pot. and charge density distribution 0-88642
 MOS structures of small-gap semicond., capacitance, effect of quantising mag. field 0-84513
 narrow gap semiconductor, modification of Einstein relation for inversion layers in strong elec. field 0-96959
 semiconducting surface inversion layers, exchange and correl. 0-75618
 semiconductor, surface depletion and inversion, arbitrary doping profile, theory 0-107912
 semiconductor surface space charge layers, subband struct., perturbation theory 0-84497
 Si, mobility temp. depend., Coulomb and surface roughness scatt. 0-80390
 solar cells, numerical modelling 0-81444
 p-CdTe-Langmuir film interface, prep., characters. and MIS struct. 0-92998
 Hg_{1-x}Cd_xTe, Einstein relation for inversion layers 0-103706
 InP and InGa_{1-x}As_xP_{1-y} binary and quaternary cpds., surface and dielec. semicond. interface props. 0-93001
 InP inversion-type MISFET with SiO₂ gate insulation interface props., elec. drift 0-93002
 InP-Si₃N₄ (SiO₂), interface props., plasma deposited dielectrics, n-channel MOSFET action 0-93003
 InSb, Einstein relation for inversion layers 0-103706

inversion layers continued

- InSb MOS struct., capacitance of n-channel inversion layers, elec. field effects 0-80393
 n-inversion layers, (001), K_1 -depend. of subband energies 0-103738
 n-Si, (111) inversion layers, valley splitting, Shubnikov de Haas oscils. 0-65698
 Si, (100) inversion layer, electromigration in two dimensional electron gas, driving force 0-84441
 p-Si, (100)-oriented, n-channel inversion layers, MOS field-effect devices, mag. quantisation effect on surface capacitance 0-70834
 n-Si channel (100) inversion layer MOSFET, valley splitting, conductivity 0-70840
 n-Si inversion layers, electronic g-factor, spin-split Landau levels 0-80346
 Si inversion layers, harmonic generation due to hot electrons 0-65694
 Si, inversion layers, nonmetallic cond. at low temp. 0-70833
 Si MIS-inversion layer solar cells 0-76632
 n-Si MOSFET, resist. temp. depend. at liq. He temps. 0-80391
 Si MOSFET, surface quantum states, two-dimensionality of many-body effects 0-103740
 p-Si, n-channel inversion layers, mag. susceptibility of electrons in presence of quantising mag. field. 0-75650
 Si, phase diagram in strong mag. fields 0-88492
 Si surface, MOS struct. band structure, minigaps, magnetoresistance, cond., space charge layers 0-92980
 Si, thermally oxidised surfaces, electron mobility in inversion and accumulation layers, MOS devices 0-103753
 Si, velocity-field curves for surface free carriers, meas. on IGFET 0-60095
 Si-SiO₂ boundary, surface charge transport in valence band of Si 0-70789
 Si-SiO₂ in MOSFETs, inversion layer carrier mobility, theory 0-60094
 Si-SiO₂ interface, (001) vicinal planes, minigaps in inversion layers, far IR absorpt. meas. 0-107919
 Si-SiO₂ interface, remote polar phonon scatt. in Si inversion layers 0-80095
 Si-SiO₂ inversion layer, n-channel, anomalous magnetoresist., model 0-96996
 Si-SiO₂ MIS systems, dynamic props. of switching, appl. to charge transfer devices 0-92997
 Si-Sn heterojunction, RHEED, Mossbauer spectroscopy and I-V characts. 0-70828
 Ta₂O₅ inversion layers for Si solar cells 0-94075
 ZnO-grainboundary-ZnO junction in ceramic varistor, capacitance-voltage characts. 0-65689

invertors

- solar energy DC-AC inverter design, effect of meteorological conditions, computer simulation 0-61373
 variable speed wind power generator, control strategy for 3-phase output (French) 0-76591

iodine

- see also nuclei with*
²³⁵I/¹²⁷I early solar system chronometer 0-62043
 adsorbed on Ag(111), photoelectron diff. aximuthal patterns, struct. sensitivity 0-107644
 adsorption on W(100) at room temp., LEED and AES study 0-84389
 air monitoring systems for radioiodine and inert gases, evaluation 0-95480
 atom, He (I) photoelectron spectrum by I₂ photodissoc. 0-83325
 atomic vapour, self-induced transparency and reson. self focusing 0-64114
 atoms, Mossbauer isotopes, isomer shift 0-78573
 chemisorbed on Au surface, AES and LEED study 0-100405
 chemisorbed on zeolites, Raman spectra 0-93301
 chemisorption, on Ag clusters, UPS obs. 0-84830
 diffusion in copper phthalocyanine polycryst., amorphous cpd. prep. (Russian) 0-66016
 impurity in Li aluminosilicate glasses, ESR spectra 0-66027
 laser, methyl iodide photodissoc., kinetic model, cross-section calcs. 0-58530
 laser, photodissociated by nucl. induced excimer fluoresc. 0-78846
 laser, photodissociation, characts. of dye comps. for passive switches 0-91826
 laser, three-level, pumped by CW dye laser 0-63993
 laser radiation, 2nd, 3rd and 4th harmonic generation 0-91844
 lead phthalocyanine:O₂(I), Schottky barrier effect on AC current response 0-75623
 liquid, static structure factor, neutron diffraction 0-103236
 metallic, mol. and monatomic phase, elec. resist. at high press. and low temp. 0-65638
 molecular ion cluster emission in SIMS, parity rule applics. (French) 0-63882
 molecular laser, optically pumped, review 0-58519
 molecular static polarisability, ab initio SCF wave functions 0-74106
 molecular vapour, saturable absorpt., self-focusing and nonlinear susceptibility 0-83647
 molecule, B-X fluoresc. band system, intensity and relative band strengths meas. 0-102540
 molecule, B-X lines, Franck-Condon factors, Ar⁺, Kr⁺ and He-Ne laser excitation 0-58320
 molecule, B-X system, mol. const. and Dunham expansion parameters 0-87095
 molecule, B-X transitions, rot.-vibr. hyperfine coupling const., extension to other levels 0-63625
 molecule, fluorescence, CW dye laser emission wavelength locking by intracavity gain 0-99721
 molecule, high-resolution saturated absorpt. spectroscopy with short light pulse coherent trains 0-64110
 molecule, in Ar, emission spectrum interpretation 0-95634
 molecule, laser fluoresc. state selected and detected mol. beam mag. reson., hyperfine transitions 0-63731
 molecule, model potential SCF calcs. 0-95528
 molecule, photodissoc., atomic He (I) photoelectron spectrum 0-83325
 molecule, photolytic cage effect in gas phase 0-81345
 molecule, polarisability anisotropy, laser assisted mol. beam spectroscopy 0-78646
 molecule, RF optically heterodyned saturation spectroscopy, reson. degenerate four-wave mixing 0-74211
 molecule, vac. UV absorpt. cross section 0-91574
 nonlinear spectroscopy, coherent background noise elimination from saturation spectrosc. signals using freq. offset pump 0-62733

iodine continued

- polyacetylene:I₂, synthesis, elec. cond., thermoelec. power 0-60016
 polyacetylene:I, dc microwave cond., permittivity 0-107843
 polyacetylene:I, electronic excitations, momentum depend., EELS study 0-76121
 polyacetylene:I, electronic structure, XPS and UPS meas. 0-66385
 polyacetylene:I, NMR struct. investigation 0-108082
 polyacetylene:I, reson. Raman spectroscopy 0-66208
 polyethylene:I₂, films, electron-beam induced carrier mobility and elec. breakdown 0-80429
 polystyrene:I₂, films, electron-beam induced carrier mobility and elec. breakdown 0-80429
 polystyrene:I, films, thermally stimulated discharge, I conc. and polarisation temp. depend. 0-107937
 polyvinylquinazoline-I₂ complexes, absorpt. spectra and elect. cond. 0-92891
 radioisotope adsorption by minerals 0-83203
 reactor poison, stress corrosion cracking of Zircaloy LWR fuel rod cladding 0-71810
 thyroid, accumulation curve of radioiodine and its role in diagnostics (Hungarian) 0-94341
 thyroid gland, X-ray fluoresc. tomography 0-61664
 Zircaloy cladding stress corrosion cracking due to I (Japanese) 0-78361
 Ar⁺ and Ar⁺-Kr⁺ ion lasers, I₂ stabilized, beat frequency 0-95916
 Ar⁺ laser 582 THz stabilisation by I₂ cell, improvements 0-102741
 BWR, primary containment vessel, spray I₂ removal characteristics 0-73972
 Fe-I system, photochemical conversion efficiency 0-71923
 He-Ne laser stabilisation, I₂ absorption cell power densities 0-99767
 He-Ne laser stabilisation by I₂, 612 nm saturated absorption 0-99765
 He-Ne laser stabilisation by I₂, 611.8 nm saturated absorption 0-99766
 Hg-Tl-I discharges, 50 Hz, axial segregation effect on elec. field strength 0-59320
 I II, reson. lines, oscill. strengths determ. by absorption method 0-58214
 I⁻, 3d⁴f config., collapse of 4f electron, X-ray spectral obs. (Russian) 0-58204
 I⁻, photo-oxidation at n-TiO₂ electrode 0-81331
 I-CdI₂ mixture, molten, nuclear spin relax. 0-88887
 I⁻-He laser discharge, positive column, particle densities 0-103215
 2I+He-I₂+He, energy transfer mechanisms studied using trajectory calcs. and Monte Carlo method 0-66785
 I₂, efficient laser action on 342 nm band, ArF laser pumping 0-99703
 I₂ molecule B-X electron transition during Cu vapour laser optical pumping (Russian) 0-78845
 I₂, quenching of laser-excited O₂ 0-99515
 I₂ seeded in supersonic free jet, collision-induced rotational relax. 0-102556
¹²⁹I₂, energy levels near B-state dissociation limit, two-photon spectrosc. obs. 0-106367
¹²⁹I₂, frozen soln. in o- or p-xylene, Mossbauer effect obs. 0-78637
 I₂-benzene, π - σ charge-transfer complex, frozen soln., Mossbauer spectra obs. 0-91655
 I₂-methylated benzene, π - σ charge transfer complex, frozen soln., Mossbauer spectra obs. 0-91655
 I₂-pyridine, n- σ charge-transfer complex, frozen soln., Mossbauer spectra obs. 0-91655
 I₂-triethylamine, n- σ charge-transfer complex, frozen soln., Mossbauer spectra obs. 0-91655
 I₂+acetylene, laser-induced 1,2-diiodoethylene form., isomerisation 0-85157
 I₂+Cu(²D), beam-gas chemiluminesc. reactions 0-85151
 I₂+K₂(C₂), ionisation reactions, absolute cross sections 0-99565
 I₂(I₂⁺)(I₂⁻), HF and SCF calcs., pot. curves, electron affinity and quadrupole moment determ. 0-95527
 I(²P_{1/2,3/2}), from ICN A-state photolysis, branching ratio wavelength depend. 0-81335
¹²⁷I, A=123, 125, labelling of cyclosporin A, prep. and biodistrib. 0-85496
¹²⁷I, A=131-2, comparative effects in rat thyroid glands 0-104670
¹²³I, prep. from gaseous TeF₆, nuclear medicine appl. (French) 0-98137
¹²³I prod. from ¹²⁷(p,n)¹²³Xe-¹²³I, at 58 MeV 0-94369
¹²³I, production in LASL radiochemistry hot cells 0-72326
¹²³I-Na, thyroid scintigraphy, clinical comparative study with ^{99m}TcO₄⁻ (Japanese) 0-81728
¹²³I, determ. of exposure rate constant using a scintillation detector 0-89863
¹²³I in the thyroid, 2-probe meas. method 0-81718
¹²³I, intramol. effects of decay in o-iodotyrosine 0-108973
¹²³I, intranuclear atoms not bound to DNA, radiotoxicity 0-104655
¹²³I labelled estradiol, a γ -emitting estradiol analogue that binds to the estrogen receptor 0-61697
¹²³I labelled estrogen derivatives 0-81734
¹²³I labelled human serum albumin, geometrical dilution (French) 0-104742
¹²³I labelled prostaglandins (Hungarian) 0-94368
¹²³I photons, absorbed fractions in the thyroid 0-109032
¹²³I, release in autoclave sterilization of radioimmunoassay kit (Japanese) 0-81727
¹²³I seed implants in prostatic cancer, preoperative extended field radiation 0-72303
¹²³I, shielding of (Japanese) 0-63404
¹²³I, variation of γ -counting efficiency with sample composition 0-83238
¹²⁷I₂, Doppler-free optoacoustic spectroscopy 0-57396
¹²⁷I₂ rovibronic absorpt. lines, hyperfine struct. 0-78596
 I₂, saturated absorption for He-Ne laser stabilisation, wavelength inter-nal comparisons 0-95872
¹²⁷I, stabilised He-Ne laser 0-106544
¹²⁷I, stabilised ion laser, beat freq. intercomparisons at 514.5 nm 0-74338
¹²⁷I, hyperfine struct. and isotope shift of 1.3 μ m transition 0-102486
¹²⁷I in bovine thyroid glands, activation anal. obs. 0-94380
¹²⁷I, mag. hyperfine field in Fe, press. depend., nucl. gamma reson. 0-71256
¹²⁹I photons, absorbed fractions in the thyroid 0-109032
¹²⁹I radioactive waste, fixation with Portland cement, radiation stability tests 0-83200
¹²⁹I, tandem accelerator mass spectrometry 0-86494
¹²⁹I₂, ¹²⁹I₂, ¹²⁷I₂, high resolution saturated absorption spectra at 633 nm using He-Ne laser 0-95637
¹²⁹I₂, complete hyperfine spectrum obs. at 612 nm 0-95638

iodine continued

- ¹²⁹I₂, selective excitation and separation in I₂+C₂H₂ laser induced chem. reaction 0-68962
¹²⁹I₂, rovibronic absorpt. lines, hyperfine struct. 0-78596
¹³¹I, age-related radiosensitivity obs. of guinea pig thyroid glands 0-104671
¹³¹I, behaviour during rinsing in in-pile loop after fission product release expt. 0-73879
¹³¹I concentrations in air, milk and antelope thyroids in southeastern Idaho 0-89871
¹³¹I, estimation of γ dose to gastric wall after administration of isotope (Japanese) 0-98141
¹³¹I manipulated in syringes, radiation exposure obs. 0-67252
¹³¹I produced radiation, low-dose, somatic mutations induction in *Tradescantia* 0-72266
¹³¹I, thyroid uptake determ. (Hungarian) 0-94339
¹³¹I treated patients, monitoring of I excretions and used materials 0-89873
¹³¹I-ortho-iodhippurate absorbed kidney dose calc., literature review 0-76841
I₂⁺+He, low energy collisions, energy redistrib. 0-63765
I₂⁺+He(Ne), energy depend. of collision induced intramolecular energy transfer 0-83470
KBr:I⁻, OH⁻, luminesc. of interstitial atomic H 0-89062
KCl:I⁻, interstitial atomic H centres, formation kinetics and struct., MO calcs. and EPR studies 0-75854
KCl:I⁻, low-temp. heat capacity enhancement due to impurities 0-107442
RbBr:I⁻, OH⁻, luminesc. of interstitial atomic H 0-89062
RbCl:I⁻, interstitial atomic H centres, formation kinetics and struct., MO calc. and EPR studies 0-75854
Se:I, vitreous, crystn, kinetics determ. (German) 0-79936

iodine compounds

- copper phthalocyanine-iodine, amorphous cpd. prep. by I₂ diffusion in polycryst., triplet EPR signals obs. (Russian) 0-66016
hydration complexes, gas phase, electrostatic calcs. 0-100055
iodide, charge transfer to solvent spectra, spectral shift data, Madelung const. determ. 0-85204
I+H₂, gas phase H-atom transfer reactions, struct.-reactivity correl., pot. energy surfaces 0-104433
I₂-quinoline (pyridine) complexes, stability const. determ. by spectrophotometric methods 0-87056
I,Ar⁺, product state distrib. and binding energy 0-63857
IBr, B⁺II(0⁺) excited state, laser-induced fluoresc. 0-58309
IBr-benzene in n-decane soln., IR line broadening by chemical exchange 0-87111
ICN, A-state photolysis, I(²P_{1/2,3/2}) branching ratio wavelength depend. 0-81335
ICl A⁺II(1), excited, laser induced fluorescence, quantum-resolved dynamics of excited states 0-69178
ICl(Br), rot. spectra in millimeter wave region, rot. transitions obs., equil. const. determ. 0-78607
IF emission spectrum and form. kinetics in electron-beam-produced plasma 0-102533
IF, in solid Ar, emission and excitation visible spectra at 12K 0-87137
I₂He⁺, product state distrib. and binding energy 0-63857
I₂He⁺ Van der Waals complex, vibr. relax. processes and decomposition 0-63765
I₂Ne⁺, product state distrib. and binding energy 0-63857
IO, free radical, Ar matrix absorpt. and emission spectra, mol. vibronic states obs., spectroscopic const. determ. 0-83387
IO₃⁻, adsorption desorption by TiO₂ suspension, kinetics, relax. technique 0-93804
Mg(IO₃)₂.4H₂O, crystal struct., unit cell, X-ray study 0-59447
Ni-I single crystals, mag. and dielectric props. 0-93095

ion-atom collisions see atom-ion collisions

ion beam effects

- see also ion-surface impact; ionoluminescence; plasma-beam interactions
accelerator irradiation, heavy ion irradiation damage 0-100291
amorphisation due to ion bombardment, SRO struct. 0-79844
atomic transport and conc. profiles 0-59723
brain, irradiation with C ions, recovery from pot. lethal damage, rat expts. 0-72234
crystal, electron-positron pair production coherent effect 0-88222
crystal surface morphology development during sputter erosion 0-88414
CTR first wall, high power ion-irrad. test 0-78443
diamond, accelerator irradiation, heavy ion irradiation damage 0-100291
electron gas coding influence in ion-bombarded layers 0-108272
electron-collision cross-section data for atom or molecule, rel. to radiation physics 0-63829
energy spike development and quenching depend. on thermal diffusion 0-88367
fast molecular ions, transmission through thin foils 0-65065
field-ion microscope specimens, field corrosion caused by polymer gaskets 0-57425
garnet epitaxial films, easy magnetisation axis orientation, ion bombard. effects 0-60383
graphite, conditioning of surface by atomic H 0-93665
graphite, ion bombarded, light gases, structural study using TEM 0-92570
heavy ion induced collective electron emission 0-80926
heavy ion stopping, prediction using ion effective charges 0-88229
heavy ions, low vel., channelling stopping power oscils. 0-103404
heavy ions in solids, electronic stopping cross-section, Z₂-oscills., target struct. effects 0-70285
intense ion beam propag. in z-discharge plasma channels, straight and tapered 0-83948
ion acoustic solitons in beam plasma system with nonisothermal electrons generated by ion-beam 0-103151
ion impact induced shock processes in solids 0-89104
isocitrate dehydrogenase from *Azotobacter vinelandii*, essential amino-acid residues identification 0-76538
kidney cells, inactivation by high-energy monoenergetic heavy-ion beams 0-72256
magnetically insulated coaxial line, ion beam effects 0-87297
mammalian cells, cultured, interpretation of mutation and inactivation obs. 0-72229
material modification, conf., Budapest, Hungary (Sept. 78) 0-86038
metal, blister formation due to the ion irrad. 0-65072

ion beam effects continued

- metal, heavy ion bombard., void conc., effect of implanted He (Russian) 0-88213
metal, light element implantation, radiation damage review 0-88219
metals, energy loss of heavy nonrelativistic ions in matter, semiclassical theory 0-84224
metals, irradi., mechanism of formation of vacancy dislocation loops (Russian) 0-65053
metals, mixed dumbbells, ion channelling studies 0-70277
mica, nuclear track microfilters, prod. and props. 0-96574
milling, anomalous sputter yield behaviour 0-108624
oscillatory wake, fast ion in solid, trapped electron binding energy, RPA calc. 0-96575
particle accelerator target heating by ion beam, thermal characts. (Japanese) 0-99374
polystyrene, energy losses and straggling for H⁺ and He⁺ beams (Russian) 0-84226
Pyrex, ion bombardment, form. of cpds., IR spectrosc. exam. (German) 0-88173
recoil atoms of heavy ion reactions, local lattice damage, TDPAD meas. 0-84220
recoil mixing in solids by energetic ion beams 0-59531
soliton solution in the wake interaction due to virtual plasmon exchange 0-65108
sputtering induced topography on solids, energetics and kinetics 0-88220
stainless steel, machine faceted, low-energy ion erosion studies 0-80923
steel, mild, surface hardness improvement by dynamic recoil implantation 0-61008
steel, stainless, stress corrosion cracking and microhardness, effect of bombardment by He⁺, Ni⁺ and Cr⁺ 0-85087
steel, stainless, type EP838 ion irradiated, surface structure changes during post-irradiation heating (Russian) 0-75272
steel, stainless 316, Fokker-Planck eqn. describing evolution of interstitial loop microstruct. during irradiation 0-107215
steel, stainless 316, soln. annealed, cavity alignment and precipitation during dual ion bombardment 0-70273
steel, stainless type 316, in-situ HVEM studies under ion beam irradiation 0-103396
Tokamak plasma, beam driven currents, trapped electrons effect 0-70011
toroidal plasmas, beam driven currents, trapped electrons effect 0-70011
transient magnetic field effects on particles slowing in solids 0-65106
V79-spheroids, survival and kinetic response after heavy ion beam exposure 0-104651
Vicia faba growth reduction, RBE of d(50)-Be neutrons and 650-MeV He²⁺ 0-98025
void, and interstitial loop evolution in pulsed fusion reactors 0-84217
yeast cells, dried, inactivation by accelerated heavy ions of very high LET 0-108965
Ag, energy losses and straggling for H⁺ and He⁺ beams (Russian) 0-84226
Ag films, effect of Ar- and N-ion bombardment on texture (Russian) 0-107338
Ag-Ni supersaturated metastable solid solns. formed by ion beam mixing 0-107425
Ag-Pd alloys, inert gas ion bombardment, dynamic surface composition changes, AES obs. 0-60745
Al, Al ion irradiated, void swelling and annealing of voids, electron microscopy study 0-88216
Al, annealed and powder sintered (SAP 895), sputtering under D⁺ and ⁴He⁺ bombardment, microstruct. effects study 0-84821
Al, energy losses and straggling for H⁺ and He⁺ beams (Russian) 0-84226
Al film, deform. under He ion bombardment 0-65073
Al-Ge (0.1 wt.%), channelling meas. of Al interstitial atom trapping by Ge atoms 0-59537
Al-Mg, Si alloy, void form. under different precip. conditions, after Al ion irrad. 0-59529
Au, energy losses and straggling for H⁺ and He⁺ beams (Russian) 0-84226
Au film, surface craters induced by displacement cascades 0-107344
Au, heavy ion irrad., cascade energy density effect on defect cluster type 0-107340
Au-Ag (35 at.%), dechannelling of energetic He ions at dislocations 0-70275
Be, blisters due to He irrad., proton backscatt. study 0-75273
Be, irradiated with He⁺ at 20 keV, surface damage and gas trapping profile meas. (French) 0-84218
C, thin foil, irradiation with 1.2 MeV Ar⁺, electron diffraction study 0-103397
CdS, defect struct. and config. produced by irrad., elastic scatt. expts. 0-84178
CdS, electron-hole pairs behaviour in energetic ion tracks 0-65457
Cr film, evaporated, concurrent ion bombard. effects 0-80142
Cr film, obtained by thermo ionic precipitation, phase composition, lattice parameters (Russian) 0-96756
Cu, blisters due to He irrad., proton backscatt. study 0-75273
Cu, crystalline reorientation following ion bombard. 0-70269
Cu, energy losses and straggling for H⁺ and He⁺ beams (Russian) 0-84226
Cu, ion bombard. by 5 keV Ar⁺, sub-surface damage 0-103399
Cu, irradiated with 20 keV He⁺, surface damage and gas trapping profile meas. (French) 0-84219
Cu, irradiation with O₂ ions, defect production and annealing 0-88214
Cu, pyramidal structures, development on ion bombarded surfaces 0-84177
Cu, surface topographical features formed by ion bombard., crystallographic depend. 0-70266
Cu, vacuum deposited layer, ion bombardment induced preferential orientation 0-100290
CuCl, electron-hole pairs behaviour in energetic ion tracks 0-65457
Fe-B amorphous alloy, fast neutron and ²³⁵U fission fragment irrad. 0-100288
Fe-Cr-Ni (19, 13 wt.%), austenitic, Ni⁺ ion irradiated, multiple dislocation loops (French) 0-65064
GaAs, electroluminescent study of irrad. induced struct. damage, athermal annealing 0-108280
GaAs, ion damage, TEM study of laser annealing 0-88215
GaAs, surface cryst. regularity by X-ray photoelectron diff. 0-89112
(Gd, Bi), (Fe, Ga), O₁₂ magneto-optic LPE garnet films, high-energy heavy ion irrad., props. 0-71390

ion beam effects continued

- Gd, energy loss and straggling of $^4\text{He}^+$ ions in vacuum-evaporated films 0-88231
- Gd-Co based amorphous sputtered films, microstruct. variability and mag. anisotropy, implanted ion effects 0-88459
- Ge, ion beam irradi., defects prod. by individual displacement cascades, TEM study 0-70265
- Ge, radiation damage by 0.5 to 10 keV ions 0-100285
- Ge thin films on glass substrates, annealing by Ar ion bombardment 0-80136
- Ge:Pb, ion implanted damaged layer, laser induced reorder 0-84201
- H species, on C foil, 800 keV amu^{-1} , electron loss and capture cross-sections 0-65066
- H_2O ice, erosion by H and He ions, energy depend. 0-65067
- He species, on C foil, 800 keV amu^{-1} , electron loss and capture cross-sections 0-65066
- InSb, ion implantation, anomalous radiation disordering 0-92553
- InSb, morphological and structural changes due to ion bombardment 0-79843
- InSb, single crystal, chem. and ion etching, surface changes (French) 0-108614
- InSb:Cd (Zn) (Ge), ion-irradiated, p-n conversion during heat treatment 0-96558
- $\text{In}_{2-x}\text{Sn}_x\text{O}_{3-y}$ -poly Si SIS solar cells 0-97787
- LiNbO_3 surfaces, ion and electron bombard., photoelectron spectroscopy and electronic props. 0-71559
- Mo alloys (MChVP and TSM10VD), erosion, effect of ion bombardment dose and previous surface treatment 0-89419
- Mo cryst., radiation induced vacancies and D_2^+ implantation 0-65076
- Mo, H_2 diffusion enhanced by self-interstitial atoms, surface reaction const. determ. 0-75386
- Mo, irradi., defect anal., electron microscopy, appl. of theory of non-edge loop image contrast 0-70200
- Mo surface, rolled, H^+ ion bombard, large blister form. 0-75274
- Mo-base alloy, TZM, blistering under He ion bombard. 0-92567
- N^+ , electronic stopping power in solids, range distrib. energy depend. 0-92575
- N_2 , ion pair creation by high-energy ions, meas. of average energy required 0-103105
- NaCl , Ne^+ , Ar^+ , Kr^+ bombard., sputtering and ionoluminescence 0-96583
- $\text{Na}_2\text{O-SiO}_2$ glass, ion bombardment, form. of cpds., IR spectrosc. exam. (German) 0-88173
- Nb, blisters due to He irradi., proton backscatt. study 0-75273
- Nb, He blistering, large swelling meas., gas press. model 0-88218
- Nb, ion bombard, by 5 keV Ar^+ , sub-surface damage 0-103399
- $\text{Nb}_{40}\text{Ni}_{60}$, amorphous, produced by Ni^+ implantation, damage distrib. 0-107062
- Nb_3Sn multifilamentary composite supercond. wires, transverse sections prep., ion milling, TEM obs. of grain size 0-101000
- NbTi films, effect of Ar- and N-ion bombardment on texture (Russian) 0-107338
- Ni (001) surface, Ar ion bombarded, enhancement of oxidation, AES study 0-97644
- Ni and alloys, heavy ion irradi., defect cluster obs. 0-107341
- Ni, cavity coalescence following $^4\text{He}^+$ irradi. 0-70272
- Ni dilute alloys, implant profiles modification by radiation enhanced diffusion and segregation 0-88217
- Ni, in situ rare gas ion irradi., cluster creation obs. by electron microscopy 0-107343
- Ni, irradi. with 20 and 500 keV $^4\text{He}^+$, depth distrib. of cavities and dislocation damage 0-107346
- Ni-Al(Si) foils, irradi., surface effects on precip. morphology 0-104168
- Ni(O1) surface N adsorption due to ion beam irradi., surface struct. LEED study (Chinese) 0-84364
- O_2 chemisorption enhancement on Cu(110) during Ne^+ bombard. 0-65070
- Pt, irradi. damage, temp. depend., electron microscopy obs. of defect kinetics 0-107339
- Pt_3Co , radiation damage profiles from low energy Ne^+ , bombard. 0-70268
- Pu, oxidation, binding energies, Auger and X-ray photoelectron spectra study 0-76550
- Si (111), ion bombard., struct. changes, AES obs. 0-79842
- Si, blistering due to 400 to 1800 keV $^4\text{He}^+$ ions, modal range determ. 0-100289
- Si, collision cascade following ion bombard. 0-65069
- Si, etching in He-F_2 plasma, etch rates, mass spectra, direct ion sampling study 0-79510
- Si film, amorphous, hopping cond. control by ion bombard. induced struct. modification 0-92898
- Si film, ion bombarded, crystalline-to-amorphous transition, defect-rich film prep. 0-65071
- Si, gettering by ion damage, minority carrier lifetime and backscatt. study 0-100286
- Si, heavy ion induced disorder in surface and at shallow depths 0-59535
- Si, high dose self-irradi., spatial correl. between primary and secondary defect profiles 0-59536
- Si, implanted, complex annealing behaviour of amorphous layers, TEM obs. of defect struct. 0-107299
- Si, implanted, damage struct. obs. using TEM and cross section specimens 0-107298
- Si, implanted, defect struct., dislocation loops and elongated defects 0-107300
- Si, ion beam irradi., defects prod. by individual displacement cascades, TEM study 0-70265
- Si, ion bombardment, anomalous surface damage from channelling-backscatt. meas. 0-84222
- Si, ion bombardment induced defect distrib., IR and electron diff. study 0-65074
- Si, ion damage TEM study of laser annealing 0-88215
- Si, ion implanted, annealing of heavy ion cascade damage, channelling meas. 0-89255
- Si, ion implanted, annealing by ion beam heating 0-103382
- Si, ion implanted, self implanted, self annealing using high ion current density treatment 0-89254
- Si, oxidation induced by ion or electron bombardment, AES-SIMS study 0-108606
- Si, radiation damage by 0.5 to 10 keV ions 0-100285
- Si, reactive ion beam etching expts., selectivity, anisotropy 0-104308

ion beam effects continued

- Si surface, ion bombardment enhanced mixing of Ag layers, Rutherford backscatt. meas. 0-65034
- Si:As, CW CO_2 -laser annealing, comparison with thermal annealing 0-84193
- Si:As, ion implanted, pulsed ion beam annealing 0-103395
- Si:B, $^4\text{He}^+$ irradiation-induced diffusion, effect on impurity distrib. 0-70470
- Si:B (0.2 wt.%) ion implanted, B atom displacement due to low temp. irradi. 0-88234
- Si:B ion implanted, strain profiles from X-ray rocking curves 0-107290
- Si:B(Be)(Li) ion implanted, channelling and random equivalent depth distrib. 0-100293
- Si:Bi, implanted, channelling obs. of pulsed Q-switched ruby laser annealing 0-59542
- Si:P, ion implanted, subsurface damage, TEM and channelled Rutherford backscatt. study 0-107337
- Si-SiO₂ interface, thermal SiO₂ sputter induced roughness, Auger sputter profiling study 0-75424
- SiC, blistering and flaking due to light ion bombardment (Japanese) 0-70264
- SiC, radiation defect annealing, recovery of LEED maxima 0-65075
- α -SiC(6H), radiation defect distrib. anisotropy near (0001) surface, LEED study 0-96577
- Si₃N₄, Si(LVV) Auger spectra, ion bombardment, electron energy loss spectra 0-80911
- SiO₂ amorphous film, Si(LVV) Auger spectra, ion bombardment, electron energy loss spectra 0-80911
- SiO₂, etching in He-F_2 plasma, etch rates, mass spectra, direct ion sampling study 0-79510
- SiO₂ glass, ion bombardment, form. of cpds., IR spectrosc. exam. (German) 0-88173
- SiO₂ glass, low loss optical fibre, radiation-induced IR absorpt. 0-87521
- SiO₂, reactive ion beam etching expts., selectivity, anisotropy 0-104308
- SiO₂ thermal film, freon ion beam etching, IR study (Russian) 0-76095
- Si(111), ion-bombard., O_2 adsorption, SIMS study 0-70522
- Ta ion induced continuum emission 0-89025
- Ta thin film, elec. cond., strain gauge factor, ion bombardment effects 0-80417
- Ti-Al-V (6.4 wt.%) ion irradiated, microstruct. study using TEM 0-96572
- Ti-Fe-C-N, ion irradiated, microstruct. study using TEM 0-96572
- VO₂, metal-insulator transition and electronic struct., ion bombard. effects 0-92948
- W, low-energy ion bombardment, depth of sputtering damage obs. by FIM 0-60734
- Zn-Mn, Kondo-system, ion implantation as method for study 0-70241
- ZnO polar surfaces, H and O_2 exposed, ion irradi., and heat treated, cond., EELS study 0-71525
- ZnS ion beam etching, topographic changes, amorphisation, luminescence study 0-76078
- Zr, foil bending by in situ ion irradi., neutron damage simulation, room temp. oxide growth 0-107342
- Zr₃Al, deformed and irradi., lattice defects obs., superlattice dislocations and defect clusters 0-107261
- Zr₃Al ordered alloy, ion bombardment damage, TEM 0-100287

ion beams

- see also beam-foil spectra; beam-foil spectroscopy; energy loss of particles; ion beam effects; ion optics; ion-surface impact; mass spectrometers; particle accelerators; sputtering
- beamlet steering by aperture displacement in ion sources with large acceleration-deceleration ratio 0-63430
- clinical beams, light-ion flux mixed with collimated fast-neutron beams 0-81723
- cluster ion beams, mass anal. by Wien filter 0-86493
- co-ordinate monitor, induced noise-like signals processing 0-102607
- conference on electron, ion and proton beam technology, conf., Boston, MA, USA (29 May-1 June, 1979) 0-67927
- conical application to thin film technology (Russian) 0-76383
- deceleration across mag. fields, expt. 0-99384
- energy broadening, Boersch effect 0-69308
- energy measurement using radiative recomb. of ions in electron beam 0-74293
- fusion reactor, TFTR, high energy heat sink, ion beam dump and calorimeter 0-99394
- generation increase through moving plasma boundary 0-63439
- heavy, wide-range reaction products magnetic analyser 0-86491
- high current, from reflection triode, operating characts. (Russian) 0-83230
- high-current, prod. in triode 0-99372
- intense, production and postacc. in magnetically insulated gaps 0-74041
- ISX-B neutral beam injector expt. on prototype beam line 0-74039
- magnetically insulated diode as ion beam source 0-95491
- merged electron-ion beam experiment, determ. overlap integral from differential-scanning meas. 0-87282
- metal target preparation for stopping power meas. of channelled ions in low energy region 0-63431
- MIN, negative ion injector, Na charge exchange cell 0-99386
- nuclear physics, use of heavy ion beams (French) 0-78182
- overlapping, use for intercal confinement fusion 0-91242
- positive ion beam dynamic decompensation in absence of mag. field (Russian) 0-106993
- proton beam characts. control by laser-induced selective multistep processes 0-61122
- pulseline driven neutralised linear ion accelerators, longit. instabilities 0-78459
- quadrupole mass/filter, transmission (French) 0-101877
- QUISTOR, ion kinetic energy calc., survey 0-78468
- solar wind, diffusion upstream ions origin rel. to solar wind deceleration upstream of Earth bow shock 0-98528
- steering of beamlets by aperture displacement in 2-stage accelerator, experimental study 0-68998
- surface crystallography, ion beam, channelling and blocking effects, double alignment backscattering 0-65350
- thermal particle motion effect on autoresonance acceleration process (Russian) 0-69007
- transport of low energy divergent H_2 beam at 300 eV by permanent magnets 0-69001
- C^{6+} , microdosimetric measurements of pretherapeutic heavy ion beams 0-72337

ion beams continued

- Cs⁺ ion source, CW monoenergetic, by photoionisation 0-63910
- H⁺, energetic beam direct cryosorption pumping 0-105655
- H₂⁺ ion beam prod. by coaxial electron impact ion source 0-62795
- He²⁺, microdosimetric measurements of pretherapeutic heavy ion beams 0-72337
- He⁺ ion beam prod. by coaxial electron impact ion source 0-62795
- HeH⁺ ion beam prod. by coaxial electron impact ion source 0-62795
- Ne¹⁰⁺, microdosimetric measurements of pretherapeutic heavy ion beams 0-72337
- Ni film, amorphous layer covered, target prep. for channelled ion stopping power meas. 0-63431

ion chambers *see ionisation chambers***ion counters** *see counters***ion cyclotron resonance heating** *see plasma heating***ion cyclotron resonance spectra** *see mass spectra***ion cyclotron resonance spectroscopy** *see mass spectroscopy***ion density**

- see also plasma density*
- D-region, ion composition at midlatitude in quiet conditions, model 0-109307
- discharges in gases, pulsed, theoretical and expt. study 0-92416
- F₁-layer at nighttime, ion composition near mag. equator 0-72683
- ionosphere, International Reference 1978 rel. to Vertical¹-6 rocket meas. 0-90285
- ionosphere-satellite interaction, ion density in wake of O⁺ plasma 0-82136
- quadrupole ion store, spatial distribution of ions derived by phase space anal. 0-95185
- solar corona, proton density effects on H like ions reson. lines components intensity ratio 0-101581
- upper atmosphere, Vertical-6 rocket flight results 0-90268
- O⁺/electron density ratio in 140-200 km height range of atmosphere 0-105102

ion emission

- see also field ion emission; secondary ion emission; thermionic ion emission*
- plasma, laser-generated, ion beam production from interaction with Nd:YAG laser radiation bursts 0-106939
- surface layers, photon induced ion desorption, surface atom core ionisation, Auger decay 0-59809
- CaO:Bi surface, O₂ chemisorpt., positive ion emission determ. 0-92785
- LiF, ion and electron emission following ion impact 0-100729
- LiF, laser irradi., Li⁺ emission, time and energy characts. 0-100710
- NaCl, ion and electron emission following ion impact 0-100729
- Si, ion and electron emission following ion impact 0-100729

ion engines

- see also aerospace propulsion; rockets*
- solar power satellite engine, ion beam injection into magnetosphere 0-82149

ion etching *see sputter etching***ion exchange**

- artificial membranes, transport regulation by environmental H⁺ conc. 0-89725
- colour positive developer consumption, bromine ion extraction from over-flow using ion exchange resins (*Russian*) 0-105733
- fibre-optic planar multimode coupling structure fabrication 0-64233
- force-flow chromatography, alkaline earth ions detected by photometric method 0-71965
- glass, refractive index gradients, form. using ion exchange diffusion 0-64227
- ice, cubic, D₂O isolated, H⁺ exchange and Bjerrum defect migration, direct spectroscopic obs. 0-88356
- membrane, electroosmotic energy conversion efficiency 0-61430
- Nafion per fluorosulphonic acid ion exchange membranes, Mossbauer spectroscopy 0-80659
- Pyrex glass, cation exchange and interdiffusion 0-80002
- refractive index variation from field-assisted ion exchange 0-74447
- Selfoc lens, aberration improvement by glass composition and ion exchange process parameter choice 0-69486
- steam turbine condensates, ion-exchange polishing analysis (*Russian*) 0-89487
- transition metal ferrocyanide selective sorbents for alkali metals, sorptive props. w.r.t. struct. 0-101051
- waveguide, graded-index surface or buried, realized by ion exchange in glass 0-69499
- waveguide fabrication in glass, optical, by low-temperature diffusion process 0-102867
- waveguides, stripe, Ag⁺/Na ion exchanged, propag. characts. 0-83664
- zeolite, hydrated Na-Y, ²³Na pulsed NMR free induction decay 0-84660
- Fe, purification, recrystn. temp. and elec. resistivity (*Japanese*) 0-100780
- KNO₃ in alkali halides tablets, phase transition and ion exchange, IR spectra 0-79937
- Li-ion conductors in solid electrolytes 0-71610
- LiAlSiO₄:Cu, β -eucryptite solid electrolyte, Cu²⁺ EPR obs. of ion exchange props. 0-108056
- Li₂O-Na₂O-B₂O₃-Al₂O₃-SiO₂ glass, Young's modulus and density, ion exchange effects 0-84982
- LiTaO₃ optical waveguides, Ag-Li and Ti-Li ion exchange effects 0-58791
- LiTaO₃ optical waveguide, Ag-Li ion exchange 0-91888
- xMnO₂(100-x)[19TeO₂.PbO] glasses, EPR studies of Mn²⁺ ion distribution 0-71167
- Na₂O-Al₂O₃-SiO₂(-K₂) glasses, ion exchange kinetics and interdiffusion mechanisms 0-80003
- Na₂O-B₂O₃-SiO₂ two-phase, stresses arising during leaching 0-81086
- Na₂O-CaO glass, abrasion-resistant, high strength 0-76369
- Na₂O-K₂O-Al₂O₃-SiO₂ structure of modified surface layer, internal friction method 0-103238
- Sb₂O₃-nH₂O acid membranes, synthesis and characterisation 0-81027
- (TiNbO₃)₂ oxide layers, intercalation of alkylammonium ions 0-64985
- Zr(HPO₄)₂.H₂O, Na⁺ transport, gas-solid and solid-solid reaction kinetics 0-61086

ion exchanging *see ion exchange***ion excited X-ray emission** *see ion microprobe analysis***ion implantation**

- see also semiconductor doping*
- alloys, ion-implanted, integral Gaussian profile determ. method 0-107313
- alloys, props. and application 0-79824

ion implantation continued

- backscattering and implantation, H and He ions, computer simulation, comparison of MARLOWE and TRIM codes 0-66350
- bubble garnet film, non-implanted, surface mag. struct. 0-84628
- chemical and electrochem. aspects, review 0-100271
- conference on electron, ion and proton beam technology, conf., Boston, MA, USA (29 May-1 June, 1979) 0-67927
- depth distrib., analytical calcs. using inhomogeneous equations 0-84203
- depth distrib., secondary ion mass spectra 0-79829
- depth distribution of vacancies produced by ion implantation 0-65024
- diamond:Sb, implanted, radiation damage and annealing study 0-100263
- elemental semiconductors, group IV, Mossbauer spectroscopy of defects, radiation damage and deep levels 0-59533
- garnet epitaxial films, easy magnetisation axis orientation, ion implantation effects 0-60383
- high current ion implanter with hybrid scanning 0-79826
- highly doped, behaviour of buried O₂ implanted layers 0-59499
- indirect recoil implantation following nuclear reactions, theory and appl. 0-75256
- inert gas crystal, lattice vibrs. and radiative transitions of implanted ions (*Russian*) 0-69098
- integrated optics high quantum efficiency waveguide coupled photodetectors on Si substrate 0-58805
- ion implanted layers, complex refr. index profile, ellipsometric meas. 0-93262
- Josephson junction fabrication by ion implantation, electron beam lithography and dry etching 0-88693
- laser applications in materials processing, seminar, San Diego, CA, USA (Aug. 79) 0-90609
- laser-plasma ion source for ion implantation in solids 0-78474
- magnet design for high-current implanters or small isotope separators 0-68222
- metal, heavy ion bombard., void conc., effect of implanted He (*Russian*) 0-88213
- metal, ion implanted H(D), interstitial positions and vibr. amplitudes, fast ion channelling study, review 0-79848
- metal, light element implantation, radiation damage review 0-88219
- MOS structure implanted with B ions, radiation defects and impurity activation 0-103757
- n⁺-p-p⁺ bifacial back surface field solar cells, optimisation of p⁺ doping level by ion implantation 0-97784
- Pearson IV distrib., appl. to ion implanted depth profiles 0-88195
- polyacetylene:Br(Pd), ion implantation effect on elec. props. 0-65026
- Pyrex, ion bombardment, form. of cpds., IR spectrosc. exam. (*German*) 0-88173
- quartz, effects of He ion implantation on SAW propag. 0-75421
- range parameters, nucl. stopping power, ion backscatt. determ. 0-88232
- recoil atoms, theory 0-92545
- recoil density resulting from ion implantation 0-88175
- recoil implantation theory 0-103378
- recoil mixing in high-fluence ion implantation 0-65095
- semiconductor annealing, pulsed laser and electron beam heating comparison 0-92547
- semiconductor counter for neutron detection 0-69030
- semiconductor devices, ion implantation with controlled nonuniformity 0-100261
- semiconductor epitaxial regrowth, laser annealing dynamics 0-92548
- semiconductor microstructure fabrication, ion channelling effects 0-70230
- semiconductor thin films, ion implanted, optical and luminesc. props. 0-60699
- semiconductors, ion implanted, laser annealing 0-65023
- semiconductors, ion-implanted, laser pulse annealing, TEM and channelling study 0-100264
- Si, ion implanted by high energy C ions structural and optical props. 0-107292
- solar cells, ion implantation and annealing technology 0-93996
- steel, austenitic, Cr-Ni, ion-implanted N, chem. state study by AES and XPS 0-79825
- steel, austenitic stainless, Cr-Ni (20, 25 wt.%), Nb stabilized, oxidation behaviour in CO₂, surface ion implantation effect 0-71791
- steel, low C, type 38NCD4, fatigue life improvement by N ion implantation, dose depend. 0-76328
- steel, mild, surface hardness improvement by dynamic recoil implantation 0-61008
- steel, stainless, D₂⁺ diffusion and permeation, ion beam meas. 0-59492
- steel, stainless, Fe-Cr-Al (15, 4 wt.%) FeCrAlloy, oxidation behaviour, Al and Y surface ion implantation effect 0-71790
- steel surface hardening, ion-carbo-nitriding in CO-N₂-H₂ gas mixtures, expt. (*Japanese*) 0-71670
- surface-ion impact, luminesc. accompanied by ion implantation 0-60683
- Teflon FEP, N implanted, TSC spectra 0-88912
- vacuum technique problems, with modern semiconductor processes (*German*) 0-86330
- Al, corrosion, general and pitting, Mo and Ar ion implantation effects 0-71794
- Al, defect structures depend. on Ca and Ga implanted species 0-59494
- Al films, resistance changes due to bombardment by N, C, or Ar ions 0-103670
- Al granular films, self-ion implantation, supercond. transition temp. enhancement 0-103774
- Al, implanted Xe behaviour during anodic oxidation 0-71800
- Al, polycrystalline, high dose implanted with Cu and Pb, doping profile after laser pulse irradiation 0-88194
- Al, polycrystalline film, trapping of ³He and ⁴He ions at room temp. 0-84221
- Al, single crystal, ¹⁸O⁺ ion implantation in channelling directions, expt. conditions and range profile obs. 0-65022
- Al single crystal, ¹⁸O⁺ ions implantation in channelling directions, stopping power meas. from max. range 0-65078
- Al:Ga, pulsed electron-beam annealing, lattice site location improvement 0-107303
- Al:Sb(Zn), ion implanted electron beam annealing, ion backscatt. and TEM meas. 0-59500
- Al-Zn-Mg-Cu (5.6, 2.5, 1.6 wt.%), corrosion, general and pitting, Mo and Ar ion implantation effects 0-71794
- Al₂O₃, anodic film, trapping of ³He and ⁴He ions at room temp. 0-84221
- Au lattice location in Zn, gamma-spectral study 0-80227
- Au-Fe ion implanted alloy, Mossbauer conversion electron scatt. 0-88898
- Au-ZnS electrolum. Schottky barrier diode, S⁺-implanted, blue emission 0-76082

ion implantation continued

- BP:Zn(Se)(Cd), epitaxial layers, ion implantation, defects and lattice locations, channelling obs. 0-88179
 Be, ion-implanted, impurity lattice location, channelling meas., Monte Carlo calc. 0-107291
 BeO, anodic film, trapping of ^3He and ^4He ions at room temp. 0-84221
 BeO film, 5 keV D implantation 0-100268
 Bi films, resistance changes due to bombardment by N, C, or Ar ions 0-103670
 (BiTm)(FeGa) $_2\text{O}_{12}$ ion implanted epitaxial garnet film, bubble domains, cryst. struct. disorder 0-93150
 CC Si:B, layer resist. depend. on implanting and annealing conditions (German) 0-96551
 Cd $_2$ Hg $_{0.8}$ Te, ion implantation doping for realisation of IR detectors, responsivity meas., ion range straggling 0-73452
 CdTe:As(P), ion implanted, elec. props. 0-65021
 Co implantation in Al, replacement collision probability at 4.2K 0-70237
 Cu, corrosion protection by ion implantation of Al and Cr 0-71789
 Cu films, resistance changes due to bombardment by N, C, or Ar ions 0-103670
 Cu, implanted with Cu $^{+}$, effect on cryst. orientation, Kr penetration meas. 0-88174
 Cu single crystals Au ion implanted, pulsed electron beam irradiation 0-65019
 Cu:In, He, lattice defect struct., PAC meas. 0-70190
 Cu:O single crystal, $^{18}\text{O}^{+}$ ion implantation in channelling directions, expt. conditions and range profile obs. 0-65022
 Cu:O single crystal, $^{18}\text{O}^{+}$ ion implantation in channelling directions, stopping power meas. from max. range 0-65078
 D trapping in C target, model 0-65025
 Fe, corrosion behaviour in H $_2$ SO $_4$ soln., ion implantation effect 0-71793
 Fe surface hardening, ion-carbo-nitriding in CO-N $_2$ -H $_2$ gas mixtures, expt. (Japanese) 0-71670
 Fe:Y, ion implanted, deep D traps due to Y-vacancy complex 0-103372
 Fe-Cr-Al-Y, oxidation resistance, heat treatment and Al $^{+}$ ion implantation 0-71785
 α -Fe-Ti, ion implanted, microstruct., ion beam anal. and TEM study 0-107294
 α -Fe-Ti, ion implanted, with C impurity, microstruct. of TiC precip. 0-66513
 Fe $_2$ B $_{10}$, metallic glass, ion implanted, UPS meas. 0-97411
 ^{57}Fe , hyperfine interactions in implanted metals, Mossbauer spectra 0-108141
 (GaAl)As:Be DH stripe geometry lasers with current confinement structure 0-58592
 (GaAl)As:Be implanted DH stripe geometry laser 0-64044
 Ga $_{1-x}$ Al $_x$ P:N epitaxial films, ion implanted, cathodoluminescence study 0-60684
 GaAs, amorphous layers, ion-implanted, low-temp. epitaxial regrowth 0-92790
 GaAs device isolation with deuteron bombardment 0-75248
 GaAs devices, ion implantation damage, characterisation and appl. 0-92551
 GaAs epitaxial layers, surface impurity gradients, Schottky barrier capacitance meas. 0-70782
 GaAs epitaxial layers, doping profile degradation due to ion implantation 0-84194
 GaAs, H ion bombard., carrier removal effects 0-92542
 GaAs heavily doped n-type layers, formation by multiple ion implantation 0-59491
 GaAs, ion beam induced annealing effects 0-59530
 GaAs, ion implantation review 0-88184
 GaAs, ion implanted, capless annealed and dielectrically annealed, comparison of doping profiles 0-100278
 GaAs, ion implanted, laser annealing 0-107296
 GaAs, ion-implantation induced damage profile, ellipsometric study, annealing 0-103400
 GaAs, ion-implanted layers, close contact capless annealing, elec. props. 0-84192
 GaAs, n-type layers, heavily doped, formation by multiple ion implantation 0-88187
 GaAs oxide film form., ion implantation effects 0-100266
 GaAs semiinsulating materials, role of substrate in elec. props. 0-59488
 GaAs: $^{119}\text{In}^{+}$, Mossbauer study of resulting ^{119}Sn impurity-defect complex 0-59486
 GaAs:Cr, ion implanted, implantation damage profiles, laser annealing, ellipsometry study 0-79819
 GaAs:Cr, semi-insulating, Cr redistrib. during thermal annealing as function of encapsulant and implant fluence 0-84199
 GaAs:Cr, semi-insulating, damage gettering of Cr during annealing of Cr and S implants 0-107304
 GaAs:Cr,Se, ion-implanted, semi-insulating effects of Cr redistrib. on elec. charact. 0-59982
 n-GaAs:H(D), ion implanted, carrier removal, capacitance-voltage profiling 0-84195
 GaAs:P $^{+}$, implantation profiles, backscatt. meas. 0-70238
 GaAs:Se, Ga, dual species ion implantation, elec. charact. 0-103377
 GaAs:Se, low dose Se $^{+}$ ions implanted, DLTS study of laser annealing 0-80204
 GaAs:Se ion implanted samples, Q-switched ruby laser annealing, improvement in elec. props. 0-100460
 GaAs:Se ohmic contacts, pulsed electron beam annealing donor density, mobility 0-65678
 GaAs:Se(Si), ion-implanted, capless annealing by melt-controlled ambient technique 0-75251
 GaAs:Si, ion implantation, thermal annealing, Hall meas., SIMS atomic profile meas. 0-75243
 GaAs:Si, transferred-electron devices by low-level ion implantation 0-92543
 GaAs:Si(Sn), ion implanted, laser annealed, high doping levels 0-88181
 GaAs:Si(s), generation of high mobility n layers, SIMS 0-103375
 GaAs:Te(Cd)(Mg)(B), ion implant depth distrib., AES and glow discharge optical spectroscopy meas. 0-65028
 GaAs:V, ion implanted, luminesc., level splitting 0-97338
 GaAs:Zn, implanted, furnace annealed, electrical, Rutherford backscattering and TEM meas. 0-100272
 GaAs:Zn, implanted, laser annealing, elect., Rutherford backscattering and SEM meas. 0-100273
 GaAs:Zn, ion implanted, TEM study after laser and furnace annealing 0-70234
 GaAs-based mixed cryst. form. by ion beam synthesis, vibr. anal. 0-103376

ion implantation continued

- GaAs-GaAlAs injection lasers, narrow-stripe proton-implanted, high bit-rate modulation 0-91824
 GaAs-InP heterojunction laser output wavelength control 0-74384
 GaAs-Si ion implanted, impurity profiles elec. props. 0-96550
 GaAs $_{1-x}$ P $_x$ N, photolum. and electrochem. study of N isoelectronic traps 0-89061
 GaP, complex ^{119}Sn impurity-defect, Mossbauer study 0-75898
 Ge epitaxial film, ion implantation and electron beam anneal effects on carrier conc. 0-75255
 Ge: ^{199}Au , impurity lattice dynamics, Mossbauer spectra, Debye temp. 0-84262
 Ge:Pb, ion implanted damaged layer, laser induced reorder 0-84201
 Ge:Sn, ion implantation of radioactive ^{119}Sn 0-59495
 ^4He stopping power, 0.15 to 1 MeV, backscatt. determ. 0-88233
 Hg electric field gradients at different Be lattice sites, gamma-spectral study 0-80224
 Hg, quadrupole interactions in Zn, lattice location, gamma spectral study 0-80227
 HgCdTe epitaxial material, ion implantation, junction form. 0-100260
 Hg $_2$ Cd $_2$ Te, implanted with Hg, Al, damage and lattice location study 0-103381
 InAs:S(Mg), ion implanted, photocond., photo-EMF, and optical absorpt. spectra 0-70763
 In $_3$ Ga $_2$ P, N free and implanted, photoluminescence study 0-97322
 InP, ion-implanted layers, close contact capless annealing, elec. props. 0-84192
 InSb, ion implantation, anomalous radiation disordering 0-92553
 InSb, ion implanted, ellipsometric study 0-60537
 InSb, morphological and structural changes due to ion bombardment 0-79843
 KBr, heavy metal ion implantation, mol. unit form. 0-100267
 KCl, heavy metal ion implantation, mol. unit form. 0-100267
 K $_2$ MX $_6$ (M=Sn, Re, Os, Ir, Pt; X=Cl, Br), heavy metal ion implantation, mol. unit form. 0-100267
 LiF, alkali ion implantation, migration, segregation, effect on optical props. 0-100269
 LiF:In, optical absorption effects of ion implantation 0-70239
 LiNbO $_3$, effects of He ion implantation on SAW propag. 0-75421
 LiNbO $_3$, optical waveguides by ion implantation 0-106622
 LiNbO $_3$:Ti single-mode optical waveguide, fabrication by sequential combination of Ti diffusion and masked ion-implantation 0-58785
 Mg-Ag, ion implanted, recovery stage characterisation by electron irradiation 0-107295
 Mo cryst., D $_2^{+}$ implantation and radiation induced vacancies 0-65076
 Mo, D and ^3He trapping and mutual replacement 0-59493
 MoSi $_2$ refractory formation by As $^{+}$ ion beam bombardment 0-107286
 Na $_2$ O-SiO $_2$ glass, ion bombardment, form. of cpds., IR spectrosc. exam. (German) 0-88173
 Nb, He blistering, large swelling meas., gas press. model 0-88218
 Nb, ion-implanted bridge with thick Pb banks, fabrication and characterisation of film parameters 0-100569
 Nb layer, ion bombarded, supercond. props. and struct. 0-88671
 NbC $_x$, supercond. transition temp., light element implantation effect 0-107951
 Nb $_2$ N, supercond. props. and structural phase transform. induced by C $^{+}$ and N $^{+}$ implantation 0-107942
 Nb $_{40}$ Ni $_{60}$, amorphous, produced by Ni $^{+}$ implantation, damage distrib. 0-107062
 Ni, ion-implanted and virgin, laser irradiation effect, epitaxial lattice regrowth 0-108306
 Ni, self implantation damaged, crit. behaviour, perturbed ang. distrib. meas. anal. 0-60476
 Ni:In, He, lattice defect struct., PAC meas. 0-70190
 Ni:O, single crystal, $^{18}\text{O}^{+}$ ion implantation in channelling directions, expt. conditions and range profile obs. 0-65022
 Ni:O single crystal, $^{18}\text{O}^{+}$ ions implantation in channelling directions, stopping power meas. from max. range 0-65078
 Ni-Cr films implanted with N ions, electric properties (Russian) 0-107927
 Ni-Cu(Zn)(In), implantation damaged, crit. behaviour, perturbed ang. distrib. meas. anal. 0-60476
 Ni-P, amorphous, prod. by ion implantation 0-75257
 NiO, diffusion of ion-implanted ^{18}O 0-107494
 PLZT ceramic, proton implanted, photoferroelectric effect for image storage and display devices 0-80315
 PLZT ceramics photosensitivity enhancement by H- and He-ion implantation 0-96934
 Pb $_{0.97}$ Hg $_{0.03}$ Te photovoltaic detector produced by Sb $^{+}$ ion implantation 0-82821
 Pt, polycrystalline film, trapping of ^3He and ^4He ions at room temp. 0-84221
 (SN) $_2$:Br, ion implantation effect on elec. props. 0-65026
 Si, advanced material for space solar cell 0-94007
 Si, amorphous, elec. props., ion implantation effects 0-79828
 Si, amorphous, implanted, recrystn. induced by scanning CW laser, reaction rates, analytical model 0-66334
 Si amorphous, ion implantation, negative magnetoresist., localised mag. states 0-70731
 Si, amorphous, ion implantation method, B and P ions 0-100274
 Si, amorphous, laser epitaxial recrystallisation threshold energy 0-70571
 Si, amorphous, sputtered, resist. control by ion implantation 0-100262
 Si, amorphous, substrate orientation effect on regrowth by laser pulses, channelling, backscatter 0-84409
 Si, amorphous layer prod. by ion implantation, diffusion broadening, ESR study 0-92552
 Si, CW laser annealing 0-92550
 Si, carrier lifetime depth distrib. due to Ar ion implantation 0-70232
 Si, complex annealing behaviour of amorphous layers, TEM obs. of defect struct. 0-107299
 Si, damage struct. obs. using TEM and cross section specimens 0-107298
 Si, defect struct., dislocation loops and elongated defects 0-107300
 Si, diffusion coefficient determ. from carrier conc. depth profile 0-107566
 Si, furnace preannealed (111) ion implanted, laser irradiation 0-65015
 Si, heavy ion induced disorder in surface and at shallow depths 0-59535
 Si, high dose self-irrad., spatial correl. between primary and secondary defect profiles 0-59536
 Si, high-dose Ar implantation, X-ray topographic obs. of strains and damage 0-59496

ion implantation continued

Si, implanted crystal, laser induced annealing and diffusion behaviour 0-88202
 Si, implanted semiconductors, laser annealing, review 0-107301
 Si, implanted with low solubility dopants, laser annealing, TEM study 0-70233
 Si, interstitial generation and loop form. during annealing in oxidising medium 0-107225
 Si, ion bombardment induced defect distrib., IR and electron diffr. study 0-65074
 Si, ion implantation, channelled, through metal silicide film 0-70231
 Si, ion implantation, channelling, alignment effects 0-88183
 Si, ion implantation, high dose, solid phase epitaxial regrowth 0-103380
 Si, ion implantation by laser annealing, characterisation, solar cell applications 0-70247
 Si ion implanted, amorphous to crystalline transition due to laser irradi. 0-103451
 Si, ion implanted, annealing of heavy ion cascade damage, channelling meas. 0-89255
 Si, ion implanted, annealing by ion beam heating 0-103382
 Si, ion implanted, damage profiles, Rutherford backscattering 0-100733
 Si, ion implanted, dopant depend. of oxidation rate 0-89384
 Si, ion implanted, electron beam annealing, surface struct. study using SEM 0-70235
 Si, ion implanted, radiation defect production at different temps. 0-103398
 Si, ion implanted, self implanted, self annealing using high ion current density treatment 0-89254
 Si, ion penetration, computer program 0-88185
 Si, ion-implanted, annealing using scanning CW laser system 0-100265
 n-Si, ion-implanted, elec. characts. after laser annealing 0-88562
 Si, ion-implanted, impurity activation monitoring by SAW techniques 0-65020
 Si ion-implanted dopant redistribution under laser annealing 0-70242
 Si ion-implanted laser-annealed solar cells 0-93881
 Si, ion-implanted layers, crystn. by ns laser pulses, TEM and RHEED 0-100421
 Si, ion-implanted layers, epitaxial regrowth by laser beam and flash annealing 0-100420
 Si ion-implanted solar cells, factors controlling efficiency 0-81451
 Si laser annealed, nonequilibrium solubility and segregation 0-84296
 a-Si, laser induced crystallisation mechanism, epitaxial regrowth 0-84962
 Si layer, on buried SiO₂ layer formed by high-dose, O ion implantation, TEM, AES, and XPS obs. 0-88172
 Si layers amorphized by molecular ions, laser annealing 0-103379
 Si, lifetime in Ar⁺ ion implant damage getterred, MOS voltage ramping 0-75247
 Si, on sapphire, epitaxial, crystalline quality improvement by ion implantation and furnace regrowth 0-88452
 Si, P implanted low pressure CVD polycryst. films, elect. characts. 0-60114
 Si, scanning CW and pulsed laser annealing 0-92549
 Si, single crystal solar cell manufacturing process, laser annealing of implanted area, energy saving 0-97791
 Si, slip dislocation nucleation during laser annealing 0-84179
 Si solar cell processing, pulsed laser techniques for annealing ion-implantation damage 0-81453
 Si solar cells, fabrication using continuous or pulsed lasers (*French*) 0-61350
 Si solar cells, high open circuit voltage, P implantation 0-89642
 Si solar cells, ion implanted grating type 0-101102
 Si solar cells, ion-implanted 0-81452
 Si solar cells, ion-implanted, expt. study of efficiency controlling factor 0-93997
 Si solar cells, low cost processes for fabrication 0-94013
 Si, standard for TEM, EELS 0-99017
 Si substrate thickness, device design, solar cell processing, empirical study of interaction 0-93995
 Si, surface, pulsed electron beam processing, doping, annealing 0-75254
 Si thin film, polycryst., CVD, elec. props. 0-107934
 Si wafer, ion implanted, electron beam annealing, computer simulation 0-96569
 Si wafer, thin surface layers, amorphous to cryst. transform., obs. technique 0-107288
 Si:As(Pb), high-dose ion implanted and annealed, implant redistribution 0-107309
 Si:^{119m}Sn, impurity lattice dynamics, Mossbauer spectra, Debye temp. 0-84262
 Si:⁵⁷Co(⁵⁷Fe), implanted, Mossbauer spectra, study of dose dependence 0-75900
 Si:Ar, As, ion implanted, laser annealing, doping profiles, channelling 0-97506
 Si:Ar, ion-implanted, epitaxial regrowth by laser annealing, microstruct. 0-84404
 Si:Ar(Ne)(O)(N), ion-implanted, defect reverse annealing, 550-650°C 0-88875
 Si:As, CW CO₂-laser annealing, comparison with thermal annealing 0-84193
 Si:As, ion implanted, formation of As complexes 0-59511
 Si:As, ion implanted, laser annealed, lattice defects, epitaxial regrowth 0-103334
 Si:As, ion implanted, low temp. thermal annealing 0-96552
 Si:As, ion implanted, pulsed ion beam annealing 0-103395
 Si:As, ion implanted, pulsed laser annealing, partial solid-state regrowth 0-103591
 Si:As, MBE with simultaneous ion implant doping 0-66432
 Si:As, scanning electron beam annealing, spreading resistance, junction depth 0-75267
 Si:As, shallow junctions by high-dose implants 0-96694
 Si:As high-dose implanted single crystals, pulsed electron-beam annealing 0-103373
 Si:As ion implanted layers, annealing by CO₂ laser, doping profile shift 0-84965
 Si:As ion implanted shallow junction 0-70228
 Si:As laser annealing, heat and mass transport model 0-92546
 Si:As⁺, implanted, CW laser annealing, electron-beam induced current 0-100709
 Si:As⁺(P⁺) ion implanted, laser annealed, correlation of struct. and elec. props 0-70855
 Si:As(B), heavy-doping effects and impurity segregation during high-pres. oxidation 0-65014

ion implantation continued

Si:As(P), ion implanted, TEM study after laser and furnace annealing 0-70234
 Si:As(Pb), ion-implanted, impurity redistrib. during laser irradi. 0-100280
 Si:As(Sb), ion implanted, lattice location of impurities after pulsed laser annealing 0-88196
 Si:B, anomalous B profiles prod. by BF₃ implantation 0-75252
 Si:B, high conc. effects in ion implantation 0-75245
 Si:B, implanted laser annealed, lattice strain, X-ray study 0-96554
 Si:B, ion implanted, structure defects formation and behaviour under annealing in various ambients 0-65033
 Si:B, P, long range enhancement of B diffusivity by P diffusion 0-103386
 Si:B (0.2 wt.%) ion implanted, B atom displacement due to low temp. irradi. 0-88234
 Si:B implanted wafers, ionis. assisted annealing and effects 0-100257
 Si:B ion implanted, strain profiles from X-ray rocking curves 0-107290
 Si:B ion implanted grating-type solar cells, var. of junction depth, collection efficiencies 0-93934
 Si:B ion implanted layers, light refl. and transmission coeffs., computer program 0-66316
 Si:B radiation damage and minority carrier lifetime, SEM-EBIC obs. 0-96573
 Si:BF₃⁺, appl. in semicond. devices production 0-103383
 Si:B(Be)(Li) ion implanted, channelling and random equivalent depth distrib. 0-100293
 Si:B(P), ion implanted crystalline and amorphous laser annealing 0-97509
 Si:Be, ion implanted, correl. of atomic distrib. and implantation induced damage profiler 0-88199
 Si:Bi, channelling obs. of pulsed Q-switched ruby laser annealing 0-59542
 Si:Bi, ion-implanted, solid phase epitaxial growth during annealing, super-saturated solid soln. form. 0-103384
 Si:Co, ion implanted, Co lattice location, channelling meas. 0-88201
 Si:Fe, ion implanted, laser annealing studies using Mossbauer spectroscopy 0-79827
 Si:Ge, recryst. after implantation using different temp. and energy sequences 0-84196
 Si:He, B ion implantation 0-96559
 p-Si:In, ion implanted, doping profiles from capacitance-voltage characts. 0-88203
 Si:Mn,Bi, standard, doubly implanted, Rutherford backscattering meas. at MeV energies, screening corrections 0-88204
 Si:N, high energy ion implantation of buried insulating layers 0-88188
 Si:N, ion implanted, oxidation characts. 0-89385
 Si:N, laser-annealed, Jahn-Teller distorted donor, EPR meas. 0-84642
 Si:N wafers, Si₃N₄ layer growth by high dose implantation and annealing, elec. props. 0-70227
 Si:N(P), ion implanted, IR transmission and rel. spectra study 0-108244
 Si:O(C), implant redistribution, annealing effects, SIMS meas. 0-96561
 Si:P, annealing after ion implantation, ellipsometric study 0-65018
 Si:P, implanted low temp. annealed, elec. activation, damage depend. 0-88182
 Si:P, ion implanted, regrowth of damage structs. by laser annealing 0-107289
 Si:P, ion implanted, subsurface damage, TEM and channelled Rutherford backscatt. study 0-107337
 Si:P, ion implanted with small doses, defect annealing by nanosecond laser pulses 0-107297
 Si:P, multiscaning electron beam annealing 0-75242
 Si:P, polycryst., channelling of implanted P during MOS device processing 0-65017
 p-Si:P implanted films, piezoresist. stress tensors, ion dose depend., -80 to 120°C 0-100538
 Si:P(As)(B), nonequilibrium solid solutions obtained by heavy ion implantation and laser annealing 0-92544
 Si:Pt, implanted and laser annealed, segregation and increased dopant solubility 0-65016
 Si:S, deep level characterisation, implantation predeposition technique 0-100444
 Si:Sb, high dose Sb ion implantation, buried layer appls. 0-88186
 Si:Sb, ion implanted, Sb diffusion during oxidation, snow-plough effect 0-88366
 Si:Sb, ion implanted and annealed, influence of implantation temp. on dislocation generation 0-88158
 Si:Sb, low energy ion implantation, profile determ. 0-88176
 Si:Sb, low energy ion implantation Schottky barrier diodes and resistors 0-88177
 Si:Sb, Mossbauer spectra of ¹¹⁹Sn defect struct. 0-97174
 Si:Sb, produced by ion implantation and laser annealing, Sb behaviour above solid solubility 0-88200
 Si:Sb,P, double implants, residual defect reduction after damage anneal 0-88170
 Si:Sn, Mossbauer study of defects due to ¹¹⁹In implantation 0-80641
 Si:Te, laser melting, surface Te atom accumulation, profiles 0-100258
 Si:Te, Mossbauer spectra of ¹¹⁹Sn defect struct. 0-97175
 Si/Pd system, solid phase epitaxial growth control by C ion implantation 0-75466
 Si-Au system, ion implanted induced giant gettering, annealing effects 0-88221
 Si-refractory metal structs., interface modification by ion implantation 0-70475
 Si:SiO₂, ion implantation through SiO₂ film, recoil implantation of O, EPR study 0-88180
 Si:SiO₂, recoil implanted O profile after ion implantation through SiO₂ 0-88198
 Si:SiO₂, two layer system, P⁺-ion penetration tails, expt. and computer anal. 0-75249
 Si:SiO₂, abrupt interface form. by very high dose O⁺ ion implantation 0-75253
 Si:SiO₂, laminar ion-implanted systems, struct. change investig. by MSSI method (*Russian*) 0-107918
 Si:SiO₂, structures, B ions implanted, energy spectra of shallow traps at various implantation energies 0-80392
 SiC ion implanted, laser induced ordering and defects 0-84754
 Si₃N₄ layers produced by ion implantation, oxidation inhibition and etching 0-103374
 SiO₂, As-implanted, electron trapping and detrapping characts. 0-65692
 SiO₂ coatings on SiO₂ substrate, cathodoluminescence spectra, electron irradi. 0-76085

ion implantation continued

- SiO₂ film, on GaP substrate, N ion implantation, optical refl. and EPR meas. 0-84197
 SiO₂, fused, surface crystn. by Li⁺ ion implantation and annealing 0-89383
 SiO₂ glass, ion bombardment, form. of cpds., IR spectrosc. exam. (*German*) 0-88173
 SiO₂, implanted, in MOS capacitor, direct current/voltage relns. as function of oxide doping 0-88635
 SiO₂ ion implanted, radiation defects and optical props. 0-107293
 SiO₂:As⁺ implanted layers in MOS struct., electron trapping and detrapping characs. 0-92982
 SiO₂:Au(Ag)(Cu), XPS line broadening and extra-atomic relax. energies 0-71561
 SiO₂:F(BF₃), ion implanted, F influence on oxidation-induced stacking faults 0-65011
 Si(111):Pb ion implanted amorphous layers, recrystallisation, impurity out-diffusion model (*Chinese*) 0-88363
 Sn film, metastable supercond. alloys, produced by low temp. ion implantation 0-88670
 α-Sn, ion implanted, defect struct., Mossbauer spectra 0-80214
 α-Sn:^{119m}Sn, impurity lattice dynamics, Mossbauer spectra, Debye temp. 0-84262
 Sn-Cu film, metastable supercond. alloys produced by low temp. ion implantation 0-88670
 TaSi₂ refractory formation by As⁺ ion beam bombardment 0-107286
 Te-Au film, metastable supercond. alloys, produced by low temp. ion implantation 0-88670
 Ti metal-metal interface, adhesion energy, surface treatment and ion implantation effects 0-107660
 Ti:D, implanted, deuterium imaging using scanning Auger spectroscopy 0-89092
 Ti:D, implanted, nucleation and growth of TiD₂ 0-97717
 Ti:D, ion implanted, depth profiles, temp. depend. 0-100270
 Ti:Pd, ion implanted, corrosion behaviour and Rutherford backscatt. anal. 0-71792
 W:³He, implanted ion positions, determ. using mol. deuteron beam 0-70240
 WSi₂ refractory formation by As⁺ ion beam bombardment 0-107286
 YIG:La(Ga) films, ferromagnetic resonance, ion implantation effect 0-97145
 Y₈₅La_{0.15}Fe_{3.75}Ga_{1.25}O₁₂ LPE films, ion implantation effect on spin waves 0-71124
 Y₈₅La_{0.15}Fe_{3.85}Ga_{1.15}O₁₂ garnet, mag. props., ion implantation effect, Mossbauer study 0-97166
 Y_{3-x}Sm_xFe₅O₁₂:⁵⁷Fe film, ion implanted, Mossbauer conversion spectra study 0-80663
 Zn:Al, ion implantation, temp. and time depend. 0-65013
 Zn-Mn, Kondo-system, ion implantation as method for study 0-70241
 ZnSn ion beam etching, topographic changes, amorphisation, luminescence study 0-76078
 ZnS, ion implantation effects on luminesc., thermo-EMF 0-88178
 ZnTe, ion implantation defect introduction, cathodolum. studies 0-75250
 ZnTe:P(As), ion implanted, cathodoluminescence emission spectrum 0-108281
 Zr, H(D) implanted, superconductivity enhancement obs. 0-70884
 Zr, ion-implanted polycryst., thermal oxidation 0-71786

ion lasers

- applications and laser principles (*French*) 0-83590
 book, gaseous electronics and gas lasers 0-73120
 book, quantum electronics 0-105442
 confined plasma column, soft X-ray lasing action conditions 0-74346
 hollow cathode discharge with variable voltage 0-59336
 hollow cathode discharges for gas lasers, review 0-99717
 hollow cathode discharges for gas lasers 0-83599
 inert gas ion laser, high voltage-low press. discharges, stationary props. 0-92400
 inert gas mixture, hollow cathode, CW operation and excitation mechanism 0-69363
 metal ion lasers, hollow cathode 0-99708
 metal vapour lasers, hollow cathode discharge, review 0-99717
 noise, low frequency 0-69364
 plasma column, multiple confinement, radial and axial arrangement 0-83974
 relativistic ion beam laser, continuously IR to X-ray tunable, in negative temp. state (*Chinese*) 0-87373
 review, excitation mechanisms and characs., book contrib. 0-106512
 soft X-ray population inversion in laser plasmas, reson. photoexcitation, photon-assisted processes 0-87378
 tube design, cathode fall theory studies 0-58560
 Al II near IR laser transitions, large diameter hollow cathode Ne-Al discharge 0-102715
 Ar, high-power, construction of side cathode 0-99742
 Ar laser and appls. (*French*) 0-83590
 Ar laser with passively locked modes, excitation of dye laser for picosecond pulse generation 0-95930
 Ar⁺ and Ar⁺-Kr⁺ ion lasers, I₂ stabilized, beat frequency 0-95916
 Ar⁺ ion laser, active mode locking study 0-91827
 Ar⁺ laser 582 THz stabilisation by I₂ cell, improvements 0-102741
 Au hollow cathode laser, ion laser transitions 0-69366
 Cd hollow cathode laser, ion laser transitions 0-69366
 Cd laser produced plasma recombination laser, power output enhancement by plasma confinement 0-63989
 Cd vapour laser, hollow-cathode white light, new design concept 0-87405
 Cr vapour, laser transitions in near IR 0-99704
 Cu hollow cathode laser, ion laser transitions 0-69366
 Cu II laser with cylindrical hollow cathodes, UV performance 0-102709
 Fe group elements, singly ionised, charge transfer, rel. to laser action 0-74246
 He-Cd vapour excitation in hollow cathode discharge 0-64815
 He-Cd vapour laser, continuous wave, intensity fluctuations investig. 0-83593
 He-Kr hollow cathode CW laser, Kr II 4584 Å generation 0-58510
 He-metal vapour lasers, positive column electron densities, experimental study (*Japanese*) 0-69376
 He-Se, vapour laser, continuous wave, intensity fluctuations investig. 0-83593
 He-Sr laser, possibility of nucl. pumping, 4305 Å Sr II transition 0-58518
 He²⁺+Li collisions, soft X-ray emission obs. 0-83591

ion lasers continued

- ¹²¹I₂ stabilised, beat freq. intercomparisons at 514.5 nm 0-74338
 Kr⁺ mode-locked ion laser, pulse width and linewidth meas. 0-102696
 N₂ travelling wave excitation 0-91774
 N₂-He ion nuclear pumped lasers feasibility study and quenching 0-64001
 Sn hollow cathode laser, emission obs. from Sn II, I transitions 0-106509
- ion lenses** *see lenses*
- ion microanalysis**
see also ion microprobe analysis
 ANL HVEM-TANDEM accelerator facilities 0-101896
 plane retarding potential analyzer, effect of total transparency of field inhomogeneity 0-99003
 second-generation ion microanalyser description and performance (*French*) 0-101055
 surface anal. by ion scattering spectrometry and secondary ion mass spectrometry 0-103541
 surface anal. tools review 0-103540
 Al-Nb superimposed metallic layers, ionic movements during anodization, Rutherford backscatt. and nuclear microanal. 0-71913
 Nb-Al superimposed metallic layers, ionic movements during anodization, Rutherford backscatt. and nuclear microanal. 0-71913
 Nb-Ta superimposed metallic layers, ionic movements during anodization, Rutherford backscatt. and nuclear microanal. 0-71913
 Ta-Nb superimposed metallic layers, ionic movements during anodization, Rutherford backscatt. and nuclear microanal. 0-71913
- ion microprobe analysers** *see ion microprobe analysis*
- ion microprobe analysis**
see also ion microanalysis
 air pollution monitoring, PIXE and NRA studies using lichen indicator 0-61744
 alloys, ion-implanted, integral Gaussian profile determ. method 0-107313
 atomic transport and conc. profiles 0-59723
 catalyst design and evaluation using PIXE 0-61201
 crystalline solids, electronic industry, chem. anal. instrumental methods progress 0-66903
 hair, human, PIXE analysis, correction factor, rel. to pollution monitoring 0-61743
 Incoloy 800, steam oxidised, oxide coating anal. 0-89399
 k-shell ionizations in proton induced X-ray emission analysis 0-101054
 laser microprobe mass analyser, achievements and appls. 0-73536
 lung pathology, appl. of PIXE 0-61691
 minerals, sputtering rates, implications for abundances of solar elements in lunar samples 0-61797
 phosphosilicate glasses, P content determ. by Rutherford backscatt., PIXE, and activation anal. (*Hungarian*) 0-85233
 PIXE, biomedical appls. 0-61691
 PIXE, technique with external beam, and its appl. to study of valuable relics 0-61198
 PIXE, use of liposomes to reduce enhancement-absorption effects 0-101053
 PIXE set-up for routine analyses 0-104488
 PIXE-PIGME system, automated, appl. to artefact obs. 0-61199
 protein analysis using PIXE 0-61691
 steel, industrial, surface chem. characterisation by SIMS, glow discharge spectrometry and other techniques 0-66907
 steel, stainless, D₂⁺ diffusion and permeation, ion beam meas. 0-59492
 surface analysis, new uses of ion beams (*Japanese*) 0-90934
 zircaloy, nuclear microprobe methods for investigating oxidative corrosion 0-71787
 Al sheet surfaces, chem. characterisation by SIMS, glow discharge spectrometry and other techniques 0-66907
 Al, single crystal, ¹⁸O⁺ ion implantation in channelling directions, expt. conditions and range profile obs. 0-65022
 Al single crystal, ¹⁸O⁺ ions implantation in channelling directions, stopping power meas. from max. range 0-65078
 Al, sputter deposit PIXE expt. 0-61196
 Al₂O₃, single crystal, O self diffusion, ion-probe meas. 0-59701
 Cu, sputter deposit PIXE expt. 0-61196
 Cu:O single crystal, ¹⁸O⁺ ion implantation in channelling directions, expt. conditions and range profile obs. 0-65022
 Cu:O single crystal, ¹⁸O⁺ ions implantation in channelling directions, stopping power meas. from max. range 0-65078
 Fe-Cr (9 wt.%), oxidation studied using C¹⁸O₂ and D₂O tracers 0-71784
 Fe-Ni-Cr (44, 17 wt.%), nuclear microprobe methods for investigating oxidative corrosion 0-71787
 Hg_{1-x}Cd_xTe, implanted with Hg, Al, damage and lattice location study 0-103381
 InP, Zn diffused single-crystal, substitutional dopant and hole conc. meas. 0-75260
 Mo, D and ³He trapping and mutual replacement 0-59493
 Ni:O, single crystal, ¹⁸O⁺ ion implantation in channelling directions, expt. conditions and range profile obs. 0-65022
 Ni:O single crystal, ¹⁸O⁺ ions implantation in channelling directions, stopping power meas. from max. range 0-65078
 Si-SiO₂, two layer system, P⁺ ion penetration tails, expt. and computer anal. 0-75249
 SiC particles in EFG ribbon solar cells, EBIC and ion microprobe anal. 0-93838
 Zr, ion-implanted polycryst., thermal oxidation 0-71786
- ion microscopes**
see also field emission ion microscopes; ion microscopy
 scanning, atomic resolution capability 0-101878
- ion microscopy**
see also field emission ion microscopy; ion microscopes
 diffusible ion localization, comparison of chemically prepared and fast frozen freeze dried, unfixed liver sections 0-95189
 lithography, heavy ion, tool for object investigation and replication 0-90931
 microscopic equipment, methods, appls. and related topics, bibliography 0-73124
 radioactive ion microscopy 0-101884
- ion mobility**
see also electrolytic ion mobility; ionic conduction in solids
 acetone, macroscopic model for solvated ion dynamics, cation conductance calcs. 0-65261
 acetonitrile, macroscopic model for solvated ion dynamics, cation conductance calcs. 0-65261
 dielectric liquids, ion mobility meas. and breakdown process, optical methods 0-84692

ion mobility continued
free burning arc characteristic formulae 0-70068
high-current free burning arcs, approximate model 0-70069
liquid dielectric, Sumoto effect under transient conditions 0-97198
optoelectronics, appl. in measuring gas discharge phenomena 0-107007
pyridine, macroscopic model for solvated ion dynamics, cation conductance calcs. 0-65261
AgCl, ionic mobility, diffusion coeffs., defect mobility energies 0-65284
Ar⁺ ions, mobilities in He gas at 82K 0-75023
F⁻ ions in Kr and Xe; mobilities and diffusion coeffs. determ. 0-100048
H⁺ ion mobility in He, expt. 0-96337
³He, liq., ion mobility, temp. and freq. depend. 0-70493
³He, negative ion mobility, theory 0-107598
³He, superfluid A-phase, ion mobility tensor, ion-quasiparticle scatt. 0-59753
LiCl-RbCl, molten, Chemla effect, mol. dynamics simulation, self exchange vel. 0-79967
Na⁺, mobility and long, diff. diffusion coeffs. in Kr and Xe 0-106866
Ne⁺ ions, mobilities in He gas at 82K 0-75023
SF₆-N₂ mixtures, attachment coeffs. and ionic mobilities, 1.2-4 eV 0-96338

ion-molecule collisions
see also charge exchange; ion-molecule reactions
drift tube technique in ion-neutral collisions, cross sections determ. 0-63748
electronic and at. collisions, conf., Kyoto, Japan (Aug.-Sept. 1979) 0-57011
electronic and at. collisions, conference, Kyoto, Japan (Aug.-Sept. 1979) 0-62394
hydroxonium complexes, produced by collisional dissoc. method, mass spectrometric study, dissoc. energies determ. 0-95707
ion+polar molecule collision, low-energy, rot. state approach 0-74224
ion-dipole capture in noncentral field, variational and trajectory investigation 0-63739
negative ions, at. and mol. collisions electron detachment for energies near threshold 0-63797
polar mol.+ion, statistical and thermodynamic theory 0-99562
polar molecules, long range dipole interaction effect 0-102558
Ar⁶⁺+H₂ collisions, ionisation and excitation resulting from electron capture 0-78683
Br⁻+H₂(D₂)(O₂)(N₂)(CO)(CO₂)(methane), total electron detachment cross sections for energies around threshold 0-99550
C-H, A²Δ-X²Π, dissociative excitation, form. environment and parent mol. effects 0-78682
C₂H₃⁺+HF, interaction, struct. and stability, ab initio calcs. 0-58347
CO₂+H⁺(D⁺), vibr. excitation, isotope and time effects 0-63773
Cl⁻+H₂(D₂)(O₂)(N₂)(CO)(CO₂)(methane), total electron detachment cross sections for energies around threshold 0-99550
H⁺+D₂, collisional complex form. 0-58339
H⁺+H₂, rot. and vibr. excitation, energy loss obs. 0-63773
H⁺+H₂, vibr. excitation, ab initio CI pot. energy surface calcs. 0-74228
H⁺+H₂, vibr.-rot excitation, ab initio CI pot. energy surface calcs. 0-74229
H⁺+H₂(CO₂), vibr. excitation, 10-30 meV 0-58358
H⁺+He(1s²), K-shell electron capture collision, static pot. effect 0-91660
H⁺+N₂, total ionis. cross section and stopping power for protons 0-69228
H₂+C⁺(N⁺)(O⁺), reactant ion electronic states, effect on charge transfer cross sections 0-63809
H₂+Li⁺, exponential gap relation, rot. inelasticity 0-78693
H₂+Xeⁿ⁺(Arⁿ⁺)(Feⁿ⁺), electron capture by heavy multicharged ions at low velocities total cross sections meas. 0-99548
H₂⁺+H₂→H₃⁺+H, state-selected ion-molecule reactions threshold electron-secondary ion coincidence technique obs. 0-85166
H₃⁺(D₃⁺)+H₂(D₂) collisions, slow ion production, charge transfer cross sections 0-106378
H₂O vapour ionised by He⁺ and He²⁺, secondary electron emission yield obs. 0-102562
He⁺+H₂(N₂)(O₂)(CO₂)(methane)(ethane)(propane), 0.7-2 MeV, charge-changing collisions, electron capture 0-58372
He⁺+N₂, collisional excitation processes, visible emission, cross-sections 0-99571
Kr⁺+molecule, ²P_{3/2}(²P_{1/2}) doublet ground state reactions at 300K 0-108702
Li⁺+CO₂, collisional excitation, quasiclassical trajectory calcs. 0-83467
N⁺+O₂, branching ratio kinetic energy depend. 0-97703
Ne⁺+D₂(H₂), energy-loss scaling in 0.5-3.5 keV 0-63768
O⁺+N₂(O₂), excited ion reactions, charge transfer coeffs. at thermal energy 0-95721
O₄⁺(O₃⁺)(O₆⁺)(O₂+H₂O) 0-95707
O⁺+O₂(N₂), metastable ion reactions, rate consts. and ion mobility at 300K 0-95722
reactant ion electronic states, effect on charge transfer cross sections 0-63809
SF₆+Li⁺(H⁺), mode selective vibr. excitation 0-58351
UF₆⁺+Ar, UF₆⁺ internal excitation 0-106386
Xe⁺+molecules, ²P_{3/2}(²P_{1/2}) doublet ground state reactions at 300K 0-108702

ion-molecule reactions
association density of quantum states and temp. depend. of rate coeff. 0-101015
association rate calc. for ion-molecule reaction 0-81282
atmospheric ion chemistry 0-61885
benzene cation+benzene, trapped ion mass spectra 0-89470
butene, isomers, ion-mol. reactions, photoionisation mass spectra 0-81298
2-butene ion, fragmentation, angular momentum in ion-mol. reacts., RRKM calc. 0-66773
clusters, small, formation, struct. and props. 0-58437
collision system, pot. curves at low collision energies, beam studies 0-61088
electric field effect on reactions in dilute gases and solutions 0-81315
ethyl cation+alkane reaction, temp. and kinetic energy relative rate consts. determ. 0-81299
fast nucleus+molecule, atom capture, quantum calcs. 0-71911
1-5-hexadiyne ion+neutral 1,5-hexadiene, trapped-ion mass spectrometry 0-97694
interstellar molecules synthesis, laboratory studies of ion-atom reactions 0-67812
ion kinetics in high-pressure laser plasmas 0-64002

ion-molecule reactions continued
ion-dipole capture in noncentral field, variational and trajectory investigation 0-63739
low energy, dipole interaction influence 0-89475
methyl cation+NH₃, reaction kinetics, 0.04-1 eV (*French*) 0-66768
methyl ion+H₂O(He) ternary association reaction in energy range 0.04-0.1 eV 0-71896
phenyl cation, struct., ion-molecule reactions studied by trapped ion mass spectroscopy 0-102586
polar molecules, long range dipole interaction effect 0-102558
propynyl cation+propyne, reactant structure effects 0-89469
tetra-n-butylammonium halides in benzene, chloroform, CCl₄, far IR spectra, ion-ion, ion-mol. interactions 0-60562
weakly ionised gas non-ideal behaviour, virial eqn. of state and fugacity coeffs. 0-79424
Ba⁺+D₂→D+BaD⁺, sequential impulse model, prod. bond dissoc. energy and cross section 0-81295
C+O⁺ ion-molecule reaction, 15 eV energy O⁺ production system 0-84817
CD⁺+H₂(HD)(D₂), isotopic exchange, interstellar implications 0-61087
CH₃⁺+H₂(HD)(D₂), isotopic exchange, interstellar implications 0-61087
CO+¹³C⁺(HCO⁺), isotopic exchange, interstellar implications 0-61087
CO⁺+D₂, state selected reaction cross-sections, coincidence technique obs. 0-66797
CO₂+N₂+He, glow discharge positive ion species identification (*Russian*) 0-84014
CO₂⁺+ethylene, rate coeffs. and product distribution determ. 0-97693
CO₂, CO₂⁺+ethylene, rate coeffs. and product distribution determ., dissoc. energy and heat of form. 0-97693
Cl⁻+HBr(HI)→HCl+Br⁻(I⁻), vibr. product state distrib., IR chemiluminesc. obs. 0-81309
Cl⁺+molecule, reactions at room temp. 0-93749
D₂O⁺(D₂O)+H₂O(NH₃), binary reactions, rate coeffs. and product ion distributions determ. 0-81305
H⁺+methane→H₃⁺+methyl radical, quantum 0-71911
H₂⁺+D₂→H₂+H, product angular and vel. vector distributions meas. by crossed beam expt. 0-101012
H₂⁺+H₂, state selected reaction cross sections, coincidence technique obs. 0-66797
H₂⁺+H₂→H₃⁺+H, state-selected ion-molecule reactions threshold electron-secondary ion coincidence technique obs. 0-85166
H₂⁺+methanol, dissoc. charge transfer reaction studied at rel. translational energies from 600 eV to 5000 eV 0-104432
H₂O⁺+NO₂(O₂)(NO)(CO)(H₂)(ethylene)(methane), rate constants determ. as function of relative kinetic energy 0-81292
H₃O⁺(H₂O)_n+D₂O(NH₃), binary reactions, rate coeffs. and product ion distributions determ. 0-81305
He⁺+H₂(D₂), dissociative charge transfer, 78-300K 0-61079
He⁺+methanol, dissoc. charge transfer reaction studied at rel. translational energies from 600 eV to 5000 eV 0-104432
Kr⁺+molecule, ²P_{3/2}(²P_{1/2}) doublet ground state reactions at 300K 0-108702
Kr⁺+H₂(N₂)(O₂)(CO)(CO₂)(methane), charge transfer reactions, rate coeffs. and product-ion distributions meas. 0-104431
N⁺+O₂, branching ratio kinetic energy depend. 0-97703
Ne⁺+H₂(N₂)(O₂)(CO)(CO₂)(methane), charge transfer reactions, rate coeffs. and product-ion distributions meas. 0-104431
Ne⁺+atom (molecule), bimolecular and termolecular reaction rate coeffs. 0-81308
Ni⁺+H₂(HD)(D₂), endothermic reactions, investig. 0-97692
O⁻+O₂→O₃⁻+O, cross section kinetic energy depend., rate consts. meas. and Monte Carlo calcs. 0-78701
O²⁺+H in planetary nebula NGC 7662, effects on emission-line spectrum 0-62233
O⁺(²D)+N₂, thermal rate coeff., products and branching ratios in ionosphere 0-82117
O⁺(²D)+N₂, charge exchange, rate coeff. temp. depend. 0-77179
O⁺(⁴S)+N₂(X¹Σ_g⁺)→NO⁺(X¹Σ⁺)+N(⁴S), MCSCF potential energy surface for collinear ⁴Σ pathway 0-63540
O⁺+N₂, metastable ion reactions, rate consts. and ion mobility at 300K 0-95722
S interstellar molecule formation, ion-molecule schemes inefficient 0-101632
U⁺+O₂(CO)(CO₂)(COS)(CS₂)(D₂O), reaction cross-sections, ion beam apparatus study 0-97691
UO⁺+O₂(CO)(CO₂)(COS)(CS₂)(D₂O), reaction cross-sections, ion beam apparatus study 0-97691
Xe⁺+molecules, ²P_{3/2}(²P_{1/2}) doublet ground state reactions at 300K 0-108702

ion optics
see also ion beams; ion microscopes; mass spectrometers
in air, ion trajectories due to electric field, calc. (*Slovenian*) 0-78760
charged particle beam-surface impact at glancing angles, reflection (*Russian*) 0-108316
cylindrical capacitor with oblique ends, ion optical coefficients determ., first-order focusing 0-63912
cylindrical radiofrequency mass analyser, low resolution mass filter 0-73519
ion beams, intense, production and postaccel. in magnetically insulated gaps 0-74041
ion optical props., aberration, crossed toroidal elec., mag. fields as mass spectrometer (*Chinese*) 0-82843
ISX-B neutral beam injector expt. on prototype beam line 0-74039
pulsed ion beam incident on mag. barrier, virtual anode form. 0-103131
quadrupole doublet, optical props., rot. of elements, effects 0-74292
second-generation ion microanalyser description and performance (*French*) 0-101055
second-order coeffs. for sector mag. analyzer, compact notation 0-63911
Ga ionisation mechanism on W field emitter 0-76156

ion plating
evaporation sources, gaseous media, and transport modes 0-80984
interface broadening during ion plating 0-65405
ionic nitriding thermochemical process, equipment, process details and advantages and prospects (*French*) 0-108641
AlN films, RF reactive ion-plating, struct. and morphology 0-104074
Fe-Cr-Mo and Fe-Cr-Mo-Si alloys, amorphous films, corrosion resist. and ion plating use 0-89423
Fe₃₂N₁₃₆Cr₁₄P₁₂B₆, Metglas amorphous films, corrosion resist. and ion plating use 0-89423

ion plating continued

- Mo ion-plated orthopaedic En58J stainless steel, corrosion fatigue 0-66694
 Nb, ion plated with Pd and Ni, prep., H_2 absorption and desorption rate (Japanese) 0-108358
 Si:H, amorphous thin film, ion plating, IR absorpt. meas. 0-84857
 Ta, ion plated with Pd and Ni, prep., H_2 absorption and desorption rate (Japanese) 0-108358
 TiO_2 film, ion plated, DC cond. study 0-100457

ion probe analysers *see ion microprobe analysis***ion probe microanalysis** *see ion microprobe analysis***ion pumps**

- bakeable ion-cryopumped ultrahigh vac. system 0-77802
 orbitron device, optimum injection condition for electrons, influence of end effects 0-82784
 TEM vacuum system, simplified low-cost design for use with ZEISS microscope 0-99012
 ultrahigh vacuum system for ISABELLE full cell 0-77798

ion recombination

- ambient gas, electron-ion recomb., classical theory 0-91623
 electron impact detachment, ionisation, excitation, dissociation and recombination 0-63832
 ethynyl cation, dissociative recomb. cross section determ., merged beam obs. 0-78715
 halide ions, recombination, exciplex or excimer form. in plasma 0-75026
 inert gas mixtures, high-press., collisional radiative recomb. 0-63595
 ion trajectories in weak electrolytes, dissociation and recomb. of ions 0-85189
 ionosphere, effect of recomb. processes and plasma nonisothermability on thermal parametric instability 0-61967
 ionospheres, ionic reactions in lab. and planetary atmospheres 0-59168
 ionospheric records over Shanghai, March 1953 to June 1955, effective coefficient of recombination (Chinese) 0-77192
 laser plasma, high press. ion kinetics 0-64002
 molecular, indirect dissociative recomb., T-matrix element, Feshbach's projection operator technique 0-58114
 molecule, photodissociation, recomb. afterglow, quenching var., activator penetration to region inaccessible to quencher 0-64813
 planetary nebulae, radio recomb. lines and mol. emission lines obs. 0-109526
 planetary nebulae, recomb. time rel. to effects of He shell flashes in nuclei 0-73021
 planetary nebulae, recombination model rel. to optical spectrum and continuum 0-109522
 planetary nebulae, theory of physical processes in hydrogenic recomb. spectra 0-109527
 plasma, recomb. press. leading to compression and plasma phase change 0-64799
 Rydberg atom, electron collisions 0-63833
 three body ion-ion recombination probability, Monte Carlo simulation 0-85160
 universe, anisotropic, recomb. dynamics rel. to relic radiation polarisation and anisotropy 0-67917
 vinyl cation, dissociative recomb. cross section determ., merged beam obs. 0-78715
 C_2^+ , dissociative recomb. cross section determ., merged beam obs. 0-78715
 $C_2H_2^+$, dissociative recomb. cross section determ., merged beam obs. 0-78715
 Fe IX, X, XI, effective dielectronic recombination rates in H plasma, emission time histories 0-79570
 Fe XXII, XXIV, XXV, charge exchange recomb. in Princeton large torus during beam heating 0-100067
 H^- form. by surface and vol. processes, neg. ion source appl., review 0-58375
 H_2^+ , dissoc. recombination, doubly excited Rydberg states 0-83506
 H_2O^+ (D_2O^+), plasma dissociative ion electron recomb., rate coeffs. 0-63747
 $^A H, A=1,2,3$, β radiative atomic recombination, antiprotonic atoms 0-83527
 He, hollow-cathode type discharge, spectroscopic obs., laser light source appl. 0-59335
 He^+ , dielectronic recomb. in a mag. field 0-91662
 He^+ recombination in planetary nebulae, He II Ly α photons absorpt. and forbidden lines intensities 0-67833
 $He+CS_2$, metastable atoms, energy transfer processes 0-83466
 He^+ high press. afterglows, reviews 0-64823
 3He -Xe nuclear pumped laser, small signal gain coeff. and power output, theory comparison with expt. 0-63983
 $Kr^+ + F^- + Ar$, three body ion-ion recombination probability, Monte Carlo simulation 0-85160
 Mg XI dielectronic recombination line, atomic parameters for reson. line satellite lines 0-78567
 N_2^+ , recomb. energy determ. from pot. curves 0-58335
 $Ne+CS_2$, metastable atoms, energy transfer processes 0-83466
 O_2 electron capture rate from geminate ion recombination fluoresc. data 0-74245
 Sr-Cs mixture, laser induced collisional two-photon ionisation, fluoresc. monitoring 0-91515
 Ti XX 0-100067
 $Xe^+ + Cl^- + Ne$, three body ion-ion recombination probability, Monte Carlo simulation 0-85160
- ion solvation** *see solvation*
- ion sources**
see also ion emission
 broad beam ion source used for sputtering and etching of Ar, Kr, O_2 and N_2 gases 0-69002
 charge exchange of metal atoms, ion source for twin mass spectrometer 0-106215
 coaxial electron impact, H_3^+ , HeH^+ and He_2^+ beam prod. 0-62795
 cold-cathode ion gun for sputter-etching, discharge characts. and improvements 0-105748
 conference on nuclear spectroscopy of fission products, Grenoble, France (May 1979) 0-77546
 CRYEBIS ion sources for Saturne synchrotron (French) 0-63432
 current trends (Hungarian) 0-57786
 deuteron source, laser-plasma 0-78475
 DITE Phase II ion source, characteristics 0-83223
 electron beam type, producing low-vel. highly charged heavy ions 0-58017

ion sources continued

- electron bombardment type, for use with mass spectrom. 0-77909
 electron cyclotron reson. ion source with permanent mags., plasma-wall interaction expts. 0-99378
 extraction element design for long pulse multi-megawatt neutral beam 0-102373
 FEBIAD ion source for fission fragment isotope separation 0-78483
 flowing afterglow plasma ion source, appls. 0-87955
 fusion reactor, 1000-kV arc power supply 0-99396
 fusion reactor, ASDEX, neutral beam injection, beam line design 0-99395
 fusion reactor, DITE-II, neutral beam ion source particle beam identification 0-99397
 fusion reactor, Heliotron E, neutral beam injector ion source power supply 0-99333
 fusion reactor, long pulse high current ion source electrode cooling 0-91360
 fusion reactor, MFTF, neutral beam source development 0-102368
 fusion reactor, neutral beam injector mag. cusp plasma source, design and fabrication 0-99377
 fusion reactor, PDX, neutral beam elec. power system, ion source supply upgrade 0-102330
 fusion reactor, PDX neutral beam injector, ion accel. structural anal. 0-102375
 fusion reactor, PDX neutral beam injector development 0-99375
 fusion reactor, rectangular plasma generator, advanced ion source for ion injectors 0-99376
 fusion reactor neutral beam injection, 120 keV, ion source 0-91357
 fusion reactor neutral beam source, 40 kV for TMX, engineering design 0-91358
 fusion reactor PDX, ORNL prototype neutral beam injection system, ion source development 0-99391
 fusion reactor stationary ion source construction 0-91359
 heavy-ion fusion preaccelerator, 1.5 MeV, fibre-optic remote control system 0-73993
 HF, proton yield increase, influence of He, Na, Ar, Kr, Xe and N_2 admixtures to H_2 obs. 0-57422
 high temperature, for on-line isotope separation appl. 0-74063
 inverse reflex tetrode, high power ion beam generation 0-68986
 ion source fission product separators 0-78479
 ISOLDE as a source of neutron-rich nuclei 0-78480
 Kaufman, appl. to low energy ion erosion expts. on fusion reactor materials 0-68942
 large diameter source for neutral beam injection, permanent magnet and coil combination 0-74066
 laser ion source, appl. in mass spectrometry 0-89564
 laser-plasma ion source for ion implantation in solids 0-78474
 liquid metal sources, positive ion emission characts. under high electric fields 0-99369
 long pulse extraction from modified duopIGatron for neutral beam fusion reactor system 0-91355
 magnetic multipole source, electron energy distrib. 0-74058
 magnetically insulated diode as ion beam source 0-95491
 magnetically insulated ion diode 0-106213
 mass spectrometer, MI-1305, cooling attachment using liquid N_2 0-105744
 mass spectrometer ion-field source emitter, influence of laser irradiation on ion current 0-101874
 Micromafios, multicharged ion source, electron cyclotron resonance (French) 0-68997
 Micromafios, multiply charged heavy ion source, radial emittance meas. 0-102365
 MIN, negative ion injector, Na charge exchange cell 0-99386
 multicusp negative ion source for high-energy neutral beam production 0-87009
 multiply charged ion interactions with Al surface, laser induced plasma 0-70007
 negative ion source, nucleated boiling water cooled cathode, design and testing 0-102370
 neutral beam, continuously operating, convectively cooled ion accelerator, mech. design and fabrication 0-102374
 neutral beam injector, continuous operation, water cooled U-tube extraction grid 0-99392
 neutral beam ion source, core snubber network design, fabrication and testing 0-102378
 neutral beam source manufacturing at Lawrence Livermore Laboratory 0-102377
 Nier-type electron impact ion source, repeller curve interpretation 0-57421
 OSIRIS, target/ion source system for isotope separation in on-line mass separator, mol. ion prod. 0-99366
 PDX neutral beam injector, multi-aperture ion accel. electrodes thermal anal. 0-102371
 periplasmatron ion source for intense neutral beam 0-99380
 PICPAB source on Spacelab spacecraft charging problems 0-85840
 PIG source with end extraction, lifetime extension 0-78472
 plasma sources, cooling pattern of acceleration grids meas. by IR scanning 0-86303
 positive ion formation energetics by negative ion charge stripping 0-78700
 positive ion source, hollow cathode design 0-99399
 quasi-DC extraction of 70 keV, 5 A ion beam 0-87010
 QUISTOR, ion kinetic energy calc., survey 0-78468
 QUISTOR, RF mass selective excitation, resonant ion ejection 0-99363
 radio-frequency trap with semi-spherical electrodes, ion storage 0-101869
 reflection triode, prod. of high current ion beams (Russian) 0-83230
 resonance ionization source for mass spectroscopy appl. isotope anal. and time of flight spectrometer 0-81380
 spark in vacuum, ion acceleration mechanisms 0-92417
 spark source mass spectrograph, modification of ion source to reduce residual gas effects 0-98996
 spark source quadrupole mass spectrometry, development, appls. 0-62789
 sputter source design for TEM fine grained coating specimen prep. 0-99015
 stripped N beam ECR ion source (French) 0-68988
 surface ionization source for heavy ions 0-68999
 thermal negative, principle, surface mats., operating conditions (Japanese) 0-91350
 triode, high current ion beam prod. 0-99372
 triode extractors with large acceleration-deceleration ratio, beamlet steering by aperture displacement 0-63430

ion sources continued

- TRISTAN II mass separator, ion source, beam optics, computer system 0-78481
 Au, liq., ion source fabrication and emission characts. 0-68995
 Bi, liquid, field ion source emission characts. 0-74059
 C- ion source for radiocarbon dating using tandem accelerators 0-94620
¹⁴C, prod. of intense negative beam from graphite 0-102361
 Cs, pulsed vapour source for ion sources in heavy ion accelerators 0-63423
 Cs⁺ ion source, CW monoenergetic, by photoionisation 0-63910
 D⁺ ion source for high voltage neutral beams for fusion reactors 0-99379
 Ga, high intensity, emission characts., atom-probe FIM obs. 0-80950
 Ga, liquid, emission characts. obs. 0-62810
 Ga, liquid, field ion source emission characts. 0-74059
 Ga liquid metal ion source, energy distrib. meas. 0-95493
 H⁻ form. by surface and vol. processes, neg. ion source appl., review 0-58375
 H₂ and rare gas field ion source with high angular current 0-68996
 He⁺ high current source of 70 mA at 10.5 kV 0-95495
 LaB₆, hollow cathode mag. multiple ion source 0-102369
 Mo, extraction grid for high power ion source 0-102372
 O, low-energy highly-stripped, double-tandem accelerator-decelerator for O⁹⁺ + He charge exchange measurements 0-81317

ion-surface impact

- see also particle backscattering; sputtering
 adhesion, surface anal. techniques appl. 0-65381
 atom ejection studies by classical trajectory simulation 0-108311
 Auger electrons upon bombardment of solids by ions of moderate energies 0-100730
 Auger spectra induced by ion impact on metals 0-71545
 backscattering analysis, Rutherford scattering cross section correction 0-66369
 backscattering and implantation, H and He ions, computer simulation, comparison of MARLOWE and TRIM codes 0-66350
 channelling, 180° ion scattering, on solid targets, evidence for yield enhancement 0-70281
 charge composition of light ions scattered by a metal surface 0-100724
 charged particle beam-surface impact at glancing angles, reflection (*Russian*) 0-108316
 conference, atomic collisions in solids, Hamilton, Canada (Aug. 1979) 0-62375
 electron capture, atomic excited state polarisation, optical detection 0-58377
 electron emission energy and angular spectra 0-71547
 electron emission yields 0-71544
 electronic material and device characterisation using surface-sensitive analytical techniques 0-65341
 electronic polarization in solids probed by dissociation of fast molecular ions 0-71530
 electrostatic deposition of thin particulate layer, resistivity meas. under ion bombardment 0-68218
 fast molecular ions, break-up on collision with solids 0-66353
 fast molecular ions, collision induced fragmentation 0-66354
 fast molecular ions collisionally induced dissociation, struct. determ. 0-66357
 fission fragment and alpha recoil induced secondary ion ejection 0-71533
 grazing incidence obs. 0-71539
 heavy ion neutralization behaviour in the 30-130 keV energy regime 0-71542
 heavy ions, low energy total backscattering 0-71535
 III-V compounds, surface comp., low-energy ion scatt. spectrometry 0-100382
 III-V semiconductor, and related cpds., low energy ion scattering spectrometry (*French*) 0-71551
 Inconel 625, electron yields under ion bombardment for clean and oxidised surfaces 0-66368
 inelastic effects in low energy scatt. 0-71534
 ion bombardment, three-dimensional surface 0-104029
 K-electron ionisation probabilities by heavy relativistic particles 0-84824
 low energy surface scatt., inelastic energy loss 0-70278
 low-atomic-mass solids, high precision depth profiling of light isotopes 0-66902
 luminescence of solid surfaces accompanied by ion implantation 0-60683
 metal, ion beam induced desorption of overlayers 0-59786
 metal surface, heterogeneous cluster ion bombardment, secondary electron emission 0-60742
 metals high density collision emission cascades following heavy ion bombard. 0-71531
 molecular deexcitation radiation obs. during keV ion-solid bombard. 0-71494
 negative ions, sputtered, characteristic electronic and vibrational temp., laser photoelectron spectral meas. 0-66346
 one-electron resonant processes in presence of surface sub-monolayer 0-93445
 polycrystal, heavy ion scatt., model 0-100731
 recoil atoms, double scatt. effect 0-100725
 secondary electron emission, threshold studies 0-66360
 secondary electron kinetic emission from electron and ion bombardment 0-66342
 segregated surface, low energy Ne⁺ scatt. 0-71538
 solid surface, H⁻ ion backscatt. due to proton bombardment 0-99554
 solid-target atoms, ejection angles of ions after double scattering 0-93446
 sputtered excited states, secondary photon emission, role of transition probability 0-102483
 stainless steel, machine faceted, low-energy ion erosion studies 0-80923
 steel, stainless, retention and re-emission of 0.125-1 keV D⁺ ions 0-66349
 surface analysis techniques and appls., symposium, Dayton, USA (Jun. 1979) 0-62363
 surface analytical techniques, quantification, review 0-65342
 surface semichannel effects on fast ion recoil energy distrib. 0-65092
 surface treatment by the low-energy ions of plasma accelerators 0-97608
 thin films, surface anal., survey of ESCA, AES, SIMS and ISS (*Hungarian*) 0-70544
 trajectory focusing effects on total reflection coeff., computer studies 0-89102
 transition metal sulphides, ion bombardment damage, XPS obs. 0-97404
 wake-bound electron contrib. to convoy electron vel. distrib., effect of ionic field 0-60729

ion-surface impact continued

- yield comparison for excited neutrals and positive ions 0-71548
 Ag, sputtering by heavy atomic and molecular ion bombard. 0-71532
 Al, Auger spectra induced by 100 keV Ar⁺ impact 0-84820
 Al, ion-induced electron emission, ion charge depend. 0-108315
 Al surface bombardment by fast H⁺ 0-66376
 Al+He(C)(N)(O), inner-shell multiple ionisation systematics, X-ray obs. 0-63790
 AlF₃, ⁴He⁺ ion scatt. spectrometry below 5 keV 0-108313
 Au, backscattering of H(He) positive ions, fraction reflected 0-60741
 Au film, integrated condensation coeff. on NaCl cleavage faces, Rutherford ion backscatt. obs. 0-59827
 Au, ion bombardment by Ar⁺, focused ejection 0-104028
 Au-C, light ion large angle scatt. in weakly screened Rutherford region 0-84823
 BaCO₃, excited Ba emission by Ar⁺ impact 0-100727
 BaTiO₃, ceramic surface, neutralisation of bombarding ion beam 0-71528
 BaTiO₃, surface study using AES and ion scatt. spectroscopy 0-65339
 Be, Auger spectra induced by 100 keV Ar⁺ impact 0-84820
 Be, secondary photon emission following ion bombard. 0-71493
 Bi-Zn, light ion large angle scatt. in weakly screened Rutherford region 0-84823
 C foil, He⁺ and HeH⁺ impact, quantum beat pattern depend. on foil thickness 0-58343
 C foil, Kr⁺ incident, equilb. charge state distrib. and multiple scatt. angles 0-59532
 C+O⁺ ion-molecule reaction, 15 eV energy O⁺ production system 0-84817
 CH₄⁺, Jahn-Teller distortion, energy and angular distrib. of collisional dissociation fragment 0-66356
 CdS, surface energy struct. changes during ion cleaning and thermal annealing 0-92962
 Cs, backscattering of H(He) positive ions, fraction reflected 0-60741
 Cs⁺ photon spectrum emitted from W surface 0-100726
 Cu, Ar sputtered, surface morphology influence on sputtered yield angular distribution 0-65338
 Cu film, on Au substrate, oxidation and interfacial behaviour, ion scatt. spectroscopy study 0-66691
 Cu, inert gas ion irradi., fast ionised recoils, blocking effect 0-71550
 Cu surface, Ar ion bombardment, fast ionised recoils, thermal lattice vibr. effects 0-100737
 D₂⁺, dissociation on impact with mylar foil 0-67164
 F, K-shell X-ray spectra from light ion bombard. studies 0-71518
 Gd₂(MoO₄)₃, surface study using AES and ion scatt. spectroscopy 0-65339
 Ge surface, (111), ion-bombarded and annealed, spectroscopic ellipsometry study 0-103543
 Ge thin films on glass substrates, annealing by Ar ion bombardment 0-80136
 H, backscatt. from Au, charge fraction ang. depend. 0-71540
 H species, on C foil, 800 keV amu⁻¹, electron loss and capture cross-sections 0-65066
 H⁺ production in foil breakup of H₂⁺, inhibition effect 0-99549
 H⁺, 5 and 15 keV, energy distrib. and recoil angles 0-71537
 H⁺, neutralisation in low energy surface scatt. by polycryst. graphite 0-71541
 H₂⁺, internuclear separations distrib. in 3.0 MeV collisions with C foils 0-71529
 H₂⁺, polarised Balmer radiation due to scatt. from Nb surface, adsorbed O₂ effects 0-99569
 H₂⁺, transmission yield through thin C-foil meas. 0-100732
 Hc, backscatt. from Au, charge fraction ang. depend. 0-71540
 He species, on C foil, 800 keV amu⁻¹, electron loss and capture cross-sections 0-65066
 He⁺, isotope effects in elastic surface scatt. on sol. and liq. Ga 0-71536
 He⁺ reflection from Pt surface, 10 to 35 keV 0-71543
 HeH⁺, foil induced dissociation, H⁰ prod. 0-66355
 HeH⁺, internuclear separations distrib. in 3.0 MeV collisions with C foils 0-71529
 K⁺, low energy small angle scatt. from Ni(001) 0-66367
 LaB₆ (100), (110), and (111), surface structs. and work functions 0-70512
 LiF, ion and electron emission following ion impact 0-100729
 MgF₂, ⁴He⁺ ion scatt. spectrometry below 5 keV 0-108313
¹⁹N II, 2p3p ¹P₁, hyperfine struct. after ion beam surface impact at grazing incidence 0-58403
 Na, Auger electron emission due to ion collisions with solid targets (*French*) 0-104031
 NaCl, ⁴He⁺ ion scatt. spectrometry below 5 keV 0-108313
 NaCl, ion and electron emission following ion impact 0-100729
 NaF, ⁴He⁺ ion scatt. spectrometry below 5 keV 0-108313
 Ne, Auger electron emission due to ion collisions with solid targets (*French*) 0-104031
 Ne⁺, isotope effects in elastic surface scatt. on sol. and liq. Ga 0-71536
 Ni (001), azimuthal anisotropies of ejected dimer ions, SIMS expt. 0-60730
 Ni (110), surface damage induced by bombard. with 3-30 keV noble gas ions 0-60728
 Ni (110) clean surface, low energy Li⁺ and He⁺ ion scatt. 0-104026
 Ni {100} and Ni {100} with O overlayer, crystallographic effects in low energy ion scatt., local ion-atom neutralisation 0-84377
 Ni, ion-implanted and virgin, laser irradi. effect, Rutherford backscatt. and channelling obs. 0-108306
 OH⁺, Coulomb explosion in 11.2 MeV collisions with C foils 0-66358
 Pt (111), surface and subsurface adsorbed O, low energy ion scatt. obs. 0-65372
 Pt (997) surface, partial faceting, He beam scatt. and LEED study 0-103547
 Pt, adsorption of O₂ on (110) surface, Ar⁺ bombardment effects on reactivity 0-89099
 Re surface, interaction with N₂⁺ beam, reaction dynamics studied by XPS and thermal desorp. spectrometry 0-93797
 Si (001) surface struct., high energy ion scatt. study 0-59772
 Si (111), O and CO sorption, ion scatt. obs. 0-59810
 Si, amorphous, ion bombard., etch pit and ripple struct. formation mechanisms 0-66366
 Si, Auger electron emission, ion induced and secondary ion emission 0-71546
 Si, Auger spectra induced by 100 keV Ar⁺ impact 0-84820
 Si, ion and electron emission following ion impact 0-100729

ion-surface impact continued

- Si, oxidation induced by ion or electron bombardment, AES-SIMS study 0-108606
 Si:Ga(As), laser-doped, impurity distrib., Rutherford backscatt. and channelling anal. 0-59507
 Si-metal interface, silicide formation, interface marker technique obs. 0-59734
 SiO₂, proton induced ionisation, energy dependence of K_β/K_α intensity ratio 0-60716
 Si(111)-√3×√3-Ag structure, atomic arrangement, low energy ion scatt. spectroscopy 0-96724
 Sn+He(C)(N)(O), inner-shell multiple ionisation systematics, X-ray obs. 0-63790
 Th, L and M X-ray emission following H and O ion impact, parameter depend. 0-66327
 W, (110) surface, low energy ion scatt. features, inelastic loss and surface crystallography 0-66371
 W dispenser cathodes, Ba-activated, surface characts., ion scatt. spectrometry and SIMS study 0-66377
 W, O₂-covered, electron emission induced by slow Ar ions 0-60740
 W surface self-diffusion, ion impact induced, FIM study 0-103549

ion thrusters *see* ion engines

ionic conduction in solids

see also superionic conducting materials

- AgPS₃-AgX (X=I, Br), glass-forming regions, struct. model (French) 0-100464
 alkali glasses, rapidly quenched, alkali ion cond. 0-107559
 alkali halide crystals, defect fermion properties, ionic cond. calcs. 0-59457
 alkali halide thin films, high-field electron injection, ionic cond., photocond. 0-75665
 alkali halides, matter transport rel. to point defect parameters 0-107488
 alkali ion conductors with sheet structures, ion mobility and influences 0-107522
 alkali metal compounds, ASbO₃·1/6AF, dielec. spectroscopy study, 100 Hz to 10 MHz, 238 to 417K (German) 0-108144
 alkaline earth fluoride based solid solns., ion transport 0-107545
 ceramic materials for ion-selective membrane electrodes development, Ag⁺ and F⁻ based materials appl. (Japanese) 0-61203
 coal slag, elec. props. 0-107476
 dielectric-semiconductor structures, surface ion migration, theoretical analysis 0-65700
 excluded volume model, for superionic conduction 0-107543
 fast ion transport in solids, conf., Lake Geneva, USA (May 1979) 0-57006
 fast ion transport in solids, conf., Lake Geneva, USA (May 1979) 0-105427
 Feynman-Hellmann theorem and oscillator strengths, force on atom in electrostatic field 0-65275
 fluoride solid electrolytes 0-70464
 glass, commercial, high field cond., weak electrolyte theory appl. 0-107475
 glass, electrical relax., Debye-Falkenhagen theory 0-108155
 glass, electrothermal props. in structural transform. zones (French) 0-88047
 glass, high-field ionic and polaronic cond., dielec. relax., Poole-Frenkel theory 0-100351
 glasses, elec., mag., and optical props., conference, Troy, NY, USA (Aug. 1979) 0-105417
 glassy polymers, elec. resist., corresponding states relationship 0-59704
 high field, non simultaneous place exchange mech. 0-70456
 hopping conductivity, freq. depend., model calcs. 0-107507
 ice, cubic, D₂O isolated, H⁺ exchange and Bjerrum defect migration, direct spectroscopic obs. 0-88356
 intercalation and substitution-intercalation cpds. in dichalcogenide hosts, factors affecting ion mobility 0-59707
 intercalation compound electrodes, thermodynamic and transport props. 0-66963
 interfacial charge transfer, coupling with bulk transport in ionic crystals 0-79986
 metal halides, fluoride structure, retarded ionic motion 0-88361
 metal oxide thick film growth, fund. theory 0-89391
 NASICON solid electrolyte, processing and phys. props. 0-60820
 polypropyleneimide film, elec. cond., 120-180°C 0-60124
 polyvinylidene fluoride, dielec. breakdown and elec. cond., room temp. to 150°C 0-60500
 superionic conductor, with fluoride struct., activation vol. 0-107557
 ternary fluorides, high anionic cond. of new solid electrolytes 0-107546
 thermally stimulated relaxation in solids, transport phenomena, book 0-77553
 (Ag,Na)Br, ionic transport numbers, polarization cell method 0-59705
 (Ag,Na)Cl solid solns., ionic transport numbers, polarization cell method 0-59705
 Ag halides, matter transport rel. to point defect parameters 0-107488
 AgBr emulsion grains, edge length depend. of ionic cond., space charge characteristics 0-88360
 AgCl, ionic mobility, diffusion coeffs., defect mobility energies 0-65284
 AgCl(Br), enhanced defect form., mean field theory 0-107220
 AgF, diffusion, elec. cond. and ¹⁹F relax. T_{1ρ} meas. 0-92718
 Ag₂HgI₄, Raman line shape and ionic cond., coupled mode model 0-66171
 α-Agl, structural and dynamical behaviour 0-107544
 AgI:Cd, polycrystalline, thermoelectric power meas. 0-59698
 AgI/Ag oxy salt system, vitreous solid electrolytes, conductance mechanism 0-107560
 (AgI)₂(Ag₂O B₂O₃)_{1-x}, amorphous superionic compound, ¹¹B lineshape and relaxation 0-108107
 AgPO₃-AgX (X=I, Br), glass-forming regions, struct. model (French) 0-100464
 Ag₂SBr, ionic conductivity in temp. range 93-573K, X-ray diff. and DTA 0-79988
 Ag₂SI, ionic conductivity in temp. range 93-573K, X-ray diff. and DTA 0-79988
 Ag₂Sb₂O₃F₂, ionic conductivity, comparative study with pyrochlore phase AgSbO₃ (French) 0-103701
 Ag₂Se thin film, switching and Ag movement, point contact technique 0-60107
 AgX-Ag₂O-P₂O₅ (X=I, Br, Cl), glass formation and ionic conductivity 0-65290

ionic conduction in solids continued

- β-Al₂O₃, conduction and dielec. loss mechanisms, paired interstitialcy model 0-107468
 Al₂O₃ polycrystalline, effects of space charge, grain-boundary segregation and mobility differences on conductivity 0-79979
 β'-Al₂O₃-Na₂O solid electrolyte, processing and phys. props. 0-60820
 BaF₂, ionic cond., activation vols., freq. depend. cond., press. effects 0-100354
 Ba_{1-x}La_xF_{2+3x}, enhanced ionic motion in solid solutions 0-107491
 Ba(PO₃)₂-AlF₃-CaF₂ glass, elec. cond. and IR spectra 0-89005
 Ba(PO₃)₂-AlF₃-MgF₂ glass, elec. cond. and IR spectra 0-89005
 Ba(PO₃)₂-fluoride glass, elec. cond., struct. 0-88056
 BeF₂, vitreous, ionic transport and defect struct. 0-107472
 δ-Bi₂O₃, thermoelectric power rel. to fast ionic conduction 0-107549
 Bi₂O₃-PbO, glass, cond. meas. using complex impedance anal. (French) 0-92707
 δ-(Bi₂O₃)_{1-x}(Y₂O₃)_x, thermoelectric power rel. to fast ionic conduction 0-107549
 Bi₂WO₆, ferroelectric, dielectric props., elec. cond. and relaxation phenomena obs. 0-80692
 CaF₂, ionic cond., activation vols., freq. depend. cond., press. effects 0-100354
 CaF₂, mol. dynamics studies of superionic conductors 0-107547
 CaF₂:Y³⁺, ionic cond. and thermal depolarisation obs. of defect clustering 0-71298
 CdF₂, electrical transport limitation by electrodes, polarisation effects 0-96689
 CdF₂, ionic cond., activation vols., freq. depend. cond., press. effects 0-100354
 CdF₂, ionic conducting fluoride fluorite, US velocity meas. 0-107381
 CdF₂:Na(Nd), ionic cond. investigation by complex admittance method 0-100352
 CeO₂:CaO(Y₂O₃), oxygen ion cond. and defect struct. 0-107553
 CsClO₄, electrical conductivity, frequency dependence 0-65288
 Cu₂In₂Zr_{1-x}S₂ system, struct. and cond. meas. (French) 0-88354
 Gd₂O₃, B-type monoclinic, DC(AC) elec. cond., thermoelectric power, dielectric const., temp. depends. 0-59980
 Gd₂Zr_{1-x}O_{2-x/2}, elec. cond. of ceramic solid solutions 0-107554
 Gd₂Zr_{1-x}O_{2-x/2}, fluorite and pyrochlore solid solutions, electrical conductivity meas. 0-65287
 GeO₂-Na₂O, Na⁺ partial dissociation investigated by elec. meas. 0-92716
 GeO₂-Na₂O glasses, equivalent cond., temp. depend., weak electrolyte theory appl. 0-107475
 H_{2n-2}O₂(IO₃)_n·4H₂O, n=0.5 to 2.0, high proton cond. 0-107562
 IrO₂, anodic films, electrochromism and ionic cond., model 0-59706
 KBr, cation defects creation mechanism 0-75224
 KCl, ionic cond., defect parameters, diffusion coeffs. 0-79978
 KCl:Pb²⁺, pure and doped, electrolytically coloured, elec. cond. and optical absorpt. meas. 0-100668
 KCl:S²⁺(SO₄²⁻), ionic cond., defect parameters, diffusion coeffs. 0-79978
 KCl:S²⁺(SO₄²⁻) 0-107487
 KClO₄, electrical conductivity, frequency dependence 0-65288
 KClO₄:CrO₄²⁻(SO₄²⁻), AC electrical conductivity meas. between temp. range 25-325°C, automated technique 0-59699
 KHSO₄:Fe³⁺, DC cond. meas., mechanism 0-65285
 K₂O-Na₂O-B₂O₃-SiO₂ glass character of elec. cond. 0-103516
 K₂O-SiO₂, impurity H⁺ ion motion, ³⁵Cl NQR obs., 77 and 298K 0-60451
 K_{1+x}Ta_{1-x}W_{1-x}O₆ pyrochlore system, comp. depend. of ionic cond. 0-107517
 LaF₃, ionic transport, NMR and cond. studies 0-107555
 La₂Ag₂-Ag₂S-Ga₂S₃ glass system, prep., thermal and elec. props. (French) 0-89192
 Li incorporated transition metal oxides, topochem. reactions, chem. prep. and characterisation 0-61115
 Li⁺-rich borate glasses, ionic cond. and activation energy 0-107561
 LiF:Mg, Z₂- and associated Z-centres, elec. cond., ionic thermocurrent, and optical absorpt. meas. 0-107229
 LiF:Mg,Ti, defect states, ESR and ionic cond. study 0-108058
 LiNH₄SO₄, DC elec. cond. 0-88603
 LiNbO₃-SiO₂:Fe₂O₃ glasses, Li⁺ ion cond. 0-107471
 Li₂O-Al₂O₃, rapidly quenched glasses, Li ion cond., elec. cond. 0-100346
 Li₂O-BaO-SiO₂ glasses, elec. cond., room temp. to 450°C 0-107473
 Li₂O-Bi₂O₃, rapidly quenched glasses, Li ion cond., elec. cond. 0-100346
 Li₂O-Ga₂O₃, rapidly quenched glasses, Li ion cond., elec. cond. 0-100346
 Li₂O-LiX-B₂O₃ glass, X=halogen, high anionic cond. of new solid electrolytes 0-107546
 Li₂O-SiO₂ glass, protonated, field-driven guest proton redistrib. 0-107474
 Li₂S-GeS₂ glass forming region, struct. and ionic cond. 0-88358
 Li₂S(O), cation diffusion NMR investigation up to 800°C 0-108092
 Li_{1/2}Zn_{1/2}(GeO₄)₄ LISICON system, Li ionic conductivity (Chinese) 0-88350
 MgAl₂O₄, pure and Fe-doped spinel, elec. cond. 0-59702
 MgCr₂O₄-TiO₂, porous ceramics, humidity-sensitive electrical conduction 0-107782
 MgF₂:Li⁺, atom transport, diffusion and ionic cond. meas. 0-107492
 MgO single crystals, impurity effects on cationic cond. (French) 0-65286
 Mg₂SiO₂:SiO₂, elec. and dielec. props. 400-900°C 0-104953
 ND₂D₂AsO₄, protonic cond. near antiferroelec. Neel temp. 0-59703
 Na₂-β-Al₂O₃, far IR absorpt., Beavers-Ross sites, interstitials 0-66241
 NaCl: Cd²⁺ dielectric loss following plastic deform. 0-84690
 NaCl:Mn²⁺, Mg²⁺, doubly doped, ionic thermocurrent study of linear dimer 0-79977
 NaCl(Br), X-ray or UV irradiated, cation defects creation mechanism 0-75224
 Na₃Cr₂(PO₄)₃, crystallographic data, ionic conductivity (French) 0-88077
 Na₃Cr₃(PO₄)₄, crystallographic data, ionic conductivity (French) 0-88077
 Na₃Fe₂(PO₄)₃, crystallographic data, ionic conductivity (French) 0-88077
 NaGdSi₃O₈, single cryst. data and ionic cond. 0-84158
 NaI:Ca²⁺, pure and doped, ionic thermocurrents meas. 0-80677
 NaI:Ca²⁺, pure and doped, lattice defects, entropy and enthalpy of formation and migration 0-96687
 Na₂O-B₂O₃-Bi₂O₃ glass with metallic Bi granules, elec. cond. 0-84493
 Na₂O-SiO₂ glass, conduction and dielec. loss mechanisms, paired interstitialcy model 0-107468
 Na₂O-SiO₂-MgO(CaO)(BaO) glasses, elec. cond., room temp. to 450°C 0-107473
 Na₂S-P₂S₅, glass forming region, struct. and ionic cond. 0-88358

ionic conduction in solids continued

Na₂S-SiS₃(GeS₂)(P₂S₅), synthesis, structure and ionic conduction (*French*) 0-65291
Na₂S-XS₂, X=Si, Ge, glass forming region, struct. and ionic cond. 0-65358
Na₂S(O), cation diffusion NMR investigation up to 800°C 0-108092
Na_{1+x}Ta_{1-x}W_{1-x}O₆ pyrochlore system, comp. depend. of ionic cond. 0-107517
Na₄YSiO₄, Na₃YSiO₇, Na₃YSiO₉ and Na₅YSi₄O₁₂, single cryst. data and ionic cond. 0-84158
Na₂Y₂Zr_{1-x}S₃ ionic cond. and NMR mobility obs., comp. depend. (*French*) 0-70459
Nd,Zr_{1-x}O_{2-x/2}, elec. cond. of ceramic solid solutions 0-107554
Nd,Zr_{1-x}O_{2-x/2} fluorite and pyrochlore solid solutions, electrical conductivity meas. 0-65287
Ni-Si melt refining by electric fields, ionic conduction of Ni, Si (*Russian*) 0-65273
PbBr₂(Cl₂)(I₂), ionic cond. and activation volumes, high press. effects 0-100353
PbF₂ based solid solns., ion transport 0-107545
PbF₂, ionic cond., activation volumes and high press. phase transitions 0-70461
PbF₂:Mn, mag. tagging of ion diffusion, ¹⁹F NMR meas. 0-108106
PbO-B₂O₃-Bi₂O₃, glass with metallic Bi granules, elec. cond. 0-84493
PbO-SiO₂ glass, reduced channel-plate, variable range hopping conductivity 0-107466
PbSnF₄, anionic conductor, thin films and ceramics 0-107556
PbSnF₄, high anionic cond. of new solid electrolytes 0-107546
RbCl:CoCl₂ system, precipitate form., ionic cond. meas. 0-96653
RbCl(Br), cation defects creation mechanism 0-75224
RbClO₄, electrical conductivity, frequency dependence 0-65288
Sb₂O₃-nH₂O acid membranes, synthesis and characterisation 0-81027
SiO₂-Li₂O-Li₂SO₄, glass-forming region, struct. and ionic cond. 0-84320
Sm₂O₃, B-type monoclinic, DC(AC) elec. cond., thermoelectric power, dielectric const., temp. depends. 0-59980
SrCl₂, fast ion transport 0-107558
SrCl₂, ionic cond., activation volumes and high press. phase transitions 0-70461
SrCl₂, mass and charge transport 0-100347
SrCl₂, point defect parameters, ionic cond. study 0-107490
SrCl₂, self-diffusion and ionic cond. 0-107489
SrF₂, ionic cond., activation vols., freq. depend. cond., press. effects 0-100354
Tb₂O₃, B-type monoclinic, DC(AC) elec. cond., thermoelectric power, dielectric const., temp. depends. 0-59980
ThO₂-CaO, and ThO₂-YO_{1.5}, solid solns., defective oxides, ionic cond. 0-107548
Ti_{1-x}Ta_{1-x}W_{1-x}O₆ pyrochlore system, comp. depend. of ionic cond. 0-107517
WO₃ thin film, partial ionic conc. of Li, appl. of AC techniques 0-70468
WO₃-P₂O₅ glass, AC cond. and dielec. props. 0-92717
ZrF₄-BaF₂-ThF₄-NaF(RF₃) (R=rare-earth) glass system, anion cond. 0-70460
ZrF₄-based glasses, elec. transport props. 0-79983
Zr_{1-x}In_{2x}O_{2-x}, ionic conductivity, lattice const. 0-96688
Zr(KPO₃)₂, cryst., ionic cond., layered struct. 0-92710
Zr(LiPO₃)₂, cryst., ionic cond., layered struct. 0-92710
Zr(NaPO₃)₂, cryst., ionic cond., layered struct. 0-92710
ZrO₂, doped, theoretical model 0-107552
ZrO₂-CaO, and ZrO₂-YO_{1.5}, solid solns., defective oxides, ionic cond. 0-107548
ZrO₂-YO_{1.5}-TaO_{2.5}, cubic fluorite phase, elec. cond. 0-107551

ionic conductivity in solids see ionic conduction in solids

ionic thermocurrents see thermally stimulated currents

ionisation

see also associative ionisation; autoionisation; charge exchange; electron attachment; electron capture; field ionisation; ion recombination; ionisation of atoms; ionisation of gases; ionisation of liquids; ionisation of molecules; ionisation of solids; ionisation potential; Penning ionisation; photoionisation; surface ionisation
interstellar medium, H ionisation rate due to OB-type stars rel. to inter-stellar clouds form. 0-109506
interstellar medium, local, ionisation state 0-90502
nova envelopes, dust form. and ionisation theory 0-98678
planetary nebulae, ionisation models 0-109529
planetary nebulae ionisation, influence of He shell flashes in nuclei 0-73021
planetary nebulae ionisation structure, atomic and mol. data 0-109528
Sun, ionisation phenomena rel. to use of MHD pulses as diagnostic technique 0-109405
D pellets, ionisation by Nd laser radiation 0-70015
H II regions, statistical approach to density and ionisation fluctuations 0-77468

ionisation chambers

A-150 plastic-equivalent gas, dosimetry appl. 0-81745
air ionisation probe for α , β , γ hand and shoe monitor 0-58084
Bragg-Gray theory corollaries, comparison to fast-neutron cavity ionisation meas. at 14.8 MeV 0-91370
calibration of dose to water for ⁶⁰Co γ -radiation 0-74032
coaxial cables used with ionisation chambers, expt. investigation 0-78489
dose meter unit for emergency operations (*French*) 0-57977
electrostatic relay, investigation of dosimetric characts., dosimeters IK-5B and IK-14 (USSR) 0-57966
fission reactor loss of coolant studies, gamma densitometer detector comparison 0-57881
gamma ray appl. to fluid density meas., theory, practices and appl. 0-73325
gas proportional scintillation detectors with uniform electric fields, secondary scintillation model 0-74087
gas purity under measuring conditions, W-value determ. (*German*) 0-104489
gaseous detectors, evolutionary steps 0-58041
guarded-wall free-air, field distortion 0-83234
high density projection chamber 0-58027
high-speed transmission avalanche counter 0-91372
laser induced ionisation tracks, formation and apps. 0-102393
liquid Ar cylindrical pulsed, 200 cm³ working vol. 0-87015
mixed β - γ dosimetry, ionisation and scintillation counters 0-57975
multi needle counter with cathode focusing 0-58039

ionisation chambers continued

multistep avalanche chamber, far UV Cherenkov photon detection appl. 0-58042
parallel plate, thin-walled, for use with photon and electron beam dosimetry 0-78490
parallel plate avalanche counters for registration of light charged particles 0-91369
parallel plate ionisation chamber, absorbed dose meas. in polystyrene phantoms 0-72335
parallel-plate, collection efficiency in pulsed X-ray field 0-99407
photon dosimetry in phantoms, effective meas. point 0-78453
photon position monitors for CHESS synchrotron source, using split photoelectron detectors and ionisation chamber 0-91336
plane-parallel chamber, pulsed electron beam irradi., ion losses 0-99421
ring imaging Cherenkov detection using multi-needle cathodic focusing detector 0-58040
variable selectivity photoionisation analyser, hydrocarbon vapour detection 0-81511
Ar-CH₄ proportional counter, light emission obs. 0-78488
³He gridded fast neutron ionisation chambers, Monte Carlo calc., of energy dependent efficiency 0-99417
³He, high pressure, improved time resolution in n- γ coincidence meas. 0-99416
³He transit time neutron spectrometry 0-63441
Kr photo-ionization proportional scintillation chamber 0-58056
O₂ in liquid Xe, electron capture 0-102402
Xe-containing fast gas mixtures for gas-filled detectors, electron drift velocities 0-74089

ionisation gauges

appearance pot. spectrometer design, demonstrations 0-105477
Bayard-Alpert gauge, three-grid modulated, mode B operation 0-105667
flame, detector for meas. fluctuating conc., turbulent flows 0-92240
high pressure gauges used in standards intercomparison, 8 \times 10⁻³-8 \times 10⁻² Pa 0-86333
modulated Bayard-Alpert gauge design 0-77805
orbitron device, optimum injection condition for electrons, influence of end effects 0-82784
self-modulating 0-82786

ionisation of atoms

see also atomic electron impact ionisation
6p levels, two-photon excitation, time resolved fluoresc., quenching, lifetimes and photoionisation cross section 0-78587
alkali metal, near-resonant two-photon ionis., non-Coulomb phase shifts of photoelectron partial waves 0-106302
alkali metal atoms, spin-polarised, near-reson. two-photon ionis., light polarisation effects 0-106308
atom+atom, collisional ionisation review 0-63801
atom+atom, two photon ionisation, radiative collision effect 0-106388
atom+H⁺, emission electron angular and energy distribution 0-87222
atom+ion impact ionisation, inner shell alignment calcs. 0-83473
atomic photoionisation anal. using relativistic random phase approximation and multichannel quantum defect theory 0-63602
atoms, polarisation of electrons and nuclei in resonant multiphoton ionisation 0-99486
chemical ionisation, classical description, complex interaction pot., exponential representation 0-99570
collisional ionisation, Penning and associative ionisation produced by laser field 0-63802
collisional ionisation, Penning ionisation, laser induced, two step optical collisional perturbation sequence 0-63778
electronic and at. collisions, conference, Kyoto, Japan (Aug.-Sept. 1979) 0-62394
excited atom ionisation due to collisions in their own gas (*Russian*) 0-91654
fast projectile electron loss forward peak oscill. struct. as autoionisation 0-69227
H like atoms, photoionisation in homogeneous elec. field (*Russian*) 0-106309
heavy atom+light ion, inner-shell ionisation, adiabatic effects 0-99561
high-Z atoms (Z=48-104), electron impact, K-shell ionisation cross sections calcs. 0-63827
inert gas, atomic photoionisation, Dirac-Fock calcs., branching ratios and angular distrib. in p shells 0-63601
inner-shell vacancy creation, ionised fragments probability distrib. 0-83274
lanthanides' ionisation pot. calc., T-value and number of 4f electrons linear correlation (*Chinese*) 0-63850
laser-induced selective multistep processes: impact on nuclear physics, chemistry and biology 0-61122
metastable atomic or molecular species, multiphoton transition detection 0-58231
multiphoton absorption above ionisation threshold 0-58224
multiphoton ionisation, effects of self-induced reson. 0-91519
multiphoton ionisation, reson. effects, light coherence effects 0-58232
multiphoton ionisation dynamics 0-91517
multiphoton ionisation processes, resonance and laser coherence effects 0-74208
multiply charged ion+H, electron capture, unitarised distorted wave approx. 0-63814
multistage ionisation in strong EM fields, Thomas-Fermi calcs. (*Russian*) 0-58226
Na, fluoresc. study, reson. radiation illum. 0-83314
near threshold struct. in K-shell spectra, photoionisation or fast charged particle ionisation 0-87064
nonresonant multiphoton atomic ionisation in stochastic EM field (*Russian*) 0-99490
photoelectron ang. distrib. and spin polarisation, theory 0-91618
photoionisation, absolute cross-sections, expt. meas. techniques 0-63598
photoionisation, fluoresc. radiation polarisation 0-87076
photoionisation, polarisation of photoelectrons, review 0-78584
photoionisation, selective, use in laser isotope separation and spectroscopy, review 0-83332
power broadened two-photon ionisation, reson. lineshape and photoelectron spectra 0-58229
resonance ionization source for mass spectroscopy appl. isotope anal. and time of flight spectrometer 0-81380
resonant ionisation spectroscopy, chem.-physics apps. 0-68259
resonant phenomena, complex stabilisation method 0-78515
singlet-triplet energy difference and singlet generalised oscillator strength, Lassetre-Dillon relation 0-63508

heat transfer continued

- tubes, nucleate pool boiling, critical heat flux, ferric oxide scale effects 0-64343
- tubes, straight and coiled, boiling heat transfer with low pressure water flows 0-74856
- tubes, temp. and heat transfer coeff. variation upon boiling mode changes 0-69629
- tubes in closely spaced in-line bank, heat transfer in cross-flow 0-59026
- tubular cover solar collectors, performance calcs., transmittance and radiosity 0-61415
- turbogenerator rotor and stator core thermal conductivity solution using integral representation method (*Russian*) 0-100451
- turbogenerators, high capacity, heating reduction measures for enhanced reliability and interval between maintenance (*Russian*) 0-96175
- turbulent boundary layer with suction under nonisothermal conditions, heat and mass transfer 0-92125
- turbulent flow in pipes, temp. field struct. 0-69923
- turbulent heat transfer from flat plates, facing curved wall effects (*Japanese*) 0-83799
- turbulent jet impinging on cylinder wall (*Japanese*) 0-83800
- turbulent pipe flow with suction or injection, high Prandtl no. heat and mass transfer 0-74857
- two moderately rotating porous discs, heat transfer 0-103028
- two parallel corotating discs, laminar flow and heat transfer, shear pump appl. (*German*) 0-69840
- vaporisation channels, rough and smooth, heat transfer in post dry-out region 0-96255
- vertical surface, cooling by liquid spray, heat transfer 0-74711
- viscoelastic boundary layer flow, second order, at stagnation point, heat transfer 0-103025
- viscous flow, unsteady, around elliptic cylinder, heat transfer, finite difference method (*Japanese*) 0-69831
- viscous fluid in pipes, nonisothermal flow, crit. phenomena 0-103074
- viscous fluid under cyclic deform., self-heating, hydrodynamic thermal explosion 0-58993
- water, boiling and heat transfer on horizontal pipes with annular fins 0-74855
- water boundary layer along heated cylinder, buoyancy and variable viscosity effects 0-79256
- water droplets, ebullition under steady-state superheated conditions 0-74928
- water droplets, ebullition under transient superheated conditions 0-74929
- water films, subcooled, flowing down vertical tube, heat transfer 0-79318
- water flow, nondimensional heat transfer law for a slanted hot film 0-74853
- water-in-oil emulsion, boiling, bubble formation, cinemicrophotography 0-74961
- Al plate calorimeter, meas. of local convective heat transfer coeff. by polarisation interferometry 0-82809
- Ar arc heating, high-pressure complex heat exchange expt. (*Russian*) 0-75112
- CO₂ laser amplifiers, porous tube generated flow field, heat and mass diffusion 0-63969
- CaSO₄ crystallisation, from liq. solns. as heat-transfer surface 0-100772
- CO₂ flow in heated tubes, with near critical parameters, turbulent flow, heat transfer 0-59022
- GaAs crystal growth, thermal and elastic const. evaluation 0-92586
- H₂, dissociated, heat transfer to catalytic surfaces, shock tube investigation 0-64551
- H₂ storage using hydride beds, thermal transport enhancement using high conductivity materials 0-61466
- H₂O flow in heated tubes, with near critical parameters, turbulent flow, heat transfer 0-59022
- He cooling systems, forced flow, numerical anal. of heat-induced transients 0-82773
- He, supercritical, free convection heat transfer 0-79296
- He, supercritical, turbulent pipe flow, heat transfer by Melik-Pashayev technique 0-74860
- Hg gravity fed heat pipe for production of high purity fixed density of Hg atoms 0-69627
- Li, liquid, transverse flow around tube bundle, heat transfer 0-64537
- N₂, critical heat flux in horizontal tube, up to critical press. (*German*) 0-99921
- N₂O₄, fission reactor coolant, heat transfer on condensation (*Russian*) 0-57860
- N₂O₄, turbulent dissoc. flow, along heated tubes, heat transfer 0-63225
- Na evaporation from slot type capillary structs., crit. heat fluxes 0-74854
- Na, liquid, evaporation from capillary-porous struct., capillary restriction in initial stages 0-107609
- NaCl gas-droplet counterflow heat exchanger, numerical model (*French*) 0-61396
- NbTi-Cu, supercond. composite, use in temp. and heat transfer coeff. meas. 0-77780
- Si sheet, high speed growth, heat treatment analysis 0-107669

heat treatment

- see also annealing; normalising; quenching (thermal); spheroidizing; tempering; thermomagnetic treatment; thermomechanical treatment
- alkali silicate glasses, struct. and thermal props. 0-84075
- alkali-borosilicate glasses, antireflection film production by heat and chem. treatment 0-66677
- alloys, rapidly quenched crystalline, struct., and heat treatment effects 0-76292
- brass, Cu-Zn (39/40 wt.%), shape memory effect and martensitic transform. depend. on heating-cooling cycles (*Russian*) 0-97482
- brass, recrystallization during induction heating 0-97511
- ceramics, development from organosilicon polymers by heat treatment 0-81014
- chemicothermal treatment, mathematical modelling 0-100955
- clays, heat treatment, effect on rheological props. of enamel slips 0-60809
- coke, shrinkage kinetics during calcination 0-93572
- electromagnetic quality inspection with specified intensity of internal field 0-108677
- electroslag welding, using plate electrodes for Al busbar component parts welding 0-81083
- epoxy EDT-10, rigid polymer, thermal stress isothermal relaxation 0-71683
- FBR oxide fuels, dynamic response of grain boundary cavities to stress and temperature changes under conditions of continuous gas generation 0-66544

heat treatment continued

- ferrites type 1500 NMZ and 2000 NMI, mag. susceptibility depend. on heating (*Russian*) 0-108603
- fibre reinforced polymer, soaking, wetting and compounding of materials during production (*German*) 0-93535
- fusion welding of Al alloys, weld susceptibility to hot cracking 0-81143
- glass, photochromic, thermochemical effects 0-87448
- glass, viscous deformation during heating and cooling 0-89314
- E-glass fibre, silane coupling agent deposited on surface, hydrolysis and drying effect on siloxane bonds 0-85072
- glass reinforced polyamide 6, fatigue strength after heat treatment, ageing and coating of Al-containing lacquer (*Polish*) 0-89347
- graphite fibre, surface anal. by XPS and polar/dispersive free energy anal. 0-65340
- graphite surface, adsorbed Cs, dissolution, lamellar cpd. form. (*French*) 0-100399
- graphitised viscose fibre, fluorination, change in struct. 0-88039
- n-hexatriacontane film, vacuum deposited on alkali halide crystals, structure and heat treatment 0-103600
- Inconel 600, thermal treatment, grain boundary microstruct. and SCC resistance 0-71675
- interface study by Auger spectroscopy 0-76587
- Invar film, superfine mag. struct. (*Russian*) 0-80572
- invariant system with switched element, design and evaluation for heat processes control during extrusion of plastic materials (*Russian*) 0-100854
- knife-edge flange, sealing after high temp. vacuum firing 0-77793
- low C steel, explosive-thermal treatment, sulphide cracking decrease, hydrogen embrittlement (*Russian*) 0-108477
- LPE growth method to reduce thermal degradation of substrates, appl. to LED fabrication 0-104061
- metal, oxidizable, laser heating in air by obliquely incident radiation 0-71815
- metal oxides and binary metal oxides, spinel struct., isoelectric point meas. 0-88609
- metal strips, welded, aged, reduction of deformations (*Russian*) 0-97508
- metal submicron particle heating in hot gas, plasma metallurgy 0-81092
- metals, electron beam appl. (*French*) 0-66558
- Ni, adsorption residual C removal by electron beam irradiation and heat treatment (*Chinese*) 0-88421
- Ni-Co, H₂ embrittlement, heat treatment and impurities effect 0-76331
- phosphate glass-Al alloy seals, elec. and mech. props., glass transition 0-81018
- phthalocyanine polymer, dynamic mech. props. and fracture energy 0-100866
- piezoelectric radiators, heat-treatment method for improved resoln. 0-104196
- PMMA, reactor irradiation, growth of macroscopic radiolytic gas bubbles, diffusion model 0-65058
- PMMA, rigid polymer, thermal stress isothermal relaxation 0-71683
- polycarbonate, bisphenol A, WAXS pattern, temp. effect and thermal history 0-93583
- polymorphic transformations kinetics model, computer modelling (*Russian*) 0-97478
- polypropylene, (Moplen) influence of temp. and mol. wt. on high speed fracture mechanics 0-76341
- polystyrene, plasma polymerised, free radicals, transient elec. current, EPR, heat treatment 0-71178
- post weld during power station construction and maintenance 0-93574
- refractories in contact with transformer steel during high-temp. heat treatment, resistance 0-66554
- steel, 12Cr1MoV, thermal fatigue and creep effect in fracture 0-104297
- steel, (0.36 wt.% C) Ni-Cr-Mo, electroslag refined, fracture toughness and fatigue behaviour 0-81171
- steel, alloy, hardened, electrochem. characts. and stress corrosion cracking, ageing and cold treatment effects 0-108639
- steel, austenitic, Cr-Mn-B-N, phase composition and struct. transformations 0-104171
- steel, austenitic, explosive-thermal treatment, sulphide cracking decrease, hydrogen embrittlement (*Russian*) 0-108477
- steel, austenitic, heavily doped, linear expansion meas. 0-103501
- steel, austenitic, KO 34 samples, electron beam welded, Charpy test expts. (*Hungarian*) 0-104252
- steel, austenitic 30KhGSA, white phases structure after heat treatment 0-76281
- steel, austenitic (03KH18N10T), heat treatment for fission reactor appls. 0-66454
- steel, austenitic stainless, corrosion resistance testing, urea plant applications (*Czech*) 0-61012
- steel, BN extraction, and identification, IR anal. 0-85254
- steel, C, hardened by HF current, mech. testing method 0-61053
- steel, C, magnetomechanical acoustic emission for residual stress NDT 0-71149
- steel, C, quenched, restoration of austenite grains during rapid heating (*Russian*) 0-76272
- steel, C, rolling contact fatigue, tufftriding effect on 0.2% C cylindrical specimen 0-100954
- steel, chemicothermal treatment, diffusional basis 0-104343
- steel, Cr, carburising kinetics, in endothermal atm. 0-76410
- steel, Cr-Mo-P (2.25, 1 wt.%), stress relief cracking, effect of P segregation 0-89324
- steel, Cr-Mo, effect of Mo on high-temp. props. 0-85005
- steel, Cr-Mo weld metal, reheat cracking, residual elements and microstruct. influence 0-66553
- steel, Cr-Mo-V, stress rupture, notch influence, temp. depend. (*German*) 0-60945
- steel, Cr-Ni-(Mo), cast, intercritical heat treatment (*Czech*) 0-89268
- steel, Cr-Ni-Mn, adiabatic shear band determ. by surface obs. 0-97579
- steel, Cr-Ni-Mo-V, austenite form. during heating, influence of recrystn. during tempering (*Russian*) 0-104188
- steel, Cr-W-Mo-Co, high-speed, from atomised powders, mech. and cutting props. 0-66556
- steel, creep rate mismatch interaction in stress relief cracking 0-97578
- steel, Fe-V-C (1, 0.2 wt.%), austenite formation 0-84927
- steel, ferritic, magnetomechanical acoustic emission for residual stress NDT 0-71149
- steel, heat resistance, thermal stability, stress-rupture strength, and creep 0-81194
- steel, heating effect on phase composition, microstruct. and mech. props. 0-100859

heat treatment continued

- steel, high and low C, wires, electroheated, thermal cycling and corrosion behaviour 0-61006
 steel, high Mn austenitic, creep rupture, p addition and two-step soln. heat treatment effects (*Korean*) 0-93646
 steel, high strength, failure stress, structural relationships 0-81190
 steel, high-C, carburising kinetics, in endothermal atm. 0-76410
 steel, high-speed tool, properties, powder metallurgy prep. method (*Czech*) 0-60800
 steel, high-strength tool steel D7KhFN, remelting effect on mech. props. 0-76284
 steel, low C, dual-phase, law of mixtures, applicability 0-89346
 steel, low C, low alloy, ferritic-pearlitic, high temp. mech. treatment, cooling effect 0-104193
 steel, low-alloy, bearing, mech. props., carbide behaviour effect (*Korean*) 0-93615
 steel, maraging 18%Ni, calorimetric anal. of ageing (*Japanese*) 0-89264
 steel, martensitic, heavily doped, linear expansion meas. 0-103501
 steel, medium C, 40MnB, dissoln. and precipitation of $M_{23}(C,B)_6$ (*Chinese*) 0-66511
 steel, medium C, Cr-Mn-Mo, austenising temp. effect on microstruct. and fracture toughness (*Chinese*) 0-66542
 steel, Ni-P plated, electrodeless, fatigue strength and plated layer microstruct. (*Japanese*) 0-93645
 steel, pearlitic, creep-induced micropore healing kinetics of 12MKh and 15KhM1F, TEM obs. (*Russian*) 0-71690
 steel, pearlitic, struct. variations under plastic strain and subsequent heating, cementite decomp. (*Russian*) 0-84954
 steel, pearlitic structural, austenite grains, growth rate during heating 0-100860
 steel, restorational carbonisation in one and two phase states (*Russian*) 0-65225
 steel, segregation and adsorption of S, influence on carburisation and nitrogenation 0-66701
 steel, stainless, heat treated, oxide comp. and corrosion susceptibility of grades 410 and 430, AES study 0-66692
 steel, stainless 304, metallurgical factors on the corrosion and mass transfer in liq. Na (*Japanese*) 0-71804
 steel, stainless type 304, fabrication-related sensitisation 0-60887
 steel, surface Si reinforced type U8, metastable phase, composition, struct. (*Russian*) 0-92599
 steel, transformer, high-temp. heat treatment, resist. of refractories in contact 0-66554
 steel, type AC/HT-2, grain diameters, US attenuation 0-89429
 steel, type AISI 316, thermal passivation in controlled vacuum 0-76276
 steel, US critical angle reflectivity, near-surface metallic prop. gradient effect 0-70516
 steel, W-Mo-Cr-V tool, laser surface melted, struct., heat treatment effect 0-76424
 steel carburisation process, diffusion modelling 0-108632
 steel fracture mode, determ. from shear lip width 0-60968
 steels, with yield pt. of about 420 to 720 N/mm², correlation between yield pt./tensile strength ratio and toughness (*German*) 0-66615
 steels ShKh15 and 12KhN3A, white phases structure after heat treatment 0-76281
 thermally induced structural changes, specimen surface influence 0-103559
 vacuum, efficiency 0-81089
 Ag-Ni (10 wt.%) wire, plastically deformed, fracture struct. (*German*) 0-71744
 AgCl:Pd⁺, ESR spectrum, quasistatic Jahn-Teller effect 0-71170
 Al, thermal desorption of oxide film, influence of grain boundaries and recrystn. 0-61023
 Al-Cu(Si)(Mg) binary and ternary alloys, dimensional changes in heat treatment. 0-89271
 Al-Mg-Si alloy, Mg₂Si dispersion hardened US waveguides, concentrators (*Polish*) 0-89237
 Al-Si (0.57 at.%), Si precipitate dissolution kinetics 0-84935
 Al-SiO₂-Si MOS structures, charge motion, TSC meas. 0-100534
 Al-Zn-Mg, age-hardenable, precipitation and dissolution processes, positron annihilation and X-ray small-angle scattering comparison 0-89238
 Al-Zn-Mg alloys, grain boundary segregation, implications to stress corrosion cracking 0-84936
 Al₂O₃, derived from boehmite, phase transformations and microstruct. 0-60857
 η -Al₂O₃ outgassed at 400, 650°C, heat of adsorp. of pyridines from soln., surface acidity 0-61154
 Al₂O₃, sintering as function of phase comp. 0-66464
 β -Al₂O₃-Na₂O solid electrolyte, heat treatment effects on ionic cond. and microstruct. 0-65293
 Al₂O₃-SiO₂ glass ceramic, surface streaks and blisters, UV fluoresc. study 0-84347
 As-Se-Ge(-S), photostructural change in Urbach tail 0-76021
 As₂S₃, vitreous, thermal capacity, 300 to 600K 0-103492
 As₂Se₃, vitreous, thermal capacity, 300 to 600K 0-103492
 As₂Te₃, vitreous, thermal capacity, 300 to 600K 0-103492
 Au/GaSb (110) interface, heat-treated, struct. and chem. state, angle-resolved XPS 0-97400
 Au-Si thin film double layer, silicide form., electron diffr. study 0-80005
 Au₂Mn, heat treated, short-range order, diffuse X-ray diffr. study (*German*) 0-88092
 B:H amorphous films, optical band gap, thermal treatment effect 0-93415
 B₂O₃-SiO₂ glass, crack growth, phase separation effects 0-89336
 C chars, thermally activated paramagnetism, mag. susceptibility meas. 0-75709
 C fibre, metal-coated with Cu, Co or Ni, coating struct., SEM study 0-97605
 C fibre, tensile strength, heat treatment and flaw effects 0-81173
 C fibres, engineering applications, production requirements and mech. props. 0-89168
 C, hard, heat-treated under pressure, characterisation of carbon phase by electron microscope 0-60855
 C reinforced plastic, degraded, study of strain, 20 to 1000°C 0-71680
 C-S, influence of polymorphic transform. on sinter stability (*Russian*) 0-66503
 CaO-SiO₂ glass prep. by gel method 0-100824
 CaO-V₂O₅-SiO₂ system, compatibility triangles 0-81037
 12CaO.7Al₂O₃, composition of gases released on heating, crystallisation (*Russian*) 0-93820
 Cd, creep, low-temp., thermal heating and quantum mechanisms 0-79868

heat treatment continued

- Cd, single crystals., plasticity study during deformation by twisting (*Russian*) 0-93597
 CdGeAs₂ crystals, Bridgman grown, optical props. rel. to O₂ content of starting materials 0-81213
 Cd,Hg_{1-x}Te, elec. characs., impurity effects 0-92890
 Cd,Hg_{1-x}Te, dislocation motion, effect of lattice defects on microhardness (*Russian*) 0-70220
 CdS-CuInSe₂ solar cell, polycrystalline thin film, high photocurrent, characs., effect of heat treatment 0-61339
 p-CdTe, nondoped, heat treatment in vacuum, dissociation obs. effects on struct. and props. (*Japanese*) 0-60662
 Cd₂Zn_{1-x}S films, chem. sprayed, carrier density and mobility 0-60121
 Co base alloy, creep-fatigue interaction in aligned eutectic and solid soln. 0-108554
 Co-P, electrodeposited alloys, heat-induced structural changes (*Japanese*) 0-89263
 Co-W alloy electrolytic coatings, heat treatment effects on coercivity, hysteresis and structure (*Russian*) 0-60381
 CoPd, single crystals, domain struct., temp. and field depend. 0-71085
 Cr-Mo steel types JIS SCMV 2, SCMV 3 and SCMV 4, high-temp. high-cycle fatigue props., press. vessel appls. (*Japanese*) 0-93650
 Cu-Al-Co liquid alloys, constant Co-content of 5 wt.%, mag. props. (*German*) 0-88720
 Cu-Cu₂Y eutectic alloy, cast and directionally solidified, struct. and props. (*Russian*) 0-104138
 Cu-Ni, evaporation limited segregation 0-70513
 Cu-Ni (30-90 wt.%), elect. resist. rel. to cold working and heat treatment 0-71765
 Cu-Ni-Co, mag. props. of system of disperse ferromag. particles, 73 to 673K (*Russian*) 0-65968
 Cu-Sn-Al, deform at high temps. (*Polish*) 0-89284
 Cu₂S-CdS heterojunctions, role of deep levels in controlling photovoltaic props. 0-92941
 Cu₂S-CdS solar cells with interdigitated grid, current-voltage analysis 0-93981
 Fe, Armco, carburising kinetics, in endothermal atm. 0-76410
 Fe, magnetomechanical acoustic emission for residual stress NDT 0-71149
 Fe rich micas, X-ray absorpt., heat treatment effects, chem. and struct. interpretation 0-84806
 Fe, segregation and adsorption of S, influence on carburisation and nitrogenation 0-66701
 Fe, volume changes and defect healing due to plastic deform. (*Russian*) 0-81139
 Fe-Al, domain struct. and magnetostriction, heat treatment effect 0-60398
 Fe-B, amorphous, induced anisotropy by heat treatment in mag. field and under applied mech. stress 0-75758
 Fe-B-C amorphous alloys with high saturation induction 0-84617
 Fe-C-Mn-V, austenite microstruct. memory (*German*) 0-84977
 Fe-Co-Al-Cu-Ti (40, 14, 7.5, 4.5 wt.%), metastable equilibrium, high coercive state (*Russian*) 0-66476
 Fe-Co-Mo-Nb(Ta) semihard mag. alloy, mag. props., thermal expansion, elec. resistivity and hardness (*Japanese*) 0-88789
 Fe-Cr-Al-Y, oxidation resistance, heat treatment and Al⁺ ion implantation 0-71785
 Fe-Cr-Co alloy, coercive force mechanism 0-71103
 Fe-Cr-Co-Mo high energy permanent magnets, mag. props. 0-97119
 Fe-Cr-Mo alloy castings, thick-section, factors affecting 0-108374
 Fe-Cr(W)-M, (M=Si,Mo,Ni,Mn,P,Cr), cellular growth of S-pearlite formed by carburisation 0-108486
 Fe-M, (M=Cr,W,Mo,V,Ti), morphology and growth kinetics of δ -pearlite formed by carburisation 0-108485
 Fe-Mn-B, B effect on intergranular embrittlement 0-108555
 Fe-Ni alloy, martensitic transform., influence of thermal and electron irradiation treatment of austenite (*Russian*) 0-66509
 Fe-Ni-B-Si, amorphous, mag. props., heat treatment effects 0-89370
 Fe-Si, grain oriented, phosphate coating anal. by IR spectroscopy 0-89570
 Fe₄₀Ni₁₈Mo₂B₁₈, amorphous, mag. anisotropy, Mossbauer study 0-65864
 Fe₂O₃ haematite platelets, growth and cross-connection in consolidation of haematite pellet (*Chinese*) 0-104186
 Fe₂O₃ thin films, reactively sputtered, mechanical stresses rel. to deposition conditions 0-80146
 Fe₂Pt austenite, long range order parameter, temp. depend. discussion 0-97481
 Fe₂Pt austenitising conditions on M_s temp. 0-81088
 FeSi, single crystals, domain struct., temp. and field depend. 0-71085
 FeTi, surface and mag. props., heat treatment and hydrogenation effects 0-75447
 GaAs:Cr, Cr distrib. and heat-treatment migration studies by SIMS 0-107305
 GaAs:Cr semi-insulating wafer, heat treatment technique for no thermal conversion 0-10857
 GaAs:Si, stacking fault prod. during heat treatment in As vapour 0-96547
 GaP, IR absorpt. spectra depend. on compensating defects and thermal treatment (*Russian*) 0-71465
 Gd-Co, amorphous films, mag. props. ferromag. reson. meas., 20-520°C (*Russian*) 0-97144
 GdCu, electrical resistivity and length changes with temp., hysteretic behaviour 0-97600
 Ge, compensated by thermal defects, recomb. and optical props. 0-64989
 Ge, high-doped single crystals., impurity atom distrib. changes around growth dislocations in thermocyclic treatment (*Russian*) 0-107307
 In₂O₃-SnO₂-InP solar cell junctions, efficiency, InP surface props. 0-85288
 InSb:Cd (Zn) (Ge), ion-irradiated, p-n conversion during heat treatment 0-96558
 KCl:Pb, impurity distrib., light scatt. and microhardness study, heat treatment 0-96562
 La₂C₃, solid solution, lattice const. and superconducting transition temp. (*Russian*) 0-92496
 La₃NbO₇, synthesis and cryst. growth 0-71590
 Li matrix ferrites, coercivity, synthesis, thermostability control 0-80569
 Li_{0.5}Mn_{0.5}Fe_{2.5}O₄ ferrite cores with rectangular hysteresis loops, pulse parameters, effect of Fe₂O₃ heat treatment 0-60370
 LiNbO₃:Fe spatial holograms, ageing limitation (*Russian*) 0-74311
 LiO₂-Al₂O₃-SiO₂, glass containing ZrO₂, cryst. process 0-103253

ionisation potential continued

- methanol, dissociation mechanism, correlation diagram approach, mass spectra obs., metastable processes 0-95728
 methanol, processes of photoionisation studied using ion-electron coincidence method 0-74204
 methyl ethyl ketone, processes of photoionisation studied using ion-electron coincidence method 0-74204
 molecules containing C, N, O and H atoms, electron affinities and ionisation pot., semiempirical calcs. 0-78535
 polyatomic molecules, visible and UV photoionisation and fragmentation 0-69195
 pyrene, mol. ionisation pot., two photon ionisation, micellar interface effects on ionisation threshold 0-91609
 second-row atoms, atomic X_α calcs. 0-83280
 semiconductors, ionisation coeffs. of electron and hole multiplication, empirical fit to Baraff's curves 0-96897
 Tamm-Dancoff approximation, 2p-h, rel. to other self energy approximants 0-83243
 transition metal compounds, reduced ionisation potentials as parameters in superconducting transition temp. calcs. 0-75671
 trifluoroacetic acid, monomer and dimer, photoelectron spectrosc. 0-87172
 Ag latent image particles, electronic effects 0-82840
 BF, isoelectronic sequence, Rydberg transitions, term value-ionisation pot. correl. 0-58276
 BF₂ radical, thermomechanical studies by mass spectrometry, enthalpy of form. and ionisation pot. determ., chem. bonds 0-81382
 BrF₃, electronic struct. and ionisation pot., SCF DV X α method 0-69057
 BrF₃, electronic struct. and ionisation pot., SCF DV X α method 0-69057
 CO, isoelectronic sequence, Rydberg transitions, term value-ionisation pot. correl. 0-58276
 ClO₂⁻, ionisation energies, SCF-X α transition state calcs. 0-74115
 Cr(NO)₃, XPS and UV photoelectron spectra, compared to NO data 0-58317
 Cs I, n²S_{1/2} and n²D_{3/2,5/2} states, energies 0-87066
 Cu IV, wavelength region 700-1200 Å, extended analysis 0-99473
 F₂O, geometry, electron spectrum, vert. ionis. pot. ab initio calc. 0-58187
 FeBr₂, transient species, He(I) photoelectron spectrosc. calcs., relativistic corrections 0-95677
 H ionisation potential and energies in mag. field 0-99585
 H₂, vertical ionis. pot., many-body Green's function calcs. 0-102439
 HF, orbital relax. energy for single and double ionis. from valence shells 0-106253
 HNF₂ and DNF₂, photoelectron spectra, vibr. struct. obs, ionisation pot. determ., ab initio calcs. of ionic geometry 0-83418
 HNF₂, vertical ionisation pot. calc. by perturbation corrections to Koopmans' theorem 0-83520
 HNO, isomerism, low lying electronic states, ab initio MRD-CI calcs. 0-83291
 H₂O, orbital relax. energy for single and double ionis. from valence shells 0-106253
 H₂O, relative ionisation energies, Tamm-Dancoff approx. calcs. 0-83243
 H₂O, vertical valence ionis. pot. calc. by perturbation, CI and CPA techniques 0-69263
 Kr VIII, excited state energies and lifetimes, beam foil spectra 0-63591
 Mg, I-XII, energy levels and optical spectra 0-87065
 N₂, isoelectronic sequence, Rydberg transitions, term value-ionisation pot. correl. 0-58276
 N₂, relative ionisation energies, Tamm-Dancoff approx. calcs. 0-83243
 N₂, vertical valence ionis. pot. calc. perturbation, CI and CPA techniques 0-69263
 NH₃, orbital relax. energy for single and double ionis. from valence shells 0-106253
 NO₂, single and double ionisation by electron impact, ionisation pot. determ. 0-95730
 NOH isomerism, low lying electronic states, ab initio MRD-CI calcs. 0-83291
 Ne, electron impact K-shell excitation, EELS 0-106396
 Ne, vertical valence ionis. pot. calc. by perturbation, CI and CPA techniques 0-69263
 PO₄³⁻, ionisation energies, SCF-X α transition state calcs. 0-74115
 SO₄²⁻, ionisation energies, SCF-X α transition state calcs. 0-74115
 SeH, isotope effects, Rydberg levels-ground state transitions, rot. const., VUV spectra obs. 0-58279
 TeCl₂, transient species, He(I) photoelectron spectrosc. calcs., relativistic corrections 0-95677
 Xe, autoionising reson., Stark effect 0-58198
 Xe²⁺(Xe³⁺)(Xe⁴⁺), molecular electron impact ionisation 0-102582
 ZnTe, elec. field and impurity conc. effects on ionisation energy of impurities, appl. to acceptors 0-88514

ionisation time *see* ionisation**ionogen** *see* electrolytes**ionoluminescence**

- molecular deexcitation radiation obs. during keV ion-solid bombard. 0-71494
 sputtered excited states, secondary photon emission, role of transition probability 0-102483
 surface-ion impact, luminesc. accompanied by ion implantation 0-60683
 Au, ion bombardment-induced photon emission as function of target temp. 0-100698
 Be, foil, ion bombardment, secondary photon emission, ion energy depend. 0-97346
 Be, secondary photon emission following ion bombard. 0-71493
 Cr, photon emission due to Ar⁺ ion bombard., adsorbed and recoil-implanted O effect 0-80872
 CsI:Ti(Na), light yield under charged-particle bombardment 0-93409
 Cu, ion bombardment-induced photon emission as function of target temp. 0-100698
 GaAs:Te(Cd)(Mg)(B), ion implant depth distrib., AES and glow discharge optical spectroscopy meas. 0-65028
 Ge, ion bombardment-induced photon emission as function of target temp. 0-100698
 KBr, decay and time resolved emission spectra from σ -excitons produced by heavy-ion irradiation 0-89071
 Mo, ion bombard., ion and photon yields, CO adsorption effect 0-89098
 NaCl, Ne⁺, Ar⁺, Kr⁺ bombard., sputtering and ionoluminescence 0-96583

ionoluminescence continued

- Ni, ion bombard., ion and photon yields, CO adsorption effect 0-89098
 Ni, photon emission due to Ar⁺ ion bombard., adsorbed and recoil-implanted O effect 0-80872
 Pb, ion bombardment-induced photon emission near melting point 0-100699
 RbI, luminesc. spectra induced by pulsed Ne⁺ and electron beams and X-rays 0-80851
 Si, photon emission due to Ar⁺ ion bombard., adsorbed and recoil-implanted O effect 0-80872
 Sn, ion bombardment-induced photon emission near melting point 0-100699
 Ti, photon emission due to Ar⁺ ion bombard., adsorbed and recoil-implanted O effect 0-80872
 Xe, liq., α -particle and electron excited luminesc., time depend., specific ionisation density effect 0-71495
 Zr, photon emission due to Ar⁺ ion bombard., adsorbed and recoil-implanted O effect 0-80872

ionosondes *see* ionospheric measuring apparatus**ionosphere**

- see also D-region; E-region; F-region; ionospheric electromagnetic wave propagation; ionospheric techniques; sporadic-E layer*
 artificial aurora, conjugate to a Hawaiian launched electron accelerator 0-82124
 aurora, pulsations of electron and ion intensity 0-61934
 aurora irregularities, overnight north-south movements obs. at 42 MHz 0-67449
 aurora modelling, time-depend. study 0-72672
 auroral arc electric fields, radar obs. 0-72692
 auroral arcs global formation, numerical simulation in three-dimensionally coupled ionosphere magnetosphere 0-67446
 auroral elec. field, non-neutral field-aligned current sheet, theory 0-77196
 auroral electric field obs., comparative rocket obs. 0-85789
 auroral electrojets, movements during high-latitude substorms 0-109315
 auroral electron bunching near artificial electron beam 0-98511
 auroral electron energy distrib., secondary peaks driving instability 0-82135
 auroral electron flux, rel. to field aligned elec. pot. difference 0-72684
 auroral electron flux obs. 0-67466
 auroral electron transport and energy degradation 0-77219
 auroral hiss, nearly reson. whistler amplified Cherenkov radiation, limitations 0-101482
 auroral oval, dayside, elec. fields meas. 0-98501
 auroral oval, dayside, evidence for parallel elec. field particle accel. 0-98503
 auroral oval, dayside, rocket-borne VLF and ELF waves meas. 0-98504
 auroral oval, dayside, ULF elec. field fluctuations obs. 0-98505
 auroral oval, morning, solar wind ion injections 0-98502
 auroral zone, electrodynamic struct. of evening sector 0-72691
 auroral zone, nighttime scintillation localised enhancements struct. 0-98506
 auroral zone currents, obs. in morning sector pass 0-98510
 auroral zone ionosphere irregularities, simultaneous rocket probe, scintillation and incoherent scatter radar obs. 0-94640
 auroral zone precipitation and convection reversal, satellite obs. 0-101479
 balloon and rocket programs, conf. Bournemouth, England (1980, Aug.) 0-105433
 Birkeland currents and auroral structure 0-77209
 bubbles in equatorial spread F, nonlinear evolution 0-85801
 bubbles seen in topside soundings of spread F, characts. 0-85800
 combined ground and satellite measurements, IRI model extension 0-61911
 counter electrojet caused by vertical wind, equator region 0-85795
 current convective instability in auroral F-region 0-72680
 cusp region on dayside, field line topography, precipitation implications 0-85822
 daily mag. variations meas. in Alaska, atmos. current system 0-85590
 dayside cleft aurora and ionosphere effects, review 0-94633
 diffuse aurora equatorward boundary, electron precipitation interpretation 0-72668
 disturbance dynamo, caused by thermospheric wind 0-82134
 disturbances in mid-latitudes, magnetospheric convection intensification effects 0-105122
 eastward electrojet over auroral arc, rocket obs. of N. edge 0-101481
 electric current and atmospheric motion in lower thermosphere, symposium, Seattle, Washington, 1977 August to September 0-62371
 electric current sources, field-aligned, in high-latitude ionosphere 0-72674
 electric current system inferred from S_p obs. in Alaska 0-85813
 electric currents, obs. by S-310-5 rocket (*Japanese*) 0-94635
 electric field, midlatitude obs. of ALADDIN rocket 0-101488
 electric field configuration, Ps 6 mag. disturbances seasonal and diurnal var. 0-67477
 electric field observations, indicating magnetosphere electricity at mid-latitude 0-77230
 electric fields and currents, global distrib. produced by magnetospheric field-aligned currents 0-109303
 electric fields induced by ion drag and substorms 0-77199
 electrical coupling to lower atmos., quasi-static model 0-61865
 electrodynamic coupling, global scale of high and low latitude regions 0-77194
 electrojet during isolated substorm event 0-105132
 electron accelerator expt. on POLAR-5 sounding rocket, evidence of elec. charge accumulation 0-77213
 electron accelerator expt. on POLAR-5 sounding rocket, for use within aurora 0-77170
 electron beam scattering in atoms, sounding rocket expt. (POLAR-5) 0-77212
 electron concentration profile, vert. struct. 0-61936
 electron density depletion due to mag. storm 0-85784
 electron density equatorial anomaly, dissimilar forms in E. Asia and India 0-109301
 electron distrib. rel. to production rate and heating 0-105103
 electron flux in topside region, excitation of SAR arc event 0-77217
 electron gas effective energy reception per created ion electron pair 0-67463
 electron precipitation during substorm, modulation by hydromagnetic waves 0-105113
 electron precipitation pulsating aurora 0-85794

ionosphere continued

- electron temp. and density, calc. technique for ground and satellite obs. 0-90275
- electron temp. enhanced by suprathermal electron beam passage, auroral zone 0-85803
- electron temperature in topside ionosphere, models for low and medium solar activity conditions 0-67460
- electrons, thermal, in winter ionosphere, energy distrib. obs. by S-310-5 rocket (*Japanese*) 0-94636
- ELF radio signals are auroral ionosphere, generation by LF and MF transmissions nonlinear demodulation 0-94639
- EM wave propagation, evidence for reflecting layer below classical D-region 0-98508
- equatorial bubbles, model computations of assoc. radio wave scintillation 0-94641
- equatorial counter-electrojet, electron drift vel., radar obs. 0-82126
- equatorial electrojet, three metre irregularities depend. on Zenith angle, radar obs. 0-105109
- equatorial electrojet, type 1 radar echoes with double-peaked Doppler spectra 0-67458
- equatorial hiss in topside ionosphere, obs. 0-61939
- equatorial ionosphere, features assoc. with radio scintillations 0-77191
- equatorial ionosphere, long-term 1.5 GHz amplitude scintillation meas. 0-85792
- equatorial irregularity patches, form., motion and decay 0-67456
- escape of ions to space, ion chem. and low altitude accel. effects 0-85798
- field aligned current above auroral arc, e^- and H^+ precipitation obs. 0-77215
- field-aligned current closure and Joule heating near Harang discontinuity 0-72682
- field-aligned currents and plasma drift vels., simultaneous obs. by Atmosphere Explorer C 0-72681
- field-aligned currents at subauroral latitude, assoc. with convection elec. fields 0-90278
- fine structure at low latitude from impedance obs. at 406 kHz 0-67468
- geomagnetic daily variations influenced by interplanetary field 0-85591
- gravity wave-plasma interaction, elec. field and current prod. 0-61957
- gravity waves revealed by radar obs. of electron density 0-77182
- HF heating enhancing plasma line 0-82140
- high-latit. ionosphere, average parallel elec. field from perpendicular elec. field vars. below 8000 km 0-72706
- hiss associated with active auroral arcs, sounding rocket obs. 0-98512
- holographic interpretation of radiowave sounding data 0-77200
- induced elec. fields in ionosphere-magnetosphere system, review 0-94647
- inhomogeneities revealed by VLF propag., auroral zone 0-105107
- inhomogeneity formation, influence of elec. field temporal variation 0-105105
- International Reference Ionosphere 1978 rel. to Vertical-6 rocket meas. 0-90285
- interplanetary magnetic fields influencing atmos. elec. currents 0-105126
- ion drag, influence on winds in N Polar Cap thermosphere 0-67445
- ion heating in auroral zone, by electrostatic ion cyclotron waves 0-72686
- ion-cyclotron noise in topside 0-101470
- ionic reactions in lab. and planetary atmospheres 0-59168
- ionisation irregularity drift motion from spaced fading and scintillation obs. 0-82133
- ionosphere total electron content, nighttime enhancements at low latits. 0-72677
- IRI lower ionosphere model compared to radiowave propagation data 0-61948
- lower ionosphere, electron density profile from radiowave data 0-67462
- magnetically active quasistationary ionosphere, decametric freq. shift of magnetoionic component 0-105104
- magnetosphere boundary layer, model involving interaction with ionosphere 0-85808
- magnetosphere-ionosphere coupling during mag. storm 0-85821
- magnetosphere-ionosphere coupling flux, VLF whistler obs. 0-77239
- magnetosphere-ionosphere current system, generating Pi ULF waves 0-85819
- magnetosphere-ionosphere electrical coupling, two-dimens. model 0-61938
- magnetotelluric apparent resistivity, effect of localised source 0-72429
- mid-latitude trough, discovery in bottomside ionosphere 0-109300
- mixed mode echo of vertical-incidence ionogram, mixed-path mechanism 0-61942
- mixed-mode echo obs. during vertical sounding 0-61943
- model of midlatitude ionosphere and plasmasphere 0-105120
- nighttime global zones of energetic particle precipitation 0-61947
- palaeofield weak dipole epochs, nondipole component effect on auroral zone config. 0-105098
- Pc5 pulsation theory, consequences of ionosphere Hall current 0-105129
- Pc5 pulsation theory, consequences of N. and S. hemispheres ionosphere electricity 0-109316
- Pc5 pulsations, model of magnetosphere and ionosphere elec. and mag. fields 0-77234
- perturbations caused by mag. storms, review of obs. 0-98495
- photoelectron flux determination from plasma line obs. by radar 0-105117
- plasma, effect on obs. of solar type III radio bursts 0-72904
- plasma, ionospheric ions population in open model magnetosphere 0-90295
- plasma, lower hybrid drift instabilities, electron collisional effects 0-101484
- plasma bubbles, spatial relationship with 1 m equatorial spread-F irregularities 0-67457
- plasma bubbles in nighttime equator region, field-aligned characts. 0-109308
- plasma convection at high latitudes, model rel. to incoherent scatter obs. 0-72687
- plasma instability, prompt striation of Ba cloud 0-72685
- plasma line, meas. at Chatanika with high-speed correlator and filter bank 0-98507
- plasma parameters, incoherent scatt. of EM waves, EISCAT project (*French*) 0-82142
- plasma processes in lower ionosphere, rel. to atmosphere mass distrib. by latitude 0-90115
- plasma props. around S. Atlantic geomagnetic anomaly region (*Japanese*) 0-72695
- plasma wave spectrum, meas. via satellite-borne cross-power spectrum analysers 0-94621
- plasma pause, electron density profile meas. stimulated plasma wave results (*Japanese*) 0-94650

ionosphere continued

- plasma pause, fluctuations of drift wave type 0-82137
- plasma pause, MHD surface wave rel. to mini-substorm and long-period Pi 2 event (*Japanese*) 0-94653
- plasma pause crossing by JIKIKEN (EXOS-B) satellite, detect. by VLF Doppler shift crossing (*Japanese*) 0-94651
- plasmasphere, large scale elec. fields and currents, related geomag. vars., review 0-105121
- plasmasphere, magnetospheric and ionospheric elec. field simultaneous obs. 0-105110
- plasmasphere, nighttime electron content, geophysical disturbance effects, 1974 August to November 0-94642
- plasmasphere, simulated plasma wave expts. by JIKIKEN (EXOS-B) satellite (*Japanese*) 0-94649
- polar wind morphology in mag. quiet conditions 0-72713
- polarisation electric field vert. distrib. in topside 0-61935
- primary ion-electron prod. rates, change with solar EUV flux 0-72675
- pulsating aurora, the importance of the ionosphere 0-85787
- radio aurora (diffuse), rel. to field-aligned currents and particle precipitation 0-105119
- records over Shanghai, March 1953 to June 1955 (*Chinese*) 0-77192
- response to sudden storm commencements (*Japanese*) 0-101490
- S_z variation, magnetosphere or ionosphere dynamo? 0-109090
- satellite wake, assessment of ion current distrib. in wake 0-101527
- satellite wake ion density, for probe meas. in O^+ plasma 0-82136
- SID phenomena, peculiar events of non-XUV origin 0-109309
- SITEC disturbances (1966-1977), rel. to solar flare occurrence 0-90276
- Sq current variability affecting magnetosphere ring current 0-72714
- Sq currents of N. and S. hemispheres affecting equator mag. variations 0-76904
- sudden phase anomalies, correl. to solar X-ray bursts 0-98513
- thermal parametric instability, effect of recomb. processes and plasma nonisothermability 0-61967
- thermosphere, lower, ionospheric sublayers form. 0-61956
- topside ion transport, obs. of H^+ and O^+ ions 0-61940
- topside ionosphere, features of parasanceous whistlers 0-67455
- total electron content, ATS-6 radio beacon obs. over Europe and USA 0-77201
- total electron content models, for European and Mediterranean regions 0-98516
- turbulent fluctuations, rel. to strong turbulence in partially ionised plasmas 0-79499
- UV fluoresc. excited by electron beam, POLAR-5 rocket expt. at 391.4 nm 0-77214
- Vertical-6 rocket flight results 0-90268
- VLF hiss from auroral zone, direction find method and obs. 0-85777
- wind in lower ionosphere, obs. by Kyoto meteor radar 0-67444
- O^+ and H^+ equal ionisation level, during max. of solar activity 0-90280
- O^+ /electron density ratio in 140-200 km height range 0-105102
- $O^+ + N_2$, charge exchange collision, rate coeff. and ionosphere implications 0-87224
- $O^+ + O_2$, charge exchange collision, rate coeff. and ionosphere implications 0-87224
- $O^+ (^2D)$, quenching by electrons 0-94630
- $O^+ (^2D)$, ionisation freq. vars. during solar cycle 21 from airglow meas. 0-77195

ionospheric electromagnetic wave propagation*see also atmospherics*

- A1 absorption measurements at 2.4 and 5.6 MHz 0-82132
- absorption, global meas. on board ships 0-98500
- amplitude scintillation at 1.5 GHz, long-term meas. at mag. equator 0-85792
- asymmetry between N. and S. hemisphere radiowave absorpt. in winter 0-101485
- ATS-6 radio beacon data, rel. to geophysical disturbance effects on mid-latit. plasmasphere nighttime electron content 0-94642
- aurora irregularities, overnight north-south movements obs. at 42 MHz 0-67449
- aurora large scale structure, by riometer radiowave absorpt. 0-72670
- auroral oval, dayside, rocket-borne VLF and ELF waves meas. 0-98504
- auroral radio backscatter at 42 MHz, amplitude rel. to Doppler shift 0-61955
- auroral substorm expansion riometer absorpt. of spikes obs. 0-85799
- auroral zone, nighttime scintillation localised enhancements struct. 0-98506
- auroral zone activity coupled to mid-latitude radiowave absorpt. 0-61945
- complex refractive index, application of Appleton-Hartree formula (*Chinese*) 0-105100
- cosmic radio noise 'absorbed' by E-region plasma waves 0-82139
- cosmic radio-noise absorpt., impulsive quasi-periodic variations 0-105116
- D-region, enhanced electron conc. at mid-latitude, positive-ion model 0-105115
- D-region, radiowave heating at HF, consequent MF absorpt. effects 0-94646
- D-region, steerable beam radar obs., angular variation obs. 0-101487
- D-region ion chemistry during intense radiowave heating 0-61952
- daytime effect on radioastronomical intensity meas. and interferometry 0-67450
- decametric freq. shift of magnetoionic component in quasistationary ionosphere 0-105104
- decametric wave propagation, ionosphere conditions forecasting by CNET, in France (*French*) 0-85790
- deuteron whistlers in topside ionosphere, trans-equatorial propag. 0-77203
- Dynasonde virtual height meas. methods, comparisons, accuracy and interpretation 0-94643
- E_s -layer, reflection coefficient at high latitude 0-61922
- E-region, appl. of group and phase height meas. to electron density profile distortion meas. 0-109299
- Earth-ionosphere waveguide, program to compute EM fields in irreg. spheroidal model 0-94638
- EISCAT project, plasma parameter determ. (*French*) 0-82142
- electron density over Delhi and latitudinal depend., INTASAT Faraday fading obs. 0-109293
- electrons heating in lower ionosphere by horizontal lightning discharges 0-90283
- ELF band, sporadic-E affecting nighttime propag. 0-77202
- ELF propag. in nonstratified Earth-ionosphere waveguide, integral eqn. method 0-61959

ionospheric electromagnetic wave propagation continued

- ELF sferics in polar region during solar proton event, June 1968 Antarctic obs. 0-90291
- ELF waves in Earth-ionosphere cavity, field eqn. for inhomogeneous ionosphere 0-61950
- equatorial electrojet, type 1 radar echoes with double-peaked Doppler spectra 0-67458
- equatorial ionosphere, dissimilar forms of electron content anomaly in E-Asia and India from Faraday rot. 0-109301
- equatorial ionosphere, scintillation obs. rel. to irregularity patch form., motion and decay 0-67456
- equatorial spread-F irregularities, spatial relationship with plasma bubbles 0-67457
- equatorial spread-F meas. by Altair incoherent scatter radar 0-61927
- F₂-layer, seasonal difference in ionisation and height due to neutrals 0-61951
- F-layer, large-scale artificial inhomogeneity spectrum 0-98515
- F-region, critical freq. rel. to ionosphere global scale electrodynamic coupling of high and low latit. regions 0-77194
- F-region, equatorial f₀ affected by strong mag. storms 0-77197
- F-region, equatorial irregularities and electron density, radar obs. 0-77222
- F-region, generalized magnetoionic formulae for radiowave propag. 0-61963
- fading, obs. E- and F-regions 0-101478
- fading from spaced receiver obs. at Thumba 0-109296
- fading obs. in E-region refl. near equatorial electrojet 0-101473
- Faraday effect, meas. at 140 MHz using two-channel polarimeter, first results 0-61912
- geostationary satellites signals, severe scintillation of VHF and GHz waves during mag. storm 0-109302
- global radiowave absorpt., temporal and spatial variation by empirical formula 0-77204
- HF heating of ionosphere, enhancing of plasma line 0-82140
- HF radio waves, power losses and Doppler shifts rel. to bottomside mid-latit. trough 0-109300
- holographic interpretation of reflected radiowave data 0-77155
- hydromagnetic wave rotation between magnetosphere and ground 0-61969
- incoherent scattering, total cross section 0-72690
- layered plasma, use of Fuchsian differential eqns. 0-75060
- LF radiowave absorpt., variation during solar cycle 0-77193
- LF/MF radio transmissions, non-linear demodulation in auroral ionosphere rel. to ELF signals generation 0-94639
- long-delay echoes, 28 MHz amateur band obs. 0-90277
- Loran-C 100 kHz signals, possible effect of atmospheric gravity waves 0-109304
- low latitude whistlers, lower and upper freq. cut-off explanation 0-82131
- lower ionosphere, electron density profile from radiowave data 0-67462
- lower ionosphere, IRI model compared to radiowave propagation data 0-61948
- magneto-active plasma, group-vel. direction 0-59201
- magnetoactive collisional plasma, dielectric tensor, refl. index and attenuation 0-59202
- magnetoplasma, refr. index profiles in layered media, extraordinary mode 0-77223
- micropulsations, obs. at ground, ionosphere control 0-77207
- microwave radiation from solar power satellite, theoretical anal. of non-linear interaction with ionosphere (Japanese) 0-94634
- Mitra-type fading near travelling ionospheric disturbances, cross spectral anal. 0-82128
- mixed mode echo of vertical-incidence ionogram, mixed-path mechanism 0-61942
- mixed-mode echo obs. during vertical sounding 0-61943
- paramesonance (PR) whistlers, features 0-67455
- plasma line, meas. at Chatanika with high-speed correlator and filter bank 0-98507
- polar slant-E condition, rel. to polar cap plasma flow entry region longit. position 0-67472
- radio aurora (diffuse), rel. to field-aligned currents and particle precipitation 0-105119
- radio pulse dispersion and virtual height determ. 0-61954
- radio wave echo from ionospheric sublayers in lower thermosphere 0-61956
- radio wave scintillation caused by equatorial ionospheric bubbles, model computations 0-94641
- radio waves, time struct. of transionospheric signals scintillation 0-90281
- radio waves transionospheric propag., appl. to total electron content comparative study 0-98516
- radio window theory, transmission coeff. 0-61953
- radiowave propagation, ray trajectory props. in irregular ionospheric waveguide 0-90284
- radiowave scintillation by ionosphere, statistical study 0-109306
- radiowave self-focusing instability in oblique ionosonde meas. 0-105101
- ray trajectories in ionospheric waveguide, influence of inhomogeneities 0-61966
- reflection, evidence for reflecting layer below classical D-region 0-98508
- scattering in whispering gallery type mode 0-98514
- scintillation, power law phase screen model, strong scatt. 0-61962
- scintillation, power law phase screen model, weak scatt. 0-61961
- scintillation in equatorial region, 100 MHz to 10 GHz, theory 0-61946
- scintillations, assoc. with features of equatorial ionosphere 0-77191
- short wave radio absorpt. in winter, rel. to O₂ aigrow 0-77184
- sporadic-E layer, VHF fading evidence for F-region disturbances 0-101475
- spread-F, equatorial, seasonal and solar cycle vars. in American zone 0-109298
- spread-F, range and frequency spread occurrence at Kodaikanal 0-72676
- spread-F in equatorial ionosphere, assoc. with radio scintillations 0-77191
- sudden phase anomalies, correl. to solar X-ray bursts 0-98513
- SW reception effects 0-67451
- time dispersion of EM pulses 0-94645
- trajectory in Earth-satellite transmission, electron density determ. in ionosphere 0-72679
- transequatorial radiowave propag. in freq. range 28 to 432MHz, amateur bands, obs. and expts. 0-101491
- transequatorial radiowave propag. over 21 year period, VHF/UHF signals, theories 0-109311
- UHF waves reflected from ionosphere, angle-of-arrival fluctuations 0-109291
- ULF noise emission, ion-cyclotron waves 0-101470

ionospheric electromagnetic wave propagation continued

- VHF forward scattering, role of metallic ions of meteor origin effect, also contrib. as sporadic-E form. 0-67461
- VHF noise field strength at 95 MHz over India, meas. techniques and obs. 0-109294
- VHF radar aurora and strong HF backscatt. comparison 0-61960
- VHF scintillation, assoc. with reversal of horiz. elec. field 0-101489
- VHF scintillation at high-latitude, analytical formulas 0-77224
- VHF scintillation at high-latitude near 70°W 0-77221
- VHF signal scintillation, from ETS-2 satellite, obs. of Waltair and Calcutta 0-109295
- virtual height-freq. curves, nocturnal, reduction method using ionisation models (Chinese) 0-105099
- VLF and LF propagation and eigenmode scatt. relations 0-61944
- VLF atmospheric anomalies, rel. to rainy days over Calcutta 0-82127
- VLF focusing during solar eclipse 0-61965
- VLF propagation, revealing inhomogeneities in auroral zone 0-105107
- VLF propagation, theory of rays and foci in magneto-ionic medium 0-105135
- whistler banded struct. origin, on refl. from ionosphere 0-101476
- whistler mode, interpretation of 6-component measurements 0-83921
- whistlers, absence at equatorial Earth surface 0-77216
- winter absorption anomaly, implications of eddy diffusion models for mesosphere and lower thermosphere 0-109198
- winter absorption anomaly at middle latits., morphological features 0-67459
- ionospheric measuring apparatus**
- Altair incoherent scatter radar for equatorial spread-F meas. 0-61927
- cross-power spectrum analysers, satellite-borne, appl. to ionospheric plasma wave meas. 0-94621
- electron accelerator expt. on POLAR-5 sounding rocket, for use within aurora 0-77170
- ELF antenna, ferrite rod, for Magion satellite for 0.1 to 16 kHz freq. range (Czech) 0-85775
- Hadamard energy spectrometer, appl. to F-region energetic electrons spectra meas. (Japanese) 0-94637
- ion temperature probes, boarded on space sounding rockets, system designs (Japanese) 0-85838
- plasma line filter bank and high-speed correlator appl. to plasma line meas. at Chatanika 0-98507
- plasma resonance probe applications (Chinese) 0-90226
- polarimeter, two-channel, for ionospheric Faraday effect meas. at 140 MHz, first results 0-61912
- UV fluoresc. excited by electron beam, POLAR-5 rocket expt. at 391.4 nm 0-77214
- VHF noise field strength at 95 MHz over India, meas. techniques and obs. 0-109294
- ionospheric measuring instruments** *see ionospheric measuring apparatus*
- ionospheric propagation** *see ionospheric electromagnetic wave propagation*
- ionospheric techniques**
- see also electron density; ion density*
- combined ground and satellite measurements, IRI model extension 0-61911
- drift measurement of Ba cloud, spaced receiver technique 0-72678
- Dynasonde virtual height meas. methods, comparisons, accuracy and interpretation 0-94643
- E_s-layer, method to meas. refl. coeff. 0-61922
- electron accelerator expt. on POLAR-5 sounding rocket, evidence of elec. charge accumulation 0-77213
- electron accelerator expt. on POLAR-5 sounding rocket, for use within aurora 0-77170
- electron beam emission, laboratory studies of rocket payload charge neutralisation 0-77258
- electron beam scattering in atoms, sounding rocket expt. (POLAR-5) 0-77212
- electron conc. determ. by regularisation method 0-72679
- electron temp. and density, calc. technique for ground and satellite obs. 0-90275
- holographic interpretation of radiowave sounding data 0-77200
- holographic interpretation of reflected radiowave data 0-77155
- lower ionosphere research, Dive and Ascent Satellite programme 0-77252
- magnetotelluric methods, methods to study crust cond. beneath magnetometer array, review 0-98486
- plasma resonance probe applications (Chinese) 0-90226
- rocket observational methods, comparison for aurora elec. field meas. 0-85789
- satellite wake ion density, for probe meas. in O⁺ plasma 0-82136
- ULF wave generation by peninsular loop currents 0-90247
- UV fluoresc. excited by electron beam, POLAR-5 rocket expt. at 391.4 nm 0-77214
- VHF noise field strength at 95 MHz over India, meas. techniques and obs. 0-109294
- virtual height radio pulse dispersion, computer simulation 0-61954
- virtual height-freq. curves, nocturnal, reduction method using ionisation models (Chinese) 0-105099
- VLF hiss from auroral zone, direction find method and obs. 0-85777
- wave measurement, via satellite-borne cross-power spectrum analysers 0-94621
- iontophoresis** *see electrophoresis*
- ions**
- see also atoms; electrolytic ions; hydrogen ions; negative ions*
- No entries
- i.r. astronomy** *see infrared astronomy*
- i.r. detectors** *see infrared detectors*
- IR drop** *see electric potential*
- i.r. imaging** *see infrared imaging*
- i.r. sources** *see infrared sources*
- irasers** *see lasers*
- iridium**
- see also nuclei with*
- Auger spectra, N_{4s}N_{6s}N_{6p} and N_{4s}N_{6s}O_{4s} 0-89094
- chemisorption of H₂, adsorption and desorption kinetics, struct. of overlayer 0-84367
- energy band structure, X-ray emission spectra, APW calc. 0-92811
- field emission spectrosc. from (111) flat and stepped planes 0-76157
- film, CO oxidation, IR absorpt. spectroscopy 0-71398
- lattice dynamics, phonon/wave vector dispersion relations, Debye temp., modified axial symmetric model 0-70339
- surface, (100), reconstruction, superstruct., model 0-103551

iridium continued

- surface, (111), chemisorbed NH_3 , mol. adsorbate structs. from angular-resolved photoemission 0-76141
 surface, (111), decomp. of hydrazine, N_2 emission, ang. depend. 0-97731
 surface, adsorbed gases, field desorption from field ion tips 0-59793
 surface, CO chemisorpt., mol. cluster calc. 0-100407
 thermophysical props. at temps. up to 7000K 0-103497
 wear coefficients determ. using pin-on-disc apparatus 0-76366
¹⁹²Ir source for radiographic inspection method 0-71861
 NaCl_4 on Pt and Ir surfaces, adsorption kinetics 0-84393
 Re:Ir, electric quadrupole orientation of ^{186,188-190}Ir 0-78140

iridium alloys

- see also iridium compounds*
 rare earth-Sn-X, X=Rh, Ir, Ru, Co, cryst. growth and cryst.-chem. invest. supercond./mag. ternary cpds. 0-100777
 Be-Ir, dil., elec. field gradient, Mossbauer meas. 0-80665
 Cr-Ir, magnetic transformations, triple point (*Russian*) 0-88747
 Dy₃Ir₂, cryst. struct. 0-96473
 Er₃Ir₂, cryst. struct. 0-96473
 Gd₃Ir₂, cryst. struct. 0-96473
 Hf-Ir, dil., elec. field gradient at ¹⁹³Ir, Mossbauer meas. 0-66090
 Ho₃Ir₂, cryst. struct. 0-96473
 Ir-Fe, dil., local magnetisation, Mossbauer meas. 0-66091
 Ir-Fe, spin fluctuation alloy, thermopower peak diffusion origin 0-88542
 Ir-Sn-M, M=Mg, Ca, Sr, Sc, Y, Zn, Cd, In or Ti, cryst. growth and cryst.-chem. invest. supercond./mag. ternary cpds. 0-100777
 Ir-W (0.3%), grain boundary comp., trace element additions effect 0-66661
 Ir-Y eutectic alloy, supercond. transition enhancement due to lattice softening 0-103775
 Lu-Ir, dil., elec. field gradient at ¹⁹³Ir, Mossbauer meas. 0-66090
 Nd₃Ir₂, cryst. struct. 0-96473
 PrIr₃, hyperfine sp. ht. and magnetisation meas. at 4.2K 0-75775
 PrIr₃, sp. ht., differential susceptibility and elec. resist. meas., 1.4-40K 0-71063
 Pr₂Ir₃, cryst. struct. 0-96473
 Sc-Ir, dil., elec. field gradient at ¹⁹³Ir, Mossbauer meas. 0-66090
 Sm₃Ir₂, cryst. struct. 0-96473
 Tb₃Ir₂, cryst. struct. 0-96473
 Ti-Ir, dil., elec. field gradient at ¹⁹³Ir, Mossbauer meas. 0-66090
 Y-Ir, dil., elec. field gradient at ¹⁹³Ir, Mossbauer meas. 0-66090
 Y₂Ir₃, cryst. struct. 0-96473
 Zr-Ir, dil., elec. field gradient at ¹⁹³Ir, Mossbauer meas. 0-66090

iridium compounds

- see also iridium alloys*
 (111) surface states, surface Umklapp effects, photoelectron spectra 0-93457
 borides, M₃Ir₂B₃ (M=L, Th, U), supercond. and mag. props. 0-97028
 Ho₃(IrRh_{1-x})₄B₈ pseudoternary system, supercond. and mag. ordering 0-70876
 IrO₂ anodic films, electrochromism, anion mechanism 0-100647
 IrO₂ film, A-C response 0-107926
 IrO₂ anodic film electrochromic cell, fabrication and display device use 0-61320
 IrO₂ anodic films, electrochromism and ionic cond., model 0-59706
 IrO₂ anodic films, electrochromic props. and device uses 0-61319
 IrO₂ anodically grown film as electrochromic material 0-71377
 IrO₂, electrochromic, oxidation state changes and struct. 0-100950

iron

- see also nuclei with*
 Abel 1060 galaxy cluster, Fe X-ray emission feature obs. and abundance 0-82518
 adsorption, of O₂, oxidation 0-108730
 adsorption, segregation and reactions of non-metal atoms, LEED and AES obs. 0-59783
 adsorption and desorption of CO and H₂ on (100), C, O, S and K adlayer effects 0-71573
 adsorption of acetic acid and ethylenediamine, XPS study 0-76132
 adsorption of C(O)(S)(K), on (100) surface, adsorbate coverage determ. by LEED, AES and XPS 0-103566
 adsorption of K on Fe(110), UPS and XPS meas. 0-95675
 anodic behaviour in 1M H₂SO₄, influence of straining 0-97612
 Armco, Bauschinger effect, computerised evaluation method 0-93625
 Armco, carburising kinetics, in endothermal atm. 0-76410
 Armco, dynamic $\alpha \rightarrow \epsilon$ transform., stress gauge meas. 0-96594
 Armco, fatigue crack propag., influence of specimen thickness (*German*) 0-66669
 Armco, grain size and strength depend. on nonmetallic inclusions (*Russian*) 0-100894
 Armco, oxide films, passivating, transient growth kinetics 0-93672
 Armco, phosphate coating, Fourier transform IR absorpt.-reflection spectra 0-71500
 Armco, plastic zone around fatigue crack, vac. effect 0-100914
 Armco, Young's modulus of Fe₃C phase (*Russian*) 0-76297
 Armco Fe, ground, residual stresses, X-ray evaluation 0-79863
 Armco Fe, microflow and strain hardening under cyclic loading 0-104182
 atom, fine struct. levels fitting, config. interaction effect, spin-orbit and electrostatic interaction parameters 0-69248
 atom, inner-shell vacancies, cascade decay, multiple ionisation and X-ray emission calcs. 0-87072
 atom, K α satellite lines following electron bombardment 0-69097
 atom, L-shell internal excitation accompanying L-capture 0-95726
 atoms, metastable states, hyperfine struct. meas. by laser RF double-resonance 0-58404
 BCC, high field Knight shift and hyperfine anisotropy of ⁵⁷Fe 0-71205
 BCC crystal, anisotropic spin-pair correlation function, neutron mag. crit. scatt. cross-section 0-60194
 biomedical meas., Fe stored in human tissue, in vivo, using susceptometer 0-101245
 boring of high purity Fe with cryst. B powder 0-84951
 Brillouin-Mandelstam scattering from thermal and excited magnons 0-70980
 burning particles, flashes, spectrographic obs. 0-89078
 carbonyl powder, specific elec. conductivity, 5 to 200 MPa (*German*) 0-70664
 cast, molten, design and field test. of radiation pyrometer (*Japanese*) 0-98917
 cast with spheroidal graphite, fine cryst. struct. on tempering (*Russian*) 0-96476
 catalyst, gasification of graphite, electron. microscopy 0-104358
 cathodic charging effect, on creep and tensile deformation 0-76320
 cementation, of Cu, deposit struct., reaction rates, SEM 0-104421
 Centaurus galaxy cluster, Fe X-ray emission feature obs. and abundance 0-82518
 chemisorbed CO, low energy vibr. modes studied by tunnelling spectroscopy 0-78590
 coadsorption of K and O₂ on (110) surface, XPS, UPS, AES, and LEED study 0-80084
 corrosion, colloid chem. appls. 0-89541
 corrosion, indoor, rate meas. 0-76404
 corrosion and passivation in LiCl soln., peripheral velocity effect 0-61000
 corrosion behaviour in H₂SO₄ soln., ion implantation effect 0-71793
 corrosion due to V₂O₅ melts (*Japanese*) 0-93691
 corrosion in aq. H₂S, FeS polymorph form. 0-81231
 corrosion protection by organic coatings, qualitative, ellipsometric-electrochem. approach 0-104344
 creep at 77, 295K, formation of five struct. 0-60926
 Debye-Waller factors, extended de Launay model calcs. 0-70352
 density and thermal expansion in liq. and solid states 0-96698
 desorption of H into ultrahigh vac. system, using permeation cell 0-86326
 determinations, effect of surface changes in Pt crucibles 0-61192
 dislocation relaxation peaks under low temp. deform., pure specimen (*French*) 0-100867
 dislocation velocity, thermal activation exam. of applied stress and temp. depend., expt. methods (*French*) 0-59474
 dissolution and passivation kinetics in solns. containing O 0-76547
 dissolution kinetics, and passivation depend. on temp. and ionic strength 0-97626
 dissolution kinetics and diffusion coefficients in molten Al 0-59666
 domain walls, 90°, stable orientations, theory and X-ray observations (*Japanese*) 0-60359
 ductile, influence of crack tip sharpness and morphology of graphite on K_{1c} (*Chinese*) 0-81144
 dynamic exponent, crossover obs., TDPAC meas. 0-108021
 electrochemical behaviour, in molten V₂O₅ (*Japanese*) 0-89498
 electrochemical nucleation and growth, of Cu, TEM 0-104451
 electrode reactions with molten glass 0-85186
 electrolytic coated medium C steel, distrib. of bounded fatigue limits 0-81198
 electron irradi., mag. aftereffect 0-88838
 electron irradiated pure Fe, annealed, magnetoresistance at 20K (*French*) 0-103677
 electron tunnelling into ferromagnetic metals 0-60104
 electron-phonon coupling, point contact spectroscopy obs. (*Russian*) 0-70342
 energy band dispersion and mag. exchange splitting, angle-resolved photoemission meas. 0-71567
 energy loss of heavy nonrelativistic ions in matter, semiclassical theory 0-84224
 epitaxial films, even magneto-optical effects 0-76007
 epitaxial growth on Au platelets, dislocations 0-96760
 extrinsic grain boundary dislocations, study in thin foils, C content influence 0-107273
 FCC film, epitaxial growth on CuAu (111) surfaces, strong ferromagnetism 0-70557
 Fermi surface under press., de Haas-van Alphen effect meas. 0-75499
 ferromagnet, dynamic susceptibility calc. 0-80488
 ferromagnetic, cold work aftereffects 0-88830
 ferromagnetic, partial circular polarisation of thermal emission in mag. field 0-71387
 ferromagnetic domain theory, quasi-dislocation theory appl. (*Japanese*) 0-60358
 ferromagnetic film, surface states, surface magnetisation and electron spin polarisation 0-65648
 ferromagnetic metals, spin fluctuation theory, Curie temp., mag. susceptibility 0-65937
 ferromagnetic micropowder, cryst. struct., coercivity, remanence, saturation 0-65967
 ferromagnetic properties, book contrib. 0-75724
 film, coated, interface magnetism by Mossbauer spectroscopy 0-75890
 film, EELS, anomalous L_{2,3}/L₁ white-line ratios 0-93444
 film, evaporated, adsorbed acetylacetone, XPS study 0-76133
 film, evaporated at oblique incidence, columnar grains inclination angle 0-75468
 film, nuclear spin system dynamics Mossbauer study in FMR conditions (*Russian*) 0-80651
 film, on PMMA, mag. behaviour during mech. stress cycles (*German*) 0-80581
 films, ferromagnetic reson., photoacoustic detection 0-80613
 films, thickness variations in extraordinary and spontaneous Hall coeffs. 0-97013
 fracture-mechanisms, tensile specimens 0-85039
 Gibbs energy in BCC and liquid states rel. to FCC, Fe-C and Fe-N phase diagrams 0-60846
 grain growth, normal and abnormal, statistical distrib. of linear grain sizes 0-93581
 hot shortness, high-temp. embrittlement, residual and trace elements influence 0-66644
 hydrogen embrittlement and H₂ adsorption 0-89401
 hydrogen permeation, rel. to embrittlement, organic inhibitors, surface treatment 0-108635
 hyperfine interactions in implanted metals, Mossbauer spectra 0-108141
 impure, Snoek peak figures in various strain amplitude ranges 0-66562
 impurity, in Pd-H, Mossbauer study of local environment of substitutional impurities 0-60475
 impurity segregation, physico-chemical aspects (*Czech*) 0-60866
 intercell exchange energy, Hartree-Fock approx. 0-60239
 internal friction in plastic deformation process (*Chinese*) 0-88259
 interstitial site determ., μ SR technique 0-71287
 ions, Li-like Auger contribs. to electron impact ionisation 0-87231
 itinerant electron ferromagnet, magnetovolume effects 0-60397
 liquid, Hall effect, band struct. and exchange scatt. 0-80250
 liquid, N solubility depend. on added elements, mechanism (*Russian*) 0-65223
 liquid impact erosion and cavitation erosion comparison 0-104302
 liver overloaded with iron diagnosis, SQUID biomedical appl. 0-101244
 magnetic aftereffect, phenomenological description 0-88835
 magnetic breakdown and Hall resist. theory and model calcs. 0-75552

heavy ion-nucleus scattering continued

- ⁴⁴Ca(⁷Li, ⁷Li), 34 MeV, ang. distrib., cross sections, double folding model anal. 0-78313
- ⁴⁴Cd(¹⁶O, ¹⁶O), 44 MeV, A=112, 114, O₂⁺, O₃⁺ state collectivity, E0 and E2 decay, T_{1/2} 0-73784
- ¹⁶⁴Er(¹³⁶Xe, ¹³⁶Xe), 547-620 MeV, high spin props. in multiple band crossing region 0-83023
- ⁵⁸Fe(⁷Li, ⁷Li), 34 MeV, ang. distrib., cross sections, double folding model anal. 0-78313
- ⁴Gd(²⁸Si, ²⁸Si), 108-144 MeV, A=144, 146, 147, 148, high spin isomer g-factors yrast traps 0-78146
- (⁷Li, ⁷Li), 30, 88 MeV, M3Y folding model eval., model indep. anal. 0-78317
- (⁷Li, ⁷Li), 99 MeV, A=12-208, ang. distrib. from double folding model pots. 0-106074
- ²⁴Mg(¹³C, ¹³C), 35 MeV, 2⁺ population probab., spin-flip and spin orbit pots., coupled channel anal. 0-99125
- ²⁴Mg(¹⁶O, ¹⁶O), ⁴⁰Ca composite system, heavy ion resonances 0-86874
- ²⁴Mg(¹⁶O, ¹⁶O), 24-40 MeV, backward angles, excitation functions, ang. distrib. and resonant behaviour 0-86822
- ⁴¹Ni(⁷Li, ⁷Li), A=58, 60, 34 MeV, ang. distrib., cross sections, double folding model anal. 0-78313
- ⁵⁸Ni(⁷Li, ⁷Li), 14.22 MeV, alignment axis orientation depend. of cross section, mass quadrupole moment alignment 0-68638
- ⁵⁸Ni(⁶Li, ⁶Li), 71 MeV, excited states deformation lengths, DWBA and coupled channels anal. 0-68541
- ⁵⁸Ni(⁶Li, ⁶Li), elastic and inelastic, 74 MeV, folding optical model parameters 0-102201
- (¹⁶O, ¹⁶O), M3Y folding model eval., model indep. anal. 0-78317
- ¹⁶O(¹²C, ¹²C), 18-26 MeV, molecular structure, projection operator anal., differential cross sections 0-106033
- ¹⁶O(¹²C, ¹²C), perturbed stationary state method, low energy collision and mol. reions. 0-78320
- ¹⁶O(¹⁶O, ¹⁶O), 10-41 MeV, molecular resonances γ -yield, band crossing model 0-106032
- ¹⁶O(¹⁶O, ¹⁶O), elastic scatt., l-window formalism 0-68684
- ¹⁶O(¹⁶O, ¹⁶O), optical pot., nuclear matter approach, energy density matter [-] 0-83112
- ¹⁶O(¹⁶O, ¹⁶O), perturbed stationary state method, low energy collision and mol. reions. 0-78320
- ²⁰⁸Pb(¹⁴N, ¹⁴N), 266 MeV, giant resonance excitation 0-78253
- ²⁰⁸Pb(⁴⁰Ar, ⁴⁰Ar), 40-48 MeV, optical model anal., strong absorption radius (*Russian*) 0-68697
- ²⁰⁸Pb(⁴⁰Ar, ⁴⁰Ar), optical model anal., strong absorption radius (*Russian*) 0-68697
- ²⁰⁸Pb(⁴⁸Ti, ⁴⁸Ti), optical model anal., strong absorption radius (*Russian*) 0-68697
- ²⁰⁸Pb(⁶Li, ⁶Li), elastic and inelastic, 74 MeV, folding optical model parameters 0-102201
- ¹⁰⁷Ru(¹⁶O, ¹⁶O), 38-42 MeV, Coulomb excitation, 2⁺ state electric quadrupole moment 0-73793
- ²⁸Si(¹²C, ¹²C), ⁴⁰Ca composite system, heavy ion resonances 0-86874
- ²⁸Si(¹⁶O, ¹⁶O), radial sensitivity of optical pot. 0-86869
- ²⁸Si(⁶Li, ⁶Li), 154 MeV, differential cross section ang. distrib., optical anal. 0-63201
- ²⁸Si(⁹Be, ⁹Be), 45, 60 MeV, low lying collective states, ang. distrib., DWBA, double folding pot. anal. 0-78113
- ²⁸Si(⁹Be, ⁹Be), 121-201.6 MeV, strong absorption dominance, global optical model anal., fusion barrier 0-83116
- ⁴⁸Sm(¹⁶O, ¹⁶O), A=150, 152, hyperfine dynamic mag. field effects 0-68689
- ⁴⁸Sm(³²S, ³²S), A=150, 152, hyperfine dynamic mag. field effects 0-68689
- ⁴⁸Sm(³⁵Cl, ³⁵Cl), 108 MeV, A=112-124 even isotopes, 2₁⁺ mag. moments and shell model struct. 0-86805
- ¹²⁴Sn(⁶Li, ⁶Li), elastic and inelastic, 74 MeV, folding optical model parameters 0-102201
- ¹⁸⁴W(¹²C, ¹²C), 70 MeV, 4⁺ state excitation ang. distrib., hexadecapole deformation length effects 0-68521
- ⁹⁰Zr(³⁵Cl, ³⁵Cl), 90 MeV, A=92, 94, 2⁺ levels mag. moments 0-105968
- ⁹⁰Zr(⁶Li, ⁶Li), elastic and inelastic, 74 MeV, folding optical model parameters 0-102201

heavy leptons

- decay, spin 3/2 intermediate vector boson corrections 0-73761
- discovery, basic relations and remaining problems (*Czech*) 0-73762
- flavour changing neutral currents with b quarks and/or τ leptons 0-73656
- grand unification, neutron oscillations and massive neutral Majorana leptons, baryon number 0-91033
- hadron leptonproduction, nucleon targets, quark-nucleon inclusive cross section, heavy lepton pairs 0-57607
- prediction in weak interaction theories 0-73657
- sequential charged lepton, semileptonic branching ratio and lifetime 0-57578
- stable method heavy leptons, astrophysical mass constraint, condensation in stars and galaxies (*Russian*) 0-72768
- e^+e^- annihilation, 12-31.6 GeV, τ production and decay branching ratios, lifetime 0-78052
- e^+e^- annihilation, hadron and lepton prod., τ -lepton decay, K[±], p, \bar{p} yields, quark flavours 0-73725
- $e^+e^- \rightarrow \tau^+\tau^- H^0$, Higgs scalar boson production, Weinberg model calcs. (*Russian*) 0-68442
- eN, deep inelastic scatt., heavy lepton mixings, Weinberg-Salam model 0-62992
- μ N, deep inelastic scatt., heavy lepton mixings, Weinberg-Salam model 0-62992
- ν production, prompt sources, and axion decays and interactions, pN beam-dump experiment 0-63028
- $\nu(\bar{\nu})$ N, heavy lepton prod. and decay, differential cross sections (*Russian*) 0-105940
- pp, heavy lepton prod. and decay, supersymmetrical model of weak and EM interactions (*Russian*) 0-86748
- τ , properties and searches 0-73763
- $\tau \rightarrow K^*\mu\nu$, in e^+e^- annihilation, T-odd asymmetry in CP violation model (*Russian*) 0-105885
- $\tau \rightarrow \mu\mu e$, flavour changing neutral current search 0-105836
- $\tau \rightarrow \nu_\tau + \text{hadron}(s)$, decay modes and ν_τ -mass 0-63057
- $\tau \rightarrow \nu_\tau \pi$, T-violation effects, neutrino mass (*Russian*) 0-95294
- $\tau \rightarrow \nu_\tau \rho^0 \pi$, spin parity anal. 0-105941

heavy leptons continued

- τ properties, $e^+e^- \rightarrow$ heavy particle pair \rightarrow secondary particle + X, energy spectrum and angular distrib. 0-62960
- $\tau \rightarrow \rho\nu_\tau$, quark model, current algebra model, divergence of axial vector current 0-57655
- τ^- , decays, SPEAR, Mark II detectors, recent results 0-74045
- $\tau^- \rightarrow \nu_\tau \pi^0 \gamma$, π form factors, axial-vector and structure dependent, vector meson dominance model 0-62989
- τ decay as QCD test 0-102006
- heavy water**
- amorphisation by NaOD in solution, collective excitations in liquid and amorphous state, 77 to 300K 0-92636
- chemisorption on SrTiO₃, oxidation and reduction, isotope exchange study 0-104461
- dielectric constant meas. over temp. range 473K to 643K 0-103912
- IR spectrometric method for meas. of slight heavy water enrichment in natural water (*French*) 0-104718
- laser, 385 μ m, CO₂ laser pumping, dispersion 0-87375
- laser, emission characteristics at 50, 66, 83, 111 and 116 μ m 0-58525
- laser, far IR, intracavity pumped by TE CO₂ laser 0-87382
- laser, phase locking to freq. standard, CO₂-OsO₄ laser freq. meas. 0-95080
- laser, synchronous pumping, ultrashort pulse generation at 385, 66 μ m 0-102705
- laser oscillator, efficient high-power, at 385 μ m 0-69422
- liquid, volumetric and derived thermal characteristics at low temp. and high pressure 0-107352
- positronium formation, isotope effects 0-93432
- pulsed opto-acoustic spectroscopy 0-62743
- Raman spectra of O-H and O-A stretching vibrations of ices II and IX 0-66166
- surface tension from Skeleton table (*German*) 0-75407
- US velocities in superheated ordinary and heavy water, thermodynamic props. 0-65156
- H⁺(D⁺) exchange rates, ¹⁷O NMR linewidths, pH depend. 0-91661
- H₂O⁺(H₂O)_{0.12}+D₂O reactions, SIFT studies, review 0-58435
- HEED** see high energy electron diffraction
- height measurement**
- Geos 3, altimeter data on coincident orbits rel. to ocean transients 0-72535
- step height determ. by two-wavelength speckle pattern method 0-105614
- Venus microrelief irregularities mean height, determination from radio transillumination data 0-72807
- Heisenberg model**
- amorphous ferromagnet, magnetisation and Curie temp., CPA calc. 0-75703
- anisotropic Heisenberg chain, nonlinear excitations 0-70927
- anisotropic spin system, S=1/2, frustration effects 0-65763
- antiferromagnet, anisotropic, finite cell calcs. 0-60164
- antiferromagnet, Green function theory 0-107975
- antiferromagnet, impure, impurity banding and mag. reson., theory 0-93181
- antiferromagnet, one-dimens., autocorrelation function, low freq., temp. and field depend. 0-65929
- antiferromagnet, one-dimens., impure, mag. susceptibility 0-60168
- antiferromagnet, s=1/2 linear Heisenberg, zero-temp dynamics in mag. field 0-65764
- antiferromagnet, two-dimensional, expansion for susceptibilities 0-70963
- antiferromagnet chain, renormalisation group nearest neighbour interactions 0-60357
- antiferromagnetic chain, alternating Heisenberg, appl. of zero temp. quantum renormalisation group 0-80526
- antiferromagnetic insulators, lattice thermal cond. 0-65319
- antiferromagnetism in amorphous Heisenberg magnet, ground state and frustration, theory 0-65766
- antiferromagnets, pseudo-one-dimens., thermodynamic variables 0-65935
- asperomagnetism, short-range order, in Heisenberg magnet 0-65941
- bicritical points in antiferromagnets, universality tests 0-84604
- α -bis (N-methylsilylaldiminato) copper II, one-dimens. spin-1/2 Heisenberg antiferromag., high-field spin dynamics 0-71224
- chain, continuous, quantum solitons as magnon bound states 0-60162
- classical, with three or four spin interactions, linear chain 0-70923
- classical amorphous chain, thermodynamics 0-108022
- classical anisotropic Heisenberg chain, scaling theory 0-80515
- classical continuous Heisenberg chain, magnon-soliton phase shift 0-107998
- classical Heisenberg chain, energy fluctuations 0-80472
- classical Heisenberg chain, solitons and magnons 0-60161
- classical Heisenberg model, infinite, nonlinear dynamics, quantum time evolution 0-100576
- classical impure Heisenberg chain, dynamics near T=0 for low impurity conc. 0-71055
- classical nearest-neighbour Heisenberg chain, low temp. dynamics 0-80524
- compressible classical Heisenberg chain, phonon dynamics and sound velocity 0-96604
- computer simulations of mag. model systems 0-65924
- copper, benzoate, one-dimens. antiferromag., heat capacity, field-induced crossover of spin-dimensionality 0-97099
- copper benzoate, low-dimensional Heisenberg antiferromag., high field magnetisation 0-80558
- copper tetraamine sulphate, two-dimensional Heisenberg antiferromag., high field magnetisation 0-80558
- correlation theory of static and dynamic properties 0-65765
- diethylammonium manganese chloride, Heisenberg magnet, spin diffusion, EPR study 0-66019
- diluted systems with competing interactions, mag. ordering, appl. to Eu, Sr_{1-x}S 0-65914
- dimethylammonium manganese trichloride: Cd(Cu), impurities in quasi-one-dimens. Heisenberg systems, anisotropy effect 0-80502
- disordered ferromagnetic states, random exchange integrals 0-80550
- disordered Heisenberg spin model, magnetisation calc. 0-60167
- disordered magnetic system, spin waves, Heisenberg model 0-71064
- ferromagnet, anisotropic, collective Green's function, dynamical RPA 0-70925
- ferromagnet, classical, with dipole-dipole interaction, renormalisation group and crit. exponents 0-60351
- ferromagnet, correlation functions in ferromagnetic and paramagnetic regions, RPA 0-71075
- ferromagnet, critical dynamics of impurity spin below T_c 0-71076

Heisenberg model continued

- ferromagnet, critical dynamics spin wave theory, dynamic scaling hypothesis failure 0-97082
- ferromagnet, cubic, with next nearest neighbour interactions, two-magnon bound states 0-70977
- ferromagnet, disordered, phase transitions, mol. field and Landau-Ginzburg theories 0-93118
- ferromagnet, disordered two-dimens., CPA theory of bond model 0-60163
- ferromagnet, linear, with applied mag. field, second-magnon like excitations 0-65837
- ferromagnet, magnon renormalisation 0-65849
- ferromagnet, point singularities in micromagnetic systems with radial symmetry 0-107976
- ferromagnet, random quenched, crit. behaviour, effective exponents, renormalisation 0-60326
- ferromagnet, spin-wave renormalisation, $S \geq 1$ 0-71070
- ferromagnet, surface magnetisation profile and localised magnons 0-70985
- ferromagnet, two-magnon reson. in absence of bound states, calc. 0-60423
- ferromagnet two-dimensional soln. 0-60166
- ferromagnet with easy-plane anisotropy, HF magnon energies, kinematic consistency 0-93097
- ferromagnetic alloys, surface spin waves, cluster Bethe lattice approach 0-70983
- ferromagnetic Heisenberg chain, weakly bound magnon states (*Russian*) 0-100591
- ferromagnetic slab, finite thickness, spin correl. functions 0-80522
- Gaussian-to-Heisenberg crossover, specific heat, renormalised perturbation theory 0-60356
- ground state energy for linear antiferromagnetic Heisenberg chain, neighbour interactions 0-84606
- Heisenberg ferromagnetic system with biquadratic exchange interactions, spin wave theory (*Chinese*) 0-88755
- Heisenberg multi-quadratic isotropic model, LRO, phase transf., exchange interactions (*Chinese*) 0-88756
- Heisenberg-Ising spin chain quantum inverse scatt. method, Jordan-Wigner transformation 0-93068
- ideal Heisenberg ferromagnet, phonon renormalisation and spin waves 0-88754
- impurity band resonance at OK, theory 0-66041
- inhomogeneous mixture of Ising and Heisenberg substances, quenched system, critical temp. 0-88770
- interactions, spirals and phase transitions with and without long range order 0-60350
- liquid metals and alloys, mag. model 0-88719
- magnetization reversal of the two-dimensional Heisenberg ferromagnet with weak Ising anisotropy 0-107977
- metamagnet, collinear, mag. phase diagram 0-71035
- metamagnetic transition in absence of mag. field, model 0-97092
- mixed-spin paramagnet, dynamics 0-60173
- nearest-neighbour spin-spin correl. functions calc. 0-80537
- nitroxide spin probes, unresolved hyperfine broadening convection in EPR, linewidth and Heisenberg spin exchange freq. determ. 0-71180
- noncollinear magnetic order and spin wave spectrum in presence of competing exchange interactions 0-65834
- O(n) Heisenberg model close to $n=d=2$ 0-98862
- one dimensional anisotropic Heisenberg model, spin 1/2, Ising like antiferromag., dynamic correlation function 0-75704
- one dimensional classical magnet, energy fluctuations 0-70924
- one dimensional uniaxial classical Heisenberg ferromagnet, transfer integral, collective coordinate results for free energy 0-93067
- one-dimensional magnet, classical, nonlinear dynamics 0-71056
- one-dimensional magnet, in mag. field, dynamic correlations 0-70926
- operator equation, nonlinear differential form, auxiliary constraint 0-65762
- quantum spin systems, $S=1/2$, manifestation of frustration effect 0-65767
- quasi-one-dimensional systems, spin-lattice Peierls instabilities, static and dynamic aspects 0-71052
- quinolinium (TCNQ)₂, random exchange Neisenberg antiferromag. chain, intermediate field magnetisation meas. 0-103857
- random one-dimensional classical Heisenberg magnet, spin dynamics, neutron scatt. cross section 0-60312
- randomly dilute, renormalisation group calcs. 0-60321
- specific heat, high-temperature (*Russian*) 0-88757
- spin anisotropic Ising-Heisenberg chain, appl. of zero temp. quantum renormalisation group 0-80526
- spin glass, calc. 0-60301
- spin glass, excitation spectra, numerical studies 0-60300
- spin glass, five-dimensional, Edwards-Anderson ordering possibility 0-60295
- spin glass, Heisenberg mode, RPA approx. 0-65904
- spin glass, X-Y and Heisenberg, below four dimensions, vanishing of Edwards-Anderson order parameter 0-60347
- thermal excitations in Heisenberg-xy systems 0-97047
- TMMC, Cu-substituted, spin dynamics, neutron scatt. cross section 0-60312
- trimethylammonium manganese trichloride, Heisenberg antiferromag. chain, specific heat and EPR 0-65931
- two-dimensional, crit. temp. 0-71039
- two-dimensional Ising system, crossing over to two-dimensional Heisenberg system 0-93123
- CsMnCl₃·2H₂O, thermal cond. in mag. field 0-70481
- CsMn_{1-x}Cu_xCl₃·2H₂O, impurities in quasi-one-dimens. Heisenberg systems, anisotropy effect 0-80502
- CsNiF₃, anisotropic Heisenberg chain, nonlinear excitations 0-70927
- CsNiF₃, longit. paramag. susceptibility, reaction field approx. 0-97059
- CsNiF₃, one-dimensional ferromagnet, optical absorpt. and static spin correlation functions 0-71415
- Cu_{0.98}Ni_{0.02}, spin glass, Heisenberg mode, RPA approx. 0-65904
- EuO, magnetic susceptibility critical exponent, corrections to scaling 0-103846
- Eu, Sr_{1-x}S, Heisenberg spin glass system, excitations 0-84610
- Eu, Sr_{1-x}S, paramag. susceptibility, expt. and comparison with high temp. series expansion 0-60176
- Fe₂Pt, ordered ferromagnetic alloy, magnetic excitation obs. 0-70978
- FeF₂·Mn, Heisenberg model, impurity band resonance at OK, theory 0-66041

Heisenberg model continued

- KCuF₂, linear chain Heisenberg antiferromag., nearest neighbour correl. function, birefr. expts. 0-71386
- KCuF₃, one-dimens. antiferromag., spin waves, neutron scatt. study 0-65848
- KMn₂Mg_{1-x}F₃, randomly diluted Heisenberg paramag. nucl. relax. 0-60444
- KMnF₃, specific heat near Neel temp. (*Russian*) 0-100340
- MnP, ferro-spiral transition, neutron scatt. studies 0-65876
- RbMnCl₃, specific heat near Neel temp. (*Russian*) 0-100340
- RbNiF₃, spin lattice, susceptibility, Heisenberg model (*Russian*) 0-65893
- TiMnCl₃, specific heat near Neel temp. (*Russian*) 0-100340

Heising modulation see amplitude modulation**helical dislocations see screw dislocations****helicity (elementary particles)**

- isolation of definite naturality exchanges: the general solution 0-101954
- s-channel resonance prod. in πN scatt., amplitude zeros in Mandelstam plane 0-73686
- SU(3)×U(1) gauge theory, electro-weak interaction, helicity mixed representation 0-78013
- supergravity, global supersymmetry transformations of noninteracting massless particles 0-95015
- γ circular polarisation, neutral current effect in bremsstrahlung and pair production 0-73655
- $\gamma d \rightarrow pn$, 250 to 800 MeV, model using $\gamma N \rightarrow \pi N$ helicity amplitudes 0-78081
- $\gamma N \rightarrow \pi N$ helicity amplitude, used in model for $\gamma d \rightarrow pn$ 0-78081
- $\gamma\gamma$, Compton scattering, 375 to 1150 MeV, differential cross section 0-57604
- $\pi\pi \rightarrow NN$, helicity amplitude, extrapolation of $S^{1=0}$ wave 0-91112

helicons**see also solid-state plasma**

- ferromagnetic semiconductors with hot electrons, instability of coupled spin-helical waves 0-107841
- magnetic semiconductor, helicon wave propag., hyperfine interaction effect 0-80307
- monopolar crystals, quasi-helicon waves instability 0-70741
- piezoelectric semiconductor-plasma, parametric excitation of helicon and acoustic waves 0-107837
- semiconductor plasma, surface helicons, theory 0-60019
- InSb, helicon beam form. during microwave transmission in mag. field 0-80308
- n-InSb, quasi-helicon waves instability 0-70741

helicopters

- environmental noise impact obs. and evaluation 0-104539
- noise level meas., development of proposed impulse correction 0-96107
- rotors, sound radiation props. for free field and near absorptive plane surface 0-102885

heliotron see plasma devices**heliports see airports****helium****see also nuclei with**

- see also helium atoms; helium films; liquid helium; solid helium**
- abundance in chaotic Friedmann Universe 0-67920
- adsorbed on graphite, band struct. and thermodynamic props. 0-80349
- adsorbed on graphite, surface band splitting, theory 0-60058
- adsorbed on W, accommodation coeffs. calcs. 0-66866
- adsorption on graphite (0001), selective, level crossings 0-71556
- backscattering from solid surfaces, positive charge fractions 0-66375
- blistering of Nb, large swelling meas., gas press. model 0-88218
- bubble alignment in α -irrad. Al foils during deform. 0-107345
- cavity depth distribution in 20 and 500 keV ⁴He⁺ irradiation. Ni 0-107346
- [cc] He-Ne laser scanning system, for video record player, information identification (*German*) 0-106557
- chloropentafluoroethane-He, multiphoton dissociation, ¹³C enrichment factor, CO₂ laser wavelength and fluence depend. 0-58331
- Clausius-Mossotti second virial coefficient 0-79426
- collisional excitation transfer for 3¹P and D states 0-106387
- cryosorption pumping of He by charcoal, cryopump design for fusion reactor 0-105654
- discharge, hollow-cathode type, spectroscopic obs., laser light source appl. 0-59335
- 30 Doradus nebular complex, He/H abundance ratio 0-62226
- Earth composition, He incorporated from immature Sun (*Russian*) 0-81856
- earthquake, precursory soil He changes, He diurnal variation limitation 0-94469
- electron localisation, mobility in dense low temp. gas 0-92247
- exhaled, Schlieren photography of exhaled air, detection of abnormal nasal escape 0-64145
- exospheres of Mercury and Venus, He atoms vel. distrib. Monte Carlo simulation 0-67588
- field adsorption on W (111), array model 0-59800
- field desorption and field ionisation on metal surface 0-104047
- fission gas release from UO₂-Zr high burnup nuclear fuel rods 0-57846
- gas, compressed, Rayleigh-Brillouin spectrum, hydrodynamic region 0-100063
- gas, compressed, Rayleigh-Buillouin spectrum, scaling 0-100062
- gas, heated, elec. breakdown parameters 0-103202
- gas, pulsed breakdown at low temp. 0-103216
- gas, second virial coeff., acoustic determ., 1.28-2.13K 0-69965
- gas thermometer secondary standard for 0.5 to 40K 0-82762
- gaseous, positron mobility edge 0-83880
- globular cluster stars, He settling and effect on inferred ages 0-73013
- glow discharge, cryogenic, effect of laser radiation (10.6 μ m) 0-64803
- Hall accelerator, variations in performance when using He gas (*Russian*) 0-103195
- injection into liquid through porous plate, squeezing out of liq. 0-64622
- interstellar neutral gas interaction with solar wind, after gravit. focusing 0-105144
- ion, energy and ang. distrib. in passing through C, Cu, Ag films 0-100292
- ion irradiation of metals, blister form. and bubble growth 0-65072
- ion source, HF, proton yield increase, influence of various admixtures to H₂ obs. 0-57422
- isoelectronic sequence, $\delta(r_1)$ matrix elements using spatially distrib. operators 0-102445
- laser-induced breakdown 0-96339
- low press. discharge, electron free streaming waves expansion 0-79595

iron alloys continued

- Au-Fe, spin glass, transition temp., freq. depend. 0-97113
 Au-Fe, spin glasses, alternating susceptibility 0-65912
 Au-Fe, UPS study, localised states 0-93449
 Au-Fe (1 at.%), spin glass, specific heat 0-60355
 Au-Fe (4 at.%), spin glass, magnetisation and energy relax. below T_g 0-65921
 Au-Fe (4.2 at.%), spin glass, DC magnetisation, field depend. 0-97103
 Au-Fe alloys, magnetism and atomic clustering 0-103810
 Au-Fe alloys, spin correlations, neutron diff. meas. 0-80482
 Au-Fe ion implanted alloy, Mossbauer conversion electron scatt. 0-88898
 AuFe spin glass, μ^+ zero-field spin relax. probe for spin dynamics 0-97177
 Au₈Fe₁₅, and Au₈₂Fe₁₈, mag. props. 0-84592
 CC Fe-Ni-Cr (35, 15 wt.%): Nb(Ti)(Mo), corrosion in HTGR He environment 0-61021
 Ce-Mg-Fe master-alloy inoculated cast Fe, struct. and props. 0-100843
 (Ce,Y_{1-x})Fe₃, mag. susceptibility and Mossbauer meas., lattice parameters 0-97068
 (Co,Fe)₈₀B₂₀ glass, induced anisotropy and time changes of permeability 0-75815
 Co-Fe, dendritic segregation 0-76260
 Co-Fe, dil., hyperfine mag. fields, press. effect, Mossbauer meas. 0-71277
 Co-Fe, dil., magnetocrystalline anisotropy anomalous temp. depend. 0-71007
 Co-Fe, soft mag. props. rel. to metallurgical aspects 0-88810
 Co-Fe amorphous alloys, worked, permivar type mag. hysteresis loop, longit. Kerr effect obs. 0-65958
 Co-Fe-B, amorphous, crystn. and thermal stability 0-107057
 Co-Fe-Si-B, decomp. of amorphous state during annealing below recryst. temp., electron microscope study (Russian) 0-75164
 Co-Fe-Si-B, ferromag., magneto-optical spectra in amorphous and cryst. states (Russian) 0-84749
 Co-Fe-V-Ni, mag. and mech. props., heat treatment and stress effects 0-60363
 Co-Mn-Ni-Fe-Si-B amorphous alloys, mag. props., low magnetostriction 0-75832
 Co-Ti-Fe (3, 1 to 2 wt.%), spinodal decomposition 0-100839
 Co₂Fe_{1-x}, ferromagnetism and spatial long-range order 0-60159
 (Co_{0.93}Fe_{0.07})_{75-x}Cr₂Si₁₅B₁₀ amorphous alloy, thermal stability, Cr conc. effects, DTA expts. 0-59395
 (Co_{0.89}Fe_{0.11})₇₂Mo₂Si₁₅B₁₀, metallic glass, strain- and field-induced mag. anisotropy 0-108004
 Co₇₅Fe₂₅Ni₁₀(Si,B)₂₈, amorphous, soft mag. props., switched-mode power supply appls. 0-88850
 Co₇₀Fe₃₀Si₁₅B₁₀, amorphous, crystn. and thermal stability 0-107057
 Co₇₀Fe₃₀Si₁₅B₁₀, amorphous, mag. aftereffect spectra and annealing props. 0-88831
 Co₂Ga_{2-x}Fe_x, elec. resist., temp. and mag. field depend., mag. contrib. 0-96846
 Co₂Ga_{2-x}Fe_x, mag. field depend. of resist., 5.80K 0-70676
 Cr-Co-Fe, low Co, phase separation, TEM and Mossbauer spectra obs. 0-71269
 Cr-Fe, dil., antiferromag., elec. resist. min., press. and impurity effects 0-59970
 Cr-Fe, dil., magnetisation, Fe local moments 0-60215
 Cr-Fe, dil., spin correlations and neutron scatt. near crit. conc., theory 0-60327
 Cr-Fe, elastic moduli, electron conc., pulse echo overlap meas. 0-59550
 Cr-Fe (6.5 wt.%), atomic clustering and mag. defects, mag. moments 0-60246
 Cr-Fe-C (28.4, 9.1 wt.%) prep. from FeCr₂O₄ chromite 0-100804
 Cr-Fe-Ni, γ -solid soln., thermodynamic activity determ. at 1500K 0-108397
 Cr-Fe-Ni alloys, claddings, chemical compatibility with UC nuclear fuels, thermodynamic model 0-63263
 Cr-Fe-Ni-Si, ternary phase equilibria for Cr-Fe-Ni rich portion, lattice stabilities 0-71628
 Cr-Ni-Fe, ternary phase diagrams, interactive computer program 0-71629
 Cr_{2.8}V_{0.2}Fe₃C₃, stacking fault study, morphology, comp. and struct. 0-84190
 Cu-Au-Fe, ferromag. ordering in FCC γ -Fe precipitates, Mossbauer study 0-71267
 Cu-Fe, dil., valence and core level spectra, XPS study 0-84838
 Cu-Fe, explosive plasma sputtered coatings, struct. and props. (Russian) 0-100783
 Cu-Fe, liq., thermodynamic props. (Polish) 0-89199
 Cu-Fe (1.5 wt.%), precipitation-effect on void formation during electron irradiation 0-84211
 Cu-Fe (1.5 wt.%), void form. during irradi. in HVEM, reactor irradi. simulation and ageing effects 0-107327
 Cu-Fe group, dil., NMR satellite data calc., struct. of mag. impurities 0-103894
 Cu-Fe system, ageing and reversion phenomena study 0-89274
 Cu-Ni-Fe, cast, strength and hot ductility, Fe effect 0-66595
 Cu-Ni-Fe, magnetic properties, heat treatment and compressive stress effects 0-60367
 CuFe, dil., anisotropic hyperfine coupling, NMR study 0-65784
 CuFe solid solns., quenched from vap. phase, mag. props. 0-60307
 DyFe₂ and Dy₂Fe₂₃, magnetostriction, room temp. to 80K 0-65993
 DyFe₂ hydrides, desorption isotherms 0-103565
 DyFe₂, domain structures and anisotropy constant. 0-93136
 DyFe₂H_x, thermodynamic props., H₂ desorption isotherm meas. 0-89516
 Dy,Tb_{1-x}Fe₂, single crystal, torque meas. 0-65877
 ErFe₂, mag. excitations, RPA theory 0-65830
 ErFe₂YFe₂, and ErFe₂LuFe₂, mag. props., 80-1300K (Russian) 0-75750
 ErFe₂ and Er₂Fe₂₃, magnetostriction, room temp. to 80K 0-65993
 Er₂Fe₂₃, magnetostriction, temp. depend., 20 to 350K 0-65994
 ErFe₂H_x, multiplet absorpt. isotherms, theory 0-103564
 ErFe₂H_x, thermodynamic props., H₂ desorption isotherm meas. 0-89516
 FE-Zn, prep. and phase diagrams (French) 0-76231
 (Fe,Co,Ni)-(Si,B), amorphous mag. alloy, magnetostriction rel. to soft mag. props. 0-84633
 Fe base superalloy, type A-286, elevated temp. fracture toughness testing of thin section irradi. materials 0-61063
 Fe, cast flake and nodular, rupture strength, circumferential notch (Japanese) 0-93649
 Fe^{48V}, nucl. orientation of ⁴⁸V, γ -ray anisotropy obs. and NMR meas. 0-97169

iron alloys continued

- Fe-(Co)-B, amorphous, crystn. 0-79704
 Fe-Ag (50 wt.%), plastic behaviour in compression, deform. rate effect (French) 0-71711
 Fe-Al, domain struct. and magnetostriction, heat treatment effect 0-60398
 Fe-Al, ordered, superlattice fringe images, computer simulation 0-103296
 Fe-Al, planar faults, faint electron microscopic image contrast obs. 0-107283
 Fe-Al, single crystals, deform. at high temps. 0-81125
 Fe-Al (4 wt.%), mag. anisotropy induced by cold rolling (Russian) 0-84595
 Fe-Al (40 at.%) and Fe-Al (50.5 at.%) ordered alloys, 20K neutron irradi. effects, stoichiometry depend., resist. obs. (French) 0-84215
 Fe-Al-Si (6.22, 9.63 wt.%), bending test under high press., high temp. 0-85057
 Fe-Al(Ti), O containing, mag. aftereffect and disaccommodation meas., time depend., activation energy, and ageing props. 0-88836
 Fe-Al(24.3 at.%)C alloy, magnetic permeability disaccommodation, 260-400K 0-93144
 Fe-As melts, surface tension, density, adsorption (Russian) 0-92757
 Fe-As system, mag. props., Mossbauer study 0-88897
 Fe-B, amorphous, anomalous thermal expansion, ΔE effect, Invar and Elinvir characts., delay time 0-80589
 Fe-B, amorphous, crystn., metal or metalloid exchange influence 0-75172
 Fe-B, amorphous, induced anisotropy, development by mag. annealing and under applied mech. stress 0-65868
 Fe-B, amorphous, induced anisotropy by heat treatment in mag. field and under applied mech. stress 0-75758
 Fe-B, amorphous, mag. aftereffect, initial susceptibility time depend. 0-88829
 Fe-B, amorphous alloy, mag. props. 0-84618
 Fe-B, amorphous alloys, compositional study on short-range struct. 0-84095
 Fe-B, amorphous ferromag., temp. depend. of resist., appl. of extended Ziman theory 0-59950
 Fe-B, for infiltration of Fe compacts 0-60806
 Fe-B, liq., mag. susceptibility meas. 0-75740
 Fe-B, metallic glasses and vapour deposited films, amorphous to cryst. transition 0-88048
 Fe-B, rapidly quenched, metastable phases 0-76234
 Fe-B amorphous alloy, annealed, microstruct. and mag. domain changes 0-75790
 Fe-B amorphous alloy, fast neutron and ²³⁵U fission fragment irradi. 0-100288
 Fe-B amorphous alloys, mag. aftereffect 0-65970
 Fe-B amorphous ribbons formation, high-speed photography investigation 0-76216
 Fe-B metallic glass, X-ray diff. meas., semi-empirical struct. model 0-107059
 Fe-B metallic glasses, diffusion coeffs. from primary crystn. data 0-100345
 Fe-B metallic glasses, struct., stability and crystn. 0-75173
 Fe-B metallic ribbons, correl. between quenching temp. and mech. and mag. props. 0-89373
 Fe-B phase ferromag. amorphous alloys, stiffening below Curie temp., pole effect (Japanese) 0-84632
 Fe-B ribbon, microhardness, and static coercive force, melt overheating effect 0-84978
 Fe-B-C, amorphous, effects of replacement of B by C on mag. props. 0-84621
 Fe-B-C amorphous alloy, formation, mag. props., thermal stability and density 0-75796
 Fe-B-C amorphous alloys for use in power transformers 0-88808
 Fe-B-C amorphous alloys with high saturation induction 0-84617
 Fe-B-Cr(Mo), metallic glasses, mag. struct., and elec. props. 0-88751
 Fe-B-Cr(Si) thin film glasses, mag. props. and corrosion resist. 0-80576
 Fe-B-Si amorphous alloy, liq. quenched, elec. resist. and cyclic deform. 0-59949
 Fe-B-Si-C amorphous alloys, prep. and props. 0-88748
 Fe-B-Si, glassy, field-induced mag. anisotropy near eutectic comp. 0-93110
 Fe-B-Si alloy filaments produced by glass-coated melt spinning 0-76213
 Fe-C, electron-irradiated, positron lifetime meas. 0-93431
 Fe-C, lenticular martensite growth by transformation wave propag. 0-81055
 Fe-C (0.64 wt.%), fatigue crack bifurcation 0-71748
 Fe-C (1.6 wt.%) martensite habit plane poles, statistical TEM trace anal. 0-97494
 Fe-C (graphite, 0.3 wt.%), powder-forged, elastic constns., density depend. 0-84987
 Fe-C alloys abrasion resist. materials, review 0-108586
 Fe-C eutectic, irregular, branching limited growth 0-81042
 Fe-C system, FCC, austenite field thermodynamics, re-anal. 0-89201
 Fe-C-Mn-V, austenite microstruct. memory (German) 0-84977
 Fe-C-Si, high purity, vacuum melted, nodular graphite form. 0-108452
 Fe-C-X, glasses and metastable cryst. phases, third element effect 0-75171
 Fe-Ci (3 wt.%), local magnetisation losses, grain orientation effect 0-88817
 Fe-Co, 3d ferromagnet nuclear spin-lattice relaxation 0-80627
 Fe-Co, ferromagnetic micropowder, cryst. struct., coercivity, remanence, saturation 0-65967
 Fe-Co, Hall effect, anomalous, residual coeff. calcs. using coherent pot. method (Russian) 0-80249
 Fe-Co-Al-Cu-Ti (40, 14, 7.5, 4.5 wt.%), metastable equilibrium, high coercive state (Russian) 0-66476
 Fe-Co-Mo, phase relations in system at 1100°C 0-108392
 Fe-Co-Mo-C, amorphous alloys, med. props. and thermal stability (Japanese) 0-85049
 Fe-Co-Mo-Nb-Ta) semihard mag. alloy, mag. props., thermal expansion, elec. resistivity and hardness (Japanese) 0-88789
 Fe-Co-Ni Perminvar, mag. props. singularities in region of mag. anisotropy (Russian) 0-84614
 Fe-Co-Ni-C, activity coeff. of C at 1273K 0-96667
 Fe-Co-Si-B, amorphous soft ferromagnet with high mag. induction 0-84619
 Fe-Co-Si-B, zero magnetostrictive amorphous alloy with high saturation induction, mag. annealing 0-60362

iron alloys continued

- Fe-Co-Si(B), amorphous ferromagnet, mag. after effect on soft mag. props. 0-84626
 Fe-Co-Ti-Al alloy type YuNDK magnets, metallographic method of distinguishing cracks 0-85096
 Fe-Co-Ti(V)(Cr)(Mn), sp. ht. in ordered and disordered phases 0-71061
 Fe-Co-V(Ni), annealing effect on microstruct. rel. to mag. and mech. props. 0-89267
 Fe-Co-2 V, (49, 2 wt.%), solid soln., rheological study of crystallographic order on creep (*French*) 0-97548
 Fe-Cr, BCC, local moments in Mossbauer study 0-108125
 Fe-Cr, crystallisation temp., overcooling temp. (*Russian*) 0-97472
 Fe-Cr, dil., spin density wave under high press., neutron diffr. study 0-65798
 Fe-Cr, high-temp. oxidation, borate inhibitors 0-66705
 Fe-Cr, hyperfine magnetic fields, Mossbauer spectra 0-97165
 Fe-Cr, influence of annealing on hyperfine interaction parameters, Mossbauer effect 0-71263
 Fe-Cr, random ferromag. alloys, local mag. moment calc. 0-70974
 Fe-Cr, specific heat enhancement and electron-phonon interaction 0-65242
 Fe-Cr (12 wt.%), corrosion in o-phosphoric acid 0-97622
 Fe-Cr (9 wt.%), extrinsic grain boundary dislocations, low C content influence 0-107273
 Fe-Cr (9 wt.%), oxidation studied using $C^{18}O_2$ and D_2O tracers 0-71784
 Fe-Cr alloy, N solubility investigation (*Russian*) 0-92675
 Fe-Cr alloy, sputter etching oxide film, comp. profile, quantitative AES 0-81383
 Fe-Cr alloys, cold worked, internal friction due to H (*Japanese*) 0-70305
 Fe-Cr alloys, in acid and neutral solns., thickness and optical constants of passive and transpassive films 0-66698
 Fe-Cr-Al, HOS 875, oxidation, cyclic, role of thermal shock 0-97640
 Fe-Cr-Al, Kanthal films, vac. deposited, evaporation characts., comp., struct. and elec. props. 0-88646
 Fe-Cr-Al, scales, $\alpha-Al_2O_3$, early stages development at high temp. 0-89413
 Fe-Cr-Al (12, 3 wt.%), internal friction and rigidity modulus, strain amplitude depend. (*Japanese*) 0-92606
 Fe-Cr-Al (7, 5 wt.%), expt. stainless alloys, phys. and mech. props. 0-97637
 Fe-Cr-Al-Y, oxidation resistance, heat treatment and Al^+ ion implantation 0-71785
 Fe-Cr-Al-Y, scales, $\alpha-Al_2O_3$, early stages development at high temp. 0-89413
 Fe-Cr-Co, ductile magnet alloys, mech. props. 0-85001
 Fe-Cr-Co, elastic props. anisotropy at room temp. (*Russian*) 0-89279
 Fe-Cr-Co, magnetic domain walls, Lorentz microscopy 0-103854
 Fe-Cr-Co, metallic magnets investigation, present state (*Polish*) 0-107987
 Fe-Cr-Co (28, 10.5 wt.%) ductile magnet alloy, humidity-induced H_2 embrittlement 0-89406
 Fe-Cr-Co alloy, coercive force mechanism 0-71103
 Fe-Cr-Co alloy, spinodally decomposed, micro-twinning 0-92537
 Fe-Cr-Co alloys, (5-9 wt.% Co), obtained by slow cooling under mag. field, permanent magnet props. 0-75797
 Fe-Cr-Co permanent magnet system, miscibility gap, microstruct. and mag. props. obs. 0-76228
 Fe-Cr-Co-Mo high energy permanent magnets, mag. props. 0-97119
 Fe-Cr-Mo, white cast, optimising fracture toughness and abrasion resist. 0-85042
 Fe-Cr-Mo alloy castings, thick-section, factors affecting 0-108374
 Fe-Cr-Mo and Fe-Cr-Mo-Si, amorphous films, corrosion resist. and ion plating use 0-89423
 Fe-Cr-Ni, corrosion behaviour in hot conc. NaOH soln. (*Japanese*) 0-85082
 Fe-Cr-Ni, foil, in situ oxidation in HVEM 0-104354
 Fe-Cr-Ni (12, 15 wt.%) austenitic alloy, Ni^{6+} irradiated, void swelling and phase stability, Si and Ti effects 0-65055
 Fe-Cr-Ni (18, 14 wt.%), γ to ϵ to α martensitic transform., external stress effect, double tensile deform. exam. 0-108438
 Fe-Cr-Ni (19, 13 wt.%), austenitic, Ni^{1+} ion irradiated, multiple dislocation loops (*French*) 0-65064
 Fe-Cr-Ni based alloys, surface oxides at high temps., backscattering Raman spectroscopy 0-93291
 Fe-Cr-O system, phase relations at 1200°C using diffusion couple technique 0-89205
 Fe-Cr-Si, heat resistive films prepared by sputtering, lifetime meas. 0-80132
 Fe-Cr-Si, oxidation resist. in high pressure CO_2 , Si effect 0-66704
 Fe-Cr-Ti (18, 0.1-0.9 wt.%), high temp. oxidation (*Japanese*) 0-71806
 Fe-Cr-Ti-Mo- TiO_2 (13, 3.5, 1.5, 2 wt.%) dispersion hardened, void swelling 0-65046
 Fe-Cr-Ti(Al) liquid alloy, thermodynamical anal. of O_2 solubility (*Russian*) 0-92676
 Fe-Cr(W)-M, (M=Si, Mo, Ni, Mn, P, Cr), cellular growth of S-pearlite formed by carburisation 0-108486
 Fe-Cu, lath martensite habit planes, TEM study 0-84942
 Fe-Cu (4.54 wt.%) alloy, scaling behaviour, 700-1000°C, 1 atm. O_2 0-93679
 Fe-Cu liquid alloy, heats of mixing, mixing entropies (*Russian*) 0-65224
 Fe-Cu-C, phase equilibria, 950 to 1500°C 0-60836
 Fe-Cu-C sintered porous materials, machinability 0-66457
 Fe-Cu-Zn, high-temperature phase diagrams (*German*) 0-108390
 Fe-Gd film, magneto-optic coeff. and refr. index, ellipsometric determ. 0-71501
 Fe-Ge, amorphous, atomic struct., neutron diffr. study 0-59392
 Fe-M, (M=Cr, W, Mo, V, Ti), morphology and growth kinetics of δ -pearlite formed by carburisation 0-108485
 Fe-M, dil., M=transition metal, impurity electronic struct., multiple scatt. approach 0-92856
 Fe-M-(I) (M=Ni, Cr, V, Ti, Mo; I=Sb, P), co-segregation at free surfaces studied by Auger spectroscopy 0-59767
 Fe-Mn, as cast, pseudo-composite struct. resulting from interdendritic segregation, cryogenic materials appl. (*French*) 0-93556
 Fe-Mn, ϵ -martensite, preferred orientation and constitution, reverse pole figures (*Russian*) 0-104178
 Fe-Mn, mechanical twinning of close-packed hexagonal ϵ -phase during plastic deform. (*Russian*) 0-60909
 Fe-Mn (0.5 wt.%), Burgers vector of dislocation determ. by weak-beam image in HVEM 0-103351
 Fe-Mn (1 at.%), strain age hardening 0-108472

iron alloys continued

- Fe-Mn cast alloys, homogenisation annealing and chemical diffusion (*Czech*) 0-66551
 Fe-Mn-B, B effect on intergranular embrittlement 0-108555
 Fe-Mn-C, struct. superplasticity 0-76317
 Fe-Mn-Ni-V-C (0.5, 3.0, 1.0, 0.2 wt.%), austenite decomp., isothermal transform. characts. 0-97477
 Fe-Mn-V-C (0.5, 1.0, 0.2 wt.%), austenite decomp., isothermal transform. characts. 0-97477
 Fe-Mn-Zn, high-temperature phase diagram (*German*) 0-108390
 Fe-Mo (13-20 at.%) binary alloys, spinodal decomp. on ageing, TEM and X-ray diffr. study 0-97503
 Fe-Mo system, thermoelec. props. 0-89208
 Fe-Mo-B metallic glass ribbons, tensile strength, crystn. temp. 0-89173
 Fe-Mo-C (0 to 4, 1 wt.%), phase equilibria at 1143, 1198 and 1253K 0-60835
 Fe-Mo-CaF₂ sintered composite, struct. and mech. props., heat treatment effect 0-66526
 Fe-Mo-Ta, ternary Laves phase strengthening 0-108466
 Fe-Mo (4.1 wt.%), steady state creep at high temps. 0-89316
 Fe-MuS eutectics, unidirectional solidification (*German*) 0-100827
 Fe-N, single cryst., solid soln. softening, effect of interstitial N 0-97496
 α -Fe-N, supersaturated solid solns., N atom precip. kinetics, resist. meas. 0-60864
 Fe-N alloys, secondary ion emission, phase transforms. effect (*Russian*) 0-66347
 Fe-N single crystals, plastic deform. in temp. range 4.2 to 300K 0-76321
 Fe-Nb-V-C-N, equilibrium comp. and solubility in steels, model of ideal solns. (*Russian*) 0-60832
 Fe-Ni, crystallisation temp., overcooling temp. (*Russian*) 0-97472
 Fe-Ni, dilute, irradiation softening effect on yield stress 0-76319
 Fe-Ni, electronic struct. calc., effects of chemisorption; contact pot. and surface magnetisation 0-103734
 Fe-Ni, clinvac comp., props. of materials used in electromechanical filter resonators (*Czech*) 0-76318
 Fe-Ni, grain boundary segregation, X-ray microanal. by STEM 0-66740
 Fe-Ni, Hall effect, anomalous, residual coeff. calcs. using coherent pot. method (*Russian*) 0-80249
 Fe-Ni, interference microscopy, for colour development and phase separation 0-100976
 Fe-Ni, lenticular martensite growth by transformation wave propag. 0-81055
 γ -Fe-Ni, local magnetisation of Fe atoms, Mossbauer effect meas. 0-75891
 Fe-Ni, magnetisation calc. method based on moments of density of states 0-65770
 Fe-Ni, reverse martensitic transform., shape deform. reversibility 0-66506
 Fe-Ni, secondary recrystallisation singularities (*Russian*) 0-66528
 Fe-Ni, secondary recrystn. and mag. props. 0-89247
 Fe-Ni, sintered, porosity determ. by US attenuation and sound vel. meas. (*German*) 0-76437
 Fe-Ni (25 to 50%), FCC, meteorites and thermodynamic equilb., Mossbauer and X-ray diffr. study 0-88087
 Fe-Ni (28 at.%), martensitic transformations, Mossbauer scattering evidence of soft modes 0-93223
 α -Fe-Ni (3-12 wt.%), structure and γ - α polymorphic transform. kinetics 0-71645
 Fe-Ni (32 wt.%), EMF appearance during γ - α transform. (*Russian*) 0-89215
 Fe-Ni (32.3 at.%), mag. struct. in commensurate approx., neutron diffr. study 0-60212
 Fe-Ni (33-38 at.%), low-angle neutron diffr., anomalous crit. scatt. (*Russian*) 0-60193
 Fe-Ni (4 wt.%), extrinsic grain boundary dislocations, low C content influence 0-107273
 Fe-Ni (50 wt.%), surface comp. and oxide film thickness after various surface treatments, AES study 0-66693
 Fe-Ni (6-8 wt.%), solution of ^{119}Sn , study by Mossbauer spectroscopy 0-75888
 Fe-Ni alloy, martensitic transform., influence of thermal and electron irradi. treatment of austenite (*Russian*) 0-66509
 Fe-Ni alloy type YuNDK25B, anomalous magnetocaloric effect 0-60278
 Fe-Ni alloys, heat treatment variations effect on surface conditions and on Hg wetted switch behaviour 0-66547
 Fe-Ni based metallic glass, Metglas 2826 MB, Mossbauer study 0-75897
 Fe-Ni film, amorphous, martensite form. time and struct. 0-104159
 Fe-Ni films, on glass substrate, thermoelec. effect 0-107769
 Fe-Ni fluorination kinetics and fluoride film form., chem. nature obs. 0-101035
 Fe-Ni Metglas type, ohmic and Hall resist., 100-700K, mag. behaviour obs. 0-80254
 Fe-Ni-Al-Co-Cu-Ti YuNDK type, S effect on mech. props. 0-60927
 Fe-Ni-Al-(Cu) (12, 0.5, 0.5 to 3 wt.%), Cu addition strengthening at 77K, mech. props. 0-60875
 Fe-Ni-B glassy ribbons melt spinning, gas boundary layer effects 0-76217
 Fe-Ni-B metallic glass, X-ray diffr. meas., semi-empirical struct. model 0-107059
 Fe-Ni-B-Mo, crystn. temp. and elec. cond. correl., Mo effect 0-75179
 Fe-Ni-B-Si, amorphous, mag. props., heat treatment effects 0-89370
 Fe-Ni-B-(P), ferromag., magneto-optical spectra in amorphous and cryst. states (*Russian*) 0-84749
 Fe-Ni-B(P), amorphous, crystn. 0-79704
 Fe-Ni-C, intercrystalline embrittlement in tempered martensite, elimination by reautenitization (*Slovak*) 0-108548
 Fe-Ni-C, quenched martensite, annealing during cathodic hydrogenation, 200°C (*French*) 0-93573
 Fe-Ni-C (25, 0.2 wt.%), strain-induced martensite (*Korean*) 0-71646
 Fe-Ni-C (30, 0.5 wt.%) single cryst., stress induced martensitic transform. 0-60860
 Fe-Ni-C (31.9, 0.02 wt.%) alloy, hardness of martensite-austenite mixtures 0-60959
 Fe-Ni-C (31.9, 0.02 wt.%), determ. of number and size distrib. of martensitic plates 0-76255
 Fe-Ni-C alloy with single-component martensite texture, α - γ transform., changes in shape (*Russian*) 0-104152
 Fe-Ni-C austenitic alloy, banded struct. formed by deform. 0-71713
 Fe-Ni-C martensite morphology, butterfly-lenticular transition temp., Cr addition effect (*Japanese*) 0-81053

iron alloys continued

- Fe-Ni-Co-Cu-Ti YuNDKT alloys, impaired mag. props. with C and S additions 0-60368
- Fe-Ni-Co-Ti, coherent particles effect inherited by martensite on $\alpha \rightarrow \gamma$ transformation (*Russian*) 0-108443
- Fe-Ni-Co-W(Mo) (18.65, 8.99, 4.87 wt.%), ageing charact., 380-530°C 0-60876
- Fe-Ni-Cr, carbide form. by C diffusion, precip. distrib. and morphology 0-104164
- Fe-Ni-Cr, heavy ion irradiat., defect cluster obs. 0-107341
- Fe-Ni-Cr, mag. props. in weak mag. fields (*Russian*) 0-75771
- Fe-Ni-Cr (30.6, 21.3 wt.%), Alloy 800, high temp. oxidation at low O₂ press., SEM, AES and electron probe microanal. study 0-93688
- Fe-Ni-Cr (35, 15 wt.%) superalloy, stress rupture and tensile props., C and B additions effect (*Chinese*) 0-104244
- Fe-Ni-Cr (44, 17 wt.%), nuclear microprobe methods for investigating oxidative corrosion 0-71787
- Fe-Ni-Cr based alloy, KhN35VTYu, temp. depend. of energy of fracture, influence of γ' phase (*Russian*) 0-81147
- Fe-Ni-Cr-Al-Ti-W-Mo (35, 15, 2.4, 2.3, 2.2 wt.%) wrought superalloy, freckles (*Chinese*) 0-104137
- Fe-Ni-Cr-Al-Y, oxidation mechanism, Y addition effect on kinetics and oxide adherence 0-97623
- Fe-Ni-Cr-Ti-Al, with thermoelastic control coeff., comp. and heat treatment influence on props. (*French*) 0-81074
- Fe-Ni-Cr-Y, Y addition effect on selective oxidation/diffusion phenomena relationship (*French*) 0-108623
- Fe-Ni-Mn (20, 5 wt.%), rel. orientation between adjacent martensite laths 0-76254
- γ -Fe-Ni-Mn alloys, spin glass state, short and long range order investigation 0-65808
- Fe-Ni-Mo, martensitic transformation, annealing, influence on struct. of austenite (*Russian*) 0-81057
- Fe-Ni-Mo, phase relations in system at 1100°C 0-108392
- Fe-Ni-Mo-C, amorphous alloys, med. props. and thermal stability (*Japanese*) 0-85049
- Fe-Ni-Mo(Si), austenite, annealing effect on atom redistrib., Mossbauer anal. (*Russian*) 0-66529
- Fe-Ni-P-B, amorphous, crystn. and struct. 0-75175
- Fe-Ni-P-B, metallic glasses, struct. relax., annealing effects on mag. props. 0-89261
- Fe-Ni-P-B amorphous ribbons, form. by melt spin technique 0-76215
- Fe-Ni-P-B metallic glass, crystallisation temperature values from isothermal transformation times 0-59397
- Fe-Ni-Ti, preaged martensite, shear strain magnitude, X-ray diffr. method 0-93592
- Fe-Ni-Ti-(Cu) (12, 0.25, 2 wt.%), Cu addition strengthening at 77K, mech. props. 0-60875
- Fe-Ni-V-(Cu) (12, 2, 2 wt.%), Cu addition strengthening at 77K, mech. props. 0-60875
- Fe-Ni-(Cu) (12, 0.5 to 3 wt.%), Cu addition strengthening at 77K, mech. props. 0-60875
- Fe-Ni-(P), phase diagram determ., 700 to 300°C 0-108399
- Fe-Ni(Al), mag. aftereffect meas., phenomenological description 0-88835
- Fe-P, amorphous, anomalous thermal expansion, ΔE effect, Invar and Elinvar charact., delay time 0-80589
- Fe-P electrodeposited foil, amorphous, mag. domains 0-75821
- Fe-P-C, amorphous, crystn. and struct. 0-75175
- Fe-P(Ga)(As)(Sb), dil., short range order, NMR study 0-71237
- Fe-Pd, magnetic after-effect of H isotopes 0-75817
- Fe-Pd (1-2 wt.%), solution of ¹¹⁹Sn, study by Mossbauer spectroscopy 0-75888
- Fe-Pd (31.2 wt.%), thermoelastic FCC-FCT martensitic transformation 0-104156
- Fe-Pt (Ni), itinerant electron ferromagnet, magnetovolume effects 0-60397
- Fe-Sb amorphous films, Mossbauer effect study 0-75896
- Fe-Sb-Ni(Cr), dil., short range order, NMR study 0-71237
- Fe-Sb-Ti(V)(Cr)(Mn)(Co)(Ni), interactions and segregations, Mossbauer and X-ray diffr. study 0-70415
- Fe-Si, (110) [001] oriented, mag. props., compressive stress effects 0-60392
- Fe-Si, dilute, irradiation softening effect on yield stress 0-76319
- Fe-Si, fatigue fracture fractography in broad strain-amplitude range, in air and vacuum 0-81186
- Fe-Si, grain oriented, misorientation effects on mag. props 0-88792
- Fe-Si, grain oriented, phosphate coating anal. by IR spectroscopy 0-89570
- Fe-Si, grain oriented sheet, grain struct. by computer mapping 0-88168
- Fe-Si, grain oriented sheet, AC hysteresis, surface struct. and elastic stress effects 0-88791
- Fe-Si, grain oriented transformer sheets, permeability and magnetostriction, tensile stress effects 0-88843
- Fe-Si, grain-oriented sheets, high permeability, low losses, review 0-88790
- Fe-Si, loss meas. at high flux densities 0-88799
- Fe-Si, mag. props., stress and reannealing effects 0-88844
- Fe-Si, microflow and strain hardening under cyclic loading 0-104182
- Fe-Si, non-oriented sheets, production and props. 0-88797
- Fe-Si, power loss and permeability meas. by means of Hall probes and stochastic ergodic correl. 0-86350
- Fe-Si, rapid cracks self-arrest potential, -196.0°C 0-100911
- Fe-Si, single cryst., mag. domain wall motion, X-ray topography study 0-65953
- Fe-Si, spreading behaviour of liq. Al 0-84345
- Fe-Si, stator core, grain-oriented and non-oriented, magnetic flux and loss distrib. 0-88798
- Fe-Si, transformer steel, high-temp. heat treatment, resist. of refractories in contact 0-66554
- Fe-Si (2-8 wt.%), single crystals, growth striations, X-ray studies 0-79774
- Fe-Si (2.6 wt.%) single cryst., crack propag., controlled plastic crack tip opening rate 0-60943
- Fe-Si (3 at%), deformation and electron bombardment, influence on dislocation struct., 20-500°C (*Russian*) 0-92536
- Fe-Si (3 to 5 wt.%) sinters, mag. props., Si and Fe-Si additions effect 0-71104
- Fe-Si (3 wt.%), behaviour of disperse inclusions, influence of recrystn. processes (*Russian*) 0-66519
- Fe-Si (3 wt.%), domain wall spacing and core loss, forsterite and stress coatings effect 0-88780

iron alloys continued

- Fe-Si (3 wt.%), electron irradiated, yield strength and elongation 0-76325
- Fe-Si (3 wt.%), ferromag. domains, imaging by neutron interferometry 0-71087
- Fe-Si (3 wt.%), grain oriented, mag. props., effect of decarburizing (*Chinese*) 0-103821
- Fe-Si (3 wt.%), grain-oriented, domain struct. regulation and power loss reduction 0-88779
- Fe-Si (3 wt.%), grain-oriented, domain wall profiles throughout magnetisation cycle 0-88781
- Fe-Si (3 wt.%), grain-oriented, stacking effect on power loss, mag. props. 0-88795
- Fe-Si (3 wt.%), grain-oriented, power loss and domain wall variation with lamination thickness 0-88814
- Fe-Si (3 wt.%), grain-oriented, energy loss reduction by lowering sheet thickness 0-88816
- Fe-Si (3 wt.%), high permeability, use in transformer cores 0-88793
- Fe-Si (3 wt.%), internal friction, instantaneous, depend. on phase of torsional oscils. (*Russian*) 0-71142
- Fe-Si (3 wt.%), losses, demagnetisation freq. and grain orientation depend. 0-88796
- Fe-Si (3 wt.%), mag. anisotropy induced by cold rolling (*Russian*) 0-84595
- Fe-Si (3 wt.%), mag. domain wall contrast in synchrotron X-ray topographs 0-75792
- Fe-Si (3 wt.%), mag. loss and magnetostriction, DC flux alternation effects 0-88794
- Fe-Si (3 wt.%), magnetisation variation during bending oscils., rel. to ΔE effect (*Russian*) 0-65983
- Fe-Si (3 wt.%), nonoriented sheets, magnetisation, tensile stress effects 0-88845
- Fe-Si (3 wt.%), oriented, losses and domains, mech. stress effects 0-88852
- Fe-Si (3 wt.%), power losses at extremely low freqs. 0-88815
- Fe-Si (3 wt.%), stripe domain structure, dynamic behaviour at high max. induction values (*Russian*) 0-80553
- Fe-Si (3 wt.%), struct. and preferred orientation, annealing parameters influence (*Czech*) 0-89248
- Fe-Si (3 wt.%), texture, Mossbauer expts. 0-71262
- Fe-Si (3 wt.%) high-permeability grain-oriented steel, quenching effect on primary recrystn. texture development 0-84956
- Fe-Si (3 wt.%) laminations, magnetostriction behaviour associated with closure domain spikes 0-75834
- Fe-Si (3 wt.%) laminations, grain oriented, plastically deformed, anomalous losses 0-88853
- Fe-Si (3.25 wt.%), single cryst. with (007) planes, domain struct. influence on mag. torque 0-108034
- Fe-Si (3wt.%), grain-oriented, secondary recryst., grain growth inhibition 0-89245
- Fe-Si (6.5 wt.%) filament, formation by modified Taylor technique, and mag. props. 0-75795
- Fe-Si (6.5 wt.%) ribbon, splat-cooled, mag. props. 0-88805
- Fe-Si cast alloy with spheroidal graphite, transform. investigation during tempering (*Russian*) 0-97479
- Fe-Si gas-flame spray deposited protective coating, for C steel heat exchanger 0-61025
- Fe-Si system, melting equilibria study (*German*) 0-66473
- Fe-Si-Al, Sendust, ribbon-form, prep. by rapid quenching, mech. and mag. props. 0-71611
- Fe-Si-Al, surface oxide layer struct., AES study 0-89396
- Fe-Si-Al (2.8-3.4, 0-0.86 wt.%) oxidation, annealing 0-89395
- Fe-Si-Al (9.6, 5.4 wt.%), ribbon-form Sendust alloy, mag. props., annealing effects 0-88800
- Fe-Si-Al ribbon-form Sendust alloy made by rapid roll quenching, mag. props., recording head appls. 0-81001
- Fe-Si-B, high induction, hot rolling treatment 0-89266
- Fe-Si-B, magnetic metallic glasses, mag. props. 0-84620
- Fe-Si-B amorphous alloys, Mossbauer spectroscopy (*French*) 0-80653
- Fe-Si-B glassy alloys, mag. props., comp. effects 0-88752
- Fe-Si-C, austenitic, C diffusivity (*German*) 0-92705
- Fe-Si-C mixed powder, cast Fe powder sintering study (*Japanese*) 0-108373
- Fe-Si-Cr magnetic films, sputtered, corrosion reduction, effect of Cr obs. 0-80573
- Fe-Si-Zn, influence of trace elements on morphology (*German*) 0-108390
- Fe-Ta, nuclear mag. moment of ¹⁸²Ta NMR-ON study 0-78139
- Fe-Tb, magnetoelastic hysteresis, elastic stress and mag. field depend. (*Russian*) 0-65982
- Fe-Tb film, magneto-optic coeff. and refr. index, ellipsometric determ. 0-71501
- α -Fe-Ti, ion implanted, microstruct., ion beam anal. and TEM study 0-107294
- α -Fe-Ti, ion implanted, with C impurity, microstruct. of TiC precip. 0-66513
- Fe-Ti, magnetism and H₂ storage 0-70941
- Fe-Ti, solubility and diffusivity of H and D in mixed crystal phase, elec. cond. meas. (*German*) 0-107575
- Fe-Ti, Ti as H trap for embrittlement control 0-66662
- Fe-Ti (V)(W), dil., thermophysical props. and elec. cond., temp. depend. 0-96842
- Fe-Ti (0.15 wt.%), Ti distrib., segregation, FIM anal. 0-84200
- Fe-Ti-C, rapidly quenched by splat-cooling 0-84923
- Fe-Ti-V-C-N, equilibrium comp. and solubility in steels, model of ideal solns. (*Russian*) 0-60832
- Fe-TiC pseudofused composite magnetoabrasive powders, props. 0-100926
- Fe-V, ⁵⁹Fe self-diffusion (*Czech*) 0-88352
- Fe-V, dilute, irradiation softening effect on yield stress 0-76319
- Fe-V, ferromag. struct. in nucl. spin echoes 0-60453
- Fe-W, Gibbs energy of form. of phases (*German*) 0-97724
- Fe-W-Cr-Mo system, mag. and mech. props. rel. to production methods (*Japanese*) 0-71107
- Fe-X-C (X=Cr, Mo, W), quenched rapidly from melts, nonequilib. phases (*Japanese*) 0-71630
- Fe-Zn, coercive force anisotropy after cold plastic deform. (*Bulgarian*) 0-75809
- Fe-Zn, galvanization study (*French*) 0-66447
- Fe-Zn, homogeneous phases, Gibbs free energies of form., Knudsen effusion method 0-66481
- Fe-Zn, physical-chemical metallurgy (*German*) 0-108390

iron alloys continued

- Fe-Zn, quenched, martensite struct. and hardness, electron microscope exam. (*Russian*) 0-66619
- Fe-Zr, amorphous phase form. in Zr-poor region, hardness and fracture strength (*Japanese*) 0-84914
- Fe₂-Al, solid soln., rheological study of crystallographic order on creep (*French*) 0-97548
- (Fe-Ni-Mo)₈₀(P-B)₂₀, amorphous, mag. aftereffects and struct. instabilities 0-88833
- Fe₂Al, alloys, superlattice-fringe imaging theory, images formed from two beams 0-79649
- Fe₂Al, electrical resistivity and LRO, energy gap formation in Fermi surface 0-88533
- Fe₂Al, electronic structure, X-ray spectra comparison with band struct. calcs. 0-97383
- Fe₂Al, electronic structure, magnetic moments 0-107695
- Fe_{1-x}B_x, amorphous, hyperfine fields and local mag. moments, Mossbauer study 0-75895
- Fe_{100-x}B_x, amorphous, mag. saturation, spin wave stiffness, temp. depend. 0-75741
- Fe_{100-x}B_x, amorphous, mag. struct., mag. susceptibility meas. 0-80485
- Fe₇₅ metallic glass, nonisothermal meas. evaluation, non-existence of dynamic correction term 0-107406
- Fe₈₀B₂₀, amorphous, Brillouin scatt. from magnons, ferromag. reson. 0-65844
- Fe₈₀B₂₀, amorphous, cold neutron scatt., local and extended defects 0-84089
- Fe₈₀B₂₀, amorphous, crystn. 0-75187
- Fe₈₀B₂₀, amorphous, mag. permeability aftereffect during annealing 0-88834
- Fe₈₀B₂₀, amorphous ferromagnet, Mossbauer hyperfine fields, mag. struct. 0-75894
- Fe₈₀B₂₀, amorphous ribbon, initial susceptibility time lag 0-100579
- Fe₈₀B₂₀, amorphous struct., Mossbauer spectroscopy investigation 0-84677
- Fe₈₀B₂₀, amorphous wire, crystn. by annealing at 780°C 0-100177
- Fe₈₀B₂₀ film, amorphous metallic, standing spin waves, Brillouin scatt. obs. 0-97291
- Fe₈₀B₂₀ glass, magnetisation reorientation, Mossbauer effect 0-66092
- Fe₈₀B₂₀, metallic glass, Doppler broadening of positron annihilation γ -radiation and elec. resist. 0-66321
- Fe₈₀B₂₀ metallic glass, crystn. and struct. relax., Mossbauer effect study 0-75182
- Fe₈₀B₂₀ metallic glass, crystn. kinetics 0-84083
- Fe₈₀B₂₀, metallic glass, optical and magneto-optical props. 0-84728
- Fe₈₀B₂₀, metallic glasses, stability and transforms. 0-75174
- Fe₈₀B₂₀, Metglas 2605, amorphous ribbon, power loss variation with freq. and applied stress 0-88849
- Fe₈₀B₂₀, Metglas 2605, Young's modulus meas. using piezoelectric US composite oscillator technique 0-108656
- Fe_{83.4}Fe_{16.6}, amorphous, mag. props. and microstruct., cooling rate and melt overheating effects 0-65965
- Fe_{83.4}Fe_{16.6}, amorphous, mag. props., melt overheating and cooling rate effects 0-89371
- Fe₈₄B₁₆, metallic glass, electrical resistivity and crystallisation 0-88526
- Fe₈₄B₁₆, metallic glass, ion implanted, UPS meas. 0-97411
- Fe₈₄B_{16-x}C_x, amorphous, mag. saturation, spin wave stiffness, temp. depend. 0-75741
- Fe₈₀B_{20-x}Ge_x, amorphous, mag. saturation, spin wave stiffness, temp. depend. 0-75741
- Fe₈₀B₄₀P₁₄B₆, Metglas 2826, amorphous ribbon, power loss variation with freq. and applied stress 0-88849
- Fe₈₀B_{20-x}Si_x, amorphous, mag. saturation, spin wave stiffness, temp. depend. 0-75741
- Fe₈₄B₁₃Si₃, metallic glass, electrical resistivity and crystallisation 0-88526
- Fe₈₀(C_{1-x}B_x)₂₀, amorphous alloy, α -Fe crystn., morphology 0-70129
- FeCo, ferromag., surface spin waves, cluster Bethe lattice approach 0-70983
- FeCo, planar faults, faint electron microscopic image contrast obs. 0-107283
- Fe_{1-x}Co_xAl, site preference and local environment effects, Mossbauer and NMR meas. 0-71264
- (Fe_{0.5}Co_{0.5})_{1-x}B_x, amorphous, hyperfine fields and local mag. moments, Mossbauer study 0-75895
- Fe₂Co₇B₂₀, amorphous, magnetisation reversal and domain boundary configs. 0-88809
- Fe₃Co₂B₂₀Si₁₀Al₁, stress-induced variation in magnetisation and dynamic magnetostrictive charact. 0-88855
- Fe_{0.5}Co_{0.5-x}Cr_x films, vacuum-deposited cryst. and mag. struct. (*Russian*) 0-93081
- (Fe_{0.9}Co_{0.93})_{75-x}Cr_xSi₁₀B₁₀, amorphous, disaccommodation of mag. permeability and induced anisotropy 0-88741
- (Fe_{0.95}Co_{0.95})₇₅Si₈B₁₄, amorphous ribbon, anomalous mag. aftereffect 0-100602
- (Fe_{1-x}Co_x)₇₅Si₁₀B₁₂, amorphous, roll mag. anisotropy 0-75757
- (Fe₂Co_{1-x})₇₅Si₈B₁₄, amorphous, saturation magnetostriction, strain modulated FMR obs. 0-75863
- Fe₂Cr_{1-x}, spin-wave evolution crossing from ferromag. to spin-glass regime 0-97080
- Fe₈Cr₂Ni₄B₁₂B₈, amorphous X-ray absorpt. spectra, effective co-ordination charges 0-84805
- (Fe₈Cr₂)₇₉P₁B₈ and (Fe₈Cr₄)₇₉P₁₃B₈, amorphous, low temp. sp. ht., mag. contribs. 0-80552
- Fe₂Ga, L₁, ordered alloy, positive temp. depend. on strength, phase destabilization 0-81203
- FeGe₂, antiferromag., Fermi surface, stress effects, oscillatory magnetostriiction and torque meas. 0-103616
- β -Fe₂Ge₃ formation in isothermal sintering, phase transition kinetics 0-89197
- Fe_{83-x}M_xB₁₇ and Fe_{78-x}M_xSi₁₀B₁₂ (M=refractory metal), glass form. and thermal stability 0-79703
- Fe_{3-x}Mn_xAl, ordering of Fe atoms, X-ray diff. meas. and mid gamma reson. anal. (*Russian*) 0-96469
- Fe_{1-x}Mn_xSn, spin reorientation, Mossbauer study, 77 to 400K 0-97172
- Fe₄₉Mn_{0.1}Ti_{0.1}H₂, localised vibrs., sp. ht. obs., room temp. 0-65248
- (Fe_{1-x}Mn_x)₂Y(B), Mn effect on Fe mag. moments, Mossbauer and mag. meas. 0-71016
- Fe₇₈Mo₂B₂₀, amorphous ribbons, magnetoelastic effects in as-quenched and stress-relieved states 0-80588
- Fe₇₈Mo₂B₂₀, metallic glass, Doppler broadening of positron annihilation γ -radiation and elec. resist. 0-66321

iron alloys continued

- Fe₂N growth kinetics in Fe-N system (*Korean*) 0-93540
- FeNi amorphous films, fast phase transition investigation by TEM method 0-107029
- (Fe_{0.5}Ni_{0.5})_{100-x}B_x and (Fe_{100-x}Ni_x)₈₀B₂₀ amorphous alloys, X-ray diff. struct. determ. 0-64906
- (Fe_{1-x}Ni_x)₈₃B₁₇, amorphous alloys ferromagnetic resonance 0-108080
- (Fe_{100-x}Ni_x)₈₃B₁₇, amorphous, crystn. 0-75176
- Fe₄₀Ni₄₀B₂₀, amorphous, phase transforms., resistometric anal. 0-75538
- Fe₄₀Ni₄₀B₂₀, amorphous, RF annealing effects 0-108037
- Fe₄₀Ni₄₀B₂₀, amorphous ribbon, power loss variation with freq. and applied stress 0-88849
- Fe₄₀Ni₄₀B₂₀ and Fe₄₀Ni₄₀P₁₄B₆, amorphous, mag. aftereffect spectra and annealing props. 0-88831
- Fe_{80-x}Ni_xB₂₀ and Fe_{80-x}Ni_xP₁₄B₆ amorphous alloys, microhardness correl. with mag. props. 0-88826
- Fe₂Ni_{80-x}B₂₀ and Fe₂Ni_{80-x}P₁₄B₆ metallic glasses, low temp. resist. and galvanomag. effects, mag. state influence 0-84461
- Fe₂Ni_{80-x}B₂₀ glass, resist., magnetoresist., and thermoelec. power 0-70681
- (Fe_{1-x}Ni_x)₈₀B_{20-x}P_x, amorphous, hyperfine fields and local mag. moments, Mossbauer study 0-75895
- Fe₁₆Ni_{78.4}B₁₀P₁₀ metallic glass, superparamag. behaviour, chem. inhomogeneities role 0-84625
- Fe₄₀Ni₄₀B_{20-x}P_x, amorphous, mag. saturation, spin wave stiffness, temp. depend. 0-75741
- Fe₄₀Ni₄₀B_{20-x}P_x metallic glasses, local struct. and dynamic disorder of Fe and Ni, EXAFS obs. 0-89088
- Fe_{80-x}Ni_xB_{20-y}P_y, amorphous, Rayleigh region and coercive force 0-88806
- (FeNi)₈₀Bi_{17.5}Al₂Si_{0.5}, stress-induced variation in magnetisation and dynamic magnetostrictive charact. 0-88855
- Fe₃₂Ni₃₆Cr₁₄P₁₂B₆, metallic glass, Doppler broadening of positron annihilation γ -radiation and elec. resist. 0-66321
- Fe₃₂Ni₃₆Cr₁₄P₁₂B₆ metallic glasses, crystn. kinetics by TEM 0-75186
- Fe₃₂Ni₃₆Cr₁₄P₁₂B₆, Metglas 2826A, EPR at 20 GHz 0-75848
- Fe₃₂Ni₃₆Cr₁₄P₁₂B₆, Metglas, bending deform., shear band form., high-speed cinematographic obs. 0-89322
- Fe₃₂Ni₃₆Cr₁₄P₁₂B₆, Metglas amorphous films, corrosion resist. and ion plating use 0-89423
- Fe₃₂Ni₃₆Cr₁₄P₁₂B₆ metallic glass, effect of pre-ageing on glass transition temp. 0-100326
- Fe₆₅Ni₂₈Mn₁, disordered, mag. struct. near ferro-antiferromagnetic transition 0-60211
- Fe₄₀Ni₄₀(Mo,Si,B)₂₀, amorphous, soft mag. props., switched-mode power supply appls. 0-88850
- Fe₄₀Ni₃₈Mo₄B₁₈ amorphous ribbons, magnetoelastic effects in as-quenched and stress-relieved states 0-80588
- Fe₄₀Ni₃₈Mo₄B₁₈, amorphous, mag. anisotropy, Mossbauer study 0-65864
- Fe₄₀Ni₃₈Mo₄B₁₈, amorphous, reversible enhancement of mag. directional ordering rate 0-103829
- (Fe_{1-x}Ni_x)₈₀P₂₀, amorphous, ferromagnetic alloys, mag. anomalies of Invar type (*Russian*) 0-93089
- (FeNi)PB amorphous wires, surface oxidation and annealing influence on induced anisotropy 0-100957
- Fe₄₀Ni₄₀P₁₄B₆, amorphous, resistometric study of short-range ordering rel. to heat treatment 0-70140
- Fe₄₀Ni₄₀P₁₄B₆, amorphous ferromagnet, Mossbauer hyperfine fields, mag. struct. 0-75894
- Fe₄₀Ni₄₀P₁₄B₆ amorphous alloy, temper embrittlement 0-76295
- Fe₄₀Ni₄₀P₁₄B₆, amorphous, mag. polarisation in approach to ferromag. saturation 0-80560
- Fe₄₀Ni₄₀P₁₄B₆, amorphous, steady-state creep rate, cryst. effect 0-81102
- Fe₄₀Ni₄₀P₁₄B₆, amorphous, mag. permeability aftereffect during annealing 0-88834
- Fe₄₀Ni₄₀P₁₄B₆, amorphous ferromag., spin wave excitations 0-97079
- Fe₄₀Ni₄₀P₁₄B₆ amorphous ribbon, mag. domains and anisotropy distrib. 0-108029
- Fe₄₀Ni₄₀P₁₄B₆ glass, viscosity near T_g, using rapid heating, and fusion characts. 0-70438
- Fe₄₀Ni₄₀P₁₄B₆ metallic glass, crystn. 0-70127
- Fe₄₀Ni₄₀P₁₄B₆, metallic glass, glass transition, viscous flow and differential scanning calorimetry meas. 0-96635
- Fe₄₀Ni₄₀P₁₄B₆, metallic glass, bending tests, evidence of ideal elastic-plastic deform. 0-97543
- Fe₄₀Ni₄₀P₁₄B₆, Metglas 2826, hot forming 0-84980
- Fe₄₀Ni₄₀P₁₄B₆, Metglas 2826, amorphous ribbon under tension, mag. domain walls and pulsed magnetisation reversal 0-88825
- (Fe₂Ni_{1-x})₈₀P₁₀B₁₀, amorphous, magnetisation reversal and domain boundary configs. 0-88809
- Fe₂Ni_{80-x}P₁₄B₆ glass, resist., magnetoresist., and thermoelec. power 0-70681
- Fe₂Ni_{80-x}P₁₄B₆, metallic glass, low temp. sp. ht. for spin-glass and spin-cluster-glass regime 0-71071
- (Fe₂Ni_{100-y})₇₉P₁₃B₈, metallic glass, low temp. sp. ht. for spin-glass and spin-cluster-glass regime 0-71071
- (Fe₆₅Ni₃₃)₇₅P₁₅B₈Al₃, amorphous, crystn. temp., press. and heating rate depend. 0-70132
- (Fe_{1-x}Ni_x)₇₅Si₁₀B₁₃, amorphous, Landau-Ginzburg theory, magnetisation and Curie temp. 0-75700
- (Fe_{1-x}Ni_x)₇₅Si₁₀B₁₃ amorphous alloys, cold rolled and as-quenched, mag. anisotropy 0-97089
- Fe_{1-x}(P,B)_x, amorphous and crystalline, photoemission and band structure 0-60754
- Fe_{100-x}P_x, structural analysis of models for amorphous metallic alloys 0-103249
- Fe₂P, spin wave excitations meas. 0-65831
- Fe₇₅P₂₅ amorphous alloy, atomic struct., computer simulation 0-88043
- Fe₇₆P₂₄, amorphous alloy, electronic struct., KKR calc. 0-96775
- Fe₇₉P₁₃B₈ amorphous alloys, splat cooled, Mn, Cr and V substituted, mag. and transport props. 0-84593
- FePC molten and amorphous alloys, struct. factors 0-79674
- Fe₈₀(P_{1-x}Bi_x)_{20-y}Si_y(Si_{1-y}), density, microhardness, and crystn. temp., comp. depend. 0-84093
- Fe₈₀20-xC_x(Si_{1-x}Ge_x), amorphous, size effect of metalloids on mag. props. 0-84594
- Fe₅₀Pd₅₀, order-disorder transition, Mossbauer study 0-71268
- Fe₂Pd_{80-x}Si₂₀, amorphous, structural and mag. heterogeneities 0-80484
- Fe₂Pd_{82-x}Si₁₈ metallic glass, long range interaction and spin wave interactions 0-65949

iron alloys continued

- Fe₃Pd₃₋₅-Si₁₈ metallic glass, mag. transitions, weak ferromagnetism 0-100583
 FePt, metamagnetic transitions in external fields 0-60272
 FePt, atomic thermal vibr. anisotropy, martensitic transform. model (French) 0-70355
 Fe₃Pt austenite, long range order parameter, temp. depend. discussion 0-97481
 Fe₃Pt austenites, ordering kinetics 0-104155
 Fe₃Pt austenitising conditions on M₂ temp. 0-81088
 FeSi picture frame single cryst., domain wall motion and magnetisation reversal, time-depend. neutron depolarisation study 0-88782
 FeSi, single crystals, domain struct., temp. and field depend. 0-71085
 FeSi-Ca-V complex alloy oxidation of steel, nonmetallic additions (Russian) 0-93685
 α -Fe_{1-x}Si_x, vacancy ordering, cryst. stabilisation energy aspects 0-103325
 Fe₃Si, electronic structure, X-ray spectra comparison with band struct. calcs. 0-97383
 Fe₃Si, electronic structure, magnetic moments 0-107695
 Fe₃Si_{1-x}, amorphous film, magneto-optic Kerr effect 0-66158
 Fe₃₀Si₇₀B₁₀, amorphous, soft mag. props. and potential uses 0-88807
 (Fe_{1-x}Si_x)_{1-x}By, metallic glass, mag. props., crystallisation 0-65885
 Fe₃Sn_{1-x}, amorphous alloy, elec. resist. 0-80246
 Fe₃Sn_{1-x}, amorphous film, struct. and mag. props. 0-65972
 FeTi, surface and mag. props., heat treatment and hydrogenation effects 0-75447
 FeTiH, solar energy storage by metal hydride 0-61455
 FeV (2 at.%), NMR spin echoes, domain wall effects 0-75883
 Fe₉₀B₁₀Co₂₀Si₄(Ge₂), amorphous, size effect of metalloids on mag. props. 0-84594
 Gd-Fe amorphous films, stress contrib. to perpendicular anisotropy 0-75819
 Gd(Al_{1-x}Fe_x)₂, intermetallic compounds, pseudobinary, Mossbauer studies 0-75887
 Gd_{1-x}Fe_x amorphous foil, EELS as analytical tool, data handling and processing 0-81407
 Gd(Fe_{1-x}Al_x)₂, magnetic behavior 0-108079
 (Gd_{0.5}Fe_{0.5})₉₀B₁₀, amorphous, mag. props., Mossbauer study 0-93093
 GdFeBi, amorphous ferrimag. films, magneto-optical props., optical spectra 0-76008
 GdZrFe₂, hyperfine field at Gd, TDPAC meas. 0-93214
 Hf-Fe, amorphous, thermal stability, crystn., DSC and elec. resist. study 0-107060
 Hf_{1-x}Fe_x amorphous alloys, formation, crystallisation and electrical resistivity 0-96838
 HoCo_{5-x}Fe_x, cryst. struct. and mag. props. 0-75800
 HoFe₂ and Ho₂Fe₁₇, magnetostriction, room temp. to 80K 0-65993
 Ho₂Fe₁₇, magnetostriction, temp. depend., 20 to 350K 0-65994
 (Ho_{0.38}Tb_{0.2}Dy_{0.22})Fe₂, microwave mag. props. 0-65860
 Ir-Fe, dil., local magnetisation, Mossbauer meas. 0-66091
 Ir-Fe, spin fluctuation alloy, thermopower peak diffusion origin 0-88542
 La-Fe alloy, amorphous, sputtered at high rate, mag. props. 0-75753
 LaNi₄Fe, H₂ absorpt. cracking, acoustic emission characts. (Japanese) 0-66631
 LuFe₂, ferromag., magnetisation density, neutron diff. study 0-60217
 LuFe₂, mag. props. changes upon H₂ absorpt. 0-71270
 Mn_{5-x}Fe_xSi₃, elec. resist. and mag. susceptibility, ferromag. to antiferromag. transition 0-80504
 Nb₄₀Fe₆₀P₁₄B₆, metallic glass, explosive compaction, mech. props. 0-89176
 NdFe₂, high field Mossbauer study 0-75893
 Ni-Cr-Fe, radiation enhanced precip. and dissolution of precipitates, point defect kinetics and dislocation obs. 0-108467
 Ni-Cr-Fe, stress corrosion cracking, factors influencing susceptibility 0-97617
 Ni-Fe, adsorption of O₂, oxidation 0-108730
 Ni-Fe, dil., hyperfine mag. fields, press. effect, Mossbauer meas. 0-71277
 Ni-Fe, dil., optical absorpt., electronic struct. 0-108227
 Ni-Fe, high-field susceptibility, spin-wave spectrum, CPA calc. 0-65818
 Ni-Fe, matrix effect in SIMS anal. using O₂⁺ primary beam 0-76576
 Ni-Fe, orientation aftereffect 0-88830
 Ni-Fe, power losses at extremely low freqs. 0-88815
 Ni-Fe, soft mag. props. rel. to metallurgical aspects 0-88810
 Ni-Fe, thermal fluctuation aftereffect meas. by pulse field method 0-88837
 Ni-Fe (19 wt.%), mag. anisotropy induced by cold rolling (Russian) 0-84595
 Ni-Fe (36 to 50 wt.%), initial permeability, domain struct. model 0-88811
 Ni-Fe based metallic glasses, Curie pt. anomalies 0-60256
 Ni-Fe film, thermally activated domain wall motion 0-88777
 Ni-Fe films, energy change of Bloch wall with angle to easy axis, calc. (Slovak) 0-103863
 Ni-Fe-Co-Ti, electron microscopy and mag. meas. 0-71097
 Ni-Fe-Cr superalloy type 718, heat treatment effect on room temp. and elevated temp. fracture toughness response 0-100922
 Ni-Fe-Cr-Mo-Ti-Al, PE 16, thermally activated domain wall motion 0-88777
 Ni-Fe-H, hydride formation in high press. range 0-65235
 Ni-Fe-Nb-Al (11.2, 8.09, 79.66 wt.%), modulated struct. growth process rel. to ageing (Chinese) 0-66541
 Ni-Fe-Nb-Mo-Al, head material for mag. recording, DC and AC mag. props. 0-88812
 Ni(Fe,Cr), electron states density model and mag. characts. calcs. (Russian) 0-92804
 Ni_{1-x}(Fe,Cr), electron states density model and mag. characts. calc. (Russian) 0-92804
 NiFe film, domain wall mass and relax. time from forced oscils. 0-71133
 NiFe, magnetising energy, anisotropic effects 0-88743
 NiFe, single and multilayer thin films, strip domains, inplane magnetisation 0-103866
 NiFe thin films, magnetoresistance, quasi-static characts. 0-107766
 Ni₃Fe, change of H₂ diffusivity with order-disorder transformation 0-59729
 Ni₃Fe, compression induced magnetic anisotropy, annealing effect 0-93112
 Ni₃Fe, disaccommodation meas. after low temp. electron and neutron irradiat. 0-88832
 Ni₃Fe, domain struct. after tensile deform., dislocation effects 0-71083

iron alloys continued

- Ni₃Fe, low-temperature specific heat, long and short range order effects 0-100339
 Ni₃Fe, magnetocryst. anisotropy, annealing temp. depend. 0-103828
 Ni₃Fe, mono- and polycryst., strain hardening, test temp. effects (Russian) 0-66531
 Ni₃Fe, polycrystalline alloy evolution of slip-line pattern during straining 0-107362
 Ni₃Fe single crystals, longitudinal magnetoresist. meas. 0-70675
 Ni₃₆Fe₃₂Cr₁₄P₁₂B₈ metallic glass, mech. props. and thermal stability 0-76362
 Ni₃(Fe_{1-x}Nb_x), temp. and conc. depend. of anomalous Hall effect (Russian) 0-70674
 (Ni₉₉Fe₁)₇₉P₁₀B₈, amorphous, low temp. sp. ht., mag. contribs. 0-80552
 (Ni₄Fe_{1-x})₈₀P₁₀B₁₀, amorphous, Curie temp., press. effect 0-75833
 NiFe, mag. film, pulse switching at low temp. 0-103868
 Ni₃Ge-Fe solid soln., flow stress, transition from positive to negative temp. depend. 0-60906
 Pb-Fe, liq., thermodynamic props. (Polish) 0-89199
 Pd-Fe, dilute ferromagnets, press. effect on Curie temp. 0-65873
 Pd-Fe, magnetic anisotropy near Curie point, quasi domain struct. (Russian) 0-65867
 Pd-Fe, normal Hall effect (Russian) 0-103676
 Pd-Fe, very dil., Mossbauer emission spectra, relax. effects 0-66084
 Pd-Fe (0.54-8.0 at.%), thermo EMF at 4.2-300K (Russian) 0-92881
 Pd-Fe-Mn, ferromagnet-spin glass, thermal expansion forced, magnetotri- and magnetisation under high press. 0-65255
 (Pd₈₀Al₂₀Si₁₃)₇₀Fe₃₀, compositionally modulated amorphous film, diffusion, struct. relax. 0-103518
 PdFe (4.7 at.%), effect of alloying on activation energy of H₂ diffusion 0-107571
 Pd_{0.98}Fe_{0.01}Gd_{0.01}, Pd-Gd exchange const., neutron diffuse scatt. meas. 0-71002
 (Pd_{0.996}Fe_{0.0035})_{1-x}Mn_x, mag. behaviour at Fe sites, Mossbauer effect meas. 0-66085
 PdH_{0.003}, Kondo system, local moments, hyperfine fields, Mossbauer study 0-80478
 (Pd₈₆Si₁₅)₆₁(Fe₆₅B₁₂)₃₉, compositionally modulated amorphous film, diffusion, struct. relax. 0-103518
 PrFe₂, high field Mossbauer study 0-75893
 PrFe₂, Laves phase, mag. props., Mossbauer spectra, crystalline field mag. anisotropy 0-65851
 Pt-Fe, dil., breakdown of ferromag. order, magnetoresist. obs. 0-71046
 Pt-Fe, dil., skew scatt. Hall effect, magnetoresist. and mag. anisotropy, orbital magnetism of impurity 0-70678
 Pt-Fe, dilute ferromagnets, press. effect on Curie temp. 0-65873
 Pt-Fe, very dil., Mossbauer emission spectra, relax. effects 0-66084
 Pt-Fe alloy, ordered, T-c phase diagram, antiferro- and ferromagnetism (Russian) 0-65871
 Pt-Fe ordered alloy, multiply mag. phase transitions 0-60264
 Ru-Fe, dil., local magnetisation, Mossbauer meas. 0-66091
 Ru₂FeSn, ferromag. Heusler alloys, hyperfine fields at nonmagnetic atoms in various sites, Mossbauer effect and NMR meas. 0-66089
 Sc-Fe, dil., elec. field gradient, Mossbauer meas. 0-80665
 ScFe₂, Mossbauer effect of ⁵⁷Fe 0-75903
 ScFe₂H₃, Mossbauer effect of ⁵⁷Fe 0-75903
 Si-Fe-W, dil. alloy, compositional changes on sputtering, projectile energy depend. 0-66362
 SiFe sheets, grain-oriented, stray field meas. 0-88775
 Si_{1-x}Fe_{100-x} polycryst. ribbon, prep. by rapid quenching, and props. 0-75803
 SmFe₂ and Sm₂Fe₁₇, magnetostriction, room temp. to 80K 0-65993
 Sm₆Mn₂₃₋₁Fe₁, magnetic behaviour, temp. and comp. depend. 0-93090
 Sm_{0.91}Tb_{0.09}(Co_{0.68}Cu_{0.10}Fe_{0.22})_{6.7}, alloy permanent magnet, coercive force (Russian) 0-65966
 (Tb,Dy)-Fe amorphous films prep. by cosputtering, magnetoelastic props. 0-97429
 Tb-Fe amorphous thin films, magnetic after-effect, Kerr magneto-optic effect obs. 0-97123
 Tb_{0.2}Dy_{0.73}Fe₂, vertically zoned, magnetomechanical coupling and magnetostriction 0-65999
 Tb_{0.3}Dy_{0.7}Fe₂, prep. by powder metallurgy, magnetostrictive props. 0-75826
 TbFe₂ and Tb₂Fe₁₇, magnetostriction, room temp. to 80K 0-65993
 Te-Fe, dil., local magnetisation, Mossbauer meas. 0-66091
 α -Ti/Fe, retrograde solid solubility 0-79950
 Ti-Al-V-Fe-Cu, melt-extracted polycryst., mech. props. 0-76360
 Ti-Fe, equiatomic, heats of form., influence of short-range order (Russian) 0-81354
 Ti-Fe, H storage material, Mossbauer surface studies, Fe clusters 0-97167
 Ti-Fe (1.4 wt.%), polymorphic transform. due to plastic deform., positron annihilation 0-79939
 Ti-Fe-Al(Mn), homogeneity and lattice parameters, Mn and Al effect on hydriding compd. FeTi 0-108400
 Ti-Fe-C-N, ion irradiated, microstruct. study using TEM 0-96572
 Ti-Fe-Ni (67, 30, 3 wt.%), reversible shape alteration (Russian) 0-71647
 Ti-Mo-V-Al-Cr-Fe (4.8, 4.7, 5.2, 1.1, 1.0 wt.%), structural changes during heating up to 1000°C, DTA study (Russian) 0-93552
 Ti-Nb-Zr-Fe, supercond. and paramag. props., effect of Fe additions (Russian) 0-65730
 Ti-Ni-Fe, multiplicity of structural transitions, phase diagrams, elec. cond. meas. 0-71649
 Ti-V-Fe-Al (10, 2, 3 wt.%), fracture toughness and stress corrosion resistance 0-100904
 Ti(Fe, Co), off-stoichiometric alloy, inverse mag. susceptibility rel. to defect conc. 0-60216
 Ti(Fe,Co)H₁, mag. and ⁵⁷Fe Mossbauer studies 0-71272
 TiFe hydrides for bulk H₂ storage 0-61463
 Ti(Fe,Co)₂, itinerant electron ferromagnet, magnetovolume effects 0-60397
 Ti₇₀Fe₃₀B₁₀, amorphous alloys, crystn. behaviour, TEM study (Japanese) 0-84087
 TiFe_{0.8}Be_{0.2} alloys for H₂ storage 0-97817
 TiFe_{1-x}Co_x, electronic struct. and mag. moment calcs. 0-65821
 TiFe_{0.8}Co_{0.2}, thermal expansion and magnetoelastic effects 0-80585
 TmFe₂, ¹⁶⁹Tm Mossbauer effect 0-71261
 TmFe₃ and Tm₂Fe₁₇, magnetostriction, room temp. to 80K 0-65993
 U-Fe metallic glasses, glass form. and thermal stability 0-75183
 U(Co_{1-x}Fe_x)₂, ferromag. onset, susceptibility and resist. meas. 0-70967

iron alloys continued

- UFe₂, giant magnetoelastic deform. of cryst. struct. mag. props. (*Russian*) 0-93159
 W-Ni-Fe system, reduction kinetics and alloy form. 0-60801
 W₅₀Fe₅₀ glassy alloy, refractory, triode sputtered 0-75185
 Y-Fe, amorphous, thermal stability, crystn., DSC and elec. resist. study 0-107060
 Y₂Fe₂₃, magnetostriction, temp. depend., 20 to 350K 0-65994
 Y(Fe_{1-x}Co_x)₂, NMR study 0-75882
 Y(Fe_{1-x}Co_x)₂, x≤0.2, mag. props. and Mossbauer meas. 0-75798
 Y₂(Fe_{1-x}Mn_x)₂₃, Mn-rich compounds, Mossbauer effect study 0-71276
 YMn_{2-x}Fe_xH₁₂, mag. props., ordering temps. 0-71028
 YbFe₂, cryst. elec. field and exchange interac., ¹⁷⁰Yb Mossbauer obs., magnetostriction contrib. 0-108124
 YbFe₂, high field Mossbauer study 0-75893
 Zircaloy-4, deformation behaviour between 77 and 900K 0-71686
 Zr-Fe metallic glasses, glass form. and thermal stability 0-75177
 Zr-Sn-Fe-Ni (1.5, 0.1, 0.15 wt.%), electron irradiation damage, direct obs. 0-84212
 Zr-Sn(Fe)(Ni) (0.15 wt.%), electron irradiation damage, direct obs. 0-84212
 Zr(Cr_{1-x}Fe_x)₂, mag. props. H absorpt. effect 0-88821
 Zr₇₀Fe₃₀ amorphous alloys, struct. factors and radial distrib. functions 0-84096
 Zr(FeCo)₂, itinerant electron ferromagnet, magnetovolume effects 0-60397
 Zr(Fe_{1-x}Al_x)₂, Curie temp., magnetisation, and cryst. struct., conc. depend. 0-75730
 Zr(Fe_{1-x}Co_x)₂, ferromag. and micromag., thermal expansion and forced volume magnetostriction 0-75830
 Zr(Fe_{1-x}Co_x)₂, NMR study 0-75882
 Zr(M_xFe_{1-x})₂ (M=V, Cr, Mn), H₂ absorpt. capacity 0-88433
 (Zr_{1-x}Nb_x)Fe₂, antiferromag. spin struct., Mossbauer effect study 0-66086

iron compounds

- see also ferrites; iron alloys
 biotite, Mossbauer and optical spectra, Fe²⁺-Fe³⁺ interactions 0-60470
 carbides, oxidation of H₂ 0-104462
 crystal growth from fused oxides, flow method, simple and economical apparatus (*Italian*) 0-80960
 δ-FeOOH (feroxyhyte), possible occurrence on surface of Mars 0-85879
 ferrous nitrosylhaemoglobin, NO binding, spin distrib., orbital model and mag. props. 0-81534
 formate dihydrate, mag. sp. ht., S_d-term 0-60289
 formate dihydrate, paramagnetic specific heat, decoration iteration transformation anal. 0-70938
 haematite, degree of reduction, potential relaxation due to cracks (*Russian*) 0-66770
 haematite reduction to magnetite, stress development mechanism (*Russian*) 0-93553
 intercalation, electron microscopy 0-84164
 internal motion, mol. vibr. calcs. 0-106323
 (iron, chromium) carboxylates, heteronuclear trimer exchange clusters, ESR spectra 0-80603
 magnetite, electrode, polycrystn., differential capacitance 0-66136
 mantle related, thermodynamic props. at high press. and temp. 0-81874
 Mossbauer ⁵⁷Fe spectra, ferrous charact., cryst. field interactions 0-108133
 myoglobins, Fe-substituted, O₂ binding, comparison with Co-substituted myoglobins, thermodynamic investig. 0-67030
 ore super-concentrate, deep drawing props. by integrated powder technology route 0-100806
 oxide reduction by electron cyclotron reson. plasma of H, model study on discharge cleaning 0-76548
 oxide reduction processes by gases, mathematical modelling (*Russian*) 0-93742
 oxides, phase equilibrium and microstructure interpretation 0-60847
 silicate glasses, local order around Fe, exam. using X-ray absorpt. spectrometry 0-79701
 titanomagnetites, temp. depend. cation distrib., mag. prop. obs. 0-85647
 zeolite-A, reduction, mag. and Mossbauer study 0-71115
 Fe₂O₃-Bi₂O₃ sintered material, elec. switching effects due to thermal ionic breakdown (*Korean*) 0-70776
 Al/AlCl₃-NaCl/FeS₂ secondary cell, preliminary study 0-108793
 Al₂O₃-SiO₂-MO-Fe₂O₃ glass, M=Ca, Mg, Ba, Sr, UV and EPR absorpt. spectra 0-89018
 B₂O₃-PbO-GeO₂-Fe₂O₃ glasses, mag. props. and Mossbauer spectra, speromag. order at low temps. 0-80530
 BaO-Fe₂O₃-B₂O₃(Na₂O) glasses, high Fe₂O₃ content, micromagnetic props. 0-65916
 BaO-Fe₂O₃-(Na₂O) glass, rapidly quenched, mag. and ferrimag. props. 0-75744
 BaO.6Fe₂O₃, solubility of CaO 0-100333
 BaTiO₃-Fe₂O₃, photoacoustic effect, first order phase transitions at increasing and decreasing temp. 0-70320
 (BiTm)₂(FeGa)₂O₁₂ ion implanted epitaxial garnet film, bubble domains, cryst. struct. disorder 0-93150
 CaFe²⁺Fe²⁺(Si₃O₇)₂(OH), ilvaite, electronic struct., press. and temp. depend. of ⁵⁷Fe Mossbauer spectrum 0-108129
 Ca₃Fe₂Ge₂O₁₂ garnet, light absorpt. spectral study 0-93322
 CaO-Al₂O₃-B₂O₃-SiO₂-FeO, glass, IR spectra at room and melt temp. 0-88986
 CoO-Fe₂O₃, isoelectric point meas. 0-88609
 Cr_{1-x}Fe_xOOH, 0≤x≤10, prep., Mossbauer effect, Neel temp. 0-108134
 CsGa_{3-x}Fe_xSe₈, tetrahedrally coordinated Fe atoms in low spin state, mag. props. and neutron diff. study (*German*) 0-88714
 CsLi_{0.5}(Al,Fe)_{1.5}F₆ pyrochlore, Mossbauer contrib. to exam. of cationic order (*French*) 0-93224
 CsLi_{0.5}F₆ pyrochlore, Mossbauer contrib. to exam. of cationic order (*French*) 0-93224
 CsNiFe₆ pyrochlore, Mossbauer contrib. to exam. of cationic order (*French*) 0-93224
 CuFeS₂, chalcopyrite, ionic diffusion obs., use of cathodolum. and AES 0-71497
 Cu₂FeS₄ bornite, cathodolum. and AES, ionic diffusion obs. 0-71497
 CuO-Fe₂O₃, isoelectric point meas. 0-88609
 β-FeOOH, Mossbauer spectra obs., chemical and thermal anal., X-ray diff., saturation magnetisation 0-88896
 Fe_{1-x}O, wustite, X-ray struct. anal. (*French*) 0-70175

iron compounds continued

- Fe complex, Fe(1,2,4-triazole)₂(NCS)₂, quasi-2-dimens. S=1/2 antiferromag., mag. props., hidden canting 0-107986
 Fe complex, nitrile nonacarbonyl, crystn., mol. structs. 0-64967
 Fe complex, nitrile nonacarbonyl cryst., mol. struct. 0-64968
 Fe complex (2, 9-dimethylphenanthroline) sulphate, mag. props., Mossbauer spectra 0-66081
 Fe garnets, sublattice magnetisation curves, Mossbauer study 0-75808
 Fe ore, cold bound pellets, reduction using H₂ gas, 700 to 900°C (*Japanese*) 0-71907
 Fe ore, reduction degree, chemical anal. calcs. (*Russian*) 0-66769
 Fe²⁺ and Fe³⁺ hydrate clusters, aq. electron exchange reaction, ab initio RHF MO calc. of inner shell reorganisations, vibr. freq. 0-102564
 Fe³⁺ solutions, UV absorption spectrosc. obs. of equilib. 0-93812
 Fe-C phase diagram, thermodynamic anal. 0-60846
 Fe-Cu: graphite-BaSO₄-CuSO₄, friction material, solid state sintering kinetics 0-104096
 Fe-I boracite, pyroelec. coeff. meas. 0-75951
 Fe-N phase diagram, thermodynamic anal. 0-60846
 Fe-O system, thermodynamics of viustite-haematite alloy melt (*Russian*) 0-65249
 Fe-O-Ca-Al system, inclusion precipitation diagram 0-108415
 Fe-W-O(C), Gibbs energy of form. of phases (*German*) 0-97724
 Fe_{0.394}Ti_{0.606}-O-S subsystem, equil. phase data under reducing conditions rel. to ilmenite upgrading 0-76240
 (Fe_{6-x}Al_x)O₉, IR spectra, lacunar γ-phase to corundum α-phase transform. 0-108199
 FeB and Fe₂B, ESCA and mag. spin data, electronic struct., isomer shifts, valence bands and chemical bonding 0-75489
 FeBO₃, Brillouin-Mandelstam scattering from thermal and excited magnons 0-70980
 FeBO₃, dynamical diffraction of gamma rays, enhanced nuclear reson. scatt. 0-108127
 FeBO₃, mag. linear dichroism and absorpt. spectra, exciton-magnon absorpt. mechanism 0-66160
 FeBO₃, magnetically tunable ultrasonic transducers for shear waves 0-74682
 FeBO₃, nuclear reaction suppression, Mossbauer spectra for Laue diff. (*Russian*) 0-66093
 FeBO₃, parametric echo, magnetoelastic NMR excitation (*Russian*) 0-66072
 FeBO₃, size effect during parametric spin wave excitations (*Russian*) 0-103824
 FeBO₃, spin-reorientation phase transition (*Russian*) 0-93122
 FeBO₃, suppression effect under hyperfine quadrupole splitting, Mossbauer study (*Russian*) 0-75906
 Fe₂BO₆, Faraday rotation and birefringence 0-100650
 Fe₂BO₆, orthorhombic cryst., birefr. and refr. index determ., refl. method 0-86380
 Fe₂B₂O₇Br(Cl)(I), boracite, single cryst. prep. and phys. props. 0-100763
 Fe₂B₂O₇I, boracite single cryst., nucleation control density growth 0-80955
 Fe₂B₂O₇I₃, cubic, approx. nonlinear optical susceptibility 0-78904
 Fe₂B₂O₇I₃, ferroelec. 43m-mm2 phase transition, molar heat capacity meas. 0-93249
 Fe₂B₂O₇I₃, improper ferroelectric, dielectric props., IR radiation pyroelectric detection 0-80711
 FeBr₂ metanagnet, unusual phase diagram, theory 0-93119
 Fe₂Cr₂Cr₂-NiC₂, stainless steel carbide, solar selective surface, fabrication, magnetron sputtering system description 0-80967
 Fe₂Cr₂Cr₂-NiC₂, stainless steel carbide, graded solar selective surface, magnetron sputtered 0-81485
 Fe₂Cr₂Cr₂-NiC₂, stainless steel carbide, sputtered solar selective surface, grading profile 0-81486
 Fe₂C, in Fe and its alloys, Young's modulus (*Russian*) 0-76297
 Fe(CN)₃^{3/4-}, redox reaction on CdTe and ZnTe electrodes (*French*) 0-89482
 Fe(CN)₆³⁻/Fe(CN)₆⁴⁻, ionic mass transfer in narrow rectangular conduits 0-61105
 Fe(CN)₆⁴⁻-Fe(CN)₆³⁻, redox reactions, mass transfer at vibr. spheres 0-57220
 Fe(CO)₅, multiphoton ionis. spectra, at Fe transitions 0-106361
 Fe(CO)₅+Ar₄(Ne^{*}) chemiionisation and chemiluminescence reactions, Penning ionisation and fluoresc. obs. 0-97689
 FeCl₂, antiferromag., magnon-phonon interactions in thermal cond. 0-65315
 FeCl₂, collinear metanagnet, mag. phase diagram 0-71035
 FeCl₂, cryst., self-consistent band struct., intersecting spheres model 0-75505
 FeCl₂, EXAFS amplitudes, many-body effects 0-97379
 FeCl₂, internal motion, mol. vibr. calcs. 0-106323
 FeCl₂, logarithmic corrections to tricritical scaling 0-65940
 FeCl₂, magnetic transition and sublattice mag. moment rotation nonequivalence (*Russian*) 0-100586
 FeCl₂, metanagnet, scaling props. of magnetisation and heat capacity, test of tricritical scaling 0-60336
 FeCl₂, reorientation of mag. moments under mech. stresses at OK 0-93153
 FeCl₂, intercalated with graphite, stage 1, dielec. response and intraband plasmon dispersion 0-59902
 FeCl₃, internal motion, mol. vibr. calcs. 0-106323
 FeCl₃, intramolecular force fields, compliance const. and vibr. amplitudes 0-58234
 FeCl₄, internal motion, mol. vibr. calcs. 0-106323
 FeCl₂(pyrazole)₂, linear-chain cpd., low-temp. mag. behaviour 0-71253
 FeCo_{1-x}Cl_x, metanagnet, mag. phase diagram by mag. induced light scatt. 0-65883
 Fe_{1-x}Co_xCl₂.2H₂O, random mixture with competing spin anisotropies, tetracrit. behaviour 0-60324
 Fe_{0.2}Co_{0.8}S₂, narrow-band ferromag., high press. effect on anomalous elec. resist. 0-70698
 Fe_{1-x}Co_xSi solid solution, semiconductor-metal transition 0-103627
 (Fe₂Cr_{4-x}Al_x)O₉, IR spectra, lacunar γ-phase to corundum α-phase transform. 0-108199
 (Fe_{1-x}Cr_x)₂O₃, yH₂O crystal growth, characterisation by Mossbauer spectroscopy, mag. meas. and electron microscopy (*French*) 0-80655
 (Fe_{6-x}Cr_x)O₉, IR spectra, lacunar γ-phase to corundum α-phase transform. 0-108199
 (Fe,Cr_{1-x})₂O₃, corundum-type solid solution single crystal growth, chem. vapour transport 0-93465

high-pressure effects in solids continued

microorganisms, lack of intracellular bubble formation at very high gas saturations 0-81562
 molybdenum chalcogenides, multicomponent, physical props. 0-84577
 Mossbauer effect, second order Doppler shift, press. depend. 0-66088
 Nylon 6 film, prior high-press. treatment effects, weight swelling, density, IR crystallinity, X-ray and viscosity obs. 0-81025
 polyacetylene, pristine and doped, press. effects on resist. 0-103698
 polyethylene terephthalate, press. effects on compressibility and crystn., thermodynamic interpret. 0-84102
 α -quartz 0-72490
 rare earth alloys, RM, (R=La, Ce, Pr, Er, M=Co, Ni), H(D) sorption at press. up to 1500 atm. 0-97819
 rare earth compounds, pressure effect on mag. ordering temp. 0-100584 (Rochelle salt)- γ -(ammonium Rochelle salt) α , phase transitions, hydrostatic press. effects 0-93246
 rocks, longit. waves vel. press. depend. rel. to rocks mineral comp. prediction at great depths (*Russian*) 0-104956
 stability under shear stress, hydrostatic press. 0-59462
 steel, high-strength low alloy, H₂ attack, 350-510°C 0-97636
 superionic conductor, with fluorite struct., activation vol. 0-107557
 thiourea, polycryst., mol. dynamics under hydrostatic press., NMR study 0-80619
 X-ray diffraction, diamond anvil cell, high press., pseudo-Kossel lines 0-79623
 X-ray diffraction patterns, high-press., nonuniform line broadening 0-79629
 AgNa(NO₃)₂, order-disorder ferroelec., influence of hydrostatic press. on polarisation dynamics 0-103913
 γ -Ag₅Zn₃, high pressure effect on brass struct. 0-107108
 Al, constitutive equation for porous materials with strength, press. effects 0-79875
 Al, melting curve and Gruneisen coeff. at high press. 0-65200
 Al, shock compression at high press. (*Russian*) 0-92608
 Al, US velocity, temp. depend., stress effects 0-75307
 Al-Zn, X-ray diff. after omnidirectional compression (*Russian*) 0-88262
 Al₂O₃, semisintered, shear strength at high press. 0-76308
 As metal, electric field gradient, temp. and press. variation 0-93205
 a-As, second and third order elastic consts., ultrasonic velocity meas. 0-103408
 (Ba,Sr)TiO₃, ferroelec. props., press. depend., anharmonic oscillator model 0-80716
 BaF₂, ionic cond., activation vols., freq. depend. cond., press. effects 0-100354
 Be, Fermi surface, stress-induced changes 0-96770
 Bi, superconducting modification obtained by impact compression (*Russian*) 0-93020
 CO₂, solid, Fermi reson. press. tuning, Raman spectra 0-93293
 CO₂, solid, high press. mol. libration calc. with Kihara core pots., Gruneisen parameter and lattice 0-65173
 CaF₂, ionic cond., activation vols., freq. depend. cond., press. effects 0-100354
 Cd, Fermi surface, stress-induced changes 0-96770
 CdF₂, ionic cond., activation vols., freq. depend. cond., press. effects 0-100354
 CdF₂·Eu²⁺, EPR spectra, hydrostatic press. and temp. effects 0-84648
 CdS, rock-salt type high-press. phase synthesis using metal sulphide additives 0-104084
 p-CdSAs, heavily doped, elec. transport props. under elastic deformation 0-96915
 γ -Ce, Kondo-like anomaly 0-96857
 CeAl₂, resistivity and volumetric meas., phase diagrams, comparison with CeS 0-107789
 CeS, resistivity and volumetric meas., phase diagrams, comparison with CeAl₂ 0-107789
 Cr-Co, dil., antiferromag., elec. resist. min., press. and impurity effects 0-59970
 Cr-Fe, dil., antiferromag., elec. resist. min., press. and impurity effects 0-59970
 Cs₂AuCl₆, electronic state of Au at high press., Mossbauer spectra 0-60467
 Cu, compressed powder, thermal cond. meas. (*German*) 0-70669
 Cu, US velocity, temp. depend., stress effects 0-75307
 Cu-mild steel explosively welded interface, SEM examination (*German, English*) 0-96746
 γ -Cu₂Zn₉, high pressure effect on brass struct. 0-107108
 Cu₄₀Zr₆₀, amorphous alloys, supercond. transition temp., press. depend. 0-84524
 DyPO₄, mag. transitions under hydrostatic press., neutron diffr. study 0-71030
 EuB₆, resistivity press. variation, lattice consts. 0-100456
 EuB₆, valence state of Eu, X-ray line displacement meas. 0-70633
 Fe, carbonyl powder, specific elec. conductivity, 5 to 200 MPa (*German*) 0-70664
 Fe, positive muon diffusion, press. depend. 0-75907
 Fe₂O₃, semisintered, shear strength at high press. 0-76308
 FeS, pressure effect on elec. resist. and thermoelec. power 0-70308
 GaAs, electron irradi. induced defect levels, hydrostatic press. effect 0-92858
 GaSe, press. induced metallic and supercond. state 0-75666
 GaTe, transport properties under hydrostatic pressure 0-75589
 Ge, dislocation electron states, from press. depend. of photocond. 0-96819
 Ge, EXAFS at high press. 0-97376
 Ge, lattice dynamics under press 0-92627
 p-Ge, negative magnetoresist. and Hall effect, press. and field depend. 0-70733
 Ge, supercond. at high press., crit. temp. 0-60130
 He, melting at room temp. and high-press. 0-80025
 InP, photoluminescence meas. using diamond-anvil press. cell 0-108256
 InSb, thermal cond., elec. cond., and thermoelec. power, press. depend. 0-59744
 KCl, cryst. isolated pore healing under press., dislocation struct. evolution (*Russian*) 0-100245
 KH₂PO₄, single crystal neutron diffraction study at high pressure 0-92497
 KHSO₄, phase diagram of 3.2 GPa, 450°C 0-76237
 KTa_{0.7}Nb_{0.3}O₃, pressure-induced resistance and colour change obs. 0-75608
 (Mg,Fe)₂SiO₄, dislocation recovery rate affected by high-press. 0-94515
 (Mg,Fe)₂SiO₄, shock deform. expts., Hugoniot data implications 0-94497

high-pressure effects in solids continued

MgO, bonding, pressure effects in lower mantle 0-72491
 MgO, semisintered, shear strength at high press. 0-76308
 NaBr, EXAFS at high press. 0-97376
 NaCl, dislocation mobility under high press., temp. depend. 0-75235
 NaCl, eqn. of state to 32 kbar and 500°C, length change meas. 0-70361
 NaF, isothermal compression at 673K, up to 10 GPa, X-ray diffr. study 0-59565
 NaF, thermal cond. meas. at high press. 0-75392
 Na₂WO₄, 0.22<x<0.84, low temp. struct., press. effects, NMR study 0-59443
 Na_{1-x}Zr_xSi_{3-x}O₁₂, press. and comp. effect on fast Na⁺ ion transport 0-107516
 Nb₃Si, Al₁₅ phase from amorphous Nb-Si alloys, high-press. synthesis 0-93516
 NdP₂O₁₂, ferroelastic, hydrostatic press. effect on phase transition temp. 0-70293
 Ni, positive muon diffusion, press. depend. 0-75907
 (Pb,Sr)TiO₃, ferroelec. props., press. depend., anharmonic oscillator model 0-80716
 Pb, shock compression at high press. (*Russian*) 0-92608
 Pb-Si superconducting solutions, effect of hydrostatic compression on tunnelling (*Russian*) 0-65746
 PbBr₂(Cl₂)(I₂), ionic cond. and activation volumes, high press. effects 0-100353
 PbHPO₄, crystals, ferroelec. phase transition, hydrostatic press. influence, dielec. meas. 0-88936
 Pb_{1-x}Sn_xTe:Ge, anomalous behaviour of impurity centres under press. (*Russian*) 0-65491
 Pd₂Sn_y (x=0.95, y=0.05; x=3, y=1), Mossbauer spectra, high press. effects, force consts. 0-84669
 Pd₃₀Zr₇₀, amorphous alloys, supercond. transition temp., press. depend. 0-84524
 ReO₃, mag. breakdown above compressibility collapse transition 0-103617
 S-Ni-Fe system containing monosulphide solid soln., elec. and struct. relations 0-90038
 Se, electronic struct. of cryst. phases and hydrostatic press. effects 0-59865
 Se, metallic state, press. induced, elec. cond. meas. 0-96949
 p-Si, elec. resist., shock wave compression effects 0-80265
 Si, lattice dynamics under press 0-92627
 Si, metallic state, press. induced, elec. cond. meas. 0-96949
 Si, p-n junction, current-voltage characts., misfit dislocations, high press. effects 0-65671
 SiO₂, shock compression at high press. (*Russian*) 0-92608
 SmB₆, resistivity press. variation, lattice consts. 0-100456
 Sn₂P₂S₆, investigation of p-T diagram near a singular point (*Russian*) 0-88937
 SrF₂, ionic cond., activation vols., freq. depend. cond., press. effects 0-100354
 Ta-Ga, crystal struct. at high press., polymorphism 0-88112
 Te, electronic struct. of cryst. phases and hydrostatic press. effects 0-59865
 Te, high-press. metallic, supercond. transition temp. press. depend. 0-80435
 Te, metallic state, press. induced, elec. cond. meas. 0-96949
 Th-Cr, supercond., press. meas. to 20 kbar 0-88667
 Ti alloys, hydrogenation at 200-600°C and up to 10000 kPa 0-107435
 Ti-Mo (3 to 35 wt.%), high pressure influence on transition temp. to supercond. 0-107952
 U, Hugoniot data, ultrahigh press. (TPa) shockwave from underground nuclear explosion 0-59580
 U₃P₄, press. effects on elec. resist. and Curie temp. 0-75559
 YbB₆, resistivity press. variation, lattice consts. 0-100456
 ZnS, cubic, compression 0-107358
 ZnS(Se)(Te), thermal expansion and lattice dynamics under press. 0-100316
 ZrO₂, semisintered, shear strength at high press. 0-76308

high-pressure phenomena and effects

see also high-pressure effects in solids
 benzene, liq., mol. motion at high press. 0-103509
 CaO-SiO₂-CO₂, subsolidus and liquidus phase relationships to 30 kbar 0-85643
 cardiovascular system, haemodynamic obs. in awake rabbits during hyperbaric He-O₂ exposure 0-101200
 CBNA, nematic-isotropic transition at high press., turbidity meas. 0-92655
 CBOOA, smectic-A reentrant nematic transition under press., X-ray obs. 0-59637
 cyclopropane, liq., mol. dynamics, Raman and NMR studies of orientational motion 0-93296
 dense plasma ionisation and cohesion, critical density and press., approx. formulas 0-59253
 1,1-difluoroethane, nucl. recoil ¹⁸F chemistry at high press. 0-89510
 Earth mantle elements compounds and modifications, high press. and temp. thermodynamics 0-81874
 EBBA, nematic-isotropic transition at high press., turbidity meas. 0-92655
 gas, high press. breakdown in strong static elec. field, plasma mechanism 0-79614
 matter under very high pressure, 10³ to 10⁶ kbars, high pressure meas. and phenomena (*French*) 0-90811
 MBBA, nematic-isotropic transition at high press., turbidity meas. 0-92655
 molecular electronic spectra, high pressure effects, Morse potential formulation 0-63617
 organic molecules, long-chain, diffusion through polymer matrix, hydrostatic press. effect on diffusion coeff. 0-92697
 phase equilibria, computational methods 0-75329
 phase equilibria in mixtures, computational effects 0-75330
 polyethylene terephthalate, molten, press. effects on compressibility and crystn., thermodynamic interpret. 0-84102
 trans-1,4-polyisoprene crystals, press. effect on growth rate 0-88064
 trans-1,4-polyisoprene crystals, press. effect on melting temp. and lamellar thickness, press. crystn. 0-88302
 polyethylsiloxane-2, liq., thermodynamic props. at high press., US prog. meas. (*Russian*) 0-65157
 porous glass:In, effect of press. on transition temp. 0-97027
 seawater, eqn. of state at high press. 0-101369

high-pressure phenomena and effects continued

- silica, fused, temp. in high-pressure shock state 0-72490
 steel, high-strength low alloy, H₂ attack, 350-510°C 0-97636
 supersonic air flow through high press. gas valves into atm., noise and flow pattern obs. 0-59067
 water, liq., thermal conductivity at high pressures, meas. with Ag co-axial cylinder cell (*Japanese*) 0-80007
 water, shock compression at press. approaching 1 Mbar (*Russian*) 0-79851
 Al, solidification, high press. effects 0-66499
 Al-Si (25.4 wt.%), solidification, high press. effects 0-66499
 Ar arc heating, high-pressure complex heat exchange expt. (*Russian*) 0-75112
 Ar, thermal cond. 0-103099
 Ar, viscosity meas. at very high press. 0-59155
 Ar-H₂(Ne) liquid solution, dielectric props., intermolecular interactions (*Russian*) 0-88904
 CaO.6Al₂O₃, thermodynamic stability, reaction with Ti, Cr and Zr oxides 0-92687
 Cs, high press. melting curve maximum 0-75337
 CuFeS₂, cubanite polymorph, synthesis above 200°C and 1 GPa, lattice constants 0-108367
 H₂, fluid, Raman meas., 0.2-630 kbar, at room temp. 0-58269
 H₂O, shock compression at high press. (*Russian*) 0-92608
 He, 3rd level, excitation and decay study up to high press. pumped by intense relativistic electron beam 0-74250
 He, thermal cond. 0-103099
³He-⁴He, mixture, isotropic phase separation temp. press. depend. 0-92751
 Hg melting line, pressures up to 1200 MPa 0-84281
 Hg, supercritical, elec. cond., four electrode method 0-62685
 Kr, thermal cond. 0-103099
 LiCl, concentrated aqueous soln., IR absorpt. to high press. and temps. 0-80803
 Mg SiO₃ melt, instantaneous struct. under high press., simulation by mol. dynamics 0-84049
 Mg-AgCl seawater battery, performance and EMF at great ocean depths 0-76623
 N₂⁻, high press. IR vibr. spectroscopy (*German*) 0-74170
 NO₂⁻, high press. IR vibr. spectroscopy (*German*) 0-74170
 Na₂R(XO₄)₂ (R=rare earth; X=P, As, V), pressure synthesis (*French*) 0-93509
 Ne, thermal cond. 0-103099
 PbI₂, high press. phase diagram to 3.5 GPa 0-104126
 Se, liq., electronic transport props., equation of state, to 1900K and 1800 bars 0-65574
 Ti-Se, liquid mixtures, press. effect on two-phase region 0-75347
 Xe, thermal cond. 0-103099

high-pressure solid-state phase transformations

- alkali hydrides, structural transition from NaCl to CsCl type under high press. 0-96458
 alkali metal halides, ionic crystals, impulse compression temps. 0-100307
 condensed gases, solid phase transition, optical meas. in diamond-anvil cells 0-73381
 crystal lattice stability and deform. phase transitions under press. 0-59624
 fluorite-type dioxides 0-101363
 graphite to diamond, probability under high temp. and press. (*Chinese*) 0-65220
 graphite-diamond, shock induced transform. anal., post shock graphitisation 0-79933
 Gruneisen parameter and eqn. of state determ. 0-90031
 ice VI, shock compression expts. for Hugoniot function 0-84248
 lanthanum ethyl sulphate:Pr, phase transition under pressure, absorpt. spectra (*Russian*) 0-92667
 methane, crystalline, struct. and compression at high press., room temp. 0-107199
 oxides, ABO₄ type, high press. phase transforms. and struct. types, cryst. chem. aspects 0-79940
 polyethylene, high press. phase, US, DTA, and X-ray diff. study 0-75188
 praseodymium ethyl sulphate, phase transition under pressure, absorpt. spectra (*Russian*) 0-92667
 quartz-coesite equilibrium curve for high-temp. calibration of solid-phase cell 0-105669
 steel, high-strength, dynamic yield strengths, phase transition press. and Hugoniot parameters 0-75331
 tetramethylammonium tetrachlorocobaltate, ferroelec., pressure-temp. phase diagrams 0-97205
 tetramethylammonium tetrachloroferrate, press. induced ferroelectricity, dielec. and DTA meas. 0-80722
 tetramethylammonium tetrachlorozincate, ferroelec., pressure-temp. phase diagrams 0-97205
 1,1,1-trichloroethane, polymorphism under high pressure (*French*) 0-96644
 tris-sarcosine calcium chloride, phase transition, hydrostatic press. effect, dielec. const. meas. 0-71327
 AgNa(NO₂)₂, crit. dynamics, hydrostatic press. effect, dielec. props. meas. 0-71328
 Am, X-ray diff. obs. 0-107422
 BN, conversion of wurtzite into cubic form, stress state effect 0-64943
 Ba, phase transitions under high press. 0-96641
 β-BaF₂, stress wave profiles 0-96593
 Ba₂NaNb₂O₁₅, high press. phase transitions, Raman scatt. studies 0-71402
 BaSi₃, trimorphic, transform. of three-connected Si nets, press.-temp. phase diagram, 40 kbar and 1000°C 0-75198
 Bi, phase transformation due to high press. and shear stress 0-75357
 Bi, phase transitions under high press. 0-96641
 BiVO₄, ferroelastic phase transition, birefringence meas. at simultaneous high pressure and temp. 0-80743
 C, hard, heat-treated under pressure, characterisation of carbon phase by electron microscope 0-60855
 CaAl₂O₄, high pressure modifications 0-104149
 CaGa₂O₄, high pressure modifications 0-104149
 CaO, B1-B2 transition, Earth mantle implications 0-79876
 CaO, eqn. of state at high press., appl. to Earth core and mantle 0-109122
 CaO high pressure metallisation, tentative evidence 0-84427
 Ca₃(PO₄)₂:Cu²⁺, ESR, high press. struct. transition 0-97134
high-pressure solid-state phase transformations continued
 Cd-Sn binary system, high press. study 0-93539
 Cd-Tl binary alloy system at high press. 0-97461
 CdHg alloy, ω phase, mag. susceptibility anisotropy w.r.t. uniform compression (*Russian*) 0-71143
 CdS(Se)(Te), determ. of wurtzite, zincblende and rocksalt phases 0-100219
 Ce, high pressure phase transition, anomalous Gruneisen parameter behaviour 0-79934
 Ce_{1-x}La_x, dil., γ-α transition temp. and press., elec. resist. meas. up to 10 kbar 0-59643
 CrAs, high press. paramag. antiferromag. transitions, elec. props., band model development (*Russian*) 0-60277
 Cs, supercond., elec. resist. and phase transforms. under high press. (*German*) 0-107763
 CsSbF₆, high press. phase relations, vibr. spectra, and cryst. chemistry 0-108200
 CuCl, pressure depend. of structural, chemical, elec. and mag. props. 0-96596
 Fe, Armco, dynamic α↔ε transform., stress gauge meas. 0-96594
 FeO, eqn. of state at high press., appl. to Earth core and mantle 0-109122
 α-Fe₂O₃, elec. resist. and phase transition under shock compression 0-72496
 Ga II, superconducting high pressure phase, sp. ht. 0-70894
 GaAs(P), semiconductor-metal transition, press. calibration above 100 kbars fixed points 0-77808
 GaNbO₄, polymorphic transition under high press. 0-100835
⁴He, solid-fluid, eqn. of state, melting props. under press. 0-96721
 HfO₂, high pressure polymorphism 0-59429
 Hg₂Cl₂, p-T phase diagram, pressure effect on phase transition 0-107370
 HgSe, elec. resist., high press. phase transform., band gap 0-70707
 In-Sb, cryst. struct. after appl. of high press., supercond. transition temp. 0-70169
 InP, depend. of phonon spectrum on hydrostatic press., Raman spectra 0-93315
 InP, press. depend. of direct absorption edge, up to high press. phase transition 0-93365
 KAg₂I₃, superionic cond., pressure effect on phase transitions 0-70405
 K₂C₂₀, press. induced staging transition 0-79938
 K₂Fe(CN)₆-KCl, press. induced reduction, IR spectra after pressurization 0-66776
 KH₂AsO₄, ferroelectric phase transition under high hydrostatic press., mol. dynamics, NQR study 0-75880
 KNO₃ in alkali halides tablets, phase transition and ion exchange, IR spectra 0-79937
 K₂SeO₄, incommensurate to ferroelec. transition, hydrostatic press. effects, neutron scatt. study 0-108166
 K₂[Pt(CN)₄]Br₃·3H₂O, high press. structs. and phase transitions 0-107423
 Mg₂SiO₄, temp. in high-pressure shock state 0-72490
 Mn-Bi micromagnetic alloy, mag., elec. and elastic props. (*Russian*) 0-108028
 ND₄I, Raman spectrum, press. effects 0-97261
 NH₄Ag₂, superionic cond., pressure effect on phase transitions 0-70405
 NH₄Cl Raman spectra, pressure effects 0-97268
 NH₄I, Raman spectrum, press. effects 0-97261
 NH₄LiSO₄, point group symm. at high press. phase 0-70150
 NaCl, phase transformation due to high press. and shear stress 0-75357
 NaH₂(SeO₃)₂, β to δ ferroelec. transition under press. Raman spectra study 0-80725
 NaNbO₃, hydrostatic press. effect on permittivity, phase transition, hysteresis 0-80670
 Na₂R(XO₄)₂ (R=rare earth; X=P, As, V), pressure synthesis (*French*) 0-93509
 PbF₂, ionic cond., activation volumes and high press. phase transitions 0-70461
 PbF₂, US vel. near press. induced cubic-to-orthorhombic transform. 0-103476
 PbI₂, ionic cond. and activation volumes, high press. effects 0-100353
 Pr, localised 4f shell breakdown under press. 0-70411
 Rb, elec. resist. and phase transforms. under high press. (*German*) 0-107763
 RbCaF₃, shift of first order transition under hydrostatic press. 0-59649
 Sb, phase transformation due to high press. and shear stress 0-75357
 Sb₂Te₃, thermoelectric properties and phase transition, under hydrostatic pressure up to 9 GPa 0-65609
 Sc₂C₃, superconducting phase synthesis at high press. and temp., critical field (*Russian*) 0-65732
 Se, trigonal, Raman scatt. at very high press. 0-60566
 Si, metallic, superconducting transition temp., press. effects, elec. cond. 0-103777
 Si, static compression in [100] and [111] directions, elec. resist. obs. 0-65637
 SiO₂, temp. in high-pressure shock state 0-72490
 SrB₂O₇:Eu³⁺, luminesc. of high-pressure phases 0-100680
 Sr₂Ba_{1-x}Nb₂O₆, high press. phase transitions, Raman scatt. studies 0-71402
 SrCl₂, ionic cond., activation volumes and high press. phase transitions 0-70461
 Sr₂Nb₂O₇, high press. phase transitions, Raman scatt. studies 0-71402
 (TSeT)₂Cl complex, phase transform. under press., cond. (*Russian*) 0-92674
 TTF-TCNQ, high press. structural transitions, neutron scatt. study 0-96647
 TTT₂I₂+ complex, influence of press. on metal-dielectric phase transition (*Russian*) 0-92818
 TaSe₂, (2H) CDW, reentrant lock in transition at high press. 0-88320
 Te, Mossbauer spectra under press. up to 8000 MPa 0-80647
 Te, trigonal, Raman scatt. at very high press. 0-60566
 Ti-Mo alloys, structural stability under high-pressure soaking 0-104151
 Ti-Mo(V), metastable diffusionless equilibria, high press. conditions 0-71627
 Ti-V (10 at.%), α-ω transformation, electron diff. evidence of intermediate BCC phase 0-81051
 TiO₂, rutile, Raman study at high press. 0-89002
 TiO₂, rutile phase, shock induced phase transition anisotropic behaviour 0-103475
 Tl, phase diagram and high press. phase transforms., DTA study (*Russian*) 0-66474
 TmSe and its mixed crystals, valence instabilities, phase diagram 0-70651

Ising model continued

- antiferromagnetic triangular cactus tree, bond-diluted, ordered phase 0-71037
 antiferromagnets, disordered spin flop, bicritical behaviour, critical experiments 0-65899
 block spins, defined by random field, convergence 0-101759
 bond dilute, bond-dil. two-dimens., phase transition 0-60320
 clusters and Ising critical droplets, global phase diagram 0-100575
 commensurate phases, spatially modulated, in simple Ising model 0-79909
 compressible dilute Ising systems, critical behaviour 0-108017
 computer simulations of mag. model systems 0-65924
 constant-coupling approx., successive phase transitions 0-97108
 correlation quadratic identities, discrete-time Toda eqn. 0-105582
 critical dynamics, time-dependent real-space renormalisation group 0-60282
 critical properties and exact results 0-93129
 critical systems, wall effects, scaling theory 0-80539
 critical temperature, modulated Pade approximant 0-84605
 critical wall perturbations and a local free energy functional for spin $1/2$ Ising model strip 0-80533
 Devil's staircase and harmless staircase, oscillating interactions through elastic stairs or other harmonic fields 0-88296
 diffusion in the one-dimensional Ising model 0-77719
 diluted systems with competing interactions, mag. ordering, appl. to $\text{Eu}_x\text{Sr}_{1-x}\text{S}$ 0-65914
 double Ising chain, transverse susceptibility (*Russian*) 0-88727
 duality relations and replica method 0-77722
 Edwards-Anderson spin glass model in two dimensions, numerical results 0-97100
 FCC Blume-Capel model, Monte Carlo study 0-103453
 ferrodistoritive spin-phonon systems, crit. props. 0-88315
 ferroelectric, H-bonded, central peak, thermal cond. 0-93250
 ferroelectric, uniaxial, crit. behaviour, electrostrictive coupling role 0-71329
 ferroelectrics, central peak in Ising model in transverse field, mode-coupling theory 0-75987
 ferroelectrics, order-disorder, pseudo-one-dimens. kinetic Ising model 0-71333
 ferromagnet, anisotropic, in external mag. field, continuous phase transition existence 0-108011
 ferromagnet, diamond lattice, phase transition, crit. props. 0-93127
 ferromagnet, gaussian fluctuations of mol. field, magnetisation and free energy 0-70918
 ferromagnet, linearisation assumption, crit. correlation function 0-60158
 ferromagnet, one-dimens., with phase transition, thermodynamic props. calc. 0-80536
 ferromagnet, phase coexistence, translation invariance and stability 0-80513
 ferromagnet, randomly dilute, conc. expansion study 0-60315
 ferromagnet, rel. to plane rotor 0-60348
 ferromagnet, two-dimens., order parameter and induced susceptibility 0-71036
 ferromagnet and antiferromagnet, two-dimens. square, ground state, apparent 3-spin interactions 0-88709
 ferromagnet-spin glass transition, Monte Carlo calc. 0-60287
 ferromagnetic, band-mixed square-lattice, approx. crit. surface 0-70921
 ferromagnetic and antiferromagnetic susceptibilities, with transverse field 0-60160
 ferromagnetic half-plane, surface, pinned domain wall, free energy and magnetisation profile 0-60361
 ferromagnetic Ising model, spin-one three dimensional, single-ion anisotropy, crit. behaviour 0-80540
 ferromagnetic-antiferromag. mixture, triangular cactus tree, statistical theory of bond-random Ising model 0-75702
 first order phase transitions, droplet models, renormalisation, singularities 0-95050
 fluctuations and FKGI inequalities 0-77712
 fractal lattices, crit. phenomena 0-105587
 Ginibre inequality, positivity and monotonicity 0-68141
 Heisenberg-Ising spin chain quantum inverse scatt. method, Jordan-Wigner transformation 0-93068
 inhomogeneous mixture of Ising and Heisenberg substances, quenched system, critical temp. 0-88770
 interacting linear Ising spin chain, phase transitions (*Russian*) 0-70920
 Ising spin glass, glass, Edwards-Anderson order parameter instability 0-71043
 Ising spin system, coupled to acoustic and optic lattice modes, critical behaviour 0-71044
 kinetic, reliability of real space renormalisation approach 0-90793
 kinetic chain relaxation, randomly signed exchange 0-70919
 kinetic processes, 1-D chain, magnetic relaxation, quantum stat. mechs. 0-80471
 kinetic processes, reduction of statistical description of system during evolution 0-80470
 layered two dimensional Ising lattice, phase transitions, spin glasses (*Russian*) 0-65945
 liquid crystals, generalised Suzuki formula application (*Chinese*) 0-107045
 local magnetisation, semi-infinite 2-D Ising model 0-71074
 long-range interaction in Ising model, dynamical props. 0-100593
 magnet coupled to isotropic elastic medium first order transition, renormalisation method 0-68151
 magnetic alloy, binary, spinodal decomp. modelling at interface 0-84913
 magnetization reversal of the two-dimensional Heisenberg ferromagnet with weak Ising anisotropy 0-107977
 Mattis model, modified, mag. relax. 0-65947
 maximum susceptibility locus crit. behaviour 0-71040
 metamagnet, compressible, renormalisation group theory of pseudocritical point 0-60337
 metastable, in negative field, near criticality 0-84608
 modulated phase with solitons, phasons and devil's staircase 0-95044
 nonlinear excitation and coherent states, Ising model in transverse field 0-68143
 one dimensional anisotropic Heisenberg model, spin $1/2$, Ising like antiferromag., dynamic correlation function 0-75704
 one dimensional randomly dilute Ising ferromagnet, dynamics 0-70922
 one-dimensional spin system, with next-nearest neighbour interactions, mag. responses to spin-Peierls transition 0-71054
 one-dimensional transverse-field, in complex longitudinal field, real-space renormalization group method, $T=0$ 0-103806

Ising model continued

- order, disorder and generalized statistics 0-99055
 partition functions in terms of infinite determinants 0-62593
 phase boundary, line of analytic singularities 0-60283
 phase transition, Monte Carlo method in Ising system with biquadratic interactions 0-60352
 phonon relaxation for transverse field model, soft mode and central peak roles 0-59615
 planar, scaling analytic corrections universality 0-105586
 planar Ising ferromagnet solvable model with roughening transitions 0-71069
 planar spin system with annealed bond disorder 0-57212
 quantum compressible Ising model, critical behaviour 0-108016
 quantum Ising chain, in real or complex field, real space renormalisation group method 0-71050
 quantum spin systems, $S=1/2$, manifestation of frustration effect 0-65767
 quenched-bond disorder, cluster extension of effective-interaction approximation 0-93130
 random anisotropy model in Ising model, Monte Carlo simulation 0-80546
 random band square lattice, frustrated plaquettes distrib. 0-108015
 random binary Ising system with transverse field, Curie temp., paramagnetic susceptibility 0-65938
 random bond Ising chain, low temp. behaviour 0-57211
 random Glauber chain, relax. of magnetisation, numerical studies 0-60313
 random spin systems, gauge symm., phase transitions (*Russian*) 0-77929
 random-bond, upper bond to sp. ht. on Nishimori's line 0-71068
 real-space renormalisation group method, continuous-variable Ising model 0-100589
 recurrence technique for confluent singularity analysis of power series 0-73277
 spatially modulated phase, with competing interactions 0-60334
 spatially nonhomogeneous, correl. functions 0-60314
 spherical random field model, low dimensionality for transition 0-68150
 spin anisotropic Ising-Heisenberg chain, appl. of zero temp. quantum renormalisation group 0-80526
 spin glass, d-dimensional, frustration effect 0-108019
 spin glass, d-dimensional, frustration effect and dilution problems 0-108018
 spin glass, dil., conc. expansions at zero temp., Ising model 0-60303
 spin glass, five-dimensional, Edwards-Anderson ordering possibility 0-60295
 spin glass, frustration model, ground states 0-60294
 spin glass, one dimens. ideal, dynamical susceptibility and relax. behaviour 0-65950
 spin glass, principle of minimum free energy 0-88773
 spin glass, Sherrington-Kirkpatrick, white and weighted averages over solns. of Thouless-Anderson-Palmer eqns. 0-108012
 spin glass, three-dimensional mag. correlations 0-103849
 spin glass transition, lower crit. dimensionality 0-60291
 spin glasses, dilute, at zero temperature, low concentration series expansion 0-93131
 spin glasses, in effective interaction approx. 0-60288
 spin glasses, random mixture of Ising systems, phase boundaries 0-60285
 spin-one, bilinear and biquadratic interactions, phase diagram 0-75772
 square lattice, two-spin correlation functions of an Ising model with continuous exponents 0-57216
 subdominant critical indices for the ferromagnetic susceptibility of the spin- $1/2$ Ising model 0-100574
 surface crit. behaviour, layer and local susceptibility 0-71058
 thin film alloys, surface magnetism props., Curie temp., Ising model 0-108039
 three-dimensional, with four-spin interaction, exact soln. 0-88711
 3d-transition metal complexes, low spin-high spin paramag. transition, Ising model calc. 0-93073
 two dimensional, nonlinear partial difference eqns., two point function 0-101762
 two-dimensional, in transverse mag. field, renormalisation group studies 0-71042
 two-dimensional, three-spin correlation functions 0-84583
 two-dimensional Ising system, crossing over to two-dimensional Heisenberg system 0-93123
 two-dimensional kinetic, dynamic correlation functions, real space renormalisation group approach 0-62589
 Union Jack lattices, non-universal Ising spin systems 0-68145
 $Z(2)(3)$ Ising spin systems, Hamiltonian formulation in 1+1 dimens. 0-57491
 $\text{AgNa}(\text{NO}_2)_2$, order-disorder ferroelec., influence of hydrostatic press. on polarisation dynamics 0-103913
 $\text{CoCl}_2 \cdot 2\text{H}_2\text{O}$, Ising antiferromag., high field transverse magnetisation meas. 0-93143
 $\text{Co}(\text{urea}) \cdot \text{Cl}_2 \cdot 2\text{H}_2\text{O}$, two-dimens. mag. props., cryst. struct., specific heat 0-75777
 CsCoBr_3 , quasi 1D Ising antiferromag., polarised Raman scatt. from mag. excitations 0-66182
 $\text{CsFeCl}_3 \cdot 2\text{H}_2\text{O}$, rectangular Ising cpd., Mossbauer meas. 0-71252
 DyPO_4 , mag. transitions under hydrostatic press., neutron diffr. study 0-71030
 Fe complex, $\text{Fe}(1,2,4\text{-triazole})_2(\text{NCS})_2$, quasi-2-dimens. $S=1/2$ antiferromag., mag. props., hidden canting 0-107986
 K_2CoF_6 , two-dimens. Ising antiferromag., nearest neighbour correl. function, birefr. expts. 0-71386
 $\text{ND}_2\text{D}_2\text{PO}_4$, cryst., transverse and longit. elec. susceptibilities, modified Ising model calcs. 0-97203
 $\text{NH}_4\text{H}_2\text{PO}_4$, cryst., transverse and longit. elec. susceptibilities, modified Ising model calcs. 0-97203
 $\text{RbFeCl}_3 \cdot 2\text{H}_2\text{O}$, pseudo-one-dimensional canted Ising antiferromag., spin-cluster excitations 0-70989
 $\text{RbFeCl}_3 \cdot 2\text{H}_2\text{O}$, rectangular Ising cpd., Mossbauer meas. 0-71252
- island-like metallic thin films** see *discontinuous metallic thin films*
islet-like metallic thin films see *discontinuous metallic thin films*
isobaric analogue resonances
 see also *nuclear collective states and giant resonances*
 analogue states and resonances in semimicroscopic shell model (*Russian*) 0-68872
 (p.p.), statistical significance of spreading widths for doorway states, reply to comments 0-63147
 (π, π), intermediate energies, collective isobaric resonance 0-63208

isobaric analogue resonances continued

- ²⁷Al isobaric analogue resonances, spectroscopic factors and γ -rays from (p,p), (p, γ) 0-86873
²⁰⁸Pb M1 isobaric analogue resonances and giant spinflip resonances from (p,n) 0-106030
⁵⁶Fe isobaric analogue resonance levels, branching ratios, from ⁵⁵Mn(p, γ) 0-68617
⁵⁶Fe(p,p), 6 MeV, elastic and inelastic, quadrupole deformation, IAR excitation, optical pots. (*Russian*) 0-63149
⁵³Mn fragmented $g_{9/2}$ isobaric analogue resonance, γ -spectra and excitation functions from $g_{9/2}$ Cr(p, γ) 0-68627
Mo(p,p' γ), odd isotopes, excited d-states from analogue resonances and p- γ correlations 0-68546
⁹⁰Nb giant particle hole resonances, Gamow-Teller strength from ⁹⁰Zr(p,n) 0-68877
¹⁴⁰Pr isobaric analogue resonances, de-excitation cascade, K-shell ionisation, spin depend. from ¹⁴⁰Ce(p,n) 0-78202
⁴⁹Ti(p, γ), 0.74-3.25 MeV, cross section and thermonuclear reaction rates, nucleosynthesis, IAR effects 0-102187
Zr(p,p' γ), odd isotopes, excited d-states from analogue resonances and p- γ correlations 0-68546

isobaric analogue states

- see also *isobaric analogue resonances*
analogue states and resonances in semimicroscopic shell model (*Russian*) 0-68672
asymmetric nuclear matter, isospin waves, IAS and giant Gamow-Teller resonance 0-91142
doorway states, fragmented, micro-resonances, strength functions, K-matrix width 0-57754
pion-nucleus single charge exchange and inelastic scatt. cross sections relationship 0-102204
(π^+ , π^0), isobaric analogue state obs. in CH₂, ⁷Li, ¹³C, ²⁷Al, ⁵⁸Ni, ⁹⁰Zr, ¹²⁰Sn, ²⁰⁸Pb 0-106078
²⁶Al 1⁺T=0 states, isobaric analogue state, spin-isospin effective interaction from ²⁶Mg(p,n) 0-68553
²⁶Al excited states, isobaric analogues, spins, DWBA anal. of ²⁷Al(³He, α) 0-105981
²⁰⁸Pb, 0⁺ IAS, spreading width and isospin impurity, isovector monopole state influence 0-78155
⁶C(p, π^+), A=12.13, 200 MeV, analogue and nonanalogue state cross sections 0-99130
⁴⁹Cr ground analogue state fine struct., I=3 states differential cross section from ⁵⁰Cr(p,d) 0-63152
⁵¹Cr levels, spectroscopic function and analogue states, PWBA anal. of ⁵²Cr(³He, α) 0-68547
⁴¹K nucleus 11.36 MeV analog state total angular momentum from ⁴⁰Ar(p,p) reaction (*Russian*) 0-102169
¹⁸O(e,e'), isovector mag. dipole and quadrupole transitions, analogues, (π , γ) relation 0-106010
²⁰⁸Pb(n,p) reaction, isobar analogue state excitation (*Russian*) 0-102124
²⁰⁸Pb, isobaric analogue states, effects of Coulomb isospin coupling, random-phase method (*Russian*) 0-86808

isobars see *atmospheric pressure and density***isoelectronic series**

- atomic systems, elastic X-ray scatt. intensity, rel. to average electron density, isoelectronic changes 0-91424
atoms, Politzer's energy rel. determ. using HF data 0-91425
diatomic mol., electronic transition probabilities, isoelectronic, isovalent corrls. for transition strength and vibr. consts. 0-87182
Group IV tetrabromides, intramol. force fields and mean vibr. amplitudes 0-106316
hexahalo ions, octahedral, mol. consts. calcs. 0-106317
hydrogenic ions, break-up processes, eikonal approach 0-91676
isoelectronic sequence, X-ray spectra 0-87071
total electronic energy, atoms and mol., SCF binding energy, Z⁻¹ perturbation theory 0-83268
two-electron atoms, doubly excited resonances assoc. with N=4 hydrogenic threshold 0-106283
Ag I isoelectronic sequence identification of W radiation generation in Tokamak 0-83981
Ar-like atoms, gradient expansion of atomic kinetic energy functional 0-95530
BF, isoelectronic sequence, Rydberg transitions, term value-ionisation pot. corrl. 0-58276
Be, excited states, oscill. strengths calcs., influence of wave function determ. method 0-99478
Be I like ions, resonant-scatt. contributions to excitation rates 0-58393
Be isoelectronic sequence, electron impact excitation of reson. transitions 0-63825
CO, isoelectronic sequence, Rydberg transitions, term value-ionisation pot. corrl. 0-58276
Cu-like ions, 4s-4p reson. lines and transitions obs. by means of laser prod. plasma, appl. to Tokamaks 0-99468
F, isoelectronic sequence, X-ray spectra 0-87071
H isoelectronic sequence, electron impact ionisation cross section 0-91688
H-like atoms, dipole polarisability of arbitrary hybrid bound states 0-87237
H-like ions, n=2 \rightarrow 1 transitions, collision strength Z-dependence 0-91675
He, $\delta(r)$ matrix elements using spatially distrib. operators 0-102445
He, isoelectronic sequence, E1 and E2 oscillator strengths, MCHF calcs. 0-106292
He like atoms, dipole transitions, transition integral cancellation 0-69052
He-like atoms and ions, gradient expansion of atomic kinetic energy functional 0-95530
He-like ions, n=2 \rightarrow 1 transitions, collision strength Z-dependence 0-91675
He-like ions, triplet-state, electron impact excitation cross sections obtained by Coulomb Ochkur Rudge approx. 0-102576
He-like ions of third sequence elements, blue satellite to resonance lines 0-70013
K I isoelectronic sequence, transition probabilities, cancellations 0-91503
Li isoelectronic sequence, self-consistent relativistic density-functional theory 0-91441
Li isoelectronic sequence, electron impact ionisation cross section 0-91688
Li isoelectronic sequence of three electron atoms, pair correlation study 0-74096
Mg isoelectronic sequence, electron impact excitation of reson. transitions 0-63825

isoelectronic series continued

- Mg isoelectronic sequence, static dipole quadrupole polarisabilities and shielding factors calc. using HF scheme 0-99450
N₂, isoelectronic sequence, Rydberg transitions, term value-ionisation pot. corrl. 0-58276
NaI, isoelectronic sequence, X-ray spectra 0-87071
Ne isoelectronic series, second order corrl. energy, Z depend. of irreducible-pair energies 0-91417
Ne-like atoms and ions, gradient expansion of atomic kinetic energy functional 0-95530
O I, isoelectronic sequence, X-ray spectra 0-87071
O isoelectronic sequence, optical oscillator strengths 0-63589
Xe like ions (I⁻, Cs⁺, Ba²⁺, La³⁺) 3d⁴4f config., collapse of 4f electron, X-ray spectral obs. (*Russian*) 0-58204
Zn isoelectronic sequence, electron impact excitation of reson. transitions 0-63825
Zn, isoelectronic sequence, oscill. strength and MCHF wavefunctions, outer corrl. 0-91505
Zn-like ions, 4s-4p reson. lines and transitions obs. by means of laser prod. plasma, appl. to Tokamaks 0-99468
Zr IV, energy levels, spectrum obs. 440 to 2670 Å 0-99470

isomer shift

- ⁵⁷Fe, isomer-shift calibration by lifetime variations in electron capture decays of ⁵²Fe 0-75902
glass: ⁵⁷Fe, 2-parameter distrib. analysis using general inversion method 0-66079
magnetic metals, hyperfine mag. fields at ¹¹⁹Sn nuclei 0-60248
Mossbauer ⁵⁷Fe spectra, ferrous charact., cryst. field interactions 0-108133
Mossbauer spectroscopy, isomer shift cancellation with resonant detectors 0-80664
niobates, mixed metal, Eu oxidation state, mag. props., Mossbauer study 0-66080
tantulates, mixed metal, Eu oxidation state, mag. props., Mossbauer study 0-66080
transition metal intermetallic cpds., H absorption and mag. props. 0-60224
Au-transition metal alloys, ¹⁹⁷Au Mossbauer isomer shift cellular atomic model 0-84673
Ba₃Ru₂Mo₃ (M=Mg, Ca, Sr, Co, Ni, Cu, Zn, Ca), Mossbauer spectra 0-108136
BaSr₂Ca_{1-x}Fe₂O₈, substituted hexagonal ferrites, mag. split Mossbauer spectra obs. and X-ray struct. data 0-71250
Co-Fe, dil., hyperfine mag. fields, press. effect, Mossbauer meas. 0-71277
Cs₂AuCl₆, electronic state of Au at high press., Mossbauer spectra 0-60467
CuFe₂O₄, Jahn-Teller type crystal distortions 0-103904
Cu₂MnAl_{1-x}Sn_x, Mossbauer effect study 0-60473
EuPt₃ compounds, partial valence change, ¹⁵¹Eu Mossbauer and magnetisation obs. 0-70167
Fe complex (2, 9-dimethylphenanthroline) sulphate, mag. props., Mossbauer spectra 0-66081
 α -Fe, uniaxial stress effect on Mossbauer spectrum 0-71244
Fe-As system, mag. props., Mossbauer study 0-88897
Fe-Cr, influence of annealing on hyperfine interaction parameters, Mossbauer effect 0-71263
 γ -Fe-Ni, local magnetisation of Fe atoms, Mossbauer effect meas. 0-75891
FeB and Fe₂B, ESCA and mag. spin data, electronic struct., isomer shifts, valence bands and chemical bonding 0-75489
Fe_{1-x}B_x, amorphous, hyperfine fields and local mag. moments, Mossbauer study 0-75895
(Fe_{0.3}Co_{0.5})_{1-x}B_x, amorphous, hyperfine fields and local mag. moments, Mossbauer study 0-75895
FeLu₂S₄, structural study, X-ray diffr., Mossbauer spectroscopy 0-107159
Fe_{0.33}NbS₂, lattice dynamics and hyperfine interactions, Mossbauer spectra study 0-108135
(Fe_{1-x}Ni_x)_{0.8}B_{0.2-x}X_x, amorphous, hyperfine fields and local mag. moments, Mossbauer study 0-75895
Fe(Sb_{1-x}Te_x)₃ system cpds., prep., cryst. struct., elec. and mag. characteris. 0-108349
Fe₂TiS₂, lattice dynamics and hyperfine interactions, Mossbauer spectra study 0-108135
FeX₄ (X=F, Cl and Br), electronic struct. and isomer shift 0-63545
FeYb₂S₄, structural study, X-ray diffr., Mossbauer spectroscopy 0-107159
⁵⁷Fe, hyperfine interactions in implanted metals, Mossbauer spectra 0-108141
GdRh₂H₄, GdRu₂H₄, struct. and mag. props., Mossbauer and magnetisation meas. 0-71271
I, atoms, Mossbauer isotopes, isomer shift 0-78573
LaCo₂, mag. props. changes upon H₂ absorpt. 0-71270
LuFe₂, mag. props. changes upon H₂ absorpt. 0-71270
Na₂(Fe,Mg)₂Si₂O₇(OH)₂, riebeckite, low temp. Mossbauer obs. of oriented single cryst. behaviour and mag. props. 0-84674
Ni-Fe, dil., hyperfine mag. fields, press. effect, Mossbauer meas. 0-71277
ScAl-Eu, intermediate valence on Eu ions, Mossbauer isomer shift 0-84587
ScFe₂, Mossbauer effect of ⁵⁷Fe 0-75903
ScFe₂H₂, Mossbauer effect of ⁵⁷Fe 0-75903
SiSb, Mossbauer spectra of ¹¹⁹Sn defect struct. 0-97174
SiTe, Mossbauer spectra of ¹¹⁹Sn defect struct. 0-97175
 α -Sn, ion implanted, defect struct., Mossbauer spectra 0-80214
Sn_{1-x}Pb_x(SeTe) films, Mossbauer effect of ¹¹⁹Sn, spectral charact., conc. depend. 0-103903
SnTe, mechanochem. and thermal oxidation comparison, Mossbauer obs. 0-104310
¹¹⁹Sn temp. depend. isomer shift, pseudopot. approach 0-84675
Te, Mossbauer spectra under press. up to 8000 MPa 0-80647
UF₆B₂(B₄), Mossbauer effect of ⁵⁷Fe nuclei, mag. props. 0-103907
⁶⁷Zn Mossbauer spectroscopy with 93 keV reson. 0-66095

isomerisation

- acetone, adsorbed on ZnO, decomp., IR and kinetic obs. 0-59780
acrolein, s-trans and s-cis, trapping from thermal mol. beams and UV-induced isomerisation in Ar matrices, enthalpy determ. 0-97688
bis(9-anthryloxy)polyoxaalkanes, intramolecular excimer form. and photodimerisation, kinetic anal., rate constants determ. 0-66800
bacteriorhodopsin chromophore, light-induced isomerisation 0-108956

isomerisation continued

- benzene-Dewar benzene, lower excited states pot. energy surfaces for isomerisation 0-104429
 1-butene, adsorbed on δ - Al_2O_3 , isomerisation, IR study 0-76554
 butene, isomers, ion-mol. reactions, photoionisation mass spectra 0-81298
 1-butene adsorption on delta alumina, microgravimetric-IR study 0-75432
 1-cyano-2-methyl-3-(cis-propenyl) cyclopropanes, rotational propensities and bond rupture identity 0-104437
 1,2-diiodoethylene, form. from 1,3-acetylene, isomerisation 0-85157
 DNA, torsionally stressed, transitions between B- and Z-conformations, theoretical anal. 0-94166
 2-fluoro ethanol, Ar matrix, induced conformational isomerisation by IR irradi. 0-101010
 fluoroformaldehyde, pot. energy surface characts., substitution effect 0-89505
 1,5-hexadiyne, time-depend. mass spectra, ionisation efficiency and breakdown curves 0-95747
 highly excited molecular systems, high energy photochem. 0-66831
 hydroxymethyl radical + O_2 , rate coefficient meas. by laser magnetic resonance flow tube method 0-66767
 isopropyl alcohol, adsorbed on ZnO, decomp., IR and kinetic obs. 0-59780
 isovaline radioracemization, cosmochemical implications 0-62087
 methyl isocyanide, laser induced thermal isomerisation, obs. by new time resolved IR photographic technique 0-57400
 methyl isocyanide photoisomerisation, laser isotope separation, C-isotope enrichment by one-photon vibr. photochemistry 0-81336
 norbornadiene-quadracyclic photoisomeric interconversion for solar energy chemical conversion and storage 0-89664
 polyacetylene, soliton formation and cis trans isomerization 0-76505
 cis-polyacetylene film, unpaired electrons, isomerisation, EPR obs. 0-60405
 polyenes, photoisomerisation, triplet pot. energy surfaces and normal mode anal. 0-108700
 polyphenylacetylene cis-trans isomers, rel. mol. wt. distrib., heating effect 0-106409
 solar energy chemical storage, photosensitization mechanisms for energy storing isomerizations 0-89679
 solar energy chemical storage using novel photocyclization reactions of 1-alkenyl-2-pyridones 0-89680
 stilbene, cis and trans, transient spectra, radiative lifetimes and quantum yields 0-78640
 stilbene anion radicals, photoinduced isomerisation, 77K 0-66818
 thermal electrocyclic reactions, anal. using topological model 0-78512
 thioindigo adsorbed on Al_2O_3 , photoisomerisation 0-89503
 CH_3PF_4 , nonrigid mol., tunnelling mechanisms, spectrosc. theory 0-78605
 CIPF_4 , nonrigid mol., tunnelling mechanisms, spectrosc. theory 0-78605
 HPN-HNP, isomerisation energies, ab initio MRD-CI calcs. 0-106271
 HSO-HOS, isomerisation energies, ab initio MRD-CI calcs. 0-106271
 HSiC-HCSI, isomerisation energies, ab initio MRD-CI calcs. 0-106271

isomerism

- see also isomerisation; nuclear isomerism; rotational isomerism*
 adenine, hydroxy and methoxy derivatives, absorption UV spectroscopy and electronic struct. of ionic and tautomeric forms 0-74177
 allylamine, N-cis lone electron pair trans isomer, total dipole moment, rel. orientation 0-69259
 aminopyrazine, far IR spectra, barrier to planarity, pot. function and energy levels 0-69137
 n-butane, trans or gauche, solute mol., solvent mol. distrib. 0-96433
 carborane, ortho- and para-, phase transition and mol. reorientation, isomer effects, PMR obs. 0-80628
 chain mols., conformational transition kinetics 0-83339
 chlorobenzaldehyde, $a^3A'' \rightarrow X^1A'$ phosphoresc., conformations and ground state fundamentals 0-78642
 2-cyanoaziridine, microwave rot. spectrum, assignments 0-91546
 cyclic mol. struct., topological characterisation 0-74254
 cytosine, hydroxy and methoxy, derivatives, absorption UV spectroscopy and electronic struct. of ionic and tautomeric forms 0-74177
 2,4-diamino-6-hydroxy-pyrimidine, IR absorption spectrum, vibr. anal., tautomerism 0-58253
 dicyanoketene, and isomeric forms, heat of form., ab initio STO-3G calcs. 0-58190
 dithiocarbamate complexes of Cr, Mn, Sn and Pb IR, electronic and mass spectra, mag. susceptibility, cond. meas. 0-97270
 hexanes, isomeric, unimol. decomp. processes following field ionisation, temp. depend. 0-95733
 hydrides, first row, bending pot. calc. using MINDO approx., force const., equilib. geometry 0-95544
 hydrocarbons, liq., Compton profiles, bond additivity 0-93423
 2-iodoacetamide, mol. struct., electron diff. obs. 0-63819
 Kruszewski's rule, for stability of isomeric polycyclic conjugated cpds., proof 0-106249
 lactams, N-methylated, cis-trans isomerism, ^1H and ^{13}C NMR obs. 0-106335
 methyl ethyl ether, charact. vibrs., isomer and isotope effects, rel. to reverse spectral problem 0-63613
 nonracemic mixtures, theory of chirality functions, concept of qualitative completeness 0-69255
 optical isomer crystal, energy difference due to parity nonconservation (Russian) 0-106405
 phenylnaphthalenes isomers, fluoresc. lifetime difference and mol. geometry 0-69176
 poly-p-chlorophenyl glycidyl ether, struct., tacticity and addition isomerism, ^{13}C NMR 0-58427
 porphin, hypersurface of adiabatic pot. calc. by CNDO/2 method, vibr. freqs., absorpt. spectra calc. 0-95543
 pyrimidines, substituted analogues, absorption UV spectroscopy and electronic struct. of ionic and tautomeric forms 0-74177
 9-cis retinal, visual pigment chromophore, twisting mechanism 0-58333
 11-cis retinal visual pigment chromophore, twisting mechanism 0-58333
 tautomerism and alternating bonds, representation, Chemical Abstracts Systems 0-63851
 thioureas, alkyl and phenyl groups trisubstituted, conformation, steric and stacking interaction 0-95587
 trialkylthioureas, N-H stretching vibrs. and conformation 0-95586
 triazastilbenes, photoelectron spectrosc. 0-106353
 ureas, alkyl and phenyl groups trisubstituted, conformation, steric and stacking interaction 0-95587

isomerism continued

- GeH_3^+ , electronic struct., electron affinity, inversion barrier, ab initio SCF Gaussian basis calc. 0-63552
 H_2 , cryst. ortho-para mixtures, vibr. coherence decay 0-78903
 $p\text{-H}_2 + ^4\text{He}$, vibr. relax., analytical approx. 0-63761
 HNO , isomerism, low lying electronic states, ab initio MRD-CI calcs. 0-83291
 $^{129}\text{I}_2$, frozen soln. in o- or p-xylene, Mossbauer effect obs. 0-78637
 NOH isomerism, low lying electronic states, ab initio MRD-CI calcs. 0-83291
 O_3H^+ , isomeric struct., ab initio MO calcs. 0-83270
 $\text{Sr Nb}_2\text{O}_6$, crystallography, polymorphism and isomerism, X-ray diff. and DTA study 0-100216
 XeF_5^+ , pseudopot. SCF MO studies, steric aspects of struct. and force fields, Jahn-Teller effect 0-99444
 XeF_6 , pseudopot. SCF MO studies, steric aspects of struct. and force fields, Jahn-Teller effect 0-99444

isomorphism

- hysteresis processes, characterisation by isomorphic transform method (Russian) 0-80562
 perfect isomorphism, predictiveness of tolerance spaces for atoms in binary and complex systems 0-107094

isothermal transformations

- binary system, isobaric and isothermal phase transform., exchange processes, entropy meas. (German) 0-90798
 steel, Cr (10 wt.%), precip. free ferrite form., STEM 0-84941
 steel, eutectoid, Si partitioning during pearlite transform., analytical electron microscopy applic. 0-108458
 Fe-Mn-Ni-V-C (0.5, 3.0, 1.0, 0.2 wt.%), austenite decomp., isothermal transform. characts. 0-97477
 Fe-Mn-V-C (0.5, 1.0, 0.2 wt.%), austenite decomp., isothermal transform. characts. 0-97477
 Ni-S incongruently subliming system, SEM and TEM obs. of high temp. transitions, temp.-comp. diagrams 0-104136

isotope detection

- see also mass spectra*
 ^{14}C dating of small samples via proportional counting 0-82102
 ^{14}Cl , Li isotopic comp. determ. by mass spectrometry 0-66899
 ^{18}O isotopic anomalies from different ore deposits, LAMMA determ. 0-61800
 S isotopic composition in CS, spectroscopic meas. (Russian) 0-91696

isotope effects

- see also isotope shifts*
 acetaldehyde, carbonyl addition, model transition states, vibr. anal. 0-71898
 acetic acid- $^{13}\text{C}_1$, in nematic phase soln., dipole-dipole couplings, selective spin population transfer investig. 0-60427
 acetone, vibr. dephasing theories, test using selective coherent ps. Stokes scatt. 0-59609
 acetonitrile- d_3 , ^2H NMR spectra, vibr. and asymmetry corrections to quadrupole coupling consts. 0-74184
 acetylene- d_0 (- d_1)(- d_2) metastable state, mol. beam elec. deflection obs. 0-74137
 alkali halides, solubility press. coeffs. and solvent isotope effect 0-96649
 allylamine, N-cis lone electron pair trans isomer, total dipole moment, rel. orientation 0-69259
 benzaldehyde gas, nonradiative electronic transition 0-83413
 benzene, isotope-mass effects in self-diffusion 0-92695
 benzene- d_0 (- d_1), radiationless triplet decay, non-Condon effects 0-83405
 benzene- d_1 , ^2H NMR spectra, vibr. and asymmetry corrections to quadrupole coupling consts. 0-74184
 bromobenzene- $-d_0$ (- d_1) radical cation, electron impact dissoci., secondary isotope effect 0-63836
 carboxylic acid systems, H(D) complexes and dimers, ν_{CO} IR band intensities 0-63715
 chemical reactions, Brownian dynamics simulation in soln. 0-104422
 cyclohexane, isotope-mass effects in self-diffusion 0-92695
 diacetylene derivatives, solid-state polymerisation, isotope effects 0-66799
 p-diazines, polycyclic, $T_1(\pi\pi^*) \rightarrow S_0$ intersystem crossing, isotope effects, ODMR and phosphoresc. obs. 0-91586
 dimethylbenzaldehydes, in durenene single cryst., zero-field splitting, guest and host isotope effects 0-107752
 ethanol- d_1 (- d_2)(- d_3), glassy state, solvated electron geometry, electron spin echo modulation obs. 0-66009
 ethylene + HBr, low temp. chain hydrobromination, kinetics and mechanism 0-93735
 ferroelectrics, displacive and order-disorder type, thermal cond. at low temps. 0-75391
 formaldehyde- $-d_0$ (- d_2), S_1 single rot. level lifetimes, isotope, elec. field and vibr. state depend. 0-78655
 formic acid, ^{16}O , ^{18}O , microwave spectra and centrifugal distortion consts. 0-83352
 graphite (0001), scattering and selective adsorption of H_2 (D_2) 0-71553
 guanine nucleotides, purinic 8-CH exchange kinetic isotope effect, Raman spectral study 0-83381
 linear chain, isotope effect on lattice const. 0-103306
 lysine, aq. solns., H^+ (D^+) exchange rates, ^{17}O NMR linewidths, pH depend. 0-91661
 meson capture, chemical, hydrogen and H isotope effects 0-69277
 metals, BCC and FCC, H-diffusion and trapping 0-70447
 metals, dissolution of interstitial H_2 and D_2 , diffusion coeffs., reverse isotope effect (Russian) 0-83868
 metals, FCC, H_2 diffusion, isotope depend. 0-59727
 methane, ^{13}C and ^{12}C , line strength ratios of $2\nu_3$ singlet 0-78616
 methane- $-d_4$, solid, rot. tunnelling, neutron scatt. obs., isotope effect 0-92468
 methanol, vibr. dephasing theories, test using selective coherent ps. Stokes scatt. 0-59609
 methanol- $-d_1$, CH_2DOH optically pumped CW far IR laser lines and frequencies 0-102707
 methyl bromide, NQR and A_1 - A_2 splitting, RF spectrosc. inside laser cavity 0-91579
 methyl ethyl ether, charact. vibrs., isomer and isotope effects, rel. to reverse spectral problem 0-63613
 muon spin rotation method, review (Polish) 0-88901
 muonic radicals, μSR spectra obs. 0-69279
 naphthalene- $-d_0$ (- d_8), radiationless triplet decay, non-Condon effects 0-83405
 nuclear spin isotope effects 0-69167

isotope effects continued

- PAA-di, nematic liquid crystal, NMR data, appl. of Landau-de Gennes theory 0-64893
 pentacene in naphthalene (p-terphenyl), mol. mixed crystals, optical dephasing and vibronic relax. 0-95957
 plasma magnetic confinement system, surface problems caused by dissolved H_2 0-57946
 polymer film, glassy and rubbery, isotope effect in H_2 and D_2 diffusion, T_g region behaviour 0-84327
 propyne- d_0 (- d_3), absolute and integrated IR intensities of fundamental modes 0-87179
 superconductors with energy depend. electronic density of states, gap and crit. temp. 0-84538
 trifluoroethene- d_0 , d_1 , mol. struct., microwave and electron diffraction. obs. 0-58384
 trifluoromethyl bromide, microwave spectra, mol. rot., isotopic variation in bond lengths, Stark meas., dipole moments determ. 0-74165
 trifluoromethyl iodide, microwave spectra, mol. rot., isotopic variation in bond lengths, Stark meas., dipole moments determ. 0-74165
 vapour pressure isotope effects, bibliography 0-77558
 water molecules, isotopic, vibr. intensities, ab initio and empirical calcs., band strengths 0-78593
 water molecules, isotopic 0-78592
 water-methanol mixtures, viscosity at 25°C, isotope substitution effects 0-92700
 Al, film, superconducting transition temp. and lattice dynamics 0-93028
 ArHBr, ArHCl, and isotopic forms, rot. spectra, mol. struct., mol. consts. 0-58246
 $BX_2 \cdot NCS$ (X=Cl, Br, I), soln., force fields and normal modes, vibr. spectra, IR and Raman obs. (French) 0-58266
 CO, Dunham vibration-rotation coefficients, isotope dependence 0-83518
 CO laser output power, active species and buffer He isotope effects (Russian) 0-63986
 CO-myoglobin, mol. tunnelling, isotope effect, time resolved IR Fourier transform obs. 0-72126
 CO_2 enriched in ^{17}O , diode laser spectroscopy of Q branches 0-78621
 $CO_2 + H^+(D^+)$, vibr. excitation, 10-30 meV 0-58358
 $CO_2 + H^+(D^+)$, vibr. excitation, isotope and time effects 0-63773
 $^{12}C^{34}S_2$, $^{13}C^{34}S_2$, high resolution IR spectra (French) 0-58249
 CaF_2 , cation jump freq., isotope effect, lattice dynamical calc. 0-88357
 CaO , formation of surface O_2^- ion by O_2 adsorption, EPR 0-61155
 $CdF_2(FCI)(FBR)$, matrix isolated IR and Raman spectra, assignments, force consts., isotope effects and thermodynamic props. 0-63631
 Ce, getting of H, mass spectrometry and microgravimetry study, rel. to HTGR gas purification 0-73374
 CoII salen complexes, O binding, reson. Raman obs. 0-58267
 CoO, isotope effects in CoO diffusion rel. to vacancies 0-84319
 Cu, H_2 diffusion, isotope depend. 0-59727
 D+H $_2$ reaction, transition state theory calculations, kinetic isotope effect explanation 0-66784
 $D_2 + Y$, high temp. equilib. meas. 0-66780
 DF, vibr. relax., isotope effect, quantum model 0-91460
 D_2O , $H^+(D^+)$ exchange rates, ^{17}O NMR linewidths, pH depend. 0-91661
 F+H $_2$ (D_2), rate consts., temp. depend. 0-81302
 FCP, microwave spectrum, struct., dipole moment and vibr.-rot. props. obs. 0-91549
 Fe meteorites, radial distrib. of spallogenic K, Ca, Cr, Ti, V and Mn isotopes 0-67488
 Fe_3O_4 , magnetite, cation diffusion, correlation and isotope effects 0-96686
 H+D $_2$ reaction, transition state theory calculations, kinetic isotope effect explanation 0-66784
 H+H $_2$ (D_2)(T_2) reactions, accurate pot. energy surface, isotope effects, quasiclassical trajectory study 0-97698
 H $_2$ +H(D)(T) reactions, accurate pot. energy surface, isotope effects, quasiclassical trajectory study 0-97698
 H $_2$ +Y, high temp. equilib. meas. 0-66780
 $H_{2-n}D_n$ Se(n=0, 1 and 2), ^{77}Se NMR on XL-100 spectrometer, isotope effects and spin-lattice relaxation 0-71211
 H $_2O$ dimer, partially deuterated, microwave spectra and struct. 0-74212
 H $_2O$, $H^+(D^+)$ exchange rates, ^{17}O NMR linewidths, pH depend. 0-91661
 H $_2O$ -HF heterodimer, H bonding, microwave rot. spectrum, mol. geometry and moment 0-99501
 H_3O^+ (D_3O^+), plasma dissociative ion electron recomb., rate coeffs. 0-63747
 H $_2O$ (D_2O), positronium formation, isotope effects 0-93432
 He $^+$, isotope effects in elastic surface scatt. on sol. and liq. Ga 0-71536
 He-Xe 3.51 μ laser mode competition in axial mag. field 0-63974
 Hg complex, methylthynylmercury(II)(- d_1 ,- d_3 ,- d_4), vibr. spectra and normal coord. calcs. 0-58259
 HgF $_2(FCI)(FBR)$, matrix isolated IR and Raman spectra, assignments, force consts., isotope effects and thermodynamic props. 0-63631
 $^{129}I_2$, $^{129}I_2$, $^{127}I_2$, high resolution saturated absorption spectra at 633 nm using He-Ne laser 0-95637
 KCl:H, ENDOR and ESR study of anion sites 0-108118
 $KDy(MoO_4)_2$, polarised IR and Raman struct., $^{92}Mo/^{100}Mo$ isotope effect 0-108198
 $K_2H(SO_4)_2$ and $K_2D(SO_4)_2$, dielec. props. and phase transitions 0-60482
 KrHBr, KrCHI, and isotopic forms, rot. spectra, mol. struct., mol. consts. 0-58246
 LiH, cryst., specific heat at const. vol., isotopic modifications effects 0-103490
 LiH(D), isotope effect on Wannier-Mott exciton levels 0-103633
 LiH $_2$ (LiD $_2$)(LiT $_2$), pot. surfaces, fundamental freqs. and thermodynamic functions 0-69205
 Li $_2$ H(Li $_2$ D)(Li $_2$ T), pot. surfaces, fundamental freqs. and thermodynamic functions 0-69205
 NH(ND) $X^2\Sigma^+$, in inert gas solid, vibr. relax., matrix and isotope effects 0-95713
 NH $_3$ (ND $_3$) in solid Ar, UV absorption spectra, temp. depend. of matrix spectra 0-63652
 NO, Fourier transform spectra, intensity and self-broadening coeff. meas. 0-102503
 $^{15}N_2$, predissoc. rot. struct. in 2490 Å band 0-87192
 Nb, diffusion of H $_2$, crystal field stabilisation 0-59728
 Nb, elec. resist. due to interstitial H (D) 0-96848
 Nb-D-H, equilib. H/D separation factors 0-95668

isotope effects continued

- Nb-H(D)(T) system, BCC, US vel. changes caused by H isotope dissolution 0-65117
 Ne $^+$, isotope effects in elastic surface scatt. on sol. and liq. Ga 0-71536
 Ni $^+$ +H $_2$ (HD)(D $_2$), endothermic reactions, investig. 0-97692
 Ni $_3$ M $_2$, M=impurity metal, formation of MH(D)-complexes 0-65236
 OH, isotope effects, Zeeman effect, far IR laser mag-reson. spectra obs. 0-63674
 $O_2(b^2\Sigma^+)$, temp. dependent quenching, photochemical study by H $_2$ -VUV laser 0-63702
 Pb and Pb alloys, interstitial substitutional model for anomalous diffusion 0-84330
 Pb stable isotopes, 2-photon spectroscopy, isotope shift of $6-2^3P_0-7^3P_0$ transition 0-87070
 Pd, elec. resist. due to interstitial H (D) 0-96848
 Pd-D-H, equilib. H/D separation factors 0-59668
 PdH $_x$, superconducting transition temp., inverse isotope effect, Einstein model 0-65734
 PdH(D $_2$), supercond. transition temps. (Russian) 0-88665
 Pt (111) and Pt (S)-12(111)X(111) surfaces, adsorption of O, thermal desorption, AES, XPS, and LEED study 0-70534
 Rb+methane (and deuterates), $5^2P_{1/2} \rightarrow 5^2P_{3/2}$ excitation transfer, isotope effects, temp. depend. 0-91630
 Rb $_3$ H(SO $_4$) $_2$ and Rb $_3$ D(SO $_4$) $_2$, dielec. props. and phase transitions 0-60482
 $^{85,87}Rb$, first excited D-level, hyperfine struct. meas. by cascade, fluoresc. spectrosc. 0-69101
 $^{99,101}RuO_2$, NQR spectroscopy 0-63664
 SeH, isotope effects, Rydberg levels-ground state transitions, rot. const., VUV spectra obs. 0-58279
 SiS, chemiluminescent flame spectra, electronic states and rot. struct. obs., vibr. assignments, Franck-Condon factors determ. 0-85179
 Sm, and isotopes, hfs, laser-RF double reson. spectroscopy 0-58170
 T $_2$ +Y, high temp. equilib. meas. 0-66780
 Ta, diffusion of H $_2$, crystal field stabilisation 0-59728
 Ta, elec. resist. due to interstitial H (D) 0-96848
 Ti, getting of H, mass spectrometry and microgravimetry study, rel. to HTGR gas purification 0-73374
 V, diffusion of H $_2$, crystal field stabilisation 0-59728
 V, elec. resist. due to interstitial H (D) 0-96848
 V-H(D), anelasticity due to long-range diffusion 0-60904
 V-H(D)(T) system, BCC, US vel. changes caused by H isotope dissolution 0-65117
 Yb, $4f^{14}6s6p^3P_1$ and 1P_1 levels, Stark effect, tensor polarisabilities 0-87080
 ZnF $_2(FCI)(FBR)$, matrix isolated IR and Raman spectra, assignments, force consts., isotope effects and thermodynamic props. 0-63631
 Zr, getting of H, mass spectrometry and microgravimetry study, rel. to HTGR gas purification 0-73374
 Zr, H(D) implanted, superconductivity enhancement obs. 0-70884

isotope exchanges

- cluster ions, formation and reactions, SIFT study, review 0-58435
 methyl(- d_3) ions, association reactions, isotopic exchanges, SIFT study, review 0-58435
 pyridine-3,4,5- d_3 , vibr. spectra, IR and Raman, H exchange rates meas. 0-102518
 pyridine-3,5- d_2 , vibr. spectra, IR and Raman, H exchange rates meas. 0-102518
 C $^+$, association reactions, isotopic exchange, SIFT study, review 0-58435
 $C_n^+ + H_2(HD)(D_2)$, isotopic exchange, interstellar implications 0-61087
 $CH_n^+ + H_2(HD)(D_2)$, isotopic exchange, interstellar implications 0-61087
 CO+ $^{13}C^+$ (HCO $^+$), isotopic exchange, interstellar implications 0-61087
 $D_2O^+(D_2O)_n + H_2O$, binary reactions, rate coeffs. and product ion distributions determ. 0-81305
 $D_2O^+(H_2O)_{0.1,2} + H_2O$ reactions, SIFT studies, review 0-58435
 $H_3O^+(H_2O) + D_2O$ reactions, SIFT studies, review 0-58435
 $H_3O^+(H_2O)_n + D_2O(NH_3)$, binary reactions, rate coeffs. and product ion distributions determ. 0-81305
 $KDy(MoO_4)_2$, polarised IR and Raman struct., $^{92}Mo/^{100}Mo$ isotope effect 0-108198
 Li $_2$ O-SiO $_2$ glasses, Li self-diffusion, mass spectrometric method 0-79982
 $^{18}O + ^{16}O$, fractionation by chemical equilib. 0-89513
 $^{18}O + ^{16}O$, fractionation by chemical equilib. 0-89513
 SrTiO $_3$ surface oxidation and reduction by D $_2O$, D $_2$, H $_2^{18}O$, isotope exchange study 0-104461

isotope relative abundance

- see also element relative abundance*
 $^{13}C^{16}O/^{12}C^{16}O$ double ratio, isotopic fractionation evidence in interstellar dark clouds 0-73017
 $^{29}I/^{127}I$ early solar system chronometer 0-62043
 Allende C3 chondrite, search for Xe fission fragment recoil 0-62083
 Allende meteorite, evidence for isotopically and chemically distinct form. reservoir for inclusion HAL 0-109399
 Bruderheim L6 chondrite, Pb isotopic abundances rel. to U-Pb age and 500 Ma shock event 0-98616
 Caledonian granites of Scotland, Nd and Sr isotope study rel. to provenance 0-109146
 carbonaceous chondrite Kr and Xe isotopes, studies of ^{248}Cm and ^{250}Cf spontaneous fission products 0-63215
 cosmic rays from supernovae, cosmogenic isotope obs. 0-101503
 dibenzylketone, photolysis in micellar soln., quantum yield and ^{13}C enrichment 0-97711
 digital isotope ratio meas. system, using programmable calculator with double collector mass spectrometer 0-63845
 Donegal granite, Ireland, emplacement age by isotope chronology 0-67356
 Duxbury massif (2.5 Ga), Quebec, initial $^{87}Sr/^{86}Sr$ rel. to remobilised pre 3.0 Ga sialic basement hypothesis 0-76970
 Earth crust, isotopic ratios rel. to rel. to mantle chemical evolution 0-90043
 Earth mantle, Nd-Sr isotope correl. and constraints on continental crust comp. and nature of lower crust 0-94498
 fission reactor fissile materials safeguards, quantity and isotopic comp. meas. (Russian) 0-63287
 fumarole B isotope composition, Satsuma Iwo-Jima, Japan 0-67358
 Galaxy, distrib. from interstellar mol. obs. 0-109550
 granitoid rocks, Nd-Sr isotopic relationship and continental crust development, chemical approach to orogenesis 0-94522
 Grenville series of Ontario, palaeomag. rel. to Ar isotope dating 0-98232

isotope relative abundance continued

- hexamethylethane, ^{13}C - ^{13}C dipolar interaction, NMR longit. cross relax. 0-93196
 limestone cave deposits, O isotopes for palaeotemp. of mid-Wisconsin 0-82069
 lunar soil samples from Luna 24, inert gas element and isotope composition 0-67593
 lunar soil samples from Luna 24 and Apollo 16, natural radioactivity meas. 0-67595
 mantle Nd and Sr isotopes, differentiation occurring in episodes 0-67352
 methane isotopic mixtures, enrichment of D using vibrationally sensitized reaction 0-76532
 molecular isotope partition function ratios, perturbation calcs., convergence 0-87239
 natural waters of Mt. Everest, mass spectrometric chem. anal. of D, ^{17}O and ^{18}O (Chinese) 0-77016
 non-destructive assay techniques for irradiated fissile material in extended configurations 0-71872
 nondestructive measurement of U and Th conc. and quantities using XFA and gamma spectrometry 0-71877
 nuclear materials analysis using plasma desorption mass spectrometry, isotope ratio determ. using TOF mass spectrometry 0-78375
 nuclear materials safeguarding; 0-68835
 nuclear materials safeguarding, determ. of U and Pu content of fuels using isotope correl. tech. 0-68834
 nuclear materials safeguarding, isotopic correl. tech., R and D by ESRADA 0-68836
 nuclear materials safeguarding, isotopic correlations in irradiated fuel from VVER power reactors (Russian) 0-68838
 nuclear materials safeguarding, isotopic inventory prediction employing a Monte Carlo Dancoff factor 0-73924
 ophiolite petrogenesis in oceanic crust, Nd and Sr isotope study 0-61782
 orogenic therzolitite petrogenesis in oceanic crust, Nd and Sr isotope study 0-61782
 rare gases in volcanic rocks, isotopes mass fractionation as indicator of gas transport to or from magma 0-98292
 resonance ionization source for mass spectroscopy appl. isotope anal. and time of flight spectrometer 0-81380
 rinneite, Rb-Sr dating of potash salt deposits 0-67429
 rock chem. weathering rate, meas. new with U isotope method 0-77142
 solar particles, isotope composition, form., effect of ion-sonic turbulence 0-101574
 solar system s-process elements, isotopic ratios rel. to ^{22}Ne neutron source model 0-72926
 stainless steel, neutron dose determ., from isotope abundance ratio, mass spectra obs. 0-61220
 transuranic trace analysis using resonance ionisation spectroscopy of inert gases 0-93833
 ^{107}Ag excesses in Santa Clara and Pinon Fe meteorites, meas. 0-85902
 Al isotopes, yield from C and Ne zones of massive star supernova 0-90406
 $\text{Al}^{26}/\text{Al}^{27}$, prod. or collapse of stellar core (Russian) 0-77285
 Al_2O_3 , single cryst., self-diffusion of O, isotope exchange investig. 0-100348
 $^{26}\text{Al}/^{27}\text{Al}$, ratio from ^{26}Al synthesis in explosive H burning 0-85929
 $^{26}\text{Al}/^{27}\text{Al}$ and ^{26}Al nucleosynthesis in novae and supernovae outbursts 0-62143
 $^{26}\text{Al}/^{27}\text{Al}$ in unstable He shell in red giant stars 0-67712
 Ar in ancient atmos., degassing from shungite 0-85749
 $^{36}\text{Ar}/^{40}\text{Ar}$ in Alpine biotites, rel. to excess Ar evolution 0-94521
 $^{40}\text{Ar}/^{36}\text{Ar}/^{39}\text{Ar}$ in Type I diamond from Arkansas 0-94493
 $^{40}\text{Ar}/^{39}\text{Ar}$, IIE iron meteorites, Weekeroo Station and Netschaevo 0-77360
 $^{40}\text{Ar}/^{39}\text{Ar}$ age and thermal history of Kirin H5 chondrite meteorite 0-101567
 $\text{BCl}_3 + \text{N}(\text{CH}_3)_3 \rightarrow \text{BCl}_2\text{N}(\text{CH}_3)_3$, complex formation, reaction product isotopic composition change (Russian) 0-81316
 ^7Be as a tracer for helio-geophysical phenomena 0-98525
 $^{10}\text{Be}/^9\text{Be}$ in North Pacific during Pliocene 0-101356
 $^{10}\text{Be}/^9\text{Be}$ ratio meas. using electrostatic tandem accelerator 0-76579
 CNO isotopes abundances in giant stars, role of mag. mixing rel. to α Boötis (Arcturus) problem 0-105229
 $^{12}\text{C}/^{13}\text{C}$ in Population I giant stars, theoretical surface abundances 0-94796
 $^{12}\text{CH}^+ / ^{13}\text{CH}^+$, interstellar abundance ratio, meas. 0-67809
 $^{13}\text{C}/^{12}\text{C}$ in atmosphere CO_2 , vars. in last 22 yrs. 0-104530
 ^{14}C in atmosphere, variability due to variable Sun 0-85730
 ^{14}C in groundwater, possible subsurface prod. rel. to dating 0-85690
 ^{14}C in wines, abundance vars. with 11-year solar cycle, (1909 to 1952) 0-109249
 ^{14}C measurement in known age specimens, cosmic ray intensity determ. 0-101516
 ^{14}C pollution of Atlantic from nucl. weapons tests 0-89683
 Ca, isotopic anal. using double vaporizer 0-106398
 $^{116}\text{Cd}/^{106}\text{Cd}$, isotope fractionation in fractions of H3 chondrites Tieschitz and Brownfield 0-94764
 ^{247}Cm in early Solar System, Allende $^{238}\text{U}/^{235}\text{U}$ ratio evidence 0-90347
 ^{56}Co , synthesis in Type II supernovae, determ. from light curves analytic solns. 0-77427
 $^{137}\text{Cs}/^{134}\text{Cs}$ radioisotopes in seawater, Cs-selective resin determ. 0-94137
 D universal abundance 0-62356
 D/H ratio for Jupiter from 8-9 μm IR spectrum 0-67638
 D/H ratio in Uranus atm. from visible spectra obs. 0-82296
 Fe nuclei in galactic cosmic rays, isotopic comp. 0-72729
 He in Earth interior, incorporated from immature Sun (Russian) 0-81856
 ^3He excess in Mid-Atlantic Ridge bottom waters, hydrothermal activity 0-101383
 $^3\text{He}/^4\text{He}$, ratio in mantle volatiles injected into Gulf of California, meas. in Guaymas Basin 0-85640
 $^3\text{He}/^4\text{He}$ in heavy-ion-rich solar energetic particle events, energy depend. and temporal evolution 0-90299
 $^3\text{He}/^4\text{He}$ in solar cosmic rays, ^3He rich events during 1976 November to December 0-61972
 $^3\text{He}/^4\text{He}$ solar cosmic ray isotopic composition from Venera 9 obs. 0-72725
 ^4He production, nonzero neutrino rest mass effects 0-105413
 $^{82}\text{Kr}/^{86}\text{Kr}$ in Murchison C2 chondrite, presolar gas component evidence 0-85904
 $^{86}\text{Kr}/^{84}\text{Kr}$ in Murchison meteorite, rel. to s-process neutron capture time scale 0-73080

isotope relative abundance continued

- ^6Li , determination using nuclear track techniques 0-95504
 Mg isotopes, yield from C and Ne zones of massive star supernova 0-90406
 Mg isotopic anomalies in meteorites, role of ^{26}Al synthesis in explosive H burning 0-85929
 $^{24}\text{Mg}/^{25}\text{Mg}/^{26}\text{Mg}$ of interplanetary dust particles 0-72879
 $^{15}\text{N}/^{14}\text{N}$ ratio in lunar microbreccias indicating ancient solar wind composition 0-62046
 Nd, in flood basalts, Earth struct. models 0-72475
 $^{143}\text{Nd}/^{144}\text{Nd}$, ratios in Cretaceous mid-ocean ridge basalt (MORB) from DSDP Holes 417D and 418A 0-94520
 $^{143}\text{Nd}/^{144}\text{Nd}$ in Bay of Islands ophiolite complex, rel. to midocean ridge basalts source evolution 0-85651
 $^{143}\text{Nd}/^{144}\text{Nd}$ in Kerguelen Islands igneous rocks, inferences on enriched oceanic mantle sources 0-98319
 $^{143}\text{Nd}/^{144}\text{Nd}$ in mantle xenoliths, equilibrated isotopic comp. meas. with unequilibrated Sr isotopes 0-98321
 $^{143}\text{Nd}/^{144}\text{Nd}$ in Norwegian eclogites, rel. to crustal origin 0-76978
 $^{20}\text{Ne}/^{21}\text{Ne}/^{22}\text{Ne}$ in Murchison C2 chondrite, presolar gas component evidence 0-85904
 $^{20}\text{Ne}/^{22}\text{Ne}$ and ^{22}Ne nucleosynthesis in novae and supernovae outbursts 0-62143
 O isotope study of lower crust xenoliths 0-89992
 $^{17}\text{O} + ^{16}\text{O}$, fractionation by chemical equilib. 0-89513
 $^{18}\text{O} + ^{16}\text{O}$, fractionation by chemical equilib. 0-89513
 $^{18}\text{O}/^{16}\text{O}$ ratio in Allende meteorite inclusion HAL, possible member of FUN family 0-105211
 ^{18}O concentration in Amazon Basin water, evidence for recycling 0-81955
 $^{18}\text{O}/^{16}\text{O}$ ratio in precipitation, correl. with temp. and altitude 0-77067
 $^{18}\text{O}/^{16}\text{O}$ variations in deep sea carbonate shells from East Pacific Rise hydrothermal field 0-109173
 ^{18}O isotopic anomalies from different ore deposits, LAMMA determ. 0-61800
 $^{18}\text{O}/^{16}\text{O}$ in terrestrial samples, rel. to use of O $_2$ isotopes as petrogenetic and geological tracers 0-89989
 Pb isotopes struct. of basic-ultrabasic layered complex 0-81847
 Pb, Sr, Nd isotopic correl. and chemistry of N.Atlantic mantle 0-90023
 $^{206}\text{Pb}/^{207}\text{Pb}$ ratio and Pb conc. in subalpine pond sediments, anthropogenic source var. 0-85315
 Pu accountability, computerised gamma spectrometer system for meas. isotopic and total Pu conc. in solns. 0-63363
 Pu, assay and accountability using neutron correlation meas. tech. 0-69015
 Pu, assay of large samples using portable neutron coincidence counter 0-69041
 Pu, calorimetric nondestructive assay for in-field meas. 0-71874
 Pu content in nuclear fuels, appl. of isotopic safeguards tech. 0-99210
 Pu, isotope composition, determ. using gamma spectrometry 0-66915
 Pu, isotopic analysis by resin-bead mass spectrometry for materials safeguards 0-78392
 Pu, isotopic composition, determ. using thermal ionisation spectrometry with automatic data eval. 0-66913
 Pu, isotopic composition, determ. using precise absolute gamma spectroscopic meas. 0-66916
 Pu, isotopic composition, nondestructive anal. using gamma spectrometry 0-63392
 Pu, nondestructive assay of large samples 0-71871
 Pu, nondestructive element and isotope assay in nuclear materials 0-71870
 Pu passive assay using Euratom variable dead-time neutron counter 0-69042
 Pu safeguards, product soln. gamma-ray NDA using K-absorption edge densitometer 0-83162
 Pu safeguards accountability, gamma-ray meas. of Pu and Am in molten salt residues 0-83165
 Pu safeguards assay, isotopic meas. by gamma ray spectrometry using two-detector method 0-83161
 ^{239}Pu , (U,Pu) O_2 fuels 0-71873
 ^{34}S in troilite, enrichment rel. to lunar soil 0-77303
 Sr, in flood basalts, Earth struct. models 0-72475
 Sr isotopes of rhyolitic ignimbrites, Batopilas area, Mexico 0-94501
 $^{87}\text{Sr}/^{86}\text{Sr}$, initial ratios in Archaean rocks of English River subprovince, NW Ontario, rel. to crust form. 0-94486
 $^{87}\text{Sr}/^{86}\text{Sr}$, ratios in Cretaceous mid-ocean ridge basalt (MORB) from DSDP Holes 417D and 418A 0-94520
 $^{87}\text{Sr}/^{86}\text{Sr}$, ancient seawater composition, Jurassic to Pleistocene, Israel groundwater obs. 0-61804
 $^{87}\text{Sr}/^{86}\text{Sr}$ in Bay of Islands ophiolite complex, rel. to midocean ridge basalts source evolution 0-85651
 $^{87}\text{Sr}/^{86}\text{Sr}$ in Kerguelen Islands igneous rocks, inferences on enriched oceanic mantle sources 0-98319
 $^{87}\text{Sr}/^{86}\text{Sr}$ in mantle xenoliths, unequilibrated isotopic comp. meas. with equilibrated Nd isotopes 0-98321
 $^{87}\text{Sr}/^{86}\text{Sr}$ in Norwegian eclogites, rel. to crustal origin 0-76978
 $^{87}\text{Sr}/^{86}\text{Sr}$ initial ratios and Rb-Sr ages, from Oxford Lake-Knee Lake greenstone belt, N.Manitoba 0-94485
 $^{87}\text{Sr}/^{86}\text{Sr}$ ratios in calc-alkaline volcanic rocks from Cerro Galan, NW Argentina, evidence for crustal contamination 0-98318
 U in rocks isotope disequilibrium, due to α -recoil and soln. effects 0-98314
 U, isotopic analysis by resin-bead mass spectrometry for materials safeguards 0-78392
 U, isotopic composition, determ. using thermal ionisation spectrometry with automatic data eval. 0-66913
 U, isotopic composition, determ. using thermal ionisation mass spectrometry 0-66914
 U, nondestructive element and isotope assay in nuclear materials 0-71870
 ^{235}U safeguards, expt. nondestructive assay using a random driver 0-83164
 $^{234}\text{U}/^{238}\text{U}$, ratio in Edwards carbonate aquifer, Texas, rel. to aquifer oxidation/reduction state 0-98362
 ^{235}U burn-up determ. by mass spectrochemical anal. 0-71989
 ^{235}U in Uf_6 , mass spectrometric determ. 0-68961
 ^{235}U , nondestructive active assay in (U,Pu) O_2 fuels 0-71873
 $^{235}\text{U}/^{238}\text{U}$ isotope ratio determ. in Uf_6 samples using gas quadrupole mass spectroscopy 0-78376
 $^{238}\text{U}/^{235}\text{U}$ in Allende meteorite rel. to early Solar System ^{247}Cm 0-90347
 $^{238}\text{U}/^{235}\text{U}$ in chondritic meteorites, search for isotopic anomalies 0-85903

isotope relative abundance continued

- Xe in Murray carbonaceous chondrite meteorite, evidence for multiple trapped Xe components 0-98618
¹³⁶Xe/¹³²Xe/¹³⁶Xe in Murchison C2 chondrite, presolar gas component evidence 0-85904

isotope separation

- see also *isotope exchanges; laser isotope separation; radiochemistry*
 centrifuge, crossed-field, ion wind effect on separation 0-79591
 chlorotrifluoromethane, multiphoton dissociation, ¹³C enrichment (French) 0-91615
 conference on nuclear spectroscopy of fission products, Grenoble, France (May 1979) 0-77546
 cosmic ray telescope, solid state, detection system for heavy ions, element and isotope separation 0-67563
 FEBIAD ion source for fission fragment isotope separation 0-78483
 fluoromethane, deuterium separation at high press. by ns CO₂ laser multiple-photon dissociation 0-91616
 formaldehyde, selective laser photolysis for ¹⁴C enrichment 0-108720
 Freon 123, deuterium separation at high press. by ns CO₂ laser multiple-photon dissociation 0-91616
 gas mixture-isotope inertial gas-kinetic separation 0-69927
 He-jet fed online mass separator for recoil atom mass spectroscopic anal. 0-98998
 inert gas isotope separation in RF discharge in travelling magnetic field 0-78719
 ion source fission product separators 0-78479
 ion sources, high temperature, for on-line isotope separation appl. 0-74063
 ISOLDE as a source of neutron-rich nuclei 0-78480
 laser-induced selective multiplet processes: impact on nuclear physics, chemistry and biology 0-61122
 light induced diffusion of gases, isomer, isotope separation (Russian) 0-79430
 magnet design for high-current implanters or small isotope separators 0-68222
 mass separation by weakly ionised plasma centrifuge 0-106985
 methane isotopic mixtures, enrichment of D using vibrationally sensitized reaction 0-76532
 methyl isocyanide photoisomerisation, laser isotope separation, C-isotope enrichment by one-photon vibr. photochemistry 0-81336
 neutron rich nuclei, beta decay half lives, expt. techniques 0-78224
 nuclear fuel cycle, extraction, concentration, UF₆ conversion, isotope separation (French) 0-63544
 nuclear fuel production, continuous gas flow control simulation (German) 0-78416
 on-line isotope separation facility HELIOS at the Mainz reactor 0-102350
 on-line mass separator for fission-produced alkali isotopes 0-98997
 online isotope separator, SOLIS, communication channel between data acquisition system and computer 0-74030
 OSIRIS, target/ion source system for isotope separation in on-line mass separator, mol. ion prod. 0-99366
 polyatomic molecules, multistage IR dissociation, collisionless energy-gathering process 0-99526
 Princeton Cyclotron data acquisition system 0-102415
 rapid automated nuclear chemistry, short lived fission products, reactor safety 0-81353
 rare gases in volcanic rocks, isotopes mass fractionation as indicator of gas transport to or from magma 0-98292
 SIRIUS facility for neutron rich fission fragment studies 0-78484
 SISAK 2, chemical separation method for short lived fission products in spectroscopic studies 0-74068
 trifluoriodomethane, highly excited, intermol. vibr. energy transfer, transient UV absorpt. spectra 0-106381
 TRISTAN II mass separator, ion source, beam optics, computer system 0-78481
 TRISTAN II mass separator at Brookhaven HFBR, research programme for fission products 0-78482
 unsolved fission product separators, gas filled JOSEF, parabola LOHENGRIN 0-78478
 Warsaw University isotope separator, machine parameters (Polish) 0-86987
 B₂O₃ laser-produced plasmas, isotopic enhancement 0-92349
 Ca, isotopic anal. using double vaporizer 0-106398
 Cd vapour, RF discharge, isotope separation 0-79619
¹⁵¹Eu (¹⁵³Eu) excitation transfer, effect on selective photoionisation 0-99538
 H₂-D₂ isotope separation by permeation through Pd membrane 0-68959
 He-jet online mass separator, improvements in total yield 0-98999
¹²³I, production in LASL radiochemistry hot cells 0-72326
 K isotope separation in solution by thermal diffusion 0-87236
 KOH gas-crystal system, isotopic equilibrium near phase transition points (Russian) 0-91697
⁷⁶Kr/⁸⁶Kr, by thermal diffusion (Rumanian) 0-86988
 NaOH gas-crystal system, isotopic equilibrium near phase transition points (Russian) 0-91697
 Ne, isotope separation by cataphoresis in DC gas discharge 0-103213
 Pu accumulation in Purex process, first extraction, computer simulation, SEPHIS code 0-68907

isotope shifts

- see also *atomic spectra*
 alkali metal radioisotopes, hyperfine spectroscopy, nucl. props. 0-57677
 3-cyanothiophene-³⁴S(-¹⁵N), partial r₀-struct., microwave spectra 0-91552
 formamide, force consts. and dipole moment derivatives, ab initio MO calcs. 0-95521
 formic acid, cryst., H bonded, IR spectrum computer simulation 0-97253
 formic acid-d₁(-d₁)(-d₂), vibr. spectra, CNDO/2 interpretation (French) 0-58155
 methane, ¹²C and ¹⁴C, line parameters for ν₂ and ν₄ bands, isotope shifts, appln. to planetary atmospheres 0-95622
 methoxy radical and deuterate, vibronic level fluoresc. spectrum 0-58305
 methyl isocyanide photoisomerisation, laser isotope separation, C-isotope enrichment by one-photon vibr. photochemistry 0-81336
 methyl orange, aq. soln., reson. Raman spectra of D and ¹⁴N isotopes 0-91566
 semicarbazide hydrochloride, vibr. spectra, normal coord. anal. 0-58255
 semicarbazide-d₀, -d₄, vibr. spectra, normal coord. anal. 0-58255
 semiconductors, shallow impurity centre spectra, isotopic shift of zero-phonon lines 0-66249

isotope shifts continued

- vibrational frequencies, band intensities and Coriolis coupling const., isotopic sum rule derivation 0-83343
 Al₂Cl₆, matrix isolated, vibr. spectra, isotopic fine struct. and valence force field calcs. 0-58258
 Ar-acetylene van der Waals molecule, radiofreq. spectroscopy and Stark effect meas., equilib. struct. and props. 0-91543
³⁹Ar, low abundant, isotope shift meas., time averaging using dye laser spectrometer 0-101850
 BCl₃, in solid Ar, Kr, high resolution IR absorpt. spectra, isotopic splitting 0-87109
 BCl₂F, in solid Ar, Kr, high resolution IR absorpt. spectra, isotopic splitting 0-87109
 Ba, atomic beam and resonance spectroscopy 0-58180
 Ba, hyperfine splitting and isotope shift of high lying levels, Doppler-free 2-photon laser spectroscopy 0-58215
 Ba II, 5d²D_{3/2,5/2}, isotope shifts, hyperfine struct., collinear fast beam laser spectroscopy 0-83310
 Ba, radioisotopes, at. beam laser spectroscopy, hyperfine struct., nucl. moments and radii 0-57678
 BaI resonance transitions, hyperfine struct. and isotope shifts, atomic beam laser spectroscopy 0-102141
 C, ¹³S-³²P₂ and ³²S-³²P₁ transitions, ¹³C isotope shift 0-58201
 Ca, stable and radioisotopes, hfs, isotope shifts, dye laser saturation spectroscopy, beam expt. 0-58169
⁴Ca, A=40 to 46.48, nuclear charge distrib., from isotope shift of 6573 angstrom line 0-57674
⁴³Ca, atomic beam and resonance spectroscopy 0-58180
 D, 1S Lamb shift and 1S-2S isotope shift 0-91464
 Dy, isotope shift meas. using laser atomic beam technique specific mass shift determ. 0-91497
 DyO, UV emission spectrum, high resolution, band systems and isotopic shifts 0-87146
 H, 1S Lamb shift and 1S-2S isotope shift 0-91464
 He, Doppler-free two-photon high resolution spectroscopy 0-58197
³He atom forbidden singlet-triplet anticrossings, D levels 0-99491
¹²⁹I, hyperfine struct. and isotope shift of 1.3 μm transition 0-102486
 K, isotope shifts of individual nS and nD levels 0-102489
 KD₂H₂₁₋₃PO₄ crystals, 0<x<0.98, light scatt. by polaritons 0-96802
^{138,139}La, Fourier transform NMR 0-57354
 LiH₂PO₄, Raman and IR spectra of transverse and longitudinal modes (French) 0-60573
⁴Lu, A=175,176, 5d6s²D_{3/2}-5d6s6p⁴F_{3/2} transition, isotope shift and hyperfine struct. 0-83309
 Mg⁺ laser cooled ions bound in Penning trap, high-resolution optical spectra 0-102487
 Nd I, isotope shifts in energy levels of neutral Nd atom 0-69095
 Ni I isotope shift for stable isotopes, nuclear charge radii 0-99484
 OCS, millimeter wave rot. spectra, isotope shifts, freqs. and mol. consts. 0-78611
 OCS, T₂ relax. meas. using budge-type superhet. microwave spectrometer 0-91551
¹⁶O/¹²C/³⁴S and ¹⁶O/¹³C/³⁴S, IR spectra, ν₃ band anal. 0-95620
¹⁸O isotope shift in ¹³C NMR, struct. depend. 0-69165
 SO₂, T₂ relax. meas. using budge-type superhet. microwave spectrometer 0-91551
 Sml, laser atomic beam spectroscopy, isotope shifts, hyperfine struct., transitions 0-102468
 Ul, precision isotope shifts meas. in visible, near IR 0-63587
 Yb I isotope shift studies in 3900 to 6500 Å region 0-74144

isotopes

see also *radioisotopes*

No entries

isotopic generators see *radioactive sources*

isotopic spin (elementary particles)

see also *baryon spin and parity; lepton spin and parity*

- hadron isospin classification, same finite group for mesons and baryons (Chinese) 0-62887
 kinematics of relativistic particles with isotopic spin, geometric quantisation 0-62871
 SU(5) grand unification, spin from isospin, half integer spin charge monopoles 0-68406
 D⁺ nonleptonic and semileptonic decays, isospin selection rule tests 0-73700
 K⁰-K⁰, SU(3) and isospin symmetry breaking effects 0-95272
 π⁻→e⁻γ, isospin-breaking, chiral limit, conserved-vector-current violation, σ model 0-62988
 ψ', ψ decay branching ratios, isospin and flavour symmetry breaking 0-95264

iteration methods see *iterative methods*

iterative methods

see also *predictor-corrector methods*

- anisotropic source flux iteration techniques, interpolation schemes 0-99200
 coherent optical iterative extrapolation of 2-D band-limited signals 0-78780
 computer-generated hologram spectrum shaping and image reconstruction 0-106475
 computerised tomographic image boundary finding and complex object localisation 0-109016
 DH stripe geometry lasers, three-dimensional anal. of mode props. 0-64020
 diffraction theory, iterative method based on spectral domain approach for corner diffr. coeff. 0-87304
 dynamical local field corrections in dielectric function 0-88500
 electronic structure calcs., self-consistent, accelerating convergence of iterative process 0-87037
 ferromagnetic plates eddy current phenomena numerical computation method (German) 0-65952
 finitely conducting cross grating theory 0-106635
 flat plate module design evolution, influence of module requirements 0-94065
 flow, supersonic, parabolic Navier-Stokes equations, implicit finite-difference method using fractional steps technique 0-69866
 fluid dynamics, free boundary flow, surface tension effects, finite element fluid flow simulators 0-82647
 fluid dynamics, groundwater flow, finite element eqns., Newton iteration and modified conjugate gradient method 0-77622
 fluid dynamics, stationary Navier-Stokes eqn., discretisation, splitting of linear operators, iterative methods 0-69755

iterative methods continued

- hologram construction from X-ray views or acoustic views 0-69339
 holography, rel. to phase problem in electron microscopy 0-99681
 hyperviral scaling iterative method 0-73196
 inelastic electron scattering in crystals, extension of Yoshioka theory 0-103219
 inhomogeneous medium, effective cond., iteration series and variational estimates, Herring method 0-70663
 MHD equilibrium equations, convergence of iterative schemes 0-59115
 NMR, high resolution, automated anal., principles and computational strategy 0-58287
 nuclear potential energy surfaces, folded Yukawa-plus-exponential model 0-86816
 optical imager, linearly degraded, iterative restoration 0-95807
 optical images, linearly degraded, iterative restoration, reblurring procedure 0-99640
 optimal restoration filter for Poisson noise impaired and linearly blurred images 0-106481
 orientation distribution function analysis from incomplete pole figures normalised by iterative method 0-59344
 physiological compartment tracer flow modelling and digital imaging 0-101257
 plano-plano interferometer modes, FFT computation, Fresnel numbers 0-86392
 random digital scene generation with specified statistics 0-99666
 rod, thin elastic, with causally mixed inputs, iterative numerical soln. 0-79161
 scattering amplitude phase construction by iteration of bounds from unitary integral 0-57142
 scattering length 0-86100
 SCF iterative sequences, convergence accel. 0-91435
 static electric field determ., numerical methods, monodielec./multidielec. regions, iterative solns. (*Spanish*) 0-106419
 superharmonic approximation for quantum crystal 0-92615
 swarm transport coefficients, iterative method calcs. 0-96336
 Tokamak equilibrium, inverse problem, iterative metric method 0-106883
 torsional vibration analysis, change of stiffness method 0-74589
 two-electron integral transformations for 2nd order multiconfig. Hartree-Fock method 0-87045
 unbounded Hermitian operators, low-lying eigenstates, method 0-98812
 wave equation, reduced, fixed incident field, inverse problem 0-62484
 H_2 , electron scatt., iterative approach to Schwinger variational principle 0-99580
 LiH, direct optimisation of orbitals for multiconfiguration self-consistent field theory by unitary transformations 0-63544
 SF_6 , arc, temp. determ. accounting for demixing 0-70057

itinerant model of magnetism *see band model of magnetism*

IV-VI semiconductors

- ferroelectric, vibronic model of lattice instability 0-80723
 structural phase transitions, anomalous resist., electron-soft phonon interactions 0-108167
 $Gd_2Se_3/PbTe$, N type selenide segmented element fabrication, thermoelectric props. 0-107835
 $Ge-Bi-Te$ system, thermal cond. change during phase transitions 0-100368
 GeS , absorpt. spectra, electron-phonon interactions 0-80810
 GeS , anisotropic EXAFS, cryst. struct. determ. 0-66323
 $p-GeS$, crystalline, photoelectric props. 0-70769
 GeS , physical basis for Urbach's rule 0-93366
 GeS , Urbach's rule, absorption edges 0-97224
 $GeSe_2$ amorphous film, laser induced oscillatory phenomena 0-84711
 $GeSe_2$ powdered crystalline, photoluminescence intensity under continuous excitation 0-71480
 $GeTe$, bond orbital model of band struct. 0-59853
 $GeTe$, effective masses for cond., density of states 0-88472
 $GeTe$, Hall coeff., temp. depend. rel. to order parameter 0-96921
 $p-GeTe$, reflectance, and thermoref. spectra 0-80814
 $GeTe$, stoichiometry deviations influence on mech. props., 25-500°C 0-103410
 $GeTe$, supercond., metal-insulator transition, electron pairing, effect on optical props. 0-60139
 $GeTe-Sb_2Te_3$, solid solutions, cond., density of states 0-88472
 Pb chalcogenides, Auger recomb., theory 0-65586
 Pb salt tunable diode laser-integrating sphere system, output intensity characs. 0-78881
 $p-Pb_{1-x}Ge_xTe$ film, cyclotron reson. above and below struct. phase transition 0-88879
 $Pb_{1-x}Ge_xTe$ magnetoplasma reflectivity and transmission spectra 0-71428
 $Pb_{1-x}Ge_xTe$ solid solns., phase transition influence on elec. props., 77 to 450K 0-103689
 $Pb_{1-x}Hg_xS-Si$ heterojunctions, elect. props. 0-100513
 $Pb_{0.97}Hg_{0.03}Te$ photovoltaic detector produced by Sb^+ ion implantation 0-82821
 PbS , anomalous magnetoresist. 0-107813
 PbS , chem. deposited thin film, effect of morphological struct. on photosensitivity 0-70760
 PbS , electrodeposition, using nonaqueous solvents 0-76200
 PbS , energy gap and dielec. props., 77 to 373K 0-66100
 PbS , film, total current spectrum and energy struct. 0-100719
 PbS films, polycryst. and epitaxial, small-angle X-ray scatt. and electron density inhomogeneities 0-96758
 PbS islands, vacuum deposited, electron microscope obs. 0-103601
 PbS , photosensitive film, electron bombard. effect on elec. cond. 0-93019
 PbS , vacuum deposited film, orientation axis tilt rel. to vapour angle of incidence 0-88456
 PbS , valence band struct. determ. by optical absorpt., size quantization effects 0-59871
 $PbS:TI$, self-compensation of acceptors by vacancies, Hall coeff. meas. 0-92913
 PbS -base photodetectors, struct. invest. by proton irradi. 0-104388
 $PbS-In_2S_3$, phase investigation 0-66488
 $PbS-PbO$ vacuum evaporated films, elec. cond. and photocond. 0-75656
 $PbS-PbSe$ epitaxial bicrystals, direct scatt. of channelled He ions at dislocations 0-65110
 $PbS-Si$ heterojunction, chem. struct., AES anal. 0-76115
 $PbS-Si$ heterojunction, related optical and IR detector props. 0-77866
 $PbS-Si$ heterojunction, space charge capacitance, $PbSn$ film thickness depend. 0-88630
 $PbS-Si$ heterojunction, PbS film growth and struct. 0-96762
- IV-VI semiconductors continued
 $PbS-Si$ p-n heterojunctions, AC admittance meas. 0-96979
 $PbS_{0.9}Se_{0.9}$ 4.6 μm LED, room temp., band gap and electrolum. 0-66302
 $PbS_{1-x}Se_x$ ($X=0.18$) homojunction injection lasers, near-field emission 0-95896
 $PbS_{1-x}Se_x$ diode laser, contact degradation due to diffusion 0-102734
 $PbS_{1-x}Se_x$ thin film, stimulated emission, temp. depend. 0-66232
 $PbS, Se_{1-x}Te_x$ multispectral photovoltaic IR detectors 0-105710
 $PbS(Se)(Te)$, bond orbital model of band struct. 0-59853
 $PbS(Se)(Te)$, strongly anisotropic polar semicond., electron-hole liq. in mag. field 0-59890
 $PbSe$, energy gap and dielec. props., 77 to 373K 0-66100
 $PbSe$ films, current carrier conc. and type control, elec. cond., synthesis process (*Russian*) 0-100412
 $PbSe$, valence band struct. determ. by optical absorpt., size quantization effects 0-59871
 $PbSe:TI$, self-compensation of acceptors by vacancies, Hall coeff. meas. 0-92913
 $Pb_{1-x}Sn_x$ epitaxial layers, radiative and nonradiative recomb. processes 0-60670
 $Pb_{1-x}Sn_xSe$ epitaxial layers obtained by LPE, growth conditions correl. with morphology 0-104079
 $Pb_{1-x}Sn_xSe$ solid solns., photoluminesc. spectra, energy band parameter determ. 0-71484
 $Pb_{1-x}Sn_xSe$, transport phenomena in solid solutions with band inversion 0-107792
 $Pb_{1-x}Sn_xSe$, $X=0.03-0.07$, monocrystal film, edge of intrinsic absorpt. (*Russian*) 0-71368
 $Pb, Sn_{1-x}Se_x$ multispectral photovoltaic IR detectors 0-105710
 $PbSnTe$, anomalous avalanche breakdown 0-80284
 $PbSnTe$, optical dielectric const. variation with carrier conc. 0-84709
 $Pb_{0.7}Sn_{0.22}Te$, $Pb_{0.91}Sn_{0.09}Se$, radiative and nonradiative recombination 0-80849
 $Pb_{0.9}Sn_{0.1}Te$:Cd, influence of Cd doping on high field magnetoresist. and Hall effect 0-75590
 $Pb_{0.8}Sn_{0.2}Te$:La, evaporated thin films, low carrier conc. 0-65414
 $Pb_{0.82}Sn_{0.18}Te$ film, effect of hydrostatic pressure on props. 0-70862
 $Pb_{0.82}Sn_{0.18}Te$ layers on mica substrate, Hall constant peculiarities 0-75588
 $Pb_{1-x}Sn_xTe$ diode laser, contact degradation due to diffusion 0-102734
 $Pb_{1-x}Sn_xTe$ epitaxial films, adsorption-induced accumulation layer form. on surface 0-60117
 $Pb_{1-x}Sn_xTe$, growth of epitaxial layers, activation by UV and IR radiation 0-71598
 $Pb_{1-x}Sn_xTe$, hole effective mass near zero bandgap, IR refl. study 0-108205
 $Pb_{1-x}Sn_xTe$, lattice and electronic props. and g-value 0-80161
 $Pb_{1-x}Sn_xTe$, narrow gap semicond., theory of mag. susceptibility 0-93070
 $Pb_{1-x}Sn_xTe$, thermoelectric effects, characteristics at low temps. 0-107831
 $Pb_{1-x}Sn_xTe$, $x=0.2$, monocrystal, photoelectric props. of p-n structures (*Russian*) 0-70808
 $Pb_{1-x}Sn_xTe$, $X=0.2$, monocrystal, edge of intrinsic absorpt. (*Russian*) 0-71368
 $Pb_{1-x}Sn_xTe$:Cd(In), solid solutions, impurity states in photoluminescence spectra (*Russian*) 0-97333
 $Pb_{1-x}Sn_xTe$:Ge, anomalous behaviour of impurity centres under press. (*Russian*) 0-65491
 $Pb_{1-x}Sn_xTe$:In, Hall effect and photoconductivity (*Russian*) 0-103720
 $Pb_{1-x}Sn_xTe$:In, impurity influence on photoluminescence at large excitation levels (*Russian*) 0-93384
 $Pb_{1-x}Sn_xTe$:In, tunnelling impurity self-localisation, anomalous props. nature (*Russian*) 0-59915
 $Pb_{1-x}Sn_xTe/PbTe_{1-x}Se_x$ lattice-matched buried heterostructure lasers with CW single mode output 0-74386
 $Pb_{1-x}Sn_xTe-PbTe$ heterostructures, MBE produced on mica and $LiNbO_3$, elec. props. study 0-88629
 $Pb_{1-x}Sn_xTe_{1-x}Se_x$ quaternary solid solns. with const. lattice parameter, cryst. growth and characs. 0-108332
 $Pb_{1-x}Sn_xTe_{1-x}Se_x$ solid solutions with constant lattice parameter, phase comp. 0-108417
 $PbTe$ and solid solns., optimal synthesis conditions for single cryst. growth 0-100776
 $PbTe$, diffusion of Ag, effect of gamma irradiation 0-59515
 $PbTe$, electrochemical surface reactions 0-76389
 $PbTe$, energy gap and dielec. props., 77 to 373K 0-66100
 $PbTe$, far IR magnetoref., band struct. 0-76010
 $PbTe$ film, electronic thermal cond. and thermoelec. power 0-93018
 $PbTe$, growth of epitaxial layers, activation by UV and IR radiation 0-71598
 $PbTe$ homogeneity region investig. in $Pb-Te$ system, equil. consts. of quasi-chem. reactions 0-108405
 $n-PbTe$, low temperature electrical transport, Hall effect 0-84478
 $n-PbTe$, noncubic (111) oriented epitaxial films, weak field magnetoresistance 0-75584
 $PbTe$, nonstoichiometric, evap. and growth of epitaxial layers 0-104072
 $PbTe$ photovoltaic detector, detectivity limits 0-105709
 $PbTe$ single crystals, growth from vapour phase under micro-gravity conditions 0-80957
 $PbTe$ thermoelectric alloys, phase diagrams, and imperfection chemistry 0-108422
 $PbTe$ thermoelectric materials, microstructure anal. using SEM X-ray microanalysis 0-107211
 $PbTe$, two photon magnetooptical absorption (*Russian*) 0-60553
 $PbTe:Fe$, single crystals, state and behaviour of Fe, mag. props. 0-93080
 $PbTe:In$, electron mobility, temp.-independent part, Hall effect and elec. cond. meas. 0-92914
 $PbTe:In$, mag. susceptibility, temp. depend., 4.2 to 200K 0-65773
 $PbTe:In$, Shubnikov-de Haas oscillatory effects, quasilocal impurity level 0-92912
 $PbTe-CdTe$ heterojunctions, fabrication and characterisation (*German*) 0-89151
 $PbTe-Ga_2Te_3$, phase interaction, DTA, XPA and microstructural anal. 0-96625
 $PbTe-In$ contacts, fabrication and props. 0-60078
 $n-PbTe-p-Pb_{1-x}Sn_xTe$ heterojunctions, heavily doped, current-flow mechanisms 0-96974
 $PbTe-Pb_{1-x}Sn_xTe$ p-n⁺ heterojunction photodetector, hot wall evaporation technique 0-65673

IV-VI semiconductors continued

- Pb_{1-x}Te-Pb_{1-x}Sn_xTe (x,y≤0.3), double heterostruct., LPE growth, heterointerface morphology 0-70550
 Si-Te system, phase diagrams 0-89209
 Sn_{1-x}Pb_xSe(Te) films, Mossbauer effect of ¹¹⁹Sn, spectral charact., conc. depend. 0-103903
 Sn_{1-x}Pb_xSe(Te) films, oxidation rel. to annealing temp. and time, Mossbauer spectra, X-ray and microstruct. obs. 0-104311
 Sn(S_{1-x}Se_x)₂, valence band states, composition depend., photoemission spectra study 0-100434
 SnTe, annealed, iodide method of prep., props. meas. 0-71591
 SnTe, bond orbital model of band struct. 0-59853
 SnTe, diffusion of ¹²⁵Te 0-84325
 SnTe, dispersive transform., interband electron-phonon interactions, phase diagram 0-93252
 SnTe, strongly anisotropic polar semicond., electron-hole liq. in mag. field 0-59890
 SnTe, structural phase transition threshold instability in strong EM field 0-103477
 SnTe, supercond., metal-insulator transition, electron pairing, effect on optical props. 0-60139

J particles see psi mesons

Jahn-Teller effect

- alkali metal halide crystals, g-tensor anal. of S⁻ and Se⁻ centres, ESR 0-84650
 benzene, first-ionisation Rydberg spectrum assignment via Jahn-Teller splitting 0-69155
 commensurate and incommensurate structural phase transitions in Jahn-Teller system 0-70403
 cooperative Jahn-Teller phase transition, crit. behaviour 0-108016
 cooperative phase transitions, crit. diffuse scatt. 0-59930
 cooperative T-(e+t) Jahn-Teller system, thermal cond. 0-70479
 cooperative T-systems, dynamics, elastic props. 0-65511
 cubic crystal, Jahn-Teller effect, soft mode influence 0-59937
 diamond, GR1 band, anal. of satellite lines by quadratic Jahn-Teller computing 0-97295
 diamond, Jahn-Teller coupling at neutral vacancy 0-71453
 dielectric crystal, APR and phonon spectroscopy to study paramagnetic ions 0-84634
 dynamic Jahn-Teller effect in ESR spectra, Green's functions calcs. 0-84643
 ferroelectrics and antiferroelectrics, elastic and dielec. anomalies, microscopical model 0-71332
 haemoglobin, Jahn-Teller pseudo effect rel. to Fe release and conformational changes 0-76701
 halobenzene cations, in solid Ne matrix, slow vibr. relax., fluoresc. obs. 0-74194
 Ham factors in multi-mode system 0-100446
 hydrides, first row, bending pot. calc. using MINDO approx., force const., equilb. geometry 0-95544
 interacting systems, predominant states and matrix elements 0-89033
 linear pseudo-Jahn-Teller effect, in strong coupling, anal. formulae for props. 0-92863
 magnetic insulators with Jahn-Teller ions, temp. depend. of exchange integrals 0-103827
 methane, mol. cations, struct., Jahn-Teller effect, MINDO/3 calcs. 0-74135
 methoxy, Jahn-Teller induced rovibronic effect, nuclear spin-electron spin hyperfine Hamiltonian 0-83298
 molecule, pre-reson. Raman scatt. by t-type mode near A—T electronic transition 0-82821
 Mossbauer ⁵⁷Fe spectra, ferrous charact., cryst. field interactions 0-108133
 phonon spectroscopy, HF, using supercond. tunnel junctions 0-65178
 quasi-Jahn-Teller optical absorption line shape due to transition from A_{1g} to (A_{1g}+T_{1g})×T_{1u} system 0-92862
 rare earth zirconos, Jahn-Teller cooperative phase transition, crossover effects 0-88316
 strongly coupled Jahn-Teller system, cluster model for optical absorption spectrum 0-89034
 thermodynamic properties, internal stress' effects in Jahn-Teller system 0-59679
 trichlorobenzene cations, Jahn-Teller distortions, quadratic and mode mixing effects., distortion geometry determ. 0-91462
 symtrifluorobenzene cation, Jahn-Teller effects, intermode interactions and intensity anomalies 0-78553
 sym-trifluorobenzene cation, Jahn-Teller effects, quadrupole coupling 0-78554
 trifluorobenzene cations, Jahn-Teller distortions, quadratic and mode mixing effects., distortion geometry determ. 0-91462
 tris(trimethylstannyl)amine, gas phase electron diffraction 0-106401
 AgCl:Pd²⁺, ESR spectrum, quasistatic Jahn-Teller effect 0-71170
 Al₂O₃:Cr³⁺, Jahn-Teller system, zero-phonon line broadening due to non-radiative transitions 0-108258
 Al₂O₃:Mn²⁺, Jahn-Teller Mn²⁺ ions, phonon spectroscopy and thermal cond. meas. 0-88282
 Al₂O₃:Mn²⁺ under uniaxial stress, Jahn-Teller model 0-88521
 Al₂O₃:V³⁺, Jahn-Teller effects, ground state 0-75528
 BaF₂:Pb²⁺, band struct., Jahn-Teller effect, UV luminesc. and optical absorpt. spectra 0-66243
 CH₄⁺, Jahn-Teller distortion, energy and angular distrib. of collisional dissociation fragment 0-66356
 CaF₂:Pb²⁺, band struct., Jahn-Teller effect, UV luminesc. and optical absorpt. spectra 0-66243
 Co complex, Co(NO₂)₆⁴⁻, bond. props. and Jahn-Teller distortion, INDO-LCAO-MO calcs. 0-75532
 CsCrCl₃, Jahn-Teller induced phase transitions 0-70391
 CsCrI₃, neutron diff. expts. at 300, 77 and 1.2K 0-107163
 CsCuCl₃, Jahn-Teller induced phase transitions 0-70391
 Cs₂MX₆ (M=Se, Te, X=Cl, Br), Γ₄⁻(³T_{1u}) state, Jahn-Teller effect, luminesc. obs. 0-60650
 CsMnF₄, planar ferromag., cryst. and mag. struct., Jahn-Teller effect 0-75715
 Cs₂PbCu(NO₂)₆, incommensurate Jahn-Teller transition, Huang scatt. 0-70401
 Cs₂PbCu(NO₂)₆, low-temp. γ-modification, struct., powder neutron diff. study, 160K 0-84151
 Cs₂TiF₆:Mn⁴⁺, spin-orbit and field splitting, Jahn-Teller effect, Zeeman meas. 0-80234
- Jahn-Teller effect continued**
 Cu complex, Cu(NO₂)₆⁴⁻, bond. props. and Jahn-Teller distortion, INDO-LCAO-MO calcs. 0-75532
 Cu_{2-x}Se, nonstoichiometric, diamag. and paramag. props., susceptibility meas. 0-70936
 DyAsO₄, first order Jahn-Teller phase transition, sp. ht. and refr. index meas. 0-59645
 DyAsO₄, phase transitions obs. 0-70412
 DyVO₄, cooperative Jahn-Teller phase transition, linear birefr. meas. 0-88960
 DyVO₄, Jahn-Teller crystal, deform. induced transitions, elastic and dielectric charact. (Russian) 0-80726
 DyVO₄, phase transitions obs. 0-70412
 Fe group, mol. Jahn-Teller reson. states as possible antecedents to magnetism 0-75701
 FeBO₃, mag. linear dichroism and absorpt. spectra, exciton-magnon absorpt. mechanism 0-66160
 Fe₂TiO₄, cooperative Jahn-Teller phase transition, crit. diffuse scatt. 0-59930
 GaAs:Cr, semi-insulating, Zeeman studies of 0.839 eV emission 0-103987
 GaAs:Cr²⁺, Jahn-Teller effect for ion impurities 0-107753
 Gd(OH)₃, dynamical effects of interaction between 4f electrons and optical phonons 0-108196
 InAs:Mn²⁺, Jahn-Teller effect for ion impurities 0-107753
 InP:Cr²⁺, Jahn-Teller effect for ion impurities 0-107753
 KCl(Br)(I):Ga³⁺, polarisation of Ga³⁺ centre A_T emission, temp. depend. 0-80842
 KI, perturbed by Jahn-Teller centres, lattice dynamics 0-107394
 KMgF₃:Co²⁺, ⁴T₁-²T₂ transition, zero-phonon lines intensities 0-75529
 K₂NaGaF₆:Cr³⁺, magneto-optical study of ²T_{1g}, ⁴T_{2g}, ²E_g-A_{2g} transitions 0-71384
 K₂PbCu(NO₂)₆, incommensurate Jahn-Teller transition, Huang scatt. 0-70401
 KZn₂, exchange interactions of transition metal ions in orbitally degenerated excited states 0-65512
 LaAlO₃, exchange interactions of transition metal ions in orbitally degenerated excited states 0-65512
 MgO:Co²⁺, weak dynamic Jahn-Teller coupling, neutron inelastic scatt. obs. 0-59934
 MgO:V²⁺, Jahn-Teller system, zero-phonon line broadening due to non-radiative transitions 0-108258
 Mg₂TiO₄:Cu(Ni), ESR of Cu²⁺ and Ni³⁺ 0-97131
 γ-MnAl, estimated theoretical limit of mag. moment 0-97072
 Nd₂Br:Cu²⁺, pseudo-Jahn-Teller effect manifestation in ESR spectrum 0-71168
 NH₃⁺, two-mode Jahn-Teller effect calcs. 0-83297
 NaCl:Ga³⁺, polarisation of Ga³⁺ centre A_T emission, temp. depend. 0-80842
 Nd(OH)₃, dynamical effects of interaction between 4f electrons and optical phonons 0-108196
 NiZn ferrite, dielec. props., Jahn-Teller ion effects 0-97181
 O₂ monolayers, on graphite, mag. α-phase and α-β-phase transition 0-70530
 RbCrCl₃, Jahn-Teller induced phase transitions 0-70391
 RbMnF₃, Jahn-Teller coupling const., LCAO calc. 0-59940
 Rb₂PbCu(NO₂)₆, incommensurate Jahn-Teller transition, Huang scatt. 0-70401
 p-Si, vacancy, charge states, Jahn-Teller stabilisation energy 0-80209
 Si:Co²⁺(Mn²⁺), spin-lattice relax. of Jahn-Teller centres, coexistence of minima with different symmetries 0-80602
 Si:N, laser-annealed, Jahn-Teller distorted donor, EPR meas. 0-84642
 SrF₂:Pb²⁺, band struct., Jahn-Teller effect, UV luminesc. and optical absorpt. spectra 0-66243
 SrO:Ni²⁺, EPR line splitting rel. to Jahn-Teller coupling and soft localised mode 0-66022
 Tb(OH)₃, dynamical effects of interaction between 4f electrons and optical phonons 0-108196
 TbVO₄, co-operative Jahn-Teller transition, low freq. dynamics, light scatt. study 0-88317
 Ti₂PbCu(NO₂)₆, incommensurate Jahn-Teller transition, Huang scatt. 0-70401
 UF₆, matrix isolated, vibronic fine struct. in fluorenc. spectrum 0-83406
 XeF₅⁺, pseudopot. SCF MO studies, steric aspects of struct. and force fields, Jahn-Teller effect 0-99444
 XeF₆ molecules with Jahn-Teller pseudo-effect, ang. depend. of inelastic scatt. of electrons 0-69246
 XeF₆, pseudopot. SCF MO studies, steric aspects of struct. and force fields, Jahn-Teller effect 0-99444
 Y(OH)₃, dynamical effects of interaction between 4f electrons and optical phonons 0-108196
 Zn₂Cu₁₀Fe_{2.9-x}O₄, ferromag. reson., g-factors, Jahn-Teller ion effects 0-66043
 Zn₂Fe_{3-x}O₄, ferromag. reson., g-factors, Jahn-Teller ion effects 0-66043
- jellies see gels**
jellium
 adsorbed CO, surface plasmon relax. energies 0-70537
 CDW in two- and three-dimens. jellium, appl. to liq. He surface and semiconductors 0-65476
 chemisorption, effective-medium theory of chem. binding 0-65367
 electromigration, driving force, strong-coupling theory 0-65300
 metallic surface, self-consistent electron theory, review 0-88616
 oscillating dipole-metal surface interaction, jellium model and random phase approx. 0-92955
 screening of proton, Anderson model calc. 0-59895
 surface-atom polarisability derivation from field-ion energy deficits 0-76155
 Al (001), enhanced photoexcitation 0-80937
- jet stream see atmospheric movements**
jets
 see also plasma jets; sprays
 acoustically excited jet, discrete noise spectrum, vortex pairing 0-74847
 Agulhas Current, topographically induced changes in struct. of inertial coastal jet 0-72545
 air jets with suspended polystyrene spheres, effect of particle proximity on drag force 0-96306
 AMTE/OUEL underwater jet noise rig, working report for 1977/78 0-79286
 AMTE/OUEL underwater jet noise rig, working report for 1978/79 0-79287

jets continued

annular, small inner diameter, investigation of vortices by schlieren photography 0-74935
 attached jet characteristics, aspect ratio effect (*Japanese*) 0-87791
 axisymmetric jets, coherent struts. using optical technique, convection vel. 0-69888
 axisymmetric swirling jets, stationary flows in surrounding inviscid medium (*Russian*) 0-69892
 axisymmetric turbulent jet initial region, annular free shear layer 0-106826
 bounded coaxial jets, convective heat transfer in turbulent mixing, swirling 0-64541
 break-up effect of nonlinear concentration profiles on jets undergoing mass transfer 0-79371
 capillary oscillations, meas. 0-96291
 circular impinging jet, heat transfer characts., stagnation point, boundary layers 0-79303
 circular jets with crossflow, inline and staggered arrays, heat transfer coeff. variations 0-74873
 conduit with lateral outlet, two-dimens. flow past barrier 0-64642
 confined coaxial jets with and without swirl, vel. characts., recirculation regions 0-103055
 confined turbulent coaxial jet, vel. characts. 0-64601
 core noise and jet noise separation, mean square pressures 0-69779
 curved wall power fluidics characts. 0-103053
 dispersive compressible fluid, steady two-dimens. jet flow 0-64598
 dissipation rate for turbulent plane and circular jets 0-69889
 eddies, large, numerical model for axisymmetric jet 0-79375
 edgetone sound, prediction of amplitude 0-74568
 excess noise from supersonic underexpanded jets in flight 0-69815
 flat surface, jet impingement, rotational flow model calcs. 0-64596
 flow characteristics for jets normal to the crossflow 0-64597
 flow hydrodynamic model, three-dimensional 0-79369
 flow visualization of cavitation in water jets and nuclei distribution measurement by holography 0-106862
 free turbulent jet directed against a flat surface, phenomena accompanying the impact, diversion, and distribution (*German*) 0-106827
 Freon electrohydrodynamic flow, jet dynamic pressure obs. (*Russian*) 0-59117
 gas, acoustic wave generation, Hartmann whistle 0-87695
 gas jet blowing into supersonic flow without 3-dimens. boundary layer separation, nozzle shape 0-100009
 gas mixture-isotope inertial gas-kinetic separation 0-69927
 heat transfer and hydrodynamics of an array of round impinging jets with one-sided exhaust of the spent air 0-79374
 heated circular jet, outer part, temp. and vel. simultaneous meas. errors 0-87830
 horizontal cylinder with different end temps., natural convection, jets 0-99996
 hydrodynamic cumulation regimes during lining collapse, cumulative jet 0-69891
 hydromagnetic capillary instability of a liquid jet with an axial flow 0-74990
 injector with distrib. multijet liquid supply, efficiency and performance 0-74939
 irrotational strain dissipation eqn. sensitisation 0-106794
 jet noise, cross-spectral densities, extension of Ribner's theory 0-69804
 laminar vertical round jets, weak buoyancy effects due to temp. differences (*German*) 0-64595
 liquid jet vacuum seal, inflow, rel. to electron beam emergence into atmosphere 0-78469
 locally elliptic calculation procedure 0-103054
 low frequency sound radiation due to the interaction of unsteady flows with a jet pipe 0-69787
 Mach wave radiation of hot supersonic jets 0-69894
 magnetisable liquid, stability 0-83831
 Meksyn's method applied to jet flows 0-96292
 melt reacting with gas jet, heat and mass transfer, mathematical modeling 0-87819
 mixing layer, free, axisymmetric, turbulent spot, data processing 0-79280
 mixing layer, free, axisymmetric, turbulent spot, vorticity and Reynolds stress 0-79281
 Newtonian jet, axisymmetric, die-swell, Galerkin finite element method 0-83830
 noise generation by jet mixing, eval. of Lighthill analogy using LV turbulence, source location and spectral noise data 0-69803
 noise in flight, prediction, importance of jet temp. 0-69814
 noise prediction, nonlinear Lilley equation 0-69805
 non-Newtonian liquid with power-law behaviour, flat submerged jet theory 0-59078
 nonequilibrium free jet expansion, rotational temp. meas for N_2 0-69890
 nonequilibrium free jet expansion, translational temp. meas. in N_2 0-64600
 nonisothermal turbulent heterogeneous jet entering air filled half space 0-64599
 nozzle in different jet regimes, internal and external flows, separation and wakes 0-100023
 ocean coastal jet and warm front propagation, theory with appl. to Sagami Bay Kyucho phenomenon 0-94538
 parallel flows of unmixed reactants, temp. and conc. distrib. in reaction region 0-92236
 parallel jets exhausting from ducts, acoustic wave propag. 0-64257
 perforated plate, axisymmetric jet array, transverse vel. profiles 0-92195
 permeable contour in flow with jet separation, impulses and impact effects 0-92196
 phthalocyanine, free base, fluoresc. excitation spectrum, cooling in supersonic free jet 0-95670
 pipe-exit flow visualisation using high-speed photography 0-106863
 pipes and bends, structure-borne sound behind a jet nozzle (*German*) 0-87804
 plane turbulent buoyant jet, parameter calcs. (*Russian*) 0-79373
 plane jet, heated, ventilated, heat transfer to plane wall 0-59025
 plane jet, stability and autooscillations from channel anal. 0-100018
 plate with impinging hot gas jet with low Re, convective heat transfer 0-96256
 polymer solution, elastic, load bearing capacity of squeeze film flow 0-103051
 pulsations at discrete freq., Navier-Stokes eqns. for fluid behind plate in channel (*Russian*) 0-74979

jets continued

pulse-jet fabric filter, high vel., dust retention effect on pressure drop 0-103072
 pulsed, flowing out of supersonic nozzles, wave struct. in nonstationary flow stage 0-59094
 radiation properties of a turbulent jet excited by a sinusoidal acoustic disturbance 0-69789
 rapidly rot. gas, free jet expansion, Newtonian thin shock layer approx. 0-74888
 reaction, turbojet engine internal noise 0-87644
 reactive gas mass spectrometric analysis with free-jet expansion sampling 0-89566
 reversed flow characteristics due to jet issuing from dead end channel (*Japanese*) 0-100021
 rotating hollow gas jets, nozzle exit flow angle and pressure forces effects (*German*) 0-69887
 round free jet, aerodynamic noise, propagation of wavelike disturbances 0-69806
 shear layer instability noise produced by various jet nozzle configurations 0-69791
 shield-hot turbulent jet interaction, nonstationary heat transfer 0-92136
 slightly heated small perturbation jets and wakes in press. grad., self-preservation 0-96290
 slow EM wave theory in conducting jets 0-91731
 slowly spreading jets, MHD instability 0-87818
 sound generation by flow-acoustic coupling 0-69793
 sound generation in flows, conf. Gottingen, Germany (Aug. 1979) 0-67937
 sound generator, vortex, separation of acoustic energy and spent-air jets 0-102953
 sound radiation by instability waves of a compressible axisymmetric jet 0-69792
 sound radiation from a simulated jet flow, calc. of vortex configuration and sound field 0-69786
 sound sinks in flows, low freq. sound absorpt. of jets 0-69788
 sound spectra radiated by gas jets, influence of closely located solid surfaces 0-69800
 spouted beds of spherical particles, spout termination, parameters 0-64621
 stratified liquid, free convective flow struct. over point heat source 0-79323
 Strouhal number influence on flight effects on jet noise radiated from convecting quadrupoles 0-69784
 submerged gas injection into liquids, flow regimes 0-59101
 submerged jet cone angle from bubble theory 0-79372
 submerged jets impinging on baffle, flow and mass transfer, polymer additive effects 0-92194
 submerged water jet, interaction of US waves with turbulence 0-87619
 subsonic, jet-mainstream interaction 0-79271
 subsonic jet in simulated motion, sound radiation 0-74846
 superheated liquid discharge from nozzle, pressure calc. 0-92199
 supersonic and sonic annular jets, 0-100019
 surface discharging heated turbulent jet, 3D finite difference model, turbulent diffusivities 0-74845
 surface noise from turbulent hot jet, temperature effects 0-69782
 transformer oil electrohydrodynamic flow, jet dynamic pressure obs. (*Russian*) 0-59117
 triple correlation of the pressure in subsonic circular jets and nonlinear interaction of instability waves 0-69893
 turbulence, laser velocimeter correlation meas. 0-106785
 turbulence generated noise at edges 0-103020
 turbulent flow, film cooling performance 0-79272
 turbulent jet flow, aeroacoustic interaction, review 0-87765
 turbulent jet impinging on cylinder wall, heat transfer and fluid mechanism study (*Japanese*) 0-83800
 turbulent jets, influence of drag reducing polymers on cavitation inception 0-106823
 two-dimensional water, sensitive to sound, behaviour (*Japanese*) 0-79376
 upstream acoustic disturbances, effects of upstream tones on the large scale instability waves and noise of jets 0-69790
 vertical jet, 2-D, under gravity integral equation method of soln. 0-59093
 vortex pairing in jet noise generation 0-69807
 wall jet, axisymmetric radialwise, flow pattern on impinged wall 0-79370
 wall jet flow, compliant walls, influences of flow convection and refraction on sound radiation 0-74595
 water jets sensitive to sound, two-dimensional, velocity fluctuations behaviour (*Japanese*) 0-100020
 Ar, nonequilibrium condensation and surface tension in supersonic jet flow (*Russian*) 0-65210
 CO, rot. distrib. in supersonic beam, IR bolometry using tunable diode laser 0-63869
 I_2 seeded in supersonic free jet, collision-induced rotational relax. 0-102556
 N_2 , freely expanding, quantum effects in rot. relax. 0-58355
 N_2 gas jet injection into Hg, interaction at submerged orifice 0-59102

j.f.e.t. see junction gate field effect transistors

Johnsen-Rahbek effect see adhesion; electrostatics

Johnson noise see thermal noise

joining processes

see also brazing; cable jointing; soldering; welding
 powder layer on steel backing plate, joint form. kinetics for hot pressing 0-100961
 Si, joining and recrystallisation using thermomigration process 0-65298
 SiC, dense, joining by hot pressing, and bond strength 0-66458

jointing, cable see cable jointing

jointing (electric connectors) see electric connectors

Jordan-Thiry field see cosmology; general relativity

Josephson effect

bridges, electric field penetration and collective oscillations, review 0-88678
 DC, spin-glass phase transition exam. 0-100594
 films with periodic thickness modulation, pinning effects 0-88702
 FIR detectors, Josephson-junction direct devices and transition edge bolometers, review 0-77865
 fluxons on a Josephson line with loss and bias 0-103794
 granular films as weak link in Josephson devices 0-88685
 granular metal, supercond. transition, increased resistance rel. to quasiparticle tunnelling 0-88689

Josephson effect continued

granular superconductors, coherence transition, structural disorder effects 0-88657
 granulated superconductors, phase transitions, Josephson energy (*Russian*) 0-84540
 HF theory, electronic analogue prototype 0-100560
 higher harmonics, flux tunnelling, thermodynamic free energy 0-60147
 hybrid Josephson FET, feasibility 0-80451
 inelastic tunnelling, pair-quasiparticle interference current 0-84566
 inhomogeneous superconductivity, Ginzburg-Landau theory 0-88672
 interferometers, large arrays, device parameter meas. 0-75682
 interferometers, symmetric two-junction, self-induced reson., theory 0-107962
 Josephson AC effect applications in precision metrology and novel voltage source (*German*) 0-70902
 Josephson coupled layered supercond., upper critical field (*Russian*) 0-100551
 Josephson element principles, applications to precision meas. of electric potential and magnetic flux at high freq. (*Norwegian*) 0-80447
 Josephson junction interferometer, loop inductance 0-97034
 Josephson junctions, applications in plasma physics 0-103194
 Josephson tunnel junction, nonresonant vortex motion 0-97037
 Josephson-junction capacitor, QED theory 0-93049
 junction, coherent radiation induced bistability 0-80453
 junction, current biased, eigenstates and eigenvalues 0-60148
 junction, fabricated by RF plasma oxidation, IV characts. (*Japanese*) 0-84564
 junction, space appl. 0-85836
 junction, with linear periodic current-phase relations, phase locking and microwave impedance 0-93043
 junction array, granular supercond., phase transitions 0-88684
 junction fabrication by ion implantation, electron beam lithography and dry etching 0-88693
 junction with matched RF source, analogue simulation 0-75683
 junctions, coupled, I-V charact., model calc. 0-84559
 junctions fabrication, tunnelling through edge-grown barriers 0-100567
 laser frequency measurement using supercond. point contacts 0-90824
 layered superconductors, Josephson coupling effects, review 0-84554
 light-sensitive junctions, locally lowered tunnelling barriers 0-100558
 metal, granular superconductivity, instability 0-103796
 metal inhomogeneous granular, superconductivity 0-103795
 microbridge, high-resistance, with Bi crosspiece 0-93050
 microbridges, with paramag. impurities, Josephson steady-state effect (*Russian*) 0-93042
 multiple flux quantum transitions, comparison with I-U characts. using Nb-point contacts 0-60149
 oscillator, current-drive, quantum modelling 0-75687
 pair transfer, quantum-mechanical description, commutator and anticommutator of collective operators 0-60146
 parametric amplifiers, gain-dependent noise temp. 0-84552
 parametrically coupled Josephson bridges, resistive state, proximity effect (*Russian*) 0-100550
 plasmon states in ultrasmall Josephson junction, dynamic Stark splitting 0-103790
 point contacts, three-dimens. assembly, crit. currents and penetration depth 0-84560
 proximity Kondo alloys, DC Josephson effect 0-88690
 proximity systems with magnetic impurities, DC Josephson effect 0-100554
 pulsars emission mechanism, AC Josephson effect hypothesis 0-82404
 quasi-two-dimensional dirty superconductor, nonstationary Josephson effect (*Russian*) 0-100556
 scattering model 0-93046
 sine-Gordon solitons, boundary effects 0-62481
 SQUID, thermodynamic equilibrium fluctuations generation by Josephson junction, Werthamer theory 0-100564
 SQUID magnetometers, AC-biased, macroscopically quantised, higher harmonics in Josephson effect 0-98952
 superconducting loop broken by damped Josephson junction, anomalous flux penetration 0-97033
 superconductivity characterisation, non-equilibrium 0-100557
 superconductors, type I, mixed state, Josephson condition, phase jumps (*Russian*) 0-107967
 thin film technology, appls. in energy, optics, and electronics, review 0-78932
 tunnel junction, paramag. impurities effect on Josephson current (*Russian*) 0-70903
 tunnel junctions of nonuniform width, max DC Josephson current vs. external mag. field charact. calc. 0-65747
 ultrahigh resolution sampling system 0-90828
 ultrashort current pulse generation and meas. with Josephson devices 0-90827
 voltage response of Josephson junctions, functional relation, extrapolation technique for accelerating computation 0-107963
 voltage standard, Josephson effect, at zero current bias 0-57245
 weak links, quasiparticle-injected, simple-heating-induced Josephson effects 0-70904
 Al granular films, inhomogeneous supercond. transitions, microwave meas. 0-103789
 Au/In proximity effect bridges, square arrays, transition temps. 0-84557
 Au/Pb/In-oxide-PbBi tunnel junctions, supercurrent interference patterns and excess currents 0-100563
 Cu-Cr, Kondo alloy, Josephson tunnelling effect 0-60145
 In film, Josephson arrays, proximity effect junctions 0-84553
 In whiskers from Sn-In alloys, current carrying, superconductivity breakdown 0-60133
 In-In_{0.9}O_{0.1}Pb, tunnel junction fabrication for MM-wave detector 0-100427
 Mo₂PbS₃ embedded in resin, composite supercond., high transition temp. 0-88660
 Nb superconducting point contact, singularities of I-V curve and voltage fluctuations 0-93044
 Nb thin film microbridge, video detection of far IR radiation (*Japanese*) 0-97038
 Nb thin-film Josephson tunnel junctions, fabrication and props., in situ ellipsometric meas. 0-65749
 Nb-Cu-Nb junctions, Josephson effect meas., critical current, temp. depend. 0-93041
 Nb-Nb Josephson junctions, submicron, thermally recyclable, fabrication and characts. 0-100566
 Nb-Nb₂O₅-Pb Josephson junction formed on Nb film edge 0-107960

Josephson effect continued

Nb-Nb₂O₅-Pb(In) Josephson junctions, props. of Nb₂O₅ thermally grown tunnel barriers 0-100568
 Nb-Nb₂O₅-Pb Josephson junction current-biased on Fiske steps, mag. field depend. 0-84567
 Nb-NbO₂-Pb Josephson junctions with high current densities, critical current 0-100552
 Nb-NbO₂-Pb tunnel junction, temp. depend. of effective Nb energy gap 0-80454
 Nb-Pb, long, magnetic field behaviour of zero field steps 0-100561
 Nb-Pb tunnel junction, crit. Josephson current, proximity effect model 0-93047
 Nb-Te-Pb Josephson junctions, prep. and props. 0-65754
 Nb₂Ge, bridge contact, Josephson effect 0-70906
 NbN embedded in resin, composite supercond., high transition temp. 0-88660
 NbN granular microbridges, Josephson effects 0-84556
 NbN weak links, granular, Josephson behaviour 0-75681
 Pb granular film, Josephson coupled, resistive transition 0-88683
 Pb-alloy Josephson tunnel junctions, effect of process variables on elec. props., cryogenic memory appls. 0-65748
 Pb-Bi counterelectrode Pb alloy Josephson junctions 0-65743
 Pb-In-(Au) base electrode film Josephson junctions, tunnel barrier oxide struct. 0-65750
 Pb-PbO₂-Pb small supercond. tunnel junctions, effect of capacitance in I-V characts., high-freq. obs. 0-80448
 Pb-PbO-Pb, tunnel junction fabrication for MM-wave detector 0-100427
 Pb-Te oxide-Pb Josephson junctions, prep. and props. 0-65754
 Sn-Sn₂O₃-Sn long Josephson tunnel junction, flux flow, crit. conditions 0-80452
 TaS₂ intercalated with methylamine, supercond. layer cpd., crit. field enhancement and reduced dimensionality 0-60152
 V-CdS-In preparation and behaviour obs. Josephson junctions 0-100559
 V₃Si embedded in resin, composite supercond., high transition temp. 0-88660
 V₃Si-SiO₂-Mo₂Re₂ supercond. tunnel junctions 0-107961

Joshi effect *see glow discharges*

Joule-Thomson effect
 No entries

junction gate field effect transistors
 semiconductor depth profiling by electron beam induced junction current meas. 0-96977

junction lasers *see semiconductor junction lasers*

junctions, waveguide *see waveguide couplers*

Jupiter
 1979 J 1 discovery by Voyager 2 camera 0-77334
 1979 J 1-3, satellite periods from Voyager 1 and 2 data 0-105196
 1980 LB, 2:1 resonance with Jupiter 0-82259
 Amalthea, effect of proximity to Roche limit on dynamical behaviour of ejecta 0-98592
 astrometric position determ. (*French*) 0-77326
 astrometric position determ. 0-77327
 astrometry using image photometric anal. technique (*French*) 0-85880
 atmosphere, greenhouse effect 0-101544
 atmosphere, response to heat sources and perturbations (*Chinese*) 0-85748
 atmosphere, wind vector, eddy mmtm. and energy conversion obs. 0-72851
 atmosphere constituents, comparison with Saturn, visible spectra obs. (*French*) 0-101550
 atmosphere disturbances and dislocations, triggering factors 0-72867
 atmosphere map at 2400 Å from Voyager 2 obs. 0-77336
 atmospheric constitution, struct. and dynamics 0-105186
 atmospheric VHF refraction 0-98608
 aurora due to protons, nightside 0-85890
 brightness coefficient of disc features, phase effect 0-98602
 Callisto, evolution from derived crustal description 0-82265
 Callisto, IR emission spectra 0-82264
 centre location in Voyager image transformation 0-101534
 close encounter with planet crossing objects, orbit changes 0-77329
 close encounters with minor bodies, importance of nearly tangent orbits 0-82248
 colour distrib. between Voyager 1 and 2 missions, 5 micron obs. 0-77345
 colour pictures from Voyager space probes, 800 line scan TV system, land based receiver systems (*German*) 0-101549
 cosmic ray electrons originating from Jupiter 0-72726
 current disc of magnetosphere, modeled using Pioneer 10 data 0-101551
 decametric radio emission, dynamic spectrum modulation lines origin 0-67643
 decametric and hectometric radio emission obs. 0-67644
 decametric radiation, non-Lo associated, obs. at freqs. above 30 MHz 0-85886
 decametric radio emission, similarity with pulsar emission (*Russian*) 0-77333
 electron flux propagation to Earth orbit 0-90357
 Galilean satellites, improved ephemerides for Voyager mission 0-62066
 Galilean satellites, photometry of Io, Europa and Callisto, 1976 to 1979, possible solar variability detect. 0-98623
 Galilean satellites, water ice existence, IR spectral reflectance obs. 0-82263
 Galileo Jupiter Orbiter Mission CCD camera 0-85859
 Ganymede, atmosphere erosion by radiation belt energetic atomic particles 0-72736
 Ganymede, surface model and characts. from radar obs. 0-90359
 Ganymede disturbing Jovian magnetosphere 0-72856
 Great Red Spot, atmosphere baroclinic model, solitary waves on unsymmetric shear flow 0-82266
 interior Vashchenko Zubarev formula for Gruneisen parameter 0-90030
 Io, 'volcanic' outbursts, elec. current origin explanation 0-82276
 Io, form. of Na clouds and regolith by micrometeoroid impact 0-77330
 Io, global SO₂ abundance upper limit 0-77332
 Io, interaction with plasma torus 0-98604
 Io, local gas emission mechanism (*Russian*) 0-82275
 Io, non-linear standing Alfvén wave current system 0-72869
 Io, plasma torus, ion density spatial distrib. 0-72861
 Io, SO₂ frost IR spectra and deposition processes 0-77331
 Io, SO₂ model atmos. and ionosphere 0-72853
 Io, volcanic activity model based on plasma obs. 0-72870
 Io's torus, charged particle radial diffusion 0-72859

Jupiter continued

- to interaction with environment, Jupiter Voyager imagery analysis 0-105197
- to plasma disc, model of plasma injection 0-72860
- to plasma torus, radiative cooling and spectra 0-72850
- to plasma torus props. from Voyager EUV data 0-82262
- to torus, latitudinal plasma oscils. 0-85892
- ion fluxes, Voyager 1 and 2 obs. out to 1200 Jupiter radii 0-94667
- ionosphere, spectral broadening meas. by Pioneers 10 and (11) 0-109391
- ionosphere, Voyager 2 occultation, radio obs. 0-77337
- IR spatial scans 0-82268
- kilometric radiation, ray tracing 0-72866
- kilometric radiation, spatial and temporal studies 0-77328
- low energy charged particle flux, Voyager LEP results 0-98605
- Lyman α albedo rel. to solar activity 0-98601
- Lyman alpha albedo, calc. from hydrocarbon and H I photochemistry 0-105194
- magnetosheath sunward flow, depend. on solar wind press. 0-72857
- magnetosphere, electrostatic waves obs. 0-72865
- magnetosphere, energetic ions and electron, Voyager 2 obs. 0-77342
- middle magnetosphere, equatorial protons instability 0-67642
- magnetosphere, plasma cloud injection from Io, S and O ions discontinuities 0-90358
- magnetosphere, plasma corotation lag from Voyager 1 obs. 0-90361
- magnetosphere, plasma waves from Voyager 2, radio obs. 0-77343
- magnetosphere, tailward directed ion beam 0-72854
- magnetosphere, Voyager 2 obs. of hot plasma environment 0-77341
- magnetosphere 0-72858
- magnetosphere and bow shock, plasma densities from Voyager 2 obs. 0-77340
- magnetosphere and bow shock, Voyager 2 magnetometer obs. 0-77339
- magnetosphere Birkeland currents and Io plasma torus, model 0-105198
- magnetosphere dust derived from Io volcanoes 0-85889
- magnetosphere HF and LF events from Voyager obs. 0-77344
- magnetosphere low energy plasma, Voyager obs. 0-72855
- magnetosphere shape and field, model 0-72868
- magnetosphere trapped energetic particle spectrum 0-72711
- magnetotail structure inferred from plasma obs. 0-72864
- methane and NH₃ bands, longitudinal variability, visible obs. 0-82270
- methane line profiles near 1.1 μ , as probe of cloud struct. and C/H ratio 0-62067
- near IR mapping spectrometer design and testing for Galileo Jupiter Orbiter 0-90336
- Neptune occultation, 1613 January 4, prediction rel. to obs. by Galileo 0-105485
- North Temperate Current C, fast moving bright spot obs. 0-67640
- polar moment of inertia determ. 0-94694
- position determ. in 1978 using Double Zeiss Astrograph, Belgian obs. (French) 0-72809
- radiation belts, 21 cm maps from all rot. aspects 0-105195
- radio emission, Stokes parameters obs. at 11 and 18 cm wavelength 0-67637
- radio emission, study at 2.7 GHz with Cambridge 5 km telescope 0-82272
- radioemission at 100 kHz, from magnetosphere 0-85891
- resonance with Periodic Comet Boethin (1975 I), libration 0-72883
- ring, dust EM scatt. lifetimes 0-82273
- ring system, summary of recent research 0-72875
- ring system dust, derived from Io volcanoes 0-85889
- rings, Voyager I obs. (French) 0-82281
- S-bursts, freq. drift meas. at different freqs. throughout several storms 0-85888
- S-bursts radio emission, occurrence with L-bursts and freq. upper limit 0-85887
- satellite orbits, three dims. periodic orbit determ. 0-67526
- satellites, atmosphereless, micrometeorite impact, ion emission 0-77362
- satellites 1979 J 1 and 2, Voyager 1 imagery analysis 0-67639
- spacecraft braking problem in Jupiter atmosphere, ballistic and navigation aspects 0-61981
- structure and evolution, effect of dense cores 0-98603
- triple shadow phenomena caused by Galilean satellites (AD 1900-2100) ephemerides 0-67641
- Voyager 1 data summary (Russian) 0-82274
- Voyager 2 encounter, trajectory and sequence modifications 0-77265
- Voyager 2 imaging science results of planet and Galilean satellites 0-72871
- Voyager 2 IR obs. 0-77335
- whistler mode chorus obs. and Io torus implications 0-72862
- whistler propagation in magnetosphere, theory 0-72863
- C/H and D/H ratios from 8-9 μ m IR spectrum 0-67638
- H I Lyman α albedo, Copernicus UV obs. 0-94747
- H I Lyman α emission and Io torus, Voyager 2 EUV obs. 0-77338
- H Lyman- α brightness, longit. asymm. 0-72852
- NH₃ abundance from visible obs. 0-82269
- NH₃ vertical density profiles from IR and radioelectric emissivity data 0-82267
- S II forbidden line emission nebula studies 0-67636
- S II forbidden line emission round planet, distrib. and intensity 0-85885
- S II ring, var. in characts., link with Io, visible obs. 0-90360
- S II torus, longitudinal asymmetry visible spectra 0-82271

K-capture see nuclear electron capture

K mesons see kaons

K-N interactions see kaon-nucleon interactions

Kalman filters

- adaptive beam forming processor formulation 0-91967
- adaptive filter structures, for seismic signals deconvolution 0-98451
- air pollution episodes in Venetian region, real-time forecasting via Kalman predictor 0-82046
- computed tomography, limited data, image reconstruction using polar pixel Kalman filter 0-80905
- deconvolution smoother, for reflection seismograms simultaneous spherical divergence correction and optimal deconvolution 0-98258
- digital, phasemeter appl., synthesis with a priori uncertainty of data 0-98934
- digital speech processing, linear prediction parameter estimation using Kalman filtering (German) 0-96134
- HTGR fuel rod fabrication, estimation and control 0-83215

Kalman filters continued

- road traffic noise abatement, noise propag. characts. identification under different conditions, appl. (German) 0-99896
- visual evoked cortical potential meas., signal optimisation using Kalman filter (Japanese) 0-72348

kaon-baryon interactions

- see also kaon-baryon scattering; kaon-hyperon interactions; kaon-nucleon interactions
- No entries

kaon-baryon scattering

- see also kaon-baryon interactions; kaon-hyperon scattering; kaon-nucleon scattering
- No entries

kaon decay

- see also kaon hadronic decay; kaon leptonic decay
- current algebra approach, symmetry-breaking Hamiltonian, chiral SU(3)×SU(3) or SU(4)×SU(4) 0-68450
- Higgs boson couplings, charged, K_L-K_S mass differences 0-62917
- K $\rightarrow\pi(\mu)\gamma$, quark mass ratios 0-105884
- K $\rightarrow\pi\mu\nu$, μ polarisation and T-odd correlations, Weinberg model of CP violation (Russian) 0-62969
- K $\rightarrow\mu e$, flavour changing neutral current search 0-105836
- K $\rightarrow\pi^0\mu^+\mu^-$, K $\rightarrow\pi^0$ decay spectrum and form factors 0-57587
- K $\rightarrow\pi^+\pi^-e^+e^-$, neutral-current process, strong interaction corrections 0-62968
- K $\rightarrow\gamma\gamma$, ($\pi^+\pi^-\gamma$), chiral quark model anal. (Russian) 0-105900
- K $\rightarrow\pi^+\pi^-\mu^+\mu^-$, transverse polarisation of μ , violation of time-reversal invariance 0-68448
- K $\rightarrow\pi^0\pi^+\pi^-\nu$, form factors 4-momentum depend., μe universality (Russian) 0-68449
- K₁₄ decay vector form factor (Russian) 0-105900
- K $\rightarrow K^*\gamma$, quark loop model, SU(3) splitting of quark masses 0-62990
- K $\rightarrow\pi^0 K^*\gamma$, SU(3) and isospin symmetry breaking effects 0-95272
- K $\rightarrow\pi^0 e^+ e^-$, six-quark model, CP violation 0-78055

kaon hadronic decay

- see also kaon regeneration
- K $\rightarrow 3\pi$, relativistic quark model anal. 0-99096
- K $\rightarrow 0^-k\pi$, k=2 or 3, Racah time reversal, a C,P,T scheme 0-78056
- K $\rightarrow\pi^+\pi^-\pi^0$, SU(3) and isospin symmetry breaking effects 0-95272
- K $\rightarrow\pi^0\pi^+\pi^-$, CP violation parameters in six quark model (Russian) 0-62974
- K $\rightarrow 0^+K^*\gamma$ and Primakoff conversion of K_L $\rightarrow K_S^0$ 0-73695

kaon-hyperon interactions

- see also kaon-hyperon scattering
- No entries

kaon-hyperon scattering

- see also kaon-hyperon interactions
- No entries

kaon interactions see kaon-baryon interactions; kaon-nucleus reactions; lepton-hadron interactions; meson-meson interactions; photon-hadron interactions

kaon leptonic decay

- No entries

kaon-nucleon interactions

- see also kaon-nucleon scattering; kaon-proton interactions
- Adler-Weisberger sum rule and the σ -commutator for the kaon-neutron system 0-101957
- KN, 50-200 GeV/c, multiparticle production, multiplicities, cross sections and ang. distrib. 0-86768
- KN, kaonic H atom and $\Delta(1405)$ 0-68479
- Kn total cross sections from Kp and kaon-nucleus scatt. data 0-102069
- K $\rightarrow N^-\mu^+\mu^+ X$, K $\rightarrow\pi^0$ structure function ratio using Drell-Yan process 0-86718
- K π^+ inelastic charge exchange scatt., diffraction approach, convergent polynomial expansion, scaling 0-78095

kaon-nucleon scattering

- see also kaon-nucleon interactions; kaon-proton scattering
- resonance region, t-channel couplings, hyperbolic dispersion relations 0-57643
- K π^+ n, QCD, one-gluon-exchange, resonating group method, soft-core approx. 0-63025
- K π^+ elastic scatt., 0.851-1.351 GeV/c, polarisation parameter 0-68478

kaon-nucleus reactions

- for inelastic kaon-nucleus scattering, see "kaon-nucleus scattering"
- see also kaon-nucleon interactions
- low energy, nuclear density shape optical pot. kaonic atom level shifts 0-63213
- (K π)₂, emulsion, 1.8 GeV/c, ^6Li , A=10, 11, double hypernuclei, prod. and decay 0-57718
- $^9\text{Be}(K^-, \pi^-)$, 720 MeV/c, Sigma hypernuclei prod., missing mass spectrum 0-57721
- $^9\text{Be}(K^-, \pi^- p)$, stopped K π^- , ^6Li possible γ -transition 0-106002
- ^6Li , supermultiplet struct. and decay props. of hypernuclear 1 $^+$ resonances from (K π^-) 0-78186

kaon-nucleus scattering

- see also kaon-nucleon scattering
- universality of the ω intercept and Inelastic rescattering of kaons in nuclei 0-102212
- (K,K), isobar doorway model, optical pot., Δ -nuclear matter binding energy 0-106079
- (K π^+ , K π^0) from Be, C, Al, Cu, Sn, Pb, 70, 125, 175 GeV/c 0-83128
- $^{12}\text{C}(K^+, K^+)$, form factors, cross sections, interior probing capability 0-73866
- $^{12}\text{C}(K^+, K^+)$, 100-1000 MeV, differential and total cross sections, nucleon motion 0-102206

kaon production

- relativistic nuclear collisions, K prod. in multiple collision model 0-99157
- D $\rightarrow K^+\pi^-$, charm-changing weak hadronic current, models 0-57585
- D $\rightarrow K^+\pi^-$, quark total number conservation, D $^+$ lifetime longer than D 0 0-57590
- D $^0\rightarrow K^0\pi^0$, $\Delta T=1$ constraints and final state interactions 0-95267
- D $^0\rightarrow K^0\pi^0$, quark total number conservation, D $^+$ lifetime longer than D 0 0-57590
- D $^+$ $\rightarrow K^0\pi^+$, quark total number conservation, D $^+$ lifetime longer than D 0 0-57590
- e $^+e^-$, hadron production, inclusive study, momentum distrib., energy and multiplicity 0-57613
- e $^+e^-$ —hadrons, 12, 30 GeV, π, k, p, \bar{p} production 0-105916
- e $^+e^-$ inclusive hadron prod., polarisation and p nonconservation asymmetries, π, K^{\pm}, D^{\pm} prod. 0-78084

kaon production continued

- $e^+e^- \rightarrow \pi^+\pi^-$ (K^+K^-), $\sqrt{s}=1.5$ GeV, EM timelike form factors for π and K 0-91089
 $\gamma p \rightarrow K^+K^-p$, 20-36 GeV, $\Phi(1019)$ prod., cross sections 0-105907
 $\gamma p \rightarrow K^+K^-p$, 20-70 GeV, K^+K^- threshold enhancement 0-78076
 Kp , 70 GeV/c, total and differential cross-sections for π and K production 0-63050
 K^-p , 32 GeV/c, exclusive reactions, diffractive dissociation processes, $\pi^+\pi^-$ and K^+K^- prod. 0-86760
 $K^-p \rightarrow K^0\pi^+\pi^-n$, 6 GeV/c, K^* and Q_2 signals, partial wave anal. 0-86754
 $\mu p \rightarrow K^0X$, 225 GeV, deep inelastic scatt., strange neutral particle prod. 0-105902
 pN , K^0 and π^- prod. rates, SU(3) symmetry violation in quark jet 0-82966
 (p,X) , 400 GeV, $A=6-180$, $\pi^+\pi^-$ and K^\pm backward prod., invariant cross sections 0-102188
 pd , 70 GeV, π^\pm , K^\pm , p , \bar{p} prod. with 0.5-2.2 GeV/c transverse momenta, yield ratio, QCD (Russian) 0-83012
 pN , 67 GeV/c, in Be, Al, Cu, inclusive π^\pm , K^\pm , p , \bar{p} prod. cross sections (Russian) 0-86769
 pN , 67 GeV/c, nuclear targets, π^\pm , K^\pm , p , \bar{p} yields (Russian) 0-68501
 pp , 300 GeV/c, inclusive prod. of K^0 , Λ^0 , K^{*0} (890) and Σ^\pm (1385) 0-95290
 pp , 70 GeV, π^\pm , K^\pm , p , \bar{p} prod. cross sections, QCD-parton model anal. (Russian) 0-63044
 pp , D, B, K prod., QCD model for heavy flavour prod., two gluon annihilation 0-86744
 $pp \rightarrow K^{*0}(892)X$, 12 and 24 GeV/c 0-86765
 $pp \rightarrow K^{*0}(892)X$, 3.6 GeV, factorisation hypothesis test 0-102055
 π^-p , 100, 200, 360 GeV/c, inclusive prod. of π^0 , K_S^0 , Λ^0 , $\bar{\Lambda}^0$, cross sections 0-73745
 $\pi^-p \rightarrow K^0K^+\pi^-n$, 3.95 GeV/c, E(1420) quantum numbers and branching ratio 0-95286
 $\pi^-p \rightarrow K^0\Lambda$, 3.5 GeV/c, Λ polarisation, high statistics meas. 0-57637
 $\pi^-p \rightarrow K^0\Sigma^0$, 1395 to 2375 MeV/c, differential cross-section and polarisation 0-57635
 $\pi^-p \rightarrow K^+K^-n$, 62 GeV, spin-5 boson resonance at 2300 MeV 0-102078
 $\pi^-p \rightarrow K^0(890)\Lambda^0\Sigma^0$, 10 GeV/c, K^0 polarisation meas. in hypercharge exchange reaction 0-63017
 $\pi^-p \rightarrow \Delta K$, low energy, amplitude anal., Lagrangian model 0-82995
 $\pi^-p \rightarrow K^+\Sigma^+$ and $K^+\pi^+\Sigma^+$, exchange degeneracy 0-57634
 $\pi^-p \rightarrow K^+\Sigma^+$, $Y^+=\Sigma^+$ or $Y^+=\Sigma^+$, 7 GeV/c, hypercharge exchange in line-reversed π^+p and K^-p 0-82998
 $\pi^-p \rightarrow K^+(890)Y^+$, $Y^+=\Sigma^+$ or $Y^+=\Sigma^+$ (1385), 7 and 11.5 GeV/c, hyperon polarisation, vector meson decay angular distrib. 0-82997
 $\pi^-p \rightarrow K^{*0}(892)X$, 16 GeV/c 0-86765
 e^+e^- annihilation, 30 GeV, inclusive K^0 prod. $K^0K^+/\mu^+\mu^-$ prod. ratio 0-91103
 $\gamma p \rightarrow K^+\lambda(\Sigma^0)$, π^+n , π^-p , $K^+\Lambda$, $K^+\Sigma^0$ final state comparisons above resonance region 0-105906

kaon-proton interactions

- see also kaon-proton scattering
 Adler-Weisberger sum rule and the σ -commutator for the kaon-proton system 0-101956
 Kp , 70 GeV/c, total and differential cross-sections for π and K production 0-63050
 kp , large P_T pion⁰ prod., meson structure functions, quark distrib. functions 0-86714
 K^-p , 10, 16 GeV/c, Σ^+ , Σ^- inclusive prod. Λ prod. comparison 0-86766
 K^-p , 110 GeV/c, charged multiplicity distrib. 0-78101
 K^-p , 32 GeV/c, exclusive reaction anal. in terms of multiparticle variables (Russian) 0-86757
 K^-p , 32 GeV/c, exclusive reactions, diffractive dissociation processes, $\pi^+\pi^-$ and K^+K^- prod. 0-86760
 $K^-p \rightarrow B^+Y^+(1385)$, 8.25 GeV/c, quasi-two-body channel data 0-63023
 $K^-p \rightarrow \Delta^+X$, 32 GeV, inclusive and total cross sections 0-105936
 $K^-p \rightarrow K^0\pi^+\pi^-n$, 6 GeV/c, K^* and Q_2 signals, partial wave anal. 0-86754
 $K^-p \rightarrow K^0\pi^-p$, 4.2 GeV/c, multichannel anal. 0-73736
 $K^-p \rightarrow \Delta^+X$, 32 GeV/c, total and differential cross sections, energy dependence 0-63048
 $K^-p \rightarrow \Delta\eta$, 6 GeV/c, baryon exchange reactions, ηNN coupling constant, Λ polarisation, nucleon-Regge exchange 0-78098
 $K^-p \rightarrow \Delta\pi^0$, 6 GeV/c, baryon exchange reactions, ηNN coupling constant, Λ polarisation, nucleon-Regge exchange 0-78098
 $K^-p \rightarrow \Delta\pi^0$, baryon Regge exchange, FESR anal. 0-63022
 $K^-p \rightarrow \pi^+\Sigma^+$ and line reversed reaction $\pi^+p \rightarrow K^+\Sigma^+$, simple Regge pole model 0-78093
 $K^-p \rightarrow \pi^+\Sigma^+$ and $\pi^+p \rightarrow K^+\Sigma^+$, exchange degeneracy 0-57634
 $K^-p \rightarrow \pi^+Y^+$, $Y^+=\Sigma^+$ or $Y^+=\Sigma^+$ (1385), 7 GeV/c, hypercharge exchange in line-reversed π^+p and K^-p 0-82998
 $K^-p \rightarrow \pi^+\Sigma^+$, box diagram calcs. unitarity corrections in strong interactions 0-91110
 $K^-p \rightarrow \pi^+\pi^-\pi^+\Lambda$, Dalitz arrays for $\omega\phi A_2$ resonances 0-105924
 $K^-p \rightarrow \pi^+\pi^-\pi^+\Sigma^-$, Dalitz array for A_1 resonance 0-105924
 $K^-p \rightarrow \rho^+Y^+$, $Y^+=\Sigma^+$ or $Y^+=\Sigma^+$ (1385), 7 and 11.5 GeV/c, hyperon polarisation, vector meson decay angular distrib. 0-82997
 $K^-p \rightarrow \Sigma^+\pi^+$, backward differential cross section 0-63024
 $K^-p \rightarrow \Sigma^+\pi^+\pi^-$, 4.15 GeV/c, nondiffractive A_1 production, double-Regge model 0-78097
 $K^-p \rightarrow \sigma^\pm$ (1385)X, 32 GeV, inclusive and total cross sections 0-105936
 K^+p , 147 GeV/c, inclusive Δ^{++} prod., cross section energy depend. 0-57651
 K^+p , 32 GeV/c, use of Hough-Powell digitizer for processing film from bubble chamber Mirabelle 0-69040
 K^+p , 70 GeV/c, cross sections and charged multiplicity distrib. 0-63053
 k^+ , multiple production processes regularities, Monte Carlo model 0-102082
 $K^+p \rightarrow K^+K^+\pi^-$, 2.7 to 32 GeV/c, impact parameter bounds, energy and effective mass dependence 0-57640
 $K^+p \rightarrow \pi^+X$, 32 GeV/c, two-pion correlations, Monte Carlo model 0-83008
 $K^\pm p$, 130, 200 GeV, jet prod. cross sections, QCD anal. and scale breaking 0-99111
 $K^\pm p$, fireball model, universal scaling function 0-57646
 $K^\pm p$, inelastic charge exchange scatt., diffraction approach, convergent polynomial expansion, scaling 0-78095
 $K^\pm p$, π^0/π^- inclusive ratio in quark recombination model 0-102022
 $K^\pm p \rightarrow K^\pm X$, triple Pomeron coupling, Reggeon treatment 0-68488

kaon-proton interactions continued

- $K_1^0 p \rightarrow Q^0(Q^0)p$, differential cross section slope, further Deck model anal. 0-73737
 $K^+p \rightarrow \pi^+\pi^+X$, 32 GeV, topological cross sections 0-102085
- kaon-proton scattering**
 see also kaon-proton interactions
 K^-p , backward elastic scattering, backward differential cross section 0-63024
 K^-p elastic scatt., 0.955-1.272 GeV/c, polarisation parameter 0-86753
 K^+p , QCD, one-gluon-exchange, resonating group method, soft-core approx. 0-63025
 $K^\pm p$, 32.1 GeV, elastic scatt. cross section 0-102076
 $K^\pm p$, elastic scatt. and diffractive dissociation, Regge model with $a_p(0)>1$ (Russian) 0-57630
- kaon regeneration**
 universality of the ω intercept and Inelastic rescattering of kaons in nuclei 0-102212
- kaon resonances** see meson resonances
- kaon scattering** see kaon-baryon scattering; kaon-nucleus scattering; lepton hadron scattering; meson-meson scattering; photon-hadron scattering
- kaons**
 see also kaon regeneration
 bound state relativistic effective range approx., EM form factors and charge radii 0-95270
 charge radius, coloured quark field theory 0-62945
 deep inelastic structure functions in massive quark model 0-86717
 $K^0 \rightarrow K^0$ transition in the standard SU(3) \otimes SU(2) \otimes U(1) scheme (Russian) 0-82951
 structure functions from inclusive prod. data, nonstrange quark distrib. 0-86715
 SU(2)_c \times U(1), strong CP-violating phase, one-loop corrections, Higgs particles 0-62910
 $e^+e^- \rightarrow \pi^+\pi^-$ (K^+K^-), $\sqrt{s}=1.5$ GeV, EM timelike form factors for π and K 0-91089
 K^- EM form factor direct meas. from elastic scatt. cross section 0-86716
 $K^0 \rightarrow K^0$ mixing, strong interaction corrections in six quark model, QCD calcs. 0-82957
 $K^{*0} \rightarrow K_S^{*0}$ and Primakoff conversion of K_1^0 to K_S^{*0} 0-73695
 $K^0 \rightarrow K^0$, weak neutral current diagonality, mixing amplitude, multi-quark gauge model (Russian) 0-68414
- Kapitza-Dirac effect**
 see also Schwarz-Hora effect
 atom scattering effectiveness, standing light wave field, quasiclassical approx. 0-83334
- Kapitza resistance**
 quartz-liquid ^4He interface, saturation effects in phonon refl. 0-92736
 Ag- ^4He interface, Kapitza cond. and enhanced power anomaly, 1-2K 0-88378
 ^3He , liq., interface with nonmag. solid, Kapitza resist., quantum perturbation treatment 0-88385
 ^4He , liq., Kapitza heat-transfer model for boundary with solid 0-107591
 ^4He , liquid-solid boundary, capillary sound motion, Kapitza resistance (Russian) 0-92737
 ^4He , superfluid, Kapitza resist. meas. using second sound (Russian) 0-88375
- KDP** see potassium compounds
- Kelvin-Helmholtz instability** see flow instability
- Kennelly-Heaviside layer** see E-region; ionosphere
- keratin** see proteins
- Kerr electro-optical effect**
 α -amino acids, naturally occurring, in aq. soln., Kerr constants 0-85353
 dye laser amplifier, DC elec. field effects 0-64006
 glycerol, highly viscous state, static and dynamic Kerr effect obs. 0-60545
 macromolecular solution rigid ellipsoidal macromols. in cond. soln. at low ionic strength, specific Kerr consts. 0-84718
 macromolecular solutions, electric field-induced optical rectification, rel. to electro-optic Kerr effect 0-84726
 p-methoxybenzoate- p - n -pentyl benzene, slow non-critical mol. reorientation in isotropic phase 0-84062
 nonpolar molecule solutions, birefr. kinetics 0-100648
 organic liquid systems, dielectric and dynamic Kerr-effect studies 0-60496
 pentyl cyanobiphenyl, laser and electric field induced Kerr effect 0-84061
 plane-parallel absorbing layer, nonlinear optical props. 0-58631
 PMMA, birefringence in elec. field 0-88962
 PMMA, relative phase retardation meas. in elec. stressed samples between crossed polarisers using He-Ne laser 0-84716
 polyethylene, relative phase retardation meas. in elec. stressed samples between crossed polarisers using He-Ne laser 0-84716
 polypeptide, conformational change induced by strong elec. field 0-85336
 polypropylene glycol melt, mol. motion, dielectric and Kerr effect relax. obs. 0-60498
 propionitrile-hydrocarbon systems, critical solns., Kerr electrooptical Kerr effect meas. 0-100645
- Kerr magneto-optical effect**
 magnetic material domain structure obs. by Kerr-magneto-optical effect, laser speckle suppression 0-85093
 measurement of magneto-optic rotation and ellipticity, spinning analyser ellipsometer (Japanese) 0-73419
 Co-Fe amorphous alloys, worked, perminvar type mag. hysteresis loop, longit. Kerr effect obs. 0-65958
 Fe thin layers, vacuum coated on PMMA, mag. behaviour during mech. stress cycles (German) 0-80581
 Fe-P electrodeposited foil, amorphous, mag. domains 0-75821
 $\text{Fe}_{80}\text{B}_{20}$, metallic glass, optical and magneto-optical props. 0-84728
 Fe_2O_3 , dielec. function and polar Kerr rotation, 0.5-3.6 eV 0-66221
 Fe_2O_3 , polar Kerr effect invisible and near IR spectral regions 0-108187
 FeSi_{1-x} , amorphous film, magneto-optic Kerr effect 0-66158
 GdFeBi, amorphous ferrimag. films, magneto-optical props., optical spectra 0-76008
 $\text{Li}_{0.5}\text{Fe}_{2.5}\text{O}_4$, magneto-optical Kerr effect, reflectivity spectra 0-66157
 $\text{Mn}_2\text{Fe}_{1-x}\text{O}_4$, dielec. function and polar Kerr rotation, 0.5-3.6 eV 0-66221
 Ni_3Fe , domain struct. after tensile deform., dislocation effects 0-71083
 Tb-Fe amorphous thin films, magnetic after-effect, Kerr magneto-optical effect obs. 0-97123

Kerr magneto-optical effect continued

- YIG, magneto-optical Kerr effect, reflectivity spectra 0-66157
YIG:Ga(Se), magneto-optical Kerr effect, reflectivity spectra 0-66157

kicksorters *see counting circuits***kidney**

- artificial, automatic extrasomatic dialysis system 0-98177
cells, inactivation by high-energy monoenergetic heavy-ion beams 0-72256
computerised tomographic image boundary finding and complex object localisation 0-109016
counterflow system modelling, numerical soln. by multiple shooting 0-104609
diseases, value of computerised tomography (*German*) 0-76832
electron microscopic diagnosis using clinical pathology liver and kidney samples, computer assisted 0-85485
glomerular filtration rate meas., comparison of 4 commercial preps. of $^{99m}\text{Tc}(\text{Sn})\text{DTPA}$ 0-81704
hollow fibre dialyser, mass transfer 0-66873
microwave imagery of isolated canine kidney, use of orthogonal polarisations 0-81783
physiological compartment tracer flow modelling and digital imaging 0-101257
renography, comparative study in hydration and dehydration (*Japanese*) 0-81726
six-tube vasa recta model as test problem 0-104610
stenosis of renal artery, effect on renovascular hypertension 0-108934
uptake measurements using $^{197}\text{HgCl}_2$, single tracer method for background subtraction 0-67217
US renal volumetry in children, accuracy and simplicity of the method 0-98044
X-irradiation and induced autoallergic glomerulonephritis effects, rat obs. 0-76793
Cd conc. in kidney and liver, neutron activation anal., organ depth determ. 0-72321
 ^{131}I -ortho-iodohippurate absorbed kidney dose calc., literature review 0-76841
 ^{99m}Tc methylene diphosphonate, immediate renal imaging and renography, clinical evaluation 0-98126

Kikuchi lines *see electron diffraction crystallography***kinematic viscosity** *see viscosity***kinematics**

- see also acceleration; ballistics*
Centaurus I cluster of galaxies, resolution into two velocity systems 0-77499
education, momentum flow as force, alternative conceptualisation for teaching mechanics 0-67993
education, speed, Galilean and Einsteinian concepts, vel., rapidity and celerity 0-73130
Galaxy central region, barlike model of inner Galaxy gas based on improved H I data 0-67845
granular materials, rolling, granule kinematics 0-84875
Iceland, continuum model of crustal generation, kinematic aspects 0-90059
LMC, kinematics and dynamics compared to galaxies of Magellanic type (*German*) 0-105348
NGC 4945, late-type spiral galaxy, excited gas kinematics, obs. 0-109547
planetary nebulae, spatial and vel. distrib. statistics 0-109518
planetary nebulae in M31 (Andromeda galaxy) and companions, rel. to vel. dispersions and virial masses 0-109520
Sa spiral galaxies, internal vel. dispersions from H I study 0-98714

kinematography *see cinematography***kinescope** *see television picture tubes***kinetic theory**

- see also Boltzmann equation; collision processes; intermolecular mechanics; kinetic theory of gases*
convective diffusion to a particle in a fluid with linear kinetics 0-69943
crystal growth, multi-component, master equations in lattice model 0-75194
crystal growth from melt, multi-component, kinetic equation theory 0-79721
dense plasmas transport coefficients, kinetic theory 0-77280
fluids, one and two dimensional, hydrodynamics, viscosity, heat conductivity, kinetics (*Russian*) 0-79972
Klein-Gordon particles, charged, quantum kinetic theory, Feynman rules and thermal eqn. 0-57177
Klein-Gordon particles, charged, quantum kinetic theory, linear kinetic eqn. 0-57178
liquids, associated, mechanism of structural dielectric relaxation 0-107034
molten metal binary mixtures with wide immiscibility range, gravitational layering of components (*Russian*) 0-104092
multi-component crystal growth, binary system crystallisation 0-88071
neutrino systems, relativistic kinetic theory of transport processes 0-73283
plasma, self-consistent kinetic theory of stochasticity 0-59179
relativistic Boltzmann kinetic eqn. derivation 0-68161
sine-Gordon chain, displacement fluctuations, long-time behaviour and dynamic scaling props. 0-101764
sulphate aerosol, stratospheric, kinetics of growth by condensation in homogeneous medium (*Russian*) 0-94566
virial inequalities, quantum and relativistic 0-62609

kinetic theory of gases

- see also Brownian motion; collision processes; equations of state; intermolecular mechanics; Joule-Thomson effect*
BBGKY system, irreversibility, velocity correlations and non-Hamiltonian dynamics 0-77686
bi-particle correlations in gas, relax. time 0-83875
binary gas mixture, drop thermophoresis 0-93806
classical Boltzmann kinetic theory justification using Liouville theory 0-87838
dense gases, vel. autocorrelation function, memory function 0-59154
dilute gas, kinetic perturbation theory 0-100051
electron motion in weakly ionised gases, stochastic theory of homogeneous systems, review 0-77735
gas flow over cylinder at low speeds under constant force, kinetic theory description 0-79354
gas flows, entropy prod. determ. using Boltzmann's H-theorem, Knudsen effusion 0-106867

kinetic theory of gases continued

- hard sphere gas mixture, vel. autocorrelation function calc. 0-75019
hard sphere gas with step repulsive barrier, generalised Enskog eqn. 0-87836
heavy ions in light gases in electric field, limits of Kihara distrib. 0-87837
hole-burning in at. vel. distrib. by EM radiation 0-64674
inhomogeneous Boltzmann gas, lumped phase space, non-linear diffusion approx., stochastic hydrodynamic theory 0-64666
interionic force pot. in ideal dipolar gas 0-96330
light induced kinetic effects in gases (*Russian*) 0-92244
Maxwellian molecule gas, heat transfer between parallel plates, Navier-Stokes eqns. 0-87839
moderately dense gas, Bhatnagar, Gross and Krook model from Chapman-Enskog equations 0-106864
non-Maxwell molecular interaction model, integrable representation 0-100050
nonequilibrium gas, small fluctuations, theory (*Russian*) 0-69962
nonisothermal gas motion in plane channel, S-model kinetic eqn. 0-83816
one-dimensional hard sphere gas, initial value problem, exact soln. 0-92243
plasma, nonequilib., kinetic theory of spectral line broadening 0-59187
relativistic electron beam relaxation in dense gas, radiative energy transfer 0-69968
two particle distribution function, Bogoliubov eqn. soln. 0-96332
very low pressure pyrolysis, gas-gas and gas-wall average energy transfer 0-93739
Xe, gas, two-body time correl., Van Hove scatt. function meas. 0-100053

kinetic theory of liquids *see kinetic theory; liquid theory***kinetics of chemical reactions** *see reaction kinetics***kink bands**

- camphor, rhombohedral, polycryst., compressive deform. and dynamic recrystn. 0-71698
ice, dislocation vel. theory, glide plane influence 0-79805
Nb, deformed polycryst., γ -peak obs. and interpret. in internal friction, 300-500K 0-81098

kinofoms *see computer-generated holography***Kirkendall effect** *see diffusion in solids***kitchen appliances** *see domestic appliances***KKR calculations**

- disordered system electron energy system, calc. methods 0-75485
fundamental Korringa-Kohn-Rostoker eqn. version of coherent potential approx. 0-59847
HEED atomic string approximation use in obtaining dispersion surfaces 0-100143
structure constants, electronic struct., KKR calc. 0-80152
Ag, electronic and mag. structure calcs. of mag. impurities 0-80213
Ag-transition metal, dil., mag. impurities, electronic struct., KKR-Green's function calc. 0-65783
Cu, electronic and mag. structure calcs. of mag. impurities 0-80213
Cu-transition metal, dil., mag. impurities, electronic struct., KKR-Green's function calc. 0-65783
 Fe_2P_{24} , amorphous alloy, electronic struct., KKR calc. 0-96775
 $\text{HfC}_x\text{N}_{1-x}$, X-ray valence photoelectron spectrum, 4f signal calc. 0-66391
Pd-Cu compound, KKR electronic struct. 0-59864
Sc, band structure, density of states, absorpt. spectra, KKRZ calc. 0-70593
 $\text{TiC}_{1-x}\text{N}_x$, (O_{1-x}), electronic struct., KKR-ATA method 0-65447
 $\text{TiN}_{1-x}\text{O}_x$, electronic struct., KKR-ATA method 0-65447
 $\text{U}_3\text{Th}_{1-x}\text{As}$ (Sb), electronic struct., relativistic KKR-averaged T-matrix approx. method 0-107702
 ZrB_3 , self-consistent band struct., XPS, reflectance, NQR, Hall effect and density of states meas. 0-107689

klystrons*see also reflex klystrons*

- laser frequency measurement using supercond. point contacts 0-90824
UHF, 600 kW, for particle acceleration and plasma heating (*German*) 0-106211

Knight shift*see also nuclear magnetic resonance*

- alkali metals, magnetic property volume depend., Knight shifts, electron spin response 0-88729
alloys, d-metal, magnetic susceptibility and Knight shift meas. 0-66055
Ni-Pt-P, metallic glass, electronic structure, pulsed NMR study 0-75869
(rare-earth) Al_2Ga_2 , synthesis, NMR and X-ray absorpt. studies 0-108083
 Ag_2F , NMR of ^{109}Ag and ^{19}F , modified Korringa relation in two-dimens. metal 0-93199
Be, electronic struct., NMR study 0-108085
 $\text{Be}_{1-x}\text{Mn}_x$, Be-rich, NMR and paramag. susceptibility 0-71206
 BeNi , dil., electronic struct., NMR study 0-108085
 $\text{Co}_2\text{Ga}_{1-x}$, NMR expts. interpretation 0-75870
Cu-Cr, dil., spin-density magnetisation near Cr atoms, NMR study 0-80626
Cu-Fe group, dil., NMR satellite data calc., struct. of mag. impurities 0-103894
Fe, BCC, high field Knight shift and hyperfine anisotropy of ^{57}Fe 0-71205
 GdRh_2B_4 , magnetic and electrostatic props., NMR study 0-93195
 H_2MoO_3 bronze, proton shift tensors PMR meas. 0-71202
 $\text{HfV}_2\text{H}_{21}$, proton NMR relax. time and Knight shifts, diffusional activation energies meas., sorption props. 0-75871
InBi single crystals, Knight shifts and quadrupole interaction 0-84662
Li, Knight shift volume depend. 0-84663
Li-Cd alloy, liq., elec. resist. and Knight shift 0-75537
 Li-NH_3 concentrated solution, NMR relaxation of ^7Li 0-108084
 LuRh_2B_4 , magnetic and electrostatic props., NMR study 0-93195
 α -Mn, localised spin fluctuations, Knight shift obs. 0-60181
Mo-Co Kondo alloy, Co impurity susceptibilities, Knight shift 0-88721
 $\text{Mo}_2\text{S}_3\text{N}$, triple chalcogenide, NMR spectra in supercond. state (*Russian*) 0-93194
 $\text{Mo}_2\text{Se}_3\text{N}$, triple chalcogenide, NMR spectra in supercond. state (*Russian*) 0-93194
Ni-Pd-P, metallic glass, electronic structure, pulsed NMR study 0-75869
 NiSe_2 , paramag. props., NMR, mag. susceptibility 0-60175
P+Nb, dil. alloy, NMR obs. of ^{93}Nb 0-71203
Pd, metallic, positive muon Knight shift 0-71280

Knight shift continued

- PdNb, dilute, NMR obs. of ^{93}Nb 0-71203
 PtV, dil. alloys, NMR obs. of ^{51}V 0-71203
 SmB_6 , intermediate valence, ^{11}B NMR study 0-93193
 Sn, white, nuclear acoustic reson., Knight shift 0-71204
 SnTe:Mn , NMR shift meas. 0-97154
 ThC_2N_y , NMR, Knight shift and spin-lattice relax. 0-100621
 VB, nuclear quadrupole parameters 0-103896
 $\text{V}_2(\text{Hf,Zr})$, NMR and mag. susceptibility, density of states determ. (*Russian*) 0-66053
 $\text{V}_{2-x}\text{Nb}_x\text{Hf}$, NMR of ^{51}V and mag. susceptibility, 20-300K (*Russian*) 0-93192
 V_2S_3 and V_2S_5 , itinerant antiferromag. spin fluctuations, NMR studies 0-93198
 ZrMn_2H_x , proton NMR relax. time and Knight shifts, diffusional activation energies meas., sorption props. 0-75871
 ZrV_2 , Knight shift vs. susceptibility plot 0-75712

Knudsen flow

- aerosol, high Knudsen number, coagulation rate measurement 0-71954
 gas dynamics eqn. boundary conditions in Chapman-Enskog Boltzmann eqn. soln. 0-96284
 gas flow over cylinder at low speeds under constant force, kinetic theory description 0-79354
 gas flows, entropy prod. determ. using Boltzmann's H-theorem, Knudsen effusion 0-106867
 nonequilibrium free jet expansion, rotational temp. meas for N_2 0-69890
 nonisothermal gas motion in plane channel, S-model kinetic eqn. 0-83816
 pipes with const. annular cross section, mol. cond. calc. method 0-79353
 porous solids, diffusion of gases, Monte Carlo simulation 0-65299
 spontaneously condensing and wet steam discontinuous flows in steam turbines, subsonic, transonic and supersonic, numerical investigation (*Russian*) 0-87800
 Fe-Zn, homogeneous phases, Gibbs free energies of form., Knudsen effusion method 0-66481

Knudsen number *see Knudsen flow***Kohn effect** *see lattice dynamics***Kondo effect**

- alloys, magnetic localisation and charge oscillations 0-75781
 amorphous alloys, mag. and nonmag., thermoelec. power, 15 to 580K 0-80255
 concentrated magnetic alloys, density of states, Kondo effect, theory 0-65780
 DC Josephson effect for superconducting proximity Kondo alloys 0-88690
 dilute alloy, perturbation expansion for the asymmetric Anderson Hamiltonian 0-80202
 Hamiltonians diagonalisation, zero-temp. mag. susceptibility 0-93078
 impurity interactions, ground state calc., impurity conc. effect 0-65782
 metallic glasses, tunnelling two-level system, Kondo-like state 0-88547
 metals, Kondo effect, Anderson Hamiltonian 0-60187
 order parameter spatial variation near Kondo impurity 0-103813
 rare earth alloys and cpds., intermediate valence, models for anomalous systems 0-96827
 rare earth systems, Kondo singularity, Anderson-Smith model 0-80479
 rare earth-transition metal alloys, amorphous, electronic and mag. props. 0-93093
 resonant level model, for soln. of Kondo problem 0-60190
 AgCr, dil., specific heat, impurity contrib. Kondo temp. 0-65903
 Au-Cr, dil., elec. resist., generalised phase shift anal. of Kondo effect 0-75556
 Au-Yb thin films, ESR spectra, strain effects 0-71172
 (Ce, La)In₃, heat capacity and elec. resist. 0-71049
 γ -Ce, Kondo-like anomaly 0-96857
 CeAl_2 , antiferromag. ordering and Kondo behaviour, ^{27}Al NQR study 0-71231
 CeAl_2 , pure and $\text{LaAl}_2(\text{YAl}_2)$ diluted, collective phenomena 0-65933
 CeAl_3 , sp. ht., Kondo effect and ferromag. order coexistence 0-65927
 $\text{Ce}_3\text{Al}_{11}$, Kondo system, competition between ferro- and antiferromag. interactions 0-60258
 CeAl_{11} , sp. ht., Kondo effect and ferromag. order coexistence 0-65927
 CeB_6 , mag. and electronic props. 0-71048
 CeB_6 , magnetostriction, US absorpt. and thermal expansion 0-66004
 $\text{Ce}(\text{In, Sn})_3$, heat capacity and elec. resist. 0-71049
 Cr-Co, dil., antiferromag., elec. resist. min., press. and impurity effects 0-59970
 Cr-Fe, dil., antiferromag., elec. resist. min., press. and impurity effects 0-59970
 Cu-Al-Mn liq. alloys, susceptibility behaviour 0-93077
 Cu-Cr, dil., spin-density magnetisation near Cr atoms, NMR study 0-80626
 Cu-Cr, Kondo alloy, Josephson tunnelling effect 0-60145
 CuCr, dil., specific heat, impurity contrib. Kondo temp. 0-65903
 $\text{Cu}(\text{Rh}_{1-x}\text{Cr}_x)_2\text{S}_4$, spinel system, susceptibility and metallic resistivity, anomalies due to s-d interaction 0-70958
 $\text{EuLa}_{1-x}\text{Al}_2$, cryst. fields and exchange parameters, ESR meas. 0-71175
 Fe_2NbSe_7 , transport props. and mag. ordering 0-65527
 $\text{Fe}_{0.5}\text{Ni}_{2.5}\text{Mn}_1$, disordered, mag. struct. near ferro-antiferromagnetic transition 0-60211
 $\text{GdLa}_{1-x}\text{Al}_2$, cryst. fields and exchange parameters, ESR meas. 0-71175
 LaNdSn_3 , reverse Kondo effect in presence of crystalline elec. field splitting 0-103684
 $(\text{La,Y})\text{Ce}$, dil., Kondo supercond., transition temp., susceptibility and resist. 0-65733
 Mo-Co Kondo alloy, Co impurity susceptibilities, Knight shift 0-88721
 Pd-Cr, dil., temp. dependent scatt. 0-59973
 Pd $_{1-x}\text{Cr}_x$, resistive Kondo behaviour as function of Cr and H conc. 0-59971
 $\text{PdHFe}_{0.003}$, Kondo system, local moments, hyperfine fields, Mossbauer study 0-80478
 Pt-Co, dil., skew scatt. Hall effect, magnetoresist. and mag. anisotropy, orbital magnetism of impurity 0-70678
 Sc-Gd, dil., reverse resist. anomaly and negative magnetoresist. 0-84459
 Th-Cr, supercond., press. meas. to 20 kbar 0-88667
 TmSe, Kondo lattice model 0-97063
 Y-Gd, dil., reverse resist. anomaly and negative magnetoresist. 0-84459
 Zn-Mn, Kondo-system, ion implantation as method for study 0-70241

Korringa-Kohn-Rostoker calculations *see KKR calculations***Koster effect** *see dislocation damping***k.p. calculations**

- zero-gap semiconductors, anisotropy of IR absorpt. coeff., k.p. calc. 0-97285
 BiSb, alloys, semimetallic, camera, dispersion relations 0-59854
 Si, phonon-assisted Auger recomb., direct calc. of overlap integrals 0-107808

Kramers-Kronig relations

- alkali halides, refractive index calculation 0-88949
 anthracene-pyrometallitic dianhydride cryst., refl. and absorpt. spectra of singlet charge transfer excitons 0-71442
 ellipsometric function, Kramers-Kronig relations and sum rules, Lorentz oscillator model 0-102617
 films, optical constants, reflection spectra by Kramers Kronig method 0-76099
 optical constants calculation (*Russian*) 0-80740
 resonance Raman spectrum, rel. to Kramers-Kronig relations 0-97267
 CdCr_2S_4 , ferromag. semicond., IR refl. spectra, phonon props. and dielec. function 0-66191
 CdGa_2S_4 , IR refl. spectra 0-60604
 CdSe , undoped and Cr doped, far IR transmission and reflectance spectra 0-71429
 Co, X-ray refl. near $L_{2,3}$ absorpt. edge 0-71513
 Dy_2S_3 , optical props. and electronic struct. in fund. absorpt. region 0-80817
 FeF_2 , dielectric properties, IR spectra, lattice dynamics (*French*) 0-76026
 $\text{Ga}_{1-x}\text{In}_x\text{As}$, IR reflectivity, cluster effect on optical phonons 0-97259
 $\text{GaSb}_{1-x}\text{Se}_x$, mixed crystals, IR reflectivity spectra 0-66204
 p-GeTe, reflectance, and thermorefl. spectra 0-80814
 K double fluorides, IR refl. spectra, vibr. modes, optical vibr. freq., Kramers Kronig anal. 0-66190
 La_2S_3 , optical props. and electronic struct. in fund. absorpt. region 0-80817
 Nd_2S_3 , optical props. and electronic struct. in fund. absorpt. region 0-80817
 SbSBr glass, IR reflectivity spectra 0-71403
 SiO evaporated film, dielec. function 8 to 33 μm , spectrophotometric and refl. meas. 0-80883
 SiO_2 deposited on Ge, optical constants, reflection spectra by Kramers Kronig method 0-76099
 Ti, X-ray refl. near $L_{2,3}$ absorpt. edge 0-71513
 V_6O_{13} , semicond., IR vibration spectra 0-88997

Kramers systems *see determinants***Kromayer lamps** *see mercury vapour lamps***Kronig-Penney model**

- channeling in Kronig-Penney pot., band struct. and Bloch wavefunctions 0-65112
 education, deep one-dimens. periodic pot., zero energy gaps, Kronig-Penney model 0-62426
 energy bands, low-lying, Mathieu and Kronig-Penney potentials comparisons 0-70583
 polytypes, one-dimens. Kronig-Penney model and calcs. 0-75494
 GaAs-AlAs superlattice, folded acoustic phonons obs., Raman scatt. 0-88996

krypton

- see also nuclei with*
 adsorbed on graphite, commensurate-incommensurate transitions, low temp. theory 0-103582
 adsorbed on graphite, overlayer-substrate spacing, LEED determ. 0-103579
 atom, 6p levels, two-photon excitation, time resolved fluoresc., quenching, lifetimes and photoionisation cross section 0-78587
 atom, approximate relativistic Hartree-Fock eqns., soln. using Slater-type functions 0-58168
 atom, first excited config., intermediate coupling coeff. 0-83450
 atom, incoherent scatt. factors calc. by direct integration over impulse approx. Compton profiles 0-102475
 atom, outer $p_{1/2}$ subshell photoionisation, polarised electrons, relativistic RPA calcs. 0-83331
 atom, photoelectron asymmetry parameters 0-95684
 atom, photoionisation, absolute cross-sections, exptl. meas. techniques 0-63598
 atom, spin-polarised photoelectrons by circularly polarised synchrotron radiation 0-91516
 atom+H(D), ion pair formation, curve crossing model 0-87216
 atoms, absorpt. spectra, field induced autoionisation near ionisation threshold 0-106301
 atoms, inner-shell level energies, absorpt. spectroscopy with synchrotron radiation 0-95583
 atoms in Ne matrix, radiative and nonradiative lifetimes in excited states 0-69106
 broad beam ion source used for sputtering and etching 0-69002
 clustering, in W (100) He desorption spectrometry 0-77908
 diffusion coefficients and mobilities of F⁻ ions in Kr and Xe 0-100048
 dilute gas, transport props., simple pair pot. model 0-87835
 excited atom+ molecules reactions, electronically excited atoms and alkali metal atoms analogy 0-76490
 filament lamps, Kr-Ag-N gas mixture, thermal conduction coefficient calculational methods (*Russian*) 0-96335
 fission gas release from UO_2 -Zr high burnup nuclear fuel rods 0-57846
 gas, ion mobility and longit. diffusion coeff. of Na^+ 0-106866
 gas, liquid, solid, refractive index, density and dielectric const. 0-66138
 gas, nonlinear susceptibility meas. via third harmonic generation, Lyman- α 1216 Å source 0-95947
 gas atoms, electron thermalization time and position distribution meas. 0-93771
 ion source, HF, proton yield increase, influence of various admixtures to H₂ obs. 0-57422
 laser, new IR laser transitions, 3.725 to 17.233 μm 0-87374
 Lennard Jones (12,6) pot. distance parameter, transport props. calc. 0-79423
 liquid, comparison on interaction induced light scatt. and IR absorption 0-60561
 low-pressure glow discharge, elec. chars. of positive column 0-100112
 mass spectroscopic chemical anal. using quadrupole mass spectrometer for fissile material accounting 0-63300
 methanol+Kr, methoxy radical prod., UV emission spectra 0-91572
 physisorbed monolayer on graphite, neutron scatt. studies 0-107655

hydrogen ions continued

- H^+ + methane- H_2^+ + methyl radical, quantum 0-71911
 H^+ + N_2 collision, total ionis. cross section and stopping power for protons 0-69228
 H^+ + SF_6 , mode selective vibr. excitation 0-58351
 H_2^+ , free free absorpt. coeffs. dipole length formulation and two centre close coupling calc. 0-83345
 H_2^+ , bound states in strong mag. field 0-99438
 H_2^+ , differential cross section rel. to charge exchange cross sections of fragments 0-78704
 H_2^+ , dissociation, doubly excited Rydberg states 0-83506
 H_2^+ , electron elastic scatt., phaseshifts, quantum defect and two electron excited states 0-91671
 H_2^+ , exchange perturbation theory 0-63518
 H_2^+ , ground state, pot. energy curves, 1/R expansion coeff. calcs. 0-91472
 H_2^+ , mol. electron density distrib., binding/antibinding anal. 0-95534
 H_2^+ , photodissoc., mass spectra 0-86489
 H_2^+ , polarised Balmer radiation due to scatt. from Nb surface, adsorbed O_2 effects 0-99569
 H_2^+ , transmission yield through thin C-foil meas. 0-100732
 H_2^+ + Ar, endothermic charge transfer reaction, low energy crossed beam study 0-95720
 H_2^+ + Ar, low energy proton transfer reactions, crossed beam studies 0-108697
 H_2^+ + D_2 → H + H , product angular and vel. vector distributions meas. by crossed beam expt. 0-101012
 H_2^+ + H_2 , state selected reaction cross sections, coincidence technique obs. 0-66797
 H_2^+ + methanol, dissociation charge transfer reaction studied at rel. translational energies from 600 eV to 5000 eV 0-104432
 H_2^+ , IR spectrum, ν_2 band obs. 0-99506
 H_2^+ , ion beam prod. by coaxial electron impact ion source 0-62795
 H_2^+ , rot.-vibr. spectrum, ab initio calcs. 0-95595
 H_2^+ , vibr. excitation, ab initio CI pot. energy surface calcs. 0-74228
 HD^+ , Hellmann-Feynman theorem anomaly 0-63510
 $H_2^+(D_2^+)$ + $H_2(D_2)$ collisions, slow ion production, charge transfer cross sections 0-106378
 $H125\alpha$ recomb. line in M82, SHF obs. 0-82486
 $Li + H^+$, Li core excitation cross section, correlation and reorganisation effect 0-87215
 $Na + H^+$, $2p^3s^2P_{3/2}$ state alignment, collisionally induced, impact parameter calc. 0-83474
 $Ne + H^-(D^-)$, electron detachment, dynamical phenomenon 0-106305

hydrogen neutral atoms

- 1S Lamb shift and 1S-2S isotope shift 0-91464
 1S resonance, stabilisation method calcs., convergence 0-91492
 adsorbed on He surface, Bose condensation, adsorption isotherms and stability 0-107638
 adsorption, on graphite (0001) surface, vibr. spectrum, at. beam scatt. obs. 0-92779
 atoms produced by IR multiphoton dissociation of alkenes, IR detection 0-83356
 Balmer γ line profiles and masses of DA white dwarf stars 0-77399
 Balmer lines, formation in bright prominences spectra (Russian) 0-77377
 bombardment of graphite surface 0-93665
 bound states in strong mag. field 0-99438
 chemisorbed, surface charge fluctuations effect on spectral density 0-65368
 chemisorbed on cluster, indirect interactions, Grimley-Pisani model and tight-binding calc. 0-65370
 Cherenkov line radiation, QSO emission-like spectra (Chinese) 0-105378
 collapsing pre-galactic gas cloud, local stability, linear perturbation anal. 0-82513
 conversion by electron impact, eikonal exchange amplitude in Coulomb break-up processes 0-87232
 detection by resonance fluoresc., coherent tunable VUV generation near Ly- β transition 0-99798
 diffusion coeff., in H_2 , luminesc. intensity meas. 0-103098
 dilute hard-sphere Bose-gas model, low-density atomic H gas property-calc. 0-87194
 Dirac atom, relativistic, energy level splitting 0-77938
 Dirac field, self-interacting, charged nonlinear spinor field in Coulomb-like potential, localised solns. 0-68351
 double-quantum saturation spectroscopy, laser and RF 0-77880
 elastic electron scatt., 20-50 eV, Born calcs. of differential cross section 0-102571
 elastic electron scattering, pseudostates wave functions determ. in modified close-coupling calcs. 0-99572
 elastic scattering of electrons, optical model approach, polarisation effects 0-58382
 electron capture by fast multiply charged ions, q^3 scaling 0-91658
 electron elastic scatt., exchange perturbation theory 0-78709
 electron elastic scatt., at low intermediate energies 0-106393
 electron excitation, matrix elements by Faddeev approach 0-78714
 electron impact, 1s-2s and 1s-2p excitation, electron-photon coincidence meas. 0-87233
 electron impact excitation, 1s-2s transition, exact second Born amplitude 0-102572
 electron impact excitation, cross-sections, multipole moments, quasiclassical calcs. 0-63828
 electron impact excitation, electron-photon coincidence, large angle expt. 0-83500
 electron impact excitation of $n=2$ to $n=3$ transition, algebraic variational method close coupling calcs. 0-91678
 electron impact ionisation, polarised Coulomb-projected Born approx. 0-106395
 electron scatt., atomic optical potential model 0-99578
 electron scatt. information obtained using symmetrically coupled partial differential eqn. 0-102574
 electron scattering, elastic, $E_0 \geq 100$ eV, ang. distrib. calc. 0-74248
 electron scattering, optical pot. methods 0-102569
 electron-photon angular correlation meas. for excitation of 2P state 0-91636
 EM vacuum fluctuations, ground state energy in multiply connected universes 0-87050
 emission-line spectrum from a slab of hydrogen at moderate to high densities 0-72759
 energy levels and bound-bound transitions in strong mag. field 0-58134

hydrogen neutral atoms continued

- energy spectra, angular distrib. from HeH^+ collisions with thin foils 0-66355
 Fermi contact interaction, spin density calcs., Hiller Sucher Feinberg identity 0-69061
 fine structure $3^2S_{1/2}$ - $3^2D_{5/2}$ interval, separated oscillatory field meas. 0-99482
 finite chains, HF solns. stability and symmetry breaking, independent particle model calcs. 0-87035
 form factor for arbitrary states, dipole moment component matrix element calcs. (Russian) 0-58143
 fusion reactor neutral beam injection, 24 MW 400 keV H beam 0-91356
 galaxies, IR magnitude/H I vel. width relation rel. to distance scale and Universe expansion rate outside Local Supercluster 0-105325
 gaseous, high-resolution mag. reson. study, 1 to 1.3K 0-95560
 $H + FH(FD)$, low barrier quantum model, vibr. deactivation 0-69216
 hydrogenlike atoms, spin-orbit terms derivation 0-73148
 hyperfine splitting inside paraboloidal surfaces 0-99445
 interplanetary H I, $L\alpha$ emission profiles reanal. rel. to local interstellar gas temp. and vel. 0-105141
 interstellar absorption in galactic centre direction 0-77465
 ionisation in AC and DC elec. fields, time depend. 0-63585
 ionisation potential and energies in mag. field 0-99585
 Jupiter atmosphere, hydrocarbon and H I photochemistry rel. to Lyman α albedo 0-105194
 Kepler problem for n-dimensional atoms, dynamical symmetries 0-58121
 line profiles in RY Persei spectra, visible obs. 0-67795
 longit. excited states in intense mag. fields, rel. to pulsars 0-91469
 Lyman α albedo of Jupiter, Copernicus UV obs. 0-94747
 Lyman α albedo of Jupiter rel. to solar activity 0-98601
 Lyman α effect on non-LTE model atmospheres of A-type stars 0-90422
 Lyman α emission from Jupiter, Voyager 2 EUV obs. 0-77338
 inner M101 galaxy group, H I obs. 0-67885
 mesic, atomic X-ray yields 1s and 2p level shifts and widths, cascades, calc. 0-78730
 mesonic atoms, formation in mixtures of lightest elements 0-87252
 mesosphere and thermosphere composition UV dayglow Lyman α and β obs. 0-109290
 multiphoton ionisation of H like atoms, Pade-Sturmian approach 0-87089
 muonic, formation at extremely low press. 0-74263
 muonic atom + Y, muon transfer mechanism from free muonic hydrogen 0-69218
 negative mesons in H, atomic capture 0-69276
 NGC 1023 galaxy group, H I obs. and possible intergalactic H I cloud discovery 0-67886
 NGC 1052, elliptical galaxy, field, H I emission mapping and line profiles 0-98719
 NGC 7538 and Shapless 159, H II region/mol. cloud complex, H I aperture synthesis obs. 0-90510
 in NGC 925, barred spiral galaxy, high-resolution H I obs. 0-105329
 one-dimens., $\Psi(x) = \Psi(-x)$ even states, teaching 0-90638
 optical harmonic coefficients, third order, at low freqs. 0-78905
 Orion Nebula, radio obs. of nearby H I distrib. and vel. 0-105322
 oscillator, four-dimensional, rot. invariance of coordinate transform., appln. to Stark problem 0-99436
 perturbation theory and Pade approx. in electric field 0-91493
 photoionisation, absolute cross-sections, expt. meas. techniques 0-63598
 photoionisation in homogeneous elec. field (Russian) 0-106309
 photon emission, Bohr theory covariant eqns., teaching 0-105482
 pulsar crust, crust, infinitely magnetised H atom theory 0-77282
 quasars, large-red shift, spectra, implications of neutrino rest mass for H I obs. problem (Russian) 0-105414
 quasi-stationary states in field of strong monochromatic wave, perturbation theory calcs. (Russian) 0-58145
 redshifted H I 21 cm line assoc. with Stephan's Quintet of galaxies 0-67882
 relativistic energy levels in strong mag. fields 0-102454
 Rydberg consts., saturated absorpt., spectroscopy meas. 0-105604
 in Sa spiral galaxies, H I study 0-98714
 Shapless 159 and NGC 7538, H II region/mol. cloud complex, H I aperture synthesis obs. 0-90510
 spin-polarised, Bose condensation, phenomenological description 0-77699
 spin-polarised, Bose-Einstein condensation 0-77698
 Stark and photoabsorption spectrum, density of oscillator strengths, atom c.f. semiconductor spectra 0-83318
 Stark effect, high orders of perturbation theory for excited states 0-87079
 Stark effect, iteration procedure for any field strength 0-69104
 Stark effect, second order correction for energy (Rumanian) 0-74147
 Stark effect studied by scattering theory methods 0-63586
 Stark spectrum and field ionisation, density of continuum states, normalised wavefunctions 0-83317
 in static multipole field, logarithmic perturbation expansion 0-91431
 superpermeability, in interaction with Pd membrane 0-81365
 trapping and thermal detection using superconducting magnet at low temp. 0-73396
 Virgo cluster spiral galaxies, H I deficiency from 21 cm obs. 0-62277
 VUV radiation, narrowband tunable, at Lyman- α wavelength 0-78907
 $K^+ p$ atom and $\Lambda(1405)$, KN interaction model 0-68479
 $\mu p + p$, elastic scattering cross section of muonic H atoms 0-69278
 β radiative atomic recombination, antiprotonic atoms 0-83527
 $Ar^* + H$, collisional quenching rates 0-95548
 Ge, heterodiffusion due to H atom surface recombination stimulation, Cu, Zn, In coated (Russian) 0-59726
 H, degenerate 3s-3d levels, in mag. field, eigenvalues, Bender-Wu formulas 0-83275
 H I α observations of Algol type stars 0-109484
 H I halo round Seyfert galaxy Markarian 348, 21 cm obs. 0-82504
 H I halo round Seyfert galaxy Markarian 348, rel. to nucl. activity 0-82505
 H-like atoms, dipole polarisability of arbitrary hybrid bound states 0-87237
 H + alkali metal atom, interaction potentials 0-63736
 H + Ar, $H\alpha$ and $H\beta$ emission cross sections 0-63782
 H + $Ar^*(Ne^*)$, assoc. ionis., rovibronic struct. in electron energy spectrum 0-106380
 H + Ar(Kr)(Xe), ion pair formation, curve crossing model 0-87216
 H + $B^{3+}(C^{4+})(N^{5+})(O^{6+})$, ($2 \leq q \leq 4, 5$), cross sections at keV energies 0-78705
 H + Br $_2$ reaction, Br prod., matrix isolated ESR 0-106336

hydrogen neutral atoms continued

- H+CF₂, IR matrix isolation spectra 0-97706
H+CN(NC)(NSi), bimolecular exchange reactions, dynamical-statistical method calcs. 0-104435
H+C₂, pot. energy surfaces, inversion calcs. 0-93734
H+C₂, stochastic-collision complex model theory 0-108696
H+Cl—HCl+e, associative reaction, product vibr. state distrib. 0-66794
H+Cs(Rb)(K)(Na), single-electron capture total cross sections 0-91656
H+D, close coupling calc., resonant spin-flip process, Ramsauer-Townsend effects 0-99547
H+D₂, collinear motion, energy transfer and dissociation, collision dynamics 0-99563
H+D₂ reaction, transition state theory calculations, kinetic isotope effect explanation 0-66784
H+e (e⁻), elastic and inelastic scatt., relativistic spin-dependent amplitude, Glauber approx. 0-63818
H+H, electron loss cross section, four-body trajectory calcs. 0-99566
H+H, spin-exchange and freq. shift cross sections at low temps. 0-83452
H+H interaction, second order dispersion energy, Borel integral investigation 0-74218
H+H₂, collinear quantum mech. reactive scatt., hyperspherical coords. 0-108694
H+H₂, collinear reaction, Delves radial coord. S-matrix propag. calcs. 0-108695
H+H₂, exponential gap relation, rot. inelasticity 0-78693
H+H₂, reaction probability, max. entropy derivation, statistical theories 0-66781
H+H₂, reactions and collisions in IR laser field, collision-induced absorpt. spectra 0-76499
H+H₂, scatt. wave function modal struct. and global behaviour 0-81307
H+H₂, sudden rot. reactive scatt., 3-dimens., approx. quantum mech. calcs. 0-76498
H+H₂(Cl₂), reactivity-selectivity, bounds derivation 0-66763
H+H₂(D₂)(T₂) reactions, accurate pot. energy surface, isotope effects, quasiclassical trajectory study 0-97698
H+H₂(ν=1), exchange reaction, integral and differential cross sections determ. 0-85153
H+H₂→H₂+H three dims. chem. reaction, distorted-wave calcs. 0-81294
H+H⁺, electron detachment in adiabatic regime, mechanisms 0-63800
H+H⁺, H excitation, angular differential cross sections 0-63784
H+H⁺, ionisation and electron capture to continuum 0-58366
H+HCO→H₂+CO, classical trajectory study 0-93750
H+HCl, semi-empirical pot. energy surfaces calc. by diatomics-in-molecules method 0-95556
H+HCl, vibr. relaxation and reaction rates determ. 0-108698
H+HF, low barrier quantum model, vibr. deactivation 0-69216
H+H⁺, electron loss cross section, four-body trajectory calcs. 0-99566
H+He²⁺, electron transfer, plane-wave factor, mol. state treatment 0-63807
H+He(Ar), collisional coherent excitation, meas. of Lyman α-photons 0-99552
H+LiF, laser-induced nonadiabatic collision process, classical model 0-97701
H+methane, abstraction and exchange reaction, barrier height calc. using POL-Cl wave functions 0-81304
H+multiply charged ion, electron capture, unitarised distorted wave approx. 0-63814
H+N³⁺, multicharged ion thermal charge exchange reaction, rel. to astrophysics 0-63815
H+NF, electronically-excited free radical reactions 0-97707
H+NF₂, electronically-excited free radical reactions 0-97707
H+Ne(Ar), electron energy loss 0-87217
H+O₂+Ar, HO₂ free radical prod., rate const. calc. 0-101026
H+O₂(N₂), collisional coherent excitation, meas. of Lyman α-photons 0-99552
H+O₂→HO₂+O(³P), yields 0-71900
H+O⁸⁺(N⁸⁺)(Cⁿ⁺)(Bⁿ⁺), charge transfer cross sections, oscillatory behaviour in low-energy collisions 0-63806
H+OH→H₂+hν, radiative association reaction for mol. synthesis in interstellar clouds 0-90509
H+T₂, H-exchange studied by crossed molecular beam experiments 0-93747
H+Xe²⁺(Ar⁹⁺)(Fe⁹⁺), electron capture by heavy multicharged ions at low velocities total cross sections meas. 0-99548
H⁰+C₂ collisions, H⁻ production cross section 0-78698
H⁰+N³⁺, electron loss cross section 0-63805
H⁺+H high energy collision, excitation multipole moments, classical trajectory approx. 0-106389
H₂+Cl(Br)(I)(F), gas phase H-atom transfer reactions, struct.-reactivity correl., pot. energy surfaces 0-104433
H₂ and H_β spectral profiles from neutral beams and plasmas in high mag. fields 0-83999
H_β dynamic Stark effect for elec. field-strength meas. in waveguide 0-69103
H(S)+Ar(³P_{0,2}), energy transfer collisions, Lyman-α emission profile obs., in microwave discharge and reaction cell 0-58359
¹H, pionic, pion mass high accuracy meas. from transitions 0-106406
H⁺+H(Li), resonant ionisation, cross section and ionisation probability 0-63785
H10α radio recomb. line in galactic radio sources, SHF obs. 0-77472
H(1s) electron scattering, variable-charge Coulomb-projected Born approximation 0-58392
H(1s)+Cs, differential electron attachment and elastic scatt., 30-528 eV 0-63745
H(2S)+He(N)(Ar), excitation and ionisation contributions to sum-rule Born cross sections 0-99551
Hα and Hβ, Stark profiles, ion-motion effect 0-63592
NH₃+H₂, NH₃ inversion transition, linewidths and T₁/T₂ ratio 0-99499
Ne:H, exciton states and L_αL_β emission 0-93372

hydrogen neutral molecules

- ¹Σ and ³Σ state pots., diatomic transition operators, L² basis expansions 0-63519
ab initio SCF intermolecular interaction energy calcs. 0-78537
adsorption on Rh-TiO₂ catalyst., surface states, NMR spectrosc. investig. 0-103891
chloropentafluoroethane-H₂, multiphoton dissoc., ¹³C enrichment factor, CO₂ laser wavelength and fluence depend. 0-58331

hydrogen neutral molecules continued

- classical many-body collision model incorporating Heisenberg and Pauli principles 0-63511
contamination in He plasma, satellites of He 492.2 nm line, fine struct. interpretation 0-59235
dynamic dipole polarisabilities calcs. 0-74110
E,F¹Σ_g⁺ state, collisional and radiative props. 0-58357
electron degradation spectrum, statistical anal. of ionisation yield 0-99581
electron dissociative attachment 0-91694
electron impact dissoc. ionisation 0-83510
electron impact excitation, H_α and H_β lines emission, intensity decay curves meas. 0-83505
electron impact excitation, low energy, distorted wave approx. cross-sections 0-83511
electron impact excitation, to high Rydberg states, by threshold energy collision 0-83509
electron impact H⁺ prod., kinetic energy, ang. distrib. 0-63838
electron impact ionisation cross section 0-78718
electron repulsion matrix elements, asymptotic form, adiabatic representation 0-87038
electron repulsion potentials calcs. 0-91427
electron scatt., absolute total cross-sections, 0.2-100 eV 0-91674
electron scatt., elastic and inelastic, Glauber approx. 0-91695
electron scatt., low energy, multichannel variational calcs., static exchange approx. 0-83483
electron scatt., Schwinger variational principle, static-exchange approx. 0-63820
electron scattering, Gaussian basis Glauber approx., elastic and vibrational excitation cross sections 0-58399
electron scattering, iterative approach to Schwinger variational principle 0-99580
electron scattering, total cross section meas. at very low energies 0-58398
electron scattering elastic, 100-2000 eV, scatt. amplitude and cross-section 0-87228
electronic chemical pot., natural orbitals occupation numbers and electronegativity 0-63509
electronic struct., valence bond model, pairwise correlation 0-78543
four-body system, adiabatic representation 0-91530
infrared spectrum of matrix isolated H₂, mol. rot. and vibr. const. determ. 0-78617
interstellar gas clouds, spherically symm., gravitational collapse, effect of H₂ form. 0-101628
interstellar H₂, collisional excitation of linear mols. CO, OCS, SiO, HCN and HC₃N in ²Σ state 0-109508
interstellar H₂, OH rot. excitation rel. to maser emission 0-62232
interstellar H₂ form. in diffuse clouds, influence of Lyman band absorpt. of UV radiation (Russian) 0-73026
liquid, muon capture rate meas. 0-69275
lowest singlet and triplet states, interactions, electronic force calcs. 0-63742
magnetic susceptibility calcs. vector pot. variation method, effective selection of gradient transform. functions 0-69258
microwave absorption in atmosphere of giant planets induced by collisions of H molecules 0-90350
NGC 7027, planetary nebula, H₂ emission spatial distrib. obs. 0-98698
nonadiabatic coupling matrix elements by Hellmann-Feynman theory and HF 0-83263
ortho-para conversion, magneto-catalytic reaction, quantum formulation 0-108750
photoelectron asymmetry parameters 0-95684
photoelectron spectra, rot. intensity distrib. 0-91605
polarisabilities, variation-perturbation calcs. 0-87243
polarisability, dipole, coupled perturbed Hartree-Fock method improvement 0-58148
predissoc., interference effects, lineshape obs. 0-83432
preionis. and predissoc., rel. to spectral line shape 0-63724
relativistic Dirac-Fock multiconfig. SCF calcs. 0-99455
relativistic Dirac-Fock multiconfig. SCF calcs. 0-99456
singlet superexcited levels, radiative emission 0-83415
solid, fundamentals, static props., review 0-75403
states velocity auto-correl. function, relax. time, neutron scatt. obs. 0-58401
static polarisability, ab initio SCF wave functions 0-74106
sticking and accommodation on low-temp. substrate, mol. beam expts. 0-84368
valence bond orbital method for understanding electronic struct. 0-106268
vertical ionis. pot., many-body Green's function calcs. 0-102439
vibrational and rotational transitions, CARS, optical Stark effect 0-99512
Zeeman effect, Bender-Wu formula and SO(4,2) dynamical group, perturbation coeffs. determ. 0-95674
Ar⁺(²P₁)+H₂, Ar⁺ two spin orbit state, reaction cross section, direct determ. 0-93748
Br+H₂, proximity induced electric dipole moment effect in laser field 0-83456
Cs-H₂ vapour, resonant character of laser induced formation of particles 0-89481
¹⁸F+H₂, hot atom reaction, nonequilib. time-depend. theory 0-61126
H⁺+He(1s²), K-shell electron capture collision, static pot. effect 0-91660
H₂, field ionisation under nonequilibrium conditions 0-74244
H₂, high resolution electron spectroscopy 0-62740
H₂ in Ar, vibr. energy relax. 0-106384
H₂, optical polarisation following electron impact 0-63831
H₂, rotational Raman intensities and polarisability anisotropy change meas. with internuclear distance 0-63641
H₂, triplet state, molecular polarisability, ab initio calcs. 0-63860
H₂, vibrationally excited 2 μm lines toward molecular clouds 0-94853
H₂-Ar, states velocity auto-correl. function, relax time, neutron scatt. obs. 0-58401
H₂-H₂ dimers, hyperfine struct. in zero mag. field 0-95700
H₂-H₂ intermol. pair pot., ab initio SCF-Cl surface 0-91457
H₂+⁴He, inelastic collision, R-matrix study 0-87204
p-H₂+⁴He, vibr. relax., analytical approx. 0-63761
H₂+Ar⁶⁺, collisions, ionisation and excitation resulting from electron capture 0-78683
H₂+C⁺(N⁺)(O⁺), reactant ion electronic states, effect on charge transfer cross sections 0-63809
H₂+CH₄⁺, isotopic exchange, interstellar implications 0-61087

laminar flow continued

liquid metals laminar flow in curved channels, transversely applied mag. field, flow anal. 0-59116
 Lorenz model, Feigenbaum sequence of bifurcations 0-83783
 low Mach number duct flows, combustion noise generation by chemical inhomogeneities 0-92237
 MHD, sink flow with transverse mag. field, boundary layer thickness 0-69940
 MHD laminar flow, longitudinal dynamic effects determination for Na, Al, Sn and Hg (*Rumanian*) 0-64792
 MHD pulsating viscous flow superposed on steady laminar motion 0-92228
 moving horizontal flat plate, laminar boundary layer, buoyancy effects 0-74877
 natural laminar convection about isothermal cylinder, Navier-Stokes eqn. soln. 0-92143
 Newtonian fluid, recirculating flow in rectangular cavity, free convective flow in enclosed container 0-74852
 nonlinear effects in laminar stability theory (*French*) 0-103012
 nose separation for laminar boundary layers on body of revolution 0-59091
 oscillating source flow of ducting fluid between parallel discs 0-99986
 periodic wavy surface, laminar boundary layer, nonlinear anal. for long waves, separation 0-87759
 pipe flow, curved pipes, fully developed oscillatory flow 0-83846
 pipe flow, curved pipes, oscillatory flow development 0-79400
 pipe flow, low Reynolds number, in vicinity of three dimensional obstacles 0-74981
 pipe flow heat transfer, simultaneous wall and fluid axial conduction 0-74870
 plate, heated, semiinfinite, vertical, with heat sources and sinks natural convection 0-59035
 plate, vertical, free convection boundary layers and heat transfer 0-59002
 plate and laminar slug flow with periodically changing temp., transient heat transfer 0-74872
 plate with nonsteady temp. on lower surface, laminar flow, conjugate heat transfer 0-74879
 polyethylene oxide, dilute solution, flow round circular cylinder 0-69882
 polymer melts, laminar and melt fracture flow through successive capillaries 0-59085
 polymer solutions, aqueous, diffusion and mass transfer from rotating disc 0-83827
 porous media, laminar flow, velocity and longitudinal dispersion, deterministic model 0-83842
 porous medium, laminar isothermal flow of two immiscible compressible fluid phases 0-69919
 porous pipe in a pipe heat exchanger, laminar flow, vel. changes 0-64512
 power law fluid, laminar flow heat transfer in helical coils 0-59030
 rectangular body, laminar flow, separation bubble and stagnation line 0-64514
 round tube flow, laminar dispersion 0-64638
 simple law of wall formulation for Newtonian fluid, unified time mean velocity profile model 0-103017
 solid reacting particles, ordered system at high Peclet numbers, mass transfer, convection 0-69830
 solid spheres, reacting, in periodic array, convective mass transfer in liq. laminar flow 0-96176
 spherical particle in circular tube flows, lateral migration 0-92221
 steady laminar flow through channel with symmetrical constriction in step form 0-100036
 steady viscous flow past circular cylinder, numerical study, vortices and separation 0-92108
 steady-state in turbulence amplifier, numerical integration (*Bulgarian*) 0-106779
 steady-state recirculating flows, finite difference schemes, practical evaluation 0-106776
 steel pipe corrosion, mass transfer coeffs. under isothermal flow conditions 0-97628
 stream flow over right circular cone, method of singular perturbations 0-69763
 supersonic flow over compression ramp, laminar separation, second order asymptotic soln. 0-83828
 suspension in inclined channel, two dimensional model 0-106834
 suspensions, flow in cylindrical pipe, using ultrasonic debitometry Doppler spectra (*French*) 0-96303
 suspensions of charged particles, laminar tube flow, entrance deposition 0-59100
 T-junction laminar flow, partially elliptic flow numerical calcs., recirculation 0-64632
 Taylor vortex flow with imposed laminar axial flow and isothermal surface heat transfer, velocity profiles 0-103031
 tracer gas axial dispersion through tube constrictions 0-64625
 tube flow, gravitational deposition of growing aerosol particles 0-59099
 two parallel corotating discs, laminar flow and heat transfer, shear pump appl. (*German*) 0-69840
 two-phase pressure driven stratified laminar pipe flow 0-64609
 unstable laminar boundary layers, nonlinear evolution and breakdown 0-92109
 unsteady laminar boundary layer flows induced by impulsive accelerating motion (*Japanese*) 0-69765
 unsteady laminar boundary layers behind blast waves, num. soln. 0-69776
 unsteady laminar separation and stall from aerodynamic surfaces 0-59090
 velocity profile for boundary layer flow along a rectangular corner (*Japanese*) 0-74832
 vertical natural laminar convection flows in cold water, buoyancy force reversals 0-59034
 vertical plate, laminar natural convection heat transfer, supercritical CO₂ and He 0-64544
 vertical plate with uniform blowing, laminar combined forced and free convection 0-74876
 viscoelastic laminar flow, combined generalised measure approach, pseudo-plasticity 0-64586
 viscous flow down an open inclined channel with naturally permeable bed 0-69764
 viscous flow through rough wall cracks, friction factor formula (*Rumanian*) 0-69925
 viscous fluid, laminar flow, Navier-Stokes eqns., central difference scheme 0-69762
 viscous fluid in toroidal tube, oscillations 0-79253

laminar flow continued

viscous incompressible fluid, laminar divergent flow through porous cone (*French*) 0-83838
 viscous incompressible fluid flow through partially filled cylinder 0-74973
 viscous liquid film instability under the influence of an adjacent gas flow 0-92110
 water boundary layer along heated cylinder, buoyancy and variable viscosity effects 0-79256
 water jets sensitive to sound, two-dimensional, velocity fluctuations behaviour (*Japanese*) 0-100020
 TiO₂ suspension in glycerine, Bingham plastic flow through annuli 0-64521

laminar to turbulent transitions
 body of revolution with heating and cooling, boundary layer transition and separation 0-64518
 Couette flow, laminar to turbulent transition spectrum evolution 0-103034
 Couette-Taylor flow, laser Doppler velocimetry obs. of transition to turbulence 0-92163
 critical Reynolds numbers for Newtonian flow in concentric annuli 0-64517
 crossflow developing in boundary layer during longit. flow around right dihedral angle 0-59049
 doubly periodic flows, transition to turbulence 0-83790
 dynamical systems, dissipative, intermittent transition to turbulence 0-79132
 early nonperiodic transitions in Couette flow 0-59056
 external noise effect on transition to turbulent convection 0-96263
 finite amplitude wave propagation in nearly parallel flow 0-74899
 free convection heat transfer from vertical thin wire to air, laminar-turbulent transitions (*Japanese*) 0-92152
 heated flat plate in water, critical Reynolds number, heat transfer 0-69766
 hydrodynamic calculations for container pipeline systems with non-Newtonian liquids 0-106817
 incompressible separated boundary layers including viscous-inviscid interaction, transition bubble 0-64515
 intermittent transitions to turbulence, intermittency in dissipative dynamical systems 0-106781
 leading edge bubble formation, peaky airfoil (*French*) 0-64524
 Lorenz model, Feigenbaum sequence of bifurcations 0-83783
 nonlinear interaction of two waves in boundary-layer flows 0-59016
 rotating disc boundary layer transition regime, spiral vortices 0-59040
 round tubes, non-Newtonian fluid transition and turbulent flow regions (*Russian*) 0-59077
 three dimensional parallel shear flows, stability and transition for rot. disc 0-74887
 tubes, viscous liquid turbulent unsteady flow, pressure drop in transition region 0-74978
 unstable laminar boundary layers, nonlinear evolution and breakdown 0-92109
 Hg, transition and turbulent flow in curved channels under transverse mag. field 0-79396

laminates

analysis, desktop calculator library module appl. 0-77764
 angle ply laminates, 3D finite difference soln. of free edge effect 0-79152
 anisotropic shells, nonlinear eqns. of Timoshenko-type theory 0-69669
 ceramic multilayer capacitors, fracture mechanics approach to structural reliability assessment 0-89328
 composite laminates, proof test and fatigue study 0-93643
 cord-rubber laminates, two-ply balanced, interlaminar-shear strain study 0-97526
 cross-ply, symmetric composites, edge effects, traction-free-edge condition satisfaction 0-79151
 cylinder, thin-walled, laminated, non-uniform, elastic equilib. with surface loads and displacements 0-69671
 cylindrical shell, reinforced laminar, intrinsic oscill. 0-99957
 damage zone failure analysis 0-85059
 elastic reinforced shells, stability 0-58948
 elastomeric bearings, high-capacity, laminated, finite-element anal. 0-96197
 EM wave propag., bonding material influence 0-91726
 fatigue damage anal. 0-104253
 fibre cross-reinforced, moment effects in plane problem 0-64393
 fibre reinforced epoxy, interlaminar failure 0-81207
 fibre reinforced laminated hybrid, tensile first cracking strain and strength 0-81175
 glass fibre reinforced epoxy laminate, metallization by Cu and chem. treatment by H₂CrO₄ (*German*) 0-93670
 glass fibre reinforced epoxy laminates, exp. determ. of nonlinear shear behaviour 0-66575
 glass fibre reinforced epoxy resin laminate, sliding behaviour against Cu or Al spheres at cryogenic temps. 0-66671
 glass fibre reinforced plastic, cemented joint of cylindrical shell with cover, stressed state 0-69668
 glass fibre reinforced plastic, strength and deformability, artificial ageing effect 0-60893
 glass fibre reinforced plastic laminates, failure models, reinforcement struct. effect 0-66641
 graphite fibre epoxy laminates, low thermal expansivity, design considerations 0-81031
 graphite fibre filled phthalocyanine composites, cure cycle investigation 0-81030
 graphite fibre filled polyimide composite laminates, space environment, phys. and mech. response 0-81140
 graphite fibre filled polyimide composite prepreg laminates, room-temp. ageing effect 0-81093
 graphite/epoxy 5208/300, proof test and fatigue study 0-93643
 graphite/epoxy laminate, T300/5208, proof testing under cyclic tension-tension fatigue 0-81249
 graphite/epoxy laminates, statistical fatigue, high load effect 0-93642
 graphite/epoxy laminates, stress wave damage 0-93611
 isotropic plane sandwich plates, constant shear theory 0-99943
 metal-composite rods, compressed, delamination 0-64396
 metal-polymer, ply-separation resist. polymer polarity effect (*Russian*) 0-61064
 Mylar film/adhesive/Al foil laminate, mech. interactions 0-81112
 orthotropic laminates, torsion strength and shear modulus determ. 0-92587

laminates continued

- periodically layered composites in plane strain, dispersion eqn. for waves 0-79212
- plates, laminated, cylindrical bending, random loading, dynamic response 0-58902
- plates, laminated anisotropic composite, penalty plate bending element 0-96200
- plates, rectangular cross-ply laminated, with nonlinear stress-strain behaviour, buckling 0-64415
- plates, symmetric, specially orthotropic, thermoelastic anal. 0-92058
- polyester laminates, glass fibre reinforced, enhanced elasticity, chem. resist. tests (*Polish*) 0-60901
- polyester resin, Polimal 109, open pore density and content (*Polish*) 0-59665
- polymer blends, selective staining method for TEM obs. of morphology 0-84103
- polymer multilayer composites, wire-reinforced, dynamically loaded, crack propagation and arrest 0-97567
- rectangular laminated plate, free vibrs., freq. and shape determ., complex boundary conditions 0-79203
- residual thermoelastic stresses 0-106721
- shell, cylindrical, three-layered, stress-strain state (*Russian*) 0-90677
- single ply, thickness effect on percolation and conductivity 0-92953
- steel, sheets bonded with low density polyethylene, static fatigue (*French*) 0-108522
- steel laminate, acoustic emission rel. to fracture at 77K (*Russian*) 0-93633
- structural elements, stress intensity factors determ. 0-99973
- thermal NDT using liquid crystals, fibreglass laminates 0-93709
- thermoviscoelastic laminate beam, stress anal. (*German*) 0-106727
- thick multilayer laminates, hybrid-stress finite element formulation 0-92043
- thin, optimal struct. and strength in two-dimens. stress state 0-64395
- three phase laminated composite, longitudinal heat propag. at low exciting freqs. 0-58889
- three-layer plates, circular, stability 0-79188
- Young's modulus determination, dynamic high-speed method (*German*) 0-85123
- C fabric reinforced plastic laminates, tensile and compressive strength determ., 20-1500°C 0-100880
- Mn-Cr-Ti layers on low C steel, composite, residual stresses rel. to arc-spraying parameters (*German*) 0-104077
- Mo-TiC lamellar eutectic composite, deformation and strength, room temp. to 2073K (*Japanese*) 0-71702
- PLZT/TFPD thermal/flash protective lens assembly, polarised delamination investigation 0-78929

laminations

- ethylene-vinyl acetate lamination, solar cell encapsulation, double vac. technique 0-93510
- Fe-Si, mag. props., stress and reannealing effects 0-88844
- Fe-Si (3 wt.%), grain-oriented, stacking effect on power loss, mag. props. 0-88795
- Fe-Si (3 wt.%), grain-oriented, power loss and domain wall variation with lamination thickness 0-88814
- Fe-Si (3 wt.%) laminations, magnetostriction behaviour associated with closure domain spikes 0-75834
- Fe-Si (3 wt.%) laminations, grain oriented, plastically deformed, anomalous losses 0-88853

lamp accessories

see also lamps

- photographic flashlamp trigger circuit 0-62750

lamps

see also discharge lamps; filament lamps; light sources

- illumination system, optical design 0-64135
- slit lamp photodocumentation of ocular structure 0-67181
- UV emitting lamps, method for estimation of O₃ concs. in vicinity 0-81765

Landau levels

- degenerate semiconductor, conduction electron acoustic spin resonance, oscillations of absorbed power 0-108075
- excitonic insulator in mag. field, two-band model 0-80192
- MIS, magneto-optic absorption by electron gas, optical phonon effects 0-97248
- MOSFET, two-dimens. electron gas, determ. of fine struct. const. based on quantised Hall resist. 0-96997
- nonequilibrium electrons, thermalisation and linear response 0-65422
- polar semiconductors, secondary cyclotron emission giant oscillations of intensity and line shape 0-66192
- quasi-local level, line shape induced by impurity 0-100441
- semiconductor, magnetophonon resonance oscills., peak shape, theory 0-107824
- semiconductors, light induced electron drift, two-photon transitions (*Russian*) 0-107853
- semiconductors, two-dimensional, Mott exciton formation in high mag. fields (*Russian*) 0-65467
- semimetal, degenerate, conduction electron acoustic spin resonance, oscillations of absorbed power 0-108075
- Bi, gas-liquid type transform. and sound attenuation in strong mag. fields, electron-hole correl. effects 0-88598
- Bi, giant quantum attenuation anomalies of sound waves at high mag. field, temp. and freq. depend. 0-70587
- Bi, giant quantum attenuation anomalies of sound waves at high mag. field, extra attenuation peaks 0-70588
- Bi, quantum-EM excitations 0-88471
- Cd_{1-x}Mn_xTe, semimagnetic, exchange interactions between localised and delocalised electrons 0-97245
- Ge, mag. field luminesc. lifetime, quantum oscills., phonon wind effects 0-93385
- He liq. surface, cyclotron reson. of two-dimens. electrons (*Russian*) 0-88374
- ⁴He superfluid, phonon-rotor excitation 0-107586
- Hg_{1-x}Mn_xTe, semimagnetic, exchange interactions between localised and delocalised electrons 0-97245
- InAs-GaSb superlattices, mag. field induced semimetal-semicond. transition 0-65656
- n-InSb, spin polarisation, anisotropic size effect, effect on CESR signal 0-70743
- n-Si channel (100) inversion layer MOSFET, valley splitting, conductivity 0-70840

Landau levels continued

- n-Si inversion layers, electronic g-factor, spin-split Landau levels 0-80346
- TlBr, resonant polaron coupling and excitons under mag. field 0-71383
- Landé g-factor** see g-factor
- Landé splitting factor** see g-factor
- landing fields** see airports
- Langmuir films**
 - anisotropic optical waveguides based on Langmuir organic films 0-64177
 - anthracene, lightly substituted, AC and DC cond. 0-80425
 - barium stearate single-layer Langmuir films, elastic and inelastic tunnelling 0-80403
 - cadmium arachidate mixed with cyanine dyes, mol. layers, photoelec. props. 0-80401
 - cadmium stearate based, deposition on p-CdTe, characts. and MIS struct. 0-92998
 - chlorophyll a, Langmuir-Blodgett films, deposition onto SnO₂ optically transparent electrode 0-80093
 - chromophore phospholipid Langmuir films, photoeffects 0-80409
 - diacetylene monocarboxylic acids, multilayers, struct. phase transitions and polymerisability 0-80129
 - dye-sensitized, anisotropic photocond. 0-80327
 - electrical and photoelec. transport props. of Langmuir-Blodgett films, device appl. 0-80431
 - esters, long-chain, X- and Y-type multilayers, form. conditions and struct. characterisation 0-80127
 - lead stearate, Langmuir-Blodgett multilayers, comp. and transfer mechanism 0-80125
 - lightguiding in Langmuir-Blodgett films 0-79006
 - manganese stearate: cadmium stearate, dil. quasi two-dimensional, ESR line width 0-71155
 - manganese stearate, Langmuir-Blodgett layers, high resolution X-ray diffr. 0-80126
 - manganese stearate, two-dimensional mag. struct. 0-108040
 - monolayer to multilayer, Langmuir-Blodgett 0-80031
 - multilayer films with and without dye-sensitisers, elec. props. 0-97006
 - sodium stearate, Langmuir-Blodgett multilayers, comp. and transfer mechanism 0-80125
 - tetramethylsiloxane dicarboxylic acid Langmuir films on Cu surface, surface EM wave absorpt. study 0-97359
 - Cu surfaces, with Langmuir films, surface EM wave absorpt. using CO₂ laser excitation 0-97365
 - InP substrate for Langmuir film growth, surface chemistry, ESCA study 0-103552
 - p-type InP/Langmuir film MIS diodes, characts. 0-80384

Langmuir probes

see also plasma diagnostics

- ion acoustic waves method of plasma potential meas. 0-59289
- sputtering, plasma characts. by Langmuir probe technique 0-80929
- Tokamak, large magnetic field ripples, electric probe meas. 0-83976

lanthanides see rare earth metals**lanthanons** see rare earth metals**lanthanum**

see also nuclei with

- addition to Cr-Mo and Ni-Cr-Mo-V low-alloy steels, remedy for temper brittleness 0-66659
- addition to Ni-Cr austenitic stainless steel, effect on heat resist. and comp. of non-metallic inclusions 0-76315
- coadsorption with B on W, field emission and field ion microscopy 0-104049
- heat capacity and supercond. props. 0-65247
- surface and volume props., flow props., surface layer thickness (*Russian*) 0-59760
- BaF₂:La³⁺, phonon reson. and IR absorpt. 0-84752
- BaF₂:La³⁺, thermal depolarisation of La³⁺-F₂⁻ defect dipoles 0-75926
- CaF₂:La³⁺, thermal depolarisation of La³⁺-F₂⁻ defect dipoles 0-75926
- (Ce,La)_{1-x}Al_x, Mg₂(NO₃)₆·24H₂O, adiabatic demagnetisation temp., mag. entropy (*Russian*) 0-65892
- EuO:La, photothreshold changes below mag. ordering temp. 0-97406
- GdAlO₃:La, antiferromag., random-field crit. and multicritical behaviour 0-65939
- GdAlO₃:La, random antiferromagnets, crit. and multicritical props. 0-60332
- La³⁺ 3d⁴f config., collapse of 4f electron, X-ray spectra obs. (*Russian*) 0-58204
- La:Eu²⁺, liquid, γ-ray spectra observation of exchange interaction 0-84672
- ¹³⁹La II 5d² 3F₄-5d4f² 3F₂⁰, hyperfine structure, ΔF=±2 transitions, three-quantum process 0-63848
- Pb_{0.8}Sn_{0.2}Te:La, evaporated thin films, low carrier conc. 0-65414
- SrF₂:La, type-I dipole reorientation, activation vol. determ. from dielec. const. 0-88916
- SrF₂:La³⁺, thermal depolarisation of La³⁺-F₂⁻ defect dipoles 0-75926
- YIG:La,Ga, film, LPE-grown, Ga incorporation, depend. of magnetisation on growth rate 0-84627
- ZnO:La, electrolum. brightness, field strength and freq. depend. 0-100696

lanthanum alloys

see also lanthanum compounds

- steel, low alloy, Mn-P, temper brittleness, rare earth mischmetal effect (*Chinese*) 0-104249
- thermoelectric materials, B₂C_x and (B,Si)₂C_x P-type LaS_x N-type alloys, fabrication and thermoelectric props. 0-107771
- (Ce,La)Al₂, collective phenomena 0-65933
- (Ce,La)In₃, heat capacity and elec. resist. 0-71049
- Ce_{1-x}Al_x, dil., γ-α transition temp. and press., elec. resist. meas. up to 10 kbar 0-59643
- Ce_{0.9-x}La_{0.1}, mixed valence state, static and dynamic mag. response 0-103816
- Co-mischmetal system, phase relations, microstruct., mag. props. 0-104118
- Cu₂La_{1-x}, splat-cooled, phase diagram and supercond. props. 0-70881
- Er-La, HCP, mag. phase diagram, neutron diffr. meas. 0-70950
- Er₂La_{1-x}Be₁₃, ESR studies 0-108064
- Er₂La_{1-x}Be₁₃, mag. sp. ht. and ESR, cryst. field interactions 0-60290
- Eu₂La_{1-x}Al₂, cryst. fields and exchange parameters, ESR meas. 0-71175
- Eu₂La_{1-x}Al₂, dil. EPR, cryst. fields and effective exchange interaction 0-66029
- Eu_{1-x}La_x, electron struct., lattice const., X-ray spectral study (*Russian*) 0-100432

lanthanum alloys continued

- Gd-La_{1-x}Al_x, cryst. fields and exchange parameters, ESR meas. 0-71175
 Ho-La HCP, mag. phase diagram, neutron diffr. meas. 0-70950
 (La,Gd)Al₃, spin glass materials, mag. field dependence of susceptibility peak 0-103840
 (La,Gd)Al₃, spin glasses, time depend. mag. props. 0-65909
 (La,Nd)Sn₃, reverse Kondo effect in presence of crystalline elec. field splitting 0-103684
 (La,Y)Ce, dil., Kondo supercond., transition temp., susceptibility and resist. 0-65733
 La-Ag alloys, amorphous, elec. resist. and supercond. 0-70885
 La-Al amorphous alloys, internal friction, relaxation process 0-92607
 La-Au, splat-quenched, Mossbauer effect and elec. resist., amorphous struct. 0-84676
 La-B, amorphous, B-rich, low freq. modes, Raman scatt. obs. 0-108202
 La-Fe alloy, amorphous, sputtered at high rate, mag. props. 0-75753
 La-Gd, exchange-coupled localised moments, Korringa relaxation rate 0-75851
 La-Gd (8 at.%), FCC, under hydrostatic pressure, resistivity meas., comparison with positive-J spin glasses 0-59958
 La-rare earth metal/AlO_x/Al tunnel junctions, cond. meas., cryst. field effects 0-88694
 La-Sm-Au, amorphous, surface effects on Sm valence, XPS and X-ray absorption meas. 0-108325
 LaAg₁₁Ni₁₁, phonon dispersion, elastic consts. and struct. instability, soft mode behaviour 0-103436
 LaAl₂, calc. of energy band-structure and Fermi surface by APW method 0-70590
 LaAl₂, doped with Tb, Nd, or Pr, crystal field effects, tunnelling within mK range 0-70907
 LaAl₂, electronic struct., APW method and local-spin-density approx. 0-65434
 LaAl₂, supercond. and normal states, anomalous US attenuation and velocity change 0-80446
 LaAl₂Ga₂, synthesis, NMR and X-ray absorpt. studies 0-108083
 La₇₆Au₂₄, disordered ribbons, production of quenched samples using arc furnace 0-71612
 LaB₆-Cu, form. by wetting of LaB₆ with Cu 0-100813
 LaBe₁₃, lattice spacings and susceptibilities 0-65778
 LaCo₂, sorption at press. up to 1500 atm. 0-97819
 La_{1-x}Co_x, amorphous alloys, thermal stability, elec. cond. enthalpy 0-100172
 La₂Co₇, mag. props. changes upon H₂ absorpt. 0-71270
 La(Co_{1-x}Ni_x)₅, distrib. of Co and Ni atoms, neutron diffr. obs. (Russian) 0-64954
 La₃Co₂Sn₇, prep. and crystal structure (German) 0-84138
 La₇₀Cu₃₀, disordered ribbons, production of quenched samples using arc furnace 0-71612
 La₉₂Eu₁₀/Ni₄₈Mn₄₀, absorption-desorption props. of H₂, degradation mechanism, Mossbauer study 0-88431
 La₇Ga₂₅, amorphous, local symmetry around glass-former sites, elec. quadrupole effects, NMR 0-80618
 LaM₂-Gd, M=transition metal, correl. between g-shift and stability, EPR study 0-88874
 LaMg, Pauli paramagnet, mag. susceptibility, nonlinear band behaviour 0-75706
 LaNi₅, H₂ absorpt. kinetics (Chinese) 0-103561
 LaNi₅, H₂ absorption in thin film hydriding alloys 0-65238
 LaNi₅, Haucke compounds, low temp. heat capacity, Debye temp. 0-96663
 LaNi₅ hydrides, 4.2K paramag. susceptibility 0-70934
 LaNi₅ hydrides (Al, Ga, In, Si, Ge and Sn substituted) appl. in chemical heat pumps for solar energy conversion 0-89667
 LaNi₅, magnetism and H₂ storage 0-70941
 LaNi₅/H system, thermodynamics of H trapping 0-107444
 LaNi₅, sorption at press. up to 1500 atm. 0-97819
 LaNi₄Al, solubility and sorption props. of H₂, effect of Al 0-103482
 LaNi_{5-x}Al_x, HYCSOS chemical heat pump, low grade heat enhancement using 0-61467
 LaNi_{5-x}Al_x, use in hydride conversion and storage system chemical heat pump 0-72077
 LaNi₄Be₆, H₂ absorpt. props. 0-88432
 LaNi₄Fe₆, H₂ absorpt. cracking, acoustic emission characs. (Japanese) 0-66631
 LaNi₆H₆, solar energy storage by metal hydride 0-61455
 LaOs, cryst. struct. 0-96474
 LaPb₃, doped with Tb, Nd, or Pr, crystal field effects, tunnelling within mK range 0-70907
 La_{80-x}Pr_xAu₂₀, amorphous, mag. and supercond. props. 0-75713
 LaSn₃, doped with Tb, Nd, or Pr, crystal field effects, tunnelling within mK range 0-70907
 La_{1-x}Tb_xAl₂, competing paramag. anisotropy from cryst. field and indirect quadrupolar coupling 0-60180
 Mg-La, appl. to H₂ storage 0-72093
 Pr_{1-x}La_xAu₂₀, amorphous, low temp. excitations, specific heat 0-100337
 (Pr_{1-x}La_x)₂In, mag. props. 0-108009
 Sm_{1-x}La_xS₂, electron struct., lattice consts., X-ray spectral study (Russian) 0-100432
 Sn-La system, heats of form. 0-89517
 (Tb_{1-x}La_x)Be₁₃, mag. struct., cryst. field effects, neutron diffr. study 0-65789

lanthanum compounds

see also lanthanum alloys

- dihydrides, struct. and stabilities 0-107146
 disc LaB₆ cathode for plasma production in magnetic field 0-106951
 ethylsulphate:Gd³⁺, zero-field splitting, contributory mechanism 0-80231
 ferrite, hexagonal, with M, W and Y structures containing Fe²⁺ and Fe³⁺ mag. ions, saturation moment and anisotropy 0-71009
 high current discharge from cold LaB₆ cathode 0-107011
 lanthanum ethyl sulphate:Pr, phase transition under pressure, absorpt. spectra (Russian) 0-92667
 lanthanum nicotinate dihydrate, cryst., nucl. quadrupole interactions, D atom coords., ENDOR obs. 0-97161
 PLTZ coarse-grained solid solutions, electro-optical processes induced by longitudinal electric field (Russian) 0-80750
 Ba_{1-x}La_xF_{2+x}, enhanced ionic motion in solid solutions 0-107491
 BaO-La₂O₃-B₂O₃, glass, refraction, refractive index from 0.365 to 2.50 μ m 0-88953
 BiFeO₃-LaFeO₃, solid solns., antiferroelec.-antiferromag., magnetoelectric effect at antiferroelec. transition 0-100637

lanthanum compounds continued

- CaLaFeO₄, two-dimens. mag. props. rel. to cryst. struct. 0-75776
 Eu₂La_{1-x}Ta_xO₁₀, polycryst., luminesc. and excitation spectra 0-60659
 Gd₂La_{1-x}B_x, solid solns., mag. susceptibility, 80 to 1000K (Russian) 0-88713
 HfF₄-BaF₂-LaF₃ glass system, IR transmitting, synthesis and props. 0-71623
 KLa(MoO₄)₂, solubility in aq. K₂MoO₄ solns., hydrothermal conditions 0-96651
 La₂F₃-CaF₂ membrane electrode development, ion selective (Japanese) 0-61203
 (La,Nd)₃PO₇, IR and Raman spectra, vibr. assignments, cryst. struct. characs. 0-97258
 La ferrite, composition and mag. props., anisotropy field, magnetisation 0-71109
 La-D, phase transition, NMR meas. 0-66508
 La-H, ordered struct. near LaH_{2.65} at 250K, NMR 0-66508
 La-H, phase equilibria 0-66492
 La-H(D), lattice parameters 0-64982
 La-Si-As ternary cpd., synthesis, stoichiometry 0-104083
 La_{2-x}A_{1+x}Cu₂O_{6-x/2} (A=Ca, Sr), synthesis and characterisation (French) 0-104085
 LaAlO₃, exchange interactions of transition metal ions in orbitally degenerated excited states 0-65512
 LaB₆ (100), (110), and (111), surface structs. and work functions 0-70512
 LaB₆ (210) surface, work function, struct. and chemisorpt. stability, XPS, UPS and LEED 0-65344
 LaB₆ cathode, thermal, illumination systems for round beam electron probe systems 0-57436
 LaB₆ cathodes, mounting methods and operating characs. 0-57437
 LaB₆ cathodes, single crystal, of <100> and <110> orientations, brightness meas. from 1500 to 1950K 0-62808
 LaB₆ cathodes for Kohler illum. and brightness meas. 0-68296
 LaB₆ crystals, zone refined, chem. characterisation 0-93821
 LaB₆, de Haas-van Alphen effect, low-field 0-75497
 LaB₆, direct recomb. and Auger deexcitation channels of La 4d to 4f reson. excitations, photoemission spectra 0-66395
 LaB₆, electronic struct., APW method and local-spin-density approx. 0-65434
 LaB₆, FIM study 0-71578
 LaB₆, gun, 100 kV, combined CTEM and STEM 0-86516
 LaB₆, hollow cathode mag. multiple ion source 0-102369
 LaB₆ single cryst. tips with [100], [110], [111] and [210] orientations, thermionic emission patterns 0-66379
 LaB₆ single crystal cathode, thermionic emission, surface struct. 0-97395
 LaB₆ surfaces, (100), (110) and (111), electron states, UPS study 0-100752
 LaB₆ synthesis by heating BN with lanthanum citrate hydrate 0-100819
 LaB₆, thermal expansion, X-ray method, room temp. to 1300 C 0-96670
 LaB₆, transverse magnetoresistance meas. 0-107764
 LaB₆C₂, ordering of B and C atoms in struct. 0-96481
 LaB₆Er, ESR, appl. of exchange induced broadening in low lying crystalline field system 0-108062
 La₂B₆O₉Nd³⁺ (Pr³⁺), cryst. growth, spectral and laser properties in $\frac{F_2}{2} \rightarrow \frac{F_1}{2}$ and $\frac{F_3}{2} \rightarrow \frac{F_1}{2}$ transitions 0-80853
 LaBr₃Np³⁺, energy level anal., polarised absorpt. and fluoresc. spectra 0-76056
 La₂C₃, solid solution, lattice const. and superconducting transition temp. (Russian) 0-92496
 (La_{0.8}Ca_{0.2})MnO_{3+x}, mag. props., Faraday method meas. 0-103832
 (La_{0.8}Ca_{0.2})MnO_{3+x}, non-stoichiometry and lattice consts. 0-100212
 LaCl₃Np³⁺, energy level anal., polarised absorpt. and fluoresc. spectra 0-76056
 LaCl₃Np³⁺, phonon-induced relax. in excited optical states, linewidth temp. depend. meas. 0-100688
 LaCl₃Pr³⁺, coherent transients by optical phase switching 0-95962
 LaCl₃U³⁺, cryst., spectrum anal., cryst. field parameters 0-76057
 LaCoO₃, Mott isolator, paramag. props., calc. 0-93071
 La₂CoO₄, mag. behaviour obs. 0-70971
 La₂Co₃-Cr ceramic, prep., phase comp. and elec. cond. (Polish) 0-71621
 LaCrO₃-MgO, LC20M electrode material in open cycle MHD systems, thermionic emission characs. 0-97394
 LaCrO₃-W(Mo)(Cr) eutectics, eutectics, prep. and microstruct. 0-108380
 LaCrO₃, X-ray cryst. struct. anal. (French) 0-92484
 La₂CuO₄, magnetic properties obs. 0-70937
 LaCu₃Ru₄O₁₂, synthesis, cryst. struct., mag. and elec. props. (French) 0-107151
 LaD₃, stoichiometric, structural phase transform., neutron diffraction evidence 0-88319
 La₂Eu_{1-x}B₆ solid solns., thermal cond., 300 to 2000K 0-59741
 LaF₃, electronic spectra, rot. anal. and orbital configurations 0-83240
 LaF₃, ¹⁹F NMR study, relaxation times meas. 0-108093
 LaF₃, high-frequency phonon lifetimes 0-70338
 LaF₃, ionic transport, NMR and cond. studies 0-107555
 LaF₃ superionic conductor insulating layer, used for photocapacitive detectors 0-92976
 LaF₃, VUV luminescence, conference, Moscow, USSR (Apr. 1978) 0-62378
 LaF₃Ce, optically pumped laser at 286 nm 0-99738
 LaF₃Er³⁺, optically excited, direct-process spin-lattice relaxation 0-93378
 LaF₃Pr³⁺, optical coherence storage in spin states, echo lifetime 0-58649
 LaF₃Pr³⁺, optical meas. of spin-lattice relaxation of dilute nuclei 0-93212
 LaF₃Pr³⁺, ultraslow optical dephasing 0-58648
 LaF₃Pr³⁺, ultraslow opt. dephasing at 2K 0-91864
 LaF₃R³⁺, R=rare earths, crystal field anal., intensity calcs. 0-100670
 LaFeAs₁₂, synthesis and cryst. struct. 0-84154
 LaFeSb₁₂, prep. and cryst. struct. 0-100211
 LaGaS₃Ce³⁺, phosphor, luminesc. props. 0-103979
 LaH_{2.69} two-phase behaviour, ¹H-NMR evidence 0-93189
 LaIr₂B₂, supercond. and mag. props. 0-97028
 La₂Li₃Co₃O₄ phase, intermediate electronic configuration 0-80226
 La₂Li₃Ir₃O₃, perovskite, prep. and mag. study 0-80486
 La₂MnRuO₆ (M=Mg, Co, Ni, Zn), cubic ordered perovskites Mossbauer obs. and absence of mag. order 0-75889
 La₂MnFeS₄, antiferromag., mag. props. and mag. struct., neutron diffr. and magnetisation meas. 0-65801
 LaMnO₃, phase diagram, mag. moments, neutron diffr. study 0-108414

lanthanum compounds continued

- LaMnO₃, stoichiometric manganite form. reaction, thermodynamic char- acts. 0-108727
 La₂MoO₆, paramag. resonance and struct. 0-84162
 LaN, form. conditions 0-101019
 LaN, miscibility with UC (*German*) 0-96654
 LaNbO₄, room temp. form., symmetry determ. by convergent beam elec- tron diffr. 0-79723
 La₂NbO₇, synthesis and cryst. growth 0-71590
 LaNi_{1-x}Fe_xO₃, magnetisation meas. and ⁵⁷Fe Mossbauer studies 0-93217
 La₂NiO₄, magnetic properties obs. 0-70937
 LaO, Franck-Condon factors rot. depend. 0-58319
 La₂O₃, cryst. struct., X-ray powder diffr. and electron diffr. study 0-107161
 La₂O₃-GeO₂ system cpds., physicochem. characts. 0-97469
 (La₂O₃)_{1-x}(CeO₂)_x:Mn, valence state of Mn, effect of annealing in H₂ atm., ESR obs. (*French*) 0-71164
 (La₂O₃)_{0.95}(CeO₂)_{0.05}:Mn²⁺, X-band EPR study 0-60409
 La₂O₃:Eu, high press. effect on luminesc. efficiency and lifetime, charge transfer absorpt. 0-66266
 La₂O₃:Eu, slow phosphoresc., high press. study 0-80839
 LaOsAs₁₂, synthesis and cryst. struct. 0-84154
 LaOsB₁₂, prep. and cryst. struct. 0-100211
 LaPO₄ catalyst crystals, high resolution electron microscopy, morphological characts. rel. to catalytic activity 0-107193
 LaP₂O₁₄, continuous ferroelastic transition elastic and mechanical props. 0-92668
 LaP₂O₁₄, coupling effects between soft optic and acoustic modes at ferro- elastic transition 0-70358
 LaRu₄As₁₂, synthesis and cryst. struct. 0-84154
 La_{3-x}Ru_xO₁₃, perovskite-type cryst. struct., X-ray determ. (*French*) 0-75206
 LaRu₄Sb₁₂, prep. and cryst. struct. 0-100211
 LaS_{1.500}-LaS_{1.333}, solid soln. region, density meas. 0-95075
 La₂S₃, unsaturated and saturated vapour press., 673-1173K, thermal disso- c. pattern 0-104457
 La₂S₃ glass (*French*) 0-71369
 La₂S₃, optical props. and electronic struct. in fund. absorpt. region 0-80817
 La₂S₃, vibr. spectra, factor-group anal. 0-80793
 La₂S₃-Ag₂S-Ga₂S₃ glass system, prep., thermal and elec. props. (*French*) 0-89192
 La₂S₄, structural transitions, symm. anal. 0-92671
 La₂(SO₄)₃·9H₂O:Gd³⁺, single cryst., EPR study, spin Hamiltonians 0-80606
 La₂Se₆, structural transitions, symm. anal. 0-92671
 La₂Si₂O₇, single cryst. growth by floating zone method with SiO₂-Si₃N₄ additions 0-93481
 La_{0.38}Sm_{0.42}B₆, FIM study 0-71578
 La₂SnMo₆S₈, supercond. props. 0-97023
 La_{1-x}Sr_xCoO₃, (0.5 ≤ x ≤ 0.9), ferromag., elec. props., itinerant electron model 0-107785
 La_{2-x}Sr_xCoO₄, mag. behaviour obs. 0-70971
 La_{1-x}Sr_xVO₃, Anderson transition, elec. resist. and thermopower meas. 0-100488
 La₂Ti₂O₇, ferroelec., layer type struct., cryst. growth 0-108348
 La₂Ti₂O₇, layered ferroelectric anomalous photovoltaic effect, photovoltaic current 0-75603
 (LaTmCa)₃(FeGe)₂O₁₂, mag. loss and domain wall mobility 0-65980
 La_{0.9}Tm_{0.1}Se, sp. ht. meas., 1.6 to 20K, mag. contrib. 0-65934
 LaVO₃, successive phase transitions, X-ray anal. 0-108437
 La₁₀W₂O₂₁, enthalpy and heat capacity at high temp. 0-70424
 α-La₂WO₆, enthalpy and heat capacity at high temp. 0-70424
 La₂W₂O₁₅, enthalpy and heat capacity at high temp. 0-70424
 Li-La phosphate glass, Nd, Cr activated, Nd luminesc. quantum efficiency meas., Nd-Cr nonradiative transfer 0-66296
 La₃Fe₅S₁₄, antiferromag., neutron diffr. study 0-70954
 Na-La_{1-x}Ce_xTb_{1-x}(PO₃)₂, optical props. (*French*) 0-103991
 Nd³⁺:LaCl₃, laser-induced fluoresc., hyperfine structs. 0-100677
 Nd³⁺:LaCl₃, laser-induced fluoresc. energy transfer effects 0-100678
 PLZT ceramic, ageing, dielec. props. 0-88940
 PLZT ceramic, bonded lens assembly manufacture 0-79018
 PLZT ceramic, proton implanted, photoferroelectric effect for image stor- age and display devices 0-80315
 PLZT ceramic, thin wafer electrode slotting process 0-79017
 PLZT ceramic, thin wafer production polishing process 0-81214
 PLZT ceramic, visible light scatt. depend. on photoferroelectric space charge fields 0-80806
 PLZT ceramics, modified by Ca²⁺(Sr²⁺)(Nd³⁺)(Y³⁺), dielec. behaviour 0-60519
 PLZT, diffuse phase transitions, Curie temp., dielectric props. 0-75979
 PLZT electro-optic shutter stereoscopic display applications 0-90826
 PLZT, mech. and elec. losses, correl., theory and expt. 0-66133
 PLZT modified high voltage dielectric, permittivity, Curie temp., loss meas. 0-80720
 PLZT powder preparation, hydrolysis ball mixing 0-81006
 PLZT slim-loop and linear ceramics, longit. electrooptic effects, display appl. 0-80751
 PLZT slugs, powder hot pressing technique 0-81007
 PLZT thermal, flash, ferroelectric protective goggles 0-81746
 PLZT/TFPD thermal/flash protective lens assembly, polarised delamina- tion investigation 0-78929
 SiO₂-Al₂O₃-Y₂O₃-La₂O₃-TiO₂ glasses with high elastic moduli, alkaline durability 0-85071
 Sm_{1-x}La_xB₆, valence transition, lattice parameter and mag. susceptibility meas. 0-59929
 Sm_{1-x}La_xS, magnetoresist. in semicond. and metallic phases 0-96914
 SrF₂-LaF₃, tentative phase diagram 0-71633
 SrLaFeO₄, two-dimens. mag. props. rel. to cryst. struct. 0-75776
 Sr_{0.5}La_{0.5}Fe_{0.5}O₄, high spin configuration stabilisation for Fe⁴⁺ (*French*) 0-88519
 (U,La)C, U self-diffusion 0-92711
 YIG-La, films, ferromagnetic resonance, ion implantation effect 0-97145
 Y_{2.85}La_{0.15}Fe_{3.75}Ga_{1.25}O₁₂ LPE films, ion implantation effect on spin waves 0-71124
 Y_{2.85}La_{0.15}Fe_{3.85}Ga_{1.15}O₁₂ garnet, mag. props., ion implantation effect, Mossbauer study 0-97166
 Y₂-La₂Fe₂O₁₂, mag. props. rel. to ionic struct. 0-75756
 ZnO-La₂O₃-B₂O₃, glass, refraction, refractive index from 0.365 to 2.50 μm 0-88953
 ZrF₄-BaF₂-LaF₃ F⁻ ion cond. glasses, cond. process 0-107477

Laplace transforms

- cascade flow problem reduction of part-channel of varying width 0-83843
 cracks, penny-shaped, ductile, dynamic effects in propagation, Hankel and Laplace transform methods 0-87741
 LANDSAT geoevaluation, digital mosaicking and lineament enhancement (*Japanese*) 0-82169
 numerical inversion method and relax. distrib. function approx. 0-84720
 planetary finite atmospheres, radiative transfer key eqn. exact soln. 0-67536
 quantum mechanics, Feynman path integrals with Gaussian measure, Laplace transform method 0-62522
 radiative transfer, time-dependent, exact soln. of integro-differential eqn. via Laplace transform 0-94703
 radiative transfer in finite atmosphere, exact soln. of basic eqn. via Laplace transform 0-94702
 reversible reactions, first order, time depend. behaviour 0-97699
 stellar finite atmosphere, radiative transfer key eqn. exact soln. 0-72762
 tube with variable boundary conditions, heat transfer, Laplace transform appl. 0-74859
 viscoelastic bar, transient wave propag. 0-106745
 viscoelastic materials, stress waves generated by internal heating in Voigt and Maxwell materials (*Japanese*) 0-69693
 viscoelastic wave propagation, integration contour deform. for Laplace transform inversion 0-74801
 Zn single cryst., dislocation velocity and plastic deform. 0-64998

large scale integration

- contactless measurement of sheet conductivity and mobility of semiconduc- tor wafer by using eddy current 0-62693
 counters, digitisers of time and pulse height, monolithic flash A/D conver- tor 0-63475
 electron beam lithography, triple slit scheme for high current variable- shaped beam forming 0-68290
 epitaxial films, model for autotuning lateral variation 0-103595
 function testing with stroboscopic microcomputer-controlled SEM 0-68294
 NMOS VLSI circuits manufacture process and problems (*Norwegian*) 0-60090
 surface analytical techniques applied to electronic components [Si LSI chip inspection] 0-81392
 Al and Al alloy metallisation surface preparation for VLSI 0-66429
 SiO₂ layers in LSI cct. device, cathodoluminesc. obs. 0-80867

laser accessories

- acousto-optic mode locking device, for Nd garnet ring laser with return mirror 0-99764
 alignment fixtures for laser beams 0-74414
 alignment system for Antares CO₂ fusion laser beams 0-74422
 alignment system for Helios CO₂ fusion laser 0-74420
 alkali metal vapour arc lamp, source for Nd³⁺:YAG laser pumping 0-78924
 antireflection coating, two-layer, error considerations in design 0-74477
 aplanatic waxicon insensitive to tilt errors, for high power laser beam transport 0-74460
 attenuator of CO₂ laser radiation, using multilayer Dacron filters 0-58616
 autocorrelator, rapid-scan, for monitoring CW mode-locked dye laser pul- ses 0-87421
 beam expander design corrected for Petzval curvature 0-74461
 beam expander for short cavity dye laser 0-87532
 beam simultaneity system for CO₂, Helios fusion laser 0-74419
 benzene derivatives, monohalogenated, saturable absorpt. of CO₂ laser 0-69465
 calorimeter types and techniques 0-69441
 compact 5×10¹² A/s rail-gun pulser for laser plasma shutter 0-70017
 compact cold cathode electron beam gun, appl. CO₂ laser (*German*) 0-86501
 cone absorption calorimeter for pulsed laser meas. 0-98980
 conical optics for radiation conversion from laser with unstable resonator 0-91831
 control element, external, for CW laser radiation power stabilisation 0-91832
 coupling arrangement, for tunable diode lasers far-IR spectroscopic light sources appl. 0-73481
 cuvette for Cu laser with excitation by transverse discharge 0-106532
 CW X-ray preioniser for high-repetition-rate gas lasers, appl. to HF pulsed laser 0-64037
 deformable mirror design for wavefront correction in CO₂ laser fusion system 0-74427
 deformable mirror for wavefront error correction in Gemini CO₂ laser fusion system 0-74426
 dichroic beam splitters, high-performance, for DF chem. lasers 0-95932
 digital beam switch for 10.6 μm laser radar 0-102836
 digital beam switch for agile beam laser radar 0-58620
 diode laser output stabilization by bevelled-end fibre coupling 0-91806
 discharge gap characts., laser-radiation-triggered, influence of discharge medium, electrooptic switch control appls. 0-64818
 dye compositions bleachable by I laser, for passive Q-switching 0-91826
 electron beam system for laser excitation, coaxial diode 0-86509
 far IR laser hybrid output couplers, metal mesh dielectric mirror design and fabrication 0-58554
 Faraday rotator using low Verdet constant material 0-69520
 field meas. Fourier transform spectrometer 0-86470
 filter for altering spectrum of multiple-frequency lasers 0-58553
 flashlamps, coaxial and preionised linear, comparison as pumping sources for high power dye lasers 0-102730
 flat top beam profile production for high energy lasers 0-58618
 gas mixture, absorbing, for isolation between amplifiers in TEA CO₂ laser 0-95911
 high speed rot. mech. shutter design for pre-pulse protection 0-96032
 high-pressure laser cell with a transverse excitation scheme 0-78859
 IR coating nonuniformity effect on precision optical systems, compensation by auxiliary laser 0-78926
 IR optical components and aspherics, 10.6 μm interferometric testing 0-74523
 IR Smart interferometer, alignment tool for CO₂ laser fusion systems 0-74425
 KS glasses for passive shutters of ruby laser for generating subnanosec. pulses 0-102728
 lightwave pulse regenerator for triggerable semiconductor lasers 0-69408
 low-level pulse meas. system at 1.064 μm, transfer standards 0-86253

laser accessories continued

- magnetic mirrors in gas lasers with non-self-sustaining discharge (*Russian*) 0-106530
 magneto-optical switch for synchronization of CO₂ and red laser beams 0-58615
 metal oxide/fluoride mirror coatings, light scatt. and optical strength in UV range 0-106595
 Michelson output coupler with one-dimensional grid, for optically pumped near MM laser 0-58555
 MIM point-contact diode harmonic generators and mixers 0-60105
 mirror grating mount, compact stepping motor design 0-87402
 mirror quality specifications for CO₂; Antares laser system 0-74423
 mirror surfaces degradation on 10000 hr. lifetime tests on CW hetero-lasers 0-106542
 multicomponent gaseous saturable absorber for CO₂ laser Helios system, optimisation 0-74393
 multistage interference-polarization filter for wavelength selection in dye lasers 0-64091
 optical delay lines to control solid state laser output characts. 0-99758
 paper, yellow and white bond, as inexpensive detector for CO₂ laser 0-78880
 picosecond pulse generation scheme for injection lasers 0-87418
 piezoelectric transducer as monitor for optically pumped far IR laser 0-102729
 plasma shutter for multichannel Nd:glass laser 0-64088
 plasma tube impedance changes for CO₂ laser power variation detection 0-69437
 Pockels cells, optically timed, electrooptic prepulse suppression for fusion laser systems 0-102743
 point contact IR detector tunnelling and rectification characteristics, geometrical and multiple image interactions 0-57376
 porous structures for cooling laser reflectors, theoretical study 0-91809
 power-per-line analyser for real-time display of laser spectra on oscilloscope 0-58552
 pump system, analytical theory 0-106540
 pyroelectric detector for subnanosecond CO₂ laser pulse meas. 0-78884
 Q-switch, ultrasonic, for Nd:glass laser 0-64034
 resonant chopper performance characteristics and limitations 0-64084
 retroreflective array as resonator mirror 0-95973
 shutter for laser pulse shaping, Pockels cell with programmable transmission control 0-64162
 side cathode for high-power Ar laser 0-99742
 skimming discharges for pulsed gas-discharge laser preionisation, spectral characts. 0-99740
 spatial profile meas. by pyroelectric vidicon camera 0-87425
 spring-loaded partial kinematic mount 0-74518
 stimulated Brillouin scatt. complex conjugate mirror for ruby laser 0-87438
 target positioning system for Helios CO₂ fusion laser beams 0-74421
 thermal neutron traps description 0-64041
 tracking system testing by 1 m unobscured IR collimator 0-78991
 two-scatter-plate low-speckle-noise integrator for atmospheric laser beam transmission meas. 0-90252
 UV high-power laser material, refractive props. and optical constants 0-106555
 UV light source, surface spark discharge type, for H₂/F₂ laser initiation 0-78923
 CO₂ laser Antares fusion system power amplifier optics 0-74394
 CaCO₃ calcite linear polarizer, role in laser technology 0-64165
 CdTe crystal Pockels modulator, PCM of CO₂ TEA laser pulse 0-102742
 CdTe linear electro-optic translation of IR laser wavelengths 0-78878
 Cu halide laser driving ccts., parametric study 0-83610
 Cu-Sn(Al)(Ga) reflecting surface absorpt. coeffs. at 10.6 μ m 0-95984
 GaAs 400 MHz TW laser modulator 0-87541
 He, hollow-cathode type discharge, spectroscopic obs., laser light source appl. 0-59335
 KCl:ReO₄⁻ nonlinear absorption for CO₂ laser pulse compression and mode locking 0-74443
 KD₂PO₄ crystal, electro-optical extraction of Nd:YAG laser pulses (*German*) 0-87416
 LiNbO₃ crystal in laser resonator, thermo-optical effect (*Chinese*) 0-106546
 LiNbO₃-Ge acousto-optic modulator for 10.6 μ m CO₂ laser 0-99776
 NaCl 46 cm window optical evaluation facility 0-74526
 NaCl Czochralski crystal growth for large CO₂ laser windows 0-74525
 NaCl large window continuous polishing 0-74527
 NaCl window production for Antares CO₂ laser system 0-74524
 Si Fabry-Perot couplers for optically pumped far IR lasers 0-69404
 Si position-sensitive detector for CW and pulsed laser beams 0-78883
 SiO₂ facet coating film effect on self-sustained pulsation suppression in GaAlAs DH lasers 0-95894
 TeO₂ acousto-optic laser beam deflector using shear wave propag. slightly off (110) crystal axis (*Japanese*) 0-102818
 TlI laser window films, stoichiometry, Rutherford backscatt. study 0-59831
 W-Ni(Co) point-contact diodes as harmonic generators and mixers, DC bias dependence 0-75653
 Xe flashlamp efficiency for photoinitiation of HF pulsed laser 0-69403
 ZnSe laser windows, AR coated, photoacoustic chopping freq. studies using CO₂ laser 0-83629
 ZnSe laser windows, photoacoustic signal var. with chopping freq. 0-75309

laser beam applications

- see also *holography; integrated optics; laser beam machining; laser beam welding; laser isotope separation; matrix isolation spectroscopy; measurement by laser beam; modulation spectroscopy; optical communication; optical radar; patient treatment; plasma production and heating by laser beam; Raman spectra; Raman spectroscopy; remote sensing by laser beam; spectroscopy; surgery; two-photon spectroscopy*
 accelerator diagnostics using laser beam 0-95497
 acoustic fields in quartz, LiIO₃ and quartz piezoelectric transducers 0-97231
 acoustic transducer-receiver activation, flexible configuration 0-83724
 adhesion determination, thin films 0-71833
 aerosols, monodisperse, mass concentration, laser monitoring 0-98878
 air pollution, laser-Raman microprobe anal. of suspended particulates 0-76687
 alloy surface composition modification by high-power CW lasers 0-93699

laser beam applications continued

- annealing Au diffusion barrier, at metal-semiconductor on metal-metal interface 0-80373
 automatic inspection of materials 0-66734
 beacons, increase of range of visibility in fog using coaxial beams technique 0-101434
 Brillouin ring laser, fibre-optic, use for inertial sensing 0-87411
 [cc] He-Ne laser scanning system, for video record player, information identification (*German*) 0-106557
 ceramic powder synthesis from laser-heated gas phase reactants 0-93525
 charged particle beams, energy spread reduction, laser pulse technique 0-87279
 chemical analysis, industrial appl. of lasers 0-87427
 conference, laser and electro-optical systems, San Diego, CA, USA (Feb. 1980) 0-62392
 conference, Masnuy-St-Jean, Mons, Belgium, Oct. 1979 0-82570
 CVD using focused laser beam 0-93493
 CW laser apps. 0-58550
 diameter meas. by laser scanned gauge (*Chinese*) 0-77756
 diffraction gratings, laser produced, review (*Rumanian*) 0-87542
 direct picture printers on photographic paper, appl. in life sciences (*French*) 0-72119
 discharge gap characts., laser-radiation-triggered, influence of discharge medium, electrooptic switch control apps. 0-64818
 discotheque light effects, safety considerations with respect to output power and exposure time, regulations and recommendations (*German*) 0-101224
 dynamic range measurements on streak cameras 0-73490
 electron-beam exposure system, distortion correction and deflection calibration by laser interferometry 0-69310
 electrophoresis, laser Doppler, high current-density electrodes 0-89500
 EPR spectrometer, high temp., CO₂ laser-heated 0-68233
 flame temperature meas. using laser induced fluoresc. spectrosc. of OH 0-90839
 Fourier transform spectrosc., new developments—passive heterodyne spectrosc. and diode laser absorpt. spectrosc. 0-95148
 n-GaAs-Ge laser alloying to from ohmic contacts 0-58546
 gas laser and its apps. (*French*) 0-83590
 geodesy, artificial satellite laser ranging, high precision, earthquake anal. 0-98215
 glass, laser decoration technology 0-84810
 high resolution two-photon FM laser spectroscopy of gas atoms, free of Doppler broadening 0-95748
 high-temperature laser microscope; design details 0-90891
 hydrophobic, optical interferometric, with homodyne detection, signal stabilization by light source tuning 0-87477
 image storage mass memory 0-102752
 inert gas halides, laser mechanism, excitation methods and apps. 0-95871
 interferometer, prism optics testing, interf. meas. 0-105698
 ion source, appl. in mass spectrometry, review 0-89564
 laser range-differencing, Earth pole posn. and rotation determ. 0-101312
 LASSO experiment on Spiro-2 spacecraft laser synchronisation from stationary orbit 0-82211
 lens, optical axis designation method 0-102798
 light-coupled logic with triggerable semicond. laser 0-74360
 low jitter spark gap triggering through fibre optics 0-107000
 magnetic material domain structure obs. by Kerr-magneto-optical effect, laser speckle suppression 0-85093
 mass spectroscopic analysis of gaseous impurity microconcentrations in nonconducting materials 0-73518
 materials processing, seminar, San Diego, CA, USA (Aug. 79) 0-90609
 medical, 1980 development trends 0-85464
 metal thin film, preheating as aid to laser recording 0-102753
 Michelson interferometer, active stabilization by electrooptically tuned laser 0-86386
 microprobe mass analyser achievements and apps. 0-73536
 Microprobe Mole/plasma chromatograph system, for anal. of compounds on micron scale 0-101049
 microscopic equipment, methods, apps. and related topics, bibliography 0-73124
 microspectral analysis, forensic appl. 0-81385
 movie camera, laser based, operation and applications 0-57405
 noncontact material testing using laser energy deposition and interferometry 0-71846
 nuclear orientation, laser-induced ^{24m}Na appl. 0-57680
 nuclear physics applications, review, book contrib. 0-68504
 optoacoustic imaging and image processing 0-95143
 optoacoustic material probing and imaging, far IR 0-83559
 optoacoustic sound focusing device using YAG laser 0-87692
 organic surface contaminants, anal. by plasma chromatography-mass spectroscopy, and Raman microprobe technique 0-108773
 particle accelerator, laser focusing, phase-adjusted 0-63434
 phasometric method of measuring the thicknesses of transparent recording carriers and substrates (*Russian*) 0-73514
 photoexcitation effects during laser trimming on thin film resistors on Si 0-64093
 photographic paper quality improvement, colour spots detection (*German*) 0-57412
 plasma sprayed coating consolidation by laser remelting 0-93697
 printer scanning system with f- θ lens 0-78942
 projection microscope, transmitted light, Cu vapour laser as image amplifier 0-73446
 projection microscope, with brightness amplifier for biology and medicine 0-76875
 projection microscope with image-brightness amplifier using Pb and Mn vapour 0-106541
 proton beam characts. control by laser-induced selective multistep processes 0-61122
 quantum electronics, conf., New York, USA (Jun. 1980) 0-90614
 reaction kinetics measurement and control using laser technology, free electron laser appl. 0-81349
 recording and information handling, seminar, San Diego, CA, USA (Aug. 1979) 0-101663
 review in brief 0-91807
 ribbon growth using scanned focused CO₂ laser beams 0-66417
 SAW generation using CW laser, NDT appl. 0-87683
 SAW study, optical heterodyne method (*Russian*) 0-64271
 scanning optical microscope for semicond. materials and devices 0-95136
 semiconductor amorphous film, laser crystallisation, for production of large grained sheets for solar cells 0-93570

laser beam applications continued

semiconductor laser screens, scanning optical microscopy appl. 0-86398
 semiconductors, ion implanted, laser annealing 0-65023
 SHG, computer controlled intracavity, in CW ring dye laser 0-91841
 silicate glass surface, photodichroic for laser recording 0-102785
 solar cell defects detection, optical scanning technique 0-81460
 solar cell fabrication, laser-induced p-n junction formation 0-93880
 solar cells, fabrication using continuous or pulsed lasers (*French*) 0-61350
 spectrometer, diode laser dual-beam, long-term temporal and scanning characts. 0-90902
 spectroscopy methods based on laser light's props. 0-62739
 stainless steel, laser surface melting for corrosion protection 0-93698
 stethoscope for respiratory sounds meas., comparison with acoustical method (*German*) 0-98058
 strain measurement, photoresist grating and diffraction pattern method (*German*) 0-68195
 stratosphere, trace constituents, laser heterodyne spectroscopy 0-109257
 surface transformation hardening, heat flow model for cylinder 0-93700
 surgery, laser medicine in Japan, current status (*German*) 0-98059
 therapeutic applications of lasers (*French*) 0-108996
 thermonuclear power plant, conceptual design study 0-78441
 thin film optical circuit fabrication using CO₂ laser 0-99881
 tracking system testing by 1 m unobscured IR collimator 0-78991
 triggered vacuum gap for high energy appl. 0-78888
 triggering lightning by pulsed laser 0-72626
 tunable, principles, characts., and appl. review (*Japanese*) 0-74330
 TV scanner, rotating mirror, development programme (*Japanese*) 0-74369
 wideband optical disc data recorder systems 0-102751
 Al aircraft alloy, fatigue resistance improvement by laser shock 0-93654
 n-BaTiO₃, ohmic contact form. 0-92969
 Cr ^{P₀} state, radiative lifetime in matrices, meas. using laser ablation and selective excitation 0-71959
 Cr film, pattern generation by laser-induced oxidation 0-61009
 GaAs, laser-induced microscopic etching 0-76379
 GaAs:Zn, implanted, laser annealing, elect., Rutherford backscattering and SEM meas. 0-100273
 InP, laser-induced microscopic etching 0-76379
 InP:Cd, doping by UV laser photodeposition 0-84191
 p-InP-Cd(Zn), ohmic contact formation on InP by laser photochemical doping 0-80369
 MgO, atomic C anal. by laserflash induced mass spectrometry 0-108767
 Nd:YAG laser integration into optical systems 0-78887
 Re film, prep. by laser melting 0-84859
 SF₆, multiwavelength phase conjugation using multiine CO₂ TEA laser 0-91847
 SF₆, spark gap, KrF laser triggered, low jitter timing 0-106999
 SO₂, absorption spectrum, meas. using frequency doubled pulsed dye laser 0-87144
 SO₂, absorption spectrum, meas. using frequency doubled CW dye laser 0-87145
 Si amorphous layer recrystallisation 0-93566
 Si, cast polycryst., annealing for solar cell appl. 0-93918
 Si film, polycryst., laser-induced CVD growth from SiCl₄ 0-84852
 Si ribbon growth by laser zone melting 0-93482
 Si ribbon solar cells, defect anal. using laser scanner 0-94089
 Si solar cell processing, pulsed laser techniques for annealing ion-implantation damage 0-81453
 Si solar cells, laser annealing, conversion efficiency improvement (*French*) 0-66976
 Si solar cells, preparation using laser processing 0-81454
 Si solar cells, realisation by laser induced diffusion of deposited Sb 0-93998
 TiC, laser CVD, coating characterisation 0-93494

laser beam effects

see also *plasma-beam interactions; plasma production and heating by laser beam*
 absorbing film, damage by high-power optical pulses, two-phase model 0-93438
 adenine, nucleic acid component, selective action by ps light pulses 0-72213
 air, plasma, slow burning gasdynamics, due to Nd laser beam (*Russian*) 0-108715
 amorphous materials, laser irradi., electronic struct., one-electron approx. 0-70576
 amorphous semiconductor film, laser induced nucleation, long wavelength instability 0-84126
 annealing mechanisms, continuous and pulsed laser impact, melting 0-84964
 atomic beam deceleration and monochromatisation laser radiation press. 0-102491
 benzene, liq., laser pulsation kinetics, optical damage effects 0-58614
 biological, laser medicine in Japan, current status (*German*) 0-98059
 cavitation in liquid crystals. 0-87633
 cell flagella, laser damage, high speed cinematography 0-81785
 conference, Masny-St-Jean, Mons, Belgium, Oct. 1979 0-82570
 corneal damage induced by near-UV laser, cumulative effects 0-85448
 corneal temperature range, implications in prediction of laser thermal damage 0-108848
 diamond, homogeneous formation in gas phase, laser beam effects (*Russian*) 0-104052
 dielectric breakdown with picosecond laser pulses, SHG sharp increase 0-102769
 DNA light induced diffusion in solutions due to laser cutting (*Russian*) 0-81646
 dosimeter glass, radiophotoluminescence intensity change by intense laser light 0-89050
 dye proflavine bound to synthetic polynucleotides, selective laser photodamage 0-99525
 elastic wave excitation by laser beam, through thermoelastic effect 0-103503
 electron scatt. in laser field, photon correl. effects 0-83481
 ferroelectric, tetragonal, irradiated by laser pulses, spatial temp. and bound-charge distrib. 0-103927
 fibre optic elements, laser radiation damage 0-102747
 fog, droplets evaporation rel. to laser beacons visibility range extension 0-101434
 gas breakdown, laser-supported, finite absorpt. length model 0-107005
 gas stream, chem. reacting, thermal crisis suppression by laser radiation reson. interaction 0-75000

laser beam effects continued

gases, optical breakdown, mol. ion reactions influence 0-96341
 glass, laser induced damage 0-66335
 graded-index antireflection coatings, high laser damage threshold 0-83628
 graphite vapour cloud, laser-prod., temp. conditions investig. 0-59290
 heterogeneous photocondensation process initiation by laser radiation 0-67410
 hydrodynamic effects in laser radiation action on condensed medium 0-93439
 insulator, wide-gap, damage by UV laser radiation 0-76110
 ion, electromagnetically confined, laser cooled, double resonance and optical pumping 0-87155
 ion emission from laser-driven implosions, routine monitoring using multi-channel digitizer 0-57268
 ion implantation by laser annealing, characterisation, solar cell applications 0-70247
 Josephson junction, coherent radiation induced bistability 0-80453
 liquid, absorbing intense IR radiation, behaviour of pressure 0-102749
 liquids, highly volatile light beam interaction, photohydraulic effect (*Russian*) 0-69440
 liquids, laser pulsation kinetics, optical damage effects 0-58614
 macromolecules, nonlinear laser photomodification, radiation damage 0-61120
 mass spectrometer ion-field source emitter, influence of laser irradiation on ion current 0-101874
 materials processing, seminar, San Diego, CA, USA (Aug. 79) 0-90609
 mechanical response to giant laser pulse, recoil impulse meas. 0-80910
 metal, laser-photoinduced etching, photodissociation of dissolved complexed halogens in soln. 0-100929
 metal, oxidizable, laser heating in air by obliquely incident radiation 0-71815
 metal film vapourisation by laser, vapourisation front relativistic velocities (*Russian*) 0-66337
 metal oxide/fluoride mirror coatings, light scatt. and optical strength in UV range 0-106595
 metal particle, ultra-fine, form., pulsed laser breakdown of carbonyl vapours 0-84881
 metal reflectance changes during laser irradi. 0-93261
 metal surface laser beam irradi., effective absorpt. coeff., temp. field determ. (*Russian*) 0-76108
 metal targets, laser radiation absorption in craters 0-97386
 metallised coating on polyethylene terephthalate film, fracture under laser irradi. (*Russian*) 0-76333
 metals, optimal heating, in oxidised medium, by CW CO₂ laser radiation 0-69445
 metals, specular refl. anomalous behaviour after 10.6 μ pulsed laser irradi. 0-93260
 metals in water, light beam interaction, photohydraulic effect (*Russian*) 0-69440
 mirrors with temperature-dependent absorptance, laser-induced thermal runaway 0-91882
 molecular ion formation on molecular cryst. surface UV laser irradi. (*Russian*) 0-71521
 molecular nonsteady-state luminesc. behaviour under narrowband laser excitation 0-87159
 molecules in degenerate electronic state, IR laser radiation effects 0-81351
 multilayer, electric field distrib. and laser damage reduction 0-87420
 nonequilibrium phase transformation theory homogeneous fluctuation effect 0-84277
 nonspherical particle, optical levitation for light scattering obs. 0-58455
 octyl-cyano-biphenyl, influence of laser light wave field on nematic phase (*Russian*) 0-92456
 optical fibre, parabolic index, selective excitation by Gaussian beams 0-95992
 optical glass, coloured, laser damage threshold, optical absorpt. influence 0-91830
 particle properties, particle heating by radiation absorption, effect of radiation press. (*German*) 0-106556
 particle properties, radiation pressure effect on particle motion (*German*) 0-102755
 phase T7, inactivation by visible laser light (*German*) 0-98010
 phosphate glasses, optical breakdown rel. to microscopic inhomogeneous struct. 0-102784
 photoexcitation effects during laser trimming on thin film resistors on Si 0-64093
 plane evaporation boundary instability in laser radiation-matter interactions (*Russian*) 0-76111
 PMMA, absorbing defect role in laser damage 0-108308
 PMMA, laser damage threshold, freq. and size depend. 0-104018
 polymers, transparent, absorbing defect/role in laser damage 0-108308
 polymers with various atomic composition and viscoelastic props., laser damage 0-104017
 pulsed heating profile width and total coupling changes with pulse length and press. 0-71520
 pulsed laser atom-probe FIM, development and appls. 0-66402
 retinal damage from a white-light laser, thresholds and mechanisms, rhesus monkey obs. 0-108955
 ruby, structural defects due to laser irradi. (*Russian*) 0-100303
 sapphire constant diameter cryst., laser heated float zone growth, meniscus angle meas. 0-108347
 segregation, nonequilibrium, during pulsed laser annealing, model 0-108451
 semiconductor, ion implanted, epitaxial regrowth, laser annealing dynamics 0-92548
 semiconductor, ion implanted, pulsed laser and electron beam annealing comparison 0-92547
 semiconductor, laser-photoinduced etching, photodissociation of dissolved complexed halogens in soln. 0-100929
 semiconductor, optical heating, coupled diffusion eqns. for heat and excess carrier density 0-60718
 semiconductors, ion-implanted, laser pulse annealing, TEM and channelling study 0-100264
 semiconductors and insulators, nonequilib. electron Coulomb collisions during optical pulse interband interaction 0-76049
 shock wave, implosive spherical, produced by laser pulses, shadowgraphic detection 0-87529
 shock wave optical diagnostic system 0-79421
 solid phase reactions induced by scanning CW laser, reaction rates, analytical model 0-66334

laser beam effects continued

- solid surface, mol. dynamic processes interaction with laser radiation 0-71943
 solid surfaces under laser irradi., electronic struct. and chemisorption 0-84812
 soot conglomerate destruction dynamics in pulsed laser radiation field 0-58617
 sound generation by moving pulsed photoacoustic sources 0-87634
 speckle dynamic statistical props. due to diffuse object longit. motion under Gaussian beam illum. 0-99628
 spherically symmetric molecules, many-photon excitation in IR laser field 0-95596
 spinach chloroplasts, laser photoinduced changes in high freq. dielectric constant 0-85449
 steel, stainless, CW CO₂ laser radiation coupling coeffs. 0-84811
 steel, stainless, laser induced damage 0-66335
 steel, stainless, O₂ desorpt. during laser irradi., etching, AES study 0-66338
 steel, W-Mo-Cr-V tool, laser surface melted, struct., heat treatment effect 0-76424
 surface thermal working by laser, laser annealing parameters (*Russian*) 0-100848
 surfaces, laser-annealed, characterisation by ellipsometry 0-103544
 tendon, rat-tail, coherent optical SHG 0-89796
 thermal coupling of 2.8- μ m laser radiation to metal targets 0-76107
 thermo-optical excitation of acoustic fields in liquid by periodic train of laser pulses 0-103945
 thermo-optical sound source in liquid, anal. of wave zone 0-87631
 thermo-optical US generation due to moving laser source in liquid 0-102903
 thin absorbing films, laser-induced removal, two-phase mechanism 0-97384
 thin absorbing films, laser-induced removal, two-phase mechanism 0-97385
 thin film, laser damage, photoacoustic study 0-80098
 tissue, significance of blood flow in temp. calcs. 0-104563
 transparent dielectric, laser induced plasma at surface 0-79531
 transparent solid optical materials, laser damage statistics rel. to structural defect statistics 0-91829
 trapped ion, laser cooling, theory 0-58414
 two-level atom, radiation by intense laser beam, resonance fluorescence, photon antibunching, Doppler shift 0-74146
 uracil, nucleic acid component, selective action by ps light pulses 0-72213
 Ag film, inertialess glow induced by picosecond laser pulses (*Russian*) 0-100714
 Ag-Cu surface alloyed films, laser melt quenched, microstruct. 0-76423
 AgBr, Herschel effect, latent image centre struct. changes under laser irradi. 0-77900
 Al foil, laser irradi., fracture props. (*Russian*) 0-108523
 Al, laser strengthening, struct., hardness and dislocation density (*Russian*) 0-76399
 Al, polycrystalline, high dose implanted with Cu and Pb, doping profile after laser pulse irradiation 0-88194
 Al, rhodamine 6G laser radiation interaction 0-97387
 Al target interaction with pulsed CO₂ laser beam, pulse shape importance 0-108307
 AlSiB, laser pulse annealing, induced nucleation, crystal growth 0-84966
 Au film, inertialess glow induced by picosecond laser pulses (*Russian*) 0-100714
 Au, metallised coating on polyethylene terephthalate film, fracture under laser irradi. (*Russian*) 0-76333
 Ba atom, laser excited, ionisation studies 0-83330
 CO-haemoprotein photolysis, transient Raman study, quantum yield origin 0-67155
 CO₂ laser irradiation at 10.6 micron, irreversible damage threshold meas. 0-83627
 CO₂ laser pulse induced vaporisation and thermoelastic press. in water 0-84227
 Ca atom, laser excited, ionisation studies 0-83330
 CdSb:Al, p-n junction formation by laser emission, photoelectric effects (*Russian*) 0-70815
 CdSb:Al(In)(Ga)(Te), p-n junction formation by laser radiation 0-96983
 n-CdSe, laser excited stimulated emission, optical gain spectrum 0-76050
 Cr foil, laser irradiated, low-angle X-ray scatt., angular block misalignment and hardness (*Russian*) 0-103413
 Cs cell, laser beam excitation, multipass, optical pumping and weak neutral current parity violation 0-58207
 Cu film, inertialess glow induced by picosecond laser pulses (*Russian*) 0-100714
 Cu foil, laser irradiated, low-angle X-ray scatt., angular block misalignment and hardness (*Russian*) 0-103413
 Cu, metallised coating on polyethylene terephthalate film, fracture under laser irradi. (*Russian*) 0-76333
 Cu-Cr alloy, laser irradi., structural changes (*Russian*) 0-100247
 CuO, desorpt. of ions by low power laser beam 0-80092
 GaAs, ion damage, TEM study of laser annealing 0-88215
 GaAs, ion implanted, laser annealing 0-107296
 GaAs, ion-implantation induced damage profile, ellipsometric study, annealing 0-103400
 GaAs, laser heating of lightly damaged material, carrier diffusion effect 0-84809
 GaAs, point defects, laser annealing 0-107224
 GaAs single crystals, laser damage statistics rel. to structural defect statistics 0-91829
 GaAs:Cr, redistrib. of Cr during laser annealing 0-88192
 GaAs:Se ion implanted samples, Q-switched ruby laser annealing, improvement in elec. props. 0-100460
 GaAs:Si(Sn), ion implanted, laser annealed, high doping levels 0-88181
 GaAs:Zn, ion implanted, TEM study after laser and furnace annealing 0-70234
 GaP films on Si, epitaxial crystallisation by nanosecond laser pulses 0-107674
 Ge amorphous film, crystn. front velocity during scanned laser crystn. 0-107662
 Ge, amorphous film, persistent photoconductivity, dangling bonds 0-84487
 n-Ge, laser irradi., accumulation of defects, effect on elec. props. 0-107317
 Ge, laser pulse annealing, induced nucleation, crystal growth 0-84966
 Ge:Pb, ion implanted damaged layer, laser induced reorder 0-84201

laser beam effects continued

- GeSe₂ amorphous film, laser induced oscillatory phenomena 0-84711
 He, laser-induced breakdown 0-96339
 InSb, Auger-governed decay of laser-induced plasma, optical probing 0-76105
 InSe, photoconductivity anisotropy at high optical excitation levels (*Russian*) 0-103721
 K vapour, mag. props. changes under laser irradi., induced EMF obs. 0-100059
 KBr, colour centre form. under polarised UV irradi., dichroism in absorption spectra 0-107232
 KD₂PO₄, transparent dielec., thermal analysis of laser-induced damage 0-66336
 KH₂PO₄ crystal, laser freq. conversion to produce UV coherent pulse, 45 GW, for laser fusion 0-69450
 Kr-Ar, phase matched, generation of Lyman- α radiation 0-91845
 Kr-Xe, phase matched, generation of Lyman- α radiation 0-91845
 LiF, laser irradi., Li⁺ emission, time and energy characts. 0-100710
 LiNbO₃, light induced ultrasonic wave velocity change, refractive index 0-97236
 Mo single cryst., laser induced dislocation struct. 0-70210
 N₂ cryogenic liq., laser sonoluminesc., at elevated hydrostatic press. 0-71498
 Na atom, cyclic interaction with circularly polarised laser radiation 0-75881
 Na atoms cooling by resonant laser radiation (*Russian*) 0-74155
 Na+Na, crossed-beam collision, laser-induced Penning and assoc. ionisation, struct. obs. 0-83476
 NaCl, F-centers, laser irradi., optical bleaching kinetics 0-66244
 NaCl, optical strength, effect of irradi. in mechanically stressed state 0-80695
 Na₂O-CaO-SiO₂, glass, formation of colour centres, linear absorption of UV radiation 0-103328
 Nb films, ion beam sputtered, supercond., laser annealing effects 0-97024
 Nd laser, excited stimulated Mendelev-B Brillouin scatt. phase fluctuations (*Russian*) 0-89014
 Ni, ion-implanted and virgin, laser irradi. effect, epitaxial lattice regrowth 0-108306
 Ni, metallised coating on polyethylene terephthalate film, fracture under laser irradi. (*Russian*) 0-76333
 PbMoO₄, elastic wave excitation and amplification by laser radiation 0-103419
 Pd coated Si wafers, interference effects on irradi. with laser beam 0-66332
 Pd, silicide formation due to laser and electron beam annealing 0-84849
 Pd-Si, amorphous thin films, laser irradi., metastable phases 0-96622
 Pt, silicide formation due to laser and electron beam annealing 0-84849
 Pt-Si, amorphous thin films, laser irradi., metastable phases 0-96622
 Pt-Si Schottky barriers on Si, laser formation and characts. 0-60079
 Pt-Si:As, silicide form. during laser irradi., p-n junctions and ohmic contacts 0-84397
 Rb vapour, mag. props. changes under laser irradi., induced EMF obs. 0-100059
 SF₆, surface ionisation on W cathode, laser irradi. effects 0-93440
 Se_{1-x}Te_x, amorphous film, photo-crystallisation 0-59839
 Si, amorphous, substrate orientation effect on regrowth by laser pulses, channeling, backscatter 0-84409
 Si, amorphous and crystalline, heating by Q-switched laser radiation 0-84963
 Si, amorphous film, selective laser recrystn. over heavily doped lines 0-84947
 Si amorphous layers, glow-discharge, laser-annealed, elec. props. 0-75661
 Si, amorphous layers, RF-sputtered on sapphire, crystallisation by CW ion laser annealing 0-80109
 Si, amorphous layers, recrystallisation, pulsed laser annealing 0-65404
 Si, annealing, using laser pulses, impurity incorporation at melt-cryst. interface 0-59504
 Si, crucible grown, virgin and implanted laser irradiation effects on surface struct. 0-92768
 Si, dense plasma dynamics during pulsed laser annealing, carrier density, recombination 0-84479
 Si epitaxial layer regrowth due to laser annealing mechanism, liquid and solid phase regimes 0-100712
 Si, furnace preannealed (111) ion implanted, laser irradi. 0-65015
 Si, graphoepitaxy on fused SiO₂, using surface micropatterns and laser crystn. 0-70554
 Si high efficiency solar cells, laser annealing, reviews 0-93976
 Si, hydrogenated amorphous, laser annealing 0-100713
 Si, implanted crystal, laser induced annealing and diffusion behaviour 0-88202
 Si, implanted semiconductors, laser annealing, review 0-107301
 Si, implanted with low solubility dopants, laser annealing, TEM study 0-70233
 Si, impurity solubility limit after laser induced melting 0-107426
 Si, ion damage TEM study of laser annealing 0-88215
 Si ion implanted, amorphous to crystalline transition due to laser irradi. 0-103451
 Si, ion implanted, CW laser annealing 0-92550
 Si, ion implanted, scanning CW and pulsed laser annealing 0-92549
 Si, ion-implanted, annealing using scanning CW laser system 0-100265
 n-Si, ion-implanted, elec. characts. after laser annealing 0-88562
 Si, ion-implanted amorphous, laser epitaxial recrystallisation threshold energy 0-70571
 Si ion-implanted dopant redistribution under laser annealing 0-70242
 Si ion-implanted laser-annealed solar cells 0-93881
 Si, ion-implanted layers, crystn. by ns laser pulses, TEM and RHEED 0-100421
 Si, ion-implanted layers, epitaxial regrowth by laser beam and flash annealing 0-100420
 Si, laser annealing, nonlinear dynamic transport processes 0-93437
 Si, laser annealing for improved stacked-struct. oxide quality 0-65386
 Si, laser annealing mechanisms, disordered overlayers, crystalln. 0-84967
 Si, laser annealing of point defects 0-107224
 Si, laser heating of lightly damaged material, carrier diffusion effect 0-84809
 a-Si, laser induced crystallisation mechanism, epitaxial regrowth 0-84962
 Si, laser induced dense plasma, dynamics 0-65612
 p-Si, laser irradi., accumulation of defects, effect on elec. props. 0-107317
 Si, laser pulsed heating, lattice temp., Raman meas. 0-80780
 Si layers amorphized by molecular ions, laser annealing 0-103379

laser beam effects continued

- Si, minority carrier lifetime improvement through laser damage gettering 0-65589
- Si, non thermal laser induced ordering, plasma life time, phonon interactions 0-84481
- Si on sapphire, stress-relieved regrowth by laser annealing 0-65389
- Si on sapphire film, laser annealing non-thermal theory expt. test 0-89273
- Si, plasma effects during pulsed laser annealing 0-84480
- Si, point defects, H passivation 0-75515
- Si polycrystalline film resistivity reduction by Nd:YAG laser annealing 0-100539
- Si processing technology, appls. of scanning CW lasers and electron beams 0-100932
- Si, reflectivity time dependence during pulsed laser annealing 0-66214
- Si single crystals, laser damage statistics rel. to structural defect statistics 0-91829
- Si, slip dislocation nucleation during laser annealing 0-84179
- Si, solar cell, open-circuit voltage at ultrahigh light intensities, plasma reflection effects 0-96928
- Si surface formation during etching of thin thermally grown oxide layers, ellipsometric control (*Russian*) 0-104315
- Si, surface topography changes due to pulsed laser annealing 0-84348
- Si, temperature during CW laser heating, Raman scatt. meas. 0-76109
- Si wafer processing, CO₂ laser heating dynamics 0-76106
- Si:Ar, As, ion implanted, laser annealing, doping profiles, channelling 0-97506
- Si:Ar, ion-implanted, epitaxial regrowth by laser annealing, microstruct. 0-84404
- Si:As, CW CO₂-laser annealing, comparison with thermal annealing 0-84193
- Si:As, diffused, laser irradi., stability study 0-65547
- Si:As, ion implanted, laser annealed, lattice defects, epitaxial regrowth 0-103334
- Si:As, ion implanted, pulsed laser annealing, partial solid-state regrowth 0-103591
- Si:As ion implanted layers, annealing by CO₂ laser, doping profile shift 0-84965
- Si:As laser annealing, heat and mass transport model 0-92546
- Si:As⁺, implanted, CW laser annealing, electron-beam induced current 0-100709
- Si:As⁺ (P⁺) ion implanted, laser annealed, correlation of struct. and elec. props 0-70855
- Si:As(P), ion implanted, TEM study after laser and furnace annealing 0-70234
- Si:As(Pb), ion-implanted, impurity redistrib. during laser irradi. 0-100280
- Si:As(Sb), ion implanted, lattice location of impurities after pulsed laser annealing 0-88196
- Si:B, implanted laser annealed, lattice strain, X-ray study 0-96554
- Si:B(P), ion implanted crystalline and amorphous laser annealing 0-97509
- Si:B(P)(As)(Sb)(Cu)(Fe), ion implanted, doping profile, pulsed laser annealing effects 0-88197
- Si:Bi, ion implanted, channelling obs. of pulsed Q-switched ruby laser annealing 0-59542
- Si:Fe, ion implanted, laser annealing studies using Mossbauer spectroscopy 0-79827
- n-Si:Ga laser doped, segregation, Rutherford backscattering 0-103483
- Si:Ga(As), laser-doped, impurity distrib., Rutherford backscatt. and channelling anal. 0-59507
- Si:N, laser-annealed, Jahn-Teller distorted donor, EPR meas. 0-84642
- Si:O, incorporation of O during pulsed-laser irradi. 0-96557
- Si:O(C), implant redistribution, annealing effects, SIMS meas. 0-96561
- Si:P, ion implanted, regrowth of damage structs. by laser annealing 0-107289
- Si:P, ion implanted with small doses, defect annealing by nanosecond laser pulses 0-107297
- Si:P, polycrystalline laser recrystallised film on Si substrate, cryst. struct., thermal oxidation 0-65391
- Si:P(As)(B), nonequilibrium solid solutions obtained by heavy ion implantation and laser annealing 0-92544
- Si:Pt, implanted and laser annealed, segregation and increased dopant solubility 0-65016
- Si:Sb, laser doping, evaporation loss and diffusion of Sb, under pulsed laser irradi. 0-59508
- Si:Sb(Ga)(Bi)(In), dopant solubility limit, laser irradi. effects 0-84295
- Si:Te, laser melting, surface Te atom accumulation, profiles 0-100258
- SiC ion implanted, laser induced ordering and defects 0-84754
- Si₃N₄, surface etching by laser-generated free radicals 0-71772
- SiO₂, cryst. and amorphous, laser-induced breakdown, electron avalanche damage mechanism 0-100711
- SiO₂, surface etching by laser-generated free radicals 0-71772
- U extraction by transfer between liq. phases, laser radiation effect 0-66795
- UF₆, laser chemistry 0-69198
- W, laser heating in air by obliquely incident radiation 0-71815
- XeCl discharge, KrF laser induced preionization 0-84020
- ZnSe/water, interface, laser-induced damage in ZnSe 0-102746
- ZnTe, secondary emission, transient behaviour under band-to-band excitation 0-108266
- ZnTe:Bi, laser annealing, channelling, reflectivity spectra 0-66215

laser beam machining

- instrumentation engineering, laser beam appls. in drilling, welding, cutting, definite abrasion and surface treatment (*German*) 0-108608
- lasers as modern machine tools for hardening, glazing, boring welding and cutting (*Dutch*) 0-91808
- optical communication fibre endface preparation by AC discharge heating and stretching 0-64232
- YAG laser trimmer for wafer level products 0-87428

laser beam welding

- heat transfer model for CW laser material processing 0-64336
- instrumentation engineering, laser beam appls. in drilling, welding, cutting, definite abrasion and surface treatment (*German*) 0-108608
- lasers as modern machine tools for hardening, glazing, boring welding and cutting (*Dutch*) 0-91808

laser beams

- see also holography; laser frequency stability; Schwarz-Hora effect
- active medium, EM field self-focusing, laser transverse struct. form. 0-87442
- alignment fixtures 0-74414

laser beams continued

- alignment of pulsed or CW beam by Si position-sensitive detector 0-78883
- amplifier system, small-scale self-focusing 0-106580
- amplitude fluctuation statistics in turbulent atmosphere 0-106458
- atmosphere propagation, IR radiation attenuation by ice platelets 0-66141
- atmosphere radiative transfer, nonlinear propag. effects, conference, San Diego, California (1979 August 29 to 30) 0-62376
- atmospheric aerosol extinction measurements, multiple scatt. corrections 0-98445
- attenuation for spatial profiling of small focal spots 0-99780
- autocorrelation by optical processing of Fabry-Perot spectrograms 0-58465
- automatic target alignment of Helios CO₂ laser system 0-74416
- beam expander for short cavity dye laser 0-87532
- beam splitting device for use with smoke chamber ray optics demonstrations 0-67990
- coherence and divergence (*Spanish*) 0-87424
- coherent fast IR wavefront aberration sensor interference problems 0-74499
- coherent Gaussian beam in laser Doppler velocimeter, interference 0-69444
- collimated laser radiation, directivity pattern axis spatial location 0-102748
- conical optics for radiation conversion from laser with unstable resonator 0-91831
- CW laser radiation power stabilisation by external control element 0-91832
- dark laser wavelength monitoring using fibre interferometer 0-74413
- deflection angle determ. from holographic shear interference patterns 0-95848
- diameter measurement of laser beams using a grating 0-102745
- difference frequency generation, Gaussian intensity profile effect 0-78906
- diffraction of high intensity light by ultrasound in nonlinear liquids 0-64270
- digital beam switch for agile beam laser radar 0-58620
- divergence influence on axicon axial intensity distrib., Kirchhoff-Fresnel integral soln. 0-95934
- dosimeter, health physics evaluation of operating conditions at laser installations 0-76835
- dye laser, second harmonic pulse structure and cavity length determ. 0-95935
- dye laser picosecond pulse generation, excitation by passively mode locked Ar laser 0-95930
- education, laser beam UHF and audio freq. difference heats 0-73139
- electrooptic prepulse suppression for fusion laser systems, using optically timed Pockels cells 0-102743
- energy meter (*French*) 0-102790
- energy meters for calibrations at most principal laser wavelengths 0-99741
- errors in mode parameters determ. of spatial distribution of radiation 0-95055
- evanescent wave holography using Gaussian beam, recording geometry and colour sensitivity 0-58473
- expander design corrected for Petzval curvature 0-74461
- far IR CW optically pumped lasers, simple accurate method for wavelength meas. 0-106554
- far IR laser intracavity polarisation modulation by CdTe AC Faraday rotation 0-58613
- flat top beam profile production for high energy lasers 0-58618
- fluctuations of laser beam diameter of single-mode laser, lens effect 0-64090
- focused beam ray tracing for laser fusion 0-83218
- focused light beams, phase anomaly, intuitive explanation 0-99622
- free electron laser, intense-beam, beam quality expts. 0-58619
- fusion system beam quality, Laser Optical Train Simulation code 0-78886
- gas, resonance four-photon shift, optimal focusing of high-power pumping 0-95574
- Gaussian, Fraunhofer diff., by single slits 0-87298
- Gaussian, transverse self-focusing and self-trapping investig., moment method 0-58652
- Gaussian instability growth 0-69469
- Gaussian light beam, diff. by plane acoustic waves at oblique incidence 0-69326
- heat flux and power profiling, using swept null point calorimetry 0-69439
- Hermite Gaussian beam, spot size and divergence 0-69436
- heterodyne optical radar S/N ratio in atmospheric turbulence 0-106558
- holographic elements, moving, laser beam deflection appl. (*Russian*) 0-63956
- image-bearing, nonuniformly polarized, generation of time-reversed replica 0-69459
- intensity distribution meas., Bragg diffraction of light 0-64092
- intensity fluctuations in rainfall, statistical characts. 0-101433
- interferometric wavelength meas. with post-detection signal processing 0-105699
- laser, double-current-confinement channelled-substrate struct., near-field and beam-waist position 0-106553
- lineshape, non-Lorentzian, reversed peak asymmetry in double optical reson. 0-69443
- low-level laser pulse meas. at 1.664 μ m, transfer standards 0-86253
- magneto-optical switch for synchronization of CO₂ and red laser beams 0-58615
- magnetoplasma, laser beam self-focusing 0-102778
- multithier hillclimbing adaptive optical system, secondary intensity maxima correction 0-106593
- multiphoton detectors of laser radiation, statistical characts. 0-86408
- nanosecond laser pulse stretch meas. in underwater propagation 0-87426
- nonlinear optical technique for laser focus movement 0-74446
- off-axis propag. in low visibility weather conditions, non-small-angle scatt. 0-102621
- optical propag. through turbulent atmosphere, He-Ne laser transmitter/receiver 0-98450
- optical rectification effect, meas. of power, polarisation and profile of laser pulses 0-91835
- optical waveguide, parabolic index with random dielectric constant gradient, Gaussian beam propag. 0-58698
- Osterberg problem and wave propag. in inhomogeneous plasma, numerical study 0-63925

laser beams continued

- phase compensation of thermal defocusing of light beams 0-64121
polarization of intense beam propag. in liquid, DC elec. field influence 0-91828
pulse amplification through energy exchange with electron beam via nonlinear radiation press. effects 0-95776
pulse energy, picoseconds order meas. (*French*) 0-74412
pulse generation, double, gradual cutting-off resonator losses 0-69433
pulse shape in cavity filled with Kerr dielectric, bistable behaviour 0-99787
pulsed laser radiation intensity fluctuations, thermal selfinteraction in turbulent medium 0-102781
random medium, finite beam propagation 0-91748
refraction at spherical surface, distortion, geometrical optics calc. 0-95929
regenerative compression of mode-locked laser pulses using saturable dye 0-95925
self-focusing stability in isotropic phase of liquid crystal 0-99812
in snowfall, intensity fluctuations (*Russian*) 0-94602
spatial coherence control by progressive US wave 0-78885
spatial distribution of laser radiation control 0-64086
speckle, non-Gaussian, contrast variation 0-83554
speckle reduction in image plane by US modulation of spatial coherence 0-106459
stimulated Brillouin scatt., three dimensional, for focused Gaussian beam 0-69456
thermal blooming, continuum-lens model 0-78918
thermal blooming cell design for use in evaluating adaptive optics 0-102780
thermal blooming in a diagonal wind 0-95965
thermal blooming in axial pipe flow: comment [and reply] 0-95966
thermal self-focusing of laser beams in moving media 0-64122
transformation of space-angular characteristics of the Gaussian beams by means of phase masks (*Ukrainian*) 0-69438
turbulent absorbing liq. medium, laser radiation thermal self-interaction 0-91868
turbulent atmosphere, beam props. of partially coherent curved beam waves 0-95798
ultrashort light pulse formation optimisation 0-64085
volume attenuation coeff., invalidity 0-95791
wavefront correlation transformations (*Russian*) 0-99778
wavefront rotation for light beam nonlinear deformation compensation (*Russian*) 0-64094
waveguide propag. in frozen gaseous layers at 4.2K 0-64168
wavelength calibration using optogalvanic effect, atlas 0-62727
CO₂ laser Antares fusion system beam alignment 0-74422
CO₂ laser Antares fusion system optical diffraction computation 0-74424
CO₂ laser beam Al target interaction, pulse shape importance 0-108307
CO₂ laser beam-diagnostics techniques, laser beam parameter monitoring 0-64089
CO₂ laser fusion system phase conjugation 0-74429
CO₂ laser Helios fusion system, beam simultaneity system 0-74419
CO₂ laser Helios fusion system alignment 0-74420
CO₂ laser Helios fusion target positioning with orthogonal telescopes 0-74421
CO₂ laser Helios fusion system beam diagnostics 0-78882
CO₂ laser pulse, nonlinear propagation, computer simulation (*Japanese*) 0-95963
CO₂ laser pulse meas., pyroelectric detector development 0-78884
CO₂ laser radiation, intracavity modulation of polarization direction 0-102744
CO₂ TEA Laser pulse, PCM with CdTe crystal Pockels modulator 0-102742
CO₂ ultrashort pulse generation by free-induction decay in KCl:KREO₄ 0-74444
CO₂ waveguide laser pulse shaping on multiple rot. lines 0-78879
CO₂-He-N₂, absorpt. coeff. for 10.6 μ m CO₂ laser radiation, 295 to 650 K 0-92252
CdTe linear electro-optic translation of IR laser wavelengths 0-78878
(GaAl)As low-beam-divergence CW DH laser, grown by low press. metal-organic CVD 0-74376
GaAs:Zn optically pumped ribbon-whisker laser, picosecond pulses 0-99771
GaAs-AlGaAs DH injection laser with stripe contacts, radiation pulse stepped shape 0-91799
GaAs-GaAlAs injection laser, radiation divergence reduction by non-waveguide mode excitation 0-91797
He-Ne lasers, wavefront curvature and diffraction effects in high precision wavelength comparisons with a Michelson interferometer 0-99781
KrF 1J avalanche discharge laser unstable resonator expts., beam divergence 0-74404
KrF* tunable ultrahigh spectral brightness excimer laser source 0-64046
Nd:glass, subnanosecond pulse oscillator, investigation by high-speed oscillography 0-74411
Nd:glass laser, stable ultrashort light pulses generation (*German*) 0-91823
Nd:glass laser in Tl vapour, output conversion from 1.06 micron to 388.1 nm 0-91850
Nd:glass laser radiation, spatial coherence of fundamental and second harmonic 0-69442
Nd:glass laser six beam system, output characts. (*Chinese*) 0-83612
Nd:glass laser system, beam spatial profile optimization in amplifier channel 0-74407
Nd:YAG, electro-optical extraction of ps laser pulse (*German*) 0-87416
Nd:YAG laser, high repetition rate stimulated Raman scatt., thermal blooming in liquid N₂ 0-91865
Nd:YAG passively locked laser, pulse width meas. by SHG method (*Chinese*) 0-87432
Pb salt tunable diode laser-integrating sphere system, output intensity characts. 0-78881
XeCl, high-energy subnanosecond pulse amplification 0-99770

laser cavity resonators

- annular, adaptive mirror effects on performance 0-58596
annular HSURIA resonators, testing with CO₂ laser, polarisation effects 0-58599
beam expander for short cavity dye laser 0-87532
complex resonator with internal diaphragm, diff. losses and field distrib., integral eqns. 0-95921
coupled laser oscillators, injection modulation 0-99773
coupled transitions with arbitrary polarization of radiation 0-78827

laser cavity resonators continued

- 3,3-diethyl thiadibocarbocyanine iodide dye, stimulated fluoresc. and stimulated reson. Raman scatt. relationship 0-91853
diffraction experiment in cavity with 1-D diaphragm 0-95920
diffraction losses for symmetrically tilted plane reflectors in open resonators 0-58598
diode laser in external cavity, linearized theory 0-69391
dye laser, CW, pumped, stable multifreq. picosecond pulse emission, phase-locked radiation pumping 0-91789
dye laser, double grazing-incidence single-mode type 0-95906
dye laser, emission locking on to wavelength of 1₂ mol. fluoresc. 0-99721
dye laser, flash lamp pumped, tuning by grazing incidence grating technique 0-95914
dye laser, mode-locked, synchronously pumped, pulse-width stabilization 0-83622
dye laser, second harmonic pulse structure and cavity length determ. 0-95935
dye laser, synchronously mode-locked CW, intracavity SHG in thin NH₄H₂PO₄ cryst. 0-95945
dye laser, tunable, N₂-laser pumped, using single prism beam expander (*Chinese*) 0-74389
dye laser characteristics with forced mode synchronisation, intracavity absorpt. effect 0-78873
dye laser spectral props., hole-burning effects 0-102718
dye lasers, book contrib. 0-106517
dye lasers, freq. locking by injection, CW and delta pulse regime anal. 0-87389
exact cavity eqns. for lasers with large output coupling 0-64079
excimer laser, with elec. discharge pumping, model 0-58516
External cavity operation with complete removal of sub-cavity effects for mode-locking injection lasers 0-58545
F₂-centre, pulsed tunable laser, IR spectral characts., 1.1-1.26 μ region 0-91805
far IR laser, intracavity pumped by TE CO₂ laser 0-87382
far IR laser intracavity polarisation modulation by CdTe AC Faraday rotation 0-58613
fibre Raman lasers 0-102767
field distribution, Rensch finite difference method calcs. (*Chinese*) 0-87412
filled telescopic resonator, steady-state lasing, oscillation modes 0-95922
fluctuations of laser beam diameter of single-mode laser, lens effect 0-64090
fluoromethane TEM₀₀ far IR laser-with integrated pump laser 0-58578
FM mode locked laser, dispersion effect 0-74406
fourth harmonic generation cascade process (*Russian*) 0-99797
Gardner-Fresnel-Kirchhoff propag. algorithm 0-83621
gas laser, polaris. effects 0-58605
gas laser, resonator parameters effect on mode volume (*Hungarian*) 0-58603
gas laser and its appls. (*French*) 0-83590
gaussian beam resonator, optical nutation 0-99807
HF chemical laser, CW, with unstable telescopic resonator, radiation field structure 0-91786
homogeneously broadened with constant loss, optimum output efficiency 0-74403
injection laser with composite resonator, active region internal parameters determ. 0-106548
intracavity resonance asymmetries, nonlinear freq. depend. diffraction effect 0-99760
intracavity absorption spectroscopy in plasma jet, laser stimulation optimisation 0-77881
introductory concepts and results, book contrib. 0-106504
Israel Physical Society 1980 annual meeting, Rehovot, Israel (April 1980) 0-94909
losses, phase polarisation method in lasing regime 0-87413
methanol laser, optically pumped, use of crystalline reflector in cavity 0-64080
methyl alcohol submm wave laser, optically pumped, intracavity double resonance obs. 0-58522
methyl fluoride, deuterated, optically pumped near-MM laser 0-69379
misalignment, anal. by ray contour method 0-58602
misalignment characteristics, resonator formed by 90° cone and mirror 0-99757
molecular lasers, laser pumping, dispersion 0-87375
monolithically integrated lasers and amplifiers using cleaved substrate technique 0-58590
multipass amplifier, theory and numerical anal. 0-78872
nonlinear resonators, radiation excitation, review 0-69462
open cavity, Slater method validity 0-69428
open resonators with aperture coupling, multimode interaction effects 0-58608
organic solution laser, unstable resonator calculation 0-58600
passive resonant ring laser gyroscope design 0-99768
periodic laser with unstable resonator, single-pulse emission characts., active-medium inhomogeneities effect 0-74365
phase conjugate mirror component for optical cavity, Gaussian transverse modes 0-58595
phase conjugate mirror forming optical cavity, Hermite-Gaussian higher-order reson. modes 0-58594
phase-conjugate resonator using 4-wave geometry conjugate mirrors 0-58650
POPOP solution dye lasers, multilayer reflectors 0-83606
pulse generation, double, gradual cutting-off resonator losses 0-69433
Q-switched Nd:YAG oscillator for stable time-tunable operation in nanosec. regime 0-99759
Q-switching mechanism by intracavity stimulated Brillouin scatt. 0-106552
radiation density, field strength superposition calcs. (*Chinese*) 0-83618
Raman laser, Nd³⁺:YAG with quartz lightguide resonator 0-99735
rectilinear optical resonators for curved metallic waveguides 0-69425
resonance phase transition in two-level lattice system, thermodynamics 0-69351
retroreflective array as resonator mirror 0-95973
ring laser, open cavity matrix eqns. in diffraction theory 0-69429
rotating anharmonic oscillators in resonator, stimulated emission power 0-99689
ruby laser, double mode locking using dye saturable absorber 0-99763
ruby laser with electrooptical shutter, emission spectrum narrowing and single freq. giant pulse lasing 0-78877
semiconductor injection laser, external optical feedback effect on props. 0-58535

laser cavity resonators continued

- semiconductor injection lasers, output depend. on inhomogeneous bonding 0-64015
 semiconductor laser, electron beam pumped, use of periodic struts. with special profiles 0-95923
 single mode laser, intracavity spectrosc., enhancement calc. 0-69426
 solid laser, multimode, with modulated resonator losses, radiation intensity fluctuations 0-74367
 solid laser characts. control using optical delay lines, resonator effective length increase 0-99758
 spatial distribution of laser radiation control 0-64086
 stimulated combined scattering of light, effect of generation of 'hot' vibrs. 0-58601
 TOPOT vapour dye lasers with multiplate reflectors 0-83606
 transverse structure of radiation from a laser with an additional mirror 0-58604
 unstable resonator, half-symmetric, with coated rear cone, polarisation effects 0-74402
 unstable resonator laser, conical optics for radiation conversion 0-91831
 unstable-resonator laser performance at near MM wavelengths 0-58607
 wavefront correlation transformations (*Russian*) 0-99778
 AlGaAs DH laser epilayer struct. optimization for integrated optical circuits 0-99879
 AlGaAs injection laser, large optical cavity, with multiple active regions 0-106538
 AlGaAs lasers, CW high-power single-mode constricted DH lasers with large optical cavity 0-64076
 (AlGa)As strip buried heterostructure lasers, mode locking using external cavity 0-91791
 Al_{1-x}Ga_xAs-GaAs DH injection laser, active region internal parameters determ., composite resonator use 0-106548
 Ar⁺ laser 582 THz stabilisation by I₂ cell, improvements 0-102741
 CO₂ laser, water-sealed, efficiency increase by reducing resonator losses 0-64081
 CO₂ high-power pulsed laser, wave-optical resonator modelling, gain saturation law 0-99693
 CO₂ high-power pump laser, direct narrow-line tuning 0-58579
 CO₂ inverted, wavefront reversal, high efficiency 0-74436
 CO₂ laser, high-pressure, CW, output power fluctuations 0-74333
 CO₂ laser, mode locking obs. by intracavity plasma injection 0-83624
 CO₂ laser, TEA, single longit. mode, double unstable resonator 0-106547
 CO₂ laser cavity and Ge phase-conjugate 10 μ m reflection expts. 0-78894
 CO₂ laser discharge tube, phase distortions due to heating differential 0-95865
 CO₂ laser modulation, plasma injection into cavity 0-83626
 CO₂ laser power variation detection via plasma tube impedance changes 0-69437
 CO₂ laser pulse compression and mode locking using KCl:ReO₄ nonlinear absorpt. 0-74443
 CO₂ lasers, optically pumped, use of crystalline reflector in cavity 0-64080
 CO₂ rotating-mirror Q-switched TEA laser, mode sweeping effects 0-99769
 CO₂ TEA laser, mode-locked, cavity-dumping 0-87415
 CO₂ waveguide laser, CW, optical pumping of far-IR molecular lasers 0-83615
 CO₂ waveguide laser, tunability calc. (*Rumanian*) 0-87371
 CO₂ waveguide laser with pulsed high-freq. discharge 0-99755
 CO₂-N₂ fast-flow laser with unstable resonator, self-oscillation instability 0-95870
 CdS crystals, one-photon pumping, active layer structure, light amplification 0-78858
 CdS monocrystal petal lasers, single-photon excitation (*Russian*) 0-99736
 CdS platelet laser, emission spectra, optical coupling between partial resonators 0-69400
 CdS_{1-x}Se_x monocrystal petal lasers, single-photon excitation (*Russian*) 0-99736
 D₂O laser, 66 μ m, with unstable reststrahlen resonator 0-83619
 GaAlAs DH injection laser, half-ring, room temp. operation 0-58558
 (GaAl)As injection lasers operating with optical fibre external resonator, characts. 0-58544
 (GaAl)As injection laser operating in external cavity, intensity self-pulsations 0-64013
 (GaAl)As injection lasers operating with optical fibre resonators 0-91812
 GaAlAs mode stabilised separated multilayer stripe geometry DH laser, optical waveguide 0-64051
 GaAs DH laser diodes stabilised using self-apertured facet coatings 0-58609
 GaAs, semi-insulating substrates, whispering gallery lasers 0-69405
 GaAs:Zn optically pumped laser, ribbon whisker between highly refl. dielec. mirrors 0-99771
 GaAs-(GaAl)As DH injection laser with pillbox resonator, characts. and fabrication 0-58581
 GaAs-Al_{0.3}Ga_{0.7}As laser diode, spontaneous radiation transfer 0-91796
 GaAs-GaAlAs DH injection lasers, external cavity operated angled-stripe geometry, CW operation 0-64078
 GaAs-GaAlAs injection laser, radiation divergence reduction by non-waveguide mode excitation 0-91797
 GaInAsP-InP stripe laser, etched mirrors fabricated by wet chem. etch 0-99744
 Ge complanar X-ray resonator circulating beam, high symm. multiple wave configurations (*Russian*) 0-78875
 HF CW chemical laser, longit. and transverse mode competition in stable, unstable resonators 0-95917
 HF CW chemical laser, spatial homogeneity of radiation improvement using telescopic resonator 0-106549
 He-Ne laser, cavity losses, phase polarisation method in lasing regime 0-87413
 He-Ne laser modal configuration, interference spectrometer study (*Spanish*) 0-86458
 He-Ne laser model LG-10, design (*Rumanian*) 0-87407
 He-Ne laser stabilisation, I₂ absorption cell power densities 0-99767
 He-Ne laser stabilisation by I₂ 612 nm saturated absorption 0-99765
 He-Ne laser stabilisation by I₂ 611.8 nm saturated absorption 0-99766
 InGaAsP DH lasers with etched reflectors, fabrication, current density 0-64050
 KrF IJ avalanche discharge laser unstable resonator expts., beam divergence 0-74404
 KrF mini-laser operation at high repetition rate 0-74396

laser cavity resonators continued

- LiNbO₃ crystal in laser resonator, thermo-optical effect (*Chinese*) 0-106546
 LiNbO₃ intracavity upconverter for IR detect., limits to low noise equivalent power operation 0-74430
 Nd:glass laser with active mode locking, ultrashort pulses 0-64087
 Nd:YAG, electro-optical extraction of ps laser pulse (*German*) 0-87416
 Nd:YAG crystal, orientation influence on thermally induced birefringence (*Chinese*) 0-88958
 Nd:YAG laser, intracavity freq. doubling by LiIO₃ long pulse emission 0-102736
 Nd:YAG laser, Q-switched, pulse stretching using Pockels cell 0-95927
 Nd:YAG pumped tunable sources, appl. to spectroscopy 0-58576
 Nd:YAG laser reflection resonator with hole coupling 0-58597
 Nd³⁺:YAG, with LiNbO₃ or Ba₂Nb₂O₇ crystals, AM of optical second harmonic 0-78908
 Nd³⁺:YAG laser, high repetition rate electrooptic Q-switching, birefringence 0-69430
 n-Pb_{0.88}Sn_{0.12}Te spin flip Raman laser pumped by TE CO₂ laser, characts. 0-87397
 XeCl mini-laser operation at high repetition rate 0-74396
 Zn,Cd_{1-x}S monocrystal petal lasers, single-photon excitation (*Russian*) 0-99736

laser frequency stability

- carbon tetrafluoride laser with optical pumping, freq. tuning and stabilisation 0-99706
 diode laser in external cavity, linearized theory 0-69391
 diode laser output stabilization by bevelled-end fibre coupling 0-91806
 dye laser, double grazing-incidence single-mode type 0-95906
 dye laser, mode-locked, synchronously pumped, pulse-width stabilization 0-83622
 F₂-centre, pulsed tunable laser, IR spectral characts., 1.1-1.26 μ region 0-91805
 far IR laser, injection phase locking 0-69431
 fibre-optic communication system performance at 1.55 μ m with single-longitudinal-mode laser 0-87556
 FIR lasers stabilizations, fast modulation technique 0-99777
 high intensity laser oscillator, output characts., stability criteria, semiclassical density matrix approach 0-63968
 hydrophone, optical interferometric, with homodyne detection, signal stabilization by light source tuning 0-87477
 interferometry, multimode fibre optic, applications 0-86387
 ion laser, ¹²⁷I₂ stabilised, beat freq. intercomparisons at 514.5 nm 0-74338
 periodic laser with unstable resonator, single-pulse emission characts., active-medium inhomogeneities effect 0-74365
 rhodamine 6G dye laser, induced radiation spectral characts., effect of vibr. relax. 0-64008
 ring gas laser, freq. synchronisation region of colliding waves 0-83620
 ruby laser, operation in free-generation mode 0-58566
 saturable absorber-laser semiclassical model, stability 0-78828
 superconducting point contacts for laser freq. meas. 0-90824
 unstable-resonator laser performance at near MM wavelengths 0-58607
 Ar⁺ laser 582 THz stabilisation by I₂ cell, improvements 0-102741
 CO₂ laser, freq. stabilization by fluorescence of CO₂ gas 0-102693
 CO₂ laser, frequency stabilisation method, phase-locking 0-74401
 CO₂ pulse-periodic TEA laser freq. stabilisation by low press. CW laser signal injection 0-74408
 CO₂-OsO₄ laser frequency meas., D₂O laser phase locking to freq. standard 0-95080
 D₂O laser phase locking to freq. standard, CO₂-OsO₄ laser freq. meas. 0-95080
 GaAlAs laser diode, for heterodyne communication systems, high frequency stability 0-99727
 He-Ne, scheme for automatic fine frequency tuning along the Lamb depression 0-74385
 He-Ne 3.39 μ m laser, FM eliminated CH₄ locked freq. stabilisation in dual feedback control 0-99772
 He-Ne CH₄ locked laser, freq. stability meas. 0-87422
 He-Ne laser, ¹²⁷I₂ stabilised, length or freq. standard 0-106544
 He-Ne laser, methane-stabilized at 88 THz 0-73304
 He-Ne laser stabilisation, I₂ absorption cell power densities 0-99767
 He-Ne laser stabilisation by I₂ 612 nm saturated absorption 0-99765
 He-Ne laser stabilisation by I₂ 611.8 nm saturated absorption 0-99766
 He-Ne laser stabilised by methane E-component, reference source freq. reproducibility 0-106507
 He-Ne lasers, transverse microwave freq. gas-discharge pumping 0-74339
 He-Ne ring laser, methane stabilised, nonlinear resonance freq. shift due to back scatt. (*Russian*) 0-78874
 He-Ne/CH₄ FM eliminated laser, freq. stability meas. 0-87423
 He-Ne-methane ring laser, freq. synchronisation interval for oppositely directed waves 0-99762
 KrCl laser, lifetime extension by H addition 0-91773
 Nd³⁺:YAG continuous laser, radiation freq. stabilisation system using Fabry-Perot interferometer 0-78871
 Nd³⁺:YAG laser frequency stability improvement using active interferometer (*Russian*) 0-64043
 Nd³⁺:YAG multimode laser radiation noise 0-74366
 XeCl laser, lifetime extension by H addition 0-91773

laser isotope separation

- chloropentafluoroethane-(He)(Xe)(O₂)(H₂)(NO), multiphoton dissoc., ¹³C enrichment factor, CO₂ laser wavelength and fluence depend. 0-58331
 conference, laser and electro-optical systems, San Diego, CA, USA (Feb. 1980) 0-62392
 large-scale, generalised concepts, appl. to D 0-68958
 mixtures, two-component, two photon isotope separation, dynamics 0-102584
 non equilibrium light gas, heavy impurity thermal diffusion under laser irradi. 0-64667
 photochemistry two-photon, photo-fragment distrib., isotope separation appl. 0-81344
 photoinisation, selective, use in laser isotope separation and spectrosc., review 0-83332
 purification of materials with overlapping absorpt. spectra 0-78452
 BCl₃-N₂ mixtures, thermomodification props., effect of resonant excitation of mol. vibr. by laser, isotope separation 0-100047
 Dy atom isotope separation, laser excitation, charge exchange with Cs⁺ ions 0-83512
¹²⁹I₂, selective excitation and separation in I₂+C₂H₂ laser induced chem. reaction 0-68962

laser isotope separation continued

- Os isotopic anomalies from different ore deposits, LAMMA determ. 0-61800
- U enrichment (*Japanese*) 0-68960
- U enrichment by photochemical laser, two-phase flow with condensation, mathematical model (*French*) 0-74029
- UF₆ molecule dissociation in two-frequency IR laser field 0-66855
- ²³⁵U, recovery from enrichment plant tailings appl. 0-83212

laser magnetic resonance

- hydroxymethyl radical + O₂, rate coefficient meas. by laser magnetic resonance flow tube method 0-66767
- methoxy radical, LMR spectra anal. 0-63677
- spectral line narrowing of triplet state, in laser excited experiments 0-63703
- HO₂ + O₃, reaction kinetics, laser mag. reson. obs. 0-102528
- NH₂, ν_2 band, laser mag. reson. 0-83523
- OH, isotope effects, Zeeman effect, far IR laser mag-reson. spectra obs. 0-63674

laser modes

- annular HSURIA resonators, testing with CO₂ laser, polarisation effects 0-58599
- atom two step reson. photoionisation, multimode and level degeneracy effects 0-78583
- buried heterostructure laser, DH multilayer LPE growth on etched substrate, optical read-out appls., longitudinal mode operation 0-99749
- CH stripe laser, spatial coherence and modal struct. 0-87531
- coupled laser oscillators, injection modulation 0-99773
- DH stripe geometry lasers, three-dimensional anal. of mode props. 0-64020
- diffraction experiment in cavity with 1-D diaphragm 0-95920
- diode laser, mode locking to external resonator, theory 0-106550
- distributed feedback laser, two-mode operation, index and gain grating configurations 0-69357
- dye laser, CW single-mode tunable 0-106534
- dye laser, DFB, single-mode operation 0-74409
- dye laser, double grazing-incidence single-mode type 0-95906
- dye laser, double mode-locked CW, pulse cross-correlation studies 0-69389
- dye laser, internally pumped mode-locked CW, theory 0-91787
- dye laser, mode-locked, synchronously pumped, pulse-width stabilization 0-83622
- dye laser, synchronously mode-locked CW, intracavity SHG in thin NH₄H₂PO₄ cryst. 0-95945
- dye laser characteristics with forced mode synchronisation, intraresonator absorpt. effect 0-78873
- education, laser beam UHF and audio freq. difference heats 0-73139
- errors in mode parameters determ. of spatial distribution of radiation 0-95055
- fibre-optic communication system performance at 1.55 μ m with single-longitudinal-mode laser 0-87556
- fibre-optic transmission by laser diode analogue baseband modulation 0-58738
- filled telescopic resonator, steady-state lasing, oscillation modes 0-95922
- fluoromethane optically pumped molecular laser, relax. oscils. 0-95875
- fluoromethane-¹³C optically pumped molecular laser, relax. oscils. 0-95875
- FM mode locked laser, dispersion effect 0-74406
- free electron laser, coherent states in single mode and multimode cases 0-102689
- gas laser, polaris. effects 0-58605
- gas laser, resonator parameters effect on mode volume (*Hungarian*) 0-58603
- gas lasers, mode interactions in longit. mag. field, active medium dispersion effects 0-63967
- Goldstone mode in stationary state of non-equilibrium dissipative system (*Chinese*) 0-87365
- injection laser diode mode structure enhancement by backface plating 0-64056
- injection laser harmonic distortion analysis 0-58537
- introductory concepts and results, Q-switching and mode-locking, book contrib. 0-106504
- multimode laser containing saturable absorbers, bistable operation 0-91862
- multimode laser steady-state stimulated Raman scatt. 0-99796
- narrow double-current-confinement channelled-substrate-planar laser fabrication by double etching 0-64073
- open cavity, Slater method validity 0-69428
- open resonators with aperture coupling, multimode interaction effects 0-58608
- parasitic oscillations in the static centered two-aperture limit 0-95861
- phase conjugate mirror component for optical cavity, Gaussian transverse modes 0-58595
- plasma, collisional, mixed mode operation, cross-focusing 0-83945
- POPOP solution dye lasers, multiplate reflectors 0-83606
- Raman-Nath standing-wave mode-locking switch, modulation index 0-78980
- regenerative compression of mode-locked laser pulses using saturable dye 0-95925
- resonator, stimulated combined scattering of light, effect of generation of "hot" vibrs. 0-58601
- rhodamine 6G dye laser, induced radiation spectral characts., effect of vibr. relax. 0-64008
- rhodamine-6G mode locked dye laser pulse width monitoring by rapid scan autocorrelator 0-87421
- ring laser, travelling wave, mode self-synchronisation 0-83605
- ring laser, unidirectional, modes 0-91818
- ring laser mode competition and anticorrelation calc. and expt. 0-102740
- ruby laser, double mode locking using dye saturable absorber 0-99763
- ruby ring laser with forced mode locking 0-95915
- saturable absorber mode locking of pair of laser amplifiers, periodic pulse soln. 0-83623
- self-synchronisation in dye laser with continuous pumping 0-83605
- semiconductor heterojunction lasers, partially homogeneous broadening and saturation, non-oscillating mode suppression 0-99775
- semiconductor injection lasers, simplified theory for mode locking 0-64021
- semiconductor laser, self-sustained pulsations 0-106522
- semiconductor laser intrinsic noise in optical communication systems 0-69394

laser modes continued

- semiconductor laser radiation, frequency self-modulation interpretation 0-64028
- semiconductor super-DFB single-mode laser with periodic stripe width variations 0-58574
- solid laser, multimode, with modulated resonator losses, radiation intensity fluctuations 0-74367
- solid laser characts. control, using optical delay lines, free-generation, Q-switching and mode-locking regimes 0-99758
- spatial distribution of laser radiation control 0-64086
- stripe geometry semiconductor lasers, transverse mode stabilisation 0-99774
- subharmonic lasers, quantum theory, first order non-equilib. phase transition 0-83584
- superradiance waveguide laser, stimulated emission spectrum, leaky modes (*Russian*) 0-87400
- terrace substrate DH laser, fundamental transverse mode oscillation (*Japanese*) 0-78856
- TOPOT vapour dye lasers with multiplate reflectors 0-83606
- transverse structure of radiation from a laser with an additional mirror 0-58604
- two-level system in resonant multifrequency field with structureless noise (*Russian*) 0-91766
- AlGaAs semiconductor lasers, single-mode stabilisation by traps 0-95893
- (AlGa)As strip buried heterostructure lasers, mode locking using external cavity 0-91791
- AlGaAs transverse junction stripe laser with distributed Bragg reflector 0-106535
- Al,Ga_{1-x}As CW multiwavelength TJS laser, MBE, single-longitudinal modes 0-64049
- Ar laser with passively locked modes, excitation of dye laser for picosecond pulse generation 0-95930
- Ar⁺ ion laser, active mode locking study 0-91827
- CO₂ CW laser, vibr. temp., dissociation and gain limitation determ., new technique 0-87369
- CO₂ high-power pump laser, direct narrow-line tuning 0-58579
- CO₂ laser, detuning effects of FM mode-locking 0-69434
- CO₂ laser, mode locking obs. by intracavity plasma injection 0-83624
- CO₂ laser, TEA, single longit. mode, various prod. techniques 0-106547
- CO₂ laser gain switch, pulse characts., approx. evaluation 0-58504
- CO₂ laser modulation, plasma injection into cavity 0-83626
- CO₂ laser pulse compression and mode locking using KCl:ReO₄ nonlinear absorpt. 0-74443
- CO₂ lasers, IR saturable absorpt. in benzene, chlorobenzene and bromobenzene 0-69465
- CO₂ long-pulse 2 GW single longit. mode source for laser-matter expts. 0-78860
- CO₂ rotating-mirror Q-switched TEA laser, mode sweeping effects 0-99769
- CO₂ TEA laser, injection tuning and mode locking on low gain rot. lines 0-95928
- CO₂ TEA laser, mode-locked, cavity-dumping 0-87415
- CO₂ TEA laser system, 20-J nanosecond pulse, based on injection-mode-locked oscillator 0-99752
- CO₂-N₂ He electroinjection laser, freq. mode, lasing conditions 0-63970
- CdS crystals, one-photon pumping, active layer structure, light amplification 0-78858
- GaAlAs actively mode-locked laser, bandwidth limited picosecond pulses 0-95905
- GaAlAs DH injection laser, half-ring, room temp. operation 0-58558
- GaAlAs mode stabilised separated multilayer stripe geometry DH laser, optical waveguide 0-64051
- GaAlAs terraced substrate laser, visible-light-emitting, characts. 0-106523
- GaAs DH laser diodes stabilised using self-apertured facet coatings 0-58609
- GaAs injection lasers, direct modulation enhancement effect of HF noise 0-83608
- GaAs laser diode, spontaneous emission reduction 0-95904
- GaAs/GaInP DH, MBE grown, optically pumped laser action at 77K 0-95890
- GaAs-GaAlAs injection laser, radiation divergence reduction by non-waveguide mode excitation 0-91797
- GaInAsP/InP 1.5-1.6 micron integrated twin-guide lasers with distributed Bragg reflectors 0-74380
- GaInAsP/InP integrated twin-guide lasers with distributed Bragg reflector, spectral behaviour 0-74381
- GaInAsP/InP narrow planar stripe lasers, lasing characts. 0-95897
- GaInAsP/InP terraced substrate DH lasers, fabrication and single transverse mode operation 0-58580
- HF CW chemical laser, longit. and transverse mode competition in stable, unstable resonators 0-95917
- He-Ne laser, beat freq., high displacement sensitivity meas. 0-95926
- He-Ne laser modal configuration, interference spectrometer study (*Spanish*) 0-86458
- He-Ne laser wavelength drift 0-67978
- He-Ne ring laser, unidirectional, modes 0-91818
- He-Xe 3.51 μ laser mode competition in axial mag. field 0-63974
- Ho:LiYF₄ laser, TEM₀₀ mode and Q-switched operation 0-74395
- I laser radiation, 2nd, 3rd and 4th harmonic generation 0-91844
- InGaAsP single-mode CW ridge-waveguide laser emitting at 1.55 micron 0-58584
- InGaAsP-InP DH lasers, spatial hole burning, spontaneous emission saturation, direct obs. 0-95892
- Kr⁺ mode-locked ion laser, pulse width and linewidth meas. 0-102696
- LiF, picosecond generation on F₂⁺ colour centres, induced mode synchronisation (*Russian*) 0-64033
- LiNbO₃ crystal in laser resonator, thermo-optical effect (*Chinese*) 0-106546
- LiNdP₂O₁₂ laser, relaxation oscillations and mode spectra, high density pumping effect 0-69396
- NH₃ laser transitions, CW, two-photon pumped 0-99702
- Nd garnet ring laser, with return mirror, mode locking 0-99764
- Nd:glass laser, blue tunable picosecond pulse generation by synchronous mixing with sideband radiation in NH₄H₂PO₄ 0-87431
- Nd:glass laser with active mode locking, ultrashort pulses 0-64087
- Nd:YAG CW laser, mode locking, 30 W average power 0-87419
- Nd:YAG CW mode-locked laser, negative feedback power stabilization 0-69435
- Nd:YAG laser, CW mode-locked and intracavity freq. doubled, anal. 0-58548

laser modes continued

- Nd:YAG laser, subnanosecond pulse generation at 100K 0-74397
 Nd:YAG passively locked laser, pulse width meas. by SHG method (Chinese) 0-87432
 Nd:YAG regenerative amplifier, expt. studies 0-95909
 Nd³⁺:YAG CW laser, intensity fluctuations in single-freq. mode 0-91802
 Nd³⁺:YAG multimode laser radiation noise 0-74366
 Pb_{1-x}Sn_xTe/PbTe_{1-x}Se, lattice-matched buried heterostructure lasers with CW single mode output 0-74386

laser radar *see optical radar***laser theory**

- see also laser transitions; population inversion; stimulated emission*
 20 years of development 0-58501
 active medium, EM field self-focusing, laser transverse struct. form. 0-87442
 atomic collisional gas-discharge laser feasibility 0-91779
 benzoxazole, aromatic derivatives, spectral luminesc. and lasing props. rel. to electronic struct. 0-99519
 book, quantum electronics 0-105442
 chemical lasers oscillating on rot., vibr. and electronic transitions, review 0-102716
 correlation function of single-mode radiation in a quasi-classical approximation 0-95815
 coupled laser oscillators, injection modulation 0-99773
 coupled transitions with arbitrary polarization of radiation 0-78827
 cylindrical active element with sheath, radiation intensity distrib. calc. 0-58531
 DH Injection lasers, single and dual-filament, self-sustained oscillations, theoretical model 0-64023
 DH lasers, phase and group indices 0-64016
 DH stripe geometry lasers, three-dimensional anal. of mode props. 0-64020
 DH stripe-geometry lasers, thermal props., interpretation of thermal resistance measurements 0-64017
 distributed feedback laser, two-mode operation, index and gain grating configurations 0-69357
 double resonance Raman amplifier, theory 0-87434
 dye laser deterioration, effect on performance 0-83602
 dye laser output coupling, optimisation by consideration of spatial gain distrib. 0-83603
 dye lasers, metastable state relaxation time determ. 0-102719
 electron beam self-bunching in resonantly absorbing medium, radiation amplification feasibility 0-102605
 far IR oscillator, optically pumped, parametric study 0-95862
 filled telescopic resonator, steady-state lasing, oscillation modes 0-95922
 fluoromethane optically pumped molecular laser, relax. oscills. 0-95875
 fluoromethane-¹³C optically pumped molecular laser, relax. oscills. 0-95875
 Fokker-Planck equation solutions, polynomial expansion method 0-91771
 free electron laser, coherent dynamics, conservation law, small signal theory and gain-spread relation 0-83582
 free electron laser, coherent dynamics with arbitrary magnet geometry 0-83581
 free electron laser, coherent states in single mode and multimode cases 0-102689
 free electron laser, multiphoton analysis 0-78826
 free electron laser, quantum theory for strong fields 0-83583
 free electron laser, small signal theory for gain in strong axial mag. field 0-78825
 free electron laser dynamics, coherent picosecond pulse propag. calcs. 0-95860
 free electron laser dynamics with space charge and wiggler effects 0-58500
 free electron laser with nonuniform wigglers, small signal gain 0-58499
 free electron lasers, classical theory, saturation, perturbation calcs. 0-83580
 free electron lasers, energy transfer, computer simulation 0-83578
 free electron lasers, low gain, analytic soln. of quasi-Bloch eqns. 0-87363
 free electron lasers, nonlinear saturation, thermal effects using EM pump 0-87364
 free electron lasers, quantum mechanical and classical theories 0-83579
 Fresnel formulas and law of stimulated emission 0-58489
 gamma lasers, kinetics, quasi-classical approach (Russian) 0-74332
 gas laser three-level gain medium, semiclassical theory, population pulsations and interf. effects 0-95863
 gas lasers, mode interactions in longit. mag. field, active medium dispersion effects 0-63967
 gas nuclear pumped laser simulation experiments 0-64042
 gaseous dipolar media, semiclassical theory, appl. to gas laser 0-83586
 Goldstone mode in stationary state of non-equilibrium dissipative system (Chinese) 0-87365
 HF chemical laser, CW, with unstable telescopic resonator, radiation field structure 0-91786
 high intensity laser oscillator, output characts., stability criteria, semiclassical density matrix approach 0-63968
 homogeneously broadened CW lasers with nonsaturating lasers, optical extraction characts. 0-91770
 homogeneously broadened with constant loss, optimum output efficiency 0-74403
 inert gas nuclear pumped lasers, prod. efficiency of excited states 0-63998
 injection laser, comprehensive model, current depend. of spontaneous and coherent emission 0-74361
 injection laser transients, phase-plane anal., effects of absorbing sections 0-64022
 injection lasers, output depend. on inhomogeneous bonding 0-64015
 introductory concepts and results, book contrib. 0-106504
 laser, optical excitation by photodissoc. wave propag. in dense gas 0-74352
 Lorentz equation derivation for unstable dispersive physical systems 0-83786
 molecular laser, optical pumping in damped photodissoc. wave propag. in dense gas 0-99714
 molecular lasers, laser pumping, dispersion 0-87375
 monochromatic waves in amplifying two-level system 0-74331
 near MM wave laser synchronous pumping, ultrashort pulse generation 0-69385
 negative light absorption by medium with selective freq. modulation of quantum oscillators 0-106501

laser theory continued

- nonlinear active medium in Gaussian random optical field, stimulated emission statistics 0-58488
 nonlinear optical amplifier, coherent radiation statistical props. 0-99691
 optically pumped laser three-photon transition theory 0-102690
 parasitic oscillations in the static centered two-aperture limit 0-95861
 periodic laser with unstable resonator, single-pulse emission characts., active-medium inhomogeneities effect 0-74365
 POPOP vapour lasing, buffer gases influence, theory 0-91790
 power as function of level of optical signal synchronisation 0-69359
 pulse amplification through energy exchange with electron beam via nonlinear radiation press. effects 0-95776
 pulse generation, double, gradual cutting-off resonator losses 0-69433
 pumping, quasi-reson. energy and charge exchange processes, new transitions 0-58526
 pumping system, thermodynamic calc. method 0-58551
 relativistic ion beam laser, continuously IR to X-ray tunable, in negative temp. state (Chinese) 0-87373
 resonance phase transition in two-level lattice system, thermodynamics 0-69351
 resonator, sensitivity to misalignment, anal. by ray contour method 0-58602
 resonator, stimulated combined scattering of light, effect of generation of 'hot' vibrs. 0-58601
 rhodamine 6G dye laser, induced radiation spectral characts., effect of vibr. relax. 0-64008
 rotating anharmonic oscillators in resonator, stimulated emission power 0-99689
 saturable absorber, analogy with convective instability in two-component liquid layer heated from below 0-79319
 saturable absorber-laser semiclassical model, stability 0-78828
 self-induced distributed feedback, stability, in system without resonator 0-87368
 semiconductor DH lasers, current-crowded carrier confinement 0-78854
 semiconductor heterojunction lasers, partially homogeneous broadening and saturation, non-oscillating mode suppression 0-99775
 semiconductor injection lasers, simplified theory for mode locking 0-64021
 semiconductor lasers, triggerable, light-coupled logic appl. 0-74360
 short-wave emission, initial plasma parameters 0-99692
 solid laser, fluctuations in laser theories 0-83587
 solid laser, multimode, with modulated resonator losses, radiation intensity fluctuations 0-74367
 solid-state ring laser, single-freq., spontaneous antiphase fluctuations, theory 0-91821
 subharmonic lasers, quantum theory, first order non-equilib. phase transition 0-83584
 successive oscillatory fields, molecular beam resonance method 0-91706
 superradiance waveguide laser, stimulated emission spectrum, leaky modes (Russian) 0-87400
 three-level laser, rate equations 0-69356
 three-level molecular laser pumping and dispersion eqns. 0-69384
 two-level system, in strong reson. field, saturation, temp. and spectrum characts. 0-99690
 two-level system, Rabi oscillations in partially coherent field 0-102688
 two-level system, spontaneous emission, non-Markovian effects 0-58487
 two-level system in resonant multifrequency field with structureless noise (Russian) 0-91766
 unstable resonator calculation, laser operating on organic compound solution 0-58600
 unstable state decay, trajectory time spread, laser photon statistics 0-83585
 van der Pol oscillator, RPA for linewidth 0-68138
 CO laser, analytical theory, multilevel cascade emission (Chinese) 0-102702
 CO lasers, scaling laws 0-95878
 CO₂ high-power pulsed laser, wave-optical resonator modelling, gain saturation law 0-99693
 CO₂ laser, output characts. at high pump levels 0-58509
 CO₂ laser discharge tube, phase distortions due to heating differential 0-95865
 CO₂ laser gain switch, pulse characts., approx. evaluation 0-58504
 CO₂ laser short pulse propagation and energy extraction 0-74335
 CO₂ multi-rotational line TEA laser, theoretical model 0-69361
 CO₂ stability of parallel pin electrode laser discharges, theoretical investigation 0-83588
 CO₂-N₂ fast-flow laser with unstable resonator, self-oscillation instability 0-95870
 Cu vapour laser, rate processes, computer simulation 0-69371
 CuCl vapour laser, output power limiting processes 0-91776
 GaAlAs DH lasers, SiO₂ insulated, characts. and near field 0-64019
 HF/UF₆-H₂ nuclear pumped laser, characts. 0-78847
 He-Ne methane system, narrow nonlinear resonances in three level system (Russian) 0-78898
³He-Ar volumetric nucl. pumped laser, dominating processes and reaction physics 0-63981
³He-Ar(Xe)(Kr)(Cl), nucl. lasing, population inversion mechanism 0-63980
³He-Xe nuclear pumped laser, small signal gain coeff. and power output, theory comparison with expt. 0-63983
 I, methyl iodide photodissoc. laser, kinetic model, cross-section calcs. 0-58530
 InGaAsP-InP DH lasers, interfacial recomb., influence on oscill. characts. 0-87393
 KrF laser, kinetic model, limiting behaviour and scaling 0-78838
 KrF* nuclear pumped lasers, excited state prod. rate and fission power pulse shape matching 0-63998
 Li₂⁺, ²Σ_g⁺-²Σ_u⁺ excimer emission, ab initio calcs. 0-91608
 N₂, IR laser transition, excitation mechanism (Japanese) 0-83594
 Na₂⁺, ²Σ_g⁺-²Σ_u⁺ excimer emission, ab initio calcs. 0-91608
 Nd:YAG laser, CW mode-locked and intracavity freq. doubled, anal. 0-58548
 Nd³⁺:YAG multimode laser radiation noise 0-74366
 Xe₂ excimer laser, electron beam excitation, VUV fluoresc., lasing 0-87379
 XeF, ground state kinetics, multilevel model of energy transfer 0-99707

laser transitions

- see also laser theory*
 acetylene-d₂, 17 to 21 μm laser lines generated using CO₂ laser pump 0-69375

laser transitions continued

bromotrifluoromethane 823 laser line, simple accurate method for wavelength meas. 0-106554
 carbon tetrafluoride $^{12}\text{CF}_4$ laser, Doppler-limited absorption spectroscopy 0-74347
 carbon tetrafluoride laser, CF_4 molecule $\nu_3 + \nu_4$ band optical pumping 0-74349
 chemical lasers oscillating on rot., vibr. and electronic transitions, review 0-102716
 chlorodifluoromethane subMM wave laser, optically pumped 0-87376
 collective processes in slightly inverted and absorbing media 0-87367
 confined plasma column, soft X-ray lasing action conditions 0-74346
 coupled transitions with arbitrary polarization of radiation 0-78827
 9,10-dichloroanthracene with iso-amy acetate or esters as solvents, dye laser material 0-74354
 cis-1,2-difluoroethene, CO_2 laser pumped, CW far IR laser lines 0-69372
 cis-1,2-difluoroethylene laser, far IR CW optically pumped 0-69368
 1,1-difluoroethylene submillimetric wave emission assignments 0-102708
 difluoromethane, optically pumped, CW far IR laser line frequencies 0-102706
 difluoromethane far IR laser gas, CW laser pumped, gain 0-69367
 ethyl iodide submillimeter wave laser, optically pumped 0-87376
 far IR CW optically pumped lasers, simple accurate method for wavelength meas. 0-106554
 fluoromethane, $^{12}\text{CH}_3\text{F}$, far IR Raman laser line obs., CO_2 laser pumping 0-69381
 fluoromethane, near-MM-wave laser synchronous pumping, ultrashort pulse generation at 496, 193 μm 0-102705
 fluoromethane- ^{13}C , pulsed far IR emission 0-69370
 fluoromethane- SF_6 , 496- μm optically pumped laser, energy-transfer mechanisms 0-99712
 formaldehyde-d (d_2) submillimetre lasers, optically pumped, assignment of laser lines 0-58513
 gas, resonance four-photon shift, optimal focusing of high-power pumping 0-95574
 inert gas mixture ion lasers, hollow cathode, CW operation and excitation mechanism 0-69363
 ion laser, $^{127}\text{I}_2$ stabilised, beat freq. intercomparisons at 514.5 nm 0-74338
 IR, for 16 μm range, review (*Rumanian*) 0-87408
 metal-vapour recombination lasers using segmented plasma excitation 0-74370
 methanol, 118 μm , diagnostic experiments and modelling 0-58515
 methanol, far IR laser, intracavity pumped by TE CO_2 laser 0-87382
 methanol, optically pumped CW for IR laser lines, freq. meas. 0-58514
 methanol, optically pumped CW subMM emission lines 0-95876
 methanol 118 μm laser line, simple accurate method for wavelength meas. 0-106554
 methanol 70 and 118 μm laser line diagnostic expts. 0-69387
 methanol far IR laser emission spectroscopy 0-58524
 methanol far IR laser gas, CW laser pumped, gain 0-69367
 methanol laser, CW, optically pumped, 170- μm emission, press. shift 0-106510
 methanol optically pumped 118.8 μm laser line, Stark splitting obs. 0-102710
 methanol subMM laser line obs. 0-58523
 methanol- d_1 , CH_3DOH optically pumped CW far IR laser lines and frequencies 0-102707
 methanol-d, optically pumped CW subMM emission lines 0-95876
 methyl cyanide, far IR laser line assignments 0-69380
 methyl fluoride, deuterated, optically pumped near-MM laser 0-69379
 methyl mercaptan, CW subMM emission lines, optical pumping 0-87381
 methyl nitrile CW for IR mol. laser, optical pumping with $^{16}\text{CO}_2$ and $^{18}\text{CO}_2$ lasers 0-74343
 methylfluoride, CW for IR mol. laser, optical pumping with $^{16}\text{CO}_2$ and $^{18}\text{CO}_2$ lasers 0-74343
 optically pumped laser three-photon transition theory 0-102690
 propynal, CW for IR mol. laser, optical pumping with $^{16}\text{CO}_2$ and $^{18}\text{CO}_2$ lasers 0-74343
 pumping, quasi-reson. energy and charge exchange processes, new transitions 0-58526
 rhodamine 6G dye laser, induced radiation spectral characts., effect of vibr. relax. 0-64008
 semiconductor diode laser, IR, for 16 μm range, review (*Rumanian*) 0-87408
 solid state lasers, book contrib. 0-106529
 tetrafluoromethane molecule, laser spectrosc. and optical pumping from CO_2 laser 0-74202
 Al II near IR laser transitions, large diameter hollow cathode Ne-Al discharge 0-102715
 Ar laser, new IR laser transitions, 3.725 to 17.233 μm , 5.804 μm laser line identification 0-87374
 Ar- N_2 mixture, electron beam pumped, lasing obs. at 337, 358, 380 and 406 nm 0-102700
 Ar- N_2 mixture, lasing at four lines 0-99713
 Ar-Xe high press. transverse discharge laser using Xe IR transitions 0-63978
 Au hollow cathode laser, ion laser transitions 0-69366
 Au vapour brightness amplifier at 627.8 nm, for projection microscope 0-83616
 Ba-Tl laser optically pumped by pair-absorption transitions, 1.5 μm emission obs. 0-58517
 CF_4 laser, for 16 μm range, review (*Rumanian*) 0-87408
 CO laser, analytical theory, multilevel cascade emission (*Chinese*) 0-102702
 CO laser, CW, with RF excitation in supersonic flow 0-74375
 CO room temperature nuclear pumped laser, parameter optimisation and spectral props. obs. 0-63995
 CO ; $00^0 1-10^0$ transition in $\text{CO}-\text{N}_2\text{O}$ reacting gas mixture, gain 0-74337
 CO ; gasdynamic laser, 16 μm radiation, modified Anderson's time-depend. anal. 0-106505
 CO ; laser, for 16 μm range, review (*Rumanian*) 0-87408
 CO ; laser, transitions, linewidth, temp. depend. 0-69360
 CO ; laser small-signal gain coefficient calc. 0-78831
 CO ; laser transitions, absolute freq. meas. by multiplication of CO_2 difference freq. 0-105618
 CO ; multi-rotational line TEA laser, theoretical model 0-69361
 CO ; TEA laser, sequence band effect on 10.4 μm band multiline oscillation 0-74334
 C^{12}I_2 effective lifetime in N and air 0-102704
 CS_2 laser, for 16 μm range, review (*Rumanian*) 0-87408

laser transitions continued

Cd hollow cathode laser, ion laser transitions 0-69366
 Ce:LaF $_3$ 286 nm laser, optically pumped 0-99738
 ClO_2 , CW for IR mol. laser, optical pumping with $^{16}\text{CO}_2$ and $^{18}\text{CO}_2$ lasers 0-74343
 Cr vapour, laser transitions in near IR 0-99704
 Cs-Xe solar-pumped MHD excimer laser, modelling 0-95873
 Cu hollow cathode laser, ion laser transitions 0-69366
 Cu II laser, UV, operating period extension by Ar admixture 0-74342
 Cu II laser with cylindrical hollow cathodes, UV performance 0-102709
 DCN waveguide lasers, optimised 190/195 μm , amplifying medium characts. 0-99709
 D_2O , far IR laser, intracavity pumped by TE CO_2 laser 0-87382
 D_2O laser, emission characteristics at 50, 66, 83, 111 and 116 μm 0-58525
 D_2O vapour high-power 385 μm laser oscillator 0-69422
 D_2O , near-MM-wave laser synchronous pumping, ultrashort pulse generation at 385, 66 μm 0-102705
 $\text{Er}_3\text{Al}_{15}\text{Ga}_2\text{O}_{12}$, LPE, spectroscopic props. 0-93419
 FCN, CW for IR mol. laser, optical pumping with $^{16}\text{CO}_2$ and $^{18}\text{CO}_2$ lasers 0-74343
 GaInAsP/InP DH lasers emitting at 1.3 μm , growth and characts. 0-64057
 GaInAsP/InP DH stripe geometry lasers emitting at 1.3 μm , growth characterisation 0-69410
 GaInAsP/InP DH lasers, 1.3 μm wavelength, LPE growth and characterisation 0-69411
 GaInAsP-InP buried heterostructure lasers, 1.6 μm wavelength 0-64055
 GeF, use in chemical lasers 0-64004
 HCCF, CW for IR mol. laser, optical pumping with $^{16}\text{CO}_2$ and $^{18}\text{CO}_2$ lasers 0-74343
 HF chemical TE laser, 16 μm emission 0-83600
 HF in absorption, anomalous dispersion meas. 0-95881
 HF premixed chain reaction CW laser, spectral output 0-95882
 He-Kr hollow cathode CW laser, Kr II 4584 \AA generation 0-58510
 He-metal vapour lasers, positive column electron densities, experimental study (*Japanese*) 0-69376
 He-Ne laser, operating on 0.63, 3.39 μm coupled transitions, intensity modulation 0-69365
 He-Ne lasers, in hollow Cu cathode, 632.8 nm output characts. 0-63975
 He-Ne ring laser, nonlinear spectroscopic technique 0-91819
 He-Sr laser, possibility of nucl. pumping, 4305 \AA Sr II transition 0-58518
 He-Zn hollow cathode laser discharge, radiative cascade excitation effect on upper laser levels 0-102697
 $^3\text{He}-\text{Ar}$ (Xe)(Kr)(Cl), volume pumped nuclear laser, survey of lasing 0-63979
 HgBr(B-X), vibr. relax., level deactivation 0-63697
 HgTl excimer laser, kinetics, optical excitation obs. 0-58527
 I_2 , efficient laser action on 342 nm band, ArF laser pumping 0-99703
 I_2 laser, three-level, pumped by CW dye laser 0-63993
 I_2 molecule B-X electron transition during Cu vapour laser optical pumping (*Russian*) 0-78845
 InGaAsP single-mode CW ridge-waveguide laser emitting at 1.55 micron 0-58584
 Kr laser, new IR laser transitions, 3.725 to 17.233 μm 0-87374
 KrF, electron beam pumped laser medium, time depend. fluoresc. spectrum in high current density range 0-78842
 Li I laser, 207 \AA , oscillator strengths 0-83598
 N_2 , IR, excitation mechanism (*Japanese*) 0-83594
 N_2 , IR laser transition, excitation process 0-87383
 N_2 laser, 406 nm emission on C-B band 0-64047
 N_2 laser 337.1 nm transition, rotational struct. variation 0-78836
 NH_3 CW far IR laser lines, CO_2 laser pumping and Stark tuning 0-69382
 NH_3 CW far IR laser lines, CO_2 laser pumping and Stark tuning 0-106508
 NH_3 , far IR emissions by IR pumping using N_2O laser 0-74345
 NH_3 laser, for 16 μm range, review (*Rumanian*) 0-87408
 NH_3 , near-MM-wave laser synchronous pumping, ultrashort pulse generation at 151 μm 0-102705
 $^{15}\text{NH}_3$ far IR laser emission at 153, 375 μm , optically pumped by $^{13}\text{C}^{16}\text{O}_2$ laser 0-58507
 NOCl laser, for 16 μm range, review (*Rumanian*) 0-87408
 OCS laser, for 16 μm range, review (*Rumanian*) 0-87408
 OCS, optically pumped CW subMM emission lines 0-95876
 Pb atomic photodissociation laser, 405.8, 368.3, 364.0 nm emission lines 0-87387
 PrF_3 , laser action of Pr^{3+} 0-95901
 SF_6 laser, for 16 μm range, review (*Rumanian*) 0-87408
 SiF, use in chemical lasers 0-64004
 Sn hollow cathode laser, emission obs. from Sn II, I transitions 0-106509
 SnF, use in chemical lasers 0-64004
 Tl-Hg, excimer band emission from electron beam initiated discharge in TlI-Hg 0-78841
 Tl-Xe, excimer band emission from electron beam initiated discharge in TlI-Xe 0-78840
 Xe 3.51 μm laser amplifiers, spectral narrowing and saturation induced rebroadening optical heterodyne obs. 0-63976
 Xe laser, new IR laser transitions, 3.725 to 17.233 μm 0-87374
 Xe-He, 3.51 μm laser amplifiers, spectral narrowing and saturation induced rebroadening optical heterodyne obs. 0-63976
 XeCl laser, B-X, form. and quenching kinetics 0-74341
 Xe, Cl, triatomic excimer, transient gain meas. at 488.0, 497.6, 514.5 nm 0-58511
 XeF, direct pumping by electron beam pulses, gain and laser oscill. obs. in blue-green 0-102699
 XeF electron-beam-pumped laser, characts., 300-600K 0-78839
 XeF laser performance, ground state population effect 0-63987

laser tuning

carbon tetrafluoride laser with optical pumping, freq. tuning and stabilisation 0-99706
 colour centre laser pumped by flashlamp-pumped dye laser, 2.4 to 3.3 μm wavelength range 0-102737
 diode laser, pressure-tuned, appl. to high-resolution spectroscopy 0-82835
 diode laser calibration by IR spectra of OCS 0-83363
 diode lasers, tunable IR, appls. to high resolution spectroscopy 0-58562
 dye activated CLC, distributed feedback, tunable radiation generation (*Russian*) 0-102720
 dye laser, CW single-mode tunable 0-106534

laser tuning continued

- dye laser, flash lamp pumped, tuning by grazing incidence grating technique 0-95914
 dye laser, high power narrowband pulsed oscillator-amplifier system 0-58570
 dye laser, tunable, 545-680 nm radiation efficient conversion to 360-415 nm UV range 0-74439
 dye laser, tunable, N₂-laser pumped, using single prism beam expander (Chinese) 0-74389
 dye laser, tunable ultrashort pulse generation 0-58612
 dye laser, tuning by multistage interference polarisation filter 0-64091
 F₂-centre, pulsed tunable laser, IR spectral characts., 1.1-1.26 μ region 0-91805
 fluoromethane, ¹²CH₃F, far IR Raman laser line obs., CO₂ laser pumping 0-69381
 fluoromethane high-power laser, tuning behaviour 0-63994
 high-resolution spectroscopy using tunable lasers 0-101849
 hydrophone, optical interferometric, with homodyne detection, signal stabilization by light source tuning 0-87477
 Michelson interferometer, active stabilization by electrooptically tuned laser 0-86386
 molecular laser, optically pumped, review 0-58519
 POPOP solution dye lasers, multilayer reflectors 0-83606
 relativistic ion beam laser, continuously IR to X-ray tunable, in negative temp. state (Chinese) 0-87373
 rhodamine 6G dye in quartz glass microcomp. matrix, as tunable solid laser 0-99734
 rhodamine 6G-safranin-T mixed dye laser energy transfer, 31 nm tuning range 0-58532
 single-sideband generation in IR 0-78876
 three-stage birefringent filter, tuning over visible region 0-58667
 TOPOT vapour dye lasers with multilayer reflectors 0-83606
 CO₂ high-power pump laser, direct narrow-line tuning 0-58579
 CO₂ laser, detuning effects of FM mode-locking 0-69434
 CO₂ laser, pulsed, high-pressure, high-power, electron-beam-controlled, continuously tunable 0-64065
 CO₂ multiatmosphere laser tuning for methyl fluoride laser pumping 0-69421
 CO₂ TEA laser, injection tuning and mode locking on low gain rot. lines 0-95928
 CO₂ waveguide laser, tunability calc. (Rumanian) 0-87371
 Ce:LaF₃ 286 nm laser, optically pumped, 275 to 315 nm pot. tuning range 0-99738
 Co:MgF₂ tunable transition-metal-doped solid state lasers 0-58549
 Ga_{0.95}In_{0.05}As_{0.95}Sb_{0.05} tunable electron-beam-pumped laser parameters 0-106524
 He-Ne, scheme for automatic fine frequency tuning along the Lamb depression 0-74385
 Ho³⁺:LiEr_{0.95}Tm_{0.05}Ho_{0.005}F₄ laser, tuning at 2.06 μ m 0-83611
 I₂ molecule B-X electron transition during Cu vapour laser optical pumping (Russian) 0-78845
 K atomic Rydberg state tunable subMM laser 0-69378
 KrF* laser, generation of high-spectral-brightness tunable XUV radiation at 83 nm 0-91846
 KrF* tunable ultrahigh spectral brightness excimer laser source 0-64046
 NH₃ CW far IR laser lines, CO₂ laser pumping and Stark tuning 0-69382
 NH₃ CW far IR laser lines, CO₂ laser pumping and Stark tuning 0-106508
 NH₃ laser, high-power efficient optically pumped, tunable over 770 to 890 cm⁻¹ range 0-91780
 NaF, F₂⁺-like colour centre, room temp. stable, CW laser, 0.99-1.22 μ m tunable 0-69399
 Nd:YAG pumped tunable sources, appl. to spectroscopy 0-58576
 Ni:MgF₂ tunable transition-metal-doped solid state lasers 0-58549
 n-Pb_{0.95}Sn_{0.05}Te spin flip Raman laser pumped by TE CO₂ laser, characts. 0-87397
 XeCl frequency-tuned laser, coherent tunable vacuum UV near H Ly- β transition 0-99798

laser velocimeters

- airflow through cascade of turbine blades, laser anemometry 0-59146
 anemometer, laser Doppler, meas. of turbulent vortex flow 0-79412
 anemometry, fundamental limitation and accuracy 0-87829
 coherent Gaussian beam in laser Doppler velocimeter, interference 0-69444
 correlation technique for surface speed measurement, industrial paper machine test (French) 0-95082
 cross-beam rate correlation, advances 0-58621
 Doppler, for charged dust particles vel. meas. in high elec. field 0-95083
 Doppler anemometer, directionally sensitive two-component 0-75004
 Doppler anemometry, periodic sampling in periodic fluid flow measurement 0-64657
 Doppler anemometry, velocity and photomultiplier bias effects 0-59140
 Doppler for turbine-vane passage velocity meas. 0-95086
 Doppler microscope, vel. measuring device 0-68251
 Doppler velocimetry of transition to turbulence in Couette-Taylor flow 0-92163
 droplet size and falling velocity meas. using laser Doppler velocimeter 0-68185
 electrostatic precipitator, particle velocity, laser Doppler anemometry study 0-59144
 fluid mechanics, photon correlation techniques, conf., Cambridge, England (March 1979) 0-56998
 fluid section flow pattern speckle photography 0-103096
 follow-up-type Doppler velocimeter, using single-mode optical fibres 0-74476
 jet turbulence, laser velocimeter correlation meas. 0-106785
 laser-Doppler anemometry and photon correlation for turbulence length scales 0-87828
 particle measuring system, for size and density simultaneous determ. 0-98880
 projection optics, afocal 0-75011
 reflected-beam laser anemometry using photon correlator 0-106861
 resonant hydraulic circuit pulsatile water flow meas. using laser Doppler velocimeter 0-103091
 spark discharge particle generator for Doppler measurements in turbulent flames 0-59139
 spectral analysis of signals from a laser Doppler anemometer operating in the burst mode 0-100041

laser velocimeters continued

- stabilized model-fitting approach to the processing of laser anemometry and other photon-correlation data 0-58622
 time-differentiated laser speckles, vel. meas. by first order statistics 0-82750
 tracking laser Doppler velocimeter with direct spectral anal. 0-99782
 transit anemometer signals, semiclassical processing 0-59145
 vaneless diffuser of centrifugal compressor, flow velocity meas. using laser Doppler anemometer 0-59147
 CO₂ IR laser velocimetry, processing techniques and applications 0-87831
 CO₂ performance of acousto-optic freq. shifter 0-100042
- lasers**
 see also chemical lasers; distributed Bragg reflector lasers; distributed feedback lasers; dye lasers; excimer lasers; free electron lasers; gas lasers; laser beams; laser frequency stability; laser tuning; liquid lasers; nuclear pumped lasers; Raman lasers; ring lasers; solid lasers; X-ray lasers
 educational course in modern optics and lasers at San Diego State University 0-62423
 energy research and laser development (Japanese) 0-91813
 modern machine tools for hardening, glazing, boring welding and cutting (Dutch) 0-91808
 operating mechanisms, characteristics and applications 0-64039
 optics conference, Los Alamos, NM, USA (May 79) 0-73095
 physics, working principles, and historical evolution 0-91807
 principles, construction and applications 0-106531
 quantum electronics, conf., New York, USA (Jun. 1980) 0-90614
 technology developments, power gains wavelength extensions (Danish) 0-64038
 tunable, principles, characts. and appl. review (Japanese) 0-74330
- latent heat**
 see also heat of fusion; heat of sublimation; heat of vaporisation
 rutile structure fluorides, high temp. polymorphism and thermal props. 0-75199
 solar energy collection and storage, latent heat diode walls, space heating (French) 0-61298
 storage, physical and chemical processes at low temps. 0-72091
 thermal storage in density stratified fluids and phase change materials 0-67003
- latent heat of adsorption** see heat of adsorption
latent heat of combustion see heat of combustion
latent heat of crystallisation see heat of crystallisation
latent heat of dissociation see heat of dissociation
latent heat of formation see heat of formation
latent heat of fusion see heat of fusion
latent heat of mixing see heat of mixing
latent heat of reaction see heat of reaction
latent heat of solution see heat of solution
latent heat of sublimation see heat of sublimation
latent heat of transformation see heat of transformation
latent heat of vaporisation see heat of vaporisation
latent image see photographic process
- lattice constants**
 see also crystal atomic structure
 alkali halide solid solns., lattice parameter and heat of form. 0-79739
 chaoite, a new allotropic form of carbon, produced by shock compression 0-80997
 cholesteryl ethyl carbonate, unit-cell dimensions and space group 0-84165
 crystal Hartree-Fock theory, ab initio effective potentials 0-103290
 cubic crystals, response to (111) loading, internal energy, elastic moduli 0-84230
 dioctadecyl hydrogen maleate crystals, X-ray spectroscopic true 2d₀₁ value, 'effective' 2d value concept of Bragg spectrometer crystals 0-70081
 disperse systems, solubility increase, phase composition, size effect calcs. 0-70418
 drift and lattice const. determ., graphic method (Chinese) 0-87985
 equivalent neighbour model, generalised, derivation of high temp. lattice consts 0-77721
 II-VI quaternary semiconductor alloys, energy bandgap and lattice constant contours 0-103622
 Invar, Fe-Ni (36 wt.%), alloy 36N, effect of melting conditions on thermal expansion coeff. 0-65256
 Invar, phase stability, spinodal decomposition 0-88327
 Kossel technique in SEM for crystallographic orientation 0-75133
 linear chain, isotope effect on lattice const. 0-103306
 metal, textured cubic, residual stress evaluation 0-89435
 metals, electron-deformation interaction, lattice contraction, Hubbard model calcs. (Russian) 0-59592
 PbO-Nb₂O₅ system, X-ray and electron microscopic phase and struct. determ. (French) 0-92508
 (rare-earth) Fe₂(BO₃)₄ cryst. growth from soln.-melt, props. 0-108337
 steel, stainless, wire, axial texture after electroplastic drawing, X-ray struct. investigation (Russian) 0-104177
 steel, W-Co-Mo-Cr-V-C (8.5, 8.1, 4.5, 3.5, 2.2, 1.02 wt.%), phase composition, struct. and props. 0-104163
 TBBA liquid crystal, monoclinic cell parameters of solid, smectic and metastable phases, temp. dependence 0-70122
 transition metal 3d monoxides, specific vol. and mag. moment calcs. 0-65822
 transition metal alloys, cohesive properties and press.-vol. relation 0-92476
 triptycene hydrogenation products, ACC and TCC, cryst. data 0-100224
 tris (3-mercaptop-1, 3-diphenyl-2-propen-1-onato) Co(III), multiple twinning 0-100250
 urea molecule, bond-length corrections for external and internal vibrs. 0-106402
 vanadocene, order-disorder phase transition, sp. ht. and crystallographic study (French) 0-84131
 X-ray spectrometer, double-beam triple-crystal, high sensitivity, for lattice parameter and topographic meas. 0-77915
 α -Ag-In solid solutions, lattice dynamics parameters (Russian) 0-96477
 Ag-Ni supersaturated metastable solid solns. formed by ion beam mixing 0-107425
 AgCl-AgBr mixed crystals, elastic consts. and cryst. symm. 0-70290
 AgGaS₂-AgGaSe₂ system, phase diagram, lattice consts., and IR spectra 0-60841

lattice constants continued

- AgMg two phase bicrystal, growth by solid state diffusion couple method 0-60773
- Al/Cu thin film couples, TEM study of intermetallic nucleation at interface 0-65305
- Al-C interstitial solid solns., atomic static displacements and deform. interaction (*Russian*) 0-64953
- β -AlO₃-(Na,Li)₂O, NMR, Raman and IR spectra, and X-ray diff., heat treatment induced changes 0-107508
- Au, fine particles, gas evaporation technique for prep., X-ray diff. study 0-75327
- Au, fine particles, gas evaporation technique of prep., X-ray diff. study, charact. temp. 0-75328
- Au₂Si₃ metastable phase, substruct. unit cell (*German*) 0-88091
- BaFe₂O₉, powder, milled and annealed, phase composition, lattice const. and crystallite size 0-71677
- Ba₃FeTa₂O₉, Mossbauer and X-ray diff. studies 0-103905
- BaGd₂X₂O₁₇ (X=Si,Ge), cell const., luminesc. of various rare-earth activators 0-93376
- BAR₂(MoO₄)₄, R=rare-earth, struct., optical, mech., spectral and physicochem. props. 0-84161
- BaTiO₃, polycryst., phase transition obs. in -170 to 220°C range (*Russian*) 0-103474
- Ba₂Ti₂O₇ single crystals, prep. and unit-cell parameters 0-103302
- BaY₂X₂O₁₇ (X=Si,Ge), cell const., luminesc. of various rare-earth activators 0-93376
- Be intermetallics, MB₂ (M=Y, La, Ce, Lu, Th), lattice spacings and susceptibilities 0-65778
- CaAl₂O₄, high pressure modifications 0-104149
- CaGa₂O₄, high pressure modifications 0-104149
- Ca₂Gd_{2-x}Sn_{2-x}Sb₂O₇, pyrochlore struct. form. 0-92504
- Ca₂Ni_{1-x}Fe₂O₄, X-ray struct. anal., determ. of lattice constant and interplanar distances (*French*) 0-96487
- Ca₂SiO₄, structurally related phases, high-temp. X-ray powder diff. 0-81050
- CdS, rock-salt type high-press. phase synthesis using metal sulphide additives 0-104084
- p-CdTe, nondoped, heat treatment in vacuum, dissociation obs. effects on struct. and props. (*Japanese*) 0-60662
- Ce-M intermetallic cpds., M=3d transition metal, sorption of H₂, structural charges 0-88429
- CeNi₂-CePt₂ system, structural and mag. studies on valence behaviour of Ce 0-103809
- Ce_{1-x}Sc_xPd₃, intermediate valence of Ce, susceptibility, lattice const., ESR meas. 0-103648
- (Ce₂Y_{1-x})Fe₂, mag. susceptibility and Mossbauer meas., lattice parameters 0-97068
- Co-Ga binary system, lattice const., phase transform (*Chinese*) 0-88108
- Co-Ni-Zn, diagram of state, crystalline lattice const., microhardness (*Russian*) 0-66479
- Co-WC hard alloys, rapidly quenched struct. 0-76233
- CoO-ZnO-MgO ternary systems, solid solns., struct. charact. 0-60629
- Cr condensates, lattice const., internal stresses (*Russian*) 0-107141
- Cr, electronic struct., spin-density functional calcs. 0-88476
- Cr film, obtained by thermo ionic precipitation, phase composition, lattice parameters (*Russian*) 0-96756
- Cr, lattice dynamics, improved Fiekel model 0-59598
- Cr_{1-x}Fe_xOOH, 0≤x≤10, prep., Mossbauer effect, Neel temp. 0-108134
- CsDy₂F₇ and Cs₂DyF₆, cryst. symm. and cell parameters (*French*) 0-81040
- CsSbO₃, solid state synthesis (*French*) 0-104438
- Cu extended X-ray fine struct., lattice const. 0-89085
- Cu, plastically deformed, lattice strain distrib. (*German*) 0-85012
- Cu, wire, axial texture after electroplastic drawing, X-ray struct. investigation (*Russian*) 0-104177
- Cu-Ag (3 at.%), plastically deformed, lattice strain distrib. (*German*) 0-85012
- Cu₂Ag_{1-x}I crystals, layer struct., X-ray diff. studies 0-96457
- Cu_{1-x}Cr_xSe₄, influence of excess Cu on physical props. 0-103836
- CuFe₂S₃, cubanite polymorph, synthesis above 200°C and 1 GPa, lattice constants 0-108367
- CuGaSe₂, thermal expansion obs. 0-70432
- Cu₂Mo₂S₈, constitution diagram, 11-2000K 0-108407
- Dy₂O₃-ZrO₂ phase diagram and long range ordering 0-93542
- DyRh_{1-x}Sn₃, new supercond./mag. cpds., X-ray powder diff. data 0-100215
- ErRh_{1-x}Sn₃, new supercond./mag. cpds., X-ray powder diff. data 0-100215
- EuB₆, resistivity press. variation, lattice const. 0-100456
- Eu_{1-x}La_xS, electron struct., lattice const., X-ray spectral study (*Russian*) 0-100432
- (EuLu)₃(FeAl)₂O₁₂, film epitaxial growth on Gd₃GaO₁₂ substrate, mag. props. 0-65402
- Eu_{1-x}R_xO₂ (R=Nd, Eu, Gd), lattice parameters, mag. and elec. props. 0-100578
- γ-Fe, FCC film, epitaxial growth on CuAu (111) surfaces, strong ferromagnetism 0-70557
- Fe-Pd (31.2 wt.%), thermoelastic FCC-FCT martensitic transformation 0-104156
- Fe-Pd Invar alloys, elec. and mag. props. and thermal expansion 0-75732
- Fe-Ti-C, rapidly quenched by splat-cooling 0-84923
- Fe_{1-x}Mg_{1-x}Zn₂Ti₂O₄ spinel system, X-ray diffraction, Fe Mossbauer effect 0-88900
- Fe₂O₄, lattice parameters, NMR freqs., and magnetoelec. pots. near 12K 0-71146
- Fe_{0.54}Sb, temperature effect on lattice const., Mossbauer spectra and density 0-88124
- GaBO₃:Fe³⁺, ESR spectra, lattice parameters 0-93170
- Ga_{1-x}In_xAs_{1-y}P_y/GaAs structure, LPE growth and lattice const. matching conditions 0-59822
- Ga_{1-x}In_xP MBE layers, comp., Rutherford scatt. and X-ray diff. meas. 0-75457
- Gd films, electrical props. correlation with microstructure 0-97009
- Gd_{3-x}S₄, ferromag., elec. props. near Curie temp. 0-107788
- Ge, EXAFS at high press. 0-97376
- p-H₂, solid, neutron diff. studies up to 5 kbar 0-59436
- HfO₂, high pressure polymorphism 0-59429
- InBO₃:Fe³⁺, ESR spectra, lattice parameters 0-93170
- InGaAsP-InP layers, grown by LPE techniques, lattice const., bandgap, thickness and surface morphology meas. 0-59818

lattice constants continued

- InP, depend. of phonon spectrum on hydrostatic press., Raman spectra 0-93315
- Ir borides, MIr₂B₂ (M=La, Th, U), supercond. and mag. props. 0-97028
- KCl crystals, Eu²⁺ concentration effect on lattice parameter and density of crystals 0-88169
- K₂Li₂Nb₂O₇ films for optical waveguides epitaxial growth and characterisation 0-79016
- KMn_{1-x}Me_xF₃ (Me=Mg²⁺, Fe²⁺, Co²⁺ and Ni²⁺) Bridgman growth, 0-60764
- K₂Sb₂O₇, solid state synthesis (*French*) 0-104438
- LaB₆ crystals, zone refined, chem. characterisation 0-93821
- La₂C₃, solid solution, lattice const. and superconducting transition temp. (*Russian*) 0-92496
- (La_{0.8}Ca_{0.2})MnO_{3+y}, non-stoichiometry and lattice const. 0-100212
- La₂Ir₂O₇, perovskite, prep. and mag. study 0-80486
- LaSiAs₃, F-type phase synthesis 0-104083
- LaVO₃, successive phase transitions, X-ray anal. 0-108437
- LiGd₂(MoO₄)₃, single crystals, cryst. growth, optical props. 0-60763
- Li₂GeO₃-Zn₂GeO₄, solid electrolyte system, phase diagram 0-66489
- Li₂O-MgO-Al₂O₃ system, subsolidus phase equilibria 0-81036
- Li_{1-x}Ta_{1-x}Ti_{2x}O₆ (0≤x≤0.028), non-stoichiometric phase, crystallographic and dielec. props. 0-75212
- LuBO₃:Fe³⁺, ESR spectra, lattice parameters 0-93170
- Mg-Nd-Zn dilute alloy, metallography and precip. kinetics 0-71655
- Mn-Ni, thermal expansion, mag. susceptibility, lattice const. 0-100341
- Mn₂O₄, hausmannite, tetragonal-cubic transform, X-ray anal. 0-103288
- MnSi_{1-x}Cr_x, crystal growth and characterisation 0-93474
- Mo, lattice dynamics, improved Fiekel model 0-59598
- Mo_{6-x}Rh_xTe₆, synthesis, struct., and elec. props. 0-92877
- Mo₆Ru₂Se₈(Te₂), synthesis, struct., and elec. props. 0-92877
- Mo_{0.5}W_{0.5}Se₂, single crystal, vapour growth, characterisation 0-93466
- Na, equilibrium struct. and phys. props., pseudopot. method 0-96778
- NaBr, EXAFS at high press. 0-97376
- NaCl with divalent impurities, lattice relax. from density meas. 0-70226
- Na₃R(XO₄)₂ (R=rare earth; X=P, As, V), pressure synthesis (*French*) 0-93509
- Nb films, ion beam sputtered, supercond., laser annealing effects 0-97024
- Nb₃Al, supercond. props. and lattice parameter, comp. and neutron irradiation effects 0-70880
- Nb₃N, supercond. props. and structural phase transform. induced by C⁺ and N⁺ implantation 0-107942
- Nb₃Nb_{1-x}Si_x(Ge)_x, impurity stabilised A15 supercond., transition temp., lattice const., specific heat 0-93026
- Nb₃Si A15 phase from amorphous Nb-Si alloys, high-press. synthesis 0-93516
- NdRh_{1-x}Sn₃, new supercond./mag. cpds., X-ray powder diff. data 0-100215
- Ni, cold-rolled, anomalous effects during X-ray stress meas. (*German*) 0-104184
- Ni precipitates, isothermal annealing influence on structural state, X-ray diff. anal. (*Russian*) 0-100849
- Ni-Al(Si), diffusion, lattice parameter, microhardness, and constitution, effect of Si additions (*Russian*) 0-84316
- Ni-Co, lattice parameter measurement, C precipitation in Ni-Co-C solid solution, Ni₃Co ordering (*Czech*) 0-60867
- Ni-Co-Al alloys, continuous precip., SEM, TEM, X-ray diff. study 0-89220
- Ni-Cr-Ta system, phase equilib. of Ni rich region at 1523 and 1273K 0-93541
- Ni-Cu-X (X=Sn, Nb, Ti), spinodal decomp. alloys, linear expansion coeff. influence on morphological anisotropy (*Japanese*) 0-70431
- Ni-Pd-Mn ternary alloys, mag. characts., use for thermosed 0-107995
- NiO, bulk props., initial state MO Ni₄O₄ and Ni₃O₄, cluster model, lattice and force const., photoemission and CT absorpt. spectra 0-84828
- Ni_{1-x}Sb_x, temperature effect on lattice const., Mossbauer spectra and density 0-88124
- NpCo₂Si₂, mag. struct., neutron diff. determ. 0-93084
- NpCu₂Si₂, mag. struct., neutron diff. determ. 0-93084
- Os borides, MO₂B₂ (M=Lu, U), supercond. and mag. props. 0-97028
- Pb-Au, interstitial and substitutional distrib. 0-84204
- PbSc_{2/3}Ti_{1/3}O₃-PbSc_{2/3}W_{1/3}O₃(PbFe_{2/3}Te_{1/3}O₃) ferroelec. props. and lattice const. 0-60520
- Pb_{1-x}Sn_xTe_{1-x}Se_x, solid solutions with constant lattice parameter, phase comp. 0-108417
- Pb_{0.95}Sn_{0.05}(Zr_{1-x}Ti_x)O₃-Nb₂O₅, phase coexistence range, lattice const. 0-92680
- Pb(Ti,Zr)O₃ solid solutions, phase coexistence discrepancies 0-96662
- PbZrTi_{1-x}O₃ ceramics, morphotrophic phase boundary 0-81035
- Pd alloy-H system, α-β phase transformations, hysteresis of press., elec. resistance, review 0-60859
- Pd alloys, effect of alloying on activation energy of H₂ diffusion 0-107571
- Pd-D, crystallite size effects, simultaneous sorption and X-ray study 0-65237
- Pd-H system, α-β phase transformations, hysteresis of press., elec. resistance, review 0-60859
- Pd-Si and PdSi films, on Si, stress obs. 0-80145
- PdSi films, on Si, stress obs. 0-80145
- RbCaF₃, first order improper ferroelastic phase transition at 194K, phenomenological description 0-70397
- RbDy₂F₁₀, RbDy₂F₇ and Rb₂DyF₆, cryst. symm. and cell parameters (*French*) 0-81040
- RbNbW₂O₉ crystals, growth and props. 0-104054
- Rb₂Sb₂O₇, solid state synthesis (*French*) 0-104438
- Rb₂ZnCl₄, phase transitions, thermal expansion coeff. 0-100638
- Rh borides, RRh₂B₂ (R=rare earth), supercond. and mag. props. 0-97028
- Ru borides, RRu₂B₂ (R=rare earth, Y, Th, or U), supercond. and mag. props. 0-97028
- ScBO₃:Fe³⁺, ESR spectra, lattice parameters 0-93170
- ScFe₂, Mossbauer effect of ⁵⁷Fe 0-75903
- ScFe₂H₂, Mossbauer effect of ⁵⁷Fe 0-75903
- Si, ground state props. in density-functional pseudopot. approach 0-92803
- Si, total energy calcs. by r-space method, Wannier functions 0-88503
- β-SiC, sintering, B transport and lattice parameter change 0-108370
- Sm, electron radiation damage, elec. resistivity change rates 0-59954
- Smb₆, resistivity press. variation, lattice const. 0-100456

lattice constants continued

- Sm_{1-x}Ba_x, valence transition induced by alloying 0-96829
 Sm_{1-x}La_xB₂, valence transition, lattice parameter and mag. susceptibility meas. 0-59929
 Sm_{1-x}La_xS, electron struct., lattice consts., X-ray spectral study (*Russian*) 0-100432
 (SmLu)₂(FeAl)₂O₁₂, film epitaxial growth on Gd₃Ga₅O₁₂ substrate, mag. props. lattice mismatch 0-65402
 SmS, physical and physicochem. props., review 0-96875
 Sm_{1-x}Yb_xB₂, valence transition, lattice parameter and mag. susceptibility meas. 0-59929
 Sn ternary intermetallic systems, new supercond./mag. cpds., X-ray powder diffr. data 0-100215
 SnTe, annealed, iodide method of prep., props. meas. 0-71591
 Sr₂FeTa₂O₈, Mossbauer and X-ray diffr. studies 0-103905
 (Tb_{1-x}Gd_x)₂Co, intermetallic cpd. mag. props., phase transform, and mag. hysteresis (*Russian*) 0-93113
 Ti-Fe-Al(Mn), homogeneity and lattice parameters, Mn and Al effect on hydriding compd. FeTi 0-108400
 Ti-C composites, hot pressed, thermophys. props. at high temps. 0-59675
 TiC-N₂, powder preparation, physical, chemical props. (*Russian*) 0-76212
 Ti_{1-x}V_x-H₂ system, reaction and press.-composition isotherms meas. 0-108391
 TiCl₃, ground-state props., Wannier functions, and electronic struct., ab initio self-consistent calc. 0-80178
 Tm_{1-x}Eu_xSe, semicond. with valence instabilities, cryst. chem. considerations 0-100213
 TmSe_{1-x}Te_x, semicond. with valence instabilities, cryst. chem. considerations 0-100213
 UAs, search for lattice distortions at low temps. 0-79759
 UC, miscibility with rare earth nitrides (*German*) 0-96654
 UFe₂, giant magnetoelastic deform. of cryst. struct. mag. props. (*Russian*) 0-93159
 UN, search for lattice distortions at low temps. 0-79759
 USb, search for lattice distortions at low temps. 0-79759
 V₂Ga, A15 cpd., hydrogenation effects on supercond. transition temp., lattice parameters 0-103772
 V₂Ge, A15 cpd., hydrogenation effects on supercond. transition temp., lattice parameters 0-103772
 V₂O₃, impurity doping effects, elec. props. obs. 0-75609
 VSe₂-S_x (0 < x < 2) solid solutions, characterisation 0-88730
 V₂Si, A15 cpd., hydrogenation effects on supercond. transition temp., lattice parameters 0-103772
 (V_{1-x}Ti_x)O₅, unit cell dimensions 0-70970
 Xe, crystalline, lattice constant at insulator-metal transition 0-107706
 Y, electron radiation damage, elec. resistivity change rates 0-59954
 Y-M intermetallic cpds., M=3d transition metal, sorption of H₂, structural charges 0-88429
 Y₂(CO₃)₃.nH₂O, tenerite, single cryst. hydrothermal growth 0-97417
 YIG:Ca, oxidising effects of high temp. annealing in reducing atmosphere 0-66696
 Y(OH)CO₃, ancylite like phase, hydrothermal cryst. growth (*French*) 0-108340
 Yb, electron radiation damage, elec. resistivity change rates 0-59954
 YbB₆, resistivity press. variation, lattice consts. 0-100456
 α-ZnF₂, lattice parameters and thermal expansion, 80-320K, X-ray obs. 0-57373
 ZnS, cubic, compression 0-107358
 ZrC-C composites, hot pressed, thermophys. props. at high temps. 0-59675
 Zr_{1-x}La_x, high-temp. enthalpy, X-ray powder diffr. data 0-107446
 Zr_{1-x}In_xO_{2-x}, ionic conductivity, lattice const. 0-96688
 ZrO₂, high pressure polymorphism 0-59429

lattice defects see crystal defects

lattice diffusion see diffusion in solids

lattice dynamics

see also crystal surface and interface vibrations; displacive transformations; Gruneisen coefficient; lattice dynamics of covalent crystals; lattice dynamics of ferroelectric crystals; lattice dynamics of ionic crystals; lattice dynamics of metallic crystals; lattice dynamics of molecular crystals; lattice localised modes; lattice phonons; soft modes; vibrational states in disordered systems

- alkali metal acid oscallates, neutron inelastic scatt. spectra in 2200-200 cm⁻¹ range 0-70327
 anharmonic crystals with complex lattice, equations of state 0-107399
 antimonates, columbite or trirutile struct., force fields rel. to cryst. struct. (*French*) 0-107104
 classical crystal optics, lattice dynamical background, review 0-97221
 Coulombic interaction summation in Gaussian basis 0-70575
 crystal lattice oscillations and molecular oscillation, change in bond length and angles as coordinates 0-107385
 electron-ion system, effective ion interaction and force consts. 0-65185
 electronic structure and solid props., rel. to chemical bonding, book 0-86044
 equations of state of crystals with strong sixth-order anharmonicity 0-92637
 exciton-phonon coupled-mode excitations in cryst., relax. rates, theory 0-59881
 fracture theory based on lattice instability 0-84244
 graphite, frequency distribution based on unfolding technique 0-92619
 graphite-Br₂ stage 2 intercalation cpds., Raman spectra 0-80787
 half space layered cryst., vibr. spectrum, Brillouin zone (*Russian*) 0-100313
 heat capacity of crystals and the vibrational spectrum, historical review 0-57071
 II-VI and III-V compounds, eight-parameter bond-bonding forces model 0-70334
 impurity centres, electron-phonon coupling from structured optical spectra, review 0-89038
 impurity molecules in solids, vibrational relaxation, anharmonic dynamics role (*Russian*) 0-75323
 impurity relaxation in nonresonance field, phonon amplification (*Russian*) 0-100310
 incommensurate structure, Debye-Waller factors, modulation wave thermal fluctuations 0-84274
 Ising spin system, coupled to acoustic and optic lattice modes, critical behaviour 0-71044
 layered crystal, low freq. vibr. spectra peculiarities, normal mode density at low temp. (*Russian*) 0-70332

lattice dynamics continued

- magnetic order coexistence with charge density waves 0-97096
 metals, electron-deformation interaction, lattice contraction, Hubbard model calcs. (*Russian*) 0-59592
 molybdates, alkaline earth, U activated, scheelite struct. luminesc. props. vibr. modes and quenching temp. 0-60651
 monatomic three dimensional FCC lattice, solitary wave effect on shock profile 0-79874
 niobates, columbite or trirutile struct., force fields rel. to cryst. struct. (*French*) 0-107104
 optical activity, lattice dynamical background 0-93267
 Peierls one dimensional model, exact solution, electron spectra, static lattice deformation (*Russian*) 0-70609
 polar semiconductors, two-phonon resonance Raman scattering 0-108204
 self-trapping of powerful light pulses, role of TO and LO lattice vibr. modes 0-99809
 semiconductors, force variation due to charged defects 0-92634
 spinel compounds, AB₂C₄, Urey-Bradley force constants 0-59587
 strain driven thermoelastic instability toward brittle fracture 0-103415
 structural phase transitions, Landau theory 0-92639
 superconductivity and lattice instability 0-88663
 superharmonic approximation for quantum crystal 0-92615
 superionic conductor, hydrodynamic theory for collective excitations 0-70530
 tantalates, columbite or trirutile struct., force fields rel. to cryst. struct. (*French*) 0-107104
 trimethylammonium cadmium trichloride, struct. phase transitions, low-freq. Raman scatt. obs. 0-80783
 tungstates, alkaline earth, U activated, scheelite struct. luminesc. props. vibr. modes and quenching temp. 0-60651
 valence force field, rel. to tensor force consts. 0-79888
 wurtzite-type crystals, lattice dynamics including the effect of electronic extension 0-59586
 X-ray diffraction and lattice dynamics, early work by I. Waller 0-62439
 α-AgI, dynamic cage effect 0-107541
 AgI, lattice dynamics of binary superionic conductors 0-107393
 Al₂(WO₄)₃:Cr(Eu), and undoped crystals, luminesc. obs. 0-89047
 As₂Se₃, monoclinic, chem. bonds rel. to electronic and vibr. states 0-64951
 BN, ¹⁵N zero point vibr. energy from nuclear photon scattering 0-59593
 BeO, wurtzite-type crystals, lattice dynamics including the effect of electronic extension 0-59586
 CdF₂, ionic conducting fluoride fluorite, US velocity meas. 0-107381
 CdIn₂S₄, partial inverse spinel struct., detection by Fourier transform spectroscopy 0-108197
 CdTe, lattice dynamics and phonon parameters bond bending force model 0-59595
 Cs halides, Gruneisen and Anderson-Gruneisen parameter determ. 0-59611
 Cs₂PbCu(NO₂)₆, incommensurate Jahn-Teller transition, Huang scatt. 0-70401
 Cu halides, lattice dynamics of binary superionic conductors 0-107393
 Cu-Be solid solutions, local oscill. conc. depend., impurity bands (*Russian*) 0-75318
 CuBr(Cl)(I), LF light scatt. spectra in superionic cond. phases, ion motion obs. 0-108217
 Cu₂PS₃Br, cryst. struct. at 293 and 473K, thermal parameters, neutron diffr. obs. 0-59450
 Fe_{0.33}NbS₂, lattice dynamics and hyperfine interactions, Mossbauer spectra study 0-108135
 Fe₂TiS₂, lattice dynamics and hyperfine interactions, Mossbauer spectra study 0-108135
 GaAs, lattice dynamics, phonon freq., bond bending force model calcs. 0-70335
 GaP, lattice dynamics and phonon parameters bond bending force model 0-59595
 GaS_{1-x}Se_x, mixed crystals, IR reflectivity spectra 0-66204
 GaSb, lattice dynamics, phonon freq., bond bending force model calcs. 0-70335
 GaSe, lattice dynamics and elastic props., Born-von Karman model study 0-70337
 GaTe, layer crystal., polarised IR refl. spectra 0-97279
 GaTe monocystal, far IR polarised complex reflectivity obs. 0-60609
 Hg_{1-x}As_xF₃, one-dimens. lattice dynamics, X-ray scatt. study 0-75317
 HgI₂, IR lattice vibr. and dielec. dispersion 0-76018
 In_{1-x}Ga_xAs_{1-y}P_{1-y} epitaxial layer, far IR refl. spectra, lattice vibrs. 0-97282
 InP, lattice dynamics and phonon parameters bond bending force model 0-59595
 K double fluorides, IR refl. spectra, vibr. modes, optical vibr. freq., Kramers Kronig anal. 0-66190
 KDy(MoO₄)₂, polarised IR and Raman struct., ⁹²Mo/¹⁰⁰Mo isotope effect 0-108198
 K₂PbCu(NO₂)₆, incommensurate Jahn-Teller transition, Huang scatt. 0-70401
 K₂Pt(CN)₄Br₃·3H₂O, CDW system, nonlinear amplitude-phase interaction 0-88490
 α-LiIO₃, pot. energy distrib. and force const. variations with temp. 0-79894
 Li₃N, interstitial sites and anharmonic thermal vibrs. in cryst. struct., ionic cond. mechanism 0-107190
 Lu₂(WO₄)₃:Cr(Eu), and undoped crystals, luminesc. obs. 0-89047
 MnCl₂, lattice dynamics, density of states and sp. ht. calc. 0-92624
 Nd₂IO₄, Raman spectra, libration lattice modes 0-60575
 NH₄Cl, ¹⁵N zero point vibr. energy from nuclear photon scattering 0-59593
 NH₄IO₄, Raman spectra, libration lattice modes 0-60575
 NaNO₃, lattice vibrs., order-disorder transform., IR spectra study 0-65176
 Ni_{0.85}Cr_{0.15}, phonons with disorder caused by force consts., neutron diffr. obs. and CPA calc. 0-96602
 PbF₂, anion disorder at high temps., neutron diffr. obs. 0-59614
 PbNb₂O₆, IR absorpt. spectra and diffuse Raman scatt., normal coord. anal. (*French*) 0-66198
 PbTa₂O₆, IR absorpt. spectra and diffuse Raman scatt., normal coord. anal. (*French*) 0-66198
 PdH₁, superconducting transition temp., inverse isotope effect, Einstein model 0-65734
 Rb halides, role of quantum effects in lattice dynamics, Debye temp., shell model calcs. 0-70336
 α-RbAgI₂, dynamic cage effect 0-107541

lattice dynamics continued

- RbAg₁₅, single particle excitations, inelastic neutron scatt. obs. 0-59599
 RbCaCl₃, Raman scatt. study of phase transitions 0-71411
 RbCrCl₃ crystals, β - γ structural phase transition, lattice dynamical anal. 0-84291
 Rb₂PbCu(NO₃)₆, incommensurate Jahn-Teller transition, Huang scatt. 0-70401
 ReO₃, cubic lattice stability, screening effect on vibr. 0-75356
 Se₂(WO₄)₃:Cr(Eu), and undoped crystals, luminesc. obs. 0-89047
 Se, trigonal, normal mode calcs. 0-84259
 SmS, electron-phonon interaction, lattice dynamical model 0-96610
¹¹⁹Sn temp. depend. isomer shift, pseudopot. approach 0-84675
 SrCl₂, anion disorder at high temps., neutron diffr. obs. 0-59614
 SrCl₂, anion motion at high temps., quasielastic neutron scatt. obs. 0-59715
 TiO₂, rutile, first order Raman spectrum, uniaxial stress effects 0-66196
 TiSe₂ (1T), Raman studies of lattice dynamics 0-103962
 Ti₂PbCu(NO₃)₆, incommensurate Jahn-Teller transition, Huang scatt. 0-70401
 V₂O₁₃, semicond., IR vibration spectra 0-88997
 WO₃, electronically induced lattice distortion, screening effect on vibr. 0-75356
 ZnIn₂S₄, vibr. spectrum, Raman study 0-97278
 ZnS, cubic, thermal vibr. temp. depend., anharmonic models 0-92618
 ZnS, lattice dynamics, phonon freq., bond bending force model calcs. 0-70335
 ZnS(Se)(Te), thermal expansion and lattice dynamics under press. 0-100316
 ZnTe, lattice dynamics and phonon parameters, bond bending force model lattice dynamics and phonon parameters bond bending force model 0-59595

lattice dynamics of covalent crystals

- diamond, Cosserat continuum model, elastic props., lattice dynamics 0-59552
 diamond, effective ion interaction and force consts., model of Si point defect 0-65185
 semiconductors, displacement correlations, adiabatic bond charge model 0-70350
 Ge, lattice dynamics under press 0-92627
 Ge:¹¹⁹Sn, impurity lattice dynamics, Mossbauer spectra, Debye temp. 0-84262
 Se, trigonal and vitreous, sp. ht. and thermal cond., 3 to 300K 0-59676
 Si, lattice dynamics under press 0-92627
 n-Si, phonon-phonon relaxation 0-96609
 Si, stretched, lattice vibr. anharmonicity, influence of stress on elastic moduli, Raman spectra 0-80791
 n-Si, vibr. excitation conditions, vol. charge redistrib. effect (Russian) 0-103427
 Si:¹¹⁹Sn, impurity lattice dynamics, Mossbauer spectra, Debye temp. 0-84262

lattice dynamics of ferroelectric crystals

- see also *displacive transformations*; *soft modes*
 displacive and order-disorder type, thermal cond. at low temps. 0-75391
 ferroelectric-elastic phase transition, modelling, appl. to KH₂PO₄ and LiNH₂C₄H₄O₆·2H₂O (Russian) 0-75961
 ferroelectrics, order-disorder, displacive transformations, tunnelling, phonons 0-75975
 ferroelectrics with hydrogen bonds, phase transition into coherent state, two-level proton calcs. (Russian) 0-71356
 Ising model in transverse field, mode-coupling theory for central peak 0-75987
 IV-VI semiconductor, vibronic model of lattice instability 0-80723
 large-gap type, vibronic theory and opt. props., anomalous bulk photovoltaic effect 0-103939
 Rochelle salt, ferroelec. phase transition, Raman scatt. study 0-97211
 Rochelle salt, ferroelectric, Raman and IR study 0-71406
 squaric acid, two-dimens. phase transition, Raman scatt. study 0-71401
 TGS, nitroaniline admixture effect on thermal parameters 0-107580
 thiourea, ferroelectric, Raman and IR study 0-71406
 Ag₂AsS₃, proustite, phonons and soft modes at ferroelec. transition 0-60524
 AgNa(NO₃)₂, ferroelec., Raman scatt. and phase transitions 0-71349
 As_{0.5}Sb_{0.5}SI cryst., ferroelec., soft mode Raman and IR spectroscopy 0-76016
 BaMgF₂:Mn²⁺ ferroelec., EPR and ENDOR study, cryst. field tensor 0-71162
 BaTiO₃, displacive ferroelectric, effective charge determ. 0-97212
 BaTiO₃, elastooptic effect near ferroelec. transition, temp. depend. 0-97233
 BaTiO₃, mean square atomic displacement temp. depend., sublattice vibration anharmonicity 0-79890
 BaTiO₃, paraelec. phase, stabilisation of soft mode 0-75985
 BaTiO₃, polycrystalline ferroelectric, grain-size dependent props. 0-71352
 BaTiO₃, vibronic theory and opt. props. 0-103939
 KD₂PO₄, neutron scattering from coupled polar-elastic waves 0-92623
 KH₂AsO₄, ferroelectric phase transition under high hydrostatic press., mol. dynamics, NQR study 0-75880
 KH₂AsO₄, NQR of ⁷⁵As, press. and temp. depend., 77K to Curie temp. 0-71227
 K(H₁D₃)₂P₄, polarised impurity cluster effects in light scatt. expts. 0-71431
 KNO₃, Raman and IR spectra and lattice vibr. 0-60565
 KNbO₃, cubic, temp. depend. of intensity of X-ray interference 0-59613
 KNbO₃, displacive ferroelectric, effective charge determ. 0-97212
 K₂SeO₄, hexagonal-orthorhombic transition, Brillouin scatt. study 0-97208
 LiNbO₃, ferroelec., displacive type phase transition, far IR reflection spectra 0-71339
 LiTaO₃, displacive ferroelectric, effective charge determ. 0-97212
 LiTaO₃, ferroelec., displacive type phase transition, far IR reflection spectra 0-71339
 Pb₂GeO₁₁, lattice dynamics parameters anisotropy, X-ray diffr. study 0-59612
 PbTiO₃, vibronic theory and opt. props. 0-103939
 Pb(Zr_{0.5}Ti_{0.48})O₃, polycrystalline ferroelectric, grain-size dependent props. 0-71352
 Rb₂ZnBr₄, soft modes at phase transforms., far IR spectrum study 0-107398
 SbSI-SbSBr system, ferroelec., anharmonic effects in far IR reflectivity spectra 0-76014

lattice dynamics of ferroelectric crystals continued

- Sn₂P₂S₆, ferroelec. semicond., phase transition and lattice dynamics 0-60526
 Sn₂P₂S₆, soft mode props., Raman scatt. study 0-60525
 SrTiO₃, ceramic, electrocaloric effects for refrigeration at cryogenic temp. 0-77789
 SrTiO₃, disorder manifestation, light scatt. spectra, high temp. 0-76017
 SrTiO₃, mean square atomic displacement temp. depend., sublattice vibration anharmonicity 0-79890
- lattice dynamics of ionic crystals**
- alkali halide crystals, long wavelength optical mode frequencies and Anderson-Gruneisen parameter 0-65182
 alkali halide crystals, mixed, impurity centre local vibr., comp. depend. of spectral parameters 0-79898
 alkali halides, lattice dynamics using breathing shell model 0-88285
 alkali halides, mixed, U-centre localised modes 0-100319
 alkali halides, Poisson ratio and Gruneisen parameter, vol. depend. anal. 0-96614
 alkali halides, V_K-centres, vibr. modes, calc. 0-84269
 alkali hydrides, lattice props. from interaction pot. energy function 0-100199
 alkaline earth oxides, cohesive and thermophysical props., role of three-body interactions 0-92477
 Anderson-Gruneisen parameter, interaction approach 0-88291
 centrosymmetric ionic crystals, stimulated excitation of second harmonic, microscopic theory 0-91849
 Gruneisen and Anderson-Gruneisen parameters, interatomic forces 0-79904
 polar crystal, Frenkel exciton effective mass temp. depend., lattice displacement interactions (Chinese) 0-84429
 transition metal dihalides, layer struct., lattice dynamics, calc. 0-65177
 β -AgI, thermal expansion, 4 to 270K 0-79961
 CaF₂, anion motion at high temps., quasielastic neutron scatt. obs. 0-59715
 CaF₂, cation jump freq., isotope effect, lattice dynamical calc. 0-88357
 CaF₂, high-frequency phonon lifetimes 0-70338
 K halides, lattice dynamics in five parameter model 0-107382
 KBr, defect modes due to H⁻D⁻ pair impurities 0-59602
 KBr, transverse optic mode self-energy at 100 and 300K, expt. determ. 0-84265
 KBr:CN⁻, neutron scatt. studies of (CN)⁻ defects 0-92620
 KCl, defect modes due to H⁻D⁻ pair impurities 0-59602
 KCl_{1-x}Br_x, impurity centre local vibr., comp. depend. of spectral parameters 0-79898
 KI, perturbed by Jahn-Teller centres, lattice dynamics 0-107394
 K_{1-x}Na_xCl and K_{1-x}Rb_xCl, impurity centre local vibr., comp. depend. of spectral parameters 0-79898
 LiI, long-range three centre potentials, influence on lattice dynamics 0-96605
 LiF, γ -irrad. pure and Mg-doped, phonon scatt. and interstitial clusters 0-70254
 Li₂SO₄·H₂O, far IR spectra, H₂O flipping motion, lattice modes 0-84258
 NH₄Cl Raman spectra, pressure effects 0-97268
 PbF₂, fast ion conductor, phonon freq. distrib., temp. variation 0-84264
 SrF₂, high-frequency phonon lifetimes 0-70338
- lattice dynamics of metallic crystals**
- alkali metals, dispersion curves using second-order perturbation theory 0-79893
 alkali metals, effective ion-ion potential, compressibility and force consts. 0-70158
 alkali metals, Gruneisen parameters, influence of press. on lattice anharmonicity and temp. depend. 0-79905
 alkali metals, lattice excitation dispersion relations 0-100314
 alkali metals, phonon dispersion binding energy, compressibility, elastic consts. electron screening and Ashcroft pot. calcs. 0-65174
 BCC metals, effective valence, from phonon data, rel. to vacancy formation energies 0-79781
 BCC metals, noncentral ionic interaction 0-65172
 BCC transition metals, tensor force model, lattice dynamics 0-103428
 generalised Gruneisen tensor from solid nonlinearity parameters 0-84275
 HCP lattices, angular forces in lattice dynamics 0-107383
 metals, BCC and FCC, H-diffusion and trapping 0-70447
 pseudoharmonic effects of phonons in heat conductivity of metals 0-70326
 Ag, Debye temp., X-ray diffr. determ., anharmonic parameters of pot. function 0-100320
 Ag, lattice dynamics on Kreh's model 0-59594
 Al, Debye temp., X-ray diffr. determ., anharmonic parameters of pot. function 0-100320
 Al, film, superconducting transition temp. and lattice dynamics 0-93028
 Al, polycryst., density fluctuations, neutron scatt. anal. 0-70349
 Al, tilt boundary, $\Sigma=5$, struct. and atomic vibr., computer simulation 0-70223
 Au, fine particles, gas evaporation technique of prep., X-ray diffr. study, charact. temp. 0-75328
 Au, lattice dynamics on Kreh's model 0-59594
 Bi, optical phonon anharmonicity and melting, light scatt. study 0-60621
 CeSn₃, intermediate valence cpd., search for phonon anomalies, inelastic neutron scatt. 0-100317
 Co, Debye-Waller factor and Lindemann parameter, temp. depend., lattice dynamical model calcs. 0-59610
 Cr, lattice dynamics, improved Fiekle model 0-59598
 Cu surface, Ar ion bombardment, fast ionized recoils, thermal lattice vibr. effects 0-100737
 Cu-Al(Au) alloys, HV electron microscopy, crit. voltages depend. on comp., temp. and short-range order 0-100146
 Cu-Pt system, phonon dispersion relations, force constant disorder effect 0-84263
 Cu-Zn-Al martensite, phonon branches meas. 0-88286
 Er, Debye-Waller factor and Lindemann parameter, temp. depend., lattice dynamical model calcs. 0-59610
 Fe₂Pt, atomic thermal vibr. anisotropy, martensitic transform. model (French) 0-70355
 Hf, lattice dynamics, phonon dispersion, mode softening 0-107390
 In, lattice dynamics, pseudopot. computation (Russian) 0-92617
 Ir, phonon/wave vector dispersion relations, Debye temp., modified axial symmetric model 0-70339
 K, Gruneisen parameter, press. depend. 0-65184
 Li, anharmonicity and low temp. phase struct., neutron diffr. study 0-107105

lattice dynamics of metallic crystals continued

- Mo, lattice dynamics, improved Fiekle model 0-59598
 Na, equilibrium struct. and phys. props., pseudopot. method 0-96778
 Na, Grüneisen parameter, press. depend. 0-65184
 Nb, phonon dispersion curves, extended screened-shell model 0-96601
 Nb, pure and N doped, neutron diffuse-scatt. intensities 0-59597
 Nb-H system, local frequency spectrum, mean thermal displacement of H 0-59604
 NdH_{2.572.62}, optical vibr. spectra of H, inelastic neutron scatt. study 0-107391
 Pd-H system, local frequency spectrum, mean thermal displacement of H 0-59604
 Pd₂Sn₂ (x=0.95, y=0.05; x=3, y=1), Mossbauer spectra, high press. effects, force const. 0-84669
 Pr H_{2.8}, optical vibr. spectra of H, inelastic neutron scatt. study 0-107391
 Ru, Debye-Waller factor and Lindemann parameter, temp. depend., lattice dynamical model calcs. 0-59610
 Sb, optical phonon anharmonicity and melting, light scatt. study 0-60621
 Sc, Debye-Waller factor and Lindemann parameter, temp. depend., lattice dynamical model calcs. 0-59610
 α -Sn, lattice dynamics 0-107389
 α -Sn:^{119m}Sn, impurity lattice dynamics, Mossbauer spectra, Debye temp. 0-84262
 Ta-H system, local frequency spectrum, mean thermal displacement of H 0-59604
 Th, phonon dispersion relations, non-central electron fluid model 0-100312
 α -Ti, strain driven thermoelastic instability toward brittle fracture 0-103415
 V-H system, local frequency spectrum, mean thermal displacement of H 0-59604
 Zn, mean square displacement of atoms in cryst. lattice, rel. to sp. ht. (German) 0-79902
 Zn, optical phonon anharmonicity and melting, light scatt. study 0-60621
 Zr, BCC, phonon dispersion relations, d-electron contrib. to Cauchy discrepancy 0-92628
 β -Zr, phonon dispersion, modified Sharma-Joshi model 0-100311

lattice dynamics of molecular crystals

- acetic acid-d₃(-d₁), Fermi reson., IR spectra band profiles 0-60569
 anthracene, metastable triclinic phase 0-59452
 anthracene, orientationally disordered cryst., lattice relax. effect 0-107278
 anthracene crystal, dynamical matrix eigenvectors from Raman scatt. 0-100315
 anthracene-phenanthrene-tetracyanobenzene, CT-cryst., mini-excitons and lattice dynamics, ESR, optical and Raman spectra 0-60406
 anthracene-pyromellitic dianhydride cryst., refl. and absorpt. spectra of singlet charge transfer excitons 0-71442
 dipolar coupling and phonon symm. (Chinese) 0-103437
 IR spectral line shape and polarisation temp. depend. 0-88991
 molecular solid, intermolecular interactions, laser induced phonon probe 0-79891
 myoglobin, atomic vibr. mean square displacement, Rayleigh scatt. of Mossbauer radiation meas. (Russian) 0-100665
 naphthalene, doped, role of nonequilibrium phonons in stimulated radiation emission 0-103971
 naphthalene, surface dynamics, calc. 0-92772
 naphthalene crystal, dynamical matrix eigenvectors from Raman scatt. 0-100315
 naphthalene-d₈, cryst., phonon dispersion curves calcs., low temp. 0-96599
 one-dimensional conductor, lattice stability, phonon dispersion, Kohn anomaly 0-96603
 organic molecular crystals, use of atom-atom pots. in interpreting behaviour, book contrib. 0-84136
 organic solids, vibr. relax. and dephasing Raman spectra, review 0-88987
 ortho-para mixtures, vibr. coherence decay 0-78903
 paradichlorobenzene, NQR study of the lattice dynamics (Russian) 0-97160
 pentacene in p-terphenyl, intermolecular interactions, laser induced phonon probe 0-79891
 perylene, intermolecular interactions, laser induced phonon probe 0-79891
 sym-trioxane, phase transition, polarised Raman spectra obs. 0-84742
 symmetrised valence and relative motion coords., force const. 0-84134
 1,2,4,5-tetrachlorobenzene, mol. solid, heat pulses, phonon-induced delocalisation of trapped excited triplet states 0-89053
 thiourea, polycryst., mol. dynamics under hydrostatic press., NMR study 0-80619
 CS₂, second order Raman spectrum in condensed phase 0-93299
 Hg(CN)₂, phonon freq. anomalous press. depend., mol. struct. distortion 0-88981
 KBr_{1-x}(CN)_x, mixed mol.-cryst., coupled rot. and translational modes 0-84267
 KCN, inelastic neutron scatt. by coupled rot. and translational modes 0-79895
 γ -O₂, mol.-dynamic study of struct., dynamics 0-96467
 β -O₂, thermodynamics of mol. libration motion (Russian) 0-70328
 RbClO₃/RbBrO₃ mixed crystals, internal optic modes obs., Raman and IR reflectance spectra 0-76024

lattice energy

- see also binding energy*
 alkali halides, photoemission, energies and lineshapes 0-89119
 alkali halides, repulsive hardness parameters, crystal-independent 0-64947
 alkali metal halides, interionic repulsive short-range interaction pot., lattice energy calc. 0-96466
 alkaline earth chalcogenides, interionic repulsive short-range interaction pot., lattice energy calc. 0-96466
 ammonium Rochelle salt, thermodynamics of ferroelectric transition 0-84702
 harmonic crystals, Helmholtz free energy, vacancy defects interactions calc. by cell cluster method 0-107443
 HCP lattice, Ewald potential calc. 0-64948
 ionic crystal, repulsive short-range interaction pot., lattice energy calc. 0-96466
 metal complexes, lattice energies calc. methods 0-107099
 metal oxides, ESCA, Madelung pot. effects 0-104036

lattice energy continued

- organic molecular crystals, use of atom-atom pots. in interpreting behaviour, book contrib. 0-84136
 polyatomic ions, charge distributions, rel. with cohesive energies of ionic crystals 0-70161
 transition metal halides and oxides, cryst. field stabilisation and lattice energy 0-75201
 transition metals, many-electron systems, self-interaction corrected approach, beyond local spin density approx. 0-92844
 Wigner crystal, electrostatic energy, Fuchs method 0-79744
 Wigner solid, electrostatic energy, Fuchs calc. 0-79743
 Wigner solids and Coulomb lattices, Fuchs energy, theory 0-79745
 Al, energy and elastic constants 0-59435
 Al, stability and strength of FCC metal using Morse pot. 0-59430
 α -Al₂O₃, charge distribution determ., SCF calc., Slater-type orbitals, Madelung type const. 0-107100
 β -Al₂O₃, Madelung pot. determ. by Ewald method 0-92475
 BaTiO₃, reduction inhibition by impurity ions 0-101018
 CO₂, solid, high press. mol. libration calc. with Kihara core pots., Grüneisen parameter and lattice 0-65173
 Cr-Fe-Ni-Si, ternary phase equilibria for Cr-Fe-Ni rich portion, lattice stabilities 0-71628
 CsCl, Madelung pot. determ. by Ewald method 0-92475
 DyCl₃, vapour press. and sublimation thermodynamics, mass loss effusion meas. 0-88313
 GdCl₃, vapour press. and sublimation thermodynamics, mass loss effusion meas. 0-88313
 LaM₂-Gd, M=transition metal, correl. between g-shift and stability, EPR study 0-88874
 Li, energy and elastic constants 0-59435
 LiNbO₃, optical absorption of hole centres, polaron model 0-97314
 NaCl, Madelung pot. determ. by Ewald method 0-92475
 NiO, bulk props., initial state MO Ni₂O₄ and Ni₁₁O₁₄, cluster model, lattice and force const., photoemission and CT absorpt. spectra 0-84828
 PbMoO₄, optical absorption of hole centres, polaron model 0-97314
 ScO₂, order-disorder transition, ionic model appl. 0-107096
 TTF stacks, intermolecular energy and struct. from atom-atom potentials 0-79738
 TlCl₃, vapour press. and sublimation thermodynamics, mass loss effusion meas. 0-88313
 TiO₂, interionic repulsive short-range interaction pot., lattice energy calc. 0-96466
 YAG, optical absorption of hole centres, polaron model 0-97314
 LaM₂-Gd, M=transition metal, correl. between g-shift and stability, EPR study 0-88874
- lattice gas** *see lattice theory and statistics*
- lattice localised modes**
see also phonon-defect interactions; phonon-impurity interactions
 alkali halide:H⁻(D⁻), local modes and colour centre absorpt. bands, analogy 0-60632
 alkali halide crystals, mixed, impurity centre local vibrs., comp. depend. of spectral parameters 0-79898
 alkali halides, mixed, U-centre localised modes 0-100319
 alkali halides, V_K-centres, vibr. modes, calc. 0-84269
 anisotropic crystal, vibr. characteristics at low temp., effect of substitution impurities (Russian) 0-103439
 anisotropic crystals, long-wave vibrs. localised near dislocations 0-59603
 BCC crystal lattice containing interstitial atom in split config., reson. and localised vibrs. (Russian) 0-84268
 diamond, van Hove singularities, absorpt. and luminesc. electronic-vibr. spectra 0-70639
 dislocation wall, localised cryst. vibrs. 0-70346
 homopolary crystals, imperfect, lattice dynamics 0-59601
 impurity atom in solid, reson. fluoresc., transient spectrum, intensity, and intensity correl. 0-84777
 impurity interactions with local vibrs., effect on spectral distrib. 0-96613
 inert gas crystal, lattice vibrs. and radiative transitions of implanted ions (Russian) 0-69098
 isotropic medium, elastic vibrations localised near dislocation 0-79897
 KBr(l):D, inelastic light scattering of localised vibration of interstitial H atom in alkali halides 0-88998
 metal-H system, inelastic neutron scattering meas. of optical vibr. freq. distrib. 0-59605
 metals, BCC and FCC, H-diffusion and trapping 0-70447
 metals, dynamical props. of point defects, book contrib. 0-103317
 metals, point defect dynamic props. and diffusion controlled reactions, book 0-101674
 organic solids, vibr. relax. and dephasing Raman spectra, review 0-88987
 semiconductor, Zincblende struct., localised vibrs. due to defect complexes, Green's function study 0-79896
 semiconductors, force variation due to charged defects 0-92634
 semiconductors, localised transition metal impurities, lattice relaxation in optical transition (Polish) 0-70345
 semiconductors, shallow impurity centre spectra, isotopic shift of zero-phonon lines 0-66249
 superionic conductor, statics and local dynamics near phase transition 0-107542
 tetrahedral lattice sites, selection rules for multiphonon transitions 0-92632
 Al, tilt boundary, $\Sigma=5$, struct. and atomic vibr., computer simulation 0-70223
 β -AlO₂-(Na,Li)₂O, NMR, Raman and IR spectra, and X-ray diffr., heat treatment induced changes 0-107508
 β -Al₂O₃:NH₄⁺(Nd³⁺), polarised Raman scatt. 0-103947
 β -Al₂O₃-(Na,Li)₂O, β -Al₂O₃-(K,Li)₂O and β -Al₂O₃-(K,Sr)₂O, ionic cond. and Raman spectra 0-107509
 β -Al₂O₃-Ag₂O(K₂O)(Li₂O)(Na₂O), low-energy excitation spectra, localised modes 0-59606
 β -Al₂O₃-Ag₂O(K₂O)(Li₂O)(Na₂O)(Rb₂O), single cryst. Raman scatt., cond. mechanism and cryst. struct. 0-66209
 β -Al₂O₃-Na₂O, NMR of ²³Na, elec. quad. interaction, 185 to 419K, ion motion obs. 0-108110
 Be-Cu, thermal expansion, vibr. characteristics at low temp., effect of substitution impurities (Russian) 0-103439
 Bi₂SiO₅:Sn(Mo), Raman scatt. spectra, impurity effect 0-80795
 CdTe:Si(Cl), force variation due to charged defects 0-92634
 γ -Ce, FCC, localised vibration of interstitial H impurities 0-75322
 Fe-Ni(28 at.%), Mossbauer scattering, martensitic transformation, evidence of soft modes 0-93223

lattice localised modes continued

- Fe_{0.49}Mn_{0.01}Ti_{0.5}H_{1.5}, localised vibr., sp. ht. obs., room temp. 0-65248
 n-GaAs:Si, B, IR absorpt. spectra, reson. and localised modes 0-66172
 GaAs:Si, IR absorpt. bands, localised modes, Si-related defects 0-76054
 GaAs:Si, Li, IR absorpt., microstruct., charge compensation 0-107565
 Ge-Si alloys, imperfect homopolar crystals, lattice dynamics 0-59601
 In pnictides, mixed, impurity induced Raman scatt. spectra 0-88983
 In_{1-x}Ga_xAs, P_{1-y}As_y, far IR reflection spectrum 0-60612
 KBr, defect modes due to H⁻-D⁻ pair impurities 0-59602
 KCl, defect modes due to H⁻-D⁻ pair impurities 0-59602
 KCl:H, ENDOR and ESR study of anion sites 0-108118
 KCl_{1-x}Br_x, impurity centre local vibr., comp. depend. of spectral parameters 0-79898
 KI, perturbed by Jahn-Teller centres, lattice dynamics 0-107394
 K_{1-x}Na_xCl and K_{1-x}Rb_xCl, impurity centre local vibr., comp. depend. of spectral parameters 0-79898
 NH₄Cl, acoustic absorption by soft modes of defects 0-59584
 NaCl, inelastic light scattering of localised vibration of interstitial H atom in alkali halides 0-88998
 Nb-H system, lattice dynamics, local frequency spectrum, mean thermal displacement of H 0-59604
 Nb_{0.85}, localised D vibr., temp. depend., neutron inelastic scatt. study 0-107395
 NbH_{0.87}, localised H vibr., temp. depend., neutron inelastic scatt. study 0-107395
 Pd-H system, lattice dynamics, local frequency spectrum, mean thermal displacement of H 0-59604
 PdH₁, inelastic neutron scattering meas. of optical vibr. freq. distrib. 0-59605
 Rb₂WO₆, low lying phonon dispersion curves, neutron scatt. study 0-92622
 Si:N(P), ion implanted, IR transmission and rel. spectra study 0-108244
 SnS₂-Se₂, layer cryst., Raman active modes 0-80767
 SrO:Ni²⁺, EPR line splitting rel. to Jahn-Teller coupling and soft localised mode 0-66022
 SrTiO₃, monodomain, O-D and O-H stretching vibr., IR spectra 0-71449
 Ta-H system, lattice dynamics, local frequency spectrum, mean thermal displacement of H 0-59604
 ThC_{0.063}, cryst. struct. and lattice dynamics 0-88088
 TiC_{1.8}, H and D soln., enthalpy, solubility and mol. vibr. determ., comparison with soln. in metals and binary alloys 0-79951
 V-H system, lattice dynamics, local frequency spectrum, mean thermal displacement of H 0-59604
 α-VD_{0.7}, vibrations of interstitial D, coherent neutron scatt. 0-96612
 α-V_{0.9}O_{0.03} solid soln., impurity vibr., inelastic neutron scatt. study 0-92635

lattice mechanics *see* **lattice dynamics****lattice phonons**

- see also electron-phonon interactions; lattice dynamics of covalent crystals; lattice dynamics of ferroelectric crystals; lattice dynamics of ionic crystals; lattice dynamics of metallic crystals; lattice dynamics of molecular crystals; lattice localised modes; phonon-defect interactions; phonon dispersion relations; phonon drag; phonon-exciton interactions; phonon-impurity interactions; phonon-magnon interactions; phonon-phonon interactions; phonon-plasmon interactions; polaritons; soft modes; spin-phonon interactions; tunnelling spectra; tunnelling spectroscopy*
 acentric crystals, optical phonons, small oscillator strength meas. from frequency-angular polariton spectra 0-92629
 adsorbed monolayers, acoustic phonons, obs. method using Brillouin scatt. 0-59804
 alkali halides, photoemission, energies and lineshapes 0-89119
 alkali metal halides, elastic consts., anomalous temp. depend., phonon-lattice interaction 0-107354
 alkali metals, Grüneisen parameters, influence of press. on lattice anharmonicity and temp. depend. 0-79905
 anthracene, cryst., heat pulse propag., exciton condensation, time-resolved fluoresc. spectra 0-84771
 anthracene, nonequilibrium phonon propag. with freq. down-conversion 0-84260
 anthracene films, optical props., comparison between free and optical contact mounting 0-89079
 atomic chain, loaded, phonon model of breaking 0-70301
 benzil, cryst., excited triplet state spin-lattice relax. probabilities, temp. depend. (Russian) 0-88860
 Brillouin scattering by Stoneley waves, elasto-optic and surface ripple mechanisms 0-71435
 compressible classical Heisenberg chain, phonon dynamics and sound velocity 0-96604
 defect-free crystals, dielec. losses due to phonon system perturb. in elec. field 0-80693
 diatomic crystals, phonon spectra calc. by recursion method 0-59596
 p-dibromo-tetrafluorobenzene mol. cryst., in commensurate phase, quasi-elastic neutron scatt. 0-107386
 dielectric, regulated, thermal capacity, strong US waves effects (Russian) 0-65240
 dielectric crystal, APR and phonon spectroscopy to study paramagnetic ions 0-84634
 dielectric plate, dimensional effects in ultrasonic wave absorpt. coeff. (Russian) 0-70321
 dispersive transitions, continuum ϕ^4 equation, kink-phonon and kink-kink interactions 0-70354
 echo, recent trends in physical acoustics (Japanese) 0-79889
 electron-hole droplet phonon wind 0-107707
 ferroelectrics, H-bonded, phonon relax. mechanism 0-79906
 ferroelectrics, order-disorder, dispersive transformations, tunnelling, phonons 0-75975
 ferromagnetic, thick film, reson. transmission of EM energy via phonons 0-60382
 focusing phenomena, catastrophe theory 0-59591
 frequency crossing techniques appl. to high resolution phonon spectroscopy 0-107392
 half space layered cryst., vibr. spectrum, Brillouin zone (Russian) 0-100313
 III-V semiconductors, radiative recomb., optical evaluation review 0-60647
 impure metals at low temperatures, conductivity 0-103669
 impurity molecules in solids, vibrational relaxation, anharmonic dynamics role (Russian) 0-75323

lattice phonons continued

- impurity relaxation in nonresonance field, phonon amplification (Russian) 0-100310
 incommensurate crystals, first order Raman scatt. from unbounded phonons 0-88990
 interacting systems, predominant states and matrix elements 0-89033
 ionic crystals, centrosymmetric, stimulated excitation of second harmonic, microscopic theory 0-91849
 Ising chain of alternating spins of 1/2, and general S, appl. of transfer matrix method 0-80529
 Jahn-Teller multimode system, Ham factors 0-100446
 light scattering near phase transition pts. in pure and defect containing cryst., review 0-93361
 lithium formate, optical phonons, small oscillator strength meas. from frequency-angular polariton spectra 0-92629
 lithium thallium tartrate, sp. ht., 0.3 to 25K, second-order ferroelec. transition 0-59674
 magneto-optic Raman scattering of Raman-inactive phonon polaritons 0-91843
 magnetocrystalline anisotropy constants, phonon-induced temp. depend. 0-65858
 metals, BCC, diffusion of H₂ and its isotopes, phonon-assisted quantum-mechanical tunnelling of interstitials 0-59730
 metals, electrical and thermal resistance, influence of static atomic displacements 0-103674
 metals, melting theory for small particles, Helmholtz free energy 0-59629
 metals, phonon-phonon scatt. role in lattice thermal cond., phonon drag, elec. cond. 0-70483
 metals, struct. of d²I/dV² characts. of point contacts 0-96975
 metals, surface positronium formation, stopping distance, positron-phonon interactions 0-96582
 molecular crystal IR spectral line shape and polarisation temp. depend. 0-88991
 molecular crystals, dipolar coupling and phonon symm. (Chinese) 0-103437
 molecular solid, intermolecular interactions, laser induced phonon probe 0-79891
 β-Na₂O-Al₂O₃, low temp. ultrasonic vel. meas., temp. depend. 0-79885
 naphthalene, doped, role of nonequilibrium phonons in stimulated radiation emission 0-103971
 naphthalene, external mode one-density states, low freq. Raman scatt. spectra (French) 0-76012
 narrow gap semiconductors, recombination mechanisms, review 0-96905
 narrow-gap ferroelectric, phase transition due to strong mag. field 0-103924
 neutron scattering from equilibrium and non-equilibrium phonons, excitons and polaritons 0-84032
 non-equilibrium phonon distrib., in cryst., spectral line shape theory 0-60530
 nondegenerate semiconductor, thermomagnetic phenomena in quantising mag. field (Russian) 0-60014
 one-component plasma, crystallized, dynamics and energy, self-consistent-phonon theory 0-107384
 optical detection of acoustic phonons at THz freqs. 0-75320
 oxide crystals, Fourier transform IR spectroscopy of vibr. states at high temp. 0-97256
 paradichlorobenzene, NQR study of the lattice dynamics (Russian) 0-97160
 pentacene in p-terphenyl, intermolecular interactions, laser induced phonon probe 0-79891
 perylene, intermolecular interactions, laser induced phonon probe 0-79891
 piezoelectric powders, phonon echoes and long-time storage (Japanese) 0-70330
 porous glass:In, effect of press. on transition temp. 0-97027
 quartz, Fourier transform IR spectroscopy of vibr. states at high temp. 0-97256
 α-quartz, high-frequency phonon lifetimes 0-70338
 Raman scatt. cross sections in simple solids 0-93334
 Raman spectra, vibr. anal. 0-93312
 reorienting or tunnelling molecular groups in solids, symmetry of rotor part of rotor-phonon interaction 0-84114
 ruby, phonon spectrum, thermal pulses under diffuse phonon propagation conditions 0-103434
 ruby R₁, zero phonon line, resonance fluoresc. meas. 0-89055
 sapphire, optical detection of acoustic phonons at THz freqs. 0-75320
 β-Sb₂O₃, Raman spectra, vibr. anal. 0-93312
 semiconductor, nonequilibrium acoustic phonons, generation by interband light absorption 0-96607
 semiconductor, phonon conduction and relaxation times 0-107585
 semiconductor, possible phonon generation by EM wave 0-96606
 semiconductors, degenerate, resonance Raman scatt., Green's function method 0-80781
 semiconductors, electron-hole drop formation, phonon wind influence (Russian) 0-92825
 semiconductors, electron-phonon interactions, combined phonon resonance (Russian) 0-75321
 semiconductors, optical props. due to phonons, book contrib. 0-80805
 semiconductors, polar, resonance electron-phonon Raman scatt., cross-section oscills. 0-60598
 semiconductors, van Hove critical point region, electron-phonon interactions, dispersion law 0-70344
 sine-Gordon system with winding-number density, low temp. soliton gas phenomenology 0-105589
 solids, acoustic wave emission, absorpt. and propag. in THz range 0-65164
 spectroscopy, HF⁺, using supercond. tunnel junctions 0-65178
 strongly coupled Jahn-Teller system, cluster model for optical absorption spectrum 0-89034
 structural phase transitions, crit. dynamics and quasi-elastic scatt. 0-92641
 superconducting transition critical temperature, BCS theory, phonon spectra, review (Spanish) 0-84535
 superconducting tunnel junction, nonequilibrium phonon effect on supercond. states with 2 coexisting energy gaps 0-84561
 superconductivity and phonons, review 0-84543
 superionic conductors, theoretical models, review 0-107465
 surface, adsorbed atoms thermal desorption, one dimens. microscopic model, weak binding case 0-96729
 sym-trioxane, phase transition, polarised Raman spectra obs. 0-84742

lattice phonons continued

- TCNQ salt, decamethylferrocenium, monomeric and dimeric, optical and EELS study 0-100660
 tetrahedral lattice sites, selection rules for multiphonon transitions 0-92632
 TGS, ferroelec. single crystal, low freq. nonlinear effects 0-84490
 TGS and deuterated cpd., ferroelec. US relax. time constant 0-84257
 thermal conductivity, anomalous temp. behaviour near structural phase transition (*Russian*) 0-75394
 thermal desorption and dissociation catalyzed by a solid surface 0-108734
 thin optical irradiated superconductors, phonon spectrum and phonon temp. definition 0-93037
 transition metal dihalides, layer struct., lattice dynamics, calc. 0-65177
 transition metals, paramagnetic susceptibility, phonon instability, mixed localised-collective electron states 0-103811
 Ag_2AsS_3 , and Ag_2SbS_3 , Raman spectra obs. of low-temp. phases 0-93327
 Ag_2O , exciton luminesc. spectra, mag. field influence 0-80860
 Al, Brillouin spectra, light scatt. cross section for surface ripples 0-71434
 Al, film, superconducting transition temp. and lattice dynamics 0-93028
 Al, metallic, phonon freq., binding energy, compressibility, elastic const. and energy band gap calcs., linear pot. 0-88284
 Al, polycryst., density fluctuations, neutron scatt. anal. 0-70349
 $\text{AlGa}_{1-x}\text{As-GaAs}$ heterostructure, quantum-well, hot electrons and phonons 0-84505
 $\text{AlGa}_{1-x}\text{As-GaAs}$ quantum-well heterostruct., exciton in recomb. 0-103990
 AlN, luminesc. excitation spectrum and band struct. 0-84783
 Al_2O_3 , corundum, Fourier transform IR spectroscopy of vibr. states at high temp. 0-97256
 Al_2O_3 , high-frequency phonon lifetimes 0-70338
 $\alpha\text{-Al}_2\text{O}_3$, polarised luminescence in neutron- and proton-irradiated single crystals 0-66271
 $\alpha\text{-Al}_2\text{O}_3$, single crystal transmission and reflectance IR phonon spectra, polariton dispersion 0-66170
 $\text{Al}_2\text{O}_3\text{:Cr}^{3+}$, HF phonon spectroscopy using supercond. tunnel junctions 0-65178
 $\text{Al}_2\text{O}_3\text{:Cr}^{3+}$, ruby, reson. scatt. and trapping of 29 cm^{-1} acoustic phonons 0-93403
 $\beta\text{-Al}_2\text{O}_3\text{:NH}_4^+(\text{Nd}^{4+})$, polarised Raman scatt. 0-103947
 $\text{Al}_2\text{O}_3\text{:V}^{3+}(\text{Fe}^{2+})$, hyperfine splitting and magnetoelastic const., freq. crossing spectroscopy 0-107392
 $\text{As}_2\text{Sb}_{1-x}\text{SI}$ mixed crystals, phonon coupling, ferroelectric phase transition, Raman study 0-108165
 As_2Se_3 , cryst., electroabsorption on indirect gap 0-80812
 Au, tilt boundary, $\Sigma=11$, simulated and observed struct., vibr. of individual atoms at grain boundary 0-88167
 BaF_2 , F^- interstitial and substitutional trivalent cations, phonon reson. and IR absorpt. 0-84752
 BaF_2 , strain induced splitting and oscillator strength anisotropy of IR transverse optic phonon 0-92625
 $\text{Bi}_{1-x}\text{Sb}_x$, magnetophonon effect on hot electrons (*Russian*) 0-107814
 CS_2 , second order Raman spectrum in condensed phase 0-93299
 CaF_2 , high-frequency phonon lifetimes 0-70338
 CaF_2 , optical detection of acoustic phonons at THz freqs. 0-75320
 CaF_2 , strain induced splitting and oscillator strength anisotropy of IR transverse optic phonon 0-92625
 $\text{CaF}_2\text{:Eu}^{2+}$, Sm^{3+} , relaxed resonance acoustic phonons in vibronic anti-Stokes luminescence (*Russian*) 0-93404
 CdCrS_4 , ferromag. semicond., IR refl. spectra, phonon props. and dielec. function 0-66191
 CdGa_2S_4 , IR refl. spectra 0-60604
 $\text{Cd}_{1-x}\text{Mn}_x\text{Te}$ mixed crystals, Raman spectra 0-103961
 CdS , stimulated Mandelstam-Brillouin scatt. on acoustic phonon amplification (*Russian*) 0-71437
 CeH_3 , phonon features in IR and Raman spectra 0-93310
 CoCO_3 , light scatt. from magnons and phonons excited by microwave pumping 0-66213
 CrCl_3 , electronic struct. and struct. phase transition 0-59644
 CsCoBr_3 , 1D Ising antiferromagnet, spin dependent Raman scattering from phonons and electronic excitations 0-103948
 CsCoBr_3 , quasi 1D Ising antiferromag., polarised Raman scatt. from mag. excitations 0-66182
 CsNiF_3 , 1D ferromag., optical absorption and spin dynamics 0-71417
 Cu-Be solid solutions, local oscil. conc. depend., impurity bands (*Russian*) 0-75318
 Cu_2O , exciton luminesc. spectra, mag. field influence 0-80860
 Cu_2VS_4 , Raman linewidth of A_1 mode under high press., reson. effects 0-108210
 Dy_2S_3 , vibr. spectra, factor-group anal. 0-80793
 DyVO_4 , Jahn-Teller crystal, deform. induced transitions, elastic and dielectric characts. (*Russian*) 0-80726
 EuTe , mag. 'Bragg' scatt. obs. through Raman scatt. 0-66179
 FeF_2 , dielectric properties, IR spectra, lattice dynamics (*French*) 0-76026
 GaAs , Brillouin spectra, light scatt. cross section for surface ripples 0-71434
 GaAs , Raman scattering from nonequilibrium LO phonons with picosecond resolution 0-80779
 GaAs:Cr , zero-phonon struct. in Cr^{2+} ($3d^4$) optical absorption 0-60640
 GaAs-AlAs superlattice, folded acoustic phonons obs., Raman scatt. 0-88996
 GaAs -based mixed cryst. form. by ion beam synthesis, vibr. anal. 0-103376
 $\text{GaAs}_{1-x}\text{P}_x$, indirect-gap, evidence for exciton localization by alloy fluctuations, photolum. 0-66276
 $\text{Ga}_{1-x}\text{In}_x\text{As}$, IR reflectivity, cluster effect on optical phonons 0-97259
 GaP , light scatt. by LO phonons, high-resolution study 0-80798
 p-GaP , spin-flip Raman scattering, review 0-108209
 GaP , thermal expansion below room temp., press. depend. of elastic stiffness const. and phonon frequencies 0-79963
 GaS , infrared optical props., polarisation depend., vibr. modes 0-100658
 GaS(Se) , layer compound, long-wavelength phonons and elastic const. 0-65175
 GaSb based eutectics, thermal cond. and diffusivity, 300-700K, phonon mechanism 0-103526
 GaSe films, optical props. at lattice vibr. freqs., IR and Raman spectra 0-60696
 GaSe , lattice dynamics and elastic props., Born-von Karman model study 0-70337
 $\alpha\text{-GaSe}$, long-wavelength lattice vibr. 0-92631

lattice phonons continued

- $\alpha\text{-GaSe}$, Raman scatt., hydrostatic press. effect 0-84745
 $\text{GaSe}_{1-x}\text{Te}_x$, Raman scatt., optical phonons and phase transition 0-66202
 $\text{GaSe}_{1-x}\text{Te}_x$, Raman spectra, phonon freq. 0-97286
 $\alpha\text{-GaTe}$, single cryst., Raman scatt. 0-60599
 GaI , Brillouin spectra, light scatt. cross section for surface ripples 0-71434
 Ge , electron-hole drop drag, interaction with thermal pulses 0-103631
 Ge , electron-hole droplet cloud kinetics, thermalisation phonons 0-88483
 Ge , electron-hole droplets distrib. and phonon wind 0-103629
 Ge , mag. field luminesc. lifetime, quantum oscil., phonon wind effects 0-93385
 Ge , thermal conductivity of semiconductors, quantum acoustical method, thermal phonon lifetimes 0-65312
 $\text{Ge}_{1-x}\text{Sn}_x$, impurity lattice dynamics, Mossbauer spectra, Debye temp. 0-84262
 Ge:P , charact. temp. and lattice thermal cond. 0-59743
 Ge-Si alloys, hot-pressed, fine-grained, boundary scatt. of phonons, lattice thermal cond. 0-107583
 Ge-Si alloys, hot-pressed, fine-grained, boundary scatt. of phonons, theory 0-107584
 GeSe_2 , multimode layer cryst., far IR transmission and reflection spectrosc., comparative merits 0-76019
 Hg(CN)_2 , phonon freq. anomalous press. depend., mol. struct. distortion 0-88981
 Hg_2Cl_2 , neutron and Raman scatt. studies, ferroelastic transitions 0-76015
 In pnictides, mixed, impurity induced Raman scatt. spectra 0-88983
 $\text{In}_{1-x}\text{Ga}_x\text{P}_{1-x}\text{As}_x\text{In}_{1-x}\text{Ga}_x\text{P}_{1-x}\text{As}_x$, visible spectrum multiple-quantum-well heterostruct. lasers 0-106537
 InP , depend. of phonon spectrum on hydrostatic press., Raman spectra 0-93315
 InP , model for $\sim 1.10\text{ eV}$ emission band 0-66289
 InSb based eutectics, thermal cond. and diffusivity, 300-700K, phonon mechanism 0-103526
 InSb , spin-flip Raman scattering, review 0-108209
 InSe , layer compound, long-wavelength phonons and elastic const. 0-65175
 K halides, spin-lattice relax. of O_2^- centre 0-88863
 KAgI_3 , superionic phase transition, dynamical and crit. pt. props. 0-107535
 $\text{KBrl}_x(\text{CN})_x$, mixed mol. cryst., coupled rot. and translational modes 0-84267
 KBr(I) , inelastic light scattering of localised vibration of interstitial H atom in alkali halides 0-88998
 KCN , inelastic neutron scatt. by coupled rot. and translational modes 0-79895
 KCN , Raman diffusion spectra, IR absorpt. in phases II and III (*French*) 0-84741
 $\text{KD}_2\text{H}_{2(1-x)}\text{PO}_4$ crystals, $0 < x < 0.98$, light scatt. by polaritons 0-96802
 $\text{KMg}(\text{SeO}_3)_2$, phase transition, neutron scatt. study 0-75351
 $\text{KMgF}_2\text{:Cr}^{3+}$, HF phonon spectroscopy using supercond. tunnel junctions 0-65178
 $\text{KMgF}_2\text{:Ni}^{2+}$, acoustic Faraday and Cotton-Mouton effects, theory 0-65987
 KMnF_3 , critical dynamics of sound 0-103424
 LaF_3 , high-frequency phonon lifetimes 0-70338
 La_2S_3 , vibr. spectra, factor-group anal. 0-80793
 Li , phonon limited resistivity struct. depend., Umklapp scatt., elastic const. 0-88532
 LiNbO_3 , parametric phonon echo obs. 0-59588
 $\text{MgO:Cr}^{2+}(\text{Mn}^{3+})(\text{V}^{3+})$, HF phonon spectroscopy using supercond. tunnel junctions 0-65178
 MgO:Ni^{2+} , near IR luminesc. from isolated and exchange-coupled Ni^{2+} ion pairs, temp. depend. 0-93382
 $\text{Mn}_2\text{Cd}_{1-x}\text{Te}$, lattice vibrs., Raman and IR spectra meas. 0-93311
 $\text{Mn}_2\text{Cd}_{1-x}\text{Te}$, phonons, Raman scatt. and IR absorpt. meas. (*French*) 0-92775
 NH_4AgI_3 , superionic phase transition, dynamical and crit. pt. props. 0-107535
 $(\text{NH}_4)_2\text{M}(\text{SO}_4)_2 \cdot 6\text{H}_2\text{O}$, $\text{M}=\text{Ni, Co, Mg}$, IR spectra 0-97280
 Na , equilibrium struct. and phys. props., pseudopot. method 0-96778
 Na , phonon limited resistivity struct. depend., Umklapp scatt., elastic const. 0-88532
 NaCN , Raman diffusion spectra, IR absorpt. in phases II and III (*French*) 0-84741
 Na^{15}N , $^{14}\text{N}_2$, O_3 mixed crystal, Raman spectra determ. of phonon density of states (*Russian*) 0-93313
 NaNO_2 , incommensurate antiferroelec. phase, Brillouin scatt. freq. shift 0-93349
 $\text{NbS}_2\text{Cl}_2(\text{Br}_2)(\text{I}_2)$, absorpt. edge spectrum, fine struct. 0-66219
 NbSe_2 (2H), Raman scatt. by supercond. gap excitations, coupling to CDWs 0-103956
 $\text{NdH}_{2.572.62}$, optical vibr. spectra of H, inelastic neutron scatt. study 0-107391
 Nd_2S_3 , vibr. spectra, factor-group anal. 0-80793
 Ni , Brillouin spectra, light scatt. cross section for surface ripples 0-71434
 Ni , phonon density of states determ. from thermodynamic functions 0-96616
 $\text{NiS}_{1-x}\text{Se}_x$, first-order Raman scattering 0-108206
 PbF_2 , US vel. near press. induced cubic-to-orthorhombic transform. 0-103476
 $\text{Pb}_{1-x}\text{Sn}_x\text{Te}$, lattice and electronic props. and g-value 0-80161
 Pd , phonon density of states determ. from thermodynamic functions 0-96616
 PdH , superconducting transition critical temperature, BCS theory, phonon spectra (*Spanish*) 0-84535
 PdH_x , local, soft modes, superconductivity thermal neutron inelastic scatt. (*Chinese*) 0-70331
 Pr H_2 , optical vibr. spectra of H, inelastic neutron scatt. study 0-107391
 Pt , phonon density of states determ. from thermodynamic functions 0-96616
 Rb halides, spin lattice relaxation meas. of O_2^- centre 0-88863
 RbAgI_3 , superionic phase transition, dynamical and crit. pt. props. 0-107535
 Si , dense plasma dynamics during pulsed laser annealing, carrier density, recombination 0-84479
 Si , phonon-assisted Auger recomb., direct calc. of overlap integrals 0-107808
 $\text{n}^+\text{nn}^+\text{Si}$ planar device, hot electron flicker noise at 78K 0-103732

impurity and defect absorption spectra of solids

- see also *impurity and defect absorption spectra of inorganic solids*
 anthracene:tetracene, electronic absorpt. spectrum, host-cryst. field effect 0-100669
 antiferromagnet, IR absorption on impurity excitations near upper edge of spin-wave band 0-80829
 atom pairs in solids, cooperative two-photon absorpt. lineshape 0-84706
 benzene cryst., electron irradi., phenylcyclohexadienyl radical form., absorpt. and fluoresc. spectra study 0-89035
 biphenyl:tetracene, electronic absorpt. spectrum, host-cryst. field effect 0-100669
 carbazole:tetracene, electronic absorpt. spectrum, host-cryst. field effect 0-100669
 o-chlorobenzoic acid: Nd^{3+} (Pr^{3+}) solid, vibrational spectra 0-84758
 disordered crystal, biphonon spectra, light absorpt. coeff. and density of states, CPA calc. 0-84271
 dispersive medium, many-photon scatt. of light by impurity centres 0-60622
 electron-phonon coupling from structured optical spectra, review 0-89038
 naphthalene:tetracene, electronic absorpt. spectrum, host-cryst. field effect 0-100669
 naphthalene molecule in durene and xylene crystals, vibronic interactions 0-84755
 naphthalene- β -naphthol, concentration effects in exciton absorption region 0-108241
 non-equilibrium phonon distrib., in cryst., spectral line shape theory 0-60530
 optical fibres, glass and plastic, neutron irradiated, optical absorpt. spectra 0.7 to 1.1 μm 0-58762
 organic molecular crystal, doped, two-particle electronic excitation, optical cooperative excitation 0-93368
 polarised light absorpt. spectra, forbidden transitions and discrete saturation 0-71464
 pressure effects of optical spectra of impurity centers in solids 0-108231
 quinzarin in alcohol glasses, electron-phonon coupling, photochemical hole burning 0-97265
 semiconductor, deep impurity centres, elastic light scattering 0-97315
 semiconductor, donor-acceptor system, weak wave absorpt. in reson. laser radiation field 0-66252
 semiconductor, doped, metal-insulator transition, anal. 0-88478
 semiconductor, interimpurity absorption in strong EM wave field (*Russian*) 0-60631
 semiconductors, localised transition metal impurities, lattice relaxation in optical transition (*Polish*) 0-70345
 semiconductors, shallow impurity centre spectra, isotopic shift of zero-phonon lines 0-66249
 strongly coupled Jahn-Teller system, cluster model for optical absorption spectrum 0-89034
 TGS, effect of Fe^{3+} admixture on phys. props. 0-76052

impurity clustering see *segregation***impurity-defect interactions**

- see also *impurity-dislocation interactions; impurity-vacancy interactions*
 homopolar crystals, imperfect, lattice dynamics 0-59601
 metal, electron irradi., selfinterstitial atomic defect interaction radii, recovery expts. and error sources 0-65049
 metals, μ^+ diffusion, LAMPP results 0-71285
 non-metallic crystals, electric field influence on defect creation mechanism 0-70251
 p-Ge: Au, Sb, Hg (Zn), radiation-defect form., Au influence 0-92911
 LiF: OH, Mg, γ -irrad. induced oxyhydride complexes 0-92555
 MgO: Li, mech. deformed crystals, imprinting of slip bands using Li impurities 0-59473
 Si, grain boundary elec. props./impurity correl. using surface anal. of multigrained samples by SIMS and AES 0-79816
 Si, neutron and electron bombard., radiation defect recomb., photoelec. props. meas. 0-60039
 V, electron-irradiated, positron annihilation study 0-70259

impurity-dislocation interactions

- see also *dislocation locking; dislocation pinning*
 charged impurity influence on dislocation motion in cryst. 0-103333
 dislocation percolation through absolute obstacles in impurity crystals (*Russian*) 0-70196
 gettering of impurities, by intentional double diffusion 0-75383
 metals, reversible H embrittlement 0-104292
 Al dilute alloys, cold worked, internal friction peaks 0-97520
 Al-Ag (7.27 wt.%), peculiarities exhibited during fatigue loading (*Chinese*) 0-71723
 Cd, single crystals, plasticity study during deformation by twisting (*Russian*) 0-93597
 Fe, pure, dislocation relaxation peaks under low temp. deform. (*French*) 0-100867
 GaAs: Sn (Te), epitaxial film, influence of impurities on stacking fault energy 0-103371
 Ge, heavily doped, microcreep breakdown 0-97549
 Nb-O (N), dislocation pinning, impurity interactions, strengthening (*Russian*) 0-92532
 Pd-H (D), elastic energy dissipation peak 0-60905
 Si, crystal defects and impurities interaction obs. by electron microscopic methods 0-65003
 Si, heavily doped, microcreep breakdown 0-97549
 Si(111): Pb ion implanted amorphous layers, recrystallisation, impurity out-diffusion model (*Chinese*) 0-88363
 Ta-O (N), dislocation pinning, impurity interactions, strengthening (*Russian*) 0-92532
 V-O, dislocation pinning, impurity interactions, strengthening (*Russian*) 0-92532
 Y, plastic deformation props., deformation ageing, plastic flow, dislocation-impurity interactions (*Russian*) 0-66582

impurity distribution

- see also *doping profiles; segregation*
 alloy melt, impurity conc. field model, growth by Czochralski method (*Russian*) 0-75191
 alloys, ion-implanted, integral Gaussian profile determ. method 0-107313
 alloys, surface composition after fabrication by SIMS 0-65351
 calcite, luminescence spectral anal. of polycyclic aromatic hydrocarbon impurities 0-71483
 composite material, matrix impurity distrib. in melt crystallisation (*Russian*) 0-100277
 corundum, defect cryst. struct. study 0-103316
 crystal growth, cylindrical pores growth, numerical calcs. 0-92471

impurity distribution continued

- crystal growth, modified Czochralski method, variations of impurity distrib. 0-88193
 Czochralski growth, fluctuating growth rates effect on segregation, back-melting 0-59413
 depth profiling, dynamic range of 10^6 0-107302
 emerald, artificial single crystal, distrib. of Cr^{3+} impurity 0-59505
 epitaxial films, condensed from vapour or molecular ion beams, impurity distrib. 0-65032
 epitaxial films, model for autodoping lateral variation 0-103595
 Fick's equations solutions for impurity diffusion, dislocations, interstitials, vacancies 0-70469
 glass, diffusion coefficient equation 0-103521
 graphite, chemisorption of O_2 , influence of Fe as impurity 0-96732
 III-V compounds, surface comp., low-energy ion scatt. spectrometry 0-100382
 III-V semiconductors, during epitaxial growth from liq. phase 0-88443
 impurity relaxation in nonresonance field, phonon amplification (*Russian*) 0-100310
 ion beam induced atomic transport and conc. profiles 0-59723
 ion implantation, range parameters, nucl. stopping power, ion backscatt. determ. 0-88232
 metal-semiconductor contacts with thin interfacial films 0-96969
 metals and alloys, segregation studies by imaging atom probe microscopy 0-66911
 metals and alloys, trace element detection by atom probe microanalysis 0-66910
 quartz, synthetic, Al centres conc. and anomalous pleochroism depend. on crystn. parameters 0-107311
 quartz glass, Ge and B dopants, OH impurities, preform material and fibre optic waveguide struct. 0-64173
 semiconductor, doping reduction using zone recrystn. with temp. gradient 0-104062
 semiconductor, ion implanted, pulsed laser and electron beam annealing comparison 0-92547
 semiconductor, lightly doped compensated, electric fields at impurity centres (*Russian*) 0-84198
 semiconductors, charge neutrality produced by impurity diffusion 0-59724
 steel, Cr-Mo, ferritic, grain boundary segregation, X-ray microanal. by STEM 0-66740
 steel, grain boundary P segregation, effect after quenching and tempering (*Russian*) 0-81145
 three-phase system, diffusion laws 0-107310
 vicinal faces grown from dil. soln., impurity incorporation, interface model 0-84127
 Ag-In melt system, conc. depend. of component and impurity diffusion coeffs., radioactive isotope method (*Russian*) 0-107454
 Al: Ga, pulsed electron-beam annealing, lattice site location improvement 0-107303
 Al: Sb (Zn), ion implanted electron beam annealing, ion backscatt. and TEM meas. 0-59500
 Al-Bi (Cd) (Pb)-Ti, containing low-melting pt. inclusions, mech. props. 0-93632
 Al₂Ga_{1-x}P, proportional ingredient content determ. by X-ray fluoroscopy 0-97747
 Al₂O₃ anodic films, H conc. profiles meas. 0-75261
 Be, ion-implanted, impurity lattice location, channelling meas., Monte Carlo calc. 0-107291
 Bi and Bi-Sb (12 at.%), cryst. growth from melt, impurity distrib. control by electrotransfer method (*Russian*) 0-66418
 CaF₂: Eu, CaF₂: Eu, Mn (Gd), single crystal predisintegration phenomena, SEM cathodolum. obs. 0-59502
 CaF₂: Mn, CaF₂: Eu, Mn, single crystal predisintegration phenomena, SEM cathodolum. obs. 0-59502
 CdS, charged impurity centres, drift during passage of photocurrent 0-70767
 Cu, high purity, identification of imperfections by thermal resistivity meas. 0-59951
 Cu single crystals Au ion implanted, pulsed electron beam irradi. 0-65019
 Cu-Be solid solutions, local oscill. conc. depend., impurity bands (*Russian*) 0-75318
 EuTe, high-temperature evaporation and reactivity 0-103469
 Fe, cast hypoeutectic, Ce distrib. in graphite grains 0-100279
 Fe, segregation of impurities, physico-chemical aspects (*Czech*) 0-60866
 Fe-Ni, grain boundary segregation, X-ray microanal. by STEM 0-66740
 Fe-Ti (0.15 wt.%), Ti distrib., segregation, FIM anal. 0-84200
 GaAs epitaxial layers, surface impurity gradients, Schottky barrier capacitance meas. 0-70782
 GaAs: B, incorporation of B during growth 0-93471
 GaAs: Cr, Cr distrib. and heat-treatment migration studies by SIMS 0-107305
 GaAs: Cr, redistrib. of Cr during laser annealing 0-88192
 GaAs: Cr, semi-insulating, Cr redistrib. during thermal annealing as function of encapsulant and implant fluence 0-84199
 GaAs: Cr, semi-insulating, damage gettering of Cr during annealing of Cr and S implants 0-107304
 GaAs: Si p-n junction LED, electroluminesc. efficiency 0-71491
 GaAs: Sn (Te), epitaxial film, influence of impurities on stacking fault energy 0-103371
 Ge, high-doped single crystals, impurity atom distrib. changes around growth dislocations in thermocyclic treatment (*Russian*) 0-107307
 Ge p^+n^- structures, charge transport under impurity freezeout conditions 0-92965
 In₂Al_{1-x}P, proportional ingredient content determ. by X-ray fluoroscopy 0-97747
 n-InAs, photoelectric props., inhomogeneous impurity distrib. 0-107867
 In₂Ga_{1-x}P, proportional ingredient content determ. by X-ray fluoroscopy 0-97747
 InP, Zn diffused single-crystal, substitutional dopant and hole conc. meas. 0-75260
 InSb, during epitaxial growth from liq. phase 0-88443
 InSb, undoped and Te-doped, anomalous impurity segregation, Hall and mass spectrum meas. (*Chinese*) 0-59501
 InSb: Cr, Zn and InSb: Zn, impurity centre behaviour, impurity conc. and Hall coeff. meas. 0-65490
 InSb: Te, cryst. growth from melt, pulling method, US effects on facet growth 0-76169
 KCl: Pb, impurity distrib., light scatt. and microhardness study, heat treatment 0-96562

impurity distribution continued

- LiF, alkali ion implantation, migration, segregation, effect on optical props. 0-100269
 $\text{Li}_2\text{O-Al}_2\text{O}_3\text{-SiO}_2\text{-Cd}^+$, glass, ESR study 0-103879
 Mo, D and ^3He trapping and mutual replacement 0-59493
 Mo films, sputtered from cylindrical-post magnetron with Ne, Ar, Kr and Xe, compressive stress and presence of inert-gas obs. 0-80140
 $\text{NH}_4\text{H}_2\text{PO}_4\text{-}^{57}\text{Fe}$, Mossbauer study, Fe^{3+} effect in habit 0-100627
 Nb, O impurity distrib. determ. by neutron activation anal. (*Russian*) 0-70243
 Pb-Au, interstitial and substitutional distrib. 0-84204
 $\text{PbF}_2\text{-Mn}$, mag. tagging of ion diffusion, ^{19}F NMR meas. 0-108106
 Pd-H, Mossbauer study of local environment of substitutional Co and Fe impurities 0-60475
 Pt-Si:As, silicide form. during laser irradi., p-n junctions and ohmic contacts 0-84397
 Sb_2S_3 spherulite crystals, direct lattice resolution obs. of defect struct. 0-107255
 ScH, Er, proton distrib. and site energies, ESR meas. 0-59509
 Si, amorphous, ion implantation method, B and P ions 0-100274
 Si, amorphous film, EELS microanalysis 0-100722
 Si, annealing, using laser pulses, impurity incorporation at melt-cryst. interface 0-59504
 Si, crystal growth, for electronic devices 0-66419
 p-Si, Czochralski grown, microdistrib. of O, SEM and spreading resist. obs. 0-79830
 Si diode, impurity profiles, scanning electron microprobe anal. 0-79832
 Si, doping impurity distrib., during cryst. growth by Czochralski method (*Russian*) 0-100276
 Si, EFG ribbon, characterisation by ion beam tech. 0-79833
 Si, effect of disorder on H content 0-75258
 Si epitaxial layers, grown in vac. at low temps. P and Sb doping 0-88189
 Si epitaxial layers, vacuum deposited, conditions for impurity migration from B, P, Sb doped sources (*Russian*) 0-107570
 Si, impurity content characterisation, exciton luminesc. 0-60653
 Si ion-implanted laser-annealed solar cells 0-93881
 Si large grain films on metallurgical Si substrates, metallic impurity distrib. and conc. 0-61357
 Si, melt grown crystals, impurity incorporation, calcs. 0-79718
 Si n/n^+ epitaxial layers, anomalies of Sb distrib. 0-65035
 Si ribbon, EFG, C contaminant conc. determ. by nuclear techniques and SIMS 0-59506
 Si ribbons grown by capillary action shaping technique, surface quality and impurity distrib. 0-108343
 Si single crystal ingot growth from metallurgical grade Si, inhomogeneities 0-59416
 Si surface, ion bombardment enhanced mixing of Ag layers, Rutherford backscatt. meas. 0-65034
 Si:Al(Ga), O_2 diffusion, conc. profile meas. 0-79990
 Si:As, shallow junctions by high-dose implants 0-96694
 Si:As, solid solubility and thermal behaviour of metastable 0-75359
 Si:Au, P-induced point defects influence on Au gettering mechanism 0-65030
 Si:B, implanted laser annealed, lattice strain, X-ray study 0-96554
 Si:B, ion implanted, structure defects formation and behaviour under annealing in various ambients 0-65033
 Si:B ion implanted, strain profiles from X-ray rocking curves 0-107290
 Si:BF $^+$, ion implantation appl. in semicond. device production 0-103383
 Si:B(Be)(Li) ion implanted, channelling and random equivalent depth distrib. 0-100293
 Si:B(P), ion implanted crystalline and amorphous laser annealing 0-97509
 Si:Bi, ion-implanted, solid phase epitaxial growth during annealing, super-saturated solid soln. form. 0-103384
 a-Si:H film, glow discharge deposited, H profiles, doping level 0-84202
 Si:In, clustering and precipitation, time-dependent perturbed ang. correlation meas. 0-65234
 Si:O, Czochralski crystal, oxygen striation and thermally induced microdefects 0-100275
 Si:Pt, implanted and laser annealed, segregation and increased dopant solubility 0-65016
 Si:Sb, ion implanted, Sb diffusion during oxidation, snow-plough effect 0-88366
 Si:Te, laser melting, surface Te atom accumulation, profiles 0-100258
 $\text{SiO}_2\text{-Na}_2\text{O-CaO-MgO}$ float glass, surface SnO_2 distrib., ellipsometry and XPS study 0-84346
 $\text{SiO}_2\text{-P}_2\text{O}_5$ glass film, CVD, P conc. profile by etch rate technique 0-96450
 Ti:D, ion implanted, depth profiles, temp. depend. 0-100270
 W: ^3He , implanted ion positions, determ. using mol. deuteron beam 0-70240
 $\text{YFe}_{3-x}\text{Al}_x\text{O}_{12}$, impurity redistrib. kinetics, temp. depend., vacancy effects 0-75263
 $\text{Y}_3\text{Fe}_{5-x}\text{Al}_x\text{O}_{12}$, mixed garnet, cation distrib., temp. depend., magnetisation study 0-79831
 $\text{YFe}_{3-x}\text{Ga}_x\text{O}_{12}$, impurity redistrib. kinetics, temp. depend., vacancy effects 0-75263
 $\text{Y}_3\text{Fe}_{5-x}\text{Ga}_x\text{O}_{12}$, mixed garnet, cation distrib., temp. depend., magnetisation study 0-79831
 YH, Er, proton distrib. and site energies, ESR meas. 0-59509
 YbTe, high-temperature evaporation and reactivity 0-103469
 ZnS ion beam etching, topographic changes, amorphisation, luminescence study 0-76078

impurity electron states

- see also A-centres; Anderson model; charge compensation; deep levels; electron traps; heavily doped semiconductors; impurity scattering; OH $^-$ -centres; U-centres; Z-centres
 acceptors, randomly distributed, direct energy transfer via exchange from excited donor 0-65483
 adatom density of states, impurity atom effects 0-92958
 alkali halides, polarization, photoinduced, rel. to exchange between vacancy and impurity 0-59914
 Anderson model, impurity pair interactions, local moment form., var. method 0-92854
 Anderson model, non-orthogonal elec. resist. 0-59947
 bulk trap energetic distribution props., space charge limited current meas. use 0-80293
 CdS, green edge luminescence spectrum, temp. depend. 0-108274
 diamond, ion-doped with Li electron transport 0-92917

impurity electron states continued

- diamond, van Hove singularities, absorpt. and luminesc. electronic-vibr. spectra 0-70639
 disordered condensed media, with impurities, energy transfer 0-80217
 doped semiconductor, potential fluctuations, random impurity distribution 0-88512
 electron gas, uniform, electronic props. of H and He impurities 0-96807
 excitation migration effect on luminesc. spectrum with inhomogeneous broadening 0-60676
 ferrocene films, plasma-polymerised, carrier trapping, elec. cond. meas., 300 to 525K 0-100543
 finite chain, with random dil. impurities, localisation characts., amplitude anal. 0-96825
 gapless semiconductor, magnetic field resonance states (*Polish*) 0-88508
 heavily doped semicond., photoemission lineshapes of impurity levels, p-wave resonance 0-76154
 heavily doped semiconductor, carrier Debye screening length, temp. depend. 0-88504
 III-V semiconductors, optical transitions, effect of perturbed k-selection and gap shrinkage 0-66257
 III-V semiconductors, radiative recomb., optical evaluation review 0-60647
 impurity centres, electron-phonon coupling from structured optical spectra, review 0-89038
 many-valley semiconductors, donor impurity levels and excitons, shallow-deep instabilities 0-75520
 metal, electron density behaviour near impurity charge 0-75518
 metals, Kondo effect, Anderson hamiltonian 0-60187
 mixed valence model, spinless, isolated f-level problem 0-107750
 molecular crystals, disordered, incoherent, electronic energy transfer in impurity band 0-75525
 naphthalene: pentacene, intermol. interaction dynamics and optical dephasing 0-64112
 naphthalene, doped, role of nonequilibrium phonons in stimulated radiation emission 0-103971
 naphthalene, in naphthalene- d_8 , Anderson-Mott transition model for excitation transport 0-96812
 naphthalene, in naphthalene- d_8 , energy trapping from localised states 0-100440
 near-surface, adiabatic potential, symmetry props., group theory methods 0-70786
 nonradiative electron transitions in crystal, impurity molecule vibr. 0-103645
 nonrigid impurity centres, symmetry groups (*Russian*) 0-65498
 p-n tunnel junctions, phototransitions accompanied by impurity scatt. 0-107901
 photoelasticity, nonlinear, in impure crystals, theory 0-108179
 polyacetylene, lightly doped, phenomenological theory of soliton formation 0-103644
 quasi-local level, line shape induced by impurity 0-100441
 quasifree excitons and electrons impurity trapping, finite coherence effects 0-59880
 rare earth metal impurity in metallic host, exchange interaction, electrical resistivity 0-84453
 recursion method for the extended impurity problem 0-96814
 resonance fluorescence of impurity atom in solid, transient spectrum, intensity, and intensity correl. 0-84777
 resonant secondary emissions by impurities in crystals 0-93335
 semiconductor, defect electronic structure and lattice config., MO approaches 0-65495
 semiconductor, direct band gap, electronic Raman scatt. of polarised light on donor levels 0-93309
 semiconductor, direct band gap type, polarization theory of reson. electronic Raman scatt. on neutral donor levels 0-108194
 semiconductor, donor-acceptor system, weak wave absorpt. in reson. laser radiation field 0-66252
 semiconductor, doped, impurity band density in atomic limit 0-107735
 semiconductor, doped, metal-insulator transition, anal. 0-88478
 semiconductor, electron-hole liquid, 'neutrality' question of impurities 0-92822
 semiconductor, heavily doped, long range fluctuations in impurity pot. effects 0-93356
 semiconductor, impurity characterisation from thermal carrier meas. 0-65595
 semiconductor, impurity ion pot., approx. equivalence of Csavinsky and Resta models 0-59901
 semiconductor, impurity ion screening charge density expansion 0-107780
 semiconductor, large-band-gap, self-compensation, role of impurities 0-92850
 semiconductor, lightly doped, compensated, percolation level, Monte Carlo calc. 0-59923
 semiconductor, localised states near displacive transition 0-70644
 semiconductor, n-type, donor-polarizability enhancement as the insulator-metal transition is approached from the insulating side 0-80184
 semiconductor, shielding by electron gas in magnetic field 0-107727
 semiconductor, three-impurity clusters, ionisation energies and electron affinities 0-65496
 semiconductor, with defects or impurities, local density of electron states 0-92857
 semiconductor, wurtzite structure, effect of local strain fields on shallow acceptor states 0-96821
 semiconductor with transition metal impurity states, EPR linewidth calc. 0-80599
 semiconductors, deep level impurity photoionisation cross-section 0-65485
 semiconductors, doped, shallow impurity states, Hubbard bands and donor excitonic states, HF calc. 0-100443
 semiconductors, exciton-impurity state with low binding energy 0-103646
 semiconductors, impurity electron scatt., resonance scatt., Hall and drift mobility 0-65487
 semiconductors, impurity photoionisation, quantum-defect, billiard-ball model comparison 0-65486
 semiconductors, localised magnetic moment of transition metal impurities 0-60192
 semiconductors, two-dimensional, Mott exciton formation in high mag. fields (*Russian*) 0-65467
 semiconductors, weakly doped compensated IR light absorption by small scale fluctuations (*Russian*) 0-66255
 transition metal-H systems, energy and electron density of states, improvements to theory 0-70636
 transition metals, ferromag., dil. H electronic struct. 0-70638

lead continued

- ion bombardment-induced photon emission near melting point 0-100699
ion implanted in Al, doping profile after laser pulse irradiation 0-88194
lake, Pb conc., rel. to boating activities and sediment interactions 0-104523
leading in glazed ceramics, colorimetric method (*Spanish*) 0-73414
liq., elec. resist. calcs., pseudopot. depend. 0-96840
liquid, collective excitations, neutron inelastic scatt. obs. 0-75148
liquid, ISSEC selection for fusion reactor 0-57950
liquid, thermal conductivity meas. in Spacelab, measuring cell design and testing (*German*) 0-57303
liquid, thermoelectric power, pseudopotential calc. 0-59959
melting, changes in electron image contrast 0-100147
melting theory for small particles, Helmholtz free energy 0-59629
molten, thermal expansion meas. to 1300K 0-65254
monolayer, double layer with Sn, growth on Al (111), struct. 0-70567
plastic properties over wide range of strain rates 0-71693
poisoning in human teeth, determ. using alpha-sensitive plastic track detector 0-94433
power cables, HV, Rb coverings quality estimation using mechanical tests (*Polish*) 0-97525
quench-condensed films, superconducting transition temp., elastic stress and strain effects 0-70883
radioactive tracer for Pu nuclear fuel input accountability in reprocessing plants 0-73919
recycling, effect on comp. 0-66455
shock compression at high press. (*Russian*) 0-92608
short range order amongst cond. electrons 0-107040
stable isotopes, 2-photon spectroscopy, isotope shift of $6^{-2} \text{ } ^3\text{P}_0\text{-}7\text{p } ^3\text{P}_0$ transition 0-87070
strength loss in supercond. state, size factor effect (*Russian*) 0-88677
subshell photoelectron branching ratio meas., using synchrotron radiation 0-66397
superconducting film, spatially inhomogeneous state appearance under laser pumping conditions 0-93053
superconducting slabs, magnetisation and migration field, reversible stage 0-65737
superconductor, effect of changes in $\alpha^2(\Omega)F(\Omega)$ on the zero-temp. energy gap 0-97025
surface, (111), vacuum deposition of Ag, Cu, substrate diffusion effects, RHEED, LEED, AES 0-65410
teeth, human, determ. of Pb distrib. by charged particle activation anal. 0-101303
thin films, single and polytextured, band struct., tunnelling spectroscopy 0-80169
traces in human blood plasma, atomic absorpt. anal., nonspecific absorpt. correction using Zeeman effect 0-76881
underpotential adsorption, cathodic deposition, on Ag(111) and (100) (*German*) 0-108363
vapour, use in laser projection microscope with image-brightness amplifier 0-106541
X-ray absorption, discontinuities and limits, chem. combination effects 0-93435
Young's modulus and internal friction, 20°C to melting point (*Russian*) 0-89278
Z dependence of thick target β -ray backscattering 0-76118
Al-Al₂O₃-Pb contacts, tunnelling spectroscopy, band struct. of Pb 0-80169
BaCl₂:Pb crystal phosphor, emission spectra 0-66298
BaF₂:Pb²⁺, band struct., Jahn-Teller effect, UV luminesc. and optical absorpt. spectra 0-66243
CaF₂:Pb²⁺, band struct., Jahn-Teller effect, UV luminesc. and optical absorpt. spectra 0-66243
GaP-Pd contact system, low temp. alloyed contact formation 0-100519
Ge:Pb, ion implanted damaged layer, laser induced reorder 0-84201
KCl:Pb, impurity distrib., light scatt. and microhardness study, heat treatment 0-96562
KCl:Pb²⁺, electrolytically coloured, elec. cond. and optical absorpt. meas. 0-100668
KCl:Pb²⁺, ion energetic parameters comparison with alkaline earth fluoride crystals 0-66243
KCl:Pb²⁺, X-ray irradi., electron-trapped centres, Pb⁺ and Pb⁰, optical absorpt. spectra 0-71461
Kl:Pb, absorpt. spectra of Pb⁺⁺ centres 0-76058
LiI:Pb, absorpt. spectra of Pb⁺⁺ centres 0-76058
LuPO₄:Pb³⁺, EPR, hyperfine interactions 0-108050
NaI:Pb, absorpt. spectra of Pb⁺⁺ centres 0-76058
Nb-Nb₂O₅-Pb Josephson junctions, props. of Nb₂O₅ thermally grown tunnel barriers 0-100568
Nb-Nb₂O₅-Pb Josephson junction formed on Nb film edge 0-107960
Nb-NbO₂-Pb Josephson junctions with high current densities, critical current 0-100552
Nb-NbO₂-Pb superconductive tunnel junctions, oxide tunnelling barriers, ESCA characterisation 0-65745
Nb-Pb supercond. tunnel junction proximity effect, theory 0-65752
Nb-Pb tunnel junction, crit. Josephson current, proximity effect model 0-93047
Nb-Te-Pb Josephson junctions, prep. and props. 0-65754
Ng-Pb Josephson junctions, magnetic field behaviour of zero field steps 0-100561
Pb II homologous ions series, Stark broadening trends 0-105157
Pb-O, thin film, microstruct. and thermal stress, doping effects 0-88458
Pb-acid cells, PbO₂ formation on Pb and antimonial Pb alloy 0-76628
Pb-Cd-Pb, supercond.-normal-metal-supercond. junction, crit. currents 0-107965
Pb-Cd-Pb junctions, pair pot., mag. field depend., crit. currents meas. 0-84555
Pb-Cu(Ag) double layers, intermetallic boundary effects, tunnelling 0-88692
Pb-formvar-Al tunnel junction, excitonic superconductivity, BCS theory, generalised jellium model 0-75684
Pb-Nb₂O₅-Nb Josephson junction current-biased on Fiske steps, mag. field depend. 0-84567
Pb-Nb-Pb bridge, fabrication technique and film parameters meas. 0-100569
Pb-Nb-Pb bridged, variable thickness, ion implant, coherent vortex motion props. obs. 0-100562
Pb-NbO₂-Nb tunnel junction, temp. depend. of effective Nb energy gap 0-80454
Pb-PbO₂-Pb small supercond. tunnel junctions, effect of capacitance in I-V characts., high-freq. obs. 0-80448

lead continued

- Pb-PbO-Pb, Josephson tunnel junction fabrication for Mm-wave detector 0-100427
Pb-Si heterojunction, RHEED, Mossbauer spectroscopy and I-V characts. 0-70828
Pb-Te-Te oxide-Pb Josephson junctions, prep. and props. 0-65754
Pb+Cb, 1s² excitation probability, scaling law, breakdown at very small internuclear distances 0-58365
Pb³⁺+Ne, highly charged very slow Ne recoil ions, K X-ray transition 0-91649
Pb₃, three photon excitation, Pb Rydberg series 0-106280
²⁰⁴Pb, muonic, first excited 2⁺ state, isomer shift of E2 transition 0-91950
²⁰⁶Pb/²⁰⁷Pb ratio and Pb conc. in subalpine pond sediments, anthropogenic source var. 0-85315
²⁰⁷Pb muonic isomer shifts, neutron hole anomalous moment contribs. 0-78728
²¹⁰Pb determination in sediment core from ocean floor off Californian coast 0-72101
RbI:Pb, absorpt. spectra of Pb⁺⁺ centres 0-76058
Si:Pb, high-dose ion implanted and annealed, implant redistribution 0-107309
Si:Pb, ion-implanted, impurity redistrib. during laser irradi. 0-100280
Si(111):Pb ion implanted amorphous layers, recrystallisation, impurity out-diffusion model (*Chinese*) 0-88363
SrF₂:Pb²⁺, band struct., Jahn-Teller effect, UV luminesc. and optical absorpt. spectra 0-66243
YPO₄:Pb³⁺, EPR, hyperfine interactions 0-108050
ZnS:Pb, blue luminesc., photoexcited EPR spectrum 0-108070

lead alloys

see also lead compounds

- dilute, diffusion thermopower, inelastic electron-phonon interaction 0-96851
interstitial substitutional model for anomalous diffusion 0-84330
ion-selective membrane electrodes development, Ag ion conduction ceramic systems (*Japanese*) 0-61203
Josephson tunnel junctions, effect of process variables on elec. props., cryogenic memory appls. 0-65748
Al-Bi(Cd)(Pb)-Ti, containing low-melting pt. inclusions, mech. props. 0-93632
In-Pb, small κ supercond., phase transitions higher than second order 0-88668
In-Pb (7 at.%), supercond. cylinder, magnetisation change induced by current near upper crit. field 0-70890
LaPb₃, doped with Tb, Nd, or Pr, crystal field effects, tunnelling within mK range 0-70907
Li-Pb eutectic alloys for fusion reactor solid breeder blankets, reactions with water 0-102297
Li-Pb liquid alloys, elec. resistivity, negative temp. coeff. 0-88527
Li-Pb liquid compound forming alloy, entropy of mixing 0-88328
Li-Pb-cooled blanket for tandem mirror fusion reactor, neutronic anal. 0-99273
LiPb alloy, compound-forming, vol. of mixing, conc. depend. 0-103484
Mo,PbS₈ embedded in resin, composite supercond., high transition temp. 0-88660
NaPb alloy, compound-forming, vol. of mixing, conc. depend. 0-103484
Pb-Ag (0.068 wt.%), Ag precipitation kinetics and activation energy 0-66517
Pb-As (~0.01 wt.%), enhanced precip. phenomena, invest. of mechanism by elec. resist. meas. 0-104162
Pb-Au, interstitial and substitutional distrib. 0-84204
Pb-Bi, creep, low-temp., thermal heating and quantum mechanisms, supercond. transition effects 0-79868
Pb-Bi, supercond., crit. mag. fields, influence of parameters 0-75691
Pb-Bi, supercond. T_c evaluation, from ab initio band struct. calcs. on Pb 0-75502
Pb-Bi, temp. regime of crystn. on rapid cooling (*Russian*) 0-66495
Pb-Bi counterelectrode Pb alloy Josephson junctions 0-65743
Pb-Bi liquid alloy, Pb and Bi diffusivities, temp. and conc. depend. (*German*) 0-84311
Pb-Bi-Tl, supercond., crit. mag. fields, influence of parameters 0-75691
Pb-Fe(Cu), liq., thermodynamic props. (*Polish*) 0-89199
Pb-I(Au) base electrode film Josephson junctions, tunnel barrier oxide struct. 0-65750
Pb-In film, superconducting tunnel junction, pulsed quasiparticle injection 0-84565
Pb-Na (8.4 at.%), supercond., surface flux pinning, crit. state model 0-97044
Pb-Ni, creep, low-temp., thermal heating and quantum mechanisms, supercond. transition effects 0-79868
Pb-Sb, thermal analysis in non-faceted/faceted eutectic systems 0-71637
Pb-Sb-As (1.1-1.8, ~0.01 wt.%), enhanced precip. phenomena, invest. of mechanism by elec. resist. meas. 0-104162
Pb-Si superconducting solutions, effect of hydrostatic compression on tunnelling (*Russian*) 0-65746
Pb-Sn (20wt.%), eddy current study of solidification 0-104141
Pb-Sn binary alloy, unidirectional solidification, convective and interfacial instabilities 0-80851
Pb-Sn(Bi)(Ni), strength loss in supercond. transition, nonmag. and paramag. impurities influence (*Russian*) 0-70875
Pb-Tl, supercond., crit. mag. fields, influence of parameters 0-75691
Pb-Zn, unmixing alloys, mathematical model for solidification process (*Russian*) 0-81047
Pb_{1-x}Li_x(As)(Ag)(In)(Sn)(Sb)(Te)(Au)(Ti)(Bi), liquid alloys, local fluctuations and quadrupolar relaxation 0-66060
Pb(Ag) alloys, effect of Ag content on yield strength 0-76322
PbBi-Al superconducting tunnel junctions, optically illuminated, quasiparticle energy distribution 0-75688
PbBi_{1-x}, quench-condensed films, superconducting transition temp., elastic stress and strain effects 0-70883
PbIn films strengthening, by preventing formation of misfit dislocations 0-84858
Pb₂Li, eutectic, ISSEC selection for fusion reactor 0-57950
Pd_{1-x}MnSb Heusler alloys, magnetic hyperfine fields on ¹¹¹Cd, TDPAC and magnetisation meas. 0-93219
Pd,Pb, Li₂ ordered alloy, positive temp. depend. on strength, phase destabilization 0-81203
PdPb₂, crystal structure (*German*) 0-96472
Pd_{1-x}Pb_x, cryst. struct., X-ray study 0-103293
PtPb_{0.7}Bi_{1.3}, crystal structure (*German*) 0-84139

lead alloys continued

- Pt₁PbBi₇, cryst. struct. (*German*) 0-107113
 Rh₂MnPb, hyperfine fields, ferromag., NMR and Mossbauer effect studies 0-71259
 Sn-Cd-Pb system, contacting layer struct. and phase composition (*Russian*) 0-66475
 Sn-Pb, temp. regime of crystn. on rapid cooling (*Russian*) 0-66495
 Sn-Pb (26%), liq. eutectic alloy Seebeck coeff. 0-84463
 Sn-Pb alloys electroplating, comparison with Au (*French*) 0-89158
 Sn-Pb solder, wettability on Cu and mild steel plates (*Japanese*) 0-89244
 Sn-Pb surfaces ageing, detrimental effect in PC fabrication 0-108625
 Sn-Pb-Bi-(Cd) infiltrated Ti base composite sintered bearing material, antifricition props. 0-60981
 Sn-Pb-(Bi) infiltrated Ti base composite sintered bearing material, antifricition props. 0-60981
 Ti-Pb, in solid and liquid state, specific electric resistance 0-103662

lead bonding

- Ti/Cu/(Au) thin films thermocompression bonds degradation by thermal ageing 0-66546

lead compounds

- see also *lead alloys*
 chalcogenides, Auger recomb., theory 0-65586
 displacive phase transition, S ion spin Hamiltonian parameter dependence on order parameter 0-70356
 eutectics, HgTe-PbTe and Au-PbTe, prep. and thermoelectric behaviour characts. 0-107774
 niobates, pyrochlore block structs., cryst. struct. determ. (*German*) 0-70178
 oxides, X-ray absorption, discontinuities and limits, chem. combination effects 0-93435
 PbO-Nb₂O₅ system, X-ray and electron microscopic phase and struct. determ. (*French*) 0-92508
 perovskites, ordered cubic, cationic effect on intramolecular forces, stretching force const. 0-88979
 PLZT coarse-grained solid solutions, electro-optical processes induced by longitudinal electric field (*Russian*) 0-80750
 PZT ceramics, ferroelec. energy conversion under shock loading 0-108163
 rare earth substituted lead apatites, Pb₁₀₋₂R₂M₂(PO₄)₆Z₂, M=Na or K and Z=F or Cl, cryst. struct. and IR spectra 0-107167
 stearate, Langmuir-Blodgett multilayers, comp. and transfer mechanism 0-80125
 B₂O₃-PbO-GeO₂-Fe₂O₃ glasses, mag. props. and Mossbauer spectra, speromag. order at low temps 0-80530
 Bi₂O₃-PbO, glass, cond. meas. using complex impedance anal. (*French*) 0-92707
 Fe₂O₃-PbO-V₂O₅ fluxed melt system, solubility and relative supersaturation meas. 0-64934
 Gd₂Se₃/PbTe, N type selenide segmented element fabrication, thermoelectric props. 0-107835
 Ge-Pb-S, glassy, photoconductivity dependences applied elec. field 0-107857
 K₂O-PbO-SiO₂, glass, effect of DC on corrosion of SnO₂ electrodes 0-85075
 xMnO₂(100-x)[19TeO₂.PbO], EPR studies of Mn²⁺ ion distribution 0-71167
 Na₂O-PbO-SiO₂, molten glass, reactions with conducting materials 0-85186
 Na₂O-PbO-SiO₂ glass-ceramic composite, directionally crystallised 0-107058
 PLZT ceramic, ageing, dielec. props. 0-88940
 PLZT ceramic, bonded lens assembly manufacture 0-79018
 PLZT ceramic, modulator for optical communication 0-78964
 PLZT ceramic, proton implanted, photoferroelectric effect for image storage and display devices 0-80315
 PLZT ceramic, thin wave electrode slotting process 0-79017
 PLZT ceramic, thin wafer production polishing process 0-81214
 PLZT ceramic, visible light scatt. depend. on photoferroelectric space charge fields 0-80806
 PLZT ceramics, elastooptic effect, stress induced birefr. 0-60543
 PLZT ceramics, modified by Ca¹⁺(Sr²⁺)(Nd³⁺)(Y³⁺), dielec. behaviour 0-60519
 PLZT ceramics photosensitivity enhancement by H- and He-ion implantation 0-96934
 PLZT, diffuse phase transitions, Curie temp., dielectric props. 0-75979
 PLZT electro-optic shutter stereoscopic display applications 0-90826
 PLZT ferroelectric thin films, epitaxial growth and optical props. 0-70543
 PLZT, mech. and elec. losses, correl., theory and expt. 0-66133
 PLZT modified high voltage dielectric, permittivity, Curie temp., loss meas. 0-80720
 PLZT, photoferroelectric image storage in antiferroelectric-phase PLZT ceramics 0-71353
 PLZT powder preparation, hydrolysis ball mixing 0-81006
 PLZT pyroelectric detectors, delayed onset of piezoelec. oscils. 0-75953
 PLZT slim-loop and linear ceramics, longit. electrooptic effects, display appl. 0-80751
 PLZT slugs, powder hot pressing technique 0-81007
 PLZT thermal, flash, ferroelectric protective goggles 0-81746
 PLZT, thin, elec. cond. and pyroelectric behaviour 0-75954
 PLZT/TFPD thermal/flash protective lens assembly, polarised delamination investigation 0-78929
 (Pb,Ba)(Zr,Ti)O₃, diffuse phase transitions, Curie temp., dielectric props. 0-75979
 (Pb, Sr)₂Ge₂O₁₁, single crystals, growth and X-ray and dielec. investigations 0-88127
 (Pb,Sr)TiO₃, ferroelec. props., press. depend., anharmonic oscillator model 0-80716
 Pb glass counter, automated calibration system 0-106233
 Pb Mg_{1/3}Nb_{2/3}O₃ ferroelectric semiconductors, electro-optical and elasto-optical props., appl. to optical storage (*Russian*) 0-80749
 Pb salt tunable diode laser-integrating sphere system, output intensity characts. 0-78881
 Pb salts, inorganic 0-77081
 Pb-PbO-Pb small supercond. tunnel junctions, effect of capacitance in I-V characts., high-freq. obs. 0-80448
 Pb-PbO-Pb, Josephson tunnel junction fabrication for Mm-wave detector 0-100427
 PbAl₂Se₄, X-ray cryst. struct. determ. (*German*) 0-107174

lead compounds continued

- (Pb_{1-x}Ba_x)₂Ge₂O₁₁, ferroelec. phase transition, dielec. const. and quasi-elastic light scatt. 0-71289
 Pb_{0.94-x/2}Ba_{0.6}Nb₂Zr_{1-x/2}O₃, Nb dopant morphology effect on microstructure 0-81005
 Pb_{1-x}Bi_xF_{2+x}, solid soln., struct. and ionic cond. correl., neutron diff. study (*French*) 0-84324
 PbBr₂, ionic cond. and activation volumes, high press. effects 0-100353
 Pb, Ca_{1-x}MoO₄, growth and props. 0-71588
 PbCl₂, ionic cond. and activation volumes, high press. effects 0-100353
 PbCl₂, struct. comparison with Co₂Si, Co₂P, and SbSi (*French*) 0-84155
 PbCl_{2-2x}Br_{2x}, luminesc. and reflection spectra (*Russian*) 0-84762
 PbCo_{1/2}Te_{1/2}O₃, antiferroelec., high-frequency permittivity, temp. depend. 0-71325
 Pb_{2-x}(Cs, Bi)_xGe₂O₁₁ 0-75960
 PbF₂, anion disorder at high temps., neutron diff. obs. 0-59614
 PbF₂ based solid solns., ion transport 0-107545
 PbF₂, fast ion conductor, phonon freq. distrib., temp. variation 0-84264
 PbF₂, ionic cond., activation volumes and high press. phase transitions 0-70461
 PbF₂, sp. ht. meas., Schottky-type diffuse phase transitions, defect form. energies and entropies 0-107441
 PbF₂, US vel. near press. induced cubic-to-orthorhombic transform. 0-103476
 PbF₂:Fe³⁺, F⁻ motion, ESR study 0-66023
 PbF₂:Mn, mag. tagging of ion diffusion, ¹⁹F NMR meas. 0-108106
 PbF₂-ZnSe multilayer 16 μm dichroic mirror, 16 μm region, mech. stress compensation 0-74465
 PbFe₂O₉, bubble and stripe lattice domain wall oscils. 0-97115
 PbFe₂O₉, dislocation etch pit morphology study (*Chinese*) 0-88150
 PbFe₂O₉, single crystal, Mossbauer spectra 0-84670
 Pb₂Ga₂S₅, X-ray cryst. struct. determ. and refinement (*French*) 0-107130
 PbGa₂Se₄, X-ray cryst. struct. determ. (*German*) 0-107174
 Pb₁₁GeO₈, X-ray powder cryst. data, struct. rel. to PbO₁₁GeO₈ and PbO 0-84146
 Pb₂GeO₁₁, elastic nonlinearity and acoustic losses 0-59554
 Pb₂GeO₁₁, Czochralski-grown oxide crystals, fluid-flow effect on gas-bubble entrapment 0-84121
 Pb₂Ge₂O₁₁, ferroelec. transition, US and elasto-optic props. 0-60527
 Pb₂Ge₂O₁₁, lattice dynamics parameters anisotropy, X-ray diff. study 0-59612
 Pb₂Ge₂O₁₁, pulsed polarisation switching process depend. on illumination 0-93253
 Pb₂Ge₂O₁₁, sputtered ferroelec. films, prep. struct. and dielec. props. 0-75452
 Pb₂Ge₂O₁₁:Gd³⁺, ferroelec. transition, temp. depend., EPR study 0-66127
 Pb₂GeO₈, X-ray powder cryst. data, struct. rel. to Pb₁₁Ge₂O₁₇ and PbO 0-84146
 Pb₂(GeO₄)(PO₄)₂, crystals, acousto-optical props. 0-100644
 xPb₂(GeO₄)(VO₄)₂, (1-x)Pb₂SiO₄(VO₄)₂, solid solution of centrosymmetric crystals, electrically induced optical activity 0-108180
 Pb₂(GeO₄)(VO₄)₂, crystals, acousto-optical props. 0-100644
 Pb₂(GeO₄)(VO₄)₂, elastic nonlinearity and acoustic losses 0-59554
 Pb₂(Ge_{1-x}Si_x)O₁₁, electrogyration, phase transition and dielectric props. 0-93269
 p-Pb_{1-x}Ge_xTe film, cyclotron reson. above and below struct. phase transition 0-88879
 Pb_{1-x}Ge_xTe magnetoplasma reflectivity and transmission spectra 0-71428
 Pb_{1-x}Ge_xTe solid solns., phase transition influence on elec. props., 77 to 450K 0-103689
 PbHPO₄, crystals, ferroelec. phase transition, hydrostatic press. influence, dielec. meas. 0-88936
 PbHPO₄, phase transitions study, role of cryst. struct. determ. 0-75197
 Pb_{1-x}Hg_xS-Si heterojunctions, elect. props. 0-100513
 Pb_{0.97}Hg_{0.03}Te photovoltaic detector produced by Sb⁺ ion implantation 0-82821
 PbI₂, 2H polytype, optical mode inversion near M-critical point, neutron scatt. mass 0-103432
 PbI₂, dielectric props., elec. cond., space charge polarisation 0-100631
 PbI₂, direct gap polar semicond., electron hole liquid phase diagram (*Russian*) 0-93314
 PbI₂, first-order 2H-4H polytype transition, exciton spectroscopic study 0-59647
 PbI₂, high press. phase diagram to 3.5 GPa 0-104126
 PbI₂, ionic cond. and activation volumes, high press. effects 0-100353
 PbI₂, multiphoton cross-section determination by means of luminescence experiments 0-93377
 PbI₂, photo-EMF, effect on photolysis of PbI₂-Ag (*Russian*) 0-92939
 PbI₂, photoexciton interaction, luminescence spectra, polariton dispersion diagram 0-93397
 PbI₂ single crystal growth, modified gel technique improved design 0-84842
 PbI₂ suspension, chem. sensitization 0-73492
 PbI₂:KI alloys, fundamental abs. edge, potential as solar convertor 0-101128
 PbI₂-Ag, photographic mat., photolysis, effect of PbI₂ photo-EMF effect (*Russian*) 0-92939
 PbI₂-Ag(Au)(Cu), light sensitive, internal photoelectric emission 0-107910
 PbI₂-PbBr₂, mixed systems, cryst. growth, struct. and optical props. (*German*) 0-96499
 PbI₂-piperidine(aniline)(pyridine), intercalation cpds., heat capacity of low temp., intercalation effect (*Russian*) 0-92682
 PbIn_{0.5}Nb_{0.5}O₃, ferroelectric, dielectric props. 0-103923
 PbIn₂S₄, vap. press., computer-automated meas. by simultaneous Knudsen torsion-effusion method 0-73334
 PbIn₂S₄, X-ray powder cryst. struct. determ. 0-66488
 PbIn₂O₂₁, X-ray powder cryst. struct. determ. 0-66488
 PbLi, gas phase thermodynamics, Knudsen effusion mass spectrosc. 0-100057
 PbMO₃S₈, supercond., upper crit. field meas. up to 600 kG 0-93057
 Pb(Mg_{1/3}Nb_{2/3})O₃-PbTiO₃-PbZrO₃ ceramics, HF filters appl. additives effect obs. (*Japanese*) 0-60507
 Pb(Mg_{1/3}Nb_{2/3})O₃, cation disordered perovskite, elastic const. and thermal expansion 0-96587
 Pb(Mg_{1/3}Nb_{2/3})O₃, electrostrictive effect 0-66113
 PbMg_{1/3}Nb_{2/3}O₃, photolum. and carrier drift mobility at ferroelec. transition 0-71469

lead compounds continued

- Pb(Mg_{1/3}Nb_{2/3})O₃:PbTiO₃, ceramic dielectric, electrostriction, relaxation, polarisation 0-80700
- Pb₂MgNb₂O₉, photoelectric states in real time spatial light modulators, photorefractive effect 0-80676
- Pb₃MgNb₂O₉-PbTiO₃, relaxor ferroelectrics, electrostrictive effects 0-66112
- PbMg_{1/3}Ta_{2/3}O₃ ferroelectric semiconductors, electro-optical and elastooptical props., appl. to optical storage (*Russian*) 0-80749
- PbMnFeF₃, vitreous, insulating, evidence of spin-glass transition 0-97112
- Pb₂MnFeF₃, vitreous, insulating, evidence of spin-glass transition 0-97112
- Pb_{1-x}Mn_xTe, photovoltaic effect, p-n junction, energy gap determ. 0-92931
- PbMoO₄, centrosymmetric cryst., linear electrogyration study 0-60540
- PbMoO₄, doped and undoped single crystals, polarisation of luminesc. and assignments 0-76069
- PbMoO₄, elastic wave excitation and amplification by laser radiation 0-103419
- PbMoO₄, optical absorption of hole centres, polaron model 0-97314
- PbMoO₄:Mn²⁺, zero-field splitting of Mn²⁺, EPR 0-75531
- PbMo₂S₈, supercond. Chevrel phase, electron tunnelling spectroscopy expts. (*German*) 0-107966
- PbMo₂S₈ wire, powder processed, crit. current density and field 0-80466
- PbMo₂S₈:Fe, elec. cond. anomalous temp. depend., mag. moments (*Russian*) 0-92878
- Pb₂Mo₂S₈ Chevrel phase, synthesis, stability and characts. 0-71608
- PbMo₂S₈O₂, O-containing Chevrel phases, synthesis and props. 0-108368
- Pb(NO₃)₂, Nd laser second harmonic stimulated Raman scatt., efficiency in calcite, nitrate crystals 0-95949
- Pb(NO₃)₂, thermal expansion study to test sensitivity of X-ray powder goniometer (*French*) 0-79631
- PbNb₂O₆, IR absorpt. spectra and diffuse Raman scatt., normal coord. anal. (*French*) 0-66198
- Pb_{1-x}Nd_xGe₂O₁₁, ferroelec. props. 0-75960
- PbO, laser excitation IR spectra, photoluminescence obs., rot. anal., rot. const. determ. 0-95619
- PbO layer vapour deposition, structure, and props. 0-65408
- PbO, reactively evaporated, photocond., H₂O induced phase transform. 0-60122
- PbO, single crystals, exciton and impurity luminesc. 0-60674
- PbO, standard free energy of formation, by EMF method with solid oxide electrolyte at low temps. (*Japanese*) 0-88338
- PbO, visible absorpt. spectra rel. to indirect excitation transitions 0-60628
- PbO, X-ray powder cryst. data, struct. rel. to Pb₂GeO₃ and Pb₁₁Ge₂O₁₇ 0-84146
- PbO-B₂O₃ glass-forming melt, specific volume and viscosity, temp. depend. 0-84073
- PbO-B₂O₃ glasses, microhardness 0-66612
- PbO-B₂O₃ phase-separated glass, fracture toughness, Vickers indentation method 0-85023
- PbO-B₂O₃-Bi₂O₃ glass with metallic Bi granules, elec. cond. 0-84493
- PbO-B₂O₃(SiO₂) glasses, structure toughness-composition relationship 0-104257
- PbO-containing binary systems, acoustooptic props. from comp. and density 0-76000
- PbO-GeO₂ glass, structure of anionic network, IR spectra 0-103256
- PbO-MoO₃-MO and PbO-WO₃-MO systems, M=Ca, Ba, Mg, Sr, perovskite type cpds. detection 0-108404
- PbO-P₂O₅ glass, ESR of VO²⁺ ions 0-100610
- PbO-SiO₂, melt, elec. cond. and struct. 0-88020
- PbO-SiO₂, melt, polymer equilibria 0-88019
- PbO-SiO₂ glass, acoustic and thermal Gruneisen parameters 0-59608
- PbO-SiO₂ glass, reduced channel-plate, variable range hopping conductivity 0-107466
- PbO-SiO₂ glass, trimethylsilylation method for silicate ion anal. (*Japanese*) 0-71975
- PbO-SiO₂ glasses, density-of-states and structural forms, Raman spectra study 0-97255
- PbO-SiO₂ glasses, high temp. ESR of Fe(III) 0-60410
- 2PbO-SiO₂-xSO₃ melts, crystn. 0-59400
- 2PbO-SiO₂, melt, coding rate influence on constitution of silicate anions, crystn. kinetics 0-103248
- 12PbO.6SiO₂.PbSO₄, crystn. from 2PbO-SiO₂-xSO₃ melts, struct. and vibr. spectra 0-59400
- Pb₃(PO₄)₂, ferroelastic, dielectric anomalies, phase transitions, permittivity, relaxation (*Russian*) 0-71293
- Pb₃(PO₄)₂, X-ray cryst. struct. determ. and refinement 0-103300
- Pb₃(P_{0.95}V_{0.05}O₄)₂, ferroelastic transition, soft mode, inelastic neutron scatt. study 0-70357
- Pb₃(P_{1-x}V_xO₄)₂, ferroelastic phase transition, DTA, dilatometric and Brillouin scatt. study 0-70398
- Pb₃Rh₂O₁₅, struct. study, X-ray diff. (*French*) 0-88100
- PbS, ab initio SCF calcs. using relativistic effective core pot. 0-95524
- PbS, anomalous magnetoresist. 0-107813
- PbS, bond orbital model of band struct. 0-59853
- PbS, chem. deposited thin film, effect of morphological struct. on photosensitivity 0-70760
- PbS, crystals, relation of struct. and bond type to slip geometry 0-88165
- PbS, electrodeposition, using nonaqueous solvents 0-76200
- PbS, energy gap and dielec. props., 77 to 373K 0-66100
- PbS, film, total current spectrum and energy struct. 0-100719
- PbS films, polycryst. and epitaxial, small-angle X-ray scatt. and electron density inhomogeneities 0-96758
- PbS islands, vacuum deposited, electron microscope obs. 0-103601
- PbS, photosensitive film, electron bombard. effect on elec. cond. 0-93019
- PbS, superficial degradation in air and water, XPS obs. (*French*) 0-89110
- PbS, vacuum deposited film, orientation axis tilt rel. to vapour angle of incidence 0-88456
- PbS, valence band struct. determ. by optical absorpt., size quantization effects 0-59871
- PbS:Ti, self-compensation of acceptors by vacancies, Hall coeff. meas. 0-92913
- PbS-base photodetectors, struct. invest. by proton irradi. 0-104388
- PbS-CuS, black Zn-dust pigmented solar selective coatings for solar photo-thermal conversion 0-66997
- PbS-In₂S₃, phase investigation 0-66488
- PbS-PbO vacuum evaporated films, elec. cond. and photocond. 0-75656
- PbS-PbSe epitaxial bicrystals, direct scatt. of channelled He ions at dislocations 0-65110

lead compounds continued

- PbS-Sb₂S₃ semicond., optical and photoelec. behaviour 0-96938
- PbS-Si heterojunction, chem. struct., AES anal. 0-76115
- PbS-Si heterojunction, related optical and IR detector props. 0-77866
- PbS-Si heterojunction, space charge capacitance, PbSn film thickness depend. 0-88630
- PbS-Si heterojunction, PbS film growth and struct. 0-96762
- PbS-Si p-n heterojunctions, AC admittance meas. 0-96979
- PbS_{0.9}Se_{0.1} 4.6 μm LED, room temp., band gap and electrolum. 0-66302
- PbS_{1-x}Se_x (X=0.18) homojunction injection lasers, near-field emission 0-95896
- PbS_{1-x}Se_x diode laser, contact degradation due to diffusion 0-102734
- PbS_{1-x}Se_x thin film, stimulated emission, temp. depend. 0-66232
- PbS, Se_{1-x}, multispectral photovoltaic IR detectors 0-105710
- PbS(Se)(Te), strongly anisotropic polar semicond., electron-hole liq. in mag. field 0-59890
- PbS_{0.5}Nb_{0.5}O₃, single cryst., dielec. props. 0-66126
- PbSc_{2/3}Ti_{1/3}O₃, ferroelec., high-frequency permittivity, temp. depend. 0-71325
- PbSc_{2/3}Ti_{1/3}O₃-PbSc_{2/3}W_{1/3}O₃(PbFe_{2/3}Te_{1/3}O₃) ferroelec. props. and lattice consts. 0-60520
- PbSe, ab initio SCF calcs. using relativistic effective core pot. 0-95524
- PbSe, bond orbital model of band struct. 0-59853
- PbSe, energy gap and dielec. props., 77 to 373K 0-66100
- PbSe film, soln. growth 0-66437
- PbSe films, current carrier conc. and type control, elec. cond., synthesis process (*Russian*) 0-100412
- PbSe, valence band struct. determ. by optical absorpt., size quantization effects 0-59871
- PbSe:Ti, self-compensation of acceptors by vacancies, Hall coeff. meas. 0-92913
- Pb₃(SiO₄)(VO₄)₂, crystals, acousto-optical props. 0-100644
- Pb₃(SiO₄)(VO₄)₂, elastic nonlinearity and acoustic losses 0-59554
- PbSnF₄, allotropic transformations 0-84926
- PbSnF₄, anionic conductor, thin films and ceramics 0-107556
- PbSnF₄, high anionic cond. of new solid electrolytes 0-107546
- Pb_{0.9}Sn_{0.1}F₂, NMR study of F atom motion (*French*) 0-100622
- Pb_{1-x}Sn_xO₂, single soln., struct. evolutions (*French*) 0-96488
- Pb_{1-x}Sn_xO₂:Sb films, DC sputtered, elec. props. 0-80426
- Pb_{1-x}Sn_xSe epitaxial layers, radiative and nonradiative recomb. processes 0-60670
- Pb_{1-x}Sn_xSe epitaxial layers obtained by LPE, growth conditions correl. with morphology 0-104079
- Pb_{1-x}Sn_xSe solid solns., photoluminesc. spectra, energy band parameter determ. 0-71484
- Pb_{1-x}Sn_xSe, transport phenomena in solid solutions with band inversion 0-107792
- Pb_{1-x}Sn_xSe, X=0.03-0.07, monocrystal film, edge of intrinsic absorpt. (*Russian*) 0-71368
- Pb₃Sn_{1-y}Se, multispectral photovoltaic IR detectors 0-105710
- PbSnTe, anomalous avalanche breakdown 0-80284
- PbSnTe, optical dielectric const. variation with carrier conc. 0-84709
- Pb_{0.78}Sn_{0.22}Te, Pb_{0.91}Sn_{0.09}Se, radiative and nonradiative recombination 0-80849
- Pb_{0.8}Sn_{0.2}Te crystals, Bridgman grown, X-ray perfection study 0-107018
- Pb_{0.8}Sn_{0.2}Te:Cd, influence of Cd doping on high field magnetoresist. and Hall effect 0-75590
- Pb_{0.8}Sn_{0.2}Te:La, evaporated thin films, low carrier conc. 0-65414
- Pb_{0.82}Sn_{0.18}Te, film, effect of hydrostatic pressure on props. 0-70862
- Pb_{0.82}Sn_{0.18}Te, layers on mica substrate, Hall constant peculiarities 0-75588
- Pb_{0.85}Sn_{0.15}Te homostructure diode laser, LPE growth, with controlled carrier conc. 0-95903
- n-Pb_{0.88}Sn_{0.12}Te spin flip Raman laser pumped by TE CO₂ laser, characts. 0-87397
- Pb_{1-x}Sn_xTe diode laser, contact degradation due to diffusion 0-102734
- Pb_{1-x}Sn_xTe epitaxial films, adsorption-induced accumulation layer form. on surface 0-60117
- Pb_{1-x}Sn_xTe, growth of epitaxial layers, activation by UV and IR radiation 0-71598
- Pb_{1-x}Sn_xTe, hole effective mass near zero bandgap, IR refl. study 0-108205
- Pb_{1-x}Sn_xTe LPE film IR detector performance 0-86422
- Pb_{1-x}Sn_xTe, lattice and electronic props. and g-value 0-80161
- Pb_{1-x}Sn_xTe, narrow gap semicond., theory of mag. susceptibility 0-93070
- Pb_{1-x}Sn_xTe, thermoelectric effects, characteristics at low temps. 0-107831
- Pb_{1-x}Sn_xTe, x=0.2, monocrystal, photoelectric props. of p-n structures (*Russian*) 0-70808
- Pb_{1-x}Sn_xTe, X=0.2, monocrystal, edge of intrinsic absorpt. (*Russian*) 0-71368
- Pb_{1-x}Sn_xTe:Cd(In), solid solutions, impurity states in photoluminescence spectra (*Russian*) 0-97333
- Pb_{1-x}Sn_xTe:Ge, anomalous behaviour of impurity centres under press. (*Russian*) 0-65491
- Pb_{1-x}Sn_xTe:In, dielectric state, avalanche breakdown in strong elec. fields (*Russian*) 0-92901
- Pb_{1-x}Sn_xTe:In, Hall effect and photoconductivity (*Russian*) 0-103720
- Pb_{1-x}Sn_xTe:In, impurity influence on photoluminescence at large excitation levels (*Russian*) 0-93384
- Pb_{1-x}Sn_xTe:In, tunnelling impurity self-localisation, anomalous props. nature (*Russian*) 0-59915
- Pb_{1-x}Sn_xTe/PbTe_{1-x}Se, lattice-matched buried heterostructure lasers with CW single mode output 0-74386
- Pb_{1-x}Sn_xTe-PbTe heterostructures, MBE produced on mica and LiNbO₃, elec. props. study 0-88629
- Pb_{1-x}Sn_xTe_{1-y}Se_y, quaternary solid solns. with const. lattice parameter, cryst. growth and characts. 0-108332
- Pb_{1-x}Sn_xTe_{1-y}Se_y, solid solutions with constant lattice parameter, phase comp. 0-108417
- Pb_{0.94}Sn_{0.06}Ti_{0.47}Zr_{0.53}O₃, piezoelectric ceramic, stress relax., time depend. deformation 0-60899
- Pb₃Sr_{1-x}(Zr,Ti,Nb)O₃, hydrophone ceramic, effect of one-dimensional uniaxial stress 0-80705
- Pb_{0.95}Sn_{0.05}(Zr_xTi_{1-x})O₃-Nb₂O₅, phase coexistence range, lattice consts. 0-92680
- PbTaO₆, IR absorpt. spectra and diffuse Raman scatt., normal coord. anal. (*French*) 0-66198
- PbTe and solid solns., optimal synthesis conditions for single cryst. growth 0-100776

lead compounds continued

PbTe, bond orbital model of band struct. 0-59853
PbTe, diffusion of Ag, effect of gamma irradiation 0-59515
PbTe, effect of pressing and sintering, study of induced defects by SEM 0-59983
PbTe, electrochemical surface reactions 0-76389
PbTe, energy gap and dielec. props. 77 to 373K 0-66100
PbTe, far IR magnetoref., band struct. 0-76010
PbTe film, electronic thermal cond. and thermoelec. power 0-93018
PbTe, growth of epitaxial layers, activation by UV and IR radiation 0-71598
PbTe homogeneity region investig. in Pb-Te system, equil. const. of quasi-chem. reactions 0-108405
n-PbTe, low temperature electrical transport, Hall effect 0-84478
n-PbTe, noncubic (111) oriented epitaxial films, weak field magnetoresistance 0-75584
PbTe, nonstoichiometric, evap. and growth of epitaxial layers 0-104072
PbTe photovoltaic detector, detectivity limits 0-105709
PbTe single crystals, growth from vapour phase under micro-gravity conditions 0-80957
PbTe, thermoelectric alloys, phase diagrams, and imperfection chemistry 0-108422
PbTe thermoelectric materials, microstructure anal. using SEM X-ray microanalysis 0-107211
PbTe, two photon magnetoabsorption (Russian) 0-60553
PbTe:Fe, single crystals, state and behaviour of Fe, mag. props. 0-93080
PbTe:In, electron mobility, temp.-independent part, Hall effect and elec. cond. meas. 0-92914
PbTe:In, mag. susceptibility, temp. depend., 4.2 to 200K 0-65773
PbTe:In, Shubnikov-de Haas oscillatory effects, quasilocal impurity level 0-92912
n-PbTe:In(Cu) epitaxial films, elec. transport props. 0-75659
PbTe:Ti, absorpt. coeff. spectral depend. 0-93370
PbTe-CdTe heterojunctions, fabrication and characterisation (German) 0-89151
PbTe-Ga₂Te₃, phase interaction, DTA, XPA and microstructural anal. 0-96625
PbTe-In contacts, fabrication and props. 0-60078
PbTe-InTe system, phase interactions and solid soln. form., physicochem. and elec. characteris. 0-104129
n-PbTe-p-Pb_{1-x}Sn_xTe, heterojunctions, heavily doped, current-flow mechanisms 0-96974
PbTe-Pb_{1-x}Sn_xTe n-p⁺ heterojunction photodetector, hot wall evaporation technique 0-65673
Pb_{1-x}Te-Pb_{1-x}Sn_xTe (x,y≤0.3), double heterostruct., LPE growth, heterointerface morphology 0-70550
Pb(Ti,Zr)O₃ solid solutions, phase coexistence discrepancies 0-96662
PbTiO₃, amorphous, crystallisation process, DTA and Raman spectroscopy meas. 0-75161
PbTiO₃, optical birefringence in low temp. region 0-93276
PbTiO₃, phase transform., different kinetic types 0-71347
PbTiO₃, photolum. and carrier drift mobility at ferroelec. transition 0-71469
PbTiO₃, vibronic theory and opt. props. 0-103939
xPbTiO₃ + (1-x)PbCd_{1/3}Nb_{2/3}O₃, phase transition spread, polarisation relaxation, dielectric susceptibility (Russian) 0-75922
Pb₃UO₄Cl₄ melts and mixtures, thermogravimetric determ. of uranyl cation state 0-101050
Pb₃(VO₄)₂, ferroelastic, phase transitions, boundary walls 0-107419
PbWO₄, doped and undoped single crystals, polarisation of luminesc. and assignments 0-76069
PbWO₄:Mn²⁺, zero-field splitting of Mn²⁺, EPR 0-75531
Pb(WO₄)_{1-x}(MoO₄)_x, growth and props. 0-71588
Pb(Zr,Ti,Mg,W)O₃, low-Q ceramics, props. and transducer appl. 0-75944
Pb(Zn,Ti)O₃ piezoelectric electrically deformable diffraction grating 0-78963
Pb(Zn_{1/3}Nb_{2/3})O₃, cation disordered perovskite, elastic const. and thermal expansion 0-96587
PbZn_{1/3}Nb_{2/3}O₃ ferroelectric semiconductors, electro-optical and elastooptical props., appl. to optical storage (Russian) 0-80749
Pb(Zn_{1/3}Nb_{2/3})O₃ single crystal, pyroelec. props., meas. under laser beam illum. 0-66117
Pb(Zn_{1/3}Nb_{2/3})O₃-PbTiO₃-PbZrO₃ ceramics, HF filters appl. additives effect obs. (Japanese) 0-60507
Pb(Zr,Ri)O₃:Ni-silicon rubber flexible composite pyroelectric, dielectric props. 0-80704
Pb(Zr,Ti)O₂ ceramic, surface barrier electroreflectance, hysteresis, ageing 0-80752
Pb(Zr,Ti)O₃ ceramics, low temp. sintering, elec. and mech. props. 0-71616
Pb(Zr,Ti)O₃ ceramics with ladder type struct., prep. and props. 0-75945
Pb(Zr,Ti)O₃ ceramics, DC field sintering preparation, piezoelectric props., ageing behaviour 0-81211
Pb(Zr,Ti)O₃, ferroic materials, fracture processes 0-79869
Pb(Zr,Ti)O₃ fibre arrays in epoxy cement, ferroelectric ceramic-plastic composites 0-81015
Pb(Zr,Ti)O₃ films, ferroelec., ion beam deposition sputtered from multi-component targets 0-80974
Pb(Zr,Ti)O₃, fracture and deform. 0-79870
Pb(Zr,Ti)O₃ internally electroded multilayers, piezoelectric props., permittivity, transducers 0-80672
Pb(Zr,Ti)O₃, internally electroded with Pt, resonance behaviour 0-84701
Pb(Zr,Ti)O₃, PCD ceramic, pyroelectric props. 0-100635
Pb(Zr,Ti)O₃, piezoelectric ceramics, low fluence neutron irradi. effects 0-92564
Pb(Zr,Ti)O₃, porosity-permittivity relations, depolarising factors determ. and pore effects (Japanese) 0-97189
Pb(Zr,Ti)O₃, research grade, hydrophone ceramic, effect of one-dimensional uniaxial stress 0-80705
Pb(Zr,Ti)O₃, shock depoled ferroelec. ceramic, anal. of ideal response 0-60511
Pb(Zr,Ti)O₃, tetragonal ferroelec. ceramic, 90° domain-rot. fraction after polarisation, X-ray determ. 0-75992
Pb(Zr,Ti)O₃:Ba, paraelectric ceramic, electrostrictive effect 0-80701
Pb(Zr,Ti)O₃:Cr₂O₃ ceramics, reson. freq. comp. and temp. depend. 0-70413
Pb(Zr,Ti)O₃:Fe(Nb) ceramic, elec. and electromechanical props., depend. on dopants 0-81212
PbZrO₃, ferroelec., crystallographic shear planes as nonstoichiometric defects 0-59484

lead compounds continued

PbZrO₃, ferroelec. solid solns., atom shifts, polarisation and Curie temps. 0-100636
PbZrO₃:La, appl. in sub-100 ps pyroelec. detectors, 10.6 μm damage threshold meas. 0-77859
Pb(Zr,Ti)O₃ ceramic transducer for generation and detection of unipolar stress pulses 0-64328
Pb(Zr_{0.52}Ti_{0.48})O₃, polycrystalline ferroelectric, grain-size dependent props. 0-71352
Pb(Zr_{1-x}Ti_x)O₃ solid solution, piezoelectric ceramic, prop. improvement by multiple substitution 0-80702
PbZr_{1-x}Ti_xO₃:Nb₂O₅ ceramic, ferroelec. transitions, polarisation meas. (French) 0-66124
PbZr_{1-x}Ti_xO₃ ceramics, morphotropic phase boundary 0-81035
Pb(Zr,Ti_{1-x})O₃ films, deposition by focused ion beam sputtering 0-76177
Pb(Zr,Ti_{1-x})O₃, meas. of Hugoniot curve with commercial manganin stress gauges 0-70362
Pb₂(As₂O₅), paulmooreite, crystal struct., dimeric arsenite groups 0-84143
Si-PbS heterojunction, effect of Si substrate orientation on struct. and interface props. 0-80097
SiO₂-PbO-B₂O₃-Al₂O₃-CaO-Na₂O-K₂O glaze, interaction with aluminosilicate glass-ceramics 0-84398
(SiTe)_{1-x}(PbTe)_x, solid soln., mag. susceptibility meas. (Russian) 0-70933
Sn_{1-x}Pb_xSe(Te) films, Mossbauer effect of ¹¹⁹Sn, spectral characts., conc. depend. 0-103903
Sn_{1-x}Pb_xSe(Te) films, oxidation rel. to annealing temp. and time, Mossbauer spectra, X-ray and microstruct. obs. 0-104311
Te-PbTe system eutectics, crystn. rate effect on electrophys. props. mutual solubility effect 0-60774
Te₈₀Ge₁₅Pb₅, DSC sensitivity to controlled ageing in glass transition region 0-71673
Te₈₀Si₂₀-Pb₅ glasses, phase separation, double T_g presence 0-88306
Ti₂Te₂Ti₄SnTe₂Ti₄PbTe₂, phase equilib., DTA, SPA and microhardness meas. 0-96628
V₂O₅-As₂O₅-PbO, semicond. glass, electronic props. 0-88557

leak detection

airtightness monitoring, classification of high performance equipment 0-104397
chromatographic method of calibrating leaks 0-77800
device for checking airtightness by parameter changes in object and medium 0-104404
LMFBR, chemical leak detection, effects of NaOH in Na 0-63326
mass spectrometer, meas. range extension 0-73375
pressure changes in interconnected chambers, mathematical model 0-108678
search gas testing methods, He leak detectors with mass spectrometer anal. (German) 0-101802
US, threshold sensitivity eval. criteria 0-104401
H₂ meter, diffusion type, Na coolant loop, LMFBR 0-68728
He, mass spectrometer leak detectors, probe with He-permeable membrane 0-98994
¹³³Xe charcoal traps, simple leak tests, nuclear medicine appl. 0-104734

leakage, magnetic see magnetic leakage

leakage currents

bipolar cell stacks, simulation program 0-76526
electromedical equipment, safety by monitoring leakage currents (German) 0-81749
SiO₂, stacked-struct. improved quality by laser annealing of Si 0-65386

learning systems

see also adaptive systems; cognitive systems; self-adjusting systems
computer learning prediction systems appl. 0-108048
continuous speech recognition system for data base consultation 0-91990

least squares approximations

astronomy, generalisation of method of least squares 0-62028
atoms, 5f^N and 5f^N7s config., parametric study 0-91444
blood pressure automated control in dogs using microprocessor 0-81797
disturbed measuring systems, estimation of signal parameters, autoregressive-linear models (German) 0-68165
electron scattering by simple Yukawa and static pots., S-wave phase shifts 0-106374
event location by recursive least squares prediction 0-96131
formaldehyde, force field calcs., damped least-squares method 0-91533
gravity anomaly inverse problem, least-squares soln. 0-98214
hologram interferometry, sensitivity vector determ., two known object rats. 0-95840
impact toughness test results, cold brittleness crit. temps. determ. 0-100980
inverse scatt., Newton's method modification at fixed energy 0-73207
lens design, least squares fitting of Zernike's polynomials to wave aberration function 0-83660
limit of applicability, modification for large errors in independent variable 0-73301
linear prediction in least-squares scheme, algorithms 0-98464
linear prediction in least-squares scheme for max. entropy spectra, Fortran subroutines 0-98465
molecular force field calcs., damped least-squares method 0-91533
optical rib waveguide with trapezoidal cross section, numerical analysis 0-96009
pocket calculator program with variable precision for least square fitting of data 0-67976
polystyrene solns., correlations of network model parameters 0-106772
rotated hamiltonians, complex-coordinate rotation and least-squares variational method 0-68075
Rowland circle, corrected, least-squares method derivation 0-64161
smoke/dust cloud temporal analysis algorithm 0-98484
Voigt functions, nonlinear least square algorithm 0-90900
wavefront estimation from wavefront slope meas., least-squares curve fitting model 0-106467
X-ray line shape broadening anal., least squares method 0-63588
CN free radical, A²Π-X²Σ⁺ Red system, perturbation analysis 0-87247
CO₂, dipole moment functions 0-87094
Cu IV, wavelength region 700-1200 Å, extended analysis 0-99473
N₂O, dipole moment functions 0-87094
NaCl 46 cm window optical evaluation facility 0-74526

leather *see materials*

Lee model

Callan-Symanzik functions and asymptotic freedom 0-73659
(π , π), scattering theory testing using Lee model 0-78325

LEED *see low energy electron diffraction*

legislation

medical measurements, law (Croatian) 0-104797
nuclear generating station, waste disposal and licensing (German)
0-99222
nuclear power plant safety, West German policy (German) 0-57865
nuclear power stations, licensing procedure, public participation under
Atomic Energy Act (German) 0-102256
spent fuel storage and disposal and plant building and operating legisla-
ture (German) 0-99223
USA Quiet Communities Act (1978), implementation by Environmental
Protection Agency 0-72113

length measurement

see also micrometry
automatic optical length meas., defocusing effects (Japanese) 0-68174
centre-distance meter, gear testing 0-62632
distance between hole centres, instrum. 0-57258
end-standards and ruled scales using laser sources (German) 0-86251
force optical interferometers for length, temp., pressure and force meas.
0-98971
gauge blocks, errors associated with checking by interferometric methods
0-105613
gauges, microscopes with IZV-21 and IZV-23 meas. heads (USSR)
0-57257
human step length measurement apparatus 0-67271
IC photomask and wafer linewidth meas. using optical spatial coherence
0-77850
interferometric length measurement with curved wavefronts (German)
0-77752
interferometry, heterodyne, principles and appls. (German) 0-68181
laser interferometric auto-correcting system of high precision thread
grinder 0-90830
metre, new definition proposal using 88 THz stabilized He-Ne laser
0-73304
microcomputer based laser interferometer for instrument graduation
(Polish) 0-90816
optical interferometry, wavelength stabilisation (German) 0-57250
pneumatic linear dimension testing device, output pressure converted to
frequency signal 0-62631
standard meas. procedures of GDR Bureau of Standards (German)
0-57246
steel gauge blocks, linear coeff. of thermal expansion (German) 0-68171
two-colour length measurement scheme using CO₂ laser 0-99747
He-Ne 3.39 μ m laser interferometer, length and refr. index meas.
0-68172

length standards *see measurement standards*

Lennard-Jones and Devonshire theory *see liquid theory*

Lennard-Jones potential

acetylene, cryst., semiempirical atom-atom pots. appls. 0-100200
binary dense gaseous mixtures, struct. and thermodynamic props., mole-
cular dynamics study 0-64866
binary fluid, molecular dynamics, critical mixing point region 0-88014
binary liquid solutions, struct. and thermodynamic props., molecular
dynamics study 0-64866
Brillouin scatt. and refr. index measurements 0-76035
compressed gas, radial distrib. function hard sphere model 0-69961
elastic sphere, deformation and sticking to a rigid plane, mol. force effect
0-106720
fermion-boson isotopic mixture, ground state configuration, theory
0-107601
fluid, cavity-biased (T,V, μ) Monte Carlo method, computer simulation
0-92434
fluid, critical lengths and spinodal region 0-84045
fluid, two-centre, perturbation theory appl. using spherically averaged
reference potential 0-64860
four term WKB approx., appl. to Varshni V and Lennard-Jones pot.
0-58113
glass and glass-forming liq., viscoelastic properties, comparison with Len-
nard-Jones model 0-84983
graphite, ⁴He interaction and scatt. 0-60732
hard core fluid with two-Yukawa tail, appl. to Ar 0-59618
inert gas mixture, dipole autocorrelation function, Lennard-Jones and
exponential dipole pots., classical calc. 0-64665
interatomic potentials, Regge poles positions and residues, inverse power
pots. 0-83439
liquid mixture, binary, equimolar, static (dynamic) props., mol. dynamics
calc. 0-64857
liquid structure, S-D periodic particle-particle/particle-mesh program
P3M3DP 0-84041
liquids, diatomic, hard and soft core, free energy difference, Monte Carlo
calcs. 0-92436
Moelwyn-Hughes parameter calc. from US data for pure liqs. and liq.
alloys 0-59375
molecular dynamics, nonequilibrium, $\tau^{-3/2}$ long-time tail for stress-stress
time correlation 0-70100
molecular solids, melting curves, Lennard-Jones Devonshire theory
0-65201
Mori theory evaluation, molecular dynamics simulation 0-92443
multipole gases, second virial coeff. meas. 0-69959
nonuniform one dimensional classical fluids, Lennard-Jones pot. interac-
tions, Percus Yevick approx. and density functional calcs. 0-64864
n-octane fluid, spontaneous cavitation 0-69886
phase transitions in two-dimensional Lennard-Jones system, calc. 0-59621
polymer chain statics and dynamics, Lennard-Jones interaction, calcs.
0-58425
polymer chains with rigid bonds, local relax. times, mol. dynamics study
(Russian) 0-59373
polymer fluid, static bulk props., reptation Monte Carlo method, LJ pot.
0-64868
polymer solutions, scaling theories for general interaction potentials
0-99592
second virial coeff. inversion for complete pot. energy functions 0-91628
second virial coefficient, functional equations 0-103442
simple fluids, hard and soft-core eqns. of state, termination temps., Kihara
pot. 0-70360

Lennard-Jones potential continued

simple liqs. with repulsive forces, thermodynamically selfconsistent theory
0-75139
soft discs, two-dimens. melting, phase transition boundary 0-96629
AgI surface, adsorption of water, effective pair pot. model 0-100394
ArHBr, ArHCl, and isotopic forms, rot. spectra, mol. struct., mol. consts.
0-58246
CaF₂, mol. dynamics studies of superionic conductors 0-107547
Cu₅₇Zr₄₃, amorphous alloy, computer simulation of atomic structure
0-70125
He II, excitation spectrum and second virial coefficient calc. 0-102549
³He, liq., polarisation effect on mag. ordering, melting curve 0-80021
⁴He ground state binding energy, near threshold behaviour in 2 and 3
dimens. 0-91716
⁴He, superfluid, elementary excitation, structure factor and phase velocity
0-80012
⁴He, threshold condition for forming atomic trimer 0-63741
Kr, Lennard Jones (12,6) pot. distance parameter, transport props. calc.
0-79423
KrHBr, KrCHI, and isotopic forms, rot. spectra, mol. struct., mol. consts.
0-58246
N₂ structural second virial coeff., intermol. pot. and mag. scatt. 0-78678
Ne, Lennard Jones (12,6) pot. distance parameter, transport props. calc.
0-79423
Ne-Xe, equilibrium of coexisting phases 0-87197
Ne+Ne, (He) low pressure broadening and shift of Ne line, Lennard-
Jones pot. 0-102554
O₂, structural second virial coeff., intermol. pot. and mag. scatt. 0-78678
TiI, atomic fluorescence, D₂ pressure effect on width and shift 0-99475
Xe, Lennard Jones (12,6) pot. distance parameter, transport props. calc.
0-79423

lenses

see also aberrations; aspherical lenses; contact lenses; electron lenses;
electrostatic lenses; focusing; magnetic lenses; photographic lenses
acoustic elliptic lenses, history 0-96158
afocal projection optics, for laser velocimeter 0-75011
annular aperture, light distrib. from diffr., aberration correction using
mirror lenses (German) 0-69325
annular HSURIA resonators, testing with CO₂ laser, polarisation effects
0-58599
array characts. on illuminated intensity distribution (Russian) 0-106591
astigmatic spectacle lenses, technological construction (Russian) 0-99817
catadioptric objective, development (German) 0-102796
caustic point displacement due to generalised bending, third-order approx.
0-83656
centrally obstructed objective, resolution limit (German) 0-95811
chirped grating, anal. 0-87563
chromatic aberrations of real rays, role of each lens in optical system
0-102655
coherent Gaussian beam in laser Doppler velocimeter, interference
0-69444
coherent information processing by a pair of lenses in spherical wave
illumination 0-95816
coma corrector for parabolic reflector telescope off-axis guiding 0-82196
coronagraph objective component surface scatt. angular distrib. obs.
0-74463
design, applied optics conf., Oakland, CA, USA (May-June 1980)
0-101661
design, least squares fitting of Zernike's polynomials to wave aberration
function 0-83660
design with simultaneous image spot, optical path difference, diffraction
MTF and Seidel aberration minimisation 0-74459
distortion by means of numerical transformation (German) 0-64132
double Gaussian objective, design (German) 0-64134
education, geometrical optics, lens Fourier transform properties 0-57024
education, lateral-angular magnification relationship for simple magnifier
0-57031
electron microscope optical model, design and use 0-86534
eyepieces, imaginary front focal planes, negative collection lens, design
considerations 0-64139
fabrications of lens blanks having reduced finishing allowances 0-74541
field corrector for parabolic reflector, design method (Chinese) 0-85857
flat image focussing spherical lens, used for Si light detector 0-91880
flight simulator viewing, triplet lens system design 0-74457
Fourier transform lens, spatial invariance test 0-69492
Fresnel lens, appl. in local reducer for stellar photometry 0-67568
Fresnel lenses, fabrication techniques 0-91939
Fresnel lenses in BaO optical waveguides 0-96034
frustrated total internal reflection element, adjustable as a function of the
incidence angle of highly collimated light beams 0-96022
generalised ray tracing, caustic surfaces, bending and merit function for
optical design 0-102612
geodesic lens formation in diffusion fabricated optical waveguides
0-91937
geodesic lenses, anal. by beam propag. method 0-58686
gradient index optical elements and system design 0-106594
gradient-index fibre array, unevenness of illuminance 0-69482
gradient-index fibre lens, radiometric props. 0-69481
gradient-index imaging, theory 0-69331
gradient-index optics: a review 0-69478
gradient-index rod, aberrations in multimode optical fibre devices
0-69487
gradient-index rod, appl. in optical fibre communication systems 0-69488
gradient-index rod, evaluation by imaging 0-69485
gradient-index spherical, design for optical pickup systems 0-69483
gratings characts. control by interference pattern (Russian) 0-87461
hologram lens, axial, on spherical substrate with remote pupil, aberrations
0-95849
holographic lateral shear interferometer for differential interference con-
trast method 0-63947
holographic lens recording techniques for IR wavelengths 0-95847
holographic optical elements, third-order aberration theory and generalised
aplanatic condition 0-74314
holography, twin-image, chromatic lens system, astron. appls. 0-87346
hyperchromatic lens, expressions for first order chromatic aberrations
0-91879
illumination system, optical design 0-64135
intensity fluctuations behind lens, receiving aperture shape effect
0-95980

lenses continued
interferometer, lateral shear, using twin three-beam holograms, lens tests appl. 0-99673
interferometric examination of lenses, mirrors and optical systems, 3D display 0-69497
laser beam expander for short cavity dye laser 0-87532
laser beam printer scanning system with f- θ lens 0-78942
laser light source for spectroscopy, far-IR, optical coupling arrangements 0-73481
lens guide, low-loss image transmission 0-91872
light wave propagation 0-78947
light-flux generated by single-lens illuminator, spectral composition for UV region 0-87450
linear Fresnel lens with grooves of finite size, solar radiation concentration 0-106592
Luneburg lens, turning point of rays 0-83659
mass production yield estimation by centering tolerance simulation 0-78941
micro-optics testing, width meas. of slit test objects 0-64223
microscope, scanning, multiple traversing of the object 0-90890
military optical system temperature effects and counter-measures 0-78938
MTF tolerancing computer program 0-78934
multiple lens experiment 0-82596
multiple point hologram lens array generation, appl. to micro-electronic mask making 0-95842
nodal slide, experimental and theoretical thick lens parameters comparison 0-67998
nonastigmatic spectacle, structural design parameters (*Russian*) 0-87460
nonsymmetrical optical system, matrix representation 0-64130
nontracking solar collectors, wide-angle lenses and image collapsing subreflectors 0-76603
objective, two-channel device for meas. transmission coeff. 0-106642
objectives, tolerancing of refr. index heterogeneity 0-78948
ophthalmic correcting cylinder axis, ophthalmometric prediction 0-98174
ophthalmic lenses, longit. spherical aberration and its effect on visual acuity 0-99816
optical axis designation method 0-102798
optical fibre coupling using graded-index rod lenses 0-91891
optical fibre hemispherical microlens tip fabrication for high efficiency coupling to InGaAsP laser 0-69505
optical fibre high index hemispherical microlens tip melt fabrication for coupling to GaAlAs laser 0-69506
optometry, perceptual effects of low-power plus lenses in emmetropic observers 0-67084
optotransducers, electronic compensation for dirty lenses 0-68189
pancratic objectives, aberration stabilisation during focusing 0-102799
paraxial eqn. dimensional analysis 0-74462
planar acoustic microscope lens using Rayleigh to compressional conversion 0-87668
production technology advances, seminar, London, England (April 1979) 0-67938
projection, 35 mm cinema projections 0-87469
radial gradient-index, with zero Petzval aberration, third-order aberrations 0-69484
resonator, annular, adaptive mirror effects on performance 0-58596
self-centring technique for mounting microsphere coupling lens on fibre 0-74517
Selfoc lens, aberration improvement by glass composition and ion exchange process parameter choice 0-69486
Selfoc lens as imaging system, chromatic aberration 0-69480
silicone-glass hybrid Fresnel lens for solar energy concentration 0-61303
slit image seen in total internal reflection (*French*) 0-95810
speckle interference fringes, lens aberration effects 0-105700
spectacle, image quality (*Russian*) 0-87463
spectacle, surface grinding and polishing, using automatic and semi-automatic machines (*French*) 0-58822
spectacle lenses, hard resin, comparative study of bitoric effect 0-91877
spherical cementing fixtures for holding lenses by rigid method 0-96043
spherical surfaces shape deviation determ., using sphere-interferometer (*Czech*) 0-58821
spherical-cylindrical lens combination, combined 1-D image-orthogonal Fourier transform processing 0-58658
superachromatic triplets, design method 0-64133
systematisation of mirror lenses according to extent of central obstruction (*German*) 0-102795
telescope, two-mirror objective systems, field lens group corrector 0-78945
Tessar-type lens, aberrations, automatic correction routine 0-58464
testing, MTF-based optical sensitivity and tolerancing computer programs 0-83686
three-lens cemented component calcs., reduced secondary spectrum 0-102800
variable-scale single-lens optical transform systems 0-58656
wavefront aberration, interferometric examination techniques 0-69498
Wolter lens component replication 0-95972
Ge, polycrystalline thermal-imaging lens, optical requirements 0-69495

lepton-deuteron interactions
see also lepton-deuteron scattering
ed, deep inelastic scatt., quark-parton model with logarithmic scaling violation 0-78071
ed-pn, disintegration and Coulomb excitation cross sections in channelled nuclei 0-59539
e⁺d-e⁻np, polarised, parity violating asymmetry 0-78080
Ld- Δ IX, deep inelastic scatt., isobar admixture possibility (*Russian*) 0-91095
vd- Δ c⁺X, high energy charmed baryon prod. obs. 0-105881
ed-e⁻pn, 1180 MeV electrons, proton distribution, neutron momentum distribution (*Russian*) 0-68652

lepton-deuteron scattering
see also lepton-deuteron interactions
ed-ed, nucleon forces, meson exchange current effects, impulse approx., review 0-57603
ed-ed*, dibaryon resonance production 0-78070
ed elastic scatt. at high momentum transfer 0-82977

lepton-hadron interactions
see also lepton-hadron scattering; lepton-nucleon interactions
(ϕ^3)₀ field theory, deep inelastic lepton-hadron scatt., cut vertex theory and reciprocity relation 0-57466

lepton-hadron interactions continued
conference, lepton-hadron physics, Karlsruhe, Germany (Sep. 1978) 0-73098
deep inelastic lepton-hadron scatt., semiinclusive hadron prod., quark fragmentation function corrections, QCD 0-63013
deep inelastic processes, QCD predictions 0-73677
deep inelastic scatt., proton struct. function higher order asymptotic freedom corrections 0-105905
deep inelastic scattering 0-73717
lepton pair production, QCD jets 0-62994
polarised deep inelastic scatt., parton transverse momenta role, struct. function, QCD evolution 0-78034
QCD phenomenology of deep-inelastic scattering 0-73660
quark fragmentation functions for inclusive hadron production, Regge formalism 0-68462
in deep inelastic scattering, quark jet as trigger for gluon jet 0-62996

lepton-hadron scattering
see also lepton-hadron interactions; lepton-nucleon scattering
U(1) \times SU_L(2) \times SU(3) theory, integer charge quarks, lepton hadronic processes (*Russian*) 0-86653

lepton interactions *see lepton-deuteron interactions; lepton-lepton interactions; photon-lepton interactions*

lepton-lepton interactions
see also electron-electron interactions; electron-positron interactions; lepton-lepton scattering; neutrino-electron interactions; neutrino-neutrino interactions
unpolarised lepton-lepton collisions, photon 3rd struct. function, QCD implications 0-73708

lepton-lepton scattering
see also electron-electron scattering; electron-positron scattering; lepton-lepton interactions; neutrino-electron scattering; neutrino-neutrino scattering
 $\nu_e e^- \rightarrow \nu_e e^-$, weak and EM radiative corrections, sensitivity test 0-105880

lepton mass
E₆ model of unified interactions, asymptotically free, mass relations and interactions 0-73642
electroweak symmetry group, B-L U(1) generator and quark-lepton symmetry 0-57549
heavy lepton decay, spin $3/2$, intermediate vector boson corrections 0-73761
minimal O(10) grand unification, ν mass 0-57546
muon-electron mass ratio in a semi-classical model 0-91072
neutrino mass problem, gauge hierarchy 0-90989
neutrino oscillations, mass and mixing scales 0-105823
neutrino rest mass, effects on Universe density perturbations spectrum and microwave background small-scale fluctuations (*Russian*) 0-109576
neutrino rest mass, implications for Universe density perturbations evolution and galaxy clusters hidden mass (*Russian*) 0-105414
neutrinos, rest mass rel. to mass density and age of Universe (*Russian*) 0-109575
stable method heavy leptons, astrophysical mass constraint, condensation in stars and galaxies (*Russian*) 0-72768
SU(2)_L \otimes SU(2)_R \otimes U(1) weak model, ν mass and spontaneous P nonconservation 0-62884
SU(2) \times U(1) gauge model, chiral SU(2) \times SU(2) symmetry and electron mass 0-57542
SU(5) \times SU(2) unification, horizontal symmetry due to quantised motion along internal axes 0-62905
unification of EM, weak and strong interactions, quark and lepton mass, quark fractional charge, baryon asymmetry 0-73637
 μ -e mass quotient, modified Weinberg-Salam model calcs. (*French*) 0-82926
 $\bar{\nu}_e$ mass from ^3H β -decay spectrum (*Russian*) 0-91159
 ν_e mass from ^3H β -spectrum in valine molecule 0-91158

lepton-nucleon interactions
see also electron-nucleon interactions; lepton-nucleon scattering; muon-nucleon interactions; neutrino-nucleon interactions
deep inelastic scattering and asymptotic freedom, Q² dependence of moments 0-82978
hadron leptoproduction, nuclear targets, quark-nucleon inclusive cross section, heavy lepton pairs 0-57607
nuclear matter, leptoproduced high energy particles, nuclear attenuation, hadronisation time 0-102182
quark and gluon jets, Breit frame, QCD 0-62995
n, structure function nonsinglet moments from deep inelastic lepton scatt., QCD 0-62980
p, structure function nonsinglet moments from deep inelastic lepton scatt., QCD 0-62980

lepton-nucleon scattering
see also electron-nucleon scattering; lepton-nucleon interactions; muon-nucleon scattering; neutrino-nucleon scattering
No entries

lepton production
see also electron pair production; muon production; neutrino production
dilepton charge production cross section for ν and $\bar{\nu}$, parton model 0-62966
direct lepton generation in strong interactions, unified model, colour quark state (*Russian*) 0-82933
hadron collisions, lepton pair production, qq annihilation within same hadron, structure function anal. validity 0-57622
hadronic lepton pair production, QCD jets 0-62994
heavy vector meson annihilation to lepton pairs, hadronic corrections 0-68424
high energy lepton pair prod. with pol. hadrons, P and C violations 0-99068
lepton pair prod. struct. functions, QCD improved quark-parton model 0-73671
massive lepton pair production as a test of models for particle production on nuclei 0-102213
multilepton production in neutrino expts. 0-91081
pair photoproduction from protons, P violating asymmetry 0-105901
pair production, QCD and hard-scatt. model, spin-spin asymmetries 0-63014
prompt lepton sources from hadronic collisions 0-73726
QCD corrections at Z₀ for hadron initiated lepton pair prod., renormalisation appl. 0-86678
D \rightarrow K π ν , charm-changing weak hadronic current, models 0-57585
e⁺e⁻ annihilation, hadron and lepton prod., τ -lepton decay, K⁺, p, p yields, quark flavours 0-73725

lepton production continued

- eN, deep inelastic scatt., heavy lepton mixings, Weinberg-Salam model 0-62992
 γ +hadron \rightarrow lepton pair, perturbative QCD, twist-2 photon operator, parton subprocesses 0-73716
 $h_1h_2\rightarrow l\bar{l}X$, massive lepton pair prod., polarisation and spin effects 0-105929
 μ N, deep inelastic scatt., heavy lepton mixings, Weinberg-Salam model 0-62992
 μ p deep inelastic scatt., inclusive cross section, lepton pair EM prod. contrib. (Russian) 0-105904
 $\nu(\bar{\nu})N$, heavy lepton prod. and decay, differential cross sections (Russian) 0-105940
 $Pn\rightarrow l^+l^-X$, scaling predictions, Drell-Yan model 0-73756
 $\bar{p}p$, heavy lepton prod. and decay, supersymmetrical model of weak and EM interactions (Russian) 0-86748
 $\bar{p}p$, massive lepton pair prod., pion exchange model anal., quark parton interpretation (Russian) 0-82993
 $\bar{p}p$ scatt., Drell-Yan process, quark-quark contrib. 0-73731
 πp , massive lepton pair prod., pion exchange model anal., quark parton interpretation (Russian) 0-82993
 π^-p , 70 GeV/c, directly produced electrons from charmed D particle decay, cross sections 0-73755

lepton scattering see *lepton-deuteron scattering; lepton-hadron scattering; lepton-lepton scattering; photon-lepton scattering*

lepton spin and parity

No entries

leptonic decays

see also *baryon leptonic decay; meson leptonic decay; muon decay*

- heavy lepton decay, intermediate vector boson corrections 0-73761
 intermediate vector boson decay, QED and QCD radiative corrections, hadronic jets 0-73759
 $SU_2\times U_1$ and the origin of the Cabibbo angle, charged gauge boson mixing 0-73639
 e^+e^- annihilation, 12-31.6 GeV, τ production and decay branching ratios, lifetime 0-78052
 e^+e^- annihilation, hadron and lepton prod., τ -lepton decay, K^+ , p , \bar{p} yields, quark flavours 0-73725
 $Z\rightarrow l^+l^-$, deviations from lepton universality in renormalisable gauge models 0-91122

leptons

see also *electrons; heavy leptons; lepton spin and parity; muons; neutrinos; positrons*

- bootstrap geometrical approach 0-95258
 bootstrap topological approach to quarks and leptons 0-95253
 composite leptons and quarks, anomalous mag. moment, flavour as dynamical quantum number 0-105854
 composite leptons and quarks, mag. moment 0-105896
 composite quarks and leptons, mag. moments 0-91056
 distribution of masses of leptons and hadrons 0-99093
 division of matter, confinement of quarks and gluons (Polish) 0-68417
 eight-lepton and eight-quark unification based on Grassmann algebra 0-105824
 EM fine struct., Fermi weak coupling, Newtonian grav. constants, unified relation 0-101974
 exotic atoms, conf., Erice, Sicily, (1979) 0-67939
 fine-structure constant, coupled Maxwell and Dirac eqns., QED 0-62894
 fourth generation of quarks and leptons, mass formula 0-105876
 grand unified wave function for quarks and leptons 0-91034
 internal quantum numbers for quarks and leptons in bootstrap approach 0-95254
 LEP, design, tests of unified field theories and quark properties, search for new quarks and leptons 0-74048
 lh theory of leptons and hadrons, unification in GA_{LR} gauge 0-86639
 new elementary particles, quark and composite models (German) 0-57570
 number conservation, forbidden processes 0-68654
 PETRA results for fluons, nuclear forces, t-quarks and quark-lepton symmetry 0-86731
 properties, review from particle data group 0-67944
 QDD, quantum dath dynamics, $SU(3)$ model for composite quarks and leptons 0-91055
 relativistic cosmology, interactions with quarks 0-90590
 rishon model, topological bootstrap approach 0-78046
 rishon model for quarks and leptons, topological bootstrap approach 0-78047
 rishon model of quarks and leptons with double $SU(2)$ symmetry and Dirac magnetic moments 0-82943
 $SO(10)$ unification, composite structs., quark and lepton composite models 0-57547
 space-time properties, unified gauge theory of gravitational and strong interactions 0-95016
 stellar gravitational collapse, neutronisation and lepton escape rel. to hydrodynamics 0-77388
 structure model 0-91063
 $SU(3)$ electroweak theory 0-86638
 $SU(5)$, unification of weak, EM and strong interactions, review 0-105814
 $SU(5)$ without symmetry constraints, unified model of quarks and leptons, conservation laws 0-101968
 subcomponent models of quarks and leptons in $SU(3)$ subcolour, proton decay 0-78035
 subquark model of leptons and quarks, unification, currents and exotic states 0-86683
 supergrand exceptional unification and quark-lepton constituents 0-91030
 supergrand unification in E_8 , quark-lepton assignments, symmetry breaking scheme 0-68408
 tumbling gauge theories with chiral fermion fields, symmetry breaking 0-99042
 unified field theories, proton and neutron disintegration, concepts of leptons and quarks (French) 0-91038
 unified models of quarks and leptons, B-L conservation and B nonconservation 0-95229
 $e^+e^-\rightarrow$ hadrons, R problem, QED and QCD corrections, quarks and leptons 0-95281
 $\bar{\nu}_e$ annihilation in Weinberg-Salam model, number of quarks and leptons (Russian) 0-102041

level crossing (energy) see *energy level crossing*

level measurement

- acoustic pulse-reflection meter, nuclear waste liquor tanks 0-86265
 automatic monitoring of liquid N_2 level, in Dewar flasks 0-57309
 contact cryogenic fluid level sensor 0-73371

level measurement continued

- hydrostatic method of level measurement (Polish) 0-101779
 light reflection liquid level sensor 0-82741
 linearisation of scale eqn. for resonance level gauges (Russian) 0-68176
 liquids, cascade transistor cct., level to freq. converter 0-73310
 sensor for conductive liquids using array of point sensors 0-68177
 sinter machine charging, potentiometric level detector (Russian) 0-90813
 tank gauging, automatic, using density transducers 0-95067
 US, liquid level measurements using longitudinal, shear extensional and torsional waves 0-77757
 water, twin-wire wave height probe with calibration stabilized for changes in water conductivity 0-57280
 He, liq., appl. of gas oscillation to pressurisation in storage vessel 0-57305

level meters

see also *power measurement*

- Bose section, commercial instruments survey (French) 0-83871
 sinter machine charging, potentiometric level detector (Russian) 0-90813
 He level gauge, with semiconductor sensor 0-57277

levels, energy see *energy states*

levitation, magnetic see *magnetic levitation*

librarianship see *information science*

libraries

- computer information, conference, London, England (Nov. 1979) 0-90599
 NOAA meteorological library and information services, description 0-109180

library mechanisation

British National Meteorological Library 0-82068

library science see *information science*

LIDAR see *optical radar*

Lie groups

see also *elementary particle symmetry*

- A(0,n) Lie superalgebra, Fock space representation 0-86606
 algebras, semi-simple with centre but no outer derivation (Japanese) 0-68386
 Bose statistics, para-, Lie superalgebra, osp(1,2n), creation and annihilation operators 0-62572
 Boussinesq equation, group theoretical approach 0-82914
 broken symmetry of transformation generating general relativistic theories 0-98836
 cohomology of graded Lie algebras and non rational Poincare-Betti series (French) 0-95222
 compact simple Lie groups, rank 2, irreducible representations (Chinese) 0-68391
 compact simple Lie groups of rank 2, irreducible representations of B_2 and G_2 (Chinese) 0-101949
 complex Lie groups, connected regular compactifications, homogeneous Hopf manifolds, and bundles (French) 0-73617
 contact structure, deformation of Lie algebra, of infinitesimal automorphisms (French) 0-62867
 contact transformations and brackets in classical thermodynamics 0-95048
 cosmology, Lagrangian or Hamiltonian formulations, shift vector field restrictions, symmetry group 0-67923
 deformation cohomology of truncated Lie algebra (French) 0-57077
 diffusion equation, nonlinear, invariance props., Lie-Backlund groups 0-62596
 Dirac Lorentz's equations, relativistic and nonrelativistic, maximally extensive local group of invariance 0-77946
 dynamical groups, symmetries and constants of motion for electric and mag. charges 0-101945
 Euclidean space, spherically symmetric self-dual eqns., representation theory and integration 0-77936
 forced harmonic oscillator, complete symmetry group 0-90705
 free particle, Hamiltonian mechanics, Lie theory of extended groups 0-77982
 Galilean invariant Schrodinger eqn., relativistic wave eqn. derivation, Lie algebra 0-105555
 Galilean formulation of spin, explicit realisations 0-62505
 gauging Lie superalgebras 0-73618
 generalised Liouville equation from Lie derivative 0-77981
 geometrical properties of spinor structure 0-95226
 Hamiltonian mechanics, Lie theory of extended groups 0-77982
 Higgs and gauge fields, group actions on principle bundles and dimensional reduction 0-105770
 hypergeometric functions, two-variable, Lie theory and separation of variables 0-73189
 identical particle indistinguishability, field quantisation Lie algebraic approach 0-77984
 invariance algebras of Schrodinger and Dirac eqns. (Russian) 0-68081
 isometries, 2-parameter groups, commutation properties 0-62879
 Klein-Gordon equation, Lie-Backlund transformation group 0-68371
 Korteweg-de Vries equation prolongation Lie algebra 0-62501
 linearisation program for nonlinear field eqns., Lie groups 0-105784
 Micu-type invariants of exceptional simple Lie algebras 0-86609
 nilpotency class of Lie algebras satisfying the Engel condition (Russian) 0-68394
 nilpotent Lie groups, smooth functions Fourier transforms 0-99067
 nilpotent two step groups, hypoelectricity and differential operator solvability (French) 0-62868
 nonstationary quantum systems, $SU(2)$ coherent states (Russian) 0-90693
 nuclear collective models, moment map 0-91138
 $O(2N)$ Gross-Neveu model, $O(8)$ Dynkin diagram P_3 symmetry 0-77968
 particle under repulsive oscillator, $Sl(3,R)$ complete symmetry group, Lie group 0-86602
 projective covering group versus representation groups 0-62874
 quantum mechanics, Heisenberg/Lie/symplectic formulations, problematic aspects 0-62497
 quantum structures, Lie-admissible symmetry, representation theory 0-62870
 quasiparticle formalism, atomic shell operators, Lie algebra 0-91414
 real simple Lie superalgebras, finite-dimens., classification 0-57516
 self-adjoint systems, Lie-admissible deformation 0-101941
 semi-simple Lie groups, Casimir operator eigenvalues, symmetric power sum expansions 0-86604
 semigroup compactifications of topological groups 0-73620

Lie groups continued

- semisimple groups, $O(n)$, $U(n)$, raising and lowering operators, infinitesimal approach 0-62875
- SL(2,R) dynamical Lie group, hyperbolic transforms 0-57515
- SL(n,C) actions, analytic, real, on spheres and complex projective spaces 0-68382
- SO(4,2), Delaunay similar elements in eccentric anomaly (*German*) 0-57507
- spinor field theory, generalized spin structures on 4-D space-times 0-62564
- SU(2,1), graded Lie algebra, irreducible representations 0-82913
- SU(2) supergroups, Yang-Mills, Lie groups, chiral coeffs., Baker-Campbell-Hausdorff formula 0-68355
- subgroups, linear, connected, in locally convex space, infinitesimal transformations 0-68381
- superalgebras, generalised, Jordan- and Lie-admissibility 0-101942
- symplectic collective model, irreducible $U(3)$ tensor interactions 0-83048
- Wigner-Eckart theorem for an arbitrary group of Lie algebra 0-86124
- zero-mass representations of Poincare supersymmetries with arbitrary spinor generators 0-99065
- ²⁴Mg rotational band collectivity, shell model excitation in Sp(4, R) symmetry 0-102095
- ¹⁶O, rotational band collectivity, shell model excitation in Sp(4, R) symmetry 0-102095

ligand field theory *see bonds (chemical); crystal field interactions; molecular energy levels*

light

- see also airglow; optics; sunlight; zodiacal light*
- gravitational deflection of light, meas. at 1919 May 29 solar eclipse 0-67553
- gravitational lens effect, EM wave diffr. in Schwarzschild space-time 0-90750
- gravitational lens effect, focusing by slowly rotating relativistic spherical mass 0-105155
- gravitational lens effect formed by spherical galaxies, multiple image prod. 0-90532
- gravitational lens hypothesis, appl. to triple QSO (PG 1115+08) 0-86012
- gravitational lens in double quasar 0957+561A, B due to intervening galaxy, IR obs. 0-73065
- non-classical effects in the statistical properties of light, review 0-99686
- wave and particle descriptions of light, equivalence, rel. to radar freq. shift 0-101692

light absorption

- see also atmospheric optics; densitometry; light transmission; optical constants; optical films; optical filters; pleochroism; spectra*
- aerosol, solar radiation absorpt., visual photometric meas. technique 0-85750
- alkali hydrides, lattice props. from interaction pot. energy function 0-100199
- alloys, substitutionally disordered, optical cond., intraband transitions 0-103933
- amplitude-phase holograms, optical parameter dispersion 0-58481
- atmosphere, absorpt. effects wavelength depend. rel. to anomalous gray shades in DMSP visible imagery 0-77111
- atmosphere, in situ meas. of aerosol absorpt. coeff./extinction coeff. ratio 0-90217
- atmosphere, IR absorpt. rel. to total O_3 content determ. using satellite meas. 0-77027
- atmosphere, IR radiation attenuation by ice platelets 0-66141
- atmosphere, light absorpt. and scatt. rel. to direct beam solar irradiance and illuminance 0-90174
- atmosphere, solar UV radiation absorpt. in mesosphere and stratosphere 0-109248
- atmosphere, true absorpt. rel. to polarised light transfer 0-67561
- atmosphere aerosol absorpt. and scatt. effects rel. to satellite retrieved temp. profiles error 0-98449
- atomic vapours, three-level system, collisional effects in saturation spectroscopy, appl. to Na 0-78579
- Auger recombination of carriers bound to centres involving phonons 0-107805
- beam volume attenuation coeff., invalidity 0-95791
- breather generation, inverse scatt. technique 0-78913
- cholesteric films, absorpt. and contrast in dichroic liq. cryst. displays 0-75155
- cholesteric liquid crystals optical properties, diffraction nature, review 0-70123
- cirrus clouds, visible and IR absorpt. calc. from lidar and radiometer meas. 0-82060
- classical crystal optics, lattice dynamical background, review 0-97221
- coatings, absorptive, at normal incidence, program for TI-59 calculator 0-84793
- compound glass rod absorption coeff. calorimetry 0-106631
- cone absorption calorimeter for pulsed laser meas. 0-98980
- crystal optical characteristics, relax. processes exciton dispersion 0-107709
- crystalline material optical absorption meas. 0-105718
- crystalline optical material props., symmetries and tensorial relationships 0-108174
- diamond:Sb, implanted, radiation damage and annealing study 0-100263
- dichlorodifluoromethane, absorpt. meas., laser power density depend. 0-92251
- disordered crystal, biphonon spectra, light absorpt. coeff. and density of states, CPA calc. 0-84271
- double-beam photometer for meas. small changes in optical absorption 0-62709
- enzyme-linked immunosorbent assay, apparatus for meas. light absorbance of small vols. of liquids 0-72387
- ethidium bromide E-DNA, intercalated birefringent fibres, microspectrophotometric invstg. (*German*) 0-57392
- ethylammoniumtetrachlorochromate, optical absorption intensity, short-range spin correlation 0-108185
- fibre attenuation and pulse dispersion due to neutron irradiation 0-58730
- filter, multilayer frustrated-total-internal-refl., spatially limited 0-96014
- galactic IR sources, 3μ extinction feature identification 0-62227
- galaxies, nearby, interstellar reddening law and dust content (*German*) 0-67850
- gaseous medium, two-photon-absorbing, polarised light propag., quantum effects 0-103107

light absorption continued

- HD 200775, Be star, optical and UV extinction by dust in (NGC 7023) 0-109515
- inert gases, electron-beam excited, transient absorpt. at XeF laser wavelengths 0-83592
- inert gases, photoabsorption, local field effects, density-functional formalism 0-78766
- interstellar extinction, 2200 Å extinction hump prod. by porous graphite grains 0-62228
- interstellar extinction, 2200 Å feature anomalous strength in Cassiopeia-Taurus association stars 0-77469
- interstellar extinction, 2200 Å feature obs. in Orion Nebula by long-slit spectroscopy 0-105297
- interstellar large globules, absorpt. meas. rel. to struct. and dynamics 0-62246
- interstellar medium, total/selective extinction ratio rel. to grain growth 0-67834
- interstellar reddening in near IR, new results from JHK photometry of reddened stars 0-94857
- interstellar reddening in solar neighbourhood, anal. 0-62239
- ionic crystal, anharmonism effect on exciton peak broadening in absorpt. spectra (*Russian*) 0-97317
- jacketed and cabled optical fibre low-temp. attenuation increase 0-58732
- Langmuir films on Cu surface, surface EM wave absorpt. study 0-97359
- lattices, FCC and BCC, optical transitions, dipole selection rules 0-97409
- layer crystals, exciton absorption of light 0-70623
- layered crystal, wave functions, exciton spectrum, light absorpt. (*Russian*) 0-100436
- liquid crystal matrix, orientational distrib. coeffs. from UV and circular dichroism meas. 0-92452
- liquids, photoacoustic and photorefractive detect. of small absorpts., electrostrictive limits 0-108171
- magnetic semiconductors, critical behaviour of electronic properties, theory 0-96861
- metal surface laser beam irradi., effective absorpt. coeff., temp. field determ. (*Russian*) 0-76108
- metal targets, laser radiation absorption in craters 0-97386
- metallic thin films (*French*) 0-60692
- methylammoniumtetrachlorochromate, optical absorption intensity, short-range spin correlation 0-108185
- middle atmosphere, solar UV radiation absorpt. rel. to numerical model of zonal mean circulation 0-109218
- mirrors, dielectric multilayer, reflectance under slight absorpt. conditions 0-83655
- mirrors with temperature-dependent absorptance, laser-induced thermal runaway 0-91882
- multilayer coatings, high-refl. or antirefl., vol., interface absorpt. and scatt. losses 0-63915
- negative light absorption by medium with selective freq. modulation of quantum oscillators 0-106501
- nematic-chiral-dye mixture, circular dichroism, selective light scatt. (*Russian*) 0-103944
- Neptune atmosphere, UV absorpt. sources from UV albedo meas. 0-82295
- neutral absorbers of NS glass, meas. of transmission when irradiated with laser radiation 0-105692
- nucleic acids and their aggregates, optical activity, review, book contrib. 0-108847
- ocean, absorpt. model for diurnal var. of underwater irradiances on horizontal surfaces 0-72549
- optical fibre attenuation charact. meas. by backscatter technique (*Italian*) 0-106600
- optical fibres, basic terms, properties, uses (*Dutch*) 0-64166
- optical glass, coloured, laser damage threshold, optical absorpt. influence 0-91830
- optical material absorpt. meas., real time holographic interferometry 0-83569
- particle shape effect on low freq. absorpt. 0-99626
- particle size dispersion, effect on IR radiation in Venus clouds 0-109384
- photothermal deflection technique for absorpt. meas. in optically thin media, thermal lens effect comparison 0-105717
- polarisation constants for light interaction with absorbing crystal plates 0-78765
- polymethine dye lasers, optical absorpt. 0-64009
- polyvinyl alcohol film containing Cu^{2+} complexes, photoconductivity 0-107849
- QSOs, absorpt. from clouds in emission-line regions 0-62308
- quarter-wave mirrors, oblique incidence reflection coefficient, small absorption of layers effect 0-64140
- radiation chemistry, photoabsorption data appls. 0-93778
- relaxation times in solid-state theory and one-dimensional molecular systems (*Russian*) 0-100640
- rough surfaces, discontinuous films, heterogeneous materials, optical props., review 0-103935
- Schiff base azo dyes in nematic liq. cryst. hosts, order parameters, optical density meas. 0-84055
- seawater, meas. technique for irradiance attenuation coefficient in a stratified ocean 0-98325
- self pulsing in absorptive optical bistability, analytical description 0-78891
- semiconductor, IR absorpt. and optical relax. time of free carriers 0-66206
- semiconductor, nonequilibrium acoustic phonons, generation by interband light absorption 0-96607
- semiconductor, optical absorpt. coeff. and minority-carrier diffusion length, differential photocurrent method of meas. 0-96896
- semiconductor, p-type, intervalence-band transitions, saturation, theory 0-75997
- semiconductors, intervalley electron-electron scattering effect on optical transitions 0-108267
- semiconductors, weakly doped compensated IR light absorption by small scale fluctuations (*Russian*) 0-66255
- silica based optical fibre dopants for 1 to 1.8 μm communications 0-91930
- silicate smokes, vapour-condensed, 800 to 130 nm extinction and interstellar extinction curve 0-82180
- skin, in vivo, light absorpt. and scatt., theoretical and expt. study 0-101219
- SMC, ratio between total and selective interstellar absorpt. (*German*) 0-67851

light absorption continued

- smoke aerosols, optical absorption to extinction ratio, photoacoustic determ. 0-58459
 sphere, totally reflecting, light extinction 0-95784
 superconductor, metal-insulator transition, electron pairing, effect on optical props. 0-60139
 translucent three-dimensional holograms, mode theory taking account of the absorption 0-91757
 unpolarised monochromatic light, total absorption by crossed grating 0-106448
 Uranus atmosphere, UV absorpt. sources from UV albedo meas. 0-82295
 UV radiation field in interstellar clouds, attenuation theory (*Russian*) 0-73026
 vegetation canopies, solar radiation absorpt. simulation 0-104635
 water, backscatter and absorption coeffs., simultaneous determ. 0-82074
 waveguide, lossy, Brewster phenomena, cut-off thickness 0-87524
 zero gap semiconductor, thin layer, dielec. response 0-103635
 zero-gap semiconductors, anisotropy of IR absorpt. coeff., k.p. calc. 0-97285
 BiI₃ film, exciton-phonon interaction, optical consts., Faraday effect., permitt. 0-59884
 C, amorphous grains, extinction coeffs., 0.21-340 μm , lab. meas. rel. to interstellar grains 0-73020
 C smokes, vapour-condensed, 800 to 130 nm extinction and interstellar extinction curve 0-82180
 CO₂-He-N₂, absorpt. coeff. for 10.6 μm CO₂ laser radiation, 295 to 650 K 0-92252
 Ca₂Fe₂Ge₂O₁₂ garnet, light absorpt. spectral study 0-93322
 CdCr₂Se₄, Mott ferromagnetic semiconductor, optical absorption edge, critical behaviour 0-97226
 CdS/Cu₂S, polycryst. thin film photovoltaic materials, photon loss anal., expt. determ. 0-93888
 CdSe, fundamental absorpt. edge, influence of laser radiation intensity (*Russian*) 0-71445
 Cu-Sn(Al)(Ga) reflecting surface absorpt. coeffs. at 10.6 μm 0-95984
 CuCl, optical absorpt. meas., evidence against intrinsic electron-hole supercond. 0-108172
 Cu₂S-CdS solar cells, optical absorption coefficient changes in Cu₂S 0-93980
 Ge₂₀Bi_{80-x}, semicond. glass, resist., thermoelec. power, optical absorpt. 0-88555
 Ge₂₀Bi_{80-x}Te₁₀, semicond. glass, resist., thermoelec. power, optical absorpt. 0-88555
 GeS, Urbach's rule, absorption edges 0-97224
 InP, compensation ratio, electron mobility and free-carrier absorpt. 0-80261
 InSb, refractive index and absorpt. coeff., cryst. orientation depend. 0-60536
 LiNbO₃, optical waveguides by ion implantation 0-106622
 N₂, liq., photoacoustic and photorefractive detect. of small absorpts., electrostrictive limits 0-108171
 α -O₂ crystals, spin ordering effect on light absorpt. (*Russian*) 0-89029
 O₃, in atmosphere, Chappuis-band absorpt. rel. to conc. determ. 0-77063
 PtO, films, electronic struct., reduction processes, photoemission, optical absorpt. and resist. meas. 0-80931
 Rb₂CrCl₄, optical absorption intensity, short-range spin correlation 0-108185
 SbSI, absorption edge, elec. field effect rel. to ferroelec. props. 0-97240
 Si-H amorphous, solar cell structure, optical absorption by gap states 0-94052
 Si-SiO₂ interface, (001) vicinal planes, minigaps in inversion layers, far IR absorpt. meas. 0-107919
 SiC smokes, vapour-condensed, 800 to 130 nm extinction and interstellar extinction curve 0-82180
 Si_{1-x}H_xAl, amorphous, co-sputtered Al modification, electronic and optical props. 0-100461
 Zn_{1-x}Cd_xS, thin solid soln. films, vapour deposited, elec. and optical chars. 0-60110

light absorption spectra *see spectra***light amplifiers** *see image intensifiers***light attenuation** *see light absorption; light scattering; light transmission; optical dispersion***light coherence***see also laser beams; lasers*

- applications, seminar, San Diego, CA, USA (Aug. 1979) 0-77542
 atmosphere optics, phase correlation scale effects rel. to atmospheric imaging chars. 0-94604
 atmospheric turbulence and aerosol effects 0-82064
 atmospheric turbulence structural chars., meas. using spatially limited laser beam 0-98413
 atoms, multiphoton ionisation, reson. effects, light coherence effects 0-58232
 bilinearly distorted image linear restoration using Wiener filters 0-83557
 bipolar spatial filtering, incoherent, review 0-102822
 birefringent optical pulse compression 0-106437
 breather generation, inverse scatt. technique 0-78913
 CH stripe laser, spatial coherence and modal struct. 0-87531
 complex spatial coherence meas. by sinusoidal phase modulation 0-106446
 concentrator, compound parabolic, phase space conservation for incoherent propag. 0-69491
 CW VUV radiation generation 0-58640
 diffracting periodic structure generation by coherent beam interference 0-69570
 difluoromethane far IR laser gas, CW laser pumped, gain 0-69367
 fast IR wavefront aberration sensor interference problems 0-74499
 fibre optics testing techniques 0-78992
 four-point field coherence function, strong fluctuations of wave intensity 0-63927
 four-wave mixing spectroscopy, coherent cancellation of background 0-91842
 free electron laser, coherent states in single mode and multimode cases 0-102689
 free-space propagation model for coherence-separable broadband optical fields 0-78763
 Gaussian beam in laser Doppler velocimeter, interference 0-69444
 Gaussian-Lorentzian light, photon counting distrib. factorial moment, spatial coherence 0-83571
 generalised matched filters for coherent optical pattern recognition 0-99654
 light coherence continued
 generalised optical theorem for partially coherent interfering beams 0-106447
 holographic image contrast degradation with partially coherent light reconstruction 0-102678
 holographic movie camera and projection system 0-78808
 holography and coherent optics, information theory, book 0-98764
 holography in partially coherent light, using Michelson interferometer 0-58480
 IC photomask and wafer linewidth meas. using optical spatial coherence 0-77850
 image registration and differencing by coherent optical pattern recognition 0-99648
 image weak modulation detection in film grain noise with partially coherent illumination 0-77897
 imagery of extended objects 0-106465
 imaging system point spread function determ. by scatt. of two monochromatic beams 0-87316
 inhomogeneous media, coherent states and light propag., graded-index waveguide coupling 0-102625
 injection laser, comprehensive model, current depend. of spontaneous and coherent emission 0-74361
 intensity fluctuations and fourth-order coherence function in random media 0-78774
 interference transfer function with quadratic detect., coherent illum. 0-78782
 laser beam coherence and divergence (*Spanish*) 0-87424
 laser beam spatial coherence control by progressive US wave 0-78885
 lower limits of degree of coherence, limiting forms of density operator and distrib. function 0-87300
 methanol far IR laser gas, CW laser pumped, gain 0-69367
 microdensitometer performance, effective incoherence and flare tradeoff 0-77851
 microscope, polarizing, with crossed polarizers, incoherent diff. imagery 0-101838
 modulation by US waves, partial coherence depend. on US parameters 0-58453
 multilevel system, group theoretical method for coherent effects calc. 0-106502
 nonlinear optical amplifier, coherent radiation statistical props. 0-99691
 nonlinear spectroscopy, coherent background noise elimination from saturation spectrosc. signals using freq. offset pump 0-62733
 optical fibre, spatial coherence and modal struct. 0-87531
 optical instrument design, partial coherence effects 0-78767
 optical processing appls., beam coherence modification by transparencies 0-78769
 optical systems, entropy and negentropy (*French*) 0-102608
 partial spatial coherence blur correction by postdetection image processing 0-78792
 partially coherent beam intensity fluctuation calc. in turbulent atmosphere 0-78775
 partially coherent perpendicularly polarized vibrs., anisotropic photographic recording, interferograms 0-57364
 partially coherent radiation, optical heterodyne detection 0-77871
 partially coherent source radiant intensity, theorems and expts. 0-78768
 partially coherent sources with phase profile, Van Cittert-Zernike theorem 0-63919
 particle cluster, coherent light scatt., spatial correl. function calcs. 0-99632
 pattern recognition using normalised invariant moments 0-99653
 periodic structure with coherent illum., resolution depend. on number of elements, wavelength and focal length 0-63941
 phase conjugation by degenerate four-wave mixing, coherence effects 0-64101
 photographic film grain noise in partially coherent imaging 0-101860
 projection system, wavelength and coherence effects 0-64136
 pseudocolour density encoding, white-light, using contrast reversal 0-83560
 radiometry, fundamental quantities and partial coherence effects 0-77838
 Raman spin-flip laser, multiply pumped, coherence effects 0-87398
 real-time incoherent subtraction of irradiance 0-74301
 retrieval problem in coherence theory, moment estimator approach 0-95785
 ruby crystal, radiation amplification, spatial coherence 0-99737
 scattering object, coherently illuminated, speckle pattern statistics in diff. field 0-63924
 signal processing, time-integrating, acousto-optic 0-102641
 solitons in the theory of guided lightwaves 0-58760
 space-variant coherent optical processing 0-102638
 spatial coherence meas. by correlated diffusers 0-74296
 spatial pattern recognition by spectral feature classification and coherent optical correlation 0-99644
 speckle reduction in image plane by US modulation of spatial coherence 0-106459
 speckle statistical props. and coherence aspects 0-78773
 spot size estimate in diff. pattern of scattered field 0-95789
 storage of optical coherence, stimulated optically induced nucl. spin polaris. 0-58649
 superfluorescence temporal and spatial coherence, from independ. SF beams interference obs. 0-58492
 superluminescence, spatial coherence 0-99683
 superposed coherent and chaotic radiation, computer simulation 0-58485
 temporal coherence rel. to optical noise, partially coherent imaging 0-102611
 tendon, rat-tail, coherent optical SHG 0-89796
 three level system, coherently pumped, cooperative relax. 0-78816
 turbulent atmosphere, beam props. of partially coherent curved beam waves 0-95798
 turbulent medium, four-point coherence function strong intensity fluctuations region 0-87319
 turbulent medium, pulsed laser radiation intensity fluctuations during thermal selfinteraction 0-102781
 UV coherent pulse, 45 GW, for laser fusion 0-69450
 wavefront reversal, transverse enhancement of coherence of scatt. field 0-95952
 white light image speckle statistical props. 0-106461
 AlGaAs DH injection phase-locked laser, coherence 0-102726
 As₂S₃ film, optical recording, light scatt. enhancement due to coherence 0-97362
 GaAlAs DH laser coherent light, propagating in multimode optical fibre, speckle contrast 0-78978

light coherence continued

- He-Xe 3.51 μ laser mode competition in axial mag. field 0-63974
- LiNbO₃:Ti diffused channel waveguide, optical parametric amplification 0-106564
- Nd:glass laser radiation, spatial coherence of fundamental and second harmonic 0-69442

light communication *see optical communication***light cones**

see also current algebra

- hadrons, extended, Lorentz deformation props., O(4) and light-cone coordinate systems 0-68354
- left-flat space-times, null tetrad and restrictive conditions 0-62545
- parton model interpretation of cut vertex formalism 0-86566
- QCD calcs., non-singlet quark struct. function 0-57464
- renormalised perturbation theory, light cone expansion 0-99045
- Wightman function, two-point, asymptotic behaviour 0-73614

light diffraction

see also holography; optical zone plates

- aberrated diffraction pattern obs. with computer-generated holograms 0-102681
- aberrational diffraction images, computation accuracy 0-87328
- aberrations, scalar diffraction theory, exact solns. 0-78778
- acousto-optic deflector, bandwidth increase method 0-99861
- acousto-optical diffraction, multifrequency, in optically birefringent media 0-74300
- acoustooptical interaction in strong field 0-95790
- amplitude filtering for superresolution, maximum central irradiance under energy constraint 0-91914
- annular aperture, light distrib. from diffr., aberration correction using mirror lenses (*German*) 0-69325
- apertures, multiple circular, located on circle, resolution 0-102615
- apertures with triangular and assoc. filters, variable apodisation 0-63914
- apodization, optimal, by means of coupled calc. of pupil function and shape 0-95788
- aspheric, testing in reflected light using blazed synthetic holograms 0-91881
- bilinearly distorted image linear restoration using Wiener filters 0-83557
- bipolar spatial filtering, incoherent, review 0-102822
- cellular deformability, diffractometric method for meas. 0-98187
- cholesteric liquid crystal, blue phase, struct., Bragg diffr. of visible and UV light 0-59385
- coherent information processing by a pair of lenses in spherical wave illumination 0-95816
- complex resonator with internal diaphragm, diffr. losses and field distrib., integral eqns. 0-95921
- copper phthalocyanine, chlorinated, radiation damage mechanism 0-88000
- coronagraph diffraction limit problems and design approaches 0-82200
- correlation filtering for increasing diffr. efficiency 0-96028
- correlators, diffr. optics based, invariant to optical element shifts 0-106471
- cross-shaped aperture, Fresnel and Fraunhofer diffraction 0-106436
- crossed slits, Fresnel and Fraunhofer diffraction 0-106436
- crossed-beam volume gratings, three dims., diffr. characts. 0-78975
- cylindrical light wave diffr. by complex spectral composition US 0-95939
- deep dielectric gratings, light diffr., transform. props. 0-99835
- defect crystal structure determination 0-103316
- diffraction gratings, theoretical method, numerical appl. 0-95786
- diffuse object longitudinal motion under Gaussian beam illum., laser speckle dynamic statistical props. 0-99628
- domain lattice of transparent crystal regular birefr. regions, optical wave diffr. divergence 0-102616
- dynamic self-diffraction of coherent light beams, review 0-102777
- field diffraction with light shadow boundary on wedge and half-plane, calc. (*Ukrainian*) 0-69324
- focused field, symmetry props. 0-83550
- Foucault, phase edge and wire optical test 0-96046
- Fraunhofer diffraction patterns, from apertures illuminated with nonparallel light 0-67983
- Fraunhofer diffraction patterns, phase reversal effect 0-101691
- Fresnel lenses in BaO optical waveguides 0-96034
- Fresnel plane interference fringe generation by correlated speckle patterns 0-106462
- Gaussian laser beams, Fraunhofer diffr. by single slits 0-87298
- Gaussian light beam, diffr. by plane acoustic waves at oblique incidence 0-69326
- grating, reflective, high efficiency, scattering types 0-99619
- high intensity light, ultrasound in nonlinear liquids 0-64270
- holograms, rainbow, demonstration of diffraction and interference of light (*Polish*) 0-68001
- holography and coherent optics, information theory, book 0-98764
- homogeneous medium, Gaussian light beam propag., diffr. effects described using complex-ray method 0-78770
- ice crystals, diffr. theory for forward scatt. pattern (*Russian*) 0-94601
- image intensity fluctuations in turbulent atm. after refl., Huygens-Kirchhoff principle calcs. 0-63926
- intracavity resonance asymmetries, nonlinear freq. depend. diffraction effect 0-99760
- inverse theory of scalar diffr., eigenvalue formulation 0-102613
- isolated surface circular defect diameter determ. based on Fraunhofer diffr. 0-73307
- Lamb wave optical detect. in fused SiO₂ 0-106690
- large-aperture optical system, energy distrib. calc. in diffr. image of point 0-74305
- laser beam coherence and divergence (*Spanish*) 0-87424
- laser cavity diffraction experiment with 1-D diaphragm 0-95920
- laser pulse autocorrelation by optical processing of Fabry-Perot spectrograms 0-58465
- laser radiation intensity distrib. meas. using Bragg diffraction of light 0-64092
- lens design with simultaneous image spot, optical path difference, diffraction MTF and Seidel aberration minimisation 0-74459
- locally deformed slab waveguide propagation and diffraction patterns 0-106630
- Luneberg apodization problem 0-87302
- 3-methylpentane-nitroethane critical binary liquid mixture, US absorpt. 0-107376
- microscope, polarizing, with crossed polarizers, incoherent diffr. imagery 0-101838

light diffraction continued

- microscopical and Ewald dynamical diffraction theories, refl. and transmission, spatial dispersive dielec. slab 0-83548
 - multielement acoustic array characterisation by acousto-optic diffraction 0-99911
 - muscle, cross-striated fibres, efficiency of light diffr. under stretch and isometric contract 0-85440
 - nuclear track detectors, glass and plastic laser diffr. appl. to determ. of etched track parameters 0-95499
 - open cavity, Slater method validity 0-69428
 - optical pattern recognition by diffraction pattern sampling 0-99643
 - optical system, diffraction and aberration effects, wave optical calc. 0-83549
 - optical system tolerancing, encircled energy performance prediction 0-78935
 - optical systems with pupils of non-uniform transmittance 0-87470
 - parallel plane diffr. grating with periodic structure, diffr. of plane wave 0-102620
 - periodic object single sideband Fresnel diffr. pattern studies 0-106440
 - point-diffraction interferometer principles and applications 0-74530
 - Q-switch, ultrasonic, for Nd:glass laser 0-64034
 - rainbow phenomena and the detection of nonsphericity in drops 0-58456
 - real stationary ultrasonic field in liquid, temporal modulation of light beam 0-83551
 - regularized object restoration, resolution beyond the diffr. limit 0-87324
 - resonance atom, spontaneous diffr. of light 0-91512
 - resonator, Gardner-Fresnel-Kirchhoff propag. algorithm 0-83621
 - ring laser, open cavity matrix eqns. in diffraction theory 0-69429
 - ring laser diffraction theory, perturbation method 0-95919
 - rough surface, random, reflectance derived with Fresnel approx. 0-87309
 - scattering object, coherently illuminated, speckle pattern statistics in diffr. field 0-63924
 - scatterplate interferometer, scalar diffraction theory 0-73432
 - shaded circular apertures, encircled energy in diffr. pattern, super-resolving and apodising props. 0-95787
 - single mode fibre near- and far-field characteristics, profile-independent representation 0-58739
 - single slit diffraction, theory testing expt. 0-77568
 - solid bodies, optic-geometric method calc. of diffraction patterns (*Russian*) 0-91746
 - speckle, dynamic props., zero-crossing study 0-63923
 - sphere, evanescent wave contrib. to diffracted amplitude 0-74295
 - spheroidal particles, colloidal dispersions, refractive index 0-106454
 - spot size estimate in diffr. pattern of scattered field 0-95789
 - striated muscle diffraction patterns, data acquisition and anal. 0-89918
 - strips illuminated at grazing incidence, uniform geometrical theory of diffr. soln. 0-58447
 - thermal self-action problems and their compensation 0-106579
 - thick layers with regular domain structure, magnetooptical diffr. of light 0-108188
 - thick planar grating, Bragg diffr. of finite beams, coupled-wave theory 0-63917
 - two coord. deflector, anisotropic diffraction and wide band scatt. 0-91920
 - ultrasound, phase geometry variation analysis 0-106441
 - US beams, diffraction of perpendicular light beam 0-87629
 - volume phase grating, angular depend. of width of Bragg peak 0-78811
 - volume phase grating, TM and TE mode diffr. efficiency, comparison 0-74507
 - Woods anomaly angular alignment gratings 0-69503
 - CO₂ laser Antares fusion system optical diffraction computation 0-74424
 - EuO film threshold characteristics in holographic and bit recording (*Russian*) 0-63944
 - NH₄Br, dislocation influence on phase transition and light scatt. (*Russian*) 0-59648
 - Pb₂Ge₂O₁₁, ferroelec. transition, US and elasto-optic props. 0-60527
 - TeO₂, two coord. deflector, anisotropic diffraction and wide band scatt. 0-91920
- light diffusion** *see light scattering*
- light dispersion** *see optical dispersion*
- light emitting devices**
see also light emitting diodes; light sources; luminescent devices
 ZnS powder phosphors electroluminescent cells, AC electrolum. characts. (*Japanese*) 0-71489
- light emitting diodes**
see also semiconductor junction lasers
 alternative scanned light sources 0-69477
 colour masters evaluation, using reflection coupling device (*German*) 0-95123
 glass fibre long wavelength optical communication, materials and devices, review 0-99854
 high radiance semiconductor light source for fibre optical communication 0-58653
 IR emitting diodes and injection lasers, optical communication appls. 0-58563
 light panel, spatial frequency analysis with incoherent optical approach 0-78779
 LPE growth method to reduce thermal degradation of substrates, appl. to LED fabrication 0-104061
 matching of semiconductor sources to thin-film planar and stripe waveguides 0-64174
 near IR (1 to 2 μ m) optical communications, colloquium, London, England (May 1980) 0-86040
 optical communications systems, components, review 0-87539
 optical coupler, low loss, for coupling LED to fibre-optic system 0-91907
 optical fibre sources and detectors (*Italian*) 0-69390
 optical fibre transmission system devices (*Japanese*) 0-58693
 optical parameter meas. using Si, photovoltaic cell, absolute spectral sensitivity calibration, radiometry, photometry (*Chinese*) 0-86367
 optoelectronic devices development 0-91902
 photographic print timer, using ring of LEDs 0-77899
 point source emitter 0-73150
 radition therapy, thin Pb sheets as tissue compensators for larger field irradi. 0-104736
 red, luminance-brightness discrepancy 0-91942
 scintillation spectrometer stabilisation using LED reference light source 0-91365
 SEM study of charge collection and cathodoluminesc. 0-65661
 transmission system, semiconductor device reliability tests 0-58573
 GaAs:Si p-n junction LED, electroluminesc. efficiency 0-71491

light emitting diodes continued

- GaAs-Ga_{1-x}Al_xAs DH LED, for optical fibre communication (*Japanese*) 0-78976
 GaAs-GaAlAs wafers, defects and degradation, transmission cathodolum. evaluation 0-65395
 GaAs-GaInAs structure, dislocation struct., TEM anal., appl. as IR LED 0-70206
 Ga_{1-x}In_xAs epitaxial layer growth by organometallic pyrolysis, homojunction LED prep. 0-76194
 GaInAsP LEDs, 1.3-1.6 µm, appl. in long haul high data rate fibre optic communication systems 0-102854
 GaN, VPE growth rate influence on elec. and luminesc. props. 0-100702
 GaP electroluminescent diode struct. prep. by SSD and Czochralski methods, dynamic props. (*Czech*) 0-97425
 GaP, VPE layer structures for LED's, SEM, and TEM obs. of dislocation density reduction expt. 0-100425
 GaP-N LED structures, local dopant conc. determ. using SEM cathodolum. spectra 0-101057
 GaP:S, defect-struct. and tetrahedral precipitates, TEM study 0-107246
 pGaP:Zn-electrolyte interface, electrochemical LED, luminescence obs. 0-84507
 InGaAsP LED sources, for near-IR absorpt. meas. 0-77135
 InGaAsP-InP DH LED, high temp. aged, dark-spot defects, TEM obs. 0-66300
 InP-InGaPAs heterojunction lasers and LEDs, 1.0 to 1.2 µm 0-74362
 PbS_{0.1}Se_{0.9} 4.6 µm LED, room temp., band gap and electrolum. 0-66302
 SiC (6H), blue-emitting diodes by CVD 0-97439
 SiC, defect luminesc. 0-89069
 SiC devices, epitaxial layer growth techniques 0-108360
 SiC LEDs prepared by overcompensation method, photon assisted tunnelling 0-97341
 SiC p-n junction, electroluminesc. 0-97343
 ZnSe, low resistance ohmic contacts using In-Ga liquid alloy, LED fabrication appl. 0-70823
 ZnTe, low voltage green LED, struct. double diffusion procedure 0-100697

light filters *see optical filters***light intensifiers** *see image intensifiers***light interference**

- see also light interferometers; light interferometry; Moire fringes*
 acoustic sensor, fibre-optic, modulation processes 0-58771
 adaptive focusing of light in inhomogeneous nonlinear medium, interf. criteria 0-99633
 algorithm for fast digital analysis of interference fringes 0-73426
 aspheric, testing in reflected light using blazed synthetic holograms 0-91881
 birefringent object film effect on interf. pattern, construction of multi-capacity matched filters 0-74478
 coherent fast IR wavefront aberration sensor interference problems 0-74499
 coherent Gaussian beam in laser Doppler velocimeter, interference 0-69444
 diffracting periodic structure generation by coherent beam interference 0-69570
 electro-optical polarisation conversion and interference tunable filters 0-102829
 fibre, single-mode systems, instability due to interference and polarization effects 0-58774
 Fresnel plane interference fringe generation by correlated speckle patterns 0-106462
 fringe intensity distrib. of elliptically polarised beam near critical angle 0-106449
 fringes, separation between maxima, evaluation from difference record of interference fringes 0-62731
 fringes of Fresnel double mirror, localised and unlocalised, theory extended to wedge 0-67960
 generalised optical theorem for partially coherent interfering beams 0-106447
 hologram interference fringe bending analysis and expt. 0-106494
 holograms, rainbow, demonstration of diffraction and interference of light (*Polish*) 0-68001
 holography and coherent optics, information theory, book 0-98764
 image subtraction through speckle modulated by Young fringes 0-95813
 laser beam coherence and divergence (*Spanish*) 0-87424
 laser speckle and surface roughness 0-102622
 liquid, extinction coefficient meas. using coaxial dual channel laser system 0-73425
 localised interference fringes, teaching 0-101680
 microscopic interference obs. by reflection contrast 0-68248
 multimode fibre link, modal noise 0-87536
 nematic liquid crystals, refractive index and birefringence by interference method 0-96440
 nonlinear crystals, interference of optical harmonics 0-64102
 nonlinear interference mirror, reflection of light 0-102761
 optical surface contract interaction zone, thickness calc. and distance meas. methodology (*Russian*) 0-99889
 OTF measurement using autocorrelation method 0-58469
 partially coherent light, lecture demonstrations 0-101700
 pattern electronic heterodyne recording 0-74316
 plane parallel optical layer interference props. for radiation parameters control 0-83547
 polarimeter, photoelectric, effect on accuracy of light interference in bi-quartz modulator 0-62713
 prism optics testing for laser interferometer, interf. meas. 0-105698
 rainbow phenomena and the detection of nonsphericity in drops 0-58456
 single slit diffraction, theory testing expt. 0-77568
 spectrometer, diode laser dual-beam, long-term temporal and scanning characts. 0-90902
 superfluorescence temporal and spatial coherence, from independ. SF beams interference obs. 0-58492
 synchrotron radiation interference effects 0-63906
 transfer function with quadratic detect., coherent illum. 0-78782
 p-Si, heavily doped contact layers on IR detectors, IR transmissivity 0-108190
 SnS₂ thin layer, far IR refractive index 0-93421

light interferometers

- see also light interferometry*
 aspheric, testing in reflected light using blazed synthetic holograms 0-91881

light interferometers continued

- birefringent element, analogue, built from polarising wide field Michelson interferometer 0-91895
 birefringent fibre interferometric secondary light source 0-105702
 bistable optical device development from integrated two-arm interferometer, appls. (*French*) 0-69555
 channel waveguide interferometric modulator for EM field detection 0-74498
 chevron beam-splitter, double-pass 0-73431
 complex Fourier spectra, interferometric determ. 0-87327
 confocal Fabry-Perot feedback system, partial differential eqn. analog soln. 0-102630
 contactless laser interferometer sweep gauge for diamond-turned surfaces 0-73441
 correlator with matched filtering using band-limited illumination 0-69531
 data handling in high vibration environment 0-95132
 design, construction and interferogram processing, optical testing appl. 0-79020
 design for high vibration environment 0-95131
 digital beam switch for 10.6 µm laser radar 0-102836
 digital beam switch for agile beam laser radar 0-58620
 diode laser wavelength monitoring using fibre interferometer 0-74413
 double beam interferometer for background suppression and spectral detection 0-95129
 electro-optical linear interferometric modulator for electromagnetic field detection 0-58782
 Fabry-Perot, piezoelectrically scanned, microcomputer-based data acquisition and stabilization system 0-62719
 Fabry-Perot, ruby laser frequency selection and stabilisation 0-58566
 Fabry-Perot etalon, optically contacted, stability to cosmic radiation 0-98544
 Fabry-Perot etalon, tunable spatial filtering 0-58668
 Fabry-Perot imaging device TAURUS for radial velocity field maps 0-82205
 Fabry-Perot interferometer, multiple-zone aperture design for airglow temp. 0-82075
 Fabry-Perot interferometer, optical bistability, inhomogeneous broadening, mean field approx. 0-90885
 Fabry-Perot interferometer instrumental function for short light pulses 0-105704
 Fabry-Perot nonlinear interferometer, beam profile hysteresis variations 0-86393
 Fabry-Perot pressure scanning interferometer, expt. construction (*Japanese*) 0-77848
 Fabry-Perot resonator with plane-parallel mirror, polaris. effects in gas lasers 0-58605
 Fabry-Perot scanning interferometer, far IR performance 0-86388
 Fabry-Perot spectrometer for solar vel. field meas. 0-90333
 Fabry-Perot-interferometer imaging system for thermospheric temp. and wind meas. 0-101441
 far IR interferometers with wire-grid beam dividers, freq. response 0-57365
 fibre optic interferometric sensor for acoustic detect., thermally induced optical phase effects 0-74479
 fibre optic Mach-Zehnder interferometer as mag. field sensor 0-69510
 fibre optic rotation sensor, all-waveguide configuration, key element tests 0-58796
 fibre optic rotation sensor with low drift 0-69530
 fibre optical interferometers for length, temp., pressure and force meas. 0-98971
 fibre-optic interferometer gyro, thermally induced nonreciprocity 0-58665
 Fizeau interferometer, spherical-wave, direct phase meas. 0-95126
 Fourier spectroscopy, far IR, spectrum distortion by multiple reflections using Michelson interferometer 0-82837
 IR laser interferometer operation and testing 0-73433
 IR lateral shearing, as optical testing tools 0-68244
 IR Smartt interferometer, alignment tool for CO₂ laser fusion systems 0-74425
 large-aperture interferometer with low-resolution holographic corrector plate 0-74315
 laser, gyromagnetic ratio of proton and fine-structure constant redeterm. 0-74253
 laser, microcomputer-based, for angular displacement meas. in instrument graduation (*Polish*) 0-90816
 laser, calibration and measurement standard, high precision (*German*) 0-78862
 laser interferometer, 500-m base, Earth surface deform. detect. 0-105087
 laser interferometer, prism optics testing, interf. meas. 0-105698
 laser interferometer systems, theory and application 0-73435
 laser interferometers, AM and FM operation and applications (*German*) 0-86389
 laser probe for measurement of vibrations of very small amplitude, in US transducers 0-73443
 laser unequal path interferometer with electro-optical camera and mini-computer, fabrication/test appl. 0-77847
 Mach-Zehnder interferometric optical switches for integrated stable optical multivibrator 0-87560
 methanol far IR laser, twin optically pumped, for plasma diagnostics 0-59306
 Michelson, for holography in partially coherent light 0-58480
 Michelson interferometer, active stabilization by electrooptically tuned laser 0-86386
 Michelson interferometer, cryogenic, rocket-borne, for EXCEDE II expt. 0-95133
 Michelson interferometer, polarizing, for far IR and MM regions 0-73427
 Michelson interferometer, residual path difference depend. on mirror setting ang. errors 0-77845
 Michelson interferometer for wavelength comparisons 0-98969
 Michelson laser interferometers, noise limitations 0-82808
 microprocessor-based interferometric data reduction system versatility 0-73439
 microscope, interference, with freq. shift, for glass fibre refr. index profile meas. 0-64175
 mirror fiducial system compatible with computer-controlled polishing facility 0-74539
 modified Michelson interferometer for hologram prod., undergraduate expt. 0-105473
 modulated fibre ring interferometer, laser appl. 0-74506
 multiple-beam wedge-shaped, for high-speed laser Doppler velocimeter 0-99782

light interferometers continued

- optoelectronic-mechanical instrum. for evaluating dynamic stress-optical coeffs. and ratio of Poisson's ratio to modulus of elasticity 0-86394
 phase-switching of a dispersive non-linear interferometer 0-82810
 phase-tracking stellar interferometer, first fringe meas. 0-82215
 picosecond optical sampling, cascade of waveguide interferometers driven by microwaves 0-99849
 point-diffraction interferometer principles and applications 0-74530
 preprocessor, use in Earth-resources satellites 0-67430
 quasiquadrature interferometer for plasma density radial profile measurements, with 10-channel operation 0-70038
 radial grating lateral shear heterodyne interferometer, adaptive optics appl. 0-77843
 rapid-scan polarising Michelson interferometer and InSb detector calibration 0-59305
 scatterplate, in uncommon path mode, for null testing 0-79015
 scatterplate interferometer, scalar diffraction theory 0-73432
 scatterplate interferometer principles, limitations and tolerances 0-73436
 second-harmonic interferometers 0-101833
 semiconductor etalon, optical bistability and ns modulation 0-64096
 semiconductor Fabry-Perot interferometer retuning by optical excitation (*Russian*) 0-98970
 Shack interferometer for optical shop use 0-73434
 shearing interferometer for dense laser prod. inhomogeneous plasma (*Russian*) 0-83994
 single mode optical fibre, small phase shift meas. 0-57366
 solar rotation induced Doppler spectral shift meas. by scanning Fabry-Perot interferometer 0-77298
 space-borne interferometers, astrometry and planetary detection 0-109357
 specimen holder for transmission dispersive far IR Fourier transform spectroscopy 0-86468
 spherical optical surfaces testing, shape deviation determ. (*Czech*) 0-58821
 Tokamak, JET, far IR interferometer design 0-59295
 Zygo interferometer system 0-73437
 $\text{Al}_{0.42}\text{Ga}_{0.58}\text{As-GaAs-Al}_{0.42}\text{Ga}_{0.58}\text{As}$, etalon, optical bistability and modulation 0-58628
 He-Ne $^{121}\text{I}_2$ stabilised laser source for Michelson interferometer, optical feedback obs. 0-106545
 Nd^{3+} :YAG laser frequency stability improvement using active interferometer (*Russian*) 0-64043
 Si Fabry-Perot couplers for optically pumped far IR lasers 0-69404

light interferometry

- see also *holographic interferometry*; *Moire fringes*
 air at Ti surface, optical breakdown, interferometric investigation 0-100064
 algorithm for fast digital analysis of interference fringes 0-73426
 anomalous dispersion meas. using 4-beam Rozhdestvenskii interferometer 0-68245
 astronomical speckle interferogram masking, holography and phase flipping 0-109373
 binary stars, obs. by speckle interferometry 0-90477
 binary stars, speckle interferometric obs. with Haute-Provence 1.93 m telescope 0-90475
 biological objects, electronic speckle pattern interferometry in vivo 0-109083
 bonded interface defect testing by differential interferometric Stoneley wave meas. 0-76444
 capacitive excitation of elastic oscillations 0-71862
 complex aspheric mirror testing by phase meas. interferometry 0-74467
 complex spatial coherence meas. by sinusoidal phase modulation 0-106446
 concave paraboloidal mirror, prod. method, interferogram tests 0-58823
 contactless thermal expansion meas. by double Michelson interferometer 0-73317
 correlative data processing system using semiconductor injection laser 0-74307
 cylindrical mirror and lens optical figure characterisation with conventional interferometer 0-78944
 defect crystal structure determination 0-103316
 diamond turned surface production, interferometric test repeatability 0-74538
 dielectric film, refractive index and thickness meas. by optical method 0-82806
 dielectric relaxation spectroscopy of polar fluids in microwave region, double beam interferometry method (*German*) 0-71309
 double beam interferometer, meas. of background suppression and spectral detection 0-95130
 dual-mode optical fibre, spatial technique for modal delay difference meas. 0-78950
 electron irradiated solid, dynamic and dosimetric charact., laser and holographic interferometry obs. (*Rumanian*) 0-90886
 electronic phase meas. techniques in optical testing 0-106643
 Fabry-Perot, consequences of piezoelectric ceramic LF charact. 0-86390
 filter, interferometric, illum. with convergent beam, spectral response optimisation (*French*) 0-99868
 Fourier spectroscopy, ghostline intensity in far IR 0-73480
 functional group analysis of interferometric data from GC Fourier transform spectroscopy 0-89548
 geodesic interference distance meas. using semicond. lasers 0-77175
 high-current arc electrode vapour influence and estimation 0-70070
 high-pressure gas equation-of-state meas. 0-77810
 holography, twin-image, chromatic lens system, astron. appls. 0-87346
 hydrophone, optical interferometric, with homodyne detection, signal stabilization by light source tuning 0-87477
 interference microscopy, for colour development and phase separation 0-100976
 interferometric examination techniques 0-69498
 Interphako interference microscopy, refr. index profile determ. of light focusing rod 0-101832
 IR, dual beam Fourier transform spectrometer, sensitivity improvement by using Digilab 496 interferometer 0-90910
 IR optical components and aspherics, $10.6\ \mu\text{m}$ interferometric testing 0-74523
 laboratory's absolute velocity meas. 0-95081
 laser, fluid props. meas. 0-75018
 laser, use in analytical ultracentrifuges, background suppression of multiplexer-gated modulatable laser 0-73430
 laser beam expander for short cavity dye laser 0-87532

light interferometry continued

- laser fusion cryogenic target characterisation by wavefront shearing interferometer 0-74008
 laser interferometric auto-correcting system of high precision thread grinder 0-90830
 laser speckles, bibliography (1976 to 1978) 0-82593
 laser system, interferometric optical anal. 0-87401
 laser wavelength meas. with post-detection signal processing 0-105699
 length meas. of gauge blocks, sources of random errors 0-105613
 length meas. with curved wavefronts (*German*) 0-77752
 length measurement with heterodyne interferometry (*German*) 0-68181
 lens wavefront aberration, interferometric examination techniques 0-69498
 leucosapphire, unique polishing features of hard crystals 0-64225
 liquids, diffusion coeff. meas. and refractive index depend. on concentration at different wavelengths 0-88346
 long-radius concave optical surface curvature meas., differential technique 0-74534
 2,6-lutidine-water thick films, interferometric obs. of crit. behaviour 0-93266
 machine tool position feedback by laser interferometer 0-73438
 metals, coated, IR surface wave interferometry 0-63913
 methanol trace detection using phase fluctuation optical heterodyne spectroscopy 0-68266
 mirror, single-point diamond-turned, performance before and after polishing 0-74466
 mirrors, plane, spatially separated, adjustment to coplanarity, interferometric technique 0-95974
 MTF, two-dimensional, meas. by second order speckle statistics calc. 0-63937
 multimode fibre optic interferometry, applications 0-86387
 multiplex image coding, astronomical IR speckle interferometry appl. (*French*) 0-67580
 NGC 604, H II region in M 33, H β photometry and Fabry-Perot interferometry rel. to core-halo struct. 0-85984
 noncontact material testing using laser energy deposition and interferometry 0-71846
 optical fibre, γ -irrad., differential interferometric meas. of refr. index changes 0-78952
 optical fibre preform rod, refractive index profile meas. by transverse differential interferometer 0-64141
 optical shop computer-controlled interferometry, in-process production tool 0-74531
 optical shop interferometric instrumentation as a cost-effective production tool 0-74535
 optical system acceptance testing with interferometer 0-95987
 optical testing status and prospects 0-74529
 organic compounds, nonlinear refr. index meas. by time integrating interferometry 0-102758
 parabolic mirror testing by vibration-insensitive laser unequal path interferometer 0-74537
 parabolic mirror testing during fabrication by long-wavelength interferometer 0-74536
 partially coherent perpendicularly polarized vibr., anisotropic photographic recording, interferograms 0-57364
 plano-plano interferometer modes, FFT computation, Fresnel numbers 0-86392
 polarisation interferometer, meas. of local convective heat transfer coeff. for plate calorimeter 0-82809
 polarisation props., optically active samples in ring interferometers (*German*) 0-77846
 precision optical element testing by phase meas. interferometry 0-74520
 precision optical evaluation by phase meas. interferometry 0-74533
 precision optical testing, using laser interferometers, microprocessors and computers 0-69563
 quick precision alignment of equipment, calibration against external goniometers 0-73429
 random-phase screens, deep, interferometric anal. 0-101834
 refractometry, precision automatic vee block, for glass refr. index meas. 0-68243
 retroreflector alignment, simple interferometric technique 0-95125
 ring laser interferometry, test of preferred frame cosmologies 0-77531
 rough surface interferometry at $10.6\ \mu\text{m}$ 0-86385
 ruby, unique polishing features of hard crystals 0-64225
 seismic microvibration frequency analysis by 50 m interferometer 0-109276
 seminar, San Diego, CA, USA (Aug. 1979) 0-73096
 signal processing, time-integrating, acousto-optic 0-102641
 silicone elastomers, dental impression materials, dimens. stability, holographic and interferometric study 0-67204
 single-mode optical fibre interferometry 0-73442
 spatial coherence meas. by correlated diffusers 0-74296
 speckle interference fringes, lens aberration effects 0-105700
 speckle interferometric analysis of transient phenomena 0-105701
 speckle interferometry image processing technique requiring no reference point 0-98556
 speckle pattern interferometry, electronic, using digital image processing techniques 0-87322
 speckle photography, double exposure, anal. technique 0-62718
 sphericity standards, interferometric meas. (*German*) 0-87569
 step height determ. by two-wavelength speckle pattern method 0-105614
 surface topography quantitative determ. by Nomarski differential interference contrast microscopy 0-73318
 testplate testing interferometry in precision optical shop 0-74532
 tetrafluoroethane, specific refractivity, interferometric meas. 0-95124
 tetrafluoromethane, specific refractivity, interferometric meas. 0-95124
 thermal expansion, speckle interferometric meas. apparatus 0-68170
 three-dimensional display interferometry of lenses, mirrors, and optical systems 0-69497
 time-wavelength coordinates obtained using spectrograph, time scan 0-62717
 truss joint strain meas. by modified Michelson interferometer 0-74821
 tunable laser interferometry, oscillator strength meas. 0-105697
 two wave interferogram sensitivity improvement process (*French*) 0-98968
 two-beam interference fringe interpolation method 0-105703
 two-beam interference pattern monitoring by phase modulation 0-77844
 two-dimensional optical system MTF meas. by second-order speckle statistics computation 0-74304
 vertical surface melting, heat transfer interferometric meas., convection effects 0-64339

light interferometry continued

- vibration measuring system using interf. fringes TV detect. and electronic image processing 0-103004
- video interferogram analysis by TV camera-microprocessor system 0-73440
- wavefront interpretation with Zernike polynomials 0-78776
- wavelength comparisons with primary Kr standard using Michelson interferometer 0-98969
- wavelength stabilisation, review of decade of work in Switzerland (*German*) 0-57250
- X-ray mirror profile meas. machine 0-69496
- Al plate, thermal strain meas. by one-beam laser speckle interferometry 0-103005
- CO₂ laser fusion system optical design and analysis 0-74391
- Fe-Ni, interference microscopy, for colour development and phase separation 0-100976
- He-Ne 3.39 μ m laser interferometer, length and refr. index meas. 0-68172
- He-Ne lasers, wavefront curvature and diffraction effects in high precision wavelength comparisons with a Michelson interferometer 0-99781
- LiNbO₃:Ti single mode electrooptic waveguide modulator, high-speed operation 0-91915
- NaCl 46 cm window optical evaluation facility 0-74526
- Ni alloys, cast, interference microscopy, for colour development and phase separation 0-100976
- Ni, magnetostrictive vibr. obs. by laser interferometric technique 0-66000
- SF₆, trace detection using phase fluctuation optical heterodyne spectroscopy 0-68266
- Se films, Ag diffusion, effect on interferometric thickness meas. 0-96695
- Si guided-wave acousto-optical devices 0-102864

light meters see *photometers*

light modulation see *optical modulation*

light polarisation

- see also *birefringence; optical rotation; photoelasticity; polarimetry*
- 2A 0311-227, AM Herculis type binary star, IR photometry and polarimetry 0-77517
- absorbing anisotropic and gyrotropic slab between crossed polarisers, transmitted intensity patterns 0-78762
- absorbing crystal plate light interaction, polarisation consts. 0-78765
- altazimuth sky scanner optical system, polarization characters. 0-77123
- analogue data processing systems, polarised modulation of light (*Russian*) 0-91884
- α Andromedae, shell star, lack of linear polarisation variability 0-62157
- aniline, liq., depolarised light scatt. from shear waves 0-97288
- anisotropic particles, light scatt. struct. coeff., angular depend. 0-103964
- anisotropic transition layer, surface polariton spectra in presence of resonance 0-88484
- annular HSURIA resonators, testing with CO₂ laser, polarisation effects 0-58599
- atmosphere, multiple scatt. theory for dispersive media with spherical particles (*Russian*) 0-94599
- atmosphere model, scatt. light intensity and polarisation degree, mol. anisotropy effect 0-77104
- Be stars, mag. fields determ. via linear polarisation spectrum (*Russian*) 0-90344
- beam, image-bearing, nonuniformly polarized, generation of time-reversed replica 0-69459
- benzene, liquid, polarised light two photon thermal blooming near UV spectra 0-66216
- birefringent element, analogue, built from polarising wide field Michelson interferometer 0-91895
- birefringent object, isopachics meas. using immersion method polarisation holography 0-99672
- borosilicate glass single-polarisation single-mode fibres 0-64205
- canted magnetic structured materials, exciton spectra, optical props. 0-70622
- γ Cassiopeiae, Be star, rapid linear polarisation variability (*Russian*) 0-77417
- cataclysmic binary stars (CBS), critique of polarimetric evidence on physical parameters and orbital inclination 0-109486
- α Ceti (Mira) at 1978 max., visible spectropolarimetry 0-94799
- Charlier approximation in photocount statistics 0-74328
- chiral substances, electro-optical responses, Jones matrix, meas. system for rot. anisotropy 0-84723
- chloromethane gas, linear electro-optical effect 0-87843
- circular cylinders, single scatt. phase matrix, ray optics and wave theory comparison 0-102610
- circumstellar dust shells, polarisation by Mie scatt., Monte Carlo anal. 0-98650
- circumstellar envelopes, Monte Carlo analysis of polarization by Thomson scattering 0-85931
- coherent light beam shifts on reflection at plane interfaces between isotropic media 0-102609
- computer-generated polarisation holography system and reconstructed image quality 0-102677
- conjugate interfaces: interfaces between transparent media of the same reflection coefficient for the parallel polarization at the same angle of incidence 0-87299
- corrugated waveguides, effective index approach to distrib. feedback, TE polarisation 0-102859
- cubic crystals, electro-optical effect rel. to spatial dispersion of permittivity 0-66151
- V1668 Cygni (Nova 1978), multifilter photometry and polarimetry 0-90454
- Cygnus X-1, critique of polarimetric evidence on physical parameters and orbital inclination 0-109486
- Cygnus X-1 (V1357 Cygni), V-band polarisation excursions during X-ray high state 0-90578
- Cygnus X-1 (V1357 Cygni), V-band polarisation vars. during X-ray high state 0-109560
- defect crystal structure determination, light interference, diffraction and scattering 0-103316
- demonstration, using rubber tubing model, classical analogy 0-77576
- dense stars, continuum spectrum polarisation in intense mag. fields, atomic physics theory 0-105160
- β,β' -dichloroethyl ether-iso-octane, critical indices, allowance for light double scatt. (*Russian*) 0-60624
- dielectric film, refractive index and thickness meas. by optical method 0-82806
- dielectric waveguide, corrugated, light emission 0-96027

light polarisation continued

- differential absorption at high modulation frequencies using a Fourier transform infrared spectrometer 0-95160
- diffraction grating, concave, polarisation anomalies 0-69519
- discrete deflector, matrix method anal. (*Russian*) 0-91747
- discrimination techniques used in realization of acousto-optical processors 0-74310
- dispersive media, theory of multiple light scatt. by spherical particles (*Russian*) 0-94599
- education, Brewster angle in semi-infinite dielectric moving perpendicularly to interface 0-57034
- electric dichroism measurement instrument with digital processing 0-82800
- electro-optic, polarisation-conversion wavelength-selective fibre switches 0-58736
- electro-optical polarisation conversion and interference tunable filters 0-102829
- electron impact excited line radiation, polarisation, long-range electron correls. effects 0-91683
- electronic spectra of molecules, pure elec. quadrupole transition polaris. 0-63691
- electrooptic polarization modulated injection laser 0-58591
- ellipsometric characters. of optical surfaces, determ. using nanosecond laser pulses 0-101822
- ellipsometry, Mueller-Stokes calculus, conventions and formulas 0-102618
- ellipsometry of transparent films on transparent substrates, theory 0-104007
- far IR laser intracavity polarisation modulation by CdTe AC Faraday rotation 0-58613
- fibre, single-mode systems, instability due to interference and polarization effects 0-58774
- fibre loss, dispersion and polarisation meas. by acousto-optical tunable filter 0-102855
- fibre optic devices, single-mode, fractional wave devices and polarisation controllers 0-106606
- fibre optic rotation sensor with low drift 0-69530
- fibre signal polarisation statistical meas. 0-99877
- fibre-optic polariser, in-line, formation and props. 0-106603
- fibres characters, single-mode, VAD, long-length 0-106604
- fluids, simple, light scatt., particle-hole model 0-60613
- foil, HeH⁺ impact, disocc., emitted light polarisation meas. 0-58361
- Fresnel coefficients of light refl. at interfaces between transparent media 0-106438
- gas concentration meas. using Raman intensity depend. on giant pulse laser polarization 0-98986
- gas laser, linearly polarized waves, interaction with longitudinal mag. field 0-95936
- gas laser, polaris. effects 0-58605
- gas superluminescence in high-current discharge, polarisation due to Zeeman splitting 0-100060
- gaseous medium, two-photon-absorbing, polarised light propag., quantum effects 0-103107
- grating type monochromators, spectrophotometry and colorimetry errors caused by polarisation of meas. system (*Japanese*) 0-101815
- grid polarisers for IR Fourier spectrometers 0-105724
- HD 50896, Wolf-Rayet star, linear polarisation periodic vars. rel. to binary star nature 0-72972
- helically ruled optical filter, spherical refl. characters. 0-64171
- AM Herculis (3U 1809+50), polarimetry and spectrophotometry rel. to mag. field 0-94835
- hologram grating, polarizing properties 0-69342
- inhomogeneously magnetised media, Faraday effect, polarisation plane rotation (*Russian*) 0-66154
- interference fringe intensity distrib. of elliptically polarised beam near critical angle 0-106449
- interstellar polarisation, rel. to grain growth in dark clouds 0-67834
- ion collisions, electron capture, atomic excited state polarisation, optical detection 0-58377
- IR spectrophotometers, meas. errors of polarising objects 0-86471
- isotropic adsorbing medium bounded, light beam splitting 0-99623
- Lamb wave optical detect. in fused SiO₂ 0-106690
- laser based on coupled transitions with arbitrary polarization of radiation 0-78827
- laser beam propagating in liquid, polarization, DC elec. field influence 0-91828
- laser cavity losses, phase polarisation method in lasing regime 0-87413
- CW Leonis (IRC+10216), IR C star, intrinsic polarisation origin 0-67730
- lidar target calibration, backscatter refl. for circularly polarised radiation 0-102750
- linearly polarised light depolarisation effective ellipse phase and amplitude 0-86381
- liquid crystal image transducer, optical props. at normal incidence, off-state behaviour 0-64160
- liquid crystal thin layer, polarised light ellipticity after passage 0-88036
- long-period variable stars in S.hemisphere, narrowband polarimetry 0-98666
- M82, optical polarisation wavelengths depend. of galaxy 0-67861
- magnetic DA white dwarfs, spectral line and circular polarisation profiles 0-62123
- magnetic fluids, light scattering and polarisation 0-60616
- Markarian 3, 231, Seyfert galaxies, optical polarisation obs. 0-90533
- methanol, optically pumped CW for IR laser lines, freq. meas. 0-58514
- methyl mercaptan, CW subMM emission lines, optical pumping 0-87381
- Michelson interferometer, polarizing, for far IR and MM regions 0-73427
- Michelson output coupler with one-dimensional grid, for optically pumped near MM laser 0-58555
- microscope, polarizing, with crossed polarizers, incoherent diff. imagery 0-101838
- modulated-Mueller-matrix photopolarimetry [MMMP]: a technique for the study of elastic light scattering by depolarizing temporally modulated media and surfaces 0-90882
- modulators, photoelastic radiation polarisation, review 0-102846
- molecular lasers, optically pumped, polarisation phenomena appl. 0-87384
- Mueller matrix meas. of polarised light interactions, using electrooptic modulator polarimeter 0-73417
- multilayer coating design achieving a broadband 90° phase shift 0-102801

light polarisation continued

- multilayer highly reflective coating design for wideband 90° phase shift 0-74464
- NGC 1999, reflection nebula, optical polarisation map and struct. 0-94856
- NGC 3227, 3516, Seyfert galaxies, optical polarisation obs. 0-90533
- nonlinear active medium in Gaussian random optical field, stimulated emission statistics 0-58488
- optical constant measurement at two incidence angle values 0-101831
- optical constants meas. method using polarised light refl. coeffs., accuracy 0-73423
- optical fibre, current measurement appl. 0-96015
- optical fibre, single-mode, single-polarisation, with refractive-index pits on both sides of core 0-99846
- optical fibres, single-mode, tension-coiled, high birefr. 0-99858
- optical multilayer filters, non normal incidence, optical monitoring, allowable tolerances (*French*) 0-87526
- parabolic-index fibre modes, propag. characts., linearly polarised approx. 0-78972
- partially coherent perpendicularly polarized vibrs., anisotropic photographic recording, interferograms 0-57364
- photon echo, identification of transitions 0-78915
- planar aromatic hydrocarbons in polymer films, polarisation data interpretations, photoelectron spectroscopy appl. 0-58302
- planetary atmosphere, F_N method for polarisation studies 0-98540
- plasma interaction with laser radiation, light press. nonlinear force, polarisation influence 0-100078
- Pockels cell modulator, max. depth of light modulation 0-102819
- polished glass surface, reflected light phase rotation 0-66147
- L_2 Puppis, semiregular variable, Ca I uneven distrib. from narrowband polarimetry 0-98666
- quarter-wave mirrors, oblique incidence reflection coefficient, small absorption of layers effect 0-64140
- quinoline, liq., depolarised light scatt. from shear waves 0-97288
- radiative transfer problems of polarised light in presence of absorpt. soln. 0-67561
- Rayleigh-scattering absorbing atmosphere, polarised radiation intensity meas. for single-scatt. albedo determ. 0-94704
- reflected light, polarisation, apparatus for obs. 0-62434
- ring interferometers, optically active samples, polarisation props. (*German*) 0-77846
- scattering by irregular absorbing particles, polarisation and scatt. functions 0-67543
- semiconductors polarised light nonlinear rotation 0-93268
- single mode fibre analysis and fabrication for low polarisation birefringence 0-58722
- single mode fibre polarisation stabilisation 0-58724
- single mode optical fibre, polarisation modulation 0-64176
- single-mode fibres, electro-optical polarisation control 0-91899
- single-polarisation single-mode fibre, exposed cladding fabrication 0-58725
- solar resonance line polarisation, non-mag., centre-to-limb var. 0-67678
- specular sphere scatt. radiance matrix, refl. standard for polarised beam scatt. meas. 0-74299
- spheroidal particles, randomly oriented, light scatt. 0-58461
- starlight interstellar polarisation, fluctuation theory 0-82442
- Stokes parameters and mag. field vector profiles (*Chinese*) 0-77386
- strip-guides, polarisation filtering 0-102861
- superconductor Faraday effect obs. in polarising microscope 0-70892
- suspension of absorbing particles, simultaneous meas. of dichroism and birefringence in elec. field., photocurrent signal obs. 0-82801
- † Tauri, Be star, rapid linear polarisation variability (*Russian*) 0-77417
- tetramethyl pyrazine in durene, phosphorescent mol., quantum beats in triplet states 0-58312
- thermal light with orthogonally polarised multiple-peak spectrum, intensity fluctuations 0-87303
- three-dimensional objects in polarised light, refl. characts. 0-87305
- three-stage birefringent filter, tuning over visible region 0-58667
- time domain reflectometry, optical fibre technique 0-78959
- twisted elliptical optical fibre, polarisation coupling 0-99831
- uniaxial liq. crystal polarised fluoresc. emission 0-80838
- unstable resonator, half-symmetric, with coated rear cone, polarisation effects 0-74402
- Venus polarisation, wavelength depend. obs. rel. to UV cloud model 0-82250
- vision, Macular pigment, role in polarised light detect., meas. technique 0-61560
- α -Al₂O₃, polarised luminescence in neutron- and proton-irradiated single crystals 0-66271
- Ar, liquid, depolarized Rayleigh scatt. at triple point, mol. dynamics simulation 0-60617
- As₂S₃ film, hologram recording using total-internal-refl., polarisation depend. 0-106491
- Au/Al thin film, Al diffusion studied by attenuated total reflection method 0-92722
- CO₂ laser radiation, intracavity modulation of polarization direction 0-102744
- CO₂, multiple scattering contribs. to depolarisation of scattered light 0-87842
- Ca II H-K and Na I D-lines, non-mag. polarisation 0-63569
- CaCO₃, calcite linear polarizer, role in laser technology 0-64165
- CdInGaS₄, crystal, Raman scattering spectra, polarisation meas. (*Russian*) 0-71410
- CdS crystals, electron-hole plasma, carrier optical orientation 0-100689
- CdS platelet lasers, optically pumped, spatial and spectral distribution of laser emission 0-64032
- CdS:Li, single crystals, anisotropic luminesc. centres 0-80857
- CdTc:Mn²⁺, luminesc. and magneto-optic reson., mag. field effect 0-93390
- Cu film, diffuse optical scattering from variable roughness surfaces 0-100704
- Fe, ferromagnetic, partial circular polarisation of thermal emission in mag. field 0-71387
- Fe, monocryst. and polycryst., thermal emission, magneto-optic circular polarisation obs. 0-70435
- GaAs-Al_xGa_{1-x}As electro-optic frequency- and polarisation-modulated injection laser 0-91810
- GaAs-Al_xGa_{1-x}As MOS rib waveguide polarizers 0-64207
- GaAs-Al_xGa_{1-x}As MOS rib waveguide polariser, modulator and isolator 0-64217

light polarisation continued

- GaP-GaAsP planar heterostructure strip ridged waveguide under mech. load, polarisation modulation 0-96038
- GaS, infrared optical props., polarisation depend., vibr. modes 0-100658
- H₂, optical polarisation following electron impact 0-63831
- H₂⁺, polarised Balmer radiation due to scatt. from Nb surface, adsorbed O₂ effects 0-99569
- He, depolarising collision cross sections, quantum beat obs. 0-87203
- He-Xe 3.51 μ laser mode competition in axial mag. field 0-63974
- He(2s-3p transitions), beam foil spectra, emitted light polarisation, depend. on foil tilt angle 0-63786
- HgBr₂, photofragment fluoresc. polarisation, press. depend. 0-63720
- KBr, colour centre form. under polarised UV irradi., dichroism in absorption spectra 0-107232
- KCl(Br), F-centre emission, mag. circular polarisation 0-108251
- KCl(Br)(I):Ga⁺, polarisation of Ga⁺ centre A_T emission, temp. depend. 0-80842
- KI:TI, polarised luminesc. of (TI⁺)₂ centres 0-71473
- Na atom, cyclic interaction with circularly polarised laser radiation 0-78581
- Na vapour, Zeeman coherence, transient and stationary, polarisation spectroscopy 0-58212
- NaCl:Ga⁺, polarisation of Ga⁺ centre A_T emission, temp. depend. 0-80842
- Nd³⁺:YAG laser active element, linearly polarised light depolarisation due to thermally induced birefr. 0-106528
- Ni, polycryst., thermal emission, magneto-optic circular polarisation obs. 0-70435
- PLZT/TFPD thermal/flash protective lens assembly, polarised delamination investigation 0-78929
- Rb, superrad. between degenerate levels, polaris. characts., coupled transitions 0-58493
- RbCl(Br), F-centre emission, mag. circular polarisation 0-108251
- SiO₂-LiO₂-Al₂O₃ glass, luminesc., polarisation degree distrib. 0-108257
- Sml, Zeeman coherence, transient and stationary, polarisation spectroscopy 0-58212
- TeO₂ shear wave acousto-optical device with polarisation filtering 0-106619
- TiBr-TiI(Cl) crystals, photoelastic moduli 0-97230
- V₂O₁₃, semicond., IR vibration spectra 0-88997
- W-halogen quartz envelope lamp, polarization characteristics 0-95970
- Xe, multiple scattering contribs. to depolarisation of scattered light 0-87842
- XeF laser, output control by injection locking 0-74405
- ZnGeP₂, p-n homodiode, polarisation photosensitivity and photopleochroism spectra 0-107866
- light propagation**
see also atmospheric light propagation; guided light propagation
 beam volume attenuation coeff., invalidity 0-95791
 coherent probe light pulse, in medium with chem. reaction wave 0-61190
 dispersion relations with finite propagation speed 0-99606
 dispersive media, theory of multiple light scatt. by spherical particles (*Russian*) 0-94599
 focusing of light beam optimisation, in moving nonlinear media, using gradient method 0-106578
 free-space propagation model for coherence-separable broadband optical fields 0-78763
 gaseous medium, two-photon-absorbing, polarised light propag., quantum effects 0-103107
 Gaussian beam propagation in 3-layered dielec. medium (*Japanese*) 0-87306
 homogeneous medium, Gaussian light beam propag., diff. effects described using complex-ray method 0-78770
 inhomogeneous media, coherent states and light propag., graded-index waveguide coupling 0-102625
 lens systems 0-78947
 nanosecond laser pulse stretch meas. in underwater propagation 0-87426
 nonlocality effects on optical phenomena in bounded solids, developments 0-93328
 nonreciprocal effect, during light passage through US beam 0-106443
 optical wave, log-amplitude fluctuations spectra, turbulence spectra parameters determ. 0-95797
 quadratic structure functions describing random tilted phase fields 0-95799
 random medium, finite beam propagation 0-91748
 random nonuniform medium, covariance function computation of light wave intensity 0-58463
 random phase screens, probability density for intensity of plane waves 0-87317
 randomly inhomogeneous media, strong fluctuations of optical beam fields 0-99634
 randomly inhomogeneous medium, fluctuations in phase arrival angle and freq. correl. of spherical waves 0-106456
 scattering medium, stratified, narrow beam propagation theory 0-106455
 scintillation meas. in turbulent propagation, detector aperture effect (*Slovak*) 0-63921
 supersonic boundary layers interacting with cooling wall jets, turbulent and optical characteristics 0-106792
 thermal self-action problems and their compensation 0-106579
 turbulent medium, four-point coherence function strong intensity fluctuations region 0-87319
 two-level resonant medium, light pulses propag. 0-64119
- light propagation in plasma**
 Brillouin and dielectric sidescatter of 10- μ m light by a plasma 0-103156
 collision-dominated plasma, laser scatt. intensity 0-83905
 collisional plasma, mixed mode operation, cross-focusing 0-83945
 CW far-infrared laser scattering from a laboratory plasma ion acoustic wave 0-106974
 electron density meas. by far IR laser beam deflection 0-59296
 Gaussian laser beam, transverse self-focusing and self-trapping investig., moment method 0-58652
 inert gas plasma, electron-beam produced, laser action of ionized and neutral atomic lines 0-106929
 Langmuir and ion acoustic wave coupling, turbulence spectra, light absorption 0-87902
 laser beam self-focused in turbulent plasma, average field 0-79505
 laser plasma, convective parametric decay instability 0-64722
 laser radiation absorption by spherical plasma, geometrical optics 0-59189
 laser radiation in plasma, oscillating two-stream instability 0-92328

light propagation in plasma continued

- magnetoplasma, laser beam self-focusing 0-102778
- non-uniform laser plasma, stimulated Raman light scatt. spectrum (*Russian*) 0-106926
- nonlinear force of light press. in laser interaction with thin plasma, polarisation influence 0-100078
- optical transparency evaluation, line broadening effect 0-79453
- Osterberg problem and wave propag. in inhomogeneous plasma, numerical study 0-63925
- radiation absorption in magnetoplasma, rel. to laser fusion 0-92273
- short-pulse laser backscatter from gas target 0-79454
- CO₂ laser beam scatt. by microscopic fluctuations in plasma density 0-79574
- CO₂-laser (long pulse)-plasma interactions, classical absorpt. and heat conduction in low-irradiance 0-75059
- He continuum radiation, 109 to 540 nm, meas. in arc plasma (*German*) 0-106932

light reflection

see also mirrors; optical films

- airport control tower cab, optical design 0-58661
- amplifying medium, spatially nonuniform 0-106444
- analogue model, light reflection and refraction, teaching 0-67948
- anisotropic continuum, with anisotropic surface layer, coeff. of attenuated total reflection 0-60535
- anisotropic frustrated-total-internal-refl. filter, space limited 0-102821
- anisotropic semiconductors, light reflection in interband transition freq. (*Russian*) 0-88945
- aspheric, testing in reflected light using blazed synthetic holograms 0-91881
- asteroids, IR reflectance spectra obs. and search for water of hydration 0-77318
- asteroids, similarity of opposition effect 0-62064
- beam splitting device for use with smoke chamber ray optics demonstrations 0-67990
- Brewster angle determ. by dithered laser beam synchronous detection 0-73422
- canted magnetic structured materials, exciton spectra, optical props. 0-70622
- cholesteric liquid crystals, gamma-ray irradi. effects, dosimetry, thermography appls. (*Spanish*) 0-92457
- circular cylinders, single scatt. phase matrix, ray optics and wave theory comparison 0-102610
- clouds, light pulse reflection, height meas. (*Russian*) 0-82056
- clouds, mathematical model for reflected and transmitted radiation 0-90215
- coatings, absorptive, at normal incidence, program for TI-59 calculator 0-84793
- coatings, textured, crystallites faces determ. 0-64846
- coherent light beam shifts on reflection at plane interfaces between isotropic media 0-102609
- coherent optics methods appl. to acoustic field investigations 0-106691
- critical light reflection at a plastic/glass interface and appl. to foot press. meas. 0-81681
- crystal optical characteristics, relax. processes exciton dispersion 0-107709
- dark-field surface inspection using total internal reflection 0-74519
- deflection effect of light reflected from moving mirror in ether theory 0-91749
- dielectric film, refractive index and thickness meas. by optical method 0-82806
- diffraction image intensity fluctuations in turbulent atm. after refl., Huygens-Kirchhoff principle calcs. 0-63926
- diffuse reflection problem, invariance principles and integral eqns. for radiation fields in plane atmosphere 0-67559
- diffuse reflectors, light collection and dissemination 0-83658
- diffused channel waveguides, direct index meas. 0-87562
- Earth surface UV reflectance, meas. from airborne platform 0-98453
- electrode surface, anisotropy of optical props. 0-60534
- ellipsometric meas., single-element rotating-polarizer ellipsometer 0-101823
- ellipsometry of transparent films on transparent substrates, theory 0-104007
- Fourier spectroscopy, far IR, spectrum distortion by multiple reflections using Michelson interferometer 0-82837
- Fresnel's eqn. for light reflection and refraction, teaching 0-101688
- Fresnel coefficients of light refl. at interfaces between transparent media 0-106438
- Fresnel formulas and law of stimulated emission 0-58489
- frustrated total internal reflection element, adjustable as a function of the incidence angle of highly collimated light beams 0-96022
- guided-beam splitter, refl. meas., fabrication method 0-74473
- gyrotropic absorbing crystals, nonorthogonal eigenwave refl. 0-99624
- helically ruled optical filter, spherical refl. characts. 0-64171
- histological and cytological reflection contrast microscopy 0-72389
- holographic plates, rear refl. elimination technique 0-73145
- holography, white light refl., developer compositions compared 0-102669
- Iapetus, relative reflectance meas. at 1.6 and 2.2 μ m 0-98607
- illumination system, optical design 0-64135
- integrating sphere accessory, spectrosc. meas. of horizontal surface from above 0-86443
- Jupiter disc features spectral reflectivity, phase effect 0-98602
- laser beam coherence and divergence (*Spanish*) 0-87424
- laser beam expander for short cavity dye laser 0-87532
- laser cavity diffraction experiment with 1-D diaphragm 0-95920
- lidar target calibration, backscatter refl. for circularly polarised radiation 0-102750
- limited light beam, nonlinear reflections and transmission 0-58624
- liquid crystal image transducer, optical props. at normal incidence, off-state behaviour 0-64160
- liquid level sensor using parallel polarised light 0-82741
- locally deformed slab waveguide propagation and diffraction patterns 0-106630
- longitudinal static spin wave struct., magnetotropic interaction of light (*Russian*) 0-93285
- Mars, reflectance spectroscopy rel. to surface comp. 0-72834
- metal surface electrodynamics, optical refl. coeffs. and surface plasmon dispersion law 0-75619
- microscopic interference obs. by reflection contrast 0-68248
- microscopical and Ewald dynamical diffraction theories, refl. and transmission, spatial dispersive dielec. slab 0-83548

light reflection continued

- multi-layer optical system, reflection and transmission coeffs. calcs., computer program 0-66316
- multilayered structure, refr. index difference between adjacent layers, meas. technique 0-101829
- multilayers, ultrathin, optical characts. 0-104005
- nematic liquid crystal, total internal reflection, review 0-96445
- nonlinear interference mirror, reflection of light 0-102761
- nonlocality effects on optical phenomena in bounded solids, developments 0-93328
- ocean surface UV reflectance, meas. from airborne platform 0-98453
- optical constant measurement at two incidence angle values 0-101831
- optical constants meas. method using polarised light refl. coeffs., accuracy 0-73423
- optical fibre, beam to fibre coupling with low standing wave ratio 0-99822
- optical surface contract interaction zone, thickness calc. and distance meas. methodology (*Russian*) 0-99889
- Osterberg problem and wave propag. in inhomogeneous plasma, numerical study 0-63925
- paraboloid mirror with coaxial linear source, intensity distribution 0-74456
- photographic papers, polarised light refl. 0-64127
- plane parallel optical layer interference props. for radiation parameters control 0-83547
- plane-parallel plate, with spatial dispersion, light refl. and transmission coeffs. 0-88951
- planetary atmosphere, transfer eqn. 0-82184
- planets, light refl. laws rel. to photometric props. 0-67601
- polarisation constants for light interaction with absorbing crystal plates 0-78765
- polarisation of reflected light, apparatus for obs. 0-62434
- polished glass surface, reflected light phase rotation 0-66147
- pyrocarbon coatings, refl. anisotropy and struct. determ. by perpendicular incidence microellipsometer 0-101824
- quarter-wave mirrors, oblique incidence reflection coefficient, small absorption of layers effect 0-64140
- radiative transfer, synthetic scattering phase function 0-98541
- Ramsey resonance, of two-level mols. in three separated fields produced by corner reflector, theory 0-74166
- reflective glass colour standards 0-90878
- reflective light valve projector efficiency and image uniformity improvement 0-87459
- retroreflectance measurements, unified coordinate system 0-73408
- retroreflecting material metrology, errors in luminous refl., chromaticity meas. 0-68235
- retroreflective material chromaticity meas. under nighttime geometry 0-73411
- retroreflectometer, NBS reference 0-73410
- retroreflector alignment, simple interferometric technique 0-95125
- retroreflector photometric and goniometric accuracy 0-86375
- retroreflector photometry, meas. error rel. to aperture size 0-73409
- rough metal surfaces, diffuse and specular refl., empirical representation 0-87315
- rough metal surfaces, empirical representation 0-87314
- rough surface, random, reflectance derived with Fresnel approx. 0-87309
- rough surfaces, reflection light, division into specular and diffuse components (*Japanese*) 0-106457
- Sahel region, Africa, surface albedo vars. investigation during recent drought (1967 to 1974) 0-76981
- Saturn disc centre spectral reflectivity, phase effect 0-98602
- shadow methods for studying turbulence using reflection from a mirror in the medium 0-95801
- slit image seen in total internal reflection (*French*) 0-95810
- spectrometer, diode laser dual-beam, long-term temporal and scanning characts. 0-90902
- specular reflectometer-spectrophotometer, NBS reference, mirror refl. meas. 0-68236
- specular sphere scatt. radiance matrix, refl. standard for polarised beam scatt. meas. 0-74299
- sphere, totally reflecting, light extinction 0-95784
- Sun glitter on sea, correl. function appl. to sea surface slope distrib. function determ. (*Russian*) 0-94611
- surface profile from horizontal light source reflection, calc. from observed image 0-101777
- surface profile from horizontal light source reflection, image calc. 0-101776
- thick layers, refl., transmission and brightness coeffs. 0-63918
- three-dimensional objects in polarised refl. characts. 0-87305
- total internal refl., Poynting vector theory, light beam shifts 0-78764
- uniaxial crystals, refl. ellipsometry nonlinear eqn. inversion 0-95120
- water mass, nonzero subsurface 670 nm irradiance reflection of Lake Ontario 0-101387
- waveguide, lossy, Brewster phenomena, cut-off thickness 0-87524
- As₂S₃ film, hologram recording using total-internal-refl., polarisation depend. 0-106491
- BaSO₄ tablet, reciprocity of reflection values for geometries 45/0 and 0/45 (*German*) 0-71370
- CO₂, inverted, wavefront reversal, high efficiency 0-74436
- Ge in TEA CO₂ laser cavity, wavefront reversal, high efficiency 0-74436
- In₂O₃ films, electron beam evaporation, elec. and optical props. (*Japanese*) 0-60784
- InSb, Auger-governed decay of laser-induced plasma, optical probing 0-76105
- LiIO₃ single crystal, surface acoustic wave parameter meas., coherent optics method 0-106691
- (NH₄)₂BeF₄, linear and nonlinear optical props. in incommensurate phase 0-69452
- Si amorphous film, anisotropic etching phenomenon, appl. as solar selective absorber surfaces 0-72054
- p-Si, heavily doped contact layers on IR detectors, IR transmissivity 0-108190
- Si:B ion implanted layers, light refl. and transmission coeffs., computer program 0-66316

light reflection spectra see reflectivity; spectra**light refraction**

see also birefringence

- analogue model, light reflection and refraction, teaching 0-67948
- angular spectra of optical radiation, side wave meas. 0-69327
- aquatic eyes, retinoscopy, refractive error considerations 0-61750

light refraction continued

- atmosphere boundary layer, refr. index structural charact. (*Russian*) 0-94597
 circular cylinders, single scatt. phase matrix, ray optics and wave theory comparison 0-102610
 conical refraction in sulphur crystals 0-95792
 conjugate interfaces: interfaces between transparent media of the same reflection coefficient for the parallel polarization at the same angle of incidence 0-87299
 eye, refractive state of ground squirrel 0-67070
 eye chromatic aberration rel. to accommodation, meas. using dynamic laser speckle pattern 0-81582
 eye refractive error meas. using dynamic laser speckle pattern 0-81583
 Fresnel's eqn. for light reflection and refraction, teaching 0-101688
 grazing light ray refraction in dispersion zone above optically homogeneous media interface 0-74297
 illumination system, optical design 0-64135
 isotropic adsorbing medium boundary, light beam splitting 0-99623
 laser beam refraction at spherical surface, distortion, geometrical optics calc. 0-95929
 limited light beam, nonlinear reflections and transmission 0-58624
 optical glass, thermally tempered, surface stress meas. by crit. ray method 0-106766
 prism cut from anisotropic media, ray refr., appl. to atm. optics haloes 0-63916
 rainbow phenomena and the detection of nonsphericity in drops 0-58456
 refracted beam formation during light ray motion along optically homogeneous media interface 0-74298
 refracting objectives for 8 to 13 μm 0-86421
 Snell's law for light rays in moving isotropic dielectrics 0-58458
 supersonic boundary layers interacting with cooling wall jets, turbulent and optical characteristics 0-106792
 thin film glass lightguide boundary refraction expts. 0-106639
 BaO-B₂O₃ glass, refraction, refractive index from 0.365 to 2.50 μm 0-88953
 BaO-La₂O₃-B₂O₃ glass, refraction, refractive index from 0.365 to 2.50 μm 0-88953
 K₂O-CaO-BaO-B₂O₃ glass, refraction, refractive index from 0.365 to 2.50 μm 0-88953
 LiIO₃ crystal, SHG, thermoelastic stresses and nonlinear refract. effect 0-74437
 ZnO-B₂O₃ glass, refraction, refractive index from 0.365 to 2.50 μm 0-88953
 ZnO-La₂O₃-B₂O₃ glass, refraction, refractive index from 0.365 to 2.50 μm 0-88953

light scattering

- see also Brillouin spectra; opalescence; Raman spectra; Rayleigh scattering; stimulated scattering
 acousto-optic multiple plane-wave scatt., explicit formalism 0-99621
 acousto-optical interaction efficiency calc. 0-103940
 active and passive particles, extinction 0-102684
 active particles, Lorenz-Mie scatt. theory paradox 0-74324
 active particles, Lorenz-Mie scatt. theory paradox 0-102683
 aerosol, single droplet, size and mass meas. using electrodynamic balance 0-89535
 aerosol particle size measuring device, using spectral transparency and small angle scatt. methods 0-95069
 aerosol scattering indicatrices under clear sky conditions in 0.55 to 2.4 μm spectral region, determ. (*Russian*) 0-94600
 aerosol size distribution by inverting spectral turbidity data 0-95796
 aerosols, differential scatt. coeff. to mass conc. ratio, spectrophotometer, cascade impactor obs. 0-72628
 aerosols, dispersity analysis, automatic photoelec. analyser for size range 0.3-40 μm 0-57251
 aerosols, monodisperse, mass concentration, laser monitoring 0-98878
 aerosols, scattering function determ. with telephotometer 0-105055
 aniline, liq., depolarised light scatt. from shear waves 0-97288
 anisotropic inhomogeneous medium, elastic light scatt., orientation characterization 0-83553
 anisotropic medium, inhomogeneity, orientation characterization by elastic light scatt. 0-83552
 anisotropic particles, light scatt. struct. coeff., angular depend. 0-103964
 arbitrarily shaped dielectric particles, multiple scatt. approach 0-87312
 atmosphere, IR radiation attenuation by ice platelets 0-66141
 atmosphere, large particle scatt. coeffs. approximation for total O₃ determ. 0-82091
 atmosphere, light absorpt. and scatt. rel. to direct beam solar irradiance and illuminance 0-90174
 atmosphere, mol. and aerosol scatt. rel. to effects of diffuse radiation on O₃ photodissoc. 0-109210
 atmosphere, mol. scatt. rel. to polarised light transfer 0-67561
 atmosphere, multiple scatt. theory for dispersive media with spherical particles (*Russian*) 0-94599
 atmosphere, particle optical constants and disperse aerosol comp., phase scattering function (*Russian*) 0-61898
 atmosphere, scatt. effects wavelength depend. rel. to anomalous gray shades in DMSP visible imagery 0-77111
 atmosphere aerosol absorpt. and scatt. effects rel. to satellite retrieved temp. profiles error 0-98449
 atmosphere model, scatt. light intensity and polarisation degree, mol. anisotropy effect 0-77104
 atmospheric aerosol extinction measurements, multiple scatt. corrections 0-98445
 atmospheric nonspherical aerosol particle characterisation with electrooptical nephelometry 0-77106
 atmospheric optical props., appl. to satellite remote sensing of phytoplankton 0-77105
 atom, resonance light scattering, intensity effects 0-91511
 atomic levels, two-photon transitions 0-83333
 bacteria E.coli strains in aq. suspension, polarisability anisotropy and aminoglycoside antibiotic effects 0-85441
 bacteriophages T4B and T7, determ. of rotational diffusion coeff. by depolarised dynamic light scattering 0-85549
 Baltic Sea, estuary region, suspension distrib. under river drifts influence (*Russian*) 0-98345
 beam volume attenuation coeff., invalidity 0-95791
 biological cell size meas. by static light scatt. Fourier transform 0-81793
 blood suspension aggregation in Couette flow (*French*) 0-97991
 borosilicate glass, birefringent, X-ray and light scatt. study 0-103937
 breather generation, inverse scatt. technique 0-78913

light scattering continued

- ceramic translucent systems, absorpt. and scatt. coeffs for visible light, Kubelka-Munk theory 0-60627
 chloromethane gas, linear electro-optical effect 0-87843
 cholesteric liquid crystals optical properties, diffraction nature, review 0-70123
 cholesteryl laurate-cholesteryl caprylate (75 wt.%), polymorphic behaviour, optical, elec. and dielec. meas. 0-65208
 circular cylinders, single scatt. phase matrix, ray optics and wave theory comparison 0-102610
 circumstellar envelopes, Monte Carlo analysis of polarization by Thomson scattering 0-85931
 classical crystal optics, lattice dynamical background, review 0-97221
 cloud extinction coefficient, estimation from multiwavelength lidar backscatter meas. 0-98446
 clouds, scatt. function in mathematical model for reflected and transmitted radiation 0-90215
 clouds, thick, light pulse propag., pulse width expression for scatt. slab 0-82059
 coherently illuminated scattering object, speckle pattern statistics in diff. field 0-63924
 compound glass optical fibres, total and scatt. loss coefficient meas. 0-69536
 coronagraph objective component surface scatt. angular distrib. obs. 0-74463
 critical mixtures, shear and critical fluctuations, instantaneous mapping of velocity gradients 0-79420
 cylinder, infinite tilted, linearly polarised incidence at arbitrary angle 0-58457
 Debye generalised fluid model, dielectric relax., depolarised dynamic light scatt. 0-108156
 defect crystal structure determination 0-103316
 dense scattering media, anisotropy factor 0-87307
 β,β' -dichloroethyl ether-isooctane, critical indices, allowance for light double scatt. (*Russian*) 0-60624
 dielectric fibres, transversely incident beam wave scatt. 0-96004
 dielectric gratings, arbitrary profiles, scatt. and guiding of EM waves 0-96005
 diffraction grating, reflective, high efficiency, scattering types 0-99619
 diffuse light scattering, mathematical modelling 0-106450
 diffuse medium, reduced effective velocity of light 0-69329
 diffuser, weak, speckle pattern, spherical aberration effect 0-87476
 diffusing surface optical autocorrelation 0-99646
 diffusion equation derived from space-time transport equation 0-78772
 disperse particles, determ. of spectrum of diameters from scattering of light 0-61169
 dispersion relations, two dimens., phase problem appl. 0-102631
 dispersive media, theory of multiple light scatt. by spherical particles (*Russian*) 0-94599
 dispersive medium, many-photon scatt. of light by impurity centres 0-60622
 DNA, radiation induced mol. size change, electron irradiated, effect of p-nitroacetophenone 0-89807
 EM radiation in media with spatial dispersion, spatial coherence formation and polarisation increase 0-106442
 expanding envelopes, Lyman α quanta scattering (*Russian*) 0-67556
 eye, aerial image modulation lowering, contribs. of retina and eye optical system 0-81584
 fatty acid monolayers, light scatt. meas. 0-89011
 ferroelectric crystals, polariton light scatt. freq.-angle spectra, nonlinear susceptibility interference (*Russian*) 0-92834
 ferromagnetic slab, light scattering from bulk and surface spin waves, theory 0-71389
 fibre attenuation meas. by backscattering method, effect of noise 0-102824
 fibre connector loss evaluation by backscattering 0-58721
 fibre splice insertion loss meas., backscattering method 0-58720
 fibrinogen, bovine, high energy-induced aggregation, time resolved spectra 0-61655
 fine-grained bleached emulsion scatt. model and expt. 0-102670
 fluid system, quasielastic light scattering spectroscopy, bispectral anal. 0-93347
 fluids, simple, light scatt., particle-hole model 0-60613
 fly ash particles, water accretion, refract. index and accreted layer thickness 0-58462
 Freon-113, correlation properties near phase-separation boundary, gravitational field effect 0-107410
 generalised optical theorem for partially coherent interfering beams 0-106447
 glass, tempered, stress analysis, oblique incidence light scattering, birefringence (*Polish*) 0-71374
 glass fibre reinforced plastic, fatigue fracture kinetics studied by diffusion scatt. of luminous fluxes 0-76446
 haemoglobin, mutual and tracer diffusion coeffs., photon correl. obs. 0-72123
 highly anisotropic scatt. medium, luminesc. of layer 0-100685
 holographic correlometer with phase modulation, viscous, superviscous light scatt. media study 0-74321
 hygroscopic particle humidification process, electrooptic scatt. meas. 0-77107
 ice crystals, light scatt. expts. (*Russian*) 0-94601
 imaging system point spread function determ. by scatt. of two monochromatic beams 0-87316
 immunoglobulin, human, high energy-induced aggregation, time resolved spectra 0-61655
 immunological reaction monitor using laser light scatt. 0-85463
 incommensurate phase, light scatt., order parameter fluctuation (*Russian*) 0-93354
 integrating sphere accessory, spectrosc. meas. of horizontal surface from above 0-86443
 interacting Brownian particles, light multiple scatt. by correlation spectroscopy 0-87313
 interferometry, multimode fibre optic, applications 0-86387
 interplanetary dust, density and phase function determ. 0-109324
 ion, electromagnetically confined, laser cooled, double resonance and optical pumping 0-87155
 IR back-scattered from vaginal tissue, self-stabilising meas. system 0-72281
 irregular absorbing particles, new scatt. model rel. to zodiacal light 0-67543

infrared spectra of organic molecules and substances continued

- propylene, He-Ne laser line, high temp. absorpt., anal. by high resolution IR spectra 0-91554
propylene and ethylene adsorbed on Ag, enhanced Raman spectra obs. 0-95607
propynal, IR-microwave double reson. and two-photon expts. 0-83396
propynal, rovibronic populations, collisionless IR multiphoton spectra, energy deposition, photoacoustic determ. 0-83354
propynal-d, in ground vibrational state, IR microwave double resonance spectra, rot. and centrifugal distortion const. determ. 0-83358
propyne-d₃, absolute and integrated IR intensities of fundamental modes 0-87179
PTFE, γ -ray effects on 19 and 30°C phase transitions, Fourier transform IR spectroscopy 0-103387
pyridine, deuterium substituted, Raman and IR vibr. spectra 0-84739
pyridine-2,3,5,6-d₄, vibr. spectra, IR and Raman, assignment 0-102519
pyridine-3,4,5-d₃, vibr. spectra, IR and Raman, H exchange rates meas. 0-102518
pyridine-3,5-d₂, vibr. spectra, IR and Raman, H exchange rates meas. 0-102518
pyridine-d₅, vibr. spectra, IR and Raman, assignment 0-102519
semicarbazide hydrochloride, vibr. spectra, normal coord. anal. 0-58255
semicarbazide-d₉, vibr. spectra, normal coord. anal. 0-58255
silane coupling agent deposited on E-glass fibre, hydrolysis and drying effect on siloxane bonds 0-85072
TCNQ ion radical salt, DECA(TCNQ)₂, IR absorpt. spectra obs. of first-order transition 0-71397
TCNQ salt, decamethylferrocenium, monomeric and dimeric, optical and EELS study 0-100660
TCNQ salt, MeDABCO(TCNQ)₂, optical, elec., and mag. props. 0-65539
TCNQ salt, n-methyl-n-ethylmorpholinium, unpaired electron states, IR refl. study 0-75491
tetra-n-butylammonium halides in benzene, chloroform, CCl₄, far IR spectra, ion-ion, ion-mol. interactions 0-60562
tetrafluoromethane, $\nu_2 + \nu_4$ band, high resolution diode laser spectra 0-69138
tetrafluoromethane+He gas mixture, collision induced for IR translational spectra 0-83353
tetrafluoromethane molecule, laser spectrosc. and optical pumping from CO₂ laser 0-74202
tetramethylsiloxane dicarboxylic acid Langmuir films on Cu surface, surface EM wave absorpt. study 0-97359
tetraphenylarsonium, Raman and IR spectra of the dicyanoidate (I) ion 0-60572
tetraphenylphosphonium, Raman and IR spectra of the dicyanoidate (I) ion 0-60572
thiurene-d₆-(d₁)-(d₂), IR spectra, normal coordinate anal. 0-87107
2-thio alkyl (allyl, benzyl) pyrimidines, IR and Raman spectra anal., mol. vibr. and symmetry (French) 0-87123
thioformaldehyde, $\tilde{\nu}_2$, $\tilde{\nu}_3$, IR absorpt. spectra 0-83362
thiones, N-H-S weak and medium strong H bonds, IR spectra 0-69132
toluene, in benzene soln., mol. motion, correl. functions 0-96431
toluene-sulphonate-diacyetylene, thermal polymerisation, near IR absorpt. and low lying states obs. 0-71399
2,4,6-tribromophenol, Raman and IR spectra, hydrogen bonds 0-84735
trichloroanilines in solutions, IR absorpt. spectra 0-69136
trichloromethane-d₀-d₁, soln., far IR spectra, band shape and moment anal. 0-58252
2,4,6-trichlorophenol, Raman and IR spectra, hydrogen bonds 0-84735
trifluoroacetic acid, soln., polarisable H bonds, IR spectrosc. obs. 0-58408
trifluoriodomethane, laser microwave double reson. spectroscopy with CO₂ laser lines 0-87156
trifluoromethane, IR spectra, spectral bandshape and intensity of C-H chromophore 0-83355
trifluoromethyl hypochlorite, vibr. spectra and normal coord. anal. 0-102517
trifluoromethyl hypofluorite, vibr. spectra and normal coord. anal. 0-102517
trimethylaminegallane, microwave, IR and Raman spectra, struct., vibr. assignment 0-95600
trimethylcarbinol complexes in soln., weakly H-bonded, IR bandshapes 0-106354
trimethylvinylsilane, IR spectra, struct., vibr. assignment, barriers to internal rot. calc. 0-87102
triphenylcarbinol complexes in soln., weakly H-bonded, IR bandshapes 0-106354
vinylloxane, Raman and IR vibr. spectra and conformations 0-83379
XH-Y complexes, IR absorpt. spectra, intramol. coupling influence, pot. energy surfaces derivation 0-91624
Ag complexes of 2-amino-5-methyl-1,3,4-thiadiazole and 2,5-dimethyl-1,3,4-thiadiazole, conductometric and IR meas. 0-87121
BCl₃NCO, soln., force fields and normal modes, vibr. spectra, IR and Raman obs. (French) 0-58266
BX₂⁺NCS⁻ (X=Cl, Br, I), soln., force fields and normal modes, vibr. spectra, IR and Raman obs. (French) 0-58266
CH₃, CH₂ and CH deformation vibration group frequencies and MO electron densities, interaction force const. 0-87101
Cl+formaldehyde, photolysis, Fourier transform IR studies, metastable species detection 0-81293
Cl+vinyl bromide-d₃ reaction, IR chemiluminesc. 0-102506
ClH-dimethyl ether, vibr.-rot. IR spectra, quantum and classical mechanics 0-91561
Cu complexes of 2-amino-5-methyl-1,3,4-thiadiazole and 2,5-dimethyl-1,3,4-thiadiazole, conductometric and IR meas. 0-87121
F+ethylene (benzene) derivatives, deuterated, IR chemiluminesc. 0-102506
FCO, form. in Ar matrix, vibr. and electronic spectra, valence force potential determ., mol. photodissoc. obs. 0-85170
H-bonded systems, frequency shift rel. to IR bandwidth 0-99502
IBr-benzene in n-decane soln., IR line broadening by chemical exchange 0-87111
K salt of β -ketoaldehyde, configurations of anions in solutions studied by IR spectroscopy, H-bond form. 0-87117
K⁺CF₃SeO₂⁻, IR and Raman spectra, normal coordinate anal. for CF₃SeO₂⁻ anion 0-87122
Li salt of β -ketoaldehyde, configurations of anions in solutions studied by IR spectroscopy, H-bond form. 0-87117
methane ν_4 - ν_4 and ν_2 + ν_4 - ν_2 hot bands, difference bands 0-63632

infrared spectra of organic molecules and substances continued

- NH₄⁺CF₃SeO₂⁻, IR and Raman spectra, normal coordinate anal. for CF₃SeO₂⁻ anion 0-87122
Na salt of β -ketoaldehydes, configurations of anions in solutions studied by IR spectroscopy, H-bond form. 0-87117
NaK, laser induced D¹¹A² fluorescence, mol. vibr. 0-87160
Ni catalyst, chemisorption of ethylene-(d), Raman and vibr. spectra 0-108747
PbO, laser excitation IR spectra, photoluminescence obs., rot. anal., rot. const. determ. 0-95619
Rb⁺CF₃SeO₂⁻, IR and Raman spectra, normal coordinate anal. for CF₃SeO₂⁻ anion 0-87122
- infrared spectra of polyatomic inorganic molecules**
gases, high resolution vibr. spectra by Fourier transform far IR spectroscopy 0-86461
HCl-inert gas mixtures, van der Waals molecules, far IR spectra 0-95610
high temp. molecules, matrix isolation studies, review 0-57399
IR bands transmission functions 0-106324
uranyl complexes, IR spectra and bond distances 0-74167
water vapour continuum absorption (3.5 to 4 μ) temp. dependence obs. 0-61903
XH-Y complexes, IR absorpt. spectra, intramol. coupling influence, pot. energy surfaces derivation 0-91624
Al₂Cl₆, matrix isolated, vibr. spectra, isotopic fine struct. and valence force field calcs. 0-58258
BCl₃, in solid Ar, Kr, high resolution IR absorpt. spectra, isotopic splitting 0-87109
BCl₃F, in solid Ar, Kr, high resolution IR absorpt. spectra, isotopic splitting 0-87109
CF₃+H, IR matrix isolation spectra 0-97706
CO, catalytic oxidation on ferrites, IR spectrosc. investig. 0-89524
CO₂, enriched in ¹⁷, ¹⁸O, diode laser spectroscopy of Q branches 0-78621
CO₂, IR band intensity 0-83425
CO₂, IR bands transmission functions 0-106324
CO₂, laser small-signal gain coefficient calc. 0-78831
CO₂, R-branch line intensities and press.-broadened line widths at 15 μ m 0-102508
¹²C¹⁶O₂, ν_2 band, IR single line strength 0-83370
¹³C¹⁶O₂, IR line strength 0-83371
CS₂, ν_2 bending fundamental, high resolution IR spectrum 0-91559
¹²C³⁴S₂, ¹³C³⁴S₂, high resolution IR spectra (French) 0-58249
CdF₂(FCl)(FBr), matrix-isolated IR and Raman spectra, assignments, force consts., isotope effects and thermodynamic props. 0-63631
CDO₃, formed by matrix reactions, IR, Raman and visible spectra 0-87110
CrO₂Cl₂, multiphoton induced inverse electronic relax. 0-66836
CsBrCN, Raman and IR vibr. spectra, struct. 0-102513
CsClCN, Raman and IR vibr. spectra, struct. 0-102513
CsI₂CN, Raman and IR vibr. spectra, struct. 0-102513
CsReO₄, IR matrix-isolation spectra 0-87108
D₂⁺, IR spectrum, vibr.-rot. assignment 0-95627
D₂⁺, rot.-vibr. spectrum, ab initio calcs. 0-95595
DNSO, IR spectra obs., mole. vibr., anharmonicity constant determ. 0-83357
⁷⁴GeH₄, mol. vibr., IR and CARS spectra (Russian) 0-102509
H-bonded systems, frequency shift rel. to IR bandwidth 0-99502
H₂⁺, IR spectrum, ν_2 band obs. 0-99506
H₂⁺, rot.-vibr. spectrum, ab initio calcs. 0-95595
HBO₂, band strengths, shock tube IR spectrosc. meas. 0-106358
HCN in smoke, tunable diode laser meas. 0-89559
HCN, J=4-3 354 GHz transition in Orion Molecular Cloud 0-101636
HDSe, high resolution IR spectra, anal. of 2 ν_1 band, rot. ground state const. determ. 0-95616
HNCO, rot. spectrum, ground and vibr. state reson., centrifugal distortion coupling 0-83364
HNO₃ IR spectra, 865.5-871.0 and 884.5-887.0 cm⁻¹ regions, equiv. width meas., atm. spectrum appl. (French) 0-87114
HO₂+HO₂, gas phase reaction mechanism, FT IR spectrosc. obs. 0-85163
H₂O dimer, continuum absorpt. spectra in 8-13 μ m range (Chinese) 0-109237
H₂O, Pt catalytic oxidation of H₂ and D₂, matrix isolation and laser fluoresc. obs. of prods. 0-66865
H₂O, Raman and IR spectrum in overtone OH stretching region 0-58263
H₂O vapour and liquid far IR spectroscopy 0-60610
H₂O, weak spectral absorpt. of vap., visible and near IR 0-82062
H₂S, absorpt. coeffs. meas. in Nd laser emission band 0-78620
Hg complex, methylethynylmercury(II)-(d₁-d₃-d₄), vibr. spectra and normal coord. calcs. 0-58259
Hg(CN)₂ ion, CN and HgC stretching vibrations and HgCN bending vibration assignments 0-69140
HgF₂(FCl)(FBr), matrix isolated IR and Raman spectra, assignments, force consts., isotope effects and thermodynamic props. 0-63631
LiReO₄, IR matrix-isolation spectra 0-87108
MoF₆, in Ar matrix, photolysis, MoF₅ form., IR spectrum 0-87115
N₃⁺, high press. IR vibr. spectroscopy (German) 0-74170
NH₂, ν_2 band, laser mag. reson. 0-83523
NH₃, absorpt. coeffs. meas. in Nd laser emission band 0-78620
NH₃, absorpt. cross sections at CO₂ laser wavelengths, temp. and press. depend. 0-78613
NH₃, high-resolution absorpt. spectra obs. using pressure-tuned diode laser 0-82835
NH₃, IR spectra, fine struct. of rot.-vibr. bands 0-102504
NH₃, lone pair contributions to the IR intensities, ab initio calcs. 0-63630
NH₃, weak IR absorpt. meas. using double-beam Fourier spectrometer 0-105725
NH₄NO₃, IR spectra and vibr. bands 0-69144
NO, IR emission Fourier transform spectroscopy, mol. rot.-vibr., RKR potential curve calc. 0-95618
NO₂⁺, high press. IR vibr. spectroscopy (German) 0-74170
N₂O, 12 μ m band lines, precise meas. with compact vacuum IR spectrometer 0-95157
N₂O, ν_3 and 2 ν_3 IR bandshape and dipole correl. functions 0-91560
N₂O₂ gaseous, integrated band intensity data, spherotrophic detection implications 0-58250
NaPO₂, mol. identification by matrix isolation IR spectrosc. 0-104485
NaPO₃, mol. identification by matrix isolation IR spectrosc. 0-104485

infrared spectra of polyatomic inorganic molecules continued

- O₃, line and band strengths in IR spectra, variational calcs. 0-87112
 O₃, line position and intensities of $2\nu_3$, $\nu_1 + \nu_3$ bands 0-87181
 OBF, band strengths, shock tube IR spectrosc. meas. 0-106358
 OCS, IR spectra, diode laser calibration 0-83363
¹⁶O/¹²C/³⁴S and ¹⁶O/¹³C/³⁴S, IR spectra, ν_3 band anal. 0-95620
 OSiF₂ prod. from SiO + F₂, matrix reactions, IR spectra and force consts. calcs. (*German*) 0-97718
 RbReO₄, IR matrix-isolation spectra 0-87108
 SbBr₃, Si₂, matrix isolated, IR spectra 0-58254
 SF₆, CW CO₂ laser spectroscopy 0-83367
 SF₆, Doppler-limited spectroscopy of $3\nu_3$ band, rot. const. and anharmonic parameters calcs., mol. photodissoc. 0-83361
 SF₆, IR laser radiation multiphoton absorpt. direct meas. by pyroelec. detector 0-102545
 SF₆, IR spectra, fine struct. of rot.-vibr. bands 0-102504
 SF₆, matrix isolated, IR spectrosc., temp. reversible site structural changes 0-95613
 SF₆, multiphoton-excited, $\nu_2 + \nu_6$ absorption and emission 0-63626
 SF₆, multiple photon absorpt., laser pulse intensity and collisions influence 0-95699
 SF₆, partial saturation of ν_3 ladder in IR absorpt., rate process model 0-58645
³²SF₆, point group symmetry breakdown, vibr.-rot. state, saturation spectroscopy 0-87116
 SO₂, IR multiphoton excitation and inverse electronic relax., mol. vibr. and fluoresc. 0-106349
 SO₂, IR spectra, Coriolis intensity perturbations 0-95617
 SeF₆, in Kr matrix, temp. reversible IR spectral changes, site struct. dynamics 0-102505
 SiF₄, integrated IR band intensities and transition moments 0-95611
 TeO₂, Cl₂ thermal decomposition, matrix isolation IR and mass spectra 0-81306
 Ti₂F₂(Cl₂), assignment of vibr. Raman and IR spectra bands 0-58268
 TiReO₄, IR matrix-isolation spectra 0-87108
 UF₆, CW CO₂ laser spectroscopy 0-83367
 ZrF₄, CW CO₂ laser spectroscopy 0-83367
 ZnF₂(FCl)(FBr), matrix isolated IR and Raman spectra, assignments, force consts., isotope effects and thermodynamic props. 0-63631
 ZnO₂, formed by matrix reactions, IR, Raman and visible spectra 0-87110

infrared telescopes *see telescopes*

infrared transmitters *see infrared sources*

infrasonic waves *see acoustic waves*

initial value problems

- Boltzmann equation, nonlinear, with soft potential, spatially periodic problems 0-77731
 Boltzmann equation in an exterior domain 0-90797
 Einstein field equations, characteristic initial value problem in general relativity 0-73238
 elastodynamics, linear, discrete time approx. of initial boundary value problems, error estimates 0-73175
 evolution systems and convection-diffusion, stiffness and stability, Gershgorin theory 0-77626
 fins, nonlinear problems, 1-D conduction, initial value problem 0-83726
 fluid dynamics, plane Couette flow, resonance mechanism, small 3-D disturbances 0-79269
 fluid dynamics, Rayleigh-Benard convection, randomly forced 0-79314
 fluids, Newtonian, eqns. of motion, initial value problem 0-62477
 KdV equation, perturbative expansion and initial value problem 0-62487
 Maxwell's initial boundary value problem, horizontal line (Rothé) method, convergence and error estimates 0-94957
 rotating dust sphere, slow rotation limit, maximal slicing condition 0-73246
 summed progressing wave formalism for initial value problem calcs. 0-92039
 thermal elastoplastic stress analysis based on initial strain method (*Japanese*) 0-77620
 wave equation in several space dimensions, Rothé method 0-82651
 wave interaction, resonant, three-wave, separable initial-value problem of initially nonoverlapping envelopes 0-68058

injection lasers *see semiconductor junction lasers*

injury by radiation *see biological effects of radiation*

inorganic insulators *see insulating materials*

inorganic molecule configurations

- see also isomerism*
 conference, Crystal XII, Canberra, Australia (Jan.-Feb. 1980) 0-62388
 Faraday effect measurement in pulsed mag. field 0-80758
 hydrides, first row, bending pot. calc. using MINDO approx., force const., equilb. geometry 0-95544
 pyrophosphatase, inorganic, of yeast, cryst. growth, derivatives formation, heavy atoms positions 0-108842
 tetramethyl-p-benzoquinone, mol. struct., gas phase electron diff. obs. 0-58386
 [Cl₃PNPCL₃][PCl₄], X-ray cryst. struct. determ. 0-88095
 Al₂ (Al₂)₂(Al₂)₂ configurations, ab initio study, LCAO, STO, MO-SCF and CI calcs., binding energy (*French*) 0-91447
 Al³⁺(H₂O)_n (n=1,2,4,6), FSGO-pair-pot. calcs. (*German*) 0-74278
 ArHBr, ArHCl, and isotopic forms, rot. spectra, mol. struct., mol. consts. 0-58246
 ArSO₃, weakly bound complex, struct., MBER obs. 0-95701
 AsF₃, inversion barrier, STO SCF calc. 0-63567
 BH₃, electronic wave function determ., genealogical technique using Clebsch-Gordan coeff. 0-95529
 BH₄⁺, pot. energy surfaces and mol. deform. induced by external cation 0-106285
 B₂O₃, bipyramidal struct., stability, ab initio SCF-MO calcs. 0-99446
 Ba₂SbS₁₁, cryst. struct., selenoantimonate (III) anions (*German*) 0-103305
 BeBH₄, H bridged system, floating spherical Gaussian model 0-78518
 Be²⁺(H₂O)_n (n=1,2,3,4,6), FSGO-pair-pot. calcs. (*German*) 0-74277
 BeOH, struct. and electronic props., ab initio calcs. 0-74113
 CO, photoelectron ang. distributions, wavelength and vibr. state depend., reson. effects, asymmetry parameters 0-91602
 CO₂, asymmetry parameter, angle resolved photoelectron spectra, multiple scatt. method 0-63708
 C₂O₂, semirigid bender, rot.-vibr. energy level separations obs., struct. and pot. functions determ. 0-83446

inorganic molecule configurations continued

- COS, asymmetry parameter, angle resolved photoelectron spectra, multiple scatt. method 0-63708
 CS₂, asymmetry parameter, angle resolved photoelectron spectra, multiple scatt. method 0-63708
 ClCO radical, struct. and props. calcs. 0-74112
 CINSO, ground state geometry, ab initio calcs. 0-106259
 ClO_n⁺, ClO_n and ClO_n⁻ (n=1 to 3), ab initio calcs., localised MO and nature of Cl-O bond 0-69070
 ClOO radical, struct. and props. calcs. 0-74112
 Cl₂Si(CH₃)_{4-n}, ³⁵Cl NQR, geminal and vicinal interactions on substituents electronic effect 0-63663
 Cl₂Si(OCH₃)_{4-n}, ³⁵Cl NQR, geminal and vicinal interactions on substituents electronic effect 0-63663
 Co complex, O₂CoCl₄ and O₂CoCl₄NH₃²⁻, struct. and bonding model, CNDO-UHF calcs. 0-95541
 Co complexes, Co II tetraphenylporphyrins, constraint, ESR and optical detect. 0-83394
 Cr(NO)₄, XPS and UV photoelectron spectra, compared to NO data 0-58317
 CsBrICN, Raman and IR vibr. spectra, struct. 0-102513
 CsClICN, Raman and IR vibr. spectra, struct. 0-102513
 CsI₂CN, Raman and IR vibr. spectra, struct. 0-102513
 Cu complex, Cu(NH₃)₂(NCX)₂, X=O, S, electronic struct., stereochem. 0-58156
 FCO, radical, struct. and props. calcs. 0-74112
 F⁻(H₂O)_n(n=1,2), FSGO-pair-pot. calcs. (*German*) 0-74278
 FNNF, mol. struct., cis effect 0-91434
 F₂O, geometry, electron spectrum, vert. ionis. pot. ab initio calc. 0-58187
 FOO radical, struct. and props. calcs. 0-74112
 FSO (FOS), struct. and props., SCF calcs. 0-106260
 FSS, struct. and props., SCF calcs. 0-106260
 GeH₂, struct. determ., restricted HF calcs. 0-87030
 H⁺+CO (¹Σ), ground state pot. energy surface, ab initio SCF calc., protonated equilb. geometry 0-83301
 H₂-H₂ dimers, hyperfine struct. in zero mag. field 0-95700
 H₄, pot. energy surfaces, valence bond calcs. 0-74129
 HBF₂ and DBF₂, harmonic force field and ground-state average struct. determ. 0-83342
 HBr, photoelectron angular distrib. 0-58318
 HCN, Fermi and Coulomb correl. holes, SCF and CI wave functions 0-69085
 HCN, intravalence triplet-triplet electronic transition, geometrical struct. and rel. energies determ. 0-99586
 HI, photoelectron angular distrib. 0-58318
 HNNN, substitution struct., rot. consts. calcs. 0-91534
 HO₂, struct. and props., SCF calcs. 0-106260
 H₂O dimer, partially deuterated, microwave spectra and struct. 0-74212
 H₂O⁺, ab initio potential energy surface study by CI techniques, equilibrium conform. determ., mol. dissoci. pathways 0-78550
 H₂O⁺, spin and rot. fine struct., orbital angular momentum 0-83247
 H₂O-HF heterodimer, H bonding, microwave rot. spectrum, mol. geometry and moment 0-99501
 (H₂O)₂, struct. studied by CNDO/2 method 0-69081
 (H₂O)₃, geometric config. energies, SCF LCAO MO calcs. 0-63551
 H₂O⁺ inversion barrier, high-order replacements inclusion in CI calcs. 0-63504
 HSO (HOS), struct. and props., SCF calcs. 0-106260
 HSS, struct. and props., SCF calcs. 0-106260
 Hg complex, methylethynylmercury(II)(-d₁, -d₃, -d₄), vibr. spectra and normal coord. calcs. 0-58259
 Hg(CN)₂, phonon freq. anomalous press. depend., mol. struct. distortion 0-88981
 KPbI₂, 2H₂O, X-ray cryst. struct. determ. 0-64958
 KrHBr, KrCHI, and isotopic forms, rot. spectra, mol. struct., mol. consts. 0-58246
 LaF⁺, electronic spectra, rot. anal. and orbital configurations 0-83240
 LiBF₄, nonrigid mol. struct. and stability, ab initio calcs. 0-83259
 LiBH₄, H bridged system, floating spherical Gaussian model 0-78518
 LiBeF₃, pot. energy surface, struct., stability and internuclear distances, ab initio calc. 0-58147
 LiBeH₃, H bridged system, floating spherical Gaussian model 0-78518
 LiCH₃, H bridged system, floating spherical Gaussian model 0-78518
 Li₂F₂, struct., force fields and normal mode freqs., ab initio calcs. 0-83260
 Li₂F₂, struct., internuclear-distances and mean amplitude of vibr. determ. by electron diff. 0-69252
 LiH-NH₃, struct. and props., SCF ab initio calcs. 0-106250
 (LiH)₃ complex, SCF interaction energy nonadditivity 0-91437
 Li⁺(H₂O)_n (n=1,2,3,4,6), FSGO-pair-pot. calcs. (*German*) 0-74277
 Mg²⁺(H₂O)_n (n=1,2,4,6), FSGO-pair-pot. calcs. (*German*) 0-74278
 MgOH, struct. and electronic props., ab initio calcs. 0-74113
 N₂, asymmetry parameter, angle resolved photoelectron spectra, multiple scatt. method 0-63708
 NH₂, spin and rot. fine struct., orbital angular momentum 0-83247
 NH₃, vibr. excitation in soft X-ray emission and core ESCA spectra 0-69163
 NH₄NO₃ crystals, NH₄⁺ ion symmetry in phases II-V, Raman spectra obs. 0-66200
 NH₄PbI₃·2H₂O, X-ray cryst. struct. determ. 0-64958
 NO₂ hydrate clusters, ground-state HF pot., Monte Carlo simulation, energy surfaces and rot. barriers 0-106412
¹⁵N/¹⁴N₂, predissoc. rot. struct. in 2490 Å band 0-87192
 N₂O, satellite struct. and momentum distrib., binary (e,2e) spectroscopy 0-69125
 N₂Br₂, ⁸¹Br NQR, conformation investig. 0-63665
 Na⁺(H₂O)_n (n=1,2,4,6), FSGO-pair-pot. calcs. (*German*) 0-74278
 Ni₃, in solid Ar, reson. Raman spectra 0-63638
 O₂, symmetry adapted wave function generation using group theoretical projection operators 0-102428
 O₂⁻, hypothetical, mol. self-consistent study, possible prep. method (*French*) 0-91717
 O₂H⁺, isomeric structs., ab initio MO calcs. 0-83270
 OPBr₃, mol. struct., electron diff. and spectroscopic vibr. amplitude 0-58387
 RbPbI₃·2H₂O, X-ray cryst. struct. determ. 0-64958
³²SF₆, point group symmetry breakdown, vibr.-rot. state, saturation spectroscopy 0-87116
 SPBr₃, mol. struct., electron diff. and spectroscopic vibr. amplitude 0-58387
 SnH₂, struct. determ., restricted HF calcs. 0-87030

light transmission continued

- clouds, mathematical model for reflected and transmitted radiation 0-90215
 coatings, absorptive, at normal incidence, program for TI-59 calculator 0-84793
 crystalline slab of point molecules, dielec. theory 0-97222
 β,β' -dichloroethyl ether-iso-octane, critical indices, allowance for light double scatt. (*Russian*) 0-60624
 diffraction patterns for optical systems with pupils of non-uniform transmittance 0-87470
 domain lattice of transparent crystal regular birefr. regions, optical wave diff. divergence 0-102616
 dusty IR Test-1 lidar obs., transmission meas. 0-99625
 Fabry-Perot etalon, optically contacted, stability to cosmic radiation 0-98544
 filament waveguides for signal transmission in far IR region (*Czech*) 0-96017
 Fresnel's eqn. for light reflection and refraction, teaching 0-101688
 gas, inhomogeneous layer, transmission calc. for spectral line with Voigt profile 0-59164
 glass fibre reinforced plastics, ageing by boiling in water, effect on physico-mech. props. 0-60892
 glass transmission and other props. 0-84712
 glasses, high vol. low cost, as solar reflectors, compositions and weathering effects 0-106589
 illuminating fibre bundles, improved characts. due to glasses type VS 1637 and VO 720 0-102844
 limited light beam, nonlinear reflections and transmission 0-58624
 liquid crystal image transducer, optical props. at normal incidence, off-state behaviour 0-64160
 longitudinal static spin wave struct., magnetotropic interaction of light (*Russian*) 0-93285
 meniscus collimator viewfinder, optimisation of mirror light transmission coeffs. 0-74469
 metal-dielectric interference filters in transmitted light 0-96013
 microcantilever electrostatic deflection system for transmission optical modulator array 0-87512
 microscopic interference obs. by reflection contrast 0-68248
 microscopical and Ewald dynamical diffraction theories, refl. and transmission, spatial dispersive dielec. slab 0-83548
 multi-layer optical system, reflection and transmission coeffs. calcs., computer program 0-66316
 multilayer superlattice stacks, very thin nonideal, wavelength variation of transmissivity, refl. 0-100701
 multilayers, ultrathin, optical characts. 0-104005
 nematic liquid crystal display, twisted, ang. and voltage depend. of light transmission, two-layer model 0-76006
 nematic liquid crystals, light transmission meas. 0-88025
 neutral absorbers of NS glass, meas. of transmission when irradiated with laser radiation 0-105692
 nitrocellulose fibres, polarised light study 0-80736
 objective lenses, two-channel device for meas. transmission coeff. 0-106642
 optical fibre, secondary coating rel. to transmission loss 0-58704
 plane-parallel plate, with spatial dispersion, light refl. and transmission coeffs. 0-88951
 polarisation constants for light interaction with absorbing crystal plates 0-78765
 polyacetylene films, doping investigation, insulator-metal transition, optical transmission meas. 0-103729
 quartz high-transmittance antirefl. film, vacuum-etched 0-74449
 quartz in metamorphic rocks, transmission spectra rel. to c-axis fabrics anal. 0-101456
 radiative transfer, synthetic scattering phase function 0-98541
 SF_6 , buffered, 10.6 μm transmission props. for nanosecond pulses 0-58644
 smoke aerosols, optical absorption to extinction ratio, photoacoustic determ. 0-58459
 solar collector glazings, effective beam rad. incidence angles for determ. of diffuse rad. transmittance 0-94112
 spectrophotometer, SF-26, stray radiation level during 280 to 350 nm region operation 0-101852
 thick layers, refl., transmission and brightness coeffs. 0-63918
 thick planar films, transmission method for index meas., modal effects 0-102862
 thin films, optical transmittance and reflectance, bulk optical props. determ. 0-88954
 Ag film, granular, transmission and reflection spectra, validity of sum rule 0-97358
 Ag halide optical fibres, extrusion, visible and IR transmission 0-58829
 Ag halide polycrystalline fibre, 10.6 μm transmission loss obs. 0-64197
 Al_2O_3 , integrally coloured oxide films on Al, optical properties 0-93420
 $\alpha\text{-Al}_2\text{O}_3$, single crystal transmission and reflectance IR phonon spectra, polariton dispersion 0-66170
 Al_2O_3 , transparent hot-pressed, transparent and translucent properties 0-60533
 $\text{As}_2\text{S}_3\text{Se}_3$ glassy semiconductors, electronic props. 0-103712
 Au film, granular, transmission and reflection spectra, validity of sum rule 0-97358
 CdO-SnO_2 DC reactively sputtered films, elec. and optical props. 0-103763
 CuGaTe_2 , refr. indices meas. 0-93259
 CuInSe_2 , refr. indices meas. 0-93259
 CuInTe_2 , refr. indices meas. 0-93259
 GaSe , thin layers, far IR refractive index 0-80799
 Ge amorphous film, crystn. front velocity during scanned laser crystn. 0-107662
 Ge-As-Se IR transmitting glass composition, prep. and props. 0-69474
 GeS_2 , single crystal, far IR transmission 0-80800
 $\text{In}_2\text{O}_3\text{:Sn}$, RF magnetron sputtered film, elec. and optical props. 0-104065
 In_2O_3 films, activated reactive evaporation technique of prep. 0-80989
 In_2O_3 films, electron beam evaporation, elec. and optical props. (*Japanese*) 0-60784
 In_2O_3 , thin film, sputter deposition form., optical and elec. props. 0-60123
 $\text{In}_2\text{O}_3\text{:Sn}$ films, activated reactive evaporation technique of prep. 0-80989
 InSb , Auger-governed decay of laser-induced plasma, optical probing 0-76105

light transmission continued

- $\text{In}_2\text{Si}_2\text{O}_7$, thin film, sputter deposition form., optical and elec. props. 0-60123
 LiF , refractive index, effect of ageing, wavelength range 460-1000 nm 0-84707
 $\text{LiO}_2\text{-Al}_2\text{O}_3\text{-SiO}_2$, glass containing ZrO_2 , cryst. process 0-103253
 $\text{NaF-SrF}_2\text{-CrF}_3$, glass transition, crystn. and melting temps., optical transmission (*French*) 0-64910
 p-Si, heavily doped contact layers on IR detectors, IR transmissivity 0-108190
 Si wafer processing, CO_2 laser heating dynamics 0-76106
 Si:B ion implanted layers, light refl. and transmission coeffs., computer program 0-66316
 SiO amorphous film, optical transmittance and reflectance, bulk optical props. determ. 0-88954
 SiO evaporated film, dielec. function 8 to 33 μm , spectrophotometric and refl. meas. 0-80883
 SiO_2 films, Si-rich, amorphous Si region obs. 0-84400
 SnS_2 thin layer, far IR refractive index 0-93421
 SrF_2 , thin film, optical props., spectral dependence, 460-1000 nm 0-76094
 YAG:Nd crystal, orientation influence on thermally induced birefringence (*Chinese*) 0-88958
 ZnS CVD IR window, optical and physical characteristics 0-106620

light velocity

- diffuse medium, reduced effective velocity of light 0-69329
 isotropy of light velocity convention, teaching 0-101689
 relativity, special, dilatational degree of freedom, six-dimensional space V_6 0-57088
 simultaneity, distant, conventionality, standard synchronisation 0-77612
 vacuum, quantised space, special relativity and relativistic field theories 0-82869

light velocity measurement

- demonstration apparatus using two dollar rotators 0-77578
 fibre optic wink-around expt. 0-90628
 Foucault's rotating mirror method for meas. speed of light 0-67996
 Mossbauer meas., isotropy 0-95026
 nuclear timing technique 0-90637
 one-way velocity of light, and light signal synchronisation 0-82644
 rotating axle expt., oscilloscopic and absolute 'coupled-shutters' variants 0-68234

light water see water**lighting**

- airport control tower cab, optical design 0-58661
 film copying techniques, colour (*German*) 0-62751
 illumination system, optical design 0-64135
 return stroke models 0-77050
 spectral eye fatigue, school lighting effects 0-76732
 veiling reflections and reflected glare from glossy paper, lighting conditions for visual comfort 0-76733
 InAsSb/GaSb broad-spectral-band IR detector, backside-illum. heterostructure approach 0-73450
- lightning**
- ball, energy condensation, comparison with exciton droplet (*Russian*) 0-107712
 ball lightning, forms and energy density 0-98402
 ball lightning, radiation, electrical and magnetic props. 0-77086
 clear air triggered lightning, movie film obs. 0-90166
 conductivity charges in cloud and energy losses 0-61867
 direction finding at close range, VHF method 0-98481
 direction to lightning channel, mag. direction finding method 0-77078
 discharges, parameters, protection of electrical systems 0-94590
 electrons heating in lower ionosphere by horizontal lightning discharges 0-90283
 electrostatic charges meas. and localisation, neutralised during lightning flashes 0-77097
 ground flashes at Port Moresby, Papua New Guinea 0-67393
 ground wave atmospherics generated by lightning return strokes, initial peaks, model 0-61876
 long arc simulated lightning attachment testing using 150 kW Tesla coil 0-70074
 optical radiations, simultaneous obs. from above and below clouds 0-85698
 physical mechanisms, present and future research (*French*) 0-82015
 precipitation observed immediately after lighting, within thundercloud 0-77055
 return strokes, latitude dependence 0-67394
 RF radiation generation, elec. field var. obs. 0-98401
 strokes, artificial, experimental station in France (*French*) 0-61841
 survey of research, definitions, unresolved problems 0-61868
 triggering lightning by pulsed laser 0-72626
 tropical regions, atm. noise data 0-61875
 tropical thunderstorms, cloud to ground and intracloud discharge 0-85705
 N fixation by lightning 0-90147
 N fixation in lightning channels, theory 0-90148
 NO_x production by lightning, shock and channel heating methods 0-72581

lightning conductors see lightning protection**lightning protection**

- see also surge protection
 discharges, parameters, protection of electrical systems 0-94590
 fusion reactor, JT-60, grounding system pot. rise during lightning strike, anal. 0-102314
 photovoltaic terrestrial systems, protection from lightning effects 0-89648
 survey of research, definitions, unresolved problems 0-61868

lightning rods see lightning protection**limit, elastic see elastic limit****limit cycles**

- dynamical system, limit cycles and symmetries 0-62462
 plasma-electron beam system, high-power, relax. oscillations 0-64744
 symmetric, bifurcation to asymmetric limit cycle, simple model 0-57080

limited space charge accumulation

- see also Gunn effect; negative resistance effects; space-charge limited devices
 No entries

linear accelerators

- see also collective accelerators; electrostatic accelerators
 beam profile scanner, medical appls. 0-101267

linear accelerators continued

- biomedical, 4 MV, use for whole-body irradiation 0-109001
- biomedical, field separation between lateral and anterior fields, dose distribution 0-94336
- electron accelerator, linear, for 1-mA average current, 10 μ sec duration 0-68978
- functional generator of controlling voltage of energy modulator for injector 0-68975
- induction linacs, efficiency calcs. 0-99357
- ion beams, intense, production and postaccel. in magnetically insulated gaps 0-74041
- ion transport in linear accelerators by electron neutralisation 0-58014
- Kharkov linear electron accelerator for obtaining beam of quasicromatic linearly polarized photons, 2-crystal goniometric setup 0-68976
- LAMPF, Monitor remote handling system update 0-68979
- low energy (250 keV, 2.5 mA) for neutron production 0-99354
- LWR fuel regeneration and waste transmutation using proton linac 0-63365
- medical electron accelerator, radioactive and toxic gas production 0-94378
- nanosecond beam dynamics in linear electron accelerator 0-86996
- NDT application in industrial products inspection 0-81267
- particle trajectory distortion by strong focusing fields 0-83228
- proton beam cooling channel for injection into linear accelerator 0-68973
- pulse amplifier with digital gain control 0-68977
- pulseline driven neutralised linear ion accelerators, longit. instabilities 0-78459
- radiotherapy, SL 75-20 accelerator, neutron and gamma doses in entrance mazes of treatment rooms 0-85500
- radiotherapy with electrons, up to 20 MeV, phys. aspects 0-85474
- resonator sensor for the parameter of charged-particle beams 0-68991
- S-band subharmonic prebuncher for picosecond single electron pulse (Japanese) 0-78460
- shielding, local absorber in accelerating section to reduce radiation level 0-83229
- short pulse accelerators, resistive wall coating's parameter determ. 0-63418
- travelling wave linac., magnetic-gun igniter for controlled thermonuclear fusion 0-91238
- ultrahigh-power ion accelerator, pulsed, operating regimes 0-78462
- X-ray beam energy at off-axis points, calc. technique for correct. 0-81742
- X-ray beams, off-axis beam quality change 0-78461
- π production and properties, LAMPF linear proton accelerator (French) 0-63417

linear algebra

- see also *determinants; eigenvalues and eigenfunctions; matrix algebra; tensors; vectors*
- oil-bearing layer with input parameter correction, discrete dynamic model 0-83778
- optical imager, linearly degraded, iterative restoration 0-95807
- optical images, linearly degraded, iterative restoration, reblurring procedure 0-99640

linear combination of atomic orbitals calculations see *LCAO calculations***linear differential equations**

- conserved densities, Hamiltonian systems 0-90682
- coupled, second-order, hybrid soln. method 0-94968

linear integrated circuits

- TEM image and electron energy loss spectrum display by self-scanned linear Si photodiode arrays 0-68330

linear motors

- asynchronous motor drive system, for rotating optical components inside vac. system 0-102874

linear programming

- education, linear programming, introduction and appl. to simple cct. 0-73136
- energy system modelling, New Zealand appl. 0-76590
- intracavity implant therapy, appl. of linear programming to dose optimisation 0-72329
- national energy policy anal. and planning models 0-101071
- plastic anal. of thin-walled beams of open cross section, finite-element model 0-74767
- respiratory mechanical behaviour lumped parameter models evaluation using simplex algorithm 0-89783

linear rectification see *rectification***linear rectifiers** see *rectifiers***linear systems**

- aerodynamic stability of Timoshenko bar, time- and space-harmonic balance (German) 0-83812
- catheter pressure meas., transducer smearing correction using microprocessor based discrete deconvolution 0-67275
- mean square response to nonstationary random excitation 0-57085
- nondelta-correlated parameter fluctuations, statistical anal. 0-95036
- statistical analysis of system acted upon by Poisson processes 0-57196

linear vibrations see *vibrations***lines (telephone)** see *telephone lines***linewidths (spectral)** see *spectral line breadth***linkages (electric connectors)** see *electric connectors***linking** see *joining processes***Liouville equation**

- see also *Vlasov equation*
- Brownian fluid affected by potential, Maxwell-Boltzmann distrib. in infinite-time limit 0-105573
- correlation function, long time asymptotic behaviour, influence of waves on relax. processes (Chinese) 0-59195
- Enskog quasiparticle, non-Hamiltonian dynamics 0-101750
- generalised Liouville equation from Lie derivative 0-77981
- Goursat problem regular solns. 0-105795
- inverse Liouville problem, quasi-particle dynamics from a given kinetic eqn. 0-101749
- magnetised plasma, Vlasov theory coherent state approach 0-64675
- N interacting particle canonical distrib. from kinetic theory 0-105569
- superalgebra in (0,1) integration of supersymmetrical Liouville eqn. (Russian) 0-101947

lip microphones see *microphones***lipid bilayers**

- alkane solubility modified by elec. field 0-97874
- n-alkanes, adsorption into bimolecular lipid layers 0-88435

lipid bilayers continued

- cation-phospholipid-induced shape changes in lipid bilayer couple 0-108855
- current pulse-induced voltage variations in bilayer membranes, apparatus 0-94420
- cyanine-dye adsorption, spectrophotometric and elec. correls. 0-85358
- dielectric constant of phospholipid bilayer rel. to ion permeability 0-81364
- 1,2-dimyristoyl-sn-glycero-3-phosphoserine multilayers, phase transitions, temp. depend., ellipsometric study 0-108846
- 1,2-dipalmitoyl-sn-glycero-3-phosphocholine multilayers, phase transitions, temp. depend., ellipsometric study 0-108846
- dipalmitoylphosphatidylcholine, changes in vol. mag. susceptibility at the phase transition 0-76770
- dodecanate/decyltrimethylammonium micelles, type II mesophase, bilayer struct., NMR spectra study 0-75149
- elastic props. changes on exposure to different agents, elec. and chem. 0-81548
- electrical breakdown 0-81552
- hydrocarbon chains, conformational anal. 0-81532
- intramembrane potential jump meas. by potentiodynamic method 0-81778
- membrane bilayers, quasitwo dimens., theoretical models 0-76713
- nerve action pot., lipid bilayer local phase transition 0-89744
- nonpolar molecules, adsorption into lipid bilayer membranes 0-61517
- permeability behaviours, steady-state, induced by cyanine dyes 0-85357
- phase transition, cholesterol effect 0-85361
- phosphatidylcholine, lateral mobility of bound amphipathic apolipoprotein ApoC-III 0-97884
- phosphatidylcholine bilayers, fluidity changes and phase transitions, intramol. excimer fluoresc. obs. 0-85342
- phospholipid, one- and two-component, main phase transition, Landau phenomenological theory 0-97872
- phospholipid bilayers, carbonyl groups dynamics, ^{13}C chem. shift anisotropy obs. 0-85326
- phospholipid bilayers, low temp. transition from fluid state 0-97871
- phospholipid cell membranes, at mol. resoln., introduction 0-104841
- photosynthetic reaction centre functional reconstitution in planar lipid bilayers 0-97881
- protein membrane multilayers, thickness depend. of props. 0-89726
- structural order of lipids and proteins, fluoresc. anisotropy data eval. 0-97873

liquefaction of gases

- He, automatic multirange liquefaction plant 0-57306

liquid alloyssee also *liquid metals*

- alloy melt, impurity conc. field model, growth by Czochralski method (Russian) 0-75191
- alloy melt, temperature distribution during cryst. growth by Czochralski method (Russian) 0-75192
- binary metallic systems, rule for surface enrichment 0-75406
- brass, liquid, thermodynamic props. (German) 0-66482
- crystallisation front interaction with turbulent alloy melt stream, heat exchange (Russian) 0-74708
- liquid alloys, positron annihilation due to vacancy trapping, simplified model (Russian) 0-71511
- melts, of a congruently melting substance, single struct. model 0-103233
- molten, compound-forming, vol. of mixing, conc. depend. 0-103484
- quadrupole relaxation rate temp. depend. 0-88884
- ternary and higher order, activity coeff. of nonmetallic solutes 0-107433
- Ag-Bi, liq. alloys, thermodynamic investigation 0-70428
- Ag-Ge eutectic alloy, heat capacity meas. over temp. range 800-1200K (French) 0-88331
- Ag-In melt system, conc. depend. of component and impurity diffusion coeffs., radioactive isotope method (Russian) 0-107454
- Ag-Sn, liquid alloys, thermodynamic props. (Japanese) 0-108396
- Ag-Zn, molten, EMF meas. of activities using ZrO_2 solid electrolytes (Japanese) 0-88339
- Al-Cu, liq. alloys, with zero superheat, fluidity 0-70289
- Al-Cu, molten, showering cryst. form. in mould cooled from top (Japanese) 0-66498
- Al-Cu dilute alloys, vein closing mechanism in fluidity tests 0-84924
- Al-Ni solid, liquid mixture, diffusion processes (Russian) 0-107563
- Al-Si melt, microheterogeneity (Russian) 0-103238
- Al-Si melts, spreading behaviour on Fe 0-84345
- Al-Ti, molten, showering cryst. form. in mould cooled from top (Japanese) 0-66498
- Al, Mg_{1-x} , vols. and entropies of mixing, calc. 0-75363
- Au-Ge-Si, influence of struct. on elec. resist. of glass forming alloys 0-65518
- Au-Zn, molten, EMF meas. of activities using ZrO_2 solid electrolytes (Japanese) 0-88339
- Au(Ag)(Cu)-Sn liquid, optical reflectivity spectra of virtual bound states 0-89021
- $\text{Au}_{71}\text{Ge}_{13}\text{Si}_{16}$, heat of crystn. and viscous behaviour 0-75166
- Bi-Sb-Te melt, Sb and Te distribution coeffs. during crystallisation (Russian) 0-93472
- Cd-Zn binary systems, melts, elec. resist., 0-700°C 0-65517
- Ce-Cu, liquid, normal spectral emissivity 0-103506
- Co-Ca, liq. alloy form. kinetics (French) 0-96652
- Cs-Au, liq., molar vol. meas. 0-59546
- Cs-Au liq. alloy, formation of localised electronic states, NMR obs. 0-93201
- CsAu, molten, equimolar, structural evidence of ionic nature 0-64882
- Cu alloys, molten, gas content meas., reduced pressure test (Chinese) 0-81390
- Cu alloys, thermal cond. and elec. resistivity 0-103661
- Cu-Al-Co liquid alloys, constant Co-content of 5 wt.%, mag. props. (German) 0-88720
- Cu-Al-Mn liq. alloys, susceptibility behaviour 0-93077
- Cu-Al(Ga)(In) alloys, elec. cond., temp. and conc. depend., model interpret. and alloy struct. (Russian) 0-88528
- Cu-M-O ternary alloys, thermochem. calcs. 0-85209
- Cu-Ni, liq., surface conc. profile and surface energy 0-84350
- Cu-Ni-S, molten, thermodynamic props. 0-104122
- Cu-O (0.05 to 0.1 wt.%) liquid alloy, deoxidation kinetics by rotating graphite cylinders 0-61084
- Cu-Pb (Fe), liq., thermodynamic props. (Polish) 0-89199
- Cu-Sn, thermodynamics of Cu and Sn solns. using copper β -alumina solid electrolyte, 800-1100K 0-107502

liquid alloys continued

- Cu-Sb binary system, wettability and interaction between solids and liqs. (*Japanese*) 0-92760
 Cu-Ti-Al(Ga)(Au)(In)(Ag)(Ni), wetting of Al_2O_3 , alloying effects 0-107617
 Fe-As melts, surface tension, density, adsorption (*Russian*) 0-92757
 Fe-B, liq., mag. susceptibility meas. 0-75740
 Fe-Cr-Ti(Al) liquid alloys, thermodynamical anal. of O_2 solubility (*Russian*) 0-92676
 Fe-Cu liquid alloy, heats of mixing, mixing entropies (*Russian*) 0-65224
 FePc molten and amorphous alloys, struct. factors 0-79674
 Ga liquid spreading over Ag thin film, kinetic eqn. (*Russian*) 0-59376
 Ga-Ge-Zn ternary alloys, thermodynamic props., EMF meas. 0-81033
 In-Ga liquid alloy, low-resistance ohmic contacts in ZnSe, LED fabrication appl. 0-70823
 In-Sb liquid alloy, mixing enthalpy, temp. depend. (*German*) 0-84298
 In-Zn binary system, melts, elec. resist., 0-700°C 0-65517
 Li-Cd, elec. resist. and Knight shift 0-75537
 Li-Mn, form factor effects, pseudopotentials resist. calc. 0-103608
 Li-Pb liquid alloys, elec. resistivity, negative temp. coeff. 0-88527
 Li-Pb liquid compound forming alloy, entropy of mixing 0-88328
 Na-Cs, struct. factor, free energy of mixing, and electrochem. pot., thermodynamic calc. 0-96436
 Na-K liq. alloy, Moolwyn-Hughes parameter calc. from US data 0-59375
 Na-K liquid alloys, struct., X-ray and neutron diffr. meas. 0-107041
 Na-K liquid alloys, triplet correlation functions and thermodynamics, solute partial structure factor 0-64881
 Pb-Bi liquid alloy, Pb and Bi diffusivities, temp. and conc. depend. (*German*) 0-84311
 Pb-Fe(Cu), liq., thermodynamic props. (*Polish*) 0-89199
 Pb-Sn (20wt.%), eddy current study of solidification 0-104141
 $\text{Pb}_{1-x}\text{Li}_x$ (As)(Ag)(In)(Sn)(Sb)(Te)(Au)(Ti)(Bi), liquid alloys, local fluctuations and quadrupolar relaxation 0-66060
 Pd-Au-Si, influence of struct. on elec. resist. of glass forming alloys 0-65518
 $\text{Pd}_{77}\text{Cu}_{16.5}\text{Si}_{6.5}$, heat of crystn. and viscous behaviour 0-75166
 Se-Tl-S alloys, liq., dielectric relax. and elec. cond. 0-108150
 Sn-Pb (26%), liq. eutectic alloy Seebeck coeff. 0-84463
 Sn-Te, molten, elec. cond. and phase diagram 0-84454
 Tl-Se, liquid mixtures, press. effect on two-phase region 0-75347
 Zn-Bi, liquid, inconsistent conjugated liquidus 0-76232
 Zn-Cd alloys, liq. and solid, ultrasound speed and compressibility meas. 0-102941

liquid crystal devices

- acoustic imaging with nematic liquid crystals (*French*) 0-69617
 acousto-optical image and hologram convertor using nematic liq. crystals. 0-76002
 active optical devices, seminar, San Diego, CA, USA (August 1979) 0-101664
 anthraquinone pleochroic dyes in liq. cryst. soln., photostability, appl. to liq. cryst. displays 0-88961
 cholesteric films, absorpt. and contrast in dichroic liq. cryst. displays 0-75155
 cholesteric sheet heat detector thermographic photographic characterisation of US intensity patterns 0-106689
 cholesteryl nonanoate-MBBA, liq. cryst. mixture, two colour display device 0-70116
 conference, Minneapolis, MN, USA (June 1979) 0-77535
 cyanobiphenyl liquid crystal IR modulator expts. 0-102837
 dielectric waveguide, flow detection using UHF EM field pattern display 0-104378
 display elements, principles and applications (*German*) 0-86277
 dye laser oscillator and amplifier in liq. cryst. matrix, anisotropic props. 0-74355
 electro-optic switch, four-port, for unpolarized fibre light 0-58715
 hybrid field-effect liquid-crystal light valve, optical data processing performance 0-99860
 image transducer, normal incidence, on-state optical performance 0-99852
 image transducer, optical props. at normal incidence, off-state behaviour 0-64160
 image transducer, performance effects of liquid crystal thickness 0-102838
 joint transform correlator performance rel. to wavefront modulator characteristics 0-102651
 light flux attenuators, use of liq. cryst. cells exhibiting dynamic scatt. 0-102845
 light modulator using piezoelectric effect 0-83679
 light valve, nonlinear optical processing in real time 0-87338
 light valve, optical feedback in incoherently illuminated systems 0-87336
 MBBA-EBBA, controllable liq. cryst. transparency, electrooptical chars. 0-78996
 MIS photosensitive high resolution struct., spatial light modulation with liq. cryst. 0-96026
 multiplexed liquid cryst. display, use of cholesteric-nematic phase change 0-107408
 nematic liquid cryst., ZhK-440, transparency, electrooptical chars. 0-78996
 nematic liquid crystal display, twisted, ang. and voltage depend. of light transmission, two-layer model 0-76006
 nematic liquid crystal transducers, dynamic scatt., pre-excitation 0-88021
 nematic reversely pretilted cell, conformation of molecular orientation 0-59388
 nematic twist cell, dynamic props., voltage depend. 0-70117
 optical fibre temp. probe rel. to thermometry and dosimetry of heat 0-98204
 optical logic with variable-grating-mode liquid-crystal devices 0-106613
 optical modulator, time depend. of conductivity under dynamic scatt. conditions 0-64178
 orientational bistability, nematic storage effects 0-70112
 real-time optical processing using the liquid crystal light valve 0-63936
 scattering indicatrix determination for coherent and incoherent radiation (*Russian*) 0-64897
 smectic C liquid crystals, ferroelec., fundamentals and display appl. 0-79676
 twisted nematic display with cholesteric dopant, transmission characteristic temp. depend. compensation 0-103934
 $\text{In}_2\text{O}_3/\text{Sn}$ transparent conducting films, homeotropic orientation of liquid crystals (*Russian*) 0-108181

liquid crystal phase transformations

- 4-alkoxyphenyl-4'-alkylbenzoates, mesomorphic props., terminal alkyl chain length effect 0-88024
 alkyl-cyanobiphenyl homologues, isotropic-nematic phase, optical Kerr effect 0-91866
 4-4-n-alkyloxybenzoyloxy-benzylidene-4'-cyanoanilines, reentrant nematic and smectic phases 0-88308
 N-4-n-alkyloxybenzylidene-4-n-alkylanilines, smectic polymorphism, calorimetric study 0-88307
 2-4-n-alkylphenyl-5-(4-n-alkyloxyphenyl)-pyrimidines, smectic polymorphism, calorimetric study 0-88307
 binary mixtures, phase transitions, entropy, relation to smectic plane tilt angle 0-65203
 biphenyl mixtures with cholesteryl chloride, static and dynamic electro-optical props., cholesteric-nematic transition 0-100646
 biphenyls, cholesteric blue phases, struct. and props. 0-103243
 butyloxybenzylidene octylaniline, liq. cryst., phase transitions, calorimetric obs. 0-103466
 butyloxybenzylidene octylaniline, liq. cryst. film, smectic B-A transition, mech. meas. 0-79918
 CBNA, nematic-isotropic transition at high press., turbidity meas. 0-92655
 CBOOA, smectic-A reentrant nematic transition under press., X-ray obs. 0-59637
 cellulose acetate, solvent effect on lyotropic mesomorphism 0-70121
 cholesteric blue phase, BCC struct., theory 0-59380
 cholesteric liq. crystals, isotropic phase, pretransitional viscosity 0-84312
 cholesteric liquid cryst., guest mol. fluoresc. in stat. state 0-63698
 cholesteryl decanoate, optical activity in blue phase 0-100641
 cholesteryl laurate-cholesteryl caprylate (75 wt.%), polymorphic behaviour, optical, elec. and dielec. meas. 0-65208
 cholesteryl myristate, smectic A-cholesteric transition, tricritical behaviour, DTA and DSC study 0-65206
 COC, cholesteric liq. cryst., positron lifetimes and phase transitions 0-59383
 colloidal solution, flow alignment, transition from isotropic to nematic phase 0-84060
 4-cyano-4'-n-pentylbiphenyl, refr. index meas. and isotropic-nematic phase transition study, surface plasmon technique 0-84282
 cyano-biphenyl LC alignment on obliquely evaporated SiO_2 films 0-79677
 4-cyanobenzoyloxy-4'-pentylstilbene, nematic, smectic A, and orthogonal smectic B phases 0-64890
 cyanobiphenyl liquid crystal IR modulator expts. 0-102837
 cybotactic nematic mesophase, X-ray scatt. 0-92454
 DOBAMBC, chiral smectic, ferroelec., press. and solute effects 0-103920
 DOBAMBC, smectic A and ferroelec. smectic phases, ^{13}C NMR study 0-75153
 p-nododocoyloxy benzylidene p-azophenyl aniline, smectic phases, mol. order, EPR study 0-79693
 EBBA, nematic-isotropic transition at high press., turbidity meas. 0-92655
 EBBA, orientational order in glassy and nematic phases, IR dichroism meas. 0-64891
 EBBA, nematic, EPR investig. 0-108077
 ethyl-p-azoxybenzoate, far IR and Raman spectra, smectic polymorphism 0-76022
 hard-particle fluids, general scaled-particle-like descriptions 0-103231
 hard-particle fluids, general y-expansion-like descriptions 0-107032
 p-p'-n-heptyl-cyanobiphenyl-isotropic solute systems, nematic-isotropic phase transformation, volumetric study 0-92653
 isotropic phase, self-focusing stability of laser beam 0-99812
 light generation at impurity atoms in ferroelectrics and LC, fluctuation effects (*Russian*) 0-91767
 MBBA, nematic liq. cryst., nonlinear optical amplification above Frederiks transition 0-95937
 MBBA, nematic-isotropic transition at high press., turbidity meas. 0-92655
 MBBA, orientational order in glassy and nematic phases, IR dichroism meas. 0-64891
 MBBA, proton spin-lattice relax. in crit. regime 0-80631
 p-methoxybenzoate-p'-n-pentylbenzene, isotropic phase nematogen optical Kerr const. 0-78919
 p-methoxybenzoate-p'-n-pentyl benzene, slow non-critical mol. reorientation in isotropic phase 0-84062
 monomer-dimer system with attractive interactions on square lattice, nematic ordering 0-79681
 multiplexed liquid cryst. display, use of cholesteric-nematic phase change 0-107408
 nematic and smectic phases, X-ray diffr. studies, review 0-100166
 nematic liquid cryst., two-dimensional, Monte Carlo simulation 0-100168
 nematic liquid crystals, orientation fluctuations in high mag. field, quenching, birefringence effects 0-64892
 nematic reentrant mesophases, phase diagrams 0-103467
 nematic to isotropic transition, effect of quasispherical and chainlike solutes 0-65202
 nematic-chiral-dye mixture, circular dichroism, selective light scatt. (*Russian*) 0-103944
 nematic-isotropic phase transition character, molecular bending fluctuations critical growth (*Russian*) 0-79919
 nematic-isotropic transition, thermodynamic props. calc. 0-103464
 nematic-smectic A(C) transitions, NMR spin-lattice relax. time 0-71222
 nematics, uniaxial and biaxial, formed by non-cylindrically symm. mols., computer simulation 0-79680
 octylcyanobiphenyl, crit. heat. capacity near nematic-smectic A transition 0-100323
 p-n-octyloxy benzylidene-p-toluidine, mol. order, EPR VAAC probe 0-70114
 trans-p-n-octyloxy- α -methyl-p'-cyanophenyl cinnamate, mag. and elec. birefr. in isotropic phase 0-80744
 octyloxycyanobiphenyl, nematic-smectic A transition, heat capacity study 0-88033
 4-n-octyloxyphenyl 4-n-pentylbenzoate, permittivity, microwave dielectric relaxation 0-80671
 PAA-di, nematic liquid crystal, NMR data, appl. of Landau-de Gennes theory 0-64893
 PEBAB, nematic, EPR investig. 0-108077
 pentyl cyanobiphenyl, laser and electric field induced Kerr effect 0-84061
 4-n-pentyl-phenylthiol-4'-n-octyloxybenzoate, smectic A-smectic C phase transition, high-resolution X-ray study 0-79921

liquid crystal phase transformations continued

- 4-n-pentylbenzenethio-4'-n-alkoxybenzoates, birefr., crit. behaviour near smectic A-C transition 0-80745
 N-4-n-pentyloxybenzylidene-4-n-hexylaniline (50.6), unclassified smectic phase 0-75157
 phenylene derivatives, effect of substitution on liq. crystalline props. 0-70113
 phosphatidylcholine bilayers, fluidity changes and phase transitions, intramol. excimer fluoresc. obs. 0-85342
 poly- γ -benzyl-L-glutamate, soln., liquid crystal transitions anal. 0-65207
 polydisperse solution of rodlike particles, isotropic-nematic phase transition, Onsager theory 0-100324
 polymer liquid-crystalline solns., struct. 0-103235
 polypeptides, helical, conc. solns., rheological behaviour and liq. cryst. order 0-83771
 potassium laurate-1-decanol-water mixtures, biaxial nematic phase obs. 0-107409
 N-p-propoxybenzylidene-p-pentylaniline, orientational order in glassy and nematic phases, IR dichroism meas. 0-64891
 re-entrant nematic phase, orientational order, electron reson. study 0-103242
 smectic A-nematic phase transform., liq. cryst. binary mixture, birefringence study 0-59638
 smectic film, two-dimens. melting, dislocation-mediated theory predictions, light scatt. use as probe 0-92651
 smectic layers with tilted molecules, solid and fluid phases 0-96444
 smectic-C film, mol. orientation fluctuations in two-dimens., light scatt. obs. 0-93355
 sodium undecanoate/water system, lyotropic liq. cryst. struct. change due to polymerisation of amphiphilic component 0-59386
 terephthalylidene-bis-(4-n-alkylanilines), smectic polymorphism, calorimetric study 0-88307
 TV screens, use of cholesteric-nematic phase transitions (*Chinese*) 0-79922
 unified model for bulk smectic-A, nematic and isotropic phases 0-79692
 viscosity, anomalous properties near $N \rightarrow S_A$ transition point (*Chinese*) 0-84052
 X-ray and light scattering obs., high resolution 0-92460
 MBBA + optically active substance, pretransition optical rotation in isotropic phase (*Russian*) 0-92657

liquid crystals

- see also cholesteric liquid crystals; liquid crystal phase transformations; nematic liquid crystals; smectic liquid crystals
 alignment films prod. by RF plasma beam technique 0-76198
 4-n-alkyl-4'-cyanobiphenyls, synthesis method from biphenyl 0-79684
 p-n-butyl-p'-heptanoyloxazobenzene oriented on NaCl MgF₂ coated NaCl, surface phenomena and IR spectra 0-79678
 carbonaceous mesophase and disc-like liquid crystals 0-79687
 cellulose acetate, solvent effect on lyotropic mesomorphism 0-70121
 central rigid cores, mesogenic power, depolarised Rayleigh scatt. study 0-89012
 collective molecular motion from depolarised light scatt. 0-60614
 copolymer globule model, orientationally-ordered liq. cryst. state (*Russian*) 0-59389
 cyano-biphenyl LC alignment on obliquely evaporated SiO₂ films 0-79677
 dipalmitoyl lecithin bilayer, mol. tilt, X-ray diffraction obs. in gel phase 0-84059
 elastic continuum theory (*Chinese*) 0-79697
 electro-optical phenomena in lyotropic liquid crystals 0-107050
 free energy derivation (*Chinese*) 0-79696
 generalised Suzuki formula application (*Chinese*) 0-107045
 hexagonal, developable domains 0-92453
 hexatic, nonlinear hydrodynamic props., theory 0-100169
 interface total reflection and surface wave obs. 0-108292
 isotropic phase, self-focusing stability of laser beam 0-99812
 layer, thin, symmetry defects and solitons, topological classif. 0-107044
 MBBA, isotropic, surface-induced ordering 0-108176
 mesogenic materials, tails or smear effects in X-ray diffr. photographs 0-96438
 NMR magic echo by sample reorientation 0-103899
 NMR spin-lattice relax. time near phase transitions 0-71222
 nonlinear, use of dissipation functions 0-84054
 ordering and theory of mol. dispersion forces and pair pots. 0-64886
 orientational distrib. coeffs. for liq. cryst. matrix 0-92452
 orientational order parameter, optical birefr. meas., polarisation field problems 0-79688
 phosphatidylcholine bilayers, fluidity changes and phase transitions, intramol. excimer fluoresc. obs. 0-85342
 phospholipid bilayers, carbonyl groups dynamics, ¹³C chem. shift anisotropy obs. 0-85326
 physical props. and sample prep., book 0-105444
 review, cyclobiphenyl compounds, crystal display 0-67962
 scattering indicatrix determination for coherent and incoherent radiation (*Russian*) 0-64897
 sodium undecanoate/water system, lyotropic liq. cryst. struct. change due to polymerisation of amphiphilic component 0-59386
 tetramethylammonium perfluorooctanoate-water, lamellar lyotropic liq. cryst., neutron diffr. struct. obs. 0-64888
 thermo-optical effects used to visualise EM fields 0-62723
 thin layer, polarised light ellipticity after passage 0-88036
 triphenylene derivatives, hexasubstituted, disc-like cpd., mol. conform. and arrangement, semiempirical calcs. 0-107048
 two-dimensional systems, order parameter from chemical shift anisotropy patterns 0-80624
 uniaxial liq. crystal polarised fluoresc. emission 0-80838
 uroporphyrin I octa-n-dodecyl ester, discotic phase 0-103240
 US and laser cavitation phenomena 0-87633
 water-in-oil microemulsions, structural relaxation by thermal current anal. 0-107049

liquid drop model (nuclear) see nuclear liquid drop model**liquid films**

- see also adsorbed layers; helium films; liquid helium; superfluidity; surface tension
 aqueous film, plane-parallel symmetrical, stability, non-spreading oil droplet effect 0-107620
 black foam films stability, review 0-104463
 boundary layers, struct. and thermodynamic peculiarities 0-88408
 butyloxybenzylidene octylaniline, liq. cryst. film, smectic B-A transition, mech. meas. 0-79918

liquid films continued

- cholesteric liquid crystal coatings, superimposed left- and right-handed, peak refl. and colour gamut 0-74472
 condensation of moving vapour on horizontal cylinder, exptl. dependences 0-58892
 confining substrate for micron thick liquid films, semicond. films 0-96722
 dipalmitoyl lecithin bilayer, mol. tilt, X-ray diffraction obs. in gel phase 0-84059
 dynamic behaviour, surface mobility effects 0-88409
 falling, laminar, gas adsorpt. with zero order react. in entrance region 0-64652
 flow down vertical or inclined surface, surface tension effects 0-106778
 flow speed measurement, electromagnetic pipeline system 0-79417
 freely flowing liquid film, cooling, heat transfer, turbulent transport model calcs. 0-64560
 heated horizontal channel, heat transfer and dry patch formation 0-64554
 highly viscous fluid emerging from slit onto plate, flow development and meas. 0-59142
 hydrodynamic contacts, films, elastic properties 0-88239
 hydrodynamic squeeze film between porous circular disks with velocity slip 0-74997
 infinite plate, thin liquid film evaporation, surface temp. and heat transfer 0-64346
 instability on surface of rot. sphere 0-59006
 insulating layer, cellular deformation mechanism, charge flux (*French*) 0-70507
 irregular wavy flow of a liquid film down a vertical plane 0-106808
 laminar falling liquid films, mass transfer with heat transfer and interfacial shear 0-80033
 liquid crystal, dislocation-mediated theory of two-dimens. melting predictions, light scatt. use as probe 0-92651
 2,6-lutidine-water thick films, interferometric obs. of crit. behaviour 0-93266
 Newton black film, line tension, determ. by cnt. bubble method 0-88406
 Newton black films, line tension determ. by diminishing bubble method 0-88407
 polymer solution, elastic, load bearing capacity of squeeze film flow 0-103051
 rupture in laminar and turbulent lubrication, inertia forces effect 0-74813
 simple fluids, small strain oscillatory squeeze film flow, polymeric liquids 0-92765
 smectic C liq. cryst. film, mol. orientation fluctuations in two-dimens., light scatt. obs. 0-93355
 thickness measurement, conductometric method 0-77751
 thin, break-up due to mass transfer intensity in absorption 0-80032
 thin films with extensive evaporation, heat transfer (*German*) 0-99920
 thin liquid film flows, boiling crisis models 0-74710
 thin liquid films in emulsions, contact angles 0-92761
 thin nonplane liquid films, existence and stability 0-92764
 transient thermocapillary flow in thin liquid layers 0-92226
 viscous, between two nearly parallel walls, temp. distrib., convection effects 0-83801
 viscous liquid film instability under the influence of an adjacent gas flow 0-92110
 water film on Fe surface, stability 0-75408
 water films, subcooled, flowing down vertical tube, heat transfer 0-79318
³He-⁴He mixture superfluid thin film, third sound vel. calc. 0-107602
 Xe adsorbed on graphite (0001) surface, monolayer liquid and solid struct. 0-65400

liquid flow coaxial cables see coaxial cables**liquid He see liquid helium****liquid helium**

- see also helium films; liquid helium-3; liquid helium-4; liquid helium sound propagation; ripples; vortices
 contact cryogenic fluid level sensor 0-73371
 cooling system, forced flow, for superconducting magnet, numerical anal. of heat-induced transients 0-82773
 cryogenic He cycles, minimal losses due to thermodynamic irreversibility 0-86320
 electron solid on surface, self-consistent Debye-Waller factors 0-84337
 free convection heat transfer in supercritical He 0-79296
 fusion reactors, Large Coil Test Facility, liq. He cooling system 0-102321
 interface with Ce₂Mg₃(NO)₁₂, effect on spin-lattice relax. 0-66011
 level gauge, with semiconductor sensor 0-57277
 multiphonon boundary of excitation spectrum, neutron and inelastic light scatt. 0-92740
 phonon coupling of two-dimens. Wigner cryst. with second surface sound (*Russian*) 0-92756
 plane surface layer, density profiles and pair correlation asymptotics (*Russian*) 0-88371
 positronium and electron bubbles, density-functional theory 0-80016
 superconducting bolometer operation obs., high-speed superconducting bolometer appl. 0-57368
 surface, cyclotron reson. of two-dimens. electrons (*Russian*) 0-88374
 surface, electron liq., high freq. cond. electron correlation effects 0-107589
 surface, liquid-crystal transition in two dimensional electronic system 0-88303
 surface, local disorder, for IR transmittance meas. 0-75395
 surface, quasi-one dimensional electron chain instability, string-zig zag transition (*Russian*) 0-65335
 surface, two-dimens., electronic cryst., dynamic props. in strong mag. field (*Russian*) 0-92755
 surface, two-dimens. Wigner cryst., electron-ripplon reson. anomalies (*Russian*) 0-92754
 surface, two-dimensional electron gas, CDW 0-65476
 two-phase mixture, circulation using jet pumps 0-82771
 vertical plate, laminar natural convection heat transfer, supercritical CO₂ and He 0-64544

liquid helium-3

- see also fermion systems; superfluid helium-3
 binding energy, variational calcs. by Pandharipande's method 0-101752
 binding energy and effective interactions, variational calcs. 0-107596
 Chakravarty-Woo eqn., extension and appl. to liq. ⁴He, liq. ³He, and nucl. matter 0-68124

liquid helium-3 continued

- electrostatic image force depend. on spatial dispersion, energy spectrum (Russian) 0-107593
 elementary excitations, density and spin density, zero sound mode, press. depend. RPA model calcs. 0-59749
 exchange model, antiferromagnetic exchange field, susceptibility-specific heat ratio (French) 0-80019
 exchange model 0-88387
 ground state of polarised and unpolarised fluid, Monte Carlo calcs. 0-92748
 interface with nonmagnetic solid, Kapitza resist., quantum perturbation treatment 0-88385
 ion mobility, temp. and freq. depend. 0-70493
 low and ultralow temp. cryogenic coolers for space missions 0-77790
 momentum distrib., Fermi-hypernetted-chain theory 0-82716
 polarisation effect on mag. ordering, melting curve 0-80021
 polarisation potentials, viscosity, thermal cond., spin diffusion 0-88389
 sound propag. at elevated densities, 0.35 to 1.4K (Russian) 0-92741
 strongly polarised, from rapid melting of polarised solid 0-70495
 superfluid transition temp. calcs. 0-103530
 surface fluctuation influence on free energy, surface tension (Russian) 0-92746
 thermal conductivity at very low temps., press. depend. 0-92742
 zero sound lifetime, neutron inelastic scatt. study 0-65329
 zero sound with velocity less than Fermi velocity (Russian) 0-92747
 ^3He , liquid, K X-ray transition energies and Lorentzian widths 0-78727
 ^3He /solid interface, refl. of transverse zero sound (Russian) 0-70492

liquid helium 3-4 mixtures

- adsorbed film, systematic exptl. study 0-107603
 bound impurity pair effect on surface tension (Russian) 0-65332
 convection in dil. solns. of ^4He superfluid ^4He 0-107600
 dilution refrigeration system, choice of tube lengths and diameters 0-57308
 dilution refrigerator, with superfluid ^4He circulation 0-57304
 films, 2-D interface excitation spectrum 0-96718
 ground state configuration of isotopic mixture, theory 0-107601
 homogeneous phase separation obs. 0-107599
 low and ultralow temp. cryogenic coolers for space missions 0-77790
 normal solution, size effect influence on capillary mass transport (Russian) 0-70497
 periodic inhomogeneities, excitation in external mag. field parallel to temp. gradient 0-88392
 positive ion mobility, wetting-nonwetting transition analogy 0-103532
 stability and stratification of quantum liq. mixture 0-59754
 superfluid, fifth sound mode 0-75398
 superfluid ^3He , in ^3He superfluid ^4He solns., mag. phases 0-59755
 superfluid thin film, third sound vel. calc. 0-107602
 tricritical mixture universality under press. 0-103533
 ^3He - ^4He mixture films, unsaturated, third sound and decay of persistent currents obs. 0-75402
 ^3He - ^4He II dilute solution, fourth sound velocity 0-70498

liquid helium-4

- see also boson systems; superfluid helium-4
 anharmonic effects in US propagation near λ transition 0-96707
 atomic trimer formation, threshold condition 0-63741
 binding energy, variational calcs. by Pandharipande's method 0-101752
 Chakravarty-Woo eqn., extension and appl. to liq. ^4He , liq. ^3He , and nucl. matter 0-68124
 cryostat design for supercond. tunnelling study (Spanish) 0-73347
 cyclotron reson. of hot electrons 0-88377
 electrostatic image force depend. on spatial dispersion, energy spectrum (Russian) 0-107593
 excited states, variational calcs. 0-80017
 film, hypernetted chain generalised eqn. optimal solns. 0-75396
 first sound nonlinear wave distrib. (Russian) 0-107588
 ground state, self-consistent description of long- and short-range correlations 0-107592
 ground state, self-consistent description of long-range and short-range correlations 0-70491
 heat capacity of liquids and dense gases at low temps. (Russian) 0-65324
 Kapitza heat-transfer model, liq. ^4He -solid interface 0-107591
 lambda point, light scatt. props., static and dynamic scaling phenomena 0-92739
 liquid-solid boundary, capillary sound motion, Kapitza resistance (Russian) 0-92737
 localised ion states, effective mass, binding energy, surface displacement 0-84333
 melting kinetics, sound transmission at liq.-solid interface 0-92734
 paired phonon model at low temp., condensate fraction 0-80018
 phonon excitation, long-wavelength, series expansion 0-88372
 quartz-liquid ^4He interface, saturation effects in phonon reflection 0-92736
 Rayleigh-Benard experiment (French) 0-80013
 solid-liquid interface mobility under 1 MHz sound wave (French) 0-100373
 static struct. factor and pair correls., neutron diff. study, 1.00 to 4.27K 0-80010
 static structure factor and pair correlation function, at saturated vapour press. 0-64878
 structure factor meas. in range 5.5 to 7K 0-80011
 supercritical, turbulent pipe flow, heat transfer by Melik-Pashayev technique 0-74860
 supercritical He I , heat transfer to turbulent flow 0-69631
 supercritical He I , heat transfer to turbulent pipe flow 0-64348
 US finite amplitude wave propag. 0-80024
 vaporisation critical point region, p - ρ - T data (Russian) 0-88373
 variational Monte Carlo calcs. with three body correl. 0-96711
 ^4He , normal liq., collective excitations, neutron inelastic scatt. study 0-107590

liquid helium sound propagation

- see also second sound; zero sound
 He , sound transmission at liq. solid interface, probe of melting kinetics 0-92734
 ^3He , sound propag. at elevated densities, 0.35 to 1.4K (Russian) 0-92741
 ^3He , superfluid, B-phase, first-sound attenuation and viscosity 0-75401
 ^3He , superfluid, size effect influence on fluid density and transition temp., fourth sound meas. 0-80022
 ^3He , superfluid B-phase, HF sound propag. meas. 0-88391
 ^3He - ^4He mixture films, unsaturated, third sound and decay of persistent currents obs. 0-75402

liquid helium sound propagation continued

- ^3He - ^4He mixture superfluid thin film, third sound vel. calc. 0-107602
 ^3He and ^3He - ^4He mixtures, superfluid, fifth sound mode 0-75398
 ^4He , anharmonic effects in US propagation near λ transition 0-96707
 ^4He film, superfluid, dynamics 0-59748
 ^4He , Kapitza heat-transfer model for boundary with solid 0-107591
 ^4He , liquid, first sound nonlinear wave distrib. (Russian) 0-107588
 ^4He , liquid-solid boundary, capillary sound motion, Kapitza resistance (Russian) 0-92737
 ^4He , normal liq., collective excitations, neutron inelastic scatt. study 0-107590
 ^4He , superfluid, fifth sound 0-88379
 ^4He , superfluid, fourth sound phenomenon under adiabatic and isothermal conditions 0-100369
 ^4He , superfluid, fourth sound attenuation 0-100370
 ^4He , superfluid, sound conversion phenomena at free surface, acoustic coeffs. 0-96709
 ^4He , superfluid, two- and three-dimens., energy spectrum and phase vel. 0-70489
 ^4He , superfluid film, compressible and layered, third sound 0-65325
 ^4He , superfluid film, solitons at low temps., Korteweg-de Vries eqn. 0-96717
 ^4He , superfluid film, third sound propag. and attenuation (Russian) 0-92733
 ^4He , US finite amplitude wave propag. 0-80024

liquid lasers

- see also dye lasers
 Er^{3+} in SeOCl_2 solvent, Racah and Judd-Ofelt parameters in laser liqs. 0-106516
 $\text{Eu}^{3+} + \text{UO}_2^{2+}$ solution, nuclear pumped liq. lasers, LASL program 0-64011
 Nd^{3+} in SeOCl_2 solvent, Racah and Judd-Ofelt parameters in laser liqs. 0-106516
 $\text{Nd}^{3+} + \text{UO}_2^{2+}$ solution, nuclear pumped liq. lasers, LASL program 0-64011
 $\text{Pm}^{3+} + \text{UO}_2^{2+}$ solution, nuclear pumped liq. lasers, LASL program 0-64011
 Pr^{3+} in SeOCl_2 solvent, Racah and Judd-Ofelt parameters in laser liqs. 0-106516
 $\text{Pr}^{3+}:\text{POCl}_3$, fluoresc. and lifetimes of excited states 0-71466
 $\text{Th}^{3+} + \text{UO}_2^{2+}$ solution, nuclear pumped liq. lasers, LASL program 0-64011

liquid metal embrittlement

- micromechanisms of crack growth, review 0-108637
 steel, stainless, liq. Li corrosion rate expressions, 600-1000°C 0-93682
 steels, types SS41, SB42, SM50A, STK55, liq. Zn embrittlement (Japanese) 0-81164
 Al-Bi(Cd)(Pb)-Ti, containing low-melting pt. inclusions, mech. props. 0-93632

liquid metals

- see also electron energy states of liquid metals; liquid alloys; mercury (metal)
 alkali, reactions with refractory metals and oxides, relevance to reactor technology 0-85173
 alkali metals, crystalline and alkaline, eqns. of state, zero compression isotherms (Russian) 0-103446
 alkali metals, liquid, O_2 pot. and O_2 distrib. coeffs. between alkali and struct. metals 0-65231
 cavitation bubble collapse and erosion intensity in constant mag. field (Russian) 0-60987
 clean metal magnetoresistance in solid and liquid phases (Russian) 0-107767
 diffusivity and solubility of oxygen, electrochem. obs. using solid oxide electrolytes 0-59669
 dipole dipole-dispersion coeffs. calcs. 0-70109
 eddy current response to solidification in one dimension 0-104140
 flow in curved channels under transverse mag. field, transition and turbulent flows 0-79396
 Hg, hot-film vel. meas. in MHD duct flow 0-75009
 incipient boiling superheats, heat flux effects 0-74697
 infiltration in medium with interconnected pores, during passage of elec. current 0-100033
 interface heat transfer of horizontal co-current liquid metal- H_2O stratified flow 0-92131
 isothermal compressibility and eqn. of state at m.p. 0-79673
 laminar flow in curved channels, transversely applied mag. field, flow anal. 0-59116
 liquid metal, electronic density of states, pseudopotential calcs. 0-70578
 LMFBF structure materials in liquid Na, capsule type creep tester (Japanese) 0-108653
 Lorentz number, Wiedemann-Franz ratio 0-80243
 magnetic model 0-88719
 melts, of a congruently melting substance, single struct. model 0-103233
 meltspinning, theoretical anal. of ribbon thickness formation 0-104143
 MHD generator channel, liquid metal piston dynamics, math. model (Russian) 0-74996
 MHD laminar flow, longitudinal dynamic effects determination for Na, Al, Sn and Hg (Rumanian) 0-64792
 Moelwyn-Hughes parameter calc. from US data for Cu, Ag, Zn, Cd, Hg, Al, Ga, In, Sn, Pb, Bi 0-59375
 optical properties by spectroscopic ellipsometry, review 0-103929
 perturbation theory extension to dense partially ionised plasmas 0-75500
 rare earths, heavy, mag. susceptibility meas. 0-75740
 solubility of H rel. to that in solid phase (Russian) 0-65222
 sound vel. meas., pulse-echo overlap technique 0-99906
 spectrometer for soft X-ray emission studies of liquid metals and metallic vapours 0-73564
 steel, interaction with $\text{Al}_2\text{O}_3/\text{Zr}$ ceramic 0-104305
 steels, types SS41, SB42, SM50A, STK55, liq. Zn embrittlement (Japanese) 0-81164
 strong binding model, electronic density of states, Green's function calcs. (Russian) 0-70111
 structural micro-inhomogeneity, Brownian motion studies (Russian) 0-92426
 structure and interatomic interaction, pseudopotential method 0-107042
 surface dipole layer and surface tension 0-70505
 surface tension and width, density functional theory 0-103537
 surface tension measurement apparatus 0-59759
 thermoelectric power, pseudopotential calc., groups IIB, IIIB, and IV 0-59959

liquid metals continued

- viscosity determination by oscillating vessel method (*Japanese*) 0-70439
 viscosity measurement apparatus 0-59759
 viscous flow due to high overheating, quasipolycrystalline model 0-70110
 Al, density fluctuations, neutron scatt. anal. 0-70349
 Al, liquid, dynamical struct. factor calc. 0-64880
 Al, liquid, structural details, molecular dynamics calcs. (*Russian*) 0-64879
 Al melt-NaF filter material interaction mechanism (*Russian*) 0-108743
 Al, molten, dissoln. kinetics and diffusion coeffs. of Fe, Co and Ni 0-59666
 Al, molten, showering cryst. form. in mould cooled from top (*Japanese*) 0-66498
 Al, molten, thermal expansion meas. to 1300K 0-65254
 Al, reaction kinetics with B_2C 0-84344
 Al, short range order amongst con. electrons 0-107040
 Al, spreading behaviour on Fe-Si 0-84345
 alkali metals, liquid, internal energy, heat of mixing, entropy, dielectric function 0-88340
 Au, ion source fabrication and emission characts. 0-68995
 Bi, liquid, field ion source emission characts. 0-74059
 Bi solid and liquid, positron annihilation temp. depend. 0-108296
 Ce, surface and volume props., flow props., surface layer thickness (*Russian*) 0-59760
 Co, liquid, Hall effect, band struct. and exchange scatt. 0-80250
 Co, liquid, N solubility depend. on added elements, mechanism (*Russian*) 0-65223
 Cu, liq., deoxidation rates by CO_2 -CO gas mixture (*Japanese*) 0-89394
 Cu, liquid, dissolved O below 0.02 wt.% effect on surface tension 0-107618
 Cu, liquid, impurity diffusion, shear cell assembly meas. (*French*) 0-75375
 Cu liquid, thermodynamic study of O_2 0-88342
 Cu, thermal cond. and elec. resistivity 0-103661
 Eu, electrical resistivity of solid and liquid phases, thermopower, melting temp. 0-59955
 Fe, liquid, Hall effect, band struct. and exchange scatt. 0-80250
 Fe, liquid, N solubility depend. on added elements, mechanism (*Russian*) 0-65223
 Fe, reaction kinetics with B_2C 0-84344
 Fe-O system, thermodynamics of viustite-haematite alloy melt (*Russian*) 0-65249
 Ga ion source, emission characts. obs. 0-62810
 Ga ion source, high intensity, emission characts. 0-80950
 Ga, liquid, field ion source emission characts. 0-74059
 Ga liquid metal field emission ion source, characts. 0-108326
 Ga liquid metal ion source, energy distrib. meas. 0-95493
 Ga solid and liquid, positron annihilation temp. depend. 0-108296
 Ga, thermal props. at high temp. 0-75336
 Hf, liquid, viscosity at melting point, free energy (*Russian*) 0-92699
 Hg quadrupole relaxation rate temp. depend 0-88884
 Hg, supercritical, elec. cond., four electrode method 0-62685
 In, O_2 activity from electrochemical meas. 0-104123
 In, thermal conductivity meas. in Spacelab, design and terrestrial testing of measuring cell (*German*) 0-57303
 In, thermal props. at high temp. 0-75536
 Ir, thermophysical props. at temps. up to 7000K 0-103497
 K, density, at near critical temp. 0-103407
 K, liquid, interionic interaction theory, pseudopotential calcs. (*Russian*) 0-79675
 K, mean spherical approx. and effective pair pots. 0-70099
 La, surface and volume props., flow props., surface layer thickness (*Russian*) 0-59760
 La:Eu³⁺, liquid, γ -ray spectra observation of exchange interaction 0-84672
 Li, cooling system of fusion reactor, corrosion inhibition by Al addition 0-108646
 Li, ISSECE selection for fusion reactor 0-57950
 Li liq., deuteron activated, shielding 0-99286
 Li liq. blanket, T removal by Y for fusion reactor recovery 0-95434
 Li, liquid, transverse flow around tube bundle, heat transfer 0-64537
 Li, X-ray scatt. factor, solid state effect 0-70163
 Mo, elec. resist., melting pt. to boiling pt., temp. depend. 0-96839
 Na, boiling hazard in LMFBRS (*French*) 0-78402
 Na, diffusion coefficient for model potentials through mean square displacement 0-70098
 Na, evaporation from capillary-porous struct., capillary restriction in initial stages 0-107609
 Na, linear pot. and elec. resist., calcs. 0-65519
 Na liquid, interionic interaction theory, pseudopotential calcs. (*Russian*) 0-79675
 Na MHD generators, optimisation for maximum electrical efficiency, output and power factor (*Rumanian*) 0-64793
 Na, mean spherical approx. and effective pair pots. 0-70099
 NaK natural convection under transverse magnetic field 0-69827
 Nb, liq. and solid, enthalpy meas. by levitation calorimetry 0-103499
 Nd, surface and volume props., flow props., surface layer thickness (*Russian*) 0-59760
 Ni, liquid, Hall effect, band struct. and exchange scatt. 0-80250
 Ni, liquid, N solubility depend. on added elements, mechanism (*Russian*) 0-65223
 Ni, reaction kinetics with B_2C 0-84344
 Ni(s, l) + NiO(s) + NiX₂O₄ (X=Al, Ga), chem. potential and solubility of O_2 0-92679
 Pb, collective excitations, neutron inelastic scatt. obs. 0-75148
 Pb, ISSECE selection for fusion reactor 0-57950
 Pb, liq., elec. resist. calcs., pseudopot. depend. 0-96840
 Pb, molten, thermal expansion meas. to 1300K 0-65254
 Pb, short range order amongst con. electrons 0-107040
 Pb, thermal conductivity meas. in Spacelab, design and terrestrial testing of measuring cell (*German*) 0-57303
 Pr, surface and volume props., flow props., surface layer thickness (*Russian*) 0-59760
 Pt, thermodynamic characterisation, by isobaric expansion meas. 0-103494
 Rb, density fluctuations from mol. dynamics simulations 0-100161
 Sn, diffusion coeff. of ¹¹⁵Sn, ¹¹⁷Sb, ¹¹⁹Ag, and ¹⁹³Au 0-96676
 Sn, liquid, impurity diffusion, shear cell assembly meas. (*French*) 0-75375
 Sn, molten, thermal expansion meas. to 1300K 0-65254
 Sn, optical props., 0.62-3.7 eV 0-75996
 Sn, optical props. by spectroscopic ellipsometry, review 0-103929

liquid metals continued

- Ti, elec. resist., melting pt. to boiling pt., temp. depend. 0-96839
 Ti, liquid, viscosity at melting point, free energy (*Russian*) 0-92699
 Ti, O_2 activity from electrochemical meas. 0-104123
 Ti, thermal props. at high temp. 0-75536
 V, elec. resist., melting pt. to boiling pt., temp. depend. 0-96839
 V, liquid, viscosity at melting point, free energy (*Russian*) 0-92699
 V, thermophysical props. at temps. up to 7000K 0-103497
 W, elec. resist., melting pt. to boiling pt., temp. depend. 0-96839
 W, molten drop break up in gas flow, surface drag, capillary excitation (*Russian*) 0-100024
 Y, electrical resistivity of solid and liquid phases, thermopower, melting temp. 0-59955
 Zn, liquid, viscosity determination by oscillating vessel method (*Japanese*) 0-70439
 Zn, thermal conductivity meas. in Spacelab, design and terrestrial testing of measuring cell (*German*) 0-57303
 Zr, liquid, viscosity at melting point, free energy (*Russian*) 0-92699

liquid oscillations

see also liquid waves

- carbon tetrachloride drops falling through H_2O , surfactants rel. to deform., oscill. (*French*) 0-66880
 container subjected to forced pitching oscillation, liquid motion, nonlinear anal. 0-96270
 damping, hydraulic torsional vibration damper (*Russian*) 0-92164
 drop of viscous liquid, in immiscible liquid, normal-mode anal. of oscillations 0-74932
 dusty fluid, flow past wavy moving wall 0-96299
 flow in U-tube manometers, effect of drag reducing polymer additives 0-64584
 fluid structure vibr. eigenvalue problems, finite elements, modal methods 0-96269
 free liquid surface oscillations, gas bubble motion 0-100025
 free oscillations in U-tube, slip boundary conditions (*Russian*) 0-79338
 ocean, wind-induced turbulence energy distrib. rel. to mixed layer evolution (*Russian*) 0-94529
 oscillating vessel with liquid containing compressible sphere, finely disperse inclusion motion 0-74963
 periodic MHD oscillations, stability, perturbation theory 0-83858
 pipe flow, curved pipes, fully developed oscillatory flow 0-83846
 pipe flow, curved pipes, oscillatory flow development 0-79400
 plane jet, stability and autooscillations from channel anal. 0-100018
 polyethylene melt, high density, oscillating flow during extrusion, model anal. 0-100016
 reversed flow characteristics due to jet issuing from dead end channel (*Japanese*) 0-100021
 shell of revolution immersed in liquid, freq. distribution function 0-69587
 source flow of conducting fluid between parallel discs 0-99986
 Stokes problem, effects of free convection on oscillatory flow past infinite porous vertical limiting surface 0-109348
 streaming in vicinity of plate possessing propagating longitudinal strain wave 0-87758
 sub-Rayleigh oscill. convection 0-87774
 viscous fluid in toroidal tube, oscillations 0-79253
 viscous fluid under cyclic deform., self-heating, hydrodynamic thermal explosion 0-58993
 water-air two phase flow, oscillatory flow instabilities 0-83833

liquid permeability see permeability

liquid phase epitaxial growth

- buried heterostructure laser, DH multilayer LPE growth on etched substrate, optical read-out apps., longitudinal mode operation 0-99749
 III-V compounds, Stefan problem, exact soln. describing growth rate with linear cooling 0-59411
 III-V semiconductors, impurity distribution, during epitaxial growth from liq. phase 0-88443
 III-V semiconductors prep. (*Czech*) 0-89131
 multi-layer, furnace design and fabrication (*Japanese*) 0-108366
 multicomponent systems, electroepitaxy, theoretical model 0-65396
 photocathode structures, TEM obs. of dislocations generated 0-100241
 source materials, for LPE, weighing method 0-66439
 Stefan problem, exact soln. describing growth rate of binary III-V compounds with linear cooling 0-59411
 thermal degradation of substrates, reduction method, appl. to LED fabrication 0-104061
 thermoelectric recrystallisation, epitaxial film growth rate 0-100424
 vapour-liquid-solid growth mechanism (*Russian*) 0-107074
 AlGaAs heterojunction laser, lightwave sources and detectors 0-64068
 AlGaAs p-n diodes, I-V characts., tunnelling 0-100510
 Al_{1-x}Ga_xAs, electron mobility illumination, compensation, space charge regions, carrier scatt. 0-70691
 AlGaAsSb LPE growth, lattice-matched to GaSb, characterisation 0-60794
 Al_{1-x}Ga_xAsZn-GaAs solar cells by LPE, open circuit voltage, fill factor 0-101108
 Al_{1-x}Ga_xSb-Pd contacts, struct., preparation elec. props. 0-65684
 Cd_{1-x}Hg_xTe, epitaxial growth from stoichiometric melt, crystn. and diffusion 0-75475
 CdTe/Hg_{1-x}Cd_xTe multilayers, LPE growth 0-80104
 CdTe-In system, equilib. phase diagram and liq. phase epitaxial growth of CdTe from In soln. (*Japanese*) 0-71634
 Co ferrite films, Mn-, Ni- and Al-substituted, LPE growth 0-96752
 Er_{1-x}Al_xO₁₂ spectroscopic props. 0-93419
 (EuLu)₃(FeAl)₂O₁₂, film epitaxial growth on Gd₂GaO₁₂ substrate, mag. props. 0-65402
 (GaAl)As, LPE, GaAs dissolution kinetic in undersaturated isothermal solns. in Ga-Al-As system 0-80106
 GaAlAs-GaAs lasers, channelled substrate, prepared by combination of organometallic pyrolysis and LPE 0-99745
 Ga_{1-x}Al_xAs, appl. of theory of electroepitaxy of multicomponent systems 0-65396
 Ga_{1-x}Al_xAs heterostructure, LPE prep., growth and dissolution kinetics, thermodynamic and kinetic models 0-75456
 Ga_{1-x}Al_xAs-GaAs p-n and p-p-n heterojunction solar cells, high efficiency, prep., eval. and characters (*Japanese*) 0-61342
 Ga_{1-x}Al_xAs, photodetector diode on GaAs substrate dark currents, tunnelling, energy gaps, effective masses 0-70805
 GaAlAsSb-GaSb low bandgap solar subcell for high efficiency multiband-gap convertors, LPE growth 0-93927
 Ga_{1-x}Al_xP varigap structs., crystallation 0-80993

liquid phase epitaxial growth continued

- GaAs epitaxial layers on polycryst. GaAs substrates, LPE growth characts. 0-75471
- GaAs, LPE, temperature instability effect, report 0-66446
- GaAs LPE from Ga soln., carrier conc., growth condition depend. 0-71584
- GaAs, multilayer liquid phase epitaxy, transition to faceting 0-96750
- GaAs, undoped epitaxial layer growth from nonstoichiometric solns., O₂ contamination sources 0-108362
- GaAs:Se ohmic contacts, pulsed electron beam annealing donor density, mobility 0-65678
- n-GaAs:Sn-p-GaAs:Ge-p-Al_{0.1}Ga_{0.9}As:Ge heterostructure solar cells, LPE growth techniques 0-66977
- GaAs-Al_{0.1}Ga_{0.9}As buried-heterostructure lasers, current injection confinement, MBE/LPE hybrid technique 0-74374
- GaAs-Ga_{0.7}Al_{0.3}As:Be, LPE, diffusion of Be into GaAs substrate 0-103517
- GaAs_{1-x}P_x heterostructure, LPE prep., growth and dissolution kinetics, thermodynamic and kinetic models 0-75456
- GaAsSb/GaAlAsSb DH lasers, growth and props. 0-69412
- GaAs_{1-x}Sb_x layer on GaAs, dislocation density reduction by improved LPE growth method 0-76202
- Ga_{0.47}In_{0.53}As, photodetector applications 0-95140
- Ga_{0.47}In_{0.53}As:Mn grown by LPE, elect. props. 0-100541
- Ga_{0.1}In_{0.9}As, on (111)B InP, LPE growth, characterisation of high purity lattice 0-104082
- GaInAsP/InP DH lasers emitting at 1.3 μ m, growth and characts. 0-64057
- GaInAsP/InP DH stripe geometry lasers emitting at 1.3 μ m 0-69410
- GaInAsP/InP DH lasers, 1.3 μ m wavelength, LPE growth and characterisation 0-69411
- (100)GaInAsP/InP DH lasers, 1.5-1.6 μ m wavelength, two phase soln. LPE technique using anti-meltback layer 0-99750
- GaInAsP/InP lasers, LPE grown, effect of p-doping on carrier lifetime and threshold current density 0-99726
- Ga_{0.1}In_{0.9}As_{0.1}P_{0.9}/GaAs structure, LPE growth and lattice consts. matching conditions 0-59822
- Ga_{0.1}In_{0.9}As_{0.1}P_{0.9}, LPE growth 0-66440
- Ga_{0.1}In_{0.9}P solid solns., isothermal liq. epitaxy 0-60793
- Ga_{0.1}In_{0.9}P_{0.1}As_{0.9}/InP DFB injection laser, one-step LPE 0-58575
- GaSb, electroliquid epitaxial growth 0-89160
- (Gd,Tm,Y)_{1-x}(Fe,Ga)_xO₂ LPE garnet thin films, magnetocrystalline anisotropy 0-93147
- HgCdTe photodiodes formed by double-layer LPE 0-104078
- HgCdTe-CdTe photodiode, 1.33 μ m, grown by LPE, phys. props. 0-107892
- Hg_{0.6}Cd_{0.4}Te LPE layer growth from Te-, Hg-, and HgTe-rich solns., comparison 0-76199
- Hg_{1-x}Cd_xTe epitaxial layers, elec. props. 0-96910
- In-Ga-P ternary system, low temp. phase diagram rel. to epitaxial growth 0-84916
- InAsSb/GaSb broad-spectral-band IR detector, backside-illum. heterostructure approach 0-73450
- InGaAs, LPE, diffusion-limited step-cooling technique, layer thickness and composition 0-84402
- In_{0.53}Ga_{0.47}As p-i-n photodiode-FET photoreceiver for 1.0 to 1.7 μ m wavelength optical fibre communications systems 0-58794
- In_{1-x}Ga_xAs layer on InP, misfit dislocation free, LPE growth 0-108364
- In_{0.1}Ga_{0.9}As:Zn, lattice matching to InP, LPE growth conditions 0-70541
- InGaAsP, anodic oxidation, refractive indices 0-97601
- InGaAsP DH lasers with etched reflectors, fabrication, current density 0-64050
- InGaAsP, LPE, diffusion-limited step-cooling technique, layer thickness and composition 0-84402
- InGaAsP LPE heterostructs., interface grading, Auger depth profile 0-103585
- InGaAsP/InP phototransistors, fabrication by LPE, photodetectors 0-95139
- InGaAsP-InP DH laser, 1.55 μ m, low temp. LPE growth for room-temp. CW operation 0-64045
- InGaAsP-InP DH lasers, perturbed InP growth, photoluminesc. study 0-106518
- InGaAsP-InP layers, grown by LPE techniques, lattice const., bandgap, thickness and surface morphology meas. 0-59818
- In_{1-x}Ga_xAs_{0.1}P_{0.9}/InP 1.5 μ m room-temp. CW laser fabrication and operation 0-64070
- In_{0.1}Ga_{0.9}As_{0.1}P_{0.9} photodetector diode on InP substrate dark currents, tunnelling, energy gaps, effective masses 0-70805
- In_{0.1}Ga_{0.9}P, N free and implanted, photoluminescence study 0-97322
- In_{1-x}Ga_xP, compositional inhomogeneity 0-88444
- InGaAsP LPE layers, compositional inhomogeneity, photoluminesc. obs. 0-75451
- In_{1-x}Ga_xP_{1-y}As_y lattice-matched epitaxial layers, LPE growth on GaAs(100), characterisation 0-75465
- In_{1-x}Ga_xP_{1-y}As_y-In_{1-x}Ga_xP_{1-z}As_z visible spectrum multiple-quantum-well heterostruct. lasers 0-106537
- InP grown by LPE, method for free In removal from surface 0-84860
- InP n⁺-p-p⁺ homojunction solar cells, high efficiency, LPE layer growth, photolithographic fabrication 0-93929
- InP surface decomposition prevention in LPE growth 0-96749
- InP-GaInAsP buried heterostructure lasers of 1.5 μ m region, fabrication and characts. 0-74388
- InP-In_{1-x}Ga_xAs_{0.1}P_{0.9}-InP 1.53 μ m single-mode CW ridge-waveguide laser 0-64072
- InSb, impurity distribution, during epitaxial growth from liq. phase 0-88443
- K₁Li₂Nb₂O₁₅ films for optical waveguides epitaxial growth and characterisation 0-79016
- Li(Nb,Ta)O₃/LiTaO₃, multi-layer optical waveguide fabrication by LPE 0-71605
- LiNbO₃:Na structure field stability limits, LPE film growth, SAW velocity 0-80102
- Ni electrodeposition on Cu (001), three-dimens. epitaxial crystallites, TEM image contrast 0-84457
- Pb, underpotential adsorption, cathodic deposition, on Ag(111) and (100) (German) 0-108363
- Pb_{1-x}Sn_xSe layers, growth conditions correl. with morphology 0-104079
- Pb_{1-x}Sn_xTe LPE film IR detector performance 0-86422
- Pb_{1-x}Te-Pb_{1-y}Sn_yTe (x,y<0.3), double heterostruct., LPE growth, heterointerface morphology 0-70550

liquid phase epitaxial growth continued

- Si, ion-implanted layers, epitaxial regrowth by laser beam and flash annealing 0-100420
- Si junction diodes, fabrication by LPE on Si:B substrates, and characts. 0-80363
- Si laser annealed, nonequilibrium solubility and segregation 0-84296
- a-Si, laser induced crystallisation mechanism, epitaxial regrowth 0-84962
- Si, slip dislocation nucleation during laser annealing 0-84179
- Si solar cells, metallurgical-grade, fabrication by epitaxial growth or direct diffusion 0-101104
- SiC epitaxial layers, growth techniques 0-108360
- p⁺-Si_{1-x}Ge_x-nSi junction diodes, lattice misfit effects on I-V characts. 0-70804
- (SmLu)₂(FeAl)₂O₁₂, film epitaxial growth on Gd₂Ga₂O₁₂ substrate, mag. props. lattice mismatch 0-65402
- SrFe₈Al₄O₁₉, thin film LPE growth and mag. props. 0-80992
- Tl, underpotential adsorption, cathodic deposition, on Ag(111) and (100) (German) 0-108363
- (Y,Sm,Ca)₃(Fe,Ge)₂O₁₂ epitaxial films, mag. props., growth condition effects 0-97124
- Y₁Fe₂O₁₂ LPE growth on Gd₂Ga₂O₁₂ substrates, substrate orientation effect 0-66438
- YIG:Co film, influence of stress induced anisotropy on domain struct. 0-100605
- YIG:La,Ga, film, LPE-grown, Ga incorporation, depend. of magnetisation on growth rate 0-84627
- (YSmLuCa)₃(FeGe)₂O₁₂ epitaxial films, LPE grown, annealing effects on mag. anisotropy 0-66548
- Zn electrodeposition, on Zn and Al single crystals, from H₂SO₄ bath, SEM obs. (Japanese) 0-93502
- Zn film deposition on Al, TEM and electron diff. obs. 0-75460

liquid semiconductor

- see also *electron energy states of liquid semiconductors*
- Hall conductivity in random-phase model 0-65599
- Hall effect measurement 0-65594
- Cd₂As₂ and CdAs₂, molten, thermal expansion and atomic bond strength parameters 0-65257
- GaP(As), liquid interaction parameters determ., 580-670°C 0-65197
- GeSe₂-As₂Se₃-Sb₂Se₃, elec. cond. over wide range of temp. 0-88564
- InP(As), liquid interaction parameters determ., 580-670°C 0-65197
- Se, electronic transport props., equation of state, to 1900K and 1800 bars 0-65574
- Se, mol. structure, local atomic arrangement at intrinsic bonding defects 0-59374
- Se, Raman spectra, crystn. processes 0-60608
- Si, dissolution of quartz, effect of C, rel. to melt growth 0-70414
- Si, reaction kinetics with B₂C 0-84344
- Te, Raman spectra, crystn. processes 0-60608
- Te-Se liquid mixtures, sound vel. meas., adiabatic compressibility determ. 0-65161
- Zn₃As₂ and ZnAs₂, molten, thermal expansion and atomic bond strength parameters 0-65257

liquid-solid transformations see *solid-liquid transformations***liquid structure**

- see also *classical theories of fluid structure; long-range order; quantum theories of fluid structure; short-range order; X-ray diffraction examination of liquids*
- α,β -trifluoroacetone, liq.-liq. transition rel. to mol. motion, NMR study 0-70383
- acetone-toluene-tetrachloromethane, mol. interaction and thermodynamic props. 0-71935
- acetonitrile-toluene-benzene, mol. interaction and thermodynamic props. 0-71935
- acrylonitrile, NMR and relax. props., liq.-liq. transition rel. to mol. motion 0-70382
- alkali halides, molten, mode coupling theory of charge fluctuation spectrum 0-92451
- n-alkane, polymer, liq., mol. arrangement, computer model 0-92446
- alkanes, liq., mol. struct., selective deuteration and IR, vibr. spectra 0-96432
- benzene, mean free path meas., US relax. 0-59585
- binary liquid solutions, struct. and thermodynamic props., molecular dynamics study 0-64866
- biphenyls, cholesteric blue phases, struct. and props. 0-103243
- n-butane, trans or gauche, solute mol., solvent mol. distrib. 0-96433
- butyloxypolyethylene octylaniline, two- and three-dimensional smectic B liq. cryst. film, long range order 0-96442
- charged particles, two-component liquid, in equilib. with vapour, surface dipole layer and surface tension 0-70505
- Debye generalised fluid model, dielectric relax., depolarised dynamic light scatt. 0-108156
- dense fluids, solvation forces between two solids 0-64855
- dextrans, branched, in soln., cross-section factor correction in small-angle X-ray scatt. data 0-84048
- dichloromethane, mean free path meas., US relax. 0-59585
- dilute fluid mixtures, spherical mols., struct. and permittivity 0-92433
- electrolyte, soln. and cryst. (German) 0-80804
- electron diffraction pattern evaluation, single beam microdensitometer 0-86370
- uran, mean free path meas., US relax. 0-59585
- ionic liquid, binary, mode coupling theory of charge fluctuation spectrum 0-92451
- ionic liquids, S-D periodic particle-particle/particle-mesh program P3M3DP 0-84041
- ionic liquids, structural props., review 0-96430
- Lennard-Jones fluid, critical lengths and spinodal region 0-84045
- Lennard-Jones fluid, two-centre, perturbation theory appl. using spherically averaged reference potential 0-64860
- Lennard-Jones liquids, S-D periodic particle-particle/particle-mesh program P3M3DP 0-84041
- liquid metals, strong binding model, electronic density of states, Green's function calcs. (Russian) 0-70111
- mean spherical approx. and effective pair pots. 0-70099
- melts, of a congruently melting substance, single struct. model 0-103233
- metallic melts, viscous flow due to high overheating, quasipolycrystalline model 0-70110
- metals, liq., dipole dipole-dispersion coeffs. calcs. 0-70109
- metals, liquid, structural micro-inhomogeneity, Brownian motion studies (Russian) 0-92426

liquid structure continued

- metals, structure and interatomic interaction, pseudopotential method 0-107042
- mixed ion-dipole system, binary distribution function calcs., dipole orientations (*Russian*) 0-79664
- molecular fluid mixtures, equilibrium props. 0-64867
- monatomic liquids, quasi-crystalline structure, role of vacancies in dynamics 0-92438
- 2(4)-monoxypyrimidines, gaseous, matrix, soln., tautomeric equilb., IR and UV absorpt. spectra 0-58256
- nucleic acids, bases and base pairs, water struct. in soln., Monte Carlo simulation 0-76709
- polymer liquid-crystalline solns., struct. 0-103235
- polymeric liquids, constitutive eqn. with factorised memory function 0-70105
- polyolefine, liq., memory effect 0-103268
- pyridine, mean free path meas., US relax. 0-59585
- quantum liquid mixture, stability and stratification 0-59754
- simple fluids, fluctuation expressions for nonequilib. distrib. functions in adiabatic flows 0-92441
- simple liquids, internal pressure and cohesive energy density, Gruneisen parameter 0-88007
- simple liquids, simplified WCA theory 0-84042
- solvent, at polarisable interfaces, mol. models, review 0-59359
- Stockmayer molecular fluid, 2-dimens., permittivity and dynamic props. 0-103910
- surface, free, charged, isolated, exptl. study of deform. (*French*) 0-88240
- surface tension and width, density functional theory, appl. to liq. metals 0-103537
- tetrachloromethane, liq. struct. and dynamics 0-79669
- thermodynamically self-consistent theories, radial distrib. function, functional derivative 0-92435
- thiophene, mean free path meas., US relax. 0-59585
- US velocity, repulsive exponent, Rao's and Kuczera's relations 0-79878
- water, coherent Raman ellipsometry, vibr. stretching region and liq. struct. obs. 0-93341
- water, Monte Carlo simulation of struct. and thermodynamic props. 0-88017
- water, physical props., two-state model approach 0-75144
- water, relax. compressibility and heat capacity 0-92580
- water, supercooled, sound vel. dispersion, struct. relax. effect, Brillouin scatt. obs. 0-107375
- water-water, pair pot. near H bonded equilb. config., amorphous and crystalline solid and liq. 0-64946
- Al, density fluctuations, neutron scatt. anal. 0-70349
- Al, liquid, dynamical struct. factor calc. 0-64880
- Al, liquid, structural details, molecular dynamics calcs. (*Russian*) 0-64879
- Al, short range order amongst cond. electrons 0-107040
- Al-Si melt, microheterogeneity (*Russian*) 0-103238
- Ar modified droplet model, mean droplet interaction below T_c 0-70363
- As-S, melt struct., orientation birefr., viscosity, refr. index, and density 0-84713
- Au-Ge-Si, influence of struct. on elec. resist. of glass forming alloys 0-65518
- CSe₂, liq., partial struct. factor, neutron diffraction meas. 0-79672
- CsAu, molten, equimolar, structural evidence of ionic nature 0-64882
- Cu-Al(Ga)(In) alloys, elec. cond., temp. and conc. depend., model interpret. and alloy struct. (*Russian*) 0-88528
- CuBr₂(Cl₂), aq. soln., structural transition, neutron diffr. study 0-64872
- Cl₂(Br₂), aq. solns., EXAFS meas. 0-60714
- GeBr₄, liq., reference interaction site model and struct. 0-70106
- H₂, metallic, ground-state energies of liq. and solid phases, variational and Monte Carlo methods 0-70502
- HCl, liquid, struct. and mol. dynamics studied using intermolecular force models 0-83445
- H₂O, modified droplet model, mean droplet interaction below T_c 0-70363
- ⁴He, fluid struct. factor meas. in range 5.5 to 7.0K 0-80011
- ⁴He, liq., static struct. factor and pair correls., neutron diffr. study, 1.00 to 4.27K 0-80010
- ⁴He, liq., static structure factor and pair correlation function, at saturated vapour press. 0-64878
- ⁴He, normal liq., collective excitations; neutron inelastic scatt. study 0-107590
- ⁴He, superfluid, elementary excitation, structure factor and phase velocity 0-80012
- Hg liquid, quadrupole relaxation rate temp. depend 0-88884
- I₂ liq., static structure factor, neutron diffraction 0-103236
- ¹₂-_x mixtures, high-temp. solids and melts, struct., thermodynamic props., Raman spectra obs. 0-66174
- K, mean spherical approx. and effective pair pots. 0-70099
- Li, X-ray scatt. factor, solid state effect 0-70163
- LiCl-KCl, molten mixture, struct., diffusion, cond., mol. dynamics calc. 0-64871
- Mg SiO₃ melt, instantaneous struct. simulated by mol. dynamics 0-84049
- MgCl₂-alkali metal chloride system, solid and molten states, struct. props., Raman spectra 0-76011
- N₂, liq., atom pair pots., X-ray diff. 0-100158
- N₂+O₂, molecular fluid mixtures, equilibrium props. 0-64867
- NH₃ vapour, supercrit. and subcrit. 0-59162
- Na, mean spherical approx. and effective pair pots. 0-70099
- Na-Cs, struct. factor, free energy of mixing, and electrochem. pot., thermodynamic calc. 0-96436
- Na-K liquid alloys, struct., X-ray and neutron diffr. meas. 0-107041
- Na-K liquid alloys, triplet correlation functions and thermodynamics, solute partial structure factor 0-64881
- NaCo(CO)₄, soln., ion sites, cryptand C221 doping effects 0-70102
- NaNO₃, aqueous soln., X-ray diffraction, radial functions and positional correl. 0-79665
- NiCl₂, aq. soln., structural transition, neutron diffr. study 0-64872
- NiCl₂(Br₂), aq. solns., EXAFS meas. 0-60714
- O₂, modified droplet model, mean droplet interaction below T_c 0-70363
- O₂, mol.-dynamic study of struct., dynamics 0-96467
- Pb, collective excitations, neutron inelastic scatt. obs. 0-75148
- Pb, short range order amongst cond. electrons 0-107040
- PbO-SiO₂, melt, elec. cond. and struct. 0-88020
- PbO-SiO₂, melt, polymer equilibria 0-88019
- Pd-Au-Si, influence of struct. on elec. resist. of glass forming alloys 0-65518
- Rb, density fluctuations from mol. dynamics simulations 0-100161
- SbCl₃/AlCl₃ molten mixtures, Raman spectra 0-93305

liquid structure continued

- Se, liquid and amorphous, struct. modelling using Monte Carlo method 0-59391
- Se, mol. structure, local atomic arrangement at intrinsic bonding defects 0-59374
- Se, Raman spectra, crystn. processes 0-60608
- SrBr₂, aq. solns., EXAFS meas. 0-60714
- Te, Raman spectra, crystn. processes 0-60608
- ZnBr₂, aq. solns., EXAFS meas. 0-60714
- ZnCl₂, aq. soln., structural transition, neutron diffr. study 0-64872
- ZnCl₂, glassy and liq. EXAFS obs. of struct., comparison with vitreous GeO₂ 0-70133
- ZnCl₂-LiCl(NaCl)(KCl)(CsCl), molten, US velocity, thermodynamic quantities and struct. (*Japanese*) 0-88270

liquid surface waves *see surface waves (fluid)***liquid theory**

- see also classical theories of fluid structure; equations of state of liquids; quantum theories of fluid structure*
- acetone, vibr. dephasing theories, test using selective coherent ps. Stokes scatt. 0-59609
- aqueous electrolyte solutions, vel. correls., improved representation 0-59360
- aqueous non-electrolytes, excess internal pressure and Gruneisen parameter behaviour 0-88015
- associated liquids, mechanism of structural dielectric relaxation 0-107034
- atomic liquids, shear viscosity determ. by nonequilib. mol. dynamics 0-79971
- benzene, equation of state studied using statistical theory results 0-84276
- binary fluid, molecular dynamics, critical mixing point region 0-88014
- binary fluid system, Onsager coeffs., steady state soln. for Benard convection 0-64851
- Born-Green-Yvon eqn., deduction involving ang. distrib. function 0-64863
- butane, flexible chain molecules, momentum space diffusion eqns. 0-75142
- carbon tetrachloride, equation of state studied using statistical theory results 0-84276
- charged hard-sphere fluid, electrified interface pot., extended mean spherical approx. calcs. 0-84502
- cluster expansion for fluids with long-range interactions 0-92440
- collective molecular motion from depolarized light scatt. 0-60614
- correlation function, long time asymptotic behaviour, influence of waves on relax. processes (*Chinese*) 0-59195
- critical binary mixtures, sound propag., mode coupling theory, validity breakdown 0-65159
- Debye generalised liquid model, dielectric relax., depolarised dynamic light scatt. 0-108156
- dense fluid, collective modes and neutron scatt. 0-92442
- dense fluids, relative motion of atomic pairs investigated in short-time regime 0-96426
- dense fluids, statistical mechanics, using hard sphere model 0-59364
- diatomic liquids, hard and soft core, free energy difference, Monte Carlo calcs. 0-92436
- dielectric relax. time rel. to single particle correl. time 0-97193
- dilute fluid mixtures, spherical pots., struct. and permittivity 0-92433
- dipolar hard sphere solvent with charged hard spheres, hypernetted chain approx. 0-61130
- dipolar liquid time-variation of dispersion and absorption of third-order electric polarisation, mol. relax. times 0-60487
- direct correlation function, factorisation 0-96427
- dynamic critical exponents, inequalities 0-79662
- electrical double layers, repulsive electrostatic interaction, statistical mech. theory 0-92432
- electrolytic aqueous media, ion-pairing, hard sphere model 0-96428
- electronic structure, structured medium approx. 0-84421
- electrostatic interactions in liquid state, effect on frontier orbitals and chem. reactivity 0-84046
- flexible mols., constrained dynamics computer simulation 0-92437
- fluid near critical point, spin-lattice relaxation time 0-80630
- fluids, one and two dimensional, hydrodynamics, viscosity, heat conductivity, kinetics (*Russian*) 0-79972
- fluids, perturbation theory and thermodynamic props., CRIS model 0-92430
- fluids, perturbation theory and thermodynamic props., inverse power and 6-12 pots. 0-92431
- fluids, perturbation theory and thermodynamic props. 0-92429
- free asymmetric rotors, classical system, second rank tensors, ang. correl. functions 0-64865
- glass forming liquids, vol. relax. 0-96429
- Gruneisen parameter rel. to Rao's acoustical parameter 0-92581
- hard dumbbell fluids, RAM and BLIP function theories 0-79658
- hard rods, attractive interactions, scaled particle theory 0-82735
- hard sphere, surface tension, compressibility, bulk modulus press. coeffs. and Rao's acoustical parameter 0-80027
- hard sphere fluid near hard wall, diffusion coefficient, mol. dynamics simulation 0-64858
- hard sphere system in equilibrium 0-86225
- hard sphere system in equilibrium, two-dimens. hard disk system 0-107033
- hard sphere system in three dimensions, thermodynamic props. 0-86226
- hard spheres in thermal eqn., time correlation functions in low-density limit 0-64859
- hard spheres mixtures, equations of state for calc. thermodynamic props. 0-84301
- homonuclear diatomic mols., force-torque correls. 0-87196
- hydrodynamic interactions and pair correl. functions on reaction kinetics, dynamic effect 0-97684
- inhomogeneous charged fluids, density functional theory, rel. to molten salts surfaces 0-79660
- ionic systems, weakly screened, evaluation of convolution integrals appearing in integral eqn. describing pair correlations 0-84044
- Kirkwood instability, mean field theory 0-84043
- Lennard-Jones fluid, nonequilibrium molecular dynamics, $t^{-3/2}$ long-time tail for stress-stress time correlation 0-70100
- Lennard-Jones fluid, two-centre, perturbation theory appl. using spherically averaged reference potential 0-64860
- Lennard-Jones mixture, binary, equimolar, static (dynamic) props., mol. dynamics calc. 0-64857
- mean spherical model for hard ion and dipoles, thermodynamics and correlations 0-103230
- memory functions for ang. motions 0-59358

liquid theory continued

- metallic glass, heat of crystn. and viscous behaviour 0-75166
 metallic glass, stability, hole theory of liquids appl. 0-100174
 metals, isothermal compressibility and eqn. of state at m.p. 0-79673
 methanol, vibr. dephasing theories, test using selective coherent ps. Stokes scatt. 0-59609
 Moelwyn-Hughes parameter calc. from US data for pure liqs. and liq. alloys 0-59375
 molecular motions in liquids, review and anal., hydrodynamics 0-59356
 molecular relaxation processes, symposium, London, England (Dec. 1976) 0-56993
 monomer-dimer system with attractive interactions on square lattice, nematic ordering 0-79681
 Mori theory evaluation, molecular dynamics simulation 0-92443
 nonergodic hard parallel squares, with Maxwellian vel. distrib., mol. dynamics calcs. 0-100156
 nonpolar polarisable fluids, effective field of a dipole, rel. to mol. polaris. 0-79659
 n-octane fluid, spontaneous cavitation 0-69886
 order parameter model, appl. to dielec. relax. 0-108151
 order parameter model, vol. and enthalpy relax. 0-88008
 organic ternary liquid systems, intermolecular interaction, US vel. meas. 0-79879
 polar liqs. permittivity, computer simulation with hard sphere point dipole pot. 0-103911
 polar mol. rot. relax., dielectric friction, Onsager cavity model 0-64664
 polar solvent, nonlocal screening, spatial correl. calcs. 0-59361
 polyelectrolyte soln., counterion condensate around line charge as δ -function, nonlinear Poisson-Boltzmann theory 0-85184
 polymer solution, osmotic pressure, correlation functions, in grand canonical formalism 0-100159
 polymers in poor solvent, loop expansion of irreducible diagrams 0-100160
 primitive model electrolytes, grand canonical Monte Carlo calculations 0-92427
 primitive model electrolytes, symmetrical, canonical Monte Carlo calcs. 0-92428
 radical pairs recombination probability in liqs., HF mag. field, reson. effect 0-93737
 Raman band profile, vibr. dephasing and intermolecular interactions 0-60556
 reference hypernetted chain equation, derivation 0-59363
 rod-shaped molecules, restricted rot. diffusion, time correl. functions 0-79655
 rotational relaxation, molecular hydrodynamics, long time tails 0-59357
 simple fluid, struct. and thermodynamics, Monte Carlo calcs. 0-59365
 simple fluids, hard and soft-core eqns. of state, termination temps., Kihara pot. 0-70360
 simple fluids, light scatt., particle-hole model 0-60613
 simple liqs. with repulsive forces, thermodynamically selfconsistent theory 0-75139
 simple liquids, corresponding states correl. and triple point solid vol. 0-92649
 soft-sphere dense fluid, bulk viscosity, nonequilib. and equilib. mol. dynamics calcs. 0-79663
 solvent structure, at polarisable interfaces, mol. models, review 0-59359
 square well fluid, eqn. of state well width depend., Monte Carlo calc. 0-64853
 square-well fluid, viscosity below critical density, molecular dynamical calcs. 0-79661
 Stockmayer fluids with dipoles and quadrupoles, spherical harmonic coeffs., dielec. const. and Kerr factor calcs. 0-84678
 Stockmayer molecular fluid, 2-dimens., permittivity and dynamic props. 0-103910
 structure of the BBGKY hierarchy near phase transition 0-88013
 surface tension and width, density functional theory, appl. to liq. metals 0-103537
 tetrahedral mol. fluids, collision induced light scatt. intensity 0-103955
 thermodynamically self-consistent theories, radial distrib. function, functional derivative 0-92435
 time-dependent pair distrib. function, const. accel. approx. 0-59362
 triangular well potential, optimised cluster theory 0-70101
 two-centre Lennard-Jones liquids, free energy, perturbation theory 0-79656
 vibr. energy relax., nonMarkovian effects 0-74230
 water, random network model, entropy calc. 0-64870
 water, random network model, liq. and ice polymorphs enthalpy and heat content 0-64869
 Ar, diffusion coefficient for model potentials through mean square displacement 0-70098
 Ar, hole theory, compressional viscosity and vibrational relaxation 0-70311
 Ar, liq., compressed, excess electron mobility theory 0-80338
 Ar, liq., equation of state studied using statistical theory results 0-84276
 Ar, liquid, binary non-additive particle interaction, self diffusion and at. motion, mol. dynamics method 0-59372
 Ar, liquid, depolarised Rayleigh scatt. at triple point, mol. dynamics simulation 0-60617
 Ar, relative motions in molecular dynamics investigation 0-92439
 BaCl₂ aq. soln., vel. correl., time integral calcs. 0-59360
 CaCl₂ aq. soln., vel. correl., time integral calcs. 0-59360
 Cu, liq., electronic structure, structured medium approx. 0-84421
 F, hard sphere model with attractive interactions 0-96434
 HCL, fluid states, mol. dynamics simulation 0-79671
 HCL liq., time correlation function, computer simulation 0-79670
 HCL, polar liqs. models, mol. polarisability effect 0-92444
 HF, polar liqs. models, mol. polarisability effect 0-92444
 LiCl aq. soln., vel. correl., time integral calcs. 0-59360
 LiCl-RbCl, molten, Chemla effect, mol. dynamics simulation, self exchange vel. 0-79967
 Na, diffusion coefficient for model potentials through mean square displacement 0-70098
 NaCl aq. soln., vel. correl., time integral calcs. 0-59360

liquid-vapour transformations

- see also boiling; condensation; evaporation; liquefaction of gases*
 alcohols, vapour-liq. equilib. and heats of mixing, simplified group method anal. 0-96637
 alkanes, vapour-liq. equilib. and heats of mixing, simplified group method anal. 0-96637
 alloys, spinodal decomposition, review 0-96657

liquid-vapour transformations continued

- benzonitrile-isooctane mixture, dielec. const. near consolute point, temp. and freq. depend. meas. 0-71292
 binary liquid mixtures, spinodal decomposition, review 0-96657
 binary mixtures, near critical, metastable, phase separation and nucleation and drop growth, rate eqns. 0-65232
 binary mixtures near critical state, gravitational distrib. of thermodynamic props. (Russian) 0-88241
 carbon tetrachloride, surface study, ellipticity coeff., ellipsometric method 0-84343
 chloroalkanes, vapour-liq. equilib. and heats of mixing, simplified group method anal. 0-96637
 critical props. for pure liqs. and mixtures 0-65213
 dielectric fluid, Debye absorption at crit. liq.-vapour transition 0-100322
 dynamic scaling and crit. point universality of fluids 0-88297
 equilibrium, cell design for use below 300K and to 9 MPa press. 0-62821
 glasses, spinodal decomposition, review 0-96657
 lattice gas model, nonsingular diameter without particle-hole symmetry 0-88311
 mixtures, showing phase splitting, modified Wilson eqn., phase equilib. prediction 0-96636
 natural gas mixtures, simulated, enthalpy and phase equil., correl. with modified Starling eqn. 0-61127
 non-Ising-like effects, eqn. of state, renormalisation group calc. 0-84286
 nucleation theory and first order phase transition dynamics near critical points 0-84284
 pentane-benzene solution, vapour-liquid equilibrium study, vaporisation critical state (Russian) 0-79931
 quantum mechanical effects, theory 0-103452
 singularity in coexistence curve diameter, non-Ising like effects 0-79929
 supersaturated vapour, critical clusters, theory and Monte Carlo simulation, review 0-82734
 transition metals, thermophysical data at high temps., submicrosecond-pulse-heating method 0-103459
 US velocity in crit. region water 0-59582
 vapour-liquid coexistence and correlations in interface 0-65212
 Ar, liq., critical exponent, η , X-ray scatt. 0-92660
 Ar, liquid, surface study, ellipticity coeff., ellipsometric method 0-84343
 Ar, liquid-vapour interface, surface of tension near triple point, theory 0-100375
 CO₂-2,2-dimethylpropane, liquid, -vapour equilib., 220 to 300K and 6.7 MPa 0-62821
 Li-LiH liq.-vap. equilib., activity coeff. 0-103468
 Li-LiH system, H isotope solubility thermodynamic singularities 0-81356
- liquid waves**
see also capillary waves; ocean waves; surface waves (fluid)
 aniline, liq., depolarised light scatt. from shear waves 0-97288
 finite, amplitude disturbance, hydraulic jumps, extension of Rayleigh's approach 0-69854
 forward diffraction of Stokes waves by a thin wedge 0-92167
 immiscible incompressible fluids, interfacial convective instability, diffusional exchanges, adsorption-desorption processes 0-70504
 inclined open channel, stability of permanent roll waves 0-64629
 incompressible irrot. flow, water waves and Korteweg-de Vries eqns. 0-69850
 internal solitary waves in stratified flows, cubic and quadratic nonlinearity 0-69856
 internal wave generation in stratified fluid collapse (Russian) 0-74942
 irregular wavy flow of a liquid film down a vertical plane 0-106808
 Lorenz attractor behaviour in a continuously stratified baroclinic fluid 0-83806
 non-rigid bed, water wave attenuation 0-69851
 quinoline, liq., depolarised light scatt. from shear waves 0-97288
 regular wave interactions with body in canal, wave power absorption appl. 0-96271
 ripples on carrier waves, distrib. and steepness 0-72548
 rotating fluids, Rossby and Kelvin waves, open boundary conditions 0-61810
 shallow water solitary waves, shelves and Korteweg-de Vries eqn. 0-92166
 shallow water waves with quasi-periodic boundary conditions, eigensolutions of elliptic problem 0-83804
 shell of revolution immersed in liquid, freq. distribution function 0-69587
 shoaling of finite-amplitude surface waves on water of slowly-varying depth 0-69853
 underwater ridge, wave guide properties for surface waves 0-96268
 water, finite depth, half-immersed circ. cylinder, long-wave behaviour of virtual mass 0-83810
 water, finite depth, half-immersed cylinder, virtual mass, integral equation method 0-87783
- liquids**
for generalities only; for specific aspects see appropriate headings
see also liquid structure; liquid theory; solutions
 refractometer laser detector for anal. of liquids 0-101830
- literature**
 Indian scientific and technical Journals critical evaluation 0-94906
- literature reviews** *see reviews*
- lithium**
see also nuclei with
 abundance in Luna 24 soil samples 0-67590
 abundance in tektites and impact glasses 0-61799
 anharmonicity and low temp. phase struct., neutron diffr. study 0-107105
 arc lamp, heat-pipe, as spectroscopic source 0-102787
 atom, 2s²2p double Auger rate 0-99489
 atom, damping const. in acetylene-air flame, Lorentz collisions, mag. field effects 0-66805
 atom, effective potentials, energy levels 0-106263
 atom, electron elastic scatt., two-pot. eikonal approx. calcs. 0-99573
 atom, electron excitation cross section calc., Born approx. with Slater wave functions 0-69243
 atom, ground state, HFS 0-91699
 atom, inelastic Feshbach resons., quasi projection operator calc. 0-58395
 atom, long range and temp. depend. interaction with Re surface, theory 0-59802
 atom, optical oscill. strengths calcs. 0-91495
 atom, positronium formation in highly excited states, first Born approx. 0-58420
 atom, two photon ionisation in presence of one photon ionisation, cross section calc. 0-83327

lithium continued

atoms, classical many-body collision model incorporating Heisenberg and Pauli principles 0-63511
 cells, electrochemistry of amorphous V_2S_5 0-76626
 chemisorption on GaAs, charge injection into space charge layers 0-100496
 classical plasma frequency in long-wavelength limit, quantum correction 0-107728
 concentration determination using nuclear track techniques 0-95504
 cross-relaxation processes, polarised β -active nuclei 0-60431
 diamond:Li, electron transport character 0-92917
 diffusion in Mo, W, vacancy mechanism (*Russian*) 0-70472
 diffusion in WO_3 thin film, appl. of AC techniques 0-70468
 dislocation behaviour, rel. to temp. between 90 and 300K 0-88146
 electrochemical injection kinetics into WO_3 film, LF AC meas. 0-57339
 electron microprobe local anal. of light elements, ultrasoft X-ray spectroscopy 0-99027
 electronic impact excitation, energy level calcs. (*Chinese*) 0-83488
 energy and elastic constants 0-59435
 exchange current in LiCl-KCl eutectic melt at 400°C for Li-S secondary cells 0-93867
 Fermi surface and quasiparticle props., density functional approx. 0-96771
 film exposed to methanol, identification of methoxide species by He(I) photoelectron spectra, MO calcs. 0-83417
 fusion reactor Li liq., deuterium activated, shielding 0-99286
 fusion reactors, liquid Li, safety anal. and support facilities 0-63380
 ground state of solids, spin density functional method, binding energy, compressibility 0-65477
 intercalated atoms, host lattice strain effects 0-88082
 ion source using surface ionisation process 0-68999
 isoelectronic sequence, electron impact ionisation cross section 0-91688
 isoelectronic sequence, self-consistent relativistic density-functional theory 0-91441
 isoelectronic sequence of three electron atoms, pair correlation study 0-74096
 isotopic composition in LiCl, determ. by mass spectrometry 0-66899
 Knight shift volume depend. 0-84663
 liquid, fusion reactor blanket, removal of T 0-95434
 liquid, fusion reactor Li cooling system, corrosion inhibition by Al additions 0-108646
 liquid, ISSEC selection for fusion reactor 0-57950
 liquid, O₂ pot. and O₂ distrib. coeffs. between alkali and struct. metals 0-65231
 liquid, transverse flow around tube bundle, heat transfer 0-64537
 M-type supergiants, Li abundance in atmospheres (*Russian*) 0-72950
 magnetic property volume depend., Knight shifts, electron spin response 0-88729
 martensitic phase transformation in single cryst., US attenuation and vel. measurements 0-75358
 molecular laser, optically pumped, review 0-58519
 optical properties by spectroscopic ellipsometry, review 0-103929
 particle size distrib. meas. by SEM 0-101775
 phonon limited resistivity struct. depend., Umklapp scatt., elastic consts. 0-88532
 plasma, elec. cond. at 12.5-50 MPa, (7-50) $\times 10^3$ K 0-64685
 plasmon satellite struct. in (e,2e) process 0-96809
 precipitation of Al(OH)₃ from solutions containing lithium ions, X-ray diff. pattern and comp. determ. 0-76502
 red cell membrane, Li transport in manic depressives 0-61525
 secondary cells, solid cathode, Li cloboranes as electrolytes 0-108794
 spectral lines intensity and plasma parameters dependence on Li additive 0-73478
 sputtered excited states, secondary photon emission, role of transition probability 0-102483
 sputtering, kinetic energies of sputtered excited atoms 0-66373
 steel, stainless, liq. Li corrosion rate expressions, 600-1000°C 0-93682
 surface characterization of film growth by SEM, EDS and ESCA 0-81240
 Tokamak breeding blankets, T breeding perform. comparative eval. 0-95398
 valence band Auger spectra, surface effect 0-80915
 X-ray scatt. factor, solid state effect 0-70163
 AgBr:Li⁺, correlated diffusion of impurities, nuclear spin relax. meas. 0-108094
 Al₂O₃:Li, TSEE, Li doping effects 0-80953
 CaCO₃:Li, synthetic calcite, (CO₂Li)²⁺-Li⁺ defect after X-irrad., EPR study 0-75852
 CdS:Li, complex luminescence centres, recombination-stimulated conversion 0-108268
 CdS:Li, electrodifussion of shallow donors, photocurrent, TSC, and exciton luminesc. meas. 0-79992
 CdS:Li, green edge luminesc., complex nature of centres 0-60671
 CdS:Li, luminescence bands, photocurrent spectra (*Russian*) 0-60677
 CdS:Li, single crystals, anisotropic luminesc. centres 0-80857
 CdSe:Li, reson. Raman and Brillouin scatt., elastic excitation-defect scatt. 0-80788
 CdTe:Li, acceptor states study by donor acceptor pair excitation luminesc. 0-100683
 CsF:Li, F-centres, saddle-point configuration, molecular model parameter 0-107234
 GaAs:Si, Li, IR absorpt., microstruct., charge compensation 0-107565
 He+Li⁺ autoionisation, electron spectra 0-91653
 KCl:Li, (F₂⁺)_A centres, optical props. 0-89026
 KCl:Li, X-irrad., F_A centres, thermolum. studies 0-80878
 KCl:Li (F₂⁺)_A centres, tunable CW laser action 0-87399
 KCl:Li F_A(II) centre laser, pumped by flashlamp-pumped dye laser 0-102737
 KCl:Li⁺, single-pulse excitation of paraelectric induction and echo signals 0-80732
 KTaO₃:Li, ferroelec. transition and atomic motions, ⁷Li NMR study 0-75872
 Li core excited even parity ²P states, fluoresc. 0-69100
 Li, cryst. wave function deter., muffin-tin method 0-65436
 Li I laser, 207 Å, oscillator strengths 0-53598
 Li II, electron impact excitation, distorted wave approx. 0-91689
 Li metal for battery industry, sources and preparation 0-97781
 Li⁺, core excited bound states in beam foil expts., CI calcs. 0-78559
 Li⁺, core-excited bound states 0-91468
 Li⁺, optical transition between bound states, beam-foil spectrosc. obs. 0-91476

lithium continued

Li⁺, ³P and ³S states, fine (hyperfine) struct., dye laser saturation spectroscopy, beam expt. 0-58169
 Li⁺ diffusion and ion-neutral interactions, laser sounding of upper atmosphere (*French*) 0-82115
 Li⁺, electron scatt., inelastic Feshbach resons., quasi projection operator calc. 0-58395
 Li⁺, H₂O affinity, ab initio SCF calcs. 0-58125
 Li⁺, low energy ion scatt. from clean Ni (110) surface 0-104026
 Li/SO₂ cells, DTA, safety studies 0-81428
 Li/SO₂ cells, safety studies, kinetics of Li-organic solvent exothermic reactions 0-72030
 Li/SOCl₂ cells, high rate discharge characts. 0-72021
 Li/SOCl₂ primary cells, SOCl₂ reduction mech. in supporting electrolyte 0-108792
 Li/TiS₂ cell with solvate melt, discharge characts. and lack of rechargeability 0-72022
 Li-D equation of state under extreme conditions, solid state to plasma region 0-69976
 Li-LiH liq.-vap. equilib., activity coeff. 0-103468
 Li-MnO₂ batteries development, Sanyo, with high energy densities 0-85272
 Li-NH₃ concentrated solution, NMR relaxation of ⁷Li 0-108084
 Li-Si, electrode pot., Li utilisation determ. 0-81427
 Li⁺-affinities of methylamine, ab initio SCF calculations 0-102443
 Li⁺-affinities of NH₃, ab initio SCF calculations 0-102443
 Li⁺-H₂O complex, charge transfer theory, Mulliken population, ab initio calc., multiconfiguration scheme 0-106392
 Li+doubly charged ions, electron capture excitation, theoretical predictions in fusion plasma 0-63810
 Li+H₂, exponential gap relation, rot. inelasticity 0-78693
 Li+H⁺, Li core excitation cross section, correlation and reorganisation effect 0-87215
 Li+HF→LiF+H, pot. energy surface, SCF and CI calcs. 0-71904
 Li+He²⁺, collisions, soft X-ray emission obs. 0-83591
 Li+Li⁺(H⁺), resonant ionisation, cross section and ionisation probability 0-63785
 Li⁺+CO₂, collisional excitation, quasiclassical trajectory calcs. 0-83467
 Li⁺+ether(thioether)(amide), pair pots., ab initio LCAO SCF MO calcs. 0-58184
 Li⁺+H₂, exponential gap relation, rot. inelasticity 0-78693
 Li⁺+H₂, sudden approx. of Cross, computational tests, cross section factorisation, scatt. phenomena 0-58352
 Li⁺+H⁺, charge transfer and ionisation, total cross sections for production of Li²⁺ determ. 0-91657
 Li⁺+Ne collisions, vel. dependence of Ne 2s and 2p, vacancy production, electron spectroscopy 0-58344
 Li⁺+SF₆, mode selective vibr. excitation 0-58351
 Li₂, ²_g, ³_g, ⁴_g excimer emission, ab initio calcs. 0-91608
 Li₂, MCSCF and CI calcs. 0-95526
 Li₂, relativistic Dirac-Fock multiconfig. SCF calcs. 0-99456
 Li₂⁺, nonadiabatic coupling matrix elements by Hellmann-Feynman theory and HF 0-83263
 Li₃, electronic struct., SCF and SCF-CI calcs. 0-87044
 Li₃⁺, electronic struct., SCF and SCF-CI calcs. 0-87044
 Li₃⁺, electronic struct., SCF and SCF-CI calcs. 0-87044
 Li₄, MCSCF and CI calcs. 0-95526
⁶Li, determination using nuclear track techniques 0-95504
 Li⁺(2²P_{1/2})+H₂(D₂), collision induced quenching and fine struct. transition rate coefficients meas. 0-74221
 Li⁺(2²P_{1/2})+He(Ne)(Ar)(Kr)(Xe), collision induced fine struct. transition rate coefficients determ. 0-74220
 Li(2²P_{1/2,3/2}), laser induced flame chemistry, saturated mode fluoresc. meas. 0-89491
 Li(2p)+H₂(N₂), Li(2p) excitation, alignment and orientation obs. 0-63794
 MgF₂:Li⁺, atom transport, diffusion and ionic cond. meas. 0-107492
 MgO:(Li), polycrystn., internal friction (*German*) 0-59577
 MgO:Li, mech. deformed crystals, imprinting of slip bands using Li impurities 0-59473
 MnO₂:Li, Zn²⁺ ion specific adsorpt. kinetics, ⁶⁵Zn γ -ray scintillation investig. 0-70529
 RbCl:Li F_A(II) centre laser, pumped by flashlamp-pumped dye laser 0-102737
 RbF:Li, F-centres, saddle-point configuration, molecular model parameter 0-107234
 Si:H, Li, amorphous, photoluminescence obs. 0-66280
 Si:Li, bound-exciton excited states, uniaxial anal. 0-71475
 Si:Li, defect electronic struct. and config., semi-empirical calc. 0-107739
 Si:Li, electron-phonon scatt., in intermediate conc. region 0-65180
 Si:Li, photolum. of bound exciton and bound multiexciton complex, Zeeman effect 0-108265
 Si:Li, thermal cond., low temp. phonon scatt., internal strain effects 0-96706
 Si:Li ion implanted, channelling and random equivalent depth distrib. 0-100293
 Si:Li n⁺-p solar cells, electron beam irradi. damage 0-94000
 SiO₂:Li⁺, surface crystn. of fused SiO₂ by ion implantation and annealing 0-89383
 ZnTe:Li, electron-phonon interactions in Raman scatt. 0-60594
 ZnTe:Li, O, Hagemark theory, O modification isoelectronic trap 0-75517
 ZnTe:Li, Zeeman splitting of ground and excited acceptor states, selective pair luminesc. 0-84780

lithium alloys

Al-Cu-Mg-Li alloy extrusions, microstruct., embrittlement and fracture props. 0-60965
 Al-Li-Mg-Be alloys, phase composition of surface films, oxidation protection mechanism (*Russian*) 0-65417
 Al-Li-Mn (2.8, 0.3 wt.%), recrystallised sheet, fracture behaviour, SEM and TEM study 0-97566
 Al-Mg-Li alloy, metastable S'-phase, struct. (*Russian*) 0-103291
 Li-Al system, Li solubility and chem. diffusion in Al, electrochem. study 0-107432
 Li-Cd, phys. props. of liq. phase and LiCd solid cpd. 0-75537
 Li-Mg, Mathiessen's rule, elec. and thermal deviations, impurity scatt. 0-88536
 Li-Mn liquid alloys, form factor effects, pseudopotentials, resist. calc. 0-103608
 Li-Pb eutectic alloys for fusion reactor solid breeder blankets, reactions with water 0-102297

internal friction continued

- Ti-Ni, internal friction and US props. (*Russian*) 0-84247
 V, dehydrogenation by annealing with Zr foils, internal friction meas. 0-96736
 V wire, deformed in torsion, internal friction, H effect 0-76300
 Zn, internal friction anomalies in temp. initiated brittle-plastic transition (*Russian*) 0-96648

internal friction of liquids *see viscosity of liquids***internal mechanics, molecular** *see molecular vibration***internal mechanics of atoms** *see atomic structure***internal modes** *see molecular vibration in solids***internal stresses**

- alkali halides, thermally stimulated depolarisation of NCO⁻ centres 0-80678
 amorphous solid, structural defects, computer simulation study 0-88040
 anelasticity influence, on internal stress meas. in creep 0-70306
 bearings, plain, fracture 0-81170
 bicrystal, elastic incompatibility stresses (*Japanese*) 0-107361
 bounded domain undergoing sequential crystallisation, stress and strain investigation 0-100183
 cemented carbides, physical and chem. nature 0-76265
 coated optical fibre cable unit, internal stress due to compressive loads, optimum design 0-58717
 component hydropressing, residual stress distrib. (*Russian*) 0-93567
 composite three-layer cylindrical shells, initial stressed and deformed state 0-102974
 corundum, defect cryst. struct. study 0-103316
 crystal defects, elastic interaction under high hydrostatic press. 0-96512
 crystal growth, creation of stress and dislocations (*Russian*) 0-103277
 cubic crystals, response to (111) loading, internal energy, elastic moduli 0-84230
 cylinder with oblate spheroidal cavity or internal penny shaped crack under tension, stresses 0-69736
 diffusion motions of macroscopic inclusions in nonuniform compressive stress fields (*Russian*) 0-88351
 discs, circularly symmetric, rupture, ductile-brittle creep 0-69735
 FCC alloy, hardening by spinodal modulated structure 0-60874
 glass rods, compressively clad, residual stresses, comparison of optical and fractographic meas. 0-108539
 Jahn-Teller system, thermodynamic properties, internal stress effects 0-59679
 laminates, residual thermoelastic stresses 0-106721
 measurement, high-temp. 0-64498
 measurement, X-ray diffr. equipment, comparison 0-82858
 metal, textured cubic, residual stress evaluation 0-89435
 metals, dislocation-core movement and frictional stress 0-92529
 metals, inelastic cyclic strain under nonuniform stress state conditions, residual stresses effect 0-81132
 metals, residual stress on drawing calcs. by stress state changes variational principle (*Russian*) 0-65125
 mirror/flat-size relations, residual contact stresses effect 0-107363
 multilayer cylindrical parts, residual stresses determ. 0-96206
 optical fibre, refractive index profile distortion, stress-induced 0-91889
 optical fibre, single mode, bending induced birefringence 0-87537
 PET films, dyed, local mech. stresses, IR spectrosc. determ. 0-65418
 PMMA, shock loaded, lateral compressive stresses meas. using Yb piezoresist. gauges 0-103007
 polyamide-polyurethane copolymer dispersions, structuring and relax. props., coating from props. 0-76559
 polycarbonate, ductile, large strain cyclic deform. 0-85000
 polyethylene, high density, ductile, large strain cyclic deform. 0-85000
 polyethylene film minimum running thickness, critical rupture stress 0-100993
 polypropylene, ductile, large strain cyclic deform. 0-85000
 pyrographite, initial stress state, neutron irradiation effect 0-97555
 rings, multilayer, circumferential residual stresses (*Russian*) 0-74729
 single crystals, internal stresses determ. with multicryst. X-ray spectrometer 0-64832
 solid solutions, dislocation-core movement and frictional stress 0-92529
 solidification front propagation, residual stress levels, polymerisation 0-59635
 steel, austenitic stainless, type SUS 304, welded joint, polarisation behaviour, boiling MgCl₂ soln. (*Japanese*) 0-93695
 steel, C, magnetomechanical acoustic emission for residual stress NDT 0-71149
 steel, C-Cr (1.0, 1.5 wt.%), 52100 bearing steel, control of surface residual stress by heat treatment 0-97501
 steel, carburized and quenched, residual stresses (*Japanese*) 0-89262
 steel, Cr plated, factors influencing durability 0-108643
 steel, Cr-Mo-P (2.25, 1 wt.%), stress relief cracking, effect of P segregation 0-89324
 steel, ferritic, magnetomechanical acoustic emission for residual stress NDT 0-71149
 steel, low alloy, high strength, fatigue crack growth, in presence of welding residual stresses (*Russian*) 0-71739
 steel, martensitic, ageing, effect of H₂ on stresses in process of $\gamma \rightarrow \alpha$ transformation (*Russian*) 0-76252
 steel, martensitic transform., stress calcs. using statistical model (*Russian*) 0-93557
 steel, medium, C, US attenuation, mag. field effect 0-89428
 steel, medium C, ground, residual stresses, X-ray evaluation 0-79863
 steel, Ni, 11.6%, quenched cylinder residual stresses, boring/turning and X-ray diffr. obs. (*German*) 0-93586
 steel, Si-Mn-P-S-Ni-Cr, residual stress meas. by X-ray diffr. 0-71688
 steel, stainless, fast neutron irradiated, solution annealed tubing, residual stress behaviour 0-65054
 steel, steam pipes, 12Cr1MoV, selection of allowable stresses based on minimum possible strength data 0-104237
 steel, strain-hardened subsurface layer, residual stress change in fatigue 0-81185
 steel, US strengthening treatment effect on fatigue resistance 0-81193
 steel bearing, surface-ground, residual stress fatigue property comparison 0-60975
 steel bearing rings, optimisation of thermomechanical working parameters (*Russian*) 0-93579
 steel plates, explosively clad, fatigue crack propagation behaviour (*Japanese*) 0-104262
 steels, alloy, stress relax. data anal. using total strain-time parametric method (*Japanese*) 0-104198

internal stresses continued

- Stepanov method shaped cryst. growth, physical problems, thermoelastic stresses 0-103279
 stochastic model for dip test in steady-state creep 0-58915
 styrene-butadiene-styrene block copolymer, stress relax. following steady-state flow, residual shear stress development 0-83772
 surface dislocations, universal concept, rel. to disclinations and grain boundaries 0-100231
 welds, residual stresses, evaluation by Barkhausen noise meas. 0-76436
 X-ray stress meas., computer-aided system (*Japanese*) 0-104366
 zincblende-type crystals, sublattice displacement from elect. or mech. deform. 0-81123
 Ag film, intrinsic stress meas. 0-71696
 Ag film deposition, thermal effects, influence on internal stress meas. 0-96767
 Ag powder, ultrafine, sintering, coalescence growth stage 0-89174
 Ag-Sn, splat-quenched, X-ray diffr. study 0-81094
 Al bicrystal, plastically deformed, slip heterogeneities 0-79858
 Al film, deform. under He ion bombardment 0-65073
 Al film, H incorporation effect on stress and electromigration 0-80139
 Al film, intrinsic stress meas. 0-71696
 Al, plastic deformation thermal activation parameters from creep kinetics and stress relaxation 0-71717
 Al thin films 1/f noise, depend. on internal mech. stresses 0-65711
 Al-Si alloy, eutectic, quasistatic 0-79165
 Al-Zn, type 7075-T6, coldworked hole specimens, residual stresses, fracture mech. anal. 0-97587
 Al-Zn-Mg-Cu alloys, heat treatment optimisation 0-60888
 Al_{0.9}Ga_{0.1}As:Cu, variable-gap semicond., impurity props., carrier recomb. 0-96907
 Au, electrodeposited and sputtered, hard, reactive softening, X-ray diffr. studies 0-100414
 Au film deposition, thermal effects, influence on internal stress meas. 0-96767
 Au film electrodeposition, substrate effects on film props. 0-81329
 Au powder, ultrafine, sintering, coalescence growth stage 0-89174
 Au-Ni, surface segregation, strain effects 0-80042
 BaTiO₃, ferroelectric ceramic, internal stress and strength, failure mechanism 0-66128
 BaTiO₃, ferroic materials, fracture processes 0-79869
 Cd films, struct. and props., X-ray diffr. spectra anal. 0-80119
 Cr condensates, lattice const., internal stresses (*Russian*) 0-107141
 Cr film, evaporated, concurrent ion bombard. effects 0-80142
 Cu film deposition, thermal effects, influence on internal stress meas. 0-96767
 Cu, plastic deformation thermal activation parameters from creep kinetics and stress relaxation 0-71717
 Cu-Ni (10 at.%), creep, substruct. and internal stresses (*Russian*) 0-97527
 Fe, Armo, ground, residual stresses, X-ray evaluation 0-79863
 Fe, magnetomechanical acoustic emission for residual stress NDT 0-71149
 α -Fe, nitrided, aging at room temp. 0-71679
 Fe-Mo (4.1 wt.%), steady state creep at high temps. 0-89316
 (FeNi)PB amorphous wires, surface oxidation and annealing influence on induced anisotropy 0-100957
 Fe₂O₃ thin films, reactively sputtered, mechanical stresses rel. to deposition conditions 0-80146
 n-GaAs epitaxial film, radiative recomb. under influence of mech. stresses 0-66291
 Ga_{1-x}Al_xAs laser diode, hetero-isolation stripe geometry for IR and visible radiation (*Japanese*) 0-83607
 GaAs-GaAlAs DH lasers, strain-enhanced luminesc. degradation, photoluminesc. obs. 0-69392
 GaAs-GaP heterostructure, radiative recomb. under influence of mech. stresses 0-66291
 Gd-Fe amorphous films, stress contrib. to perpendicular anisotropy 0-75819
 LiF film, intrinsic stress meas. 0-71696
 Li₂O-Al₂O₃-SiO₂ glass, study of elastic props. 0-104205
 Li₂O-Al₂O₃-SiO₂ glass, crystallised, grain size and internal strain 0-103259
 Mg films, struct. and props., X-ray diffr. spectra anal. 0-80119
 MgCd wire, elongation during disorder-order transform. (*Russian*) 0-104148
 Mn-Cr-Ti layers on low C steel, composite, residual stresses rel. to arc-spraying parameters (*German*) 0-104077
 Mo alloys, intercryst. fracture in ductile-brittle transition region, local internal stresses effect 0-81200
 Mo fibre reinforced Cu, rule of mixtures of deform. parameters in stage III 0-97532
 Mo films, sputtered from cylindrical-post magnetron with Ne, Ar, Kr and Xe, compressive stress and presence of inert-gas obs. 0-80140
 Na₂O-B₂O₃-SiO₂ glass, fracture toughness, effect of microheterogeneous struct. 0-104256
 Nb₃Sn, supercond. composite, residual stress state, crit. currents 0-80468
 Ni, creep, substruct. and internal stresses (*Russian*) 0-97527
 Ni, dislocation structure evolution after hydroextrusion (*Russian*) 0-96530
 Ni, electrodeposited film, thermal anal., occlusion of gases rel. to mag. props. 0-59823
 Ni electrodeposition, structure-internal stress relationship 0-70561
 Ni-Fe (36 to 50 wt.%), initial permeability, domain struct. model 0-88811
 Ni-P, electrodeposited film, thermal anal., occlusion of gases rel. to mag. props. 0-59823
 Ni-S, electrodeposited film, thermal anal., occlusion of gases rel. to mag. props. 0-59823
 NiPt, quenched, ordering kinetics and domain struct. form. during isothermal tempering (*Russian*) 0-66502
 Pb(Ti,Zr)O₃ solid solutions, phase coexistence discrepancies 0-96662
 Pb(Zr,Ti)O₃ ceramics, DC field sintering preparation, piezoelectric props., ageing behaviour 0-81211
 Pb(Zr,Ti)O₃, ferroic materials, fracture processes 0-79869
 Pd-Si and PdSi films, on Si, stress obs. 0-80145
 PtSi films, on Si, stress obs. 0-80145
 Si, high-dose Ar implantation, X-ray topographic obs. of strains and damage 0-59496
 Si, polycrystalline, thermal oxide anomalous stress 0-93661
 Si, residual stress and defects induced by scribing 0-60990
 Si:B, implanted laser annealed, lattice strain, X-ray study 0-96554

internal stresses continued

- Si-Li, thermal cond., low temp. phonon scatt., internal strain effects 0-96706
- Si₃N₄/ZrO₂, hot-pressed, compressive surface stresses developed by oxidation induced phase change 0-60992
- SiO₂ film, prep. using high press. O₂, residual stress, chemical etch rate, refr. index and density meas. 0-71768
- W fibre reinforced Cu composites, correl. between thermal cycling-induced microstructural changes at interphase boundaries and tensile behaviour (*Japanese*) 0-71674
- ZnS, film, intrinsic stress meas. 0-71696

internuclear double resonance *see* **INDOR****interplanetary magnetic fields**

- see also interplanetary matter*
- A₂-index, 1964-1976, rel. to geomag. field and interplanetary field states 0-104866
- auroral electrojet, empirical relations to interplanetary parameters 0-105118
- B₁ and B₂ components, origin (*Russian*) 0-98611
- B_z-component sign rel. to longit. position of magnetosphere polar cap plasma flow entry region 0-67472
- B_z component, direction rel. to Earth bow shock three-dimensional shape 0-85832
- correlation with interplanetary cosmic ray protons 0-77243
- direction, influence on magnetosphere hydromag. energy spectra 0-67476
- Earth atmosphere elec. current systems and interplanetary field 0-105126
- Earth bow shock, DC mag. field obs. 0-90306
- Earth bow shock, initial ISEE mag. field obs. 0-90307
- Earth bow shock, theory of magnetic shocks in collisionless plasma 0-85854
- Earth bow shock interaction, backstreaming ions and interplanetary mag. field 0-101500
- Earth bow shock region, mag. field topology rel. to upstream particle events 0-77247
- Earth bow shock tangential mag. field line rel. to upstream energetic electrons 0-90308
- Earth bow shock vicinity, low-freq. waves obs. 0-90311
- Earth magnetosphere interaction, mag. curl in front of magnetosphere boundary 0-85804
- Earth satellite observations by Isee-1 and -3, reliability of method 0-85895
- geomagnetic activity, cyclical nature due to interplanetary field 0-81813
- geomagnetic daily variations influenced by interplanetary field 0-85591
- geomagnetic pulsations affected by interplanetary medium 0-77228
- Halley-Venus mission, Planet-A project for mag. meas. in interplanetary space (*Japanese*) 0-94672
- heliosphere magnetic field configuration, three-dimensional model 0-94670
- intensity, vars. during geomag. storms with gradual commencements (*Russian*) 0-105127
- magnetosheath, high latit., mag. field lines rel. to ≤ 2 MeV electrons transport 0-90296
- magnetosheath, mag. field direction rel. to obs. of energetic electrons of magnetospheric origin 0-90310
- magnetosphere interaction, correl. with auroral convection over ($60^\circ \leq \Delta \leq 75^\circ$) 0-67454
- magnetosphere merging with interplanetary field, half-wave rectifier response 0-72710
- magnetosphere-solar wind dynamo affected by IMF vector 0-85824
- north-south component in 1972 rel. to geomagnetic bays and geomagnetic activity 0-105124
- north-south field component, solar cycle dependent configurations in solar wind interaction regions 0-98529
- northward magnetic field, assoc. convection in magnetosphere polar cap 0-94658
- sector boundaries, rel. to Swan Cloud in Comet Kohoutek (1973 XII) and cometary plasma tails general morphology 0-98612
- sector boundaries at 1 AU, (1971-1973) 0-94668
- sector boundary passage effect on equatorial geomagnetic field, daily variations 0-67335
- sector structure, form. by large scale spiral waves in solar wind 0-85831
- sector structure, rel. to ionosphere global scale electrodynamic coupling of high and low latit. regions 0-77194
- sector structure (1926-1970), deduced from geomagnetic data 0-90368
- sector structure and anisotropy of 50-1000 GV cosmic rays 0-62072
- shock wave, 1978 January 3 to 4, Prognoz-6 energetic particle and solar wind meas. 0-90315
- shock waves, collisionless, mag. structs. thickness 0-90314
- solar wind, dynamic mag. struct. of large amplitude Alfvénic vars. 0-72734
- solar wind, mag. field direction rel. to obs. of energetic electrons of magnetospheric origin 0-90310
- solar wind, mag. field fluctuations rel. to plasmadynamical processes (*German*) 0-109323
- solar wind, mag. field rel. to Alfvén wave accel. 0-85923
- solar wind, mag. field rel. to plasma irregularities anisotropic struct. 0-67489
- solar wind, magnetic data anal. rel. to MHD turbulence 0-61977
- solar wind, obs. of fully developed anisotropic MHD turbulence 0-94669
- solar wind corotating interaction regions, energetic particles shock accel. 0-82159
- southward component, correl. with plasma sheet thinning during magnetospheric substorms 0-72705
- turbulence, character rel. to mean free path of low-rigidity cosmic rays 0-98524
- variation effects on solar flare cosmic ray particle intensity 0-77372
- Venus magnetic tail interaction, unipolar induction effects 0-62060
- vertical component origin and recurrency 0-90369

interplanetary matter

- see also comets; cosmic dust; interplanetary magnetic fields*
- acceleration effect on solar cosmic rays, soln. to Fokker Planck eqn. 0-77242
- circumsolar dust cloud, inner F-corona, model and composition 0-82162
- circumsolar plasma, Venera 10 radio signal spectral meas. 0-109326
- cold-cloud aggregates, chemical energy and meteorite chondrule origin 0-105210
- collisional growth to planetesimals, relative vel. 0-82247
- corotating energetic particle events, origin 0-82161
- cosmic ray protons, 1-4.5 MeV, spectral anal. and correl. study 0-77243
- cosmic rays, flow lines and energy changes 0-82158

interplanetary matter continued

- cosmic rays, low-rigidity, weak turbulence diffusion theory rel. to mean free paths 0-98524
- cosmic rays propagation, rel. to large amplitude wave-trains of neutron intensity 0-94660
- dust, light scatt. intensity, theory 0-109324
- dust complex, azimuthal asymmetry mechanism from restricted three-body problem 0-85843
- dust components in inner Solar System 0-85914
- dust grain trace element anal., stratosphere collected particle 0-82319
- dust in stratosphere, visible absorpt. spectra 0-101554
- dust origin and evolution 0-101555
- dust particles, Mg isotopic composition 0-72879
- Earth bow shock, conference, Strasbourg, France (1978 August 31 to September 1) 0-82573
- Earth bow shock, first evidence and early studies, historical introduction 0-85816
- Earth bow shock, initial ISEE mag. field obs. 0-90307
- Earth bow shock, kinetic models of shocks in collisionless plasmas 0-90330
- Earth bow shock, obs. of backstreaming protons in upstream solar wind 0-90309
- Earth bow shock, review of upstream energetic-particle meas. 0-90308
- Earth bow shock, theory of magnetic shocks in collisionless plasma 0-85854
- Earth bow shock, three-dimensional shape 0-85832
- Earth bow shock plasma, possible generation mechanisms of low-freq. waves (≤ 50 Hz) 0-90312
- Earth bow shock vicinity, low-freq. waves obs. 0-90311
- electric currents, generation by solar activity rel. to solar wind energy source 0-94768
- electrons, energetic, of magnetospheric origin in magnetosheath and solar wind, obs. 0-90310
- heliosphere, model of mag. field configuration 0-94670
- ion fluxes from Jupiter, Voyager 1 and 2 obs. 0-94667
- Jupiter as source of electrons observed at Earth orbit 0-90357
- magnetic measurement in interplanetary space during Halley-Venus mission, Planet-A project (*Japanese*) 0-94672
- magnetosheath, Prognoz 4 obs. of ≤ 2 MeV electrons and cold plasma 0-90296
- magnetospheric storm, interplanetary shock wave with increased solar wind energy deposition 0-77237
- piston problem, one-dimensional, in non-ideal gas, time-dependent soln. 0-82185
- plasma, collisionless, stability of contact discontinuity, solar wind and magnetosphere boundary appls. 0-62002
- protoplanetary nebula formation of inhomogeneous Earth 0-90348
- scintillation, appl. to solar wind recurrence determ. at high heliographic latit. 0-62106
- scintillation spectra, radio spectrograph obs. rel. to electron density vars. physical form 0-72741
- scintillations, obs. rel. to solar wind plasma irregularities anisotropic struct. 0-67489
- shock wave, 1978 January 3 to 4, Prognoz-6 energetic particle and solar wind meas. 0-90315
- shock waves, collisionless, mag. structs. thickness 0-90314
- shock waves, collisionless shocks simulation and laboratory expts. 0-87893
- solar wind, He⁺ flux after interplanetary shock, Imp 7 obs. 0-101520
- solar wind, low freq. continuum from ISEE 3, thermal electrostatic noise, LF obs. 0-101519
- solar wind, plasmadynamical processes review (*German*) 0-109323
- solar wind corotating structures, MHD model 0-90304
- solar wind interaction regions, N-S mag. field component solar cycle dependent configurations 0-98529
- solar wind sputtering rate 0-85835
- solar wind turbulent plasma, radio wave propag. meas. using three satellites 0-101518
- solar wind velocity determ. from interplanetary scintillation effects on 3C 279, SHF obs. (*Russian*) 0-77248
- Sun and heliosphere, conference, London, England (1979 April 3 to 4) 0-82574
- travelling interplanetary phenomena, space expts. related to Solar Maximum Year project 0-90404
- velocity distrib. from scintillation obs. 0-105143
- Venus environment, plasma wave investigation by Pioneer Venus Orbiter 0-67497
- zodiacal dust cloud, thermal emission at 11 and 20 microns 0-90367
- zodiacal light, new model for scatt. by irregular absorbing particles 0-67543
- H atoms from heliosphere, ionis. in near Sun region 0-105145
- H I, interstellar, interaction with solar wind 0-101506
- H I, Ly α emission profiles reanal. rel. to local interstellar gas temp. and vel. 0-105141
- He I, interstellar, obs. with gas absorpt. cell, implications for local interstellar medium struct. 0-62234
- He, interaction of solar wind with Sun's gravity focused He 0-105144
- He⁺, obs. in driver gas of interplanetary shock wave 0-72735

interplanetary medium *see* **interplanetary matter****interpolation**

- see also function approximation*
- biomedical surface mapping 0-81750
- computerised tomography, fan-beam to parallel-beam conversion by rubber sheet transformation 0-109009
- formant frequency and bandwidth conversion to reflection coefficients 0-91975
- two-beam interference fringe interpolation method 0-105703

interstellar dust *see* **cosmic dust****interstellar magnetic fields**

- see also interstellar matter*
- 3C 219, double radio galaxy, mag. field configurations from obs. at 1.48 and 4.89 GHz 0-77500
- 3C 31, radio galaxy, mag. field struct. in radio jets 0-82526
- 3C 58, supernova remnant, radioemission from mag. field interaction with relativistic electrons 0-73023
- Cassiopeia A, mag. field decrease rel. to radio spectrum secular flattening 0-101637
- direction correlation with planetary nebula major axes, hydromagnetic model 0-82473

lithium compounds continued

- LiNbO₃, electrooptic photorefractive crystals for optical information processing 0-74313
 LiNbO₃, ferroelec., displacive type phase transition, far IR reflection spectra 0-71339
 LiNbO₃, Fe diffused, single-mode waveguide, comparison of bending losses in integrated optical circuits 0-83684
 Y-Z LiNbO₃, filamentary defects visualisation at wafer inspection stage 0-75315
 LiNbO₃, finite difference anal. of SAW 0-75423
 LiNbO₃, for reflective dot array pulse compression filters 0-74623
 LiNbO₃, Fourier transform IR spectroscopy of vibr. states at high temp. 0-97256
 LiNbO₃, grating-tuned picosecond IR source with CdSe down-conversion 0-74435
 LiNbO₃, hologram recording, γ radiation effect 0-78812
 LiNbO₃, hologram storage depend. on envelope field, space charge field 0-78801
 LiNbO₃, holographic storage, effects of nonstoichiometry and Fe-doping 0-69344
 LiNbO₃, holographic storage and retrieval 0-99669
 LiNbO₃, intracavity upconverter for IR detect., limits to low noise equivalent power operation 0-74430
 LiNbO₃ layers, Li out-diffused, SHG phase matching temp. variation 0-69455
 LiNbO₃ lenses, diamond-turned aspheric geodesic waveguide lenses 0-58804
 LiNbO₃, light induced ultrasonic wave velocity change, refractive index 0-97236
 LiNbO₃, luminesc. props., Li/Nb ratio effect 0-97323
 LiNbO₃, nonlinear crystals, interference of optical harmonics 0-64102
 LiNbO₃, optical absorption of hole centres, polaron model 0-97314
 LiNbO₃, optical waveguides, Ag-Li and Ti-Li ion exchange effects 0-58791
 LiNbO₃, optical waveguide surface, acoustooptical interaction for TE modes, metallisation effect 0-69541
 LiNbO₃, optical waveguides by ion implantation 0-106622
 LiNbO₃, parametric phonon echo obs. 0-59588
 LiNbO₃, photoinduced surface storage of SAW patterns 0-74309
 LiNbO₃, photorefractive crystals for computer interfaced optical memory system, hologram characterisation 0-58475
 LiNbO₃, piezoelec., SAW interaction with secondary electrons 0-80708
 LiNbO₃, piezoelectric material for electrostatic voltage sensors (*Japanese*) 0-105632
 LiNbO₃, planar lightguide, optical mode interaction with standing elastic surface waves 0-99836
 LiNbO₃ pure and Fe doped, IR induced acousto-photorefractive memory effect 0-80746
 LiNbO₃, pure and Fe doped, two-photon photorefractivity 0-80753
 LiNbO₃, SAW, suppression of harmonic generation by ZnO thin-film loading 0-84355
 LiNbO₃, SAW propag., effects of He ion implantation 0-75421
 LiNbO₃, SAW propag. velocity meas. 0-92003
 LiNbO₃ sensor for elec. hygrometer (*Japanese*) 0-95103
 LiNbO₃ single crystals, growth from melt, Czochralski method (*Chinese*) 0-76171
 LiNbO₃ single crystals grown by automatic diameter control, power striations (*Chinese*) 0-81080
 LiNbO₃ single crystals, wetted-die growth technique 0-97426
 LiNbO₃, spontaneous polarisation, low temp. meas. 0-75921
 LiNbO₃ substrate, covered with metal or quartz powder, dynamic SAW reflecting struct. 0-74565
 LiNbO₃ substrate, Pb_{1-x}Nb_xTe-PbTe heterostructures produced by MBE 0-88629
 LiNbO₃ substrates for integrated passive optical rotation sensors using guided waves, developments 0-58781
 LiNbO₃ surfaces, ion and electron bombard., photoelectron spectroscopy and electronic props. 0-71559
 LiNbO₃, temp. coeff. of freq. determ. 0-75316
 LiNbO₃, thermionic emission characts. 0-104034
 LiNbO₃, two-photon absorption spectra, energy struct. anal. 0-99785
 LiNbO₃, valence band UPS and partial p and d density of states 0-71560
 LiNbO₃, very high throughput damage resistant waveguide modulator 0-58788
 LiNbO₃ waveguide, diffusion fabricated, angular variation calcs. using mode propag. consts. 0-69540
 LiNbO₃ waveguide, electrooptic surface prism laser deflector 0-87492
 LiNbO₃ waveguide, planar electro-optic prism array beam splitter 0-64209
 LiNbO₃ waveguide, Y-cut, for fabrication of wideband guided-wave acousto-optic Bragg deflector 0-74510
 LiNbO₃ waveguide modulators and switches, Ti-diffused, fabrication on directional coupler principle 0-83678
 LiNbO₃ waveguides, diffused channel, multimode and single mode, direct index meas. 0-87562
 LiNbO₃ waveguides, optical scattering phenomena 0-58786
 LiNbO₃, XPS and UPS from surface defects 0-76136
 LiNbO₃ Y-cut four-mode waveguide, generalised parameters describing acoustooptical interaction 0-91924
 LiNbO₃, YZ-cut, coated with SiO₂ thin film, SAW props. 0-84356
 LiNbO₃/Cu(Fe), light induced charge transport, photovoltaic effects, impurity states 0-80317
 LiNbO₃/Fe, elec. resist., temp. and conc. depend. 0-80275
 LiNbO₃/Fe, electro-optic cryst., light induced charge transport, holographic obs. 0-70747
 LiNbO₃/Fe, exoelectron emission in pyroeffect regime 0-76158
 LiNbO₃/Fe, holography appl., comparison with KNbO₃, w.r.t. recording and erasure sensitivity (*Russian*) 0-78795
 LiNbO₃/Fe, holographic recording and thermal fixing, invest. of mechanisms 0-78810
 LiNbO₃/Fe, impurity charge states after UV irradiation 0-60462
 LiNbO₃/Fe, photoinduced refractive index discontinuities at surface 0-75999
 LiNbO₃/Fe, photoinduced scatt. and bleaching effect 0-95959
 LiNbO₃/Fe, white-light image processing 0-87321
 LiNbO₃/Fe (0.05%), hologram recording γ radiation effect 0-78812
 LiNbO₃/Fe spatial holograms, ageing mechanism and thermal fixing (*Russian*) 0-74311
 LiNbO₃/Fe³⁺, X-ray absorpt. 0-108299

lithium compounds continued

- LiNbO₃/Fe(Nb), SHG, phase-matching temp., impurity influence 0-69463
 LiNbO₃/Na structure field stability limits, LPE film growth, SAW velocity 0-80102
 LiNbO₃/Na⁺ (Co²⁺, Zr⁴⁺) film, improvement in temp. stability and SAW device appl. 0-75939
 LiNbO₃/Ni optical absorpt. spectra 0-71450
 LiNbO₃/Rh, Czochralski-grown oxide crystals, fluid-flow effect on gas-bubble entrapment 0-84121
 LiNbO₃/Ti, coupled waveguided TE/TM mode splitter 0-64142
 LiNbO₃/Ti, planar and channel optical waveguides, anisotropic diffusion expts. 0-64200
 LiNbO₃/Ti, planar optical waveguides, processing and props. 0-78965
 LiNbO₃/Ti 3-dB optical waveguide mode convertor using chirped gratings, power transfer 0-79014
 LiNbO₃/Ti channel waveguide high-speed cutoff modulator 0-64195
 LiNbO₃/Ti diffused optical waveguide, guided light scatt. sources 0-78966
 LiNbO₃/Ti diffused optical waveguide, efficient tapered gap prism coupling 0-78967
 LiNbO₃/Ti diffused strip waveguide, optical propag. losses and coupling losses 0-58664
 LiNbO₃/Ti digitally driven integrated optics amplitude modulator 0-58808
 LiNbO₃/Ti electro-optic TE-TM mode convertor structure 0-64215
 LiNbO₃/Ti electro-optic branching waveguide, characts. 0-83681
 LiNbO₃/Ti in-diffused waveguide, refractive index profile calc. from measured coupling angles 0-78954
 LiNbO₃/Ti optical waveguide electrooptic devices polarisation independ. directional coupler switch and wavelength filters 0-58783
 LiNbO₃/Ti optical waveguides and crystals, absorption loss and photorefractive index changes 0-58787
 LiNbO₃/Ti optical waveguides, Ti diffusion process and control, waveguide characts. 0-58790
 LiNbO₃/Ti optical waveguide, surface wave mode conversion, static strain-optic effect 0-87561
 LiNbO₃/Ti phase-matched waveguide electro-optic TE=TM mode convertor 0-58749
 LiNbO₃/Ti planar waveguide, edge coupling to GaAlAs DH laser diode 0-87559
 LiNbO₃/Ti single mode electrooptic waveguide modulator, high-speed operation 0-91915
 LiNbO₃/Ti single-mode optical waveguide, fabrication by sequential combination of Ti diffusion and masked ion-implantation 0-58785
 LiNbO₃/Ti single-mode waveguides, losses due directional changes 0-58789
 LiNbO₃/Ti strip waveguide, SHG 0-102773
 LiNbO₃/Ti waveguide, ps signal processing with planar, nonlinear integrated optics 0-64208
 LiNbO₃/Ti waveguide electro-optic TE=TM mode converter-wavelength filter 0-64210
 LiNbO₃/Ti Z-cut crystals, Ti diffusion process parameters 0-102849
 LiNbO₃-CdS system, expt. investigation of nonlinear Rayleigh wave interaction 0-102946
 LiNbO₃-CdSe layer structure, SAW absorpt., elec. field effects 0-65355
 LiNbO₃-gap coupled Schottky diode memory correlator, grating coupled optical imaging 0-64143
 LiNbO₃-Ge acousto-optic modulator for 10.6 μ m CO₂ laser 0-99776
 LiNbO₃-Ge acoustooptic modulator (*Japanese*) 0-69542
 LiNbO₃-pn-diode airgap convolver struct. optical scanner using single SAW pulse 0-64144
 LiNbO₃-Si, acoustoelectronic memory, effect of band-bending 0-70771
 LiNbO₃-SiO₂-Fe₂O₃ glasses, Li⁺ ion cond. 0-107471
 LiNDP-O₂ laser, relaxation oscillations and mode spectra, high density pumping effect 0-69396
 LiO₂-Al₂O₃-SiO₂ glass containing ZrO₂, cryst. process 0-103253
 LiO₂-SiO₂ glass ceramic mineralogy 0-60826
 Li₂O, cation diffusion NMR investigation up to 800°C 0-108092
 Li₂O, neutron irradiat. effects, optical absorpt. spectra 0-75271
 Li₂O pellets, neutron irradiated, temp. distrib. 0-86968
 Li₂O pellets, sintered, neutron irradiated, ESR study 0-92566
 Li₂O, porosity, dependence on thermal diffusivity and thermal conductivity, 200-900°C 0-92726
 Li₂O single cryst., ⁶Li(n,α)³H, 2.7 MeV triton recoil range 0-63372
 Li₂O, single crystal synthesis using vacuum fusion technique 0-71585
 Li₂O Tokamak breeding blankets, T breeding perform. comparative eval. 0-95398
 Li₂O-2SiO₂ glass, DTA study, Kissinger plot 0-84084
 Li₂O-Al₂O₃, rapidly quenched glasses, Li ion cond., elec. cond. 0-100346
 Li₂O-Al₂O₃-Cr₂O₃ system, subsolidus equilibria 0-60843
 Li₂O-Al₂O₃-GeO₂ glass, interdiffusion coeffs. of Li and Na 0-88369
 Li₂O-Al₂O₃-SiO₂ glass, study of elastic props. 0-104205
 Li₂O-Al₂O₃-SiO₂ phase separation of initial stages of sialitisation 0-88053
 Li₂O-Al₂O₃-SiO₂ glass-ceramic, near-zero thermal-expansion heat treatment effect in fracture behaviour 0-66537
 Li₂O-Al₂O₃-SiO₂ glasses, crystallised, grain size and internal strain 0-103259
 Li₂O-Al₂O₃-SiO₂:Cd²⁺ glass, ESR study 0-103879
 Li₂O-Al₂O₃-SiO₂-TiO₂ system glasses, Raman spectra obs. of glass-ceramics form. 0-60825
 Li₂O-Al₂O₃-SiO₂(P₂O₅):Cd²⁺ glasses, γ -irrad., EPR study 0-84639
 Li₂O-B₂O₃ glass struct. study using ¹⁰B NMR 0-84658
 Li₂O-B₂O₃ glasses, fast ion transport 0-107470
 Li₂O-B₂O₃ glasses, low Li₂O content, ⁷Li NMR study 0-84657
 Li₂O-B₂O₃:Cr³⁺ glass, absorpt. spectra, Pano antireson. and vibronic Lamb shift 0-71458
 Li₂O-B₂O₃-P₂O₅ glass, mech. and elec. props 0-84228
 Li₂O-BaO-SiO₂ glasses, elec. cond., room temp. to 450°C 0-107473
 Li₂O-Bi₂O₃, rapidly quenched glasses, Li ion cond., elec. cond. 0-100346
 Li₂O-Ga₂O₃, rapidly quenched glasses, Li ion cond., elec. cond. 0-100346
 Li₂O-GeO₂-Ga₂O₃ glass, electrode props., dissolution kinetics 0-89387
 Li₂O-LiF-B₂O₃ glasses, fast Li⁺ conduction 0-79984
 Li₂O-LiF-B₂O₃-Li₂SO₄ glasses, DC cond. and secondary struct. relax. 0-107469
 Li₂O-LiX-B₂O₃ glass, X=halogen, high anionic cond. of new solid electrolytes 0-107546
 Li₂O-MgO-Al₂O₃ system, subsolidus phase equilibria 0-81036
 Li₂O-MgO-Al₂O₃-SiO₂ glass scintillator for pulsed neutron detection 0-87019

lithium compounds continued

- Li₂O-Na₂O-B₂O₃-Al₂O₃-SiO₂ glass, Young's modulus and density, ion exchange effects 0-84982
 Li₂O-P₂O₅ glass, ESR of VO²⁺ ions 0-100610
 Li₂O-P₂O₅-Cd²⁺ glass, γ -irrad., EPR study 0-84639
 Li₂O-SiO₂, corrosion behaviour in aq. solns. of Al compounds 0-66679
 Li₂O-SiO₂ glass, protonated, field-driven guest proton redistrib. 0-107474
 Li₂O-SiO₂ glass, thermotransport props. 0-79985
 Li₂O-SiO₂ glasses, Li self-diffusion, mass spectrometric method 0-79982
 Li₂O-SiO₂-P₂O₅ glass ceramic fibres, heat treatment, crystn., tensile strength 0-84995
 Li₂O-TiO₂, pseudobinary phase rotations, DTA and X-ray anal. 0-108411
 Li₂O-TiO₂-Al₂O₃-SiO₂ glass, γ -irrad., struct. position of Ti, EPR study 0-84644
 LiOH, hydrolysed surface of LiH, effect on IR absorption, X-ray luminesc. and EPR spectra 0-60660
 Li₂O.2SiO₂, ceramic, prep. of oriented microstructure by unidirectional solidification of melts 0-71614
 Li₂O.2SiO₂, prep. from film forming soln. 0-60811
 Li₂O.2SiO₂, short range struct. by pulsed neutron scatt. 0-59396
 Li_{1+x}P₃O₃₊₁, polyphosphate, melting and crystallisation 0-70376
 Li-Pb, T breeding fusion blanket with boiling water coolant 0-99274
 Li-Pb, Tokamak breeding blankets, T breeding perform. comparative eval. 0-95398
 LiRbSO₄, order-disorder phase transitions with many-minimum potential, thermodynamic props. 0-96623
 LiReO₄, IR matrix-isolation spectra 0-87108
 Li₂S, cation diffusion NMR investigation up to 800°C 0-108092
 Li₂S-GeS₂, glass forming region, struct. and ionic cond. 0-88358
 Li₂S-P₂S₅-LiI, ionic cond. meas. from room temp. to glass transition temp. (French) 0-88355
 Li₂SO₄ based solid electrolytes, FCC phase transport mechanism studies and uses 0-107525
 Li₂SO₄, fast ion conductors, X-ray diff., neutron diff., and Brillouin scatt. study 0-107170
 Li₂SO₄, high temp. fast ion cond. phases, neutron diff. obs. of struct. 0-107512
 Li₂SO₄.H₂O, far IR spectra, H₂O flipping motion, lattice modes 0-84258
 LiSbO₃.1/6LiF, dielec. spectroscopy study, 100 Hz to 10 MHz, 238 to 417K (German) 0-108144
 Li₃Si, cryst. struct. and electrochem. anal. (German) 0-88132
 Li₂SiO₄, piezoelectric glass ceramic, recrystallisation, pyroelectric response, permittivity 0-80703
 Li₂Si₂O₅, pyroelectric glass-ceramics 0-75950
 LiTaO₃, appl. in sub-100 ps pyroelec. detectors, 10.6 μ m damage threshold meas. 0-77859
 LiTaO₃, crystals for commercial SAW TV IF filters, fabrication 0-80961
 LiTaO₃, Czochralski-grown oxide crystals, fluid-flow effect on gas-bubble entrapment 0-84121
 LiTaO₃, dispersive ferroelectric, effective charge determ. 0-97212
 LiTaO₃, ferroelec., dispersive type phase transition, far IR reflection spectra 0-71339
 LiTaO₃, Fourier transform IR spectroscopy of vibr. states at high temp. 0-97256
 LiTaO₃, interdigital transducer on piezoelectric half space, spectrum of emanating acoustic waves 0-79044
 LiTaO₃, monolithic pyroelectric array, IR detectors 0-77857
 LiTaO₃ optical waveguides, Ag-Li and Ti-Li ion exchange effects 0-58791
 LiTaO₃ optical waveguide, Ag-Li ion exchange 0-91888
 LiTaO₃, propagation of SAW, arbitrary cut (Japanese) 0-92769
 LiTaO₃, single cryst. prep. for surface acoustic wave device appls. (Japanese) 0-60772
 LiTaO₃:Cu(Fe), light induced charge transport, photovoltaic effects, impurity states 0-80317
 LiTaO₃:Fe, electro-optic cryst., light induced charge transport, holographic obs. 0-70747
 LiTaO₃/CCD hybrid focal plane, IR imaging and detection, crosstalk 0-77856
 Li₂Ta₂S₇ and Li₂Ti₂S₇, chem. diffusivity of Li at 30°C 0-59737
 Li_{1+x}Ta_{1.5y}Ti_{0.5y}O₃ (0≤y≤0.028), non-stoichiometric phase, crystallographic and dielec. props. 0-75212
 LiTbF₄, cryst. field parameters, mag. susceptibility meas., 0.3 to 100K 0-60214
 LiTbF₄, uniaxial dipolar ferromag., critical behaviour, mag. susceptibility meas. 0-80528
 LiTbO₃.Y_{0.5}F₄, uniaxial dipolar ferromag., critical behaviour, mag. susceptibility meas., effect of Y³⁺ dilution 0-80528
 Li_{1+x}Ti_{2-x}O₄, high temp. spinel-Ramsdellite transform. 0-70407
 Li₂Ti₂S₇, alkali ion ordering, X-ray study 0-107165
 Li₂TiS₂, electrodes, thermodynamic and transport props. 0-66963
 LiTmF₄, van-Vleck paramagnet, giant magnetostriction (Russian) 0-103872
 LiTmF₄, rare earth, EPR spectra, elec. field effects, cryst. field interactions 0-71176
 Li₂UO₄, energy transfer, cryst. struct. and chemical composition effect 0-108248
 Li₂UO₅, energy transfer, cryst. struct. and chemical composition effect 0-108248
 Li₂UO₅.Cl₄ melts and mixtures, thermogravimetric determ. of uranyl cation state 0-101050
 LiVO₃:Cr³⁺, study of ESR spectra 0-80601
 β -Li₂V₂O₇, heat of form. and sp. ht., 450 to 900K 0-61129
 β -Li₂V₂O₇, bronze, thermodynamics of ordering 0-84302
 Li₂VSe₂, intercalation cpds., electron chem., ionicity 0-89501
 Li₂WO₄:Li₂TiS₂, cyclable organic electrolyte cell, using 2 intercalation electrodes 0-76625
 Li₂WO₃, electrochem. and chem. Li incorporation, cryst. struct. 0-88131
 Li₂WO₄(IV), cryst. struct. rel. to wolframite-type struct. 0-92505
 LiYF₄, ESR spectra of non Kramers ions, elec. field influence 0-103884
 LiYF₄, electron-irrad. induced defects, optical and EPR study, impurity effects 0-66238
 LiYF₄:Ho laser, TEM₀₀ mode and Q-switched operation 0-74395
 LiYF₄:Pr, NMR meas. of hyperfine const. of Pr³⁺ excited state 0-88895
 LiYF₄:rare earth, EPR spectra, elec. field effects, cryst. field interactions 0-71176
 LiY(MoO₄)₂, X-ray cryst. struct. determ. 0-107124
 LiYbF₄:Ho³⁺, active medium for Nd laser freq. convertor, cascade stimulated emission 0-102727
 LiZn ferrosilicates, mol. field. coeff. conc. depend. 0-97114

lithium compounds continued

- Li_{1/2}Zn_{1/2}(GeO₄)₄ LISICON system, Li⁺ ionic conductivity (Chinese) 0-88350
 Li_{1/2}Zn(GeO₄)₄, LISICON, AC meas. of ionic cond., 298 to 573K 0-107526
 Li₂Zr(MoO₄)₃, X-ray cryst. struct. determ. 0-88125
⁶LiD, polarised target material, DNP 0-87007
 Mg(NO₃)₂.RNO₃ (R=Li, Na, K), thermogravimetric anal. of dehydration processes (Japanese) 0-66791
 Na_{2-x}Li_xErSi₄O₁₂, solid electrolytes for Na/TiS₂ cells, synthesis, characts. and utilisation 0-107518
 Na_{1-x}Li_xNbO₃ mixture, ferroelec.-paraelec. transitions, dielec. props. meas. 0-66125
 NaLiSO₄, anhydrous, struct. relationships w.r.t. fast ion cond. 0-107188
 Na₂O-Li₂O-Al₂O₃, local electrode current density and flow decoration 0-100935
 Na₂O-Li₂O- β -Al₂O₃.H₂O, water mol. vibrs., IR and Raman spectra 0-89006
 Ni-ferrite powders, form. in presence of Li₂SO₄-Na₂SO₄ molten salts, prep. and characts. 0-84869
 SiO₂-B₂O₃-Li₂O-Al₂O₃ (28, 2, 1 wt.%) glass, dielec. const. at 3 GHz 0-93233
 SiO₂-Li₂O, glass, layers near surface, anal. using SIMS 0-88041
 SiO₂-Li₂O-Li₂SO₄, glass-forming region, struct. and ionic cond. 0-84320
 SiO₂-Li₂O-Al₂O₃ glass, luminesc., polarisation degree distrib. 0-108257

lithospace see Earth crust**lithosphere see Earth crust****liver**

- carcinoma, VX2, improved detectability in the rabbit with contrast enhancement in computerised tomography 0-98118
 electron microscopic diagnosis using clinical pathology liver and kidney samples, computer assisted 0-85485
 functional reserve capacity meas. by organ-reflectance spectrometry (Japanese) 0-94313
 gamma-camera images, improvement using physiological gating mechanism 0-98065
 hepatobiliary imaging, clinical evaluation of ^{99m}Tc-(p-butyl) iminodiacetic acid (Japanese) 0-67236
 hepatobiliary scintigraphy, characts. of ^{99m}Tc-E-HIDA (Japanese) 0-81729
 intrahepatic lithiasis detection, sequential scintiphotography with ^{99m}Tc pyridoxylidene-glutamate 0-72309
 magnetic susceptibility measurement, living rats 0-72391
 membranes, mouse, X-irrad., dose-rate effects 0-94293
 metastases, γ -scan accuracy for detect., comparative study with grey scale ultrasonography (French) 0-104741
 metastases diagnosis, conf., Brussels, Belgium (Nov.-Dec. 78) 0-82568
 microsomes, γ -induced lipid peroxidation and membrane-bound enzymes 0-104660
 Mossbauer spectrometry of Fe in hepatic and splenic tissues 0-81544
 NMR observations, pulsed, spin-lattice relax. values 0-94171
 pathology characterisation, clinical appl. of a US attenuation coeff. estimation technique 0-76813
 physiological compartment tracer flow modelling and digital imaging 0-101257
 RBE of cyclotron fast neutrons and γ -rays for late hepatic injury in rats 0-108975
 subtraction scintigraphy with ⁶⁷Ga-citrate and ^{99m}Tc-colloid in the diagnosis of intrahepatic masses 0-104752
 US scattering struct., theoretical modelling 0-89785
 US signals in diffuse liver disease, computer anal. 0-67173
 Cd conc. in kidney and liver, neutron activation anal., organ depth determ. 0-72321
 Fe overload, non-invasive diagnosis, SQUID appl. 0-101244
^{99m}Tc-hepatobiliary agents, absorbed dose estimation 0-72330

livestock see farming**living systems**

- see also biocybernetics; brain models; extraterrestrial life; physiological models
 nonequilibrium linear behaviour, enzyme-mediated multidimensional inflection points 0-72122
 review of ecology and systematics (book) 0-67945

load control see load regulation**load regulation**

- energy storage options, Na/S battery development program at GEC 0-61327
 power system that includes wind energy generators, model based 0-61256
 underground pressurised saturated hot water storage for peak loading appls. 0-76653

lobes (distribution) see antenna radiation patterns**local moments in dilute systems**

- alloys, magnetic localisation and charge oscillations 0-75781
 Anderson model, ground state, var. trial function approach 0-59913
 Anderson model, impurity pair interactions, local moment form., var. method 0-92854
 ferromagnetism onset, mag. inhomogeneity 0-75774
 itinerant magnets, band struct., mag. props. and local moments 0-70929
 metal, indirect coupling between localised mag. moments by narrow band electrons 0-70942
 metal-insulator transition and local moment-formation, spin-density functional approach 0-65451
 metals, ESR of localised moments 0-71153
 metals, spin and charge polarisation around mag. impurities 0-75714
 semiconductors, doped, local spin-density-functional method, appl. to metal-insulator transition 0-96789
 semiconductors, indirect exchange interaction between localised moments 0-93079
 semiconductors, localised magnetic moment of transition metal impurities 0-60192
 variational method for mag. impurities in metals 0-103814
 Wolff model, thermodynamic props., local moments in dil. alloys, var. method 0-65781
 Ag, electronic and mag. structure calcs. of mag. impurities 0-80213
 Ag-transition metal, dil., mag. impurities, electronic struct., KKR-Green's function calc. 0-65783
 Au-Cr, dil., elec. resist., generalised phase shift anal. of Kondo effect 0-75556
 Au-Cr, dil. alloys, elec. resist., deviations from Matthiessen's rule 0-75541
 Au-Er, dil., EPR at 100 mK to 1K 0-66028

local moments in dilute systems continued

- Au-Gd(Y), dil., conduction electron-local moment exchange interaction meas. 0-60191
 Au-Yb, dil., EPR at 100 mK to 1K 0-66028
 Cd_{1-x}Mn_xTe, indirect exchange interaction 0-97087
 Cr-Fe, dil., magnetisation, Fe local moments 0-60215
 CrCo, dil., low temp. specific heat meas., 1.5 to 4K 0-60328
 Cu, electronic and mag. structure calcs. of mag. impurities 0-80213
 Cu-Al-Mn liq. alloys, susceptibility behaviour 0-93077
 Cu-Fe group, dil., NMR satellite data calc., struct. of mag. impurities 0-103894
 Cu-Mn, exchange-coupled localised moments, Korringa relaxation rate 0-75851
 Cu-transition metal, dil., mag. impurities, electronic struct., KKR-Green's function calc. 0-65783
 CuCr(Fe)(Mn), dil., anisotropic hyperfine coupling, NMR study 0-65784
 Hg_{1-x}Mn_xTe, indirect exchange interaction 0-97087
 Ir-Fe, dil., local magnetisation, Mossbauer meas. 0-66091
 La-Gd, exchange-coupled localised moments, Korringa relaxation rate 0-75851
 LiZn ferromagnets, mol. field. coeff. conc. depend. 0-97114
 Mg-Tb(Dy)(Ho)(Tm), dil., macroscopic shape effect due to quadrupole orientation, magnetostriction and thermal expansion meas. 0-60396
 Ni-Mn alloy, mag. moment distrib. and environmental effects, neutron scatt. obs. 0-60247
 PbTe:Fe, single crystals, state and behaviour of Fe, mag. props. 0-93080
 Pd-Mn (1-10 wt.%), mag. ordering, influence on resistivity 0-75557
 PdH_{1-x}Fe_{0.003x}, Kondo system, local moments, hyperfine fields, Mossbauer study 0-80478
 Ru-Fe, dil., local magnetisation, Mossbauer meas. 0-66091
 SnTe:Mn, NMR shift meas. 0-97154
 SrO:Ni²⁺, EPR line splitting rel. to Jahn-Teller coupling and soft localised mode 0-66022
 Te-Fe, dil., local magnetisation, Mossbauer meas. 0-66091
 (Ti_{1-x}V_x)₂O₃, 0 < x < 0.1, magnetisation and mag. moments 0-65772
 Ti_{1-x}V_xSe₂, mag. susceptibility, 4.2-300K 0-60188
 VO₂, metal-insulator transition, electron correls. and spin dimerization, thermodynamical study 0-70615

localised electron states

- see also Anderson model; charge-ordered states; charge transfer states; Wigner crystal*
 actinide compounds, neutron scatt. studies 0-75716
 amorphous semiconductor, cond. mechanism and localised states (Japanese) 0-84467
 Anderson localisation, mean field theory and ϵ -expansion 0-80203
 Boltzmann electron gas in Gaussian random potential, mean field approach 0-107721
 cancellation effects in localised theories 0-84445
 chain with light emitting ends, radiative lifetime, recombination kinetics 0-108260
 chalcogenide glasses, optical versus transport processes. 0-84449
 disordered alloy, electron localisation, temp. depend. 0-80219
 disordered electronic systems, near two-dimens., noncompact σ models and existence of mobility edge 0-92860
 disordered Fermi systems, in two dimensions, interaction effects 0-75655
 disordered system, low-freq. cond. due to variable range hopping, cluster approx. 0-92886
 disordered system, one-dimens., density of states and wavefunction shape, periodic boundary condition influence 0-80223
 disordered system in mag. field, frequency dependence of conductivity tensor, theoretical investigation 0-70725
 disordered system with n orbital per site, Lagrange formulation, hyperbolic symm., Goldstone modes 0-80222
 electronic localised state at edge dislocations, parabolic dispersion law (Russian) 0-65479
 ferromagnetic semiconductor, surface localised low energy electron-magnon states (Russian) 0-88734
 finite chain, with random dil. impurities, localisation characts., amplitude anal. 0-96825
 glasses, electron scavenging, hopping controlled time-depend. reaction rates 0-108723
 hopping conduction in disordered insulator, continuous-time random walk model 0-96863
 hopping transport kinetic theory, localised state separation, Pauli master eqn. 0-80276
 metal, plasmon satellite struct. in (e,2e) process 0-96809
 metal, US attenuation, quantum oscills. with dislocations under press. (Russian) 0-88273
 metal surface chemisorption theory, electron localisation, surface interactions 0-84376
 metals, electronic struct. and magnetism, review 0-70573
 3-methylpentane glassy matrix, localised electrons, cavity model 0-107743
 minimal metallic cond., localisation scaling theory (Russian) 0-103671
 mixed valence model, spinless, coherent-hybridisation states and virtual-bound states 0-107749
 mixed valence model, spinless, isolated f-level problem 0-107750
 Mossbauer ⁵⁷Fe spectra, ferrous charact., cryst. field interactions 0-108133
 naphthalene: pentacene, intermol. interaction dynamics and optical dephasing 0-64112
 naphthalene, in naphthalene-d₈, Anderson-Mott transition model for excitation transport 0-96812
 naphthalene, in naphthalene-d₈, energy trapping from localised states 0-100440
 one dimensional disordered system, cond. and electron localisation 0-103658
 photoelectron spectra, localised and delocalised calcs. 0-63709
 polydiacetylene-toluenesulphonate, photocond. meas., 0.62-3.1 eV 0-70757
 polymer, conjugated and saturated chain, electronic struct., review 0-59860
 polymer metal contact, charge transfer and contact charge spectroscopy 0-65680
 polymer metal contact, charge transfer and contact charge spectroscopy 0-65681
 quasi-local level, line shape induced by impurity 0-100441
 random potential, electron localisation, random walk analogue 0-107733
 random systems, localisation 0-80218

localised electron states continued

- rare earths cpds., Fano-resonances, surface and bulk effects in photoemission 0-97405
 solid electrolyte, mobility paths for MI₄⁻³ clusters, ab initio electronic struct. calcs. 0-70458
 spin-dependent correlated atomic pseudopotentials 0-107686
 superconductivity-ferromagnetism coexistence in two-band model (Russian) 0-84539
 p-terphenyl, hopping cond. among localised states 0-70861
 p-terphenyl film, polycryst., charge carrier transport and DC cond. 0-70858
 tetracene, hopping cond. among localised states 0-70861
 tetramethylammonium(0), Li(CH₃NH₂)₄, existence, conduction- and localised-electron spin reson. 0-66035
 transition metals, alloys, and cpds., XPS asymmetry of core electrons and electronic struct. parameters 0-93460
 transition metals, itinerant and localised d-electrons, positron annihilation data 0-93428
 two-dimensional impurity bands, carrier-density dependence of activation energies associated with hopping 0-88561
 Ag particles embedded in dielec. KCl medium, search for maximum metallic resist. 0-107756
 Al, film, granular, transition to localisation, elec. resist. 0-70877
 Al, granular supercond., normal state cond. 0-88529
 β -Al₂O₃:Na₂O, colour centre ESR by localised tunnelling states 0-108073
 As-Se amorphous system, photocond. props. 0-88587
 As₂S₃ film, evaporated, switching effects 0-96952
 As₂S₃(Se_{0.00-x}), localised states density near valence band edge (Russian) 0-103638
 As₂Se₃, amorphous radiative interband recombination 0-66286
 Au-3d transition metal alloys, UPS study, localised states 0-93449
 Ba₂NaNb₂O₁₅, ferroelectric, local states, thermoluminesc. study 0-60690
 Bi₂Sb_{1-x}Te_x, single crystal, dispersion of magnetoplasma waves (Russian) 0-70739
 CdSiP₂, electronic struct., X-ray spectroscopic investigation 0-108300
 CdTe:Cl, semi-insulating, impurity photocond. spectra, local state distrib. in band gap 0-107865
 CePd₃, mixed-valence, 3d and 4d core levels, XPS study 0-89111
 Co₂Ga_{1-x}Fe_x, elec. resist., temp. and mag. field depend., mag. contrib. 0-96846
 CoS₂(Se_x), core-level and valence-band XPS 0-93450
 Cs-Au liq. alloy, formation of localised electronic states, NMR obs. 0-93201
 EuO(S), ferromagnetic electronic structure, absorption, thermoreflexion and thermotransmission spectra (French) 0-97300
 FeS₂, core-level and valence-band XPS 0-93450
 Ge-Si, electronic structure, short-range order effects, calc. 0-92861
 H₂O, crystalline ice, localised excess electrons yield studied as function of dose rate 0-97712
⁴He, electron localisation, mobility in dense low temp. gas 0-92247
 LaCoO₃, Mott isolator, paramag. props., calc. 0-93071
 Li, plasmon satellite struct. in (e,2e) process 0-96809
 MgSiP₂, electronic struct., X-ray spectroscopic investigation 0-108300
 MnS₂(Se_x), core-level and valence-band XPS 0-93450
 Na, plasmon satellite struct. in (e,2e) process 0-96809
 Na₂O-B₂O₃-SiO₂-As₂O₃(As₂O₃) glasses, DC and AC resist., bipolaronic hopping cond. 0-88558
 Ni, photoemission spectra, valence band and core level satellite due to excitation of d electron 0-97408
 Ni_{1-x}Co_xS₂, elec. cond., thermoelec. power and optical meas. 0-59986
 NiS₂(Se_x), core-level and valence-band XPS 0-93450
 Pb granular film, Josephson coupled, resistive transition 0-88683
 Pb_{1-x}Sn_xTe:In, tunnelling impurity self-localisation, anomalous props. nature (Russian) 0-59915
 Pd, photoemission spectra, valence band and core level satellite due to excitation of d electron 0-97408
 Pr, localised 4f shell breakdown under press. 0-70411
 Se, amorphous layer, localised states in band gap 0-59928
 Se, glassy, localised electronic states, photoluminesc. and ESR studies 0-65501
 Se-Te-Sb glasses, electronic transport 0-88579
 Si, amorphous, glow discharge deposited, mobility edge calc. 0-80220
 Si amorphous, ion implantation, negative magnetoresist., localised mag. states 0-70731
 Si, amorphous, rel. to transport results, interpretation 0-80260
 Si, amorphous film, TSC, density of localised states distrib. 0-65587
 Si, impurity states, localised orbital approach 0-92851
 a-Si:H, depletion width determ. by analytical model 0-100445
 Si:H,B, amorphous, field effect and thermoelec. power 0-96924
 a-Si:H:F, depletion width determ. by analytical model 0-100445
 Si-SiO₂ interface, unwanted effects of ions in SiO₂ layers, review 0-92985
 SiO₂, thin film dielec., in MIM struct., interfacial props. rel. to non-stoichiometry 0-80399
 TiO₂, core levels, cryst.-field splitting, X-ray emission study 0-66328
 Ti, core level binding energies, UPS obs. 0-66388
 UO₂, electronic distributions by X-ray spectroscopy 0-97407
 UO₂, Mg K α and He(II) photoelectron spectra, origin from multi-configurational Dirac-Fock calcs. 0-66387
 V-Ti-C, high temp. carbide form., electron microscopy study 0-89228
 V₂O₅, core levels, cryst.-field splitting, X-ray emission study 0-66328
 V₂O₅:CuO-BaO glass, unpaired electron localisation, ESR study 0-66026
 W-Re amorphous alloys, phase-slip and localisation diffusion lengths 0-107747
 Zn, core levels, cryst.-field splitting, X-ray emission study 0-66328
 ZnSiP₂, electronic struct., X-ray spectroscopic investigation 0-108300
- localised modes in crystals** *see lattice localised modes*
localised states, electron *see localised electron states*
locomotives
see also railways
 wheel temperature in railroad service, effect of brake shoes 0-93660
loggers *see data loggers; recorders*
logging (recording) *see recording*
logic, formal *see formal logic*
logic circuit elements *see logic devices*
logic circuits
see also flip-flops; formal logic; logic devices
 nuclear radiation pulse counter control cct. (Spanish) 0-95508

logic design

truth-table look-up optical processing utilizing binary and residue arithmetic 0-69334

logic devices

optical logic with variable-grating-mode liquid-crystal devices 0-106613
 optical using nonlinear coherent coupler 0-58630
 semiconductor lasers, triggerable, light-coupled logic appl. 0-74360

long-range order

see also order-disorder transformations

p-alkoxybenzylidene-p-n-butylanilines, IR absorpt. spectra, elec. field effects, orientational order parameter determ. by IR dichroism 0-80778
 p-alkoxybenzylidene-p-aminocyananilines, IR absorpt. spectra, elec. field effect, orientational order parameter determ. by IR dichroism 0-80777
 alloy, binary, magnetic, interface struct., Monte Carlo simulation 0-60317
 alloys, binary, ferromagnetism and spatial long-range order 0-60159
 alloys, substitutional, electrical resist., long and short range orders effect 0-107761

cholesterol nonanoate, cyclohexanone admixture effect on mesophase order parameter, refr. index meas. 0-100165
 colouring problem on randomly ordered lattice, critical conc. existence for long range order 0-80519
 Coulomb systems, absence of long-range order with long-range potentials 0-70157

4-cyanobiphenyl/4-cyano-p-terphenyl liq. cryst. mixture, order parameters of dissolved dyes 0-100167
 cyanooctylbiphenyl, smectic A phase, X-ray diffr. study 0-79690
 EBBA, IR absorpt. spectra, elec. field effects, orientational order parameter determ. by IR dichroism, bend elastic consts. 0-80778
 EBBA, nematic, orientational order, effect of hexa-n-alkoxy-triphenylene disc-like solutes 0-79682

EBBA, orientational order in glassy and nematic phases, IR dichroism meas. 0-64891
 EBBA, Tsvetkov parameter, temp. depend. 0-88035
 Heisenberg multi-quadratic isotropic model, LRO, phase transf., exchange interactions (*Chinese*) 0-88756

α -In₂Te₃, 1 phase, order-disorder transform. for DO₂₂ struct., thermodynamic study 0-70155

interfaces, co-segregation of metallic and non-metallic impurities 0-60868
 Ising model, with long-range interactions, dynamical props. 0-100593
 liquid crystals, orientational order parameter, optical birefr. meas., polarisation field problems 0-79688

magnetic system, interactions, spirals and phase transitions with and without long range order 0-60350
 MBBA, IR absorpt. spectra, elec. field effects, orientational order parameter determ. by IR dichroism, bend elastic consts. 0-80778
 MBBA, nematic, flexibility gradient of fatty acid spin labels, EPR study 0-71181

MBBA, orientational order in glassy and nematic phases, IR dichroism meas. 0-64891
 MBBA, Tsvetkov parameter, temp. depend. 0-88035

ordered regions near macroscopic defects and percolation phase transform. in crystals (*Russian*) 0-92665
 PAA, Tsvetkov parameter, temp. depend. 0-88035
 PAP, Tsvetkov parameter, temp. depend. 0-88035

N-p-propoxybenzylidene-p-pentylaniline, orientational order in glassy and nematic phases, IR dichroism meas. 0-64891
 spinel compounds, 1:3 octahedral order, order-disorder transition, review 0-88079

two dimensional system of electrons in uniform neutralizing positive background, absence of cryst. order 0-103610
 Al superconducting film, transition to zero vorticity, long-range topological order 0-93039

Cr, lattice dynamics, improved Fieiek model 0-59598
 CsLi_{0.5}(Al,Fe)_{1.5}F₆ pyrochlore, Mossbauer contrib. to exam. of cationic order (*French*) 0-93224

Cu-Au alloys, vacancy and divacancy migration activation energies, elec. cond. meas. 0-88140
 Cu-Zn, rheological study of crystallographic order on creep (*French*) 0-97548

Cu₃Au, alloys, superlattice-fringe imaging theory, images formed from two beams 0-79649
 Cu₃Au, electrical resistivity and LRO, energy gap formation in Fermi surface 0-88533
 Cu₃Au, neutron irradi., displacement cascades, direct obs. method 0-107335

CuInS₈, sulphospinel electron diffr. and electron microscopy study, order-disorder transform obs. 0-88080
 Dy₂O₃-ZrO₂ phase diagram and long range ordering 0-93542
 Fe-Co-V(Ni), annealing effect on microstruct. rel. to mag. and mech. props. 0-89267

γ -Fe-Ni-Mn alloys, spin glass state, short and long range order investigation 0-65808
 Fe₃Al, alloys, superlattice-fringe imaging theory, images formed from two beams 0-79649

Fe₃Al, electrical resistivity and LRO, energy gap formation in Fermi surface 0-88533
 Fe₃Pt austenite, long range order parameter, temp. depend. discussion 0-97481

LaB₆C₂, ordering of B and C atoms in struct. 0-96481
 Mo, lattice dynamics, improved Fieiek model 0-59598
 3Nb₂O₇.8WO₃, circular diffuse scattering studied by 1 MV high resolution electron microscopy 0-59350

Nb₃Sn, powder metallurgically produced, microstruct. characts. 0-89233
 Ni₃Fe alloys, low-temperature specific heat, long and short range order effects 0-100339

Ni₃Fe, magnetocryst. anisotropy, annealing temp. depend. 0-103828
 V₁₂, mag. struct., long- and short-range order and Mossbauer spectroscopy 0-65803

Zr₂Al, deformed and irradi., lattice defects obs., superlattice dislocations and defect clusters 0-107261

Lorentz transformation

acceleration in Lorentz transformation, teaching 0-90639

contraction of metric standards 0-82638

EM transmission structures, relativistic foundation and network formalisms 0-58446
 fluxoid motion for Lorentz transform law with EM fields 0-67954
 hadronic jet phenomenon and Lorentz deformation 0-105806
 hadrons, extended, Lorentz deformation props., O(4) and light-cone coordinate systems 0-68354

light clock, special-relativistic slowing of clock rates 0-77613

Lorentz transformation continued

massless Euclidean Thirring field, four point Schwinger function, Lorentz group invariant forms (*German*) 0-90980
 massless particle fields, arbitrary spin, Lorentz transformation laws (*French*) 0-62823

O(3,1) Lorentz group, generating functions, integrity bases (*French*) 0-105803

physical system, model of space-time from set theory concepts 0-82660
 quantum fields in Lorentz basis 0-86565
 relativistic motion in a plane, teaching 0-101686

relativistic two fermion equations, Lorentz, parity and charge conjugation invariance 0-90976
 spinor theory via involutions, Lorentz group representation appl. 0-86607

string moving in uniform static external field, 2-D space-time surface 0-57087
 superluminal boost in x-direction in complex Minkowski space, tachyonic connections 0-105497

superluminal Lorentz transformations, imaginary units, motion of tachyon 0-86082
 vector laws of physics, reformulation 0-68036

vector product formulation of special relativity and electromagnetism 0-105496

Lorenz number

metals, liq., Wiedemann-Franz ratio 0-80243

semiconductor, Seebeck and Hall coeffs. Lorenz number, anisotropy, theory (*German*) 0-65608
 semimetals, degenerate, heat conduction, thermal EMF, Lorenz number anisotropy at low temp. 0-75549

spin glasses, elec. resist., thermal resist. and thermopower 0-65542
 thermal props. at high temp. 0-75536
 Ag, low temp. resist. and thermoelec. ratio, electron-electron scatt. contrib. 0-70670

Al, low temp. resist. and thermoelec. ratio, electron-electron scatt. contrib. 0-70670
 Au, low temp. resist. and thermoelec. ratio, electron-electron scatt. contrib. 0-70670

Cu alloys, liq., thermal cond. and elec. resistivity 0-103661
 Cu, liq., thermal cond. and elec. resistivity 0-103661
 Cu, low temp. resist. and thermoelec. ratio, electron-electron scatt. contrib. 0-70670

Cu powder, sp. ht. cond. and sp. elec. cond. meas., Wiedemann Franz Lorenz law (*German*) 0-92872
 In, liq., thermal props. at high temp. 0-75536
 K, low temp. resist. and thermoelec. ratio, electron-electron scatt. contrib. 0-70670

RuO₂, thermal conductivity meas., rel. to elec. cond. 0-65317
 Tl, liq., thermal props. at high temp. 0-75536

Loschmidt number *see constants***loss angle**

see also dielectric losses

Cd(NO₃)₂, phase transition, SHG, optical and dielec. meas. 0-71334

loss angle, dielectric *see dielectric losses***loss measurement**

compound glass optical fibres, total and scatt. loss coefficient meas. 0-69536
 epoxy/E-glass continuous fibre composite type 3M Scotchply, complex moduli, comparison of meas. with estimated bounds 0-93590

optical, of multi-mode fibres, non-destructive method 0-69550
 optical fibre cable vibration characteristics, fibre strain and optical loss meas. 0-99870

optical fibre connector loss evaluation by backscattering 0-58721
 optical fibre loss, dispersion and polarisation meas. by acousto-optical tunable filter 0-102855

optical fibre loss estimation using backscatter technique, time domain reflectometry theoretical assumptions 0-74508
 optical fibre splice insertion loss meas., backscattering method 0-58720
 optical fibre total loss spectra, precise meas., automatic meas. system 0-64169

optical fibres, backscattering method for attenuation and connection insertion loss meas., anal. 0-58675
 optical waveguide, loss measurement, nondestructive, using three prisms 0-106596

polyester/E-glass chopped fibre composites types PPG SMC-R25 and PPG SMC-R65, complex moduli, comparison of meas. with estimated bounds 0-93590

polyester/E-glass hybrid chopped/continuous fibre composite type PPG XMC-3, complex moduli, comparison of meas. with estimated bounds 0-93590

power loss of mag. materials under sinusoidal flux conditions 0-85348
 solar receiver radiative loss and eye hazard evaluation by Net-Radiometer 0-89673

superconducting magnets, analogue digital double integration joulemeter 0-57325
 Fe-Si, power loss and permeability meas. by means of Hall probes and stochastic ergodic correl. 0-86350

losses

see also dielectric losses; eddy current losses; heat losses; loss angle; magnetic leakage

alkali lime germanosilicate GRIN fibre prep., losses and geometrical props. 0-69560
 electro-optical light modulator with small nonactive losses 0-78981

fibre, single-mode, numerical aperture effects 0-69548
 glass, high GeO₂, zero material dispersion wavelength and waveguide props. 0-58733

image contrast loss in presence of chromatic magnification difference, numerical estimate 0-95823
 laser, homogeneously broadened with constant loss, optimum output efficiency 0-74403

lasers, homogeneously broadened CW type with nonsaturating lasers, optical extraction characts. 0-91770
 lens, gradient-index rod, aberrations in multimode optical fibre devices 0-69487

lens, gradient-index rod, appl. in optical fibre communication systems 0-69488
 lens guide, low-loss image transmission 0-91872

low-loss graded-index fibre, 3 km and 10 km preform design and modified CVD method 0-58746
 methylundecanhydride hardened phenol formaldehyde resin, hardening kinetics and mech. losses 0-66520

inversion layers continued

- InSb MOS struct., capacitance of n-channel inversion layers, elec. field effects 0-80393
 n-inversion layers, (001), K_1 -depend. of subband energies 0-103738
 n-Si, (111) inversion layers, valley splitting, Shubnikov de Haas oscils. 0-65698
 Si, (100) inversion layer, electromigration in two dimensional electron gas, driving force 0-84441
 p-Si, (100)-oriented, n-channel inversion layers, MOS field-effect devices, mag. quantisation effect on surface capacitance 0-70834
 n-Si channel (100) inversion layer MOSFET, valley splitting, conductivity 0-70840
 n-Si inversion layers, electronic g-factor, spin-split Landau levels 0-80346
 Si inversion layers, harmonic generation due to hot electrons 0-65694
 Si, inversion layers, nonmetallic cond. at low temp. 0-70833
 Si MIS-inversion layer solar cells 0-76632
 n-Si MOSFET, resist. temp. depend. at liq. He temps. 0-80391
 Si MOSFET, surface quantum states, two-dimensionality of many-body effects 0-103740
 p-Si, n-channel inversion layers, mag. susceptibility of electrons in presence of quantising mag. field. 0-75650
 Si, phase diagram in strong mag. fields 0-88492
 Si surface, MOS struct. band structure, minigaps, magnetoresistance, cond., space charge layers 0-92980
 Si, thermally oxidised surfaces, electron mobility in inversion and accumulation layers, MOS devices 0-103753
 Si, velocity-field curves for surface free carriers, meas. on IGFET 0-60095
 Si-SiO₂ boundary, surface charge transport in valence band of Si 0-70789
 Si-SiO₂ in MOSFETs, inversion layer carrier mobility, theory 0-60094
 Si-SiO₂ interface, (001) vicinal planes, minigaps in inversion layers, far IR absorpt. meas. 0-107919
 Si-SiO₂ interface, remote polar phonon scatt. in Si inversion layers 0-80095
 Si-SiO₂ inversion layer, n-channel, anomalous magnetoresist., model 0-96996
 Si-SiO₂ MIS systems, dynamic props. of switching, appl. to charge transfer devices 0-92997
 Si-Sn heterojunction, RHEED, Mossbauer spectroscopy and I-V characts. 0-70828
 Ta₂O₅ inversion layers for Si solar cells 0-94075
 ZnO-grainboundary-ZnO junction in ceramic varistor, capacitance-voltage characts. 0-65689

invertors

- solar energy DC-AC inverter design, effect of meteorological conditions, computer simulation 0-61373
 variable speed wind power generator, control strategy for 3-phase output (French) 0-76591

iodine

- see also nuclei with
²⁹¹I¹²⁷ early solar system chronometer 0-62043
 adsorbed on Ag(111), photoelectron diff. aximuthal patterns, struct. sensitivity 0-107644
 adsorption on W(100) at room temp., LEED and AES study 0-84389
 air monitoring systems for radioiodine and inert gases, evaluation 0-95480
 atom, He (I) photoelectron spectrum by I₂ photodissoc. 0-83325
 atomic vapour, self-induced transparency and reson. self focusing 0-64114
 atoms, Mossbauer isotopes, isomer shift 0-78573
 chemisorbed on Au surface, AES and LEED study 0-100405
 chemisorbed on zeolites, Raman spectra 0-93301
 chemisorption, on Ag clusters, UPS obs. 0-84830
 diffusion in copper phthalocyanine polycryst., amorphous cpd. prep. (Russian) 0-66016
 impurity in Li aluminosilicate glasses, ESR spectra 0-66027
 laser, methyl iodide photodissoc., kinetic model, cross-section calcs. 0-58530
 laser, photodissociated by nucl. induced excimer fluoresc. 0-78846
 laser, photodissociation, characts. of dye comps. for passive switches 0-91826
 laser, three-level, pumped by CW dye laser 0-63993
 laser radiation, 2nd, 3rd and 4th harmonic generation 0-91844
 lead phthalocyanine-O₂(I), Schottky barrier effect on AC current response 0-75623
 liquid, static structure factor, neutron diffraction 0-103236
 metallic, mol. and monatomic phase, elec. resist. at high press. and low temp. 0-65638
 molecular ion cluster emission in SIMS, parity rule applies. (French) 0-63882
 molecular laser, optically pumped, review 0-58519
 molecular static polarisability, ab initio SCF wave functions 0-74106
 molecular vapour, saturable absorpt., self-focusing and nonlinear susceptibility 0-83647
 molecule, B-X fluoresc. band system, intensity and relative band strengths meas. 0-102540
 molecule, B-X lines, Franck-Condon factors, Ar⁺, Kr⁺ and He-Ne laser excitation 0-58320
 molecule, B-X system, mol. const. and Dunham expansion parameters 0-87095
 molecule, B-X transitions, rot-vibr. hyperfine coupling const., extension to other levels 0-63625
 molecule, fluorescence, CW dye laser emission wavelength locking by intracavity gain 0-99721
 molecule, high-resolution saturated absorpt. spectroscopy with short light pulse coherent trains 0-64110
 molecule, in Ar, emission spectrum interpretation 0-95634
 molecule, laser fluoresc. state selected and detected mol. beam mag. reson., hyperfine transitions 0-63731
 molecule, model potential SCF calcs. 0-95528
 molecule, photodissoc., atomic He (I) photoelectron spectrum 0-83325
 molecule, photolytic cage effect in gas phase 0-81345
 molecule, polarisability anisotropy, laser assisted mol. beam spectroscopy 0-78646
 molecule, RF optically heterodyned saturation spectroscopy, reson. degenerate four-wave mixing 0-74211
 molecule, vac. UV absorpt. cross section 0-91574
 nonlinear spectroscopy, coherent background noise elimination from saturation spectrosc. signals using freq. offset pump 0-62733

iodine continued

- polyacetylene-I₂, synthesis, elec. cond., thermoelec. power 0-60016
 polyacetylene-I₂, dc microwave cond., permittivity 0-107843
 polyacetylene-I₂, electronic excitations, momentum depend., EELS study 0-76121
 polyacetylene-I₂, electronic structure, XPS and UPS meas. 0-66385
 polyacetylene-I₂, NMR struct. investigation 0-108082
 polyacetylene-I₂, reson. Raman spectroscopy 0-66208
 polyethylene-I₂, films, electron-beam induced carrier mobility and elec. breakdown 0-80429
 polystyrene-I₂, films, electron-beam induced carrier mobility and elec. breakdown 0-80429
 polystyrene-I₂ films, thermally stimulated discharge, I conc. and polarisation temp. depend. 0-107937
 polyvinylquinazoline-I₂ complexes, absorpt. spectra and elect. cond. 0-92891
 radioisotope adsorption by minerals 0-83203
 reactor poison, stress corrosion cracking of Zircaloy LWR fuel rod cladding 0-71810
 thyroid, accumulation curve of radioiodine and its role in diagnostics (Hungarian) 0-94341
 thyroid gland, X-ray fluoresc. tomography 0-61664
 Zircaloy cladding stress corrosion cracking due to I (Japanese) 0-78361
 Ar⁺ and Ar⁺-Kr⁺ ion lasers, I₂ stabilized, beat frequency 0-95916
 Ar⁺ laser 582 THz stabilisation by I₂ cell, improvements 0-102741
 BWR, primary containment vessel, spray I₂ removal characteristics 0-73972
 Fe-I system, photochemical conversion efficiency 0-71923
 He-Ne laser stabilisation, I₂ absorption cell power densities 0-99767
 He-Ne laser stabilisation by I₂ 612 nm saturated absorption 0-99765
 He-Ne laser stabilisation by I₂ 611.8 nm saturated absorption 0-99766
 Hg-Tl-I discharges, 50 Hz, axial segregation effect on elec. field strength 0-59320
 I II, reson. lines, oscil. strengths determ. by absorption method 0-58214
 I⁻, 3d⁵4f config., collapse of 4f electron, X-ray spectral obs. (Russian) 0-58204
 I⁻, photo-oxidation at n-TiO₂ electrode 0-81331
 I-CdI₂ mixture, molten, nuclear spin relax. 0-88887
 I⁺-He laser discharge, positive column, particle densities 0-103215
 2I+He→I₂+He, energy transfer mechanisms studied using trajectory calcs. and Monte Carlo method 0-66785
 I₂, efficient laser action on 342 nm band, ArF laser pumping 0-99703
 I₂ molecule B-X electron transition, during Cu vapour laser optical pumping (Russian) 0-78845
 I₂, quenching of laser-excited O₂ 0-99515
 I₂ seeded in supersonic free jet, collision-induced rotational relax. 0-102556
¹²⁹I₂, energy levels near B-state dissociation limit, two-photon spectrosc. obs. 0-106367
¹²⁹I₂, frozen soln. in o- or p-xylene, Mossbauer effect obs. 0-78637
 I₂-benzene, π - σ charge-transfer complex, frozen soln., Mossbauer spectra obs. 0-91655
 I₂-methylated benzene, π - σ charge transfer complex, frozen soln., Mossbauer spectra obs. 0-91655
 I₂-pyridine, π - σ charge-transfer complex, frozen soln., Mossbauer spectra obs. 0-91655
 I₂-triethylamine, n - σ charge-transfer complex, frozen soln., Mossbauer spectra obs. 0-91655
 I₂+acetylene, laser-induced 1,2-diiodoethylene form., isomerisation 0-85157
 I₂+Cu(²D), beam-gas chemiluminesc. reactions 0-85151
 I₂+K₂(C₂), ionisation reactions, absolute cross sections 0-99565
 I₂(I₂⁺)(I₂⁻), HF and SCF calcs., pot. curves, electron affinity and quadrupole moment determ. 0-95527
 I(²P_{1/2,3/2}), from ICN A-state photolysis, branching ratio wavelength depend. 0-81335
¹²⁷I, A=123, 125, labelling of cyclosporin A, prep. and biodistrib. 0-85496
¹²⁷I, A=131-2, comparative effects in rat thyroid glands 0-104670
¹²⁷I, prep. from gaseous TeF₆, nuclear medicine appl. (French) 0-98137
¹²⁷I prod. from ¹²⁷(p,n)¹²³Xe→¹²⁷I, at 58 MeV 0-94369
¹²⁷I, production in LASL radiochemistry hot cells 0-72326
¹²⁷I-Na, thyroid scintigraphy, clinical comparative study with ^{99m}TcO₄⁻ (Japanese) 0-81728
¹²⁷I, determ. of exposure rate constant using a scintillation detector 0-89863
¹²⁷I in the thyroid, 2-probe meas. method 0-81718
¹²⁵I, intramol. effects of decay in o-iodotyrosine 0-108973
¹²⁵I, intranuclear atoms not bound to DNA, radiotoxicity 0-104655
¹²⁵I labelled estradiol, a γ -emitting estradiol analogue that binds to the estrogen receptor 0-61697
¹²⁵I labelled estrogen derivatives 0-81734
¹²⁵I labelled human serum albumin, geometrical dilution (French) 0-104742
¹²⁵I labelled prostaglandins (Hungarian) 0-94368
¹²⁵I photons, absorbed fractions in the thyroid 0-109032
¹²⁵I, release in autoclave sterilization of radioimmunoassay kit (Japanese) 0-81727
¹²⁵I seed implants in prostatic cancer, preoperative extended field radiation 0-72303
¹²⁵I, shielding of (Japanese) 0-63404
¹²⁵I, variation of γ -counting efficiency with sample composition 0-83238
¹²⁷I₂, Doppler-free optoacoustic spectroscopy 0-57396
¹²⁷I₂ rovibronic absorpt. lines, hyperfine struct. 0-78596
¹²⁷I₂ saturated absorption for He-Ne laser stabilisation, wavelength international comparisons 0-95872
¹²⁷I₂ stabilised He-Ne laser 0-106544
¹²⁷I₂ stabilised ion laser, beat freq. intercomparisons at 514.5 nm 0-74338
¹²⁹I, hyperfine struct. and isotope shift of 1.3 μ m transition 0-102486
¹²⁹I in bovine thyroid glands, activation anal. obs. 0-94380
¹²⁹I, mag. hyperfine field in Fe, press. depend., nucl. gamma reson. 0-71256
¹²⁹I photons, absorbed fractions in the thyroid 0-109032
¹²⁹I radioactive waste, fixation with Portland cement, radiation stability tests 0-83200
¹²⁹I, tandem accelerator mass spectrometry 0-86494
¹²⁹I₂, ¹²⁷I₂, ¹²⁷I₂ high resolution saturated absorption spectra at 633 nm using He-Ne laser 0-95637
¹²⁷I₂, complete hyperfine spectrum obs. at 612 nm 0-95638

iodine continued

- ¹²⁹I₂, selective excitation and separation in I₂+C₂H₂ laser induced chem. reaction 0-68962
¹²⁹I₂, rovibronic absorpt. lines, hyperfine struct. 0-78596
¹³¹I, age-related radiosensitivity obs. of guinea pig thyroid glands 0-104671
¹³¹I, behaviour during rinsing in in-pile loop after fission product release expt. 0-73879
¹³¹I concentrations in air, milk and antelope thyroids in southeastern Idaho 0-89871
¹³¹I, estimation of γ dose to gastric wall after administration of isotope (Japanese) 0-98141
¹³¹I manipulated in syringes, radiation exposure obs. 0-67252
¹³¹I produced radiation, low-dose, somatic mutations induction in Tradescantia 0-72266
¹³¹I, thyroid uptake determ. (Hungarian) 0-94339
¹³¹I treated patients, monitoring of I excretions and used materials 0-89873
¹³¹I-ortho-iodohippurate absorbed kidney dose calc., literature review 0-76841
I₂⁺+He, low energy collisions, energy redistrib. 0-63765
I₂⁺+He(Ne), energy depend. of collision induced intramolecular energy transfer 0-83470
KBr:I⁻, OH⁻, luminesc. of interstitial atomic H 0-89062
KCl:I⁻, interstitial atomic H centres, formation kinetics and struct., MO calcs. and EPR studies 0-75854
KCl:I⁻, low-temp. heat capacity enhancement due to impurities 0-107442
RbBr:I⁻, OH⁻, luminesc. of interstitial atomic H 0-89062
RbCl:I⁻, interstitial atomic H centres, formation kinetics and struct., MO calc. and EPR studies 0-75854
Se:I, vitreous, crystn, kinetics determ. (German) 0-79936

iodine compounds

- copper phthalocyanine-iodine, amorphous cpd. prep. by I₂ diffusion in polycryst., triplet EPR signals obs. (Russian) 0-66016
hydration complexes, gas phase, electrostatic calcs. 0-100055
iodide, charge transfer to solvent spectra, spectral shift data, Madelung const. determ. 0-85204
I+H₂, gas phase H-atom transfer reactions, struct.-reactivity correl., pot. energy surfaces 0-104433
I₂-quinoline (pyridine) complexes, stability const. determ. by spectrophotometric methods 0-87056
I, Ar⁺, product state distrib. and binding energy 0-63857
I Br, B² Π (O⁺) excited state, laser-induced fluoresc. 0-58309
I Br-benzene in n-decane soln., IR line broadening by chemical exchange 0-87111
ICN, A-state photolysis, I(²P_{1/2,3/2}) branching ratio wavelength depend. 0-81335
ICl A² Π (1), excited, laser induced fluorescence, quantum-resolved dynamics of excited states 0-69178
ICl(Br), rot. spectra in millimeter wave region, rot. transitions obs., equil. const. determ. 0-78607
IF emission spectrum and form. kinetics in electron-beam-produced plasma 0-102533
IF, in solid Ar, emission and excitation visible spectra at 12K 0-87137
I, He⁺, product state distrib. and binding energy 0-63857
I, He⁺ Van der Waals complex, vibr. relax. processes and decomposition 0-63765
I, Ne⁺, product state distrib. and binding energy 0-63857
IO, free radical, Ar matrix absorpt. and emission spectra, mol. vibronic states obs., spectroscopic const. determ. 0-83387
IO₂⁺, adsorption desorption by TiO₂ suspension, kinetics, relax. technique 0-93804
Mg(IO₃)₂.4H₂O, crystal struct., unit cell, X-ray study 0-59447
Ni-I single crystals, mag. and dielectric props. 0-93095

ion-atom collisions see atom-ion collisions

ion beam effects

- see also ion-surface impact; ionoluminescence; plasma-beam interactions
accelerator irradiation, heavy ion irradiation damage 0-100291
amorphisation due to ion bombardment, SRO struct. 0-79844
atomic transport and conc. profiles 0-59723
brain, irradiation with C ions, recovery from pot. lethal damage, rat expts. 0-72234
crystal, electron-positron pair production coherent effect 0-88222
crystal surface morphology development during sputter erosion 0-88414
CTR first wall, high power ion-irrad. test 0-78443
diamond, accelerator irradiation, heavy ion irradiation damage 0-100291
electron gas coding influence in ion-bombarded layers 0-108272
electron-collision cross-section data for atom or molecule, rel. to radiation physics 0-63829
energy spike development and quenching depend. on thermal diffusion 0-88367
fast molecular ions, transmission through thin foils 0-65065
field-ion microscope specimens, field corrosion caused by polymer gaskets 0-57425
garnet epitaxial films, easy magnetisation axis orientation, ion bombard. effects 0-60383
graphite, conditioning of surface by atomic H 0-93665
graphite, ion bombarded, light gases, structural study using TEM 0-92570
heavy ion induced collective electron emission 0-80926
heavy ion stopping, prediction using ion effective charges 0-88229
heavy ions, low vel., channelling stopping power oscils. 0-103404
heavy ions in solids, electronic stopping cross-section, Z₂-oscils., target struct. effects 0-70285
intense ion beam propag. in z-discharge plasma channels, straight and tapered 0-83948
ion acoustic solitons in beam plasma system with nonisothermal electrons generated by ion-beam 0-103151
ion impact induced shock processes in solids 0-89104
isocitrate dehydrogenase from Azotobacter vinelandii, essential amino-acid residues identification 0-76538
kidney cells, inactivation by high-energy monoenergetic heavy-ion beams 0-72256
magnetically insulated coaxial line, ion beam effects 0-87297
mammalian cells, cultured, interpretation of mutation and inactivation obs. 0-72229
material modification, conf., Budapest, Hungary (Sept. 78) 0-86038
metal, blister formation due to the ion irrad. 0-65072

ion beam effects continued

- metal, heavy ion bombard., void conc., effect of implanted He (Russian) 0-88213
metal, light element implantation, radiation damage review 0-88219
metals, energy loss of heavy nonrelativistic ions in matter, semiclassical theory 0-84224
metals, irradi., mechanism of formation of vacancy dislocation loops (Russian) 0-65053
metals, mixed dumbbells, ion channelling studies 0-70277
mica, nuclear track microfilters, prod. and props. 0-96574
milling, anomalous sputter yield behaviour 0-108624
oscillatory wake, fast ion in solid, trapped electron binding energy, RPA calc. 0-96575
particle accelerator target heating by ion beam, thermal characts. (Japanese) 0-99374
polystyrene, energy losses and straggling for H⁺ and He⁺ beams (Russian) 0-84226
Pyrex, ion bombardment, form. of cpds., IR spectrosc. exam. (German) 0-88173
recoil atoms of heavy ion reactions, local lattice damage, TDPAD meas. 0-84220
recoil mixing in solids by energetic ion beams 0-59531
soliton solution in the wake interaction due to virtual plasmon exchange 0-65108
sputtering induced topography on solids, energetics and kinetics 0-88220
stainless steel, machine faceted, low-energy ion erosion studies 0-80923
steel, mild, surface hardness improvement by dynamic recoil implantation 0-61008
steel, stainless, stress corrosion cracking and microhardness, effect of bombardment by He⁺, Ni⁺ and Cr⁺ 0-85087
steel, stainless, type EP838 ion irradiated, surface structure changes during post-irradiation heating (Russian) 0-75272
steel, stainless 316, Fokker-Planck eqn. describing evolution of interstitial loop microstruct. during irradiation 0-107215
steel, stainless 316, soln. annealed, cavity alignment and precipitation during dual ion bombardment 0-70273
steel, stainless type 316, in-situ HVEM studies under ion beam irradiation 0-103396
Tokamak plasma, beam driven currents, trapped electrons effect 0-70011
toroidal plasmas, beam driven currents, trapped electrons effect 0-70011
transient magnetic field effects on particles slowing in solids 0-65106
V79-spheroids, survival and kinetic response after heavy ion beam exposure 0-104651
Vicia faba growth reduction, RBE of d(50)-Be neutrons and 650-MeV He²⁺ 0-98025
void, and interstitial loop evolution in pulsed fusion reactors 0-84217
yeast cells, dried, inactivation by accelerated heavy ions of very high LET 0-108965
Ag, energy losses and straggling for H⁺ and He⁺ beams (Russian) 0-84226
Ag films, effect of Ar- and N-ion bombardment on texture (Russian) 0-107338
Ag-Ni supersaturated metastable solid solns. formed by ion beam mixing 0-107425
Ag-Pd alloys, inert gas ion bombardment, dynamic surface composition changes, AES obs. 0-60745
Al, Al ion irradiated, void swelling and annealing of voids, electron microscopy study 0-88216
Al, annealed and powder sintered (SAP 895), sputtering under D⁺ and ⁴He⁺ bombardment, microstruct. effects study 0-84821
Al, energy losses and straggling for H⁺ and He⁺ beams (Russian) 0-84226
Al film, deform. under He ion bombardment 0-65073
Al-Ge (0.1 wt.%), channelling meas. of Al interstitial atom trapping by Ge atoms 0-59537
Al-Mg, Si alloy, void form. under different precip. conditions, after Al ion irrad. 0-59529
Au, energy losses and straggling for H⁺ and He⁺ beams (Russian) 0-84226
Au film, surface craters induced by displacement cascades 0-107344
Au, heavy ion irradiated, cascade energy density effect on defect cluster type 0-107340
Au-Ag (35 at.%), dechannelling of energetic He ions at dislocations 0-70275
Be, blisters due to He irrad., proton backscatt. study 0-75273
Be, irradiated with He⁺ at 20 keV, surface damage and gas trapping profile meas. (French) 0-84218
C thin foil, irradiation with 1.2 MeV Ar⁺, electron diffraction study 0-103397
CdS, defect struct. and config. produced by irrad., elastic scatt. expts. 0-84178
CdS, electron-hole pairs behaviour in energetic ion tracks 0-65457
Cr film, evaporated, concurrent ion bombard. effects 0-80142
Cr film, obtained by thermo ionic precipitation, phase composition, lattice parameters (Russian) 0-96756
Cu, blisters due to He irrad., proton backscatt. study 0-75273
Cu, crystalline reorientation following ion bombard. 0-70269
Cu, energy losses and straggling for H⁺ and He⁺ beams (Russian) 0-84226
Cu, ion bombard. by 5 keV Ar⁺, sub-surface damage 0-103399
Cu, irradiated with 20 keV He⁺, surface damage and gas trapping profile meas. (French) 0-84219
Cu, irradiation with O₂ ions, defect production and annealing 0-88214
Cu, pyramidal structures, development on ion bombarded surfaces 0-84177
Cu, surface topographical features formed by ion bombard., crystallographic depend. 0-70266
Cu, vacuum deposited layer, ion bombardment induced preferential orientation 0-100290
CuCl, electron-hole pairs behaviour in energetic ion tracks 0-65457
Fe-B amorphous alloy, fast neutron and ²³⁵U fission fragment irrad. 0-100288
Fe-Cr-Ni (19, 13 wt.%), austenitic, Ni⁺ ion irradiated, multiple dislocation loops (French) 0-65064
GaAs, electroluminescent study of irrad. induced struct. damage, athermal annealing 0-108280
GaAs, ion damage, TEM study of laser annealing 0-88215
GaAs, surface cryst. regularity by X-ray photoelectron diff. 0-89112
(Gd, Bi)₂ (Fe, Ga)₂O₁₂ magneto-optic LPE garnet films, high-energy heavy ion irrad., props. 0-71390

low-temperature techniques continued

- TEM, analytical, contamination reduction using liq. N₂ cold trap assembly 0-101056
 thermal conductance measurement apparatus, for insulating mechanical supports 0-82772
 thermal conductivity meas. under uniaxial compression 0-105653
 tissue temperature simulation in cryosurgery 0-85355
 C resistors for low temp. thermometry 0-86308
 CePd₃-Er, dil., low field mag. susceptibility, electro-nuclear effects, rel. to thermometry 0-60189
 Ge and Ge-diamond bolometers operated at 4.2, 2.0, 1.2, 0.3, 0.1K, design and construction 0-77868
 H₂ atoms trapping and thermal detection using superconducting magnet of low temp. 0-73396
 He cooling systems, forced flow, numerical anal. of heat-induced transients 0-82773
 He level gauge, with semiconductor sensor 0-57277
 He, liq., appl. of gas oscillation to pressurisation in storage vessel 0-57305
 He liquefiers and refrigerators, cryogenics of Sulzer, Switzerland 0-82769
³He gas thermometer secondary standard for 0.5 to 40K 0-82762
 N₂ liq., decanting siphon using self-opening valve 0-57310
 NbTi-Cu, supercond. composite, use in temp. and heat transfer coeff. meas. 0-77780
¹¹⁷Sn, ¹¹⁹Sn, low temp. NMR thermometry 0-82775

LPE see liquid phase epitaxial growth

LS coupling see Russell-Saunders coupling

LSA see limited space charge accumulation

LSI see large scale integration

lubrication

see also friction

- bearings, strength and damping coeffs. of lubricating oils, vibration diagnostics (*Russian*) 0-97592
 boundary lubrication characteristics, of lubricants used in cold rolling of steel, SEM 0-85068
 composite materials, water lubrication, wear studies 0-60984
 contact, frictionally heated, thermoelastic deform. 0-83764
 cutting fluid, hydrolysed polyacrylonitrile based, operational characteristics 0-89359
 cylinders in elastohydrodynamic contact, lubricant layer thickness and resistance to rolling 0-96236
 deformation broaching of difficult-to-form metals 0-108473
 dry film, parylene (vacuum deposited polymeric coating) appl. 0-108607
 elastohydrodynamic lubrication, 2-D random surface model for asperity contact 0-66675
 elastohydrodynamic lubrication, non-Newtonian effects of volume relaxation 0-103009
 elastohydrodynamic traction, granular behaviour 0-103008
 elastohydrodynamic traction, non-Newtonian thermo-viscoelastic, from combined slip and spin 0-103043
 film rupture in laminar and turbulent lubrication, inertia forces effect 0-74813
 hydrodynamic contacts, films, elastic properties 0-88239
 hydrodynamic lubrication, free boundary problem, variational inequalities 0-62475
 hydromagnetic squeeze film between porous circular disks with velocity slip 0-74997
 liquid-friction bearing tester, description and improvements over existing designs 0-64503
 machine bearings, turbogenerator, with hybrid hydrostatic hydrodynamic lubrication, behaviour in laminar and turbulent conditions (*Italian*) 0-81208
 metalworking, role of friction, and energy saving in deep drawing 0-76271
 oil film formation, techniques 0-97597
 oil seal, static contact shape and kinetic behaviour 0-97598
 polymer-containing metal-filled lubricant, tribological study on steel 0-104301
 porous boundaries, Reynolds eqn., generalised form. 0-87803
 Reynolds equation at very low spacing, compressible, numerical soln., factored implicit scheme, mag. recording appl. 0-92183
 self-excited vibrations in lubricated friction 0-58984
 steel, friction and wear during hot forging 0-89358
 steel, mild and type EN31, eval. of cold rolling oils and boundary lubrication characts. by SEM 0-85068
 steel bearing, surface-ground, residual stress fatigue property comparison 0-60975
 testing, test machine 0-76452
 thin film, viscous, between two nearly parallel walls, temp. distrib., convection effects 0-83801
 tribology, material aspects in manufacturing processes 0-81210
 turbogenerator bearing oil film damping and stiffness coefficients determ. for dynamic behaviour stability study (*Italian*) 0-106762
 viscoelastic fluid lubrication, slider-bearing config., non-Newtonian normal stresses 0-69753
 wear, lubricated, contrib. to theory 0-88257
 wear debris examination, oil anal. techniques, appl. to plain bearing materials study 0-97596
 zinc dialkyldithiophosphate surface film, prep. and nature 0-104300
 Al alloy granules, lubricants for rolling 0-60980
 Al boundary lubrication, inelastic electron tunnelling spectroscopic study 0-70302
 Au contact surface by plasma-deposited thin films of fluorocarbon polymer 0-89157
 Cd film, dry lubrication on C steel, tribological behaviour 0-89364
 Cu pin-on-disc friction and wear under boundary lubrication, dissolved O₂ effect 0-76365
 MoS₂, solid lubricant, antifriction and elec. props. depend. on oxidation temp., dopant influence 0-108584
 NbSe₂, solid lubricant, antifriction and elec. props. depend. on oxidation temp., dopant influence 0-108584
 Si wafers, saw damage reduction in lubricant environment 0-108585
 Ti alloys, lubrication by chloroparaffins, friction and wear (*Russian*) 0-93657
 WS₂, solid lubricant, antifriction and elec. props. depend. on oxidation temp., dopant influence 0-108584

Luder's bands

- Zircaloy, annealed, neutron irradiated, inhomogeneous deform. behaviour 0-85014

Luder's bands continued

- Al bicrystals, isoxial, fatigue crack initiation in grain boundary affected regions (*Japanese*) 0-89338
 Cu-Ni-Al (5, 2.5 at.%), precip. hardening (*Japanese*) 0-71663
- Ludwig-Soret effect** see diffusion in solids
- luminescence** see brightness
- luminescence**
 see also cathodoluminescence; chemiluminescence; electroluminescence; fluorescence; fluorescent screens; ionoluminescence; luminescence of gases; luminescence of liquids and solutions; luminescence of solids; luminescent devices; phosphorescence; phosphors; photoluminescence; sonoluminescence; stimulated emission; superradiance; thermoluminescence; triboluminescence
 bacterial single cells, bioluminesc. obs. 0-108860
 benzoxazole, aromatic derivatives, spectral luminesc. and lasing props. rel. to electronic struct. 0-99519
 bifurcated fibre luminometer for inaccessible or hazardous location 0-62712
 bioluminescence of firefly larva, circular polarisation 0-94441
 circularly polarised, from model molecular system 0-63705
 low temperature luminescence spectroscopy using pulsed dye laser (*Czech*) 0-86445
 molecular electronic spectra, pure elec. quadrupole transition polaris. 0-63691
 moving acceptors, direct energy transfer, decay law 0-89045
 spectroscopy, refractive index correction, quantum efficiencies calc. 0-86444
 two-chromophore systems, circularly polarised luminescence 0-63705
 Ca²⁺+HCl, reaction performed under high resolution, luminescence obs. 0-95662
 Sr²⁺+HCl, reaction performed under high resolution, luminescence obs. 0-95662
- luminescence chambers** see scintillation chambers
- luminescence of gases**
 2,5-diphenyl-1,3,4-oxadiazole, vapour, spectral, fluoresc., photochem. and laser props. 0-106344
 2,5-diphenyl-1,3-oxazole vapour, spectral, fluoresc., photochem. and laser props. 0-106344
 2,5-diphenylfuran vapour, spectral, fluoresc., photochem. and laser props. 0-106344
 luminous flares, heat of radiation calcs. (*German*) 0-68154
 POPOP vapour, spectral, fluoresc., photochem. and laser props. 0-106344
 pyrimidine, vapour, phosphoresc. 0-83408
 smear samples, simple and rapid meas. of α -rays using air luminesc. 0-106243
 p-terphenyl vapour, spectral, fluoresc., photochem. and laser props. 0-106344
 Ar, excitation by pulsed electric discharge, luminescence obs., time resolved spectra meas. 0-102482
 H, diffusion coeff., in H₂, luminesc. intensity meas. 0-103098
- luminescence of inorganic solids**
 alkali cyanides, mol. excitons, X-ray excited emission spectra obs. 0-66287
 alkali halide, dynamics of nonrelaxed and self-trapped holes (*Russian*) 0-80607
 alkali halide crystals, activated, physical phenomena and optical data processing appl. (*Russian*) 0-80819
 alkali halide crystals, triboluminesc. spectra 0-66312
 alkali halides, emission band of F-centre 0-76071
 alkali halides, irradiated, formation of Z centre 0-103326
 alkali halides, Z₁-centres, peculiarities of thermolum. 0-103999
 alkali metal halides, X-ray induced colour centre and halogen aggregate form. 0-96565
 alkali-alumino-phosphate:U, rontgenoluminesc. and fluoresc., radiative transitions obs. 0-103977
 alkaline earth halides:Eu²⁺, fluorescence lifetime and quantum efficiency for 5d-4f transitions 0-100681
 alkaline earth oxide, photon multiplication and secondary electron-hole pairs generation (*Russian*) 0-66262
 CdS, green edge luminescence spectrum, temp. depend. 0-108274
 ceramic materials, thermoluminesc. dating, comparison of results 0-84791
 chalcogenide glasses, Luminescence, temp. depend. rel. to nonradiative transitions 0-71485
 chalcogenide glasses, optical versus transport processes. 0-84449
 diamond, Jahn-Teller coupling at neutral vacancy 0-71453
 diamond, natural type-IIb, single dislocations, cathodoluminescence obs. by STEM 0-80871
 diamond, van Hove singularities, absorpt. and luminesc. electronic-vibr. spectra 0-70639
 diamonds, synthetic, polarised infra-red cathodoluminescence 0-89073
 direct gap semiconductors, gain spectrum of electron-hole liquid 0-66279
 dosimeter glass, radiophotoluminescence intensity change by intense laser light 0-89050
 exciton condensation, light scatt. by electron-hole drops 0-84435
 exoemission phenomena, TSC, thermionic emission, book contribution 0-80954
 glass:Nd³⁺, spectral props. (*Chinese*) 0-60645
 glass, electron migration and spectral relax., random-walk model 0-80280
 glasses, elec., mag., and optical props., conference, Troy, NY, USA (Aug. 1979) 0-105417
 glasses, non-radiative recombination at valence-alternation pairs 0-89048
 II-VI semiconductor, resonant secondary emission spectra, relax. of energy and polarisation 0-93331
 III-V multilayer structure, as-grown, assessment of defects by differentiated cathodolum. topography 0-59819
 III-V semiconductors, optical transitions, effect of perturbed k-selection and gap shrinkage 0-66257
 III-V semiconductors, radiative recomb., optical evaluation review 0-60647
 III-V semiconductors epitaxial structures as wide-gap substrates, minority carrier diffusion length determ. by photoluminesc. 0-103992
 inert gas crystal, lattice vibr. and radiative transitions of implanted ions (*Russian*) 0-69098
 ion-surface collisions, luminesc. accompanied by ion implantation 0-60683
 ionic crystal, fundamental luminescence at high ionisation levels (*Russian*) 0-103985
 metaphosphate glass: Nd³⁺, Yb³⁺, luminesc., energy transmission and migration between Nd³⁺ and Yb³⁺ 0-66297

luminescence of inorganic solids continued

- MIM cathode, local electron emission and electroluminescence patterns obs. 0-108327
- mixed fluoride crystals, nucl. radiation effects 0-80831
- molybdates, alkaline earth, U activated, scheelite struct. luminesc. props. vibr. modes and quenching temp. 0-60651
- optical fibre, neutron and gamma induced transient absorpt. and luminesc. 0-58763
- phosphate glass: Yb³⁺, luminesc. band struct., chronoscopic study at 4.2K 0-60663
- phosphors, cathodoluminesc. investig., appl. to cathode ray tube screening 0-108282
- photographic emulsion, luminescence rel. to latent image 0-73498
- quartz, luminescence centres at 396 and 280 nm 0-103996
- rare earth double orthophosphates with alkali metals, conc. depend. of luminesc. props. 0-100673
- rare earth double orthophosphates with alkali metals, spectroscopic obs., struct. and chem. nature 0-100674
- rare earth germanates, K₂O₃-GeO₂ system cpds., physicochem. characts. 0-97469
- rare earth oxyhalides: Eu³⁺, fluorescence spectra obs. (French) 0-89042
- rare gas, crystal, quasi-atomic and quasi-molecular exciton states (Russian) 0-103628
- ruby, luminescence, absorption of R and N lines, effect of mag. field 0-60550
- ruby, quantum efficiency, photoacoustic meas. 0-73472
- ruby, radiation-induced optical processes, impurity effects 0-66310
- ruby R₁ zero phonon line, resonance fluoresc. meas. 0-89055
- sapphire, neutron bombard., F-centre fluorescence, photoluminescence 0-100676
- sapphire, optical detection of acoustic phonons at THz freqs. 0-75320
- semiconductor, biexcitons, one-photon radiative recomb. 0-70621
- semiconductor, single-quantum radiative recomb. of biexcitons due to biexciton-exciton interactions 0-96793
- semiconductor, STEM spectroscopic techniques for simultaneous electronic and defect obs. 0-100145
- semiconductors, amorphous, luminescence 0-80862
- semiconductors, electron beam or optically excited, quasi-equilib. approx. 0-84779
- semiconductors, exciton and domain luminesc., book 0-82588
- semiconductors, intervalley electron-electron scattering effect on optical transitions 0-108267
- semiconductors, thermally stimulated conductivity luminescence, defect levels, traps, book contribution 0-80296
- semiconductors, thermally stimulated relaxation processes, book contribution 0-80295
- sphalerite, hydrothermal single crystals, feasibility of optical methods for quality control 0-89065
- steel, trace element UV emission, spectrochem. anal. (French) 0-71997
- thermally stimulated luminescence application, radiation dosimetry, book contribution 0-80882
- thermally stimulated relaxation in solids, transport phenomena, book 0-77553
- tungstates, U activated, scheelite struct. luminesc. props. vibr. modes and quenching temp. 0-60651
- tungstates, U-doped, perovskite struct., luminesc. quenching, QMSCC calcs. 0-71470
- uniaxially compressed crystal, exciton molecule radiation (Russian) 0-108264
- Ag halide, visible luminescence obs. at or below 77K 0-108263
- Ag halide emulsions, primitive and AgNO₃-digested, IR luminescence obs. at 77K 0-103983
- AgBr, connection between the topography of luminescence centres and the latent image (Russian) 0-62785
- AgBr microcrystals, spectrally sensitised, luminesc., effect of hydrophobic organic compounds 0-97331
- AgBr, photoluminesc. study of excitons in high mag. fields 0-80843
- AgCl, luminescence fatigue, adsorbed Ag atoms 0-66281
- Ag₂HgI₄, preparation, optical and luminescence spectra 0-104064
- AgI, connection between the topography of luminescence centres and the latent image (Russian) 0-62785
- Ag₂O, exciton luminesc. spectra, mag. field influence 0-80860
- Ag₂S sols, red-IR photoluminescence obs. at 77K 0-103982
- (Al,Ga)As DH lasers, superlinear emission characts., negative resist. obs. 0-95895
- AlGaAs heterojunctions, nonradiative recomb. vel. estimate from edge luminesc. props. 0-65668
- AlGaAs heterojunction photocell with luminesc. wavelength converter 0-108800
- n-Al,Ga_{1-x}As, ion implanted films, optical and luminesc. props. 0-60699
- Al,Ga_{1-x}As, pure and Ge doped, shallow acceptor photoluminescence 0-76064
- Al,Ga_{1-x}As:Cu, variable-gap semicond., impurity props., carrier recomb. 0-96907
- Al,Ga_{1-x}As-GaAs heterostruct., varizional, parameter determ. by photoluminescence method (Russian) 0-108291
- Al,Ga_{1-x}As-GaAs quantum-well heterostruct., exciton in recomb. 0-103990
- Al,Ga_{1-x}P, LPE, crystallographic obs. and electrolum. 0-88445
- Al,Ga_{1-x}Sb, soln.-grown, photolum. 0-71476
- AlN, luminesc. excitation spectrum and band struct. 0-84783
- Al₂O₃ and double oxides, photon multiplication and secondary electron-hole pairs generation (Russian) 0-66262
- α -Al₂O₃, polarised luminescence in neutron- and proton-irradiated single crystals 0-66271
- α -Al₂O₃, recombination luminescence mechanism 0-71477
- Al₂O₃:Cr photoexcited crystals, cooperative thermoluminescence quenching (Russian) 0-80881
- Al₂O₃:Cr³⁺, ruby, reson. scatt. and trapping of 29 cm⁻¹ acoustic phonons 0-93403
- Al₂O₃-SiO₂ glass ceramic, surface streaks and blisters, UV fluoresc. study 0-84347
- Al₂(WO₄)₃:Cr(Eu), and undoped crystals, luminesc. obs. 0-89047
- As chalcogenides, deep levels, photoluminesc. and photocond. 0-70641
- As₂S₃, amorphous, time resolved luminesc. 0-66288
- a-As₂S₃, time-resolved photoluminescence study 0-89057
- As₂S₃, amorphous, struct., vibr. and electronic spectra 0-64908
- As₂Se₃, amorphous radiative interband recombination 0-66286
- As₂₀Se₈₀ and As₂₀Se₈₀ semicond. glasses, densified, photoluminesc., inelastic deform. effect 0-66293
- Au discontinuous film, electroluminescence obs. 0-103998

luminescence of inorganic solids continued

- Au, ion bombardment-induced photon emission as function of target temp. 0-100698
- BaCl₂, Sn-activated, luminescence studies 0-108246
- BaCl₂:Pb crystal phosphor, emission spectra 0-66298
- BaF₂:Pb²⁺, band struct., Jahn-Teller effect, UV luminesc. and optical absorpt. spectra 0-66243
- BaGd₂Si₂O₇, cell const., luminesc. of various 'rare-earth activators' 0-93376
- Ba₂NaNb₂O₇, ferroelectric, local states, thermoluminesc. study 0-60690
- BaNd₂(MoO₄)₄, luminescence spectra 0-84161
- Ba₂SiO₄Br₂:Eu, blue emitting X-ray luminescent material for intensifying screens (French) 0-66260
- BaTiO₃, intrinsic luminesc. 0-71467
- BaTiO₃, pure and Fe doped, ferroelec., switching and electrolum. 0-76079
- BaY₂Si₂O₇, cell const., luminesc. of various rare-earth activators 0-93376
- Be, foil, ion bombardment, secondary photon emission, ion energy depend. 0-97346
- BeF₂:Eu³⁺ glass, luminesc. of Eu³⁺, transition probabilities 0-80845
- BeF₂:Eu³⁺ glass, struct., Monte Carlo simulations 0-96448
- BeF₂:KF-CaF₂-AlF₃-EuF₃ fluoroberyllate glass, Eu³⁺ fluoresc. linewidth 0-66285
- Bi₂Al₂O₃, luminesc. expts. 0-60656
- Bi₂GeO₅:Dy(Ho)(Er), luminesc., emission and excitation spectra 0-103975
- CaCO₃, luminesc. under N₂ laser excitation, and appl. to archaeological dating 0-60685
- CaF₂, optical detection of acoustic phonons at THz freqs. 0-75320
- CaF₂:Dy, TLD-200, thermolum. phosphor, photolum. and absorpt. spectra, thermolum. mechanisms 0-97321
- CaF₂:Eu, CaF₂:Eu,Mn(Gd), single crystal predisintegration phenomena, SEM cathodolum. obs. 0-59502
- CaF₂:Eu²⁺, photoluminesc. mag. circ. polaris. 0-89056
- CaF₂:Eu²⁺, Sm²⁺, relaxed resonance acoustic phonons in vibronic anti-Stokes luminescence (Russian) 0-93404
- CaF₂:Mn, CaF₂:Eu,Mn, single crystal predisintegration phenomena, SEM cathodolum. obs. 0-59502
- CaF₂:Mn, low temp. X-irrad., Mn centres, optical absorpt. and emission props. 0-60635
- CaF₂:Mn(Co)(Ni), X-irrad., thermolum. 0-60686
- CaF₂:Pb²⁺, band struct., Jahn-Teller effect, UV luminesc. and optical absorpt. spectra 0-66243
- CaO, photoionisation of F-centre, luminesc. and photocond. meas. 0-66270
- CaO:Ce³⁺, Gd³⁺, sensitization of Ce³⁺ luminesc. by Gd³⁺ 0-97326
- CaO:Eu³⁺, influence of crystal field on luminesc. (Russian) 0-80834
- CaS, atomic and mol. centres of O, ESR and luminesc. methods (Russian) 0-84764
- CaS:Ce, Na phosphor, photoluminescence and excitation spectra 0-89049
- CaS:Cu, colour centres, optical and thermal depths determ. 0-66275
- CaS:Pd phosphors, trap and luminescent centre location, photo- and electroluminescence studies 0-71482
- CaSO₄:Dy, phototransferred TL studies 0-80875
- CaSO₄:Dy, TLD-900, thermolum. stability at low radiation doses 0-101272
- CaSO₄:Dy, thermoluminescent glow peaks, post γ -irrad. annealing study 0-89077
- CaSO₄:Dy ribbon, dosimetric props. study 0-63395
- CaSO₄:Dy sintered pellets, thermolum. response 0-93411
- CaSO₄:Dy(Tm), thermolum. thermolum. phosphor, photolum. and absorpt. spectra, thermolum. mechanisms 0-97321
- CaSO₄:Sm phosphors, X-irrad., thermoluminesc., charge compensation effects 0-97351
- Ca_{1-x}Sr_xEr³⁺ mixed crystal, luminesc. transition, inhomogeneous line broadening calc. 0-97332
- CdF₂:Er³⁺, Tm³⁺, evidence for Er³⁺→Tm³⁺ energy transfers, fluoresc. expts. 0-60655
- CdF₂:NaF thin films, electroluminescence obs. at 77K (French) 0-80866
- CdF₂:Sm³⁺, photoconverted, thermally stimulated relax. 0-84476
- CdIn₂S₄ single crystals, recombination process and localised levels 0-93383
- Cd_{1-x}Mn_xTe, exchange induced ionization of bound excitons, luminesc. meas. 0-97328
- Cd₂Nb₂O₇, photolum. and carrier drift mobility at ferroelec. transition 0-71469
- CdS crystals, electron-hole plasma, carrier optical orientation 0-100689
- CdS crystals, radiative recombination, high excitation rates 0-108269
- CdS, electron and hole trapped centres, EPR, photoluminescence, photoconductivity study 0-108071
- CdS epitaxial layers on sapphire, exciton struct. of absorpt., photoluminesc. and photocond. spectra 0-89027
- CdS, multiphoton cross-section determination by means of luminescence experiments 0-93377
- CdS, single crystals, US luminesc. obs. 0-76092
- CdS, spectroscopic study of local centre interaction, change with external illumination 0-80323
- CdS thin films, growth and evaluation for fabrication of high performance photovoltaic solar cells 0-93501
- CdS:Cu, photocurrent, elec. field effect on recombination processes (Russian) 0-100484
- CdS:Ga crystal cathodoluminescence, SEM analysis 0-97349
- CdS:In(Cl) concentration quenching mechanism of luminescence 0-97336
- CdS:Li, complex luminescence centres, recombination-stimulated conversion 0-108268
- CdS:Li, luminescence bands, photocurrent spectra (Russian) 0-60677
- CdS:Li, pure and doped, green edge luminesc., complex nature of centres 0-60671
- CdS:Li, single crystals, anisotropic luminesc. centres 0-80857
- CdS:Li(Cu), pure and doped, electrodiffusion of shallow donors, photocurrent, TSC, and exciton luminesc. meas. 0-79992
- CdS:Na, Hagemark theory, green edge emission line intensity 0-75517
- CdS_{1-x}Se_x, chem. comp. and luminescence obs. 0-80869
- CdS_{1-x}Se_x, mixed crystals, deformation effects on free excitons 0-76073
- CdSe, recombination mechanism at dislocations, photoluminescence 0-103993
- CdSe, single crystals, luminesc. of electron-hole plasma 0-60675
- CdTe crystals, excitation luminescence spectra rel. to shallow impurity conc. 0-97335

luminescence of inorganic solids continued

- p-CdTe, nondoped, heat treatment in vacuum, dissociation obs. effects on struct. and props. (*Japanese*) 0-60662
 p-CdTe, photocond., photoluminesc., spectral studies 0-88593
 CdTe, recombination radiation due to high-density excitons 0-93392
 CdTe, vapour-phase-grown, cathodoluminesc. study 0-76086
 CdTe:Li(Cl), acceptor states study by donor-acceptor pair excitation luminesc. 0-100683
 CdTe:Mn²⁺, luminesc. and magneto-optic reson., mag. field effect 0-93390
 CdTe(Se):Co, impurity luminescence no phonon line depend. on temp., Debye temp. 0-66273
 CdZnS thin films, growth and evaluation for fabrication of high performance photovoltaic solar cells 0-93501
 Cd_{1-x}Zn_x heteroepitaxial single-cryst. layers, photoluminesc. props. 0-100692
 Ce³⁺ impurities in cubic crystals, 5d→4f radiative transition probability calc. 0-71474
 Cr, photon emission due to Ar⁺ ion bombard., adsorbed and recoil-implanted O effect 0-80872
 Cs halides:H, luminesc. of interstitial atomic H 0-103986
 CsBr:Cu⁺, excitation and absorpt. spectra 0-108255
 CsBr(Cl):Cu⁺, γ-irradiated, thermolum. emission 0-104001
 CsCl, luminesc. in vac. UV range above and below phase transition temp. 0-93399
 CsI:Na⁺ (K⁺), luminesc. processes 0-103989
 CsI:Tl(Na), light yield under charged-particle bombardment 0-93409
 Cs₂MX₄ (M=Se, Te, X=Cl, Br), Γ₄⁻(³T_{1u}) state, Jahn-Teller effect, luminesc. obs. 0-60650
 CsMnCl₂·2H₂O, antiferromag. insulator, self-trapping of excitons 0-70619
 CsMnF₆, exciton migration, excitation and luminesc. study (*Russian*) 0-66264
 CsMnF₆, exciton-magnon interactions in optical transition, absorpt. and emission spectra meas. 0-70981
 Cs₂NaYCl₆:Bi³⁺, luminescence props., emission and excitation spectra 0-108262
 α-CsNd(PO₃)₄, single cryst. struct. and spectral-luminescent props. 0-96490
 CsPbCl₃, electronic struct. and optical props. in fundamental absorpt. region 0-93367
 Cu, hot cathodoluminescence study, electron-hole recombination 0-93410
 Cu, ion bombardment-induced photon emission as function of target temp. 0-100698
 CuCl crystal resonant Raman scatt. and luminescence competition (*Japanese*) 0-80770
 CuGaSe₂, evidence of donor-acceptor type transition 0-93375
 CuI, single crystals, growth and optical props. 0-93470
 Cu₂O, exciton luminesc. spectra, mag. field influence 0-80860
 Eu double metaphosphates with alkali metals or H, luminesc. props. 0-100675
 Eu²⁺ impurities in cubic crystals, 5d→4f radiative transition probability calc. 0-71474
 Eu_{1-x}La_xTa₂O₁₀, polycryst., luminesc. and excitation spectra 0-60659
 EuNa₂Mg₂(VO₄)₃, disordered, thermal quenching of luminesc. 0-71472
 EuP₂O₁₄, luminesc. of Eu³⁺, transition probabilities 0-80845
 Eu₂Sr_{1-x}S, magneto-optical redshift in absorpt. and photoluminesc., mag. short-range order 0-71388
 Fe, ferromagnetic, partial circular polarisation of thermal emission in mag. field 0-71387
 Fe₂O₃, semicond. anode in aq. electrolyte, electrochem. and electrochem. 0-76080
 (Ga,Al)As:Si(Ge), epitaxial layers, radiative recomb., compensation, cathodolum. study 0-66307
 n-GaAs epitaxial film, radiative recomb. under influence of mech. stresses 0-66291
 (GaAl)As DH laser wafer, photoluminesc. improvement with buffer layer 0-64014
 GaAlAs, luminescence circular polarisation, electron optical orientation resonant variation (*Russian*) 0-84782
 Ga_{1-x}Al_xAs, epitaxial, radiative deep states 0-76061
 Ga_{1-x}Al_xAs structures, STEM and scanning deep level transient spectroscopy in defect centre anal. cathodoluminesc. techniques 0-103642
 Ga_{1-x}Al_xN heteroepitaxial films, photoluminesc., cathodoluminesc. 0-66292
 Ga_{1-x}Al_xP:N epitaxial films, ion implanted, cathodoluminescence study 0-60684
 Ga(As,P):N, isoelectronic impurity states, long-range, short-range model 0-75524
 GaAs, electroluminescent study of irradiation induced struct. damage, athermal annealing 0-108280
 GaAs, electron-spin relaxation and recomb. kinetics, time-resolved luminesc. study 0-108074
 GaAs epitaxial films on strongly doped substrate, basic parameter meas. utilising magnetoresist. and SEM techniques under parameter meas. conditions 0-65728
 GaAs, excited luminescence, influence of IR illumination 0-76072
 GaAs, exciton effects in photocond., photoluminesc. 0-96797
 GaAs, γ- and electron irradiation, influence on recomb. charact. near surface 0-71478
 GaAs, hot photoluminescence spectrum on pumping across the L-valley (*Russian*) 0-103984
 n-GaAs, ion implanted films, optical and luminesc. props. 0-60699
 GaAs, luminescence emitted from deep centres, plastic deform. effect on internal quantum efficiency 0-60672
 p-GaAs, MBE grown, As₂ and As₃ effects on photolum. 0-103974
 GaAs on Ga₂Al_{1-x}As, electron scatt., cathodoluminesc., loss spectra 0-104023
 GaAs, photoluminescence electron gas coding influence in ion-bombarded layers 0-108272
 GaAs, spin-depend. recomb., photoluminesc. obs. 0-60666
 GaAs:Cr, 0.84 eV n-phonon luminesc., fine struct. and origin 0-103980
 GaAs:Cr, photoluminescence in strong electric fields 0-108270
 GaAs:Cr, semi-insulating, Zeeman studies of 0.839 eV emission 0-103987
 GaAs:Cr semi-insulating wafer, heat treatment technique for no thermal conversion 0-100857
 n-GaAs:Ge, film, substrate temp. depend. of Ge incorporation during MBE 0-76196
 GaAs:O, electrochem., photolum., negative differential resist. rel. to recomb. processes 0-66304

luminescence of inorganic solids continued

- GaAs:Se cathodoluminescence decay obs. with SEM and streak camera, 90 to 300K 0-97348
 GaAs:Si, accelerated growth rate effect on MBE, Hall mobility and photolum. meas. 0-104067
 GaAs:Si, influence of stoichiometry on recomb. processes 0-93396
 GaAs:Si p-n junction LED, electroluminesc. efficiency 0-71491
 GaAs:Te(Cd)(Mg)(B), ion implant depth distrib., AES and glow discharge optical spectroscopy meas. 0-65028
 GaAs:V, ion implanted, luminesc., level splitting 0-97338
 GaAs:W²⁺, radiative transitions, photoluminesc. obs. 0-108271
 GaAs/(Ga,Al)As, DH laser diode, electroluminescence near 1 eV 0-60682
 GaAs-Cu:Ti, cathode luminescence spectra, Hall effect, cryst. defects 0-76087
 GaAs-Ga₂Al_{1-x}As DH laser material crystal cathodoluminescence, SEM analysis 0-97349
 GaAs-GaAlAs DH lasers, strain-enhanced luminesc. degradation, photoluminesc. obs. 0-69392
 GaAs-GaAlAs wafers, defects and degradation, transmission cathodolum. evaluation 0-65395
 GaAs-GaP heterostructure, radiative recomb. under influence of mech. stresses 0-66291
 GaAs_{1-x}P_x, indirect-gap, evidence for exciton localization by alloy fluctuations, photolum. 0-66276
 GaAs_{1-x}P_xN, photolum. and electrochem. study of N isoelectronic traps 0-89061
 GaAs_{1-x}P_x(Te), bound exciton stress depend., piezoluminescence, photoluminescence 0-80206
 GaAs_{1-x}Sb_x, (x≤0.05), band gap, temp. depend., from edge photolum. meas. 0-71486
 GaInAs-InP, growth by low-pressure metalorganic CVD 0-71595
 GaN epitaxial films, cathodoluminesc. spectra 0-71496
 GaN, luminesc. centres 0-93405
 GaN, photoluminesc. spectra, energy distrib. 0-97339
 GaN, polarised electroluminescence emission, microstructure investigations 0-97344
 GaN, VPE growth rate influence on elec. and luminesc. props. 0-100702
 GaN:Zn, n-i struct., anomalous luminesc. 0-80865
 GaP, green cathodolum. from cryst. defects, SEM, TEM study 0-80870
 n-GaP, ion implanted films, optical and luminesc. props. 0-60699
 GaP:Bi,N, photoluminesc., electroluminesc., 4.2 to 300K, excitons and hole traps 0-108275
 GaP:Ce(Dy)(Pr) epitaxial films, photoluminesc. spectra 0-66294
 GaP:Co, optical spectra and Zeeman anal. of Co 3d⁷ state 0-66247
 GaP:Co(Ni), photolum. excitation spectroscopy 0-80841
 GaP:N LED structures, local dopant conc. determ. using SEM cathodolum. spectra 0-101057
 GaP:S(Se), donor bound exciton excited states 0-66284
 GaP:Zn, O, influence of impurity-absorbed illumination on luminesc. 0-93395
 p-GaP:Zn,S, spin polarisation of donors and acceptors in mag. field, optical and microwave study 0-93393
 GaPAs_{1-x}N_x, luminesc. of N bound state excitons, local-environment effects 0-100691
 GaSb:Sn, p-n junction, electroluminesc. and photoluminesc. 0-66306
 GaSe, deep free and constrained excitons and biexcitons, collective interactions (*Russian*) 0-66282
 GaSe, exciton luminesc. kinetics, intermediate electron-hole states 0-93389
 GaSe, exciton-phonon quasibound states, photocond. and luminesc. study 0-96800
 Gd₂(MoO₄)₃, ferroelec.-ferroelastic, photolum. and photocond. meas. 0-84768
 Ge, electron-hole droplets distrib., and phonon wind 0-103629
 Ge, ion bombardment-induced photon emission as function of target temp. 0-100698
 Ge, mag. field luminesc. lifetime, quantum oscill., phonon wind effects 0-93385
 Ge, nonequilibrium charge carrier-mag. field interaction electron-hole drops, recombination (*Russian*) 0-75511
 Ge:B(Al)(Ga), shallow acceptor spectral line intensities 0-88517
 Ge:In (Sb) and pure cryst., kinetics of strain-confined large electron-hole drop and its clinging excitation system 0-75508
 Ge:Sb, electron-hole drop lifetime, quenching temp. influence 0-59889
 GeSb, far IR emission stimulation by impact ionisation 0-66301
 GeSe₂, glassy, powdered and bulk, fatigue of photolum. 0-80855
 GeSe₂, powdered crystalline, photoluminescence intensity under continuous excitation 0-71480
 Hg_{1-x}Cd_xTe, near band-gap photoluminesc., bound exciton luminesc. obs. 0-103973
 InAs and solid solutions, recombination mechanisms of excess carriers, luminesc. obs. 0-97337
 p-In_{0.53}Ga_{0.47}As:Zn on InP, elec. and optical props. 0-75662
 In_{1-x}Ga_xAs:Si p-n structures, electrochem. spectra, 77 to 300K 0-93408
 InGaAsP, band-gap energy by electroreflectance and photoluminesc. spectra 0-107700
 InGaAsP DH, luminesc., quantum efficiency determ. 0-108273
 InGaAsP-InP DH LED, high temp. aged, dark-spot defects, TEM obs. 0-66300
 InGaAsP-InP DH lasers, perturbed InP growth, photoluminesc. study 0-106518
 In_{0.3}Ga_{0.7}P, N free and implanted, photoluminescence study 0-97322
 n-In_{1-x}Ga_xP, direct-gap semiconductor, cathodoluminesc., electron irradiation effects 0-108283
 InGaPAs LPE layers, compositional inhomogeneity, photoluminesc. obs. 0-75451
 In_{1-x}Ga_xP_{1-y}As_y, lattice-matched epitaxial layers, LPE growth on GaAs(100), characterisation 0-75465
 In₂O₃-SnO₂-CdTe:P, p-n homojunction solar cell, elec., photovoltaic props., photoluminescence 0-81463
 InP films, organometallic VPE grown, props. 0-96753
 InP, luminescence, hot electron effects 0-66277
 InP, model for ~1.10 eV emission band 0-66289
 InP, photolum. meas. using diamond-anvil press. cell 0-108256
 InP, press. depend. of direct absorption edge 0-93365
 InP, VPE growth for MESFET's 0-103602
 InSb, reabsorbed radiative recomb. and photon recycling 0-76076
 InTa_{1-x}Nb_xO₄ system, structural and luminescent props. 0-84769
 KBr, cation defects creation mechanism 0-75224

luminescence of inorganic solids continued

- KBr, decay and time resolved emission spectra from σ -excitons produced by heavy-ion irradiation 0-89071
 KBr, F-centre lifetime, perturbation effects, luminesc. meas. 0-108252
 KBr, self-trapped exciton form. via thermally induced defect reactions 0-60687
 KBr: Γ^- , OH $^-$, luminesc. of interstitial atomic H 0-89062
 KBr: Sr^{2+} , Cu $^+$, thermolum. response, extension of two-step reaction model 0-89075
 KBr:Ti, 480K thermal glow peak, Ti $^+$ centres 0-108284
 KBr:Ti, electroluminescence, spectra and quantum yield activator conc. depend., cond. changes 0-89070
 KBr:Ti, luminesc., decay model for A $_T$ and A $_X$ emissions 0-93379
 KBr(I), photostimulated recomb., electron spin polarisation 0-60673
 KCl, thermoluminesc., halogen and alkali impurity effects 0-93752
 KCl:Ag $_x$, X-irrad., thermoluminesc. study of Ag centres 0-80874
 KCl:Ca $^{2+}$, Z-centre thermolum. 0-80879
 KCl:Eu $^{2+}$ crystals, photostimulated afterglow investigation at room temp. 0-108259
 KCl:Li, X-irrad., F $_A$ centres, thermolum. studies 0-80878
 KCl:SnCl $_2$, photostimulated hole recombination luminesc. (Russian) 0-80833
 KCl:Sr crystal, Z $_4$ colour centre, luminesc. study 0-64993
 KCl:Sr $^{2+}$, Cu $^+$, thermolum. response, extension of two-step reaction model 0-89075
 KCl:Ti, electroluminescence, spectra and quantum yield activator conc. depend., cond. changes 0-89070
 KCl:Ti, temp. depend. of cathodolum. (Russian) 0-80868
 KCl:Ti (0.003 to 0.27 mol.%), electrolum. 0-71490
 KCl(Br), F-centre emission, mag. circular polarisation 0-108251
 KCl:Br $_{1-x}$, mixed crystals, thermolum. and optical absorption studies 0-104000
 KCl(Br)(I):Ga $^+$, polarisation of Ga $^+$ centre A $_T$ emission, temp. depend. 0-80842
 KI, growth time of π emission in picosecond range 0-76067
 KI, self trapped exciton form. time at $^1\Sigma_u^+$ state under pulsed electron beam in ps range 0-97347
 KI, self-trapped exciton form. via thermally induced defect reactions 0-60687
 KI:Ti, decay of fast component of impurity luminesc. excitation in A-absorption band (Russian) 0-84767
 KI:Ti, polarised luminesc. of (Ti $^{3+}$), centres 0-71473
 K $_2$ NaGaF $_6$:Cr $^{3+}$, magneto-optical study of $^2T_{1g}$, 2E_g , 4A_g transitions 0-71384
 Li $_2$ UO $_4$, energy transfer, cryst. struct. and chemical composition effect 0-108248
 La $_2$ Be $_2$ O $_7$:Nd $^{3+}$ (Pr $^{3+}$), cryst. growth, spectral and laser properties in $^4F_{3/2}$ - $^4I_{13/2}$ and $^4F_{3/2}$ - $^4I_{13/2}$ transitions 0-80853
 LaBr $_3$:Np $^{3+}$, energy level anal., polarised absorpt. and fluoresc. spectra 0-76056
 LaCl $_3$:Np $^{3+}$, energy level anal., polarised absorpt. and fluoresc. spectra 0-76056
 LaCl $_3$:Np $^{3+}$, phonon-induced relax. in excited optical states, linewidth temp. depend. meas. 0-100688
 LaCl $_3$:U $^{3+}$, cryst., spectrum anal., cryst. field parameters 0-76057
 LaF $_3$, VUV luminescence, conference, Moscow, USSR (Apr. 1978) 0-62378
 LaF $_3$:Er $^{3+}$, optically excited, direct-process spin-lattice relaxation 0-93378
 LaGaS $_3$:Ce $^{3+}$, phosphor, luminesc. props. 0-103979
 La $_2$ O $_3$:Eu, high press. effect on luminesc. efficiency and lifetime, charge transfer absorpt. 0-66266
 La $_2$ O $_3$:Eu, slow phosphoresc., high press. study 0-80839
 Li-La phosphate glass, Nd, Cr activated, Nd luminesc. quantum efficiency meas., Nd-Cr nonradiative transfer 0-66296
 Li $_2$ B $_4$ O $_7$:Mn, thermolum. response to pions 0-101270
 LiCl, radiation effects on decay time of F-centre emission 0-93381
 LiCl single crystals, γ -irrad., thermolum. meas. 0-80880
 LiCl, thermolum., order of kinetics 0-89074
 LiCl:Ag, fluoresc. and UV absorpt. spectra 0-80844
 LiF, cryst., triboluminesc. spectra 0-66312
 LiF crystal, contact damage obs. by cathodoluminesc. 0-71728
 LiF TLD phosphor, γ -irrad. induced sensitisation, UV effects 0-108286
 LiF TLD phosphor, residual thermoluminescence effect on sensitisation 0-108287
 LiF, thermolum., trapping mechanism based on Z-centres 0-76089
 LiF, thermolum. response to pions 0-101270
 LiF:Mg, TLD-100, thermolum. phosphor, photolum. and absorpt. spectra, thermolum. mechanisms 0-97321
 LiF:Mg,Ti, defect states, ESR and ionic cond. study 0-108058
 LiF(TLD-600), unannealed, fading for thermal neutrons and γ -rays 0-83225
 LiH, defect form. at low temp., EPR, thermolum. and TSC study 0-107222
 LiH, effect of surface hydrolysis to LiOH on IR absorption, X-ray luminesc. and EPR spectra 0-60660
 LiH, formation and annihilation of Li colloids and H bubbles 0-107228
 LiInS $_2$, blue-band emission 0-76062
 LiNbO $_3$, luminesc. props., Li/Nb ratio effect 0-97323
 Lisd $_4$ UO $_5$, energy transfer, cryst. struct. and chemical composition effect 0-108248
 Lu $_2$ -Si $_2$ O $_7$:Eu, synthesis and spectroscopic study 0-84846
 Lu $_2$ (WO $_4$):Cr(Eu), and undoped crystals, luminesc. obs. 0-89047
 LuYSO $_4$:Er $^{3+}$ (Tm $^{3+}$)(Ho $^{3+}$), thermolum. meas. 0-97354
 MgAl $_2$ O $_4$, γ -irradiated crystal, TSC, thermolec. power, thermolum. and afterglow 0-75583
 MgO crystal, contact damage obs. by cathodoluminesc. 0-71728
 MgO crystal cathodoluminescence, SEM analysis 0-97349
 MgO doped powder phosphors, photo- and thermostimulated luminesc. obs. (Russian) 0-66263
 MgO, photoluminesc. during mechanical deform. 0-60665
 MgO:Al, and nominally pure single crystal, thermally stimulated luminesc. rel. to temp. and EPR (Russian) 0-84789
 MgO:Cr $^{3+}$, emission and excitation spectra 0-93387
 MgO:Cr $^{3+}$, optical excitation transfer 0-97325
 MgO:Ni $^{2+}$, near IR luminesc. from isolated and exchange-coupled Ni $^{2+}$ ion pairs, temp. depend. 0-93382
 MgO-Al $_2$ O $_3$ -P $_2$ O $_5$ system glass, heat treatment of aluminium metaphosphate influence on thermolum. 0-108285
 MgS:Ce $^{3+}$ phosphors, emission and excitation spectra (French) 0-93380

luminescence of inorganic solids continued

- Mg $_2$ SiO $_4$:Tb, thermolum. phosphor, photolum. and absorpt. spectra, thermolum. mechanisms 0-97321
 MgUO $_4$, energy transfer, cryst. struct. and chemical composition effect 0-108248
 Mn complex, with 4-benzylpyridine hydrochloride, photoluminesc. props. 0-89044
 Mn $_2$ Cd $_{1-x}$ Se single crystals, photoluminesc., composition depend. 0-80854
 Mo, ion bombard., ion and photon yields, CO adsorption effect 0-89098
 N $_2$ film, on metal or sapphire substrates, luminescence and nonradiative energy transfer to surfaces 0-97350
 NH $_4$ Br:Cu $^+$, luminesc., orientation phase transition 0-100687
 NH $_4$ Br:Ti, and pure crystals, luminesc., VUV irradiated at 80K (Russian) 0-84763
 Na $_4$ Al $_3$ Si $_3$ O $_{24}$:(NaX) $_{2n}$, X=Cl, Br or I, sodalites, thermal destruction of colour centres (Russian) 0-84169
 Na $_3$ Al $_2$ Si $_2$ O $_{10}$:Cl(Br)(I), cathodochromic sodalites, coloured crystals, tunnel and recomb. luminesc., temp. depend. (Russian) 0-66261
 NaBr(I), optically activated F $^-$ -F $^+$ centre conversion in mag. field 0-108253
 NaBrO $_3$, cryst., mechanoluminesc. spectra 0-97355
 NaCl, cryst., triboluminesc. spectra 0-66312
 NaCl, migration of nonrelaxed holes, self-trapping, ESR and luminesc. obs. (Russian) 0-66033
 NaCl, pure and doped, 20K X-ray irradiation, thermolum. and recovery processes 0-93412
 NaCl, self-trapped exciton form. via thermally induced defect reactions 0-60687
 NaCl:Ga $^{3+}$, polarisation of Ga $^{3+}$ centre A $_T$ emission, temp. depend. 0-80842
 NaCl:Mn $^{2+}$, thermolum. spectra, mechanisms 0-80873
 NaCl(Br), X-ray or UV irradiated, cation defects creation mechanism 0-75224
 NaClO $_3$, cryst., mechanoluminesc. spectra 0-97355
 NaF, X-irrad., colour centres and thermolum. 0-84790
 NaF:Mn, role of Mn $^{2+}$ in thermolum. 0-97353
 NaF:U, luminesc. spectra, Vibr. struct. 0-80840
 Na $_3$ La $_{1-x-y}$ Ce $_x$ Tb $_y$ (PO $_4$) $_2$, optical props. (French) 0-103991
 NaMgF $_3$, defects induced by X- and vacuum UV irradi., optical and elec. study 0-107319
 NaMnCl $_3$, antiferromag. insulator, self-trapping of excitons 0-70619
 Na $_2$ O-P $_2$ O $_5$ -Y $_2$ O $_3$ -Tb $_2$ O $_3$ glass, conc. quenching of luminesc. in disordered system with dipolar interaction 0-89059
 Na $_2$ O-SiO $_2$ glasses, elementary electronic excitations, refl., luminesc., and photoemission meas. 0-84778
 NaPO $_3$:Eu $^{3+}$, luminesc. of Eu $^{3+}$, transition probabilities 0-80845
 Na $_2$ S $_2$ O $_3$ digested AgX emulsions, red-IR photoluminescence obs. at 77K 0-103982
 NaY $_{1-x}$ Sm $_x$ F $_4$, luminesc. expt. suggesting Sm $^{3+}$ ion pairing 0-76065
 NaZnGeO $_4$:Mn, electrolum., ionisation domains 0-84787
 Nd:silicate glass, resonance laser excitation, inhomogeneously broadened emission spectra 0-66295
 Nd $^{3+}$ glass luminesc. band profile deform. under free-oscillation conditions 0-71487
 Nd $^{3+}$:LaCl $_3$, laser-induced fluoresc., hyperfine structs. 0-100677
 Nd $^{3+}$:LaCl $_3$, laser-induced fluoresc. energy transfer effects 0-100678
 NdP $_2$ O $_7$, fluoresc. lifetime meas., IR and photoacoustic spectroscopy 0-60652
 Ne:H, exciton states and L $_{\alpha}$ L $_{\beta}$ emission 0-93372
 Ni, ion bombard., ion and photon yields, CO adsorption effect 0-89098
 Ni, photon emission due to Ar $^+$ ion bombard., adsorbed and recoil-implanted O effect 0-80872
 P $_2$ O $_5$ -R $_2$ O $_3$ -M $_2$ O(M'O), (M=alkali metal, M'=alkaline earth, R=Y or rare earth), metaphosphate glass phosphors, fluoresc. props., activation conc. effect 0-89058
 Pb, ion bombardment-induced photon emission near melting point 0-100699
 PbCl $_{2-x}$ Br $_x$, luminesc. and reflection spectra (Russian) 0-84762
 PbI $_2$, first-order 2H-4H polytype transition, exciton spectroscopic study 0-59647
 PbI $_2$, multiphoton cross-section determination by means of luminescence experiments 0-93377
 PbI $_2$, photoexciton interaction, luminescence spectra, polariton dispersion diagram 0-93397
 PbMg $_{1/3}$ Nb $_{2/3}$ O $_3$, photolum. and carrier drift mobility at ferroelec. transition 0-71484
 PbMoO $_4$, doped and undoped single crystals, polarisation of luminesc. and assignments 0-76069
 PbO, single crystals, exciton and impurity luminesc. 0-60674
 PbS $_{1-x}$ Se $_x$ thin film, stimulated emission, temp. depend. 0-66232
 Pb $_{1-x}$ Sn $_x$ Se epitaxial layers, radiative and nonradiative recomb. processes 0-60670
 Pb $_{1-x}$ Sn $_x$ Se solid solns., photoluminesc. spectra, energy band parameter determ. 0-71484
 Pb $_{0.78}$ Sn $_{0.22}$ Te, Pb $_{0.91}$ Sn $_{0.09}$ Se, radiative and nonradiative recombination 0-80849
 Pb $_{1-x}$ Sn $_x$ Te:Ce(In), solid solutions, impurity states in photoluminescence spectra (Russian) 0-97333
 Pb $_{1-x}$ Sn $_x$ Te:In, impurity influence on photoluminescence at large excitation levels (Russian) 0-93384
 PbTiO $_3$, photolum. and carrier drift mobility at ferroelec. transition 0-71469
 PbWO $_4$, doped and undoped single crystals, polarisation of luminesc. and assignments 0-76069
 RbBr, self trapped exciton form. time at $^1\Sigma_u^+$ state under pulsed electron beam in ps range 0-97347
 RbBr: Γ^- , OH $^-$, luminesc. of interstitial atomic H 0-89062
 RbCl:Ca $^{2+}$, thermolum. and optical absorption studies 0-104002
 RbCl(Br), cation defects creation mechanism 0-75224
 RbCl(Br), F-centre emission, mag. circular polarisation 0-108251
 RbI, luminesc. spectra induced by pulsed Ne $^+$ and electron beams and X-rays 0-80851
 RbI, photostimulated recomb., electron spin polarisation 0-60673
 RbMnF $_3$:Er $^{3+}$, absorption, emission, excitation and lifetime meas. 0-71460
 RbMnF $_3$:Fr, pure and doped, unirradiated and electron irradi., energy transfer 0-108254
 SbSI, photolum. spectra in ferroelec. phase, 600-800 nm., 14-100K 0-71468
 Se $_2$ O $_3$ and double oxides, photon multiplication and secondary electron-hole pairs generation (Russian) 0-66262

ion implantation continued

- SiO₂ film, on GaP substrate, N ion implantation, optical refl. and EPR meas. 0-84197
 SiO₂, fused, surface crystn. by Li⁺ ion implantation and annealing 0-89383
 SiO₂ glass, ion bombardment, form. of cpds., IR spectrosc. exam. (*German*) 0-88173
 SiO₂, implanted, in MOS capacitor, direct current/voltage relns. as function of oxide doping 0-88635
 SiO₂, ion implanted, radiation defects and optical props. 0-107293
 SiO₂:As⁺ implanted layers in MOS struct., electron trapping and detrapping characts. 0-92982
 SiO₂:Au(Ag)(Cu), XPS line broadening and extra-atomic relax. energies 0-71561
 SiO₂:F(BF₃), ion implanted, F influence on oxidation-induced stacking faults 0-65011
 Si(111):Pb ion implanted amorphous layers, recrystallisation, impurity out-diffusion model (*Chinese*) 0-88363
 Sn film, metastable supercond. alloys, produced by low temp. ion implantation 0-88670
 α-Sn, ion implanted, defect struct., Mossbauer spectra 0-80214
 α-Sn:^{119m}Sn, impurity lattice dynamics, Mossbauer spectra, Debye temp. 0-84262
 Sn-Cu film, metastable supercond. alloys produced by low temp. ion implantation 0-88670
 TaSi₂ refractory formation by As⁺ ion beam bombardment 0-107286
 Te-Au film, metastable supercond. alloys, produced by low temp. ion implantation 0-88670
 Ti metal-metal interface, adhesion energy, surface treatment and ion implantation effects 0-107660
 Ti:D, implanted, deuteride imaging using scanning Auger spectroscopy 0-89092
 Ti:D, implanted, nucleation and growth of TiD₂ 0-97717
 Ti:D, ion implanted, depth profiles, temp. depend. 0-100270
 Ti:Pd, ion implanted, corrosion behaviour and Rutherford backscatt. anal. 0-71792
 W:³He, implanted ion positions, determ. using mol. deuteron beam 0-70240
 WSi₂ refractory formation by As⁺ ion beam bombardment 0-107286
 YIG:La(Ga) films, ferromagnetic resonance, ion implantation effect 0-97145
 Y_{2.85}La_{0.15}Fe_{3.75}Ga_{1.25}O₁₂ LPE films, ion implantation effect on spin waves 0-71124
 Y_{2.85}La_{0.15}Fe_{3.85}Ga_{1.15}O₁₂ garnet, mag. props., ion implantation effect, Mossbauer study 0-97166
 Y_{3-x}Sm_xFe₅O₁₂:⁵⁷Fe film, ion implanted, Mossbauer conversion spectra study 0-80663
 Zn:Al, ion implantation, temp. and time depend. 0-65013
 Zn-Mn, Kondo-system, ion implantation as method for study 0-70241
 ZnS ion beam etching, topographic changes, amorphisation, luminescence study 0-76078
 ZnS, ion implantation effects on luminesc., thermo-EMF 0-88178
 ZnTe, ion implantation defect introduction, cathodolum. studies 0-75250
 ZnTe:P(As), ion implanted, cathodoluminescence emission spectrum 0-108281
 Zr, H(D) implanted, superconductivity enhancement obs. 0-70884
 Zr, ion-implanted polycryst., thermal oxidation 0-71786

ion lasers

- applications and laser principles (*French*) 0-83590
 book, gaseous electronics and gas lasers 0-73120
 book, quantum electronics 0-105442
 confined plasma column, soft X-ray lasing action conditions 0-74346
 hollow cathode discharge with variable voltage 0-59336
 hollow cathode discharges for gas lasers, review 0-99717
 hollow cathode discharges for gas lasers 0-83599
 inert gas ion laser, high voltage-low press. discharges, stationary props. 0-92400
 inert gas mixture, hollow cathode, CW operation and excitation mechanism 0-69363
 metal ion lasers, hollow cathode 0-99708
 metal vapour lasers, hollow cathode discharge, review 0-99717
 noise, low frequency 0-69364
 plasma column, multipole confinement, radial and axial arrangement 0-83974
 relativistic ion beam laser, continuously IR to X-ray tunable, in negative temp. state (*Chinese*) 0-87373
 review, excitation mechanisms and characts., book contrib. 0-106512
 soft X-ray population inversion in laser plasmas, reson. photoexcitation, photon-assisted processes 0-87378
 tube design, cathode fall theory studies 0-58560
 Al I near IR laser transitions, large diameter hollow cathode Ne-Al discharge 0-102715
 Ar, high-power, construction of side cathode 0-99742
 Ar laser and appls. (*French*) 0-83590
 Ar laser with passively locked modes, excitation of dye laser for picosecond pulse generation 0-95930
 Ar⁺ and Ar⁺-Kr⁺ ion lasers, I₂ stabilized, beat frequency 0-95916
 Ar⁺ ion laser, active mode locking study 0-91827
 Ar⁺ laser 582 THz stabilisation by I₂ cell, improvements 0-102741
 Au hollow cathode laser, ion laser transitions 0-69366
 Cd hollow cathode laser, ion laser transitions 0-69366
 Cd laser produced plasma recombination laser, power output enhancement by plasma confinement 0-63989
 Cd vapour laser, hollow-cathode white light, new design concept 0-87405
 Cr vapour, laser transitions in near IR 0-99704
 Cu hollow cathode laser, ion laser transitions 0-69366
 Cu II laser with cylindrical hollow cathodes, UV performance 0-102709
 Fe group elements, singly ionised, charge transfer, rel. to laser action 0-74246
 He-Cd vapour excitation in hollow cathode discharge 0-64815
 He-Cd vapour laser, continuous wave, intensity fluctuations investig. 0-83593
 He-Kr hollow cathode CW laser, Kr II 4584 Å generation 0-58510
 He-metal vapour lasers, positive column electron densities, experimental study (*Japanese*) 0-69376
 He-Se, vapour laser, continuous wave, intensity fluctuations investig. 0-83593
 He-Sr laser, possibility of nucl. pumping, 4305 Å Sr II transition 0-58518
 He²⁺+Li collisions, soft X-ray emission obs. 0-83591

ion lasers continued

- ¹²⁷I₂ stabilised, beat freq. intercomparisons at 514.5 nm 0-74338
 Kr⁺ mode-locked ion laser, pulse width and linewidth meas. 0-102696
 N, travelling wave excitation 0-91774
 N₂-He ion nuclear pumped lasers feasibility study and quenching 0-64001
 Sn hollow cathode laser, emission obs. from Sn II, I transitions 0-106509
- ion lenses** *see* *lenses*
- ion microanalysis**
see also ion microprobe analysis
 ANL HVEM-TANDEM accelerator facilities 0-101896
 plane retarding potential analyzer, effect of total transparency of field inhomogeneity 0-99003
 second-generation ion microanalyser description and performance (*French*) 0-101055
 surface anal. by ion scattering spectrometry and secondary ion mass spectrometry 0-103541
 surface anal. tools review 0-103540
 Al-Nb superimposed metallic layers, ionic movements during anodization, Rutherford backscatt. and nuclear microanal. 0-71913
 Nb-Al superimposed metallic layers, ionic movements during anodization, Rutherford backscatt. and nuclear microanal. 0-71913
 Nb-Ta superimposed metallic layers, ionic movements during anodization, Rutherford backscatt. and nuclear microanal. 0-71913
 Ta-Nb superimposed metallic layers, ionic movements during anodization, Rutherford backscatt. and nuclear microanal. 0-71913
- ion microprobe analysers** *see* *ion microprobe analysis*
- ion microprobe analysis**
see also ion microanalysis
 air pollution monitoring, PIXE and NRA studies using lichen indicator 0-61744
 alloys, ion-implanted, integral Gaussian profile determ. method 0-107313
 atomic transport and conc. profiles 0-59723
 catalyst design and evaluation using PIXE 0-61201
 crystalline solids, electronic industry, chem. anal. instrumental methods progress 0-66903
 hair, human, PIXE analysis, correction factor, rel. to pollution monitoring 0-61743
 Incoloy 800, steam oxidised, oxide coating anal. 0-89399
 k-shell ionizations in proton induced X-ray emission analysis 0-101054
 laser microprobe mass analyser, achievements and appls. 0-73536
 lung pathology, appl. of PIXE 0-61691
 minerals, sputtering rates, implications for abundances of solar elements in lunar samples 0-61797
 phosphosilicate glasses, P content determ. by Rutherford backscatt., PIXE, and activation anal. (*Hungarian*) 0-85233
 PIXE, biomedical appls. 0-61691
 PIXE, technique with external beam, and its appl. to study of valuable relics 0-61198
 PIXE, use of liposomes to reduce enhancement-absorption effects 0-101053
 PIXE set-up for routine analyses 0-104488
 PIXE-PIGME system, automated, appl. to artefact obs. 0-61199
 protein analysis using PIXE 0-61691
 steel, industrial, surface chem. characterisation by SIMS, glow discharge spectrometry and other techniques 0-66907
 steel, stainless, D₂⁺ diffusion and permeation, ion beam meas. 0-59492
 surface analysis, new uses of ion beams (*Japanese*) 0-90934
 zircaloy, nuclear microprobe methods for investigating oxidative corrosion 0-71787
 Al sheet surfaces, chem. characterisation by SIMS, glow discharge spectrometry and other techniques 0-66907
 Al, single crystal, ¹⁸O⁺ ion implantation in channelling directions, expt. conditions and range profile obs. 0-65022
 Al single crystal, ¹⁸O⁺ ions implantation in channelling directions, stopping power meas. from max. range 0-65078
 Al, sputter deposit PIXE expt. 0-61196
 Al₂O₃, single cryst., O self diffusion, ion-probe meas. 0-59701
 Cu, sputter deposit PIXE expt. 0-61196
 Cu:O single crystal, ¹⁸O⁺ ion implantation in channelling directions, expt. conditions and range profile obs. 0-65022
 Cu:O single crystal, ¹⁸O⁺ ions implantation in channelling directions, stopping power meas. from max. range 0-65078
 Fe-Cr (9 wt.%), oxidation studied using C¹⁸O₂ and D₂O tracers 0-71784
 Fe-Ni-Cr (44, 17 wt.%), nuclear microprobe methods for investigating oxidative corrosion 0-71787
 Hg_{1-x}Cd_xTe, implanted with Hg, Al, damage and lattice location study 0-103381
 InP, Zn diffused single-crystal, substitutional dopant and hole conc. meas. 0-75260
 Mo, D and ³He trapping and mutual replacement 0-59493
 NiO, single crystal, ¹⁸O⁺ ion implantation in channelling directions, expt. conditions and range profile obs. 0-65022
 Ni:O single crystal, ¹⁸O⁺ ions implantation in channelling directions, stopping power meas. from max. range 0-65078
 Si-SiO₂, two layer system, P⁺-ion penetration tails, expt. and computer anal. 0-75249
 SiC particles in EFG ribbon solar cells, EBIC and ion microprobe anal. 0-93838
 Zr, ion-implanted polycryst., thermal oxidation 0-71786
- ion microscopes**
see also field emission ion microscopes; ion microscopy
 scanning, atomic resolution capability 0-101878
- ion microscopy**
see also field emission ion microscopy; ion microscopes
 diffusible ion localization, comparison of chemically prepared and fast frozen freeze dried, unfixed liver sections 0-95189
 lithography, heavy ion, tool for object investigation and replication 0-90931
 microscopic equipment, methods, appls. and related topics, bibliography 0-73124
 radioactive ion microscopy 0-101884
- ion mobility**
see also electrolytic ion mobility; ionic conduction in solids
 acetone, macroscopic model for solvated ion dynamics, cation conductance calcs. 0-65261
 acetonitrile, macroscopic model for solvated ion dynamics, cation conductance calcs. 0-65261
 dielectric liquids, ion mobility meas. and breakdown process, optical methods 0-84692

ion mobility continued

free burning arc characteristic formulae 0-70068
high-current free burning arcs, approximate model 0-70069
liquid dielectric, Sumoto effect under transient conditions 0-97198
optoelectronics, appl. in measuring gas discharge phenomena 0-107007
pyridine, macroscopic model for solvated ion dynamics, cation conductance calcs. 0-65261
AgCl, ionic mobility, diffusion coeffs., defect mobility energies 0-65284
Ar⁺ ions, mobilities in He gas at 82K 0-75023
F⁻ ions in Kr and Xe; mobilities and diffusion coeffs. determ. 0-100048
H⁺ ion mobility in He, expt. 0-96337
³He, liq., ion mobility, temp. and freq. depend. 0-70493
³He, negative ion mobility, theory 0-107598
³He, superfluid A-phase, ion mobility tensor, ion-quasiparticle scatt. 0-59753
LiCl-RbCl, molten, Chemla effect, mol. dynamics simulation, self exchange vel. 0-79967
Na⁺, mobility and longit. diffusion coeffs. in Kr and Xe 0-106866
Ne⁺ ions, mobilities in He gas at 82K 0-75023
SF₆-N₂ mixtures, attachment coeffs. and ionic mobilities, 1.2-4 eV 0-96338

ion-molecule collisions

see also charge exchange; ion-molecule reactions
drift tube technique in ion-neutral collisions, cross sections determ. 0-63748
electronic and at. collisions, conf., Kyoto, Japan (Aug.-Sept. 1979) 0-57011
electronic and at. collisions, conference, Kyoto, Japan (Aug.-Sept. 1979) 0-62394
hydroxonium complexes, produced by collisional dissoc. method, mass spectrometric study, dissoc. energies determ. 0-95707
ion+polar molecule collision, low-energy, rot. state approach 0-74224
ion-dipole capture in noncentral field, variational and trajectory investigation 0-63739
negative ions, at. and mol. collisions electron detachment for energies near threshold 0-63797
polar mol. + ion, statistical and thermodynamic theory 0-99562
polar molecules, long range dipole interaction effect 0-102558
Ar⁸⁺+H₂ collisions, ionisation and excitation resulting from electron capture 0-78683
Br⁺+H₂(D₂)(O₂)(N₂)(CO)(CO₂)(methane), total electron detachment cross sections for energies around threshold 0-99550
C-H, A²Δ-X²Π, dissociative excitation, form. environment and parent mol. effects 0-78682
C₂H₃⁺+HF, interaction, struct. and stability, ab initio calcs. 0-58347
CO₂+H⁺(D⁺), vibr. excitation, isotope and time effects 0-63773
Cl⁺+H₂(D₂)(O₂)(N₂)(CO)(CO₂)(methane), total electron detachment cross sections for energies around threshold 0-99550
H⁺+D₂, collisional complex form. 0-58339
H⁺+H₂, rot. and vibr. excitation, energy loss obs. 0-63773
H⁺+H₂, vibr. excitation, ab initio CI pot. energy surface calcs. 0-74228
H⁺+H₂, vibr.-rot excitation, ab initio CI pot. energy surface calcs. 0-74229
H⁺+H₂(CO₂), vibr. excitation, 10-30 meV 0-58358
H⁺+He(1s⁺), K-shell electron capture collision, static pot. effect 0-91660
H⁺+N₂, total ionis. cross section and stopping power for protons 0-69228
H₂+C⁺(N⁺)(O⁺), reactant ion electronic states, effect on charge transfer cross sections 0-63809
H₂+Li⁺, exponential gap relation, rot. inelasticity 0-78693
H₂+Xeⁿ⁺(Arⁿ⁺)(Feⁿ⁺), electron capture by heavy multicharged ions at low velocities total cross sections meas. 0-99548
H₂⁺+H₂→H₃⁺+H, state-selected ion-molecule reactions threshold electron-secondary ion coincidence technique obs. 0-85166
H₃⁺(D₃⁺)+H₂(D₂) collisions, slow ion production, charge transfer cross sections 0-106378
H₂O vapour ionised by He⁺ and He²⁺, secondary electron emission yield obs. 0-102562
He⁺+H₂(N₂)(O₂)(CO₂)(methane)(ethane)(propane), 0.7-2 MeV, charge-changing collisions, electron capture 0-58372
He⁺+N₂, collisional excitation processes, visible emission, cross-sections 0-99571
Kr⁺+molecule, ²P_{3/2}(²P_{1/2}) doublet ground state reactions at 300K 0-108702
Li⁺+CO₂, collisional excitation, quasiclassical trajectory calcs. 0-83467
N⁺+O₂, branching ratio kinetic energy depend. 0-97703
Ne⁺+D₂(H₂), energy-loss scaling in 0.5-3.5 keV 0-63768
O⁺+N₂(O₂), excited ion reactions, charge transfer coeffs. at thermal energy 0-95721
O₄⁺(O₃⁺)(O₆⁺)(O₂⁺+H₂O) 0-95707
O⁺+O₂(N₂), metastable ion reactions, rate consts. and ion mobility at 300K 0-95722
reactant ion electronic states, effect on charge transfer cross sections 0-63809
SF₆+Li⁺(H⁺), mode selective vibr. excitation 0-58351
UF₆⁻+Ar, UF₆⁻ internal excitation 0-106386
Xe⁺+molecules, ²P_{3/2}(²P_{1/2}) doublet ground state reactions at 300K 0-108702

ion-molecule reactions

association density of quantum states and temp. depend. of rate coeff. 0-101015
association rate calc. for ion-molecule reaction 0-81282
atmospheric ion chemistry 0-61885
benzene cation+benzene, trapped ion mass spectra 0-89470
butene, isomers, ion-mol. reactions, photoionisation mass spectra 0-81298
2-butene ion, fragmentation, angular momentum in ion-mol. react., RRKM calc. 0-66773
clusters, small, formation, struct. and props. 0-58437
collision system, pot. curves at low collision energies, beam studies 0-61088
electric field effect on reactions in dilute gases and solutions 0-81315
ethyl cation+alkane reaction, temp. and kinetic energy relative rate consts. determ. 0-81299
fast nucleus+molecule, atom capture, quantum calcs. 0-71911
1-5hexadiyne ion+neutral 1,5-hexadiyne, trapped-ion mass spectrometry 0-97694
interstellar molecules synthesis, laboratory studies of ion-atom reactions 0-67812
ion kinetics in high-pressure laser plasmas 0-64002

ion-molecule reactions continued

ion-dipole capture in noncentral field, variational and trajectory investigation 0-63739
low energy, dipole interaction influence 0-89475
methyl cation+NH₃, reaction kinetics, 0.04-1 eV (French) 0-66768
methyl ion+H₂O(He) ternary association reaction in energy range 0.04-0.1 eV 0-71896
phenyl cation, struct., ion-molecule reactions studied by trapped ion mass spectroscopy 0-102586
polar molecules, long range dipole interaction effect 0-102558
propynyl cation+propyne, reactant structure effects 0-89469
tetra-n-butylammonium halides in benzene, chloroform, CCl₄, far IR spectra, ion-ion, ion-mol. interactions 0-60562
weakly ionised gas non-ideal behaviour, virial eqn. of state and fugacity coeffs. 0-79424
Ba⁺+D₂→D+BaD⁺, sequential impulse model, prod. bond dissoc. energy and cross section 0-81295
C+O⁺ ion-molecule reaction, 15 eV energy O⁺ production system 0-84817
CD₄⁺+H₂(HD)(D₂), isotopic exchange, interstellar implications 0-61087
CH₃⁺+H₂(HD)(D₂), isotopic exchange, interstellar implications 0-61087
CO⁺+¹³C⁺(HCO⁺), isotopic exchange, interstellar implications 0-61087
CO⁺+D₂, state selected reaction cross-sections, coincidence technique obs. 0-66797
CO₂+N₂+He, glow discharge positive ion species identification (Russian) 0-84014
CO₂⁺+ethylene, rate coeffs. and product distribution determ. 0-97693
CO₂CO₂⁺+ethylene, rate coeffs. and product distribution determ., dissoc. energy and heat of form. 0-97693
Cl⁺+HBr(HI)→HCl+Br⁺(I⁺), vibr. product state distrib., IR chemiluminesc. obs. 0-81309
Cl⁺+molecule, reactions at room temp. 0-93749
D₃O⁺(D₂O)_n+H₂O(NH₃), binary reactions, rate coeffs. and product ion distributions determ. 0-81305
H⁺+methane→H₃⁺+methyl radical, quantum 0-71911
H₃⁺+D₂→H₂⁺+H, product angular and vel. vector distributions meas. by crossed beam expt. 0-101012
H₂⁺+H₂, state selected reaction cross sections, coincidence technique obs. 0-66797
H₂⁺+H₂→H₃⁺+H, state-selected ion-molecule reactions threshold electron-secondary ion coincidence technique obs. 0-85166
H₂⁺+methanol, dissoc. charge transfer reaction studied at rel. translational energies from 600 eV to 5000 eV 0-104432
H₂O⁺+NO₂(O₂)(NO)(CO₂)(H₂)(ethylene)(methane), rate constants determ. as function of relative kinetic energy 0-81292
H₂O⁺(H₂O)_n+D₂O(NH₃), binary reactions, rate coeffs. and product ion distributions determ. 0-81305
He⁺+H₂(D₂), dissociative charge transfer, 78-330K 0-61079
He⁺+methanol, dissoc. charge transfer reaction studied at rel. translational energies from 600 eV to 5000 eV 0-104432
Kr⁺+molecule, ²P_{3/2}(²P_{1/2}) doublet ground state reactions at 300K 0-108702
Kr²⁺+H₂(N₂)(O₂)(CO)(CO₂)(methane), charge transfer reactions, rate coeffs. and product-ion distributions meas. 0-104431
N⁺+O₂, branching ratio kinetic energy depend. 0-97703
Ne²⁺+H₂(N₂)(O₂)(CO)(CO₂)(methane), charge transfer reactions, rate coeffs. and product-ion distributions meas. 0-104431
Ne⁺+atom (molecule), bimolecular and termolecular reaction rate coeffs. 0-81308
Ni⁺+H₂(HD)(D₂), endothermic reactions, investig. 0-97692
O⁺+O₂→O₃⁺+O, cross section kinetic energy depend., rate consts. meas. and Monte Carlo calcs. 0-78701
O²⁺+H in planetary nebula NGC 7662, effects on emission-line spectrum 0-62233
O⁺(²D)+N₂, thermal rate coeff., products and branching ratios in ionosphere 0-82117
O⁺(²D)+N₂, charge exchange, rate coeff. temp. depend. 0-77179
O⁺(⁴S)+N₂(X²Σ_g⁺)→NO⁺(X¹Σ⁺)+N(⁴S), MCSCF potential energy surface for collinear ⁴Σ pathway 0-63540
O⁺+N₂, metastable ion reactions, rate consts. and ion mobility at 300K 0-95722
S interstellar molecule formation, ion-molecule schemes inefficient 0-101632
U⁺+O₂(CO)(CO₂)(COS)(CS₂)(D₂O), reaction cross-sections, ion beam apparatus study 0-97691
UO⁺+O₂(CO)(CO₂)(COS)(CS₂)(D₂O), reaction cross-sections, ion beam apparatus study 0-97691
Xe⁺+molecules, ²P_{3/2}(²P_{1/2}) doublet ground state reactions at 300K 0-108702

ion optics

see also ion beams; ion microscopes; mass spectrometers
in air, ion trajectories due to electric field, calc. (Slovenian) 0-78760
charged particle beam-surface impact at glancing angles, reflection (Russian) 0-108316
cylindrical capacitor with oblique ends, ion optical coefficients determ., first-order focusing 0-63912
cylindrical radiofrequency mass analyser, low resolution mass filter 0-73519
ion beams, intense, production and postaccel. in magnetically insulated gaps 0-74041
ion optical props., aberration, crossed toroidal elec., mag. fields as mass spectrometer (Chinese) 0-82843
ISX-B neutral beam injector expt. on prototype beam line 0-74039
pulsed ion beam incident on mag. barrier, virtual anode form. 0-103131
quadrupole doublet, optical props., rot. of elements, effects 0-74292
second-generation ion microanalyser description and performance (French) 0-101055
second-order coeffs. for sector mag. analyzer, compact notation 0-63911
Ga ionisation mechanism on W field emitter 0-76156

ion plating

evaporation sources, gaseous media, and transport modes 0-80984
interface broadening during ion plating 0-65405
ionic nitriding thermochemical process, equipment, process details and advantages and prospects (French) 0-108641
AlN films, RF reactive ion-plating, struct. and morphology 0-104074
Fe-Cr-Mo and Fe-Cr-Mo-Si alloys, amorphous films, corrosion resist. and ion plating use 0-89423
Fe₃Ni₃Cr₁₄P₁₂B₆, Metglas amorphous films, corrosion resist. and ion plating use 0-89423

lunar rocks and minerals continued

- elemental abundances, implications from sputtering rates of minerals 0-61797
- glass globules, origin of shapes 0-62048
- highlands rocks, origin and comp. and effects of meteorite bombardment 0-109381
- impact microcraters, diameter to depth ratio dependence 0-94765
- ion beam analysis 0-62089
- Luna 24 basalts, irradi. history and $^{40}\text{Ar}/^{39}\text{Ar}$ age determ. 0-82245
- Luna 24 core, fragment mineralogy and petrology 0-82243
- Luna 24 core sample, solar flare exposure and thermolum. obs. 0-82246
- Luna 24 core sample L24125, optical excitation spectroscopy 0-82244
- Luna 24 core samples, separation and distrib. 0-82241
- Luna 24 soil samples, metal and phosphide phases 0-82242
- microcrater and accretionary grain populations, development from lunar surface and Apollo samples obs. 0-94732
- microcrater and accretionary grain populations, temporal development under meteoroid and solar wind bombardment 0-94731
- pyroxenes from planetary basalt, silicate mineralogy study 0-72802
- regolith interaction with lunar exosphere, Monte Carlo simulation methods 0-67588
- regolith microbreccias $^{15}\text{N}/^{14}\text{N}$ ratio indicating ancient solar wind composition 0-62046
- regolith radioactivity in Mare Crisium, orbital and laboratory estimates comparison 0-62045
- regolith reprocessing by cratering, erosion of material layer which loses charact. props. 0-62053
- regolith samples from Luna-24, element abundance determ., neutron activation obs. 0-67597
- regolith samples from Luna-24, X-ray diffr. and thermogravimetric obs. 0-67598
- soil, surface refl. characts. for radar, obs. from Luna spacecraft 0-72798
- soil column from Luna-24, grain size separates from particle track anal. 0-67599
- soil grains from Luna 24 drill core samples, surface exposure duration 0-67592
- soil samples from Luna 24, inert gas element and isotope composition 0-67593
- soil samples from Luna 24 and Apollo 16, natural radioactivity meas. 0-67595
- soil samples from Luna-24, N_2 abundance neutron activation obs. 0-67594
- soil samples from Luna-24, radioactivity and cosmic ray dose rate, thermolum. obs. 0-67596
- soils, Li abundance in Luna 24 soil samples 0-67590
- solar wind effects, in-situ meas. review 0-77556
- solar wind interactions with surface grains, O^{+} role 0-62050
- troilite, ^{34}S enrichment mechanism, appl. to lunar soil 0-77303
- ^3He content meas., method for solar flare cosmic ray proton flux determ. 0-98576
- K-rich globules in Luna 20 soil, SEM obs. 0-67591
- S contents, neutron capture gamma-ray spectroscopy 0-94728
- Ti rich basalt geology of Oceanus Procellarum, Flamsteed region 0-105183

lunar seismology

- thermal history, present state and tectonics, fission origin model 0-98582

lunar structure

- see also lunar rocks and minerals; Moon*
- blocky craters rel. to megaregolith 0-62051
- density structure, max. entropy inversion 0-67602
- force function, third and higher harmonics rel. to peculiarities of trans-latory-rotatory motion (*Russian*) 0-90349
- gravitational field model, harmonic anal. 0-72799
- highlands crust 0-109381
- mare domes, classification and origin 0-77305
- Mare Serenitatis multiringed basin, struct. and selenology 0-77304
- mascon basins: lava filling, tectonics and origin, review 0-98583
- moment of inertia and gravity field, study of Earth-Moon system 0-105184
- regolith reprocessing by cratering, erosion of material layer which loses charact. props. 0-62053
- relief and selenoid deform., harmonic anal. 0-72800
- solar wind ion bombardment, lunar surface modification 0-109325
- surface, Luna 16-24 3 cm radar obs. 0-77302
- surface features, absolute heights from photographs, computer processing technique (*Russian*) 0-109380
- thermal history, present state and tectonics, fission origin model 0-98582
- Fe and Ti surface distrib., orbital γ -ray spectra 0-94727

lung

- see also pneumodynamics*
- airway smooth muscle, contracted, hysteresis, dog expts. 0-81634
- airway transepithelial elec. pot. in vivo, species and regional diffs. 0-98208
- albumin flux, differential permeability of endothelial and epithelial barriers, sheep expts. 0-81553
- alveolar epithelium transport of albumin and sucrose, conc. diff. effect 0-67329
- alveolar macrophages, effect of X-irrad. in mice 0-98024
- arteries, small, pulmonary, elasticity in the cat 0-108942
- Bayer map evaluation in ^{57}Co -bleomycin scintigraphy (*Japanese*) 0-72319
- beta-emitting particles, fraction of energy absorbed, rat obs. 0-104641
- blood flow, spatial distrib. in dogs with PEEP ventilation 0-72191
- blood flow in isolated perfused dog lung lobes, effect of oedema 0-97975
- bronchogenic cancer, small cell, undifferentiated, role of radiation therapy in treatment 0-67226
- bronchogenic carcinoma among former U mine workers at Port Radium, Canada 0-98802
- bronchoscopic tumour localisation, small radiation detector probes, scintillation and semiconductor detectors 0-61676
- cancer, interstitial brachytherapy, 20 year experience 0-72302
- cancer rel. to Rn in dwellings 0-89870
- carcinogenic effect of localised fission fragment irradi., rat expts. 0-81656
- carcinoma, extended fractionation radiation therapy study 0-72305
- cardiovascular system, mathematical models and identification problems 0-89780
- cells, mouse, radiosensitivity, in vitro colony method obs. 0-101230
- circulation, density dilution method appl. to obs. of fast osmotic fluid shifts 0-104781
- death due to inhalation of β -emitters, probability estimation 0-89801
- degassing, evaluation of 2 methods 0-101294

lung continued

- density, Compton scatt. meas., multiple photon interactions 0-67146
- dolphin, lung collapse and intramuscular circulation during diving 0-81643
- dose distribution calculation method for bone- and lung-equivalent material, diagnostic X-rays (*German*) 0-61704
- dose in half body radiotherapy, determ. by computerised tomography 0-104763
- epithelial cells, type 2, proliferative response after X-rays and fission neutrons 0-108974
- extravascular lung thermal vol., reappraisal as meas. of pulmonary oedema 0-97867
- fibrosing disease diagnosis, histological section SEM and energy-dispersive X-ray microanalysis 0-72314
- finite element model for macroscopic deform. 0-108945
- interstitial fluid space compliance, estimation in isolated perfused rabbit lung 0-104605
- lesions evaluation, comparison of ^{67}Ga -citrate, ^{111}In -bleomycin and $^{99\text{m}}\text{Tc}$ -citrate 0-94327
- lymph transport increase without heart failure after coronary ligation in sheep 0-67122
- macroscopic deformation, finite element model 0-89781
- magnetic field meas., comparison between two methods 0-104712
- magnetopneumographic measurement, localised-fluid, freeze-dried lungs 0-104714
- magnetopneumography, analytic methods 0-104713
- mean caliper diameter of lung nuclei determ. 0-98189
- microvascular filtration, comparison of characts. in isolated and intact lungs, dog expts. 0-97974
- mucociliary transport mechs. 0-97956
- mucociliary tracheal clearance vel., radiological method for determ. 0-104727
- nuclear medical imaging, estimates of radiation absorbed doses from radionuclides 0-101269
- oedema diagnosis by a surgically noninvasive microwave technique 0-61659
- oedema of intact dogs, meas. by transthoracic γ -ray attenuation 0-81787
- parenchyma, math. model 0-108940
- parenchyma irradiated by inhaled $^{238}\text{PuO}_2$ particles, collagen localisation, Syrian hamsters 0-72252
- pathology, appl. of PIXE 0-61691
- percutaneous cricothyroid bronchography (*Dutch*) 0-85471
- peribronchial fluid pressure rel. to vascular and airway press. and interstitial oedema 0-97971
- radiographical visibility and sharpness of lung struct. at 90, 140 and 350 kV 0-98124
- shape during normal gravity and weightlessness, radiographic comparison, human 0-67260
- small cell carcinoma, low dose elective brain irradi. 0-67253
- sputum viscoelasticity, meas. using conventional dynamic and raised cosine pulse methods (*Japanese*) 0-67132
- SQUID fluxgate magnetometers, magnetopneumographic meas. 0-104711
- sublobar atelectasis and regional pulmonary blood flow, pig expts. 0-81633
- surfactant early release following lung irradi. of alveolar type II cells 0-94291
- tracheal ciliary beat, improved device for freq. recording 0-109070
- tracheal epithelium, dog, interdependence of Na^+ and Cl^- transport 0-61519
- tracheal muco-ciliary transport, theoretical and expt. study 0-97958
- transvascular fluid shifts in zone I lungs, rabbit obs. 0-101198
- tumour induction in RFM mice after localised X- or neutron irradi. 0-72260
- tumorigenesis from particulate sources of ^{147}Pm β -radiation 0-72247
- vascular interdependence in excised dog lobes 0-97976
- vascular permeability after microemboli, effect of platelet depletion, sheep obs. 0-97972
- vessel pressure-diameter behaviour, pigs, effect of parenchyma and length changes 0-67116
- volume measurement from supine portable chest radiographs 0-81703
- X-irradiation, single dose, sequence of histological changes, mouse obs. 0-98019
- CO_2 single breath diffusing capacity, theoretical anal. 0-67328
- $^{144}\text{CeO}_2$, effects of repeated inhalation exposure, mouse obs. 0-104676
- $^{144}\text{CeO}_2$, repeated inhalation exposure of mice, retention and dosimetry 0-109034
- Pu burdens in Austrian residents 0-109042
- Pu dose to lung and bone from contaminated soils, statistical uncertainties 0-109028

lutecium *see* lutetium**lutetium**

- see also nuclei with*
- Lu I, $5d6s6p$ -config., laser spectrosc. investig. 0-69096
- Lu III, $6s^2 5f_{12} 6p^2$ $^2\text{P}_{3/2}$ transition, relativistic oscillator strengths, influence of core polarisation 0-58132
- ^ALu , $A=175,176$, $5d6s^2 5f_{12} 6p^2$ $^2\text{F}_{3/2}$ transition, isotope shift and hyperfine struct. 0-83309

lutetium alloys

- Ag-Lu, dil., virtual bound states, transport props. obs. 0-70667
- Au-Lu, dil., virtual bound states, transport props. obs. 0-70667
- Lu-Ir, dil., elec. field gradient at ^{191}Ir , Mossbauer meas. 0-66090
- LuBe_{13} , lattice spacings and susceptibilities 0-65778
- LuFe_2 , ErFe_2 - LuFe_2 (10, 90 wt.%), mag. props., 80-1300K (*Russian*) 0-75750
- LuFe_2 , ferromag., magnetisation density, neutron diffr. study 0-60217
- LuFe_2 , mag. props. changes upon H_2 absorpt. 0-71270
- Lu_2Ir_3 , cryst. struct. 0-96473
- $\text{Pr}_2\text{Lu}_{10}\text{Ag}_{50}$, amorphous, mag. props. 0-60182
- Th-Lu (1 at.%), Heisenberg exchange, residual resist. meas. 0-75558

lutetium compounds

- see also lutetium alloys*
- diphalocyanine, solid-state anion migration in anodic oxidation 0-60994
- $(\text{EuLu}_3(\text{FeAl})_2\text{O}_{12})_x$, film epitaxial growth on $\text{Gd}_3\text{GaO}_{12}$ substrate, mag. props. 0-65402
- $\text{KLu}(\text{WO}_4)_2\text{Er}^{3+}$, room temp. stimulated emission obs. 0-106527
- LuAG , electrostatic model of cryst. field 0-59945
- $\text{Lu}_3\text{Al}_2\text{O}_4\text{Ho}^{3+}$, stimulated emission at low temps. 0-106526
- $\text{LuBO}_3\text{Fe}^{3+}$, ESR spectra, lattice parameters 0-93170
- LuBiTe_3 , prep., elec. props., and crystallographic date 0-59981
- $\text{LuCrO}_3\text{Er}^{3+}$, doping effect on ^{53}Cr NMR in domain walls 0-71219

lutetium compounds continued

- Lu₂Ir₂O₇, pyrochlore, sp. ht. below 20K, Debye temp. 0-65241
- LuOs₂B₂, supercond. and mag. props. 0-97028
- LuPO₄Gd³⁺, zircon struct. EPR investig., rel. to radiation resistance 0-97138
- LuPO₄Pb³⁺, EPR, hyperfine interactions 0-108050
- LuRh₂B₄, magnetic and electrostatic props., NMR study 0-93195
- LuRhO₃, elec., mag. and photoelectrochemical props. 0-96925
- Lu₂Si₂O₇Eu₂, synthesis and spectroscopic study 0-84846
- Lu₂Sn₂Mo₂S₃, supercond. props. 0-97023
- Lu₂(WO₄)₃Cr(Eu), and undoped crystals, luminesc. obs. 0-89047
- LuYScO₄Er³⁺(Tm³⁺)(Ho³⁺), thermolum. meas. 0-97354
- (SmLu)₃(FeAl)₂O₁₂, film epitaxial growth on Gd₃Ga₂O₁₂ substrate, mag. props. lattice mismatch 0-65402
- Tm_{1-x}Lu_xVO₄, Jahn-Teller system, thermodynamic properties, internal stress effects 0-59679
- (YLuSmCa)₃(FeGe)₂O₁₂ garnet film, bubble domain expansion, fuzzy wall struct. 0-71128
- (YLuSmCa)₃(GeFe)₂O₁₂ garnet films, bubble expansion saturation vel., sampling optical photography 0-75820

Luxemburg effect see ionospheric electromagnetic wave propagation

Lyapunov methods

- asymptotic stability of unsteady inviscid stratified flows 0-83832
- characteristic exponents and stochasticity 0-59177
- characteristic numbers and Kolmogorov entropy, stochasticity of dynamical systems 0-59178
- mechanical systems, follower load type, time invariant functionals 0-77609
- multidimensional systems oscillations of mechanical systems that do not become linear when the parameter vanishes 0-68032
- nonequilibrium steady states, irreversible processes, Lyapunov functions 0-95049
- one dimensional distributed parameter system parameter and state estimation, heat conduction experimental result (Japanese) 0-83727
- stability of constant Laplace solutions of the unrestricted three-body problem 0-68030
- three rigid bodies problem, particular solns. for translational motion (Russian) 0-61999

CUMULATIVE INDEXES

Card index of the entire PA 1980-1981, 1982-1983, 1984-1985, 1986-1987, 1988-1989, 1990-1991, 1992-1993, 1994-1995, 1996-1997, 1998-1999, 2000-2001, 2002-2003, 2004-2005, 2006-2007, 2008-2009, 2010-2011, 2012-2013, 2014-2015, 2016-2017, 2018-2019, 2020-2021, 2022-2023, 2024-2025, 2026-2027, 2028-2029, 2030-2031, 2032-2033, 2034-2035, 2036-2037, 2038-2039, 2040-2041, 2042-2043, 2044-2045, 2046-2047, 2048-2049, 2050-2051, 2052-2053, 2054-2055, 2056-2057, 2058-2059, 2060-2061, 2062-2063, 2064-2065, 2066-2067, 2068-2069, 2070-2071, 2072-2073, 2074-2075, 2076-2077, 2078-2079, 2080-2081, 2082-2083, 2084-2085, 2086-2087, 2088-2089, 2090-2091, 2092-2093, 2094-2095, 2096-2097, 2098-2099, 2100-2101, 2102-2103, 2104-2105, 2106-2107, 2108-2109, 2110-2111, 2112-2113, 2114-2115, 2116-2117, 2118-2119, 2120-2121, 2122-2123, 2124-2125, 2126-2127, 2128-2129, 2130-2131, 2132-2133, 2134-2135, 2136-2137, 2138-2139, 2140-2141, 2142-2143, 2144-2145, 2146-2147, 2148-2149, 2150-2151, 2152-2153, 2154-2155, 2156-2157, 2158-2159, 2160-2161, 2162-2163, 2164-2165, 2166-2167, 2168-2169, 2170-2171, 2172-2173, 2174-2175, 2176-2177, 2178-2179, 2180-2181, 2182-2183, 2184-2185, 2186-2187, 2188-2189, 2190-2191, 2192-2193, 2194-2195, 2196-2197, 2198-2199, 2200-2201, 2202-2203, 2204-2205, 2206-2207, 2208-2209, 2210-2211, 2212-2213, 2214-2215, 2216-2217, 2218-2219, 2220-2221, 2222-2223, 2224-2225, 2226-2227, 2228-2229, 2230-2231, 2232-2233, 2234-2235, 2236-2237, 2238-2239, 2240-2241, 2242-2243, 2244-2245, 2246-2247, 2248-2249, 2250-2251, 2252-2253, 2254-2255, 2256-2257, 2258-2259, 2260-2261, 2262-2263, 2264-2265, 2266-2267, 2268-2269, 2270-2271, 2272-2273, 2274-2275, 2276-2277, 2278-2279, 2280-2281, 2282-2283, 2284-2285, 2286-2287, 2288-2289, 2290-2291, 2292-2293, 2294-2295, 2296-2297, 2298-2299, 2300-2301, 2302-2303, 2304-2305, 2306-2307, 2308-2309, 2310-2311, 2312-2313, 2314-2315, 2316-2317, 2318-2319, 2320-2321, 2322-2323, 2324-2325, 2326-2327, 2328-2329, 2330-2331, 2332-2333, 2334-2335, 2336-2337, 2338-2339, 2340-2341, 2342-2343, 2344-2345, 2346-2347, 2348-2349, 2350-2351, 2352-2353, 2354-2355, 2356-2357, 2358-2359, 2360-2361, 2362-2363, 2364-2365, 2366-2367, 2368-2369, 2370-2371, 2372-2373, 2374-2375, 2376-2377, 2378-2379, 2380-2381, 2382-2383, 2384-2385, 2386-2387, 2388-2389, 2390-2391, 2392-2393, 2394-2395, 2396-2397, 2398-2399, 2400-2401, 2402-2403, 2404-2405, 2406-2407, 2408-2409, 2410-2411, 2412-2413, 2414-2415, 2416-2417, 2418-2419, 2420-2421, 2422-2423, 2424-2425, 2426-2427, 2428-2429, 2430-2431, 2432-2433, 2434-2435, 2436-2437, 2438-2439, 2440-2441, 2442-2443, 2444-2445, 2446-2447, 2448-2449, 2450-2451, 2452-2453, 2454-2455, 2456-2457, 2458-2459, 2460-2461, 2462-2463, 2464-2465, 2466-2467, 2468-2469, 2470-2471, 2472-2473, 2474-2475, 2476-2477, 2478-2479, 2480-2481, 2482-2483, 2484-2485, 2486-2487, 2488-2489, 2490-2491, 2492-2493, 2494-2495, 2496-2497, 2498-2499, 2500-2501, 2502-2503, 2504-2505, 2506-2507, 2508-2509, 2510-2511, 2512-2513, 2514-2515, 2516-2517, 2518-2519, 2520-2521, 2522-2523, 2524-2525, 2526-2527, 2528-2529, 2530-2531, 2532-2533, 2534-2535, 2536-2537, 2538-2539, 2540-2541, 2542-2543, 2544-2545, 2546-2547, 2548-2549, 2550-2551, 2552-2553, 2554-2555, 2556-2557, 2558-2559, 2560-2561, 2562-2563, 2564-2565, 2566-2567, 2568-2569, 2570-2571, 2572-2573, 2574-2575, 2576-2577, 2578-2579, 2580-2581, 2582-2583, 2584-2585, 2586-2587, 2588-2589, 2590-2591, 2592-2593, 2594-2595, 2596-2597, 2598-2599, 2600-2601, 2602-2603, 2604-2605, 2606-2607, 2608-2609, 2610-2611, 2612-2613, 2614-2615, 2616-2617, 2618-2619, 2620-2621, 2622-2623, 2624-2625, 2626-2627, 2628-2629, 2630-2631, 2632-2633, 2634-2635, 2636-2637, 2638-2639, 2640-2641, 2642-2643, 2644-2645, 2646-2647, 2648-2649, 2650-2651, 2652-2653, 2654-2655, 2656-2657, 2658-2659, 2660-2661, 2662-2663, 2664-2665, 2666-2667, 2668-2669, 2670-2671, 2672-2673, 2674-2675, 2676-2677, 2678-2679, 2680-2681, 2682-2683, 2684-2685, 2686-2687, 2688-2689, 2690-2691, 2692-2693, 2694-2695, 2696-2697, 2698-2699, 2700-2701, 2702-2703, 2704-2705, 2706-2707, 2708-2709, 2710-2711, 2712-2713, 2714-2715, 2716-2717, 2718-2719, 2720-2721, 2722-2723, 2724-2725, 2726-2727, 2728-2729, 2730-2731, 2732-2733, 2734-2735, 2736-2737, 2738-2739, 2740-2741, 2742-2743, 2744-2745, 2746-2747, 2748-2749, 2750-2751, 2752-2753, 2754-2755, 2756-2757, 2758-2759, 2760-2761, 2762-2763, 2764-2765, 2766-2767, 2768-2769, 2770-2771, 2772-2773, 2774-2775, 2776-2777, 2778-2779, 2780-2781, 2782-2783, 2784-2785, 2786-2787, 2788-2789, 2790-2791, 2792-2793, 2794-2795, 2796-2797, 2798-2799, 2800-2801, 2802-2803, 2804-2805, 2806-2807, 2808-2809, 2810-2811, 2812-2813, 2814-2815, 2816-2817, 2818-2819, 2820-2821, 2822-2823, 2824-2825, 2826-2827, 2828-2829, 2830-2831, 2832-2833, 2834-2835, 2836-2837, 2838-2839, 2840-2841, 2842-2843, 2844-2845, 2846-2847, 2848-2849, 2850-2851, 2852-2853, 2854-2855, 2856-2857, 2858-2859, 2860-2861, 2862-2863, 2864-2865, 2866-2867, 2868-2869, 2870-2871, 2872-2873, 2874-2875, 2876-2877, 2878-2879, 2880-2881, 2882-2883, 2884-2885, 2886-2887, 2888-2889, 2890-2891, 2892-2893, 2894-2895, 2896-2897, 2898-2899, 2900-2901, 2902-2903, 2904-2905, 2906-2907, 2908-2909, 2910-2911, 2912-2913, 2914-2915, 2916-2917, 2918-2919, 2920-2921, 2922-2923, 2924-2925, 2926-2927, 2928-2929, 2930-2931, 2932-2933, 2934-2935, 2936-2937, 2938-2939, 2940-2941, 2942-2943, 2944-2945, 2946-2947, 2948-2949, 2950-2951, 2952-2953, 2954-2955, 2956-2957, 2958-2959, 2960-2961, 2962-2963, 2964-2965, 2966-2967, 2968-2969, 2970-2971, 2972-2973, 2974-2975, 2976-2977, 2978-2979, 2980-2981, 2982-2983, 2984-2985, 2986-2987, 2988-2989, 2990-2991, 2992-2993, 2994-2995, 2996-2997, 2998-2999, 3000-3001, 3002-3003, 3004-3005, 3006-3007, 3008-3009, 3010-3011, 3012-3013, 3014-3015, 3016-3017, 3018-3019, 3020-3021, 3022-3023, 3024-3025, 3026-3027, 3028-3029, 3030-3031, 3032-3033, 3034-3035, 3036-3037, 3038-3039, 3040-3041, 3042-3043, 3044-3045, 3046-3047, 3048-3049, 3050-3051, 3052-3053, 3054-3055, 3056-3057, 3058-3059, 3060-3061, 3062-3063, 3064-3065, 3066-3067, 3068-3069, 3070-3071, 3072-3073, 3074-3075, 3076-3077, 3078-3079, 3080-3081, 3082-3083, 3084-3085, 3086-3087, 3088-3089, 3090-3091, 3092-3093, 3094-3095, 3096-3097, 3098-3099, 3100-3101, 3102-3103, 3104-3105, 3106-3107, 3108-3109, 3110-3111, 3112-3113, 3114-3115, 3116-3117, 3118-3119, 3120-3121, 3122-3123, 3124-3125, 3126-3127, 3128-3129, 3130-3131, 3132-3133, 3134-3135, 3136-3137, 3138-3139, 3140-3141, 3142-3143, 3144-3145, 3146-3147, 3148-3149, 3150-3151, 3152-3153, 3154-3155, 3156-3157, 3158-3159, 3160-3161, 3162-3163, 3164-3165, 3166-3167, 3168-3169, 3170-3171, 3172-3173, 3174-3175, 3176-3177, 3178-3179, 3180-3181, 3182-3183, 3184-3185, 3186-3187, 3188-3189, 3190-3191, 3192-3193, 3194-3195, 3196-3197, 3198-3199, 3200-3201, 3202-3203, 3204-3205, 3206-3207, 3208-3209, 3210-3211, 3212-3213, 3214-3215, 3216-3217, 3218-3219, 3220-3221, 3222-3223, 3224-3225, 3226-3227, 3228-3229, 3230-3231, 3232-3233, 3234-3235, 3236-3237, 3238-3239, 3240-3241, 3242-3243, 3244-3245, 3246-3247, 3248-3249, 3250-3251, 3252-3253, 3254-3255, 3256-3257, 3258-3259, 3260-3261, 3262-3263, 3264-3265, 3266-3267, 3268-3269, 3270-3271, 3272-3273, 3274-3275, 3276-3277, 3278-3279, 3280-3281, 3282-3283, 3284-3285, 3286-3287, 3288-3289, 3290-3291, 3292-3293, 3294-3295, 3296-3297, 3298-3299, 3300-3301, 3302-3303, 3304-3305, 3306-3307, 3308-3309, 3310-3311, 3312-3313, 3314-3315, 3316-3317, 3318-3319, 3320-3321, 3322-3323, 3324-3325, 3326-3327, 3328-3329, 3330-3331, 3332-3333, 3334-3335, 3336-3337, 3338-3339, 3340-3341, 3342-3343, 3344-3345, 3346-3347, 3348-3349, 3350-3351, 3352-3353, 3354-3355, 3356-3357, 3358-3359, 3360-3361, 3362-3363, 3364-3365, 3366-3367, 3368-3369, 3370-3371, 3372-3373, 3374-3375, 3376-3377, 3378-3379, 3380-3381, 3382-3383, 3384-3385, 3386-3387, 3388-3389, 3390-3391, 3392-3393, 3394-3395, 3396-3397, 3398-3399, 3400-3401, 3402-3403, 3404-3405, 3406-3407, 3408-3409, 3410-3411, 3412-3413, 3414-3415, 3416-3417, 3418-3419, 3420-3421, 3422-3423, 3424-3425, 3426-3427, 3428-3429, 3430-3431, 3432-3433, 3434-3435, 3436-3437, 3438-3439, 3440-3441, 3442-3443, 3444-3445, 3446-3447, 3448-3449, 3450-3451, 3452-3453, 3454-3455, 3456-3457, 3458-3459, 3460-3461, 3462-3463, 3464-3465, 3466-3467, 3468-3469, 3470-3471, 3472-3473, 3474-3475, 3476-3477, 3478-3479, 3480-3481, 3482-3483, 3484-3485, 3486-3487, 3488-3489, 3490-3491, 3492-3493, 3494-3495, 3496-3497, 3498-3499, 3500-3501, 3502-3503, 3504-3505, 3506-3507, 3508-3509, 3510-3511, 3512-3513, 3514-3515, 3516-3517, 3518-3519, 3520-3521, 3522-3523, 3524-3525, 3526-3527, 3528-3529, 3530-3531, 3532-3533, 3534-3535, 3536-3537, 3538-3539, 3540-3541, 3542-3543, 3544-3545, 3546-3547, 3548-3549, 3550-3551, 3552-3553, 3554-3555, 3556-3557, 3558-3559, 3560-3561, 3562-3563, 3564-3565, 3566-3567, 3568-3569, 3570-3571, 3572-3573, 3574-3575, 3576-3577, 3578-3579, 3580-3581, 3582-3583, 3584-3585, 3586-3587, 3588-3589, 3590-3591, 3592-3593, 3594-3595, 3596-3597, 3598-3599, 3600-3601, 3602-3603, 3604-3605, 3606-3607, 3608-3609, 3610-3611, 3612-3613, 3614-3615, 3616-3617, 3618-3619, 3620-3621, 3622-3623, 3624-3625, 3626-3627, 3628-3629, 3630-3631, 3632-3633, 3634-3635, 3636-3637, 3638-3639, 3640-3641, 3642-3643, 3644-3645, 3646-3647, 3648-3649, 3650-3651, 3652-3653, 3654-3655, 3656-3657, 3658-3659, 3660-3661, 3662-3663, 3664-3665, 3666-3667, 3668-3669, 3670-3671, 3672-3673, 3674-3675, 3676-3677, 3678-3679, 3680-3681, 3682-3683, 3684-3685, 3686-3687, 3688-3689, 3690-3691, 3692-3693, 3694-3695, 3696-3697, 3698-3699, 3700-3701, 3702-3703, 3704-3705, 3706-3707, 3708-3709, 3710-3711, 3712-3713, 3714-3715, 3716-3717, 3718-3719, 3720-3721, 3722-3723, 3724-3725, 3726-3727, 3728-3729, 3730-3731, 3732-3733, 3734-3735, 3736-3737, 3738-3739, 3740-3741, 3742-3743, 3744-3745, 3746-3747, 3748-3749, 3750-3751, 3752-3753, 3754-3755, 3756-3757, 3758-3759, 3760-3761, 3762-3763, 3764-3765, 3766-3767, 3768-3769, 3770-3771, 3772-3773, 3774-3775, 3776-3777, 3778-3779, 3780-3781, 3782-3783, 3784-3785, 3786-3787, 3788-3789, 3790-3791, 3792-3793, 3794-3795, 3796-3797, 3798-3799, 3800-3801, 3802-3803, 3804-3805, 3806-3807, 3808-3809, 3810-3811, 3812-3813, 3814-3815, 3816-3817, 3818-3819, 3820-3821, 3822-3823, 3824-3825, 3826-3827, 3828-3829, 3830-3831, 3832-3833, 3834-3835, 3836-3837, 3838-3839, 3840-3841, 3842-3843, 3844-3845, 3846-3847, 3848-3849, 3850-3851, 3852-3853, 3854-3855, 3856-3857, 3858-3859, 3860-3861, 3862-3863, 3864-3865, 3866-3867, 3868-3869, 3870-3871, 3872-3873, 3874-3875, 3876-3877, 3878-3879, 3880-3881, 3882-3883, 3884-3885, 3886-3887, 3888-3889, 3890-3891, 3892-3893, 3894-3895, 3896-3897, 3898-3899, 3900-3901, 3902-3903, 3904-3905, 3906-3907, 3908-3909, 3910-3911, 3912-3913, 3914-3915, 3916-3917, 3918-3919, 3920-3921, 3922-3923, 3924-3925, 3926-3927, 3928-3929, 3930-3931, 3932-3933, 3934-3935, 3936-3937, 3938-3939, 3940-3941, 3942-3943, 3944-3945, 3946-3947, 3948-3949, 3950-3951, 3952-3953, 3954-3955, 3956-3957, 3958-3959, 3960-3961, 3962-3963, 3964-3965, 3966-3967, 3968-3969, 3970-3971, 3972-3973, 3974-3975, 3976-3977, 3978-3979, 3980-3981, 3982-3983, 3984-3985, 3986-3987, 3988-3989, 3990-3991, 3992-3993, 3994-3995, 3996-3997, 3998-3999, 4000

ABSTRACTS AND CURRENT PAPERS JOURNALS

SUBSCRIPTION PRICES

	USA \$	UK £	ROW £	JAPAN ¥
PHYSICS ABSTRACTS				
Paper or Microfiche.....	1105	440	565	452,000
Paper and Microfiche.....	1658	660	848	678,000
2nd and subsequent copies.....	480	250	250	200,000
ELECTRICAL & ELECTRONICS ABSTRACTS				
Paper or Microfiche.....	820	375	450	360,000
Paper and Microfiche.....	1230	562	675	540,000
COMPUTER & CONTROL ABSTRACTS				
Paper or Microfiche.....	495	230	290	232,000
Paper and Microfiche.....	742	345	435	348,000
PA/EEA/CCA COMBINED SUBSCRIPTION				
Paper or Microfiche.....	2150	915	1165	932,000
Paper and Microfiche.....	3225	1372	1748	1,398,000
EEA/CCA COMBINED SUBSCRIPTION				
Paper or Microfiche.....	1200	535	675	540,000
Paper and Microfiche.....	1800	802	1012	810,000
CURRENT PAPERS IN PHYSICS				
Member rate.....	60	30	30	—
Non-Member rate.....	140	80	80	64,000
CURRENT PAPERS IN ELECTRICAL & ELECTRONICS ENGINEERING				
Member rate.....	55	30	30	—
Non-Member rate.....	118	65	65	52,000
CURRENT PAPERS ON COMPUTERS & CONTROL				
Member rate.....	55	30	30	—
Non-Member rate.....	118	65	65	52,000
KEY ABSTRACTS				
Member rate*.....	30	15	15	—
Non-Member rate.....	65	30	30	24,000
KEY ABSTRACTS EMI/PMI COMBINED.....	—	50	50	40,000

*The Key Abstracts Member rate is available to Members of the IEE and IEEE only.

CUMULATIVE INDEXES

Cumulative indexes are available for *Physics Abstracts*, *Electrical & Electronics Abstracts* and *Computer & Control Abstracts*, for both

authors and subjects. These cumulations generally cover a period of four years, with the exception of *Computer & Control Abstracts*

where the initial volume covered the period 1966-68. The table below shows the prices and periods for the two types of cumulative index.

	PHYSICS ABSTRACTS		ELECTRICAL & ELECTRONICS ABSTRACTS		COMPUTER & CONTROL ABSTRACTS	
	Subject	Author	Subject	Author	Subject	Author
	£	£	£	£	£	£
1955-59	20	20	15	20	—	—
1960-64	40	17	20	12	—	—
1965-68	63	25	35	20	—	—
1969-72	—	—	72	64	48	30
1973-76	600	300	250	150	150	75
1966-68	—	—	—	—	15	

For US\$ and Yen prices please contact the appropriate address below

ORDERING PROCEDURE

THE AMERICAS

North (including Canada), Central and South

All orders from the above areas, and orders from members of Institute of Electrical and Electronics Engineers Inc. anywhere in the world, should be sent to Fulfillment Manager, Institute of Electrical & Electronics Engineers Inc., 445 Hoes Lane, Piscataway, N.J. 08854, USA.

日本のお客様にご案内申し上げます

日本国内に於ける INSPEC の購入価格はすべて円建てとなっております。また刊行物はすべて航空便で配達されます。INSPEC 刊行物の価格その他についてのお問い合わせは最寄の洋書取扱専門店または輸入総代理店（ユー・エス・エシヤテック カンパニー 〒105 東京都港区新橋 1-13-12、TEL 03 (502) 6471 までご連絡ください。

REMAINDER OF THE WORLD

All remaining subscriptions should be sent to INSPEC Marketing Department, P.O. Box 26, Hitchin, Herts SG5 7RS, England. Telephone Hitchin 53331, Telex 825962, Telegrams IEE G.

OTHER INSPEC SERVICES

SDI

(Selective Dissemination of Information.) This is a service individually tailored to the requirements and interests of the engineer or research worker. Details of information relevant to the interest profile of the individual subscriber are selected from the data being processed for the INSPEC database. Information is dispatched weekly on 150 mm × 100 mm (6" × 4") cards.

TOPICS

This is an SDI service based on standard profiles. There are over 70 subjects covering high-activity areas of research and development. This is an inexpensive card service designed to alert engineers and researchers to the availability of literature within their subject area.

MAGNETIC TAPES

Tapes containing all the information included in the INSPEC publications are issued twice monthly. They enable the larger research and development organisations to produce their own internal information and current-awareness services.

articles from
literature you
do not hold ?

BOSTON SPA

Can help you

Over 43000 current periodicals available*

Most of the papers listed in INSPEC services
are held at the British Library Lending Division (BLLD)

REQUESTS DEALT WITH IN 48 HOURS*

Write for further information to:

The Director General
The British Library Lending Division
Boston Spa
Wetherby
West Yorkshire LS23 7BQ
England

*Photocopies of papers are available for research or private study to organisations in the UK registered as users of the BLLD. Where individuals in the UK do not belong to an organisation registered with the BLLD they should apply via their public library. In case of difficulty please contact the BLLD.

All requests from outside the UK should be made via the BLLD Overseas Photocopy Service.